ACTA CHEMICA SCANDINAVICA 14 (1960) 1—8

Characterization of Three Different Hog Intestinal Maltases

ARNE DAHLQVIST

Department of Physiological Chemistry, University of Lund, Lund, Sweden

Hog intestinal maltase activity was recently separated into three fractions (maltase I—III) with different heat stability and different K_s values. The characterization of these maltases with respect to their optimum pH, transglycosylase activity, and specificity, is now reported.

Generally, *maltase I* showed properties markedly different from those of *maltases II and III*. The two last maltases, on the other side, had very similar properties except their different sensibility to heat.

All three maltases were found to be α-D-*glucopyranosidases* (glucosido-maltases). *Maltase I* hydrolyzed *sucrose* with a rate 1.7 times the rate for maltose hydrolysis. However, it did not hydrolyze *iso*maltose or phenyl α-D-glucopyranoside. *Maltases II and III* hydrolyzed *isomaltose* and *phenyl α-D-glucopyranoside* but not sucrose. All three maltases hydrolyzed *maltosucrose* (α-D-glucopyranosyl(1→4)α-D-glucopyranosyl(1→2) β-D-fructofuranoside).

Hog intestinal maltase activity was recently separated into three fractions by the method of heat inactivation combined with ion exchange chromatography [1,2]. One of these fractions (maltase III) was not inactivated even when heated in 0.01 M phosphate buffer pH 6.0 at 70°C for 1 h. The other two fractions were more heat-labile, and were rapidly inactivated at 60°C. However, a small difference in heat stability was found also between these two fractions (maltases I and II), which was utilized for the purification of the maltase II fraction [2].

The three maltase fractions are all derived from the microsomes of the intestinal mucosa [1]. Each one of them contributes to about one third of the total maltase activity of the mucosa [1].

The three hog intestinal maltases were found to have different K_s values, which supports the theory that they are different enzymes [2]. In the present paper the optimum pH, the transglycosylase property, and the specificity of the three different maltases are recorded, and their characterization as three different enzymes is discussed.

MATERIALS AND METHODS

Hog intestinal maltases

Maltase preparations were the same fractions from mutual displacement chromatography as were used earlier for K_s determinations [2]. In the text these fractions are referred to as *maltase I, II,* and *III* [1,2]. The specific maltase activity (units of maltase per mg of protein [2]) of the preparations used were 175 for maltase I, 100 for maltase II, and 200 for maltase III.

Substrates

Maltose (monohydrate), cryst., was obtained from Merck A. G. (Germany). For maltase determinations the commercial preparation was used without further purification. In paper chromatography, however, it formed some spots which moved more slowly than maltose. For K_s determinations and for transglycosylase activity studies, therefore, maltose was used which had been purified upon carbon-celite columns [3], and which only formed one spot in paper chromatography. *Isomaltose* (6(α-D-glucopyranosyl) D-glucose) was prepared by enzymatic hydrolysis of dextran, as will be described elsewhere [4]. The hydrolysis of maltose and *iso*maltose was determined with acid copper reagent as described earlier for maltose [2].

Sucrose, cryst., was obtained from J. T. Baker Co. and *αα-trehalose (dihydrate)*, chemically pure, from Pfanstiehl Inc. The hydrolysis of these sugars was determined with the 3,5-dinitrosalicylic acid method [3].

Phenyl-α-D-glucopyranoside. The tetraacetate was obtained by condensation of α-pentaacetylglucose (obtained from Nutritional Biochemicals Corp.) and phenol in the presence of $ZnCl_2$ [5,6]. It had $[\alpha]_D^{20}$ +168.0° (7.2 % in $CHCl_3$) and m. p. 113—114°C. Deacetylation was performed as described elsewhere [7], and the product was crystallized from water. Drying at 50°C *in vacuo* over P_2O_5 yielded anhydrous phenyl α-D-glucopyranoside with $[\alpha]_D^{20}$ +186.0° (3 % in water).

The hydrolysis of phenyl α-D-glucopyranoside was measured at 0.1388 M substrate concentration as in the case of the other substrates. The enzyme solution, therefore, was mixed with an equal volume of 0.2776 M phenyl α-D-glucopyranoside solution. Such a concentrated solution, however, crystallizes at room temperature. It was therefore heated in a boiling water-bath until it became clear, and was then placed in a test-tube in a water-bath at 37°C for 3—5 min before it was mixed with the enzyme solution. The amount of glucose produced was determined with the method of Somogyi and Nelson [8,9] after precipitation of the proteins with the Zn-Ba-reagents of Somogyi [10].

Maltosucrose (α-D-glucopyranosyl(1 → 4) α-D-glucopyranosyl(1→2) β-D-fructofuranoside) was prepared as described earlier [3]. The hydrolysis of this sugar, too, was measured with the method of Somogyi and Nelson.

The rate of hydrolysis of all substrates was measured at 37°C at 0.1388 M substrate concentration in the presence of 0.05 M maleate buffer pH 6.5. When the *initial rate of reaction* was measured, the degree of hydrolysis was not allowed to exceed 10 %. One unit of maltase activity during these conditions produces 1 mg of glucose (= 1 % of hydrolysis in 2 ml of reaction mixture) in 1 h. For comparison of the rate of hydrolysis of different substrates the number of molecules of the different substrates that were hydrolyzed per time unit, was calculated. For a trisaccharide, such as maltosucrose, either the number of glycosylic linkages hydrolyzed or the number of molecules totally hydrolyzed may be calculated [11].

Paper chromatography of sugars was performed as described earlier [3].

^{14}C-Labelled glucose was obtained from the Radiochemical Centre (England). The ^{14}C-labelled sugars were localized on paper chromatograms as described earlier [3].

RESULTS AND DISCUSSION

Optimum pH

The pH activity curves for the three different intestinal maltases are seen in Fig. 1. The optimum pH for the *maltase I* activity was 6.5 with a fairly

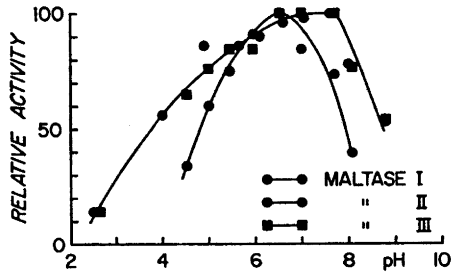

Fig. 1. Influence of pH on the activity of the three different maltases from hog intestinal mucosa. The reaction mixtures contained 5 units of maltase/ml. Buffers: 0.05 M citrate pH 2.5, 0.05 M acetate pH 4.0—5.0, 0.05 M maleate pH 5.5—6.5, 0.025 M veronal pH 7.0—9.0. The pH of the reaction mixtures was measured with a glass electrode.

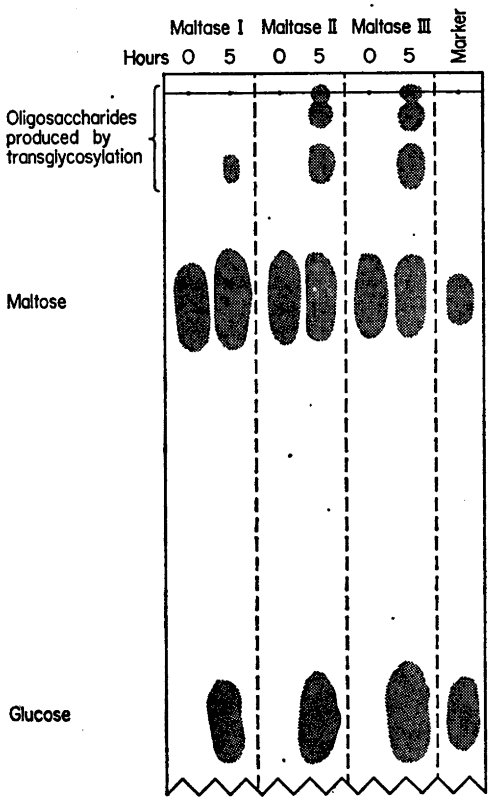

Fig. 2. Formation of oligosaccharides by transglycosylation by the three different hog intestinal maltases. The reaction mixture in all cases contained 50 units of maltase/ml 0.833 M maltose (= 30 % maltose monohydrate), 0.05 M maleate buffer pH 6.5, and a few drops of toluene in each tube. Of the reaction mixtures, 5 µl spots were applied to a paper chromatogram which was run for 60 h. Maltase I produced only one oligosaccharide spot, while maltases II and III produced at least three different oligosaccharide spots.

narrow peak. The shape of this curve coincides with that for the intestinal *invertase* activity [4], which it has not been possible to separate from the maltase I fraction [1,2]. *Maltases II and III* had broader pH activity curves, with optima at pH 6.5—7.5. No difference was found in the shape of the curves for the maltase II and III fractions.

Transglycosylase activity

All three fractions produced slower moving oligosaccharides in a concentrated maltose solution. With *maltase I* only one oligosaccharide spot was found on the paper chromatogram, but with *maltases II and III* a series of at least three different oligosaccharides was formed (Fig. 2).

The transglycosylase activity with ^{14}C-labelled glucose as receptor was also studied. All three maltases incorporated ^{14}C-labelled glucose into the maltose spot (Fig. 3). The rate for this reaction, however, compared with the rate for liberation of glucose, was greater with maltase II and III activities than with maltase I. With maltase I no detectable amount of ^{14}C-labelled glucose was incorporated into the oligosaccharide with slower chromatographic mobility than maltose, but with maltases II and III a great part of the ^{14}C-labelled glucose was incorporated into the oligosaccharides as well (Fig. 3).

The incorporation of ^{14}C-labelled glucose into maltose is *not* caused by the combination of two free glucose molecules. In a 1.65 M (= 30 %) * solution of glucose, under the corresponding experimental conditions, no detectable amount of maltose was formed in 5 h. (When the reaction time was extended to 23 h, however, a faint spot with the same chromatographic mobility as maltose was formed by maltases II and III, but not by maltase I. The reason for the difference is not known. Since the reaction mixture in all cases contained the same number of maltase units per ml, it should have been expected that the reverse reaction (the synthesis of maltose), too, would proceed with the same rate in all three cases. It is well known that the kinetics of the hydrolysis of maltose are such that detectable amounts of maltose are present at equilibrium [12].) In the experiment shown in Fig. 3, therefore, the incorporation of ^{14}C-labelled glucose into maltose (and other oligosaccharides) must be the result of a *transglycosylation*.

Maltases II and III seem to have a stronger transglycosylase activity in relation to their hydrolytic activity than maltase I, since a greater amount of ^{14}C-labelled glucose was incorporated into maltose by maltases II and III than by maltase I under the same experimental conditions. No difference in the transglycosylase activity of maltase II and that of maltase III could be detected.

Rate for the liberation of glucose in concentrated substrate solutions. The amount of glucose liberated (as measured with the acid copper reagent [2]) per time unit by *maltase I* increased with increasing substrate concentration up to more than 5 % (0.1388 M) maltose (monohydrate) (Table 1). With *maltase II and III*, however, the optimal substrate concentration was 1 % (0.0278 M),

* Per cent means gram of solute in 100 ml of solution.

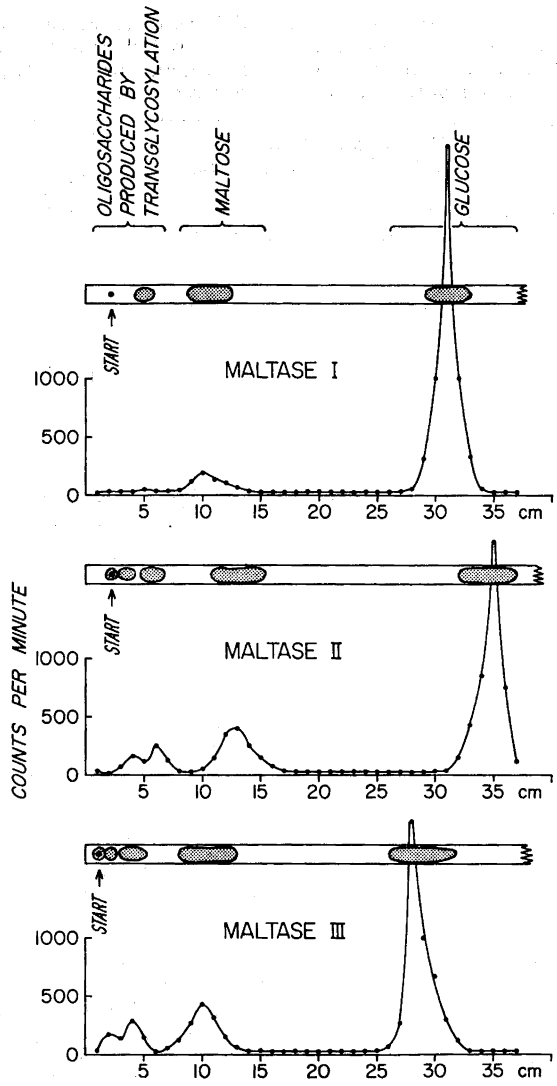

Fig. 3. Transglycosylation by the three different hog intestinal maltases with ^{14}C-glucose as receptor. The reaction mixture contained 50 units of maltase/ml, 0.833 M maltose, 1 mg of ^{14}C-labelled glucose (1 250 000 c.p.m.)/ml, 0.05 M maleate buffer pH 6.5, and one drop of toluene. After 5 h at 37°C the reaction was interrupted by boiling in a water-bath for 2 min, and 5 μl spots of the reaction mixtures were applied to paper chromatograms which were run for 2 days. Each spot contained 6 250 c.p.m. of ^{14}C-labelled sugars. Counting and chemical localization of the sugars were performed on the same paper strip [3]. With *maltase I* 500 c.p.m. (8 % of the total activity) was incorporated into the maltose spot and no detectable amount into the oligosaccharide spot. With *maltase II* 1 250 c.p.m. (20 %) was incorporated into the maltose and 650 c.p.m. (10.4 %) into the other oligosaccharides produced. With *maltase III* 1 250 c.p.m. (20 %) was incorporated into the maltose and 600 c.p.m. (9.6 %) into the other oligosaccharides.

Table 1. The rate of liberation of glucose by three different intestinal maltases in 1 % (0.0278 M) and 5 % (0.1388 M) maltose solutions. The reaction was performed at 37°C in the presence of 0.05 M maleate buffer pH 6.5. The amount of glucose produced was measured with the acid copper reagent.

	Mg of glucose in 1 h per 2 ml of react. mixt.		rate in 1 % maltose / rate in 5 % maltose
	1 % maltose (monohydrate)	5 % maltose (monohydrate)	
Maltase I	6.0	7.5	0.8
Maltase II	6.2	5.3	1.2
Maltase III	11.4	9.5	1.2

and at higher substrate concentration the amount of glucose liberated decreased (Table 1). This effect is possibly caused by the stronger transglycosylase activity of maltases II and III as compared with maltase I.

Specificity of hog intestinal maltases

Sucrose was hydrolyzed by *maltase I* with a rate that was 1.7 times the rate for the hydrolysis of maltose. The invertase and maltase activities of this fraction were not separable by ion exchange chromatography or by heat inactivation, performed in a series of buffers of different pH values [1]. There is strong evidence, therefore, that these two activities are caused by the same enzyme *. *Maltase II* and *maltase III*, on the other hand, did not hydrolyze sucrose. Under the experimental conditions used, a hydrolysis of sucrose with only 1/100 of the rate for maltose hydrolysis would have been detected.

αα-Trehalose (1-(α-D-glucopyranosyl) α-D-glucopyranoside) was *not* hydrolyzed by any of the three maltase fractions. A hydrolysis with only 1/100 of the rate for maltose hydrolysis would have been detected.

Isomaltose (6-(α-D-glucopyranosyl) D-glucose) was *not* hydrolyzed by *maltase I*. A hydrolysis with only 1/200 of the rate for maltose hydrolysis would have been detected. *Maltase II* hydrolyzed iso-maltose with 0.02 times and *maltase III* with 0.05 times the rate for maltose hydrolysis. When heated in the presence of 0.01 M phosphate buffer pH 6.0, the *iso*maltase activity of the maltase II preparation was destroyed below 60°C, while the *iso*maltase activity of the maltase III preparation was not inactivated below 70°C. The inactivation of the *iso*maltase activity of the two preparations ran parallel with that of the maltase activity. It seems probable, therefore, that the *iso*-maltase activity of these two preparations is caused by the same enzyme as the maltase activity.

* Experiments which will be reported in a later paper demonstrate that sucrose and maltose act as competitive inhibitors for each others with this enzyme fraction, which clearly shows that hog intestinal *invertase* is identical with *maltase I*.

Phenyl α-D-glucopyranoside was *not* hydrolyzed by *maltase I*. A hydrolysis with only 1/1 000 of the rate for maltose hydrolysis would have been detected. *Maltase II* hydrolyzed phenyl α-D-glucopyranoside with 0.03, and *maltase III* with 0.05 times the rate for maltose hydrolysis (calculated as the number of molecules hydrolyzed per time unit). As was the case with the *iso*maltase activity of the maltase II and III fractions, phenyl α-D-glucopyranosidase activity had the same sensitivity to heat as had the maltase activity.

Maltosucrose (α-D-glucopyranosyl(1→4)α-D-glucopyranosyl(1→2)β-D-fructofuranoside) was hydrolyzed by all three maltase fractions. By *maltase I* it was hydrolyzed *completely* into glucose and fructose. Calculated as the number of glycosylic linkages hydrolyzed per time unit, the rate for hydrolysis of maltosucrose was 0.8 times the rate for maltose hydrolysis. With the aid of paper chromatography, sucrose was found to be the intermediary product during the hydrolysis of maltosucrose. The trisaccharide is therefore first hydrolyzed into one molecule of glucose and one molecule of sucrose, and then the sucrose molecule is hydrolyzed into glucose and fructose. *Maltase II* and *maltase III* both hydrolyzed maltosucrose into glucose and sucrose, *i.e.* only the *maltose* linkage of the trisaccharide was hydrolyzed. When calculated as the number of glycosylic linkages hydrolyzed per time unit, the rate for hydrolysis of maltosucrose was 0.4 times the rate for maltose hydrolysis for both fractions. The heat inactivation of the maltosucrase activity of these two fractions ran parallel with the inactivation of the maltase activity.

The specificity of *maltase I*, thus, differs markedly from the specificity of *maltase II* and *maltase III*. No difference in specificity was found between the last-mentioned two fractions, however, except that they hydrolyzed *iso*-maltose and phenyl α-D-glucopyranoside at a slightly different rate. All three fractions may be classified as α-D-glucopyranosidases (glucosido-maltases) * since they hydrolyze a number of other α-D-glucopyranosides in addition to maltose.

Possibility of a heat-stabilizing factor

There is no doubt that *maltase I* is an enzyme which differs from the two other fractions. *Maltase II* and *maltase III*, on the other side, are very similar. Except the great difference in their sensitivity to heat [1], the only differences were a small difference in the K_s value for maltose [2], and a slightly different relative rate of hydrolysis of *iso*maltose and phenyl α-D-glucopyranoside. The K_s value as well as the relative rate of hydrolysis of different substrates may be influenced by contaminants in the enzyme preparation, which react with the enzyme. The question therefore arises if the difference in heat sensitivity may be an artifact.

During studies on yeast invertase Myrbäck [14] observed that the course of the heat inactivation did not always follow the kinetics of a first order reaction. The course of the heat inactivation of some preparations should coincide with the existence in them of two different invertases with different

* Leibowitz [13] once postulated the exixtence of *gluco-maltases*, which, in contrast to glucosido-maltases, should have their specificity directed towards the *reducing* component of the maltose molecule. Later workers, however, have not been able to verify the existence of gluco-maltases [12].

heat stability. The K_s value for the invertase activity was not altered, however, during partial heat inactivation, which would have been expected if there really had been two different invertases in the preparation. In order to explain the course of the heat inactivation, therefore, the existence was proposed, not of two different invertases, but of a *heat-stabilizing factor* in a small amount, insufficient to protect the whole enzyme [15].

In order to find out if the maltase III preparation contained a heat-stabilizing factor, an experiment was made for the purpose of showing if the presence of a maltase III preparation, the maltase activity of which had been completely inactivated, could protect maltase II against heat inactivation. A small amount of a *maltase III* preparation, with 216 units/ml of maltase, was heated for 10 min at 100°C. The maltase activity was found to be completely destroyed by this procedure. After cooling, 0.5 ml of the inactivated enzyme preparation was mixed with 0.5 ml of a *maltase II* preparation with 160 units/ml of maltase. When this mixture was heated at 60°C, for 45 min., the maltase activity was found to be completely destroyed. (Before the experiment, both maltase preparations had been dialyzed against 0.01 M phosphate buffer pH 6.0) Thus no heat-stabilizing factor could be demonstrated in the heat-stable maltase preparation.

If maltase II and maltase III are really different enzymes, however, the structural difference between them is probably very small since they are so similar in action and so difficult to separate from each other.

Acknowledgment. The author's thanks are due to Professor Bengt Borgström for his interest in my work and for valuable discussions.

This work has been supported by grants from the *Medical Faculty of the University of Lund.*

The skilful technical assistance of Mrs. K. Hagebris is gratefully acknowledged.

REFERENCES

1. Dahlqvist, A. *Acta Chem. Scand.* **13** (1959) 945.
2. Dahlqvist, A. *Acta Chem. Scand.* **13** (1959) 1817.
3. Dahlqvist, A. and Borgström, B. *Acta Chem. Scand.* **13** (1959) 1659.
4. Dahlqvist, A. *To be published.*
5. Helferich, B. und Schmitz-Hillebrecht, E. *Ber.* **66** (1933) 378.
6. Montgomery, E. M., Richtmyer, Nelson, K. and Hudson, C. S. *J. Am. Chem. Soc.* **64** (1942) 690.
7. Dahlqvist, A. *Acta Chem. Scand.* **14** (1960) 9.
8. Somogyi, M. *J. Biol. Chem.* **195** (1952) 19.
9. Nelson, N. *J. Biol. Chem.* **153** (1944) 375.
10. Somogyi, M. *J. Biol. Chem.* **160** (1945) 69.
11. Dahlqvist, A. *Acta Chem. Scand.* **12** (1958) 2012.
12. Gottschalk, A. in Sumner, J. B. and Myrbäck, K. (Ed.) *The Enzymes*, Vol. I., part 1, New York 1950.
13. Leibowitz, J. und Mechlinski, P. *Z. physiol. Chem. Hoppe-Seyler* **154** (1926) 64.
14. Myrbäck, K. *Z. physiol. Chem. Hoppe-Seyler* **130** (1923) 97.
15. Myrbäck, K. *Personal communication.*

Received September 9, 1959.

ACTA CHEMICA SCANDINAVICA 14 (1960) 9—16

Characterization of Hog Intestinal Trehalase

ARNE DAHLQVIST

Department of Physiological Chemistry, University of Lund, Lund, Sweden

Hog intestinal trehalase is a specific enzyme, separable from the intestinal invertase, maltase, and *iso*maltase activities. In the present paper the partial purification and the characteristics of hog intestinal trehalase will be described.

In contrast to the hog intestinal invertase and maltase activities, hog intestinal trehalase had *no* transglycosylase activity. Nor could any synthesis of trehalose be detected.

Hog intestinal trehalase has very high specificity for *aa*-trehalose. The preparation did not hydrolyze sucrose, maltose, *iso*maltose, phenyl α-D-glucopyranoside, or *ββ*-trehalose. It hydrolyzed *αβ*-trehalose slowly, but heat inactivation revealed that this sugar was *not* hydrolyzed by the same enzyme as *aa*-trehalose.

The high specificity and the lack of transglycosylase activity makes it probable that hog intestinal trehalase acts upon its substrate in a more symmetrical way than do the other glycosidases.

That intestinal mucosa from certain mammals (rabbit, horse, cow) has trehalase activity *, has been known since the end of the 19th century [1–3]. Until recently it has not been known, however, if the intestinal trehalase activity is caused by a specific enzyme, or if it is only one activity of an intestinal α-D-glucopyranosidase which acts on many different substrates, as proposed by Weidenhagen [3,4].

In the course of a study of hog intentinal α-D-glucopyranosidase activities it was recently observed, however, that the hog intestinal trehalase activity was separable from the hog intestinal invertase and maltase activities. The trehalase activity was inactivated by exposure to ethanol, and it appeared as a separate peak in chromatography upon DEAE-cellulose [5]. The hog intestinal trehalase activity could also be separated from the invertase and maltase activities by heat inactivation [6]. Hog intestinal trehalase, therefore, is a specific enzyme, as has earlier been reported in the case of trehalase from fungi (*Aspergillus niger* [7], yeast [3]) and insect larvae (*Galleria mellonella* [8]).

In the present paper the partial purification of trehalase from hog intestinal mucosa and some characteristics of hog intestinal trehalase will be described.

* *Trehalase* activity (without prefix) means hydrolytic activity against the *naturally* occurring trehalose, *aa*-trehalose (1(α-D-glucopyranosyl) α-D-glucopyranoside).

MATERIALS AND METHODS

Hog intestinal mucosa was obtained from the slaughterhouse immediately after slaughter, and was chilled with crushed ice during the transport to the laboratory.

Substrates. *αα-Trehalose* (1-(α-D-glucopyranosyl) α-D-glucopyranoside) (dihydrate) of analytical grade purity, with $[\alpha]_D^{20}$ +178.3°, was obtained from Pfanstiehl Chemical Co. *Sucrose*, cryst., was obtained from J. T. Baker Co. and *maltose* (monohydrate), cryst., from Merck A. G. (Germany).

αβ-Trehalose (1-(α-D-glucopyranosyl) β-D-glucopyranoside, *neo*trehalose) and *ββ-trehalose* (1-(β-D-glucopyranosyl) β-D-glucopyranoside, *iso*trehalose) were obtained as their *octaacetates*, a generous gift from *Professor H. Bredereck* (Technische Hochschule, Stuttgart) [9]. Deacetylation was performed by shaking with excess of NaOH (200 mg of trehalose octaacetate and 40 ml of 0.1 N NaOH) at room temp. for 16 h. The Na-acetate formed and the excess of NaOH were removed by filtration through a column with 2 cm diam., containing 4 g of Dowex 2 (OH-form), 4 g of Dowex 50 (H-form), and 4 g of Dowex 2 (OH-form) as separate layers. The flow rate was 0.5 ml/min. The column was washed with 150 ml of water. The neutral filtrate was evaporated at reduced pressure to a volume of about 10 ml, lyophilized and dried *in vacuo* at 50°C over P_2O_5. About 90 mg of each sugar was obtained.

The sugars obtained did not reduce Somogyi's copper reagent. They had the same mobility as αα-trehalose on the paper chromatogram. $[\alpha]_D^{20}$ was +79.0° for αβ-trehalose (3 % in water) and −41.4° for ββ-trehalose (4.2 % in water).

Phenyl-α-D-glucopyranoside was obtained as its *tetraacetate* by the method of *Helferich* [10] as modified by *Montgomery et al.*[11] $[\alpha]_D^{20}$ of the tetraacetate was +168.0° (7.2 % in $CHCl_3$), m. p. 113−114°C (reported [10] $[\alpha]_D^{20}$ +168°, m. p. 115−116°C). Deacetylation was performed as described above in the case of trehalose octaacetates. The phenyl-α-D-glucopyranoside was crystallized from water and dried *in vacuo* at 50°C over P_2O_5. $[\alpha]_D^{20}$ was +186.0° (anhydrous, 3 % in water).

Isomaltose (6(α-D-glucopyranosyl) D-glucose) was obtained by enzymatic hydrolysis of dextran (kindly supplied by *A. B. Pharmacia*) as described elsewhere [12].

Determination of trehalase activity was performed at 0.1388 M substrate concentration at 37°C in the presence of 0.05 M maleate buffer pH 6.0. 1 ml of enzyme solution (containing 0.5−3 units of trehalase) was mixed with 1 ml of substrate solution (10.5 % * αα-trehalose (dihydrate) in 0.1 M maleate buffer pH 6.0 with a few ml of toluene per litre as a preservative). After 60 min. at 37°C the reaction was interrupted by the addition of 2 ml of Sumner's 3,5-dinitrosalicylic acid reagent [13]. A blank was prepared with the same composition, but the 3,5-dinitrosalicylic acid reagent was added *before* the substrate solution. The tubes were boiled in a water-bath for 10 min, chilled with tap water, and diluted with 20 ml of distilled water. The red colour was measured in a Beckman B spectrophotometer at 530 mμ. The colour was stable for at least 20 h. The amount of glucose produced was calculated from a standard curve with known amounts of glucose. One unit of trehalase is the amount which produces 1 mg of glucose (= 1 % hydrolysis in 2 ml of reaction mixture) during the conditions used.

Determination of K_s for trehalase activity was made by measuring the rate of hydrolysis in 0.0500−0.0007 M trehalose solutions. The degree of hydrolysis was never allowed to exceed 10 %. The amount of glucose produced in these dilute substrate solutions was determined with the method of Somogyi and Nelson [14,15] after deproteinization with Somogyi's Zn-Ba reagents [16]. Calculation of K_s was performed as described earlier [17].

The hydrolysis of sucrose, maltose, isomaltose, and phenyl-α-D-glucopyranoside was measured at 0.1388 M substrate concentration at 37°C in the presence of 0.05 M maleate buffer pH 6.0. The amount of glucose produced from these substrates was determined with the methods described elsewhere [12,18].

The hydrolysis of αβ-trehalose and ββ-trehalose was measured at 0.0139 M substrate concentration at 37°C in the presence of 0.05 M maleate buffer pH 6.0. The amount of glucose produced was determined with the reagents of Somogyi and Nelson [14,15] after deproteinization with the Zn-Ba-reagents [16].

* Per cent means gram of solute in 100 ml of solution.

Determination of protein was made with the method of Lowry et al. [19] by use of human serum albumin (kindly supplied by *A. B. Kabi*) as a standard.

Determination of inorganic phosphate was made with the method of King [20]. The blue colour produced was measured with a Beckman B spectrophotometer at 700 mμ.

Paper chromatography of sugars was performed as described earlier [21].

^{14}C-Labelled glucose was obtained from the *Radiochemical Centre* (England). The distribution of the radioactivity on paper chromatograms was measured as described earlier [21].

Crystalline trypsin (Trypure Novo) was kindly supplied by *A. B. Ferrosan.*

RESULTS AND DISCUSSION

As the source of trehalase hog intestinal mucosa was used. While the mucosa of the duodenum and the proximal jejunum had a strong trehalase activity (trehalase/invertase activity quotient 0.50—0.75), the trehalase activity of the distal part of the small intestine was weak (trehalase/invertase activity quotient about 0.10). For the preparation of trehalase the proximal 100 cm of the small intestine was therefore used.

Solubilization and purification of trehalase. The mucosa and the intestinal contents of the proximal part of the small intestine were squeezed out manually within a few minutes after the slaughter. From 10 pigs (about 10 metres of small intestine) 200 ml of viscous liquid was thus obtained, which yielded 55 mg/ml of protein, 96 units/ml of trehalase, 140 units/ml of invertase, and 210 units/ml of maltase. For solubilization of the glycosidases 30 mg of crystalline trypsin, freshly dissolved in 20 ml of water, was added during stirring [5]. After 4 h at room temperature the solution was centrifuged at 600 *g* for 10 min and the supernatant was filtered through a bed of Solkafloc cellulose powder SW 40 A. The filtrate was dialyzed against 0.01 M phosphate buffer pH 6.0.

The solution was then applied to a 6 × 20 cm column, containing 80 g (dry weight) of DEAE-cellulose [5], equilibrated with 0.01 M phosphate buffer pH 6.0. The column operations were performed at +4°C. The column was first eluted with 4 l of 0.01 M phosphate buffer pH 6.0, which eluted 40 % of the protein applied to the column, but only 8 % of the trehalase activity. This fraction was discarded. The main part (80 %) of the trehalase activity, together with 5 % of the protein, was eluted with 4 l of 0.05 M phosphate buffer pH 6.0. This buffer did not elute the invertase and maltase activities from the column.

For concentration of the enzyme, this fraction was diluted with 4 vol. of distilled water, and filtered through a column containing 10 g (dry weight) of DEAE-cellulose, equilibrated with 0.01 M phosphate buffer pH 6.0. All the trehalase activity was adsorbed to the column. The enzyme was eluted with 200 ml of 0.20 M phosphate buffer pH 6.0, dialyzed against distilled water and lyophilized. Since the powder obtained was found to contain considerable amounts of inorganic phosphate, it was dissolved in 25 ml of distilled water and again dialyzed against distilled water. On lyophilization of the dialyzed solution 160 mg of a white powder, with a trehalase, activity of 34 units/mg, was obtained. This corresponds to 25 % of the trehalase activity of the original solution. The powder had the same absorption coefficient according to Lowry's method for protein determination as pure human serum

Table 1. Hydrolysis of *aa*-trehalose by hog intestinal trehalase. Course of the reaction. The reaction mixture contained 0.1388 M *aa*-trehalose, 0.05 M maleate buffer pH 6.0, 1 mg/ml of purified trehalase containing 1 mg of protein and 34 units of trehalase per mg. The temperature was 37°C. — Up to between 15 and 20 % hydrolysis the reaction followed zero order kinetics.

t Time, h	x per cent of hydrolysis	k_{zero} x/t
0.083	5.3	63.7
0.166	10.6	63.7
0.250	15.9	63.7
0.333	20.5	61.4
0.500	30.5	61.0
0.667	39.3	58.9
0.833	48.3	58.0
1.000	52.9	52.9
2.000	80.3	40.1
3.000	91.7	30.6
4.000	97.3	24.4

albumin. The specific trehalase activity of the powder (trehalase activity/mg of protein) was 20 times that of the original solution.

Stability of hog intestinal trehalase activity. In crude hog intestinal glycosidase preparations the trehalase activity, in contrast to the invertase and maltase activities, was not stable when stored at low temperature. After storage at —16°C for a month, the trehalase activity of a crude preparation had decreased by 25 %. At higher temperatures the decrease was more rapid. After storage at —16°C for 6 months, no more than about 15 % of the trehalase activity remained, while the invertase and maltase activities were unaffected.

The trehalase activity of the purified, lyophilized powder, however, was very stable. After storage at —16°C for 6 months, *no* decrease of the trehalase activity of this preparation could be detected.

Kinetics of hog intestinal trehalase. Hog intestinal trehalase had its optimum pH around 6.0 (Fig. 1). The hydrolysis of *aa*-trehalose by hog intestinal trehalase proceeded to completion with glucose as the only product. Up to 20 % hydrolysis the reaction followed zero order kinetics (Table 1). Within wide limits the initial velocity of the reaction was proportional to the amount of enzyme present (Fig. 2).

The K_s value was determined at 3.0×10^{-3} M *aa*-trehalose (at 37°C in the presence of 0.05 M maleate buffer pH 6.0). The V_{max} was 1.02 times the initial velocity at 0.1388 M substrate concentration.

Influence of inorganic phosphate on hog intestinal trehalase activity. The trehalase activity by extracts from some *insects* is stimulated by the presence of inorganic phosphate, which has led to the conclusion that a phosphorolysis may be involved in the trehalase action by these preparations [23]. Later researchers, however, found that the hydrolysis of trehalose by insect trehalase proceeds to completion with glucose as the sole product. Since their preparations had no activity on glucose-1-phosphate, the cleavage of trehalose by their preparations must be a purely hydrolytic reaction [8].

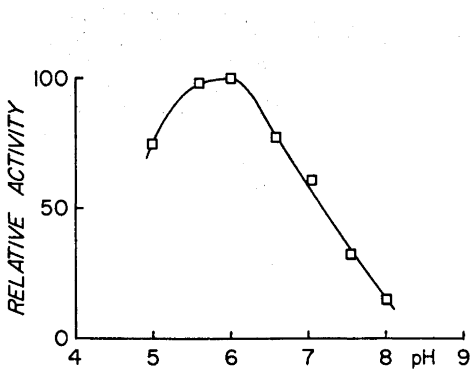

Fig. 1. Influence of pH on the hydrolysis of *aa*-trehalose by hog intestinal trehalase. Buffers: 0.05 M acetate pH 5.0, 0.05 M maleate pH 5.5—6.5, 0.025 M veronal pH 7.0—8.0. Temperature 37°C. Substrate concentration 0.1388 M.

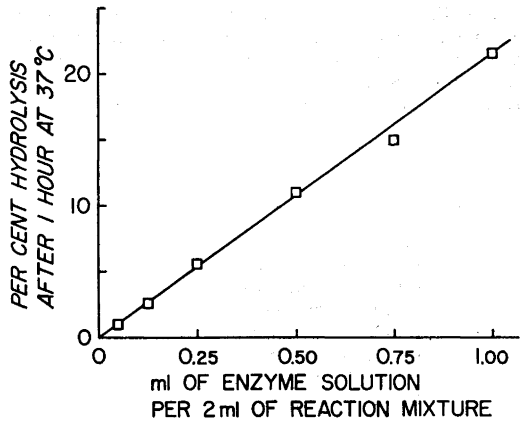

Fig. 2. Proportionality between the degree of hydrolysis after 1 h and the amount of enzyme added. Experimental conditions: 0.1388 M *aa*-trehalose solution in the presence of 0.05 M maleate buffer pH 6.0. The enzyme solution was a purified preparation of hog intestinal trehalase, containing 0.65 mg of protein and 22 units of trehalase per ml. Up to 20 % hydrolysis, the degree of hydrolysis after 1 h was proportional to the amount of enzyme added.

The influence of inorganic phosphate on the hog intestinal trehalase activity was studied with the results seen in Table 2. The reaction mixture contained 25 μg/ml of the lyophilized trehalase preparation, 0.1388 M *aa*-trehalose, and varying amounts of phosphate or maleate buffer pH 6.0. Without addition of phosphate buffer, the reaction mixture was found to contain less than 0.2 μg/ml of inorganic phosphorous. The trehalase activity was *not* stimulated by the addition of phosphate buffer. The presence of concentrated phosphate buffer rather decreased the rate of hydrolysis to some extent.

Transglycosylation properties of hog intestinal trehalase. Most glycosidases are known to have transglycosylase activity, *i.e.* they are able to transfer the glycosyl residue of their substrate to some receptor other than water [24]. In a concentrated substrate solution the substrate may itself act as receptor, which results in the formation of oligosaccharides. Also other compounds, containing a free alcohol group, may act as receptors. If the substrate is a disaccharide, the transfer of the glycosylic residue to a free hexose may lead to the regeneration of the substrate or the production of other disaccharides [21,24].

A reaction mixture, containing 30 % (= g/100 ml) of *aa*-trehalose (dihydrate) and 41 units/ml of hog intestinal trehalase in 0.05 M maleate buffer pH 6.0 with toluene as preservative, was incubated at 37°C for 23 h. When 5 μl spots of the reaction mixture were chromatographed, only glucose and trehalose were found (Fig. 3). Thus no oligosaccharide formation could be

Table 2. Influence of inorganic phosphate on the activity of hog intestinal trehalase. Experimental conditions: 0.1388 M substrate concentration, pH 6.0, temperature 37°C, and time of reaction 60 min. The reaction mixture contained 25 μg/ml of purified hog intestinal trehalase. The degree of hydrolysis was determined with the 3,5-dinitrosalicylic acid reagent. — The presence of phosphate did *not* stimulate the trehalase activity.

Buffer	Degree of hydrolysis, %
No buffer	1.79
0.010 M maleate	1.80
0.025 M maleate	1.85
0.050 M maleate	1.83
0.005 M phosphate	1.86
0.025 M phosphate	1.85
0.050 M phosphate	1.74
0.100 M phosphate	1.59

demonstrated. During the corresponding conditions, hog intestinal invertase and hog intestinal maltases produce a series of oligosaccharides in addition to their hydrolysis products [12,21].

In another experiment 1 mg/ml of ^{14}C-labelled glucose was added to a reaction mixture with the same composition as above. After 5 and 23 h at 37°C 5 μl samples of the reaction mixture were applied to a paper chromatogram. After run for 2 days, the distribution of the radioactivity on the chromatogram was measured as described earlier [21]. Each 5 μl spot contained 6 250 c.p.m. of ^{14}C-labelled sugar as measured with the counter. All the radioactivity was localized in the *glucose* spot. Glucose is therefore *not* incorporated into trehalose or other oligosaccharides by intestinal trehalase. During the corresponding conditions the intestinal maltases form ^{14}C-labelled maltose and other oligosaccharides [12], and intestinal invertase, too, forms a ^{14}C-labelled disaccharide [21].

That hog intestinal trehalase has no transglycosylase activity was also indicated by the fact that the rate of glucose formation (as measured with the 3,5-dinitrosalicylic acid reagent) did not decrease when the substrate concentration was increased to 0.794 M (30 % *aa*-trehalose dihydrate). The

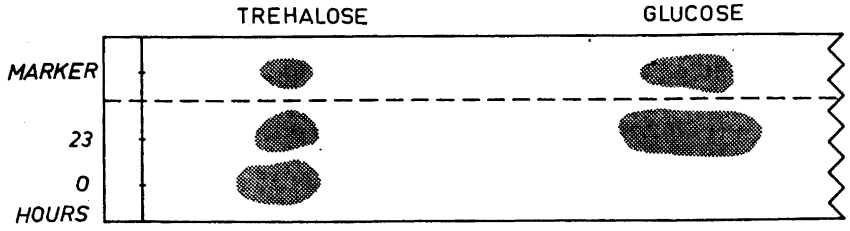

Fig. 3. Hydrolysis of a 30 % solution of *aa*-trehalose (dihydrate) by hog intestinal trehalase. Experimental conditions, see text. The chromatogram was developed for 2 days. In contrast to the other intestinal glycosidases, trehalase did *not* form any oligosaccharides by transglycosylation.

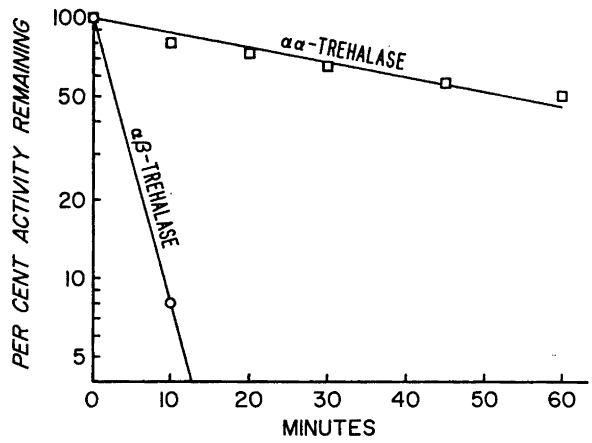

Fig. 4. Separation of $\alpha\beta$-trehalase and $\alpha\alpha$-trehalase activity by heat inactivation. A solution of purified hog intestinal trehalase, containing 5 mg/ml of protein in 0.01 M phosphate buffer pH 6.0, with 165 units/ml of $\alpha\alpha$-trehalase and 1 unit/ml of $\alpha\beta$-trehalase, was heated at 65°C. While the $\alpha\beta$-trehalase activity was rapidly inactivated, the $\alpha\alpha$-trehalase activity only decreased slowly.

hog intestinal invertase and maltase activities decrease in concentrated substrate solutions, probably owing to their transglycosylase activity [12,17,21].

In some cases, the equilibrium for reactions catalyzed by glycosidases has been found to be such that the synthesis of the substrates from the hydrolysis products could be demonstrated [22]. A solution containing 30 % glucose and 41 units/ml of trehalase in 0.05 M maleate buffer pH 6.0 and with toluene as a preservative was incubated at 37°C. After 23h only glucose was found on a paper chromatogram. The equilibrium for the reaction catalyzed, therefore, must be far to the side of hydrolysis.

Specificity of hog intestinal trehalase. The trehalase preparation had no hydrolytic activity on *sucrose*, *maltose*, *isomaltose*, *phenyl* α-D-*glucopyranoside*, or *ββ-trehalose*. The experimental conditions were such that a hydrolysis with a rate only 1/100 of that for the hydrolysis of $\alpha\alpha$-trehalose would have been detected with sucrose, maltose and *iso*maltose as substrates, and only 1/1 000 with phenyl α-D-glucopyranoside and $\beta\beta$-trehalose.

The preparation hydrolyzed *αβ-trehalose* with a rate which was 0.006 times the rate for the hydrolysis of $\alpha\alpha$-trehalose. The hydrolysis of $\alpha\beta$-trehalose proceeded *to completion*. The K_s for the hydrolysis of $\alpha\beta$-trehalose was determined at 9.1×10^{-3} and the V_{max} at 1.65 times the rate of hydrolysis at 0.0139 M substrate concentration. — Heat inactivation at 65°C (performed as described earlier [6]), however, revealed that $\alpha\alpha$-trehalose and $\alpha\beta$-trehalose were hydrolyzed by different enzymes (Fig. 4). The hydrolytic activity on $\alpha\beta$-trehalose was completely destroyed after 20 min while 73 % of the original $\alpha\alpha$-trehalase activity persisted after that time. Hog intestinal trehalase, therefore, has *no* activity on $\alpha\beta$-trehalose. The specificity of the contaminating enzyme, which hydrolyzed $\alpha\beta$-trehalose, is not known.

Mode of action upon the substrate. Glycosidases generally act upon their substrates asymmetrically, *i.e.* they are more firmly bound to the *glycon* component (the glycosyl residue) of their substrates than to the *aglycon*. This appears from their greater specificity for the glycon [4,17,22] and by the phenomenon of transglycosylation [24]. This fact is particularly apparent in the case of invertases. In sucrose either the glucosylic or the fructosylic part may be regarded as glycon and aglycon, respectively. Consequently, there are two kinds of invertases, namely, glucosido- and fructosidoinvertases, with activity on different α-D-glucopyranosides or β-D-fructofuranosides, and with transglucosylase or transfructosylase activity, respectively [4,17,21,24].

Hog intestinal trehalase, on the other hand, has no transglycosylase activity. Nor does it seem to be able to hydrolyze any other α-D-glucopyranoside than αα-trehalose. These facts make it probable that hog intestinal trehalase has a more symmetrical way of attacking its substrate than have the other glycosidases. This property is possibly common to many different trehalases, since trehalases from many different sources seem to have a marked specificity for their substrate [3,8,22].

Acknowledgment. The author's thanks are due to Professor Bengt Borgström for his interest in my work and for valuable discussions.

This work has been supported by grants from the *Medical Faculty of the University of Lund.*

The skilful technical assistance of Mrs. K. Hagebris is gratefully acknowledged.

REFERENCES

1. Bourquelot, E. and Gley, E. *Compt. rend. soc. biol.* **47** (1895) 555.
2. Fischer, E. and Niebel, W. *Sitzber. Preuss. Akad. Wiss.* **75** (1895) 73.
3. Myrbäck, K. *Ergeb. Enzymforsch.* **10** (1949) 168.
4. Weidenhagen, R. in Nord F. F. and Weidenhagen, R. (Ed) *Handbuch der Enzymologie*, Vol. 1 Leipzig 1940.
5. Borgström, B. and Dahlqvist, A. *Acta Chem. Scand.* **12** (1958) 1997.
6. Dahlqvist, A. *Acta Chem. Scand.* **13** (1959) 945.
7. Bourquelot, E. *Compt. rend.* **116** (1893) 826.
8. Kalf, G. H. and Rieder, S. W. *J. Biol. Chem.* **230** (1958) 691.
9. Bredereck H., Höschele, G. and Ruck, K. *Chem. Ber.* **86** (1953) 1277.
10. Helferich, B. and Schmitz-Hillebrecht, E. *Chem. Ber.* **66** (1933) 378.
11. Montgomery, E. M., Richtmyer, N. K. and Hudson, C. S. *J. Am. Chem. Soc.* **64** (1942) 690.
12. Dahlqvist, A. *To be published.*
13. Sumner, J. B. *J. Biol. Chem.* **62** (1924) 287.
14. Somogyi, M. *J. Biol. Chem.* **195** (1952) 19.
15. Nelson, N. *J. Biol. Chem.* **153** (1944) 375.
16. Somogyi, M. *J. Biol. Chem.* **160** (1945) 69.
17. Dahlqvist, A. *Acta Chem. Scand.* **12** (1958) 2012.
18. Dahlqvist, A. *Acta Chem. Scand.* **13** (1959) 1817.
19. Lowry, O. H., Rosebrough, N. J., Farr, A. L. and Randall, R. J. *J. Biol. Chem.* **193** (1951) 265.
20. King, E. J. *Biochem. J.* **26** (1932) 292.
21. Dahlqvist, A. and Borgström, B. *Acta Chem. Scand.* **13** (1959) 1659.
22. Gottschalk, A. in Sumner J. B. and Myrbäck, K. The Enzymes, Vol. I, Part 1, New York 1950.
23. Frèrejacque, M. *Compt. rend.* **213** (1941) 88.
24. Edelman, J. *Advances in Enzymol.* **17** (1956) 189.

Received September 7, 1959.

ACTA CHEMICA SCANDINAVICA 14 (1960) 17—20

Preparation of Ursodeoxycholic Acid and 3α,7β,12α-Trihydroxycholanic Acid

Bile Acids and Steroids 94

BENGT SAMUELSSON

Department of Chemistry, Karolinska Institutet, Stockholm, Sweden

The compounds have been prepared through reduction of the corresponding 7-ketoacids with sodium in *n*-propanol. Reversed phase partition chromatography of the reduction products revealed that the epimeric 7β- and 7α-hydroxycompounds are formed in the proportion of about 3:1.

Ursodeoxycholic acid (3 α,7β-dihydroxycholanic acid) is found in the bile of certain bear species [1] and in the coypu [1]. Traces of this acid has recently also been reported to occur in the rat [2] and man [3]. Urxodeoxycholic acid has previously been prepared synthetically through reduction of 7-ketolithocholic acid (3α-hydroxy-7-ketocholanic acid) with sodium ethoxide and through catalytic hydrogenation in acidic medium. The yield of the 7β-epimer was only about 10 % [4]. Sodium borohydride reduction of 7-ketocholanic acids and derivatives produces specifically the corresponding 7α-hydroxycompounds [5-8]. The 7-ketone in the bile acid series has been reported to be almost resistent to reduction with aluminium *iso*propoxide [8,9]. In one case, however, a successful reduction, which gave predominately the axial epimer (7α), has been described [10]. These authors also reported the preparation of ursodeoxycholic acid in 95 % yield by reduction of 7-ketolithocholic acid with sodium in *n*-propanol. When this method was used in the present investigation and the reaction product separated by reversed phase partition chromatography, it appeared that the reduction gives a mixture consisting of the equatorial 7β- and axial 7α-hydroxyepimers in the approximate proportion of 3:1.

3α,7β,12α-trihydroxycholanic acid has never been synthesized or isolated before. Recently, however, an acid with identical chromatographic properties and sulfuric acid spectrum has been isolated as a metabolite of cholic acid-24-^{14}C in the rat [11] and has been detected in samples of human bile [3].

3α,7β,12α-trihydroxycholanic acid was obtained by reduction of 7-ketodeoxycholic acid (3α,12α-dihydroxy-7-ketocholanic acid) by the same method

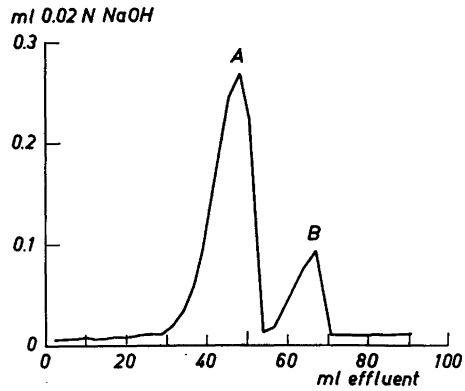

Fig. 1. Chromatography of an aliquot of the reaction product obtained by reduction of 7-ketolithocholic acid with sodium in *n*-propanol. Column: 4.5 g of hydrophobic SuperCel. Moving phase: 55 % (v/v) aqueous methanol. Stationary phase: 10 % (v/v)-heptane in chloroform. A: Ursodeoxycholic acid. B: Chenodeoxycholic acid.

as above. The two epimers, separated chromatographically, were found in the same proportion as in the reduction of 7-ketolithocholic acid. The methyl ester of 3α,7β,12α-trihydroxycholanic acid yielded a tri-*p*-nitrobenzoate on acylation with *p*-nitrobenzoyl chloride in pyridine. Under similar conditions methyl cholate only gives the 3α-mono-*p*-nitrobenzoate [12].

EXPERIMENTAL

Ursodeoxycholic acid. 7-Ketolithocholic acid (m. p. 200—202°) was prepared through sodium dichromate oxidation of methyl 3α-cathyloxy-7α-hydroxycholanate followed by hydrolysis [13,14]. A solution of 0.5 g of the ketoacid in 10 ml of anhydrous *n*-propanol was refluxed with 1 g of sodium for 3 h. The solution was diluted with water, acidified with hydrochloric acid and extracted with ethylacetate. After evaporation to dryness *in vacuo* the residue was chromatographed on hydrophobic Super Cel with 55 % (v/v) methanol as moving phase and 10 % (v/v) heptane in chloroform as stationary phase [15] (Fig. 1).

No unchanged ketoacid could be detected and of the two peaks which appeared, the first one (77 %) was crystallized from ethylacetate/light petroleum. Yield: 0.32 g, m. p. 201—202°. There was no depression of the m. p. on admixture with authentic ursodeoxycholic acid that was kindly supplied by Prof. G. A. D. Haslewood. $[\alpha]_D^{25} = +57 \pm 2°$ (*c* 1.02, dioxane). (Found: C 73.1; H 10.3. Calc. for $C_{24}H_{40}O_4$: C 73.4; H 10.3).

The material in the second peak (23 %) with an elution volume characteristic of chenodeoxycholic acid was crystallized from ethylacetate/light petroleum. M. p. 141—142°, undepressed by authentic chenodeoxycholic acid.

3α, 7β, 12α-trihydroxycholanic acid. Methylcholate was oxidized with N-bromosuccinimide [16] to methyl-7-ketodeoxycholate, purified *via* the diacetate [17] (m. p. 118—118.5°) and saponified. 7-Ketodeoxycholic acid was crystallized according to the directions given by Hoehn and Linsk [18]; m. p. 198—199°. The ketoacid was reduced as described above and the reaction product was separated by reversed phase partition chromatography on hydrophobic Super Cel. Aqueous methanol (50 % (v/v)) was used as the moving phase and *iso*octanol-chloroform (1:1) as stationary phase [19]. (Fig. 2.) The more hydrophilic compound (72 %), 3α,7β,12α-trihydroxycholanic acid (0.2 g), was dissolved in 3 ml methanol, neutralized with 0.1 N NaOH and added slowly to 100 ml of cold

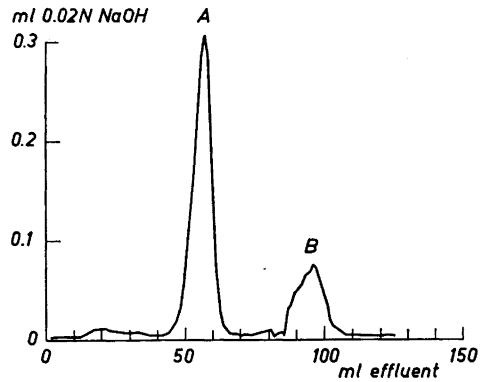

Fig. 2. Chromatography of an aliquot of the reaction product obtained by reduction of 7-ketodeoxycholic acid with sodium in *n*-propanol. Column: 4.5 g of hydrophobic Super Cel. Moving phase: 50 % (v/v) aqueous methanol. Stationary phase: *iso*octanol / chloroform (1:1). A: 3α,7β,12α-trihydroxycholanic acid. B: Cholic acid.

0.05 N HCl, with vigorous stirring. The precipitated acid crystallized after standing 12 h at +4°. 0.155 g (56 % yield calculated on 7-ketodeoxycholic acid) was obtained after filtration, washing with water and drying; m. p. 127—129°. The m. p. was not changed after repeated recrystallizations by this method. $[\alpha]_D^{25} = +62 \pm 2°$ (*c* 1.13, dioxane). (Found C 70.3; H 10.0. Calc. for $C_{24}H_{40}O_5$: C 70.5; H 9.9.)

A sample of this acid was crystallized from ethylacetate/heptane and dried at 130° at 0.001 mm Hg for 24 h; m. p. 157—158° (decomp.). $[\alpha]_D^{25} = +57 \pm 2°$ (*c* 1.06, dioxane). The elemental analysis indicated that the acid had formed a complex with heptane. (Found C 72.7; H 10.4. Calc. for $C_{24}H_{40}O_5 + C_7H_{16}$: C 73.2; H 11.1). Several other organic solvents were tried for recrystallization without success.

Methyl 3α,7β,12α-trihydroxycholanate-tri-p-nitrobenzoate. The method of Borsche [12] was followed. A solution of 75 mg of methyl 3α,7β,12α-trihydroxycholanate, prepared with diazomethane, was dissolved in 2 ml of dry pyridine and cooled to 0°. 180 mg of *p*-nitrobenzoylchloride in 2 ml of pyridine was added. After standing at room temperature for 12 h the reaction mixture was transferred to a mixture of ether, ethylacetate, ice and 2 N HCl. The ether layer was washed successively with 2 N HCl, 5 % aqueous sodium carbonate and water. After evaporation to dryness *in vacuo* the residue was crystallized from ethylacetate/ethanol to yield 121 mg of fine needles, m. p. 188—189°. The concentrated mother liquor gave an additional 24 mg of crystals with the same m. p. Total yield: 94 % $[\alpha]_D^{25} = +140 \pm 3°$ (*c* 1.19, dioxane). (Found C 63.5; H 6.0; N 4.8. Calc. for $C_{46}H_{51}O_{14}N_3$: C 63.5; H 5.9; N 4.8).

The second compound (B in Fig. 2) comprising about 28 % of the two epimers, was eluted at the place of cholic acid. It was crystallized from ethylacetate, m. p. 197—198°, undepressed by authentic cholic acid.

Acknowledgements. The technical assistence of Miss I. Lindell is gratefully acknowledged. This work is part of investigations supported by a research grant (H 2842) to Prof. Sune Bergström from the *National Institutes of Health. United States Public Health Service*, Bethesda, Maryland and by *Karolinska Institutets Reservationsanslag.*

REFERENCES

1. Haslewood, G. A. D. *Physiol. Rev.* **35** (1955) 178.
2. Mahowald, T. A., Yin, M. W., Matschiner, J. T., Hsia, S. L., Doisy, E. A. Jr., Elliott, W. H. and Doisy, E. A. *J. Biol. Chem.* **230** (1958) 581.
3. Sjövall, J. *Acta Chem. Scand.* **13** (1959) 711.
4. Miyazi, S. *Z. Physiol. Chem. Hoppe-Seyler* **250** (1937) 31.
5. Mosbach, E. H., Meyer, W. and Kendall, F. E. *J. Am. Chem. Soc.* **76** (1954) 5799.
6. Samuelsson, B. *Acta Chem. Scand.* **13** (1959). 976.
7. Bergström, S., Lindstedt, S. and Samuelsson, B. *J. Biol. Chem.* **234** (1959) 2022.
8. Hsia, S. L., Matschiner, J. T., Mahowald, T. A., Elliott, W. H., Doisy, E. A. Jr., Thayer, S. A. and Doisy, E. A. *J. Biol. Chem.* **225** (1957) 811.
9. Tukamoto, M. *J. Biochem. (Japan)* **32** (1940) 461.
10. Kanazawa, T., Shimazaki, A. Sato, T. and Hoshino, T. *Proc. Japan Acad.* **30** (1954) 391.
11. Norman, A. and Sjövall, J. *J. Biol. Chem.* **233** (1958) 872.
12. Borsche, W. *Ber.* **57** (1924) 1620.
13. Fieser, L. F., Herz, J. E. Klohs, M. W., Romero, M. A. and Utne, T. *J. Am. Chem. Soc.* **74** (1952) 3309.
14. Samuelsson, B. *Acta Chem. Scand.* **13** (1959) 236.
15. Bergström, S. and Sjövall, J. *Acta Chem. Scand.* **5** (1951) 1267.
16. Fieser, L. F. and Rajagopalan, S. *J. Am. Chem. Soc.* **71** (1949) 3935.
17. Corey, E. J. *J. Am. Chem. Soc.* **76** (1954) 175.
18. Hoehn, W. M. and Linsk, J. *J. Am. Chem. Soc.* **67** (1945) 312.
19. Norman, A. *Acta Chem. Scand.* **7** (1953) 1413.

Received September 10, 1959.

ACTA CHEMICA SCANDINAVICA 14 (1960) 21—27

Metabolism of 3α,7β,12α-Trihydroxycholanic Acid in the Rat

Bile Acids and Steroids 95

BENGT SAMUELSSON

Department of Chemistry, Karolinska Institutet, Stockholm, Sweden

Tritium labelled 3α, 7β, 12α-trihydroxycholanic acid has been prepared. The metabolism of this acid after intraperitoneal or intracecal injection into bile fistula rats has been studied. It is not attacked by the liver enzymes but is extensively transformed by the intestinal microorganisms. Deoxycholic- and 12-ketolithocholic acids were identified in the feces and cecum and cholic, deoxycholic and 12-ketolithocholic acids in the bile.

In a recent investigation on the transformation of cholic acid-24-^{14}C in the rat during the enterohepatic circulation a metabolite was isolated with properties identical with 3α, 7β, 12α-trihydroxycholanic acid. Material with the same chromatographic behaviour and sulfuric acid spectrum was also isolated from human bile samples [2]. 3α, 7β, 12α-Trihydroxycholanic acid is probably only formed by reduction of a bacterial metabolite of cholic acid, 7-ketodeoxycholic acid (3α, 12α-dihydroxy-7-ketocholanic acid) in the liver [3].

The metabolism of randomly tritium labelled 3α, 7β, 12α-trihydroxycholanic acid in the rat liver and intestine and the liver metabolism of the intestinal metabolites has been studied in the present investigation.

EXPERIMENTAL

Bile acid samples

Tritium labelled 3α, 7β, 12α-trihydroxycholanic acid. The inactive acid [4] (5 mg) was exposed to tritium gas [5] (2 Curie, 99 % pure, 200 mm Hg. Purchased from Isotope Division, A. E. R. E. Harwell, England) at room temperature for 4 days. The tritium labelled product was purified by chromatography with solvent system C3 after dilution with 30 mg of inactive 3α, 7β, 12α-trihydroxycholanic acid. It was crystallized by acidification of an aqueous solution of the sodium salt, yielding 19 mg, m. p. 126—128°. Specific activity: 20 μC/mg. The radioactivity of this sample was further checked by recrystallizations of the free acid with inactive material and after conversion of the methylester to the tri-*p*-nitrobenzoate [4].

7-Ketodeoxycholic acid was prepared according to the method of Hoehn and Linsk [6], m. p. 197–198°.

12-Ketolithocholic acid (3α-hydroxy-12-ketocholanic acid) was prepared according to the method of Bergström and Haslewood [7], m. p. 160–161°.

Animal experiments

Bile duct cannulated rats (Sprague-Dawley strain, 200–250 g, male) were prepared as described earlier [8]. The sodium salt of the labelled bile acid in 0.9 % aqueous NaCl was injected intraperitoneally 12 h after the bile duct cannulation. The bile was collected in ethanol. The excreted radioactive products represent the pure liver metabolites of the administered acid. In another series of experiments the labelled bile acid was administered by intracecal injection during the operation [1]. The rats were killed after 36 h. Labelled material present in feces and the large intestine of these animals represents transformation products of the injected acid by the intestinal microorganisms. The radioactive compounds excreted in the bile during this period consist of the intestinal metabolites, absorbed from the large intestine as well as the products formed by the action of liver enzymes on these metabolites.

Isolation procedures and chromatographic methods

The bile was filtered, evaporated and hydrolyzed with 2 N NaOH for 8 h at 120° in a closed steel tube. The solution was acidified with hydrochloric acid and extracted with ether.

Feces and intestinal contents were refluxed twice with 80 % aqueous ethanol. After evaporation the residue was hydrolyzed, acidified and extracted with ether. The residue from the ether extracts was distributed between equal volumes of 70 % ethanol and light petroleum by a 3-stage counter-current extraction. The residue from the combined aqueous phases was chromatographed.

Separation of the free bile acids was made by reversed phase partition chromatography as described by Bergström and Sjövall [9] and Norman and Sjövall [1].

Solvent system	Moving phase	(ml)	Stationary phase	(ml)
F (Ref.[9])	Mathanol-water	165: 135	Chloroform-heptane	45 : 5
C3 (Ref.[1])	Methanol-water	140 : 160	Chloroform-isooctanol	15 : 15

4 ml of the stationary phase was supported on 4.5 g of hydrophobic Super Cel. Temperature 23°.

The radioactivity of the fractions collected from the column was determined by counting of an aliquot in an infinitely thin layer on aluminium planchets. A gas flow counter Frieseke Hoepfner FH 51, was used.

RESULTS

Intraperitoneal injection of tritium labelled 3α, 7β, 12α-trihydroxycholanic acid to bile duct cannulated rats. Bile fistulas were made on two rats and tritium labelled 3α, 7β, 12α-trihydroxycholanic acid (0.2 mg) injected intraperitoneally 12 h after the operation. Of the administered ^3H 78–92 % was excreted in the bile within the first 24 h. The hydrolyzed bile was chromatographed with solvent system C3. The only radioactive material, eluted, consisted of unchanged 3α, 7β, 12α-trihydroxycholanic acid as judged by rechromatography together with the inactive acid and by isotope-dilution. The stationary phase retained less than 1 % of the chromatographed ^3H.

Intracecal injection of tritium labelled 3α, 7β, 12α-trihydroxycholanic acid into bile duct cannulated rats. Tritium labelled 3α, 7β, 12α-trihydroxycholanic

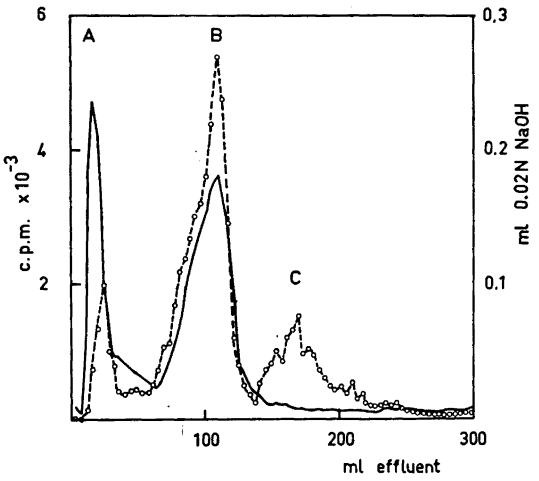

Fig. 1. Chromatographic separation of labelled products in the large intestine and feces after injection of 0.5 mg of ^{3}H labelled 3α, 7β, 12α-trihydroxycholanic acid into the cecum of a bile fistula rat. Inactive deoxycholic acid (15 mg) was added. Column: 9 g of hydrophobic Super Cel. Solvent system: F. ———— Titration values; - - - - - - - Radioactivity.

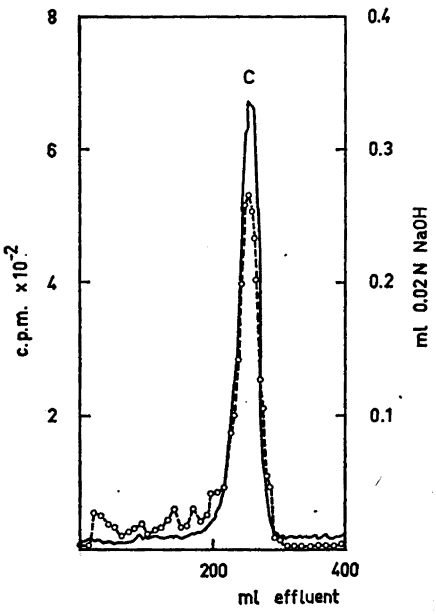

Fig. 2. Chromatographic separation of peak C of the chromatogram shown in Fig. 1 Inactive 12-ketolithocholic acid (15 mg) was added. Column: 9 g of hydrophobic Super Cel. Solvent system: F. ———— Titration values; - - - - - - - Radioactivity.

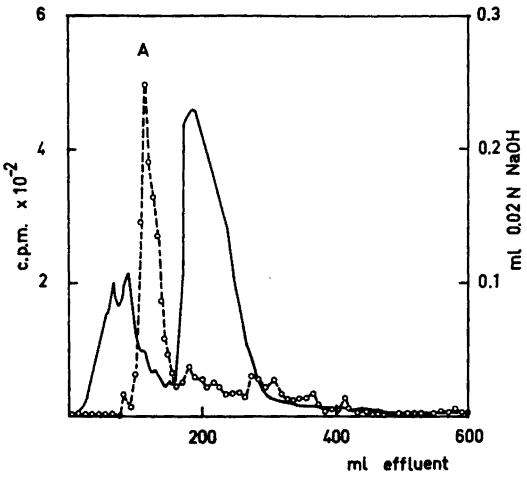

Fig. 3. Chromatographic separation of peak A of the chromatogram shown in Fig. 1 Inactive 7-ketodeoxycholic acid (15 mg) was added. Column: 9 g of hydrophobic Super Cel. Solvent system: C 3. ———— Titration values; - - - - - - - Radioactivity.

acid (0.5 mg to each of three rats) was injected into the cecum immediately after cannulation of the bile duct. The rats (RI, RII, RIII) were killed after 36 h.

Metabolites in the large intestine and feces. The labelled material (15 % (RI), 32 % (RII) and 36 % (RIII) of the injected ^3H) present in the large

Table 1. Recrystallizations of radioactive bands isolated by chromatography from the large intestine and feces or from the bile after intracecal administration of tritium labelled 3α, 7β, 12α-trihydroxycholanic acid to bile fistula rats.

Sample	Inactive bile acid added	Crystallizing solvent	Weight mg	*c. p. m.* mg
Dihydroxycholanic acid band from the large intestine and feces (Fig. 1)	Deoxycholic acid		100	7 300
		Aqueous acetic acid	87	7 650
		Ethyl acetate	70	7 600
		Aqueous ethanol	47	7 900
		Aqueous acetic acid	34	7 700
12-Ketolithocholic acid band from the large intestine and feces (Fig. 2)	12-Ketolithocholic acid		100	1 230
		Ethyl acetate	83	1 320
		Aqueous ethanol	61	1 160
		Aqueous acetone	44	1 060
		Ethylacetate	32	1 280
Cholic acid band from the bile (Fig. 4)	Cholic acid		100	4 700
		Aqueous acetic acid	80	4 920
		Ethyl acetate	68	4 840
		Ethyl acetate	53	4 720
		Aqueous ethanol	37	5 020

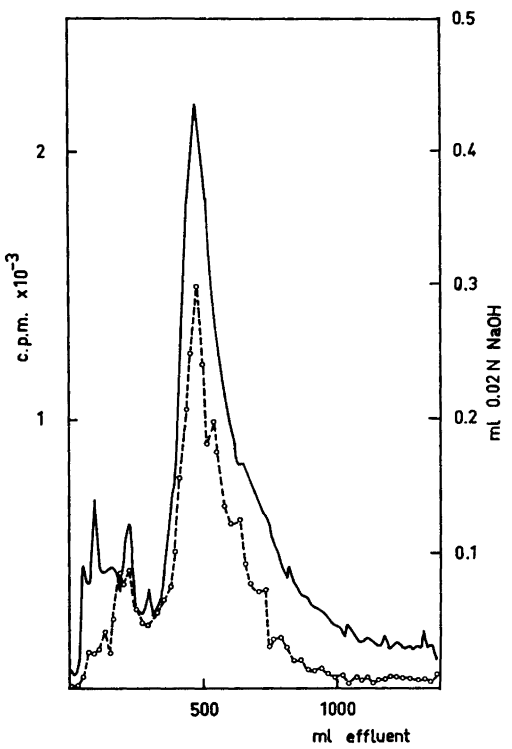

Fig. 4. Chromatographic separation of acids from hydrolyzed bile, excreted during 36 h following intracecal administration of 0.5 mg of ^{3}H-labelled 3α, 7β, 12α-trihydroxycholanic acid. Column: 13.5 g of hydrophobic Super Cel. Solvent system: C 3. ——— Titration values; - - - - - - - Radioactivity.

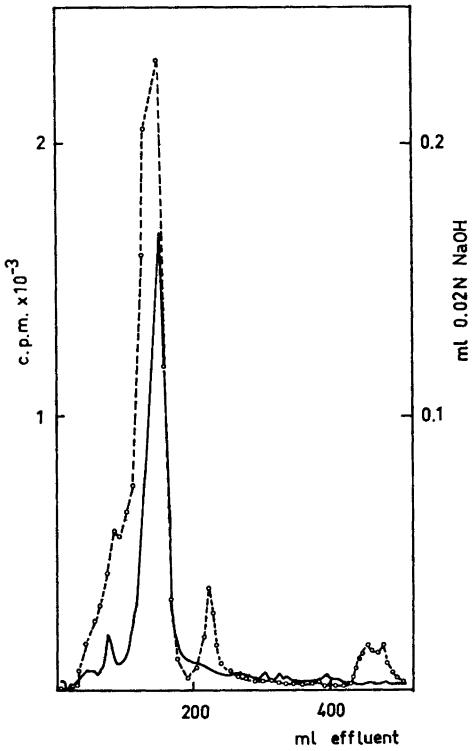

Fig. 5. Chromatographic separation of acids remaining in the stationary phase of the chromatogram shown in Fig. 4. Inactive deoxycholic acid (19 mg) was added. Column: 9 g of hydrophobic Super Cel. Solvent system: F. ——— Titration values; - - - - - - - Radioactivity.

intestine and feces was first chromatographed together with inactive deoxycholic acid with solvent system F. A chromatogram from one of the rats is shown in Fig. 1. (1.5 % of the chromatographed radioactivity remained in the stationary phase). The main peak of radioactivity (B) coincides with the titration peak caused by added inactive deoxycholic acid. The identity was established by recrystallizations with unlabelled deoxycholic acid in different solvents (Table 1). The third radioactive peak (C) was rerun together with unlabelled 12-ketolithocholic acid (Fig. 2). The identity was prooved by isotope dilution (Table 1). The radioactivity being eluted almost with the front (A in Fig. 1) was rechromatographed with the more polar solvent system C3 together with unlabelled 7-ketodeoxycholic acid (Fig. 3). The main part of the radioactivity appeared at the position of 3α, 7β, 12α-trihydroxycholanic

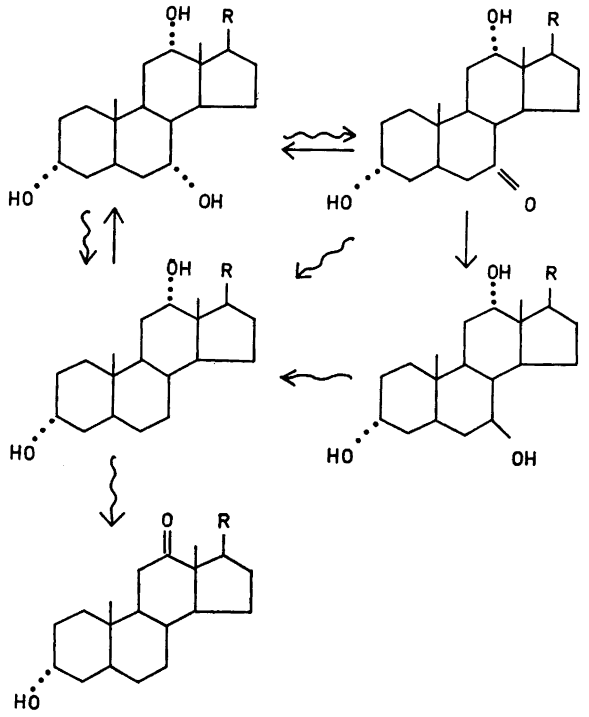

Fig. 6. ——→ Reaction caused by liver enzymes. ~~→ Reaction caused by intestinal microorganisms.

acid as shown by rechromatography with the unlabelled compound. No significant amount of tritium was eluted at the position of 7-ketodeoxycholic acid (160—280 ml effluent) or cholic acid (300—450 ml effluent).

Metabolites excreted in the bile. The hydrolyzed bile (containing 53 % (RI), 44 % (RII) and 38 % (RIII) of the injected ^3H) was chromatographed with solvent system C3 (Fig. 4). The main part of the radioactivity coincides with the titration peak (350—750 ml effluent) of the inactive cholic acid present in the bile. The identity was established by isotope dilution (Table 1). Traces of radioactivity appear at the position of 3α, 7β, 12α-trihydroxycholanic acid. The material remaining in the stationary phase was chromatographed with solvent system F together with unlabelled deoxycholic acid (Fig. 5). The main peak of radioactivity is eluted at the same position as the added inactive deoxycholic acid. At the beginning of this peak, however, contaminating labelled material of unknown nature is eluted. This could be removed by rechromatography with the same solvent system. The identity of labelled deoxycholic acid was established by isotope dilution. The following radioactive band (200—240 ml effluent) was identified as 12-ketolithocholic acid. The structure of the least hydrophilic compound (440—500 ml effluent) has not been determined.

DISCUSSION

When tritium labelled 3α, 7β, 12α-trihydroxycholanic acid was administered intraperitoneally to bile fistula rats it was excreted unchanged in the bile. In the large intestine, however, when administered by intracecal injection it was extensively transformed. The identified metabolites consisted of deoxycholic acid and 12-ketolithocholic acid. The labelled products excreted in the bile in these experiments, were identified as cholic, deoxycholic and 12-ketolithocholic acids. The labelled cholic acid found in the bile is most probably only formed by 7α-hydroxylation of deoxycholic acid absorbed from the intestine.

The numerous possibilities of converting cholic, deoxycholic, 7-ketodeoxycholic and 3α, 7β, 12α-trihydroxycholanic acids into each other are summarized in Fig. 6. Thus, different oxygen functions at C7 (ketone, α- and β-hydroxyl groups) in bile acids with the parent structure of deoxycholic acid are eliminated by microorganisms in the rat. Results available at present are not sufficient to establish whether cholic acid is the common denominator in the microbiological formation of deoxycholic acid by the following reactions:

$$7\alpha\text{-ol} \rightleftharpoons \text{7-ketone} \rightleftharpoons 7\beta\text{-ol}$$

or if the different functions are eliminated *per se*.

From experiments [10] with cholic acid-7-^{3}H-24-^{14}C, it is known that deoxycholic acid is synthesized *in vivo* with a negligibly intermediate formation of 7-ketodeoxycholic acid and that the dehydrogenation of cholic acid to 7-ketodeoxycholic acid is reversible in suspensions of *E. coli* [11].

Acknowledgements. The technical assistance of Miss H. Rytz is gratefully acknowledged. This work is part of an investigation supported by a research grant (H2842) to Prof. Sune Bergström from the *National Institutes of Health, United States Public Health Service,* Bethesda, Maryland, and by *Karolinska Institutets Reservationsanslag.*

REFERENCES

1. Norman, A. and Sjövall, J. *J. Biol. Chem.* **233** (1958) 872.
2. Sjövall, J. *Acta Chem. Scand.* **13** (1959) 711.
3. Gustafson, B., Norman, A. and Sjövall, J. *Acta Chem. Scand.* **14** (1960) 17.
4. Samuelsson, B. *Acta Chem. Scand.* **14** (1960) 17.
5. Wilzbach, K. E. *J. Am. Chem. Soc.* **79** (1957) 1013.
6. Hoehn, W. M. and Linsk, J. *J. Am. Chem. Soc.* **67** (1945) 312.
7. Bergström, S. and Haslewood, G. A. D. *J. Chem. Soc.* (1939) 540.
8. Bergström, S., Sjövall, J. and Voltz, J. *Acta Physiol. Scand.* **30** (1953) 22.
9. Bergström, S. and Sjövall, J. *Acta Chem. Scand.* **5** (1951) 1267.
10. Bergström, S., Lindstedt, S. and Samuelsson, B. *J. Biol. Chem.* **234** (1959) 2022.
11. Samuelsson, B. *Unpublished observation.*

Received September 10, 1959.

ACTA CHEMICA SCANDINAVICA 14 (1960) 28—42

On Vitamins in Sewage Sludge

XI. Further Studies on the Production of Vitamin B_{12} by Some Enrichment Cultures of Methane Bacteria

HALINA Y. NEUJAHR

Royal Institute of Technology, Division of Food Chemistry, Stockholm 70, Sweden

Fermentations with a methanol-fermenting and vitamin B_{12}-producing enrichment culture of methane bacteria were performed in order to find the most favourable conditions for obtaining high yields of vitamin B_{12}.

Stirring was not favourable for high yields of *E. coli* activity but, on the other hand, it resulted in the formation of only one vitamin B_{12} factor which seems to be the clinically active factor III of Bernhauer [5] or/and factor W[4], which has in earlier investigations been found to be active for *Ochromonas malhamensis*.

The conversion of the different vitamin B_{12} factors formed in non-stirred cultures to cyanocobalamin could not be achieved by adding greater than previously used amounts of 5,6-dimethyl benziminazole at the start or smaller amounts at a later stage of the fermentation. Concentrations of 10 μg benziminazole per ml medium inhibited the growth of the culture.

Under certain conditions, the addition of glucose was found to stimulate both the evolution of gas and the production of vitamin B_{12} activity. As far as could be observed, the carbohydrate had no effect upon the kind of vitamin B_{12} factors formed in synthetic media.

The addition of certain nitrogenous materials, *e. g.* corn steep liquor or casein hydrolyzates together with glucose, or casein hydrolyzates together with glucose and yeast extract, resulted in a greatly diminished synthesis of vitamin B_{12}. The possible reasons for this phenomenon are discussed.

The addition of sterilized sewage to the medium was found to have a favourable effect on vitamin B_{12} synthesis and can successfully replace the Bactopeptone (Difco) used in earlier experiments.

The greatest utilization of methanol was found to take place in media containing sterilized sewage.

It seems that vitamin B_{12} begins to accumulate in the cells when their metabolic activity (juged by gas evolution and methanol utilization) tends to decrease. However, no correlation between the utilization of methanol and the production of gas and vitamin B_{12} activity could finally be concluded, so far.

It has been reported earlier from this laboratory that enrichment cultures of methane bacteria produce varying amounts of vitamin B_{12} activity [1-3]. The enrichment culture producing the highest activity was the one obtained in a methanol-containing medium [3]. The present investigation is concerned with a further study of the conditions under which such a culture should be grown in order to obtain high yields of the vitamin. Fermentations were carried out in two liter vessels. The intensity of gas evolution was used as an indicator for the intensity of growth since other changes in the culture, *e.g.* turbidity, dry solids content, *etc.* were difficult to follow for reasons discussed elsewhere [1]. In one series of experiments, the influence of stirring was studied both with the enrichment culture obtained in the medium containing ethanol and consisting mainly of *Mb. omelianskii* [1], and with the enrichment culture obtained in the methanol-containing medium [3]. In the rest of the experiments, certain modifications of the earlier adopted medium [3] were studied using only the culture obtained in the methanol-containing medium. The following points were studied: 1. addition of greater than earlier used amounts of 5,6-dimethyl benziminazole (DMB) and variation of the time of this addition; 2. addition of organic nutrients, notably casein hydrolyzates, corn steep liquor, sterilized sewage, whey and glucose; 3. adjustment of the pH every day to the optimum value; 4. adjustment of the methanol concentration in the medium several times during the fermentation period.

Using certain modifications of the medium, it has been possible to obtain *E. coli* activities higher than 10 μg/ml calculated as cyanocobalamin in cup plate assay. These high activities represented, however, mixtures of several vitamin B_{12} factors. Attempts to get all these factors converted by the cultures to cyanocobalamin have not yet been successful, even if the yield of cyanocobalamin could be improved. The dominating factor(s) in the cultures was (were) probably factor W[4] earlier isolated from digested sludge in this laboratory and (or) factor III of Bernhauer[5]. The former factor was found to be active for *Ochromonas malhamensis* [4], which indicates that it may also be active for higher animals. The clinical activity of factor III has been proved [6]. It thus seems to be of considerable interest that the enrichment cultures of the methanol-fermenting organism can produce such high amounts of this(these)physiologically active factor(s).

EXPERIMENTAL

The fermentations were carried out in 2 l conical flasks provided with stoppered outlets at the bottom through which samples could be removed by means of a syringe. The tops of the flasks were closed with rubber stoppers provided with glass tubes containing sterile cotton wool filters, by means of which the flasks were connected, using rubber tubing, with devices for collecting and measuring the evolved gas. The gas collecting devices consisted of scaled cylindrical vessels of 1 l capacity, provided with two outlets, one at the bottom and one at the top. The top outlet was connected to the fermentation vessel whereas the bottom outlet was connected to a separating funnel, which functioned as a levelling flask. The gas was collected over a saturated aqueous solution of NaCl. The apparatus is shown schematically in Fig. 1. Up to six fermentations could be run simultaneously. The fermentation flasks were filled with media, only a little space being left above. The basal medium used in all experiments with the methanol-fermenting organism was the one previously used [3] and had the following composition:

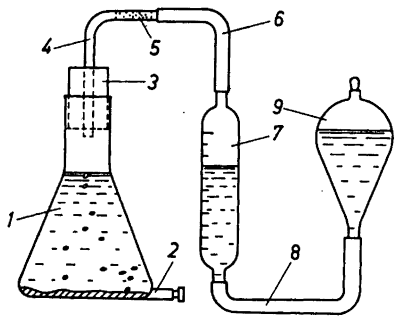

Fig. 1. Apparatus used in fermentations with a methanol-fermenting enrichment culture of methane bacteria. 1 fermentation flask; 2 outlet for taking samples; 3 pierced rubber tap; 4 bent glass tube; 5 cotton wool filter; 6 rubber tubing; 7 calibrated gas collection vessel; 8 rubber tubing; 9 levelling flask.

NH_4Cl	—	1.0 g
K_2HPO_4	—	0.4 g
$MgCl_2 . 6H_2O$	—	0.1 g
$CoCl_2 . 6H_2O$	—	10 mg
CH_3OH	—	10 ml
$CaCO_3$	—	15 g
Asbestos powder	—	5 g
Tap water	—	1 000 ml

Each fermentation flask was filled with 1 600 ml of this medium and, in addition, 160 ml of a separately sterilized solution consisting of 32 ml 1 % $Na_2S . 9H_2O$ solution + 128 ml of 5 % $Na_2CO_3 . 10H_2O$ solution, was added while the medium was still hot after autoclaving. If not otherwise stated, the methanol was autoclaved together with the medium. The pH of the final medium M was adjusted with separately sterilized HCl (1:5) to 6.5—7.5. The flasks were cooled in a nitrogen atmosphere, inoculated with 100 ml of the actively growing enrichment culture and incubated at 37°C for 2—3 weeks. Samples were removed every day and assayed for vitamin B_{12} activity as described elsewhere [7]. The gas evolved and the pH of the medium were also measured daily in all fermentations. The gas evolution is given in the tables and figures as the number of ml evolved from a 2 l vessel in 1 h. The vitamin B_{12} activity is given as the activity for *E. coli* 113-3 calculated as cyanocobalamin in the plate assay. In some experiments, determinations of reducing substances [8] and of methanol according to the *Official Methods of Analysis* [9] were performed. In some experiments, certain fractions of sterilized sewage were used as a substrate after supplementation with the components of medium M.

Further details of the different experiments are given below.

I. *Influence of stirring.* The influence of stirring was studied *a.* with the methanol-fermenting organism, and *b.* with the ethanol-fermenting one. The stirring was achieved by means of a magnete. Media: *a.* (M) supplemented with Bactopeptone, 0.25 %; *b.* Barker's medium (used already in earlier experiments [1]). In some vessels, the fermenting medium was covered with a layer of paraffin oil. The results are given in Tables 1 and 2.

II. *Influence of DMB.* The influence of DMB was studied only with the methanol-fermenting organism.

The purpose of this experiment was to investigate whether concentrations of DMB greater than those previously used or adding the DMB at a later stage of fermentation could lead to greater yields of cyanocobalamin at the expense of the other vitamin B_{12} factors. Medium: M supplemented with 0.25 % Bactopeptone and with *a.* 1 μg or 10 μg DMB/ml medium added at the beginning of the fermentation, or *b.* 1 μg DMB added after 8 days' fermentation. The results are shown in Figs. 2a and 2b.

III. *Influence of carbohydrates.* The influence of carbohydrates was studied only with the methanol-fermenting organism.

a. Glucose (10 g/l) was added to the medium M and its content as well as the pH were readjusted to their initial values four times during the fermentation period. DMB

was present in the medium from the beginning at a level of 1 μg/ml. *b.* Glucose was added to the medium M as in *a*, and its content as well as the pH were readjusted to their initial values every day. Methanol was added aseptically and its content readjusted to 1 % several times during the fermentation period. DMB was added after eight days' fermentation at a level of 1 μg/ml. *c.* Milk whey was mixed with sterilized sewage in the proportion 1:1. Methanol was added aseptically and its content readjusted several times to 1 %. DMB was present in the medium from the beginning.

For comparison parallel fermentations in all three cases, *a*, *b*, and *c*, were performed without the addition of carbohydrate. The results of these experiments are given in Figs. 3a, 3b and in Table 3.

IV. *Influence of organic nitrogen sources and yeast extract.* The influence of these materials was studied only with the methanol-fermenting organism.

In all fermentations of this series, methanol was sterilized separately and its content in the medium adjusted four times during the fermentation period. If not otherwise stated, DMB was added after 8 days' fermentation at a level of 1 μg/ml medium. The different supplements to the medium M were as follows:

a. Bactopeptone (Difco) 0.25 %; DMB.
b. Corn steep liquor added at a level corresponding to 0.4 % total nitrogen or ~0.2 % available nitrogen; DMB added at the beginning of the fermentation.
c. Acid hydrolyzed casein (Casaminoacids Vitaminfree, Difco) added at a level corresponding to 0.11 % total nitrogen; trypsin hydrolyzed casein (Bactogen, Vitrum) added at a level corresponding to 0.16 % total nitrogen; glucose 1 %; DMB added at the beginning of the fermentation.
d. Nitrogen sources and glucose as in *c.*; Yeast Extract (Difco) 0.25 %; DMB.
e. The medium consisted of sterilized sewage supplemented with the components of medium M and with DMB.
f. Medium as in *e*, further supplemented with glucose 1 % and Yeast Extract (Difco) 0.25 %.

The results of this experiment are shown in Figs. 4a, 4b, 4c, 4d, 4e and 4f.

V. *Utilization of methanol.* Fermentations were performed as in the other experiments using the methanol-fermenting organism and six different modifications of the basal medium M. The modifications used are given in Table 4. The amounts of the different materials added to medium M were the same as in corresponding additions applied in

Table 1. The influence of stirring on the gas production and vitamin B_{12} activity of an enrichment culture of a methanol-fermenting methane organism. Experimental details in text.

Time of fermentation h	Gas evolution ml/h *			*E. coli* activity μg/ml **		
	stirring	stirring + oil layer	no stirring	stirring	stirring + oil layer	no stirring
0	0	0	0	0	0	0
20	17	14	34		0.1	
25	22	25	50	0.1	0.1	0.5
28	23		53			
44	32	30	70	0.3	0.3	1.0
53	35		80			
92	30	22	70	0.8	0.8	4.6
116	25	20	60	0.9	0.8	4.6
140	23		50	1.0		4.6
164	17	24	46	1.0	0.9	4.6

* evolved in a 2 liter fermentation flask
** calculated as cyanocobalamin in plate assay

the experimental series III and IV. In all fermentations in this series, DMB was added after 8 days. MeOH was added aseptically to the sterile medium and its content determined three times during the fermentation period. After each determination, the level of the methanol in the medium was readjusted to its initial value (1 %). The results of these experiments can be seen in Table 4.

RESULTS AND DISCUSSION

I. *Influence of stirring.* It seems from Table 1 that stirring is unfavourable for both gas evolution and production of vitamin B_{12} in fermentations with the methanol-fermenting organism. In fermentations with *Mb. omelianskii* (see Table 2) the use of stirring together with a covering oil layer gave higher values for the *E. coli* activity than those obtained with stirring alone. This may be explained by the fact that stirring facilitates the distribution of the oxygen which has diffused in from the surrounding air and which is harmful to the growth and, thus also, to the production of vitamin B_{12}. Since the evolution of gas in this fermentation is very slow, the diffusion of oxygen from the air may be quite important if oil is not used. The *E. coli* activity values obtained in the fermentations with *Mb. omelianskii* are so small that no further conclusions can be made about the influence of stirring.

In the methanol fermentation (see Table 1) an oil layer together with stirring does not give a higher gas evolution than that obtained with stirring alone whereas the stationary fermentation gives the highest gas evolution and vitamin B_{12} activity. Thus the unfavourable effect of stirring upon the production of gas and vitamin B_{12} activity cannot be explained by the distribution throughout the medium of the diffused oxygen. Besides, the evolution of gas is so strong in this fermentation that a diffusion of oxygen into

Table 2. The influence of stirring on the gas production and vitamin B_{12} activity of an enrichment culture of *Mb. omelianskii.* Experimental details in text.

Time of fermentation h	Gas evolution ml/*h* *			*E. coli* activity μg/ml **		
	stirring	stirring + oil layer	no stirring	stirring	stirring + oil layer	no stirring
20	6	1	6			
28	14	7	8			
42	9	4	9	0.001	0.001	0.001
50	7	5	2			
66	4	8	2			
74	1	11	1			
90	0.5	8	1	0.001	0.003	0.001
115	0.1	2	0.6			
137	0.2	0.2	0.2	0.001	0.003	0.001
162	0.2	0.1	0			
166	0.2	0.2	0.1	0.002	0.004	0.001
190	0.2	0.3	0.2			
215	0	0	0	0.002	0.004	0.002

* evolved in a 2 liter fermentation flask

** calculated as cyanocobalamin in plate assay

the medium is not probable since an overpressure in the medium is established very soon after the start of the fermentation. The reasons for the unfavourable effect of stirring could thus not be deduced. Possibly, the stirring causes a disintegration of some complexes or configurations of the medium components which are favourable for the growth of the organism. It would be interesting to investigate whether the same effect is produced at different stirring rates. This, however, could not be done in the present investigation. Still, it cannot be understood why stirring had such distinctly different effects on two different enrichment cultures of methane organisms.

Chromatographic and electrophoretic studies were performed only with the methanol-fermenting culture since the enrichment culture of *Mb. omelianskii* produced such small amounts of *E. coli* activity. The results of these studies indicate that stirring, although not favourable for the production of gas and *E. coli* activity, may cause a different distribution of the activity between the various vitamin B_{12} factors than is the case in a stationary fermentation. Thus stirring seems to favour the formation of vitamin B_{12} substances which upon chromatography and electrophoresis give only one spot. The position of the spot indicates that it may be identical with factor III (Bernhauer) [5] and/or factor W (Neujahr) [4] and possibly other factors with R_c-values in the range 0.6—0.7 (*cf.* Ref.[4]). The phenomenon could be noticed even if DMB (1 μg/ml) was present in the medium. In the stationary fermentations, on the other hand, the *E. coli* activity formed could always be separated by chromatography into three spots if DMB had not been added to the medium and into four spots if it had been added. The four spots corresponded to the following factors: spot 1 - factor B (Ford) [10] spot 2 - cyanocobalamin, spot 3 - factor III (Bernhauer) [5] and/or factor W (Neujahr) [4] and possibly other factors with R_c-values in the range 0.6—0.7 (*cf.* Ref.[4]), spot 4 - factors Z (Neujahr) [4]. The distribution of *E. coli* activity between the different factors

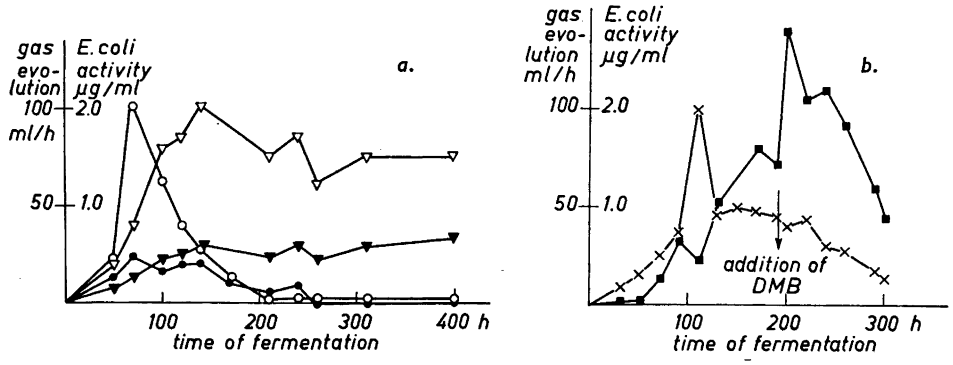

Fig. 2. Influence of 5,6-dimethyl benziminazole (DMB) on the gas production and *E. coli* activity of a methanol fermenting enrichment culture of methane bacteria. a. DMB added at the beginning: O—O—O gas evolution, ▽-▽-▽ *E. coli* activity in a fermentation with 1 μg DMB/ml medium; ●—●—● gas evolution, ▼—▼—▼ *E. coli* activity in a fermentation with 10 μg DMB/ml medium. b. 1 μg DMB/ml medium added after 192 h of fermentation: X—X—X gas evolution, ■—■—■ *E. coli* activity.

as found in this experiment is in agreement with previous experience [3]. Since stirring did not seem to give higher yields of vitamin B_{12}, not even when applied together with a covering oil layer, only stationary fermentations were carried out in the following experiments. For convenience no oil layer was employed.

II. *Influence of DMB.* It can be seen in Fig. 2a that the addition of 10 μg instead of 1 μg DMB per ml medium has a strongly inhibiting effect on both evolution of gas and production of vitamin B_{12} activity. A similar inhibitory effect of DMB on the enrichment culture of *Mb. omelianskii* has been reported earlier from this laboratory [1]. The inhibitory effect of benziminazoles upon the growth of several microorganisms is well known and attributed to its competition with adenine or guanine [11]. The inhibitory effect of benziminazoles may be influenced by vitamin B_{12} [12]. On the other hand, Pawelkiewicz [13] has used amounts of 20 μg DMB per ml medium in his fermentations with *Propionibacterium shermannii* for production of vitamin B_{12} without reporting any inhibition of the bacterial growth. Bernhauer [14] reports the use of amounts up to 40 μg DMB per ml medium in similar fermentations without mentioning any inhibitory effect on growth. In fermentations with *Propionibacterium shermannii* carried out in our laboratory [15], in which large additions of DMB (30 μg/ml) were used together with glucose and different modifications of the conventional medium, no such effect could be noticed. Thus it seems that the effect of DMB on cultures of vitamin B_{12}-producing methane bacteria differs from its effect on cultures of vitamin B_{12}-producing propionic acid bacteria. The following conclusions could be made at this point:

1) DMB seems to inhibit the growth of the methanol-fermenting organism, at least when added at a level of 10 μg/ml.

2) In the presence of DMB, on the other hand, cyanocobalamin is formed in preference to other vitamin B_{12} factors [3].

3) In the presence of DMB, several vitamin B_{12} factors could be converted to cyanocobalamin by an enrichment culture of another methane organism, viz. *Mb. omelianskii.*

Starting from the above three statements, a fermentation was made in which the methanol-fermenting culture was allowed to grow without added DMB for 192 h, after which time DMB was added to the medium at a level of 1 μg/ml. It was hoped that the amply formed vitamin B_{12} factors would then be converted to cyanocobalamin. The course of this fermentation can be seen in Fig. 2b. A comparison of Figs. 2a and 2b leads to the following conclusions: Fermentation without added DMB seems to proceed somewhat more slowly than in the presence of 1 μg DMB/ml medium. This is in agreement with previous experience with the methanol-fermenting organism [3]. Adding 1 μg DMB/ml medium after 192 h of fermentation results in a sudden increase of *E. coli* activity to a value which is about 50 % higher than the highest value in the corresponding fermentation with DMB added at the beginning. However, this higher *E. coli* activity decreases again very rapidly contrarily to what is the case in the fermentation with DMB added at the beginning. Chromatographic studies revealed further that the addition of DMB after 192 h results in the formation of a considerably smaller amount of cyanocobalamin than is the case in the fermentation in which DMB is added at the

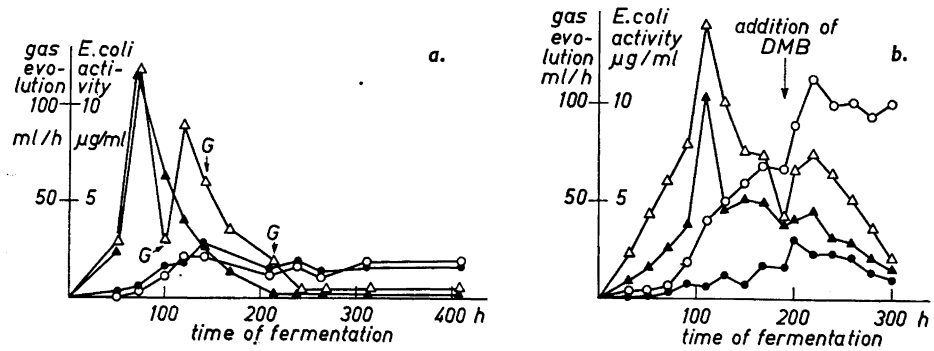

Fig. 3. Influence of glucose on the gas production and *E. coli* activity of a methanol-fermenting enrichment culture of methane bacteria. ▲—▲—▲ gas evolution, ●—●—● *E. coli* activity in the fermentation without glucose; △—△—△ gas evolution, O—O—O *E. coli* activity in the fermentation with glucose. a. DMB added at the beginning, methanol level not adjusted: G readjustment of the glucose level. b. DMB added after 192 h, methanol level adjusted, glucose level and pH readjusted daily.

beginning. Thus the conversion of the different vitamin B_{12} factors to cyanocobalamin cannot be achieved by this method, at least not with the level of DMB used. The factors predominantly produced in such fermentation are again factor III or/and factor W together with only smaller amounts of cyanocobalamin, factor B and factors Z.

It seems from above that smaller amounts of DMB (1 µg/ml) may be favourable for the fermentation, especially in its initial phase, whereas higher amounts of DMB (10 µg/ml) are harmful to the fermentation. This harmful effect depends probably on the known antimetabolic effect of benziminazoles [10,11] whereas the favourable effect of small amounts of DMB may depend on the fact that it is a precursor of cyanocobalamin and at a low concentration — 1 µg/ml — may not produce the antimetabolic effect.

III. *Influence of carbohydrates. a.* The course of two fermentations, in which DMB was added at the beginning and the level of methanol not adjusted during the fermentation time, is shown in Fig. 3a. In one of the fermentations glucose was present and its level adjusted 3 times during the fermentation period. It seems from Fig. 3a that, under the conditions stated above, glucose may stimulate the evolution of gas if added at a relatively early stage of the fermentation. Thus the adjustment of the glucose level (to 1 %) after 100 h results in a considerably increased gas evolution whereas repeated readjustments of glucose after both 140 h and 214 h have no longer such an effect. It should be mentioned that the last two readjustments necessitated the addition of approximately the same amounts of glucose as the first one. The glucose was thus being consumed in the medium all the time.

The production of vitamin B_{12} activity does not seem to be affected by the addition of glucose under the conditions described above.

b. Two other fermentations were performed in which DMB was added after 192 h and methanol added aseptically to the sterilized medium and its

level readjusted to the initial value (1 %) several times during the fermentation. In one of the fermentations, glucose was also present and its level was determined and readjusted to the initial value (1 %) every day. The course of these two fermentations is represented in Fig. 3b. It is evident from Fig. 3b that, under the new and more carefully controlled conditions, the addition of glucose very distinctly stimulates the formation of both gas and vitamin B_{12} activity. The highest *E. coli* activity obtained in this fermentation, *viz.* 11 μg/ml calculated as cyanocobalamin in the plate assay, is higher than any other activity obtained in fermentations of this kind. Moreover, in the fermentation in which the level of glucose was adjusted every day to 1 %, the vitamin B_{12} activity once formed is not destroyed again as is the case in the corresponding fermentation without glucose. Since the favourable effect of glucose appears only when the level of methanol is maintained at a somewhat constant value, it may be assumed that both substances are necessary for the high production of gas and vitamin B_{12}. The favourable effect of low molecular carbohydrates upon the production of vitamin B_{12} in septic methane fermentations of sewage sludge with *Mb. omelianskii* has been reported also by Cserei-Pehany [16].

c. In a separate experiment in this series, an attempt was made to use milk whey instead of glucose as a source of carbohydrate. The results are given in Table 3. It can be seen there that the addition of whey leads to a somewhat lower gas production but a consistently higher production of vitamin B_{12} activity throughout the fermentation than is the case in the corresponding fermentation without added carbohydrate. The highest *E. coli* activity obtained in the fermentation with whey is of the order of 3—4 μg/ml, calculated

Table 3. The influence of milk whey on the gas production and vitamin B_{12} activity of an enrichment culture of a methanol-fermenting methane organism.

Time of fermentation h	Medium supplemented with whey		Medium not supplemented	
	Gas evolution ml/h *	*E. coli activity* μg/ml **	Gas evolution ml/*h* *	*E. coli* activity μg/ml **
38	0		2	
62	0	0.1	16	0.02
90	12		15	
111	12	0.9	28	0.1
158	45	2.4	42	0.6
182	28		42	
209	37	3.1	44	1.5
233	42	3.1	48	1.9
258	33		50	
278	3	3.0	25	2.1
326	2	3.4	22	3.1
350	0	3.9	3	2.6
380	0		3	
405	0	3.2	12	2.8

* evolved in a 2 l fermentation flask
** calculated as cyanocobalamin in plate assay

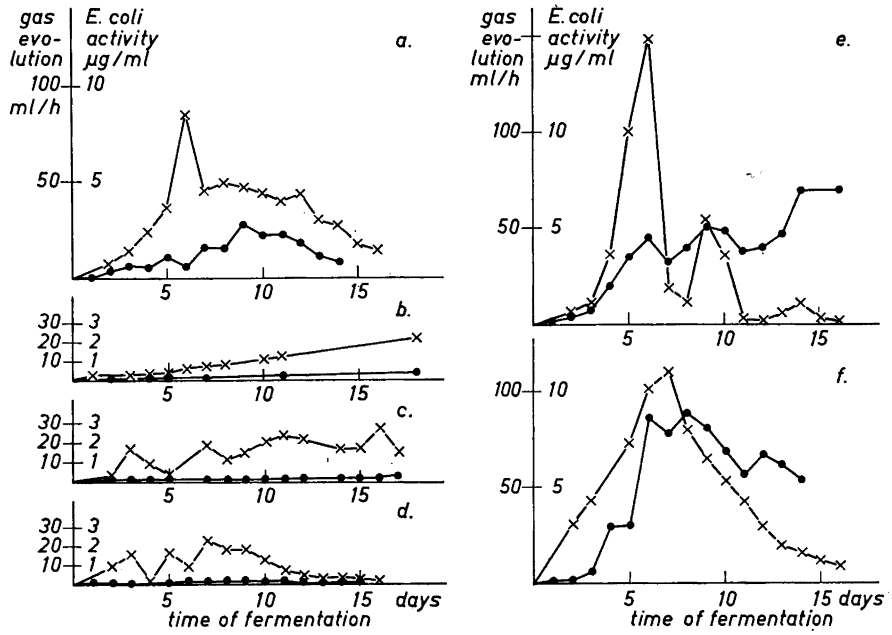

Fig. 4. Influence of certain nitrogenous materials on the gas production and vitamin B_{12} activity of a methanol-fermenting enrichment culture of methane bacteria. X—X—X evolution of gas, ●—●—● *E. coli* activity calculated as cyanocobalamin in plate assay. Basal medium containing. a. Bactopeptone. b. corn steep liquor. c. casein hydrolyzates + glucose. d. casein hydrolyzates + glucose + yeast extract. e. sterilized sewage. f. sterilized sewage + glucose.

as cyanocobalamin in the plate assay. These values are not directly comparable with those of the fermentations with glucose since, as described in Experimental, a different medium was used in the fermentations with whey and only fermentations with DMB added at the beginning were carried out.

Chromatographic and electrophoretic studies of the *E. coli* activity did not reveal any differences between the kind of factors formed in fermentations with and without the addition of carbohydrate to the basal medium. Chromatography gave spots corresponding to the following factors (listed in order of decreasing amounts): factor W[4] and/or III [5], factor B[10], cyanocobalamin, factors Z [4]. In the fermentations performed under more carefully controlled conditions, *i.e.* repeated readjustments of the glucose content, pH and methanol, a certain regularity in the occurrence of factors Z, B and W and/or III could be observed. Thus, during the first two or three days of the fermentation, there occurred a chromatographically almost immobile factor, different from factors Z2 + Z3 [4]. The behaviour of this factor was similar to that of factor C_2[17] (*cf.* Ref.[4]). This factor disappeared simultaneously as factors Z2 + Z3 appeared in the medium. The latter factors could usually be observed for the following two or three days, after which time their content

decreased markedly and they finally disappeared. Simultaneously with the disappearance of factors Z2 + Z3, factor B began to appear. Factors W and/or III were present all the time. A similar sequence for the appearance of factors C_2, C_1[17] (which may possibly be identical with factor Z3) and B has been observed earlier in anaerobically decomposing sewage sludge [18].

IV. *Influence of organic nitrogen sources and yeast extract.* It has been found in an earlier investigation [3] that the addition of Bactopeptone (Difco) stimulated both the production of gas and the vitamin B_{12} activity. An attempt was now made to elucidate whether other nitrogenous sources may have a similar and possibly more pronounced effect since the use of *a.* Bactopeptone, is very expensive. It can be seen in Fig. 4 that the addition of *b.* corn steep liquor (Fig. 4b), *c.* casein hydrolyzates together with glucose (Fig. 4c), and *d.* casein hydrolyzates together with glucose and yeast extract (Fig. 4d) results in a greatly diminished production of gas and vitamin B_{12} activity as compared with the fermentation with Bactopeptone (Fig. 4a). The shape of the gas evolution curves in Figs. 4b, 4c, and 4d is also quite different from the shape of the corresponding curve in Fig. 4a and the corresponding curves in Figs. 2a, 2b, 3a, 3b. Thus, the maximum in the gas evolution, which usually occurs between 70—110 h in the fermentations with the methanol-fermenting organism, is missing in those fermentations in which the above mentioned modifications of the conventional medium were employed. In the fermentations with casein hydrolyzates (Fig. 4c and 4d), the gas evolution curve has instead a "pulsating" character and the maximum gas evolution values are 4—5 times lower than the maximum values in other fermentations of this kind. A suspicion has arisen that, in the fermentations with media modified according to *b*, *c*, and *d*, some other organisms present in the enrichment culture of methane bacteria have developed due to the fact that the modified media might not have been any longer selective for the methanol-fermenting organism. At least in so far as the fermentations with casein hydrolyzates (Figs. 4c and 4d) are concerned, such a suspicion was jutified by the results of microscopic studies, by the putrefactive odour produced in these fermentations and also by the "pulsating" character of the gas evolution. In these fermentations, motile, possibly rod shaped organisms seemed to be present together with the coccoidal forms and the immobile rods usually present in fermentations of this kind [3]. Some of the motile forms may possibly have had the characteristic shape of *Clostridia*. However, the microscopic studies were rendered very difficult by the fact that methane bacteria grow mostly in the sediment [1] (*i.e.* the asbestos powder, calcium carbonate and sediment produced during the fermentation) the particles of which were very difficult to separate from the bacterial cells. Thus, under the microscope, the bacteria always appeared imbedded in a bulky precipitate and no definite conclusions about their shape could be made. There remains, however, the fact that certain motile forms were present in the cultures which was inconsistent with the immobile character of methane bacteria.

Further support for the suspicion that some *Clostridia* developed in the fermentations with casein hydrolyzates came from the results of chromatographic and electrophoretic studies. The *E. coli* activity produced in these fermentations was found to contain ψ-B_{12} together with factors W [4] and/or

III [5], B^{10} and cyanocobalamin. None of the methane bacteria studied so far was found to produce ψ-B_{12}[1,3]. On the other hand, certain strains of *Clostridia* were found, in a separate study, to produce ψ-B_{12}[10].

In the fermentation with corn steep liquor (Fig. 4b), the shape of the gas evolution curve is still more different from the gas evolution curves usually obtained in the fermentations with methane bacteria. Not only are the gas evolution maxima missing — at least during the period investigated — but also the gas evolution is extremely slow (2—3 ml/h) during the first five days of fermentation after which it increases slowly but steadily and, after eighteen days, still shows a tendency to increase. It should further be mentioned that, during the first five days, which were characterized by an extremely slow gas evolution (*cf.* Fig. 4b), the pH of the medium decreased considerably (to 6.5—6.7) after each of the daily readjustments to its optimum value (7.2) whereas, during the following period of time, characterized by a steady increase in gas evolution, the changes of pH were less pronounced and limited to the range 6.7—6.9 even without readjustments which were therefore no longer undertaken after 7 days of fermentation.

Microscopic examinations did not indicate that other organisms than the methanol-fermenting methane bacteria may have developed in the fermentation. Neither could any putrefactive odour be detected in the fermentation flask as was the case in the fermentations with casein hydrolyzates.

Knivett in England who has succeeded in growing a methane organism in a continuous culture [20] suggests that "a starved cell, which has to synthesize cell material from the simplest materials, may need to produce a lot of B_{12} coenzyme to do this whilst a cell adequately supplied with growth factors, amino acids etc., has no need to synthesize them and its coenzyme requirement may be less"[20]. Corn steep liquor is considered to be a source of most essential nutrients. According to the attractive suggestion of Knivett, the addition of corn steep liquor would thus result in a considerably diminished synthesis of vitamin B_{12} until the supply of the nutrients was exhausted in the medium. But can a similar relation apply also to the production of gas? (*cf.* Fig. 4b), *i.e.*, can the adequately supplied cells of the methanol-fermenting methane organism satisfy their growth requirements in a different way than by producing methane gas? (*cf.* also the above mentioned changes of pH!). The results of the present investigation are, however, much too preliminary to permit speculations of this kind. It should further be remembered that an enrichment and *not* a pure culture of the methanol-fermenting organism was used in the experiment. Bactopeptone is also an excellent source of different nutrients but it was found to stimulate both the production of gas and vitamin B_{12} activity in cultures of the methanol-fermenting organism [3]. On the other hand, the mutual relation of gas evolution and vitamin B_{12} activity curves in most fermentations with the enrichment culture can be plausibly interpreted by the suggestion of Knivett [20]. It can be seen for instance in Figs. 2a, 2b, 3a, 3b, 4a that the maximum in *E. coli* activity always comes *after* the maximum in gas evolution. It seems that the vitamin B_{12} content of the cells begins to increase as their metabolic activity — judged by the gas evolution — tends to decrease, probably due to the exhaustion of certain nutrients in the medium.

It can be seen in Fig. 4e that the use of sterilized sewage in the medium greatly stimulates the evolution of gas and production of vitamin B_{12} activity as compared for instance with Bactopeptone. The maximum gas evolution obtained in this fermentation is much greater than with most other modifications of the basal medium and comparable perhaps only with the medium containing glucose, DMB added after 8 days in the fermentation with regularly adjusted pH and methanol content (Fig. 3b). As in the fermentations with casein hydrolyzates (*cf.* Figs. 4c and 4d), the gas evolution curve has three maxima. However, here the second maximum is much smaller than the first and the third much smaller than the second. No indications could be found that other organisms than the methanol-fermenting one had developed in the culture. The curve for *E. coli* activity (Fig. 4e) shows a steady tendency to increase apart from two less pronounced maxima which seem to correspond to the first two maxima of the gas evolution curve. Between the 14th and 16th day of fermentation, the *E. coli* activity remains at the level of 7 μg/ml which is very high compared with the yields obtained in the fermentations in which nitrogenous materials were added (*cf.* Figs. 4a, 4b, 4c and 4d).

A still higher yield of *E. coli* activity, *viz.* 9 μg/ml, was obtained in a similar fermentation with sterilized sewage in which, however, the medium was further supplemented with glucose and yeast extract (Fig. 4f). The maximum value of *E. coli* activity was obtained after only 8 days of fermentation, after which time the activity tended to decrease again.

Chromatographic and electrophoretic studies revealed that the *E. coli* activity produced in the fermentations with sterilized sewage was mainly due to factors W[4] and/or III [5]. Roughly estimated, at least 70 % of the *E. coli* activity was contributed by these factors. Cyanocobalamin was present in much smaller amounts than the above factors. Factors B and Z were present only in trace amounts. In the fermentations with sterilized sewage, in which the medium was further supplemented with glucose and yeast extract, the dominant factors were factor W[4] or/and III[5] and factor B[10]. Cyanocobalamin was present in much smaller amounts than in the fermentations with sterilized sewage only. Thus the higher *E. coli* activity obtained in the further supplemented medium (Fig. 4f), *viz.* 9 μg/ml instead of 7 μg/ml (Fig. 4e) in the medium containing only sterilized sewage, may not reflect a really higher yield of vitamin B_{12} obtained in the richer medium since, according to previous experience [4], factor B gives much greater growth zones than cyanocobalamin when assayed by the plate method. Very small amounts of factors Z[4] and of some not identified factors were also produced in the fermentation with sterilized sewage, glucose and yeast extract.

It seems from the above that sterilized sewage, supplemented in an appropriate way provides a very good medium for obtaining high yields of vitamin B_{12} activity in fermentations with the methanol-fermenting enrichment culture of methane bacteria. It has also been successfully used in this laboratory for the cultivation of other vitamin B_{12}-producing organisms [15]. As described above (*cf.* p. 36), the addition of glucose to the basal medium M may lead to even higher yields of *E. coli* activity (Fig. 3b), *viz.* 11 μg/ml, than is the case in the fermentation with sterilized sewage (Fig. 4e). However, with glucose, greater amounts of factor B are formed and this makes un-

Table 4. Gas evolution, vitamin B_{12} production and utilization of methanol by an enrichment culture of a methanol-fermenting organism grown in different media. Experimental details in text.

Media / ıe of nen-on h	M + BP + DMB			M + BP + DMB + G			M+BP+ +DMB + G +Cas.ac. + Bactogen + YE			SM + YE			SM + DMB			SM + DMB + G + YE		
	Gas	B_{12}	MeOH	Gas	B_{12}	MeOH	Gas	B_{12}	MeOH	Gas	B_{12}	MeOH	Gas	B_{12}	MeOH	Gas	B_{12}	MeOH
0	0	0.2	0	0	0.2	0	0	0.2	0	0	0.2	0	0	0.2	0	0	0.2	0
10	85	0.5	0.09	140	4.6	0.11	10	0.05	0.07	116	4.4	0.15	150	2.0	0.09	104	2.5	0.11
30	36	2.3	0.08	72	10	0.14	5	0.15	0.04	30	4.4	0.05	4	4.4	0.18	25	6.4	0.03
50	0	0.8	0.02	0	10	0.07	0	0.15	0.03	0	7.4	0.08	0	7.0	0	0	5.4	0

M — basal medium described in the text
BP — Bactopeptone (Difco, 0.25 %)
DMB — 5,6-dimethyl-benziminazole,1 μg/ml
G — glucose, 1 %
Cas.ac. — Casaminoacids Vitaminfree (Difco)
Bactogen — trypsin hydrolyzed casein (Vitrum)
YE — yeast extract (Difco)
SM — sterilized sewage, supplemented with components of medium M

Gas — ml/h in a 2 l fermentation flask
B_{12} — μg/ml calculated as cyanocobalamin in plate assay
MeOH — ml methanol used/h in a 2 l fermentation flask

certain, once again, a direct comparison of the *E. coli* activity values obtained in the fermentations with glucose with those obtained in the fermentations with sterilized sewage. It should also be mentioned that the sterilized sewage contained only negligible amounts of reducing sugars.

V. *Utilization of methanol.* It can be seen in Table 4 that the greatest utilization of methanol took place in the fermentations with sterilized sewage in the medium. A somewhat lower utilization of methanol can be noticed in the media to which glucose had been added while the lowest utilization was observed in the media containing Bactopeptone or casein hydrolyzates. The latter finding may provide an interesting contribution to the discussion on p. 39. However, no conclusions concerning the relation between utilization of methanol and an adequate supply of preformed cell material can so far be made for various reasons — *viz.* partly because the values for methanol utilization, given in Table 4, are too few, and also because no sure correlation between utilization of methanol, production of gas and production of vitamin B_{12} activity can be deduced from Table 4 even if in most cases the vitamin B_{12} activity tends to increase when the utilization of methanol begins to decrease.

VI. *Maintainance of optimum pH.* As was described above, certain fermentations were performed with a daily readjustment of the pH to its optimum value for the methanol-fermenting organism (7.2). However, it was found that, in the media not containing glucose, the changes in pH were very small. After a few days of fermentation, these media exhibited in addition a very strong buffering capacity in the range 6.8—7.0. On the other hand, the fermentations in media containing glucose were characterized by considerable daily decreases in pH.

Acknowledgements. The author wishes to thank Professor H. Lundin, Head of the Division, for his encouraging interest in this work and Assistant Professor N. Nielsen, AB Kabi, Stockholm, for the generous gift of corn steep liquor and kind information about its chemical composition. The valuable technical assistance of Ing. Giancarlo Rossi-Ricci is gratefully acknowledged.

REFERENCES

1. Neujahr, H. Y. and Callieri, D. A. *Acta Chem. Scand.* **12** (1958) 1153.
2. Neujahr, H. Y. and Callieri, D. A. *Acta Chem. Scand.* **12** (1958) 1167.
3. Neujahr, H. Y. and Callieri, D. A. *Acta Chem. Scand.* **13** (1959) 1453.
4. Neujahr, H. Y. *Acta Chem. Scand.* **10** (1956) 917.
5. Friedrich, W. and Bernhauer, K. *Angew. Chem.* **65** (1953) 627.
6. Bernhauer, K., Blumberger, Kj. and Petrides, P. *Arzneimittel-Forsch.* **5** (1955) 442.
7. Neujahr, H. Y. *Acta Chem. Scand.* **11** (1957) 1191.
8. *Tekniska meddelanden.* Svenska Pappers och Cellulosa Ingenjörsfören. *C. C. A.* **11** (1942).
9. *Off. Meth. An. Ass. Off. Agric. Chem.* 8th ed., 1955, p. 142.
10. Ford, J. E., Kon, S. K. and Porter, J. W. G. *Biochem. J.* **50** (1951) ix.
11. Woolley, D. W. *A Study of Antimetabolites*, John Wiley & Sons, N. Y. 1952, p. 56.
12. Funk, H. B. and Nathan, H. A. *Proc. Soc. Exptl. Biol. Med.* **99** (1958) 394.
13. Pawelkiewicz, J. *Acta Biochim. Polon.* **1** (1954) 313.
14. Bernhauer, K., Becher, E. and Wilharm, G. *Abstracts VII*th Intern. Congr. Microbiol. Stockholm 1958, p. 400.
15. Neujahr, H. Y., Kurz, W. G. and Rossi-Ricci, G. *Arkiv Kemi. In press.*
16. Cserei-Pehany, E. and Richter, G. *Abstracts VII*th *Intern.* Congr. Microbiol. Stockholm 1958, p. 377.
17. Kon, S. K. *Biochem. Soc. Symposia Cambridge, Engl.* No **13** (1955) 23.
18. Neujahr, H. Y. *Acta Chem. Scand.* **9** (1955) 622.
19. Neujahr, H. Y. and Rossi-Ricci, G. *Acta Chem. Scand.* **14** (1960) 43.
20. Knivett, V. A. *Private communication.*

Received August 20, 1959.

ACTA CHEMICA SCANDINAVICA 14 (1960) 43—47

On Vitamins in Sewage Sludge

XII. Production of Vitamin B_{12} by Certain *Clostridia*

HALINA Y. NEUJAHR and GIANCARLO ROSSI-RICCI

Royal Institute of Technology, Division of Food Chemistry, Stockholm 70, Sweden

The ability to produce vitamin B_{12} was investigated in three strains of *Clostridia*.

The strains were found to produce amounts of *E. coli* activity ranging from 16—60 mμg/ml medium, calculated as cyanocobalamin in plate assay. These amounts are considerably smaller than those obtained in this laboratory with certain methane bacteria [6,7].

The addition of Co^{2+} was found to have only a negligible effect on the production of *E. coli* activity.

The factors mainly produced by the strains are factor A and ψ-B_{12}. If the medium is supplemented with 5,6-dimethyl benzimidazole, however, cyanocobalamin is produced almost exclusively.

As reported from this laboratory [1] and by several other authors [2–4], digested sewage sludge contains considerable amounts of vitamin B_{12} activity. It has also been reported earlier from this laboratory that the formation of vitamin B_{12} activity during the anaerobic decomposition of sewage sludge proceeds in several stages and seems to be caused by several different microorganisms [5]. The initial stages of the anaerobic sludge fermentation imply the decomposition of high molecular organic matter (proteins, fats and carbohydrates) to low molecular compounds (alcohols and fatty acids). The latter compounds are utilized during the final stages of the anaerobic sludge decomposition by methane bacteria with a simultaneous formation of large amounts of methane and carbon dioxide.

It was found in this laboratory that several of the methane organisms active during the final stages of the anaerobic sludge decomposition produce vitamin B_{12} activity [6]. Some of the methane organisms were found to produce considerable amounts of certain vitamin B_{12} factors when grown in appropriate media [7]. It was therefore considered to be of interest to investigate also whether the organisms active during the initial stages of the anaerobic sludge decomposition produce vitamin B_{12} activity and, if that is the case, which particular vitamin B_{12} factors are synthesized.

According to Enebo [8], the quantitatively most important group of organic materials in municipal sewage are high molecular carbohydrates. The organisms known to decompose such carbohydrates under anaerobic conditions are *Clostridia*. Three available strains of *Clostridia*, which presumably are active also during the anaerobic decomposition of sewage sludge, were grown in a medium containing maize meal, yeast autolyzate and phosphates both with and without the addition of Co^{2+} and 5,6-dimethyl benziminazole. The ability of these strains to produce vitamin B_{12} activity was investigated.

EXPERIMENTAL

The three strains of *Clostridia* investigated were

1. *Clostridium acetobutylicum* Weizmann (AB)
2. *Clostridium butylicum* (B4)
3. *Clostridium butylicum* (B6)

The cultures were maintained in the form of spores in soil.

Basal medium. Maize meal 70 g, yeast antolyzate (12 h at 50–60°C) 25 ml, $NH_4H_2PO_4$ 5 g, KH_2PO_4 1 g, dist. water 1 000 ml. The maize meal was boiled for about 30 min and mixed with the yeast autolyzate and salts. The pH was adjusted to 6 with NaOH and finally with $CaCO_3$ and the medium autoclaved for 1 h at 120°C and steamed the following day.

Preparation of the inocula. 10 ml portions of the sterile medium in test tubes (18 × 200 mm) were inoculated with 2 ml of a soil-spore suspension in a sterile saline solution which had been submitted to a heat shock (2 min in boiling water). The test tubes were incubated at 37°C for 24 h in evacuated vessels containing an alkaline pyrogallol solution. After this time, a considerable gas evolution usually took place.

Fermentations for determining the ability of Clostridia to produce vitamin B_{12}. 20 ml portions of the sterile medium in 50 ml E-flasks were inoculated with 5 ml of inoculum prepared as described above. The flasks were incubated at 37°C for either 7 or 14 days in evacuated vessels containing alkaline pyrogallol solution. Six simultaneous fermentations were performed with each strain according to the following scheme:

No. of flasks	Additions to the basal medium	Time of fermentation days
1	none	7
1	»	14
1	Co^{2+}, 2.5 μg/ml	7
1	» 2.5 »	14
1	Co^{2+}, 2.5 μg/ml + 5,6-dimethyl benziminazole, 1 μg/ml	7
1	—»— —»—	14

The Co^{2+} was supplied as a 0.1 % solution of $CoCl_2 \cdot 6H_2O$.

Vitamin B_{12} activity was determined by the cup plate method using *E. coli 113-3* as described elsewhere [5]. Chromatographic determinations were performed in solvent system I[9] and paper electrophoresis according to Holdsworth [10] using 2 M HAc containing 0.01 % KCN, pH 2.5, 10 V/cm, 18 h at +4°C. In both the chromatographic and electrophoretic determinations, bioautography on *E. coli 113-3* plates was used to reveal the spots obtained.

The results of this investigation are given in Table 1.

Table 1. Production of vitamin B_{12} by certain *Clostridia*

Co, 2.5 μg Co^{2+}/ml medium
DMB, 1 μg 5,6-dimethyl benziminazole/ml medium
AB, *Cl. acetobutylicum* Weizmann
B4, *Cl. butylicum*
B6, *Cl. butylicum*
ψ, ψ-B_{12}
Cy, cyanocobalamin
A, factor A
Brackets mean that the factor in question is present in much smaller amounts than the other factors.

Strain	Additions to the basal medium	Time of ferment. days	pH	*E. coli* activity		
				μg/ml *	Vitamin B_{12} factors present as identified by	
					chromatography	electrophoresis
AB	none	7	4.9	53	A + ψ	A; ψ
»	Co	7	4.9	60	A + ψ	A; ψ; (?)
»	Co + DMB	7	4.9	35	Cy	Cy; (B?)
»	none	14	4.9	46	A + ψ	A; ψ
»	Co	14	4.9	54	A + ψ; (Z?)	A; ψ; (?)
»	Co + DMB	14	4.9	18	Cy; (Z?)	Cy
B4	none	7	4.9	24	A + ψ	A; ψ
»	Co	7	4.9	30	A + ψ	A; ψ; (?)
»	Co + DMB	7	4.9	13	Cy	Cy; (B?)
»	none	14	4.9	33	A + ψ	A; ψ
»	Co	14	4.9	46	A + ψ; (Z?)	A; ψ; (?)
»	Co + DMB	14	4.9	18	Cy	Cy; (B?)
B6	none	7		16	A + ψ	A; ψ
»	Co	7		growth typical for methionine		
»	Co + DMB	7		24	Cy; (Z?)	Cy
»	none	14	5.0	40	A + ψ	A; ψ
»	Co	14	5.0	50	A + ψ	A; ψ; (?)
»	Co + DMB	14	5.0	24	Cy; (Z?)	Cy

* calculated as cyanocobalamin in plate assay.

RESULTS AND DISCUSSION

In all of the flasks, an intensive fermentation must have taken place during the first 4—5 days of incubation judging by the vigorous gas evolution and the decrease of pH from its initial value (6.0) to 4.9—5.0 (see Table 1). It can further be seen in Table 1 that in all flasks, except one, there was a production of *E. coli* activity in amounts ranging from 16 to 60 mμg/ml calculated as cyanocobalamin in plate assay. A prolonged time of fermentation (14 days instead of 7 days) seemed to increase the total *E. coli* activity produced in fermentations with strains B4 and B6 whereas the reverse may be true for strain AB. In one flask, *viz.* the fermentation with strain B6 in the basal medium supplemented with Co^{2+} and interrupted after 7 days, considerable amounts of

methionine seemed to be present instead of vitamin B_{12} activity. The reasons for this discrepancy could not be deduced.

The *E. coli* activity produced in the fermentations of the basal medium, not further supplemented, was due to factor A and ψ-B_{12} as shown by both chromatography and electrophoresis. The situation was the same with all three strains after both 7 and 14 days of fermentation. The addition of Co^{2+} had only negligible effect on the total amount of *E. coli* activity obtained and only a very slight effect on the kind of vitamin B_{12} factors produced which, with all three strains, were once again mainly factor A and ψ-B_{12} together with only trace amounts of a factor neutral on electrophoresis at pH 2.5. After 14 days of fermentation, small amounts of a factor ressembling the factors Z[10] could be detected by chromatography in fermentations with strains AB and B4 but not with strain B6. This factor moved still more slowly, upon chromatography in solvent system I[8], than factor Z3[11]. Its presence could not be confirmed by electrophoresis. The nature of this factor was not further investigated since it was present in much smaller amounts than the other two factors, *viz.* factors A and ψ-B_{12}.

The addition of DMB together with Co^{2+} resulted in a considerable decrease in the values for total *E. coli* activity produced in fermentations with all three strains as compared with the fermentations in the unsupplemented basal medium or this medium supplemented with Co^{2+} alone. The decrease may, however, be only an apparent one since the addition of DMB led the synthesis of vitamin B_{12} activity in all fermentations towards the formation of mainly cyanocobalamin instead of factors A and ψ-B_{12}. As discussed elsewhere [5,12], cyanocobalamin gives much smaller growth zones on *E. coli* plates than several other vitamin B_{12} factors. In certain cases (cf. Table 1), very small amounts of the above mentioned factor Z was formed together with cyanocobalamin as revealed by chromatography but not confirmed by electrophoresis. In other cases, very small amounts of a factor ressembling factor B seemed to be present as judged by the results of paper electrophoresis but not confirmed by chromatography. Again, the nature of these factors was not further investigated since they were present only in very small amounts.

The following conclusions concerning the three strains of *Clostridia* can be made on the basis of the present investigation.

1. *Clostridia* seem to produce amounts of vitamin B_{12} activity which are considerably smaller than those obtained in fermentations with certain methane bacteria [6,7].

2. *Clostridia* seem to produce mainly factor A and ψ-B_{12} in the basal medium not supplemented with 5,6-dimethyl benziminazole. However, with this compound added to the medium they produce almost exclusively cyanocobalamin. It should be mentioned that none of the hitherto investigated methane bacteria was found to produce ψ-B_{12} or factor A[6,13].

3. The presence of centain amounts of ψ-B_{12} and factor A in digested sludge could thus be attributed to ***inter alia*** the activity of *Clostridia*.

Acknowledgements. The authors are greatly indebted to Dr. L. Enebo of the Division of Fermentations, Royal Institute of Technology, Stockholm 70, for providing us with the strains of *Clostridia* and to Dr. C. Carenberg for advice concerning the performing

of the fermentations. The authors wish to thank Professor Harry Lundin, Head of the Division, for his encouraging interest in this work.

REFERENCES

1. Sjöström, A. G. M., Neujahr, H. Y. and Lundin, H. *Acta Chem. Scand.* **7** (1953) 1036.
2. Bernhauer, K. and Friedrich, W. *Angew. Chem.* **65** (1953) 627; **66** (1954) 776.
3. Janicki, J., Pawetkiewicz, J. and Nowakowska, K. *Acta Biochim. Polon.* **3** (1956) 161.
4. Kamikubo, T. *Vitamins (Kyoto)* **11** (1956) 206, 210.
5. Neujahr, H. Y. *Acta Chem. Scand.* **9** (1955) 622.
6. Neujahr, H. Y. and Callieri, D. A. *Acta Chem. Scand.* **13** (1959) 1453.
7. Neujahr, H. Y. *Acta Chem. Scand.* **14** (1960) 28.
8. Enebo, L. *Svensk Kem. Tidskr.* **70** (1958) 465.
9. Neujahr, H. Y. *Acta Chem. Scand.* **11** (1957) 1191.
10. Holdsworth, E. S. *Nature* **171** (1953) 148.
11. Neujahr, H. Y. *Acta Chem. Scand.* **10** (1956) 917.
12. Neujahr, H. Y. *Acta Chem. Scand.* **13** (1959) 1960.
13. Neujahr, H. Y. and Callieri, D. A. *Acta Chem. Scand.* **12** (1958) 1163, 1167.

Received August 25, 1959.

ACTA CHEMICA SCANDINAVICA 14 (1960) 48—62

Transfer of Triplet State Energy in Fluid Solutions

I. Sensitized Phosphorescence and Its Application to the Determination of Triplet State Lifetimes

HANS L. J. BÄCKSTRÖM and KJELL SANDROS

Institutionen för fysikalisk kemi, Chalmers Tekniska Högskola, Göteborg, Sweden

The photo-luminescence spectra of biacetyl, benzil, and anisil, in oxygen-free benzene solutions at room temperature have been determined, using the mercury line at 366 mμ as exciting light. All three substances show mainly phosphorescence, with a mean lifetime exceeding 5×10^{-5} sec, but also measurable fluorescence. Addition of an efficient phosphorescence quencher makes it possible to study the fluorescence spectra separately.

Measurements on solutions containing both benzophenone and one of the three substances mentioned have shown that the latter may be excited to luminescence also by light primarily absorbed by benzophenone. The spectrum of this sensitized luminescence shows it to be pure phosphorescence. This proves that the sensitization takes place by a transfer of triplet state energy from sensitizer to acceptor.

The triplet energy level of benzophenone lies 4 000 cm^{-1} above that of biacetyl. This difference is sufficiently large to justify the assumption that the transfer of triplet state energy is a diffusion controlled process. On this basis the mean life of benzophenone in its triplet state may be calculated from measurements of the intensity of sensitized biacetyl phosphorescence as a function of the concentration of biacetyl. The following values were obtained: in benzene solution at 20°C, 1.9×10^{-6} sec, in *iso*propanol solution, 5.7×10^{-6} sec at 20°C, and 4.6×10^{-6} sec at 25°C. The latter figure is in satisfactory agreement with a previous value calculated from the kinetics of a photochemical reaction involving triplet state benzophenone.

Comparative intensity measurements of sensitized and unsensitized biacetyl phosphorescence indicated that the internal conversion from the excited singlet state to the triplet state is virtually complete in fluid solution. It is suggested that the low phosphorescence yield in biacetyl vapour is due to radiationless transitions to the ground state from higher vibrational levels of the triplet state.

In a previous paper [1] we presented the results of a study of the quenching effect of different types of compounds on the long-lived fluorescence of biacetyl in solution. As shown by Lewis and Kasha [2], this luminescence accompanies the spin-forbidden transition of an excited biacetyl molecule

from its lowest triplet state to the singlet ground level. In the nomenclature proposed by these authors [3] it should therefore be termed phosphorescence to distinguish it from normal fluorescence, which is a spin-allowed transition (generally singlet → singlet). In the present paper we have adopted this nomenclature.

One result of our study [1] was the discovery of a class of quenchers, consisting of unsaturated and aromatic compounds, that were assumed to act by a transfer of excitation energy resulting in a triplet → singlet transition in the biacetyl molecule and the reverse transition in the quencher. This type of energy transfer has been shown by Terenin and Ermolaev [4] to explain the phenomenon of sensitized phosphorescence observed in solid solutions at liquid air temperature. Broadly speaking, the necessary condition for the transfer to be possible is that the triplet energy level of the sensitizer (donor) must lie above that of the acceptor. As pointed out in our previous paper, the same process of energy transfer may be expected to take place in fluid solutions at ordinary temperatures. Substances with triplet levels lying below that of biacetyl should therefore act as quenchers of biacetyl phosphorescence. This interpretation of our results receives strong support from further work on phosphorescence quenching, to be published shortly.

On the other hand, substances with triplet levels lying *above* that of biacetyl, should be able to function as sensitizers of biacetyl phosphorescence in solution. The present paper gives the results of experiments designed to test this conclusion. The experiments were extended to two other substances showing phosphorescence in solution, namely benzil and anisil.

EXPERIMENTAL

Apparatus

For measuring *luminescence spectra* the optical system of a Beckman DU spectrophotometer was used. The cell compartment mounting block, containing the entrance mirror, was replaced by a similar metal block into which a sealed Pyrex tube (outer diameter 8 mm), containing the degassed solution to be studied, could be introduced from below directly in front of the entrance slit An opening in the metal block permitted the tube to be illuminated from the side. Light from a water-cooled 80-watt A.C. mercury lamp, Hanau S 81, was filtered through a 2 mm Schott UG 2 glass and focused on the tube with a lense. The exciting light was therefore mainly of wavelength 366 mμ. A Sorensen voltage regulator was used to keep the lamp voltage constant.

From the exit slit of the instrument the light beam passed through a hole (diameter 12.5 mm) in the metal block and struck the photocathode of a multiplier phototube of the head-on type. The latter was enclosed in a light-tight housing screwed on to the back of the metal block. Two different multiplier tubes were used, RCA 5819 and RCA 6217. The latter tube has a spectral sensitivity curve extending farther into the red wavelength region, but also a less favourable signal to noise ratio. The tube was connected to a stabilized adjustable voltage supply and the current was read on a sensitive light-spot galvanometer (Norma Model 251 J). The voltage was chosen so as to give satisfactory results with a low slit width. For biacetyl luminescence a slit width of 0.2 mm was used, corresponding to a half-intensity band width of 4 mμ at the wavelength 500 mμ. For benzil and anisil the slit width had to be increased to 0.3 mm owing to the lower luminescence yield.

In determining a spectrum, readings were taken at different settings of the wavelength selector. Repeated readings at the wavelength corresponding to the maximum in the luminescence curve served as a check on the constancy of the exciting light. Using the

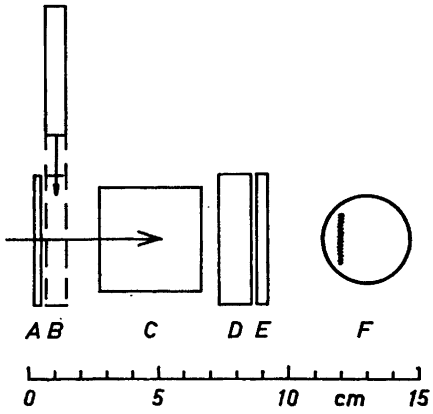

Fig. 1. Schematic diagram of experimental arrangement for measuring relative luminescence intensities. (A) Light filter (Schott UG2, 2 mm). (B) Uranyl glass. (C) Cylindrical glass cell, 4 × 4 cm. (D) Quartz cell with 0.5 M sodium nitrite solution. (E) Light filter (Chance OY3, 4 mm). (F) Multiplier phototube, RCA 931 A. — A light-tight box with an opening for the exciting beam enclosed parts C—F. The measurements were made in a darkened room.

spectral sensitivity curves of the multiplier phototubes, as given by the manufacturers, and the dispersion data for the Beckman spectrophotometer, relative intensity values at different wavelengths were calculated. No correction was made for the variation of reflexion losses with wavelength. The curve thus obtained was finally recalculated to give relative numbers of light quanta emitted at different wave-numbers.

For all three substances studied luminescence curves were determined with both photomultiplier tubes, covering the range from the onset of luminescence at about 470 mμ to the limit (about 610 mμ) where the normal sensitivity of tube 5819 has dropped to 10 % of its maximum value. The results with the two tubes showed no systematic deviations. The curves shown in Figs. 4—6 are based on measurements made with tube 6217 for wavelengths above 600 mμ and with tube 5819 for shorter wavelengths.

The experimental arrangement for measuring *relative luminescence intensities* is shown schematically in Fig. 1. The degassed solution was contained in the cylindrical glass cell C (shown in more detail in Ref.[1], Fig. 2). It was excited to luminescence by a light beam of wavelength 366 mμ from the exit slit of a Bausch and Lomb grating monochromator (1 200 grooves per mm, focal length 500 mm). The light source was an A.C. mercury lamp. Fluctuations in line voltage were eliminated with a Sorensen voltage regulator. The luminescence light reaching the cathode of the photomultiplier tube (F) was limited by the filter combination D + E to wavelengths > approximately 510 mμ. The stabilized voltage applied to the multiplier tube was adjusted to give a current of suitable magnitude within one of the two lowest measuring ranges of a certified high-resistance light-spot galvanometer (Norma Model 251 J). The sensitivity in these ranges was 1.975×10^{-9} and 1.975×10^{-8} A per scale division, respectively.

The fluorescent uranyl glass (B) was used to obtain a measure of the intensity of the exciting light. With C removed and B in the path of the light beam, in an accurately fixed position, the photocurrent produced by the fluorescence light was determined. This current was in the third measuring range of the galvanometer (1.975×10^{-7} A per scale division). Determinations made before and after a luminescence measurement showed that the intensity of the exciting light was constant to better than 1 % during an experiment.

In order to minimize photochemical changes in the solutions they were exposed to light as little as possible.

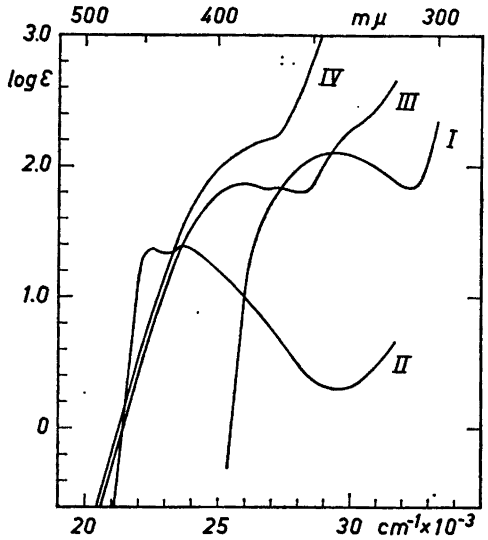

Fig. 2. Absorption spectra in benzene solution, log ε *vs.* wave number in cm^{-1}. (I) Benzophenone. (II) Biacetyl. (III) Benzil. (IV) Anisil.

Materials

Anisil (*p,p'*-dimethoxybenzil) was prepared from anisoin according to the directions of Biltz and Arnd [5]. It was recrystallized three times from ethanol.

All other chemicals were of the highest purity obtainable commercially. *Biacetyl* was further purified and stored as described earlier [1]. *Benzil* was recrystallized three times from ethanol. *Benzophenone* was recrystallized twice from an ethanol-water mixture and once from a methanol-water mixture. *Benzene* and *isopropanol* were fractionally distilled using a column corresponding to 15 theoretical plates.

All solutions were degassed as described earlier [1]. The phosphorescence lifetime for biacetyl in dilute benzene solution at 20°C was generally found to be only about 700 μsec as against 1 000 μsec in our earlier work [1]. This shows that we did not succeed in obtaining the benzene as pure as earlier although the raw-material was from the same source and the method of purification was the same.

RESULTS AND DISCUSSION

Luminescence spectra

The substance used as sensitizer was benzophenone. Its long-wave absorption band in benzene solution at room temperature is shown in Fig. 2, together with the corresponding spectra of the acceptors studied. The molar decadic extinction coefficients at 366 mμ were found to have the following values: benzophenone 67, biacetyl 4.5, benzil 68, anisil 180.

Energy level diagrams for benzophenone and biacetyl are shown in Fig. 3. Only the lowest excited levels are included as being the only ones of interest in the present connection. Since liquid solutions of benzophenone do not show

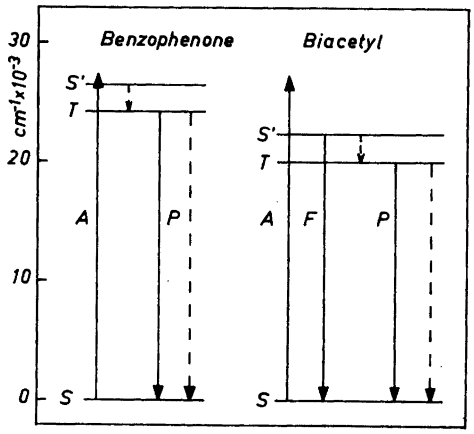

Fig. 3. Electronic energy level diagrams for benzophenone and biacetyl, showing the energy above the ground level (S), expressed in wave numbers, of the first excited singlet level (S') and the lowest triplet level (T). Solid arrows represent transitions involving radiation: (A) absorption of light of wavelength 366 mμ, (F) fluorescence, (P) phosphorescence. Dashed arrows represent radiationless transitions.

measureable phosphorescence, the position of its lowest triplet level is known only from its phosphorescence spectrum in solid solutions at liquid air temperature. For this reason the diagrams are based entirely on absorption and luminescence measurements made under those conditions [4,6-8]. The spectral changes produced by changing the temperature or the solvent are small enough to be unimportant in the present discussion.

Only the zero-point vibrational levels are shown, in order not to complicate the diagrams *. It will be noted that no radiative S' → S transition is indicated in the case of benzophenone. Benzophenone shows no fluorescence, only phosphorescence, which proves [10] that the radiationless transition to the slightly lower lying triplet level is essentially complete. This means that the lifetime of benzophenone in its excited singlet state must be so short that transfer of energy to the acceptor from benzophenone molecules in this state may be ruled out as a possibility. This is one of the advantages of using benzophenone as a sensitizer in the present case.

The value reported [7] for the quantum efficiency of phosphorescence in solid solution at 77°K, 0.84 ± 10 %, shows that under these conditions radiationless transition to the ground state must be of minor importance. The rate of decay of phosphorescence under the same conditions [7] corresponds to a mean life of the triplet state of 0.008 sec. In liquid solution at ordinary temperature, collisional deactivation or chemical reaction with the solvent reduces the lifetime to a small fraction of this value (See p. 59).

* In accordance with the Franck-Condon principle, molecular spectra are largely determined by the higher vibrational levels. See, *e.g.*, Förster [9]. The absorption and luminescence spectra of benzophenone have recently been discussed by Dörr [6].

Biacetyl shows fluorescence as well as phosphorescence, and the same is true of the other two substances studied as acceptors in the present work. As found by Groh [11], irradiation of biacetyl vapour with light of wavelength 366 mμ leads to the emission of a "fast" fluorescence of low intensity and with a spectrum lying mostly between 400 and 500 mμ, in addition to the previously known slow fluorescence (phosphorescence) whose spectrum lies mostly at wavelengths > 500 mμ. Similarly, Sidman and McClure [8] found that the photoluminescence of biacetyl crystals at low temperatures contains a weak blue component. An analysis of its band spectrum showed it to be true fluorescence.

For the purpose of the present investigation, the most important difference between benzophenone and biacetyl is that the latter compound shows strong phosphorescence even in liquid solution in a suitable solvent. No measurements of quantum efficiency either in solid or in liquid solution have been made, but already the existence of fluorescence shows that the internal conversion $S' \rightarrow T$ cannot be complete. However, molecules that have reached the triplet state exhibit remarkable stability toward deactivating influences. This is shown by the fact that the triplet state lifetime in benzene solution at 20°C may amount to [1] as much as 1.0×10^{-3} sec, which is 45 % of the value found in solid solution at liquid air temperature.

As regards the relative positions of the energy levels of the two substances, Fig. 3 shows that the S′ level of benzophenone lies above that of biacetyl. From this point of view an energy transfer: $D_{S'} + A_S = D_S + A_{S'}$ (D donor, A acceptor) would be possible. For the reason mentioned above this possibility may, however, be excluded. That this is not the mechanism of the sensitized luminescence observed is confirmed by the experimental results. As shown below, the sensitized luminescence is pure phosphorescence, whereas raising the acceptor to the S′ level by direct light absorption produces both fluores-

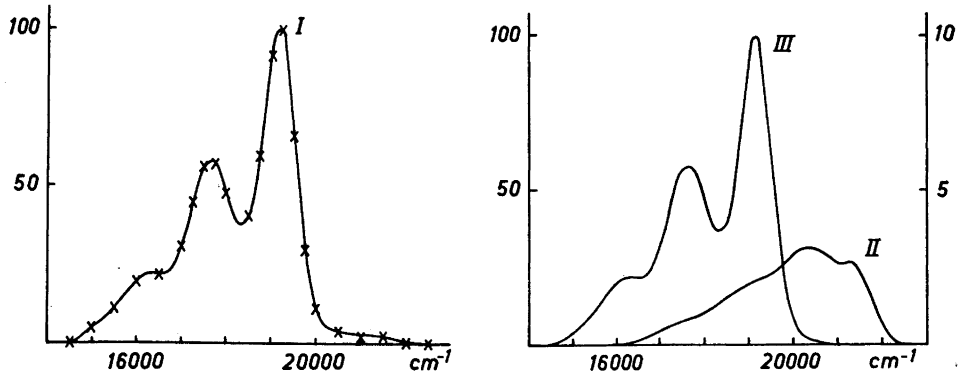

Fig. 4, a and *b*. Luminescence spectra of biacetyl in benzene solution, showing relative numbers of light quanta emitted *vs.* wave number in cm^{-1}. (I) Unsensitized luminescence. Biacetyl 0.222 M, observed values. (X) Calculated values. (II) Fluorescence (scale to the right). Biacetyl 0.222 M, pyrene 4.4×10^{-4} M. (III) Sensitized luminescence (scale to the left). Benzophenone 2.64×10^{-2} M, biacetyl 7.0×10^{-3} M.

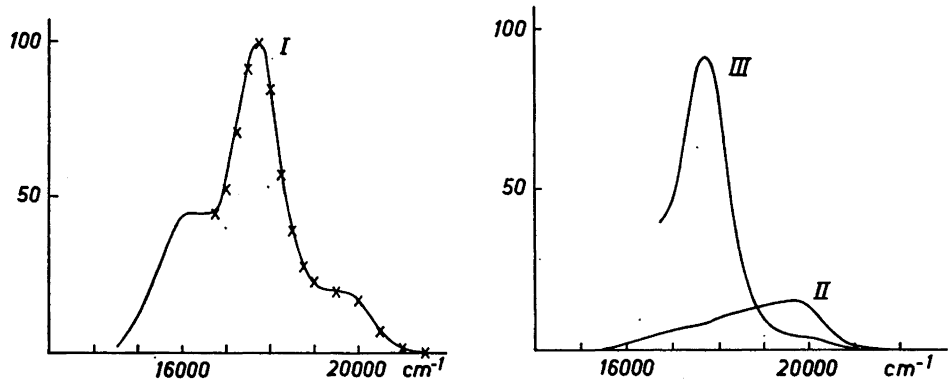

Fig. 5, a and *b*. Luminescence spectra of benzil. (I) Unsensitized luminescence. Benzil 2.14×10^{-2} M, observed values. (X) Calculated values. (II) Fluorescence. Benzil 2.75×10^{-2} M, pyrene 2.7×10^{-4} M. (III) Sensitized luminescence. Benzophenone 3.43×10^{-2} M, benzil 1.49×10^{-2} M. — The measurements represented by curve III met with difficulties and were only pursued as far as shown. Apparently a photochemical reaction took place, leading to a change in the spectrum.

cence and phosphorescence. There can be no doubt, therefore, that the sensitization takes place by a process: $D_T + A_S = D_S + A_T$. That this process is energetically possible is shown by the relative position of the triplet levels.

The results obtained with the three acceptors studied are given in graphical form in Figs. 4—6, the relative number of light quanta emitted being plotted in arbitrary units against the wave-number in cm^{-1}. In each case, curve I represents the spectrum obtained on irradiating a pure solution of the acceptor in benzene with light of wavelength 366 mμ. This spectrum is partly fluorescence, partly phosphorescence. The curves marked II represent the pure fluorescence spectrum as obtained by eliminating the phosphorescence by the addition of a small quantity of pyrene, which is a strong phosphorescence quencher [1]. The fact that pyrene itself shows fluorescence made it necessary to apply a slight correction. The fluorescence of pyrene in very dilute solutions [12] lies mainly in the ultraviolet but extends into the visible with decreasing intensity. The magnitude of the correction was obtained from the observed fluorescence in the region 23 000—25 000 cm^{-1} where the acceptors themselves show no luminescence, as is evident from curves I.

The curves marked III represent the luminescence spectra of solutions containing both benzophenone and a low concentration of acceptor. The concentrations were such that only a small fraction (2—7 %) of the absorbed light went to the acceptor, the rest being absorbed by the benzophenone. Nevertheless, visual comparison showed that the luminescence intensity was much higher than that obtained when the acceptor was present alone in the same low concentration. This was confirmed by quantitative intensity measurements of biacetyl luminescence that will be presented in a later section (p. 60).

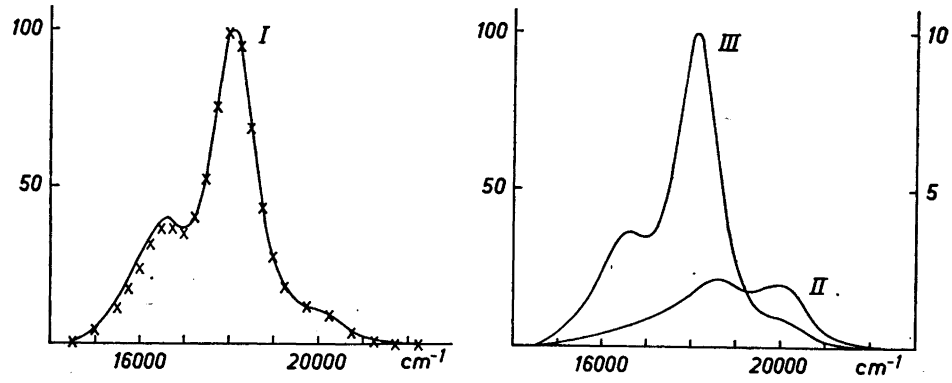

Fig. 6, a and *b*. Luminescence spectra of anisil. (I) Unsensitized luminescence. Anisil 6.9×10^{-3} M, observed values. (X) Calculated values. (II) Fluorescence (scale to the right). Anisil 1.27×10^{-2} M, pyrene 2.7×10^{-4} M. (III) Sensitized luminescence (scale to the left). Benzophenone 2.64×10^{-2} M, anisil 7.8×10^{-4} M.

There is thus no doubt that radiation absorbed by benzophenone gives rise to a sensitized luminescence of the acceptor. The spectrum of this luminescence differs from that obtained on direct excitation of the acceptor. Curve I for benzil shows a hump which coincides with the maximum in the fluorescence spectrum (curve II) and which is absent in curve III. Similarly curve I for biacetyl extends to higher wave-numbers than curve III. In the case of anisil the difference is less apparent which can be connected with the position and low intensity of its fluorescence. The conclusion seems inevitable that fluorescence is absent from the sensitized luminescence, which therefore represents pure phosphorescence. In agreement with this it is found that by multiplying the experimental intensity values for sensitized luminescence and for fluorescence by suitably chosen factors, one for each kind of luminescence, curves are obtained that, when added together, reproduce the directly excited luminescence (curve I) of the acceptor in question. In the figures, curves II and III have been drawn in this manner, and the result of the addition is represented by the crosses in Figs. 4a, 5a and 6a. By determining the areas under the curves it is found that the ratio between the quantum efficiencies of phosphorescence and of fluorescence under our experimental conditions was 20:1 for biacetyl, 4.0:1 for benzil, and 25:1 for anisil.

Obviously, very different values may be expected under other conditions. Thus it has been reported by Ermolaev [13], who studied the luminescence of different carbonyl compounds, including benzil, in solid solutions at −195°C, that their luminescence, within an error of 2—3 %, consisted entirely of long-lived radiation. For benzil he found a mean life of this radiation of 4.4×10^{-3} sec. Under our conditions it was only 7×10^{-5} sec, which shows that the phosphorescence yield had been reduced in the ratio of 60:1. The fluorescence yield, on the other hand, probably changes relatively little with temperature. Our results are therefore not incompatible with those of Ermolaev.

Table 1. Intensity of sensitized biacetyl phosphorescence in benzene solution at 20°C as a function of biacetyl concentration. Sensitizer: benzophenone, 1.65×10^{-2} mole/l.

[A] mole/l	I, scale divisions	τ_A μsec	τ_A/I observed	τ_A/I calculated
2.76×10^{-3}	90.5	489	5.40	5.35
2.73×10^{-4}	71.5	445	6.22	6.28
5.07×10^{-5}	39.5	440	11.1	10.8
2.39×10^{-5}	31.0	528	17.0	17.0
1.64×10^{-5}	21.1	440	20.9	22.4

For benzil and anisil, phosphorescence in fluid solution has not been reported previously. The following values of the phosphorescence mean life were determined as described earlier [1]: Benzil in benzene, 5.9×10^{-3} M, $\tau = 71$ μsec, benzil in carbon tetrachloride, 4.7×10^{-3} M, $\tau = 141$ μsec, anisil in benzene, 1.4×10^{-3} M, $\tau = 60$ μsec.

The intensity of sensitized phosphorescence as a function of the acceptor concentration. The triplet state lifetime of the sensitizer

With benzophenone as sensitizer and biacetyl as acceptor, the intensity of the sensitized phosphorescence was studied as a function of the acceptor concentration, using the method described above. In one series of measurements the solvent was benzene, in two others, *iso*propanol. In each series the voltage applied to the photomultiplier tube was adjusted so that the fluorescence of the uranyl glass always gave the same photocurrent. The phosphorescence photocurrents observed were therefore directly comparable. Before a measurement the solution was brought to the desired temperature. For every solution the phosphorescence mean life was determined at 20°C.

The results for benzene solutions at 20°C are given in Table 1, those for *iso*propanol solutions at 20 and 25°C in Fig. 7. They can be accounted for on the following reaction scheme. In addition to the processes indicated in the energy level diagram, Fig. 2, the scheme includes possible chemical reactions with the solvent (L) (steps 3 and 7).

$$D_S + h\nu \rightarrow D_{S'} \rightarrow D_T \quad (1)$$

$$D_T \rightarrow D_S \text{ (radiationless deactivation)} \quad (2)$$

$$D_T + L \rightarrow \text{Reaction products} \quad (3)$$

$$D_T + A_S \rightarrow D_S + A_T \quad (4)$$

$$A_T \rightarrow A_S + h\nu' \text{ (phosphorescence)} \quad (5)$$

$$A_T \rightarrow A_S \text{ (radiationless deactivation)} \quad (6)$$

$$A_T + L \rightarrow \text{Reaction products} \quad (7)$$

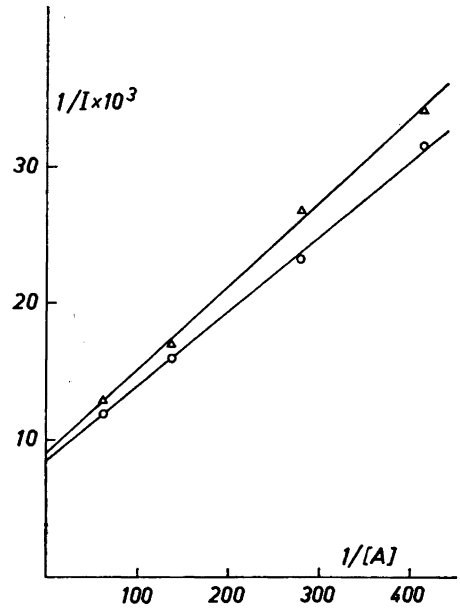

Fig. 7. Sensitized phosphorescence of biacetyl in *iso*propanol solution, $1/I$ *vs.* $1/[A]$. I = phosphorescence intensity in scale divisions, [A] = biacetyl concentration in mole/l. Sensitizer benzophenone, 3.74×10^{-3} M. ⊙ 20°C, △ 25°C.

The assumption that, in the case of benzophenone, step (1) has a quantum efficiency = 1, seems to be supported by all known facts *. Triplet state acceptor molecules will then be formed with the quantum efficiency

$$\varphi_4 = \frac{k_4[A_S]}{k_2 + k_3[L] + k_4[A_S]}$$

The probability for radiative transition of A_T to the ground state is equal to

$$\frac{k_5}{k_5 + k_6 + k_7[L]}$$

The quantum efficiency of phosphorescence therefore becomes

$$\varphi_5 = \frac{k_4[A_S]}{k_2 + k_3[L] + k_4[A_S]} \cdot \frac{k_5}{k_5 + k_6 + k_7[L]}$$

The natural mean lifetime of the acceptor in its triplet state, τ_A^N, its mean lifetime in the solution, τ_A, and the triplet state lifetime of the donor in the absence of acceptor, τ_D°, are given by:

$$\tau_A^N = \frac{1}{k_5}; \quad \tau_A = \frac{1}{k_5 + k_6 + k_7[L]}; \quad \tau_D^\circ = \frac{1}{k_2 + k_3[L]}$$

$$\text{Hence: } \frac{1}{\varphi_5} = \frac{\tau_A^N}{\tau_A}\left(1 + \frac{1}{k_4[A]\tau_D^\circ}\right) \tag{8}$$

where [A] denotes the concentration of the acceptor.

* For a discussion of this point, see Bäckström, H. L. J., Steneryr, A. and Perlmann, P. *This Journal* 12 (1958) 8.

Provided that the experimental conditions are such that the photocurrent (I) may be assumed to be proportional to φ_5, the following relations should hold: $I = a\varphi_5$, where a is a constant, and

$$\frac{\tau_A}{I} = K\left(1 + \frac{1}{k_4[A]\tau_D^\circ}\right), \text{ where } K = \frac{\tau_A^N}{a}$$

The values of τ_A/I given in the last column of Table 1 were calculated from a formula of this type, namely,

$$\frac{\tau_A}{I} = 5.25\left(1 + \frac{1}{1.87 \times 10^4[A]}\right)$$

The high value of the mean lifetime of triplet state biacetyl in benzene solutions makes it very susceptible to deactivation by impurities accidentally present. This is probably the explanation of the variations in τ_A in Table 1. It may easily be shown that eqn (8) should be valid also if a deactivation of this kind is included in the reaction scheme. The necessary condition is only that the impurity should not change the value of τ_D°. However, the much shorter lifetime of benzophenone in its triplet state makes it much less susceptible to deactivating influences.

In *iso*propanol solutions the lifetime of biacetyl in its triplet state is considerably reduced by reaction with the solvent (step 7). Within limits of error the same value of τ_A was found in all cases (21 μsec at 20°C). The results of the intensity measurements are given in graphical form in Fig. 7, $1/I$ being plotted against 1/[A]. The straight lines correspond to the formulas

$$\frac{1}{I} = 8.43 \times 10^{-3}\left(1 + \frac{1}{153\,[A]}\right) \text{ at } 20°C, \text{ and}$$

$$\frac{1}{I} = 9.02 \times 10^{-3}\left(1 + \frac{1}{147\,[A]}\right) \text{ at } 25°C.$$

The reaction scheme rests on the assumption that the light is absorbed exclusively by the sensitizer. This was very nearly the case in the benzene experiments, but less so in the *iso*propanol experiments where the lower value of τ_D° made it necessary to use higher biacetyl concentrations. However, the fraction of the light absorbed by the biacetyl never exceeded 5 %.

Step 4 is a transfer of triplet state energy. The triplet level of biacetyl is 4 000 cm^{-1} lower than that of benzophenone, corresponding to an energy difference of $>$ 11 kcal/mole. The results on phosphorescence quenching given in Ref.[1], Table 2, indicate that this energy difference is sufficient to make the process diffusion controlled, and this is confirmed by later results. The rate constant may therefore be estimated by a formula derived by Debye [14] on the assumption that the molecules may be regarded as spheres. If the molecular diameters of the reacting species are assumed equal the result is:

$$k = \frac{8RT}{3\,000\,\eta} \text{ l mole}^{-1} \text{ sec}^{-1}$$

where η is the viscosity in dyne-sec/cm^2 and $R = 8.31 \times 10^7$ erg/°K. This simplified form of the equation is the one generally used. However, if the diameters (d_1 and d_2) are not equal the result should be multiplied by a factor

$$\frac{1}{4}\left(2 + \frac{d_1}{d_2} + \frac{d_2}{d_1}\right)$$

For benzene solutions at 20°C the simplified formula gives 1.0×10^{10} l mole^{-1} sec^{-1}. Our results in this solvent thus indicate a mean life of benzophenone in its triplet state of about 1.9×10^{-6} sec. The results of the low-temperature work of Gilmore, Gibson, and McClure [7], mentioned on p. 52, show that the natural lifetime is about 0.01 sec. Accordingly the phosphorescence yield under our experimental conditions must have been about 0.02 %. A weak blue luminescence could be seen when an oxygen-free solution of benzophenone in benzene was irradiated with light of wavelength 366 mμ. As was to be expected [15], saturation of the solution with air caused a marked reduction in luminescence intensity.

As regards the measurements in *iso*propanol solution, some results of Forster [16] point to a possible source of error. In a study of the visible absorption spectrum of biacetyl he found that the extinction coefficients of solutions in certain alcohols decrease with time and approach an equilibrium value while the spectral shape is unchanged. This indicates a reaction with the solvent, leading to the formation of a colourless reaction product. In agreement with this we found that the extinctions of a solution of biacetyl in *iso*propanol at wavelengths in the visible and near ultraviolet decreased with time whereas their ratio remained unchanged. At the same time the extinctions at shorter wavelengths ($<$330 mμ) increased. However, the reaction was so slow that the decrease in concentration of unchanged biacetyl during the time required for a measurement of the intensity of sensitized phosphorescence (about 2 h) was of the order of 1 %.

For solutions in *iso*propanol, the rate constant given by the simplified Debye formula is 2.7×10^9 l mole^{-1} sec^{-1} at 20°C and 3.2×10^9 l mole^{-1} sec^{-1} at 25°C. With these values for k_4 the experimental results at the two temperatures give 5.7×10^{-8} sec and 4.6×10^{-8} sec, respectively, for the triplet state lifetime (τ_D°) of benzophenone in *iso*propanol solution. An independent value of the same quantity at 25°C has previously been obtained by an entirely different method [15]. A study of the retarding effect of nitric oxide on the photochemical reaction between nitric oxide and *iso*propanol, sensitized by benzophenone, yielded a value of 252 for the product $k \times \tau^\circ$, where k is the rate constant for the deactivation of excited benzophenone molecules in their triplet state by nitric oxide. There is reason to believe that this is also a diffusion controlled process [15]. Assuming $k = 3.2 \times 10^9$ l mole^{-1} sec^{-1}, τ° becomes 7.9×10^{-8}sec. However, this is a case where the molecules taking part in the diffusion controlled process are very different in size. According to the complete Debye formula this leads to an increase in the rate constant and a corresponding decrease in the calculated value of τ°. Since the molecules are far from spherical it is not possible to calculate the magnitude of this effect. The conclusion seems justified, however, that the results of the two determinations of τ° agree within the probable limits of error. This agreement furnishes a very

direct proof that the biradical state of benzophenone appearing as an intermediate in its photochemical reactions is identical with the triplet state responsible for its phosphorescence at low temperatures [15].

Comparison of the values of τ_D° in benzene and in *iso*propanol shows that the latter value is determined almost entirely by the reaction with the solvent (step 3). The same is true of τ_A in *iso*propanol (21 μsec). Hence $k_3/k_7 \sim 350$, *i.e.*, biacetyl in the triplet state reacts much more slowly with *iso*propanol than does benzophenone.

Intensity measurements on sensitized and unsensitized phosphorescence

The following experiments were made in order to demonstrate the existence of sensitized phosphorescence by intensity measurements, and to compare the quantum efficiencies of sensitized and unsensitized phosphorescence in the case of biacetyl. The sensitizer was benzophenone, the solvent benzene. The experimental arrangements were the same as in the previous section.

1. A 3.07×10^{-3} M solution of biacetyl, with a calculated light absorption at 366 mμ of 12.0 %, gave a galvanometer deflection of 11.5 scale divisions. The phosphorescence decay rate corresponded to a triplet state lifetime of 796 μsec.

2. 3.46×10^{-3} M biacetyl + 7.74×10^{-3} M benzophenone. Calculated total light absorption 99.3 %, 2.9 % absorbed by biacetyl and the rest by benzophenone. Galvanometer deflection 98.0 scale divisions, $\tau = 756$ μsec.

Obviously most of the luminescence in this case must be sensitized phosphorescence.

3. A 0.1226 M solution of biacetyl gave an extinction at 366 mμ of 0.515, corresponding to a light absorption of 99.1 % in a layer thickness of 4 cm. It gave a galvanometer deflection of 21.0 scale divisions, and $\tau = 154$ μsec. The low value of τ is due to the high concentration ("self-quenching") [1].

In experiments 2 and 3, the solutions had very nearly the same extinctions. The galvanometer deflections observed may therefore be assumed to be strictly proportional to the phosphorescence yields.

As will appear from the following, no appreciable error is introduced if the phosphorescence observed in experiment 2 is assumed to be entirely sensitized. Its quantum yield (φ_2) will then be given by eqn (8). As regards the quantum yield in experiment 3 (φ_3), it follows from the reaction scheme that

$$\varphi_3 = \frac{(\tau_A)_3}{\tau_A^N} \cdot P$$

where P denotes the probability under our experimental conditions for the internal conversion of singlet excited biacetyl to the triplet state (*Cf.* Fig. 3). With the value of $k_4\tau_D^\circ$ found above in benzene solution, 1.87×10^4 l mole^{-1}, and with [A] = 3.46×10^{-3} mole/l, the factor within parentheses in eqn (8) becomes 1.015. Hence

$$P = \frac{756}{154} \times \frac{21.0}{98.0} \times \frac{1}{1.015} = 1.04$$

Experiments 2 and 3 were repeated under almost identical conditions but with a fresh sample of biacetyl. The resulting value of P was 1.10.

These results indicate that when biacetyl is excited by light absorption in solution, the internal conversion to the triplet state is practically complete. The fraction of the singlet excited biacetyl molecules returning to the ground state with the emission of fluorescence may be estimated at about 0.22 %. This figure is based on the ratio between phosphorescence and fluorescence found above (p. 55) for a 0.222 M solution, an estimate of the triplet state lifetime in that solution (100 ± 10 μsec), and assuming the natural lifetime to be equal to the phosphorescence lifetime, 2.25×10^{-3} sec, in a solid solution at 77°K [17].

The phosphorescence quantum yield of biacetyl in the vapour state at 27°C has been determined by Almy and Gillette [18]. When the wavelength of the exciting light is 366 mμ the phosphorescence yield rises with pressure, apparently from zero at zero pressure, and seems to approach a value almost as great as that obtained when the mercury lines at 405 or 436 mμ are used as exciting light. This value, 0.145 ± 0.030, is nearly constant in the pressure range investigated (2—45 mm).

Under the same conditions the integrated intensity ratio of phosphorescence to fluorescence has been found by Okabe and Noyes [19] to be 58.4 ± 2.5:1, independent of pressure and incident wavelength. Recalculated to relative numbers of quanta the ratio becomes 64:1, giving a fluorescence quantum yield of $0.145/64 = 0.23$ %, *i.e.* within limits of error the same value as in solution. This indicates that the yield of fluorescence from the low lying vibrational levels of the excited singlet state is determined entirely by the relative rates of light emission and of internal conversion to the triplet state, and that the latter rate is not affected by the presence of the solvent. (*Cf.* Ref.[17], p. 906).

On this basis the efficiency of the internal conversion to the triplet state from the low lying vibrational levels of the excited singlet state should be 99.8 % both in the vapour and in solution. Since the phosphorescence lifetime of biacetyl in the vapour state at 25°C has been found [20] to be 1.80×10^{-3} sec, whereas the natural lifetime may be assumed [17] to be about 2.25×10^{-3} sec, the phosphorescence yield observed by Almy and Gillette corresponds to a conversion efficiency of only about 20 %. This must be due to a radiationless process which originates in the higher vibrational levels of the triplet state and which will therefore be suppressed in solution, where the excess vibrational energy is rapidly removed by collisions with solvent molecules. On the other hand, the process must be sufficiently rapid to compete with collisional deactivation in a gas at low pressures. Dissociation may be excluded as a possibility both on the basis of the photochemical data [21] and because the available energy, 64 kcal/mole, is too low. Probably, therefore, the explanation of the discrepancy is the occurrence of radiationless transitions to the ground state. The theoretical treatment of such processes [22] has shown that they are possible only if the two electronic states differ in some essential way, for instance in multiplicity, as in the present case. Furthermore they may be expected to be favoured by atomic oscillations that cause the molecule to become distorted.

REFERENCES

1. Bäckström, H. L. J. and Sandros, K. *Acta Chem. Scand.* **12** (1958) 823.
2. Lewis, G. N. and Kasha, M. *J. Am. Chem. Soc.* **67** (1945) 994.
3. Lewis, G. N. and Kasha, M. *Ibid.* **66** (1944) 2100.
4. Terenin, A. N. and Ermolaev, V. L. *Trans. Faraday Soc.* **52** (1956) 1042.
5. Biltz, H. and Arnd, Th. *Ann.* **339** (1905) 267.
6. Dörr, F. *Z. Elektrochem.* **61** (1957) 950.
7. Gilmore, E. H., Gibson, G. E. and McClure, D. S. *J. Chem. Phys.* **20** (1952) 829; **23** (1955) 399.
8. Sidman, J. W. and McClure, D. S. *J. Am. Chem. Soc.* **77** (1955) 6461.
9. Förster, Th. *Fluoreszenz organischer Verbindungen*, Vandenhoeck & Ruprecht, Göttingen 1951, p. 209.
10. Kasha, M. *Discussions Faraday Soc.* **No. 9** (1950) 14.
11. Groh, H. J. *J. Chem. Phys.* **21** (1953) 674.
12. Förster, Th. and Kasper, K. *Z. Elektrochem.* **59** (1955) 976.
13. Ermolaev, V. L. *Optika i Spektroskopiya* **1** (1956) 523.
14. Debye, P. *Trans. Electrochem. Soc.* **82** (1942) 265.
15. Bäckström, H. L. J., Steneryr, A. and Perlmann, P. *Acta Chem. Scand.* **12** (1958) 8.
16. Forster, L. S. *J. Am. Chem. Soc.* **77** (1955) 1417.
17. McClure, D. S. *J. Chem. Phys.* **17** (1949) 905.
18. Almy, G. N. and Gillette, P. R. *J. Chem. Phys.* **11** (1943) 188.
19. Okabe, H. and Noyes, W. A. *J. Am. Chem. Soc.* **79** (1957) 801.
20. Kaskan, W. E. and Duncan, A. B. F. *J. Chem. Phys.* **18** (1950) 427.
21. Sheats, G. F. and Noyes, W. A. *J. Am. Chem. Soc.* **77** (1955) 1421.
22. Teller, E. *J. Phys. Chem.* **41** (1937) 109; Franck, J. and Livingston, R. *Revs. Modern Phys.* **21** (1949) 505; Franck, J. and Sponer, H. Volume commemoratif Victor Henri: *Contribution à l'Étude de la Structure Moléculaire*, 1948, p. 169.

Received September 9, 1959.

ACTA CHEMICA SCANDINAVICA 14 (1960) 63—71

Characterization of Hog Intestinal Invertase as a Glucosido-Invertase

III. Specificity of Purified Invertase

ARNE DAHLQVIST

Department of Physiological Chemistry, University of Lund, Lund, Sweden

The specificity of purified hog intestinal invertase has been studied.

Hog intestinal invertase, purified by mutual displacement chromatography on TEAE-cellulose, hydrolyzed *sucrose* and *turanose* (3-(α-D-glucopyranosyl)-D-fructose). Heat inactivation and inhibition experiments indicated that a single enzyme in this preparation hydrolyzed both sucrose and turanose.

Maltose was also hydrolyzed by the purified hog intestinal invertase. Maltose and sucrose inhibited the hydrolysis of each other competitively, and the values of K_i for maltose and sucrose as inhibitors for each other agreed with the values of K_s for each sugar as substrate, indicating the hydrolysis of each of these sugars by the same enzyme.

The purified invertase, however, is responsible for only 1/2 of the total turanase activity and 1/3 of the total maltase activity of crude hog intestinal glycosidase preparations.

Melezitose (α-D-glucopyranosyl (1→3) β-D-fructofuranosyl-(2→1)α-D-glucopyranoside) was *not* hydrolyzed by the purified enzyme preparation. Crude hog intestinal glycosidase preparations have melezitase activity caused by two other α-D-glucopyranosidases, but these enzymes have no invertase activity.

The characterization of hog intestinal invertase as a *glucosido-invertase* (α-D-glucopyranosidase) was recently confirmed by a study of the transglycosylation catalyzed by this enzyme [1]. It may therefore be expected that hog intestinal invertase should hydrolyze, in addition to sucrose, a number of other α-D-glucopyranosides, *e.g. maltose*, *isomaltose* (6-(α-D-glucopyranosyl)-D-glucose), *trehalose* (1-(α-D-glucopyranosyl)-α-D-glucopyranoside), *melezitose* (α-D-glucopyranosyl (1 → 3) β-D-fructofuranosyl (2 → 1) α-D-glucopyranoside), *turanose* (3-(α-D-glucopyranosyl)-D-fructose), *phenyl-α-D-glucopyranoside*, or *methyl-α-D-glucopyranoside*.

Methyl-α-D-glucopyranoside is *not* hydrolyzed by crude hog intestinal preparations [2,3], and is therefore *not* a substrate for hog intestinal invertase.

The hydrolysis of *melezitose* and *turanose* by crude hog intestinal preparations has been reported previously [4]. Since the preparation used contained several different α-D-glucopyranosidases [5-10], however, these findings do *not* prove that melezitose and turanose are hydrolyzed by intestinal *invertase*.

Hog intestinal invertase was recently purified by ion exchange chromatography, and was then separated from all the *trehalase*, *isomaltase* and *phenyl-α-D-glucopyranosidase* activity of the original preparation [5,8,9]. These glucosides are therefore not substrates for hog intestinal invertase. The invertase was also separated from 2/3 of the *maltase* activity of the original preparation [6,7,9]. However, 1/3 of the original maltase activity accompanied the invertase activity during its purification, and was not separable from the invertase activity by heat inactivation at varying pH-values or by ion exchange chromatography [6,7]. The question therefore arises, if this part of the maltase activity is caused by the same enzyme as the invertase activity.

In the present paper will be reported a study of the specificity of purified intestinal invertase. The aim the study was to answer the following two questions:

1) Is the hydrolysis of *melezitose* and *turanose* by crude hog intestinal preparations caused by the same enzyme as is responsible for the invertase activity?

2) Is that part of the *maltase* activity (= 1/3 of the total maltase activity), which it was not possible to separate from the invertase activity, caused by the same enzyme as the invertase activity?

MATERIALS AND METHODS

Enzyme preparations

Purified hog intestinal invertase was obtained by mutual displacement chromatography upon TEAE-cellulose [7]. The preparation had maltase activity which was 0.6 times the invertase activity, and was identical with the *purified hog intestinal maltase I* described in previous papers [7,9]. The specific invertase activity of the preparation was 292 units per mg of protein. One unit of glycosidase activity is the activity which causes 1 % of hydrolysis in 2 ml of reaction mixture in 1 h at 37°C under the conditions used.

Purified hog intestinal maltase II and *purified hog intestinal maltase III* were the same preparations as have been described in previous papers [7,9]. The specific maltase activity of these preparations was 100 and 200 units per mg of protein, respectively. These two maltase preparations had no invertase activity [9].

Crude hog intestinal glycosidase preparation was obtained as described earlier [5]. This preparation contained all the hog intestinal glycosidase activities observed earlier [4-10]. The specific invertase activity of the crude preparation was 20 units per mg of protein. The maltase activity of the crude preparation was 2 times the invertase activity, and it contained maltase I, II, and III in about equal proportions, expressed as number of units per ml.

Substrates

Sucrose, cryst., was obtained from J. T. Baker Co. *Maltose* (monohydrate), cryst., was obtained from Merck A.G. (Germany). Since the commercial maltose was found to contain contaminating sugars, which moved slower than maltose in paper chromatography (higher homologues), it was purified on carbon-celite columns [1,7]. The product was chromatographically pure. *Melezitose* (dihydrate) was obtained from Pfanstiehl Chemical Co., and *turanose* from Nutritional Biochemicals Corporation. All substrates used were chromatographically homogenous.

Activity determination

Determination of glycosidase activity was performed at 0.1388 M substrate concentration in the presence of 0.05 M maleate buffer pH 6.5. The degree of hydrolysis of the different substrates was determined with the methods described earlier [4,7]. (In order to spare enzyme, the 3,5-dinitrosalicylic acid method in some cases was replaced by the more sensitive Somogyi-Nelson method [4] for the determination of the hydrolysis of melezitose. The values obtained by these two methods agreed very well.)

Determination of the hydrolysis of sucrose and maltose in mixture. For the separate determination of the hydrolysis of sucrose and maltose, when the reaction solution contained these two substrates *in mixture*, it was necessary to determine the amounts of glucose and fructose liberated by quantitative paper chromatography. One molecule of sucrose hydrolyzed liberates one molecule of fructose and one molecule of glucose. One molecule of maltose hydrolyzed liberates two molecules of glucose. The number of sucrose and maltose molecules, respectively, which are hydrolyzed in a mixture of these two substrates therefore may be calculated.

The quantitative determination of glucose and fructose on paper chromatograms was performed with 5 μl spots of the reaction mixture as described earlier [1].

RESULTS AND DISCUSSION

Invertase activity

The invertase activity of the purified hog intestinal invertase preparation had the same characteristics as that of a crude hog intestinal glycosidase preparation. The optimum pH was 6.5 (Fig. 3) in accordance with that for a crude preparation [4]. The K_s was determined at 2.6×10^{-2}, which may be compared with the value 2.5×10^{-2} obtained for a crude preparation [4]. It has been demonstrated earlier that the K_s value for the invertase activity was the

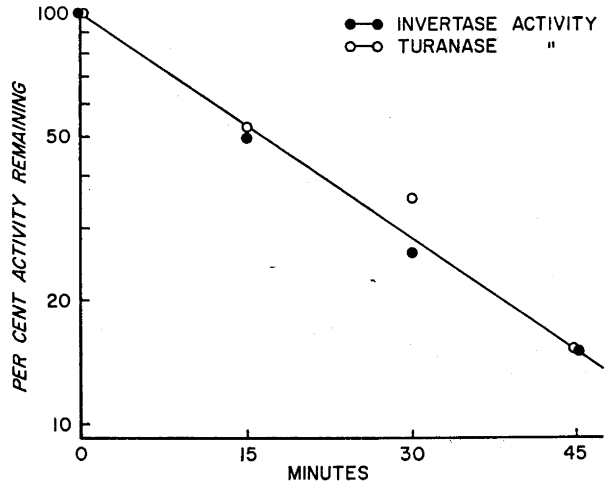

Fig 1. Heat inactivation of purified hog intestinal invertase in 0.01 M phosphate buffer pH 6.0 at 48°C. The solution contained 305 units/ml of invertase, 23 units/ml of turanase and 1.05 mg/ml of protein. The inactivation of the invertase and turanase activities ran parallel.

Table 1. Action of purified hog intestinal invertase upon sucrose and turanose alone and in mixture. The reaction mixture contained 0.01 mg/ml of protein. After incubation at 37°C for 1 h, the amount of glucose liberated was determined with glucose oxidase [4].

Concentration of substrate	Mg of glucose produced in 2 ml of reaction mixture
0.10 M sucrose	3.2
0.05 M sucrose	2.5
0.10 M turanose	<0.5
0.05 M turanose	<0.5
0.05 M sucrose +0.05 M turanose	1.4

same in different fractions of the single invertase peak obtained by anion exchange chromatography of a solubilized hog intestinal glycosidase preparation [7]. These facts indicate that the invertase activity of hog intestinal glycosidase preparations is exerted by one single enzyme.

Turanase activity

The purified invertase preparation had turanase activity which was 7.5 % of the invertase activity, whereas a crude hog intestinal glycosidase preparation had turanase activity which was 15 % of the invertase activity [4].

The K_s for the turanase activity of the purified invertase preparation was determined at 1.0×10^{-2}, which is lower than the value obtained [4] with a crude glycosidase preparation (2.8×10^{-2}). When the purified invertase was inactivated at 48°C in the presence of 0.01 M phosphate buffer pH 6.0, the inactivation of the turanase activity ran completely parallel with the inactivation of the invertase activity (Fig. 1), which supports the theory that the invertase and turanase activities of this fraction are caused by the same enzyme. This theory was also supported by the fact that the amount of monosaccharides produced by a certain amount of the enzyme acting upon the two substrates *in mixture* was less than the sum of the amounts of monosaccharides produced when the same amount of enzyme in separate experiments was acting upon each substrate alone (Table 1).*

* In a later experiment the inhibition of the hydrolysis of a series of sucrose solutions (0.025—0.100 M) by the presence of turanose (0.025 M) was determined. The amount of glucose liberated in the reaction mixtures was determined with glucose oxidase as described earlier for turanose [4]. Since turanose is hydrolyzed considerably slower than sucrose, the approximation was made that all the glucose liberated was produced from sucrose. (This approximation will cause the K_i value measured to be somewhat *too high*. From the relative rates of hydrolysis of turanose and sucrose and the K_s values for these activities the error to be expected was calculated at about 1/3 of the K_i value). It was found that turanose inhibited the hydrolysis of sucrose *competitively* and K_i for turanose as inhibitor was calculated at 1.2×10^{-2} which accords with the K_s value for the hydrolysis of turanose. This strongly supports the theory that sucrose and turanose are hydrolyzed by the same enzyme in the preparation studied. (For definitions and calculations see the experiments with sucrose and maltose described below.).

The remainder of the turanase activity of the crude glycosidase preparation appeared to be present in the *maltase II* and *maltase III* fractions [9]. The turanase activity of these fractions showed the same heat inactivation patterns as did the maltase activity [6,9]. At 72°C, the inactivation of the turanase activity of the maltase III preparation ran parallel to that of the maltase activity (Fig. 2). The turanase activity was 4 % of the maltase activity for maltase II and 6 % for maltase III. This means that the turanase activity of a crude preparation [4] quantitatively fits very well with the sum of the turanase activities of the invertase (= maltase I), maltase II and maltase III in the crude preparation. (In the calculation it is assumed that the activities of the maltase I, II and III in the crude preparation were equal, and that the maltase/invertase activity quotient was 2.0.)

Melezitase activity

The purified invertase had *no measurable melezitase activity.* With the conditions used, this means that the amount of monosaccharides produced from melezitose was less than 0.05 % of that produced from sucrose. All of the melezitase activity of the crude preparation [4] could be shown to reside in the maltase II and maltase III fractions.

The purified *maltase III* hydrolyzed melezitose *to glucose and sucrose* as demonstrated by paper chromatography. Only the turanose link of the trisaccharide was hydrolyzed. *Maltase II*, too, had some melezitase activity (with glucose and sucrose as the hydrolysis products), but this activity was weaker in relation to the maltase activity than that of maltase III. The melezitase activities followed the same heat inactivation patterns as did the maltase activities [9] of these two fractions. At 72°C the inactivation of the melezitase activity of a maltase III preparation ran parallel with that of the maltase activity (Fig. 2). The melezitase activity * was 0.1 % of the maltase activity for maltase II and 0.4 % for maltase III. With the same assumptions as made above in calculating the turanase activity, these enzymes would cause a melezitase activity of the crude preparation 0.17 % of the (total) maltase activity, which is somewhat higher than the value obtained, 0.10 % **, in earlier experiments [4]. Maltase II and III, therefore, are the only

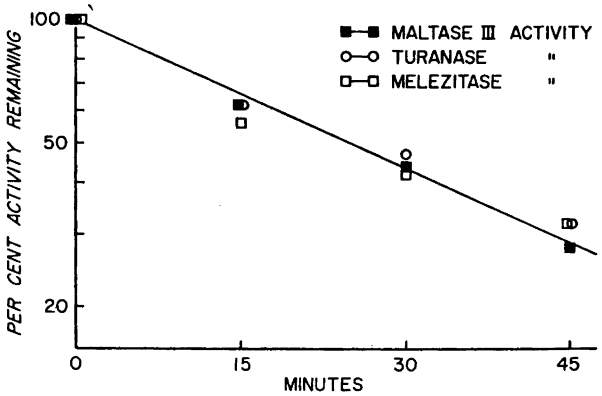

Fig. 2. Inactivation of a purified hog intestinal maltase III preparation at 72°C in the presence of 0.01 M phosphate buffer pH 6.0. The solution contained 235 units/ml of maltase III, 14 units/ml of turanase, 0.9 units/ml of melezitase and 1.18 mg/ml of protein. The inactivation of the maltase, turanase and melezitase activities ran parallel.

* Calculated as number of melezitose molecules hydrolyzed to glucose and sucrose, compared with the number of maltose molecules hydrolyzed by the same amount of enzyme.

** Calculated as number of melezitose molecules *completely* hydrolyzed [4].

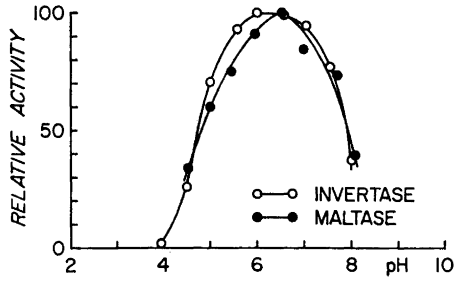

Fig. 3. pH activity curves for the invertase and maltase (I) activities of a purified hog intestinal invertase preparation. Temperature 37°C, 0.1388 M substrate concentration. Buffers: 0.05 M acetate pH 4.0—5.0, 0.05 M maleate pH 5.5—6.5, 0.025 M veronal pH 7.0—8.0. pH was measured with a glass electrode.

enzymes in crude hog intestinal glycosidase preparations which hydrolyze melezitose. When a crude glycosidase preparation was heated at 60°C, in the presence of 0.01 M phosphate buffer pH 6.0, the amount of reducing sugars produced from melezitose per time unit decreased by 70 % within 30 min but was then not further diminished. After heating, the invertase (= maltase I) and maltase II (containing weak melezitase activity) are inactivated, but maltase III (containing the majority of melezitase activity) remains unaffected. This marked decrease in the amount of reducing sugars liberated from melezitose is chiefly caused by the inactivation of *invertase*. Although the invertase has no melezitase activity *per se*, it hydrolyzes the sucrose formed from melezitose hydrolysis to two molecules of reducing sugar. In the absence of invertase, melezitose is hydrolyzed by maltase III only to glucose and sucrose, and one molecule, rather than three, of reducing sugar is released for each melezitose molecule hydrolyzed.

Maltase activity

The purified hog intestinal invertase preparation had maltase activity (= maltase I) which was 0.6 times the invertase activity. This activity represents 1/3 of the total maltase activity of crude preparations. Attempts to separate the maltase (I) activity of the purified invertase preparation from the invertase activity were not sucessful. With rechromatography on ion exchange columns the two activities formed a homogenous peak [6]. When the preparation was exposed to heat, the two activities were inactivated completely similarly, even when such experiments were performed in a series of buffers of varying pH [6]. In frontal analysis the maltase I and invertase activities appeared as one common, homogeneous front [7], and they were not separable by mutual displacement chromatography [7]. The pH activity curve of the maltase I activity was similar to that of the invertase activity (Fig. 3) but differed from those of the maltase II and III activities [9].

All these facts support the theory, that the maltase I activity is caused by same enzyme as the invertase activity. The ability to independently determine the hydrolysis of sucrose and maltose, by quantitative paper chromatography of the hydrolysis products, when these two substrates are mixed with each other, offers one additional method for proving the identity of the maltase I

and invertase activities. If one enzyme catalyzes the hydrolysis of two different substrates, these two substrates must act as competitive inhibitors for each other. The invertase activity should be competitively inhibited by maltose, and the maltase I activity competitively inhibited by sucrose. In addition the inhibitor constant (K_i) for maltose as a competitive inhibitor for the invertase must have the same value as the substrate constant (K_s) for maltose as substrate for maltase I, and vice-versa, if it possible to ascribe the invertase and maltase I activities to the same enzyme.

Definitions. K_s = the dissociation constant for the enzyme-substrate complex (Michaeli's constant). K_s is measured as the substrate concentration at which the initial velocity of reaction is half of the V_{max} (provided no (competitive) inhibitor is present) *.

K_i = the dissociation constant for the enzyme-inhibitor complex. When the inhibition is *competitive*, K_i is calculated from the influence of the presence of the inhibitor upon the *apparent* K_s value for the substrate.

v = the measured initial velocity for the hydrolysis of the substrate.

V_{max} = the initial velocity for the hydrolysis of the substrate when the enzyme is 100 % saturated with substrate.

[s] = the substrate concentration
[i] = the inhibitor concentration.

The constants were obtained graphically by the method of Lineweaver and Burk [11] as modified by Dixon [12,13] (Fig. 4).

Experimental conditions. The reaction mixture contained 0.05 M maleate buffer pH 6.5, and the incubation of the substrate with the enzyme was performed for 60 min at 37°C. After this time the reaction was interrupted by boiling in a water-bath for 2 min.

The enzyme used was the purified invertase preparation. The substrate concentration varied within the range of 0.10—0.01 M, and the inhibitor concentration was 0.0139 or 0.0278 M in the experiments where inhibitor was present. In each experiment the hydrolysis at a series of different substrate concentrations was measured, at a constant concentration of inhibitor. The degree of hydrolysis was never allowed to exceed 20 % at the lowest substrate concentration used in the experiment. The quantitative determination of glucose and fructose, after elution from the paper chromatograms, was made with amounts of 1—8 μg.

It is essential for the accuracy of the results that no transglycosylation [1] occurs. In the experiments with sucrose as substrate, without maltose present, there was no measurable difference between the amount of glucose and the amount of fructose liberated, and this demonstrates that no transglycosylation occurs at the substrate concentrations used.

Inhibition of invertase activity. In one series of experiments *sucrose* was used as *substrate*. One such experiment is illustrated in Fig. 4. Without inhibitor present, the K_s for the invertase activity was determined at 2×10^{-2}

* Measured in this way, the K_s is not the true dissociation constant for the enzyme-substrate complex, but with most enzymes it has probably approximately the same value [13].

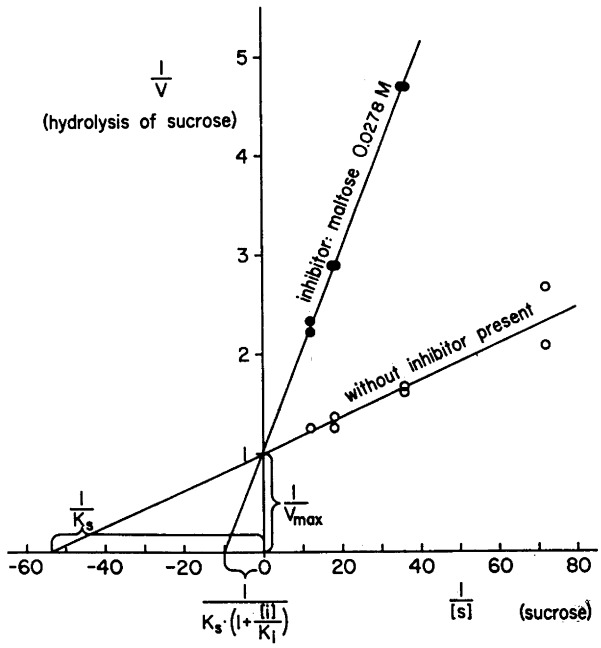

Fig. 4. Inhibition of the invertase activity of a purified hog intestinal invertase preparation by maltose. The V_{max} for the hydrolysis of *sucrose* was unaltered by the addition of inhibitor (maltose) which demonstrates that the inhibition was *competitive*. The K_s (for sucrose) and the K_i (for maltose as inhibitor of the invertase activity) were calculated from the intercept with the abscissa as seen in the figure.

with the chromatographic method, which may be compared with the value 2.6×10^{-2} earlier obtained with the 3,5-dinitrosalicylic acid method [7]. Maltose was found to inhibit the invertase activity competitively with a K_i value at about 1×10^{-2}, which agrees with the value for K_s for maltase I obtained earlier (1.1×10^{-2}) with another method [7].

Inhibition of maltase I activity. In another series of experiments *maltose* was used as *substrate*. Without the presence of sucrose the K_s for the maltase I activity was determined at 1×10^{-2}. Sucrose inhibited the maltase I activity competitively with K_i at 2×10^{-2}, which agrees with the K_s value for the invertase activity obtained earlier.

These results clearly demonstrate that the *maltase I* activity, which represents one third of the total maltase activity of crude preparations, and which closely follows the *invertase* activity during its purification, is exerted by the same enzyme as the invertase activity.

Acknowledgment. The author's thanks are due to Professor Bengt Borgström for his interest in my work and for valuable discussions. This work has been supported by grants from the *Medical Faculty of the University of Lund.* The skillful technical assistance of Mrs. K. Hagebris is gratefully acknowledged.

REFERENCES

1. Dahlqvist, A. and Borgström, B. *Acta Chem. Scand.* **13** (1959) 1659.
2. Myrbäck, K. and Myrbäck, S. *Svensk Kem. Tidskr.* **48** (1936) 64.
3. Steensholt, G. and Veibel, S. *Acta Physiol. Scand.* **6** (1943) 62.
4. Dahlqvist, A. *Acta Chem. Scand.* **12** (1958) 2012.
5. Borgström, B. and Dahlqvist, A. *Acta Chem. Scand.* **12** (1958) 1997.
6. Dahlqvist, A. *Acta Chem. Scand.* **13** (1959) 945.
7. Dahlqvist, A. *Acta Chem. Scand.* **13** (1959) 1817.
8. Dahlqvist, A. *Acta Chem. Scand.* **14** (1960) 9.
9. Dahlqvist, A. *Acta Chem. Scand.* **14** (1960) 1.
10. Dahlqvist, A. *Acta Chem. Scand.* **14** (1960) 72.
11. Lineweaver, H. and Burk, C. *J. Am. Chem. Soc.* **56** (1934) 658.
12. Dixon, M. *Biochem. J.* **55** (1953) 170.
13. Dixon, M. and Webb, E. C. *Enzymes*, Longmans, Green & Co., London 1958.

Received November 10, 1959.

ACTA CHEMICA SCANDINAVICA 14 (1960) 72—80

Hog Intestinal Isomaltase Activity

ARNE DAHLQVIST

Department of Physiological Chemistry, University of Lund, Lund, Sweden

Homogenates of hog intestinal mucosa have *isomaltase* activity, caused by at least three different enzymes.

About 3/4 of the total isomaltase activity is caused by an enzyme (or enzymes) which seems to have mainly isomaltase activity. This enzyme has no invertase or maltase activity, but it possibly hydrolyzes phenyl-α-D-glucopyranoside. The name *specific isomaltase* is suggested for this enzyme.

The remainder of the isomaltase activity is caused by two hog intestinal maltases, which hydrolyze isomaltose slowly.

Separation of the specific isomaltase from the other hog intestinal α-D-glucopyranosidases was not successful. It could be stated, however, that the specific isomaltase has transglycosylase properties which clearly differ from those of the isomaltase activity accompanying the two maltases.

The influence of freezing and thawing upon the specific isomaltase activity is complex, and involves a decrease as well as an increase of this activity.

The hydrolysis of *isomaltose* (6-α(-D-glucopyranosyl)-D-glucose) by enzyme preparations from hog intestinal mucosa has recently been studied by Larner, Mc Nickle and Gillespie [1-7]. These authors postulated that isomaltose and maltose were hydrolyzed by two different enzymes in these preparations, although they were able to separate these two activities only partially. A hog intestinal maltase preparation was obtained, which had no demonstrable isomaltase activity, but the isomaltase activity* was never purified from maltase activity [3,6].

More recently, however, it has been demonstrated that hog intestinal *maltase* activity is not caused by a single enzyme, but can be separated into three different fractions (maltase I—III) with different enzymatic properties.[8-10] One of these fractions, maltase I, had no detectable isomaltase activity, while the other two, maltase II and III, hydrolyzed isomaltose slowly [10].

The present investigation was undertaken to elucidate further the relation between the *maltase* and *isomaltase* activities of hog intestinal mucosa.

* Larner *et al.* name this activity *oligo-1,6-glucosidase* (to distinguish it from *amylo*-1,6-glucosidase). It seems more logical to call it *isomaltase* activity in agreement with general nomenclature used for other glycosidase activities.

MATERIALS AND METHODS

Enzyme preparations

Crude hog intestinal glycosidase preparations. Pieces of hog small intestine were cut within a few minutes after slaughter and chilled with crushed ice during the transport to the laboratory. In some experiments the mucosa was scraped off (as done by Larner *et al.*[3]) and homogenized for 2 min in an "Ultra-Turrax" homogenizer with an equal volume of saline or buffer. In other experiments the mucosa was squeezed out manually and solubilized as described earlier [11]. Whichever procedure was used, the relation of the isomaltase activity to the invertase and maltase activity of the preparation obtained was the same.

Purified hog intestinal maltase II and purified hog intestinal maltase III were obtained by mutual displacement chromatography of solubilized hog intestinal glycosidase preparations as described earlier [9].

Substrates

Isomaltose (6-(α-D-glucopyranosyl)-D-glucose) was prepared by enzymatic hydrolysis of dextran as described by Jeanes *et al.*[12] *Dextran* (average molecular weight M_w (end group analysis) 17 600, M_n (light scattering) 40 400) was obtained as a gift from A. B. Pharmacia (Uppsala, Sweden). *Penicillium funiculosum* was obtained from Centraalbureau voor Schimmelkultures (Baarn, Nederland). The mold was cultured on a solution containing 2 % dextran and 3 % yeast extract (from Difco Lab., Detroit, Mich.) at room temp. for 9—10 days during shaking. The culture filtrate had dextranase activity of 18 units/ml (determined essentially as described by Tsuchiya *et al.*[13], but the amount of reducing sugar produced was measured with the 3,5-dinitrosalicylic acid reagent [17] instead of Somogyi's copper reagent).

For preparations of isomaltose 4 g of dextran was dissolved in 40 ml of water. To this solution was added 20 ml of 0.1 N acetate buffer pH 5.1, 20 ml of culture filtrate from *Penicillium funiculosum*, and 5 ml of toluene. After 23 h, at 37°C the reducing power of the solution corresponded to 77 % of hydrolysis to isomaltose. After removing toluene, the solution was boiled for a few minutes to interrupt the enzymatic hydrolysis. The solution was then poured onto a 9 × 25 cm carbon-celite column [14]. The glucose was eluted with 5 l of distilled water, and then the isomaltose was eluted with 5 l of 5 % (by vol.) ethanol. The isomaltose fraction was evaporated at reduced pressure to a volume of about 50 ml and then lyophilized (the sugar was markedly hygroscopic and crystallization was not successful). The powder obtained was dried *in vacuo* over P_2O_5 at 50°C. The yield was 1.75 g of chromatographically homogeneous sugar (when 1 mg of the sugar was run on a paper chromatogram it formed only one spot). The chromatographic mobility was somewhat lower than that of maltose, R_M value (mobility/mobility of maltose) 0.75 in ethyl acetate: acetic acid : water 9:2:2 (v/v). The molecular weight of the sugar was determined at 325 by cryoscopy (calcd. for $C_{12}H_{22}O_{11}$ 342.3). The optical rotation agreed well with that reported for isomaltose, measured $[\alpha]_D^{20}$ +117.5° (10 % in water), reported for isomaltose +122.0° [12], +103.2° (amorphous) [15], +120° (cryst.) [15]. Acetylation with sodium acetate as catalyst yielded the β-octaacetate (amorphous, in spite of several attempts crystallization was not achieved) which had $[\alpha]_D^{20}$ +97.5° (2 % in $CHCl_3$), reported for isomaltose-β-octaacetate +96.9° [12,16].

Phenyl-α-D-glucopyranoside was prepared as described earlier [10]. The other substrates used were commercial preparations of analytical grade purity [11].

Determination of glycosidase activity

The reaction mixture in all cases had 0.1388 M substrate concentration and contained 0.05 M maleate buffer pH 6.5 and small amount of toluene as preservative. The degree of hydrolysis was determined with the methods described earlier [9-10]. One unit of glycosidase activity is the amount which causes 1 % of hydrolysis in 2 ml of reaction mixture in 1 h at 37°C during these conditions. The degree of hydrolysis was not allowed to exceed 10 %.

The hydrolysis of isomaltose was determined with Tauber and Kleiner's acid copper reagent as described earlier for maltose [9]. Since isomaltose had stronger reducing power with this reagent than maltose, the sugar determination was made with 1.0 mg of isomaltose instead of 2.5 mg of maltose. The modified copper reagent (Caputto's reagent) which was used for K_s and optimum pH determinations with maltose could not be used for isomaltase determinations, because isomaltose, itself, reduced this reagent too strongly.

Adsorbents

Cellulose ion exchangers. DEAE-cellulose was prepared from Solkafloc cellulose powder SW 40 A by the method of Peterson and Sober [20]. The product contained 0.8 mequiv. titrable hydroxyl groups per gram dry weight. *TEAE-cellulose* was prepared from DEAE-cellulose by ethylation as described by Porath [21]. CM-cellulose was prepared from Whatman cellulose powder by the method of Peterson and Sober [20]. It contained 0.3 mequiv. titrable acid groups per gram dry weight.

Alumina Cγ-gel was prepared as described by Willstätter and Kraut [22]. The gel was stored, suspended in distilled water, for six months at room temperature before use. The amount of gel used in the experiments will be expressed as mg dry weight, determined after drying to constant weight at 100°C.

Calcium phosphate gel (for column chromatography) was prepared by the method of Tiselius et al.[23]

Paper chromatography of sugars was performed as described earlier [14].

RESULTS AND DISCUSSION

Freshley prepared homogenates of hog small intestinal mucosa hydrolyzed *isomaltose* with a rate which was 8—10 % of the rate for the hydrolysis of maltose. The relation between the isomaltase and maltase activities was the same in all parts of the small intestine. Some different α-D-glucopyranosidase activities of a representative homogenate from hog small intestine are recorded in Table 1.

The separation of several different hog intestinal α-D-glucopyranosidases has been reported previously [8–10,17]. Two of the different α-D-glucopyranosidases separated had *isomaltase* activity, namely maltase II and maltase III.

Table 1. Some α-D-glucopyranosidase activities of a freshly prepared homogenate (1:2 in saline) of hog intestinal mucosa. The protein content of the homogenate was 9.5 mg/ml.

	Units/ml
Invertase	32
Maltase (total)	62
Maltase I *	19
Maltase II	21
Maltase III **	22
Isomaltase	6.8
Phenyl-α-D-glucopyranosidase	3.6

* Calculated as 0.6 times the invertase activity [10].

** Determined after inactivation of maltase I and II by heat [9].

The rate for the hydrolysis of isomaltose by these fractions was 2 and 5 %, respectively, of the rate for the hydrolysis of maltose [10]. Since each of the maltase II and III contributes only 1/3 to the total maltase activity of crude preparations, the isomaltase activity of these purified maltase fractions can contribute only 1/4 of the total isomaltase activity of the crude preparation. The existence therein of a *specific hog intestinal isomaltase* therefore was postulated.

The question then arises, if the isomaltase activity of the purified maltase II and III preparations really is caused by these enzymes *per se*, or if is caused by contamination with the specific isomaltase.

In order to study the properties of the specific hog intestinal isomaltase, attempts were made to separate this enzyme from the other intestinal α-D-glucopyranosidases.

Solubilization. Like the other hog intestinal glycosidase activities, the isomaltase activity is localized to the microsome fraction, obtained by differential centrifugation [6,11]. Like the invertase and maltase activities, the isomaltase activity could be solubilized with trypsin (in the presence of phosphate buffer) and precipitated with ethanol in the same way as described earlier for the other activities [11], without losses of isomaltase activity.

It has been reported that hog intestinal isomaltase is inactivated by high speed centrifugation [6]. This, however, could not be verified. Even when homogenates of intestinal mucosa (in the presence of 0.01 M veronal buffer pH 7.5) were centrifuged at 100 000 × *g* for 3 h (Spinco preparative ultracentrifuge, rotor 40) no losses of isomaltase activity were recorded. All the activity was found in the sediment, when fresh homogenates were used, or in the supernatant, when solubilized preparations were used.

Ion exchange chromatography. Chromatography of the solubilized glycosidase preparations on DEAE-cellulose or TEAE-cellulose, which has earlier been used for the separation of the other hog intestinal α-D-glucopyranosidases [9,11], was associated with losses of more than 50 % of the isomaltase activity. When adsorption to TEAE-columns, however, was performed at +4°C and elution completed within 60 min, 90—100 % of the isomaltase activity was eluted with 0.07—0.15 M phosphate buffer (pH 6.0) together with the invertase and maltase activities. DEAE- and TEAE-cellulose, therefore, were not useful for the purification of hog intestinal iso-maltase.

Neither the isomaltase, invertase or maltase activities were adsorbed to CM-cellulose in 0.01 M phosphate buffer pH 6.5, although 50 % of the protein content of the glycosidase preparation was adsorbed.

Adsorption to alumina Cγ-gel. At pH 5.0 (in 0.02 M acetate buffer) the invertase, maltase and isomaltase activities were adsorbed to alumina Cγ-gel. When pH was increased, the activities were released all together, and at pH 6.0 (0.02 M phosphate buffer) no adsorption occured.

The influence of varying the amount of adsorbent in the presence of 0.02 M acetate buffer pH 5.0 was studied (Table 2). The activities investigated, however, showed no difference in their degree of adsorption during these conditions which was sufficiently great to be used for their separation.

Adsorption to calcium phosphate gel. This adsorbent was used in columns, as described by Tiselius *et al.*[23], and the experiments were performed in the

Table 2. Adsorption of intestinal α-D-glucopyranosidases on alumina Cγ-gel in 0.02 M acetate buffer, pH 5.0. The solution contained 0.8 mg/ml of protein, 10 units/ml of invertase, 21 units/ml of maltase, 2.5 units/ml of isomaltase and 0.9—7.2 mg/ml (dry weight) of alumina Cγ-gel. After shaking for 30 min at room temperatur, the solution was centrifuged and the supernatant analyzed.

Mg/ml of alumina C γ-gel	Per cent adsorbed			
	Protein	Invertase activity	Maltase activity	Isomaltase activity
0.9	35	40	23	40
1.8	53	83	65	75
3.6	66	96	90	95
7.2	70	100	96	95

presence of phosphate buffer pH 6.8. The invertase, maltase and isomaltase activities were weakly adsorbed to calcium phosphate, for the adsorption step it was necessary to use 0.001 M buffer. Whether gradient elution or step-wise elution was used, the invertase, maltase and isomaltase activities were eluted all together with 0.002—0.005 M buffer. Calcium phosphate is therefore no suitable adsorbent for the separation of these activities. (The trehalase activity, however, was not eluted until the buffer concentration exceeded 0.005 M, and was therefore separated from the other activities. The separation of hog intestinal trehalase on ion exchange columns has been reported earlier [11,17]).

Heat inactivation. The isomaltase activities of the purified maltase II and III preparations followed the same heat inactivation patterns as the maltase activities, *i.e.* that of the maltase II fraction was rapidly inactivated at 60°C, while that of the maltase III fraction was not inactivated at temperatures below 70°C (in presence of 0.01 M phosphate buffer pH 6.0) [10].

In one experiment, a crude solubilized glycosidase preparation, after dialysis against 0.01 M phosphate buffer pH 6.0, was heated at 60°C. The preparation had protein content 5.2 mg/ml and contained 38.5 units/ml of invertase, 97 units/ml of total maltase and 7.6 units/ml of isomaltase. During heating, all the invertase activity and 62 % of the total maltase activity were abolished within 20 min. The remaining 38 % of the maltase activity (*i.e.* maltase III [8]) was not affected during heating for 60 min. The isomaltase activity decreased by 74 % within 20 min. but was then not further diminished. Apparently the specific isomaltase was inactivated (together with the weak isomaltase activity of maltase II) within the first 20 min. The quotient between that isomaltase activity which survived heating and the maltase activity which was not abolished, fits well with the isomaltase/maltase activity quotient of a purified maltase III preparation [10].

Transglycosylation properties. The purified maltase II and maltase III as well as a crude glycosidase preparation, formed a number of oligosaccharide spots when acting in a concentrated (30 %*) isomaltose solution. The oligosaccharides formed by the crude preparation were, however, not identical with those formed by the purified maltase preparations.

* Per cent means g of solute per 100 ml of solution.

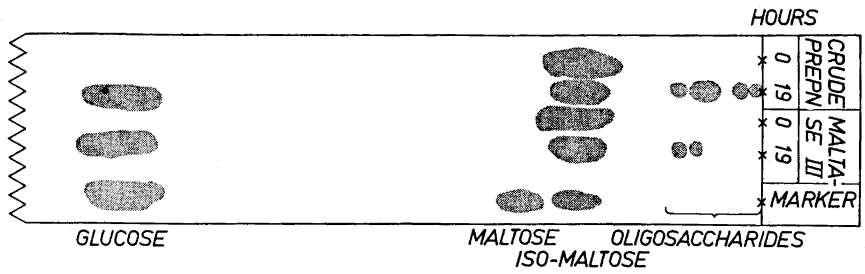

Fig. 1. Oliogosaccharides produced by transglycosylation by hog intestinal isomaltase. The *crude preparation* was a freshly prepared solubilized hog intestinal glycosidase preparation. In this case the reaction mixture contained 12 units of isomaltase, 108 units of (total) maltase and 15 mg of protein/ml. In the other case a *purified maltase III preparation* was used, and the reaction mixture contained 12 units of isomaltase, 263 units of maltase (III) and 1.5 mg of protein/ml. In both cases the reaction mixture containe 30 % isomaltose, 0.05 M maleate buffer and a few drops of toluene/ml. Before incubation and after incubation at 37°C for 19 hours 5 μl spots of the reaction mixture were applied to a chromatogram, which was developed with ethyl acetate: acetic acid: water (v/v) for 3 days.

In Fig. 1. is shown a chromatogram from one such experiment. In one case the reaction mixture contained a crude preparation, yielding 12 units/ml of isomaltase, 108 units/ml of (total) maltase and 15 mg/ml of protein. In the other case it contained a purified maltase III preparation, yielding 12 units/ml of isomaltase, 263 units/ml of maltase and 1.5 mg/ml of protein. In both cases the reaction mixture contained 30 % isomaltose, 0.05 M maleate buffer pH 6.5 and a few drops of toluene/ml. After different time of incubation at 37°C, 5 μl spots were applied to a paper chromatogram, which was developed for 3 days.

After the reaction had proceeded for 19 h, the reaction mixture with the crude glycosidase preparation contained *four* different oligosaccharides, formed by transglycosylation, which were separated on the paper chromatogram. In the reaction mixture with the purified maltase III, however, only *two* oligosaccharides could be detected (Fig. 1), although the reaction mixture in both cases contained equally many units of isomaltase activity per ml. Even when the reaction time was extended to two and three days, only two oligosaccharides could be detected in the reaction mixture which contained purified maltase III. A purified maltase II preparation showed the same behaviour as maltase III. It is therefore apparent that the specific isomaltase which is present in crude preparations, is able to form some oligosaccharides by transglycosylation which cannot be formed by the purified maltase II and III. This indicates that the isomaltase activity precent in the purified maltase II and maltase III preparations is *not* caused by contamination with specific isomaltase.

After a crude preparation had been heated at 60°C for 1 h (inactivating the specific isomaltase and maltase II but not the maltase III) it formed only two oligosaccharides in a 30 % isomaltose solution. These oligosaccharides had

the same mobility as those formed by the purified maltase II and maltase III preparations.

Effect of freezing. It has been reported by Larner *et al.*[6] that freezing and thawing of particulate intestinal glycosidase preparations *increases* the isomaltase and maltase activities by more than 200 %. In another paper [3], however, the same authors state that freezing and thawing *reduces* the isomaltase activity of crude preparations.

The present author has *not* observed any remarkable change of the maltase or invertase activities of either particulate or solubilized intestinal glycosidase preparations, although these preparations usually were stored in the frozen state in order to preserve their activity. Nor was any change of these activities observed when intestinal microsomes were frozen and thawed repeatedly as an attempt to solubilize the glycosidases [11].

For studing the effect of freezing and thawing upon hog intestinal isomaltase activity a solubilized crude glycosidase preparation was used which contained 15 mg/ml of protein in 0.01 M phosphate buffer pH 6.0. About 5 ml of the solution in a test tube was frozen by dipping the tube into a mixture of dry ice and ethanol at −80°C. After freezing, which took less than one min, the tube was held in the freezing mixture for 10 min, and then thawed in a water-bath at 37°C. As is seen in Table 3, the isomaltase activity had decreased by 1/3 after repeating this procedure three times. By further repeating of the freezing and thawing the isomaltase activity was, however, not further decreased, although the isomaltase activity still was three times that which could be caused by the isomaltase activity of maltase II and maltase III in the preparation. It was also found that the preparation after this treatment still formed all the four oligosaccharides in a 30 % isomaltose solution which were formed by the crude preparation before freezing. It is therefore not possible to *completely* inactivate the specific isomaltase by repeated freezing and thawing.

Exactly the same resultes were obtained when the freezing mixture consisted of sodium chloride and ice at −15°C. The temperature used seems therefore to be without importance for the results.

The effect of keeping the preparation in the frozen state for a longer time was also studied. The same enzyme preparation was used, but in this case the preparation was distributed in a series of test tubes, so that the content of each tube was frozen and thawed only once. The tubes were stored at −16°C

Table 3. Effect of repeated freezing and thawing upon some hog intestinal α-D-glucopyranosidase activities. For experimental conditions, see text.

	Activity (units per ml)			
	Isomaltase	Maltase	Invertase	Phenyl-α-D-glucopyranosidase
Before freezing	13.6	130	61	8.3
Frozen and thawed once	11.8	131	62	8.8
Frozen and thawed three times	9.1	115	62	8.2

Table 4. Effect of storage in the frozen state upon some hog intestinal α-D-glucopyranosidase activities. For experimental conditions, see text.

	Activity (units per ml)			
	Isomaltase	Maltase	Invertase	Phenyl-α-D-glucopyranosidase
Before freezing	13.6	130	61	8.3
After 4 days at −16°C	11.0	135	55	8.0
After 12 days at −16°C	8.2	148	55	7.0
After 33 days at −16°C	18.0	165	57	8.5

and each tube was thawed just before analysis. The effect of storage in the frozen state upon the different α-D-glucopyranosidase activities is shown in Table 4. The iso-maltase activity decreased by a little more than 1/3 within the first two weeks, but then *increased* to 1/3 more than its original value. In this experiment the maltase activity, too, increased somewhat, but not so much as reported by Larner *et al.*[6]

The effect of freezing during a still longer time was studied by analysis of a solubilized glycosidase preparation which had been dialyzed against distilled water and kept frozen at −16°C for eight months. This preparation contained 23.5 units/ml of invertase and 45 units/ml of maltase, *i.e.* the maltase/invertase activity quotient was 1.9, which agrees well with that of fresh preparations. The isomaltase activity of the preparation which had been frozen for eight months was 5.5 units/ml, *i.e.* the isomaltase activity was 12 % of the maltase activity, which is somewhat higher than the value usually obtained with fresh preparations (8—10 %). When acting in a 30 % solution of isomaltose, this preparation formed all the four different oligosaccharides which are formed by a fresh crude intestinal glycosidase preparation.

The isomaltase activities of *purified maltase II and maltase III preparations* were not changed by storage in the frozen state.

The procedure of freezing apparently has a complex effect upon the isomaltase activity of hog intestinal mucosa, with an initial *decrease* of the isomaltase activity followed by a more slow *increase* of this activity. A more thorough investigation of this phenomenon must wait until a method has been found for the purification of the specific isomaltase of hog intestinal mucosa. One explanation may be that the specific isomaltase is a mixture of several different enzymes which are influenced in different ways by freezing, but no other indications for such a heterogenity have appeared.

Phenyl-α-D-glucopyranosidase activity was studied in some experiments. Of the different hog intestinal α-D-glucopyranosidases separated earlier, two had phenyl-α-D-glucopyranosidase activity, namely maltase II and maltase III. The phenyl-α-D-glucopyranosidase activity of these fractions was 3 and 5 %, respectively, of their maltase activity (calculated as number of molecules hydrolyzed per time unit) [10]. Fresh mucosa homogenates had phenyl-α-D-glucopyranosidase activity about 6 % of their (total) maltase activity. This means that the phenyl-α-D-glucopyranosidase activity of the maltases II and III in the homogenates can contribute only 1/2 to the total phenyl-α-D-

glucopyranosidase activity. The remainder of the phenyl-α-D-glucopyranosidase activity may be caused by the specific isomaltase.

During heating at 60°C, the major part (about 2/3) of the phenyl-α-D-glucopyranosidase activity of crude preparations was abolished together with the invertase (= maltase I), maltase II and specific isomaltase. After heating the preparation had phenyl-α-D-glucopyranosidase/maltase (III) activity quotient which was the same as that of a purified maltase III preparation.

The effect of freezing and thawing upon the phenyl-α-D-glucopyranosidase activity of crude preparations varied somewhat. In some experiments slightly decreased activity was observed on freezing and thawing (Table 4) while in other cases no change could be stated (Table 3). It can not at present be stated whether that part of the phenyl-α-D-glucopyranosidase activity which is not caused by maltase II and maltase III is caused by the specific isomaltase or by some other enzyme.

Acknowledgment. The author's thanks are due to Professor Bengt Borgström for his interest in my work and for valuable discussions.

This work has been supported by grants from the *Medical Faculty of the University of Lund.*

The skillful technical assistance of Mrs. K. Hagebris is gratefully acknowledged.

REFERENCES

1. Larner, J. and Mc Nickle, C. M. *J. Am. Chem. Soc.* **76** (1954) 4747.
2. Larner, J. and Gillespie, R. E. *Arch. Biochem. Biophys.* **58** (1955) 252.
3. Larner, J. and Mc Nickle, C. M. *J. Biol. Chem.* **215** (1955) 723.
4. Larner, J. *J. Am. Chem. Soc.* **77** (1955) 6385.
5. Larner, J. and Gillespie, R. E. *J. Am. Chem. Soc.* **78** (1956) 882.
6. Larner, J. and Gillespie, R. E. *J. Biol. Chem.* **223** (1956) 709.
7. Larner, J. and Gillespie, R. E. *J. Biol. Chem.* **225** (1957) 279.
8. Dahlqvist, A. *Acta Chem. Scand.* **13** (1959) 945.
9. Dahlqvist, A. *Acta Chem. Scand.* **13** (1959) 1817.
10. Dahlqvist, A. *Acta Chem. Scand.* **14** (1960) 1.
11. Borgström, B. and Dahlqvist, A. *Acta Chem. Scand.* **12** (1958) 1997.
12. Jeanes, A., Wilham, C. A., Jones, R. W., Tsuchiya, H. M. and Rist, C. E. *J. Am. Chem. Soc.* **75** (1953) 5911.
13. Tsuchiya, H. M., Jeanes, A., Bricker, H. M. and Wilson, C. A. *J. Bact.* **64** (1952) 513.
14. Dahlqvist, A. and Borgström, B. *Acta Chem. Scand.* **13** (1959) 1659.
15. Pigman, W. W. (Ed.) *The Carbohydrates*, New York 1957.
16. Wolfrom, M. L., Georges, L. W. and Miller, I. L. *J. Am. Chem. Soc.* **71** (1949) 125.
17. Dahlqvist, A. *Acta Chem. Scand.* **14** (1960) 9.
18. Tauber, H. and Kleiner, I. S. *J. Biol. Chem.* **99** (1932) 249.
19. Somogyi, M. *J. Biol. Chem.* **160** (1945) 69.
20. Peterson, E. A. and Sober, H. A. *J. Am. Chem. Soc.* **78** (1956) 751.
21. Porath, J. *Arkiv Kemi* **11** (1957) 97.
22. Willstätter, R. und Kraut, H. *Ber.* **56** (1923) 1117.
23. Tiselius, A., Hjertén, S. and Levin, Ö. *Arch. Biochem. Biophys.* **65** (1956) 132.

Received November 26, 1959.

ACTA CHEMICA SCANDINAVICA 14 (1960) 81—85

The Chemistry of the Natural Order Cupressales

XXIV.* Heartwood Constituents of *Chamaecyparis thyoides* (L) Britt.

C. ENZELL

Organisk-kemiska Institutionen, Kungl. Tekniska Högskolan, Stockholm, Sweden

The heartwood of *Chamaecyparis thyoides* was found to contain carvacrol methyl ether, α-cedrene, cuparene, thujopsene (widdrene), cedrol, widdrol, cuparenic acid, hinokiic acid (widdrenic acid) and "Widdringtonia acid II"; no tropolones were detected.

The family *Cupressaceae* has been subdivided by botanists into about twenty genera, most of which are monotypic or include only a few species. Both chemical and botanical aspects of the relationship between the different genera and the various species of the larger genera have been discussed in a recent review [1].

The present investigation was undertaken to provide a chemical characterisation of *Chamaecyparis thyoides*, a tree endemic to the south-eastern part of North America. Zavarin and Anderson [2], in a survey of the occurrence of tropolones, have previously examined an extract from this tree by paper chromatography and have reported the presence of α-, β- and γ-thujaplicins.

The heartwood of *Chamaecyparis thyoides*, very kindly provided by Dr. J. P. Bain, Glidden Co., Jacksonville, Florida, was extracted with acetone and the light petroleum-soluble part of this extract was separated into acidic and neutral fractions. The neutral part, after a preliminary distillation, was fractionated through a high efficiency column giving a forerun, which contained mainly carvacrol methyl ether, and three main fractions with practically constant boiling points.

The first fraction was a mixture of sesquiterpene hydrocarbons, which according to gas chromatographic examination contained two main components in about equal amounts. Oxidation of the hydrocarbon mixture with selenium dioxide furnished an oil, from which widdrenal [3] was isolated in crystalline form. The non-crystalline material on further oxidation with silver oxide and chromatography on dimethyl sulphoxide-impregnated silica gel gave cedrene carboxylic acid and hinokiic acid. The oxidation product of widdrenal, "widdrenic acid" [3], has recently been shown [4] to be identical with hinokiic

* Part XXIII. *Acta Chem. Scand.* **13** (1959) 1395.

acid. The hydrocarbon fraction thus contains α-cedrene and thujopsene. The optical rotation and the infra-red absorption (1 647 and 885 cm^{-1}) of this fraction were, however, consistent with the presence of a minor constituent of more positive rotation containing a $RR'C=CH_2$-group, possibly the so-called β-cedrene [5].

Hirose and Nakatsuka [6] have shown that the "thujopsene" originally isolated by Kawamura [7] from *Thujopsis dolobrata* (Linneus, f) Sieb. et Zucc., on oxidation with selenium dioxide furnished a crystalline aldehyde which was identical with the widdrenal previously obtained by Erdtman and co-workers [3,8] from "widdrene", a hydrocarbon isolated from several *Widdringtonia* species and from *Biota orientalis*. Recently Erdtman and Norin [4] obtained pure "widdrene" from *Thujopsis dolobrata* and suggested that the name thujopsene should be retained for this hydrocarbon. Although it was clear that several of the oils containing thujopsene also contained a second component this had not been identified. It now seems probable that many of these oils are mixtures of thujopsene and α-cedrene and that similar mixtures are of frequent occurence.

Sesquichamene (b.p. 122—123°/12 mm, d_4^{28} 0.9277, n_D^{28} 1.5021, $[\alpha]_D^{28}$ —89.85°), isolated by Kafuku and Nozoe [9] from the leaves of *Chamaecyparis obtusa*, Sieb. et Zucc. and later by Katsura [10] from the leaves of *Chamaecyparis formosensis*, Mats. on oxidation with potassium permanganate, gave a glycol $C_{15}H_{26}O_2$, m.p. 89—91°, and a ketoaldehyde, $C_{14}H_{20}O_2$, disemicarbazone m.p. 233°. It has been suggested [11] that sesquichamene is identical with α-cedrene, but the physical constants of sesquichamene and the similarity of the melting points of the oxidation products to those of thujopsene glycol [12] (92—93°) and cedrene ketoaldehyde disemicarbazone (233°) makes it probable that it was in fact a mixture containing mainly thujopsene and α-cedrene.

The main component of the second fraction from *Chamaecyparis thyoides* was the aromatic sesquiterpene hydrocarbon cuparene. The isolation of this compound and the elucidation of its structure have been described in a previous paper [13].

The third fraction was a crystalline mixture of the sesquiterpene alcohols cedrol and widdrol [3], which were separated by chromatography on alumina. Widdrol is apparently frequently associated with cedrol [3,14]; its structure is at present being investigated.

On standing, the acidic fraction from *Chamaecyparis thyoides* deposited crystalline material, which after recrystallisation gave pure "Widdringtonia acid II" [3], m.p. 191—193°. The remainder of the material on distillation gave a small amount of low-boiling forerun and a higher-boiling, crystalline main fraction. According to paper chromatographic results, the low-boiling material contained at least five components, but no tropolones and no carvacrol were detected. The crystalline main fraction gave hinokiic acid on crystallisation and the remaining mixture was separated into hinokiic acid and cuparenic acid [13] by chromatography on dimethyl sulphoxide-impregnated paper.

The absence of tropolones from the sample of wood examined in this investigation is not in accordance with the results obtained by Zavarin and Anderson[2], but this divergence is probably due to the variations not infrequent in biological material.

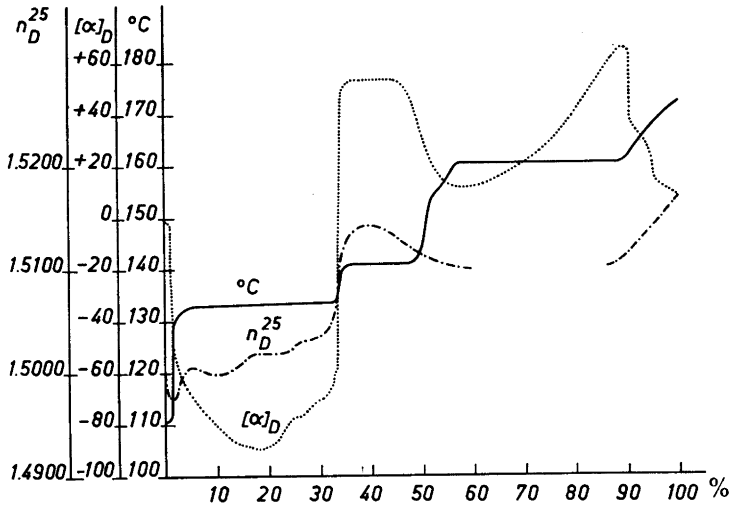

Fig. 1. Distillation of the main neutral fraction, ——— b. p. (°C/20 mm), ····· $[\alpha]_D$, —·—·—·— n_D^{25}.

The results of the present study show a pattern of heartwood constituents which is remarkably similar to that of the Southern hemisphere genus *Widdringtonia* [3]. Any detailed comparison with the patterns of heartwood constituents of other species of *Chamaecyparis* and with those of other genera of the Cupressaceae is however impeded by the lack of sufficient data [1].

EXPERIMENTAL

Melting points were taken on a Kofler micro hot stage (uncorr). Unless stated to the contrary, rotations were measured in chloroform. Infrared spectra were recorded on a Perkin-Elmer No 21 instrument (NaCl-prism; liquids, pure oils in an 0.025 mm NaCl-cell). Light petroleum refers to a fraction b.p. 35—60°, unless otherwise stated. Microanalyses by Dr. A. Benhardt, Mülheim.

Extraction. Finely milled air-dry heartwood of *Chamaecyparis thyoides* (9.9 kg) was extracted with acetone for 48 h. The extract was filtered, concentrated to small volume and poured with vigorous stirring into a tenfold volume of ether. The precipitate (25 g) was filtered off, washed with ether and set aside.

The combined ether solutions were concentrated and poured into light petroleum in the same way. This precipitate (50 g) after extraction with light petroleum was also set aside. The light petroleum solution was concentrated to one litre, extracted successively with aqueous potassium hydroxide (5 % and then 10 %) and washed with water. The alkaline solutions were combined, washed with light petroleum, acidified with dilute sulphuric acid (10 %) and extracted with light petroleum. The combined neutral solution and the acidic solution gave, after drying (Na_2SO_4) and evaporation of the solvent, a neutral fraction, a yellow oil (340 g, 3.5 % of the wood), and an acidic fraction, a redbrown oil (37 g, 0.4 % of the wood).

The neutral oil (340 g) was distilled to give a fraction, b.p. 120°/50 mm-180°/6 mm (260 g). The residue (80 g) gave two crystalline compounds in very small amounts, a "C_{15}-ketone", m. p. 108—109°, $[\alpha]_D$ +73°, 2,4-dinitrophenylhydrazone, m. p. 198—199° (Found: N 14.2. $C_{21}H_{22}N_4O_4$ requires N 14.5), and a substance, m. p. 140—141°, $[\alpha]_D$ +58° (Found: C 68.3; H 10.4. $C_{21}H_{38}O_5$ requires C 68.1; H 10.3), but it has not yet been further investigated.

The main part of the distillate was fractionally distilled through a vacuum-jacketed, packed column and where necessary refractionated through a spinning band column.

Curves for the distillation of the main neutral fraction showing boiling point (20 mm), refractive index and rotation plotted against percentage of material distilled are given in Fig. 1. There were three main fractions and a small forerun.

The forerun (0 → 1 %), according to its infrared absorption, contained mainly carvacrol methyl ether. Demethylation with hydrogen bromide (30 %, 1.5 h) followed by etherification with ethyl chloroacetate and saponification of the ester gave carvacroxyacetic acid (50 %), m. p. and mixed m. p. 152—153°.

The fraction b. p. 131—133° (2 → 32 %) was a mixture of sesquiterpene hydrocarbons. A gas chromatogram on a Perkin-Elmer vapour fractometer model 154 B (two metre column, 2,4-dinitrophenyl-2-naphthyl ether (20 %) on celite; column temp. 156°; flow rate 50 ml/min of helium; charge 5 μl) showed two peaks with elution times of 14 and 15 min and percentage of total area 48 and 52, respectively. This mixture (2.0 g) was oxidised with selenium dioxide (1.2 g) in ethanol (30 ml) for 3 h at reflux temperature. Evaporation of the solvent followed by repeated distillation of the product and recrystallisation from light petroleum gave widdrenal (0.2 g), m. p. and mixed m. p. 75—76°; infrared spectrum identical with that of authentic material. The non-crystalline part of the oxidation product (1.1 g) was added to a suspension of silver oxide (silver nitrate, 1.6 g, and sodium hydroxide 0.8 g) in water (15 ml) and the mixture was stirred vigorously for 2 h at 100°. The reaction mixture was separated into a neutral fraction (0.4 g) and an acid fraction (0.6 g). The chloroform-soluble part (0.2 g) of the acid fraction was chromatographed on dimethyl sulphoxide-impregnated silica gel.

This dimethyl sulphoxide-impregnated silica gel column was prepared by a method developed by Lindberg and Wickberg [15] for the separation of acetylated sugars. Dried, acid-washed silica gel (0.03—0.08 mm, 30 ml) was suspended in a solution of dimethyl sulphoxide in chloroform (5 %, 100 ml). The suspension was kept under reduced pressure in a vacuum desiccator for a short time and then transferred to a separatory funnel fitted on the top of a chromatogram tube that was completely filled with the same chloroform solution. Moderate pressure was applied to the top of the separatory funnel and the taps were opened to allow the suspension to replace the solution in the tube. The silica gel (1.5 × 24 cm) was saturated with dimethyl sulphoxide by passing a solution of dimethyl sulphoxide in ether (5 %, 150 ml). This was followed by a small volume of pure ether (5 ml), to prevent precipitation of dimethyl sulphoxide by the eluant to be used, and finally by the eluant (100 ml).

The acid mixture (0.2 g) was absorbed on the column and eluted with a mixture of light petroleum (b. p. 60—71°) and *iso*propyl ether (2:1, 6 ml fractions). The separation was most conveniently followed by the test chromatograms of the eluate on dimethyl sulphoxide-impregnated paper [18] with light petroleum and using a mixed indicator as spray reagent. The acids were found in fractions 15—18 and 20—26. The first acid (0.1 g) after sublimation had m. p. 122—124°, $[\alpha]_D$ −68° (*c* 2.2) (*cf.* authentic cedrenecarboxylic acid, m. p. 122°). Cedrol (8.4 g) was dehydrated with formic acid, refluxed with methanolic potassium hydroxide (10 %, 0.5 h) and filtered through alumina (200 g) in light petroleum to give α-cedrene [16] (7.0 g), $[\alpha]_D$ −91° (pure oil), d_{20}^{20} 0.9371, n_D^{25} 1.4968. It was gas chromatographically homogeneous (conditions as above, elution time 14 min) and the infrared spectrum indicated that there was no exocyclic methylene group present.

α-Cedrene (4 g) was oxidised with selenium dioxide in ethanol to give cedrenal [17] (3.8 g) and a part (0.6 g) of this aldehyde was treated with an aqueous silver oxide suspension at reflux temperature for 15 h giving cedrene carboxylic acid [17] (0.3 g). The infrared spectra of the two acids were superimposable and the mixed m. p. was undepressed, 122—124°. The second acid (0.1 g), m. p. 169—170°, was identified as hinokiic acid, mixed m. p. undepressed, infrared spectra identical.

The fraction b. p. approx. 141° (34 → 47 %) after purification as described in a previous paper [13] gave pure cuparene (b. p. 138°/19 mm, d_{21}^{21} 0.9374, $[\alpha]_D$ +65°, n_D^{25} 1.5202) in 45 % yield. It was further characterised by oxidation with chromic acid to cuparenic acid, m. p. 158—160°, $[\alpha]_D$ +63° (*c* 2.4).

The fraction b. p. approx. 161° (56 → 89 %) was a crystalline mixture of sesquiterpene alcohols. A sample of this mixture (3.0 g) was separated by chromatography on alumina (200 g); elution with benzene gave cedrol (1.8 g), m. p. and mixed m. p. 87—88°, $[\alpha]_D$ +10° (*c* 2.1); further elution with benzene-ether (9:1) gave widdrol (1.0 g), m. p. and mixed m. p. 97—98°, $[\alpha]_D$ +105° (*c* 2.9).

The acidic fraction (37 g) on standing deposited crystalline material (6 g) which was filtered off, washed with light petroleum and recrystallised from methanol giving pure "Widdringtonia acid II", m. p. and mixed m. p. 191—193°, $[\alpha]_D$ −96° (*c* 1.9), infrared spectrum identical with that of authentic material. A part (12 g) of the remaining oil on quick distillation gave a low-boiling forerun (1.9 g, 90—125°/4 mm), a higher-boiling main fraction (8.3 g, 145—170°/4 mm) and a residue (1.6 g, discarded). The forerun showed five distinct spots when chromatographed on dimethyl sulphoxide-impregnated paper[18], but none of these compounds were obtained in a crystalline state when eluted from a preparative (60 mg) chromatogram and this fraction was not further investigated. The higher-boiling, main fraction crystallised on standing. After repeated crystallisation from light petroleum it gave pure hinokiic acid (1.5 g), m. p. and mixed m. p. 169—171°, $[\alpha]_D$ −85° (*c* 2.1) infrared spectrum identical with that of authentic material. The remaining material, a constant melting mixture (135—138°) was conveniently separated by preparative paper chromatography. A sheet of paper (23 × 50 cm, Whatman 3MM) was impregnated with a mixture of dimethyl sulphoxide and benzene (3:2), dried in an oven (60°, 3 min) and then placed between glass plates to protect it from atmospheric moisture while the acid mixture was being applied. A chromatogram of the acid mixture (70 mg) was run on this paper in light petroleum (b. p. 60—71°) for 7 h. Two bands, at 12 and 20 cm from the starting line, were detected when the chromatogram was sprayed with water. These bands were cut out, extracted with ether and the ether solutions obtained were washed with water, dried (Na_2SO_4) and the ether was evaporated. The slow moving acid (20 mg) was identified as cuparenic acid, m. p. and mixed m. p. 158—160°, $[\alpha]_D$ +63° (*c* 2.1), infrared absorption identical with that of authentic material. The fast moving acid was hinokiic acid which was identified in the same way.

No tropolones could be detected in the total acidic fraction, in the distilled acidic fractions or in the ether or light petroleum-insoluble fractions of the acetone extract when these were chromatographed according to the method of Wachtmeister and Wickberg [19].

Acknowledgements. Thanks are due to Professor H. Erdtman for his interest and encouragement, to Miss Gurli Hammarberg for skilful assistance, to Dr. B. R. Thomas for valuable discussions, to Dr. J. Bain., Jacksonville, Fla, for supplying the wood used in this study and to the *Swedish Technical Research Council* for financial support.

REFERENCES

1. Erdtman, H. *Fourth International Congress of Biochemistry.* Vol. II — *Biochemistry of Wood* (1958).
2. Zavarin, E. and Anderson, A. B. *J. Org. Chem.* **21** (1956) 332.
3. Erdtman, H. and Thomas, B. R. *Acta Chem. Scand.* **12** (1958) 267.
4. Erdtman, H. and Norin, T. *Acta Chem. Scand.* **13** (1959) 1124.
5. Simonsen, J. and Barton, D. H. R. *The Terpenes* (2nd Ed.) Vol. III, Cambridge 1951, p. 75.
6. Hirose, Y. and Nakatsuka, T. *Gakkaishi Mokuzai* **4** (1958) 26.
7. Kawamura, J. *Bull. Imp. Forestry Expt. Sta, Japan* **30** (1930) 59, from Aikawa, T. and Tanaka, J. *Quart. J. Osaka Techn. Expt. Sta.* **8** (1958) 197.
8. Erdtman, H. and Pelchowicz, Z. *Ber.* **89** (1956) 341.
9. Nozoe, T. and Kafuku, K. *Bull. Chem. Soc. Japan* **6** (1931) 111.
10. Katsura *J. Chem. Soc. Japan* **63** (1942) 1483, from *Chem. Abstracts* **41** (1947) 3449.
11. Simonsen, J. and Barton, D. H. R. *The Terpenes* (2nd Ed.) Vol. III, Cambridge 1951, p. 113.
12. Kawamura, J. *Bull. Govt. Forestry Expt. Sta. Japan* **30** (1930) 59, from Akiyoshi, S. and Nagahama, S. *Bull. Chem. Soc. Japan* **30** (1957) 886.
13. Enzell, C. and Erdtman, H. *Tetrahedron* **4** (1958) 361.
14. Runeberg, J. *To be published shortly in Acta Chem. Scand.*
15. Lindberg, B. and Wickberg, B. *Arkiv Kemi* **13** (1959) 447.
16. Bluman, A. and Schulz, L. *Ber.* **64** (1931) 1540.
17. Treibs, W. *Ber.* **70** (1937) 2060.
18. Wickberg, B. *Acta Chem. Scand.* **14** (1960) *In the press.*
19. Wachtmeister, C.A. and Wickberg, B. *Acta Chem. Scand.* **12** (1958) 1335.

Received August 14, 1959.

ACTA CHEMICA SCANDINAVICA 14 (1960) 86—94

Studies on the Hydrolysis of Metal Ions

26. Application of a Liquid Distribution Method to the Study of the Hydrolysis of Ag^+

P. J. ANTIKAINEN* and D. DYRSSEN

Department of Inorganic Chemistry, Royal Institute of Technology, Stockholm 70, Sweden

The distribution of silver at 25°C between solutions of quinoline (Q) in benzene and 3 M $Na(ClO_4,OH)$ has been studied as a function of $[Q]_{org}$, $[OH^-]$ and the silver concentration. In these experiments the reaction

$$Ag^+ (aq) + 2\ Q\ (org) + ClO_4^- (aq) \rightleftharpoons AgQ_2ClO_4\ (org)$$

(eq. const. $\log K = 3.23 \pm 0.02$) was used for the study of the hydrolysis of Ag^+ in 3 M $NaClO_4$ at low concentrations of silver. The data provide no evidence for the presence of significant amounts of polynuclear complexes. Furthermore, the data indicate that AgOH is not formed to any large extent in 3 M $Na(ClO_4, OH)$. The value of $\log K_1K_2 = \log[Ag(OH)_2^-][Ag^+]^{-1}[OH^-]^{-2}$ was calculated to be 3.50 ± 0.10 in 3 M $Na(ClO_4, OH)$. No evidence was found for $Ag(OH)_3^{2-}$ in solutions less alkaline than 0.5 M.

These conclusions are supported by measurements of the solubility of Ag_2O in 3 M $Na(ClO_4,OH)$. The value of $\log K_{s2} = \log [Ag(OH)_2^-][OH^-]^{-1}$ was determined to be -3.82 ± 0.06. Together with the solubility product, $K_{s0} = 10^{-7.42 \pm 0.02}$, determined by Hietanen [7] we obtained $\log K_1K_2 = 3.60 \pm 0.08$. The pH of the solubility minimum of Ag_2O is determined by this constant.

In connection with the distribution experiments the distribution constant, K_d, of quinoline between various organic solvents and 3 M $NaClO_4$ has been determined (Table 1).

The hydrolysis of silver ions, Ag^+, has been studied by several people. The data hitherto obtained have been collected together with values of K_{s0}, the solubility product, in Part II of the compilation of stability constants by Bjerrum, Schwarzenbach, and Sillén [1]. Rather different values of the equilibrium constants for the formation of AgOH and $Ag(OH)_2^-$ have been given. Moreover some authors have in addition suggested the hydroxo complexes

* Present address: Institute of Chemistry, University of Helsinki, Helsinki, Finland.

Ag_2OH^+ and $Ag(OH)_3^{2-}$. There seems to be some uncertainty about the existence of AgOH in solution. In a recent paper by Pleskov and Kabanov [2] a trinuclear complex, $Ag_3O(OH)_2^-$, has been claimed from emf data in alkaline solutions of Ag_2O. A critical discussion of available data will be presented in a subsequent paper by Biedermann and Sillén [9].

The purpose of this work was to apply the liquid distribution method to the study of the hydrolysis of Ag^+ in 3 M $Na(ClO_4,OH)$. The method allows the use of very low concentrations of silver in the aqueous phase; this would favor the mononuclear reactions. Also one usually does not obtain slow equilibria as with systems where a solid phase is present. In addition, a few measurements have been made of the solubility of silver oxide in 3 M $Na(ClO_4,OH)$. These solubility data are compared with data obtained from the distribution measurements.

EXPERIMENTAL

Determination of $[Ag]_{tot}$ *and* $[OH^-]$. The experiments were carried out in a room thermostated at 25°C. The Na^+ concentration in the aqueous phase was kept constant at 3 M using $NaClO_4$ and NaOH. The distribution between the organic phase, quinoline in benzene, and the aqueous phase, was measured by liquid counting using ^{110m}Ag as a tracer. 20th Century Electronic M6 liquid counter tubes (volume 10 ml, wall thickness approx. 30 mg/cm^2) and Tracerlab Scalers were used for the radiometric determinations. In the solubility measurements the silver concentration of the aqueous phase was likewise determined radiometrically. Equilibration was attained by slow tilting (20—25 revolutions per min) of the solutions in glass-stoppered Pyrex centrifuge tubes; 1 h in the liquid distribution experiments, at least 2 days in the solubility measurements. The volume of the two phases in the liquid distribution measurements was 15 ml each. For the determination of the solubility of silver oxide, 15—40 ml 3 M $Na(ClO_4,OH)$ was used. After shaking, the phases were separated by centrifugation. Samples for liquid counting were withdrawn with 10 ml pipettes; in the solubility measurements the contamination by solid particles was avoided by sucking the solution through a capillary tube. The correction factor for the effect of the solvent composition on the counting rate was found to be 0.964 for the solvent pair quinoline-benzene/3 M $Na(ClO_4,OH)$; 2.96×10^{-4} M silver from sample 1 gave 19 604 cpm in the quinoline-benzene phase, but only 18 895 cpm in the aqueous phase. The determination of $-\log [OH^-]$ was carried out analytically in most cases; lower concentrations were measured potentiometrically with a Beckman glass electrode (Type 1190-72) using a solution of 0.01 M NaOH + 2.99 M $NaClO_4$ as reference ($-\log [OH^-] = 2.00$).

Choice of extracting system. It has been shown by Dyrssen, Krasovec, and Sillén [4] that Ag^+ can be extracted with chloroform from acid or neutral perchlorate solutions as $Ag(quinoline)_3ClO_4$. As quinoline does not react with alkali, it was thought that a two-phase system with quinoline and perchlorate would be very suitable for the determination of $[Ag^+]$ in an aqueous alkaline solution. However, chloroform is known to react with alkali forming, among other products, chloride ions. (It was found that a 0.1 M NaOH + 2.9 M $NaClO_4$ solution became 0.03 M in Cl^- after contact with chloroform for 24 h). A separate investigation by Mrs. Solweig Ekberg (*cf.* Table 1) showed that benzene could be a good choice as a diluent for quinoline and extracting solvent for $Ag(quinoline)_3ClO_4$. Benzene is a sufficiently stable organic solvent also. A few preliminary experiments with acridine showed that the solubility of its silver perchlorate complex was too low.

Reagents. Some insoluble matter was precipitated when the quinoline-benzene solutions, prepared from pure analytical grade products, were shaken with aqueous solutions containing silver. The quinoline solutions in benzene (0.5—0.8 M) had to be purified therefore by shaking them with a dilute solution of $AgClO_4$ (3×10^{-4} M) in distilled, chloride-free water. Traces of silver in the benzene phase were then removed by shaking with water repeatedly (at least six times). Still we obtained some losses of silver in the distribution experiments in the alkaline range, which were due probably to the collection

Table 1. Distribution constant, K_d, of quinoline between equal volumes of various organic solvents and 3 M $NaClO_4$ (0.001 M in NaOH). The concentration of quinoline in the aqueous phase after equilibration was determined spectrophotometrically at 273–283 mμ (except for hexone) and at the peak value around 312 mμ. 3 M $NaClO_4$ (with 0.001 M NaOH) saturated with the organic solvent were used as blanks. K_d was calculated as $[Q]'_{org}[Q]^{-1}_{aq} - 1$.

Solvent	Initial conc. of quinoline in the organic phase, $[Q]'_{org}$ M	log K_d
Chloroform	0.1	2.784 ± 0.020
Benzene	0.01	2.146 ± 0.002
Tri-n-butyl phosphate	0.02	2.123 ± 0.023
Methyl isobutyl carbinol	0.02	2.104 ± 0.023
Methyl isobutyl ketone	0.02	1.951 ± 0.001
Carbon tetrachloride	0.01	1.887 ± 0.056
*Iso*propylether	0.02	1.537 ± 0.018
n-Hexane	0.01–0.002	1.159 ± 0.018

of insoluble silver in the interphase. Although this seemed not to have any influence on the distribution ratio, it might have been worthwhile to have treated the organic phase with a solution of Ag_2O in, *e. g.*, 0.1 M NaOH in order to remove impurities that might react with silver in alkaline solutions only. The quinoline concentration in the benzene phase was determined spectrophotometrically at 312.5 mμ by Mrs. Ekberg.

The $NaClO_4$ was made from doubly recrystallized Na_2CO_3 p. a. and conc. $HClO_4$ p. a. The $NaClO_4$ was crystallized twice from distilled, chloride-free water according to a technique used by our colleagues at this laboratory [5]. The molarity of the $NaClO_4$ solution was determined from the specific gravity of the solution and the weight of $NaClO_4$ (dried at 110°C) per gram of the solution. The NaOH was of finest Merck quality and contained negligible amounts of chloride.

The radioactive isotope of silver was obtained by thermal neutron irradiation of a weighed piece of pure silver at A.E.R.E., Harwell, England. The silver was dissolved in nitric acid and the silver concentration was checked gravimetrically as AgCl. The initial specific activities of the two silver samples used were 1.2 and 12 mC per gram Ag, respectively. Stock solutions of the radioactive silver were prepared in 3 M $NaClO_4$.

APPLICATION OF THE LAW OF MASS ACTION TO THE DATA

Symbols. The following symbols and definitions are used:

$[\ ]$ concentrations in the aqueous phase
$[\ ]_{org}$ concentrations in the benzene phase
Q quinoline
$K_1 = [AgOH][Ag^+]^{-1}[OH^-]^{-1}$
$K_2 = [Ag(OH)_2^-][AgOH]^{-1}[OH^-]^{-1}$

With two liquid phases:

$K = [AgQ_2ClO_4]_{org}[Ag^+]^{-1}[Q]^{-2}_{org}[ClO_4^-]^{-1}$ (equil. constant)
$q = [Ag]_{total,\ org}[Ag]^{-1}_{total,\ aq}$ (net distribution ratio)
$\varphi = q[Q]^{-2}_{org}[ClO_4^-]^{-1}$ and $y = -\log \varphi\ [OH^-]$ (auxiliary functions)

In equilibrium with Ag_2O:

$K_{s0} = [Ag^+][OH^-]$
$K_{s1} = [AgOH] = K_{s0}K_1$
$K_{s2} = [Ag(OH)_2^-][OH^-]^{-1} = K_{s0}K_1K_2 = K_{s1}K_2$

Distribution measurements. The quantity measured in the distribution experiments is the net distribution ratio

$$q = [Ag]_{total,org}[Ag]^{-1}_{total,\ aq}$$

It may be seen from Table 2 ($[OH^-] \approx 10^{-7}$ M, $[ClO_4^-] = 3$ M) that $q[Q]^{-2}_{org}$ is constant for a range of values of $[Q]_{org}$ and silver concentration in both phases. This is a strong indication that silver is extracted as monomeric AgQ_2ClO_4. As the concentration of quinoline in the aqueous phase was low due to a high value of the distribution constant (*cf.* Table 1), silver complexes with quinoline were not likely to be formed in the aqueous phase in any appreciable amount. Furthermore, it was shown by Dyrssen, Krašovec, and Sillén [4] that the distribution of silver between quinoline in chloroform and perchlorate solutions in the range pH 3—10 was function of $[Q]^2_{org}[ClO_4^-]$ only. Thus we may assume that the extraction of silver takes place by the following reaction (eq. const. K):

$$Ag^+ \text{ (aq)} + 2\ Q \text{ (org)} + ClO_4^- \text{ (aq)} \rightleftharpoons AgQ_2ClO_4 \text{ (org)}$$

In the presence of a complexing ion like OH^- the expression for q will be

$$q = \frac{[AgQ_2ClO_4]_{org}}{[Ag^+] + [AgOH] + [Ag(OH)_2^-] + [\text{other hydroxo complexes}]} \quad (1a)$$

or

$$\log q = \log K\,[Q]^2_{org}\,[ClO_4^-] - \log\,(1 + K_1[OH^-] + K_1K_2[OH^-]^2 + \ldots.) \quad (1b)$$

Other hydroxo complexes would appear in eqn. (1b) as terms with higher powers of $[OH^-]$ (*e.g.* $Ag(OH)_3^{2-}$) or of $[Ag^+]$ (*e.g.* $Ag_2(OH)_2$). Further the equation presupposes that silver is not extracted as AgQ_2OH. In fact, at the silver concentrations used practically no silver was found to be extracted by a solution of quinoline in benzene from a solution of Ag(I) in 0.5 M NaOH as long as no ClO_4^- was present.

Eqn. (1b) may be written as

$$y = \log\,(q^{-1}[Q]^2_{org}[ClO_4^-]\,[OH^-]^{-1}) = -\log\,\varphi\,[OH^-] = \log\,K^{-1}K_1 + \\ + \log\,(K_1^{-1}[OH^-]^{-1} + 1 + K_2[OH^-]) \quad (1c)$$

The curve $y = -\log\,\varphi\,[OH^-]$ against $\log\,[OH^-]$ will have two asymptotes, namely

$$[OH^-] \to 0;\ y = -\log\,[OH^-] - \log\,K;\ \textit{i.e.}\ \varphi = K \quad (2a)$$

$$[OH^-] \to \infty;\ y = \log\,[OH^-] + \log\,K_1K_2 - \log\,K \quad (2b)$$

The intersection of the asymptotes at

$$[OH^-] = [OH^-]_0 \text{ and } y = y_0$$

gives

$$-\,2\,\log\,[OH^-]_0 = \log\,K_1K_2 \quad (3a)$$

and

$$y_0 = \log\,(K^{-1}K_1{}^{1/2}K_2{}^{1/2}) \quad (3b)$$

The point at $[OH^-] = [OH^-]_0$ on the distribution curve is

$$y'_0 = \log K^{-1}K_1(K_1^{-\frac{1}{2}}K_2^{\frac{1}{2}} + 1 + K_1^{-\frac{1}{2}}K_2^{\frac{1}{2}}) \quad (4)$$

The difference between this point and the point of intersection of the asymptotes is

$$y'_0 - y_0 = \log (1 + \log K_1^{\frac{1}{2}}K_2^{-\frac{1}{2}} + 1) \quad (5)$$

i.e., this quantity is determined by $K_1K_2^{-1}$, the ratio between the two consecutive constants. The smallest value of $y'_0 - y_0$ is log 2, which corresponds to the case when AgOH may be neglected ($K_1 = 0$, see Fig. 1).

Solubility measurements. It is not possible to determine from solubility measurements whether silver oxide dissolves in water as polynuclear fractions of the solid phase, *e.g.* $Ag_2(OH)_2$, as the concentrations of such species will not vary with the composition of the solvent. Assuming the same species to exist in the aqueous phase as previously in the distribution experiments, we obtain

$$[Ag]_{total} = [Ag^+] + [AgOH] + [Ag(OH)_2^-] \quad (6a)$$

or

$$[Ag]_{total} = [AgOH](K_1^{-1}[OH^-]^{-1} + 1 + K_2[OH^-]) \quad (6b)$$

[AgOH] is constant ($= K_{s1}$) in the presence of solid Ag_2O.
The curve log $[Ag]_{total}$ against log $[OH^-]$ will have the same form as the curve $y = -\log \varphi$ $[OH^-]$ against log $[OH^-]$ for the distribution data (eqn. 1c). Eqns. 2—5 will be the same except that K_{s1} must be substituted for $K^{-1}K_1$, and

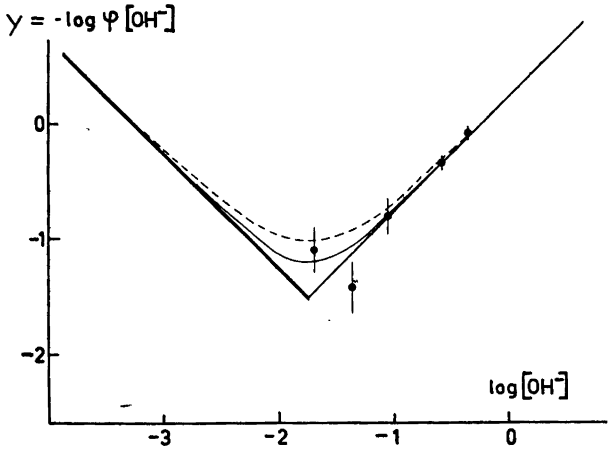

Fig. 1. The distribution of Ag — ^{110m}Ag between solutions of quinoline in benzene and 3 M $Na(ClO_4,OH)$ plotted as $y = -\log \varphi$ $[OH^-]$ against log $[OH^-]$. The data are taken from Table 2. The equations for the curves with their two asymptotes are given in the text. The full-drawn curve has been calculated for $K_1 = 0$ and the dashed curve for $K_1 = K_2$. The position of the asymptote will slope −1 is calculated from values of φ in Table 2, where the hydrolysis of Ag^+ has no influence on the distribution ($[OH^-] \approx 10^{-7}$ M).
The point of intersection of the two asymptotes gives log $K_1K_2 = 3.50 \pm 0.10$.

Table 2. Distribution of Ag-^{110m}Ag between quinoline in benzene and 3 M Na(ClO_4,OH) solutions as a function of the concentrations of quinoline, silver, NaOH, and $NaClO_4$.

$-\log [Q]_{org}$	$-\log [Ag]_{tot, org}$	$-\log [Ag]_{tot, aq}$	$\log q$	$\log \varphi$
$[OH^-] \approx 10^{-7}$ M, $[ClO_4^-] = 3$ M				
1.227	5.000	6.235	1.235	3.212
1.403	5.022	5.939	0.917	3.246
1.558	5.094	5.702	0.608	3.247
1.704	5.184	5.473	0.289	3.220
2.102	5.620	5.151	−0.489	3.238
		mean value:	$\log \varphi = 3.23 \pm 0.02$ (= $\log K$)	
$[OH^-] = 10^{-1.70}$ M, $[ClO_4^-] = 10^{0.474}$ M				
0.584	5.079	7.078	1.999	2.693
0.584	4.650	6.978	2.328	3.022
0.806	5.198	6.681	1.483	2.621
0.806	4.767	6.480	1.713	2.851
		mean value:	$\log \varphi = 2.80 \pm 0.20$	
$[OH^-] = 10^{-1.37}$ M, $[ClO_4^-] = 10^{0.472}$ M				
0.584	5.349	7.280	1.931	2.627
0.584	5.057	7.133	2.076	2.772
0.584	4.765	6.960	2.195	2.891
0.584	3.967	6.277	2.310	3.006
0.584	3.599	5.346	1.747	2.443
0.584	3.338	5.663	2.325	3.021
		mean value:	$\log \varphi = 2.79 \pm 0.23$	
$[OH^-] = 10^{-1.06}$ M, $[ClO_4^-] = 10^{0.464}$ M				
0.584	4.813	5.947	1.134	1.838
0.584	3.956	5.113	1.157	1.861
0.584	3.731	4.856	1.125	1.829
0.584	3.610	4.851	1.241	1.945
0.637	6.052	6.835	0.783	1.593
0.637	5.777	6.798	1.021	1.831
0.637	5.368	6.427	1.059	1.869
0.637	4.974	6.242	1.268	2.078
0.637	4.692	5.730	1.038	1.848
0.637	4.530	5.760	1.230	2.040
		mean value:	$\log \varphi = 1.87 \pm 0.16$	
$[OH^-] = 10^{-0.594}$ M, $[ClO_4^-] = 10^{0.438}$ M				
0.584	5.861	6.012	0.151	0.881
0.584	5.643	5.861	0.218	0.948
0.584	4.281	4.543	0.262	0.992
		mean value:	$\log \varphi = 0.94 \pm 0.07$	
$[OH^-] = 10^{-0.363}$ M, $[ClO_4^-] = 10^{0.409}$ M				
0.584	6.570	6.408	0.162	0.597
0.584	6.348	6.087	0.261	0.498
0.584	6.114	5.771	0.343	0.416
0.584	5.553	5.256	0.297	0.462
0.584	4.401	4.239	0.162	0.597
0.584	4.376	4.169	0.207	0.552
0.584	4.358	4.109	0.249	0.510
		mean value:	$\log \varphi = 0.45 \pm 0.06$	

Table 3. The solubility of Ag_2O in 3 M $Na(ClO_4,OH)$ measured radiometrically at 25°C with ^{110m}Ag. Determination of log K_{s2} = log $[Ag(OH)_2^-][OH^-]^{-1}$ for $[OH^-] > 0.1$ M.

log $[OH^-]$	log $[Ag]_{total}$	log $[Ag]_{total}[OH^-]^{-1}$
−1.42	−5.08	(−3.66)
−1.04	−4.76	(−3.72)
−0.883	−4.65	−3.77
−0.827	−4.60	−3.77
−0.578	−4.50	−3.92
−0.461	−4.30	−3.84
−0.248	−4.06	−3.81
	mean value:	−3.82 ± 0.06

log $[Ag]_{total}$ for −log φ $[OH^-]$. The value of $[OH^-]$ of the solubility minimum of Ag_2O is thus given by

$$-2 \log [OH^-]_0 = \log K_1K_2 \qquad (3'a)$$

The constants in these equations may found by fitting normalized curves to the data [3].

RESULTS

Distribution data. The data on the distribution of silver between solutions of quinoline in benzene and 3 M $NaClO_4$-NaOH solutions, with varying amounts of NaOH are given in Table 2 and plotted in Fig. 1. The two curves in Fig. 1

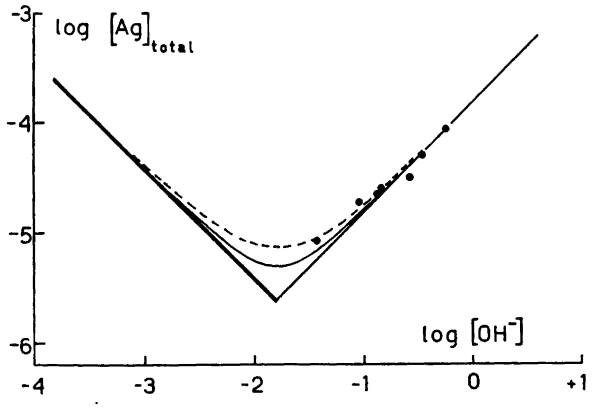

Fig. 2. The solubility of Ag_2O in 3 M $Na(ClO_4, OH)$ as a function of $[OH^-]$. The data are given in Table 3. The equations for the curves are given in the text and are the same as for the curves in Fig. 1. The full-drawn curve has been calculated for $K_1 = 0$ and the dashed curve for $K_1 = K_2$. The position of the left-hand asymptote with slope −1 is given by the solubility product, K_{s0}. The point of intersection of the two asymptotes gives log $K_1K_2 = 2$ (1.80 ± 0.04) = 3.60 ± 0.08.

correspond to the assumptions $K_1 = 0$ (full-drawn curve) and $K_1 = K_2$ (dashed curve). In spite of the rather large limits of error it can be said that $K_1 < K_2$. The point of intersection of the two asymptotes at log $[OH^-] = -1.75 \pm 0.05$ gives

$$\log K_1K_2 = 3.50 \pm 0.10$$

There is no evidence of a third complex below 0.5 M NaOH. The equilibrium constant K for the reaction

$$Ag^+ \text{ (aq)} + 2 \text{ Q (org)} + ClO_4^- \text{ (aq)} \rightleftharpoons AgQ_2ClO_4 \text{ (aq)}$$

can be calculated from Table 1 ($[ClO_4^-] = 3$ M, $[OH^-] \approx 10^{-7}$ M) to be log $K = 3.23 \pm 0.02$. This constant determines the left-hand asymptote in Fig. 1 rather accurately.

It can also be seen from Table 2 that the value of q (or φ) is independent of the silver concentration at the low amounts of silver used in these experiments. As silver certainly is monomeric in the organic phase (*cf.* φ at $[OH^-] \approx 10^{-7}$ M) this proves that no appreciable amounts of polynuclear complexes are present in the aqueous phase.

It was mentioned under "Experimental" that losses of silver occured in the distribution experiments in spite of the purification of the reagents. However, the loss of silver did not seem to correlate with any change in q (or φ). It was also found that the losses could be kept at a minimum using a rather large concentration of quinoline in benzene.

Solubility data. The data in Table 3 are plotted in Fig. 2 as log $[Ag]_{total}$ against log $[OH^-]$. It was shown above that the same curves as in Fig. 1 then apply to the solubility data too. The position of the left-hand asymptote with slope -1 is given by the solubility product, K_{s0}; log $[Ag]_{total} = \log K_{s0} - \log [OH^-]$. A value of this constant, log $K_{s0} = 7.42 \pm 0.02$, was determined from potentiometric determinations of $[Ag^+]$ and $[H^+]$ by Hietanen [7]. The right-hand asymptote is determined by log K_{s2}, which was calculated to be -3.82 ± 0.06 in Table 3. The point of intersection of the asymptotes gives

$$\log K_1K_2 = 3.60 \pm 0.08$$

This value is not very different from the value determined from the distribution data. Nor do the solubility data provide any evidence of appreciable amounts of AgOH or $Ag(OH)_3^{2-}$; we conclude $K_1 < K_2$ and $K_3 \ll K_2$ in 3 M $NaClO_4$ from these experiments too. It might be pointed out that a study of the solubility of Ag_2O in solutions less alkaline than 0.01 M gives rather uncertain values due to the fact that the buffer capacity of such solutions is low.

CONCLUSIONS

The hydrolysis of silver in water, examined at low concentrations of silver in 3 M $NaClO_4$ at 25°C by the distribution and solubility methods described above, can be explained by the following two reactions:

$$Ag^+ + OH^- \rightleftharpoons AgOH \qquad K_1$$

$$AgOH + OH^- \rightleftharpoons Ag(OH)_2^- \qquad K_2$$

The data indicate that $K_1 < K_2$, *i.e.* that in 3 M $Na(ClO_4,OH)$ [AgOH] is never as much as 1/3 of the total silver. The value of $\log K_1K_2$ was determined as 3.6 ± 0.1. The hydrolysis of Ag^+ thus seems to resemble that of Hg^{2+} as determined by Hietanen and Sillén [6]. No evidence is found for the existence of $Ag(OH)_3^{2-}$ below $[OH^-] = 0.5$ M.

The distribution method allows a full variation of the concentration of all silver species. However, no influence of the silver concentration on the distribution ratio could be detected at $[Ag^+][OH^-] < K_{s0}$. This does not preclude the possibility that polynuclear hydroxo complexes can be proved to exist in solutions with higher silver concentrations, *e.g.* 1 M $AgNO_3$ or 5 M KOH saturated with Ag_2O. In the former case titration with HNO_3 in 1 M $AgNO_3$ would reveal any $Ag_m(OH)_n$ and in the second case a potentiometric determination of $[Ag^+]$ (*cf.* Ref.[2]) on dilution with 5 M KOH should reveal any polynuclear species. Results on such solutions will be reported in following papers [7,8].

Acknowledgements. The present investigation has been supported by *the Swedish Council for Atomic Research*, the *Air Force Office of Scientific Research of the ARDC, USAF* through its European Office on contract no AF 61 (052)-162 and by a grant from the University of Helsinki. The work has been carried out in cooperation with Professor Lars Gunnar Sillén, Dr. George Biedermann, and Dr. Sirkka Hietanen. The English has been revised by Mr. David Martin.

REFERENCES

1. Bjerrum, J., Schwarzenbach, G. and Sillén, L. G. *Stability Constants*, part II, The Chemical Society, London, 1958, Spec. Publication No 7.
2. Pleskov, Yu. V. and Kabanov, B. N. *Zhur. Neorg. Khim.* **2** (1957) 1807.
3. Sillén, L. G. *Acta Chem. Scand.* **10** (1956) 186.
4. Dyrssen, D., Krašovec, F. and Sillén, L. G. *Int. Conf. on Coordination Chemistry*, London 1959.
5. "*Some laboratory methods* . . ., Department of Inorganic Chemistry, Royal Institute of Technology, Stockholm", manuscript, 1959.
6. Hietanen, S. and Sillén, L. G. *Acta Chem. Scand.* **6** (1952) 747.
7. Antikainen, P. J., Hietanen, S. and Sillén; L. G. *Acta Chem. Scand.* **14** (1960) 95.
8. Biedermann, G. and Hietanen, S. *Acta Chem. Scand.* **14** (1960) *In press.*
9. Biedermann, G. and Sillén, L. G. *Acta Chem. Scand.* **14** (1960) *In press.*

Received August 27, 1959.

ACTA CHEMICA SCANDINAVICA 14 (1960) 95—101

Studies on the Hydrolysis of Metal Ions

27. Potentiometric Study of the Argentate(I) Complex in Alkaline Solution

P. J. ANTIKAINEN*, SIRKKA HIETANEN and LARS GUNNAR SILLÉN

Department of Inorganic Chemistry, Royal Institute of Technology, Stockholm 70, Sweden

The composition of the argentate(I) complex formed in alkaline solutions of silver oxide has been studied by emf titrations with constant ionic medium (0.95 and 12.6 M NaOH, 1.15 and 11.5 M KOH) using Ag-AgI electrodes. The data indicate that only mononuclear complexes are formed; from this result, together with the solubility data of other workers, it is concluded that the formula of the complex is $Ag(OH)_2^-$. No evidence has been found for the presence of the polynuclear argentate complexes proposed by some previous workers [5].

The solubility product of $Ag_2O(s)$ in 3 M $Na(ClO_4)$ at 25°C was determined as $\log K_{s0} = \log [Ag^+][OH^-] = -7.42 \pm 0.02$.

Silver oxide is appreciably more soluble in strongly alkaline solutions than in water, which proves that one or more argentate species are formed. The formula of the argentate species is the problem of the present work.

The solubility of Ag_2O in NaOH (0.1 to 5.3 M) was studied by Laue [1] in 1927. The solubility, which we may express as a total concentration of B_s moles Ag/l in a saturated solution, was approximately proportional to $[OH^-]$, more nearly so after an activity correction. Laue concluded that the formula of the complex formed is AgO^-. We shall use instead the equivalent formula $Ag(OH)_2^-$; from equilibrium studies in aqueous solutions it is hard to distinguish between formulas that differ only by the content of H_2O and we shall keep to the convention of writing OH complexes if there is no definite evidence for other formulas.

In 1933, Johnston, Čůta and Garrett [2] published their data on the solubility of Ag_2O in NaOH (0.001 to 6.6 M) and KOH (0.0005 to 5.2 M). Like Laue, whose work they do not seem to have seen, they found a solubility minimum at 0.015 M OH^-, and a linear course of B_s with higher $[OH^-]$. They explained their data assuming the species AgOH and AgO^-; in addition, they found evidence for an unknown species, perhaps Ag_2OH^+, besides Ag^+, in solutions on the acid side of the solubility minimum.

* Present address: Institute of Chemistry, University of Helsinki, Helsinki, Finland.

Their data [2] have later been discussed by Reynolds and Argersinger [3] and by Beck [4], who used the position of the solubility minimum to calculate the equilibrium constants. Neither quotes the work of Laue [1], in spite of its high quality.

The fact that the solubility, B_s, is proportional to $[OH^-]$ may be explained by assuming the predominant complex to be $Ag(OH)_2^-$ (or AgO^-), as was done by the authors quoted [1-4]. However, the same result would be obtained with any argentate complex of the charge -1. For instance, we have, with the general formula:

$$\frac{n}{2}\,Ag_2O(s) + \frac{m}{2}\,H_2O + OH^- \rightleftharpoons Ag_nO_{\frac{1}{2}(n-m)}(OH)^-_{m+1}$$

$$B_s = n[Ag_nO_{\frac{1}{2}(n-m)}(OH)^-_{m+1}] = nKf^{-1}_{cpx}f_{OH}\{H_2O\}^{m/2}[OH^-] \approx \text{const}\ [OH^-] \quad (1)$$

Here K is the equilibrium constant for (1), f_{cpx} is the activity factor of the argentate complex and f_{OH} that of the OH^- ion. The two activity factors may approximately cancel each other out. The "conventional" formula for the complex, $Ag_n(OH)^-_{n+1}$, is obtained by setting $m = n$.

The fact that $B_s/[OH^-]$ must be constant for any value of n in (1) was realized by Pleskov and Kabanov [5], who measured the solubility of Ag_2O in KOH (3 to 15 M). For the logarithm of the ratio, $\log (B_s[OH^-]^{-1}) = \log nK$, at 25°C, Laue gave -3.76, Johnston *et al.* -3.71, and Pleskov and Kabanov ≈ -3.8. From the variation of the solubility with water activity, Pleskov and Kabanov moreover concluded $m = 1$ in eqn. (1)

Pleskov and Kabanov tried to determine the number of Ag atoms, n, in the argentate ion by studying the emf:s of silver concentration cells with various total concentrations, B, of Ag. Applying the Nernst equation (eqn. 3 or 6a below), they concluded that $n = 3$. The complex would then be trinuclear, $Ag_3(OH)^-_4$ or rather $Ag_3O(OH)^-_2$.

Recently, Antikainen and Dyrssen [6] studied the distribution equilibria of silver(I) between 3 M $Na(ClO_4,OH)$, and benzene solutions of quinoline. Their data, however, indicate that the predominant complex is the mononuclear $Ag(OH)^-_2$. Because of this apparent contradiction between the distribution [6] and emf [5] data, it was thought necessary to make a new emf investigation as a check of the Russian work.

The cell used in the present investigation had the following composition:

$$-Ag/I\ M\ M^+OH^-, B_+M\ Ag/I\ M\ M^+OH^-\ \text{with}\ B_0\ M\ Ag/Ag+ \quad (2)$$

In our experiments, M^+ was Na^+ or K^+, and the concentration, I, was about 1 or 12 M. Pleskov and Kabanov used 6 and 16 M KOH.

According to the Nernst equation, the emf of this cell (2) is given by the ratio between the concentrations of free Ag^+ in the two half-cells. Now, B is always very small as compared with I, and so the liquid junction potential in (2) is certainly negligible, and the activity factors may be assumed to be the same on both sides. Thus we have

$$E = 59.15\ \log\ ([Ag^+]_+[Ag^+]_-^{-1}) \quad (3)$$

For any dissolved species, $Ag_n(OH)_{n+r}^{r-}$, the law of mass action gives (β = equilibrium constant):

$$[Ag_n(OH)_{n+r}^{r-}] = \beta[Ag^+]^n[OH^-]^{n+r} \quad (4)$$

Now let us assume that, in the solutions with I M OH^-, one single complex of this type predominates and that the concentrations of all other species, including Ag^+, are much smaller. The concentration of the predominating species, $[Ag_n(OH)_{n+r}^{r-}]$, is then equal to B/n, and so eqn. (4) becomes

$$B/n = \beta[Ag^+]^n I^{n+r} \quad (5)$$

The activity factors are included in the equilibrium constant, β ,in eqns. (4) and (5); this can be done, provided that only experiments at the same I are compared.

In our cell (2) we have on both sides the same values for β and I and so it follows from eqns. (3) and (5)

$$E = \frac{59.15}{n} \log B_+/B_- \quad (6)$$

Here, B_+ and B_- are the total concentrations of silver at the two electrodes.

In the present work, B_+ was kept constant at the value B_0, whereas B_- was varied; it is denoted by B. In practice the two solutions were prepared by mixing the same stock solution — an almost saturated solution of Ag_2O in I M MOH — with various amounts of pure I M MOH; thus the ratio B_0/B is known with better accuracy than the separate values of B_0 and B.

We then have

$$E = \frac{59.15}{n} \log (B_0/B) \quad (6a)$$

EXPERIMENTAL

Sodium hydroxide solutions were prepared as usual here (see, *e.g.*, Ref. [7]), starting from a 50 % solution of the commercial *p.a.* reagent, which was kept in a polythene bottle. To prepare the 12.6 M solution, the 50 % solution (which is 18 M) was filtered through a G4 Jena glass filter funnel into a Büchner flask of Jena glass and diluted. In the making of the 0.957 M NaOH solution, recrystallized $Ba(OH)_2$ was added to the 50 % NaOH to remove the last trace of carbonate before the solution was filtered and diluted as before.

Potassium hydroxide, 11.5 M, was prepared from commercial *p.a.* reagent, which was dissolved in distilled water, after which $Ba(OH)_2$ was added. The 1.15 M KOH solution was prepared by simple dilution.

Silver oxide was prepared from recrystallized $Ba(OH)_2$ and $AgNO_3$. It was first washed carefully with de-aerated water until Ba could not be detected with sulfuric acid. The silver oxide was then washed three times with I M MOH and finally suspended in I M MOH and transferred to a polythene flask. The flask was shaken for 19 — 48 h and the solution so obtained, which may not have been quite saturated ($B_0 \leqq B_S$) was the starting solution of concentration B_0.

Some polythene flasks were found to reduce alkaline argentate(I) solutions, forming metallic silver; usually Polva polythene flasks, which do not seem to reduce silver, were used.

The *total silver concentration*, B_0, in the argentate solutions was determined as follows: the 12.6 M NaOH was diluted, hydrazinium sulfate was added, the metallic Ag was filtered off, washed, dissolved in HNO_3 and titrated with KCNS in the usual way. $B_0 = 0.7 \pm 0.2$

mM was found. To 11.5 M KOH, $HClO_4$ was added, $KClO_4$ was filtered off, and Ag^+ in the filtrate was titrated with KCNS. Result: $B_0 = 0.6 \pm 0.1$ mM. From the diagram of Pleskov and Kabanov we may read the solubility B_s between 0.60 and 0.65 mM Ag in 11.5 M KOH, which indicates that our solutions were close to saturation.

With 1 M NaOH, $B_0 = 0.12 \pm 0.01$ mM was found, which is somewhat less than the solubility ≈ 0.18 mM found from Johnston's, Čůta's and Garrett's data.

For our equation (6a) we do not need an accurate value for B_0 but only for B_0/B which is obtained, with all the accuracy necessary, from the volume ratio of dilution. Even the approximate values for B_0 show that in our experiments we have used the same range of B_0 and B as have Pleskov and Kabanov.

Nitrogen gas was bubbled through 10 % H_2SO_4, 10 % NaOH, and finally through the ionic medium, I M MOH.

Electrodes. Some preliminary experiments were made with Ag, AgCl-electrodes; however, the emf was found to drift as much as 4 mV in 1.5 h, probably because of the dissolution of AgCl. If the AgCl was first washed away with conc NH_3, and then with water, E showed no continous drift but rather small jumps so that the accuracy was not more than $\pm$ 1 mV.

For all the following experiments, Ag, AgI-electrodes were used. Pt coils were covered with Ag and then electrolyzed as anodes in 0.1 M NaI (30 min, 0.3 mA). Even with them a drift around 1 mV/h was noticed, in 1 M NaOH (KOH) solution.

In 12.6 M NaOH, E was more constant and the difference between two Ag, AgI-electrodes in the same solution was at most 0.3 mV in one experiment; between different solutions the deviations were sometimes as high as 1 mV. One had to wait 15—60 min for a stable potential.

In 11.5 M KOH, the emf was somewhat less stable than in 12.6 M NaOH.

The cell (2) consisted of a reference half-cell with $B = B_0$ and the "titration" half-cell with B variable. The reference half-cell, in the final experiments, was always a "Wilhelm" apparatus [9]; for the 1 M MOH experiments it was shortened by leaving out the middle part of the salt bridge. Some attempts were made to use polythene bridges of different constructions, but so great were the difficulties met with — solution was pumped out or in through the flexibility of polythene, silver was reduced — that a glass "Wilhelm" was finally used. Changes within the reference electrode may account for the fact that the line constructed on eqn. (6a) does not always pass through the origin. See especially 0.957 M NaOH, where the reference electrode was Ag, AgCl which had been kept for a day in the "Wilhelm"; in all other experiments the reference electrode was Ag, AgI.

For the titration half cell, a vessel of Jena glass was used with 1 M MOH, and one of polythene with 12 M MOH. To check whether the reduction of Ag made any perceptible difference, a glass vessel was also used in some of the experiments with 12 M MOH. No difference was found.

Table 1 shows, for each titration, the order in which the additions were made. A known amount of I M MOH with B_0 M Ag was added through a pipet and the emf measured. The solution was then diluted by addition of several portions of I M MOH without Ag (denoted as "0") and E was measured after each portion. All additions were made by means of pipets, which were filled with nitrogen before the solution was sucked up into them. In the course of the titration, a certain amount of solution was withdrawn with a pipet (denoted by "—" in the table) to keep the total volume within reasonable limits. At the end, a "back-titration" was made by adding again one or several portions of the B_0 solution.

Two electrodes were used in the titration cell in all experiments with 12 M MOH. The difference between them was in general less than 0.2—0.3 mV (see table and figs.).

The whole cell was kept in a thermostat room at 25 $\pm$ 0.2°C, and the emf was measured with a Cambridge type K potentiometer.

RESULTS

Table 1 gives our data in a short-hand form which we hope will be easily understood. The corresponding graphs, E *versus* log (B_0/B), are given in the four fields of Fig. 1. In each field are also given lines with slopes corresponding to

Table 1. Results of emf measurements. For each experiment ("titration"), first the various additions in ml are given; "0" stands for I M MOH without Ag, "B_0" for the stock solution, I M MOH with B_0 M Ag. The figures given are then $\log(B_0/B)$ and E in mV (sometimes for two different electrodes).

a) 0.957 M NaOH

I. 49.89 ml B_0 + 3 · 9.95 ml 0—49.89 ml + 4 · 9.95 ml 0 + 9.95 ml B_0.

$\log(B_0/B)$, E : 0.000 −18.7; 0.079 −14.3; 0.146 −10.3; 0.203 −6.4; 0.328 0.3; 0.426 4.8; 0.505 8.9; 0.572 13.4; 0.444 6.8 (9.6 after 5 h).

II. 29.63 ml B_0 + 2 · 5.00 ml 0 + 10 ml 0 + 2 · 5.00 ml 0 — 29.63 ml + 3 · 10.00 ml 0 + 20.00 ml B.

$\log(B_0/B)$, E : 0.000 −17.1; 0.068 −13.1; 0.126 −9.6: 0.224 −3.2; 0.266 −0.5; 0.304 2.2; 0.429 10.1; 0.526 16.1; 0.605 22.3; 0.360 6.0;

b) 12.6 M NaOH

I. 29.25 ml B_0 + 2 · 4.91 ml 0 + 2 · 9.75 ml 0—29.63 ml + 4.91 ml 0 + 9.75 ml 0 + 4.91 ml B_0 + 19.85 ml B_0.

$\log(B_0/B)$, E(two electrodes): 0.000 −0.3 0.3; 0.068 3.2 3.5; 0.126 6.2 6.6; 0.223 12.0 12.4; 0.301 16.8 17.0; 0.370 21.1 21.2; 0.479 27.4 27.1; 0.399 23.3 23.3; 0.241 14.2 14.5;

II. 29.25 ml B_0 + 2 · 4.91 ml 0 + 2 · 9.75 ml 0—29.63 ml + 2 · 9.75 ml 0 + 3 · 9.75 ml B_0.

$\log(B_0/B)$,E(two electrodes): 0.000 0.8 1.1; 0.068 4.5 4.7; 0.126 7.8 8.1; 0.223 13.5 13.2; 0.301 18.6 17.7; 0.427 27.1 25.7; 0.524 34.2 32.7; 0.381 24.7 24.3; 0.301 18.9 17.7; 0.250 15.7 14.6;

c) 1.15 M KOH

I. 29.63 ml B_0 + 2 · 5.00 ml 0 + 2 · 10.00 ml 0—29.63 ml + 10.00 ml 0 + 2 · 10.00 ml B_0 + 9.90 ml 0.

$\log(B_0/B)$ E: 0.000—4.1; 0.066 0.4; 0.125 3.9; 0.222 9.5; 0.301 15.6; 0.426 24.4; 0.301 16.2; 0.234 11.6; 0.301 16.2.

II. Same as I except that last point is left out:

0.000 2.1; 0.066 6.3; 0.125 10.6; 0.222 17.1; 0.301 23.2; 0.426 31.4; 0.301 23.8; 0.234 19.3

d) 11.5 M KOH

I. 29.25 ml B_0 + 4.91 ml 0 + 2 · 9.75 ml 0 + 4.91 ml 0—29.63 ml + 2 · 9.75 ml 0 + 2 . 9.75 ml B_0.

$\log(B_0/B)$, E(two electrodes): 0.000 0.8 0.9; 0.067 4.3 4.5; 0.177 9.7 9.7; 0.264 14.0 13.9; 0.302 17.2 17.0; 0.428 23.0 22.6; 0.525 26.3 25.7; 0.428 21.1 20.9; 0.301 17.5 17.3.

II. 29.25 ml B_0 + 4.91 ml 0 + 2 · 9.75 ml 0 + 4.91 ml 0—29.63 ml + 9.75 ml 0 + 19.85 ml B_0 + 9.75 ml B_0.

log (B_0/B), E (two electrodes): 0.000 0.9 0.5; 0.067 4.6 4.0; 0.177 9.7 9.1; 0.264 14.0 12.8; 0.302 15.2 15.9; 0.428 20.6 21.4; 0.232 12.4 12.6; 0.190 10.4 10.5.

n = 1, 2, and 3, according to eqn. (6a). Obviously, the slope of the present data is not compatible with n = 2 or n = 3 but agrees fairly well with n = 1.

Admittedly, the silver electrodes do not behave very well in these solutions. It is seen, however, from the "back titrations" that the emfs are fairly reproducible; a small drift of the order of 1 or 2 mV would not affect the general conclusions.

The conclusions are the same for ~1 M and ~12 M alkali, as could be expected from the equilibrium condition, eqn. (1): in a saturated solution, the ratios between the species, say, $Ag(OH)_2^-/Ag_3(OH)_4^-/OH^-$ would be practically independent of $[OH^-]$. Thus, if the trinuclear complex predominates at low I, it should do so at high I too; if it is insignificant (as it seems to be) at low I, one could not increase its importance by increasing I.

One may ask why Pleskov and Kabanov got a so much lower slope, that it would correspond to n = 3. We would think that the main cause is in the electrodes. They seem to have used silver wires (instead of electrolytically

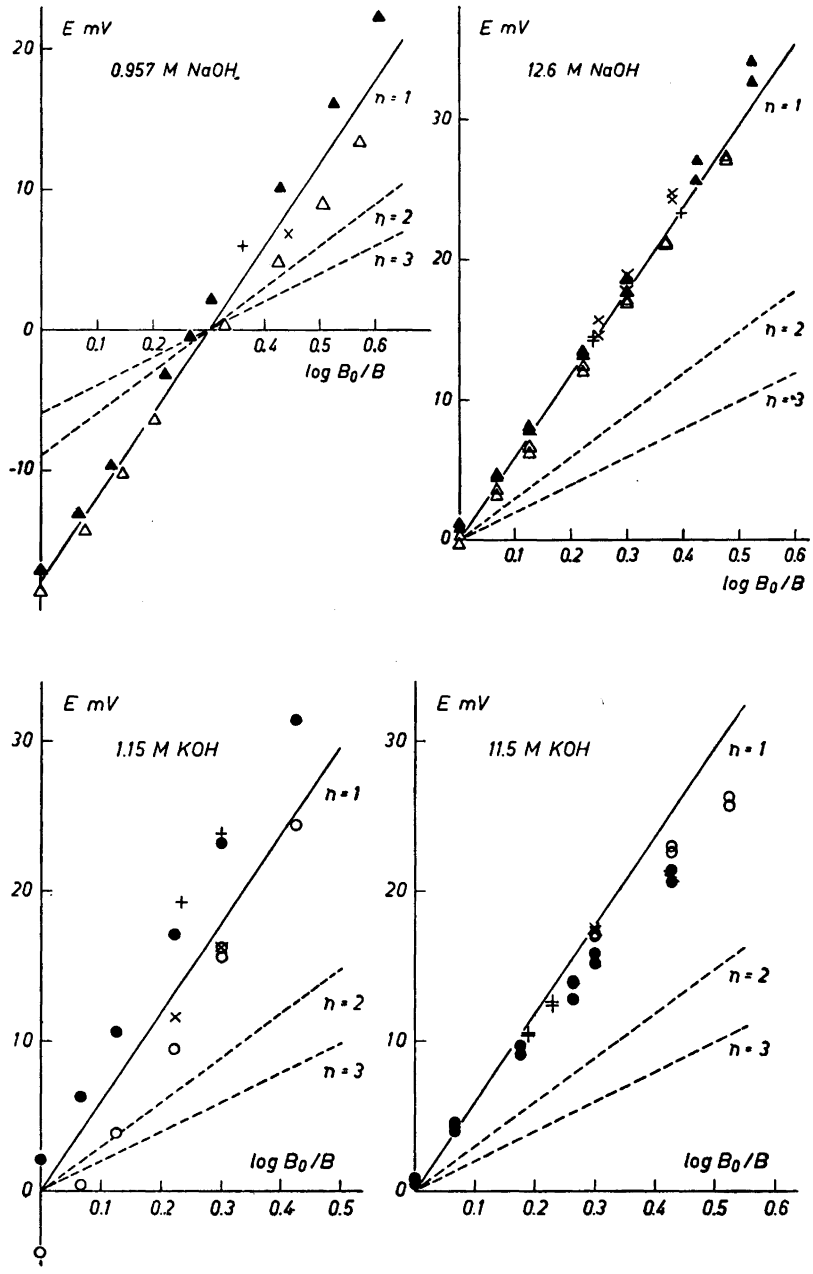

Fig. 1. Experimental results, plotted as E (mV) *versus* $\log(B_0/B)$. Full-drawn line: calculated with eqn. (6a) and $n = 1$; dotted lines calculated with eqn. (6a) and $n = 2$ or 30 Different runs, or electrodes, are denoted by different symbols.

precipitated silver), which, according to our experience, can give rise to emf:s somewhat different from the standard emf:s for pure silver; the deviations are especially great at low $[Ag^+]$. Covering the silver electrolytically with an oxide "Ag_2O_2" layer and then reducing it (method not mentioned) [5], might lead to difficulties. If solid Ag_2O is left on the silver surface, it is likely to dissolve in a unsaturated solution and the actual concentration of Ag^+ would be higher than calculated from the dilution, the emf measured would be less than expected and so would the slope.

It is apparent from the present work how important is the treatment of the electrodes. It should be mentioned that, in a few of our preliminary experiments, the apparent slope would have corresponded to $n \sim 1.5$.

In conclusion, our present data give no reason to assume any polynuclear species in argentate solutions. In the region where the solubility is proportional to $[OH^-]$, the formula of the predominant species can be simply written as $Ag(OH)_2^-$. At very high alkalinities, >5 M OH^-, other species such as $Ag(OH)_3^{2-}$ may perhaps occur; the bend in the solubility curve is however not upward, as would be expected from terms for higher complexes, but downward, presumably because of activity factors.

SOLUBILITY PRODUCT OF Ag_2O

In connection with other work [6], the solubility product of AgOH was determined in the medium 3 M $(Na)ClO_4$. Silver electrodes were used for determining $[Ag^+]$; they were standardized against acid solutions of known Ag^+. Three titrations were carried out, starting with acid silver solution and adding alkali. A glass electrode was used as a check, but $[OH^-]$ was taken from the analytical composition of the solution. The average value obtained was

$$\tfrac{1}{2}Ag_2O(s) + \tfrac{1}{2}H_2O \rightleftharpoons Ag^+ \pm OH^-; \log K_{s0} = -7.42 \pm 0.02 \ (25°C, 3\ M\ (Na)ClO_4)$$

The measurements could have been made more accurate but the precision sufficed for our needs.

Acknowledgements. This work has been supported in part by the *Air Force Office of Scientific Research of the Air Research Development Command, United States Air Force,* through its European Office.

Dr. George Biedermann has given valuable aid in the preparation of very pure Ag_2O. Professor Robert Connick has been kind enough to read the manuscript and to give helpful comments on it.

REFERENCES

1. Laue, E. *Z. anorg. Chem.* **165** (1927) 325.
2. Johnston, H. L., Čůta, F. and Garrett, A. B. *J. Am. Chem. Soc.* **55** (9133) 2311.
3. Reynolds, C. A. and Argersinger, W. J. Jr. *J. Phys. Chem.* **56** (1952) 417.
4. Beck, M. T. *Acta Chim. Acad. Sci. Hung.* **4** (1954) 227.
5. Pleskov, Ju. V. and Kabanov, B. M. *Zhur. neorg. Khim.* **2** (1957) 1807.
6. Antikainen, P. J. and Dyrssen, D. AFOSR-TN 59—664. *Acta Chem. Scand.* **14** (1960) 86.
7. Ingri, N., Lagerström, G., Frydman, M., and Sillén, L. G. *Acta Chem. Scand.* **11** (1957) 1034.
8. Brown, A. S. *J. Am. Chem. Soc.* **56** (1934) 646.
9. Forsling, W., Hietanen, S., and Sillén, L. G. *Acta Chem. Scand.* **6** (1952) 901.

Received September 29, 1959.

ACTA CHEMICA SCANDINAVICA 14 (1960) 102–106

On the Biosynthesis of the Pigments from *Penicillium islandicum* I

STEN GATENBECK

Institute of Biochemistry, University of Lund, Lund, Sweden

The biochemical interrelationships of the pigments iridoskyrin, islandicin, rubroskyrin, luteoskyrin and skyrin in the mould *Penicillium islandicum* have been investigated. The specific radioactivity / time curves of the pigments have been determined after feeding the mould for a short time with ^{14}C-labelled acetate. Analysis of these curves indicates that the pigments are formed independently of each other.

The mould *Penicillium islandium* Sopp produces a set of various pigments of very close structural relationship to each other when grown on a medium with glucose as the sole carbon source. All the pigments are polycyclic compounds and have furthermore the anthracene structure in common. The dominant compounds are skyrin, rubroskyrin, luteoskyrin, iridoskyrin and islandicin. From the structures of these compounds (Fig. 1) one would anticipate a biological interconversion. Rubroskyrin and luteoskyrin are easily transformed *in vitro* by dehydrating agents or dithionite [1] to iridoskyrin so it is reasonable to assume them to be the biological precursors of iridoskyrin.

As shown in earlier papers [2,3] the actual pigments originate from acetate. In order to investigate their interconvertibility a series of experiments has been carried out on the incorporation of ^{14}C-labelled acetate into these pigments in addition to studying the production sequence of the pigments (expt. A). The variations in time of their specific radioactivities were followed (expt. B). In other experiments (C and D) the specific radioactivities were determined after replacement of the labelled substrate with normal Czapek-Dox medium.

EXPERIMENTAL

Experiment A. A Petri dish (5 × 15 cm) containing 100 ml of Czapek-Dox medium was sterilized and inoculated with a spore suspension of *Penicillium islandicum* Sopp, N.R.R.L. 1036. After two days the whole surface of the medium was covered by a white mycelium. At eight hourly intervals a piece of the mycelium (*ca.* 3 × 3 cm) was cut out and thoroughly extracted with acetone. A portion of the acetone solution was developed on a paper chromatogram in a solvent containing benzene-2 % formic acid (10:1). The

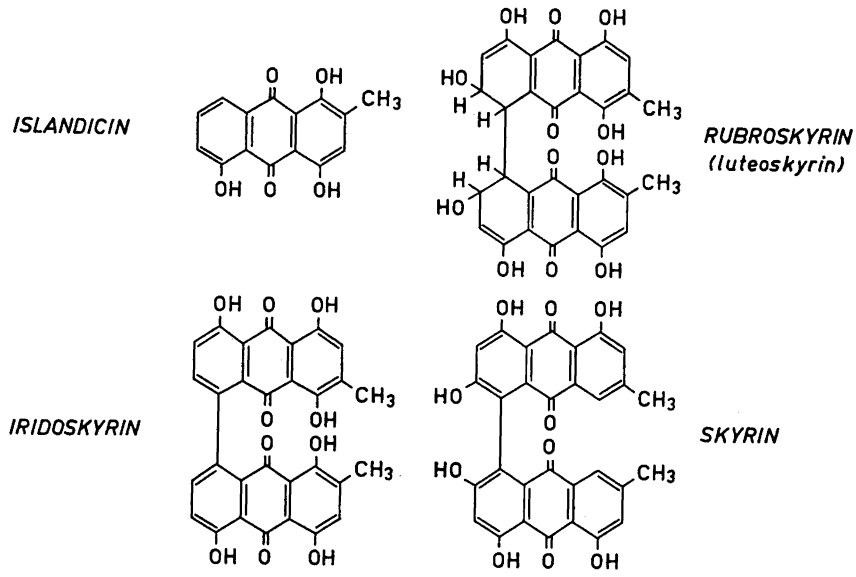

Fig. 1.

different pigments were identified by their R_F-values, color and color reactions with methanolic magnesium acetate solution (Table 1). The pigment that appeared first was skyrin. It was not possible to detect any other pigment until 24 h after the appearance of skyrin. The experiment was repeated with shorter intervals between the withdrawals of the test samples but even with one hourly intervals it was not possible to determine any production order in time of rubroskyrin, luteoskyrin, iridoskyrin and islandicin.

Experiment B. A culture was grown for seven days in the same way as in experiment A. After the addition of 0.25 mC $CH_3{}^{14}COONa$ (5 mC/mmole) samples were taken from the mycelium at different times as described above. Every sample was extracted with acetone, the acetone solution evaporated to dryness and the residue triturated several times with petroleum ether (b. p. 40—60°C) in order to remove the lipids. After dissolving the pigments in acetone, two equal portions were withdrawn, one of which was then developed on a paper chromatogram. The total radioactivity of the iridoskyrin-islandicin spot was measured directly on the paper. The pigments were extracted from the paper with 3 ml of HCl-acidified acetone. Their concentration was measured in a Hilger Uvispek spectrophotometer at 492 mμ. Iridoskyrin and islandicin have their absorption maxima at the same wavelengths but the molar extinction coefficient of iridoskyrin is twice that of islandicin (log ε_{492} 4.09). The molar specific radioactivity of the mixture iridoskyrin-islandicin was calculated, the amount being expressed as islandicin.

The other portion of the acetone solution was evaporated to dryness and 1 ml of concentrated H_2SO_4 added. After keeping at room temperature for 20 h it was diluted with water and exhaustively extracted with ether. The extract was concentrated to a small volume and developed on a paper chromatogram in the same solvent as above. The radioactivity and the amount of the mixture of the natural iridoskyrin-islandicin and the iridoskyrin obtained from rubroskyrin and luteoskyrin by the treatment with H_2SO_4 was measured as above. After subtraction of the radioactivity and the amount of natural iridoskyrin-islandicin, the specific radioactivity of rubroskyrin-luteoskyrin was calculated. The values are given in Fig. 2.

Table 1.

Compound	R_F-value (benzene-formic acid	Color	Color with meth. Mg-acetate
Islandicin	1.00	Pink	Purple
Iridoskyrin	0.95	Pink	Purple
Skyrin	0.15	Yellow	Violet
Rubroskyrin	0.20	Red	Green
Luteoskyrin	0.30	Yellow	—

It was also desirable to know the molar specific radioactivity of skyrin. In the solvent used, skyrin and rubroskyrin overlap on the paper chromatogram and no other solvent could be found which would separate them completely. In order to obtain a true value of the specific radioactivity, skyrin was cleaved to emodin which is easily separated from the other pigments by paper chromatography. The cleavage was performed according to Raistrick [4] by dissolving an aliquot of the acetone extract in 1 N NaOH and treating the solution with sodium dithionite for one hour at room temperature. After acidification with concentrated HCl the solution was extracted with ether and the ether phase developed on a paper chromatogram in benzene-formic acid. The radioactivity and the amount of emodin was then determined as above (log ε_{437} 4.10).

Experiment C. The mould was cultured in a Petri dish as described in experiment A. After seven days an aqueous solution of 0.25 mC of $CH_3{}^{14}COONa$ was added to the medium. The radioactive medium was withdrawn with a pipette after half an hour and fresh Czapek-Dox solution added after washing the mycelium three times with sterilized, distilled water by injecting the water beneath the mycelium. Test samples were taken from the mycelium over a period of 10 h. The pieces of mycelium were extracted with acetone, the lipids removed and the extract developed on a paper chromatogram as above. The molar specific radioactivity of iridoskyrin-islandicin was determined. The region on the paper containing rubroskyrin and luteoskyrin was cut out and the pigment extracted from the paper with acetone. The acetone solution was evaporated to dryness, treated with concentrated H_2SO_4 for 20 h and the molar specific radioactivity determined after further chromatographing as in expt. B. The values are given in Fig. 3.

Experiment D. Expt. C was repeated with the modification that islandicin was separated from iridoskyrin by sublimation in vacuum at 160°C. The residue from the sublimation consisting of iridoskyrin was resublimed in vacuum at 270°C. The molar specific radioactivities of islandicin and iridoskyrin were then determined separately. As the culture in this experiment produced unusally large amount of luteoskyrin this pigment was isolated by paper chromatography and its molar specific radioactivity determined without prior conversion to iridoskyrin. The concentration of luteoskyrin was measured at 447.5 mμ (log ε 4.46). The results of expt. D are shown in Fig. 4.

RESULTS AND DISCUSSION

The values in Fig. 2 show that the molar specific radioactivity of naturally occurring iridoskyrin-islandicin is definitely higher than that of rubroskyrin-luteoskyrin. If rubroskyrin-luteoskyrin were precursors of iridoskyrin-islandicin they should have a higher specific radioactivity than iridoskyrin-islandicin or at least the same. While the results of expt. B immediately exclude this possibility they do not argue against the reverse mechanism.

Although expt. C shows a rather high incorporation of labelled acetate after half an hour, experiment A and repeated experiments of the same type indicate that the radioactivity of the pigments has not reached the steady state within this time.

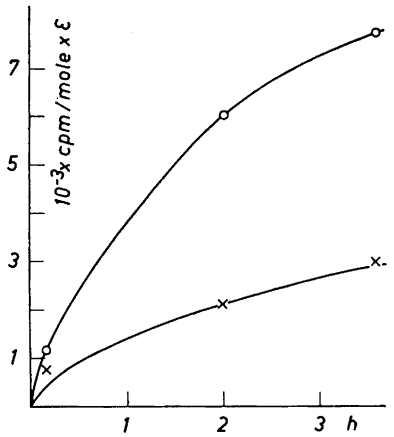

Fig. 2. Specific radioactivity/time curves, iridoskyrin-islandicin O———O, rubroskyrin-luteoskyrin ×———×.

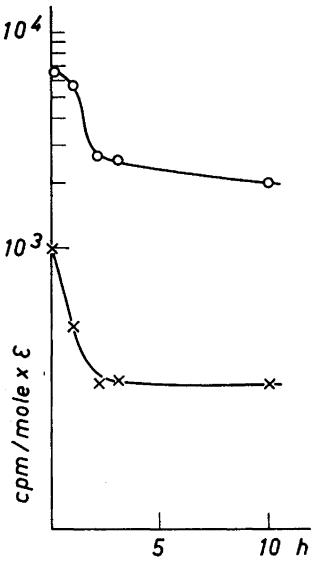

Fig. 3. Specific radioactivity/time curves, iridoskyrin-islandicin O———O, rubroskyrin-luteoskyrin ×———×.

If the iridoskyrin-islandicin mixture was transformed to rubroskyrin-luteoskyrin by a hydration reaction, the specific radioactivity of the former should decrease relative to that of the latter. As seen from Fig. 3 the specific radioactivities of iridoskyrin-islandicin and rubroskyrin-luteoskyrin decrease almost at the same rate and this result has been obtained in several repeated

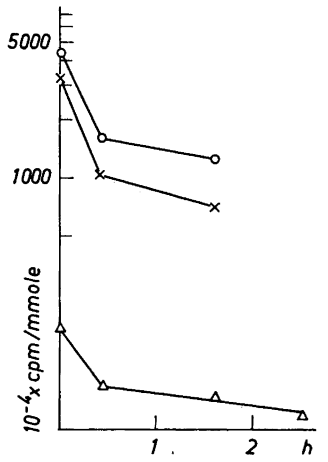

Fig. 4. Specific radioactivity/time curves, islandicin O———O, iridoskyrin ×———×, luteoskyrin △———△.

experiments. This is in accord with the independent formation of these pigments.

Expt. D confirms the conclusions derived from expt. C that there is no interconvertibility of the anthraquinones and their hydrated forms. Furthermore, expt. D gives the surprising result that islandicin is not the immediate precursor of its dimer, iridoskyrin. The parallel specific radioactivity/time curves of these compounds in Fig. 4 indicate that the biosynthesis of one pigment is wholly independent of the production of the other one.

Emodin, which is equivalent to skyrin, has about the same specific radioactivity as rubroskyrin-luteoskyrin and is consequently not a precursor of iridoskyrin-islandicin. The early formation of skyrin indicates that it has a separate position in the biosynthesis of the pigments. As skyrin occurs in other strains of *Penicillium islandicum*[4] and in other moulds, *e.g. P. rugulosum*[5], *P. wortmanni*[5], *Endothia parasitica* and *E. fluens*[6], which do not produce rubroskyrin or luteoskyrin, it is assumed, that skyrin has no connection with these pigments.

REFERENCES

1. Howard, B. H. and Raistrick, H. *Biochem. J.* **57** (1954) 212.
2. Gatenbeck, S. *Acta Chem. Scand.* **12** (1958) 1211.
3. Gatenbeck, S. *Acta Chem. Scand.* **12** (1958) 1985.
4. Howard, B. H. and Raistrick, H. *Biochem. J.* **56** (1954) 56.
5. Breen, J., Dacre, J. C., Raistrick, H. and Smith, G. *Biochem. J.* **60** (1955) 618.
6. Shibata, S., Tanaka, O., Chihara, G. and Mitsuhashi, H. *Pharm. Bull. Japan* **1** (1953) 302.

Received September 16, 1959.

ACTA CHEMICA SCANDINAVICA 14 (1960) 107–110

On Observable Discontinuities and Coherence in the Kinetics of Enzymically Reacting Systems

J. A. CHRISTIANSEN

Sundvænget 9, Hellerup, Denmark

It is shown that there are thermodynamic arguments for the belief, that the cyclic transformations which the individual molecules of an enzyme in a macroscopic reacting system are forced to run through during their action as catalysts are in phase, are coherent. A necessary consequence of this behaviour is, that the reaction proceeds in observable jumps, whose magnitude is determined by the amount of enzyme present in the system. Experimental evidence, which seems to support this view is quoted.

This paper contains an extension of considerations from former papers of the author [1-3].

In most mechanical or even quantum-mechanical pictures of an elementary chemical reaction the process is considered to be a continuous one. The picture may be more ore less refined, but the fundamental assumption is always the one due to Arrhenius, that a molecule or a complex of molecules to react must pass a state in which its energy is maximum.

Arrhenius [4] called this state the active one. Later on R. Marcelin [5] denoted it as the critical state, while J. N. Brønsted [6] in a paper in German used the name "Übergangszustand". The corresponding name in English "transition state" was used by M. Polanyi and M. G. Evans [7], and this name has since been used exclusively by H. Eyring and his school.

But even if the single elementary reaction be described as proceeding continuously, it is evident that statistically an elementary reaction must be considered as practically speaking discontinuous. This is so, because the life times of the reactants and the resultants are immensely much larger than that of the intermediate complex. Therefore we commit only a very small error if we state that a molecule or a complex of molecules is either in the reactant state or in the resultant state. Or we may say, that the reaction takes place in a jump from one state to the other through the transition state. However, in a macroscopic system, containing an immense number of reacting molecules

the jumps are randomly distributed in time, and the discontinuity is therefore not observable. But this statement may not be true in the case where a reaction is catalyzed, *e.g.* by an enzyme.

Let a reaction, which has a positive affinity from the left to the right

$$B_1 + B_2 + B_3 = A_2 + A_3 + A_1 \qquad (B)$$

be catalyzed by an enzyme in three elementary steps:

$$\begin{array}{ll} B_1 + X_1 = X_2 + A_2 & (+1) \\ B_2 + X_2 = X_3 + A_3 & (+2) \\ B_3 + X_3 = X_1 + A_1 & (+3) \end{array} \qquad (A)$$

X_1, X_2, and X_3 being three different forms or compounds with the substrates (B_i, A_i) of the enzyme.

The sequence (A) means, that the reaction (B) forces the enzyme to undergo a cyclic transformation in the order 1231. What we observe is the occurrence or the disappearence of one species of the resultants or the reactants respectively. To fix our ideas let us assume, that we observe the occurrence of A_1 which may be, *e.g.*, a (hydrated) hydrogen ion.

The liberation of this takes place in the moment when X_3 is transformed into X_1 which, according to the foregoing, is a sudden event, so long as only one molecule of the enzyme is considered. Or in other words, we may state that the enzyme molecule must be at a certain time in one of its three possible states.

Consider now the realistic case, where there are many molecules of the enzyme within a certain volume element. May we then assume that the different molecules are simultaneously in the same state or may we not? Or expressed in another way, is the instantaneous distribution of the enzyme on its different states the same everywhere in the reacting system?

According to thermodynamics it seems, that the answer to the latter question must be yes, because we know that, to change the state of the whole system from one in which the distribution is the same everywhere to one in which it is not, requires work. Therefore the former state of the system is more probable than the latter and, as usual in statistical thermodynamics, so much more so that it is, practically speaking, the only possibility. We may therefore say that the cyclic transformations of the individual enzyme molecules must always be in phase or, that the system is coherent in respect of transformations of the enzyme.

This coherence would have an important consequence: As mentioned above the transformation of an X_3 into an X_1 is accompanied by a liberation of A_1. If now coherence exists this means, that all the enzyme molecules X_3 react simultaneously that is, an amount of A_1 which is stoichiometrically equivalent to the amount of enzyme in the system is suddenly released. If, therefore, the liberation of A_1 in our system is observed and taken as a measure of the extent of the overall reaction (B) it is evident, that we observe a discontinuous progress of the reaction. Or, in other words, the reaction is observed to proceed in consecutive jumps, each representing the same number of individual reactions according to (B). It must be added, however, that the author is not

able at present to indicate a mechanism, by means of which the coherence is maintained. It is evidently a question of great importance whether or not the peculiar behaviour described above of a reaction catalyzed by an enzyme has ever been found, and the answer seems to be in the affirmative: It is an experimental fact [8], that certain (by no means all) nerves in their endings spontaneously generate electrical impulses which are transmitted through the nerve and which can be observed oscillographically by means of electrodes connected to the nerve in a suitable way. The signals as we may call them appear periodically, the period, which is often of the order of 0.01 to 0.1 s, being constant so long as the corresponding sense organ is not stimulated. Furthermore, and this is what mostly interests us here, the duration of the signal is only a small fraction of the distance in time between two consecutive signals. We thus get the impression, that periodically an outburst of "something" takes place which causes the electrical disturbance. Evidently this phenomenon might be understood on the lines described above if an enzyme catalyzing a chemical (metabolic?) reaction were located in the nerve ending, the substrates being supplied from its surroundings. This again would be a corroboration of the widely accepted assumption, that everything which happens in a living organism is caused by chemical reactions. It may be added that it is a fact that chemical reactions go on in nerves as in other cells of the living organism.

Besides this to a certain extent direct evidence for the existence of discontinuities in the course of an enzymic reaction, evidence of a more indirect nature seems to exist: In most (not in all) cases of enzymic reactions it can be shown that steady state is arrived at in the course of an exceedingly short time. In such cases a function φ of the extent of reaction ξ can always be found, which obeys the equation

$$t = \varphi(\xi)$$

where t is the time at which the extent of reaction has reached the value ξ. If now, as hitherto assumed, ξ increases continuously with time, it must be possible to determine the rate of the reaction with an accuracy which is only limited by the inaccuracy of the experiments. If, however, the reaction proceeds in observable jumps it may well happen, that the accuracy obtained is less than that estimated from the properties of the experimental procedure. We have had in the institute of physical chemistry of the university of Copenhagen indications of such a situation. However, as we might have overestimated the accuracy of our measurements, the results were not published. Then a Russian colleague, S. E. Shnoll, referring to the present authors paper [2], sent him a paper in Russian [9], in whose English summary Shnoll explicitly states, that his determinations of the rate of a certain reaction show deviations, which certainly cannot be explained by inaccuracies in the experimental procedure.

The different pieces of evidence mentioned above may not seem sufficiently convincing when they are taken separately. But when taken together they seem to point out that reactions of the types mentioned show discontinuities which are macroscopically observable. Or as we may say, the single cyclic transformations in the macroscopic system are in phase, are coherent.

REFERENCES

1. Christiansen, J. A. *Acta Chem. Scand.* **11** (1957) 1436.
2. Christiansen, J. A. *Z. Elektrochem.* **62** (1958) 225.
3. Christiansen, J. A. *Acta Chem. Scand.* **12** (1958) 352.
4. Arrhenius, S. *Z. physik. Chem.* **4** (1889) 226.
5. Marcelin, R. *Ann. phys.* **3** [9] (1915) 120.
6. Brønsted, J. N. *Z. physik. Chem.* **102** (1922) 169.
7. Polanyi, M. and Evans, M. G. *Trans. Faraday Soc.* **31** (1935) 875.
8. *Cf.* Ref.[2], p. 225.
9. Shnoll, S. E. *Voprosy Med. Khim.* **4** (1958) 443.

Received September 24, 1959.

ACTA CHEMICA SCANDINAVICA 14 (1960) 111–125

The Bacteriostatic Action of Benzoic and Salicylic Acids

II. The Effect on Acetate Metabolism

INGMAR BOSUND*

Swedish Institute for Food Preservation Research, Gothenburg, Sweden, and State Dairy Research Station, Alnarp, Sweden

The effect of benzoic and salicylic acids on the acetate metabolism of resting cells of *Proteus vulgaris* was investigated by the Warburg technique.

The oxidation of acetate by washed cells previously grown in a medium containing glucose and amino acids was inhibited by both acids. Small amounts of succinate added simultaneously with the acetate in these respiration studies decreased the inhibition caused by benzoic acid considerably.

In similar experiments with cells previously grown in a medium with acetate as the sole carbon source, the effect of benzoic acid on the rate of acetate oxidation was much less, while that of salicylic acid was as before.

Both inhibitors had a tendency to increase the total amount of CO_2 evolved per mole of substrate added in experiments with washed cells previously grown in the acetate medium. Such an increase in CO_2 output from acetate induced by benzoic acid was further investigated in experiments with labelled acetate and shown to be derived mainly from the methyl group of the acetate molecule.

Neither of the acids had any appreciable effect on pyruvate dismutation with cell-free extracts of *Escherichia coli*.

In a previous investigation [1] the oxidation of glucose and pyruvate by resting cells of *Proteus vulgaris* was found to be completely inhibited at the oxidation level of acetate by 0.01 M benzoic acid or 0.003 M salicylic acid at pH 6.0. It was further shown that these concentrations of the two acids are necessary for complete suppression of growth of this organism at the pH mentioned. It was considered that the inhibition of acetate oxidation might have something to do with the bacteriostatic effect.

This paper is concerned with the influence of benzoic and salicylic acids on the oxidation of acetate by resting cells of *P. vulgaris* and with the effect of these acids on acetyl phosphate formation with extracts of *Escherichia coli*.

* Present address: State Dairy Research Station, Alnarp, Sweden.

EXPERIMENTAL

Organisms. The same strain of *Proteus vulgaris* was used as before. The extract in the experiments on acetyl phosphate formation was prepared from cells of *Escherichia coli*.

Growth conditions. Cell suspensions for respiration studies with *P. vulgaris* were prepared from cultures grown either in a fairly rich medium containing glucose and amino acids (medium A) or in a poor medium with acetate as the sole carbon source (medium B). In the case of medium B the inoculation was made with cells previously adapted to growth in this medium. Medium A: glucose, 10.0 g; casein hydrolysate (Difco vitamin-free casamino acids), 1.0 g; NH_4Cl, 1.0 g; nicotinamide, 0.2 mg; K_2HPO_4, 9.5 g; KH_2PO_4, 1.5 g; $MgSO_4 \cdot 7H_2O$, 0.1 g; distilled water to 1 l; adjusted to pH 7.0. Medium B: $CH_3COONa \cdot 3H_2O$, 1.0 g; NH_4Cl, 1.0 g; nicotinamide 0.2 mg; $Na_2HPO_4 \cdot 2H_2O$, 6.0 g; KH_2PO_4, 3.0 g; $MgSO_4 \cdot 7H_2O$, 0.1 g; distilled water to 1 l; adjusted to pH 7.0. The cultures were grown at 37°C in Kluyver flasks with sufficient aeration to ensure maximum growth rate or, in some experiments using medium A, in Erlenmeyer flasks without aeration or shaking. In some experiments the cells were harvested early in the logarithmic growth phase, and then the medium was inoculated with a heavy suspension of washed cells. When necessary, growth was followed by turbidity measurements in a Beckman spectrophotometer at 425 mμ.

Methods. Oxygen consumption and production of carbon dioxide was measured by the conventional Warburg technique as described in the first paper of this series. The data recorded in the figures and tables have been corrected for endogenous respiration. In the experiments with labelled acetate the oxidation was terminated by addition of 0.3 ml of 5 N H_2SO_4 when the rate of oxygen consumption had decreased to the value of the endogenous respiration. The cells were collected by centrifugation, washed three times with distilled water and dried at 110°C. The media and the washings were pooled, neutralized with 2 N NaOH and evaporated to dryness over night by freeze drying. The total amount of carbon in the cells and in the media was then converted into CO_2 by the wet decomposition method of van Slyke and Folch [2]. The CO_2 was collected as $BaCO_3$ in centrifuge tubes containing a saturated solution of $Ba(OH)_2$ in water. The precipitates were washed twice with distilled water, dried at 125°C and weighed. The respiratory CO_2, which was absorbed during the experiment in 10 % KOH in the center wells of the Warburg flasks was carefully transferred, together with the KOH, into a flask containing a known amount of K_2CO_3 dissolved in distilled water. The carbonate was collected as $BaCO_3$ by addition of 0.2 M $BaCl_2$, and the precipitate was washed, dried and weighed in the way described. The total amount of radioactivity in the three samples of $BaCO_3$, from cells, media and respiratory CO_2 was then determined by plating the carbonate on aluminium dishes and counting in a Geiger-Müller counter. In each experiment it was checked that the sum of the radioactivities recovered in the three samples of $BaCO_3$ corresponded to the amount added with the acetate.

Preparation of E. coli extract. The soluble enzyme system used in the experiments on acetyl phosphate formation was prepared from cells of *E. coli* grown in a medium containing lactose, meat extract, yeast extract, trypton and phosphate. The cells were harvested by use of a Sharples centrifuge, washed twice with 0.9 % KCl-solution and freeze dried. The extract was prepared from the dry powder in the way described by Korkes *et al.*[3]

Reagents. The reagents used were commercial preparations with the exception of acetyl phosphate, which was synthesized from *iso*propenyl acetate and phosphoric acid by the method of Stadtman and Lipmann [4]. DPN * and CoA were supplied by Pabst Laboratories; DPT and lactic dehydrogenase, by Sigma Chemical Company; and methyl and carboxyl labelled samples of sodium acetate, by The Radiochemical Centre, Amersham, England.

RESULTS

The effect of benzoic acid on acetate oxidation by washed cells previously grown in medium A. Preliminary respiration studies showed that the acetate oxidiz-

* Abbreviations: DPN = diphosphopyridine nucleotide, CoA = coenzyme A and DPT = diphosphothiamine.

Table 1. Influence of growth conditions, increasing physiological age of the cells at the time of harvesting and the presence of small amounts of succinate on the rate of acetate oxidation in respiration studies with washed cells of *P. vulgaris*.

Expt. No.	Growth at time of harvesting, mg dry weight/ml growth medium	Growth medium and growth phase at time of harvesting	Oxygen consumption during acetate oxidation, μl/mg dry weight and hour (Q_{O_2})		b/a
			a without succinate	b with addition of small amounts of succinate	
1	1.50	Medium A. Stationary phase. No aeration.	0	0	—
2	0.72	Medium A. Log phase. Aeration only during one generation of growth before harvesting.	0	0	—
3	0.14	Medium A. Log phase. Aerated.	30	34	1.1
4	0.23	Medium A. Log phase. Aerated.	22	31	1.4
5	0.56	Medium A. Log phase. Aerated.	17	29	1.7
6	1.30	Medium A. Very slow growth. Aerated.	8	26	3.2
7	2.00	Medium A. Stationary phase. Aerated.	1.5	15	10.0
8	0.17	Medium B. Log phase. Aerated.	125	125	1.0

Each vessel contained 5—10 mg dry weight of washed cells, 133 μmoles of potassium phosphate, 7 μmoles of sodium acetate and 0.2 μmoles of sodium succinate (when present). Temp. 37°C; pH 6.0. In these experiments the rate of oxygen consumption generally became constant about 20 min after addition of substrate. The Q_{O_2} values recorded are based on measurements made after this initial period. In all experiments the oxygen consumption due to succinate oxidation was completed about 15 min after addition of substrate as determined in separate flasks where only succinate was added. This oxygen uptake could thus have no influence on the Q_{O_2} values shown in the table. Moreover, the theoretical amount of oxygen for complete oxidation of 0.2 μmole of succinate is only 15.7 μl (generally about 10 μl was consumed in these experiments) whereas the total oxygen consumption due to acetate oxidation during the experimental period was more than 200 μl.

ing capacity of *P. vulgaris* cells, isolated from the growth medium by centrifugation and washed as described in the experimental part, varies with the growth conditions and with the physiological age of the cells at the time of harvesting. The influence of such factors in the pre-history of the cells on the rate of oxygen consumption after addition of acetate to washed cell suspensions is shown in Table 1 (see also Table 6). In these tables the increase in the rate of acetate oxidation, caused by the addition of small amounts of succinate together with the acetate is clearly demonstrated. It is probable that this stimulating

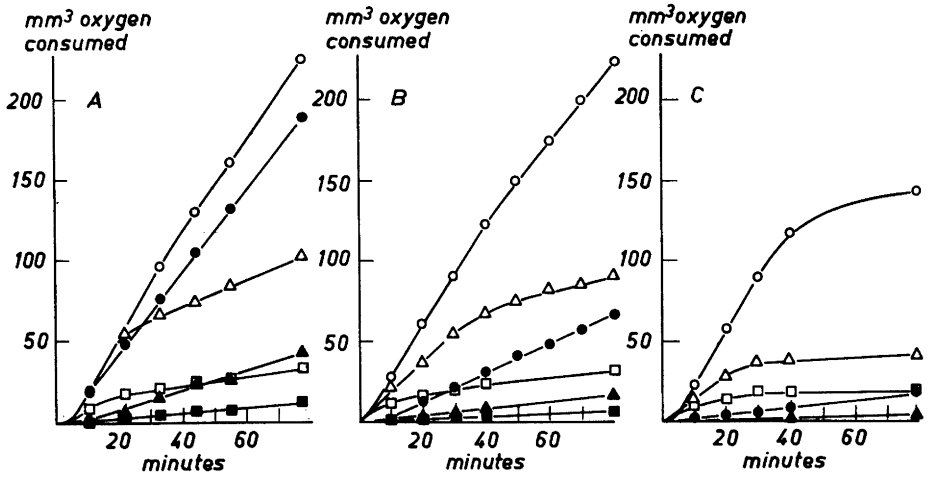

Fig. 1. Influence of benzoic acid on acetate oxidation by washed *P. vulgaris* cells previously grown with aeration in medium A. A — cells harvested in the logarithmic growth phase, B — cells harvested early in the stationary phase, and C — cells harvested after 8 h in the stationary phase. The vessels contained besides 7 mg dry wt. of cells, 133 μmoles of potassium phosphate and 10 μmoles of sodium acetate: ●———● no further additions; ▲———▲ 3.5 mM sodium benzoate; ■———■ 7.0 mM sodium benzoate; ○———○ 0.2 μmoles of sodium succinate; △———△ 0.2 μmoles of sodium succinate and 3.5 mM sodium benzoate; □———□ 0.2 μmoles of sodium succinate and 7 mM sodium benzoate. Temp. 37°C; pH 6.0. The values recorded have been corrected for the oxygen uptake attributable to the succinate oxidation (10—15 μl).

effect is due either to conversion of succinate to oxalacetate, which serves as a condensing partner for oxidation of acetate through the Krebs cycle or to the functioning of succinate as a readily utilizable source of energy for the ATP-generated activation of acetate.

It is evident from the table that only cells pre-grown with adequate aeration oxidize acetate to any appreciable extent and at a rate decreasing with increasing age of the cells when harvested (Expts. Nos. 3—7). Cells, harvested after growth without aeration, or with aeration for only one or two generations, did not oxidize acetate (Expts. Nos. 1—2). The great acetate oxidizing capacity of washed cells pre-cultivated in medium B is apparent from Expt. No. 8.

For the cultivation of cells in medium B, the Kluyver flasks were inoculated with cells previously adapted to the growth medium employed, but unaccustomed to excessive aeration. Therefore, in order to obviate any consequent delay in growth (Dagley, Dawes and Morrison [5] or Lwoff and Monod [6]), the medium was inoculated with a fairly large amount of cells.

In some experiments *P. vulgaris* was studied with regard to its ability to oxidize other fatty acids, such as propionic and butyric acids. No oxygen consumption attributable to such an oxidation was, however, noticed, not even in the presence of succinate.

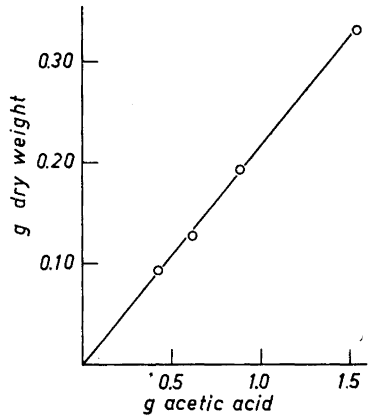

Fig. 2. Total growth of *P. vulgaris* in medium B as a function of the amount of acetic acid available.

As is shown in Fig. 1 A, B and C benzoic acid completely inhibited acetate oxidation by washed *P. vulgaris* cells, pre-grown in medium A, at concentrations previously found not to influence the initial rate of glucose and pyruvate oxidation by this organism. The degree of inhibition was approximately the same whether the cells were harvested in the logarithmic or in the stationary phase. Simultaneous oxidation of a comparatively small amount (0.2 μmole) of succinate markedly reduced the inhibitory effect of 3.5 mM benzoic acid for the first 20—30 min. In parallel experiments with omission of acetate the same amount of succinate was oxidized with consumption of 10—15 μl of oxygen during this period, after which the rate of the oxygen uptake decreased to that of the endogenous respiration (see the text to Table 1). The succinate oxidation was not inhibited by benzoic acid in the concentrations used.

In a similar study (unpublished) with salicylic acid, which in a concentration of about 1—2 mM completely inhibited any acetate oxidation, addition of succinate did not markedly reduce the inhibition produced. Salicylic acid in the same concentration range was previously found [1] to block glucose and pyruvate oxidation at the acetate level in experiments where the initial rate of glucose oxidation was actually stimulated.

Adaptation of P. vulgaris to growth on acetate as the sole carbon source. The comparatively strong inhibitory effect of benzoic acid on acetate oxidation as revealed by the experiments discussed above was further investigated, but now with cells grown on acetate as the sole carbon source (apart from CO_2). The same strain of *P. vulgaris*, but acetate-adapted, was used as before. The strain was adapted to acetate by successive inoculation in test tubes with medium B containing decreasing amounts of glucose or some other readily utilizable carbon source. pH values above 6.5 proved best for the adaptation process which resulted in a rather slow growth, even of fully adapted cells, owing to lack of aeration. The adapted cells behaved in the same way as the original cells in bacteriological standard tests and were, as before, dependent on addition of nicotinamide for growth. Cells for respiration studies were cultured in Kluyver flasks inoculated with adapted cells and adequately

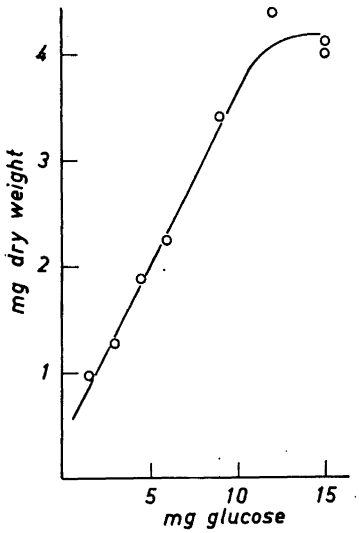

Fig. 3. Total growth of acetate adapted *P. vulgaris* in medium B containing butyrate instead of acetate and supplemented with varying amounts of glucose. When growth had ceased in the different flasks the content of volatile acids in the culture media was determined by steam-distillation and paper chromatography of the distillates. Butyric acid was quantitatively recovered from all the distillates. In flasks where relatively much glucose had been added, additional amounts of volatile acids (probably acetic and formic) were found.

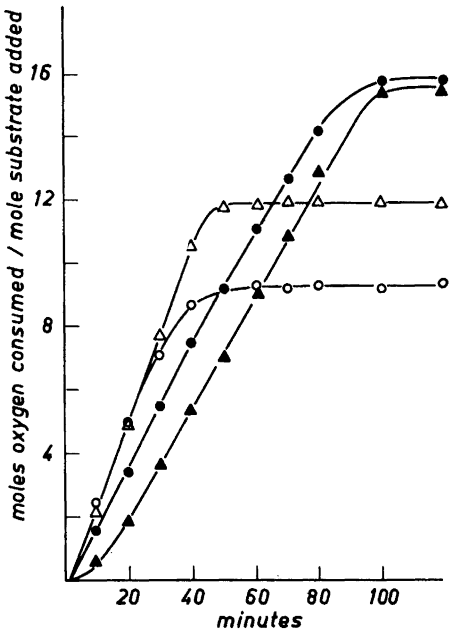

Fig. 4. Effect of benzoic acid on pyruvate and acetate oxidation by washed *P. vulgaris* cells previously grown in medium B. Each vessel contained 2.2 mg dry wt. of cells and 133 μmoles of potassium phosphate. O——O 7 μmoles of sodium pyruvate; ●——● 7 μmoles of sodium pyruvate and 8 mM sodium benzoate; △——△ 7 μmoles of sodium acetate; ▲——▲ 7 μmoles of sodium acetate and 8 mM sodium benzoate. Temp. 37°C; pH 6.0; final volume 2.5 ml.

aerated. As mentioned above, it was necessary to start with heavy inoculation to avoid unduly long lag phases. The cells were therefore allowed to multiply for 24—48 h before aeration was started.

During these conditions the total yield of bacterial growth obtained varied with the amount of acetate added as shown in Fig. 2. The mean generation time during aeration was 3—4 h. Attempts to adapt the strain to growth on butyrate as the sole carbon source proved unsuccessful. Fig. 3 shows an experiment demonstrating the inability of acetate adapted cells to utilize butyrate when grown in a butyrate medium containing various amounts of glucose to support growth.

The effect of benzoic acid and salicylic acid on acetate and pyruvate oxidation by washed cells pre-grown in the acetate medium. The highest rate of oxygen

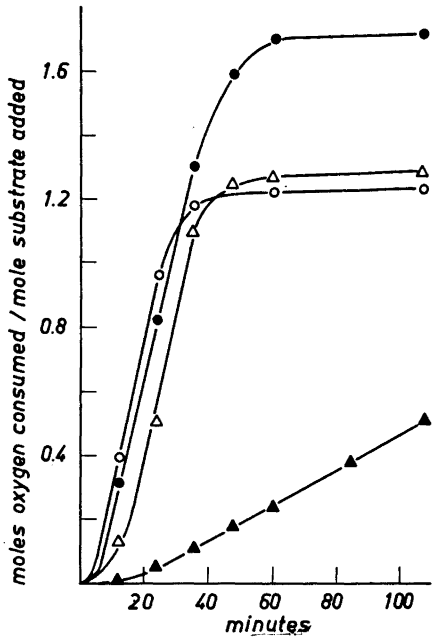

Fig. 5. Effect of salicylic acid on pyruvate and acetate oxidation by washed *P. vulgaris* cells previously grown in medium B. Each vessel contained 3.6 mg dry wt. of cells and 133 μmoles of potassium phosphate. O——O 7 μmoles of sodium pyruvate, ●——● 7 μmoles of sodium pyruvate and 2 mM sodium salicylate, △——△ 7 μmoles of sodium acetate, ▲——▲ 7 μmoles of sodium acetate and 1 mM sodium salicylate. Temp. 37°C; pH 6.0; final volume 2.5 ml.

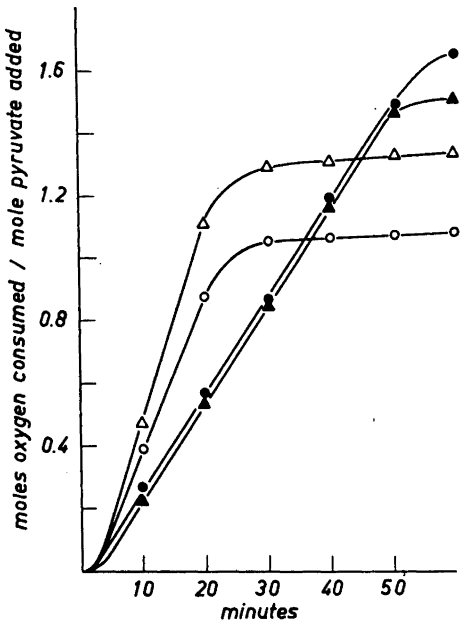

Fig. 6. Effect of benzoic acid on pyruvate oxidation in presence and absence of ammonium ions by washed *P. vulgaris* cells previously grown in medium B. Each vessel contained 3.2 mg dry wt. of cells, 133 μmoles of potassium phosphate and 7 μmoles of sodium pyruvate. O——O no further additions, ●——● 8 mM sodium benzoate, △——△ 20 μmoles of ammonium chloride, ▲——▲ 20 μmoles of ammonium chloride and 8 mM sodium benzoate. Temp. 37°C; pH 6.0; final volume 2.5 ml.

consumption during acetate oxidation with washed cells previously grown on glucose and amino acids was about 30 μl oxygen per mg dry weight and hour (Table 1). The corresponding values found in similar experiments in which the cells had been grown on acetate and harvested in the logarithmic phase generally ranged between 100 and 200. These latter experiments also showed (Figs. 4 and 5) that the rate of oxygen consumption was approximately the same whether acetate or pyruvate was used as substrate; the total amount of oxygen taken up per mole substrate was somewhat greater for acetate.

Figs. 4 and 5 illustrate the effect of benzoic and salicylic acids on acetate and pyruvate oxidation by washed cells previously grown on acetate. The most striking feature in these results compared with those obtained in a previous study is the absence of any specific inhibiting effect on the pyruvate

Table 2. Influence of benzoic and salicylic acids on the extent and rate of pyruvate and acetate oxidation by washed *P. vulgaris* cells previously grown in medium B. The experiments were similar to those in Figs. 4 and 5.

Substrate	Benzoate experiments			Salicylate experiments			
	Moles of oxygen consumed per mole substrate (4 experiments)		Benzoate conc. giving 50 % inhibition of oxidation rate, mM	Moles of oxygen consumed per mole substrate (2 experiments)			Salicylate conc. giving 50 % inhibition of oxidation rate, mM
	No inhibitor	8 mM benzoate		No inhibitor	0.4mM salicylate	4 mM salicylate	
Pyruvate	1.00	1.60	15	1.10	—	1.70	4
Acetate	1.25	1.60	10	1.25	1.35	—	0.4

oxidation at the oxidation level of acetate in the presence of benzoic or salicylic acid. On the contrary these acids considerably increase the *total amount* of oxygen consumed per mole of substrate. The magnitude of this increase is shown in Table 2 together with the approximate concentrations at which the two acids produced 50 % reduction in the *rate* of oxygen consumption. These figures show that the rate of acetate oxidation by washed cells grown in medium B is much more sensitive to salicylic acid than is that of pyruvate oxidation. The difference is also apparent from the experiment illustrated in Fig. 5 where 2 mM salicylic acid produced no demonstrable effect on the rate of pyruvate oxidation, whereas half this concentration caused 90 % inhibition of the rate of acetate oxidation. The influence of salicylic acid on the amount of oxygen consumed per mole of acetate could thus be studied only at rather low concentrations. At these concentrations no significant increase was observed.

The above effects of benzoic acid on the pyruvate and acetate oxidations were further studied in some experiments in which ammonium ions were added to the cell suspension simultaneously with the substrate. The presence of ammonium ions caused the oxygen consumption per mole pyruvate to decrease in the presence of benzoic acid and to increase in the absence of inhibitor (Fig. 6). A similar tendency, though less marked, was also noticed in some experiments with acetate.

The results suggested an enhanced release of CO_2 from pyruvate and acetate in the presence of benzoic acid and from pyruvate in the case of salicylic acid. This was demonstrated more directly by actual measurement of CO_2 production and furthermore in experiments with labelled acetate, which were carried out in Warburg vessels in the same way as those with unlabelled substrates. The total amount of radioactivity in cells, medium and respiratory CO_2 after oxidation of the same amounts of methyl and carboxyl labelled acetate was measured in the way described in the experimental part. Table 3

Table 3. Effect of benzoic acid on radioactivity of CO_2, medium and cells after oxidation of methyl and carboxyl labelled acetate by *P. vulgaris*.

Fraction	$^{14}CH_3COOH$ experiment Distribution of radioactivity in per cent of total		$CH_3{}^{14}COOH$ experiment Distribution of radioactivity in per cent of total	
	No inhibitor	With 6 mM benzoate	No inhibitor	With 6 mM benzoate
Respiratory CO_2	48	75	76	81
Medium	42	16	14	11
Cells	10	9	10	8

shows the result of a typical experiment with washed cells harvested from an actively growing culture in medium B. From the values of the distribution of radioactivity recorded in this table it can be calculated that the amount of CO_2 evolved per mole of acetate increased from 1.24 to 1.56 in the presence of benzoic acid. These values are in excellent agreement with those obtained by direct measurement of the CO_2 evolved. Such measurements, performed in separate experiments, showed that the molar amount of CO_2 evolved per mole of acetate increased from 1.25 in the absence to 1.60 in the presence of benzoic acid. It is noteworthy that the additional CO_2 production caused by benzoic acid originates almost entirely from the methyl group of the acetate molecule, and that the incorporation of both the methyl and carboxyl carbon in the cells is almost uneffected by benzoic acid.

Table 4 shows the distribution of methyl carbon in cells, media and respiratory CO_2 after acetate oxidation with and without addition of ammonium ions and the effect of benzoic acid on this distribution. In the absence of ammonium ions the quantitative values differ somewhat from those in Table 3, but the tendency is the same. Addition of ammonium ions resulted in increased incorporation of carbon in the cell, both in the presence and in the absence of benzoic acid. However, this increase was somewhat larger when the oxidation

Table 4. Effect of benzoic acid on radioactivity of CO_2, medium and cells after oxidation of methyl labelled acetate by *P. vulgaris* in presence and absence of ammonium ions.

Fraction	$^{14}CH_3COOH$ experiment Acetate oxidation in absence of ammonium ions Distribution of radioactivity in per cent of total		$^{14}CH_3COOH$ experiment Acetate oxidation in presence of ammonium ions Distribution of radioactivity in per cent of total	
	No inhibitor	With 6 mM benzoate	No inhibitor	With 6 mM benzoate
Respiratory CO_2	54	71	47	63
Medium	29	14	21	14
Cells	17	15	32	23

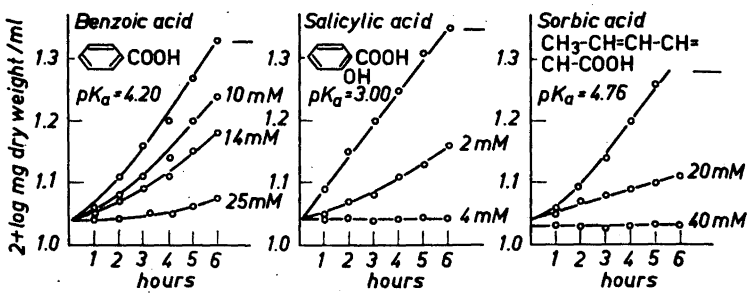

Fig. 7. Effect of benzoic, salicylic and sorbic acids on growth of *P. vulgaris* in medium B. Inhibitor concentrations as indicated. The experiments were performed at 30—35°C in aerated Kluyver flasks.

proceeded without inhibitor and the additional amount incorporated in this case was balanced by a decrease in the radioactivity of the medium.

Growth experiments with acetate adapted cells. * The results set forth above prompted investigations of the effect of benzoic and salicylic acids on the growth of *P. vulgaris* in medium B, in which all cell material must be synthesized from the acetyl group. Unfortunately these experiments had to be carried out at neutral pH values, at which the effect of benzoic and salicylic acids is rather low, since, as mentioned, the adapted strain did not grow rapidly in the acetate medium at pH values lower than 6.5. The experimental arrangement consisted of a battery of equally aerated Kluyver flasks containing 400 ml of the acetate medium at pH 7.0. The flasks were inoculated with adapted cells in the presence of varying amounts of inhibitor and the growth was followed turbidimetrically. Readings were taken continually for the first seven hours during which the pH rose from 7.0 to 7.3 in the absence of inhibitor. As might be expected from the experiments on acetate oxidation with adapted cells reported above, in acetate medium salicylic acid proved to be a much stronger inhibitor than benzoic acid. In this connection it was considered worthwhile to test the efficiency of some aliphatic fatty acid with growth inhibiting effect in the simple acetate medium under investigation. For this reason some experiments with sorbic acid were performed. As shown in Fig. 7, benzoic acid and sorbic acid seemed to be equally strong inhibitors, at least when compared without considering the difference in the dissociation constants, while salicylic acid proved much stronger.

In another series of experiments the effect of benzoic acid was studied on growth in medium A inoculated either with washed cells previously grown in this medium or with washed cells adapted to medium B. Since adaptation to acetate medium had strongly improved the ability of the cells to oxidize acetate in the presence of benzoic acid, it was tempting to imagine that the growth of such cells might be less sensitive to this inhibitor than the growth of unadapted cells, but no such difference could be demonstrated.

* This investigation was carried out in close collaboration with Miss Inger Erichsen, Swedish Institute for Food Preservation Research, who actually performed most of the experiments. For this valuable help I am greatly indebted.

The effect of benzoic and salicylic acids on pyruvate dismutation in extracts from E. coli. The preparation of extracts from *E. coli* and *Streptococcus faecalis* catalyzing the dismutation of 2 molecules of pyruvate to acetyl phosphate, carbon dioxide, and lactate in the presence of ortho-phosphate was described by Korkes *et al.* [3] The soluble enzyme system involved in this process seemed to be suitable for further investigation of the effect of benzoic and salicylic acids on pyruvate and acetate oxidation. The first preparations were made from cells of the *P. vulgaris* strain used in this investigation and resulted in extracts with much lower activity than those obtained by Korkes *et al.* from *E. coli.* However, since experiments (to be published) with resting cells of *E. coli*, similar to those with *P. vulgaris* previously reported, showed essentially the same effects of benzoic and salicylic acids on this organism, the present experiments on pyruvate dismutation could be performed equally well on extracts from *E. coli.* On the whole, there seems to be great similarities between the pyruvate metabolism in *E. coli* and in *P. vulgaris* (Razzell and Gunsalus [7]). The extracts were prepared in the way described above and assayed for activity in the system proposed by Korkes *et al.* The activity of our preparations ranged between 230 and 260 units per ml of dialyzed extract (1 unit = 1.0 mm^3 of CO_2 per hour at pH 6.0 and 25°C), compared with 270 units for that of Korkes *et al.* The influence of benzoic and salicylic acids on the evolution of CO_2 and the formation of acetyl phosphate during pyruvate dismutation was studied at pH 6.0. The enzyme activity at this pH was only about 60 % of that obtained at pH 7.4, but the lower pH was nevertheless preferred because of the known increase of metabolic activity of weak acids with decreasing pH.

Table 5 shows the influence of rather large amounts of benzoic and salicylic acids on pyruvate dismutation in cell free extracts. It is evident that the effect is weak, especially since the bacterial cell membrane usually believed

Table 5. Effect of benzoic and salicylic acids on pyruvate dismutation in cell free extracts of *E. coli.*

Additions of inhibitor	μmoles of CO_2 formed a	μmoles of acetyl phosphate formed b	b/a
—	4.54	1.58	0.35
3.5 mM benzoate	3.89	1.42	0.36
7.0 mM benzoate	3.33	1.33	0.40
14.0 mM benzoate	3.22	1.15	0.36
3.5 mM salicylate	3.34	1.49	0.45
7.0 mM salicylate	2.28	1.49	0.65
14.0 mM salicylate	2.31	1.85	0.80

Each vessel contained: 500 μl dialyzed extract, 50 μmoles of potassium phosphate, 2.4 μmoles of $MgCl_2$, 1.6 μmoles of $MnCl_2$, 0.1 μmoles of DPT, 50 μg of CoA, 0.15 μmoles of DPN and 2 μl of lactic dehydrogenase in the main compartment and 50 μmoles of sodium pyruvate together with the inhibitor in the side arm. Final volume 1.22 ml. Temp. 30°C; pH 6.0; gas phase, nitrogen. CO_2 evolution was measured 20 and 40 min after addition of pyruvate and inhibitor to the enzyme extract.

to prevent penetration of the inhibitors studied had been removed. The evolution of CO_2 from pyruvate in nitrogen atmosphere with intact cells at pH 6.0 is much more sensitive to benzoic and salicylic acids as revealed by experiments (not shown here) with washed cells identical with those from which the extracts were prepared. It is further clear from Table 5 that benzoic acid had no influence on the amount of acetyl phosphate formed per mole of CO_2 produced. On the other hand, salicylic acid seemed to increase this value. This effect was not further investigated because of the relatively high concentrations of inhibitor required.

Experiments with acetyl phosphate and intact cells. The sensitivity of acetate oxidation (at least by intact cells) to benzoic and salicylic acids and the protective effect of small amounts of succinate suggested that the inhibition might be overcome by simultaneous energy producing reactions. With this in mind, acetyl phosphate, in itself an energy-rich compound, should be a better starting point for acetate oxidation than the acetate molecule. However, when acetyl phosphate was added to intact cells of *P. vulgaris* or baker's yeast, the rate of oxygen consumption was very slow. Parallel experiments showed that the oxygen consumed could be ascribed to oxidation of acetate after chemical decomposition of the acetyl phosphate added.

DISCUSSION

Addition of acetate to a suspension of washed *Proteus vulgaris* cells in phosphate buffer is followed by increased oxygen consumption due to oxidation of the acetate. The rate of this oxygen consumption is determined by the pre-history of the cells. In the present work the influence of three factors in this pre-history on the acetate oxidizing ability has, to some extent, been investigated: 1. the composition of the growth medium employed in cultivating the cells, 2. aeration during growth, and 3. the physiological age of the cells at the time of harvesting. It is important to note that the term "acetate oxidizing ability" used above, refers to the rate of the oxygen consumption following the addition of acetate to cells isolated from the growth medium by centrifugation and washing. A survey of the experiments discussed is shown in Table 6.

This investigation shows that the rate of acetate oxidation by washed *P. vulgaris* cells varies considerably with the conditions prevailing during cultivation of the cells. The ability to oxidize acetate, at least by cells grown in a glucose-casein hydrolysate medium (medium A), thus seems to be dependent upon aeration during growth. When such a medium is inoculated with a small amount of cells and aerated, a lag phase occurs before growth begins. It is possible that the ability to oxidize acetate at any appreciable rate is acquired during this period. If large inocula are used, the lag phase is almost completely abolished and no acetate oxidizing power seems to be acquired, at least not by the first generation (Table 6:II).

The rate of acetate oxidation by washed cells previously grown in medium A decrease steadily with increasing age of the cells at the time of harvesting and becomes insignificant after some hours in the stationary phase (Table

Table 6. Summary of the effects of benzoic and salicylic acids on acetate and pyruvate oxidation by washed *P. vulgaris* cells.

		I	II	III	IV
Pre-history of the cells used in the respiration studies	Cultivation	Growth in medium A. No aeration. ↓	Growth in medium A. No aeration ↓ Transfer of the washed cells to fresh medium A and aeration during the time required for the cell material to double ↓	Growth in medium A. Aeration started immediately after inoculation. ↓	Growth in medium B without aeration for 24—48 h ↓ Growth in medium B with aeration. ↓
	Harvesting and washing.	Harvesting in the stationary phase. Washing once in phosphate buffer.	Harvesting in the logarithmic growth phase. Washing once in phosphate buffer.	Harvesting at different ages of the cultures. Washing once in phosphate buffer. Increasing age of the culture →	Harvesting in the logarithmic growth phase. Washing once in phosphate buffer.
Results of the respiration studies.	Qo_2 after addition of acetate (Table 1).	0	0	30 22 17 8 1.5	125
	Qo_2 after addition of acetate + small amounts of succinate (Table 1)	0	0	34 31 29 26 15	125
	Influence of benzoic acid on the oxidation of acetate.	—	—	Strong inhibition, partly abolished by small amounts of succinate.	The rate reduced to 50% by 10 mM benzoic acid. Increased total substrate breakdown.
	Influence of benzoic acid on the oxidation of pyruvate.	—	—	Specific inhibition at the oxidation level of acetate (Bosund [1]).	The rate reduced to 50% by 15 mM benzoic acid. Increased total substrate breakdown.
	Influence of salicylic acid on the oxidation of acetate	—	—	Strong inhibition, largely unaffected by succinate addition.	The rate reduced to 50% by 0.4 mM salicylic acid. No increase in total substrate breakdown at this concentration.
	Influence of salicylic acid on the oxidation of pyruvate.	—	—	Specific inhibition at the oxidation level of acetate (Bosund [1]).	The rate reduced to 50% by 4 mM salicylic acid. Increased total substrate breakdown.

6:III and Table 1). If the cultures are not too old when harvested, most of the activity can, however, be restored by adding a small amount of succinate together with the acetate in the respiration experiments. This seems to indicate that the decreasing oxidation rate is due either to lack of Krebs cycle intermediates or to a low level of energy-rich compounds in the cells. The latter explanation would be consistent with the marked increase in the rate of acetate oxidation observed after addition of succinate in the presence of benzoic acid if, as suggested in the first part of this series, this inhibitor interferes with the ATP-generated acetate activation. The absence of an equally marked effect in the case of salicylic acid may be due to the specific uncoupling of oxidative phosphorylation produced by this acid [8].

So far, only experiments with cells cultivated in medium A have been discussed. In such a fairly rich medium much of the energy requirements for growth can be met by ATP-generation at the substrate level. In medium B where acetate is the sole carbon source oxidative phosphorylation is of prime importance especially since the acetate molecule must be activated in an ATP-requiring process before it can be metabolized. It is therefore highly probable that the enzyme systems involved both in the acetate activation and in the generation of ATP from the acetate oxidation exist in larger amounts in cells grown in medium B than in cells grown in medium A. It may further be assumed that cells grown in medium B contain only small amounts of the acetate generating pyruvate oxidase (Stumpf [9], Moyed and O'Kane [10]), which significance in relation to the results previously obtained with cells grown in medium A was discussed in the first paper of this series.

It is consistent with this view that the characteristic feature of the action of benzoic and salicylic acids on cells grown in the glucose-casein hydrolysate medium, *i.e.* the blocking of pyruvate oxidation at the oxidation level of acetate, is not observed in experiments with cells grown in the acetate medium. Furthermore, the sensitivity of acetate oxidation to benzoic acid when the acetate is added directly as substrate is similarly less in experiments with cells grown in the acetate medium (the concentration of benzoic acid required for complete inhibition is increased 4—5 fold). It is noteworthy that this is true only with benzoic acid; salicylic acid in a concentration of 1—2 mM completely inhibits acetate oxidation by both kinds of cells although, as mentioned above, the blocking of pyruvate oxidation at the oxidation level of acetate is abolished, even in this case, by growing the cells in the acetate medium.

The most characteristic effect of benzoic and salicylic acids on acetate-adapted cells is the increased substrate breakdown induced in the presence of these acids. A stimulation of oxygen consumption and CO_2 production is generally observed in the presence of substances impairing the formation of energy-rich compounds and such an effect by salicylic acid agrees with the action of this substance on oxidative phosphorylation [8]. The similarity between the effects of benzoic and salicylic acids in the present experiments is noteworthy, though the inhibition of oxidative phosphorylation by benzoic acid is weak, at least in experiments with rat liver mitochondria [11].

Salicylate has for some years been known [12, 13] to produce effects on carbohydrate metabolism in the rat, which agrees well with the present find-

ings. In recent experiments with salicylate [14] an increased output of total CO_2 and $^{14}CO_2$ was observed in rats given acetate-2-^{14}C and a corresponding inhibition of isotope incorporation into liver glycogen and liver fatty acids.

The increase in the output of CO_2 from acetate observed in the presence of benzoic acid was further investigated in respiration studies with labelled acetate (Tables 3 and 4). These studies confirm the results obtained in the experiments in which the CO_2 evolution was actually measured and indicate that the increase in CO_2 production induced by benzoic acid is derived mainly from the methyl group of the acetate molecule. When acetate is oxidized in absence of inhibitor, a corresponding amount of methyl carbon accumulates in the medium. The incorporation of ^{14}C-compounds into the cells is largely uninfluenced by benzoic acid. The results could tentatively be explained by assuming that a keto acid, derived mainly from the methyl group of the original acetate molecule accumulates in the medium in the absence of benzoic acid. If the acetate oxidation occurs in the presence of ammonium ions, as in the experiment showed in Table 4, such a keto acid may be incorporated in the cell material after conversion to the corresponding amino acid. Further research is, however, necessary before any valid interpretation can be made on this point.

Acknowledgements. This work is part of an investigation supported by the *Swedish Natural Science Research Council* and the *Swedish Technical Research Council.*

I am greatly indebted to Professor G. Lindeberg, Agricultural College of Norway, Vollebekk, Norway, and to Professor E. Adler, Chalmers University of Technology, Gothenburg, Sweden, for continued and encouraging interest in this work. I also wish to express my sincere gratitude to Professor G. Ehrensvärd and his collaborators at the Institute of Biochemistry, Lund, Sweden, for stimulating discussions and valuable help with the isotope technique.

REFERENCES

1. Bosund, I. *Acta Chem. Scand.* **13** (1959) 803.
2. van Slyke, D. D. and Folch, J. *J. Biol. Chem.* **136** (1940) 509.
3. Korkes, S., del Campillo, A., Gunsalus, I. C. and Ochoa, S. *J. Biol. Chem.* **193** (1951) 721.
4. Stadtman, E. R. and Lipmann, F. *J. Biol. Chem.* **185** (1950) 549.
5. Dagley, S., Dawes, E. A. and Morrison, G. A. *J. Gen. Microbiol.* **4** (1950) 437.
6. Lwoff, A. and Monod, J. *Ann. Inst. Pasteur* **73** (1947) 323.
7. Razzell, W. E. and Gunsalus, I. C. *Bacteriol. Proc.* **1954** 97.
8. Penniall, R., Kalnitsky, G. and Routh, J. I. *Arch. Biochem. Biophys.* **64** (1956) 390.
9. Stumpf, P. K. *J. Biol. Chem.* **159** (1945) 529.
10. Moyed, H. S. and O'Kane, D. J. *J. Biol. Chem.* **218** (1956) 831.
11. Bosund, I. *Acta Chem. Scand.* **11** (1957) 541.
12. Lutwak-Mann, C. *Bioehem. J.* **36** (1942) 706.
13. Smith, M. J. H. *Biochem. J.* **59** (1955) 52.
14. Smith, M. J. H. *J. Biol. Chem.* **234** (1959) 144.

Received September 2, 1959.

ACTA CHEMICA SCANDINAVICA 14 (1960) 126–150

Studies on the Hydrolysis of Metal Ions

25. The Hydrolysis of Lead(II) in Perchlorate Medium

ÅKE OLIN

Department of inorganic chemistry, the Royal Institute of Technology, Stockholm 70, Sweden

The hydrolysis of lead(II) has been studied at 25°C by the inert medium method using 3 M or 0.3 M $(Na)ClO_4$ and the cells

– Pb-Hg / S / ref. +
– glass / S / ref. +

S had the general composition
B M Pb(II), H M H^+, $(I-2B-H)$ M Na^+, I M ClO_4^-

The experimental data Z (average number of OH^- bound per lead (II)) and η (log $[Pb(II)]_{tot}$ / $[Pb^{2+}]_{free}$) as functions of log h can be explained by the following reactions and equilibrium constants.

		Equilibrium constants	
		3 M $(Na)ClO_4$	0.3 M $(Na)ClO_4$
$Pb^{2+} + H_2O \rightleftharpoons PbOH^+ + H^+$	$\log \beta_{11}$	-7.9 ± 0.1	-7.8 ± 0.1
$4Pb^{2+} + 4H_2O \rightleftharpoons Pb_4(OH)_4^{4+} + 4H^+$	$\log \beta_{4,4}$	-19.25 ± 0.1	-19.90 ± 0.1
$3Pb^{2+} + 4H_2O \rightleftharpoons Pb_3(OH)_4^{2+} + 4H^+$	$\log \beta_{4,3}$	-22.87 ± 0.1	-23.35 ± 0.1
$6Pb^{2+} + 8H_2O \rightleftharpoons Pb_6(OH)_8^{4+} + 8H^+$	$\log \beta_{8,6}$	-42.14 ± 0.1	-42.66 ± 0.1

SURVEY OF PREVIOUS WORK

The two most complete investigations on the hydrolysis of Pb(II) hitherto published are those of Pedersen [1] and Faucherre [2]. Pedersen carried out potentiometric titrations of $Pb(NO_3)_2$ solutions to which NaOH was added and log h followed with a glass electrode. The experimental data could be explained by the formation of the complexes Pb_2OH^{3+}, $PbOH^+$ and $Pb_4(OH)_4^{4+}$. However, the nitrate is not very suitable for this type of investigation since the basic lead nitrates have so low solubility that only one percent of the total Pb(II) was hydrolysed before precipitation started.

This led Faucherre to study lead(II) perchlorate solutions instead, which allow the addition of 4/3 OH^- per Pb(II) before precipitation starts. Potentiometric titrations, where NaOH was added and log h followed with a glass

electrode, were interpreted as follows. In solutions where less than one OH^- per lead(II) had been added the complex $Pb_4(OH)_4^{4+}$ was formed. On further addition of alkali the complex $Pb_9(OH)_{12}^{6+}$ started to form. When 4/3 OH^- per lead(II) had been added precipitation started. Spectrophotometric and cryoscopic measurements on solutions containing less than one OH^- per lead(II) indicated the complex $Pb_4(OH)_4^{4+}$ also. Faucherre followed the change in log h of $Pb(NO_3)_2$ solutions upon dilution. These measurements also indicated the complex $Pb_4(OH)_4^{4+}$. In addition $PbOH^+$ was indicated in dilute solutions.

Most of the other previous works on the hydrolysis of Pb(II) have been done with so called pure salt solutions, notably with solutions of $Pb(NO_3)_2$. Kullgren [3] measured the acidity of $Pb(NO_3)_2$ kinetically at 100°C and 85.5°C. He could explain his data by the reaction $Pb^{2+} + H_2O \rightleftharpoons PbOH^+ + H^+$ ($\beta_{11} = 1.02 \times 10^{-6}$). Denham and Marris [4] measured the acidity of $Pb(NO_3)_2$ and $PbCl_2$ solutions with the quinhydrone electrode but did not attempt to explain their findings in terms of a hydrolysis reaction. Cranston and Brown [5] made similar experiments with the glass electrode and assuming only the first mononuclear step, calculated from their data $\beta_{11} = 1.7 \times 10^{-8}$ at 15°C and from the earlier data by Denham and Marris $\beta_{11} = 3.8 \times 10^{-8}$ at 25°C. Guiter [6] followed colorimetrically the change of log h in a $Pb(NO_3)_2$ solution on dilution. He suggested that the ions $Pb_2(OH)_2^{2+}$, $PbOH^+$ and their nitrato complexes were formed, but apparently some of his results contradict the law of mass action.

Reiff and Müller [7] suggested the complex $Pb_2(OH)_2^{2+}$. Their measurements of the concentration of Pb^{2+} by lead amalgam in solutions of analytical composition $PbOHClO_4$ showed that $[Pb^{2+}]$ was not negligibly small. Therefore they suggested that the complex was partly dissociated to Pb^{2+}, $PbOH^+$ and $Pb(OH)_2$. From a study of the solubility of $Pb(IO_3)_2$ in $HClO_4$-$NaClO_4$ mixtures and PbO in $HClO_4$, Misra and Pani [8] and Pattanaik and Pani [9] claimed the existence of $PbOH^+$. They interpreted the increase of the solubility of the iodate with increasing acidity as due to the formation of $PbOH^+$ which contradicts the law of mass action; a more reasonable explanation is the formation of undissociated iodic acid. See also Ref. [10] where the increase of the solubility of $Cu(IO_3)_2$ with acidity was used to determine the dissociation constant for iodic acid. The fact that they were able to dissolve PbO in $HClO_4$ in a 1:1 ratio is not very convincing evidence for the formation of $PbOH^+$ since any species $(PbOH^+)_n$ would give the same result. The formation of $PbOH^+$ and $Pb(OH)_2$ has been suggested by Goward [11] from polarographic measurements.

Finally we might cite a report on ultracentrifuge work on lead perchlorate solutions by Johnson and Kraus [12]. "Preliminary ultracentrifugation studies of Pb(II) in perchlorate solution indicate that low-molecular weight polymers are formed in the range of hydrolysis studied, between hydroxyl numbers (n) about 0.5 and 1.4. Interpretation by a simple monomer-tetramer equilibrium does not seem adequate, however, since degrees of polymerization higher than 4 are found for $n = 1.4$. Near $n = 1$ the weight average degree of polymerization is about 4, but existence of a predominant tetrameric species has not yet been established".

From the above survey we might conclude that there is good evidence for the complexes $PbOH^+$ and $Pb_4(OH)_4^{4+}$ but comparatively little quantitative work has been done on solutions with a $OH^-/Pb(II)$ ratio > 1. The electrometric measurements have been done almost exclusively with log h-sensitive electrodes. It was therefore considered worthwhile to reinvestigate the hydrolysis of Pb(II) in perchlorate solution using both the glass electrode and the amalgam electrode.

SYMBOLS

The commoner symbols used in the text are defined below for reference.

B total Pb(II) concentration
b concentration of Pb^{2+}
H analytical hydrogen ion concentration
h actual hydrogen ion concentration
Z average number of hydrogen ions split off by one Pb(II)
ν average number of OH^- groups bound to one Pb(II) in a complex (5)
η log B/b
$\beta_{p,q}$ formation constant of $Pb_q(OH)_p^{(2q-p)+}$ from Pb^{2+} and H_2O.

$$q\ Pb^{2+} + p H_2O \rightleftharpoons Pb_q(OH)_p^{(2q-p)+} + p H^+$$

$$BZ = h - H = \Sigma\, p\beta_{p,q}\, b^q h^{-p}$$

$$10\eta = 1 + \Sigma\, q\beta_{p,q}\, b^{q-1} h^{-p}$$

$y(x)_v$ y as a function of x at constant v

Other symbols used are defined where they appear in the text. All concentrations in tables and figures are expressed in M (moles/l) and equilibrium constants are given on the M scale. In the text, however, the more convenient unit mM will be used frequently.

In the following we shall describe in detail only the experiments done with 3 M $(Na)ClO_4$ as medium and their interpretation. The interpretation of the data with 0.3 M $(Na)ClO_4$ will be discussed briefly at the end of the chapter dealing with the calculations on the 3 M $(Na)ClO_4$ data.

METHOD OF INVESTIGATION

The experiments have been carried out as potentiometric titrations. The analytical hydrogen ion concentration of lead(II) perchlorate solutions with 3 M $(Na)ClO_4$ as the ionic medium was varied by adding sodium hydroxide or perchloric acid. The total lead concentration, B, was kept constant in each run and the hydrogen ion concentration, h, and the concentration of Pb^{2+}, b, were measured with the cells

— glass/equilibrium solution/ ref. + (I)

$$E = E_g^\circ - 59.15 \log h - E_j \quad (1)$$

— Pb-Hg/equilibrium solution/ ref. + (II)

$$E = E_{am}^\circ - 29.58 \log b - E_j \quad (2)$$

Eqns. (1) and (2) have been written on the assumption that the activity factors keep constant so that they may be included as constants in the E°'s. However, this is only approximately correct since E°_{am} is not independent of the total lead concentration, B, for B larger than 10 mM. The change in E°_{am} when b was lowered from 80 mM to 5 mM was -0.3 mV but from 5 mM down to 0.5 mM no further change in E°_{am} was observed. No similar trend in E°_{g} was noted. This may be due to the fact that E°_{g} cannot be determined with sufficient accuracy (± 0.2 mV). A thorough investigation of these changes in the activity factors has been omitted deliberately since such an investigation by G. Biedermann is now under way at this Institute.

The composition of the solutions measured can be written

$$[\mathrm{Pb(II)}] = B \text{ M}, [\mathrm{H^+}] = H \text{ M}, [\mathrm{Na^+}] = (3-2B-H) \text{ M}, [\mathrm{ClO_4^-}] = 3 \text{ M}$$

where H is the analytical hydrogen ion concentration. In the present case H is usually a negative number, so that the solutions are deficient in hydrogen ions.

Apparatus

The measurements were performed in an oil thermostat at 25° ± 0.1°C using the salt bridge described by Forsling, Hietanen and Sillén [13]. The reference half-cell was

$$3 \text{ M } \mathrm{NaClO_4}/3 \text{ M } \mathrm{ClO_4^-}, 2.99 \text{ M } \mathrm{Na^+}, 0.01 \text{ M } \mathrm{Ag^+}/\mathrm{AgCl}, \mathrm{Ag} \qquad \text{(III)}$$

Much trouble was experienced before we found a glass electrode which could be used without too large corrections in the log h range (-2 to -8.5) studied. The glass electrodes were tested against the hydrogen electrode in a series of buffers made up by gradually adding NaOH in 3 M $\mathrm{NaClO_4}$ to a solution, S, containing 0.005 M $\mathrm{HClO_4}$, 0.005 M HAc, 0.005 M $\mathrm{H_3PO_4}$, 0.005 M $\mathrm{H_3BO_3}$, 3 M $\mathrm{NaClO_4}$. The emfs of the cells

$$-\ \mathrm{Pt}/\mathrm{H_2}/\mathrm{S}/\ \mathrm{ref}\ +\ (E_H) \qquad \text{(IV)}$$

$$-\ \mathrm{glass}\ /\mathrm{S}/\ \mathrm{ref}\ +\ (E_g) \qquad \text{(V)}$$

were measured. Actually the glass and $\mathrm{H_2}$ electrodes were kept in the same solution. The difference $\Delta E = E_H - E_g$ was thus obtained for different log h values, which were calculated from E_g and eqn. (1) using an E°_{g} determined with mixtures of $\mathrm{HClO_4}$ and 3 M (Na)$\mathrm{ClO_4}$. The glass electrode finally selected for the measurements was a Beckman electrode (No. 1190—808) which gave a constant ΔE down to log $h \simeq -7.5$, thus behaving like a hydrogen electrode. From log $h \simeq -7.5$ to -8.5 ΔE gradually increased and the corresponding change in ΔE was applied as a correction to the glass electrode. The largest correction (at log $h = -8.5$) was + 0.5 mV.

The emf of cell (I) was recorded to ± 0.2 mV on a Radiometer valve potentiometer (PHM4). The amalgam emf was measured to ± 0.01 mV by a Cambridge potentiometer.

Experimental details of the emf measurements and titration procedure

The liquid junction potential, E_j, and an estimate of the beginning of the hydrolysis of Pb(II) was obtained in a titration, where standard NaOH was added to a solution containing 10 mM Pb^{2+} and 100 mM $HClO_4$ in 3 M $(Na)ClO_4$. Treating the data as an ordinary acid-base titration using Gran's extrapolation method [14] a straight line was obtained almost the whole way down to the equivalence point. This indicates that the hydrolysis of Pb(II) at moderate concentrations is small until an excess of OH^- has been added.

The amalgam and glass electrode potentials were also used to determine E_j by the procedure described by Biedermann and Sillén [15]. The results obtained were in complete agreement with their findings and E_j has been calculated as $-16.7\ h$ mV in subsequent titrations.

E_g^o and E_{am}^o were determined from the potentials in acid solution inserting the analytical concentrations for h and b in eqns. (1) and (2), which is permissible since the hydrolysis is negligible for $H > 2$ mM. For $B > 5$ mM the titrations were started from $H \simeq 20$ mM and the $E^{o\prime}$s calculated from the first points of each titration. This procedure becomes less satisfactory for lower values of B since then most of the alkali added is consumed to neutralize the acid added for the determination of the $E^{o\prime}$s, which is undesirable when Z is to be determined accurately. When B was 5 mM or less the titration was started from the H^+ concentration ($\simeq 0.3\ B$) associated with the lead perchlorate stock solution, NaOH gradually added and the hydrolysis followed till precipitation started. Afterwards a strong perchloric acid solution was introduced to give H values between 5 and 20 mM and E_g^o and E_{am}^o determined from the potentials. In one of the 2.5 mM titrations both methods were used as a check. The values for E_g^o agreed to $\pm$ 0.1 mV and those for E_{am}^o to $\pm$ 0.05 mV which is as good as can be expected.

In general after each addition of alkali the glass and amalgam emfs took about 20 min to attain a constant value. The time increased somewhat as the degree of hydrolysis increased. Also it was somewhat longer at the lowest B (1.25 mM) measured. A local excess of OH^- could not be avoided upon addition of the alkali and a precipitate was formed. The precipitate dissolved rapidly and completely at the beginning of a run but in the most hydrolysed solutions small amounts remained undissolved. This small residue apparently dissolved very slowly, since the potentials remained constant. It may consist of basic lead carbonates formed from the inevitable carbonate content (*ca.* 0.1 % of total OH^-) of the sodium hydroxide.

In general, the titrations had to be discontinued when Z had reached $\simeq 1.3$ since the solutions became permanently turbid owing to the precipitate of basic lead perchlorates. In the 80 and 40 mM titrations, where rather strong alkali had to be used, the amount of precipitate formed was appreciable when Z had reached 1 and the hydrolysis could not be followed further. The lowest B value that could be used satisfactorily was 1.25 mM. When 0.625 mM was tried reproducible values could not be obtained. When the same lead solution was titrated with the same alkali different results were obtained on different

days. The nonreproducibility occured with 0.625 mM Pb(II) only and in hydrolysed solution. In acid solution the agreement between different titrations was still good.

The measurements on $B = 0.625$ mM revealed an impurity in the sodium perchlorate. When the very weak NaOH solution used for this titration was standardized potentiometrically against $HClO_4$, both solutions containing 3 M $(Na)ClO_4$, it was found that the Gran extrapolation was not linear near the equivalence point. The 3 M $(Na)ClO_4$ behaved as if it contained a weak acid (concentration $\simeq 3 \times 10^{-5}$ M). By making the same standardization in 0.3 M $(Na)ClO_4$, it was established that the disturbance was connected with the $NaClO_4$. In this medium the disturbance almost disappeared. The Z measurements in 3 M $(Na)ClO_4$ have been corrected for this buffer capacity of the ionic medium on the assumption that it is a function of log h only and not affected by the presence of lead. With the exception of the last few points of the 1.25 and 2.5 mM titrations the correction is less than 1 % in Z. This impurity was not detected until the measurements in 3 M $(Na)ClO_4$ were almost completed. It was therefore decided to extend the measurements to 0.3 M $(Na)ClO_4$ to avoid the uncertainty in the Z values for small values of B caused by the impurity.

The reversibility of the hydrolysis reactions was tested by carrying out some back titrations. The results from these titrations in general agreed to better than $\pm$ 0.005 in Z and η with those from the forward titrations, thus indicating that true equilibria were measured.

Materials and analysis

Sodium perchlorate was prepared and analysed as described previously [16]. The determination of free, strong acid or base in the product has been somewhat modified. Since the method employed can also be advantageously used to determine the analytical hydrogen ion concentration in solutions of metal salts, which do not hydrolyse too strongly, it may be worth a short description. The following solutions are employed

S_1 Metal salt solution of concentration B M and ionic medium I M
S_2 Metal salt solution of concentration $2B$ M and ionic medium $2I$ M
S_3 Solution containing acid or base of known concentration H M

When the acidity of the ionic medium is determined S_1 and S_2 of course, do not contain the metal salt. To a known volume (V_0) of solution S_1 are added equal volumes (V) of solutions S_2 and S_3, and log h is measured as a function of V. If the acidity of solution S_1 is δ, it is 2 δ in solution S_2, so that the acidity in each point is given by;

$$h = \frac{V_o\delta + 2V\delta + VH}{V_o + 2V} = \delta + \frac{VH}{V_o + 2V} \quad (3)$$

From the measured emf we get;

$$E = E^o + 59.15 \log h + E_j;\ 10^{(E-Ej)/59.15} = h\ 10^{E^o/59.15} = \text{const} \cdot h = \text{const} \cdot \left(\delta + \frac{VH}{V_o + 2V}\right) \quad (4)$$

If we plot $10^{(E-Ej)/59.15}$ as a function of $VH/(V_o + 2V)$ a straight line is obtained which, when extrapolated to $10^{(E-Ej)/59.15} = 0$ gives $-\delta$ on the horizontal axis. The method is a version of the usual Gran extrapolation [14], and a special case of a more general expression derived by Berecki-Biedermann [17].

Perchloric acid solutions were prepared and analysed as described previously [16].

Sodium hydroxide was prepared either from 50 % NaOH by dilution or by the method described by Han and Chao [18] adding $Ba(OH)_2$. No difference was observed between titrations carried out with NaOH prepared in either way. Base solutions stronger than *ca.*

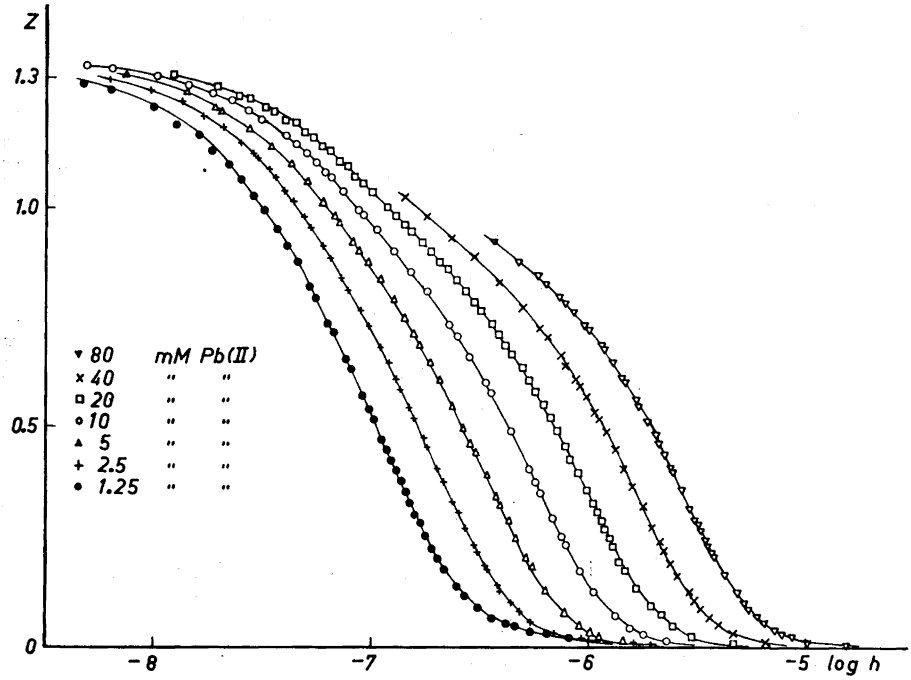

Fig. 1. Average number, Z, of OH^- bound per Pb(II) as a function of log h with 3 M $(Na)ClO_4$ as medium. The curves are calculated with the equilibrium constants given in the text.

25 mM were standardized visually against standard acid. Less strong solutions were standardized potentiometrically using Gran's method to determine the end point.

Lead (II) perchlorate solutions were prepared from two different lead sources. One solution was prepared from PbO (Baker p.a.) which was dissolved in perchloric acid and small amounts of tetravalent lead present in the oxide destroyed by H_2O_2. The other solution was prepared from lead metal (Merck silberfrei) which was dissolved in nitric acid and the nitric acid dispelled by fuming with perchloric acid. Due to the very great solubility of lead perchlorate, this salt could not be satisfactorily recrystallised from water but had to be used without further purification. The Z and η data obtained from solutions made up from the two stock solutions were consistent which would indicate that no impurities were present. Lead was determined as lead sulfate [19] or as lead iodate [20]. Both methods gave the same results to ± 0.1 %. The analytical hydrogen ion concentration was determined potentiometrically using a Gran extrapolation to obtain the equivalence point.

Lead amalgam was prepared by dissolving lead metal (Merck silberfrei) in mercury. The amalgam was stored under 25 mM $HClO_4$ in a N_2 atmosphere and the lead concentration in the amalgam was *ca.* 0.7 % (weight).

RESULTS AND CALCULATIONS

The experimental data are presented in Figs 1, 2, 3 and 4 and in Tables 1 and 2 giving Z and η as functions of log h and B. $Z = (h-H)/B$, *i. e.* the average number of OH^- groups bound per lead(II), and $\eta = \log B/b$.

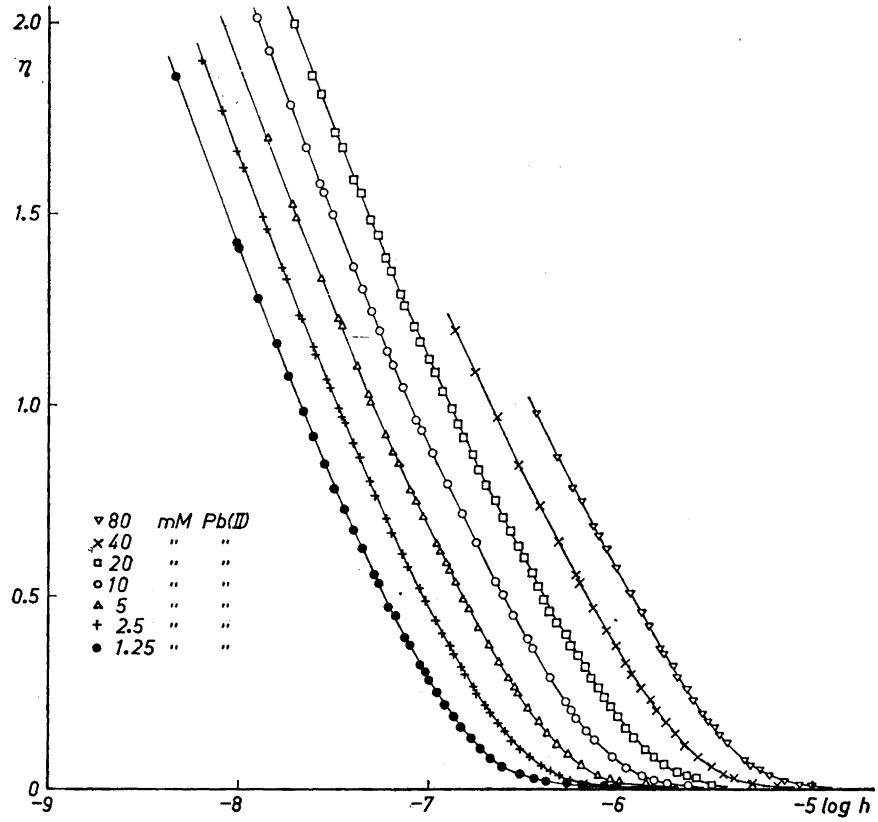

Fig. 2. η = log B/b as a function of log h with 3 M (Na)ClO_4 as medium. The curves are calculated with the equilibrium constants given in the text.

In those earlier studies, published from this Institute, where it has been possible to determine experimentally both η and Z, these have been treated separately to find the formulas of the hydrolysis products and their formation constants (see for example Ref. [21]). The fact that the two sets of data have given the same results may be taken as additional evidence for the correctness of the hydrolysis mechanism proposed.

With lead(II), such a procedure certainly would give the main complexes formed, but it is somewhat more difficult to establish the minor products with certainty. When deriving the composition of the complexes formed, we shall prefer to combine the two sets of data. This mode of approach greatly simplifies our task, although we lose the double-check of the previous method. As a check on systematic errors in either set of data the equilibrium constants will be determined from the Z and η data separately.

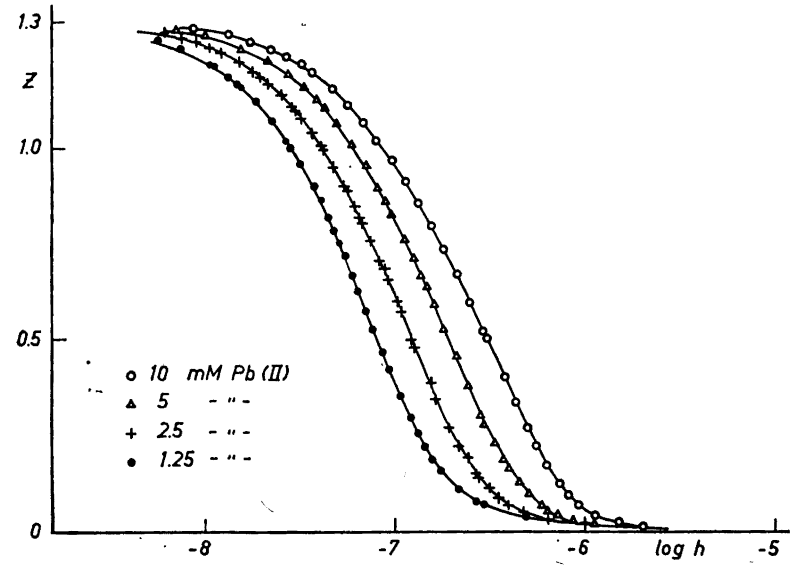

Fig. 3. Z as a function of log h with 0.3 M $(Na)ClO_4$ as medium. The curves are calculated with the equilibrium constants given in the text.

It is apparent that polynuclear complexes are formed since Z and η are functions of both B and log h. It is also apparent that more than one complex is formed. The lower the value of B is, the steeper are the Z and η curves. This would indicate that when B is lowered, complexes with a higher OH^-/Pb(II) ratio are formed at increasingly early stages of the hydrolysis. The limiting value of this ratio is 4/3 as indicated by the $Z_{lim} \simeq 1.3$ and $\lim_{b \to 0} (\Delta\eta/\Delta\log h)_B \simeq -1.3$.

Determination of the products of hydrolysis in the region where $\nu = 1$. By combining the Z and η data we can calculate the number of OH^- groups bound per hydrolysed Pb(II), ν,

$$\nu = \frac{h-H}{B-b} \tag{5}$$

This quantity gives an average value of the ratio OH^-/Pb(II) in the complexes formed. On calculation from Tables 1 and 2, ν is found to have the value 1.00 ± 0.02 in the initial stages of hydrolysis for B values larger than 2.5 mM. After the halt at 1.0, ν steadily increases with -log h and the largest value of ν registered was 1.33.

For the two lowest concentrations, however, the initial ν values showed irregularities indicating that the data from these concentrations are less reliable at small values of Z. Usually ν started from a value of *ca.* 1.2 and then decreased to *ca.* 1.05. Afterwards it steadily increased again in a regular manner. These irregularities are probably connected with the impurity in the $NaClO_4$, since they are less pronounced with 0.3 M $(Na)ClO_4$. But even with this medium the values for the lowest concentrations do not show the

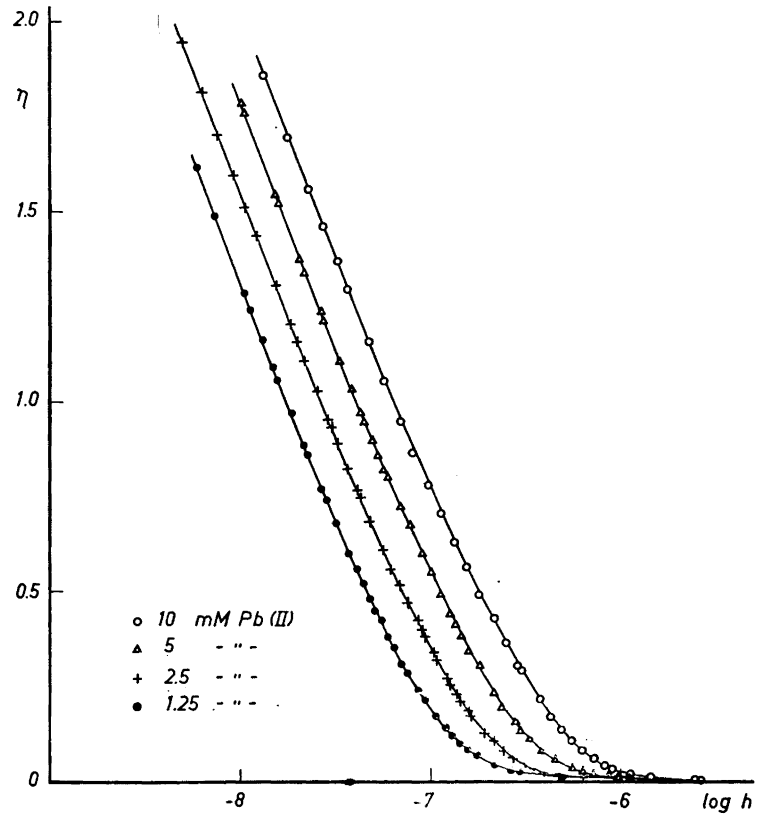

Fig. 4. η as a function of log h with 0.3 M $(Na)ClO_4$ as medium. The curves are calculated with the equilibrium constants given in the text.

regular behaviour of those found for the higher values of B. However, it must be pointed out that ν is very sensitive to experimental errors since H and $(B-b)$ are both obtained as differences between numbers which are about equal in magnitude. It is reasonable to assume that even for the two lowest values of B, complexes with a OH^-/Pb(II) ratio = 1 are formed in the initial stages of hydrolysis.

We shall start with a determination of the formulas of the complexes formed in the region where $\nu = 1$. In this region complexes with the general composition $(PbOH^+)_n$ apparently predominate. However, their range of predominance varies greatly with B. For $B = 80$ mM it extends to $Z \simeq 0.8$. but for $B = 5$ mM ν deviates significantly from 1 when $Z > 0.3$. An inspection of the curves for $B \geq 5$ mM shows that they are parallel and that the spacing along the log h axis

$$\left(\frac{\Delta \log B}{\Delta \log h}\right)_\eta \simeq \left(\frac{\Delta \log B}{\Delta \log h}\right)_z = 1.33 \pm 0.03 \qquad (6)$$

Table 1.

Corresponding values of —log h, Z and η with 3 M $(Na)ClO_4$ medium.

∇ B = 0.080 M: Run I. —log h, Z, η; 4.962, 0.011, 0.0049; 5.108, 0.030, 0.0147; 5.174, 0.050, 0.0238; 5.223, 0.069, 0.0333; 5.260, 0.088, 0.0424; 5.317, 0.125, 0.0617; 5.361, 0.160, 0.0799; 5.422, 0.211, 0.1086; 5.443, 0.228, 0.1174; 5.475, 0.260, 0.1364; 5.507, 0.291, 0.1556; 5.563, 0.351, 0.1935; 5.620, 0.407, 0.2337; 5.674, 0.459, 0.2743; 5.727, 0.509, 0.3169; 5.781, 0.557, 0.3612; 5.836, 0.602, 0.4068; 5.890, 0.644, 0.4552; 5.948, 0.685, 0.5072; 6.007, 0.723, 0.5617; 6.071, 0.760, 0.6201; 6.139, 0.795, 0.6823; 6.207, 0.829, 0.7483; 6.244, 0.845, 0.7834.

Run II. 4.812, 0.004, 0.0025; 4.990, 0.013, 0.0059; 5.059, 0.021, 0.0109; 5.137, 0.037, 0.0184; 5.182, 0.053, 0.0251; 5.221, 0.067, 0.0322; 5.277, 0.096, 0.0461; 5.317, 0.123, 0.0596; 5.351, 0.149, 0.0742; 5.410, 0.196, 0.0992; 5.459, 0.238, 0.1239; 5.495, 0.277, 0.1479; 5.532, 0.312, 0.1692; 5.574, 0.356, 0.1979; 5.615, 0.397, 0.2263; 5.652, 0.436, 0.2557; 5.691, 0.480, 0.2875; 5.770, 0.546, 0.3500; 5.852, 0.612, 0.4190; 5.936, 0.674, 0.4910; 6.022, 0.730, 0.5731; 6.114, 0.784, 0.6573; 6.218, 0.833, 0.7557; 6.330, 0.880, 0.8642; 6.445, 0.924, 0.9798.

$\times$ B = 0.040 M: Run I. —log h, Z, η; 5.182, 0.011, 0.0051; 5.334, 0.031, 0.0145; 5.404, 0.051, 0.0237; 5.453, 0.070, 0.0328; 5.486, 0.088, 0.0419; 5.515, 0.106, 0.0511; 5.541, 0.124, 0.0592; 5.588, 0.157, 0.0761; 5.623, 0.188, 0.0926; 5.656, 0.217, 0.1089; 5.683, 0.246, 0.1251; 5.710, 0.272, 0.1403; 5.760, 0.322, 0.1704; 5.804, 0.366, 0.1998; 5.845, 0.407, 0.2289; 5.890, 0.451, 0.2627; 5.933, 0.493, 0.2968; 5.977, 0.534, 0.3320; 6.019, 0.572, 0.3688; 6.068, 0.609, 0.4077; 6.114, 0.645, 0.4486; 6.208, 0.713, 0.5355; 6.311, 0.755, 0.6308; 6.421, 0.832, 0.7350; 6.533, 0.887, 0.8492; 6.646, 0.936, 0.9672; 6.759, 0.984, 1.0859; 6.864, 1.029, 1.1961.

Run II; 5.160, 0.010, 0.0049; 5.304, 0.025, 0.0122; 5.366, 0.039, 0.0189; 5,443, 0.067, 0.0300; 5.527, 0.117, 0.0554; 5.590, 0.163, 0.0788; 5.637, 0.203, 0.1018; 5.676, 0.240, 0.1224; 5.710, 0.274, 0.1420; 5.759, 0.321, 0.1714; 5.845, 0.408, 0.2309; 5.929, 0.488, 0.2939; 5.967, 0.526, 0.3269; 6.049, 0.598, 0.3966; 6.137, 0.664, 0.4723; 6.227, 0.725, 0.5538; 6.322, 0.783, 0.6437; 6.426, 0.836, 0.7417; 6.529, 0.886, 0.8472; 6.641, 0.934, 0.9567.

$\square$ B = 0.020 M: Run I. —log h, Z, η; 5.333, 0.009, 0.0035; 5.497, 0.023, 0.0096; 5.600, 0.045, 0.0197; 5.656, 0.067, 0.0299; 5.703, 0.088, 0.0400; 5.769, 0.130, 0.0603; 5.821, 0.171, 0.0806; 5.868, 0.210, 0.1015, 5.907, 0.249, 0.1228; 5.943, 0.287, 0.1448; 6.012, 0.358, 0.1901; 6.080, 0.426, 0.2371; 6.147, 0.490, 0.2875; 6.212, 0.551, 0.3426; 6.360, 0.664, 0.4606; 6.497, 0.766, 0.5975; 6.651, 0.859, 0.7506; 6.813, 0.944, 0.9176; 6.971, 1.022, 1.0861; 7.123, 1.094, 1.2594; 7.199, 1.129, 1.3510; 7.278, 1.161, 1.4477; 7.361, 1.193, 1.5569; 7.457, 1.223, 1.6742; 7.571, 1.251, 1.8179, 7.716, 1.279, 2.0015; 7.919, 1.306; 2.2658.

Run II; 5.512, 0.022, 0.0109; 5.606, 0.044, 0.0204; 5.708, 0.087, 0.0404; 5.774, 0.129, 0.0610; 5.825, 0,170, 0.0819; 5.848, 0.190, 0.0924; 5.889, 0.229, 0.1140; 5.929, 0.267, 0.1353; 5.967, 0.304, 0.1580; 5.983, 0.322, 0.1688; 6.051, 0.391, 0.2148; 6.115, 0.456, 0.2631; 6.178, 0.518, 0.3145; 6.245, 0.578, 0.3690; 6.279, 0.606, 0.3984; 6.311, 0.634, 0.4274; 6.384, 0.687, 0.4903; 6.420, 0.712, 0.5231; 6.457, 0.737, 0.5576; 6.528, 0.786, 0.6303; 6.570, 0.810, 0.6681; 6.609, 0.832, 0.7070; 6.690, 0.877, 0.7871; 6.729, 0.898, 0.8270; 6.771, 0.919, 0.8676; 6.847, 0.959, 0.9514; 6.886, 0.979, 0.9930; 6.927, 0.998, 1.0364; 7.001, 1.035, 1.1195; 7.043, 1.053, 1.1627; 7.079, 1.071, 1.2063; 7.155, 1.105, 1.2939; 7.231, 1.139, 1.3852; 7.310, 1.171, 1.4839; 7.397, 1.202, 1.5924; 7.495, 1.230, 1.7165; 7.617, 1.258, 1.8676.

$\circ$ B = 0.010 M: Run I. —log h, Z, η; 5.831, 0.051, 0.0226; 5.963, 0.114, 0.0527; 6.043, 0.176, 0.0828; 6.110, 0.236, 0.1159; 6.171, 0.295, 0.1497; 6.227, 0.352, 0.1865; 6.281, 0.408, 0.2251; 6.369, 0.495, 0.2910, 6.458, 0.578, 0.3640; 6.556, 0.662, 0.4512; 6.648, 0.736, 0.5380; 6.751, 0.811, 0.6394; 6.893, 0.900, 0.7807; 7.042, 0.985, 0.9368; 7.187, 1.067, 1.1061; 7.353, 1.145, 1.3055; 7.561, 1.220, 1.5610; 7.916, 1.292, 2.0193; 8.327, 1.325, 2.5596.

Run II. 5.644, 0.013, 0.0064; 5.748, 0.027, 0.0128; 5.808, 0.041, 0.0186; 5.884, 0.068, 0.0318; 5.978, 0.122, 0.0581; 6.129, 0.251, 0.1267; 6.251, 0.376, 0.2031; 6.362, 0.492, 0.2896; 6.480, 0.602, 0.3890; 6.612, 0.707, 0.5056; 6.753, 0.807, 0.6416; 6.827, 0.855, 0.7144; 6.903, 0.902, 0.7932; 6.982, 0.948, 0.8753; 7.062, 0.995, 0.9598; 7.136, 1.039, 1.0480; 7.221, 1.082, 1.1433; 7.261, 1.102, 1.1930; 7.304, 1.123, 1.2447; 7.400, 1.164, 1.3626; 7.510, 1.204, 1.5002; 7.578, 1.224, 1.5823; 7.650, 1.243, 1.6749; 7.736, 1.262, 1.7888; 7.847, 1.280, 1.9290; 7.990, 1.299, 2.1206; 8.197, 1.137, 2.4008; 8.335, 1.324, 2.5720.

$\triangle$ B = 0.005 M: Run I. —log h, Z, η; 5.836, 0.014, 0.0070; 5.999, 0.037, 0.0168; 6.109, 0.071, 0.0327; 6.203, 0.127, 0.0601; 6.274, 0.182, 0.0874; 6.340, 0.243, 0.1206; 6.386, 0.290, 0.1456; 6.436, 0.343, 0.1780; 6.487, 0.395, 0.2115; 6.536, 0.447, 0.2480; 6.587, 0.498, 0.2879;

Table 1. Continued.

6.636, 0.547, 0.3281; 6.688, 0.596, 0.3731; 6.741, 0.645, 0.4201; 6.793, 0.688, 0.4695; 7.162, 0.969, 0.8488; 7.233, 1.013, 0.9262; 7.307, 1.056, 1.0117; 7.381, 1.098, 1.1037; 7.469, 1.140, 1.2095; 7.571, 1.181, 1.3319; 7.699, 1.221, 1.4928; 7.859, 1.261, 1.7010; 8.134, 1.299, 2.0580.

Run II. 5.858, 0.013, 0.0073; 5.955, 0.025, 0.0137; 6.051, 0.047, 0.0239; 6.207, 0.126, 0.0614; 6.337, 0.235, 0.1175; 6.536, 0.446, 0.2521; 6.742, 0.643, 0.4235; 6.974, 0.833, 0.6463; 7.033, 0.876, 0.7115; 7.097, 0.919, 0.7788; 7.163, 0.967, 0.8515; 7.229, 1.011, 0.9282; 7.571, 1.179, 1.3336; 7.856, 1.258, 1.7010; 8.318, 1.310, 2.3024; 7.729, 1.228, 1.5317; 7.488, 1.142 1.2318; 7.324, 1.063, 1.0320; 7.190, 0.982, 0.8768; 7.075, 0.903, 0.7487; 6.966, 0.825, 0.6368; 6.913, 0.789, 0.5857; 6.867, 0.751, 0.5398; 6.822, 0.714, 0.4962; 6.698, 0.603, 0.3829; 6.555, 0.461, 0.2636; 6.426, 0.328, 0.1720; 6.296, 0.198, 0.0979; 6.115, 0.074, 0.0367.

+ B = 0.0025 M: Run I. —log h, Z, η; 5.708, 0.007, 0.0030; 6.152, 0.033, 0.0135; 6.264, 0.057, 0.0250; 6.325, 0.081, 0.0362; 6.371, 0.105, 0.0463; 6.409, 0.128, 0.0578; 6.470, 0.173, 0.0794; 6.519, 0.217, 0.1007; 6.562, 0.259, 0.1231; 6.604, 0.300, 0.1467; 6.676, 0.378, 0.1954; 6.744, 0.452, 0.2448; 6.808, 0.518, 0.2961; 6.869, 0.583, 0.3479; 6.928, 0.644, 0.4020; 7.020, 0.729, 0.4861; 7.109, 0.808, 0.5740; 7.195, 0.880, 0.6656; 7.282, 0.948, 0.7620; 7.366, 1.010, 0.8624; 7.462, 1.068, 0.9689; 7.527, 1.105, 1.0456; 7.595, 1.140, 1.1312; 7.673, 1.172, 1.2245; 7.758, 1.203, 1.3327; 7.862, 1.233, 1.4621; 7.985, 1.261, 1.6264.

Run II. 5.797, 0.010, 0.0041; 6.029, 0.020, 0.0074; 6.127, 0.030, 0.0115; 6.252, 0.060, 0.0226; 6.316, 0.079, 0.0331; 6.365, 0.102, 0.0443; 6.423, 0.139, 0.0619; 6.482, 0.184, 0.0842; 6.528, 0.227, 0.1072; 6.573, 0.268, 0.1302, 6.633, 0.328, 0.1656; 6.700, 0.405, 0.2137; 6.766, 0.474, 0.2633; 6.827, 0.541, 0.3151; 6.889, 0.604, 0.3675; 6.962, 0.678, 0.4351; 7.053, 0.760, 0.5206; 7.141, 0.836, 0.6092; 7.226, 0.906, 0.7018; 7.312, 0.972, 0.7978; 7.398, 1.034, 0.9003; 7.446, 1.061, 0.9530; 7.476, 1.080, 0.9895; 7.544, 1.116, 1.0673; 7.612, 1.150, 1.1525; 7.689, 1.182, 1.2485; 7.778, 1.212, 1.3597; 7.881, 1.242, 1.4949; 8.016, 1.269, 1.6673; 8.099, 1.282, 1.7724; 8.201, 1.294, 1.9057.

● B = 0.00125 M: Run I. —log h, Z, η; 6.078, 0.022, 0.0063; 6.271, 0.033, 0.0114; 6.345, 0.042, 0.0158; 6.450, 0.064, 0.0249; 6.514, 0.085, 0.0347; 6.582, 0.115, 0.0499; 6.631, 0.148, 0.0648; 6.698, 0.200, 0.0905; 3.753, 0.251, 0.1168; 6.803, 0.299, 0.1456; 6.847, 0.351, 0.1743; 6.889, 0.400, 0.2041; 6.933, 0.446, 0.2348; 7.016, 0.538, 0.3021; 7.097, 0.628, 0.3721; 7.175, 0.713, 0.4495; 7.260, 0.796, 0.5333; 7.348, 0.876, 0.6263; 7.441, 0.953, 0.7287; 7.547, 1.029, 0.8461; 7.662, 1.099, 0.9860; 7.806, 1.166, 1.1625; 8.002, 1.228, 1.4130; 8.348, 1.282, 1.8623.

Run II. 5.478, 0.011, 0.0016; 6.196, 0.029, 0.0090; 6.387, 0.050, 0.0178; 6.470, 0.072, 0.0266; 6.526, 0.093, 0.0360; 6.573, 0.114, 0.0459; 6.609, 0.136, 0.0557; 6.670, 0.175, 0.0763; 6.727, 0.224, 0.1016; 6.778, 0.278, 0.1283; 6.829, 0.326, 0.1564; 6.871, 0.375, 0.1858; 6.915, 0.422, 0.2162; 6.959, 0.469, 0.2477; 6.996, 0.514, 0.2791; 7.045, 0.568, 0.3204; 7.128, 0.656, 0.3927; 7.209, 0.738, 0.4711; 7.292, 0.819, 0.5570; 7.395, 0.913, 0.6713; 7.493, 0.995, 0.7805; 7.611, 1.066, 0.9191; 7.743, 1.129, 1.0753; 7.902, 1.191, 1.2795.

in the range where $\nu = 1$. This means that the complexes formed can be written as $Pb(Pb(OH)_{1.33 \pm 0.03})_n$ (Ref. [22]), where n is variable and unknown and may assume any value which fulfills the requirements that $n(1.33 \pm 0.03)$ are whole numbers. The restriction that the complexes should give a value $\nu = 1$ gives as the only possibility $n = 3$, from the relation $n(1.33 \pm 0.03)/(n + 1) = 1$. Hence the complex formed is $Pb_4(OH)_4^{4+}$.

In this derivation we have not made use of the shapes of the Z and η curves for the complex. It is therefore necessary to make a comparison with theoretical curves for $Pb_4(OH)_4^{4+}$ to see if the experimental $Z(\log h)_B$ and η $(\log h)_B$ curves are of the correct shapes. At the same time the equilibrium constant for the reaction

$$4\,Pb^{2+} + 4\,H_2O \rightleftharpoons Pb_4(OH)_4^{4+} + 4\,H^+ \qquad (7)$$

is determined.

Table 2.

Corresponding values of $-\log h$, Z and η with 0.3 M $(Na)ClO_4$ medium.

○ B = 0.010 M: Run I. $-\log h, Z, \eta$; 5.696, 0.012, 0.0051; 5.943, 0.040, 0.0176; 6.032, 0.067, 0.294; 6.132, 0.119, 0.0558; 6.200, 0.170, 0.0808; 6.303, 0.266, 0.1342; 6.428, 0.399, 0.2167; 6.538, 0.521, 0.3029; 6.675, 0.667, 0.4290; 6.812, 0.796, 0.561; 6.947, 0.912, 0.7035; 7.094, 1.018, 0.8621; 7.244, 1.113, 1.0527; 7.434, 1.200, 1.2951; 7.569, 1.240, 1.4594; 7.752, 1.279, 1.6971; 8.063, 1.316, 2.1045.

Run II. 5.674, 0.012, 0.0037; 5.836, 0.023, 0.0095; 6.087, 0.093, 0.0416; 6.256, 0.219, 0.1051; 6.367, 0.334, 0.1711; 6.521, 0.501, 0.2884; 6.607, 0.596, 0.3631; 6.742, 0.733, 0.4915; 6.878, 0.856, 0.6282; 7.013, 0.967, 0.7765; 7.165, 1.066, 0.9469; 7.331, 1.157, 1.1548; 7.434, 1.200, 1.2884; 7.495, 1.220, 1.3675; 7.647, 1,260, 1.5602; 7.875, 1.298, 1.8594.

△ B = 0.005 M: Run I. $-\log h, Z, \eta$; 6.061, 0.029, 0.0134; 6.247, 0.079, 0.0357; 6.343, 0.126, 0.0584; 6.540, 0.302, 0.1507; 6.676, 0.455, 0.2460; 6.796, 0.592, 0.3454; 6.901, 0.713, 0.4478; 7.004, 0.822, 0.5546; 7.113, 0.921, 0.6736; 7.224, 1.010, 0.8011; 7.270, 1.041, 0.8538; 7.344, 1.092, 0.9478; 7.413, 1.129, 1.0333; 7.491, 1.166, 1.1270; 7.579, 1.201, 1.2389; 7.682, 1.234, 1.3728; 4.817, 1.266, 1.5459; 8.003, 1.297, 1.7872.

Run II. 6.525, 0.276, 0.1338; 6.617, 0.378, 0.1939; 6.747, 0.528, 0.3021; 6.868, 0.666, 0.4127; 7.020, 0.826, 0.5631; 7.184, 0.966, 0.7369; 7.351, 1.089, 0.9444; 7.588, 1.199, 1.2335; 7.474, 1.154, 1.0932; 7.388, 1.109, 0.9857; 7.251, 1.021, 0.8197; 7,099, 0.892, 0.6388; 6.967, 0.767, 0.5016; 6.817, 0.607, 0.3596; 6.681, 0.453, 0.2463; 6.556, 0.305, 0.1544; 6.408, 0.163, 0.0776; 6.066, 0.026, 0.0134.

\+ B = 0.0025 M: Run I. $-\log h, Z, \eta$; 6.004, 0.018, 0.0081; 6.406, 0.068, 0.0297; 6.504, 0.108, 0.0490; 6.617, 0.192, 0.0821; 6.783, 0.346, 0.1727; 6.895, 0.481, 0.2559; 6.986, 0.601, 0.3404; 7.079, 0.708, 0.4273; 7.165, 0.805, 0.5169; 7.248, 0.892, 0.6122; 7.385, 1.009, 0.7677; 7.490, 1.078, 0.8871; 7.596, 1.142, 1.0270; 7.735, 1.202, 1.2045; 7.917, 1.255, 1.4388; 8.309, 1.317, 1.9517.

Run II. 6.193, 0.031, 0.0129; 6.328, 0.050, 0.0193; 6.457, 0.086, 0.0375; 6.578, 0.151, 0.0693; 6.715, 0.271, 0.1305; 6.842, 0.415, 0.2133; 6.969, 0.575, 0.3212; 7.035, 0.655, 0.3827; 7.121, 0.758, 0.4702; 7.167, 0.805, 0.5155; 7.209, 0.850, 0.5622; 7.320, 0.952, 0.6859; 7.385, 1.009, 0.7664; 7.432, 1.045, 0.8228; 7.540, 1.111, 0.9503; 7.598, 1.142, 1.0254; 7.664, 1.172, 1.1061; 7.817, 1.228, 1.3070; 7.919, 1.255, 1.4369; 7.978, 1.268, 1.5125; 8.039, 1.281, 1.5967; 8.122, 1.293, 1.7022.

● B = 0.00125 M: Run I. $-\log h, Z, \eta$; 6.308, 0.035, 0.0147; 6.577, 0.076, 0.0337; 6.756, 0.154, 0.0699; 6.922, 0.295, 0.1412; 7.022, 0.420, 0.2125; 7.119, 0.531, 0.2835; 7.197, 0.629, 0.3535; 7.266, 0.719, 0.4245; 7.353, 0.818, 0.5171; 7.439, 0.907, 0.6131; 7.552, 1.001, 0.7389; 7.667, 1.083, 0.8846; 7.806, 1.158, 1.0587; 7.978, 1.223, 1.2832; 8.134, 1.263, 1.4877.

Run II. 6.529, 0.067, 0.0276; 6.663, 0.107, 0.0462; 6.744, 0.145, 0.0648; 6.842, 0.217, 0.0996; 6.972, 0.351, 0.1720; 7.069, 0.468, 0.2413; 7.151, 0.572, 0.3102; 7.222, 0.666, 0.3792; 7.292, 0.751, 0.4502; 7.358, 0.827, 0.5232; 7.427, 0.898, 0.6013; 7.501, 0.962, 0.6821; 7.572, 1.020, 0.7680; 7.648, 1.074, 0.8619; 7.730, 1.124, 0.9711; 7.829, 1.170, 1.0908; 7.883, 1.192, 1.1621; 7.948, 1.214, 1.2399.

This is accomplished in the following way. We start from the equations

$$B = b + 4\beta_{4,4}b^4h^{-4} \tag{8}$$

$$BZ = 4\beta_{4,4}b^4h^{-4} \tag{9}$$

$$10\eta = B/b = 1 + 4\beta_{4,4}b^3h^{-4} \tag{10}$$

and introduce

$$\beta^3 = 4\beta_{4,4} \text{ and } v = \beta\ B\ h^{-4/3} \tag{11, 11a}$$

We find after elimination of b

$$\log v = \log B - 4/3 \log h + \log \beta =$$
$$= \eta + 1/3 \log (10\eta - 1) = 1/3 \log Z - 4/3 \log (1 - Z) \tag{12}$$

According to these equations plots of Z and η as functions of (log B — 4/3 log h) should give single curves independent of B. Then these are compared with the theoretical η (log v) and Z(log v) curves and examined for a fit. The difference on the log v and (log B — 4/3 log h) axes in this position gives log β and from eqn. (11) log $\beta_{4,4}$.

For $B \geq 5$ mM the experimental points in the region with $v = 1$ fell on single curves, which had the shape required by the theoretical curves. The value of the equilibrium constant found from the Z and η data was the same

$$\log\beta_{4,4} = -19.25 \pm 0.03$$

The 2.5 and 1.25 mM curves showed deviations in a direction which indicated that species smaller than $Pb_4(OH)_4^{4+}$ were also present. However, the deviations are not very large.

In order to obtain information about the cause of these deviations the terms for the $Pb_4(OH)_4^{4+}$ ion were subtracted from B and BZ. The following quantities were calculated and plotted as functions of log h

$$\eta_c = \log \frac{B_c}{b} \quad \text{and} \quad Z_c = \frac{BZ - 4\beta_{4,4}b^4h^{-4}}{B_c} \qquad (13,\ 13a)$$

where B_c, a corrected B, is defined by

$$B_c = B - 4\beta_{4,4}b^4h^{-4} \qquad (14)$$

These plots showed that η_c and Z_c were independent of B_c and were functions of log h only, which indicates that the mononuclear complex $PbOH^+$ is formed. In fact a satisfactory fit was obtained with normalized curves according to Sillén [23]. The equilibrium constant for the reaction

$$Pb^{2+} + H_2O \rightleftharpoons PbOH^+ + H^+ \qquad (15)$$

was found to be

$$\log \beta_{11} = -7.90 \pm 0.05$$

The equilibrium constants $\beta_{4,4}$ and β_{11} were also determined simultaneously from projection maps by the method described by Biedermann and Sillén [24] with (log B — 4/3 log h) and log h as variables on the axes. This approach gave the same values for the equilibrium constants as before, but indicated that the uncertainty in log β_{11} should be increased to ± 0.1 logarithmic unit.

Determination of the products of hydrolysis in the region where $v > 1$. Now we turn to the upper parts of the Z(log h)$_B$ and η (log h)$_B$ curves. The calculations to be described in the following were made on the Z and η data for $B < 40$ mM. (In the 40 and 80 mM titrations $Pb_4(OH)_4^{4+}$ is so predominant that little information can be found about the other species present). As has already been mentioned both the Z and η data indicate that complexes with a OH^-/Pb(II) ratio = 4/3 are formed. By calculating the concentrations of $Pb_4(OH)_4^{4+}$ and $PbOH^+$ for each experimental point and subtracting the terms for these

ions we can find the average number of OH^- groups bound to each Pb(II) in the unknown complexes. This quantity remained constant at 1.33 ± 0.03 in the region where it could be calculated with sufficient accuracy. This region covered more than one log h unit for each value of B. It is therefore apparent that the complexes predominating in the upper parts of the curves are of the form $(Pb(OH)_{4/3}^{2/3+})_n$ and the formulas of the complexes have been determined on this assumption.

Approach I. Information about possible species written as $Pb(Pb(OH)_t)_n$ is found from the difference quotient $(\Delta \log B/\Delta \log h)_\eta = t$. If one only of the above complexes predominated, we would have $t = 2.0$ for $Pb_3(OH)_4^{2+}$, $t = 1.6$ for $Pb_6(OH)_8^{4+}$, $t = 1.5$ for $Pb_9(OH)_{12}^{6+}$, *etc.* The spacing along the log h axis between the experimental η (log h)$_B$ curves for $B = 20$, 10 and 5 mM gave a t value close to 1.6, but for the two lower concentrations t was somewhat higher. Since the presence of $PbOH^+$ could be expected to cause such an effect, it was considered possible that the data could be explained by the formation of $Pb_6(OH)_8^{4+}$ only. To test the hypothesis the following equations were used. We start from

$$B = b + \beta_{11} b h^{-1} + 4\beta_{4,4} b^4 h^{-4} + 6\beta_{8,6} b^6 h^{-8} \quad (16)$$

$$BZ = \beta_{11} b h^{-1} + 4\beta_{4,4} b^4 h^{-4} + 8\beta_{8,6} b^6 h^{-8} \quad (17)$$

$$B/b = 10\eta = 1 + \beta_{11} h^{-1} + 4\beta_{4,4} b^3 h^{-4} + 6\beta_{8,6} b^5 h^{-8} \quad (18)$$

and introduce the corrected dependent variables B_c, η_c and Z_c by

$$B_c = B - \beta_{11} b h^{-1} - 4\beta_{4,4} b^4 h^{-4} = b + 6\beta_{8,6} b^6 h^{-8} \quad (19)$$

$$B_c Z_c = BZ - \beta_{11} b h^{-1} - 4\beta_{4,4} b^4 h^{-4} = 8\beta_{8,6} b^6 h^{-8} \quad (20)$$

$$B_c/b = 10\eta_c = 1 + 6\beta_{8,6} b^5 h^{-8} \quad (21)$$

With the parameters

$$6\beta_{8,6} = \alpha^5 \text{ and } 8\beta_{8,6} = \gamma^5 \quad (22, 22a)$$

and the variables

$$\alpha B_c h^{-1.6} = v \text{ and } \gamma B_c h^{-1.6} = u \quad (23, 23a)$$

we get

$$\log v = \log B_c - 1.6 \log h + \log \alpha = \eta_c + 0.2 \log (10\eta_c - 1) \quad (24)$$

and

$$\log u = \log B_c - 1.6 \log h + \log \gamma = 0.2 \log Z_c - 1.2 \log (1 - 0.75 Z_c) \quad (25)$$

If the hypothesis is valid each of the Z_c and η_c according to eqns. (24) and (25) should give a single curve when plotted as a function of (log B_c − 1.6 log h). The terms for $PbOH^+$ and $Pb_4(OH)_4^{4+}$ were calculated with the equilibrium constants already determined.

The plots showed that $Pb_6(OH)_8^{4+}$ alone did not suffice to explain the data. The data for the three highest concentrations fulfilled the requirements for the formation of $Pb_6(OH)_8^{4+}$ at large values of Z_c and η_c well, but the t value used was too small to bring the data from the 2.5 and 1.25 mM titrations on to the η_c, $Z_c(\log B_c - 1.6 \log h)$ curves formed at the higher concentrations. Moreover at low Z_c and η_c the shapes of the experimental and theoretical curves were a little different. The fact that we have to use a larger t value for the lower concentrations to bring the data on to the same curve indicates the presence of $Pb_3(OH)_4^{2+}$. $Pb_3(OH)_4^{2+}$ is the only complex with $\nu = 4/3$ and a t value > 1.6.

From the above discussion it may be considered likely that the data could be explained by the formation of $Pb_6(OH)_8^{4+}$ and $Pb_3(OH)_4^{2+}$. However, we shall start with the more general assumption that all members of the series $(Pb(OH)_{4/3}^{2/3+})_n$ may be present. In order to determine the equilibrium constant for the first member of the series, $Pb_3(OH)_4^{2+}$, two methods were used.

Approach II. We start from the equations

$$B = b + [PbOH^+] + 4[Pb_4(OH)_4^{4+}] + 3[Pb_3(OH)_4^{2+}] + 6[Pb_6(OH)_8^{4+}] + - \quad (26)$$

$$B_c = B - b - [PbOH^+] - 4[Pb_4(OH)_4^{4+}] = 3\beta_{4,3}b^3h^{-4} + 6\beta_{8,6}b^6h^{-8} - - - =$$

$$= 3\beta_{4,3}x + 6\beta_{8,6}x^2 + - - - \quad (27)$$

$$b^3h^{-4} = x \quad (28)$$

We can calculate $[Pb_4(OH)_4^{4+}]$ and $[PbOH^+]$ for each experimental point from the potentials and the equilibrium constants already determined. In addition we can find $b^3h^{-4} = x$. With this quantity as the independent variable, B_c becomes a function of x only.

$$B_c = 3\beta_{4,3}x + 6\beta_{8,6}x^2 + - - - \text{ or } B_cx^{-1} = 3\beta_{4,3} + 6\beta_{8,6}x + - - - \quad (27, 27a)$$

The first two coefficients of the above series are found by plotting B_cx^{-1} as function of x. If the first two complexes only are present a straight line should be obtained. The presence of higher complexes should give the line a curvature for the higher x values. The plot is shown in Fig. 5. The points fall with good approximation on a straight line and there appears to be no indication of the presence of $Pb_9(OH)_{12}^{6+}$ or higher complexes. The intercept and the slope of the line give the following equilibrium constants.

$$\log \beta_{4.3} = - 22.89 \pm 0.1$$
$$\log \beta_{8.6} = - 42.13 \pm 0.1$$

corresponding to the equilibria

$$3\ Pb^{2+} + 4H_2O \rightleftharpoons Pb_3(OH)_4^{2+} + 4\ H^+$$
$$6\ Pb^{2+} + 8\ H_2O \rightleftharpoons Pb_6(OH)_8^{4+} + 8\ H^+$$

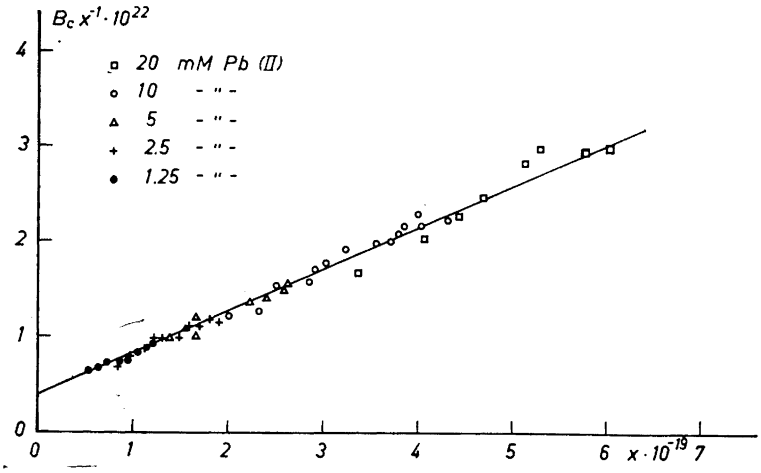

Fig. 5. Determination of log $\beta_{4,3}$ (and log $\beta_{8,6}$) from eqn. (27). B_c; terms for $Pb_4(OH)_4^{4+}$ and $PbOH^+$ have been subtracted. The drawn line yields log $\beta_{4,3} = -22.89$ (and log $\beta_{8,6} = -42.13$).

Approach III. The above calculations were made on the assumption that $Pb_4(OH)_4^{4+}$ and $PbOH^+$ were formed in the initial stages of hydrolysis. If we combine the amalgam data with the Z data the members of the series can be found on the more general assumption, which is strongly supported by the initial ν values, that only complexes of the general type $(PbOH)_n^{n+}$ occur beside $(PbOH_{4/3})_n^{2/3n+}$ species. The following equations are valid.

$$B = b + \Sigma\, n\beta_{n,n}b^n h^{-n} + 3\beta_{4,3}b^3h^{-4} + 6\beta_{8,6}b^6h^{-8} + - - - \qquad (29)$$

$$BZ = \Sigma\, n\beta_{n,n}b^n h^{-n} + 4\beta_{4,3}b^3h^{-4} + 8\beta_{8,6}b^6h^{-8} + - - - - - \qquad (30)$$

Subtracting and rearranging we get

$$(BZ + b - B)\, x^{-1} = \beta_{4,3} + 2\,\beta_{8,6}x + - - - \qquad (31)$$

The plot $(BZ + b - B)x^{-1}$ versus x yields a straight line (Fig. 6) and the equilibrium constants are found to be

$$\log \beta_{4,3} = -22.85 \pm 0.1$$

$$\log \beta_{8,6} = -42.15 \pm 0.1$$

From Figs. 5 and 6 we find that the data for each total lead(II) concentration are gathered in different parts of the lines and do not overlap to any great extent, nor do they cover a broad range in x. This is due to the nature of the functions used. They are based on the concentrations of the $(Pb(OH)_{4/3}^{2/3+})_n$ species obtained from the difference between B and the concentrations of the other species present. Of course, when the latter predominate this difference

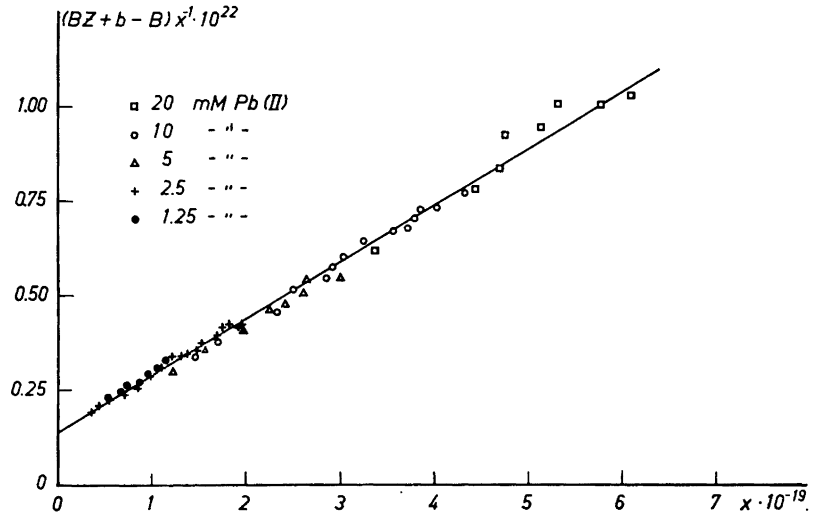

Fig. 6. Determination of log $\beta_{4,3}$ (and log $\beta_{8,6}$) from eqn. (31). The drawn line yields log $\beta_{4,3} = -22.85$ (and log $\beta_{8,6} = -42.15$).

is not very accurate. This leads to a quite narrow x range where the difference is of sufficient accuracy. Therefore any curvature of the lines may not show up. The value found for log $\beta_{4,3}$ will be accepted as being correct, but we shall still doubt the value found for log $\beta_{8,6}$ since higher complexes may also be present.

Now we can subtract the term for $Pb_3(OH)_4^{2+}$ in eqns. (19,20,21) and obtain

$$B_c Z_c = \Sigma\, p\beta_{p,q} b^q h^{-p} \tag{32}$$

$$10^{\eta_c} = 1 + \Sigma\, q\beta_{p,q} b^{q-1} h^{-p} \tag{33}$$

where the sums represent the terms for the unknown complexes. Since the plots in Figs. 5 and 6 strongly indicated that the term for $Pb_6(OH)_8^{4+}$ predominates in the sums above we started with the assumption that $p = 8$ and $q = 6$ and eqns. (24) and (25) were used to test it. From Figs. 7 and 8 it is seen that Z_c and η_c are functions of (log B_c — 1.6 log h) only as required by the hypothesis. The agreement between the experimental and normalized curves is also good. Hence there is no reason to introduce more new complexes other than $Pb_3(OH)_4^{2+}$ and $Pb_6(OH)_8^{4+}$ to explain the upper parts of the η (log $h)_B$ and Z(log $h)_B$ curves. Log $\beta_{8,6}$ was found from eqns. (24, 25) and the difference between the coordinates on the (log B_c — 1.6 log h) and the log v and log u axes when the experimental and normalized curves overlap.

$$\log \beta_{8,6} = -42.15 \pm 0.1\ (\eta \text{ data}) \text{ and } -42.13 \pm 0.1\ (Z \text{ data})$$

Final values for $\beta_{4,4}$ and β_{11}. Thus having established the complexes which predominate in the low log h region and their equilibrium constants it must be remembered that these findings were based partly on the hypothesis that

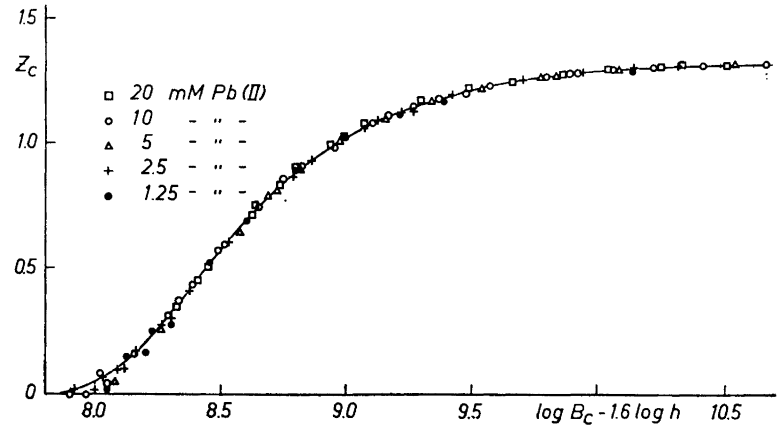

Fig. 7. Z_c as a function of (log B_c −1.6 log h) according to eqn. (25). Z_c, B_c; terms for $Pb_4(OH)_4^{4+}$, $Pb_3(OH)_4^{2+}$ and $PbOH^+$ have been subtracted. Drawn curve represents normalized curve, calculated from eqn. (25), in position of best fit and giving log $\beta_{8,6} = -42.13$.

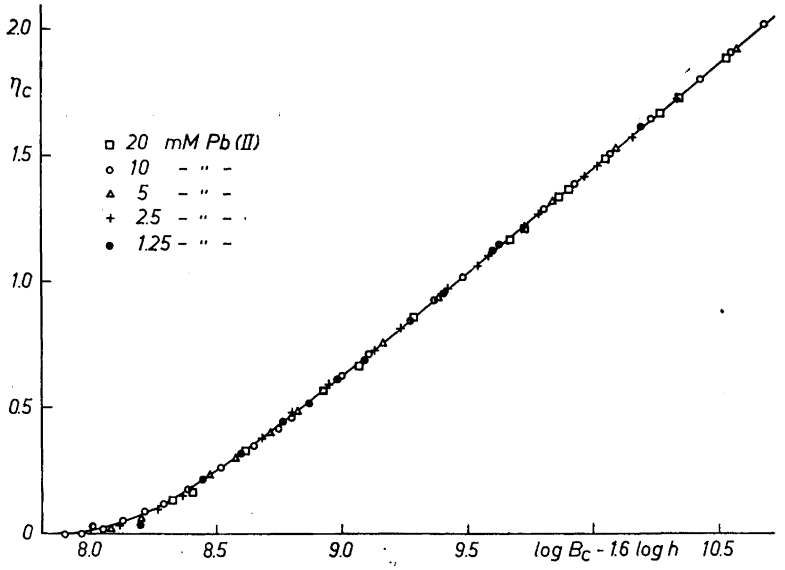

Fig. 8. η_c as a function of (log B_c −1.6 log h) according to eqn. (24). η_c, B_c; terms for $Pb_4(OH)_4^{4+}$, $Pb_3(OH)_4^{2+}$ and $PbOH^+$ have been subtracted. Drawn curve represents normalized curve, calculated from eqn. (24), in position of best fit and giving log $\beta_{8,6} = -42.15$.

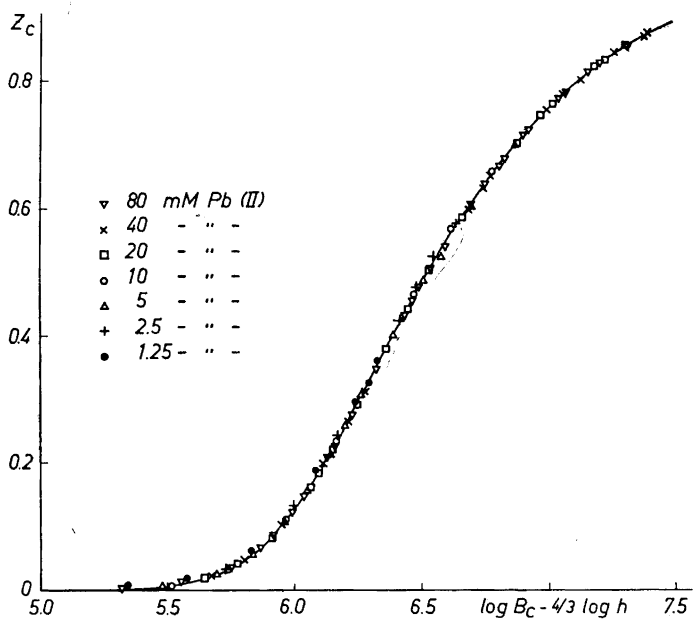

Fig. 9. Z_c as a function of (log B_c −4/3 log h) according to eqn. (12). Z_c, B_c; terms for $Pb_6(OH)_8^{4+}$, $Pb_3(OH)_4^{2+}$ and $PbOH^+$ have been subtracted. Drawn curve represents normalized curve, calculated from eqn. (12), in position of best fit and giving log $\beta_{4,4} = -19.26$.

$Pb_4(OH)_4^{4+}$ and $PbOH^+$ were formed as the initial hydrolysis products. Therefore it was considered necessary to recalculate the data in the high log h region to see that this hypothesis in not upset by disturbances from the new complexes. A calculation of the concentrations of $Pb_3(OH)_4^{2+}$ and $Pb_6(OH)_8^{4+}$ showed that they give only a small contribution in this region.

In order to follow, separately, the formation curve of $Pb_4(OH)_4^{4+}$ at low B values and into the region where the contribution of $Pb_3(OH)_4^{2+}$ and $Pb_6(OH)_8^{4+}$ is not negligible the following equations were derived

$$B_cZ_c = BZ - \beta_{11}bh^{-1} - 4\beta_{4,3}b^3h^{-4} - 8\beta_{8,6}b^6h^{-8} = 4\beta_{4,4}b^4h^{-4} \quad (34)$$

$$10^{\eta_c} = (B - \beta_{11}bh^{-1} - 3\beta_{4,3}b^3h^{-4} - 6\beta_{8,6}b^6h^{-8})\, b^{-1} = 1 + 4\beta_{4,4}b^3h^{-4} \quad (35)$$

By subtracting the terms for the other complexes, calculated with the equilibrium constants already determined, we have arrived at equations identical to (9, 10) and the equilibrium constant is determined as described there (Figs. 9, 10). The value found was

$$\log \beta_{4,4} = -19.25 \pm 0.03 \ (\eta \text{ data}) \text{ and } -19.26 \pm 0.03 \ (Z \text{ data})$$

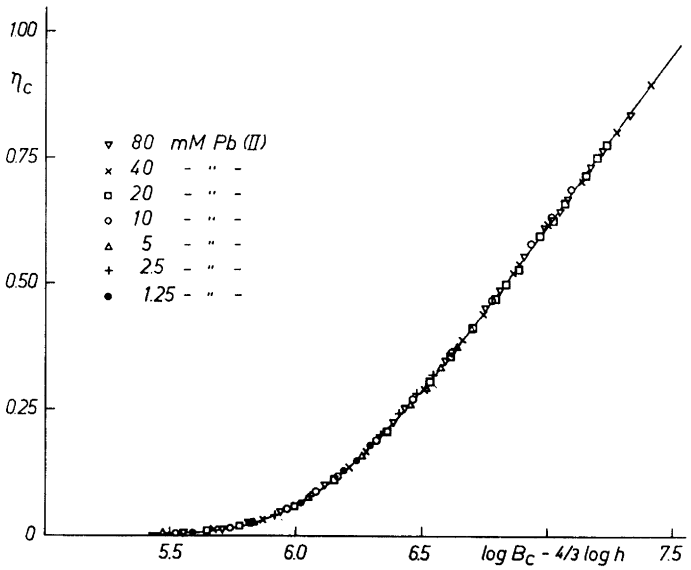

Fig. 10. η_c as a function of (log B_c $-4/3$ log h) according to eqn. (12). η_c, B_c; terms for $Pb_6(OH)_8^{4+}$, $Pb_3(OH)_4^{2+}$ and $PbOH^+$ have been subtracted. Drawn curve represents normalized curve, calculated from eqn. (12), in position of best fit and giving log $\beta_{4,4} = -19.25$.

Determination of the equilibrium constants in 0.3 M (Na)ClO_4. With 0.3 M (Na)ClO_4 as medium the Pb(II) concentrations 10, 5, 2.5 and 1.25 mM were investigated. The interpretation of the data has not been carried out independent of the results which were obtained from the 3 M (Na)ClO_4 data. We have tested only to see if they could be explained by the same mechanism. The calculations were started from eqn. (31) which gave a good straight line from which the equilibrium constants were found as

$$\log \beta_{4,3} = -23.35 \pm 0.1$$

$$\log \beta_{8,6} = -42.66 \pm 0.1$$

Knowing these constants the quantities

$$B_cZ_c = BZ - 4\beta_{4,3}b^3h^{-4} - 8\beta_{8,6}b^6h^{-8} \quad (36)$$

$$10^{\eta_c} = (B - 3\beta_{4,3}b^3h^{-4} - 6\beta_{8,6}b^6h^{-8})b^{-1} \quad (37)$$

were calculated and Z_c and η_c plotted as functions of (log B_c $-$ 4/3 log h). The data from the 10 and 5 mM titrations fell on the same curve as required by the formation of $Pb_4(OH)_4^{4+}$, but the data for the other two values of B were slightly off the curve. This is not unexpected since the Z and η curves

for these concentrations clearly indicate the presence of mononuclear species. Log $\beta_{4,4}$ was determined from the 10 and 5 mM titrations by curve-fitting according to eqn. (12) and found to be

$$\log \beta_{4,4} = -19.89 \pm 0.05 \ (\eta \text{ data}) \text{ and } -19.91 \pm 0.05 \ (Z \text{ data})$$

With these values for log $\beta_{4,4}$, new $B_c Z_c$ and η_c functions were calculated where the terms for $Pb_4(OH)_4^{4+}$ had also been subtracted. Plots of Z_c and η_c as functions of log h gave single curves, which fitted the normalized curves for $PbOH^+$ well. Log β_{11} was found to be

$$\log \beta_{11} = -7.75 \pm 0.1$$

Log β_{11} was estimated also from the lower parts of the Z and η curves of the 2.5 and 1.25 mM titrations. The value found was log $\beta_{11} = -7.8 \pm 0.1$. With this value for log β_{11} the terms for $PbOH^+$ were also subtracted in eqns. (36) and (37). The new plots of Z_c and η_c as functions of (log B − 4/3 log h) fell on the same curves for all concentrations and the plots gave good agreement with the normalized curves for the formation of $Pb_4(OH)_4^{4+}$.

With the help of the equilibrium constants thus found theoretical Z $(\log h)_B$ and η $(\log h)_B$ curves were calculated for all values of B both in 3 M and 0.3 M (Na)ClO_4. In general very good agreement was found between the experimental and theoretical curves as is seen from Figs. 1, 2, 3 and 4. However, there are two questions that need some discussion.

The first question is concerned with the Z data from the titrations at low values of B. As has been mentioned already the 3 M (Na)ClO_4 contained an acidic impurity. The Z data used in the previous calculation have been corrected for this impurity. If for the moment we assume that the correction is not valid, ν values as high as 1.37 are found for $B = 1.25$ mM. Thus complexes with a OH^-/Pb(II) ratio $> 4/3$ must also be present. It is likely that these complexes contain only a few Pb atoms since otherwise the deviations could be expected to be most pronounced at the highest values of B. The simplest explanation that might be suggested is the formation of $Pb(OH)_2$. We have

$$BZ' - (\beta_{11} b h^{-1} + 4\beta_{4,4} b^4 h^{-4} + 4\beta_{4,3} b^3 h^{-4} + 8\beta_{8,6} b^6 h^{-8}) = p\beta_{p,q} b^q h^{-p} \qquad (38)$$

Z' is the Z value which is obtained if no correction is applied for the acidity in the $NaClO_4$. The quantity in the parenthesis was calculated as a function of log h using the previously determined equilibrium constants and neglecting the term $q\beta_{p,q} b^q h^{-p}$ in B. This approximation was employed since exact calculations would be very time-consuming. Using eqn. (38) log $\beta_{2,1}$ ($p = 2$, $q = 1$) was estimated from the 1.25 and 2.5 mM titrations. The value found was log $\beta_{2,1} \simeq -16$. No other hypotheses were tested.

A value of $\beta_{2,1}$ around 10^{-16} would make the acidity constants of Pb^{2+} and $PbOH^+$ about equal. This unusual situation has been observed for other metal

ions including Hg^{2+} (Ref. [27]), Tl^{3+} (Ref. [25]), Fe^{3+} (Ref. [26]), In^{3+} (Ref. [28]) and Sc^{3+} (Ref. [29]). The η data do not show any deviation from the calculated curves either in 3 M or 0.3 M (Na)ClO_4. In 0.3 M (Na)ClO_4 medium, where no correction has been applied for the acidity in the $NaClO_4$, there is almost no discrepancy between the experimental and calculated Z (log $h)_B$ curves, which would indicate the validity of the correction applied to the measurements with 3 M (Na)ClO_4 as medium. Since the presence of $Pb(OH)_2$ in the investigated log h region is dubious it has not been included in the explanation of the data.

The second question is concerned with the data at low Z for the 80 and 40 mM titrations. In this region ν is found to be < 1. It starts from *ca.* 0.9 and increases to 1.00 ± 0.02. The deviations from $\nu = 1$ for the first points appear to be outside the limits of the experimental error and would indicate the presence of complexes with a OH^-/Pb(II) ratio < 1, for instance Pb_2OH^{3+}. This is not unlikely since a high value of B and log h favours the formation of such complexes. The disturbance might be caused by the complex Pb_2OH^{3+}, for which Pedersen [1] found evidence in concentrated $Pb(NO_3)_2$ solutions. A search for this complex is now being made by studying the hydrolysis in concentrated $Pb(ClO_4)_2$ solutions.

To sum up we propose the following reactions and equilibrium constants to explain the data.

		Equilibrium constants	
		3 M (Na)ClO_4	0.3 M (Na)ClO_4
$Pb^{2+} + H_2O \rightleftharpoons PbOH^+ + H^+$	log β_{11}	-7.9 ± 0.1	-7.8 ± 0.1
$4Pb^{2+} + 4H_2O \rightleftharpoons Pb_4(OH)_4^{4+} + 4H^+$	log $\beta_{4,4}$	-19.25 ± 0.1	-19.90 ± 0.1
$3Pb^{2+} + 4H_2O \rightleftharpoons Pb_3(OH)_4^{2+} + 4H^+$	log $\beta_{4,3}$	-22.87 ± 0.1	-23.35 ± 0.1
$6Pb^{2+} + 8H_2O \rightleftharpoons Pb_6(OH)_8^{4+} + 8H^+$	log $\beta_{8,6}$	-42.14 ± 0.1	-42.66 ± 0.1

DISCUSSION

The present investigation agrees with the earlier works by Pedersen [1] and Faucherre [2] in so far as they also found evidence for the complexes $Pb_4(OH)_4^{4+}$ and $PbOH^+$. The numerical values of the equilibrium constants seem to agree less satisfactorily. However, they have often been determined in different media and are therefore not directly comparable.

Faucherre's values for $\beta_{4,4}$ were obtained from his measurements on $Pb(NO_3)_2$ solutions, which also contained $Ba(NO_3)_2$ to make the ionic strength, I, 0.6 or 0.06. Pedersen also determined $\beta_{4,4}$ in mixtures of $Pb(NO_3)_2$ and $Ba(NO_3)_2$ at different I and has given a formula from which log $\beta_{4,4}$ can be calculated knowing I. In the table below the results of these authors are compared.

I	log $\beta_{4,4}$ (Faucherre)	log $\beta_{4,4}$ (Pedersen)
0.6	-18.75	-20.81
0.06	-18.05	-20.61

In perchlorate medium Faucherre did not determine $\beta_{4,4}$ directly. He calculated theoretical Z curves for $Pb_4(OH)_4^{4+}$ with $\log \beta_{4,4} = -18.75$ obtained with nitrate medium, and from the fact that these curves satisfactorily pass through his experimental points in 1 M $NaClO_4$ the value in this medium must be close to -18.75. This value differs by 0.5 units from our value in 3 M $NaClO_4$.

The lower value for $\beta_{4,4}$ in nitrate medium, found by Pedersen, is reasonable considering the complex formation between Pb^{2+} and NO_3^-. The values found by Faucherre with the same medium, therefore, seem to be somewhat in error.

The discrepancy between the results obtained by Faucherre and us from measurements on solutions with $Z > 1$ is probably due mainly to his mode of calculation. His calculations were based on the assumption that the lead(II) at $Z = 1$ is present solely as $Pb_4(OH)_4^{4+}$, which is not correct.

The values for $\log \beta_{11}$ found in the literature range between -6.2 and -8.7. There is, however, no value from perchlorate solutions.

The complexes found probably have closed structures but we shall at the present stage refrain from any structure proposals.

Acknowledgements. The author is indebted to Professor Lars Gunnar Sillén for his continual interest in this work and to Professor Robert E. Connick, Univ. of Calif., for valuable criticism of the manuscript. He also wishes to thank Dr. George Biedermann for discussions on practical aspects of the research and for comments in the manuscript. Thanks are also due to Mr. György Patzauer for skilful help with some of the measurements and calculations and to Mr. Frans Eriksson for construction of the apparatus. The English of this paper has been corrected by Mr. David Martin. This work has been supported by *Statens Tekniska Forskningsråd (Swedish Technical Research Council)* and the *Air Force Office of Scientific Research of the Air Research and Development Command, United States Air Force,* through its European Office.

REFERENCES

1. Pedersen, K. J. *Kgl. Danske Videnskab. Selskab, Mat.-fys. Medd.* (1945) 22:10.
2. Faucherre, J. *Bull. soc. chim. France* **1954** 128.
3. Kullgren, C. *Z. physik. Chem.* **85** (1913) 466.
4. Denham, H. G. and Marris, N. A. *Trans. Faraday Soc.* **24** (1928) 515.
5. Cranston, J. A. and Brown, H. F. *J. Roy. Tech. Coll. (Glasgow)* **4** (1937) 54.
6. Guiter, H. *Bull. soc. chim. France* **1947** 269.
7. Reiff, F. and Müller, A. *Z. anorg. allgem. Chem.* **229** (1936) 285.
8. Misra, R. N. and Pani, S. *J. Indian Chem. Soc.* **34** (1957) 387.
9. Pattanaik, R. K. and Pani, S. *J. Indian Chem. Soc.* **34** (1957) 709.
10. Ramette, R. W. *J. Chem. Educ.* **36** (1959) 191.
11. Goward, G. W. *Thesis.* Princeton Univ. 1954, Univ. Microfilms 9414.
12. Johnson, J. S. and Kraus, K. A. *ORNL-2386,* **1957** 99.
13. Forsling, W., Hietanen, S. and Sillén, L. G. *Acta Chem. Scand.* **6** (1952) 901.
14. Gran, G. *Analyst* **77** (1952) 661.
15. Biedermann, G. and Sillén, L. G. *Arkiv Kemi* **5** (1953) 425.
16. Olin, Å. *Acta Chem. Scand.* **11** (1957) 1445.
17. Berecki-Biedermann, C. *Arkiv Kemi* **9** (1956) 175.
18. Han, J. E. S. and Chao, T. Y. *Ind. Eng. Chem. Anal. Ed.* **4** (1932) 229.
19. Scott, W. W. *Standard Methods of Chemical Analysis,* 5th Ed. p. 500.
20. Gentry, C. H. R. and Sherrington, L. G. *Analyst* **71** (1946) 31.
21. Tobias, R. S. *Acta Chem. Scand.* **12** (1958) 198.

22. Sillén, L. G. *Acta Chem. Scand.* **8** (1954) 299.
23. Sillén, L. G. *Acta Chem. Scand.* **10** (1956) 186.
24. Biedermann, G. and Sillén, L. G. *Acta Chem. Scand.* **10** (1956) 1011.
25. Hietanen, S. and Sillén, L. G. *Acta Chem. Scand.* **6** (1952) 747.
26. Biedermann, G. *Arkiv Kemi* **5** (1953) 441.
27. Hedström, B. O. A. *Arkiv Kemi* **6** (1953) 1.
28. Biedermann, G. *Arkiv Kemi* **9** (1956) 277.
29. Biedermann, G., Kilpatrick, M., Pokras, L. and Sillén, L. G. *Acta Chem. Scand.* **10** (1956) 1327.

Received August 25, 1959.

ACTA CHEMICA SCANDINAVICA 14 (1960) 151–156

Conjugate Additions of Grignard Reagents to alpha,beta-Unsaturated Esters

VII. Additions to Acetylenic Esters

CLAUS BRETTING, JON MUNCH-PETERSEN, PEER MØLLER JØRGENSEN and SUSANNE REFN

Organisk-kemisk Laboratorium, Polyteknisk Læreanstalt, Copenhagen, Denmark

The reactions of *n*-butylmagnesium bromide with esters of phenylpropiolic, tetrolic and acetylenedicarboxylic acids have been investigated. With *sec*-butyl phenylpropiolate and tetrolate conjugate addition takes place if the reaction is catalyzed by cuprous chloride; otherwise tertiary acetylenic alcohols are formed. Diethyl acetylenedicarboxylate gave a small yield of conjugate addition product when the reaction was uncatalyzed and the reaction time very short. The ethyl ester of phenylpropiolic acid gave unsatisfactory results. The general reactivity of the triple bond is considered.

Isolated carbon-carbon triple bonds are in general more reactive towards nucleophilic reagents than are double bonds. Thus, alcohols are added, in the presence of the corresponding alkoxides, to alkynes but not to alkenes. Sometimes electrophilic catalysts, such as certain metallic salts, must be present in order to secure addition, *e.g.* the additions of water and hydrogen cyanide to acetylene in the presence of mercuric sulfate and cuprous chloride, respectively. As in the case of the ethylenic bond, a carbonyl group in conjugation with the multiple bond will enhance the reactivity towards nucleophilic reagents and, conversely, reduce the reactivity towards electrophilic reagents. Thus, α,β-acetylenic esters are known to add nucleophilic reagents without the presence of a catalyst:

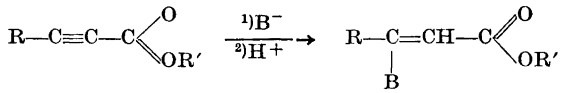

Several Michael-type condensations with malonic and cyanoacetic esters are described in the literature [1] for the cases of phenylpropiolic, tetrolic, propiolic and acetylenedicarboxylic esters. Other nucleophilic reagents, such as

ammonia [2] and phenylhydrazine [2,3], have also been added to the triple bond of α,β-acetylenic esters. Recently, the addition of methyl thioglycolate to dimethyl acetylenedicarboxylate has been described [4]. In this, as well as some of the above cases, the primarily formed products undergo further reactions under certain conditions.

Also reactions of Grignard reagents with α,β-acetylenic esters are described in the literature. Wilson and Hyslop [5] found that only normal tertiary alcohols were formed from ethyl phenylpropiolate and methyl- and phenylmagnesium bromides. No yields were reported. Hurd and Cohen [6], however, were able to obtain the ketone (phenylpropiolophenone) from ethyl phenylpropiolate and phenylmagnesium bromide in 85 % yield. Thus in these as well as in some other cases [7] only 1,2-additions (to the carbonyl group) have been encountered.

With acetylenic ketones Kohler [8] has found that benzoyl-phenylacetylene with phenylmagnesium bromide gives exclusively 1,2-addition under conditions where the corresponding ethylenic compound, benzalacetophenone, gives chiefly 1,4-addition. However, Fuson and Meek [9] have found that with mesitoyl-phenylacetylene, in which the carbonyl group is sterically hindered, 1,4-addition of methyl- and mesitylmagnesium bromides takes place in good yields, although the yield with phenylmagnesium bromide is only 20 %.

In the present investigation certain α,β-acetylenic esters have been subjected to the action of *n*-butylmagnesium bromide under conditions which have previously been found favourable for conjugate addition to α,β-ethylenic esters, uncatalyzed [10] as well as catalyzed by cuprous chloride [11]. The results are given in Table 1.

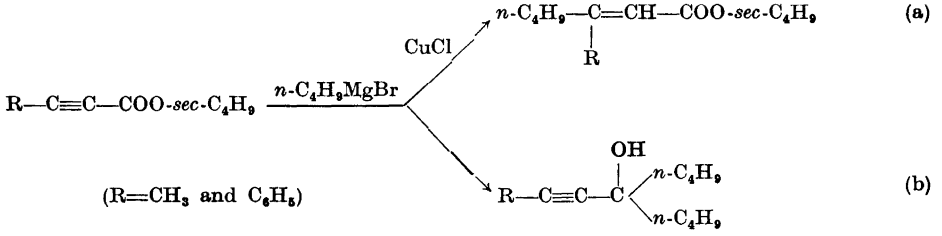

In the uncatalyzed reactions (*b*) *sec*-butyl tetrolate and phenylpropiolate, in contrast to the corresponding ethylenic compounds, do not give conjugate addition products but carbonyl addition products (*i.e.* tertiary alcohols) *. These results prove the triple bond of acetylenic esters to be less reactive towards Grignard reagents than the double bond in ethylenic esters.

This is in agreement with other evidence that a triple bond to a much less degree than a double bond is able to participate in conjugation with other multiple bonds [12]. For example, the methyl group of ethyl tetrolate does not

* The yield of tertiary alcohol from phenylpropiolic ester (also the ethyl ester, *cf.* below) is diminished by the formation of varying quantities of a lower boiling (106—107°/5 mm) product with higher refractive index (n_D^{25} 1. 5392). This compound, which rather quickly turns into a viscous yellow syrup, may be an elimination product from the tertiary alcohol. It contains oxygen, but shows no infra-red absorption for either carbonyl or hydroxyl groups.

Table 1. Type of products and yields from reactions of α,β-acetylenic esters with *n*-butylmagnesium bromide.

	No catalyst	CuCl-catalyst
sec-Butyl phenylpropiolate	Tertiary alcohol [a] (1,2-addition) 28–47 % [b]	Ethylenic ester [c] (1,4-addition) 55 %
Ethyl phenylpropiolate	Tertiary alcohol [a] (1,2-addition) 21–37 % [b]	High-boiling, non-destillable product
sec-Butyl tetrolate	Tertiary alcohol [d] (1,2-addition) 63 %	Ethylenic ester [e] (1,4-addition) 73 %
Di-*sec*-butyl acetylenedicarboxylate (crude)		High-boiling, non-distillable product. Tar
Diethyl acetylenedicarboxylate [f]	Diethyl di-*n*-butylsuccinate [g] 15 % Mostly high-boiling residue	High-boiling, non-distillable product [h]

[a] Phenylethynyl-di-*n*-butylcarbinol, b.p. 131°/0.9 mm, n_D^{25} 1.5213. (Found: C 83.50; H 9.69. Calc. for $C_{17}H_{24}O$ (244.36): C 83.55; H 9.90). [b] *cf.* foot-note, page 152. [c] *sec*-Butyl β-*n*-butylcinnamate, b.p. 124.5°/0.8 mm, n_D^{20} 1.5072. (Found: C 78.40; H 9.19. Calc. for $C_{17}H_{24}O_2$ (260.36): C 78.42; H 9.29). [d] 1-Propynyl-di-*n*-butylcarbinol, b.p. 108°/11 mm, n_D^{20} 1.4562. (Found: C 79.15; H 12.07. Calc. for $C_{12}H_{22}O$ (182.30): C 79.06; H 12.16). [e] *sec*-Butyl 3-methylhept-2-enoate (β-*n*-butylcrotonate), b.p. 104–105°/13 mm, n_D^{20} 1.4478. (Found: C 72.65; H 10.96. Calc. for $C_{12}H_{22}O_2$ (198.30): C 72.68; H 11.18). [f] Ester added during ½ h only, and worked up immediately. [g] B.p. 97–102°/0.7 mm, n_D^{25} 1.4379. (Found: C 67.15; H 10.30. Calc. for $C_{16}H_{30}O_4$ (286.40): C 67.09; H. 10.56). [h] This result was obtained also when the addition time for the ester was reduced to ½ h.

show any reactivity towards carbonyl groups in condensation processes of the aldol or Claisen types as compared with ethyl crotonate, which is the vinylog of ethyl acetate [13]. Furthermore, it has been found by G. Østrup of this department [14] that, in the preparation of tetrolyl chloride from the acid and thionyl chloride, addition of hydrogen chloride to the multiple bond takes place to a considerable degree, whereas this is not the case in the analogous preparation of crotonyl chloride, in which the reactivity of the double bond towards electrophilic reagents is strongly reduced by conjugation with the carbonyl group.

The mechanism which has been proposed for conjugate addition af Grignard reagents to α,β-ethylenic systems [15] involves a cyclic synchronous electron

shift within a six-membered ephemeral ring, the energy of activation thereby being especially low. In the corresponding reaction with acetylenic esters, however, the conditions for such a mechanism is much less favourable, since the linearity of the triple bond prevents the formation of a regular hexagon.

The presence of cuprous chloride (*a*, above) has the drastic effect of changing completely the direction of addition from 1,2- to 1,4-addition, the sole products now being the *sec*-butyl esters of *β*-*n*-butyl-*α*,*β*-ethylenic acids. This is in agreement with the above-mentioned catalytic effect of metallic salts on additions to the triple bond, and also with the previously described general effect of cuprous chloride that the presence of this compound promotes conjugate additions of Grignard reagents to *α*,*β*-unsaturated esters in competition with carbonyl addition reactions [11].

Diethyl acetylenedicarboxylate was used besides the *sec*-butyl ester, since the latter proved to be difficult to obtain in a pure state, probably due to elimination and decarboxylation during the distillation. Both esters were found to give only tarry or high-boiling products when the standard cuprous chloride catalyzed procedure was followed. A similar result has apparently been obtained by Gilman and Robinson [16] in the uncatalyzed reaction of diethyl acetylenedicarboxylate and phenylmagnesium bromide. On the other hand, Michael [17] has reported the formation in 20—25 % yield of diethyl ethylfumarate by treating diethyl acetylenedicarboxylate for a long period with ethyl iodide in the presence of zinc. No details are given.

We have found that when the addition of *n*-butylmagnesium bromide was uncatalyzed and performed quickly a small yield of a well-defined product could be obtained. This proved to be a di-*n*-butylsuccinic ester, which was presumably formed by two 1,4-additions to the triple bond. For sterical reasons one would expect the product to be an *α*,*α*′-isomer, but previous investigations of conjugate additions to citraconic and mesaconic esters [18] have shown that in such cases mixtures of isomers may be formed. No attempts were made during the present work to determine the structure of the dibutylsuccinic ester.

In the above-mentioned addition of methyl thioglycolate to dimethyl acetylenedicarboxylate [4], the use of piperidine as a catalyst likewise resulted in two 1,4-additions, the *α*,*α*′-product presumably being formed.

Apparently acetylenedicarboxylic esters are far more reactive than the mono-carboxylic esters, and in the presence of cuprous chloride polymerisation takes place. This was also the case with ethyl phenylpropiolate, when cuprous chloride was present, whereas the *sec*-butyl ester under these conditions did give the 1,4-addition product. The uncatalyzed reaction with ethyl phenylpropiolate gives the same products as does the *sec*-butyl ester.

EXPERIMENTAL

Microanalyses are by Mr. Preben Hansen, Microanalytical Division, The Chemical Laboratory, The University of Copenhagen. Fractional distillations were through a simple 45 cm × 8 mm Podbielniak type column with a tantalum wire spiral, a heated jacket and a partial reflux head.

Preparations of α,β-acetylenic acids

Phenylpropiolic acid [19] and *acetylenedicarboxylic acid* [20] were obtained according to the directions in *Organic Syntheses*.

Tetrolic acid. But-2-yn-1-ol was prepared as described in *Organic Syntheses* [21]: 1,3-dichlorobut-2-ene (Eastman, technical) * was hydrolyzed to 3-chlorobut-2-en-1-ol and from this hydrogen chloride was eliminated by means of sodium amide in liquid ammonia. The butynol, dissolved in acetone, was oxidized with chromic anhydride in sulfuric acid as described for the preparation of propiolic [22] and γ-chlorotetrolic [23] acids. The yield of of tetrolic acid, b. p. 93—98°/15 mm, m. p. 72—73° (from ligroin) was 40 %. The overall yield from 1,3-dichlorobut-2-ene was about 20 %, but could probably be improved.

Preparations of α,β-acetylenic esters

sec-*Butyl esters* were prepared by esterification of the acids as previously described [24]: sec-*Butyl phenylpropiolate*, b. p. 112—113°/1 mm, n_D^{20} 1.5368, yield 58 %. (Found: C 77.10; H 6.80. Calc. for $C_{13}H_{14}O_2$ (202.34): C 77.20; H 6.98.) sec-*Butyl tetrolate*, b.p. 72—73°/12 mm, n_D^{25} 1.4392, yield 59 %. (Found: 68.70; H 8.66. Calc. for $C_8H_{12}O_2$ (140.18): C 68.54; H 8.63.) *Di*-sec-*butyl acetylenedicarboxylate;* by the distillation gas-evolution took place, and the pressure and boiling point were fluctuating. The main fraction passed over at 110—113°/1.4—1.8 mm, n_D^{20} 1.4479; the yield was only about 20 % and the analysis was slightly incorrect (about 1 % in carbon).

Diethyl acetylenedicarboxylate was prepared by an esterification procedure similar to that described in *Organic Syntheses* for the dimethyl ester [25]; b. p. 63—64°/1 mm, n_D^{25} 1.4418. (Found: C 56.50; H 5.92. Calc. for $C_8H_{10}O_4$ (170.16): C 56.46; H 5.92.)

Ethyl phenylpropiolate was obtained by sulfuric acid catalyzed esterification of the acid with excess of ethanol under reflux for 8 h; b. p. 87—89°/0.8 mm (rep.[5] 104°/1.5 mm), n_D^{20} 1.5534, yield 76 %. (Found: C 75.90; H 5.86. Calc. for $C_{11}H_{10}O_2$ (174.19): C 75.84; H 5.79).

Addition reactions

These were carried out as previously described [10,11], except in one case with diethyl acetylenedicarboxylate (see Table 1).

The identity of the reaction products were further checked by *infra-red spectroscopy*. The spectra were measured with a Beckman IR2 spectrophotometer with sodium chloride prisms, using 5 % solutions in carbon tetrachloride. The alcohols were identified by their hydroxyl band in the 3 μ regicn and by the absence of a carbonyl absorption. The spectra of the esters showed an absorption at 1 715 cm^{-1} within the carbonyl region for α,β-unsaturated esters, as well as a somewhat weaker band around 1 650 cm^{-1} (C=C stretching vibration). Furthermore, the *sec*-butyl esters also showed the group of absorption bands around 1 111 cm^{-1}, which has previously been found in the spectra of other *sec*-butyl carboxylates [18]. The diethyl di-*n*-butylsuccinate (from diethyl acetylenedicarboxylate) showed the normal carbonyl band for saturated ester at 1 730 cm^{-1}, but no absorption for conjugated C=O, C=C or OH.

The authors want to express their gratitude towards *Otto Mønsteds Fond* and *Det Teknisk-Videnskabelige Forskningsraad* for financial support.

* The authors are indebted to *Dansk Esso A/S*, Copenhagen, for the generous gift of this chemical.

REFERENCES

1. Gidvani, B. S., Kon, G. A. R. and Clifford, R. W. *J. Chem. Soc.* **1932** 1027; Gidvani, B. S. and Kon, G. A. R. *J. Chem. Soc.* **1932** 2443; Farmer, E. H., Ghosal, S. C. and Kon, G. A. R. *J. Chem. Soc.* **1936** 1804; Michael, A. *J. Org. Chem.* **2** (1937) 303.
2. Feist, F. *Ann.* **345** (1906) 110 [Henecka, H. *Chemie der beta-Dicarbonylverbindungen*, Springer Verlag, Berlin 1950, p. 193].
3. Buchner, E. *Ber.* **22** (1889) 2929.
4. Fiesselmann, H. and Schipprak, P. *Chem. Ber.* **87** (1954) 835.
5. Wilson, F. J. and Hyslop, W. McNinck *J. Chem. Soc.* **123** (1923) 2612.
6. Hurd, C. D. and Cohen, F. L. *J. Am. Chem. Soc.* **53** (1931) 1073.
7. Vassiliades, C. and Capatos, L. *Compt. rend.* **194** (1932) 1830 [*Chem. Abstracts* **26** (1932) 4306]; Dufraisse, C. and Monier, J.-A. *Compt. rend.* **196** (1933) 1327 [*Chem. Abstracts* **27** (1933) 3471]; Dufraisse, C. and Rocher, H. *Bull. soc. chim. France* [5] **2** (1935) 2235.
8. Kohler, E. P. *Am. Chem. J.* **38** (1907) 511 [*Chem. Abstracts* **2** (1908) 826].
9. Fuson, R. C. and Meek, J. S. *J. Org. Chem.* **10** (1945) 551.
10. Munch-Petersen, J. *Acta Chem. Scand.* **12** (1958) 967.
11. Munch-Petersen, J. *Acta Chem. Scand.* **12** (1958) 2007, 2046.
12. See also Staab, H. A. *Einführung in die theoretische organische Chemie*, Verlag Chemie, Weinheim 1959, p. 139 and 350; Royals, E. E. *Advanced Organic Chemistry*, Prentice-Hall, Englewood Cliffs, N. J. 1954, p. 514.
13. Feist, F. *Ann.* **345** (1906) 100; Ingold, E. H. *J. Chem. Soc.* **127** (1925) 1199. *Cf.* Wislicenus, W. and Schöllkopf, K. *J. prakt. Chem.* [2] **95** (1917) 269. [*Chem. Zentr.* **1917 II**, 803].
14. Østrup, G. *Unpublished observation.*
15. For references, see Ref.[18]
16. Gilman, H. and Robinson, J. D. *Bull. soc. chim. France* [4] **45** (1929) 636.
17. Michael, A. *Ber.* **29** (1896) 1791.
18. Bjerl Nielsen, E., Munch-Petersen, J., Møller Jørgensen, P. and Refn, S. *Acta Chem. Scand.* **13** (1959) 1943.
19. Abbott, T. W. *Organic Syntheses, Coll. Vol.* **II** (1943) 515.
20. Abbott, T. W., Arnold, R. T. and Thompson, R. B. *Organic Syntheses, Coll. Vol.* **II** (1943) 10.
21. Ashworth, P. J., Mansfield, G. H. and Whiting, M. C. *Organic Syntheses* **35** (1955) 20.
22. Wolf, V. *Chem. Ber.* **86** (1953) 735.
23. Olomucki, M. *Compt. rend.* **246** (1958) 1877 [*Chem. Abstracts* **52** (1958) 17096 g].
24. Munch-Petersen, J. *J. Org. Chem.* **22** (1957) 170.
25. Fones, W. S. *Organic Syntheses* **32** (1952) 55.

Received September 9, 1959.

ACTA CHEMICA SCANDINAVICA 14 (1960) 157–179

Least Squares Calculations of Equilibrium Constants for some Metal Complexes *

JAN RYDBERG**

Chemistry Division, Argonne National Laboratory, Lemont, Illinois, U.S.A.

The least squares technique demonstrated in an earlier paper [1] has been applied to complexes formed between a number of different organic ligands and rare earth and actinide metals. The consequences of various weighing procedures are discussed and demonstrated in the examples. A comparison is carried out between the results of the least squares calculations and the results of earlier (usually graphical) computations, and the reasons for the discrepancies are discussed.

In a recent paper [1] it was demonstrated how equilibrium constants could be calculated from solvent extraction data by the methods of least squares and using high-speed digital computers. These calculations rapidly yielded the maximum number of equilibrium constants and their precision. On the other hand it was also indicated that — in the absence of very precise experimental data — the earlier graphical methods gave equilibrium constants, which cannot be supported by the results of the least squares calculations.

It was therefore felt to be of value to make a more comprehensive comparison between various methods of calculating equilibrium constants from solvent extraction data. For that purpose, a series of papers by Bernström, Dyrssen, Rydberg, *et al.* [2–14] was selected, in which a number of different graphical computations of equilibrium constants have been used.

The principles of the various computational methods are briefly outlined below, together with the relation between the primary parameters obtained and the equilibrium constants calculated from them. The least squares method will not be described in any detail, because its use in this kind of investigations has been fully treated in earlier papers [1,15]. The result of this investigation is summarized in Table 1, where equilibrium constants computed by the least squares method can be compared with the constants determined by earlier methods.

* Based on work performed under the auspices of the U. S. Atomic Energy Commission.

** On leave from the University of Stockholm, and the Research Institute of National Defense, Stockholm, Sweden.

OUTLINE OF VARIOUS COMPUTATIONAL PROCEDURES

The most commonly used methods for calculation of equilibrium constants from solvent extraction data are the ligand number method (sometimes called the Bjerrum method; *e.g.* Refs.[2,16,17]) the limiting value method (sometimes called the Leden method; *e.g.* Refs.[2,17,18]) and the two-parameter method (sometimes called the Dyrssen-Sillén method [14]).

The basic equation for all the solvent extraction work discussed here is [2]

$$Q = \frac{\lambda_\nu \beta_\nu [\mathrm{A}]^\nu}{\sum_0^N \beta_n [\mathrm{A}]^n} \qquad (1)^*$$

where Q is the distribution ratio between the organic and aqueous phases of all mononuclear forms of the metal (charge $+\nu$) at constant activity factors for all species involved, [A] is the concentration of free (uncomplexed) ligand ion (here assumed to be monovalent), λ_ν is the partition constant of the uncharged MA_ν complex between the two solvents, and β_n is the gross complexity constant as defined by

$$\beta_n = \frac{[\mathrm{MA}_n]}{[\mathrm{M}]\ [\mathrm{A}]^n} = \prod_0^n k_n \qquad (2)$$

where by definition $\beta_0 = k_0 = 1$, and k_n is the stepwise complexity constant. For simplicity the charges of the ions have been omitted. N is the maximum coordination number of A for M.

1. *The ligand number method.* It has been shown [2] that

$$\frac{\mathrm{d} \log Q}{\mathrm{d} \log [\mathrm{A}]} = \nu - \bar{n} \qquad (3)$$

where $\bar{n}$ is the mean ligand number defined by [16]

$$\bar{n} = \frac{\sum_1^N n[\mathrm{MA}_n]}{\sum_0^N [\mathrm{MA}_n]} \qquad (4)$$

Since ν is known, the graphical derivation of the curve log Q *versus* log [A] will yield $\bar{n}$. Eqn. 4 can be rearranged to

$$\sum_0^N (\bar{n} - n)\ \beta_n\ [\mathrm{A}]^n = 0. \qquad (5)$$

* The symbols used here conform with those in Refs. [1,15], and differ slightly from those in Refs. [2-14]

By choosing N number of points $\bar{n}_i([A]_i)$ on the curve $\bar{n}$ *versus* log [A], preferably at $\bar{n}_i = 0.5, 1.5, \ldots\ldots N-0.5$, a set of N equations are obtained. The solution of this set of equations by determinants using Cramer's rule is straightforward.

2. *The limiting value method.* Equation 1 can be rearranged to

$$Q^{-1} = \frac{1}{\lambda_\nu} \sum_{N}^{0} \varphi_{\nu-n}[A]^{n-\nu} \tag{6}$$

If, *e.g.* for $\nu = N$, Q^{-1} is plotted against $[A]^{-1}$, the limiting value when $[A]^{-1} \to 0$ of the resulting curve will yield

$$\lim_{[A]^{-1} \to 0} Q^{-1} = \frac{\psi_0}{\lambda_\nu} + \frac{\psi_1}{\lambda_\nu} [A]^{-1} (+ \ldots.)$$

Since $\psi_0 = 1$, the intercept on the Q^{-1} axes will be $1/\lambda_\nu$, and the slope at the intercept will be ψ_1/λ_ν. By then setting $F_1 = \left(\frac{\lambda_\nu}{Q} - 1\right)[A]$ and taking the limiting value of F_1 when $[A]^{-1} \to 0$, the new intercept value will be ψ_1 and the corresponding slope ψ_2; similarly all ψ_n and λ_ν can be determined. The relation between ψ and β is given by

$$\psi_{\nu-n} = \beta_n/\beta_\nu \tag{7}$$

3. *The two-parameter method.* It is assumed [14] that the relation between the equilibrium constants can be approximated to

$$\log \beta_N = Np_1 \tag{8}$$

and

$$\log k_n/k_{n+1} = 2p_2 \tag{9}$$

Here 10^{p_1} is called the mean complexity constant, and 10^{2p_2} is called the mean spreading factor.

When these relations are introduced into eqn. 1, it becomes

$$Q = \frac{\lambda_\nu [A]^\nu \, 10^{\nu[p_1+p_2(N-\nu)]}}{\sum_{0}^{N} [A]^n 10^{n[p_1+p_2(N-n)]}} \tag{10}$$

It is seen that in addition to λ_ν this equation only contains two unknown parameters, p_1 and p_2. For a given combination of ν and N (which are known parameters) a family of curves log Q/λ_ν as a function of log ([A] + p_1) can be constructed, each curve representing a specific p_2 value. By placing this family of curves (*e.g.* suitably etched on a clear plastic ruler) over the experimental points log Q *versus* log [A], the curve with the best fit can be found; from the curvature and intercepts on the two axes, the parameters λ_ν, p_1 and p_2 are obtained.

4. *The least squares method.*
Eqn. 1 can be rearranged to

$$z = \sum_{0}^{N} a_n [\mathrm{A}]^n \tag{11}$$

where

$$z = [\mathrm{A}]^p/Q \tag{12}$$

and

$$a_n = \beta_n/\lambda_p\beta_p \tag{13}$$

Eqn. 11 can be solved by the method of weighted least squares using high speed digital computers [1,15] to cut down on the computation time. It will then yield $a_n \pm \sigma_{a_n}$, where σ_{a_n} is the standard deviation in a_n. The weight, which has to be assigned to the z_i values, depends on the precision of the measurements of Q_i.

Several kinds of standard errors in Q have been tested here for solvent extraction data: (1) errors in Q (or in I_{org} and I_{aq}, which represent measured standardized radioactivities of the organic and aqueous phases) given in the original paper, (2) a counting error in Q, called $\sigma_Q(I)$, based on the assumption that the number of measured counts is 5 times that given for the intensities (5 min. measurement if I is given in counts per min., cpm) and that the background error is ± 1 (thus, *e.g.* $\sigma(I_{aq}) \approx 1 + \sqrt{I_{aq}/5}$), (3) a constant percentage (**P**) error, called $\sigma_Q(\%)$, making $\sigma_Q(\%) = \mathbf{P}\ Q$, (4) errors in Q caused by errors in the determination of the free ligand concentration. These kinds of errors are more extensively discussed elsewhere [1].

Since the weight of a point $z_i(x_i)$ is defined here as one over the variance σ_i^2 of the z_i value, *i.e.* $\omega_i = 1/\sigma_i^2$, the weight of all points can be changed by multiplying the variance with a constant factor. This will not change the $a_n \pm \sigma_{a_n}$ values, *cf.* Ref.[15], but will alter the χ^2 values (*e.g.* Ref.[20]), which also are calculated in the computer program [1,15]. Since the ratio χ^2/k should be within the range 0.5—1.5 for a reasonable consistency between the experimental data and the equations used for computing a_n, χ^2/k can be brought into this range by changing the weights of the data. This procedure is used all through this investigation to see what size of standard error should have been assigned to the original data. The k value is the number of degrees of freedom in the computations and is equal to $L-N-1$ for eqn. 11; L is the number of experimental points.

It is obvious that when $\sigma_{a_n} > a_n$, the a_n value is of little statistical significance. If such an a_n value is obtained, it is omitted from eqn. 11 and the least squares computations are repeated without it. Though this means mathematically that the particular a_n value is put equal to zero, it should be interpreted only as a way of removing parameters from the calculations which can only be determined very inaccurately; this usually causes only small changes in the remainning parameters (see paragraphs a and d below). Similarly, negative a_n values are omitted, because in the deductions of the basic solvent extraction equations only positive concentrations of the complexes are assumed to exist.

Table 1. Survey of the investigated systems.

§	System	Original method *		Least squares method	
		Primary parameters	Equilibrium constants	Primary parameters	Equilibrium constants
a	Th(IV)-acetylacetone-benzene-0.01M $NaClO_4$	$\psi_1 \times 10^5 = 1.0 \pm 0.1$ $\psi_2 \times 10^{12} = 5.4 \pm 0.3$ $\psi_3 \times 10^{19} = 1.0 \pm 0.2$ $\psi_4 \times 10^{27} = 1.5 \pm 0.5$ $\lambda_4 = 330 \pm 30$	$(\log k_1 = 7.82 \pm 0.16)$ $(\log k_2 = 7.73 \pm 0.09)$ $\log k_3 = 6.27 \pm 0.05$ $\log k_4 = 5.00 \pm 0.04$ $\log \lambda_4 = 2.52 \pm 0.04$	$a_0\ 10^{30} = 4.89 \pm 0.93$ $a_2\ 10^{14} = 1.81 \pm 0.07$ $a_3\ 10^8 = 2.53 \pm 0.22$ $a_4\ 10^3 = 3.41 \pm 0.45$	$\log k_1k_2 = 15.57 \pm 0.08$ $\log k_3 = 6.15 \pm 0.04$ $\log k_4 = 5.14 \pm 0.07$ $\log \lambda_4 = 2.48 \pm 0.06$
b	Th(IV)-acetylacetone-chloroform-0.1 M $NaClO_4$	$\beta_1 = 1.0 \times 10^8$ $\beta_2 = 3.0 \times 10^{15}$ $\beta_3 = 3.0 \times 10^{21}$ $\beta_4 = 6.0 \times 10^{26}$ $\lambda_4 = 350 \pm 20$	** $\log k_1 = 8.00 \pm 0.17$ $\log k_2 = 7.48 \pm 0.14$ $\log k_3 = 6.00 \pm 0.11$ $\log k_4 = 5.30 \pm 0.05$ $\log \lambda_4 = 2.55 \pm 0.03$	$a_1\ 10^{22} = 7.2 \pm 3.2$ $a_2\ 10^{14} = 1.96 \pm 0.44$ $a_3\ 10^8 = 1.32 \pm 1.13$ $a_4\ 10^3 = 2.95 \pm 1.33$	$\log k_2 = 7.43 \pm 0.21$ $\log k_3 = 5.83 \pm 0.39$ $\log k_4 = 5.35 \pm 0.42$ $\log \lambda_4 = 2.53 \pm 0.20$
c	U(IV)-acetylacetone-benzene-0.1 M $NaClO_4$	p_1, p_2 } Not given in original paper $\log \lambda_4 = 3.62 \pm 0.05$	$\log k_1 = 9.05 \pm 0.10$ $\log k_2 = 7.97 \pm 0.17$ $\log k_3 = 6.90 \pm 0.18$ $\log k_4 = 5.84 \pm 0.11$ $\log \lambda_4 = 3.62 \pm 0.05$	$a_0 \times 10^{34} = 3.9 \pm 2.2$ $a_1 \times 10^{25} = 4.0 \pm 1.3$ $a_2 \times 10^{17} = 7.3 \pm 1.0$ $a_3 \times 10^{10} = 2.40 \pm 0.45$ $a_4 \times 10^4 = 2.29 \pm 0.13$	$\log k_1 = 9.02 \pm 0.29$ $\log k_2 = 8.26 \pm 0.15$ $\log k_3 = 6.52 \pm 0.09$ $\log k_4 = 5.98 \pm 0.09$ $\log \lambda_4 = 3.64 \pm 0.025$
d	Pu(IV)-acetylacetone-benzene-0.1 M $NaClO_4$	ψ_1, ψ_2, ψ_3, ψ_4, λ_4 } Not given in original paper	$\log k_1 = 10.8 \pm 1.0$? $\log k_2 = 8.6\ (\pm 0.2)$ $\log k_3 = 8.6\ (\pm 0.3)$ $\log k_4 = 6.0\ (\pm 0.3)$ $\log \lambda_4 = 2.56\ (\pm 0.2)$		
		$\beta_1 = 1.3 \times 10^{10}$ $\beta_2 = 1.6 \times 10^{19}$ $\beta_3 = 5.0 \times 10^{27}$ $\beta_4 = 8.0 \times 10^{33}$ $\log \lambda_4 = 2.50$	$\log k_1 = 10.0\ (\pm 1)$ $\log k_2 = 9.1\ (\pm 0.2)$ $\log k_3 = 8.5\ (\pm 0.3)$ $\log k_4 = 5.9\ (\pm 0.3)$ $\log \lambda_4 = 2.50\ (\pm 0.2)$	$a_1 \times 10^{27} = 6.1 \pm 1.5$ $a_3 \times 10^9 = 3.6 \pm 0.5$ $a_4 \times 10^3 = 2.9 \pm 0.5$	$\log k_2k_3 = 17.77 \pm 0.12$ $\log k_4 = 5.91 \pm 0.09$ $\log \lambda_4 = 2.54 \pm 0.07$
		$p_1 = 8.5\ (\pm 0.1)$ $p_2 = 0.8\ (\pm 0.1)$ $\log \lambda_4 = 2.44\ (\pm 0.1)$	$\log k_1 = 10.9\ (\pm 0.18)$ $\log k_2 = 9.3\ (\pm 0.14)$ $\log k_3 = 7.7\ (\pm 0.14)$ $\log k_4 = 6.1\ (\pm 0.18)$ $\log \lambda_4 = 2.44\ (\pm 0.1)$		

e	Th(IV)-cinnamic acid-hexone-0.1 M $NaClO_4$	$p_1 = 3.6$ $p_2 = 0.2$ $\log \lambda_4 \approx 3.7$	$\log k_1 = 4.2$ $\log k_2 = 3.8$ $\log k_3 = 3.4$ $\log k_4 = 3.0$ $\log \lambda_4 \approx 3.7$	$a_1 \times 10^{14} = 2.52 \pm 0.93$ $a_4 \times 10^4 = 6.61 \pm 2.02$	$\log k_2k_3k_4 = 10.42 \pm 0.21$ $\log \lambda_4 = 3.18 \pm 0.13$
f	Th(IV)-cinnamic acid-chloroform-0.1 M $NaClO_4$	$p_1 = 3.6$ $p_2 = 0.2$ $\log \lambda_4 \approx 3.2$	$\log k_1 = 4.2$ $\log k_2 = 3.8$ $\log k_3 = 3.4$ $\log k_4 = 3.0$ $\log \lambda_4 \approx 3.2$	$a_1 \times 10^{14} = 7.7 \pm 2.7$ $a_3 \times 10^6 = 1.40 \pm 0.46$	$\log k_2k_3 = 7.15 \pm 0.15$ $\log k_4\lambda_4 = 5.85 \pm 0.15$
g	La(III)-cupferron-hexone-0.1 M $NaClO_4$	$p_1 = 4.30$ $p_2 = 0.50$ $\log \lambda_3 = 0.75$	$(\log k_1 = 5.30)$ $(\log k_2 = 4.30)$ $(\log k_3 = 3.30)$ $\log k_1k_2k_3 = 12.90$ $\log \lambda_3 = 0.75$	$a_1 \times 10^9 = 4.9 \pm 1.0$ $a_2 \times 10^5 = 5.8 \pm 4.3$ $a_3 \times 10 = 2.4 \pm 0.5$ — $(a_1 \times 10^9 = 7.7 \pm 2.2)$ $(a_3 \times 10 = 2.19 \pm 0.15)$	$\log k_2 = 4.07 \pm 0.34$ $\log k_3 = 3.61 \pm 0.34$ $\log \lambda_3 = 0.65 \pm 0.09$
h	Sm(III)-cupferron-hexone-0.1 M $NaClO_4$	$p_1 = 4.75$ $p_2 = 0.50$ $\log \lambda_3 = 1.40$	$(\log k_1 = 5.75)$ $(\log k_2 = 4.75)$ $(\log k_3 = 3.75)$ $\log k_1k_2k_3 = 14.25$ $\log \lambda_3 = 1.40$	$a_1 \times 10^{10} = 1.35 \pm 0.14$ (1.39 ± 0.17) $a_2 \times 10^5 = 0.91 \pm 0.11$ (0.72 ± 0.19) $a_3 \times 10^2 = 4.60 \pm 0.50$ (4.60 ± 0.47)	$\log k_2 = 4.83 \pm 0.07$ $\log k_3 = 3.70 \pm 0.07$ $\log \lambda_3 = 1.34 \pm 0.05$
i	Th(IV)-cupferron-chloroform-0.1 M $NaClO_4$	$p_1 = 6.75$ $p_2 = 0.20$ $\log \lambda_4 = 2.79 \pm 0.08$	$\log k_1 = 7.35$ $\log k_2 = 6.95$ $\log k_3 = 6.55$ $\log k_4 = 6.15$ $\log \lambda_4 = 2.79 \pm 0.08$	$a_0 \times 10^{30} = 1.68 \pm 0.32$ $a_2 \times 10^{16} = 6.4 \pm 1.3$ $a_4 \times 10^3 = 2.0 \pm 1.5$	$\log k_1k_2 = 14.58 \pm 0.12$ $\log k_3k_4 = 12.50 \pm 0.33$ $\log \lambda_4 = 2.69 \pm 0.32$
j	Th(IV)-dichloro-oxine-hexol-0.1 M $NaClO_4$	$p_1 = 9.90 \pm 0.10$ $p_2 = 0.50$ $\log \lambda_4 = 2.72$	$(\log k_1 = 11.40)$ $(\log k_2 = 10.40)$ $(\log k_3 = 9.40)$ $(\log k_4 = 8.40)$ $\log k_1k_2k_3k_4 = 39.6$ $\log \lambda_4 = 2.72$	$a_1 \times 10^{31} = 1.80 \pm 0.14$ $a_3 \times 10^{11} = 1.14 \pm 0.24$ $a_4 \times 10^3 = 1.51 \pm 0.78$	$\log k_2k_3 = 19.80 \pm 0.10$ $\log k_4 = 8.12 \pm 0.24$ $\log \lambda_4 = 2.82 \pm 0.22$

m	Th(IV)-1-nitroso-2-naphtol-hexone-0.1 M $NaClO_4$	$p_1 = 8.50 \pm 0.10$ $p_2 = 0.70$ $\log \lambda_4 = 2.05$	$(\log k_1 = 10.60)$ $(\log k_2 = 9.20)$ $(\log k_3 = 7.80)$ $(\log k_4 = 6.40)$ $\log k_1k_2k_3k_4 = 34.0 \pm 0.4$ $\log \lambda_4 = 2.05$	$a_1 \times 10^{26} = 5.5 \pm 0.3$ $a_2 \times 10^{17} = 5.7 \pm 0.9$ $a_3 \times 10^{9} = 4.5 \pm 0.5$ $a_4 \times 10^{3} = 8.1 \pm 1.5$	$\log k_2 = 9.02 \pm 0.08$ $\log k_3 = 7.89 \pm 0.09$ $\log k_4 = 6.26 \pm 0.10$ $\log \lambda_4 = 2.09 \pm 0.08$
n	Th(IV)-2-nitroso-1-naphtol-hexone-0.1 M $NaClO_4$	$p_1 = 8.30 \pm 0.10$ $p_2 = 0.70$ $\log \lambda_4 = 2.10$	$(\log k_1 = 10.40)$ $(\log k_2 = 9.00)$ $(\log k_3 = 7.60)$ $(\log k_4 = 6.20)$ $\log k_1k_2k_3k_4 = 33.2 \pm 0.4$ $\log \lambda_4 = 2.10$	$a_2 \times 10^{16} = 1.49 \pm 0.16$ $a_3 \times 10^{9} = 4.7 \pm 1.0$ $a_4 \times 10^{3} = 7.8 \pm 2.0$	$\log k_3 = 7.50 \pm 0.10$ $\log k_4 = 6.22 \pm 0.15$ $\log \lambda_4 = 2.11 \pm 0.11$
o	Sr(II)-oxine-chloroform-0.1 M $NaClO_4$	$2p_1 = 3.23 \pm 0.12$ $2p_2 = 1.55 \pm 0.12$ $\log \lambda_2'' = 2.01 \pm 0.24$	$\log k_1 = 2.39 \pm 0.06$ $\log k_2 = 0.84 \pm 0.06$ $\log \lambda_2'' = 2.01 \pm 0.24$	$a_0 \times 10^{6} = 3.5 \pm 0.6$ $a_1 \times 10^{3} = 1.7 \pm 0.1$	$\log k_1 = 2.7 \pm 0.1$ $\log k_2\lambda_2'' = 2.77 \pm 0.03$
p	La(III)-oxine-chloroform-0.1 M $NaClO_4$	$p_1 = 5.65$ $p_2 = 0.10$ $\lambda_3 = 2.57$	$(\log k_1 = 5.85)$ $(\log k_2 = 5.65)$ $(\log k_3 = 5.45)$ $\log k_1k_2k_3 = 16.95$ $\log \lambda_3 = 2.57$	$a_1 \times 10^{14} = 6.1 \pm 0.8$ $a_3 \times 10^{3} = 1.53 \pm 1.12$	$\log k_2k_3 = 10.4 \pm 0.3$ $\log \lambda_3 = 2.8 \pm 0.3$
q	Sm(III)-oxine-chloroform-0.1 M $NaClO_4$	$p_1 = 6.50$ $p_2 = 0.15$ $\log \lambda_3 = 2.45$	$(\log k_1 = 6.8)$ $(\log k_2 = 6.5)$ $(\log k_3 = 6.2)$ $\log k_1k_2k_3 = 19.50$ $\log \lambda_3 = 2.45$	$a_1 \times 10^{15} = 1.64 \pm 0.31$ $a_3 \times 10^{3} = 1.94 \pm 0.43$	$\log k_2k_3 = 12.07 \pm 0.13$ $\log \lambda_3 = 2.7 \pm 0.1$
r	Th(IV)-oxine-chloroform-0.1 M $NaClO_4$	$p_1 = 9.70$ $p_2 = 0.25$ $\log \lambda_4 = 2.39 \pm 0.09$ $p_1' = 1.40$ $p_2' = 0.40$	$\log k_1 = 10.45$ $\log k_2 = 9.95$ $\log k_3 = 9.45$ $\log k_4 = 8.95$ $\log \lambda_4 = 2.39 \pm 0.09$ $\log k_5 = 2.60$ $\log k_6 = 1.80$	*Split I ($\sigma_Q(I)$)* $a_2 \times 10^{21} = 2.1 \pm 0.4$ $a_3 \times 10^{12} = 14 \pm 4$ $a_4 \times 10^{3} = 1.5 \pm 1.0$ *Split I ($\sigma_Q(\%)$)* $(a_0 \times 10^{42} = 1.4 \pm 2.4)$ $a_2 \times 10^{21} = 2.5 \pm 0.7$ $a_3 \times 10^{12} = 6.5 \pm 2.9$ $a_4 \times 10^{3} = 1.7 \pm 0.4$ *Split II ($\sigma_Q(\%)$)* $a_4 \times 10^{3} = 1.9 \pm 0.3$ $a_5 = 2.9 \pm 0.9$	$(\log k_1k_2 = 21.3 \pm 0.9)$ $\log k_3 = 9.42 \pm 0.23$ $\log k_4 = 8.41 \pm 0.22$ $\log \lambda_4 = 2.77 \pm 0.10$ $\log k_5 = 3.18 \pm 0.15$

s	Th(IV)-N-phenyl-benzohydroxamic acid-chloroform-0.1 M $NaClO_4$	$p_1 = 9.45 \pm \sim 0.05$ $p_2 = 0.45 \pm \sim 0.05$ $\log \lambda_4 = 3.45 \pm 0.03$	$(\log k_1 = 10.40 \pm 0.15)$ $(\log k_2 = 9.90 \pm 0.07)$ $(\log k_3 = 9.00 \pm 0.07)$ $(\log k_4 = 8.10 \pm 0.15)$ $\log k_1k_2k_3k_4 = 37.8 \pm \sim 0.2$ $\log \lambda_4 = 3.45 \pm 0.03$	$a_0 \times 10^{30} = 1.72 \pm 1.16$ $a_2 \times 10^{15} = 6.65 \pm 0.80$ $a_4 \times 10^4 = 3.9 \pm 1.3$	$\log k_1k_2 = 15.59 \pm 0.30$ $\log k_3k_4 = 10.77 \pm 0.16$ $\log \lambda_4 = 3.41 \pm 0.15$
t	Th(IV)-salicylic acid hexone-0.1 M $NaClO_4$	$p_1 = 2.9$ $p_2 = 0.45$ $\log \lambda_4' = 5.7$	$\log k_1 = 4.25$ $\log k_2 = 3.35$ $\log k_3 = 2.45$ $\log k_4 = 1.55$ $\log \lambda_4' = 5.7$	$a_0 \times 10^{18} = 7.6 \pm 1.4$ $a_2 \times 10^{10} = 3.58 \pm 0.26$ $a_4 \times 10^6 = 3.16 \pm 0.33$	$\log k_1k_2 = 7.67 \pm 0.08$ $\log k_3k_4 = 3.94 \pm 0.06$ $\log \lambda_4' = 5.50 \pm 0.05$
u	Th(IV)-tropolone-chloroform-0.1 M $NaClO_4$	$p_1 = 8.14$ $p_2 = 0.49$ $\log \lambda_4 = 3.16$ $p_1' = 2.08$ $p_2' = 0.21$	$\log k_1 = 9.61$ $\log k_2 = 8.63$ $\log k_3 = 7.65$ $\log k_4 = 6.67$ $\log \lambda_4 = 3.16$ $\log k_5 = 2.29$ $\log k_6 = 1.87$	*Split I* (σ_Q (%)) $a_1 \times 10^{27} = 1.91 \pm 0.61$ $a_2 \times 10^{18} = 5.04 \pm 0.56$ $a_4 \times 10^4 = 4.47 \pm 0.69$ *Split I* ($\sigma_Q(I)$) $a_1 \times 10^{27} = 2.79 \pm 0.88$ $a_2 \times 10^{18} = 7.56 \pm 0.88$ $a_4 \times 10^4 = 6.84 \pm 2.37$ *Split II* (σ_Q (%)) $a_4 \times 10^4 = 4.54 \pm 0.73$ $a_6 = 9.87 \pm 3.04$	$\log k_2 = 9.43 \pm 0.15$ $(\log k_2 = 9.42 \pm 0.15)$ $\log k_3k_4 = 13.96 \pm 0.16$ $(\log k_3k_4 = 13.95 \pm 0.08)$ $\log \lambda_4 = 3.17 \pm 0.15$ $(\log \lambda_4 = 3.35 \pm 0.07)$ $\log k_5k_6 = 4.34 \pm 0.15$

* The original parameters of the limiting value method are φ_n and λ_ν
„ „ „ „ „ ligand number „ „ β_n and λ_ν
„ „ „ „ „ two-parameter „ „ p_1, p_2 and λ_ν

** Corrected for error in log [A] in original paper.

RESULTS

The solvent extraction systems investigated here are given in alphabetical order of the ligand in Table 1, which contains the computed primary parameters and the equilibrium constants obtained from them. Sometimes only the primary parameters are given in the original papers and usually without any indication of the sizes of the standard deviations. In order to facilitate a comparison between the least squares calculations and the results of the other methods in these cases, equilibrium constants have been computed from the parameters and standard deviations estimated when possible; those values which are not found in the original paper are given within parenthesis in the table.

In all systems, the least squares parameters a_n have been used to calculate log Q as a function of log [A] according to

$$Q = [A]^p / \sum_0^N a_n [A]^n. \qquad (14)$$

If nothing particular is said in the text accompanying the Tables, it is understood that the curve thus obtained goes smoothly through the experimental points with about equally many points on both sides of the curve (see also Discussion).

a. *The Th(IV)-acetylacetone-benzene-0.01 M $NaClO_4$ system* [2]. The least squares computations on this system have been discussed before [1]. Regardless of the kinds of errors tested for the primary data, the parameter a_1 came out negative. Omitting a_1 and using a certain combination of counting and pH error (see Ref.[1]), the a_n values in Table 1a were obtained. (The corresponding a_n values with *all* parameters are: a_0 $10^{30} = 6.4 \pm 1.7$, a_1 $10^{22} = -1.3 \pm 1.3$, a_2 $10^{14} = 1.94 \pm 0.15$, a_3 $10^8 = 2.34 \pm 0.29$ and a_4 $10^3 = 3.53 \pm 0.49$; omitting a_1, the changes in the remaining parameters are rather small, see Table 1a).

Though the requilibrium constants of the two computational procedures are in good agreement, the spread of the experimental data (an average standard deviation of about 25 %) prevents a separation of k_1 from k_2. With the limiting value method more constants have been calculated than are justifiable. The precision of the equilibrium constants of the limiting value method is based on graphical estimates and are obviously in good agreement with the corresponding least squares data.

b. The Th(IV)-acetylacetone-chloroform-0.1 M $NaClO_4$ system.[3] In the original paper, the standard deviations of the primary data I_{org} and I_{aq} are given. Using these deviations, the least squares procedure yields a negative value of a_0 and with a standard deviation of > 100 %. Omitting this parameter, a χ^2/k value of 39 is obtained, indicating that the weights assigned from the errors in the primary data are incorrect (*cf.* Ref.[1]).

Following the procedure discussed in Ref.[1] for the Th-acetylacetone-benzene case, both a counting error (σ_Q(I)) and a ligand error (σ_Q(A)) was tried, separately as well as combined. With a weighing factor of 6 times the original counting error, and a ligand error corresponding to $\pm$ 0.01 log units,

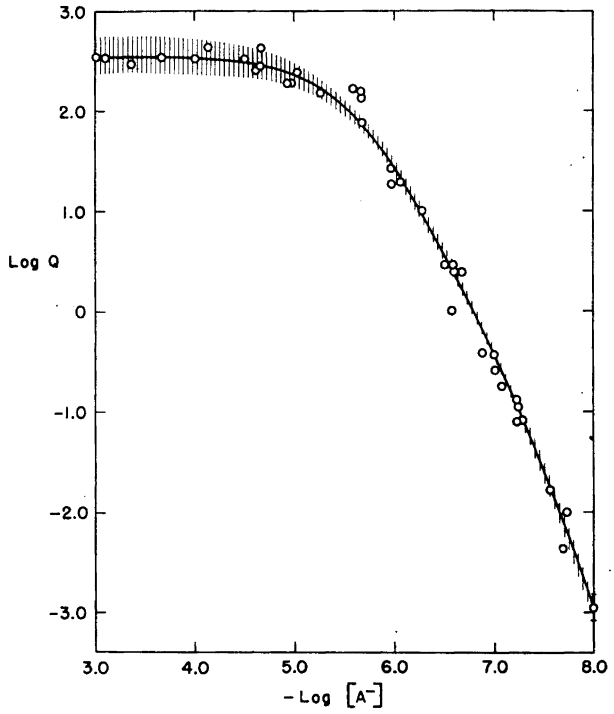

Fig. 1. The Th(IV)-acetylacetone-chloroform-0.1 M $NaClO_4$ system. The curve is computed from the least squares parameters in Table 1 b. The shaded area indicates the precision of the curve.

$\chi^2/k = 1.5$ was obtained; the a_n values for this combination are given in Table 1b. The fact that so much larger errors had to be assigned to the data indicates that the solvent extraction procedure may involve large errors, which were not originally accounted for.

Table 1b shows that though the numerical values of the equilibrium constants obtained with the two computational methods agree fairly well, the least squares method indicates that the experimental data do not allow a calculation of k_1. This is also clear from Fig. 1, where the curve computed without k_1 obviously fit the data very well. The broad band around the curve in Fig. 1 gives the precision of the curve as obtained with the least squares method. From Table 1b it is also seen that the estimated errors given for the equilibrium constants of the ligand number method are far too small.

c. The U(IV)-acetylacetone-benzene-0.1 M $NaClO_4$ system [4,19]. The least squares treatment of this system has recently been described [19]. The results are summarized in Table 1c, where comparison is made only with the results of the two-parameter method, though the ligand number method was also used in the original paper [4].

Table 2. Comparison between a_n parameter values obtained by the least squares calculations and those computed from graphically obtained equilibrium constants for the Pu(IV) acetylacetone system.

Method	Parameter values					
	χ^2/k	$a_0 \times 10^{37}$	$a_1 \times 10^{26}$	$a_2 \times 10^{17}$	$a_3 \times 10^{9}$	$a_4 \times 10^{3}$
limiting value	—	2.8	1.7	6.9	2.8	2.8
ligand number	—	1.0	1.0	1.3	4.0	3.2
two-parameter	—	3.6	2.9	5.8	2.9	3.6
least squares (5 parameters)	0.91	-17 ± 10	1.9 ± 0.8	-0.046 ± 0.53	3.3 ± 0.6	2.9 ± 0.4
least squares (3 parameters)	1.07	—	0.61 ± 0.15	—	3.6 ± 0.5	2.9 ± 0.5
Parameters refer to the following equilibria (no index means aqueous phase):		$\frac{[M]\,[A]^4}{[MA_4]_{org}}$	$\frac{[MA]\,[A]^3}{[MA_4]_{org}}$	$\frac{[MA_2]\,[A]^2}{[MA_4]_{org}}$	$\frac{[MA_3]\,[A]}{[MA_4]_{org}}$	$\frac{[MA_4]}{[MA_4]_{org}}$

This system is the only one in the present investigation where significant values have been obtained for all possible parameters using the least squares method. The agreement between the results of the two computational methods is fair. The precision of the equilibrium constants of the two parameter method is based on graphical estimates [19].

d. The Pu(IV)-acetylacetone-benzene-0.1 M $NaClO_4$ system [5]. From the spread of the experimental points, the standard deviations in Q were assumed to be 20 %. With the least squares method this produced a χ^2/k value of 0.91 and the parameter values in Table 2. Omitting the negative parameters, a χ^2/k of 1.07 was obtained, indicating that the 20 % error is a reasonable estimate.

Table 1d contains the primary parameters and the equilibrium constants computed from them, including those of all three different methods given in the original paper. The precision values given within parenthesis are, for the limiting value and ligand number methods, estimates from the differences in β_n-values obtained with these two methods. In the two-parameter method, the precision in the primary parameters are here assumed to be $\pm$ 0.1.

It is seen from Table 2 that a_0 is negative with $\sigma_{a_0} < |a_0|$, which should mean that negative concentrations of either Pu^{4+} or $PuAa_4$ exist. Since this cannot be true, a_0 had to be omitted with the consequences that no k_1 value can be calculated. The difficulty encountered in calculating k_1 with the limiting value method also supports that the calculation of such a value (as has been done with the ligand number and two-parameter methods) is dubious. Thus in contradiction to the graphical methods, the least squares result clearly indicates that the experimental data do not permit a calculation of k_1, the reason probably being that the concentration of Pu^{4+} in the experiments is too low to have any serious influence on the measurements. (It is obvious that the omission of a_0 does not mean that Pu^{4+} does not exist! *cf.* p. 160).

Since a_2 was negative and was associated with a very large standard error it was also omitted. Of the a_2 values computed from the graphically obtained equilibrium constants (see Table 2), it is seen that the ligand number value is much smaller than those of the other two methods. In the original paper [5], a plot of $\bar{n}$ against log [A] for Pu(IV) showed a steeper slope at $\bar{n} = 2$ than was the case for the similar Th(IV) and U(IV) systems [2-4], thus indicating an unexpectedly low concentration of the PuA_2^{2+} complex. The numerically low and highly uncertain value of a_2 obtained by the least squares calculation agrees well with these more visual findings on the $\bar{n}$ curve. It must therefore be concluded that in the Pu(IV) acetylacetone system the formation of the second complex, PuA_2^{2+}, seems to be hindered. A "regular" behaviour of the system would give an a_2 value of about 6×10^{-17} (the two-parameter value), while its real value probably is $< 0.5 \times 10^{-17}$. A use of the a_2 value obtained by the two-parameter or limiting value methods is therefore probably very misleading.

On the other hand, it should be mentioned that both Th(IV) and U(IV) show an unusually high stability for their second acetylacetonate complex, as judged by the regular principles of the two-parameter method. The only explanation that would remove the conclusions above about the PuA_2^{2+} complex is that systematic errors are involved in the Pu(IV) system which do not appear in the Th(IV) and U(IV) systems, or vice versa. Investigations by other methods than solvent extraction may settle this question; such experiments are being planned.

e. The Th(IV)-cinnamicacid-hexone-0.1 M $NaClO_4$-system.[6] As pointed out in the original paper, the data are badly scattered which makes accurate calculations of the equilibrium constants difficult. By choosing $\sigma_Q(\%) = 0.7\ Q$, $\chi^2/k = 0.99$ was obtained with two negative parameters (a_0 and a_3) and two parameters having standard deviations > 100 % (a_2 and a_3). Omitting these three parameters, $\chi^2/k = 1.03$ is obtained with the a_n values in Table 1e.

Thus the least squares method only yields two parameters, while the two-parameter method yields three parameters, that is one parameter more than the experimental data permit. Though the $k_1k_2k_3$ values of the two computations agree, the λ_4 values show a rather large discrepancy.

f. The Th(IV)-cinnamic acid-chloroform-0.1 M $NaClO_4$ system.[6] In the least squares treatment, the parameters a_0, a_2, and a_4 came out negative. With these parameters omitted and $\sigma_Q(\%) = 0.7\ Q$, a $\chi^2/k = 0.85$ was obtained; the corresponding a_n values are given in Table 1f.

In the original paper [6], three parameters are obtained: p_1, p_2, and λ_4. Fig. 2 shows the curve in the original paper given with these three parameters and also the curve computed with the a_1 and a_3 parameters. It is obvious that the equilibrium constants calculated from the least squares parameters give all the information which can be obtained from the experimental data.

g. The La(III)-cupferron-hexone-0.1 M $NaClO_4$ system.[7] Two kinds of errors were tested on this system: a counting error $\sigma_Q(\mathrm{I})$ and a percentage error $\sigma_Q(\%)$. With 1 "$\sigma_Q(\mathrm{I})$" the least squares method gave $\chi^2/k = 412$, and of the four parameters a_0 came out negative, and a_0 and a_2 with standard deviations > 100 %; $\chi^2/k = 2\,791$ was obtained when only a_0 was omitted. Reasonable value of χ^2/k (0.95) was obtained from a weighing factor corresponding

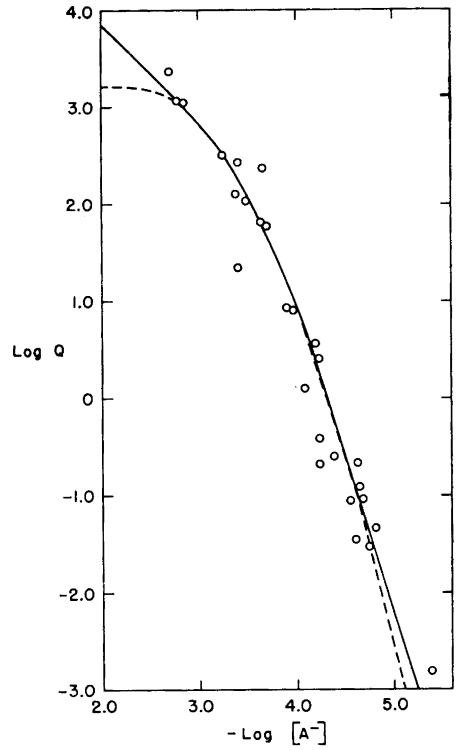

Fig. 2. The Th(IV)-cinnamic acid-chloroform-0.1 M $NaClO_4$ system. The solid curve (———) is computed with the least squares parameters in Table 1 f. The dashed curve (- - - - -) was obtained with the parameters of the two-parameter method.

to 20 times "σ_Q(I)", indicating that the experiments involved much larger than the estimated counting errors.

When tested with the σ_Q(%) error, a_0 came out negative, and both a_0 and a_2 had standard deviations > 100 %. However, omitting a_0 only, a_2 came out with only a 75 % standard deviation. Thus there is some support in the data for significance of the a_2 parameter. Reasonable $\chi^2/k = (0.91)$ was obtained for $\sigma_Q(\%) = 0.4\ Q$.

In Fig. 3 is plotted the experimental data and two curves, one obtained with the counting error and 2 parameters, and the other with the percentage error and 3 parameters. The shaded areas are the standard deviations in Q due to the standard deviation in a_n. The two areas overlap each other. Since the curve with 3 parameters seems to fit the experimental data somewhat better, its parameter values are given in Table 1g together with the equilibrium constants calculated from them. Within parenthesis, the a_n values for the "σ_Q(I)" computation are also given; it is seen that the two pairs of a_1 and a_3 values overlap each other.

h. The Sm(III)-cupferron-hexone-0.1 M $NaClO_4$ system.[7] Both with a counting and a percentage error the least squares computations yielded a negative a_0 with a standard deviation > 100 %. A weight corresponding to 7 "σ_Q(I)" produced $\chi^2/k = 0.82$, and a 20 % σ_Q(%) error produced $\chi^2/k = 1.29$,

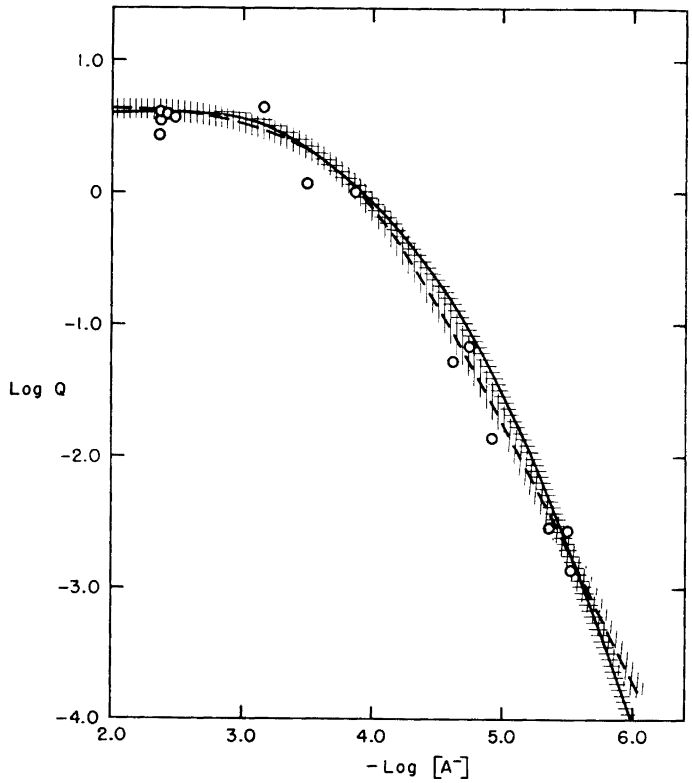

Fig. 3. The La(III)-cupferron-hexone-0.1 M $NaClO_4$ system. The solid curve (———) is obtained for a σ_Q(I) error and 2 parameters, and the dashed curve (- - - - -) for a σ_Q(%) error and 3 parameters; see Table 1 g. The shaded areas indicate the precision of the curves.

both cases with a_0 omitted. In Table 1h the parameters for the counting error are given with those for the percentage error within parenthesis; the differences between the two sets of parameters is negligible.

The least squares calculations indicate (in contradiction to the two-parameter method) that the experimental data do not allow a calculation of a k_1 value.

i. The Th(IV)-cupferron-chloroform-0.1 M $NaClO_4$ system. [8] The least squares calculations were performed only with a counting error. A 10 "σ_Q(I)" weight * gave $\chi^2/k = 1.66$ with the parameter a_1 negative, and a_1 and a_3 having standard deviations > 100 %. With a_1 and a_3 omitted, χ^2/k became 1.50; the corresponding a_n values are given in Table 1i.

A comparison between the results of the two computational methods shows that more equilibrium constants than the data permit are calculated with the

* With 10 "σ_Q(I)" weight, we mean a weight of $1/(10\ \text{"}\sigma_Q\text{(I)"})^2$.

two-parameter method, and also that the precision of the λ_4 constant is overestimated.

j. The Th(IV)-dichlorooxine-hexol-0.1 M $NaClO_4$ system. [9] Using a counting error in the least squares treatment, the parameters a_0 and a_2 came out with standard deviations > 100 %. For a 6"σ_Q(I)" weight, χ^2/k became 1.06. The parameters obtained are given in Table 1j. The comments in paragraph h about the k_1 value are applicable also to this case.

k. The Th(IV)*-methoxybenzoic acid-chloroform-0.1 M $NaClO_4$ system.* [6] The least squares procedure using a 1 "σ_Q(I)" weight gave $\chi^2/k = 1.6 \times 10^6$ and all parameters with standard deviations in excess of 100 %. Therefore the weight of the points was decreased to correspond to a 40 "σ_Q(I)" weight, where $\chi^2/k = 4.5$ was obtained. With this weight all parameters except a_4 were negative or had standard deviations > 100 %. All combinations of 2, 3, and 4 parameters were tested; in no case was it possible to obtain a combination of only positive parameters with standard deviations < 100 %.

Since it was unreasonable to decrease the weight of the points further with this kind of error, the system was further investigated with a constant percentage error in Q. For $\sigma_Q(\%) = 0.7\ Q$, $\chi^2/k = 1.4$ was obtained; of the five parameters only 2 were positive, but had standard deviations > 100 %. Again all possible combinations were run, and again no combination with only positive parameters with standard deviations < 100 % could be obtained.

Obviously the experimental data are too poor to make possible *any* calculation of equilibrium constants with the least squares procedure and the present methods of weighing the data.

l. The Th(IV)-methoxybenzoic acid-hexone-0.1 M $NaClO_4$ system. [6] The least squares procedure with a 30 "σ_Q(I)" weight produced a $\chi^2/k = 1.24$ with one parameter (a_1) negative and one with a standard deviation close to 100 % (a_3). The system was therefore run, first with a_1 omitted, and then with all possible combinations of 2 and 3 omitted parameters. As a result, a number of possible combinations were obtained, all with a 30 "σ_Q(I)" weight as shown in Table 3.

From this table it is seen that χ^2/k increases with decreasing number of parameters. Though the χ^2/k values in the last three cases is > 1.5, they could rather easily be brought down to < 1.5 by a slight decrease in weight; they are therefore worth being included in the Table.

Table 3. Possible parameter combinations for the Th(IV)-methoxybenzoic acid-hexone-0.1 M $NaClO_4$ system when tested with a 30 "σ_Q(I)" weight (see paragraph l).

χ^2/k	$a_0 \times 10^{13}$	$a_1 \times 10^9$	$a_2 \times 10^6$	$a_3 \times 10^4$	$a_4 \times 10^2$	Average stand. dev. in a_n
1.21	1.04 ± 0.39	–	1.25 ± 0.34	5.39 ± 0.21	3.9 ± 1.8	38 %
1.35	–	0.87 ± 0.17	–	8.63 ± 1.51	2.7 ± 1.8	35 »
1.62	0.80 ± 0.44	–	1.94 ± 0.25	–	7.4 ± 1.4	29 »
1.65	–	–	1.61 ± 0.37	4.07 ± 2.35	4.5 ± 2.1	43 »
1.83	–	–	2.10 ± 0.25	–	7.2 ± 1.5	17 »

Considering both the χ^2/k values and the average standard deviations of all the a_n values, some slight preference may be given to the combination yielding $\chi^2/k = 1.35$. A plot of the curves obtained with the various parameter combinations will show that the curves for 3 and 4 parameters fit the experimental points about equally well. In view of the scatter of the data, the least squares method and the χ^2 test cannot in this case distinguish between different functional models, and therefore no reliable equilibrium constants can be computed.

m. The Th(IV)-1-nitroso-2-naphtol-hexone-0.1 M $NaClO_4$ system.[10] Using a counting error with the least squares method, a_0 was obtained with a standard deviation > 100 %. With the other 4 parameters and a 5 "σ_Q(I)" weight, $\chi^2/k = 1.1$ was obtained. The corresponding parameter values are given in Table 1m.

In this case, like in some of the earlier ones, it is possible to omit an additional parameter and still obtain real values for the remaining parameters. The result, using the same weight is: $\chi^2/k = 3.2$, $a_1 \times 10^{26} = 19.1 \pm 3.5$, $a_3 \times 10^9 = 6 \pm 1$, and $a_4 \times 10^3 = 6.4 \pm 3.7$. Since χ^2/k is considerably increased and the average standard deviation in the parameters is here 31 % compared to 13 % for the case with 4 parameters, it is concluded that, from a statistical point, the system is most correctly described with 4 parameters.

n. The Th(IV)-2-nitroso-1-naphtol-hexone-0.1 M $NaClO_4$ system.[10] In all least squares tests, some parameters came out negative or with standard deviations > 100 %. The only possibly significant combination was obtained with the omission of a_0 and a_1, which gave $\chi^2/k = 0.7$ for a 6 "σ_Q(I)" weight. The parameters are given in Table 1n.

If also a_3 is omitted, one obtains for the same weights $\chi^2/k = 2.9$ and the parameter values $a_2 \times 10^{16} = 2.12 \pm 0.21$ and $a_4 \times 10^3 = 10.1 \pm 3.9$. Since χ^2/k as well as the average standard deviation in a_n is greater with this parameter combination, the earlier results with 3 parameters are of greater statistical significance. However, a detailed analyses of the data shows that a higher statistical significance can be obtained using two parameters, a_2 and a_4, if the weight of one single point (at -log [A] = 6.41) is considerably decreased. The least squares method does not allow a calculation of k_1 (*cf.* paragraph h).

o. The Sr(II)-oxine-chloroform-0.1 M $NaClO_4$ system.[11] In the original paper it is assumed that the organic phase only contains the complex $SrA_2.2HA$. On this assumption the following polynomial is developed:

$$\frac{[A]^2}{Q}[HA]^2_{org} = \frac{1}{\beta_2\lambda_2''} + \frac{\beta_1}{\beta_2\lambda_2''}[A] + \frac{\beta_2}{\beta_2\lambda_2''}[A]^2$$

Using this expression in the least squares treatment, the parameters will become $a_0 = 1/\beta_2\lambda_2''$, $a_1 = \beta_1/\beta_2\lambda_2''$ and $a_2 = 1/\lambda_2''$, where λ_2'' is the partition constant for the $SrA_2.2HA$ complex. For $\sigma_Q(\%) = 0.3\,[HA]^2_{org}/Q$, χ^2/k is 0.89 and the following parameter values are found: $a_0 \times 10^3 = 3.6 \pm 0.7$, $a_1 = 1.7 \pm 0.2$ and $a_2 \times 10^3 = 1.0 \pm 6.0$. Since the standard deviation in a_2 is > 100 %, runs were made with a_2 omitted, yielding $\chi^2/k = 0.86$ and the a_1 and a_0 values in Table 1o; the a_0 and a_1 values are almost identical to those obtained with three parameters.

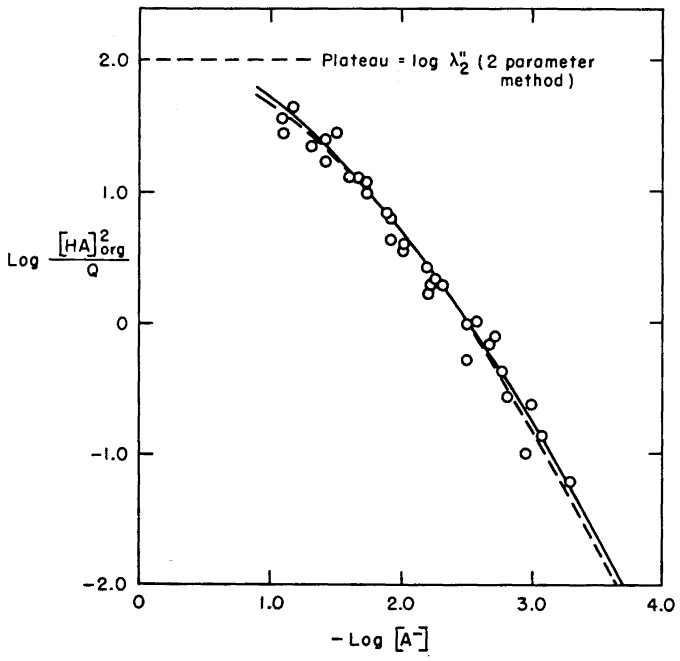

Fig. 4. The Sr(II)-oxine-chloroform-0.1 M $NaClO_4$ system. The solid curve (———) is obtained with the least squares parameters in Table 1 o, and the dashed curve (- - - - -) with the parameters of the two-parameter method.

From a_0 and a_1 only two equilibrium constants can be computed k_1 and $k_2\lambda_2''$. With these 2 parameters, the solid curve in Fig. 4 is calculated. Since the curve goes smoothly through the experimental points, with about equally many points on both sides and without any tendency to level out into a sort of plateau, it is obvious that the data do not allow a separate calculation of the λ_2'' value, as has been done with the two-parameter method.

p. The La (III)-oxine-chloroform-0.1 M $NaClO_4$ system.[7] All least squares computations using counting as well as percentage errors gave negative a_0, and a_0 and a_2 having standard errors > 100 %. Omitting these parameters, $\chi^2/k = 1.08$ was obtained for a 20 "σ_Q(I)" weight; the same χ^2/k value was obtained for a 70 % error in Q. The parameters are given in Table 1p. A comparison with the results of the two-parameter computation shows considerable discrepancies.

Fig. 5 gives the curves calculated with the parameters of the two computational methods. It is seen that the two-parameter curve has about equally many points on each side, while the least squares curve has about twice as many points below as above the curve. However, with badly scattered data the log scale is misleading, because in such a plot the average value will always be closer to the higher points (*e. g.* $y_1 = 5$, $y_2 = 15$ and thus $\bar{y} = 10$; therefore log $y_1 = 0.7$, log $y_2 = 1.18$, and log $\bar{y} = 1.0$ and not $(0.7 + 1.18)/2 = 0.94$).

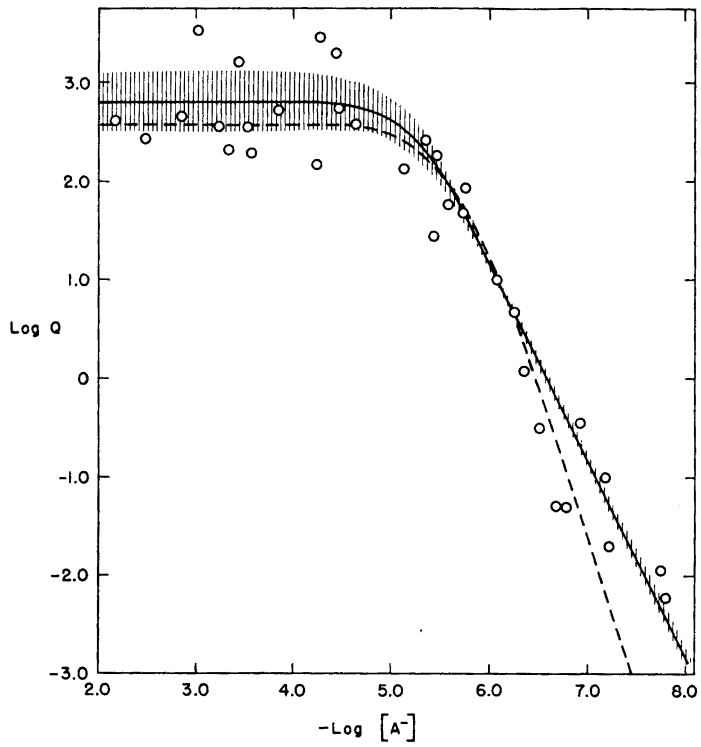

Fig. 5. The La(III)-oxine-chloroform-0.1 M $NaClO_4$ system. The solid curve (———) is obtained with the least squares parameters of Table 1 p (using 2 parameters), and the dashed curve (- - - - -) with the parameters of the two-parameter method (using 3 parameters). The shaded area indicates the precision of the least squares curve.

When the higher values are given a less weight than the lower ones the average curve will move closer to the lower points; this effect of weighing is not sufficiently pronounced in Fig. 5 to move the least squares curve down to the two-parameter curve (the author of the original paper has obviously weighted the higher points still less than the present author).

q. The Sm(III)-oxine-chloroform-0.1 M $NaClO_4$ system. [7] Using percentage and counting errors for the least squares treatment, the parameters a_0 and a_2 came out negative and with standard deviations > 100 %. Omitting these parameters, the standard deviation in a_3 turned out to be > 100 % when the counting error was used, but not with the percentage error. With $\sigma_Q(\%) = 0.5Q$, a χ^2/k value of 1.35 was obtained. The corresponding a_n values are given in Table 1q. The discrepancies between the results of the two-parameter method and the least squares method are again quite large.

r. The Th(IV)-oxine-chloroform-0.1 M $NaClO_4$ system. [8] Because of the big range of free ligand concentration ($10^{-1} \gtrsim [A] \gtrsim 10^{-11}$), the GEORGE computer could not handle the whole problem for $N = 6$. It was therefore decided

to split it into two parts and run these two separately with overlapping [A] values (the same principle of splitting was used in the original paper with the two-parameter method). This splitting can be justified, because the Q values are almost independent of [A] in the range $10^{-4} > [A] > 10^{-8}$, which means that in the presence of negatively charged complexes one can neglect the positively charged ones, and vice versa. Considering the experimental data in the original paper, the problem was divided in the two following parts:

Split I: $z = \sum_{0}^{4} a_n x^n$, run on the IBM 704 for $x < 10^{-3}$.

Split II: $z = \sum_{0}^{2} a_{n+4} x^n$, run on the GEORGE for $x > 10^{-9}$.

Using a percentage as well as a counting error in the Split I case, a_1 came out negative. Omitting this parameter, a_0 was obtained with a standard deviation > 100 % (this a_0 is given within parenthesis in Table 1r; it is used for computing an approximate k_1k_2 value). Omitting both a_0 and a_1, the parameters in Table 1r were obtained; the 70 % error in Q yielded a $\chi^2/k = 0.83$, and the 17 "σ_Q(I)" weight $\chi^2/k = 0.98$.

Only a 70 % error was tested in the Split II case, which first yielded a negative a_6 value with standard deviation > 100 %. With this parameter omitted, the a_4 and a_5 values in Table 1r were obtained with a $\chi^2/k = 0.73$. The good agreement between the χ^2/k and a_4 values of Split I (σ_Q(%)) and Split II (σ_Q(%)) indicates consistency between the two split cases.

The equilibrium constants in Table 1r are computed from the σ_Q(%) data, λ_4 being taken from a_4 of Split I (σ_Q(%)). A comparison between the results of the two computational methods indicates that more parameters (and more equilibrium constants) are given by the two-parameter method than the experimental data justify. Particularly dubious is the calculation by that method of a k_1 value, because in the concentration range where the first complex, MA^{3+}, is supposed to exist, the scatter of the experimental data is tremendous (*e. g.* for $-\log [A^-] = 10.53 \pm 0.01$ the spread in log Q is 1.75, *i. e.* over a factor of 50 in Q).

Because of the generally very great scatter of experimental data in this system, the comments in § p about the distortion of the log scale is particularly applicable to this case.

s. The Th(IV)-N-phenylbenzohydroxamic acid-chloroform-0.1 M $NaClO_4$ system. [12] With a counting error, the least squares calculations yielded a negative a_1, and a_1 and a_3 with standard deviations > 100 %. Omitting these parameters, a $\chi^2/k = 0.91$ was obtained with a 20 "σ_Q(I)" weight; the resulting parameters are given in Table 1s.

The average standard errors given for p_1 and p_2 is somewhat above 12 %, while for a_0 and a_2 it is about 40 %. Similarily, for λ_4 the two-parameter method gives a standard error of about 7 %, while the least squares method gives about

33 %. The high precision given for the two-parameter method seems therefore overestimated.

t. The Th(IV)-salicylic acid-hexone-0.1 M $NaClO_4$ system. [6] Whith the functional form given for this system in the original paper, the same equations as before can be used in the least squares treatment, provided Q is replaced by $Q/[H_2A]_{aq}$ and the partition constant λ_4 is replaced by

$$\lambda_4' = \frac{[Th(HA)_4H_2A]_{org}}{[Th(HA)_4]_{aq}[H_2A]_{aq}}$$

where H_2A stands for undissociated salicylic acid. With the least squares treatment using a percentage error in Q, the parameters a_1 and a_3 came out with standard deviations > 100 %. Omitting them and using $\sigma_Q(\%) = 0.3.Q$, a χ^2/k value of 0.94 and the parameter values in Table 1t were obtained. The table indicates that more equilibrium constants have been computed from the two-parameter results than the experimental data permit.

u. The Th(IV)-tropolone-chloroform-0.1 M $NaClO_4$ system. [13] With this system the same mathematical difficulties were encountered as with the Th(IV)-oxine system in § r, and the same splitting procedure was used to get around these difficulties; Split I was used for $[A] < 10^{-2}$, and Split II for $[A] > 10^{-7}$.

Using a percentage and a counting error, a_0 and a_3 came out negative, and a_3 with a standard deviation > 100 %. Omitting a_0 and a_3, the parameters a_1, a_2 and a_4 given in Table 1u were obtained; for a 70 % error in Q, $\chi^2/k = 0.51$ was obtained, while a counting error corresponding to 15 "$\sigma_Q(I)$" gave $\chi^2/k = 0.73$. It is seen in the table that the equilibrium constants k_2 and k_3k_4 computed from the two Split I data agree well (the values within parenthesis are computed from the Split I ($\sigma_Q(\%)$) data), while the precision of the k_3k_4 and λ_4 values obtained from the Split I ($\sigma_Q(I)$) data is less good.

The Split II case was only run with a percentage error in Q, which gave an a_5 value with a standard deviation > 100 %. Omitting a_5 and using a $\sigma_Q(\%) = 0.7\ Q$ error, a χ^2/k value of 0.56 and the parameters a_4 and a_6 in Table 1u were obtained; log k_5k_6 in the table is computed from these a_4 and a_6 values. It is seen that the 70 % error in Q used in both Split I ($\sigma_Q(\%)$) and Split II ($\sigma_Q(\%)$) give approximately identical $a_n \pm \sigma_{a_n}$ and χ^2/k, demonstrating good consistency between the two treatments.

With the equilibrium constants of the least squares procedure, a curve $Q([A])$ can be computed which goes smoothly through the experimental points. Thus, with the present spread in the experimental data, the Th(IV)-tropolone system can be completely explained by only 4 equilibrium constants.

DISCUSSION

With good data, the ligand number and limiting value methods should give the same equilibrium constants as the least squares method; *cf.* Ref. [15] This is also true for the two-parameter method as long as only two complexes are present in the system studied.

Though only the least squares method yields true standard deviations of the constants, rather good estimates of precision can be made with the limiting value method; these two methods are the only ones here discussed where the experimental data are used directly for computing the parameters. On the other hand, precision estimates are very hard to make with the ligand number method, because the calculation of the complexity constants are based on points $\bar{n}$ ([A]) taken from a smoothed curve through the experimental points (*cf.* discussion in connection with eqn. 5). This is rather pointedly illustrated by comparing the dissertations of J. Bjerrum [16] (ligand number method and few estimates of precision) and I. Leden [18] (limiting value method and almost all constants with precision estimates). Good estimates of precision are also hard to make with the two-parameter method.

With very scattered data, as has been the case in the solvent extraction work here investigated, different results may be anticipated with different computational methods.

In the ligand number method, the graphical differentiation of the smooth curve through the experimental points may introduce errors which in the later computations cannot be detected; this method may therefore sometimes lead to the calculation of more constants than the original data would permit (see Tables 1b and d, and Ref. [1]).

The limiting value method is sensitive to large spread of the experimental data. With poor data it is extremely hazardous to extrapolate curves through the measured or calculated points to zero. Further, the errors obtained in one constant propagates to the successive constants. If the computations are not carried out carefully, such a propagated error may in a later step turn up as a "constant". Though the limiting value method makes more direct use of the experimental data than any of the other graphical methods, its use should be limited to rather good data.

With very poor data, the visual judgement of the two-parameter method may be the only way to get information about the system. In such a case one should realize that the method is entirely qualitative (see paragraphs k and l in the experimental part).

The two-parameter method is based on the assumption that the experimental data fall on a curve with two asymptotes, one with slope zero (when the aqueous phase contains almost only the uncharged complex MA_ν) and one with slope ν (when the aqueous phase contains almost only uncomplexed metal ions $M^{\nu+}$).* When this method is carelessly applied to data which do not closely approach these asymptotes, dubious results may be obtained. This is demonstrated in a great number of tables above, where from the two-parameter results partition constants (q's) and k_1 or $k_1k_2.....k_N$ have been calculated, while the least squares method shows that there is no support in the experimental data for significant values of these constants. ** Thus improper application of the two-parameter method may produce more parameters than the experimental data allow (Tables 1e, f, o, p, q, r and u); on the other hand,

* The principles of the two-parameter method can be used with the assumption that the first measurable complex is MA_r, giving an asymptote of slope $\nu - r$; however, this has never been done.

** By definition (see equations 2 and 8) $k_1k_1 ..... k_N = 10^{N\rho_1}$.

with very good data the method does not always permit the evaluation of all parameters involved (Tables 1c and m).

A draw-back of the two-parameter method is also the difficulty in relating the parameters to any specific equilibrium constants (*cf.* Tables 1i, s and t, where the two different computational methods have produced the same number of parameters, and k_1 and λ_ν both exist). Though there is some experimental support for the existence of a constant spreading factor, *cf.e.g.* Ref. [16,18], certainly not all systems are of the regular type indicated by eqn. 9. The calculation of step-wise equilibrium constants from the parameters of the two-parameter method must therefore be based on additional information about the system than the experimental data alone provide. In fact, such a calculation is in contradiction to the original purpose of the two-parameter method [14].

The simultaneous consideration of all experimental data in the least squares method leads to the computation of the maximum number of significant equilibrium constants and their precision; in this respect this method is superior to any of the graphical methods.

However, graphical plots must be made before the least squares calculations are begun, in order to see if any curve at all can be fitted to the experimental points; it is also advisable to check the results of the computations with the input data, so that errors in making up the programs, *etc.* are disclosed, *cf.* Ref. [15]

When parameters are omitted in the least squares calculations (because they are negative or their standard deviations exceed the parameter value) this does not necessarily mean that the corresponding complexes do not exist, but only that the equilibrium constants cannot be calculated because of uncertanties in the experimental data (*cf.* paragraph d).

Since the laborius manual computations of the least squares method are now overcome by the use of high speed digital computers, it is hoped that this method will be more used in the future.

The present investigation also indicates the need for more refined technique in solvent extraction work.

Acknowledgement. The author wishes to thank Drs. J. C. Hindman and J. C. Sullivan of the Chemistry Division, and Dr. W. Miller, Mr. W. Greenhow and Mrs. M. Hanson of the Applied Mathematics Division, for their extensive cooperation in this investigation. He is also most grateful to Dr. W. M. Manning, Head of the Chemistry Division, for his interest in this work and for the research appointment which made it possible.

REFERENCES

1. Rydberg, J. and Sullivan, J. C. *Acta Chem. Scand.* **13** (1959) 2057.
2. Rydberg, J. *Acta Chem. Scand.* **4** (1950) 1503.
3. Rydberg, J. *Arkiv Kemi* **5** (1953) 413.
4. Rydberg, J. and Rydberg, B. *Arkiv Kemi* **9** (1956) 81.
5. Rydberg, J. *Arkiv Kemi* **9** (1956) 109.
6. Hök-Bernström, B. *Acta Chem. Scand.* **10** (1956) 174.
7. Dyrssen, D. *Svensk Kem. Tidskr.* **66** (1954) 234.
8. Dyrssen, D. *Svensk Kem. Tidskr.* **65** (1953) 43.
9. Dyrssen, D., Dyrssen, M. and Johansson, E. *Acta Chem. Scand.* **10** (1956) 341.
10. Dyrssen, D., Dyrssen, M. and Johansson, E. *Acta Chem. Scand.* **10** (1956) 106.

11. Dyrssen, D. *Svensk Kem. Tidskr.* **67** (1955) 311.
12. Dyrssen, D. *Acta Chem. Scand.* **10** (1956) 353.
13. Dyrssen, D. *Acta Chem. Scand.* **9** (1955) 1567.
14. Dyrssen, D. and Sillén, L. G. *Acta Chem. Scand.* **7** (1953) 663.
15. Sullivan, J. C., Rydberg, J. and Miller, W. *Acta Chem. Scand.* **13** (1959) 2023.
16. Bjerrum, J. *Metal Ammine Formation in Aqueous Solutions*, Diss. Copenhagen 1941.
17. Sullivan, J. C. and Hindman, J. C. *J. Am. Chem. Soc.* **74** (1952) 6091.
18. Leden, I. *Potentiometrisk undersökning av några kadmiumsalters komplexitet*, Diss. Lund 1943.
19. Rydberg, J. and Sullivan, J. C. *Acta Chem. Scand.* **13** (1959) 186.
20. Deming, W. E. *Statistical Adjustment of Data.* J. Wiley & Sons, New York 1948.

Received August 6, 1959.

ACTA CHEMICA SCANDINAVICA 14 (1960) 180–188

Heats of Combustion of Butanal and Some Related Compounds

JAN TJEBBES

*Thermochemistry Laboratory *, University of Lund, Sweden*

Heats of combustion values have been determined and from these, heat of formation data at 25°C calculated in kcal.mole^{-1} for the following six carbon-hydrogen-oxygen compounds: 2-butenal ($\Delta H_f^\circ = -34.45 \pm 0.09$), butanal ($\Delta H_f^\circ = -57.06 \pm 0.17$), butanol-1 ($\Delta H_f^\circ = -79.55 \pm 0.10$), 2-ethyl-2-hexenal ($\Delta H_f^\circ = -62.46 \pm 0.17$), 2-ethyl-hexanal ($\Delta H_f^\circ = -83.32 \pm 0.18$), 2-ethyl-hexanol-1 ($\Delta H_f^\circ = -103.46 \pm 0.19$).

Precise data on heats of combustion of aliphatic aldehydes are lacking in the literature, and since the appearance of Kharasch's compilation [1] no further determinations have been published. Therefore it was judged of interest to study a number of aliphatic aldehydes, the choice of compounds being mainly governed by an interest in the aldol condensation reaction and associated processes for butanal.

Verkade and Coops [2] have accurately determined the heats of combustion of the lower 1-alkanols. However, a redetermination for butanol-1 was performed in order to ascertain the internal consistency within this investigation **. No value of the heat of combustion of 2-ethyl-hexanol-1 has been found in the literature.

SAMPLE PURITY

It was found difficult to obtain the aldehydes in a very pure state. Before describing the special problems met with in handling the aldehydes, the general procedure for preparing the samples for combustion will be given.

* Sponsored by the *Swedish Natural Science Research Council* and the *Swedish Technical Research Council*.

** Verkade and Coops' value recalculated [3] to present day units is ΔH_c°(butanol-1) = − 638.25 ± 0.32 kcal.mole^{-1}, and the value given in this paper is ΔH_c°(butanol-1) = − 638.25 ± 0.10 kcal.mole^{-1}.

Table 1. Density of butanal *versus* water content.

Water %	d_4^{25} g · ml^{-1}
x	$0.7966_0 \pm 0.0000_2$
$x + 0.275$	$0.7976_1 \pm 0.0000_5$
$x + 0.551$	$0.7988_3 \pm 0.0000_5$

Procedure. All six substances used in this investigation were prepared and carefully purified by the Research Laboratory, Mo och Domsjö AB, Örnsköldsvik, Sweden. After the final distillation in a Podbielniak column with 50—70 theoretical plates, samples of the main fraction were enclosed in sealed Pyrex-glass ampoules in an atmosphere of carbon dioxide or helium. The purity was established using gas-liquid chromatographic technique on the contents of one of these ampoules, and a number of ampoules were sent to our laboratory. Immediately upon arrival (2—3 days later) a distillation was performed at room temperature under reduced pressure. All samples were handled in a nitrogen atmosphere and great care was taken to exclude air. The middle fraction from this distillation (about one third of the total sample) was collected in a receiver where *ca.* 10 combustion ampoules (made from soft glass) had been placed in advance, and then the ampoules were filled [4] immediately. At the same time ampoules were filled with samples for gas-liquid chromatographic analysis and for density determination. The combustions were made as soon as possible, and in no case did more than six days elapse between ampoule filling and combustion. In the case of butanal all experiments were carried out within two days. Analysis (by Mo & Domsjö) and density determination were performed so as to coincide in time with the middle experiment in the combustion series.

The gas-liquid chromatographic analysis was done in order to determine the amount of impurities, especially water. For all substances except butanal the area under the water peak of the chromatogram was proportional to the water content of the sample, which was found from calibration experiments with known amounts of water added to the sample. The linearity implies that no reaction leading to the formation of water occurred on the column. In the

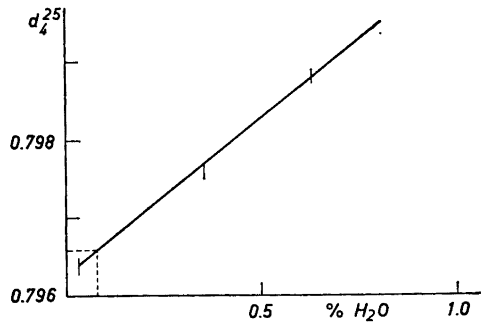

Fig. 1. Density of butanal *versus* water content.

case of butanal, however, a reaction took place on the column forming water and organic impurities.

The water content of the butanal sample was evaluated using the observation that the density of a sample of this compound was found to vary linearly with the water content, at least within a small interval. A sample of butanal was prepared exactly as the material for combustion. This sample was divided into three parts and water was added to two of them, increasing the amount of water by 0.275 resp. 0.551 %. The densities of the three parts were determined, Table 1. The slope of the line, density *versus* per cent water, was calculated, and the line was drawn (Fig. 1) using the value of Smith and Bronner[5]: $d_4^{25} = 0.7964$ at 0.03 % water. As indicated by dotted lines in the diagram the density 0.7966 then corresponds to a water content of 0.08 ± 0.02 %.

Special problems. The unsaturated aldehydes studied were found to be stable during storage in Pyrex-glass ampoules for two weeks. However, distillation at temperatures higher than *ca.* 50°C caused rapid decomposition. These compounds were found to be very sensitive to oxidation; and it was therefore necessary to exclude all traces of air in handling them.

Butanal was found to be unstable even when every precaution was taken in storing the samples. The decomposition was followed by measuring the density, and an increase in d_4^{25} of 0.00003 per day was observed. Distillation of butanal above room temperature caused an increase in water content and in amounts of other impurities. When distillation was performed at room temperature with the receiver kept at −40 to −80°C, the distillate showed a marked tendency to polymerize to solid products. A few successful distillations were performed with the receiver kept at −20°C and the distilling flask at 35°C (pressure 40—50 mm Hg).

In a number of cases condensation of butanal took place within the sealed combustion ampoule, which then invariably burst *. This was shown by the following series of experiments. Twelve ampoules (of the combustion type) were filled with butanal and left to stand for some days. During this time several ampoules burst and now and then one of the intact ampoules was opened. The refractive index ** of the content was immediately determined for both cases and was found unchanged for all intact ampoules, but altered for every broken ampoule, usually about 0.002 units.

The handling of 2-ethyl-hexanal offered the same kind of difficulties as did butanal but to a much smaller extent. Distillation could be performed at 85°C and 35 mm Hg, and gas-liquid chromatography was successfully run at 150°C. With the alcohols of this investigation no special problems were met, and the analyses showed that perfect purity was obtained in both cases.

Results of purity determinations. In Table 2 values of densities and amounts of impurities have been summarized. As a comparison, density values found in the literature have also been given.

* In a few cases the ampoule burst in the bomb during filling with oxygen. The butanal then exploded, and in a separate experiment it was found that oxygen caused the butanal to explode at a pressure of 12 atm.

** The small amount of substance in an ampoule made a density determination impossible, and therefore refractive indices were chosen as an aid to follow the purity.

Table 2. Sample purity.

Substance	d_4^{20} g · ml^{-1}	d_4^{25} g · ml^{-1}	H_2O %	Org.matter %	Literature
2-Butenal	0.8526	0.8475	0.02	0.05	$d^{17.3}$ = 0.8557 [6]
Butanal	—	0.7966	0.08	—	d_4^{25} = 0.7964/0.03 % H_2O [5]
Butanol-1	0.8099	0.8059	0	0	d_4^{25} = 0.8057 [7]
2-Ethyl-2-hexenal	0.8522	0.8461	0.014	0.4	d_4^{25} = 0.8528 [8]
2-Ethyl-hexanal	0.8201	0.8156	0.03	0.7	d_4^{18} = 0.8231 [9]
2-Ethyl-hexanol-1	0.8332	0.8291	0	0	d_4^{20} = 0.8328 [10]

The organic impurity of 2-butenal was small enough to be neglected, but this was not the case with 2-ethyl-2-hexenal. Three organic impurities gave traces on the chromatogram, but one of them made up for 75 % of the total amount. This one was isolated with the aid of a preparative column and examined by infrared spectroscopy. The spectrogram was compared with that of 2-ethyl-2-hexenal and differences were found on three frequencies, namely 979 cm^{-1} had changed to 969 cm^{-1}; 1 202 cm^{-1} to 1 180 cm^{-1} and at 1 730 cm^{-1} a new absorption peak appeared. The impurity was most certainly 2-ethyl-3-hexenal, and its presence would not affect the heat of combustion value to a noticeable extent. The organic impurity found in 2-ethyl-hexanal was thought to be formed during analysis. The peak on the chromatogram corresponding to this impurity was always found when analysing samples from different steps of the purification process and was always of the same relative size, while all other impurity-peaks gradually disappeared. As the purification involved distillations at different pressures, the presence of an azeotropic mixture was not likely.

COMBUSTION CALORIMETRY

All calorimetric quantities are expressed in terms of the defined calorie which is equal to 4.1840 absolute joules. All weighings have been reduced to mass. The molecular weight for each compound has been given in the Tables and is based upon the 1954 International Atomic Weights.

In this work the symbols introduced by Hubbard, Scott and Waddington [11] have been used.

Apparatus and method. The calorimetric system of Bjellerup [12] was used with the difference that his rotating bomb was replaced by a static one of the same construction. The aldehydes showed a marked tendency for splashing upon ignition, and therefore a platinum baffle was used together with a platinum shield [4]. Paraffin oil of known heat of combustion [13] was used as an ignition aid. The amount of HNO_3 formed was determined by titration with NaOH.

In each experiment the calorimeter vessel was filled with water until a fixed total weight of calorimeter with mounted bomb was reached, and the energy equivalent of the system was calculated using the following principles [12]. The result of the calibration (see below) is reported as ε° which is the theoretical energy equivalent (in cal.deg^{-1}) of the calorimeter with mounted, empty,

Table 3. Calibration.

t_h = 25.0°C, t_i = 24.1°C, P^i(Gas) = 30.0 atm, V(Bomb) = 0.2751 l, V^i(water) = 0.000820 l, $\Delta E_c/M$ (Benzoic acid) = −6 317.83 ± 0.62 cal · g^{-1}, m(Pt) = 29.790 g, $\Delta E_c^\circ/M$(Fuse) = 3 971 ± 4 cal · g^{-1}

m' g	m''' g	m^i(cont) g	Δt deg	$\Delta E(HNO_3)$ cal	ε°(calor) cal · deg^{-1}
0.824826	0.005553	42.23	0.88885	1.13	5 927.08
0.826326	0.005858	42.20	0.89059	0.78	5 927.16
0.826176	0.005785	42.20	0.89034	1.39	5 928.10
0.825124	0.005468	42.20	0.88899	1.44	5 928.21
0.825980	0.005809	42.20	0.88996	0.40	5 928.29
0.824832	0.005695	42.20	0.88894	0.72	5 926.67
0.825694	0.005692	42.20	0.88979	1.40	5 927.91
				Mean	5 927.63
ε°(calor) = 5 927.63 ± 0.24 cal · deg^{-1}				Stand. dev. of mean	0.24

bomb and filled with water until the fixed total weight. In an actual experiment m^i(Cont) grams (total substance, oxygen, ampoule, water and loose platinum parts) are introduced into the bomb, and the amount of calorimeter water must be reduced accordingly in order to maintain the fixed total weight. The energy equivalent of the system is thus diminished by $C_p(H_2O)\cdot m^i$ (Cont) cal.deg^{-1}, and at the same time the energy equivalent ε^i (Cont) of the added bomb content must be taken into account. The total energy equivalent of the calorimetric system will therefore be:

$$\varepsilon^\circ(\text{calor}) \; - \; C_p(H_2O)\cdot m^i(\text{Cont}) \; + \; \varepsilon\,(\text{Cont}) \quad \text{cal.deg}^{-1}$$

Calibration. The calorimetric system was calibrated by burning benzoic acid (National Bureau of Standards Standard Sample 39 g) under specified conditions [14], and the calibration combustions are reported in Table 3.

Heats of combustion and formation. The six combustion series are reported Tables 4 to 9. The found heat of combustion value for a sample containing x % water was called $\Delta E_c'/M$ (in cal.g^{-1}) and the heat of combustion of the pure compound has been calculated thus:

$$\Delta E_c^\circ/M = \frac{100}{100 - x} \cdot \Delta E_c'/M \;\; \text{cal.g}^{-1}$$

Washburn corrections were applied as described by Hubbard, Scott and Waddington [11]. No accurate information concerning the heat capacities of the substances was available. For butanol-1 the value 0.7 cal.g^{-1}.deg^{-1} was used and for the other five compounds 0.5 cal.g^{-1}.deg^{-1}. Anticipating an error in these values of 0.2 cal.g^{-1}.deg^{-1} a value of the uncertainty introduced into the heat of combustion determinations was found to be 0.05 cal per combustion, *i.e.* 0.1 cal.g^{-1} in the $\Delta E_c^\circ/M$ values. This uncertainty could therefore be neglected in the calculations.

Table 4. 2-Butenal (containing 0.02 % water).

t_h = 25.0°C, t_i = 24.1°C, P^i(Gas) = 28.5 atm, V(Bomb) = 0.2751 l, V^i(water) = 0.000820 l, ε°(calor) = 5 927.63 ± 0.24 cal . deg^{-1}, m(Pt) = 29.762 g, $\Delta E_c^\circ/M$ (Oil) = −1 0979.6± 0.9 cal · g^{-1}, $\Delta E°/M$ (Fuse) = −3 971 ± 4 cal · g^{-1}, ΔE_Σ = 2.18 cal, M' = 70.092 g · mole^{-1}.

m' g	m'' g	m''' g	m^i(cont) g	Δt deg	$\Delta E(HNO_3)$ cal	$-\Delta E_c'/M$ cal · g^{-1}
0.420223	0.175318	0.005772	41.73	0.88735	2.79	7 790.10
0.416744	0.179539	0.005815	41.66	0.89040	2.21	7 788.19
0.408634	0.178871	0.005343	41.62	0.87792	0.76	7 789.02
0.415021	0.176115	0.005425	41.65	0.88137	1.06	7 789.46
0.441231	0.159940	0.005605	41.65	0.88633	2.17	7 791.34
0.435677	0.157640	0.005594	41.69	0.87459	1.65	7 791.14

Mean 7 789.88
Stand. dev. of mean 0.50

$\Delta E_c'/M$ = −7 789.9 cal · g^{-1}
$\Delta E_c^\circ/M$ = −7 791.4 cal · g^{-1}

Table 5. Butanal (containing 0.08 % water).

t_h = 25.0°C, t_i = 24.1°C, P^i(Gas) = 30.0 atm, V(Bomb) = 0.2751 l, V^i(water) = 0.000820 l, ε°(calor) = 5 927.63 ± 0.24 cal · deg^{-1}, m(Pt) = 29.692 g, $\Delta E_c^\circ/M$ (Oil) = −1 0979.6 ± 0.9 cal · g^{-1}, $\Delta E_c^\circ/M$ (Fuse) = −3 971 ± 4 cal · g^{-1}, ΔE_Σ = 1.72 cal, M' = 72.108 g · mole^{-1}

m' g	m'' g	m''' g	m^i(cont) g	Δt deg	$\Delta E(HNO_3)$ cal	$-\Delta E_c'/M$ cal · g^{-1}
0.417289	0.163881	0.004594	42.11	0.88990	1.36	8 196.91
0.407458	0.171305	0.004868	42.12	0.89038	1.51	8 198.56
0.372048	0.193951	0.004177	42.11	0.88255	1.14	8 194.94

Mean 8 196.80
Stand. dev. of mean 1.13 *

$\Delta E_c'/M$ = −8 196.8 cal · g^{-1}
$\Delta E_c^\circ/M$ = −8 203.4 cal · g^{-1}

* Another series using less pure substance gave the same precision, so it was felt permissible to use only three values for obtaining the standard deviation.

ΔH_c° values were computed from the ΔE_c° values. If the combustion reaction is:

$$C_aH_bO_c(l) + (a + b/4 - c/2)\, O_2(g) \rightarrow a\, CO_2(g) + b/2\, H_2O(l)$$

this relation holds:

$$-\Delta H_c^\circ = -\Delta E_c^\circ - (b/4 - c/2)\cdot 0.592 \text{ kcal.mole}^{-1}$$

Table 6. Butanol-1.

t_h = 25.0°C, t_i = 24.1°C, P^i(Gas) = 30.0 atm, V(Bomb) = 0.2751 l, V^i(water) = 0.000820 l, ε°(calor) = 5 927.63 ± 0.24 cal · deg^{-1}, m(Pt) = 29.762 g, $\Delta E_c^\circ/M$ (Oil) = −1 0979.6 ± 0.9 cal · g^{-1}, $\Delta E_c^\circ/M$ (Fuse) = −3 971 ± 4 cal · g^{-1}, ΔE_Σ = 1.49 cal, M' = 74.124 g · mole^{-1}

m' g	m'' g	m''' g	m^i(cont) g	Δt deg	$\Delta E(HNO_3)$ cal	$-\Delta E_c/M$ cal · g^{-1}
0.385950	0.168523	0.005271	42.21	0.88161	2.96	8 593.34
0.365678	0.181195	0.005454	42.16	0.87557	1.01	8 595.43
0.390181	0.166171	0.005834	42.18	0.88379	2.39	8 595.06
				Mean		8 594.61
$\Delta E_c^\circ/M$ = −8 594.6 cal · g^{-1}				Stand. dev. of mean		0.64

Table 7. 2-Ethyl-2-hexenal (containing 0.014 % water).

t_h = 25.0°C, t_i = 24.1°C, P^i(Gas) = 30.0 atm, V(Bomb) = 0.2751 l, V^i(water) = 0.000820 l, ε°(calor) = 5 927.63 ± 0.24 cal · deg^{-1}, m(Pt) = 29.764 g, $\Delta E_c^\circ/M$ (Oil) = −1 0979.6 ± 0.9 cal · g^{-1}, $\Delta E_c^\circ/M$ (Fuse) = −3 971 ± 4 cal · g^{-1}, ΔE_Σ = 1.88 cal, M' = 126.200 g · mole^{-1}

m' g	m'' g	m''' g	m^i(cont) g	Δt deg	$\Delta E(HNO_3)$ cal	$-\Delta E_c'/M$ cal · g^{-1}
0.454216	0.088487	0.005031	42.16	0.88147	1.87	9 238.25
0.489861	0.063730	0.005127	42.18	0.89155	1.10	9 242.87
0.469287	0.078639	0.005934	42.17	0.88752	1.26	9 240.40
0.459681	0.087428	0.005704	42.18	0.88864	1.24	9 241.10
0.467358	0.082095	0.005348	42.17	0.89054	1.14	9 241.78
0.457202	0.089691	0.005328	42.18	0.88879	1.14	9 242.28
				Mean		9 241.11
$\Delta E_c'/M$ = −9 241.1 cal · g^{-1}				Stand. dev. of mean		0.67
$\Delta E_c^\circ/M$ = −9 242.4 cal · g^{-1}						

Heats of formation were calculated using the heat of formation values at 25°C[15]:

for CO_2(g): ΔH_f° = − 94.0518 kcal.mole^{-1}
for H_2O(l): ΔH_f° = − 68.3174 kcal.mole^{-1}

Final overall standard deviations were computed by the method of Bjellerup [16] and include the errors of (i) the heat of combustion value for benzoic acid, (ii) the calibration experiments, (iii) the paraffin oil combustions, (iv) the determination of mass including water analysis and finally (v) the standard deviation of the actual combustion series.

Table 8. 2-Ethyl-hexanal (containing 0.03 % water).

t_h = 25.0°C, t_i = 24.1°C, P^i(Gas) = 30.0 atm, V(Bomb) = 0.2751 l, V^i(water) = 0.000820 l, $\varepsilon°$(calor) = 5 927.63 ± 0.24 cal · deg^{-1} in all experiments except the fourth where $\varepsilon°$(calor) = 5 935.48 ± 0.24 cal · deg^{-1}, m(Pt) = 29.516 g, $\Delta E_c^°/M$ (Oil) = −1 0979.6 ± 0.9 cal · g^{-1}, $\Delta E_c^°/M$ (Fuse) = −3 971 ± 4 cal · g^{-1}, ΔE_Σ = 1.70 cal, M' = 128.216 g · mole^{-1}

m' g	m'' g	m''' g	m^i(cont) g	Δt deg	$\Delta E(HNO_3)$ cal	$-\Delta E_c'/M$ cal · g^{-1}
0.409769	0.113481	0.004335	41.87	0.87338	1.18	9 463.74
0.435605	0.093896	0.004083	41.87	0.87808	1.27	9 461.74
0.446309	0.085515	0.004645	41.90	0.88011	1.21	9 462.86
0.422621	0.107697	0.004037	41.87	0.88172	1.38	9 461.17
0.433487	0.094669	0.004231	41.90	0.87634	1.82	9 462.06
0.443856	0.090238	0.004371	41.87	0.88488	1.55	9 463.36
0.413009	0.115624	0.004799	41.86	0.88260	1.58	9 458.61
0.439658	0.108168	0.004788	41.89	0.91189	2.55	9 461.79
0.439684	0.089070	0.004654	41.87	0.87641	2.48	9 464.18
				Mean		9 462.17
$\Delta E_c'/M$ = −9 462.2 cal · g^{-1}				Stand. dev. of mean		0.56
$\Delta E_c^°/M$ = −9 465.0 cal · g^{-1}						

Table 9. 2-Ethyl-hexanol-1.

t_h = 25.0°C, t_i = 24.1°C, P^i(Gas) = 30.0 atm, V(Bomb) = 0.2751 l, V^i(water) = 0.000820 l, $\varepsilon°$(calor) = 5 927.63 ± 0.24 cal · deg^{-1}, m(Pt) = 29.758 g, $\Delta E_c^°/M$ (Oil) = −1 0979.6 ± 0.9 cal · g^{-1}, $\Delta E_c^°/M$ (Fuse) = −3 971 ± 4 cal · g^{-1}, ΔE_Σ = 1.31 cal, M' = 130.232 g · mole^{-1}

m' g	m'' g	m''' g	m^i(cont) g	Δt deg	$\Delta E(HNO_3)$ cal	$-\Delta E_c^°/M$ cal · g^{-1}
0.427374	0.100038	0.004245	42.11	0.89256	1.42	9 684.30
0.401689	0.114704	0.004867	42.10	0.87829	1.45	9 687.24
0.459568	0.062875	0.004255	42.10	0.87654	1.32	9 688.60
0.459179	0.064999	0.004276	41.85	0.87974	1.22	9 687.57
0.450269	0.079140	0.004574	41.87	0.89176	1.74	9 687.88
0.447457	0.076646	0.004430	41.88	0.88214	1.85	9 684.34
0.407624	0.100577	0.004097	41.85	0.86099	2.17	9 682.99
				Mean		9 686.13
$\Delta E_c^°/M$ = −9 686.1 cal · g^{-1}				Stand. dev. of mean		0.83

Table 10. Thermochemical data, referring to the liquid standard state at 25°C.

Compound	$-\Delta E_c^°/M$ cal · g^{-1}	$-\Delta E_c^°$ kcal · mole^{-1}	$-\Delta H_c^°$ kcal · mole^{-1}	$-\Delta H_f^°$ kcal · mole^{-1}
2-Butenal	7 791.4 ± 1.2	546.12 ± 0.09	546.71 ± 0.09	34.45 ± 0.09
Butanal	8 203.4 ± 2.3	591.53 ± 0.17	592.42 ± 0.17	57.06 ± 0.17
Butanol-1	8 594.6 ± 1.3	637.07 ± 0.10	638.25 ± 0.10	79.55 ± 0.10
2-Ethyl-2-hexenal	9 242.4 ± 1.3	1 166.39 ± 0.17	1 168.17 ± 0.17	62.46 ± 0.17
2-Ethyl-hexanal	9 465.0 ± 1.4	1 213.56 ± 0.18	1 215.63 ± 0.18	83.32 ± 0.18
2-Ethyl-hexanol-1	9 686.1 ± 1.4	1 261.44 ± 0.19	1 263.81 ± 0.19	103.46 ± 0.19

The uncertainties given are the final overall standard deviations.

Acknowledgements. The author wishes to express his sincere gratitude to the Mo och Domsjö AB, especially Dr. B. Nycander for a most stimulating cooperation in performing this investigation.

REFERENCES

1. Kharasch, M. S. *J. Research Natl. Bur. Standards* **2** (1929) 359—430.
2. Verkade, P. E. and Coops, J. *Rec. trav. chim.* **46** (1927) 903.
3. Rossini, F. D. *J. Research Natl. Bur. Standards* **13** (1934) 189.
4. Sunner, S. *Studies in Combustion Calorimetry Applied to Organo-sulphur Compounds (Diss.)*, Lund 1949.
5. Smith, T. and Bronner, R. *Ind. Eng. Chem.* **43** (1951) 1169.
6. Auwers, K. and Eisenlohr, F. *J. prakt. Chem.* **82** (1910) 115.
7. Brunjes, A. and Bogart, M. *Ind. Eng. Chem.* **34** (1943) 255.
8. Batalin, V. S. and Slavina, S. E. *J. Gen. Chem. (USSR)* **7** (1937) 202.
9. Häusermann, M. *Helv. Chim. Acta* **35** (1951) 1211.
10. Levene, P. A. and Taylor, F. A. *J. Biol. Chem.* **54** (1922) 351.
11. Hubbard, W. N., Scott, D. W. and Waddington, G. *Standard States and Corrections for Combustions in a Bomb at Constant Volume* Chapter 5 of Rossini, F. D. (Ed.) *Experimental Thermochemistry*, New York 1956.
12. Bjellerup, L. *Acta Chem. Scand.* **13** (1959) 1511.
13. Bjellerup, L. and Tjebbes, J. *Unpublished measurements.*
14. Coops, J., Jessup, R. S. and van Nes, K. *Calibration of Calorimeters for Reactions in a Bomb at Constant Volume* Chapter 3 of Rossini, F. D. (Ed.) *Experimental Thermochemistry*, New York 1956.
15. Selected Values of Chemical Thermodynamic Properties, *Circular of Natl. Bur. Standards 500*, Washington D. C. 1952.
16. Bjellerup, L. *Acta Chem. Scand.* **14** (1960). *In press.*

Received September 24, 1959.

ACTA CHEMICA SCANDINAVICA 14 (1960) 189–193

Polymorphs and Conformations of the Cytidylic Acids

S. FURBERG

Institute of Chemistry, University of Oslo, Blindern-Oslo, Norway

Unit cell dimensions and space groups have been determined for three polymorphs of cytidylic acid "a" and two polymorphs of cytidylic acid "b". The conformations of the molecules are discussed.

It was shown by Harris *et al.*[1] that cytidylic acid "a" (cytidine-2-phosphate) and cytidylic acid "b" (cytidine-3-phosphate) both exist in two stable crystalline forms called the alc-form and the H_2O-form. The different polymorphs were characterized by their infra-red spectra, but crystal data were not given. In connection with other X-ray crystallographic studies of nucleic acid components, we have determined unit cell dimensions of the polymorphs, thus providing an additional method for their identification. A third polymorphic form of the "a"-isomer, which is metastable, was also examined.

Crystal data were derived from oscillation and Weissenberg diagrams taken with Cu radiation ($\lambda = 1.542$ Å). The cell dimensions given are believed to be accurate to within 1 %. The space groups were determined from systematic absences and the densities measured by the flotation method. None of the crystal forms contain water of crystallization [1].

Cytidylic acid "b". Following the procedure described by Harris *et al.*, the two polymorphs were obtained together by letting a saturated aqueous solution evaporate on a watch-glass.

The *alc-form* crystallizes in the monoclinic system, with $a = 5.94$ Å, $b = 16.96$ Å, $c = 6.89$ Å and $\beta = 118°$. The space group is $P2_1$ and the unit cell contains two molecules. The observed density is 1.73 g/cm^3, the calculated value 1.75 g/cm^3. This polymorphic form was found to occur in a variety of different crystal habits. Short polar needles elongated along b with c lying in the predominant face were observed, but usually the crystals are elongated along the diagonal [101], being either rod-like, or developed as flat plates (010). The length of this diagonal is 6.66 Å.

The *H_2O-form* is readily obtained as big flat plates several mm of extension. In general, they are somewhat elongated along c, with (010) as the dominating face. Forms {011}, {001}, {100}, and {110} were also observed. The crystals are biaxial positive with (001) as the optic axial plane. They crystallize in the

orthorhombic system, with unit cell dimensions $a = 8.80$ Å, $b = 21.7$ Å and $c = 6.85$ Å. The space group is $P2_12_12$, and there are four molecules in the unit cell. The density was found to be 1.66 g/cm³ (calculated 1.64 g/cm³).

Cytidylic acid "a". A sample of the *alc-form* was kindly supplied by Dr. R.J.C. Harris of the Central Laboratories, Imperial Cancer Research Fund. It consisted of very small needles with b as the needle axis. On the basis of a number of weak oscillation diagrams taken around the needle axis it was concluded that the crystals are monoclinic, with $a = 16.97$ Å, $b = 7.50$ Å, $c = 11.80$ and $\beta = 119°$. The space group is $C2$, as reflexions with $h + k$ odd are absent and the molecules are optically active. The calculated density assuming four molecules per unit cell, is 1.68 g/cm³.

By letting a saturated aqueous solution evaporate on a watch-glass, two other polymorphic forms were obtained, one as a crust at the edge and one deposited from the middle of the solution. The latter is probably the H_2O-form of Harris *et al.* The former is metastable and is transformed into the alc-form described above in the course of a few days. The transformation is made evident by the loss of extinction and by changes in the X-ray diagrams.

The *metastable* form yields needle-shaped crystals elongated along the c axis. The crystals grow either together in spherulitic formations of needles, or alternatively well-developed crystals with (100) as the dominating face are formed. They give straight extinction and may be recognized under the microscope by the angle of 57° between (010) and (021). The crystals are monoclinic, with $a = 9.32$ Å, $b = 22.8$ Å, $c = 7.38$ Å and $\beta = 95°$. Space group $P2_1$. Four molecules in the unit cell give a calculated density of 1.38 g/cm³. This density is much lower than that of the four other crystalline cytidylic acids, for which values between 1.64 and 1.75 g/cm³ are found. The packing of the molecules must be a very loose one and it is not surprising that the crystals are less stable than those of the other polymorphs.

The crystals of the *H_2O-form* were extremely small, and only feeble diffraction patterns were obtained. These show that the crystals probably are orthorhombic, with $a = 7.35$ Å, $b = 25.2$ Å and $c = 6.66$ Å. The extinctions indicate the space group $P2_12_12_1$ or $P2_12_12$. The calculated density is 1.74 g/cm³. The crystals have the shape of flat prisms elongated along c. Faces (100), (001) and (010) were observed, the latter being predominant.

Identification. The data given above provide a method for identification of extremely small quantities of the different polymorphs and isomorphs of of cytidylic acids. One single crystal of dimensions greater than say 0.05 mm will suffice with ordinary cameras and X-ray sources.

In general, the crystals are more or less elongated along one direction and the crystals may be identified by taking an oscillation diagram around this axis. The polymorphs are distinguishable by the length of the corresponding crystallographic axis, and by the symmetry, where some of them give diagrams with a plane of symmetry perpendicular to the axis of oscillation, others not (denoted "plane" and "no plane", respectively, in Table 1). Table 1 may serve as a key for the identification.

All the crystals give straight extinction when lying on the predominant face, except some of the habits of "b" alc and the metastable form.

Table 1. The characteristics of oscillation diagrams of crystals of cytidylic acid.

Length of axis, Å	Symmetry	Polymorph
6.66	No plane	"b" alc.
6.66	Plane	"a" H_2O
6.85	Plane	"b" H_2O
7.38	No plane	"a" metastable
7.50	Plane	"a" alc.
16.96	Plane	"b" alc.

Molecular shape. The molecular structure of nucleotides is a problem of considerable interest because of its relation to the structure of nucleic acids. We have carried out a complete structure analysis of the "b" H_2O polymorph and determined the molecular structure [2]. In the crystals the NH_2-group in one molecule is connected by hydrogen bonds to PO_4-groups in neighbouring molecules and the molecular axis is roughly parallel to *b*, the longest cell edge. It seems reasonable to assume that the amino and phosphate groups are linked together by hydrogen bonds also in the other polymorphic forms. Taking also the unit cell dimensions and the space group into account, this permits some conclusions to be drawn about the general shape of the molecules and their orientation in the crystals.

Considering first the "b"-isomer the molecular dimensions in the known structure ("b" H_2O) are roughly 4.5 × 7 × 11 Å, whereas in the "b" alc form the molecule probably extends only about 8.5 Å in the *b* direction. This indicates a considerably shorter molecule, and it seems likely that the molecule exhibits different shapes in the two polymorphic crystal forms.

Two main factors govern the general shape of the cytidylic acid molecule, namely (i) at the conformation of the ribose ring and (ii) the orientation of the phosphate group. From the crystal structure analysis of cytidine and cytidylic acid "b" H_2O two different ribose conformations are known to occur, one with $C_{2'}$ out of the plane of the four other atoms, and one with $C_{3'}$ out of the plane [2]. As for the orientation of the phosphate group, one would expect a staggered arrangement of the bonds around the $C_{3'}—O_{3'}$ linkage. There are three such orientations, but one of these corresponds to a *cis* relation between phosphate and ribose and would seem to be less favourable than the other two. Thus the molecule may be expected to occur in four general shapes:

(1) $C_{2'}$ out of the plane; $P—O_{3'}$ nearly parallel to $C_{2'}—C_{3'}$
(2) » » » » » » » » » $C_{3'}—C_{4'}$
(3) $C_{3'}$ » » » » » » » » $C_{2'}—C_{3'}$
(4) » » » » » » » » » $C_{3'}—C_{4'}$

Conformations (1) and (2) are shown in Fig. 1. The length of the molecule, as measured by the distance $P—N_6$, is about 9.8 Å, 8.8 Å, 9.1 Å and 8.5 Å in the four conformations, respectively. These values are based on bond lengths and angles derived by the X-ray analysis of cytidylic acid "b" H_2O. Minor

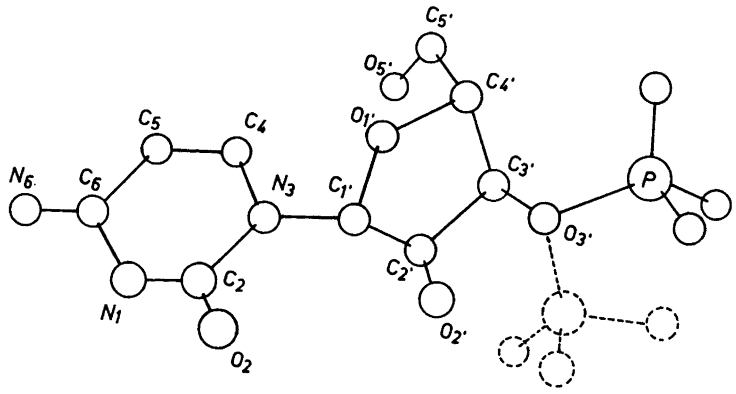

Fig. 1. Conformations of cytidylic acid "b" with atom $C_{2'}$ out of the ring plane.

variations in molecular shape may also be obtained by rotation around the bonds $N_3—C_{1'}$ and $P—O_{3'}$, but these changes do not alter the length of the molecule and need not be considered in this connection.

In the known structure of the H_2O polymorph the molecule has conformation (1), the most extended one. As stated above, the molecule would seem to be less extended in the alc polymorph and one of the other three conformations occurs. It may also be mentioned that current models of DNA are based on a nucleotide conformation of type (4).

Turning now to cytidylic acid "a", there are also in this case four stable conformations. It is seen from models, however, that the molecule is less extended than that of the "b" isomer, the amino and phosphate groups being in closer proximity. The $P—N_6$ distances are 7.5 Å and 5.8 Å, respectively, with $C_{2'}$ out of the plane, and 7.3 Å and 8.0 Å with $C_{3'}$ out of the plane. In the three first-mentioned conformations the molecule is very roughly equally extended in all directions, in agreement with the cell dimensions of the H_2O form, which may be interpreted as indicating four molecules of dimensions $7 \times 7 \times 6$ Å along the *b* axis. Similar molecular dimensions may be derived from the data obtained for the alc-form. On the basis of the data given above it is not possible to decide whether or not the molecule has the same conformation in the two cases. As for the unstable modification, the low density of this form makes a comparison with the other polymorphs difficult.

Finally, it may be remarked that the discussion of the conformations of the cytidylic acids given above is valid also for other 2' and 3' nucleotides. For each isomer there should be four conformations as far as variations in ribose puckering and orientation of the phosphate group are concerned. In the case of the 5' -nucleotides, there are more conformations because of the additional single bond $C_{4'}—C_{5'}$.

The author wishes to thank Dr. W. E. Cohn of the Oak Ridge National Laboratories and Dr. R. J. C. Harris of the Central Laboratories, Imperial Cancer Research Fund, for supplying samples of the isomers. The investigation was supported by *Norsk Hydros fond.*

REFERENCES

1. Harris, R. J. C., Orr, S. F. D., Roe, E. M. F. and Thomas, J. F. *J. Chem. Soc.* **1953** 489.
2. Alver, E. and Furberg, S. *Acta Chem. Scand.* **13** (1959) 910.

Received September 8, 1959.

ACTA CHEMICA SCANDINAVICA 14 (1960) 194–196

Association of Zn-free Insulin

KJELD MARCKER

Universitetets Fysisk-Kemiske Institut, Copenhagen, Denmark

In this investigation the association of Zn-free insulin in dependence on concentration and pH has been investigated by means of osmometry. The minimum molecular weight at acid pH has been found to 12 000, and at basic pH to 6 000. The association monomer to dimer seems to proceed by a reaction which is different from the one leading to association of dimers to higher degrees of association.

Molecular weights for insulin determined by several methods have already been published.[1–6] In these investigations it has been observed that the molecular weight of insulin is dependent upon pH, temperature, ionic strength and protein concentration of the solution.

The insulin used in these experiments was crystalline Zn-insulin and therefore it seemed worth while to investigate the association of Zn-free insulin in aqueous solution. Fredericq [5] has found indications of association of insulin molecules by means of Zn-ions. On account of this finding it was therefore expected that a difference between crystalline Zn-insulin and Zn-free insulin would exist, and this was found to be the case.

The insulin used was Zn-free pig insulin prepared from crystalline Zn-insulin by precipitation at pH 2 with NaCl. The colloid osmotic pressures were measured by means of the inverted micro-osmometer described by Christiansen and Jensen [7]. The semipermeable membranes were made according to Adair [8]. The membranes prepared by this method have proved to be impermeable to molecules with molecular weights as low as five to six thousands. The collodion solution used was made in the following way: 4 g of completely dry pyroxolin (Parlodion Mallinckrodt) were dissolved in a mixture of 50 ml of anhydrous alcohol and 50 ml of anhydrous ether; to this mixture were added 6 ml of anhydrous ethylene glycol. The preparation of the semipermeable membranes turned out to be a difficult problem. In the drying process the membranes shrink, thus giving rise to tensions in the membranes. Besides the membranes lose their elasticity which makes it very difficult to place them on the capillary. In order to avoid these difficulties smaller modifications in the membrane making procedure have been tried, but unfortunately without success. On account of the above mentioned irregularities about 50 % of the membranes had to be discarded. The tension in the membranes could easily be detected, because in the case of tension it was impossible to obtain a straight line in the interpolation diagram.

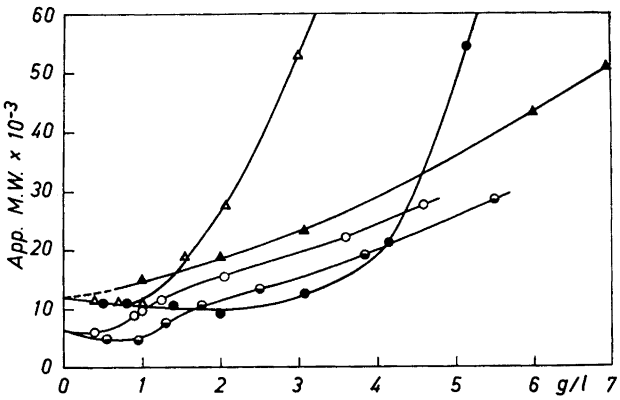

Fig. 1. Association of Zn-free insulin: Ordinate: Apparent molecular weight; Abscissa: Concentration in g/l. △ pH = 2.10; ● pH = 2.98; ▲ pH = 7.70; ○ pH = 8.31; ◒ pH = 9.10. Temp. 20°C.

Fredericq [5] and Gutfreund [3] have observed a specific anion effect upon the association of crystalline Zn-insulin. In this investigation no attempt has been made to evaluate a possible anion effect upon the association of Zn-free insulin.

The buffers used were: HCl-KCl, citrate-HCl and veronal-HCl. All buffers were adjusted to the ionic strength 0.2 with KCl. According to our experience the influence of the Donnan-effect is then negligible. The results are shown in Fig. 1.

It should be mentioned that the points in the diagram refer to apparent molecular weights and not to the true molecular weights. On account of the association it is impossible to extrapolate to infinite dilution in order to obtain the true molecular weight. The difference, however, between the true and the apparent molecular weight is probably not great, because of the relatively small electrical charge on the insulin molecule.

The surprisingly high degree of association in the acid region might be explained as a "salting out" effect. At pH 2 and 3 insulin is easily precipitated by KCl. At acid pH Fredericq [5] has obtained evidence for the existence of the insulin monomer in very dilute solution. In the present investigation there is no indication for the existence of the monomer at acid pH. On the contrary the results strongly support the generally accepted view that the minimum molecular weight in acid solution is 12 000 which corresponds to the dimer. In nearly neutral solution crystalline zinc insulin is reported to have a molecular weight of 36 000. The results of this investigation show that this is not the case with zinc-free insulin. The results reported here indicate a molecular weight of 12 000 at a pH about 7.7. Schlichtkrull [9] has shown that the minimum amount of zinc in crystalline zinc insulin is two atoms pr 36 000. It therefore seems reasonable to assume that three molecules having a molecular weight of 12 000 are associated by means of two zinc ions. Until recently it was generally accepted that the monomer insulin molecule did not exist in aqueous solution. By sedimentation experiments at pH 9 and 10 Fredericq [4],

however, demonstrated the presence of the monomer in dilute aqueous solution. The results reported here are in agreement with the findings of Fredericq as they clearly show that in dilute basic solution insulin molecules exist as monomers. By closer examination of the curves representing the results obtained at pH 8.31 and pH 9.10, a difference in the course of the curves in the concentration range 0 to 1.5 g/l compared to that from 1.5 g/l to higher values is apparent. This might indicate that the reaction of monomers to dimers is different from the reaction of dimers to higher association compounds.

Acknowledgements. The authors thanks are due to Professor J. A. Christiansen and Dr. J. Schlichtkrull for their kind interest and many valuable suggestions.

Financial support from *Novo Terapeutisk Laboratorium* and *Købmand i Odense Johann og Hanne Weimann, født Seedorf's Foundation* is gratefully acknowledged.

REFERENCES

1. Gutfreund, H. *Biochem. J.* **40** (1946) 432.
2. Gutfreund, H. *Ibid.* **42** (1948) 544.
3. Gutfreund, H. *Ibid.* **50** (1952) 564.
4. Fredericq, E. *Nature* **171** (1953) 570.
5. Fredericq, E. *Arch. Biochem. Biophys.* **65** (1956) 218.
6. Tietze, F. and Neurath, H. *J. Biol. Chem.* **194** (1952) 1.
7. Christiansen, J. A. and Jensen, C. E. *Acta Chem. Scand.* **7** (1953) 1247.
8. Adair, G. S. *Biochem. J.* **62** (1955) XXVI.
9. Schlichtkrull, J. *Acta Chem. Scand.* **10** (1956) 1455.

Received September 10, 1959.

ACTA CHEMICA SCANDINAVICA 14 (1960) 197–210

Alkaline Hydrolysis of Some Local Anaesthetic Esters

BO KARLÉN and ALLAN ÅGREN

Department of Chemistry, Royal Pharmaceutical Institute, Stockholm, Sweden

The alkaline hydrolysis of the following local anaesthetic esters has been studied: benzocaine, butyl benzocaine, tetracaine, procaine, panthesine and *o*-hydroxyprocaine.

The velocity constants are determined photometrically in water solution at 25.0, 35.0 and 45.0°C. The influence of substituents on the activation energy and the frequency factor is discussed.

A knowledge of the behaviour of the local anaesthetics on alkaline hydrolysis is of interest not only from a theoretical point of view but also practically. For example the deterioration of pharmaceutical preparations may be estimated and the possibility of heat sterilization predicted. Further, the duration and toxicity of intravenous injected preparations is said to be connected with the speed of hydrolysis by blood serum [1]. In the thesis of Terp [2] the hydrolysis of procaine influenced by procaine esterase is discussed. Obviously, other physical and chemical factors will also affect the physiological effect of local anaesthetics, *e.g.* their solubility. However, this property has not been studied in this work.

Some of the substances which we have studied have also been investigated by other authors. The purpose of most of the earlier investigations published has been to make clear the stability of pharmaceutical preparations under special conditions and the authors have not been interested in the kinetic problems from a theoretical point of view. Among these publications the following may be mentioned [3–8]. Only a few investigations have been found in the literature, where the kinetic aspects on the alkaline hydrolysis of local anaesthetic esters have been thoroughly studied. In Table 1 a survey of the results from other authors is found. The authors all have found, that the process in strongly alkaline solution is a bimolecular reaction and thus can be written

$$\text{ester} + \text{OH}^- \rightarrow \text{alcohol} + \text{acid}$$

and the velocity constant, k_2, is defined by the equation

$$\mathrm{d}x/\mathrm{d}t = k_2\,(\text{OH}^-)\,(\text{ester})$$

Table 1. Previous work.

Compound	k_2 lit/mole/min	Temp. °C	Medium	E kcal	A lit/mole/min	Ref.
Benzocaine	7.53×10^{-4}	25	85 % ethanol	20.00	11.50	9
	5.04×10^{-3}	25	56 % acetone	16.70	10.00	10
	1.14×10^{-3}	30	88 % ethanol	—	—	13
	2.52×10^{-1}	30	water	—	—	15
	1.85×10^{-1}	25	water	12.6	8.5	this work
Procaine	4.8×10^{-2}	40	60 % acetone	—	—	11
	6.6×10^{-1}	40	water	13.80	9.38	12
	7.84×10^{-1}	37	water	—	—	14
	3.14×10^{-1}	25	water	14.2	9.9	this work

In the table all the values of k_2 are given in litre/mole/min. In some of the investigations the hydrolysis has been studied at several temperatures so that the activation energy, E, and the frequency factor, A, could be calculated. In the calculations the Arrhenius formula has been used

$$k_2 = PZ \times e^{-E/RT}$$

and

$$\log (PZ) = A$$

A great number of investigations have been published, where esters of different kinds have been studied in this respect. To be mentioned are the following authors, namely Tommila [16], Tommila and Hinshelwood [10], Newling and Hinshelwood [17], Kindler [13], Jones and Robinson [18], Ingold and Nathan [9] *etc.*

Among the many local anaesthetic esters only benzocaine and procaine seem to have been kinetically studied, and thus the present work will elucidate the properties of some other of the most used local anaesthetic esters.

Many of the authors mentioned have studied the end products of the hydrolysis. Some have found that the first produced acid is later on broken down by decarboxylation, but this has only been found in acidic solutions. In the present work no further decomposition of the acid has been found, at least during the relatively short time the process has been followed. Hydroxy procaine is hydrolyzed to *p*-amino salicylic acid. Not even this rather unstable acid has been decomposed under the conditions and short time used by us.

METHODS

Some authors [1-3,6] have followed the ester hydrolysis by a chemical separation of one of the hydrolysis products, and then the amount of this substance or the ester left has been estimated, for instance photometrically. Another method being used is a titration of the hydroxyl ion. In order to make this method possible the amount of the reacting species must be rather great and this gives a rather high velocity. Further, the investigation has to be made in a suitable solvent as the water solubility of the esters is small. As solvent, acetone-water has been used by Tommila [16] and Armstrong [11], ethanol-water by Ingold [9] and Kindler [13].

We have preferred to use a direct method also used by Higuchi [12,15] and others. All the esters studied in this work have a strong absorption in the UV. The acid formed has the maximum absorption shifted to another wavelength and the molecular extinction at this wavelength is lower than for the ester. Thus the concentration of the ester may be measured photometrically without separating it from the acid. The alcohol has a very low extinction in the same wavelength region. Thanks to the strong absorption, very low concentrations can be used, and thus water is suitable as a solvent.

Figs. 1—6 show the extinction curves of the esters and the corresponding acids. In the hydrolysis experiments all measurements are made at the wavelength where the extinction of the ester has its maximum. We have used the method given by Higuchi [12]:

A 0.1000 % water solution of the ester or its salt was warmed up to the temperature at which the hydrolysis was to be made. (Butyl benzocaine is sparingly soluble in water and in this case a saturated solution was made.) From this stock solution a certain volume was added to a solution of sodium hydroxide in water free from carbon dioxide. The volumes were so chosen that the concentration of the ester was 0.01000 % and the pH of the solution was exactly 12.00. This mixture was kept in one bottle in a water bath, the temperature of which was known within 0.1°. At different times samples were

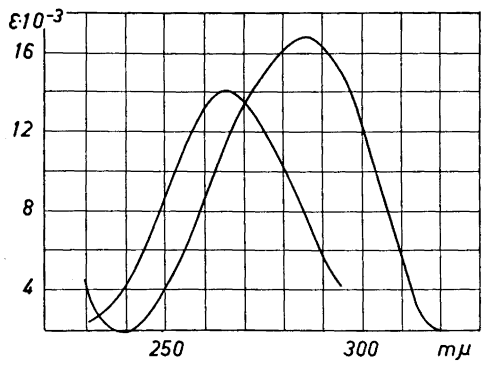

Fig. 1. Molecular extinction *vs.* wave length. Benzocaine (ε_{max} = 16 850 at 286 mμ) and *p*-amino benzoic acid (ε_{max} = 13 980 at 265 mμ). pH = 9.5

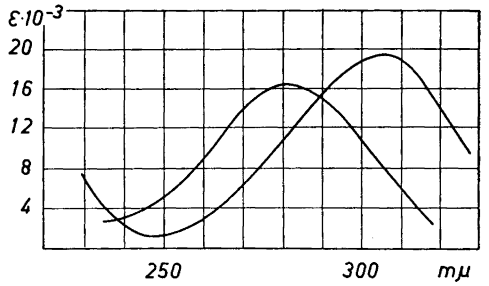

Fig. 2. Molecular extinction *vs.* wave length. Butyl benzocaine (ε_{max} = 19 450 at 305 mμ) and *p*-butyl amino benzoic acid (ε_{max} = 16 640 at 280 mμ). pH = 9.5

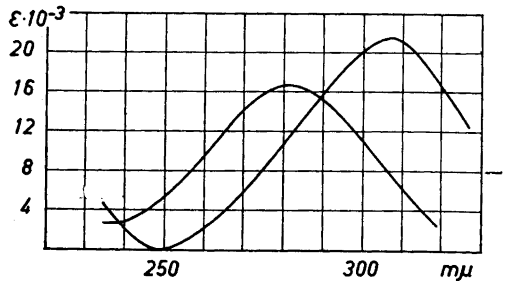

Fig. 3. Molecular extinction *vs.* wave length. Tetracaine (ε_{max} = 21 340 at 307 mμ) and *p*-butyl amino benzoic acid (ε_{max} = 16 640 at 280 mμ). pH = 9.5

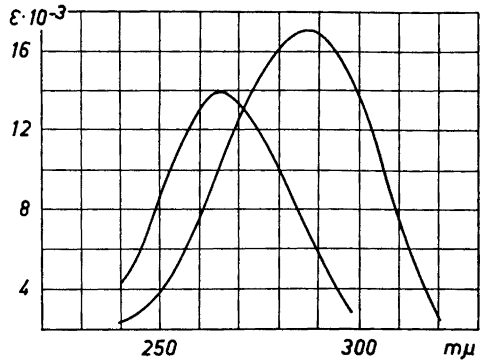

Fig. 4. Molecular extinction *vs.* wave length. Procaine (ε_{max} = 17 050 at 287 mμ) and *p*-amino benzoic acid (ε_{max} = 13 980 at 265 mμ). pH = 9.5

taken from the mixture and added to a borate buffer solution with a pH = 9.5, which was made according to the Swedish Pharmacopeia Ed. XI. The extinction of the resulting solution was measured with a Beckmann photometer model DU in 1 cm cuvettes.

In order to avoid the influence of the carbon dioxide of the air, some experiments were made in a slightly different manner. The reaction mixture was dispensed in a number of bottles closed with glass stoppers. The content of each bottle was used only for one measurement. However, it was found that the results from these experiments agreed with the other ones.

The reaction mixture contained about 30 times the theoretically necessary amount of sodium hydroxide to hydrolyse the total amount of ester. This means that the concentration of hydroxyl ions is hardly changed during the experiment. It was found that the pH of the solutions was diminished by 0.02 units at the end of the experiments. Thus, the reactions could be treated as monomolecular.

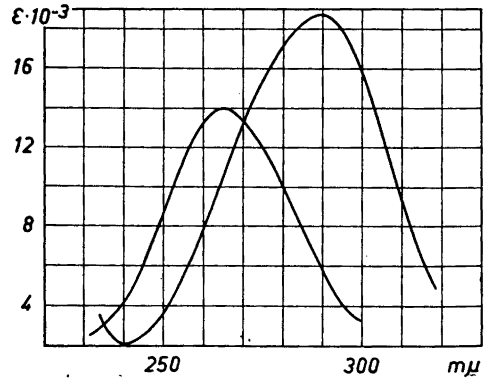

Fig. 5. Molecular extinction *vs.* wave length. Panthesine (ε_{max} = 18 680 at 289 mμ) and *p*-amino benzoic acid (ε_{max} = 13 980 at 265 mμ). pH = 9.5

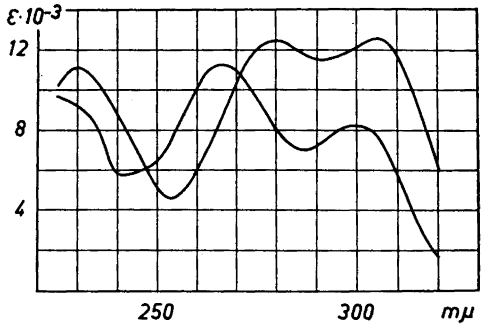

Fig. 6. Molecular extinction *vs.* wave length. Hydroxy procaine (ε_{max} = 12 550 at 305 mμ) and *p*-amino salicylic acid (ε_{max} = 8 290 at 300 mμ). pH = 9.5

Table 2. Hydrolysis of benzocaine. Starting conc. of ester = 6.054×10^{-4} mole/lit. λ = 286 mμ

Temp.	Time (min)	E_t	$E_t - E_s$	log (% ester left)
25°	0	1.020	0.563	2.0000
	65	0.955	0.498	1.9467
	120	0.905	0.448	1.9008
	210	0.845	0.388	1.8383
	240	0.835	0.378	1.8270
	315	0.762	0.305	1.7338
	"infin."	0.457	0.000	—
35°	0	1.020	0.563	2.0000
	30	0.970	0.513	1.9596
	55	0.934	0.477	1.9280
	135	0.805	0.348	1.7911
	180	0.760	0.303	1.7309
	"infin."	0.457	0.000	—
45°	0	1.020	0.563	2.0000
	15	0.960	0.503	1.9511
	40	0.885	0.428	1.8809
	60	0.828	0.371	1.8189
	82	0.773	0.316	1.7492
	120	0.730	0.273	1.6857
	225	0.572	0.115	1.3102
	340	0.509	0.052	0.9655
	"infin."	0.457	0.000	—

All the esters studied in this investigation were examined at 25.0, 35.0 and 45.0°C.

Chemicals. Commercial benzocaine, tetracaine hydrochloride, procaine hydrochloride, and panthesine methane sulfonate were used without any further purification.

Hydroxy procaine hydrochloride was synthesized from *p*-amino salicylic acid and β-chloroethyl diethylamine hydrochloride. The latter was synthesized according to Gough and King [20]. The acid was suspended in acetone and then β-chloroethyl diethylamine hydrochloride was added. The mixture was refluxed for 20 h. *Iso*propyl alcohol containing 10 % hydrogen chloride was then added to the filtered solution [19]. The precipitate was washed with acetone and recrystallized from ethanol. The melting point was 153.5—154°C. The water content was determined by K. Fischer titration to be 1.8 %.

Butyl benzocaine was synthesized from butyl bromide and benzocaine [21]. Its melting point was 68°C. The other chemicals used were of analytical grade.

RESULTS

The results of the experiments are reported in Tables 2—7. E_t is the extinction of the reaction mixture when added to the buffer solution. E_o, the extinction at the beginning of an experiment, was determined by measuring the ester in the same buffer solution but without any alkali. E_s, the extinction after "infinite" time, was determined by measuring the corresponding acid dissolved in the buffer solution.

Table 3. Hydrolysis of butyl benzocaine.

Starting conc. of ester = 4.190×10^{-5} (25°) mole/lit. $\lambda = 305$ mμ
4.370×10^{-5} (35°) »
4.113×10^{-5} (45°) »

Temp.	Time (min)	E_t	$E_t - E_s$	log (% ester left)
25°	0	0.815	0.453	2.0000
	70	0.756	0.394	1.9394
	125	0.730	0.368	1.9098
	225	0.700	0.338	1.8728
	275	0.683	0.321	1.8504
	350	0.661	0.299	1.8196
	465	0.622	0.260	1.7589
	"infin."	0.362	0.000	—
35°	0	0.850	0.473	2.0000
	70	0.730	0.353	1.8729
	120	0.690	0.313	1.8207
	225	0.629	0.252	1.7265
	275	0.583	0.206	1.6390
	350	0.560	0.183	1.5876
	465	0.514	0.137	1.4619
	"infin."	0.377	0.000	—
45°	0	0.800	0.445	2.0000
	60	0.668	0.313	1.8472
	115	0.630	0.275	1.7910
	215	0.500	0.145	1.5130
	265	0.475	0.120	1.4308
	340	0.434	0.079	1.2493
	"infin."	0.355	0.000	—

From the experimental results, the concentration of ester in each measurement could be calculated by the formula

$$\% \text{ ester left} = \frac{E_t - E_s}{E_o - E_s} \times 100$$

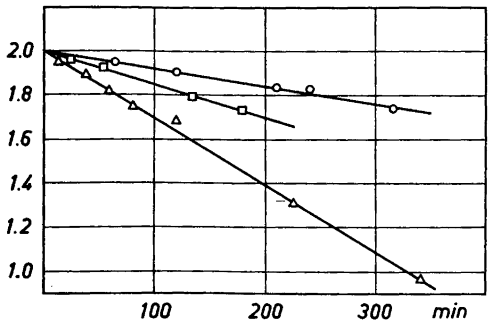

Fig. 7. Hydrolysis of benzocaine. log (% ester left) *vs.* time.

Table 4. Hydrolysis of tetracaine HCl.

Starting conc. of ester = 3.028×10^{-4} (25°) mole/lit. $\lambda = 307$ mμ
3.304×10^{-4} (35°) »
3.304×10^{-4} (45°) »

Temp.	Time (min)	E_t	$E_t - E_s$	log (% ester left)
25°	0	0.646	0.428	2.0000
	60	0.612	0.394	1.9640
	120	0.558	0.340	1.8890
	180	0.530	0.312	1.8627
	230	0.497	0.279	1.8142
	300	0.468	0.250	1.7665
	360	0.454	0.236	1.7415
	430	0.433	0.215	1.7010
	"infin."	0.218	0.000	—
35°	0	0.705	0.467	2.0000
	50	0.647	0.409	1.9424
	70	0.607	0.369	1.8977
	140	0.523	0.285	1.7855
	185	0.484	0.246	1.7216
	240	0.443	0.205	1.6425
	"infin."	0.238	0.000	—
45°	0	0.705	0.467	2.0000
	45	0.578	0.340	1.8622
	65	0.532	0.294	1.7990
	135	0.405	0.167	1.5534
	180	0.359	0.121	1.4135
	235	0.318	0.080	1.2338
	"infin."	0.238	0.000	—

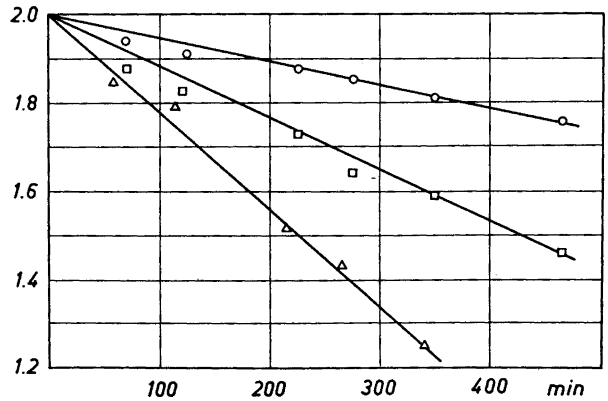

Fig. 8. Hydrolysis of butyl benzocaine. log (% ester left) *vs.* time.

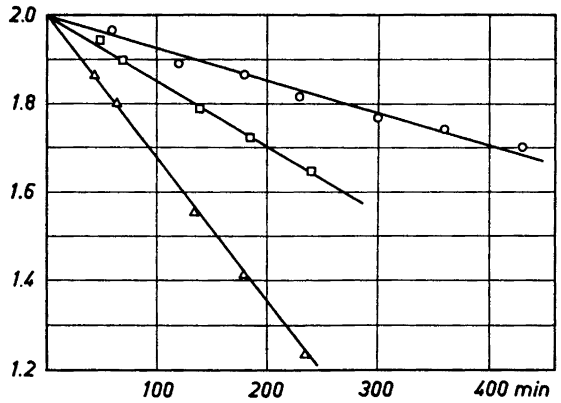

Fig. 9. Hydrolysis of tetracaine. log (% ester left) *vs.* time.

If the logarithm of this number is plotted against the time, straight lines should be obtained. These are found in Figs. 7—12. From the slope of the lines the velocity constant, k_1, may be calculated. k_1 refers to the "monomolecular" reaction:

$$k_1 \cdot t = \ln \frac{E_o - E_s}{E_t - E_s}$$

or

$$\frac{k_1 \cdot t}{2.303} = 2 - \log (\% \text{ ester left})$$

However, the reaction rate is

$$dx/dt = k_1 (\text{ester}) = k_2 (\text{ester}) (OH^-)$$

where k_2 is the bimolecular reaction rate constant. Thus the following equations are valid

$$k_2 = k_1/(OH^-)$$

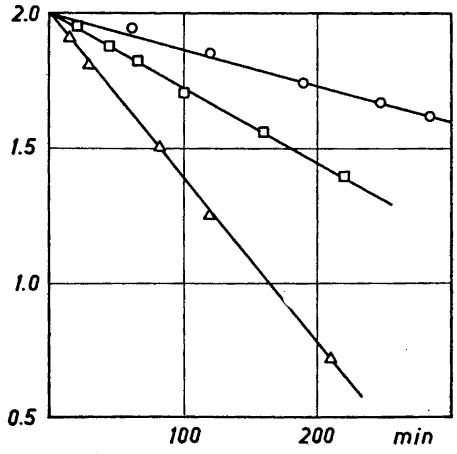

Fig. 10. Hydrolysis of procaine. log (% ester left) *vs.* time.

Table 5. Hydrolysis of procaine HCl.

Starting conc. of ester = 3.667×10^{-4} mole/lit. $\lambda = 287$ mμ

Temp.	Time (min)	E_t	$E_t - E_s$	log (% ester left)
25°	0	0.625	0.364	2.0000
	60	0.582	0.321	1.9453
	120	0.522	0.261	1.8555
	195	0.462	0.201	1.7421
	247	0.430	0.169	1.6668
	285	0.412	0.151	1.6179
	"infin."	0.261	0.000	—
35°	0	0.627	0.365	2.0000
	20	0.596	0.334	1.9615
	45	0.537	0.275	1.8770
	65	0.504	0.242	1.8215
	100	0.448	0.186	1.7046
	160	0.395	0.133	1.5615
	220	0.353	0.091	1.3967
	"infin."	0.262	0.000	—
45°	0	0.625	0.364	2.0000
	15	0.558	0.297	1.9116
	30	0.498	0.237	1.8136
	82	0.378	0.117	1.5070
	120	0.326	0.065	1.2518
	210	0.280	0.019	0.7177
	"infin."	0.261	0.000	—

Table 6. Hydrolysis of panthesine methane sulfonate.

Starting conc. of ester = 1.239×10^{-4} mole/lit. $\lambda = 289$ mμ

Temp.	Time (min)	E_t	$E_t - E_s$	log (% ester left)
25°	0	0.463	0.311	2.0000
	35	0.445	0.293	1.9741
	65	0.429	0.277	1.9497
	120	0.394	0.242	1.8911
	215	0.354	0.202	1.8126
	270	0.323	0.171	1.7402
	"infin."	0.152	0.000	—
35°	0	0.463	0.311	2.0000
	40	0.422	0.270	1.9386
	65	0.388	0.236	1.8802
	90	0.355	0.203	1.8147
	120	0.320	0.168	1.7325
	250	0.243	0.091	1.4663
	"infin."	0.152	0.000	—
45°	0	0.463	0.311	2.0000
	30	0.372	0.220	1.8497
	50	0.338	0.186	1.7767
	95	0.267	0.115	1.5679
	130	0.232	0.080	1.3931
	150	0.213	0.061	1.2926
	"infin."	0.152	0.000	—

Table 7. Hydrolysis of hydroxy procaine HCl.

Starting conc. of ester = 3.394×10^{-4} mole/lit. $\lambda = 305$ mμ

Temp.	Time (min)	E_t	$E_t - E_s$	log (% ester left)
25°	0	0.433	0.1745	2.0000
	60	0.426	0.1675	1.9823
	120	0.421	0.1625	1.9689
	240	0.407	0.1485	1.9299
	300	0.399	0.1405	1.9058
	360	0.391	0.1325	1.8802
	420	0.385	0.1265	1.8603
	480	0.379	0.1205	1.8392
	795	0.348	0.0895	1.7101
	840	0.344	0.0855	1.6902
	900	0.338	0.0795	1.6586
	"infin."	0.2585	0.0000	—
35°	0	0.433	0.1745	2.0000
	30	0.426	0.1675	1.9823
	60	0.417	0.1585	1.9582
	90	0.409	0.1505	1.9358
	120	0.399	0.1405	1.9059
	150	0.389	0.1305	1.8738
	180	0.378	0.1195	1.8352
	240	0.365	0.1065	1.7855
	270	0.358	0.0995	1.7560
	300	0.352	0.0935	1.7290
	330	0.346	0.0875	1.7002
	360	0.341	0.0825	1.6747
	420	0.332	0.0735	1.6245
	480	0.325	0.0665	1.5810
	"infin."	0.2585	0.0000	—
45°	0	0.449	0.1905	2.0000
	23	0.424	0.1655	1.9389
	40	0.403	0.1445	1.8900
	60	0.386	0.1275	1.8256
	83	0.369	0.1105	1.7634
	120	0.350	0.0915	1.6815
	150	0.336	0.0775	1.6094
	180	0.322	0.0635	1.5228
	210	0.311	0.0525	1.4403
	240	0.303	0.0445	1.3685
	270	0.297	0.0385	1.3056
	300	0.293	0.0345	1.2579
	330	0.289	0.0305	1.2044
	"infin."	0.2585	0.0000	—

or when pH = 12.00 and $(OH^-) = 0.01$

$$k_2 = 100\, k_1$$

k_2 is given in litre/mole/min. The results are surveyed in Table 8.

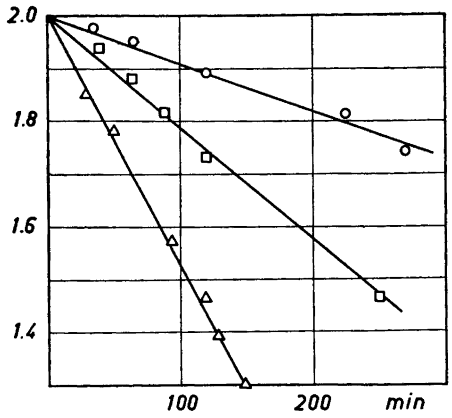

Fig. 11. Hydrolysis of panthesine. log (% ester left) *vs.* time.

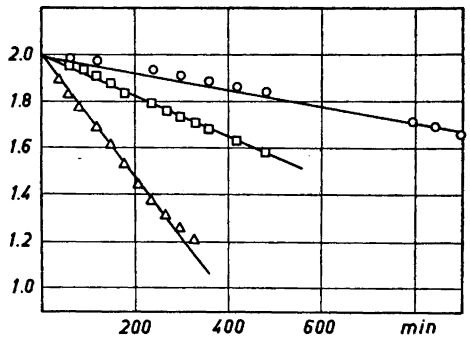

Fig. 12. Hydrolysis of hydroxy procaine. log (% ester left) *vs.* time.

The equation of Arrhenius is transformed to

$$\ln k_2 = \ln (PZ) - E/RT$$

or, when $\log (PZ) = A$

$$\log k_2 = A - \frac{E}{2.303\ RT}$$

Thus, if $\log k_2$ is plotted against $1/T$ a straight line should be obtained. The slope of the line, multiplied by 2.303 R, is the activation energy, E, and the intercept the frequency factor, A. In Fig. 13 these straight lines are shown. Table 9 shows the values obtained in this manner. The numbers are calculated by means of the method of least squares.

DISCUSSION

In alkaline medium the ester hydrolysis is due to the action of the nucleophilic reagent OH^- upon the carbon atom of the carbonyl group. This carbon atom has a partial positive charge due to the electrophilic character of the oxygen atom:

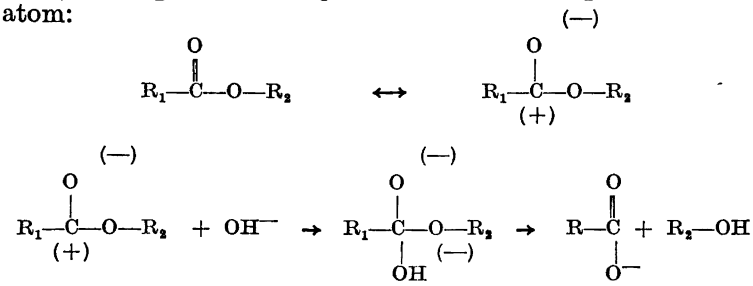

Table 8. Survey of results.

Name	k_2 lit/mole/min.		
	25.0°	35.0°	45.0°
Benzocaine	0.185	0.352	0.701
Butyl benzocaine	0.122	0.269	0.509
Tetracaine	0.173	0.344	0.743
Procaine	0.314	0.631	1.416
Panthesine	0.206	0.482	1.080
Hydroxy procaine	0.0825	0.204	0.613

By substitution in the acidic or the alcoholic part of the ester molecule the positive charge of the carbonyl carbon may be increased or decreased, which leads to a faster or slower hydrolysis. The ease with which the hydrolysis takes place may be expressed by the activation energy, E, of the process. A high value of E means a slow reaction and a low value of E means a fast reaction (provided that the value of the frequency factor A is unchanged).

The facts presented in this work are still too few to draw definite conclusions. However, it seems to be possible to make some preliminary observations.

The introduction of a butyl group causes, as expected, an electron releasing effect. This is apparent by a comparison of the activation energies of benzocaine and butyl benzocaine. Here the butyl group diminishes the positive charge of the carbonyl carbon and thus the activation energy is increased by

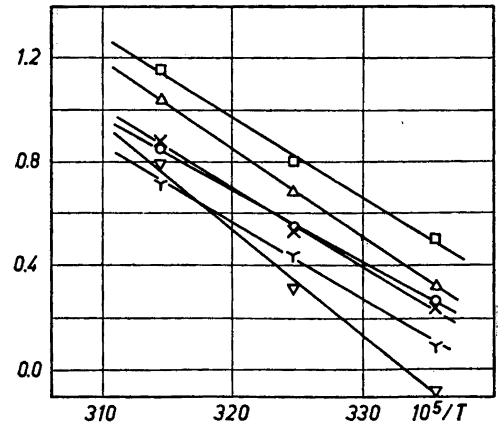

Fig. 13. (1 + log k_2) *vs.* 1/T.

Benzocaine	O	Procaine	□
Butyl benzocaine	Y	Panthesine	△
Tetracaine	×	Hydroxy procaine	▽

Table 9. Survey of results calculated from Fig. 13.

No.	Name	Formula	*E* kcal.	*A* lit/mole/min.
1	Benzocaine	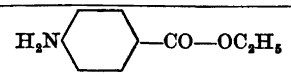	12.6	8.5
2	Butyl benzocaine	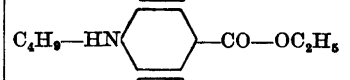	13.5	9.0
3	Tetracaine	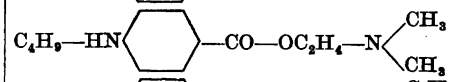	13.8	9.3
4	Procaine	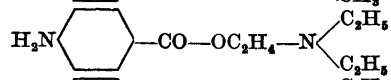	14.2	9.9
5	Panthesine	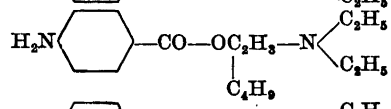	15.7	10.8
6	Hydroxy procaine	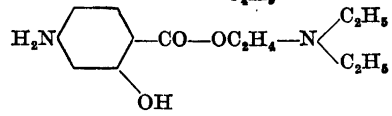	18.9	12.8

0.9 kcal. A comparison of procaine and panthesine shows that the butyl group, when placed in the β-position of the alcohol, increases the E value by 1.5 kcal. In both cases the frequency factor is increased at the same time.

The introduction of a tertiary amino group in the alcoholic part of the ester has a rather vague effect. By comparing benzocaine and procaine it can be seen that the amino group increases E by 1.6 kcal, but by comparing butyl benzocaine and tetracaine it is found that there is an increase by only 0.3 kcal. At the same time there is a change in the frequency factor.

However, the introduction of a hydroxy group in the *ortho*-position in the benzene ring has the most striking effect. By a comparison of procaine and hydroxy procaine it is found that the OH group causes an increase in E by 4.7 kcal and in A by 2.9 units. The increase of the activation energy may be understood by the resonance effect, which is followed by an *o*-hydroxy group and which is visualized by the formula

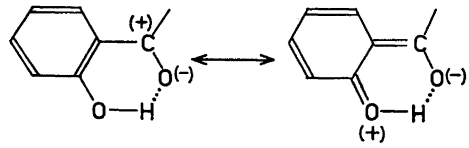

(The dotted line represents a hydrogen bond.) By this resonance the charge on the carbonyl carbon is diminished.

The increase in A is opposite to the effect which is found in other cases of *ortho* substitution of esters of benzoic acid [9]. This effect may be understood by the following reasoning.

In esters of benzoic acid and *p*-amino benzoic acid there is a free rotation of the bond between the benzene ring and the carboxylic group. The reagent OH^- may rather easily attack the carbonyl carbon, which leads to hydrolysis. When there is an *ortho* group such as CH_3, Cl or NO_2 the carboxyl group will prefer to be in a plane which is perpendicular to the plane of the benzene ring. This means that the hydroxyl ion must attack from that side of the molecule which is opposite to the *ortho* substituent, and this fact makes the attack more difficult from steric reasons. This is indicated by a low value of A.

Ortho substitution by the hydroxy group seems to have an opposite effect. The hydroxy group is bound to the carbonyl group with a hydrogen bond, and thus the carboxyl group is held in the same plane as the benzene ring. The reagent OH^- will attack in a direction which is perpendicular to the benzene ring plane. From a steric point of view this attack seems to be easier than from another angle and this is indicated by a high value of A. However, at the same time there is a decrease in E.

Acknowledgement. Our thanks are due to Dr. F. Holmes who corrected the English text.

REFERENCES

1. Hazard, R. and Ravasse, J. *Compt. rend. soc. biol.* **139** (1945) 13.
2. Terp, P. *Prokain*, Thesis, Copenhagen 1953.
3. Schou, S. A. and Abildgaard, J. *Pharm. Acta Helv.* **10** (1935) 38.
4. Dietzel, R. *Pharm. Zentralhalle* **79** (1938) 321.
5. Biggs, A. I. *J. Pharm. Pharmacol.* **4** (1952) 479.
6. Vastagh, G. and Zöllner, E. *Pharm. Zentralhalle* **93** (1954) 334; **94** (1955) 3.
7. Heim, F. and Neff, V. *Arzneimittel-Forsch.* **5** (1955) 587.
8. v. Ooteghem, M. and Steiger, K. *Pharm. Weekblad* **7** (1958) 325.
9. Ingold, C. K. and Nathan, W. S. *J. Chem. Soc.* **1936** 222.
10. Tommila, E. and Hinshelwood, C. N. *J. Chem. Soc.* **1938** 1801.
11. Armstrong, M. R. *Dissertation Abstr.* **15** (1955) 37.
12. Higuchi, T., Havinga, A. and Busse, L. W. *J. Am. Pharm. Assoc. Sci. Ed.* **39** (1950) 405.
13. Kindler, K. *Ann.* **450** (1926) 1.
14. Aven, M. and Foldes, F. F. *Science* **114** (1951) 206.
15. Higuchi, T. and Lachman, L. *J. Am. Pharm. Assoc. Sci. Ed.* **44** (1955) 521.
16. Tommila, E. *Ann. Acad. Sci. Fennicae* **A 57** (1941) No. 13. **A 59** (1943) Nos. 3, 4.
17. Newling, W. B. S. and Hinshelwood, C. N. *J. Chem. Soc.* **1936** 1357.
18. Jones, B. and Robinson, J. *J. Chem. Soc.* **1955** 3845.
19. Brit. Pat. 739, 210.
20. Gough, G. A. C. and King, H. *J. Chem. Soc.* **1928** 2437.
21. Brit. Pat. 571, 410.

Received September 15, 1959.

ACTA CHEMICA SCANDINAVICA 14 (1960) 211–232

Short Communications

The Structure of the Products Formed in the Reaction of β-Dialkylaminoethyl Chlorides with 2-Hydroxythiazoles

RICHARD DAHLBOM

Research Laboratories, AB Astra, Södertälje, Sweden

In a paper from these laboratories some years ago [1] a series of compounds were described, which were prepared by the reaction of a β-dialkylaminoethyl chloride with the sodium salt of a 2-hydroxythiazole (thiazol-2-one). The reaction products were thought to be 2-(β-dialkylaminoethoxy)-thiazoles (I).

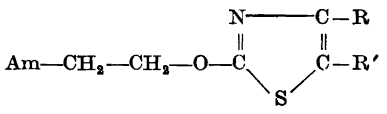

I

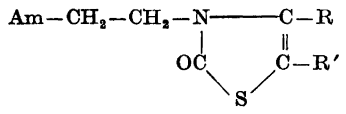

II

Am = $(CH_3)_2N-$, $(C_2H_5)_2N-$, 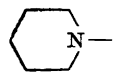

R = CH_3, C_6H_5 R′ = H, CH_3, C_6H_5

However, later work in this field [2,3] has indicated that in alkylations of this type the alkyl residue enters the 3-position in the thiazole nucleus, the reaction product being an N-substituted thiazol-2-one (II). The structure of the products formed in the above reaction was therefore reinvestigated using infrared spectroscopy.

It was found that all compounds in this series showed a very strong absorbtion band in the range 1 655 – 1 640 cm^{-1}, which can only be due to a carbonyl group. No absorbtion bands were observed near 1 250 cm^{-1} and in the 1 150 – 1 060 cm^{-1} region which are characteristic for aryl ethers [4] and which are found in the infrared spectrum of 2-methoxythiazole [2].

It can therefore be concluded that the products formed in the reaction of β-dialkylaminoethyl chlorides with the sodium salt of a 2-hydroxythiazole are 3-(β-dialkylaminoethyl)-thiazol-2-ones (II) and not 2-(β-dialkylaminoethoxy)-thiazoles (I).

The infrared spectra were recorded in KCl discs on a Perkin-Elmer No. 21 instrument with an NaCl prism.

1. Dahlbom, R. *Acta Chem. Scand.* **7** (1953) 374.
2. Klein, G. and Prijs, B. *Helv. Chim. Acta* **37** (1954) 2057.
3. DeStevens, G., Frutchey, A., Halamandaris, A. and Luts, H. A. *J. Am. Chem. Soc.* **79** (1957) 5263.
4. Bellamy, L. J. *The infra-red spectra of complex molecules*, 2nd Ed., Methuen & Co, London 1958, p. 117.

Received December 5, 1959.

A New Apparatus for Separation of Chemical Compounds by Liquid-Liquid Extraction

PENTTI K. HIETALA

Laboratory of the Foundation for Chemical Research, Biochemical Institute, Helsinki, Finland

Partition between two immiscible or partially miscible solvents has in recent years become a very valuable tool for the isolation, determination and characterization of chemical substances. The first apparatus for "countercurrent" extraction was the one described by Jantzen [1]. Other workers have subsequently built apparatus on the same principle. The first laboratory-scale device with continuous flow of solvents was the column of Cornish *et al.* [2] The excellent work of Craig and his associates [3,4] has made the counter-current distribution technique a useful routine method. Another apparatus working on the same principle is that described by v. Metzsch [5]. For the large number of other works reference should be made to more comprehensive reviews on the subject [6,7].

In this laboratory there has been a need for methods for the isolation, determination and characterization of different chemical substances of plant origin. For this purpose I have developed a new type of counter-current apparatus with 100 distribution tubes, using continuous solvent flow. This may be regarded as an improved modification of an apparatus developed by Weygand *et al.* [8] The new apparatus is intended for the separation of one substance from a mixture by solvent distribution. It has the following advantages:

1) The construction is extremely simple. There are no complicated mechanical or glass parts. This makes the operation very reliable. The building of the apparatus is not very costly.

2) The apparatus works precisely according to theoretical calculations. This has usually not been true of earlier apparatus with continuous solvent flow, which has been a serious objection by comparison with apparatus functioning after the "decanting" principle.

3) There are no limiting factors in the use of different solvent systems. The apparatus has been loaded with large amounts of raw unpurified plant extracts without stable emulsions being produced.

4) The apparatus has 100 tubes, but in principle the number of tubes is unlimited.

5) It is possible to run the apparatus with either flowing upper phase or flowing lower phase, these flowing in opposite directions. This can be done with successively smaller amounts of both phases, which increases considerably the effective number of tubes in the isolation of a substance. In this way the apparatus corresponds theoretically to about 1 100 distribution tubes without recycling for a 99.7 % yield and approximately 2 500 tubes for a 95.5 % yield. In practice, distributions corresponding to some hundred "transfers" can be conveniently made.

An important defect is that work with this apparatus is somewhat more time-consuming than with apparatus using the "decanting" principle.

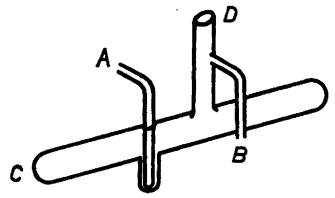

Fig. 1. See text.

The design of one distribution unit is seen in Fig. 1. Tube A is the inlet tube for the upper phase, tube B corresponds to tube A in the next cell. Ten such units are fused together into one piece, and these are connected to each other with suitable plastic tubing. In runs where lower phase flows in the reverse direction, it enters through tube B and leaves the unit through A. The equilibration is made by a continuous swinging movement of the main tube C in its length-wise direction through an angle of $\pm 30°$. The tubes are filled through D. Tubes D are closed with stoppers. In the two end tubes there are stopcocks for changing the solvent and the direction of flow. The whole row of 100 tubes is mounted on a suitable bar and made to swing by an electric motor. The frequency and amplitude of the strokes can be adjusted. The flow rate of solvents is controlled with Mariotte's flasks at both ends of the apparatus. The apparatus is used with a fraction collector having a moving center arm. The fraction collector is shifted from one end to the other if the solvent and direction of flow are changed.

Table 1. Distribution constants and recoveries in the distribution of oxalic, succinic and glutaric acid mixture presented in Fig. 2.

Acid	K, determined in separatory funnels	Conc. in the upper phase, normality	K, calc. from distr. curves	Substance weighed mequiv.	Substance found from distribution	Recovery %
Oxalic	0.24—0.22	0.02—0.002	0.23	5.85	5.89	100.8
Succinic	1.09—1.02	0.05—0.004	1.08	4.95	4.91	99.3
Glutaric	2.05—1.80	0.06—0.002	1.90	4.91	4.96	101

The volume of one tube is 86 ml. The relative amounts of the upper and lower phases can be varied over at least the ratios 3—0.33.

The theory of the apparatus cannot be presented here in detail. Stene [9] *e. g.* has made theoretical calculations concerning distribution in apparatus functioning after this principle. The distribution, presented as a function of tube number, of the mass of a solute A introduced into the first tube at the beginning of the distribution, forms a Poisson distribution curve known from statistics. When the tube number is large, it can be approximated by a standard error curve. In this apparatus the standard deviation δ of the normal error curve is $\delta = \sqrt{x}$, where x is the number of those tubes through which the maximum of the solute A has passed. When the solute A has passed through the whole apparatus and has been collected in fractions, the amount of effluent corresponding to δ is approximately $\sqrt{x(v + KV)}$, where v is the amount of the flowing phase and V the amount of the stationary phase in one distribution unit. K is the distribution coefficient of the substance.

Fig. 2 shows the distribution of a known mixture of oxalic, succinic and glutaric acids in the solvent system *n*-butanol-water. These acids are known to have distribution coefficients which are relatively concentration-independent. Table 1 shows numerical values concerning the distribution.

As an example of the fractionation of substances of biological origin Fig. 3 shows distribution of three sulfur-containing glucosides from turnip seeds.

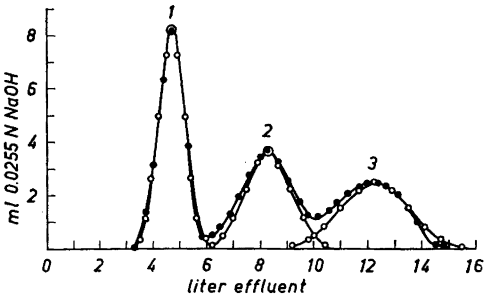

Fig. 2. Distribution of oxalic, succinic and glutaric acids in a solvent system *n*-butanol-water at 20°C. Run in one direction only with the lower phase flowing. Volume ratio 1:1. Flow speed 6 ml/min. ●———● experimental curve by titration O———O calculated curves, 1, oxalic acid, 2, succinic acid, 3, glutaric acid.

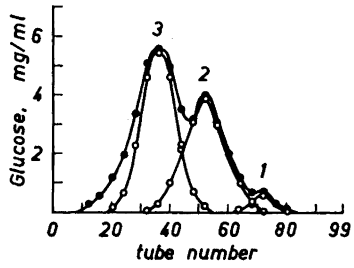

Fig. 3. The distribution of three sulfur-containing glucosides from turnip seeds in a solvent system *n*-butanol-ethanol-water (4:1:4) at 20°C. Volume ratio 46:40. The points of the curve represent samples from the tubes of the apparatus after 22.5 liters of the upper phase had flown through with a speed of 10—15 ml/min. Ordinate: Glucose as determined quantitatively by the anthron method. Abscissa: Tube number. ●———● experimental curve. Curve 1: Gluconapin, K 0.148; Curve 2: Gluconasturtin, K 0.104; Curve 3: Progoitrin, K 0.066. The deviation of the last curve depends on dissociation-association phenomena of the last substance in the unbuffered solvent system. The whole amount of substance was about 8 g dry weight.

The exact mathematical and theoretical treatment and technical details omitted from this preliminary note will be presented in a further paper.

I wish to thank Professor Artturi I. Virtanen, Director of the Biochemical Institute, for his encouragement, for valuable suggestions during this work and for the excellent facilities put at my disposal in the laboratory of the Foundation for Chemical Research. I also wish to thank Dr. Matti Kreula for his valuable help and suggestions in planning and building the mechanical parts of this counter-current apparatus.

This work has been supported partly by the *Rockefeller Foundation* and partly it belongs to the research project under U. S. Public Law No. 480, 83rd Congress.

1. Jantzen, E. *Dechema-Monographie 48*, Verlag Chemie, Berlin 1932.
2. Cornish, R. E., Archibald, R. C., Murphy, E. A. and Evans, H. M. *Ind. Eng. Chem.* **26** (1934) 397.
3. Craig, L. C. *J. Biol. Chem.* **155** (1944) 519.
4. Craig, L. C., Hausmann, W., Ahrens, Jr., E. H. and Harfenist, E. J. *Anal. Chem.* **23** (1951) 1326.
5. v. Metzsch, F. A. *Chem. Ing. Tech.* **25** (1953) 66.
6. Rauen, H. M. and Stamm, W. *Gegenstromverteilung*, Springer-Verlag, Berlin-Göttingen-Heidelberg 1953.
7. Hecker, E. *Verteilungsverfahren im Laboratorium*, Verlag Chemie, Weinheim 1955.
8. Weygand, F., Wacker, A. and Dellwegg, H. *Z. Naturforsch.* **6B** (1951) 130.
9. Stene, S. *Arkiv Kemi, Mineral. Geol.* **18A** (1945) 18.

Received December 4, 1959.

Ozonisation of 3-Methyl*cyclo*pent-2-en-2-ol-1-one

JOHAN B.SON BREDENBERG

Department of Chemistry, Institute of Technology, Helsingfors, Finland

In a previous paper[1] it was shown by physical methods that 3-methyl*cyclo*penta-1,2-dione exists as the enol 3-methyl*cyclo*pent-2-en-2-ol-1-one. This structure should be readily attacked by ozone to yield laevulic acid. The other possible enol structure for the compound, 5-methyl*cyclo*pent-2-en-2-ol-1-one, should, on the other hand, give methylsuccinic acid. The enol structure can therefore be confirmed also by ozonisation of the compound.

The compound was ozonised in aqueous solution at room temperature and the water evaporated. The evaporation residue, which had an infrared spectrum of almost pure laevulic acid, but with a small amount of starting material, was distilled and gave a high yield of pure laevulic acid, b.p. 103 —105°/1 mm, identified by its infrared spectrum and its phenylhydrazone, m.p. 105—106°, and 2,4-dinitrophenylhydrazone, m.p. 207—208°. The result consequently corroborated the evidence obtained by physical methods.

Experimental. 3-Methyl*cyclo*pent-2-en-2-ol-1-one (Fluka A.-G.) (3.73 g) was dissolved in water (150 ml) and ozonised at room temperature for 2 h (5.1 % O_3, 15.7 mg O_3/min). The solution was left to stand for two days, after which the water was evaporated under diminished pressure at 20°. The evaporation residue, an almost colourless oil, was distilled under reduced pressure and gave two fractions. The first fraction, b.p. 80—103°/1 mm, (0.53 g) which partly crystallised, consisted, according to the infrared spectrum, of the starting material and laevulic acid. The second fraction, b. p. 103—105°/1 mm, (2.94 g) had the infrared spectrum of pure laevulic acid. The fraction yielded a phenylhydrazone, m. p. 105—106°, and a 2,4-dinitrophenylhydrazone, m. p. 207—208°, both prepared in the usual way[2,3]. Neither derivative gave any m. p. depression with authentic material from pure laevulic acid.

1. Bredenberg, J. B. *Acta Chem. Scand.* **13** (1959) 1733.
2. Fischer, E. *Ann.* **236** (1886) 126.
3. Cowley, M. A. and Schuette, H. A. *J. Am. Chem. Soc.* **55** (1933) 3463.

Received December 16, 1959.

The exact mathematical and theoretical treatment and technical details omitted from this preliminary note will be presented in a further paper.

I wish to thank Professor Artturi I. Virtanen, Director of the Biochemical Institute, for his encouragement, for valuable suggestions during this work and for the excellent facilities put at my disposal in the laboratory of the Foundation for Chemical Research. I also wish to thank Dr. Matti Kreula for his valuable help and suggestions in planning and building the mechanical parts of this counter-current apparatus.

This work has been supported partly by the *Rockefeller Foundation* and partly it belongs to the research project under U. S. Public Law No. 480, 83rd Congress.

1. Jantzen, E. *Dechema-Monographie 48*, Verlag Chemie, Berlin 1932.
2. Cornish, R. E., Archibald, R. C., Murphy, E. A. and Evans, H. M. *Ind. Eng. Chem.* **26** (1934) 397.
3. Craig, L. C. *J. Biol. Chem.* **155** (1944) 519.
4. Craig, L. C., Hausmann, W., Ahrens, Jr., E. H. and Harfenist, E. J. *Anal. Chem.* **23** (1951) 1326.
5. v. Metzsch, F. A. *Chem. Ing. Tech.* **25** (1953) 66.
6. Rauen, H. M. and Stamm, W. *Gegenstromverteilung*, Springer-Verlag, Berlin-Göttingen-Heidelberg 1953.
7. Hecker, E. *Verteilungsverfahren im Laboratorium*, Verlag Chemie, Weinheim 1955.
8. Weygand, F., Wacker, A. and Dellwegg, H. *Z. Naturforsch.* **6B** (1951) 130.
9. Stene, S. *Arkiv Kemi, Mineral. Geol.* **18A** (1945) 18.

Received December 4, 1959.

Ozonisation of 3-Methyl*cyclo*pent-2-en-2-ol-1-one

JOHAN B.SON BREDENBERG

Department of Chemistry, Institute of Technology, Helsingfors, Finland

In a previous paper[1] it was shown by physical methods that 3-methyl*cyclo*penta-1,2-dione exists as the enol 3-methyl*cyclo*pent-2-en-2-ol-1-one. This structure should be readily attacked by ozone to yield laevulic acid. The other possible enol structure for the compound, 5-methyl*cyclo*pent-2-en-2-ol-1-one, should, on the other hand, give methylsuccinic acid. The enol structure can therefore be confirmed also by ozonisation of the compound.

The compound was ozonised in aqueous solution at room temperature and the water evaporated. The evaporation residue, which had an infrared spectrum of almost pure laevulic acid, but with a small amount of starting material, was distilled and gave a high yield of pure laevulic acid, b.p. 103 —105°/1 mm, identified by its infrared spectrum and its phenylhydrazone, m.p. 105—106°, and 2,4-dinitrophenylhydrazone, m.p. 207—208°. The result consequently corroborated the evidence obtained by physical methods.

Experimental. 3-Methyl*cyclo*pent-2-en-2-ol-1-one (Fluka A.-G.) (3.73 g) was dissolved in water (150 ml) and ozonised at room temperature for 2 h (5.1 % O_3, 15.7 mg O_3/min). The solution was left to stand for two days, after which the water was evaporated under diminished pressure at 20°. The evaporation residue, an almost colourless oil, was distilled under reduced pressure and gave two fractions. The first fraction, b.p. 80—103°/1 mm, (0.53 g) which partly crystallised, consisted, according to the infrared spectrum, of the starting material and laevulic acid. The second fraction, b. p. 103—105°/1 mm, (2.94 g) had the infrared spectrum of pure laevulic acid. The fraction yielded a phenylhydrazone, m. p. 105—106°, and a 2,4-dinitrophenylhydrazone, m. p. 207—208°, both prepared in the usual way[2,3]. Neither derivative gave any m. p. depression with authentic material from pure laevulic acid.

1. Bredenberg, J. B. *Acta Chem. Scand.* **13** (1959) 1733.
2. Fischer, E. *Ann.* **236** (1886) 126.
3. Cowley, M. A. and Schuette, H. A. *J. Am. Chem. Soc.* **55** (1933) 3463.

Received December 16, 1959.

*iso*Thiocyanates XXXVII *. Rotatory Dispersion Studies of Optically Active Sulphoxides Derivable from *iso*Thiocyanates of Natural Origin

W. KLYNE and JANET DAY

Postgraduate Medical School, University of London, England

ANDERS KJÆR

Organic Chemical Laboratory, Royal Veterinary and Agricultural College, Copenhagen, Denmark

Within the group of naturally occurring sulphoxides, in which optical activity can be partly or wholly attributed to the presence of an asymmetric sulphur atom (*cf. e.g.* Refs. [1,4]), a homologous series of *iso*thiocyanates presents an interesting stereochemical problem. In 1948, Schmid and Karrer [2] assigned the structure $CH_3SOCH=CHCH_2CH_2NCS$ to sulphoraphen, a strongly *laevo*rotatory mustard oil, isolated from radish seed. This finding was soon followed by the isolation by Schultz and Gmelin [3] of the glucoside, glucoiberin, enzymically hydrolyzed to another sulphoxide-mustard oil, for which the structure $CH_3SO(CH_2)_3NCS$ was suggested [3] and later proved [4]. More recently, Kjær *et al.* [4,6-8] reported the isolation of additional sulphoxide-mustard oils, subsequent to enzymic hydrolysis of glucosides present in various crucifers. Thus, alyssin [4,5] ($CH_3SO(CH_2)_5NCS$), hirsutin [6] ($CH_3SO(CH_2)_6NCS$), arabin [7] ($CH_3SO(CH_2)_9NCS$) and camelinin [8] ($CH_3SO(CH_2)_{10}NCS$) were encountered as species of natural provenance. Lately, Procházka [9] added sulphoraphan, (−)-$CH_3SO(CH_2)_4NCS$, the saturated compound corresponding to sulphoraphen [2], to the above series (*cf.* also Ref. [6]).

Identical configuration around the asymmetric sulphur atom in the homologous series of naturally derived sulphoxide-mustard oils was suggested by the fact that the optical rotations at 589 mμ [4] of the *iso*thiocyanates measured, as well as of various thiourea derivatives*, were all negative and of comparable magnitude.

In order to substantiate this conclusion, a rather unusual and extensive series of homologous, naturally derived sulphoxides of the general structural type (I) was subjected to rotatory dispersion studies in methanol solution.

$$CH_3S(CH_2)_nNHCXNHY$$
$$\downarrow$$
$$O$$

I

X = O, or S
Y = H, C_6H_5, or $C_6H_5CH_2$
n = 3, 4, 5, 8, 9, or 10

In all cases the rotation becomes *more negative* as one moves to shorter wave lengths (negative plain curves; for nomenclature, see Djerassi and Klyne [10]). Except

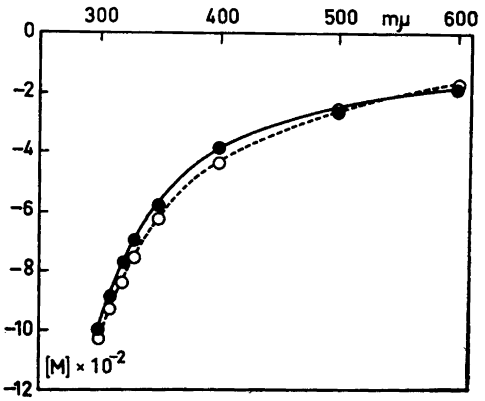

Fig. 1. Rotatory dispersion curve of straight-chain N-(ω-methylsulphinylalkyl)-thioureas, $CH_3SO(CH_2)_nNHCSNH_2$, in methanol. - - - - : n = 5; ——— : n = 10.

* Part XXXVI of this series: *Acta Chem. Scand.* 13 (1959) 1575.

* No rotation was reported for the aromatic thiourea-derivatives employed in the characterisation of sulphoraphan [9]. A small specimen of the phenylthiourea, kindly placed at our disposal by Dr. Procházka, Prague, was measured in the laboratory of one of the authors (A.K.) and gave: $[\alpha]_D^{25}$ −54° (*c* 1.8, 96 % EtOH, microtube).

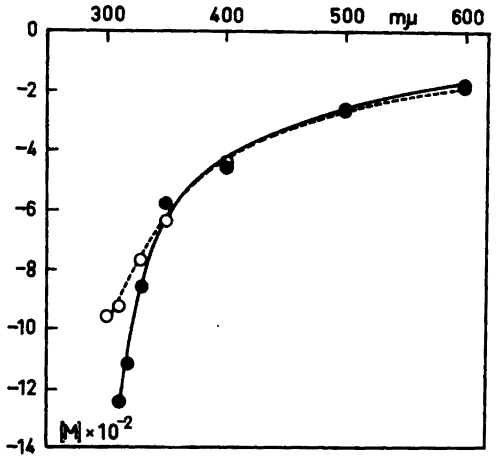

Fig. 2. Rotatory dispersion curve of straight-chain, N-substituted N′-(ω-methylsulphinylalkyl)-thioureas, $CH_3SO(CH_2)_nNHCSNHR$, in methanol. ———: n = 5, R=C_6H_5 - - - -: n = 10, R=$C_6H_5CH_2$.

for a few points in the region of 300 mμ, the curves, when plotted as molecular rotations, are very closely similar, and some are almost superimposable. Representative examples are reproduced in Figs. 1 and 2. In Table 1, the values determined at 600 mμ, 500 mμ, 400 mμ and 300 mμ, are listed for all the compounds investigated.

Clearly, the rotatory dispersion curves provide a much better means of allotting configuration at the asymmetric sulphur atom of the compounds (I), than do "monochromatic" rotation analogies. From the present results it seems safe to conclude that all sulphoxide-*iso*thiocyanates encountered in Nature thus far, possess identical configurations. Their spatial relationship to (+)-*S*-methyl-L-cysteine sulphoxide, the sole sulphoxide of established absolute configuration [11], remains to be determined.

From the present rotatory dispersion curves it is evident that the presence of an aromatic nucleus at a considerable distance from the asymmetric sulphur atom in eleven of the compounds apparently has a negligible effect on the dispersion curve down to 300 mμ. In the phenylthiourea-derivative of sulphoraphen, with a double bond located αβ to the sulphur atom, a slight deviation in the rotatory dispersion curve is noticed at about 300 mμ, compared with those of the saturated series.

Table 1. Molecular rotations in methanol at various wave lengths of compounds represented by formula (I).

Formula	Mol. weight	Concn. (mg/ml)	Molecular rotations at λ 300 mμ	400 mμ	500 mμ	600 mμ
			(ALL VALUES NEGATIVE)			
$CH_3SO(CH_2)_3NHCSNHCH_2C_6H_5$ [4,c]	270	0.1	670	360	280	160
$CH_3SO(CH_2)_4NHCSNHC_6H_5$ [9]	270	0.1	630 (320) [d]	330	250	160
$CH_3SOCH=CH(CH_2)_2NHCSNHC_6H_5$ [b]	268	0.1	1 040	460	300	200
$CH_3SO(CH_2)_5NHCSNH_2$ [4]	208	1	1 030	440	250	180
$CH_3SO(CH_2)_5NHCSNHC_6H_5$ [4]	284	0.1	1 250 (310)	450	260	180
$CH_3SO(CH_2)_8NHCSNH_2$ [6]	250	1	1 000	400	210	80
$CH_3SO(CH_2)_8NHCSNHC_6H_5$ [6]	327	1 and 0.1	820 (310)	420	270	170
$CH_3SO(CH_2)_9NHCSNH_2$ [7]	264	1	980	410	250	160
$CH_3SO(CH_2)_9NHCSNHC_6H_5$ [7]	341	1 and 0.1	610 (330) ?	400	210	150
$CH_3SO(CH_2)_9NHCSNHCH_2C_6H_5$ [7]	355	0.1	1 080	570	370	150
$CH_3SO(CH_2)_9NHCONHCH_2C_6H_5$ [7]	339	0.5	940	430	250	190
$CH_3SO(CH_2)_{10}NHCSNH_2$ [8]	279	1	1 000	380	270	190
$CH_3SO(CH_2)_{10}NHCSNHC_6H_5$ [8]	355	0.2	990 (320)	420	230	150
$CH_3SO(CH_2)_{10}NHCSNHCH_2C_6H_5$ [c]	369	1	950	450	250	170
$CH_3SO(CH_2)_{10}NHCONHCH_2C_6H_5$ [8]	352	0.5	1 040	440	250	150

[a] Determined at 25°. [b] A specimen prepared from sulphoraphen as described [3]. [c] A non-analyzed specimen [8]. [d] Lowest wave-length recorded, when not 300 mμ.

Optical rotations were measured with a Rudolph photoelectric spectropolarimeter using a tube of 1 dm length. For the details, see Ref.[12]. The experimental error is probably ±20° for molecular rotations (*cf.* Ref.[12]). In some cases it was impossible to make measurements down to 300 mμ because of intense light absorption by the compound under study. The course of a typical curve for $CH_3SO(CH_2)_5NHCSNH_2$ between 350 and 300 mμ is indicated by the following values; [M], and λ in parentheses; −625 (350), −755 (330), −840 (320), −930 (310), −1 030 (300 mμ).

The work in Copenhagen is part of investigations supported by *Statens Almindelige Videnskabsfond (The Danish State Research Foundation)* and *Carlsbergfondet (The Carlsberg Foundation)*.

The rotatory dispersion work in London is supported by a contract from *U. S. Army Research and Development Group* and a grant from *The Department of Scientific and Industrial Research* (United Kingdom). The polarimeter is a generous loan to one of us (W.K.) from *The Wellcome Trust* (London).

1. Kjær, A. *Handbuch der Pflanzenphysiologie*, Springer-Verlag, Berlin-Göttingen-Heidelberg 1958, vol. **IX**, p. 70 f.f. —*Fortschr. Chem. org. Naturstoffe.* **18** (1960). *In press.*
2. Schmid, H. and Karrer, P. *Helv. Chim. Acta* **31** (1948) 1017.
3. Schultz, O.-E. and Gmelin, R. *Arch. Pharm.* **287/59** (1954) 404.
4. Kjær, A. and Gmelin, R. *Acta Chem. Scand.* **10** (1956) 1100.
5. Schultz, O.-E. and Wagner, W. *Z. Naturforsch.* **11b** (1956) 417.
6. Kjær, A. and Christensen, B. *Acta Chem. Scand.* **12** (1958) 833.
7. Kjær, A. and Gmelin, R. *Acta Chem. Scand.* **10** (1956) 1358.
8. Kjær, A., Gmelin, R. and Boe Jensen, R. *Acta Chem. Scand.* **10** (1956) 1614.
9. Procházka, Ž. *Collection Czechoslov. Chem. Communs.* **24** (1959) 2429.
10. Djerassi, C. and Klyne, W. *Proc. Chem. Soc.* **1957**, 55.
11. Hine, R. and Rogers, D. *Chem. & Ind. London* **1956** 1428.
12. Jones, P. M. and Klyne, W. *J. Chem. Soc.* **1960** 871.

Received December 10, 1959.

Purification of Human Plasminogen on DEAE-cellulose

PER WALLÉN and KURT BERGSTRÖM

Kemiska Institutionen II, Karolinska Institutet, Stockholm, Sweden

In a recent communication a method for the purification of human plasminogen was outlined [1]. The most important step of this method was an adsorption of a partially purified plasminogen preparation on columns of DEAE-cellulose equilibrated with an ammonium acetate buffer, pH 9.0, containing lysine to a concentration of 0.01 M. Under these conditions about 80 % of the protein was adsorbed, whereas 60—80 % of the plasminogen passed through the column in the frontal fraction together with about 20 % of the protein. We were prompted to use lysine in this connection by the observation of Alkjaersig, Fletcher and Sherry [2], who found that ε-aminocaproic acid and lysine increased the solubility of plasminogen and plasmin preparations at neutral reaction, probably due to a dissolution of a protein complex.

As starting material we used a plasminogen preparation obtained from Cohn's fraction III by dialysis against a phosphate buffer of pH 7.0 and low ionic strength. The specific activity ranged from 8 to 20 times that of fraction III. This variability was shown to be caused by the poor reproducibility of the first step. Therefore we now have excluded this step.

Plasminogen is easily adsorbed on DEAE-cellulose, previously equilibrated with ammonium acetate buffer, pH 9.0, but if lysine is added to the buffer it is not adsorbed. Thus it was near at hand first to adsorb plasminogen to DEAE-cellulose from a weakly alkaline buffer without lysine and then to try to elute the activity with the same buffer to which lysine had been added. In the following a method based on this principle is outlined.

A preparation obtained from Cohn's fraction II + III by precipitating the plasminogen at low ionic strength and pH 5.3 was used as starting material. Preparations of this type have almost the same specific activity as fraction III and the yields are higher. About 35 g DEAE-cellulose (Brown Comp. New Hampshire, U.S.A.) were suspended in 0.04 M ammonium acetate buffer pH 9.0. The slurry was poured in a column with a diameter of 4 cm and packed with

Optical rotations were measured with a Rudolph photoelectric spectropolarimeter using a tube of 1 dm length. For the details, see Ref.[12]. The experimental error is probably ±20° for molecular rotations (*cf.* Ref.[12]). In some cases it was impossible to make measurements down to 300 mμ because of intense light absorption by the compound under study. The course of a typical curve for $CH_3SO(CH_2)_5NHCSNH_2$ between 350 and 300 mμ is indicated by the following values; [M], and λ in parentheses; −625 (350), −755 (330), −840 (320), −930 (310), −1 030 (300 mμ).

The work in Copenhagen is part of investigations supported by *Statens Almindelige Videnskabsfond (The Danish State Research Foundation)* and *Carlsbergfondet (The Carlsberg Foundation)*.

The rotatory dispersion work in London is supported by a contract from *U. S. Army Research and Development Group* and a grant from *The Department of Scientific and Industrial Research* (United Kingdom). The polarimeter is a generous loan to one of us (W.K.) from *The Wellcome Trust* (London).

1. Kjær, A. *Handbuch der Pflanzenphysiologie*, Springer-Verlag, Berlin-Göttingen-Heidelberg 1958, vol. **IX**, p. 70 f.f. —*Fortschr. Chem. org. Naturstoffe.* **18** (1960). *In press.*
2. Schmid, H. and Karrer, P. *Helv. Chim. Acta* **31** (1948) 1017.
3. Schultz, O.-E. and Gmelin, R. *Arch. Pharm.* **287/59** (1954) 404.
4. Kjær, A. and Gmelin, R. *Acta Chem. Scand.* **10** (1956) 1100.
5. Schultz, O.-E. and Wagner, W. *Z. Naturforsch.* **11b** (1956) 417.
6. Kjær, A. and Christensen, B. *Acta Chem. Scand.* **12** (1958) 833.
7. Kjær, A. and Gmelin, R. *Acta Chem. Scand.* **10** (1956) 1358.
8. Kjær, A., Gmelin, R. and Boe Jensen, R. *Acta Chem. Scand.* **10** (1956) 1614.
9. Procházka, Ž. *Collection Czechoslov. Chem. Communs.* **24** (1959) 2429.
10. Djerassi, C. and Klyne, W. *Proc. Chem. Soc.* **1957**, 55.
11. Hine, R. and Rogers, D. *Chem. & Ind. London* **1956** 1428.
12. Jones, P. M. and Klyne, W. *J. Chem. Soc.* **1960** 871.

Received December 10, 1959.

Purification of Human Plasminogen on DEAE-cellulose

PER WALLÉN and KURT BERGSTRÖM

Kemiska Institutionen II, Karolinska Institutet, Stockholm, Sweden

In a recent communication a method for the purification of human plasminogen was outlined [1]. The most important step of this method was an adsorption of a partially purified plasminogen preparation on columns of DEAE-cellulose equilibrated with an ammonium acetate buffer, pH 9.0, containing lysine to a concentration of 0.01 M. Under these conditions about 80 % of the protein was adsorbed, whereas 60—80 % of the plasminogen passed through the column in the frontal fraction together with about 20 % of the protein. We were prompted to use lysine in this connection by the observation of Alkjaersig, Fletcher and Sherry [2], who found that ε-aminocaproic acid and lysine increased the solubility of plasminogen and plasmin preparations at neutral reaction, probably due to a dissolution of a protein complex.

As starting material we used a plasminogen preparation obtained from Cohn's fraction III by dialysis against a phosphate buffer of pH 7.0 and low ionic strength. The specific activity ranged from 8 to 20 times that of fraction III. This variability was shown to be caused by the poor reproducibility of the first step. Therefore we now have excluded this step.

Plasminogen is easily adsorbed on DEAE-cellulose, previously equilibrated with ammonium acetate buffer, pH 9.0, but if lysine is added to the buffer it is not adsorbed. Thus it was near at hand first to adsorb plasminogen to DEAE-cellulose from a weakly alkaline buffer without lysine and then to try to elute the activity with the same buffer to which lysine had been added. In the following a method based on this principle is outlined.

A preparation obtained from Cohn's fraction II + III by precipitating the plasminogen at low ionic strength and pH 5.3 was used as starting material. Preparations of this type have almost the same specific activity as fraction III and the yields are higher. About 35 g DEAE-cellulose (Brown Comp. New Hampshire, U.S.A.) were suspended in 0.04 M ammonium acetate buffer pH 9.0. The slurry was poured in a column with a diameter of 4 cm and packed with

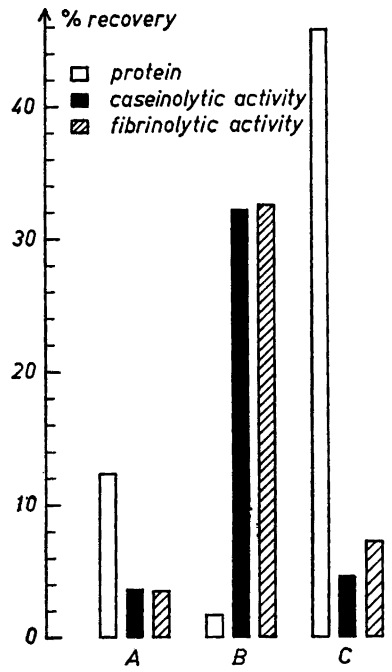

Fig. 1. Adsorption and step-wise elution of human plasminogen on DEAE-cellulose. The buffers are:

A) 0.04 M ammonium acetate, pH 9.0.
B) 0.04 M ammonium acetate, pH 9.0 containing lysine to a concentration of 0.01 M.
C) 0.04 M ammonium acetate, pH 4.0 containing lysine to a concentration of 0.01 M.

an excess air pressure of about 50 mm Hg. The column was equilibrated with the same buffer. 10 g of the starting material was suspended in 500 ml of the equilibration buffer and dialysed against the same buffer during 6—8 h. Some of the material did not dissolve and was removed by centrifugation. The opalescent supernatant was applied to the column, which was then developed with about 1 000 ml of the equilibration buffer. The elution was then performed stepwise with 0.04 M ammonium acetate buffer, pH 9.0 and 4.0, both buffers containing lysine to a concentration of 0.01 M. The protein concentration in the effluent was followed by measuring the optical density at 280 mμ in a Beckman DU photometer.

The fractions were acidified with hydrochloric acid to pH 3.5, dialysed against distilled water and precipitated with cold acetone at a concentration of 40 % at −15°C. The precipitates were lyophilized and the fractions tested with the caseinolytic method of Müllertz [3] and the fibrinolytic method of Christensen [4].

The result of such an experiment is shown in Fig. 1, where the amount of lyophilized protein, caseinolytic and fibrinolytic activity in the fractions are expressed as per cent of the starting material. In the frontal peak appears about 12 % of the protein but only 4 % of the plasminogen. The main part of the plasminogen thus has been adsorbed to the ion exchanger. When the column is eluted with the same buffer, to which lysine has been added, a small peak appears containing only about 1—2 % of the protein but about 30—35 % of the activity, which means a purification of about 20 times as compared to the starting material. With the acidic buffer, finally, 40 % of the protein material and 5 % of the plasminogen is eluted. Five preparations have been made according to the method outlined. The increase in specific activity in the second fraction (B in Fig. 1) has ranged from 20 to 30 times as compared to the starting material and the yield has ranged from 30 to 35 %.

1. Wallén, P. and Bergström, K. *Acta Chem. Scand.* **13** (1959) 1464.
2. Alkjaersig, N., Fletcher, P. and Sherry, S. *J. Biol. Chem.* **234** (1959) 832.
3. Müllertz, S. *Biochem. J.* **61** (1955) 424.
4. Christensen, L. R. *J. Clin. Invest.* **28** (1949) 163.

Received January 14, 1960.

Influence of Steric Hindrance on the Isotope Effect in Aromatic Substitution

PHILIP C. MYHRE*

Nobel Institute of Chemistry, Stockholm 50, Sweden

As part of an investigation of the effect of steric hindrance on the mechanism of aromatic substitution, isotope effects in the nitration and bromination reactions of the highly hindered hydrocarbon, 1,3,5-tri-*t*-butylbenzene, have been measured. No isotope effect could be detected when this hydrocarbon was nitrated in acetic acid — acetic anhydride solution in the presence or absence of sulfuric acid catalyst. However, a "full" isotope effect ($k_T/k_H \sim 0.1$) is observed when the same tritium labeled hydrocarbon is brominated in acetic acid — dioxane solution with bromine, silver perchlorate and perchloric acid. The brominating agent in this reaction is believed to be "positive" bromine or a "positive" bromine carrier [1]. Hydrogen exchange was shown to be absent during these reactions.

The nitration of tri-*t*-butylbenzene was effected in essentially quantitative yield using the method of Wepster, Verkade *et al.* [2] Possible fractionation of tritium in the reactant as well as the derivative was investigated in some experiments by using less than the stoichiometric amount of nitric acid and recovering both the nitro derivative and the unreacted hydrocarbon.

Normal bromination of tri-*t*-butylbenzene apparently proceeds only in the presence of a "positive" brominating agent. When the classical catalyst, iron powder, is used, it is reported that only the dealkylated 1-bromo-2,5-di-*t*-butylbenzene (I) is isolated in 70 % yield [3]. Barclay and Betts [4] report a 67 % yield of 1-bromo-2,4,6-tri-*t*-butylbenzene (II) by bromination in aqueous acetic acid with silver nitrate and nitric acid. The brominating conditions used in the present measurements yield a mixture of the desired product (II) and the dealkylated product (I). These compounds were identified by comparison of their infrared spectra with the spectra of known samples.

A typical reaction was performed by adding bromine (2.4 g, 15 mmole) to a well stirred solution of tri-*t*-butylbenzene [5] (2.4 g, 10 mmole), silver perchlorate (3.0 g, 15 mmole) and perchloric acid (1.0 ml, 11 mmole) in 60 ml of acetic acid-dioxane (5:1 by volume) and allowing the mixture to stand with stirring for about 16 h. The product was isolated by filtration of the silver salts, addition of water to the filtrate and extraction of the organic product with pentane. The following material balance was obtained by infrared analysis of the crude product: I, 21 %; II, 68 %; unreacted hydrocarbon, 8 %. The infrared spectrum of a synthetic mixture of pure components compounded in this ratio agreed well with the spectrum of the crude reaction product. II was isolated by repeated crystallization from ethanol and sublimation *in vacuo*, m. p. 173—174°.

Activity measurements were made in the usual manner [6] by inside counting of hydrogen obtained from the combustion water of the reactants and derivatives.

A general expression [6,7] for aromatic substitution in compounds possessing a symmetry similar to tri-*t*-butylbenzene which relates the molar activity in the derivative and that in the initial reactant to the kinetic isotope effect (k_T/k_H), the extent of reaction and the relative rate of side reactions is

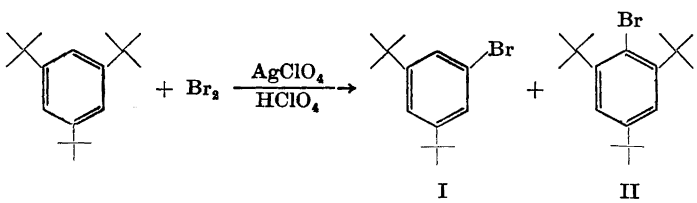

* U. S. National Science Foundation Postdoctoral Fellow, 1958—1960.

$$\frac{d}{r_0} = \frac{2 + 2q}{2 + \beta + 3q} \cdot \frac{1}{x}\left[1 - (1 - x)^{(2+\beta+3q)/(3+3q)}\right]$$

where d is the molar activity in the derivative measured after separation from the by-product, r_0 is the molar activity in the initial reactant, β is the ratio k_T/k_H, q is the ratio of the specific rates of dealkylation and substitution and x is the extent of reaction. It is assumed that isotopic hydrogen only influences the reaction rate at its own position.

where r is the molar activity in the unconsumed reactant. The other symbols retain their previous meanings. For nitration q vanishes since no evidence of side reactions can be detected. On the basis of product analysis q is assigned a value of 1/3 for the bromination reaction.

All experimentally determined values of the isotope effect for the nitration of tri-*t*-butylbenzene, as shown in Table 1, fall within the interval 1.0 ± 0.1.

Table 1. Isotope effects in nitration of 2,4,6-tri-*t*-butylbenzene in acetic acid — acetic anhydride solution at about 25°.

	Number of experiments	% Yield derivative	Calculated mean k_T/k_H with maximum experimental deviations
Uncatalyzed nitration (nitro derivative)	3	>97 %	$0.98 \begin{matrix}+ 0.05 \\ - 0.06\end{matrix}$
Catalyzed nitration [a] (nitro derivative)	2	80–83 %	$1.04 \begin{matrix}+ 0.06 \\ - 0.06\end{matrix}$
(recovered reactant)	2	80–83 %	$1.04 \begin{matrix}+ 0.01 \\ - 0.02\end{matrix}$

[a] H_2SO_4 concentration, 0.02 % by weight; mole ratio acid to hydrocarbon, 1:100.

The function relating the molar activity in the unconsumed reactant and the molar activity in the initial reactant to the kinetic isotope effect is

$$\log \frac{r}{r_0} = \frac{1 - \beta}{3 + 3q}\left[-\log(1 - x)\right]$$

In Fig. 1 the average value of d/r_0 obtained from duplicate counting of two separate bromination runs is compared with the theoretical function $f(x,\beta,q)$ where $q = 1/3$. The experimental data

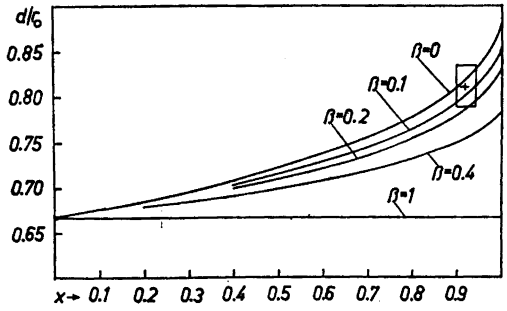

Fig. 1. Tritium content of 1-bromo-2,4,6-tri-*t*-butylbenzene relative to initial hydrocarbon. Curves show the function $f(x,\beta,q)$ for certain values of β.

indicate that β is less than 0.2. The most probable value appears to be 0.1 or less. More experimental work is necessary in order to ascertain the value of β with greater accuracy.

The isotope effect investigations made by Zollinger [8,9] of the azo coupling reaction and Schubert *et al.* [10,11] of the acid-catalyzed decarbonylation of 2,4,6-trialkylbenzaldehydes clearly show that in these reactions steric hindrance around the site of electrophilic substitution increases the kinetic importance of the aromatic C—H bond breaking. Their observations are readily explicable in terms of the generally accepted two-step reaction mechanism of aromatic substitution, and, in fact, constitute very strong evidence in favor of this mechanism. Analysis

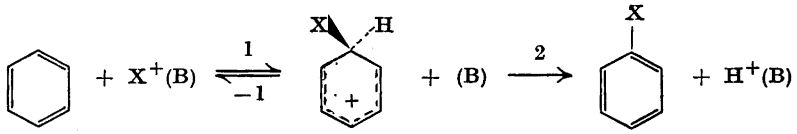

of the general rate equation of this mechanism reveals that step 2 will be rate-controlling and a hydrogen isotope effect will be observed when the velocity ratio (v_{-1}/v_2) is large. Such a condition should be facilitated when bulky substituents are located *ortho* to the reaction site since the contribution to the total energy of the transition state due to steric repulsion should be larger for step 2 than for step -1. If other factors affecting v_{-1}/v_2 do not counterbalance the steric effects, step 2 should become rate-controlling when a highly hindered compound is subjected to an electrophilic substitution even though an isotope effect is not observed when an unhindered compound is allowed to undergo the same reaction.

The absence of an isotope effect in the nitration of relatively unhindered aromatic compounds is well documented [1,6]. The present work shows this effect is absent even under conditions approaching maximum hindrance. It is concluded that for aromatic nitration other energetic considerations are of far greater importance than steric factors in determining the velocity ratio (v_{-1}/v_2).

There appears to be no isotope effect in the bromination of benzene by hypobromous acid [12] or bromine with iodine catalyst [6]. These results may be contrasted with the strong isotope effect found in the bromination of tri-*t*-butylbenzene and the previously reported isotope effects in the bromination of 2-naphthol-6,8-disulphonic acid ($k_D/k_H = 0.50$)[8] and dimethylaniline ($k_D/k_H = 0.53$)[13]. Although the situation at present is not altogether clear-cut, it would appear that in the aromatic bromination reaction steric hindrance is able to profoundly influence the velocity ratio (v_{-1}/v_2).

Further discussion will be deferred until investigations concerning the isotope effects in the bromination of aromatic hydrocarbons possessing intermediate hindrance and the importance of basic and solvent species on the isotope effect have been completed. The investigations reported here will be published in full detail at a later date.

1. De La Mare, P. B. D. and Ridd, J. H. *Aromatic Substitution* Butterworths Scientific Publications, London, 1959.
2. Burgers, J. Hoefnagel, M. A., Verkade, P. E., Visser, H. and Wepster, B. M. *Rec. trav. chim.* **77** (1958) 491.
3. Bartlett, P. D., Roha, M. and Stiles, R. M. *J. Am. Chem. Soc.* **76** (1954) 2349.
4. Betts, E. E. and Barclay, L. R. C. *Can. J. Chem.* **33** (1955) 1768.
5. Barclay, L. R. C. and Betts, E. E. *Can. J. Chem.* **33** (1955) 672.
6. Melander, L. *Arkiv Kemi* **2** (1950) 211.
7. Halvarson, K. and Melander, L. *Arkiv Kemi* **11** (1957) 77.
8. Zollinger, H. *Helv. Chim. Acta* **38** (1955) 1597, 1608, 1617, 1624.
9. Zollinger, H. *Experientia* **12** (1956) 165.
10. Schubert, W. M. and Burkett, H. *J. Am. Chem. Soc.* **78** (1956) 64.
11. Schubert, W. M. and Myhre, P. C. *J. Am. Chem. Soc.* **80** (1958) 1755.
12. De La Mare, P. B. D., Dunn, T. M. and Harvey, J. T. *J. Chem. Soc.* **1957** 923.
13. Farrell, P. G. and Mason, S. F. *Nature* **183** (1959) 250.

Received January 3, 1960.

The UV-Absorption of some 1α, 5α-Epidithio-steroids

GÖRAN BERGSON and BERNDT SJÖBERG

Chemical Institute, University of Uppsala, Sweden

ROBERT C. TWEIT and R. M. DODSON

The Chemical Research Division of G. D. Searle & Co. Chicago, Illinois, USA.

Recently Tweit and Dodson [1] isolated a disulfide from the reaction of 1,4-androstadiene-3,17-dione with hydrogen sulfide and sulfur in pyridine. For various reasons the disulfide linkage was proposed to be between carbon atoms one and five, and the disulfide bridge was placed on the α-side of the molecule. The compound is thus 1α, 5α-epidithioandrostane-3,17-dione (I) which implies that the molecule contains the five-membered 1,2-dithiolane ring.

From a study of molecular models it appeared that the dihedral angle of the disulfide group in I, as in other dithiolane derivatives, cannot be very far from zero. In 1,2-dithiolane-4-carboxylic acid the dihedral angle has been found [2] to be 27°. Furthermore it can be concluded, that the sulfur-sulfur bond distance is certainly larger than the usual (2.08 ± 0.03 Å) since otherwise a large departure from the principle of maximum overlap for the carbon-sulfur bonds must be assumed. Since 1,2-dithiolane and many of its derivatives have an absorption band in the ultraviolet with maximum at about 330 mμ and since Bergson [3] has shown that an increase in the sulfur-sulfur bond distance might be expected to decrease the excitation energy, the thiosteroid I might have

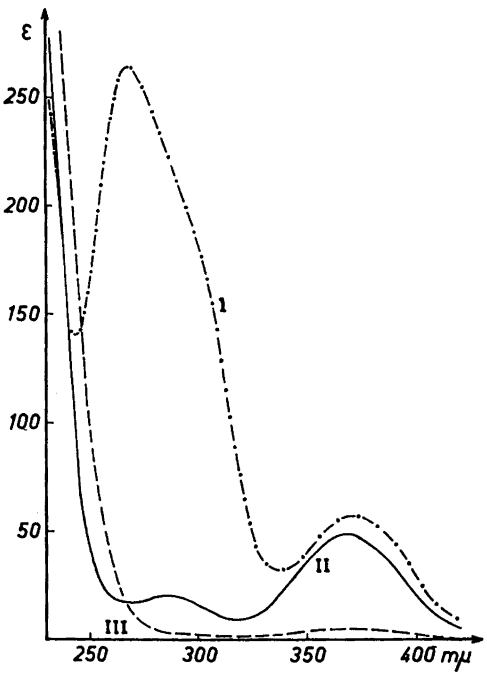

Fig. 1. Ultraviolet absorption in methanol of:
I: 1α,5α-epidithioandrostane-3,17-dione.
II: 1α,5α-epidithioandrostane-3α,17β-diol.
III: 3α,17β-dihydroxyandrostane-1α,5α-dithiol.

an absorption band at longer wavelengths than 330 mμ. The ultraviolet spectrum of 1α,5α-epidithioandrostane-3,17-dione (I) and its reduction products 1α,5α-epidithioandrostane-3α,17β-diol (II) and 3α,17β-dihydroxyandrostane-1α,5α-dithiol (III) have therefore been reinvestigated in

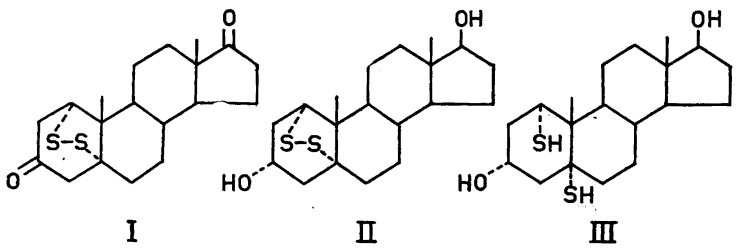

I II III

detail. The results are given in Fig. 1. The disulfides I and II have a maximum at 371 mμ ($\varepsilon_{max} = 58$) and 369 mμ ($\varepsilon_{max} = 49$), respectively. We think that this band is due to a transition from the antibonding 3pπ-orbital to the antibonding σ-orbital of the disulfide group [3,4]. This is in harmony with its almost complete disappearance in the dithiol III; the very small remaining absorption is certainly due to the precense of a trace of II formed by the unavoidable oxidation of III. We cannot at present give a precise interpretation of the absorption at the shorter wave-lengths. Remarkable is the strong absorption maximum at 268 mμ for the keto-compound (I). This cannot be due solely to the keto-groups. It may possibly be due to a trans-annular interaction of the 3-keto-group and the disulfide bridge (*cf.* Leonard *et al.* [5])

1. Tweit, R. C. and Dodson, R. M. *J. Am. Chem. Soc.* **81** (1959) 4409.
2. Foss, O. and Tjomsland, O. *Acta Chem. Scand.* **11** (1957) 1426.
3. Bergson, G. *To be published.*
4. Bergson, G. *Arkiv Kemi* **12** (1958) 233.
5. Leonard, N. J., Brown, T. L. and Milligan, T. W. *J. Am. Chem. Soc.* **81** (1959) 504.

Received December 16, 1959.

Studies on the Zirconium-Aluminium and Hafnium-Aluminium Systems

LARS-ERIK EDSHAMMAR and STEN ANDERSSON

Institute of Inorganic and Physical Chemistry, University of Stockholm, Stockholm, Sweden

The following phases have been observed in the zirconium-aluminium system: Zr_3Al, Zr_2Al, Zr_5Al_3, Zr_3Al_2, Zr_4Al_3, ZrAl, Zr_2Al_3, $ZrAl_2$ and $ZrAl_3$[1]. The crystal structures have been reported for Zr_3Al[2], Zr_5Al_3[3], $ZrAl_2$[4] and $ZrAl_3$[5].

In the present investigation, metals of high purity were used, *viz.* aluminium (99.99 %) and zirconium (iodide zirconium 99.9 %, oxygen 260 ppm, Foote Mineral Company). The alloys were prepared by melting in an electric arc furnace under an argon atmosphere and heat-treated in sealed evacuated silica tubes. Tantalum foils protected the alloys from reacting with the silica.

The phase analyses were performed by means of X-ray powder patterns taken in a Guinier camera, potassium chloride being added to the specimens as an internal standard [6]. Single crystal data were obtained in a Weissenberg camera with Cu*K* radiation.

While the crystal structures of Zr_5Al_3 and $ZrAl_2$ were being studied at this Institute, Wilson *et al.*[3,4] published the structures of these compounds. Thus, Zr_5Al_3 was reported to have the **D8*s*** type of structure while $ZrAl_2$ was found to be of the **C14** type. The data given for $ZrAl_2$ are in perfect agreement with our results but this is, however, not the case with Zr_5Al_3.

Single crystals of Zr_5Al_3 could be obtained from a melt of the approximate composition $ZrAl_{0.50}$. The single crystal and powder data showed the structure to be tetragonal with the following unit cell axes:

$$a = 11.049 \text{ Å}, \qquad c = 5.396 \text{ Å}.$$

The Patterson projections along[001] and [100] were calculated and the following structure was derived:

Unit cell content: 4 Zr_5Al_3.

Space-group: *I*4/*mcm* (No. 140)

		x	*y*	*z*
16 Zr in	16 (*k*)	0.077	0.218	0
4 Zr in	4 (*b*)	0	½	1/4
8 Al in	8 (*h*)	0.16	0.66	0
4 Al in	4 (*a*)	0	0	1/4

This structure of the **D8*m*** type is represented by W_5Si_3 (Aronsson [7]). It may be that the occurrence of the **D8*s*** and the **D8*m*** structures depends on the heat-treatment of the sample. It has, however, been suggested that the Me_5X_3 phases with the **D8*s*** type of structure are stabilized by the prescence of impurities such as boron, carbon, nitrogen and oxygen [8-10]. This interesting hypothesis seems to be supported by the observation that a mixture of zirconium, aluminium and aluminium oxide with a composition close to the formula $Zr_{10}Al_6O$ upon melting gave a product with a pure **D8*s*** structure. The powder pattern was found to give the following parameters for the hexagonal unit cell:

$$a = 8.177 \text{ Å}, \qquad c = 5.674 \text{ Å}.$$

The axes reported by Wilson *et al.*[3] for the **D8*s*** phase are 8.184 and 5.702 Å, respectively.

detail. The results are given in Fig. 1. The disulfides I and II have a maximum at 371 mμ ($\varepsilon_{max} = 58$) and 369 mμ ($\varepsilon_{max} = 49$), respectively. We think that this band is due to a transition from the antibonding 3pπ-orbital to the antibonding σ-orbital of the disulfide group [3,4]. This is in harmony with its almost complete disappearance in the dithiol III; the very small remaining absorption is certainly due to the precense of a trace of II formed by the unavoidable oxidation of III. We cannot at present give a precise interpretation of the absorption at the shorter wave-lengths. Remarkable is the strong absorption maximum at 268 mμ for the keto-compound (I). This cannot be due solely to the keto-groups. It may possibly be due to a trans-annular interaction of the 3-keto-group and the disulfide bridge (*cf.* Leonard *et al.* [5])

1. Tweit, R. C. and Dodson, R. M. *J. Am. Chem. Soc.* **81** (1959) 4409.
2. Foss, O. and Tjomsland, O. *Acta Chem. Scand.* **11** (1957) 1426.
3. Bergson, G. *To be published.*
4. Bergson, G. *Arkiv Kemi* **12** (1958) 233.
5. Leonard, N. J., Brown, T. L. and Milligan, T. W. *J. Am. Chem. Soc.* **81** (1959) 504.

Received December 16, 1959.

Studies on the Zirconium-Aluminium and Hafnium-Aluminium Systems

LARS-ERIK EDSHAMMAR and STEN ANDERSSON

Institute of Inorganic and Physical Chemistry, University of Stockholm, Stockholm, Sweden

The following phases have been observed in the zirconium-aluminium system: Zr_3Al, Zr_2Al, Zr_5Al_3, Zr_3Al_2, Zr_4Al_3, ZrAl, Zr_2Al_3, $ZrAl_2$ and $ZrAl_3$[1]. The crystal structures have been reported for Zr_3Al[2], Zr_5Al_3[3], $ZrAl_2$[4] and $ZrAl_3$[5].

In the present investigation, metals of high purity were used, *viz.* aluminium (99.99 %) and zirconium (iodide zirconium 99.9 %, oxygen 260 ppm, Foote Mineral Company). The alloys were prepared by melting in an electric arc furnace under an argon atmosphere and heat-treated in sealed evacuated silica tubes. Tantalum foils protected the alloys from reacting with the silica.

The phase analyses were performed by means of X-ray powder patterns taken in a Guinier camera, potassium chloride being added to the specimens as an internal standard [6]. Single crystal data were obtained in a Weissenberg camera with Cu*K* radiation.

While the crystal structures of Zr_5Al_3 and $ZrAl_2$ were being studied at this Institute, Wilson *et al.*[3,4] published the structures of these compounds. Thus, Zr_5Al_3 was reported to have the **D8*s*** type of structure while $ZrAl_2$ was found to be of the **C14** type. The data given for $ZrAl_2$ are in perfect agreement with our results but this is, however, not the case with Zr_5Al_3.

Single crystals of Zr_5Al_3 could be obtained from a melt of the approximate composition $ZrAl_{0.50}$. The single crystal and powder data showed the structure to be tetragonal with the following unit cell axes:

$$a = 11.049 \text{ Å}, \qquad c = 5.396 \text{ Å}.$$

The Patterson projections along[001] and [100] were calculated and the following structure was derived:

Unit cell content: 4 Zr_5Al_3.

Space-group: *I*4/*mcm* (No. 140)

		x	*y*	*z*
16 Zr in	16 (*k*)	0.077	0.218	0
4 Zr in	4 (*b*)	0	½	1/4
8 Al in	8 (*h*)	0.16	0.66	0
4 Al in	4 (*a*)	0	0	1/4

This structure of the **D8*m*** type is represented by W_5Si_3 (Aronsson [7]). It may be that the occurrence of the **D8*s*** and the **D8*m*** structures depends on the heat-treatment of the sample. It has, however, been suggested that the Me_5X_3 phases with the **D8*s*** type of structure are stabilized by the prescence of impurities such as boron, carbon, nitrogen and oxygen [8-10]. This interesting hypothesis seems to be supported by the observation that a mixture of zirconium, aluminium and aluminium oxide with a composition close to the formula $Zr_{10}Al_6O$ upon melting gave a product with a pure **D8*s*** structure. The powder pattern was found to give the following parameters for the hexagonal unit cell:

$$a = 8.177 \text{ Å}, \qquad c = 5.674 \text{ Å}.$$

The axes reported by Wilson *et al.*[3] for the **D8*s*** phase are 8.184 and 5.702 Å, respectively.

The powder pattern of Zr_4Al_3 was obtained from a sample annealed at 850°C for several days. It was possible to index it it with the following hexagonal unit cell dimensions:

$$a = 5.430 \text{ Å}, \qquad c = 5.389 \text{ Å}.$$

The observed density, 5.32 g cm^{-3}, is in good agreement with the value, 5.37 g cm^{-3}, calculated for a cell content of one formula unit Zr_4Al_3. The intensity data suggest that the structure contains chains of zirconium atoms (Zr—Zr = $\frac{1}{2}$ c) similar to those present in the Zr_5Al_3 phase.

Further studies on these structures are in progress.

In connection with the investigations on the zirconium-aluminium system, the aluminium-rich region of the hafnium-aluminium system has also been studied. Thus, three compounds, *viz.* Hf_2Al_3, $HfAl_2$ and $HfAl_3$, have been prepared so far. The X-ray powder patterns demonstrate clearly that they are all isomorphous with the corresponding phases in the zirconium-aluminium system.

$HfAl_3$ has a hexagonal **C14** type of structure with the unit cell axes:

$$a = 5.288 \text{ Å}, \qquad c = 8.739 \text{ Å}$$

$HfAl_3$ has a tetragonal $\mathbf{D0_{23}}$ type of structure with the unit cell axes:

$$a = 4.010 \text{ Å}, \qquad c = 17.310 \text{ Å}$$

For valuable discussions and a continuous interest in this research work, the authors are much indebted to Dr. Arne Magnéli.

1. Mc. Pherson, D. J. and Hansen, M. *Trans. Am. Soc. Metals* **46** (1954) 354.
2. Keeler, J. H. and Mallery, J. H. *J. Metals* **7** (1955) 394.
3. Wilson, C. G., Sams, D. and Renouf, T. J. *Acta Cryst.* **12** (1959) 947.
4. Wilson, C. G. *Acta Cryst.* **12** (1959) 660.
5. Brauer, G. *Z. anorg. Chem.* **1** (1939) 242.
6. Westman, S. and Magnéli, A. *Acta Chem. Scand.* **11** (1957) 1587.
7. Aronsson, B. *Acta Chem. Scand.* **9** (1955) 1107.
8. Nowotny, H. and Parthé, E. *Planseeber. Pulvermet.* **2** (1954) 34.
9. Nowotny, H., Parthé, E., Kieffer, R. and Benesovsky, F. *Monatsh.* **85** (1954) 255.
10. Brewer, L. and Krikorian, O. *UCRL 2544, University of California 1954.*

Received January 15, 1960.

Ozonolysis of *p*-Benzoquinone. III. Counter-current Ozonisation

ERLING BERNATEK and KRISTIAN VALEN

Universitetets Kjemiske Institutt, Blindern-Oslo, Norway

On two previous occasions [1,2] we have reported on the ozonolysis of *p*-benzoquinone and discussed some of the possible reaction paths. Anomalous ozonolysis and/or rearrangement of normal ozonides occurred to a large extent. This was to be expected since in quinone two carbonyl groups are conjugated with the double bonds attacked by ozone.

The experimental procedure employed — being a batch procedure — had the drawback that the primary reaction products were in contact with ozone for a comparably long time. Consequently some of the isolated products could have been formed by further oxidation. In order to avoid this and especially to investigate closer the formation of a monozonide and its decomposition products, we adopted a counter-current procedure similar to that of Pummerer and Richtzenhain [3] which allowed a brief contact between the quinone solution and ozone, rapidly followed by hydrolysis.

Previous experiments with the batch procedure has shown that even if quinone was present in excess to the amount of ozone required for mono-ozonolysis only minor amounts of reaction products originating from cleavage of one double bond were found. It thus seems that secondary reactions proceed about as fast as the initial ozonolysis.

In Table 1 is summarised some of the relationships between the amount of applied ozone per mole of quinone, % reacted quinone and consumed ozone as found by the counter-current method. Finally the theoretically possible amount of monozonide (or products from mono-ozonolysis) in moles per mole of quinone is calculated.

When about one mole of ozone is applied per mole of quinone 65 % of the latter is attacked. A substantial part of the quinone must therefore have consumed two molecules of ozone. From the last column it is clear that mono-ozonolysis occurs in increasing amounts with decreasing ozone-quinone ratio.

The powder pattern of Zr_4Al_3 was obtained from a sample annealed at 850°C for several days. It was possible to index it it with the following hexagonal unit cell dimensions:

$$a = 5.430 \text{ Å}, \qquad c = 5.389 \text{ Å}.$$

The observed density, 5.32 g cm^{-3}, is in good agreement with the value, 5.37 g cm^{-3}, calculated for a cell content of one formula unit Zr_4Al_3. The intensity data suggest that the structure contains chains of zirconium atoms (Zr—Zr = $\frac{1}{2}$ c) similar to those present in the Zr_5Al_3 phase.

Further studies on these structures are in progress.

In connection with the investigations on the zirconium-aluminium system, the aluminium-rich region of the hafnium-aluminium system has also been studied. Thus, three compounds, *viz.* Hf_2Al_3, $HfAl_2$ and $HfAl_3$, have been prepared so far. The X-ray powder patterns demonstrate clearly that they are all isomorphous with the corresponding phases in the zirconium-aluminium system.

$HfAl_3$ has a hexagonal **C14** type of structure with the unit cell axes:

$$a = 5.288 \text{ Å}, \qquad c = 8.739 \text{ Å}$$

$HfAl_3$ has a tetragonal $\mathbf{D0_{23}}$ type of structure with the unit cell axes:

$$a = 4.010 \text{ Å}, \qquad c = 17.310 \text{ Å}$$

For valuable discussions and a continuous interest in this research work, the authors are much indebted to Dr. Arne Magnéli.

1. Mc. Pherson, D. J. and Hansen, M. *Trans. Am. Soc. Metals* **46** (1954) 354.
2. Keeler, J. H. and Mallery, J. H. *J. Metals* **7** (1955) 394.
3. Wilson, C. G., Sams, D. and Renouf, T. J. *Acta Cryst.* **12** (1959) 947.
4. Wilson, C. G. *Acta Cryst.* **12** (1959) 660.
5. Brauer, G. *Z. anorg. Chem.* **1** (1939) 242.
6. Westman, S. and Magnéli, A. *Acta Chem. Scand.* **11** (1957) 1587.
7. Aronsson, B. *Acta Chem. Scand.* **9** (1955) 1107.
8. Nowotny, H. and Parthé, E. *Planseeber. Pulvermet.* **2** (1954) 34.
9. Nowotny, H., Parthé, E., Kieffer, R. and Benesovsky, F. *Monatsh.* **85** (1954) 255.
10. Brewer, L. and Krikorian, O. *UCRL 2544, University of California 1954.*

Received January 15, 1960.

Ozonolysis of *p*-Benzoquinone. III. Counter-current Ozonisation

ERLING BERNATEK and KRISTIAN VALEN

Universitetets Kjemiske Institutt, Blindern-Oslo, Norway

On two previous occasions [1,2] we have reported on the ozonolysis of *p*-benzoquinone and discussed some of the possible reaction paths. Anomalous ozonolysis and/or rearrangement of normal ozonides occurred to a large extent. This was to be expected since in quinone two carbonyl groups are conjugated with the double bonds attacked by ozone.

The experimental procedure employed — being a batch procedure — had the drawback that the primary reaction products were in contact with ozone for a comparably long time. Consequently some of the isolated products could have been formed by further oxidation. In order to avoid this and especially to investigate closer the formation of a monozonide and its decomposition products, we adopted a counter-current procedure similar to that of Pummerer and Richtzenhain [3] which allowed a brief contact between the quinone solution and ozone, rapidly followed by hydrolysis.

Previous experiments with the batch procedure has shown that even if quinone was present in excess to the amount of ozone required for mono-ozonolysis only minor amounts of reaction products originating from cleavage of one double bond were found. It thus seems that secondary reactions proceed about as fast as the initial ozonolysis.

In Table 1 is summarised some of the relationships between the amount of applied ozone per mole of quinone, % reacted quinone and consumed ozone as found by the counter-current method. Finally the theoretically possible amount of monozonide (or products from mono-ozonolysis) in moles per mole of quinone is calculated.

When about one mole of ozone is applied per mole of quinone 65 % of the latter is attacked. A substantial part of the quinone must therefore have consumed two molecules of ozone. From the last column it is clear that mono-ozonolysis occurs in increasing amounts with decreasing ozone-quinone ratio.

Table 1.

Run	Moles O_3 / quinone	% Reacted quinone	% Reacted O_3	Moles monozonide / quinone
1	2.17	95.4	86.8	0.06
2	1.74	83.8	88.2	0.17
3	1.43	79.4	97.7	0.24
4	1.05	67.2	~ 100	0.44
5	1.01	65.0	100	0.45
6	0.98	60.3	100	0.37
7	0.82	56.9	100	0.56
8	0.80	57.5	100	0.61

Oxidation of the aqueous decomposition solution with hydrogen peroxide and analysis for maleic acid constituted another method to determine the degree of mono-ozonolysis. For run 7 and 8 it was found *ca.* 0.20 moles of maleic acid per mole of reacted quinone, the calculated amount of mono-ozonolysis products being *ca.* 0.6 mole. This large difference must have significance and is most likely due to the inability of some mono-ozonolysis products to form maleic acid on oxidation with hydrogen peroxide. It must be remarked, however, that maleic acid is not entirely stable towards hydrogen peroxide under the prevailing conditions and the obtained results are therefore probably rather low.

In the later runs we always kept the ratio between ozone and quinone close to 0.80. The aqueous decomposition solution had an acidic reaction, gave a precipitate with 2,4-dinitrophenylhydrazine and reduced Tollens reagent. Oxalic and maleic acids could not be detected. Formic acid was produced in an amount of 0.78 moles per mole of reacted quinone. Some fractionation of the carbonyl compounds could be achieved by means of a weakly basic ion-exchange column. Neutral components were eluted with water and acidic components with 5 % aqueous formic acid.

The neutral eluate contained glyoxal as identified through its *p*-nitrophenylhydrazone. Mesoxalic dialdehyde was not present in detectable amounts.

From the acidic eluate was precipitated a complex mixture of dinitrophenylhydrazones. This could be separated into three fractions: Glyoxylic acid dinitrophenylhydrazone (from one run only), some red crystals (DNP I) and yellowish crystals (DNP II). The infra-red solid-state spectra of DNP I and II were very similar differing mainly in the relative intensities of some bands. Absorptions at 1 720 cm^{-1} and 1 425 cm^{-1} probably represent a free carboxyl group while the presence of an unreacted carbonyl group seems less probable but cannot be entirely excluded. In composition, however, the two derivatives differ somewhat and none of them corresponds very closely to a rational formula. Closest comes DNP II to the formula $C_{17}H_{12}N_8O_{10}$ which could represent a bis-dinitrophenylhydrazone of a conceivable mono-ozonolysis product $CHO-CH=CH-CO-COOH$. Our only possible conclusion for the present is therefore that in the acidic eluate there are carbonyl compounds resulting from mono-ozonolysis and of a rather complicated nature.

Experimental. Ozonisation procedure. The ozonisation apparatus was essentially that of Pummerer and Richtzenhain [3] with only minor modifications. The reaction column proper was 60 by 2 cm and filled with Fenske helices. Surrounding this was a cooling mantle, during the runs filled with ice. *p*-Benzoquinone in chloroform was trickled down the reactor while ozone was let in at the bottom. After ozonisation the reaction mixture passed into a flask containing continously agitated water. A liquid seal prevented ozone from entering the decomposition vessel. After completion of the ozonisation the apparatus was rinsed briefly with chloroform.

Ozone in the oxygen from the ozone generator and in the effluent gases from the counter-current reactor was determined by absorption in neutral potassium iodide and titration with standard thiosulphate after acidification.

In all the experiments the rate of flow of ozonised oxygen was kept constant at 20 l/h which gave 1.68 g O_3/h. Variations in experimental procedure was therefore effected through varying the concentration of *p*-benzoquinone in chloroform and the flow of this solution.

After ozonisation and decomposition the liquid layers were separated and the chloroform phase exhaustively extracted with water. Some unreacted *p*-benzoquinone went into the water and the combined aqueous extracts were therefore extracted with a small amount fresh chloroform. The unreacted quinone was determined iodometrically in the combined chloroform solutions.

Maleic acid. The aqueous decomposition solution was evaporated to a small volume and barium chloride added. In none of the runs thus investigated any barium maleinate separated. Due to a slight solubility of this salt a minor amount of maleic acid may have escaped detection.

Decomposition solutions from runs 7 and 8 were mixed with 3 ml 30 % hydrogen peroxide and evaporated to dryness on a water-bath. The residues consisted of white, somewhat sticky crystals which were indentified as maleic acid. In the runs 0.935 g and 1.153 g *p*-benzoquinone reacted with ozone and gave 199 mg and 228 mg maleic acid, respectively. Controls by precipitating the dissolved residues with barium chloride were satisfactory.

Formic acid. Aliquots of the decomposition solutions were distilled *in vacuo* to dryness. The distillate was taken up in standard sodium hydroxide and backtitrated with hydrochloric acid. The capillary was connected to a sodium hydroxide-asbestos tube to prevent the entrance of carbon dioxide. Substituting the air in the distilling apparatus with nitrogen did not alter the titration values significantly.

Ion-exchange chromatography. The decomposition solution was passed through a column of De-acidite G and washed with water. The neutral washings which reduced ammoniacal silver solution were combined and precipitated with *p*-nitrophenylhydrazine. This precipitate was extracted with glacial acetic acid and recrystallised from nitrobenzene m. p. *ca.* 270° (decomp.). Through its infra-red spectrum it was identified as glyoxal *p*-nitrophenylosazone. Further elution was performed with 5 % formic acid when more aldehydic material appeared. The acidic eluate was precipitated with 2,4-dinitrophenylhydrazine and the material extracted with boiling water. In one case there separated yellow needles from the aqueous extracts, m. p. 190°, identified as glyoxylic acid dinitrophenylhydrazone. The residue from the extraction was partially soluble in hot glacial acetic acid. From the acetic acid separated red crystals, m. p. 226° (decomp.). (Found: C 43.9; H 3.2; N 20.6.) The insoluble part was recrystallised from nitrobenzene. Yellowish crystals, m. p. 255° (decomp.). (Found: C 41.6; H 2.7; N 22.4. Calc. for $C_{17}H_{12}N_8O_{16}$: C 41.8; H 2.5; N 22.9.)

1. Bernatek, E. *Acta Chem. Scand.* **8** (1954) 1943.
2. Bernatek, E. and Straumsgård, K. A. *Acta Chem. Scand.* **13** (1959) 178.
3. Pummerer, R. and Richtzenhain, H. *Ann.* **529** (1937) 50.

Received December 12, 1959.

The Structure of Dinitropinoresinol

JARL GRIPENBERG and INGEGERD PETRELL

Department of Chemistry, Finland Institute of Technology, Helsingfors, Finland

Some years ago the preparation of dinitropinoresinol was reported [1]. Its structure was not determined, but it was assumed to be I in analogy with dinitropinoresinol dimethylether. Dinitropinoresinol gives, however, upon treatment with nitric acid 4,6-dinitroguaiacol, m.p. 122°, and must therefore have structure II

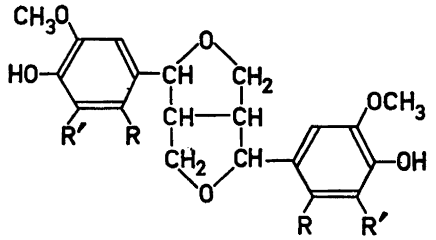

I R = NO_2; R′ = H
II R = H ; R′ = NO_2

The aim of the earlier work [1] was the degradation of the aromatic rings of pinoresinol to carboxylic groups. We have now attempted to achieve this by ozonolysis (*cf.* Ref.[2]), but the desired acid could not be obtained. The only products that could be identified were oxalic acid and in some experiments where the reaction time was kept very short, maleic acid.

In connection with this work we had to prepare relatively large amounts of pinoresinol and we found that when the crude pinoresinol from the potassium salt [3] was treated with dioxan it immediately crystallised. The crystals contain 1 molecule of dioxan, which can readily be removed by heating under vacuum on a boiling water bath. This method of purification is more convenient than the customary one *via* the acetate [3].

1. Gripenberg, J. and Lindahl, B. *Acta Chem. Scand.* **6** (1952) 1147.
2. Carnmalm, B. *Acta Chem. Scand.* **10** (1956) 477.
3. Erdtman, H. *Svensk Kem. Tidskr.* **46** (1934) 229.

Received January 18, 1960.

Decomposition solutions from runs 7 and 8 were mixed with 3 ml 30 % hydrogen peroxide and evaporated to dryness on a water-bath. The residues consisted of white, somewhat sticky crystals which were indentified as maleic acid. In the runs 0.935 g and 1.153 g *p*-benzoquinone reacted with ozone and gave 199 mg and 228 mg maleic acid, respectively. Controls by precipitating the dissolved residues with barium chloride were satisfactory.

Formic acid. Aliquots of the decomposition solutions were distilled *in vacuo* to dryness. The distillate was taken up in standard sodium hydroxide and backtitrated with hydrochloric acid. The capillary was connected to a sodium hydroxide-asbestos tube to prevent the entrance of carbon dioxide. Substituting the air in the distilling apparatus with nitrogen did not alter the titration values significantly.

Ion-exchange chromatography. The decomposition solution was passed through a column of De-acidite G and washed with water. The neutral washings which reduced ammoniacal silver solution were combined and precipitated with *p*-nitrophenylhydrazine. This precipitate was extracted with glacial acetic acid and recrystallised from nitrobenzene m. p. *ca.* 270° (decomp.). Through its infra-red spectrum it was identified as glyoxal *p*-nitrophenylosazone. Further elution was performed with 5 % formic acid when more aldehydic material appeared. The acidic eluate was precipitated with 2,4-dinitrophenylhydrazine and the material extracted with boiling water. In one case there separated yellow needles from the aqueous extracts, m. p. 190°, identified as glyoxylic acid dinitrophenylhydrazone. The residue from the extraction was partially soluble in hot glacial acetic acid. From the acetic acid separated red crystals, m. p. 226° (decomp.). (Found: C 43.9; H 3.2; N 20.6.) The insoluble part was recrystallised from nitrobenzene. Yellowish crystals, m. p. 255° (decomp.). (Found: C 41.6; H 2.7; N 22.4. Calc. for $C_{17}H_{12}N_8O_{16}$: C 41.8; H 2.5; N 22.9.)

1. Bernatek, E. *Acta Chem. Scand.* **8** (1954) 1943.
2. Bernatek, E. and Straumsgård, K. A. *Acta Chem. Scand.* **13** (1959) 178.
3. Pummerer, R. and Richtzenhain, H. *Ann.* **529** (1937) 50.

Received December 12, 1959.

The Structure of Dinitropinoresinol

JARL GRIPENBERG and INGEGERD PETRELL

Department of Chemistry, Finland Institute of Technology, Helsingfors, Finland

Some years ago the preparation of dinitropinoresinol was reported [1]. Its structure was not determined, but it was assumed to be I in analogy with dinitropinoresinol dimethylether. Dinitropinoresinol gives, however, upon treatment with nitric acid 4,6-dinitroguaiacol, m.p. 122°, and must therefore have structure II

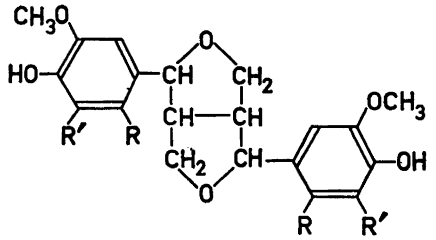

I R = NO_2; R′ = H
II R = H ; R′ = NO_2

The aim of the earlier work [1] was the degradation of the aromatic rings of pinoresinol to carboxylic groups. We have now attempted to achieve this by ozonolysis (*cf.* Ref.[2]), but the desired acid could not be obtained. The only products that could be identified were oxalic acid and in some experiments where the reaction time was kept very short, maleic acid.

In connection with this work we had to prepare relatively large amounts of pinoresinol and we found that when the crude pinoresinol from the potassium salt [3] was treated with dioxan it immediately crystallised. The crystals contain 1 molecule of dioxan, which can readily be removed by heating under vacuum on a boiling water bath. This method of purification is more convenient than the customary one *via* the acetate [3].

1. Gripenberg, J. and Lindahl, B. *Acta Chem. Scand.* **6** (1952) 1147.
2. Carnmalm, B. *Acta Chem. Scand.* **10** (1956) 477.
3. Erdtman, H. *Svensk Kem. Tidskr.* **46** (1934) 229.

Received January 18, 1960.

The Inverse Relationship between Tryptophan and Hydroxyproline in Animal Tissues

OLLE DAHL

Scan's Centrallaboratorium, Malmö, Sweden

During recent years several contributions have increased our knowledge of the amino acid composition of proteins and in particular their content of essential amino acids.

Tryptophan is an essential amino acid typical of high-quality animal proteins and may often, although not always, be considered a special feature of this kind of protein. Blood protein is an example of a protein high in tryptophan but low in the essential amino acid methionine [1]. This is in contrast to, for instance, striated muscular tissue, milk, and egg protein.

An amino acid typical of the low-quality protein present in connective tissue is hydroxyproline, the assessment of which has acquired increased importance over the past few years. Since connective tissue is practically devoid of tryptophan and, on the other hand, striated muscular tissue contains very little hydroxyproline, there is an indication of an inverse relationship between tryptophan and hydroxyproline. The present study was undertaken to assess, whether this relationship is a general characteristic of animal tissues or is subject to limitations. In particular, unstriated muscular tissue, *i.e.* the tissue found in stomach, intestine etc., was investigated.

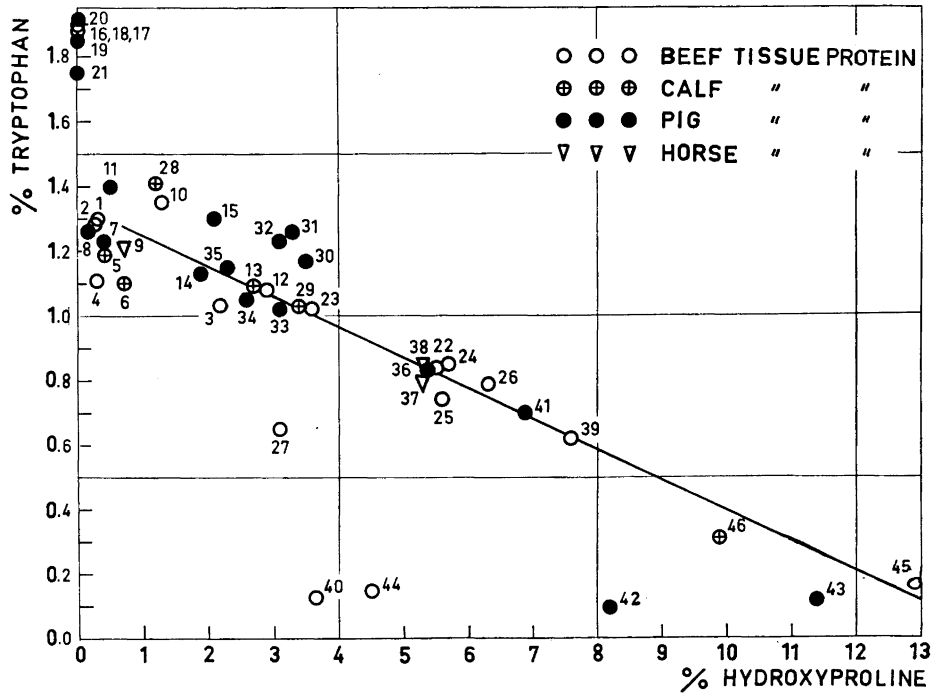

Fig. 1. Relation between the content of tryptophan (T) and hydroxyproline (H) in various animal tissues. The proportions of the two amino acids are given as percentages of total protein (N × 6.25).

The regression line drawn, T = −0.0950 · H +1.345 has been calculated on the basis of all the data except those indicated in the text; coefficient of correlation −0.949, significant at more than the 99.9 % level.

Key to Fig. 1:

1. Longiss. dorsi (1); heifer, 26 months, grade expr.
2. Longiss. dorsi (1); cow, 8 years, grade 3+.
3. Beef meat, assortment III (fairly rich in connective tissue); cow, 7 years, grade 2+.
4. Longiss. dorsi (1); bull, 11 years, grade expr.
5. Longiss. dorsi (2); calf (fattened, male), 9 weeks, grade 1+.
6. Longiss. dorsi (2); calf (newly born, male), < 1 week.
7. Longiss. dorsi (3); bacon pig (hog), 6½ months, grade expr.
8. Longiss. dorsi (3); sow, 2 years, grade 1.
9. Horse meat, assortment II (fairly poor in connective tissue); animal 11 years old, grade 1.
10. Spleen, cow
11. » pig
12. Lungs, cow
13. » calf (fattened)
14. » pig sample No. 1
15. » pig sample No. 2
16. Blood, beef
17. Blood plasma, beef
18. Blood corpuscles (4), beef
19. Blood, pig
20. Blood plasma, pig
21. Blood corpuscles (4), pig
22. Rumen, cow
23. Omasum, cow
24. Fat end (Rectum anal end), cow
25. Udder, cow
26. Mouths (without skin), cow
27. Glands from cow's head
28. Small intestine (round), calves (fattened)
29. Fat ends (Rectum anal ends), calves (fattened)
30. Stomach (maw), pig, sample No. 1
31. » (»), » » » 2
32. » (»), sow
33. Caps (Caecum), pig
34. Chitterlings (large intestine, colon), pig, sample No. 1
35. Chitterlings (large intestine, colon), pig, sample No. 2
36. Bladders, pig
37. Stomach, horse
38. Bung (Caecum), horse
39. Cracklings (connective tissue) from wet rendered beef tallow (5)
40. Cracklings (connective tisue), residue from solvent extracted perinephric beef tallow
41. Cracklings (connective tissue), from wet rendered pig fat (5)
42. Cracklings (connective tissue), residue from solvent extracted pig's back fat
43. Back rind, pig
44. Neck tendon (ligamentum nuchae), cow
45. Achilles tendon, cow
46. Achilles tendon, calves (fattened, male)

---

(1) From the last rib to the second lumbar vertebra.
(2) From the last dorsal vertebra to the second lumbar vertebra.
(3) Between the last three (12th to 14th) dorsal vertebra.
(4) Residue after separation of blood into plasma and corpuscles [proportion of plasma to corpuscles 7:3 (beef blood) and 6:3 (pig blood), respectively].
(5) Commercial fatty raw material containing intestinal glands.

This kind of tissue, which is of a considerable interest from a nutritional and also physiological point of view, has not been previously investigated for its tryptophan and hydroxyproline contents.

Tryptophan was determined on the minced tissue without previous hydrolysis according to the widely used method of Bates essentially as described by Graham *et al.*[3] Hydroxyproline was assessed according to the method of Neuman and Logan as modified by Stegemann [3]. This was compared with the modification of Lollar [4] for different kind of tissues. The agreement between the methods was good. The results appear in Fig. 1.

With a few exceptions a close linear, negative correlation was found to exist between the contents of tryptophan and hydroxyproline. The regression line was calculated on the basis of all the data except those of the blood and blood fractions (samples Nos. 16—21), which are very high in tryptophan but contain no hydroxyproline, and the samples No. 27 (glands), Nos. 40 and 42 (cracklings from fatty tissue), and No. 44 (*ligamentum nuchae*).

The inverse relationship between tryptophan and hydroxyproline could best be explained by assuming tryptophan to be related to true cellular, and hydroxyproline to connective tissue content. This point is being investigated, as is the unforeseen difference in hydroxyproline between young and old animals (*cf.* samples Nos. 45 and 46).

The contents of tryptophan and hydroxyproline in unstriated tissues (Nos. 28—38) are intermediate. This is, among other

things, of interest from a nutritional point of view, since stomachs, intestines, and udders are used by some food manufacturers either alone or mixed with other ingredients in various chopped meat products.

The assistance of Mrs. Siv Olsson, and Mrs. Anni Esping is gratefully acknowledged.

1. Block, R. J. and Weiss, K. W. *Amino Acid Handbook*, Charles C. Thomas, Publisher, Springfield, Illinois, U.S.A.; 1956.
2. Graham, C. E., Smith, E. P., Hier, S. W. and Klein, D. *J. Biol. Chem.* **168** (1947) 711.
3. Stegemann, H. *Z. Physiol. Chem. Hoppe-Seyler* **311** (1958) 41.
4. Lollar, R. M. *J. Am. Leather Chemists' Ass.* **53** (1958) 2.

Received January 18, 1960.

The Solubility and the Salt Sensitivity of Yeast D- and L-Lactic Cytochrome c Reductase

AGNAR P. NYGAARD

Johan Throne Holst's Institutt for Ernæringsforsking, Blindern, Oslo, Norway

Homogenates of aerobic yeast have been found to contain D- and L-lactic cytochrome c reductase in the ratio 1:2 [1,2]. Using our extraction method / (15—30°), mainly the L-enzyme was solubilized. At low temperatures (0—5°) both enzymes were obtained in the particulate fraction. Half or more of the L-activity was readily extracted from the particles at 30° with 0.2 M disodium phosphate, whereas the D-enzyme remained insoluble. The extracted particles contained D- and L-lactic cytochrome c reductase in the ratio 1:1. Further mechanical desintegration with ballotini beads gave rise to soluble D-lactic cytochorme c reductase; very little of the L-enzyme was obtained. Complete extraction was not achieved for any of the two enzymes. It is concluded that one part of the L-activity was more firmly bound to the particulate fraction than the other.

Following the described method [3], three fractions of lactic cytochrome c reductase were obtained [2,4]. Fractions I, II, and III were eluted in that order from a N,N-diethylaminoethyl-cellulose column. Fractions I and II were specific for L-lactic acid. Fraction III was D-specific (D-LDH III). However, small amounts of a L-specific enzyme has now been found in some of the fractions III (L-LDH III).

The D- and the L-enzyme of the cell homogenate were both salt sensitive. The D-enzyme was more salt sensitive than the isolated D-LDH III [2]. The L-enzyme was inhibited 50 % when the phosphate concentration (pH 7.1) was increased from 0.01 to 0.08 μ.

The activity of fractions I and II, which represented most of the L-LDH activity of the purified solution, was quite the same in phosphate of ionic strength 0.01 and 0.08. In contrast, both D- and L-LDH III were inhibited 70—90 % when the buffer concentration was increased from μ 0.01 to 0.08. The inhibition of L-LDH III was the same with low and high concentrations of cytochrome c, whereas the inhibition of D-LDH III was less at high concentrations of the acceptor [2].

The strong effect of salt on L-LDH of the cell homogenate suggests that fair amounts of the salt sensitive enzyme is present in the cell. In this connection it is interesting that L-LDH obtained by the method of Boeri *et al.*[6] is very salt sensitive.

To the authors' knowledge, the effect of salts on D- and L-LDH III is stronger than for any other enzymes described. From other relationships D-lactic cytochrome c reductase has been proposed as intermediate in the formation of the L-enzyme [1,5].

D- and L-LDH III were eluted together with ribonucleic acids [7]. Furthermore, the enzymes precipitated together with nucleic acids when the eluate was dialyzed against water. A charge aggregate between protein and nucleic acid might explain both the salt sensitivity and the high negative charge which these two enzymes have available to the anion exchanger.

1. Nygaard, A. P. *Arch. Biochem. Biophys. In press.*
2. Nygaard, A. P. *Biochim. et Biophys. Acta. In press.*
3. Nygaard, A. P. *Biochim. et Biophys. Acta* **33** (1959) 517.
4. Nygaard, A. P. *Biochim. et Biophys. Acta* **35** (1959) 212.
5. Nygaard, A. P. *Arch. Biochem. Biophys. In press.*
6. Boeri, E. and Tosi, L. *Arch. Biochem. Biophys.* **60** (1956) 463.
7. Nygaard, A. P. *Biochim. et Biophys. Acta* **30** (1958) 450.

Received January 2, 1960.

things, of interest from a nutritional point of view, since stomachs, intestines, and udders are used by some food manufacturers either alone or mixed with other ingredients in various chopped meat products.

The assistance of Mrs. Siv Olsson, and Mrs. Anni Esping is gratefully acknowledged.

1. Block, R. J. and Weiss, K. W. *Amino Acid Handbook*, Charles C. Thomas, Publisher, Springfield, Illinois, U.S.A.; 1956.
2. Graham, C. E., Smith, E. P., Hier, S. W. and Klein, D. *J. Biol. Chem.* **168** (1947) 711.
3. Stegemann, H. *Z. Physiol. Chem. Hoppe-Seyler* **311** (1958) 41.
4. Lollar, R. M. *J. Am. Leather Chemists' Ass.* **53** (1958) 2.

Received January 18, 1960.

The Solubility and the Salt Sensitivity of Yeast D- and L-Lactic Cytochrome c Reductase

AGNAR P. NYGAARD

Johan Throne Holst's Institutt for Ernæringsforsking, Blindern, Oslo, Norway

Homogenates of aerobic yeast have been found to contain D- and L-lactic cytochrome c reductase in the ratio 1:2 [1,2]. Using our extraction method / (15—30°), mainly the L-enzyme was solubilized. At low temperatures (0—5°) both enzymes were obtained in the particulate fraction. Half or more of the L-activity was readily extracted from the particles at 30° with 0.2 M disodium phosphate, whereas the D-enzyme remained insoluble. The extracted particles contained D- and L-lactic cytochrome c reductase in the ratio 1:1. Further mechanical desintegration with ballotini beads gave rise to soluble D-lactic cytochorme c reductase; very little of the L-enzyme was obtained. Complete extraction was not achieved for any of the two enzymes. It is concluded that one part of the L-activity was more firmly bound to the particulate fraction than the other.

Following the described method [3], three fractions of lactic cytochrome c reductase were obtained [2,4]. Fractions I, II, and III were eluted in that order from a N,N-diethylaminoethyl-cellulose column. Fractions I and II were specific for L-lactic acid. Fraction III was D-specific (D-LDH III). However, small amounts of a L-specific enzyme has now been found in some of the fractions III (L-LDH III).

The D- and the L-enzyme of the cell homogenate were both salt sensitive. The D-enzyme was more salt sensitive than the isolated D-LDH III [2]. The L-enzyme was inhibited 50 % when the phosphate concentration (pH 7.1) was increased from 0.01 to 0.08 μ.

The activity of fractions I and II, which represented most of the L-LDH activity of the purified solution, was quite the same in phosphate of ionic strength 0.01 and 0.08. In contrast, both D- and L-LDH III were inhibited 70—90 % when the buffer concentration was increased from μ 0.01 to 0.08. The inhibition of L-LDH III was the same with low and high concentrations of cytochrome c, whereas the inhibition of D-LDH III was less at high concentrations of the acceptor [2].

The strong effect of salt on L-LDH of the cell homogenate suggests that fair amounts of the salt sensitive enzyme is present in the cell. In this connection it is interesting that L-LDH obtained by the method of Boeri *et al.*[6] is very salt sensitive.

To the authors' knowledge, the effect of salts on D- and L-LDH III is stronger than for any other enzymes described. From other relationships D-lactic cytochrome c reductase has been proposed as intermediate in the formation of the L-enzyme [1,5].

D- and L-LDH III were eluted together with ribonucleic acids [7]. Furthermore, the enzymes precipitated together with nucleic acids when the eluate was dialyzed against water. A charge aggregate between protein and nucleic acid might explain both the salt sensitivity and the high negative charge which these two enzymes have available to the anion exchanger.

1. Nygaard, A. P. *Arch. Biochem. Biophys. In press.*
2. Nygaard, A. P. *Biochim. et Biophys. Acta. In press.*
3. Nygaard, A. P. *Biochim. et Biophys. Acta* **33** (1959) 517.
4. Nygaard, A. P. *Biochim. et Biophys. Acta* **35** (1959) 212.
5. Nygaard, A. P. *Arch. Biochem. Biophys. In press.*
6. Boeri, E. and Tosi, L. *Arch. Biochem. Biophys.* **60** (1956) 463.
7. Nygaard, A. P. *Biochim. et Biophys. Acta* **30** (1958) 450.

Received January 2, 1960.

On the Biosynthesis of the Pigments of *Penicillium islandicum* III

STEN GATENBECK

Institute of Biochemistry, University of Lund, Sweden

PETER BARBESGÅRD

Institute of Genetics, University of Copenhagen, Denmark

In the studies of the biosynthesis of anthraquinones, approximately 50 UV-induced mutants of *Penicillium islandicum* Sopp N.R.R.L. 1036 have been isolated, in the hope that some of the mutants would accumulate an intermediate metabolite because a step in the reaction chain leading to the formation of anthraquinones had been blocked by mutation. The mutants investigated were selected on the basis of their visually abnormal pigment production as compared with the wild type, and a series of strains was obtained varying in colour from pigment-free to dark brown. Paper chromatographic analysis of the pigments of the mycelia and of the aromatic substances occurring in the culture media showed that only variations with respect to the quantities of the normally produced individual substances had been induced by the UV treatment. In the pigment-free mutants no aromatic compounds were detectable with the reagents used.

The principal anthraquinone pigments produced by *P. islandicum* as skyrin, rubroskyrin, iridoskyrin and islandicin, are formed from acetate units by head to tail couplings [1,2] and, despite their close structural relationships, they are not interconvertible *in vivo* but seem to be derived from a common prearomatic stage. The failure to block the formation of any one of these pigments by mutation is in accordance with related findings, published elsewhere [3]. Evidently, the only way to effect a change of the aromate production is to interfere with the acetate condensing enzyme(s) resulting in a general blocking of the aromate production. Consequently, the biogenesis of the anthraquinones should not take place by stepwise formations of defined intermediates such as benzene derivatives, but be dependent throughout on the participating of activated acetate. The increased production of individual pigments has been utilized in investigations published previously [4,5].

Experimental. *Preparation of the mutants.* The culture media used were Czapek-Dox solution (minimal medium) and Czapek-Dox solution supplemented with hydrolyzed casein, B-vitamins, nucleic acid hydrolyzate, Difco malt extract and yeast extract (complete medium). Both media were adjusted to pH 4.5 and 2.5 % Difco agar was added. A suspension of condiaspores in sterile, distilled water was irradiated with a Westinghouse steril-lamp, and then filtered through sterilized filter paper to remove spore clusters and mycelia fragments. The irradiation was done in a small, open petri dish with 5 ml of spore suspension with 10^5 spores per ml. The distance from the UV-lamp was 11.5 cm and the spores were irradiated for 90 sec. After dilution to 10^4 spores per ml, 0.1 ml of the suspension was plated on each of 50 petri dishes containing complete medium. The untreated control was plated on 10 petri dishes, 50 spores per plate. After having grown for 6 days at 28°C, the colonies on the plates were counted, and it was found that the irradiated plates showed, on the average, 1 % survival of the conidiaspores. Among the treated colonies, 50 were selected, which on visual inspection showed an abnormal pigmentation as compared with the wild type. They were transferred to slants of complete medium and each strain was re-isolated by plating on complete medium. From a single colony, spores were transferred to minimum as well as to complete medium to decide whether some of the strains showed different pigmentation when cultivated on the two media. This was not the case.

All the re-isolated strains were grown in culture flasks containing 150 ml of Czapek-Dox liquid medium, two flasks for each strain. These cultures were utilized in the chemical investigations described below.

Chemical analysis of the mutants. The cultures were harvested after two and three weeks' growth, respectively, and the mycelia were separated from the media by filtration. Each mycelium was mechanically disintegrated in 25 ml of acetone, and after centrifugation, 0.5 ml of the supernatant was developed on a paper chromatogram with benzene-formic acid (2 %) (10:1) as the solvent. The pigments were recognized by their R_F values and colour reactions with alcoholic magnesium acetate.

	Skyrin	Rubro-skyrin	Irido-skyrin	Islan-dicin
R_F	0.15	0.25	0.90	0.95
			blue	blue
Colour	violet	green	violet	violet

The relative quantities of the different pigments were visually estimated by a direct comparison with the amounts produced by the wild type.

The culture medium was extracted with ether, the residue after evaporation redissolved in acetone, and one third of the solution used for paper chromatographic analysis. After running in a solvent consisting of chloroform-methanol-formic acid (4 %) (10:1:1) the paper was sprayed with alcoholic ferric chloride, dibromoquinone chloroimide, diazotized sulfanilic acid and phosphomolybdic acid. The culture media of the mutants, with the exception of the pigment-free ones, contained in varying amounts the aromatic compounds normally produced by the wild type.

The only difference observed between the cultures grown for three weeks and two weeks, respectively, was a higher production of the substances investigated in the former.

One of the authors (P.B.) wishes to thank *The Danish State Research Foundation* for financial support.

1. Gatenbeck, S. *Acta Chem. Scand.* **12** (1958) 1211.
2. Gatenbeck, S. *Ibid.* **14** (1960) 102.
3. Gatenbeck, S. *Ibid.* **14** (1960) *In press.*
4. Gatenbeck, S. *Ibid.* **12** (1958) 1985.
5. Gatenbeck, S. *Ibid.* **13** (1959) 386.

Received January 25, 1960.

A Note on Proton Magnetic Resonance Spectra of Alcohols in Carbon Tetrachloride

STURE FORSÉN*

Research Group for NMR, Division of Physical Chemistry, The Royal Institute of Technology, Stockholm 70, Sweden

In the high resolution proton magnetic resonance (PMR) spectra of the pure forms of most primary and secondary alifatic alcohols, the signal from the OH-protons are obtained as multiplets. When such an alcohol, *e.g.* ethanol, is diluted with a nonpolar solvent such as *cyclo*hexane or *per*--deuterocyclohexane, the OH-triplet is found to persist down to concentrations where the noise level no longer permits observations. The addition of small amounts of carbon tetrachloride to pure ethanol, however, changes the triplet into a sharp singlet [1]. This is rather unexpected since carbon tetrachloride is generally assumed to be about as nonpolar as *cyclo*hexane. We have, however, found that if commercially available carbon tetrachloride of *pro analysi* quality, which in mixtures with ethanol produces OH-singlets, was first washed with a 0.01 M solution of sodium hydroxide and then with three or four portions of water and thereafter kept away from direct or indirect sunlight, the addition of this product to a purified alcohol, *e.g.* ethanol, did not affect the splitting of the OH-signal, *i.e.* this signal was displayed as a triplet down to concentrations where the noise level no longer permitted direct observations (mole fraction alcohol *ca.* 0.02). In Fig. 1 the PMR spectrum at mole fraction alcohol 0.1 is shown (*cf.* PMR spectrum in Ref.[1], p. 3).

Exposure of a mixture of ethanol and purified carbon tetrachloride (mole fraction alcohol 0.8) to ultraviolet light or sunlight 5—30 sec. was, however, found to be sufficient to produce a sharp OH-singlet from the triplet. The extreme sen-

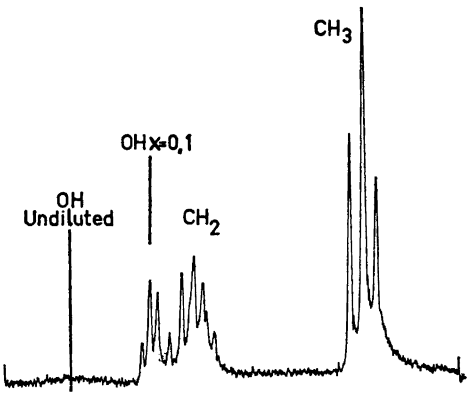

Fig. 1. PMR spectrum of ethanol in carbon tetrachloride purified according to text. Mole-fraction ethanol = 0.1. The position of the OH-triplet in pure ethanol is indicated (*cf.* spectrum in Ref.[1], p. 3).

* Present address: Atomic Energy Department, ASEA, Västerås, Sweden.

	Skyrin	Rubro-skyrin	Irido-skyrin	Islan-dicin
R_F	0.15	0.25	0.90	0.95
			blue	blue
Colour	violet	green	violet	violet

The relative quantities of the different pigments were visually estimated by a direct comparison with the amounts produced by the wild type.

The culture medium was extracted with ether, the residue after evaporation redissolved in acetone, and one third of the solution used for paper chromatographic analysis. After running in a solvent consisting of chloroform-methanol-formic acid (4 %) (10:1:1) the paper was sprayed with alcoholic ferric chloride, dibromoquinone chloroimide, diazotized sulfanilic acid and phosphomolybdic acid. The culture media of the mutants, with the exception of the pigment-free ones, contained in varying amounts the aromatic compounds normally produced by the wild type.

The only difference observed between the cultures grown for three weeks and two weeks, respectively, was a higher production of the substances investigated in the former.

One of the authors (P.B.) wishes to thank *The Danish State Research Foundation* for financial support.

1. Gatenbeck, S. *Acta Chem. Scand.* **12** (1958) 1211.
2. Gatenbeck, S. *Ibid.* **14** (1960) 102.
3. Gatenbeck, S. *Ibid.* **14** (1960) *In press.*
4. Gatenbeck, S. *Ibid.* **12** (1958) 1985.
5. Gatenbeck, S. *Ibid.* **13** (1959) 386.

Received January 25, 1960.

A Note on Proton Magnetic Resonance Spectra of Alcohols in Carbon Tetrachloride

STURE FORSÉN*

Research Group for NMR, Division of Physical Chemistry, The Royal Institute of Technology, Stockholm 70, Sweden

In the high resolution proton magnetic resonance (PMR) spectra of the pure forms of most primary and secondary alifatic alcohols, the signal from the OH-protons are obtained as multiplets. When such an alcohol, *e.g.* ethanol, is diluted with a nonpolar solvent such as *cyclo*hexane or *per*--deuterocyclohexane, the OH-triplet is found to persist down to concentrations where the noise level no longer permits observations. The addition of small amounts of carbon tetrachloride to pure ethanol, however, changes the triplet into a sharp singlet [1]. This is rather unexpected since carbon tetrachloride is generally assumed to be about as nonpolar as *cyclo*hexane. We have, however, found that if commercially available carbon tetrachloride of *pro analysi* quality, which in mixtures with ethanol produces OH-singlets, was first washed with a 0.01 M solution of sodium hydroxide and then with three or four portions of water and thereafter kept away from direct or indirect sunlight, the addition of this product to a purified alcohol, *e.g.* ethanol, did not affect the splitting of the OH-signal, *i.e.* this signal was displayed as a triplet down to concentrations where the noise level no longer permitted direct observations (mole fraction alcohol *ca.* 0.02). In Fig. 1 the PMR spectrum at mole fraction alcohol 0.1 is shown (*cf.* PMR spectrum in Ref.[1], p. 3).

Exposure of a mixture of ethanol and purified carbon tetrachloride (mole fraction alcohol 0.8) to ultraviolet light or sunlight 5—30 sec. was, however, found to be sufficient to produce a sharp OH-singlet from the triplet. The extreme sen-

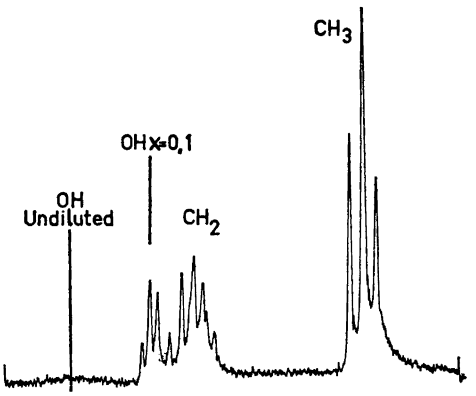

Fig. 1. PMR spectrum of ethanol in carbon tetrachloride purified according to text. Mole-fraction ethanol = 0.1. The position of the OH-triplet in pure ethanol is indicated (*cf.* spectrum in Ref.[1], p. 3).

* Present address: Atomic Energy Department, ASEA, Västerås, Sweden.

sitivity towards hydrochloric acid of the shape of the OH-signal from ethanol, as shown by Arnold [2], would indicate that small amounts of hydrochloric acid are formed photolytically in the solution and that this is the cause of the observed alteration in the OH-signal. Further evidence for this assumption is the fact that careful addition of minute amounts of alkali to a irradiated mixture of ethanol and carbon tetrachloride brought back the OH-triplet which, upon further irradiation of the mixture, again turned to a singlet.

In addition, another observation of interest was made. When a small amount of water was added to a mixture of ethanol and carbon tetrachloride (mole fraction ethanol 0.85; water 0.05) a separate water line could be seen in the PMR spectrum to the high field side of the OH-triplet. The mixture was then irradiated for a few seconds in ultraviolet light and the PMR spectrum now revealed a complete coalescence of the water and OH-signals into one broad signal. This coalescence is normally only observed at much higher concentrations of water (mole fraction water 0.40—0.50) [3]. Careful addition of a small amount alkali made the coalesced line again separate into a OH-triplet and a separate water line. Repetition of the procedure revealed the coalescence and the separation to be completely reversible. The observation is clearly in line with the suggestion that hydrochloric acid accelerates the proton exchange in ethanol.[2]

From the observation in Ref.[1] and our own dilution experiments with commercial, unwashed carbon tetrachloride, it would appear that small amounts of hydrochloric acid are usually present in the commercial product (for an exception see Ref.[4]).

Carbon tetrachloride purified according to above should be a convenient nonpolar solvent when spin-coupling effects are to be studied in dilute solutions in which the effect of the proton exchange between the OH-groups is reduced.

The spectrometer used in this work is a Varian 4300 B NMR Spectrometer operated at 40 Mc and equipped with a V-K 3506 Flux Stabilizer.

The author wishes to thank the head of the Division, Professor Ole Lamm, Dr Torbjörn Westermark who orginally suggested this work, and the head of the NMR Group, Dr Erik Forslind, for many stimulating discussions at the blackboard.

1. Becker, E. D., Liddel, U. and Shoolery, J. N. *J. Mol. Spectroscopy* **2** (1958) 1.
2. Arnold, J. T. *Phys. Rev.* **102** (1956) 136.
3. Weinberg, I. and Zimmerman, J. R. *J. Chem. Phys.* **23** (1955) 748.
4. Saunders, M. and Hyne, J. B. *J. Chem. Phys.* **29** (1958) 1319.

Received January 25, 1960.

ACTA CHEMICA SCANDINAVICA 14 (1960) 233–246

Adenosine Triphosphatase Activity in Chloroplasts

J. S. C. WESSELS

Philips Research Laboratories, N. V. Philips' Gloeilampenfabrieken, Eindhoven, Netherlands

and

HERRICK BALTSCHEFFSKY

Wenner-Gren Institute, University of Stockholm, Sweden

The ATP-ase * activity of isolated spinach chloroplasts has been studied. Two distinct systems with ATP-ase activity are observed in this material. They are different in their pH optima and their response to $MgCl_2$ and chlorpromazine.

At pH 7.5 the ATP-ase activity is rather constant in different chloroplast preparations. It is strongly stimulated by $MgCl_2$ and inhibited by chlorpromazine. The pyrophosphatase activity at pH 7.5 is very low under the conditions of the ATP-ase activity measurements. Thus it can be excluded that the release of phosphate from ATP at pH 7.5 involves a liberation and a subsequent hydrolysis of inorganic pyrophosphate. Dinitrophenol does not stimulate the ATP-ase activity, either in intact or in broken chloroplasts.

At pH 5.5 a variable ATP-ase activity is found. It is unaffected by $MgCl_2$ and chlorpromazine and parallels the pyrophosphatase activity at this pH.

Results of kinetic experiments on the Mg^{++}-stimulated ATP-ase activity of spinach chloroplasts are given.

It is discussed whether the ATP-ase activity of chloroplasts has a functional relationship to the enzymatic mechanism by which phosphorylation of ADP is coupled to electron transport during light-induced phosphorylation.

ATP-ase activity becomes evident in rat liver mitochondria when either DNP is added or their structure is disrupted in some way, *e.g.* by making the mitochondrial suspension hypotonic, by ageing, or by treatment with detergents [1–7]. Addition of Mg^{++}-ions stimulates the ATP-ase activity of disrupted mitochondria. DNP-induced ATP-ase activity is obtained in mito-

* Abbreviations: AMP, adenosine monophosphate; ADP, adenosine diphosphate; ATP, adenosine triphosphate; ATP-ase, adenosine triphosphatase; FMN, flavin mononucleotide; FAD, flavinadenine dinucleotide; DNP, 2,4-dinitrophenol; P, inorganic phosphate; PP, inorganic pyrophosphate; Tris, tris(hydroxy-methyl)-aminomethane.

chondria when they are in an "intact" state and disappears when the mitochondria lose their structural integrity. The disappearance of the "intact" mitochondrial structure, involving a loss of the capability to carry out oxidative phosphorylation and of the stimulation of ATP-ase activity with DNP, is concomitant with the development of Mg^{++}-stimulated ATP-ase activity [7].

ATP-ase activity of animal mitochondria is supposed to be a reversal of part of the reaction sequence involved in ATP formation by oxidative phosphorylation [5, 7-15]. The Mg^{++}-activated ATP-ase may involve a one-step transfer of phosphate from ATP to an unknown carrier, followed by a hydrolysis of the compound so formed, whereas the DNP-activated ATP-ase may consist of two consecutive transfer steps, one identical with that involved in the Mg^{++}-activated ATP-ase, and a second yielding a high-energy compound which is subsequently split due to the presence of DNP [7].

Arnon [16] has reported that chloroplasts seem to be rather free of ATP-hydrolyzing enzymes. Avron and Jagendorf [17-18] did not observe any ATP-ase activity in chloroplasts under a large variety of conditions. Baltscheffsky [19], on the other hand, has recently shown that chloroplasts exhibit ATP-ase activity in the presence of added Mg^{++}-ions.

In this paper detailed results of our studies on the ATP-ase activity of spinach chloroplasts are presented. Attention has been directed towards the possibility that this activity is an expression of reversed reactions in light-induced phosphorylation and that information may be obtained about a possible similarity between the mechanisms for generation of ATP in oxidative phosphorylation and in light-induced phosphorylation.

METHODS

Broken spinach chloroplasts were prepared according to the method of Wessels [20]. As no significant difference in ATP-ase activity was found between once washed and four times washed chloroplasts (the activity decreased only 10 % after four washings), they were washed only once. The chlorophyll content of the chloroplast suspension was determined by the method of Arnon [21].

ATP-ase activity was measured by estimating colorimetrically the inorganic phosphate liberated from ATP. The incubation medium, containing ATP and $MgCl_2$ as indicated in the individual experiments, and distilled water to bring the volume up to 1.5 ml, was warmed to 30°. Then 1 ml of a suspension of chloroplasts in 0.1 M Tris buffer, previously warmed rapidly to 30°, was added with stirring. The contents of the tube were incubated in the dark at 30°. The reaction was stopped by the addition of 2 ml of the reaction mixture to 4 ml of ice-cold 9 % trichloroacetic acid. After filtering an aliquot (3 ml) was taken for the estimation of inorganic phosphate by the method of Fiske and Subbarow [22]. The amount of phosphate split from ATP was determined by subtracting (from the values obtained) the phosphate content of a reaction mixture of the same composition, in which the reaction had been quenched directly after the mixture had been made up.

In the pyrophosphatase activity measurements, ATP was replaced by sodium pyrophosphate. Both the ATP and the pyrophosphate solutions were brought to the pH desired in the experiment before being added to the reaction mixture.

ATP, ADP, AMP, FMN and FAD were products of the Sigma Chemical Company.

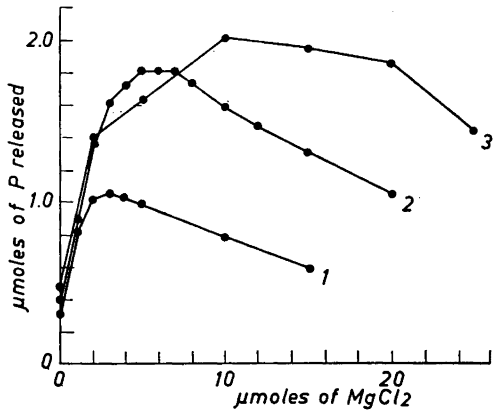

Fig. 1. ATP-ase activity as a function of $MgCl_2$ concentration. The reaction mixture contained, in addition to $MgCl_2$, 5 µmoles of ATP (1), 10 µmoles of ATP (2) or 20 µmoles of ATP (3), and 1 ml of a suspension of chloroplasts in 0.1 M Tris buffer pH 7.5, containing 0.5 mg chlorophyll. Reaction time, 20 min at 30°.

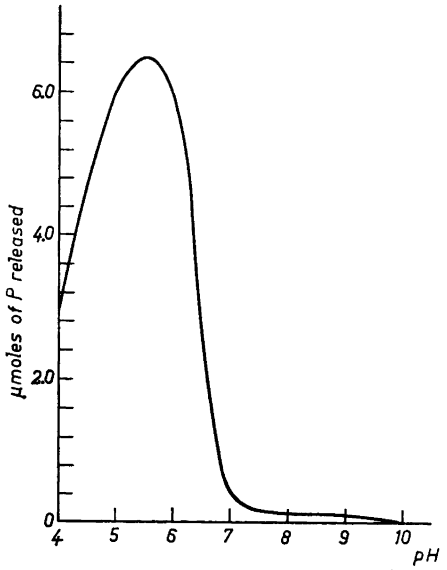

Fig. 2. Effect of pH on ATP-ase activity in the absence of $MgCl_2$. Reaction mixture: 10 µmoles of ATP and 1 ml of a suspension of chloroplasts in 0.1 M buffer, containing 0.5 mg chlorophyll. Reaction time, 15 min at 30°.

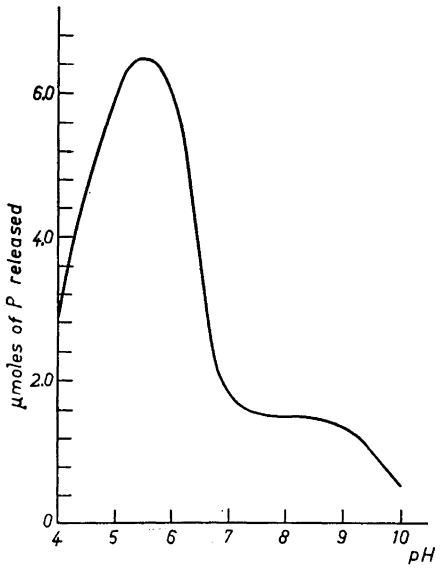

Fig. 3. Effect of pH on ATP-ase activity in the presence of $MgCl_2$. Reaction mixture: 10 µmoles of ATP, 5 µmoles of $MgCl_2$ and 1 ml of a suspension of chloroplasts in 0.1 M buffer, containing 0.5 mg chlorophyll. Reaction time, 15 min at 30°.

RESULTS

Fig. 1 confirms the finding of Baltscheffsky [19] that isolated spinach chloroplasts exhibit a Mg^{++}-dependent ATP-ase activity at pH 7.5. The optimal $MgCl_2$ concentration is 0.5—0.7 times the concentration of ATP.

Figs. 2 and 3 show the dependence of ATP-ase activity on pH in the absence and in the presence of added $MgCl_2$. As buffers we used glycine-NaOH (pH 8.5—10), Tris-HCl (pH 7—9), Tris-maleate-NaOH (pH 5.2—8.6) and phthalate-NaOH (pH 4—6). If possible, measurements were performed with two or more different buffers at each pH so as to prevent errors due to the effect of the buffer on the ATP-ase activity.

It must be stressed that the height of the maximum at pH 5.5 was found to be variable, ranging from one to six times the activity at pH 7.5. The amount of ATP split per unit time per unit chlorophyll at pH 7.5, on the other hand, was nearly constant, *viz.* 8—12 μmoles/h/mg chlorophyll. The ATP-ase activity at pH 5.5 was particularly high in chloroplasts from spinach grown in a greenhouse. The maximum at pH 5.5 cannot be ascribed to an impurity of the particular chloroplast preparation, because it did not disappear either after more washings or after digitonin treatment of the chloroplasts. In the latter case the chloroplasts were suspended in a 1 % digitonin solution. The suspension was allowed to stand for 30 min at 0°, and was then centrifuged for 7 min at 1 000 × *g*. The residue was discarded and the supernatant centrifuged for 30 min at 20 000 × *g*. The precipitated chloroplast fragments

Table 1. ATP-ase activity of two chloroplast preparations having extremely high (A) and extremely low (B) activity at pH 5.5 as compared to the ATP-ase activity at pH 7.5.

Chloroplast preparation	Additions (μmoles), unless otherwise indicated	pH	μmoles of P released
A	10 ATP	5.5	8.4
A	10 ATP + 5 $MgCl_2$	5.5	8.6
A	10 ATP + 5 × 10^{-4} M chlorpromazine	5.5	8.4
A	10 ATP + 5 $MgCl_2$ + 5 × 10^{-4} M chlorpromazine	5.5	8.3
B	10 ATP	5.5	1.1
B	10 ATP + 5 $MgCl_2$	5.5	1.6
B	10 ATP + 5 × 10^{-4} M chlorpromazine	5.5	1.1
B	10 ATP + 5 $MgCl_2$ + 5 × 10^{-4} M chlorpromazine	5.5	1.1
A or B	10 ATP	7.5	0.26
A or B	10 ATP + 5 $MgCl_2$	7.5	1.5
A or B	10 ATP + 5 × 10^{-4} M chlorpromazine	7.5	0.11
A or B	10 ATP + 5 $MgCl_2$ + 2 × 10^{-3} M chlorpromazine	7.5	0.20
A or B	10 ATP + 5 $MgCl_2$ + 5 × 10^{-4} M chlorpromazine	7.5	0.44
A or B	10 ATP + 5 $MgCl_2$ + 2 × 10^{-4} M chlorpromazine	7.5	0.89
A or B	10 ATP + 5 $MgCl_2$ + 6 × 10^{-5} M chlorpromazine	7.5	1.2

Chlorophyll concentration, 0.5 mg per sample. Reaction time, 15 min at 30°. The data for "A or B" represent a mean value obtained with a great number of chloroplast preparations of type A or B and of intermediate type. At pH 7.5 no significant difference was found between the mean values for the different types.

Table 2. Effect of inhibitors on ATP-ase activity.

Additions (μmoles), unless otherwise indicated	pH	μmoles of P released
10 ATP + 5 $MgCl_2$	7.5	1.4
10 ATP + 5 $MgCl_2$ + 10 ADP	7.5	1.0
10 ATP + 5 $MgCl_2$ + 10 AMP	7.5	0.88
10 ADP	7.5	0.28
10 ADP + 5 $MgCl_2$	7.5	0.50
10 ADP + 5 $MgCl_2$ + 2×10^{-4} M chlorpromazine	7.5	0.29
10 AMP + 5 $MgCl_2$	7.5	0.02
10 ATP	7.5	0.31
10 ATP + 3×10^{-4} M DNP	7.5	0.30
10 ATP + 5 $MgCl_2$	7.5	1.3
10 ATP + 5 $MgCl_2$ + 6×10^{-5} M DNP	7.5	1.3
10 ATP + 5 $MgCl_2$ + 3×10^{-4} M DNP	7.5	1.3
10 ATP + 5 $MgCl_2$ + 0.01 M KCN	7.5	1.3
10 ATP + 5 $MgCl_2$ + 2 FMN	7.5	1.4
10 ATP + 5 $MgCl_2$ + 10 FMN	7.5	1.4
10 ATP + 5 $MgCl_2$ + 0.01 M NaF	7.5	0.59
10 ATP + 5 $MgCl_2$ + 10^{-4} M *p*-chloromercuribenzoate	7.5	0.49
10 ATP + 5 $MgCl_2$ + 10^{-3} M $Na_2S_2O_4$	7.5	1.9
10 ATP + 5 $MgCl_2$ + 10^{-3} M $Na_2S_2O_4$ + 10^{-3} M KCN	7.5	1.9
10 ATP + 5 $MgCl_2$ + 5×10^{-3} M NaN_3	7.5	0.60
10 ATP + 5 $MgCl_2$ + 10^{-3} M $(NH_4)_2SO_4$	7.5	1.3
10 ATP + 5 $MgCl_2$ + 0.01 M succinate	7.5	1.3
10 ATP + 5 $MgCl_2$ + 5×10^{-3} M atebrin	7.5	0.78
10 ATP + 5 $MgCl_2$ + 0.03 M arsenate	7.5	0.91
10 ATP + 5 $MgCl_2$ + 10 P	7.5	1.1
10 ATP	5.5	5.0
10 ATP + 3×10^{-4} M DNP	5.5	5.0
10 ATP + 5 $MgCl_2$	5.5	5.4
10 ATP + 5 $MgCl_2$ + 3×10^{-4} M DNP	5.5	5.2

Chlorophyll concentration, 0.5 mg per sample. Reaction time, 15 min at 30°.

were resuspended in buffer and diluted to a concentration of 0.5 mg of chlorophyll/ml.

The ATP-ase activities at pH 5.5 and pH 7.5 differed with respect to their response to $MgCl_2$ and chlorpromazine. At pH 5.5 both $MgCl_2$ and chlorpromazine had only a slight effect, especially when the activity was high. At pH 7.5, on the other hand, the ATP-ase activity could be raised 4—10 fold by adding $MgCl_2$ to the reaction mixture. Addition of chlorpromazine resulted in inhibition at pH 7.5, which could not be reversed by FMN or FAD. In Table 1 two extreme types of results obtained with various chloroplast preparations are given:

a) High ATP-ase activity at pH 5.5, showing low response to $MgCl_2$ and chloropromazine as compared to the ATP-ase activity at pH 7.5.

b) Low ATP-ase activity at pH 5.5, showing stimulation by $MgCl_2$ and inhibition by chlorpromazine in the presence of $MgCl_2$.

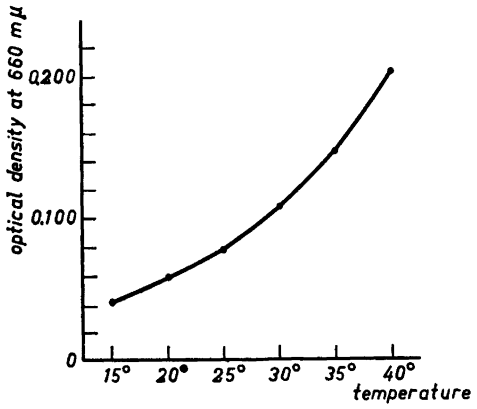

Fig. 4. Effect of temperature on ATP-ase activity (expressed as optical density at 660 mμ). The reaction mixture contained: 10 μmoles of ATP, 5 μmoles of $MgCl_2$ and 1 ml of a suspension of chloroplasts in 0.1 Tris buffer pH 7.5, containing 0.5 mg chlorophyll. Reaction time, 20 min.

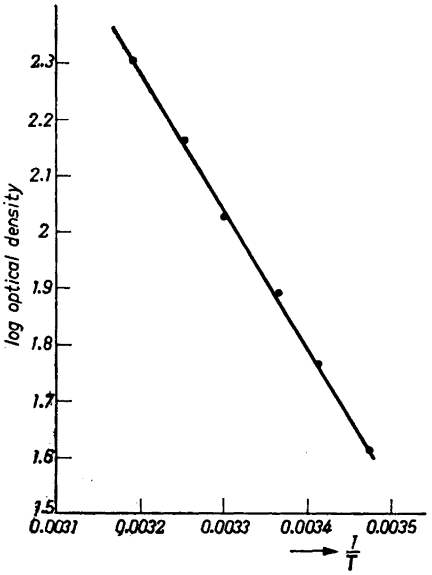

Fig. 5. Arrhenius plot of data of Fig. 4.

Other chloroplast preparations gave results intermediate between those represented in Table 1. The results indicate that chloroplasts contain two enzymes (or enzyme systems) having ATP-ase activity. One enzyme (system) is present in chloroplasts in a rather constant amount, has a broad pH optimum, is strongly stimulated by $MgCl_2$ and inhibited by chlorpromazine. The content of the other enzyme (system) varies in different chloroplast preparations. This enzyme (system) has a pH optimum of 5.5, is not stimulated by $MgCl_2$ and is resistant to chlorpromazine.

As shown in Table 2, ATP-ase activity at pH 7.5 is inhibited by AMP, fluoride, *p*-chloromercuribenzoate, azide, atebrin, arsenate and phosphate. The inhibition by ADP is variable. $(NH_4)_2SO_4$, DNP and KCN had no effect, whereas addition of FMN caused a slight stimulation. A marked stimulation of the ATP-ase activity was observed upon addition of dithionite to the reaction mixture.

Chloroplasts were found to release inorganic phosphate from ADP, but not from AMP. The liberation of inorganic phosphate from ADP at pH 7.5, like the splitting of ATP, was stimulated by $MgCl_2$ and inhibited by chlorpromazine. The release of inorganic phosphate from ADP, the rate of which varied between 20 and 80 % of that of the splitting of ATP, is probably due to the myokinase activity of the chloroplasts. Mazelis [23] has shown that spinach chloroplasts have a high myokinase activity.

It should be noted that with whole chloroplasts similar results were obtained as with broken ones, and that no stimulating effect of DNP could be observed.

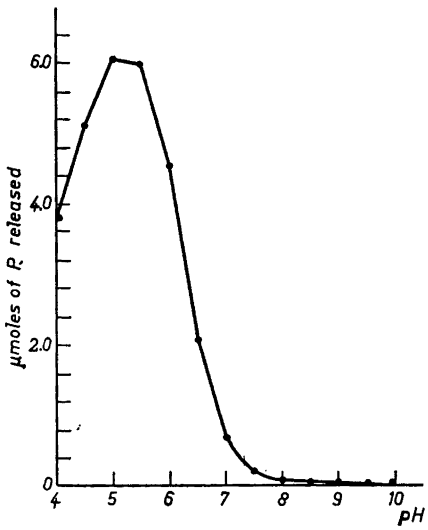

Fig. 6. Effect of pH on pyrophosphatase activity in the absence of $MgCl_2$. Reaction mixture: 10 µmoles of sodium pyrophosphate and 1 ml of a suspension of chloroplasts in 0.1 M buffer, containing 0.5 mg chlorophyll. Reaction time, 15 min at 30°.

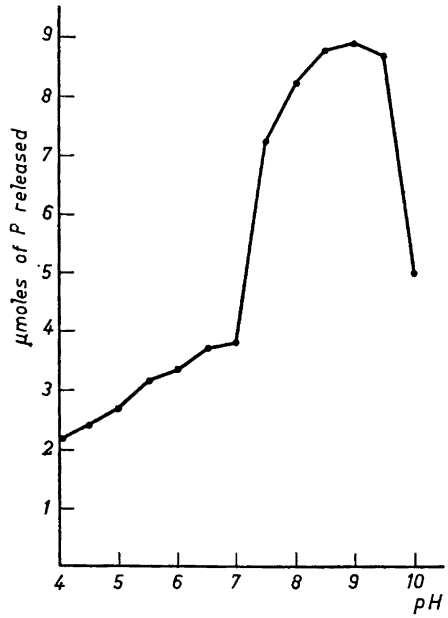

Fig. 7. Effect of pH on pyrophosphatase activity in the presence of $MgCl_2$. Reaction mixture: 10 µmoles of sodium pyrophosphate, 50 µmoles of $MgCl_2$ and 1 ml of a suspension of chloroplasts in 0.1 M buffer, containing 0.5 mg chlorophyll. Reaction time, 10 min at 30°.

An increase in temperature resulted in an acceleration of ATP-ase activity (Fig. 4). Fig. 5 shows that a straight line is obtained on plotting the logarithm of the reaction velocity against the reciprocal of the absolute temperature. The value of the activation energy was calculated from the slope and was found to be about 11 500 cal over the temperature range studied.

In order to test whether the cleavage of ATP could be due to apyrase activity, we have investigated the pyrophosphatase activity of spinach chloroplasts at different pH's. Chloroplasts were found to contain two pyrophosphatases which can be distinguished by pH optima and response to $MgCl_2$. One enzyme has a pH optimum of 5.0—5.5 and does not require Mg^{++}. The other enzyme has a pH optimum of 8.5—9.0 and a requirement for high concentrations of added $MgCl_2$ (Figs. 6 and 7; Table 3). These results resemble those of Naganna *et al.*[24] who have reported that green leaves contain both an acid pyrophosphatase and an alkaline pyrophosphatase, the latter being active only in the presence of $MgCl_2$. The pyrophosphatases were found to be insensitive to 5×10^{-4} M chlorpromazine.

The pyrophosphatase activity at pH 5.5 was sufficient to account for the ATP-ase activity of chloroplasts at this pH. This possibility is supported by

Table 3. Pyrophosphatase activity of spinach chloroplasts.

Additions (μmoles), unless otherwise indicated	pH	μmoles of P released
10 ATP	5.5	6.1
10 ATP + 5 $MgCl_2$	5.5	6.0
10 ATP + 30 $MgCl_2$	5.5	4.5
10 PP	5.5	12
10 PP + 5 $MgCl_2$	5.5	11
10 PP + 30 $MgCl_2$	5.5	7.8
10 PP + 5×10^{-4} M chlorpromazine	5.5	12
10 ATP	7.5	0.29
10 ATP + 5 $MgCl_2$	7.5	1.5
10 ATP + 30 $MgCl_2$	7.5	1.2
10 PP	7.5	0.18
10 PP + 5 $MgCl_2$	7.5	0.24
10 PP + 10 $MgCl_2$	7.5	0.81
10 PP + 20 $MgCl_2$	7.5	5.7
10 PP + 30 $MgCl_2$	7.5	8.5
10 PP + 40 $MgCl_2$	7.5	8.9
10 PP + 50 $MgCl_2$	7.5	9.1
10 PP + 30 $MgCl_2$ + 5×10^{-4} M chlorpromazine	7.5	9.0
10 ATP *	5.5	2.9
10 ATP + 10 PP *	5.5	6.6
10 PP *	5.5	6.5

Chlorophyll concentration, 0.5 mg per sample.

our finding that there exists a correlation between pyrophosphatase activity and ATP-ase activity at pH 5.5 in different chloroplast preparations. As a rule the amount of inorganic phosphate released from pyrophosphate was found to be about twice that split from ATP at pH 5.5. As shown in Table 3, addition of ATP did not increase the release of inogranic phosphate from pyrophosphate at pH 5.5.

At pH 7.5, however, the pyrophosphatase activity of spinach chloroplasts in the presence of 5 μmoles of $MgCl_2$ is much lower than the ATP-ase activity. The amount of inorganic phosphate formed by cleavage of pyrophosphate was found to be 10—20 % of the amount split from ATP by the same chloroplast preparation. This indicates that the splitting of ATP at pH 7.5 does not proceed by way of an apyrase, but is caused by a true ATP-ase activity.

KINETICS OF THE ATP-ase ACTIVITY AT pH 7.5

Fig. 8 represents the increase of inorganic phosphate as a function of time in a medium containing 10 μmoles of ATP, 5 μmoles of $MgCl_2$ and 1 ml of a suspension of chloroplasts in 0.1 M Tris buffer, pH 7.5, (0.5 mg chlorophyll). It

* 0.2 mg of chlorophyll per sample. Reaction time, 15 min at 30°.

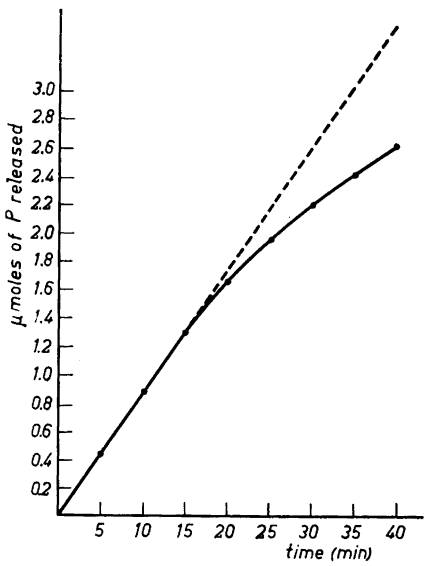

Fig. 8. ATP-ase activity as a function of time. The reaction mixture contained: 10 μmoles of ATP, 5 μmoles of $MgCl_2$ and 1 ml of a suspension of chloroplasts in 0.1 M Tris buffer pH 7.5, containing 0.5 mg chlorophyll. Temperature 30°.

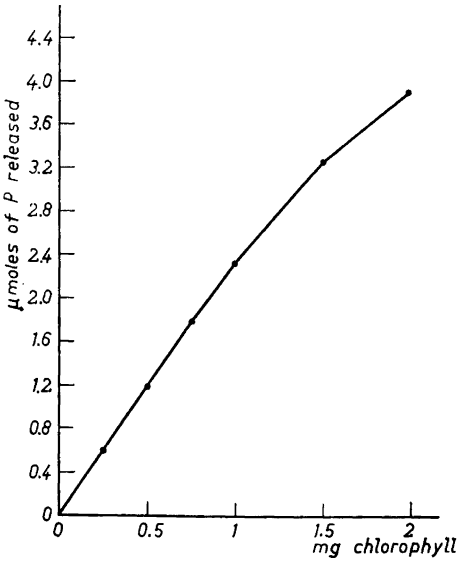

Fig. 9. Effect of varying the amount of chloroplast preparation on the ATP-ase activity. The reaction mixture contained: 10 μmoles of ATP, 5 μmoles of $MgCl_2$ and 1 ml of a suspension of chloroplasts in 0.1 M Tris buffer pH 7.5. Reaction time, 15 min at 30°.

is seen that the reaction rate is constant during the first 15 min of the reaction. In some preparations constancy has been obtained for more than 30 min. As shown in Fig. 9, the rate of ATP cleavage is proportional to the chlorophyll concentration up to 1 mg chlorophyll per sample.

In Fig. 10 the effect of ATP concentration on the velocity of ATP-ase activity is presented, showing the general type of curve obtained with enzyme reactions. For each concentration of ATP the optimal concentration of $MgCl_2$ was added, *viz.* μmoles ATP: μmoles $MgCl_2$ = 2:1. In Fig. 11 the reciprocal of the ATP concentration was plotted against the reciprocal of the rate of production of inorganic phosphate (expressed as optical density at 660 mμ) according to the method of Lineweaver and Burk [25]. The Michaelis constant was calculated from the intercept on the extended 1/S axis and was found to be 1.2×10^{-3} M.

Fig. 12 illustrates the effect of temperature on the maximum velocity (V_{max}) of ATP cleavage, which was calculated from the intercept on the $1/v$ axis of Lineweaver-Burk plots at different temperatures. When log V_{max} is plotted against the reciprocal of the absolute temperature ($1/T$) a straight line is obtained (Fig. 13). The value of the activation energy was calculated from the slope and was found to be 12 800 cal over the temperature range studied. We were unable to study the inhibition of ATP-ase activity by ADP

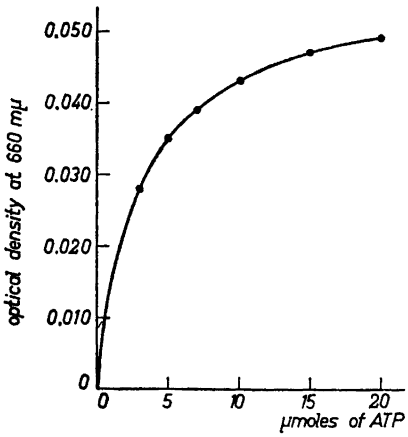

Fig. 10. Effect of ATP concentration on ATP-ase activity (expressed as optical density at 660 mμ). The reaction mixture contained, in addition to ATP, $MgCl_2$ (μmoles $MgCl_2$: μmoles ATP = 1:2) and 1 ml of a suspension of chloroplasts in 0.1 M Tris buffer pH 7.5, containing 0.5 mg chlorophyll. Reaction time, 10 min at 30°.

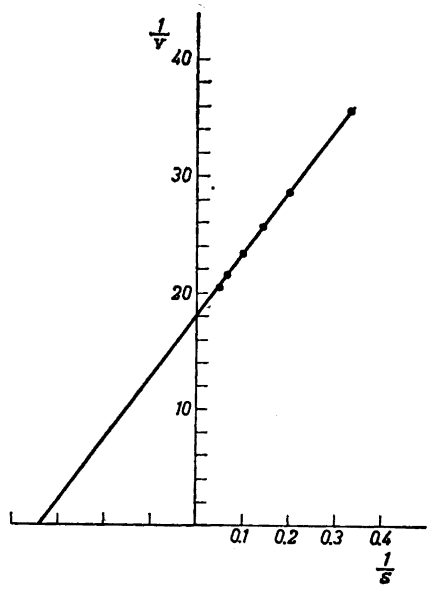

Fig. 11. Lineweaver-Burk plot of the data of Fig. 10. Reciprocal of ATP concentration (1/S) *vs.* reciprocal of optical density at 660 mμ (1/*v*).

kinetically, because of the myokinase activity of the chloroplasts. A kinetic investigation of the inhibition by AMP, on the other hand, was quite possible. Fig. 14 represents the rate of ATP cleavage as a function of ATP concentration in the presence and in the absence of 10 μmoles of AMP. When these data are plotted as 1/*v* against 1/S, as illustrated in Fig. 15, the slope but not the intercept with the 1/*v* axis is found to increase upon addition of AMP. This indicates that AMP inhibits the ATP-ase activity competitively.

DISCUSSION

Lehninger *et al.*[26] have postulated the following reaction scheme for oxidative phosphorylation in mitochondria:

$$\text{Carrier}_{red} + X \longrightarrow \text{Carrier}_{ox} \sim X + 2\ e \quad (1)$$

$$\text{Carrier}_{ox} \sim X + P \rightleftharpoons \text{Carrier}_{ox} + P \sim X \quad (2)$$

$$P \sim X + ADP \rightleftharpoons ATP + X \quad (3)$$

X is an enzyme capable of undergoing reversible phosphorylation. This type of scheme is rather widely accepted, at least as a framework for a general reaction mechanism (recently, however, the necessity of an X-compound between the electron carrier and P has been questioned by Löv *et al.*[27]). The DNP-induced ATP-ase reaction is assumed to involve the splitting of ATP

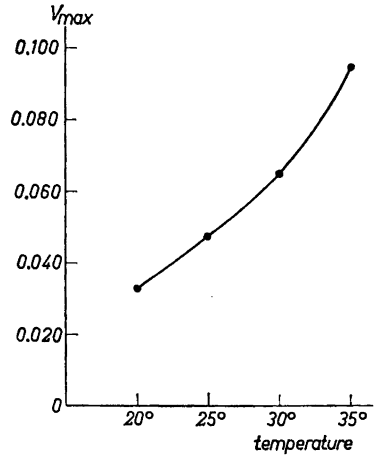

Fig. 12. Effect of temperature on the maximum velocity of ATP cleavage (expressed as optical density at 660 mμ). V_{max} was calculated from Lineweaver-Burk plots at 20, 25, 30 and 35°. The reaction mixture contained, in addition to ATP and $MgCl_2$ in a ratio of 2:1, 1 ml of a suspension of chloroplasts in 0.1 M Tris buffer pH 7.5, containing 0.7 mg chlorophyll. Reaction time, 10 min.

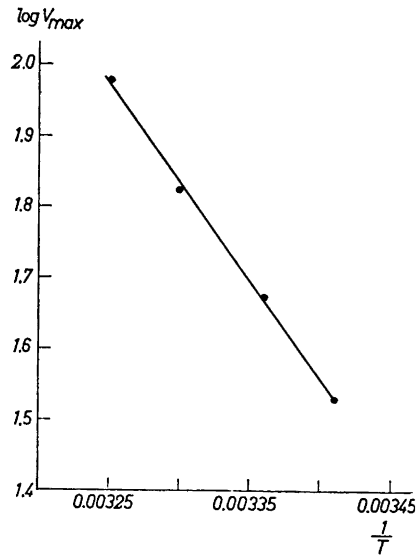

Fig. 13. Arrhenius plot of data of Fig. 12.

by reversal of reactions (3) and (2), followed by a rapid hydrolytic decomposition of $carrier_{ox} \sim X$. Siekevitz *et al.*[7] obtained data supporting the conclusion that the mitochondrial Mg^{++}-activated ATP-ase reaction constitutes a part of the reaction sequence involved in the DNP-induced ATP-ase and is not due to a separate enzyme. The finding by Kielley and Bronk [28] that DNP stimulates ATP-ase activity in phosphorylating fragments of rat liver mitochondria only in the presence of Mg^{++} is in agreement with this view. The Mg^{++}-activated ATP-ase reaction may be a reversal of reaction (3), followed by decomposition of $P \sim X$.

Our results indicate that chloroplasts exhibit two systems with ATP-hydrolyzing activity, one of which is dependent on added Mg^{++}. Contrary to the results obtained with "intact" liver mitochondria, the phosphorylating whole spinach chloroplasts isolated by us consistently show Mg^{++}-stimulated ATP-ase activity. In this respect they resemble phosphorylating heart muscle mitochondria, which are isolated according to Holton *et al.*[29] and are reported to always have a moderately high ATP-ase activity. It is an open question whether the Mg^{++}-stimulated ATP-ase activity should be regarded as an expression of damage in the isolated chloroplasts or as an inherent property of the system. In liver mitochondria the development of Mg^{++}-stimulated ATP-ase activity is paralleled by a loss of the capability to carry out oxidative phosphorylation. In chloroplasts, on the other hand, the Mg^{++}-

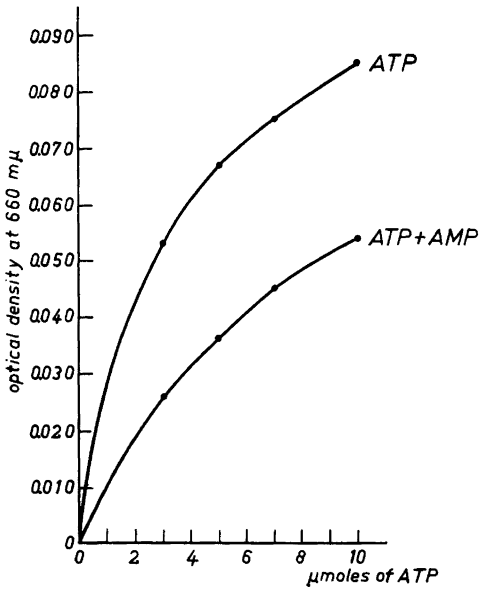

Fig. 14. Inhibition of ATP-ase activity by AMP. Reaction rate (expressed as optical density at 660 mμ) as a function of ATP concentration in the absence and in the presence of 10 μmoles of AMP. The reaction mixture contained, in addition to ATP and $MgCl_2$ in a ratio of 2:1, 1 ml of a suspension of cloroplasts in 0.1 M Tris buffer pH 7.5, containing 0.8 mg chlorophyll. Reaction time, 10 min at 30°.

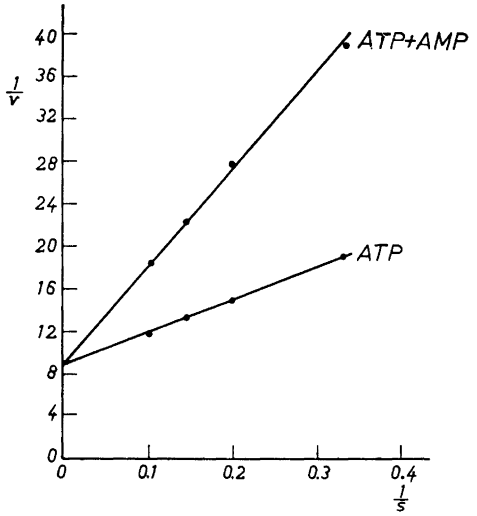

Fig. 15. Lineweaver-Burk plot of the data of Fig. 14, illustrating competitive inhibition of ATP-ase activity by AMP. Reciprocal of ATP concentration (1/S) *vs.* reciprocal of optical density at 660 mμ (1/*v*).

stimulated ATP-ase activity does not increase as light-induced phosphorylation falls off.

Light-induced phosphorylation is not much inhibited by low concentrations of DNP, in contrast to oxidative phosphorylation [30-33]. In fact it was found that DNP can catalyze the generation of ATP by illuminated chloroplasts in the absence of exogenous eletron carriers [34]. The mechanisms of light-induced and respiratory generation of ATP thus seem different in at least one respect. The finding that DNP does not induce ATP-ase activity in spinach chloroplasts may be another reflection of the same difference.

The reported lack of ATP-ase activity and of an exchange reaction between ATP and ^{32}P are according to Avron and Jagendorf [18] confirmatory evidence for the view that the last step in ATP formation in light-induced phosphorylation is an irreversible one. Löw *et al.*[27] have shown that a close relationship seems to exist between the P—ATP exchange and the DNP-induced ATP-ase reactions in isolated mitochondria. Our finding that no DNP-induced ATP-ase reaction could be obtained in chloroplasts may be interpreted to mean, by

comparison, that a P—ATP exchange reaction should not be expected in isolated chloroplasts.

Though the amount of inorganic phosphate released in the ATP-ase reaction of the isolated chloroplasts is rather low (8—12 μmoles/h/mg chlorophyll) as compared to the rate of light-induced phosphorylation in the particular chloroplast preparations (60—80 μmoles ATP formed/h/mg chlorophyll, anaerobic conditions, cofactor 2×10^{-4} M vitamin K_3), there are two reasons to believe that the Mg^{++}-stimulated ATP-ase activity is not due to mitochondrial contamination. First, the chloroplast preparations showed no measurable respiratory activity and second, repeated washings of the chloroplasts did not significantly affect the ATP-ase activity. Arnon's [16] statement that chloroplasts seem to be rather free of ATP-hydrolyzing enzymes has not been supported by any published experiments. The failure of Avron and Jagendorf [17,18] to detect any ATP-ase activity may have been due to the combined effect of short reaction time, low concentration of chloroplasts (*cf.* Ref.[18] Table I), high concentration of $MgCl_2$ and low temperature, as compared to our conditions.

The Mg^{++}-activated ATP-ase activities in spinach chloroplasts and in liver mitochondria were found to be similar in their response to azide, *p*-chloromercuribenzoate, fluoride, AMP, ADP, chlorpromazine and atebrin, which were inhibitory and also to dithionite, which had a stimulating effect (*cf.* Refs.[7,10,35,36]). In spinach chloroplasts KCN had no significant effect, whereas in mitochondria a small but significant stimulation of the Mg^{++}-activated ATP-ase reaction has been reported [35]. $(NH_4)_2SO_4$, which recently was found to be an uncoupler of light-induced phosphorylation in chloroplasts [37], did not influence the ATP-ase activity.

Löw [35,36] has shown that the flavin antagonists atebrin [38-40] and chlorpromazine [41] affect the DNP-induced ATP-ase activity of "intact" liver mitochondria as well as the Mg^{++}-stimulated ATP-ase activity of structurally disorganized mitochondria. He concluded that both of these ATP-ases involve the participation of diaphorase flavin. In chloroplasts, those concentrations of chlorpromazine (3×10^{-4} M) and atebrin (5×10^{-3} M), which inhibited the Mg^{++}-stimulated ATP-ase activity by 50 % also caused a precipitation of chloroplast material. In chloroplasts light-induced phosphorylation in the presence of vitamin K_3 or FMN, as well as the phosphorylation coupled to the reduction of ferricyanide were found to be inhibited by much lower concentrations of chlorpromazine and atebrin (50 % inhibition by 5×10^{-5} M chlorpromazine and 5×10^{-5} M atebrin) than the ATP-ase activity. Thus we are not certain that these agents inhibit chloroplast ATP-ase by a specific action towards flavin.

Summarizing it may be said that the Mg^{++}-stimulated ATP-ase reaction of chloroplasts in several respects is similar to that of disrupted liver mitochondria. Our data do not permit, however, to draw a definite conclusion as to whether the Mg^{++}-stimulated ATP-ase reaction is a reversal of ATP forming reactions in light-induced phosphorylation in chloroplasts.

REFERENCES

1. Hunter, F. E. in Mc Elroy, W. D. and Glass, B. *Phosphorus Metabolism* **1** (1951) 297.
2. Potter, V. R. and Recknagel, R. O. in Mc Elroy, W. D. and Glass, B. *Phosphorus Metabolism* **1** (1951) 377.
3. Potter, V. R., Siekevitz, P. and Simonson, H. C. *J. Biol. Chem.* **205** (1953) 893.
4. Kielley, W. W. and Kielley, R. K. *J. Biol. Chem.* **191** (1951) 485.
5. Lardy, H. A. and Wellman, H. J. *J. Biol. Chem.* **201** (1953) 357.
6. Pressman, B. C. and Lardy, H. A. *Biochim et. Biophys. Acta* **21** (1956) 458.
7. Siekevitz, P., Löw, H., Ernster, L. and Lindberg, O. *Biochim et. Biophys. Acta* **29** (1958) 378.
8. Lee, K. H. and Eiler, J. J. *J. Biol. Chem.* **203** (1953) 705.
9. Myers, D. K. and Slater, E. C. *Nature* **179** (1957) 363.
10. Myers, D. K. and Slater, E. C. *Biochem. J.* **67** (1957) 558, 572.
11. Lardy, H. A. and Wellman, H. *J. Biol. Chem.* **195** (1952) 215.
12. Slater, E. C. *Nature* **172** (1953) 975.
13. Boyer, P. D., Falcone, A. B. and Harrison, W. H. *Nature* **174** (1954) 401.
14. Cooper, C. and Lehninger, A. L. *J. Biol. Chem.* **224** (1957) 547, 561.
15. Bronk, J. R. and Kielley, W. W. *Biochim et. Biophys. Acta* **29** (1958) 369.
16. Arnon, D. I. *Ann. Rev. Plant Physiol.* **7** (1956) 325.
17. Avron, M. and Jagendorf, A. T. *Plant Physiol.* **33** (1958) XVIII.
18. Avron, M. and Jagendorf, A. T. *J. Biol. Chem.* **234** (1959) 967.
19. Baltscheffsky, H. *Acta Chem. Scand.* **13** (1959) 393.
20. Wessels, J. S. C. *Biochim et. Biophys. Acta* **29** (1958) 113.
21. Arnon, D. I. *Plant Physiol.* **24** (1949) 1.
22. Fiske, C. H. and Subbarow, Y. *J. Biol. Chem.* **66** (1925) 375.
23. Mazelis, M. *Plant Physiol.* **31** (1956) 37.
24. Naganna, B., Venugopal, B., Sripathi, C. E. *Biochem. J.* **60** (1955) 224.
25. Lineweaver, H. and Burk, D. *J. Am. Chem. Soc.* **56** (1934) 658.
26. Lehninger, A. L., Wadkins, C. L., Cooper, C., Devlin, T. M. and Gamble, J. L. *Science* **128** (1958) 450.
27. Löw, H., Siekevitz, P., Ernster, L. and Lindberg, O. *Biochim et. Biophys. Acta* **29** (1958) 392.
28. Kielley, W. W. and Bronk, J. R. *Proc. Intern. Symp. Enzyme Chem., Tokyo and Kyoto*, Maruzen, Tokyo, 1958, p. 286.
29. Holton, F. A., Hülsmann, W. C., Myers, D. K. and Slater, E. C. *Biochem. J.* **67** (1957) 579.
30. Wessels, J. S. C. *Biochim et. Biophys. Acta* **33** (1959) 53.
31. Arnon, D. I., Whatley, F. R. and Allen, M. B. *Science* **127** (1958) 1026.
32. Whatley, F. R., Allen, M. B. and Arnon, D. I. *Biochim et. Biophys. Acta* **32** (1959) 32.
33. Ohmura, T. *J. Biochem. Tokyo* **45** (1958) 319.
34. Wessels, J. S. C. *Biochim et. Biophys. Acta* **36** (1959) 264.
35. Löw, H. *Biochim et. Biophys. Acta* **32** (1959) 1.
36. Löw, H. *Biochim et. Biophys. Acta* **32** (1959) 11.
37. Jagendorf, A. T. *Brookhaven Symposia in Biol.* **11** (1958) 236.
38. Wright, C. I. and Sabine, J. C. *J. Biol. Chem.* **155** (1944) 315.
39. Haas, E. *J. Biol. Chem.* **155** (1944) 321.
40. Hellerman, L., Lindsay, A. and Bovarnick, M. R. *J. Biol. Chem.* **163** (1946) 553.
41. Yagi, K., Nagatsu, T. and Ozawa, T. *Nature* **177** (1956) 891.

Received December 15, 1959.

ACTA CHEMICA SCANDINAVICA 14 (1960) 247–256

Preparation and Some Properties of Sub-Mitochondrial, Reduced Diphosphopyridine Nucleotide Oxidizing Particles from Isolated Mitochondria

HERRICK BALTSCHEFFSKY, MOLLY FUDGE and BARBRO ARWIDSSON

Wenner-Gren Institute, University of Stockholm, Sweden

A simple method for preparation and isolation of sub-mitochondrial particles from isolated rat or guinea-pig liver mitochondria is described. It consists of grinding the mitochondria with Al_2O_3 in a mortar and subsequent differential centrifugation. Some properties of a fraction, which is centrifuged down at 100 000 *g* (60 min centrifugation), are described.

The fraction oxidizes reduced diphosphopyridine nucleotide at a much higher rate than reduced triphosphopyridine nucleotide, both with oxygen and with cytochrome c as electron acceptors. The oxidation of succinate with cytochrome c is strongly stimulated by phenazine methosulfate. Antimycin A inhibits the oxidation of succinate in the absence of phenazine methosulfate, which can mediate electron transport from succinate to cytochrome c around the antimycin A-sensitive site. When a catalytic amount of diphosphopyridine nucleotide is added, β-hydroxybutyrate is oxidized by added cytochrome c in the presence of the sub-mitochondrial fraction whereas glutamate oxidation occurs only when also the final supernatant is added. This indicates that mitochondrial dehydrogenases are differently distributed in the sub-mitochondrial fractions.

The methods employed for preparation of sub-mitochondrial particles from isolated animal mitochondria [1–10] are of two kinds with respect to the disruption of the mitochondrial structure, chemical [1–6] and physical or mechanical [7–10]. Three physical methods have been reported: use of a Waring blendor[7], sonic vibration [8–9] and grinding with alumina [10]. This paper describes the method of preparation and some properties of sub-mitochondrial DPNH-oxidizing * particles obtained from isolated liver mito-

* Abbreviations: ATP, adenosine triphosphate; ATP-ase, adenosine triphosphatase; DPN, diphosphopyridine nucleotide; DPNH, reduced diphosphopyridine nucleotide; TPN, triphosphopyridine nucleotide; TPNH, reduced triphosphopyridine nucleotide; DNP, 2,4-dinitrophenol; PMS, phenazine methosulfate; HOQNO, 2-*n*-heptyl-4-hydroxyquinoline-N-oxide; M, moles per liter.

chondria by grinding with alumina. Earlier communications on this method have been in note or abstract form [10-13].

MATERIALS AND METHODS

The pyridine nucleotides, PMS, cytochrome c and antimycin A were obtained from Sigma Chemical Co., St. Louis, Mo., U.S.A. HOQNO was obtained from Dr. J. W. Cornforth, National Institute for Medical Research, London, England, this gift is gratefully acknowledged. Antimycin A and HOQNO were dissolved in ethanol. The stock solutions were kept in a deep-freeze. The molecular weight of antimycin A was taken as 548, in agreement with the formula $C_{28}H_{40}O_9N_2$ [14] (*cf.* Ref.[15]).

Liver mitochondria were prepared in 0.25 M sucrose, essentially according to the method of Schneider and Hogeboom [16] as modified by Ernster and Löw [17]. For one preparation 4—8 white male rats, each weighing 200—300 g or 2—4 male guinea-pigs, each weighing 300—400 g were used. After decapitation of an animal, the liver was removed, weighed, cut into small pieces and rinsed once or twice with sucrose. The homogenization was carried out on a 30—40 % tissue suspension as rapidly as possible (in between 15 and 30 sec) in a Potter-Elvehjem homogenizer with a loosely fitting Teflon Pestle. When all the livers were homogenized a dilution to a 15—20 % suspension was made. The material was centrifuged 10 min at 800 *g* * in an International Refrigerated Centrifuge, model PR-1, head no. 840. The pellet was discarded and the supernatant centrifuged 20 min at 4 100 *g*. The mitochondrial pellet was suspended in sucrose to the same volume as before the centrifugation and recentrifuged at 4 100 *g*, now for 15 min. The supernatant was discarded and the mitochondrial pellet suspended in a small volume of sucrose (1—2 ml per 5 g of liver). The material was centrifuged 8 min at 20 000 *g* in a Spinco Ultracentrifuge, model L, head no. 40, which was also used for the subsequent centrifugations. In this centrifugation the resulting pellet was sharply divided into two parts. The upper part, small in volume, was the remaining "fluffy layer" [18] which was thoroughly swirled off from the densely packed mitochondrial layer and discarded. The remaining layer contained mitochondria of high ("intact") quality, as judged by the criteria of P/O ratios and respiratory control. It was used for preparation of the sub-mitochondrial particles, according to one of the following two methods.

Method I: The mitochondrial layer was suspended in a small volume of 0.03 M phosphate buffer, pH 7.0, and centrifuged 5 min at 25 000 *g*. The supernatant was discarded. The pellet was mixed in a mortar with 20 mg Al_2O_3 (Alcoa A-301) per gram liver and ground for 6 min. The mixture was transferred to a centrifugation tube with small volumes of the phosphate buffer and centrifuged 10 min at 25 000 *g*. The pellet contained Al_2O_3 and "heavier fragments". The supernatant was centrifuged 60 min at 100 000 *g*. The pellet from this centrifugation was suspended in a small volume of the phosphate buffer. The resulting yellow, translucent suspension contained "DPNH-oxidase particles".

Method II: The mitochondrial layer was mixed in a mortar with 20 mg Al_2O_3 (Alcoa A-301) per gram liver and ground for 6 min. The mixture was transferred to a centrifugation tube with small volumes of 0.25 M sucrose. From this on, the method was the same as method I, except that 0.25 M sucrose was used throughout.

The "heavier fragments" could be separated from the alumina with a glass rod. This fraction was obtained by transfer to an empty tube with the aid of phosphate or sucrose medium, 10 min centrifugation at 25 000 *g* and suspension of the pellet in the medium desired.

All operations were carried out at as near to 0°C as possible. Delays between the individual steps were avoided.

The solutions were made with deionized water and kept at 0°C.

Method II has also been used for preparation of sub-mitochondrial particles from isolated rat- or guinea pig-heart-muscle mitochondria [12].

---

* The *g* values are given for the bottom of the tubes with the International Refrigerated Centrifuge and for the middle of the tubes with the Spinco Ultracentrifuge.

Electron micrographs were taken of the isolated mitochondria, the "heavier fragments" fraction and the "DPNH-oxidase particles" *. The majority of the mitochondria appeared to be "intact" with clearly visible internal double membrane structures. Some, however, appeared to be swollen, with diminished integrity of the internal membranes. The microsomal contamination appeared to be low. Both the "heavier fragments" fraction and the DPNH-oxidase particles appeared to be more or less round vesicles with no interior structures. No "intact" mitochondria were observed in these fractions.

Measurements. Protein was determined by the biuret method. Phosphorylation was measured by the ^{32}P method recommended by Lindberg and Ernster [19], ATP-ase activity by the method of Martin and Doty [20] as described by Lindberg and Ernster [19].

Oxidase activities were measured with the Warburg technique or, for DPNH and TPNH by following the disappearance of the absorption of reduced nucleotide at 340 mμ in a Beckman Recording Spectrophotometer, model DK 2. Cytochrome c reducing activities were measured at 550 mμ, in the presence of mM KCN. The following values were used for the extinction coefficients: DPNH minus DPN and TPNH minus TPN at 340 mμ = 6.2 $cm^{-1} \times mM^{-1}$, reduced cytochrome c minus oxidized cytochrome c at 550 mμ = 19.1 $cm^{-1} \times mM^{-1}$.

RESULTS

A method similar to method I where the mitochondria were treated with 0.03 M phosphate, pH 7.0, before the grinding, was outlined in the first note [10] about this work. This medium had earlier been used for preparation of submitochondrial particles by sonic treatment of liver mitochondria [21]. Method II gave a higher yield than method I (Table 1), as was previously noted [11]. Preparations made according to method II have been used for the experiments reported below, unless otherwise indicated.

Table 1. Yield of "DPNH-oxidase particles".

Material	Method	Number of preparations	mg protein/g liver		
			lowest value	highest value	mean value
Rat liver	I	3	0.1	0.2	0.1
» »	II	9	0.5	0.9	0.7
Guinea pig liver	I	3	0.2	0.3	0.2
» » »	II	4	0.8	1.4	1.1

The higher yield obtained with method II allowed some experiments to be done in order to confirm the visual observation that 6 min was a suitable grinding time. Mitochondria were isolated from 80 g of liver. During the grinding, which was extended to 15 min, samples were removed from the mixture at suitable time intervals, weighed and put into centrifuge tubes. Two variables of the "DPNH-oxidase particles" obtained from these samples were determined: the amount of protein recovered and the DPNH-oxidase activity. Fig. 1 shows that 6 min grinding was suitable with respect to the yield of

* Thanks are due to Dr. Fritiof S. Sjöstrand of the Department of Anatomy, Karolinska Institutet, for carrying out the studies with the electron microscope.

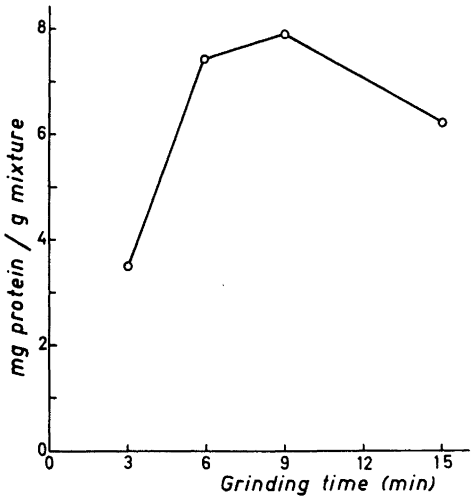

Fig. 1. Yield of protein as a function of grinding time (guinea pig).

protein. Table 2 shows that this was true also with respect to the yield of DPNH-oxidase activity. Parallel values are given in Table 2 to show that the experimental error was satisfactorily small for the purpose of the experiment.

The recovery of mitochondrial protein is shown in Table 3. With both methods of preparation the bulk of the protein was in the supernatant after the centrifugation at 100 000 *g*. Whereas method II gave a better yield of "DPNH-oxidase particles" than method I, the opposite was true for the "heavier fragments" fraction. A considerable amount of protein (6 %) was dissolved by the treatment of the "intact" mitochondria with phosphate. As was to be expected, the amount of protein was low (2 %) in the corresponding fraction from a similar centrifugation in 0.25 M sucrose.

The efficiency of the oxidative phosphorylation obtained was very low, as was shown in a note [10]. It was true both with preparations made according to method I and method II, and likewise when versene was added or a mixture of sucrose and phosphate was used. Shortening the reaction time to

Table 2. DPNH-oxidase activity as a function of grinding time. The oxidation of DPNH was measured spectrophotometrically at 340 mμ, in 25 mM phosphate buffer pH 7.0, in the presence of 1 % serum albumin. Material: "DPNH-oxidase particles". Each given value is the mean value of two determinations from a separate sample. Reaction volume 3 ml (guinea pig).

Grinding time min	DPNH-oxidase activity μmoles DPNH oxidized/min/g mixture	
0.2	0.1	0.3
3	1.7	1.6
6	2.0	2.5
9	2.5	2.6
15	2.3	2.2

Table 3. Recovery of mitochondrial protein (rat).

Fraction	Recovery per 100 mg mitochondrial protein	
	Method I	Method II
	mg protein	mg protein
"DPNH-oxidase particles"	7	23
"Heavier fragments"	15	11
Supernatant$_{25\,000\ g}$ *	6	2
Supernatant$_{100\,000\ g}$ *	59	55
Total recovery	87	91

* Supernatant $_{25\,000\ g}$ and Supernatant $_{100\,000\ g}$ = supernatant from the centrifugation at 25 000 *g* which was performed immediately before the grinding and the centrifugation at 100 000 *g*, respectively.

2 min (measuring the rate of oxidation of DPNH at 340 mμ and at 20°C), did not result in higher P/O ratios.

The ATP-ase activity of isolated liver mitochondria is related to their state and capacity for oxidative phosphorylation. A parallel relationship exists between disappearance of mitochondrial integrity, oxidative phosphorylation and DNP-induced ATP-ase activity. When these decrease, the Mg^{++}-stimulated ATP-ase activity, on the other hand, increases [22]. Fig. 2 shows that the Mg^{++}-stimulated ATP-ase activity of the "DPNH-oxidase particles" is very high as compared to the DNP-induced ATP-ase and the endogenous ATP-ase activities.

In early preparations of "DPNH-oxidase particles" with the alumina grinding-method, DPNH was oxidized at a much higher rate than succinate with either oxygen or cytochrome c as electron acceptor [10,11]. It has been

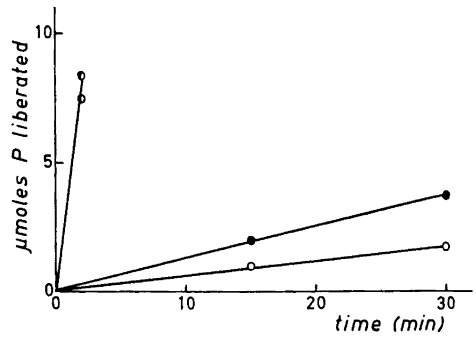

Fig. 2. Effects of Mg and DNP on the ATP-ase activity. ◐ = Mg added, ● = DNP added, O = no addition. The reaction medium contained: 0.015 M tris(hydroxymethyl)-aminomethane, pH 7.6, and 0.01 M ATP. Where added: 4 mM $MgCl_2$ or 10^{-4} M DNP. Final volume 2.0 ml. Temperature 30°C (guinea pig).

Table 4. Cytochrome c reductase activities. Spectrophotometric measurement at 550 mμ. In the reaction cuvette: "DPNH-oxidase particles", 1 mM KCN, 5×10^{-5} M cytochrome c and 30 mM phosphate buffer, pH 7.0. Where added: 6.7 mM succinate or 0.1 mM DPNH (final concentrations are given throughout). The final volume was 3 ml. Temperature 22°C. The values are given as μM cytochrome c reduced/min/mg protein (rat).

Method	Number of preparations	DPNH-cytochrome c reductase activity			Succinate-cytochrome c reductase activity			
		lowest value	highest value	mean value a	lowest value	highest value	mean value b	$\frac{a}{b}$
I	3	120	260	200	4.5	12	9.2	22
II	6	140	390	220	4.2	19	10	22

Table 5. Cytochrome c-reducing activities in "DPNH-oxidase particles". The reduction of cytochrome c was measured spectrophotometrically at 550 mμ. In the cuvette: "DPNH-oxidase particles", 1 mM KCN, 5×10^{-5} M cytochrome c and 30 mM phosphate buffer, pH 7.0, and, where added: 6.7 mM succinate, 6.7 mM glutamate, 6.7 mM β-hydroxybutyrate, 0.1 mM DPNH, 0.1 mM TPNH, 0.033 mM DPN (with glutamate and β-hydroxybutyrate), 0.01 M DPN (with TPNH), 0.33 mM PMS, 0.67 μM antimycin A, 0.2 ml supernatant (sup) containing 5.5 mg protein per ml. Temperature 22°C. The additions were made during the experiment (rat).

Substrate	Addition	Addition	μM cytochrome c reduced/min/mg protein
Succinate	—	—	5
Sup	—	—	13
Succinate	Sup	—	17
Succinate	—	—	5
Succinate	PMS **	—	45
Succinate	Antimycin A	—	0
Succinate	Antimycin A	PMS	51
DPNH			130
Glutamate	—	—	0
Glutamate	DPN	—	0
Glutamate	DPN	Sup	79
β-Hydroxybutyrate	—	—	0
β-Hydroxybutyrate	DPN	—	47
β-Hydroxybutyrate	DPN	Sup	54
TPNH *	—	—	6
TPNH *	DPN	—	30
DPNH *	—	—	115

* Experiments made on preparations according to method I.

** As PMS is autoxidizable the data with PMS may be quantitative only with respect to the reduction of cytochrome c (and not indicate an equivalent oxidation of succinate).

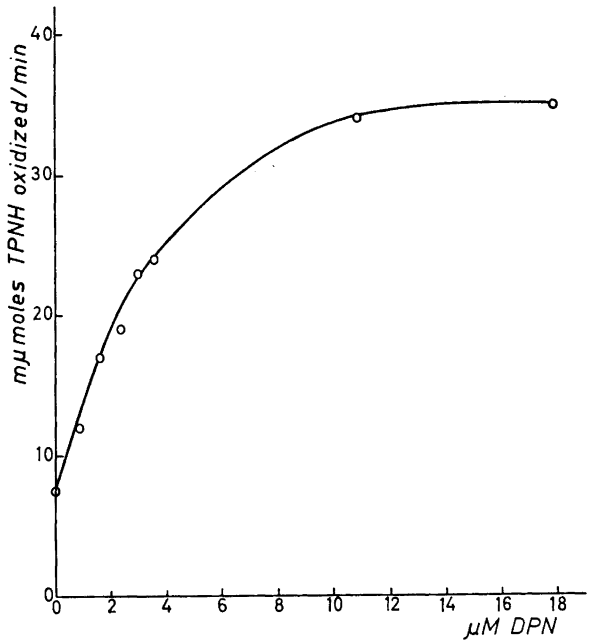

Fig. 3. Stimulation of TPNH-oxidase by DPN. The oxidation of TPNH was measured spectrophotometrically at 340 mμ. Initial concentration of phosphate buffer pH 7.0, was 27 mM. Protein content 1.9 mg. Successive additions of DPN were made. Final volume before the additions 3.0 ml. Note the rate of oxidation of TPNH (that of DPNH was, in a separate experiment, 120 mμmoles DPNH oxidized/min). (Variation of the concentration of phosphate buffer over a wide range did not influence the rate.) Temperature 20°C (rat).

found, however, that both method I and method II may give preparations where the oxidase activities were of the same order of magnitude with succinate and with DPNH as substrates. On the other hand, the difference between the rates with DPNH and succinate as substrates has constantly been great for the cytochrome c reductase activities (Table 4).

Different cytochrome c-reducing activities are shown in Table 5. The low rate of oxidation of succinate with cytochrome c is stimulated by phenazine methosulfate, which is known to accept electrons from a purified and solubilized succinic dehydrogenase preparation [23]. Antimycin A (or HOQNO) inhibits the succinate-cytochrome c reductase activity, but the stimulation due to phenazine methosulfate is unihibited. These agents have previously been reported to provide a by-pass for electrons around the antimycin A- and HOQNO-sensitive step in bacterial light-induced phosphorylation [24,25], and recently also in mitochondrial electron transport [26]. The present results demonstrate that electrons which, through the action of phenazine methosulfate, have passed around the antimycin A sensitive step may be brought back to the respiratory chain at the cytochrome c-level. Mitochondrial substrates,

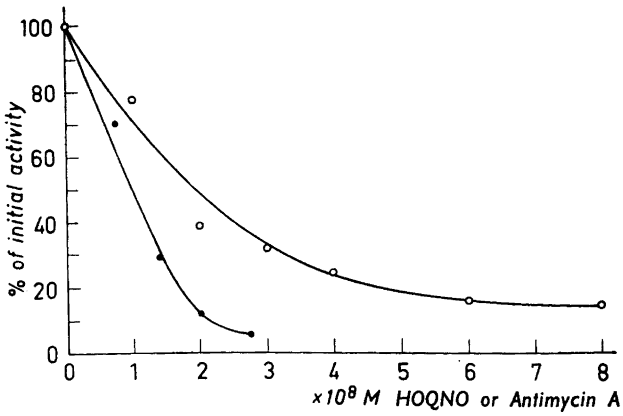

Fig. 4. Inhibition by antimycin A and HOQNO of DPNH-oxidase activity. ○ = HOQNO, ● = antimycin A. The oxidation of DPNH was measured spectrophotometrically at 340 mμ. The reaction medium contained: 25 mM phosphate buffer pH 7.0 and "DPNH-oxidase particles" containing 0.62 mg protein. Final volume 3.0 ml. Temperature 22°C (rat).

which are linked to DPN over specific dehydrogenases, may be oxidized after addition of catalytic amounts of DPN (*e.g.* β-hydroxybutyrate), or they may need addition of both DPN and the final supernatant from the preparation (*e.g.* glutamate). Mitochondrial dehydrogenases thus seem to be distributed in different sub-mitochondrial fractions. This may be a reflection of a corresponding compartmentation in the structure of the mitochondrion. The low initial rate of oxidation of TPNH can be markedly stimulated by DPN in catalytic amounts. This is shown in more detail in Fig. 3 and indicates that pyridine nucleotide transhydrogenase [27] is present in the particles.

It has been shown earlier [12] that amytal *, antimycin A, and HOQNO in "DPNH-oxidase particles" from liver inhibit only that part of the respiration which is not due to the addition of cytochrome c. Fig. 4 shows the inhibition curves for antimycin A and HOQNO in a system where no cytochrome c had been added.

DISCUSSION

Isolated "intact" mitochondria have been disrupted into smaller fragments by various chemical and mechanical means. The new, simple method described in this paper, grinding with alumina, was originally used for disruption of bacterial cells [28]. After the grinding the various sub-mitochondrial fractions are separated by differential centrifugation performed in a similar manner to that after sonic disruption [8]. The recovery of mitochondrial protein in different fractions (Table 2), with a high amount in the final supernatant, resembles the distribution shown by Kielley and Bronk [8] in the fractions obtained from sonicated mitochondria.

* 5-Ethyl-5-*iso*amylbarbiturate.

The fraction which has been termed "DPNH-oxidase particles" oxidized DPNH in previously described preparations at a much higher rate than succinate [10]. As many preparations, both with method I and method II, have given rather similar rates with the two substrates and as a marked variation between different preparations has been found, it can be stated that the alumina grinding as such does not constantly give low succinoxidase activity in the "DPNH-oxidase particles" and the absolute DPNH-oxidizing activities are governed by factors which are difficult to control. Two possible sources for this difficulty should be considered, the postulated "external" mitochondrial pathway for oxidation of DPNH [29,30], and influence of microsomes. The fact that amytal, antimycin A and HOQNO virtually completely inhibit the DPNH-oxidase activity in the absence of cytochrome c [11,12] shows that this respiration is of a mitochondrial, and not microsomal, origin. The additional respiration, which is initiated by external cytochrome c, may originate from either of the two sources mentioned above, or from both. A low microsomal contamination in the mitochondria would be percentagewise increased in the fraction containing the "DPNH-oxidase particles" because of similar sedimentation characteristics. DPNH-cytochrome c reductase activity of the microsomes may then be linked to the mitochondrial oxidase at the cytochrome c-level and by-pass a rate-limiting step between DPNH and cytochrome c. The effect would be the same as that of the postulated "external" mitochondrial pathway. A vague indication that microsomes may be responsible for at least part of the stimulating effect of added cytochrome c in preparations from liver is found from experiments with "DPNH-oxidase particles" from heart muscle [12]. In this material the increased DPNH-oxidase activity, which is due to addition of cytochrome c, is sensitive to the above-mentioned inhibitors, and the ratio DPNH- to succinate-cytochrome c reductase activity is lower than the corresponding ratio in liver material. The amount of microsomes which can be obtained from heart muscle homogenates is very low.

Glutamate was not oxidized by the DPNH-oxidase particles unless both DPN and the final supernatant were added. Thus no glutamic dehydrogenase was active in the particles. The same was reported for sub-mitochondrial particles obtained by Kielley and Bronk [8] (but not by McMurray, Maley and Lardy [9]) after sonic disruption of liver mitochondria. On the other hand, β-hydroxy-butyric dehydrogenase was present (Table 5).

Acknowledgements. Many thanks are due to Professor Olov Lindberg for valuable advice and continuous support, to Dr. Lars Ernster, Dr. Hans Löw and Dr. Thomas Conover for stimulating discussions and to Mrs. Torill Hundal for skilful technical assistance.

REFERENCES

1. Cooper, C., Devlin, T. M. and Lehninger, A. L. *Biochim. et Biophys. Acta* **18** (1955) 159.
2. Cooper, C. and Lehninger, A. L. *J. Biol. Chem.* **219** (1956) 489.
3. Siekevitz, P. and Watson, M. L. *J. Biophys. Biochem. Cytol.* **2** (1956) 653.
4. Ziegler, D., Lester, R. and Green, D. E. *Biochim. et Biophys. Acta* **21** (1956) 80.
5. Green, D. E., Mackler, B., Repaske, R. and Mahler, H. R. *Biochim. et Biophys. Acta* **15** (1954) 435.

6. Abood, L. G. and Alexander, L. *J. Biol. Chem.* **227** (1957) 717.
7. Kielley, W. W. and Kielley, R. K. *J. Biol. Chem.* **200** (1953) 123.
8. Kielley, W. W. and Bronk, J. R. *J. Biol. Chem.* **230** (1958) 521.
9. McMurray, W. C., Maley, G. F. and Lardy, H. A. *J. Biol. Chem.* **230** (1958) 219.
10. Baltscheffsky, H. *Exptl. Cell Research* **13** (1957) 630.
11. Baltscheffsky, H. *Acta Chem. Scand.* **12** (1958) 597.
12. Baltscheffsky, H. and Baltscheffsky, M. *Biochim. et Biophys. Acta* **29** (1958) 220.
13. Baltscheffsky, H. *IV Intern. Congr. Biochem., Abstracts*, Vienna, 1958, p. 67.
14. Tenner, G. M., Bumpus, F. M., Dunshee, B. R. and Strong, F. M. *J. Am. Chem. Soc.* **75** (1953) 1100.
15. Liu, Wen-chih and Strong, F. M. *J. Am. Chem. Soc.* **81** (1959) 4387.
16. Schneider, W. C. and Hogeboom, G. H. *J. Biol. Chem.* **183** (1950) 123.
17. Ernster, L. and Löw, H. *Exptl. Cell Research, Suppl.* **3** (1955) 133.
18. Lardy, H. A. and Wellman, H. *J. Biol. Chem.* **195** (1952) 215.
19. Lindberg, O. and Ernster, L. In Glick, D. *Methods of Biochemical Analysis*, Interscience, New York, 1956, Vol. **3**, p. 1.
20. Martin, J. B. and Doty, D. M. *Anal. Chem.* **21** (1949) 965.
21. Bronk, J. R. and Kielley, W. W. *Biochim. et Biophys. Acta* **24** (1957) 440.
22. Siekevitz, P., Löw, H., Ernster, L. and Lindberg, O. *Biochim. et Biophys.* Acta **29** (1958) 378.
23. Kearney, E. B. and Singer, T. P. *Biochim. et Biophys. Acta* **17** (1955) 596.
24. Geller, D. M. *Abstr. 7th Intern. Congr. for Microbiology, Stockholm* 1958, p. 73.
25. Baltscheffsky, H. and Baltscheffsky, M. *Acta Chem. Scand.* **12** (1958) 1333.
26. Kimura, T. and Singer, T. P. *Nature* **184** (1959) 791.
27. Kaplan, N. O., Colowick, S. P. and Neufeld, E. F. *J. Biol. Chem.* **205** (1953) 1.
28. McIlwain, H. *J. Gen. Microbiol.* **2** (1948) 288.
29. Lehninger, A. L. *The Harvey Lectures* 1953–1954, Academic Press Inc., New York 1955, p. 176.
30. Ernster, L. *Exptl. Cell Research* **10** (1956) 721.

Received December 29, 1959.

ACTA CHEMICA SCANDINAVICA 14 (1960) 257–263

Inhibitor Studies on Light-Induced Phosphorylation in Extracts of *Rhodospirillum rubrum*

HERRICK BALTSCHEFFSKY and MARGARETA BALTSCHEFFSKY

Wenner-Gren Institute, University of Stockholm, Sweden

Light-induced phosphorylation in extracts of the photosynthetic bacterium *Rhodospirillum rubrum* is strongly inhibited not only by 2-*n*-heptyl-4-hydroxyquinoline-N-oxide [1] and antimycin A[2] but also by gramicidin and oligomycin A in concentrations which are similar to those necessary to inhibit the reactions involved in oxidative phosphorylation in animal mitochondria. Amytal, azide and cyanide [3] have only a weak inhibitory effect. Dicumarol and especially 2,4-dinitrophenol, which both "uncouple" phosphorylation from electron transport in animal mitochondria, have a much less pronounced inhibitory effect on the light-induced phosphorylation.

The similarities between the two different electron transport phosphorylation * systems in response to various kinds of inhibitors indicate that the investigated mechanism for bacterial light-induced phosphorylation has properties similar to the mechanism for mitochondrial oxidative phosphorylation. This is true with respect not only to electron transport but also to the mechanism of coupling between electron transport and phosphate esterification and to the nature of a reaction involved in phosphate transfer. The differences show that reactions near the oxidizing and the reducing ends of the mitochondrial respiratory chain are not shared by the bacterial system for light-induced phosphorylation.

Studies with inhibitors and stimulators have provided information about the system for respiration and oxidative phosphorylation in animal mitochondria. Experimental evidence for the assumption that light-induced phosphorylation (LIP) in photosynthetic bacteria is dependent upon electron transport was first obtained with the electron transport inhibitor HOQNO [1] **. Current concepts about the electron transport system in LIP in the facultative

* The term "electron transport phosphorylation" is used to denote "phosphorylation linked to electron (or hydrogen) transport".

** Abbreviations: P, orthophosphate; ATP, adenosine triphosphate; DPN, diphosphopyridine nucleotide; DPNH, reduced diphosphopyridine nucleotide; HOQNO, 2-n-heptyl-4-hydroxyquinoline-N-oxide; DNP, 2,4-dinitrophenol; % P_{org}, percentage orthophosphate esterified; M, moles per liter.

phototroph *Rhodospirillum rubrum* are largely based on results obtained with electron transport inhibitors and stimulators [1-4]. Further results obtained with inhibitors of electron transport and phosphorylation are given and discussed in this paper.

MATERIALS AND METHODS

ATP, DPNH, PMS and antimycin A were obtained from Sigma Chemical Co., St. Louis, Mo., U.S.A. Gramicidin D was obtained from Mann Research Laboratories, New York, N.Y., U.S.A. HOQNO was obtained from Dr. J. W. Cornforth, National Institute for Medical Research, London, England, and oligomycin A from Dr. F. M. Strong, Department of Biochemistry, University of Wisconsin, Madison, Wisc., U.S.A. These gifts are gratefully acknowledged. Hexokinase was prepared and stored as in Ref.[5] Antimycin A, HOQNO, gramicidin and oligomycin A were dissolved in ethanol. The stock solutions were kept in a deep-freeze. In the reaction medium for LIP the ethanol content was kept below 1 % in order not to inhibit the LIP. The molecular weight of antimycin A was taken as 548 (*cf.* Ref.[6]).

Rhodospirillum rubrum, van Niel strain S1, was grown and harvested as has been described [4]. The method which was used for disruption of the bacteria, grinding with alumina, was first employed on bacteria by McIlwain [7]. It has been described in a previous paper [4], as well as the procedures employed for preparation of "chromatophores" and "chromatophore fragments" and for measuring yield and efficiency of LIP, and the medium used in the LIP experiments. The results reported here have been obtained with the "chromatophore fragments" fraction unless otherwise indicated. The two fractions were equally efficient in LIP but the "chromatophores" fraction showed a higher DPNH-oxidase activity than the "chromatophore fragments" fraction.

Aerobic conditions were used throughout. In all experiments 3.3×10^{-4} M * succinate was added in accordance with the finding of Frenkel [8,9] that a reducing agent in catalytic amounts is necessary to elicit full LIP activity in "purified" extracts of *R. rubrum*. Frenkel [9] has shown that the LIP process is inhibited by molecular oxygen in the absence, or at very low concentrations, of hydrogen donor. Under our conditions, with an added excess of succinate, anaerobiosis obtained with N_2 *via* a pyrogallol solution did not result in higher LIP values. In fact, a slight inhibition of the LIP as compared with aerobiosis was obtained (10 and 15 % in two separate experiments with different preparations).

RESULTS

Fig. 1 shows that the rate of LIP is a linear function of the concentration of the chromatophore extract. A time curve for LIP is given in Fig. 2.

Amytal gives only a weak inhibition of LIP, even at concentrations several times higher than those which strongly inhibit the oxidation of DPN-linked substrates in animal mitochondria [10] (Fig. 3).

Fig. 4 shows the inhibition curves for antimycin A and HOQNO, which have been shown [11] to inhibit electron transport in animal mitochondria between cytochrome b and cytochrome c_1. Fig. 5 shows that the inhibition obtained with antimycin A was by-passed by phenazine methosulfate [2,12], even at high concentrations of the inhibitor. However, with increasing concentrations of antimycin A the amount of phosphate esterified decreased.

As shown in Table 1, no marked inhibition was obtained with high concentrations of KCN and NaN_3. Mitochondrial electron transport is strongly inhibited by 5×10^{-4} M concentrations of these agents.

* Final concentrations are given throughout.

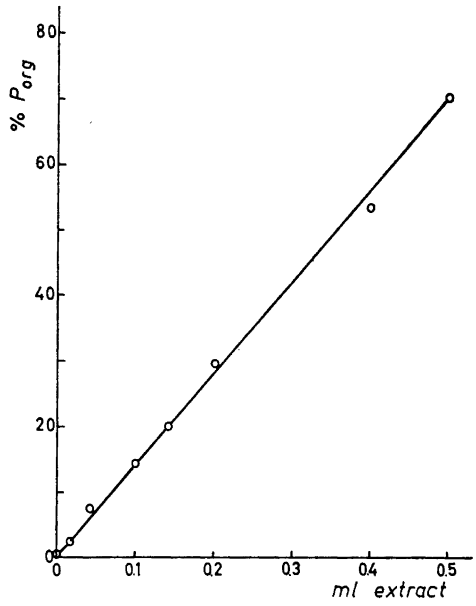

Fig. 1. LIP as a function of the amount of added "chromatophore fragments". The tubes contained 1.5 ml 0.2 M glycylglycine pH 7.4, 8 μmoles $K_2H^{32}PO_4$, 10 μmoles ATP, 1 μmole succinate, 30 μmoles $MgCl_2$, 60 μmoles glucose and an excess of yeast hexokinase. "OD_{800}" = 0.20 for a sample with 0.1 ml "chromatophore fragments" per 3.0 ml (reaction volume 3.0 ml). 20 min experiment at 30°C.

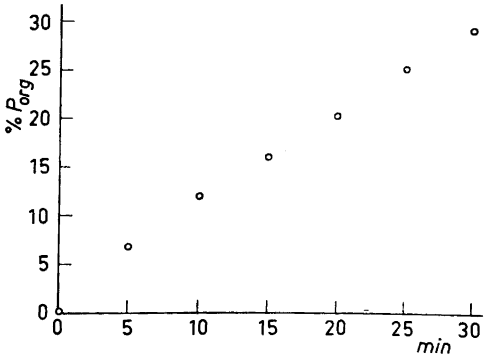

Fig. 2. Time curve for LIP. Experimental details as in Fig. 1. "OD_{800}" = 0.20.

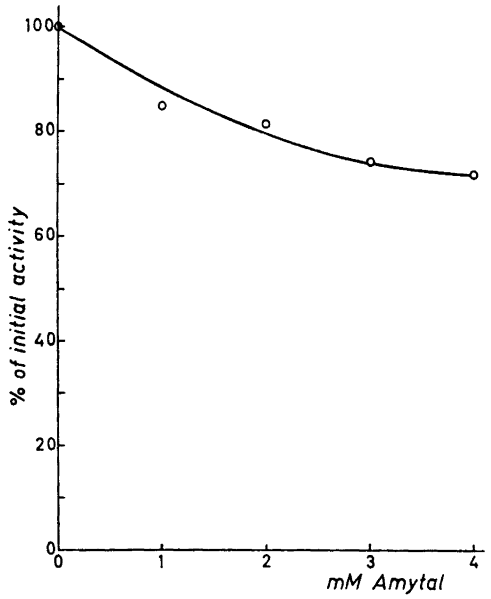

Fig. 3. Effect of amytal on LIP. Experimental details as in Fig. 1. "OD_{800}" = 0.20. 30 min experiment. 100 % initial activity = 39.4 % P_{org}.

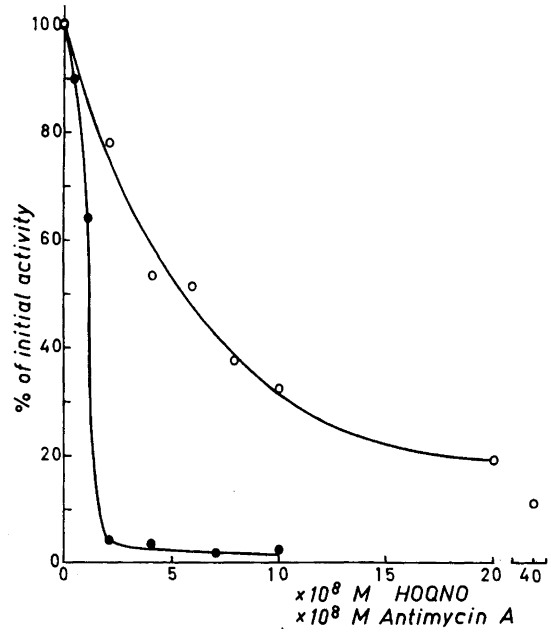

Fig. 4. Effect of antimycin A and HOQNO on LIP. Experimental details as in Fig. 1. ● = antimycin A, ○ = HOQNO. For ●, "OD_{800}" = 0.28, 100 % initial activity = 56.3 % P_{org}. For ○, "OD_{800}" = 0.32, 100 % initial activity = 62.0 % P_{org}. 30 min experiment. "Chromatophores" fraction.

The effect of two well known agents that uncouple oxidative phosphorylation in mitochondria, DNP and dicumarol, is shown in Fig. 6. Comparatively high concentrations were required to obtain an inhibitory effect on LIP. Dicumarol was much more efficient than DNP in this system.

Oligomycin A and gramicidin, which inhibit oxidative phosphorylation in animal mitochondria, also strongly inhibit LIP in extracts of *Rhodosprillium rubrum* (Figs. 7 and 8). LIP in spinach chloroplasts is inhibited by gramicidin [13,14] but not by oligomycin A in the concentrations tested [14].

DISCUSSION

A certain similarity between the mitochondrial system for oxidative phosphorylation and the system for LIP in *R. rubrum* has been indicated by the work of several investigators [1-4]. It is in the flavin and cytochrome regions that common denominators in the electron carrier systems have been suggested [3,4]. The nature of the reactions at both the reducing and the oxidizing ends of the mitochondrial electron transport chain is, however, not shared by the chromatophore system. This is shown by the fact that amytal, which inhibits electron transport in phosphorylating mitochondria between DPNH

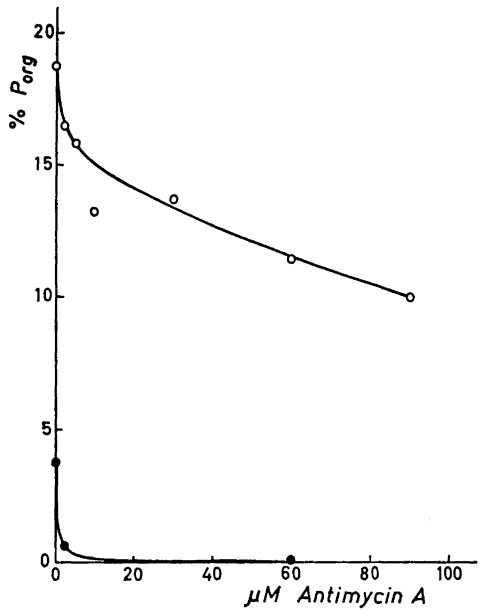

Fig. 5. Effect of antimycin A on PMS-stimulated LIP. Experimental details as in Fig. 1. O = PMS-stimulated, ● = without PMS, which curve is given as a comparison. The PMS-concentration, where added, was 3.3×10^{-4} M. "OD_{800}" = 0.50. 6 min experiment with PMS, 20 min without PMS (the values given are recalculated for 6 min assuming linearity).

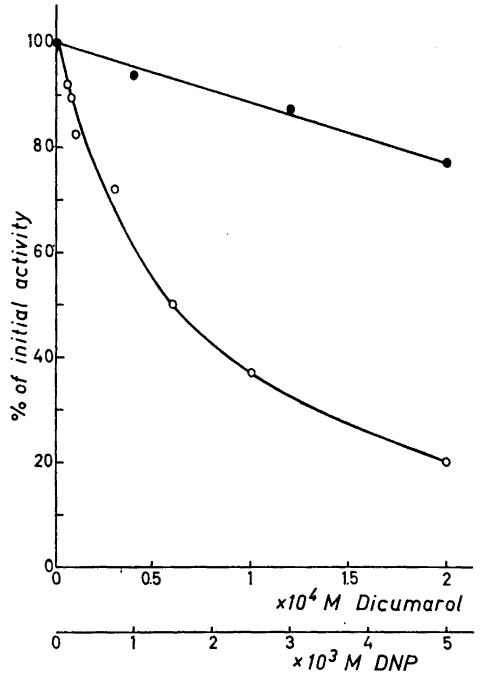

Fig. 6. Effects of dicumarol and DNP on LIP. Experimental details as in Fig. 1. O = dicumarol, ● = DNP. For O, "OD_{800}" = 0.47, 100 % initial activity = 47.5 % P_{org}, 30 min experiment. For ●, "OD_{800}" = 0.20, 100 % initial activity = 10.9 % P_{org}, 20 min experiment.

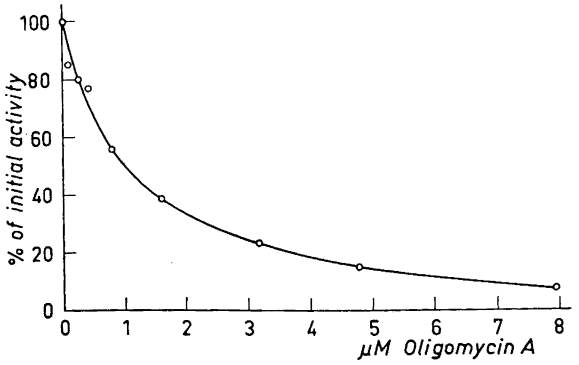

Fig. 7. Effect of oligomycin A on LIP. Experimental details as in Fig. 1. "OD_{800}" = 0.48, 100 % initial activity = 18.8 % P_{org}, 20 min experiment. "Chromatophores" fraction.

Table 1. Effects of NaN_3 and KCN on LIP. Experimental details as in Fig. 1. "OD_{800}" = 0.54, 20 min experiment.

KCN or NaN_3 concentration M	% P_{org} KCN	% P_{org} NaN_3
—	34.8	34.8
$\times 10^{-4}$	33.0	34.9
$\times 10^{-3}$	35.5	36.1
3×10^{-3}	33.1	39.9
5×10^{-3}	31.9	34.0

and flavin [15], as well as cyanide and azide, which both inhibit at the cytochrome a_3-level, have no similar effect on LIP in *R. rubrum* (Fig. 3 and Table 1).

The concentrations of antimycin A and HOQNO which were needed to inhibit LIP in *R. rubrum* (Fig. 4) were found to be almost the same as those inhibiting electron transport in mitochondrial systems [16,6]. This supports the previously formulated concept [12] that an identical or at least very similar electron carrier is acted upon in both systems.

DNP and dicumarol are "uncoupling agents" in mitochondrial oxidative phosphorylation, *i.e.* they inhibit the phosphorylation but not the respiration. In order to inhibit LIP in extracts of *R. rubrum* much higher concentrations of dicumarol and especially DNP were required than those necessary for uncoupling of the mitochondrial system [17]. It is therefore doubtful whether the inhibitory effect in the bacterial system is due to a similar mechanism as that in mitochondria. It may be appropriate to mention that at high concentration of DNP [18] and dicumarol [19] electron transport itself is inhibited in mitochondrial systems.

Also gramicidin and oligomycin A interfere with oxidative phosphorylation in animal mitochondria. Gramicidin is an "uncoupling agent" [17] and oligomycin A an inhibitor of both phosphorylation and oxidation reactions [20]. The effect of oligomycin A on respiration is especially strong with DPN-linked substrates and has been assumed to involve the inhibition of a phosphoryla-

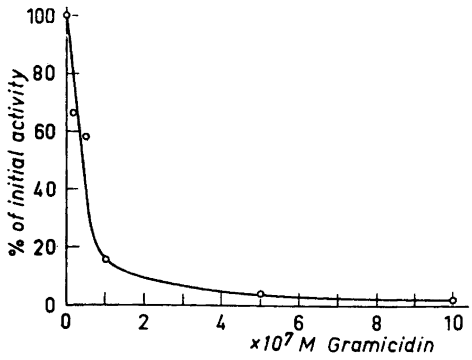

Fig. 8. Effect of gramicidin on LIP. Experimental details as in Fig. 1. "OD_{800}" = 0.20, 100 % initial activity = 13.3 % P_{org}, 20 min experiment.

tion reaction to which the respiration is obligatorily coupled [20]. The fact that both gramicidin and oligomycin A inhibited the LIP is an indication that the phosphorylation reactions proper in bacterial LIP share qualities with those of the oxidative phosphorylation reactions in animal mitochondria with respect to the mechanism of coupling between electron transport and phosphate esterification and to the nature of a reaction involved in phosphate transfer.

Acknowledgements. Thanks are due to Professor Olov Lindberg for valuable advice and continuous support, to Dr. Lars Ernster, Dr. Hans Löw and Dr. Thomas Conover for stimulating discussions and to Mrs. Torill Hundal for skilful technical assistance.

REFERENCES

1. Smith, L. and Baltscheffsky, M. *Federation Proc.* **15** (1956) 357.
2. Geller, D. M. *Abstr. 7th Intern. Congr. for Microbiology, Stockholm* 1958, p. 73.
3. Smith, L. and Baltscheffsky, M. *J. Biol. Chem.* **234** (1959) 1575.
4. Baltscheffsky, H. *Biochim. et Biophys. Acta* **40** (1960) 1.
5. Ernster, L. and Löw, H. *Exptl. Cell Research Suppl.* **3** (1955) 133.
6. Baltscheffsky, H., Fudge, M. and Arwidsson, B. *Acta Chem. Scand.* **14** (1960) 247.
7. McIlwain, H. *J. Gen. Microbiol.* **2** (1948) 288.
8. Frenkel, A. W. *J. Biol. Chem.* **222** (1956) 823.
9. Frenkel, A. W. *Plant Physiol.* **31** (1956) xxx.
10. Ernster, L., Jalling, O., Löw, H. and Lindberg, O. *Exptl. Cell Research, Suppl.* **3** (1955) 124.
11. Chance, B. in Colowick, S.P. and Kaplan, N. O. *Methods in Enzymology,* Academic Press, New York 1957, Vol. IV, p. 273.
12. Baltscheffsky, H. and Baltscheffsky, M. *Acta Chem. Scand.* **12** (1958) 1333.
13. Whatley, F. R., Allen, M. B. and Arnon, D. I. *Biochim. et Biophys. Acta* **32** (1959) 32.
14. Baltscheffsky, H. *Acta Chem. Scand.* **14** (1960) 264.
15. Chance, B., in Gaebler, O. H. *Enzymes: Units of Biological Structure and Function,* Academic Press Inc., New York 1956, p. 447.
16. Ahmad, K., Schneider, H. G. and Strong, F. M. *Arch. Biochem.* **28** (1950) 281.
17. Lehninger, A. L., in Gaebler, O. H. *Enzymes: Units of Biological Structure and Function,* Academic Press Inc., New York 1956, p. 217.
18. Loomis, W. F. and Lipmann, F. *J. Biol. Chem.* **173** (1948) 807.
19. Raw, I. and Mahler, H. R. *J. Biol. Chem.* **234** (1959) 1867.
20. Lardy, H. A., Johnson, D. and McMurray, W. C. *Arch. Biochem. Biophys.* **78** (1958) 587.

Received December 29, 1959.

ACTA CHEMICA SCANDINAVICA 14 (1960) 264–272

Inhibitor Studies on Light-Induced Phosphorylation in Isolated Spinach Chloroplasts

HERRICK BALTSCHEFFSKY

Wenner-Gren Institute, University of Stockholm, Sweden

Light-induced phosphorylation in isolated chloroplasts is greatly stimulated by the addition of several types of compounds capable of undergoing reduction and oxidation [1-3], among them flavin nucleotides. Whether the stimulatory agent is a flavin or not, 4×10^{-5} M atebrin * completely or almost completely inhibits the phosphorylation, indicating that endogenous chloroplast flavin is an obligatory participant in this system. The inhibition is not reversed by high concentrations of flavin nucleotide. In fact, flavin adenine dinucleotide (2×10^{-3} M) gives nearly complete and flavin mononucleotide (5×10^{-3} M) partial inhibition of phosphate esterification.

Amytal ** gives only slight inhibition.

Low concentrations of antimycin A, 2-*n*-heptyl-4-hydroxyquinoline-N-oxide and oligomycin A have no inhibitory effect on light-induced phosphorylation in isolated spinach chloroplasts comparable to the effects on light-induced phosphorylation in a bacterial *(Rhodospirillum rubrum)* extract and respiration and phosphorylation in animal mitochondria. The hypothesis [2] that added compounds effective as cofactors, such as FMN, menadione and phenazine methosulfate, may bridge over a gap in electron transport of the chloroplasts as they are presently isolated, is discussed.

Light-induced phosphorylation † (LIP) in isolated spinach chloroplasts is stimulated by both physiological electron carriers and non-physiological redox-compounds [1-3]. This and other evidence indicates that the phosphorylation process is linked to electron transport. Several schemes for the electron transport have been suggested [4-8]. In the present paper results of inhibitor studies on LIP in isolated spinach chloroplasts are presented and discussed.

Some data have already been given in an abstract [9].

* 3-Chloro-7-methoxy-9-(1-methyl-4-diethylamino-butylamino) acridine.

** 5-Ethyl-5-*iso*amylbarbiturate.

† This term as used here is equivalent to "cyclic photophosphorylation" [4].

MATERIALS AND METHODS

ATP *, FAD, FMN, PMS and antimycin A were obtained from Sigma Chemical Co., St. Louis, Mo., U.S.A. The FAD was of the 80–90 % pure type. Gramicidin D was obtained from Mann Research Laboratories, New York, N.Y., U.S.A. HOQNO was obtained from Dr. J. W. Cornforth, National Institute for Medical Research, London, England, and oligomycin A from Dr. F. M. Strong, Department of Biochemistry, University of Wisconsin, Madison, Wisc., U.S.A.; these gifts are gratefully acknowledged. Hexokinase was prepared and stored as in Ref.[10]. Antimycin A, HOQNO, gramicidin and oligomycin A were dissolved in ethanol. The stock solutions were kept in a deep-freeze. In the reaction medium for LIP the ethanol content was kept below 1 % in order not to inhibit the LIP. In such a medium, antimycin A occasionally did not keep solubilized when used in high concentrations, in which case the medium was discarded. The molecular weight of antimycin A was taken as 548 (*cf.* Ref.[11]).

Spinach was obtained as whole spinach plants from local growers. The chloroplasts were isolated according to Allen, Whatley and Arnon [12], with one washing and subsequent fragmentation of the whole chloroplasts by addition of hypotonic (0.035 M) NaCl. The chlorophyll content was determined according to Arnon [13]. All experiments were performed immediately after the preparation was finished. The medium employed for the phosphorylation experiments contained, unless otherwise noted, 1.0 ml 0.08 M tris-(hydroxymethyl)-aminomethane pH 8.3, 8 μmoles $K_2H^{32}PO_4$, 10 μmoles ATP, 30 μmoles $MgCl_2$, 60 μmoles glucose and an excess of yeast hexokinase. The final volume was 3.0 ml. The experiments were performed under aerobic conditions in test tubes which were immersed in a water-bath of 20°C. The light source consisted of a row of incandescent 150 W Philips lamps, adjusted to give a light intensity of about 30 000 lux at the reaction tubes. The reaction was stopped with 1 ml of 2 M perchloric acid.

Phosphorylation was measured by the ^{32}P method recommended by Lindberg and Ernster [14]. In all experiments two controls were run. In one of them the reaction was stopped at zero time. The other one was a dark control which was wrapped in aluminium foil and run parallel with the other tubes. The low amount of phosphate esterified in the dark was used as a zero for the LIP values.

Ascorbate gives a very low stimulation of LIP under aerobic conditions [15] but has nevertheless been used as a stimulatory agent in some of the experiments with inhibitors. It is also a stabilizer for the isolated chloroplasts [2,6] and has thus been added in some experiments along with other stimulating agents.

RESULTS

To obtain conveniently measurable rates of LIP in isolated spinach chloroplasts it is necessary to add one of a number of suitable stimulatory agents to the reaction medium. The following stimulatory agents have been employed in the present work: phenazine methosulfate [3], FMN [15], FAD, menadione [1], DNP [16] and ascorbate [15].

In Fig. 1 a typical time curve for LIP is given. It shows that 6 min, which has also been used by Jagendorf and Avron [3], is a suitable reaction time.

Amytal gave only a weak inhibition of LIP in chloroplasts with any of the stimulating agents used, even at concentrations several times higher than those which strongly inhibit the oxidation of DPN-linked substrates in animal mitochondria [17] (Fig. 2).

* Abbreviations: P, orthophosphate; ATP, adenosine triphosphate; FAD, flavinadenine dinucleotide; FMN, flavin mononucleotide; PMS, phenazine methosulfate; HOQNO, 2-*n*-heptyl-4-hydroxyquinoline-N-oxide; DNP, 2,4-dinitrophenol; M, moles per liter; % P_{org}, percentage ortophosphate esterified.

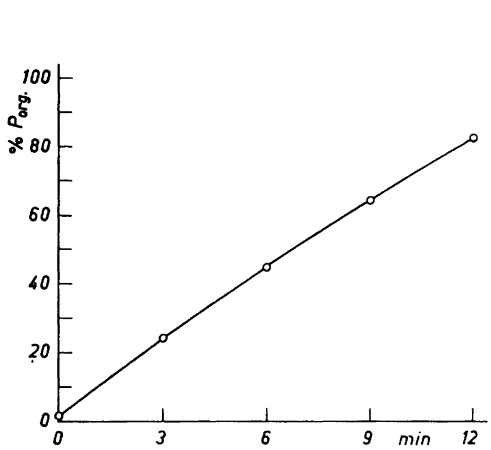

Fig. 1. Time curve of LIP stimulated by FMN. All tubes contained 30 μmoles ascorbate, 0.4 μmoles FMN and 0.16 mg chlorophyll.

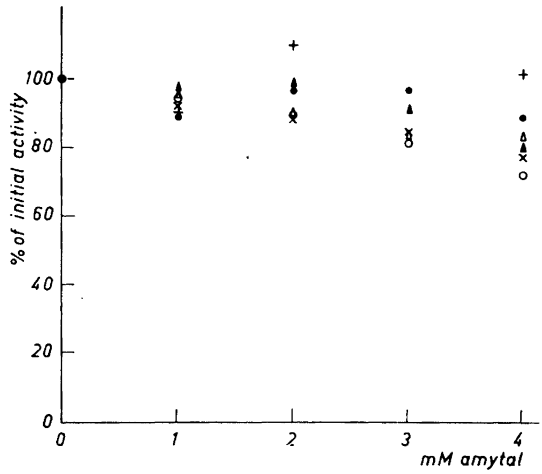

Fig. 2. The effect of amytal on LIP in the presence of various stimulatory agents. × = FMN, △ = PMS, ▲ = DNP, ○ = FAD, ● = menadione and + = ascorbate. The PMS- and menadione-series represent mean values of three, respectively two, different experiments. With the exception of the PMS-series all tubes contained 30 μmoles of ascorbate.

Atebrin, a flavoenzyme antagonist [18], inhibited LIP strongly (Fig. 3) regardless of the stimulatory agent used. The inhibition occured at concentrations of atebrin which were of the same order of magnitude as those required for inhibition of LIP in extracts of *Rhodospirillum rubrum* [19].

In extracts of *R. rubrum* the inhibition obtained with atebrin could be overcome completely with FAD and partially with FMN [19]. With chloroplasts such an effect did not appear. On the contrary it was found that the corres-

Table 1. Effects of FMN and FAD on LIP. All tubes contained 30 μmoles ascorbate. The chlorophyll content in each tube was with FAD 0.066 mg., with FMN 0.072 mg. (Repeated experiments confirmed the inhibition at 2×10^{-3} and 5×10^{-3} M FMN.)

Concentration of FMN or FAD M	% P_{org} FMN	FAD
—	5	5
5×10^{-5}	53	30
1.5×10^{-4}	51	29
6×10^{-4}	57	17
2×10^{-3}	47	7
5×10^{-3}	44	5

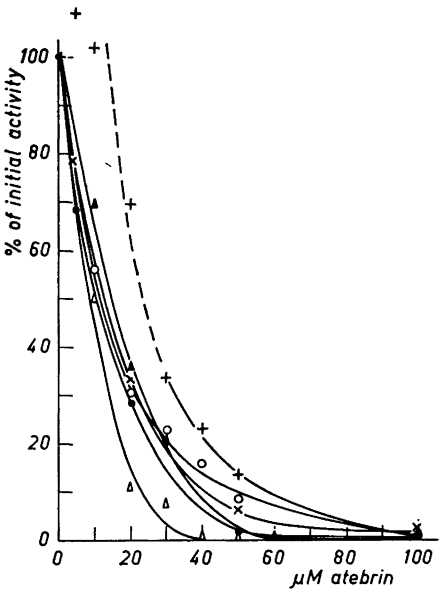

Fig. 3. The effect of atebrin on LIP in the presence of various stimulatory agents. × = FMN, △ = PMS, ▲ = DNP, O = FAD, ● = menadione and + = ascorbate. With the exception of the FAD- and PMS-series all tubes contained 30 μmoles of ascorbate.

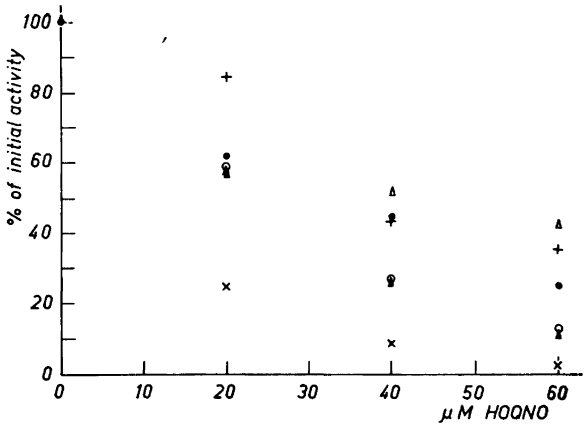

Fig. 4. The effect of HOQNO on LIP in the presence of various stimulatory agents. × = FMN, △ = PMS, ▲ = DNP, O = FAD, ● = menadione and + = ascorbate.

ponding concentrations of the flavin nucleotides inhibited the LIP in chloroplasts, the inhibition due to FAD being very strong (Table 1). The strong inhibitory effect of 2 mM FAD (Table 1) was obtained also when the LIP had been stimulated with PMS or menadione. The inhibition in one experiment was more than 95 % in the former and more than 75 % in the latter case.

Table 2. Effect of antimycin A on LIP, stimulated by FMN, PMS or menadione. With the exception of the PMS-series all tubes contained 30 μmoles ascorbate. Where added: 0.4 μmoles FMN, 0.06 μmoles PMS or 0.3 μmoles menadione. In the FMN-, PMS- and menadione-series, respectively, values for 100 % initial activity was 18, 33 and 56 % P_{org} and the chlorophyll content 0.044, 0.044 and 0.105 mg.

Concentration of antimycin A M	Percentage of initial activity		
	FMN	PMS	menadione
—	100	100	100
2×10^{-5}	83	78	—
5×10^{-5}	24	19	32

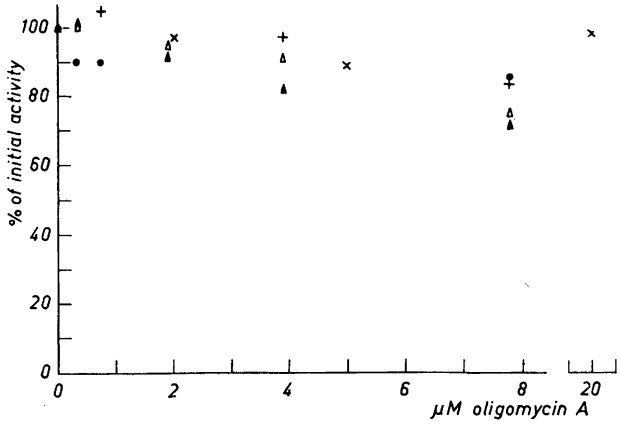

Fig. 5. The effect of oligomycin A on LIP in the presence of various stimulatory agents. △ = PMS, ▲ = DNP, ● = menadione, X = FMN and + = ascorbate. With the exception of the PMS-series all tubes contained 30 μmoles ascorbate. The chlorophyll content in each tube was for the different series taken in the above order, 0.12, 0.28, 0.10, 0.13 and 0.35 mg. The 100 % initial activity was, in the same order, 42, 48, 54, 57 and 9 % P_{org}. These values are included as examples of the rates of LIP obtained and may be regarded as representative, although the rate with menadione was unusually high and although considerable variations occured. (FAD gave rates similar to or somewhat lower than FMN.)

Antimycin A and HOQNO have been shown to inhibit LIP in extracts of *R. rubrum* [20] at similar concentrations as they inhibit electron transport in mitochondrial systems [21,11]. According to Arnon, Allen and Whatley [22] antimycin A does not inhibit LIP in spinach chloroplasts (in anaerobic experiments). No studies with HOQNO have been reported. Also under aerobic conditions LIP was unaffected by low concentrations of antimycin A as well as of HOQNO. As Table 2 and Fig. 4 show, both antimycin A and HOQNO inhibited LIP in chloroplasts at concentrations only as high as between 10^{-5} and 10^{-4} M.

Oligomycin A, which inhibits oxidative phosphorylation in animal mitochondria and the respiration connected with it, but not the respiration induced by addition of DNP [23], gave no significant inhibition of LIP in spinach chloroplasts (Fig. 5). As has been reported, oligomycin A inhibits LIP in extracts of *R. rubrum* [20].

Whatley, Allen and Arnon [24] have shown that gramicidin, which is an uncoupler of oxidative phosphorylation, strongly inhibits LIP under anaerobic conditions. Table 3 shows that inhibition occurs also under aerobic conditions.

DISCUSSION

The path of electron transport in LIP of plant chloroplasts is still essentially unknown. A comparison of various schemes which have been proposed [4-8] shows that no general agreement has been reached in this field. In a recent scheme for LIP in green plants Arnon [4] proposes three different electron trans-

Table 3. The inhibition of LIP by gramicidin. All tubes contained 30 μmoles ascorbate. Where added: 0.4 μmoles FMN or 0.3 μmoles menadione. The chlorophyll content in each tube and the values for 100 % initial activity were as follows: In the FMN-series, experiment 1, 0.090 mg chlorophyll, 46.5 % P_{org}; experiment 2, 0.116 mg chlorophyll, 36.3 % P_{org}. In the menadione-series, experiment 1, 0.089 mg chlorophyll, 15.7 % P_{org}; experiment 2, 0.116 mg chlorophyll, 16.3 % P_{org}.

Concentration of gramicidin M	Percentage of initial activity FMN		menadione	
	expt. 1	expt. 2	expt. 1	expt. 2
—	100	100	100	100
10^{-7}	64	67	54	33
10^{-6}	36	32	9	12

port pathways, all coupled to phosphorylation: (1) the cyclic electron transport system involving vitamin K and a cytochrome, (2) the cyclic electron transport system involving TPN, FMN and cytochromes and (3) the "open" non-cyclic mechanism, which transports electrons from chlorophyll to TPN. According to Wessels [6] TPN is not a member of the cyclic electron carrier chain(s). Both Wessels [25] and Whatley, Allen and Arnon [24] have reported that FMN and menadione are involved in separate pathways of electron transport in LIP under aerobic conditions. Marré, Servettaz and Forti [7] have presented a scheme with five electron carriers, among them cytochrome c, in a single electron transport chain joining the oxidizing and reducing equivalents produced by the photolysis of water. Jagendorf and Avron [3] have pointed out that FMN and menadione as well as PMS may act by bridging a gap in electron transport of the chloroplasts as they are presently isolated.

The absence of a strong inhibition by amytal indicates that no electron transport step identical with that in phosphorylating mitochondria between DPNH and flavin exists in the system studied. A similar lack of inhibition by amytal has been found for bacterial LIP [20]. Arnon, Whatley and Allen [2] have earlier shown that DPN does not seem to be involved in LIP of chloroplasts.

The fact that atebrin inhibited LIP not only when FMN or FAD were added but also when menadione, PMS, DNP or ascorbate were used indicates that chloroplast flavin participated in the electron transport regardless of the nature of the stimulatory agent. When considered together with other results listed below, this finding supports scheme (1) for representation of electron transport in LIP of isolated spinach chloroplasts:

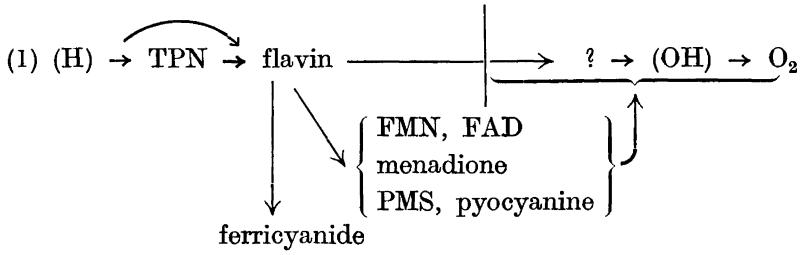

Cyclic electron transport in LIP is in this paper written in its classical form, combining reducing (H) and oxidizing (OH) equivalents from the Hill-reaction (cf Ref.[4]). The stimulatory agents in this scheme may be reoxidized by (OH) or, at least under aerobic conditions, O_2, or by any agent between these and the indicated block in the electron transport chain. Differences between the response of LIP towards various inhibitors when different stimulatory agents are employed may be due to different sites of reoxidation of the stimulatory agents (*cf.* Ref.[4]).

The following information is relevant for the scheme presented. (a) Light induces a phosphorylation concomitantly with the reduction of TPN, or of ferricyanide [26]. In both cases one molecule of ATP is reported to be formed during the transport of two electrons. For the reduction of TPN (but not for that of ferricyanide) an enzyme, photosynthetic pyridine nucleotide reductase [27,28], is necessary. This enzyme is isolated and purified from the supernatant of the chloroplast preparation. (b) Oxidation of photo-reduced TPN in chloroplasts is accomplished when any of the compounds FMN, menadione and pyocyanine is added [29]. (c) A TPNH-specific diaphorase, containing FAD [30], has been isolated from spinach chloroplasts [31]. Electrons from this diaphorase may be accepted by compounds such as potassium ferricyanide, menadione and FMN [32]. (d) High rates of LIP in spinach chloroplasts are obtained by addition of a stimulatory agent with oxidation-reduction properties, such as FMN, FAD, menadione, PMS or pyocyanine [32].

If electron transport between flavin and (OH) is blocked immediately on the oxidizing side of flavin in the isolated chloroplasts, then any physiological electron carrier between the point of inhibition and the point at which the added stimulatory agent is oxidized will remain undetected by inhibitor or spectrophotometric experiments. Four electron carriers which could be so situated have been found in chloroplasts: cyctochrome b_6[33], cytochrome f[34] (with a cytochrome c-like spectrum), vitamin K_1[35] and plastoquinone (Q_{254})[36,37] which is a quinone closely related to coenzyme Q. It is possible that such a by-pass might explain the resistence of LIP in isolated chloroplasts towards antimycin A and HOQNO. Another possibility is that the compound on which these inhibitors act in mitochondria and chromatophores is lacking in chloroplasts or has a structure modified so as to make it less sensitive to the inhibitors. They appear to act in the b-type cytochrome or coenzyme Q region in mitochondria and chromatophores, where they are effective in concentrations of less than one thousandth of what is needed to inhibit LIP in chloroplasts.

Hill [33] has reported an experiment which may support the concept of a block in electron transport of isolated chloroplasts on the reducing side of cytochrome b_6. With illuminated leaves of the "golden varieties" of certain plants he could observe the sharp absorption band of reduced cytochrome b_6 at 563 mμ. With chloroplasts prepared from such leaves, however, no reduced cytochrome b_6 was found, until the preparation was reduced with sodium dithionite.

It is to be observed that not only with respect to the effect of the electron transport inhibitors antimycin A and HOQNO does the electron transport phosphorylation system in isolated chloroplasts show differences from those

of bacterial chromatophores and of animal mitochondria. Low concentrations of oligomycin A, which is reported to block a reaction involved in phosphate transfer in mitochondrial oxidative phosphorylation [23] and inhibit LIP in bacterial chromatophores [20], have no or very small influence on LIP in isolated chloroplasts. These facts are the more remarkable as the two former systems have a similar sensitivity to these inhibitors. On the basis of present evidence it is not possible to decide whether the findings reflect inherent differences between the systems, or whether the sensitivity towards the inhibitors is lost in spinach chloroplasts during the preparation. However, the fact remains that the system for LIP in isolated plant chloroplasts differs in its response to inhibitors both of electron transport and of phosphate transfer from the system for LIP in bacterial chromatophores and the system for oxidative phosphorylation in animal mitochondria. It still seems necessary to strongly consider the possibility that the system for LIP in spinach chloroplasts is partially destroyed, as they are presently prepared.

Acknowledgements. Thanks are due to Professor Olov Lindberg for his active and supporting interest in this work, and to Dr. Lars Ernster, Dr. Thomas Conover and Mrs. Margareta Baltscheffsky for valuable help.

REFERENCES

1. Arnon, D. I., Whatley, F. R. and Allen, M. B. *Biochim. et Biophys. Acta* **16** (1955) 607.
2. Arnon, D. I., Whatley, F. R. and Allen, M. B. *Nature* **180** (1957) 182.
3. Jagendorf, A. T. and Avron, M. *J. Biol. Chem.* **231** (1958) 277.
4. Arnon, D. I. *Nature* **184** (1959) 10.
5. Wessels, J. S. C. *Biochim. et Biophys. Acta* **29** (1958) 113.
6. Wessels, J. S. C. *Biochim. et Biophys. Acta* **35** (1959) 53.
7. Marré, E., Servettaz, O. and Forti, G. *Atti del 2° Congr. Intern. di Fotobiologia*, Edizione Minerva Medica, Torino 1957, p. 329.
8. Avron, M. and Jagendorf, A. T. *J. Biol. Chem.* **234** (1959) 1315.
9. Baltscheffsky, H. *Acta Chem. Scand.* **13** (1959) 2130.
10. Ernster, L. and Löw, H. *Exptl. Cell Research. Suppl.* **3** (1955) 133.
11. Baltscheffsky., H, Fudge, M. and Arwidsson, B. *Acta Chem. Scand.* **14** (1960) 247.
12. Allen, M. B., Whatley, F. R. and Arnon, D. I. *Biochim. et Biophys. Acta* **27** (1958) 16.
13. Arnon, D. I. *Plant Physiol.* **24** (1949) 1.
14. Lindberg, O. and Ernster, L. in Glick, D. *Methods of Biochemical Analysis*, Interscience Publishers, New York 1956, Vol. *3*, p. 1.
15. Whatley, F. R., Allen, M. B. and Arnon, D. I. *Biochim. et Biophys. Acta* **16** (1955) 605.
16. Wessels, J. S. C. *Biochim. et Biophys. Acta* **36** (1959) 264.
17. Ernster, L., Jalling, O., Löw, H. and Lindberg, O. *Exptl. Cell Research Suppl. 3* (1955) 124.
18. Haas, E. *J. Biol. Chem.* **155** (1944) 321.
19. Baltscheffsky, H. *Biochim. et Biophys. Acta* **40** (1960) 1.
20. Baltscheffsky, H. and Baltscheffsky, M. *Acta Chem. Scand.* **14** (1960) 257.
21. Ahmad, K., Schneider, H. G. and Strong, F. M. *Arch. Biochem.* **28** (1950) 281.
22. Arnon, D. I., Allen, M. B. and Whatley, F. R. *Biochim. et Biophys. Acta* **20** (1956) 449.
23. Lardy, H. A., Johnson, D. and McMurray, W. C. *Arch. Biochem. Biophys.* **78** (1958) 587.
24. Whatley, F. R., Allen, M. B. and Arnon, D. I. *Biochim. et Biophys. Acta* **32** (1959) 32.
25. Wessels, J. S. C. *Biochim. et Biophys. Acta* **25** (1957) 97.
26. Arnon, D. I., Whatley, F. R. and Allen, M. B. *Science* **127** (1958) 1026.

27. San Pietro, A. and Lang, H. M. *Science* **124** (1956) 118.
28. San Pietro, A. and Lang, H. M. *J. Biol. Chem.* **231** (1958) 211.
29. Davenport, H. E. *Nature* **184** (1959) 524.
30. Avron, M. and Jagendorf, A. T. *Arch. Biochem. Biophys.* **72** (1957) 17.
31. Avron, M. and Jagendorf, A. T. *Arch. Biochem. Biophys.* **65** (1956) 475.
32. Walker, D. A. and Hill, R. *Biochem. J.* **69** (1958) 57P.
33. Hill, R. *Nature* **174** (1954) 501.
34. Hill, R. *Biochem. J.* **37** (1943) xxiii.
35. Dam, H., Glavind, J. and Nielsen, N. *Z. physiol. Chem.* **265** (1940) 80.
36. Crane, F. L. *Plant Physiol.* **34** (1959) 128.
37. Crane, F. L. *Plant Physiol.* **34** (1959) 546.

Received December 29, 1959.

ACTA CHEMICA SCANDINAVICA 14 (1960) 273–295

Stereochemical Studies

IX *. The Relationship between Optical Rotatory Dispersion and Configuration for Some Carboxylic Acids

BERNDT SJÖBERG

Department of Organic Chemistry, Chemical Institute, University of Uppsala

The optical rotatory dispersion of several series of arylsubstituted mono- and dicarboxylic acids, and acid derivatives, has been investigated. The utility of plain dispersion curves for establishing configurational relationships has been demonstrated. Attention is called to the high rotation and the steepness of the dispersion curves of anilides in these series. The advantage, and at times the necessity, of using dispersion curves instead of measurements at the D-line, when applying Freudenberg's displacement rule, has been demonstrated.

A knowledge of the configurational relationships between different types of optically active compounds is important in many branches of chemistry. Several chemical and physical methods have been developed for correlating relative configurations [1,2]. From the X-ray crystallographic investigations on sodium rubidium tartrate by Bijvoet, Peerdeman and van Bommel [3] it follows that for compounds with a configuration related to glyceraldehyde even the absolute configuration is known. Most of the methods referred to [1–3] are laborious and require a fairly large amount of optically active substance. Studies of the optical rotatory dispersion, (*i.e.* the change of optical rotation with wavelength), can be performed on as little as 0.1—2 mg of a compound, and with a modern spectropolarimeter a simple dispersion curve from 700 to 275 mμ can be produced in less than half an hour.

Measurements of optical rotatory dispersion have been made by various scientists since the phenomenon was discovered in 1817 by Biot [4]. These investigations have mainly been concerned with physico-chemical aspects of rotatory dispersion [5–7], but some workers, (for instance Tschugaeff, Rupe, Freudenberg, Kuhn and Levene), also tried to relate the observed optical rotation to molecular structure, (for reviews and references see Refs.[1,6,8–13]). It was not until Djerassi started in 1954 extensive studies of the optical rotatory

* Part VIII, *Arkiv Kemi* 15 (1960) 419.

dispersion of ketones and aldehydes that it was proved that spectropolarimetry was an extremely valuable tool for the chemist in solving structural and stereochemical problems. The work by Djerassi and collaborators has been published in the series "Optical Rotatory Dispersion Studies I[14]—XXXIV [15]", and has also been reviewed [16–18].

In order to facilitate further discussion of the application of optical rotatory dispersion in this paper, a brief description will be given of some of the physical background and of the nomenclature used. A compound possesses optical rotatory power in an isotropic medium only when the mirror images of the molecule cannot be superimposed. When plane polarized light, (which is the superposition of right and left circularly polarized components), is transmitted through an optically active medium, the two components travel with unequal velocities. A phase difference between the right and the left circularly polarized components will thus arise, producing a rotation of the plane of polarization. The angle of rotation per unit length, α, is given by the expression,

$$\alpha = \frac{\pi}{\lambda_{vac}} (n_l - n_r) \qquad (1)$$

where λ_{vac} is the wavelength of the light *in vacuo* and n_l and n_r are the refractive indices of the left and right circularly polarized waves, respectively.

Simultaneously with the optical activity produced by the difference in velocity of propagation of right and left circularly polarized waves, there is a second effect referred to as circular dichroism, arising from unequal absorption of the two waves. This is due to differential absorption of the two components of the incident linearly polarized wave so that they have different amplitudes after traversing the medium. They thus combine to give elliptically polarized light. The difference between the absorption coefficients for left and right circularly polarized light is only a small fraction of the mean absorption coefficient, and as a consequence the ellips is very elongate. Any medium that exhibits circular birefringence will simultaneously show circular dichroism and the light will then not be plane polarized, but the effect is only apparent in the immediate vicinity of an absorption band. The variation of rotation and ellipticity in the neighbourhood of an absorption band has been called the *Cotton effect.*

Several physical theories have been developed which attempt quantitatively, to relate molecular structure to optical rotatory power, examples are those based on classical mechanics by Drude [19], Born [20,21] and Kuhn [7,22,23], and based on quantum-mechanical treatment of dispersion by Rosenfeld [24]. Further theories employing quantum-mechanical considerations have been put forward by Kirkwood [25], Condon, Altar, Eyring [26,27] and by Moffitt and Moscowitz [28–30]. A clear account of some of the theories of optical rotatory power has been given by Schellman [31].

The system of nomenclature used in this context by organic chemists is outlined in Fig. 1 [32,33]. It is somewhat different from that used by physical chemists [5,34]. The term *plain* curve is used if the curve shows no maximum, (peak), or minimum, (trough), directly related to a Cotton effect. They are

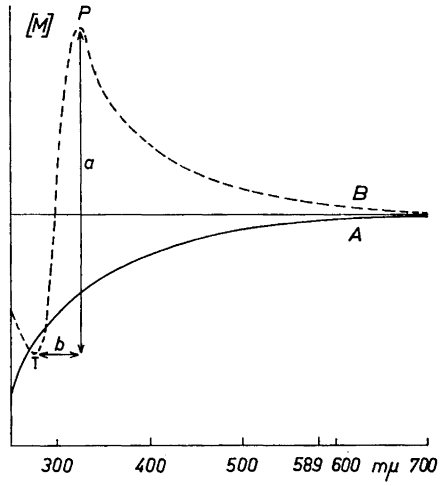

Fig. 1. Examples of a plain negative dispersion curve (A), and of a positive Cotton effect curve (B); (P, peak; T, trough; a, amplitude; b, breadth.)

called *positive* or *negative* respectively if they rise or fall towards shorter wavelengths. Other types of curves are called *anomalous* and in Fig. 1, this type is represented by a *positive single Cotton effect* curve. The Cotton effect is *positive* if the peak occurs at a longer wavelength than the corresponding absorption maximum, and the trough at a shorter wavelength.

The variation of the partial specific rotation $[\alpha]_{px}$ with wavelength outside the range of optically active absorption, can be expressed according to Drude [19]

$$[\alpha]_{px} = \frac{A_x}{\lambda^2 - \lambda_x^2} \tag{2}$$

where A_x is a molecular parameter, and λ_x is the centre of the single optically active absorption band. If more than one absorption band contributes to the rotation within the given spectral range, the general Drude equation [19] must be used:

$$[\alpha] = \sum \frac{A_i}{\lambda^2 - \lambda_i^2} \tag{3}$$

A numerical evalution of the unknown constants in eqn. 3 is extremely time-consuming even for its abbreviated forms [35].

The optical rotatory dispersion work performed recently by organic chemists has mainly been concerned with anomalous dispersion curves, and rotations have been measured in the regions of maximum absorption for the low intensity bands of, for example, ketones and aldehydes. With these compounds it is often unnecessary to calculate λ_i in the Drude equation because comparison of the rotatory dispersion curve and the electronic absorption spectrum of the substances, directly gives λ_i. It has been clearly shown that the sign, shape, and amplitude of these anomalous dispersion curves can be correlated empirically to certain structural and steric features of the compounds [16-18]. Only when more information is sought about the quantitative contributions of the

various optically active chromophores must the molecular parameters A_i, (which are related to the rotational strength [30]), be calculated.

The present paper deals with the optical rotatory dispersion of some carboxylic acids. As the carboxyl group absorbs in a region which is at present inaccessible for rotatory dispersion measurements, it was expected that only the plain part of the curves could be experimentally determined. With the compounds investigated by Djerassi [16-18] the useful information had been obtained mainly from the anomalous part of the dispersion curves. Thus two different problems arose: (a), What information can be obtained from plain dispersion curves, and (b), how can compounds with plain curves be transformed into derivatives possessing anomalous dispersion curves. Both problems are being investigated and some aspects of the second one have already been published [36]; further studies will follow. The first problem will now be discussed in more detail.

GENERAL EXPERIMENTAL PROCEDURE

The optical rotatory dispersion curves in this paper have been obtained with a Rudolph photoelectric spectropolarimeter with the exception of a few cases (the measurements were made at Wayne State University, Detroit, Michigan, USA). A detailed description of the instrument as well of its operation, scope and limitations has been given elsewhere [37], and so will only be briefly mentioned here. The spectropolarimeter unit consisted of a light source, monochromator, polarimeter with photomultiplier tube, and photometer. The light source was a glass-jacketed concentrated-arc zirconium lamp in the spectral region 700—320 mμ. For shorter wavelengths a quartz-jacketed xenon high pressure arc lamp was used. The monochromatic light was produced by means of a Beckman DU quartz monochromator. Readings were taken by the method of symmetrical angles [37,38], and the polarimeter equipped with a polarizer drive which automatically changed a chosen symmetrical angle from positive to negative to positive at four seconds periods. One photomultiplier tube was used over the spectral range covered.

The polarimeter tubes were of the centre-filling type with permanently fastened fused silica end windows. The length of the tubes was either 10 cm or 5 cm and the capacity 1.9 ml. The substance to be investigated, 1—4 mg, was weighed out in a 2.00 ml volumetric flask on a microbalance. Solutions were made up in spectro grade solvents, most measurements being made in methanol. Readings were usually performed at 700, 650, 589, 550, 525, 400—330 mμ at 10 mμ intervals, and below 330 mμ at 5 mμ intervals. Blank readings using pure solvent were taken daily. Temperatures were recorded (see experimental) for each run, but no special temperature control was used. The temperature fluctuations were those encountered in the isolated room employed only for polarimetric studies. The errors inherent in the present rotatory dispersion measurements are of such an order of magnitude, that ordinary variations of the room temperature are not significant.

The maximum error in the readings was of the order of ± 0.02° which, for a concentration c = 0.2 g/100 ml, is equivalent to a specific rotation of ± 10° (10 cm tube). This error could have been substantially decreased in the visible region by using a much higher concentration, but for the measurements at shorter wavelengths a concentration c = 0.2 g/100 ml, or even less, had to be used due to the encreased absorption both by the optical system and the compounds. For the purpose of the present investigation, information about the dispersion curves in the ultraviolet region is more important than in the visible.

RESULTS AND DISCUSSION

A great number of optically active carboxylic acids of the following types,

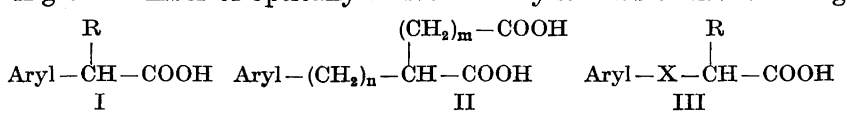

where X is CH_2, NH, O, S or Se, have previously been made in Uppsala [39-42]. The steric relationships have been established, usually by means of the Fredga quasi-racemate method [43,44]. The optical rotatory dispersion of some series of these compounds has now been studied to see if the relative configurations of compounds in special series could be derived from the dispersion curves. The investigations on compounds related to type III will be discussed in a separate paper [45]. Information about the position of the optically active absorption bands can be obtained from the Drude equation. However, it was thought likely that the same type of empirical approach as has been used by Djerassi [16-18] would be more successful, with a large number of compounds, than using a detailed analysis of the Drude equation. All the ivestigated compounds have only one asymmetric centre, and the problem of determining the configuration is thus simplified in distinguishing between the two possibilities. When the region of the Cotton effect can not be quite reached, it is of course not possible to observe all the features — sign, shape and amplitude — which have been used in the correlation of optical rotatory dispersion and molecular structure. Nevertheless, it seemed likely that for the simple compounds of types I—III, dispersion curves and configuration could be correlated if measurements were made close to the first anisotropic absorption band.

α-Aryl monocarboxylic acids and derivatives

The compounds in this series can all be derived from type I, and they may be divided into three sections. In the first, the alkyl group is methyl and the aryl group varies. Most of the dispersion curves have been produced on the D-enantiomers, and even when the actual measurements in some cases were made on the L-forms, the curves throughout this paper will refer to compounds of D-configuration.

According to the Kuhn-Freudenberg theory [1,6] each group attached to the asymmetric centre contributes to the total rotation in two ways — (a), by its own rotatory contribution and (b), by its vicinal action on the other substituents. Weak absorption bands located in the near ultraviolet region often furnish strong partial rotations. The rotation in the visible region will be particularly influenced by these absorption bands due to their proximity. The rotatory contribution from absorption bands in the far ultraviolet will not be so apparent in the visible wavelength range, even if these absorption bands have high anisotropy factors.

The compounds of type I have their aromatic nuclei directly attached to the asymmetric centre. The first absorption in the region 270 to 230 mμ will come from the aromatic group, and if any of these benzenoid absorption bands are anisotropic, the aromatic group will be dominant for the rotation in the visible and near ultraviolet region. Investigations by Kuhn and Biller [12] clearly showed that the phenyl group is highly anisotropic in mandelic acid, atrolactic acid, and some derivatives of these acids, while the anisotropy of the phenyl bands was shown to be very small for phenyl substituted carbinols and halides [12,46]. Rothen and Levene [47] studied the optical rotatory dispersion of some phenyl substituted carboxylic acids, and they found no anomaly in the 250 mμ region. Numerical evaluation of the unknown constants in the Drude

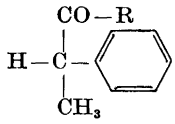

IV R = OH
V R = OCH_3
VI R = NH_2
VII R = $NH-C_6H_5$

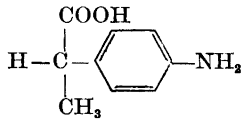

VIII

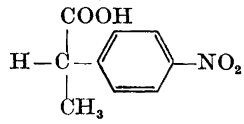

IX

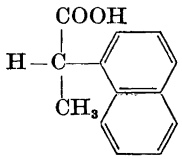

X

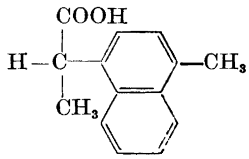

XI

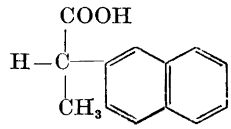

XII

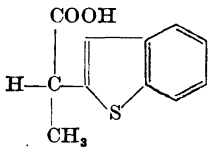

XIII

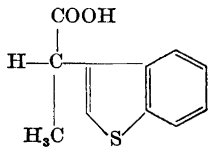

XIV

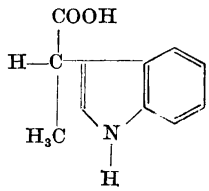

XV

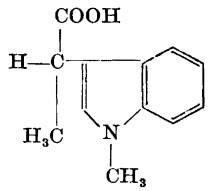

XVI

equation indicated that the first optically active absorption band should be somewhere between 205 and 235 mμ, and so these authors concluded that the phenyl absorption in the 250 mμ region is not anisotropic for phenyl substituted fatty acids.

The rotatory dispersion curve of hydratropic acid (IV) is found in Fig. 2. The rotation rapidly increases towards the region of phenyl absorption. In this way the dispersion curve of hydratropic acid resembles that of mandelic acid [12]. Measurements with a recording Rudolph spectropolarimeter could be extended further into the ultraviolet region (dotted curve), and a peak was found in the experimental dispersion curve at about 270 mμ. An anomalous dispersion curve was also obtained with a Perkin-Elmer spectropolarimeter [37]. This anomaly, however, which was found close to the limiting range of the instruments may not be real. When the direct monochromatic light is almost completely absorbed a small fraction of scattered light of higher wavelengths will result in an effectively higher wavelength than that read on the monochromator. This circumstance may have caused the decreased rotation in the experimental curve below 270 mμ. Even though Rothen and Levene explicitly stated that no anomaly had been found in the 250 mμ region, it can be seen from their own measurements that the rotation of (+)-ethylphenylacetic acid was considerably less at 241 mμ than at 275 mμ (Ref.[46], Table II), *i.e.* the dispersion curve must have had a peak between 275 and 241 mμ.

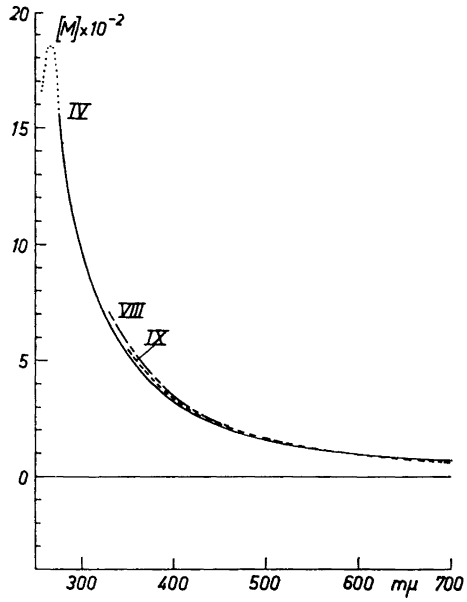

Fig. 2. Optical rotatory dispersion curves of (+)-hydratropic acid (IV), (+)-*p*-amino-hydratropic acid (VIII) and (+)-*p*-nitro-hydratropic acid (IX).

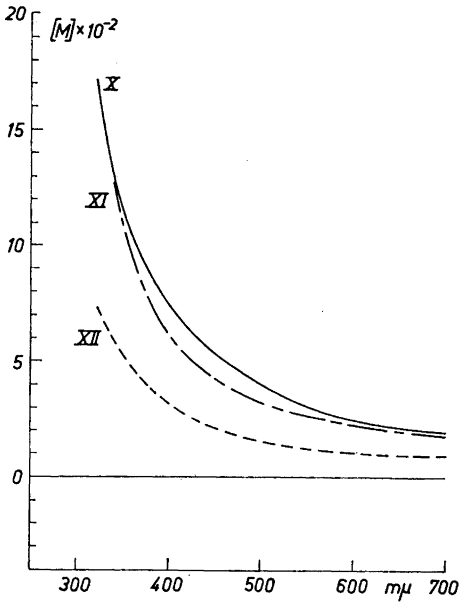

Fig. 3. Optical rotatory dispersion curves of (+)-α-(1-naphthyl)-propionic acid (X), (+)-α-(4-methyl-1-naphthyl)-propionic acid (XI) and (+)-α-(2-naphthyl)-propionic acid (XII).

The present author finds it likely that the phenyl absorption in the 250 mμ region is anisotropic and that the anisotropy factor of this absorption band has the same sign as that of the absorption at about 200 mμ, which may be the second absorption region of the phenyl group, or the first absorption region of the carboxyl group. The values of λ_i, found by Rothen and Levene may be unreliable. Heller [35] pointed out that it is easy to have a fortuitous agreement between calculated and observed [α]-values, and therefore unreliable constants in the two-term Drude equation. It is particularly difficult to calculate the constants, when two absorption bands with the same sign for the anisotropy factors are close together.

For the purpose of the present investigation it is not absolutely necessary to know if a certain absorption band is anisotropic, but it is important that the analogous compounds to be compared have similar groups which are dominant in the rotation. A certain group, for example an aromatic one, may have anisotropic bands or it may have strong vicinal action on the other groups.

The effects on the rotatory power of substitution in different aromatic systems have been studied by several investigators, by Betti [48], Nerdel *et al.*[49,50] and Singh *et al.*[51,52]. The optical rotatory dispersions of hydratropic acid (IV), *p*-aminohydratropic acid (VIII) and *p*-nitrohydratropic acid (IX) have previously been investigated by Nerdel and Würgau [53] in the visible region,

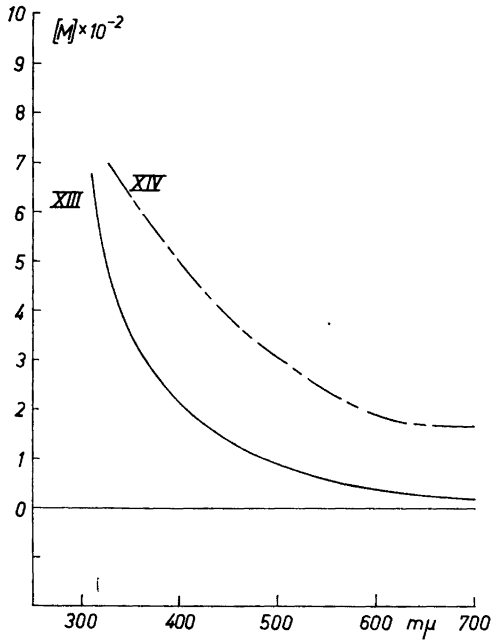

Fig. 4. Optical rotatory dispersion curves of (+)-α-(2-thianaphthenyl)-propionic acid (XIII) and (+)-α-(3-thianaphthenyl)-propionic acid (XIV).

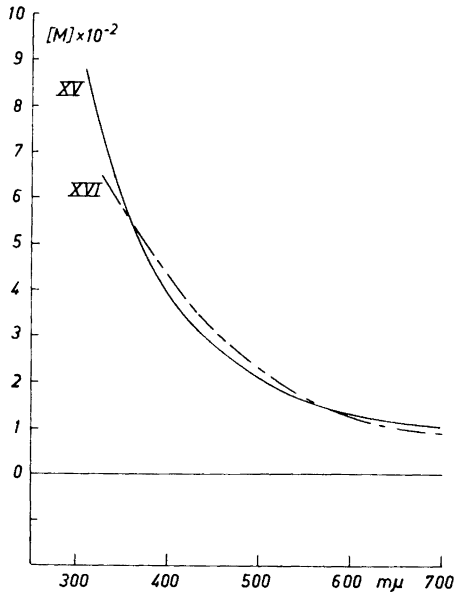

Fig. 5. Optical rotatory dispersion curves of (+)-α-(3-indolyl)-propionic acid (XV) and (+)-α-(1-methyl-3-indolyl)-propionic acid (XVI).

and now repeated and extended to the ultraviolet region, by the author. The curves are found in Fig. 2.

Introduction of an amino or a nitro group alters the benzenoid absorption bands considerably. The principal peak is displaced about 25 mμ towards longer wavelengths, and the intensity of this band is greatly increased [54]. Hydratropic acid *p*-aminohydratropic acids have almost the same molecular rotation in ethanol at the D-line, while that of *p*-nitrohydratropic acid is somewhat lower [55]. The dispersion curves are similar for the three acids; the amino and the nitro compounds having slightly higher molecular rotations towards shorter wavelengths. The dispersion curves of *p*-chlorohydratropic acid and *p*-hydroxihydratropic acid seem also to be positive for the D-forms [53].

The dispersion curves of (+)-α-(1-naphthyl)-propionic acid (X), (+)-α-(4-methyl-1-naphthyl)-propionic acid (XI) and (+)-α-(2-naphthyl)-propionic acid (XII) are found in Fig. 3. The three curves are similar and correspond well with the dispersion curve of hydratropic acid. Other aromatic systems which have been studied are the thianaphthenyl and the indolyl (Figs. 4 and 5). Phenyl, naphthyl, thianaphthenyl and indolyl groups apparently have similar influences on the rotation with this type of compound.

The second series derived from type I has been obtained by keeping the aryl group constant and varying the alkyl group. The following compounds have been investigated:

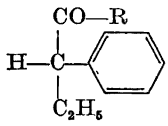

XVII R = OH
XVIII R = NH_2
XIX R = NH—C_6H_5

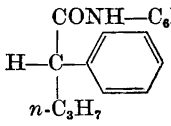

XX

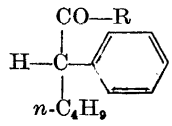

XXI R = NH_2
XXII R = NH—C_6H_5

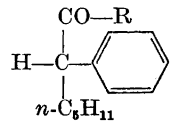

XXIII R = NH_2
XXIV R = NH—C_6H_5

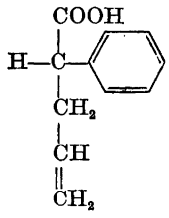

XXV

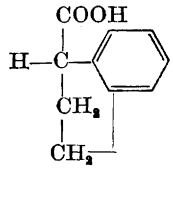

XXVI

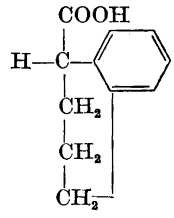

XXVII

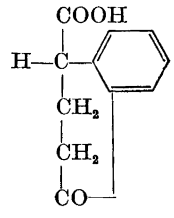

XXVIII

The configurational relationship between hydratropic acid (IV) and ethylphenylacetic acid (XVII) has been established by Levene *et al.* from optical rotatory measurements at the D-line [56], and also from rotatory dispersion measurements [47]. Pettersson [57,58] related the compounds XVII—XXIV by applying the quasi-racemate method to the amides. The relationship between hydratropic acid and glyceraldehyde has been established in several ways [41,55,59] (for references to earlier work see Ref.[55]). The configuration of allylphenylacetic acid (XXV) was established by Fredga and Westman [60].

The dispersion curves of (+)-ethylphenylacetic acid (XVII) and (+)-allylphenylacetic acid (XXV) are given in Fig. 6. These curves, are plain positive, and correspond well with the dispersion curve of hydratropic acid (Fig. 2). Changing the alkyl group from methyl to ethyl or allyl does not appreciably alter the rotatory dispersion of the acids in this series.

Fredga [61] investigated 1-indanecarboxylic acid and proved that the (—)-form belongs to the D-series. It was concluded from the higher auxin activity that (—)-1-indanecarboxylic acid (XXVI) and (—)-1,2,3,4-tetrahydro-1-naphthoic acid (XXVII), (which also shows higher activity than its enantiomer [62]), have the same configuration. More evidence was obtained from the similar shifts in rotation when the rotatory power of the acids was measured in different solvents [63]. Levorotatory 1,2,3,4-tetrahydro-1-naphthoic acid was also shown to belong to the D-series by Westman [63], who synthesized it from (+)-*a*-phenylglutaric acid *cf.* formulas XXVII and XXXIX. The optical rotatory dispersion curves of (—)-1-indanecarboxylic acid and (—)-1,2,3,4-tetrahydro-1-naphthoic acid are to be found in Fig. 7; both curves being plain negative, and show the same order of rotation.

In the series of alkylphenylacetic acids, the compounds of D-configuration have plain positive dispersion curves in the region 700—275 mμ with high rotation at lower wavelengths. However, when the acids have the alkyl

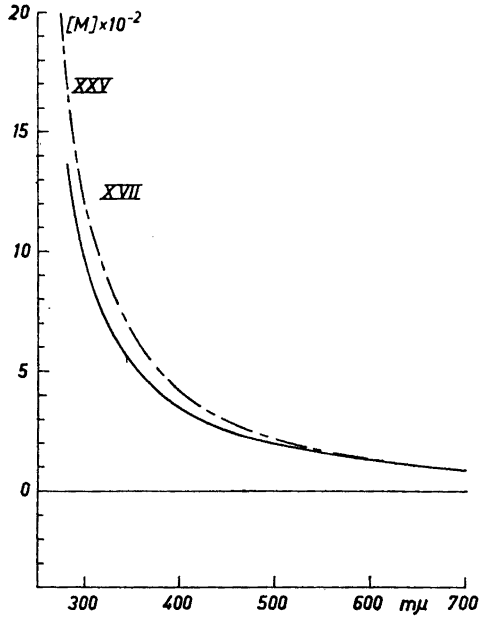

Fig. 6. Optical rotatory dispersion curves of (+)-ethylphenylacetic acid (XVII) and (+)-allylphenylacetic acid (XXV).

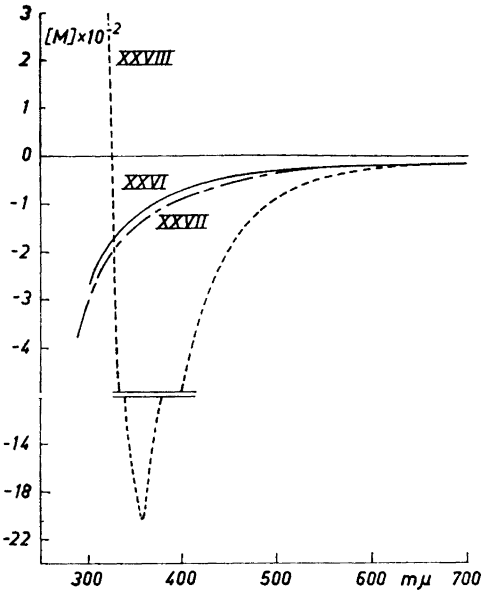

Fig. 7. Optical rotatory dispersion curves of (−)-1-indanecarboxylic acid (XXVI), (−)-1,2,3,4-tetrahydro-1-naphthoic acid (XXVII) and (−)-4-keto-1,2,3,4-tetrahydro-1-naphthoic acid (XXVIII).

group ring closed to the *ortho* position, so as to form a five or six membered ring, the D-compounds have plain negative dispersion curves of comparatively low rotation in the same wavelength region. The "ring closed forms" have only been investigated in two cases in this series; it is unlikely that the same relation between configuration and sign of the dispersion curve will be found for compounds with small, medium and large rings. Parallels to these "open and closed forms" have also been studied for phenoxy acids and phenylthio acids [45].

The third section of compounds derived from type I has been obtained by varying both the aryl and alkyl groups. The diarylpropionic acids, previously studied by Pettersson [64-66], belong to this group. The optical rotatory dispersion curves of three of the acids (XXIX—XXXI) have been investigated. The curves of benzylphenylacetic acid (XXIX) and of 2-thenylphenylacetic acid (XXX) are almost identical throughout the investigated wavelength region, while benzyl-2-thienylacetic acid (XXXI), which has a thiophene nucleus attached to the asymmetric carbon instead of a benzene nucleus, has a lower rotation in the visible region, and a somewhat steeper curve below 300 mμ (Fig. 8).

Analogous benzene and thiophene compounds are closely similar in many respects [42], and so it was expected that the three compounds XXIX—XXXI

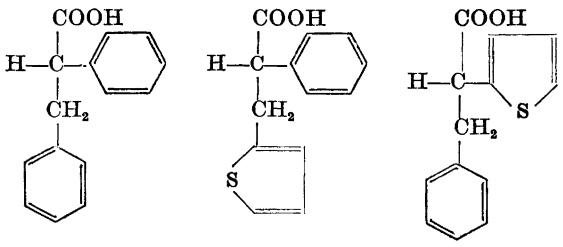

XXIX XXX XXXI

of the same configuration should have the same type of dispersion curves. The first series of ultraviolet absorption bands of thiophene is displaced by about 20 mμ towards shorter wavelengths compared to benzene [67]. Pettersson [40] investigated the optical rotation at the D-line of some 2-thienyl substituted acids; he pointed out that it was not possible to decide from these measurements if the lower rotation of the 2-thienyl compounds compared to the phenyl analogs depends on the shorter wavelength of absorption, or on a lower anisotropy of the band. The greater steepness of the dispersion curve of benzyl-2-thienylacetic acid at lower wavelengths compared to the curve of benzylphenylacetic acid, suggests instead a higher anisotropy of the 2-thienyl absorption

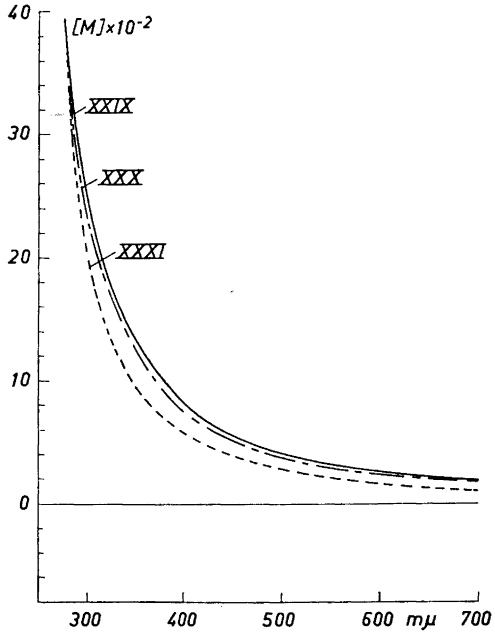

Fig. 8. Optical rotatory dispersion curves of (+)-benzylphenylacetic acid (XXIX), (+)-2-thenylphenylacetic acid (XXX) and (+)-benzyl-2-thienylactic acid (XXXI).

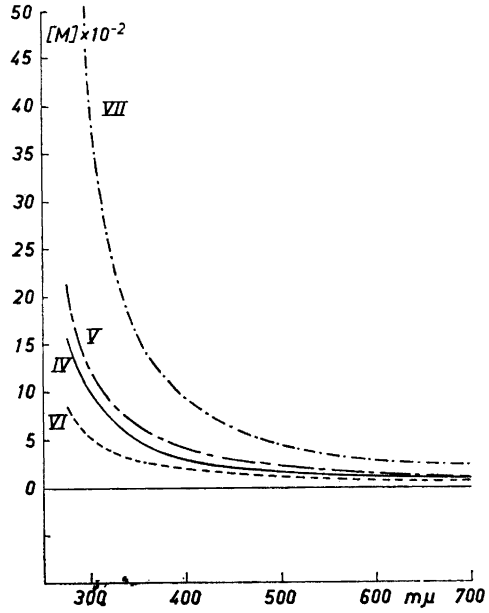

Fig. 9. Optical rotatory dispersion curves of (+)-hydratropic acid (IV), (+)-methyl hydratropate (V), (+)-hydratropamide (VI) and (+)-hydratropanilide (VII).

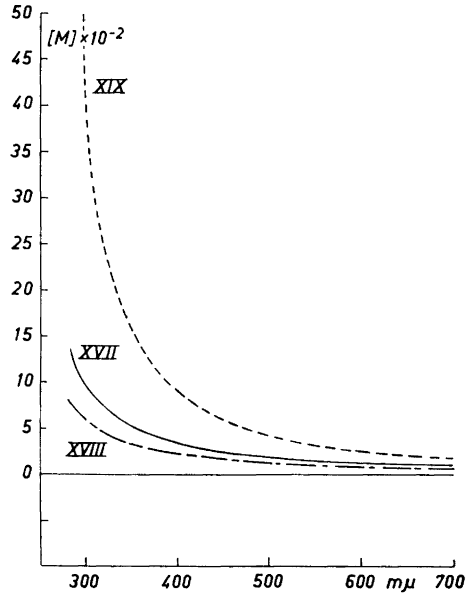

Fig. 10. Optical rotatory dispersion curves of (+)-ethylphenylacetic acid (XVII), (+)-ethylphenylacetamide (XVIII) and (+)-ethylphenylacetanilide (XIX).

band, and the lower rotation in the visible region should be due to the shorter wavelength of absorption. Definite answers regarding the anisotropy of an absorption band can only be obtained from careful calculation of the rotational strength [30], or experimentally from measurements of the circular dichroism [5,7].

The displacement rule

Optical rotation data from the sodium D-line has often been used for correlation of configurations within series of similar compounds; (for reviews see Mills and Klyne [2], and Klyne [68]). This approach is based on the application of different rules, for instance the *rule of optical superposition* and the *distance rule*. Another qualitative rule which has been more generally used is *Freudenberg's displacement rule* [11], which can be formulated: "If two similar asymmetric molecules A and B are altered in the same way to give A' and B', then the differences in molecular rotation (A'—A) and (B'—B) are of the same sign" [68]. The displacement rule follows from Kuhn's *vicinal rule* [6] which says that when a small change is made in one of the groups attached to the asymmetric centre, the anisotropy of this group suffers the most change, while the vicinal action is less affected.

The displacement rule is best used when the shifts are large. As the rotational shifts at the sodium D-line for a given structural change are nearly

always less than in the ultraviolet region, it is better to apply Freudenberg's displacement rule on data obtained as far into the ultraviolet region as possible, but without losing accuracy in the measurements. Series of similar carboxylic acids are usually converted to esters, amides or anilides, and the shifts compared. The dispersion curves of hydratropic acid (IV), its methyl ester (V), amide (VI) and anilide (VII), are compared in Fig. 9, and those of ethylphenylacetic acid (XVII), its amide (XVIII) and anilide (XIX) are given in Fig. 10. The rotations of the amides at the D-line are slightly lower than those of the corresponding acids, while the rotations of the anilides are higher; the differences in molecular rotation are enhanced in the ultraviolet region. The calculated shifts for methylphenylacetic acid (hydratropic acid) and ethylphenylacetic acid at 589 mμ (sodium D-line) and 290 mμ, are found in Table 1.

Table 1. Molecular rotational shifts for methylphenylacetic acid and ethylphenylacetic acid; Δ_1 for (amide—acid); Δ_2 for (anilide—acid).

Acid	589 mμ		290 mμ	
	Δ_1	Δ_2	Δ_1	Δ_2
Methylphenylacetic	− 30°	+ 190°	− 480°	+ 4 880°
Ethylphenylacetic	− 30°	+ 160°	− 450°	+ 4 660°

Just as the optical rotatory dispersion curves for a series of acids were compared above, the curves for (+)-methylphenylacetamide (VI), (+)-*n*-butylphenylacetamide (XXI) and for (+)-*n*-amylphenylacetamide (XXIII) are compared in Fig. 11. In Fig. 12 are the curves of (+)-*n*-propylphenylacetanilide (XX), (+)-*n*-butylphenylacetanilide (XXII) and (+)-*n*-amylphenylacetanilide (XXIV). The three amides in Fig. 11, have all plain positive dispersion curves with comparatively low rotations even in the ultraviolet region, while the anilides have very high rotations at lower wavelengths.

From the examples discussed above it can be concluded, that the configurational relationships between different members in the series of alkylphenylacetic acids can be obtained with certainty, directly from the rotatory dispersion curves of the acids, as well as from the dispersion curves of the anilides. The amides are not very suitable for comparison due to the lower rotation throughout the investigated wavelength region.

Solvent effects. The influences of external conditions, such as solvent, temperature and concentration, on optical activity has been observed, and its importance recognized, ever since Biot's early investigations on tartaric acid [69,70]. These factors produce complicated results since both chemical and physical changes may occur from the alteration in external conditions [71]. It is quite obvious that the rotatory power will usually be greatly affected by changes in solvent or temperature, if the solute constitutes an equilibrium mixture of two or more distinct molecular species. The optical rotation is also very sensitive to conformational changes, and inversion of the Cotton effect has been observed [72] on altering the polarity of the solvent. The dipole-dipole interaction between solvent and solute will not only influence the conformation of

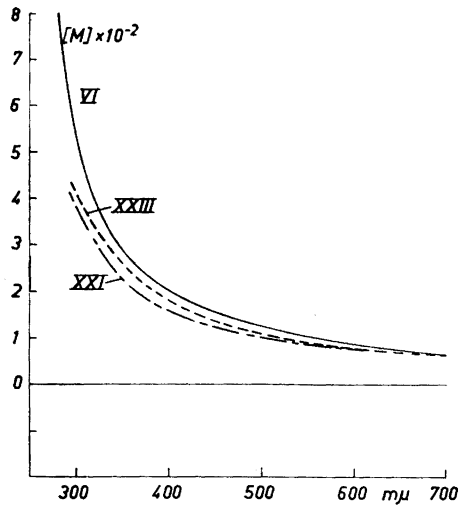

Fig. 11. Optical rotatory dispersion curves of (+)-methylphenylacetamide (VI), (+)-*n*-butylphenylacetamide (XXI) and (+)-*n*-amylphenylacetamide (XXIII).

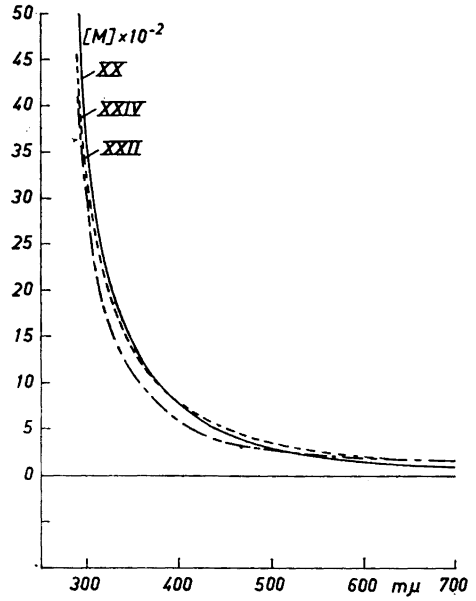

Fig. 12. Optical rotatory dispersion curves of (+)-*n*-propylphenylacetanilide (XX), (+)-*n*-butylphenylacetanilide (XXII) and (+)-*n*-amylphenylacetanilide (XXIV).

the molecules, but will also affect the local field, and in that way exert direct vicinal action on the chromophores of the optically active compounds. Furthermore, if strong bonds are formed between solvent and solute, the chromophores of the optically active molecule will change; sometimes even the solvent molecules can act as chromophoric groups.

Solvent influence on the rotation in the visible region was extensively studied by Pickard and Kenyon [73] and by Rule *et al.*[74,75] The solvent effect is especially noticeable in rotatory dispersion work [76,77], and thus when the dispersion curves of different compounds are compared, they should be made with the same solvent and at about the same concentration and temperature. Nevertheless, the solvent effect can be utilized, and comparison of the effect on similar compounds may give information regarding their steric relationship. Such investigations at the sodium D-line have been made on several compounds [39–41,78]. These studies of the rotational shifts can be considered as a special way of applying Freudenberg's displacement rule, and from the discussion above it is evident that information which is more reliable will be obtained if the rotatory dispersion curves are studied in different solvents, and not only the rotational shifts at the D-line in this way.

Pettersson [40] investigated the solvent effect on several α-arylcarboxylic acids at the D-line. Large negative shifts were observed for compounds of D-configuration when the rotation was measured in dilute sodium hydroxide solution. The rotatory dispersion curves in sodium hydroxide solution of some

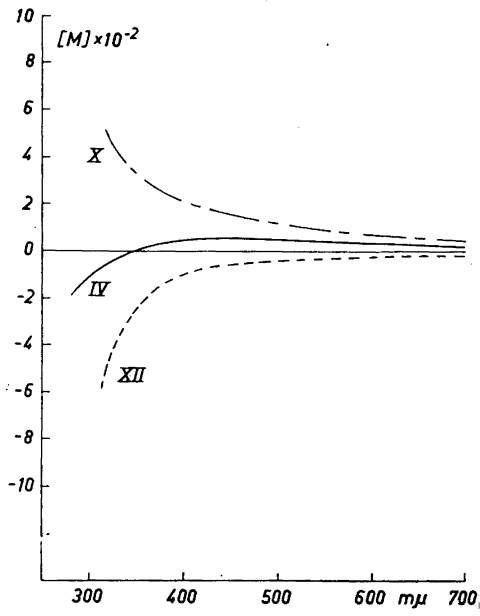

Fig. 13. Optical rotatory dispersion curves in 0.1 N sodium hydroxide of (+)-hydratropic acid (IV), (+)-α-(1-naphthyl)-propionic acid (X) and (+)-α-(2-naphthyl)-propionic acid (XII).

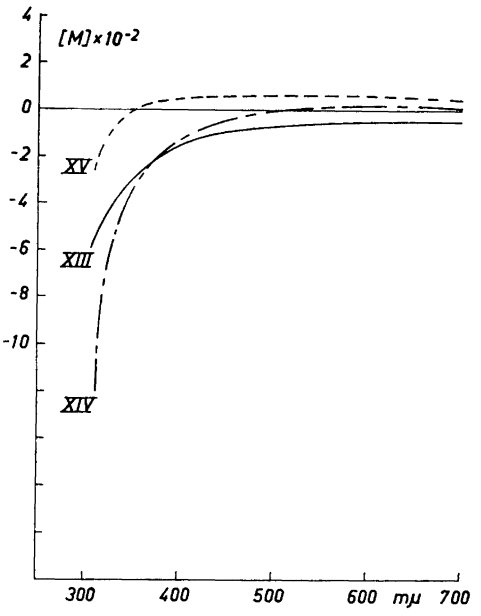

Fig. 14. Optical rotatory dispersion curves in 0.1 N sodium hydroxide of (+)-α-(2-thianaphthenyl)-propionic acid (XIII), (+)-α-(3-thianaphthenyl)-propionic acid (XIV), and (+)-α-(3-indolyl)-propionic acid (XV).

of these acids are given in Figs. 13 and 14. It can be seen that the negative shifts are very prominent in the ultraviolet region, and for all the compounds, except α-(1-naphthyl)-propionic acid (X), even the sign of the dispersion curves is reversed compared to that in methanol.

Aryl dicarboxylic acids

Oxidative degradation of natural products often yields alkyl substituted dicarboxylic acids; for example alkylsuccinic and alkylglutaric acids have been key substances in stereochemical studies on terpenes. Alkylsuccinic acids have also proved to be valuable substances in connecting aromatic compounds to the steric system of glyceraldehyde. Analogous benzene and thiophene derivatives can often be sterically related by the quasi-racemate method, and the thiophene compounds desulphurized with Raney nickel to the corresponding aliphatic compounds without racemisation [79].

In order to see if the steric relationships between different dicarboxylic acids could be found directly from their optical rotatory dispersion curves, an investigation of a large number of dicarboxylic acids was undertaken. The results on the alkylsubstituted acids will be published in a separate paper [80], and only the acids which are derived from type II will be discussed here.

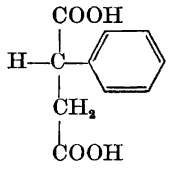

XXXII

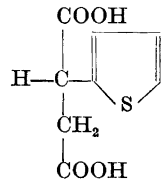

XXXIII

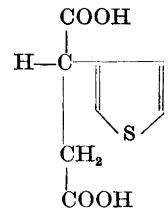

XXXIV

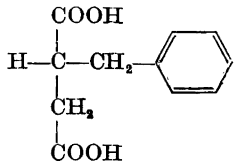

XXXV

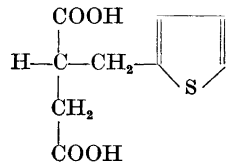

XXXVI

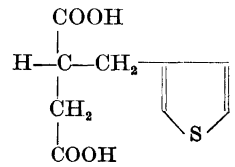

XXXVII

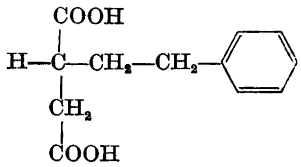

XXXVIII

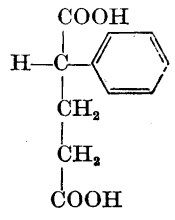

XXXIX

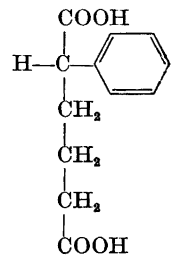

XL

The configurations of these acids have previously been determined and the dextrorotatory compounds all belong to the D-series, (references are given below). The optical rotatory dispersion curves of (+)-phenylsuccinic acid (XXXII) [81], (+)-2-thienylsuccinic acid (XXXIII) [82] and (+)-3-thienylsuccinic acid (XXXIV) [83] are shown in Fig. 15. The dispersion curves are very similar for all these compounds being plain and positive with high rotation at lower wavelengths. It is interesting to compare the dispersion curve of phenylsuccinic acid to that of hydratropic acid (Fig. 2). Substitution of a hydrogen atom in the methyl group of hydratropic acid with a carboxyl group, gives phenylsuccinic acid. It can be seen that such a substitution does not change the main character of the curve, but only causes a higher rotation. The higher rotation may either be due to the vicinal action of the carboxymethyl group on the phenyl and carboxyl groups attached to the asymmetric centre, or (and) to a positive rotatory contribution from the carboxymethyl group. It has been shown by Levene and Rothen [47,48] that a carboxymethyl group has an opposite sign for its rotatory contribution to that of a carboxyl group in some series of compounds. For example, α-phenylpropionic acid, (hydratropic acid), of D-configuration is dextrorotatory, while β-phenylbutyric acid is levorotatory. Similarly a change in sign due to the partial rotation of the carboxyl group occurs when going from α-methylbutyric acid to β-methylvaleric acid. The

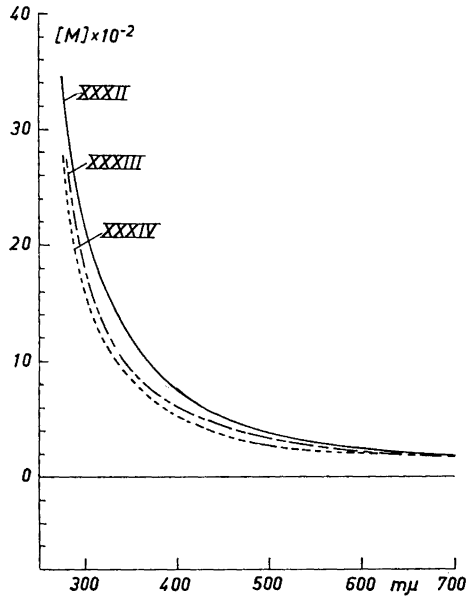

Fig. 15. Optical rotatory dispersion curves of (+)-phenylsuccinic acid (XXXII), (+)-2-thienylsuccinic acid (XXXIII) and (+)-3-thienylsuccinic acid (XXXIV).

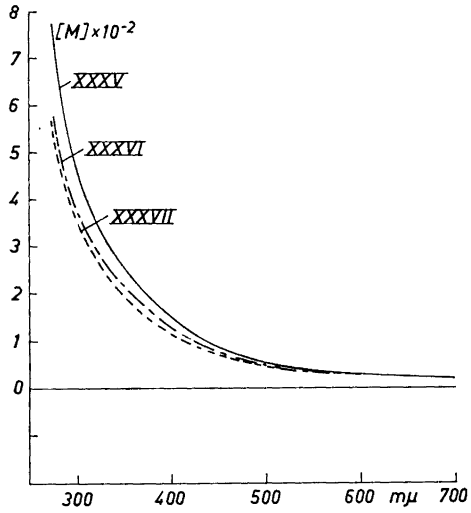

Fig. 16. Optical rotatory dispersion curves of (+)-benzylsuccinic acid (XXXV), (+)-2-thenylsuccinic acid (XXXVI) and (+)-3-thenylsuccinic acid (XXXVII).

reason that the same type of inversion is not found when going from hydratropic acid to phenylsuccinic acid, must be connected with the mutual influence of a phenyl and a carboxyl group attached to the same asymmetric centre.

The variations in the rotatory dispersion curves of some compounds belonging to type II, when n increases from 0 to 1, can be seen from a comparison of Figs. 15 and 16. Benzylsuccinic acid (XXXV) [79], 2-thenylsuccinic acid (XXXVI) [79], and 3-thenylsuccinic acid (XXXVII) [85] of D-configuration have plain positive dispersion curves, but the rotation is considerably lower than for the corresponding compounds with the aryl group directly attached to the asymmetric centre.

According to the distance rule a smaller change in rotation will be expected when n increases from 1 to 2 compared to that for an increase of n from 0 to 1. That this is so can be seen from Fig. 17, where the dispersion curves of (+)-phenylsuccinic acid (XXXII), (+)-benzylsuccinic acid (XXXV) and (+)-phenylethylsuccinic acid (XXXVIII) [86] are reproduced.

The influence on the rotatory dispersion curves of compounds belonging to type II, when n is kept constant (n = 0) and m is varied from 1 to 3, has been studied on the series (+)-phenylsuccinic acid (XXXII), (+)-α-phenylglutaric acid (XXXIX) [87] and (+)-α-phenyladipic acid (XL) [88]. The dispersion curves for these compounds, all of D-configuration, are found in Fig. 18;

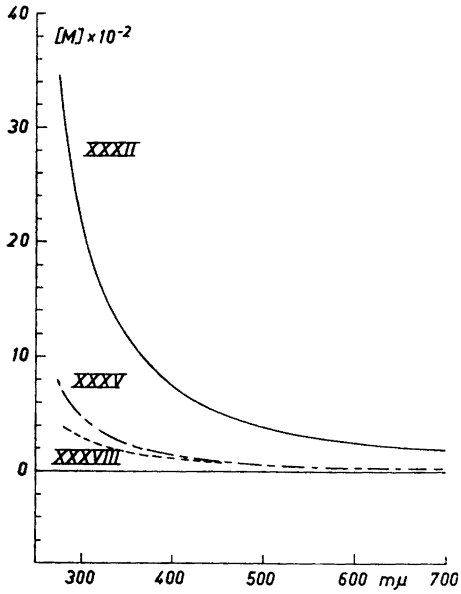

Fig. 17. Optical rotatory dispersion curves of (+)-phenylsuccinic acid (XXXII), (+)-benzylsuccinic acid (XXXV) and (+)-phenylethylsuccinic acid (XXXVIII).

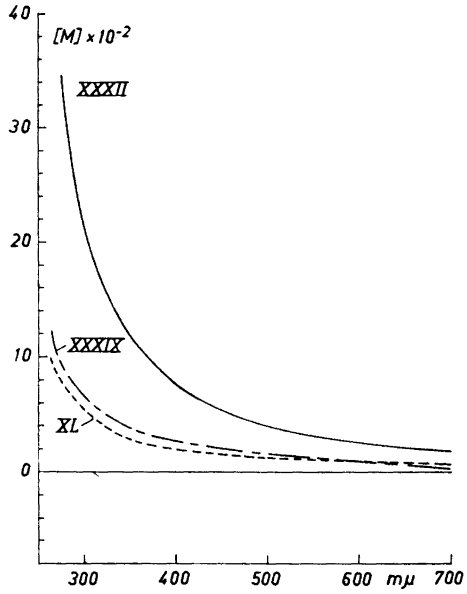

Fig. 18. Optical rotatory dispersion curves of (+)-phenylsuccinic acid (XXXII), (+)-α-phenylglutaric acid (XXXIX) and (+)-α-phenyladipic acid (XL).

the curves are all plain and positive. In the series of alkyl dicarboxylic acids the D-alkylsuccinic acids are dextrorotatory with plain positive dispersion curves, while D-α-alkylglutaric acids are levoratory with plain negative dispersion curves [80].

In the present paper all dispersion curves refer to compounds of D-configuration. All the curves, except the three of the "ring closed" compounds XXVI, XXVII and XXVIII, are plain and positive in the investigated wavelength region. It may be fortuitous, of course, that such different compounds have the same type of rotatory dispersion curves for analogous configuration, but nevertheless, the relative configurations of compounds within some series of types I and II can be obtained with great certainty using these curves. In the Aryl—$\underset{\displaystyle R}{\underset{|}{CH}}$—COOH series, where R is alkyl, an analogous configuration will give a similar dispersion curve if the aryl group is kept constant, and the alkyl group varies. If the alkyl is the same and the aryl group varies, the magnitude of the rotation may change considerably, but the dispersion curves are still of the same general type and especially sign. The last statement is probably not of unrestricted validity, as the aryl group has a dominant influence on the rotation, and very great variations in this group may be expected to reverse the sign of the dispersion curves. However, the following variations in the aryl group have not resulted in any major rotatory dispersion changes:

phenyl, *p*-aminophenyl, *p*-nitrophenyl, *p*-chlorophenyl, *p*-hydroxiphenyl, 1-naphthyl, 4-methyl-1-naphthyl, 2-naphthyl, 2-thianaphthenyl, 3-thianaphthenyl, 3-indolyl and 1-methyl-3-indolyl.

$$\text{Aryl-(CH}_2)_n\text{-CH(-(CH}_2)_m\text{-COOH)-COOH}$$

In the Aryl-$(CH_2)_n$-CH(-$(CH_2)_m$-COOH)-COOH series, the relative configuration of compounds with different aryl groups can be obtained directly from the dispersion curves if n and m are kept constant, (n equal to 0). The aryl group can probably be varied in the same way as for compounds belonging to type I (see above). It may not always be safe to compare compounds belonging to the series with m = 1 to that with m = 2, even if phenylsuccinic and *α*-phenylglutaric acid of the same configuration have the same type of dispersion curves. However, a change of m from 2 to a higher integer will have a smaller influence on the rotation, and a comparison of different acids with n = 0, m = 2 with acids having n = 0, m = 3, 4 . . . is fairly sound. When m is constant (equal to 1), and n varies from 0 to 2, as with the investigated compounds phenylsuccinic, benzylsuccinic, phenylethylsuccinic acids, the disperison curves are of the same type for analogous configuration. When m is greater than 1, these dicarboxylic acids are more similar to the series of *α*-alkyl-*ω*-phenylcarboxylic acids investigated by Levene and Rothen [47,48], which had an alternating change in the rotation at the D-line, but still had the same type of dispersion curves on movement of the phenyl group away from the asymmetric centre. The effect of separation distance of an aliphatic carbonyl function (ketone, aldehyde) on an asymmetric centre has been investigated by Djerassi and Geller [89], and they found that the sign of the Cotton effect curve is reversed when either one, or no carbon atoms are interposed.

The extensive investigations of the anomalous optical rotatory dispersion of ketones and aldehydes by Djerassi *et al.*[16–18] have clearly shown the advantages of using dispersion curves instead of only sodium D-line rotations. Compounds, such as carboxylic acids, which have their ultraviolet absorption in a presently inaccessible region for rotatory dispersion measurements, give only plain dispersion curves, but nevertheless the configurational relationship between compounds belonging to certain series of simple compounds can be obtained directly from their dispersion curves. Occasionally the plain dispersion curves cross the zero rotation line somewhere below 589 mμ [18,45,47] and then configurational assignmentes based on a single measurement at the D-line may be impossible. The displacement rule applied using D-line rotations often gives valuable information about configurational relationships, but even when this rule is used it is more reliable to make a comparison of the dispersion curves of the different derivatives. Freudenberg and Biller [90] pointed out that when the displacement rule is used, the nature of the optical activity has to be considered. Comparisons should be made with great caution if the rotational shifts, when going from one derivative to another, are more dependent on changes in the vicinal action than on changes in the direct contribution from the altered group. For example the rotatory contribution of the phenyl group in the methyl ester of mandelic acid methyl ether is negative, but positive in the dimethylamide. On the other hand, the phenyl contribution is positive in

the corresponding derivatives of atrolactic acid (α-methylmandelic acid)[12,90]. Similar changes in the rotatory contributions cannot be detected from measurements of only D-line rotations, but can at least qualitatively be observed directly in the optical rotatory dispersion curves.

Acknowledgement. The author wishes to express his sincere gratitude to Professors Arne Fredga, Carl Djerassi, and to Dr. E. J. Eisenbraun for many valuable discussions as well as for all the facilities put at his disposal. He is also indebted to Drs. Salo Gronowitz, Magnus Matell, Kurt Skagius (Pettersson) and Lars Westman for specimens of many of the optically active substances.

Financial support from, the *Swedish Natural Science Research Council*, the *Sweden-America Foundation, Smålands nation (A. M. Lundins stipendiefond)*, and the *National Cancer Institute* (grant No. CY-2919) *of the National Institutes of Health, U.S. Public Health Service*, is gratefully acknowledged.

EXPERIMENTAL

The experimental results are recorded in the manner outlined in Ref. [32]. If not otherwise stated the rotatory dispersion curves were taken in methanol. The samples were purified, usually by recrystallization, and the D-line rotations were checked to be in accordance with the literature values. As these measurements were taken in various solvents and at high concentrations, the rotations are not directly comparable with those obtained in the rotatory dispersion (R.D.) measurements, and the results are not reported. The molecular rotation values at the D-line and the previous configurational determinations can be found in the references given.

(+)-Hydratropic acid (IV) [55] R.D. (Fig. 2) in methanol (*c.* 0.0905), temp. 29°: $[M]_{589}$ + 110°, $[M]_{400}$ + 320°, $[M]_{350}$ + 500°, $[M]_{300}$ + 960°, $[M]_{275}$ + 1 560°.

R.D. (Fig. 13) in 0.1 N sodium hydroxide (*c* 0.100), temp. 27°: $[M]_{589}$ + 30°, $[M]_{400}$ + 40°, $[M]_{350}$ + 10° $[M]_{300}$ −100°, $[M]_{280}$ −290°.

(+)-Methyl hydratropate (V) Prepared from (+)-hydratropic acid using diazomethane. R.D. (Fig. 9) in methanol (*c* 0.225), temp. 25°: $[M]_{589}$ + 170°, $[M]_{400}$ + 440°, $[M]_{350}$ + 650°, $[M]_{300}$ + 1 200°, $[M]_{275}$ + 2 120°.

(+)-Hydratropamide (VI)[57] R.D. (Fig. 9) in methanol (*c* 0.120), temp. 27°: $[M]_{589}$ + 80°, $[M]_{400}$ + 200°, $[M]_{350}$ + 290°, $[M]_{300}$ + 530°, $[M]_{280}$ + 780°.

(+)-Hydratropanilide (VII) [57] R.D. (Fig. 9) in methanol (*c* 0.167), temp. 27°: $[M]_{589}$ + 300°, $[M]_{400}$ + 920°, $[M]_{350}$ + 1 600°, $[M]_{300}$ + 4 250°, $[M]_{290}$ + 5 680°.

(+)-p-Aminohydratropic acid (VIII) [55] R.D. (Fig. 2) in methanol (*c* 0.122), temp. 27°: $[M]_{589}$ + 110°, $[M]_{400}$ + 330°, $[M]_{350}$ + 540°, $[M]_{330}$ + 710°.

(+)-p-Nitrohydratropic acid (IX) [55] R.D. (Fig. 2) in methanol (*c* 0.150), temp. 29°: $[M]_{589}$ + 130°, $[M]_{400}$ + 330°, $[M]_{390}$ + 340°.

(+)-α-(1-Naphthyl)-propionic acid (X) [91] R.D. (Fig. 3) in methanol (*c* 0.094), temp. 30°: $[M]_{589}$ + 260°, $[M]_{400}$ + 740°, $[M]_{350}$ + 1 240°, $[M]_{320}$ + 1 710°.

R.D. (Fig. 13) in 0.1 N sodium hydroxide (*c* 0.090) temp. 26°: $[M]_{589}$ + 60°, $[M]_{400}$ + 230°, $[M]_{350}$ + 360°, $[M]_{315}$ + 520°.

(+)-α-(4-Methyl-1-naphthyl)-propionic acid (XI) [92] R.D. (Fig. 3) in methanol (*c* 0.096), temp. 27°: $[M]_{589}$ + 210°, $[M]_{400}$ + 590°, $[M]_{350}$ + 1 100°, $[M]_{340}$ + 1 240°.

(+)-α-(2-Naphthyl)-propionic acid (XII) [93] R.D. (Fig. 3) in methanol (*c* 0.096), temp. 27°: $[M]_{589}$ + 110°, $[M]_{400}$ + 310°, $[M]_{350}$ + 510°, $[M]_{320}$ + 720°.

R.D. (Fig. 13) in 0.1 N sodium hydroxide (*c* 0.100), temp. 24°: $[M]_{589}$ −30°, $[M]_{400}$ −90°, $[M]_{350}$ − 260°, $[M]_{315}$ − 580°.

(+)-α-(2-Thianaphthenyl)-propionic acid (XIII) [94] R.D. (Fig. 4) in methanol (*c.* 0.060), temp. 27°: $[M]_{589}$ + 40°, $[M]_{400}$ + 210°, $[M]_{350}$ + 340°, $[M]_{310}$ + 680°.

R.D. (Fig. 14) in 0.1 N sodium hydroxide (*c* 0.100), temp. 25°: $[M]_{589}$ − 60°, $[M]_{400}$ − 130°, $[M]_{350}$ − 330°, $[M]_{305}$ − 600°.

(+)-α-(3-Thianaphthenyl)-propionic acid (XIV) [95] R.D. (Fig. 4) in methanol (*c* 0.092), temp. 28°: $[M]_{589}$ + 190°, $[M]_{400}$ + 480°, $[M]_{350}$ + 650°, $[M]_{330}$ + 710°.

R.D. (Fig. 14) in 0.1 N sodium hydroxide (*c* 0.105) temp. 25°: $[M]_{589}$ + 10°, $[M]_{400}$ − 80°, $[M]_{350}$ − 300°, $[M]_{310}$ − 1 170°.

(+)-α-(3-Indolyl)-propionic acid (XV) [96] R.D. (Fig. 5) in methanol (*c* 0.120), temp. 27°: $[M]_{589}$ + 130°, $[M]_{400}$ + 390°, $[M]_{350}$ + 600°, $[M]_{310}$ + 880°.

R.D. (Fig. 14) in 0.1 N sodium hydroxide (*c* 0.179), temp. 24°: $[M]_{589}$ + 50°, $[M]_{400}$ + 50°, $[M]_{350}$ − 10°, $[M]_{310}$ − 270°.

(+)-α-(1-Methyl-3-indolyl)-propionic acid (XVI) [97,98] R.D. (Fig. 5) in methanol (*c* 0.100), temp. 23°: $[M]_{589}$ + 140°, $[M]_{400}$ + 440°, $[M]_{350}$ + 580°, $[M]_{325}$ + 630°.

(+)-Ethylphenylacetic acid (XVII) [57] R.D. (Fig. 6) in methanol (*c* 0.575), temp. 27°: $[M]_{589}$ + 130°, $[M]_{400}$ + 350°, $[M]_{350}$ + 530°, $[M]_{315}$ + 790°; (*c* 0.115): $[M]_{315}$ + 780°, $[M]_{300}$ + 970°, $[M]_{280}$ + 1 370°.

(+)-Ethylphenylacetamide (XVIII) [57] R. D. (Fig. 10) in methanol (*c* 0.130), temp. 27°: $[M]_{589}$ + 100°, $[M]_{400}$ + 240°, $[M]_{350}$ + 330°, $[M]_{300}$ + 620°, $[M]_{280}$ + 810°.

(+)-Ethylphenylacetanilide (XIX) [57] R.D. (Fig. 10) in methanol (*c* 0.170), temp. 27°: $[M]_{589}$ + 290°, $[M]_{400}$ + 890°, $[M]_{350}$ + 1 560°, $[M]_{300}$ + 4 170°, $[M]_{290}$ + 5 700°.

(+)-n-Propylphenylacetanilide (XX) [58,59] R.D. (Fig. 12) in methanol. (*c* 0.140), temp. 27°: $[M]_{589}$ + 190°, $[M]_{400}$ + 780°, $[M]_{350}$ + 1 360°, $[M]_{305}$ + 3 010°; (*c* 0.028): $[M]_{305}$ + 3 100°, $[M]_{300}$ + 3 640°, $[M]_{290}$ + 5 200°.

(+)-n-Butylphenylacetamide (XXI) [58,59] R.D. (Fig. 11) in methanol (*c* 0.142), temp. 27°: $[M]_{589}$ + 80°, $[M]_{400}$ + 160°, $[M]_{350}$ + 200°, $[M]_{320}$ + 300°; (*c* 0.071): $[M]_{320}$ + 310°, $[M]_{300}$ + 380°, $[M]_{290}$ + 420°.

(+)-n-Butylphenylacetanilide (XXII) [58,59] (Fig. 12) in methanol (*c* 0.115), temp. 27°: $[M]_{589}$ + 220°, $[M]_{400}$ + 600°, $[M]_{350}$ + 1 020°, $[M]_{310}$ + 2 210°; (*c* 0.023): $[M]_{310}$ + 2 250°, $[M]_{300}$ + 3 060°, $[M]_{290}$ + 4 100°.

(+)-n-Amylphenylacetamide (XXIII) [58,59] R.D. (Fig. 11) in methanol (*c* 0.127), temp. 27°: $[M]_{589}$ + 80°, $[M]_{400}$ + 180°, $[M]_{350}$ + 270°, $[M]_{300}$ + 420°, $[M]_{290}$ + 450°.

(+)-n-Amylphenylacetanilide (XXIV) [58,59] R.D. (Fig. 12) in methanol (*c* 0.235), temp. 28°: $[M]_{589}$ + 220°, $[M]_{400}$ + 770°, $[M]_{350}$ + 1 320°, $[M]_{300}$ + 3 240°, $[M]_{290}$ + 4 570°.

(+)-Allylphenylacetic acid (XXV) [60] R.D. (Fig. 6) in methanol (*c* 0.263), temp. 28°: $[M]_{589}$ + 150°, $[M]_{400}$ + 420°, $[M]_{350}$ + 660°, $[M]_{300}$ + 1 220°, $[M]_{275}$ + 1 980°.

(−)-1-Indanecarboxylic acid (XXVI) [61] R.D. (Fig. 7) in methanol (*c* 0.098), temp. 27°: $[M]_{589}$ − 20°, $[M]_{400}$ − 70°, $[M]_{350}$ − 120°, $[M]_{300}$ − 270°.

(−)-1.2.3.4-Tetrahydro-1-naphthoic acid (XXVII) [63] R.D. (Fig. 7) in methanol (*c* 0.257), temp. 28°: $[M]_{589}$ − 20°. $[M]_{400}$ − 90°, $[M]_{350}$ − 140°, $[M]_{310}$ − 270°; (*c* 0.0514): $[M]_{310}$ − 260°, $[M]_{300}$ − 330°, $[M]_{290}$ − 360°.

(−)-4-Keto-1,2,3,4-tetrahydro-1-naphthoic acid (XXVIII) [63] R.D. (Fig. 7) in methanol (*c* 0.105), temp. 24°: $[M]_{589}$ − 30°, $[M]_{400}$ − 470°, $[M]_{357.5}$ − 2 050° (T), $[M]_{327}$ ± 0°, $[M]_{305}$ + 1 770°.

(+)-Benzylphenylacetic acid (XXIX) [40,65] R.D. (Fig. 8) in methanol (*c* 0.125), temp. 28°: $[M]_{589}$ + 290°, $[M]_{400}$ + 800°, $[M]_{350}$ + 1 310°, $[M]_{310}$ + 2 040°; (*c* 0.0125): $[M]_{310}$ + 2 140°, $[M]_{300}$ + 2 600°, $[M]_{275}$ + 4 060°.

(+)-2-Thenylphenylacetic acid (XXX) [40,64] R.D. (Fig. 8) in methanol (*c* 0.133), temp. 27°: $[M]_{589}$ + 270°, $[M]_{400}$ + 770°, $[M]_{350}$ + 1 210°, $[M]_{310}$ + 2 020; (*c* 0.0133); $[M]_{310}$ + 2 100°, $[M]_{300}$ + 2 440°, $[M]_{275}$ + 3 950°.

(+)-Benzyl-2-thienylacetic acid (XXXI) [40,64] R.D. (Fig. 8) in methanol (*c* 0.121), temp. 28°: $[M]_{589}$ + 190°, $[M]_{400}$ + 590°, $[M]_{350}$ + 940°, $[M]_{310}$ + 1 640°; (*c* 0.0242): $[M]_{310}$ + 1 800°, $[M]_{300}$ + 2 150°, $[M]_{275}$ + 4 000°.

(+)-Phenylsuccinic acid (XXXII) [81,99] R.D. (Fig. 15) in methanol (*c* 0.120), temp. 24°: $[M]_{589}$ + 250°, $[M]_{400}$ + 750°, $[M]_{350}$ + 1 170°, $[M]_{300}$ + 2 160°, $[M]_{275}$ + 3 460°.

(+)-2-Thienylsuccinic acid (XXXIII) [82] R.D. (Fig. 15) in methanol (*c* 0.130), temp. 24°: $[M]_{589}$ + 220°, $[M]_{400}$ + 610°, $[M]_{350}$ + 950°, $[M]_{300}$ + 1 750°, $[M]_{280}$ + 2 700°.

(+)-3-Thienylsuccinic acid (XXXIV) [83] R.D. (Fig. 15) in methanol (*c* 0.143), temp. 25°: $[M]_{589}$ + 200°, $[M]_{400}$ + 530°, $[M]_{350}$ + 840°, $[M]_{300}$ + 1 560°, $[M]_{275}$ + 2 800°.

(+)-Benzylsuccinic acid (XXXV) [79,100] R.D. (Fig. 16) in methanol (*c* 0.163), temp. 24°: $[M]_{589}$ + 30°, $[M]_{400}$ + 160°, $[M]_{350}$ + 260°, $[M]_{300}$ + 440°, $[M]_{275}$ + 780°.

(+)-2-Thenylsuccinic acid (XXXVI) [79,100] R.D. (Fig. 16) in methanol (*c* 0.110), temp. 25°: $[M]_{589}$ + 20°, $[M]_{400}$ + 150°, $[M]_{350}$ + 230°, $[M]_{300}$ + 340°, $[M]_{275}$ + 570°.

(+)-3-Thenylsuccinic acid (XXXVII) [85] R.D. (Fig. 16) in methanol (*c* 0.171), temp. 25°: $[M]_{589}$ + 30°, $[M]_{400}$ + 110°, $[M]_{350}$ + 190°, $[M]_{300}$ + 330°, $[M]_{275}$ + 580°.

(+)-Phenylethylsuccinic acid (XXXVIII) [86,101] (Fig. 17) in methanol (*c* 0.100), temp. 24°: $[M]_{589}$ + 30°, $[M]_{400}$ + 100°, $[M]_{350}$ + 180°, $[M]_{300}$ + 280°, $[M]_{270}$ + 450°.

(+)-α-Phenylglutaric acid (XXXIX) [87] R.D. (Fig. 18) in methanol (c 0.100), temp. 21°: $[M]_{589}$ + 100°, $[M]_{400}$ + 230°, $[M]_{350}$ + 390°, $[M]_{300}$ + 650°, $[M]_{265}$ + 1 220°.

(+)-α-Phenyladipic acid (XL) [88] R.D. (Fig. 18) in methanol (c 0.100), temp. 21°: $[M]_{589}$ + 90°, $[M]_{400}$ + 190°, $[M]_{350}$ + 320°, $[M]_{300}$ + 550°, $[M]_{265}$ + 1 010°.

REFERENCES

1. Freudenberg, K. *Stereochemie*, Franz Deuticke, Leipzig and Wien 1933, pp. 662–720.
2. Mills, J. A. and Klyne, W. in Klyne, W. *Progress in Stereochemistry*, Butterworths Scientific Publications, London 1954, Vol. I, Chap. 5.
3. Bijvoet, J. M., Peerdeman, A. F. and van Bommel, A. J. *Nature* **168** (1951) 271.
4. Biot, J. B. *Mém. acad. sci.* Toulouse **2** (1817) 41.
5. Lowry, T. M. *Optical Rotatory Power*, Longmans, Green and Co., London 1935.
6. Kuhn, W. Ref.[1], pp. 317–434.
7. Kuhn, W. *Ann. Rev. Phys. Chem.* **9** (1958) 417.
8. Tschugaeff, L. and Pastanogoff, W. *Z. physik. Chem.* **85** (1913) 553.
9. Dahn, H. and Reichstein, T. *Helv. Chim. Acta* **35** (1952) 1.
10. Freudenberg, K. and Kuhn, W. *Ber.* **64** (1931) 703.
11. Freudenberg, K. *Ber.* **66** (1933) 177.
12. Kuhn, W. and Biller, H. *Z. physik. Chem.* **B 29** (1935) 1.
13. Levene, P. A. and Rothen, A. in Gilman, H. *Organic Chemistry*, John Wiley and Sons, New York 1938, First Ed., Vol II, Chap. 21.
14. Djerassi, C., Foltz, E. W. and Lippman, A. E. *J. Am. Chem. Soc.* **77** (1955) 4354.
15. Allinger, N. L., Hermann, R. B. and Djerassi, C. *J. Org. Chem.* **25** (1960). *In press.*
16. Djerassi, C. *Bull. soc. chim. France* **1957** 741.
17. Djerassi, C. *Record Chem. Prog.* **20** (1959) 101.
18. Djerassi, C. *Optical Rotatory Dispersion: Applications to Organic Chemistry*, McGraw-Hill Book Company, Inc., New York 1960.
19. Drude, P. *Lehrbuch der Optik*, Hirzel, Leipzig 1900, 2nd Ed. 1906.
20. Born, M. *Physik. Z.* **16** (1915) 251.
21. Born, M. *Proc. Roy. Soc. London* **A 150** (1935) 84.
22. Kuhn, W. *Z. physik. Chem.* **B 4** (1929) 14.
23. Kuhn, W. *Z. physik. Chem.* **B 30** (1935) 356.
24. Rosenfeld, L. *Z. Physik* **52** (1928) 161.
25. Kirkwood, J. G. *J. Chem. Phys.* **5** (1937) 479.
26. Condon, E. U. *Rev. Modern Phys.* **9** (1937) 432.
27. Condon, E. U., Altar, W. and Eyring, H. *J. Chem. Phys.* **5** (1937) 753.
28. Moffitt, W. *J. Chem. Phys.* **25** (1956) 1189.
29. Moffitt, W. and Moscowitz, A. *J. Chem. Phys.* **30** (1959) 648.
30. Moscowitz, A. Ref.[18], Chap. 12.
31. Schellman, J. A. *Compt. rend. trav. lab. Carlsberg, Sér. chim.* **30** (1958) 363.
32. Djerassi, C. and Klyne, W. *Proc. Chem. Soc.* **1957** 55.
33. Djerassi, C. Ref.[18], Chap. 2.
34. Lowry, T. M. *Trans. Faraday Soc.* **26** (1930) 266.
35. Heller, W. *J. Phys. Chem.* **62** (1958) 1569.
36. Sjöberg, B., Fredga, A. and Djerassi, C. *J. Am. Chem. Soc.* **81** (1959) 5002.
37. James, A. N. and Sjöberg, B. Ref.[18], Chap. 3.
38. Heller, W. in Weissberger A. *Physical Methods of Organic Chemistry*, 2nd Ed., Vol. I, Part II, Chap, XXIII, Interscience Publishers, Inc., New York 1949.
39. Matell, M. *Kgl. Lantbruks-Högskol. Ann.* **20** (1953) 205.
40. Pettersson, K. *Arkiv Kemi* **10** (1957) 297.
41. Sjöberg, B. *Arkiv Kemi* **13** (1958) 1.
42. Gronowitz, S. *Arkiv Kemi* **13** (1959) 295.
43. Fredga, A. in "*The Svedberg 1884 30/8 1944*", Almqvist and Wiksell, Uppsala 1944, p. 261.
44. Fredga, A. *Tetrahedron.* **8** (1960) 126.
45. Sjöberg, B. *Arkiv Kemi. In press.*
46. Levene, P. A. and Rothen, A. *J. Biol. Chem.* **127** (1939) 237.

47. Rothen, A. and Levene, P. A. *J. Chem. Phys.* **7** (1939) 975.
48. Betti, M. *Trans. Faraday Soc.* **26** (1930) 337.
49. Nerdel, F. and Kresse, G. *Z. Elektrochem.* **56** (1952) 234.
50. Nerdel, F. and Liebig, H. *Ann.* **621** (1959) 42.
51. Singh, B. K. and Verma, S. M. *J. Indian Chem. Soc.* **35** (1958) 179.
52. Singh, B. K. and Sarma, S. R. G. *J. Indian Chem. Soc.* **35** (1958) 463.
53. Nerdel, F. and Würgau, H. *Ann.* **621** (1959) 34.
54. Gillam, A. E. and Stern, E. S. *Electronic Absorption Spectroscopy*, Edward Arnold Ltd., London 1957.
55. Fredga, A. *Arkiv Kemi* **7** (1954) 241.
56. Levene, P. A., Marker, R. E. and Rothen, A. *J. Biol. Chem.* **100** (1933) 589.
57. Pettersson, K. *Arkiv Kemi* **10** (1956) 283.
58. Pettersson, K. *Arkiv Kemi* **9** (1956) 509.
59. Pettersson, K. and Willdeck, G. *Arkiv Kemi* **9** (1956) 333.
60. Fredga, A. and Westman, L. *Arkiv Kemi* **7** (1954) 193.
61. Fredga, A. *Chem. Ber.* **89** (1956) 322.
62. Veldstra, H. and van de Westeringh, C. *Rec. trav. chim.* **70** (1951) 1113.
63. Westman, L. *Arkiv Kemi* **12** (1958) 161.
64. Pettersson, K. *Arkiv Kemi* **7** (1954) 279.
65. Pettersson, K. *Arkiv Kemi* **7** (1954) 339.
66. Pettersson, K. *Arkiv Kemi* **8** (1955) 387.
67. Gronowitz, S. *Arkiv Kemi* **13** (1958) 239.
68. Klyne, W. in Braude, E. A. and Nachod, F. C. *Determination of Organic Structures by Physical Methods*, Academic Press Inc., New York 1955, Chap. 3.
69. Biot, J. B. *Mém. acad. sci.* Toulouse **15** (1838) 207.
70. Biot, J. B. *Ann. chim. et phys.* **10** (1844) 385.
71. Kauzmann, W. J., Walter, J. E. and Eyring, H. *Chem. Revs.* **26** (1940) 339.
72. Djerassi, C. and Geller, L. E. *Tetrahedron* **3** (1958) 319.
73. Kenyon, J. and Pickard, R. H. *J. Chem. Soc.* **107** (1915) 35.
74. Rule, H. G., Barnett, M. M. and Cunningham, J. P. *J. Chem. Soc.* **1933** 1217.
75. Chambers, A. R. and Rule, H. G. *Nature* **133** (1934) 910.
76. Kuhn, W., Freudenberg, K. and Seidler, R. *Z. physik. Chem.* **B 13** (1931) 379.
77. Hargreaves, M. K. and Richardson, P. J. *J. Chem. Soc.* **1957** 2260.
78. Fredga, A. *Studien über Selen-di-karbonsäuren und Diselen-di-karbonsäuren.* Diss. Uppsala 1935, p. 184; also in *Uppsala Universitets Årsskrift* **1935:** 5, p. 184.
79. Fredga, A. *Arkiv Kemi* **6** (1953) 277.
80. Sjöberg, B., Fredga, A., Eisenbraun, E. J. and Djerassi, C. *To be published.*
81. Pettersson, K. *Arkiv Kemi* **7** (1954) 347.
82. Pettersson, K. *Arkiv Kemi* **7** (1954) 39.
83. Gronowitz, S. *Arkiv Kemi* **11** (1957) 361.
84. Levene, P. A. and Rothen, A. *J. Org. Chem.* **1** (1936) 76.
85. Gronowitz, S. and Larsson, S. *Arkiv Kemi* **8** (1956) 567.
86. Fredga, A., Sjöberg, B. and Zeppezauer, M. *Arkiv Kemi. In press.*
87. Westman, L. *Arkiv Kemi* **11** (1957) 431.
88. Westman, L. *Arkiv Kemi* **12** (1958) 167.
89. Djerassi, C. and Geller, L. E. *J. Am. Chem. Soc.* **81** (1959) 2789.
90. Freudenberg, K. and Biller, H. *Ann.* **510** (1934) 230.
91. Fredga, A. *Arkiv Kemi* **8** (1956) 463.
92. Sjöberg, B. *Arkiv Kemi* **12** (1958) 573.
93. Sjöberg, B. *Arkiv Kemi* **9** (1956) 295.
94. Sjöberg, B. *Arkiv Kemi* **12** (1958) 565.
95. Sjöberg, B. *Arkiv Kemi* **11** (1957) 439.
96. Sjöberg, B. *Arkiv Kemi* **12** (1958) 251.
97. Fredga, A. and Agenäs, L.-B. *Arkiv Kemi.* **15** (1960) 327.
98. Sjöberg, B. *Arkiv Kemi. In press.*
99. Wren, H. and Williams, H. *J. Chem. Soc.* **109** (1916) 572.
100. Fredga, A. and Palm, O. *Arkiv Kemi, Mineral. Geol.* **26A** (1949) No. 26.
101. Porath, J. *Arkiv Kemi, Mineral. Geol.* **26 B** (1949) No. 16.

Received December 24, 1959.

ACTA CHEMICA SCANDINAVICA 14 (1960) 296–302

On the Biosynthesis of the Pigments of *Penicillium islandicum*. II

STEN GATENBECK

Institute of Biochemistry, University of Lund, Lund, Sweden

The acetate origin of islandicin from *P. islandicum* is shown by degradation after feeding the mould with ^{14}C-carboxyl labelled acetate, resulting in a strict alternate labelling of the anthracen structure.

By feeding the mould with ^{18}O-labelled acetate, three hydroxyl groups in islandicin and four in emodin are shown to be derived from the carbonyl group of acetic acid. Furthermore, the incorporation of ^{18}O in the secondary alcoholic groups of rubroskyrin indicates their formation from keto groups, originating from acetate, by hydrogenation.

The acetate origin of skyrin from *Penicillium islandicum* has been demonstrated by the incorporation of ^{14}C-labelled acetate in the molecule[1]. The ^{14}C-distribution in skyrin was experimentally established by reductive cleavage of the dianthraquinone to emodin. Oxidation of emodin to acetic acid according to Kuhn and Roth and hypobromite degradation of tetranitroemodin to bromopicrin left the radioactivities of six C-atoms out of fifteen to be measured directly. The isotope distribution of the remaining C-atoms was calculated by means of the acetate theory and the experimentally determined localizations of ^{14}C-atoms. In spite of the agreement with the theory it was desirable to complete the experiment with an investigation of a genuine anthraquinone and to make a more extensive degradation of the molecule.

Islandicin, which occurs in dominant amounts in the pigments of *P. islandicum*, was chosen as starting material. The degradation of islandicin, isolated from the mould after growing on a Czapek-Dox medium containing ^{14}C-carboxyl labelled acetate, was made according to the reaction series outlined in Fig. 1.

In the reaction series I, ring A of islandicin was obtained as 3-hydroxyphthalic acid by oxidation with hydrogen peroxide in alkali. Decarboxylation of 3-hydroxyphthalic acid yielded *m*-hydroxybenzoic acid, and the carboxyl group in position 2 as carbon dioxide. The radioactivity of the carbon dioxide, measured as barium carbonate, was 1/4 of the total radioactivity of 3-hydroxyphthalic acid. The carboxyl group in position 1 of 3-hydroxyphthalic acid

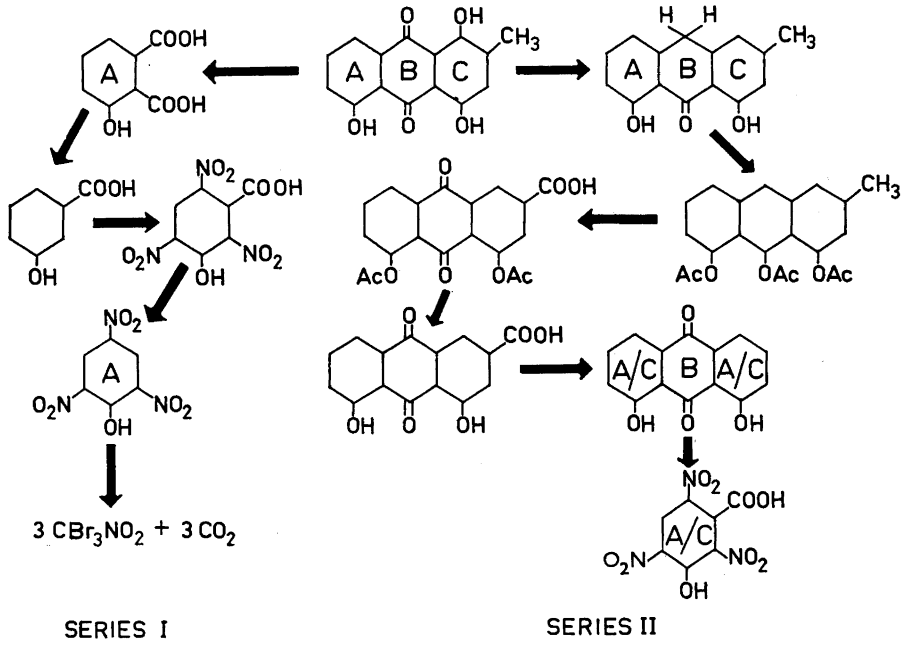

Fig. 1. Scheme of degradation of islandicin.

obtained as carbon dioxide by decarboxylation of the trinitro derivative of *m*-hydroxybenzoic acid, was shown to be nonradioactive. By treating the remaining picric acid with a barium hypobromite solution, the carbon atoms in the 2-, 4-, and 6-positions of the 3-hydroxyphthalic acid were obtained as bromopicrin which was nonradioactive. However, the barium carbonate formed during the reaction, and representing the carbon atoms in the 1-, 3-, and 5-positions, contained the other 3/4 of the total radioactivity of 3-hydroxyphthalic acid.

The ^{14}C-isotope distribution in 3-hydroxyphthalic acid obtained by oxidative cleavage of islandicin is apparently the same as that in the 3-hydroxyphthalic acid formed *in vivo* by *P. islandicum* [2].

On the presumption that the methyl group of islandicin is nonlabelled, which is later confirmed by the experiment, the specific radioactivities of the 3-hydroxyphthalic acid and the islandicin (2.37×10^4 cpm/mg C and 2.23×10^4 cpm/mg C, resp.) indicate that the radioactivity is equally distributed between the A and C rings of islandicin.

In the reaction series II, islandicin was reduced with hydriodic acid to chrysophanol anthron according to Howard and Raistrick [3]. Oxidation of the triacetyl derivative of chrysophanol anthron with chromic anhydride left diacetylrhein. After hydrolysis of the acetyl derivative, the rhein formed

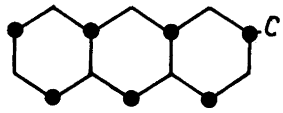

Fig. 2. ^{14}C-Distribution in anthraquinones derived from ^{14}C-carboxyl labelled acetate.

was decarboxylated and the evolved carbon dioxide shown to be nonradioactive. The symmetrical anthraquinone, chrysazin, obtained during the decarboxylation was oxidized with fuming nitric acid to trinitro-*m*-hydroxybenzoic acid. The benzene ring of this substance represents a statistical mixture of the A and C rings of islandicin. The further degradation of trinitro-*m*-hydroxybenzoic acid was performed with the same procedures as described for the degradation of 3-hydroxyphthalic acid. The ^{14}C-distribution in the benzene ring, *i.e.* the rings A + C of islandicin, was identical with that of ring A.

Combination of the ^{14}C-distributions obtained from the two reaction series gives a strict alternate labelling of the carbon atoms all over the molecule of islandicin, as shown in Fig. 2.

As shown in an earlier paper [4] ^{18}O-labelled acetic acid is an available tool for confirmation of the acetate origin of phenolic substances produced by moulds. In some cases it should also be possible to distinguish in the phenolic compound between the oxygen atoms derived from the carbonyl groups of the acetyl units and the oxygen atoms secondarily introduced.

To obtain some information of the character of the oxygen atoms in the polyhydroxyanthraquinone derivatives produced by *P. islandicum*, the mould was grown as above with acetic acid labelled with ^{14}C and ^{18}O in the carboxyl group as the tracer substrate.

Islandicin, skyrin and rubroskyrin were isolated from the mycelium. The radioactivity and the ^{18}O-content of islandicin and emodin, obtained by cleavage of skyrin, were determined.

As seen from Table 3, islandicin and emodin have approximately the same radioactivity, indicating a steady state of the ^{14}C metabolism. Under this condition the ^{18}O-content of the oxygen containing groups originating from the carboxyl group of acetic acid should be the same in islandicin and emodin.

Guided by the acetate theory, the positions of the ^{18}O-labelled groups in phenolic substances could be deduced. Islandicin will theoretically contain three ^{18}O-labelled positions (4, 5 and 10); emodin four labelled positions (4, 5, 7 and 10).

The average amounts of ^{18}O in emodin and islandicin were 0.82 atom% and 0.64 atom%, resp. By calculating the ^{18}O-content in the expected labelled positions, 1.02 atom% (emodin) and 1.07 atom% (islandicin) are obtained. The coincidence of these two values is a support of the validity of the theoretically calculated number of labelled positions in the two substances.

The localization of the labelled oxygen in emodin and islandicin is not established by the ^{18}O-analysis. Emodin anthron and chrysophanol anthron were prepared from the anthraquinones by refluxing with hydriodic acid. The two anthrons should theoretically contain only the labelled oxygen groups but ^{18}O-analysis of the two compounds, however, showed that the ^{18}O groups were interchanged with the nonlabelled aqueous medium during the reaction.

The isolated rubroskyrin was thermally decomposed at 270°C whereby the secondary alcoholic groups of rubroskyrin are split off as water. The ^{18}O-analysis of the water (0.54 atom%) indicated that the alcoholic groups originate from acetic acid and are formed from carbonyl groups by hydrogenation at some stage during the biosynthesis of rubroskyrin. The rather low value of ^{18}O compared with the expected value (1.05 atom%) taken from the ^{18}O-analysis of the anthraquinones, could be explained with a faster exchange of a secondary alcoholic group than of a phenolic hydroxyl group.

In column 7 of Table 3 are given the dilution ratios of ^{18}O and ^{14}C in the substances studied. The ratios 1 obtained for emodin and islandicin show that the activation of exogenous acetate and the formation of these anthraquinones are extremely rapid processes in *P. islandicum*.

Degradation of islandicin

EXPERIMENTAL

The culture conditions and the isolation of the islandicin used are described elsewhere [2].

Reaction series I. 104.5 mg of labelled islandicin were dissolved in 25 ml of 1 N sodium hydroxide. The solution was heated on a steam bath and an aqueous solution of 30 % hydrogen peroxide added dropwise until the islandicin solution was colourless. After cooling, the solution was acidified with hydrochloric acid and extracted exhaustively with ether. The residue, after evaporation of the ether solution, was developed on a paper chromatogram with chloroform-methanol-formic acid (4 %) (10:1:1) as the solvent. The

Table 1. ^{14}C-Distribution in 3-hydroxyphtalic acid obtained by oxidation of islandicin.

Material	Numbers of C-atoms from 3-hydroxy-phthalic acid	Radio-activity cpm	Total radio-activity of the material cpm	Number of ^{14}C-labelled positions	
				Found	Calculated
1	2	3	4	5	6
3-Hydroxyphthalic acid (total comb.)	8	483	3 864	3.99	4
COOH-Group (2-position)	1	960	960	1	1
m-Hydroxybenzoic acid (total comb.)	7	405	2 835	3.06	3
COOH-Group (1-position)	1	61	61	0.06	0
Bromopicrin (C-atoms from 2,4,6-positions)	3	0	0	0	0
CO_2 from the hypobromite degradation (C-atoms from 1,3,5-positions)	3	920	2 760	2.89	3

The numbers of ^{14}C-labelled positions in column 5 are obtained by taking the radio-activity of the COOH-group from 2-position as the basis for the calculations. This COOH-group is supposed to be derived directly from the COOH-group in acetic acid.

region of the paper containing 3-hydroxyphthalic acid (R_F *ca.* 0.15) was cut out and the phthalic acid extracted with ethanol. The yield of 3-hydroxyphthalic acid, determined spectrophotometrically (ε_{333} 1 665) was 60 %. The ethanolic solution was evaporated to dryness at room temperature and the specific radioactivity of the 3-hydroxyphthalic acid determined (2.37×10^4 cpm/mg C). To the labelled compound was added 1.5 g of non-labelled 3-hydroxyphthalic acid and the mixture recrystallized to constant radioactivity from water.

The degradation of the 3-hydroxyphthalic acid and the radioactivity measurements (Table 1) were performed as described in a previous paper [2].

Reaction series II. A mixture of 150 mg of islandicin, 3 ml of glacial acetic acid, 150 mg of red phosphorus and 0.6 ml of hydriodic acid (*d*, 1.67) was refluxed, with stirring, for 5 h. After filtration of the hot solution, chrysophanol anthron crystallized on cooling. Recrystallization from glacial acetic acid yielded 53 mg (40 %) of chrysophanol anthron, m. p. 206°C.

A mixture of the labelled anthron and 705 mg of nonlabelled chrysophanol anthron was recrystallized to constant radioactivity. After combustion of the anthron according to van Slyke and Folch [5], the radioactivity of the carbon dioxide was measured as barium carbonate (the same amount of barium carbonate (15 mg) was used throughout this work for the radioactivity measurements).

Acetylation of the anthron was made with the method described by Naylor and Gardner [6]. A mixture of 500 mg of the chrysophanol anthron, 11 ml of acetic anhydride, and 560 mg of anhydrous sodium acetate was boiled for 5 h and then poured onto crushed ice, and the precipitate formed filtered off and recrystallized from glacial acetic acid. Yield of triacetylchrysophanol anthron: 360 mg (47 %), m. p. 237°C.

The triacetylchrysophanol anthron was oxidized to diacetylrhein according to Hesse [7] by dissolving in a solution of 4 ml of glacial acetic acid and 4 ml of acetic anhydride, and heating with a solution of 750 mg of chromic anhydride in 5 ml of glacial acetic acid at 70°C for 4 h. After addition of water and boiling for a while in order to decompose the acetic anhydride, the precipitate formed was filtered off and redissolved in 1 N sodium carbonate without further purification and the unreacted triacetylchrysophanol anthron separated by filtration. The sodium carbonate solution was acidified with hydrochloric acid and the diacetylrhein sucked off and hydrolyzed with 1 N sodium hydroxide by

Table 2. ^{14}C-Distribution in islandicin.

Material	Number of C-atoms	Radio-activity cpm	Total radio-activity of the material cpm	Number of ^{14}C-labelled positions	
				Found	Calculated
1	2	3	4	5	6
Islandicin (total comb.)	15	97	1 455	7	7
Chrysazin (total comb.)	14	104	1 456	7	7
COOH-Group (rhein)	1	1	1	0	0
COOH-Group (trinitro-*m*-hydroxy-benzoic acid)	1	13	13	0.06	0
Picric acid (total comb.)	6	104	624	3.00	3
Bromopicrin	3	0	0	0	0
CO_2 from the hypobromite degradation	3	190	570	2.74	3

The numbers of ^{14}C-labelled positions in column 5 are obtained by placing seven theoretically labelled positions in chrysazin as basis for the calculations.

Table 3. ^{18}O and ^{14}C analysis.

Material	Radio-activity (total) cpm	Radio-activity of labelled C cpm	Average ^{18}O-content atom %	Theoretical number of ^{18}O-labelled positions	Calculated ^{18}O-content of labelled positions	Dilution ^{18}O *versus* ^{14}C
Sodium acetate	47 600	95 200	21.6			1
Islandicin	2 375	5 089	0.64	3	1.07	1.08
Emodin	2 300	4 928	0.82	4	1.02	1.09
Rubroskyrin			0.54 (the alcoholic group)			

boiling for 15 min. The rhein was isolated after acidification of the solution and recrystallized from glacial acetic acid. Yield 160 mg (57 %), m. p. 320°C.

The rhein was decarboxylated by heating with 5 ml of pure quinoline and 100 mg of copper chromite (prepared according to the method of Adkins and Connor [8]) at 220°C for 2 h. The radioactivity of the carbon dioxide evolved was measured as barium carbonate. After cooling, the reaction mixture was treated with excess of dilute hydrochloric acid, boiled for a few minutes and extracted with ether. The residue, after evaporation of the ether, consisting of chrysazin, was recrystallized from dilute acetic acid. Yield 128 mg (95 %), m. p. 196°C.

The labelled chrysazin was recrystallized together with 2.0 g of nonlabelled chrysazin from glacial acetic acid and the radioactivity determined after combustion as above.

The chrysazin was refluxed with nitric acid (*d*, 1.52) for 7 h and then evaporated to dryness on the steam bath. A filtered water solution of the residue was exhaustively extracted with ether after acidification with hydrochloric acid. Evaporation of the ether phase, containing trinitro-*m*-hydroxybenzoic acid and very small amounts of picric acid, and recrystallization of the residue from dilute sulfuric acid yielded 700 mg of trinitro-*m*-hydroxybenzoic acid, m. p. 186°C.

The ^{14}C-distribution in the trinitro-*m*-hydroxybenzoic acid was experimentally established with the same methods used for the degradation of 3-hydroxyphthalic acid.

The values of the radioactivities in Table 2 are transformed to the same level of dilution.

Analysis of ^{18}O-incorporation

^{18}O-Labelled sodium acetate was prepared by the reaction of 294 mg of water (containing 90 atom% ^{18}O) with an equivalent amount of acetyl chloride at 0°C. The acetic acid and the remaining hydrochloric acid formed were neutralized with 1 N sodium hydroxide. 16.8 mg (0.1 mC) of ^{14}C-carboxyl labelled sodium acetate were added and a small volume withdrawn for isotope analyses. The radioactivity of the dried substance was made after combustion as above, and the ^{14}O content measured after cracking as described earlier [4].

The culture conditions were the same as previously mentioned but with the doubly labelled acetate as the tracer substrate.

After drying at room temperature, the mycelium was extracted in a Soxhlet apparatus with petroleum ether (b. p. 40—60°C) for 3 h, and then with acetone until the extraction solvent was almost uncoloured. The acetone solution was evaporated to dryness, and the pigments separated in a column of silica gel with chloroform as solvent. Islandicin and iridoskyrin together with small amounts of lipids followed the front and a mixture of skyrin and rubroskyrin was eluted by the addition of 10 % acetone to the chloroform.

The islandicin was isolated from its evaporated fraction by sublimation at 150—160°C in vacuum and recrystallization from chloroform. Yield 115 mg, m. p. 218°C.

Skyrin and rubroskyrin were separated in a second silica gel column with ether as the solvent. Emodin, obtained by cleavage of skyrin with sodium dithionite according to Howard and Raistrick [9], was purified by sublimation at 180—190°C in vacuum and recrystallization from toluene. Yield 55 mg, m. p. 257°C.

The radioactivities and ^{18}O contents of islandicin and emodin were determined by the methods described above.

The fraction containing rubroskyrin was developed on a paper chromatogram (Whatman 3 MM) with *iso*propylether, saturated with water, as the solvent. The region containing rubroskyrin (R_F 0.40) was cut out and extracted with acetone. Evaporation of the acetone yielded 30 mg of chromatographically pure rubroskyrin, m. p. 275—280°C (decomp.).

The rubroskyrin was thermally decomposed at 270°C in the apparatus used for the preparation of carbon dioxide for ^{18}O-analysis. Special precautions were taken and test samples run to secure that no decomposition product other than water entered the cracking oven during the process.

REFERENCES

1. Gatenbeck, S. *Acta Chem. Scand.* **12** (1958) 1211.
2. Gatenbeck, S. *Acta Chem. Scand.* **12** (1958) 1985.
3. Howard, B. H. and Raistrick, H. *Biochem. J.* **44** (1949) 227.
4. Gatenbeck, S. and Mosbach, K. *Acta Chem. Scand.* **13** (1959) 1561
5. *Cf.* Calvin, Heidelberg, Reid, Tolbert and Yankwich, *Isotopic Carbon*, Wiley, New York 1949, p. 92.
6. Naylor, C. A. and Gardner, J. H. *J. Am. Chem. Soc.* **53** (1931) 4114.
7. Hesse, O. *Ann.* **388** (1912) 77.
8. Adkins, H. and Connor, R. *J. Am. Chem. Soc.* **53** (1931) 1092.
9. Howard, B. H. and Raistrick, H. *Biochem. J.* **56** (1954) 56.

Received December 5, 1959.

ACTA CHEMICA SCANDINAVICA 14 (1960) 303–311

Chromatography on ECTEOLA * of Sulfate Containing Mucopolysaccharides

NILS R. RINGERTZ and PETER REICHARD

Department of Cell Research and Department of Chemistry I, Karolinska Institutet, Stockholm 60, Sweden

The chromatographic behaviour at different pH of hyaluronic acid, chondroitinsulfuric acid and heparin on ECTEOLA cellulose columns was studied. At acid pH good separations of the three polysaccharides from each other were obtained either by step-wise or gradient elution chromatography. Heparin preparations could be fractionated into subfractions of different anticoagulant activity. When the chromatography was carried out at +4°C no detectable inactivation of heparin occurred. The recovery of polysaccharides from the columns was close to 100 %.

A great number of different methods have been used for the preparation and fractionation of acid mucopolysaccharides (see *e.g.* Ref.[1-3]). Most of these methods have involved salt or alcohol fractionation, or electrophoresis. These methods are not easily adapted for a rapid preparation of small quantities of polysaccharides, as is often desired in tracer studies and enzyme experiments. An exception in this respect is the cetylpyridinium method of Scott [2,4,5].

Paper chromatography has not been used to any large extent, probably because of difficulties in finding a system where the polysaccharides give reproducible R_F values.

Ion exchange chromatography on Dowex 1 was used by Davidson and Meyer [6] for the preparation of chondroitin.

We have previously described briefly the use of the cellulose anion exchanger ECTEOLA for the fractionation of acid mucopolysaccharides [7]. This paper reports these experiments in full and describes some further extensions from them.

ECTEOLA was originally introduced by Peterson and Sober [8] for the chromatography of proteins. So far, however, it has been used mainly in the fractionation of nucleotides and polynucleotides [9,10].

* For brevity, this anion exchanger will be referred to here simply as ECTEOLA. This designation is derived from a contraction of the words epichlorohydrin and triethanolamine.

MATERIALS AND METHODS

Polysaccharides. Several batches of polysaccharides prepared according to different methods were used in this investigation *. However, the experiments shown in Tables 2—4 were all performed with the same polysaccharides. Some analytical data for the main polysaccharide preparations studied are shown in Table 1. It can be seen that hyaluronic acid was contaminated with materials containing galactosamine and sulfate. It is likely that this was due to the presence of a small quantity of chondroitin sulfuric acid.

Packing of columns. ECTEOLA cellulose (commercial grade, 0.39 meq/g) prepared according to Peterson and Sober [9], was obtained from Brown Company, Berlin, New Hampshire, USA. Before use, about 50 g of ECTEOLA cellulose was suspended in 0.5 M NaCl and packed in a large glass column. The column was then washed with 5 liters of 0.5 M NaOH, 5 liters of 3 M NaCl and 3 liters of 0.1 M NaCl—HCl (1:1). These washings were essential, otherwise materials giving various reactions for sugars were eluted in the chromatograms. The washed resin was then resuspended in 0.1 M NaCl—HCl (1:1) and packed into smaller columns for chromatography.

Polysaccharide solutions in water were adjusted to the pH used for chromatography by the addition of small quantities of the salt solution used for starting the chromatogram. The final solutions, containing 0.5—2 mg polysaccharide/ml with a salt concentration of less than 0.05 M, were allowed to drain into the column by gravity.

Elution of columns: Four different systems were used for elution of the columns:

A. 0.1—3.0 M HCl.
B. 0.1—3.0 M NaCl—HCl (1:1), pH 1.3 **.
C. 0.1—2.5 M NaCl in 0.05 M Glycine-HCl-buffer, pH 2.9 **.
D. 0.1—2.5 M NaCl in 0.05 M Sodium acetate buffer, pH 5.0 **.

Table 1. Analytical data †of polysaccharides used.

Polysaccharide	Source	Abbrev.	% amino sugar[15]	% amino glucose amine[16]	% of sugar as galactose amine[16]	% uronic acid[17]	% S[18,19]	% N	% Moisture	Ash %
Hyaluronic acid	Umbil. cord	HYA	38.2	90.4	9.6	36.6	0.6	3.56	14.5	8.0
Chondroitin sulfuric acid A	Calf cartilage	CHS-A	25.4	<3.0	100.0	27.7	4.3	2.58	12.0	24.5
Heparin Anticoag. 100 U/mg	Beef lung	HEP 100	24.5	100.0	0	20.8	10.4	2.18	13.7	39.4
Heparin by-product Polysaccharide II Anticoag. 5 U/mg	Beef lung	HBP II	12.9	51.5	48.5				9.1	
Heparin Anticoag. 120 U/mg	Beef lung	HEP 120	23.2						13.3	

* We wish to thank Drs. A. Balasz, S. Gardell, B. Högberg, T. Laurent, J. Scott and Vitrum Company for generous gifts of polysaccharide preparations.

** pH was measured on 0.1 M solutions.

† All figures for air dry preparations.

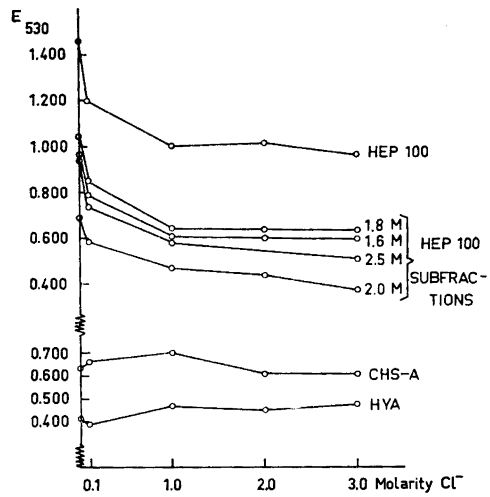

Fig. 1. Effect of different concentrations of HCl—NaCl (1:1) on the development of color in the carbazol reaction.

In a few exceptional cases when the polysaccharide was not completely eluted in these systems, the columns were at the end eluted with 0.5 M NaOH.

The columns were either eluted step-wise or by a gradient elution system which gave a linear increase in chloride concentration [11]. During step-wise elution a total of 100—150 ml of solution was used in each step with 1 × 10 cm ECTEOLA columns containing 10—15 mg of polysaccharide. The columns were eluted with the same eluent until the effluent contained less than 10 μg uronic acid/ml. In most cases 10—20 ml fractions were collected with an automatic fraction collector. The rate of elution during both gradient and step-wise chromatography was 10—20 ml/hour for a 10 × 1 cm column.

Analysis of fractions. The polysaccharides were localized in the different chromatographic fractions with the carbazol method [12]. For keratosulfate the anthrone reaction [13] was used. Salt concentration of the effluent was determined by conductivity measurements.

The influence of salt concentration on the results obtained by the carbazol method was studied in model experiments (Fig. 1). It is seen that, with heparin, increasing salt concentration (HCl—NaCl, 1:1) depressed the color development by about 40 %. No similar effect was observed for hyaluronic acid or chondroitin sulfuric acid. Instead, with hyaluronic acid a slight increase in color was observed at higher salt concentrations, while the effect on chondroitin sulfuric acid was negligable. Since high salt concentrations depressed the color development with heparin, it was considered necessary to investigate whether subfractions of heparin gave the same results. This was found to be the case (*cf.* Fig. 1), although minor quantitative differences could be observed.

The different heparin fractions were eluted at salt concentrations between 1.5 and 3.0 M Cl^- (system A), where no changes took place in the influence of salt on color development. Consequently no correction for the salt effect between different heparin fractions was necessary.

For heparin the carbazol reaction normally gives uronic acid values that are about 60 % higher than the theoretical ones [12]. The depression in color formation observed for heparin in the presence of chloride almost abolishes this anomaly and makes possible a more accurate quantitative interpretation of the carbazol reaction in the effluent. The errors in the quantitative estimation of chondroitin sulfuric acid and hyaluronic acid due to the presence of salt were found to be less than 8 %.

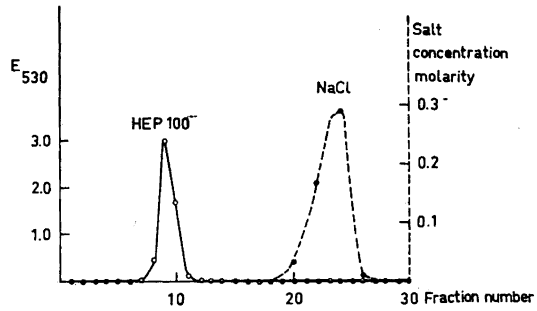

Fig. 2. Separation by gel-filtration on a Sephadex column (14 × 2 cm) of 2.5 mg of HEP 100 from 110 mg of NaCl.

Removal of salt. It was necessary to remove salts before more detailed analysis of the polysaccharide fractions could be made. This was done by dialysis at 0°C for 24 h against distilled water in tubing obtained from Visking Corporation, Chicago, Ill., USA. The solution was then neutralized to pH 7 with NaOH and evaporated under vacuum to a small volume. The polysaccharides were precipitated with 3—4 volumes of ethanol. The precipitate was then washed with 75 % ethanol, dried in a vacuum, weighed and analyzed.

When it was expected that an appreciable amount of polysaccharide would be lost during dialysis, a gel filtration technique was used [14]. This is illustrated by Fig. 2 which shows the separation of 2.5 mg of heparin (HEP 100) and 110 mg of NaCl by gel filtration on Sephadex G 25 (Pharmacia, Uppsala, Sweden). The materials were dissolved in 1 ml of water and introduced into the column by gravity. Elution was carried out with distilled water. Fractions were collected by a fraction collector (1.5 ml/30 sec). The polysaccharide could be completely separated from salt, the whole procedure being completed in less than 10 min.

Analytical methods. The total amino sugar content of the polysaccharides was determined by a modification of the Elson-Morgan procedure [15]. Glucosamine and galactosamine were separated and determined according to Gardell [16], uronic acid according to Tracey [17]. Sulfate was analyzed by the benzidine method [18] as modified by Balazs [19]. In this last modification the benzidine sulfate precipitate was collected on bacterial filters (Ra. Millipore Filter Comp., Bedford, Mass., USA.). Nitrogen was determined according to Kjeldahl. For moisture determinations the polysaccharides were dried under vacuum over P_2O_5 for 22 h at 90°C. Anticoagulant activity * was determined according to Studer and Winterstein [20].

RESULTS AND DISCUSSION

Tables 2, 3 and 4 give a survey of the chromatographic behaviour of hyaluronic acid (HYA), chondroitinssulfuric acid (CHS-A) and heparin (HEP 100) in four different chromatographic systems (*cf.* material and methods).

Hyaluronic acid (Table 2) was found to be very loosely or not at all bound to the ion exchanger in systems A and B. At the higher pH values of systems C and D it was adsorbed to the exchanger. In a gradient chromatogram with system D hyaluronic acid was eluted as a sharp peak between 0.4—0.5 M chloride.

* We wish to thank Prof. E. Jorpes, mrs Sohlberg and Vitrum Company for help with the determination of anticoagulant activities.

Table 2. Chromatographic behaviour of hyaluronic acid on ECTEOLA.

Fraction (Molarity Cl^-)	Amount of polysaccharide in % of total quantity eluted in different fractions	
	System B (and A)	System C (and D)
0.1	92	0
0.7	0	92
0.9	0	0
1.1	8	8

The calculations are based on the carbazol reaction applied directly to the eluted fractions.

The data in Tables 2—4 were obtained from chromatograms of 10—15 mg of polysaccharide on ECTEOLA columns, 1 × 10 cm.

Table 3. Chromatographic behaviour of chondroitin sulfuric acid A on ECTEOLA.

Fraction (Molarity Cl^-)	Amount of polysaccharide in % of total quantity eluted in different fractions			
	System A	System B	System C	System D
0.1	3	3	0	0
0.4	—	—	—	0
0.7	5	5	52	40
0.9	—	—	—	54
1.1	16	89	48	5
1.4	70	3	0	1
1.7	6	0	0	0
2.5	—	0	0	0
3.0	0	—	—	—

For experimental data see Table 2.

Table 4. Chromatographic behaviour of heparin (HEP 100) on ECTEOLA.

Fraction (Molarity Cl^-)	Amount of polysaccharide in % of total quantity eluted in different fractions			
	System A	System B	System C	System D
0.1	0	0	0	0
0.4	—	—	—	0
0.7	0	0	0	9
0.9	—	—	—	40
1.1	0	0	66	49
1.4	0	13	34	2
1.7	4	41	0	—
2.5	24	46	0	0
3.0	56	—	—	—
0.5 M NaOH	16	0	0	0

For experimental data see Table 2.

The different behaviour of hyaluronic acid in systems A and B on the one hand and systems C and D on the other hand was probably due to the fact that the pK of the carboxyl groups of hyaluronic acid is 3.2 [21]. The polysaccharide therefore contains hardly any negative charge at a pH below 1.5 (systems A and B). At pH values of 3 and 5 (systems C and D, respectively) the carboxyl group can be expected to be at least partially dissociated and to cause the binding of the polysaccharide to the basic groups of the ECTEOLA column.

The two sulfated polysaccharides studied showed a different behaviour. Chondroitin sulfuric acid A (Table 3) was retained by the exchanger in all four systems. For complete elution of CHS-A the highest chloride concentration was required with system A (HCl), the lowest chloride concentration with system D.

Heparin showed a behaviour similar to chondroitin sulfuric acid A with the four chromatographic systems. In system A heparin was only partially eluted even at 3.0 M HCl. Complete elution of heparin was only obtained by raising the pH (Table 4).

The behaviour of the two sulfated polysaccharides is at first sight rather unexpected. Because of the dissociation of carboxyl groups the polysaccharides would be expected to contain a higher negative net charge at pH values of 3 and 5 (systems C and D, respectively) than at pH-values below 1.5 (systems A and B). Thus one would expect that the polysaccharides would be eluted with a lower chloride concentration at the more acid pH. The reverse was found to be the case.

The sharpest separations of hyaluronic acid, chondroitin sulfuric acid and heparin from each other could be obtained with systems A and B. Since heparin was not completely eluted from the resin with 3 M HCl in system A, it was considered that system B was more suitable for elution of the polysaccharides. System B was therefore studied further.

Fig 3 shows a separation of an artificial mixture of HYA, CHS-A and Hep 120 by step-wise elution. It can be seen that a clear separation of the three polysaccharides into three main peaks was obtained. As demonstrated in

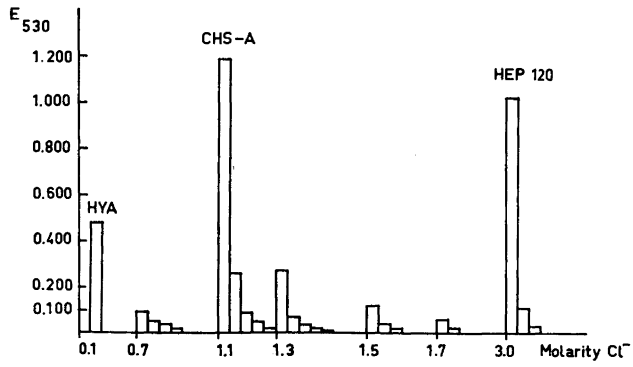

Fig. 3. Fractionation on an ECTEOLA column (1 × 12 cm) of a polysaccharide mixture containing 6 mg HYA, 14 mg CHS—A and 13 mg HEP 120. Fractions 12—15 ml/30 min.

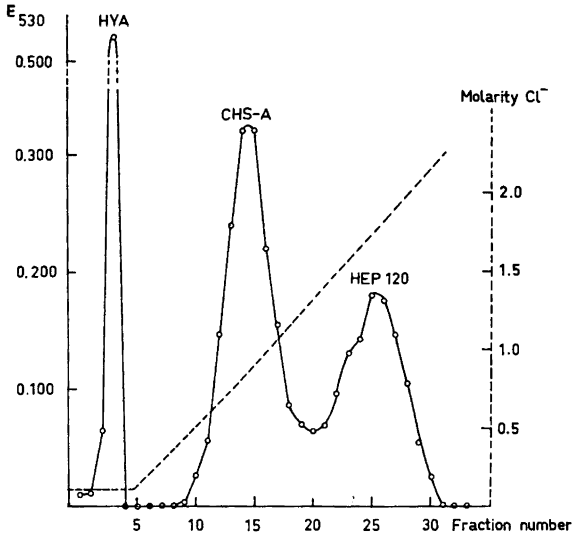

Fig. 4. Gradient chromatogram of the same mixture as in Fig. 3. Reservoir: 400 ml of 3.0 M NaCl—HCl (1:1), mixing vessel: 400 mg of 0.1 M NaCl—HCl (1:1). Fractions ca 20 ml/h. Dotted line = salt concentration.

separate experiments, materials eluted at 0.7, 1.1 and 1.3 M Cl^- originated from the CHS-A preparation, while the HEP 120 contained the material eluted in the 1.5, 1.7 and 3.0 M Cl^- fractions.

A gradient chromatography of a similar mixture of the three polysaccharides is shown in Fig. 4. Again three main peaks, correspondig to HYA, CHS-A and HEP 120 were obtained. The latter two polysaccharides were not separated completely. This behaviour was expected from the behaviour of CHS-A and HEP 120, on individual columns, and from the results obtained in the experiment shown in Fig. 3. The gradient chromatograms clearly demonstrate that the separations obtained by step-wise elution were not due to chromato-

Table 5. Fractionation of heparin into subfractions by chromatography on ECTEOLA.

	amount of material	anticoagulant activity
	mg	units/mg
Starting material	225	110
1.4 M fraction	23	50
1.6 M »	68	85
1.8 M »	30	130
2.0 M »	35	130
2.5 M »	20	140

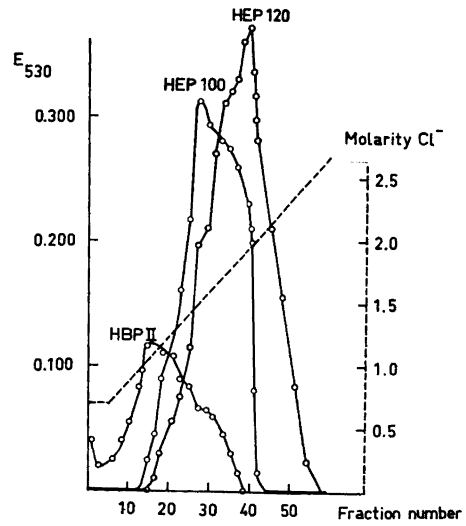

Fig. 5. Chromatography on three separate columns of "heparin" preparations of different anticoagulant activity. The three columns (1 × 5 cm) were eluted simultaneously from the same mixing vessel. Reservoir: 400 ml of 3.0 M NaCl—HCl (1:1), mixing vessel: 400 ml of 0.7 M NaCl—HCl (1:1). Fractions 3 ml/20 min, 12 mg of polysaccharide on each column.

graphic artefacts. However, step-wise elution allowed more clearcut separations and was therefore used in most experiments.

In the experiments described so far, no special attempts were made to obtain subfractions of heparin. However, it was thought of interest to see whether a commercial preparation of this polysaccharide could be further fractionated by chromatography. Such an experiment is described in Table 5.

The fractions obtained differed from each other as regards anticoagulant activity. The most active fractions were those eluted at the highest ionic strength. Fractionation of heparin into materials of different anticoagulant activity has been obtained by several authors [22], the earliest studies in this field being those of Jorpes [23].

In another set of experiments a comparison was made of the chromatographic behaviour of three "heparins" of different anticoagulant activity during gradient elution. HBP II, HEP 100 and HEP 120 were chromatographed on three separate columns of the same dimensions. The three columns were connected with the same gradient system. The results (Fig. 5) indicate that, even though considerable overlapping did occur, the three polysaccharides nevertheless showed distinct differences in their chromatographic behaviour. More material was eluted at higher salt concentrations from the HEP 120 preparation than from HEP 100. A similar difference existed between HEP 100 and HBP II. Thus in general the materials with the highest anticoagulant activities tended to show the highest affinity to the column.

As reported earlier [7] chromatography on ECTEOLA in system B was not found to cause demonstrable inactivation of heparin or loss of sulfate groups from this polysaccharide. It was also found that the recovery of polysaccharides (hyaluronic acid, chondroitin sulfuric acid A and B, and heparin) was close to 100 %. On the other hand losses of some polysaccharides occurred when salts were removed by dialysis.

Chromatography on ECTEOLA with system B has been used for the preparation from mast cell tumors of polysaccharide fractions of different chemical and biological properties [24]. The method was also easily adapted to a microscale which has permitted the fractionation of the polysaccharide from normal peritoneal mast cells in quantities less than 500 μg [25]. When used with the orcinol reaction for the demonstration of polysaccharides in the effluent the separation of 20 μg of HYA, 20 μg of CHS-A and 20 μg of HEP 120 could be followed without difficulty.

REFERENCES

1. Blix, G. and Gardell, S. *To be published.*
2. Scott, J. E. in Glick, D., Ed. *Methods of Biochemical Analysis*, Interscience Publishers Inc. New York. *To be published.*
3. Gibian, H. *Mucopolysaccharide und Mucopolysaccharidasen*, Franz Deuticke, Wien 1959.
4. Scott, J. E. *Chem. & Ind. London* **1955** 168.
5. Borelius, E. Gardell, S. and Scott, J. E. *To be published.*
6. Davidson, E. A. and Meyer, K. *J. Biol. Chem.* **211** (1954) 605.
7. Ringertz, N. R. and Reichard, P. *Acta Chem. Scand.* **13** (1959) 1467.
8. Peterson, E. A. and Sober, H. A. *J. Am. Chem. Soc.* **78** (1956) 751.
9. Bendich, A., Fresco, J. R., Rosenkrantz, H. S. and Briser, S. M. *J. Am. Chem. Soc.* **77** (1955) 3671.
10. Bendich, A., Pahl, H. B., Korngold, G. C., Rosenkranz, H. S. and Fresco, J. R. *J. Am. Chem. Soc.* **80** (1958) 3949.
11. Bock, R. M. and Ling, N. S. *Anal. Chem.* **26** (1954) 1543.
12. Dische, Z. *J. Biol. Chem.* **167** (1947) 189.
13. Scott, T. A. and Melvin, E. H. *Anal. Chem.* **25** (1953) 1656.
14. Porath, J. and Flodin, P. *Nature* **183** (1959) 1657.
15. Blix, G. *Acta Chem. Scand.* **2** (1948) 467.
16. Gardell, S. *Acta Chem. Scand.* **7** (1953) 207.
17. Tracey, M. V. *Biochem. J.* **43** (1948) 185.
18. Andersson, L. *Acta Chem. Scand.* **7** (1953) 689.
19. Balasz, A. *Unpublished.*
20. Studer, A. and Winterstein, A. *Helv. Physiol. et Pharmacol. Acta* **9** (1951) 6.
21. Laurent, T. *Thesis*, Almqvist och Wiksell, Uppsala 1957.
22. Foster, A. B. and Huggard, A. J. *Advances in Carbohydrate Chem.* **10** (1955) 335.
23. Jorpes, E. *Biochem. J.* **36** (1942) 203 and in *Heparin in the treatment of thrombosis*, Oxford Medical Publications, London 1946.
24. Ringertz, N. R. *Acta Chem. Scand.* **14** (1960) 312.
25. Bloom, G. and Ringertz, N. R. *Arkiv Kemi. In press.*

Received December 23, 1959.

ACTA CHEMICA SCANDINAVICA 14 (1960) 312–320

Acid Polysaccharides of two Mast Cell Tumors in Mice

NILS R. RINGERTZ

Department of Cell Research and Genetics, Karolinska Institutet, Stockholm 60, Sweden

Polysaccharides prepared from two mast cell tumors in mice were fractionated by chromatography on ECTEOLA cellulose. Both tumors contained heparin and also large quantities of other polysaccharides. These were present in both solid and ascites sublines of the tumors. Polysaccharide fractions from one of the tumors were analyzed and found to differ from each other in sulfate content, anticoagulant activity, and type of amino sugar present.

The first indication of the chemical nature of the metachromatic component of the mast cell granules came from the findings of Jorpes [1] that heparin contained sulfate groups and gave a strong metachromatic reaction with toluidine blue. Subsequent chemical and histological studies by Jorpes, Holmgren and Wilander [2] disclosed a close relationship between the heparin content of various tissues and the number of mast cells found therein indicating that heparin was present in the mast cells.

The histochemical significance of the metachromatic staining reaction was also pointed out by Lison [3], who showed that high molecular polysulfuric acid esters gave such a reaction.

The observations made by Jorpes, Holmgren and Wilander [2] received further support by the finding of Oliver *et al.*[4] in 1947 that a dog mast cell tumor of dermal origin contained large quantities of heparin. During the last decade the heparin content of mast cells has been further substantiated by the work of a number of authors [5,6].

In spite of the fact that several authors [7–9], have advanced theories about the participation of mast cells in the production of the metachromatic ground substance of connective tissue, little is known if other polysaccharides are present in mast cells.

Data obtained by Magnusson and Larsson [10] on a dog mastocytoma and by Korn [11] and Rodén [12] on mast cell tumors in mice, indicate that besides heparin these neoplastic mast cells also contain other polysaccharides with lower sulfate content, similar to heparin monosulfuric acid [13] and chondroitin sulfuric acids.

The aim of the present investigation was to study the total polysaccharide content of two types of mast cell tumors in order to obtain a basis for further studies on the biosynthesis of heparin in the tumor mast cells.

MATERIAL AND METHODS

Tumors. Two mast cell tumors of independent origin were used in the present investigation. One tumor was obtained in July 1957 in its 23rd transplant generation from Dr. Thelma Dunn [14], National Cancer Institute, Bethesda, Maryland, USA. It has been maintained in this laboratory by routine transplantation every 14—20 days to inbred dba, dba F_1, or dba back cross mice as a subcutaneous tumor (DMS). The tumor yield was 1—2 g (wet weight)/mouse. The tumor was easily transformed to the ascites form (DMA) upon intraperitoneal inoculation. A maximum of 1.5 ml ascites was obtained from each mouse. In these fluids 85 % of the cell population were tumor cells.

The second tumor was obtained in March 1958 from Dr. J. Furth [15], Children's Cancer Research Foundation, Harvard Medical School, Boston, Mass., USA. It has been kept in our laboratory as a solid, subcutaneous tumor in LAF_1 mice (FMS). When grown as a subcutaneous tumor a maximum of 8—17 g (wet weight) of tumor/mouse was obtained 4—8 months after inoculation. Often, however, these large tumors showed central necrotic areas and the tumors were therefore usually taken at the size of 4—6 g (*i. e.* 2—4 months after inoculation). When grown intraperitoneally 0.5—1.5 ml of ascites containing 60—80 % tumor cells was obtained from each mouse (FMA). This tumor also produced large solid infiltrates in the peritoneum and in the mesenteries. The intraperitoneal solid tumor mass thus obtained could to a large degree be dissected free from other tissues. The histology of the tumors was studied by routine examination of toluidine blue stained sections and smears.

Preparation of polysaccharide. The tumors were cut into small pieces and homogenized in 2—3 volumes of 0.1 M phosphate buffer, pH 7.8. The homogenate was boiled for 5 min and then digested with a pancreatic extract [16] (Pankreatin, Merck, Darmstadt, Germany). The digestion was performed with 10 mg of enzyme/g wet tissue for 24—48 h.

In some experiments, where a higher degree of purity of the polysaccharide material was desired, the homogenate was first digested with a crude papain preparation (10—30 mg/g wet tissue) for 16 h at 65° in 0.1 M phosphate buffer pH 6.2 containing 0.3 M NaCl, 0.005 M cysteine hydrochloride and 0.0005 M versene [17]. After digestion the preparation was precipitated with 3—4 volumes of ethanol. The precipitate was washed twice with 75 % ethanol and then dried at 50°C in a vacuum. After this the material was digested over night with a pancreatic extract as described above.

After digestion the material was boiled for 5—10 min and centrifuged. The precipitate was washed with distilled water and the combined supernatants were precipitated with 3—4 volumes of ethanol. The precipitate was washed with 75 % ethanol, redissolved in water and acidified at 0°C by the addition of 4 N perchloric acid. The precipitate was washed repeatedly with cold 0.1 N perchloric acid. The combined supernatants were neutralized with KOH and after standing for 1 h the precipitate was removed by centrifugation. The supernatant was then made 0.05 M with respect to Cl^- by the addition of HCl—NaCl (1:1).

Chromatography on ECTEOLA cellulose [18,19]. For the separation of 400 mg of polysaccharide, an ECTEOLA column 4 × 7 cm was used. For smaller quantities a correspondingly thinner column was used. Step-wise chromatography was performed with 250—300 ml of eluent for each step with a 4 × 7 cm column. Fractions were collected at 50 ml/30 min. For elution of the columns, chloride buffers containing equimolar amounts of HCl and NaCl were used. The chloride concentrations in the different elution steps were 0.1, 1.1, 1.4, 1.7 and 2.5 M, respectively. The columns were finally washed with 0.5 M NaOH. This sometimes eluted materials giving a positive carbazol reaction. The absorption spectra for these materials in the carbazol reaction, however, were not those expected for uronic acid containing compounds. These fractions were not studied further.

The chloride concentrations in the different elution steps were chosen on the basis of previous model experiments with known polysaccharides. The fractions were analyzed by the carbazol reaction [20]. Salt was removed from the effluent either by dialysis or by gel filtration on Sephadex G-25 (Pharmacia, Uppsala, Sweden) [21].

Analytical methods. Total amino sugars were determined by the Elson-Morgan reaction [22] after hydrolysis for 8 h in 6 N HCl at 100°C. Glucosamine and galactosamine were determined separately by the method of Gardell [23]. The identity of the amino sugars was checked by paper chromatography according to Gardell *et al.* [24] as modified by Stoffyn and Jeanloz [25]. Uronic acid was estimated by the carbazol reaction [20] using glucuronic acid

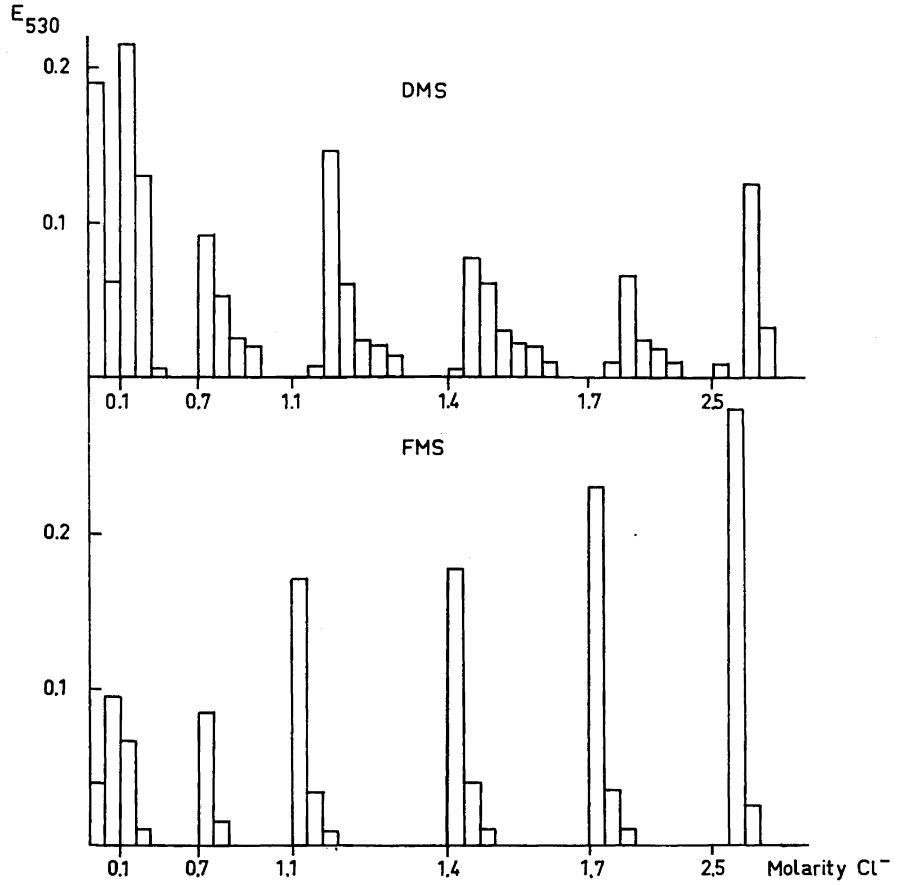

Fig. 1. Stepwise chromatography on ECTEOLA columns of polysaccharides from "pankreatin"-digested DMS and FMS subcutaneous tumors.

as standard. Nitrogen was determined according to Kjeldahl and sulfate by a benzidine method [26,27]. Optical rotation was measured on 1 % solutions in a Zeiss poalrimeter using 10 cm cuvettes.

RESULTS AND DISCUSSION

Chromatographic patterns. Fig. 1 shows the chromatograms obtained with polysaccharides from subcutaneous DMS and FMS tumors. It can be seen, that when the chloride concentration of the eluent was changed, carbazol reacting material was eluted in both chromatograms. The elution steps were chosen so that hyaluronic acid was expected to be completely eluted with the 0.1 M fraction, chondroitin sulfuric acid A and B mainly with the 1.1 M fraction, and heparin mainly with the 2.5 M fraction. From both tumors, carbazol

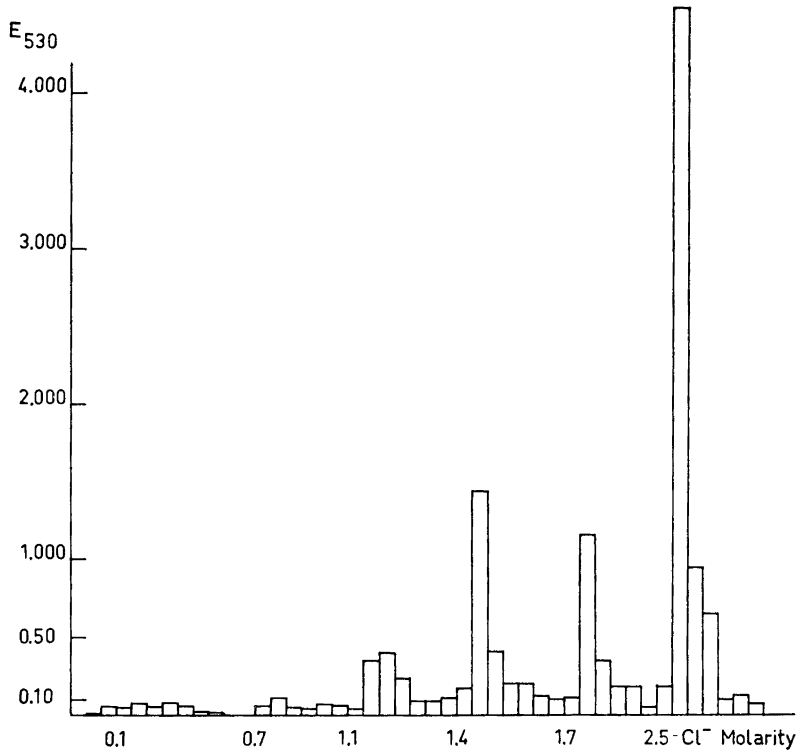

Fig. 2. Stepwise chromatography on an ECTEOLA column (4 × 8 cm) of 450 mg of polysaccharide from "pankreatin" digested solid intraperitoneal FMS tumors. Fractions: 50 ml/30 min.

reacting materials were eluted at the position of heparin, but it was also obvious that both tumors contained large quantities of other polysaccharides. The maximum total quantity of polysaccharides obtained from the FMS tumor was 3—4 mg/g wet weight of tumor tissue. The corresponding value for the DMS tumor was only about 0.5—1.0 mg.

The chromatographic patterns obtained with polysaccharide from the DMS and FMS tumors differed somewhat as to the relative quantity of carbazol reacting material eluted in the different fractions but otherwise showed great similarity. With the FMS tumor the chromatographic patterns varied with the site of growth. With intraperitoneal solid tumors relatively more polysaccharide was eluted at higher chloride concentrations than with the subcutaneous tumors (*cf.* Figs. 1 and 2).

In order to investigate whether the main part of the polysaccharides found in the solid tumors originated from the tumor cells and not from blood vessels and connective tissue, the polysaccharide content of ascites sublines of the two tumors was studied. The chromatogram obtained during the separa-

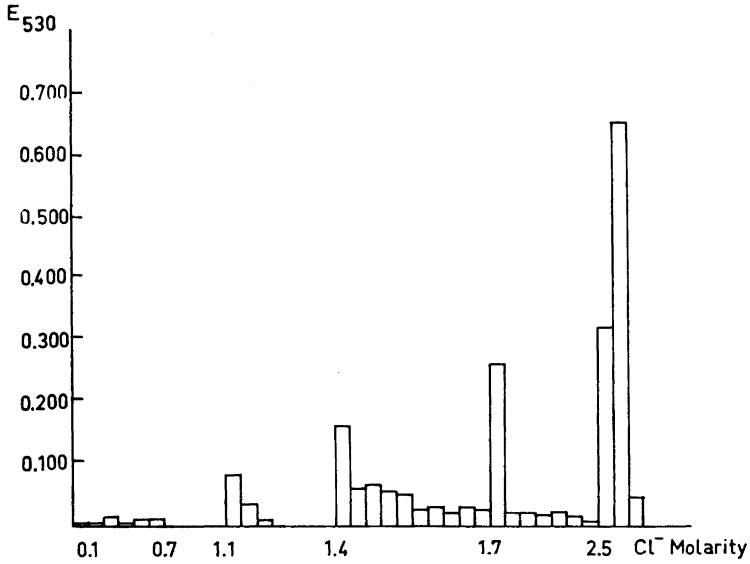

Fig. 3. Stepwise chromatography on an ECTEOLA column (2 × 8 cm) of 70 mg of polysaccharide from "pankreatin" digested FMA ascites tumor. Fractions: 8 ml/30 min.

tion of polysaccharide from the ascites line of the FMS tumor, (FMA), (Fig. 3) was closely similar to that obtained from the solid intraperitoneal tumors in the same animals (Fig. 2).

The same results were obtained with the DMS and DMA tumors except for the 1.1 M fraction, which in the DMA tumor was practically free from carbazol reacting material.

Analyses of the amino sugar type present in the unfractionated FMS and DMS polysaccharides showed that 20—40 % and 24 %, respectively, of the total amino sugars was galactosamine, the remainder being glucosamine. In the unfractionated FMA polysaccharides < 10 % of the amino sugars was galactosamine.

The results indicate that a major part of the non-heparin polysaccharides come from the tumor mast cells while the polysaccharide quantity contributed by the blood vessels and connective tissue in the solid tumors is small.

In order to obtain some information on the chemical nature of the polysaccharides prepared from the mast cell tumors the fractions obtained from the FMS tumor were analyzed. It was found difficult to obtain enough material from the DMS line because of the small size of the tumors and their low polysaccharide content.

Analysis of the 0.1 M fraction. This fraction showed a strong ultraviolet absorption at 260 and 280 mμ and gave an absorption spectrum in the carbazol reaction which was not typical of uronic acids (Fig. 4).

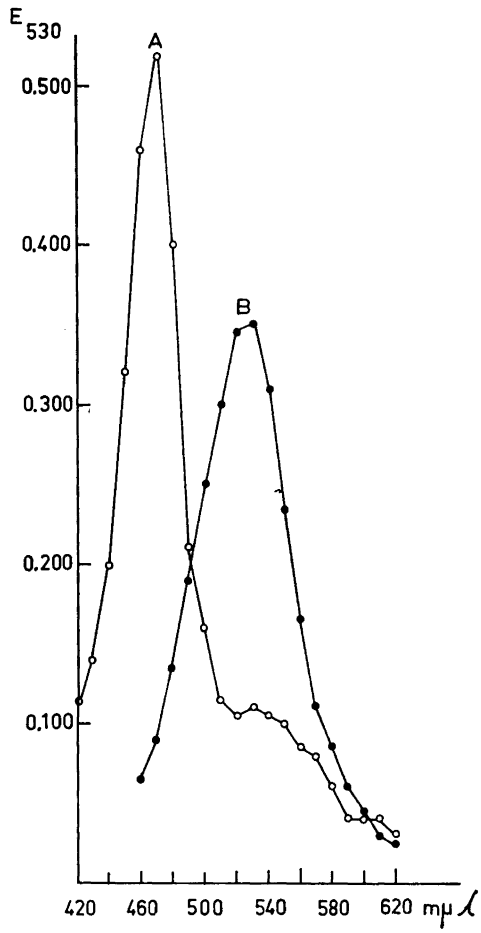

Fig. 4. Carbazol spectra for the 0.1 M fraction (A) and for the 1.1 M fraction (B) obtained in an ECTEOLA chromatogram of the type shown in Fig. 1 (FMS). Curve B is the spectrum obtained for hexuronic acid-containing polysaccharides.

In order to obtain further information about the carbazol reacting material eluted in the 0.1 M fraction, the material obtained from a chromatogram of about 400 mg of FMS tumor polysaccharide (120 g wet tumor tissue) was neutralized to pH 7 with 1 N NaOH and concentrated to 58 ml. From this material, 2 ml were added to a 2 × 14 cm Sephadex column [21]. The column was eluted with distilled water, 1.5 ml fractions being collected at 30 sec intervals. Two components giving carbazol reactions were found (Fig. 5). The main component was eluted after the void volume of the column and gave a typical uronic acid spectrum in the carbazol reaction. A smaller component was eluted close to the salt peak. In its last fractions it contained material giving a maximum at 470 mμ in the carbazol reaction. The main component contained amino sugar and traces of sulfate. The smaller component was not studied further.

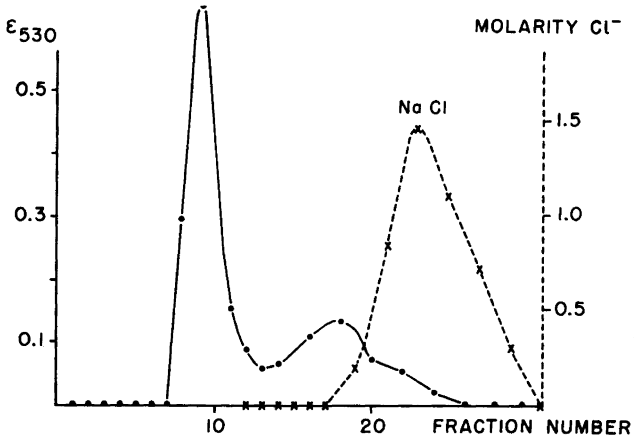

Fig. 5. Fractionation on a Sephadex gel column (2 × 14 cm) of material (= 0.7 mg of glucuronic acid) from the 0.1 M ECTEOLA fraction. The main component is eluted after the void volume of the column indicating a high molecular weight.

A similar separation into two components was obtained also by gradient chromatography on ECTEOLA at pH 5.0 [19]. The major component was eluted between 0.20 and 0.33 M Cl^- and the smaller component between 0.40 and 0.55 M Cl^-. In this chromatographic system, hyaluronic acid, prepared by different methods from cock's comb, bovine vitreus and a human mesothelioma was eluted as sharp peaks between 0.40 and 0.50 M Cl^-.

The results indicate the presence in the 0.1 M fraction of a high molecular polysaccharide with little or no sulfate and with a chromatographic behaviour different from that of high molecular hyaluronic acid.

Analysis of the 0.7—2.5 M fractions. Table 1 shows some analytical data for FMS polysaccharides eluted at higher salt concentrations. The results show that all fractions contained uronic acid, amino sugar and varying quantities of sulfate. The analytical data indicate that the fractions were contaminated with non-polysaccharide material. The nitrogen analyses are in excess of what can be expected from the amino sugar determinations suggesting that in the 1.1—2.5 M fractions 1—5 %, and in the 0.7 M fraction about 17 % of the dry weight may be due to contaminating protein.

The method used for the estimation of uronic acid is known to give values deviating from those obtained by decarboxylation methods. Heparin is thus known to give values about 50 % higher than theory [20]. As the nature of the uronic acid moiety of the different polysaccharide fractions is not known, exact calculations of the ratio of uronic acid to amino sugar is impossible. The values in Table 1, calculated on the basis of glucuronic acid standards indicate, however, that the 1.1—2.5 M fractions contained equimolar quantities of amino sugar and uronic acid.

The amino sugars in the different fractions were isolated by ion exchange chromatography according to Gardell [23]. Glucosamine and galactosamine were identified by their effluent volumes in ion exchange chromatography

Table 1. Analytical data for FMS tumor polysaccharide fractions. The values are for dry polysaccharides.

	Fraction				
	0.7 M	1.1 M	1.4 M	1.7 M	2.5 M
Amino sugar %	15.7	27.6	23.5	37.3	27.6
Galactosamine, % of total amino sugar	*	73	56	20	14
Glucosamine, % of total amino sugar	*	27	44	80	86
Uronic acid	9.8	20.0	20.1	36.5	36.5
SO_4/amino sugar, molar ratio	—	0.98	1.02	1.50	2.20
Nitrogen, %	3.91	2.36	2.64	3.28	2.34
Anticoagulant activity, U/mg	0	0	6	55	100
$[\alpha]_D^{22}$	—	+ 1°	+ 1°	+ 39°	+ 35°

and by paper chromatography after degradation with ninhydrin to arabinose and lyxose, respectively [25].

The 1.1 and 1.4 M fractions contained glucosamine and galactosamine in about equal quantities. In the 1.7 M and 2.5 M fractions glucosamine dominated over galactosamine. In the 0.7 M fraction paper chromatography indicated the presence of both amino sugars.

The fractions eluted at lower salt concentration in the chromatogram contained less sulfate than the fractions eluted later in the chromatogram. The 1.1 and 1.4 M fractions contained about 1 mole of sulfate per amino sugar molecule. The 2.5 M fraction regularly contained more than 2 sulfate groups per molecule of amino sugar. The 1.7 M fraction gave intermediate values varying between 1.4 and 1.6 sulfate groups per amino sugar.

The 1.7 and 2.5 M fractions showed marked anticoagulant activity when tested according to Studer and Winterstein [28]. These fractions also showed a strong positive optical rotation while the 1.1 and 1.4 M fractions showed no optical activity.

The analytical data show that the 2.5 and 1.7 M fractions contain heparin. The absolute value for the anticoagulant activity must, however, be interpreted with great caution as the *in vitro* assay system is based on bovine plasma and the polysaccharides tested derive from another species.

The nature of the polysaccharides eluted in the 0.7—1.4 M fractions is not altogether clear, but the results strongly suggest that these fractions may contain mixtures of heparin-like polysaccharides with a low sulfate content, and chondroitin sulfuric acid.

The finding of other polysaccharides than heparin in mast cell tumors raises the question whether these polysaccharides are present in normal mast cells. The results obtained by Schiller and Dorfman [29] indicate that heparin is the only major polysaccharide present in peritoneal mast cells in the rat. Using a micromodification of the ECTEOLA method, we [30] have obtained data on the same material which support the results of Schiller and Dorfman. The polysaccharide content of mouse mast cells is being studied.

* Identified by paper chromatography only.

Acknowledgements. The author is indebted to Drs. E. A. Balazs, T. Dunn, J. Furth, T. Laurent and J. Scott for generous gifts of tumors and of hyaluronic acid samples and to Dr. H. Danielsson for help with the determinations of optical activity.

REFERENCES

1. Jorpes, J. E. *Acta Med. Scand.* **88** (1936) 427.
2. Jorpes, J. E., Holmgren, H. and Wilander, O. *Z. mikroskop. anat. Forsch.* **42** (1937) 279.
3. Lison, L. *Arch. biol. Liége* **46** (1935) 599.
4. Oliver, J., Bloom, F. and Mangieri, C. *J. Exptl. Med.* **86** (1947) 107.
5. Riley, J. F. *The Mast Cells*, E. and F. Livingstone Ltd. Edinburgh 1959.
6. *A guide to the Literature on Heparin and Anticoagulant Therapy in Thrombosis.* Ed. Vitrum, Stockholm 1959.
7. Staemmler, M. *Frankfurt. Z. Pathol.* **25** (1921) 391.
8. Sylvén, B. *Acta Chir. Scand.* **87** (1941) Suppl. 66.
9. Asboe-Hansen, G. *Intern. Rev. Cytol.* **33** (1954) 399.
10. Magnusson, S. and Larsson, B. *Acta Chem. Scand.* **9** (1955) 534.
11. Korn, E. D. *J. Am. Chem. Soc.* **80** (1958) 1520.
12. Rodén, L. and Dorfman, A. *To be published.*
13. Jorpes, J. E. and Gardell, S. *J. Biol. Chem.* **176** (1948) 267.
14. Dunn, T. B. and Potter, M. *J. Natl. Cancer Inst.* **18** (1957) 587.
15. Furth, J., Hagen, P. and Hirsch, E. I. *Proc. Soc. Exptl. Biol. Med.* **95** (1957) 824.
16. Korn, E. D. *J. Biol. Chem.* **234** (1959) 1325.
17. Scott, J. E. in Glick, D., Ed. *Methods of Biochemical Analysis*, Interscience Publishers Inc. New York. *To be published.*
18. Ringertz, N. R and Reichard, P. *Acta Chem. Scand.* **13** (1959) 1467.
19. Ringertz, N. R. and Reichard, P. *Acta Chem. Scand. In print.*
20. Dische, Z. *J. Biol. Chem.* **167** (1947) 189.
21. Porath, J. and Flodin, P. *Nature* **183** (1959) 1657.
22. Blix, G. *Acta Chem. Scand.* **2** (1948) 467.
23. Gardell, S. *Acta Chem. Scand.* **7** (1953) 207.
24. Gardell, S., Heijkenskjöld, F. and Roch-Nordlund, A. *Acta Chem. Scand.* **4** (1950) 970.
25. Stoffyn, P. J. and Jeanloz, R. W. *Arch. Biochem. Biophys.* **52** (1954) 373.
26. Andersson, L. *Acta Chem. Scand.* **7** (1953) 689.
27. Balazs, E. A. *Unpublished.*
28. Studer, A. and Winterstein, A. *Helv. Physiol. et Pharmacol. Acta* **9** (1951) 6.
29. Schiller, S. and Dorfman, A. *Biochem. et Biophys. Acta* **31** (1959) 278.
30. Bloom, G. and Ringertz, N. R. *Arkiv Kemi. In press.*

Received December 23, 1959.

ACTA CHEMICA SCANDINAVICA 14 (1960) 321–347

Studies on Local Anesthetics XIX *

Local Anesthetic Acitivity of N-(Dialkylaminoalkyl)benzamides. Physicochemical Measurements on N-(Dialkylaminoalkyl)benzamides and Benzoic Acids

BJÖRN LÜNING

Institute of Organic Chemistry and Biochemistry, University of Stockholm, Stockholm, Sweden

Local anesthetic properties and LD50 values were evaluated for 22 N-(dialkylaminoalkyl)benzamides. Ionization constants were determined for 26 N-(dialkylaminoalkyl)benzamides, for benzoic acid and all mono-, di-, and trimethylbenzoic acids. Ultraviolet spectra were measured on 15 N-(dialkylaminoalkyl)benzamides, 5 dimethyl-, and all trimethylbenzoic acids. The oscillator strength of these compounds for the absorbtion band at 220–240 mμ was determined and a correlation between these values and the ionization constants was found. Infrared spectra were recorded for the two racemates of N-(2-diethylamino-1,2-dimethylethyl)-2-methylbenzamide.

In a previous paper [1] the syntheses of sixty-five N-(dialkylaminoalkyl)-benzamides were reported. Variations were achieved by introducing one, two, or three methyl groups in the benzene nucleus, by using different alkylene chains (R_1) between the nitrogen atoms, and by attaching methyl or ethyl groups to the terminal nitrogen atom, the general structure being defined by the formula:

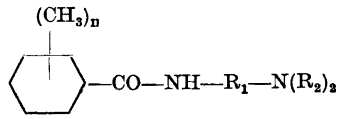

n=0, 1, 2, or 3.

A representative selection of these benzamides has been subjected to pharmacological tests, *i.e.* toxicity measurements and determinations of their local anesthetic properties. Further, a report is given on the thermodynamic ionization constants of these compounds. Since it is of interest to compare the ionization constants of the amides and the corresponding benzoic acids,

* For paper XVIII of this series see Lüning [1].

the latter compounds were also included in the measurements. Further, an investigation, *i.e.* determination of the oscillator strength, was made on the ultraviolet spectra of the amides and the acids. Infrared spectra of the two racemates of a compound containing two asymmetric carbon atoms are presented. Finally, a comparison is made between the ionization constants and the oscillator strengths.

EVALUATION OF LOCAL ANESTHETIC ACTIVITY AND LD50

The compounds were tested for their local anesthetic action on the rabbit cornea, and compared with Xylocaine ®, the technique of Wiedling [2] being followed (*cf.* also Löfgren and Tegner [3]). Xylocaine and all the other compounds were used as solutions of their hydrochlorides, made isotonic by the aid of sodium chloride. As a measure of the potency, *relative activity* (RA) was used, *i.e.* the quantity which is obtained by dividing the molarity of a standard Xylocaine solution by the molar concentration of the compound in question which gives the same duration of anesthesia as that of the Xylocaine standard. The molarity of the latter was 0.0738 (= 2 % Xylocaine · HCl solution). Before measuring the duration of anesthesia, both the solution of the actual compound and that of Xylocaine, were adjusted to the same pH, *i.e.* 6.5 *. In the toxicity investigations the LD50 values were obtained from subcutaneous injections in white mice and calculated (a) as grams of the base per kilogram of body weight and (b) as moles per kilogram of body weight ("molar" LD50 value). For these determinations, the bases were dissolved in a mixture of 1,2-propylene glycol and water (1:1, vol/vol) and the "pH" adjusted to about 6.5 by the addition of hydrochloric acid.

The ratio of the *molar* LD50 value of Xylocaine to the corresponding value for one of the other compounds is called the *relative toxicity* (RT) of the compound. For the quotient RA/RT the term *anesthetic index* (Q) will be used (*cf.* Löfgren *et al.*[5]). The *relative latency* (RL) is obtained by dividing the latency time for a solution of the compound to be tested by the latency time for a standard Xylocaine solution having the same duration of anesthesia as the test solution. To determine the RA value of a compound, 10—30 animals were used. In general, the maximum error in the RA values is about 20 %. The error in the RT values is less. The results of the pharmacological measurements are collected in Table 1. The numbering of the compounds is the same as that in the previous paper [1] where the chemical properties of the compounds are presented. The following observations can be made on the relationship between the chemical constitution and the pharmacological properties of the material.

A. From Table 1 is found that no systematic correlation can be detected between the local anesthetic activity or the toxicity and the number and positions of methyl groups in the aromatic residue of N-(dialkylaminoalkyl)-benzamides.

* Because of the low buffering effect of the solution of the hydrochloride at the pH used, and the relatively high buffering capacity of the body fluids, the pH value of the solution need not be very accurately measured.

Table 1. Pharmacolocical properties of N-(dialkylaminoalkyl)-benzamides.

Compound		LD50		RT [e]	RA [e]	RL [e]	Q[e]=RA/RT
Number [a]	Name	g/kg	mole/kg 10^{-3}				
I	N-(2-Diethylaminoethyl)-2-methylbenzamide	0.45	1.92	0.76	0 [f]	∞	—
VII	N-(2-Diethylaminoethyl)-3-methylbenzamide	0.46	1.97	0.74	0.4	4.5	0.5
XIII	N-(2-Diethylaminoethyl)-4-methylbenzamide	0.44	1.88	0.77	0 [f]	∞	—
XIX	N-(2-Diethylaminoethyl)-2,3-dimethylbenzamide	0.52	2.10	0.69	0.2	1.3	0.3
XXIII	N-(2-Diethylaminoethyl)-2,4-dimethylbenzamide	0.35	1.41	1.03	0.7	3	0.7
XXVII	N-(2-Diethylaminoethyl)-2,5-dimethylbenzamide	0.40	1.62	0.90	0.4	2.6	0.4
A	N-(2-Diethylaminoethyl)-2,6-dimethylbenzamide [b]	0.57	2.29	0.63	0.5	1.2	0.8
XXXII	N-(2-Diethylaminoethyl)-3,4-dimethylbenzamide	0.36	1.45	1.00	0.3	2.1	0.3
XXXVI	N-(2-Diethylaminoethyl)-3,5-dimethylbenzamide	0.34	1.35	1.07	0.7	2.7	0.7
XLI	N-(2-Diethylaminoethyl)-2,3,4-trimethylbenzamide	0.32	1.22	1.19	0.6	9.0	0.5
XLVI	N-(2-Diethylaminoethyl)-2,3,5-trimethylbenzamide	0.19	0.72	2.0	1.0	3.0	0.5
XLVIII	N-(2-Diethylaminoethyl)-2,3,6-trimethylbenzamide	0.33	1.26	1.15	0.7	3.0	0.6
LIII	N-(2-Diethylaminoethyl)-2,4,5-trimethylbenzamide	0.25	0.95	1.53	0.9	2.3	0.6
LVIII	N-(2-Diethylaminoethyl)-2,4,6-trimethylbenzamide	0.25	0.95	1.53	1.2	3.5	0.8
LXIII	N-(2-Diethylaminoethyl)-3,4,5-trimethylbenzamide	0.29	1.00	1.45	0.5	4.5	0.3
V*a*	N-(2-Diethylamino-1,2-dimethylethyl)-2-methylbenzamide [c]	0.54	2.06	0.70	0.6	1.5	0.9
V*b*	N-(2-Diethylamino-1,2-dimethylethyl)-2-methylbenzamide [c]	0.43	1.64	0.88	0.7	3	0.8
B	N-(3-Diethylaminopropyl)-2,6-dimethylbenzamide [b]	~0.9	~3.4	0.4	0 [f]	∞	—
C	N-(2-Diethylamino-1-methylethyl)-2,6-dimethylbenzamide [b]	0.22	0.84	1.7	2.1	—	1.2
D	N-(2-Diethylamino-2-methylethyl)-2,6-dimethylbenzamide [b]	0.23	0.88	1.6	1.8	—	1.1
E	N-(2-Diethylamino-1,2-dimethylethyl)-2,6-dimethylbenzamide [b,d]	0.075	0.27	5.2	3.4	—	0.7
XXXI	N-(3-Diethylamino-2,2-dimethylpropyl)-2,6-dimethylbenzamide	0.25	0.86	1.7	3.2	3	1.9
F	N-(3-Diethylaminopropyl)-3,5-dimethylbenzamide [b]	0.71	2.71	0.53	0.88	6	1.7
XXXVII	N-(2-Diethylamino-1-methylethyl)-3,5-dimethylbenzamide	0.30	1.15	1.26	0.6	3	0.5
XXXVIII	N-(2-Diethylamino-2-methylethyl)-3,5-dimethylbenzamide	0.22	0.84	1.7	1.0	1	0.6
XXXIX	N-(2-Diethylamino-1,2-dimethylethyl)-3,5-dimethylbenzamide [d]	0.28	1.00	1.45	1.5	2.4	1.0
XL	N-(3-Diethylamino-2,2-dimethylpropyl)-3,5-dimethylbenzamide	0.20	0.70	2.1	1.6	1	0.8
LX	N-(2-Dimethylaminoethyl)-2,4,6-trimethylbenzamide	0.62	2.65	0.55	0 [f]	∞	—
Xylocaine	α-Diethylamino-2,6-dimethylacetanilide [g]	0.34	1.45	1.0	1.0	1.0	1.0

[a] The numbering is chosen in accordance with that given for the same compounds in Lüning [1].
[b] The values given for these compounds are taken from Löfgren *et al.*[4]
[c] These are racemates of the same compound, *cf.* Lüning [1].
[d] Measurements made on mixtures of racemates obtained in the synthesis.
[e] Regarding definitions of these quantities see p. 322.
[f] The compounds, the RA-values of which are denoted as 0, give no measurable anesthesia at a concentration of 0.0738 mole/litre.
[g] See Löfgren [8].

Table 2. Change in relative anesthetic activity (RA), relative toxicity (RT), and anesthetic index for variations in the "intermediate chain" R_1 and positions of methyl groups in Ar (*cf.* formula).

$$Ar-CO-NH-R_1-N(C_2H_5)_2$$

Ar = 2,6-dimethylphenyl or 3,5-dimethylphenyl.

$$R_1{}^a = \begin{cases} -CH_2-CH_2- & (1), \\ -CH_2-CH_2-CH_2- & (2), \\ -CH(CH_3)-CH_2- & (3), \\ -CH_2-CH(CH_3)- & (4), \\ -CH(CH_3)-CH(CH_3)- & (5), \\ \text{or } -CH_2-C(CH_3)_2-CH_2- & (6). \end{cases}$$

Factor f_A, f_T and f_Q indicate the change in RA, RT, and Q respectively.

Compound			RA	f_A	RT	f_T	$Q\left(=\frac{RA}{RT}\right)$	f_Q
No.	Ar	R_1						
A. Change of R_1 from (1) to (2).								
A[b]	2,6-dimethylphenyl	(1)	0.5	0	0.6	0.7	0.8	0
B[b]	»	(2)	0		0.4		0	
XXXVI	3,5-dimethylphenyl	(1)	0.7	1.3	1.1	0.4	0.7	2.4
F[b]	»	(2)	0.9		0.5		1.7	
B. Change of R_1 from (1) to (3).								
A[b]	2,6-dimethylphenyl	(1)	0.5	4.2	0.6	2.8	0.8	1.5
C[b]	»	(3)	2.1		1.7		1.2	
XXXVI	3,5-dimethylphenyl	(1)	0.7	0.9	1.1	1.2	0.7	0.7
XXXVII	»	(3)	0.6		1.3		0.5	
C. Change of R_1 from (1) to (4).								
A[b]	2,6-dimethylphenyl	(1)	0.5	3.6	0.6	2.7	0.8	1.4
D[b]	»	(4)	1.8		1.6		1.1	
XXXVI	3,5-dimethylphenyl	(1)	0.7	1.4	1.1	1.5	0.7	0.9
XXXVIII	»	(4)	1.0		1.7		0.6	
D. Change of R_1 from (1) to (5).								
A[b]	2,6-dimethylphenyl	(1)	0.5	6.8	0.6	8.7	0.8	0.8
E[b]	»	(5)	3.4		5.2		0.7	
XXXVI	3,5-dimethylphenyl	(1)	0.7	2.1	1.1	1.4	0.7	1.4
XXXIX	»	(5)	1.5		1.5		1.0	
E. Change of R_1 from (1) to (6).								
A[b]	2,6-dimethylphenyl	(1)	0.5	6.4	0.6	2.8	0.8	2.4
XXXI	»	(6)	3.2		1.7		1.9	
XXXVI	3,5-dimethylphenyl	(1)	0.7	2.3	1.1	1.9	0.7	1.1
XL	»	(6)	1.6		2.1		0.8	

[a] The formulas of the radicals R_1 must be read in the same direction as the total formula above.

[b] The values given for these compounds are taken from Löfgren *et al.*[4]

B. The effect of variations in the intermediate chain, R_1, (*cf.* formula above) upon anesthetic activity and toxicity is surveyed in Table 2. If Ar is 2,6-dimethylphenyl, and one methyl group is attached to the intermediate chain (transitions A → C and A → D) the increase in anesthetic activity is three to fourfold. The toxicity increases about three times [4]. The corresponding structural change, when Ar is 3,5-dimethylphenyl (XXXVI → XXXVII and XXXVI → XXXVIII), is accompanied by a smaller increase (f_A* = 1.4) or even a small decrease (f_A = 0.9). The toxicity is increased by about 20—50 %.

When one methyl group is attached to each of the carbon atoms of an ethylene radical constituting the intermediate chain R_1, the anesthetic activity is increased approximately seven times if Ar is 2,6-dimethylphenyl (A → E). The toxicity is increased eight to nine times [4]. On the other hand, if Ar is 3,5-dimethylphenyl, the corresponding change (XXXVI → XXXIX) is accompanied by a doubling of the anesthetic activity. The toxicity increases only about 40 %.

The replacement of ethylene by 2,2-dimethyltrimethylene in the intermediate chain is accompanied by a six to sevenfold increase in anesthetic activity when Ar is 2,6-dimethylphenyl (A → XXXI). The toxicity increases about three times. Ar being 3,5-dimethylphenyl, the corresponding change (XXXVI → XL) is followed approximately by a doubling of the anesthetic activity. The increase in toxicity is about the same.

If R_1 is extended by one carbon atom from ethylene to trimethylene and Ar is 2,6-dimethylphenyl (A → B) [4], the activity is lost, whereas it is increased (f_A = 1.3) when Ar is 3,5-dimethylphenyl (XXXVI → F).

C. If the alkyl group (R_2) at the terminal nitrogen atom is changed from ethyl to methyl the anesthetic activity is lost (LVIII → LX).

D. N-(2-Diethylamino-1,2-dimethylethyl)-2-methylbenzamide appears as two separable racemates V*a* and V*b*. They do not differ significantly regarding toxicity or duration of anesthesia. However, the latency time of V*a* is about half of that of V*b*.

DETERMINATION OF THERMODYNAMIC IONIZATION CONSTANTS

The thermodynamic ionization constants in aqueous solution at 25°C were determined for twenty-six N-(dialkylaminoalkyl)benzamides, benzoic acid and all mono-, di-, and trimethylbenzoic acids. For the benzoic acids the equilibrium

$$BH + H_2O \rightleftharpoons B^- + H_3O^+ \qquad (1)$$

is valid. For the basic amides the corresponding expression is

$$BH^+ + H_2O \rightleftharpoons B + H_3O^+ \qquad (2)$$

From equilibrium (1) the expression

$$pK_a = pH - \log \frac{C_{cat} - C_{an} + C_{H^+} - C_{OH^-}}{C_{tot} - C_{cat} + C_{an} - C_{H^+} + C_{OH^-}} + pf_{B^-} \qquad (3)$$

* The *factor* f_A indicates the change in RA.

Table 3. Ionization constants of benzoic acid and methyl substituted benzoic acids in aqueous solution at 25°C.

Acid	$1/2\Gamma \cdot 10^3$	p/B^-	*	pH	$C_{H^+} \cdot 10^3$ mole/litre	pK_a	pK_a average
Benzoic	4.342	0.029	+0.109	4.297	0.050	4.217	4.21_6
	4.342	0.029	+0.373	4.557	0.028	4.213	
	1.998	0.021	−0.190	4.008	0.098	4.219	
2-Methylbenzoic	3.340	0.026	+0.030	3.933	0.117	3.929	3.93_4
	4.356	0.029	+0.135	4.042	0.091	3.936	
	4.699	0.030	+0.041	3.947	0.113	3.936	
3-Methylbenzoic	3.337	0.026	+0.029	4.299	0.050	4.296	4.28_9
	4.669	0.030	+0.107	4.364	0.043	4.287	
	4.379	0.029	+0.150	4.406	0.039	4.285	
4-Methylbenzoic	4.752	0.030	+0.377	4.770	0.017	4.423	4.41_3
	5.235	0.031	+0.490	4.852	0.014	4.393	
	5.581	0.032	+0.562	4.954	0.011	4.424	
2,3-Dimethylbenzoic	2.051	0.022	+0.050	3.805	0.157	3.777	3.80_0
	3.154	0.026	+0.273	4.049	0.089	3.802	
	3.370	0.026	+0.319	4.116	0.077	3.823	
2,4-Dimethylbenzoic	3.996	0.028	+0.341	4.612	0.024	4.299	4.30_2
	3.590	0.027	+0.497	4.785	0.016	4.315	
	3.696	0.027	+0.507	4.773	0.017	4.293	
2,5-Dimethylbenzoic	2.364	0.022	+0.392	4.419	0.038	4.049	4.04_0
	2.687	0.024	+0.496	4.516	0.031	4.044	
	3.343	0.026	+0.363	4.364	0.043	4.027	
2,6-Dimethylbenzoic	2.514	0.023	+0.477	3.719	0.191	3.265	3.25_5
	3.004	0.025	+0.485	3.718	0.191	3.258	
	1.978	0.021	+0.378	3.600	0.251	3.243	
3,4-Dimethylbenzoic	2.561	0.023	+0.494	4.963	0.011	4.492	4.49_6
	2.504	0.023	+0.469	4.946	0.011	4.500	
3,5-Dimethylbenzoic	2.731	0.023	+0.557	4.906	0.012	4.372	4.39_3
	2.864	0.024	+0.529	4.898	0.013	4.393	
	2.741	0.023	+0.524	4.914	0.012	4.413	
2,3,4-Trimethylbenzoic	1.665	0.019	+0.696	4.752	0.018	4.075	4.06_3
	1.858	0.020	+0.643	4.661	0.022	4.038	
	3.297	0.026	+0.916	4.965	0.011	4.075	
2,3,5-Trimethylbenzoic	1.998	0.021	+0.628	4.634	0.023	4.027	4.00_6
	1.152	0.017	+0.490	4.455	0.035	3.982	
	2.281	0.022	+0.618	4.604	0.025	4.008	
2,3,6-Trimethylbenzoic	2.018	0.022	+0.553	3.877	0.133	3.346	3.33_9
	3.393	0.026	+0.673	3.986	0.103	3.339	
	1.985	0.022	+0.232	3.541	0.288	3.331	
2,4,5-Trimethylbenzoic	3.140	0.025	+0.788	5.138	0.007	4.375	4.37_5
	3.983	0.028	+0.887	5.233	0.006	4.374	
2,4,6-Trimethylbenzoic	2.947	0.025	+0.612	4.138	0.073	3.551	3.54_5
	3.440	0.027	+0.663	4.175	0.067	3.539	
3,4,5-Trimethylbenzoic	1.842	0.020	+1.003[a]	5.519	—	4.536	4.51_9
	1.675	0.019	+1.083[a]	5.569	—	4.505	
	2.328	0.022	+1.149[a]	5.642	—	4.515	

[a] Since the solubility of the trimethylbenzoic acids, is very low (for 3,4,5-trimethylbenzoic acid 10^{-4} mole/litre) in water, the logarithms must be kept at high values.

* $\log \dfrac{C_{Na^+} - C_{Cl^-} + C_{H^+}}{C_{tot} - C_{Na^+} + C_{Cl^-} - C_{H^+}}$

Table 4. Ionization constants of N(2-diethylaminoethyl)benzamides in aqueous solution at 25°C. All compounds were weighed as hydrochlorides for these measurements; thus $C_{Cl} = C_{tot}$ and the expression for pK_a can be simplified accordingly.

Compound	$1/2\,\Gamma \cdot 10^3$	pf_{BH+}	*	pH	$C_{OH^-} \cdot 10^3$ mole/litre	pK_a	pK_a average
N-(2-Diethylamino-ethyl)-benzamide	5.775	0.032	−0.071	9.002	0.010	9.041	9.04_9
	6.920	0.035	−0.205	8.881	0.008	9.051	
	5.433	0.032	+0.193	9.279	0.019	9.054	
I	4.123	0.029	−0.314	8.584	—	8.869	8.87_5
	4.540	0.030	+0.148	9.054	0.010	8.876	
	3.279	0.025	−0.079	8.826	0.007	8.880	
VII	2.963	0.025	−0.095	8.980	0.010	9.049	9.04_7
	3.840	0.028	−0.295	8.785	0.006	9.052	
	2.345	0.022	+0.147	9.209	0.016	9.040	
XIII	3.220	0.026	−0.355	8.755	0.006	9.084	9.08_3
	3.464	0.026	+0.309	9.402	0.025	9.081	
	4.258	0.029	−0.041	9.057	0.011	9.083	
XIX	4.685	0.030	+0.388	9.278	0.019	8.860	8.86_2
	4.631	0.030	−0.125	8.767	0.006	8.862	
	7.719	0.037	−0.038	8.863	0.007	8.864	
XXIII	3.557	0.027	+0.114	9.055	0.011	8.914	8.91_7
	3.881	0.028	−0.276	8.665	0.005	8.913	
	5.145	0.031	−0.020	8.934	0.009	8.923	
XXVII	4.494	0.030	−0.374	8.533	—	8.877	8.88_5
	4.371	0.029	+0.130	9.050	0.011	8.891	
	5.740	0.032	−0.013	8.905	0.008	8.886	
A	5.463	0.032	+0.191	8.912	0.008	8.689	8.68_8
	6.553	0.034	−0.359	8.357	—	8.682	
	4.296	0.029	−0.051	8.671	0.005	8.693	
XXXII	4.227	0.029	−0.247	8.847	0.007	9.065	9.07_0
	4.701	0.030	+0.248	9.352	0.023	9.074	
	5.056	0.031	−0.010	9.092	0.012	9.071	
XXXVI	3.614	0.027	−0.238	8.834	0.007	9.045	9.04_6
	3.420	0.026	+0.139	9.210	0.016	9.045	
	4.515	0.030	−0.036	9.041	0.011	9.047	
XLI	5.230	0.032	−0.337	8.592	—	8.897	8.89_3
	5.302	0.032	+0.110	9.040	0.011	8.898	
	5.026	0.031	−0.066	8.850	0.007	8.885	
XLVI	4.243	0.029	−0.352	8.543	—	8.866	8.86_6
	4.197	0.029	+0.175	9.072	0.012	8.868	
	4.564	0.030	−0.001	8.893	0.008	8.864	
XLVIII	3.937	0.028	−0.019	8.710	0.005	8.701	8.69_9
	4.715	0.030	+0.175	8.903	0.008	8.698	
	4.203	0.029	+0.005	8.731	0.005	8.697	
LIII	4.257	0.029	−0.344	8.589	—	8.904	8.91_2
	4.544	0.030	+0.148	9.094	0.012	8.916	
	3.915	0.028	−0.001	8.944	0.009	8.917	
LVIII	3.213	0.026	−0.371	8.352	—	8.697	8.70_5
	3.770	0.027	+0.167	8.902	0.008	8.708	
	3.550	0.027	+0.033	8.771	0.006	8.711	
LXIII	3.745	0.027	−0.364	8.718	0.005	9.055	9.06_7
	4.059	0.028	+0.173	9.280	0.019	9.079	
	5.422	0.032	−0.006	9.092	0.012	9.066	

* $\log \dfrac{C_{Na^+} - C_{OH^-}}{C_{tot} - C_{Na^+} + C_{OH^-}}$

Table 5. Ionization constants of N-(dialkylaminoalkyl)-benzamides of different structures in aqueous solution at 25°C.

Compound	Prepn.	1/2 Γ $\times 10^3$	pf_{BH^+}	*	pH	$C_{OH^-} \times 10^3$	pK_a	pK_a average
V *a*[b]	Base[a]	4.074	0.029	−0.390	9.220	0.017	9.581	9.57_4
		3.826	0.028	+0.124	9.719	0.052	9.567	
		4.906	0.031	−0.035	9.569	0.037	9.573	
V *b*[b]	B HCl	1.945[c]	0.021	−0.272[c]	9.064	0.012	9.315	9.31_2
		1.981[c]	0.021	−0.143[c]	9.182	0.015	9.304	
		1.830[c]	0.020	−0.242[c]	9.094	0.012	9.316	
F	B HCl	4.916	0.031	+0.051	9.917	0.083	9.835	9.83_4
		3.956	0.028	−0.375	9.486	0.031	9.833	
XXXVII	Base[a]	4.466	0.030	−0.435	8.829	0.007	9.234	9.24_1
		4.415	0.029	+0.015	9.285	0.019	9.241	
		5.684	0.032	−0.074	9.205	0.016	9.247	
XXXVIII	B HCl	3.902	0.028	−0.204	9.237	0.017	9.413	9.40_1
		3.894	0.028	+0.407	9.822	0.066	9.387	
		4.096	0.029	−0.020	9.401	0.025	9.403	
XL	Base[a]	3.355	0.027	−0.914[c]	8.358	—	9.245	9.23_4[d]
		4.195	0.029	−1.112[c]	8.167	—	9.250	
		4.915	0.032	−1.108[c]	8.130	—	9.206	
N-(3-Diethylaminopropyl)-2,3,6-trimethylbenzamide	B HCl	3.510	0.027	−0.236	9.461	0.029	9.670	9.67_3
		5.272	0.032	−0.018	9.690	0.049	9.676	
N-(2-Dimethylaminoethyl)-2,3,6-trimethylbenzamide	B HCl	3.442	0.026	−0.348	7.738	—	8.060	8.06_5
		4.538	0.030	+0.017	8.117	—	8.070	
N-(2-Dimethylaminoethyl)-2,4,5-trimethylbenzamide	B HCl	5.560	0.032	−0.369	7.948	—	8.285	8.28_9
		5.204	0.031	+0.163	8.492	—	8.298	
		4.556	0.030	−0.009	8.306	—	8.285	
LX	B HCl	4.424	0.029	−0.366	7.592	—	7.929	7.94_6
		4.891	0.031	+0.176	8.175	—	7.968	
		3.235	0.026	−0.010	7.956	—	7.940	

* $\log \dfrac{C_{tot} - C_{Cl^-} + C_{Na^+} - C_{OH^-}}{C_{Cl^-} - C_{Na^+} + C_{OH^-}}$

[a] The base was dissolved in an excess of HCl, and then neutralized with NaOH.
[b] V *a* and V *b* are racemates of the same compound.
[c] Because of the low solubility of the base in water, it was necessary to make the measurements under conditions where the concentration of base was kept low.
[d] Since in this measurement the ratio between the acid BH^+ and the free base B is great, the accuracy is somewhat lower.

can be derived (*cf.* Lövgren [6]), whereas equilibrium (2) gives

$$pK_a = pH - \log \frac{C_{tot} - C_{an} + C_{cat} - C_{OH^-} + C_{H^+}}{C_{an} - C_{cat} + C_{OH^-} - C_{H^+}} - pf_{BH^+} \qquad (4)$$

In equation (3) C_{tot} is $C_{BH} + C_{B^-}$, whereas in equation (4) this quantity is equal to $C_{BH^+} + C_B$. The quantities C_{cat} and C_{an} represent the concentrations of cations and anions of strong electrolytes. Further,

$$pf_{B^-} = -\log f_{B^-} \; ; \qquad pf_{BH^+} = -\log f_{BH^+} \qquad (5)$$

where f_{B^-} and f_{BH^+} are the activity coefficients of the ions B^- and BH^+ respectively.

The pH values were measured by the aid of a cell of the type:
(—) Glass electrode / H^+(aq) // KCl (satd) / Hg_2Cl_2, Hg (+)

For this cell we have

$$pH = \frac{E - E'}{k} \tag{6}$$

where E is the e.m.f. of the cell and E′ is the standard potential of the cell including the liquid junction potential (assumed to be constant). At 25°C, k is 59.16 mV. Kielland [7] has calculated activity coefficients for a large number of ions at different concentrations in water at 25°C by use of the Debye-Hückel formula

$$-\log f_i = pf_i = \frac{0.358 \cdot z_i^2 \cdot \Gamma^{1/2}}{1 + 10^8 d_i \cdot 0.2325\ \Gamma^{1/2}} \tag{7}$$

where f_i is the activity coefficient of the i-th ion with valence z_i and effective diameter d_i. Γ is the ionic concentration, given by $\Gamma = \Sigma C_i z_i^2$ with C_i in moles per litre.

According to measurements by Löfgren [8], the effective diameter of the BH^+ ions was evaluated to 8×10^{-8} cm. For the B^- ions no determination of the effective diameter was made. A change in d from 5×10^{-8} to 10^{-7} alters pf_i negligibly in comparison with other errors. The values of pf_i for $d = 6 \times 10^{-8}$, $d = 7 \times 10^{-8}$, and $d = 8 \times 10^{-8}$ were plotted against $1/2\ \Gamma$ in a diagram from which pf_{BH^+} and pf_{B^-} were read off directly at any concentration *.

Since it is difficult to obtain a clear survey of the systematic errors, (above all, errors caused by liquid junction potentials) the pK_a values are given to two decimals. For mutual comparison, however, the values can be given with greater accuracy; particularly for the salts of the N-(dialkylaminoalkyl)-benzamides the maximum errors seldom exceed $\pm$ 0.005, whereas for the benzoic acids the errors are somewhat greater.

When calculating pK_a values from (3) or (4), these expressions, for special conditions, can be simplified. Thus, when working at an ionic concentration $> 2 \times 10^{-3}$ mole per litre, C_{H^+} can be neglected at pH > 5, and C_{OH^-} at pH < 9.

Experimental data from the measurements of the thermodynamic ionization constants of benzoic acids in aqueous solution at 25°C are found in Table 3. The ionization constants of the benzoic acids have been measured earlier; good surveys have been presented by Shorter *et al.*[9] and Dippy *et al.*[10,11]. The most accurate determinations given by these authors have, however, been made by conductivity measurements. Since it is essential to obtain a uniformly measured series for mutual comparison, benzoic acid, all mono-, di-, and trimethylbenzoic acids were remeasured. In Table 4 the data from the pK_a determinations of N-(2-diethylaminoethyl)benzamides are given, and in Table

* The three curves did not deviate from each other by more than 0.001 in pf below a value for $\frac{1}{2}\Gamma$ of 8×10^{-3} mole/litre.

5 pK_a values of ten N-(dialkylaminoalkyl)benzamides of different structure have been collected. In a later chapter, a few considerations upon the relationship between chemical structure and the ionization constant will be given.

ULTRAVIOLET AND INFRARED SPECTRA

Ultraviolet spectra have been recorded for methyl substituted benzoic acids and N-(2-diethylaminoethyl)benzamides in the wavelength region 218—310 mμ. In this region two bands are found, one at 220—240 mμ with $\varepsilon_{max} \simeq 10^4$, and one at 260—285 mμ with $\varepsilon_{max} \simeq 300-600$. A band with a higher extinction at about 200—210 mμ is positioned beyond the limits of proper measuring with the solvents used (the benzoic acids in ethanol, and the benzamides in cyclohexane). However, Moser *et al.*[12] have been able to measure the spectrum of benzoic acid and a few methyl substituted benzoic acids between 200 and 220 mμ in other solvents (*e.g.* a mixture of 99.5 % of water 0.5 % of ethanol). According to Hedden *et al.*[13] the band at 260—285 mμ will here be designated as the B-band (B for benzene ring absorption) and that at 220—240 mμ as the C-band (C for conjugation). Particular interest will be focussed on the intensity of the C-band.

Table 6. Wavelengths, wave numbers (ν), and oscillator strengths of maxima and inflexions of benzoic acids and N-(2-diethylaminoethyl)-benzamides for the ultraviolet absortion band at 220—240 mμ.

Positions and number of methyl groups attached to the aromatic nucleus	Benzoic acids			N-(2-Diethylaminoethyl)-benzamides		
	λ_{max} mμ	ν_{max} $cm^{-1} \times 10^{-4}$	f	λ_{max} mμ	ν_{max} $cm^{-1} \times 10^{-4}$	f
—	228[a]	4.386	0.123_7	222.5	4.494	0.099_8
2-Methyl	228[a]	4.386	0.039_9	—	—	0.000[c]
3-Methyl	232[a]	4.310	0.113_2	226	4.425	0.060_3
4-Methyl	236	4.237	0.207_5	231	4.329	0.192_1
2,3-Dimethyl	235[b]	~4.25	0.021_5	—	—	0.000[c]
2,4-Dimethyl	236	4.237	0.086_6	230[b]	~4.35	0.034_7
2,5-Dimethyl	236[b]	~4.24	0.013_1	—	—	0.000[c]
2,6-Dimethyl	228[a,b]	~4.39	0.014_4	—	—	0.000[c]
3,4-Dimethyl	235.5	4.246	0.191_0	233	4.292	0.115_3
3,5-Dimethyl	233.5	4.283	0.073_0	232	4.310	0.037_1
2,3,4-Trimethyl	237[b]	~4.22	0.036_7	233[b]	~4.29	0.010_8
2,3,5-Trimethyl	239[b]	~4.18	0.008_4	—	—	0.000[c]
2,3,6-Trimethyl	223[b]	~4.48	0.008_3	—	—	0.000[c]
2,4,5-Trimethyl	237	4.219	0.099_1	234[b]	~4.27	0.021_1
2,4,6-Trimethyl	—	—	0.000[c]	—	—	0.000[c]
3,4,5-Trimethyl	238.5	4.193	0.174_9	237	4.219	0.134_2

[a] Values calculated from curves published by Moser *et al.*[12]

[b] Inflexions; wavelengths and wavenumbers can not be given with any great accuracy.

[c] No maximum or inflexion could be observed at the expected wavelength, hence the extinction (and the oscillator strength f) is set equal to zero for the absorbtion band under consideration.

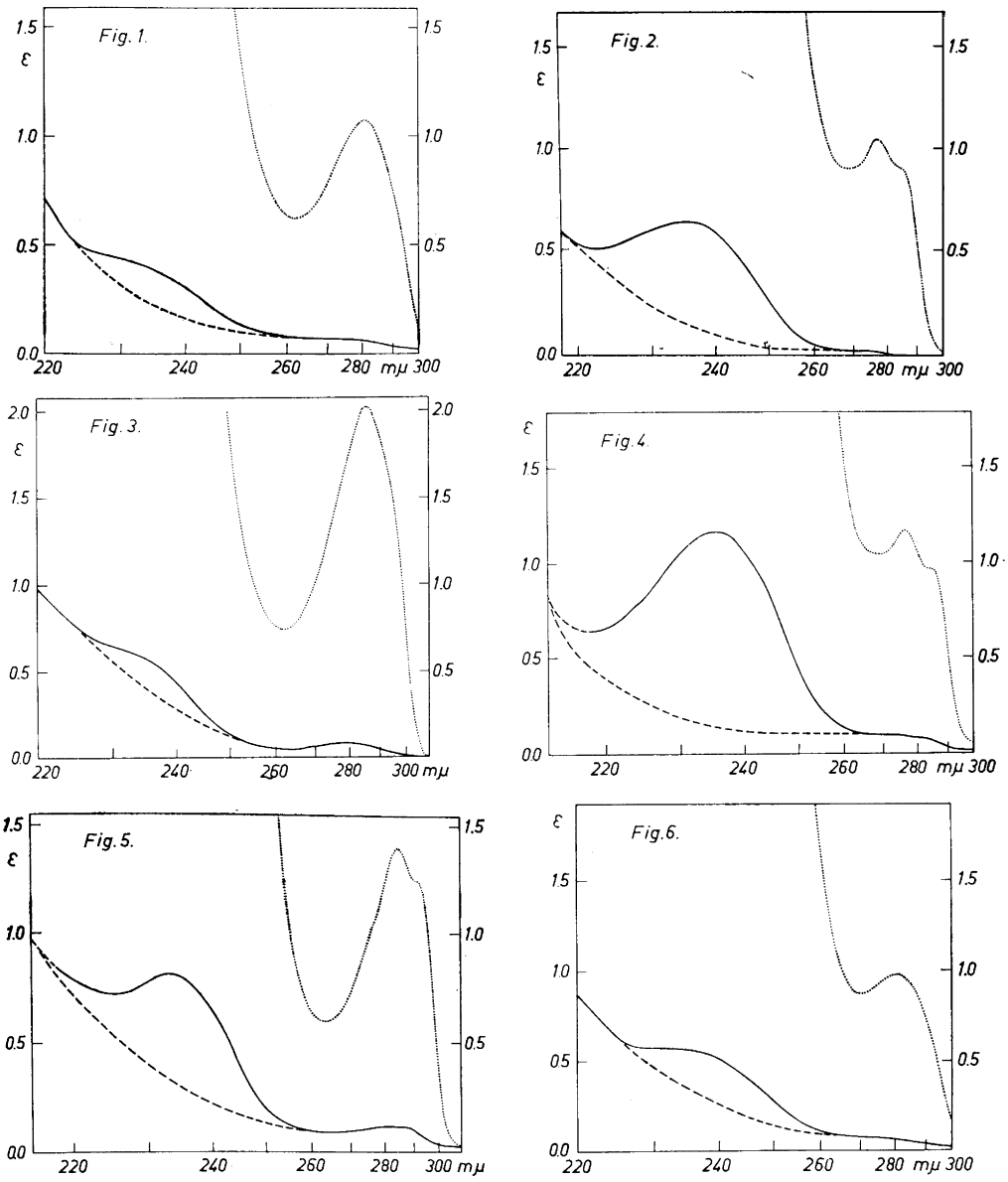

Figs. 1—6. Ultraviolet absorbtion curves of *1:* 2,3-dimethylbenzoic acid; *2:* 2,4-dimethylbenzoic acid; *3:* 2,5-dimethylbenzoic acid; *4:* 3,4-dimethylbenzoic acid; *5:* 3,5-dimethylbenzoic acid; *6:* 2,3,4-trimethylbenzoic acid *.

* The extinctions of curves drawn with dotted lines should be multiplied by 10^3, and the extinctions of curves drawn with solid or broken lines should be multiplied by 10^4. Curves drawn with broken lines are estimated, and are used as reference curves for calculation of the integrated extinction $\int \varepsilon_\nu d\nu$.

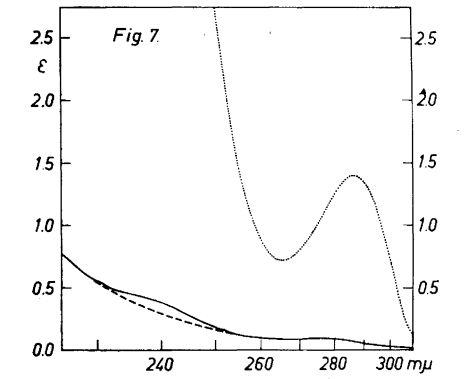

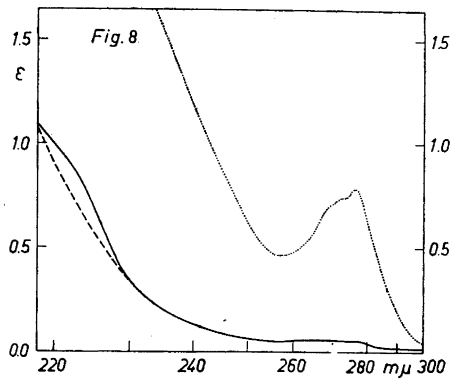

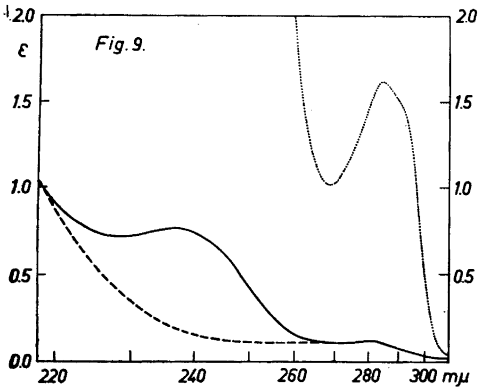

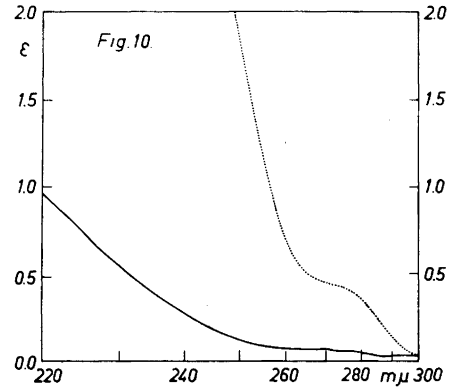

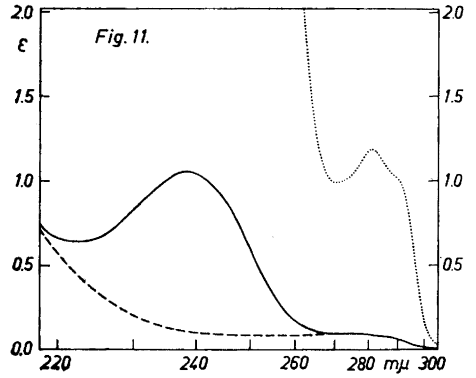

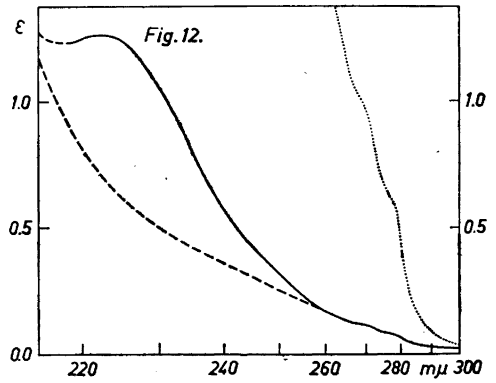

Figs. 7—12. Ultraviolet absorbtion curves of *7:* 2,3,5-trimethylbenzoic acid; *8:* 2,3,6-trimethylbenzoic acid; *9:* 2,4,5-trimethylbenzoic acid; *10:* 2,4,6-trimethylbenzoic acid; *11:* 3,4,5-trimethylbenzoic acid; *12:* N-(2-diethylaminoethyl)-benzamide *.

* For designation of the curves see note to Figs. 1—6.

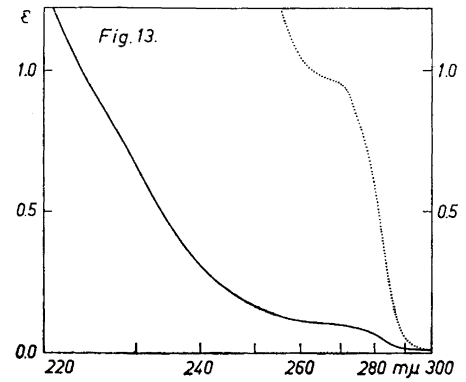

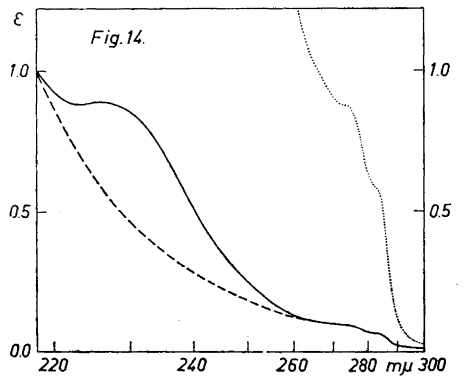

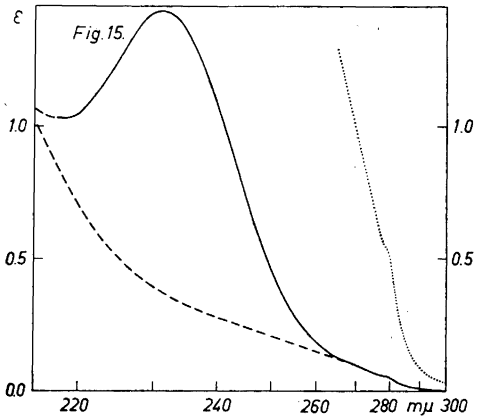

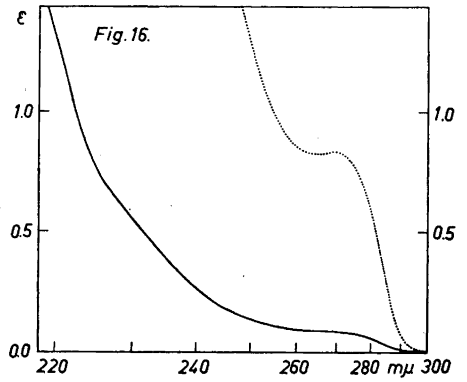

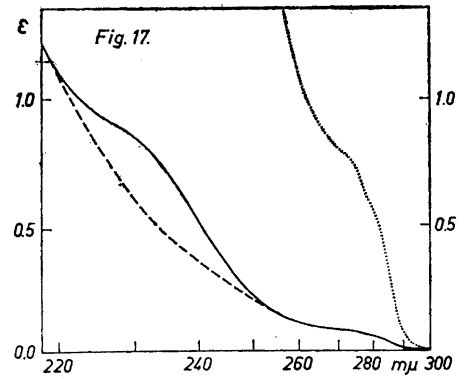

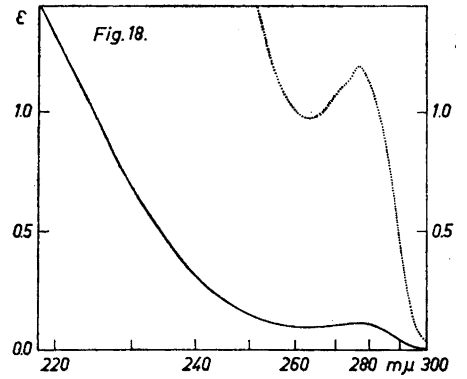

Fig.s 13—18. Ultraviolet absorbtion curves of *13:* I; *14:* VII; *15:* XIII; *16:* XIX; *17:* XXIII; *18:* XXVII *.

* For designation of the curves see note to Figs. 1—6.

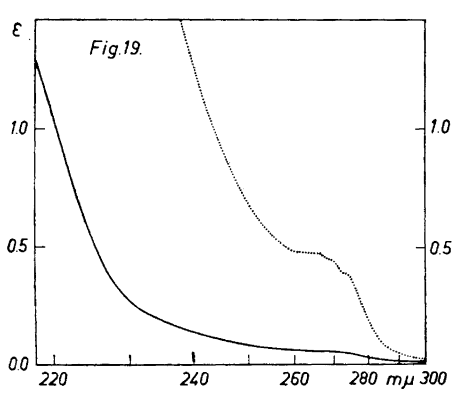

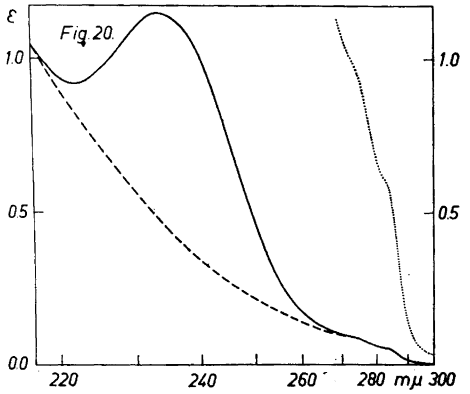

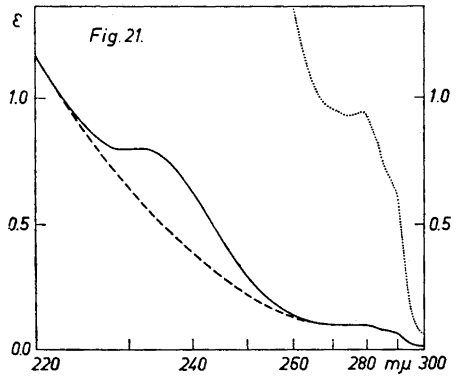

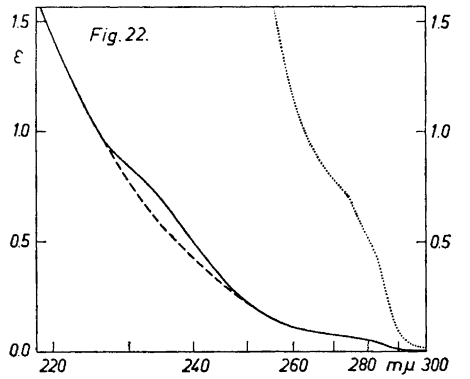

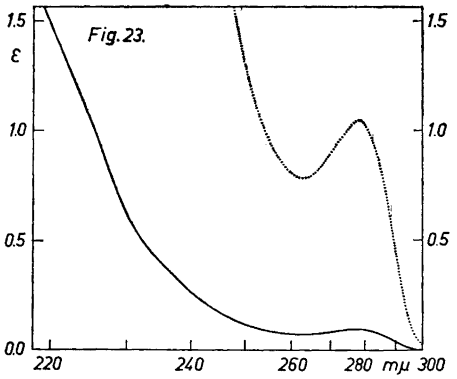

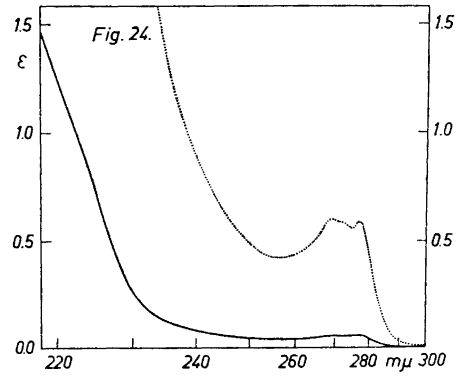

Figs. 19—24. Ultraviolet absorbtion curves of *19:* A; *20:* XXXII; *21:* XXXVI; *22:* XLI; *23:* XLVI; *24:* XLVIII *.

* For designation of the curves see note to Figs. 1—6.

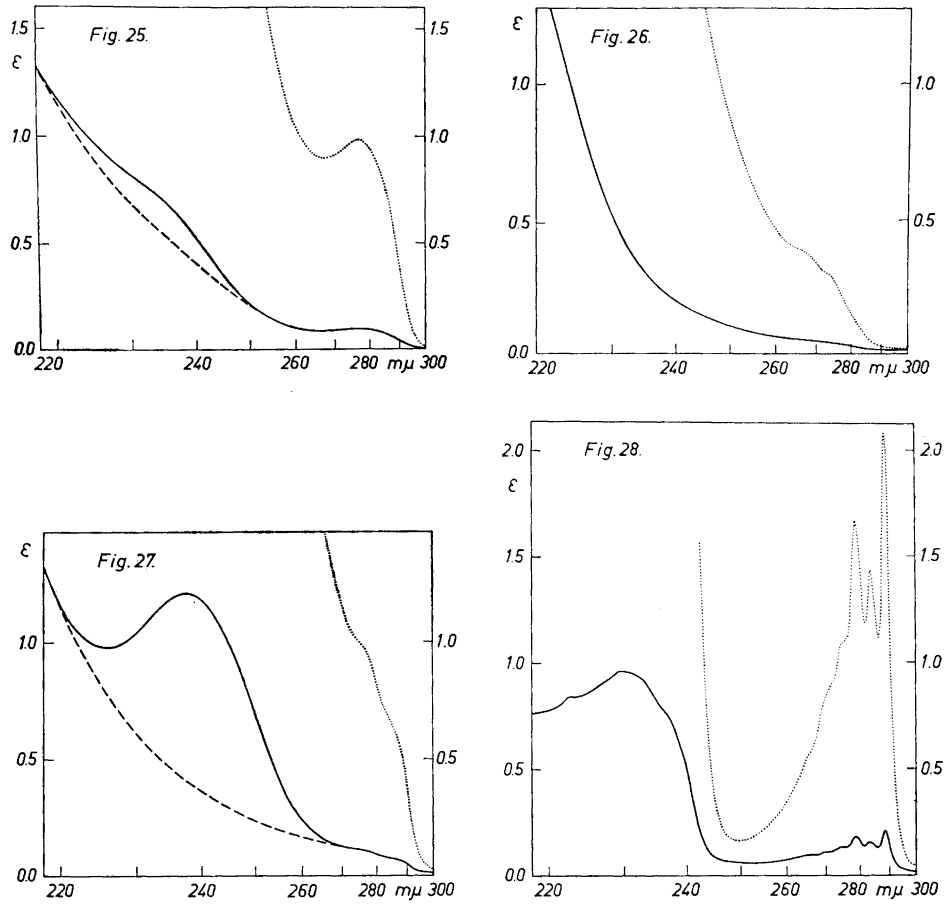

Figs. 25—28. Ultraviolet absorbtion curves of *25:* LIII; *26:* LVIII; *27:* LXIII; *28:* 2,6-dimethylbenzonitrile *.

A quantity which may give some information on the conjugation in a benzoic acid or N-(2-diethylaminoethyl)benzamide is the *oscillator strength f* (of the C-band) which is defined by [14,15]

$$f = \frac{0.1028 \cdot m \cdot c^2}{\pi \cdot e^2 \cdot n} \int_{-\infty}^{+\infty} \varepsilon_\nu d\nu = 4.32 \cdot 10^{-9} \int_{-\infty}^{+\infty} \varepsilon_\nu d\nu \qquad (8)$$

There m and c are the mass of the electron and the velocity of light respectively; and n is the number of molecules in one cm^3, e being the electronic charge,

* For designation of the curves see note to Figs. 1—6.

and $\int_{-\infty}^{+\infty} \varepsilon_\nu d\nu$ the integrated molar extinction over a whole band. Because of overlapping, the band under consideration often occurs as a slight inflexion only. Since intensities in spectra are additive, the integrated molar extinction for a given band can be defined as $\int_{-\infty}^{+\infty} \Delta\varepsilon_\nu d\nu$ in which $\Delta\varepsilon$ is the difference in extinction between the measured curve and a constructed hypothetical curve. The nature of the latter depends on adjacent bands in the spectrum and may be calculated by Fourier analysis, or — as has been done here — be visualized by arbitrary drawing * (see for instance Figs. 1—28).

* The error in the determination of the oscillator strength would of course be smaller by employing Fourier analysis to calculate the integrated extinction. However, this requires that the measurements be extended down to 190 mμ.

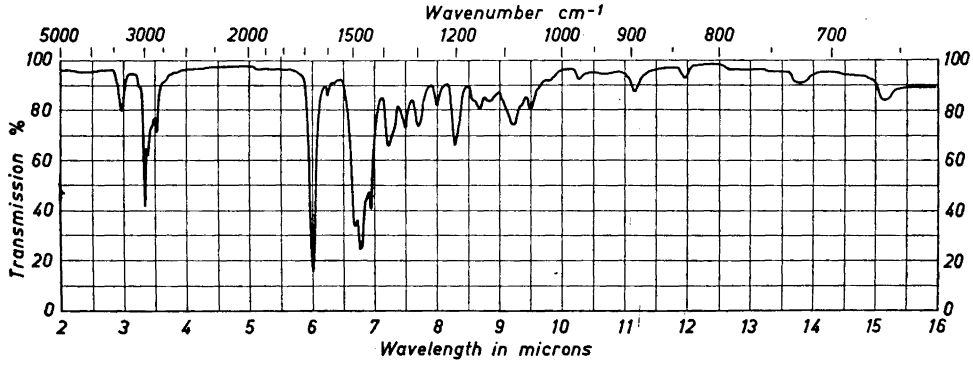

Fig. 29. Infrared spectrogram of V *a*; 4.5 % solution in CCl_4.

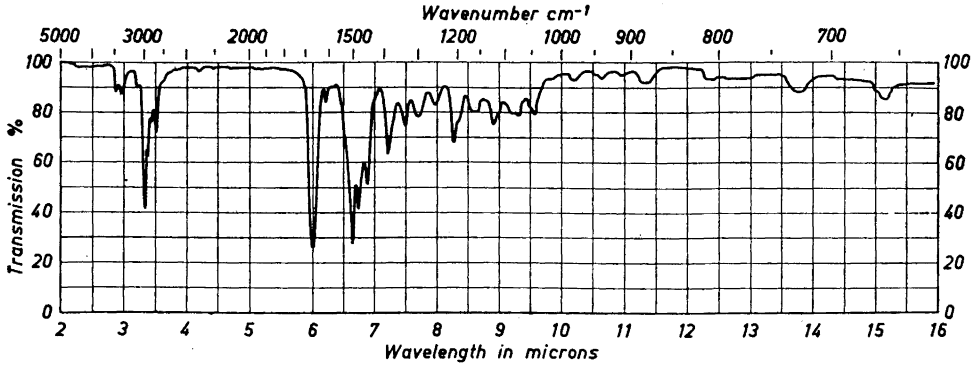

Fig. 30. Infrared spectrogram of V *b*; 4.5 % solution in CCl_4.

The experimental data from the measurements on the ultraviolet absorbtion spectra are found in Table 6 and Figs. 1—28.

Infrared spectra recorded for the two racemates of N-(2-diethylamino-1,2,-dimethylethyl)-2-methylbenzamide in CCl_4 are shown in Figs. 29 and 30. Spectra of the two racemates were also taken up in CS_2 (no diagram shown here). Both racemates showed a relatively strong band at 737 cm^{-1}.

DISCUSSION ON IONIZATION CONSTANTS AND OSCILLATOR STRENGTHS

When attaching a methyl group to the benzene nucleus of a benzoic acid or a N-(2-diethylaminoethyl)benzamide, the pK_a-value is altered in a systematic way. The introduction of a methyl group *para* to the carboxyl group of a benzoic acid is always accompanied by a decrease in acid strength (Table 7). Methyl groups in the positions *ortho* to the carboxyl group cause a marked increase in the acid strength (Table 11). Smaller effects in both directions are brought about by methyl groups in the *meta* positions (Table 9). The influence of methyl groups on the strength of a conjugate acid of the corresponding N-(2-diethylaminoethyl)benzamide is essentially the same as that of the benzoic acid (Tables 8, 10, and 12). — The present results support earlier observations on the strength in aqueous solution of simple alkyl substituted benzoic acids [10,11].

The introduction of a methyl group to the *para* position of acids which do not contain *ortho* methyl groups results in a ΔpK_a equal to $+ 0.18 \pm 0.05$ * (mean of three cases, *cf.* Table 7). This is consistent with the observations by Dippy [10] who compared the ionization constants of benzoic acid and *p*-toluic acid. However, the effect of a *para* methyl group in the presence of one or two *ortho* methyl groups is noticeably increased, *i.e.* ΔpK_a is then equal to $+ 0.31 \pm 0.02$ ** (mean of four cases).

* Maximum error.
** Probable error of the mean.

Table 7. Change in pK_a on the introduction of *p*-methyl groups into benzoic acids.

Structural change Y → Z		ΔpK_a
Y	Z	
Benzoic acid	4-methylbenzoic acid	+ 0.197
2-Methylbenzoic acid	2,4-dimethylbenzoic acid	+ 0.368
3-Methylbenzoic acid	3,4-dimethylbenzoic acid	+ 0.207
2,3-Dimethylbenzoic acid	2,3,4-trimethylbenzoic acid	+ 0.263
2,5-Dimethylbenzoic acid	2,4,5-trimethylbenzoic acid	+ 0.335
2,6-Dimethylbenzoic acid	2,4,6-trimethylbenzoic acid	+ 0.290
3,5-Dimethylbenzoic acid	3,4,5-trimethylbenzoic acid	+ 0.128
		Mean value + 0.26 ± 0.03 [a]

[a] The error given for the mean is the probable error if the number of measurements from which the mean is calculated is four or higher.

Table 8. Change in pK_a on the introduction of *p*-methyl groups into N-(2-diethylamino-ethyl)-benzamides.

Structural change Y → Z		ΔpK_a
Y	Z	
N-(2-Diethylamino-ethyl)-benzamide	XIII	+ 0.034
I	XXIII	+ 0.042
VII	XXXII	+ 0.022
XIX	XLI	+ 0.031
XXVII	LIII	+ 0.027
A	LVIII	+ 0.017
XXXVI	LXIII	+ 0.028
		Mean value + 0.029 ± 0.003[a]

[a] For the error, see note, Table 7.

The values of ΔpK_a for the introduction of *ortho* methyl groups into benzoic acids vary within wide limits (*cf.* Table 11). Exceptionally high numerical values are obtained when introducing methyl groups into the 6-position of 2-methyl substituted benzoic acids. The effect of a methyl group in the *ortho* position of a benzoic acid is also increased by the presence of a neighbouring *meta* methyl group. On the other hand, a *para* methyl group in most cases diminishes the acid strengthening effect of an *ortho* methyl group. This tendency is especially manifest in the difference in ionization constant of *p*-toluic acid and 2,4-dimethylbenzoic acid ($\Delta pK_a = -0.11$) or 3,4-dimethylbenzoic acid and 2,4,5-trimethylbenzoic acid ($\Delta pK_a = -0.12$), where no steric interactions can occur between the *ortho* methyl group and other methyl groups present in the molecule.

Table 9. Change in pK_a on the introduction of *m*-methyl groups into benzoic acids.

Structural change Y → Z		ΔpK_a
Y	Z	
Benzoic acid	3-methylbenzoic acid	+ 0.073
2-Methylbenzoic acid	2,3-dimethylbenzoic acid	− 0.134
2-Methylbenzoic acid	2,5-dimethylbenzoic acid	+ 0.106
3-Methylbenzoic acid	3,5-dimethylbenzoic acid	+ 0.104
4-Methylbenzoic acid	3,4-dimethylbenzoic acid	+ 0.083
2,3-Dimethylbenzoic acid	2,3,5-trimethylbenzoic acid	+ 0.206
2,4-Dimethylbenzoic acid	2,3,4-trimethylbenzoic acid	− 0.239
2,4-Dimethylbenzoic acid	2,4,5-trimethylbenzoic acid	+ 0.073
2,5-Dimethylbenzoic acid	2,3,5-trimethylbenzoic acid	− 0.034
2,6-Dimethylbenzoic acid	2,3,6-trimethylbenzoic acid	+ 0.084
3,4-Dimethylbenzoic acid	3,4,5-trimethylbenzoic acid	+ 0.025
		Mean value + 0.03 ± 0.04[a]

[a] For the error, see note, Table 7.

Table 10. Change in pK_a on the introduction of *m*-methyl groups into N-(2-diethylaminoethyl)-benzamides.

Structural change Y → Z		ΔpK_a
Y	Z	
N-(2-Diethylaminoethyl)-benzamide	VII	− 0.002
I	XIX	− 0.013
I	XXVII	+ 0.010
VII	XXXVI	− 0.001
XIII	XXXII	− 0.014
XIX	XLVI	+ 0.004
XXIII	XLI	− 0.024
XXIII	LIII	− 0.005
XXVII	XLVI	− 0.019
A	XLVIII	+ 0.011
XXXII	LXIII	+ 0.005
		Mean value − 0.004±0.004[a]

[a] For the error, see note, Table 7.

Table 11. Change in pK_a on the introduction of *o*-methyl groups into benzoic acids.

Structural change Y → X		ΔpK_a
First *o*-methyl group:		
Y	Z	
Benzoic acid	2-methylbenzoic acid	− 0.282
3-Methylbenzoic acid	2,3-dimethylbenzoic acid	− 0.489
3-Methylbenzoic acid	2,5-dimethylbenzoic acid	− 0.249
4-Methylbenzoic acid	2,4-dimethylbenzoic acid	− 0.111
3,4-Dimethylbenzoic acid	2,3,4-trimethylbenzoic acid	− 0.433
3,4-Dimethylbenzoic acid	2,4,5-trimethylbenzoic acid	− 0.121
3,5-Dimethylbenzoic acid	2,3,5-trimethylbenzoic acid	− 0.387
		Mean value − 0.30 ± 0.05[a]
Second *o*-methyl group:		
Y	Z	
2-Methylbenzoic acid	2,6-dimethylbenzoic acid	− 0.679
2,3-Dimethylbenzoic acid	2,3,6-trimethylbenzoic acid	− 0.461
2,4-Dimethylbenzoic acid	2,4,6-trimethylbenzoic acid	− 0.757
2,5-Dimethylbenzoic acid	2,3,6-trimethylbenzoic acid	− 0.701
		Mean value − 0.65 ± 0.07[a]

[a] For the error, see note, Table 7.

Table 12. Change in pK_a on the introduction of *o*-methyl groups into N-(2-diethylaminoethyl)-benzamides.

Structural change Y → Z		ΔpK_a
First *o*-methyl group:		
Y	Z	
N-(2-Diethylaminoethyl)-benzamide	I	− 0.174
VII	XIX	− 0.185
VII	XXVII	− 0.162
XIII	XXIII	− 0.166
XXXII	XLI	− 0.176
XXXII	LIII	− 0.157
XXXVI	XLVI	− 0.180
		Mean value − 0.171 ± 0.004 [a]
Second *o*-methyl group:		
Y	Z	
I	A	− 0.187
XIX	XLVIII	− 0.163
XXIII	LVIII	− 0.212
XXVII	XLVIII	− 0.186
		Mean value − 0.187 ± 0.010 [a]

[a] For the error, see note, Table 7.

A methyl group introduced in the *meta* position of a benzoic acid will cause a small decrease in acid strength ($\Delta pK_a = + 0.09 \pm 0.02$ *; mean of seven cases), provided that no methyl group is located in the *ortho* position between the entering methyl group and the carboxyl. A *meta* methyl group adjacent to an *ortho* methyl is often acid strengthening (*cf.* Table 9).

The effect of *meta* and *para* methyl groups in the N-(2-diethylaminoethyl)-benzamides is about 10 % of that in the corresponding benzoic acids, whereas the effect of *ortho* methyl groups in the basic amides is about 40 % of that in the benzoic acids. The variation in ΔpK_a when introducing methyl groups into the *ortho* positions of benzoic acids (*cf.* above) has not been observed in the benzamide series.

An extensive critical survey of current ideas dealing with the influence of substitution in the benzene nucleus on the ionization constant of benzoic acids has been given by Brown *et al.*[16] The acid strength of benzoic acid is governed by two factors acting in opposite directions. The inductive effect

* Probable error of the mean.

of the benzene nucleus (being electron-attracting) is acid-strengthening, and the resonance between the carboxyl group and the benzene nucleus is acid-weakening. *Para* and *meta* alkyl groups are acid-weakening by means of an electron-repelling * effect [16]. The actual observations in many cases support these theories. Deviations will be discussed below. Brown *et al.*[16] consider the effect of alkyl substituents in the *ortho* positions to be *mainly* of a steric nature. This is ascribed to a twisting of the carboxyl group out of the plane of the ring. An *ortho* methyl should be acid weakening by means of its electron-repelling effect. This is, however, outweighed by the strong effect of resonance inhibition. The more bulky the *ortho* alkyl groups, the more pronounced is the steric inhibition of resonance. Thus, *o-tert*-butylbenzoic acid is three times stronger than *o*-toluic acid, despite the electron-repelling effect of *tert*-butyl being greater than that of methyl [10,11,16].

This theory may explain the abnormal acid-strengthening effect of a *meta* methyl group adjacent to an *ortho* methyl group. The crowding of bulky substituents may enhance the twisting of the carboxyl group out of the plane of the ring. The resulting increase in acid strength is apparently large enough to compensate for the acid weakening effect of the *meta* methyl group. A similar explanation of this *ortho-meta*-effect is given by Dippy *et al.*[11]

The surprisingly large effect of *ortho* methyl groups on the pK_a of the benzamides may be due to steric interference between the bulky dialkylamino-alkyl group and the *ortho* methyl groups. The concept of steric hindrance would also explain the observation (*cf.* above) that a *para* methyl group diminishes the acid strengthening effect of an *ortho* methyl group. The effect may also be expressed as an increase in the acid weakening property of the *para* methyl group in presence of *ortho* methyl groups. Considering the influence of the *para* methyl group on the effect of the *ortho* methyl group, it seems reasonable to assume that the *para* methyl, by virtue of its electron repelling effect, counteracts the twisting of the carboxyl group out of the plane of the ring (*cf.* Dippy [11]).

As a general rule, the introduction of a *para* methyl group is accompanied by an increase in oscillator strength (f) of the ultraviolet absorption band at 220—240 mμ. Hedden *et al.*[13] give a value of + 0.04 for the change in f when a methyl group is introduced in the *para* position of acetophenones. The corresponding value in the present determinations is + 0.06 for the benzoic acids, and + 0.05 for N-(2-diethylaminoethyl)benzamides (*cf.* Tables 13 and 14). The surprisingly low f value for 2,4,6-trimethylbenzoic acid as compared with that of 2,6-dimethylbenzoic acid is consistent with the values for the corresponding acetophenones as reported by Braude [18], but not with those given by Schwartzman *et al.* [25]

When introducing a methyl group into a *meta* position of a benzoic acid or N-(2-diethylaminoethyl)benzamide, f is in most cases slightly decreased. The average change in f is −0.02 for the acids and −0.03 for the basic amides (Tables 15 and 16).

* Throughout this paper no differentiation has been made between the inductive effect of alkyl groups and the so called hyperconjugation which has recently been brought into question (*cf.* for instance Ref.[17]). Thus, when discussing the electron-repelling effect of an alkyl group, the true inductive effect and a possible "hyperconjugation" effect are included.

Table 13. Change in f on the introduction of p-methyl groups into benzoic acids.

Structural change Y → Z		Δf
Y	Z	
Benzoic acid	4-methylbenzoic acid	+ 0.0838
2-Methylbenzoic acid	2,4-dimethylbenzoic acid	+ 0.0467
3-Methylbenzoic acid	3,4-dimethylbenzoic acid	+ 0.0778
2,3-Dimethylbenzoic acid	2,3,4-trimethylbenzoic acid	+ 0.0152
2,5-Dimethylbenzoic acid	2,4,5-trimethylbenzoic acid	+ 0.0860
2,6-Dimethylbenzoic acid	2,4,6-trimethylbenzoic acid	− 0.0144 [b]
3,5-Dimethylbenzoic acid	3,4,5-trimethylbenzoic acid	+ 0.1019
		Mean value + 0.057±0.016[a]

[a] For the error, see note, Table 7.
[b] Regarding this value see text p. 341.

Table 14. Change in f on the introduction of p-methyl groups into N-(2-diethylaminoethyl)-benzamides.

Structural change Y → Z		Δf
Y	Z	
N-(2-Diethylaminoethyl)-benzamide	XIII	+ 0.0923
I	XXIII	+ 0.0347
VII	XXXII	+ 0.0550
XIX	XLI	+ 0.0108
XXVII	LIII	+ 0.0211
XXXVI	LXIII	+ 0.0971
		Mean value + 0.052±0.015[a]

[a] For the error, see note, Table 7.

The introduction of a methyl group in an *ortho* position is accompanied by a strong decrease in oscillator strength (Tables 17 and 18). The change in f — associated with the introduction of the first methyl group in the benzoic acids — had a value of −0.10. The corresponding value in the benzamide series was found to be −0.09. In the acetophenones the change of f is −0.07 when methyl groups are introduced in the *ortho* positions [13]. On introducing a methyl group in the 6-position of a 2-methyl substituted benzoic acid or N-(2-diethylaminoethyl)benzamide, the change is smaller, being −0.03. From Table 6 is seen that for most amides, *one ortho* methyl group is sufficient to diminish the oscillator strength almost to zero. For the benzoic acids, even *two ortho* methyl groups do not give such a strong effect.

The absorption band studied is considered to be associated with the conjugation between the aromatic nucleus and the carbonyl group [13,18]. The oscillator

Table 15. Change in f on the introduction of *m*-methyl groups into benzoic acids.

Structural change Y → Z		Δf
Y	Z	
Benzoic acid	3-methylbenzoic acid	− 0.0105
2-Methylbenzoic acid	2,3-dimethylbenzoic acid	− 0.0184
2-Methylbenzoic acid	2,5-dimethylbenzoic acid	− 0.0268
3-Methylbenzoic acid	3,5-dimethylbenzoic acid	− 0.0402
4-Methylbenzoic acid	3,4-dimethylbenzoic acid	− 0.0165
2,3-Dimethylbenzoic acid	2,3,5-trimethylbenzoic acid	− 0.0131
2,4-Dimethylbenzoic acid	2,4,5-trimethylbenzoic acid	+ 0.0125
2,4-Dimethylbenzoic acid	2,3,4-trimethylbenzoic acid	− 0.0499
2,5-Dimethylbenzoic acid	2,3,5-trimethylbenzoic acid	− 0.0047
2,6-Dimethylbenzoic acid	2,3,6-trimethylbenzoic acid	− 0.0061
3,4-Dimethylbenzoic acid	3,4,5-trimethylbenzoic acid	− 0.0161
		Mean value − 0.017±0.005[a]

[a] For the error, see note, Table 7.

Table 16. Change in f on the introduction of *m*-methyl groups into N-(2-diethylaminoethyl)-benzamides.

Structural change Y → Z		Δf
Y	Z	
N-(2-Diethylaminoethyl)-benzamide	VII	− 0.0395
VII	XXXVI	− 0.0232
XIII	XXXII	− 0.0768
XXIII	LIII	− 0.0136
XXIII	XLI	− 0.0239
XXXII	LXIII	+ 0.0189
		Mean value − 0.026±0.013[a]

[a] For the error, see note, Table 7.

strength gives a measure of the probability for a given transition, and hence also of the degree of conjuagtion. The low value of f when *ortho* methyl groups are present is probably due to the out-of-plane twisting of the carbonyl group (*cf.* above and Refs.[13,18,26,27]). This theory is supported by UV spectra of the benzonitriles, which do *not* show any *ortho* effect. Thus, benzonitrile [19], *o*-tolunitrile [19], and 2,6-dimethylbenzonitrile (see Fig. 28) for the actual band have about the same ε_{max} value, *i.e.* $\sim 9.5 \times 10^3$.

The effect of *meta* and *para* methyl groups upon the intesities of spectra is not yet fully understood.

Since the degree of conjugation between the carbonyl group and the benzene nucleus influences both the ionization constant and the oscillator strength,

Table 17. Change in f on the introduction of *o*-methyl groups into benzoic acids.

Structural change Y → Z		Δf
First *o*-methyl group:		
Y	Z	
Benzoic acid	2-methylbenzoic acid	− 0.0838
3-Methylbenzoic acid	2,3-dimethylbenzoic acid	− 0.0917
3-Methylbenzoic acid	2,5-dimethylbenzoic acid	− 0.1001
4-Methylbenzoic acid	2,4-dimethylbenzoic acid	− 0.1209
3,4-Dimethylbenzoic acid	2,3,4-trimethylbenzoic acid	− 0.1543
3,4-Dimethylbenzoic acid	2,4,5-trimethylbenzoic acid	− 0.0919
3,5-Dimethylbenzoic acid	2,3,5-trimethylbenzoic acid	− 0.0646
		Mean value − 0.101±0.011[a]
Second *o*-methyl group:		
Y	Z	
2-Methylbenzoic acid	2,6-Dimethylbenzoic acid	− 0.0255
2,3-Dimethylbenzoic acid	2,3,6-trimethylbenzoic acid	− 0.0132
2,5-Dimethylbenzoic acid	2,3,6-trimethylbenzoic acid	− 0.0048
2,4-Dimethylbenzoic acid	2,4,6-trimethylbenzoic acid	− 0.0866
		Mean value − 0.033±0.019[a]

[a] For the error, see note, Table 7.

a certain parallellism might occur between ΔpK_a and Δf. Hence, in Table 19 ΔpK_a and Δf for the various structural changes studied, have been listed side by side.

EXPERIMENTAL

The *N-(dialkylaminoalkyl)benzamides* and their *hydrochlorides* were analytical samples of high purity. Regarding the preparation and purification of these, see Lüning [1].

N-(2-Diethylaminoethyl)benzamide was obtained from benzoyl chloride and 1-amino-2-diethylaminoethane by the general method described by Lüning [1]. The hydrochloride was prepared and recrystallized several times from a mixture of *iso*propyl ether and methyl ethyl ketone m. p. 88°−89°. (Found: Cl 13.8. Calc. for $C_{13}H_{21}ClN_2O$: Cl 13.8.) The melting point of the hydrochloride does not agree with that given for the same compound by Hazard *et al.*[20] who give neither an acceptable method of synthesis nor any proof of the composition. The base was liberated from the hydrochloride and taken up in ether, which was evaporated, leaving the base as an oil; $n_D^{25} = 1.5281$. (Found: Equiv. wt. 223. Calc. for $C_{13}H_{20}N_2O$: Equiv. wt. 220.3.)

Concerning the preparation of *benzoic acids* see Lüning [1]. Each benzoic acid was recrystallized several times from ethanol; all the melting points agreed with those given by Smith and Stanfield [21]. The melting points of 2,3,5-trimethylbenzoic acid and 3,4,5-trimethylbenzoic acid, which were not reported by these authors, were in accordance with those given by Jannasch and Weiler [22].

Table 18. Change in f on the introduction of *o*-methyl groups into N-(2-diethylaminoethyl)-benzamides.

Structural change Y → Z		Δf
First *o*-methyl group:		
Y	Z	
N-(2-Diethylaminoethyl)-benzamide	I	− 0.0988
VII	XIX	− 0.0603
XIII	XXIII	− 0.1574
VII	XXVII	− 0.0603
XXXII	XLI	− 0.1045
XXXII	LIII	− 0.0942
XXXVI	XLVI	− 0.0371
		Mean value − 0.088±0.015[a]
Second *o*-methyl group:		
Y	Z	
XXIII	LVIII	− 0.034 $_7$

[a] For the error, see note, Table 7.

Table 19. Comparison between ΔpK_a and Δf for substitution of methyl groups into different positions in the benzene nucleus of benzoic acids and N-(2-diethylaminoethyl)-benzamides. The number of calculations underlying each mean is given in parenthesis.

Position of methyl group introduced	Benzoic acids		N-(2-Diethylaminoethyl)-benzamides	
	Δf	ΔpK_a	Δf	ΔpK_a
First *ortho* [a]	−0.101 ± 0.011 [b] (7)	−0.30±0.05[b] (7)	−0.088 ± 0.015 [b] (7)	−0.171 ± 0.004 [b] (7)
Second *ortho* [a]	−0.033 ± 0.019 [b] (4)	−0.65±0.07[b] (4)	−0.035 (1)	−0.187 ± 0.010 [b] (4)
Meta	−0.017 ± 0.005 [b] (11)	+0.03±0.04[b] (11)	−0.026 ± 0.013 [b] (6)	−0.004 ± 0.004 [b] (11)
Para	+0.057 ± 0.016 [b] (7)	+0.26±0.03[b] (7)	+0.052 ± 0.015 [b] (6)	+0.029 ± 0.003 [b] (7)

[a] The first and the second *ortho* methyl group often give rise to different variations of f and pK_a values, see also text p. 338.
[b] For the error, see note, Table 7.

2,6-Dimethylbenzonitrile was prepared from 2,6-dimethylaniline by a Sandmeyer reaction, and purified by means of sublimation.

The duration and latency time of anesthesia were measured on rabbit cornea according to the method given by Wiedling [2] *. The LD50 values were calculated by the method of Kärber [23]. For each toxicity determination, at least 60 male white mice were used. The compound, in the form of a 3 "per cent" solution (weight/volume), was injected under the dorsal skin. The base was dissolved in 1,2-propylene glycol, the equivalent amount of hydrochloric acid was added, followed by water to give the proportion propylene glycol: water equal to 1:1 (v/v). The "pH value" was adjusted to 6.5 before injection.

The solutions for pK_a determinations were prepared in four different ways: (1) Benzoic acids were dissolved in water by gentle heating for a short period, and the solutions neutralized to about 50 % with NaOH. (2) Benzoic acids were dissolved in a slight excess of carbonate-free NaOH which was then titrated back to about 50 % with HCl. (3) Hydrochlorides of bases were dissolved in water and neutralized to 30—60 % with NaOH. (4) Bases were dissolved in a slight excess of HCl which was then titrated back to about 50 % with NaOH. The pH values given in Tables 3—5 are the means of two measurements, obtained by the aid of different glass electrodes. For details in the measurements, and a diagram of the cell used, see Löfgren [8] and Lindström [24].

The ultraviolet absorbtion spectra were measured with the aid of a Beckman DK2 recording quartz spectrophotometer, using a hydrogen lamp as a light source. The wavelength scale is logarithmic. The values of $\int_{-\infty}^{+\infty} \Delta\varepsilon_\nu d\nu$ were obtained by calculation of $\sum_{-\infty}^{+\infty} \Delta\varepsilon\Delta\nu$ of the area between the recorded curve and an arbitrary reference curve, as is demonstrated in Figs. 1—28. $\Delta\varepsilon$ is the difference in molar extinction between the measured curve and the reference curve. The reference curves are included in the figures as dashed lines.

The infrared spectra were measured with the aid of a Beckman IR 5 double beam Infrared Recording Spectrophotometer, using a sodium chloride cell (0.1 mm).

The toxicity determinations were made at the *Battelle Institute*, Frankfurt, Germany, with the aid of a grant from *Aktiebolaget Astra*, Södertälje, Sweden. The measurements of the local anesthetic activity were performed in the research laboratories of *Aktiebolaget Astra*.

I wish to express my sincere gratitude to *Aktiebolaget Astra* for the invaluable help with the pharmacological measurements, and for financial support during the course of this work.

REFERENCES

1. Lüning, B. *Acta Chem. Scand.* **13** (1959) 1623.
2. Wiedling, S. *Acta Pharmacol. Toxicol.* **8** (1952) 117.
3. Löfgren, N. and Tegnér, C. *Acta Chem. Scand.* **8** (1954) 1806.
4. Löfgren, N. and Stoffel, W. *Acta Chem. Scand.* **13** (1959) 1585.
5. Löfgren, N., Tegnér, C. and Takman, B. *Acta Chem. Scand.* **11** (1957) 1724.
6. Lövgren, N. *Elementa* **22** (1939) 95.
7. Kielland, J. *J. Am. Chem. Soc.* **59** (1937) 1675.
8. Löfgren, N. *Studies on Local Anesthetics, Xylocaine a New Synthetic Drug.* Dissertation Stockholm 1948.
9. Shorter, J. and Stubbs, F. *J. Chem. Soc.* **1949** 1180.
10. Dippy, J. *Chem. Revs.* **25** (1939) 151.
11. Dippy, J., Hughes, S. and Laxton, J. *J. Chem. Soc.* **1954** 1470.
12. Moser, C. and Kohlenberg, A. *J. Chem. Soc.* **1951** 804.
13. Hedden, G. and Brown, W. *J. Am. Chem. Soc.* **75** (1953) 3744.
14. Mulliken, R. *J. Chem. Phys.* **7** (1939) 14.

* *Cf.* also Löfgren and Tegner [3].

15. Mulliken, R. and Rieke, C. *Repts. Prog. in Phys.* **8** (1941) 231.
16. Brown, H., McDaniel, D. and Häfliger, O. in Braude, E. and Nachod, F. *Determination of Organic Structures by Physical Methods.* Academic Press inc., New York, N Y, 1955, pp. 584 ff and 603—605.
17. Gray, G. *Steric Effects in Conjugated Systems.* Butterworths Scientific Publications, London 1958, pp. 114—115.
18. Braude, E., Sondheimer, F. and Forbes, W. *Nature* **173** (1954) 117.
19. Wolf, K. and Strasser, O. *Z. physik. Chem. (Leipzig)* **B 21** (1933) 389.
20. Hazard, R., Giudicelli, R., Thuillier, G., and Beauvallet, M. *Compt. rend. soc. biol.* **147** (1953) 755.
21. Smith, H. and Stanfield, J. *J. Am. Chem. Soc.* **71** (1949) 81.
22. Jannasch, P. and Weiler, M. *Ber.* **27** (1894) 3441.
23. Kärber, G. *Arch. exp. Pathhol. Pharmakol.* **162** (1931) 480.
24. Lindström, S. *Acta Chem. Scand.* **11** (1957) 962.
25. Schwartzman, L. and Corson, B. *J. Am. Chem. Soc.* **76** (1954) 781.
26. Forbes, W. and Mueller, W. *Can. J. Chem.* **33** (1955) 1145.
27. Forbes, W. and Sheratte, M. *Can. J. Chem.* **33** (1955) 1829.

Received December 22, 1959.

ACTA CHEMICA SCANDINAVICA 14 (1960) 348–352

On the Oxidation of 3α,7α,12α-Trihydroxycoprostane by Mouse and Rat Liver Homogenates

Bile Acids and Steroids 97

HENRY DANIELSSON

Department of Chemistry, Karolinska Institutet, Stockholm, Sweden

3α,7α,12α-Trihydroxycoprostane has been found to be hydroxylated to 3α, 7α, 12α, 27-tetrahydroxycoprostane in whole homogenates as well as washed mitochondria of rat liver. The same reaction occurs also in mouse liver homogenates, which in addition transform 3α, 7α, 12α-trihydroxycoprostane into acidic material, part of which has been identified as 3α, 7α, 12α-trihydroxycoprostanic acid. Mouse liver mitochondria alone effect mainly the 27-hydroxylation, while addition of 100 000 × *g* supernatant increases the formation of acidic material 3- to 4-fold. 3α, 7α, 12α, 27-Tetrahydroxycoprostane is a more efficient precursor of the coprostanic acid than 3α, 7α, 12α-trihydroxycoprostane.

The intermediate steps in the degradation of cholesterol to bile acids are not wholly known. The probable sequence of reactions has been proposed by Bergström and Lindstedt [1–4] on basis of their studies on the formation of cholic acid in bile-fistula rats from different possible intermediates. According to these investigations the steroid nucleus is hydroxylated prior to the completion of the side-chain oxidation, and one of the earliest steps appears to be the introduction of the hydroxyl-group of C_7 of the steroid molecule.

The use of *in vitro*-systems seems a reasonable approach to further investigations on the individual steps in the degradation of cholesterol to bile acids. Horning *et al.* [5,6] and Gurin *et al.* [7,8] studied the oxidation of 26-^{14}C-cholesterol to $^{14}CO_2$ in mitochondrial preparations of mouse and rat liver and characterized the cofactor requirements for maximal $^{14}CO_2$-production. Gurin *et al.* [7] also provided evidence for the formation of labeled 25-dehydrocholesterol together with a labeled C_{27}-steroid aldehyde and acid from 26-^{14}C-cholesterol in these experiments. Using the above-mentioned mitochondrial system Fredrickson [9] investigated the products formed from 4-^{14}C-cholesterol and was able to isolate labeled 25- and 26-hydroxycholesterol, neither of which was converted to cholic acid in the bile-fistula rat [10]. In addition there were formed several acidic products not identical with cholic or deoxycholic acid.

Currently the metabolism of 4-^{14}C-cholesterol in mouse and rat liver mitochondrial systems is being studied in this laboratory. With the use of reversed phase partition chromatography [11] some 10 compounds formed from cholesterol in these systems have been isolated and partly identified [12,13]. Some of these substances undoubtedly arise through autoxidation of the added cholesterol, but at least two enzymically formed labeled products have been isolated. Both these compounds, which are transformed into normal bile acids in the bile-fistula rat, are neutral steroids retaining the C_{27}-side-chain, but the detailed structures are as yet not known. In these experiments *in vitro* with 4-^{14}C-cholesterol very limited degradation of the side-chain has so far been obtained.

To study the oxidation of the side-chain we then turned to 3α,7α,12α-trihydroxycoprostane. Bergström *et al.* [14] have shown, that when this compound is injected into a bile-fistula rat, it is rapidly excreted in bile mainly as cholic acid. We have found that both rat and mouse liver homogenates are able to oxidize this compound in good radiochemical yield (50—70 %).

EXPERIMENTAL

White male mice (Danish State Serum Institute strain) weighing approx. 25 g and white male rats (Sprague-Dawley strain) weighing approx. 150 g were used. Homogenates (33 % w/v) were prepared in 0.25 M sucrose containing 3.6 mg nicotinamide/ml using a tight-fitting Potter-Elvehjem pestle. Fractionations of homogenates were carried out in a Spinco preparative ultracentrifuge in the usual manner. The mitochondrial and microsomal pellets were resuspended in the above-mentioned sucrose medium by homo-

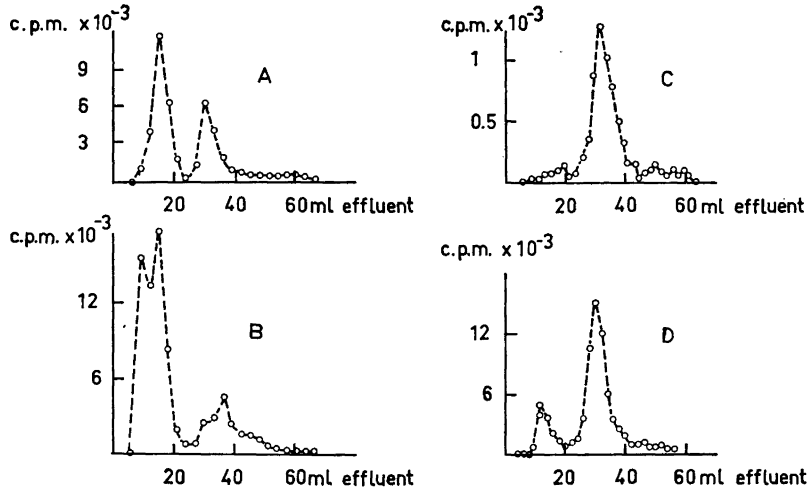

Fig. 1. Chromatograms of incubations of 3α,7α,12α-trihydroxycoprostane with mouse liver mitochondria (curve A) and with ditto plus supernatant (curve B). 4.5 g Hostalene columns. Phase system III. Curves C and D show the rechromatograms of 9—21 ml of effluent of the corresponding chromatograms (curves A and B) with phase system IV. 4.5 g hydrophobic Hyflo columns.

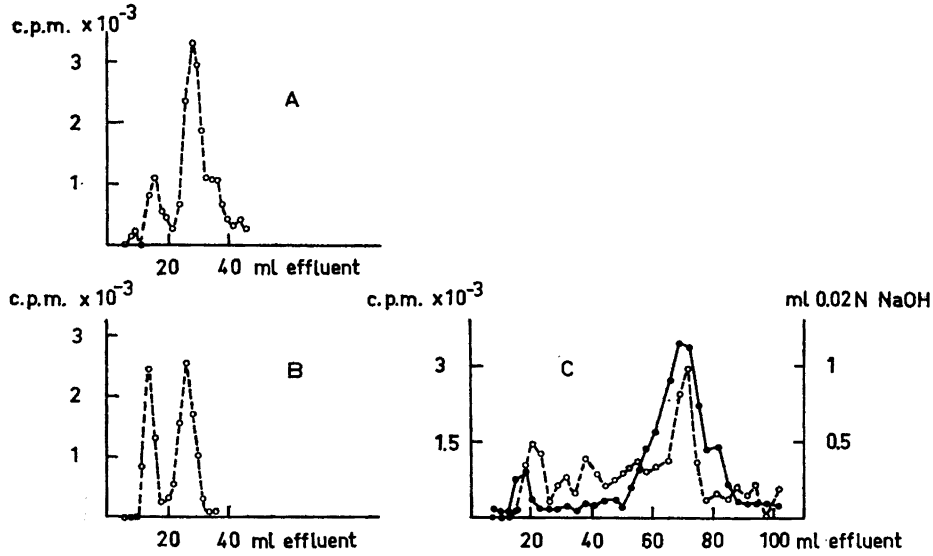

Fig. 2. Chromatograms of incubations of 3*a*,7*a*,12*a*,27-tetrahydroxycoprostane with mouse liver mitochondria (curve A) and with ditto plus supernatant (curve B). 4.5 g hydrophobic Hyflo columns. Phase system IV. Curve C shows the chromatogram of the saponified acidic material of the previous columns together with unlabeled 3*a*,7*a*,12*a*-trihydroxycoprostanic acid. 4.5 g hydrophobic Hyflo column. Phase system: 50 % aqueous methanol as moving phase, 10 % heptane in chloroform as stationary phase.

genization with a loose-fitting pestle for 10—20 sec. Incubations were run aerobically for 1 h at 37° with constant shaking.

The 3*a*,7*a*,12*a*-trihydroxycoprostane used was randomly labeled with tritium according to the method of Wilzbach [15] in the apparatus described by Bergström and Lindstedt [16]. The tritium-labeling was kindly carried out by Dr. B. Samuelsson of this laboratory. To each incubation there were added 0.8—2 μC (60—150 μg) of the labeled 3*a*,7*a*,12*a*-trihydroxycoprostane as an emulsion prepared by dissolving the compound in 0.1 ml of ethanol and diluting with 0.9 ml of a 1 % solution of bovine serum albumin in water.

The following amounts of unfractionated and fractionated homogenate were used per incubation: 3 ml whole homogenate (corresponding to approx. 1 g of liver), 3 ml mitochondria (from approx. 4 g of liver), 3 ml microsomes (from approx. 4 g of liver) and 3 ml 100 000 × *g* supernatant (from approx. 1 g of liver). To each incubation 1 ml of 0.1 M Tris-HCl buffer, pH 7.6, was added.

Incubations were terminated by addition of ethanol and after filtration and evaporation the aqueous solution was acidified and extracted twice with ether. The ether-extracts were chromatographed in the reversed phase systems described previously [11]. In addition a modification of system III was employed using 45 % aqueous *iso*propanol as moving phase (phase-system IV). Hostalene [17] or hydrophobic Hyflo Supercel [11] were used as supporting material for the stationary phase.

RESULTS AND DISCUSSION

Incubations with whole homogenates of mouse liver resulted in the conversion of about 50 % of the 3*a*,7*a*,12*a*-trihydroxycoprostane into more polar material, that could be separated into one acidic fraction and one neutral

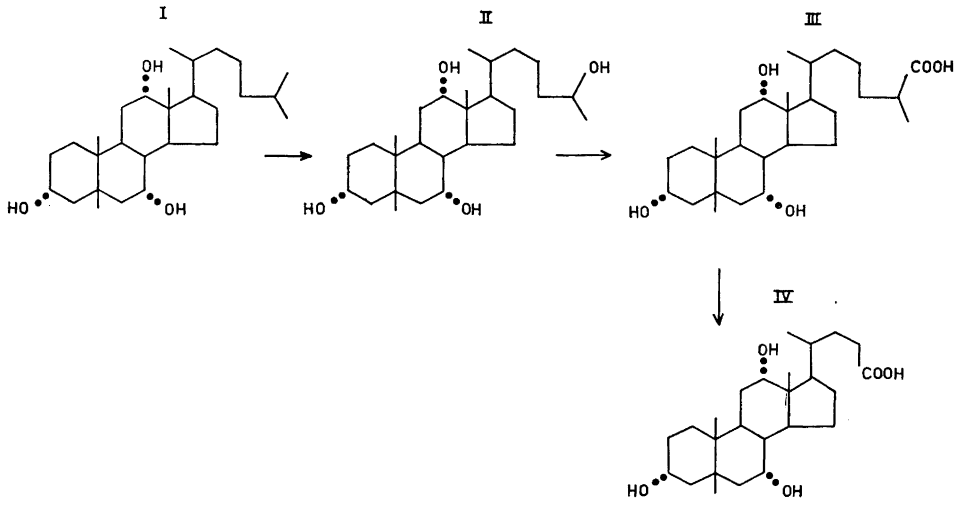

Fig. 3. Postulated sequence for the oxidation of the C_{27}-side-chain: 3α,7α,12α-trihydroxycoprostane (I), 3α,7α,12α,27-tetrahydroxycoprostane (II), 3α,7α,12α-trihydroxycoprostanic acid (III) cholic acid (IV).

tetrahydroxyl compound. Use of the whole homogenate of rat liver resulted in the formation of the tetrahydroxy fraction only. Washed mitochondria of mouse and rat liver effected mainly the formation of the tetrahydroxy compound and addition of 100 000 × *g* supernatant (hereafter called supernatant) to mouse liver mitochondria but not to rat liver mitochondria resulted in the additional formation of acidic material. Hardly any change (0—5 % conversion to more polar material) of the 3α,7α,12α-trihydroxycoprostane was observed in presence of microsomes and/or supernatant from either species.

Fig. 1 shows chromatograms using phase system III of incubations with mouse liver mitochondria (curve A) and with mouse liver mitochondria plus supernatant (curve B). The peak at 30 and 36 ml of effluent, respectively, represents unchanged 3α,7α,12α-trihydroxycoprostane. The material eluted between 9 and 21 ml of effluent in both chromatograms was rerun with phase system IV (curves C and D, Fig. 1). In the presence of mitochondria alone (curve C, Fig. 1) there is one main peak at 31 ml of effluent appearing at the position of a neutral tetrahydroxylated C_{27}-steroid and a small amount of isotope (5 % of total isotope eluted) is eluted earlier representing the acidic fraction. The addition of supernatant (curve D, Fig. 1) increases considerably the amount of isotope in the acidic fraction (18 % of total isotope eluted). The labeled material in the main peak was identified as 3α,7α,12α,27-tetrahydroxycoprostane by cocrystallization to constant specific activity with unlabeled material (m.p. 204°), obtained by $LiAlH_4$-reduction of 3α,7α,12α-trihydroxycoprostanic acid (m.p. 170—171°, reported 172—174° [18]) isolated from frog bile.

Incubation of labeled 3α,7α,12α,27-tetrahydroxycoprostane, biosynthesized *in vitro* from 3α,7α,12α-trihydroxycoprostane, with mouse liver mitochondria demonstrated that this compound was a more efficient precursor of the acidic fraction than 3α,7α,12α-trihydroxycoprostane. Fig. 2 shows the chromatograms with phase system IV of the products of these incubations. There was a 15 % conversion to acidic material by mouse liver mitochondria (curve A, Fig. 2); the addition of supernatant increased the yield of acidic material to 50 % (curve B, Fig. 2). The acidic peaks from these experiments were combined, saponified and chromatographed with unlabeled 3α,7α,12α-trihydroxycoprostanic acid (curve C, Fig. 2). Part of the radioactivity coincides with the titration peak of the added carrier and the identity was confirmed by isotope dilution. The peaks appearing earlier in the chromatogram were not identified, but it is known from the work of Bergström *et al.*[19], that 3α,7α,12α-trihydroxycoprostanic acid is converted to cholic acid also *in vitro*.

A preliminary scheme for the oxidation of the C_{27}-steroid side-chain would then entail hydroxylation of one of the terminal methylgroups and subsequent oxidation of this hydroxyl to a C_{27}-acid, which in turn is oxidized to the C_{24}-acid (*cf.* Fig. 3). It cannot be stated at present, whether the C_{24}-acid is formed by direct oxidation of the C_{27}-acid or whether a series of C_{26}-intermediates occur.

Acknowledgments. The author is very grateful to Prof. T. Kazuno for a generous gift of 3α,7α,12α-trihydroxycoprostanic acid.

The skillful technical assistance of Miss Birgitta Holmberg and Miss Electra Pascalides is gratefully acknowledged.

This work is part of investigations supported by *Statens Medicinska Forkningsråd, Knut och Alice Wallenbergs Stiftelse,* Stockholm, Sweden, and the *National Heart Institute, National Institutes of Health,* Bethesda, Maryland, USA (H 2842).

REFERENCES

1. Bergström, S. *Rec. Chem. Progr. (Kresge-Hooker Sci. Lib.)* **16** (1955) 63.
2. Bergström, S. and Lindstedt, S. *Biochim. et Biophys. Acta* **19** (1956) 556.
3. Lindstedt, S. *Acta Chem. Scand.* **11** (1957) 417.
4. Lindstedt, S. *Dissertation*, Lund, Sweden (1957).
5. Anfinsen, C. B. and Horning, M. G. *J. Am. Chem. Soc.* **75** (1953) 1511.
6. Horning, M. G., Fredrickson, D. S. and Anfinsen, C. B. *Arch. Biochem. Biophys.* **71** (1957) 266.
7. Lynn, W. S., Staple, E. and Gurin, S. *Federation Proc.* **14** (1955) 783.
8. Whitehouse, M. W., Staple, E. and Gurin, S. *J. Biol. Chem.* **234** (1959) 276.
9. Fredrickson, D. S. *J. Biol. Chem.* **222** (1956) 109.
10. Fredrickson, D. S. and Ono, K. *Biochim. et Biophys. Acta* **22** (1956) 183.
11. Danielsson, H. *Biochim. et Biophys. Acta* **27** (1958) 401.
12. Danielsson, H. and Horning, M. G. *Biochim. et Biophys. Acta* **34** (1959) 596.
13. Danielsson, H. *Acta Chem. Scand.* **14** (1960). *In press.*
14. Bergström, S., Pääbo, K. and Rumpf, J. A. *Acta Chem. Scand.* **8** (1954) 1109.
15. Wilzbach, K. E. *J. Am. Chem. Soc.* **79** (1957) 1013.
16. Bergström, S. and Lindstedt, S. *Acta Chem. Scand.* **11** (1957) 1275.
17. Bergström, S., Danielsson, H. and Göransson, Å. *Acta Chem. Scand.* **13** (1959) 776.
18. Kazuno, T. *Hiroshima J. Med. Sci.* **6** (1958) 297.
19. Bergström, S., Bridgwater, R. J. and Gloor, U. *Acta Chem. Scand.* **11** (1957) 836.

Received September 28, 1959.

ACTA CHEMICA SCANDINAVICA 14 (1960) 353–358

The Chemistry of the Natural Order Cupressales

XXV *. Heartwood Constituents of *Juniperus chinensis L.*

CLAES PILO (in part) and JARL RUNEBERG

Organisk-kemiska Institutionen, Kungl. Tekniska Högskolan, Stockholm, Sweden

From the heartwood of *Juniperus chinensis* there were isolated: thujopsene, cuparene, cedrol, widdrol, hinokiic acid, "widdringtonia acid II", carvacrol, thymohydroquinone, 3-hydroxy-thymoquinone and 3,6-dihydroxy-thymoquinone. Paper chromatographic evidence was obtained for the presence of nootkatin, α-, and β-thujaplicin and gas chromatographic evidence for the presence of α-cedrene.

Most of the genera into which the family Cupressaceae has been divided botanically are small or monotypic. The largest genus, *Juniperus*, which is found almost only in the northern hemisphere is divided into two subgenera, *Oxycedrus* and *Sabina*, with altogether some 50—60 species. It thus appears to be particularly suitable for systematic chemical investigation.

Only a few juniper woods have been investigated before and interest has been mainly directed towards the constituents of the berries, leaves and bark [1,2].

Bredenberg and Gripenberg [3–5] made the interesting discovery that the diterpene sugiol and related compounds are present in *Juniperus communis* and Nakatsuka and Hirose [6] have found tropolones (nootkatin and β-thujaplicin) in *J. chinensis*. Cedrol and "cedrene" have frequently been found in juniper woods. However, they appear to be absent from those species of the subgenus *Oxycedrus* that have been investigated and Bredenberg has suggested that cedrol and cedrene might be characteristic of the *Sabina* junipers.

Thirty years ago Ushida [7] published a note on some constituents of the wood of *J. chinensis (Sabina)* and recorded an interesting "cedrol" of abnormally high rotation $[\alpha]_D + 85.4°$. Three years ago the sesquiterpene alcohol widdrol [8] (m.p. 98°, $[\alpha]_D + 105°$) from *Widdringtonia* was isolated in this institute and one of us (C.P.), working with Professor H. Erdtman, made a preliminary study of the wood of *J. chinensis* with the intention of comparing Ushida's "cedrol" with widdrol. Cedrol of normal optical properties was

* Part XXIV. *Acta Chem. Scand.* **14** (1960) 81.

easily obtained but some fractions had a higher rotation (up to about + 60°) and may have been similar to the preparation obtained by Ushida.

Other constituents isolated during this study included thymohydroquinone, a constituent of *Tetraclinis articulata* [9] and *Libocedrus decurrens* [10] that had not previously been found among the junipers, and a crystalline acid. Ultraviolet spectra of the ligroin-soluble part of the acid fraction indicated the presence of tropolones. A more detailed study has now been made (J.R.) of the extract from a larger sample of *Juniperus chinensis* heartwood.

J. chinensis is a native of China and Japan but the wood used in these investigations came from a tree grown in the Glasnevin National Botanic Garden, Dublin. Our thanks are due to Mr. T. Walsh, keeper, for kindly putting the wood at our disposal. It should be noted that the wood came from a tree that was probably killed by a fungal infection. It is therefore possible that some of the substances found, *e.g.* the hydroxythymoquinones (see below), do not occur in sound wood. An interesting case of changed metabolism due to infection has been described by Hasegawa and Shirato [11].

The air-dried wood was extracted with acetone and the light petroleum-soluble part of the extract was separated into neutral and acid fractions with alkali.

The tropolones were concentrated by precipitation from the ligroin soluble part of the acid fraction with cupric acetate, decomposition of the crude copper salts with hydrochloric acid and steam distillation. The fraction most volatile in steam gave 3-hydroxy-thymoquinone. According to paper chromatographic analysis the next fraction contained a mixture of nootkatin and α- and β-thujaplicins but in such small amounts that a separation was not attempted (Nakatsuka and Hirose obtained 6 g nootkatin and 0.3 g β-thujaplicin from 147 kg of wood).

Fractional distillation of the tropolone-free acid portion of the oil yielded thymohydroquinone, 3,6-dihydroxy-thymoquinone and carvacrol. The high-boiling fractions gave two sesquiterpene acids. One was identified as hinokiic acid ("widdrenic acid" [12]), recently isolated from a number of *Widdringtonia* species and also prepared by oxidation of thujopsene ("widdrene"). The other was found to be identical with the "Acid II", m.p. 192—194°, $[\alpha]_D$ −94°, from the same source [8].

The neutral portion of the oil was fractionally distilled. It contained only traces of monoterpenes or compounds of similar boiling point. The lowest boiling fraction was yellow and it was therefore expected that thymoquinone would be present but this could not be confirmed.

To check the possibility that the 3- and 3,6-hydroxylated thymoquinones might have been formed from thymoquinone during isolation, a solution of thymoquinone in light petroleum was shaken with either aqueous or ethanolic alkali in the presence of air. The product was chromatographed on paper by the method developed for tropolones by Wachtmeister and Wickberg [13]; this indicated that both the hydroxylated thymoquinones were present. Even though attempts to isolate thymoquinone from the wood failed, it is thus possible that the two hydroxythymoquinones are artefacts formed during the alkali extraction of the oil or as a result of *post mortem* enzymatic oxidation in the wood.

Since the presence of carvacrol methyl ether in the neutral oil was to be expected, a sample of the lowest boiling fraction was demethylated and chromatographed on paper. No carvacrol was detected but spots corresponding to two unidentified phenols were found.

The infrared spectrum of the rather large sesquiterpene fraction that followed resembled those of corresponding fractions isolated from *Widdringtonia* [8]. According to gas chromatographic analysis, fraction 2 (Table 1, see experimental part) contained four components. The substances were present approximately in the ratio 300:90:10:1, assuming complete resolution. The principal constituent was identified as thujopsene by conversion into the corresponding aldehyde by oxidation with selenium dioxide. The next largest constituent, according to gas chromatographic evidence, was α-cedrene. Fraction 3 (Table 1) contained the two main components in a ratio of 1:4, but the minor constituents could not be detected in this fraction.

The next higher boiling fraction was redistilled and treated with ozone at low temperature. From the material unaffected by ozone cuparene [14] was isolated.

According to the infrared spectrum the highest boiling fraction of the neutral material appeared to contain alcohols and carbonyl compounds.

The compounds isolated and a very approximate estimate of the amounts present are given below. The figures are subject to the uncertainties of the estimation and to the wide variations possible in biological material. The amounts are given as a percentage of the air-dried wood. Total acetone extract 8.37, ether-soluble acetone extract 7.48, light petroleum-soluble acetone extract 5.92, sodium bicarbonate-soluble 0.058, sodium hydroxide-soluble 0.83, soluble in ethanolic potassium hydroxide 0.43, neutral 4.6. Tropolones (nootkatin, α- and β-thujaplicin) 0.007, thymohydroquinone 0.018, 3-hydroxythymoquinone 0.0009, 3,6-dihydroxy-thymoquinone 0.0003, carvacrol 0.11, hinokiic acid 0.001, "Widdringtonia acid II" 0.061, thujopsene 0.27, cuparene 0.10, cedrol 1.7, widdrol 0.14, high-boiling carbonyl compounds 0.043.

EXPERIMENTAL

Rotations were measured in chloroform. Melting points, taken on a hot stage, are uncorrected. Light petroleum refers to the fraction b. p. 40—60°.

Isolation of the oils. Ground, air-dried heartwood (6.0 kg) was continuously extracted with acetone for 48 h. The acetone was evaporated and the remaining oil was poured with stirring into ten volumes of ether. The ether solution was filtered (precipitate 54 g), evaporated, and the rest similarly poured into ten volumes of light petroleum. After filtration (precipitate 94 g) the solution was evaporated to about three l and extracted successively with a saturated solution of sodium bicarbonate, with 2 N sodium hydroxide and with 2 N ethanolic potassium hydroxide. On acidification and extraction with ether the sodium bicarbonate solution yielded a viscous oil (3.5 g) which was not further investigated. The sodium hydroxide-soluble material (50.6 g) (A) was isolated in the same way by acidification of the alkaline solution and extraction with ether. The ethanolic potassium hydroxide solution was shaken several times with light petroleum, acidified and extracted with ether. The ether extract was washed with water and gave on evaporation a reddish brown oil (39.4 g) (B). The remaining petroleum ether solution was washed with water and evaporated yielding neutral material (260.8 g) (C).

I. *Alkali-soluble fraction.* The viscous product A (19.8 g) was dissolved in acetone, poured onto cotton wool and the acetone was evaporated. This material was then

extracted with hot ligroin (b. p. 100—125°) and the extract was shaken with a saturated solution of cupric acetate; the sticky copper salts were filtered off, washed with ligroin and water and decomposed with 2 N hydrochloric acid. The product was extracted with ether and the ether solution was washed with water, dried, and evaporated affording a resin (6.8 g) (A_1) which was steam distilled.

The first 100 ml of distillate deposited a small amount (20 mg) of orange red needles which gave a strong violet colour with sodium hydroxide. This substance was recrystallised from ethanol-water and sublimed, m. p. 168—170°, undepressed when mixed with an authentic sample of *3-hydroxy-thymoquinone* prepared from 2,4-dinitrothymol *via* 2,4-diaminothymol [15]. The infrared spectra of the two samples were identical.

The next 200 ml of steam distillate was extracted with ether. The ether extract on evaporation gave a syrupy material (314 mg) which according to paper chromatographic [13] evidence contained nootkatin and *α*- and *β*-thujaplicins in amounts decreasing in this order.

The ligroin solution remaining after the removal of the copper salts was evaporated and the residue was separated by distillation into lower boiling (b. p. below 180°/2 mm, 5.7 g) (A_2) and higher boiling (b. p. 180—184°/2 mm, 4.8 g) (A_3) fractions.

The material soluble in ethanolic potassium hydroxide (B) was subjected to a quick preliminary distillation. The fraction boiling below 160°/1.5 mm (B_1) was added to fraction A_2 and the combined material (27 g) was distilled through a spinning band column. On standing the fraction boiling at 117—152°/20 mm (2.4 g) deposited a small amount (6 mg) of bright red needles, which gave a strong violet colour with sodium hydroxide. This compound was recrystallised from 95 % ethanol and sublimed, m. p. 223—224°, undepressed when mixed with synthetic *3,6-dihydroxy-thymoquinone* prepared from thymoquinone *via* 3,6-bismethylamino-thymoquinone [16].

The fraction boiling at 117—152°/20 mm was found to contain mainly *carvacrol*. After 3,6-dihydroxy-thymoquinone had been removed by filtration a sample was converted into carvacroxyacetic acid, m. p. 150.0—151.5°, undepressed by an authentic sample.

The fraction b. p. 152—165°/20 mm crystallised on standing. This was a mixture of cedrol and widdrol (see below) indicating that the separation of neutral material from weak phenols had been unsatisfactory. (It has later been found that extraction with ethanolic potassium hydroxide should be avoided.)

The fraction b. p. 166°/20 mm (3.0 g) was dissolved in ether and extracted with 2 N sodium hydroxide. Acidification of the alkaline solution furnished a product (330 mg), which was recrystallised from ether-light petroleum and sublimed, m. p. 145.0—145.5°, undepressed by an authentic sample of *thymohydroquinone*.

A part of product A (22.4 g) was fractionally distilled in a vacuum. The fraction boiling between 145—175°/0.8 mm (8.1 g) crystallised partly on standing. It was dissolved in ether and the solution was extracted with 2 N sodium carbonate. On acidification the alkaline solution afforded a substance (1.4 g) which was recrystallised from ether, m. p. 192—194°, $[\alpha]_D$ −94° (*c*, 1.3). It was identified (mixed m. p., I.R.) as *Acid II* from *Widdringtonia* [8].

Table 1. Distillation of fraction C_1. Total distillate 107 g or 79 %.

Fraction	Weight (g)	B.p./21 mm (°C)	Rotation $[\alpha]_D$	Refractive index (n_D^{21})
1	5.3	124—136	−48.7	1.4990
2	14.5	136—137	−70.5	1.5025
3	7.5	137—141	−70.8	1.5041
4	18.1	141—165	+ 8.8	1.5088
5	27.1	165—166	+13.9	—
6	28.1	166	+14.7	—
7	6.6	166	+66.7	—

In another experiment a similar fraction of the sodium hydroxide soluble oil on treatment with light petroleum partly crystallised. Recrystallisation from methanol-water afforded thymohydroquinone. The methanol-water mother liquor was evaporated and the residue combined with the material soluble in light petroleum. On standing for several months the combined oils deposited another compound (0.2 g), which was recrystallised from methanol-water, m. p. 169.5—170.5°, $[\alpha]_D$ −86° (*c*, 1.3). It was identified as *hinokiic acid* [12] (mixed m. p., I.R.).

II. *Neutral fraction:* A quick preliminary distillation of the neutral oil C afforded a product boiling below 160°/3 mm (C_1) and a higher boiling residue (C_2). C_1 on fractional distillation through a vacuum-jacketed, packed column, gave the fractions listed in Table 1.

Attempts to demonstrate the presence of thymoquinone in fraction 1 (Table 1): Fraction 1 (0.5 g) was suspended in water (20 ml) saturated with sulphur dioxide and allowed to stand for a week. The solution was extracted with ether and the ether extract was washed with water and evaporated. The residue, like the starting material, was yellow and afforded no acidic material on extraction of a solution in light petroleum with 2 N potassium hydroxide.

No phenolic material was obtained on reduction with zinc and acetic acid.

Demethylation of Fraction 1 (Table 1): Fraction 1 (1.5 g) in glacial acetic acid (6 ml) was refluxed with hydrobromic acid (48 %, 8 ml) for 1 h. The reaction mixture was extracted with light petroleum, the organic phase was extracted with 2 N ethanolic potassium hydroxide and the alkaline extract was acidified, extracted with light petroleum, washed with water dried and evaporated affording an oil (0.48 g). This was examined by paper chromatography [13]. No spot corresponding to carvacrol was found but two spots of higher R_F value were observed.

Gas chromatographic examination of the sesquiterpene fraction: A Perkin-Elmer Vapor Fractometer Model 154 was used together with a Speedomax Type G (Leeds & Northrup Co.) recorder. (Column length 2 m, internal column diameter 5 mm, stationary phase 60—80 mesh celite, impregnated with 2,4-dinitrophenyl-2-naphthyl ether (m. p. 95°C) in the proportion of 25 % by weight [17], charge 1 μl, temperature 145°, flow of helium 64 ml per minute.)

The following peaks were obtained (Recorder deflection (mV) given as a function of time (min)). Fraction 2 (Table 1): 1.1 (15.4), 4.2 (16.9). Fraction 3 (Table 1): 0.4 (11.9), 1.6 (15.4), 4.7 (16.9). Pure α-cedrene, prepared from cedrol [18] gave a peak at 15.4 min and pure thujopsene [12] gave a peak at 16.9 min.

Thujopsene: Fraction 2 (Table 1) (1.0 g) was dissolved in 95 % ethanol (20 ml) and selenium dioxide (0.6 g) was added. The solution was refluxed for 4 h, filtered and evaporated to dryness. The product on sublimation yielded a substance (160 mg) which was recrystallised from light petroleum, m. p. 74.5—75.5°. It was identified as widdrenal (mixed m. p., I.R.).

The infrared spectrum of fraction 4 (Table 1) showed medium height aromatic absorption at 1 527 cm^{-1}. This fraction (17.3 g) was redistilled through a spinning band column yielding the fractions listed in Table 2.

Table 2. Redistillation of fraction 4 (Table 1.) (17.3 g.) Total distillate 14.8 g, 86 %.

Fraction	Weight (g)	B.p./20 mm (°C)	Rotation $[\alpha]_D$	Refractive index (n_D^{21})
1	1.06	141—146	−59.8	1.5033
2	1.04	146	−60.8	1.5040
3	2.18	146—149	−26.7	1.5062
4	3.14	149—151	+18.7	1.5104
5	1.23	151	+67.5	1.5127
6	1.81	151—155	+62.0	1.5133
7	0.77	155	+27.1	1.5121
8	1.00	155—168	+13.6	1.5077
9	2.58	168	+11.4	—

Cuparene. Fractions 5 and 6 (Table 2) were combined and a sample (2.2 g) in methylene chloride (15 ml) was ozonised at −70°C until an excess of ozone was indicated by the appearance of a blue colour. The reaction mixture was then treated with hydrogen peroxide (30 %, 4 ml) in potassium hydroxide (10 %, 1.5 ml) added dropwise at room temperature. Water (30 ml) was added, the organic phase was separated and the water phase extracted with methylene chloride. The methylene chloride solution was evaporated and the residue was chromatographed on basic aluminium oxide (50 g). Light petroleum (100 ml) eluted a colourless oil (760 mg) which was fractionally distilled. The main fraction b.p. 117°/7 mm, $[\alpha]_D$ +65°, n_D^{21} 1.5230, was identified as cuparene [14] by comparison of the infrared spectrum with that of an authentic sample.

Cedrol: Fraction 6 (Table 1) was recrystallised four times from 95 % ethanol, m. p. 88.0−88.5°, $[\alpha]_D$ +10.4° (*c*, 3.2). The compound was identified as cedrol (mixed m. p., I.R.).

Widdrol: The mother liquor from the first recrystallisation of cedrol was concentrated and two further crops of crystalline material collected. The non-crystalline material (2.5 g) was chromatographed on basic aluminium oxide (200 g). Benzene eluted an oily material which was not investigated; benzene-ether (1:1) eluted mainly cedrol and ether eluted a substance, $[\alpha]_D$ +95° (*c*, 2.5), which was recrystallised from light petroleum and sublimed twice along a temperature gradient, m. p. 98.0−99.0°, $[\alpha]_D$ +105° (*c*, 1.0) identical with widdrol [8] (mixed m. p., I.R.).

The high-boiling neutral fraction: The residue from the distillation described in Table 1 was combined with the distillation residue C_2. A sample of the combined material (C_3) was fractionally distilled through a spinning band column. 65 % of the oil distilled between 143°/10 mm and 183°/5 mm. A main fraction (43 %) was obtained at 160−165°/10 mm ($[\alpha]_D$ +1.1°). According to infrared spectra all the fractions seemed to be rather complex mixtures showing strong hydroxyl and carbonyl bands.

On separation using Girard D reagent the oil C_3 gave 12 % of a mixture of carbonyl compounds. This material showed no hydroxyl absorption and on chromatography gave only liquid fractions.

The authors are indebted to Professor H. Erdtman for his interest in this work, to Miss G. Hammarberg for the infrared and ultraviolet spectra, and to *the Swedish Natural Science Research Council* for financial support.

REFERENCES

1. Bredenberg, J. B. *Acta Chem. Scand.* **11** (1957) 98.
2. Herout, V. and Sykora, V. *Tetrahedron* **4** (1958) 250.
3. Bredenberg, J. B. and Gripenberg, J. *Acta Chem. Scand.* **8** (1954) 1728.
4. Bredenberg, J. B. *Acta Chem. Scand.* **11** (1957) 927.
5. Bredenberg, J. B. *Acta Chem. Scand.* **11** (1957) 932.
6. Nakatsuka, T. and Hirose, Y. *J. Japan. Forestry Soc.* **37** (1955) 196; *Chem. Abstr.* **50** (1956) 5238 h.
7. Ushida, S. *J. Soc. Chem. Ind. Japan (Suppl.)* **31** (1928) 190 B; *Chem. Zentr.* **1928 : II** 2198.
8. Erdtman, H. and Thomas, B. R. *Acta Chem. Scand.* **12** (1958) 267.
9. Grimal, E. *Compt. rend.* **139** (1904) 927.
10. Zavarin, E. and Anderson, A. B. *J. Org. Chem.* **20** (1955) 82.
11. Hasegawa, M. and Shirato, T. *J. Japan Forestry Soc.* **41** (1959) No. 1.
12. Erdtman, H. and Norin, T. *Acta Chem. Scand.* **13** (1959) 1124.
13. Wachtmeister, C. A. and Wickberg, B. *Acta Chem. Scand.* **12** (1958) 1335.
14. Enzell, C. and Erdtman, H. *Tetrahedron* **4** (1958) 361.
15. Carstanjen, E. *J. prakt. Chem.* **2** 15 (1877) 399.
16. Zinke, Th. *Ber.* **14** (1881) 95.
17. Groth, A. B. *Svensk Papperstidn.* **61** (1958) 10, 315.
18. Naves, Y. R., Papazian, G. and Perrottet, E. *Helv. Chim. Acta* **26** (1943) 315.

Received September 30, 1959.

ACTA CHEMICA SCANDINAVICA 14 (1960) 359–378

On the Constitution of Phenolphthalein Oxime and Related Compounds

HENNING LUND

Leo Pharmaceutical Products, Ballerup, Denmark

Phenolphthalein oxime is suggested to be a *p*-hydroxyanil of *o*-(*p*-hydroxybenzoyl)benzoic acid. Chemical evidence, infrared spectra, and polarographic data supporting the proposed constitution are presented. Structures for the "pseudoanilides" and "anilides" of *o*-benzoylbenzoic acids are suggested. According to the proposed constitution of phenolphthalein oxime a new rearrangement, which ressembles that of the Lossen degradation, occurs during the formation of the compound.

Phenolphthalein reacts in alkaline solution with hydroxylamine and a yellow, insoluble compound is obtained on acidifying with acetic acid [1]. Friedländer assumed that the compound was an oxime of the quinoid form of phenolphthalein and suggested formula I accordingly. The phenolphthalein oxime was found to be hydrolysed by mineral acid to *o*-(*p*-hydroxybenzoyl)-benzoic acid and *p*-aminophenol, and the latter was assumed to be obtained by a rearrangement of the supposed primarily formed phenylhydroxylamine. Shortly after, however, Friedländer [2] abandoned the structure I, as it did not explain the behaviour of the oxime of 3',5',3'',5''-tetrabromophenolphthalein, which on acid hydrolysis yielded 2,6-dibromo-4-aminophenol instead of 3,5-dibromo-4-aminophenol expected from I.

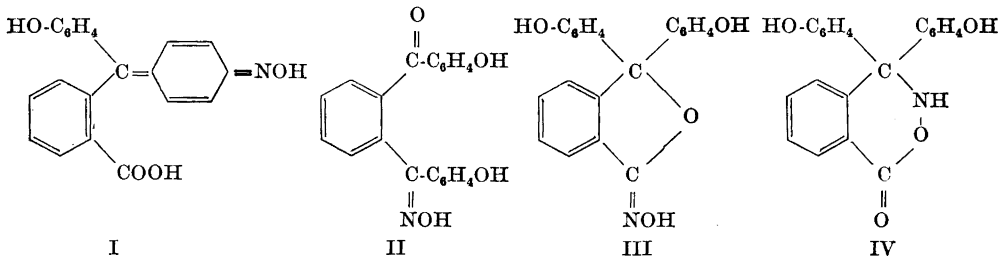

I II III IV

Later H. Meyer [3] proposed formula II and R. Meyer [4] discussed the structures III and IV without deciding between them. Orndorff and Murray [5] adopted the formula V, which H. Meyer [6] previously had considered, and this seemed to be common accepted constitution for many years. Some inconsistencies of this formulation with the experimental facts were pointed out by Lund [7] who instead proposed the structures VI, which take in consideration the tautomerism found in this series of compounds.

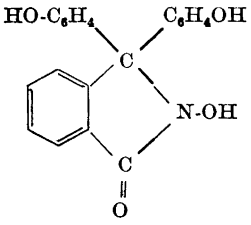

V

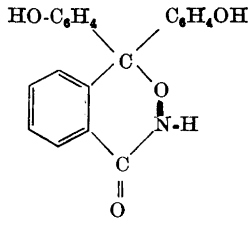

VI a

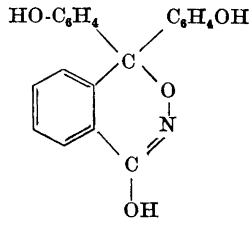

VI b

Although the proposed formulations are rather different, all but II assume that the *p*-hydroxyphenyl groups are bonded to the central carbon atom in the same manner as in phenolphthalein.

The purpose of the present investigation was to decide between the proposed structures of phenolphthalein oxime, and to this end a chemical, spectrophotometric, and polarographic investigation of the compound and derivatives thereof was undertaken.

CHEMICAL INVESTIGATION

It has long been known [8] that phenolphthalein oxime on reaction with dimethyl sulfate in alkaline solution yields a yellow trimethyl ether, which on boiling with alcoholic potassium hydroxide splits off one methyl group thus forming a dimethyl ether. This dimethyl ether can exist as a yellow and a colourless compound [7], which are readily interconvertible. On boiling with acetic anhydride it rearranges into 2-(4'-methoxybenzoyl)benz-*p*-anisidide (VIIa or VIIb, R = R' = OCH_3). On hydrolysis of the dimethyl ether with mineral acid *o*-(*p*-anisoyl) benzoic acid and *p*-anisidine are obtained.

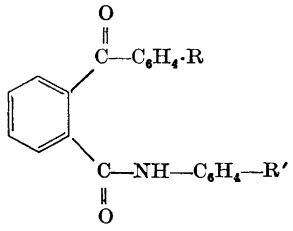

VII a

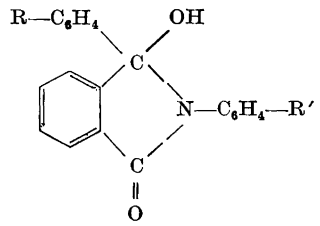

VII b

As might have been expected the mixed anhydride made from *o*-(*p*-methoxybenzoyl) benzoic acid and ethyl chloroformate reacted with *p*-anisidine yielding *o*-(*p*-methoxybenzoyl)benz-*p*-anisidide. When *o*-(*p*-methoxybenzoyl)benzoic acid, however, was treated with excess of thionyl chloride and the resulting chloride, after removing the excess of thionyl chloride *in vacuo*, reacted with *p*-anisidine in dry benzene, a compound was obtained in high yield, which proved to be phenolphthalein oxime dimethyl ether.

If it is assumed that phenolphthalein oxime dimethyl ether has one of the structures previously proposed with the two *p*-methoxyphenyl groups bonded to the central carbon atom one of the anisyl groups must have come from the anisoylbenzoic acid and the other one by some rearrangement from the *p*-anisidine. It would, however, in the phenolphthalein oxime dimethyl ether be impossible to determine which group has come from the acid and which one from the amine. Only one compound would, therefore, be expected to be formed in the reaction between *o*-(*p*-anisoyl)benzoic acid chloride and aniline and in the reaction between *o*-benzoylbenzoic acid chloride and *p*-anisidine.

When *o*-(*p*-anisoyl)benzoic acid after treatment with thionyl chloride reacted with aniline an "*o*-(*p*-anisoyl)benz-pseudoanilide" was formed with properties similar to that of phenolphthalein oxime dimethyl ether. On hydrolysis with mineral acid only *o*-(*p*-anisoyl)benzoic acid and aniline were obtained. The compound rearranged on boiling with acetic anhydride to "*o*-(*p*-anisoyl)benzanilide" with a structure represented by VII a or b (R = OCH_3, R' = H).

o-Benzoylbenzoic acid, after treatment with thionyl chloride, reacted with *p*-anisidine yielding an "*o*-benzoylbenz-pseudo-*p*-anisidide", which, too, had properties very similar to those of phenolphthalein oxime dimethyl ether. This compound had previously been obtained by H. Meyer [9] by heating a mixture of *o*-benzoylbenzoic acid and *p*-anisidine. On boiling with mineral acid *o*-benzoylbenzoic acid and *p*-anisidine were obtained, and as found by Meyer it reacted with phenylhydrazine yielding "benzoylbenzoic acid phenylhydrazone", *i.e.* 2,4-diphenyl-phthalazin-1-one. On boiling with acetic anhydride the "*o*-benzoylbenz-pseudo-*p*-anisidide" rearranged into "*o*-benzoylbenz-*p*-anisidide" (VIIa or b, R = H, R' = OCH_3).

As the "*o*-(*p*-anisoyl)benz-pseudoanilide" is not identical with "*o*-benzoylbenz-pseudo-*p*-anisidide" it follows that the two *p*-anisyl groups in phenolphthalein oxime dimethyl ether are not bonded in the same manner to the central carbon atom. None of the previously suggested structures can account for this fact and must, therefore, be rejected.

Instead are proposed the following constitutions for phenolphthalein oxime (VIII), its dimethyl ether (IXa and b; R = R' = OCH_3), and trimethyl ether (XIV). Whether the compounds VIII and IXa exist in solution as zwitterions or with an undissociated carboxyl group is not known; in the solid state the oxime is assumed to possess the zwitterion structure.

This formulation, where phenolphthalein oxime is a *p*-hydroxyanil of *o*-(*p*-hydroxybenzoyl)benzoic acid, requires that during the formation of the oxime a rearrangement, not previously described, of the type found in the Lossen degradation occurs.

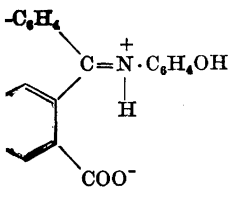

VIII

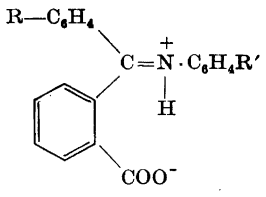

a

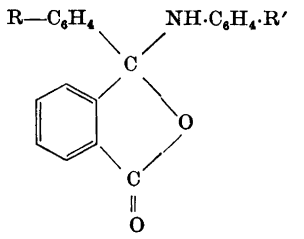

b

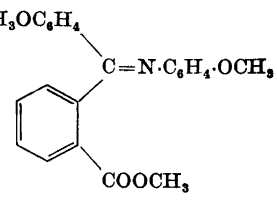

XIV

IX R = R′ = OCH_3
X R = OCH_3; R′ = H
XI R = H; R′ = OCH_3
XII R = R′ = H
XIII R = OCH_3; R′ = OH

The constitution of the oxime assumed here is in accordance with the hydrolysis of the oxime in mineral acid and alkaline solution to *o*-(*p*-hydroxybenzoyl)benzoic acid and *p*-aminophenol. The formation of 2,6-dibromo-4-aminophenol on hydrolysis of the oxime of 3',5',3'',5''-tetrabromophenolphthalein is expected from this formulation. The solubility of the phenolphthalein oxime and its dimethyl ether in alkali, the insolubility in alkali of the trimethyl ether, the alkaline hydrolysis of the trimethyl ether to the dimethyl ether, and the hydrolysis of "*o*-(*p*-anisoyl)benz-pseudoanilide" (X) to *o*-(*p*-anisoyl) benzoic acid and aniline and the hydrolysis of "*o*-benzoylbenz-pseudo-*p*-anisidide" (XI) to *o*-benzoylbenzoic acid and *p*-anisidine are readily understood from the structures VIII to XIV. The difference in colour of the phenolphthalein oxime at pH 10 and 13 [1] is explained by the successive dissociation of the three acidic groups, and the yellow and the colourless form of the phenolphthalein oxime dimethyl ether [7] correspond to IXa and b, respectively.

A titration curve of phenolphthalein oxime has not been obtained due to the insolubility of the compound at pH-values lower than 7, but on rapid titration of the hydrochloride of the dimethyl ether in 50 % alcohol with 0.1 N NaOH a pK-value of 5.8 was found for the supposed carboxyl group under conditions, where the pK-value of *o*-(*p*-anisoyl)-benzoic acid was found to be 5.0.

The solubility of phenolphthalein oxime and its ethers in mineral acid is assumed to be due to the presence of the azomethine group. Benzophenone anil and benzophenone *p*-hydroxyanil are soluble in mineral acid, and the latter is claimed by Reddelin [10] to require boiling with strong mineral acid for hydrolysis.

The phenolphthalein oxime contains one mole of water of crystallization which is not removed by drying in high vacuum at 100°C over phosphorus pentoxide for 18 h. On raising the temperature to 120°C for 18 h most of the water was removed, but still about 0.3 mole of water of crystallization was found by a Fischer-titration. This might explain the low values for carbon

and high values for hydrogen reported by Friedländer [1] for the analysis of the phenolphthalein oxime.

Phenolphthalein reacts with N-methyl hydroxylamine analogously with the reaction with hydroxylamine yielding a compound similar to phenolphthalein oxime; the compound is hydrolysed to *o*-(*p*-hydroxybenzoyl)benzoic acid and N-methylaminophenol [7]. This "phenolphthalein N-methyl-oxime" also contains one mole of water of crystallization which is difficult to remove. The yellow "phenolphthalein N-methyl-oxime" is soluble in alkali and acid yielding a yellow solution, but the solution in ether or dioxane is colourless. The yellow form is assumed to possess the structure XVa, whereas the colourless form would be represented by XVb. None of the previously suggested formulations allow the "phenolphthalein N-methyl-oxime" to exist in two forms.

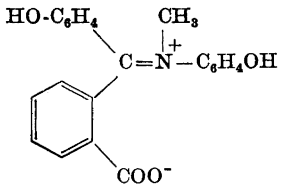

XV a

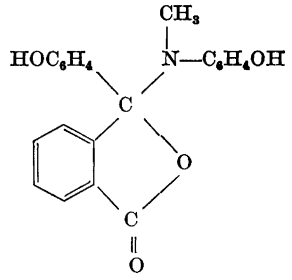

XV b

o-(*p*-Anisoyl)benzoic acid reacts after treatment with thionyl chloride with N-methylaniline yielding a white compound, which dissolves in acid with a yellow colour. The colourless form of "*o*-(*p*-anisoyl)benz-pseudo-N-methylanilide" is assumed to have a structure similar to XVb, whereas in acid solution a protonated form corresponding to XVa is likely.

From a similar reaction between the acid chloride of 2-benzoylbenzoic acid and N-methylaniline Wawzonek *et al.*[11] isolated a white compound which they assumed to be a non-cyclic normal N-methylanilide with the nitrogen bonded to the carboxyl carbon atom. In view of the similarities with the above mentioned "*o*-(*p*-anisoyl)benz-pseudo-N-methylanilide" it seems likely that the compound obtained by Wawzonek *et al.* is "*o*-benzoylbenz-pseudo-N-methylanilide" with a structure similar to XVb.

Phenolphthalein monomethylether reacts with hydroxylamine yielding a "phenolphthalein monomethylether oxime" (XIII), which is hydrolyzed on boiling with mineral acid to *o*-(*p*-anisoyl)benzoic acid and *p*-aminophenol. The same compound is formed by action of *p*-aminophenol on the chloride obtained from *o*-(*p*-anisoyl)benzoic acid on treatment with thionyl chloride.

On reaction with diazomethane in a mixture of ether and dioxane the phenolphthalein oxime yields a mixture of different methylated compounds from which phenolphthalein oxime trimethyl ether and a dimethyl ether were isolated. This dimethyl ether was different from IX as it was hydrolyzed by alcoholic potassium hydroxide to "phenolphthalein monomethylether oxime" (XIII).

A mechanism of the postulated rearrangement, which proceeds during the formation of phenolphthalein oxime, is presented below.

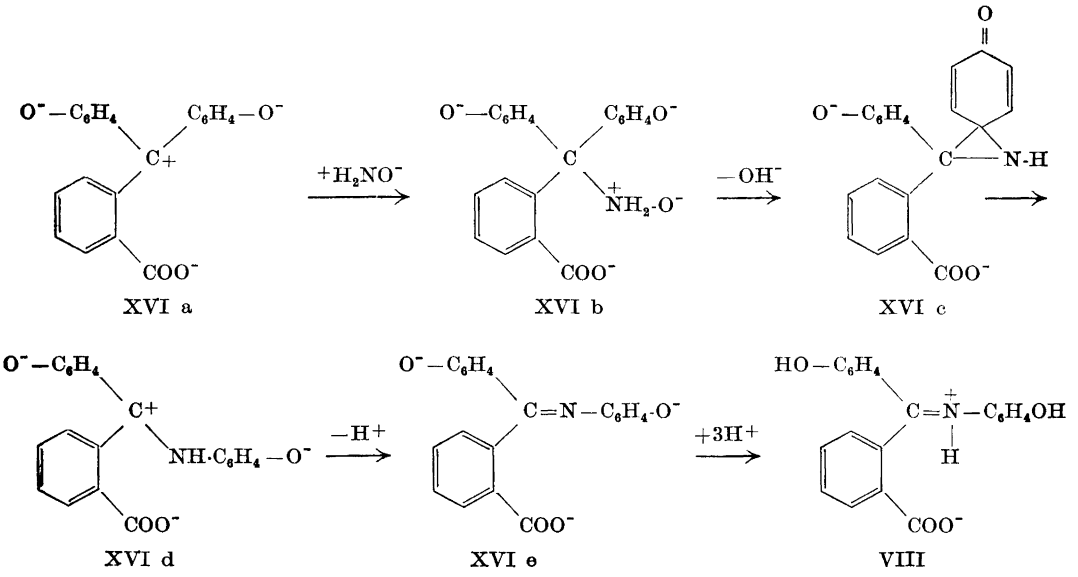

The structure XVIa is one of the resonance structures of phenolphthalein in alkaline solution. This carbonium ion is assumed to react with the anion of hydroxylamine forming a bond between carbon and nitrogen. The migration of the phenyl group requires the formation of a quinoid form of the phenyl group, and the plane of the migrating phenyl group is at a right angle to the plane of the three-membered ring. After completion of the migration the carbonium ion XVId loses a proton, and on addition of acid the phenolphthalein oxim (VIII) precipitates.

This mechanism is in agreement with many features found in the reaction between phenolphthalein and hydroxylamine. It has been found [12] that only phthaleines containing at least one *p*-hydroxyphenyl group are able to form oximes. The mechanism suggested above makes that requirement understandable. If, however, a nitro group is present *ortho* to the hydroxyl group it is found that the phthalein does not form an oxime; thus 3',3''-dinitrophenolphthalein forms no oxime, whereas 3',5'-dinitrophenolphthalein does [12]. This is explained by the formation of an *aci*-form of the nitro group in alkaline solution containing an *o*-quinoid structure, which excludes the possibility of a *p*-quinoid form of the phenyl group during the migration.

Furthermore, the formation of N-(*p*-hydroxyphenyl)phthalimide on reaction of phenolphthalein with excess of hydroxylamine can be explained by assuming that the carbonium ion XVId reacts with hydroxylamine analogously with the carbonium ion XVIa with the migration of the second *p*-hydroxyphenyl group. The compound formed would split off one mole of *p*-aminophenol and yield N-(*p*-hydroxyphenyl)phthalimide.

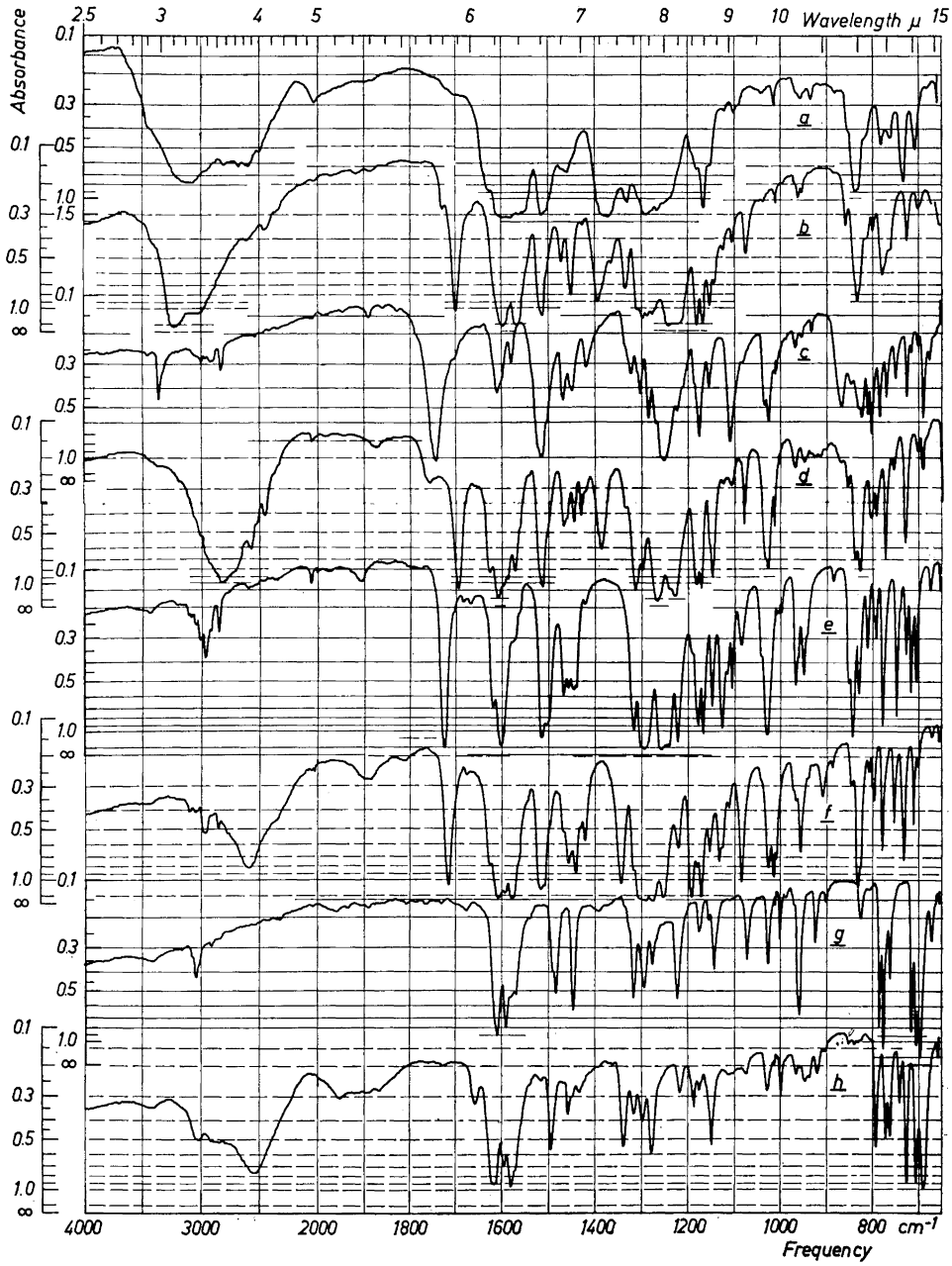

Fig. 1. Infrared spectra (potassium bromide) of phenolphthalein oxime (a), its hydrochloride (b), phenolphthalein oxime dimethyl ether (c), its hydrochloride (d), phenolphthalein oxime trimethyl ether (e), its hydrochloride (f), benzophenone anil (g), and its hydrochloride (h).

Fluorescein does not form an oxime on treatment with hydroxylamine which might be understood as a migration of one of the phenyl groups is hindered by the oxygen bridge between them. Hydroquinonephthalein [8] forms 3 "oximes" on reaction with hydroxylamine, but as they on hydrolysis with mineral acid yield hydroquinonephthalein [8] their constitution must be different from that of phenolphthalein oxime.

SPECTROPHOTOMETRIC INVESTIGATION

The infrared spectra were obtained using potassium bromide discs which had been kept at 100°C for 2—3 minutes before the spectra were recorded following the procedure of Buur Jensen [13].

The spectrum of phenolphthalein oxime (Fig. 1a) shows a strong absorption from 3 500 cm^{-1} to 2 300 cm^{-1}. The absorption between about 2 800 cm^{-1} and 2 300 cm^{-1} is believed to be an "ammonium band" [14] and the absorption about 2 040 cm^{-1} an "immonium band" [14], both of which would be expected from the structure VIII. The strong absorption from 1 615 cm^{-1} to 1 550 cm^{-1} is assumed to contain the phenyl bands and the bands of the carboxylate ion. In this respect the spectrum of the phenolphthalein oxime resembles those of many amino acids. A shoulder at 1 630 cm^{-1} may be due to the azomethine group. The absence of any absorption from 1 800 cm^{-1} to 1 640 cm^{-1} makes the structures I, II, IV, and V very unlikely, whereas III and VIb would not be expected to have absorption in this region; however, the presence of the "ammonium band" excludes III.

The hydrochloride of phenolphthalein oxime (Fig. 1b) has an absorption band at 1 700 cm^{-1} which is attributed to the presence of an unionized carboxyl group. It may be recalled [15] that the carboxyl group of the hydrochlorides of β- and γ-amino acids generally have a carbonyl absorption in the region 1 730 cm^{-1} to 1 700 cm^{-1} and aromatic carboxyl groups at 1 700 cm^{-1} to 1 680 cm^{-1}. This is in accordance with VIII, whereas it seems more difficult to accept that the hydrochloride of VIb would absorb about 1 700 cm^{-1}, when VIb as zwitterion does not do so.

The colourless form of phenolphthalein oxime dimethyl ether (Fig. 1c) has a sharp absorption peak at 3 390 cm^{-1} which is attributed to an N—H stretching frequency. A carbonyl absorption is found at 1 750 cm^{-1}, which also is present in phthalide and substituted phthalides as phenolphthalein and its dimethyl ether. Both the presence of the N—H stretching frequency and the phthalide ring is required by the suggested structure IXb and excludes the formulations I, II, III and V. The yellow form (IXa) has not been obtained free from the colourless dimethyl ether in the solid state, why no spectrum of this compound can be presented.

In the spectrum of the hydrochloride of phenolphthalein oxim dimethyl ether (Fig. 1d) a carbonyl absorption band is found at 1 700 cm^{-1} as in the hydrochloride of the oxime itself, which also would be expected from IXa.

It might be mentioned that in all the compounds containing an aryl methyl ether a band of medium intensity is found between 1 040 cm^{-1} and 1 025 cm^{-1} besides the strong ether band about 1 250 cm^{-1}. A similar observation has been made by Colthup [16].

The carbonyl absorption of phenolphthalein oxime trimethyl ether (Fig. 1e) is at 1 726 cm^{-1}. This is in accordance with the structure XIV which contains an aryl ester group, and the normal frequency for aryl esters is in the region 1 730 cm^{-1} to 1 717 cm^{-1} [15]. A band of medium intensity at 1 620 cm^{-1} might be attributed to the presence of the azomethine group. In the hydrochloride (Fig. 1f) of the trimethyl ether a similar band is found at 1 625 cm^{-1}. The carbonyl frequency at 1 717 cm^{-1} is attributed to an ester group as in XIV. The "ammonium band" and "immonium band" required by the suggested structure is found about 2 600 cm^{-1} and 1 900 cm^{-1}, respectively.

For comparison the spectra of benzophenone anil (Fig. 1g) and its hydrochloride (Fig. 1h) are presented, and the similarities in the spectra of the phenolphthalein oxime trimethyl ether and the benzophenone anil on the one hand and their hydrochlorides on the other support the proposed structures.

The spectra of "*o*-(*p*-anisoyl)benz-pseudoanilide" (X), "*o*-benzoylbenz-pseudo-*p*-anisidide" (XI) and "*o*-benzoylbenz-pseudoanilide" (XII) are similar to that of the colourless form of phenolphthalein oxime dimethyl ether in that they contain an N—H stretching frequency about 3 390 cm^{-1} and a carbonyl absorption about 1 750 cm^{-1}. They are, therefore, believed to possess structures similar to IXb in the solid state.

The yellow compound, *o*-(*p*-methoxybenzoyl)benz-pseudo-2,6-dimethyl-anilide, obtained from the action of 2,6-xylidine on the acid chloride from *o*-(*p*-anisoyl)benzoic acid and thionyl chloride, yields a spectrum without a N—H absorption about 3 400 cm^{-1} and with a carbonyl absorption at 1 711 cm^{-1}. This is attributed to an unionized carboxyl group, although the frequency is slightly higher than the usual one for aromatic carboxyl acids. The structure XVII is suggested for the compound in the solid state. The presence of the azomethine group is in accordance with the yellow colour. It is noteworthy that the two methyl groups in the xylidine nucleus prevent the formation of a phthalide structure or a zwitterion. However, the absorption from 2 800 cm^{-1} to 2 300 cm^{-1} attributed to the O—H stretching vibrations of the carboxyl group might contain an amount of "ammonium"-absorption.

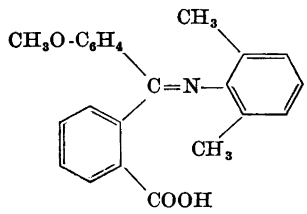

XVII

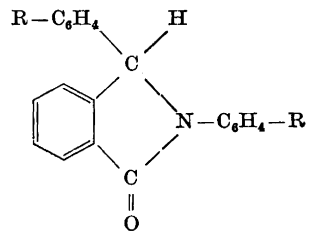

XVIII

The spectrum of "phenolphthalein N-methyl-oxime" in potassium bromide is similar to that of the phenolphthalein oxime, but in a dioxane solution, which is colourless, the spectrum is quite different. In the dioxane solution the "phenolphthalein N-methyl-oxime" shows a strong carbonyl absorption at 1 760 cm^{-1} which suggests the presence of a phthalide ring. As some absorp-

tion about 1 750 cm^{-1} is found in the spectrum obtained in potassium bromide it is possible that a certain amount of the compound contains the lactone form in the solid state. The analysis seems to exclude that the presence of the absorption at 1750 cm^{-1} (in potassium bromide) is due to a small content of unreacted phenolphthalein. The spectra are thus in accordance with the structures XVa and b.

The white compounds, "*o*-(*p*-anisoyl)benz-pseudo-N-methylanilide" and "*o*-(*p*-anisoyl)benz-pseudo-N-methyl-*p*-anisidide" contain a carbonyl absorption about 1 760 cm^{-1} and no other carbonyl absorption. A structure as that suggested by Wawzonek *et al.*[11] for "*o*-benzoylbenz-pseudo-N-methylanilide" containing a keto and an amide group is thus unlikely for these compounds, and a structure similar to XVb is suggested. This structure is also in accordance with the fact that the compounds are hydrolyzed by cold, dilute alkali, which would not be expected for a normal anilide.

The "*o*-(*p*-anisoyl)benz-*p*-anisidide", obtained from phenolphthalein oxime dimethyl ether on treatment with acetic anhydride [7], yields a spectrum containing a broad absorption around 3 250 cm^{-1}, which is attributed to the presence of a hydroxyl group. A carbonyl absorption is found at 1 675 cm^{-1} and a small shoulder is visible at 1 660 cm^{-1}. This suggests that in the solid state most of the compound is found in the cyclic form VIIb and a minor part possesses the open chain structure VIIa.

The compounds obtained on treatment of the "pseudoanilides" and "pseudoanisidides" with acetic anhydride yield similar spectra and are assumed to exist mainly in the cyclic form corresponding to VIIb with varying contents of the open chain structure. The presence of the methoxy groups seems to favour the cyclic form, and in *o*-benzoylbenzanilide the diaryl ketone group manifests itself as a band with medium intensity at 1 660 cm^{-1} indicating that an appreciable amount of this compound possesses the open chain structure.

Whereas the spectrum of *o*-(*p*-anisoyl)benz-N-*cyclo*hexylamide, obtained from the acid chloride and *cyclo*hexylamine, only suggests the presence of the cyclic structure of the amide, the *o*-benzoylbenz-N-ethylamide shows three carbonyl bands (1 689 cm^{-1}, 1 676 cm^{-1}, 1 660 cm^{-1}) indicating the presence of approximately equal amounts of both forms in the solid state.

On controlled potential reductions of phenolphthalein oxime was obtained a compound with a carbonyl absorption at 1 645 cm^{-1} which is in accordance with the structure XVIII suggested by H. Meyer [17] for the reduction product obtained from the action of zinc on phenolphthalein oxime.

The spectrum in carbon tetrachloride of the acid chloride from thionyl chloride and *o*-benzoylbenzoic acid contains a carbonyl band at 1 790 cm^{-1} and no bands between 1 760 cm^{-1} and 1 620 cm^{-1}. As no diaryl ketone thus is present it is likely that the chloride exists in the cyclic form XIX, which supports the formulation of the reaction products of the chloride and aromatic amines.

The "*o*-(*p*-anisoyl)benz-pseudo-ethyl ester", formed on reaction between the acid chloride and ethanol, shows in potassium bromide and in chloroform solution a carbonyl band at 1 765 cm^{-1} indicating the presence of a phthalide ring and the spectrum contains no absorption corresponding to a diaryl ketone. The spectrum is thus in accordance with the structure XX.

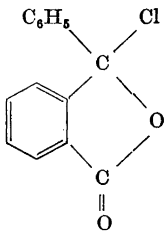

XIX

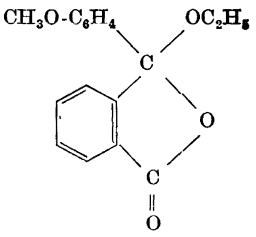

XX

The carbonyl absorption of the "α-oxime" of hydroquinonephthalein is found about 1 680 cm^{-1}. The formula proposed by Meyer [8] for this white compound contains a ring system similar to that (V) suggested by Orndorff and Murray [5] for the phenolphthalein oxime. The spectrum of the "α-oxime" seems not to exclude the structure proposed by Meyer.

The anhydride of the oxime of *o*-(*p*-anisoyl)benzoic acid, 4-(4'-methoxyphenyl)-2,3-benzoxazin-1-one, XXI has a spectrum containing a carbonyl absorption at 1 730 cm^{-1}, whereas the anhydride of the phenylhydrazone of 2-benzoylbenzoic acid, 2,4-diphenyl-phthalazin-1-one, XXII, absorbs at 1 660 cm^{-1}.

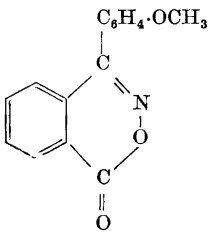

XXI

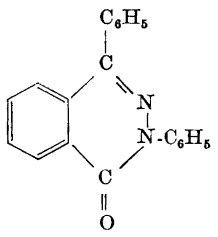

XXII

POLAROGRAPHIC INVESTIGATION

Phenolphthalein has been investigated polarographically by Kolthoff *et al.*[17,18] The compound was assumed to be reduced in a 2 electron reduction to phenolphthalin which in this investigation has been confirmed by controlled potential reduction. The wave showed in certain media a characteristic minimum, and at higher alcohol concentrations the height of the wave was dependent upon the alcohol concentration in such a way, that the wave height diminished at higher alcohol concentrations and became rate controlled [18]. It was assumed that the current below pH 7 was determined by the rate of the transformation of phenolphthalein through its anion into a quinoid form, which was reduced. Some experimental facts, however, seem to be incompatible with this assumption. It would be expected that the rate of the formation of the anion would be very much lower at pH 1 than at pH 7; furthermore,

phenolphthalein dimethyl ether is reduced at potentials similar to those of phenolphthalein, and the wave is best defined in solutions more acid than pH 1; at higher pH-values minima are found. In this case no possibility of a transformation through an anion into a quinoid form exists, and it seems more likely that the rate of a reaction which involve some kind of protonization is determining for the height of the wave. This might also be the case for phenolphthalein but the mechanism of the reduction is still not clear.

The polarographic behaviour of 2-benzoylbenzoic acid, 2-(4'-hydroxybenzoyl)benzoic acid, and 2-(4'-methoxybenzoyl)benzoic acid resembles that of pyruvic acid [19] in that the acids and their anions are reduced at different potentials. In a certain pH-region the height of the more positive wave is determined by the rate of the recombination of the anion and the proton.

By controlled potential reduction of 2-(4'-methoxybenzoyl)benzoic acid it was found that the reaction was a two-electron reduction to 3-(4'-methoxyphenyl)-phthalide.

In Table 1 are given the polarographic data of phenolphthalein oxime (VIII), its monomethyl- (XIII), dimethyl-(IX), and trimethyl ether (XIV), "*o*-(*p*-anisoyl)benz-pseudoanilide" (X), "*o*-benzoylbenz-pseudo-*p*-anisidide" (XI), "*o*-benzoylbenz-pseudoanilide" (XII), "*o*-(*p*-anisoyl)-benz-pseudo-2,6-dimethylanilide" (XVII), "phenolphthalein N-methyl-oxime", and "*o*-(*p*-anisoyl)benz-pseudo-N-methylanilide".

Table 1. Limiting currents in μA and half-wave potentials *vs* S.C.E. at different pH-values of phenolphthalein oxime (VIII), phenolphthalein monomethylether oxime (XIII), phenolphthalein oxime dimethyl ether (IX), phenolphthalein oxime trimethyl ether (XIV), "*o*-(*p*-anisoyl)benz-pseudoanilide" (X), "*o*-benzoylbenz-pseudo-*p*-anisidide" (XI), "*o*-benzoylbenz-pseudoanilide" (XII), "*o*-(*p*-anisoyl)benz-pseudo-2,6-dimethylanilide" (XVII), "phenolphthalein N-methyl-oxime" (XV), and "*o*-(*p*-anisoyl)benz-pseudo-N-methylanilide" (XXIII). Concentration 10^{-3} M. 0.01 % gelatin added as maximum suppressor.

pH	1.0		3.5		5.5		7.5		9.8		13	
	i_l	$-E_{\frac{1}{2}}$	i_l	$-E_{\frac{1}{2}}$	i_l	$-E_{\frac{1}{2}}$	i_l	$-E_{\frac{1}{2}}$	i_l	$-E_{\frac{1}{2}}$	i_l	$-E_{\frac{1}{2}}$
VIII	3.6	0.79	3.4	0.84	3.5	0.92	3.6	1.07	3.4	1.28	1.5	1.48
XIII	3.6	0.75	3.4	0.80	3.4	0.87	3.4	1.01	3.5	1.25	0.8	1.38
IX	3.8	0.75	3.8	0.79	3.7	0.87	3.9	1.00	3.9	1.25	1.2	1.37
											~1.0	~1.80
XIV[a]	3.3	0.78	3.3	0.93	3.5	1.04	3.5	1.12[b]	3.6	1.21[b]	0.5	1.37
									0.5	1.80	2.0	1.73
X	3.9	0.66	3.7	0.72	3.8	0.79	3.9	0.95	3.8	1.18[b]	0.6	1.31
			4.0	1.38					1.4	1.77	3.2	1.73
XI	4.0	0.59	4.1	0.66	4.0	0.74	4.0	0.93	4.0	1.16[b]	1.6	1.29[b]
											2.6	1.65
XII	3.7	0.53	3.7	0.64	3.6	0.71	3.8	0.89	4.1	1.09[b]	0.5	1.20
									0.6	1.65	3.4	1.54
XVII	3.7	0.78	3.6	0.87	3.6	0.95	3.7	1.08	2.9	1.30[b]	0	—
			5.8	1.28								
XV	3.4	0.77	3.4	0.82	3.6	0.90	3.6	0.99	3.9	1.17	[c]	~1.33
XXIII	4.0	0.66	3.2	0.75	3.3	0.84	3.4	0.92	3.5	1.03	[c]	~1.07

[a] 40 % dioxane. [b] Minimum. [c] The compound is hydrolyzed.

The phenolphthalein oxime yields below pH 11 a diffusion controlled, two-electron wave. The half-wave potentials are dependent upon pH with a slope of the $E_{\frac{1}{2}}$-pH curve of about 0.02 V/pH-unit below pH 5 and about 0.08 V/pH-unit between pH 5 and 10. The presence of the dissociable groups in the compound explains this behaviour. In strongly alkaline solution the height of the wave diminishes somewhat.

The half-wave potentials of phenolphthalein oxime are a little less negative than those of 2-(4'-hydroxybenzoyl)benzoic acid in accordance with the proposed structure VIII. This makes formula V very unlikely, as neither phenolphthalein imide nor benzoylhydroxamic acid are reducible in the medium used.

Controlled potential reduction in acid solution of phenolphthalein oxime showed that the reduction consumed 2 electrons per molecule, and the isolated product was 2-(4'-hydroxyphenyl)-3-(4''-hydroxyphenyl)-2,3-dihydro-2-*iso*-benzazol-1-one (XVIII, R = OH).

The compounds IX, X, XI, and XII behave below pH 10 similarly to the oxime. The "*o*-benzoylbenz-pseudoanilide" (XII) has previously been investigated by Wawzonek *et al.*[11] who from the polarographic data concluded, that the compound in acid solution contained the azomethine group in accordance with the assumption made here. In strongly alkaline solution the wave diminishes in height and another wave appears at more negative potentials. According to Wawzonek *et al.*[11] the second wave is due to the reduction of the compound with the form XIIb containing a phthalide ring. As the height of the first wave in strongly alkaline solution is almost independent of the height of the mercury reservoir it is assumed to be determined by the rate of some reaction. This might be the opening of the phthalide ring, but as IX, X, and XI are soluble in alkali yielding a yellowish solution, it is likely that the phthalide ring in these solutions is opened. It must thus be another reaction which determines the height of the first wave of these compounds.

Controlled potential reduction of phenolphthalein oxime dimethyl ether yielded both in acid and alkaline solution 2-(4'-methoxyphenyl)-3-(4''-methoxyphenyl)-2,3-dihydro-2-*iso*benzazol-1-one (XVIII, R = OCH_3). The reduction of the dimethyl ether is thus analogous with that of phenolphthalein oxime.

The reduction of the phenolphthalein oxime trimethyl ether is slightly different from that of the above mentioned compounds in that the slope of the $E_{\frac{1}{2}}$/pH-curve is about 0.08 V/pH-unit from pH 1 to 10. This is due to the methylation of the carboxyl group; no dissociable groups are thus present in the molecule. In strongly alkaline solution two waves are found, and in this case no phthalide ring, whose reduction can be due to the occurrence of the more negative wave, is present. In the reduction of oximes and other azomethine compounds [20] minima are often found in alkaline solution and in some cases a second wave is found. It is generally assumed that the height of the first wave of the oxime is dependent upon the rate of the protonization of the oxime, and the second wave is due to the reduction of the unprotonated compound. The pH at which the first wave diminishes is in the case of phenolphthalein oxime trimethyl ether considerably higher than in the case of the oximes, but possibly not high enough to exclude the occurrence of such a

protonization at the electrode surface, and at present no other explanation of the two waves in alkaline solution can be offered.

Controlled potential reduction at pH 3 and pH 5 of phenolphthalein oxime trimethyl ether yielded in a two-electron reduction the same compound (XVIII, R = OCH_3) as the reduction of the dimethyl ether. As anils generally are reduced to the aniline derivatives it is assumed that the primarily formed derivative of benzhydrylaniline reacts with the methyl ester yielding the lactam.

The *o*-(*p*-anisoyl)benz-pseudo-2,6-dimethylanilide (XVII) resembles phenolphthalein oxime dimethyl ether below pH 8. However, in the region pH 2 to 4 a second wave, probably catalytic, appeared; the nature of this wave was not investigated further. At higher pH-values the first wave diminishes in height and disappears completely in strongly alkaline solution without the appearence of a second wave. The reduction thus resembles that of many oximes, and the height of the wave is, too, in a certain pH-interval assumed to be governed by the rate of protonization of the azomethine compound at the electrode surface.

Controlled potential reduction of the "*o*-(*p*-anisoyl)benz-pseudo-2,6-dimethylanilide" at pH 0.5 showed the reduction to be a two-electron reduction. In the reaction medium was precipitated a compound, which was identified as 3-(4'-methoxyphenyl)-phthalide. Steric hindrance might be responsible for the failure to form a derivative of 2,3-dihydro-2-*iso*benzazol-1-one, analogously with the reduction product of phenolphthalein oxime dimethyl ether, and for the instability of the assumed, primarily formed, benzhydrylaniline derivative.

The "*o*-(*p*-anisoyl)benz-pseudo-N-methylanilide" (XXIII) is reduced from pH 1 to 10 in a single two-electron wave. The slope of the $E_{\frac{1}{2}}$/pH-curve is about 0.04 V/pH-unit. In strongly alkaline solution the compound is hydrolyzed and the wave of *o*-(*p*-anisoyl)benzoic acid appears.

From a controlled potential reduction in acid solution of the compound 3-(4'-methoxyphenyl)-phthalide was isolated. The reduction thus results in a cleavage of the carbon-nitrogen bond. This might be a direct reduction of the single bond or a reduction of the carbon-nitrogen double bond resulting from an opening of the phthalide ring by forming a zwitterion. As the solution in the neutral region is colourless the compound predominantly exists with the phthalide ring intact, and if the zwitterion is the reducible species the ring opening is a fast reaction. This is likely as the opening of the phthalide ring just requires a displacement of electrons without the participation of hydrogen ions.

The polarographic data of *o*-(*p*-anisoyl)benz-*p*-anisidide (VII), *o*-benzoylbenz-*p*-anisidide (XXVI), *o*-benzoylbenzanilide (XXVII), and *o*-(*p*-anisoyl)-benz-N-*cyclo*hexylamide (XXVIII) are given in Table 2. In acid solution the wave is hardly visible, but at higher pH-values the wave grows and reaches at pH 13 for some of the compounds a height to be expected of a diffusion controlled wave. At lower pH-values the height of the wave is governed by the rate of some reaction. The compounds can exist in a cyclic (VIIb) and a non-cyclic (VIIa) form. From the infrared spectra it can be concluded that the compounds in the solid state to a high degree are found in the cyclic form. As the potentials at which the compounds are reduced are not much different

Table 2. Limiting currents in μA and half-wave potentials *vs* S.C.E. at different pH-values of *o*-(*p*-anisoyl)benz-*p*-anisidide (VII), *o*-benzoylbenz-*p*-anisidide (XXVI), *o*-benzoylbenzanilide (XXVII), *o*-(*p*-anisoyl)benz-N-*cyclo*hexylamide (XXVIII), *o*-benzoylbenz-N,N-diethylamide (XXIX), and *o*-(*p*-anisoyl)benz-2,6-dimethylanilide (XXX). Concentration 10^{-3} M. 0.01 % gelatin added as maximum suppressor.

pH	1.0		3.5		5.5		7.5		9.8		13	
	i_l	$-E_{\frac{1}{2}}$	i_l	$-E_{\frac{1}{2}}$	i_l	$-E_{\frac{1}{2}}$	i_l	$-E_{\frac{1}{2}}$	i_l	$-E_{\frac{1}{2}}$	i_l	$-E_{\frac{1}{2}}$
VII	0.08	0.91	0.15	1.01	0.15	1.11	0.45	1.23	2.7	1.43	3.2	1.54
XXVI	<0.05	—	<0.05	—	<0.05	—	<0.05	—	0.9	1.49	1.7	1.60
XXVII	<0.05	—	<0.05	—	0.1	1.1	0.3	1.25	2.0	1.37	2.7	1.56
XXVIII	0.15	0.84	0.15	1.01	0.2	1.12	0.5	1.23	0.8	1.36	2.3	1.57
XXIX	4.4	0.86	4.6	1.02	4.3	1.12	4.2	1.17	4.4	1.29	4.3	1.43
XXX[a]	1.8	0.88	2.3	1.12	2.2	1.23	3.0[b]	1.36	4.2	1.54	4.1	1.56

[a] 45 % dioxane. [b] Drawn out wave.

from those of *o*-benzoylbenz-N,N-diethylamide, which from the infrared spectrum (>C = O, $\nu = 1\ 665$ cm^{-1}; —CO—N<, $\nu = 1\ 620$ cm^{-1}) can be shown to possess the non-cyclic structure, it is assumed that the wave is due to the reduction of the form containing a free keto group (VIIa). The wave height would thus be determined by the rate of the transformation of the cyclic into the non-cyclic form.

Controlled potential reduction in strongly alkaline solution of *o*-(*p*-anisoyl)-benz-*p*-anisidide showed the reduction to be a two electron reduction and the isolated product was 3-(4'-methoxyphenyl)-phthalide. If it is the non-cyclic form which is reduced the expected compound would be a benzhydrol derivative. It seems a little unexpected that the carbon-nitrogen bond in the amide group is broken under the influence of the primarily formed secondary alcohol group.

o-Benzoylbenz-N,N-diethylamide (XXIX) yields from pH 1 to 13 a diffusion controlled, two-electron wave (Table 2). Controlled potential reduction in 0.5 N sodium hydroxide showed the reduction product to be 3-phenylphthalide. In this case, too, the carbon-nitrogen bond in the amide group is cleaved.

The polarographic reduction of *o*-(*p*-anisoyl)benz-2,6-dimethylanilide (XXX) showed that the compound to a higher degree than, e.g. *o*-benzoylbenzanilide, possessed the non-cyclic structure, and/or the rate of the ring opening is higher.

Whereas phenolphthalein imide, phenolphthalein hydrazide, and hydroquinonephthalein-*a*-oxime are not polarographically reducible 4-(4'-methoxyphenyl)-2,3-benzoxazin-1-one (XXI) and 2,4-diphenyl-phthalazin-1-one (XXII) are (Table 3). The polarographic data of the oxime of 2-(4'-methoxyphenyl)-benzoic acid (XXIV) are also shown in Table 3.

The behaviour of the oxime XXIV resembles that of benzophenone oxime. In a region around the neutral point the wave due to the reduction of the compound protonated at the electrode surface diminishes in height and disappears, whereas a more negative wave becomes visible, which represents the reduction of the unprotonated oxime. In strongly alkaline solution this wave

Table 3. Limiting currents in μA and half-wave potentials *vs* S.C.E. at different pH-values for 4-(4'-methoxyphenyl)-2,3-benzoxazin-1-one (XXI), 2-(4'-methoxybenzoyl)-benzoic acid oxime (XXIV), and 2,4-diphenylphthalazin-1-one (XXII). Concentration 10^{-3} M. 0.01 % gelatin added as maximum suppressor.

pH	1.0		3.5		5.5		7.5		9.8		13	
	i_l	$-E_{\frac{1}{2}}$	i_l	$-E_{\frac{1}{2}}$	i_l	$-E_{\frac{1}{2}}$	i_l	$-E_{\frac{1}{2}}$	i_l	$-E_{\frac{1}{2}}$	i_l	$-E_{\frac{1}{2}}$
XXI	4.4	0.46	4.4	0.64	8.8	0.89	8.9	1.09	8.7	1.19	0	—
	4.3	0.69	4.3	0.80								
XXIV	8.0	0.71	7.8	0.88	7.6	1.04	3.0	1.18	4.3	1.72	0	—
XXII	4.6	0.87	3.7	1.08	3.7	1.11	2.5	1.25[a]	3.4	1.74	0	—

[a] Minimum.

disappears, probably due to a loss of a proton from the oxime group. In strongly acid solution the compound loses water and is transformed to the 2,3-benzoxazin-1-one (XXI).

This compound is in acid solution reduced in two two-electron steps, but due to the low solubility of the compound no preparative reduction has been made. From pH about 5 to 10 a single four-electron wave is found. In alkaline solution the 2,3-benzoxazin-1-one ring is opened and the oxime XXIV is formed

The 2,4-diphenyl-phthalazin-1-one is in acid solution reduced in a single wave. At higher pH-values the height of the wave diminishes and a minimum on the curve is found as in the case of many oximes and phenylhydrazones [20]. About pH 9 the first wave has disappeared and a more negative wave is found. This wave disappears, however, in strongly alkaline solution. The height of the wave corresponds to a two-electron reduction, but due to the low solubility of the compound this could not be tested in a controlled potential reduction.

Hydroquinonephthalein (XXV) is reduced (Table 4) from pH 0 to 10 in a single, two-electron wave, which at least in acid solution is diffusion controlled. At pH about 9 the oscillations due to the mercury drops are abnormal from −0.8 to −1.1 V *vs* S.C.E.; when the alcohol concentration was raised to 65 % the height of the wave about −0.7 V diminished and another wave about −1.2 V appeared. In strongly alkaline solution two waves are found both of which become smaller with time, probably due to the formation of a carbinol as in the case of phenolphthalein. It seems somewhat unexpected that hydroquinonephthalein is reducible at such positive potentials, when the phthalide ring is assumed to be reduced at about −1.9 V *vs* S.C.E. as in 3,3-(4'-hydroxydiphenyl)phthalide [21]. An explanation similar to that given by Kolthoff for the reduction of phenolphthalein is not likely as no quinoid structure can be formed after removal of a proton; the only possible quinoid structure seems to be an *ortho* quinoid form with the oxygen bridge between the phenyl groups carrying a positive charge. However, the mechanism of the reduction is not clear.

2-(4'-Methoxybenzoyl)benzoic acid pseudoethylester XX shows (Table 4) a single two-electron wave from pH 1 to 10. In more alkaline solutions the compound is hydrolyzed. From pH about 7 minima are found as in the case of phenolphthalein. On the evidence from the infrared investigation the com-

Table 4. Limiting currents in μA and half-wave potentials *vs* S.C.E. at different pH-values for 2-(4'-anisoyl)benzoic acid pseudo-ethylester (XX) and hydroquinonephthalein (XXV). Concentration 10^{-3} M. 0.01 % gelatin added as maximum suppressor.

pH	1.0		3.5		5.5		7.5		9.8		13	
	i_l	$-E_{\frac{1}{2}}$	i_l	$-E_{\frac{1}{2}}$	i_l	$-E_{\frac{1}{2}}$	i_l	$-E_{\frac{1}{2}}$	i_l	$-E_{\frac{1}{2}}$	i_l	$-E_{\frac{1}{2}}$
XX	4.1	0.75	4.2	0.91	4.1	0.98	4.2	1.08[a]	4.1	1.14[a]	—[b]	1.14
XXV	3.5	0.35	3.5	0.43	3.5	0.50	3.4	0.58	3.5	0.73[c]	—[d]	0.79
											—[d]	1.30

[a] Minimum. [b] The compound is hydrolyzed. [c] Abnormal drop oscillations. [d] The wave height diminishes with time.

pound is assumed to possess the structure XX containing a phthalide ring. As a transformation to the normal, non-cyclic ester is unlikely under the conditions employed, and the presence of the phthalide ring also is suggested by the occurrence of the minima, which would not be expected for the non-cyclic ester, it seems likely that the compound in the solution has the assigned structure XX. It is, however, unexpected that this structure would be reducible below −1.0 V *vs* S.C.E. in view of the reduction of phthalide at −2.03 V *vs* S.C.E.[21]

Controlled potential reduction at −1.2 V *vs* S.C.E. in an acetate buffer showed that the wave was due to a two-electron reduction, and the isolated product was 3-(4'-methoxyphenyl)-phthalide.

o-Benzoylbenzoic acid pseudoethyl ester is reduced in the medium used (40 % ethyl alcohol containing buffer and 1 M potassium chloride) in the same manner as XX and different from the normal ester of *o*-benzoylbenzoic acid; in 50 % dioxane containing 0.1 M tetraethylammonium iodide Wawzonek *et al.*[21] found a pH-independent wave at a much more negative potential (about −1.9 V *vs* S.C.E.) for the pseudoester, and this was confirmed in the present investigation. However, in solutions containing less dioxane than about 40 % a wave is visible about −1.1 V *vs* S.C.E. which is the higher the lower the concentration of dioxane is. In 50 % dioxane containing potassium chloride the wave about −1.1 V is found, but on addition of tetraethylammonium iodide this wave disappears. This kind of influence of the supporting electrolyte where one wave is replaced by another one in the presence of capillary-active cations has apparently not been described before and will be discussed in a later communication.

EXPERIMENTAL

The polarograph was a recording polarograph Radiometer Type PO 3a. The capillary delivered 2.16 mg of mercury at a corrected mercury column height of 48.5 cm. The drop time 3.90 sec. (H_2O, open circuit). The capillary constant $m^{2/3}t^{1/6} = 2.13$ $mg^{2/3}$ $sec^{-\frac{1}{2}}$.

The apparatus used for the controlled potential reductions was an electromechanical potentiostat of the Lingane-Jones type. The buffer solutions employed were from pH 2.5 to 8 a sodium phosphate-citric acid buffer and from pH 8 to 11 a sodium borate buffer. The medium generally used was 40 % aqueous alcohol containing 1 M potassium chloride and 0.01 % gelatin. In a few cases the alcohol was replaced by peroxide-free dioxane.

For the infrared measurements a Perkin-Elmer Model 21 infrared spectrophotometer was employed. The potassium bromide discs were heated to 100°C for 2—3 min before use [13].

Phenolphthalein oxime was prepared and purified according to Friedländer [1] and Lund [7]. The compound contained one mole water of crystallization. (Found: C 68.32; H 4.72; N 3.86; H_2O 4.43. Calc. for $C_{20}H_{15}NO_4$, H_2O: C 68.37; H 4.88; N 3.98; H_2O 5.13. After drying for 20 h at 120°C *in vacuo* was found: H_2O 1.82.) Infrared spectrum, Fig. 1a.

In a similar manner was prepared *phenolphthalein monomethyl ether oxime* from phenolphthalein monomethyl ether and hydroxylamine, m. p. 228°. (Found: C 72.24; H 4.97; N 3.94. Calc. for $C_{21}H_{17}NO_4$: C 72.16; H 4.93; N 4.03.) The same compound was prepared analogously to the phenolphthalein oxime dimethyl ether (below) from the acid chloride of 2-(4′-methoxybenzoyl)benzoic acid and *p*-aminophenol. (Found: C 72.31; H 4.91; N 4.12; OCH_3 8.72. Calc. for $C_{21}H_{17}NO_4$: C 72.16; H 4.93; N 4.03; OCH_3 8.93.)

Phenolphthalein oxime dimethyl ether: 5.0 g of *o*-(*p*-anisoyl)benzoic acid were refluxed with 15 ml redestilled thionyl chloride for 30 min. The excess of thionyl chloride was removed *in vacuo* from a water bath, $t < 80$°C. 20 ml dry benzene were added to the residue and evaporated *in vacuo*. The residue was dissolved in 40 ml dry benzene, and 5 g of *p*-anisidine + 5 g of triethylamine in 50 ml dry benzene were added. The mixture was warmed for 15 min and after cooling poured into water. By addition of acetic acid pH was lowered to about 4, and the aqueous layer was discarded. The reaction product was extracted from the benzene layer with N sodium hydroxide, and on addition of acetic acid a precipitate, 5.8 g, was obtained. It was dissolved in ether, from which a white compound, 4.0 g, precipitated, m. p. 156°—158°. It was identified as phenolphthalein oxime dimethyl ether (here suggested to be 3-(4′-methoxyphenyl)-3-(N-4″-methoxyphenylamino)-phthalide, IXb) as the infrared spectrum, the polarographic data and m. p. were identical with those of authentic phenolphthalein oxime dimethyl ether [7]. (Found: C 72.85; H 5.20; N 3.91; OCH_3 16.99. Calc. for $C_{22}H_{19}NO_4$: C 73.09; H 5.30; N 3.89; OCH_3 17.18.) Infrared spectrum, Fig. 1c.

In a similar manner were prepared the following compounds: "o-(p-*anisoyl)benz-pseudoanilide*" (3-(4′-methoxyphenyl)-3-(N-phenylamino)-phthalide, Xb), m. p. 161°. (Found: C 76.05; H 5.26; N 4.37; OCH_3 9.30. Calc. for $C_{21}H_{17}NO_3$: C 76.12; H 5.18; N 4.23; OCH_3 9.37.) "o-*Benzoylbenz-pseudo*-p-*anisidide*" (3-phenyl-3-(N-4′-methoxyphenylamino)-phthalide, XIb), m. p. 195° (198°[9]). (Found: C 76.02; H 5.25; N 3.98. Calc. for $C_{21}H_{17}NO_3$: C 76.12; H 5.18; N 4.23.) "o-*Benzoylbenz-pseudoanilide*" (3-phenyl-3-(N-phenylamino)-phthalide), m. p. 220°—221° (220°—221°[22]). (Found: C 79.49; H 4.96; N 4.51; Calc. for $C_{20}H_{15}NO_2$: C 79.72; H 5.02; N 4.65.) "o-*(p-Anisoyl)benz-pseudo-2,6-dimethylanilide*" (2,6-dimethylanil of 2-(4′-methoxybenzoyl)benzoic acid), m. p. 187°—189°. (Found: C 76.41; H 5.82; N 3.98. Calc. for $C_{23}H_{21}NO_3$: C 76.86; H 5.89; N 3.90.)

"o-(p-*Anisoyl)benz-pseudo-N-methylanilide*" (3-(4′-methoxyphenyl)-3-(N-methyl-N-phenylamino)-phthalide): 5.0 g of 2-(4′-methoxybenzoyl)benzoic acid was transformed to the acid chloride as described above. 10 ml N-methylaniline in 50 ml dry benzene were added. After reaction the mixture was poured into water. The benzene layer was washed with dilute acid (too concentrated acid extracts the compound) and dilute alkali. After drying the benzene was removed, and the residue crystallized spontaneously after some days. It was recrystallized from benzene-ligroin. M. p. 103°. (Found: C 76.52; H 5.39; N 4.13. Calc. for $C_{22}H_{19}NO_3$: C 76.50; H 5.54; N 4.07.)

In the same manner was prepared "o-(p-*Anisoyl)benz-pseudo-N-methyl*-p-*anisidide*" (3-(4′-methoxyphenyl)-3-(N-methyl-N-4″-methoxyphenylamino)-phthalide), m. p. 145°—146°. (Found: C 73.52; H 5.72; N 3.74. Calc. for $C_{23}H_{21}NO_4$: C 73.60; H 5.63; N 3.72.)

Phenolphthalein oxime trimethyl ether (4-methoxyanil of 2-(4′-methoxybenzoyl)benzoic acid methyl ester, XIV) was prepared according to Meyer and Spengler [8]. (Found: C 73.43; H 5.52; N 3.95; OCH_3 24.58. Calc. for $C_{23}H_{21}NO_4$: C 73.60; H 5.63; N 3.72; OCH_3 24.80.) Infrared spectrum, Fig. 1e.

"*Phenolphthalein N-methyl-oxime*": 10 g of phenolphthalein and 8 g of potassium hydroxide were dissolved in 40 ml water and heated to 70°. 3.0 g of N-methyl hydroxylamine oxalate in 20 ml water were added. After 5—10 min the blood-red solution was cooled, 100 ml ether added and the mixture acidified with acetic acid. The yellow precipitate dissolved in ether giving a colourless solution. The ether layer was extracted with a mixture of carbonate and bicarbonate, which was acidified with acetic acid. The yellow precipitate was recrystallized from dioxane-water. It smelted unsharply between 160°

and 165°. (Found: C 68.87; H 5.24; N 3.80. Calc. for $C_{21}H_{17}NO_4$, H_2O: C 69.03; H 5.24; N 3.83.)

o-(p-*Anisoyl)benz*-p-*anisidide* was prepared according to Lund[7] by boiling the "pseudo"-compound with acetic anhydride for 2 min., m. p. 175°—177°. In the same manner were prepared o-(p-*anisoyl)benzanilide*, m. p. 190°—192°, o-*benzoylbenz*-p-*anisidide*, m. p. 202° (204°[9]), o-*benzoylbenzanilide* m. p. 195° (195°[22]), o-(p-*anisoyl)benz*-2,6-*dimethylanilide*, m. p. 238°. (Found: C 76.83; H 6.16; N 3.82. Calc. for $C_{23}H_{21}NO_3$: C 76.86; H 5.89; N 3.90.)

2-(4′-*Methoxybenzoyl)benzoic acid pseudo ethyl ester:* 7 g of the acid was transformed to the acid chloride as described before and treated with excess of ethyl alcohol. The excess alcohol was removed under reduced pressure and the residue dissolved in ether, which was washed with bicarbonate solution; the ether was dried and removed. The residue crystallized spontaneously after some time and was recrystallized from alcohol, 3.5 g. M. p. 76°—78°. (Found: C 71.67; H 5.89. Calc. for $C_{17}H_{16}O_4$: C 71.83; H 5.67.)

Reduction of phenolphthalein oxime: 1.0 g of the compound was reduced at —0.8 V *vs* S.C.E. in a mixture of 15 ml 4 N hydrochloric acid, 10 g potassium chloride, 80 ml water, and 50 ml alcohol. The reduction consumed two electrons per molecule; the yellow colour disappeared during the reduction and some of the reduction product precipitated. After completion the reaction mixture was diluted with water and extracted with ether, which was washed with dilute acid and bicarbonate and dried. After removal of the ether the residue was recrystallized from alcohol, m. p. 254°—256°. It was identified as 2,3-bis-(*p*-hydroxyphenyl)-phthalimidine[3] (2-(4′-hydroxyphenyl)-3-(4″-hydroxyphenyl)-2,3-dihydro-2-*iso*benzazol-1-one). (Found: C 75.69; H 4.94; N 4.38. Calc. for $C_{20}H_{15}NO_3$: C 75.70; H 4.77; N 4.42.)

In a similar manner was performed the *reduction of phenolphthalein oxime dimethyl ether.* The reaction product was identified as 2-(4″-methoxyphenyl)-3-(4′-methoxyphenyl)-2,3-dihydro-2-*iso*benzazol-1-one from m. p. 130° (130°—131°[23]) and analysis. (Found: C 76.49; H 5.53; N 3.88. Calc. for $C_{22}H_{19}NO_3$: C 76.50; H 5.55; N 4.06.) The same compound was isolated from an alkaline reduction.

Reduction of phenolphthalein oxime trimethyl ether: The compound (1 g) was reduced in a mixture of 40 ml water, 100 ml methanol, 30 ml ethyl acetate, 15 ml glacial acetic acid, and 10 g potassium hydroxide. After completion of the reduction (two electrons per molecule) the reduction product was isolated as described above for the phenolphthalein oxime. The product was identical with that obtained above from the dimethyl ether as shown from the m. p. 128°—130° and infrared spectrum.

Reduction of "o-(p-*anisoyl)benz-pseudo-N-methylanilide*": A suspension of 1 g of the compound in 40 % alcoholic acetate buffer was reduced at —0.85 V *vs* S.C.E. consuming 2 electrons per molecule. The compound dissolved during the reduction. The reaction mixture was diluted with water and made acid with mineral acid. The reaction product precipitated (0.5 g); it was identified as 3-(4′-methoxyphenyl)-phthalide from the m. p. 116°—117° (117,5°—118.5°[24]) and an infrared spectrum identical with that of actual 3-(4′-methoxyphenyl)-phthalide.

Reduction of "o-(p-*anisoyl)benz-pseudo-2,6-dimethylanilide*": This compound was reduced at —0.85 V *vs* S.C.E. in 50 % alcohol containing hydrochloric acid and potassium chloride. The reduction required two electrons per molecule, and the product precipitated during the reaction. After dilution of the reaction mixture the product was filtered off and identified as 3-(4′-methoxyphenyl)-phthalide from its m. p. 117° and infrared spectrum.

Reduction of o-(p-*anisoyl)benz*-p-*anisidide:* 1 g of the compound was reduced at —1.6 V *vs* S.C.E. in 40 % dioxane containing 0.5 N potassium hydroxide. After completion of the reduction (two electrons per molecule) the reaction mixture was diluted and acidified with mineral acid. The product precipitated and was identified as 3-(4′-methoxyphenyl)-phthalide from its m. p. 117° and infrared spectrum.

Reduction of o-(p-*anisoyl)benzoic acid pseudo ethyl ester:* The compound was reduced at —1.2 V *vs* S.C.E. in 50 % alcohol containing acetate buffer. The reduction required 2 electrons per molecule, and after removing some of the alcohol the mixture was acidified with mineral acid. The product precipitated and was identified as 3-(4′-methoxyphenyl)-phthalide from the m. p. 117° and the infrared spectrum.

In a similar manner the normal ester *ethyl* o-*benzoylbenzoate* was reduced in a two-electron reduction, and the isolated product was 3-phenyl-phthalide, m. p. 115°, identified from the infrared spectrum.

Reduction of o-*benzoylbenz*-N,N-*diethylamide:* The compound was reduced in 50 % alcohol containing 0.5 N sodium hydroxide and 5 g of potassium chloride at −1.6 V *vs* S.C.E. During the electrolysis a blue colour was observed which, on interruption of the current, faded in the course of half a minute, but reappeared when electrolysis was continued. The reduction required two electrons per molecule, and on acidifying the colourless solution the product precipitated. It was identified as 3-phenyl-phthalide from the m. p. 115° and the infrared spectrum.

REFERENCES

1. Friedländer, P. *Ber.* **26** (1893) 172.
2. Friedländer, P. and Stange, A. *Ber.* **26** (1893) 2258.
3. Meyer, H. *Sitzber. Wiener Akad.* **108** (1899) 67.
4. Meyer, R. and Kissin, S. M. *Ber.* **42** (1909) 2825.
5. Orndorff, W. R. and Murray, R. R. *J. Am. Chem. Soc.* **39** (1917) 679.
6. Meyer, H. *Monatsh.* **17** (1896) 439.
7. Lund, Hakon *Acta Chem. Scand.* **8** (1954) 1307.
8. Meyer, R. and Spengler, O. *Ber.* **36** (1903) 2949.
9. Meyer, H. and Turnau, R. *Sitzber. Wiener Akad.* **118** (1909) 261.
10. Reddelien, G. *Ber.* **42** (1909) 4759.
11. Wawzonek, S., Laitinen, H. A. and Kwiatkowski, S. J. *J. Am. Chem. Soc.* **66** (1944) 830.
12. Thiel, A. and Diehl, R. *Sitzber. Marburg Akad.* **62** (1927) 471.
13. Jensen, J. B. *Dansk Tidsskr. Farm.* **32** (1958) 205.
14. Witkop, B. *Experientia* **10** (1954) 420.
15. Bellamy, L. J. *The Infra-red Spectra of Complex Molecules*, Methuen and Co. Ltd., London 1954.
16. Colthup, N. B. *J. Opt. Soc. Am.* **40** (1950) 397.
17. Kolthoff, I. M. and Lehmicke, D. J. *J. Am. Chem. Soc.* **70** (1948) 1879.
18. Kolthoff, I. M. and Lingane, J. J. *Polarography*, 2nd Ed., Interscience Publishers, New York, London, 1952.
19. Brdicka, R. and Wiesner, K. *Collection Czeschoslov. Chem. Communs.* **12** (1947) 138.
20. Lund, Henning *Acta Chem. Scand.* **13** (1959) 249.
21. Wawzonek, S., Laitinen, H. A. and Kwiatkowski, S. J. *J. Am. Chem. Soc.* **66** (1944) 827.
22. Meyer, H. *Sitzber. Wiener Akad.* **116** (1907) 1117.
23. Meyer, R. and Glikin, J. *Ber.* **40** (1907) 1454.
24. Brubaker, M. M. and Adams, R. *J. Am. Chem. Soc.* **49** (1927) 2279.

Received October 7, 1959.

ACTA CHEMICA SCANDINAVICA 14 (1960) 379–384

Dipole Moments of Guaiacol Derivatives

J. JOHAN LINDBERG

Institute of Chemistry, University of Helsingfors, Finland

The molar polarizations and dipole moments of eugenol, dehydrodi-*iso*eugenol, 2,6-dimethoxyphenol, vanillin and *o*-vanillin have been determined in benzene and dioxan solution. It is found impossible to distinguish by means of dipole moment data between a stiff configuration containing an $OH...OCH_3$-chelate and a structure with "freely" rotating substituents. The rearrangements observed in the ultraviolet spectrum of guaiacol, when changing from an inert solvent (*cyclo*hexane) to dioxan, however, indicate a loss of planarity of the molecule when going from intramolecular to intermolecular hydrogen bond formation in accordance with previous infra-red spectroscopic investigations. A marked intermolecular interaction between *o*-vanillin and dioxan is noted.

It has been observed that the association between solute and solvent due to hydrogen bonds brings about an increase of the dipole moment of the associated molecules which is higher than the pure vectorial addition of the moments of the isolated molecules [1–3]. The observed dipole moment increment grows usually with the increase of the hydrogen bond strength. An exception is made by guaiacol, which shows the same moment in inert solvent (benzene) as in hydrogen acceptor solvent (dioxan). This effect was explained by Curran [4] as being caused by the $OH...OCH_3$ chelate, which should hinder the formation of the intermolecular hydrogen bond between the phenolic hydroxyl group and the oxygen atom of dioxan. This explanation, however, is contradicted by spectroscopic evidence, which indicates that guaiacol, like phenol, forms intermolecular hydrogen bonds with proton acceptor solvents [5–7]. Furthermore a series of investigations seems to indicate that the chelate in question is very weak in nature [7–9]. Actually, Fischer and Zengin [10] concluded from measurements of relaxation times that the hydroxyl group in eugenol is completely free to rotate also in such inert solvents as carbon tetrachloride. However, in the light of investigated infra-red spectra this assumption does not seem to be justified [7].

Full clarity regarding the interpretation of the dipole data of guaiacol appears to be obtainable only by determining the dipole moments of a series of guaiacylic and related compounds in inert and proton acceptor solvents. In order to achieve this end the measurements in benzene and dioxan solutions of the dipole moments of a series of compounds related to guaiacol are reported in the present paper.

EXPERIMENTAL

The dielectric constants required in the dipole moment determinations, were measured by the heterodyne-beat method at 500 kc using an apparatus described elsewhere [11]. The cylindrical measurement cell used in the investigation was made of Pyrex glass and was of the type described by le Fevre [12]. Its volume was 50 ml and its variable capacity about 25.5 pF.

The refractivities used in the calculations of the dipole moments were partially taken from the relevant literature and partially determined experimentally using an Abbe refractometer. The molar polarization at infinite dilution was calculated by the methods developed by Halverstadt and Kumler [13] and Smith and Cleverdon [14], from the dielectric increment and the variation of the specific volume with concentration.

The dipole moments were calculated employing the usual formula

$$\mu = 0.01281\sqrt{(P_{2\infty} - [R])\ T}\quad D \qquad (1)$$

Table 1. Weight fractions, dielectric constants and specific volumes of benzene solutions at 25°C. w_2 denotes weight fraction of solute, v_2 specific volume of solution, $\alpha = \frac{\partial \varepsilon}{\partial w_2}$ and $\beta = \frac{\partial v_2}{\partial w_2}$ at infinite dilution. ε is dielectric constant of solution.

	w_2	ε	v_2	α	β
Benzene	1.00000	2.2726	1.14670		
Guaiacol	0.01638	2.360	1.1420	+5.294	−0.2620
	0.02836	2.424	1.1386		
	0.04584	2.522	1.1347		
Eugenol	0.01522	2.336	1.1428	+4.096	−0.2162
	0.02647	2.383	1.1415		
	0.04116	2.446	1.1374		
Dehydrodi*iso*-eugenol	0.004703	2.286	1.1445	+3.041	−0.483
	0.008014	2.298	1.1427		
	0.01290	2.312	1.1416		
2,6-Dimethoxy-phenol	0.009678	2.317	1.1427	+4.545	−0.3375
	0.009842	2.314	1.1438		
	0.01523	2.342	1.1407		
	0.02491	2.374	1.1386		
	0.02735	2.396	1.1371		
	0.03379	2.428	1.1356		
Vanillin	0.01118	2.336	...	+5.365	−0.4150
	0.01329	2.350	1.1410		
	0.01866	2.384	1.1391		
	0.02251	2.408	...		
	0.03397	2.491	...		
	0.02673	...	1.1356		
	0.02792	...	1.1348		
o-Vanillin	0.005961	2.334	1.1441	+10.00	−0.465
	0.008308	2.356	1.1426		
	0.01147	2.388	1.1410		
	0.01345	2.403	1.1408		
	0.01743	2.446	1.1389		
	0.01963	2.471	...		

Table 2. Weight fractions, dielectric constants and specific volumes of dioxan solutions at 25°C.

	w_2	ε	v_2	α	β
Dioxan	1.00000	2.214	0.97272		
Eugenol	0.01297	2.275	0.9724	+4.790	−0.0254
	0.02266	2.321	0.9719		
	0.03545	2.384	0.9722		
Dehydrodi*iso*-eugenol	0.002970	2.223	0.9725	+3.348	−0.1388
	0.008350	2.242	0.9723		
	0.01314	2.259	0.9709		
2,6-Dimethoxy-phenol	0.01122	2.269	0.9714	+4.903	−0.1246
	0.02044	2.314	0.9713		
	0.02972	2.353	0.9690		
Vanillin	0.009672	2.307	0.9714	+9.625	−0.1820
	0.01988	2.406	0.9686		
	0.02862	2.484	0.9679		
o-Vanillin	0.007409	2.319	0.9710	+14.13	−0.0760
	0.01165	2.382	0.9706		
	0.01967	2.502	0.9698		

Table 3. Molar polarizations and dipole moments.

Substance	Solvent	$P_{2\infty}$	$[R]$	μ	$\Delta\mu$	Author
Methanol *	Benzene	—	—	1.66	+0.25	2
	Dioxan	—	—	1.91		2
Phenol *	Benzene	—	—	1.53	+0.25	2
	Dioxan **	—	—	1.78		2
Anisol *	Benzene	—	—	1.31	+0.03	2
	Dioxan	—	—	1.34		2
Guaiacol	Benzene	156.6	34.6	2.44	±0.0	Present
	Benzene	155.2		2.41		4
	Dioxan	155.0		2.41		4
Eugenol	Benzene	172.2	48.3	2.46	+0.05	Present
	Dioxan	177.0		2.51		»
Dehydrodi*iso*-eugenol	Benzene	251.6	92.8	2.79	+0.09	»
	Dioxan	261.9		2.88		»
2,6-Dimethoxy-phenol	Benzene	169.2	41.4	2.50	−0.07	»
	Dioxan	161.9		2.43		»
Vanillin	Benzene	208.9	40.5	2.87	+0.52	»
	Dioxan	275.3		3.39		»
o-Vanillin	Benzene	317.7	41.2	3.67	+0.47	»
	Dioxan	392.2		4.14		»
Salicylaldehyde	Benzene	—	—	2.88	+0.11	4
	Dioxan	—	—	2.99		4
p-Hydroxybenz-aldehyde	Dioxan	—	—	4.19		17

* For the sake of conformity, the dipole data of methanol, phenol and anisol are taken from one and the same publication although also other data are available, cf. *e.g.* Ref.[1].

** On dilution with heptane 1.86 *D* [2].

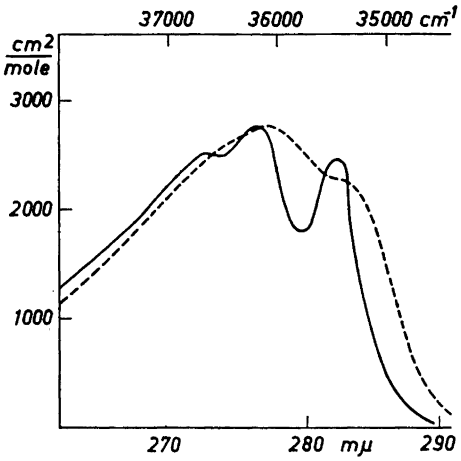

Fig. 1. Ultraviolet absorption spectrum of guaiacol at 20°C. Solvents: *Cyclo*hexane ———, dioxan -------.

No correction was made for the influence of the atomic refraction, *cf.* Ref.[15].

The ultraviolet spectra investigated were determined with a Beckmann spectrophotometer Model DU equipped with a thermostat, which was adjusted to 20.0°C.

Reagents. The investigated phenols were purified as previously described[7]. *Pro analysi* benzene (Merck AG) was distilled twice and stored over sodium. Dioxan was purified using the method given by Hess and Frahm[16] and stored over sodium. The *cyclo*hexane used was of "spectrograde" purity (Eastman Kodak).

DISCUSSION

The experimental data and the results of the investigation are found in Tables 1—3 and Fig. 1. An examination of Table 3, especially the column giving $\Delta\mu$-values, *i.e.* differences between dipole moments in dioxan and benzene solution, shows that the investigated substances, roughly taken, can be divided into three groups:

a) Substances with free hydroxyl groups (phenol, methanol), showing a moderate increase in dipole moment (about 0.3 *D*) when forming hydrogen bonds with dioxan.

b) Substances forming chelates of the type OH...OCH_3 (guaiacol, eugenol, 2,6-dimethoxyphenol and dehydrodi*iso*eugenol), having almost identical moments in benzene and dioxan solution.

c) Vanillin and *o*-vanillin, having substantially higher dipole moments in dioxan than in benzene solution (about 0.5 *D*). A small increase in the dipole moment is also shown by salicylaldehyde (0.11 *D*), which forms a strong chelate of the same type as *o*-vanillin, *i.e.* CHO...HO[8].

Below, some of the experimental results will be discussed in closer detail. Taking guaiacol as an example it is found, that in the same manner as in phenol[2], there is a marked rearrangement of the ultraviolet spectrum of guaiacol, when going from an inert solvent (*cyclo*hexane) to dioxan (*cf.* Fig. 1). Thus, counting from the band maxima there seems to be a "red shift" of the bands in the 280 mμ region of about 200—300 cm^{-1}. Furthermore a marked

deletion of spectral fine structure is observed. According to Merkel [18] such phenomena could be accounted for by an increase of the significance of polar valence structures and a decrease of the planarity of the whole molecule. In the case under review it would mean that the planar, stiff chelate structure is replaced by a less symmetric guaiacol-dioxan complex, where the positive and negative charge centers of the hydroxyl group are more separated. This interpretation is also in conformity with previous infra-red spectroscopic investigations on guaiacylic compounds and their deuterated derivatives [7,19].

According to the calculations made by Curran [4] a stiff *cis*-configuration of guaiacol (I) should cause a dipole moment of 2.45 *D*, while in the same

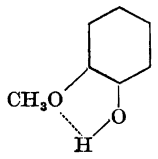

I

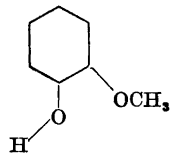

II

conditions a stiff *trans*configuration (II) should cause a moment of only 0.8 *D* in benzene and 0.9 *D* in dioxan solution. In the light of the previously discussed spectroscopic results it can be stated, that although in benzene solution a stiff *cis*-configuration can be taken for granted, it is not as likely, that a stiff structure would at all be present in dioxan solution. Using known dipole data for phenol and anisol (*cf.* Table 3) simple vector rules [20] give a moment of about 2.5 *D* for a guaiacol molecule with "freely" rotating substituents. Thus, in this case, a selection between the different possibilities must be made by other means than dipole data.

The ionization constants in water, pK (and thus also the hydrogen bond formation capacity of the hydroxyl group [7]), of phenol, guaiacol, 2,6-dimethoxyphenol and eugenol (and probably also of dehydrodi*iso*eugenol) are nearly equal and about 10, *cf.* Refs. [21, 22], whereas the pK-values of vanillin and *o*-vanillin are considerably lower, *i.e.* 7.4 and 7.9, respectively [23]. Bearing in mind the introductory discussion it would be expected that the difference between dipole moment in dioxan and benzene solution, $\Delta\mu$, should be much higher in the latter two substances than in the former ones. It is of interest to note that this is indeed the case (*cf.* Table 3).

On the other hand, the small $\Delta\mu$-value of salicylaldehyde, *i.e.* + 0.11 *D*, is worth noting. In *p*-hydroxybenzaldehyde the $\Delta\mu$-effect must be very high as indicated by the strong dipole moment in dioxan solution, *i.e.* 4.19 *D*. The great difference in behaviour between the two isomers must principally be attributed to the influence of the CHO...HO chelate in salicylaldehyde. This chelating effect seems to be of greater strength than the corresponding one in *o*-vanillin, *cf.* Refs. [21, 24], where a more marked intermolecular interaction is noted.

Summing up the results it can be concluded that it is impossible to distinguish between a stiff *cis*-structure and a structure with "freely" rotating substituents in guaiacylic compounds by means of dipole moment studies.

The absence of increase of dipole moment in guaiacylic compounds of very weak acidity (pK 10) when an intermolecular hydrogen bond is formed with a proton acceptor solvent must apparently, at least partly, be ascribed to charge rearrangements when the weak OH...OCH_3 chelate is broken.

REFERENCES

1. Mecke, R. and Reuter, A. *Z. Naturforsch.* **4a** (1949) 368.
2. Nagakura, S. and Baba, H. *J. Am. Chem. Soc.* **74** (1952) 5693.
3. Hulett, J. R., Pegg, J. A. and Sutton, L. E. *J. Chem. Soc.* **1955** 3901.
4. Curran, B. C. *J. Am. Chem. Soc.* **67** (1945) 1835.
5. Batuev, M. I. *Compt. rend. acad. sci. U.R.S.S.* **47** 97; *Doklady Akad. Nauk. S.S.S.R.* **47** (1945) 100.
6. Lindberg, J. J. *Paper and Timber (Finland)* **37** (1955) 206.
7. Lindberg, J. J. *Soc. Sci. Fennica Commentationes Phys. Math.* **XX.1**. (1957).
8. Fischer, E. *Z. Naturforsch.* **4a** (1949) 368; Lüttke, W. and Mecke, R. *Z. physik. Chem.* **196** (1951) 56; Tsuboi, M. *Bull. Chem. Soc. Japan* **25** (1952) 60; Flett, M. St. C. *Spectrochim. Acta* **108** (1957) 21.
9. Shigorin, D. N., Shemyakin, M. M., Zhukina, L. A., Kolosov, M. N. and Mendelevich, F. A. *Doklady Akad. Nauk. S.S.S.R.* **108** (1956) 672.
10. Fischer, E. and Zengin, N. *Z. Physik* **147** (1957) 113.
11. Lindberg, J. J. *Suomen Kemistilehti* **B 32** (1959) 12.
12. Le Fevre, R. J. W. *Dipole Moments*, 3rd Ed., Methuen & Co., London 1953, p. 50.
13. Halverstadt, I. F. and Kumler, W. D. *J. Am. Chem. Soc.* **64** (1942) 2988.
14. Smith, J. W. and Cleverdon, D. *Trans. Faraday Soc.* **45** (1949) 109.
15. *Loc. cit.*[12], p. 26.
16. Hess, K. and Frahm, H. *Ber.* **74** (1938) 2627.
17. *Landolt-Börnstein, Zahlenwerte und Funktionen aus Physik, Chemie, Astronomie, Geophysik und Technik.* Edited by Eucken, A. and Hellwege, K. H., Berlin 1951, Vol. I:3, II p. 424.
18. Merkel, E. *Z. Elektrochem.* **63** (1959) 373.
19. Lindberg, J. J. and Kenttämaa, J. *Suomen Kemistilehti* **B 32** (1959) 193.
20. Partington, J. R. *An Advanced Treatise on Physical Chemistry*, Longmans, Green and Co., London 1954, Vol. V, p. 447.
21. Juslén, C. and Lindberg, J. J. *Finska Kemistsamfundets Medd.* **68** (1959) 53.
22. Rao, G. G. *J. Indian Chem. Soc.* **12** (1935) 161.
23. Robinson, R. A. and Kiang, A. K. *Trans. Faraday Soc.* **51** (1955) 1398.
24. Lindberg, J. J. *Soc. Sci. Fennica Commentationes Phys. Math.* **XXI. 7.** (1958).

Received September 22, 1959.

ACTA CHEMICA SCANDINAVICA 14 (1960) 385–390

Investigations on Xanthoperol and its Precursor

JOHAN B.-SON BREDENBERG

Department of Chemistry, Institute of Technology, Helsingfors, Finland

The 11-epimer of xanthoperol has been found as a precursor. The natural 11α-configuration (Ia) has been assigned to the precursor and the 11β-configuration (IIa) to xanthoperol. The epimerisation is effected by heating in alkaline solution. The stability of the *cis*- and *trans*-forms of the A/B ring junction is discussed.

Xanthoperol has been acetylated to a diacetate, the alkaline hydrolysis of which has been studied.

Previous attempts to isolate the precursor of xanthoperol have been unfruitful. It has now been possible, by repeated chromatography, to obtain a small amount of a yellow compound, $C_{20}H_{26}O_3$, m.p. 207—210°, from the fractions containing the precursor. After boiling in sodium hydroxide solution, the yellow compound gives spectra in infrared and ultraviolet which are almost identical with the spectra of xanthoperol. The extinction values for the ultraviolet spectra are slightly lower owing to a small amount of 9-ketoferruginol which has nearly the same solubility as the compound. The compound is therefore the precursor sought. The precursor has ultraviolet spectra with the same shape as those of xanthoperol [1], with maxima at 249 and 341 mμ in neutral and 269 and 405 mμ in alkaline solution. The infrared spectrum has peaks at 3 160, 1 725 and 1 645 cm^{-1}, thus indicating the presence of a hydroxyl group and two keto groups, which latter nicely correspond to an α-diketo group conjugated with a benzene ring. The precursor has therefore the same functional groups in the same chromophore as xanthoperol and the change under the conditions employed can only be explained as an epimerisation.

Nuclear magnetic resonance investigations [2] have shown that xanthoperol has the structure of 9,10-diketoferruginol, but it is assumed that the configuration at C-11 is inverted (IIa). The inference has been drawn from the closer relationship of the nmr spectra of xanthoperol to its mono-keto reduction product than to that of 9-ketoferruginol (Ic), from which the mono-keto product differs only in the configuration at C-11, since the centre at C-12 cannot have been influenced under the conditions employed during the rapid reduction of xanthoperol. Inversion at C-12 requires more powerful reagents

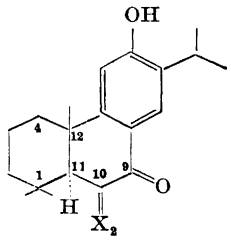

I a : $X_2 = O$
b : $X_2 = (OH)_2$
c : $X_2 = H_2$

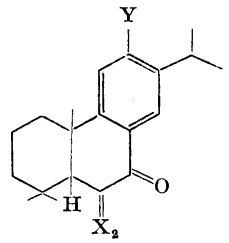

II a : $X_2 = O$ $Y = OH$
b : $X_2 = O$ $Y = OAc$
c : $X_2 = H_2$ $Y = OH$
d : $X_2 = O$ $Y = O^-$

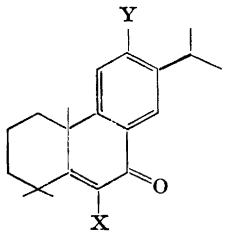

III a : $X = OAc$ $Y = OAc$
b : $X = OAc$ $Y = O^-$
c : $X = O^-$ $Y = O^-$

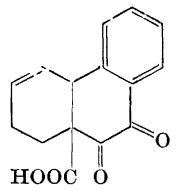

IV

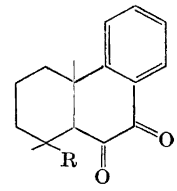

V

($AlCl_3$)[3,4]. This leaves structure IIc for the reduction product * and leads to the above assumption.

Apart from some recently investigated compounds [5,6], the natural diterpenes with an angular methyl group at C-12 have the same configuration at the rings A/B, which are *trans*-locked with the methyl group at C-12 in β-orientation [7,8]. All the diterpenes hitherto found in *Juniperus communis* L.[9,10] have this configuration and it seems therefore obvious that it should be assigned to the precursor isolated. From the foregoing it can be seen that the precursor is the less stable epimer. It has previously been found [11,12] that the A/B ring *cis* juncture is more stable than the *trans* juncture in octahydrophenanthrenes with an angular methyl group at C-12. It seems reasonable to assume that 9-keto-11 β-ferruginol (IIc) is more stable than the epimer (Ic) since it is formed under conditions that probably lead to the more stable epimer, and the *cis*-form would therefore be more stable in the 9-keto compounds also. The extension of the stability relationships to the 9,10-diketones cannot be presumed without fuller investigation but does not seem unreasonable in the light of the fact that the configuration for a *cis-syn-trans* perhydrophenanthrene with the keto group next to the *cis*-head is not inverted under the conditions normally employed for conversion [13]. The present evidence therefore strongly suggests that the precursor has the *trans*-form (Ia) and

* Wenkert and Chamberlin [11] have independently proposed this structure for the compound.

xanthoperol the *cis*-form (IIa). For it would seem very strange to assign the unnatural *cis*-form to the precursor and the natural *trans*-form to the artefact xanthoperol.

It has previously [14] been assumed that the precursor would have the same chromophore as 9-ketoferruginol. The ultraviolet spectra of the fractions containing the precursor still gave an appreciable reduction of the intensity at 280 mμ after hydrolysis but, in addition, it was found that a previously overlooked inflexion at 330 mμ had disappeared. The present evidence does not rule out the possibility of the existence of other precursors.

The ultraviolet and infrared spectra of the diketoferruginol epimers need some comment. The 10-keto group in the *trans*-form is evidently less conjugated with the 9-keto group owing to a larger angle between the keto groups [15]. The 9-keto group, on the other hand, is more strongly conjugated with the aromatic ring than the corresponding group in the *cis*-form. The cross-conjugation is therefore much stronger in the *cis*-form, as is clearly seen from the ultraviolet spectra. When the precursor is left to stand in alkaline solution at room temperature, the intensity of the maximum at 405 mμ slowly diminishes. This fall in intensity could be explained by the formation of a hydrate of the 10-keto group (I b). The same behaviour has been observed in several α-diketones [16–18]. (In methanol solution the compound IV [18] has about the same spectrum as acetophenone.) Unfortunately, the ultraviolet spectra in this connection were taken only between 355 and 500 mμ and lack of material prevented further investigation.

Several papers have recently been published in which α-diketo compounds with the general structure V are described. Wenkert and Jackson [4] have found that chromic acid oxidation of the corresponding hydrocarbons can be used as a method for determining the A/B ring junction, since only *cis*-compounds give α-diketones. Ghatak [19] has arrived at the same conclusion in a study of desoxypodocarpic acid isomers and the method has also been used by Saha *et al.*[12] The diketones readily give the enol acetate upon refluxing with acetic anhydride and sodium acetate [4,19]. This acetylation procedure was therefore applied to xanthoperol. In the crude product after 1 hour's boiling the infrared spectrum showed that the phenolic OH band had disappeared. In the region 1 800—1 630 cm^{-1} there were four bands at 1 765, 1 724, 1 685, and 1 667 cm^{-1}. When these bands were compared with the bands for xanthoperol monoacetate (IIb), the band at 1 685 could be assigned to the keto group at C-9 in the diketo compound and the band at 1 724 to the keto group at C-10. The band at 1 667 could be assigned only to the keto group at C-9 in a diacetate IIIa and the slightly broadened band at 1 765 therefore belonged to the unresolved phenol and enol acetate bands. Thus, it was found that the acetylation had only been partial and it was therefore continued for 20 h. The crude product now gave only two bands, at 1 765 and 1 665 cm^{-1}, in the afore-mentioned region and the expected diacetate was obtained as prisms, m.p. 158—159°, by crystallisation from aqueous ethanol.

On acidic hydrolysis, the diacetate afforded only mixtures but alkaline hydrolysis yielded interesting results. Short hydrolysis for 1 min with 0.5 N NaOH at room temperature gave a crude product with an infrared spectrum having bands at 3 330, 1 770 and 1 642 cm^{-1}, a side band at 1 747 and an

inflexion at 1 670 cm^{-1}. The spectrum can be nicely explained if it is assumed that the phenol acetate is rapidly hydrolysed, leaving behind the enol acetate with a small amount of diacetate. It has previously been observed that the phenol acetates of 9-ketoferruginol and xanthoperol are rapidly hydrolysed in alkaline solutions. One minute after the solution has been made alkaline, the ultraviolet spectrum of xanthoperol diacetate was of the same shape and intensity as the spectrum of 9-keto-Δ^{10}-dehydroferruginol in alkaline solution [10], thus supporting the conclusion above. The spectrum slowly changes, with isosbestic points at 400, 320 and 268 mμ, to the spectrum of xanthoperol in alkaline solution. The change in the spectra shows that only two absorbing substances are taking part in the alkaline hydrolysis and this can be explained by the reaction sequence IIIa—IIIb—IIIc—IId, where the absorbing substances are IIIb and IId. After the rapid hydrolysis of the phenol acetate group, the enol acetate group is slowly hydrolysed with the immediate formation of xanthoperol. The hydrolysed diacetate has been isolated and an infrared spectrum of the crude product gives the bands for xanthoperol. Pure xanthoperol has been crystallised from the crude product. The results obtained thus strongly support the structure IIa for xanthoperol.

The non-enolisation of the compound, which was partly responsible for erroneous conclusions [14]. has been commented on by Wenkert and Jackson [4]. They have explained it as due to steric compression. The steric conditions are, in our view, not the sole reason for the non-enolisation, but the phenol hydroxyl apparently also has an influence on it. This applies at least to alkaline solutions, in which the phenoxide ion is formed.

Kondo *et al.*[20] have recently obtained xanthoperol from the heartwood of *Cryptomeria japonica* D.Don. The bulk of the compound has been obtained after alkaline hydrolysis but a small amount has been isolated by extraction with sodium hydroxide without previous hydrolysis and the authors therefore conclude that xanthoperol is present as such in the tree. In the light of the present results it seems necessary to investigate whether the precursor is rearranged during the isolation procedure that has been used by Kondo *et al.*

EXPERIMENTAL

All m.p.s were determined with a Kofler microscope. The microanalyses were performed by Dr. A. Bernhardt, Mülheim. The infrared spectra were recorded with a Beckman IR-5 instrument, and the ultraviolet spectra with a Beckman DK-2 instrument.

9-Keto-11β-ferruginol (IIc). Clemmensen-reduced xanthoperol (0.24 g) was acetylated and the acetate oxidised with CrO_3 as before [14]. The oxidised product was hydrolysed and extracted in the usual way. Upon crystallisation from benzene, 15 mg of small prisms were obtained, m. p. 254—256°. UV spectrum: ethanol, λ_{max} 235 mμ (logε 4.20), 286 mμ (logε 4.12).

Isolation of the precursor. One hundred grams of the non-steam-volatile portion of the neutral extract from *Juniperus communis* L.[9] was chromatographed on alumina and small samples from each fraction were taken for investigation of the content of the precursor by taking the ultraviolet spectra before and after hydrolysis. The fractions containing the precursor were chromatographed anew and the spectra were taken as before. The fractions now containing the precursor were combined (0.54 g) and dissolved in 100 ml ether. The solution was extracted four times with 25 ml 2 % NaOH solution. The alkaline solutions were acidified and extracted with ether within 5 min after the extraction with alkaline solution. The ether extracts were combined and worked up as usual, leaving a crystalline

residue. This was crystallised from benzene and yielded 10 mg of small prisms, m. p. 207—210°, easily soluble in ethanol and difficultly soluble in benzene. (Found: C 77.0; H 8.2. Calc. for $C_{20}H_{26}O_3$: C 76.4; H 8.3.) UV spectrum: ethanol, λ_{max} 249 mμ (log ε 3.73), 341 mμ (log ε 3.94); 0.5 N NaOH in ethanol-water (1:1), 269 mμ (log ε 3.83) 405 mμ (log ε 4.08). IR spectrum: 1 mg/300 mg KBr, principal bands, cm^{-1}, 3 160 (s), 2 940 (s), 2 870 (m), 1 725 (m), 1 645 (s), 1 600 (s), 1 585 (s), 1 560 (s), 1 500 (s), 1 465 (m), 1 380 (m), 1 365 (m), 1 345 (m), 1 310 (s), 1 270 (s), 1 220 (m), 1 170 (m), 1 100 (m), 965 (w), 917 (w), 897 (w), 870 (m), 835 (w). The compound was contaminated with a small amount of 9-ketoferruginol.

Epimerisation of the precursor. The precursor was dissolved in 0.5 N NaOH in water (c 20 mg/l) and ultraviolet spectra were recorded in the range 500—355 mμ. The following extinction values were recorded at the maximum at 405 mμ at room temperature: a (time after solution, min), 38 (5), 36 (30), 33 (60), 27 (120), and 12 (300). The solution was thereafter heated on a water bath and the following values were recorded: λ_{max}, a (min), 410, 20 (15), 430, 19 (30), 440, 19.5 (45), and 445, 37 (120). UV spectrum of the epimerised product: ethanol, λ_{max} 251 mμ (log ε 3.74), 352 mμ (log ε 3.86); 0.5 N NaOH in ethanol-water (1:1), plateau at 260—270 mμ (log ε 3.9), max. 445 mμ (log ε 4.07) and an inflexion at 350 mμ due to the presence of a small amount of 9-ketoferruginol. IR spectrum: film on KBr, principal bands, cm^{-1}, 3 350 (broad), 2 950 (s), 2 870 (m), 1 718 (m), 1 660 (m), 1 595 (s), 1 565 (s), 1 505 (m), 1 460 (m), 1 370 (m), 1 330 (s), 1 295—1 265 (broad), 1 180 (m), 1 163 (m), 1 149 (m), 920 (w, broad), 865 (w, broad).

Xanthoperol diacetate (IIIa). Xanthoperol (140 mg) was acetylated with acetic anhydride and sodium acetate according to the procedure of Wenkert and Jackson [4]. The crude product after 1 hour's boiling had the maxima in the infrared: (film on KBr), 1 765 (s), 1 724 (m), 1 685 (s), 1 667 cm^{-1} (s), no hydroxyl band. The acetylation was completed by boiling for 20 h. The crude product was crystallised from aqueous ethanol, yielding 100 mg colourless prisms, m. p. 158—159°. By sublimation of the evaporated mother liquor a further amount (30 mg) of a colourless sublimate was obtained, m. p. 159—160°, identical with the previous crystals. (Found: C 72.0; H 7.5; O 20.3. Calc. for $C_{24}H_{30}O_5$: C 72.3; H 7.6; O 20.1.) UV spectrum: ethanol, λ_{max} 263 mμ (log ε 4.10), plateau 277 mμ (log ε 4.08). IR spectrum: 1 mg/300 mg KBr, principal bands, cm^{-1}, 2 960 (m), 2 870 (w), 1 765 (s), 1 665 (s), 1 612 (m), 1 565 (w), 1 495 (w), 1 460 (w), 1 420 (w), 1 385 (w), 1 370 (s), 1 320 (m), 1 205 (s), 1 170 (m), 1 155 (m), 1 110 (m), 1 095 (m), 1 035 (s), 932 (m), 903 (w), 885 (w), 865 (w), 795 (w).

Hydrolysis of xanthoperol diacetate. a. Acid hydrolysis. Hydrolysis with 2 N HCl gave ultraviolet and infrared spectra which showed that the hydrolysis was slow and gave a mixture of compounds.

b. Alkaline hydrolysis. 1. The diacetate (7 mg) was dissolved in ethanol (20 ml) and 1 N NaOH (20 ml) was added. The hydrolysis was stopped after 1 min at room temperature by acidification and extraction with ether. An infrared spectrum of the extracted product (film on KBr) showed bands at 3 330 (broad), 1 770 (s), 1 747 (m), 1 670 (inflexion), and 1 642 cm^{-1} (s). Attempts to obtain crystals from the crude product failed.

2. The diacetate (1.3 mg) was dissolved in ethanol (50 ml) and 1 N NaOH (50 ml) was added. A series of ultraviolet spectra were taken at 1, 5, 20, 60, 90, 120, 240, and 1 320 min at room temperature and warming for 10 min on a water bath. The spectra had isosbestic points at 268, 320 and 400 mμ, except the two last-mentioned which did not pass through the two lower points, probably owing to slow deterioration of the alkaline solutions. The first spectrum had λ_{max} 246 mμ (log ε 4.17, calc. for xanthoperol monoacetate) and 382 mμ (log ε 4.13). At the times given the high-end maximum had the following values: λ_{max} (a), 382 (38), 382 (37), 387 (35), 395 (33), 400 (33), 405 (34), 410 (34), 415 (35), and 420 (35). At the time when the experiment was interrupted the maxima were at 270 and 420 mμ in the alkaline solution and 250 and 345 mμ in the acidified solution.

3. The diacetate (4 mg) was hydrolysed for 2 h on a water bath with 1 N NaOH. After acidification and extraction the crude product gave the infrared spectrum of xanthoperol, and upon crystallisation from light petroleum-benzene, 1 mg of xanthoperol was isolated.

Xanthoperol monoacetate [14] *(IIb).* IR spectrum: 1 mg/300 mg KBr, principal bands, cm^{-1}, 2 960 (m), 2 870 (w), 1 780 (s), 1 724 (s), 1 685 (s), 1 610 (s), 1 555 (m), 1 490 (m),

1 460 (m), 1 385 (w), 1 370 (s), 1 320 (m), 1 265 (m), 1 250 (s), 1 190 (s), 1 180 (s), 1 150 (m), 1 120 (w), 1 110 (m), 1 098 (m), 1 050 (m), 1 022 (m), 1 010 (m), 970 (w), 952 (w), 928 (m), 915 (m), 882 (w), 868 (m), 846 (w), 778 (m).

The author is indebted to the late Prof. K. Alder for an ultraviolet spectrum of compound IV.

REFERENCES

1. Bredenberg, J. B. and Gripenberg, J. *Acta Chem. Scand.* **10** (1956) 1511.
2. Bredenberg, J. B. and Shoolery, J. N. *Acta Chem. Scand.* **14** (1960). *In press.*
3. Ohta, M. and Ohmori, L. *Pharm. Bull (Japan)* **5** (1957) 91, 96; *Chem. Abstracts* **51** (1957) 16390.
4. Wenkert, E. and Jackson, B. G. *J. Am. Chem. Soc.* **80** (1958) 211.
5. Cocker, J. D. and Halsall, T. G. *J. Chem. Soc.* **1956** 4262.
6. Djerassi, C., Cais, M. and Mitscher, L. A. *J. Am. Chem. Soc.* **80** (1958) 247.
7. Klyne, W. *J. Chem. Soc.* **1953** 3072.
8. Haagen-Smit, A. J. *Progr. in Chem. Org. Nat. Prods.* **12** (1955) 1.
9. Bredenberg, J. B. and Gripenberg, J. *Acta Chem. Scand.* **8** (1954) 1728.
10. Bredenberg, J. B. *Acta Chem. Scand.* **11** (1957) 932.
11. Wenkert, E. and Chamberlin, J. W. *J. Am. Chem. Soc.* **81** (1959) 688.
12. Saha, N. N., Ganguly, B. K. and Dutta, P. C. *J. Am. Chem. Soc.* **81** (1959) 3670.
13. Linstead, R. P. and Whetstone, R. R. *J. Chem. Soc.* **1950** 1428.
14. Bredenberg, J. B. *Acta Chem. Scand.* **11** (1957) 927.
15. Sandris, C. and Ourisson, G. *Bull. soc. chim. France* **1958** 350.
16. Sandris, C. and Ourisson, G. *Bull. soc. chim. France* **1958** 338.
17. Schroeder, H. D., Bencze, W., Halpern, O. and Schmid, H. *Chem. Ber.* **92** (1959) 2338.
18. Alder, K., Haydn, J. and Krüger, B. *Chem. Ber.* **86** (1953) 1372.
19. Ghatak, U. R. *Tetrahedron Letters* **1** (1959) 19.
20. Kondo, T., Imamura, H. and Suda, M. *Bull. Agr. Chem. Soc. Japan* **23** (1959) 233.

Received November 6, 1959.

ACTA CHEMICA SCANDINAVICA 14 (1960) 391–397

Crystal Structure of the 1:1 Addition Compound Trimethylamine — Iodo Monochloride

O. HASSEL and H. HOPE

Universitetets Kjemiske Institutt, Blindern-Oslo, Norway

As a part of a research programme dealing with the structures of charge transfer compounds having halogen molecules as electron acceptors the crystal structure of the 1:1 compound trimethylamine — iodo monochloride has been determined. The crystals are orthorhombic, the space group is *Pbca* and the lattice constants:

$a = 11.52$ Å $\quad b = 11.08$ Å $\quad c = 10.77$ Å

The number of molecules per unit cell is *eight*.

The nitrogen atom is tetrahedrally surrounded by the methyl groups and the I—Cl group, the N—I—Cl arrangement is at least nearly linear. The N—I distance (2.30 Å) corresponds closely to the distance previously observed in addition compounds formed by tertiary amines, the I—Cl distance of 2.52 Å is very nearly the same as that observed in the pyridine iodo monochloride compound (2.54 Å).

During the last few years crystal structure determinations of a series of charge transfer compounds have been carried out in this laboratory in which halogen molecules act as acceptors; ethers, amines and different other organic molecules as donors. The following report deals with the 1:1 compound formed by trimethylamine and iodo monochloride.

This compound (apparently first described as a simple addition compound by Pictet and Krafft [1]) is easily obtained by bringing together equimolecular quantities of the two components dissolved in a non-polar solvent like ligroin, carbon disulphide or carbon tetrachloride at temperatures below 10°C. We used the latter solvent and added the iodo monochloride solution drop by drop to the amine solution which was cooled by ice water. The yellow precipitate was dried *in vacuo* in the dark and stored at a low temperature. It was recrystallized from methylene chloride at temperatures below 10°C.

Analysis of the compound was carried out as follows: The substance was dissolved in glacial acetic acid and solid potassium iodide added, thereafter water in portions. Free iodine was titrated with a standard thiosulphate solution. The results obtained correspond within one per cent to theoretical values for $(CH_3)_3NICl$. Combustion analysis gave the following result: Found C 16.2; H 3.9. Calc. for C_3H_9NICl: C 16.3; H 4.1.

Single crystals were grown from methylene chloride solution by slowly evaporating the solvent in a refrigerator box. The most ideally developed crystals were obtained by

putting fine glass fibres into the vessel in which the crystals were grown. The crystals thus obtained were firmly fixed to the fibre and could be mounted on the goniometer head of the camera and set in the desired position. In cases where the linear extension of the crystal exceeded 0.1 mm its dimensions could be reduced by repeatedly bringing it for a short time into methylene chloride. Although the crystals are not very stable even at room temperature, the first Weissenberg pictures intended for a determination of lattice constants and space group could be obtained without cooling the crystals or putting them into sealed capillary tubes. Later exposures used for intensity measurements were performed at about −20°C in a Weissenberg camera equipped with cooling devices. The multiple film technique was employed and the intensities estimated visually. All diagrams were taken with CuK radiation.

The crystals are orthorhombic, bipyramidal in shape, the space group is *Pbca*. The lattice constants are as follows (−20°C):

$$a = 11.52 \text{ Å}; \qquad b = 11.08 \text{ Å}; \qquad c = 10.77 \text{ Å}$$

with a possible error of ± 0.5 %. Inserting the density measured at room temperature (2.10 g cm^{-3}) the calculated number of molecules in the unit cell is 7.84.

The number of observed reflexions in the *hk0* zone was 68 (theor. 82), in the *0kl* zone 69 (theor. 82) and in the *h0l* zone 61 (theor. 83).

The plane group of all three projections along the principal axes is the same, *pgm*. The first of these projections to be worked out was that along the z-axis (Fig. 1). The structure factor signs were computed on the basis of a Patterson synthesis and a Fourier synthesis subsequently worked out. The y parameter of chlorine, determined from the Fourier map, was not very accurate, however, because of overlapping, and the next step was the working out of a synthesis with projection along the x axis (Fig. 2). The coordinates of both iodine and

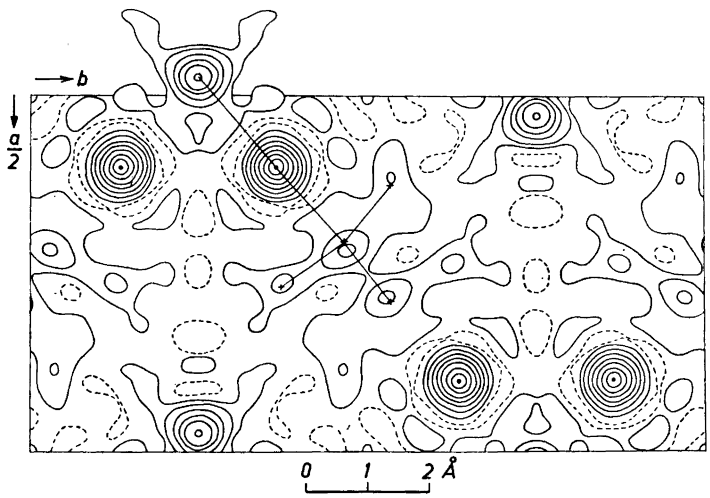

Fig. 1. Fourier projection along the z-axis. Contour lines for I at 0, 5, 20, 35, ... eÅ^{-2}, for Cl at 0, 5, 10, 20... eÅ^{-2}, for lighter atoms at 0, 5, 10, 15... eÅ^{-2}.

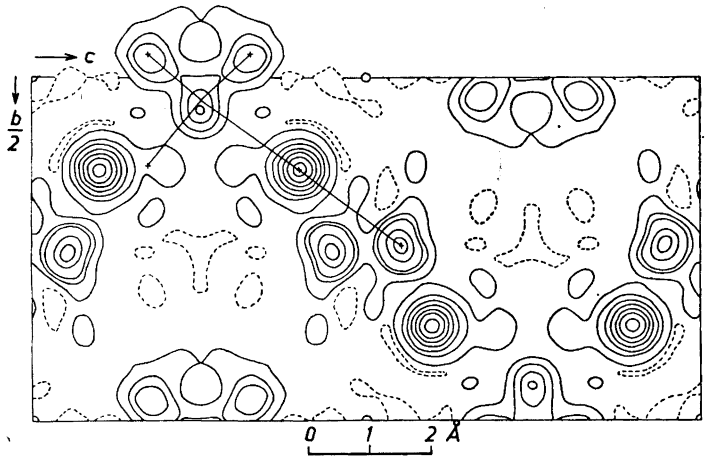

Fig. 2. Fourier projection along the x-axis. Contour lines for I at 0, 5, 20, 35... eÅ^{-2}, for all other atoms at 0, 5, 10, 15... eÅ^{-2}.

chlorine atoms were thus determined, but due to overlapping the x and z coordinates of the nitrogens were still rather uncertain and a Fourier projection along the y axis was therefore carried out inserting the structure factor signs obtained from the two first projections.

For all three projections difference Fourier projections were worked out with subtraction of the contribution from iodine.

The atomic coordinates arrived at by combining the information obtained from all the projections are listed in Table 1.

The agreement between observed and calculated structure factors may be judged by inspecting Table 2. When calculating the values listed in this table a temperature factor $B = 2.40$ was employed which was independently derived both from the xy and the yz projection. The "reliability factor" R including all observed reflexions is 0.09.

The agreement between observed and calculated intensities appears to be good enough to garantee that the iodine coordinates and even the chlorine coordinates have been determined with considerable accuracy. The coordinates

Table 1. Final coordinates of the atoms in one molecule obtained from Fourier projections.

	x	y	z
I	0.0982	0.1345	0.1005
Cl	−0.028	0.246	−0.053
N	0.205	0.033	0.248
C_1	0.270	0.126	0.330
C_2	0.126	−0.033	0.323
C_3	0.290	−0.033	0.176

Table 2. Observed and calculated structure factors. The given values are one fourth of the absolute values.

h k l	F_{obs}	F_{calc}	*h k l*	F_{obs}	F_{calc}
0 2 0	13	−13.1	4 1 0	25	−22.9
4	50	−48.7	3	33	−33.6
6	12	10.4	5	51	51.6
8	52	57.3	7	12	9.4
10	28	−32.9	9	16	−13.0
12	21	−18.7	11	<9.0	− 5.0
14	9	6.0	13	14	17.3
2 0 0	28	31.9	6 1 0	36	40.3
2	42	−43.5	3	<7.4	− 0.7
4	8	− 7.8	5	24	−23.3
6	13	−10.1	7	24	−26.5
8	24	22.5	9	20	19.1
10	14	−12.8	11	8	− 6.7
12	<8.5	3.4	8 1 0	45	49.2
14	<4.5	2.3	3	19	15.8
4 0 0	39	−40.2	5	20	−19.4
2	14	− 8.2	7	16	−15.6
4	57	60.9	9	30	34.3
6	27	−25.4	11	<6.6	− 1.7
8	22	−18.9	10 1 0	14	14.8
10	10	7.8	3	<9.6	− 5.5
12	19	17.4	5	<9.5	5.0
6 0 0	49	−50.3	7	12	− 9.1
2	<7.0	− 1.0	9	10	8.9
4	55	55.8	12 1 0	17	−14.2
6	20	−19.7	3	20	−21.3
8	26	−24.6	5	24	25.3
10	13	10.0	7	<6.4	2.7
12	15	17.1	14 1 0	9	− 6.6
8 0 0	15	14.4	3	10	−10.2
2	<8.6	− 4.1	0 0 2	21	24.7
4	13	− 9.4	4	59	−57.2
6	<9.5	1.4	6	53	−51.3
8	10	8.5	8	<7.7	1.8
10	<7.9	− 4.0	10	23	22.7
10 0 0	41	40.2	12	9	7.9
2	<9.6	1.2	2 0 2	42	45.1
4	34	−31.2	4	24	−18.7
6	15	12.9	6	27	−24.1
8	21	19.4	8	<8.0	− 3.8
10	12	−10.8	10	<8.6	5.5
12 0 0	<8.0	3.6	12	<7.1	− 5.5
2	<9.0	− 2.4	4 0 2	12	−10.0
4	18	−17.6	4	46	46.2
6	<7.3	5.1	6	29	28.5
8	<5.0	5.1	8	16	−16.8
14 0 0	13	−16.2	10	27	−31.7
2	9	8.0	12	<6.5	− 6.2
4	11	10.3	6 0 2	10	− 9.0
2 1 0	47	−55.8	4	40	41.0
3	46	−52.8	6	26	25.7
5	55	61.9	8	12	−12.6
7	14	12.0	10	22	−26.0
9	36	−33.2	12	8	− 7.1
11	<9.4	− 6.1	8 0 2	<7.7	5.3
13	20	21.7	4	11	−10.5

$h\,k\,l$	F_{obs}	F_{calc}	$h\,k\,l$	F_{obs}	F_{calc}
6	<8.6	− 3.2	8	22	−22.1
8	<9.6	− 1.7	10	32	−38.1
10	7	5.0	12	6	− 8.6
10 0 2	<8.6	6.6	0 6 2	9	− 8.9
4	26	−25.3	4	19	−17.7
6	24	−23.1	6	7	− 7.0
8	9	9.4	8	10	11.0
10	17	18.2	10	14	15.4
12 0 2	<7.9	4.4	12	7	6.3
4	10	−10.5	0 8 2	20	20.7
6	9	− 7.6	4	30	−29.1
14 0 2	10	− 9.3	6	25	−26.6
4	9	10.2	8	<8.0	0.8
1 0 2	44	−49.1	10	13	13.6
4	33	−33.1	0 10 2	12	−10.4
6	21	18.5	4	12	12.1
8	27	26.2	6	14	14.7
10	<8.6	− 2.0	8	<6.4	1.4
12	13	−12.1	0 12 2	<7.4	2.9
3 0 2	78	−82.0	4	16	15.8
4	50	−51.2	6	9	7.9
6	30	27.7	0 14 2	<3.8	3.0
8	39	36.2	0 2 1	53	−60.3
10	<8.5	− 0.9	3	69	−74.6
12	18	−18.4	5	<5.8	0.9
5 0 2	15	−13.1	7	50	51.7
4	15	−13.3	9	19	20.3
6	<7.6	− 8.0	11	16	−16.2
8	<8.5	− 1.2	13	17	−19.7
10	<8.2	1.4	0 4 1	19	12.6
12	<5.9	1.0	3	18	18.0
7 0 2	40	36.7	5	10	− 8.7
4	23	18.8	7	<7.8	− 4.6
6	31	−33.0	9	8	− 8.4
8	29	−33.6	11	7	4.5
10	<7.3	3.9	13	6	5.5
12	18	19.0	0 6 1	40	40.4
9 0 2	26	24.2	3	55	55.7
4	<8.5	0.9	5	9	− 8.7
6	15	−20.0	7	25	−24.9
8	15	−18.1	9	20	−20.3
10	<5.6	− 0.8	11	13	12.1
11 0 2	24	−20.0	0 8 1	15	−12.1
4	18	−14.1	3	20	−18.9
6	<7.3	1.3	5	8	− 5.3
8	8	6.6	7	18	18.9
13 0 2	25	−24.4	9	<7.3	2.9
4	17	−16.7	11	7	− 4.5
6	9	7.9	0 10 1	14	−17.2
0 2 2	42	−41.7	3	20	−23.0
4	8	6.7	5	<8.2	− 0.1
6	16	13.7	7	20	23.6
8	8	7.2	9	9	7.3
10	<8.5	2.8	0 12 1	10	10.1
12	7	6.9	3	14	14.1
0 4 2	13	−13.1	5	<6.2	− 4.1
4	60	60.4	7	8	−10.7
6	40	33.9	0 14 1	9	9.3

Table 3. Atomic distances and valency angles in the trimethylamine—iodo monochloride complex.

	Distance (Å)		Angle (°)
I—Cl	2.52	I—N—C_1	109
N—I	2.30	I—N—C_2	107
N—C_1	1.55	I—N—C_3	104
N—C_2	1.42	C_1—N—C_2	109
N—C_3	1.45	C_2—N—C_3	118
I—C_1	3.17	C_1—N—C_3	108
I—C_2	3.05		
I—C_3	3.00		

Table 4. N—I and I—I (resp. I—Cl) distances in addition compounds.

	N—I	I—I (I—Cl)
Pyridine · ICl	2.30	2.54
Trimethylamine · I_2	2.27	2.84
Trimethylamine · ICl	2.30	2.52

of the lighter atoms, however, are certainly less accurate. The small deviation from linearity observed for the N-I-Cl group with an angle at the I atom deviating by less than 4° from 180° may therefore not be significant. The atomic distances and bond angles derived from the coordinates listed in Table 1 are given in Table 3.

It is obvious that the type of structure found for the trimethylamine — iodo monochloride compound is closely analogous to structures previously derived for halogen addition compounds of aliphatic amines.[2] The linear arrangement nitrogen-halogen-halogen has been observed in all solid halogen addition compounds of aromatic amines so far investigated and also in the 1:1 iodine compounds of γ-picoline and quinoline which are now being investigated in this laboratory. It is interesting to note that the nitrogen-iodine bond length is very nearly the same in all these compounds, whether aliphatic or aromatic, and that the lengthening of the halogen-halogen bond as compared with the bond distance in the free iodine or iodo monochloride molecules is also practically the same (Table 4). The base property of the amine as judged from the dissociation constant in aqueous solution does not appear to be of any importance for the structure of the addition compound. The results of X-ray analyses do not substantiate Hantzsch's suggestion[3] that the solid halogen compounds of amines should be regarded as salt-like substances containing a halogen-substituted ammonium cation and a halogen anion.

Thus the evidence available from X-ray analysis of simple addition compounds formed by amines and halogens do not indicate a tendency towards the formation of ions like PyI^+. This does not mean, however, that salt-like structures cannot be formed. Some simple salts are known which must be expected to contain ions like Py_2I^+. In a recently started analysis of the crystal structure of the 1:2 compound formed by pyridine and iodine we have

actually observed the Py_2I^+ ion. According to space group requirements it has a center of symmetry. This means that the N-I-N arrangement is linear. The ion is probably at least very nearly planar. The remaining iodine atoms form an arrangement consisting of centrosymmetric I_3^- ions and iodine molecules very similar to that observed by Havinga [4] in tetra-ethylammonium heptaiodide. Additional examples of ionic compounds formed by amines and halogens will probably be found in the future.

REFERENCES

1. Pictet, A. and Krafft, G. *Bull. soc. chim. France* [3] **7** (1892) 74.
2. Eia, G. and Hassel, O. *Acta Chem. Scand.* **10** (1956) 139; Strømme, K. O. *Acta Chem. Scand.* **13** (1959) 268.
3. Hantzsch, **A.** *Ber.* **38** (1905) 2161.
4. Havinga, E. E. *Thesis*, Groningen 1957.

Received October 2, 1959.

ACTA CHEMICA SCANDINAVICA 14 (1960) 398–406

Crystal Structure of the 1:1 Molecular Compound 1,4-Dioxan, Sulphuric Acid

O. HASSEL and CHR. RØMMING

Universitetets Kjemiske Institutt, Blindern-Oslo, Norway

The 1:1 addition compound 1,4-dioxan, sulphuric acid crystallizes in the monoclinic system — space group $P2_1/c$ — with lattice parameters:

$$a = 13.22 \text{ Å}; \; b = 7.73 \text{ Å}; \; c = 7.71 \text{ Å}; \; \beta = 92°.$$

Hydrogen bonds link each sulphuric acid unit to two neighbouring dioxan molecules, thus producing endless chains of alternating dioxan and sulphuric acid molecules. Two sets of non-equivalent dioxan molecules are present in the structure, and two sets of hydrogen bonds are therefore also present. The lengths of these bonds are found equal to 2.51 and 2.59 Å, respectively.

In order to establish the crystal structure of one solid compound formed by an ether and a strong mineral acid, an X-ray analysis of the 1:1 compound 1,4-dioxan, sulphuric acid has been carried out. This compound has a melting point of 101°C (Faworski [1]). The possible structure of the isolated complex has been discussed on the basis of dipole moment measurements by Syrkin and Anisimova [2] who have concluded that both hydrogen atoms of the sulphuric acid molecule are linked to one particular ether oxygen atom. The angle between the two hydrogen bonds thus established would, however, appear to be rather small and we would therefore prefer a model in which both ether oxygen atoms are involved in hydrogen bond formation. In this case the dioxan molecule would of course be present in the »boat» form. Both models would lead to a rather high dipole moment. In the crystal the possibility of chains built up of alternating sulphuric acid and dioxan molecules would also have to be considered. In this case centrosymmetrical dioxan molecules might be expected.

EXPERIMENTAL

The compound was prepared as described by Faworski [1]. Sulphuric acid was added to a solution of dioxan in benzene and the reaction mixture cooled slowly. The needle-shaped crystals thus obtained turned out to be well fitted for X-ray examination. The

procedure of bringing a crystal into a capillary tube without admitting small traces of moisture which would eventually liquefy the crystal after the tube had been sealed, turned out to be difficult. By careful handling this could, however, be achieved. The cross section of the crystals used in the X-ray work was approximately 0.15 × 0.15 mm².

The experimental material on which the analysis was based consisted of integrated Weissenberg (Wiebenga) diagrams (CuK_α-radiation) with rotation about the *c*-axis (needle-axis) and precession diagrams (MoK_α-radiation, $\mu = 30°$) of the (*h*0*l*)- and (0*kl*)-zones. The number of reflexions recorded in the (*hk*0)-zone was 113 (theor. 135), in the (*h*0*l*)-zone 101 (theor. 129) and in the (0*kl*)-zone 49 (theor. 72). The intensities in the Wiebenga diagrams were recorded photometrically, whereas the precession diagram intensities were estimated visually. Most of the computation work was performed using a Ferranti Mercury machine.

The crystals are monoclinic, space group $P2_1/c$, and the parameters obtained are as follows:

$$a = 13.22 \text{ Å}; \; b = 7.73 \text{ Å}; \; c = 7.71 \text{ Å}; \; \beta = 92°.$$

These figures are believed to be accurate to within 0.03 Å and 0.5°. The calculated density, assuming the unit cell to contain four molecules of either kind, is 1.57.

STRUCTURE DETERMINATION

If the dioxan and sulphuric acid molecules take up fourfold general positions no symmetry requirements for the single molecules have to be fulfilled. On the other hand, the dioxan molecules may occupy two two-fold positions involving centers of symmetry, in this case two types of dioxan molecules are present in the structure.

Projection along the c*-axis.* From the Weissenberg data a two-dimensional Patterson synthesis was worked out. This synthesis made possible the localization of the sulphur atom and the determination of approximate coordinates of the sulphuric acid oxygen atoms. The atoms belonging to dioxan molecules could not be determined, but it became obvious that two non-equivalent sets of dioxan molecules are present in the structure having their centers of symmetry

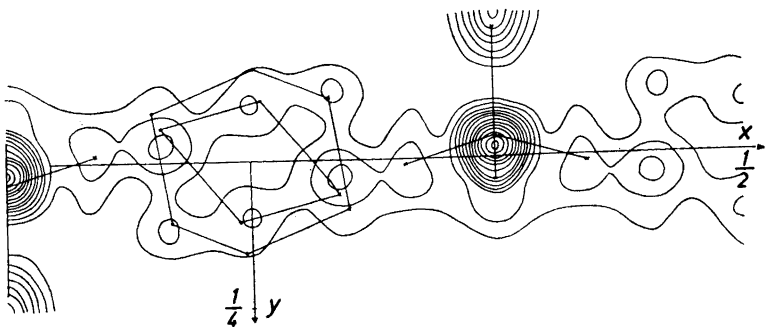

Fig. 1. Fourier map based on the (*hk*0)-reflexions using F_{hk0} with $h+k = 2n$ only.

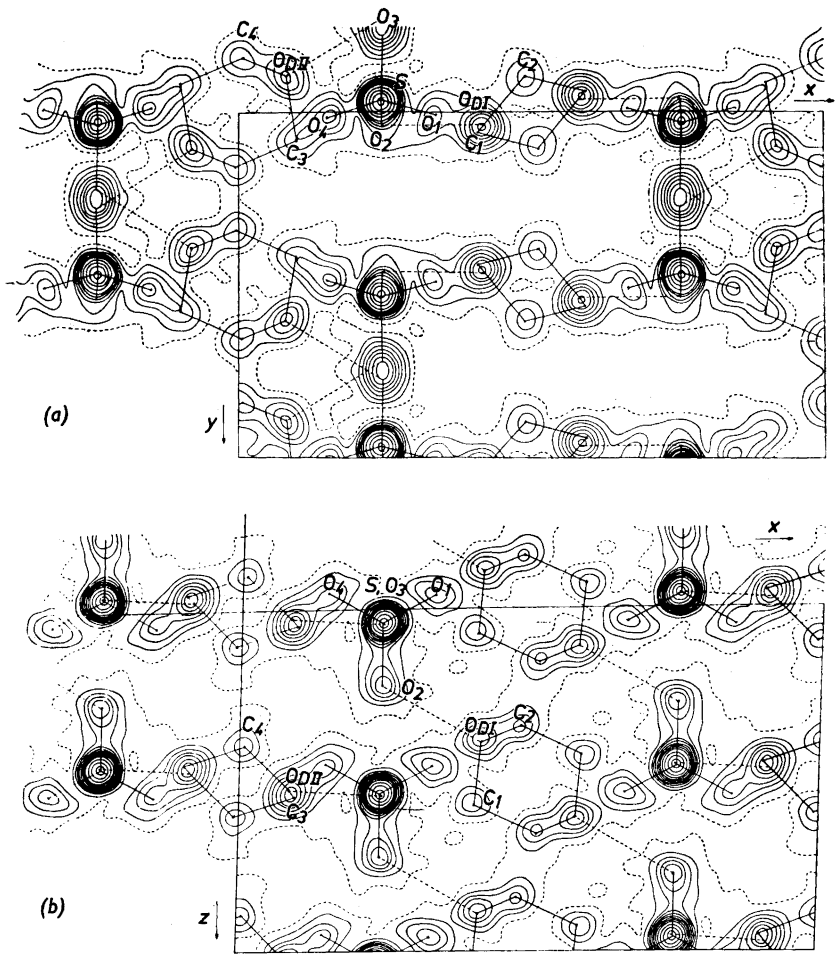

Fig. 2. Electron density projection along the *c*-axis (a) and *b*-axis (b). Contour lines at intervals of 2e. Å^{-2} from 2—16 e. Å^{-2} and 4 e. Å^{-2} from 16 e. Å^{-2} upwards.

in (0,0) and (1/2,0), respectively. The approximate coordinates of the sulphur and oxygen atoms of the sulphuric acid group were as follows: S: (0.250, —0.013) ; O_1: (0.345, 0) ; O_2: (0.250, 0) ; O_3: (0.250, —0.208) and O_4: (0.155, 0). On the basis of these coordinates only the structure factor signs of reflexions with $h + k = 2n$ could be determined. The neglection of other reflexions introduced an extra line of symmetry ($x = 1/4$) in the resulting Fourier synthesis (reproduced in Fig. 1). Here the sulphuric acid molecule therefore exhibits a symmetry line which is not real and the peaks around (0,0) indicate two overlapping dioxan molecules rather than one molecule. Using a reasonable

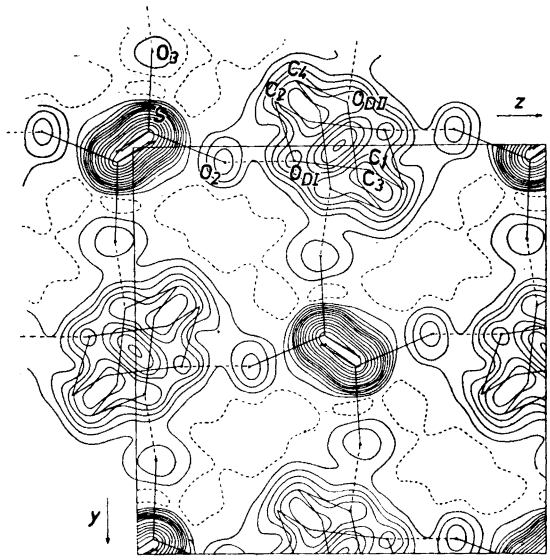

Fig. 3. Electron density projection along the *a*-axis. Contour lines as in Fig. 2.

model of the dioxan ring it was possible to split up the "double molecule" into two molecules, the centers of which were placed in (0,0) and (1/2, 0) thus bringing the symmetry in accordance with the true symmetry requirements of the plane group *pgm*. (The dioxan rings drawn in Fig. 1 are based on the ultimate, refined coordinates).

The *R* factor of the [001] projection at this preliminary stage of the analysis was 0.32. Successive refinements brought it down to 0.19 and after employing difference syntheses and least squares refinements it dropped to 0.13. At this stage further refinements of this projection were not attempted.

Projection along the b-*axis*. From a Patterson synthesis based on the (*h*0*l*) intensities and the coordinates obtained from the [001] projection a preliminary spatial model of the structure could be set up. It was assumed that hydrogen bonds are established between the hydroxy oxygens of the sulphuric acid molecules and the ether oxygen atoms of dioxan corresponding to "equatorial" directions in the dioxan molecules. After refinements the *R* factor was 0.14.

Projection along the a-*axis*. Using parameters derived from the two earlier projections the Fourier projection along the *a*-axis was refined until an *R* factor of 0.16 was obtained.

In all three projections overlapping of atoms occurred preventing further direct refinements. Nearly all coordinates could be determined, however, from at least one of the projections. Combining parameters obtained from different projections, and also (at this stage) introducing hydrogen parameters determined by projection of a model it was possible to perform least squares refinements on all three data sets alternatingly. The mean value of the atomic

Table 1. Atomic coordinates as fractions of the cell edges.

Atom	x	y	z
S	0.2446	−0.0355	0.0383
O_1	0.3354	0.0118	−0.0401
O_2	0.2450	0.0358	0.2212
O_3	0.2479	−0.2322	0.0494
O_4	0.1505	0.0133	−0.0481
O_{DI}	0.4182	0.0344	0.3894
O_{DII}	0.0830	−0.1069	0.5226
C_1	0.410	0.060	0.573
C_2	0.487	−0.106	0.343
C_3	0.098	0.072	0.559
C_4	0.008	−0.156	0.397

coordinates thus obtained are listed in Table 1. Estimates of the standard deviations [3] for the positions of resolved atoms were as follows:

Oxygen: $\sigma(x) = 0.014$ Å ; $\sigma(y) = 0.016$ Å ; $\sigma(z) = 0.018$ Å
Carbon: $\sigma(x) = 0.018$ Å ; $\sigma(y) = 0.020$ Å ; $\sigma(z) = 0.023$ Å

A comparison between observed and calculated structure factors is given in Table 3. In the calculations the analytical approximation to the atomic scattering factors computed by Forsyth and Wells [4] was employed.

The final R factors not including unobserved reflexions were as follows: $R_{hk0} = 0.09$; $R_{h0l} = 0.12$ and $R_{0kl} = 0.09$. The Fourier maps are reproduced in Figs. 2 and 3.

DISCUSSION OF THE STRUCTURE

The structure is built up of chains of alternating sulphuric acid and dioxan molecules. Two dioxan molecules are linked to a particular sulphuric acid

Table 2. Angles and interatomic distances.

$\angle$ S O_2O_{DI} = 115.8°
$\angle$ S O_3O_{DII}' = 117.1°
$\angle$ $O_{DI}'O_{DI}O_2$ = 166° } "equatorial" = 153°
$\angle$ $O_{D'II}O_{DII}O_3'$ = 172° }

Hydrogen bonds:

O_2–H– –O_{DI} : 2.59 Å
O_3'–H– – –O_{DII} : 2.51 Å

Distances in the sulphuric acid molecule:

SO_1	: 1.41 Å	O_1O_3	: 2.33 Å
SO_2	: 1.51 Å	O_1O_4	: 2.44 Å
SO_3	: 1.52 Å	O_2O_3	: 2.46 Å
SO_4	: 1.44 Å	O_2O_4	: 2.39 Å
O_1O_2	: 2.39 Å	O_3O_4	: 2.40 Å

Bond lenghts in the dioxan molecules:

$O_{DI}C_1$	: 1.44 Å	$O_{DII}C_3$	: 1.42 Å
$O_{DI}C_2$	: 1.47 Å	$O_{DII}C_4$	: 1.41 Å
$C_1'C_2$	: 1.53 Å	$C_3'C_4$	: 1.59 Å

Table 3. Observed and calculated structure factors.

hkl	F_o	F_c	*hkl*	F_o	F_c
1 0 0	6	5	7 3 0	7	6
2 0 0	51	−43	8 3 0	16	−15
3 0 0	13	−12	9 3 0	12	11
4 0 0	44	44	10. 3 0	12	−10
5 0 0	4	5	11. 3 0	< 4	1
6 0 0	63	−66	12. 3 0	< 3	− 6
7 0 0	< 3	0	13. 3 0	< 3	1
8 0 0	48	49	14. 3 0	5	6
9 0 0	15	17	15. 3 0	< 3	2
10. 0 0	21	−20	0 4 0	35	38
11. 0 0	12	−12	1 4 0	21	−20
12. 0 0	47	48	2 4 0	60	−63
13. 0 0	10	10	3 4 0	5	− 3
14. 0 0	11	−11	4 4 0	15	15
15. 0 0	6	− 7	5 4 0	23	20
16. 0 0	7	7	6 4 0	20	−19
1 1 0	27	28	7 4 0	11	11
2 1 0	17	16	8 4 0	17	15
3 1 0	31	−31	9 4 0	6	3
4 1 0	11	10	10. 4 0	27	−28
5 1 0	37	38	11. 4 0	14	−14
6 1 0	7	6	12. 4 0	10	10
7 1 0	10	− 9	13. 4 0	< 3	1
8 1 0	12	−10	14. 4 0	8	− 9
9 1 0	18	16	15. 4 0	< 2	− 1
10. 1 0	7	− 5	1 5 0	12	9
11. 1 0	8	− 7	2 5 0	7	7
12. 1 0	< 4	− 2	3 5 0	43	−43
13. 1 0	9	8	4 5 0	4	4
14. 1 0	4	5	5 5 0	18	18
15. 1 0	3	− 3	6 5 0	6	5
16. 1 0	< 2	1	7 5 0	17	−15
0 2 0	133	136	8 5 0	10	−11
1 2 0	26	−27	9 5 0	24	23
2 2 0	36	−39	10. 5 0	< 4	− 2
3 2 0	13	−14	11. 5 0	10	−12
4 2 0	18	−18	12. 5 0	< 3	− 3
5 2 0	4	4	13. 5 0	4	5
6 2 0	34	−31	14. 5 0	4	5
7 2 0	4	4	0 6 0	< 4	1
8 2 0	14	13	1 6 0	4	3
9 2 0	7	5	2 6 0	10	− 9
10. 2 0	16	−17	3 6 0	6	6
11. 2 0	15	−17	4 6 0	3	5
12. 2 0	23	23	5 6 0	16	11
13. 2 0	< 3	3	6 6 0	16	12
14. 2 0	9	− 7	7 6 0	9	9
15. 2 0	8	− 6	8 6 0	5	4
16. 2 0	< 2	0	9 6 0	6	2
1 3 0	25	−25	10. 6 0	9	− 8
2 3 0	19	18	11. 6 0	5	− 2
3 3 0	10	−11	12. 6 0	4	0
4 3 0	20	21	13. 6 0	2	3
5 3 0	7	8	1 7 0	6	6
6 3 0	9	7	2 7 0	< 4	2

hkl	F_o	F_c	*hkl*	F_o	F_c
3 7 0	22	−24	3 0 8	7	6
4 7 0	< 4	1	3 0 10	15	8
5 7 0	11	10	4 0−10	< 6	1
6 7 0	5	4	4 0− 8	< 6	2
7 7 0	11	−11	4 0− 6	7	− 3
8 7 0	4	− 5	4 0− 4	11	13
9 7 0	11	14	4 0− 2	8	− 6
10. 7 0	3	4	4 0 2	42	−34
11. 7 0	4	− 5	4 0 4	< 5	5
0 8 0	< 3	− 1	4 0 6	7	7
1 8 0	7	3	4 0 8	< 6	− 4
2 8 0	< 3	2	4 0 10	8	− 4
3 8 0	< 3	− 1	5 0−10	12	8
4 8 0	< 3	1	5 0− 8	12	12
5 8 0	< 3	− 3	5 0− 6	24	26
6 8 0	8	7	5 0− 4	16	20
7 8 0	4	− 2	5 0− 2	21	24
8 8 0	< 3	0	5 0 2	42	−38
9 8 0	2	− 2	5 0 4	66	−58
1 9 0	10	9	5 0 6	52	−52
2 9 0	3	3	5 0 8	12	−10
3 9 0	10	−10	5 0 10	< 5	− 3
4 9 0	< 3	2	6 0− 8	7	6
5 9 0	9	10	6 0− 6	7	10
6 9 0	4	2	6 0− 4	18	−20
0 0 2	122	128	6 0− 2	21	−20
0 0 4	26	24	6 0 2	47	−44
0 0 6	8	− 8	6 0 4	25	−26
0 0 8	7	− 8	6 0 6	< 6	− 3
0 0 10	9	− 6	6 0 8	< 6	0
1 0−10	8	5	7 0− 8	9	−10
1 0− 8	8	8	7 0− 6	39	−42
1 0− 6	25	31	7 0− 4	48	−52
1 0− 4	37	44	7 0− 2	46	−44
1 0− 2	57	62	7 0 2	40	36
1 0 2	< 3	3	7 0 4	16	12
1 0 4	10	8	7 0 6	19	19
1 0 6	26	−28	7 0 8	12	10
1 0 8	12	− 8	8 0− 6	< 6	− 5
1 0 10	< 6	− 3	8 0− 4	7	2
2 0−10	10	10	8 0− 2	< 5	3
2 0− 8	12	12	8 0 2	23	24
2 0− 6	< 5	1	8 0 4	26	22
2 0− 4	35	−43	8 0 6	9	5
2 0− 2	< 3	− 3	9 0− 6	6	6
2 0 2	56	−56	9 0− 4	7	9
2 0 4	59	−59	9 0− 2	22	20
2 0 6	< 5	− 4	9 0 2	< 6	4
2 0 8	< 6	3	9 0 4	< 6	1
2 0 10	< 6	1	9 0 6	9	− 9
3 0−10	9	− 5	10. 0− 6	< 6	− 1
3 0− 8	8	− 4	10. 0− 4	24	−22
3 0− 6	16	−22	10. 0− 2	16	−16
3 0− 4	< 5	− 6	10. 0 2	10	− 8
3 0− 2	36	−40	10. 0 4	17	−13
3 0 2	47	45	10. 0 6	6	− 4
3 0 4	< 5	1	11. 0− 6	9	− 8
3 0 6	< 6	4	11. 0− 4	< 6	− 2

hkl	F_o	F_c	*hkl*	F_o	F_c
11. 0— 2	11	—10	0 3 4	15	14
11. 0 2	13	8	0 3 5	16	18
11. 0 4	10	4	0 3 6	6	7
11. 0 6	12	11	0 3 7	< 5	— 4
12. 0— 6	6	— 4	0 3 8	6	8
12. 0— 4	< 6	5	0 3 9	< 5	— 3
12. 0— 2	18	20	0 4 1	4	— 6
12. 0 2	23	24	0 4 2	24	23
12. 0 4	10	10	0 4 3	17	19
12. 0 6	< 6	0	0 4 4	14	13
13. 0— 6	12	14	0 4 5	19	20
13. 0— 4	15	17	0 4 6	3	— 4
13. 0— 2	13	12	0 4 7	15	15
13. 0 2	< 6	2	0 4 8	< 5	— 4
13. 0 4	7	— 5	0 5 1	48	43
13. 0 6	14	—10	0 5 2	22	23
14. 0— 4	7	— 6	0 5 3	21	19
14. 0— 2	< 6	— 2	0 5 4	19	19
14. 0 2	11	—11	0 5 5	10	9
14. 0 4	10	—10	0 5 6	< 5	5
15. 0— 2	9	— 9	0 5 7	< 5	0
15. 0 2	9	7	0 5 8	7	6
0 1 1	12	12	0 6 1	< 4	— 4
0 1 2	6	— 4	0 6 2	< 4	2
0 1 3	50	46	0 6 3	16	16
0 1 4	14	18	0 6 4	< 5	— 2
0 1 5	34	31	0 6 5	20	20
0 1 6	9	10	0 6 6	< 5	— 4
0 1 7	5	— 6	0 6 7	14	13
0 1 8	3	6	0 7 1	< 5	4
0 1 9	< 5	— 5	0 7 2	10	11
0 2 1	23	26	0 7 3	6	5
0 2 2	50	47	0 7 4	6	10
0 2 3	30	31	0 7 5	< 5	3
0 2 4	26	23	0 7 6	< 5	2
0 2 5	9	9	0 8 1	< 5	— 1
0 2 6	< 5	— 3	0 8 2	< 5	3
0 2 7	< 5	6	0 8 3	8	6
0 2 8	5	— 5	0 8 4	< 5	0
0 2 9	< 5	2	0 8 5	9	9
0 3 1	69	68	0 9 1	< 5	1
0 3 2	7	— 5	0 9 2	6	7
0 3 3	33	31	0 9 3	< 5	2

unit by hydrogen bonds,the direction of which is roughly "equatorial" (Fig. 4). Both dioxan molecules are centrosymmetrical, but they are not crystallographically equivalent. The two O—H—O distances as computed from the coordinates listed in Table 1 are 2.51 Å and 2.59 Å, respectively, the standard deviation is 0.025 Å. It is obvious that two different types of S—O distances are present in the sulphuric acid group, one of which (involving the "keto" oxygen atom) is 1.42 Å, the other 1.51 Å. Some of the atomic distances computed have been listed in Table 2. (Compare also Fig. 5).

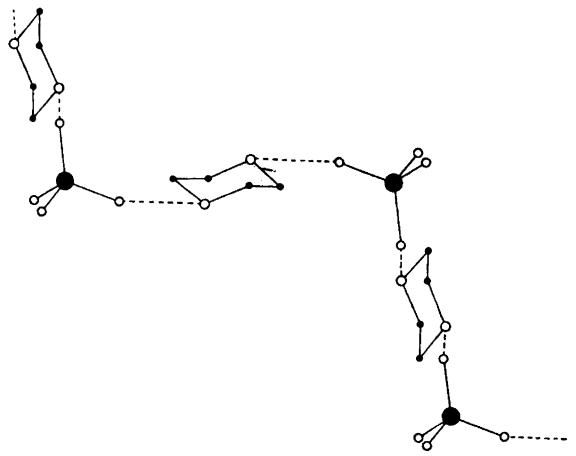

Fig. 4. Structure of the sulphuric acid-dioxan chains.

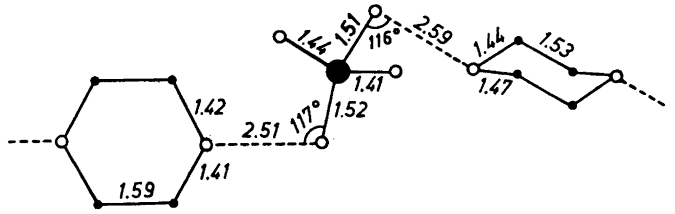

Fig. 5. Distances and angles. Open circles indicate oxygens, closed circles sulphur (large) and carbon (small) atoms.

This investigation has in part been sponsored by the *United States Air Force Development Command* under contract AF 61(052)-71.

REFERENCES

1. Faworski, A. *J. Russ. Phys.-Chem. Soc.* **38** (1906) 747. *Chem. Zentr.* **1907** I 16.
2. Syrkin, Ya.K. and Anisimova, K. M. *Doklady Akad. Nauk S.S.S.R.* **59** (1948) 1457. *Chem. Abstracts* **42** (1948) 6593 i.
3. Cruickshank, D. W. T. *Acta Cryst.* **2** (1949) 65.
4. Forsyth, T. B. and Wells, M. *Acta Cryst.* **12** (1959) 412.

Received November 6, 1959.

ACTA CHEMICA SCANDINAVICA 14 (1960) 407–427

Benzaurinstudien

III. Gleichgewichte und Reaktionskinetik des Benzaurins und des 4″-Chlor-benzaurins in wässrigen Lösungen

HANS GUSTAF HANSSON

Abteilung für anorganische und physikalische Chemie des Chemischen Instituts der Universität Lund, Schweden

In a previous paper [1] the equilibrium conditions of 3,3′,5,5′-tetrabromo-benzaurin and 3,3′-dibromo-5,5′-dimethyl-benzaurin in aqueous solutions were described. It was shown that these derivates of benzaurin constitute an equilibrium system, which consists of six different forms, three of which are coloured "anhydrous" forms in instantaneous pH-equilibrium with each other and three of which are colourless "carbinolic" forms, likewise in instantaneous pH-equilibrium. A coloured form is reversibly converted into the corresponding colourless form by taking up water, a time reaction that appears as a gradual fading of the colour of the solution. The equilibrium and velocity constants of the system were determined by light absorption measurements at different pH-values.

In the present paper the corresponding investigation of the unsubstituted benzaurin and the 4″-chloro-benzaurin is presented, and — as expected — the results can be described according to the scheme that proved valid for tetrabromo-benzaurin and dibromo-dimethyl-benzaurin [1].

The constants determined refer to the ionic strength 0.50 M and a solvent with the composition 98 % water + 2 % acetone. The temperature was 20°C.

In einem früheren Aufsatz [1] wurde über eine Untersuchung über die Gleichgewichte und die Reaktionskinetik in wässriger Lösung bei zwei Derivaten von Benzaurin, nämlich 3,3′,5,5′-Tetrabrom-benzaurin und 3,3′-Dibrom-5,5′-dimethyl-benzaurin, berichtet. Das Resultat ergab, dass bei Farbstoffen dieses Typus in wässrigen Lösungen ein Reaktionsschema vorliegt, das gewisse Ähnlichkeiten mit dem der früher von Bodforss und Cigén untersuchten basischen Triphenylmethanfarbstoffe vom Malachitgrüntypus zeigt.[2–4] Die in das Schema eingehenden Konstanten wurden bestimmt.

In der vorliegenden Arbeit werden die Resultate entsprechender Untersuchungen, teils über die unsubstituierte Stammsubstanz Benzaurin, teils

4″-Chlor-benzaurin. (Anhydrid).

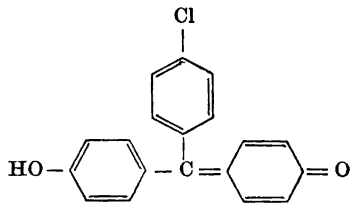

über 4″-Chlor-benzaurin, dargelegt. Wie erwartet können die Verhältnisse bei diesen mit demselben Reaktionsschema beschrieben werden. Es ist hier unten (für 4″-Chlor-benzaurin) wiedergegeben, wobei Bezeichnungen und Definitionen mit den vorher verwendeten [1,3] übereinstimmen.*

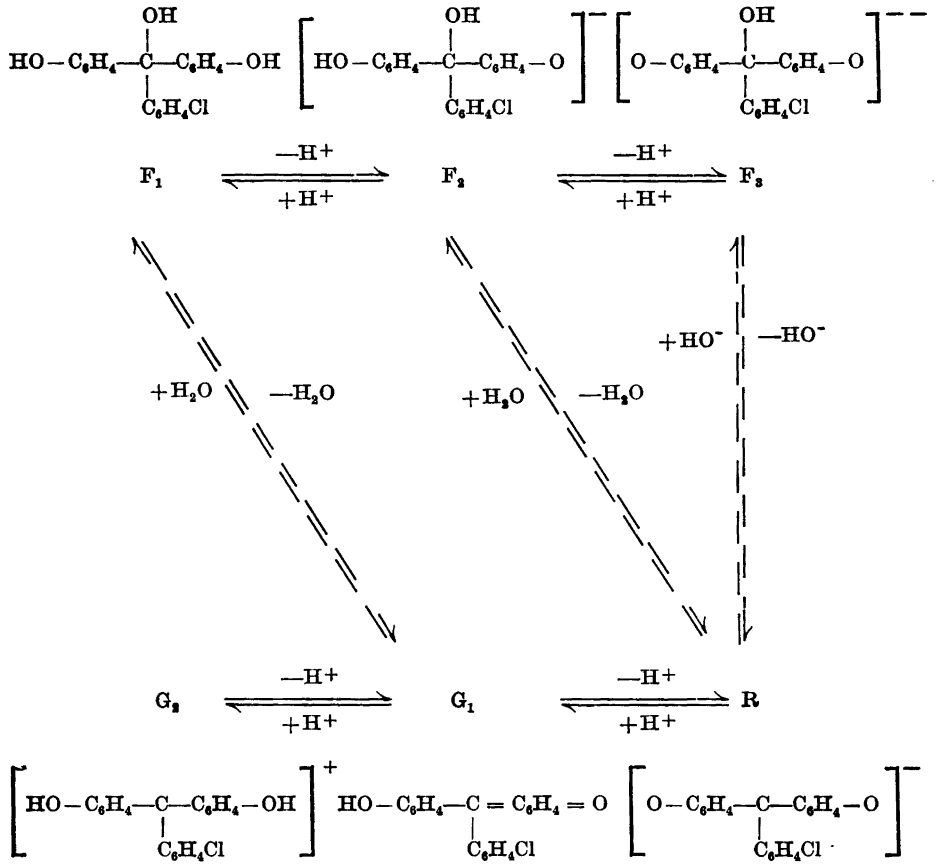

* Ausgezogene Pfeile bezeichnen momentane Reaktionen, gestrichelte Pfeile Zeitreaktionen. Sämtliche Reaktionen sind völlig reversibel.

Unter Verwendung der Bezeichnungen R, G_1 und G_2 für die gefärbten Formen und F_1, F_2 und F_3 für die farblosen (siehe das Schema oben) werden die Konstanten wie folgt definiert:

Die Protolysenkonstanten:

$$K_1 = \frac{[G_1]}{[H] \cdot [R]}\ ;\ K_7 = \frac{[H^+] \cdot [G_1]}{[G_2]}\ ;\ K_3 = \frac{[H^+] \cdot [F_2]}{[F_1]}\ ;\ K_4 = \frac{[H^+] \cdot [F_3]}{[F_2]}$$

Die Hydratationskonstanten (bei konstanter Wasseraktivität):

$$K_2 = \frac{[F_1]}{[G_1]} \quad ; \quad K_6 = \frac{[R]}{[F_2]}$$

Nach den Definitionen gilt $K_1K_2K_3K_6 = 1$. Ferner wird $K_5 = K_6/K_4$ gesetzt.

Die Geschwindigkeitskonstanten:

k_1 für die Reaktion $G_1 + H_2O \rightarrow F_1$
k_2 für die Reaktion $F_1 \rightarrow G_1 + H_2O$
k_3 für die Reaktion $R + H_2O \rightarrow F_2$ einschliesslich $R + OH^- \rightarrow F_3$
k_4 für die Reaktion $F_2 \rightarrow R + H_2O$ einschliesslich $F_3 \rightarrow R + OH^-$
k_1 und k_3 enthalten die Konzentration des Wassers. Ferner ist $k_2 = k_1/K_2$ und $k_4 = k_3 \cdot K_6$.

Aus dem Farbstoffperchlorat werden Stammlösungen in Aceton bereitet. Beim Mischen einiger ml einer solchen Stammlösung, welche die farblosen Karbinolformen F_1, F_2 und F_3 nicht enthält, mit einer geeigneten Wasserpufferlösung stellt sich das Gleichgewicht $G_1 \rightleftharpoons H^+ + R$ momentan ein *. Die Lösung hellt sich wegen der Zeitreaktionen $G_1 + H_2O \rightarrow F_1$ und $R + H_2O \rightarrow F_2$ (einschliesslich $R + OH^- \rightarrow F_3$) allmählich auf, ohne dabei ihren Farbton zu ändern, wobei ebenfalls die Gleichgewichte $F_1 \rightleftharpoons H^+ + F_2$ und $F_2 \rightleftharpoons H^+ + F_3$ sich momentan einstellen.

Durch Messen der Aufhellungsgeschwindigkeiten bei verschiedenen H^+-Konzentrationen — die Messungen werden spektrophotometrisch bei geeignet gewählter Wellenlänge ausgeführt — können teils die Geschwindigkeitskonstanten, teils durch Extrapolation auf die Zeit Null die Lichtextinktion E_0 im Augenblick des Mischens festgestellt werden. Aus der Variation von E_0 mit der $[H^+]$ kann K_1 berechnet werden. Nachdem die Aufhellung erfolgt und Gleichgewicht eingetreten ist, erhält man (mit gewissen Ausnahmen, siehe unten) einen stabilen und reproduzierbaren Wert (E_∞) der Lichtextinktion. Aus zusammengehörigen Werten von E_∞ und $[H^+]$ kann man in geeignet gewählten pH-Intervallen ** die Konstanten K_2, K_3, K_4 und K_6 und in stark sauren Lösungen (in denen die Aufhellung schnell verläuft) K_7 berechnen. Da die Formeln dieser Berechnungen schon abgeleitet worden sind[1] (abgesehen von der Berechnung von K_7), wird die Darstellung unten kurz gefasst.

Die Protolysenverläufe bei Benzaurin und 4″-Chlor-benzaurin sind im Vergleich zu denen bei Tetrabrom-benzaurin und Dibrom-dimethyl-benzaurin stark gegen niedrigere $[H^+]$ verschoben. So bildet sich die Form G_2 schon bei

* G_2 tritt erst in verhältnismässig stark sauren Lösungen auf.
** pH bedeutet $-\log[H^+]$.

mässiger Säurestärke (0,1 M HCl), weshalb K_7, im Gegensatz zum Falle beim Tetrabrom-benzaurin und beim Dibrom-dimethyl-benzaurin, bei der gewählten Ionenstärke, 0,50 M, für die Bestimmung zugänglich wird. Leider sind die Resultate bei Benzaurin und 4″-Chlor-benzaurin in einer anderen Hinsicht unvollständig. Bei Messungen in alkalischen Lösungen mit pH $>\sim$ 10 erwies es sich als unmöglich, einen stabilen und reproduzierbaren Wert von E_∞ zu erhalten. Dadurch wurde die genaue Bestimmung von K_4 unmöglich gemacht.

FORMELN

I. Berechnung von K_1 aus den Anfangsextinktionen

Für eine Reihe von Lösungen, erhalten durch Mischen einer Acetonstammlösung des Farbstoffes mit geeigneten Puffern, werden die Anfangsextinktionen E_0 bei gleicher Schichtdicke d und Gesamtkonzentration C des Farbstoffes durch Extrapolation auf die Zeit Null bestimmt. Falls die Messungen bei einer Wellenlänge stattfinden, wo nur R absorbiert, gilt [1]

$$\frac{1}{E_0} = \frac{1}{E_R} + \frac{K_1 \cdot [H^+]}{E_R} \tag{1}$$

wo E_R die Extinktion bei der betreffenden Schichtdicke für eine Lösung ist, in der $[R] = C$ ist. $1/E_0$ wird als Funktion von $[H^+]$ aufgetragen und gibt eine Gerade. Aus deren Schnittpunkt a_1 mit der Ordinate und dem Richtungskoeffizienten b_1 erhält man

$$E_R = 1/a_1 \quad ; \quad K_1 = b_1/a_1$$

II. Berechnungen aus den Gleichgewichtsextinktionen

Eine Lösung, die durch Mischung von einem Puffer mit einer Stammlösung des Farbstoffes in Aceton erhalten worden ist, enthält beim Gleichgewicht die Formen G_1, R, F_1, F_2 und F_3 (siehe Fussnote * S. 409).

A. Wenn $[H^+] \ll 1/K_1$ ist, kann $[G_1]$ vernachlässigt werden. Wenn E_∞ die Lichtextinktion beim Gleichgewicht ist und E_R wie oben (I.) definiert ist, gilt wie schon gezeigt wurde [1]:

$$E_\infty = E_R \cdot \frac{K_6}{1 + K_6 + [H^+]/K_3 + K_4/[H^+]} \tag{2}$$

und für $[H^+] = \sqrt{K_3 \times K_4}$

$$(E_\infty)_{max} = E_R \cdot \frac{K_6}{1 + K_6 + 2 \cdot \sqrt{K_4/K_3}} \tag{2a}$$

1. *Bestimmung von K_3K_6 und K_6.* In einem Gebiet, wo $[H^+] \gg K_4$ ($[F_3] \ll [F_1] + [F_2] + [R]$) ist, kann $K_4/[H^+]$ in Formel (2) vernachlässigt werden. Man bekommt dann:

$$\frac{1}{E_\infty} = \frac{1 + 1/K_6}{E_R} + \frac{1}{E_R \cdot K_3K_6} \cdot [H^+] \tag{3}$$

Die zusammengehörigen Werte von E_∞ und $[H^+]$ werden bestimmt. $1/E_\infty$ als Funktion von $[H^+]$ aufgetragen, gibt eine Gerade. Aus deren Schnittpunkt a_2 mit der Ordinate und dem Richtungskoeffizienten b_2 bekommt man:

$$K_6 = 1/(a_2 \cdot E_R - 1) \quad ; \quad K_3K_6 = 1/b_2 \cdot E_R$$

E_R erhält man entweder oben (I) und/oder/durch Extrapolation auf die Zeit Null für Lösungen mit genügend kleinen $[H^+]$-Werten. Wenn $[H^+] \ll 1/K_1$ ist, ist $E_0 = E_R$. Bei evtl. grösseren $[H^+]$-Werten muss $[G_1]$ berücksichtigt und eine entsprechende Korrektion in E_0 gemacht werden.

2. Bestimmung von $K_6/K_4 = K_5$ und K_6. Wenn $[H^+] \ll K_3$ ($[F_1] \ll [F_2] + [F_3] + [R]$) ist, kann $[H^+]/K_3$ in Formel (2) vernachlässigt werden. Man bekommt dann folgende lineare Funktion von $[H^+]$:

$$\frac{[H^+]}{E_\infty} = \frac{1}{E_R \cdot K_5} + \frac{1 + 1/K_6}{E_R} \cdot [H^+] \qquad (4)$$

Aus zusammengehörigen Werten von E_∞ und $[H^+]$ wird $[H^+]/E_\infty$ als Funktion von $[H^+]$ aufgetragen. Man erhält eine Gerade. Aus deren Schnittpunkt a_3 mit der Ordinate und dem Richtungskoeffizienten b_3 bekommt man (mit bekanntem E_R, siehe oben)

$$K_5 = 1/a_3 \cdot E_R \quad ; \quad K_6 = 1/(b_3 \cdot E_R - 1)$$

Wenn erforderlich wird bei den Berechnungen unter 1. und 2. oben E_∞ durch korrigierte Werte, und zwar durch E'_∞ oder E''_∞ unter 1. und E'''_∞ unter 2., ersetzt. Die Korrektionen, die nur einige Prozent von E_∞ betragen, und die in der bereits beschriebenen Weise[1] ausgeführt werden, berücksichtigen die geringen Konzentrationen, die nicht ganz zu vernachlässigen sind, von G_1 und F_3 bzw. F_1 in den Randgebieten bzw. im Randgebiet des betreffenden pH-Intervalls.

B. Bestimmung von K_2. Wenn $[H^+]$ grösser ist als in A und wenn es als sicher gilt, dass $[H^+] \gg K_4$ ist, hat man beim Gleichgewicht die Formen G_1, R, F_1 und F_2. ($[F_3]$ wird vernachlässigt). Aus zusammengehörigen Werten von E_∞ und $[H^+]$ und entsprechendem, bekanntem E_R kann dann K_2, wie schon gezeigt worden ist [1], aus der Formel

$$K_2 = \frac{E_R - E_\infty(1 + K_1 \cdot [H^+] + 1/K_6)}{E_\infty \cdot K_1 \cdot [H^+]} \qquad (5)$$

berechnet werden.

C. Bestimmung von K_7. Wenn HCl-Lösungen mit einer Säurestärke $> 0{,}1$ M mit einigen ml einer Stammlösung des Farbstoffes in Aceton versetzt werden, stellt sich zwischen den Formen F_1, G_1 und G_2 ein Gleichgewicht fast momentan ein. Wenn die Lichtabsorption der Lösung E und die Gesamtkonzentration des Farbstoffes C ist, gilt

$$\frac{[H^+] \cdot [G_1]}{[G_2]} = K_7 \quad ; \quad \frac{[F_1]}{[G_1]} = K_2$$

$$E = E_{G_1} \cdot [G_1]/C + E_{G_2} \cdot [G_2]/C$$

$$C = [F_1] + [G_1] + [G_2]$$

wo E_{G_1} (E_{G_2}) die Extinktion bei gleicher Schichtdicke für eine Lösung ist, in der $[G_1]$ ($[G_2]$) gleich C ist. Durch Vereinfachung erhält man

$$E = \frac{K_7 \cdot E_{G_1} + [H^+] \cdot E_{G_2}}{K_7(1 + K_2) + [H^+]} \tag{6}$$

Aus diesem Ausdruck kann man teils die Formel

$$\frac{[H^+]}{E - \frac{E_{G_1}}{1 + K_2}} = \frac{K_7(1 + K_2)}{E_{G_2} - \frac{E_{G_1}}{1 + K_2}} + \frac{[H^+]}{E_{G_2} - \frac{E_{G_1}}{1 + K_2}} \tag{7}$$

teils die Formel

$$\frac{E - \frac{E_{G_1}}{1 + K_2}}{E_{G_2} - E} = \frac{[H^+]}{K_7(1 + K_2)} \tag{8}$$

bekommen, in denen die linken Glieder lineare Funktionen von $[H^+]$ sind.

Bei der Anwendung von Formel (7) wird für zusammengehörige Werte von E und $[H^+]$ der Ausdruck $[H^+]/\left(E - \frac{E_{G_1}}{1 + K_2}\right)^*$ als Funktion von $[H^+]$ aufgetragen. Man erhält eine Gerade. Aus deren Schnittpunkt a_4 mit der Ordinate und dem Richtungskoeffizienten b_4 bekommt man

$$K_7 (1 + K_2) = a_4/b_4 \qquad (7a); \qquad E_{G_2} = 1/b_4 + \frac{E_{G_1}}{1 + K_2} \qquad (7b)$$

Die Formel (7) verlangt bei der Anwendung, dass die Messungen sich auf Wasserstoffionenkonzentrationen erstrecken, die nicht viel kleiner als $K_7 (1 + K_2)$ sind. Im vorliegenden Falle bedeutet dieses, dass die Ionenstärke 0,50 M überschritten werden muss. K_2 hat in diesem Falle einen Wert, der sich von dem früheren, bei der Ionenstärke 0,50 M bestimmten, unterscheidet. K_7 kann daher nicht aus der Formel (7a) oben berechnet werden und es wird folgendermassen verfahren. Eine Mess-serie wird bei einer höheren, konstanten Ionenstärke (1,00 M) durchgeführt und zusammengehörige Werte von E und $[H^+]$ werden graphisch nach Formel (7) dargestellt, wonach E_{G_2} nach Formel (7b) berechnet wird. Danach wird eine neue Messerie bei der Ionenstärke 0,50 M durchgeführt, wobei zusammengehörige Werte von E und $[H^+]$ nach Formel (8) graphisch dargestellt werden, unter Einsetzen des oben bestimmten Wertes von E_{G_2}. Das linke Glied der Formel wird als Funktion von $[H^+]$ aufgetragen. Man bekommt eine Gerade durch Origo mit dem Richtungskoeffizienten b_5, wo $K_7 = 1/b_5(1 + K_2)$ ist, wobei das Einestzen vom früher bestimmten K_2 die Konstante K_7 ergibt.

III. Berechnungen der Geschwindigkeitskonstanten

Beim Mischen einer Stammlösung des Farbstoffes in Aceton mit einer Pufferlösung hellt sich die Mischung wegen der Zeitreaktionen $G_1 + H_2O \rightarrow F_1$

---

* E_{G_1} ist bekannt, siehe "Messungen und Ergebnisse". Der Ausdruck $\frac{E_{G_1}}{1 + K_2}$ hat sowohl in (7) als auch in (8) den Charakter eines Korrektionsgliedes und beträgt nur einige Prozent von E. (K_2 ist gross).

und $R + H_2O \rightarrow F_2$ auf. Die Konstante k der Aufhellungsgeschwindigkeit wird durch Messung der Lichtextinktion E als Funktion der Zeit t ermittelt. Folgende Formeln [1,3,4] gelten:

$$k = \frac{1}{t} \cdot \ln \frac{E_0 - E_\infty}{E - E_\infty} \tag{9}$$

$$k = \frac{k_2 \cdot [H^+]^2 + k_4 K_3 \cdot [H^+]}{[H^+]^2 + K_3 \cdot [H^+] + K_3 K_4} + \frac{k_1 K_1 \cdot [H^+] + k_3}{1 + K_1 \cdot [H^+]} \tag{10}$$

k ist über das ganze in Frage kommende pH-Gebiet experimentell bestimmt worden, wobei E im Absorptionsmaximum von R gemessen wird, wo $[R] \geqq [G_1]$ ist, bei geringerem pH im Absorptionsmaximum von G_1. Log $(E - E_\infty)$ als Funktion von t aufgetragen ergibt eine Gerade, deren Richtungskoeffizient $= - k \cdot {}^{10}\log e$ ist.

A. Bestimmung von k_1 und k_2. In genügend sauren Lösungen, wo die Reaktion $G_1 + H_2O \rightleftharpoons F_1$ dominiert, und man von der Reaktion $R + H_2O \rightleftharpoons F_2$ absehen kann, gilt [1]

$$k = k_1 \cdot \frac{K_1 \cdot [H^+]}{1 + K_1 \cdot [H^+]} + k_2 \tag{11}$$

Da $k_2 = k_1/K_2$ ist, kann k_1, bei verschiedenen $[H^+]$-Werten, aus (11) mit zusammengehörigen Werten von k und $[H^+]$ eingesetzt, berechnet werden. Man findet wie früher [1], dass k_1 mit $[H^+]$ gemäss der Formel

$$k_1 = k_1^\circ + k_1' \cdot [H^+] \tag{12}$$

wächst, wo k_1° von Null verschieden ist. (Man bekommt k_2 aus der Relation $k_2 = k_1/K_2$.) Die Reaktion $G_1 + H_2O \rightleftharpoons F_1$ wird folglich durch die H^+-Ionen katalysiert. Die Katalyse mag einer eventuellen schnellen Reaktion $G_2 + H_2O \rightleftharpoons F_1 + H^+$ entsprechen.

B. Bestimmung von k_3 und k_4. Bei genügend hohen pH-Werten, wo von der Reaktion $G_1 + H_2O \rightleftharpoons F_1$ abgesehen werden kann, und wo ferner $[H^+] \ll K_3$ ist, gilt [1]

$$k = k_4 \frac{[H^+]}{[H^+] + K_4} + k_3 \tag{13}$$

Evtl. kann die Formel weiter vereinfacht werden, wenn bei geringen $[H^+]$-Werten der erste Ausdruck des rechten Gliedes vernachlässigt werden kann und daher $k = k_3$ wird. Die Bestimmung von k_3 $(= k)$ bei verschiedenen pH-Werten zeigt, dass k_3 wie früher [1] der Formel

$$k_3 = k_3^\circ + k_3' \cdot [OH^-] \ * \tag{14}$$

folgt. Man findet dass k_3° von Null verschieden ist. (k_4 erhält man aus der Relation $k_4 = k_3 \cdot K_6$.) Folglich wird die Reaktion $R + H_2O \rightleftharpoons F_2$ durch die OH^--Ionen katalysiert. Die Katalyse entspricht wahrscheinlich der Reaktion $R + OH^- \rightleftharpoons F_3$.

ALLGEMEINES ÜBER DEN EXPERIMENTELLEN TEIL

Die Stammlösungen des Farbstoffes in Aceton, welche durch Auflösung einer abgewogenen Menge des Perchlorats des Farbstoffes** zubereitet wurden, waren von der Stärke

* $[OH^-]$ erhält man aus $[H^+] \cdot [OH^-] = K_w$. ** G_1-Perchlorat.

4×10^{-4} M. Ohne Zusatz einer Base erwiesen sich die Stammlösungen als schlecht haltbar und sehr empfindlich gegen Spuren von Wasser, das durch Hydratation (Bildung der F-Formen) die Lösung aufhellt. Infolgedessen wurden die für die Messungen benutzten Stammlösungen bei der Zubereitung mit Triäthylamin bis zu einer Konzentration von 1×10^{-2} M versetzt. Solche Lösungen zeigten eine ausgezeichnete Haltbarkeit, was dadurch zu erklären ist, dass die Hydratation für das Gleichgewicht $R + H_2O \rightleftharpoons F_2$, das in basischen Lösungen dominiert, verhältnismässig gering ist und bedeutend geringer als beim Gleichgewicht $G_1 + H_2O \rightleftharpoons F_1$. (Vergleiche die Werte für $1/K_6$ und K_2).

Die Messlösungen wurden in Kolben aus Pyrex- oder Jenaer-Glas bereitet, dadurch dass zu 49,0 ml Puffer 1,050 ml Farbstoffstammlösung mittels einer Injektionsspritze aus Pyrex-Glas zugesetzt wurde. Das Volumen der Spritze war durch Auswägen mit Wasser ermittelt worden; die Reproduzierbarkeit betrug 0,1 %. Folglich beziehen sich die bestimmten Konstanten durchgehend auf ein Lösungsmittel von der Zusammensetzung 98 % Wasser + 2 % Aceton. Die Ionenstärke war durch Zusatz von NaCl konstant und gleich 0,50 M (siehe jedoch die Bestimmung von K_7 und die Aufnahme der E_{G_2}-Kurven). Die Temperatur betrug 20°C.

Die Messung von $[H^+]$ wurde wie früher [1] für $pH < 8$ mit Chinhydronelektroden und für $pH > 8$ mit Platin-Wasserstoffgaselektroden ausgeführt. Als Vergleichslösung diente eine HCl-NaCl-Lösung mit bekannter $[H^+]$. In den sauren Lösungen ($0 \leq pH \leq 1$), die bei der Bestimmung von K_7 zur Verwendung kamen, wurde die $[H^+]$ durch Zusatz von einer bekannten Menge HCl festgelegt. Für Messungen über die Reaktionskinetik bei $pH > 11{,}8$ wurde die $[OH^-]$ durch Zusatz von bekannter Menge NaOH festgelegt. $K_w = [H^+] \cdot [OH^-]$ ist in der früheren Arbeit [1] zu $1{,}22 \times 10^{-14}$ bestimmt worden.

Für die Messungen der Lichtextinktion wurde ein Beckman-Quarz-Spektrophotometer, Modell DU, benutzt. Die Glas- oder Quarzküvetten waren mit Schliffstopfen versehen. Von jedem Paar diente eine, mit dest. Wasser gefüllt, als Nullreferenz.

Bei den früheren Untersuchungen [1] über Tetrabrom-benzaurin und Dibrom-dimethyl-benzaurin musste die Konzentration des Farbstoffes in gewissen Mess-serien wegen der Schwerlöslichkeit der Substanzen (der Formen G_1) sehr niedrig ($3{,}5 \times 10^{-7}$ M) gehalten werden. Benzaurin und 4'-Chlor-benzaurin scheinen bedeutend leichter löslich zu sein; die Konzentration des Farbstoffes in den Messlösungen konnte durchgehend $\sim 9 \times 10^{-6}$ M betragen.

Wie schon erwähnt erwies es sich als unmöglich, reproduzierbare Werte der Lichtextinktion (E_∞) beim Gleichgewicht für $pH > \sim 10$ zu erhalten. Der Grund ist wahrscheinlich ein irreversibler Abbau des Farbstoffes in alkalischem Milieu. Messlösungen, bereitet aus Stickstoff-gesättigten, von gelöstem Saurstoff befreiten Puffern, zeigten keine Verbesserung der Reproduzierbarkeit bei E_∞. Auch nicht der Zusatz von geringen Mengen KCN führte zu einer Verbesserung. Demzufolge ist es nicht möglich gewesen, die für eine sorgfältige Bestimmung von K_4 nach Formel (4) erforderlichen Messungen auszuführen. Ebenfalls konnte nicht $(E_\infty)_{max}$ (vgl. Formel (2a)) aus den Messungen ermittelt werden. Da E_∞ verglichen mit E_0 klein ist, spielt jedoch die Unsicherheit in E_∞ keine grössere Rolle bei der Bestimmung der Geschwindigkeitskonstante k. Die Kurven über die Variation dieser Konstante mit dem pH-Wert weisen im Gegensatz zum Verhalten beim Tetrabrom-benzaurin und Dibrom-dimethyl-benzaurin [1] kein Maximum auf (Fig. 8 und 18, Formel (10)).

Die Geschwindigkeitskonstanten sind mit Brigg'schen Logarithmen berechnet worden und enthalten also die Grösse $^{10}\log e$.

Die bestimmten Konstanten sind so angegeben worden, dass die Unsicherheit normalerweise 2 – 5 Einheiten in der letzten Ziffer beträgt. Bei evtl. grösserer Unsicherheit wurde die Ziffer in Klammern gesetzt.

Die verwendeten Chemikalien waren pro-analysi-Produkte von Baker oder Merck.

MESSUNGEN UND ERGEBNISSE

I. Benzaurin

Präparat: Das Benzaurin wurde nach Döbner [5] synthetisiert. Nach Reinigung mit Bisulfit wurde der Farbstoff in reiner Form als Perchlorat hergestellt (Pfeiffer [6], Meyer und Gerloff [7]). Das Endprodukt bestand aus roten Kristallen

mit ausgeprägtem, grünem Oberflächenglanz. Die Elementaranalyse ergab folgendes Resultat: C 60,61; H 3,89; O 25,40; Cl 9,32; 9,64. Berechnet für $C_{19}H_{15}O_6Cl$: C 60,89; H 4,03; O 25,62; Cl 9,46.

Puffersubstanzen waren Dinatriumhydrogenphosphat-Natriumhydroxyd, Borsäure-Natriumhydroxyd, Natriumdihydrogenphosphat-Dinatriumhydrogenphospat, Essigsäure-Natriumacetat in folgenden ungefähren pH-Intervallen: 10,5—11,5; 8,7—9,6; 7,4—8,5; 5,1—6,7.

Die Lichtabsorptionskurven * für das rote Ion R, das gelbe Molekül G_1 und das rotgelbe Ion G_2 finden sich in Fig. 1 wieder, wo der molekulare Lichtextinktionskoeffizient ε der betreffenden Formen als Funktion der Wellenlänge λ in mμ aufgetragen ist. Die Kurve für R wurde durch Messung von E_∞ in einem Puffer mit pH = 9,58 und $C = 8{,}0 \times 10^{-6}$ M aufgenommen; d betrug 5 cm. Durch Extrapolation auf $t = 0$ wurde bei $\lambda = 550$ mμ entsprechendes E_R zu 1,90 (0,758 bei $d = 2$ cm) bestimmt. Da E_∞ bei 550 mμ zu 0,692 gemessen wurde, galt für die Lösung, dass $E_R/E_\infty = 2{,}74$ war. ε_R wurde aus

$$2{,}74\, E_\infty = \varepsilon_R \times 5 \times 8{,}0 \times 10^{-6}$$

berechnet.

Die G_1-Kurve wurde bei pH = 5,85 aufgenommen. Da der Gleichgewichtswert E_∞ klein ist (K_2 ist gross), wurden sämtliche Punkte auf der Kurve durch Extrapolationsverfahren erhalten. C war $8{,}0 \times 10^{-6}$ M und $d = 5$ cm. E_0 wurde durch Extrapolation auf $t = 0$ erhalten. Aus diesem E_0 wurde E_{G_1} gemäss der Formel

$$E_0 = \frac{[H^+]}{1/K_1 + [H^+]} \cdot E_{G_1} + \frac{1/K_1}{1/K_1 + [H^+]} \cdot E_R$$

berechnet, und ε_{G_1} nach $E_{G_1} = \varepsilon_{G_1} \times 5 \times 8{,}0 \times 10^{-6}$.

Die Kurve für G_2 wurde in einer Lösung mit $[H^+] = 0{,}825$ (Ionenstärke 1.00 M) M aufgenommen. E wurde mit $C = 8{,}1 \times 10^{-6}$ M und $d = 5$ cm gemessen. Bei der Bestimmung von K_7 unten wurde E_{G_1} bei $\lambda = 490$ mμ (und

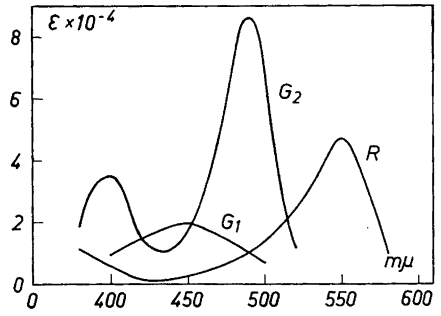

Fig. 1. Benzaurin. Lichtabsorptionskurven. R ist das rote Ion, $[(OC_6H_4)_2\ C(C_6H_5)]^+$; G_1 ist das gelbe Molekül $(HOC_6H_4)C(C_6H_5)(C_6H_4O)$; G_2 das rotgelbe Ion $[(HOC_6H_4)_2\ C(C_6H_5)]^+$.

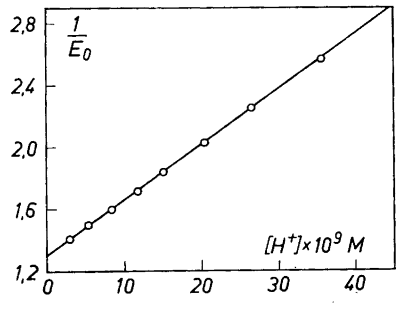

Fig. 2. Benzaurin. $1/E_0$ als Funktion von $[H^+]$ für die Bestimmung von K_1 (und E_R). $\lambda = 550$ mμ, $d = 2$ cm und $C = 8{,}0 \times 10^{-6}$ M.

* E_R, E_{G_1} und E_{G_2} sind im Kap. Formeln (I. und II.C) definiert.

$d = 2$ cm) erhalten. Aus E_{G_2} und dem bei 490 mμ gemessenen Wert von E wurde der Quotient E_{G_2}/E für die Lösung zu 2,50 berechnet. ε_{G_2} wurde also aus der Relation $2{,}50\ E = \varepsilon_{G_2} \times 5 \times 8{,}1 \times 10^{-6}$ erhalten.

Die Daten für die Maxima betrugen:

$$\begin{aligned}(\varepsilon_R)_{max} &= 4{,}7 \times 10^4 \text{ bei } \lambda \approx 550 \text{ m}\mu\\ (\varepsilon_{G_1})_{max} &= 1{,}8(8) \times 10^4 \text{ bei } \lambda \approx 450 \text{ m}\mu\\ (\varepsilon_{G_2})_{max} &= 8{,}6 \times 10^4 \text{ bei } \lambda \approx 490 \text{ m}\mu\\ (\varepsilon_{G_3})_{max} &= 3{,}5 \times 10^4 \text{ bei } \lambda \approx 400 \text{ m}\mu\end{aligned}$$

Bestimmung von K_1 aus Formel (1). Im Gebiet $7{,}4 < \text{pH} \leq 8{,}5$ wurden Messlösungen durch Mischen von 49 ml Puffer mit 1 ml Acetonstammlösung des Farbstoffes bereitet. Die Aufhellung wurde extinktiometrisch bei $\lambda = 550$ mμ verfolgt und E_0 durch Extrapolation erhalten. Die Messungen wurden bei einer Schichtdicke d von 2 cm ausgeführt; die Gesamtkonzentration C des Farbstoffes betrug $8{,}0 \times 10^{-6}$ M. In Fig. 2 ist $1/E_0$ als Funktion von $[H^+]$ dargestellt.

Resultat: $E_R = 0{,}76(6)$; $K_1 = 2{,}7(2) \times 10^7$; $1/K_1 = 3{,}7 \times 10^{-8}$

Bestimmung von K_3K_6 und K_6 aus Formel (3). Die Messlösungen wurden im Gebiet $8{,}7 < \text{pH} < 9{,}6$ bereitet. C war $9{,}3 \times 10^{-6}$ M. E_∞ wurde bei 5 cm Schichtdicke und bei der Wellenlänge 550 mμ gemessen. Entsprechendes E_R wurde bei $d = 2$ cm durch Extrapolation auf $t = 0$ für sieben Lösungen im selben pH-Gebiet bestimmt. Aus den E_0-Werten wurde, nach Korrektion für $[G_1]$, $(E_R)_{2\text{ cm}} = 0{,}876 \pm 0{,}005$ erhalten, folglich ist $(E_R)_{5\text{ cm}} = 2{,}19 \pm 0{,}01$. Fig. 3 gibt $1/E''_\infty$ als Funktion von $[H^+]$ wieder.

Resultat: $K_6 = 0{,}93$; $K_3K_6 = 3{,}4(2) \times 10^{-10}$; $K_3 = 3{,}7 \times 10^{-10}$

Die Reproduzierung der Messungen ergab das gleiche Resultat.

Bestimmung von $K_5' = K_6/K_4$ und K_6 aus Formel (4) konnte nicht durchgeführt werden, weil es, wie schon erwähnt wurde, bei einem $\text{pH} > \sim 10$ unmöglich ist, reproduzierbare Werte von E_∞ zu erhalten. Aus den Messungen wurde ein ungefährer Wert von K_4 geschätzt. $K_4 \approx 7 \times 10^{-11}$.

Bestimmung von K_2 aus Formel (5) erfolgte im Gebiet $7{,}6 \leq \text{pH} \leq 8{,}3$. Die Messlösungen waren identisch mit einigen von den Lösungen, die bei der Bestimmung von K_1 oben zur Verwendung kamen. Nachdem Gleichgewicht eingetreten war, wurde E_∞ bei $\lambda = 550$ mμ und $d = 2$ cm gemessen. Durch

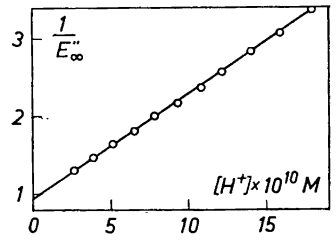

Fig. 3. Benzaurin. $1/E''_\infty$ als Funktion von $[H^+]$ für die Bestimmung von K_3K_6 und K_6. $\lambda = 550$ mμ, $d = 5$ cm und $C = 9{,}3 \times 10^{-6}$ M.

Tabelle 1. Benzaurin. Messungen bei 550 mμ zur Bestimmung von K_2; $d = 2$ cm, $C = 8{,}0 \times 10^{-6}$ M.

$[H^+] \times 10^9$ M	26,4	20,4	15,0(8)	11,7(5)	8,3(3)	5,2(6)
E_∞	0,010(0)	0,012(5)	0,017(5)	0,022(5)	0,030(5)	0,046(0)
K_2	101	103	101	99	99	100

Extrapolation bei pH = 9,58 wurde $E_R = 0{,}758$ erhalten. Für K_1 und K_6 wurden die oben bestimmten Werte verwendet. Die Resultate sind in Tabelle 1 aufgeführt. Im Mittel wurde $K_2 = 100$ erhalten.

Die oben erhaltenen Konstanten ergeben das Produkt $K_1K_2K_3K_6 = 0{,}93$.

Bestimmung von K_7. Zuerst wurde eine Mess-serie bei der Ionenstärke 1,00 M ausgeführt. $[H^+]$ variierte in den Messlösungen zwischen 0,17 und 1,00 M. C war $8{,}2 \times 10^{-6}$ M und E wurde bei der Wellenlänge 490 mμ (im Absorptionsmaximum von G_2) mit $d = 2$ cm gemessen. In Fig. 4 ist $[H^+]/(E - \frac{E_{G_1}}{1 + K_2})$ als Funktion von $[H^+]$ aufgetragen. Man bekommt (mit $E_{G_1}/(1 + K_2) = 0{,}002$)

$$E_{G_2} = 1{,}39(2); \qquad (K_7 (1 + K_2) = 1{,}21)$$

Danach wurde eine Mess-serie bei der Ionenstärke 0,50 M und mit gleichem C wie oben ausgeführt. $[H^+]$ variierte zwischen 0,085 und 0,49 M, und E wurde bei gleichem λ und d wie oben gemessen. Mit obenstehendem E_{G_2} wird in Fig. 5 $(E - \frac{E_{G_1}}{1 + K_2})/(E_{G_2} - E)$ als Funktion von $[H^+]$ wiedergegeben. Resultat *

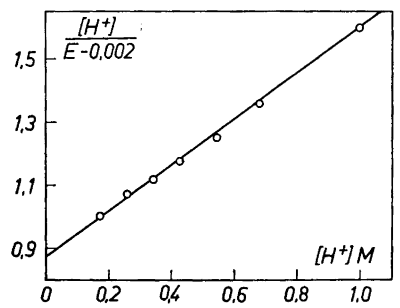

Fig. 4. Benzaurin. $[H^+]/\left(E - \frac{E_{G_1}}{1 + K_2}\right)$ als Funktion von $[H^+]$ für die Bestimmung von $E_{G_2} \cdot \lambda = 490$ mμ, $d = 2$ cm und $C = 8{,}2 \times 10^{-6}$ M.

* Eine graphische Berechnung aus der weniger genauen Formel (7) ergibt das Resultat $K_7 (1 + K_2) = 1{,}7(7)$ und $E_{G_2} = 1{,}46$.

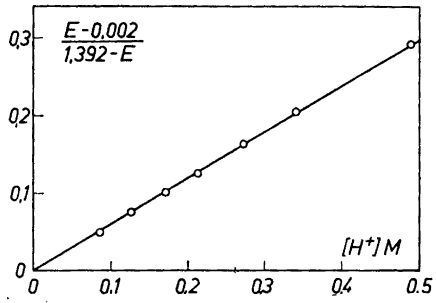

Fig. 5. Benzaurin. $\left(E - \frac{E_{G_1}}{1 + K_2}\right) / (E_{G_2} - E)$ als Funktion von [H+] für die Bestimmung von K_7. $\lambda = 490$ mμ, $d = 2$ cm und $C = 8{,}2 \times 10^{-6}$ M.

$K_7(1 + K_2) = 1{,}6(8)$. Einsetzen von $K_2 = 100$ ergibt $K_7 = 1{,}6(6) \times 10^{-2}$.

Messungen der Reaktions- (Aufhellungs-) geschwindigkeiten. Die Geschwindigkeitskonstante k wurde im Gebiet $5{,}1 < \text{pH} < 12{,}7$ bestimmt. In den Gebieten $8{,}7 < \text{pH} < 9{,}6$ und $6{,}0 < \text{pH} < 6{,}7$ war (mit einer Ausnahme) $C = 9{,}3 \times 10^{-6}$ M, für die übrigen Lösungen $8{,}0 \times 10^{-6}$ M. E wurde bei $\lambda = 450$ mμ

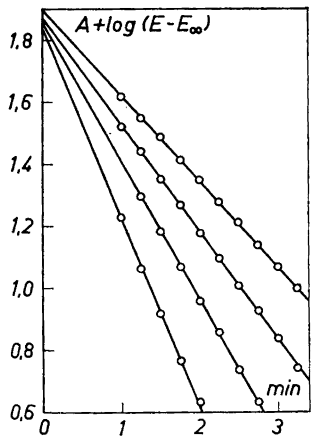

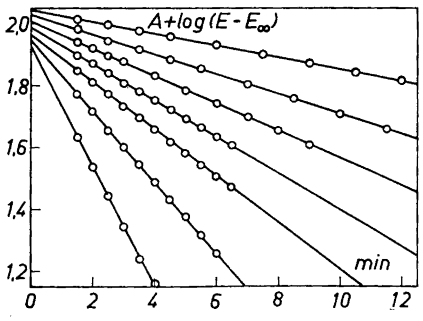

Fig. 6. Benzaurin. Reaktionskinetik bei $\lambda = 450$ mμ, $d = 5$ cm und $C = 8{,}0 \times 10^{-6}$ M. Für die Linien gelten in der Ordnung von oben nach unten die folgenden Daten:

A:	2,03	2,00	2,00	1,95
pH:	5,460	5,350	5,227	5,114

Fig. 6a. Benzaurin. Reaktionskinetik bei $\lambda = 450$ mμ und $d = 5$ cm. Für die Linien gelten in der Ordnung von oben nach unten die folgenden Daten:

A:	2,17	2,13	2,10	2,13	2,04	2,08	2,05
pH:	6,659	6,433	6,284	6,157	6,038	5,850	5,610
$C \times 10^6$ M:	9,3	9,3	9,3	8,0	9,3	8,0	8,0

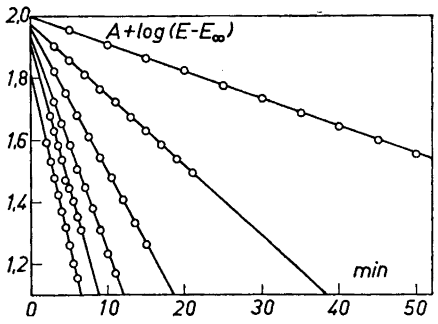

Fig. 7. Benzaurin. Reaktionskinetik bei $\lambda = 550$ mμ, $d = 2$ cm und $C = 8{,}0 \times 10^{-6}$ M. Für die Linien gelten in der Ordnung von oben nach unten die folgenden Daten:

A:	2,13	2,10	2,08	2,05	2,03	1,94
pH:	11,50(5)	11,95(5)	12,25(5)	12,43	12,55(5)	12,65

(Absorptionsmaximum von G_1)| mit $d = 5$ cm für pH < 7 gemessen, und bei $\lambda = 550$ mμ (Absorptionsmaximum von R) mit $d = 2$ cm für pH > 7 gemessen. In den Figuren 6, 6a und 7 sind die kinetischen Verläufe in den sauren und alkalischen Lösungen wiedergegeben, in welchen die Messungen der graphischen Berechnung von k_1 und k_2 bzw. k_3 und k_4 zu Grunde lagen. Fig. 8 zeigt k als Funktion des pH-Wertes. (Vergleiche Formel (10)).

Bestimmung von k_1 und k_2. Im Gebiet $5{,}1 <$ pH $< 6{,}7$ ist k_1 aus Formel (11) durch Einsetzen der Beziehung $k_2 = k_1/K_2$ und zusammengehörigen Werten von k und $[H^+]$ berechnet worden. Die Figuren 9 und 9a zeigen, dass k_1 als Funktion von $[H^+]$ eine Gerade ist. Graphische Bestimmung ergab das Resultat: $k_1^\circ = 5{,}2 \times 10^{-3}$, $k_1' = 8{,}0 \times 10^4$. Man erhält also:

$k_1 = 5(,2) \times 10^{-3} + 8{,}0 \times 10^4\ [H^+]$; $k_2 = 5(,2) \times 10^{-5} + 8{,}0 \times 10^2\ [H^+]$ (Min^{-1}); $[H^+]$ in Mol/l.

Bestimmung von k_3 und k_4. Im Gebiet pH $> 11{,}9$ gilt, dass $k = k_3$ ist. Fig. 10 zeigt, dass k_3 in diesem Gebiet eine lineare Funktion von $[OH^-]$ ist. Da k_3° klein ist, konnte es nicht graphisch ermittelt werden; k_3' wurde zu 2,0(4) bestimmt.

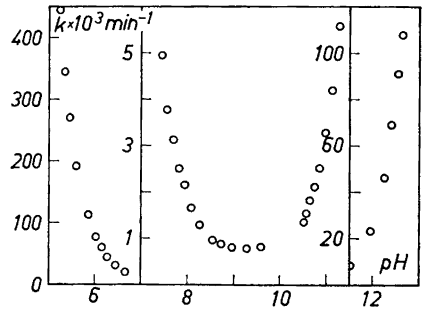

Fig. 8. Benzaurin. Die Geschwindigkeitskonstante k als Funktion von pH. O sind experimentell gefundene Werte.

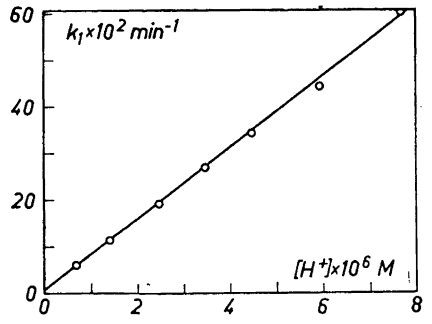

9.

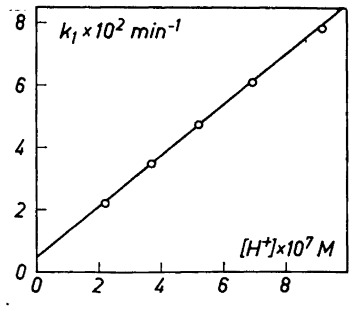

9a.

Fig. 9 und 9a. Benzaurin. Die Geschwindigkeitskonstante k_1 als Funktion von [H+].

Für die Bestimmung von $k_3°$ wurden zusammengehörige Werte von k und [H$^+$] in Formel (10) eingesetzt. k_3 wird mit den bekannten Werten von k_1, k_2, K_1, K_3, K_4 und K_6 und der Beziehung $k_4 = k_3 \cdot K_6$ berechnet. [H$^+$] wird so gewählt, dass der Ausdruck K_3K_4 in Formel (10) nur den Charakter eines Korrektionsgliedes hat, in welchem Falle der geschätzte Wert von K_4 ausreichend ist. Aus dem erhaltenen k_3 wird $k_3° = k_3 - k_3' \cdot [OH^-]$ berechnet. Folgende vier Berechnungen wurden ausgeführt:

[H+] $\times 10^9$ M	0,452	0,78(2)	1.59(2)	2,96
$k \times 10^4$ Min^{-1}	7,9(1)	7,7(5)	8.5(9)	9,6(9)
$k_3° \times 10^4$ Min^{-1}	4,5(4)	4,6(4)	5.1(2)	4,9(7)

Mittelwert: $k_3° = 4{,}8 \times 10^{-4}$ Min^{-1}.
Man erhält also
$k_3 = 4{,}8 \times 10^{-4} + 2{,}0(4)\,[OH^-]$; $k_4 = 4{,}5 \times 10^{-4} + 1{,}8(9)\,[OH^-]$ (Min^{-1}); [OH$^-$] in Mol/l.

II. 4″-Chlor-benzaurin

Als *Präparat* wurde das in einer früheren Arbeit beschriebene Perchlorat des Farbstoffes verwendet (Benzaurinstudien I.[8]).

Puffersubstanzen waren Dinatriumhydrogenphosphat-Natriumhydroxyd, Borsäure-Natriumhydroxyd, Natriumdihydrogenphosphat-Dinatriumhydrogenphosphat in den pH-Intervallen 9,8—11,5, 8,0—9,7, 5,6—7,9.

In sämtlichen unten dargelegten Messungen war die Gesamtkonzentration C des Farbstoffes in den Messlösungen $9{,}0 \times 10^{-6}$ M.

Die *Lichtabsorptionskurven* für R (rot), G_1 (gelb) und G_2 (rotgelb) finden sich in Fig. 11 wieder. Sämtliche Kurven wurden bei $d = 5$ cm aufgenommen; die R-Kurve bei pH = 9,45 mit $E_R/E_\infty = 3{,}80$, die G_1-Kurve durch Extrapolationsverfahren bei pH = 6,15 und die G_2-Kurve bei [H$^+$] = 1,015 M mit $E_{G_1}/E = 5{,}25$. Die Berechnungen von ε wurden wie beim Benzaurin ausgeführt.

Es wurden folgende Daten für die Maxima erhalten:

$(\varepsilon_R)_{max} = 4{,}0 \times 10^4$ bei $\lambda \approx 555$ mμ; $(\varepsilon_{G_1})_{max} = 1{,}6(5) \times 10^4$ bei $\lambda \approx 450$ mμ;
$(\varepsilon_{G_2})_{max} = 13(,0) \times 10^4$ bei $\lambda \approx 495$ mμ; $(\varepsilon_{G_2})_{max} = 6{,}0 \times 10^4$ bei $\lambda \approx 410$ mμ.

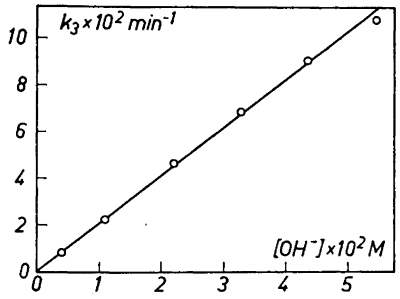

Fig. 10. Benzaurin. Die Geschwindigkeitskonstante k_3 als Funktion von $[OH^-]$.

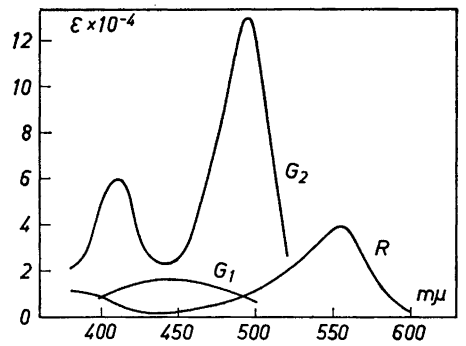

Fig. 11. 4″-Chlor-benzaurin. Lichtabsorptionskurven. R ist das rote Ion $[(OC_6H_4)_2 C(C_6H_4Cl)]^+$, G_1 das gelbe Molekül $(HOC_6H_4) C(C_6H_4Cl)(C_6H_4O)$ und G_2 das rotgelbe Ion $[(HOC_6H_4)_2 C(C_6H_4Cl)]^+$.

Bestimmung von K_1 aus Formel (1) erfolgte im Gebiet $7{,}2 < \text{pH} < 8{,}3$. Die Extinktionsmessungen wurden bei $\lambda = 550$ mμ und $d = 2$ cm ausgeführt; E_0 wurde durch Extrapolation erhalten. Fig. 12 zeigt $1/E_0$ als Funktion von $[H^+]$.

Resultat: $E_R = 0{,}69(5)$; $K_1 = 2{,}2(2) \times 10^7$; $1/K_1 = 4{,}5 \times 10^{-8}$

Bestimmung von K_3K_6 *und* K_6 aus Formel (3) im Gebiet $8{,}4 < \text{pH} < 9{,}5$. E_∞ wurde bei $d = 5$ cm und $\lambda = 550$ mμ gemessen. E_R wurde bei $d = 2$ cm durch Extrapolation für sechs Lösungen zu $0{,}692 \pm 0{,}004$ bestimmt (in guter Übereinstimmung mit dem Wert oben bei der Bestimmung von K_1). Folglich war $(E_R)_{5\text{ cm}} = 1{,}73(0)$. Fig. 13 zeigt $1/E''_\infty$ als Funktion von $[H^+]$.

Resultat: $K_6 = 0{,}90$; $K_3K_6 = 3{,}0(7) \times 10^{-10}$; $K_3 = 3{,}4 \times 10^{-10}$

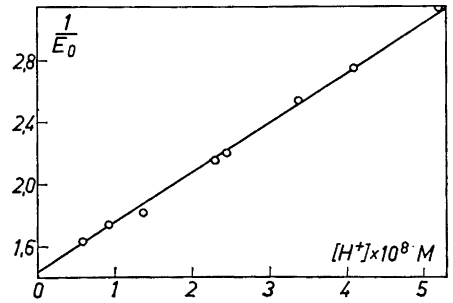

Fig. 12. 4″-Chlor-benzaurin. $1/E_0$ als Funktion von $[H^+]$ für die Bestimmung von K_1 (und E_R). $\lambda = 550$ mμ und $d = 2$ cm.

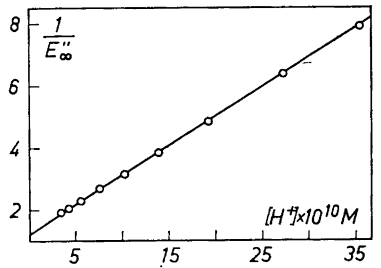

Fig. 13. 4″-Chlor-benzaurin. $1/E''_\infty$ als Funktion von $[H^+]$ für die Bestimmung von K_3K_6 und K_6. $\lambda = 550$ mμ und $d = 5$ cm.

Tabelle 2. 4″-Chlor-benzaurin. Messungen bei 550 mμ zur Bestimmung von K_2; $d = 5$ cm, $C = 9{,}0 \times 10^{-6}$ M.

$[H^+] \times 10^6$ M	41,0	33,7	24,5	23,1	13,7(3)	9,2(1)	5,9(5)
E_∞	0,014(0)	0,016(0)	0,022(5)	0,023(5)	0,042(0)	0,055(5)	0,083(5)
K_2	133	140	136	139	127	141	140

Bestimmung von $K_5 = K_6/K_4$ *und* K_6 aus Formel (4) konnte aus bereits erwähntem Grund nicht ausgeführt werden. Aus den Messungen wurde ein ungefährer Wert von K_4 geschätzt. $K_4 \approx 14 \times 10^{-11}$.

Bestimmung von K_2 aus Formel (5) im Gebiet $7{,}2 < \text{pH} < 8{,}3$. Die Messlösungen waren identisch mit denen, die bei der Bestimmung von K_1 oben verwendet wurden. E_∞ wurde bei $\lambda = 550$ mμ und $d = 5$ cm gemessen; das entsprechende E_R ist dann 1,73(0). Für K_1 und K_6 wurden die oben bestimmten Werte eingesetzt. Die Resultate sind in Tabelle 2 aufgeführt. Als Mittelwert wurde $K_2 = 137$ erhalten.

Die oben bestimmten Konstanten ergeben das Produkt $K_1K_2K_3K_6 = 0{,}93$.

Bestimmung von K_7. In der ersten Mess-serie bei der Ionenstärke 1,00 M variierte $[H^+]$ zwischen 0,25 und 1,00 M. E wurde bei $d = 5$ cm und bei $\lambda = 490$ mμ gemessen. Fig. 14 zeigt $[H^+]/\left(E - \frac{E_{G_1}}{1 + K_2}\right)$ als Funktion von $[H^+]$. Man erhält (mit $E_{G_1}/(1 + K_2) = 0{,}004$)

$$E_{G_2} = 5{,}5(9) \quad ; \quad (K_7(1 + K_2) = 4{,}3)$$

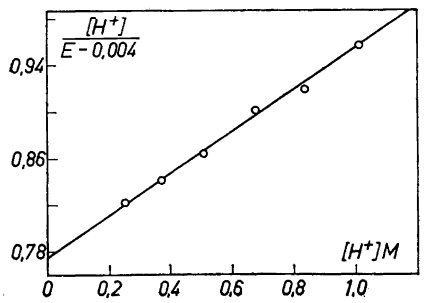

Fig. 14. 4″-Chlor-benzaurin. $[H^+]/\left(E - \frac{E_{G_1}}{1 + K_2}\right)$ als Funktion von $[H^+]$ für die Bestimmung von E_{G_2}. $\lambda = 490$ mμ und $d = 5$ cm.

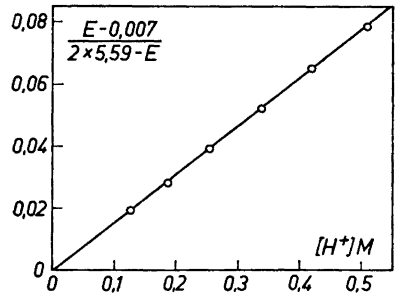

Fig. 15. 4″-Chlor-benzaurin. $\left(E - \frac{E_{G_1}}{1 + K_2}\right) / (E_{G_2} - E)$ als Funktion von [H+] für die Bestimmung von K_7. $\lambda = 490$ mμ und $d = 10$ cm.

In der zweiten Mess-serie bei der Ionenstärke 0,50 M, wo $[H^+]$ zwischen 0,12 und 0,50 M variierte, wurde E bei $d = 10$ cm gemessen. Mit $E_{G_2} = 2 \times 5{,}59$ und $E_{G_1}/(1 + K_2) = 0{,}007$ wird in Fig. 15 $(E - \frac{E_{G_1}}{1 + K_2})/(E_{G_2} - E)$ als Funktion von $[H^+]$ wiedergegeben. Man erhält $K_7(1 + K_2) = 6{,}4(4)$. Das Einsetzen von $K_2 = 137$ ergibt $K_7 = 4{,}7 \times 10^{-2}$.

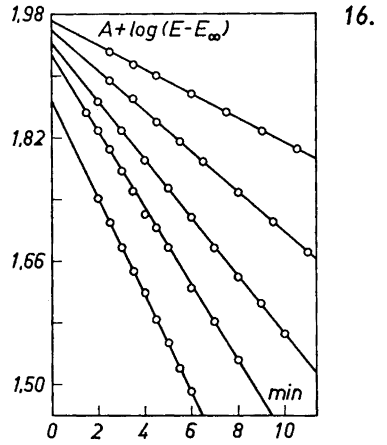

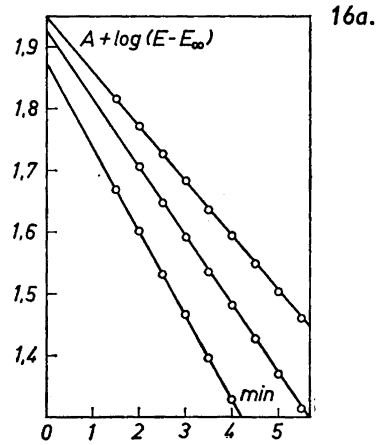

Fig. 16. 4″-Chlor-benzaurin. Reaktionskinetik bei $\lambda = 450$ mμ und $d = 5$ cm. Für die Linien gelten in der Ordnung von oben nach unten die folgenden Daten:

A:	2,17	2,14	2,11	2,08	2,02
pH:	6,555	6,313	6,151	6,003	5,915

Fig. 16a. 4″-Chlor-benzaurin. Reaktionskinetik bei $\lambda = 450$ mμ und $d = 5$ cm. Für die Linien gelten in der Ordnung von oben nach unten die folgenden Daten:

A:	2,10	2,08	2,02
pH:	5,752	5,648	5,590

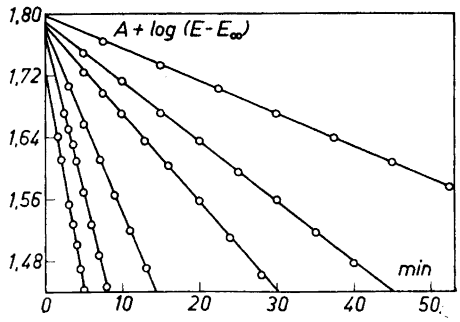

Fig. 17. 4″-Chlor-benzaurin. Reaktionskinetik bei $\lambda = 550$ mμ und $d = 2$ cm. Für die Linien gelten in der Ordnung von oben nach unten die folgenden Daten:

A:	1,98	1,96	1,95	1,94	1,93	1,88
pH:	11,03(5)	11,33	11,51(5)	11,82	12,06	12,21(5)

Messungen der Aufhellungsgeschwindigkeit. k wurde im Gebiet $5{,}5 < \text{pH} < 12{,}3$ bestimmt. Für $\text{pH} < 7$ wurde E bei $\lambda = 450$ mμ mit $d = 5$ cm gemessen; für $\text{pH} > 7$ wurde E bei $\lambda = 550$ mμ mit $d = 2$ cm gemessen. Die Figuren 16, 16a und 17 zeigen die kinetischen Verläufe in den sauren und alkalischen Lösungen, in welchen die Messungen der graphischen Berechnung von k_1 und k_2 bzw. k_3 und k_4 zu Grunde lagen. Fig. 18 zeigt k als Funktion von pH.

Bestimmung von k_1 und k_2 erfolgte im Gebiet $5{,}6 < \text{pH} < 6{,}5$, analog den Berechnungen für Benzaurin. Fig. 19 zeigt k_1 als Funktion von $[H^+]$ (eine Gerade). Man erhält $k_1^\circ = 5{,}0 \times 10^{-3}$ und $k_1' = 4{,}8 \times 10^4$. Es gilt also (mit $[H^+]$ in Mol/l):

$$k_1 = 5{,}(0) \times 10^{-3} + 4{,}8 \times 10^4\,[H^+];\; k_2 = 3{,}(65) \times 10^{-5} + 3{,}5 \times 10^2\,[H^+]\,(\text{Min}^{-1})$$

Bestimmung von k_3 und k_4. Für $\text{pH} > 11$ wächst k stark mit dem pH-Wert. Aus zusammengehörigen Werten von k und $[H^+]$ wird k_3 aus Formel (13)

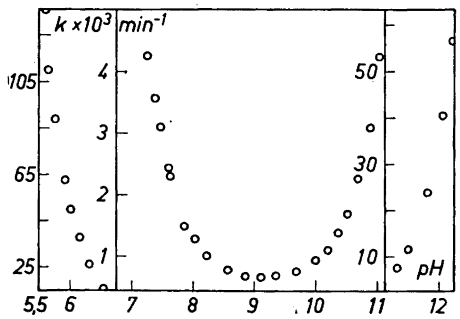

Fig. 18: 4″-Chlor-benzaurin. Die Geschwindigkeitskonstante k als Funktion von pH. O sind experimentell gefnndene Werte.

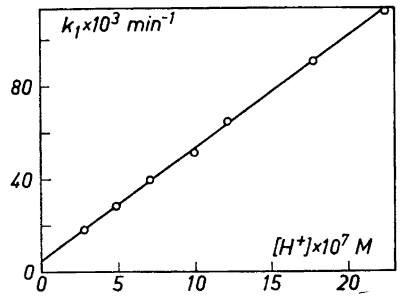

Fig. 19. 4″-Chlor-benzaurin. Die Geschwindigkeitskonstante k_1 als Funktion von $[H^+]$.

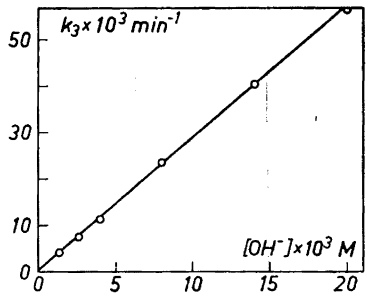

Fig. 20. 4″-Chlor-benzaurin. Die Geschwindigkeitskonstante k_3 als Funktion von [OH$^-$].

berechnet. Der Ausdruck $k_4 \cdot [H^+]/([H^+] + K_4)$ ist hier ein Korrektionsglied, weniger als 5 % von k betragend, und kann daher mit dem oben geschätzten Wert von K_4 zufriedenstellend berechnet werden (bei den höheren pH-Werten wird es vernachlässigt). Aus Fig. 20 geht hervor, dass k_3 eine lineare Funktion von [OH$^-$] ist. Wie beim Benzaurin ist $k_3°$ so klein, dass es nicht graphisch ermittelt werden kann. Man erhält $k'_3 = 2{,}8(7)$. $k_3°$ wurde wie beim Benzaurin nach untenstehenden Berechnungen bestimmt.

$[H^+] \times 10^9$ M	0.397	0,76(7)	1,39(0)	2,72
$k \times 10^4$ Min^{-1}	6.9(8)	6,6(8)	6,8(2)	7,8(1)
$k_3° \times 10^4$ Min^{-1}	3.8(5)	4,0(4)	4,1(3)	4,2(3)

Mittelwert: $k_3° = 4{,}1 \times 10^{-4}$ Min^{-1}.
Man erhält also mit [OH$^-$] in Mol/l:

$$k_3 = 4{,}1 \times 10^{-4} + 2{,}8(7)[OH^-]; \; k_4 = 3{,}7 \times 10^{-4} + 2{,}5(9)[OH^-] \; (Min^{-1})$$

DISKUSSION

Tabelle 3 enthält eine Zusammenstellung der bestimmten Konstanten für Benzaurin und 4″-Chlor-benzaurin. Es geht aus der Zusammenstellung hervor, dass eine Substitution von Wasserstoff gegen Chlor in der freien Parastellung die Konstanten des Systems wenig ändert. Nur bei drei Gleichgewichtskonstanten ist eine mit Sicherheit verifizierte Änderung vorzufinden. Die Protolysenkonstanten K_7 und $1/K_1$ sind mit den ungefähren Faktoren 2,8 bzw. 1,2 und die Hydratationskonstante K_2 mit dem ungefähren Faktor 1,4 gewachsen. Sonstige Abweichungen in den Gleichgewichtskonstanten dürfen als innerhalb der Fehlergrenzen liegend betrachtet werden. Bezüglich der Geschwindigkeitskonstanten ist es auffallend, dass $k_1°$ (ganz besonders) und $k_3°$ fast die gleichen sind. Dagegen wächst k_1 mit der [H$^+$] bedeutend schneller bei Benzaurin ($k_1' = 8{,}0 \times 10^4$) als bei 4″-Chlor-benzaurin ($k_1' = 4{,}8 \times 10^4$). (Vergleiche die Änderung in K_7.) In alkalischen Lösungen wächst k_3 mit der [OH$^-$] schneller bei 4″-Chlor-benzaurin als bei Benzaurin (k_3' ist 2,9 im Vergleich zu 2,0).

Tabelle 3. Zusammenfassung der Ergebnisse. [H+] und [OH⁻] in Mol/l.

—	K_7	$1/K_1$	K_3	K_4	K_2	K_6
Benzaurin	$1{,}6(6) \times 10^{-2}$	$3{,}7 \times 10^{-6}$	$3{,}7 \times 10^{-10}$	$\sim 7 \times 10^{-11}$	100	0,93
4″-Chlor-benzaurin	$4{,}7 \times 10^{-2}$	$4{,}5 \times 10^{-6}$	$3{,}4 \times 10^{-10}$	$\sim 14 \times 10^{-11}$	137	0,90

—	k_1 Min^{-1}	k_2 Min^{-1}
Benzaurin	$5, (2) \times 10^{-3} + 8{,}0 \times 10^{4}$ [H+]	$5, (2) \times 10^{-5} + 8{,}0 \times 10^{2}$ [H+]
4″-Chlor-benzaurin	$5, (0) \times 10^{-3} + 4{,}8 \times 10^{4}$ [H+]	$3{,}(65) \times 10^{-5} + 3{,}5 \times 10^{2}$ [H+]

—	k_3 Min^{-1}	k_4 Min^{-1}
Benzaurin	$4{,}8 \times 10^{-4} + 2{,}0(4)$ [OH⁻]	$4{,}5 \times 10^{-4} + 1{,}8(9)$ [OH⁻]
4″-Chlor-benzaurin	$4{,}1 \times 10^{-4} + 2{,}8(7)$ [OH⁻]	$3{,}7 \times 10^{-4} + 2{,}5(9)$ [OH⁻]

Das Einführen des Cl-Atoms hat die Lichtabsorptionskurven etwas geändert. Das (ε_R)-Maximum und das grosse (ε_{G_2})-Maximum sind um etwa 5 mμ und das kleine (ε_{G_1})-Maximum um cirka 10 mμ gegen rot verschoben worden.

Herrn Professor Sven Bodforss spreche ich meinen herzlichen Dank für seine wertvolle Ratschläge bei der Durchführung dieser Arbeit aus. Ebenso danke ich Herrn Professor Sture Fronæus und Herrn Dozent Rune Cigén für wertvolle Diskussionen.

Fräulein Lena Hansson war als Assistentin im Laboratorium behilflich.

Die Synthese von Benzaurinperchlorat wurde von Herrn Olle Nilsson, Lund, die Mikroelementaranalyse von Herrn Dr. Alfred Bernhardt, Max-Planck-Institut für Kohlenforschung, Mühlheim/Ruhr, ausgeführt.

Die Untersuchung wurde mit finanzieller Hilfe von *Statens Naturvetenskapliga Forskningsråd* und *Kungliga Fysiografiska Sällskapet i Lund* ausgeführt.

Die Übersetzung ins Deutsche ist von fil.mag. Ingrid Wartenberg ausgeführt.

LITERATUR

1. Hansson, H. G. *Acta Chem. Scand.* **13** (1959) 1309 (= Benzaurinstudien II.).
2. Bodforss, S. und Cigén, R. *Kgl. Fysiograf. Sällskap. Lund, Förh.* **26** (1956) No. 6.
3. Cigén, R. *Protolysengleichgewichte und Reaktionsgeschwindigkeiten einiger basischer Triphenylmethanfarbstoffe* (Diss.), Universität Lund 1956.
4. Cigén, R. *Acta Chem. Scand.* **12** (1958) 1456.
5. Döbner, O. *Ann.* **217** (1883) 223.
6. Pfeiffer, P. *Ann.* **412** (1917) 253, S. 331.
7. Meyer, R. und Gerloff, W. *Ber.* **56** (1923) 98.
8. Hansson, H. G. und Nilsson, O. *Kgl. Fysiograf. Sällskap. Lund, Förh.* **29** (1959) No. 9 (= Benzaurinstudien I.).

Eingegangen am 29. September 1959.

ACTA CHEMICA SCANDINAVICA 14 (1960) 428–436

The Measurement of Self-diffusion with a New Continuous Monitoring Method

I. Evaluation of the "Δl-Effect" in the Open-ended Capillary Method

E. BERNE and J. BERGGREN

Department of Inorganic Chemistry, Chalmers Institute of Technology, and Swedish Institute of Silicate Research Gothenburg, Sweden

A new continuous monitoring capillary method is introduced. A mathematical treatment involving only the experimental values of the activity remaining in the capillary at various times gave evidence for the existence of a constant "Δl-effect" which could be calculated.

I. INTRODUCTION

Many authors have pointed out the fact that a possible source of error with the open-ended capillary method is due to convection disturbances at the top of the capillary.

Two effects can be distinguished, both of them tending to sweep out part of the active solution of the capillary, and leading therefore to effective diffusion paths shorter than the geometric length of the capillary. Such convection disturbances may occur:

— Firstly, when the boundary between the active and the inactive solutions is broken, *i.e.* when the capillary is immersed in the inactive bath. This effect, termed "immersion error", has been tested by Mills and Kennedy [1], Krauss and Spinks [2] and Mills and Adamson [3], who found activity losses in the capillary equal to 1.3 %, 0.5 % and 1.7 %, respectively.

— Secondly, when the outer inactive solution is stirred, in order to maintain the boundary condition $c = 0$ at the mouth of the capillary (c being the concentration of the labelled particles). If the stirring is too rapid or turbulent, part of the active solution may be swept more or less continually out of the capillary during the diffusion run. Wang, who termed this latter effect the "Δl-effect", has proposed a method for measuring it by using capillaries of different lengths [4]. But this method appears to be quite unsatisfactory, since it only gives an accuracy of the same magnitude as the "Δl-effect" itself, *i.e.* $\pm$ 2 % [1,3,4].

The only way to check whether a diffusion process out of an open-ended capillary is ideal should consist in a continuous registering of the activity inside the capillary during a whole diffusion run. In this case, the diffusion process should correspond to the solution of Fick's general diffusion equation for the actual boundary conditions:

$$\frac{I}{I_0} = \frac{8}{\pi^2} \sum_0^\infty \frac{1}{(2n+1)^2} \exp[-(2n+1)^2\pi^2 Dt/4l^2] \quad (1)$$

where I = activity remaining in the capillary after a diffusion time t,
I_0 = initial activity in the capillary before diffusion
l = length of the capillary.

Mills and Godbole have recently made a first attempt in this direction by building an apparatus allowing them to make several measurements during a single diffusion run. [5] However ,the frequency of their observations (13 to 20 for a run) was not high enough for a complete and accurate survey of the whole diffusion run.

The following work was undertaken in order to observe, by continuous registering of the activity inside the capillary, how the diffusion really proceeds, when experimental techniques such as Wang's modification [6] of the initial Anderson and Saddington method [7] are used, *i.e.* with mechanical stirring of the outer inactive solution.

II. EXPERIMENTAL

1) Description of apparatus

The apparatus is shown in Fig. 1. The container for the inactive solution was a 3-liter glass beaker (A), with a lateral cylindrical connection (B) (diameter = 3.5 cm) terminated at right angles by another narrow cylindrical tube (C) (diameter = 0.8 cm) which contained the capillary. An opening (diameter = 0.8 cm) was made in tube (B), immediately above tube (C), to allow the lowering of the capillary into the cell. It could be closed with a rubber stopper (E). The solution was stirred mechanically by means of a propeller (F) placed vertically in the 3-liter beaker, and a plexiglas top (G) was laid over the beaker to prevent any evaporation. The capillaries used had internal and external diameters of 0.08 and 0.6 cm, respectively, and a length of (3.89 ± 0.01) cm.

A special G.M. tube for γ-ray counting (H), enclosed in a steel envelope, was tightly pressed to, and fixed along the wall of, the capillary. (For more details about the relative positions of capillary and G.M. tube, see further below.)

The whole diffusion cell and the G.M. tuber were immersed in a 30-liter water thermostat, kept at a temperature of (25.00 ± 0.01)°C.

The G.M. tube was connected to a counter, working on Preset Count. A special additive electronic device gave the apparatus the ability to choose, by itself, between two different preset number of counts to be registered, according to the radioactivity of the measured samples (UL and LL for high and low radioactivities, respectively). During a counting operation, the counter first worked on UL (*i.e.* it started as if it would count the higher preset number of impulses), but if the time for counting a certain number of impulses appeared to be too long, it turned over automatically to LL after 30 sec, (*i. e.* it would only count the lower preset number of impulses). Both for UL and for LL, the manipulator could select in advance one of two different preset number of counts, 10 000 and 5 000 counts for UL and 600 and 400 counts for LL, respectively.

The times corresponding to each measurement were printed on a paper roll by a registering device, connected to the counter (a number 1 or a number 2, printed before

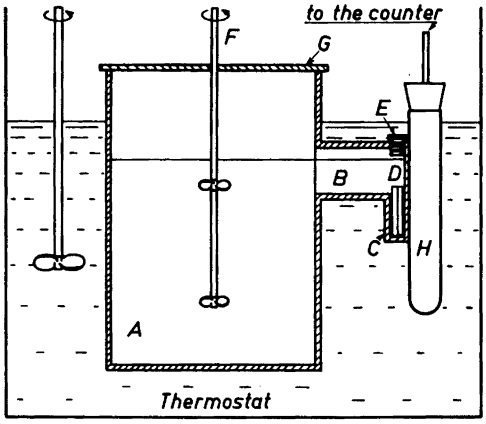

Fig. 1. Apparatus for continuous monitoring open-ended capillary method.

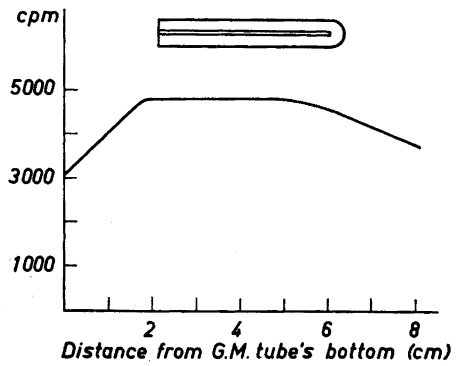

Fig. 2. Efficiency curve of the G.M.tube. The representation of the capillary, at the same scale, shows the relative positions of the G.M.tube and the capillary.

the time data in different characters, indicated whether the counter had worked on UL or on LL). After each measurement, the counter stopped for one minute, and then restarted automatically.

2) Preparation of solutions

All experiments were performed with 0.001 M sodium iodide solutions.

The radioactive solutions were prepared by adding 5 to 15 μl of a carrier-free Iodine-131 solution (specific activity = 12 mC/ml) to 25 ml of the inactive sodium iodide solution. The corresponding activities were 9 000 to 15 000 cpm for the contents of a capillary. The isotope was provided by the Isotope Division AERE, Harwell, England.

3) Experimental procedure

The capillary was filled with the radioactive solution by means of a thin micropipette, operated with a medical syringe. A small drop of active solution was left on top in order to prevent evaporation during the time necessary to reach thermal equilibrium, and also to avoid as far as possible convection disturbances when the capillary was immersed in the inactive bath. Then the capillary was put in place in the holder (C), and the inactive solution, already at 25°C, was gently poured into the cell, along the walls of the beaker (A), until its level reached to 4/5th of the height of the capillary. After 10 min, the thermal equilibrium could be considered as established, and more inactive solution was slowly poured into the cell, until its total volume was about 1 600 ml. This last operation was done just before the counter started a new measurement. After 9 000 minutes, only about 15 % of the initial activity was left in the capillary, and the experiment was stopped.

4) Preliminary experiments

a. Relative positions of capillary and G.M.tube. The counting efficiency of the G.M. tubes we used has been measured by displacing a radioactive point source along the tube, and measuring its activity at all positions. It was found in this way that the counting

efficiency for each G.M. tube was constant along a region extending on both sides of its middle point. The length of this region was comparable to that of the capillary, but somewhat shorter. Fig. 2 represents the efficiency curve of one of our G. M. tubes as well as the position which was given to the capillary.

Since the greatest concentration changes occur in the upper end of the capillary, its top was placed in the constant efficiency zone. By taking into account the efficiency gradient of the G.M. tube and the activity gradient in the capillary, it could be demonstrated mathematically that the center of gravity of the total measured radioactivity in the capillary no longer moved after a diffusion time t = 2 000 to 3 000 min. It may be noteworthy that Mills and Godbole came to the same conclusions for their own semi-continuous monitoring apparatus, with a 2 cm long capillary placed inside the hole (2 cm high) of a well-crystal of a scintillation counter [8].

b. Background. Before each diffusion run, the background was measured over a period of 15 min. It was of course impossible to check it during a run. We assumed that it kept approximately constant, and the measurement made at the beginning of each run (250 to 300 cpm) was used in the calculation.

c. Control of convection in the cell. A capillary was very accurately filled with the radioactive solution, and its contents (obtained by withdrawing them and rinsing five times with water) transferred using a micropipette into the inactive bath, right above the top of a sealed capillary in holder (C). Stirring was then started, and the radioactivity continually measured. It was found that with a stirring rate of 80 to 150 rpm, the radioactivity was evenly dispersed in the bath after 3 to 4 min. With a stirring rate of 320 rpm, uniform repartition was established in less than a minute. For our diffusion experiments, a stirring rate of 80 rpm was used.

d. Influence of the radioactive species which have diffused out from the capillary. The last experiment may be used for the determination of the constant ratio a between the number of counts per minute I'' corresponding to a certain amount of radioactivity evenly dispersed in the main body of the cell, and the number of counts I' corresponding to the same amount contained in the capillary. Five experiments yielded a mean value a = 3.8 %.

III. RESULTS AND DISCUSSION

1) The activities I_i' corresponding to the registered time data τ_i were calculated as follows:

$$I_i' = \frac{A}{\tau_i} - B \tag{2}$$

A being the number of registered counts (5 000 or 400)
B being the background.

As there was so much data, and as each individual value was known with a poor accuracy (the statistical counting accuracy), the individual values were not used for calculation, but mean values, I_i', of sets of 10 single values. It was assumed that in the case of Iodine-131, the half-life of the isotope was long enough for the radioactive decay between the measurements i and $(i + 10)$ to be neglected.

A mean diffusion time t_i, corresponding to each I_i' value was then calculated as follows:

$$t_i = \sum_{1}^{10(i-1)} (\tau_i + 1) + \frac{1}{2} \sum_{10_i-g}^{10_i} \tau_i \tag{3}$$

(it was assumed that the error arising from taking a linear mean time instead of a logarithmic one was negligible).

I_i' values were then corrected for radioactive decay over the period $t = 0$, $t = t_i$.

$$I_i'^0 = I_i'/e^{-\lambda t_i} \tag{4}$$

λ being the decay constant of the isotope.

Then $I_i'^0/I_0$ was calculated, and corrected for the contribution of the activity, I'' which had diffused out, according to eqn. (5):

$$\frac{I_i^0}{I_0} = \frac{\frac{I_i'^0}{I_0} - \alpha}{1 - \alpha} \tag{5}$$

Finally, D could be calculated from eqn. (1).

All these long calculations have been done with an electronic computer Alwac III E.

We reproduce in Fig. 3 two characteristic shapes of the curves $D = f(t)$.

It is seen that the experiments did not yield a constant value of D. It may consequently be deduced that the diffusion did not follow an ideal process.

The difference between curves (1) and (2) seems to be due to a difference in the size of the radioactive drop left on top of the capillary before immersion. Curves of type (2) were obtained when rather large drops were left (covering the whole top of the capillary tube), while curves of type (1) were obtained with smaller drops (4 to 6 % of the capillary volume).

The influence of the size of the drop may be roughly explained in the following way. When a large drop is left on top of the capillary, there may be no "immersion error". On the contrary, part of the active solution of the drop may remain for a while in the neighbourhood of the capillary, and the apparent D is then too low. After a certain time, a "Δl-effect" gradually takes place, and D increases slowly. When a smaller drop is left on top, there may be an "immersion error". The values for D found at the beginning of the run are consequently too high, but tend to decrease as the diffusion current again

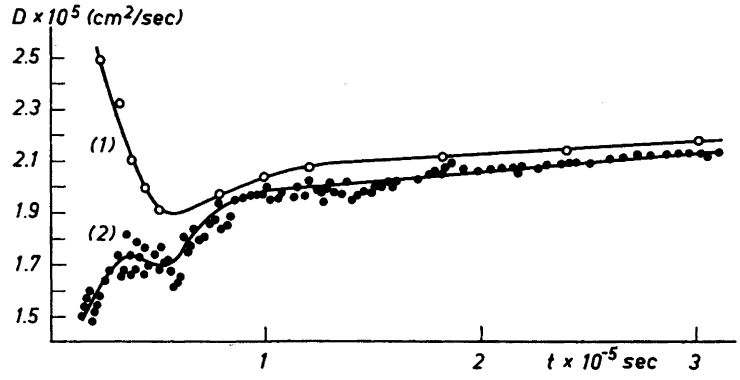

Fig. 3. Plot of D *vs.* t. O: experimental points for curve (1). ●: experimental points for curve (2).

fills the top of the capillary with radioactive solution. After a certain time, a "Δl-effect" is established, and D tends to increase again.

2) Plots similar to those of Mills and Godbole [5], *i.e.* plots of $\log (I^0/I_0)$ *vs.* t. gave approximately straight lines, as may be seen from Fig. 4. The slopes of these lines were calculated from the general equation:

$$s = \frac{\sum_{i=1}^{i=n} \log (I_i^0/I) - \sum_{i=n+1}^{i=2n} \log (I_i^0/I_0)}{\sum_{1=i}^{i=n} t_i - \sum_{i=n+1}^{i=2n} t_i} \qquad (6)$$

An example is given in Table 1, related to the curve in Fig. 4:

Table 1.

Number of points	Time interval	$D \times 10^{-5}$ (cm²/sec)
90	$2.18 \times 10^5 - 5.46 \times 10^5$	2.30
30	$2.18 \times 10^5 - 2.95 \times 10^5$	2.21
30	$2.95 \times 10^5 - 4.10 \times 10^5$	2.26
30	$4.01 \times 10^5 - 5.46 \times 10^5$	2.39

Two conclusions may be drawn from these results:

a) Obviously, the self-diffusion coefficients calculated are too high. For the very dilute solutions investigated here, they ought to be equal to the

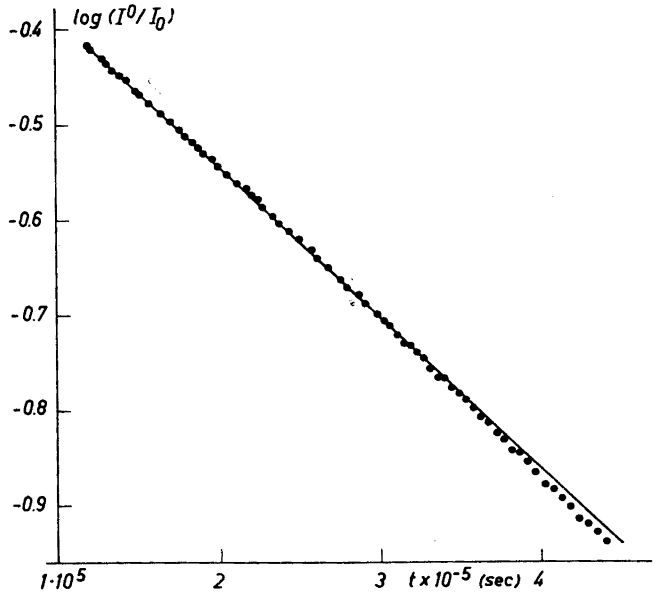

Fig. 4. Plot of $\log(I^0/I_0)$ *vs.* t. (Same experiment as Fig. 3, Curve 1.)

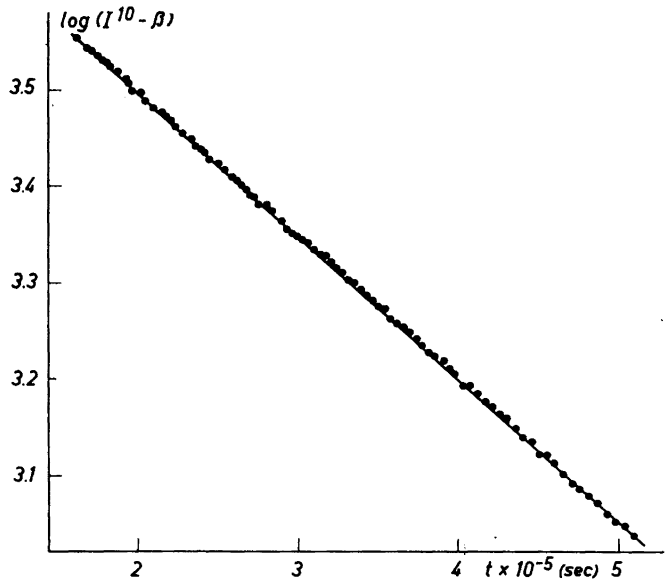

Fig. 5. Plot of $\log(I'^0-\beta)$ *vs. t.* (Same experiment as Fig. 4.)

Nernst limitimg value: $D^0 = 2.045 \times 10^{-5}$ cm²/sec. This discrepancy may be due to two factors: the poor accuracy of α and I_0, and probably the relatively high convection disturbances at the top of the capillary. This last factor is not to be regarded here as serious, since our purpose was in fact the investigation of these disturbances and their influence on the diffusion process.

b) As may be seen on Fig. 4, it is possible to draw a straight line through the experimental points of the plot $\log(I^0/I_0)$ *vs. t*, even if the diffusion process is far from being theoretical. Only calculations enable conclusions to be drawn about the diffusion process. So that it is regrettable that Mills and Godbole [5] did not report the data corresponding to their measurements during a single diffusion run. Although it is very probable that their own apparatus did not give rise to such important convection disturbances as ours, these authors have not yet given evidence that the convection disturbances were negligible.

3) We have already pointed out the fact that a source of error in the calculation of D was the poor accuracy of α and I_0.

It will be proved in the following part that if the convection disturbances at the top of the capillary have the same influence on the diffusion process as a constant "Δl-effect" *i.e.* if the experimental $I_i'^0$ values fit the case of an ideal process out of a capillary of effective length l_{eff}, shorter than its geometrical length, then it is possible to calculate the value of the product $\alpha I_0 = \beta$, by making use of only the experimental $I_i'^0$ values; this value, now exact, may then be used for the calculation of D/l^2_{eff}.

The abreviated diffusion equation

$$\frac{I_i'^0 - a\ I_0}{I_0\ (1-a)} = \frac{8}{\pi^2} \exp\ [-\pi^2 D t_i / 4 l^2_{eff}] \tag{7}$$

(which is valid with in an accuracy of 0.2 % for $Dt/l^2 > 0.2$) may also be written

$$\ln(I_i'^0 - \beta) = \frac{\pi^2 D t_i}{4\ l^2_{eff}} + C \tag{8}$$

C and β being constants.

If there exists a constant diffusion path l_{eff}, and if the apparent D does not vary with time, eqn. (8) will be satisfied by any experimental point $(I_i^{0\prime}, t_i)$. A set of 4 experimental points: $(I'_1{}^0, t_1)$, $(I'_2{}^0, t_2)$, $(I'_3{}^0, t_3)$, $(I'_4{}^0, t_4)$ will then satisfy the following equation:

$$\frac{\ln \dfrac{I'_1{}^0 - \beta}{I'_2{}^0 - \beta}}{\ln \dfrac{I'_3{}^0 - \beta}{I'_4{}^0 - \beta}} = \frac{t_2 - t_1}{t_4 - t_3} \tag{9}$$

β has been determined by a method of "trial and error" for 50 different sets of 4 points. The 50 values of β thus obtained differed from each other, as each $I_i'^0$ value is only known with the statistical counting error, but it has been verified that they followed a gaussian statistical distribution, and that they also were statistically distributed along the time axis. * An example is given in Table 2.

Table 2. $\bar{\beta} = (357 \pm 28)$ cpm. Relative dispersion $\sigma = 140$ cpm.

Interval	Frequency of β values
$\bar{\beta}-2\sigma;\ \bar{\beta}$	24
$\bar{\beta}-\sigma;\ \bar{\beta}$	10
$\bar{\beta};\ \sigma + \bar{\beta}$	10
$\bar{\beta}\ ;\ \bar{\beta} + 2\sigma$	24
$\bar{\beta}-2\sigma;\ \bar{\beta} + 2\sigma$	48 = 96 % of total amount

The good statistical repartition of the β values proves that our initial hypothesis concerning an ideal diffusion process out of a fictive capillary of length l_{eff} was correct.

The plot of log $(I'^0 - \beta)$ *vs.* t. appears to be rigorously linear, as may be seen in Fig. 5. The slope of this line, K, has been calculated for 50 sets of 2 points, and the statistical distribution of the various K values analyzed, in order to detect possible deviations from a theoretical diffusion process. An example is given in Table 3:

* This was only the case for experiments performed with relatively small drops left on top of the capillary before immersion. When larger drops were left, it was found that the positive deviations from the β mean value occurred at the beginning of the diffusion run, and the negative ones at the end.

Table 3. $\overline{K} = (1.481 \pm 0.003) \times 10^{-6}$ sec^{-1}. Relative dispersion $\sigma = 0.02 \times 10^{-6}$ sec^{-1}.

Interval	Frequency of K values
$\overline{K}-2\sigma$; $\overline{K}$	19
$\overline{K}-\sigma$; $\overline{K}$	9
$\overline{K}$; $\overline{K}+\sigma$	8
$\overline{K}$ $\overline{K}+2\sigma$	13
$\overline{K}-2\sigma$; $\overline{K}+2\sigma$	49 = 98 % of total amount

The constant ratio D/l^2_{eff} may be now calculated from the value of $\overline{K}$.

If one assumes l_{eff} to be equal to l, the diffusion coefficient obtained is somewhat too high. If, on the other hand, one assumes l_{eff} to be different from l, and D equal to the Nernst limiting value, the magnitude of the "Δl-effect" can be determined. The following results were obtained:

if $l_{\text{eff}} = l = 3.89$ cm	then $D = 2.091 \times 10^{-5}$ cm^2/sec.
if $D = 2.045 \times 10^{-5}$ cm^2/sec	then $l_{\text{eff}} = 3.84_7 = 3.85$ cm.

Thus, the present method has enabled a precise determination of the magnitude of the "Δl-effect", which was evaluated to 0.4 mm, *i.e.* 1 % of the capillary's length.

Work is proceeding in this laboratory to investigate whether the "Δl-effect" is constant for various solutions, and to what extent it depends on the viscosity of the solutions. If it were found that reasonable changes in the viscosity have no influence on its magnitude, then a capillary could be calibrated with known solutions, *i.e.* dilute solutions for which $D = D^{\circ}_{\text{Nernst}}$, and used for the study of unknown solutions.

Acknowledgments. The authors are grateful to Professor C. Brosset for his constant interest in the present work.

REFERENCES

1. Mills, R. and Kennedy, J. W. *J. Am. Chem. Soc.* **75** (1953) 6596.
2. Krauss, C. J. and Spinks, J. W. T. *Can. J. Chem.* **32** (1954) 71.
3. Mills, R. and Adamson, A. W. *J. Am. Chem. Soc.* **77** (1955) 3454.
4. Mills, R. *Ibid.* **77** (1955) 6116.
5. Mills, R. and Codbole, E. W. *Australian J. Chem.* **11** (1958) 1.
6. Wang, J. H. *J. Am. Chem. Soc.* **73** (1951) 510.
7. Anderson, J. S. and Saddington, K. *J. Chem. Soc.* **1949** 381.
8. Mills, R. and Godbole, E. W. *Australian J. Chem.* **12** (1959) 102.

Received September 19, 1959.

ACTA CHEMICA SCANDINAVICA 14 (1960) 437–440

Ribose in Meat

H. FREDHOLM

Research laboratory of the Sveriges Slakteriförbund, Stockholm 20, Sweden

Careful chromatographic methods for detection, estimation and quantitative determination of ribose in meat are described in detail. Samples of meat from the gracilis-muscle of hogs and cattle were collected and examined immediately after slaughter as well as after different kinds of storage up to 6 months.

Immediately after slaughter all samples of meat from cattle contained less than 5, probably less than 1 μg of ribose per g meat, that is, no ribose could be detected by the technique used which does not account for the ribose bound, *e. g.*, in ribonucleic acids in the samples. In a few samples of meat from hogs immediately after slaughter traces of ribose could be detected, but in most samples none.

During storage under refrigeration the ribose content of the meat, as determined by the methods described increases up to 120 μg per g meat in 16 days (meat from cattle). The increase is practically proportional to storage-time. Cold storage of meat (−20°C) shows the same result, so that a ribose content, defined as above, of 60 μg per g meat can be obtained after 1 month. If meat is frozen immediately after slaughter and then kept in cold storage, it will last much longer until ribose can be detected by the methods described.

For several reasons it seems likely that the ribose detected and determined by using the methods described is free or loosely bound.

Even very small amounts of ribose may be of importance in meat influencing its properties as a chemical system as well as a microbiological medium. Therefore it seemed to be of interest to know if "free" ribose is formed in meat from, *e.g.*, ribonucleic acids during ordinary handling and storage of meat, and if so, what quantities of ribose would be formed by different kinds of handling and storage. Possibly a method of determining "free" ribose would furnish a tool for the judging of meat in regard to certain qualities.

The term free ribose is used here for the quantity of ribose which can be detected by the mild methods developed, even if some part of this quantity might be formed, *e.g.*, from more complex products of hydrolysis of ribonucleic acids, such as mononucleotides, during analysis.

A similar investigation on deoxyribose in meat is beeing carried out, the results of which will be published later.

EXPERIMENTAL

Meat from cattle and hogs were used in this work. In order to get defined meat the raw material was obtained from the gracilis-muscle only.

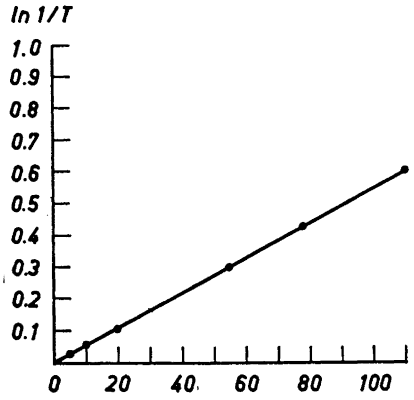

Fig. 1. Evaluation curve for ribose from light absorbance at 5 100 Å. Extinction in 10 mm cells.

First a method for detection and estimation of ribose was developed, then a method for the quantitative determination of ribose in meat was worked out. It is essential in both methods that free ribose can be extracted with no or the slightest possible hydrolysis of ribonucleid acids or other compounds containing ribose.

Detection and estimation of ribose in meat. To 30 g of finely but carefully ground sample of meat 110 ml of distilled water and 30 ml of 20 % phosphotungstic acid were added. The mixture was well stirred, then heated on a waterbath for 10 min and centrifuged. The waterphase was filtered into a glassvessel, desalted using Dowex 50, evaporated and made up to 5 ml.

Paper chromatograms were taken using the technique of Partridge [1] with modifications published later by several authors as described by Block *et al.*[2] On every chromatogram known quantities of ribose were run. As usual parallel chromatograms were carried out using other carbohydrates and related compounds which occur in meat.

Quantitative determination of ribose in meat. To 50 g of finely but carefully ground sample of meat 100 ml of distilled water and 50 ml of 20 % phosphotungstic acid were added. The mixture was then treated as described above under Detection and estimation, except that the desalted, evaporated filtrate was made up to 10 ml.

The chromatographic method, which was used by Pridham [3] for determination of aldohexoses, some aldopentoses though not ribose, hexuronic acids and 6-deoxy-aldohexoses was found to give excellent results with ribose too and therefore was used.

After the colour of the spots had been eluted from the paper with aqueous methanol containing stannous chloride (1.0 g of stannous chloride in 5 ml of water + 90 ml of absolute methanol, then filtered) the absorbances were measured in a Zeiss spectrophotometer PMQ II at 5 100 Å. At this wavelength there is an absorption maximum for the coloured compounds formed by the interaction of ribose with the *p*-anisidine-hydrochloride reagent.

The same precautions to avoid confusion were observed, as were described above under Detection and estimation. The evaluation curves obtained with known quantities of ribose on the same paper chromatograms, using the same procedure, application, development, drying, spraying with *p*-anisidine, eluting and spectrophotometric measuring show straight lines with varying amounts of ribose from 5 to 110 μg as will be seen from Fig. 1.

RESULTS

Detection of ribose in meat. Samples of meat from cattle were collected:

1. Immediately after slaughter, that is within 15 min.
2. After storage under refrigeration (+ 1 to + 4°C) for 2, 6, 8, 10, 13 and 15 days.

Table 1. Chromatography of free ribose in meat from cattle. Ribose spots.

Time Days	1 No storage	2 Storage under refr.	3 Cold storage	4 Immediately frozen, then cold storage	5 Kept minced with water	6 Kept minced with water +phospho-tungstic acid
0	None	—	—	—	—	—
1	—	—	—	None	—	—
2	—	Trace	—	—	Trace	None
3	—	—	—	None	—	—
6	—	Defined spot	—	—	Defined spot	None
7	—	—	—	None	—	—
8	—	Defined spot	—	—	Defined spot	None
10	—	Defined spot	—	—	Strong spot	None
13	—	Strong spot	—	—	Strong spot	None
14	—	Strong spot	—	None	—	—
15	—	Very strong spot	—	—	Very strong spot	None
Months						
1	—	—	—	None	—	—
2	—	—	Defined spot	—	—	—
6	—	—	Defined spot	—	—	—

Table 2. Chromatography of free ribose in meat from hogs. Ribose spots.

Time	1 No storage	2 Storage under refr.	3 Cold storage
0	None to traces	—	—
2 days	—	Defined spot	—
8 days	—	Strong spot	—
4 months	—	—	Defined to strong spots

3. After 2 and 6 months cold storage at −20°C. Carcasses handled commercially before cold storage, including refrigeration.
4. Samples collected within 15 min after slaughter, then immediately frozen (within 1 h after slaughter), then kept 1, 3, 7, 14 and 30 days at −20°C.
5. Samples collected and ground within 1 h after slaughter, then 110 ml dist. water added to 30 g ground meat. The mixture kept under refrigeration (+ 1 to + 4°C) during 2, 6, 8, 10, 13 and 15 days.
6. The same series as sub 5 but 110 ml dist. water + 30 ml 20 % phosphotungstic acid added instead of water only.

Samples of meat from hogs were collected as follows.
1. Immediately after slaughter.
2. After storage under refrigeration (+ 1 to + 4°C) for 2 and 8 days.
3. After cold storage for 4 months at −20°C.

Tables 1 and 2 contain the results of qualitative chromotogrophy.

Quantitative determination of ribose in meat. Table 3 gives the results of the quantitative measurements of ribose in meat from cattle determined as described above. Samples were collected, 1) Immediately after slaughter 2) After storage under refrigeration (+ 1 to + 4°C) for 2, 4, 6 and 16 days, 3). After cold storage at −20°C during 1 month. 0.02 ml of resulting solution applied.

Table 3. Quantities of free ribose in meat from cattle after different handling.

Samples	Number of samples	Ribose of spot μg
Immediately after slaughter	10	None
Refrigerated for:		
2 days	3	1
4 days	1	8
6 days	4	5−7
16 days	1	12
Cold storage for:		
1 month	3	6

CONCLUSIONS AND DISCUSSION

Whilst ribose cannot be detected in fresh meat from cattle immediately after slaughter, and only in traces and in some cases of such meat from hogs if the careful chromatographic methods described are used which allow detection of about 1 μg of ribose, there will appear an increasing amount of ribose *e.g.* during storage even if this storage is carried out under refrigeration or as cold storage. Immediate freezing of the meat after slaughter delays the appearence of ribose for at least 1 month.

Though it is not possible at present to decide if the quantity of ribose detected and determined by the methods described exists as free ribose or as partly bound, there are reasons to believe that this quantity of ribose is in a free or loosely bound state. The most important reason to think so seems to be the fact that all samples examined have been very finely ground in order to allow all chemical compounds therein to be uniformly distributed in the samples and free to be attacked by chemical action during analytical procedure.

REFERENCES

1. Partridge, S. M. *Nature* **164** (1949) 443.
2. Block, R. J. Durrum, E. L. and Zweig, G. *A Manual of paper chromatography and paper electrophoresis.* New York 1958, p. 170−188.
3. Pridham, J. B. *Anal. Chem.* **28** (1956) 1967.

Received October 10, 1959.

ACTA CHEMICA SCANDINAVICA 14 (1960) 441–452

The Crystal Structure of Potassium Perchromate

ROLF STOMBERG and CYRILL BROSSET

Department of Inorganic Chemistry, Chalmers University of Technology, Göteborg, Sweden

The crystal structure of potassium perchromate has been determined by two- and three-dimensional X-ray methods. The perchromate crystallizes in the space group $I\,\bar{4}2m$, with $a = 6.703 \pm 0.003$ Å and $c = 7.632 \pm 0.003$ Å The length of the bond between the two oxygen atoms in a peroxide group is 1.489 ± 0.022 Å. The oxidation number of +5 for the chromium has been confirmed.

The crystal structure of potassium perchromate, K_3CrO_8, has previously been determined by Wilson [1], who, by means of powder diffraction data, found the oxygen-oxygen single bond in the peroxide group to be 1.34 ± 0.06 Å, a rather uncertain and somewhat low value in comparison with those obtained by other authors [6,7]. This would justify a refinement of the structure. It would also be of interest to establish definitely if chromium is surrounded by four equidistant O_2^{2-}-ions and consequently has the oxidation number +5, or if it might be enclosed both by O_2^{2-} and O_2^--ions.

EXPERIMENTAL

Preparation and analysis. K_3CrO_8 was prepared according to Riesenfeld [2] by adding hydrogen peroxide to a cooled, alkaline solution of potassium chromate. The temperature did not exceed −5°C. The crystals were filtered, and dried with alcohol and ether. The chromium content was determined by converting the sample into chromate, adding KI and titrating the liberated iodine with a thiosulfate solution. The potassium content was determined as potassium perchlorate. (Found: K 39.6; Cr 17.5. Calc. for K_3CrO_8: K 39.5; Cr 17.5.)

Magnetometric measurement. K_3CrO_8 has been found to be paramagnetic and the moment was determined by the Gouy method which gave the approximate value $\chi_M = 1\,240 \pm 30$ units, clearly indicating the existence of a single unpaired electron found also by Tjabbes [4] and Klemm and Werth [5].

X-Ray methods. In order to determine the cell dimensions accurately powder photographs of Guinier type were taken using Cu $K\alpha$ radiation and with NaCl as reference substance. Due regard was taken to film shrinkage according to Hägg by copying a scale on the films before development.

The structural investigation was based on single crystal methods. Multiple-film equi-inclination Weissenberg photographs were taken with rotation about [1$\bar{1}$0] (layer lines 0, 1, 2 and 4), [100] (layer lines 0, 1, 2, and 3) and [001] (layer lines 0, 1, 2, 4 and 6) using molybdenum radiation. Thin tinfoils were placed between the films in order to increase

the absorption. The reflexion intensities were estimated by visual comparison with standard scales. A subjective correction was made for variation in spot shape. As molybdenum radiation was used and the crystals were only 0.1 mm thick no correction was made for absorption. The reflexion intensities were corrected using Lorentz and polarization factors.

As the perchromate was decomposed in a few days under the influence of the X-rays it was necessary to use new crystals after about 20 h exposure.

DETERMINATION OF THE STRUCTURE

The cell dimensions were obtained from powder diffraction data by the method of least squares. K_3CrO_8 is tetragonal with

$$a = 6.703 \pm 0.003 \text{ Å.}$$
$$c = 7.632 \pm 0.003 \text{ Å.}$$

Calculated and observed $\sin^2\Theta$-values are given in Table 1.

Table 1. X-ray powder diffraction data for K_3CrO_8.

h k l	$10^4 \cdot \sin^2\Theta_{obs}$	$10^4 \cdot \sin^2\Theta_{calc}$
1 0 1	233	234
1 1 0	265	265
0 0 2	408	408
2 0 0	530	529
1 1 2	672	673
2 1 1	763	763
2 0 2	936	937
2 2 0	1 058	1 058
3 0 1	1 290	1 292
3 1 0	1 324	1 323
2 2 2	1 465	1 466
0 0 4	1 631	1 632
3 1 2	1 730	1 731
3 2 1	1 821	1 821
4 0 0	2 118	2 116
2 0 4	2 166	2 162
3 3 0	2 381	2 382
4 0 2	2 526	2 524
4 2 0	2 645	2 645
2 2 4	2 691	2 691
3 3 2	2 789	2 789
4 1 3	3 170	3 167
4 0 4	3 750	3 749
5 1 2	3 847	3 847
5 2 1	3 940	3 938
4 2 4	4 272	4 278
6 0 0	4 762	4 761
5 3 2	4 901	4 905

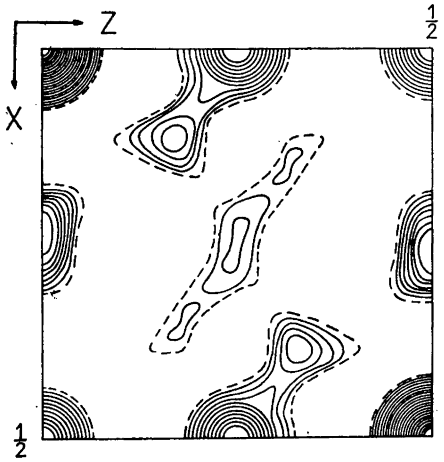

Fig. 1. Patterson projection on (010).

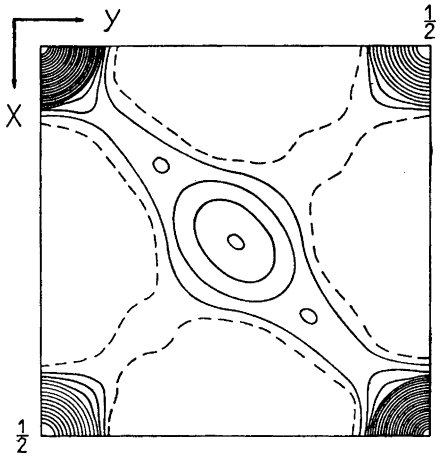

Fig. 2. Patterson projection on (001).

In all photographs only reflexions from planes of the following types were observed:

hkl	with	$h + k + l = 2n$
$hk0$	with	$h + k = 2n$
hhl	with	$l = 2n$
$0kl$	with	$k + l = 2n$
$00l$	with	$l = 2n$

The following space groups are thus possible:
$I4/mmm$ (No. 139), $I4mm$ (No. 107), $I\bar{4}m2$ (No. 119), $I\bar{4}2m$ (No. 121) and $I422$ (No. 97).

The experimentally determined density [1] is 2.79, from which the number of molecules per unit cell appears to be 2 (1.94).

From a Patterson projection on (010) (Fig. 1) it was concluded that the heavy atoms (Cr and K) are situated at (0;0), (0;$\frac{1}{4}$), (0;$\frac{1}{2}$), (0;$\frac{3}{4}$), ($\frac{1}{2}$;0), ($\frac{1}{2}$;$\frac{1}{4}$), ($\frac{1}{2}$;$\frac{1}{2}$) and ($\frac{1}{2}$;$\frac{3}{4}$), whereas the oxygen co-ordinates are of the general type.

Further information could be obtained from a Patterson projection on (001) (Fig. 2), which shows that the Cr and K atoms occupy the positions (0;0), (0;$\frac{1}{2}$), ($\frac{1}{2}$;0) and ($\frac{1}{2}$;$\frac{1}{2}$) and that the oxygen parameters seem to be of the type (x;x).

Of the possible space groups only $I\bar{4}2m$ is consistent with all these observations. According to this space group the positions of the heavy atoms will be the following

2 *a* 000
2 *b* 00 1/2
4 *d* 0 1/2 1/4, 1/2 0 1/4

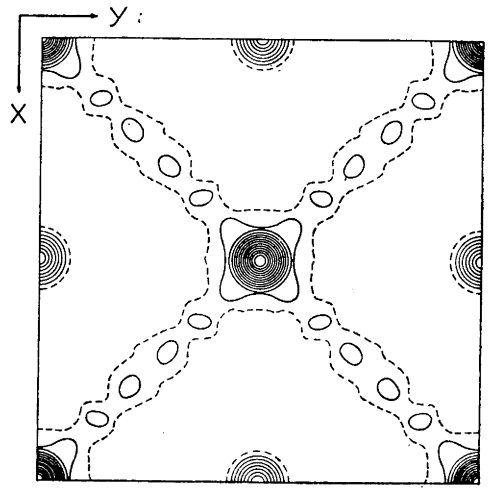

Fig. 3. Projection of the electron density in K_3CrO_8 on (001) (arbitrary units).

As no heavy peaks have appeared in the Patterson projection, except the one at origo it seemed very probable that the Cr atoms occupy the position 2 *a* and the K atoms 2 *b* and 4 *d*.

That this assumption is correct is indicated by the close agreement between observed and calculated structure factors arrived at in the final stage of the investigation.

The signs of the structure factors were calculated on the assumption that the chromium and potassium positions alone determined these. Two Fourier projections were synthesised, one (see Table 2, column 1) on (001) (Fig. 3) and one (Table 2, column 2) on (010) (Fig. 4).

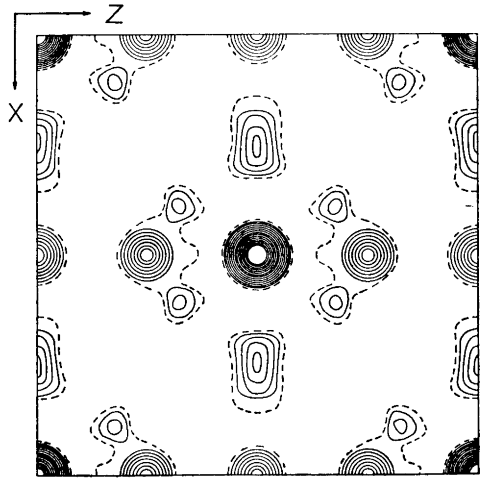

Fig. 4. Projection of the electron density in K_3CrO_8 on (010) (arbitrary units).

Table 2. Atomic parameters obtained from the various Fourier syntheses.

Atom		1	2	3	4	5	6
O_1	x	0.138	0.117	0.134	0.125	0.132	0.1355
	y	0.138	—	0.135	—	0.132	0.1355
	z	—	0.175	—	0.183	0.183	0.1825
O_2	x	0.207	0.200	0.203	0.208	0.206	0.2050
	y	0.207	—	0.204	—	0.206	0.2050
	z	—	0.000	—	0.011	0.011	0.0075

The heavy peaks all occurred at the above-mentioned positions for potassium and chromium. The oxygen parameters thus obtained are subject to great errors, however, because of the considerable differences in the electron densities between the chromium and potassium atoms on the one hand and the oxygen atoms on the other hand.

In order to attain greater accuracy two difference syntheses were produced (Table 2, columns 3 and 4) by subtracting the contributions of the chromium and potassium atoms from the structure factors with due regard to the temperature factor. The parameters obtained from these two projections were in better agreement with each other, but there was still great uncertainty in the $O_{(2)}$-position because of the overlapping. A $(F_o - F_c)$-synthesis was tried but with the aid of this it was not possible to get sufficiently exact parameter displacements. It was therefore necessary to make a three-dimensional Fourier analysis in order to resolve the peaks.

Three-dimensional refinement

The final atomic co-ordinates from the (010)- and (001)-projections, which are shown in column 5 of Table 2, were used to calculate $\sum_r f_r A_r$ and $\sum_r f_r B_r$ in the expression

$$|F(hkl)| = \{[\sum_r f_r A_r]^2 + [\sum_r f_r B_r]^2\}^{\frac{1}{2}} \quad ,$$

where the notation is that adopted in the International Tables for X-ray Crystallography [10]. The phase angle $\alpha(hkl)$ could thereafter be deduced by means of the equation

$$\alpha(hkl) = \tan^{-1}\left\{\frac{[\sum_r f_r B_r]}{[\sum_r f_r A_r]}\right\}$$

This quantity was used in the expression for the electron density

$$\varrho_{xyz} = \frac{8}{V_c} \sum_h \sum_k \sum_l |F(hkl)| \{\cos 2\pi hx \cos 2\pi ky \cos 2\pi lz \cos\alpha(hkl) -$$

$$\sin 2\pi hx \sin 2\pi ky \sin 2\pi lz \sin\alpha(hkl)\}.$$

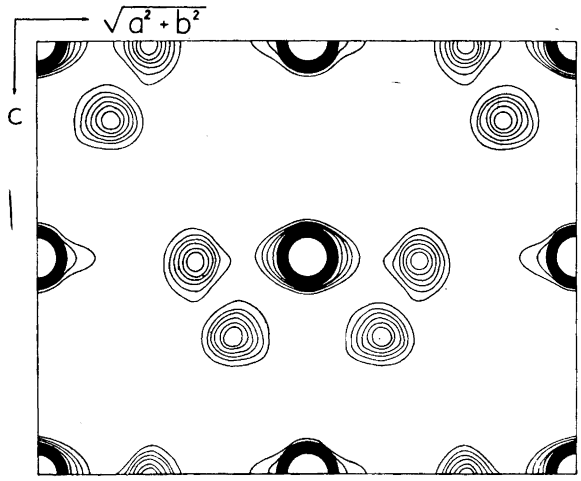

Fig. 5. The electron density of K_3CrO_8 in the plane $(1\bar{1}0)$. Contours at 2 e/Å^3. The curves are not drawn in the centers of the heavy atoms.

In the first stage of the calculation the quantities $\sum_h\sum_k |F(hkl)| \cos 2\pi hx \cos 2\pi ky \cos\alpha(hkl)$ and $\sum_h\sum_k |F(hkl)| \sin 2\pi hx \sin 2\pi ky \sin\alpha(hkl)$ were determined with $h = 0-8$, 10 and $k = 0-8$, 10, and with x taken at intervals of 1/200 of the cell side, and with y at intervals of 1/60 of the cell side. With the aid of these two-dimensional data one-dimensional Fourier syntheses were computed in the z-direction, with z taken at intervals of 1/200 of the cell side. Because $x_1 = y_1$ and $x_2 = y_2$ it was sufficient to calculate the electron density in the plane $(1\bar{1}0)$ (Fig. 5).

Final parameter values of the oxygen atoms are given in column 6 of Table 2. The arrangement of the atoms is given in Table 3. In Table 4 are

Table 3. Arrangement of the atoms in K_3CrO_8.

Atom	x	y	z	Atom	x	y	z
Cr_1	0	0	0	O_5	0.6355	0.6355	0.6825
Cr_2	1/2	1/2	1/2	O_6	0.7050	0.7050	0.5075
K_1	0	0	1/2	O_7	0.8645	0.8645	0.1825
K_2	1/2	1/2	0	O_8	0.7950	0.7950	0.0075
K_3	0	1/2	1/4	O_9	0.1355	0.8645	0.8175
K_4	1/2	0	3/4	O_{10}	0.6355	0.3645	0.3175
K_5	1/2	0	1/4	O_{11}	0.2050	0.7950	0.9925
K_6	0	1/2	3/4	O_{12}	0.7050	0.2950	0.4925
O_1	0.1355	0.1355	0.1825	O_{13}	0.8645	0.1355	0.8175
O_2	0.2050	0.2050	0.0075	O_{14}	0.7950	0.2050	0.9925
O_7	0.3645	0.3645	0.6825	O_{15}	0.3645	0.6355	0.3175
O_4	0.2950	0.2950	0.5075	O_{16}	0.2950	0.7050	0.4925

Table 4. Values of observed and calculated structure factors for K_3CrO_8 including the phase angle α(hkl).

h k l	F_{obs}	F_{calc}	$\alpha°(hkl)$
2 0 0	85	77	0
4 0 0	73	74	0
6 0 0	76	83	0
8 0 0	66	66	0
1 0 0 0	62	60	0
1 1 0	43	42	0
3 1 0	20	21	180
2 2 0	132	146	0
4 2 0	75	79	0
6 2 0	61	66	0
8 2 0	58	68	0
1 0 2 0	47	47	0
3 3 0	47	46	0
4 4 0	101	99	0
6 4 0	61	60	0
8 4 0	41	45	0
1 0 4 0	56	66	0
5 5 0	26	22	0
6 6 0	60	64	0
8 6 0	71	59	0
1 0 6 0	60	48	0
7 7 0	36	23	0
8 8 0	69	65	0
1 0 1	36	45	0
3 0 1	30	35	180
5 0 1	27	27	0
2 1 1	30	35	265
4 1 1	10	8	62
6 1 1	20	14	61
3 2 1	35	37	333
5 2 1	28	24	127
7 2 1	20	15	17
5 4 1	17	15	344
0 0 2	34	29	0
2 0 2	24	24	180
4 0 2	37	39	0
1 1 2	128	117	347
3 1 2	118	105	355
5 1 2	91	87	8
7 1 2	48	54	2
9 1 2	57	60	354
2 2 2	41	47	321
3 3 2	93	87	355
5 3 2	55	51	9
7 3 2	84	82	2
5 5 2	83	80	353
7 5 2	57	52	357
9 5 2	64	62	8
7 7 2	66	59	359
9 7 2	59	43	4
9 9 2	72	46	349
3 0 3	17	10	0

Table 4, continued.

$h\ k\ l$	F_{obs}	F_{calc}	$\alpha°(hkl)$
5 0 3	36	36	0
4 1 3	39	26	4
3 2 3	24	23	16
4 3 3	17	20	189
0 0 4	110	133	0
2 0 4	60	65	0
4 0 4	86	89	0
6 0 4	57	67	0
1 1 4	15	16	53
3 1 4	18	15	80
5 1 4	19	18	304
2 2 4	102	109	14
4 2 4	63	65	357
6 2 4	71	66	345
8 2 4	52	67	7
4 4 4	70	68	359
6 4 4	61	65	5
8 4 4	57	56	356
5 5 4	29	19	38
6 6 4	57	60	8
8 6 4	55	53	356
8 8 4	52	53	2
1 0 5	33	31	0
3 0 5	29	30	180
3 2 5	24	22	22
5 4 5	19	13	11
0 0 6	49	49	0
1 1 6	81	86	350
3 1 6	50	57	359
5 1 6	63	66	5
7 1 6	85	64	0
2 2 6	30	24	323
3 3 6	83	87	356
5 3 6	59	57	5
7 3 6	53	59	2
5 5 6	62	75	355
7 5 6	38	41	357
7 7 6	67	69	359
2 1 7	17	17	267
3 2 7	18	14	330
0 0 8	43	65	0
2 0 8	43	54	0
4 0 8	61	82	0
1 1 8	12	9	246
2 2 8	48	75	356
4 2 8	39	56	4
4 4 8	39	50	355
6 4 8	42	61	3
6 6 8	36	51	352
0 0 10	26	20	0
1 1 10	35	64	1
2 2 10	23	13	45
3 3 10	39	66	1
5 5 10	44	63	7

given observed structure factors and those calculated using the values of the atomic parameters given in Table 3. In Table 4 are also included the phase angles $\alpha(hkl)$ used in computing the electron density in the plane $(1\bar{1}0)$.

The structure factor disagreements,

$$R = \frac{\Sigma(|F_{calc}| - |F_{obs}|)}{\Sigma|F_{obs}|}$$

of the final coordinates are $R_{hkl} = 13.2$ %, $R_{hk0} = 8.4$ % and $R_{h0l} = R_{0kl} = 17.4$ %, excluding those terms too weak to be observed.

Observed structure factors have been corrected for thermal vibrations by the factor $\exp[B(\sin\Theta/\lambda)^2]$ with $B = 2.0 \times 10^{-16}$ cm^2, determined by the method of least squares from the final structure factors. An isotropic temperature factor has been applied in spite of the fact that the $(F_o - F_c)$-synthesis showed the existence of somewhat different magnitudes in the thermal vibrations in the x- and z-directions.

Accuracy of the determination

The standard deviations $\sigma(x)$ and $\sigma(z)$ of atomic coordinates were estimated from the differences ΔF between the magnitudes of observed and calculated values of the structure factors according to Cruickshank's method [3], where

$$\sigma(x) = \frac{2\pi[\Sigma h^2(F_o - F_c)^2]^{\frac{1}{2}}}{a \cdot V \cdot \frac{\partial^2\varrho}{\partial x^2}}$$

and

$$\sigma(z) = \frac{2\pi[\Sigma l^2(F_o - F_c)^2]^{\frac{1}{2}}}{c \cdot V \cdot \frac{\partial^2\varrho}{\partial z^2}};$$

here a and c are the cell edges and V the cell volume.

As proposed by Shoemaker, Donohue, Schomaker and Corey [8] these values have been increased by the factor of 1.3 as the structure has no centre of symmetry but the projections are centro-symmetric.

The values of $\frac{\partial^2\varrho}{\partial x^2}$ and $\frac{\partial^2\varrho}{\partial z^2}$ were obtained from the values of the electron density in the neighbourhood of the final Fourier peaks. Mean values for the oxygen atoms are

$$\frac{\partial^2\varrho}{\partial x^2} = 610 \text{ and } \frac{\partial^2\varrho}{\partial z^2} = 625 \text{ e/Å}^5$$

The standard deviations of the oxygen atomic positions are thus $\sigma(x) = 0.0084$ and $\sigma(z) = 0.0096$ Å. The standard deviations in the bond lengths are 0.022 Å for O_1-O_2 and 0.015 Å for K—O and Cr—O. The probable error in the bond angles is 1°.

Table 5. Interatomic distances.

Cr_1-O_1	1.895 Å
Cr_1-O_2	1.944
K_1-O_1	2.743
K_1-O_4	2.797
K_2-O_1	2.661
O_1-O_2	1.489
O_1-O_4	2.905
O_2-O_5	2.569
O_4-O_{10}	2.744
O_4-O_{12}	2.751

Description of the structure

Bond lengths and other interatomic distances are given in Table 5 and bond angles in Table 6. Fig. 6 shows the arrangement of the oxygen atoms about the chromium atom. From this figure, and from the data obtained, it follows that the chromium atom in K_3CrO_8 is surrounded by eight oxygen atoms, four being at a distance of 1.895 Å and four at 1.944 Å. The discrepancy between these two values is not significant. Thus the close agreement between the bond lengths indicates that the chromium atom is bonded to eight oxygen atoms. This 8-coordination with the symmetry $\bar{4}\ 2\ m$ has a dodecahedral configuration.

The length of the bond between the two oxygen atoms, as a peroxide ion is 1.489 Å, close to values found in other peroxy compounds [6,7]. The shortest distances between oxygen atoms not belonging to the same peroxide ion are 2.91 Å, 2.57 Å, 2.75 Å, and 2.74 Å.

The potassium atoms are also 8-coordinate, the shortest potassium-oxygen distances being 2.74 Å, 2.80 Å, and 2.66 Å.

DISCUSSION

The likely configurations for a complex ion or a molecule of formula AB_8 are four in number, [9,11] namely the cube, the Archimedean antiprism with symmetry $\bar{8}2m$, the dodecahedron with symmetry $\bar{4}2m$ and the face-centered trigonal prism. The need to use *f*-orbitals of the central atom in forming cubic bonds has been quoted as unfavourable [11], although it is believed that diketone complexes of Ce(IV), Th(IV) *etc.* have cubic arrangements [15].

Table 6. Bond angles.

$O_1-Cr_1-O_2$	45.6°
$Cr_1-O_1-O_2$	68.9
$Cr_1-O_2-O_1$	65.5
$O_4-Cr_2-O_{16}$	89.8
$O_4-Cr_2-O_{10}$	91.2
$O_3-Cr_2-O_5$	95.4
$O_3-O_{12}-O_5$	55.8
$O_1-K_1-O_4$	63.9

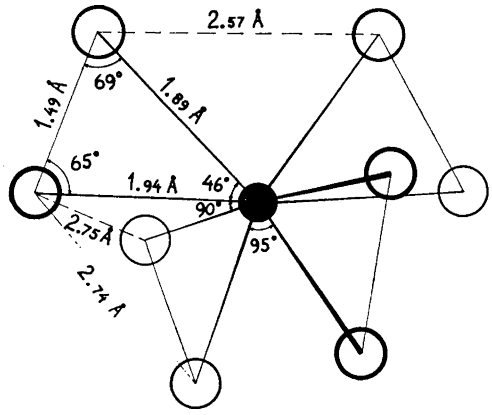

Fig. 6. Bond lengths and bond angles in K_3CrO_8.

According to the literature [14] other molecules and ions with co-ordination number 8 are 8-quinolinol chelates of tetrapositive metals; cyano- and fluoro-complexes such as $Mo(CN)_8^{4-}$, $W(CN)_8^{4-}$, and TaF_8^{3-}; and oxalato complexes such as $U(C_2O_4)_4^{4-}$. So far only the antiprismatic and the dodecahedral arrangements have been established for a discrete group AB_8.

Hoard and Nordsieck [9] have found that $Mo(CN)_8^{4-}$ has the dodecahedral arrangement with the carbon atoms at the vertices, and that the symmetry of the complex ion can be approximated to $\bar{4}2m$. The present investigation has shown that CrO_8^{3-} has the symmetry $\bar{4}2m$ and that the geometrical arrangement of the oxygen atoms surrounding the central chromium atom is dodecahedral. One would have expected the same configuration for $Mo(CN)_8^{4-}$, CrO_8^{3-} and TaF_8^{3-}, but Hoard *et al.* [12] have shown by X-ray analysis that TaF_8^{3-} has the arrangement of an Archimedean antiprism.

According to Kimball [11] the dodecahedral, antiprismatic and face-centered trigonal prismatic configurations are given by appropriate linear combinations of *spd*-orbitals, but Higman [13] has concluded that one *f*-orbital is required for the $Mo(CN)_8^{4-}$-arrangement. This conclusion does not seem adequate as there are no available *f*-orbitals in CrO_8^{3-}. It is highly probable that the bonds are d^4sp^3-hybrids because the paramagnetism of the substance is in accordance with the orbital configuration

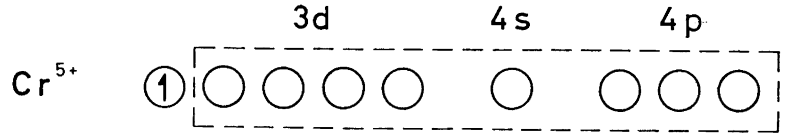

The stability of this arrangement has also been found to occur with Mo^{5+} in $Mo(CN)_8^{3-}$ which is not oxidized to $Mo(CN)_8^{2-}$. This is in contrast to other Mo(V) compounds which are readily oxidized to Mo(VI).

It is rather remarkable that the two non-isoelectronic ions $Mo(CN)_8^{4-}$ and CrO_8^{3-} have the same configuration. It should also be pointed out that the structure of the $Mo(CN)_8^{3-}$-ion, which is isoelectronic with CrO_8^{3-}, has not yet been determined.

Finally it should be mentioned that $Cr(O_2)_4^{4-}$ does not seem to exist. This may be explained by assuming that the configuration with a single electron in the 3*d* orbital has a stabilizing effect.

REFERENCES

1. Wilson, I. A. *Arkiv Kemi Mineral. Geol.* **15B** (1942) No. **5**.
2. Riesenfeld, E. H., Wohlers, H. E. und Kutsch, W. A. *Ber.* **38** (1905) 1885.
3. Cruickshank, D. W. J. *Acta Cryst.* **2** (1949) 65.
4. Tjabbes, B. Th. *Z. anorg. u. allgem. Chem.* **210** (1933) 385.
5. Klemm, W. and Werth, H. *Z. anorg. u. allgem. Chem.* **216** (1933) 127.
6. Abrahams, S. C., Collin, R. L. and Lipscomb, W. N. *Acta Cryst.* **4** (1951) 15.
7. Vannerberg, N. G. *Arkiv Kemi* **14** (1959) 17.
8. Shoemaker, D. P., Donohue, J., Schomaker, V. and Corey, R. B. *J. Am. Chem. Soc.* **72** (1950) 2328.
9. Hoard, J. L. and Nordsieck, H. H. *J. Am. Chem. Soc.* **61** (1939) 2853.
10. *International Tables for X-ray Crystallography*, The Kynock Press, Birmingham 1952, Vol I.
11. Kimball, G. E. *J. Chem. Phys.* **8** (1940) 188.
12. Hoard, J. L., Martin, W. J., Smith, M. E. and Whitney, J. F. *J. Am. Chem. Soc.* **76** (1954) 3820.
13. Higman, B. *J. Chem. Phys.* **21** (1953) 2224.
14. Moeller, T. *Inorganic Chemistry*, John Wiley & Sons, New York 1955.
15. Cartmell, E. and Fowles, G. W. A. *Valency and Molecular Structure*, Butterworths, London 1956.

Received October 6, 1959.

ACTA CHEMICA SCANDINAVICA 14 (1960) 453–456

On Relative Donor Strengths: A Thermochemical Study

INGVAR LINDQVIST and MARGARETA ZACKRISSON

Institute of Chemistry, University of Uppsala, Uppsala, Sweden

A simple method for qualitative studies of relative orders of enthalpy changes has been developed. The relative orders of donor strength of some oxide chlorides and organometalloid oxides have been established. A brief discussion of the effects of substitution has been given.

In a previous paper [1] it has been pointed out that in the study of addition compounds, the determination of the relative acceptor and donor strengths of the reacting molecules is a very important problem. In the work described there, a spectroscopic method was used for this purpose. A more direct method is to measure the heat of reaction of the adduct formation. The discussion in the earlier paper [1] about such reactions in a solvent is valid in this case too.

This paper deals with an attempt to determine the relative donor strengths of a number of molecules in reactions with $SbCl_5$ and $SnCl_4$ as acceptors by a simple thermochemical method. In most of the reactions studied here the formation of adduct molecules is probably complete but some dissociation will not influence the measured order of donor strengths because only reactions of the same type have been compared.

EXPERIMENTAL

Chemicals. 1,2-$C_2H_4Cl_2$, $(CH_3)_2SO$, $(C_6H_5)_2S$, $(CH_3)_2CO$, $CH_3COOC_2H_5$, $(C_2H_5)_2CO$, $(C_2H_5)_2O$, $POCl_3$ and $SOCl_2$ were purified by distillation. (B.p. 84°, 95°/30 mm, 92°, 57°, 77°, 103°, 35°, 105° and 80°C.) $SeOCl_2$ was repeatedly distilled until it had a final melting point of + 10.5°C. In order to obtain $(C_6H_5)_2SeO$, $(C_6H_5)_2Se$ was prepared [2] and oxidized according to a method described by Bergson [3] (for preparing selenanthren-5,10-dioxide). This method gave a hydrate which was dried at 70°/10 mm for 12 h (M.p.113°C). $(CH_3)_3PO$ and $(C_6H_5)_3PO$ were prepared as described earlier [4] (M.p. 137–139° and 152–154°C). $(CH_3)_2SO_2$ was prepared by oxidation of $(CH_3)_2SO$ according to McAllan *et al.*[5] (M.p. 108–109°C). $(C_6H_5)_2SO_2$ was prepared by Dr. B. Sjöberg whose help is gratefully acknowledged (M.p. 125°C). $(C_6H_5)_3AsO$ was friendly sent to us by Prof. S. Y. Tyree, Chapel Hill, North Carolina. $SbCl_5$ and $SnCl_4$ were purified according to Dodd and Robinson [6].

THERMOCHEMICAL MEASUREMENTS

The apparatus used for this purpose is very simple. In each of two reaction vessels of Dewar type, thermistors are placed, functioning as resistances in a Wheatstone bridge. Equal volumes of a solution of the acceptor molecule are placed in the reaction vessels. The bridge is balanced with a variable resistance, using a galvanometer as null indicator. Solutions of two different donor molecules are poured into each of the vessels simultaneously. If the heat of reaction is not the same in both of the reactions the galvanometer needle deflects, thus indicating which of the reactions has the larger change of enthalpy.

1,2-Dichlorethane has been used as a solvent and the solutions of the donor molecules have been 0.4 M. Because $SbCl_5$ in most of the cases we know gives addition compounds with one donor molecule, but $SnCl_4$ with two molecules, 0.4 M solutions of $SbCl_5$ and 0.2 M solutions of $SnCl_4$ and equal volumes of donor and acceptor solutions have been used for the reactions. We have assumed that if there is any difference in the heat capacity of the solutions at such dilutions, it must be so small that it cannot influence the results. (This has also been checked by experiments which will not be presented in this paper, because only crude qualitative experiments are described here, which cannot be influenced by such minor sources of error.)

RESULTS

The results are summarized in Table 1.

Table 1.

Acceptor: $SbCl_5$

1. $(C_6H_5)_2SeO = (C_6H_5)_3AsO > (CH_3)_3PO > (CH_3)_2SO$
2. $(C_2H_5)_2S > (CH_3)_2CO = CH_3COOC_2H_5 = (C_2H_5)_2CO = (C_2H_5)_2O$
3. $(CH_3)_2SO_2 > (C_6H_5)_2SO_2 = POCl_3 = SeOCl_2 > SOCl_2$

Acceptor: $SnCl_4$

1. $(C_6H_5)_2SeO = (C_6H_5)_3AsO > (CH_3)_3PO > (C_6H_5)_3PO$
2. $(C_2H_5)_2S > (CH_3)_2CO = CH_3COOC_2H_5 > (C_2H_5)_2CO = (C_2H_5)_2O$

The donor molecules studied fall naturally into three classes of decreasing strength. Each of the compounds of a class are of the same order of strength compared to the difference between the classes, which is especially large between class 1 and class 2. The sequence within each class is not definitely proved to be correct but the experiments strongly indicate the given order. Such a small amount of substance of $(C_6H_5)_3AsO$ was available that solutions which were only 0.04 M had to be used. The effect at this dilution is very small and the position of this donor in the sequence is thus doubtful, but its placement in class 1 is certainly correct.

$(C_6H_5)_3PO$ gives HCl-evolution and dark color with $SbCl_5$[4] even at this dilution and could not be studied with that acceptor. $(CH_3)_2SO$ could not

be studied with $SnCl_4$ as acceptor because of the formation of a precipitate. The nature of this precipitate was not further explored. The compounds of class 3 gave no measurable effect with $SnCl_4$ as acceptor. The reason is probably that the addition compounds are completely dissociated in their components at this dilution.

DISCUSSION

It is often assumed that the order of relative donor strengths of the molecules will also give information about the bond strength between the donor and the acceptor atoms of the compound formed. There are some objections against this assumption, however. In adduct formation the acceptor molecule has changed its structure completely and there might be subsequent energy changes which have been ignored in the assumption. For the determination of *relative* interaction strengths with the same acceptor molecule this complication is of importance only if the structure of the donor molecule also has changed appreciably.

Another complication is the fact that in some cases a secondary acceptor-donor interaction takes place, *e.g.* with $SeOCl_2$[7] and with sulfoxides [8]. In the detailed discussion of the order of relative donor strengths this secondary interaction might be important.

Finally it can be remarked that any attempt to subdivide the energy of a molecule into different bond energies is a rather arbitrary procedure.

The donor function of the oxygen atoms in $POCl_3$[9], $(C_6H_5)_2SO$[8], $(CH_3)_3PO$[10], and $(C_6H_5)_2SO_2$[11] with $SbCl_5$ as acceptor and in $POCl_3$[10] and $SeOCl_2$[7] with $SnCl_4$ as acceptor has recently been definitely established by X-ray work and there is no reason to suspect that the other molecules studied here, in which oxygen is bonded to the central atom of the molecule, will react differently. Concerning the ether and the sulfide it can safely be assumed that the oxygen and the sulfur atoms, respectively, are the donor atoms. In ethyl acetate it is not established which of the oxygen atoms functions as the donor atom and it should be of great interest to know.

The results show that not only the donor atom, but also the other atoms in the donor molecule are of great importance for the donor strength. All oxychlorides are much weaker as donors than the corresponding compounds with organic substituents. The larger electronegativity of chlorine compared with the organic groups causes a drift of electrons from oxygen and thus a lower tendency to donate an electron pair. In most cases we can even see the difference between molecules with the same central atom but with different organic substituents.

Other facts also seem to influence the donor strength. Sulfur in $(CH_3)_2SO$ and carbon in $(CH_3)_2CO$ have the same electronegativity (2.5). Nevertheless, $(CH_3)_2SO$ has much stronger donor properties than $(CH_3)CO$. One difference between those molecules is that the sulfur atom of the sulfoxide has a free electron pair lacking at the carbon atom in acetone.

In class 2 we can note that ethyl sulfide seems to be a stronger donor than ethyl ether. Ahrland *et al.*[12] have divided acceptor atoms into two classes and placed antimony and tin in the class which should form more stable

complexes with oxygen than with sulfur, but these experiments indicate that they are probably border-line elements.

It has been established that only one of the oxygen atoms in the sulfones is functioning as a donor atom [11] and the other oxygen atom seems to decrease the donor strength to an appreciable extent compared with methyl-sulfoxide.

Steric hindrances might also affect the strength of the acceptor-donor bond, but there is no obvious example of this among the molecules studied.

These experiments give good hope of further exploring relative donor and acceptor strengths in a simple way. We also intend to improve the apparatus and perhaps be able to give an approximative value of the magnitude of the enthalpy changes at the reactions.

A grant from the *Swedish Natural Science Research Council* is gratefully acknowledged. Finally we wish to thank Prof. G. Hägg for all facilities put at our disposal.

REFERENCES

1. Kinell, P.-O., Lindqvist, I. and Zackrisson, M. *Acta Chem. Scand.* **13** (1959) 190.
2. *Organic synthesis* Coll. Vol. II (1943) 238.
3. Bergson, G. *Acta Chem. Scand.* **11** (1957) 580.
4. Lindqvist, I. and Olofsson, G. *Acta Chem. Scand.* **11** (1959) 1753.
5. McAllan, D. T., Cullum, T. V., Dean, R. A. and Fidler, F. A. *J. Am. Chem. Soc.* **73** (1951) 3627.
6. Dodd, R. E. and Robinson, P. L. *Experimental Inorganic Chemistry*, Amsterdam 1954, p. 210, 216.
7. Hermodsson, Y. *To be published.*
8. Hansson, A. and Vänngård, M. *To be published.*
9. Lindqvist, I. and Brändén, C.-I. *Acta Cryst.* **12** (1959) 642.
10. Brändén, C. I., and Lindqvist, I. *To be published.*
11. Hansson, A. *To be published.*
12. Ahrland, S., Chatt, J. and Davies, N. R. *Quart. Revs.* **12** (1958) 265.

Received October 24, 1959.

ACTA CHEMICA SCANDINAVICA 14 (1960) 457–464

Die Biosynthese der Orsellinsäure und Penicillinsäure (1)

KLAUS MOSBACH

Biochemisches Institut der Universität Lund, Lund, Schweden

Die in Gegenwart von $CH_3{}^{14}COONa$ aus *Chaetomium cochliodes* gebildete Orsellinsäure wurde isoliert und ihre ^{14}C-Verteilung bestimmt. Es wurde gezeigt, dass das Orsellinsäuremolekül entsprechend der Acetattheorie aufgebaut wird. Das Vorkommen von Orsellinsäure in *Penicillium barnense* wurde festgestellt. Spezifisch markierte Orsellinsäure wurde als Substrat zu *Penicillium barnense* gegeben und die gebildete Penicillinsäure isoliert. Das radioaktive Markierungsmuster der Penicillinsäure entsprach dem der zugesetzten Orsellinsäure, womit gezeigt wurde, dass Orsellinsäure Precursor der Penicillinsäure ist.

Der klassische Metabolit in Schimmelpilzen, Penicillinsäure, wurde unter anderem auch in *Penicillium barnense* gefunden.[1] Es lagen auch Beweise für das Vorkommen einer aromatischen Substanz von phenolischem Charakter im Kulturmedium desselben Pilzes vor. Es wurde nun gezeigt, mit den schon einmal beschriebenen Analysenmethoden [2], dass es sich bei dieser Verbindung um Orsellinsäure handelt. Nach etwa 10 Tagen wurde der Anteil der Orsellinsäure im Kulturmedium immer geringer, wobei sich gleichzeitig der Anteil der Penicillinsäure erhöhte.

Das gemeinsame Vorkommen dieser beiden Metaboliten in derselben Spezies, ihre wechselweisen quantitativen Beziehungen zueinander sowie die strukturelle Ähnlichkeit der Orsellinsäure und Penicillinsäure lassen auf einen metabolischen Zusammenhang schliessen. Man könnte sich dabei die Penicillinsäure durch eine Ringspaltung der Orsellinsäure entstanden denken. Dieser Gedanke war schon vor einigen Jahren von Ehrensvärd [3] ausgesprochen worden und unabhängig von ihm von Birch [3].

Eine Parallele zu dieser Ringspaltung wäre der Übergang biosynthetischer ^{14}C-markierter 6-Methylsalicylsäure zu Patulin.[4,5].

Um diese Hypothese zu untersuchen, wurde spezifisch markierte Orsellinsäure, (2-^{14}C- und karboxyl-^{14}C-markiert), zum Medium von *Penicillium barnense* gegeben und die Penicillinsäure isoliert. Jedoch musste zunächst einmal festgestellt werden, inwieweit die von Birch [6] gezeigte head-to-tail-Kupplung von Acetateinheiten bei 6-Methylsalicylsäure auch für Orsellinsäure Gültigkeit hat. Dabei hat sich gezeigt, dass auch für Orsellinsäure

die Acetattheorie in vollem Umfang gilt, und dies ist somit neben der von Gatenbeck [7] gezeigten Acetatkupplung bei der 3-Hydroxyphthalsäure ein weiterer Beweis für deren Richtigkeit.

Auch der von Gatenbeck und dem Verfasser [8] gezeigte Einbau des Sauerstoffisotopen ^{18}O aus $CH_3{}^{14}CO^{18}ONa$ in die Karboxyl- und die beiden Hydroxylgruppen der Orsellinsäure kann als ein weiterer Beweis für die Acetattheorie gelten.

EXPERIMENTELLER TEIL

1). Degradation der Orsellinsäure

Kulturbedingungen: Vier Fernbachkolben mit je 500 ml Czapek-Dox-Lösung (5 % Dextrose) wurde mit Perithecien von *Chaetomium cochliodes Pall.* okuliert. Nach 12 Tagen wurde in die Kolben eine Lösung von $CH_3{}^{14}COONa$ (insgesamt 0.5 mC) pipettiert. Nach weiteren 7 Tagen wurde das Myzelium durch Filtrieren vom Medium getrennt und die Orsellinsäure in der schon beschriebenen Weise isoliert [2]. Ein kleiner Teil des Mediums wurde mit Äthyläther extrahiert und der Extrakt chromatographiert. (System: Wasser-Äthyl-Methylketon-Diäthylamin.)[9] Das Messen der Radioaktivität entlang des Papierchromatogrammes ergab nur zwei Aktivitätsspitzen, deren R_F-Werte jeweils denen der Orsellinsäure bzw. des Orcinols entsprachen. (Orsellinsäure $R_F = 30$; Orcinol $R_F = 90$.)

Oxydation der Orsellinsäure nach van Slyke-Folch: 270 mg nicht radioaktiver Orsellinsäure wurde zu 72 mg der isolierten radioaktiven Säure gegeben. Durch wiederholtes Lösen und Eindunsten in Äthyläther wurde eine homogene Mischung erhalten.

5 mg der Substanz wurden nun nach der Methode von van Slyke-Folch [10] oxydiert und das dabei gebildete Kohlendioxyd in karbonatfreiem Bariumhydroxyd aufgefangen. Das Bariumkarbonat wurde isoliert und dessen Radioaktivität gemessen. Bei allen radioaktiven Messungen wurden jeweils 15 mg/cm^2 Bariumkarbonat verwendet.

Dekarboxylierung der Orsellinsäure: 131 mg Orsellinsäure wurden in 12 ml Glyzerin durch Erwärmen im Ölbad gelöst. Das dabei gebildete Kohlendioxyd wurde durch einen durch das System geleiteten Strom von kohlendioxydfreiem Stickstoff in eine Bariumhydroxydlösung gebracht und als Bariumkarbonat isoliert.

Kuhn-Roth-Oxydation der Orsellinsäure: Die Kuhn-Roth-Oxydation von 100 mg Orsellinsäure ergab Essigsäure, die durch Wasserdampfdestillation isoliert wurde. Das während der Reaktion gebildete Kohlendioxyd wurde in Bariumhydroxid aufgefangen. Die Essigsäure wurde durch eine Schmidt-Reaktion dekarboxyliert und das Kohlendioxyd als Bariumkarbonat isoliert. Das dabei gebildete Methylamin wurde dann durch eine alkalische Permanganatlösung zu Kohlendioxyd oxydiert. Nach Ansäuern derselben wurde das dadurch freigemachte Kohlendioxyd in Baryt aufgefangen.

2,4,6-Trinitroorcinol: 75 mg Orsellinsäure wurden in 0,350 ml konz. Schwefelsäure gelöst und bei 0°C eine kalte Mischung von 0,135 ml konz. Salpetersäure und 0,27 ml konz. Schwefelsäure zugegeben. Nach einem weiteren Zusatz von 0,220 ml konz. Salpetersäure und einer halben Stunde Stehen bei Zimmertemperatur wurde die Mischung in Eiswasser gebracht. Das dabei ausgefällte 2,4,6-Trinitroorcinol wurde abfiltriert und aus Wasser umkristallisiert. (Schmelzp. 171°C.)[11]

Hypobromit-Oxydation von 2,4,6-Trinitroorcinol: Zu 33 mg Trinitroorcinol in 5 ml heissem Wasser wurden 7 ml einer gesättigten Bariumhydroxydlösung gegeben. Die auf 0°C gekühlte Suspension wurde mit einer eiskalten Bariumhypobromitlösung (0,2 ml Br_2, 1,6 g $Ba(OH)_2$, 30 ml H_2O) versetzt. Nach 5 Stunden Umrühren in einem verschlossenen Erlenmeyerkolben bei Zimmertemperatur wurde das gebildete Brompikrin mit Wasserdampf überdestilliert. Das Destillat wurde in einem vorgekühlten Zntrifugenrohr aufgefangen und abzentrifugiert. Nach Waschen mit angesäuertem destillierten Wasser wurde das Brompikrin erneut zentrifugiert und nach van Slyke-Folch zu Kohlendioxyd oxydiert. Das während der Hypobromitreaktion gebildete Bariumkarbonat wurde filtriert und mit kochendem destilliertem Wasser gewaschen. Durch Ansäuern mit Perchlorsäure wurde das Kohlendioxyd freigemacht und noch einmal als Bariumkarbonat isoliert.

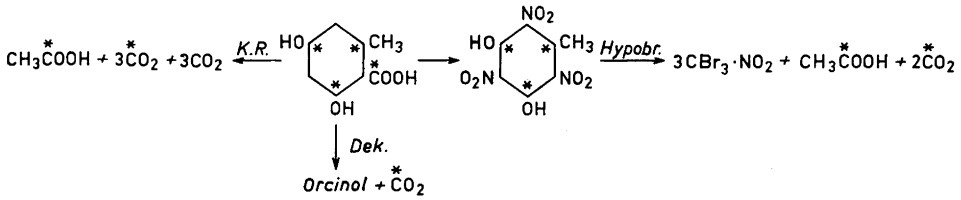

Abb. 1. Degradationsschema der Orsellinsäure.

2). Synthese von 2-^{14}C- und karboxyl-^{14}C-markierter Orsellinsäure

Äthylacetoacetat: ($CH_3{}^{14}COCH_2{}^{14}COOH$): 250 mg ^{14}C-markiertes Bariumkarbonat wurde mit Perchlorsäure versetzt und das dabei gebildete radioaktive Kohlendioxyd in eine Ätherlösung von Magnesiumjodmethyl eingeleitet und die durch Hydrolyse mit

Tabelle 1. ^{14}C-Verteilung in biosynthetischer Orsellinsäure.

Material	Anzahl C-Atome von der Orsellinsäure	Totale Radioaktivität desMateriales in Imp./Min	Anzahl der COOH-Gruppen entsprechend der Acetattheorie	
			Gef.	Theor.
(1)	(2)	(3)	(4)	(5)
Alle Kohlenatome der Orsellinsäure Oxydation nach van Slyke-Folch	8	1 370	4.03	4
Dekarboxylierung	1	346	1.01	1
Kohlenatom 6 der Orsellinsäure K-R-Oxydation (Essigsäure) *	1	340	1	1
Methylgruppe der Orsellinsäure K-R-Oxydation (Essigsäure)	1	0	0	0
Kohlenatome 1, 2, 3, 4, 5 und Karboxylgruppe der Orsellinsäure K-R-Oxydation	6	1 032	3.03	3
Kohlenatome 2 und 4 der Orsellinsäure Hypobromitoxydation von Trinitroorcinol	2	598	1.76	2
Kohlenatome 1, 3 und 5 der Orsellinsäure Brompikrin	3	0	0	0

* Die Radicaktivität der Karboxylgruppe der durch Kuhn-Roth-Oxydation erhaltenen Essigsäure ist als Basis für die Ausrechnung der theoretischen Aktivität der einzelnen Proben verwendet worden, da sie durch direktes Messen erhalten worden ist.

Wasser gebildete karboxylmarkierte Essigsäure isoliert. Das Natriumsalz der gebildeten Essigsäure wurde dann mit nicht radioaktivem Natriumacetat vermischt und durch Erwärmen mit Diäthylsulfat bei 180°C verestert. Das sich bildende Äthylacetat wurde sukzessiv abdestilliert. 25 g des gebildeten Äthylacetates wurde dann mit Natrium versetzt, um eine Kondensation zu Äthylacetoacetat zu ermöglichen [12]. Das Äthylacetoacetat wurde vom Reaktionsgemisch getrennt und schliesslich durch Destillation im Vakuum gereinigt. (Ausbeute: 6 g Äthylacetoacetat.) Dass gerade dieser Weg für die Synthese gewählt wurde, lag daran, dass die sich gleichzeitig bildende Dehydracetsäure für andere Versuche gebraucht wurde.

Dihydroorsellinsäureester: 0,69 g Natrium wurden in 10 ml abs. Äthylalkohol gelöst und 4,2 g des markierten Acetessigesters sowie 3,4 g Krotonsäureäthylester hinzugegeben [13]. Nach Erhitzen auf dem Wasserbad wurde das sich gebildete Natriumsalz des Dihydroorsellinsäureesters mit verdünnter Schwefelsäure zersetzt und der freie Ester isoliert.

Dibromorsellinsäureäthylester: 3,3 g Dihydroorsellinsäureester ergab nach Bromieren mit 8 g Br_2 Dibromorsellinsäureäthylester [14], der sich als kristalliner Brei abscheidete.

Orsellinsäureäthylester: 1,5 g markierter Dibromorsellinsäureäthylester wurde in 25 ml 2 N Natronlauge gelöst und nach Zusatz von 2 g nach Busch und Stöve bereitetem Katalysator (Palladium auf Calciumkarbonat) hydriert. Der gebildete Orsellinsäureäthylester wurde dann nach Filtrieren des Katalysators durch Ansäuern der Lösung ausgefällt und isoliert.

Orsellinsäure: Ein Teil des Esters der Osellinsäure wurde in 10 %-iger NaOH-Lösung bei Zimmertemperatur verseift und zwar während 10 Tagen. (Ausbeute: 250 mg markierte Orsellinsäure.)

Lokalisieren der Markierung in der synthetisierten Orsellinsäure: Bei der Kondensation des Krotonsäureäthylesters mit dem markierten Acetessigester zu Dihydroorsellinsäureäthylester is ausser dem in der Literatur beschriebenen Weg der Kondensation theoretisch ein weiterer möglich. Um diese Möglichkeiten zu untersuchen, wurde ein Teil der synthetischen Orsellinsäure nach van Slyke-Folch oxydiert und ein anderer zu Orcinol dekarboxyliert.

Tabelle 2. ^{14}C-Verteilung in der synthetisierten Orsellinsäure.

Material (1)	Anzahl der Kohlenatome von der (2) Orsellinsäure	Totale Radioaktivität des Materiales in Imp./Min. (3)
Orsellinsäure Oxydation nach van Slyke-Folch	8	138 480
Dekarboxylierung	1	66 900

Aus den erhaltenen Werten geht hervor, dass sich genau die Hälfte der Radioaktivität in der Karboxylgruppe befindet, welches somit die Alternative (1) der Kondensation zu Dihydroorsellinsäureäthylester bestätigt.

3). Zugabe der Orsellinsäure

Zu zwei Fernbachkolben mit 14 Tagen alten Kulturen von *Penicillium barnense* (in jedem Kolben 500 ml Czapek-Dox-Lösung) wurden je 100 mg markierte Orsellinsäure gegeben. Von einem Kolben wurde zuerst das alte Medium aufgesaugt und dann die Orsellinsäure, in 500 ml frischer Czapek-Dox-Lösung gelöst, vorsichtig unter den Myzelienteppich hineinpippetiert. Der pH-Wert der SCD-Lösung war vorher mit Natronlauge auf den Wert des alten Mediums (pH = 7,5) gebracht worden. Ausserdem wurde 1 ml abs.

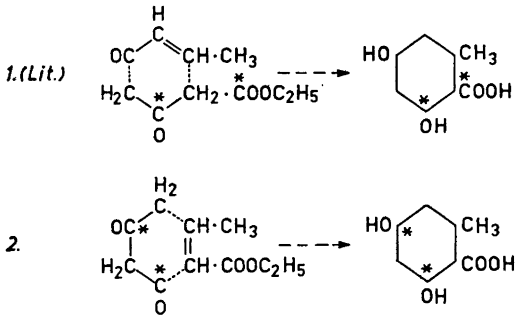

Abb. 2. Die zwei theoretisch möglichen Wege der Kondensation von Krotonsäureäthylester mit Acetessigester.

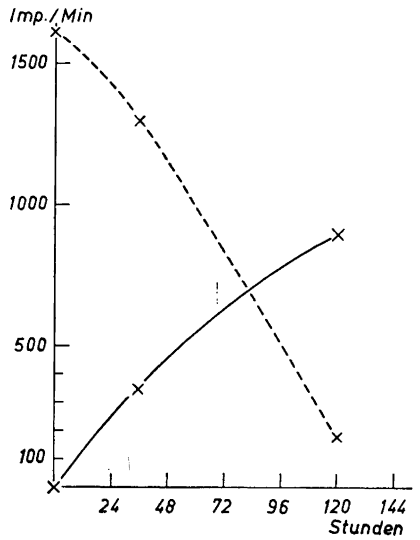

Abb. 3. Veränderung der Menge radioaktiver Orsellinsäure im Verhältnis zur Menge radioaktiver Penicillinsäure mit der Zeit. Da die zugesetzte Orsellinsäure im Gegensatz zur isolierten Penicillinsäure eine doppelte Markierung hat, sind die erhaltenen radioaktiven Werte der Orsellinsäure um die Hälfte reduziert worden, um eine direkte Vergleichsmöglichkeit zu haben.

Alkohol hinzugegeben, um die Orsellinsäure in Lösung zu bringen. In dem anderen Kolben wurde die auch hier in 1 ml abs. Alkohol gelöste Säure direkt in das alte Medium pippetiert. Es zeigte sich allerdings später im wesentlichen kein Unterschied im Produktionsbild der beiden Kulturen, weshalb in der Fortsetzung hierauf nicht mehr eingegangen wird. In einem Vorversuch war zunächst einmal gezeigt worden, dass die zugesetzte Orsellinsäure vom Organismus metabolisiert wurde. Weiterhin hatte sich ergeben, dass 6 Tage nach dem Zusatz in der Fettfraktion des Myzeliums fast keine Radioaktivität zu finden war, also keine schnelle Degradierung der Säure zu C_2-Einheiten. Um nun das eventuelle Auftreten radioaktiver Penicillinsäure zu verfolgen, wurden in gewissen Zeitabständen 25 ml-Fraktionen aus dem Medium genommen, angesäuert, mit Äther extrahiert und chromatographiert. (Lösungsmittelsystem: Benzol-Ameisensäure [9]. R_F: Orsellinsäure 0,02. R_F: Penicillinsäure 0,40.) Die Radioaktivität wurde direkt auf dem chromatographierten Papierstreifen (Whatman 3 MM) gemessen.

4). Isolierung und Degradation der Penicillinsäure.

6 Tage nach Zusatz der Orsellinsäure wurde aus dem Medium durch Ansäuern mit Salzsäure die Penicillinsäure mit Äthyläther extrahiert. Nach Zugabe von nicht radioaktiver Penicillinsäure konnte aus dem braunen Extrakt nach mehrfachem Umkristallisieren aus Benzol 550 mg chromatographisch reine Penicillinsäure von konstanter Aktivität isoliert werden.

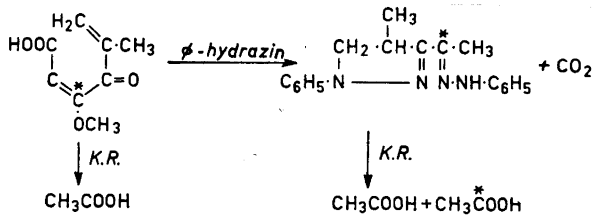

Abb. 4. Vereinfachtes Degradationsschema der isolierten Penicillinsäure.

Van Slyke-Folch-Oxydation der Penicillinsäure: 5 mg der reinen Penicillinsäure wurde nach der Methode von van Slyke-Folch oxydiert und das dabei gebildete Kohlendioxyd in eine karbonatfreie Bariumhydroxydlösung gebracht.

Kuhn-Roth-Oxydation der Penicillinsäure: 33 mg Penicillinsäure wurden oxydiert und das dabei gleichzeitig gebildete Kohlendioxyd als Bariumkarbonat isoliert. Die erhaltene Essigsäure wurde nach van Slyke-Folch totalverbrannt.

Darstellung und Degradation von 3-Acetyl-4:5-dihydro-4-methyl-1-phenylpyrazol Phenylhydrazon: 500 mg Penicillinsäure wurden zusammen mit 500 mg wasserfreiem

Tabelle 3. ^{14}C-Verteilung in der Penicillinsäure.

Material (1)	Anzahl C-Atome (2)	Radioaktivität in Imp/Min (3)	Totale Radioaktivität des Materiales in Imp/Min (4)
van Slyke-Folch-Oxydation der Penicillinsäure	8	221	1 768
van Slyke-Folch-Oxydation der durch Kuhn-Roth-Oxydation von Penicillinsäure erhaltenen Essigsäure	2	42	84
van Slyke-Folch Oxydation des Phenylhydrazones	18	95	1 710
Das bei der Phenylhyd. behandlung freigemachte CO_2	1	72	72
Kuhn-Roth-Oxydation des Phenylhydrazones, Karboxylgruppe der Essigsäure *	2	857	1 714
Kuhn-Roth-Oxydation des Phenylhydrazones, Methylgruppe der Essigsäure	2	0	0

* Da die durch Kuhn-Roth-Oxydation des Phenylhydrazones erhaltene Essigsäure zur Hälfte aus nicht radioaktiver Essigsäure (siehe Kuhn-Roth-Oxidation der Penicillinsäure) besteht, muss der erhaltene Wert von 857 Imp/Min für die totale Radioaktivität verdoppelt werden = 1 714 Imp/Min.

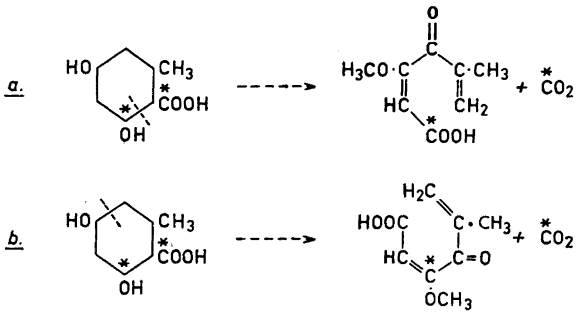

Abb. 5. Die zwei theoretisch möglichen Wege einer Ringspaltung der Orsellinsäure zu Penicillinsäure.

Natriumacetat in 3 ml Wasser durch Erwärmen gelöst. 0,41 ml Eisessig und 0,69 ml Phenylhydrazin wurden zugesetzt und das sich dabei bildende Kohlendioxyd in Baryt aufgefangen. Nach etwa einer Stunde wurde die wässrige Lösung abdekantiert und die zurückbleibende gelbe Masse aus abs. Äthylalkohol umkristallisiert. (Ausbeute: 100 mg Phenylhydrazon. Schmelzp. 176°C.)

5 mg des gebildeten Phenylhydrazones wurden nach van Slyke-Folch oxydiert und als Bariumkarbonat isoliert.

85 mg des Phenylhydrazones wurden oxydiert (Kuhn-Roth) und die Essigsäure isoliert.

Die erhaltene Essigsäure wurde dann nach Schmidt dekarboxyliert und die Karboxylgruppe als Bariumkarbonat isoliert. Das sich dabei gleichzeitig gebildete Methylamin wurde mit Stickstoff in eine 0,1 N Salzsäurelösung gebracht, eingedunstet und nach van Slyke-Folch oxidiert.

RESULTATE UND DISKUSSION

Tabelle 1 zeigt, dass die Biosynthese der Orsellinsäure *via* einer head-to-tail-Kupplung von Acetat vorsichgeht. Dies war schon vor Beginn der Versuche mit $CH_3{}^{14}CO^{18}ONa$ gezeigt worden.[8] Aus den erhaltenen Werten in Tabelle 3 geht hervor, dass die aromatische Verbindung Orsellinsäure Precursor der heterocyklischen Verbindung Penicillinsäure ist. Ausserdem ist gezeigt worden, dass von den beiden theoretisch möglichen Wegen einer Ringspaltung, der letztere Gültigkeit hat. [b.]

Die Ringspaltung der Orsellinsäure scheint durch einen hydrolytischen Vorgang vorsichzugehen. Ähnliches lässt sich auch für den Übergang 6-Methylsalicylsäure-Patulin vermuten. Versuche in Gegenwart von $H_2{}^{18}O$ könnten hierüber Auskunft geben. Auch die Präparation zellfreier Enzymextrakte kann Aufschluss über die einzelnen Schritte bei der Umwandlung der Orsellinsäure zu Penicillinsäure geben. Versuche in dieser Richtung sind im Gang.

Aus Tabelle 3 ist auch ersichtlich, dass sich in zwei weiteren Kohlenatomen der Penicillinsäure eine, allerdings schwache (knapp 5 % der totalen), Radioaktivität befindet. Diese Kohlenatome entsprechen genau dennen, die bei der Biosynthese der Penicillinsäure in Gegenwart von $CH_3{}^{14}COONa$ markiert werden.[3] Der Gedanke liegt somit nahe, dass hier ein geringer Teil der zuge-

setzten spezifisch markierten Orsellinsäure zu C_2-Einheiten degradiert worden ist, die dann als markierte Essigsäure auf dem normalen Wege zur Bildung der Penicillinsäure beigetragen hat.

Aus Abbildung 4 geht hervor, wir in einem Zeitraum von 120 Stunden die Menge der radioaktiven Orsellinsäure allmählich zugunsten der Menge der radioaktiven Penicillinsäure abnimmt.

Ich möchte Herrn Prof. Gösta Ehrensvärd, der diese Arbeit angeregt hat, für sein gezeigtes Interesse herzlich danken. Auch Herrn Dr. Sten Gatenbeck danke ich vielmals für wertvolle Diskussionen, sowie Herrn Dr. Martin Tveit.

REFERENZEN

1. Saluste, E. *persönliche Mitteilung.*
2. Mosbach, K. *Z. Naturforsch.* **14b** (1959) 69.
3. Birch, A. J., Blance, G. E. und Smith, H. J. *J. Chem. Soc.* **1958** 4582.
4. Tanenbaum, St. W. und Bassett, E. W. *J. Biol. Chem.* **234** (1959) 1861.
5. Bu'Lock, J. D. und Ryan, A. J. *Proc. Chem. Soc. London* **1958** 222.
6. Birch, A. J. *et al. Austral. J. Chem.* **8** (1955) 539.
7. Gatenbeck, S. *Acta Chem. Scand.* **12** (1958) 1211.
8. Gatenbeck, S. und Mosbach, K. *Acta Chem. Scand.* **13** (1959) 1561.
9. Reio, L. *J. Chromatography* **1** (1958) 366.
10. *Cf.* Calvin, Heidelberger, Reid, Tolbert und Yankwich, *Isotopic carbon* Wiley, New York 1949, S. 92.
11. Birch, A. J. *et al. J. Chem. Soc.* **1958** 360.
12. Gattermann-Wieland *Die Praxis des organischen Chemikers*, W. de Gruyter & Co, Berlin 1939, S. 250.
13. von Schilling, R. und Vorländer, D. *Ann.* **308** (1899) 195.
14. Sonn, A. *Ber.* **61** (1928) 926.
15. Birkinshaw, J. H. *Biochem. J.* **30** (1936) 394.

Eingegangen am 24. Oktober 1959.

ACTA CHEMICA SCANDINAVICA 14 (1960) 465–470

Phase Analysis Studies on the Vanadium — Oxygen System within the $VO_{0.25}$—$VO_{1.5}$ Region at 800° C

SVEN WESTMAN and CLAES NORDMARK

Institute of Inorganic and Physical Chemistry, University of Stockholm, Stockholm, Sweden

The lower vanadium oxides existing at 800° have been investigated by X-ray methods. Powder diffraction data are given for the two phases $VO_{0.53}$ and $VO_{1.27}$. The homogeneity range and lattice occupancy of the VO phase have been established.

The phase relations of the vanadium-oxygen system have been studied by several investigators, using various methods. The results may be summarized as follows. The solubility limit for oxygen in b.c.c. vanadium (α phase) was found, by Tucker, Seybolt and Sumsion [1], to be 3.2 at. % ($VO_{0.033}$). Rostoker and Yamamoto [2] found this to be valid only above 900°C, the solubility decreasing at lower temperatures.

The tetragonal β phase, "V_4O", obtained by Seybolt and Sumsion [3] was shown to be homogeneous between 15 and 21.8 at. % O (*i.e.* $VO_{0.17}$—$VO_{0.28}$). This was confirmed by Schönberg [4] and by Rostoker and Yamamoto [2].

Klemm and Grimm [5] found X-ray diffractograms of $VO_{0.3}$ to contain weak reflexions in addition to those given by the tetragonal phase. They ascribed this to a continuous deformation of the tetragonal lattice. From metallographic evidence, Rostoker and Yamamoto [2] postulated the existence of a δ phase which they thought to be V_2O. The phase was, however, never obtained in a pure state. The authors gave a tentative indexing of the X-ray pattern of the δ oxide, assuming a hexagonal unit cell.

The homogeneity range of the "VO" phase, which has a structure of the sodium chloride type [6], was found, by Schönberg [4] and Andersson [7], to extend from $VO_{0.80}$ to $VO_{1.20}$ at 900°C. Schönberg [4] assumed the vanadium lattice to be only partly occupied by atoms above the composition $VO_{1.0}$.

The existence of an "X phase" ($VO_{\sim 1.3}$) proposed by Klemm and Grimm [5] has not been confirmed by subsequent work.

The corundum structure of the sesquioxide was established by Goldschmidt *et al.*[8]

Phase analyses by Andersson [7] and Aebi [9] cover the higher vanadium oxides.

In connection with a wider research programme covering the oxide chemistry of several transition metals, a reinvestigation of the lower vanadium oxides was thought desirable, considering the rather incomplete evidence reviewed above.

EXPERIMENTAL

The starting materials for the preparations were vanadium metal (Fairmount Chemical Co. 99.7 % pure) and vanadium pentoxide (LKB-produkter, reagent grade). Vanadium sesquioxide was obtained by reduction of vanadium pentoxide with hydrogen [10].

Preparations of vanadium oxides with compositions between $VO_{0.25}$ – $VO_{1.5}$ were obtained by melting pressed pellets consisting of weighed amounts of vanadium metal and vanadium sesquioxide in an argon atmosphere by means of an electric arc furnace [11]. The samples were subsequently heat-treated in sealed, evacuated silica tubes at 800°C for two weeks and then quenched in water.

The preparations were analyzed for oxygen content by dissolution in cerium(IV) sulphate solution followed by back-titration with iron(II) sulphate solution. The procedure is similar to the one described by Reuter and Siewert [12]. A weighed sample (~0.1 g) of finely divided oxide was dispersed in 10 ml of 50 % sulphuric acid and dissolved by addition of $Ce(SO_4)_2$ solution in excess, so that all the vanadium was oxidized to the vanadyl state. During the dissolution process the mixture was kept hot and the sample was ground with a glass rod. After cooling and dilution, 5 ml of concentrated phosphoric acid was added, and the small amount of vanadate formed back-titrated to the vanadyl state using ferrous ammonium sulphate solution, with diphenylamine sulphonic acid as indicator.

The phase analysis was performed by means of X-ray powder photographs taken in a Guinier focusing camera of 80 mm diameter with strictly monochromatized $CuK\alpha_1$ radiation. An aluminium foil (35 μ) covering the film served to reduce the background fogging caused by fluorescent radiation from the samples. Potassium chloride (a = 6.2919 Å at 20°C [13]) was added to the specimens as an internal standard. Details of the techniques employed in the X-ray work have been given in a previous article [14].

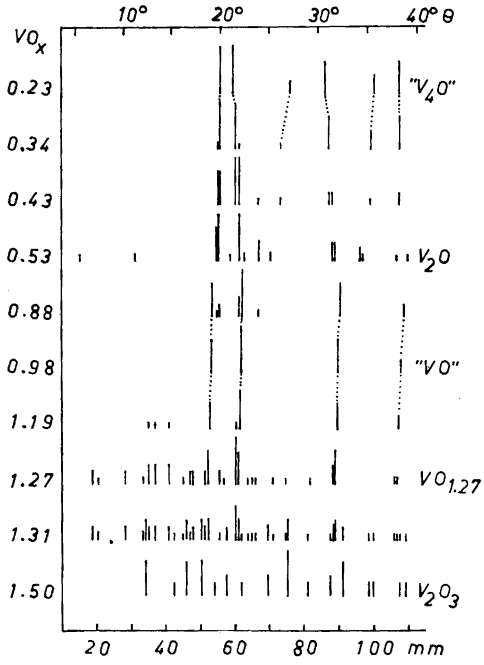

Fig. 1. Powder patterns of VO_x samples.

Table 1. Guinier powder pattern of $VO_{0.53}$. Cu$K\alpha_1$ radiation.

Intensity	$\sin^2\Theta_{obs}$
vw	0.00978
vvw	0.03920
m	0.11386
s	0.11547
vvw	0.12858
vs	0.13802
w	0.14556
m	0.16465
vw	0.18246
w	0.18439
w	0.27441
w	0.27716
w	0.32074
vw	0.32391
vw	0.38823
w	0.39216

RESULTS

The present phase analysis has established the existence of two phases with the approximate compositions $VO_{0.53}$ and $VO_{1.27}$. The results are summarized in Fig. 1. The homogeneity range of the "VO" phase and the occupancy of its vanadium and oxygen lattices have been determined.

The "V_4O" phase appears to be homogeneous up to the composition $VO_{\sim 0.3}$. No accurate determination of the phase boundary has been made however, since the result seemed to be in fairly good agreement with previously published work.

The $VO_{0.53}$ phase (possibly V_2O) seems to have an extremely narrow range of composition. X-Ray powder data are given in Table 1. It is evident from Fig. 1 that the structure of "V_2O" represents a transition between the V_4O and the VO structures. It has not been possible so far to obtain single crystals of this phase.

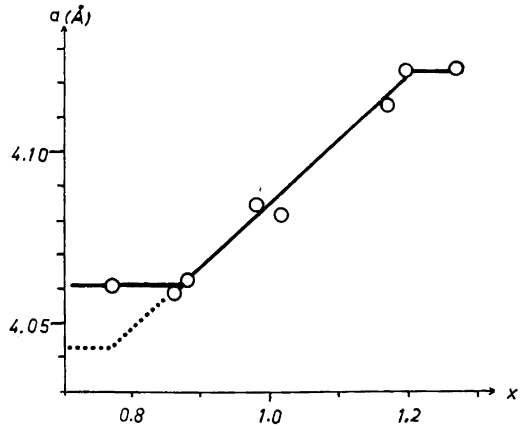

Fig. 2. Lattice parameter of VO_x (800°C).

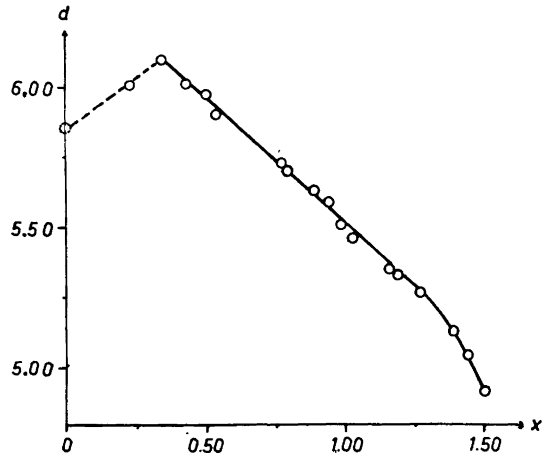

Fig. 3. Density of VO_x samples (g cm^{-3})

The cubic "VO" phase is homogeneous between the limits $VO_{0.89}$ and $VO_{1.20}$. The lattice parameter varies between $a = 4.062$ Å and $a = 4.125$ Å (Fig. 2).

Schönberg [4] found a somewhat extended homogeneity range towards lower oxygen content at 900°C (indicated by the dotted line in Fig. 2). The lattice parameter *vs.* composition curve obtained in the present investigation is, within its limits, in excellent agreement with the results of Schönberg [4] and Andersson [7].

The densities of the oxide preparations have been determined (Fig. 3) and the occupancy of the vanadium and oxygen lattices of the NaCl-type structure calculated for various compositions of the "VO" phase. The result is shown in Fig. 4.

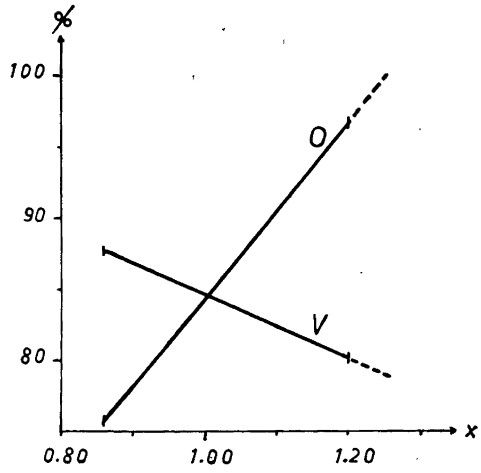

Fig. 4. Percent occupancy of atomic sites in cubic VO_x.

Table 2. Guinier powder pattern of $VO_{1.27}$. $CuKa_1$ radiation. Lattice parameters found: $a = b = 16.623 \pm 0.005$ Å; $c = 16.515 \pm 0.004$ Å.

Intensity	$h\,k\,l$	$\sin^2\Theta_{obs}$	$\sin^2\Theta_{calc}$	$(\sin^2\Theta_{obs} - \sin^2\Theta_{calc}) \times 10^5$
w	1 1 2	0.01306	0.01300	+ 6
vw	2 0 2	0.01729	0.01729	0
vw	2 1 3	0.03034	0.03031	+ 3
vw	2 0 4	0.04343	0.04339	+ 4
m	3 2 3	0.04750	0.04749	+ 1
m	2 2 4	0.05213	0.05198	+15
s	5 1 2	0.06464	0.06453	+11
vw	4 2 4	0.07780	0.07775	+ 5
vw	1 1 6	0.08283	0.08260	+23
w	6 0 2	0.08596	0.08600	− 4
w	3 1 6	0.09987	0.09978	+ 9
vs	4 4 4	0.01351	0.10351	0
vw	7 1 2	0.11614	0.11606	+ 8
vw	6 2 4	0.12088	0.12069	+19
vw	7 3 2	0.13330	0.13323	+ 7
vs	8 0 0	0.13741	0.13741	0
vs	0 0 8	0.13927	0.13922	+ 5
vw	5 3 6	0.15127	0.15131	− 4
vw	2 2 8	0.15642	0.15640	+ 2
vw	9 1 2	0.18493	0.18476	+17
vw	{9 2 3} {7 6 3}	0.20205	0.20208	− 3
vw	6 3 7	0.20310	0.20321	−11
vw	3 1 10	0.23917	0.23900	+17
s	8 8 0	0.27489	0.27483	+ 6
s	8 0 8	0.27646	0.27663	−17
vw	12 4 4	0.37832	0.37834	− 2
vw	4 4 12	0.38185	0.38195	−10
m	8 8 8	0.41389	0.41404	−15

The upper composition limit, $VO_{1.20}$, represents an almost completely occupied oxygen lattice (96 %), whereas no similar relation defines the lower phase boundary. It is noteworthy that the boundaries of the high-temperature "TiO" phase with the same type of structure ($TiO_{0.64}$—$TiO_{1.26}$) are defined by 96 % and 98 % occupancy of the Ti and O lattices, respectively [15].

The $VO_{1.27}$ phase forms below ~ 900°C and appears to have a very narrow range of homogeneity. The X-ray powder diffractogram given in Table 2 has been indexed on the basis of single crystal data. The symmetry of the phase is body-centered tetragonal with

$$a = b = 16.623 \text{ Å} = 4 \times 4.156 \text{ Å}$$
$$c = 16.515 \text{ Å} = 4 \times 4.129 \text{ Å}$$
$$V = 4\,563 \text{ Å}^3$$

The diffraction symmetry is pseudo-cubic with reflexions $h00$, $h \neq 4n$, missing. It is shown, by single crystal as well as powder data, that the crystal structure is a superstructure of a slightly deformed VO (NaCl-type) structure.

The observed density of the phase indicates that the vanadium lattice is only partly occupied. The vacancies should, on the above evidence, be

ordered; and the number per unit cell, a multiple of four. If the cell content is assumed to be $V_{204}O_{256}$, observed and calculated values of density and composition agree rather well:

obs.	*calc*
$d = 5.269$	$d = 5.272$
$VO_{1.269}$	$VO_{1.255}$

$VO_{1.27}$ ought to be the "X phase" reported by Klemm and Grimm [5]. Crystal structure studies are in progress.

Acknowledgements. The authors wish to express their gratitude to Dr. A. Magnéli for having suggested this work and for his continuing interest in the investigation. Further, we want to thank Mr. G. Kruuse and Mr. T. Karlsson for their assistance in the preparative and analytical work.

The investigation has been sponsored by the *Office, Chief of Research and Development, U.S. Department of Army* through its European Research Office.

REFERENCES

1. Tucker, C. W., Seybolt, A. U. and Sumsion, H. T. *Acta Met.* **1** (1953) 390.
2. Rostoker, W. and Yamamoto, A. S. *Trans. Am. Soc. Metals* **47** (1955) 1002.
3. Seybolt, A. U. and Sumsion, H. T. *J. Metals* **5** (1953) 292.
4. Schönberg, N. *Acta Chem. Scand.* **8** (1954) 221.
5. Klemm, W. and Grimm, L. *Z. anorg. u. allgem. Chem* **250** (1942) 42.
6. Mathewson, C. H., Spire, E. and Samans, C. H. *Trans. Am. Soc. Steel Treating* **20** (1932) 357.
7. Andersson, G. *Acta Chem. Scand.* **8** (1954) 1599.
8. Goldschmidt, V. M., Barth, T. and Lunde, G. *Skrifter Norske Videnskaps-Akad. Oslo I. Mat. Naturv. Kl.* **1925** No. 7.
9. Aebi, F. *Helv. Chim. Acta* **31** (1948) 8.
10. Brauer, G. *Handbuch der präparativen anorganischen Chemie*, Stuttgart 1954, p. 951—952.
11. Hägg, G. and Kiessling, R. *IVA* **26** (1955) 105.
12. Reuter, B. and Siewert, J. *Z. anal. Chem.* **162** (1958) 175.
13. Hambling, P. G. *Acta Cryst.* **6** (1953) 98.
14. Westman, S. and Magnéli, A. *Acta Chem. Scand.* **11** (1957) 1587.
15. Andersson, S., Collén, B., Kuylenstierna, U. and Magnéli, A. *Acta Chem. Scand.* **11** (1957) 1641.

Received October 9, 1959.

ACTA CHEMICA SCANDINAVICA 14 (1960) 471–485

The Copper(II) Complexity of O-Phosphorylethanolamine

RAGNAR ÖSTERBERG

Department of Medical Biochemistry, University of Göteborg, Göteborg, Sweden

The complex formation between copper(II) and O-phosphorylethanolamine (H_2A) ions has been studied in 0.15 M KCl medium at 25° by pH titration.

By an adaption of Hedström's method [39] the concentration of free O-phosphorylethanolamine was calculated. The experimental data could be explained by formation of the complexes: $CuHA^+$, CuA, $Cu(HA)A^-$ and CuA_2^{2-}. The corresponding equilibrium constants were computed (Table 2).

Probable coordination sites involved in the complexes are suggested, and are discussed in relation to copper(II) binding of phosphoproteins and phosphatides.

As pointed out by several authors [1–5] phosphoproteins and phosphopeptides may under physiological conditions act as strong metal binders. The great metal affinity of these compounds has been partly ascribed to the presence of phosphorus [2,4,6–9], which in view of recent investigations [2,10–18] occurs mainly as monophosphate esters linked through the hydroxyl groups of serine and threonine residues *. Informations of the metal binding power of phosphoproteins and their break-down products may, thus, be obtained from studies on O-phosphorylated model compounds. Apparent stability constants of some metal complexes of O-phosphorylserine have previously been reported [20,21]. The present paper describes the copper(II) complexity of another model compound, O-phosphorylethanolamine; this ligand itself being an important metabolite existing in living tissues both in free [22–29] and combined state [28–35].

The complex formation was measured by pH titration [36–38] at 25° in 0.15 M KCl. In this case several titrations for different ligand concentrations were carried out to allow calculation of the free ligand concentration more directly from the experimental data by graphical integration (*cf.* Ref.[39]), assuming the possible presence of any set of mononuclear equilibria including hydrogen and hydroxo copper(II) complexes of the ligand. An equation required for this calculation was derived by applying the equations formulated by Hedström [39].

* Apart from the phosphomonoester bond, the occurrence of other linkages of phosphorus has been suggested for some phosphoproteins [19].

The existing complexes and corresponding overall equilibrium constants were evaluated graphically. The pK values of the ligand, determined under the same experimental conditions [40], were used in the computations.

SYMBOLS

A O-phosphorylethanolamine with all dissociable hydrogen removed,

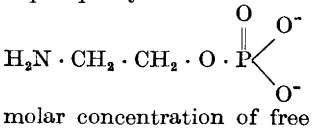

a molar concentration of free A

b_q apparent stability constant of the complex $CuA_q^{(2-2q)+}$ defined by $b_q = [CuA_q^{(2-2q)+}]\ [CuA_{q-1}^{(4-2q)+}]^{-1}\ [Cu^{2+}]^{-1}$

b_{CuHA} apparent stability constant of the complex CuHA+, defined by $b_{CuHA} = [CuHA^+]\ [HA^-]^{-1}\ [Cu^{2+}]^{-1}$

$b_{Cu(HA)A}$ apparent stability constant of the complex $Cu(HA)A^-$, defined by $b_{Cu(HA)A} = [Cu(HA)A^-]\ [CuHA^+]^{-1}\ [A^{2-}]^{-1}$

b_{CuCl} apparent stability constant of the complex CuCl+, defined analogical to b_q

C_A total molar concentration of O-phosphorylethanolamine, defined by eqn. 5

C_{Cu} total molar concentration of copper(II) ions, defined by eqn. 4

C_H total molar concentration of hydrogen ions, defined by eqn. 6

C_{Cl} total molar concentration of chloride ions

h molar concentration of free hydrogen ions

I defined by eqn. 21

j number of protons bound in the proton complex H_jA

K_{CuHA} apparent acid ionization constant of the complex CuHA+, defined by $K_{CuHA} = h\ [CuA]\ [CuHA^+]^{-1}$

$K_{Cu(HA)A}$ apparent acid ionization constant of the complex $Cu(HA)A^-$, defined by $K_{Cu(HA)A} = h[CuA_2^{3-}]\ [Cu(HA)A^-]^{-1}$

L defined by eqn. 22

M g moles/litre

p,q,r number of HA^-, A^{2-}, OH^- groups bound in the complex $Cu(HA)_pA_q(OH)_r^{(2-p-2q-r)+}$, respectively

R defined by eqn. 9

S defined by eqn. 10

Z ligand number, defined by eqn. 8

β_2 apparent complexity constant, $= b_1 b_2$

$\beta_{Cu(HA)A}$ apparent complexity constant, $= b_{CuHA} b_{Cu(HA)A}$

$\varkappa_{1,1p,0q,r}$ apparent overall equilibrium constant defined by eqn. 2

$\varkappa_{j1}$ apparent complexity constant defined by eqn. 3

φ defined on page 478

[ ] molar concentration of the species indicated

MATERIALS

O-Phosphorylethanolamine, prepared according to Baer and Stancer [41], was a generous gift from Ing. G. Fölsch of this institute. The data of analysis for the present preparation are to be found in Ref.[40] Aqueous stock solutions of this compound were standardized by potentiometric titrations. When not used, these solutions had to be kept frozen in order to obtain satisfactory reproducibility.

Aqueous stock solutions of copper(II) chloride were prepared from the British Drug Houses Ltd. (A.R.) product and was standardized by an ion exchange method [42].

Carbonate-free 0.2557 M KOH, containing 0.15 M KCl was prepared and standardized as before [17].

The other reagents used in this work were of analytical grade and were not purified further. Tripple distilled water and weighed-in pipettes were used throughout.

METHOD

The quantities, h and C_H, were varied at each pH titration, while C_{Cu} and C_A were held practically constant. This was carried out by successive delivering KOH to the titration solution, recording pH after each addition. As recording instrument a Radiometer PHM 3j valve potentiometer, equipped with a Radiometer glass electrode G 102 B, and a calomel electrode K 100 was used. The activity coefficients were assumed to be constant in the presence of 0.15 M KCl. All measurements were carried out at 25.00 ± 0.03°.

The pH meter was standardized with 0.05 M potassium biphthalate and 0.05 M borax as recommended by Hitchock *et al* [43]. The pH meter readings were transformed to values of $-\log h$ by a calculated activity coefficient [40] being 0.79 ± 0.02. It was thought to apply in the pH range, 4—7, involved in the computations below. For routine calibration of the entire measuring system, acetic acid titrations were used, *cf.* Ref.[40], the deviations never exceeding 0.01 pH units.

Assuming O-phosphorylethanolamine only to interact with copper(II) ions, when both protons are removed from the phosphoryl group, *i.e.* as HA^- and A^{2-}, the complex equilibria can be written

$$Cu^{2+} + pH^+ + (p+q)A^{2-} + rH_2O \rightleftharpoons Cu(HA)_pA_q(OH)_r^{(2-p-2q-r)+} + rH^+ \quad (1)$$

$$(p = 0,1,2,...;\ q = 0,1,2,...;\ r = 0,1,2,...;\ p+q+r = 1,2,3,...;)$$

Since H_2O is approximately constant, the system is defined by the overall equilibrium constants * (all charges omitted in the following for the sake of clarity):

$$\varkappa_{1,1p,0q,r} = \frac{[Cu(HA)_pA_q(OH)_r]}{[Cu]\ h^{p-r}\ a^{p+q}} \quad (2)$$

The quantities p,q, and r may attain any integer values given above, restricted by $(p+q+r)_{max}$, which is equal to the maximum coordination number of copper(II). Occurrence of polynuclear complexes was assumed to be negligible with the use of low values for C_A and C_{Cu}, with C_A in excess of C_{Cu}.

Analogously to eqn. 2, constants for the formation of proton complexes are defined

$$\varkappa_{j1} = \frac{[H_jA]}{h^j\ a} \qquad (j = 1,2,3) \quad (3)$$

The values of these constants, used in this work, have been re-calculated from the pK values reported earlier [40].

Due to presence of bulk electrolyte (0.15 M KCl), the species $CuCl^+$ has also to be considered. The total content of copper(II), ligand and dissociable hydrogen will thus be given by (*cf.* Ref.[38])

* The notation of these constants is simplified, when only one or two complex forming groups are bound to the central metal ion. Thus will, *e.g.*, the constants corresponding to $CuOH^+$ and CuA be written $\varkappa_{1,1}$ and $\varkappa_{1,01}$, respectively.

$$C_{Cu} = [Cu](1 + \sum \varkappa_{1,1p,0q,r} h^{p-r} a^{p+q} + b_{CuCl}[Cl]) \quad (4)$$

$$C_A = a + \sum (p+q)\varkappa_{1,1p,0q,r}[Cu]h^{p-r}a^{p+q} + \sum \varkappa_{j1} h^j a \quad (5)$$

$$C_H = h - [OH] + \sum (p-r)\varkappa_{1,1p,0q,r}[Cu]h^{p-r}a^{p+q} + \sum j\varkappa_{j1} h^j a \quad (6)$$

The summations have been carried out in respect of all stated values of p,q and r. The value of C_H for each point of titration may be calculated from

$$C_H = 2C_A - [KOH] \quad (7)$$

The figure $b_{CuCl}[Cl]$ in eqn. 4 will be constant as $[Cl] \approx C_{Cl} = 0.15$, and $[OH]$ in eqn. 6 negligible in the $-\log h$ range involved.

From eqns. 4 and 5 we obtain the ligand number defined thus (*cf.* Ref.[38])

$$Z = \frac{C_A - a - \sum \varkappa_{j1} h^j a}{C_{Cu}} = \frac{\sum (p+q)\varkappa_{1,1p,0q,r} h^{p-r} a^{p+q}}{1 + \sum \varkappa_{1,1p,0q,r} h^{p-r} a^{p+q} + b_{CuCl}[Cl]} \quad (8)$$

It follows from eqn. 8 that the constants $\varkappa_{1,1p,0q,r}$ can be determined, if Z is known as a function of h and a. As Z is given by eqn. 8, if h and a are known, we have, thus, first to compute a. This computation as well as the evaluation of p,q,r and $\varkappa_{1,1p,0q,r}$ will be described after the following section.

MEASUREMENTS

Solutions for titration of metal complexes were prepared by pipetting stock solutions of O-phosphorylethanolamine, copper(II) chloride, potassium chloride and aq. dest. in order to obtain the initial concentrations C_A, C_{Cu} and 0.15 M KCl. The titrations were continued to pH 10.5. All titration equipment was the same as that described [17]. The content (initially 10 ml) of the titration vessel was stirred and freed from carbon dioxide by bubbling nitrogen, pretreated as previously [17].

Five titrations with different C_A were carried out in this manner covering the concentration ranges $C_A = (0.8-3) \times 10^{-3}$, $C_H = (0.8-6) \times 10^{-3}$ and $C_{Cu} = 7.8 \times 10^{-4}$. Each titration could be reproduced within 0.01 in pH. The data used for the calculations below constituted a mean of at least two titrations.

At $-\log \approx 6.3$ the measuring solutions grew slightly opalescent, developing into a greenish-blue precipitate at $-\log h \approx 7$. Semi-quantitative analysis of the washed and dried precipitate, isolated from a solution of pH 7.8, showed the presence of about 4 % N and 16 % P. This apparently indicates the precipitate to be a copper(II)-O-phosphorylethanolamine compound. Due to this sparing solubility of the present system above $-\log h \approx 6.3$, the computations were not extended further than up to $-\log h = 6.10$.

The results of the measurements are shown in Fig. 1, where the titrations are represented as $-\log h(C_H)c_A$ curves.

DETERMINATION OF THE FREE O-PHOSPHORYLETHANOLAMINE CONCENTRATION

No true indications about the kind of complexes formed could be obtained from usual titration curves (as for example in the Cu(II)-O-phosphorylserine

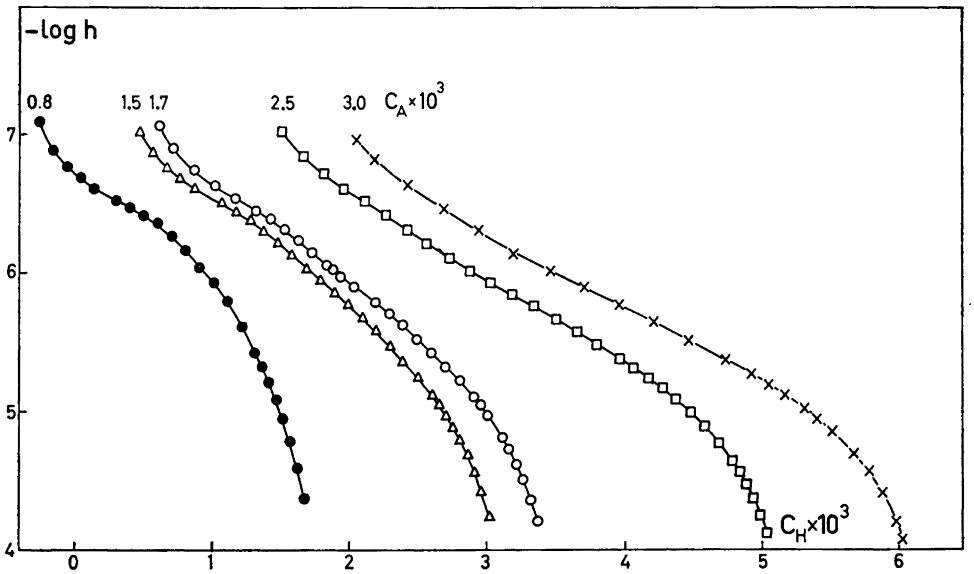

Fig. 1. The potentiometric measurements. $-\log h$ as a function of the total concentration of hydrogen ions, C_H (obtained from eqn. 7), for different total O-phosphorylethanolamine concentration, C_A.

system [21]). The free ligand concentration was therefore computed without any special assumptions about the complexes formed. For this purpose Hedström's method [39] was made applicable to measurements and equilibria of the present type.

We define the functions R and S

$$R = \sum \varkappa_{j1} h^j a = \sum [H_jA] \tag{9}$$

$$S = \sum \varkappa_{1,1p,0q,r} h^{p-r} a^{p+q} \tag{10}$$

Partial differentiation of R with respect to $\ln h$, followed by partial differentiation with respect to $\ln a$, results in

$$\left(\frac{\partial R}{\partial \ln h}\right)_a = \sum j \varkappa_{j1} h^j a \tag{11}$$

$$\left(\frac{\partial^2 R}{\partial \ln h \, \partial \ln a}\right) = \sum j \varkappa_{j1} h^j a = \left(\frac{\partial R}{\partial \ln h}\right)_a \tag{12}$$

Partial differentiation of S with respect to $\ln h$ and $\ln a$, followed by partial differentiation with respect to $\ln a$ and $\ln h$, gives

$$\left(\frac{\partial S}{\partial \ln h}\right)_a = \sum (p-r) \varkappa_{1,1p,0q,r} h^{p-r} a^{p+q} \tag{13}$$

$$\left(\frac{\partial S}{\partial \ln a}\right)_h = \sum (p+q)\varkappa_{1,1p,0q,r} h^{p-r} a^{p+q} \tag{14}$$

$$\left(\frac{\partial^2 S}{\partial \ln h\ \partial \ln a}\right) = \left(\frac{\partial^2 S}{\partial \ln a\ \partial \ln h}\right) = \sum (p-r)(p+q)\varkappa_{1,1p,0q,r} h^{p-r} a^{p+q} \tag{15}$$

We may eliminate [Cu] from eqns. 5 and 6 by extension of the expression in those equations, containing [Cu] with C_{Cu}. By substituting eqns. 9—11 and 13—14 into the resulting equations, followed by partial differentiation with respect to ln$h$ and ln$a$, respectively, we obtain

$$\left(\frac{\partial C_A}{\partial \ln h}\right)_a = C_{Cu}\left[\frac{(1 + S + b_{CuCl}[Cl])\left(\frac{\partial^2 S}{\partial \ln a\ \partial \ln h}\right) - \left(\frac{\partial S}{\partial \ln a}\right)_h\left(\frac{\partial S}{\partial \ln h}\right)_a}{(1 + S + b_{CuCl}[Cl])^2}\right] + \left(\frac{\partial R}{\partial \ln h}\right)_a \tag{16}$$

$$\left(\frac{\partial C_H}{\partial \ln a}\right)_h = C_{Cu}\left[\frac{(1 + S + b_{CuCl}[Cl])\left(\frac{\partial^2 S}{\partial \ln h\ \partial \ln h}\right) - \left(\frac{\partial S}{\partial \ln h}\right)_a\left(\frac{\partial S}{\partial \ln a}\right)_h}{(1 + S + b_{CuCl}[Cl])^2}\right] + \left(\frac{\partial^2 R}{\partial \ln h\ \partial \ln a}\right) \tag{17}$$

From eqns. 12 and 15 follows that the right hand sides of eqns. 16 and 17 are identical. Consequently

$$\left(\frac{\partial C_A}{\partial \ln h}\right)_a = \left(\frac{\partial C_H}{\partial \ln a}\right)_h \tag{18}$$

This equation may be transformed [39] to

$$\left(\frac{\partial \ln a}{\partial \ln h}\right)_{C_A} = -\left(\frac{\partial C_H}{\partial C_A}\right)_h \tag{19}$$

Solving for $-\log a$ within the range $-\log h_0$ to $-\log h$ results in

$$-\log a = -\left[\int_{-\log h_0}^{-\log h} \left(\frac{\partial C_H}{\partial C_A}\right)_h \mathrm{d}(-\log h)\right]_{C_A} + (-\log a_0) \tag{20}$$

From eqn. 20 values of $-\log a_0/a$ were determined by graphical integration [39]. The $-\log h(C_H)_{C_A}$ curves of Fig. 1 were thus cut for constant $-\log h$, and C_H drawn against C_A (Fig. 2a). The quantity $\left(\frac{\partial C_H}{\partial C_A}\right)_h$ was determined, and plotted against $-\log h$ (Fig. 2b). The area under the resulting curve from $-\log h = -\log h_0$ to $-\log h$ gave then $-\log a_0/a$. After the calculation of a_0 from

$$a_0 = C_A/(1 + \varkappa_{11} h + \varkappa_{21} h^2) \tag{5a}$$

at a $-\log h$ value ($= -\log h_0$), where no complex formation could be detected, the corresponding a values were obtained. The a values, determined in this manner, are listed in Table 1. For each a value determined the corresponding Z value was calculated; the result has been compiled in the same table.

In spite the graphical integration method [39] by Hedström usually requires many values for the known variables, the rather few C_A values of this study, seem sufficient, due to the constancy of $\left(\frac{\partial C_H}{\partial C_A}\right)_h$ in the C_A range involved (Fig. 2a).

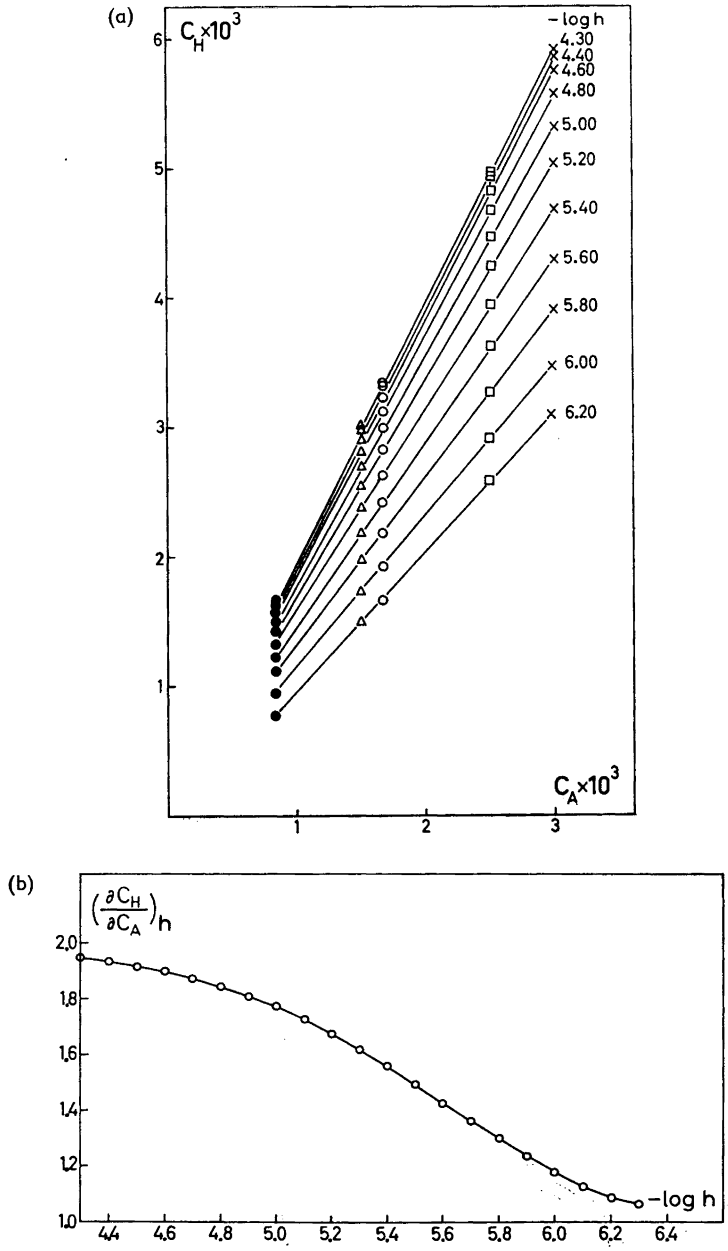

Fig. 2. Evaluation of the free O-phosphorylethanolamine concentration. (a). C_H *vs.* C_A for different $-\log h$. (b). $\left(\frac{\partial C_H}{\partial C_A}\right)_h$ *vs.* $-\log h$ for $C_A = (0.8-3) \times 10^{-3}$.

Table 1. Corresponding values of $-\log h$, C_A, C_H (obtained from $-\log h(C_H)C_A$ curves), a (obtained from eqns. 20 and 5a), and Z (from eqn. 8).
$C_{Cu} = 7.84 \times 10^{-4}$
$\varkappa_{11} = 1.259 \times 10^{10}$ M^{-1}, $\varkappa_{21} = 4.678 \times 10^{15}$ M^{-2}

	* × $C_A = 3.010 \times 10^{-3}$ $-\log h_0 = 4.30$			* □ $C_A = 2.519 \times 10^{-3}$ $-\log h_0 = 4.30$			* ○ $C_A = 1.682 \times 10^{-3}$ $-\log h_0 = 4.30$			* △ $C_A = 1.507 \times 10^{-3}$ $-\log h_0 = 4.30$			* ● $C_A = 0.834 \times 10^{-3}$ $-\log h_0 = 4.40$		
$-\log h$	$C_H \times 10^3$	$a \times 10^9$	Z	$C_H \times 10^3$	$a \times 10^9$	Z	$C_H \times 10^3$	$a \times 10^9$	Z	$C_H \times 10^3$	$a \times 10^9$	Z	$C_H \times 10^3$	$a \times 10^9$	Z
5.300	4.870	16.17	0.0973	4.080	13.535	0.0834	2.720	9.039	0.0579	2.457	8.097	0.0523	1.372	4.483	0.0297
5.400	4.687	23.31	0.1261	3.927	19.51	0.1076	2.620	13.035	0.0742	2.366	11.67	0.0671	1.324	6.464	0.0381
5.500	4.498	33.13	0.1596	3.766	27.72	0.1354	2.518	18.52	0.0932	2.270	16.59	0.0841	1.273	9.185	0.0478
5.600	4.300	46.36	0.1985	3.605	38.81	0.1688	2.410	25.92	0.1159	2.177	23.215	0.1044	1.224	12.855	0.0591
5.700	4.105	63.92	0.2455	3.435	53.49	0.2081	2.299	35.73	0.1427	2.071	32.01	0.1285	1.169	17.725	0.0728
5.800	3.904	86.83	0.2974	3.263	72.68	0.2528	2.175	48.55	0.1728	1.965	43.48	0.1555	1.109	24.075	0.0878
5.900	3.703	116.3	0.3564	3.079	97.31	0.3019	2.041	65.00	0.2056	1.850	58.22	0.1851	1.038	32.235	0.1045
6.000	3.479	153.6	0.4227	2.903	128.55	0.3583	1.907	85.86	0.2431	1.725	76.91	0.2194	0.948	42.59	0.1233
6.100	3.280	200.3	0.4947	2.729	167.65	0.4187	1.779	112.0	0.2837	1.611	100.3	0.2552	0.862	55.54	0.1428

* Initial concentration.

EVALUATION OF THE EQUILIBRIUM CONSTANTS

As can be seen from Table 1 all values of Z are below 1. To include all possibly existing complexes, $(p+q)_{max}$ was therefore in the first place assumed to equal 2. For $p = q = 0$, r was assigned to 1, but otherwise r was set equal to zero. Eqn. 8 will thus be reduced to

$$\frac{Z}{(1-Z)a}\varphi = \varkappa_{1,11}h + \varkappa_{1,01} + \frac{(2-Z)a}{(1-Z)}(\varkappa_{1,12}h^2 + \varkappa_{1,11,01}h + \varkappa_{1,02}) \qquad (8a)$$

where $\varphi = 1 + \varkappa_{1,1}h^{-1} + b_{CuCl}[Cl]$

Since the term $b_{CuCl}[Cl]$ is approximately constant in this study (*cf.* p. 474), the expression φ in eqn. 8a will be constant for constant h. Varying values of $\varkappa_{1,1}$ in this expression are reported in the literature [44]. In the present study use will therefore be made of a range of values from $10^{-7.5}$ to $10^{-8.25}$ M. From these values follow that the amount of $CuOH^+$ will be rather negligible in the present $-\log h$ range.

To identify complexes formed, $Z(1-Z)^{-1}a^{-1}$ was first plotted against h (Fig. 3). In this plot of eqn. 8a the presence of $CuHA^+$ and CuA only should give a straight line independant of C_A; existing $CuHA^+$ species making the ordinata values to decrease with h. At the occurrence of higher complexes, *i.e.* $(p+q)>1$, the plotted data should vary with C_A. As the latter case applies to Fig. 3, we may identify the higher complexes apparently present.

In Fig. 4 the quantity $Z(1-Z)^{-1}a^{-1}$ has therefore been plotted against $(2-Z)a(1-Z)^{-1}$ for constant h. As shown in the figure data are best represented by a serie of straight lines, indicating the true value of $(p+q)_{max}$ to be 2. Conse-

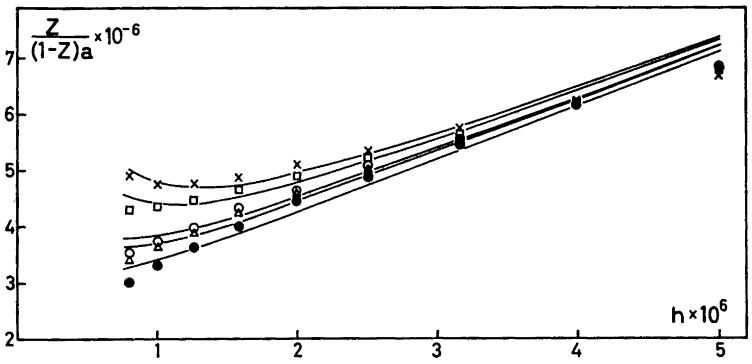

Fig. 3. $Z(1\text{-}Z)^{-1}a^{-1}$ *vs.* h for different C_A (eqn. 8 a). The curves are calculated for $\varkappa_{1,11} = 1.1 \times 10^{12}$ M^{-2}, $\varkappa_{1,01} = 2.45 \times 10^{6}$ M^{-1}, $\varkappa_{1,11,01} = 2.3 \times 10^{18}$ M^{-3}, $\varkappa_{1,02} = 2.45 \times 10^{12}$ M^{-2}; $\varkappa_{1,1} = 10^{-7.73}$M, $b_{CuCl} = 1.0$ M^{-1}. The symbols of the plotted points are those indicated in Table 1.

quently we may consider the probable existence of $Cu(HA)_2$, $Cu(HA)A^-$ and CuA_2^{2-} apart from $CuHA^+$ and CuA. In Fig. 4 there is, however, a slight upward trend for increasing C_A at high $-\log h$. For this reason the plotted points corresponding to $C_A > 2.52 \times 10^{-3}$ and $-\log h > 6.0$ were excluded at the calculation of slopes and intercepts of the straight lines.

From these intercepts (I) and slopes (L) the following functions were formed:

$$I\varphi = \varkappa_{1,11}h + \varkappa_{1,01} \tag{21}$$

$$L\varphi = \varkappa_{1,12}h^2 + \varkappa_{1,11,01}h + \varkappa_{1,02} \tag{22}$$

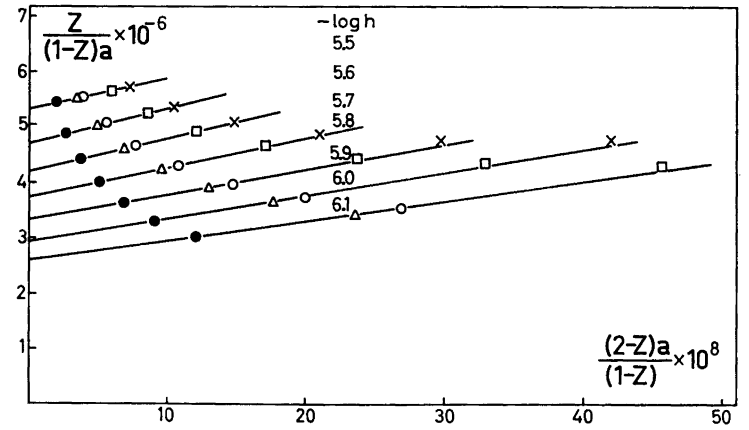

Fig. 4. $Z(1\text{-}Z)^{-1}a^{-1}$ as a function of $(2\text{-}Z)a(1\text{-}Z)^{-1}$ with h as parameter (eqn. 8a). The symbols are the same as indicated in Table 1.

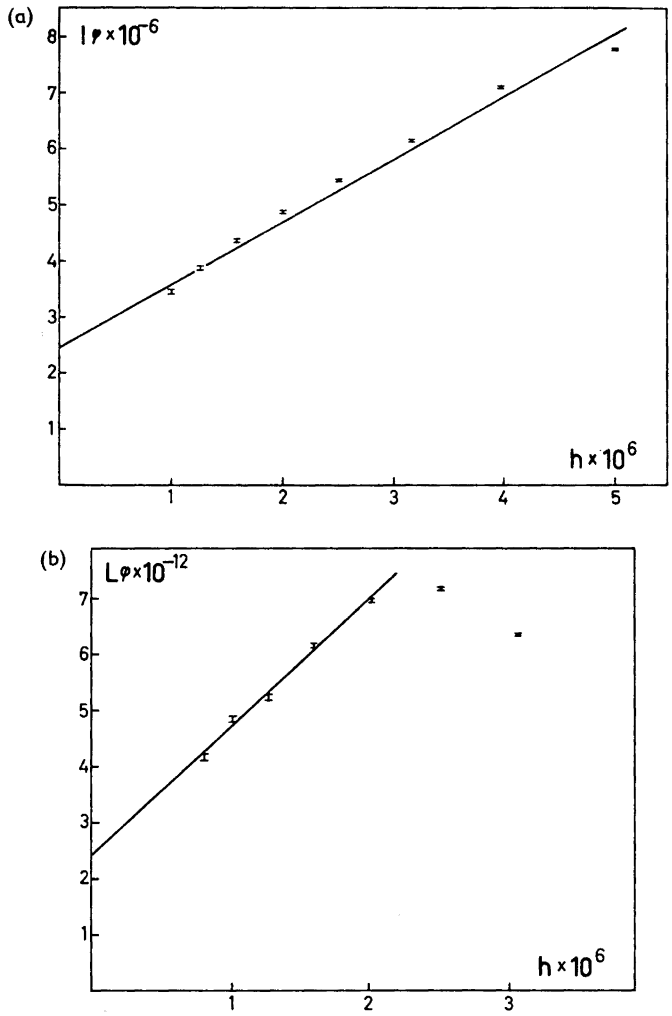

Fig. 5. Graphical evaluation of the overall equilibrium constants, assuming $\varkappa_{1,1} = 10^{-7.73}$M (indicated range $10^{-7.5}$ — $10^{-8.25}$ M) and $b_{CuCl} = 1.0$ M^{-1}.
(a) Eqn. 21 plotted as $I\varphi$ *vs.* h.
(b) Eqn. 22 plotted as $L\varphi$ *vs.* h.

In Fig. 5a, eqn. 21 is plotted as the curve $I\varphi(h)$. For each h-value the above-mentioned range of $\varkappa_{1,1}$ is indicated (mean value $10^{-7.73}$ M). The constant b_{CuCl} was set equal to 1.0 M^{-1} (Ref.[44]). As shown in the figure, data can be fitted to a straight line with finite slope and intercept. The species $CuHA^+$ and CuA are thus obviously existing. The intercept ($\varkappa_{1,01}$) and the slope ($\varkappa_{1,11}$) of the best straight line furnished the equilibrium constants:

$$\varkappa_{1,01} = (2.45 \pm 0.2) \times 10^6\ \mathrm{M}^{-1}$$
$$\varkappa_{1,11} = (1.1 \pm 0.2) \times 10^{12}\ \mathrm{M}^{-2}$$

In a similar manner $L\varphi$ has been plotted against h in Fig. 5b. Even in this case, data can be fitted to a straight line, which may provide evidence of existence of the species $Cu(HA)A^-$ and CuA_2^{2-}. Formation of $Cu(HA)_2$, in measurable quantities can reasonable be ruled out. In the present plot data should then have been represented as a parabola with its vertex downwards. The values of equilibrium constants related to $Cu(HA)A^-$ and CuA_2^{2-} were computed from the best straight line to be:

$$\varkappa_{1,02} = (2.45 \pm 0.2) \times 10^{12}\ \mathrm{M}^{-2}$$
$$\varkappa_{1,11,01} = (2.3 \pm 0.2) \times 10^{18}\ \mathrm{M}^{-3}$$

The logarithms of the computed overall equilibrium constants, $\varkappa_{1,1p,0q,r}$, were converted into logarithms of apparent stability constants and apparent complexity constants of the complexes, as well as into pK values of the hydrogen copper(II) complexes. This is evident from Table 2, where all these constants are given in logarithmic form.

DISCUSSION

As can be seen in Fig. 3, the curves calculated from the computed constants reasonably agree with the plotted data. As expected the deviations are most apparent at high h, as the pH decrements due to complex formation are least pronounced there.

The complexes evaluated as formed in this study, *i. e.* $CuHA^+$, CuA, $Cu(HA)A^-$ and CuA_2^{2-}, may not exclude the existence of other complexes for true, and at least some other possibilities may therefore be discussed.

An indication of the existence of complexes with more than two O-phosphorylethanolamine groups per central ion, thus, seems to be the upward trend of the curves of Fig. 4 at high $-\log h$. This trend is, however, too slight to allow any accurate proof of the existence of such species.

In the present computations, only a hydroxo complex $CuOH^+$ was considered, which apparently is the only inorganic hydroxo species formed in the present concentration ranges [44]. Other monohydroxo complexes, *i. e.* in the first place Cu(HA)OH and $CuA(OH)^-$, would at $-\log h = 6.1$ (the upper limit of $-\log h$ used in this work) apparently constitute less than 5 % of the corresponding species $CuHA^+$ and CuA, *cf.* Ref.[45]. These hydroxo complexes, consequently, cannot appreciably change the proposed reaction scheme. This is also evident from the curves of Figs. 3 and 5a, as the occurrence of a large amount of $CuA(OH)^-$ would have been indicated as an upward trend for decreasing h. The right hand side of eqn. 8a should then include the figure $\varkappa_{1,01,1}h^{-1}$. The presence of Cu(HA)OH on the other hand, cannot be excluded, as these measurements do not distinguish this complex from CuA.

The apparent negligible amount of these mononuclear hydroxo species may exclude the existence of *ol* complexes [7,46-50]. Polynuclear complexes, where one copper(II) ion is coordinated through either the phosphoryl and amino group of the ligand, can reasonably also be excluded. In the $-\log h$ range involved the pK value of the ligand amino group ($=10.10$) does not allow for such complex formation due to the relatively low copper(II)-ammine affinity (see, *e. g.*, $\log b_1$ for the Cu(II)-ammine system [44]), *cf.* Ref.[51]

Table 2. Logarithms of $\varkappa_{1,1p,0q,r}$ constants, apparent stability constants, and apparent complexity constants of the complexes, and apparent pK values of the acid complexes in 0.15 M KCl medium at 25°.

$C_A = (0.8-3) \times 10^{-3}$, $C_{Cu} = 7.84 \times 10^{-4}$, $-\log h = 5.30-6.10$.
$\log\varkappa_{11} = 10.10$, $\log\varkappa_{21} = 15.67$, $\varkappa_{1,1} = 10^{-7.73}$M, $b_{CuCl} = 1.0$ M^{-1}

Reaction				Log. equilibrium constant	
$Cu^{2+} + H^+ + A^{2-}$	$\rightleftharpoons$	$CuHA^+$		$\log\varkappa_{1,11}$	= 12.04
$Cu^{2+} + HA^-$	$\rightleftharpoons$	$CuHA^+$	$\log \frac{\varkappa_{1,11}}{\varkappa_{11}}$	$= \log b_{CuHA}$	= 1.94
$Cu^{2+} + A^{2-}$	$\rightleftharpoons$	CuA	$\log\varkappa_{1,01}$	$= \log b_1$	= 6.39
$Cu^{2+} + H^+ + 2A^{2-}$	$\rightleftharpoons$	$Cu(HA)A^-$		$\log\varkappa_{1,11,01}$	= 18.36
$Cu^{2+} + HA^- + A^{2-}$	$\rightleftharpoons$	$Cu(HA)A^-$	$\log \frac{\varkappa_{1,11,01}}{\varkappa_{11}}$	$= \log\beta_{Cu(HA)A}$	= 8.26
$CuHA^- + A^{2-}$	$\rightleftharpoons$	$Cu(HA)A^-$	$\log \frac{\varkappa_{1,11,01}}{\varkappa_{1,11}}$	$= \log b_{Cu(HA)A}$	= 6.32
$Cu^{2+} + 2A^{2-}$	$\rightleftharpoons$	CuA_2^{2-}	$\log\varkappa_{1,02}$	$= \log\beta_2$	= 12.39
$CuA + A^{2-}$	$\rightleftharpoons$	CuA_2^{2-}	$\log \frac{\varkappa_{1,02}}{\varkappa_{1,01}}$	$= \log b_2$	= 6.00
$CuHA^+$	$\rightleftharpoons$	$CuA + H^+$	$\log \frac{\varkappa_{1,11}}{\varkappa_{1,01}}$	$= pK_{CuHA}$	= 5.65
$Cu(HA)A^-$	$\rightleftharpoons$	$CuA_2^{2-} + H^+$	$\log \frac{\varkappa_{1,11,01}}{\varkappa_{1,02}}$	$= pK_{Cu(HA)A}$	= 5.97

The existence of $CuHA^+$ and $Cu(HA)A^-$ provides evidence for the ligand phosphoryl group to act complexing. This is in contrast to the Ag(I) — O-phosphorylethanolamine system [52], where the species AgA^- and AgA_2^{3-} only could be detected in a similar concentration range as the present. The amino group of the ligand was suggested as single coordination site for the latter species [52], which may be attributed to Ag(I) preferably forming linear complexes with this type of ligand, *cf.* Ref.[53]. The great difference between b_{CuHA} and b_1 in this work (*cf.* Table 2) indicates the ligand amino group to be introduced as dentate site, when $CuHA^+$ is converted to CuA. The species CuA and CuA_2^{2-} may, thus, be coordinated through the ligand phosphoryl and amino group or the amino group only. The former alternative is more probable, at least for CuA, as $\log b_1$ of the Cu(II)-ammine system [44] is reported to be about 2 log. units lower than that of the present. The effect of the increased net negative charge, caused by the presence of the phosphoryl group, cannot reasonable alone explain this great difference in b_1. — Due to the same fact

copper(II) reasonably interacts with the phosphoryl group also in the corresponding O-phosphorylserine 1:1 complex [21]. The central copper(II) ion is, however, in this complex apparently mainly coordinated through a five-membered chelate ring formed by the amino and carboxyl donor groups. The value of $\log b_1$ (= 9.64) in this system is about 1.5 — 2 log. units greater than $\log b_1$, in copper(II) systems of similar unphosphorylated amino acids [38,54,55].

Klotz *et al.*[6,56] studied the copper(II) binding properties of α- and β-casein. The α-casein was found to have the greater copper(II) binding capacity, being greater than that of any other protein investigated [6]. The difference in copper (II) affinity of α- and β-casein paralleled the phosphorus content of those proteins, suggested to be due to difference in net negative charge [6]. The apparent complexing action of the phosphoryl group in the present complexes, and in the O-phosphorylserine complexes [21] may indicate that the greater copper(II) binding power of these phosphoproteins is partly due to complex formation through phosphoryl groups.

In the phospholipids, phosphatidylethanolamine and phosphatidylserine, where the phosphoryl group is diesterified, the same groups are free to react as those proposed as main dentate sites in O-phosphorylethanolamine and O-phosphorylserine. Since the pK values of the amino group in these phosphatides are of the same size [57] as those of the corresponding low molecular weight phosphates [21,40], both types of compounds may at a physiological pH form copper(II) complexes of nearly the same strength. The complexes formed by those ligands will then be those, where the dissociable proton is removed from the amino nitrogen group due to the pK value of the hydrogen copper(II) complexes (*cf.* Table 2 and Ref.[21]). This gives evidence for a considerable copper(II) complexity of these phosphatides, which may have biological significance. At inhibition of tromboplastinase action by copper(II) ions [58], for instance, complexes will obviously be formed between Cu(II) ions and the tromboplastical active lipid substrate, mainly constituting phosphatidylethanolamine and phosphatidylserine [59].

Acknowledgements. The author wishes to express his gratitude to Docent Ido Leden for valuable discussions. The skilful technical assistance of Mr. Åke Lundquist is greatly acknowledged. The investigation was aided by grants from the *Medical Faculty, University of Göteborg.*

REFERENCES

1. Mellander, O. *Uppsala Läkarfören. Förh.* **52** (1947) 107.
2. Mecham, D. K. and Olcott, H. S. *J. Am. Chem. Soc.* **71** (1949) 3670.
3. Mellander, O. *Nutrition Rev.* **13** (1955) 161.
4. Halkett, J. A. E., Peters, Jr., T. and Ross, J. F. *J. Biol. Chem.* **231** (1958) 187.
5. Pantlitschko, M. and Gründig, E. *Monatsh.* **89** (1958) 489.
6. Fiess, H. A. and Klotz, I. M. *J. Am. Chem. Soc.* **74** (1952) 887.
7. Gurd, F. R. N. and Wilcox, P. E. *Advances in Protein Chem.* **11** (1956) 311.
8. Carr, C. W. and Engelstad, W. P. *Arch. Biochem. Biophys.* **77** (1958) 158.
9. Zittle, C. A., Della Monica, E. S., Rudd, R. K. and Custer, J. H. *Arch. Biochem. Biophys.* **76** (1958) 342.

10. Hipp, N. J., Groves, M. L. and McMeekin, T. L. *J. Am. Chem. Soc.* **74** (1952) 4822.
11. Sampath Kumar, K. S. V., Sundararajan, T. A. and Sarma, P. S. *Enzymologia* **18** (1957) 228.
12. Sundararajan, T. A. and Sarma, P. S. *Enzymologia* **18** (1957) 234.
13. Hofman, T. *Biochem. J.* **69** (1958) 139.
14. Peterson, R. F., Nauman, L. W. and McMeekin, T. L. *J. Am. Chem. Soc.* **80** (1958) 95.
15. Sundararajan, T. A. and Sarma, P. S. *Biochem. J.* **71** (1959) 537.
16. Kalan, E. B. and Telka, M. *Arch. Biochem. Biophys.* **79** (1959) 275.
17. Österberg, R. *Arkiv Kemi* **13** (1959) 409.
18. Williams, J. and Sanger, F. *Biochim. et Biophys. Acta* **33** (1959) 294.
19. Perlmann, G. *Advances in Protein Chem.* **10** (1955) 1.
20. Österberg, R. *Nature* **179** (1957) 476.
21. Österberg, R. *Arkiv Kemi* **13** (1959) 393.
22. Outhouse, E. L. *Biochem. J.* **30** (1936) 197; **31** (1937) 1459.
23. Colowick, S. P. and Cori, C. F. *Proc. Soc. Exptl. Biol. Med.* **40** (1939) 586.
24. Stone, W. E. *J. Biol. Chem.* **149** (1943) 29.
25. Gordon, A. H. *Biochem. J.* **45** (1949) 99.
26. Awapara, J., Landua, A. J. and Fuerst, R. *J. Biol. Chem.* **183** (1950) 545.
27. Astrup, T., Carlström, G. and Stage, A. *Acta Physiol. Scand.* **24** (1951) 202.
28. Walker, D. M. *Biochem. J.* **52** (1952) 679.
29. Tallan, H. H., Moore, S. and Stein, W. H. *J. Biol. Chem.* **211** (1954) 927.
30. Wittcoff, H. *The Phosphatides*, Reinhold Publ. Corp., N.Y. 1951, Chapter III, and other references given there.
31. Campbell, P. N. and Work, T. S. *Biochem. J.* **50** (1952) 449.
32. Roberts, E. and Lowe, I. P. *J. Biol. Chem.* **211** (1954) 1.
33. Kennedy, E. P. and Weiss, S. B. *J. Biol. Chem.* **222** (1956) 193.
34. Potter, R. L. and Buettner-Janusch, V. *J. Biol. Chem.* **233** (1958) 462.
35. Schneider, W. C. and Rotherham, J. *J. Biol. Chem.* **233** (1958) 948.
36. Bjerrum, J. *Metal Ammine Formation in Aqueous Solution*, P. Haase and Son, Copenhagen 1941.
37. Martell, A. E. and Calvin, M. *Chemistry of the Metal Chelate Compounds*, Prentice-Hall, Inc. New York 1952, pp. 78—93.
38. Bjerrum, J., Schwarzenbach, G. and Sillén, L.G. *Stability Constants, Part I: Organic Ligands. The Chemical Society, Spec. Publ.* No. 6, London 1957.
39. Hedström, B. *Acta Chem. Scand.* **9** (1955) 613.
40. Fölsch, G. and Österberg, R. *J. Biol. Chem.* **234** (1959) 2298.
41. Baer, E. and Stancer, H. C. *Can. J. Chem.* **34** (1956) 436.
42. Samuelson, O. *Ion Exchangers in Analytical Chemistry*, Almqvist & Wiksell, Uppsala 1952, Chapter VIII.
43. Hitchcock, D. I. and Taylor, A. C. *J. Am. Chem. Soc.* **59** (1937) 1812.
44. Bjerrum, J., Schwarzenbach, G. and Sillén, L.G. *Stability Constants, Part II: Inorganic Ligands. The Chemical Society Spec. Publ.* No. 7, London 1958.
45. Martell, A. E., Chaberek, Jr. S., Courtney, R. C., Westerback, S. and Hyytiainen, H. *J. Am. Chem. Soc.* **79** (1957) 3036.
46. Pedersen, K. J. *Kgl. Danske Videnskab. Selskab. Mat. fys. Medd.*, **20**:7 (1943).
47. Berecki-Biederman, C. *Arkiv Kemi* **9** (1956) 175.
48. Bailar, Jr., J. C. *The Chemistry of the Coordination Compounds*, Reinhold Publ. Corp., New York 1956, Chapter 13.
49. Courtney, R. C., Gustafson, R. L., Chaberek, Jr., S. and Martell, A. E. *J. Am. Chem. Soc.* **81** (1959) 519.
50. Gustafson, R. L. and Martell, A. E. *J. Am. Chem. Soc.* **81** (1959) 525.
51. Williams, R. J. P. *Biol. Revs. Cambridge Phil. Soc.* **28** (1953) 387—388.
52. Datta, S. P. and Grzybowski, A. K. *J. Chem. Soc.* **1959** 1091.
53. Schwarzenbach, G. *Helv. Chim. Acta* **36** (1953) 23.

54. Murphy, C. B. and Martell, A. E. *J. Biol. Chem.* **226** (1957) 37.
55. Bretton, P. *J. chim. phys.* **54** (1957) 827, 837.
56. Klotz, I. M., Faller, I. L. and Urquhart, J. M. *J. Phys. & Colloid. Chem.* **54** (1950) 18.
57. Garvin, J. E. and Karnovsky, M. L. *J. Biol. Chem.* **221** (1956) 211.
58. Feldman, D. and Ginell, R. *Proc. Soc. Exptl. Biol. Med.* **89** (1955) 13.
59. Kushner, D. J. and Feldman, D. *Biochim. et Biophys. Acta* **30** (1958) 466.

Received October 7, 1959.

ACTA CHEMICA SCANDINAVICA 14 (1960) 486–490

Studies on Local Anesthetics XX *

Synthesis of Some α-Monoalkylamino-2-methylpropionanilides. A New Useful Local Anesthetic

NILS LÖFGREN and CLAËS TEGNÉR

Institute of Organic Chemistry and Biochemistry, University of Stockholm, Stockholm, and Research Laboratories, AB Astra, Södertälje, Sweden

Five new α-monoalkylamino-2-methylpropionanilides in which the alkyl group is an ethyl, *n*-propyl, *iso*propyl, *n*-butyl or *iso*butyl group have been synthesised. All five compounds possess local anesthetic activity and one of them, the *n*-propylamino compound ("L 67"), had such valuable properties that it was subjected to clinical tests. These showed the new compound to be an effective injection anesthetic.

A review of the chemistry of local anesthetics has recently been published by Killian [2] in which the aminoacylanilides are discussed as well as other groups of anesthetics. A number of papers on the synthesis of local anesthetics of this type have been published from this institute, one of which describes the preparation of α-diethylamino-2,6-dimethylacetanilide [3] (Xylocaine®). Since its introduction into clinical use it has become the most important injection anesthetic. This paper presents a new local anesthetic, α-n-*propylamino-2-methylpropionanilide*, which in its pharmacological properties is similar to Xylocaine.

A series of compounds of the general formula

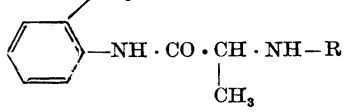

in which R is an ethyl (I), *n*-propyl (II), *iso*propyl (III), *n*-butyl (IV), or *iso*butyl (V) group were synthesised and tested pharmacologically. The inter-

* For paper XIX of this series, see Lüning [1].

mediate α-bromo-2-methylpropionanilide was prepared by reacting α-bromopropionyl bromide with *o*-toluidine in an aqueous acetate buffer [4]. One mole of the α-bromo-2-methylpropionanilide was then heated with an excess of the appropriate monoalkylamine in benzene solution.

Compounds I—V were tested for local anesthetic activity on rabbit cornea, using the technique of Wiedling [5] and the lethal doses (LD50) of each compound was determined by subcutaneous injection in white mice. The activity and toxicity values presented here are relative values referring to Xylocaine as a standard, *i.e.* the activity and toxicity of Xylocaine are both, by definition, taken as unity. Thus, a compound is characterised by its *relative anesthetic activity*, RA (for Xylocaine: RA = 1) and its *relative toxicity*, RT (for Xylocaine: RT = 1)*. For the quotient RA/RT the term *anesthetic index*, Q, is used (for Xylocaine: Q = 1). The results of the pharmacological measurements are compiled in Table 1. As can be seen from the table, compound I has the lowest activity (RA $\sim$ 0.3) being approximately 70 % lower than that of Xylocaine. Compound I has also, compared with Xylocaine, a low toxicity (RT = 0.41) and therefore its anesthetic index (Q $\sim$ 0.7) is only about 30 % lower than that of Xylocaine. Compound IV possesses the highest activity (RA = 2.2). It also has the highest toxicity (RT = 0.91), equal to or slightly less than that of Xylocaine. Since however RA is considerably higher than RT, the Q value is high (2.4). The RA values of II, III and V are 0.9, 0.7 and 0.8 respectively and since their relative toxicities are all < 0.7, they have Q values higher than that of Xylocaine. When tested for irritant properties by injection in the rabbit ear ** (aqueous solutions of the hydrochlorides), IV gave a moderate and V a strong irritant action but the other three compounds (I, II and III) did not appreciably irritate the skin. Among the three nonirritant compounds, II and III have rather good RA values (especially II) and very favourable Q values and they were therefore subjected to clinical tests.

Table 1. Local anesthetic activity (rabbit cornea) and toxicity (white mouse) of compounds I—V. For the terms relative anesthetic activity and relative toxicity, see above.

Compound	Relative anesthetic activity (RA)	Toxicity, LD50		Relative toxicity (RT)	$Q\left(=\frac{RA}{RT}\right)$
		g base/kg	moles/kg × 10^3		
Xylocaine	1.0	0.34	1.45	1.0	1.0
I	0.30	0.72	3.5	0.41	0.7
II	0.86	0.71	3.2	0.45	1.9
III	0.68	0.73	3.3	0.44	1.5
IV	2.2	0.38	1.6	0.91	2.4
V	0.82	0.55	2.3	0.63	1.3

* For further information on the meaning of the terms RA and RT, see Löfgren, Tegnér and Takman [6].

** For this technique, see Wiedling [7].

At present we are able to present briefly the clinical results for compound II, in clinical tests known as *L 67* or *Astra 1512* *. This compound, *i.e.* α-n-*-propylamino-2-methylpropionanilide*, did not produce any sign of irritation when tested for infiltration anesthesia in man **. No side effects were observed. The efficiency of the compound was studied in practically all forms of injection anesthesia (subcutaneous anesthesia of the skin, terminal anesthesia of the teeth, various forms of block anesthesia, *e.g.* sacral and mandibular anesthesia, *etc.*). From these tests it is evident that compound II has a similar action to that of Xylocaine. The two compounds produce approximately the same incidence, onset, extent and duration of anesthesia. In dental use, compound II gives a shorter anesthesia of the soft tissues than Xylocaine, *i.e.* in this respect compound II is more favourable than Xylocaine. Furthermore, as shown in Table 1, the toxicity of compound II is about 50 % lower than that of Xylocaine ***. It is thus a very promising injection anesthetic for clinical use.

EXPERIMENTAL †

α-Bromo-2-methylpropionanilide was prepared from α-bromopropionyl bromide and *o*-toluidine by the aqueous acetate buffer method given by Löfgren [4]. Colourless needles were obtained from benzene, m. p. 132—133°, yield 81 %. The melting point agrees with that observed by Tigerstedt [10] who synthesised the compound from α-bromopropionyl bromide and *o*-toluidine in a dry organic solvent.

α-Ethylamino-2-methylpropionanilide (I). A mixture of α-bromo-2-methylpropionanilide (24 g, 0.10 mole), ethylamine (12 g, 0.27 mole) and benzene (50 ml) was heated in a steel autoclave at 80° for 8 h. The reaction mixture was then diluted with absolute ether and filtered to remove the amine hydrobromide formed. After evaporation of the solvent the residue was distilled under reduced pressure and the fraction b. p. 145—147°/0.9 mm was collected as a colourless oil (16.5 g, 80 %). The oil soon solidified and was recrystallised from petroleum ether (b. p. 40—60°). Colourless crystals, solidifying point 36—37°. (Found: C 69.7; H 8.92. Calc. for $C_{12}H_{18}N_2O$ (206.3): C 69.9; H 8.79.)

α-n-*Propylamino-2-methylpropionanilide* (II). A solution of α-bromo-2-methylpropionanilide (24 g, 0.10 mole) and *n*-propylamine (16 g, 0.27 mole) in benzene (100 ml) was refluxed for 8 h. The reaction mixture was treated as described under compound I and the base was isolated as colourless needles, m. p. 37—38°, b. p. 159—162°/1 mm, n_D^{20} 1.5298†† (19 g, 87 %). (Found: C 71.0; H 8.95. Calc. for $C_{13}H_{20}N_2O$ (220.3): C 70.9; H 9.15.)

Salts of this compound were prepared by dissolving the base in dry ether and adding an ether solution or an ether-ethanol solution of the acid. The precipitated salts were recrystallised from ethanol — *iso*propyl ether. To prepare the sulphamate a different technique had to be used (see below). The following salts were prepared:

Hydrochloride. M. p. 167—168°. (Found: C 60.8; H 8.21; N 10.73. Calc. for $C_{13}H_{21}ClN_2O$ (256.8): C 60.8; H 8.24; N 10.91.)

---

* A paper on clinical results with the compound has already appeared [8]. Further results of the pharmacological and the clinical investigations will be published shortly.

** Aqueous solutions of the hydrochloride, with or without the addition of epinephrine, were used for the clinical tests.

*** In experiments carried out by Wiedling [9] both the intravenous and the intraperitoneal toxicities (white mouse) were 60—65 % of those of Xylocaine.

† All melting points are corrected.

†† supercooled liquid.

Hydrogen sulphate. M. p. 175—176°. (Found: C 49.7; H 6.95; N 8.66. Calc. for $C_{13}H_{22}N_2O_5S$ (318.4): C 49.0; H 6.97; N 8.80.)

Monohydrogen citrate. On treating 1 mole of the base with 1 mole of citric acid the dibasic citrate separated, m. p. 140—142° decomp. (Found: C 60.7; H 7.55; N 9.10. Calc. for $C_{32}H_{48}N_4O_9$ (632.8): C 60.7; H 7.65; N 8.85.)

Lactate. M. p. 133—134°. (Found: C 61.7; H 8.45; N 9.18. Calc. for $C_{16}H_{26}N_2O_4$ (310.4): C 61.9; H 8.44; N 9.03.)

Methanesulphonate. M. p. 169—171°. (Found: C 53.2; H 7.63; N 8.50. Calc. for $C_{14}H_{24}N_2O_4S$ (316.4): C 53.1; H 7.65; N 8.86.)

Sulphamate. The sulphamate of compound II was prepared in the following way:

A mixture of the base (22 g, 0.10 mole) and sulphamic acid (9.7 g, 0.10 mole) in absolute ethanol (40 ml) was boiled under reflux (condenser with calcium chloride tube) until dissolved. Dry acetone (30 ml) and then absolute ether (30 ml) were added to this clear solution through the condenser. After cooling the crystals that separated were sucked off and washed with a mixture of equal volumes of dry acetone and dry ether. Yield 24 g, 75 %. The salt thus obtained is of high purity but, if desired, it can be recrystallised from absolute ethanol-*iso*propyl ether. M. p. 130—131°. (Found: C 49.1; H 7.42; N 12.9. Calc. for $C_{13}H_{23}N_3O_4S$ (317.4): C 49.2; H 7.30; N 13.2.)

If in the procedure described above aqueous alcohol is used instead of absolute alcohol the sulphamate may be obtained in a hydrated form. However, a closer characterisation has not yet been carried out.

All the salts, described here, are readily soluble in water.

*α-Iso**propylamino-2-methylpropionanilide hydrochloride* (III). A mixture of α-bromo-2-methylpropionanilide (24 g, 0.10 mole), *iso*propylamine (16 g, 0.27 mole) and benzene (100 ml) was heated in a steel autoclave at 80° for 8 h. The reaction mixture was then diluted with dry ether and filtered to remove precipitated *iso*propylammonium bromide. The addition of a dry ethereal solution of hydrogen chloride precipitated the hydrochlorides of III and the remaining *iso*propylamine. The salts were filtered off, washed with ether and then dissolved in hot water to which had been added some activated carbon. From the filtered solution the hydrochloride of III separated as colourless crystals, m. p. 236—237° decomp. (16.5 g, 64 %). (Found: C 61.3; H 8.30; Cl (Mohr) 13.8. Calc. for $C_{13}H_{21}ClN_2O$ (256.8): C 60.8; H 8.24; Cl 13.8.)

α-n-Butylamino-2-methylpropionanilide hydrochloride (IV). α-Bromo-2-methylpropionanilide (24 g, 0.10 mole), *n*-butylamine (20 g, 0.27 mole) and benzene (100 ml) were boiled under reflux for 8 h. After dilution with dry ether the *n*-butylammonium bromide was filtered off and the filtrate evaporated to dryness. The residue was dissolved in ether and ethereal hydrogen chloride was added until no more precipitate was formed. This was filtered off and then recrystallised from absolute ethanol giving colourless crystals, m. p. 175—177° (19 g, 71 %). (Found: C 61.9; H 8.39; Cl (Mohr) 13.1. Calc. for $C_{14}H_{23}ClN_2O$ (270.8): C 62.1; H 8.56; Cl 13.1.)

*α-Iso**butylamino-2-methylpropionanilide hydrochloride* (V). The compound was obtained from α-bromo-2-methylpropionanilide and *iso*butylamine. The procedure described under compound III was followed, but instead of heating the reaction mixture in an autoclave it was boiled under reflux for 8 h. The hydrochloride was obtained from water as colourless crystals (*cf.* under compound III) and was recrystallised from the same solvent, m. p. 221—223° decomp., yield 63 %. (Found: C 61.9; H 8.29; Cl (Mohr) 13.1. Calc. for $C_{14}H_{23}ClN_2O$ (270.8): C 62.1; H 8.56; Cl 13.1.)

Thanks are due to Dr. B. Sjögren, director of research of AB Astra, for facilitating this work and to Dr. S. Wiedling for performing the pharmacological tests.

REFERENCES

1. Lüning, B. *Acta Chem. Scand.* **14** (1960) 321.
2. Killian, H. *Lokalanästesie und Lokalanästetika* Georg Thieme Verlag, Stuttgart 1959, p. 44.
3. Löfgren, N. *Arkiv Kemi, Mineral. Geol.* **22 A** (1946) No. 18.

4. Löfgren, N. *Studies on Local Anesthetics. Xylocaine, a New Synthetic Drug. Diss.* Stockholm 1948.
5. Wiedling, S. *Acta Pharmacol. Toxicol.* **8** (1952) 117.
6. Löfgren, N., Tegnér, C. and Takman, B. *Acta Chem. Scand.* **11** (1957) 1724.
7. Wiedling, S. *Acta Pharmacol. Toxicol.* **4** (1948) 351.
8. Eriksson, E. and Gordh, T. *Acta Anaesthesiol. Scand.* Suppl. **2** (1959) 81.
9. Wiedling, S. *In preparation.*
10. Tigerstedt, A. *Ber.* **25** (1892) 2919.

Received October 1, 1959.

ACTA CHEMICA SCANDINAVICA 14 (1960) 491–514

Short Communications

Reactivity of Polyvinyl Chloride

SVEN SONNERSKOG

A-B Svenskt Konstsilke, Borås, Sweden

It was shown in a previous paper [1] that the thermal instability of polyvinyl chloride, prepared in emulsion systems, is related to the presence of polymeric (hydro)peroxides, formed by the occurrence of an induction period during the initiating step, by random copolymerization with oxygen as comonomer, or by deactivation of trapped polymer radicals at grinding and drying operations. As a consequence inhibition or retardation of color formation and decomposition on heating can be achieved by the formation of a redox system, where the polymer takes part as an active component. The same principle may be used in the preparation of graft copolymers by the interaction of polymeric peroxide radicals and acrylonitrile in an aqueous suspension at 32°C.

Complementary studies have been carried out from other points of view. A summary is given below. As earlier [1], the rate of color formation and gelation in pyridine at 100°C is used to indicate the inhibitory action of coreactants or the change of thermal stability, caused by earlier operations in other media. Any discoloration arising from side reactions between solvent and additives is identified in a blank. The concentration of stabilizers in test solutions was kept high (1–10 % by wt of polymer) to make sure that an excess is at hand, compared to the amount of radical intermediates in the degradation cycle.

New types of inhibitors. a. *Carbon black.* Addition of *High Abrasion Furnace* or *Easy Processing Channel* blacks to a solution of polyvinyl chloride in pyridine gives a satisfactory inhibition of thermal degradation according to the standard schedule. This statement merely implies the nonappearance of the later steps — strong discoloration and gelation — in the degradation cycle, as a weak color formation is visually undetectable for obvious reasons. The removal of suspended inhibitor by filtration is unfeasible, because the average end to end distance of the polymer molecules far exceeds the diameter of a carbon particle.

The inhibitory properties of carbon black are known from rubber chemistry. It has been recently shown that reinforcing carbon black fillers act as radical acceptors [2]. Analogous effects have also been reported on milling of polyethylene [3].

b. *Thiophenol.* This compound gives a complete protection against thermal decomposition in pyridine. A prolonged heating beyond the standard schedule (more than 330 min) gives no other visible change but a light yellow color formation. This is expected from the type reactions of an aromatic modifier and a polymeric hydroperoxide (= POOH):

$$\begin{aligned}
&\mathrm{POOH} && \rightarrow \mathrm{PO\cdot} + \mathrm{HO\cdot}\\
&\mathrm{PO\cdot} + \mathrm{C_6H_5SH} && \rightarrow \mathrm{POH} + \mathrm{C_6H_5S\cdot}\\
&\mathrm{HO\cdot} + \mathrm{C_6H_5SH} && \rightarrow \mathrm{H_2O} + \mathrm{C_6H_5S\cdot}\\
&2\ \mathrm{C_6H_5S\cdot} && \rightarrow \mathrm{C_6H_5-S-S-C_6H_5}
\end{aligned}$$

Arylmercaptans are known to react with alkenes [4]. When peroxides are present, addition occurs contrary to the Markownikoff rule. As technical grades of polyvinyl chloride always show a low, significant degree of unsaturation, this side reaction cannot be ignored. No distinction, however, between the separate contributions is made here, as they necessarily work in the same direction of improved stability. Moreover the quantitative relations would be obscured by a conceivable combination reaction between PO· and RS· radicals.

c. *Oxalic acid.* Oxidation of oxalic acid by free radicals is a case of hydrogen abstraction, where the transfer agent acquires radical character but loses its activity in a secondary step by thermal decomposition:

$$\mathrm{POOH} + \mathrm{HOOC-COOH} \rightarrow \mathrm{POH} + \mathrm{H_2O} + 2\ \mathrm{CO_2}$$

The inhibiting action of oxalic acid is comparable to that of thiophenol. An analy-

tical grade of highest purity (oxalic acid dihydrate) was used in order to exclude catalytic effects from metallic impurities, especially ferrous compounds.

Deactivation of the polymer in an aqueous medium. Hydroperoxides may decompose by thermal dissociation, by reduction activation and by acid or base catalysis. The influence of neutral, alkaline and acid water on the polymer properties was therefore considered, preferably in the vicinity of 100°C, because such treatments are believed to occur as routine methods of purification of technically produced material. An improvement of heat stability was observed in all three cases (pH range 1—12), but the most acid medium was distinctly superior, yet insufficient to impart a complete stability to the polymer when heated in pyridine. This statement is valid for aqueous media, containing hydrochloric, sulfuric or phosphoric acid. The necessary time of reaction seems to be short. The main improvement of heat stability is obtained within 15 min, followed by a moderate change of purity and whiteness of the sample when heating is continued for arbitrary periods.

Analogous effects are obtained by adding cobaltous chloride to the water. This reduction activator operates at a satisfactory rate in a neutral medium at a moderate temperature (35°C). Its action is enhanced by the presence of sulphur dioxide. Samples of polyvinyl chloride, soaked in this way for 8 h, or more, are stable in pyridine according to the actual testing schedule.

A variety of coreactants might be mentioned here, working in the same manner. *Vinyl acetate* is active in the presence of nonionic detergents, allowing solubilization of monomer in the polymer particles. This is particularly interesting, as no indication of graft copolymerization has been found. On the contrary a strict emulsion homopolymerization of vinyl acetate takes place by use of the activator system polyvinyl chloride-ferrous chloride-sodium pyrosulphite. Separation of the two polymers is preferably carried out by filtration in standard glass equipment. The opposite case-grafting — seems to be restricted to *acrylic* monomers (acrylonitrile, acrylic esters and related derivatives, such as N,N′-methylene-*bis*(acrylamide)).

Graft copolymerization and interpolymerization in solution. a. *N-vinyl-2-pyrrolidone* is a solvent for polyvinyl chloride at elevated temperature. When such a solution is stored at 100°C for several hours in the absence of air, viscosity is gradually increased. At increasing time of reaction the water soluble fraction of the system gradually disappears, even when the weight ratio polymer/solvent is low. Practical working conditions are found in the concentration range of 2—5 %.

As no reduction activator is present, an attempt of interpretation is obscured by a number of conceivable overlapping cases. A thermally dissociating polymeric hydroperoxide would be able to initiate a graft copolymerization as well as a homopolymerization of the comonomer. The latter reaction might even be superposed by a pure thermal initiation of the monomer, resulting in an appreciable formation of water soluble homopolymer. No experimental evidence for the existence of such a fraction has been found at high extents of reaction. It is probable that growing macromolecules of this kind are deactivated by combination reaction with radical species of hydrophobic origin. The ultimate composition would then be undistinguishable from a graft copolymer, formed directly by a chain reaction between the primary components.

b. *Polyvinyl chloride-polyvinyl alcohol* interpolymers. Accumulated experience makes probable that a second vinyl polymer, added to a fresh solution of polyvinyl chloride in pyridine, would give a block copolymer on heating, provided the added compound is accessible to reactivation by hydrogen abstraction. Polyvinyl alcohol of low acetyl content was selected for this purpose. An equimolar mixture of the two components was heated at 100°C in pyridine, until turbidity had decreased to a low, constant value. At this interchange level the polyvinyl alcohol is no more extractable with water. The formation of an interpolymer is expected from previous studies [5] on reactivation of polyvinyl alcohol by free radicals.

1. Sönnerskog, S. *Acta Chem. Scand.* **13** (1959) 1634.
2. Watson, W. F. *Makromol. Chem.* **34** (1959) 240.
3. Biggs, B. S. in *Polymer Degradation Mechanisms, Natl. Bur. Standards, Circular* 525, Washington 1953, p. 137.
4. Posner, T. *Ber.* **37** (1904) 502.
5. Hartley, F. D. *J. Polymer Sci.* **34** (1959) 397.

Received December 14, 1959.

Studies on Fibrinopeptides from Different Species

BIRGER BLOMBÄCK

Chemistry Department II, Karolinska Institutet, Stockholm, Sweden, and

JOHN SJÖQUIST

Department of Physiological Chemistry, University of Lund, Lund, Sweden

Starting with the work of Bailey, Bettelheim, Lorand and Middlebrook [1] in 1951, it has now been fairly well established by these authors and by others that when bovine thrombin acts on bovine fibrinogen at least two different peptides (A and B) are released from the fibrinogen molecule revealing N-terminal glycyl residues in the fibrin (*cf.* Refs.[2-4]). Both peptides isolated from the supernatant contain arginine as the C-terminal amino acid residue [5,6]. The release of at least peptide A is followed stoichiometrically by the appearance of N-terminal glycine in the fibrin [3]. Thus peptide bonds involving arginylglycyl residues in fibrinogen are apparently hydrolyzed by thrombin.

With respect to synthetic substrates such as tosylarginine methyl ester the thrombin specificity seems to resemble that of trypsin [7]. Thrombin action differs, however, in many respects from that of trypsin [8,9] and in any case when acting on fibrinogen the proteolysis brought about by thrombin is much more limited than that by trypsin. Probably, the structure of the amino acid sequence in the vicinity of the peptide bonds hydrolyzed by thrombin or the secondary and tertiary structure of the fibrinogen molecule determines the narrow specificity of this enzyme.

Bovine thrombin also acts on fibrinogen from other species and species specific peptides seem to be released [10-13]. The characterization of these peptides may give information on the specific requirements for thrombin action. This paper gives preliminary data concerning the amino acid composition and amino acid sequences of some peptides released from human, pig and rabbit fibrinogen. The experiments which have been performed to establish the amino acid sequence of bovine peptides A and B have recently been reported elsewhere [3,6,14,15].

The different fibrinogens were mainly prepared according to a method previously described [16]. The coagulability of the fibrinogen preparations was 94—99 %. The peptides split off by bovine thrombin were isolated from the clot supernatant by column chromatography [17] on Dowex 50—X2.

From human fibrinogen two main peptides could be isolated and one of them was studied in detail. Also from each of pig and rabbit fibrinogen two main peptides could be isolated. The origin of other, smaller peptides observed on the chromatograms will not be discussed in this paper. All peptides containing tyrosine-O-sulphate have in this work been denoted as B-peptides in view of their similarity in this respect to bovine peptide B. The other peptides have tentatively been denoted as A-peptides.

The fact that the isolated peptides contain the N-terminal amino acids disappearing from the corresponding fibrinogen during the transformation to fibrin [10-12] establishes their relation to the proteolytic activity of thrombin.

The amino acid composition of the peptides (Table 1) was determined using the method recently reported [18,19]. As only small amounts of human, pig and rabbit peptides were accessible their content of cystine (or cysteine) was not determined. Peptides designated HP4-4 and KP10-A in Table 1 have not yet been analyzed for tryptophan. The other peptides do not contain tryptophan as judged from spectrophotometric readings in the ultra-violet. For comparison the amino acid residues of the bovine fibrinopeptides [6,15] are included in Table 1.

Although the amino acid compositions show remarkable differences some common features should be pointed out. Thus, all peptides in Table 1 have a high content of dicarboxylic amino acids. Furthermore, the peptides contain one or two arginine residues. In the bovine fibrinopeptides A and B the C-terminal position is occupied by arginine. The C-terminal amino acids in the other peptides have not yet been determined. It is also of interest that only one peptide, the pig peptide SP1-1, contains histidine.

Tyrosine has hitherto been found in fibrinopeptides from ox [20,17,21,4] and from rabbit fibrinogen [12]. It is also present in a fibrinopeptide from the pig. In all cases the hydroxyl group of tyrosine is esterified with sulphuric acid. The occurrence of tyrosine-O-sulphate in fibrinopeptides from

Table 1. Amino acid composition of fibrinopeptides from different species. R = residues

Species	Ox		Man		Pig				Rabbit			
Peptide	A	B	A HP 4–4		A SP 1–4		B SP 1–1		A KP 10–A		B KP 10–B	
Amino acid	R	R	μM/mg *	R	μM/mg *	R	μM/mg *	R	μM/mg *	R	μM/mg *	R
Alanine	0	1	1.05	2	0.76	2	0.62	2	0.42	1	0.78	2
Arginine	1	2	0.50	1	0.41	1	0.69	2	0.41	1	0.38	1
Aspartic acid	3	4	1.06	2	0.46	1	1.69	5	0.76	2	1.90	5
Glutamic acid	2	3	1.11	2	1.61	4	0.73	2	0.84	2	0.40	1
Glycine	5	3	2.57	5	1.60	4	0.37	1	1.24	3	—	0
Histidine	0	0	—	0	—	0	0.31	1	—	0	—	0
Leucine / *Iso*leucine	1	1	0.52	1	0.37	1	0.37	1	0.43	1	0.39	1
Lysine	0	1	—	0	0.40	1	0.36	1	—	0	—	0
Phenylalanine	1	1	0.51	1	0.35	1	—	0	0.46	1	—	0
Proline	2	2	—	0	—	0	0.36	1	0.40	1	0.40	1
Serine	2	0	0.40	1	—	0	—	0	0.42	1	—	0
Threonine	1	1	—	0	—	0	—	0	0.75	2	—	0
Tyrosine	0	1	—	0	—	0	0.32	1	—	0	0.42	1
Valine	1	1	0.53	1	0.82	2	0.74	2	0.41	1	0.42	1
Total number of residues	19	21		16		17		19		16		13

* Uncorrected for losses during acid hydrolysis. The figures refer to air-dry substances.

several species might indicate that this unique structural unit is of importance for the biological function of the protein. However, tyrosine-O-sulphate has been reported to be absent in peptide material from human fibrinogen [21]. In the peptide designated A from man tyrosine is absent (Table 1). The other main peptide present in the clot supernatant of human fibrinogen has, however, not been analyzed since it has not yet been obtained in homogeneous form.

Table 2 shows the amino acid sequences of the different peptides as determined with a modification of the phenylthiohydantoin method of Edman [15,22]. Except for bovine peptide A only partial sequences from the N-terminal end are known. All peptides with the possible exception of the bovine B-peptide seem to be made up of a single peptide chain. The partial sequences as well as the amino acid composition show clearly that these peptides are species specific.

The amino acid sequences of bovine peptides A and B have shown that the C-terminal part consists, in addition to arginine, mainly of neutral amino acid residues, whereas the dicarboxylic amino acids are displaced towards the N-terminal end of the molecule. Further elucidation of the amino acid sequences of the different peptides will show if this arrangement is a common feature.

It has been suggested that the pro · pro sequence in bovine A-peptide should be of importance in directing thrombin action [14]. This sequence, however, seems not to be a constant finding among fibrinopeptides as the peptide from man and one of the pig peptides does not contain proline.

Acknowledgement. This work has been aided by grants from the *Swedish Medical Research Council*, the *Therese and Johan Andersson Foundation and* the *Magnus Bergvall Foundation.*

1. Bailey, K., Bettelheim, F. R., Lorand, L. and Middlebrook, W. R. *Nature* **167** (1951) 233.
2. Scheraga, H. A. and Laskowski, M. Jr. *Advances in Protein Chem.* **12** (1957) 1.

Table 2. N-terminal amino acid sequences of fibrinopeptides from different species.

	N-terminal amino acid or amino acid sequences of fibrinogen and peptides.
Ox	
Peptide A	H-Glu·Asp·Gly·Ser·Asp·Pro·Pro·Ser·Gly·Asp·Phe·Leu·Thr·Glu·Gly·Gly·Gly·Val·Arg-OH
	OSO_3H
Peptide B (partial sequence. No reactive N-terminal)	(Glu, Phe, Pro, Thr) Asp·Tyr·Asp·Glu·Gly·Glu·Asp·Asp·Arg·Pro·Lys·Val·Gly·Leu·Gly·Ala·Arg-OH
Fibrinogen	Glu. Tyr.
Man	
H P 4—4 (Peptide A)	Ala·Asp·Ser·Gly·
Fibrinogen	Ala. Tyr.
Pig	
S P 1—4 (Peptide A)	Ala·Glu·Val·Asp·
S P 1—1 (Peptide B)	Ala·Leu·Asp·Tyr (or Ileu) OSO_3H
Fibrinogen	Ala. Tyr.
Rabbit	
K P 10-A (Peptide A)	Val·Asp·Pro·Gly·Glu·
K P 10-B (Peptide B)	Ala·Asp·Asp·Tyr·Gly· OSO_3H
Fibrinogen	Val. Ala. Tyr.

3. Blombäck, B. *Acta Physiol. Scand.* **43** (1958) Suppl. 148.
4. Gladner, J. A., Folk, J. E., Laki, K. and Carroll, W. R. *J. Biol. Chem.* **234** (1959) 62.
5. Gladner, J. A., Folk, J. E. and Laki, K. *Federation Proc.* **17** (1958) 229.
6. Blombäck, B., Wallén, P. and Sjöquist, J. *Acta Chem. Scand.* **13** (1959) 819.
7. Sherry, S. and Troll, W. *J. Biol. Chem.* **208** (1954) 95.
8. Bailey, K. and Bettelheim, F. R. *Biochim. et Biophys. Acta* **18** (1955) 495.
9. Bailey, K. and Bettelheim, F. R. *Brit. Med. Bull.* **11** (1955) 50.
10. Jorpes, J. E., Blombäck, G. E. B. and Yamashina, I. *Proc. Intern. Symposium Enzyme Chem.*, Tokyo and Kyoto 1957. p. 400
11. Blombäck, B. and Yamashina, I. *Arkiv Kemi* **12** (1958) 299.
12. Blombäck, B., Boström, H. and Vestermark, A. *Biochim. et Biophys. Acta* **38** (1960) 502.
13. Lorand, L. and Middlebrook, W. R. *Science* **118** (1953) 515.
14. Folk, J. E., Gladner, J. A. and Levin, Y. *J. Biol. Chem.* **234** (1959) 2317.
15. Sjöquist. J. Blombäck, B. and Wallén, P. *Arkiv Kemi. In press.*
16. Blombäck, B. and Blombäck, M. *Arkiv Kemi* **10** (1956) 415.
17. Blombäck, B. and Vestermark, A. *Arkiv Kemi* **12** (1958) 173.
18. Sjöquist, J. *Arkiv Kemi* **11** (1957) 129.
19. Sjöquist, J. *Biochim. et Biophys. Acta In press.*
20. Bettelheim, F. R. *J. Am. Chem. Soc.* **76** (1954) 2838.
21. Von Korff, R. W. and Bronfenbrenner, A. *J. Am. Chem. Soc.* **80** (1958) 5575.
22. Sjöquist, J. *Arkiv Kemi* **14** (1959) 291.

Received January 26, 1960.

Crystallographic Data of Two Pinoresinol Derivatives

EINAR WANG LUND

Kjemisk Institutt, Universitetet i Oslo, Blindern, Norway

Pinoresinol belongs to that class of naturally occurring lignans which contains the 2,6-diaryl-3,7-dioxabi*cyclo*[3.3.0]octane nucleus:

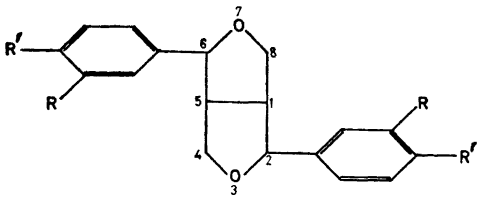

In pinoresinol R = OCH_3, R' = OH. In the same class of lignans is found a number of compounds, some of which are optical isomers or diastereoisomers.

Conclusive evidence for a *cis*-configuration of the central bi*cyclo*-octane nucleus is given by the presence of optical activity in the dilactone formed by oxydative degradation [1] and in the diol formed by opening of the tetrahydrofuran rings by mild hydrogenolysis[2]. Another argument against a *trans* configuration is that this would be a sterically highly strained structure. It has further been shown by Erdtman [3] and by Gripenberg [4] that pinoresinol is symmetrical in the respect that the substituted phenyl groups are either both in *cis* or both in *trans* position to the bridge hydrogen atoms at 1 and 5.

In order to decide which of the two possibilities is present in pinoresinol, an X-ray crystallographic investigation has been started. Compounds chosen for this study are dibromo- and diiodopinoresinol-dimethylether (R = R' = OCH_3, halogen in *para* position to R). Crystals of these two compounds have been prepared by Professor H. Erdtman and placed at the author's disposal for an X-ray study.

Both halogen derivatives crystallize in very fine needles. The crystals of the bromo-compound show monoclinic symmetry with unit cell dimensions: a = 8.25 Å, b = 26.7 Å, c = 4.83 Å, β = 103.3°. With two molecules in the unit cell the calculated density is 1.75 gcm^{-3}. Very fine thread-like crystals have been observed to float in an aqueous solution of zinc iodide of density 1.70 gcm^{-3}.

Extinctions of the reflexions $0k0$ with $k = 2n + 1$ indicate one of the space groups $P2_1/m$ or $P2_1$. With two molecules in the unit cell only the latter is possible, because a point or plane of symmetry is not compatible with what is known about the molecule.

The crystals of the iodo-compound are tetragonal with unit cell dimensions a = 21.3 Å, c = 4.86 Å. Calculated density on the basis of four molecules in the unit cell is 1.93 gcm^{-3}. The observed density of very fine, thread-like needles, determined in the same way as for the bromo-compound, is 1.96 gcm^{-3}.

Extinctions of the reflexions 001 and 003 indicate one of the space groups $P4_2/m$ or $P4_2$. The former of these requires the molecule to possess a plane of symmetry. Therefore the space group $P4_2$ is considered to be the most probable.

An important detail of the unit cell of both halogen derivatives is the short c-axis of about 4.8 Å. This fact in itself may decide between the two possibilities for the geometry of the pinoresinol molecule, because it has to be confined to a rather low-ceilinged unit cell.

From what is known about the structure of furanose compounds certain details of the five-membered rings in the nucleus can be inferred. Each ring may be characterized by a plane of reference containing the bridge C—C bond and the oxygen atom. It is highly probable that the two remaining carbon atoms of one ring are situated on each side of such a plane. With a *cis* configuration of the central nucleus the planes of the two condensed five-membered rings make an angle of about 120° with one another.

As a plane of reference of the whole molecule may be chosen one going through the two oxygen atoms and being parallel to the bridge C—C bond. Taking reasonable bond angles and interatomic distances into account, the following features of the molecular structure may be inferred with a high degree of probability. Of the two bonds at each of the carbon atoms 2 and 6, not engaged in the ring, one must be pointing nearly perpendicular to the plane of reference, being in *trans* position to the bridge hydrogen atoms at 1 and 5. The other bond at 2 and 6 is closer to being

parallel to the plane mentioned, making probably an angle near the tetrahedral with the first bond mentioned. For the molecule to be accommodated in the unit cell, the last mentioned bond must be the one occupied by the substituted phenyl group. A conclusion of these considerations is thus that the phenyl groups must be in *cis* position to the hydrogen atoms at the bridge carbons. The same conclusion is reached by Beroza [5], taking stability and intramolecular steric factors into consideration.

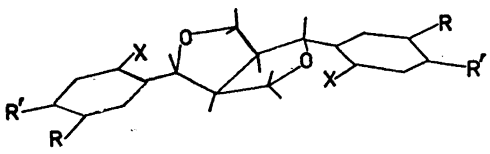

Fig. 1. A probable model of halogen derivatives of pinoresinoldimethylether. X = Br or I.

Fig. 1 shows a drawing in perspective of a probable model based on the arguments given.

A detailed structure determination of diiodopinoresinoldimethylether is in progress.

The author wishes to thank Professor H. Erdtman for placing crystals of the halogen derivatives of pinoresinoldimethylether at his disposal.

1. Erdtman, H. and Gripenberg, J. *Acta Chem. Scand.* **1** (1947) 71.
2. Haworth, R. D. and Woodcock, D. *J. Chem. Soc.* **1939** 1054.
3. Erdtman, H. *Svensk Kem. Tidskr.* **48** (1936) 236.
4. Gripenberg, J. *Suomen Kemistilehti* **19 B** (1946) 138.
5. Beroza, M. *J. Am. Chem. Soc.* **78** (1956) 5082.

Received February 9, 1960.

The Structure and Conformation of 1,2,3-Tribromo*cyclohexane* (m.p. 51° C) in the Gas Phase

V. A. ATKINSON and K. THURMANN-MOE

Universitetets Kjemiske Institutt, Blindern-Oslo, Norway

Bornubert, Rio and Senechal [1] synthesized a 1,2,3-tribromo*cyclo*hexane (m. p. 51°C) to which they assigned the *eee* conformation on grounds of the compounds reaction used. A sample of their compound was investigated by gas phase electron diffraction in Oslo in order to test the validity of the asigned conformation. The diagrams were taken using distances of 48 cm and 19 cm between the diffraction point and the photographic plate. The data was treated in our usual manner [2], using a damping factor of 0.0036. The $\sigma(r)/r$ radial distribution curve obtained is shown in Fig. 1 (a).

The peak at r = 5.72 Å can only be due to a Br (1*e*)—Br (3*e*) distance. Of the six conformations of 1,2,3-tribromo*cyclo*hexane that can be distinguished with electron diffraction, only those corresponding to *eee* and *eae* contain this distance. Theoretical radial distribution curves were therefore calculated for each of these conformations. It was found that the theoretical *eee* curve gave better agreement with the experimental curve than did the theoretical *eae* curve. However, the agreement was still not particularly good. The peaks at r = 5.72 Å and 4.27 Å in the theoretical *eee* curve were too high, and that at r = 4.63 Å too low. Since the substance is a well defined isomer, these anomalies could only be explained by assuming that in the gas phase it contains either a mixture of the *eee* and *aaa* forms, or else a mixture of the *eae* and *aea* forms. Only the *aaa* conformation would give rise to a substantial peak in the neighbourhood of r = 4.63 Å (due to the Br (1*a*)—Br (2*a*) and Br (2*a*)—Br (3*a*) distances), so it was concluded that the substance must be a mixture of the *eee* and *aaa* forms in the gas phase.

Further theoretical calculations were made using structural models based on the latest parameters for the *cyclo*-hexane ring obtained in our department: C—H=1.103 Å,

parallel to the plane mentioned, making probably an angle near the tetrahedral with the first bond mentioned. For the molecule to be accommodated in the unit cell, the last mentioned bond must be the one occupied by the substituted phenyl group. A conclusion of these considerations is thus that the phenyl groups must be in *cis* position to the hydrogen atoms at the bridge carbons. The same conclusion is reached by Beroza [5], taking stability and intramolecular steric factors into consideration.

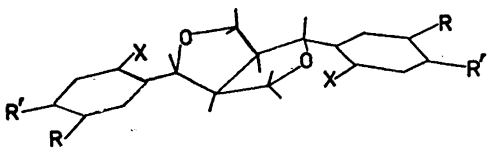

Fig. 1. A probable model of halogen derivatives of pinoresinoldimethylether. X = Br or I.

Fig. 1 shows a drawing in perspective of a probable model based on the arguments given.

A detailed structure determination of diiodopinoresinoldimethylether is in progress.

The author wishes to thank Professor H. Erdtman for placing crystals of the halogen derivatives of pinoresinoldimethylether at his disposal.

1. Erdtman, H. and Gripenberg, J. *Acta Chem. Scand.* **1** (1947) 71.
2. Haworth, R. D. and Woodcock, D. *J. Chem. Soc.* **1939** 1054.
3. Erdtman, H. *Svensk Kem. Tidskr.* **48** (1936) 236.
4. Gripenberg, J. *Suomen Kemistilehti* **19 B** (1946) 138.
5. Beroza, M. *J. Am. Chem. Soc.* **78** (1956) 5082.

Received February 9, 1960.

The Structure and Conformation of 1,2,3-Tribromo*cyclohexane* (m.p. 51° C) in the Gas Phase

V. A. ATKINSON and K. THURMANN-MOE

Universitetets Kjemiske Institutt, Blindern-Oslo, Norway

Bornubert, Rio and Senechal [1] synthesized a 1,2,3-tribromo*cyclo*hexane (m. p. 51°C) to which they assigned the *eee* conformation on grounds of the compounds reaction used. A sample of their compound was investigated by gas phase electron diffraction in Oslo in order to test the validity of the asigned conformation. The diagrams were taken using distances of 48 cm and 19 cm between the diffraction point and the photographic plate. The data was treated in our usual manner [2], using a damping factor of 0.0036. The $\sigma(r)/r$ radial distribution curve obtained is shown in Fig. 1 (a).

The peak at r = 5.72 Å can only be due to a Br (1*e*)—Br (3*e*) distance. Of the six conformations of 1,2,3-tribromo*cyclo*hexane that can be distinguished with electron diffraction, only those corresponding to *eee* and *eae* contain this distance. Theoretical radial distribution curves were therefore calculated for each of these conformations. It was found that the theoretical *eee* curve gave better agreement with the experimental curve than did the theoretical *eae* curve. However, the agreement was still not particularly good. The peaks at r = 5.72 Å and 4.27 Å in the theoretical *eee* curve were too high, and that at r = 4.63 Å too low. Since the substance is a well defined isomer, these anomalies could only be explained by assuming that in the gas phase it contains either a mixture of the *eee* and *aaa* forms, or else a mixture of the *eae* and *aea* forms. Only the *aaa* conformation would give rise to a substantial peak in the neighbourhood of r = 4.63 Å (due to the Br (1*a*)—Br (2*a*) and Br (2*a*)—Br (3*a*) distances), so it was concluded that the substance must be a mixture of the *eee* and *aaa* forms in the gas phase.

Further theoretical calculations were made using structural models based on the latest parameters for the *cyclo*-hexane ring obtained in our department: C—H=1.103 Å,

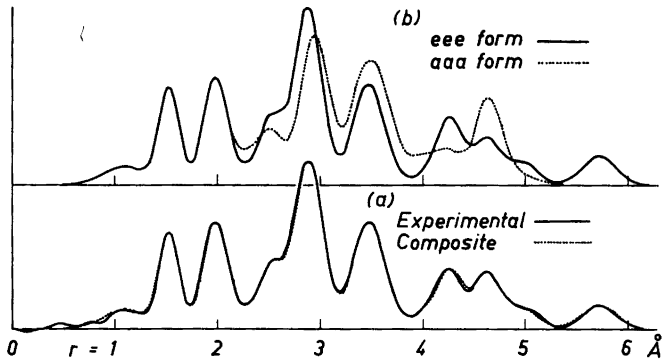

Fig. 1. Theoretical and experimental $\sigma(r)/r$ curves for the 1,2,3-tribromo*cyclo*hexane.

C–C = 1.529 Å, <CCC = 111.5°, <CCH = 110.0°, <HCH = 108.7°.

The C–Br bond distance used was 1.974 Å obtained from the experimental radial distribution curve. In order to get reasonable agreement between the experimental and theoretical curves, some distortion of the models was necessary. The well-defined peak at r = 3.48 Å suggested that this distance represented the closest approach of two non-bonded bromine atoms. This corresponds to a van der Waals radius of 1.74 Å for bromine (*cf.* Pauling's value [3] of 1.95 ± 0.1 Å). Using this value for the Br(1*e*)–Br(2*e*) and Br(1*a*)–Br(3*a*) distances, we calculated the parameters of models with the C–Br bonds distorted from the usual *cyclo*hexane positions. In the case of the *eee* model the distortion was slight; the C(1)–Br and C(3)–Br bonds were out of position by 2°, moved away from the Br(2) atom. As might be expected, the distortion of the *aaa* model was greater; the C(1)–Br and C(3)–Br bonds deviated 20° from the axial position, while the C(2)–Br bond was 9° from the axial position.

Fig. 1(b) shows the theoretical radial distribution curves for these *eee* and *aaa* conformations. Least squares procedure showed that the composite theoretical radial distribution curve giving best agreement with the experimental curve should be constructed on a basis of 19 % of the *aaa* form and 81 % of the *eee* form. In Fig. 1(a) this composite radial distribution curve is compared with the experimental curve. The dispersion of the standard deviation is 4 %.

The accuracy of the ratio between the two forms that we have derived clearly depends on the models we have used for the calculation of the theoretical radial distribution curves. It seems quite probable that small changes in the models would have given slightly different theoretical curves, which might have combined in slightly different proportions to give a composite curve agreeing as well or better with the experimental curve. For this reason we assess our possible error in the distribution ratio as high as ±5 %. The presence of 19 ± 5 % of the *aaa* form corresponds to an energy difference of 1.2 ± 0.3 kcal/mole between the two conformations.

Preliminary X-ray studies of the 1,2,3-tribromo*cyclo*hexane crystals have established a monoclinic structure, with space group $P2_1$, containing two molecules in a unit cell of dimensions: a = 6.44 Å, b = 9.22 Å, c = 7.52 Å and β = 106°.

We wish to thank Cand.real. A. Almenningen for taking the electron diffraction pictures and Prof. O. Hassel for his advice and encouragement. Thanks are also due to *Norges Teknisk-Naturvitenskapelige Forskningsråd* for financial support (V.A.A.).

1. Cornubert, R., Rio, A. and Senechal, P. *Bull. soc. chim. France* **1955** 46.
2. Almenningen, A. and Bastiansen, O. *Acta Chem. Scand.* **9** (1955) 815.
3. Pauling, L. *The Nature of the Chemical Bond.* Cornell University Press, Ithaca, New York, 1939.

Received February 11, 1960.

Precursors of Benzoxazolinone in Rye Plants

I. Precursor II, the Aglucone

ARTTURI I. VIRTANEN and
PENTTI K. HIETALA

Laboratory of the Foundation for Chemical Research, Biochemical Institute, Helsinki, Finland

When benzoxazolinone (BOA) was isolated from crushed rye seedlings, it was at first regarded as a primary substance in these plants [1]. It was, however, difficult to understand why this ether-soluble compound could not be extracted from crushed plants with ether. Before long it was found that it is formed from a precursor (precursor II) which in turn is a product of an enzymatic splitting of a compound (precursor I) found in intact rye plants [2].

Glucosides proved to be primary precursors, the enzymatic hydrolysis of which led to the formation of the corresponding aglucones after the plants were crushed, or the plant sap was pressed[3]. BOA was formed from the aglucone in rye plants and MBOA (methoxybenzoxazolinone) from the aglucone in wheat and maize plants by chemical transformation. If the enzymes are destroyed by placing intact plants in boiling water or boiling ethanol solution, or by keeping them in 70 % ethanol at −20°C for a longer time, the aglucone is no longer formed when plants are crushed. Only the glucoside (precursor I) is to be found in plants treated in this way.

When experimental results accumulated, Virtanen and Hietala [3,4] found that only the splitting off of glucose takes place in the enzymatic decomposition of the glucoside. Soon thereafter they were able to propose the probable structure for the glucoside (I) in rye and the aglucone (II) formed from it. At the same time evidence was obtained that BOA is formed from the aglucone by the liberation of formic acid.

A proof for structure II for the aglucone was obtained by reducing the oxime group to the imido group (III) [4]. This compound was synthesized by Honkanen and Virtanen [5] from *ortho*(dichloroacetamido)-phenol by heating in a dilute sodium bicarbonate solution. Recently Honkanen and Virtanen [6] also succeeded in synthesizing the aglucone, and thus proved its structure.

Wahlroos and Virtanen [7] have described the isolation of the glucoside and aglucone from maize plants and demonstrated that these precursors of MBOA have anologous structures to those of the precursors of BOA in rye plants.

The spectroscopic identification of precursor II (the aglucone) of BOA in the press juice of rye plants. 5 ml of juice were pressed from 13 g of 8-day-old rye seedlings. The juice was heated in a water bath for 2 min (the temperature rose to about 70°C) to coagulate proteins. No noticeable amount of BOA was formed by this treatment. The juice was filtered through a hard filter paper. The clear solution was pipetted into two test tubes, 2 ml into each. The one was heated in a water bath for 1 h. Both water solutions were extracted four times with 2 ml of ether. Five different samples were then obtained: 1. The original juice. 2. The ether extract obtained from the juice heated for 1 h. 3. The water solution of the above. 4. The ether extract obtained from the unheated juice. 5. The water solution of the above.

All the solutions were diluted with water to 1:100 (the ether had been evaporated before this at room temperature). The curves in Fig. 1 show the UV-absorption curves of the solutions. Water was used as control solution in all measurements.

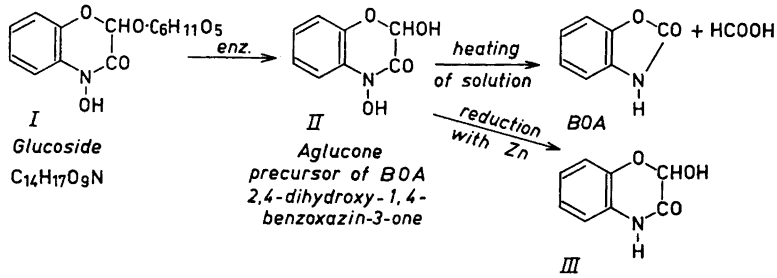

The examination of the spectra: The ether extract spectra of the heated and the unheated juice differ completely from each other. Spectrum 2 is that of BOA (max. 270 mμ and min. 245 mμ). If spectra 4 (ether extract) and 5 (water solution after ether extraction), obtained from the unheated juice, are summed, a spectrum nearly identical with spectrum 1 is obtained. This is not the case if spectra 2 and 3 are summed. Spectrum 4 is thus derived from the substance from which BOA is formed on heating the water solution.

In agreement with the spectroscopic investigation reported above, a paper chromatographic analysis (*iso*propanol:ammonia:

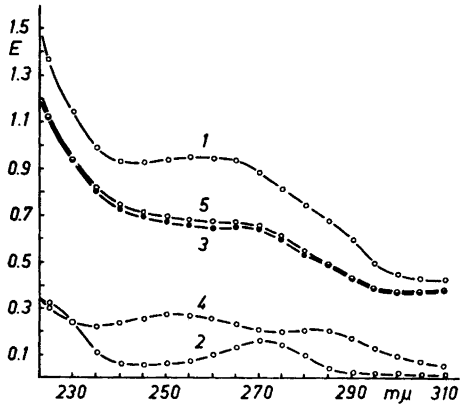

Fig. 1. UV spectra of solutions 1—5 mentioned in the text.

water 8:1:1, Whatman No. 4 paper) of solutions 1—5 showed that a substance (R_F 0.23) is found in ether extract 4. This substance had disappeared in ether extract 2, which on the other hand contained the BOA spot moving near the solvent front. When again it was found that the ether-soluble precursor II is not present in intact rye seedlings if these are placed in boiling water or ethanol, it was obvious that the substance was formed enzymatically from the primary precursor on crushing. This substance was found to be a glucoside and precursor II the aglucone formed from it.

The isolation of the aglucone. 1 190 g of rye seedlings (Pekka), grown for 7 days in the light, were ground. The mass was allowed to stand for 1 h at room temperature to ensure the enzymatic decomposition of the glucoside (in fact the hydrolysis took place very rapidly). The mass was vigorously pressed, and 850 ml of juice was obtained. The juice was kept in two bottles in a water bath for 4 min during which the temperature rose to about 70°C. The filtered, clear solution was shaken twice with ether, twice with *n*-butanol, and finally twice with ether. The combined ether and butanol solutions were evaporated to dryness *in vacuo* (the temperature did not rise above 20°C). The residue was dissolved in 100 ml of water, the solution was shaken 3 times with 100 ml of ether. The ether solutions were evaporated, and 75 ml of ether was added to the residue. The unsoluble, reddish substance was filtered off, 250 mg of active charcoal was added, the mass was shaken, and the charcoal was filtered off after standing. 40 ml of *cyclo*hexane was added to the solution, and it was evaporated *in vacuo* until crystallization began. The crystals were separated, washed with *cyclo*hexane, and dried at low temperature. They were recrystallized in the same way from a mixture of ether and *cyclo*hexane, washed with *cyclo*hexane, and finally dried at 100°C. Yield 428 mg; m. p. 152°.

Properties of the aglucone

1. *Analysis.* Found: C 53.40; H 3.98; N 7.40; O 33.15. Calc. for $C_8H_7O_4N$: C 53.04; H 3.90; N 7.73; O 35.33.

2. It gives a strong blue-violet colour with $FeCl_3$.

3. Its R_F value with *iso*propanol-ammonia-water 8:1:1 is 0.23.

4. Formic acid and BOA are rapidly formed when a dilute water solution of the aglucone is heated in a sealed tube in a water bath. A strong formic acid reaction was obtained with chromotropic acid. Formic acid was determined quantitatively by a fractionated steam distillation.

5. It does not react with 2,4-dinitrophenylhydrazine at room temperature. Upon heating a dark precipitate is formed. This has not been further investigated.

6. A potentiometric titration with 0.0200 N NaOH gave 190 as the equivalent weight and a $pK = 7.02$ (calculated from the curve). On titration with acid no clear equivalent point could be noticed and hence the aglucone does not consume acid in the pH range of the titration. This indicates that it has not a betaine structure.

7. By paper chromatography *ortho*-aminophenol was found to be formed as the main

product on strong hydrolysis with hydrochloric acid. This compound was extracted with ether from the hydrolysate neutralized with $NaHCO_3$ and identified by the UV-spectrum. *Ortho*-aminophenol was formed also on alkali fusion.

8. Hydroxylamine is a product of strong acid hydrolysis.

9. On reduction with hydrogen iodide and red phosphorus (62 mg of substance, 30 mg of red phosphorus, and 0.5 ml of hydrogen iodide, heating for 4 h at 170°C) *ortho*-aminophenol and a smaller amount of glycine (about 3 to 4 mg) were formed. Amino compounds were separated in an Amberlite IR-120 column. *Ortho*-aminophenol was separated by ether extraction from the ammonia eluate, from which ammonia was evaporated *in vacuo*, and identified by the UV-spectrum. Glycine was identified in the remaining water solution on a two-dimensional paper chromatogram. Other amino acid spots were not observed.

10. Methylation with dimethylsulphate (73 mg of substance and a five-fold excess of dimethylsulphate) led to a reaction product which after ether extraction was recrystallized from water, m. p. 84–85°. Its UV-spectrum greatly resembled that of BOA. (Found: N 9.82. Calc. for $C_8H_7O_2N$: N 9.40.) The substance obtained is probably N-methylbenzoxazolinone, the m. p. of which has been reported to be 86°.

11. Reduction with zinc and hydrochloric acid (123 mg of aglucone, 2 g of zinc dust, and 0.1 ml of 1 % ferric chloride solution; dropwise addition of concentrated hydrochloric acid until the ferric chloride reaction disappeared) led to a reduction product with m. p. 198° without recrystallization, and 201–203° (corr.)[5] after recrystallization. Mol. wt. (Rast) 167; calc. for $C_8H_7O_3N$: 165. Since the substance no longer gives any colour reaction with ferric chloride, the NOH group has apparently been reduced to NH. The UV-spectrum of the reduction product is shown in Fig. 2.

12. The aglucone did not consume hydrogen on catalytic hydrogenation with platinum in ethanol solution.

Conclusions: The results mentioned in paragraphs 7 and 9 can be understood only if nitrogen and carbon atoms outside the benzene ring are in the order —N—C—C—, and the nitrogen atom is attached to a carbon atom in the benzene ring. The formation of glycine in paragraph 9 is possible only if two oxygen atoms are bound to the terminal carbon atom.

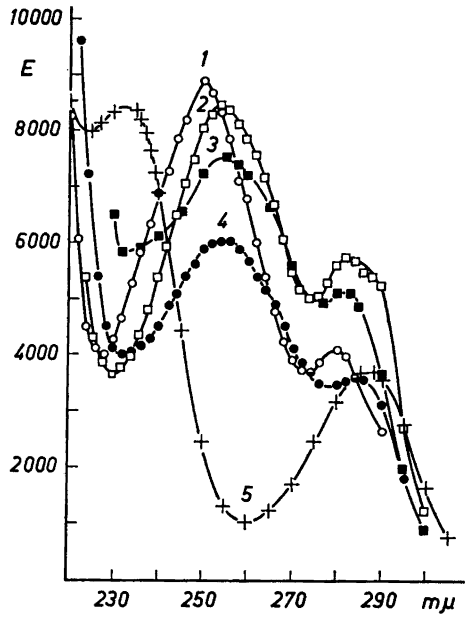

Fig. 2. UV spectra in ethanol solutions of

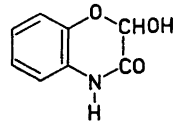

1. reduced aglucone,

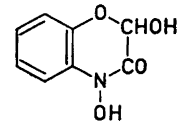

2. aglucone,

3. glucoside $C_{14}H_{17}O_9N$,

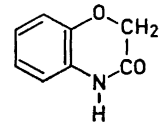

4. 2H-1,4-benzoxazin-3-(4H) one (synth.),

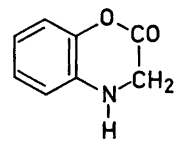

5. 3H-1,4-benzoxazin-2-(4H) one (synth.).

The formation of hydroxylamine mentioned in paragraph 8 and the positive Feigl-Amaral test [8] for an N—O bond suggests that the hydroxyl group is combined with the nitrogen atom and that the aglucone is a hydroxylamine derivative.

Taking into account these conclusions and the elementary composition of the aglucone, the possibility of an aliphatic side chain in the aglucone is ruled out, and a ring formed of nitrogen, carbon, and oxygen atoms is indicated. Structure II was suggested for the aglucone. This structure was supported by the similarity of the UV-spectra of the aglucone and its reduction product with 2H-1,4-benzoxazin-3-(4H) one synthesized by us (Fig. 2).

The structure of the aglucone could later be confirmed by synthesis by Honkanen and Virtanen [5,6], as already mentioned in this paper.

The support given by the *Rockefeller Foundation* is gratefully acknowledged.

1. Virtanen, A. I. and Hietala, P. K. *Acta Chem. Scand.* **9** (1955) 1543; Virtanen, A. I., Hietala, P. K. and Wahlroos, Ö. *Arch. Biochem. Biophys.* **69** (1957) 486; Virtanen, A. I. *Angew. Chem.* **70** (1958) 544.
2. Virtanen, A. I. and Wahlroos, Ö. *Suomen Kemistilehti B* **31** (1958) 402; Virtanen, A. I. and Hietala, P. K. *Ibid.* **32** (1959) 38.
3. Virtanen, A. I. and Hietala, P. K. *Suomen Kemistilehti B* **32** (1959) 139.
4. Virtanen, A. I. and Hietala, P. K. *Ibid.* **32** (1959) 252.
5. Honkanen, E. and Virtanen, A. I. *Ibid.* **33** (1960) 9.
6. Honkanen, E. and Virtanen, A. I. *Acta Chem. Scand.* **14** (1960) 504.
7. Wahlroos, Ö. and Virtanen, A. I. *Suomen Kemistilehti B* **32** (1959) 139.
8. Feigl, F. and Amaral, J. R. *Microchim. Acta* **1958** 337.

Received February 25, 1960.

Precursors of Benzoxazolinone in Rye Plants

II. Precursor I, the Glucoside

PENTTI K. HIETALA and
ARTTURI I. VIRTANEN

Laboratory of the Foundation for Chemical Research, Biochemical Institute, Helsinki, Finland

The identification and isolation of precursor I (the glucoside). As reported in previous communications [1], the glucoside $C_{14}H_{17}O_9N$ was isolated from rye seedlings. It is a primary compound present in intact rye plants. The aglucone $C_8H_7O_4N$ which is the immediate precursor of benzoxazolinone (BOA) is formed from the glucoside enzymatically.

225 g of 10-day-old seedlings of Pekka rye were put into 1.5 l of boiling water, the solution was decanted, filtered, and evaporated to 250 ml *in vacuo*. Ether-soluble substances were removed by extraction, and a chromatogram was made from the water solution with water-saturated butanol. 150 μl were pipetted on the starting spot. The dark spot, R_F 0.57, visible in UV light, represented the glucoside sought, from which precursor II is formed enzymatically. The spectrum of the substance is very similar to that of the aglucone.

The isolation of larger amounts of the substance was performed by counter-current extraction, using the butanol-water solvent system. In another connection, one of us (H) will give a detailed account of the isolation. The m. p. of the glucoside was 186.5—187°C (uncorr.). R_F 0.57 in water-saturated *n*-butanol. (Found: C 49.04; H 4.98; N 3.81; O 41.04. Calc. for $C_{14}H_{17}O_9N$: C 48.98; H 4.99; N 4.08; O 41.95.) UV spectrum (in ethanol). Glucoside: max. 255 mμ, ε = 7 570, max. 281 mμ, ε = 5 160. Aglucone: max. 254 mμ, ε = 8 500, max. 282 mμ, ε = 5 800. The curves of the UV spectra are presented in the paper of Virtanen and Hietala [1].

The UV spectra of the glucoside and the aglucone are very similar. Already from this it was probable that the structure of the free aglucone was the same as that bound to the sugar glucosidically. This concept was supported by all other observations. Some of these which elucidate the

The formation of hydroxylamine mentioned in paragraph 8 and the positive Feigl-Amaral test [8] for an N—O bond suggests that the hydroxyl group is combined with the nitrogen atom and that the aglucone is a hydroxylamine derivative.

Taking into account these conclusions and the elementary composition of the aglucone, the possibility of an aliphatic side chain in the aglucone is ruled out, and a ring formed of nitrogen, carbon, and oxygen atoms is indicated. Structure II was suggested for the aglucone. This structure was supported by the similarity of the UV-spectra of the aglucone and its reduction product with 2H-1,4-benzoxazin-3-(4H) one synthesized by us (Fig. 2).

The structure of the aglucone could later be confirmed by synthesis by Honkanen and Virtanen [5,6], as already mentioned in this paper.

The support given by the *Rockefeller Foundation* is gratefully acknowledged.

1. Virtanen, A. I. and Hietala, P. K. *Acta Chem. Scand.* **9** (1955) 1543; Virtanen, A. I., Hietala, P. K. and Wahlroos, Ö. *Arch. Biochem. Biophys.* **69** (1957) 486; Virtanen, A. I. *Angew. Chem.* **70** (1958) 544.
2. Virtanen, A. I. and Wahlroos, Ö. *Suomen Kemistilehti B* **31** (1958) 402; Virtanen, A. I. and Hietala, P. K. *Ibid.* **32** (1959) 38.
3. Virtanen, A. I. and Hietala, P. K. *Suomen Kemistilehti B* **32** (1959) 139.
4. Virtanen, A. I. and Hietala, P. K. *Ibid.* **32** (1959) 252.
5. Honkanen, E. and Virtanen, A. I. *Ibid.* **33** (1960) 9.
6. Honkanen, E. and Virtanen, A. I. *Acta Chem. Scand.* **14** (1960) 504.
7. Wahlroos, Ö. and Virtanen, A. I. *Suomen Kemistilehti B* **32** (1959) 139.
8. Feigl, F. and Amaral, J. R. *Microchim. Acta* **1958** 337.

Received February 25, 1960.

Precursors of Benzoxazolinone in Rye Plants

II. Precursor I, the Glucoside

PENTTI K. HIETALA and
ARTTURI I. VIRTANEN

Laboratory of the Foundation for Chemical Research, Biochemical Institute, Helsinki, Finland

The identification and isolation of precursor I (the glucoside). As reported in previous communications [1], the glucoside $C_{14}H_{17}O_9N$ was isolated from rye seedlings. It is a primary compound present in intact rye plants. The aglucone $C_8H_7O_4N$ which is the immediate precursor of benzoxazolinone (BOA) is formed from the glucoside enzymatically.

225 g of 10-day-old seedlings of Pekka rye were put into 1.5 l of boiling water, the solution was decanted, filtered, and evaporated to 250 ml *in vacuo*. Ether-soluble substances were removed by extraction, and a chromatogram was made from the water solution with water-saturated butanol. 150 μl were pipetted on the starting spot. The dark spot, R_F 0.57, visible in UV light, represented the glucoside sought, from which precursor II is formed enzymatically. The spectrum of the substance is very similar to that of the aglucone.

The isolation of larger amounts of the substance was performed by counter-current extraction, using the butanol-water solvent system. In another connection, one of us (H) will give a detailed account of the isolation. The m. p. of the glucoside was 186.5—187°C (uncorr.). R_F 0.57 in water-saturated *n*-butanol. (Found: C 49.04; H 4.98; N 3.81; O 41.04. Calc. for $C_{14}H_{17}O_9N$: C 48.98; H 4.99; N 4.08; O 41.95.) UV spectrum (in ethanol). Glucoside: max. 255 mμ, ε = 7 570, max. 281 mμ, ε = 5 160. Aglucone: max. 254 mμ, ε = 8 500, max. 282 mμ, ε = 5 800. The curves of the UV spectra are presented in the paper of Virtanen and Hietala [1].

The UV spectra of the glucoside and the aglucone are very similar. Already from this it was probable that the structure of the free aglucone was the same as that bound to the sugar glucosidically. This concept was supported by all other observations. Some of these which elucidate the

chemical nature of the glucoside are reported in the following (*cf.* the corresponding observations made on the aglucone [1]).

A potentiometric titration with 0.0200 N NaOH gave equiw.wt. 338 (calc. 343). The p*K* calculated from the curve was 6.67. Titration with acid showed that the structure of the glucoside cannot be betainic. The result was thus the same as with the aglucone.

With $FeCl_3$ the glucoside gave an intensely violet colour, as did the aglucone.

On hydrolysis with 1 N HCl (100°C, 3 h) the largest part of the glucoside remained unchanged. The glucoside is accordingly rather stable on acid hydrolysis. A sugar which gave a weak reaction with aniline phthalate on paper chromatograms was found in the solution. Using three different solvent systems (water-saturated *n*-butanol, *iso*-propanolwater 16:4, phenol-water-NH_3), this sugar travelled as glucose.

Ortho-aminophenol was formed on strong acid hydrolysis (89 mg of glucoside and 1 ml of conc. HCl in a sealed tube for 40 h at 100°C). It was extracted with ether from a solution neutralized with $NaHCO_3$. Hydroxylamine could be found in the hydrolysate, and the qualitative Feigl-Amaral reaction for the N—O bond was positive. The result was thus the same as with the aglucone.

Ortho-aminophenol was formed as the main product on alkali fusion (4.1 mg of glucoside, 371 mg of KOH, and 0.1 ml of water, the temperature was raised to 200°C in 30 min). It was isolated in crystalline form and identified by paper chromatography, mixed m. p., and UV spectrum.

The same products as with the aglucone were also obtained on reduction with HI (*d* 1.96) and red phosphorus at 170—180°C, using reaction times of 2, 4, and 10 h. *Ortho*-aminophenol was identified by the UV spectrum. Glycine was found by amino acid chromatography.

The number of acetylating hydroxyl groups was determined in a pyridine solution by titrating the acetic acid formed from the excess acetanhydride. About five OH groups per mole were found.

The hydrolysis of the glucoside by a homogenate of rye seedlings leads to the formation of the aglucone and glucose. The aglucone can be extracted from the water solution by ether.

The above observations on the glucoside indicate that no rearrangement takes place in the molecule during hydrolysis. Since on the basis of the $FeCl_3$ reaction there is still a free NOH group in the glucoside, the glucose has to be bound to the OH group which is attached to carbon atom 2 in the heterocyclic ring. The structure of the glucoside is accordingly the following.

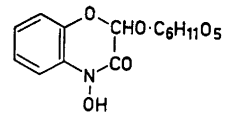

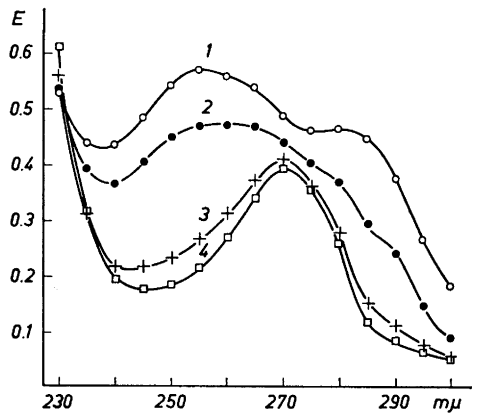

Fig. 1. UV spectra of the raw aglucone preparation from rye seedlings. A dilute solution was heated in a water bath for 2 min (2), 6 min (3), and 60 min (4). 1 was not heated.

The quantitative determination of the glucoside in rye seedlings. Since the glucoside is rapidly hydrolysed to the aglucone in crushed rye seedlings, it can be determined by the UV spectrum of the aglucone extracted by ether. A quantitative method has not, however, been developed yet for the estimation of the aglucone. On the other hand, a method has been developed by the present authors [2] for the determination of BOA formed rapidly from the aglucone at 100°C. The transfer of the aglucone into BOA in very dilute solutions is an extremely rapid reaction as shown in Fig. 1. Already at 50°C a slow formation of BOA can be observed. The kinetics of this complicated reaction has not been investigated closely, but it seems that the relative amount of BOA formed from the aglucone

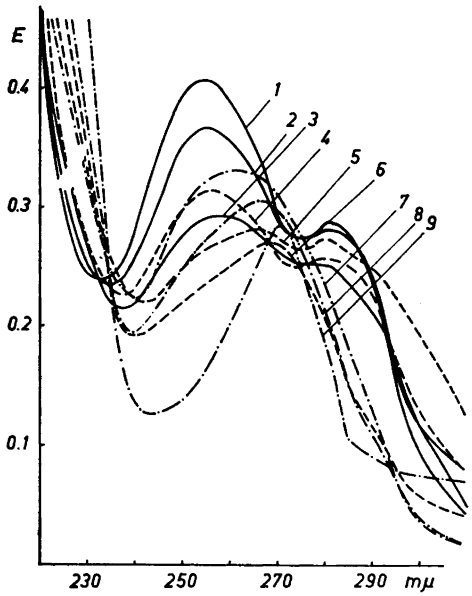

Fig. 2. UV spectra of water solutions of the aglucone of different concentrations heated at 100°C. Aglucone, max. 254 mμ, 282 mμ; BOA max. 270 mμ.

1. 10 mg/ml 5 min, *2.* 15 min, *3.* 60 min, *4.* 300μg/ml 5 min, *5.* 15 min, *6.* 60 min, *7.* 10 μg/ml 5 min, *8.* 15 min, *9.* 60 min.

decreases when the aglucone concentration rises. This is shown by the following test.

The aglucone was heated in a test tube in a boiling water bath at concentrations of 10 mg/ml, 300 μg/ml, and 10 μg/ml for 5 min, 15 min, and 1 h. For the measurement of spectra the first solution was diluted 1:1 000 and the second 1:30, and the most dilute solution was measured as such. Fig. 2 shows the changes occurring in the spectra of the different solutions.

When a relatively short reaction time is used, the formation of BOA can therefore be followed by spectrophotometry only in very dilute solutions of the aglucone.

The highest values found in this laboratory for BOA in rye seedlings have been about 1.1 mg of BOA per g fresh weight[3], corresponding to 2.8 mg of the glucoside if the yield is quantitative. The quantitativeness of the yield depends decisively on how thoroughly the plant material is crushed. A 90 % yield of BOA is more probable when plant material (0.5—1 g) is crushed in a mortar. The hydrolysis of the glucoside in a homogenate of rye seedlings is rapid. For the sake of safety it is best to allow the homogenate to stand at room temperature for 30 min before heating.

The support given by the *Rockefeller Foundation* is gratefully acknowledged.

1. *cf.* Virtanen, A. I. and Hietala, P. K. *Acta Chem. Scand.* **14** (1960) 499.
2. Hietala, P. K. and Virtanen, A. I. *Acta Chem. Scand.* **12** (1958) 119.
3. *cf.* Virtanen, A. I. *Angew. Chem.* **70** (1958) 544.

Received February 25, 1960.

The Synthesis of Precursor II of Benzoxazolinone Formed in Rye Plants, and the Enzymic Hydrolysis of Precursor I, the Glucoside

ERKKI HONKANEN and ARTTURI I. VIRTANEN

Laboratory of the Foundation for Chemical Research, Biochemical Institute, Helsinki, Finland

In earlier papers Virtanen *et al.*[1,2] have presented the structure 2,4-dihydroxy-1,4-benzoxazin-3-one (I) for the aglucone enzymatically formed in crushed rye seedlings. The structure is now confirmed by the synthesis of the aglucone itself and its reduction product (II), which is obtained by reduction with zinc dust in boiling acetic acid[3].

The starting material for the synthesis of the aglucone was *o*-(methoxymethoxy)-nitrobenzene (III), from which the corresponding phenylhydroxylamine derivative (IV) is prepared in the usual way by reduction with zinc dust in a neutral medium. By allowing this compound to react with dichloroacetylchloride, N-(*o*-methoxymethoxyphenyl)-dichloroacethydroxamic acid (V) is obtained. The methoxymethoxy group is then hydrolysed by heating in a dilute methanolic hydrochloric acid solution. Finally the compound formed (VI) is

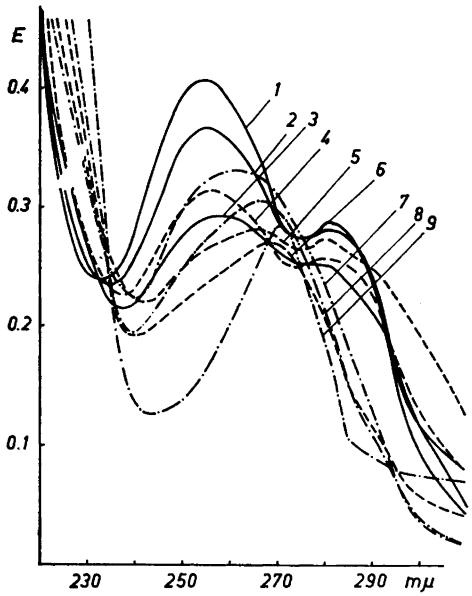

Fig. 2. UV spectra of water solutions of the aglucone of different concentrations heated at 100°C. Aglucone, max. 254 mμ, 282 mμ; BOA max. 270 mμ.

1. 10 mg/ml 5 min, *2.* 15 min, *3.* 60 min, *4.* 300μg/ml 5 min, *5.* 15 min, *6.* 60 min, *7.* 10 μg/ml 5 min, *8.* 15 min, *9.* 60 min.

decreases when the aglucone concentration rises. This is shown by the following test.

The aglucone was heated in a test tube in a boiling water bath at concentrations of 10 mg/ml, 300 μg/ml, and 10 μg/ml for 5 min, 15 min, and 1 h. For the measurement of spectra the first solution was diluted 1:1 000 and the second 1:30, and the most dilute solution was measured as such. Fig. 2 shows the changes occurring in the spectra of the different solutions.

When a relatively short reaction time is used, the formation of BOA can therefore be followed by spectrophotometry only in very dilute solutions of the aglucone.

The highest values found in this laboratory for BOA in rye seedlings have been about 1.1 mg of BOA per g fresh weight[3], corresponding to 2.8 mg of the glucoside if the yield is quantitative. The quantitativeness of the yield depends decisively on how thoroughly the plant material is crushed. A 90 % yield of BOA is more probable when plant material (0.5—1 g) is crushed in a mortar. The hydrolysis of the glucoside in a homogenate of rye seedlings is rapid. For the sake of safety it is best to allow the homogenate to stand at room temperature for 30 min before heating.

The support given by the *Rockefeller Foundation* is gratefully acknowledged.

1. *cf.* Virtanen, A. I. and Hietala, P. K. *Acta Chem. Scand.* **14** (1960) 499.
2. Hietala, P. K. and Virtanen, A. I. *Acta Chem. Scand.* **12** (1958) 119.
3. *cf.* Virtanen, A. I. *Angew. Chem.* **70** (1958) 544.

Received February 25, 1960.

The Synthesis of Precursor II of Benzoxazolinone Formed in Rye Plants, and the Enzymic Hydrolysis of Precursor I, the Glucoside

ERKKI HONKANEN and ARTTURI I. VIRTANEN

Laboratory of the Foundation for Chemical Research, Biochemical Institute, Helsinki, Finland

In earlier papers Virtanen *et al.*[1,2] have presented the structure 2,4-dihydroxy-1,4-benzoxazin-3-one (I) for the aglucone enzymatically formed in crushed rye seedlings. The structure is now confirmed by the synthesis of the aglucone itself and its reduction product (II), which is obtained by reduction with zinc dust in boiling acetic acid[3].

The starting material for the synthesis of the aglucone was *o*-(methoxymethoxy)-nitrobenzene (III), from which the corresponding phenylhydroxylamine derivative (IV) is prepared in the usual way by reduction with zinc dust in a neutral medium. By allowing this compound to react with dichloroacetylchloride, N-(*o*-methoxymethoxyphenyl)-dichloroacethydroxamic acid (V) is obtained. The methoxymethoxy group is then hydrolysed by heating in a dilute methanolic hydrochloric acid solution. Finally the compound formed (VI) is

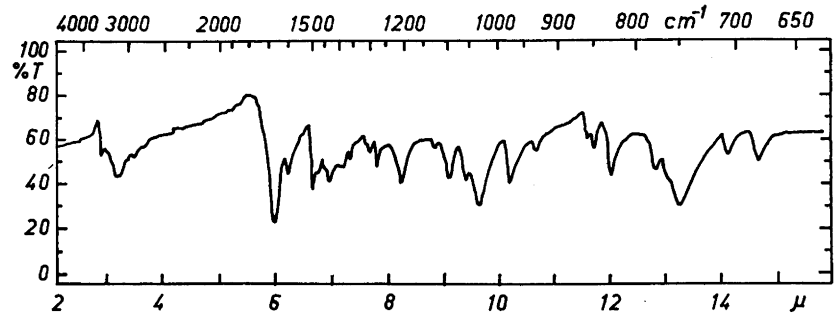

Fig. 1. The IR spectrum of the synthetic and the natural aglucone.

dissolved in a sodium hydroxide solution and allowed to stand for some time at room temperature, whereby hydrolysis and cyclisation to 2,4-dihydroxy-1,4-benzoxazin-3-one(I) occurs.

The synthesis of the reduction product [3] is carried out by an analogous procedure. The starting material was now *o*-aminophenol (VII), from which the N-dichloroacetyl derivative (VIII) is prepared. When this compound is dissolved in a dilute sodium hydrogencarbonate solution and boiled for a short time, the 2-hydroxy-1,4-benzoxazin-3-one (II) is formed.

The identity of these compounds with the aglucone and its reduction product were confirmed by the mixed melting points, the UV and the IR spectra. Fig. 1 shows the IR spectrum of the synthetic aglucone. The IR spectrum of the natural aglucone is identical with the spectrum in the figure. The spectrum is in accord with the structure proposed by Virtanen and Hietala for the aglucone.

When the glucoside, also isolated from rye seedlings, was reduced by an analogous procedure as the aglucone, a substance (X) is obtained, which also did not give any colour reaction with ferric chloride. On the basis of the similarity of its UV spectra with that of the reduction product of the aglucone, the structure (X) can be suggested for this compound and the structure (IX) for the glucoside. The attempts to synthesize the compound (X) from the reduction product (II) and acetobromoglucose failed.

All melting points are corrected.

o-(Methoxymethoxy)-nitrobenzene. A mixture of 5.31 g of dry potassium salt of *o*-nitrophenol and 2.5 g of chloromethyl-

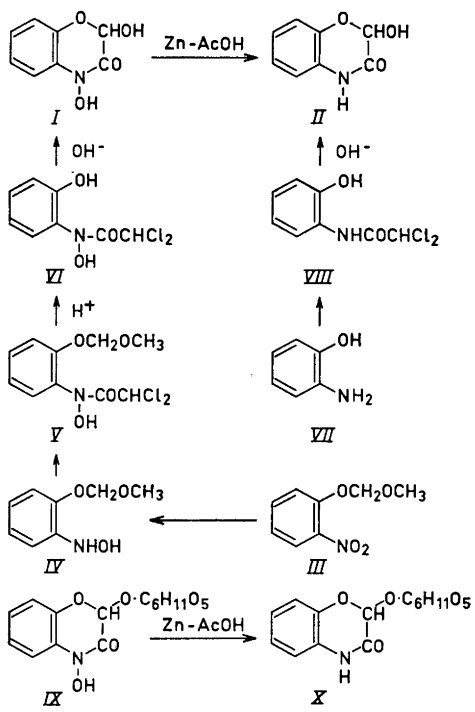

methylether [4] in 15 ml of dry benzene was refluxed for one hour. The benzene solution was then washed several times with dilute sodium hydroxide solution and dried over sodium sulphate. The solvent was evaporated and the residue distilled in a vacuum. The yield was 3.9 g (71 %). B. p. 134—135°/7 mm. (Found: N 7.74. Calc. for $C_8H_9NO_4$: N 7.65.)

o-(Methoxymethoxy)-phenylhydroxylamine. A solution of 3.66 g of *o*-(methoxymethoxy)-nitrobenzene and 2.0 g of ammonium chloride in 50 ml of 60 % alcohol was cooled below 10°C. To this solution 2.0 g of zinc dust were added in the course of half an hour with stirring. The solution was filtered and 50 ml of water were added, and then extracted with ether. The ether solution was dried and the solvent evaporated. The residue (3.3 g) was a yellow oil which did not crystallize. It was used without further purification for the following reaction.

2,4-Dihydroxy-1,4-benzoxazin-3-one. To a solution of 3.3 g of the crude *o*-(methoxymethoxy)-phenylhydroxylamine in 50 ml of dry ether 1.45 g of dichloroacetylchloride in 20 ml of ether were gradually added under cooling (0°C). The ether solution was decanted from the dark brown oil and evaporated to dryness. The residue was dissolved in 20 ml of methanol and 2 ml of 2 N hydrochloric acid and refluxed for half an hour. The solvent was evaporated under reduced pressure, and the residue was dissolved in 20 ml of 1 N sodium hydroxide solution, and allowed to stand for 2 h at room temperature. After addition of dilute hydrochloric acid to the acid reaction, the solution was filtered and extracted first several times with benzene (to remove the coloured impurities) and then with ether. The ether solution was dried and the solvent evaporated. The residue was dissolved in a few ml of 0.5 N hydrochloric acid and extracted several times with benzene. The water solution was filtered and then extracted with ether. After drying, the solvent was evaporated and the residue crystallized from a mixture of ether-benzene. The overall yield was 61 mg (3.5 %). M. p. 153–154° C, mixed m. p. 151–152°C with the aglucone (m. p. 151–152°C).

UV spectrum (in ethanol).

Synthetic product: max. 255 mμ, ε = 8 850; max. 282 mμ, ε = 5 880.

Aglucone: max. 254 mμ, ε = 8 500; max. 282 mμ, ε = 5 800.

Reduction of the aglucone: 48 mg of the aglucone were dissolved in 20 ml of glacial acetic acid, and 100 mg of zinc dust were added. The mixture was boiled for 15 min and excess zinc was filtered off. The acetic acid was evaporated under reduced pressure, and the residue was crystallized from an ether-benzene mixture. Yield 25 mg (57 %). M. p. 201–203°C. UV spectrum (in ethanol): Max. 250 mμ, ε = 8 900, max. 282 mμ, ε = 4 350. (Found: C 58.23 H 4.45; O 28.82. Calc. for $C_8H_7NO_3$: C 58.18; H 4.27; O 29.06.)

o-(Dichloroacetamido)-phenol. To a solution of 2.18 g of pure *o*-aminophenol in dry ether 1.5 g of dichloroacetylchloride in ether were added gradually. After standing for one hour at room temperature, the precipitated *o*-aminophenol hydrochloride was filtered off, and the filtrate evaporated to dryness, whereat the product crystallizes. After recrystallization from a mixture of benzene-petroleum ether the m. p. was 134–135°C and the yield 1.7 g (77 %). (Found: N 6.20. Calc. for $C_8H_7Cl_2NO_2$: N 6.37.)

The synthesis of the reduction product. 220 mg of *o*-(dichloroacetamido)-phenol and 10 ml of 0.2 M $NaHCO_3$ solution were boiled for 10 min. The solution was cooled and made slightly acid with hydrochloric acid and extracted with ether. The ether solution was dried, a few ml of benzene were added, and most of the ether was evaporated, upon which the product crystallizes. M. p. 201–203°C. Yield 124 mg (75 %). Mixed m. p. 201–203°C with the reduction product of the aglucone. UV spectrum (in ethanol): Max. 250 mμ, ε = 8 850, max. 282 mμ, ε = 4 400.

Reduction of the glucoside. To a boiling solution of 10 mg of the glucoside in 5 ml of acetic acid 25 mg of zinc dust were added. After boiling for 15 min, the excess zinc was filtered off. The acetic acid was evaporated under reduced pressure, and the residue was dissolved in a few ml of water. The zinc was then precipitated as sulphide. After filtration the solution was evaporated to dryness and the residue was dissolved in absolute alcohol. Benzene was added, and the alcohol was distilled off, upon which the product crystallized. M. p. 158–160°C. (Found: N 4.12. Calc. for $C_{14}H_{17}NO_8$: N 4.28.) UV spectrum (in ethanol): Max. 250 mμ, ε = 7 500, max. 278 mμ, ε = 3 800.

The hydrolysis of the glucoside occurs rapidly through an enzyme present in rye seedlings, as previously shown in this laboratory. The enzyme has not been purified or further investigated yet. The glucoside was not hydrolysed by yeast in our experiments. On the other hand, hydrolysis of the glucoside was observed in a homogenate of the small intestine of the rabbit, although a much weaker one than in rye seedlings. A homogenate of rat intestine had much the same effect as that

of the rabbit. From these observations we may conclude that the glucoside can be decomposed in the animal organism without the enzyme present in plants.

The support given by the *Rockefeller Foundation* is gratefully acknowledged.

1. Virtanen, A. I. and Hietala, P. K. *Suomen Kemistilehti B* **32** (1959) 252.
2. Wahlroos, Ö. and Virtanen, A. I. *Acta Chem. Scand.* **13** (1959) 1906.
3. Honkanen, E. and Virtanen, A. I. *Suomen Kemistilehti B* **33** (1960) 9.
4. Marvel, C. S. and Porter, P. K. *Org. Syntheses Coll.* **Vol. I** (1946) 377.

Received February 25, 1960.

The Enzymic Formation of Thiocyanate (SCN^-) from a Precursor(s) in *Brassica* Species

ROLF GMELIN and ARTTURI I. VIRTANEN

Laboratory of the Foundation for Chemical Research, Biochemical Institute, Helsinki, Finland

The chemical nature of the goitrogenic "*Brassica* factors" is still unclear to a great extent. This is partly due to the fact that several active factors may be involved, which are moreover formed only through enzymic reactions when plants are crushed. This has long been known in regard to the formation of the strongly goitrogenic thiooxazolidones occurring in the crushed and moistened seeds of many crucifers [1]. Recently Virtanen *et al.*[2], and Kreula and Kiesvaara [3] found the formation of vinyl-thiooxazolidone also in cabbage, kale, rape, and other fodder plants belonging to the *Cruciferae* family.

The same authors [4] have also demonstrated the transfer of this substance to milk in very small amounts (about 0.05 % of the amount fed). These quantities are so small that they cannot be expected to have any goitrogenic effect in the milk. Kreula and Kiesvaara [4] have given a detailed report on the methods used in these investigations. Somewhat later Altamura *et al.*[5] independently also demonstrated the formation of vinyl-thiooxazolidone in cabbage.

The goitrogenic effect of thiooxazolidones is due to the fact that they inhibit the synthesis of thyroid hormones. This effect cannot be overcome by high doses of iodide.

Another type of goitrogenic substances belonging to the *Brassica* factors has a primary influence on the uptake of iodide by the thyroid gland. This influence can be prevented by increasing the amount of the iodide dose. Many pieces of information given in the literature [6,7] indicate that salts of thiocyanic acid (SCN^-) represent this type in crucifers. Jirousek [8], who has investigated and reviewed the thiocyanate metabolism, found that in the animal organism SCN^- is formed endogenously from cyanides, nitriles, and sulphur-containing compounds, and that both the SCN^- brought exogenously into the organism and that formed endogenously in it have to be taken into consideration as goitrogenic factors. Michajlovskij and Langer [9,10] have performed systematic determinations on the SCN^- content in different vegetables. They found a particularly high SCN^- content in the press juice of different cabbage species (up to 50 mg %). They used the term "präformiertes Rhodanid" for the SCN^- present in food stuffs, obviously in contrast to the SCN^- formed endogenously.

Our investigations concerning the problem whether it is possible to make milk goitrogenic by feeding cows with plants, especially those belonging to the *Cruciferae*, have led to some new findings regarding the *Brassica* factors. These findings are briefly reported in the present paper.

An account was recently given about the formation of organic thiocyanates in some crucifers [11]. Benzyl thiocyanate was found to be formed enzymatically from glucotropaeolin in *Lepidium ruderale* and allyl thiocyanate from sinigrin in *Thlaspi arvense*. It was found in this laboratory that after the injection of benzyl thiocyanate into rats, the SCN^- content has risen considerably in blood serum and in different organs. This finding led us to look for thiocyanate esters also in *Brassica oleracea* species. For the present we have, however, no indications for the formation of such esters in fresh cabbage species. On the other hand, the result of these investigations was the finding that free SCN^- is formed from glucosidic precursors, present in cabbage. The thiocyanate found by Michajlovskij and Langer in the press juice of cabbage is thus not "preformed SCN^-"

of the rabbit. From these observations we may conclude that the glucoside can be decomposed in the animal organism without the enzyme present in plants.

The support given by the *Rockefeller Foundation* is gratefully acknowledged.

1. Virtanen, A. I. and Hietala, P. K. *Suomen Kemistilehti B* **32** (1959) 252.
2. Wahlroos, Ö. and Virtanen, A. I. *Acta Chem. Scand.* **13** (1959) 1906.
3. Honkanen, E. and Virtanen, A. I. *Suomen Kemistilehti B* **33** (1960) 9.
4. Marvel, C. S. and Porter, P. K. *Org. Syntheses Coll.* **Vol. I** (1946) 377.

Received February 25, 1960.

The Enzymic Formation of Thiocyanate (SCN^-) from a Precursor(s) in *Brassica* Species

ROLF GMELIN and ARTTURI I. VIRTANEN

Laboratory of the Foundation for Chemical Research, Biochemical Institute, Helsinki, Finland

The chemical nature of the goitrogenic "*Brassica* factors" is still unclear to a great extent. This is partly due to the fact that several active factors may be involved, which are moreover formed only through enzymic reactions when plants are crushed. This has long been known in regard to the formation of the strongly goitrogenic thiooxazolidones occurring in the crushed and moistened seeds of many crucifers [1]. Recently Virtanen *et al.*[2], and Kreula and Kiesvaara [3] found the formation of vinyl-thiooxazolidone also in cabbage, kale, rape, and other fodder plants belonging to the *Cruciferae* family.

The same authors [4] have also demonstrated the transfer of this substance to milk in very small amounts (about 0.05 % of the amount fed). These quantities are so small that they cannot be expected to have any goitrogenic effect in the milk. Kreula and Kiesvaara [4] have given a detailed report on the methods used in these investigations. Somewhat later Altamura *et al.*[5] independently also demonstrated the formation of vinyl-thiooxazolidone in cabbage.

The goitrogenic effect of thiooxazolidones is due to the fact that they inhibit the synthesis of thyroid hormones. This effect cannot be overcome by high doses of iodide.

Another type of goitrogenic substances belonging to the *Brassica* factors has a primary influence on the uptake of iodide by the thyroid gland. This influence can be prevented by increasing the amount of the iodide dose. Many pieces of information given in the literature [6,7] indicate that salts of thiocyanic acid (SCN^-) represent this type in crucifers. Jirousek [8], who has investigated and reviewed the thiocyanate metabolism, found that in the animal organism SCN^- is formed endogenously from cyanides, nitriles, and sulphur-containing compounds, and that both the SCN^- brought exogenously into the organism and that formed endogenously in it have to be taken into consideration as goitrogenic factors. Michajlovskij and Langer [9,10] have performed systematic determinations on the SCN^- content in different vegetables. They found a particularly high SCN^- content in the press juice of different cabbage species (up to 50 mg %). They used the term "präformiertes Rhodanid" for the SCN^- present in food stuffs, obviously in contrast to the SCN^- formed endogenously.

Our investigations concerning the problem whether it is possible to make milk goitrogenic by feeding cows with plants, especially those belonging to the *Cruciferae*, have led to some new findings regarding the *Brassica* factors. These findings are briefly reported in the present paper.

An account was recently given about the formation of organic thiocyanates in some crucifers [11]. Benzyl thiocyanate was found to be formed enzymatically from glucotropaeolin in *Lepidium ruderale* and allyl thiocyanate from sinigrin in *Thlaspi arvense*. It was found in this laboratory that after the injection of benzyl thiocyanate into rats, the SCN^- content has risen considerably in blood serum and in different organs. This finding led us to look for thiocyanate esters also in *Brassica oleracea* species. For the present we have, however, no indications for the formation of such esters in fresh cabbage species. On the other hand, the result of these investigations was the finding that free SCN^- is formed from glucosidic precursors, present in cabbage. The thiocyanate found by Michajlovskij and Langer in the press juice of cabbage is thus not "preformed SCN^-"

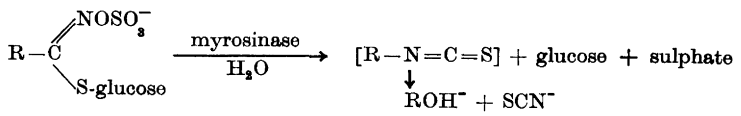

but is formed enzymatically from a glucosidic precursor(s) in cabbage. This fact was established when enzymes were destroyed in cabbage leaves by placing them intact in boiling methanol. The solution obtained was free from SCN^-. After addition of myrosinase solution to the purified extract SCN^- was formed, as determined by colour reactions for SCN^- and by paper chromatography.

The determination of SCN^- formed enzymatically in fresh plants was performed in the following way. 10 g of whole leaves of *Brassica oleracea* species were twice extracted by boiling for 15 min in 50 ml portions of methanol. The methanolic solutions were decanted. The plant material was thoroughly ground in a mortar, and was once more extracted by boiling in 50 ml of 70 % methanol. The combined extracts were evaporated *in vacuo*. The residue was taken up in water, and the solution was treated with about 0.6 ml of 20 % lead acetate solution. Filtration and washing of the filter residue with water. Excess lead ions in the filtrate were precipitated by H_2S. The filtrate was concentrated *in vacuo* to about 20 ml and brought to 25 ml (volumetric flask). 10 ml of this solution, 1 ml of myrosinase solution *, and 1 ml of phosphate buffer at pH 7 were incubated for 2 h at 37°. The solution was then brought to 100 ml. A control without addition of myrosinase solution was treated in the same way, and was used as a blank. 5 ml samples were mixed with 1 ml of Fe-reagent, measured at 500 mμ with a Klett-Summerson colorimeter, and the values compared with a standard SCN^- curve, essentially as in the method of Barker [13].

Table 1 shows the amounts of SCN^- formed in different cabbage species.

As is apparent from the list, varying amounts of SCN^- are formed in different cabbage species. The thiocyanate content of the press juices found by Langer and Michajlovskij corresponds to the amounts found by us.

* prepared according to Neuberg and Wagner [12]. SCN^- originally present in the myrosinase solution, was removed by shaking the solution for 30 min with Dowex 2 × 4 in chloride form.

Table 1. SCN^- content in cabbage species after myrosinase treatment.

Brassica species	SCN^- formation per 100 g fresh plants
Brassica oleracea * var. *sabauda* ssp. *Ulmer*	27—31 mg
Brassica oleracea * var. *gemmifera*	10 mg
Brassica oleracea * var. *capitata*	4 mg
Brassica oleracea * var. *cretica*	4 mg
Brassica napus var. *rapifera* •	8.8 mg
Brassica napus * var. spring rape	2.5 mg
Brassica rapa * var. winter turnip rape	1.7 mg

* leaves
• root

No formation of SCN^- was found in the crushed and moistened seeds of different cabbage species.

Attempts to isolate the glucosidic precursor from cabbage have been unsuccessful so far. The following findings can, however, be presented.

1. The precursor(s) of SCN^- decomposes with myrosinase so that SCN^- is liberated.
2. On spraying with $AgNO_3$ solution and heating, the precursor of SCN^- gives the same reaction on the paper chromatogram as mustard oil glucosides (gray-brown spot[14]).
3. On spraying with $FeCl_3$ solution, the precursor of SCN^- gives a brownish red spot after a short heating to 100°.
4. The position of the precursor on the paper chromatogram could be established furthermore either by spraying the paper first with myrosinase solution, and after standing for 1 h with $FeCl_3$ solution or by eluting the zones by the usual colour reactions for SCN^- after treatments of the eluates by myrosinase.

5. In a butanol-acetic acid-water system, the R_F value [15] of the SCN^- precursor was 0.76, in a pyridine-amylalcohol-water system it was 1.0.

Although the information about the chemical nature of the precursor is still scanty, we think it reasonable to publish a preliminary communication about our results at this stage. In our opinion the finding of the enzymatic formation of SCN^- is rather important, since it may help to shed light on many discrepancies about the *Brassica* factors.

If the SCN^- precursor is a mustard oil glucoside, as we suppose on the basis of the present indications, the formation of SCN^- according to the following reaction scheme seems probable, (see p. 508).

This secondary decomposition of an *iso*thiocyanate is no unknown reaction. Already in 1879 Will and Laubenheimer [16] have observed that *p*-hydroxybenzyl mustard oil (the *iso*thiocyanate formed from the glucoside sinalbin, present in white mustard) is split almost quantitatively into SCN^- by the action of alkali.

We have, however, found that considerable amounts of SCN^- are formed from glucosinalbin during the enzymatic cleavage even at pH 7. The initially present, pungent tasting *p*-hydroxybenzyl isothiocyanate decomposes gradually, loosing its irritating properties, into SCN^- and probably *p*-hydroxybenzyl alcohol. This secondary reaction seems to proceed at pH 7 at a slower rate than is the case with the SCN^- precursor of cabbage. Treatment of glucosinalbin with alkali, however, affords complete and fast fission, and permits a simple assay for the glucosinalbin content in the seeds of *Sinapis alba* by colorimetric SCN^- determination.

As long as the SCN^- precursor has not yet been isolated from *Brassica oleracea* species, the plants containing glucosinalbin (*Sinapis* species, *Bunias* species, *Lepidium campestre etc.*) may be used as suitable models for studies on the goitrogenic effect of the SCN^- precursor. Wagner-Jauregg and Koch [17] have for example observed a slight goitrogenic effect by application of myrosinase treated sinalbin solution to rabbits (sinalbin itself was without effect) but have not recognized or regarded SCN^- as the evidently responsible goitrogenic factor in this experiment.

Several thioglucosides were found in the limited number of cabbage species used so far for the attempted isolation of the SCN^- precursor: glucoraphanin, sinigrin, and glu-

Acta Chem. Scand. 14 (1960) No. 2

conapin in the fresh parts of *Brassica oleracea* var. *gemmifera;* glucoiberin and sinigrin in the fresh parts of marrow stem kale ("Chou Moellier"); glucoiberin and glucoraphanin in *Brassica oleracea* var. *cretica.* They were detected [14] directly by paper chromatography and comparison with authentic thioglucosides, or indirectly as thioureas derived from the enzymatically formed *iso*thiocyanates by the method of Kjær and Rubinstein [18] in different solvent systems.

From 500 g fresh parts of *Brassica oleracea* var. *gemmifera* 15 mg of analytically pure sulphoraphan-phenylthiourea were isolated (m. p. 145°C) *.

The presence of glucoiberin and glucoraphanin and their *iso*thiocyanates, respectively, in cabbage species becomes of special interest since Bachelard and Trikojus [20] have recently found that cheirolin (3-methylsulphonylpropyl *iso*thiocyanate) has a significant thyreostatic effect in animals. Iberin (3-methylsulphinylpropyl *iso*thiocyanate) and sulphoraphan (4-methylsulphinylbutyl *iso*thiocyanate) belong to the same isothiocyanate type as cheirolin, and may thus be considered as potential members in the group of "Brassica factors".

This investigation is a part of a research project under U.S. Public Law No. 480, 83rd Congress.

1. Astwood, E. B., Greer, M. A. and Ettlinger, M. G. *J. Biol. Chem.* **181** (1949) 121.
2. Virtanen, A. I., Kreula, M. and Kiesvaara, M. *Acta Chem. Scand.* **12** (1958) 580.
3. Kreula, M. and Kiesvaara, M. *Ibid.* **13** (1959) 1375.
4. Virtanen, A. I., Kreula, M. and Kiesvaara, M. *Ibid.* **13** (1959) 1043.
5. Altamura, M. R., Long Jr., L. and Hasselström, T. *J. Biol. Chem.* **234** (1959) 1847.
6. Greer, M. A. *Am. J. Clin. Nutrition* **5** (1957) 440.
7. Langer, P. *Nature* **185** (1960) 174.
8. Jirousek, L. *Physiol. Bohemosloven.* **5** (1956) 316.
9. Michajlovskij, N. and Langer, P. *Hoppe-Seyler's Z. physiol. Chemie* **312** (1958) 26; **317** (1959) 30.

* The presence of glucoiberin and glucoraphanin in *Brassica oleracea* species was established two months ago by the isolation of iberin-phenylthiourea and sulforaphan-phenylthiourea from a combined extract of *Brassica oleracea* var. *gemmifera* and var. *sabauda* by Procházka *et al.*[19]

10. Langer, P. and Michajlovskij, N. *Ibid.* **312** (1958) 31.
11. Gmelin, R. and Virtanen, A. I. *Suomen Kemistilehti B* **32** (1959) 236; *Acta Chem. Scand.* **13** (1959) 1474.
12. Neuberg, C. and Wagner, J. *Biochem. Z.* **174** (1926) 457.
13. Barker, H. *J. Am. Med. Assoc.* **106** (1936) 762.
14. Schultz, O. E. and Gmelin, R. *Z. Naturforsch.* **7 b** (1952) 500.
15. Schultz, O. E. and Wagner, W. *Ibid.* **11 b** (1956) 73.
16. Will, H. and Laubenheimer, A. *Ann.* **199** (1879) 150.
17. Wagner-Jauregg, Th. and Koch, J. *Z. Naturforsch.* **2 b** (1947) 13.
18. Kjær, A. and Rubinstein, K. *Acta Chem. Scand.* **7** (1953) 528.
19. Procházka, Z., Šanda, V. and Jirousek, L. *Collection Czech. Chem. Commun.* **24** (1959) 3606.
20. Bachelard, H. S. and Trikojus, V. M. *Nature* **185** (1960) 80.

Received February 20, 1960.

Isolation of an Iron-Containing Red Protein from Human Milk

BENGT JOHANSON

Department of Medical Biochemistry, University of Göteborg, Göteborg, Sweden

The presence of a red protein in bovine milk has been observed by several authors [1-4]. Sörensen and Sörensen [1] as well as Polis and Shmukler [3] performed a partial purification of this protein and recently a procedure for its isolation was described by Grooves [4]. The protein isolated by Grooves contained iron and was in certain respects similar to the iron-binding protein in blood plasma (transferrin [5] or β_1-metal-combining protein [6]). According to Schäfer [7] *human* milk assumes a red color after addition of small amounts of iron, probably due to the formation of an iron-protein complex. It has also been observed in this laboratory that crude preparations of human milk whey proteins are often salmon coloured[8]. This colour becomes more pronounced after addition of iron to the milk. A partial purification of the red component has been achieved by chromatography on calcium phosphate [9]. A method for isolation of the red protein has now been worked out and will be presented below.

Four litres of fresh human milk were defatted by centrifugation. After addition of 10 mg of Fe^{2+} (in the form of ferrous ammonium sulphate) to the milk, giving it a distinct reddish tint, solid ammonium sulphate was added to 45 % saturation and pH adjusted to 8.0 by careful addition of concentrated ammonia. When the milk was warmed to 37° for 30 min a flocculent precipitate was formed, which was removed by filtration through a fluted paper (Whatman No. 12). The rate of filtration was most often slow and the filtration had to proceed overnight at +4°C. The precipitate was discarded and the red-brown filtrate was acidified to pH 4.0 with 1 M sulfuric acid. The precipitate formed was quickly removed by gravity filtration or better by centrifugation and the pH of the filtrate (supernatant) immediately readjusted to 8.0. Ammonium sulphate was added to 80 % saturation and the red precipitate collected by filtration and dissolved in a minimal amount of distilled water. The dark red solution was dialyzed against distilled water followed by dialysis against 0.02 M sodium phosphate buffer, pH 8.0. The solution was then chromatographed on DEAE-cellulose [10] previously equilibrated with the same buffer. Under the conditions described the red protein was not sorbed on the ion-exchanger but appeared in the effluent without significant retardation. The red fraction was further chromatographed on calcium phosphate as described earlier [9], using phosphate buffers of pH 8.0 instead of 6.9. The red fraction eluted with 0.5 M phosphate buffer was dialyzed against distilled water and finally

Fig. 1. Electrophoretic pattern of the purified red protein. Glycine-NaOH buffer, pH 9.4, ionic strength 0.1. Ascending boundaries to the left, descending boundaries to the right. Duration 350 min.

10. Langer, P. and Michajlovskij, N. *Ibid.* **312** (1958) 31.
11. Gmelin, R. and Virtanen, A. I. *Suomen Kemistilehti B* **32** (1959) 236; *Acta Chem. Scand.* **13** (1959) 1474.
12. Neuberg, C. and Wagner, J. *Biochem. Z.* **174** (1926) 457.
13. Barker, H. *J. Am. Med. Assoc.* **106** (1936) 762.
14. Schultz, O. E. and Gmelin, R. *Z. Naturforsch.* **7 b** (1952) 500.
15. Schultz, O. E. and Wagner, W. *Ibid.* **11 b** (1956) 73.
16. Will, H. and Laubenheimer, A. *Ann.* **199** (1879) 150.
17. Wagner-Jauregg, Th. and Koch, J. *Z. Naturforsch.* **2 b** (1947) 13.
18. Kjær, A. and Rubinstein, K. *Acta Chem. Scand.* **7** (1953) 528.
19. Procházka, Z., Šanda, V. and Jirousek, L. *Collection Czech. Chem. Commun.* **24** (1959) 3606.
20. Bachelard, H. S. and Trikojus, V. M. *Nature* **185** (1960) 80.

Received February 20, 1960.

Isolation of an Iron-Containing Red Protein from Human Milk

BENGT JOHANSON

Department of Medical Biochemistry, University of Göteborg, Göteborg, Sweden

The presence of a red protein in bovine milk has been observed by several authors [1-4]. Sörensen and Sörensen [1] as well as Polis and Shmukler [3] performed a partial purification of this protein and recently a procedure for its isolation was described by Grooves [4]. The protein isolated by Grooves contained iron and was in certain respects similar to the iron-binding protein in blood plasma (transferrin [5] or β_1-metal-combining protein [6]). According to Schäfer [7] *human* milk assumes a red color after addition of small amounts of iron, probably due to the formation of an iron-protein complex. It has also been observed in this laboratory that crude preparations of human milk whey proteins are often salmon coloured[8]. This colour becomes more pronounced after addition of iron to the milk. A partial purification of the red component has been achieved by chromatography on calcium phosphate [9]. A method for isolation of the red protein has now been worked out and will be presented below.

Four litres of fresh human milk were defatted by centrifugation. After addition of 10 mg of Fe^{2+} (in the form of ferrous ammonium sulphate) to the milk, giving it a distinct reddish tint, solid ammonium sulphate was added to 45 % saturation and pH adjusted to 8.0 by careful addition of concentrated ammonia. When the milk was warmed to 37° for 30 min a flocculent precipitate was formed, which was removed by filtration through a fluted paper (Whatman No. 12). The rate of filtration was most often slow and the filtration had to proceed overnight at +4°C. The precipitate was discarded and the red-brown filtrate was acidified to pH 4.0 with 1 M sulfuric acid. The precipitate formed was quickly removed by gravity filtration or better by centrifugation and the pH of the filtrate (supernatant) immediately readjusted to 8.0. Ammonium sulphate was added to 80 % saturation and the red precipitate collected by filtration and dissolved in a minimal amount of distilled water. The dark red solution was dialyzed against distilled water followed by dialysis against 0.02 M sodium phosphate buffer, pH 8.0. The solution was then chromatographed on DEAE-cellulose [10] previously equilibrated with the same buffer. Under the conditions described the red protein was not sorbed on the ion-exchanger but appeared in the effluent without significant retardation. The red fraction was further chromatographed on calcium phosphate as described earlier [9], using phosphate buffers of pH 8.0 instead of 6.9. The red fraction eluted with 0.5 M phosphate buffer was dialyzed against distilled water and finally

Fig. 1. Electrophoretic pattern of the purified red protein. Glycine-NaOH buffer, pH 9.4, ionic strength 0.1. Ascending boundaries to the left, descending boundaries to the right. Duration 350 min.

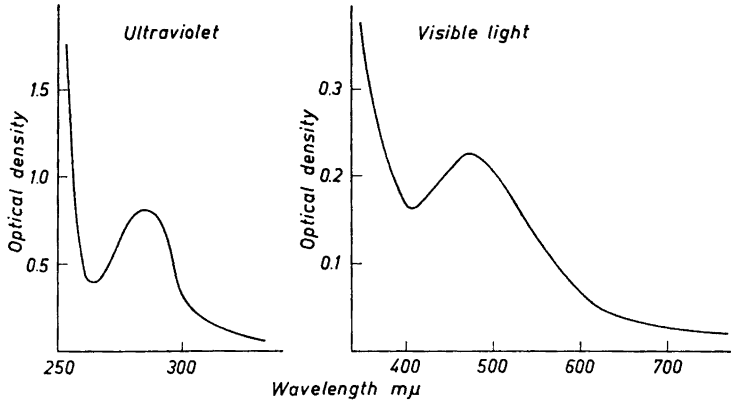

Fig. 2. Absorption spectrum of the red protein at pH 9.0.

precipitated with ammonium sulphate between 60 and 75 % saturation at pH 8.0.

The product obtained was run in moving boundary electrophoresis and found to be homogeneous in glycine-NaOH buffer of pH 9.4 and ionic strength 0.1 (Fig. 1) and also in sodium veronal-HCl buffer of pH 8.6 and ionic strength 0.1. Electrophoresis at pH 8.0, however, showed an asymmetric peak on the ascending limb that might be due to a heterogeneity of the preparation.

Analysis of the iron content according to Lorber [11] after combustion with sulfuric acid and 30 % hydrogen peroxide [12] showed the presence of 0.13—0.15 % iron in different preparations. After passage of the protein through a column with cation exchange resin (Dowex 50, X-12) at pH 8.5 the iron content was diminished to 0.10—0.11 %. The main part of the iron could thus not be removed by the resin. The light absorption was examined in the wavelength range of 225—700 mμ (Fig. 2) in a Zeiss spectrophotometer, PMQ II, using 1 cm cuvettes. In the ultraviolet region only the expected maximum around 280 mμ was found. In the region of visible light a broad maximum at 460—470 mμ and a minimum around 410 mμ were found. At a protein concentration of 1.0 % (pH 9.0) the optical density at 460 mμ varied between 0.40 and 0.45 for different preparations (1 cm light pathway). The ratio of the optical densities at 460 to 408 mμ varied between 1.30 and 1.38. The type of light absorption curves and the presence of

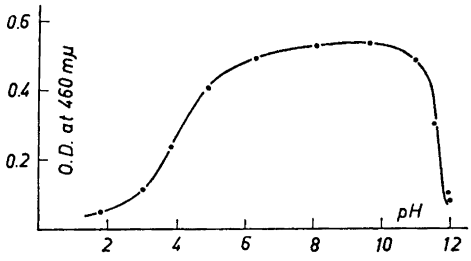

Fig. 3. The pH-dependance of the light absorption of the red protein at 460 mμ.

strongly bound iron suggests a certain similarity to blood serum transferrin. The milk protein is, however, not identical to transferrin, as there is no immunological relationship between the two proteins as determined by diffusion-in-gel analysis [13]. Furthermore the iron complex formed by the milk protein seems to be more stable in acid media than the iron-transferrin complex. The milk protein is thus not completely decolorized until pH 2 (Fig. 3) and at this pH 90—95 % of the iron is removable by passing the protein through a column of Dowex 50, X-12.

These and further studies will be reported in detail shortly.

I am indebted to Mrs Birgit Johansson and Miss Anita Wallin for skilful technical assistence. The investigation was supported by a grant from the *Medical Faculty*, University of Göteborg to the author and a grant from the *Swedish Dairies' Association* to Prof. Olof Mellander, Dr. Lars Svennerholm and the author.

1. Sörensen, M. and Sörensen, S. P. L. *Compt. rend. trav. lab. Carlsberg* **23** (1939) 55.
2. Theorell, H. and Åkeson, Å. *Arkiv Kemi, Mineral. Geol.* **18** *A* (1943) No. 7.
3. Polis, B. D. and Shmukler, H. W. *J. Biol. Chem.* **201** (1953) 475.
4. Grooves, M. L. *In manuscript.*
5. Laurell, C. B. *Acta Chem. Scand.* **7** (1953) 1407.
6. Koechlin, B. A. *J. Am. Chem. Soc.* **74** (1952) 2649.
7. Schäfer, K. H. *"V. Kongress der Europäischen Gesellschaft für Hämatologie"*, Freiburg 1956, p. 154.
8. Johansson, B. *Acta Chem. Scand.* **8** (1954) 1108.
9. Johansson, B. *Nature* **181** (1958) 996.
10. Sober, H. A., Gutter, F. J., Wyckoff, M. M. and Peterson, E. A. *J. Am. Chem. Soc.* **78** (1956) 756.
11. Lorber, F. *Biochem. Z.* **181** (1927) 391.
12. Theorell, H., Beznak, M., Bonnichsen, R., Paul, K.-G. and Åkeson, Å. *Acta Chem. Scand.* **5** (1951) 445.
13. Hanson, L. Å. and Johansson, B. *Unpublished results.*

Received March 2, 1960.

Perjodatoxydation von Phenolen VI*. Dimere *o*-Chinole aus Mesitol und 2,6-Dimethylphenol

ERICH ADLER, JOSEF DAHLÉN und GERTRUD WESTIN

Organisch-chemisches Institut, Chalmers Technische Hochschule, Göteborg, Schweden

Die Einwirkung von Natriumperjodat auf wässrige Lösungen von Mesitol bzw. 2,6-Dimethylphenol führt in rascher Reaktion zu Substanzen vom Schmp. 183° bzw. 196°, für welche die Strukturen der Dimeren V[1] bzw. VI angenommen wurden. Ihre Entstehung war verständlich mit der Annahme, dass die Phenole zunächst zu den *o*-Chinolen I bzw. II oxydiert werden, und dass die letzteren sich durch Diels-Alder-Reaktion dimerisieren. Wessely und Mitarb. hatten das Dimere vom Schmp. 183° auch bei der alkalischen Verseifung von 2,4,6-Trimethyl-*o*-chinolacetat (I, OAc statt OH) erhalten und für das Produkt ebenfalls Struktur V vermutet [2]. Direkter Vergleich der beiden Präparate bestätigte deren Identität.

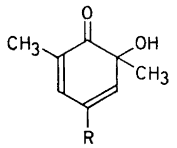

I. R = CH_3
II. R = H

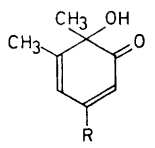

III. R = CH_3
IV. R = H

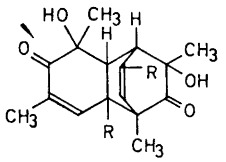

V. R = CH_3
VI. R = H

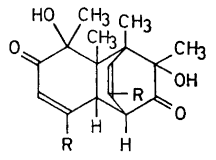

VII. R = CH_3
VIII. R = H

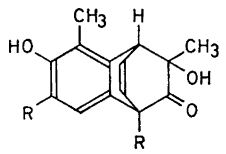

IX. R = CH_3
X. R = H

Kürzlich berichteten jedoch Wessely und Mitarb.[3] über Versuche, welche die genannten Autoren zu einer Revision der Formel V veranlasste. Man fand, dass die alkalische Verseifung von 2,4,6-Trimethyl-*o*-chinolacetat (I, OAc statt OH) neben dem Dimeren vom Schmp. 183° überraschenderweise monomeres 2,3,5-Trimethyl-*o*-chinol (III) lieferte. Im alkalischen Medium war demnach eine Acyloinumlagerung einge-

* V. Mitt.: Adler, E., Junghahn, L., Lindberg, U., Berggren, B. und Westin, G. *Acta Chem. Scand.* **14** (1960). *Im Druck.*

I am indebted to Mrs Birgit Johansson and Miss Anita Wallin for skilful technical assistence. The investigation was supported by a grant from the *Medical Faculty*, University of Göteborg to the author and a grant from the *Swedish Dairies' Association* to Prof. Olof Mellander, Dr. Lars Svennerholm and the author.

1. Sörensen, M. and Sörensen, S. P. L. *Compt. rend. trav. lab. Carlsberg* **23** (1939) 55.
2. Theorell, H. and Åkeson, Å. *Arkiv Kemi, Mineral. Geol.* **18** *A* (1943) No. 7.
3. Polis, B. D. and Shmukler, H. W. *J. Biol. Chem.* **201** (1953) 475.
4. Grooves, M. L. *In manuscript.*
5. Laurell, C. B. *Acta Chem. Scand.* **7** (1953) 1407.
6. Koechlin, B. A. *J. Am. Chem. Soc.* **74** (1952) 2649.
7. Schäfer, K. H. *"V. Kongress der Europäischen Gesellschaft für Hämatologie"*, Freiburg 1956, p. 154.
8. Johansson, B. *Acta Chem. Scand.* **8** (1954) 1108.
9. Johansson, B. *Nature* **181** (1958) 996.
10. Sober, H. A., Gutter, F. J., Wyckoff, M. M. and Peterson, E. A. *J. Am. Chem. Soc.* **78** (1956) 756.
11. Lorber, F. *Biochem. Z.* **181** (1927) 391.
12. Theorell, H., Beznak, M., Bonnichsen, R., Paul, K.-G. and Åkeson, Å. *Acta Chem. Scand.* **5** (1951) 445.
13. Hanson, L. Å. and Johansson, B. *Unpublished results.*

Received March 2, 1960.

Perjodatoxydation von Phenolen VI*. Dimere *o*-Chinole aus Mesitol und 2,6-Dimethylphenol

ERICH ADLER, JOSEF DAHLÉN und GERTRUD WESTIN

Organisch-chemisches Institut, Chalmers Technische Hochschule, Göteborg, Schweden

Die Einwirkung von Natriumperjodat auf wässrige Lösungen von Mesitol bzw. 2,6-Dimethylphenol führt in rascher Reaktion zu Substanzen vom Schmp. 183° bzw. 196°, für welche die Strukturen der Dimeren V[1] bzw. VI angenommen wurden. Ihre Entstehung war verständlich mit der Annahme, dass die Phenole zunächst zu den *o*-Chinolen I bzw. II oxydiert werden, und dass die letzteren sich durch Diels-Alder-Reaktion dimerisieren. Wessely und Mitarb. hatten das Dimere vom Schmp. 183° auch bei der alkalischen Verseifung von 2,4,6-Trimethyl-*o*-chinolacetat (I, OAc statt OH) erhalten und für das Produkt ebenfalls Struktur V vermutet [2]. Direkter Vergleich der beiden Präparate bestätigte deren Identität.

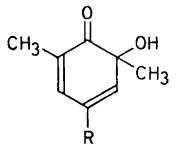

I. R = CH_3
II. R = H

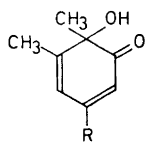

III. R = CH_3
IV. R = H

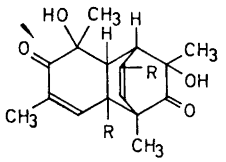

V. R = CH_3
VI. R = H

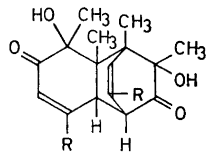

VII. R = CH_3
VIII. R = H

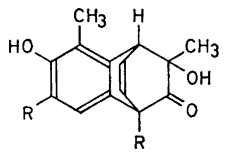

IX. R = CH_3
X. R = H

Kürzlich berichteten jedoch Wessely und Mitarb.[3] über Versuche, welche die genannten Autoren zu einer Revision der Formel V veranlasste. Man fand, dass die alkalische Verseifung von 2,4,6-Trimethyl-*o*-chinolacetat (I, OAc statt OH) neben dem Dimeren vom Schmp. 183° überraschenderweise monomeres 2,3,5-Trimethyl-*o*-chinol (III) lieferte. Im alkalischen Medium war demnach eine Acyloinumlagerung einge-

* V. Mitt.: Adler, E., Junghahn, L., Lindberg, U., Berggren, B. und Westin, G. *Acta Chem. Scand.* **14** (1960). *Im Druck.*

treten. Da ferner das Dimere vom Schmp. 183° beim Erhitzen auf 200° zum Teil unter Bildung von III zerfiel und anderseits III bei 130° wieder das genannte Dimere lieferte, nahmen Wessely und Mitarb.[3] für die Substanz vom Schmp. 183° die Formel VII eines dimeren 2,3,5-Trimethyl-*o*-chinols an. Aus ähnlichen Gründen schrieben sie einem bei Verseifung von 2,6-Dimethyl-*o*-chinolacetat (II, OAc statt OH) erhaltenen Produkt vom Schmp. 196° die Struktur eines dimeren 2,3-Dimethyl-*o*-chinols (VIII) zu. Direkter Vergleich der letztgenannten Substanz mit dem von uns aus 2,6-Dimethylphenol und Perjodat erhaltenen Produkt gleichen Schmelzpunkts ergab wiederum Identität.

Wären die von Wessely c.s.[3] für die beiden Dimeren vorgeschlagenen Strukturen VII und VIII richtig, so müsste also angenommen werden, dass auch unter den von uns angewandten Bedingungen der Perjodatoxydation die primär entstehenden *o*-Chinole I bzw. II sich in III bzw. IV umlagerten, bevor Dimerisierung eintrat. Da wir bei pH 4—5 (Zimmertemp.) arbeiteten und die Reaktion innerhalb 5 Min. abgeschlossen ist, erschien uns diese Annahme unwahrscheinlich. Aus den nachstehenden Ergebnissen folgern wir, dass den Dimeren die "normalen" Strukturen V bzw. VI zukommen.

Perjodatoxydation von 2,3,5-Trimethylphenol gab kein Dimeres, sondern (neben 2,3,5-Trimethyl-*p*-chinon) das monomere 2,3,5-Trimethyl-*o*-chinol III, das bei gewöhnlicher Temperatur stabil war. Die rasche Bildung des Dimeren vom Schmp. 183° bei der Perjodatoxydation von Mesitol kann demnach nicht über das 2,3,5-Trimethyl-*o*-chinol verlaufen.

Das Diacetylderivat (Schmp. 158°) des aus 2,6-Dimethylphenol gewonnenen Dimeren vom Schmp. 196° zerfiel beim Erhitzen auf 180° unter Bildung von 2,6-Dimethyl-*o*-chinolacetat [3,4] (II, OAc statt OH). Letzteres konnte bei 120° wieder zum Dimeracetat vom Schmp. 158° dimerisiert werden; dagegen blieb 2,3-Dimethyl-*o*-chinolacetat [5] (IV, OAc statt OH) bei 120° unverändert. Milde alkalische Verseifung des Dimerdiacetats gab neben dem Ausgangsdimeren ein Anhydrodimeres, Schmp. 176°, von phenolischem Charakter. Ganz ähnlich erhielten wir bei Verseifung des dimeren 2-Methyl-*o*-chinolacetats von Metlesics und Wessely [6] das Phenol X, dessen Struktur eindeutig festgelegt ist [6]. Das Anhydroprodukt vom Schmp. 176° ist spektral und im chemischen Verhalten mit X völlig analog; es kann ihm daher Struktur IX zugeschrieben werden. Die bei der Bildung von IX erfolgte Aromatisierung ist nur mit Struktur VI (dimeres 2,6-Dimethyl-*o*-chinol) und nicht mit Struktur VIII (dimeres 2,3-Dimethyl-*o*-chinol) für das Dimere vom Schmp. 196° in Einklang zu bringen.

Es scheint, dass die Versuchsergebnisse von Wessely c.s.[3] damit zu erklären sind, dass sowohl in Alkali wie beim trockenen Erhitzen die *o*-Chinolpaare I, III bzw. II, IV sich in Acyloinumlagerungs-Gleichgewichten befinden, und da wohl I und II, nicht aber III und IV zur Dimerisierung neigen, so werden unter den genannten Bedingungen I und II immer in dimerer Form (V und VI), III und IV immer in monomerer Form gefunden.

Ausführliche Publikation obiger und weiterer Versuche erfolgt demnächst.

Der eine von uns (E.A.) dankt Herrn Prof. Wessely, Wien, bestens für die Freundlichkeit uns von seinen Ergebnissen durch Übersendung eines Korrekturabzugs der Arbeit [3] vorzeitig zu unterrichten, sowie für sein Entgegenkommen beim Austausch der Dimerpräparate.

1. Adler, E. *Angew. Chem.* **69** (1957) 272.
2. Privatmitteilung, s. auch Siegel, A., Wessely, F., Stockhammer, P., Antony, F. und Klezl, P. *Tetrahedron* **4** (1958) 49.
3. Budzikiewicz, H., Schmidt, G., Stockhammer, P. und Wessely, F. *Monatsh.* **90** (1959) 609.
4. Cavill, G. W. K., Cole, E. R., Gilham, P. T. und McHugh, D. J. *J. Chem. Soc. (London)* **1954** 2785.
5. Wessely, F., Kotlan, J. und Metlesics, W. *Monatsh.* **85** (1954) 69.
6. Metlescis, W. und Wessely, F. *Monatsh.* **88** (1957) 108.

Eingegangen am 14. März 1960.

Corrections to „Sewage as a Substitute for Casein Hydrolyzates in Fermentations with *Propionibacterium shermannii*" *

HALINA Y. NEUJAHR

Royal Institute of Technology, Division of Food Chemistry, Stockholm 70, Sweden

The composition of the semi-synthetic medium (Footnote on p. 2159) is erroneously given and shall include calcium pantothenate, 4 mg, and biotin, 0.3 mg/l medium.

* *Acta Chem. Scand.* **13** (1959) 2158.

Received February 29, 1960.

Correction to "On Vitamins in Sewage Sludge X" *

HALINA Y. NEUJAHR

Royal Institute of Technology, Division of Food Chemistry, Stockholm 70, Sweden

In Fig. 1 (p. 1965, the right part) *for* IV + III + Met *read* W + III + Met.

* *Acta Chem. Scand.* **13** (1959) 1960.

Received February 29, 1960.

ACTA CHEMICA SCANDINAVICA 14 (1960) 515–528

Periodate Oxidation of Phenols

II *. Oxidation of 2,6-Dimethoxyphenol and 3-Methoxycatechol. Formation of a 1,2-Naphthoquinone **

ERICH ADLER, RUNE MAGNUSSON, BRITT BERGGREN and HANS THOMELIUS

Institutionen för organisk kemi, Chalmers Tekniska Högskola, Göteborg, Sweden

The action of sodium periodate on an aqueous solution of 2,6-dimethoxyphenol (I) rapidly produces coerulignone (II), 2,6-dimethoxy-*p*-quinone (III), 3-methoxy-*o*-quinone (IV), 3,8-dimethoxy-1,2-naphthoquinone (V), m. p. 198–199°, and a violet substance (VI), m. p. 205–206°, of unknown structure. Compounds IV, V, and VI were also obtained by periodate oxidation of 3-methoxycatechol (VII). A similar treatment of IV yielded V and VI.

A dimeric 3-methoxy-*o*-quinone (VIII), m. p. 139–140°, is formed in solutions of the monomer (IV) in certain organic solvents; in aqueous solutions of IV, or of VIII, a monohydrate of dimer VIII (XIII, m. p. 114–115°) is formed. Both dimer VIII and its monohydrate XIII, when treated with periodate, are degraded to the β-naphthoquinone V. Thus, V arises from phenols I or VII in aqueous periodate solution by dimerisation of the 3-methoxy-*o*-quinone (IV) first formed and degradation of the dimer.

A second dimeric 3-methoxy-*o*-quinone (m. p. 110°) was obtained from benzene solutions of the monomer. On periodate oxidation it is converted to the violet compound VI.

In Part I [1] of this series it was shown that the action of sodium periodate on monoethers of catechol results in rapid oxidative cleavage of the ether group. Guaiacol, for instance, yielded about 90 % of the calculated amount of methanol, in addition to *o*-benzoquinone. Sodium bismuthate was found [2] to act in a similar way.

Lead tetraacetate however, although largely equivalent to periodate and bismuthate as a glycol-splitting agent, differs from them in its action on guaiacol. As reported by Wessely and Kotlan [3], lead tetraacetate attacks mainly the free 4-position, yielding methoxy-*p*-benzoquinone as the major reaction product. Similarly, the pyrogallol derivative 2,6-dimethoxyphenol

* Part I, see Ref. [1].

** Preliminary report: Adler, E. *Angew. Chem.* **71** (1959) 580.

(I) is oxidised by lead tetraacetate at the position *para* to the phenolic hydroxyl group, with the formation of 2,6-dimethoxy-*p*-quinone (II) (78 %) and coerulignone (III) (10 %) [3]. The action of Fremy's salt (potassium nitrosodisulphonate, $ON(SO_3K)_2$) on guaiacol and 2,6-dimethoxyphenol resembles that of lead tetraacetate and gives methoxy-*p*-quinone and 2,6-dimethoxy-*p*-quinone, respectively, in high yields [4].

PERIODATE OXIDATION OF 2,6-DIMETHOXYPHENOL (I)

As in the case of guaiacol, periodate treatment of 2,6-dimethoxyphenol (I) in dilute aqueous solution resulted in rapid consumption of the oxidant and the liberation of nearly 1 mole of methanol per mole of phenol after a reaction time of only 1—2 min. In addition to this *ortho* oxidative demethylation, some *para* oxidation also occurred, the ratio between *ortho* and *para* oxidation being dependent on the experimental conditions used and especially on the initial concentration of the phenol.

When a reaction mixture containing 8 mmole of I and 24 mmole of $NaIO_4$ per litre was used, and the oxidation was allowed to proceed at 4° for only 2 min, the expected product of the *o*-oxidative demethylation, *i.e.*, 3-methoxy-*o*-quinone (IV), was formed in 58 % yield (Table 1, Expt. 1). In addition to this compound there were also obtained small amounts of a brilliant red compound, $C_{10}H_4O_2(OCH_3)_2$, m.p. 198—199°, and traces of a dark-violet substance (VI), m.p. 205—206°, with the same composition. As will be described in a following communication [5], the red substance has been shown to be the hitherto unknown β-naphthoquinone V (3,8-dimethoxy-1,2-naphtoquinone). The dark-violet product (VI), which, on treatment with *o*-phenylenediamine, yielded an orange phenazine, m.p. 229—230°, is believed to be the isomeric 3,5-dimethoxy-1,2-naphthoquinone. Further investigation of the structure of substance VI is in progress. As shown below, both products, V and VI, originate from the 3-methoxy-1,2-benzoquinone (IV) that is formed first.

The *para* oxidation of I also gave small amounts of coerulignone (II) and 2,6-dimethoxy-1,4-benzoquinone (III) (Scheme 1).

Increasing the reaction temperature to 20° and the time of oxidation to 10 min (Table 1, Expt. 2) reduced the yield of the *o*-benzoquinone IV, but increased the yields of the β-naphthoquinone V and of coerulignone (II). This change in the ratio of the yields of products II, IV, and V was still more pronounced when the initial concentration of the starting phenol was increased ten-fold (Expt. 3). *Para* oxidation, mainly with the formation of coerulignone (II), then occurred to a greater extent and the yield of the β-naphtoquinone V was also further increased, but the yield of the *o*-benzoquinone IV was insignificant.

The separation of the various reaction products was based on the following procedure (for details, see Experimental). Coerulignone (II), which is practically insoluble, was recovered from the reaction mixture by filtration, and the products III, IV, V, and VI were extracted from the filtrate with chloroform and separated by chromatography on alumina. Fractional elution yielded the pure products III, V, and VI, but the *o*-benzoquinone IV was irreversibly adsorbed (and destroyed) on the alumina column. The difference between

Scheme 1.

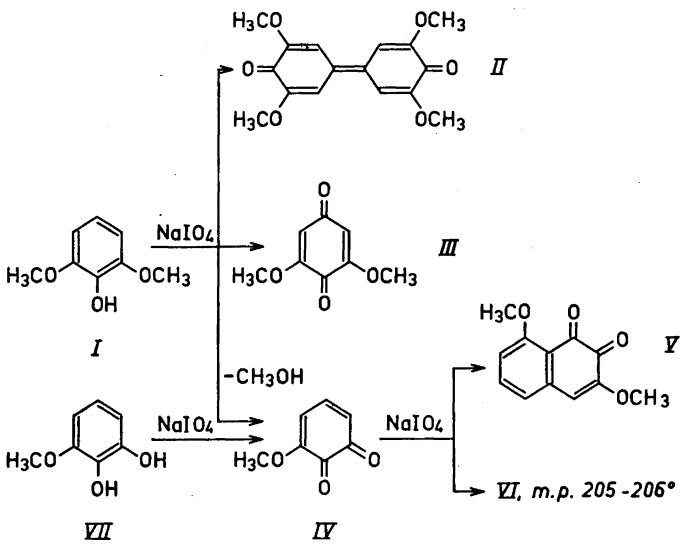

the weight of the crude residue, obtained on evaporation of the chloroform extract and the combined weights of compounds III, V, and VI, eluted from the alumina column, was taken as a measure of the amount of 3-methoxy-1,2-benzoquinone (IV) present.

The yields given for IV may thus be slightly too high, as they could include minor amounts of polymeric transformation products of IV (and their periodate oxidation products) formed in the aqueous reaction mixture. However, polymeric products of this

Table 1. Periodate oxidation of 2,6-dimethoxyphenol (I), 3-methoxycatechol (VII), and 3-methoxy-1,2-benzoquinone (IV) in water [a].

Expt. No.	Starting material		Temp. °C	Time of oxid., min	Yields of reaction products, per cent					
	Compound	Conc. in react.mixt., mmole/l			II	III	IV	V	VI	Total II to VI
1	I	8	4	2	7	5	58	7	2	79
2	I	8	20	10	12	3	35	15	7	72
3	I	80	20	10	31	3	5	25	2	66
4	VII	80	20	10	—	—	12	48	2	62
5	IV	40	20	10	—	—	21 [b]	51	2	74

[a] The ratio of starting material/$NaIO_4$ used was 1:3.
[b] Unreacted starting material and polymers.

sort are sparingly soluble in chloroform and the error due to this source should be limited. As expected, the yield of water-soluble material not extractable with chloroform (= 100 minus total yield of products II—VI, as given in Table 1, last column) increases with increasing temperature, reaction time, and phenol concentration (*cf.* Expts. 1, 2, and 3).

On recrystallisation from ether, the crude solids remaining on evaporation of the chloroform extracts from reaction mixtures similar to those given in Expts. 1 and 2 (Table 1), gave 3-methoxy-1,2-benzoquinone (IV), m.p. 110° [6], in yields of 30—40 % based on the amount of phenol I used.

OXIDATION OF 3-METHOXYCATECHOL (VII)

As reported in Part I [1], periodate oxidation of 3-methoxy catechol (VII) yielded 3-methoxy-1,2-benzoquinone (IV) (nearly 60 %), *i.e.*, the oxidation occurred preferentially at the "catechol grouping" of VII rather than at the "guaiacol grouping" which was also present in VII. The experimental conditions were comparable to those used in Expt. 1, Table 1, for the oxidation of 2,6-dimethoxyphenol (low phenol concentration, low temperature, short reaction time).

Increasing the phenol concentration, temperature or time (Table 1, Expt. 4) resulted in a remarkably high yield of 3,8-dimethoxy-1,2-naphthoquinone (V) (48 %) and a simultaneous decrease of the amount of 3-methoxy-1,2-benzoquinone (IV). This is in accordance with the results of the oxidation of 2,6-dimethoxyphenol reported above. In the case of 3-methoxycatechol no defined *para* oxidation products were detected, and the yield of the β-naphthoquinone derivative V was considerably higher than in the oxidation of 2,6-dimethoxyphenol (*cf.* Expts. 3 and 4).

THE FORMATION OF 3,8-DIMETHOXY-1,2-NAPHTHOQUINONE (V). DIMERIC 3-METHOXY-1,2-BENZOQUINONE (VIII) AND ITS MONOHYDRATE (XIII)

While the formation of the *para* oxidation products, coerulignone (II) and 2,6-dimethoxy-*p*-quinone (III), from 2,6-dimethoxyphenol (I), and the formation of 3-methoxy-1,2-benzoquinone (IV) from I or from 3-methoxycatechol (VII) are easily understood, the formation of 3,8-dimethoxy-1,2-naphthoquinone (V) from the phenols I or VII was rather surprising. It obviously involved the fusion of two molecules of the starting phenol with the loss of two carbon atoms per two molecules of the phenol, and, in the case of 2,6-dimethoxyphenol (I), the oxidative removal of one methoxyl group per molecule of the starting phenol.

Such a fusion of two C_6-entities could be assumed to arise by spontaneous dimerisation of the 3-methoxy-1,2-benzoquinone (IV) first formed by periodate oxidation of both phenols, I and VII. In fact, comparatively concentrated aqueous solutions of the *o*-benzoquinone IV when treated with periodate (Table 1, Expt. 5) were found to give the dimethoxy-1,2-naphthoquinone V in yields (about 50 %) similar to those obtained from 3-methoxycatechol (*cf.* Expt. 4). As in the case of the phenols I and VII, respectively, the formation of the β-naphtoquinone V from the *o*-benzoquinone IV was practically complete within a reaction time of 10 min.

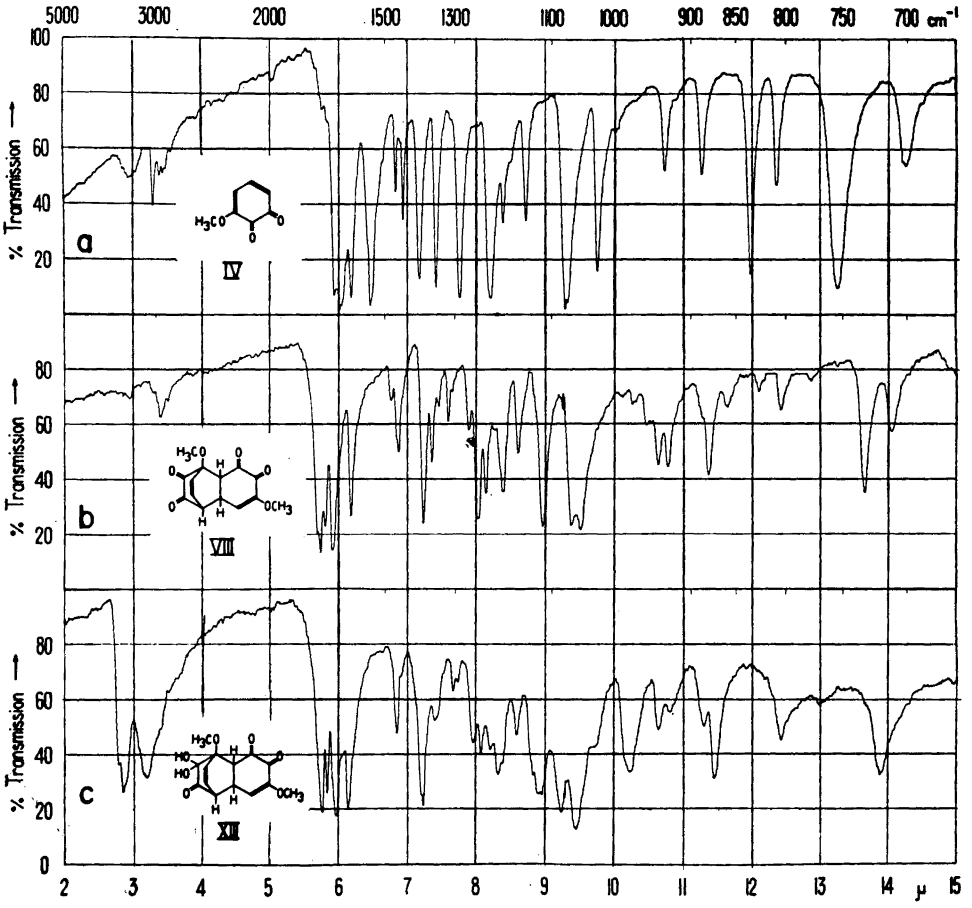

Fig. 1. Infra-red absorption spectra. a. 3-Methoxy-1,2-benzoquinone (IV). b. Dimeric 3-methoxy-1,2-benzoquinone (VIII). c. Monohydrate (XIII) of dimer VIII.

The assumption that the oxidative conversion of 3-methoxy-1,2-benzoquinone (IV) into 3,8-dimethoxy-1,2-naphthoquinone (V) involved an initial dimerisation of IV, could be examined experimentally when it was found that a dimeric 3-methoxy-1,2-benzoquinone could be easily obtained. When solutions of the monomer IV in certain solvents, such as acetone, methylene chloride, chloroform, dioxane, or ethyl acetate, were allowed to stand for a day at room temperature, a yellow product, m.p. 139—140°, was formed which had the same elemental composition as IV.

The infra-red spectrum of 3-methoxy-1,2-benzoquinone (IV) (Fig. 1a), shows very similar carbonyl absorption to that reported for the 5-ethyl homologue [7,8], but the infra-red spectrum of the yellow product (Fig. 1b) shows absorption bands at comparatively short wave-lengths, 5.69, 5.74, and

5.82 μ, indicating the presence of three isolated CO groups, and also a band at 5.93 μ, indicating an α,β-unsaturated carbonyl group. These bands, and a further band at 6.19 μ (ethylenic bond of C=C—C=O system), are practically identical with those reported by Harley-Mason and Laird [9] (*cf.* also Ref.[10]) for the yellow dimer of unsubstituted *o*-benzoquinone described by Willstätter and Müller [6], the structure of which was recently elucidated (VIII, H instead of CH_3O) [10,9,11]. Its formation by diene addition of two molecules of *o*-benzoquinone is analogous to the dimerisation of alkylated *o*-quinones clarified a few years ago [12,7,13].

Similar diene addition of 2 molecules of 3-methoxy-1,2-benzoquinone can give rise to four isomeric adducts, VIII—VIIIc:

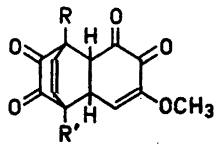

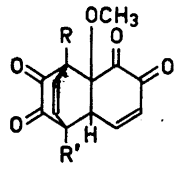

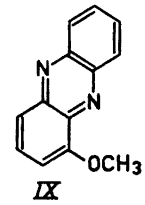

IX

VIII: R = CH_3O; R′ = H VIIIb: R = CH_3O; R′ = H

VIIIa: R = H; R′ = CH_3O VIIIc: R = H; R′ = CH_3O

The light absorption of the dimeric 3-methoxy-*o*-quinone, m.p. 139—140°, (Fig. 2, curve 1) seems to be in harmony with structures VIII or VIIIa rather than VIIIb or VIIIc. The main maximum at 300 mμ can be acsribed to the methoxyl-substituted conjugated ene-dione chromophore of VIII or VIIIa, and the broad maximum at higher wave-length will be due to the 1,2-diketo groupings present.

Treatment of dimeric 3-methoxy-*o*-quinone with *o*-phenylenediamine, in pyridine solution, gave a yellow phenazine derivative, m.p. 172—173°, which was identical with 1-methoxypenazine (IX) obtained from monomeric 3-methoxy-*o*-quinone. The yield was 90 %, indicating that both the monomer units in VIII had reacted, "retrodiene cleavage" giving rise to the phenazine derivative of the free monomer. A similar reversed diene reaction has been observed in the reaction between dimeric 4,5-dimethyl-*o*-quinone and *o*-phenylenediamine [12].

It appeared not quite impossible that 3-methoxy-*o*-quinone (IV), when treated with *o*-phenylenediamine in an organic solvent, might dimerise before condensation with the amine, and that consequently the phenazine derivative obtained from IV might be that of the dimeric rather than the monomeric *o*-quinone. However a determination of the molecular weight of the phenazine (Rast, found 224, calc. 210) confirmed that the derivative actually was that derived from the monomer.

Structures VIII—VIIIc, proposed for the dimeric 3-methoxy-*o*-quinone, clearly suggest that it should be possible to convert the substance, by periodate oxidation, into a β-naphthoquinone. In fact, treatment of the dimer with periodate gave 3,8-dimethoxy-1,2-naphthoquinone (V)[5], m.p. 198—199°, in

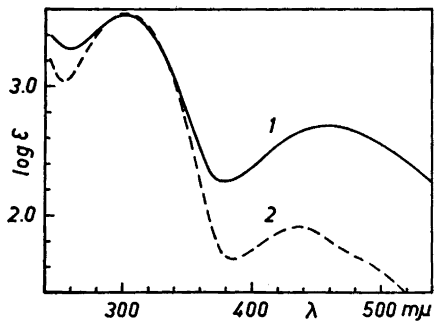

Fig. 2. Absorption spectra of dimeric 3-methoxy-1,2-benzoquinone (VIII) (curve 1), and the monohydrate XIII of dimer VIII (curve 2). Solvent: Chloroform.

87 % yield *. Together with the data reported above (analysis, IR and UV absorption), this proves structure VIII for the yellow dimer, and excludes the alternative structures VIIIa—c. The conversion VIII → V by treatment with periodate obviously involved oxidative removal of the diketo group of the bi*cyclo*octene system as well as of the two angular hydrogen atoms. The mechanism of this reaction will be discussed further in a subsequent communication [14].

The results just described strongly supported the view that the formation of β-naphthoquinone V from 3-methoxy-1,2-benzoquinone (IV) or its precursors, *i.e.* the phenols I or VII, in aqueous periodate solution, is due to dimerisation of IV followed by periodate degradation of the dimer. As mentioned above, this conversion of the *o*-benzoquinone IV into the β-naphthoquinone V proceeds very rapidly; under the conditions used (see, for instance, Table 1, Expt. 5) V could be detected already after a reaction time of 2 min, and the reaction was practically complete in 10 min.

Thus, it had to be assumed that the first step of the reaction, the dimerisation of the *o*-benzoquinone IV, proceeds in water at a comparatively high rate. This assumption, however, was not self-evident, since the dimerisation

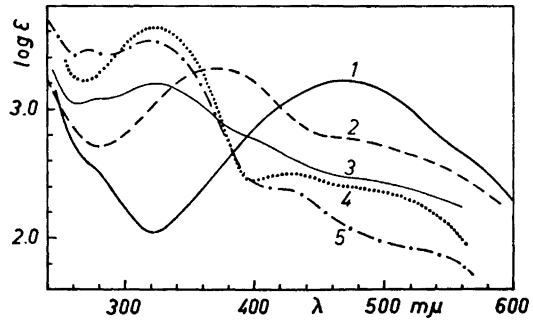

Fig. 3. Absorption spectra of 3-methoxy-1,2-benzoquinone (IV) in chloroform (curve 1), of IV dissolved in water to give a concentration of 0.6 mmole/l (curve 2), of IV dissolved in water to give a saturated solution (40 mmole/l), and then diluted to 0.6 mmole/l (curve 3) and of dimeric 3-methoxy-1,2-benzoquinone (VIII) dissolved in 25 % aqueous acetic acid (curve 4) and in water (curve 5).

* Briefly reported in Part I[1].

of IV in the organic solvents mentioned above appeared to be a comparatively slow reaction. The behaviour of 3-methoxy-1,2-benzoquinone in water — in the absence of periodate — was therefore examined in some detail.

While dilute solutions (about 1 mmole/l) of 3-methoxy-1,2-benzoquinone (IV) in chloroform show the absorption spectrum presented in Fig. 3 (curve 1, λ_{max} 468 mμ, log ε 3.23, which is very similar to the curve reported [7] for the 5-ethyl homologue of IV), a freshly prepared aqueous solution of similar concentration showed an absorption maximum at a considerably lower wavelength (Fig. 3, curve 2; λ_{max} 370 mμ, log ε 3.31). Since the absorption curve for a chloroform extract of a freshly prepared dilute aqueous solution of IV was practically identical with curve 1, the lower wavelength of the maximum in the aqueous solution could not be caused by any irreversible reaction between the methoxy-*o*-quinone and water. It might however be caused by the reversible addition of one molecule of water, forming one of the monohydrates Xa and Xb. The assumption of an equilibrium between the *o*-quinone IV and its hydrate X seems also to find support in the appearance of the long-wave branch of absorption curve 2, which has a shoulder at 460—470 mμ, *i.e.*, at the maximum position of the absorption curve of the quinone in chloroform solution (curve 1). Hydration in this way would imply the conversion of the *o*-quinonoid system of IV into an *o*-quinol-like

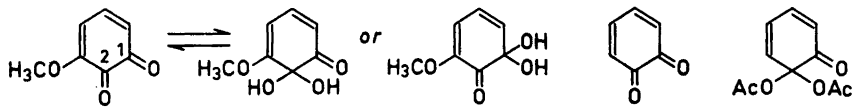

	IV	*Xa*	*Xb*	*XI*	*XII*
λ_{max}:	468	370		375	310
log ε_{max}:	3.23	3.31		3.23	3.6
Solvent:	$CHCl_3$	H_2O		$CHCl_3$	C_2H_5OH

(2,4-dienone) system (Xa or Xb), which would appear compatible with the hypsochromic shift of the absorption maximum by 98 mμ.

For comparison, absorption data for *o*-benzoquinone (XI) [7] and 2-acetoxy-*o*-quinol acetate (XII) [3] are given above; the 2,4-dienone XII has a maximum at a wavelength 65 mμ shorter than that of the *o*-quinone XI. A comparison of the pair IV and X with the pair XI and XII also shows the strongly bathochromic effect of the methoxyl substituent in the chromophoric systems involved.

Of the two isomeric hydrates Xa and b, the first seems more probable. Due to the mesomeric effect of the methoxyl group, carbon atom 1 in IV (see formula above) will be less positive than 2, and therefore less accessible to nucleophilic attack by water; furthermore, the inductive effect of the methoxyl group will strengthen the positive character of carbon atom 2. Thus, both effects will act together, and the formation of Xa will be favoured. The comparatively strong bathochromic effect of the methoxyl group, indicated by a comparison of the maxima of XII and X, would also be in harmony with formula Xa, in which the methoxyl group is at the end of the conjugated system (δ-methoxydienone).

If a freshly prepared dilute aqueous solution of 3-methoxy-1,2-benzoquinone (IV), showing absorption curve 2 (Fig. 3), is kept at room temperature, the maximum at 370 mμ gradually decreases, and new maxima at 265 and 300 mμ form during the course of a few hours. Simultaneously, the initial deep-red colour of the solution turns to brown, the material extracted by chloroform gradually decreases in amount and develops maxima at 262 and 296 mμ rather than the broad maximum at 468 mμ characteristic of the intact *o*-quinone IV. These comparatively slow transformations of the monomer in dilute aqueous solutions have not yet been further examined.

An absorption curve quite different from curve 2 in Fig. 3 (freshly prepared 0.6 mmolar aqueous solution of *o*-quinone IV) was obtained by preparation of a saturated, *i.e.*, about 40 mmolar, solution of the quinone in water and then as soon as the substance had dissolved (after about 5 min), diluting the solution with water to a concentration suitable for absorption measurement (0.6 mmolar) (Fig. 3, curve 3). The long-wave branch with a shoulder at about 470 mμ (unchanged 3-methoxy-*o*-quinone (IV)?) was markedly lower than in curve 2, and the absorption maximum of curve 2 at 370 mμ (monohydrate X?) was now only a weak inflection. A new maximum had, however, appeared at 315 mμ.

A similar maximum was also shown by aqueous and aqueous acetic acid solutions of the dimeric 3-methoxy-*o*-quinone VIII (Fig. 3, curves 5 and 4, respectively), which suggested that dimerisation of the *o*-quinone IV had taken place in the saturated aqueous solution. When the latter solution was concentrated *in vacuo*, a pale-yellow crystalline solid, m.p. 114—115° (decomp.), deposited. On treatment with periodate in aqueous acetic acid, this compound was converted, in high yield, into 3,8-dimethoxy-1,2-naphthoquinone (V). It thus behaved in the same way as dimer VIII.

The new, pale-yellow product, in an air-dry condition analysed for a dimeric methoxy-*o*-quinone containing 3 molecules of water. Two molecules of water were removed on drying at 0.04 mm Hg over phosphorus pentoxide at room temperature and can therefore be regarded as water of crystallisation, but the third molecule could not be removed. The ultra-violet absorption of the substance in chloroform solution (Fig. 2, curve 2) exhibited a maximum at 302 mμ close to that of the anhydrous dimer VIII (Fig. 2, curve 1), which indicates that the main chromophores of both compounds are similar. However, the long-wave absorption band of the new compound was markedly weaker than that of dimer VIII, indicating the presence of only one 1,2-diketo grouping.

In contrast to dimer VIII (Fig. 1b), the new product (Fig. 1c) showed a distinct hydroxyl band (2.84 μ) in the infra-red spectrum, and only three CO stretching vibration bands (5.74, 5.81, 5.95 μ) instead of the four CO bands characteristic of dimer VIII. The presence of a strong absorption band at 6.12 μ, in addition to the CO band at 5.95 μ, indicates the presence of a C=C—C=O grouping.

These data indicate that the compound, m.p. 114—115°, is a monohydrate of dimer VIII, the molecule of water being linked to VIII by covalent bonds. Since the conjugated ene-dione chromophore appears to be unaffected, the molecule of water present must have been added to one of the keto groups of the bi*cyclo*octene system. Structure XIII is therefore proposed for the substance.

Like the anhydrous dimer VIII, the hydrate XIII, when treated with *o*-phenylenediamine in pyridine, gave 1-methoxyphenazine (IX) in excellent

Scheme 2.

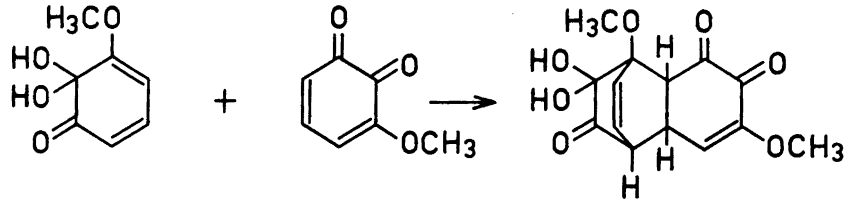

Xa *IV* *XIII*

yield (93 %), indicating that both monomer halves reacted and that a "retro-diene cleavage" had occurred. This result also supports structure XIII.

As expected, a solution of the isolated dimer hydrate XIII in water or aqueous acetic acid showed the absorption maximum at 315 mμ which had been observed in a saturated solution of 3-methoxy-*o*-benzoquinone (IV) a few minutes after it had been dissolved (*cf.* p. 523). There is therefore no doubt that XIII is formed very rapidly in aqueous solutions of IV, provided that the concentration is comparatively high, and this explains the rapid conversion of phenols I and VII and of *o*-quinone IV into β-naphthoquinone V by aqueous periodate, as described above.

The remarkably high rate of the dimerisation of 3-methoxy-*o*-quinone in water could possibly be explained as follows.It has been found earlier (preliminary report, see Ref.[15]) that *o*-quinols undergo dimerisation by Diels-Alder addition, and also that an *o*-quinol and an *o*-quinone molecule may add in a similar way, with the *o*-quinol molecule acting as a diene and the *o*-quinone molecule as a philodiene. Both types of reactions have been found to proceed very rapidly in an aqueous medium, and, in the special case studied, the *o*-quinol-*o*-quinone addition proceeded considerably faster than the self-dimerisation of the *o*-quinone involved. Monohydrate X, assumed to be formed from 3-methoxy-*o*-quinone in water (see p. 522), would be of an *o*-quinol type, and, hence, would probably possess a strong tendency to undergo a Diels-Alder reaction. The rapid formation of XIII in saturated aqueous solutions of 3-methoxy-*o*-quinone IV might then be regarded as a dimerisation of monohydrate X with subsequent loss of one molecule of water, or, alternatively, as an addition of a molecule of the *o*-quinol-like monohydrate X (diene) to a molecule of unchanged *o*-quinone IV (philodiene), as shown in Scheme 2*.

---

* *Note added in proof.* It has been found that an aqueous solution of 3-methoxy-5-methyl-1,2-benzoquinone [7] has its main absorption maximum at 370 mμ, an additional, weak band with maximum at 480 mμ also being present, whereas a single, strong band with maximum at 480 mμ is observed in chloroform solution. Although this behaviour of the compound is similar to that shown by 3-methoxy-1,2-benzoquinone (IV), the 5-methyl homologue differs from IV in being comparatively stable in aqueous solutions and showing no marked tendency to dimerisation. Therefore the view presented above (p. 524) that hydration of IV, which is believed to be the reason for the short-wave absorption in aqueous solution, might be responsible for the rapid dimerisation of this *o*-quinone in concentrated aqueous solution, seems to be contradicted by the results obtained with the 5-methyl homologue.

Alcoholic solutions of IV and its 5-methyl homologue show short-wave absorption maxima similar to those observed in water (hemiketal formation?). This behaviour is specific for 3-

There is also of course the third possibility of a diene-addition between two molecules of the *o*-quinone, followed by hydration of the dimer, which cannot be excluded.

The absorption spectrum of the dimer hydrate XIII in 25 % acetic acid was identical with that of the anhydrous dimer VIII in the same solvent (Fig. 3, curve 4), indicating that the dimer VIII, when dissolved in aqueous solvents, is converted into XIII. In fact, crystalline XIII deposited from aqueous or aqueous acetic acid solutions of VIII on concentration under reduced pressure.

The anhydrous dimer VIII dissolves rather slowly in water at room temperature, the rate of hydration probably being the limiting factor. During the time necessary for dissolution (1—2 h), the solution acquires a slightly red colour, and the absorption spectrum (Fig. 3, curve 5) differs somewhat from that of a freshly prepared, pale yellow solution in 25 % acetic acid (Fig. 3, curve 4), in which dimer VIII dissolves much more rapidly than in water; an "aged" solution in aqueous acetic acid, however, shows similar changes to those in the aqueous solution.

Neither freshly prepared nor "aged" solutions of VIII or XIII in water or in alcohols gave distinct colour reactions with ferric chloride. Heating the solutions gave dark brown-red products which were not further investigated. These also gave negative ferric chloride reactions. The dimeric 3-methoxy-*o*-quinone VIII and its monohydrate XIII thus differ from the similar dimer of unsubstituted *o*-quinone [9-11], which, on heating for a short time in water, enolises to yield the corresponding phenolic isomer. The latter gives coloured ferric complexes typical of a catechol structure.

Only one case of oxidative conversion of a phenol into a β-naphthoquinone seems to have been reported in the literature. Zincke and Francke [16] ** found that treatment of 6-bromoprotocatechuic acid with conc. nitric acid yields 3,6-dibromo-1,2-naphthoquinone-7-carboxylic acid. It can be assumed that the course of this reaction is similar to that described in the present paper.

Note: A second dimer of 3-methoxy-1,2-benzoquinone. After solutions of 3-methoxy-1,2-benzoquinone (IV) in benzene had been kept at room temperature for several hours, there could be isolated a yellow crystalline substance, m. p. 110° (decomp.). It is obviously a dimeric *o*-quinone different from the dimer VIII (m. p. 139—140°) which is formed in the (polar) organic solvents mentioned on p. 519. On treatment with *o*-phenylenediamine the new product behaved like dimer VIII (see p. 520), yielding the phenazine derivative IX of monomeric 3-methoxy-*o*-quinone (1-methoxyphenazine, m. p. 172—173°). This supports the view that the new product is formed by diene addition of 3-methoxy-*o*-quinone, in an analogous way to the formation of VIII, and reverts to the monomer when the phenazine is formed.

The dimer of m. p. 110° is still less stable than dimer VIII, and, although it was apparently obtained in a state of purity, elemental analysis has not yet given any clear results.

When treated with periodate, the new dimer is converted in high yield into the dark-violet compound (VI), m. p. 205—206°, which was obtained as a by-product in the periodate oxidation of phenols I and VII and the *o*-quinone IV in aqueous solutions (see p. 516). Thus, the dimer of m. p. 110°, or possibly a hydrate of it, appears to be formed,

---

methoxy-1,2-quinones; aqueous or alcoholic solutions of 4-methoxy-1,2-quinone and of 3-methyl- and 3-bromo-1,2-quinones, for instance, have absorption curves very similar to those found in chloroform solutions (Adler, E., Thomelius, H. and Granerus, G. *To be published*).

One of the ketonic oxygen atoms is very rapidly exchanged for ^{18}O, if 3-methoxy-5-methyl-1,2-quinone is dissolved in water enriched of $H_2{}^{18}O$, and reextracted with methylene chloride. This supports the view (see above) that rapid reversible hydration of one of the keto groups takes place (Adler, E. and Falkehag, I. *To be published*).

** Prof. H. Erdtman, Stockholm, has kindly drawn the authors' attention to this paper.

in small amounts, in aqueous solutions of *o*-quinone IV, in addition to the hydrate XIII of dimer VIII. If the assumed structure for substance VI, *i. e.*, 3,5-dimethoxy-1,2-naphthoquinone (*cf.* p. 516), is correct, the structure of the new dimer, which is the precursor of VI, will probably be represented by formula VIIIa (p. 520).

Mixtures of both dimers, VIII and VIIIa (?), were repeatedly obtained when 3-methoxy-*o*-quinone (IV) was allowed to dimerise in various organic solvents. The mixtures showed melting points between those of the pure dimers. Attempts to separate the two components by fractional crystallisation were unsuccessful and, furthermore, both dimers are adsorbed and destroyed on alumina. The presence of both dimers in these mixtures is easily demonstrated, however, by periodate oxidation and chromatographic separation of the crude oxidation product; this gives both β-naphthoquinone V and the violet substance VI in a pure state.

The dimerisation of IV in nitromethane, yielding a product with m.p. 130° (mixture of VIII and VIIIa ?), was recently reported by Horner and Dürckheimer [20].

EXPERIMENTAL

Ultra-violet spectra were measured with a Beckman DU instrument; infra-red spectra with a Perkin-Elmer instrument, model 21. Microanalyses were done by A. Bernhardt, Mülheim (Ruhr), Germany.

Periodate consumption and methanol formation were determined as described previously [17,1].

Periodate oxidation of 2,6-dimethoxyphenol (I). An ice-cooled, stirred solution of I (1.004 g = 6.52 mmole) in water (400 ml), was treated with sodium metaperiodate (4.164 g = 19.45 mmole) in ice-cold water (400 ml), added all in one lot, and the temperature of the mixture was kept at about 4°. After 2 min, excess periodate was reduced by addition of ethylene glycol (1.2 g). The dark-blue needles which had settled out during the oxidation period, were filtered off and were identified with *coerulignone (II)* by comparison with an authentic sample and by reduction with warm 50 % aqueous sodium bisulphite to dihydrocoerulignone, m. p. 190° [18]. The yield of coerulignone was 70 mg (7 %).

The dark brown-red filtrate was extracted with five 100 ml portions of chloroform. The combined dark-red chloroform solutions were dried briefly over anhydrous sodium sulphate, filtered, and divided into two equal parts, which were evaporated to dryness under reduced pressure. (Both the chloroform extraction and the evaporation were carried out as rapidly as possible in order to avoid any appreciable dimerisation of the *o*-quinone.)

a) Isolation of 3-methoxy-1,2-benzoquinone (IV). One of the crude, partially-crystalline chloroform residues (328 mg, *i.e.* 65 % yield by weight, based on I) was treated with three 150 ml portions of boiling, dry ethyl ether. The ether extracts after filtration and cooling to −80° deposited dark brown-red crystals (166 mg), m. p. 98−105°; no depression with 3-methoxy-*o*-quinone, m. p. 107−110°, prepared according to Willstätter and Müller [6]. The infra-red spectra of the two samples were essentially identical. The lower m. p. of the sample obtained by periodate oxidation was due to the presence of traces of oxidation products III and V, detected by chromatography on alumina (see below), and probably also of dimer VIII, which could not be completely removed even by repeated recrystallisation from ether.

b) *Isolation of 2,6-dimethoxy-1,4-benzoquinone (III), 3,8-dimethoxy-1,2-naphthoquinone (V) and substance VI.* The second of the two chloroform residues (325 mg) obtained above was treated with three 100 ml portions of boiling benzene. A small amount of undissolved material (2 mg) was removed by filtration, and the solution was chromatographed on a column of neutral alumina (1 × 20 cm). Elution with benzene gave the yellow 2,6-dimethoxy-*p*-quinone (III), m. p. and mixed m. p. 255−256° (31 mg, 5 % based on I), followed by the dark-violet *compound VI*, m. p. 205−206°, (12 mg, 2 %), needles from benzene-hexane. Analysis of VI indicated the composition $C_{10}H_4O_2(OCH_3)_2$. (Found: C 66.05; H 4.61; OCH_3 27.99. Calc. for $C_{12}H_{10}O_4$: C 66.05; H 4.62; OCH_3 28.44.)

Further elution of the alumina column with benzene containing 3 % ethanol eluted the red 3,8-dimethoxy-1,2-naphthoquinone (V), flat prisms or plates from benzene or acetone,

m. p. 198—199° (20 mg, 7 %). (Found: C 66.25; H 4.54; OCH_3 28.36. Calc. for $C_{12}H_{10}O_4$: C 66.05; H 4.62; OCH_3 28.44.) For derivatives of V and proof of its structure see Ref.[5].

After elution of compounds III, VI, and V, a broad black zone remained in the upper part of the column. It could not be washed out with common solvents. 3-Methoxy-1,2-benzoquinone (IV) and its dimer (VIII) both gave similar, very strongly adsorbed degradation products on alumina. The difference between the total weight of solids chromatographed (323 mg) and the combined weights of the eluted substances III, V, and VI (63 mg), *i. e.* 260 mg, was taken as a measure of the amount of *3-methoxy-1,2-benzoquinone (IV)* formed in the periodate oxidation (yield 58 %).

The experiment described above is listed as Expt. 1 in Table 1. The same procedure was used in the other experiments presented in Table 1, although neither coerulignone nor 2,6-dimethoxy-*p*-quinone were formed from 3-methoxycatechol (VII) and 3-methoxy-*o*-quinone (IV) on treatment with periodate.

Phenazine derivative obtained from VI. When the dark-violet solution of substance VI (80 mg) in pyridine (8 ml) was mixed with a solution of *o*-phenylenediamine (200 mg) in the same solvent (2 ml), the colour of the mixture immediately turned to orange. After 1 h at room temperature part of the solvent was removed under reduced pressure. Addition of water gave a crystalline precipitate which was recrystallised from methanol and methanol-water. Orange needles or prisms, m. p. 229—230°. (Found: C 74.31; H 4.84; N 9.89; OCH_3 21.09; Mol. wt. (Rast) 299. Calc. for $C_{18}H_{14}O_2N_2$: C 74.47; H 4.86; N 9.63; OCH_3 21.38; Mol. wt. 290.)

Dimeric 3-methoxy-1,2-benzoquinone, m. p. 139—140° (VIII). A solution of 3-methoxy-1,2-benzoquinone (IV) (1.6 g) in acetone (200 ml) was kept at room temperature for about 16 h. The solvent was evaporated under reduced pressure and the partially crystalline residue was washed with cold chloroform which removed unchanged monomer and brown, amorphous material. The yellow crystals remaining (yield 30—40 %), m. p. 136—138°, were dissolved in acetone with brief heating (prolonged heating in any solvent causes discoloration). Cooling to —20° yielded the dimer VIII as deep-yellow prisms, m. p. 139—140°. (Found: C 60.74; H 4.50; OCH_3 22.55. Calc. for $C_{14}H_{12}O_6$: C 60.87; H 4.31; OCH_3 22.47.)

Dimer VIII was also obtained in the same way from solutions of IV in methylene chloride, chloroform, ethyl acetate, and dioxane. Dimerisation of IV could also be carried out in the solid state. For instance, a solution of IV in methylene chloride was taken to dryness under reduced pressure in a rotating film evaporator, giving a layer of solid IV spread over the wall of the round-bottomed flask. A few millilitres of acetone or methylene chloride were then added without dissolving the major part of the solid, and the flask was stoppered. After about 16 h the initially dark-brown layer of IV had turned yellow. The crude product was purified as described above.

The product has to be stored at —20°. At room temperature and in day-light, it gradually darkens.

IR spectrum, see Fig. 1. UV spectrum, see Figs. 2 and 3.

1-Methoxyphenazine (IX) from dimer VIII. The yellow solution of dimer VIII (100 mg) in pyridine (5 ml) was mixed with a solution of *o*-phenylenediamine (130 mg) in 1 ml of the same solvent. The mixture turned orange. After 1 h at room temperature, the solvent was removed under reduced pressure and the solid residue was dissolved in chloroform. The chloroform solution was washed with 0.5 N sulphuric acid and water, and then was dried and evaporated. The yellow crystalline residue (140 mg) had m. p. 170—171°. Yield 90 %. Recrystallisation from methanol-water raised the m. p. to 172—173°, undepressed by a sample of 1-methoxyphenazine, m. p. 172—173°, (Literature [19]: 169°) obtained from 3-methoxy-*o*-quinone. The IR spectra of both samples also proved their identity.

Periodate oxidation of dimer VIII. A solution of dimer VIII (77 mg) in 50 % aqueous acetic acid (10 ml) was mixed with an aqueous solution (20 ml) of sodium metaperiodate (245 mg). After 2.5 h at room temperature, the red solution was extracted with methylene chloride. The methylene chloride solution was washed with water, dried over anhydrous calcium sulphate, and evaporated. Dark-red crystals of nearly pure 3,8-methoxy-1,2-naphthoquinone (V), m. p. 194—195°, remained. Yield 87 %. Recrystallisation from benzene raised the m. p. to 198—199°, undepressed on admixture of V, prepared as above.

Monohydrate of dimeric 3-methoxy-o-quinone (XIII). a) From 3-methoxy-o-quinone (IV). A freshly-prepared, almost saturated solution of IV (100 mg) in water (20 ml)

(36 mmole/l) was concentrated under reduced pressure to a volume of about 5 ml. On cooling in the refrigerator, a greyish yellow crystalline product deposited. Recrystallisation from acetone-hexane, ethyl acetate-hexane, or acetone-water (without heating) gave pale-yellow plates or prisms, m. p. 114—115° (decomp.). Yield 25 %.

b) *From dimer VIII.* Dimer VIII (439 mg) was dissolved in 25 % aqueous acetic acid (50 ml); the time required for it to dissolve completely (with shaking) was about 20 min. The solution was concentrated under reduced pressure to a volume of a few millilitres; water was added gradually in the final stages of the evaporation in order to reduce the amount of acetic acid in the concentrate. After cooling in the refrigerator the crystalline product which deposited, was collected. Yield 40 %. The product was identified by m. p., mixed m. p., and IR spectrum with the dimer monohydrate obtained from 3-methoxy-*o*-benzoquinone.

The methoxyl content of the air-dry product indicated that the dimer contained 3 mols. of water. (Found: OCH_3 18.52. Calc. for $C_{14}H_{12}O_6$, $3H_2O$: 18.79.) On drying over P_2O_5 for 6 h at room temperature and 0.04 mm Hg the substance lost 2 mols. of water (loss of weight found, 10.5 %, calc., 10.9 %). The dried product analysed for a monohydrate of a dimeric methoxyquinone. (Found: C 56.80; H 5.04; OCH_3 20.65. Calc. for $C_{14}H_{14}O_7$: C 57.14; H 4.80; OCH_3 21.09.) An aqueous solution of the substance was neutral. Ferric chloride colour tests for phenolic or catechol groupings were negative. The substance darkened gradually, even at low temperature. IR spectrum, Fig. 1. UV spectrum, Figs. 2 and 3.

When allowed to react with *o*-phenylenediamine in pyridine, the hydrated dimer VIII gave *1-methoxyphenazine (IX)*, m. p. 171—172°, in 93 % yield.

Treatment of an aqueous acetic acid solution of the monohydrate XIII with periodate gave *3,8-dimethoxy-1,2-naphthoquinone* (V) in about 80 % yield.

The present work has been supported financially by *Statens Naturvetenskapliga Forskningsråd* and *Statens Tekniska Forskningsråd.*

REFERENCES

1. Adler, E. and Magnusson, R. *Acta Chem. Scand.* **13** (1959) 505.
2. Adler, E. and Lindberg, C. B. *To be published.*
3. Wessely, F. and Kotlan, J. *Monatsh.* **84** (1953) 291.
4. Teuber, H.-J. and Rau, W. *Chem. Ber.* **86** (1953) 1036.
5. Adler, E., Magnusson, R. and Berggren, B. *Acta Chem. Scand.* **14** (1960) 539.
6. Willstätter, R. and Müller, E. *Ber.* **44** (1911) 2171.
7. Teuber, H.-J. and Staiger, G. *Chem. Ber.* **88** (1955) 802.
8. Otting, W. and Staiger, G. *Chem. Ber.* **88** (1955) 828.
9. Harley-Mason, J. and Laird, A. H. *J. Chem. Soc.* **1958** 1718.
10. Patchett, A. A. and Witkop, B. *J. Org. Chem.* **22** (1957) 1477.
11. Horner, L. and Dürckheimer, W. *Chem. Ber.* **91** (1958) 2532.
12. Horner, L. and Sturm, K. *Ann.* **597** (1955) 1.
13. Teuber, H.-J. *Angew. Chem.* **68** (1956) 420.
14. Adler, E. and Berggren, B. *Acta Chem. Scand.* **14** (1960) 529.
15. Adler, E. *Angew. Chem.* **69** (1957) 272, and unpublished work.
16. Zincke, Th. and Francke, B. *Ann.* **293** (1896) 120.
17. Adler, E. and Hernestam, S. *Acta Chem. Scand.* **9** (1955) 319.
18. Cybulski, C. L. *Ber.* **31** (1898) 616.
19. Wrede, F. and Strack, E. *Ber.* **62** (1929) 2053.
20. Horner, L. and Dürckheimer, W. *Z. Naturforsch.* **14b** (1959) 742.

Received October 30, 1959.

ACTA CHEMICA SCANDINAVICA 14 (1960) 529–538

Periodate Oxidation of Phenols

III. The Conversion of Dimeric *o*-Benzoquinones into β-Naphthoquinones *

ERICH ADLER and BRITT BERGGREN

Institutionen för organisk kemi, Chalmers Tekniska Högskola, Göteborg, Sweden

Dimeric *o*-benzoquinone (VI) and its phenolic isomer (VIII) both react with 3 moles of periodate to give β-naphthoquinone in 70 % yield. In the same way both dimeric 3-methoxy-*o*-benzoquinone (IV) and its monohydrate (IVa) are degraded by periodate to 3,8-dimethoxy-1,2-naphthoquinone (V). The course of these reactions was investigated. Dehydrogenation of the catechol grouping present in VIII with silver oxide gave the *o*-quinone IX, which was converted, by treatment with 2 moles of periodate, into β-naphthoquinone. Periodate cleavage of the α-diketo grouping in the diacetyl derivative of VIII, followed by alkaline hydrolysis of the product (XI), yielded 1,2-dihydroxy-5,8-dihydronaphthalene-5,8-dicarboxylic acid (XII). The latter was converted into β-naphthoquinone by treatment with periodate (2 moles) or with silver oxide. IX and XII are probable intermediates in the conversions of VI and VIII, respectively, into β-naphthoquinone.

A reaction scheme is given showing the probable course of these conversions (Scheme 3).

As reported in Part II [1] of this series, the action of excess sodium periodate on pyrogallol-1,3-dimethyl ether (I) in aqueous solution results mainly in oxidative removal of one of the methoxyl groups with the liberation of methanol and the formation of 3-methoxy-1,2-benzoquinone (II). The *o*-quinone undergoes further reactions, which are rapid when relatively high initial concentrations of phenol I are used. For instance, periodate oxidation of phenol I in 80 mM solution gave 3,8-dimethoxy-1,2-naphthoquinone (V) in 25 % yield, with a reaction time of 10 min. Under similar conditions, the β-naphthoquinone V was obtained in yields of about 50 % when pyrogallol-1-methyl ether (III) or 3-methoxy-1,2-benzoquinone (II) were treated with periodate.

* Preliminary report: Adler, E. *Angew. Chem.* **71** (1959) 580.

Scheme 1.

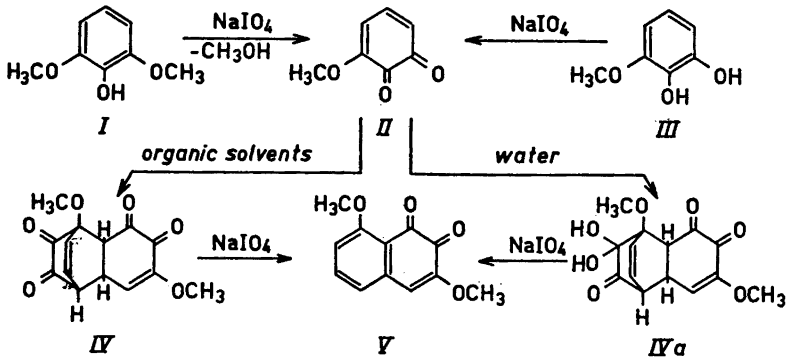

It was also found [1] that 3-methoxy-1,2-benzoquinone (II) in various organic solvents undergoes dimerisation by diene-philodiene addition, yielding the yellow dimer IV, m.p. 139—140°; in aqueous solution a monohydrate of IV, (IVa) m.p. 114—115°, is produced. Both forms of the dimeric 3-methoxy-*o*-quinone, when treated with aqueous periodate solution, were smoothly converted into the *β*-naphthoquinone V.

The formation of the 1,2-naphthoquinone V from the 1,2-benzoquinone II, in aqueous solution in the presence of periodate, is thus the result of dimerisation of II followed by periodate oxidation (*cf.* Scheme 1).

As briefly reported previously [8], the dimer of unsubstituted *o*-benzoquinone (VI) [2-5], when treated with periodate, undergoes a similar degradation, with the formation of *β*-naphthoquinone (VII). (Scheme 2).

The present communication deals with the mechanism of this oxidative conversion of dimeric 1,2-benzoquinones into 1,2-naphthoquinones. For reasons presented below, detailed studies have, as yet, only been made on the conversion of dimeric *o*-benzoquinone into *β*-naphthoquinone but probably the results obtained in these studies are also valid for the analogous reaction of the dimeric 3-methoxy-*o*-benzoquinone.

CONVERSION OF DIMERIC *o*-BENZOQUINONE (VI, VIII) INTO *β*-NAPHTHOQUINONE (VII)

Dimeric *o*-quinone (VI), dissolved in 50 % acetic acid, was found to consume nearly 3 moles of sodium periodate in about 20 min (Fig. 1, curve 1); the resulting orange solution gave *β*-naphthoquinone (VII), m.p. 145—146°, in 70 % yield.

The phenolic isomer (VIII) of dimeric *o*-quinone (VI), which is obtained by heating the quinone with ethanolic hydrochloric acid [3] or simply with water [4,5], also consumes 3 moles of periodate. In aqueous solution, the main reaction is complete after 3 min, giving *β*-naphthoquinone in 70 % yield. In 50 % acetic acid the reaction is slightly slower (Fig. 1, curves 2 and 3).

The rapid main reaction is followed by further slow periodate consumption. The similar slow oxidation of *β*-naphthoquinone itself (Fig. 1, curve 4) indicates

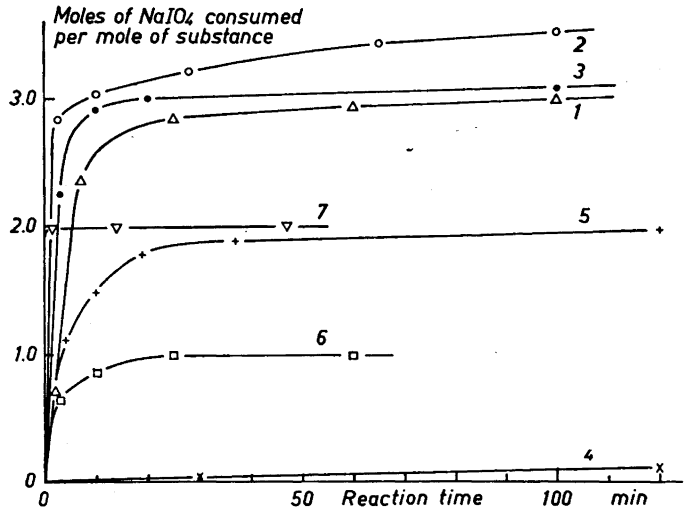

Fig. 1. Periodate consumption by dimeric *o*-quinone (VI) in 50 % aqueous acetic acid (curve 1), by the phenolic isomer VIII of dimeric *o*-quinone in water (curve 2) and in 50 % aqueous acetic acid (curve 3) and by β-naphthoquinone (VII) (curve 4), the *o*-quinone IX (curve 5), the diacetyl derivative of VIII (X) (curve 6), and 1,2-dihydroxy-5,8-dihydronaphthalene-5,8-dicarboxylic acid (XII) (curve 7), in 50 % aqueous acetic acid. The molar ratio substance/$NaIO_4$ was 1/4.

that this is due to cleavage of the 1,2-diketo grouping of the β-naphthoquinone formed in the main reaction.

When β-naphthoquinone was treated with periodate at pH 6.5 instead of the slightly acidic conditions used above (the pH value of an unbuffered aqueous solution of sodium metaperiodate is about 3.5) the oxidation proceeded at a satisfactory rate, and *o*-carboxycinnamic acid was obtained in good yield [6].

The next step in the investigation of the conversions VI → VII and VIII → VII, was the preparation of substances IX and XII, which obviously were possible intermediates.

The red *o*-quinone IX was obtained by dehydrogenating the phenolic dimer VIII with silver oxide. It has also been prepared recently by Horner and Dürckheimer [5], who used tetrachloro-*o*-quinone as dehydrogenating agent.

The dicarboxylic acid XII, m.p. 182—183°, was made by cleaving the diketo bridge of the diacetate (X) [4] of the phenolic dimer (VIII) with periodate (Fig. 1, curve 6), to give the dicarboxylic acid XI, m.p. 189—190°, and then removing the protecting acetyl groups by alkaline hydrolysis under nitrogen.

The ultra-violet and visible light absorption spectra of the ketonic dimer VI, its phenolic isomer VIII, the *o*-quinonoid substance IX, and the diacetate X are shown in Fig. 2; the spectra of the dicarboxylic acids XI and XII are shown in Fig. 3. Substances VI, VIII, IX, and X show the characteristic absorption band between 400 and 500 mμ of α-diketones. As expected, this long-wave absorption is absent from the spectra of the dicarboxylic acids XI

Scheme 2.

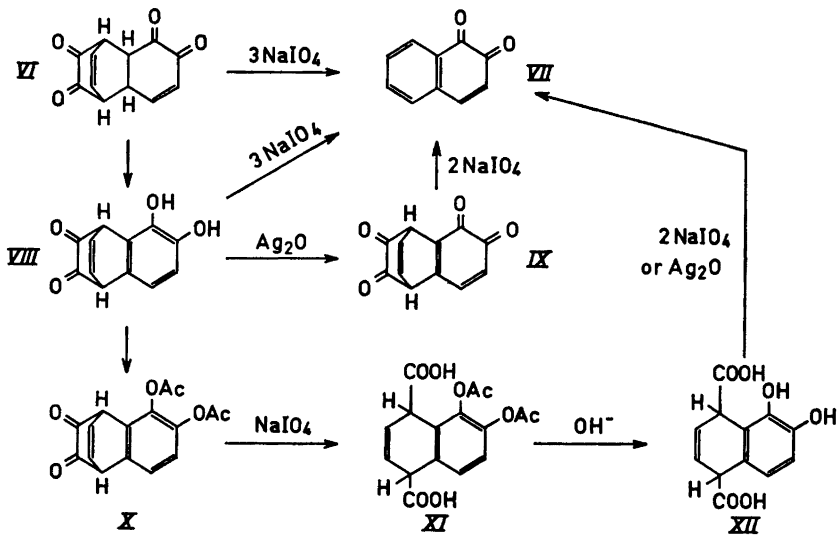

and XII. The infra-red absorption data for the acids XI and XII (see Experimental) are also in harmony with the proposed structures.

An examination was then made of the behaviour of compounds IX and XII on treatment with periodate. The *o*-quinone IX consumed 2 moles of the oxidant (Fig. 1, curve 5), and was converted into β-naphthoquinone. The dicarboxylic acid XII also consumed 2 moles of periodate very rapidly (Fig. 1, curve 7), and gave β-naphthoquinone. Surprisingly enough, the same transformation, (XII → VII), could be brought about merely by shaking a solution of XII in acetone with silver oxide.

The results described so far are summarised in Scheme 2. They suggest that the periodate oxidation of the two forms of dimeric *o*-benzoquinone (VI, VIII) giving β-naphthoquinone (VII) follows the reaction sequences shown in Scheme 3.

As indicated in Scheme 3, the primary step in the oxidation of the ketonic dimer (VI) with excess periodate can be assumed to be the cleavage of the diketo grouping of the bi*cyclo*octene system. However, attempts to isolate the expected cleavage product, *i.e.*, the diketodicarboxylic acid XIII, after treating VI (in aqueous acetic acid solution) with an equimolar amount of periodate, were without success. β-Naphthoquinone (VII) was formed, but the yield was only about a third of that obtained in experiments with excess periodate. Three moles of the oxidant were required for maximum conversion of the dimer VI into the end product, VII. This seems to indicate that the diketodicarboxylic acid (XIII) first formed, rapidly enolises to give the dihydroxydicarboxylic acid (XII), which is then converted into β-naphthoquinone (VII) with further consumption of periodate.

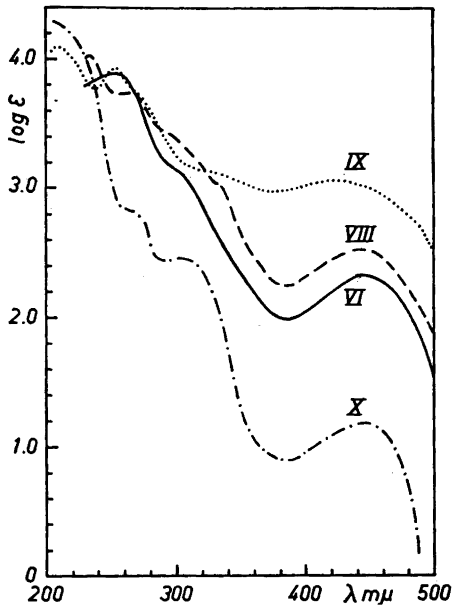

Fig. 2. Absorption spectra of dimeric *o*-quinone (VI), the phenolic isomer of dimeric *o*-quinone (VIII), the diacetyl derivative of VIII (X), and the *o*-quinone IX. Solvents: For VI and VIII, methylene chloride, for X and IX, 95 % ethanol.

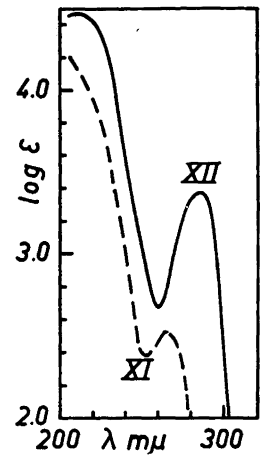

Fig. 3. Ultraviolet absorption of 1,2-dihydroxy-5,8-dihydronaphthalene-5,8-dicarboxylic acid (XII) and its diacetyl derivative (XI), in 95 % ethanol.

As described above, the dihydroxydicarboxylic acid XII is almost instantly converted into VII not only by periodate (2 moles) but also by silver oxide. This suggests that the conversion XII → VII involves dehydrogenation of the catechol grouping of XII to form an intermediate *o*-quinonoid dicarboxylic acid XIV, which immediately undergoes spontaneous decarboxylation to yield 1,2-dihydroxynaphthalene (XV), which is then dehydrogenated to give the end-product, VII. As expected, the suggested final step, XV → VII, could be shown to proceed with great ease when XV was treated either with periodate in aqueous acetic acid, in which case an equimolar amount of $NaIO_4$ was consumed almost instantly, or with silver oxide in acetone.

Starting from the phenolic form of dimeric *o*-benzoquinone (VIII), the primary step is assumed to be the dehydrogenation of the catechol grouping rather than the oxidative opening of the diketo bridge. The diketo grouping of the *o*-quinone IX thus formed would then be opened by a further mole of periodate to give the hypothetical intermediate XIV; the rapid concluding steps XIV → XV → VII are identical with those postulated above for the oxidation of the ketonic dimer VI.

The assumption of two different paths, VI → XIII → XII → XIV and VIII → IX → XIV, for the initial steps of the oxidation of the ketonic dimer

Scheme 3.

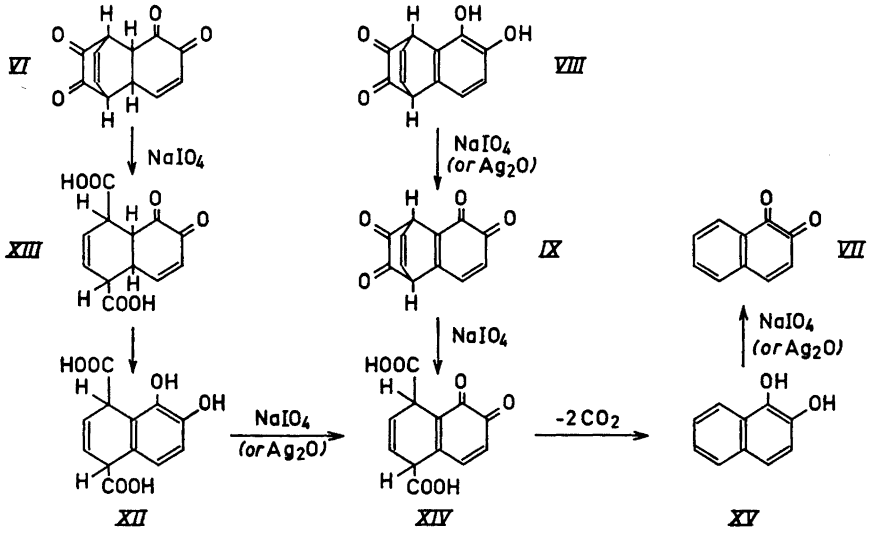

(VI) and of its phenolic isomer (VIII) might appear unnecessary. It could be supposed instead that in polar solvents the ketonic dimer VI was in equilibrium with the phenolic form VIII and that in both cases it was the phenolic form that was attacked by the periodate. However, freshly prepared solutions of the ketonic dimer VI in aqueous acetic acid or aqueous ethanol do not give the catechol colour reaction with ferric chloride, given by solutions of the phenolic dimer VIII. In these solvents the isomerisation VI → VIII proceeds so slowly at room temperature that it cannot be involved in the rapid conversion of the ketonic dimer VI into β-naphthoquinone by periodate.

It was assumed above that the hypothetical primary intermediate XIII enolises rapidly to give the partially aromatic compound XII which readily undergoes further oxidation. This assumption may seem to be in contrast to the remarkably low tendency of VI to enolise. However, an inspection of Stuart-Briegleb models indicates that the stability of VI might be explained by the greater strain shown by the bridged ring system in the enol form (VIII) than in the keto form (VI). This would cause some resistance to enolisation in the latter compound. The dihydronaphthalene derivative XII on the other hand is not more strained than XIII and enolisation of the latter would therefore be expected to proceed easily.

In dioxane or aqueous dioxane solution the enolisation VI → VIII was found to take place comparatively rapidly even at room temperature; this was indicated by the appearance of a distinct ferric chloride colour reaction immediately after dissolving the ketonic dimer (VI). The intensity of the colour increased and after about one hour approached that given by a solution of the phenolic isomer (VIII).

According to the view presented above (cf. also Scheme 3), the keto bridge carbon atoms of dimers VI and VIII are removed as carbon dioxide from the intermediate XIV, which is assumed to be formed by oxidation of both the dihydroxydicarboxylic acid (XII) and the *o*-quinone IX. Compound XIV is thus common to both pathways, VI → VII, and VIII → VII. The finding that both VI and VIII require 3 moles of periodate for conversion into β-naphthoquinone, supports this view. If, for instance, β-naphthoquinone were formed directly from the diketodicarboxylic acid XIII, by the loss of two molecules of formic acid, then one mole of periodate would have been sufficient to convert dimer VI into β-naphthoquinone.

The spontaneous rapid decarboxylation of the postulated *o*-quinonoid intermediate XIV can be attributed to the special position of the carboxylic groups, both of which are part of vinylogous β-keto acid structures (Scheme 4 A). Furthermore, a Stuart-Briegleb model of XIV suggests the possibility

Scheme 4.

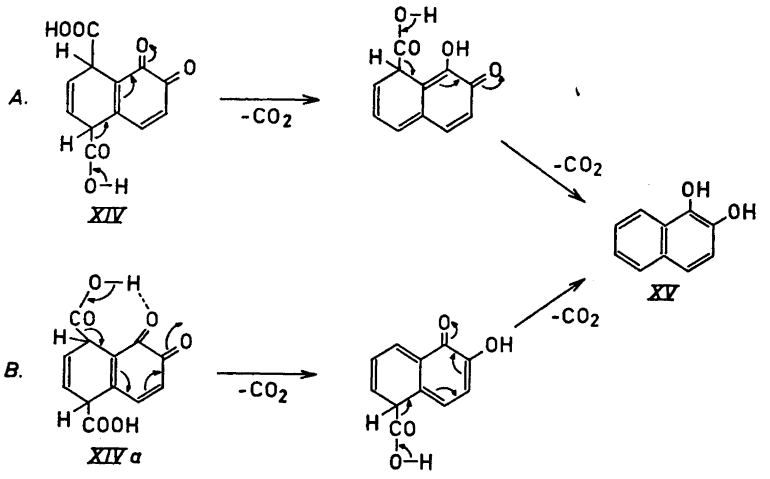

of chelation between the carboxyl group in position 8 and the keto group in position 1, as indicated in formula XIVa. This points to a mechanism for the decarboxylation of the 8-carboxyl group that is closely related to the generally accepted mechanism [7] for the decarboxylation of β-keto acids (Scheme 4 B).

CONVERSION OF DIMERIC 3-METHOXY-1,2-BENZOQUINONE (IV) AND ITS MONOHYDRATE (IVA) INTO 3,8-DIMETHOXY-1,2-NAPHTHOQUINONE(V)

As reported previously [1], treatment of dimeric 3-methoxy-1,2-benzoquinone (IV) with periodate in aqueous solution produces 3,8-dimethoxy-1,2-naphthoquinone (V) in about 85 % yield. Fig. 4, curve 1, shows the consumption of the oxidant as a function of reaction time. The comparatively rapid initial phase of the reaction seems to be completed after about 1 h. In 25 % aqueous

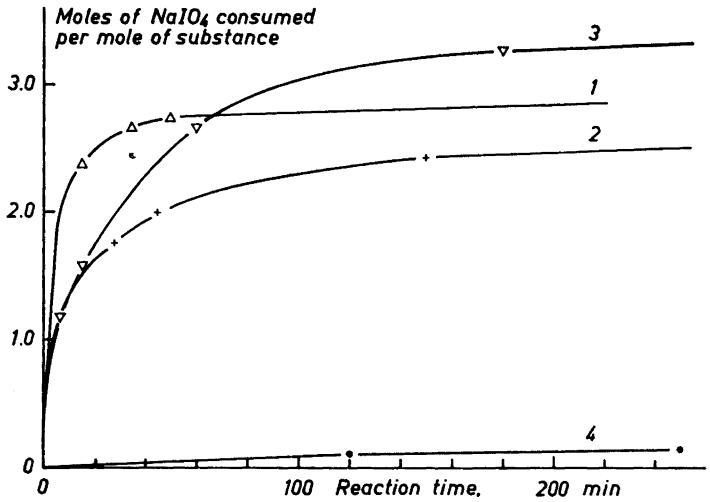

Fig. 4. Periodate consumption by dimeric 3-methoxy-1,2-benzoquinone (IV) in water (curve 1) and in 25 % aqueous acetic acid (curve 2), by the monohydrate of IV (IVa), (curve 3), and by 3,8-dimethoxy-1,2-naphthoquinone (V) in 25 % aqueous acetic acid (curve 4). Molar ratio, substance/$NaIO_4$ = 1/4.

acetic acid the reaction proceeded at a somewhat decreased rate (Fig. 4, curve 2).

The periodate consumption of the hydrated dimer IVa, in 25 % aqueous acetic acid, is shown in curve 3.

As in the degradation of dimeric *o*-quinone, further oxidation of the *β*-naphthoquinone formed was very slow; the rate of periodate consumption by isolated 3,8-dimethoxy-1,2-naphthoquinone (V) in 25 % aqueous acetic acid is shown in curve 4.

In a buffered aqueous medium (pH 6.5) the naphthoquinone V was oxidised fairly rapidly and gave 2-carboxy-3-methoxy-α-methoxycinnamic acid. This reaction was used in the elucidation of the structure of V, which will be reported in a following paper[6].

Extrapolation of curves 1 and 2 back to time zero indicates that 2,7 and 2,4 mole $NaIO_4$ per mole of dimer IV were required for the production of the naphthoquinone V, in water and dilute acetic acid, respectively. The hydrated dimer IVa however consumed about 3 mole $NaIO_4$/mole (curve 3), thus behaving in the same way as the dimeric *o*-quinone (VI, VIII, Fig. 1). The reason for the somewhat lower consumption of periodate in the case of the anhydrous dimer IV is still unknown. In spite of the differences in periodate consumption the yields of naphthoquinone V were equally high (80—85 %)[1] in the three experiments represented by curves 1, 2 and 3. Since, as reported in Part II[1], the anhydrous dimer IV, when dissolved in water, or 25 % acetic acid, is converted into the hydrate IVa, it would be expected that IV and IVa would also show the same periodate consumption. Possibly, the anhydrous

dimer to some extent undergoes some periodate-saving reaction (autoxidative cleavage of the diketo bridge?) before the hydration is complete.

Apart from the minor discrepancies just mentioned, the periodate uptake by dimeric 3-methoxy-*o*-quinone (IV, IVa) was similar to that found for dimeric *o*-quinone (VI). It therefore seems probable that the mechanism discussed above for the conversion VI → VII, will also be valid for the similar conversion IV (IVa) → V but it has not yet been possible to carry out a more detailed investigation of this reaction. The phenolic isomer of IV has not so far been obtained. Attempts to prepare its diacetate by treating IV with acetic anhydride in pyridine gave a product, which, although showing some of the properties expected, has not yet been obtained in a state of purity. For these reasons, possible intermediates corresponding to compounds IX and XII in the *o*-quinone series, have not been available for an examination of their role in the degradation of the 3-methoxy-*o*-quinone dimers (IV, IVa).

EXPERIMENTAL

Ultra-violet and visible absorption spectra were measured with a Beckman DU spectrophotometer, infra-red spectra with a Perkin-Elmer model 21 instrument (KBr). Analyses were carried out by A. Bernhardt, Mülheim (Ruhr), Germany.

Periodate consumption. In the experiments of Fig. 1 the substance (1 mmole) was dissolved (or suspended) in glacial acetic acid (50 ml) (except for curve 2, where water was used instead of HOAc), and a solution of $NaIO_4$ (4 mmole) in water (50 ml) was added. Substances VI and IX only dissolved completely about 10 min after the addition of the periodate. In the experiment of Fig. 4, curve 1, the dimeric 3-methoxy-*o*-quinone (IV) was allowed to dissolve in water, which required about 1.5 h at room temperature (hydration, *cf.* Ref.[1]), before the periodate solution was added. In the remaining experiments of Fig. 4 the samples were readily soluble in the solvents used. The concentrations were the same as given above.

Unconsumed periodate was determined on 5 ml samples of the reaction mixture as described previously [8]. The β-naphthoquinones formed were extracted before the addition of the thiosulphate-iodide mixture.

Periodate oxidation of dimeric o-*benzoquinone (VI).* A suspension of the substance (108 mg = 0.5 mmole) in glacial acetic acid (25 ml) was mixed with an aqueous solution of sodium metaperiodate (25 ml containing 440 mg = 2.0 mmole). After 30 min the clear orange-red solution was extracted with methylene chloride. The methylene chloride solution was washed with water, dried over anhydrous sodium sulphate, and taken to dryness under reduced pressure. The red crystalline residue had m.p. 144°, after recrystallisation from ether 146°, undepressed on admixture of *1,2-naphthoquinone*, m.p. 145—147° [9]. The infra-red spectra of both samples were identical. Yield of crude product, 70 %.

In the same way, *1,2-naphthoquinone* was obtained (70 %) from the *phenolic isomer VIII* by periodate oxidation in aqueous or aqueous acetic acid solution.

o-*Quinone IX.* A solution of the phenolic isomer of the dimeric *o*-quinone (VIII) [4] (300 mg) in acetone (20 ml) was shaken, in the presence of anhydrous sodium sulphate, with silver oxide (1.0 g) for 10 min. The solution was filtered and evaporated under reduced pressure. The crystalline residue was washed with cold ethyl acetate and recrystallised, without heating, from acetone-hexane. Dark-red prisms, decomposing above 220°. (Found: C 67.23; H 3.08. Calc. for $C_{12}H_6O_4$: C 67.29; H 2.83.)

The same substance has been obtained by Horner and Dürckheimer [5], who used tetrachloro-*o*-quinone as dehydrogenating agent. UV absorption see Fig. 2; the infra-red spectrum shows CO stretching vibration bands at 5.76, 5.89 and 6.02 μ. Oxidation with periodate yielded *β-naphthoquinone.*

The diacetate (X) of the phenolic form of dimeric o-*quinone*, which was previously obtained from VIII with boiling acetic anhydride [4], was prepared by treatment with acetic anhydride-pyridine at room temperature; m.p. 144°.

1,2-Diacetoxy-5,8-dihydronaphthalene-cis-*5,8-dicarboxylic acid (XI).* A solution of the diacetate X (150 mg = 0.5 mmole) in glacial acetic acid (25 ml) was mixed with an aqueous solution of $NaIO_4$ (3 mmole). After 60 min the colourless solution was extracted with methylene chloride and the extract was washed with water, dried over anhydrous Na_2SO_4 and evaporated to dryness. Colourless prisms, m.p. 189—190° after recrystallisation from ethyl acetate. Yield 70 %. (Found: C 57.47; H 4.35. Calc. for $C_{16}H_{14}O_8$: C 57.49; H 4.22.) Potentiometric titration in ethanolic solution gave two equivalence points, corresponding to equivalent weights of 342 and 170, respectively (calc.: 334 and 167).

UV-absorption spectrum see Fig. 3. IR-absorption bands: 3.2 and 3.75—4.0 μ (COOH); 5.72—5.82 μ (CO of vinyl ester and carboxyl groups); 6.17, 6.30 (both weak) and 6.72 μ (aromatic nucleus).

1,2-Dihydroxy-5,8-dihydronaphthalene-cis-*5,8-dicarboxylic acid (XII).* Diacetate XI (500 mg) was dissolved, with careful exclusion of air, in a mixture of ethanol (25 ml) and 10 % aqueous sodium hydroxide (6 ml). After 6 h, the solution was acidified with aqueous sulphuric acid. Extraction with methylene chloride removed only traces of an oily material; the solution was then extracted with ethyl acetate and the extract was washed with water, dried over anhydrous calcium sulphate and evaporated to dryness. The crystalline residue (yield 67 %) was recrystallised from ethyl acetate-hexane; colourless prisms, m.p. 182—183° (decomp.). The product contained 1/3 mole of water of crystallisation, which was not removed on drying over P_2O_5 in a high vacuum at room temperature. (Found: C 56.46; H 4.16. Calc. for $C_{12}H_{10}O_6$,1/3 H_2O: C 56.25; H 4.20). When heated for 2 h at 90° (0.1 mm Hg), the substance lost 2.30 % of its weight (calc. for 1/3 mole H_2O: 2.48 %) and then analysed for the anhydrous product. (Found: C 57.66; H 4.20. Calc. for $C_{12}H_{10}O_6$: C 57.60; H 4.03). Neutralisation equivalent of the substance before dehydration: found 128, calc. 125.

Addition of ferric chloride to an ethanolic solution of the substance produced a rather unstable dark-green colour, which turned to blue-violet on addition of aqueous sodium bicarbonate. UV absorption of the substance see Fig. 3. IR absorption bands: 2.91 μ (phenolic OH); 3.25 and 3.65—3.90 μ (COOH); 5.79 μ (COOH) and 5.91 μ (8-COOH chelated with 1-OH?); 6.14, 6.26 and 6.67 μ (aromatic nucleus).

Oxidation of XII. a) A solution of XII in 50 % aqueous acetic acid was treated with sodium periodate (3 mole/mole of XII); 2 moles $NaIO_4$ were consumed in 1—2 min (*cf.* Fig. 1). Extraction with methylene chloride gave *β-naphthoquinone* in high yield.

b) A solution of XII in acetone was shaken for 5 min with silver oxide and anhydrous Na_2SO_4. Filtration and evaporation yielded red crystals, identified as *β-naphthoquinone* by m.p. (145—146° after sublimation *in vacuo*), mixed m.p. and infra-red absorption.

Oxidation of 1,2-dihydroxynaphthalene (XV) with periodate or with silver oxide, as in the preceding experiments, also yielded *β-naphthoquinone.*

REFERENCES

1. Adler, E., Magnusson, R., Berggren, B. and Thomelius, H. *Acta Chem. Scand.* **14** (1960) 515.
2. Willstätter, R. and Müller, H. E. *Ber.* **44** (1911) 2171, p. 2187; *cf.* also Goldschmidt, S. and Graef, F. *Ibid.* **61** (1928) 1868.
3. Patchett, A. A. and Witkop, B. *J. Org. Chem.* **22** (1957) 1477.
4. Harley-Mason, J. and Laird, A. H. *J. Chem. Soc.* **1958** 1718.
5. Horner, L. and Dürckheimer, W. *Chem. Ber.* **91** (1958) 2532.
6. Adler, E., Magnusson, R. and Berggren, B. *Acta Chem. Scand.* **14** (1960) 539.
7. Westheimer, F. H. and Jones, W. A. *J. Am. Chem. Soc.* **63** (1941) 3283; Schenkel, H. and Schenkel-Rudin, M. *Helv. Chim. Acta* **31** (1948) 522.
8. Adler, E. and Magnusson, R. *Acta Chem. Scand.* **13** (1959) 505.
9. Fieser, L. F., in *Org. Syntheses* **17** (1937) 68.

Received October 30, 1959.

ACTA CHEMICA SCANDINAVICA 14 (1960) 539–549

Periodate Oxidation of Phenols

IV. Structure of the Periodate Oxidation Product of a Dimeric 3-Methoxy-*o*-quinone

ERICH ADLER, RUNE MAGNUSSON and BRITT BERGGREN

Institutionen för organisk kemi, Chalmers Tekniska Högskola, Göteborg, Sweden

The red product, m. p. 198 – 199°, formed by the action of periodate on pyrogallol-1,3-dimethyl ether, pyrogallol-1-methyl ether, 3-methoxy-*o*-quinone, and dimeric 3-methoxy-*o*-quinone (m. p. 139 – 140°), was shown to be 3,8-dimethoxy-1,2-naphthoquinone (IIIa).

In the initial step of a series of degradation reactions, IIIa was treated with periodate at pH 6.5. Although unbuffered solutions of $NaIO_4$ (pH about 4) attack the β-naphthoquinone IIIa extremely slowly, oxidative cleavage proceeded at a satisfactory rate in the buffered medium and gave 2-carboxy-3-methoxy-α-methoxycinnamic acid (VIII) in good yield. A similar periodate cleavage was carried out with 3-methoxy-1,2-naphthoquinone (XVII) and with unsubstituted β-naphthoquinone.

The cinnamic acid VIII was converted, via 7-methoxyphthalide-3-methoxyacetic acid (IX), into 8-methoxy-*iso*coumarin-3-carboxylic acid (X), which was demethylated to give the corresponding 8-hydroxy compound (XI). X was degraded by alkali to 2-methyl-6-methoxybenzoic acid (XII), which gave *m*-cresol on boiling with aqueous hydriodic acid.

2-Carboxy-α-methoxycinnamic acid (XVIII), obtained by periodate oxidation of XVII, was converted to *iso*coumarin-3-carboxylic acid (XIX) on heating.

As reported in preceding papers [1,2], the action of sodium periodate on pyrogallol-1,3-dimethyl ether, pyrogallol-1-methyl ether, and 3-methoxy-1,2-benzoquinone (I) in aqueous solutions gives, among other products, a red compound, $C_{10}H_4O_2(OCH_3)_2$, m.p. 198—199°. Its formation has been shown to be due to a dimerisation of I (which is either used as starting material or formed as an intermediate in the periodate oxidation of the pyrogallol ethers) followed by degradation of the dimer by the periodate present. A dimeric 3-methoxy-*o*-quinone, m.p. 139—140°, could be obtained from solutions of I in organic solvents, and a monohydrate of the dimer, m.p. 114—115°, was obtained from aqueous solutions of I. Both products were readily converted into the red substance, m.p. 198—199°, when treated with periodate. The present paper deals with the structure of the red oxidation product.

The isolation of a further dimer of 3-methoxy-*o*-quinone, m. p. 110°, which is formed in benzene solutions of the monomer, and the periodate degradation of this lower-melting dimer to a violet compound, m. p. 205—206°, isomeric with the red product, m. p. 198—199°, have been mentioned in a previous paper [1]. The structures of this second dimer and its oxidation product are still under investigation.

The properties of the first-mentioned dimer, m.p. 139—140°, indicated [1] that it was formed by Diels-Alder reaction between two molecules of monomer I, and probably had structure II, analogous to the structure of the dimeric *o*-quinone [3]. Due to the unsymmetrical substitution of I, its dimerisation could give rise to two isomers, IIa and IIb. The analytical composition of the red periodate oxidation product of II showed that it might be a dimethoxy-naphthoquinone, and structures IIIa or IIIb therefore seemed very probable. This paper describes experimental evidence showing that this was correct and enabling a decision to be made between IIIa and IIIb.

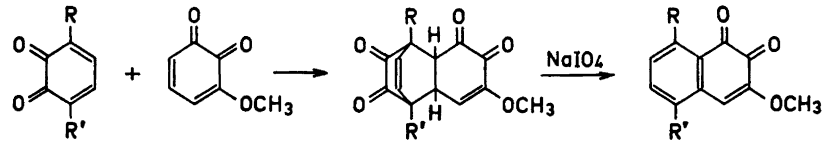

Ia, Ib *I* *IIa, IIb* *IIIa, IIIb*

Ia, IIa, IIIa: R = OCH_3, R′ = H
Ib, IIb, IIIb: R = H, R′ = OCH_3

The absorption spectra of the red compound were in harmony with the view that it was a naphthoquinone derivative. Its infra-red absorption spectrum exhibited the double carbonyl band (maxima at 5.98 and 6.03 μ) characteristic of quinones. Comparison of the absorption spectrum in the ultraviolet and visible region (Fig. 1) with the absorption spectra of known naphthoquinones [4,5] revealed a close resemblance with that reported for 3-methyl-6,8-dimethoxy-1,2-naphthoquinone [5]. Furthermore, reduction with zinc dust in acetic acid gave a leuco compound, m.p. 141—143°, which was converted into a diacetate, m.p. 152—153°, with an ultra-violet absorption (Fig. 1) typical for a naphthalene derivative. Oxidation of the red compound with permanganate gave 3-methoxyphthalic acid (VI), and treatment with *o*-phenylenediamine gave a yellow phenazine, m.p. 164—165°, the absorption spectrum of which (Fig. 1) was similar to those reported for benzo[*a*]phenazines [4]. These data clearly indicate that the red substance is a dimethoxy-1,2-naphthoquinone carrying one methoxyl group in each ring (IIIa or IIIb). The structures of the derivatives mentioned above can then be represented by formulae IV, V and VII, with the methoxyl groups arranged as in IIIa, or by corresponding formulae, in which the positions of the methoxyl groups would be those shown in IIIb.

A decision between the two possibilities IIIa and IIIb could be made by the following experiments.

Although the degradation of dimer II to β-naphthoquinone III by periodate was fast [1,2], the latter compound, although containing a 1,2-diketo grouping,

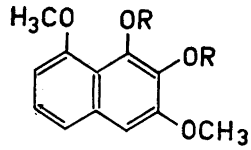

IV R=H
V R=Ac

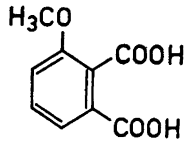

VI

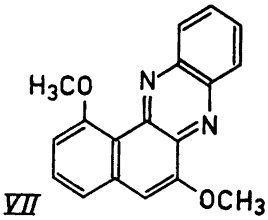

VII

was attacked only very slowly by excess of the oxidant under the conditions used, *i.e.* in aqueous or aqueous acetic acid solution. However, on treatment with an aqueous periodate solution, buffered to pH 6.5, naphthoquinone III was comparatively rapidly oxidised to a colourless acid, m.p. 142°. Its analytical composition and equivalent weight were in harmony with structure VIII, 2-carboxy-3-methoxy-α-methoxycinnamic acid, or the corresponding 6-methoxy isomer. The similarity of the ultra-violet absorption spectrum of the substance with those of 2-carboxycinnamic acid (XXII) [6,7] and 2-carboxy-α-methoxycinnamic acid (XVIII) (see below) (Fig. 2) supported this structure.

It was intended to convert the 2-carboxy-3-(or 6-) methoxy-α-methoxy cinnamic acid VIII, by heating with hydriodic acid, into either 2-carboxy-3-hydroxy-hydrocinnamic acid (XV) or its 6-hydroxy isomer. Identification of either of the latter products would have been easy, since the methyl ethers of both isomers and, as well, the lactone of the 6-hydroxy isomer had been made available by recent work of Eastham and Larkin [8]. In a preparatory attempt to demethylate 2-carboxy-3-methoxy-hydrocinnamic acid (XIV) * with hydriodic acid, the expected acid XV was decarboxylated and 3-hydroxy-hydrocinnamic acid (XVI) was formed.

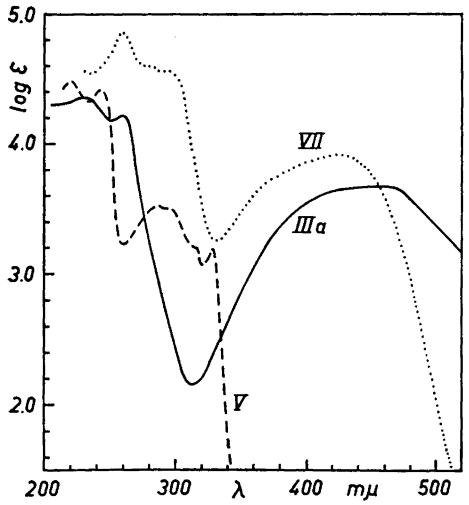

Fig. 1. Absorption spectra of 3,8-dimethoxy-1,2-naphthoquinone (IIIa), 1,2-diacetoxy-3,8-dimethoxy-naphthalene (V), and 1,6-dimethoxybenzo[*a*]phenazine (VII). Solvent: 95 % ethanol.

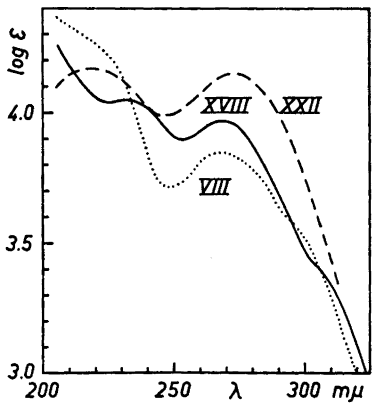

Fig. 2. Ultraviolet absorption spectra of 2-carboxycinnamic acid (XXII), 2-carboxy-α-methoxycinnamic acid (XVIII), and 2-carboxy-3-methoxy-α-methoxycinnamic acid (VIII). Solvent: 95 % ethanol.

Treatment of VIII with boiling aqueous hydriodic acid (d = 1.70) produced neither of the possible hydrocinnamic acids, but instead, gave 8-hydroxy-*iso*coumarin-3-carboxylic acid (XI) (*cf.* below).

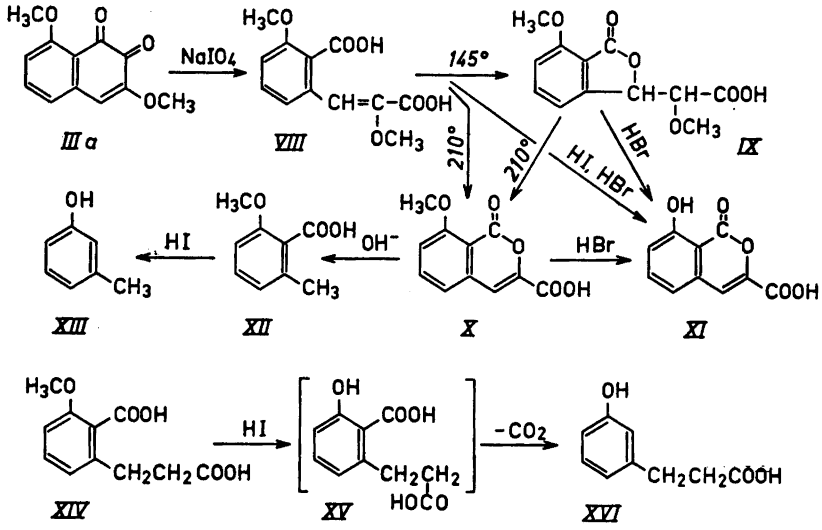

Like 2-carboxycinnamic acid (XXII)[6,7], the dimethoxy derivative VIII (or the corresponding 6-methoxy isomer?) underwent cyclisation when heated to the melting point, giving a lactone acid, m.p. 205°, which must be either 7-methoxyphthalide-3-methoxyacetic acid IX or the corresponding isomer with a methoxyl group in position 4 rather than 7. These structures are supported by infra-red data (see Experimental) as well as by the general appearance of the ultra-violet absorption curve of the substance, which is similar to that of XXIII which was obtained by cyclisation of XXII, although the long-wave maximum of IX is shifted towards higher absorbance and wave-length, which can be explained by the presence of the nuclear methoxyl substituent (Fig. 3).

The lactone acid IX melted (at 205°) with vigorous evolution of gas, and the melt solidified to yield a new compound (X), m.p. 258°. Analysis showed that the decomposition occurring at the melting point of IX was not due to decarboxylation but to the loss of one mol. of methanol. As expected, X was also obtained directly from the cinnamic acid VIII, by heating to 205—210°, the transformations VIII → IX and IX → X taking place consecutively at 145° and 205—210°, respectively.

The structure of compound X was elucidated in the following way.

3-Methoxy-1,2-naphthoquinone (XVII)[4], when treated with periodate at pH 6.5, gave 2-carboxy-α-methoxycinnamic acid (XVIII), m.p. 137° (U.V. absorption curve see Fig. 2). On melting, this substance reacted in the same way as its 3- (or 6-)methoxy derivative (VIII). The primary cyclisation pro-

* The authors are indebted to Prof. J. F. Eastham, University of Tennessee, Knoxville, U.S.A., for a gift of samples of the 3-methoxy and 6-methoxy derivatives of 2-carboxy-hydrocinnamic acid.

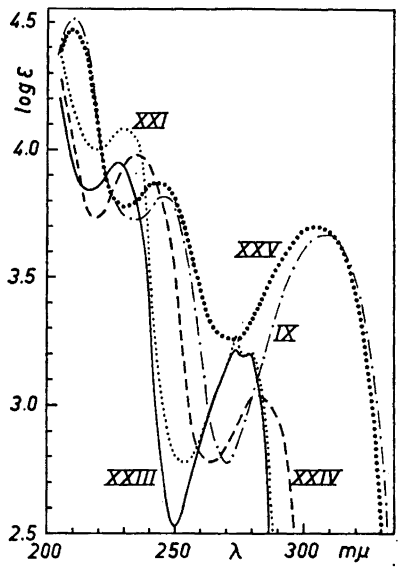

Fig. 3. Ultraviolet absorption spectra of 3-phthalide acetic acid (XXIII, ————); 7-methoxyphthalide-3-methoxyacetic acid (IX, —.—.—); γ-lactone of 2-carboxyphenylglyceric acid (XXI b, ...); 3,4-dihydro*iso*coumarin-3-carboxylic acid (XXIV, — — —); 8-methoxy-3,4-dihydro-*iso*coumarin-3-carboxylic acid (XXV, °°°°°). Solvent: 95 % ethanol.

duct, which would correspond to structure IX (H instead of the nuclear methoxyl substituent), was not isolated in this case, as the second reaction step, *i.e.*, the loss of one mole of methanol, obviously began at a temperature only slightly above the melting point of XVIII. Thus, on heating at 142—160°, a methoxyl-free lactone acid, m.p. 244—245°, was formed. As expected, it was identical with *iso*coumarin-3-carboxylic acid (XIX) obtained by Bamberger [9] and Zincke [10] from β-naphthoquinone (XX) *via* the hydroxylactone acid XXI. The ultra-violet absorption spectrum of XIX is of the same type as that of product X, although the long-wave maximum of the latter is shifted to higher absorbance and wave-length due to the presence of the methoxyl group (Fig. 4). The infra-red absorption spectra of X and XIX are very similar, both exhibiting bands typical of carboxylic OH, a lactone-CO, a carboxylic CO, and a C=C bond conjugated with carboxyl, the corresponding bands for the two compounds being situated at almost the same wave-lengths (see Experimental). On the basis of these results, the analytical composition, $C_{11}H_8O_5$, and the neutralisation equivalent (found: 205, calc.: 220), substance X can be assigned the structure 8- (or 5-)methoxy-*iso*coumarin-3-carboxylic acid.

On treatment with boiling aqueous hydrobromic acid (d = 1.49), X was converted into a phenol, m.p. 290°, which was also obtained from both VIII and IX by similar treatment, or by heating with aqueous hydriodic acid. The ultra-violet absorption curve of the phenolic substance (Fig. 4) was very similar to that of the ether X, and titration indicated that the carboxyl group had been retained. Ethanolic ferric chloride gave a stable, intense violet-blue colour, the absorption spectrum of which was comparable to that of the ferric complexes of salicylic acid and — at least in the position of the maximum — of methyl salicylate (Fig. 5). The phenolic product must therefore be 8-hydroxy-*iso*coumarin-3-carboxylic acid (XI). This implies that the methoxyl

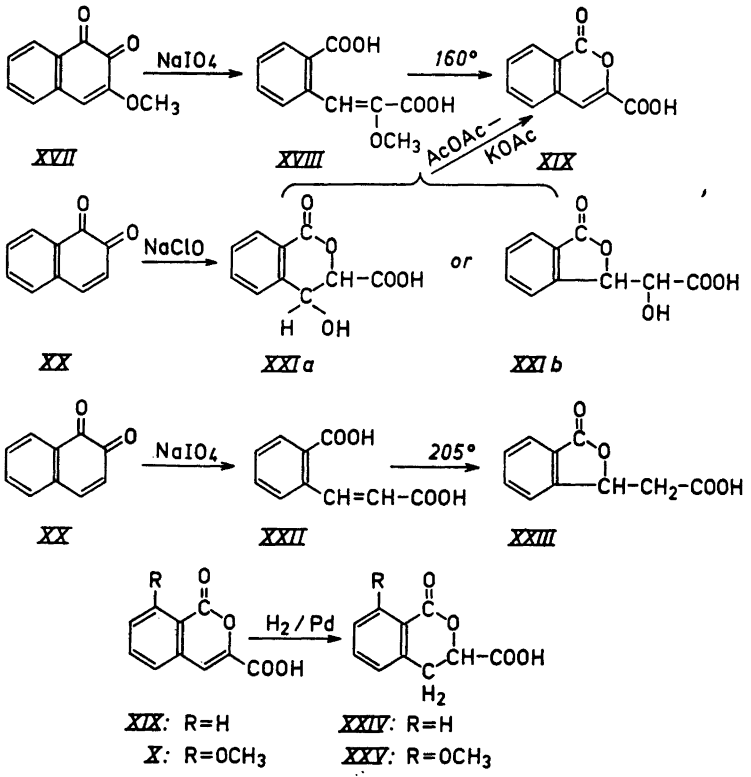

groups of β-naphthoquinone III are in the 3,8-positions (IIIa) rather than in the 3,5-positions (IIIb). Correspondingly, the positions of the nuclear methoxyl substituent in the derivatives IV, V and VII, as well as in the degradation intermediates VIII, IX and X are those given in the formulae above.

This conclusion was confirmed by further degradation of 8-methoxy-*iso*-coumarin-3-carboxylic acid (X). Bamberger [12] has shown that *iso*coumarin-3-carboxylic acid (XIX), when heated with strong alkali, is broken down to *o*-toluic acid. Compound X in this way yielded 2-methyl-6-methoxybenzoic acid (XII). On heating with hydriodic acid, acid XII was demethylated, and the expected 2-methyl-6-hydroxybenzoic acid was simultaneously decarboxylated giving *m*-cresol (XIII) as the only reaction product.

These results definitely establish structure IIIa for the starting material, and, therefore, structure IIa for the dimeric 3-methoxy-*o*-quinone.

A few remarks may be added regarding the structures of some of the compounds involved in the present work, especially the structure of the hydroxylactone acid XXI mentioned above.

The five-ring lactone (phthalide) structure of the cyclisation products IX and XXIII seems to be well established, as it is highly probable that the addition of the aryl carboxylic group to the ethylenic bond of the acrylic acid substituent in VIII and XXII will follow the general mechanism of such reactions. The six-ring enol lactone (*iso*coumarin) structure of substances X, XI and XIX is also undoubtedly correct, satisfactory evidence for the structure of XIX having been provided by the work of Bamberger [9] and Zincke [10,11].

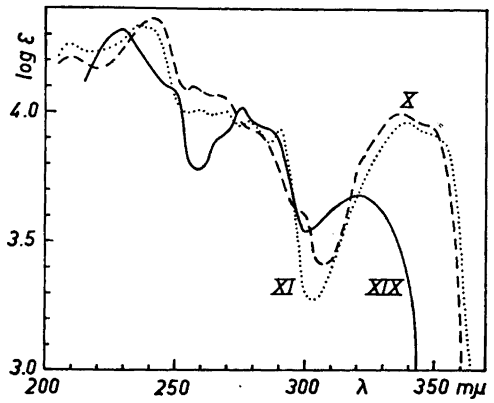

Fig. 4. Ultraviolet absorption spectra of *iso*coumarin-3-carboxylic acid (XIX, ————); 8-methoxy*iso*coumarin-3-carboxylic acid (X, — — —); 8-hydroxy*iso*coumarin-3-carboxylic acid (XI . . . . .). Solvent: 95 % ethanol.

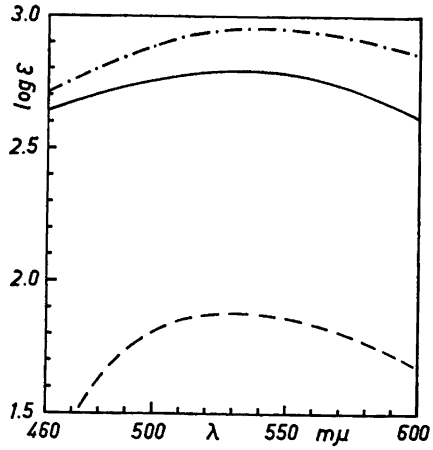

Fig. 5. Light absorption of the Fe^{3+} chelates of 8-hydroxy*iso*coumarin-3-carboxylic acid (XIX, ————); salicylic acid, —.—.—.—, methyl salicylate — — — —. The ferric chelate solutions were prepared by adding 0.2 ml of a 1 % solution of $FeCl_3$ in 96 % ethanol to 4 ml of a solution of the substance in the same solvent. The concentration of substance XIX and of salicylic acid was 1.5×10^{-3} M, that of methyl salicylate was 8.5×10^{-3} M.

However, there did not appear to be unambiguous evidence for the δ-lactone structure XXIa proposed by the latter authors for the hydroxylactone acid obtained by hypochlorite oxidation of β-naphthoquinone. The δ-lactone structure XXIa rather than a γ-lactone structure (XXIb) had been accepted [9,10] as it seemed to explain the ease with which the substance was dehydrated to give the *iso*coumarincarboxylic acid XIX when it was heated above the m. p.[10], or on heating with mineral acid [9], or with acetic anhydride [11]. As shown above, the *iso*coumarin system is, however, also readily formed from a γ-lactone (*cf.* IX → X or IX → XI) with a methoxyacetic acid substituent at position 3 of the phthalide system. By analogy, the assumption of a γ-lactone structure (XXIb) for the hydroxylactone acid of Bamberger and Zincke would also seem to be in harmony with its convertibility into the *iso*coumarin XIX.

In fact, the ultra-violet spectrum of the hydroxylactone acid XXI is very similar to that of the γ-lactone XXIII (see Fig. 3), and differs markedly from that of 3,4-dihydro-*iso*coumarin-3-carboxylic acid (XXIV) [12], a δ-lactone isomeric with the γ-lactone XXIII.

The 8-methoxyl analogue of XXIV, *i. e.*, the δ-lactone XXV, m. p. 238°, cannot be used in this comparison, as the methoxyl group present causes a hyperchromic and bathochromic shift similar to that encountered in the case of the isomeric γ-lactone IX; *cf.* Fig. 3. XXV was obtained by catalytic hydrogenation of X.

The infra-red spectrum of the hydroxylactone acid XXI shows a lactone carbonyl band at 5.67 μ, *i. e.*, at the same position as the γ-lactones IX (5.67 μ) and XXIII (5.65—5.70 μ). However, the corresponding bands of the δ-lactones XXIV (5.63—5.69 μ) and XXV (5.68—5.73 μ) are very close to these positions, and, therefore, no conclusion on the size of the lactone ring of XXI can be drawn from the position of its lactone carbonyl band.

Consideration of the ultra-violet absorption data given above, strongly suggests however that Bamberger and Zincke's hydroxylactone acid has the γ-lactone structure XXIb rather than the previously accepted δ-lactone structure XXIa.

The conversion of the γ-lactones IX and XXIb into the *iso*coumarin derivatives X and XIX, respectively, by loss of a molecule of methanol (or water) and simultaneous ring enlargement, could proceed by the following mechanism:

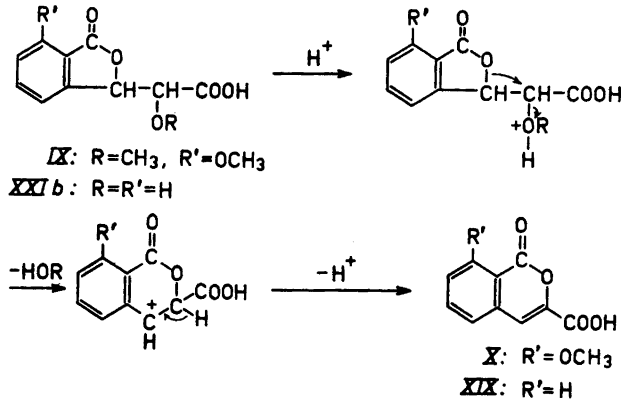

EXPERIMENTAL

Ultra-violet spectra were measured with a Beckman DU spectrophotometer. Infra-red spectra were recorded on a Perkin-Elmer model 21 instrument, using KBr discs. Microanalyses were made by Alfred Bernhardt, Mülheim.

3,8-Dimethoxy-1,2-naphthoquinone (IIIa). The isolation of this substance from reaction mixtures obtained on periodate oxidation of pyrogallol-1,3-dimethyl ether, pyrogallol-1-methyl ether, 3-methoxy-*o*-quinone (I), dimeric 3-methoxy-*o*-quinone (IIa) and the monohydrate of IIa has been described previously [1,2]. As a starting material in the present investigation the compound was prepared as follows.

An aqueous solution of sodium metaperiodate (20.6 g in 200 ml) was added to a stirred solution of pyrogallol-1-methyl ether (4.5 g) in water (200 ml), the temperature of the reaction mixture being kept below 20° by the addition of ice. After 10 min, ethylene glycol (6.0 g) was added. The reaction mixture was stirred a few minutes longer, diluted with water and extracted exhaustively with chloroform. The dark-red chloroform solution was dried over anhydrous calcium sulphate, and evaporated to dryness. The solid residue (2.3 g), after one recrystallisation from benzene, yielded 1.74 g (49.5 %) of nearly pure IIIa, brilliant red plates, m. p. 194–195°. Further recrystallisation increased the m. p. to 198–199°. Analyses see Ref.[1]. Absorption spectrum, Fig. 1.

Chromatography of the benzene mother liquors on alumina gave further amounts of IIIa and small amounts of a violet substance, m. p. 205–206° (*cf.* Ref.[1]).

1,2-Dihydroxy-3,8-dimethoxynaphthalene (IV). 3,8-Dimethoxy-1,2-naphthoquinone (IIIa) (200 mg), dissolved in glacial acetic acid (5 ml), was reduced with zinc dust giving a nearly colourless solution. After dilution with water, the mixture was filtered, and the filtrate was extracted with ether. The ethereal solution was dried over anhydrous sodium sulphate and evaporated. The crystalline residue (120 mg) was found to undergo rapid autoxidation; sublimation (120° bath temperature, 0.5 mm Hg) yielded light-red crystals. This material was recrystallised from benzene, to which ascorbic acid was added, which brought about decolorisation of the boiling solution. On cooling, slightly reddish flat prisms (97 mg) were obtained, which after a further recrystallisation from benzene had m. p. 141–143°. (Found: C 66.53; H 5.75; OCH_3 27.39. Calc. for $C_{12}H_{12}O_4$: C 65.44; H 5.49; OCH_3 28.18.) Brief treatment of IV with aqueous sodium periodate regenerated the naphthoquinone.

The *diacetate* (V) was obtained by treating freshly prepared IV with a boiling mixture of acetic anhydride and pyridine for a few minutes. Colourless prisms from ethanol, m. p. 152–153°. (Found: C 63.15; H 5.27; OCH_3 20.40. Calc. for $C_{16}H_{16}O_6$: C 63.03; H 5.26; OCH_3 20.07.)

Permanganate oxidation of 3,8-dimethoxy-1,2-naphthoquinone (IIIa). A 4 % aqueous solution of potassium permanganate (25 ml) was added slowly to a stirred suspension of IIIa (226 mg) in N sulphuric acid (25 ml). After 24 h sulphur dioxide was passed into the reaction mixture. The resulting solution, which was practically colourless, was continuously extracted with ether for 18 h. The ethereal solution was dried and evaporated, and the residue was recrystallised from ether, giving *3-methoxyphthalic acid (VI)*, (yield 23 %), m. p. 173—175°, undepressed on admixture of an authentic sample of VI (m. p. 174—176°), obtained by acid permanganate oxidation of 1,2-dimethyl-3-methoxybenzene [13]. Heating of either sample of the acid to 180°, followed by sublimation at a bath temperature of 170° (0.01 mm Hg), yielded *3-methoxyphthalic anhydride*, m. p. and mixed m. p. 164—165°. The identity of the two samples of the anhydride was confirmed by comparison of their IR absorption spectra.

1,6-Dimethoxybenzo[a]phenazine (VII). A solution of 3,8-dimethoxy-1,2-naphthoquinone (IIIa) (0.5 mmoles) in glacial acetic acid (40 ml) was mixed with a solution of *o*-phenylenediamine (1 mmole) in the same solvent (10 ml). After 30 min heating on a steam-bath the solvent was removed under reduced pressure and the residue was dissolved in methanol. Addition of water produced a voluminous precipitate of fine brownish-yellow needles, which softened at 80—100°, solidified again on further heating, and melted at 160°. Analysis of the substance after drying at room temperature, indicated the presence of 2 moles of water. (Found: C 66.75; H 5.47; N 8.45; OCH_3 18.83. Calc. for $C_{18}H_{14}O_2N_2$, $2H_2O$: C 66.25; H 5.56; N 8.58; OCH_3 19.02.)

When dried at 60° (0.01 mm Hg), the substance lost 12.65 % of its weight (calc. for 2 H_2O: 11.04 %). Recrystallisation from benzene-hexane gave golden-yellow prisms, m. p. 164—165°. (Found: C 73.94; H 4.95; N 10.07; OCH_3 21.05. Calc. for $C_{18}H_{14}O_2N_2$: C 74.47; H 4.86; N 9.63; OCH_3 21.38.) UV spectrum, Fig. 1.

2-Carboxy-3-methoxy-α-methoxycinnamic acid (VIII). 3,8-Dimethoxy-1,2-naphthoquinone (IIIa) (600 mg) was suspended in 0.5 M phosphate buffer solution (180 ml) of pH 6.5, sodium metaperiodate (3 g) in water (60 ml) was added and the mixture was shaken for 2.5 h. Some inorganic material ($NaIO_3$) was removed by filtration and the pale yellow filtrate was then acidified with 2 N HCl and thoroughly extracted with ethyl acetate. After drying over anhydrous calcium sulphate the solvent was evaporated under reduced pressure. The crystalline residue (644 mg) was recrystallised from acetone-chloroform. Colourless rods (437 mg; yield 63 %), m. p. 142—143°; the melt solidified (cyclisation product IX). On slow heating substance VIII is gradually converted to IX and may not show any sharp melting point. (Found: C 57.06; H 4.86; OCH_3 24.30. Calc. for $C_{12}H_{12}O_6$: C 57.14; H 4.79; OCH_3 24.61.) Neutralisation equivalent, found, 132, calc., 126. UV spectrum, Fig. 2. IR maxima (μ): 3.5 and 3.75—3.95 (carboxylic OH); 5.84—5.92 (CO of α,β-unsaturated carboxylic and arylcarboxylic acid); 6.12 (C=C conjugated with COOH).

7-Methoxyphthalide-3-methoxyacetic acid (IX). A sample of substance VIII (100 mg) was heated to the melting point. The melt resolidified at the melting temperature or after some cooling. Recrystallisation from ethyl acetate-hexane gave thin colourless plates (86 mg), m. p. 204—205° (gas evolution; the melt resolidified with formation of X). (Found: C 57.08; H 4.85; OCH_3 24.71. Calc. for $C_{12}H_{12}O_6$: C 57.14; H 4.79; OCH_3 24.61.) UV spectrum, Fig. 3. IR maxima (μ): 3.3 and 3.9 (broad carboxylic OH bands); 5.67 (carbonyl of α,β-unsaturated lactone); 5.87 (CO of carboxyl group); the band at 6.12 which is present in the IR spectrum of VIII was absent.

*8-Methoxy-*isocoumarin-3-carboxylic acid (X). A sample of VIII (289 mg) was heated to 205—210°. When the evolution of gas (CH_3OH) had ceased and the melt had become solid again, the product was allowed to cool. It was then treated with warm ethyl acetate; the undissolved, almost white, crystalline material (198 mg) was collected and recrystallised from methanol (charcoal) giving needles, m. p. 257—258°. Yield 75 %. The same product was obtained by heating substance IX to its melting point. The product contained about 1 mole of methanol of crystallisation, which was not completely removed unless drying was done at 100—120° (0.1 mm Hg). (Found: loss of weight, 11.75 %. Calc. for $C_{11}H_8O_5$, CH_3OH: 12.73 %. Analysis of a dried sample gave: C 60.14; H 3.65; OCH_3 14.09. Calc. for $C_{11}H_8O_5$: C 60.00; H 3.66; OCH_3 14.03.) Neutralisation equivalent, found, 205, calc., 220. UV spectrum, Fig. 4. IR maxima (μ): 3.25—3.5 and 3.8—4.0 (carboxylic OH); 5.73 (CO of unsaturated lactone); 5.85 (CO of unsaturated carboxylic acid); 6.06 (C=C conjugated with carboxyl).

8-Hydroxy-isocoumarin-3-carboxylic acid (XI). This substance was obtained by heating VIII, IX, or X with either aqueous hydriodic or hydrobromic acid. In a typical example, substance VIII (100 mg) was treated for 4 1/2 h with boiling aqueous hydriodic acid (15 ml, d = 1.70) in the presence of red phosphorus. On cooling, the reaction product deposited as a crystalline solid; it was filtered off, together with the phosphorus, and separated from the latter by elution with ethyl acetate. The ethyl acetate solution was evaporated to dryness. The residue was washed with methylene chloride, which removed some iodine, and recrystallised from ethyl acetate-hexane; colourless prisms, m. p. 290°; yield, 36 %.

In another example, substance IX (19.5 mg) was treated for 1 h with boiling aqueous hydrobromic acid (2 ml, d = 1.49). Crystals of XI were deposited, m. p. 287°, undepressed on admixture of a sample obtained as above. Yield, 68 %. (Found: C 58.40; H 3.10. Calc. for $C_{10}H_6O_5$: C 58.26; H 2.93.) Neutralisation equivalent, found, 224, calc., 206. UV spectrum, Fig. 4. Absorption spectrum of the ferric complex, Fig. 5. IR maxima (μ): 3.1—3.5 and 3.75—4.0 (phenolic and carboxylic OH); 5.74 (CO of unsaturated lactone); 5.90—6.02 (CO of unsaturated carboxylic acid, probably also some lactone carbonyl, chelated with phenolic OH); 6.09 (C=C conjugated with carboxyl)*.

Alkaline degradation of X. A solution of substance X (190 mg) in 40 % aqueous NaOH (2 ml) was refluxed for 1 h. The mixture was diluted with water and filtered, and the filtrate was acidified with dilute sulphuric acid. On cooling, the filtrate deposited colourless needles (92 mg), m. p. 141—142°, unchanged after recrystallisation from water. For *2-methyl-6-methoxybenzoic acid* (XII) Chuit and Bolsing [14] reported m. p. 139°.

m-Cresol from 2-methyl-6-methoxybenzoic acid (XII). A sample of XII (59 mg) was treated with boiling aqueous hydriodic acid (d = 1.70) and some red phosphorus for 35 min. After cooling, the phosphorus was filtered off and washed with water. The filtrate was extracted with ether and the ethereal solution was shaken with aqueous sodium bisulphite, which removed iodine, and then with aqueous sodium bicarbonate. The ether phase was dried and evaporated; the IR spectrum of the oily residue was indistinguishible from the spectrum of *m*-cresol.

The bicarbonate solution contained no organic material.

2-Carboxy-α-methoxycinnamic acid (XVIII) (G.B.) **. 3-Methoxy-1,2-naphthoquinone (XVII) [4] was oxidised with periodate at pH 6.5, as described above for similar oxidation of IIIa. The quinone colour had disappeared after about 2 h. Extraction of the filtered solution with ethyl acetate gave thin plates, m. p. 137° after recrystallisation from ethyl acetate-hexane. Yield 70 %. (Found: C 59.53; H 4.58; OCH_3 14.02. Calc. for $C_{11}H_{10}O_5$: C 59.46; H 4.54; OCH_3 13.97.) UV spectrum, Fig. 2. IR maxima (μ): 3.3—3.5 and 3.75—3.95 (carboxylic OH); 5.85 and 5.90 (CO of aryl and α,β-unsaturated carboxyl); 6.12 (C=C conjugated with carboxyl).

Isocoumarin-3-carboxylic acid (XIX) (G.B.). Substance XVIII, when heated, melted at 137° and began to decompose at a temperature only slightly above the m. p. After heating to 160° the melt solidified. Recrystallisation from water gave plates, m. p. 237°

---

* *Note added in proof.* In a recent paper, Gerd Bendz [*Arkiv Kemi* **14** (1959) 511] reports the isolation of 8-hydroxy-3-methyl*iso*coumarin from the culture medium of *Marasmius ramealis*. The compound differs from substance XI only in carrying a methyl rather than a carboxyl group in the 3-position. As expected, the UV maxima of both substances are rather similar. There is, however, a striking difference in the positions of the lactone CO peaks of the two compounds. Whereas Bendz' 3-methyl compound has a CO band at 5.95 μ, the corresponding band of the 3-carboxy compound (XI) is found at 5.73 μ. As was pointed out by Bendz, the wave-length value of 5.95 μ is within the region expected for an unsaturated six-membered ring lactone carbonyl, a similar value (5.98 mμ) being found for the 3,4-dihydro derivative of Bendz' compound. Then the value found for substance XI is unexpectedly low. Similar relationships are found for the methyl ether of Bendz' compound and its 3,4-dihydro derivative on the one hand (*cf.* also Ref.[18]) and the carboxylic compounds X, XXIV and XXV on the other hand. This seems to indicate that the 3-carboxyl substituent of the unsaturated six-membered ring lactone causes the lactone CO stretching band to be shifted to the low wave-length values observed. It may be of interest ta note that a similarly low value, 5.70 μ, has been reported [15] for 5,6,7-trimethoxy-*iso*coumarin-3-aldehyde.

** Experiments marked "G.B." were carried out by Mr. Gunnar Bergström.

(yield 70 %), identical by mixed m. p. and IR absorption spectrum with XIX, prepared from XXI according to Zincke and Schmidt[11]. The UV absorption (Fig. 4) is rather similar to that reported for *iso*coumarin [15].

Periodate oxidation of β-naphthoquinone (XX) (G.B.). On oxidation, in the same way as for the β-naphthoquinones IIIa and XVII, XX yielded *2-carboxycinnamic acid (XXII)*, m. p. 205° (lit. [6,7], 203–205°). Yield 70 %. UV absorption, Fig. 2 (see also Ref. [16]).

*3,4-Dihydro-*iso*coumarin-3-carboxylic acid (XXIV) (G.B.).* A $PdCl_2$-$BaSO_4$ catalyst (0.5 g, with 5 % $PdCl_2$) was hydrogenated in 93 % acetic acid (10 ml), a solution of substance XIX (95 mg) in the same solvent (5 ml) was added, and the mixture was stirred in a hydrogen atmosphere. The hydrogen uptake ceased when 1 mole of H_2/mole of XIX had been consumed. Evaporation of the filtered solution, and recrystallisation of the residue from benzene gave XXIV, m. p. 154–155°. For the same substance obtained by sodium amalgam reduction of XIX, Bamberger [12] reported m. p. 153.5°. UV spectrum, Fig. 3. IR maxima (μ): 3.15 and 3.85–4.05 (carboxylic OH); 5.63–5.69 (lactone CO); 5.83 (carboxylic CO).

3-Hydroxyhydrocinnamic acid (XVI). A mixture of 2-carboxy-3-methoxyhydrocinnamic acid (XIV) [8] (see Note, p. 542) (100 mg), aqueous hydriodic acid (d = 1.70) (7 ml) and a little red phosphorus was boiled under reflux for 45 min. After filtration, the solution was diluted with water, and extracted six times with ether. The ethereal solution was washed with aqueous sodium bisulphite and water, dried and evaporated. Recrystallisation of the residue from ethyl acetate-hexane gave colourless needles (34 mg), m. p. 110°. (Lit.[17], 111°.) Neutralisation equivalent, found, 170; calc. for XVI, 166.

*3,4-Dihydro-8-methoxy*iso*coumarin-3-carboxylic acid (XXV).* This substance was prepared by catalytic hydrogenation of X, as described for the preparation of XXIV from XIX. It was recrystallised from ethyl acetate-hexane, prisms, m. p. 238°. (Found: C 59.47; H 4.43; OCH_3 14.26. Calc. for $C_{11}H_{10}O_5$: C 59.46; H 4.54; OCH_3 14.97.) The UV maxima (Fig. 3) are similar to those reported for (–)-3,4-dihydro-8-hydroxy-3-methyl*iso*coumarin (= mellein) [18]. IR maxima (μ): 3.24 and 3.7–4.0 (COOH); 5.68–5.73 (lactone carbonyl; 5.84 (COOH).

Financial support from *Statens Naturvetenskapliga Forskningsråd* is gratefully acknowledged.

REFERENCES

1. Adler, E., Magnusson, R., Berggren, B. and Thomelius, H. *Acta Chem. Scand.* **14** (1960) 515.
2. Adler, E. and Berggren, B. *Acta Chem. Scand.* **14** (1960) 529.
3. Patchett, A. A. and Witkop, B. *J. Org. Chem.* **22** (1957) 1477; Harley-Mason, J. and Laird, A. H. *J. Chem. Soc.* **1957** 1718; Horner, L. and Dürckheimer, W. *Chem. Ber.* **91** (1958) 2532.
4. Teuber, H.-J. and Götz, N. *Chem. Ber.* **87** (1954) 1236.
5. Ebnöther, A., Meijer, Th. M. and Schmid, H. *Helv. Chim. Acta* **35** (1952) 911.
6. Greenspan, F. P. *Ind. Eng. Chem.* **39** (1947) 847; Fernholz, H. *Chem. Ber.* **84** (1950) 110.
7. Johnson, W. S. (Ed.) *Organic Syntheses* **34** (1954) 8.
8. Eastham, J. F. and Larkin, D. R. *J. Am. Chem. Soc.* **80** (1958) 2887.
9. Bamberger, E. and Kitschelt, M. *Ber.* **25** (1892) 888, 1138.
10. Zincke, Th. *Ber.* **25** (1892) 1493; *cf.* also Johnston, H. W., Kaslow, C. E., Langsjoen, A. and Shriner, R. L. *J. Org. Chem.* **13** (1948) 477.
11. Zincke, Th. and Schmidt, W. *Ber.* **27** (1894) 733.
12. Bamberger, E. *Ann.* **288** (1895) 134.
13. Moschner, J. *Ber.* **33** (1900) 742.
14. Chuit, Ph. and Bolsing, Fr. *Bull. soc. chim. France* [3] **35** (1906) 142.
15. Hay, J. Evelyn and Haynes, L. J. *J. Chem. Soc.* **1958**, 2231.
16. Horii, Z., Ninomiya, I. and Tamura, Y. *Pharm. Bull. (Tokyo)* **5** (1957) 6.
17. Schwenk, E. and Papa, D. *J. org. Chem.* **10** (1945) 232.
18. Blair, J. and Newbold, G. T. *J. Chem. Soc.* **1955**, 2871.

Received October 30, 1959.

ACTA CHEMICA SCANDINAVICA 14 (1960) 550–555

Effect of Temperature and Concentration of Sulphuric Acid on the Rate of Formation of the Boron 1,1′-Dianthrimide Complex

O. B. SKAAR and F. J. LANGMYHR

University of Oslo, Chemical Institute A, Blindern, Norway

The effect of temperature and concentration of sulphuric acid on the rate of formation of the boron-1,1′-dianthrimide complex has been investigated spectrophotometrically. Series of solutions containing boron, 1,1′-dianthrimide and varying amounts of water were prepared and heated at four different temperatures. At intervals solutions were removed and measured photometrically. On the basis of the extinction data velocity constants were calculated. An empirical equation was derived for the influence of temperature and concentration of sulphuric acid on the velocity constant. The velocity constant is redoubled either by an 8°C increase of temperature, or by a decrease of concentration of sulphuric acid corresponding to the difference between 100.6 % sulphuric acid and the strength of the initial acid.

In the literature qualitative indications are given on the effect of temperature and concentration of sulphuric acid on the development of the colour of the boron 1,1'-dianthrimide complex. Ellis, Zook and Baudisch [1] state that 3 h heating at 90°C or 5 h heating at 80°C is necessary to develop the colour. According to Otting [2] the rate of colour formation increases with increasing water content. In a previous paper the authors [3] have described the determinations of formula, rate of reaction and stability constant of the boron 1,1'-dianthrimide complex. The solvent applied in these investigations was 93.8 % sulphuric acid, and the rate of reaction and the stability constant were determined for solutions heated at 71° and 70°C, respectively.

The present paper describes the effect of temperature and concentration of sulphuric acid upon the rate of reaction of the complex.

EXPERIMENTAL

Instruments. Extinction measurements were made with a Klett-Summerson spectrophotometer equipped with a B 650 filter. (In the authors previous publication [3] the absorption maximum of the boron 1,1′-dianthrimide complex was found at 630 mμ.)

Reagents. The 1,1'-dianthrimide (E. Merck) was recrystallized twice from nitrobenzene before use. Boric acid, sulphuric acid (95—97 %), and other chemicals were of reagent grade quality. The strength of sulphuric acid was found to be 96.8 %. The acid was protected against absorption of water vapour and contamination with dust.

Glassware. Reagent solutions were prepared in 50 ml bottles (Jena *Geräteglas*) with ground-in glass stoppers. The solutions were heated in specially made photometric cells, prepared from ordinary soda glass tube (14 mm outer, 12 mm inner diameter). The length of these cells was about 20 cm. The cells were marked to keep them in the same position during photometric measurement.

Heat treatment. This was given in a thermostatically controlled water bath. The temperature of the bath varied regularly about the prefixed temperature, the maximum deviations being ± 2°C.

Standard solutions. 0.5715 g of boric acid were weighed out, dissolved in concentrated sulphuric acid and diluted to 1 000 ml with the same acid. From this standard solution (containing 100 μg B per ml) 50 ml were pipetted into another 1 000 ml volumetric flask and diluted to volume with concentrated sulphuric acid. From this latter solution (containing 5 μg B per ml) known amounts of boron were taken. 0.0794 g of 1,1'-dianthrimide were dissolved in concentrated sulphuric acid and diluted to 1 000 ml with the same acid.

Preparation of reacting solutions. Reaction mixtures of boron and 1,1'-dianthrimide were prepared according to the formula: X ml of distilled water + (14—X) ml of concentrated sulphuric acid + 1 ml of boron standard solution + 5 ml of 1,1'-dianthrimide standard solution. The following values of X were chosen: 0.5—1.0—1.5—2.0—2.5 and 3.0. In a series of corresponding blank solutions the volume of boron standard solution was replaced by concentrated sulphuric acid. The solutions were pipetted into 50 ml bottles and were thoroughly mixed. Suitable amounts were then transferred to the photometric cells. To prevent uptake of water vapour during the heating period the cells were fitted with rubber stoppers. Four different series of solutions were prepared according to the formula given above, each series being heated at one of the following mean temperatures: 49.5—67.0—71.0 and 79.8° C.

PHOTOMETRIC MEASUREMENTS

The six reacting solutions and their corresponding blanks (all belonging to one temperature series) were placed in the water bath. At 1 to 1.5 h intervals a solution and its corresponding blank were removed and the extinction of both was measured against distilled water. A constant time of 10 min was employed for photometric measurement. The reacting solutions were finally brought near equilibrium by heating them for an extended period of time varying with the temperature applied. (Excessive heating resulted in destruction of considerable amounts of 1,1'-dianthrimide). The extinction data obtained were corrected for the absorption of the cells (filled with distilled water) and for the absorption of the blanks. The final, corrected extinction values are given in Figs. 1a, b, c and d. The data are given in per cent of the final extinction value obtained after the heating time specified in the figures. The values in Fig. 1 given in parenthesis for zero time indicate time of preheating period.

DISCUSSION

Figs. 1a, b, c and d show that the rate of complex formation increases with the temperature and the content of water. In order to develop an approximate expression for the influence of these factors on the rate of reaction the

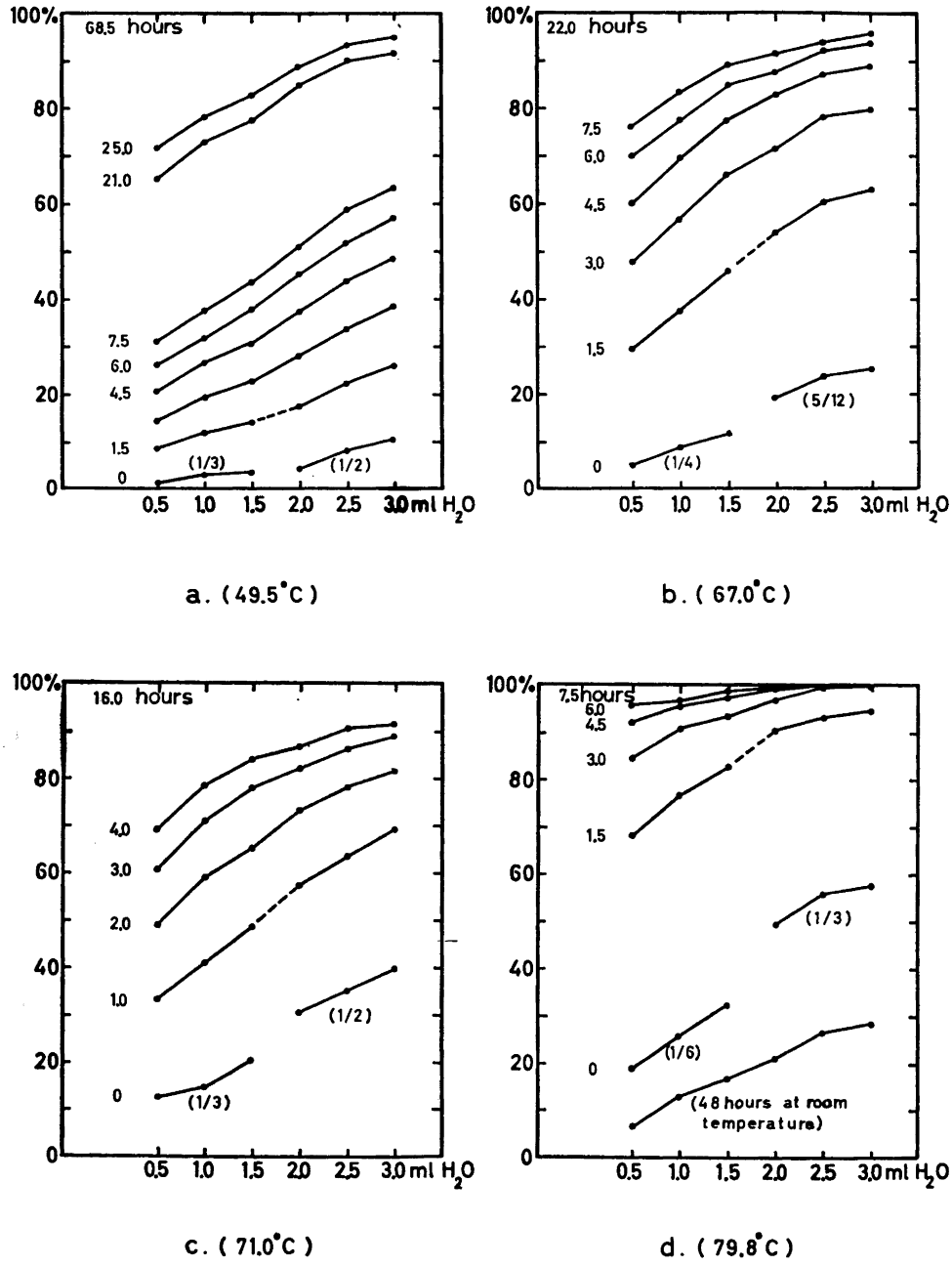

Fig. 1a, b, c and d. The effect at different temperatures and heating times of concentration of sulphuric acid on the formation of the boron 1,1′-dianthrimide complex.

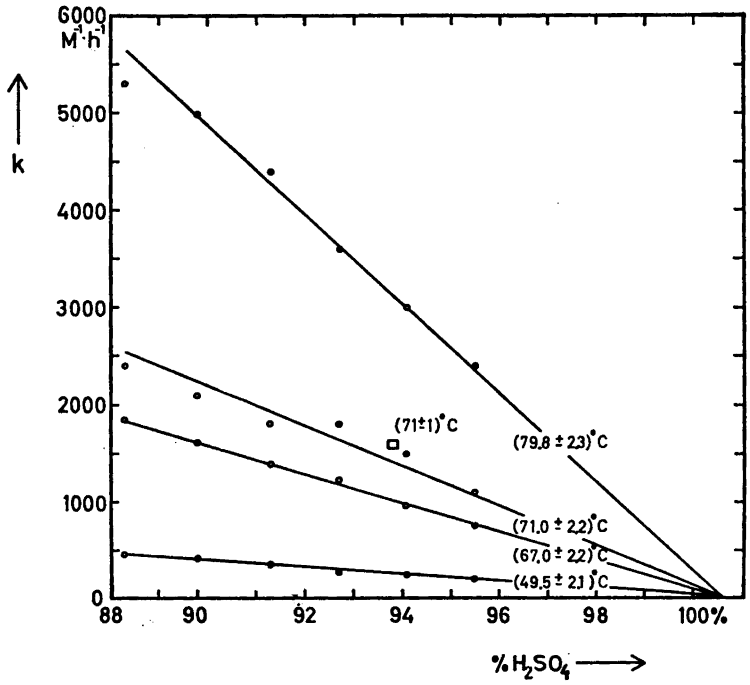

Fig. 2. The effect at different temperatures of concentration of sulphuric acid on the velocity constant of the boron 1,1'-dianthrimide complex.

following assumptions were made. The time of heating t employed in the calculations is the observed time of standing in the water bath. It was assumed that the reduced rate of reaction during photometric measurement corresponds approximately to the lowered rate of complex formation during reheating in the water bath. The assumptions were further made that equilibrium is attained at the final extinction measurements, and that the contamination of boron originating from the reagents is compensated for by subtracting the extinction of the blanks. The stability constant [3] $K = 1.4 \times 10^5$ M^{-1} was applied, and this value was considered constant within the temperature range 50°—80°C and concentration range 88.3—95.5 % sulphuric acid. All concentrations were calculated on the basis of a volume of 19.6 ml (19 ml of concentrated sulphuric acid plus 1 ml of water). In cases where the starting volume differed from 19.6 ml, corrections were made by multiplication with $19.6/V$, where V (in ml) was the volume in question. The original concentrations of boron and 1,1'-dianthrimide were 2.36×10^{-5} M and 29.7×10^{-5} M, respectively. The amount of boron not complexed at equilibrium was $2.3 \times 10^{-5} / (1.4 \times 10^5 \times 27.4 \times 10^{-5}) = 0.06 \times 10^{-5}$ M. The molar concentration of the boron 1,1'-dianthrimide complex (X) determined spectrophotometrically was $X = p\ (2.36 - 0.06) \times 10^{-5}/100$ where p is the percentage of maximum extinc-

tion. In the authors earlier publication [3] an expression for the velocity constant k was developed. Taking into consideration the assumptions made above, the original equation is transformed to:

$$k = \frac{2.303 \times V}{(t_2 - t_1) \times 19.6 \times 28.16 \times 10^{-5}\ \mathrm{M}} \log \frac{13.1 - p_2/100}{13.1 - p_1/100} \cdot \frac{100 - p_1}{100 - p_2}$$

This equation was then applied to calculate the velocity constants given in Table 1.

Due to the simplifications made, the values based on first and second extinction measurement are considered to be more reliable than those based on second and third. The values for k based on first and second measurement are also shown in Fig. 2 (the room temperature values are not included in this figure).

Table 1. Velocity constants at different temperatures and concentrations of sulphuric acid.

Temperature °C	Time interval in hours	Velocity constants in $M^{-1} \cdot h^{-1}$ at the following concentrations of sulphuric acid (%):					
		95.5	94.1	92.7	91.3	89.8	88.3
Room temperature	0 −48.0	5	10	13	16	21	23
49.5	0 − 1.5	190	240	270	360	410	460
49.5	1.5− 3.0	170	220	250	330	400	440
67.0	0 − 1.5	750	950	1 220	1 400	1 620	1 740
67.0	1.5− 3.0	760	960	1 210	1 240	1 510	1 550
71.0	0 − 1.0	1 100	1 500	1 800	1 800	2 100	2 400
71.0	1.0− 2.0	1 000	1 400	1 500	1 800	2 000	2 000
79.8	0 − 1.5	2 400	3 000	3 600	4 400	5 000	5 300
79.8	1.5− 3.0	2 000	2 500	2 600	3 100	(7 900)	(6 100)

It is seen from Fig. 2 that the k values at a constant temperature lie approximately on straight lines converging at at point corresponding to 100.6 % sulphuric acid. (The square seen in Fig. 2 indicates the value of k (1 600 M^{-1} h^{-1}) determined previously by the authors [3].)

The following empirical equation was finally derived for the influence of temperature and concentration of sulphuric acid on the velocity constant:

$$k_{t,c} = 235(100.6 - c)10^{0.038(t-71)}$$

The indexes t and c indicate the temperature and the concentration of sulphuric acid, respectively, for which the velocity constant is calculated. The formula was developed on the basis of the previously determined value for k, *viz.* $k_{71;\,93.8} = 1\,600\ M^{-1}\ h^{-1}$. In view of the approximations made, the expression for the velocity constant is assumed to be valid within the ranges $50° < t < 80°C$ and $88.3\ \% < c < 95.5\ \%$ sulphuric acid. It is seen, that the velocity con-

stant is redoubled by an 8°C increase of temperature, or by a decrease of concentration of sulphuric acid corresponding to the difference between 100.6 % sulphuric acid and the strength of the initial acid.

Acknowledgement. The authors are indebted to Professor Haakon Haraldsen for his interest in the investigation and for the facilities placed at their disposal.

REFERENCES

1. Ellis, G. H., Zook, E. G. and Baudisch, O. *Anal. Chem.* **21** (1949) 1345.
2. Otting, W. *Angew. Chem.* **64** (1952) 670.
3. Langmyhr, F. J. and Skaar, O. B. *Acta Chem. Scand.* **13** (1959). 2107.

Received October 27, 1959.

ACTA CHEMICA SCANDINAVICA 14 (1960) 556–560

Nuclear Magnetic Resonance Investigations of Xanthoperol

JOHAN B-SON BREDENBERG

Department of Chemistry, Institute of Technology, Helsingfors, Finland

and

JAMES N. SHOOLERY

Varian Associates, Palo Alto, California, U.S.A.

It has by nuclear magnetic resonance investigations been found that xanthoperol has the structure of 9,10-diketoferruginol, but with the configuration at C-11 probably inverted.

The structure I, without configurational implications, has been previously proposed for xanthoperol [1]. The evidence for this structure were indirect and it was therefore necessary to study it further, especially as the biogenetic relationship between the proposed structure and the structures of the other diterpene compounds in *Juniperus communis* L. [2,3] was obscure.

The nuclear magnetic resonance spectrum of xanthoperol in $CDCl_3$ at 60 Mc has been taken and is presented in Fig. 1. The reference is pure benzene in an external space. The peak at −51 cps arises from residual $CHCl_3$ in the solvent while the small peak immediately adjacent to the $CHCl_3$ peak is almost certainly due to residual benzene which has been used in the crystallisation of the compound. The assignments of the two benzene ring protons, H—8 at −95 cps and H—5 at −30 cps, are based on comparison of this spectrum with the spectra of a number of alkaloids [4] in which it has been found that a keto group conjugated with the ring shifts the resonance of the adjacent benzene ring proton down to the vicinity of −100 cps relative to the zero of reference. The resonance from the phenolic hydrogen, −11 cps, has been identified by its temperature dependence. The signal-to-noise ratio obtainable in this solution makes it rather difficult to see the seven lines from the C—H proton in the *iso*propyl group, but there is little doubt that they lie at about +200 cps, since a reproducible series of peaks with about the right spacing has been observed in this vicinity in several spectra. The spacing of the two peaks

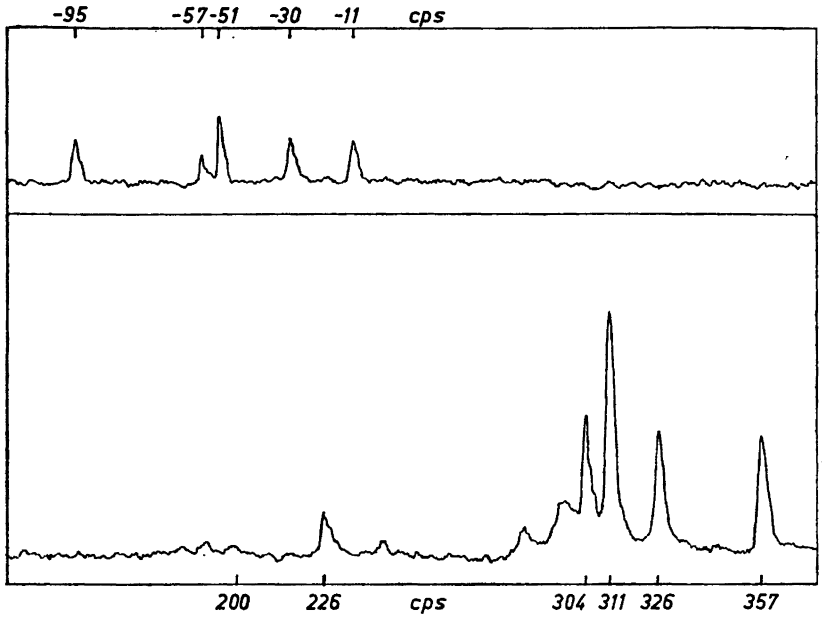

Fig. 1. Nmr-spectrum of xanthoperol in $CDCl_3$, external reference benzene. 60 Mc.

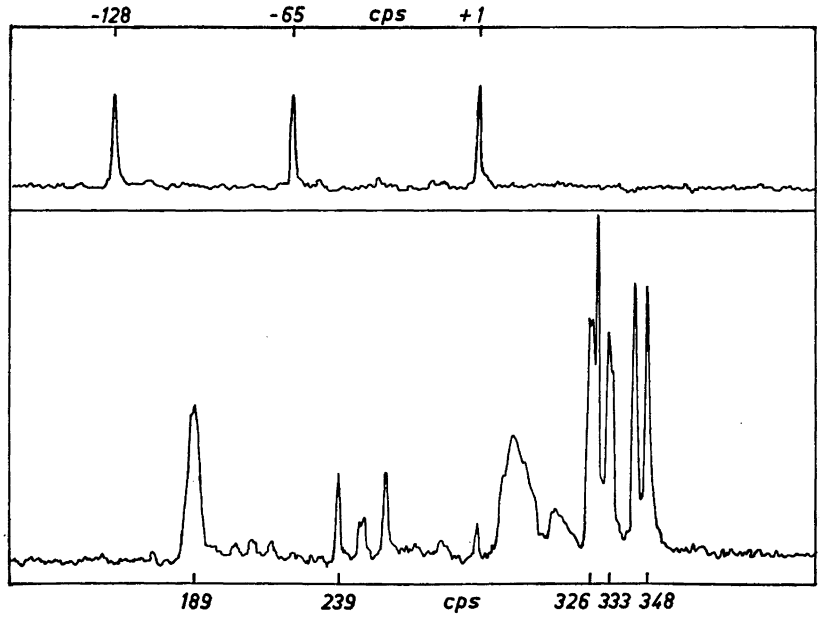

Fig. 2. Nmr-spectrum of 9-ketoferruginol in deuterated tetrahydrofuran, external reference benzene. 60 Mc.

at 304 cps and 311 cps, 7 cps apart, is on the other hand completely characteristic of the spin coupling for the *iso*propyl group methyl doublet. The fact that the line at 311 cps is twice as large as the one at 304 cps can only be explained on the basis of an accidental overlap by one other methyl group in the molecule. In addition, there are two methyl group lines at 326 and 357 cps, both of which are equally as sharp as the line at 311 cps. This fact shows that none of the methyl groups in the A-ring is attached to a carbon atom which also possesses a hydrogen, in which case the methyl group resonance would be split into a doublet. Therefore, structure I is not acceptable. These leaves two structures, II and III, with a geminal dimethyl group. The line at 357 cps is assigned to the angular methyl since angular methyl groups in steroids generally fall at higher positions than side chain methyls [5]. The lines at 311 and 326 cps therefore correspond to the *gem.*-dimethyl group.

The assignments given above have been confirmed from the spectrum of 9-ketoferruginol in fully deuterated tetrahydrofuran (Fig. 2). The spectrum shows clearly three sharp methyl group peaks and two slightly broader peaks

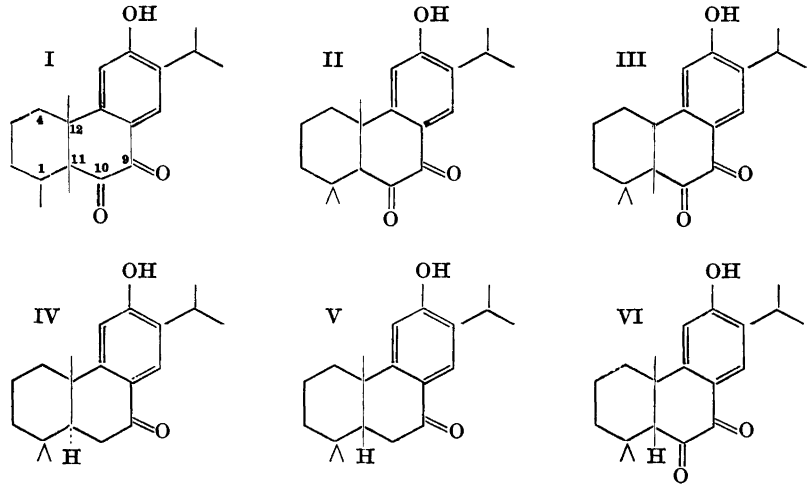

belonging to the doublet from the *iso*propyl methyl groups, all lying between 326 and 348 cps from external benzene. These numbers must all be diminished by about 25 cps to correct for the difference in the diamagnetic bulk susceptibilities of deuterated tetrahydrofuran and chloroform. One can then compare the numbers with those obtained for xanthoperol and it is found that the two peaks previously assigned to the *iso*propyl methyls in xanthoperol correspond within a few cycles to those which are assigned to the same groups in 9-ketoferruginol. The two benzene ring protons give resonances at −65 and + 1 cps and when we correct for the bulk susceptibility effect, we find that these two peaks correspond fairly well, both in position and spacing, to the two peaks in xanthoperol which were assigned to the benzene ring protons. The phenolic proton must give a resonance at −128 cps which indicates an enormous shift to low field compared with the position found in xanthoperol.

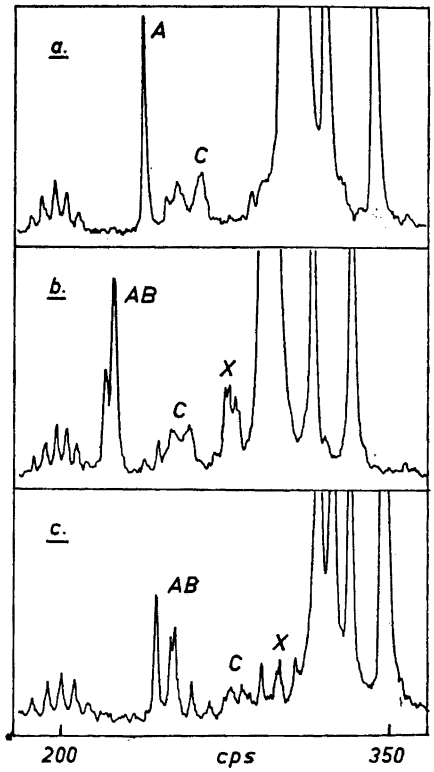

Fig. 3. The high-field end of the nmr-spectra of *a.* xanthoperol, *b.* its monoketonic reduction product, and *c.* 9-ketoferruginol. All spectra are taken in pyridine at 60 Mc with external benzene as reference.

This is probably due to formation of a strong hydrogen bond between this proton and the solvent since a shift towards lower field would be expected in that case.

The decision between structures II and III for xanthoperol must be based on a study of the peak at 226 cps (Fig. 1) which is assigned to the angular hydrogen. The position of this peak could be accounted for in a satisfactory way by either of these structures. However, only structure II places this hydrogen far enough from other hydrogen nuclei so that no spin coupling would be expected, and therefore only structure II accounts for the sharpness of this line. It is very unlikely that if the angular hydrogen were located at C-12 it would not couple its spin fairly strongly to one or the other of the two protons on C-4. For a closer study of this coupling the high-field end of the spectra of xanthoperol, its monoketonic reduction product [1] and 9-ketoferruginol have been taken in pyridine solution (Fig. 3). Unfortunately, the three spectra were not run at exactly the same scale factor and no internal reference compound was added with the result that the spectra cannot be perfectly lined up and compared directly.

The central five lines of the seven-line multiplet due to the C—H proton in the *iso*propyl side chain are now clearly seen at 200 cps. Xanthoperol

has a single sharp line labelled A which is assigned to the proton on C-11, the methyl group on C-12 accounting for its lack of spin coupling. The resonance from this proton moves toward higher fields when the adjacent keto group is reduced and becomes the pattern of four lines marked X in the mono-keto product. The four lines almost certainly arise from spin coupling to the two protons on C-10 to give an ABX pattern [6] similar to the one for 9-ketoferruginol. The AB pattern in the mono-keto reduction product is not so well defined as in 9-ketoferruginol, however, because the couplings are smaller, as can be seen in the X pattern. The shape of the AB pattern in the monoketo reduction product is predicted with $J_{AB} = 16$ cps, $J_{AX} = 5$ cps, $J_{BX} = 2.5$ cps, and $\delta_{AB} = 14$ cps at 60 Mc. The AB pattern in 9-ketoferruginol is satisfactorily described by $J_{AB} = 16$ cps, $J_{AX} = 7.2$ cps, $J_{BX} = 8.5$ cps, and $\delta_{AB} = 7$ cps at 60 Mc. The nmr spectra are, therefore, most compatible with structure II for xanthoperol, since III would not be expected to yield an ABX pattern in its mono-keto reduction product. The structure for the monoketonic reduction product accordingly has to be changed and since it differs, for reasons discussed more closely elsewhere [7], from 9-ketoferruginol (IV) only in its configuration at C-11 it must be assigned the configuration in structure V. The change from *trans* to *cis* ring fusion has therefore changed one of the spin couplings quite a lot, but left the other relatively unchanged. The configuration of xanthoperol cannot be conclusively determined from its nmr spectra but a closer examination of the region C (Fig. 3) which is tentatively assigned to the C-4 protons, and the spacing of the methyl groups seems to indicate a much closer relationship between xanthoperol and the *cis*-form characteristic of the mono-keto reduction product rather than the *trans*-form characterized by 9-ketoferruginol. This result points to the *cis*-form for xanthoperol as given by the configuration in VI.

EXPERIMENTAL

The nmr spectra were taken at Varian Associates, Palo Alto, California, with a 60 Mc High Resolution NMR Spectrometer in a field of 14 100 gauss.

The authors wish to express their thanks to Mr. L. F. Johnson for taking the nmr spectra.

REFERENCES

1. Bredenberg, J. B. *Acta Chem. Scand.* **11** (1957) 927.
2. Bredenberg, J. B. and Gripenberg, J. *Acta Chem. Scand.* **8** (1954) 1728.
3. Bredenberg, J. B. *Acta Chem. Scand.* **11** (1957) 932.
4. Goodvin, S., Shoolery, J. N. and Johnson, L. F. *J. Am. Chem. Soc.* **81** (1959) 3065.
5. Shoolery, J. N. and Rogers, M. T. *J. Am. Chem. Soc.* **80** (1958) 5121.
6. Pople, J. A., Schneider, W. G. and Bernstein, H. J. *High-resolution Nuclear Magnetic Resonance*, McGraw-Hill Book Co., New York 1959, p. 132.
7. Bredenberg, J. B. *Acta Chem. Scand.* **14** (1960) 385.

Received November 18, 1959.

ACTA CHEMICA SCANDINAVICA 14 (1960) 561–565

Heats of Hydrolysis of Phenyl Acetate and Phenyl Thiolacetate

INGEMAR WADSÖ

*Thermochemistry Laboratory *, University of Lund, Sweden*

The heats of hydrolysis of phenyl acetate and phenyl thiolacetate have been determined calorimetrically at 25°C. For the idealized, isothermal hydrolysis reactions

$$PhOAc(l) + H_2O(l) \rightarrow PhOH(s) + HOAc(l)$$

and

$$PhSAc(l) + H_2O(l) \rightarrow PhSH(l) + HOAc(l)$$

the enthalpy changes were found to be -6.86 ± 0.06 and -2.97 ± 0.08 kcal/mole, respectively.

Heat and free energy changes in transacylation from phenyl thiolacetate to thiols have been briefly discussed.

The simple phenyl thiolacetate as well as aminoacyl derivatives of thiophenol have been used extensively during recent years, as acylating agents towards thiols and amines in peptide chemistry. Also O-phenylesters, preferably nitro-substituted, have been proved to be useful in this connection [1].

Phenol and thiophenol derivatives of aminoacids and peptides can be looked upon as "active forms" of the corresponding acids. They can be condensed, under conditions that are possible in the cell, with another aminoacid or peptide, by which reaction a peptide bond is formed:

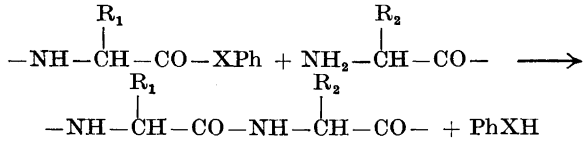

X = O, S.

The acylated phenols have been described as "energy-rich" *i.e.* their hydrolysis reactions have been supposed to proceed under release of a large amount

* Sponsored by *The Swedish Natural Science Research Council* and by *The Swedish Technical Research Council.*

Table 1. Heats of hydrolysis of phenyl acetate and phenylthiol acetate.

Substance	mmoles	ε	$10^4 \times \log R_i/R_f$	$-\Delta H$, kcal/mole
PhOAc	3.536	7 752	95.48	20.93
	3.335	7 750	89.84	20.88
	3.303	7 750	89.30	20.95
	3.228	7 750	87.08	20.91
				Mean 20.92 ± 0.02
PhSAc	3.397	7 724	94.29	21.44
	3.267	7 723	90.79	21.46
	3.228	7 723	89.85	21.50
	3.172	7 722	88.49	21.54
				Mean 21.49 ± 0.03

of free energy. As in a simple hydrolysis reaction the entropy term is small, the enthalpy change is of the same order as the free energy change. Therefore, it seemed to be of interest to determine the heats of hydrolysis of the acetic acid esters of the simple phenol and thiophenol, thereby also supplementing the recently performed measurements on alkyl acetates [2] and alkyl thiolacetates [3].

EXPERIMENTAL

Materials. Phenyl acetate was prepared from phenol and acetic anhydride [4]. The crude product was purified by distillation at different pressures in a 10-plate column, followed by fractional freezing out. The product reacted neutral. The equivalent weight, as determined by potentiometric titration of the acetic acid formed by hydrolysis, coincided with the theoretical value within the limits of experimental error. $d_4^{25} = 1.0740$, $n_D^{25} = 1.5010$.

Phenyl thiolacetate was prepared from benzene thiol and acetyl chloride [5]. The ester was purified by distillation, until the equivalent weight, as determined by iodometric titration of thethiol formed by alkaline hydrolysis [3], indicated 100.0 % purity. The product reacted neutral and did not consume any iodine. $d_4^{25} = 1.1164$, $n_D^{25} = 1.5690$.

Phenol of purum grade was purified by fractional freezing out until a colourless substance with a melting point at 41.0°C was obtained.

Benzene thiol was distilled until iodometric titration in water-ethanol gave an equivalent weight indicating 100.0 % purity.

Acetic acid was purified by fractional freezing out 4 times. Titration values proved the substance to be pure within the limits of experimental error.

Apparatus. The reactions were carried out in a metal "isothermal" calorimeter which has been described in detail elsewhere (Type D in Ref.[6]).

Calibration. The heat equivalent of the calorimeter, including its content, was determined electrically by passing a known current for a given time (240 sec) through the heating element. The calibrations were performed on the system after hydrolysis had taken place. The result of each calibration experiment was adjusted to give the heat equivalent of a "standard system", ε°, in which the calorimetric liquid contained the hydrolysis products from a certain amount of ester (450 mg). The actual heat equivalent values, ε, were obtained from ε° by applying small corrections for the variations in the amount of substance used.

Calorimetric procedure. In order to obtain a rapid reaction, the hydrolyses were performed in strong (0.8 N) sodium hydroxide, water-ethanol (2:3) solution. The calorimeter was charged with 100 ml of this solution. After equilibration, the reaction was started by breaking the sealed glass ampoule containing the ester. The thiol formed from phenyl thiolacetate was to a certain extent oxidised in the alkaline medium, as was the case with

Table 2. Heat of solution measurements.

Substance	mmoles	ε	$10^4 \times \log R_i/R_f$	$-\Delta H$, kcal/mole
PhOH	3.801	7 746	12.86	2.62
	3 360	7 745	11.35	2.62
	3.356	7 745	11.55	2.67
	3 521	7 745	11.98	2.64
				Mean 2.64 ± 0.02
PhSH	3.433	7 718	31.42	7.06
	3.115	7 716	28.74	7.12
	3.507	7 719	32.19	7.08
	3.409	7 718	31.51	7.13
				Mean 7.10 ± 0.04
HOAc	3.809	7 741	57.23	11.63
	3.499	7 740	52.36	11.58
	3.421	7 740	51.43	11.64
	3.392	7 736	50.98	11.63 *
	3.684	7 737	55.35	11.63 *
				Mean 11.62 ± 0.02
H_2O	3.470	7 738	0.92	0.21
	4.087	7 738	1.02	0.19
				Mean 0.20 ± 0.01

aliphatic thiols [3]. However, it was found that the autoxidation of benzene thiol was much slower than that observed for aliphatic thiols. In order to cancel the heat effect of autoxidation, the same technique as given in Ref.[3] had to be used. Thus the experiments on phenyl thiolacetate and benzene thiol were performed in a solution in which a small amount (0.5 ml) of benzene thiol has been substituted for the calorimetric liquid. As seen from the results given in Table 2, presence of thiol did not significantly change the heat of solution value of acetic acid.

In every case the reaction period was 8 minutes or less. The initial and final thermistor resistances (R_i and R_f, respectively) were obtained graphically.

Corrections to standard states. The ideal isothermal hydrolysis reaction V is obtained from eqns. I and IV, which correspond to the reactions taking place under actual experimental conditions.

I	$PhXAc(l) + H_2O(soln) \longrightarrow PhXH(soln) + HOAc(soln)$	ΔH_1
II	$PhXH(s/l) \longrightarrow PhXH(soln)$	ΔH_2
III	$HOAc(l) \longrightarrow HOAc(soln)$	ΔH_3
IV	$H_2O(l) \longrightarrow H_2O(soln)$	ΔH_4
V	$RXAc(l) + H_2O(l) \longrightarrow RXH(s/l) + HOAc(l)$	ΔH^0

$$\Delta H^0 = \Delta H_1 - \Delta H_2 - \Delta H_3 + \Delta H_4$$

Units of measurement. The results of the calorimetric experiments are expressed in terms of the defined calorie, equal to 4.1840 abs. joules, and refer to the isothermal process at 25°, and to the true mass. The molecular weights were computed from the 1951 table of international atomic weights [7].

* PhSH present. 99.79 ml of calorimetric liquid.

RESULTS

From four calibration experiments on the system (containing 99.79 ml of calorimetric liquid) where no benzene thiol was added, the standard heat equivalent, ε°, was found to be 7 750 $\pm$ 8 * cal/unit of log R_i/R_f. From four calibration experiments on the system (99.40 ml of calorimetric liquid) where benzene thiol was present, the ε^0-value was found to be 7 721 $\pm$ 7 cal/unit of log R_i/R_f.

In the tables the following symbols have been used:

log R_i/R_f the expression proportional to the temperature change; R_i and R_f are the corrected thermistor resistance values at the start and the end, respectively, of the main period;

ε the heat equivalent of the actual system in calories per unit of log R_i/R_f.

Table 3.

Substance	$-\Delta H_1$	$-\Delta H_2$	$-\Delta H_3$	$-\Delta H_4$	$-\Delta H^0$
PhOAc	20.92	2.64	11.62	0.20	6.86 $\pm$ 0.04
PhSAc	21.49	7.10	11.62	0.20	2.97 $\pm$ 0.06

Table 3 contains a summary of the obtained data and the heat of hydrolysis of the idealized reaction V. The uncertainties given in the table do not include possible systematic errors. As the accuracy of the titrations, by which the purity of the esters and actic acid was tested, cannot be considered to be better than $\pm$ 0.2 %, the true uncertainties are somewhat greater. Taking this into consideration, the standard heats of hydrolysis for phenyl acetate and phenyl thiolacetate will be -6.86 ± 0.06 and -2.97 ± 0.08 kcal/mole, respectively.

DISCUSSION

In a forthcoming paper, heats of hydrolysis data for some O, S and N-acetyl compounds will be discussed more generally. Here, the derived heat of hydrolysis of phenyl thiolacetate will be compared with the corresponding data for some alkyl thiolacetates (Table 4).

Table 4. ΔH^0 for the hydrolysis of some alkyl thiolacetates [2] and phenyl thiolacetate.

Substance	EtSAc	*n*-PrSAc	*n*-BuSAc	*i*-PrSAc	*t*-BuSAc	PhSAc
ΔH^0, kcal/mole	−0.95	−0.93	−1.09	−1.39	−3.00	−2.97

The enthalpy change for a transacylation reaction $R_1SAc + R_2SH \rightarrow R_1SH + R_2SAc$ is equal to the difference of the heat of hydrolysis of the two thiolesters. If all reaction participants are liquids, the entropy change must be very small, considering the symmetric nature of the reaction. The same applies to the substances in solution, provided the interactions between the

* All uncertainties given are the average deviation of the mean.

medium and the reactants, and the reaction products, respectively, are of the same magnitude. Therefore, the standard free energy change for the reaction, should in this case be very nearly the same as the standard enthalpy change. Thus, when acetylating alkyl thiols by phenyl thiolacetate, the reaction seems to be accompanied by a standard free energy change of *ca* 2 kcal/mole or less. Therefore, from an energetic point of view, phenyl thiolacetate cannot be considered as an effective acetylating agent towards alkyl thiols. This conclusion is confirmed, *e.g.*, by the experiments carried out by Wieland and Bokelmann [8], who had to use phenyl thiolacetate in a tenfold excess in order to get glutathione "completely" S-acetylated in an acid water methanol solution.

Acknowledgements. This work has been supported by a grant from *University of Lund.*

REFERENCES

1. Wieland, Th. and Heinke, B. *Ann.* **615** (1958) 184.
2. Wadsö, I. *Acta Chem. Scand.* **11** (1957) 1745.
3. Wadsö, I. *Acta Chem. Scand.* **12** (1958) 630.
4. Vogel, A. I. *Practical Organic Chemictry. Longmans, Green and Co. London 1948.*
5. Michlar, W. *Ann.* **176** (1875) 177.
6. Sunner, S. and Wadsö, I. *Acta Chem. Scand.* **13** (1959) 97.
7. Wichers, E. *J. Am. Chem. Soc.* **74** (1952) 2447.
8. Wieland, Th. and Bokelmann, E. *Angew. Chem.* **64** (1952) 59.

Received November 12, 1959.

ACTA CHEMICA SCANDINAVICA 14 (1960) 566–572

An Adiabatic Calorimeter for Measuring Heats of Vaporisation at 25° C

INGEMAR WADSÖ

*Thermochemistry Laboratory *, University of Lund, Sweden*

An adiabatic calorimeter for measuring heats of vaporisation at 25°C has been constructed. It has been designed preferably for compounds having vapour pressures between 1 and 100 mm Hg at 25°C. An adequate amount of substance for each run is 150 mg. The accuracy has been checked by remeasuring some well-known heats of vaporisation. The results indicate an accuracy of 0.5 % or better.

By combustion and reaction calorimetry it is possible to obtain very accurate heat of formation data for most kinds of substances. Unfortunately, there are many thermochemical precision data which at present cannot be used to their full extent, because of a lack of heat of vaporisation data. Calorimetric data have been obtained for many hydrocarbons, but are lacking for other substances, with very few exceptions. As a rule, heats of vaporisation data must be obtained indirectly from vapour pressure measurements by use of Clausius-Clapeyron's equation, or simply from empirical rules [1].

Several types of calorimeters for measuring heats of vaporisation have been described in the literature (see, *e.g.*, Ref.[2]). However, most of them were designed for work at a temperature higher than 25°C, and values obtained have therefore to be recalculated to the standard reference temperature. Also, in all of the methods, it is necessary to use a considerable amount of substance. It was therefore undertaken to design and build a simple but accurate calorimeter for the determination of heats of vaporisation at 25°C, using small amounts of substance.

The apparatus described in the present paper is of a very simple design and requires only *ca* 150 mg of substance per determination. The accuracy is 0.5 % or better, which for most purposes is quite satisfactory. However, the method in its present form is limited to substances having vapour pressures at 25°C in the range 1—100 mm Hg.

* Sponsored by *The Swedish Natural Science Research Council* and by *The Swedish Technical Research Council.*

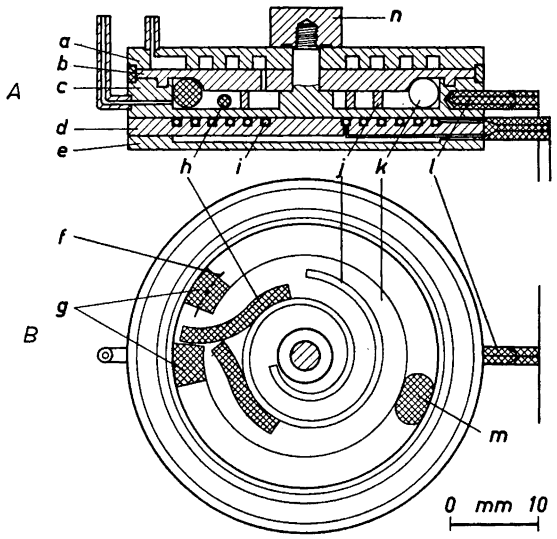

Fig. 1. A. Section through the calorimeter.
B. Disc *c* seen from above. For explanations see the text.

Principle. The evaporation of the substance is caused by a flow of nitrogen kept under reduced pressure *. The heat taken from the calorimeter is compensated electrically in such a way as to keep the temperature of the calorimeter constant and equal to that of the surrounding thermostat. From the amount of substance evaporated, as determined by weighing, and from the amount of supplied electrical energy, the molar heat of vaporisation can be calculated.

Construction. The construction of the calorimeter is shown in Fig. 1. The calorimeter body consists of five gold plated brass discs, *a*—*e*. The liquid substance to be vaporised is introduced into an ampoule placed in the cavity between discs *b* and *c*. The ampoule, *k*, consists of a bent thin-walled teflon tube, inner diameter 4 mm, closed in both ends by silicone rubber stoppers, *g*. One of these stoppers holds a capillary teflon tube, *f*, length 10 mm, inner diameter *ca* 0.3 mm. The ampoule is divided into two parts by means of a silver wool pellet, *m*. At the start of an experiment the liquid is kept between the pellet and the capillary tube, but when the pressure inside the calorimeter is lowered, the liquid will be pressed out from the ampoule and absorbed on glass fibre wicks, *h*.

The carrier gas passes from the gas inlet tube through the evaporation chamber into a spiral groove between discs *a* and *b*. The heat loss accompanying the vaporisation is compensated by electrical energy generated in the heating element *i*, which is a spiralized manganin wire lacquered and nylon spun (resistance 40 Ω), lying in a spiral groove in disc *d*. An air gap between disc

* This "carrier gas technique" has been used previously, *e. g.* by Coon and Daniels [3].

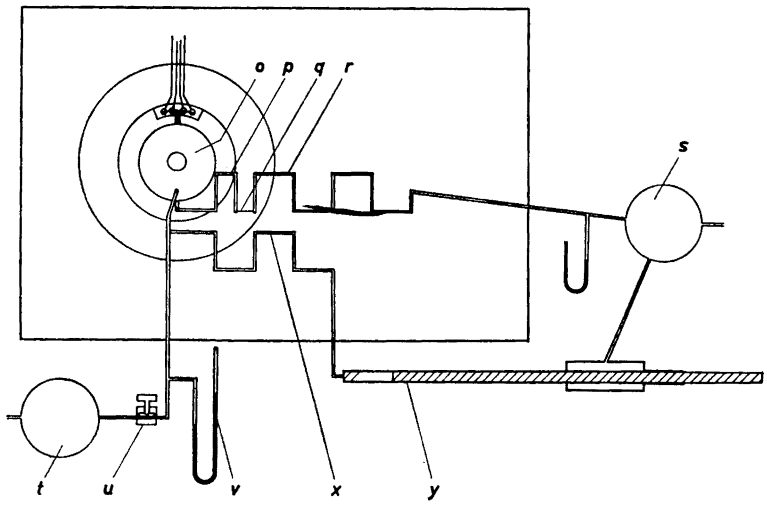

Fig. 2. Schematic view of the calorimetric equipment.

d and the bottom disc *e* prevents the bottom surface from being overheated. The saturated carrier gas is allowed to reach thermal equilibrium in the spiral duct in disc *a* before passing through the outlet tube. To ensure a good thermal contact between the gas mixture and the calorimeter, *ca* 50 mm of the spiral duct is filled by loosely packed silver wool. To improve the thermal conductivity between the discs *b* and *c*, a gold spiral, *j*, is introduced in the evaporation chamber.

A thermistor, *l*, is inserted in a drilled hole in disc *c*. The thermistor was a Stanthel, type F 2311, 2000 Ω, sealed off with a microflame *ca* 5 mm from the top, with subsequent cooling of the thermistor bead. Electrical connections from the thermistor and the heater consist of 0.4 mm platinum wires dipping into mercury cups.

In order to obtain a vacuum tight system silicone rubber gaskets had to be used between discs *a* and *c*, and between the nut *n* and disc *a*.

The calorimeter is placed on three polystyrene pegs inside a chromium plated brass can, fitted with a thin-walled lid. The can is placed in a bigger brass vessel and the space between the two cans is filled by copper chips. The outer can is immersed in a water thermostat kept at 25°C by means of a standard mercury contact thermometer fitted with an electronic relay.

The carrier gas is brought to 25°C by passing it through a copper tube (*r* in Fig. 2) inside the thermostat. In order to keep the gas flow at a suitable rate, the gas is passed through a capillary tube, *q*.

Heat effects due to the expansion of the carrier gas, after having passed the capillary tube, are avoided by allowing the gas to pass through a small silver tube, *p*, in contact with the copper chips between the two cans, before it reaches the calorimeter, *o*.

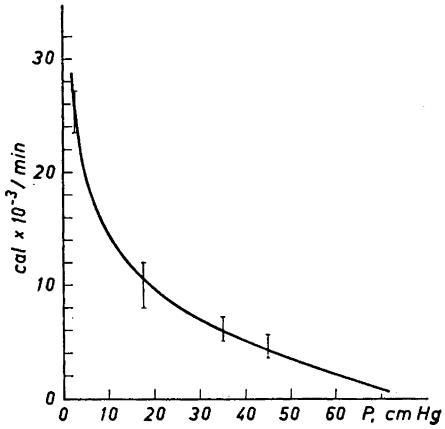

Fig. 3. The "zero" effect *versus* the pressure as shown by the manometer *v*.

By altering the pressure inside the calorimeter the flow of the carrier gas through the capillary tube, and thereby the evaporation rate, is changed. The pressure can be regulated by means of a screw clamp, *u*, and a "leakage valve", *y*. The valve consists of a metal tube and polystyrene rod as shown in Fig. 2. The rod is close fitting but movable to allow variation in the leakage from the nitrogen tank *s* to the vacuum tank *t*. By moving the rod of this valve it is possible to regulate the pressure inside the calorimeter within very small limits. The pressure in the nitrogen tank is kept slightly higher than atmospheric so that no air can reach the calorimeter by leakage through the end of the metal tube.

The temperature of the calorimeter is observed by means of the thermistor which forms one of the arms in a conventional D.C. bridge circuit. A Sullivan Spot Galvanometer (T 2001/D) with sensitivity 0.005 μA/mm, was used as a zero point instrument. The sensitivity corresponded to a temperature change of 0.0002°C, equivalent to a change in energy content of 0.002 cal.

Procedure. The ampoule was charged with *ca* 150 mg of substance and placed in the evaporation chamber. Discs *a* and *b* were fastened to discs *c*, *d* and *e*, by means of the central screw and the nut *n*. A slow stream of nitrogen was forced through the calorimeter in order to remove adsorbed water. The gas inlet and outlet tubes were closed by stoppers and the calorimeter was weighed to the nearest 0.01 mg. After being cooled to a temperature slightly below 25°C, the calorimeter was placed in the thermostat and the two gas tubes were connected to the metal tubes *p* and *x* by means of PVC tubes. The temperature of the calorimeter was raised to that of the thermostat, after which the system was allowed to equilibrate for 15 min. The vaporisation was started by opening the screw clamp *u*. A suitable voltage was applied to the heater, and by regulating the vaporisation with the leakage valve, the temperature of the calorimeter was kept equal to that of the surroundings.

By using a storage battery of high capacity (144 Ah), and by passing the current through a dummy heater circuit for *ca* half an hour before the experiment started, the variation in the current during a run was insignificant.

The current through the heater was determined by measuring the potential drop over a 10 Ω standard resistance in series with the heater, by use of a Rubicon High Precision Type B Potentiometer.

An appropriate time for the evaporation varied between *ca* 10 min for substances having vapour pressures of 100 mm Hg, to *ca* 60 min for substances having vapour pressures of 1 mm Hg. During this time *ca* 100 mg of the substance evaporated.

The experiment was finished by switching off the electrical current and closing the clamp *u*. The calorimeter was then filled with nitrogen to atmospheric pressure and the temperature was adjusted to that of the thermostat by addition of a small amount of electrical energy. The calorimeter was closed by the stoppers and the amount of substance evaporated was determined by reweighing the calorimeter. From the known resistance of the heater, and from the measured current and time, the supplied electrical energy could be calculated.

Zero effect.. When a stream of nitrogen was passed through the calorimeter, furnished with an empty ampoule, a small evolution of heat was observed, which included heat of friction and heat of expansion of the carrier gas. This heat effect could be determined by measuring the speed of the galvanometer spot when passing the zero position. As could be expected, the effect varied with the pressure (as shown by manometer *v*), that is, with the ve-

Table 1. Heats of vaporisation of some hydrocarbons.

Substance	mmoles	Q, cal	q, cal	ΔH_v, kcal/mole
*Cyclo*hexane	1.338	10.601	0.011	7.93
	1.250	9.832	0.010	7.87
	1.081	8.513	0.009	7.88
	1.020	8.087	0.008	7.94
	1.062	8.358	0.010	7.88
			Mean	7.89 ± 0.02
Methyl*cyclo*hexane	1.272	10.689	0.028	8.43
	1.193	9.958	0.026	8.37
	1.145	9.502	0.024	8.32
	1.220	10.334	0.026	8.49
	1.058	8.972	0.024	8.50
			Mean	8.42 ± 0.04
n-Octane	0.9055	8.972	0.038	9.95
	0.8329	8.204	0.035	9.89
	0.7419	7.375	0.031	9.98
	0.7648	7.594	0.031	9.97
	0.6523	6.440	0.038	9.93
			Mean	9.94 ± 0.02
Mesitylene	0.6372	7.050	0.16	11.32
	0.6909	7.676	0.17	11.36
	0.6376	7.074	0.15	11.32
	0.6657	7.406	0.16	11.37
	0.6902	7.748	0.13	11.42
			Mean	11.36 ± 0.04

locity of the nitrogen stream through the calorimeter. In Fig. 3 the mean of this "zero" effect is plotted against the pressure. Each value in the figure is a mean of five to ten separate experiments. The uncertainties, expressed as the standard deviation of the mean, are indicated by the lengths of the vertical lines. The correction due to "zero" effect amounts only to *ca* 0.1 % for compounds having a vapour pressure of 100 mm Hg, but is as much as 2 % for compounds having vapour pressures of 2 mm Hg. Heat effects due to adsorption and wetting of the interior part of the calorimeter are negligible as judged from available data in the literature [4].

The vapour of the substance leaves the calorimeter with a directed velocity and thus has acquired some kinetic energy, which corresponds to a small amount of energy withdrawn from the system. The carrier gas has almost exactly the same kinetic energy when entering the calorimeter as when leaving it, and can thus be left out of consideration. The kinetic energy of the vapour can easily be estimated. The vapour velocity is calculated to be less than 5 m per sec, and thus the correction must be in the order of 10^{-4} cal, which is insignificant.

The accuracy of the method seems mainly to be limited by the uncertainty in the weight determinations and in the "zero" effect experiments. The ampoule technique worked satisfactorily; before the experiment the weight of the calorimeter was found to be constant. After a run, however, a small vapour leakage was observed for compounds having high vapour pressures. By graphical extrapolation over the short time between the finish of the experiment and the weighing, this error could be corrected for. Corrections applied were always less than 0.2 %.

The weight difference has to be corrected in order to obtain a value of the true mass evaporated. Therefore, it is necessary to consider the amount of nitrogen replaced by the ampoule content before the experiment, and by the remaining liquid and its vapour after the experiment. As the total cavity of the calorimeter is as small as 1.5 ml, these corrections are quite small, being 0.4 % for compounds having vapour pressures in the order of 100 mm Hg.

The "carrier gas technique" makes it possible to control the speed of the vaporisation accurately and in a very simple manner. Attempts to work without carrier gas were not successful as no constant rate of vaporisation could be obtained.

The apparatus, in the simple design described here, seems to be unsuitable for compounds having vapour pressures lower than 1 mm Hg. These demand either a long time of evaporation, in which case errors from the lack of adiabatic conditions will be very significant, or a high gas velocity, in which case the results will be strongly influenced by a high uncertainty in the "zero" effect.

The calorimeter has been tested on four hydrocarbons. Each compound was purified by fractional distillation through a 25-plate column until the purity, as judged by gas chromatographic analysis (Pye Argon Chromatograph), was better than 99.5 %. The results * of the measurements are given in Table 1.

* Uncertainties are given as the standard deviation of the mean. Uncertainties due to the "zero" effect are included.

The following symbols have been used:

Q electrical energy supplied
q amount of energy due to the "zero" effect
ΔH_v heat of vaporisation at 25°C

As seen in Table 2, the results obtained in this work, are in very good agreement with accurate values found in the literature [5]. The method seems therefore, not to be impaired by any significant systematic errors.

Table 2. Comparison between literature data and values obtained in this work.

Compound	Vapour pressure in mm Hg at 25°C	ΔH_v, kcal/mole	
		Ref [5]	This work
*Cyclo*hexane	96	7.89_5	7.89 ± 0.02
Methyl*cyclo*hexane	45	8.45_1	8.42 ± 0.04
n-Octane	14	9.91_5	9.94 ± 0.02
Mesitylene	2.5	11.34_5	11.36 ± 0.04

Acknowledgements. This work has been supported by *Knut och Alice Wallenbergs Stiftelse.* Part of the experimental work was performed by Mrs A. M. Wadsö and is gratefully acknowledged.

REFERENCES

1. Janz, G. J. *Estimation of Thermodynamic Properties of Organic Compounds.* Academic Press Inc. Publishers, New York 1958; Klages, F. *Chem. Ber.* **82** (1949) 358.
2. Sturtevant, J. M. in Weissberger, A. *Physical Methods in Organic Chemistry,* **Part 1.** Interscience, New York 1949.
3. Coon, E. D. and Daniels, F. *J. Phys. Chem.* **37** (1933) 1.
4. *Int. Crit. Tables* **Vol. V.** 142. McGraw-Hill, New York 1929; Howard, F. L. and Culbertson, J. L. *J. Am. Chem. Soc.* **72** (1950) 1185.
5. *Selected Values of Properties of Hydrocarbons and Related Compounds.* American Petroleum Institute Research Proj. 44.

Received November 12, 1959.

ACTA CHEMICA SCANDINAVICA 14 (1960) 573–576

Raman and Infrared Spectra of 1,4-Dichloro-2-butyne

BØRGE BAK, J. J. CHRISTIANSEN and E. MADSEN

Chemical Laboratory of the University of Copenhagen, Copenhagen, Denmark

In order to investigate whether a barrier to internal rotation in compounds C(LMN)—C≡C—C(XYZ) is detectable by means of conventional Raman and infrared techniques, 1,4-dichloro-2-butyne was examined. The spectra show no signs of the presence of a barrier, but the existence of a *small* barrier (<100 cm^{-1}) cannot be excluded. For all 'practical' purposes the rotation may be considered as unhindered.

In the Vålådalmeeting (Sweden 1958) Pauling suggested that there might be a hindrance to the internal rotation about the bonds in compounds of the general formular C(LMN)—C≡C—C(XYZ) and that the barrier might be as high as 0.5 kcal per mole ($\sim$ 175 cm^{-1}). In an earlier investigation by Thompson *et al.*[1] the barrier in CH_3—C≡C—CH_3 has been shown to be zero. The slight chance existed, however, that a larger barrier might be present in polar compounds like CH_2Cl—C≡C—CH_2Cl (I). Electron-diffraction investigation of this compound has shown that the barrier is close to zero but admittedly this experimental procedure has no high sensitivity to fixation of the magnitude of small barriers. Of course, the experimental method *par excellence* to apply is a microwave investigation, either of (I) or, preferably, of a compound like CH_3—C≡C—CH_2Cl (II) in which no rotational isomers would exist. This investigation has already been started by Laurie and Lide [3] who found that an upper limit to the height of a small barrier actually present in (II) is 0.1 kcal per mole ($\sim$ 35 cm^{-1}). — This result is in harmony with our recent studies of the infrared and Raman spectra of (I). If the barrier were *high* (1—3 kcal per mole), the usual signs of rotational isomerism such as "extra" lines would be expected. A *lower* barrier would have a chance to make itself noticed by its low-lying "pseudo"-torsional level(s). Nothing of this happens. In fact, the number of observed fundamentals is so small that the idea of a force-field of higher symmetry than the nuclear skeleton is hard to avoid. The observed spectra are interpretable in a straightforward manner — at least within the area of the usual medium-resolved infrared and Raman spectra — if one assumes unhindered rotation.

EXPERIMENTAL

$CH_2Cl-C\equiv C-CH_2Cl$ (I) was prepared [4] from 31 g of commercial $CH_2OH-C\equiv C-CH_2OH$. Yield 30 g (b. p. 49°–51°C at 75 mm Hg). By redistillation, 3 fractions were obtained which were identical with respect to their infrared absorption curves in the 600–4 000 cm^{-1} region. The Raman and the infrared spectra to be discussed refer to spectra of the middle fraction (20 g).

The *Raman spectrum* has earlier been photographed by Valette [5]. Our Raman spectrum, given in Table 1, is more complete than Valette's. Exposure periods of 2–6 h were applied. The quality of the high-dispersion spectrograph of high light-gathering power has been described elsewhere [6]. Line positions were measured against an iron-arc spectrum on photographic enlargements (1:15). They are thought to be reliable to 1–2 cm^{-1}.

Infrared spectra were recorded on a commercial Perkin-Elmer 21 instrument using KBr, NaCl, and CaF_2 optics in the appropriate regions. A cell thickness of 0.025 mm was applied except in regions where no or only very weak lines were found. Here, cells of 0.1 and even 1.0 mm thickness were used, except for the 400–650 cm^{-1} region where only one cell thickness was available (0.025 mm). The 'Optical D' given in Table 1 for reason of comparison, is the density that would have been found if the cell thickness 0.025 mm had been applied throughout. The frequencies measured in the infrared are thought to be good to 2–3 cm^{-1}.

INTERPRETATION OF SPECTRA

A glance at Table 1 shows that we are very far from observing the 24 fundamental vibrations to be expected for a molecule with 10 atoms. Most of the observed bands are obviously combination — and overtones. In view of the fact that a thorough Raman-infrared investigation usually brings out all or nearly all of the fundamentals [7], something exceptional is at work. We believe that this is the unhindered rotation, which causes a higher symmetry for the potential function than for the nuclear skeleton. Hence, a number of normal vibrations that would usually be observed separately, degenerate.

$CH_3-C\equiv C-CH_3$, with no barrier to the internal rotation, has the instantaneous symmetry D_3, but the symmetry of the potential field, and hence of the normal vibrations, is greater than this [8]. Actually the pseudo-symmetry of dimethylacetylene is D_{3d} (*not* D_{3h}). If this description can be extended to involve (I) the vibrations would be classified in four classes: A_{1g} (4 vibrations), A_{1u} (3), E_g (4 double-degenerate), and E_u (4 double-degenerate), *i.e.* 15 distinct normal frequencies. One might, however, suspect *a priori*, that the introduction of chlorine might cause changes analogous to what happens if, *e.g.*, one or more hydrogen atoms in a highly symmetrical hydrocarbon are substituted by deuterium. If all the symmetry elements are hereby removed, all 3N-6 normal vibrations are observed (thorough work provided). According to this latter description we should be able to find 24 fundamentals in the combined Raman and infrared spectra.

Before we counted the observed normal vibrations it seemed wise to investigate whether we were reasonably sure to have all of them recorded. For this purpose approximately correct modes of vibrations were constructed for (I) in the two extreme positions, *i.e.* the *trans* and the *cis* configuration where the symmetry is high enough (C_{2h} and C_{2v}) to make such sketching possible. It appeared that probably only one low-lying frequency might have escaped

Table 1. Observed Raman and infrared spectra of liquid $CH_2Cl-C\equiv C-CH_2Cl$ at 25°C.

Line No.	Raman spectrum Frequency	Intensity	Infrared spectrum Frequency	'Optical D'	Interpretation Fundamental	Combination
0					$\nu_0 = 215$ cm^{-1} (unobserved)	
1	330*	2			$\nu_1 = 330$	
2	400—455 *	2			$\nu_2 = 425$	$2\nu_0 = 430$
3			435	0.2	$\nu_3 = 435$	
4			490	0.2	$\nu_4 = 490$	
5			545	0.03		$\nu_5=\nu_0+\nu_1=$ 545
6	700	10	700	10	$\nu_6 = 700$	$\nu_0+\nu_4=$ 705
7			750	0.03		$\nu_7=\nu_1+\nu_2=$ 755
8			778	0.2	$\nu_8 = 778$	
9	785	8			$\nu_9 = 785$	
10	903	1	903	0.05	$\nu_{10} = 903$	$\nu_2+\nu_4=$ 915
11			1 160	3	$\nu_{11}=1\,160$	
12	1 165	2			$\nu_{12}=1\,165$	
13			1 260	11	$\nu_{13}=1\,260$	
14	1 266	10			$\nu_{14}=1\,266$	
15			1 383	0.03		$\nu_{15}=\nu_0+\nu_{12}=1\,380$
16			1 425	1.1	$\nu_{16}=1\,425$	
17	1 430	6			$\nu_{17}=1\,430$	
18			1 602	0.02		$\nu_{18}=\nu_6+\nu_{10}=1\,603$
19			1 648	0.02		$\nu_{19}=\nu_0+\nu_{17}=1\,645$
20			1 653	0.02		$\nu_{20}=\nu_4+\nu_{11}=1\,650$
21			1 674	0.04		$\nu_{21}=\nu_8+\nu_{10}=1\,681$
22			1 750 *	0.01		$\nu_{22}=\nu_4+\nu_{13}=1\,750$
23			1 805	0.02		$\nu_{23}=2\nu_{10}=1\,806$
24			1 855	0.01		$\nu_{24}=\nu_2+\nu_{17}=1\,855$
25			1 944	0.01		$\nu_{25}=\nu_8+\nu_{12}=1\,943$
26			2 037	0.01		$\nu_{26}=\nu_8+\nu_{13}=2\,038$
27			2 067	0.01		$\nu_{27}=\nu_{10}+\nu_{12}=2\,068$
28			2 115	0.01		$\nu_{28}=\nu_6+\nu_{16}=2\,125$
29			2 160	0.01		$\nu_{29}=\nu_{10}+\nu_{13}=2\,163$
30			2 195	0.01		$\nu_{30}=\nu_8+\nu_{16}=2\,203$
31			2 232	0.02		$\nu_{31}=\nu_9+\nu_{17}=2\,215$
32	2 245	10			$\nu_{32}=2\,245$	
33			2 312	0.10		$\nu_{33}=2\nu_{11}=2\,320$
34			2 325	v.w.		$\nu_{34}=\nu_{11}+\nu_{12}=2\,325$
35	2 331	4				$\nu_{35}=2\nu_{12}=2\,330$
36			2 417	0.02		$\nu_{36}=\nu_{11}+\nu_{13}=2\,420$
37	2 423	0				$\nu_{37}=\nu_{12}+\nu_{13}=2\,425$
38	2 505	0				$\nu_{38}=2\nu_{14}=2\,532$
39			2 510	0.01		$\nu_{39}=2\nu_{13}=2\,520$
40			2 585	0.01		$\nu_{40}=\nu_{16}+\nu_{11}=2\,585$
41			2 831	0.05		$\nu_{41}=2\nu_{16}=2\,850$
42			2 947	0.35	$\nu_{42}=2\,947$	$\nu_6+\nu_{32}=2\,945$
45	2 954	10			$\nu_{43}=2\,954$	
44			2 990	0.45	$\nu_{44}=2\,990$	
45	2 995	3			$\nu_{45}=2\,995$	

* Broad band.

observation in harmony with the findings of Crawford[9] for $CH_3-C\equiv C-CH_3$, in the spectrum of which a low-lying level at 213 cm^{-1} was found. If we assume that we did not observe a band at 215 cm^{-1} (*outside* the region accessible to us in the infrared and *in* a region where our Raman spectrum has some background) our scheme of combination bands fits well.

Table 1, then, indicates that we have observed fundamentals at 330, 425, 435, 490, 700, 778, 785, 903, 1 160, 1 165, 1 260, 1 266, 1 425, 1 430, 2 245, 2 947, 2 954, 2 990 and 2 995 cm^{-1}, *i.e.* 19 fundamentals. However, some of the observed bands may be grouped in close pairs, *viz.* 425—435, 778—785, 1 160—1 165, 1 260—1 266, 1 425—1 430. Counting "pairs + singles" we get 14 (+ 1 unobserved = 15). Thus, a description of the molecule as freely rotating but very slightly perturbed due to the chlorines, seems rather adequate.

For the present purpose we shall refrain from giving the forms of the normal vibrations although they are rather obvious in some of the cases (C—Cl valence vibrations at 700 and 778, C—C at 903 and 1 160, CH_2 scissoring at 1 425, C≡C vibration at 2 245 and C—H vibrations at 2 947, 2 954, 2 990 and 2 995). The numbering of the frequencies in Table 1 is completely arbitrary.

Acknowledgement. The authors thank professor Langseth for permission to use the Raman spectrograph.

REFERENCES

1. Mills, I. M. and Thompson, H. W. *Proc. Roy. Soc.* **1954** 306.
2. Morino, Y., Miyagawa, I. and Wada, A. *J. Chem. Phys.* **20** (1952) 1976.
3. Laurie, V. W. and Lide, D. R. *Spectroscopia Mol.* **8** (1959) 8.
4. Johnson, A. W. *J. Chem. Soc.* **1946** 1011.
5. Valette, A. *Ann. chim. Paris* **3** (1948) 677.
6. Langseth, A. and Lord, R. *Kgl. Danske Vidensk. Selskab Mat. Fys. Medd.* **16** (1938).
7. Langseth, A. and Bak, B. *Kgl. Danske Vidensk. Selskab Mat. Fys. Medd.* **24** (1947).
8. Bauman, R. P. *J. Chem. Phys.* **24** (1956) 13.
9. Crawford, B. L. *J. Chem. Phys.* **7** (1939) 555.

Received November 20, 1959.

ACTA CHEMICA SCANDINAVICA 14 (1960) 577–585

The Kinetics of the Acid-Catalysed Hydrolysis of Alkyl Formates

PENTTI SALOMAA

Department of Chemistry, University of Turku, Turku, Finland

The acid-catalysed hydrolysis of ethyl, *sec.*-propyl and *tert.*-butyl ormates has been studied kinetically in aqueous solutions over a wide range of temperature (15°C–86°C). The rate coefficients for ethyl and *sec.*-propyl formates are in reasonable accord with the Arrhenius equation over the whole temperature range, but the plot of log k against reciprocal absolute temperature for *tert.*-butyl formate is linear only in the low temperature range. The results suggest that all three esters are hydrolysed by essentially the same mechanism, a bimolecular acyl-oxygen fission, at the low temperatures. In the case of *tert.*-butyl formate, however, another mechanism which has a higher activation energy and which presumably involves unimolecular alkyl-oxygen fission, significantly augments the rate at the higher temperatures.

The hydrolysis reactions of the same esters have also been studied at 25°C in the presence of hydrogen chloride concentrations up to 3 M. The influence of the catalyst concentration on the rate was found to be similar for all the esters, and furthermore closely resembled its influence on the rate of hydrolysis of ethyl acetate. This is also in accord with the view that the hydrolysis of the three esters takes place by an essentially similar mechanism under these conditions.

It is well known that the acid-catalysed hydrolysis reactions of formic esters proceed at appreciably higher rates than the acid-catalysed hydrolysis reactions of the corresponding acetic esters in which a bimolecular acyl-oxygen fission is assumed to take place [1]. For this reason a change to a unimolecular alkyl-oxygen fission mechanism, which becomes apparent in different ways with the acetic esters [1,2] when the alkyl groups of the esters are varied in the sequence ethyl, *sec.*-propyl and *tert.*-butyl, may be expected to be less pronounced with the formic esters. Stimson [3], for example, concluded from the values of the Arrhenius parameters for the hydrolysis of *tert.*-butyl formate in acetone-water solution (60 % acetone by volume) that the mechanism of the reaction represents a bimolecular acyl-oxygen fission. So far as the hydrolysis in aqueous acid solutions is concerned, where the proton availability is much greater than in acetone-water mixtures [4] and which may therefore

be expected to favour the unimolecular mechanism, data for *tert.*-butyl formate have not been reported. The results of a kinetic study of the hydrolysis of alkyl formates in aqueous hydrogen chloride solutions, which is an extension of an earlier study of the acid hydrolysis of aliphatic esters [2,5], are presented and discussed in the following.

EXPERIMENTAL

Materials. Ethyl and *sec.*-propyl formates were prepared by customary methods [6] and purified by efficient fractional distillation. *tert.*-Butyl formate was synthesized by a method described recently by Young and Paré [7], in which *iso*butylene is passed into anhydrous formic acid to which cation exchange resin (Dowex X 50) has been added. The *iso*butylene was prepared by adding *tert.*-butyl alcohol dropwise to a large excess of anhydrous oxalic acid at a temperature of 80—90°C. The physical constants of the *tert.*-butyl formate after it had been fractionally distilled (*b. p.* 82.8°C at 755 mm Hg, d_4^{25} 0.8694, n_D^{25} 1.3787) were in accord with those reported by Young and Paré. The purities of the esters were checked by hydrolysing known weights in dilute acid solution and determining the formic acid produced by alkalimetric titration. The consumption of base did not deviate by more than 2 % from the calculated amount.

Kinetic measurements. Depending on the conditions, three different methods were employed in following the progress of the reactions. The first method, which was used to follow the reactions at 25°C when the catalyst acid concentration was high compared to that of the ester, has previously been described by the writer [5,2] and is based on the determination of the concentration of unreacted ester in samples removed from the reaction mixture after suitable intervals. The second method, which was used when the catalyst concentration and reaction temperature were relatively low (see below), was based on the alkalimetric titration of the formic acid present in samples pipetted from the reaction mixture. In the third method, employed at temperatures where volatility was appreciable, aliquots of the reaction mixture were transferred to ampoules which were sealed by fusion to avoid volatilization and which were opened after suitable intervals for the titrimetric determination of the liberated formic acid. For temperatures of 45°C and higher, electrically heated oil thermostats regulated by mercury contact thermometers were employed, whereas at the lower temperatures similarly heated and regulated water thermostats were used. The temperatures of the thermostats remained constant within ± 0.03°C.

The time periods used when the first method was employed to analyse the unreacted ester by alkaline hydrolysis were much shorter for the formic esters than for acetic esters [2] because of the higher rates of alkaline hydrolysis of the former esters. Periods of only a few minutes were considered sufficient in the case of ethyl and *sec.*-propyl formates. With *tert.*-butyl formate, the rate of alkaline hydrolysis of which was unknown, a time of one hour was chosen and was found by separate experiments to be sufficiently long. In the above experiments, as well as in those described below, the initial ester concentration was between 0.1 and 0.16 M.

In the second method, 5 ml samples taken with a semiautomatic pipette from the reaction mixtures were run into ice-water mixtures to arrest the reaction and titrated immediately in a nitrogen atmosphere (to exclude carbon dioxide) with 0.07—0.11 N standard sodium hydroxide to the phenolphthalein endpoint. Because each sample was cooled and diluted and the titration performed rapidly, no appreciable hydrolysis of the ester took place. Zero time was chosen as the time of taking the first sample. From 8 to 10 samples were withdrawn during the reaction in addition to those taken to determine the final value.

In the third method, the reaction mixture was prepared by mixing the components at 25°C, after which twelve 5 ml aliquots were pipetted into 6—7 ml glass ampoules. After the ampoules had been sealed by fusion, they were transferred simultaneously to a thermostat, the temperature of which was usually much above 25°C. After the ampoules had warmed to the temperature in the thermostat (in separate experiments a period of 5—10 min was found sufficient for the temperatures to become uniform in the solutions when

the group of ampoules was vigorously shaken), two ampoules were removed and cooled rapidly by shaking them in ice-water. After the ampoules had been opened, the acid in the solutions was titrated as in the second method. The time when the two ampoules were immersed in the ice-water mixture was taken as zero time and the mean base consumption as the initial value in the calculation of rate coefficients. Seven further samples were taken at intervals during the course of the reaction and titrated. The total amount of acid present at the end of the reaction was determined by titrating the samples in the three remaining ampoules after a sufficiently long period of time; the mean base consumption for these samples was employed as the final value. The procedure in which initial samples are analysed under the same conditions as the other samples taken during the course of the reaction reduces the time error to a minimum and is easily applied in practice. In principle it is of no importance how far the reaction has progressed before the first sample is taken.

Since in the experiments described the concentrations were measured at 25°C, usually a much lower temperature than that at which the reaction took place, the actual concentrations were calculated using the values of the density of water at different temperatures given in the International Critical Tables [8].

The change from the second to the third method of following the reaction took place with *sec.*-propyl and *tert.*-butyl formates at 45°C and 55°C, respectively, but with ethyl formate, owing to its greater volatility, at 25 – 35°C. The second and third methods were compared using ethyl formate at 25°C; the value of the second-order rate coefficient was 0.00337 l mole^{-1} s^{-1} when the second method was employed and 0.00335 l mole^{-1} s^{-1} when the third method was employed.

Kinetic equations for low catalyst concentrations. When relatively high catalyst acid concentrations were employed, the hydrogen ion concentration in the reaction mixture remained practically constant as the reaction progressed and the first-order rate law was satisfactorily obeyed. However, as it was necessary to employ relatively low catalyst acid concentrations at the highest temperatures because of the high reaction rates, the formic acid produced catalysed the reaction and this had to be taken into account in the calculations. In extreme cases, the increase in the hydrogen ion concentration during the reaction represented the greater part of the total catalyst concentration at the end of the reaction.

The time law for the reaction is

$$\frac{dx}{dt} = k_c \, C_{H^+} \, (a-x) \tag{1}$$

where a denotes the ester concentration at zero time, x the decrease in this concentration during time t, k_c the second-order rate coefficient and C_{H^+} the hydrion concentration, which was also a function of time in the experiments. Since $x = 0$ when $t = 0$, eqn. (1) yields on integration

$$k_c = \frac{\ln [a/(a-x)]}{\int_0^t C_{H^+} \, dt} = \frac{(1/t) \ln [a/(a-x)]}{(1/t) \int_0^t C_{H^+} dt} = \frac{k_t}{(C_{H^+})_t} \tag{2}$$

where k_t is the value of the rate coefficient computed from the usual first-order rate equation. This first-order coefficient has different values at different times during the course of the reaction and the corresponding hydrion concentration

$$(C_{H^+})_t = \frac{1}{t} \int_0^t C_{H^+} dt \tag{3}$$

is the time average of the hydrion concentration over the interval (0, t). The value of the integral in eqn. (3) can be determined when the variation of the hydrion concentration with time is known. The integral was calculated as a sum of trapezoids by a method described by the writer in connection with a study of the alcoholysis of α-halogenoethers [9]. The hydrion concentration at each time of sampling was determined as follows. The initial concentration of hydrogen chloride in the reaction mixture in moles per litre

Table 1. The hydrolysis of *sec.*-propyl formate at 86.22°C. ml NaOH = ml of 0.1102 N sodium hydroxide solution consumed in the titration of the sample. Sample volume (measured at 25°C) 5.01 ml. The coefficient for the thermal expansion from 25°C to 86.22°C is 1.0301. $10^3K = 0.1206$ mole l^{-1}, $10^3c = 0.816$ mole l^{-1} (at 86.22°C).

t min.	ml NaOH	$10^6\ k_t$	$10^3\ f$	$10^3\ C_{H+}$	$10^3\ (C_{H+})_t$	$10^3\ k_c$
0	0.57	—	11.3	1.605	—	—
4	1.30	395	26.9	2.209	1.907	207
10	2.68	505	56.4	2.997	2.325	217
15	3.76	559	79.5	3.479	2.629	213
20	4.65	587	98.5	3.826	2.885	203
25	5.64	660	119.6	4.174	3.108	212
30	6.43	720	136.5	4.432	3.307	218
42	7.48	770	158.9	4.750	3.674	210
∞	8.64	—			—	—

Average $k_c = 0.211$ l mole^{-1} s^{-1}

(denoted by c) was determined when the reaction medium was prepared. The total acid concentration in the sample is given by $(c + f)$, where f is the concentration of the formic acid formed. The hydrion concentration in the reaction mixture at the time of sampling can be computed from

$$C_{H+} = \tfrac{1}{2}(c-K) + \sqrt{\tfrac{1}{4}(c-K)^2 + (c + f)K} \qquad (4)$$

where K is the acid dissociation constant of formic acid at the temperature in question. For the temperature dependence of this dissociation constant, Harned and Embree [10] have given the following equation

$$\log K = -(173.624/T) + 17.88348 \log T - 0.0280397\ T - 39.06123 \qquad (5)$$

Although this equation is based on experimental data for the temperature range from 0° to 60°C, the general thermodynamic form of the equation and the fact that the value of K varies only slightly with temperature justified the use of the equation for extrapolation to obtain the values of the constant at temperatures above 60°C. Furthermore, any error resulting from the use of the equation was the same for all the esters studied and hence the values of the rate coefficients for the latter are comparable at each temperature. In addition, the fact that the data for ethyl and *sec.*-propyl formates obeyed the Arrhenius equation with satisfactory accuracy over the temperature range where eqn. (5) was employed showed that no serious errors resulted. As far as the effect of electrolyte concentration on the values of K is concerned, this could be disregarded because the ionic strength was very low in the experiments in which eqns. (2), (3), (4) and (5) were applied.

The data in Table 1 refer to a case where the initial concentration of hydrogen chloride was lower than the hydrion concentration due to the dissociation of formic acid produced in the reaction. The large increase in the values of k_t as the reaction progressed shows that the reaction was autocatalytic. On the other hand, the calculated values of k_c at different stages of the reaction are essentially constant, which shows that the equations employed correctly represent the course of the reaction. It may be mentioned, however, that constant values would have been obtained for k_c even if values of K deviating slightly from those derived from eqn. (5) had been employed. This is due to the fact that in this extreme case the second term under the root sign in eqn. (4) primarily determines the value of the hydrion concentration. Therefore the value of k_c includes, in addition to the usual experimental errors in kinetic measurements, the error in the value of K.

Table 2. The rate coefficients of the acid-catalysed hydrolysis of alkyl formates at different temperatures and the values of the parameters of the Arrhenius equation computed from the data for the lower temperatures (15—45.5°C).

°C	10^3 k_c in 1 mole^{-1}s^{-1}		
	Ethyl formate	*sec.*-Propyl formate	*tert.*-Butyl formate
15.00	1.33	1.18	2.62
25.00	3.36	2.92	5.98
35.00	7.58	6.85	13.0
45.48	17.4	15.6	31.4
55.63			60.5
66.06			117.4
68.48	98.0		
76.15			314
86.22	294	211	683
15.00—45.48	E = 15 340 cal per mole, log A = 8.76	E = 15 440 cal per mole, log A = 8.79	E = 14 790 cal per mole, log A = 8.62

RESULTS AND DISCUSSION

The acid-catalysed hydrolysis of alkyl formates could be followed kinetically by the methods described above over the temperature range from 15 to 86°C. The results of the experiments are collected in Table 2. Rate coefficients of the acid-catalysed hydrolysis of ethyl and *sec.*-propyl formates at relatively low temperatures have been reported previously. For comparison, the following values in 1 mole^{-1}s^{-1} units referring to 25°C may be mentioned: ethyl formate, 0.00312 (Palomaa [11]), 0.00325 (Salmi [12]), 0.00307 (Tommila and Hella [13]); *sec.*-propyl formate, 0.00280 (Palomaa [11]), 0.00293 (Palomaa *et al.*[14]).

The plots of the logarithm of the rate coefficient against reciprocal absolute temperature in Fig. 1 show that the Arrhenius equation is obeyed well by the data for the three formic esters at relatively low temperatures. The values of the activation energy and frequency factor computed by the method of least squares from the data referring to the temperature range from 15 to 45.5°C are given in Table 2; in this temperature range the plots are satisfactorily linear for all three esters. Since the values of the activation energy and the frequency factor for *tert.*-butyl formate are of the same magnitude as the values for ethyl and *sec.*-propyl formate in this temperature range, there is no reason to believe that the mechanism of hydrolysis of the first-mentioned ester differs essentially from that of the last two esters, *i.e.* all three esters presumably hydrolyse under the conditions by the normal mechanism of acid-catalysed ester hydrolysis designated as $A_{AC}2$ by Ingold [1].

It will be seen from Fig. 1 that the behaviour of *tert.*-butyl formate deviates from that of the other two esters at higher temperatures in that its rate coefficient increases more rapidly with temperature than the Arrhenius parameters

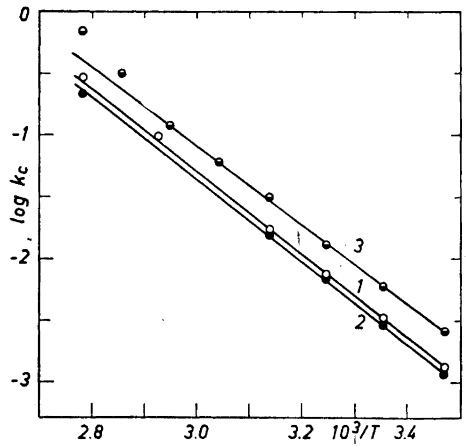

Fig. 1. Plots of log k_c against $1/T$ for the hydrolysis reactions of alkyl formates in dilute acid solution. 1. Ethyl formate. 2. *sec.*-Propyl formate. 3. *tert.*-Butyl formate. The straight lines are Arrhenius plots based on data obtained in the temperature range 15—45.5°C.

computed from the data for lower temperatures would imply. This different behaviour cannot be attributed to systematic errors in the method of following the reaction at the higher temperatures because the data obtained for ethyl and *sec.*-propyl formates by the same experimental procedure exhibit only slight deviations from the linear dependence of log k_c on reciprocal temperature.

The different behaviour of *tert.*-butyl formate at the higher temperatures suggests that under these conditions, in addition to the $A_{AC}2$ mechanism, another hydrolysis mechanism with a higher activation energy begins to contribute to the rate. This assumption is supported by the following rough estimates. If we assume that the Arrhenius equation based on the data obtained at the lower temperatures relates to the $A_{AC}2$ mechanism and also applies as far as this mechanism is concerned at the higher temperatures, as it approximately does in the case of ethyl and *sec.*-propyl formates, it is possible to determine the contribution of the $A_{AC}2$ mechanism to the rate of hydrolysis of *tert.*-butyl formate at the higher temperatures. When the rate coefficients of hydrolysis by the $A_{AC}2$ mechanism calculated for the higher temperatures are subtracted from the over-all observed rate coefficients, the resulting rate coefficients should represent the contribution of the assumed concurrent mechanism. The latter rate coefficients calculated from the data for *tert.*-butyl formate given in Table 2 are 0.261 l mole^{-1}s^{-1} at 86.22°C and 0.082 l mole^{-1}s^{-1} at 76.15°C. The values of the parameters of the Arrhenius equation derived from these rate coefficients are $E = 29$ kcal per mole and log $A = 17$ and are of such magnitudes that they can be taken to refer to the unimolecular alkyl-oxygen fission mechanism of acid-catalysed ester hydrolysis ($A_{AL}1$). For the acid-catalysed hydrolysis of *tert.*-butyl acetate, for example, which hydrolyses primarily by the unimolecular $A_{AL}1$ mechanism [1,2], the values of the parameters computed from the data reported by Palomaa *et al.*[14] are $E = 27.6$ kcal per mole and log $A = 16.34$. From the values derived for the Arrhenius parameters one can estimate the rate coefficient of the hydrolysis of *tert.*-butyl

formate by the $A_{AL}1$ mechanism to be about 10^{-4} l mole^{-1}s^{-1} at 25°C and hence this mechanism contributes very little to the over-all rate of hydrolysis, 59.8 $\times$ 10^{-4} l mole^{-1}s^{-1}, at this temperature.

It will be noted that the rates of hydrolysis by the $A_{AL}1$ mechanism of acetic esters do not differ greatly from the rates of hydrolysis of the corresponding formic esters, whereas in the case of the $A_{AC}2$ mechanism a corresponding change in structure leads to a marked change in reactivity. In water and water-alcohol mixtures, alkoxymethyl formates react by the $A_{AL}1$ mechanism only from 1.5 to 3 times as fast as the corresponding acetates [15]. If the rate coefficient for the hydrolysis of *tert.*-butyl acetate [2] in dilute acid at 25°C, 1.34 $\times$ 10^{-4} l mole^{-1}s^{-1}, can be taken to represent hydrolysis by the unimolecular $A_{AL}1$ mechanism, the magnitude of the estimated rate coefficient of the hydrolysis of *tert.*-butyl formate by the same mechanism at 25°C, 10^{-4} l mole^{-1}s^{-1}, is plausible.

One particular point of interest concerning the effect of structure on hydrolysis by the bimolecular $A_{AC}2$ mechanism is that when the alkyl group changes from ethyl to *tert.*-butyl the rate becomes smaller in the case of acetates in such a degree that the unimolecular $A_{AL}1$ mechanism begins to predominate, whereas in the case of formates the rate increases (*e.g.*, about twofold at 15°C). This latter increase in rate is not, at least not at the lower temperatures, due to a change in mechanism from $A_{AC}2$ to $A_{AL}1$, as other experimental evidence would lead one to conclude. This different effect of alkyl group structure in the hydrolysis of formates and acetates by the $A_{AC}2$ mechanism is probably due to the combined effect of several factors. One possible explanation is that the retardation of the rate of hydrolysis when a tertiary alkyl group replaces a primary alkyl group in acetic esters is primarily due to steric hindrance, and the $A_{AL}1$ mechanism, which is insensitive to steric effects, begins to predominate. In the case of the formic esters, steric hindrance is of lesser significance because in these compounds the carbonyl group is more exposed to the attack of a water molecule, and therefore the polar factors become more apparent. These assumptions are supported by the observation that at the lower temperatures where the different formic esters may be expected to react by the same mechanism the effect of structure on the rate becomes apparent primarily as a change in the activation energy

Table 3. The first-order rate coefficients k (in s^{-1}) for the hydrolysis of ethyl, *sec.*-propyl and *tert.*-butyl formates in aqueous hydrochloric acid solutions of various concentrations. Hydrochloric acid concentrations in moles per litre. 25°C.

Ethyl formate		*sec.*-Propyl formate		*tert.*-Butyl formate	
c_{HCl}	$10^3 k$	c_{HCl}	$10^3 k$	c_{HCl}	$10^3 k$
0.1512	0.503	0.1512	0.442	0.0841	0.503
0.349	1.21	0.748	3.02	0.497	3.47
1.35	6.00	1.35	6.08	1.36	11.2
2.09	9.90	2.09	10.4	2.10	21.0
2.96	13.5	2.96	14.3	2.97	33.8

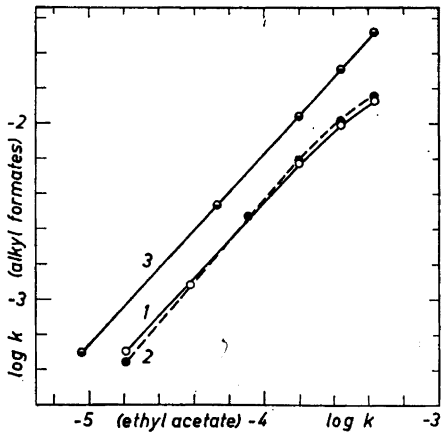

Fig. 2. Plots of the values of log k for alkyl formates against the values of log k for ethyl acetate at identical acid concentrations in aqueous hydrochloric acid solutions at 25°C. 1. Ethyl formate. 2. *sec.*-Propyl formate. 3. *tert.*-Butyl formate.

(see Table 2). The frequency factor, and hence the entropy of activation, does not vary significantly in value from one ester to the other, which suggests only slight changes in steric hindrance. A more detailed study of the effects of polar and steric factors on the acid-catalysed hydrolysis reactions of formic and acetic esters would be desirable.

Since the formic esters studied may be assumed to hydrolyse in acid solution at low temperatures by the bimolecular mechanism in which the critical complex includes a water molecule in addition to the ester molecule and a proton, these esters offered a possibility of studying the validity of the Zucker-Hammett hypothesis [16,17] by carrying out kinetic measurements of the rates of hydrolysis in moderately acid solutions by the method previously described by the author [5,2]. Measured values of the first-order rate coefficients, k, of the hydrolysis of the three formic esters in aqueous hydrochloric acid solutions of varying concentration are shown in Table 3. The data reveal that the rates fo all three esters react similarly to a change in the medium and the values of k increase slightly more rapidly than they would if they were proportional to the molar concentration of the catalyst hydrochloric acid. The curves in Fig. 2, in which the values of log k for the formic esters are plotted against the values of log k for ethyl acetate for the same hydrogen chloride concentrations (the latter values interpolated from previously reported data [5,2]), show that the effect of the acid medium on the rate is approximately the same for the formic esters as for ethyl acetate. The increase in the rate at the higher acid concentrations is, however, possibly slightly less rapid with the formic esters than with ethyl acetate. Since the rate of hydrolysis of ethyl acetate, in contrast to *tert.*-butyl acetate [2], follows more closely the acid concentration than the acidity function H_0, in qualitative agreement with the expectations based on the Zucker-Hammett hypothesis, it follows from the plots in Fig. 2 and the discussion above that this hypothesis is approximately valid also for the formic esters in the investigated media.

Acknowledgements. The writer wishes to thank Miss Raili Linnantie, Ph.M., for the preparation and purification of the materials used and for assistance in some of the kinetic runs. Thanks are also due to the *Valtion Luonnontieteellinen Toimikunta* (The State Council for Natural Sciences) for financial support.

REFERENCES

1. Ingold, C. K. *Structure and Mechanism in Organic Chemistry*, G. Bell and Sons Ltd., London 1953, Ch. XIV.
2. Salomaa, P. *Suomen Kemistilehti* **B 32** (1959) 145.
3. Stimson, V. R. *J. Chem. Soc.* **1955** 4020.
4. Braude, E. A. and Stern, E. S. *J. Chem. Soc.* **1948** 1976.
5. Salomaa, P. *Suomen Kemistilehti* **B 32** (1959) 81.
6. Vogel, A. J. *Practical Organic Chemistry*, 3rd Ed., Longmans, Green and Co., London 1956, p. 385.
7. Young, W. and Paré, E. M. *J. Org. Chem.* **23** (1958) 1772.
8. *International Critical Tables*, Mc Graw-Hill Book Co., New York 1928, Vol. III, pp. 22—24.
9. Salomaa, P. *Ann. Univ. Turkuensis* **A XIV** (1953) No. 1, pp. 39—41.
10. Harned, H. S. and Embree, N. D. *J. Am. Chem. Soc.* **56** (1934) 1042.
11. Palomaa, M. H. *Ann. Acad. Sci. Fennicae* **A IV** (1913) No. 2, p. 16.
12. Salmi, E. J. *Ann. Univ. Aboensis* **A III** (1932) No. 3, p. 108.
13. Tommila, E. and Hella, A. *Ann. Acad. Sci. Fennicae* **A II** (1954) No. 53.
14. Palomaa, M. H., Salmi, E. J., Jansson, J. I. and Salo, T. *Ber.* **68** (1935) 303.
15. Salomaa, P. *Acta Chem. Scand.* **11** (1957) 141, 239.
16. Zucker, L. and Hammett, L. P. *J. Am. Chem. Soc.* **61** (1939) 2791.
17. Long, F. A. and Paul, M. A. *Chem. Revs.* **57** (1957) 935.

Received November 14, 1959.

ACTA CHEMICA SCANDINAVICA 14 (1960) 586–593

The Acid-Catalysed Solvolysis of Alkoxymethyl Esters

Part V. Hydrolysis of β-Chloroethoxymethyl Esters

PENTTI SALOMAA and RAILI LINNANTIE

Department of Chemistry, University of Turku, Turku, Finland

The acid-catalysed hydrolysis reactions of the β-chloroethoxymethyl esters of formic and acetic acids have been studied kinetically. Evidence has been collected which shows that the formic ester hydrolyses in dilute acid solution at low temperatures predominantly by the bimolecular $A_{AC}2$ mechanism with a minor contribution by the unimolecular $A_{AL}1$ mechanism. The existence of the two reaction paths is indicated, firstly, by the actual magnitudes of the rate coefficients in comparison to the values estimated from the linear free energy relations, secondly, by the deviation from linearity of the plot of the logarithm of the rate coefficient against reciprocal temperature, and, thirdly, by the variation of the rate coefficient in moderately acid solutions. The relative contributions of the two mechanisms to the over-all rates have been estimated.

The kinetic data for β-chloroethoxymethyl acetate, on the other hand, are consistent with the assumption that this ester hydrolyses predominantly by the unimolecular $A_{AL}1$ mechanism, although there is definite indication of a simultaneous, minor contribution by the $A_{AC}2$ mechanism.

In a recent study of the hydrolysis of alkoxymethyl esters of acetic and formic acids [1], evidence based on kinetic data obtained by different experimental methods was presented which suggested that methoxymethyl and ethoxymethyl esters of acetic acid hydrolyse in aqueous acid solutions by the unimolecular $A_{AL}1$ mechanism whereas a contribution of the bimolecular $A_{AC}2$ mechanism to the over-all rate was established in the hydrolysis of methoxymethyl formate. The magnitudes of the rate coefficients of the hydrolysis of β-chloroethoxymethyl formate * at different temperatures and the computed value of the activation energy indicated as highly probable that the electron-attracting substituent chlorine retards the unimolecular mecha-

* An error was made when the rate constants for this compound reported by Palomaa and Herna [2] were cited in *Ref.*[1]. The correct value at 25°C is 0.00368 l mole^{-1}s^{-1} and the correct value of the activation energy 15 300 cal/mole. These values are, however, close to those obtained for alkyl formates and do not therefore alter the conclusions drawn.

nism to such an extent that the bimolecular mechanism dominates this reaction. The present study was undertaken to obtain a more detailed picture of the nature of this reaction and also to determine the effect of the halogen on the reaction of the corresponding ester of acetic acid. The acid components of the esters were selected in order to effect a real change in the rate by the bimolecular mechanism (*cf.*, *e.g.*, *Ref.*[3]).

HYDROLYSIS OF β-CHLOROETHOXYMETHYL FORMATE

In dilute hydrochloric acid solutions, the rate of hydrolysis of β-chloroethoxymethyl formate was found to be proportional to the molar concentration of the acid and hence the values of the second-order rate coefficients k_c, obtained by dividing the directly computed first-order rate coefficients by the acid concentration, were essentially independent of the latter. Table 1 contains the values determined for k_c in these solutions at different temperatures. The values referring to the temperatures 15°, 25° and 35°C are from 4 to 9 % lower than the values obtained earlier by Palomaa and Herna [2] who used a slightly different method of following the reaction.

Table 1. Hydrolysis of β-chloroethoxymethyl formate in dilute (0.05—0.1 M) hydrochloric acid solutions. Values of k_c (in 1 mole^{-1}s^{-1}) at different temperatures.

°C	0.88	9.00	15.00	25.00	35.00	46.00	55.83	67.60
$10^3 k_c$	0.318	0.775	1.40	3.33	7.72	22.6	[51.2	134

Although the rate coefficients at low temperatures are of the magnitude generally observed for formic esters that react by the normal type of acid-catalysed ester hydrolysis involving a bimolecular acyl-oxygen fission, certain observations suggest that the over-all rate coefficients include a minor contribution of another mechanism, the unimolecular alkyl-oxygen fission. In a recent study [4] it was shown that the solvolytic reactions of alkoxymethyl compounds that can be assumed to involve a unimolecular formation of an unstable alkoxymethyl cation in the rate-determining stage exhibit approximately linear free energy correlations when the structure of the alkoxyl group is varied. On the basis of the values of the rate coefficients, polar substituent constants and reaction constants given, it is possible to obtain an estimate, $k_c = 9 \times 10^{-4}$ l mole^{-1}s^{-1}, for the rate coefficient of the hydrolysis of β-chloroethoxymethyl formate at 25°C by the unimolecular mechanism; this amounts to one-fourth of the measured over-all rate coefficient. Although the estimated value cannot be very accurate, its magnitude shows that a concurrent reaction mechanism is highly probable.

The existence of two independent reaction paths is indicated also by the observed temperature dependence of the rate coefficients. The plot of log k_c for β-chloroethoxymethyl formate against reciprocal temperature shown in Fig. 1 reveals a satisfactory linearity in the low temperature range but increases in slope at the higher temperatures. Such a behaviour is in accord with the occurrence of two concurrent reactions with different activation energies;

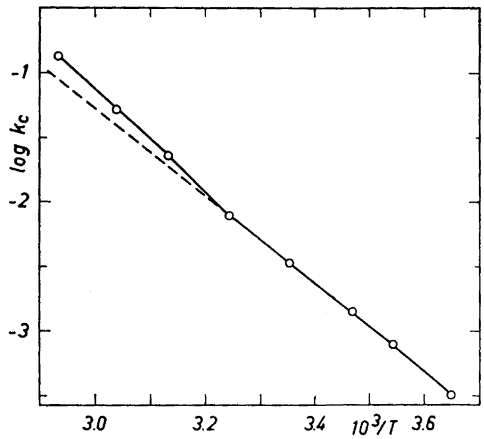

Fig. 1. Hydrolysis of β-chloroethoxymethyl formate at different temperatures. Plot of log k_c against $1/T$.

the reaction with the lower activation energy dominates in the low temperature range but the contribution of the second reaction with the higher activation energy gradually becomes more significant as the temperature rises. The situation is in principle similar to that observed with methoxymethyl formate [1].

Calculations made by the iteration method [1] assuming that the over-all rate coefficient is the sum of two rate coefficients which both vary with temperature in accordance with the Arrhenius equation, $k_c = k_1 + k_2 = A_1 \exp(-E_1/RT) + A_2 \exp(-E_2/RT)$, revealed that the following values of the four Arrhenius parameters, $E_1 = 22$ kcal/mole, $\log A_1 = 13$, $E_2 = 14.4$ kcal/mole and $\log A_2 = 8.0$, yield a plot which reasonably closely approximates the experimental plot. Although the above values of the constants include in addition to experimental errors any errors due to genuine deviations from the Arrhenius equation (the values for the reaction indicated by subscript 2 can be more reliably calculated than those for reaction 1 because the former reaction which has the lower activation energy dominates over the greater part of the temperature range), they are of the magnitudes expected for the postulated mechanisms (*cf. Ref.*[1]). From the values of the parameters it can be estimated that the contribution of the unimolecular mechanism is about one-fourth of the over-all rate at 25°C. This estimate is in good agreement with the estimate obtained above on the basis of polar substituent effects.

The third item of evidence for the simultaneous operation of two mechanisms is obtained from the kinetic data for the reaction in moderately acid solutions when the data are considered in relation to the acidity function H_0 of Hammett [5]. Although the general applicability of the Zucker-Hammett hypothesis [5,6] for a basis of criterion of reaction mechanism has recently been questioned [7-10], the hypothesis seems to be in satisfactory accord with the kinetic data for the hydrolysis reactions of aliphatic esters of different types in hydrochloric acid solutions [1,11-13]. In this connection it may be pointed out that there hardly exists any single, unequivocal experimental criterion for the determination of the molecularity of a solvolytic reaction.

In a preliminary communication [14] the authors drew attention to the fact that if the Zucker-Hammett hypothesis is valid for the types of reaction under study and these reactions involve concurrent unimolecular and bimolecular

Table 2. First-order rate coefficients k (in s^{-1}) for the hydrolysis of β-chloroethoxymethyl formate in hydrochloric acid solutions. The acid concentrations, given in moles per liter, refer to 25°C.

0.88°C		25.00°C	
c_{HCl}	10^4k	c_{HCl}	10^3k
0.1534	0.490	0.1534	0.511
0.590	2.06	0.590	2.15
0.944	3.44	0.944	3.98
1.534	5.40	1.534	8.20
2.36	11.6	2.36	14.0
3.07	19.2	3.06	21.5
3.78	28.9	3.77	38.5
4.72	63.7	4.72	67.8
6.93	421		

mechanisms, the latter mechanism will not become clearly evident when the reactions take place in hydrochloric acid solutions of moderate concentration unless its contribution happens to be the dominating one. This is because the unimolecular mechanism becomes more significant with increasing acidity and finally overweighs the bimolecular mechanism so that the latter can no longer be experimentally detected. If, however, the contribution of the bimolecular mechanism is large enough in dilute acid solution, the plot of log k against $-H_0$ will have a special form characterized by a point of inflexion. This follows from the fact that the rate increases less rapidly at low acidities where the contribution of the bimolecular mechanism is significant than at high acidities where the unimolecular mechanism assumes control.

The above behaviour expected in the case of two concurrent mechanisms was actually observed in the hydrolysis of β-chloroethoxymethyl formate[14]. The data relating to 25°C on the basis of which the plot of *Ref.*[14] was made are given in Table 2. As the bimolecular mechanism could be assumed to become even more significant at lower temperatures because of its lower activation energy, the variation of the over-all rate with increasing acidity was investigated also at 0.88°C. These results are given in Table 2 in addition to those referring to 25°C. The curve plotting the logarithm of the observed first-order rate coefficient at 0.88°C against the value of the acidity function at 25°C (Fig. 2) is similar in form to that referring to the rate measurements at 25°C, but the unusual form of the curve is more clearly evident.

The contributions of the unimolecular mechanism to the over-all rate of hydrolysis of β-chloroethoxymethyl formate in dilute hydrochloric acid at 25°C as estimated by the three different methods are given below:

Method	*Fraction of over-all rate*
Effect of structure	0.3
» » temperature	0.3
» » acidity	0.2—0.5

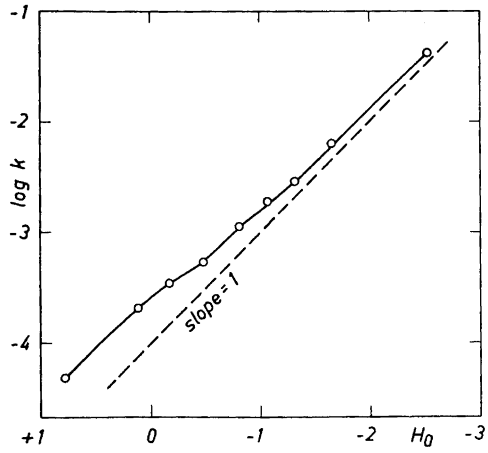

Fig. 2. Hydrolysis of β-chloroethoxymethyl formate at 0.88°C. Plot of log k against the values of the H_0 acidity function [15] at 25°C.

The estimate based on the last method [14] is the most uncertain because a more accurate result would require that the Zucker-Hammett hypothesis in its ultimate form [5] would be accurately true and not a satisfactory approximation. In view of this limitation, the above estimates are consistent.

HYDROLYSIS OF β-CHLORETHOXYMETHYL ACETATE

The second-order rate coefficients k_c of the hydrolysis of β-chloroethoxymethyl acetate at the temperatures 15°, 25° and 35°C were reported in a recent paper in connection with a study of polar effects on the reactions of alkoxymethyl compounds (*Ref.*[4], Table 3). Although the estimated substituent effect of the β-chloroethyl group conformed well with the effect of this group in other reactions of alkoxymethyl compounds which are assumed to involve the unimolecular formation of an alkoxymethyl cation, and although the values of the activation energy and frequency factor of β-chloroethoxymethyl acetate were of approximately the same magnitude as the values of other alkoxymethyl acetates studied, there is reason to suspect that the hydrolysis of β-chloroethoxymethyl acetate is a composite reation with a minor contribution due to the normal type of acid-catalysed ester hydrolysis. In other reactions of alkoxymethyl compounds the retarding effect of the β-chloroethyl group on the rate was associated with an elevated activation energy, whereas the opposite situation prevailed in the case of β-chloroethoxymethyl acetate. This exceptional observation can be explained by assuming that the over-all reaction includes a contribution of the bimolecular acyl-oxygen fission reaction with a lower activation energy that is not large enough to cause the Arrhe-

Table 3. Hydrolysis of β-chloroethoxymethyl acetate in dilute (0.05—0.1 M) hydrochloric acid solutions. Values of k_c (in 1 mole^{-1}s^{-1}) at different temperatures.

°C	0.88	6.56	15.00	25.00	35.00	49.90	64.70
$10^4 k_c$	0.119	0.251	0.711	2.41	7.56	40.4	188

Table 4. First-order rate coefficients k (in s^{-1}) for the hydrolysis of β-chloroethoxymethyl acetate in hydrochloric acid solutions. The acid concentrations, given in moles per liter, refer to 25°C.

0.88°C		25°C	
c_{HCl}	10^5k	c_{HCl}	10^4k
0.1534	0.182	0.1534	0.370
0.590	0.840	0.590	1.78
0.944	1.55	0.944	3.20
1.534	3.27	1.534	7.21
2.36	7.62	2.36	17.2
3.07	14.7	3.07	34.4
3.78	30.1	3.78	64.7
4.72	77.2	4.72	155
6.93	797		

nius plot to deviate from linearity when the temperature range is narrow. The participation of the normal type of acid-catalysed ester hydrolysis is also plausible in view of the actual magnitudes of the rate coefficients. The value (0.000241 l $mole^{-1}s^{-1}$) of the rate coefficient k_c at 25°C is only 2.2 times the value reported by Tommila and Hella [16] for methyl acetate and 6.8 times the value obtained by Euranto [17] for chloromethyl acetate under the same conditions.

The simultaneous operation o :the two mechanisms is indicated by the kinetic data relating to a wide range of temperature that are shown in Table 3. The plot of log k_c against reciprocal temperature drawn in Fig. 3

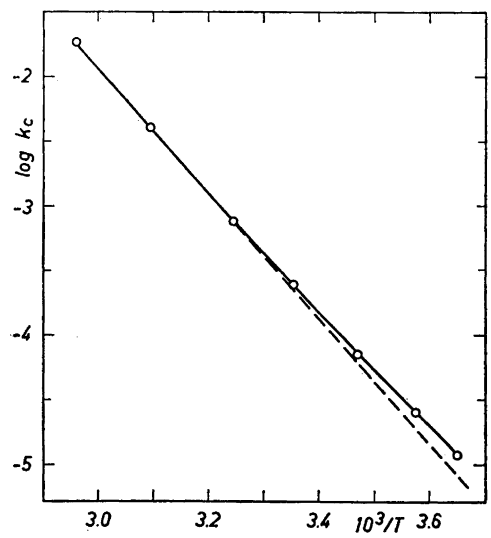

Fig. 3. Hydrolysis of β-chloroethoxymethyl acetate at different temperatures. Plot of log k_c against $1/T$.

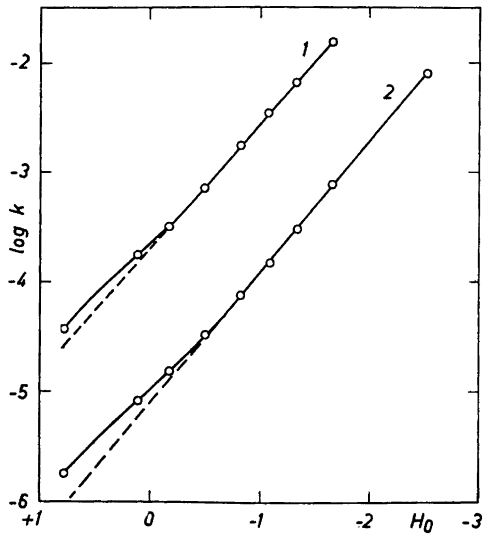

Fig. 4. Plot of log k against the values of the H_0 acidity function [15] at 25°C for the hydrolysis of β-chloroethoxymethyl acetate in hydrochloric acid solutions. 1. 25°C. 2. 0.88°C.

shows that the Arrhenius equation is not satisfactorily obeyed. Although the departure from linearity is less than in the case of methoxymethyl formate [1] and β-chloroethoxymethyl formate (see above), it is larger than could be ascribed to experimental errors or genuine deviations from the Arrhenius equation that could occur in the present type of reaction. In order to obtain a satisfactory estimate of the contribution of the bimolecular mechanism to the rate, it would be necessary to study the reaction at much lower temperatures where, owing to its lower activation energy, the mechanism would contribute more to the over-all rate.

To permit a better comparison with other alkoxymethyl esters, the hydrolysis of β-chloroethoxymethyl acetate was also studied over a wider range of hydrogen chloride concentration. The first-order rate coefficients at different acid concentrations are given in Table 4 and their logarithms are plotted as a function of the value of the acidity function H_0 in Fig. 4. The plot of the data referring to 25°C is approximately linear with a slope close to unity, the deviation from linearity being hardly greater than can be ascribed to experimental error, whereas the data referring to 0.88°C yield a plot that clearly has a smaller slope at low acidities than at high acidities. This is the expected result [14] if the Zucker-Hammett hypothesis can be assumed to be at least approximately valid for the reaction in question and if there are two concurrent reaction mechanisms which differ in their dependence on the acidity of the solution. Here the bimolecular acyl-oxygen fission with its lower activation energy can be expected to contribute more to the over-all rate at the lower temperatures.

EXPERIMENTAL

The preparation and purification of the compounds studied except β-chloroethoxymethyl formate have been described earlier [1,4]. β-Chloroethoxymethyl formate was synthesized from α-chloromethyl-β-chloroethyl ether and lead formate. It was found advantageous to use a large excess of lead formate (about 140 % of the calculated amount) to effect complete conversion of the chloroether. After the components were mixed, the mixture was heated on a water bath. The crude product was extracted with ether, the lead chloride and unreacted lead formate removed by centrifugation and the residue remaining after the ether was distilled off distilled under reduced pressure. The main ester fraction boiled at 82.5°C under a pressure of 17 mm Hg. When the purity was checked by titration of the formaldehyde formed from the ester (*cf.* Ref.[1]), 191.7 mg of the ester was equivalent to 41.16 ml of 0.0676 N iodine solution (calc. 40.93 ml).

The method of following the reactions was that used in earlier studies of alkoxymethyl esters [1]. In all cases the first-order rate equation was satisfactorily obeyed.

The authors wish to express their gratitude to the *Valtion Luonnontieteellinen Toimikunta (The Finnish State Council for Natural Sciences)* for financial aid.

REFERENCES

1. Salomaa, P. *Acta Chem. Scand.* **11** (1957) 132, 141, 235, 239.
2. Palomaa, M. H. and Herna, T. O. *Ber.* **66** (1933) 305.
3. Ingold, C. K. *Structure and Mechanism in Organic Chemistry*, G. Bell and Sons Ltd., London 1953, Ch. XIV.
4. Salomaa, P. *Suomen Kemistilehti* **B 33** (1960) 11.
5. Long, F. A. and Paul, M. A. *Chem. Revs.* **57** (1957) 935.
6. Zucker, L. and Hammett, L. P. *J. Am. Chem. Soc.* **61** (1939) 2791.
7. Taft, Jr., R. W., Deno, N. C. and Skell, P. S. *Ann. Rev. Phys. Chem.* **9** (1958) 303.
8. Koskikallio, J. and Whalley, E. *Can. J. Chem.* **37** (1959) 788.
9. Bunton, C. A., de la Mare, P. B. D. and Tillett, J. G. *J. Chem. Soc.* **1959** 1766.
10. Archer, G. and Bell, R. P. *J. Chem. Soc.* **1959** 3228.
11. Salomaa, P. *Acta Chem. Scand.* **11** (1957) 247.
12. Salomaa, P. *Suomen Kemistilehti* **B 32** (1959) 81, 145.
13. Salomaa, P. *Acta Chem. Scand.* **14** (1960) 577.
14. Salomaa, P. and Linnantie, R. *Acta Chem. Scand.* **12** (1958) 2051.
15. Paul, M. A. and Long, F. A. *Chem. Revs.* **57** (1957) 1.
16. Tommila, E. and Hella, A. *Ann. Acad. Sci. Fennicae*, **Ser. A II** (1954) No. 53.
17. Euranto, E. *Suomen Kemistilehti* **B 29** (1956) 144; *Ann. Univ. Turkuensis*, **Ser. A I** (1959) No. 31.

Received November 30, 1959.

ACTA CHEMICA SCANDINAVICA 14 (1960) 594–608

On the Equilibrium $In^{3+} + 2In(s) \rightleftharpoons 3In^{+}$

GEORGE BIEDERMANN and TOM WALLIN

Department of Inorganic Chemistry, Royal Institute of Technology, Stockholm 70, Sweden

The equilibrium between In^{3+}, indium metal and indium ions in the lower oxidation state has been studied at 25°C by bringing indium(III) perchlorate solutions into intimate contact with finely divided indium metal. After a steady state was attained in the solution a) the number of equivalents of the reducing agent formed, b) the emf of the couple and c) the emf of the In^{3+}-In(s) couple were measured. The indium(III) concentration varied between 0.01 and 0.2 M, the hydrogen ion concentration was kept ≤ 0.01 M and all solutions were made to contain 3 M ClO_4^- by the addition of $NaClO_4$.

The data can be well explained by assuming that only the In^+ ion is formed and that for $In^{3+} + 2In(s) \rightleftharpoons 3In^+$, $\log K = -8.4 \pm 0.1$. No evidence has been found for the species In^{2+}.

In the ionic medium 3 M ClO_4^- the following standard potentials have been determined at 25°C

$In^{3+} + 2e^- \rightleftharpoons In^+$	$e^\circ_{1,3} = -425.5 \pm 1$ mV
$In^{3+} + 3e^- \rightleftharpoons In(s)$	$e^\circ_{0,3} = -343 \pm 1$ mV
$In^+ + e^- \rightleftharpoons In(s)$	$e^\circ_{0,1} = -178 \pm 5$ mV

Experimental conditions influencing the rate of the reaction $In^+ + 2H^+ \rightarrow In^{3+} + H_2$ have been discussed.

The experiments of Thiel [1] in 1904 gave the first indication of the existence of the In^+ ion in water solution. Thiel found that InCl and InBr are readily dissolved in water, but that metallic indium is formed rapidly in the solution because of the reaction $3In^+ \rightarrow In^{3+} + 2In(s)$. Materials of the stoichiometric composition InX_2 (X = halogen) could not be dissolved; when these came into contact with water, decomposition to In^{3+} and InX(s) occurred immediately.

Hepler, Hugus and Latimer [2] published in 1953 the results of their investigation on the equilibrium between In^{3+}, indium metal and indium ions of the lower oxidation states. These authors attempted to equilibrate at 25°C indium(III) perchlorate solutions of $\log[H^+] = -1$ with finely divided indium, and measured the number of equivalents of the reducing agents present, after attainment of a steady state, by titrating with Ce(IV) solution. Assuming the simultaneous equilibria

$$In^{3+} + 2\,In(s) \rightleftharpoons 3\,In^{+} \qquad K_1 = [In^{+}]^3[In^{3+}]^{-1}$$
$$\text{and } 2In^{3+} + In(s) \rightleftharpoons 3\,In^{2+} \qquad K_2 = [In^{2+}]^3[In^{3+}]^{-2}$$

we have calculated from their data the constants $\log K_1 = -7.5$ and $\log K_2 = -6.4$.* These values are valid at the ionic strength 0.83; the inert salt added was $Ce(ClO_4)_3$.

Kangro and Weingärtner [3] in 1954 studied the reduction of In^{3+} by indium metal with emf measurements. These investigators measured at different temperatures the redox potential with a Pt electrode and the potential of indium metal in indium(III)sulfate solutions of $\log[H^+]$ about -2.5 which were in contact with indium metal. The equivalent concentration of the reduced ions was determined by titrating with $KMnO_4$ solution. Equilibrium could not be established under these experimental conditions because of the rapid oxidation of the indium ions in the lower oxidation state by hydrogen ions. This reaction was observed especially on the surface of the Pt foil used to measure the redox potential. By assuming that In^+ is formed exclusively and that the hydrolysis can be neglected, Kangro and Weingärtner obtained at 26.5°C with extrapolation to infinite dilution $\log K_1 = -6.917$.

EXPERIMENTAL DIFFICULTIES

The study of a redox equilibrium of this type involves a number of difficulties.

The standard potential of the indium redox couple lies at about -400 mV, the ions in the lower oxidation state are therefore unstable in respect to oxidation by hydrogen ions at $\log [H^+] > -7$. Solutions containing indium(III) in appreciable amount cannot be prepared, however, unless $\log [H^+] > -3$, because of the precipitation of indium hydroxide. The rate of oxidation by hydrogen ions may be much suppressed under suitable experimental conditions but it cannot be eliminated completely in acid solutions. The law of mass action consequently cannot be applied to a set of analytical data to ascertain the formulas of the ions formed by reduction, nor can the corresponding equilibrium constants be obtained, unless independent evidence is obtained that real equilibrium is established in the solution.

When a reversible redox electrode can be found, the correct value of the equilibrium constant can be computed by combination of the emf and the analytical data without the necessity of the attainment of a real equilibrium. The noble metals most often used to measure redox potentials are unfortunately good catalysts for oxidation reactions with hydrogen ions. If this reaction occurs with an appreciable speed on the electrode surface, the reliability of the emf measurements is impaired.

With a number of redox systems — Sn(II)—Sn(IV)[4], Cr(II)—Cr(III)[5], Ti(II)—Ti(III)[6] and V(II)—V(III)[7] — reproducible emfs have been obtained with mercury redox electrodes which were introduced by Forbes [4] in 1914. Evolution of hydrogen on the mercury surface is slow because of the high

* We have not been able to derive the constants $\log K_1 = -10.5$ and $\log K_2 = -7.7$ given in the original publication.

overvoltage but it cannot be avoided completely. Also there is always the possibility of amalgam formation when mercury electrodes are employed.

Since the In^{3+} ion is an acid of considerable strength [8] the hydrogen ion concentration of the solution should be known accurately. It is essential to choose an appropriate acidity. The concentration of the ions in the lower oxidation state is diminished if the hydrogen ion concentration is so low that hydrolyzed species of In(III) are formed in appreciable amounts, while if the acidity is high, then oxidation by hydrogen ions becomes rapid. In either case the analysis and emf measurements become more difficult.

In our experiments the concentration of the ions in the lower oxidation state varied between 0.1 and 1 mM. The accurate determination of a reducing agent at such low concentrations presents some difficulties. Visual end point indication proved to be quite unsatisfactory. The slowness of the electrode reaction in the neighborhood of the equivalence point made potentiometric methods impractical. Good results were obtained on the other hand with amperometric end point determination.

METHOD

To study the redox equilibrium, oxygen-free solutions of In^{3+} were brought into intimate contact with finely divided indium metal. The reduction started immediately and proceeded rapidly at the range of indium(III) concentrations studied in this work. The progress of the reduction was followed by a redox and an In electrode. When both these electrodes attained a steady value, which usually required 3 to 4 hours, the indium metal was removed from the solution and a known amount of an iodine solution was added. This immediately oxidized the indium ions of the lower oxidation state to In^{3+}; the excess iodine was measured with an 1 mM $Na_2S_2O_3$ solution.

The indium(III) concentration of the test solutions was varied between 0.0100 and 0.200 M. The hydrogen ion concentration was kept in the majority of the experiments at 0.0100 M; at this acidity the hydrolysis of In(III) is negligible for the indium concentrations studied [8] and the rate of oxidation of the ions in the lower oxidation state by hydrogen ions is slow. A few data were obtained also at $\log [H^+] < -2$ where hydrolyzed species of In(III) are formed in appreciable amounts.

In order to minimize the variation of the activity factors all solutions were made to contain 3 M ClO_4^- by adding $NaClO_4$. The test solutions thus had the general composition

B M In^{3+}, H M H^+, $(3.000-3B-[H^+])$ M Na^+, 3 M ClO_4^- = solution S

In each experiment three quantities were measured: 1) the number of moles of iodine reduced by one liter of the test solution in the steady state; this number will be denoted by R; 2) The emf of the redox half-cell against a standard half-cell SE; 3) The emf of the In^{3+}-In half-cell against SE. These are related to the concentrations of the ionic species present in the solution by the equations that follow.

The reaction between In^{3+} and In(s) may be generally written

$$q\ In^{3+} + (3\ p-q)\ In(s) \rightleftharpoons 3\ In_p^{q+},\ K_{p,q} = \{In_p^{q+}\}^3\ \{In^{3+}\}^{-q} \qquad (1)$$

where the symbol {} denotes activity. The standard state is defined so that the activity factors tend to unity if the solutes are present in negligible amounts in the solvent 3 M $NaClO_4$. Iodine oxidizes In_p^{q+} according to the equation

$$In_p^{q+} + \frac{3p-q}{2} I_2 \rightarrow p\ In^{3+} + (3p-q)\ I^- \quad (2)$$

thus R will be equal to

$$R = \sum \frac{3p-q}{2} [In_p^{q+}] \quad (3)$$

The electrode reaction at the indium metal may be written

$$In^{3+} + 3e^- \rightleftharpoons In(s) \quad (4)$$

and that at the redox electrode

$$p\ In^{3+} + (3p-q)e^- \rightleftharpoons In_p^{q+} \quad (5)$$

At equilibrium the emf of the cell

In/solution S/redox electrode

should be zero, hence at 25°C

$$e_r^\circ + \frac{59.15}{3p-q} \log \frac{\{In^{3+}\}^p}{\{In_p^{q+}\}} = e_{0,3}^\circ + \frac{59.15}{3} \log \{In^{3+}\} \quad (6)$$

where e_r° and $e_{0,3}^\circ$ denote the standard potentials referred to the hydrogen scale. If there are several species In_p^{q+} e_r° is of course different for each of them. From (1) and (6) we obtain

$$\log K_{p,q} = \frac{3p-q}{19.72} (e_r^\circ - e_{0,3}^\circ) \quad (7)$$

To determine the potentials of the redox and of the In^{3+}— In couples the cells

— redox electrode/solution S/SE + (A)

and — In/solution S/SE + (B)

have been employed. SE denotes the half-cell

Ag, AgCl/0.0100 M NaCl, 2.990 M $NaClO_4$/3 M $NaClO_4$/

The emf of these cells can be written at 25°C

$$E_A = e_{SE} - e_r^\circ - \frac{59.15}{3p-q} \log \frac{[In^{3+}]^p}{[In_p^{q+}]} - \frac{59.15}{3p-q} \log \frac{f^p(In^{3+})}{f(In_p^{q+})} + E_j \quad (8)$$

$$E_B = e_{SE} - e_{0,3}^\circ - 19.72 \log [In^{3+}] - 19.72 \log f\ (In^{3+}) + E_j \quad (9)$$

where $f(In^{3+})$ and $f(In_p^{q+})$ denote the activity factors, e_{SE} is a constant and E_j is the liquid junction potential between solution S and 3 M $NaClO_4$. In a previous paper [9] it has been shown that at low metal ion concentration E_j for

all practical purposes is a function of the $[H^+]$ only, namely $E_j = 16.7\,[H^+]$ mV in 3 M $NaClO_4$. The estimation of the activity factors has been treated in a separate study, and the results pertaining to our problem are discussed in a later section.

In order to eliminate the effect of the small variation of e_{SE} with time, before each E_A and E_B measurement the emf, E_C, of the cell

$$-\ \text{SE}/0.0100\ \text{M}\ H^+,\ 2.990\ \text{M}\ Na^+,\ 3\ \text{M}\ ClO_4^-,\ \text{quinhydrone (s)/Pt}\ + \qquad \text{(C)}$$

was determined. The relevant value of e_{SE} (which might vary slightly between different days) was calculated by the equation

$$E_C = e_Q^\circ + 59.15 \log [H^+] - E_j - e_{SE} \qquad (10)$$

The standard potential $e_Q^\circ = 677.7 \pm 0.1$ mV of the quinhydrone half-cell was determined using the cell

$$H_2\ (1\ \text{atm})/S_1/S_1,\ \text{quinhydrone(s)/Pt}$$

where S_1 denotes the solution: 0.0500 M H^+, 2.950 M Na^+, 3.000 M ClO_4^-.

By measuring E_A, E_B and R at a series of B values the functions $E_A\,(B, R)$ and $E_B\,(B)$ have been determined; the study of these functions is the subject of the following discussion.

MATERIALS AND ANALYSIS

Indium (III) perchlorate solutions were made from indium metal of 99.99 % purity generously provided and spectrographically examined by the Consolidated Mining and Smelting Company of Canada Ltd. The solutions were prepared and analyzed for indium and hydrogen ions as described previously [8]. A few experiments were made to determine the [In(III)] by electroanalysis but no satisfactory results were obtained. The deposition was not complete at log $[H^+]$ values greater than -2, whereas at lower log $[H^+]$ values the deposited metal contained some indium hydroxide.

Potassium iodate solutions were made from double recrystallized KIO_3, Merck p.a. This preparation was compared with recrystallized and water-free $K_2Cr_2O_7$ by titrating the same $Na_2S_2O_3$ solution with both solutions using a weight burette; the results agreed within 0.02 %.

Sodium thiosulfate solutions were prepared from $Na_2S_2O_3\,(H_2O)_5$ Merck p.a. To prevent bacterial decomposition *iso*butyl alcohol was added according to Winkler [10], and the solution was made 1 mM in Na_2CO_3 as recommended by Kolthoff [11].

Distilled water used to prepare ½ mM KIO_3 and 1 mM $Na_2S_2O_3$ solutions was first filtered through a G5 Jena glass filter, then boiled and finally made oxygen-free by bubbling nitrogen through it for 2 h. Without these precautions the dilute solutions deteriorated rapidly. *Hydrochloric acid* solutions were made from 38 % HCl Merck p.a. which was purified by distillation. *Sodium iodide* Malinckrodt p.a. was used without further purification; no traces of iodate could be detected in this preparation. *Sodium perchlorate, sodium hydrogen carbonate* and *sodium chloride* solutions were prepared and analyzed as usual in this laboratory [8]. *Carbon dioxide* and *nitrogen* were taken from cylinders and freed from oxygen by passage over hot activated copper. The gases were passed through water and 3 M $NaClO_4$ to obtain the right vapor pressure.

The *amperometric titrations* were carried out with a platinum wire as the indicator electrode and SE as the reference electrode, the solutions being stirred vigorously with a rotating magnet. The galvanometer had a sensitivity of 4×10^{-9} A/mm. The accuracy of the amperometric determination of iodine in our solutions was tested by adding a known amount of iodine to an indium perchlorate solution and titrating with thiosulfate which has been standardized against KIO_3. An accuracy of 0.2 % was obtained in the iodine concentration range 0.1 to 1 mM.

Experimental details of the emf measurements

All emf measurements were made at 25.0 ± 0.3°C in a thermostated room. The arrangement of the reference half-cell and the salt bridge is described elsewhere [12]. The emfs were measured with a valve potentiometer, Radiometer PHM 3, Copenhagen, which was calibrated against a Leeds and Northrup potentiometer of type K3. The reading accuracy was 0.1 mV.

Indium metal electrodes were prepared by electrolysis from an acid In(III) solution using a Pt gauze cathode. The deposited metal consisted of fine crystals and thus it had a large surface. This was of importance since the metal served also as the reducing agent in the test solution. Quite a thick layer of indium must be deposited because indium forms an alloy with platinum and this, in contrast to pure indium metal, is easily dissolved in $[HClO_4] \geq 10$ mM. In oxygen-free solutions and at $\log [H^+] \leq -2$ these electrodes came to equilibrium within 2–3 h and gave potentials which were constant and reproducible to within 1 mV for many hours. *Ag,AgCl electrodes* were prepared as usual in this laboratory [8].

On the measurement of the redox potential

We had considerable difficulty in finding an appropriate redox electrode. Platinum foils never attained a quite constant potential in our solutions, and the difference $E_A - E_B$ was in no case less than 20 mV. Gold, silver and mercury pool electrodes proved also to be unsatisfactory. The failure of these types of electrodes may be ascribed partly to their catalytic activities for the oxidation of In_p^{q+} by H^+ and partly to the slowness of the electrode reaction at the low R values studied in this work.

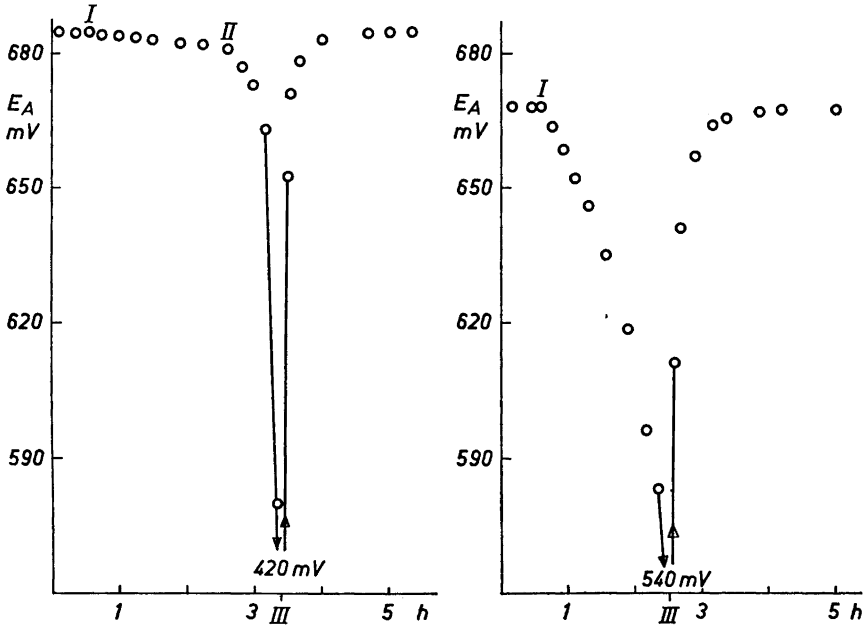

Fig. 1. Reproducibility of the redox electrodes. E_A (eqn (8)) as a function of time at $\log [H^+] = -2$ (Fig. 1a) and at $\log [H^+] = -1$ (Fig. 1b). The indium electrode was removed at point I, air was admitted at point II. At point III the indium metal electrode was reinserted and the CO_2 stream restarted.

Good results were obtained on the other hand with mercury coated platinum foils; these electrodes were found to give potentials reproducible within at least 0.5 mV and to reach a constant potential rapidly in solutions of log $[H^+] \leq -2$. The redox electrodes were made by precipitating mercury electrolytically on a platinum foil with a current density of about 5 mA cm^{-2} for about 10 min from a slightly acid $Hg(ClO_4)_2$ solution.

Several experiments were made to test these electrodes; a typical one concerning their reproducibility will now be described, *cf.* Fig. 1a. Four mercury-platinum electrodes were put into an oxygen-free solution of $B = 100$ mM and $R = 0.5$ mM which had been in contact with indium metal for several hours. The electrodes reached a constant potential within 20 min and they agreed within 0.2 mV. Now the indium metal was removed (point I in Fig. 1a), this caused a slow decrease of E_A due to the oxidation of In_p^{q+} by H^+. After 2 h the solution was brought into contact with air (point II); now of course E_A decreased rapidly. When the In metal was reinserted (point III) and the O_2 was expelled from the solution with CO_2 all the four redox electrodes had in an hour re-attained, within 0.1 mV, the constant starting potential.

In all experiments at least two but usually four electrodes were used; the potential difference between them never exceeded 0.5 mV.

Several experimental facts seem to indicate that the satisfactory function of this type of redox electrodes is to be ascribed to the formation of an alloy on the platinum surface. When a platinum foil was kept in mercury for about nine months at 25°C it was found by X-ray analysis that a substantial part of the foil had become transformed to $PtHg_4$. The crystal structure of this alloy was determined by Bauer, Nowotny and Stempfl [13], who found it to be the phase richest in mercury which can be prepared at 450 and 200°C. Our experiments give evidence that $PtHg_4$ is stable at room temperature and is the phase which is in equilibrium with liquid mercury.

No alloy formation could be detected by X-ray analysis on the redox electrodes prepared as described above. This failure is to be explained by the fact that the amount of alloy formed was too small to be detected by X-ray diffraction, it must have been less than one weight percent.

In the course of our work it was observed that the redox electrode became much less satisfactory when the electrolysis was prolonged and small drops of mercury were visible on the electrode surface. Electrodes prepared in the same way differed considerably and the potential difference between the indium and these redox electrodes was higher by several mV than that between the indium and the redox electrodes prepared by short electrolysis. A rapid alloy formation can occur on the platinum surface; when the surface is completely covered with the alloy further amounts of mercury cannot react except by diffusion through the alloy. Deposition of large amounts of mercury thus has the effect of decreasing the active surface of the electrode; perhaps some In of lower valency is also removed by amalgam formation.

In order to prepare properly functioning electrodes it was essential to boil the platinum foil in *aqua regia* before electrolysis. This treatment creates a large and active surface which can react rapidly with mercury, whereas on bright, polished platinum surfaces mercury is deposited in droplets.

Evidence for alloy formation between platinum and mercury has been found by several investigators who studied the electroanalysis of mercury [14]. When the deposited mercury is dissolved in hot concentrated nitric acid, appreciable amount of platinum(IV) can be detected in the solution and the surface of the gauze turns dark indicating the dissolution of some platinum.

Procedure

After the test solution was placed in a six-necked flask a vigorous stream of CO_2 or N_2 was passed through it for about an hour to expel oxygen. Then the indium electrode was immersed and the reference half-cell was connected. To hasten the attainment of the steady state the solution was stirred with a rotating magnet. When the indium electrode attained a constant value, which usually occurred after 2 to 3 h, two or more redox electrodes were put into the solution. These required a period of between 15 min and 2 h, depending on B, to reach a constant value. Before the final values of E_A and E_B were taken the magnetic stirring was stopped.

To determine R the indium electrode was taken out, the gas stream was stopped and a known amount of iodine was added to the solution. In a number of experiments the redox electrodes were removed before the titration. The presence of the redox electrodes was found not to influence appreciably the R value obtained. In separate experiments evidence was found that during the interval — about 1 to 2 min — which elapsed between the removal of the indium metal and the introduction of iodine no appreciable amount of the ions in the reduced form was oxidized by hydrogen ions, *cf.* Fig. 1a.

As dilute solutions of iodine are unstable the iodine was prepared just before the addition. To a 0.5 mM KIO_3 solution placed in a small separating funnel of about 50 ml capacity 10 ml of 0.2 M HCl was added and the solution was made oxygen-free by passing through CO_2 for 15 min. Now 0.2 g solid NaI was added and after 20 min the iodine solution was introduced into the flask. The titration was started immediately.

The 1 mM $Na_2S_2O_3$ solution used to measure the small excess of iodine was standardized each time immediately after the determination of R. In connection with the standardization an important point was to avoid any excess of thiosulfate when titrating the iodine which remained after the reduction with In_p^{q+}. Thiosulfate was found to decompose appreciably in our acid solutions. The excess could be avoided by plotting the current as a function of added ml thiosulfate during the titration and extrapolating the resulting line to zero current. The last increment of thiosulfate required to attain the equivalence point was calculated from this extrapolation. No appreciable error could be made in this way since the residual current was always less than 10^{-8} A, and the current as a function of ml thiosulfate proved to be strictly a straight line in the neighborhood of the equivalence point.

On the steady state and the rate of oxidation of In_p^{q+} by hydrogen ions

The data obtained in the final series of measurements are presented in Table 1. This final series was preceded by a preliminary one covering the same B range with 15 measurements. The results of this preliminary series are somewhat less trustworthy because insufficient attention was paid to a few experimental details of minor importance. These data are nevertheless in acceptable agreement with those of the final series.

Table 1. Survey of experimental data.

B M	E_A mV	E_B mV	$R \times 10^4$ M
1.000×10^{-2}	701.3	707.1	2.46_1
»	703.0	707.3	2.64_1
2.000×10^{-2}	697.5	700.1	3.29_4
»	697.8	701.1	3.30_8
» 1)	699.7	705.5	2.47_5
5.00×10^{-2}	689.3	691.9	4.86_3
»	689.9	692.4	4.53_1
»	689.2	693.8	4.40_5
1.000×10^{-1}	684.3	685.6	6.45_6
»	684.3	685.7	6.28_2
»	684.2	685.5	6.32_2
» 2)	688.9	690.2	5.01_9
2.000×10^{-2}	677.8	678.8	8.27_1
»	677.4	678.9	8.07_7

1) $\log [H^+] = -3.11$; $[In^{3+}] = 1.29 \times 10^{-2}$ M
2) $\log [H^+] = -2.90$; $[In^{3+}] = 4.52 \times 10^{-2}$ M

The $[In^{3+}]$ of the hydrolyzed solutions with log $[H^+] < -2$ was measured with an indium electrode, the equilibrium concentration of hydrogen ions was calculated from B, $[In^{3+}]$ and the analytical hydrogen ion concentration employing the hydrolysis constants determined previously [8].

The E_A and E_B values given in Table 1 indicate that true equilibrium could not be established in the bulk of our solutions. The difference $E_B - E_A$, which is a measure of the distance from the equilibrium, is 6 mV at the lowest B = 10 mM, and decreases to about 1 mV at the maximum B = 200 mM. The relatively small differences $E_B - E_A$ show that oxidation by hydrogen ions could be restrained to a great extent under the experimental conditions employed.

We may describe schematically the system consisting of the indium net, the test solution and the redox electrode as

$$In/R_e\colon\ R_s\colon\ R_A/Hg-Pt$$

where R_e is the equilibrium value of R which prevails in the layer surrounding the indium net, R_s is the value of R in the bulk of the solution and R_A is that in the vicinity of the redox electrode. These are related by the inequality

$$R_e \geq R_s \geq R_A$$

The symbol ":" denotes a concentration gradient. The steady state to which the data in Table 1 are referred is attained when the rate of diffusion of In_p^{q+} from the solution layer around the indium gauze becomes equal to the rate of the reaction

$$\overline{In}_p^{q+} + 3\,(p-q)\,H^+ \rightarrow p\,In^{3+} + \frac{3\,p-q}{2}\,H_2 \qquad (11)$$

occuring in the solution, on the wall of the flask or on the redox electrode. A similar condition holds for the layer surrounding the redox electrode and the solution if $R_s > R_A$.

The limited accuracy of the emf data does not permit a detailed study of the reaction mechanism of (11); a few interesting conclusions, however, can be drawn. The data in Table 1 give evidence that (11) is kinetically of less than first order in $[In_p^{q+}]$ at constant acidity. In the case of a first order reaction $E_B - E_A$ would be independent of $[In_p^{q+}]$, whereas if it were of a higher order, $E_B - E_A$ would increase with $[In_p^{q+}]$. An analysis of the $E_B - E_A = f(B, R)$ function indicates that (11) is retarded by In^{3+} ions. This may be explained by assuming that (11) is a heterogeneous reaction which may occur, *e.g.*, on the surface of the glass flask. As the $[In^{3+}]$ is increased a larger fraction of the surface becomes covered with adsorbed In^{3+} ions and thus the number of active centers available for (11) is decreased.

We have some evidence that (11) occurs chiefly on solid surfaces. In several experiments a solution containing In_p^{q+} was passed through a thin layer of glass wool and a fine glass capillary. A substantial decrease of R was always observed and gas bubbles could be seen on the glass wall. No difference was found between the catalytic activities of glass and polyethylene surfaces

of identical size. Metals which show a low overvoltage for hydrogen are very effective catalysts, as was discussed previously in connection with the redox electrodes.

In order to evaluate the redox potential measurements we had to assume that

$$R_s = R_A$$

i.e. reaction (11) does not occur to an appreciable extent on the Hg—Pt surface. The good reproducibility of the redox potential measurements seems to indicate that this assumption is a good approximation. When the redox potentials were measured with platinum or gold electrodes, several electrodes immersed in the same solutions differed by about 20 mV, whereas with the mercury-plated platinum electrodes the difference never exceeded 0.5 mV and usually was within 0.2 mV.

Another experimental fact seems to be in agreement with this hypothesis. Several redox potential measurements were made in the following way: after the first redox electrode attained a constant value two or three freshly prepared electrodes were put into the solution at the same time. This had no detectable effect on the potential of the first electrode. If the electrode surfaces were effective catalysts, R_s would be decreased (at least temporarily) by increase of the surface. This decrease of R_s would diminish the diffusion velocity of In_p^{q+} to the first electrode. Thus R_A would decrease, which should have been detected when measuring the redox potential.

The dependence of the reaction rate on the hydrogen ion concentration is illustrated in Fig. 2, which shows the potential difference between an indium and a redox electrode in the steady state as a function of log $[H^+]$ in a solution of $B = 100$ mM. The measurements were made with the technique described previously. The potential difference is seen to decrease rapidly with the $[H^+]$ and it attains a minimum value of about 2 mV at log $[H^+] = -2$. Substantially lower log $[H^+]$ values could not be studied because of the precipitation of indium hydroxide.

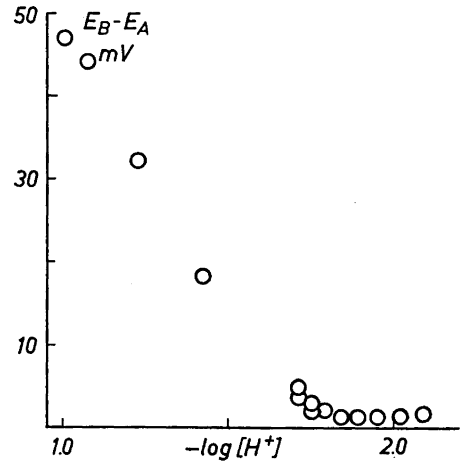

Fig. 2. Dependence of the rate of reaction (11) on log $[H^+]$. $E_B - E_A$ as a function of log $[H^+]$. The $[In(III)]_{total}$ was kept at 0.100 M.

The rapid increase of the reaction rate with increasing $[H^+]$ is also clearly demonstrated by the experiments whose results are shown in Figs. 1a and 1b. In the absence of metallic indium In_p^{q+} is seen to be oxidized rather slowly at log $[H^+] = -2$ (Fig. 1a) but very rapidly at log $[H^+] = -1$ (Fig. 1b). At log $[H^+] = -2$ the redox potential is decreased in one hour by 4 mV whereas at log $[H^+] = -1$ six minutes are sufficient for the same decrease.

RESULTS

In order to explain the data given in Table 1 we will assume in the first instance that only *one* species In_p^{q+} is formed by reduction and that the activity factors are constant. Then according to (1) and (3) the $[In_p^{q+}]$ and $[In^{3+}]$ are related to R and B by the equations

$$[In_p^{q+}] = \frac{2\,R}{3\,p-q} \tag{12}$$

and

$$B > [In^{3+}] \geq B - \frac{q}{3}\,\frac{2\,R}{3p-q} \tag{13}$$

We shall use in the following calculations the approximation

$$\log [In^{3+}] = \log B \tag{14}$$

the error made using this approximation has no appreciable influence on the results since R never exceeds 0.03 B.

The charge of the reduced species q and the number of indium atoms it contains p as well as the equilibrium constant $K_{p,q}$ can be found by using (7). When we eliminate e_r° and $e_{0,3}^\circ$ using (8) and (9), and employ (12) and (14) for $[In_p^{q+}]$ and log $[In^{3+}]$, eqn (7) will take the form

$$\log K_{p,q} = 3 \log \frac{2}{3\,p-q} + 3 \log R + \frac{3\,p-q}{19.72}\,\Delta E - q \log B \tag{15}$$

This can be rearranged to

$$3 \log R + 3\,p\,\frac{\Delta E}{19.72} = \log K_{p,q} - 3 \log \frac{2}{3\,p-q} + q\,(\log B + \frac{\Delta E}{19.72}) \tag{16}$$

where for convenience ΔE is written for $E_B - E_A$.

In (16) R, ΔE and B are determined experimentally, whereas p, q and $K_{p,q}$ are unknown. To find p and q and thus also $K_{p,q}$ we have calculated the left-hand side of (16) by assuming $p = 1$, 2, 3, and 4 and plotted the resulting values against $\log B + \frac{\Delta E}{19.72}$. For the correct value of p a straight line should result with the slope q.

The plot for $p = 1$ is given in Fig. 3a which shows that the points may be satisfactorily represented by a straight line of unit slope. In the plots for

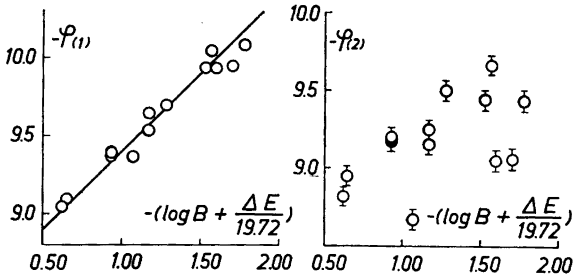

Fig. 3. Ascertainment of the species formed by reduction. $\varphi\,(p) = 3 \log R + \frac{3p\Delta E}{19.72}$ as a function of $\log B + \frac{\Delta E}{19.72}$. The line in Fig. 3a) represents the equation $3 \log R + \frac{3\Delta E}{19.72} = -8.40 + \log B + \frac{\Delta E}{19.72}$.

$p = 2$, 3, and 4, points belonging to practically the same $\log B + \frac{\Delta E}{19.72}$ but of different ΔE deviated from each other by an amount exceeding the experimental uncertainty. This indicates that the hypothesis $p > 1$ is inconsistent with (16) and cannot yield a constant value for $K_{p,q}$. The plot for $p = 2$ is shown in Fig. 3b. It was of no interest to consider higher values of p than 4 because the deviations increased rapidly as p exceeds one. We can thus conclude that our data can be explained only by assuming the formation of the species with $p = 1$ and $q = 1$, *i.e.* In^+. $\log K_{11}$ was calculated for each experimental point with (15); these are collected in Table 2. We can write as the most probable value

$$\log K_{11} = -8.4 \pm 0.1$$

The maximum uncertainty of the $\log K_{11}$ value corresponds to that of $\pm$ 1 mV in the ΔE measurements, which was sometimes found for $B < 0.05$ M. With the data of the preliminary series $\log K_{11}$ was calculated as -8.5 ± 0.2.

It should be pointed out that if true equilibrium had been attained when ΔE would equal zero, only the charge q could have been determined by emf and analytical data but not p, *cf.* (15). In such case one would have to measure the variation of the redox potential when increasing amounts of a solution containing only the oxidized form are added to the equilibrated solution.

The standard redox potential, $e^\circ_{1,3}$, may be obtained by substituting (12) and (14) into (8). The $e^\circ_{1,3}$ values calculated are summarized in Table 2. We find as the most probable value

$$e^\circ_{1,3} = -424 \pm 1.5 \text{ mV}$$

ON THE INFLUENCE OF THE ACTIVITY FACTORS

If one wishes to study ionic equilibria where the composition of the reaction products and their activity factors are not known with certainty beforehand,

Table 2. Survey of results.

B M	$-\log K_{11}$	$-e^{\circ}_{1,3}$ mV	$\log \frac{f^3(In^+)}{f(In^{3+})}$	$29.58 \log \frac{f(In^{3+})}{f(In^+)}$ mV	$-e^{\circ}_{1,3}$ mV corrected with the activity factors	$-e^{\circ}_{0,3}$ mV
1.000×10^{-2}	8.30	424.0	0.002	0.15	424.2	342.8
»	.24	3.4	0.002	0.15	3.6	2.8
2.000×10^{-2}	.49	4.6	0.004	0.31	4.9	1.7
»	.41	5.2	0.004	0.31	5.5	3.0
»	.34	—	0.004	0.31	—	—
5.00×10^{-2}	.38	3.4	0.010	0.80	4.2	2.1
»	.48	4.7	0.010	0.80	5.5	2.4
»	.30	4.6	0.010	0.80	5.4	4.0
1.000×10^{-1}	.44	3.8	0.021	1.64	5.4	2.8
»	.47	4.1	0.021	1.64	5.7	2.9
»	.47	3.4	0.021	1.64	5.0	2.2
»	.42	—	0.021	1.64	—	—
2.000×10^{-1}	.45	2.7	0.038	3.32	6.0	3.5
»	.43	3.2	0.038	3.32	6.5	4.3
Probable value	8.4 ± 0.1	424 ± 1.5	—	—	425 ± 1.5	343 ± 1

one cannot hope to find reliable results unless large changes in the activity factors of the reacting species are eliminated by using a constant ionic medium. If the concentration of the reacting ions is kept low compared with that of the inert salt *e.g.* the indium(III) concentration is less than 10 mM in 3 M ClO_4^-, the error introduced by neglecting the variation of the activity factors is inappreciable even when the experimental accuracy is high. For many investigations, however, it is inevitable that the concentrations of the reacting species are increased to high values. This is the case with our present problem since at B values lower than 10 mM almost unsurmountable experimental difficulties arise.

In work now being carried out in this laboratory by one of us the variation of the activity factors in a constant ionic medium forms the subject of an extensive experimental study. The results pertaining to our problem are taken from this work.

In order to estimate the changes of $f^3(In^+)/f(In^{3+})$ caused by the replacement of Na^+ by In^{3+} we will introduce the assumption that $f(In^+)$ varies in the same way as $f(Ag^+)$ when the two ions are present in equal concentrations in solutions otherwise identical. It is believed that this is a reasonable assumption since a considerable number of experimental results indicate that the activity factors of ions of the same charge are influenced approximately to the same extent by changes in the ionic medium.

The determination of $f^3(Ag^+)/f(In^{3+})$ was made by measuring the emf's of the cells

— In (2 % in Hg)/B M In^{3+}, 0.0100 M H^+, (3.000—3 B — [H^+]) M Na^+, 3 M ClO_4^-/SE + (D)

and

—SE/0.00100 M Ag^+, B M In^{3+}, 0.0100 M H^+, (3.000—3 B—[Ag^+]—[H^+])M Na^+, 3 M ClO_4^-/AgCl, Ag + (E)

B was varied between 0.0100 and 0.200 M. The emf's of these cells can be written at 25°C

$$E_D = E_D^\circ - 19.72 \log [In^{3+}] - 19.72 \log f(In^{3+}) + E_j \quad (17)$$

$$E_E = E_E^\circ + 59.15 \log [Ag^+] + 59.15 \log f(Ag^+) - E_j \quad (18)$$

Plotting

$$E_D + E_E - 19.72 \log \frac{[Ag^+]^3}{[In^{3+}]} \left(= E_D^\circ + E_E^\circ + 19.72 \log \frac{f^3(Ag^+)}{f(In^{3+})}\right) \quad (19)$$

against the [In^{3+}] a straight line was obtained; thus by extrapolation to [In^{3+}] = 0 the constant $E_D^\circ + E_E^\circ$ could be read. With this constant we calculated $f^3(Ag^+)f^{-1}(In^{3+})$ up to B = 200 mM. The $f^3(Ag^+)f^{-1}(In^{3+})$ values are seen, *cf.* Table 2, to be rather close to unity; at B = 200 mM $f^3(Ag^+)f^{-1}(In^{3+})$ attains the maximum value 1.09. We have not been able to determine K_{11} with so high an accuracy that a correction for the variation of the activity factors would be warranted.

It is clear that $f(In^{3+})$ and $f(In^+)$ individually cannot be evaluated from these measurements because changes in the composition of the solution involve a change in E_j also, and the activity and liquid junction terms cannot be calculated separately. Conductance measurements recently made in this laboratory in solutions of 3 M ClO_4^- indicate that changes in E_j due to the replacement of Na^+ by In^{3+} cannot make up more than a small part of the variation of E_D + 19.72 log [In^{3+}] or E_E — 59.15 log[Ag^+]. E_j is determined primarily by the hydrogen ion concentration because the mobility of H^+ exceeds by far that of all other cations; the [H^+] was kept strictly constant in all measurements.

Assuming that changes in E_j are quite negligible we calculated from the E_D and E_E measurements log $f(In^{3+})f^{-1}(In^+)$, see Table 2. If these are introduced we can estimate as the most probable value $e_{1,3}^\circ = -425 \pm 1.5$ mV.

The $e_{0,3}^\circ$ values calculated from E_B measurements with the activity factors determined with E_D give evidence, see Table 2, that our indium electrodes functioned satisfactorily, thus indium is not dissolved to an appreciable extent by H^+ under the experimental conditions used in this work. We shall accept $e_{0,3}^\circ = -343 \pm 1$ mV. At higher log [H^+] values than —2 no constant and reproducible potentials could be obtained because the rate of dissolution becomes appreciable.

Acknowledgements. This work was financially supported by *Statens Naturvetenskapliga Forskningsråd (Swedish Natural Science Research Council)*.

We are indebted to Professor Lars Gunnar Sillén for his great interest and for his valuable criticism. We should like to thank Dr. Clara Berecki-Biedermann for many valuable discussions especially concerning analytical problems, and Civilingenjör Rune Söderquist for his help in connection with the X-ray work. Professor Robert E. Connick has been kind enough to read the manuscript and to give valuable comments on it. Mr. Frans Ericson has been of great help by making many parts of our equipment.

Thanks are due to the Consolidated Mining and Smelting Company of Canada Ltd. for generously granting a large amount of indium metal of the highest purity.

REFERENCES

1. Thiel, A. *Z. anorg. Chem.* **40** (1904) 280.
2. Hepler, L. G., Hugus, Jr. Z. Z. and Latimer, W. M. *J. Am. Chem. Soc.* **75** (1953) 5652.
3. Kangro, W. and Weingärtner, F. *Z. Elektrochem.* **58** (1954) 505.
4. Forbes, G. S. and Bartlett, E. P. *J. Am. Chem. Soc.* **36** (1914) 2030.
5. Forbes, G. S. and Richter, H. W. *J. Am. Chem. Soc.* **39** (1917) 1140.
6. Forbes, G. S. and Hall, L. P. *J. Am. Chem. Soc.* **46** (1924) 385.
7. Jones, G. and Colvin, J. H. *J. Am. Chem. Soc.* **66** (1944) 1573.
8. Biedermann, G. *Arkiv Kemi* **9** (1956) 277.
9. Biedermann, G. and Sillén, L. G. *Arkiv Kemi* **5** (1953) 425.
10. Winkler, L. W. *Die chemische Analyse*, Bd 29, Ferdinand Enke Verlag, Stuttgart 1931.
11. Kolthoff, J. M. *Die Massanalyse*, Bd. 2, Julius Springer Verlag, Berlin 1928.
12. Forsling, W., Hietanen, S. and Sillén, L. G. *Acta Chem. Scand.* **6** (1952) 901.
13. Bauer, E., Nowotny, H. and Stempfl, A. *Monatsh.* **84** (1953) 692.
14. See *e.g.*, Pohland, E. and Lehl-Thalinger, M. *Quecksilber*, in *Handbuch der Analytischen Chemie*, Part III, Volume II. b, Springer-Verlag, Berlin 1945.

Received December 1, 1959.

ACTA CHEMICA SCANDINAVICA 14 (1960) 609–616

Crystalline Leghemoglobin

1. Purification Procedure

NILS ELLFOLK*

Medicinska Nobelinstitutet, Biokemiska avdelningen, Stockholm, Sweden

A procedure is described for the purification of leghemoglobin to give the two main components in a crystalline state. The different components were isolated by chromatography using diethylaminoethyl cellulose as adsorbent. The main components were crystallised from slightly acid ammonium sulphate solution. Both of the crystalline components were found to be electrophoretically homogeneous in long-time electrophoresis runs at two different pH values. The electrophoretically faster component contained 0.32 % iron, and the slower one 0.29 % iron.

In 1938 Pietz [1] reported the observation of a red pigment in the root nodules of *Vicia Faba*. He assumed this substance to be 5,6-quinone-2,3-dihydroindole-2-carboxylic acid, the red oxidation product of tyrosin or dihydroxyphenylalanin. In 1939 Kubo [2] extracted the pigment from soya bean root nodules, and fractionated it with ammonium sulphate. On the basis of his studies, Kubo concluded that the red pigment was a hemoprotein similar to hemoglobin. Burris and Haas [3] definitely showed that the pigment was a hemin compound, but disagreed with its classification as a hemoglobin-like compound. Keilin and Wang [4], as well as Virtanen [5], idependently confirmed the results of Kubo concerning the hemoglobin nature of the pigment. The same conclusion was later reached by Little and Burris [6]. Virtanen *et al.*[7] proposed that the name leghemoglobin be used for the hemoglobin-like pigments in the root nodules of leguminous plants. This name will be used in this paper.

Ellfolk and Virtanen [8] found that leghemoglobin could be fractionated by electrophoresis to give two components of equal concentration but of different hemin content. This was later confirmed by Thorogood [9], who also was able to find a third component, and probably a fourth one.

* Permanent address: Research Laboratories of the State Alcohol Monopoly, Helsinki, Finland.

The experiments to be reported here have been carried out in order to develop a technique to purify the different components. All the present studies on leghemoglobin have been done on the oxidized form, *i.e.* leghem*i*globin. A preliminary report of these results has recently been published [10].

MATERIAL

Soya bean root nodules. The soya beans were inoculated with root nodule bacteria *(Rizobium leguminosarum)*, and grown in a green-house with a relative humiditiy of 70—80 %, and a temperature of 25°C. The culture medium was sea sand. The watering solution (pH 6.5, and free from chemically bound nitrogen) had the following composition: 3.6 g $MgSO_4 \cdot 7\ H_2O$, 4.5 g KCl, 4.2 g KH_2PO_4, 4.0 g $CaSO_4$, 25 mg ferric citrate, 0.55 mg LiCl, 1.1 mg $CuSO_4 \cdot 5\ H_2O$, 1.1 mg $ZnSO_4 \cdot 7\ H_2O$, 12.3 mg H_3BO_3, 1.1 mg $Al_2(SO_4)_3$, 0.55 mg $SnCl_2$, 0.55 mg KI, 7.7 mg $MnCl_2 \cdot 4\ H_2O$, 1.1 mg $NiCl_2 \cdot 6\ H_2O$, 1.1 mg $CoCl_2 \cdot 6\ H_2O$, 0.55 mg KBr, and 60 liters of tap water. The plants were usually harvested after the first blossoms appeared (after about six weeks). The nodules were used immediately, or stored at −20°C.

Ion exchange material. An adsorbent (CM—W) [11] with carboxyl groups was prepared from Whatman cellulose powder, and an absorbent with diethylaminoethyl (DEAE) groups was prepared from Solka Flok as well as from Whatman cellulose powder [11]. The product prepared from Solka Flok was preferred for column chromatography because it resulted in a faster-flowing column.

METHODS

Iron determination. Iron was determined spectrophotometrically by the sulphosalicylic acid method [12]. Combustion of the material was performed with sulphuric acid and hydrogen peroxide. The intensity of the color that was formed in ammoniacal solution with sulphosalicylic acid was measured at 424 mμ in the spectrophotometer.

Pyridine hemochromogen was determined according to Paul, Theorell and Åkeson [13].

Column chromatography. Dry ion exchange cellulose was dispersed with rapid stirring in the buffer that was used for the first elution, and was allowed to settle. The buffer solution was changed several times until no pH change occurred. 10 cm high columns were prepared by allowing the slurry to settle under gravity in glass tubes. Tubes with an internal diameter of 1 cm were used for preliminary studies, whereas for preparative runs, tubes with an internal diameter of 2.5 cm were used. The chromatography was always performed at +3°C.

Electrophoresis. This was carried out at 0.6°C in a Tiselius electrophoresis apparatus (Beckman/Spinco Model H Electrophoresis-Diffusion Instrument). For most of the runs the 11 ml cell was used, though in some experiments the 2 ml cell was used. As the source of illumination, the 644 mμ spectral line from a Cd-Hg vapor lamp was isolated by means of a red filter. Before electrophoresis the protein was dialyzed for 48 h against 2 liters of buffer at +3°C.

The mobility was calculated by a simple equation $u = S/F$, where S is the apparent speed of the boundary, and F is the potential gradient. The latter quantity is calculated from the equation $F = i/q\varkappa$ where i is the current in amperes, q is the cross-section of the electrophoresis cell in cm^2 and $\varkappa$ is the specific conductance of the solutions.

RESULTS

Different methods were tried in an effort to separate the different components of leghemoglobin. Repeated fractionations with ammonium sulphate at small increments gave no separation of the different components as determined by paper electrophoresis. Fractionation with acetone also was unsuc-

cessful. In addition, preparative electrophoresis on a cellulose column [14], high voltage electrophoresis on paper, ion exchange chromatography on both carboxymethyl cellulose and diethylaminoethyl-cellulose were tested for their ability to separate the different components of leghemoglobin. Of these methods, only ion exchange chromatography on DEAE-cellulose could be successfully used on a preparative scale. The column was prepared at pH 5.2, which is slightly higher than the isoelectric points of the components. A lower pH was not used because of the danger of denaturation of the protein on the column. The following procedure was used for preparing crystalline fractions of the two main components:

Extraction. Frozen nodules were ground in a mortar with a small amount of distilled water, and centrifuged at + 3°C. The supernatant solution contained most of the leghemoglobin of the nodules. In order or remove all the leghemoglobin, the precipitate was extracted a second and third time with distilled water. The extracts were pooled, and fractionated at room temperature with ammonium sulphate.

Ammonium sulphate fractionation. Solid ammonium sulphate was added until the solution was 55 % saturated with respect to ammonium sulphate. The pH of the solution was kept just above pH 5 by the addition of ammonia. After 1 h, the solution was centrifuged, and the precipitate was discarded. To the clear red supernatant solution, solid ammonium sulphate was added to a saturation of 80 %. After 1 h, the crude leghemoglobin was centrifuged down, and the clear, yellow supernatant solution was discarded. The precipitate was dissolved in a small amount of 0.1 M phosphate buffer at pH 8. Further fractionation with ammonium sulphate was avoided because it was evident that the micro air bubbles formed by addition of solid ammonium sulphate had a denaturating effect on the heminprotein.

Dialysis. Before the resulting preparation was fractionated on the ion exchange column, the remaining ammonium sulphate had to be removed by dialysis. The dissolved precipitate was dialyzed for 6 h against 10^{-4} M phosphate buffer (pH 8) and for 24 h against distilled water.

Column chromatography. For preparative work, the column (2.5 cm in diameter) was loaded with 100 to 150 mg of protein in 10 to 15 ml of salt-free solution. All of the protein remained on top of the column as a sharp brown band (Fig. 1, column I). The eluation was started with acetate buffer pH 5.2, $\mu = 0.01$. With this ionic strength one band moved down the column and could easily be separated (Fig. 1, *a*). A very faint, broad band (Fig. 1, *b*) followed the first band. When fraction *b* had left the column, the ionic strength of the eluation buffer was increased to 0.02—0.03 by the addition of sodium chloride. At this ionic strength a very sharp band, followed by a small sharp band, moved down the column (Fig. 1, *c* and *d*). On the top of the column there remained a brown band (Fig. 1, *e*) which could not be quantitatively eluted even with buffers of high ionic strength (sodium chloride concentration increased to 3 M). The color of the bands was not uniform during the eluation procedure, but showed a change from red-brown to green. This was found not to depend upon the presence of any oxidized product of leghemiglobin (cholеglobin) but on the formation of a green complex between leghemiglobin and the acetic acid of the eluant.

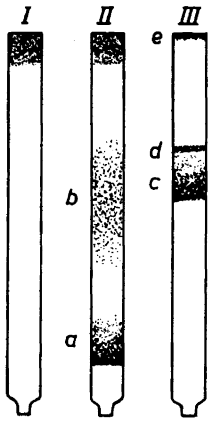

Fig. 1. Column chromatograms of leghemoglobin. Leghemoglobin adsorbed on the top of the DEAE-cellulose column (I). The chromatogram was developed with acetate buffer of pH 5.2, $\mu = 0.01$ (II), and $\mu = 0.03$ (III).

To concentrate the rather dilute fractions, the solutions were dialyzed against distilled water, and the proteins were adsorbed on the top of a short column (1.5—2 cm high). The proteins were eluted from the column by a small volume of 0.1 M phosphate buffer.

Crystallisation. The two main fractions of leghemoglobin were crystallised at + 3°C by dialysing a salt-free solution of each protein against an increasing concentration of ammonium sulphate. The dialysis was started against 55 % saturated ammonium sulphate at pH 6. The degree of saturation was increased by increments of 2.5 % every 12 h, while the pH was maintained at 6. At 60 % saturation, the pH was lowered to about 5 by the addition of sulphuric acid. The first crystals were usually obtained about 24 h later, after which the ammonium sulphate saturation was increased step-wise to 65 %.

Crystallisation of component *a* was also achieved by adding saturated ammonium sulphate solution of pH 5 to a concentrated solution of the protein until a clear "silkiness" was obtained. After keeping the solution at + 3°C for several days, crystals were formed. For some reason, crystals were not obtained from component *c* by this technique, although a silkiness could easily be produced. Fig 2A shows a photomicrograph (phase-contrast microscope) of separate needles of compound *a* and demonstrates the homogeneity of the preparation, whereas Fig. 2B shows a photomicrograph (phase-contrast microscope) of an association of these crystals to form a cluster of needles. Fig. 2C shows a photomicrograph of cyrstals of component *c* taken with an ultraviolet light microscope illuminated with light of 2 750 Å. The crystals are in the form of needles associated to form rosettes.

The photomicrographs show that the crystals of the two components have very similar forms, but that they differ in the way they associate. Both crystalline components were clearly double refracting in plane polarized light, except for the crystals in Fig. 2A which evidently were too thin to produce a double refraction.

Electrophoresis. The fractions that were crystallised (*a* and *c*), as well as fractions *b* and *d*, were examined in the Tiselius apparatus at two different pH

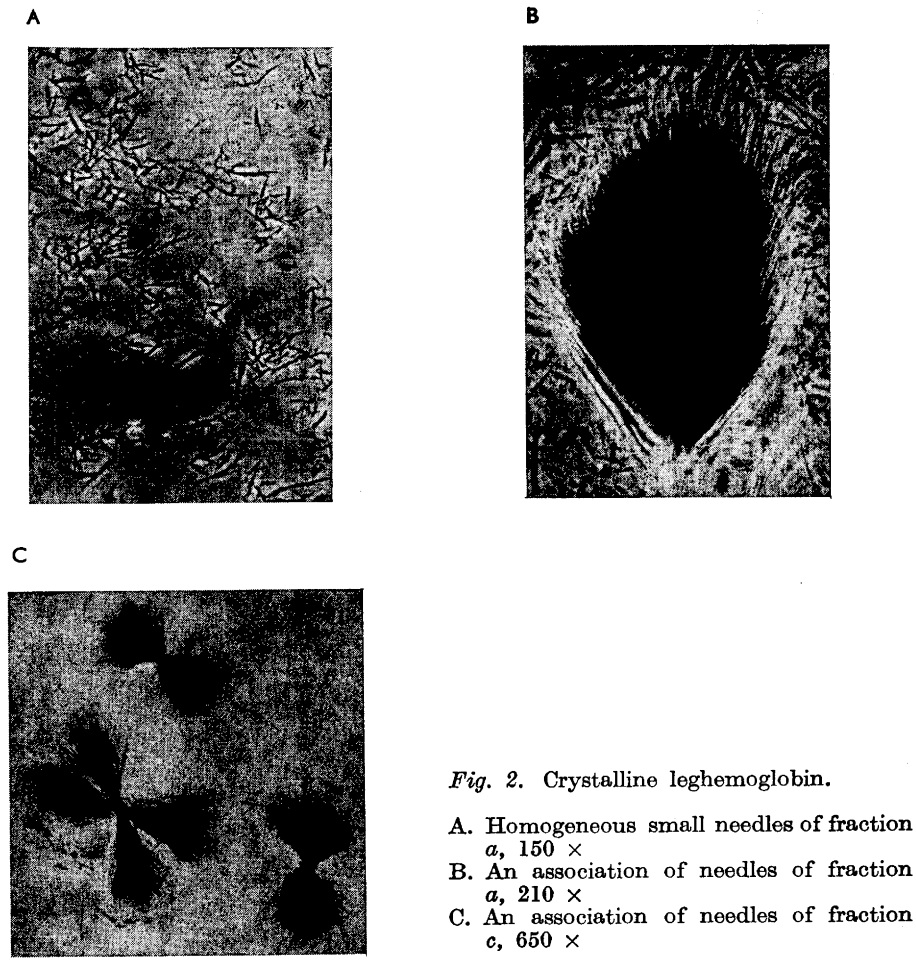

Fig. 2. Crystalline leghemoglobin.

A. Homogeneous small needles of fraction *a*, 150 ×
B. An association of needles of fraction *a*, 210 ×
C. An association of needles of fraction *c*, 650 ×

values. At pH 6.05, $\mu = 0.1$ (phosphate buffer), and at pH 9.0, $\mu = 0.1$ (veronal buffer), the two main crystallised fractions appeared to be homogeneous as determined by long run electrophoresis. Fig. 3 shows the electrophoretic patterns at pH 6.05. Similar patterns were obtained at pH 9.0 after 470 min. At both pH values the direction of migration was anodic. It can be seen that fraction *a* represents the electrophoretically slower component and fraction *c* the faster one.

During electrophoresis of fraction *b* at pH 6.05, only a very broad boundary with no distinct separate peaks was found, thereby indicating the presence of several different components. Electrophoresis of fraction *d* at pH 6.05 showed the presence of two components, one of which had the same mobility as fraction *c*, while the other had a slightly higher mobility.

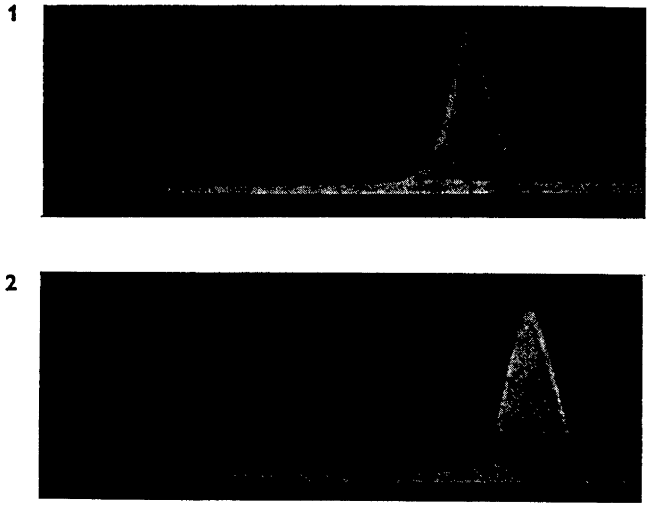

Fig. 3. Electrophoretic patterns of leghemoglobin; pH 6.05, $\mu = 0.1$ $F = 6.75$ V/cm, descending boundaries.
1) *a*, $t = 620$ min.
2) *c*, $t = 490$ min.

Iron content. Simultaneous iron and dry matter determinations were carried out on aliquots of the two main components. An average iron content of 0.32 % was found for the electrophoretically faster component (component *c*), while a value of 0.29 % was found for the slower component (component *a*).

Absorption spectra. The spectra of the components of leghemoglobin dissolved in acetate buffer were different from the spectra when the leghemoglobin was dissolved in phosphate buffer. The difference in the spectra was found to be caused by the formation of a green-colored reversible complex between leghemoglobin and acetate. Compared with the typical acid methemoglobin spectrum found for all of the different components (*a*—*d*), the spectrum of the acetate complex showed a typcial increase in absorption of the 625 mμ band accompanied by a slight shift in the absorption maximum toward the violet part of the spectrum. No quantitative differences were found in the methemoglobin spectra of the two main components (*a* and *c*). For fractions *b* and *d*, the maximum absorption in the region of 625 mμ was somewhat flattened, probably because of the presence of bile pigments. The sodium chloride extract of fraction *e* showed no maximum or minimum in the visible part of the spectrum, but showed a maximum corresponding to the Soret band in the ultraviolet region of the spectrum. The pyridine hemochromogens of the different components showed a typical peak at 557 mμ. In the case of fraction *e*, however, the ratio of absorbance at 630 mμ/557 mμ was 0.46, thereby indicating the presence of a high percentage of bile pigments or other pigments such as polyphenols.

DISCUSSION

It has been shown that leghemoglobin can be resolved into four components on a DEAE-cellulose column. The different fractions were eluted from the column in the order of increasing electrophoretic mobility so that the electrophoretically slower component was first eluted from the column. After the four bands were eluted, one band still remained on the top of the column. This evidently consisted of degradation products of leghemoglobin of different degrees of denaturation. This band was not totally eluted even if the ionic strength of the eluant was increased to $\mu = 3.0$. The band was not caused by a surface denaturation of the protein on top of the column. Rechromatographed material left no band on the top of the column after eluation of the other components.

The two electrophoretically homogeneous main components have been crystallised for the first time. The electrophoretically faster component was found to have an iron content of 0.32 %. This value compares favorably with the value of 0.34 % that was obtained previously when this component was isolated by free electrophoresis [15]. This component was earlier [15] assumed to represent pure leghemoglobin. The electrophoretically slower component, on the basis of its low iron content, was assumed to be an artefact consisting of pure leghemoglobin and an ironless protein. The present study does not support this assumption, but on the contrary shows that the electrophoretically slower component is a homogeneous individual protein.

Of the two smaller components that represent only a small percentage of the total chromoprotein, at least one represents a homogeneous individual protein (compound *d*). It is difficult to decide if component *b* contains an individual component or if it is a mixture of different oxidation products of fraction *a*. These two smaller components, however, are regularly found in different preparations of leghemoglobin. This might indicate that they represent real individual fractions, even though they contain some oxidized material (choleglobin). The existence of subfractions of proteins is known with other proteins. Crystalline myoglobin has been found to contain a main fraction and at least two subfractions in lower concentration [16]. The differences between these subfractions are very small, probably being caused by the substitution of one or more amino acids by others [17]. In a similar way it is possible that the smaller fractions of leghemoglobin might represent subfractions of the two main components.

Acknowledgments. The author wishes to express his thanks to Professor Hugo Theorell and coworkers at the Department of Biochemistry, Nobel Medical Institute, for valuable discussions and advice during the course of this work. The investigation has been supported by a grant from the *State Commission of Natural Sciences (Statens Naturvetenskapliga Kommission)* which is gratefully acknowledged.

REFERENCES

1. Pietz, J. *Zentr. Bakteriol. Parasitenk.* II, **99** (1938) 1.
2. Kubo, H. *Acta Phytochim. (Japan)* **11** (1939) 195.
3. Burris, R. H. and Haas, E. *J. Biol. Chem.* **155** (1944) 227.
4. Keilin, D. and Wang, Y. L. *Nature* **155** (1945) 227.

5. Virtanen, A. I. *Nature* **155** (1945) 747.
6. Little, H. N. and Burris, R. H. *J. Am. Chem. Soc.* **69** (1947) 83.
7. Virtanen, A. I., Jorma, J. and Laine, T. *Suomen Kemistilehti*, **18 B** (1945) 49.
8 Ellfolk, N. and Virtanen, A. I. *Acta Chem. Scand.* **4** (1950) 1014.
9. Thorogoad, E. *Science* **126** (1957) 1011.
10. Ellfolk, N. *Acta Chem. Scand.* **13** (1959) 596.
11. Peterson, E. A. and Sober, A. *J. Am. Chem. Soc.* **78** (1956) 751.
12. Lorber, F. *Biochem. Z.* **181** (1927) 391.
13. Paul, K. G., Theorell, H. and Åkeson, Å. *Acta Chem. Scand.* **7** (1953) 1284.
14. Flodin, P. and Porath, J. *Biochim. et Biophys. Acta* **13** (1954) 175.
15. Ellfolk, N. and Virtanen, A. I. *Acta Chem. Scand.* **6** (1952) 411.
16. Theorell, H. and Åkeson, Å. in "*Biochemistry of Nitrogen*", *Ann. Acad. Sci. Fennicæ Ser. A II, No.* **60** (1955) 303.
17. Åkeson, Å. and Theorell, H. *Arch. Biochem. and Biophys. In press.*

Received November 3, 1959.

ACTA CHEMICA SCANDINAVICA 14 (1960) 617–624

Reduction to Standard Heat of Combustion of Bomb Calorimetric Data for Organic Bromine Compounds

LARS BJELLERUP

Department of Organic Chemistry, University of Lund, Lund, Sweden

The rigorous Washburn reduction of combustion calorimetric data for organic bromine compounds is discussed and applied to a recent high-precision moving-bomb method.

The general scheme for the reduction is treated in two respects: (i) The accuracy of the reduction is improved by presentation of experimental data for the auxiliary numerical quantities entering some of the more important corrections. For $As_2O_3-As_2O_5-HBr$ solutions of various composition, data are thus given for, (a) the density at 20 and 25°C, (b) the heat capacity at 25°C, and (c) the solubility of carbon dioxide at 20 and 25°C. (ii) The general scheme is modified to apply specifically to the above-mentioned bomb calorimetric method.

A combustion-bomb calorimetric method for organic bromine compounds has recently been described [1] by which results of an immediate precision [2] slightly better than 0.01 % can be obtained. To take full advantage of this high precision in order to obtain high-accuracy standard heats of combustion for organic bromine compounds, the application of rigorous Washburn corrections [3] to the calorimetric data obtained is required. The original Washburn reduction [3] treated data obtained on compounds containing only carbon, hydrogen and oxygen. Later, the Washburn reduction was extended to apply to nitrogen compounds of the formula $C_aH_bO_cN_d$ [4,5] and to sulfur compounds of the formula $C_aH_bO_cS_d$ [7–9]. In Ref. [9] a complete and rigorous treatment was given not only of those corrections usually described as the "Washburn corrections", but of all other corrections that must be applied to the original calorimetric data from combustion experiments with organic sulfur compounds in order to obtain the energy of the idealized combustion reaction, *i.e.* the standard heat of combustion of the compound investigated. The corrections were treated separately and presented in a systematic computation form in which the various terms were kept separate. This mode of presentation had several advantages. One was that many of the terms, either unchanged or modified, enter into reductions to standard heat of combustion of calorimetric data obtained on organic compounds containing other elements instead of sulfur. This was illustrated by discussion of the modifications to the general computation form for sulfur compounds that had to be made to apply it to

organic nitrogen, chlorine, bromine and iodine compounds, respectively. For chlorine and bromine compounds, however, no critical selection could be made of the numerical quantities that enter into some of the more important corrections, because reliable experimental data were not available for these quantities *cf.* Refs.[9] (p. 126—127), [10] (p. 217—218) Through recent work in this laboratory, data have been obtained for the more important of these auxiliary quantities. Part of this work has been reported elsewhere [11] and the remainder is given here.

More specifically, the aim of this paper is to describe the modifications and additions that have to be made to the treatment, given in Ref.[9] (p. 114—119), of the reduction to standard heat of combustion of bomb calorimetric data for bromine compounds, to make the reduction applicable to and commensurate in accuracy with the experimental method described in Ref.[1]

MODE OF PRESENTATION. NOTATION

For convenience the same presentation and notation as in Ref.[9] is used in this paper. On only a few points, which are clearly indicated in the text, is the treatment and the notation of this paper different from those of Ref.[9]

ACTUAL BOMB PROCESS AND IDEALIZED COMBUSTION REACTION

The actual process occurring in the bomb in combustion experiments with organic bromine compounds, using the method given in Ref.[1], was discussed in detail in the cited paper.

The idealized combustion reaction, to which the standard heat of combustion of the compound is referred, is defined by eqn. 1, where reactants and products are in their thermodynamic standard states [12].

$$C_aH_bO_cBr_d(\text{c or liq}) + (a + b/4 - c/2)\ O_2(g) \longrightarrow$$
$$\longrightarrow a\ CO_2(g) + b/2\ H_2O(\text{liq}) + d/2\ Br_2(\text{liq}) \qquad (1)$$

It should be noted that this idealized combustion reaction is the same as that given in Refs. [9] (p. 118), [10] (p. 211, eqn. 3)

CALCULATION OF THE CORRECTIONS

The calculation of the standard heat of combustion from the original calorimetric data was described in Ref.[1] * Some of the corrections were treated in detail and the rest, mainly those usually described as the Washburn corrections, are discussed here. These are presented as modifications to the various items of the computation form for bromine compounds given in Ref. [9] (p. 114—119) and make the reduction applicable to data obtained with the experimental method described in Ref.[1]

* There are two obvious misprints in eqn. 29 of Ref. [1]. The equation should read:

$$-\Delta Ec^\circ/M(\text{Compound}) = \frac{1}{m'}\left\{-\Delta E_{\text{I.B.P.}} - \left[-\Delta E(\text{As}) - \Delta E(\text{Oil}) - \Delta E(\text{Fuse}) - \Delta E(CO_2) - \right.\right.$$
$$\left.\left. - \Delta E(HNO_3) - \Delta E(\text{Au}) - \Delta E(\text{Pt})\right] - \Delta E(\text{HBr}) - \Delta E_\Sigma\right\}$$

Initial and final states

(1) $C_{a'}H_{b'}O_{c'}Br_{d'}$; (2)—(6) unchanged; (7) $C_{a''}H_{b''}O_{c''}Br_{d''}$; (8)—(12) unchanged; (13) $C_{a'''}H_{b'''}O_{c'''}Br_{d'''}$; (14)—(23) unchanged; (24)—(25) these two items are entirely formal. They can be deleted and the following treatment accordingly modified; (26)—(29b) unchanged;

(29c) g^i, the ratio of the vapor pressure of H_2O over the initial solution to that over pure water. Experimental data are not available for the lowering of the vapor pressure by arsenious oxide. From data [13 (p. 294)] on comparable compounds (boric acid) however, g^i for the 0.0625 M As_2O_3 solution, used in Ref.[1], can be estimated at 0.998;

(29d) $K^{*i}(O_2)$ the solubility of O_2 in the initial bomb solution in moles per liter of solution per atm O_2 pressure. Since no data on the solubility of O_2 in aqueous As_2O_3 solutions are available the values of the solubility in pure water, given in the table on p. 84 in Ref.[9], will be used as an approximation;

(30)—(34) unchanged;

(35) $n^i(O_2 \text{ diss.}) = K^{*i}(O_2)V^i(\text{soln.})[P^i(\text{gas.}) - P^i(H_2O \text{ vap.})]$. Since, in combustion experiments with bromine compounds, N_2 is present only as a small impurity in the O_2 and since it can be treated as though it were O_2, except for the formation of HNO_3, the notation $(O_2 + N_2)$ used in Ref.[9] has been changed to (O_2) in this paper;

(36) $n^i(O_2 \text{ tot.}) = n^i(\text{gas.}) - n^i(H_2O \text{ vap.}) + n^i(O_2 \text{ diss.})$.

The stoichiometry of the isothermal bomb process can be described by the following set of equations [1]:

$$C_aH_bO_cBr_d + [a + (b-d)/4 - c/2]\ O_2 \rightarrow \\ \rightarrow a\ CO_2 + (b-d)/2\ H_2O + d\ HBr \quad (2)$$

$$As_2O_3 + O_2 \rightarrow As_2O_5 \quad (3)$$

$$1/2\ N_2 + 5/4\ O_2 + 1/2\ H_2O \rightarrow HNO_3 \quad (4)$$

$$Au + 1/4\ O_2 + 2\ HBr \rightarrow HAuBr_2 + 1/2\ H_2O \quad (5)$$

$$Pt + 1/2\ O_2 + 4\ HBr \rightarrow H_2PtBr_4 + H_2O \quad (6)$$

The amounts of HNO_3, $HAuBr_2$ and H_2PtBr_4 present in the final bomb solution are listed in the items:

(37) $n^f(HNO_3)$; (37a) $n^f(HAuBr_2)$; (37b) $n^f(H_2PtBr_4)$. Under the conditions of the experimental technique described in Ref.[1] these quantities are small enough to permit decomposition, as outlined in Ref.[9 (p. 122–123)], of the corresponding substances under actual bomb conditions immediately after Step 12 without significant loss in accuracy. This means that all terms involving $n^f(HNO_3)$, $n^f(HAuBr_2)$ and $n^f(H_2PtBr_4)$, except in items 86a, 86b and 86c, can be left out from the subsequent discussion.

(38)—(38a) unchanged; (39) $n^f(HBr) = d$; (40) $n^f(H_2O \text{ liq.}) = n^i(H_2O \text{ tot.}) + (b-d)/2 - n^i(H_2O \text{ vap.})$; (41) $m^f(\text{soln.}) = 18.016n^f(H_2O \text{ liq.}) +$

$+ 197.82n^f(As_2O_3) + 229.82n^f(As_2O_5) + 80.924n^f(HBr)$; (42) wt.%$(As_2O_3)$ = $= 19\,782n^f(As_2O_3)/m^f(soln.)$; (42a) wt.%$(As_2O_5) = 22\,982n^f(As_2O_5)/m^f(soln.)$; (42b) wt.%$(HBr) = 8092n^f(HBr)/m^f(soln.)$; (43) delete;

(44) $\varrho^f(soln.) = \varrho(H_2O) + 0.00785$ wt.%$(As_2O_3) + 0.00808$ wt.%$(As_2O_5) +$ $+ 0.00710$wt.%(HBr) g/ml. This equation has been found to represent, within an uncertainty of $\pm$ 0.0001 g/ml, experimental data [14] on the densities at 20 and 25°C of seven aqueous As_2O_3—As_2O_5—HBr solutions of various compositions within the concentration ranges 0—1.23 wt.% of As_2O_3, 0—1.28 wt.% of As_2O_5 and 0—1.79 wt.% of HBr, which are the ranges of interest in the given method [1].

(45) unchanged; (46)—(47) delete; (48)—(49) unchanged;

(50) $n^f(CO_2$ tot.$) = a$;

(51) $K(CO_2) = 0.0383_5$ and 0.0336 mole/liter atm at 20 and 25°C, respectively. The solubility of CO_2 in aqueous As_2O_3—As_2O_5—HBr solutions, similar in composition to those obtained in combustion experiments, has been measured * by use of the method given in Ref.[7] (p. 85) It was found that the solubility of CO_2 was the same in each of three investigated solutions, which had the following compositions:
(A) 0.0633 M As_2O_3; (B) 0.0475 M As_2O_3—0.0158 M As_2O_5—0.0671 M HBr; (C) 0.0317 M As_2O_3—0.0316 M As_2O_5—0.122 M HBr. Therefore the solubility values given above can be used in all combustion experiments irrespective of the HBr concentration in the final bomb solution.

(52)—(55) unchanged;

(56) $n^f(O_2$ tot.$) = n^i(O_2$ tot.$) - [a + (b-d)/4-c/2] - n^f(As_2O_5)$;

(57) $K^f(O_2)$, the solubility of O_2 in the final bomb solution in moles per liter of solution at unit fugacity (in atm) of O_2 gas. Since no data on the solubility of O_2 in As_2O_3—As_2O_5—HBr solutions are available the values of the solubility in pure water, given in Ref.[9] (p. 88), will be used as an approximation;

(58) unchanged; (59) $K^{*f}(O_2) = D(O_2)K^f(O_2)$;

(60) $$n^f(O_2 \text{ diss.}) = \frac{0.082054(t_h + 273.2)K^{*f}(O_2)V^f(soln.)/V^f(gas.)}{1 + 0.082054(t_h + 273.2)K^{*f}(O_2)V^f(soln.)/V^f(gas.)} n^f(O_2 \text{ tot.});$$

(61) $n^f(O_2$ gas.$) = n^f(O_2$ tot.$) - n^f(O_2$ diss.$)$; (62) $n^f(gas.) = n^f(O_2$ gas.$) +$ $+ n^f(CO_2$ gas.$) + n^i(H_2O$ vap.$)$; (63)—(65) unchanged;

(66) g^f, the ratio of the vapor pressure of H_2O over the final solution to that over pure H_2O. Experimental data are not available for the vapor pressure lowering of water by the mixture of As_2O_3, As_2O_5 and HBr present in the final bomb solution. As in item 29c, however, g^f for an average final bomb solution, having the composition 0.02 M As_2O_3—0.04 M As_2O_5—0.16 M HBr, was estimated at 0.993 from data [13] (p. 293—294) on comparable compounds;

(67) $n^f(H_2O$ vap.$) =$
$g^f[C_0 + \{a(O_2) + [a(CO_2) - a(O_2)]x(CO_2)\}P^f(gas.)]\ V^f(gas.)/18.016.$

* The author's thanks are due to Dr. S. Sunner, Thermochemistry Laboratory, University of Lund, for making these measurements in connection with the work reported in Ref.[7]

Energy factors and calorimetric data

(68)—(69) unchanged. For the 0.0625 M As_2O_3 solution, used as initial bomb solution in Ref.[1], a value for $(\delta V/\delta T)_P$ of 2.57×10^{-7} liter/g deg was obtained from experimental density data. In the same way $(\delta V/\delta T)_P$ values were obtained for various As_2O_3—As_2O_5—HBr solutions having compositions corresponding to combustion experiments with samples containing from 4 to 7 mgatoms of bromine. In all cases the value of $(\delta V/\delta T)_P$ was found to be virtually the same and equal to 2.35×10^{-7} liter/g deg. Therefore the following values can be used at 25°C for all combustion experiments with the method of Ref.[1]: $(\delta E/\delta P)_T^i$(soln.) = −0.00186 cal/g atm and $(\delta E/\delta P)_T^f$(soln.) = −0.00170 cal/g atm;

(70) delete;

(71) $\Delta E'_{soln.}(O_2)$ and (71a) $\Delta E''_{soln.}(O_2)$, the change of internal energy in cal/mole at t_h for the solution of O_2 in the initial and final bomb solution, respectively. Since no data are available for the heat of solution of O_2 in aqueous As_2O_3 and As_2O_3—As_2O_5—HBr solutions, the corresponding values for pure water, given in Ref.[9] (p. 100), will be used as an approximation;

(71b) $\Delta E''_{soln.}(CO_2)$, the change of internal energy in cal/mole at t_h for the solution of CO_2 in the final bomb solution. From the solubility data given above in item 51 a value for $\Delta E_{soln.}(CO_2)$ of −4 000 cal/mole at 22.5°C was obtained for the pertinent final bomb solutions. By the use of a temperature coefficient of + 44 cal/mole deg [9] (p. 99),[15] the following values were obtained for $\Delta E''_{soln.}(CO_2)$: − 4 110 and −3 890 cal/mole at 20 and 25°C;

(71c) $\Delta E_{oxid.}$(HBr), the change of internal energy in cal/mole at t_h for the oxidation of HBr in Soln. I (under a pressure of 1 atm) with O_2 (in its standard state) to water and bromine (both in their standard states) according to the equation d(HBr·nH_2O)(in Soln. I) + d/4 O_2(g) → d(n + 1/2) H_2O(liq) + + d/2 Br_2(liq). No experimental values have been obtained for the energy of this reaction and since no data are available for the energy of formation of HBr in aqueous As_2O_3—As_2O_5 solutions, it is not possible to calculate values for $\Delta E_{oxid.}$(HBr). However, the values of $\Delta E^\circ_{oxid.}$(HBr), given in Ref.[9] (p. 119) can be used as a satisfactory approximation since the error introduced thereby is almost entirely cancelled by the introduction of the same error, but with opposite sign, in the $\Delta E_{decomp.}(As_2O_5)$ value given in the following item;

(71d) unchanged. From experimental data reported [11] for the heat of the reaction [As_2O_3 + 2 H_2O](aq) + 2 Br_2(liq) → [As_2O_5 + 4 HBr](aq) a value of $-(77.4 \pm 0.1) \times 10^3$ cal/mole was calculated for the change of internal energy, $\Delta E_{oxid.}$[As_2O_3(aq)], for the reaction As_2O_3(aq) + O_2(g) → As_2O_5(aq). In this calculation, it was assumed that the energy of formation of HBr in aqueous As_2O_3—As_2O_5 solution is the same as that in pure water [12]. Thus, by using $\Delta E_{oxid.}$[As_2O_3(aq)] for $-\Delta E_{decomp.}(As_2O_5)$, the error introduced by the approximation is almost entirely cancelled by an analogous error introduced in item 71c. The value 77.4×10^3 cal/mole will therefore be used for $\Delta E_{decomp.}(As_2O_5)$ at 25°C;

(71e) unchanged. No heat of dilution data for $As_2O_3 \cdot nH_2O$ are available and therefore the corresponding correction in item 92b has to be neglected.

Since C^i(Soln.) is rather small and since the difference in concentration of As_2O_3 in Soln. III and in the initial bomb solution is also small, the error introduced by neglecting the correction in item 92b certainly will be barely significant;

(72)—(73) unchanged;

(74) ε^o(Calor.), the energy equivalent of "the standard calorimetric system". As described in Ref.[1] the energy equivalent of the calorimetric system is divided in three parts: (i) ε^o(Calor.), the energy equivalent of the whole system as assembled for a fictive experiment with no contents in the bomb ("the standard calorimetric system"), (ii) $C_P(H_2O)m^i$(Cont.), the energy equivalent of an amount of water equal in mass to the contents of the bomb (*cf.* item 74a and 74b), and (iii) ε(Cont.), the energy equivalent of the contents of the bomb, by which is understood all removable matter in the interior of the bomb, including the platinum combustion crucible and its suspension ring (*cf.* item 75 and 76);

(74a) m^i(Cont.), the mass of the contents of the bomb, is obtained from the relation $m^i(\text{Cont.}) = 32.00n^i(O_2 \text{ tot.}) + V^i(\text{soln.})\varrho^i(\text{soln.}) + m(\text{Sub.}) + m(\text{Pt}) + m(\text{glass})$;

(74b) $\varepsilon(\text{Calor.}) = \varepsilon^o(\text{Calor.}) - C_P(H_2O)m^i(\text{Cont.})$;

(75) $\varepsilon^i(\text{Cont.}) = C_V(O_2)n^i(O_2 \text{ tot.}) + A^iV^i(\text{soln.})\varrho^i(\text{soln.}) + Bn^i(H_2O \text{ vap.}) + C'_Pm' + C''_Pm'' + C'''_Pm''' + 0.0317m(\text{Pt}) + 0.17m(\text{glass})$. For 0.0624 M As_2O_3 solution under a pressure of 1 atm the heat capacity, C_P, has been found [11] to be 0.988 cal/g deg at 25°C. This value will be used as an approximation for A^i. For C_P(Pt) the value 0.0317 cal/g deg at 25°C is given in Ref.[16]

(76) $\varepsilon^f(\text{Cont.}) = C_V(O_2)n^f(O_2 \text{ tot.}) + C_V(CO_2)n^f(CO_2 \text{ tot.}) + A^f[m^f(\text{soln.}) + 18n^f(H_2O \text{ vap.})] + Bn^f(H_2O \text{ vap.}) + 0.0317m(\text{Pt}) + 0.17\ m(\text{glass})$. As in the preceding item, C_P values for final bomb solutions under a pressure of 1 atm will be used as approximations for A^f. For As_2O_3—As_2O_5—HBr solutions having compositions corresponding to combustion experiments with samples containing 5 and 6 mgatoms of bromine the heat capacities, C_P, at 1 atm and 25°C have been found * to be 0.969 and 0.964 cal/g deg, respectively;

(77) unchanged. With the method of Ref.[1] $\Delta E_{ign.}$ is incorporated into the value of ε^o(Calor.). Therefore it is formally put equal to zero in the calculations;

(78)—(79) unchanged;

(80) $\Delta t_{ex.}$. This symbol was used in Ref.[1] for "the heat exchange correction" and it will be retained here. It represents the same quantity as does the symbol $\Delta t_{corr.}$ in Ref.[9]

Changes in internal energy

(81)—(83) unchanged; (84) $\Delta E^i_{soln.}(O_2) = \Delta E'_{soln.}(O_2)n^i(O_2 \text{ diss.})$; (85) unchanged; (86) $\Delta E_{I.B.P.} = \varepsilon(\text{Calor.})(t_i - t_f + \Delta t_{ex.}) + \varepsilon^i(\text{Cont.})(t_i - t_h) + \varepsilon^f(\text{Cont.})(t_h - t_f + \Delta t_{ex.}) + \Delta E_{ign.}$;

---

* The author's thanks are due to Dr. I. Wadsö, Thermochemistry Laboratory, University of Lund, for making the heat capacity measurements.

Step 12a. The HNO_3, $HAuBr_2$ and H_2PtBr_4 are decomposed under final bomb conditions according to the reactions $HNO_3(aq) \rightarrow 1/2\ N_2(g) + 5/4\ O_2(g) + 1/2\ H_2O(liq)$, $HAuBr_2(aq) + 1/2\ H_2O(liq.) \rightarrow Au(c) + 1/4\ O_2(g) + 2HBr(aq)$ and $H_2PtBr_4(aq) + H_2O(liq) \rightarrow Pt(c) + 1/2\ O_2(g) + 4\ HBr(aq)$. As discussed in Ref.[1] the following values of ΔE, at 25°C, can be used for these reactions: $\Delta E_{\text{decomp.}}(HNO_3) = 14.18 \times 10^3$, $\Delta E_{\text{decomp.}}(HAuBr_2) = 8 \times 10^3$ and $\Delta E_{\text{decomp.}}(H_2PtBr_4) = 43.4 \times 10^3$ cal/mole. The change of energy associated with this step is the sum of the following three items:

(86a) $\Delta E^{\text{f}}_{\text{decomp.}}(HNO_3) = \Delta E_{\text{decomp.}}(HNO_3) n^{\text{f}}(HNO_3)$;

(86b) $\Delta E^{\text{f}}_{\text{decomp.}}(HAuBr_2) = \Delta E_{\text{decomp.}}(HAuBr_2) n^{\text{f}}(HAuBr_2)$;

(86c) $\Delta E^{\text{f}}_{\text{decomp.}}(H_2PtBr_4) = \Delta E_{\text{decomp.}}(H_2PtBr_4) n^{\text{f}}(H_2PtBr_4)$;

(87) unchanged; (88) $\Delta E^{\text{f}}_{\text{soln.}}(O_2) = -\Delta E''_{\text{soln.}}(O_2) n^{\text{f}}(O_2\ \text{diss.})$; (89) unchanged; (90)—(91b) delete;

Step 19. The HBr is oxidized with O_2 (in its standard state) according to the reaction d $(HBr \cdot nH_2O)$(in Soln. I) + d/4 $O_2(g) \rightarrow$ d(n + 1/2) $H_2O(liq)$ + + d/2 $Br_2(liq)$. The water and the bromine are brought to their standard states.

(92) $\Delta E^{\text{f}}_{\text{oxid.}}(HBr) = \Delta E_{\text{oxid.}}(HBr) n^{\text{f}}(HBr)$;

Step 19a. The As_2O_5 in Soln. II is decomposed to As_2O_3 in Soln. III and O_2 gas in its standard state.

(92a) $\Delta E^{\text{f}}_{\text{decomp.}}(As_2O_5) = \Delta E_{\text{decomp.}}(As_2O_5) n^{\text{f}}(As_2O_5)$;

Step 19b. Water (in its standard state) is removed from Soln. III to bring the concentration of As_2O_3 to C^{i}(soln.).

(92b) $\Delta E^{\text{f}}_{\text{diln.}}(As_2O_3) = \Delta E_{\text{diln.}}(As_2O_3) n^{\text{i}}(As_2O_3)$;

(93) $\Delta E^{\text{f}}(\text{gas.})]^{\text{o f}}_{P^{\text{f}}(\text{gas.})} = -(\delta E/\delta P)_T(O_2\ \text{gas.})\{1 + 1.69x(CO_2)[1 + x(CO_2)]\} P^{\text{f}}(\text{gas.}) n^{\text{f}}(\text{gas.})$;

(94)—(98) unchanged;

(99) $\Delta Ec^{\circ}/M(\text{Compound}) = n'\Delta Ec^{\circ}(\text{Compound})/m'$;

(100) $\Delta Ec^{\circ}(\text{Compound}) = M'\Delta Ec^{\circ}/M(\text{Compound})/1\ 000$;

By definition of the quantities $\Delta E_{\text{B}}/M(\text{Compound})$ and ΔE_{Σ} as follows: $\Delta E_{\text{B}}/M(\text{Compound}) =$ [items 86+86a+86b+86c+87+92+92a—96—97]$/m'$ $\Delta E_{\Sigma} =$ items 81 + 82 + 83 + 84 + 85 + 88 + 89 + 92b + 93 + 94, item 99 becomes

(99) $\Delta Ec^{\circ}/M(\text{Compound}) = \Delta E_{\text{B}}/M(\text{Compound}) + \Delta E_{\Sigma}/m'$. The reason for this operation is given in Ref.[9] (p. 102–103)

It is seen that the symbols $\Delta Ec^{\circ}/M(\text{Compound})$, $\Delta E_{\text{I.B.P.}}$ and ΔE_{Σ} denote the same quantities in this paper as in Ref.[1], and the symbols $\Delta E^{\text{f}}_{\text{decomp.}}(HNO_3)$, $\Delta E^{\text{f}}_{\text{decomp.}}(HAuBr_2)$, $\Delta E^{\text{f}}_{\text{decomp.}}(H_2PtBr_4)$, $\Delta E^{\text{f}}_{\text{soln.}}(CO_2)$, $\Delta E^{\text{f}}_{\text{oxid.}}(HBr)$, $\Delta E^{\text{f}}_{\text{decomp.}}(As_2O_5)$, $n''\Delta Ec^{\circ}$(Auxiliary material) and $n'''\Delta Ec^{\circ}$(Fuse) of this paper correspond with the symbols $-\Delta E(HNO_3)$, $-\Delta E(Au)$, $-\Delta E(Pt)$, $-\Delta E(CO_2)$, $+\Delta E(HBr)$, $-\Delta E(As)$, $+\Delta E(Oil)$ and $+\Delta E(Fuse)$, respectively, in Ref.[1]

The numerical ΔE_{Σ} values reported in Ref.[1] were calculated according to the scheme given in this paper.

REFERENCES

1. Bjellerup, L. *Acta Chem. Scand.* **13** (1959) 1511.
2. Rossini, F. D. and Deming, W. E. *J. Wash. Acad. Sci.* **29** (1939) 416.
3. Washburn, E. W. *Bur. Standards J. Research* **10** (1933) 525.
4. Prosen, E. J. *Determination of Heats of Combustion Using a Bomb Calorimeter. A. Carbon-Hydrogen-Oxygen Compounds. B. Nitrogen Compounds.* National Bureau of Standards Report 1119, Washington, D.C. 1951.
5. Prosen, E. J. *Combustion in a Bomb of Compounds Containing Carbon, Hydrogen, Oxygen, and Nitrogen*, Chapter 6 of Ref.[6]
6. Rossini, F. D. (Ed.) *Experimental Thermochemistry*, Interscience Publishers, Inc., New York 1956.
7. Sunner, S. *Studies in Combustion Calorimetry Applied to Organo-Sulphur Compounds* (Diss.) University, Lund 1949.
8. Hubbard, W. N., Scott, D. W. and Waddington, G. *J. Phys. Chem.* **58** (1954) 152.
9. Hubbard, W. N., Scott, D. W. and Waddington, G. *Standard States and Corrections for Combustions in a Bomb at Constant Volume*, Chapter 5 of Ref.[6]
10. Smith, L. and Bjellerup, L. *Combustion in a Bomb of Organic Bromine Compounds*, Chapter 9 of Ref.[6]
11. Bjellerup, L., Sunner, S. and Wadsö, I. *Acta Chem. Scand.* **11** (1957) 1761.
12. Rossini, F. D., Wagman, D. D., Evans, W. H., Levine, S. and Jaffe, I. *Selected Values of Chemical Thermodynamic Properties*, Circular of the National Bureau of Standards 500, U.S. Government Printing Office, Washington, D.C. 1952.
13. *International Critical Tables.* McGraw-Hill Book Company, Inc., New York 1926—33, Vol. III.
14. Bjellerup, L. *Unpublished measurements.*
15. Harned, H. S. and Davis, R. *J. Am. Chem. Soc.* **65** (1943) 2030.
16. Stull, D. R. and Sinke, G. C. *Thermodynamic Properties of the Elements*, American Chemical Society, Washington, D.C. 1956.

Received December 7, 1959.

ACTA CHEMICA SCANDINAVICA 14 (1960) 625–633

Hydrolysis of Phosphopeptides

I. Acid Hydrolysis of O-Phosphoryl-DL-serylglycine and Glycyl-(O-phosphoryl)-DL-serine. Sequence Inversion in Dilute Hydrochloric Acid

GEORG FÖLSCH, OLOF MELLANDER and LARS STRID

Department of Medical Biochemistry, University of Göteborg, Sweden

The hydrolysis of SerP-Gly * and Gly-SerP in 2 N hydrochloric acid at 100° and in conc. hydrochloric acid at 37° was studied by column chromatographic separation of the hydrolysis products on an anion exchange resin. In 2 N hydrochloric acid sequence inversion occurs with both phosphopeptides. Gly-SerP is hydrolysed faster than SerP-Gly in both conc. and 2 N acid and hydrolysis takes place almost entirely at the peptide bond. SerP-Gly is largely dephosphorylated to serylglycine.

Partial acid hydrolysis is the general method used for breaking down peptide chains to di- and tripeptide fragments. In the large amount of work done during the last deecade on the determination of amino acid sequences in polypeptides and proteins, the conditions of hydrolysis, *e.g.* temperature, time and acid strength, have been varied widely. It is known, however, that these variations can have a marked effect on the results of hydrolysis [1–4]. In the partial hydrolysis of phosphoproteins and phosphorylated polypeptides, different conditions of hydrolysis may cause still greater differences in results, since in these materials both peptide and phosphate ester bonds may be hydrolysed.

Several investigations have been reported on amino acid sequences near O-phosphorylserine residues in phosphoproteins such as casein, phosvitin, ovalbumin and pepsin [5–8]. A large amount of work has also been done on the determination of the structure around the "*active centers*" of enzymes such as trypsin, chymotrypsin, horse-liver ali esterase and phosphoglucomutase, using the technique of deactivation of the enzyme by a phosphorylating reagent, partial acid hydrolysis of the product and separation and determina-

* The following abbreviations are used here: SerP, O-phosphorylserine; SerP-Gly, O-phosphorylserylglycine; Gly-SerP, glycyl-(O-phosphoryl)-serine.

tion of the structure of the resulting peptides containing O-phosphorylserine [4,9–14].

In these investigations different concentrations of hydrochloric acid have been used for the partial hydrolysis, and it therefore appeared essential to know more about the hydrolysis of phosphorylated peptides, especially in view of the observations of Sanger and Thompson [2] and Schaffer *et al* [4], that sequence inversion may take place under certain conditions. Furthermore, a knowledge of the hydrolytic behaviour of phosphorylated peptides might assist an understanding of the action of proteolytic enzymes and phosphatases [15] on them. In the present investigation a study was therefore made of the hydrolysis of the two model peptides SerP-Gly and Gly-SerP in conc. hydrochloric acid at 37° and in 2 N hydrochloric acid at 100°.

EXPERIMENTAL

Materials

The *O-phosphoryl-*DL*-serylglycine* (SerP-Gly) and *glycyl-(O-phosphoryl)-*DL*-serine* (Gly-SerP) were samples of materials, of which the syntheses and analytical data have been described previously [16,17]. Their purity was further demonstrated by the column chromatographic results described below (Fig. 1, zero time hydrolysis).

Hydrolysis

A. In 2 N HCl: About 10 mg of phosphopeptide was dissolved in 1 ml of 2.02 N HCl (3 × glass-distilled azeotropic acid, diluted with distilled water), and 0.1 ml portions of the solution were hydrolysed in sealed tubes of 4 × 0.6 cm. Hydrolyses for 0.5 h and 1.0 h were done in boiling water, those for longer times in an oven at 100° ± 1°. After hydrolysis the tubes were immediately placed in an ice-box at −20° and kept at this temperature until just before the chromatographic analysis, when they were opened and diluted with 2 ml of water.

B. In conc. HCl: The hydrolyses in conc. HCl (Merck p.a.) were done essentially in the same way, but in an air thermostat at 37 ± 0.5°C. The sealed tubes containing the hydrolysates were kept at −20° until just before chromatography. The tube was then opened and the hydrochloric acid was removed *in vacuo* over NaOH. The dry residue was dissolved in 2 ml of water.

Chromatography

The method for the separation of phosphorylated peptides that has been described in a previous paper [18] from this laboratory was used. As only three phosphorus-containing compounds, SerP, SerP-Gly and Gly-SerP had to be separated, it was possible to decrease the height of the column and increase the solvent gradient. A column of 1.2 cm diameter was packed to a height of 20 cm with Dowex 1-X2 resin in formate form. The hydrolysate was applied and the column was eluted with 0.1 M formic acid. After 24 ml, gradient elution was started using 1.0 M pyridinium formate, pH 4.5, in the reservoir. The mixing chamber volume was 550 ml.

Fractions of 2 ml were collected in 180 × 18 mm calibrated test tubes. The flow rate was 24 ml/h, and a complete separation took 10 h. The fractions were analysed according to Moore and Stein [19] by addition of 1 ml of ninhydrin solution, dilution with 10 ml of ethanol-water (1:1) and measurement of the optical density at 575 mμ using a Bausch & Lomb monochromatic colorimeter. The peaks found were identified by their chromatographic behaviour (*cf.* Fig. 1) and by N-terminal analysis (see below). The results are shown in Tables 1 and 2.

Ninhydrin colour values. A value of 1.03 has been reported [7] for O-phosphorylserine. The colour values for SerP-Gly and Gly-SerP were determined as follows. Samples of

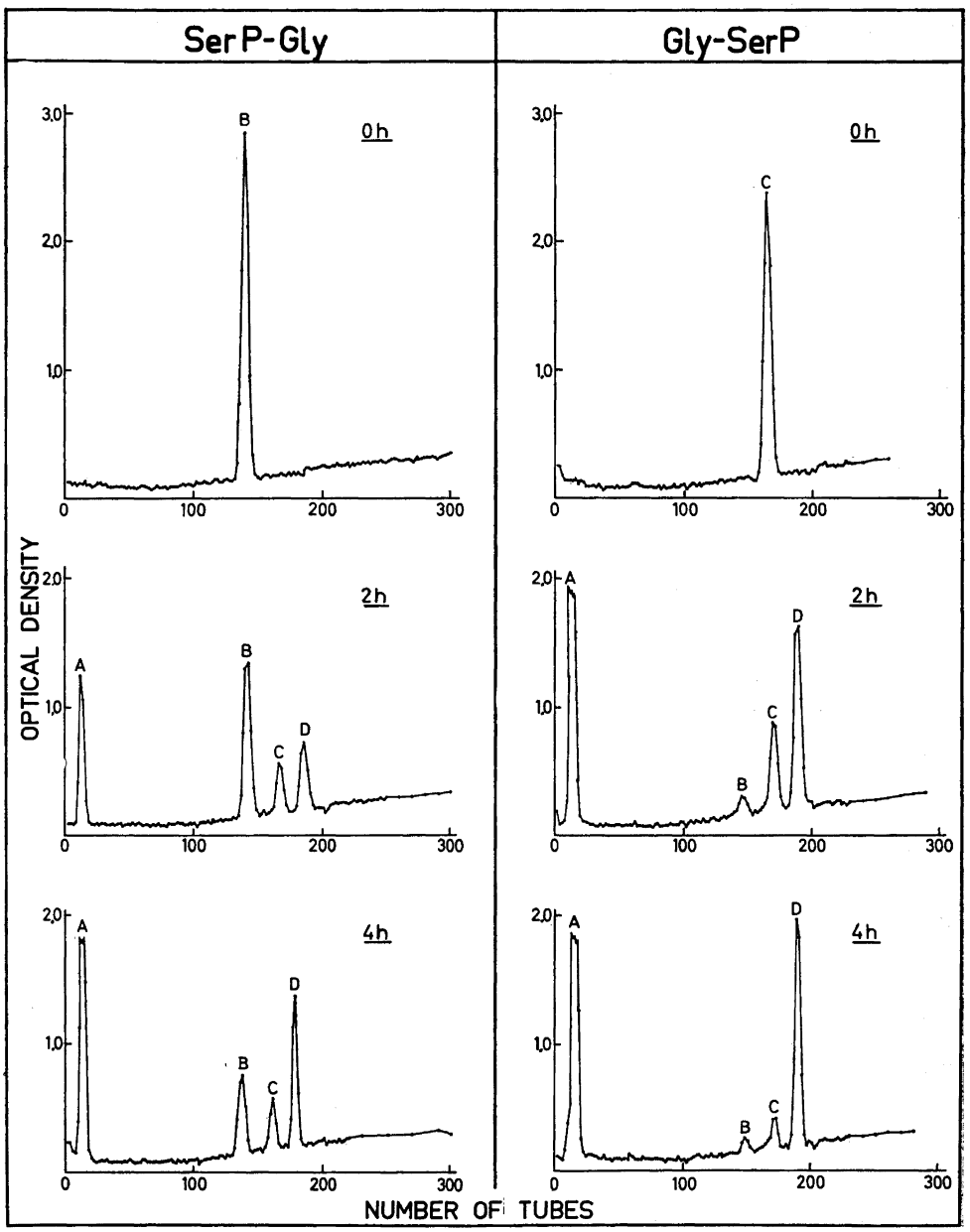

Fig. 1. Column chromatographic separation of the products of hydrolysis of SerP-Gly and Gly-SerP in 2 N HCl, 100°. Peak A contains the unphosphorylated amino acids and peptides; B is SerP-Gly; C is Gly-SerP and D is SerP.

these two compounds and of leucine were dried for 3 h at 70° *in vacuo* over P_2O_5 and 3—5 mg of each compound was dissolved in 50 ml of 0.2 M sodium citrate buffer, pH 5.0. One ml of these solutions was used for the ninhydrin reaction, and the optical density was measured with a Beckman B spectrophotometer at 570 mμ. The colour values obtained were: SerP-Gly 1.00 ± 0.02; Gly-SerP 0.98 ± 0.03.

Identification of peak B obtained from Gly-SerP as SerP-Gly by N-terminal analysis *. Fifty mg of Gly-SerP was hydrolysed for 2 h at 100° in 5 ml of 2 N HCl. After evaporation over NaOH *in vacuo* the hydrolysate was chromatographed as described above. Fractions of 2 ml were collected and 0.2 ml of each was used for ninhydrin reaction. The fractions containing peaks A and B (Fig. 1) were evaporated to dryness *in vacuo* (peak A was used for the complete hydrolysis experiment described below).

Peak B, from its position in the chromatogram was suspected to be SerP-Gly. Its N-terminal amino acid was identified by the DNP-method of Sanger as described by Janz *et al.*[13] The sample, weighing about 3 mg, was shaken for 3 h at 40° with 2 ml of 66 % ethanol containing 1 % $NaHCO_3$ and 1 % 1-fluoro-2,4-dinitrobenzene. After evaporation to dryness, the mixture was dissolved in 4 ml of water, acidified and extracted with 3 × 2 ml of ether to remove fluorodinitrobenzene and dinitrophenol. The DNP derivative of B was extracted from the water phase with 3 × 2 ml of methyl acetate and the combined extract was evporated to dryness and hydrolysed for 2 h at 100° with 2 ml of 2 N HCl. The hydrolysate was diluted with 1 ml of water and the DNP-amino acid was taken up in 3 × 2 ml of methyl acetate and identified as N-dinitrophenyl-(O-phosphoryl)-DL-serine (DNP-SerP) by paper chromatography in the solvent systems *tert*-amyl alcohol — diphthalate buffer and 1.5 M phosphate buffer, pH 6.0. Synthetic DNP-SerP prepared ** from SerP and fluorodinitrobenzene was used as reference, it had an R_F value of about 0.7 in the phosphate buffer. In the *tert*-amyl alcohol — diphthalate system, this compound had moved only 2 cm after 100 h running.

Authentic SerP-Gly, treated as peak B, gave exactly the same results.

Complete hydrolysis of peak A obtained from SerP-Gly and Gly-SerP. To determine the amount of peptide in the dephosphorylated fraction obtained from Gly-SerP, peak A from the above chromatogram was dissolved in 3 ml of water. Two samples of 1 ml were evaporated to dryness, and one of them was hydrolysed for 20 h at 110° in 0.1 ml of 6 N HCl and again evaporated to dryness. The two samples were then dissolved separately in 0.35 M sodium citrate buffer (5 ml), pH 5.28, and 2 ml of each solution was used for reaction with ninhydrin solution. The ninhydrin colour yields were:

Unhydrolysed peak A from Gly-SerP	1.88
Hydrolysed » » » »	1.96

This increase of 4 % in the ninhydrin colour is equal to about 7 % by weight of peptide in peak A.

From a 2 h hydrolysate of SerP-Gly, peak A when isolated and treated as above, gave the following ninhydrin colour yields:

Unhydrolysed peak A from SerP-Gly	0.913
Hydrolysed » » » »	1.177

Complete hydrolysis of this fraction from SerP-Gly gave an increase of 30 % in ninhydrin colour, indicating that the fraction contained about 45 % by weight of dephosphorylated peptide.

RESULTS

The rates of hydrolysis of SerP-Gly and Gly-SerP in 2 N HCl at 100° and in conc. HCl at 37° are shown in Fig. 2 as measured by the ninhydrin colour

* Schaffer *et al.*[4], by a similar procedure have demonstrated the formation of Gly-SerP from SerP-Gly in 2N HCl.

** The preparation of DNP-SerP was made by Bo Öberg in this laboratory.

Table 1. Hydrolysis of 1 mg of phosphopeptide in 0.1 ml of 2.0 N HCl at 100°.

Hours	Ninhydrin colour							
	1.0 mg SerPGly				1.1 mg GlySerP			
	Unphospho-rylated	SerPGly	GlySerP	SerP	Unphospho-rylated	SerPGly	GlySerP	SerP
0	0	8.01	0	0	0	0	7.46	0
0.5	0.56	(5.77)	0.36	0.30	1.58	0.15	5.17	1.47
1	1.48	5.64	0.76	0.84	3.36	0.40	4.86	2.75
2	2.59	4.07	1.23	1.62	6.52	0.43	2.28	4.64
4	5.90	1.93	1.03	2.75	9.55	0.31	0.72	4.82
6	7.61	0.96	0.49	3.48				
20	13.25	0	0	1.70				

Table 2. Hydrolysis of 1 mg of phosphopeptide in 0.1 ml of conc. HCl at 37°

Days	Ninhydrin colour							
	1.0 mg SerPGly				1.1 mg GlySerP			
	Unphospho-rylated	SerPGly	GlySerP	SerP	Unphospho-rylated	SerPGly	GlySerP	SerP
0	0	7.19	0	0	0	0	7.01	0
1	0.67	6.32	0	0.51	2.72	0	4.92	2.46
3	1.62	5.12	0	1.13	5.10	0	2.13	4.64
7	2.85	3.68	0	1.89	7.92	0	0.55	6.45

yield from chromatographic fractions of hydrolysates. Fig. 2 also shows the formation of a mixture of unphosphorylated amino acids and peptides (peak A), SerP (peak D) and the formation of phosphopeptide with an *inversed* amino acid sequence during hydrolysis in 2 N HCl.

The hydrolysis of Gly-SerP in 2 N HCl is appreciably faster than that of SerP-Gly, as can be seen from Fig. 2 and the following table.

Time	0	0.5	1	2	4	6	20 h
SerP-Gly	0	(27.9)	29.5	49.1	75.9 %	88	100 % hydrolysis
Gly-SerP	0	30.6	35.0	69.4	90.3 %	—	— »

In spite of the faster hydrolysis of Gly-SerP the amount of this compound formed by sequence inversion of SerP-Gly, is more than twice as large as the amount of SerP-Gly formed from Gly-SerP.

Fig. 2 also shows, that much more SerP is formed from Gly-SerP than from SerP-Gly, and that comparatively more ninhydrin colour is obtained from the dephosphorylated peaks (A) from Gly-SerP than from SerP-Gly. Since all the compounds concerned have ninhydrin colour values of 100 ± 0.05 (relative to leucine), calculation shows that peak A from Gly-SerP contains almost only the free amino acids (glycine and serine) while peak A from SerP-Gly contains large amount of dephosphorylated peptide (serylglycine) *. This was confirmed by isolation of peak A, followed by complete hydrolysis. These results show that Gly-SerP is hydrolysed mainly at the peptide bond yielding glycine and SerP, while SerP-Gly, apart from some hydrolysis at the peptide bond, to a large extent releases its phosphoric acid residue yielding serylglycine.

In conc. HCl, Gly-SerP is hydrolysed much faster than SerP-Gly:

Time	0	1	3	7	days
SerP-Gly	0	12.2	28.9	48.9	% hydrolysis
Gly-SerP	0	29.7	69.2	92.2	% »

Here also Gly-SerP is hydrolysed mainly at the peptide bond, while SerP-Gly affords a large amount of dephosphorylated peptide, as can be calculated from the colour yield. No sequence inversion was observed in conc. HCl.

DISCUSSION

Peptide bonds involving the amino groups of serine and threonine residues with their β-hydroxyl groups intact are known to be unusually labile to acid hydrolysis [1,20]. This lability is a consequence of an N→O acyl shift *via* an oxazolin [21] or, more likely, a hemiacetal [22] derivative:

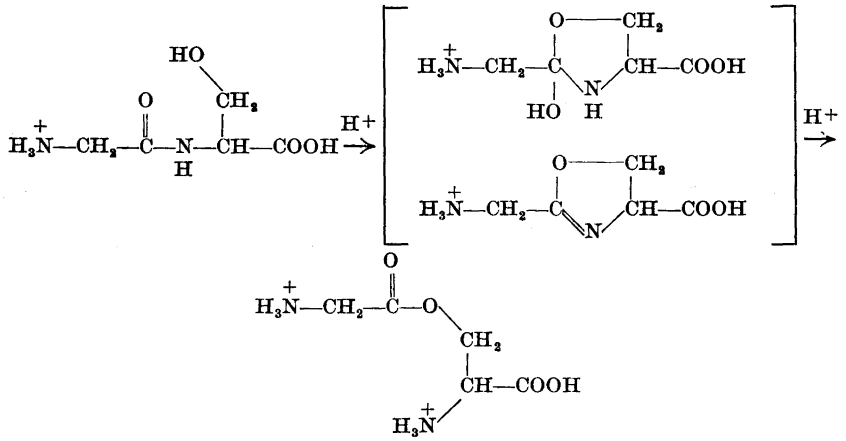

* Glycylserine may be formed by sequence inversion, but should be hydrolysed very easily, see discussion.

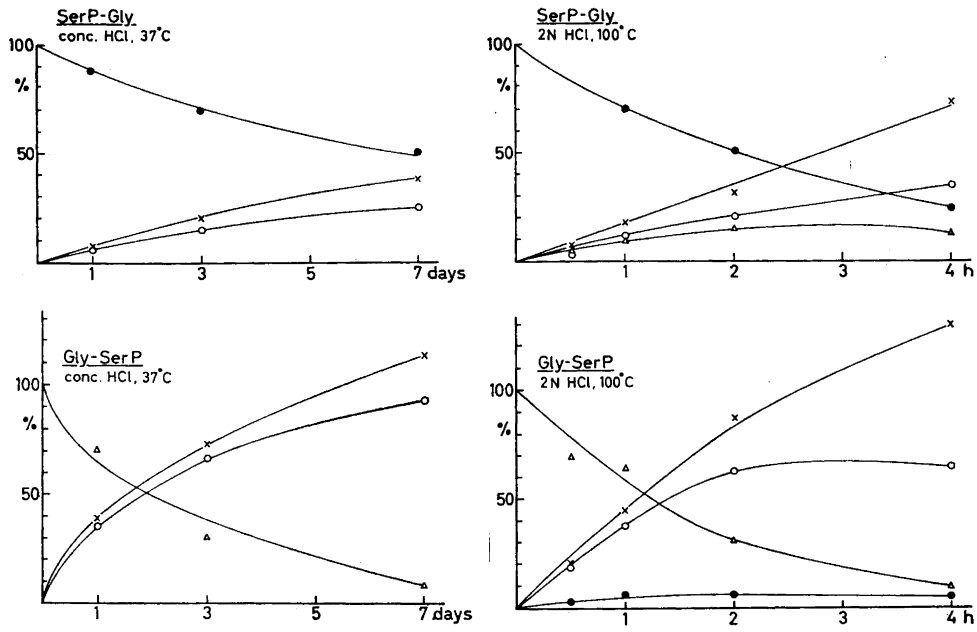

Fig. 2. Rates of hydrolysis of SerP-Gly and Gly-SerP, of formation of dephosphorylated amino acids and peptides and of SerP, and the formation of phosphopeptide with an inversed amino acid sequence. Measured as changes in ninhydrin colour; zero time colour = 100 %.

● — ● — ● SerP-Gly
△ — △ — △ Gly-SerP
○ — ○ — ○ SerP
× — × — × Unphosphorylated amino acids and peptides.

In SerP-Gly and Gly-SerP, the hydroxyl groups are esterified with phosphoric acid and, therefore, not available for this reaction. As Gly-SerP is hydrolysed almost exclusively to glycine and SerP, the acyl shift mechanism is not responsible for the higher sensitivity of this phosphopeptide to acid hydrolysis.

Martin has recently discussed the mechanism of the acid hydrolysis of dipeptides in aqueous solution, and the effects of the different side chains of the α-amino acids on the rate of hydrolysis [23]. According to Martin, the mechanism is the same as for amides in general. In the first, fast step, a proton is reversibly added to the peptide bond nitrogen atom, forming an amide cation. In the second, rate-controlling step, a water molecule is added to the carbonyl carbon atom in a bimolecular substitution. A consequence of this mechanism is, that substituents at the β-carbon atom of an N-terminal amino acid have only steric effects on the rate of hydrolysis, while substituents in the C-terminal amino acids produce mainly polar effects. According to this, Gly-SerP would be expected to be hydrolysed at the peptide bond appreciably faster

than SerP-Gly, as in fact was found experimentally. Firstly, the steric hindrance of the side chain of O-phosphorylserine should in the N-terminal position, as in SerP-Gly, keep water molecules from coming in contact with the carbonyl carbon atom of the intermediate amide cation to a much greater extent than the two hydrogen atoms of glycine in Gly-SerP; this effect is shown by the side chain of serine (Ref.[23], Table 3). Secondly, the electronattracting phosphate group of O-phosphorylserine in the C-terminal position as in Gly-SerP should increase the rate of hydrolysis as is found in the case of C-terminal dicarboxylic acid [23].

Schaffer *et al.* have shown [4] that SerP-Gly, during hydrolysis in 2 N HCl, undergoes sequence inversion to Gly-SerP to an appreciable extent. Thompson and Thompson have suggested [3] that this inversion, which is supposed to go *via* the diketopiperazine [1], leads to the more stable peptide sequence as in the conversion of glycylvaline to valylglycine [2]. However, the experimental results obtained here show, that SerP-Gly is at least as stable as Gly-SerP in hydrochloric acid, and that Gly-SerP also undergoes sequence inversion:

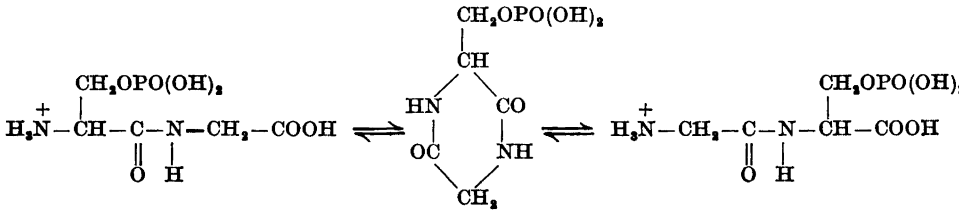

If the mechanism for the hydrolysis of dipeptides is also applicable to diketopiperazines, the intermediate above should show preferential ring-opening to give SerP-Gly. As in fact more Gly-SerP is formed by sequence inversion than SerP-Gly, the above diketopiperazine seems to be formed faster from SerP-Gly than from Gly-SerP.

The work was supported by grants from the *Swedish Medical Research Council* to Professor Olof Mellander.

REFERENCES

1. Sanger, F. *Advances in Protein Chem.* **7** (1952) 1.
2. Sanger, F. and Thompson, E. O. P. *Biochem. et Biophys. Acta* **9** (1952) 225.
3. Thompson, E. O. P. and Thompson, A. R. *Fortschr. Chem. Org. Naturstoffe* **12** (1955) 270.
4. Schaffer, N. K., Harshman, S. and Engle, R. R. *J. Biol. Chem.* **214** (1955) 799.
5. Flavin, M. *J. Biol. Chem.* **210** (1954) 771.
6. de Verdier, C.-H. *Acta Soc. Med. Upsaliensis* **60** (1955) 48.
7. Hipp, N. J., Groves, M. L. and McMeekin, T. L. *J. Am. Chem. Soc.* **79** (1957) 2559.
8. Williams, J. and Sanger, F. *Biochem. et Biophys. Acta* **33** (1959) 294.
9. Schaffer, N. K., Simet, L., Harshman, S., Engle, R. R. and Drisko, R. W. *J. Biol. Chem.* **225** (1957) 197.
10. Anderson, L. and Jollés, G. R. *Arch. Biochem. Biophys.* **70** (1957) 121.
11. Oosterbaan, R. A., Kunst, P., van Rotterdam, J. and Cohen, J. A. *Biochim. e Biophys. Acta* **27** (1958) 549; 556.
12. Dixon, G. H., Kauffman, D. L. and Neurath, H. *J. Biol. Chem.* **233** (1958) 1373.

13. Jansz, H. S., Posthumus, C. H. and Cohen, J. A. *Biochim. et Biophys. Acta* **34** (1959) 387; 396.
14. Hartley, B. S., Naughton, M. A. and Sanger, F. *Biochim. et Biophys. Acta* **34** (1959) 244.
15. Mellander, O., Bennich, H. and Fölsch, G. *Acta Soc. Med. Upsaliensis* **64** (1959) 303.
16. Fölsch, G. *Acta Chem. Scand.* **9** (1955) 1039.
17. Fölsch, G. *Acta Chem. Scand.* **12** (1958) 561.
18. Strid, L. Acta Chem. Scand. **13** (1959) 1787.
19. Moore, S. and Stein, W. H. *J. Biol. Chem.* **211** (1954) 907.
20. Gordon, A. H., Martin, A. J. P. and Synge, R. L. M. *Biochem. J.* **35** (1941) 1369.
21. Desnuelle, P. and Casal, A. *Biochim. et Biophys. Acta* **2** (1948) 64.
22. van Tamelen, E. E. *J. Am. Chem. Soc.* **73** (1951) 5773; *cf.* Konstas, S., Photaki, I. and Zervas, L. *Chem. Ber.* **92** (1959) 1288.
23. Martin, R. J. L. *Austral. J. Chem.* **10** (1957) 256.

Received December 1, 1959.

ACTA CHEMICA SCANDINAVICA 14 (1960) 634–640

Low Temperature Heat Capacities and Thermodynamic Properties of the $Ni_{1-x}Se$-Phase

FREDRIK GRØNVOLD and TORKILD THURMANN-MOE

Kjemisk Institutt A, Universitetet i Oslo, Blindern, Norway

and

EDGAR F. WESTRUM, JR. and NORMAN E. LEVITIN

Department of Chemistry, University of Michigan, Ann Arbor, Michigan, U.S.A.

Heat capacities of three nickel selenides with compositions $Ni_{0.95}Se$, $Ni_{0.875}Se$ and $Ni_{0.80}Se$, representing the $Ni_{1-x}Se$-phase with NiAs-like structure and cation vacancies, were measured in the range 5 to 350°K. No transitions or other heat-capacity anomalies were observed, except for slight upward trends in the heat-capacity values for $Ni_{0.875}Se$ and $Ni_{0.80}Se$ compared to those for $Ni_{0.95}Se$ above 250°K, which might possibly indicate the beginning of transitions. Values for the enthalpy function and entropy were calculated and tabulated for several temperatures. At 298.15°K the entropies are 8.754 eu for $Ni_{0.4872}Se_{0.5128}$ (*i. e.* $Ni_{0.95}Se$), 8.608 eu for $Ni_{0.4667}Se_{0.5333}$ (*i. e.* $Ni_{0.875}Se$ or Ni_7Se_8) and 8.506 eu for $Ni_{0.4444}Se_{0.5556}$ (*i. e.* $Ni_{0.80}Se$ or Ni_4Se_5).

The $Ni_{1-x}Se$-phase offers interesting possibilities for studying an order-disorder process as a function of composition and of temperature from a combined structural and thermodynamic point of view. It was shown by Alsén[1] that NiSe has a hexagonal structure of the NiAs-type in which each nickel atom is surrounded by six selenium atoms at the corners of a slightly irregular octahedron, or trigonal antiprism. These antiprisms are stacked on top of each other in the c-direction so that the nickel atoms form endless chains in this direction.

More recent work has shown[2] that the $Ni_{1-x}Se$-phase has a composition varying between $Ni_{0.98}Se$ and $Ni_{0.77}Se$ and that the stoichiometric 1:1 ratio is not included, at least not in the case of samples heat-treated at 550 and 400°C when examined by X-ray diffraction at room temperature. The structure is hexagonal only in the nickel-rich range, and additional, weak reflections are observed when $1-x$ is less than 0.91, indicating the presence of superstructure. For a sample with composition $Ni_{0.87}Se$ the superstructure was found to be orthorhombic with $A = a\sqrt{3}$, $B = 3a$ and $C = 3c$, where a and c are the dimen-

sions of the hexagonal unit. With further increase in the number of vacant Ni-positions below $Ni_{0.83}Se$, the basic structure changes from hexagonal to monoclinic, and at the composition $Ni_{0.80}Se$ the size of the unit cell is $A' = a\sqrt{3}$, $B' = a$, $C' = 2c$ and $\beta = 90.52°$.

A determination of the atomic arrangement in $Ni_{0.80}Se$ has ascertained[3] that there is a considerable degree of order among the vacancies after the 20 % missing nickel atoms. These vacancies are distributed in an ordered way in every other layer of metal atoms normal to the *c*-axis, while apparently almost no vacancies exist in the rest of the layers. Slight movements of nickel and selenium atoms in the vicinity of the vacancies are observed, but in general, the structure is little affected. The contraction in volume by the 5.32 % decrease in mass per unit cell is 5.26 %.

The $Ni_{1-x}Se$-phase shows metallic behavior, with a weak, almost temperature-independent paramagnetism. Thus its heat capacity behavior is expected to resemble that of the δ-phase in the nickel-tellurium system[4] which shows no magnetic transitions and rather small variations in heat capacity as a function of composition.

The nickel selenides are rather different from the iron selenides[5] in that no clear-cut separation into two-phase regions occurs within the $Ni_{1-x}Se$-phase. Therefore, it was thought of interest to carry out heat-capacity measurements on the nickel selenides in order to ascertain if the apparent absence of exsolution into phases of slightly different compositions is caused by failure of the nickel selenides to reach equilibrium (in contrast to what seems to be the case for the iron selenides), or by too small an entropy increment between ordered and slightly disordered states to cause such separation.

This requires studying a thermodynamic cycle involving free energy measurements as well as enthalpy and entropy measurements. The enthalpy of formation of the $Ni_{1-x}Se$-phase has been determined[6] at 775°C, and high-temperature heat-capacity measurements are presently in progress to study entropy changes accompanying the order-disorder process.

In this paper are reported the results of low-temperature heat-capacity measurements carried out on three single-phase samples within the homogeneity range of the $Ni_{1-x}Se$-phase, having compositions $Ni_{0.95}Se$, $Ni_{0.875}Se$ and $Ni_{0.80}Se$.

EXPERIMENTAL

A. *Preparation of the samples.* The nickel selenides were prepared by fusion of high-purity nickel and selenium. "Nickel oxide, low in cobalt and iron" from the British Drug Houses Ltd. was reduced with dry, purified hydrogen gas at 500°C for 5 h. The resulting, malleable nickel was broken into pieces and reduced again, this time at 1 000°C for 4 h. Spectrographic analysis showed the presence of the following impurities (in ppm): Al(100), Ba(1), Ca(10), Co(10), Cr(1), Cu(1), Fe(10), Mg(50), Mn(1), Si(50).

The high-purity selenium was a gift from Bolidens Gruvaktiebolag. According to their analysis it contained these impurities (in ppm): Cl(2), Fe(0.8), K(0.3), Na(0.4), non-volatile matter (12). The following elements were not detected (the numbers indicate the sensitivity limit in ppm): Ag(0.03), Al(0.3), As(1), Bi(0.1), Ca(1), Cr(0.3), Cu(0.1), Hg(0.5), Mg(0.3), Mn(0.1), Ni(0.3), Pb(0.3), S(5), Si(1), Sn(0.3), Te(1), Zn(1).

Accurately-weighed quantities of nickel and selenium corresponding to the compositions $Ni_{0.95}Se$, $Ni_{0.875}Se$ and $Ni_{0.80}Se$ were heated in evacuated and sealed vitreous silica tubes. The samples were fused for 2 h at 1 050, 1 000 and 950°C, respectively. They were

then cooled, fragmented and annealed at 550°C for seven days and cooled over a period of two more days. X-Ray powder photographs of the samples were identical to those obtained earlier[3].

B. *Cryostat and calorimeter.* The Mark I cryostat and technique employed in low-temperature adiabatic calorimetry will be described elsewhere[7]. Two different calorimeters were used, W-7 with a capacity of 40 cm³ was used for the $Ni_{0.95}Se$ and $Ni_{0.875}Se$ samples, while calorimeter W-17 with a capacity of 60 cm³ was used for the $Ni_{0.80}Se$ sample. Both calorimeters are gold-plated and have four and two vanes, respectively. Separate series of measurements were carried out to determine the heat capacities of the empty calorimeters, using the same thermometer and heater and exactly the same amount of indium-tin solder for sealing the calorimeter and Apiezon-T grease for thermal contact with the thermometer and heater. The heat capacity of the empty calorimeter W-7 represented from 17 to 25 % of the total heat capacity, and that of calorimeter W-17 from 16 to 21 %.

Temperatures were measured with a capsule-type platinum resistance thermometer (laboratory designation A-3) within an axial well in the calorimeter. The thermometer was calibrated by the National Bureau of Standards, and the temperatures were judged to correspond with the thermodynamic temperature scale within 0.1°K from 5 to 10°K, 0.03°K from 10 to 90°K and 0.04°K from 90 to 350°K. Precision is considerably better, and the temperature increments are probably accurate to 0.001°K after corrections for quasi-adiabatic drift.

The thermometer resistance and power input were measured with a calibrated White double-potentiometer, calibrated resistances and a calibrated standard cell. An electric timer, operated by a calibrated tuning fork and amplifier, was automatically started at the beginning of the heating period and stopped at the end.

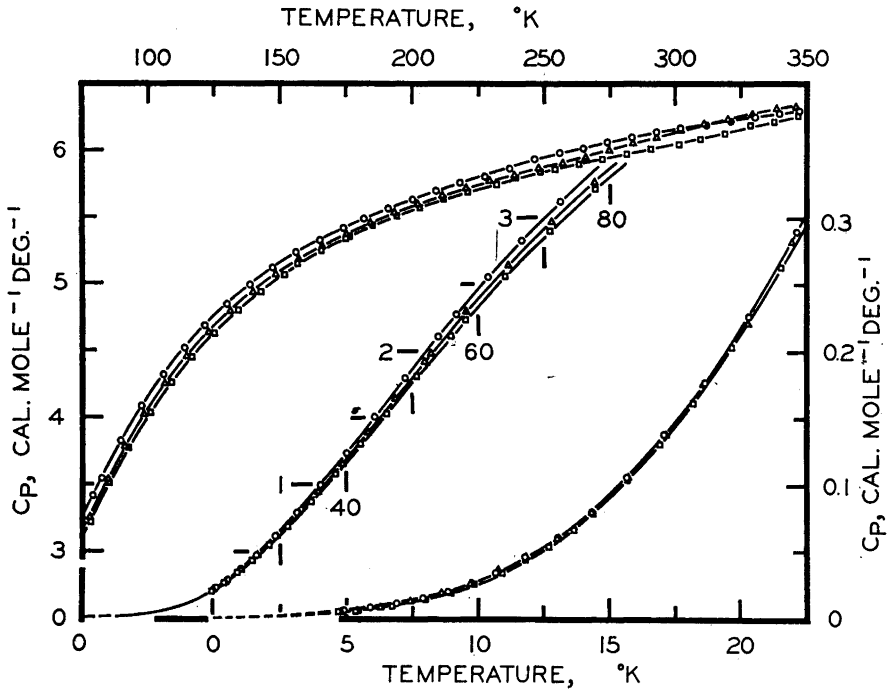

Fig. 1. Heat capacities of nickel selenides on a gram formula weight basis: O represents $Ni_{0.4872}Se_{0.5128}$, △ represents $Ni_{0.4667}Se_{0.5333}$ and □ represents $Ni_{0.4444}Se_{0.5556}$.

Table 1. Heat capacities of nickel selenides, cal °K^{-1} "mole"$^{-1}$.

T, °K	C_p	T, °K	C_p	T, °K	C_p
		$Ni_{0.950}Se$			
		(formula weight $Ni_{0.4872}Se_{0.5128}$ = 69.09 g)			
Series I		20.27	0.2266	156.18	5.234
		22.09	0.2900	165.03	5.326
56.71	2.270	24.11	0.3680	174.05	5.418
61.59	2.551	26.48	0.4719	183.04	5.498
66.77	2.821	29.29	0.6095	182.04	5.491
72.47	3.114	32.58	0.7884	191.02	5.565
78.89	3.409	36.14	0.9964	200.06	5.628
		40.01	1.233	209.17	5.696
Series II		44.32	1.503	218.35	5.756
		48.96	1.796	227.56	5.803
4.91	0.006	53.97	2.108	237.01	5.865
5.88	0.008			246.47	5.933
6.88	0.011	Series III		255.78	5.978
7.89	0.015			264.93	6.013
8.84	0.020	82.09	3.541	274.18	6.059
9.76	0.027	89.30	3.824	283.52	6.097
10.66	0.034	97.37	4.083	292.84	6.139
11.78	0.046	105.89	4.318	302.13	6.164
13.03	0.0610	113.91	4.517	311.55	6.190
14.32	0.0809	121.59	4.686	321.06	6.218
15.65	0.1050	129.88	4.846	330.48	6.247
17.08	0.1378	138.58	4.993	339.86	6.278
18.62	0.1767	147.33	5.119	347.33	6.296
		$Ni_{0.875}Se$			
		(formula weight $Ni_{0.4667}Se_{0.5333}$ = 69.51 g)			
4.82	0.005	39.40	1.155	175.18	5.371
5.39	0.007	43.27	1.394	184.20	5.452
6.28	0.008	47.41	1.645	193.28	5.530
7.42	0.013	51.88	1.917	202.40	5.598
8.60	0.019	52.95	1.981	211.59	5.659
9.70	0.026	58.25	2.295	220.65	5.716
10.76	0.036	64.59	2.642	229.79	5.767
11.84	0.047	71.20	2.966	239.01	5.813
12.98	0.0604	77.54	3.255	248.11	5.863
14.27	0.0797	84.02	3.535	257.09	5.903
15.66	0.1056	90.82	3.787	265.97	5.949
17.11	0.1379	98.27	4.023	274.98	6.002
18.57	0.1757	106.39	4.252	283.88	6.052
20.13	0.2210	114.65	4.457	292.94	6.098
21.94	0.2820	123.00	4.635	302.05	6.155
24.12	0.3644	131.36	4.795	311.05	6.200
26.66	0.4734	139.77	4.934	320.15	6.237
29.47	0.6082	148.46	5.068	329.40	6.272
32.51	0.7665	157.25	5.185	338.66	6.317
35.80	0.9489	166.19	5.283	345.99	6.327

Table 1 (continued).

$Ni_{0.800}Se$

(formula weight $Ni_{0.4444}Se_{0.5556}$ = 69.96 g)

Series I		337.72	6.214	25.77	0.4312
		346.76	6.256	28.30	0.5446
156.88	5.150			31.10	0.6830
165.84	5.250	Series II		34.58	0.8702
174.93	5.339			38.33	1.080
176.40	5.351	5.36	0.006	42.13	1.302
185.38	5.434	4.68	0.005	46.18	1.530
194.29	5.507	5.48	0.006	50.76	1.812
203.10	5.569	6.73	0.009	55.95	2.112
212.01	5.629	8.03	0.014	58.08	2.226
221.09	5.688	8.97	0.020	64.04	2.553
230.22	5.741	9.87	0.026	70.82	2.892
239.42	5.791	10.87	0.034	77.82	3.212
248.70	5.831	11.80	0.0439	84.76	3.510
254.12	5.855	12.67	0.0538	92.43	3.778
263.27	5.899	13.60	0.0669	100.64	4.035
272.43	5.937	14.38	0.0790	108.85	4.261
281.60	5.974	15.68	0.1042	116.87	4.455
290.82	6.010	16.89	0.1303	125.13	4.631
300.14	6.044	18.15	0.1615	134.31	4.803
309.57	6.083	19.63	0.2030	142.84	4.940
319.10	6.127	21.49	0.2630	151.64	5.066
328.61	6.169	23.56	0.3399		

The calorimeter was loaded with sample and evacuated, and helium added at 5 cm Hg pressure at about 25°C to provide thermal contact between calorimeter and sample. It was then placed in the cryostat and cooled. The mass of sample used was 162.675 g $Ni_{0.95}Se$, 171.863 g $Ni_{0.875}Se$ and 172.998 g $Ni_{0.80}Se$.

RESULTS

The heat-capacity determinations are listed in Table 1 in chronological order, and expressed in terms of the thermochemical calorie, defined as 4.1840 abs joules. The ice point is taken to be 273.15°K and the atomic weights of nickel and selenium as 58.71 and 78.96, respectively. The data are expressed in terms of one mole of mixture, "mole", equivalent to the gram formula weight of Ni_ySe_{1-y}, *i.e.*, 69.09 g $Ni_{0.95}Se$, 69.51 g $Ni_{0.875}Se$ and 69.96 g $Ni_{0.80}Se$. An analytically-determined curvature correction for the finite temperature increments was applied to the observed values of $\Delta H/\Delta T$. The approximate temperature increments can usually be inferred from the adjacent mean temperature values in Table 1.

The heat capacity *versus* temperature curves are shown in Fig. 1. For $Ni_{0.95}Se$ it has the usual sigmoidal shape, with no anomalies or other irregular behavior up to 350°K. For $Ni_{0.875}Se$ and $Ni_{0.80}Se$ a slight relative increase in the values compared to those of $Ni_{0.95}Se$ is observed above 250°K. This might possibly indicate the beginning of transitions.

Table 2. Thermodynamic properties of nickel selenides, cal °K^{-1} "mole"$^{-1}$.

	$Ni_{0.950}Se$			$Ni_{0.875}Se$			$Ni_{0.80}Se$		
	(formula weight $Ni_{0.4872}Se_{0.5128}$ = 69.09 g)			(formula weight $Ni_{0.4667}Se_{0.5333}$ = 69.51 g)			(formula weight $Ni_{0.4444}Se_{0.5556}$ = 69.96 g)		
T, °K	$C_p°$	$S°-S_0°$	$\frac{H°-H_0°}{T}$	$C_p°$	$S°-S_0°$	$\frac{H°-H_0°}{T}$	$C_p°$	$S°-S_0°$	$\frac{H°-H_0°}{T}$
10	0.028	0.0110	0.0080	0.029	0.0110	0.0080	0.027	0.0100	0.0073
15	0.093	0.0330	0.0241	0.093	0.0331	0.0242	0.090	0.0311	0.0229
20	0.218	0.0754	0.0556	0.217	0.0754	0.0556	0.215	0.0726	0.0540
25	0.406	0.1431	0.1059	0.401	0.1425	0.1054	0.398	0.1392	0.1036
30	0.647	0.2376	0.1753	0.634	0.2355	0.1734	0.628	0.2314	0.1712
35	0.928	0.3581	0.2624	0.903	0.3531	0.2581	0.892	0.3476	0.2550
40	1.233	0.5018	0.3645	1.195	0.4926	0.3568	1.177	0.4852	0.3523
45	1.548	0.6652	0.4785	1.499	0.6509	0.4668	1.471	0.6408	0.4603
50	1.862	0.8446	0.6012	1.803	0.8246	0.5852	1.765	0.8111	0.5761
60	2.459	1.238	0.8618	2.388	1.206	0.8376	2.327	1.183	0.8216
70	2.994	1.658	1.1290	2.914	1.614	1.0976	2.840	1.581	1.0739
80	3.455	2.088	1.3917	3.368	2.034	1.3538	3.297	1.991	1.3239
90	3.842	2.518	1.6432	3.752	2.453	1.5996	3.692	2.403	1.5657
100	4.161	2.940	1.8795	4.074	2.866	1.8314	4.022	2.809	1.7953
110	4.427	3.350	2.0994	4.345	3.267	2.0480	4.295	3.206	2.0106
120	4.652	3.745	2.3030	4.575	3.656	2.2492	4.523	3.590	2.2107
130	4.846	4.125	2.4913	4.772	4.030	2.4359	4.720	3.960	2.3963
140	5.013	4.491	2.6657	4.941	4.390	2.6089	4.895	4.316	2.5687
150	5.156	4.841	2.8270	5.087	4.736	2.7693	5.050	4.659	2.7291
160	5.277	5.178	2.9765	5.213	5.068	2.9182	5.182	4.989	2.8784
170	5.380	5.501	2.1149	5.322	5.387	3.0565	5.293	5.307	3.0173
180	5.472	5.811	3.2433	5.418	5.694	3.1850	5.387	5.612	3.1464
190	5.554	6.109	3.3628	5.503	5.990	3.3048	5.469	5.906	3.2665
200	5.630	6.396	3.4743	5.579	6.274	3.4167	5.546	6.188	3.3786
210	5.699	6.673	3.5786	5.649	6.548	3.5213	5.618	6.460	3.4835
220	5.764	6.939	3.6765	5.712	6.812	3.6195	5.683	6.723	3.5820
230	5.825	7.197	3.7686	5.770	7.067	3.7117	5.741	6.977	3.6747
240	5.886	7.446	3.8556	5.823	7.314	3.7986	5.791	7.223	3.7618
250	5.944	7.688	3.9379	5.872	7.553	3.8806	5.837	7.460	3.8439
260	5.997	7.922	4.0161	5.921	7.784	3.9581	5.883	7.690	3.9215
270	6.043	8.149	4.0904	5.971	8.008	4.0317	5.928	7.913	3.9950
280	6.085	8.369	4.1609	6.026	8.226	4.1020	5.969	8.129	4.0648
290	6.124	8.584	4.2279	6.085	8.439	4.1693	6.004	8.339	4.1310
300	6.160	8.792	4.2917	6.143	8.646	4.2342	6.044	8.543	4.1941
350	6.300	9.724	4.5689	6.288	9.610	4.5225	6.270	9.464	4.4742
273.15	6.057	8.219	4.1130	5.988	8.078	4.0542	5.942	7.982	4.0173
298.15	6.154	8.754	4.2801	6.133	8.608	4.2224	6.037	8.506	4.1826

Values of C_p, $S_0°$ and $(H°-H_0°)/T$ for the three samples at selected temratures are listed in Table 2. No values for the free energy function are given because of the uncertainty about complete ordering of the atoms and holes, just as for the iron-selenides. The enthaply and entropy increments were computed by integration of the heat-capacity equation, obtained by successive approximations on an IBM 650 calculator. The heat-capacity values are considered to have a probable error of 1 % at 10°K and 0.1 % above 25°K. The estimated probable error in the entropy and enthalpy functions is 0.1 % above 100°K. Some of the data are given to an additional digit because of its significance when the entropies or enthalpies at different temperatures or compositions are compared. The effects of nuclear spin and isotopic mixing are not included in the entropy function.

The non-applicability of the Kopp-Neumann law is immediately evident, since the "molar" heat capacity, and also the entropy, decreases with inreasing selenium content, although the heat capacity and entropy of selenium is higher than for nickel. Within the homogeneity range of the Ni_{1-x} Se-phase reasonable interpolations could have been made, but even over this narrow range of compositions deviations from additivity are observed. These deviations suggest that interpolations should be made with great caution, and might aid in the resolution of the factors contributing to the heat capacities of phases with NiAs-like structure and cation vacancies.

Acknowledgment. The partial support of the *Division of Research, U. S. Atomic Energy Commission*, and of *Norges Almenvitenskapelige Forskningsråd* are gratefully acknowledged.

The authors thank Bolidens Gruvaktiebolag for a generous supply of high-purity selenium and Bruce Justice and Elfreda Chang for assistance in the calorimetric measurements and reduction of the data.

REFERENCES

1. Alsén, N. *Geol. Fören. i Stockholm Förh.* **47** (1925) 19.
2. Grønvold, F. and Jacobsen, E. *Acta Chem. Scand.* **10** (1956) 1440.
3. Grønvold, F. *Paper presented at the 2. Nordiske Strukturmøte*, Oslo 1955.
4. Westrum, E. F. Jr., Chou, C., Machol, R. E. and Grønvold, F. *J. Chem. Phys.* **28** (1958) 497.
5. Grønvold, F. and Westrum, E. F. Jr. *Acta Chem. Scand.* **13** (1959) 241.
6. Grønvold, F. *Paper presented at the XVI International Congress of IUPAC*, Paris 1957.
7. Westrum, E. F. Jr. and Beale, A. F. Jr. *To be published.*

Received November 14, 1959.

ACTA CHEMICA SCANDINAVICA 14 (1960) 641–649

Studies on Succinic Acids

V. The Preparation and Properties of Diastereoisomers of Tetraalkylsuccinic Acids

LENNART EBERSON

Department of Organic Chemistry, Chemical Institute, University of Lund, Sweden

The diastereoisomers of three tetraalkylsuccinic acids containing two asymmetric centres, *viz.* α,α′-dimethyl-α,α′-diethyl-, α,α′-dimethyl-α,α′-dipropyl-, and α,α′-dimethyl-α,α′-di*iso*propylsuccinic acid, have been prepared. Their relative configuration is discussed on the basis of dissociation constant measurements, and in each pair the isomer with lower ratio between K_1 and K_2 is proposed to be the *meso* form.

Only a few tetraalkylsuccinic acids containing two asymmetric centres have been described in the literature [1–3]. Stefl [1] prepared α,α′-dimethyl-α,α′-diethyl- and α,α′-dimethyl-α,α′-dipropylsuccinonitrile (II, R = C_2H_5 and n-C_3H_7) by thermal decomposition of the corresponding bisazonitriles (I) and was able to isolate the diastereoisomers in a pure or almost pure state.

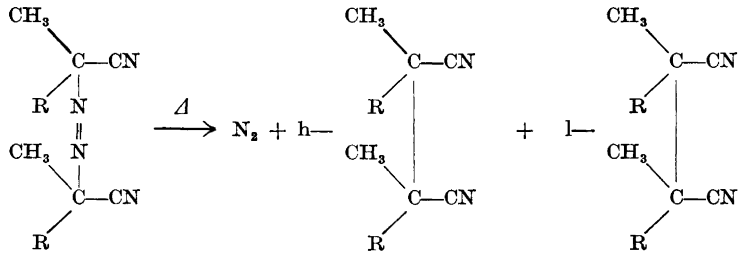

I II

(The letters h and l designate high- and low-melting, respectively). He studied the hydrolysis of these dinitriles and summarized the results in the following scheme:

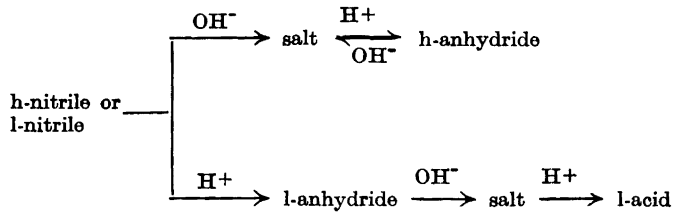

i.e. on hydrolysis both dinitriles were converted into the same anhydride, in alkaline medium into the high-melting anhydride and in acid medium into the low-melting anhydride. Furthermore, he also concluded that the h-anhydride was isomerised to the l-anhydride by treatment with concentrated hydrochloric acid at 180° for 6 h or with acetic anhydride at the boiling temperature for 12 h, whereas the inverse reaction was claimed to occur on boiling the l-anhydride with 40 % aqueous potassium hydroxide for 2—3 days *.

Dox [3] synthesised α,α′-dimethyl-α,α′-diethylsuccinic acid by the bisazonitrile method and converted it into the anhydride and the imide but did not attempt to separate it into diastereoisomers.

The present author [2] has prepared α,α′-dimethyl-α,α′-diethylsuccinic acid and α,α′-diethyl-α,α′-di*iso*propylsuccinic acid by Kolbe electrolysis of the appropriate malonic monoesters, but could not separate them into diastereoisomers by fractional crystallisation. In the latter case the ease of formation of the anhydride from the acid both in solution and in the solid state made this procedure impossible.

It is now of course apparent that the isomerisations described by Stefl are not consistent with modern theories on the mechanism of inversion at an asymmetric carbon atom, since there is no mechanism for inversion at a quaternary carbon atom which does not involve scission and recombination of a carbon to carbon bond and this possibility seems very unlikely in view of the rather mild reaction conditions that Stefl used. Another point worthy of note is the failure to isolate the h-acid, the solution of the h-acid salt giving the h-anhydride directly on acidification. Tetraalkylsuccinic acids certainly have a very strong tendency to lose water forming anhydrides [2,4,5], but both tetraethyl- and tetrapropylsuccinic acid are liberated as the free acids by acidification of solutions of their salts. It is evident that some of the results must have been misinterpreted. The present paper deals with the problem of preparing pure diastereoisomers of some α,α′-dimethyl-α,α′-dialkylsuccinic acids and with evidence on the steric relationships between the acids obtained from dissociation constant measurements.

α,α′-Dimethyl-α,α′-diethylsuccinic acid

The product of hydrolysis of dimethyl α,α′-dimethyl-α,α′-diethylsuccinate by concentrated sulphuric acid was a liquid anhydride with rapidly dissolved in boiling 10 % aqueous sodium hydroxide solution [2]. On acidification this

* The present author was not able to duplicate the last-mentioned reaction with α,α′-dimethyl-α,α′-diethylsuccinic acid prepared in a different way [2].

gave a mixture of acids, m.p. 125—40°, which could not be separated by fractional crystallisation using several different solvents and solvent pairs. The acid slowly changes into the anhydride in solution, which complicates the separation procedure, since contamination by a small amount of anhydride considerably lowers the melting points of the acid. The melting point determinations must be done in sealed capillaries and the heating rate and time must be carefully controlled in order to obtain reproducible values [2,6].

An attempt was then made to prepare the acids by the bisazonitrile method since this permits the separation of the two forms at the dinitrile stage [1], and no inversion would be expected to occur during the hydrolysis. In fact the two nitriles were easily separated by fractional crystallisation from ligroin, and were then hydrolysed according to the following scheme:

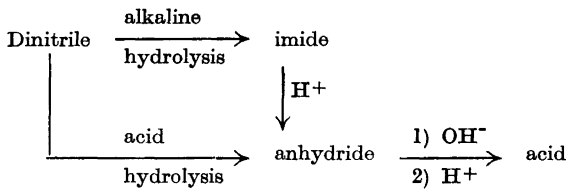

In no case was any interconversion between the two diastereoisomeric series observed. The m.p's of the various compounds are listed in Table 1.

Table 1. Melting points of diastereoisomers of α,α'-dimethyl-α,α'-diethylsuccinic acid and their derivatives

	Imide, m.p.	Anhydride, m.p.	Acid, m.p.
High-melting dinitrile, m.p. 99—101°	97—99°	32—33°	189—192°
Low-melting dinitrile, m.p. 44—45°	92—95°	40—42°	182—184°

The melting point differences between the two series are rather small for the imides, anhydrides and acids, and it is difficult to identify the diastereoisomers by melting point determinations only. In the light of these findings the results reported by Stefl are quite understandable. The "h-anhydride" must actually have been the h- and l-imide, which were mistaken for the same compound. These imides dissolve in aqueous sodium hydroxide and are precipitated by acidification, which explains why the "h-acid" was never obtained. The apparent transformation of "h-anhydride" into "l-anhydride" by concentrated hydrochloric acid was a hydrolysis of the imides to the anhydrides. The "l-anhydride" apparently was either the h- or l-anhydride (or, as the dinitriles were not always separated from each other, a mixture of the anhydrides) and similarly the "l-acid" was either h- or l-acid (or a mixture). The small differences in melting point and solubility are probably responsible for Stefl's misinterpretation, especially as he never obtained the anhydrides in the solid state and the care necessary in m.p. determinations on the acids was not fully known at that time.

α,α'-Dimethyl-α,α'-dipropylsuccinic acid

This acid was best prepared by Kolbe electrolysis of monoethyl methylpropylmalonate. The succinic ester was easily hydrolysed by treatment with warm concentrated sulphuric acid, giving a mixture of anhydrides. The acid mixture obtained by alkaline hydrolysis of the anhydride and acidification was separated into two forms by fractional crystallisation from ethyl acetate, m.p. 173—175° and 166—167°, respectively. The corresponding anhydrides were liquid. The bisazonitrile method was also used but was not superior to the Kolbe method as the over-all yield of the dinitriles was low and they were impossible to separate by fractional crystallisation. The high-melting isomer was obtained in a pure state but the other fractions obtained were always mixtures of varying composition. It was established however that the high-melting dinitrile corresponded to the high-melting acid. Stefl's results with this acid can presumably be explained in the same way as for the α,α'-dimethyl-α,α'-diethylsuccinic acid.

α,α'-Dimethyl-α,α'-di*iso*propylsuccinic acid

This pair of acids was prepared by Kolbe electrolysis of monoethyl methyl-*iso*propylmalonate and subsequent treatment in the same way as for the *n*-propyl compound. The melting points of the acids were 175—177° (anhydride 65—66°) and 130—131° (anhydride 78—79°), respectively. Again the bisazonitrile method gave a low over-all yield of dinitriles, and only the high-melting compound was obtained pure, m.p. 67—68°. This isomer corresponded to the high-melting acid.

α,α'-Dimethyl-α,α'-di-(*tert.*-butyl)-succinic acid

The dimethyl ester of this acid has been prepared by Ansell *et al.*[7] It was not possible to hydrolyse the ester with concentrated sulphuric acid, and therefore the Kolbe method could not be used. The bisazonitrile method also failed because the intermediate radicals disproportionate instead of coupling. The reaction product on hydrolysis with strong sulphuric acid gave methyl-(*tert.*-butyl)-acetic acid in low yield.

DISCUSSION

The dissociation constants of the three acid pairs were determined in 50 % (by wt). aqueous ethanol by potentiometric titration [8]. The pK_1, pK_2, and ΔpK values are given in Table 2. Corresponding values for α,α'-diethyl-, α,α'-di*iso*propyl-, tetramethyl-, and tetraethylsuccinic acid have been included for comparison.

The dissociation constants of a number of *meso* and *racemic* α,α'-dialkylsuccinic acids and tetraalkylsuccinic acids and the K_1/K_2 ratios [8,9] for these compounds indicated that: Firstly, in an α,α-'dialkylsuccinic acid the alkyl

Table 2. Thermodynamic dissociation constants of alkylsubstituted succinic acids in 50 % (by wt.) aqueous ethanol

Succinic acid	pK_1	pK_2	ΔpK
α,α'-Dimethyl-α,α'-diethyl-, m.p. 189—92° [a]	5.73	9.66	3.93
α,α'-Dimethyl-α,α'-diethyl-, m.p. 182—4° [a]	4.45	10.44	5.99
α,α'-Dimethyl-α,α'-dipropyl-, m.p. 173—5°	5.73	9.99	4.26
α,α'-Dimethyl-α,α'-dipropyl-, m.p. 166—7°	4.56	10.86	6.30
α,α'-Dimethyl-α,α'-di*iso*propyl-, m.p. 175—7°	6.92	9.32	2.40
α,α'-Dimethyl-α,α'-di*iso*propyl-, m.p. 130—1°	3.20	13.13	9.93
Racem-α,α'-diethyl-[8]	4.76	9.22	4.46
Meso-α,α'-diethyl-[8]	5.37	7.43	2.06
Racem-α,α'-di*iso*propyl-[8]	3.66	11.44	7.78
Meso-α,α'-di*iso*propyl-[8]	5.98	8.10	2.12
Tetramethyl-[8]	4.84	10.13	5.29
Tetraethyl-[8]	4.78	11.42	6.64

[a] α,α'-Dimethyl-α,α'-diethylsuccinic acid prepared by the Kolbe method gave pK_1 and pK_2 values of 4.86 and 10.16 respectively [8]. Obviously this sample was a mixture of diastereoisomers.

groups have a tendency to take up positions *trans* to each other; in the *meso* acids this brings the carboxyl groups into a *trans* configuration and in the *racemic* acid into a *gauche* configuration. In the latter case a high K_1/K_2-ratio is obtained partly due to the formation of an internal hydrogen bond in the mono-anion, partly to increased Coulomb interaction between the carboxyl groups. Secondly, the accommodation of alkyl groups in, for instance, a tetraalkylsuccinic acid molecule introduces steric strain, which would be reduced in the cyclic hydrogen-bonded structure.

It is evident that these two factors cannot always be easily distinguished. In the tetraalkylsuccinic acids of the type studied in this paper the molecule is highly strained due to the presence of the four alkyl groups, and it can be expected that the two more bulky alkyl groups will have the greater influence on the conformational equilibrium. In the hydrogen-bonded structure, for the *meso* acid mono-anion the methyl groups will lie on one side of the ring and the more bulky groups on the other side. In the other possible *meso* acid conformation all groups will be *trans* staggered and this would be energetically favoured if there was no interaction between the carboxyl groups.

In the *racemic* acid mono-anion with a cyclic structure the bulky alkyl groups will be situated *trans* to each other and this arrangement will therefore be less strained than that of the corresponding *meso* form. From these considerations it can be concluded that the *meso* acid should possess a lower K_1/K_2-ratio than the *racemic* acid since: (1) in the fully *trans* staggered conformation the Coulomb interaction between the carboxyl groups is less than that of the most favoured *racemic* acid conformation (which has the carboxyl groups *gauche*) and moreover the formation of an internal hydrogen bond is not possible, and 2) if a cyclic *meso* acid conformation is present in appreciable amounts, it must nevertheless be less stable than the corresponding *racemic*

form. On these grounds the acids with the lower ΔpK in Table 2 are ascribed the *meso* configuration. The m.p's and solubility relationships are in agreement with this.

EXPERIMENTAL

The analyses were done by the Department of Analytical Chemistry, Chemical Institute, University of Lund. Melting points were determined with a Kofler apparatus unless otherwise stated. M.p's in sealed capillaries (abbreviated s.c.) were done as described in paper II of this series.

α,α'-Dimethyl-α,α'-diethylsuccinic acid

A. *Bisazonitrile method.* Hydrazine sulphate (96 g) and sodium cyanide (75 g, 97—98 %) were dissolved in 1 500 ml of water in a three litre bottle. Methylethyl ketone (96 g) was added and the mixture was shaken for 48 h. The organic layer was then taken up in ether, the ether was removed by evaporation *in vacuo* at room temperature and the residue, a viscous oil (120 g) which did not crystallise even after standing for several days in a vacuum desiccator, was dissolved in 200 ml of acetic acid + 100 ml of concentrated hydrochloric acid. The mixture was cooled to 5°, and an equimolecular amount of bromine dissolved in 400 ml of 70 % aqueous acetic acid was added with vigorous stirring during the course of 2 min. Stirring was continued for half an hour and the reaction mixture was then poured into ice water (3 l). The precipitate was collected, washed thoroughly with water, and dried giving the crude bisazonitrile (93 g), m.p. 49—51°, m.p. after recrystallisation from light petroleum 50—51° (80 g). Stefl [1] reported m.p. 54—55°, Dox [3] 57°, and Overberger *et al.*[10] 49—51°.

The recrystallised, dry bisazonitrile (80 g) was decomposed by boiling in carbon tetrachloride (500 ml) for 20 h. The solvent was distilled off and the residue was subjected to fractional crystallisation from ligroin. The more insoluble fraction (30 g) had m.p. 70—90°. One recrystallisation from ligroin afforded pure high-melting α,α'-dimethyl-α,α'-diethylsuccinonitrile (25 g, 22 %), m.p. 99—101°. The low-melting isomer was isolated from the mother liquor, m.p. 44—45° after two recrystallisations from ligroin; the yield of pure low-melting α,α'-dimethyl-α,α'-diethylsuccinonitrile was 19.5 g (17 %). Stefl [1] reported m.p. 98—99° and 42—43°, respectively. For the high-melting form Overberger *et al.*[10] found m.p. 96—98°.

The high-melting α,α'-dimethyl-α,α'-diethylsuccinonitrile, 10 g, was hydrolysed by boiling with a mixture of concentrated sulphuric acid (50 ml), water (20 ml) and acetic acid (60 ml) for 20 h. The reaction mixture was poured into water, the organic layer was taken up in ether, the ether solution was washed with sodium carbonate solution and water, and finally the ether was distilled off. The residue was distilled *in vacuo*, b.p. 117—118°/10 mm. The main fraction (9.2 g) solidified on standing, m.p. 30—33°, and was recrystallised from light petroleum, m.p. 32—33°. According to the analysis it was an anhydride of α,α'-dimethyl-α,α'-diethylsuccinic acid. (Found: C 65.2; H 8.9; Calc. for $C_{10}H_{16}O_3$: C 65.2; H 8.8). The anhydride was dissolved in 10 % aqueous potassium hydroxide by boiling for 30 min. Addition of dilute hydrochloric acid precipitated the high-melting α,α'-dimethyl-α,α'-diethylsuccinic acid, which was crystallised from ethyl acetate, m.p. 189—192° (s.c.). (Found: C 59.5; H 9.2; equiv. wt 204. Calc. for $C_{10}H_{18}O_4$: C 59.4; H 9.0; equiv. wt 202).

The high-melting α,α'-dimethyl-α,α'-diethylsuccinonitrile was hydrolysed under alkaline conditions by boiling with 30 % aqueous potassium hydroxide for 48 h. The reaction mixture was extracted with ether to remove any remaining nitrile, and the aqueous layer was acidified with dilute hydrochloric acid. The crystalline material deposited was collected and recrystallised from ligroin, m.p. 97—99°; according to analyses this material was α,α'-dimethyl-α,α'-diethylsuccinimide. (Found: C 65.5; H 9.3; N 7.7. Calc. for $C_{10}H_{17}O_2N$: C 65.5; H 9.3; N 7.7). Dox [3] reported m.p. 93—4° for an imide of unspecified configuration. The imide was hydrolysed to the anhydride, m.p. 32—33°, by boiling for 8 h with concentrated sulphuric acid, water, and acetic acid in the same proportions as above.

Low-melting α,α'-dimethyl-α,α'-diethylsuccinonitrile (10 g) was hydrolysed in the same way as for the high-melting nitrile. The α,α'-dimethyl-α,α'-diethylsuccinic anhydride obtained (9.0 g), b.p. 124—126°/12 mm, m.p. 39—41°, was recrystallised from light petroleum, m.p. 40—42°. (Found: C 64.9; H 8.7. Calc. for $C_{10}H_{16}O_3$: C 65.2; H 8.7). Hydrolysis gave the low-melting α,α'-dimethyl-α,α'-diethylsuccinic acid, m.p. 182—184° (s.c.) after recrystallisation from ethyl acetate. (Found: C 59.3; H 9.0; equiv. wt 203. Calc. for $C_{10}H_{18}O_4$: C 59.4; H 9.0; equiv. wt 202).

Alkaline hydrolysis of the low-melting dinitrile in the same way as for the high-melting nitrile afforded an α,α'-diemethyl-α,α'-diethylsuccinimide of m.p. 92—95° after recrystallisation from ligroin. (Found: C 65.5; H 9.4; N 7.6. Calc. for $C_{10}H_{17}O_2N$: C 65.5; H 9.4; N 7.7). Acid hydrolysis of this imide gave the anhydride, m.p. 40—42°.

B. *Kolbe method.* A crude mixture of the two diastereoisomeric acids was prepared as described previously [2]. Fractional crystallisation was tried with ethyl acetate, benzene, ethyl acetate-benzene, and ethyl acetate-light petroleum, but no separation was achieved. The sample with highest m.p. melted at 173—176° (s.c.). The products isolated from the mother liquors were largely anhydrides.

α,α'-Dimethyl-α,α'-dipropylsuccinic acid

A. *Bisazonitrile method.* The bishydrazonitrile was prepared in the same way as for the methylethyl derivative from hydrazine sulphate (96 g), sodium cyanide (75 g), and methyl propyl ketone (115 g) in water (1 500 ml). The crude product (125 g) was oxidised directly with bromine in aqueous acetic acid as described above. The crystalline product obtained was contaminated with a strongly lachrymatory oil, which was removed by suction on a sintered glass-funnel. The nature of this product was not investigated. The product was recrystallised from light petroleum, m.p. 55—70°, yield 42 g. Stefl [1] reported m.p. 64° and Overberger *et al.* 73—74.5°. The bisazonitrile was decomposed by boiling in carbon tetrachloride for 24 h. The solvent was distilled off, and the residue was distilled *in vacuo*, b.p. 106—110°/0.5 mm. The main fraction (27 g, 21 %) solidified on standing over night, m.p. 40—70°. In spite of several attempts to separate the two isomers by fractional crystallisation from various solvents, only the high-melting, less soluble form was obtained in a pure state, m.p. 83—85° after three recrystallisations from ligroin. Stefl reported m.p. 84° for the high-melting form and that the other isomer was liquid. Overberger *et al.*[10] gave m.p. 83—83.5° for the high-melting form.

The mixture of dinitriles (10 g) was hydrolysed with sulphuric acid — water — acetic acid and the crude anhydride was directly hydrolysed in the same way as before. The dried acid was dissolved in the minimum of ethyl acetate and the solution was treated with decolorising carbon, filtered, and allowed to cool. The crystals were filtered off, m.p. 171—175° (s.c.) and recrystallised from ethyl acetate, m.p. 173—175° (s.c.). According to analyses this substance was an α,α'-dimethyl-α,α'-dipropylsuccinic acid. (Found: C 62.3; H 9.5; equiv. wt 228. Calc. for $C_{12}H_{22}O_4$: C 62.6; H 9.6; equiv. wt 230). The anhydride was prepared by treating the acid with excess acetyl chloride. Distillation gave the pure α,α'-dimethyl-α,α'-dipropylsuccinic anhydride, b.p. 114—116°/12 mm. (Found: C 67.7; H 9.6. Calc. for $C_{12}H_{20}O_3$: C 67.9; H 9.5).

The mother liquor from the above filtration was diluted with five volumes of light petroleum giving a precipitate of the low-melting α,α'-dimethyl-α,α'-diethylsuccinic acid, m.p. 158—162° (s.c.), which was recrystallised from acetic acid-ligroin (1:10), m.p. 166—167° (s.c.). (Found: C 62.4; H 9.4; equiv. wt 230. Calc. for $C_{12}H_{22}O_4$: C 62.6; H 9.6; equiv. wt 230). The anhydride was liquid, b.p. 115—118°/14 mm. (Found: C 67.9; H 9.5. Calc. for $C_{12}H_{20}O_3$: C 67.9; H 9.5). The amounts of pure acids isolated were 1.9 and 1.1 g, respectively, but the material could be recovered from the mother liquor as anhydride, for use in subsequent preparations.

The high-melting α,α'-dimethyl-α,α'-dipropylsuccinonitrile was found to correspond to the high-melting acid.

B. *Kolbe method.* The preparation and electrolysis of monoethyl methylpropylmalonate was done in the same way as before [2]. The product was obtained in 35 % yield, b.p. 119—120°/2 mm, n_D^{20} 1.4468, d_4^{20} 0.9704. According to analyses it was the diethyl ester. (Found: C 66.7; H 10.5; r_D 0.2752. Calc. for $C_{16}H_{30}O_4$: C 66.9; H 10.7; r_D 0.2777). The

ester was hydrolysed with concentrated sulphuric acid in the usual way, and the acids were prepared as described for the anhydride obtained from the dinitriles. The pure acids melted at 174—175° (s.c.) and 166—167° (s.c.), respectively.

α,α'-Dimethyl-α,α'-diisopropylsuccinic acid

A. *Bisazonitrile method.* The bishydrazonitrile was prepared in the same way as the methylethyl derivative from hydrazine sulphate (96 g), sodium cyanide (75 g), and methyl *iso*propyl ketone (115 g) in water (1 500 ml). The crude product (125 g) was oxidised directly as described above. In this case also a strongly lachrymatory oil was formed that had to be removed by suction on a sintered glass-funnel. The crystalline mass was recrystallised from ethanol, m.p. 64—69°, yield 44 g. Overberger *et al.* found m.p. 68.5—70°. The bisazonitrile was boiled over night in carbon tetrachloride (250 ml). Distillation yielded a mixture of dinitriles, (16.5 g, 13 %), b.p. 142—145°/14 mm, which partially solidified after standing for a few days. Attempts to separate the two forms failed, and only the high-melting α,α'-dimethyl-α,α'-di*iso*propylsuccinonitrile could be obtained pure, m.p. 67—68° after recrystallisation from light petroleum. (Found: C 74.7; H 10.4; N 14.8. Calc. for $C_{12}H_{20}N_2$: C 75.0; H 10.5; N 14.6).

The mixture of dinitriles (10 g) was hydrolysed as before. The anhydride obtained was purified by distillation, b.p. 110—111°/1.5 mm and this was converted to the acid in the usual way. The acid was dissolved in the minimum amount of boiling ethyl acetate as rapidly as possible. The high-melting α,α'-dimethyl-α,α'-di*iso*propylsuccinic acid which crystallised on cooling, was recrystallised from ethyl acetate, m.p. 169—172° (s.c.). (Found: C 62.4; H 9.6; equiv. wt 116. Calc. for $C_{12}H_{22}O_4$: C 62.6; H 9.6; equiv. wt 115). The anhydride was prepared and recrystallised from light petroleum, m.p. 65—66°. (Found: C 67.7; H 9.5; Calc. for $C_{12}H_{20}O_3$: C 67.9; H 9.5).

The mother liquor from which the high-melting acid had crystallised was rapidly evaporated to about one third of its original volume and then diluted with five volumes of light petroleum. This treatment precipitated the low-melting α,α'-dimethyl-α,α'-di*iso*propylsuccinic acid, m.p. 131—2° (s.c.), unchanged after a further recrystallisation from ethyl acetate-light petroleum (1:5). (Found: C 62.4; H 9.5; equiv. wt 229. Calc. for $C_{12}H_{22}O_4$: C 62.6; H 9.6; equiv. wt 230). The anhydride melted at 78—79° after recrystallisation from light petroleum. (Found: C 67.9; H 9.5. Calc. for $C_{12}H_{20}O_3$: C 67.9; H 9.5). The amounts of pure acids obtained were 1.0 g and 0.7 g, respectively, but the material could be recovered as anhydride from the mother liquor for use in subsequent preparations.

The high-melting α,α'-dimethyl-α,α'-di*iso*propylsuccinonitrile was found to correspond to the high-melting acid.

B. *Kolbe method.* The preparation and electrolysis of monoethyl methyl*iso*propylsuccinate was carried out as described previously [8]. The product was obtained in 24 % yield, b.p. 125—130°/4 mm, n_D^{20} 1.4558; d_4^{20} 1.0035. According to analyses it was the dimethyl ester. (Found: C 65.7; H 10.3; r_D 0.2708. Calc. for $C_{14}H_{26}O_4$: C 65.1; H 10.1; r_D 0.2722). The two acids were prepared from this ester in the usual way, m.p. 170—172° (s.c.) and 130—131° (s.c.).

Attempts to prepare α,α'-dimethyl-α,α'-di-(tert.-butyl)-succinic acid. The bisazonitrile from pinacolone was prepared according to Overberger *et al.*[11] Decomposition in carbon tetrachloride yielded a dark-brown liquid, which could not be distilled owing to the very vigorous foaming. It was therefore hydrolysed directly with sulphuric acid-water-acetic acid (4:1:3). The product was isolated by ether extraction and distilled, 90—93°/6 mm. The distillate soon solidified and was recrystallised from light petroleum, m.p. 53—57°. According to analyses it was methyl-(*tert.*-butyl)-acetic acid. (Found: C 64.5; H 10.8; equiv. wt 130.6. Calc. for $C_7H_{14}O_2$: C 64.5; H 10.9; equiv. wt 130.2). Newman *et al.*[12] reported m.p. 51—52°.

pK-measurements. The p*K* values for these acids were determined as described in paper III of this series [8].

The author wishes to express his sincere gratitude to Professor Erik Larsson for his kind interest in this work. A grant from *Matematisk-naturvetenskapliga Fakulteten* is gratefully acknowledged.

REFERENCES

1. Stefl, A. *Über Bernsteinsäure und ihre Homologen* (Diss.) München 1914.
2. Eberson, L. *Acta Chem. Scand.* **13** (1959) 40.
3. Dox, A. W. *J. Am. Chem. Soc.* **47** (1925) 1471.
4. Walker, J. and Walker, A. P. *J. Chem. Soc.* **87** (1905) 961.
5. Crichton, J. *J. Chem. Soc.* **89** (1906) 929.
6. Eberson, L *Acta Chem. Scand.* **13** (1959) 203.
7. Ansell, M. F., Hickinbottom, W. J. and Holton, P. G. *J. Chem. Soc.* **1955** 349.
8. Eberson, L. *Acta Chem. Scand.* **13** (1959) 211.
9. Eberson, L. *Svensk Kem. Tidskr.* **71** (1959) 153.
10. Overberger, C. G., O'Shaughnessy, M. T. and Shalit, H. *J. Am. Chem. Soc.* **71** (1949) 2661.
11. Overberger, C. G. and Berenbaum, M. B. *J. Am. Chem. Soc.* **73** (1951) 2618.
12. Loening, K. L., Garrett, A. B. and Newman, M. S. *J. Am. Chem. Soc.* **74** (1952) 3929.

Received November 28, 1959.

ACTA CHEMICA SCANDINAVICA 14 (1960) 650–656

The Activation of Phosphoprotein Phosphatase with Inorganic Phosphate and Surfactants

BO NORBERG

Chemical central laboratory, Sabbatsbergs sjukhus, Stockholm, Sweden

In the determination of the activity of phosphoprotein phosphatase as released inorganic phosphate, Pi, which can be precipitated with calcium at pH 9, the enzyme activity is dependent upon the concentration of Pi, so that the apparent activity approaches 0 in connection with falling Pi, attains a maximum at about 0.1 mM Pi, when the substrate is 1 % phosvitin, and sinks in connection with an even moderate excess of Pi. The enzyme activity is further increased by quaternary ammonium bases such as cetyltrimethylammonium bromide and other detergents. The activation is presumed to be connected with an increased tendency to reaction in the carbinol-group of the serine residue in the substrate.

In an earlier investigation [1] it was found that precipitation of the inorganic phosphate (Pi) released by the phosphoprotein phosphatase was necessary in order to get satisfactory reproducibility and proportionality between enzyme concentration and reaction rate. In the course of subsequent work, however, a number of apparently inexplicable irregularities were observed. Thus on one day fresh liver extract gave good activity with two casein substrates (2.17 and 3.86 units per gram liver), whereas much smaller values were obtained the next day (0 and 1.17 units per gram). Experiments with phosvitin [2] also gave unexpected results, adrenal extract giving higher activity, in 5 out of 6 experiments, than liver extract, as compared with the reverse relation when casein was used as substrate [1]. Parallel measurements of activity were then carried out with casein and phosvitin as substrate, and extract of adrenal glands, erythrocytes and liver from the rat, guinea-pig, rabbit, and cat as enzyme source. With liver in these experiments a higher apparent activity was obtained with casein substrate in 11 out of 13 tests. Adrenals and blood corpuscles, on the other hand, gave higher activity with phosvitin in 10 out of 15 experiments. Since inhibition of phosphoprotein phosphatase with Pi has been shown [1,3], and since liver is richer in Pi than are red corpuscles, the irregularities might possibly be due to the occurrence of Pi. Attempts to eliminate the excess Pi by dialysis, however, resulted regularly in a loss of activity. A more careful investigation of the effect of Pi was therefore indicated.

In the subsequent experiments human erythrocytes were chiefly used as source of enzyme. In a preliminary series with rat liver, an extract in 0.1 M acetate, of pH 5.8, gave activities of between 3.26 and 4.76 units per gram, on an average 4.07 with a standard deviation of 0.056, while an aqueous extract gave 3.88—4.87 units per gram, averaging 4.35. Systematic testing with erythrocyte extract showed optimal activity at an ionic strength of 0.04. Accordingly the erythrocytes, after 3 washings with isotonic sodium chloride were hemolyzed with distilled water, after which the hemolysate was diluted to 50 mg hemoglobin per ml and ionic strength 0.2, using sodium chloride and acetate buffer, pH 5.8. Phosvitin with about 1.1 mg protein nitrogen per ml (determined on trichloroacetic acid precipitate) was used as substrate.

Measurement of the enzyme activity was performed by incubating 1 ml extract and 4 ml substrate at 38°C, then stopping the enzyme effect with trichloroacetic acid and measuring the Pi released after precipitation with calcium at pH 9[1]. Apart from this standard method two alternatives were tried: a) direct determination of Pi in the trichloroacetic acid extract according to Fiske-Subbarow and b) extraction of directly obtained phosphomolybdate complex [4]. However, these alternative methods regularly gave lower values than did the standard method, especially at the optimal initial concentration of Pi. In 84 comparisons the standard technique gave on an average 1.61 ± 0.27 (standard deviation) times greater activity than did alternative a). The apparent difference in activity is referable to the higher blank value in the alternative methods. The preliminary explanation of this might be the occurrence of an acid-labile phosphorus linkage in the substrate. In subsequent testing only the standard technique was used.

The revovery of Pi which had been added to dialysed substrate was investigated at four phosvitin concentrations. It was found that in order to get a certain blank value more Pi was required the higher the phosvitin-content. This emerges clearly from Fig. 1, where increasing addition of phosphate does not give a rising blank value until after the addition of 100 μmole/l with approx. 1 % phosvitin, and of 200 μmole/l for 2 % phosvitin.

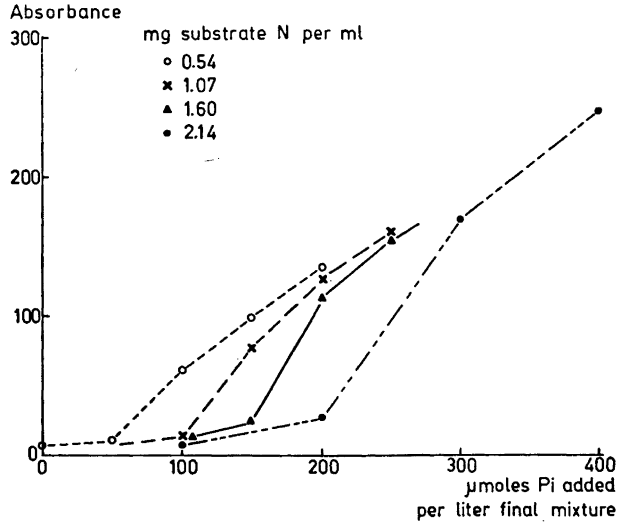

Fig. 1. Apparent inorganic phosphate (Pi, as absorbance) against total concentration of added Pi at increasing phosvitin concentrations.

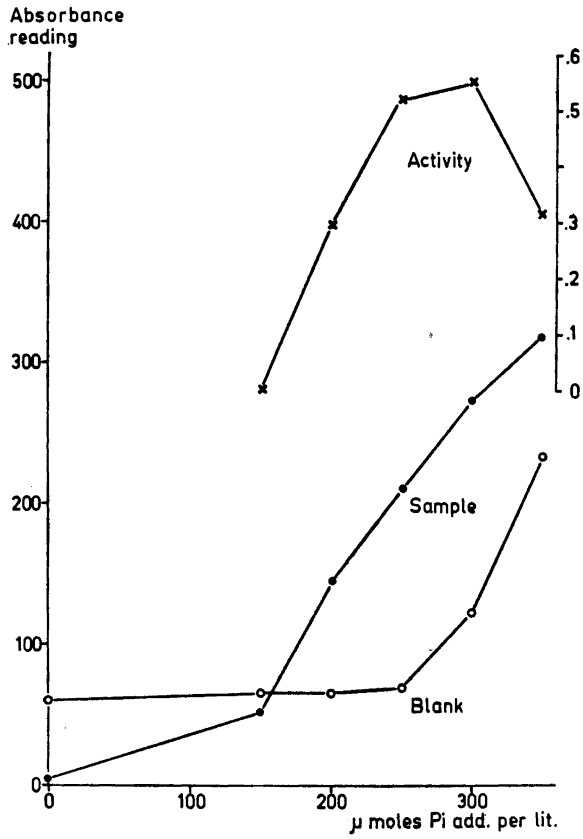

Fig. 2. Effect of addition of inorganic phosphate on blank reading and enzyme activity.

The *relation between enzyme activity and added Pi* is illustrated by the experiment shown in Fig. 2. On the addition of Pi corresponding to up to 0.15 mM no enzyme activity at all is obtained on incubation. On larger additions it increases however, reaching a maximum at the same time as the blank value begins to rise in response to a Pi-addition corresponding to a final concentration of 0.25 mM phosphate at 1.8 % phosvitin. Even slightly larger amounts of Pi result in inhibition.

In subsequent experiments 1 % phosvitin was usually used as substrate, and maximal enzyme activity was then obtained at a blank value of about 100 μM Pi. This appears from a series of experiments comprising 39 tests and reproduced in Fig. 3. When the actual concentration of Pi found in the blank value exceeds 150 μM, the activity is greatly reduced. If the initial Pi-value approaches 0, the enzyme activity disappears entirely. One must obviously determine the content of Pi in every enzyme sample and adapt the addition of Pi to the substrate so that the optimal concentration of Pi for the actual substrate is approximately reached; the interval between too little and too much is evidently very small.

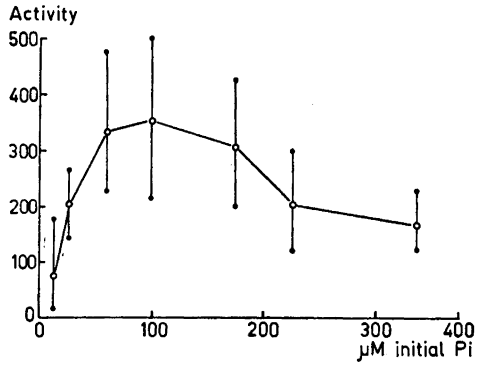

Fig. 3. Actual initial concentration of Pi at incubation and its effect on enzyme activity (mean value and range). Each mean represents 2 to 8 experiments.

Just how sensitive the enzyme reaction is to excess phosphate is shown in Fig. 4. With a rising incubation period an increasing concentration of Pi is obtained, which results in increasing inhibition; so that the apparent activity per 100 mg hemoglobin has fallen below 50 % of the highest value measured when the concentration of Pi has risen to no more than 0.4 mM. This striking sensitivity to phosphate in the incubation milieu shows clearly how difficult it is with *in vitro* experiments to throw light upon the activity of the enzyme *in vivo*.

In connection with the testing of casein as substrate, *quaternary ammonium bases* were also added in the dialysis, with the intention of preventing bacterial contamination of the substrate. This resulted, in the majority of the experiments in a not inconsiderable increase in the activity, as is exemplified in Table 1.

Similar results were also obtained with octylphenoxyethoxyethyldimethylbenzylammonium chloride ("Septin" Pharmacia, Uppsala) and cetyltrimethylammonium bromide, CTB, and also with ethylendiamine-tetraacetate, EDTA. The sensitivity of the enzyme to the phosphate ion concentration was not investigated however, and with the exception of some of these tests no attention was paid to this factor. The significance of the addition of phosphate for casein which had been dialyzed against 0.5 % CPBr with extract from fresh rat's liver as enzyme is shown in Table 2. In other casein substrates which had been dialyzed with or without addition of quaternary ammonium base an addition of phosphate corresponding to 0.12—1.05 mM Pi was required at the start of the incubation,with an average of 0.51 mM Pi for optimal effect (22 substrates with 20 mM organically bound phosphorus).

For testing with phosvitin CTB in a concentration of 10 mM was generally used. The effect of the detergent and of the addition of phosphate is shown in Table 3, which clearly indicates stimulation but also the dependence on the addition of phosphate both without and with CTB. To throw further light upon this, Table 4 shows the results of an experiment in which the phosvitin solutions were prepared directly in water and in 0.01 M CTB, respectively, without dialysis. Here the water substrate gives an apparently very low

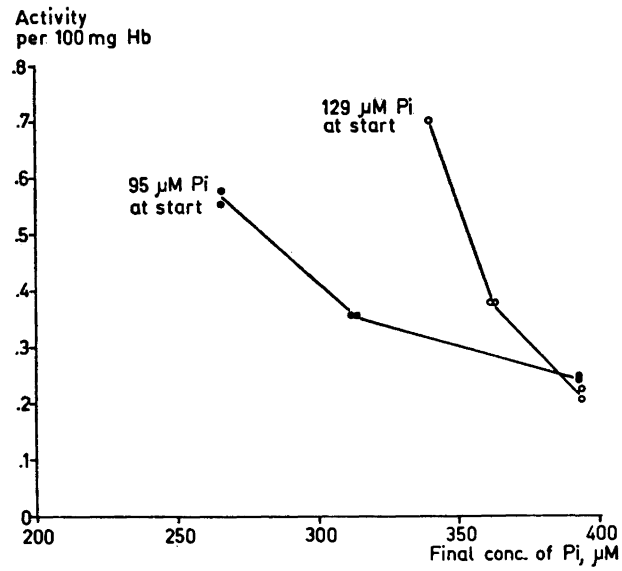

Fig. 4. Increasing inhibition of enzyme activity with rising concentration of Pi in digest. Initial concentration of Pi 95 μM (dots) and 129 μM (circles).

concentration of Pi. In the CTB-substrate, on the other hand, one obtains with increasing phosvitin-concentration a considerable Pi concentration. The optimal activity is obtained at an apparent concentration of 61 μM Pi in the substrate + 214 μM in the hemolysate. The activation, which apparently derives from the detergent, seems to be intimately connected with the Pi which is available, and at a higher substrate-concentration it turns into a faint but distinct inhibition. The interesting thing about this experiment is that the detergent appears to mobilize the labile phosphorus in the substrate, as there was no special addition of phosphate.

The results of the investigation appear to show that a certain minimal concentration of inorganic phosphorus is required to obtain the greatest possible activity with phosphoprotein phosphatase in the measuring system used. On the other hand, further inorganic phosphorus which is produced by the

Table 1. Phosphoprotein phosphatase activity of rat liver homogenate using casein dialyzed against acetate buffer with or without cetylpyridinium bromide, CPBr.

Casein No.	CPBr concentration at dialysis, mM			Maximum change, %
	None	0.26–1.3	2.6–13	
13	0.74	0.59	0.61	− 20
14	1.70	2.06	2.19	+ 29
17	0.52	3.94	4.82	+825
19	0	1.20	1.01	+∞
21	5.13	4.64		− 10
33	1.17	1.86	2.59	+120
34	10.5	11.6	—	+ 10
43	9.72	14.5	—	+ 49

Table 2. Effect of addition of inorganic phosphate, Pi, to casein dialyzed against 0.5 % CPBr on activity of liver phosphoprotein phosphatase.

Pi added corresponding to concentration at incubation, μM	Activity in units per gram of fresh liver
0	0
100	0.1
200	0.02
300	5.01
400	7.74
500	9.40
600	10.7

enzyme or which exists from the outset, results in a striking inhibition. It is evident that this phosphatase activity can be regulated with great sensitivity by Pi. A further activation through detergents also seems to occur, and the experiments appear to indicate that this effect may consist in a loosening and breaking of covalent phosphorus linkages in the substrate.

The *in vitro* system applied cannot be considered comparable with the conditions obtaining *in vivo*, but it is an interesting coincidence that at the maximal activation of the enzyme the concentration of Pi coincides with the minimal concentration required for oxidative phosphorylation in respiring mitochondria [5-7]. In contradistinction to oxidative phosphorylation and phosphorolysis [8], where Pi is included as substrate component, the activating phosphate seems rather to act as a cofactor for the phosphoprotein phosphatase, as is the case in the transformation of serine to glycine [9]. The possibility that Pi is required to overcome a solubilization effect in the precipitation of calcium phosphate [10], which is included in the analytic procedure applied, cannot be ruled out, but it seems unlikely, since the phosphate effect exists, even if more faintly, in direct phosphate analysis. On the other hand, it is not inconceivable that through dialysis the substrate loses some phosphate, which is replaced

Table 3. Effect of added KH_2PO_4 on activity of erythrocyte phosphoprotein phosphatase on phosvitin prepared in water and in 0.01 M cetyltrimetylammonium bromide, CTB.

Added Pi corresponding to final conc., μM	Activity per 100 mg hemoglobin		% increase with CTB
	1.8 % phosvitin in water	2.3 % phosvitin in 0.01 M CTB	
0	0	0	0
150	0	0.123	∞
200	0.292	0.490	68
250	0.521	0.732	40
300	0.554	0.883	60
350	0.309	0.575	86

Table 4. Comparison between activities of a hemolysate on phosvitin of different concentrations without and with 0.01 M CTB.

Substrate % phosvitin	Substrate in water		Substrate in 0.01 M CTB		% change of activity with CTB
	Apparent Pi in substrate, μM	Activity U/100 mg hemoglobin	Apparent Pi in substrate, μM	Activity U/100 mg hemoglobin	
1	7	0.128	15	0.272	+106
2	9	0.194	61	0.334	+ 72
3	13	0.199	268	0.295	+ 48
4	14	0.195	470	0.184	− 5
5	15	0.241	524	0.178	− 26
hemolysate	214				

by added Pi. A simple and rapid exchange between serine-bound phosphorus and Pi has been shown [11], and, as has been adduced above, it is conceivable that the dertegence effect is connected with a further loosening of the phosphorus-serine linkage or with activation of the carbinol-group of the serine [12]. In view of the fact that surfactants prove as a rule to be enzyme-inhibitors [13] it is also more probable that the effect here starts on the substrate; this would entail an intensification of the affinity between enzyme and substrate [14]. The inhibition of excess Pi may be a competition for the active site of the enzyme.

Acknowledgements. This investigation has been supported by the *Swedish Medical Research Council,* and by *The National Institutes of Health of the United States* (Grant H-1142) during studies at the Department of Surgical Research, Medical College of Virginia, Richmond, Va. The author is indebted to Miss Edith Andersson for devoted assistance.

REFERENCES

1. Norberg, B. *Acta Chem. Scand.* **4** (1950) 1206.
2. Mecham, D. K. and Olcott, H. S. *J. Am. Chem. Soc.* **71** (1949) 3670.
3. Singer, M. F. and Fruton, J. S. *J. Biol. Chem.* **299** (1957) 111.
4. Ernster, L., Zetterström, R. and Lindberg, O. *Acta Chem. Scand.* **4** (1952) 804.
5. Lardy, H. A. and Wellman, H. *J. Biol. Chem.* **195** (1952) 215.
6. Gatt, S. and Racker, E. *J. Biol. Chem.* **234** (1959) 1015, 1024.
7. Wadkins, C. L. and Lehninger, A. L. *J. Biol. Chem.* **234** (1959) 681.
8. Rowen, J. W. and Kornberg, A. *J. Biol. Chem.* **193** (1951) 497.
9. Wright, B. E. and Stadtman, T. C. *J. Biol. Chem.* **219** (1956) 863.
10. Mandl, I., Grauer, A. and Neuberg, C. *Biochim. et Biophys. Acta* **10** (1953) 540.
11. Ågren, G. *Acta Chem. Scand.* **13** (1959) 1048.
12. Koshland, D. E. and Erwin, M. Y. *J. Am. Chem. Soc.* **79** (1957) 2659.
13. Wills, E. D. *Biochem. J.* **60** (1955) 529.
14. Hughes, D. E. *Biochem. J.* **45** (1949) 325.

Received November 5, 1959.

ACTA CHEMICA SCANDINAVICA 14 (1960) 657–676

On the Crystal Structure of $W_2O_3(PO_4)_2$

PEDER KIERKEGAARD

Institute of Inorganic and Physical Chemistry, University of Stockholm, Stockholm, Sweden

$W_2O_3(PO_4)_2$ possesses a monoclinic unit cell which contains four formula units and has the dimensions

$a = (7.83 \pm 0.01)$ Å
$b = (12.48 \pm 0.02)$ Å
$c = (7.76 \pm 0.01)$ Å
$\beta = (91.9 \pm 0.1)°$
$V = 758$ Å^3

A structure is proposed with the symmetry No. 11, $P2_1/m$. The positions of the wolfram and phosphorus atoms in the unit cell were determined from the Patterson and Fourier electron density functions. The parameters of the oxygen atoms were deduced from geometrical considerations, using interatomic distances from previoulsy determined structures. The arrangement arrived at may be considered as an idealized structure that should be slightly distorted in order to give an explanation of the very weak reflexions with k = odd.

In $W_2O_3(PO_4)_2$, there are WO_6 octahedra joined by PO_4 tetrahedra giving a three-dimensional arrangement, the groups being joined in such a way that, firstly, every WO_6 octahedron is linked to four PO_4 tetrahedra and one WO_6 octahedron and, secondly, every PO_4 tetrahedron is linked to four WO_6 octahedra.

During the course of crystal structure studies at this Institute on phosphorus-oxygen compounds of molybdenum and wolfram, reports have been published on the structures of the phases WOP_2O_7[1] and $Mo(OH)_3PO_4$[2]. According to Schulz [3], the WO_3-P_2O_5 system contains, in addition to the former compounds, a phase of the composition 2 WO_3·P_2O_5 which is insoluble in water, acids and dilute ammonia and slowly soluble in hot dilute sodium hydroxide. In solutions of 2 WO_3·P_2O_5, only orthophosphate ion could be proved — diphosphate or polyphosphate ions were not found.

This article will describe investigations on the structure of 2 WO_3.P_2O_5.

PREPARATION OF THE CRYSTALS

A viscous, colourless solution of WO_3 (10 g) in concentrated (14.5 M) H_3PO_4 (25 ml) was prepared at about 220°C. The solution was heated at about 475°C for several hours,

after which crystals satisfactory for X-ray work were obtained (the method according to Schulz [3]). After cooling, the crystals were washed with hot water and dried in air. Under the microscope, they were seen to be colourless rods.

Analysis. A sample was fused with sodium potassium carbonate in a platinum crucible and the cake was dissolved in boiling water. From an ammoniacal solution, the *phosphorus* was precipitated (according to Kolthoff and Sandell [4]) with a magnesium solution. The precipitate was filtered off, washed with water, dissolved in hot 1 M HNO_3 and from this solution the phosphorus was finally precipitated with ammonium molybdate and weighed as $(NH_4)_3PO_4 \cdot 12\ MoO_3$. The amount of *wolfram* in the filtrate — made neutral — was determined gravimetrically by precipitation with mercury(I)nitrate according to Cumming and Kay [5] and weighing, after ignition, as WO_3. The methods of analysis were tested carefully on samples with known compositions and the errors were found to be very low.

The *density* of the crystals was determined from the apparent loss of weight in benzene.

	Calculated for $2\ WO_3 \cdot P_2O_5$	Found	
% WO_3	75.56	76.3	76.5
% P_2O_5	23.44	23.3	23.5
Density	5.30	5.02 ±	0.01

The density is calculated for 4 formula units per cell.

UNIT CELL AND SPACE GROUP

From rotation and Weissenberg photographs (*hk*0—*hk*4; *h*0*l*—*h*6*l*, 0*kl*—4*kl*), taken with CuK radiation, of small crystals of different shapes (one needle about 0.1 mm in length and about 0.04 mm in diameter rotated around the needle axis, [010], and one cube-like body with an edge of only about 0.06 mm rotated around [100] and [001]), it was concluded that the crystals are monoclinic and that the dimensions of the unit cell are about 7.7_7 Å, 12.5_3 Å, 7.8_3 Å and that the monoclinic angle is about 91°.

The reflections were recorded photographically using the multiple film technique and the relative intensities were estimated visually by comparison with an intensity scale obtained by photographing a reflection with different exposure times. The F^2 values were then calculated using the nomograms given by Lu[6]. No correction was applied for the absorption.

More accurate values for the unit cell dimensions were calculated from a powder photograph taken with strictly monochromatized Cu$K\alpha_1$ radiation in a focusing camera of Guinier type. KCl was used as an internal standard (see Table 1, p. 671).

$$a = (\ 7.83 \pm 0.01)\ \text{Å} \qquad \beta = (91.9 \pm 0.1)^\circ$$
$$b = (12.48 \pm 0.02)\ \text{Å} \qquad V = 758\ \text{Å}^3$$
$$c = (\ 7.76 \pm 0.01)\ \text{Å}$$

The value (5.02) found for the density gives $3.8 \approx 4$ formula units in the unit cell.

The reflections with k = odd are very weak but the only ones systematically absent are

$$0k0 \text{ with } k = \text{odd}$$

This is characteristic of the space groups No. 4 $P2_1$ and No. 11 $P2_1/m$. The absence of the piezo-electric effect is consistent with the latter space group and the investigation was started by examining whether the structure was consistent with this space-group with the higher symmetry.

In No. 11 $P2_1/m$, the following point positions are possible

2(*a*):000; $0\frac{1}{2}0$; 2(*b*): $\frac{1}{2}00$; $\frac{1}{2}\frac{1}{2}0$; 2(*c*): $00\frac{1}{2}$; $0\frac{1}{2}\frac{1}{2}$;
2(*d*): $\frac{1}{2}0\frac{1}{2}$; $\frac{1}{2}\frac{1}{2}\frac{1}{2}$; 2(*e*): $\pm(x\frac{1}{4}z)$;
4(*f*): $\pm(xyz)$; $\pm(x,\frac{1}{2}-y,z)$

POSITIONS OF THE WOLFRAM AND PHOSPHORUS (P_1) ATOMS

Patterson projections. In order to find the eight wolfram positions, the three Patterson projections *P*(*uvp*), *P*(*pvw*) and *P*(*upw*) were calculated (Figs. 1 and 2).

The eight wolfram atoms in the unit cell must occupy either two fourfold positions ($2 \times 4(f)$) or combinations of the twofold positions and the fourfold position or four of the twofold positions. Now, if the wolfram atoms occupy any twofold position 2(*a*)—(*e*), we will get this as a special case of the general point position 4(*f*). Therefore, we will start the examination assuming that the eight wolfram atoms occupy point positions 4(*f*).

In the point position 4(*f*), the interatomic vectors are:

$\pm[2x$	$2y$	$2z]$ weight 1
$\pm[2x$	$\frac{1}{2}$	$2z]$ » 2
$\pm[0$	$2y-\frac{1}{2}$	$0]$ » 2

By comparing this table with *P*(*uvp*) in Fig. 1, we see that at $u = 0$ there is (besides the origin maximum) only one high maximum at $v = \frac{1}{2}$, and thus we find that the *y*-coordinates will be ≈ 0 or 1/4. Now, in *P*(*uvp*) there are also pronounced peaks at $v = 1/4$ (A and B in Fig. 1). These maxima certainly correspond to W—W vectors and the position at $v = 1/4$ will exclude the possibility that all of the wolfram atoms have the same *y* coordinate. Thus we conclude that the *y*-coordinates of the wolfram atoms are 0 and 1/4, which will give

4 W_1 in 4(*f*) with $x = x_1$ $y \approx 0$ $z = z_1$
2 W_2 in 2(*e*) » $x = x_2$ $y = 1/4$ $z = z_2$

The W—W distances would then be

$\pm[0$	$\frac{1}{2}$	$0]$	weight 2
$\pm[2x_1$	$1/4 \pm 1/4$	$2z_1]$	» 2
$\pm[2x_2$	$\frac{1}{2}$	$2z_2]$	» 1
$\pm[x_1 \pm x_2$	$\pm 1/4$	$z_1 \pm z_2]$	» 2

Now in *P*(*uvp*) and *P*(*pvw*) (Fig. 1), we see that all peaks at $v = 0$ are nearly identical with the maxima at $v = \frac{1}{2}$. This is not in agreement with the

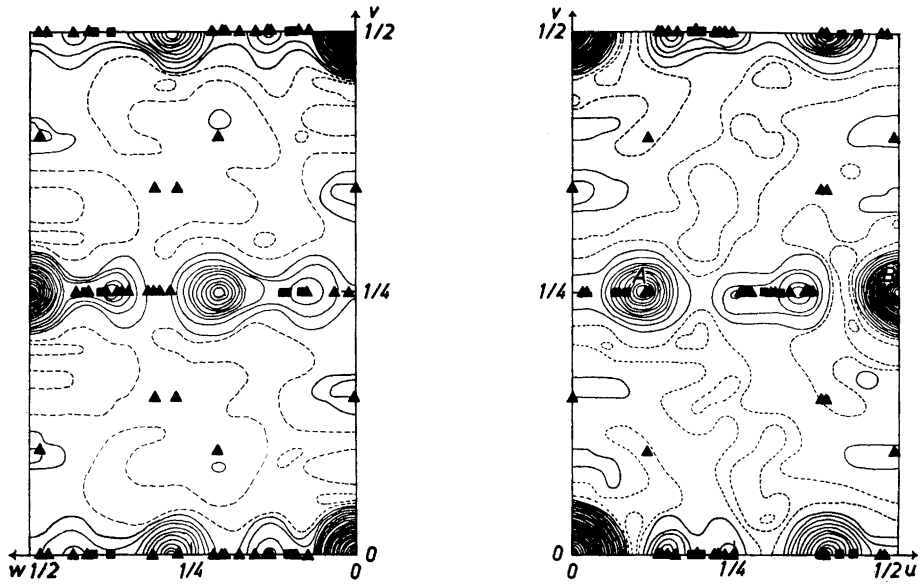

Fig. 1. The Patterson projections *P(uvp)* and *P(pvw)*. The W—P (■) and W—O (▲) vectors have been indicated for the final structure. Dashed lines indicate negative values.

table above. The only way to explain this is that the remaining two wolfram atoms (W_3) are situated in the point position 2(*e*) with $x \approx -x_2$ and $z \approx -z_2$. Thus we have

$$2\ W_3 \text{ in } 2(e) \text{ with } x \approx -x_2 \quad y = 1/4 \quad z \approx -z_2$$

The W—W distances would then be:

$\pm[0$	$\frac{1}{2}$	$0]$ weight 4
$\pm[2x_1$	$1/4 \pm 1/4$	$2z_1]$ » 2
$\pm[2x_2$	$1/4 \pm 1/4$	$2z_2]$ » 2
$\pm[x_1 \pm x_2$	$\pm 1/4$	$z_1 \pm z_2]$ » 4

The Patterson projection on the *uw* plane should therefore show (besides the origin maximum) the following maxima

I	$\pm[2x_1$,	$2z_1]$	weight 4
II	$\pm[2x_2$,	$2z_2]$	» 4
III	$\pm[x_1 + x_2$,	$z_1 + z_2]$	» 8
IV	$\pm[x_1 - x_2$,	$z_1 - z_2]$	» 8

There are two high peaks in *P(upw)* at $u = 0.39_0$, $w = 0.27_4$ (C in Fig. 2) and at $u = 0.61_4$, $w = 0.31_2$ (D in Fig. 2) and, in addition, two peaks at

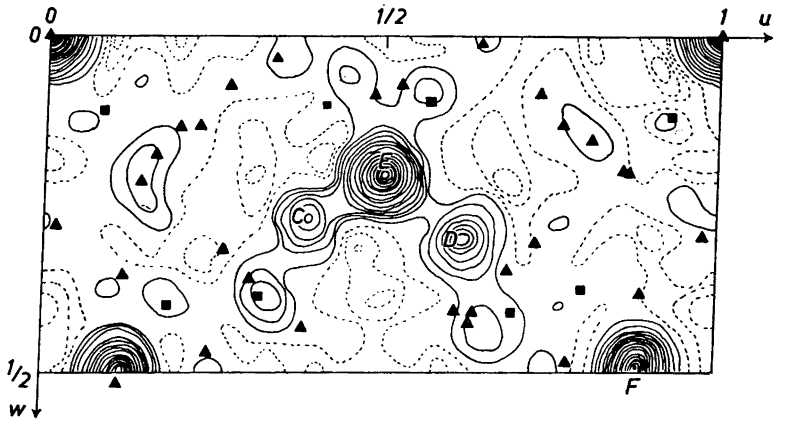

Fig. 2. The Patterson projection $P(upw)$. The positions of the vectors for the final structure have been marked as in Fig. 1. For the largest maxima (00) and (10), only every second contour has been marked. Dashed lines indicate negative values.

$u = 0.49_7$, $w = 0.20_7$ (E in Fig. 2) and at $u = 0.88_8$, $w = 0.48_1$ (F in Fig. 2) whose heights are about double those of the former. (All maxima have been located by the interpolation table given by Booth [7]). These maxima certainly correspond to the W—W wectors I—IV so the peak C must correspond to the vector I or II (and D to II or I) and the peak E to the vector III or IV (and F to IV or III). By calculating the vectors I—IV for all possible combinations of x_1, x_2, z_1 and z_2, the following two alternatives were found for the arrangement of the wolfram atoms (it is sufficient to consider the range $0 \leq x \leq \frac{1}{2}$, $0 \leq z \leq 1$):

Alt. a:	4 W_1 in	4(*f*) with	$x \approx 0.19_5$	$y \approx 0$	$z \approx 0.13_7$
	2 W_2 »	2(*e*) »	$x \approx 0.31_0$	$y = 1/4$	$z \approx 0.65_3$
	2 W_3 »	2(*e*) »	$x \approx 0.69_0$	$y = 1/4$	$z \approx 0.34_7$
Alt. b:	4 W_1 »	4(*f*) »	$x \approx 0.31_0$	$y \approx 0$	$z \approx 0.65_3$
	2 W_2 »	2(*e*) »	$x \approx 0.19_5$	$y = 1/4$	$z \approx 0.13_7$
	2 W_3 »	2(*e*) »	$x \approx 0.80_5$	$y = 1/4$	$z \approx 0.86_3$

These two sets of wolfram parameters will give identical W—W vectors and the values obtained checked well with the Patterson projections $P(uvp)$ and $P(pvw)$ in Fig. 1. The positions and heights of the maxima in these projections were found to be in good agreement with the claculated W—W-distances. The parameters obtained from $P(upw)$ should, however, be more accurate since, in the calculation of this projection, more F^2 values were used and since less overlapping occurs in this projection.

Thus, from the Patterson projections we get two alternatives for the arrangement of the wolfram atoms and, at this state of the investigation, it was not possible to rule out one of them.

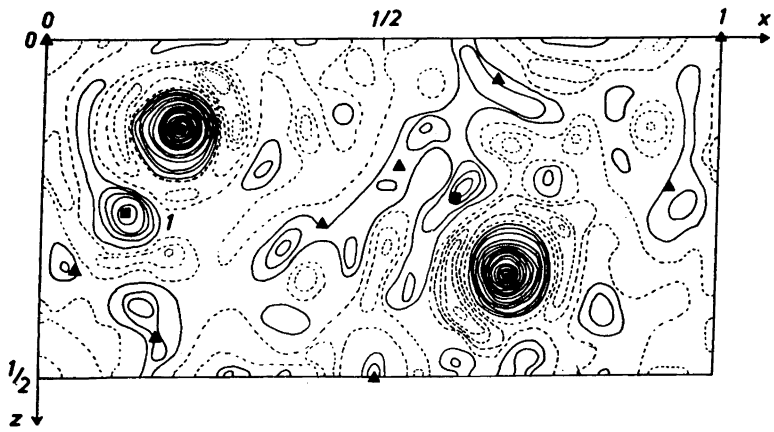

Fig. 3. Electron density projected on the *xz* plane. The final positions of the phosphorus (■) and oxygen atoms (▲) have been marked. In the wolfram peaks, only every second contour has been marked. Dashed lines indicate negative values.

However, in the Patterson projections there are, in addition to peaks corresponding to the W—W vectors, several lower maxima which perhaps could be ascribed to the W—P distances. In the unit cell, there are eight phosphorus atoms situated in 4(*f*) and/or 2(*a*)—(*e*) and consequently the corresponding possible W—P distances were calculated. From the positions of the lower maxima, situated at $v = 0$, 1/4 and ½ in Fig. 1, 2(*a*)—(*d*) can at once be ruled out as possible point positions if the peaks are real and correspond to W—P vectors. Thus the phosphorus atoms must occupy 2(*e*) and/or 4(*f*). It should now be possible to obtain possible alternatives for the parameters of the phosphorus atoms but it would be preferable to determine their sites from a map giving electron density since such a map gives maxima that are sharper and less in number than those of the corresponding vector map.

Electron density projection. For a compound of this type, the electron density projections can easily be calculated since the signs of all the F_{hkl} values can be determined from the contributions given by the wolfram atoms because of their dominant scattering factors. In this case, the projection $\varrho(xpz)$ should be favourable for calculation since the two alternatives for the wolfram arrangement will give equal F_{h0l} values. In this way, $\varrho(xpz)$ was calculated and the result is given in Fig. 3. We see that the wolfram atoms are clearly indicated at $x = 0.195$, $z = 0.137$ and at $x = 0.690$, $z = 0.347$.

Besides the very high wolfram maxima in the calculated electron density projection, there is a lower peak in ϱ (xpz) at $x = 0.12$, $z = 0.26$ (1 in Fig. 3). If this lower peak is a real maximum, and not a false one due to diffraction effects or inadequate intensity data, it is possible that two overlapping phosphorus atoms could give a peak of this height. As mentioned above, the point positions 2(*e*) and 4(*f*) were possible for the arrangement of the phosphorus atoms. If four phosphorus atoms are situated in 4(*f*), two phosphorus maxima overlap

in the *xz* projection of the electron density. Since the projection $\varrho(xpz)$ really shows one rather distinct maximum (1 in Fig. 3), which could be ascribed to overlapping phosphorus atoms, we may conclude that this peak, if real, gives the position of four phosphorus atoms (4 P_1) in 4(*f*). Now all W—P_1 distances were calculated and the lower maxima in the Patterson projections were compared with the W—P_1 vectors. From Fig. 1, we see that most of the lower peaks outside $v = \pm 1/4$ are situated in or close to the planes $v = 0$ and $\frac{1}{2}$. From this we immediately obtain $y_{P_1} \approx 0$ and thus we may conclude

$$4\ P_1 \text{ in } 4(f) \text{ with } x \approx 0.12 \qquad y \approx 0 \qquad z \approx 0.26$$

For the arrangement of the wolfram atoms we have already found two possible sets of parameters (see p. 661) and consequently we obtain two alternatives for the W—P vectors

$$\left.\begin{aligned} u &= \pm (0.195 \pm 0.12) \\ w &= \pm (0.137 \pm 0.26) \end{aligned}\right\} \quad \begin{aligned} v &= 0 \text{ and } \tfrac{1}{2} \text{ if alt. a} \\ &= 1/4 \text{ and } 3/4 \text{ if alt. b} \end{aligned}$$

$$\left.\begin{aligned} u &= \pm (0.310 \pm 0.12) \\ w &= \pm (0.653 \pm 0.26) \end{aligned}\right\} \quad \begin{aligned} v &= 1/4 \text{ and } 3/4 \text{ if alt. a} \\ &= 0 \text{ and } \tfrac{1}{2} \text{ if alt. b} \end{aligned}$$

Thus it should be possible, from the positions of the maxima corresponding to the vectors above, to decide which alternative for the wolfram coordinates is the correct one. The vectors were therefore compared with $P(uvp)$ and $P(pvw)$ in Fig. 1 and it was found that the two alternatives seemed to be about equally plausible, even if the agreement might be a little better for b than for a.

Three-dimensional Patterson calculations. By introducing three dimensional Patterson calculations, it should, however, be possible to decide which of the two sets gives the correct wolfram position in the unit cell. Therefore $P(u0w)$ and $P(u1/4w)$ were calculated using all reflexions (975) obtained with Cu*K* radiation. In order to obtain more reflexions and in this way reduce the cutting-off effects, trials were also made with Mo*K* radiation but it was found that these experiments gave no additional information. However, the data obtained with Cu*K* radiation should be sufficient, even if it would have been advantageous to get reflexions with higher *h* and *l* values than nine which was the highest index in these directions obtained with Cu*K* radiation. The results are given in Fig. 4 ($P(u0w)$) and Fig. 5 ($P(u1/4w)$).

In $P(u0w)$ there are, besides the maxima due to W—W vectors, two maxima at $w = 0.19_2$, $w = 0.41_0$ (1 in Fig. 4) and at $u = 0.56_1$, $w = 0.09_2$ (2 in Fig. 4). In $P(u1/4w)$ there are also, besides the high "wolfram" peaks, two maxima at $u = 0.32_3$, $w = 0.38_5$ (3 in Fig. 5) and at $u = 0.92_9$, $w = 0.11_9$ (4 in Fig. 5). All these maxima certainly correspond to the W—P_1 wectors given above since the positions and heights of the peaks are in good agreement with calculated data and, moreover, from the position of the peaks 1 and 2 at $v = 0$ (and 3 and 4 at $v = 1/4$) we obtain immediately that the alternative b will give the correct position of the wolfram atoms. Thus we may conclude (the values are weighted means of the parameters found in the calculated functions):

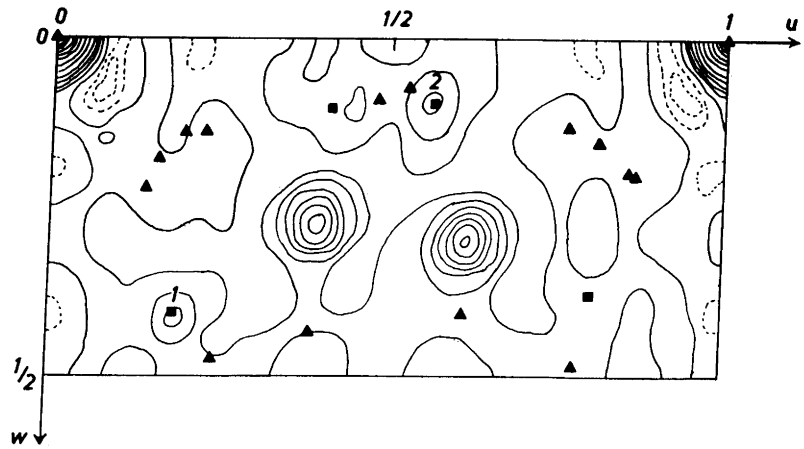

Fig. 4. The Patterson function $P(u0w)$. The positions of the vectors for the final structure have been marked as in Fig. 1. For the maxima at (00) and (10), only every second contour has been marked. Dashed lines indicate negative values.

4 W_1	in	$P2_1/m$	4(f)	with	$x = 0.310$	$y = 0$	$z = 0.653$
2 W_2	»	»	2(e)	»	$x = 0.195$	$y = 1/4$	$z = 0.137$
2 W_3	»	»	2(e)	»	$x = 0.805$	$y = 1/4$	$z = 0.863$
4 P_1	»	»	4(f)	»	$x = 0.12$	$y = 0$	$z = 0.25$

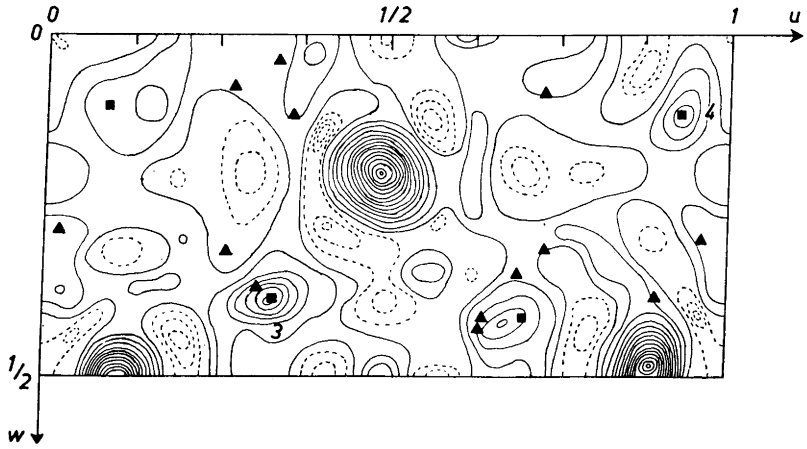

Fig. 5. The Patterson function $P(u1/4w)$. The positions of the vectors for the final structure have been marked as in Fig. 1. For the two largest maxima, only every second contour has been marked. Dashed lines indicate negative values.

Using these parameters, W—P_1 distances were calculated and these vectors have been indicated in Figs. 1 and 2. The agreement between observed and calculated data is quite good thus indicating that the coordinate values are reasonably correct.

The remaining maxima in the Patterson functions and electron density projection may correspond to W—P and W—O vectors or phosphorus and oxygen atom positions but, at this stage of the investigation, they were not considered since these peaks are about the same height as the false maxima.

POSITIONS OF THE OXYGEN ATOMS

General remarks. The light oxygen atoms do not make any appreciable contribution to the intensities of the reflections and their positions had thus to be found from considerations of the interatomic distances. The following assumptions were made:

1. The W—O distance was assumed to be not less than that found [8-10] in WO_3 and related compounds, *i.e.* 1.8_5 Å.

2. Each phosphorus atom was assumed to be surrounded by four oxygen atoms giving a tetrahedron with the bond lengths within the limits: P—O = 1.4_5 — 1.6_5 Å and O—O = 2.4_8 — 2.6_8 Å (these distances are limits for those published [11-13]).

3. The distance between two oxygen atoms not belonging to the same PO_4-group was assumed to be not less than 2.6_0 Å.

With these assumptions, the space free for oxygen atoms will be deduced as follows.

There are two symmetry planes in the unit cell at $y = \pm 1/4$. If an oxygen atom is not situated exactly in a symmetry plane, it must be at a distance of at least 1.3_0 Å (1.2_4 Å if belonging to the same PO_4-group) from it. Accordingly, the y coordinates of the atoms should be either $y = 1/4$ and $y = 3/4$ or within the limits $-0.14_5 \leq y \leq 0.14_5$, $0.35_5 \leq y \leq 0.64_5$ Moreover there are eight symmetry centres per unit cell (the point positions $2(a)-(d)$). If an oxygen does not coincide with a symmetry centre, it must be situated outside a sphere of radius 1.3_0 Å around it. For the same reason, spheres of radii 2.6_0 Å around each oxygen atom which has been located and of radii 1.8_5 Å around each wolfram atom enclose domains forbidden for the centres of other oxygen atoms.

Positions of the oxygen atoms around the phosphorus atoms (P_1). The four phosphorus atoms, the positions of which have been found above, are surrounded by four wolfram atoms at the distances: P_1-W_2; $W_2-2\,P_1 = 3.2_9$ Å; P_1-W_3, $W_3-2\,P_1 = 3.2_9$ Å; $P_1-2\,W_1$, $W_1-2\,P_1 = 3.4_2$ Å, 3.4_7 Å. The angles, W—P—W, between the phosphorus and the four neighbouring wolfram atoms are 104°, 101°, 100° and 143°. Now it seems very probable that the four oxygen atoms around the phosphorus atom P_1 will be strongly attracted by the wolfram atoms and, with the assumptions made above and from the calculated angles and W—P_1 distances, we see that it is possible for all oxygen atoms belonging to the same PO_4 tetrahedron to be in contact with four different wolfram atoms. Assuming this, which seems to be very probable, the following coordinates are obtained

4 O_1	in	$P2_1/m$	4(f)	with	$x = 0.20$	$y = 0.10_0$	$z = 0.14$
4 O_2	»	»	»	»	$x = 0.20$	$y = 0.90_0$	$z = 0.14$
4 O_3	»	»	»	»	$x = 0.17$	$y = 0$	$z = 0.44$
4 O_4	»	»	»	»	$x = 0.93$	$y = 0$	$z = 0.22$

Positions of the oxygen atoms O_5 and O_6. In this structure, the wolfram atoms are situated in pairs, W_1-W_1 and W_2-W_3, with the distances 3.8_7 Å or 3.6_6 Å. Now, in several oxygen compounds of wolfram, a similar value, about 3.75 Å, has been found [8,9,14] for the distances between wolfram atoms joined by oxygen atoms. It seems therefore very probable that the wolfram atoms mentioned above are also joined in the same way; *i.e.* by oxygen atoms. Assuming this, the parameters of the oxygen atoms O_5 and O_6 would be

2 O_5	in	$P2_1/m$	2(d)	with	$x = \frac{1}{2}$	$y = 0$	$z = \frac{1}{2}$
2 O_6	»	»	2(e)	»	$x = 0$	$y = 1/4$	$z = 0$

Positions of the oxygen atoms O_7-O_{14}. For the remaining 24 oxygen atoms in the unit cell we note, as before for the oxygen atoms O_1-O_6, that they must be strongly attracted by the wolfram atoms and, consequently, should be situated as close to them as possible. Now we have found contacts W—3 O and if all of the remaining 24 oxygen atoms are in contact with wolfram, we obtain the coordination W—6 O. A higher coordination number is excluded since spatial reasons will prevent the latter O atoms being in contact with more than one W atom. Now, in most of the oxygen compounds of wolfram the same coordination number has been reported [9,14,15] and thus, it seems very reasonable that the coordination W—6 O also occurs in $2WO_3 \cdot P_2O_5$. We must therefore investigate the possibility that all of the remaining oxygen atoms in the unit cell are in contact with wolfram. Now, the wolfram atoms W_2 and W_3 are situated in the symmetry planes ($y = \pm 1/4$) and each of them is in contact with three oxygen atoms (O_1, O_2 and O_6). Two of these oxygen atoms (O_1 and O_2) are situated outside the symmetry planes and, with the assumptions made above (see p. 665), we get immediately that the only possibility for obtaining the coordination W_2—6 O and W_3—6 O is with 12 oxygen atoms in the point position 2(e). Reasonable interatomic distances were only obtained assuming:

2 O_7	in	$P2_1/m$	2(e)	with	$x = 0.05$	$y = 1/4$	$z = 0.34$
2 O_8	»	»	»	»	$x = 0.95$	$y = 1/4$	$z = 0.66$
2 O_9	»	»	»	»	$x = 0.42$	$y = 1/4$	$z = 0.27$
2 O_{10}	»	»	»	»	$x = 0.58$	$y = 1/4$	$z = 0.73$
2 O_{11}	»	»	»	»	$x = 0.67$	$y = 1/4$	$z = 0.06$
2 O_{12}	»	»	»	»	$x = 0.33$	$y = 1/4$	$z = 0.94$

From the positions given above for the oxygen atoms O_3, O_4 and O_5 — which atoms are in contact with the wolfram atoms W_1 and situated in the same planes ($y = 0$ and $\frac{1}{2}$) — we obtain at once that the only possibility for obtaining the coordination W_1—6 O is if the remaining twelve oxygen atoms

are situated in the point position 4(*f*). It is now easy to calculate the coordinates of those atoms so that reasonable O—O and W—O distances are obtained. Thus we get

4 O_{13}	in	$P2_1/m$	4(*f*)	with	$x = 0.47$	$y = 0$	$z = 0.83$
4 O_{14}	»	»	»	»	$x = 0.31$	$y = 0.15_0$	$z = 0.65$
4 O_{15}	»	»	»	»	$x = 0.31$	$y = 0.85_0$	$z = 0.65$

POSITIONS OF PHOSPHORUS ATOMS P_2 AND P_3

Now when the positions of all oxygen atoms have been determined, the parameters of the four remaining phosphorus atoms should be obtainable. It was assumed above that the coordination figure around the phosphorus atoms is a tetrahedron. Thus it should be possible using the known oxygen positions to find the remaining phosphorus positions so that each of these atoms will be surrounded by four oxygen atoms in a tetrahedral arrangement and with the P—O distances within the limits assumed above (p. 665).

Since a PO_4-group has not a centre of symmetry as would be required in 2(*a*)—(*d*), the four phosphorus atoms must occupy the positions 4(*f*) or 2 × 2(*e*). Now, in the Patterson projections in Fig. 1, we see that most of the maxima are situated at $v = 0$, 1/4 and ½ and from this we conclude that, if the phosphorus atoms are situated in 4(*f*), the *y*-coordinate ≈ 0. Otherwise, we would have pronounced peaks due to W—P vectors outside these planes. As a matter of fact, the low maxima situated outside the planes ($v = 0$, 1/4 and ½) were found to correspond to W—O vectors (see p. 670). However, at $y = 0$ through the unit cell, there are only two tetrahedral interstices of the kind described above *viz.* those coinciding with the positions of the phosphorus atoms P_1. Thus the remaining four phosphorus atoms must be situated in the symmetry planes ($y = \pm 1/4$), *i.e.* in the position 2(*e*). The *x* and *z* coordinates of these phosphorus atoms — situated with $y = 1/4$ — are easy to determine since there are also in this section through the unit cell only two possible phosphorus positions. Thus we obtain

2 P_2	in	$P2_1/m$	2(*e*)	with	$x = 0.61$	$y = 1/4$	$z = 0.26$
2 P_3	»	»	»	»	$x = 0.39$	$y = 1/4$	$z = 0.74$

REFINEMENT OF THE PARAMETERS

The parameters found above will only give an idealized structure since the weak reflections with odd *k* remain unexplained. The appearance of these reflections could be explained by assuming a distortion of the structure in such a way that some or all of the atoms are displaced from the positions given above. A refinement of the structure was therefore started.

In order to eliminate the diffraction effects as much as possible and get more reliable *x* and *z* coordinates for the phosphorus atoms, the wolfram atoms were subtracted from the Fourier image in Fig. 3. The structure factors were then corrected by an exponential factor, $e^{-0.28 \sin^2 \Theta}$, obtained in the

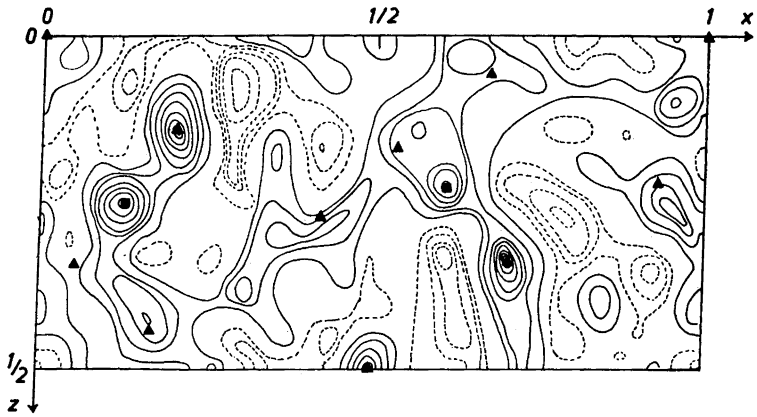

Fig. 6. Electron density projected on the *xz* plane with the wolfram atoms subtracted. The final positions of the phosphorus and oxygen atoms have been indicated as in Fig. 3. Dashed lines indicate negative values.

ordinary way for the determination of temperature factors. From Fig. 6, which shows this new electron density projection, we see the phosphorus atoms P_1 at $x = 0.11_8$, $z = 0.25_4$ and $P_2 + P_3$ at $x = 0.60_6$, $z = 0.23_7$. The four overlapping oxygen atoms are also clearly indicated at $x = 0.20$, $z = 0.15$ (O_1 and O_2) and at $x = 0.70$, $z = 0.34$ (O_{14} and O_{15}). The positions of these peaks are in good agreement with the corresponding parameters given above except for the *z*-parameter of the phosphorus atoms P_2 and P_3 which should be changed from 0.26 to 0.23 according to this new electron density projection. The positions of the oxygen atoms, belonging to the tetrahedra around P_2 P_3, consequently had to be shifted a little in order to get reasonable P—O distances. It is remarkable that most of the remaining maxima — although rather diffuse and about the same heigh as the false maxima — were found to coincide fairly well with oxygen positions. However, by means of this calculation, it was not possible to obtain any deviations which could explain the double *b* axis even if the maximum formed by the overlapping atoms P_2 and P_3 is a little elongated, indicating perhaps that x_{P_2} and z_{P_2} not are exactly equal to $\bar{x}_{P_2}$ or $\bar{z}_{P_2}$ as assumed above. An attempt to solve the structure by trial and error methods assuming a displacement of these phosphorus atoms and of the surrounding oxygen atoms was however, without success.

It was thought that three-dimensional Patterson calculations would perhaps solve the problem. Such calculations were therefore performed, firstly, in order to discover any deviation from the space group considered and, secondly, to investigate displacements like those proposed above for P_2 and P_3 or distortions produced when some of the atoms are not situated exactly in the planes $y = 0$ or $1/4$ ($\frac{1}{2}$ or $3/4$) as obtained — except in the case of the oxygen atoms O_1, O_2, O_{14} and O_{15} — in the structure investigation given above. However, all these attempts to perform a complete structure determination were in vain. Neither was it possible to solve the structure by calculating the generalized

Patterson functions using the observed values of $|F_{h1l}|^2$, $|F_{h3l}|^2$ or $|F_{h5l}|^2$. This was probably due to the poor experimental intensity material from the weak zones, *h*1*l*, *h*3*l* and *h*5*l*, obtained with Cu*K* radiation (as to Mo*K* radiation *cf.* p. 663).

Finally, attempts to solve the structure by trial and error methods assuming that the weak reflections were due to the displacement of the wolfram and some of the oxygen atoms were also without success.

FINAL STRUCTURE PROPOSITION

Thus, in spite of all the attempts to make a complete structure determination, we must restrict our conclusions to the following idealized structure for 2 $WO_3.P_2O_5$.

Space group No. 11 $P2_1/m$. Four formula units per unit cell. Atomic positions:

		x	*y*	*z*
4 W_1	in 4(*f*)	0.310 ± 0.003	0	0.653 ± 0.003
2 W_2	in 2(*e*)	0.195 ± 0.003	1/4	0.137 ± 0.003
2 W_3	in 2(*e*)	0.805 ± 0.003	1/4	0.863 ± 0.003
4 P_1	in 4(*f*)	0.12	0	0.25
2 P_2	in 2(*e*)	0.61	1/4	0.24
2 P_3	in 2(*e*)	0.39	1/4	0.76
4 O_1	in 4(*f*)	0.20	0.10_0	0.14
4 O_2	in 4(*f*)	0.20	0.90_0	0.14
4 O_3	in 4(*f*)	0.17	0	0.44
4 O_4	in 4(*f*)	0.93	0	0.22
2 O_5	in 2(*d*)	½	0	½
2 O_6	in 2(*e*)	0	1/4	0
2 O_7	in 2(*e*)	0.05	1/4	0.34
2 O_8	in 2(*e*)	0.95	1/4	0.66
2 O_9	in 2(*e*)	0.42	1/4	0.27
2 O_{10}	in 2(*e*)	0.58	1/4	0.73
2 O_{11}	in 2(*e*)	0.67	1/4	0.06
2 O_{12}	in 2(*e*)	0.33	1/4	0.94
4 O_{13}	in 4(*f*)	0.47	0	0.83
4 O_{14}	in 4(*f*)	0.31	0.15_0	0.65
4 O_{15}	in 4(*f*)	0.31	0.85_0	0.65

The accuracy of the parameters for the phosphorus and the oxygen atoms is estimated to be about ± 0.02. Using these parameters, all the structure factors *hk*0—*hk*4, 0*kl*—4*kl* and *h*0*l*—*h*6*l* were calculated, multiplied by the factor $e^{-0.28 \sin^2 \Theta}$ (*cf.* above) and compared with the observed ones. Some of the results are shown in Table 2 where the values for *hk*0, *h*0*l*, *h*2*l* and 0*kl* for even values of *k* have been listed. All the *observed* structure factors with odd *k* from *hk*0, 0*kl* and *h*1*l* have been listed in Table 3. As is seen from Table 2,

there is quite a good agreement between the observed and calculated data. The reliability index according to Booth (see Ref.[5], p. 101) was found to be 0.18 for *hk*0, 0.16 for *h*0*l* and 0.17 for 0*kl* (absent reflections not included) and 0.22, 0.21 and 0.22 for the same reflections calculated without the phosphorus and oxygen atoms. This shows that the structure should be essentially correct as regards the heavy atoms and also indicates that the proposed coordinates for the phosphorus and the oxygen atoms will give a better agreement between observed and calculated intensities than that obtained when the phosphorus and oxygen atoms are omitted from the calculations. The coordinates were also checked against the Patterson functions and the electron density projections. The positions of all W—P and W—O vectors have been indicated in Figs. 1, 2, 4 and 5 and the positions of the phosphorus and oxygen atoms have also been market in Figs. 3 and 6. From the figures, we see that the agreement between calculated maxima and observed peaks is fairly good, which also seems to indicate the coordinate values to be plausible.

In the structure determination described above, we have assumed that the structure is consistent with the space group $P2_1/m$ having the higher symmetry and, since nothing was found against this, the asumption may be correct. Nevertheless, it is of course possible that all or some of the atoms are arranged according to the low-symmetry space group $P2_1$ and this has also in part been considered since all calculations made for the structure determination are independent of the space group assumption. However, it does not seem possible to get any essential difference for the atom arrangement even if the space

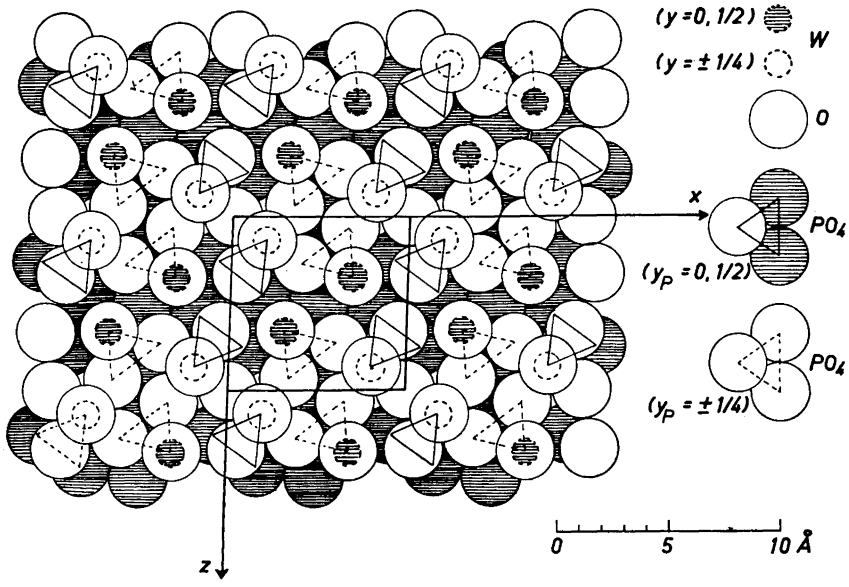

Fig. 7. Projection on the *xz* plane of the structure of $W_2O_3(PO_4)_2$.

group $P2_1$ is considered. This will perhaps increase the errors in the parameters since all of the coordinates are therefore obtained from overlapping peaks.

DESCRIPTION OF THE STRUCTURE

The structure of $2WO_3.P_2O_5$ may be described as built up of WO_6-octahedra and PO_4-tetrahedra. Every wolfram atom is in contact with four PO_4-groups and every PO_4-group with four wolfram atoms. Every wolfram atom is also in contact with one oxygen atom (O_{7-8}; O_{13}), which is bound only to this wolfram atom, and one oxygen atom (O_{5-6}) that is shared by two wolfram atoms. In this way, the crystals are built up of plane W_2O_3-groups parallel to the *xz* plane and joined by PO_4-tetrahedra so that every tetrahedron links together four W_2O_3-groups giving a threedimensional arrangement. The building principle might be expressed by the formula $W_2O_3(PO_4)_2$ and the compound should then be written according to this rather than $2WO_3 \cdot P_2O_5$. A further discussion of the structure will be given later on in a separate article.

The *xz* projection of the structure is shown in Fig. 7.

Table 1. Powder photograph of $2WO_3 \cdot P_2O_5$. Cu$K\alpha_1$-radiation. Reflections systematically absent in space group $P2_1/m$ have been omitted. KCl (a = 6.2930 Å) has been used as an internal standard.

h k l	$10^4\sin^2\Theta$ calc	$10^4\sin^2\Theta$ obs	$p F^2$ calc	I obs	*h k l*	$10^4\sin^2\Theta$ calc	$10^4\sin^2\Theta$ obs	$p F^2$ calc	I obs
1 0 0	97	96	<1	v v w	1 1 2	542	—	0	—
0 0 1	99	—	<1	—	1 3 1	545	—	0	—
1 1 0	135	—	0	—	0 2 2	547	550	5	v v w
0 1 1	137	—	0	—	0 4 0	610	607	372	v v st
0 2 0	152	—	0	—	2 2 $\bar{1}$	626	625	92	m
1 0 $\bar{1}$	189	190	12	v w	1 2 $\bar{2}$	631	—	3	—
1 0 1	202	203	10	v v w	2 2 1	652	655	122	m
1 1 $\bar{1}$	227	228	0	v v w	1 2 2	657		4	
1 1 1	240	—	0	—	1 4 0	706	697	<1	v v w
1 2 0	249	250	218	v v st	0 4 1	708	—	<1	—
0 2 1	251		242		2 3 0	731	733	0	v w
1 2 $\bar{1}$	341	342	196	v v st	0 3 2	737	—	0	—
1 2 1	354	355	192	st	2 0 $\bar{2}$	756	—	3	—
2 0 0	388	385	114	m	2 1 $\bar{2}$	794	—	0	—
0 0 2	394	396	52	w	1 4 $\bar{1}$	799	799	11	v v w
2 1 0	426	426	0	v v w	2 0 2	808	—	2	—
0 1 2	432	—	0	—	1 4 1	812	813	8	v v w
1 3 0	440	—	0	—	2 3 $\bar{1}$	816	—	0	—
0 3 1	442	—	0	—	1 3 $\bar{2}$	821	—	0	—
2 0 $\bar{1}$	473	476	147	v v st	2 3 1	842	—	0	—
1 0 $\bar{2}$	478		172		2 1 2	846	—	0	—
2 0 1	499	498	110	st	1 3 2	847	847	0	v v w
1 0 2	504	505	213	m	3 0 0	872	—	>1	—
2 1 $\bar{1}$	511	—	0	—	0 0 3	877	—	>1	—
1 1 $\bar{2}$	516	—	0	—	2 2 $\bar{2}$	908	910	212	st
2 1 1	537	540	0	v v w	3 1 0	910	—	0	—
1 3 $\bar{1}$	539		0		0 1 3	925	—	0	—
2 2 0	540		<1		3 0 $\bar{1}$	951	953	42	w

Table 2. Comparison between calculated and observed structure factors from Weissenberg photographs of $W_2O_3(PO_4)_2$. Cu*K*-radiation.

h k l	*F* calc	|*F*| obs	*h k l*	*F* calc	|*F*| obs	*h k l*	*F* calc	|*F*| obs	*h k l*	*F* cals	|*F*| obs
3 0 9	16	—	7 0 5	15	—	9 0 $\bar{3}$	21	26	0 2 9	20	33
2 0 9	26	28	6 0 5	— 89	72				1 2 $\bar{9}$	42	51
1 0 9	11	9	5 0 5	— 22	18	9 0 2	— 69	79	2 2 $\bar{9}$	— 16	—
0 0 9	31	24	4 0 5	78	70	8 0 2	4	—	3 2 $\bar{9}$	— 8	9
1 0 $\bar{9}$	— 19	21	3 0 5	16	—	7 0 2	59	67	4 2 $\bar{9}$	— 11	11
2 0 $\bar{9}$	— 67	66	2 0 5	— 35	50	6 0 2	8	—			
3 0 $\bar{9}$	27	26	1 0 5	3	—	5 0 2	— 18	8	5 2 8	— 48	52
4 0 $\bar{9}$	53	47	0 0 5	— 23	24	4 0 2	11	9	4 2 8	55	46
			1 0 $\bar{5}$	— 5	7	3 0 2	— 85	95	3 2 8	23	18
5 0 8	9	—	2 0 $\bar{5}$	80	73	2 0 2	13	29	2 2 8	— 14	15
4 0 8	18	15	3 0 $\bar{5}$	12	—	1 0 2	146	118	1 2 8	7	18
3 0 8	— 45	50	4 0 $\bar{5}$	— 86	73	0 0 2	— 72	58	0 2 8	— 28	18
2 0 8	— 41	34	5 0 $\bar{5}$	— 1	—	1 0 $\bar{2}$	—131	102	1 2 $\bar{8}$	— 20	15
1 0 8	70	71	6 0 $\bar{5}$	71	64	2 0 $\bar{2}$	17	10	2 2 $\bar{8}$	50	58
0 0 8	48	45	7 0 $\bar{5}$	1	—	3 0 $\bar{2}$	65	71	3 2 $\bar{8}$	36	33
1 0 $\bar{8}$	— 53	54				4 0 $\bar{2}$	18	21	4 2 $\bar{8}$	— 69	63
2 0 $\bar{8}$	— 11	12	8 0 4	2	—	5 0 $\bar{2}$	36	35	5 2 $\bar{8}$	— 30	26
3 0 $\bar{8}$	3	—	9 0 4	23	13	6 0 $\bar{2}$	— 4	—			
4 0 $\bar{8}$	— 14	13	8 0 4	69	65	7 0 $\bar{2}$	— 68	72	6 2 7	— 12	—
5 0 $\bar{8}$	38	30	7 0 4	— 19	30	8 0 $\bar{2}$	25	26	5 2 7	3	—
6 0 $\bar{8}$	17	—	6 0 4	— 35	37	9 0 $\bar{2}$	67	55	4 2 7	— 39	33
			5 0 4	14	—				3 2 7	— 7	—
6 0 7	12	15	4 0 4	— 44	51	9 0 1	4	14	2 2 7	71	69
5 0 7	79	69	3 0 4	41	37	8 0 1	— 15	38	1 2 7	— 15	18
4 0 7	0	6	2 0 4	101	100	7 0 1	— 40	58	0 2 7	— 77	79
3 0 7	— 63	63	1 0 4	— 64	67	6 0 1	55	62	1 2 $\bar{7}$	11	15
2 0 7	— 5	—	0 0 4	— 90	96	5 0 1	73	77	2 2 $\bar{7}$	37	45
1 0 7	0	—	1 0 $\bar{4}$	57	57	4 0 1	— 97	111	3 2 $\bar{7}$	10	—
0 0 7	— 1	9	2 0 $\bar{4}$	64	78	3 0 1	— 71	72	4 2 $\bar{7}$	13	—
1 0 $\bar{7}$	59	60	3 0 $\bar{4}$	— 31	26	2 0 1	105	104	5 2 $\bar{7}$	— 7	—
2 0 $\bar{7}$	— 6	—	4 0 $\bar{4}$	— 9	—	1 0 1	32	26	6 2 $\bar{7}$	— 54	47
3 0 $\bar{7}$	— 89	79	5 0 $\bar{4}$	— 31	35	0 0 1	8	6	7 2 $\bar{7}$	5	—
4 0 $\bar{7}$	15	11	6 0 $\bar{4}$	— 60	55	1 0 $\bar{1}$	35	26			
5 0 $\bar{7}$	67	59	7 0 $\bar{4}$	50	40	2 0 $\bar{1}$	—119	90	7 2 6	26	37
6 0 $\bar{7}$	— 18	18	8 0 $\bar{4}$	68	64	3 0 $\bar{1}$	— 65	60	6 2 6	54	55
7 0 $\bar{7}$	— 12	12	9 0 $\bar{4}$	40	38	4 0 $\bar{1}$	112	107	5 2 6	— 45	43
						5 0 $\bar{1}$	61	90	4 2 6	— 59	56
7 0 6	— 38	33	9 0 3	— 2	12	6 0 $\bar{1}$	— 60	81	3 2 6	45	48
6 0 6	17	8	8 0 3	— 12	18	7 0 $\bar{1}$	— 25	38	2 2 6	19	24
5 0 6	— 5	—	7 0 3	54	67	8 0 $\bar{1}$	15	32	1 2 6	— 28	21
4 0 6	42	33	6 0 3	55	59	9 0 $\bar{1}$	— 1	—	0 2 6	22	24
3 0 6	45	57	5 0 3	— 85	100				1 2 $\bar{6}$	— 68	56
2 0 6	— 50	59	4 0 3	— 55	52	9 0 0	8	—	2 2 $\bar{6}$	— 44	47
1 0 6	— 82	89	3 0 3	107	113	8 0 0	— 75	77	3 2 $\bar{6}$	67	68
0 0 6	56	52	2 0 3	28	30	7 0 0	— 9	—	4 2 $\bar{6}$	61	56
1 0 $\bar{6}$	67	50	1 0 3	— 19	35	6 0 0	58	63	5 2 $\bar{6}$	— 51	46
2 0 $\bar{6}$	— 34	45	0 0 3	6	—	5 0 0	2	—	6 2 $\bar{6}$	— 32	28
3 0 $\bar{6}$	— 7	—	1 0 $\bar{3}$	— 55	47	4 0 0	4	—	7 2 $\bar{6}$	15	18
4 0 $\bar{6}$	7	—	2 0 $\bar{3}$	— 39	38	3 0 0	2	—	8 2 $\bar{6}$	— 3	—
5 0 $\bar{6}$	— 32	19	3 0 $\bar{3}$	128	121	2 0 0	—107	103			
6 0 $\bar{6}$	53	40	4 0 $\bar{3}$	42	42	1 0 0	— 4	17	8 2 5	— 21	10
7 0 $\bar{6}$	40	34	5 0 $\bar{3}$	— 93	77				7 2 5	42	37
8 0 $\bar{6}$	— 53	37	6 0 $\bar{3}$	— 36	36	3 2 9	56	56	6 2 5	3	—
			7 0 $\bar{3}$	41	47	2 2 9	— 24	26	5 2 5	— 10	—
8 0 5	30	26	8 0 $\bar{3}$	— 5	—	1 2 9	— 58	61	4 2 5	6	—

h k l	F calc	|F| obs	h k l	F calc	|F| obs	h k l	F calc	|F| obs	h k l	F calc	|F| obs
3 2 5	— 14	13	7 2 2	— 11	21	5 4 0	4	—	0 4 1	6	12
2 2 5	— 54	46	6 2 2	— 80	78	6 4 0	45	51	0 6 1	— 90	82
1 2 5	121	119	5 2 2	38	39	7 4 0	— 6	—	0 8 1	5	—
0 2 5	21	18	4 2 2	115	116	8 4 0	— 61	76	0 10 1	— 52	47
1 2 $\bar{5}$	—100	99	3 2 2	— 19	21	9 4 0	5	21	0 12 1	3	—
2 2 $\bar{5}$	— 9	—	2 2 2	— 89	68				0 14 1	— 48	53
3 2 $\bar{5}$	9	25	1 2 2	— 17	21	0 6 0	0	—	0 16 1	3	14
4 2 $\bar{5}$	— 2	—	0 2 $\bar{2}$	— 15	25	1 6 0	— 35	39			
5 2 $\bar{5}$	47	51	1 2 $\bar{2}$	— 12	9	2 6 0	3	—	0 4 2	— 50	40
6 2 $\bar{5}$	2	—	2 2 $\bar{2}$	103	96	3 6 0	81	85	0 6 2	— 12	24
7 2 $\bar{5}$	— 69	44	3 2 $\bar{2}$	— 36	33	4 6 0	— 6	—	0 8 2	— 42	38
8 2 $\bar{5}$	— 9	—	4 2 $\bar{2}$	—119	102	5 6 0	—117	92	0 10 2	— 8	—
			5 2 $\bar{2}$	51	54	6 6 0	12	—	0 12 2	— 31	37
8 2 4	— 19	11	6 2 $\bar{2}$	59	73	7 6 0	48	68	0 14 2	— 7	—
7 2 4	— 51	63	7 2 $\bar{2}$	— 14	30	8 6 0	— 1	—			
6 2 4	28	38	8 2 $\bar{2}$	— 14	13	9 6 0	10	—	0 4 3	4	9
5 2 4	66	69	9 2 $\bar{2}$	— 18	11				0 6 3	89	92
4 2 4	— 34	38				0 8 0	155	136	0 8 3	4	—
3 2 4	— 85	79	9 2 1	51	61	1 8 0	— 2	—	0 10 3	55	66
2 2 4	20	21	8 2 1	53	57	2 8 0	— 67	70	0 12 3	3	—
1 2 4	36	32	7 2 1	— 64	61	3 8 0	1	—	0 14 3	56	61
0 2 4	12	21	6 2 1	— 46	52	4 8 0	1	—			
1 2 $\bar{4}$	78	77	5 2 1	— 8	26	5 8 0	2	—	0 4 4	— 56	61
2 2 $\bar{4}$	— 42	33	4 2 1	— 15	37	6 8 0	44	51	0 6 4	11	23
3 2 $\bar{4}$	— 97	94	3 2 1	49	60	7 8 0	— 6	—	0 8 4	— 60	61
4 2 $\bar{4}$	47	43	2 2 1	78	74	8 8 0	— 61	67	0 10 4	7	18
5 2 $\bar{4}$	41	45	1 2 1	— 98	92				0 12 4	— 49	62
6 2 $\bar{4}$	— 26	49	0 2 1	—110	59				0 14 4	6	15
7 2 $\bar{4}$	— 31	33	1 2 $\bar{1}$	99	77	0 10 0	0	—			
8 2 $\bar{4}$	10	18	2 2 $\bar{1}$	68	45	1 10 0	— 18	26			
9 2 $\bar{4}$	— 13	—	3 2 $\bar{1}$	44	54	2 10 0	1	—	0 4 5	— 18	24
			4 2 $\bar{1}$	1	10	3 10 0	49	58	0 6 5	18	—
9 2 3	30	37	5 2 $\bar{1}$	— 5	—	4 10 0	— 3	—	0 8 5	— 17	28
8 2 3	— 57	61	6 2 $\bar{1}$	— 39	39	5 10 0	— 79	76	0 10 5	12	—
7 2 3	— 12	—	7 2 $\bar{1}$	75	77	6 10 0	7	—	0 12 5	— 14	24
6 2 3	31	42	8 2 $\bar{1}$	35	45	7 10 0	32	52	0 14 5	11	—
5 2 3	13	—	9 2 $\bar{1}$	— 64	66						
4 2 3	20	32				0 12 0	112	111	0 4 6	39	39
3 2 3	24	24	9 2 0	12	—	1 12 0	— 1	—	0 6 6	19	21
2 2 3	—111	94	8 2 0	1	—	2 12 0	— 53	67	0 8 6	41	38
1 2 3	— 54	35	7 2 0	49	61	3 12 0	1	—	0 10 6	14	26
0 2 3	92	77	6 2 0	12	—	4 12 0	1	—	0 12 5	34	33
1 2 $\bar{3}$	48	35	5 2 0	—126	117						
2 2 $\bar{3}$	— 88	80	4 2 0	— 4	18	5 12 0	1	—	0 4 7	— 1	—
3 2 $\bar{3}$	— 4	11	3 2 0	81	73	6 12 0	36	40	0 6 7	— 73	74
4 2 $\bar{3}$	— 12	—	2 2 0	3	9				0 8 7	— 1	—
5 2 $\bar{3}$	— 15	13	1 2 0	— 33	33	0 14 0	0	—	0 10 7	— 50	52
6 2 $\bar{3}$	53	56	0 2 0	0	—	1 14 0	— 20	30			
7 2 $\bar{3}$	10	—				2 14 0	1	—	0 4 8	39	42
8 2 $\bar{3}$	— 67	76	0 4 0	193	136	3 14 0	51	54	0 6 8	— 24	21
9 2 $\bar{3}$	— 11	18	1 4 0	— 2	7	4 14 0	— 4	—	0 8 8	38	42
			2 4 0	— 64	56						
9 2 2	— 14	12	3 4 0	0	—	0 16 0	74	50	0 4 9	27	21
8 2 2	26	32	4 4 0	— 3	9	1 16 0	— 1	—	0 6 9	19	25

The distances between neighbouring atoms in $W_2O_3(PO_4)_2$ will be (in Å):

W_1-O_3	;	O_3-W_1			$=1.9_3$		
W_1-O_4	;	O_4-W_1			$=2.1_6$		
W_1-O_5	;	$O_5-2\ W_1$			$=1.9_3$		
W_1-O_{13}	;	$O_{13}-W_1$			$=1.8_5$		
W_1-O_{14}	;	$O_{14}-W_1$			$=1.8_7$		
W_1-O_{15}	;	$O_{15}-W_1$			$=1.8_7$		
$W_2-2_1O=W_3-2\ O_2$	;	O_1-W_2	;	O_2-W_3	$=1.8_7$		
$W_2-O_6=W_3-O_6$	;	O_6-W_2	;	O_6-W_3	$=1.8_3$		
$W_2-O_7=W_3-O_8$	;	O_7-W_2	;	O_8-W_3	$=1.9_5$		
$W_2-O_9=W_3-O_{10}$	;	O_9-W_2	;	$O_{10}-W_3$	$=2.0_1$		
$W_2-O_{12}=W_3-O_{11}$	;	$O_{12}-W_2$	;	$O_{11}-W_3$	$=1.9_1$		
P_1-O_1	;	O_1-P_1			$=1.6_5$		
P_1-O_2	;	O_2-P_1			$=1.6_5$		
P_1-O_3	;	O_3-P_1			$=1.5_1$		
P_1-O_4	;	O_4-P_1			$=1.5_1$		
$P_2-O_9=P_3-O_{10}$	;	O_9-P_2	;	$O_{10}-P_3$	$=1.5_1$		
$P_2-O_{11}=P_3-O_{12}$	;	$O_{11}-P_2$	;	$O_{12}-P_3$	$=1.4_9$		
$P_2-2\ O_{15}=P_3-2\ O_{14}$	;	$O_{15}-P_2$	;	$O_{14}-P_3$	$=1.6_5$		
O_1-O_2					$=2.5_0$		
$O_1-O_3=O_2-O_3$	;	O_3-O_1	;	O_3-O_2	$=2.6_6$		
$O_1-O_4=O_2-O_4$	;	O_4-O_1	;	O_4-O_2	$=2.5_5$		
$O_1-O_6=O_2-O_6$	;	$O_6-2\ O_1$	;	$O_6-2\ O_2$	$=2.6_5$		
$O_1-O_7=O_2-O_8$	;	$O_7-2\ O_1$	;	$O_8-2\ O_2$	$=2.7_2$		
$O_1-O_9=O_2-O_{10}$	;	$O_9-2\ O_1$	;	$O_{10}-2\ O_2$	$=2.7_2$		
$O_1-O_{12}=O_2-O_{11}$	;	$O_{12}-2\ O_1$	;	$O_{11}-2\ O_2$	$=2.6_6$		
$O_1-O_{13}=O_2-O_{14}$	;	$O_{13}-O_1$	;	$O_{14}-O_2$	$=2.8_7$		
O_3-O_3					$=2.8_5$		
$O_3-2\ O_4$	;	$O_4-2\ O_3$			$=2.5_0$	;	2.7_8
O_3-O_5	;	$O_5-2\ O_3$			$=2.6_1$		
$O_3-O_7=O_3-O_8$	;	$O_7-2\ O_3$	;	$O_8-2\ O_3$	$=3.3_4$		
$O_3-O_{14}=O_3-O_{15}$	;	$O_{14}-O_3$	;	$O_{15}-O_3$	$=2.6_9$		
$O_4-O_7=O_4-O_8$	;	$O_7-2\ O_4$	;	$O_8-2\ O_4$	$=3.3_8$		
O_4-O_{13}	;	$O_{13}-O_4$			$=3.1_4$		
$O_4-O_{14}=O_4-O_{15}$	;	$O_{14}-O_4$	;	$O_{15}-O_4$	$=2.8_6$		
$O_5-2\ O_{13}$	;	$O_{13}-O_5$			$=2.5_8$		
$O_5-2\ O_{14}=O_5-2\ O_{15}$	;	$O_{14}-O_5$	;	$O_{15}-O_5$	$=2.6_8$		
$O_6-O_7=O_6-O_8$	;	O_7-O_8	;	O_8-O_6	$=2.6_5$		
$O_6-O_{11}=O_6-O_{12}$	;	$O_{11}-O_6$	;	$O_{12}-O_6$	$=2.6_4$		
$O_7-O_7=O_8-O_8$					$=2.6_3$		
$O_7-O_9=O_8-O_{10}$	;	O_9-O_7	;	$O_{10}-O_8$	$=2.9_6$		
$O_9-O_{11}=O_{10}-O_{12}$	;	$O_{11}-O_9$	;	$O_{12}-O_{10}$	$=2.5_9$		
$O_9-O_{12}=O_{10}-O_{11}$	;	$O_{12}-O_9$	;	$O_{11}-O_{10}$	$=2.6_1$		
$O_9-2\ O_{13}=O_{10}-2\ O_{13}$	;	$O_{13}-O_9$	;	$O_{13}-O_{10}$	$=3.3_4$		
$O_9-2\ O_{15}=O_{10}-2\ O_{14}$	;	$O_{15}-O_9$	;	$O_{14}-O_{10}$	$=2.5_0$		
$O_{11}-O_{12}$	;	$O_{12}-O_{11}$			$=2.7_9$		

$O_{11}-2\,O_{13} = O_{12}-2\,O_{13}$; $O_{13}-O_{11}$; $O_{13}-O_{12} = 3.4_3$
$O_{11}-2\,O_{15} = O_{12}-2\,O_{14}$; $O_{15}-O_{11}$; $O_{14}-O_{12} = 2.5_7$
$O_{13}-O_{13}$ $= 2.6_6$
$O_{13}-O_{14} = O_{13}-O_{15}$; $O_{14}-O_{13}$; $O_{15}-O_{13} = 2.6_3$
$O_{14}-O_{14} = O_{15}-O_{15}$ $= 2.5_0$

The distances are all within the normal range showing that the lattice is also supported by O—O contacts. However, they may be in error by some tenths of an Ångström unit.

This investigation forms part of a research program on metal oxides and related compounds supported by the *Swedish Natural Science Research Council.*

Table 3. The observed structure factors with k = odd from Weissenberg photographs $hk0$, $0kl$, $h1l$, of $W_2O_3(PO_4)_2$. CuK-radiation.

$h\,k\,l$	$\lvert F\rvert$ obs	$h\,k\,l$	$\lvert F\rvert$ obs	$h\,k\,l$	$\lvert F\rvert$ obs	$h\,k\,l$	$\lvert F\rvert$ obs
0 1 $\bar{9}$	7	2 1 4	5	6 1 $\bar{2}$	14	7 5 0	16
2 1 $\bar{9}$	6	1 1 4	7	9 1 $\bar{2}$	9	8 5 0	9
4 1 $\bar{9}$	11	0 1 $\bar{4}$	14			9 5 0	7
		1 1 $\bar{4}$	8	9 1 1	5		
4 1 8	7	2 1 $\bar{4}$	6	8 1 1	6	2 7 0	19
0 1 8	8	3 1 $\bar{4}$	12	5 1 1	8		
2 1 $\bar{8}$	11	5 1 $\bar{4}$	13	4 1 1	12		
4 1 $\bar{8}$	6	8 1 $\bar{4}$	7	3 1 1	4	7 9 0	18
				2 1 1	16	8 9 0	20
4 1 7	7	5 1 3	11	1 1 $\bar{1}$	22		
0 1 7	8	4 1 3	5	4 1 $\bar{1}$	14	2 11 0	28
3 1 $\bar{7}$	12	3 1 3	10	7 1 $\bar{1}$	9		
5 1 $\bar{7}$	14	2 1 3	8	9 1 $\bar{1}$	16	2 15 0	18
7 1 $\bar{7}$	6	1 1 3	12				
		0 1 3	11	8 1 0	10	0 3 1	12
2 1 6	12	1 1 $\bar{3}$	9	6 1 0	13	0 3 2	5
1 1 6	13	2 1 $\bar{3}$	15	4 1 0	5	0 3 3	7
3 1 $\bar{6}$	13	5 1 $\bar{3}$	12	2 1 0	22	0 3 4	7
7 1 $\bar{6}$	6	6 1 $\bar{3}$	10			0 3 7	12
		7 1 $\bar{3}$	14	2 3 0	40	0 3 8	6
8 1 5	6	8 1 $\bar{3}$	11	3 3 0	10	0 3 9	6
6 1 5	7			4 3 0	6		
5 1 5	8	9 1 2	9	5 3 0	14	0 5 1	9
3 1 5	7	7 1 2	10	6 3 0	17	0 5 2	11
1 1 5	16	6 1 2	12	7 3 0	10	0 5 5	10
3 1 $\bar{5}$	7	5 1 2	6	8 3 0	10	0 5 7	17
4 1 $\bar{5}$	11	4 1 2	6				
5 1 $\bar{5}$	10	3 1 2	4	1 5 0	5		
6 1 $\bar{5}$	14	1 1 2	5	3 5 0	6	0 7 1	15
7 1 $\bar{5}$	11	0 1 2	8	4 5 0	5		
8 1 $\bar{5}$	5	1 1 $\bar{2}$	19	5 5 0	9	0 13 2	17
		2 1 $\bar{2}$	2				
8 1 4	9	3 1 $\bar{2}$	6	6 5 0	14	0 15 1	12

The author wishes to thank Professor Arne Ölander for his kind interest and Dr. Arne Magnéli and Dr. Georg Lundgren for valuable discussions in connection with this work. Thanks are also due to the *Swedish Board for Computing Machinery* for the use of the Calculator BESK for a considerable part of the calculating work involved in this investigation and to the author's colleagues at this Institute for access to the programs [16] used for calculations with BESK. The author is also indebted to Mr. Lundström for help with the measurement of the piezoelectric effect.

REFERENCES

1. Kierkegaard, P. *Acta Chem. Scand.* **12** (1958) 1715.
2. Kierkegaard, P. *Acta Chem. Scand.* **12** (1958) 1701.
3. Schulz, I. *Z. anorg. u. allgem. Chem.* **281** (1955) 99.
4. Kolthoff, I. M. and Sandell, E. B. *Textbook of Quantitative Inorganic Analysis*, 3rd Ed., New York 1952, p. 382.
5. Cumming, A. C. and Kay, S. A. *Quantitative Chemical Analysis*, 9th Ed., Edinburgh p. 367.
6. Lu, C. S. *Rev. Sci. Instr.* **14** (1943) 331.
7. Booth, A. D. *Fourier Technique in X-Ray Organic Structure Analysis*, Cambridge 1948, p. 64.
8. Bräkken, H. *Z. Krist.* **78** (1931) 484.
9. Magnéli, A. *Nova Acta Regiae Soc. Sci. Upsaliensis* (IV) **14** (1950) No. 8.
10. Andersson, G. *Acta Chem. Scand.* **7** (1953) 154.
11. Wells, A. F. *Structural Inorganic Chemistry*, 2nd Ed., Oxford 1950, p. 487.
12. MacLennan, G. and Beevers, C. A. *Acta Cryst.* **9** (1956) 187.
13. Davies, D. R. and Corbridge, D. E. C. *Acta Cryst.* **11** (1958) 315.
14. Hägg, G. and Magnéli, A. *Revs. Pure Appl. Chem. (Australia)* **4** (1954) 235.
15. Magnéli, A. *J. Inorg. & Nuclear Chem.* **2** (1956) 330.
16. Westman, S. Blomqvist, G., and Åsbrink, S. *Arkiv Kemi* **14** (1959) 535.

Received November 3, 1959.

ACTA CHEMICA SCANDINAVICA 14 (1960) 677–682

Optical Resolution of some Auxin-active Thiocarbamates

MAGNUS MATELL

Research Laboratory, Mo och Domsjö AB, Örnsköldsvik, Sweden *

Several thiocarbamyl-derivatives of α-hydroxy- and α-thiocarboxylic acids have been synthesized and some of them resolved into optical antipodes. The compounds are of plant physiological interest and some of them show stereochemical specificity. The structural requirements for auxin activity have been modified to fit the results of the present investigation.

An interesting type of racemization has been observed. The acids are stable in the solid state but are rapidly racemized on melting. The theoretical considerations involved in this phenomenon will be discussed in a subsequent paper.

A few years ago a new type of plant growth regulators was discovered by van der Kerk and coworkers [1]. The structures of the new compounds, thiocarbamic esters of glycolic acid (I) or thioglycolic acid (II) are in part identical with the well-known α-aryloxyalkanoic acids (V). The fundamental

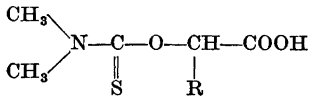

I

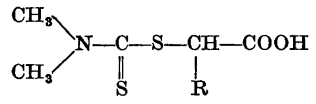

II

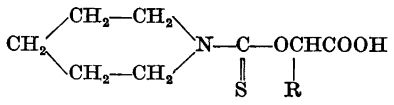

III

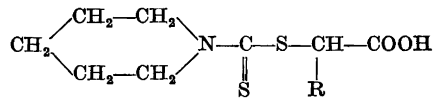

IV

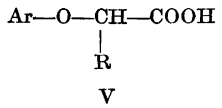

V

difference is the absence of a cyclic system in I and II; this is notable, as such a system, with a polar side-chain in a definite spatial position, has been generally accepted as a necessary requirement for auxin-activity [2].

* Present address: Berol AB, Göteborg 14, Sweden.

It has been found that the aryloxyalkanoic acids show stereochemical specificity, *i.e.* the auxin-activity is associated with a definite configuration (D—)[3-5]. It was thus of interest to find out whether the new compounds behaved in a similar way.

In the present study some acetic acids (R = H) and propionic acids (R = CH_3) of type I—IV have been synthesized. The propionic acids of type I—III have been resolved into optical antipodes. The growth-regulating properties have been studied by Professor B. Åberg. The acids of type I and II not only give typical auxin responses in several tests, but the propionic acids also show stereochemical specificity [6]. This fundamental physiological similarity between compounds of type I—II and type V may be regarded as evidence that they are all taking part in identical or similar reaction mechanisms within the cell. This view is further supported by the fact that the auxin activity is lowered when the C—O—C link in I is replaced by C—S—C. A similar lowering of the auxin activity has been found when the ether oxygen in α-(2-naphthoxy)propionic acid is replaced by sulphur [4].

In view of these facts a revision of the ring structure requirement seems to be inevitable. In fact van der Kerk *et al.* have pointed out that the C—N bond is likely to acquire some double-bond character due to internal electron shifts. A partial ring system is thus formed, with the side-chain in a distinct spatial position [1]. This argument has ben verified by infra-red investigation of a number of dithiocarbamates [7]. Some structurally similar O-alkylxanthates have been found to give physiological responses in spite of the fact that in these compounds resonance is much less probable [8]. However, the responses reported seem not to be of a true auxin type.

It is thus possible to apply the current structure-activity requirements to the new types of growth regulators, provided the ring requirement is stated as: A ring system or a partial ring system with the side-chain in a distinct spatial position.

The piperidylderivatives III and IV did not show auxin responses and the steric effects of the propionic acids were weak. For that reason the optical resolution was completed only for one of the acids.

During the optical resolution of the acids now investigated it was found that the optical activity increased very little or even decreased from one recrystallization to the next. These irregularities could be derived from thermal instability of the optically active forms. The behaviour of the antipodes was studied by melting point microscopy. In most cases new crystals were rapidly formed in the melt at a temperature just above the primary melting point. The phenomenon was not due to isomorphism, since the new crystals were optically inactive. Further, the melting points coincided with the melting points of the corresponding racemates, with which they are identical as proved by lack of melting point depression of mixtures. This racemization is rather rapid in the melt but seems not to occur in the crystalline state as the melting point is sharp and independent of the heating time. Even if racemization occurred to such a slight extent as a few percent it should be possible to detect by microscopy the formation of some eutectic melt at the lower, eutectic temperature. A racemization of this type seems not to have been reported previously. A theoretical discussion will appear in a paper to follow.

Table 1. Preparative and analytical data.

Compound				Method	Yield [a] (%)	Recryst. from	M. p.[b] (°C)	$[\alpha]_D^t$ (in acetone)	Equiv. weight	
Formula	Type	R	Isomer						Found	Calc.
$H_3)_2NCSOCH_2COOH$	I	H		A	43	BzH	115 −117.5[c]			
$_5H_{10})NCSOCH_2COOH$	III	H		A	34	aq. EtOH	118 −120.5		204.2	203.3
$H_3)_2NCSOCHCOOH$	I	CH_3	Rac.−	A	35	BzH	134 −136		175.7	177.2
			(+) −			BzH + petr.ether	122 −122.5	+75.9° (24°C)		177.2
			(−) −			» »	122 −122.5	−76.3° (20.5°C)	178.4	177.2
$_5H_{10})NCSOCHCOOH$	III	CH_3	Rac.−	A	35	aq. EtOH	145.5−147		218.8	217.3
			(+) −			BzH + petr.ether	98 − 99	+84.4° (21°C)	219.3	217.3
			(−) −			» »	98 − 99.5	−85.2° (21°C)	218.8	217.3
$H_3)_2NCS_2CH_2COOH$	II	H		B	46	Water	147 −149.3[d]			
$_5H_{10})NCS_2CH_2COOH$	IV	H		B	75	aq. EtOH	149 −151[e]		220.3	219.3
$H_3)_2NCS_2CHCOOH$	II	CH_3	Rac.−	B	38	» »	136 −138[f]		194.9	193.3
			(+) −			BzH + petr.ether		+76.9° (21°C)	195.0	193.3
			(−) −			» »	114.5−116	−77.4° (21°C)	194.4	193.3
$_5H_{10})NCS_2CHCOOH$	IV	CH_3	Rac.−	B	20	aq. EtOH	125 −130		234.1	233.4

[a] based on α-chlorocarboxylic acid in method A, on amine in method B. [b] hot stage microscope, corr. [c] Ref.[12] gives 116−117°C (uncorr.). [d] Ref.[12] gives 145−146°C (uncorr.). [e] Ref.[12] gives 145—147°C uncorr.). [f] Ref.[12] gives 134−135°C (uncorr.).

EXPERIMENTAL

The racemic acids were synthesized by one of the general procedures A and B, which are given below [9,12]. Further experimental details are found in Table 1.

Method A. An aqueous solution of 1 mole of an α-chlorocarboxylic acid is refluxed for 4 h with excess sodium carbonate in order to form the α-hydroxycarboxylic acid. After cooling to room temperature potassium hydroxide (1.2 mole) and carbon disulphide (1 mole) are added and the mixture shaken for 24−40 h. Excess carbon disulphide is removed *in vacuo* and 1 mole of chloroacetamide is added to the clear red solution. The mixture is stirred at room temperature for 6−7 h, filtered and carefully acidified with sulphuric acid. The yellow, crystalline intermediate is collected and added to an aqueous solution of 1 mole of the appropriate amine. After about 24 h at room temperature the solution is filtered and acidified with dilute hydrochloric acid to pH 2−3. The product is sometimes precipitated as an oil, which crystallizes rapidly on scratching.

Method B. Carbon disulphide (1 mole) is added to an aqueous solution of the amine (1 mole) cooled in ice. A concentrated aqueous solution of sodium hydroxide (1 mole) is added, followed by a neutralized solution of the α-chlorocarboxylic acid added at such a rate that the temperature is kept below 40°C. The solution is stirred for 2−4 h at room temperature and is then acidified. The product may come out as an oil which crystallizes on scratching.

Optical resolutions. Preliminary experiments were carried out with the following bases:

Strychnine	Quinidine	Cinchonidine
Brucine	Morphine	(+)-α-Phenethylamine
Quinine	Cinchonine	(−)-β-Phenylisopropylamine [10]

Ethyl acetate alone or with a small quantity of methanol was found to be the most effective solvent. The salt of the acid to be resolved with the optically active base was recrystallized several times. After each recrystallization a small sample of the salt was decomposed with hydrochloric acid, the acid isolated and the rotatory power determined.

Further details on the resolutions are found in Tables 2−6. The (+)-form of N-pentamethylenethiocarbamyllactic acid was obtained *via* the same base, brucine, as the (−)-form, which is notable. A small quantity of water (25 ml) was added to the mother liquor from crystallization No. 1a. A further crop of crystals was thus obtained (yield 18 %)

Table 2. Recrystallization of the (−)-β-phenyl*iso*propylamine salt of N,N-dimethylthiocarbamyllactic acid. Initial quantity: 0.07 mole.

Recryst. No.	Solvent (ml)		Yield of salt (%)	$[\alpha]_D$ of the acid
	EtAc	MeOH		
1	250	100	42.5	56.7°
2	125	75	32	65.0°
3	100	50	27	75.6°
4	80	40		74.7°
5	50	30	20	(71.4°)
6	50	30	18	74.1°

Table 3. Recrystallization of the cinchonidine salt of N,N-dimetylthiocarbamyllactic acid recovered from cryst. No. 1 and 2 above ($[\alpha]_D = -36°$). Initial quantity: 0.042 mole.

Recryst. No.	Solvent (ml)		Yield of salt (%)	$[\alpha]_D$ of the acid
	EtAc	MeOH		
1	150	15	67	−57.6°
2	150	20	49	−73.1°
3	100	18	35.5	(−70.9°)
4	75	15	22	−76.1°

Table 4. Recrystallization of the brucine salt of N-pentamethylenethiocarbamyllactic acid. Initial quantity: 0.2 mole.

Recryst. No.	EtAc (ml)	Yield of salt (%)	$[\alpha]_D$ of the acid	Note
1a	400	20	−56.7°	Cryst. No. 1 yielded two fractions; the second one (31 %) was recrystallized as No. 1b and then combined with the first one.
		31	−42.5°	
1b	200	26	−49.2°	
2	350	35	−77.1°	
3	300	31	−80.3°	
4	300	27.5	−80.3°	

Table 5. Recrystallization of the strychnine salt of N,N-dimethyldithiocarbamyllactic acid. Initial quantity: 0.075 mole.

Recryst. No.	Solvent (ml)		Yield of salt (%)	$[\alpha]_D$ of the acid
	EtAc	MeOH		
1	300	20	54	−54.4°
2	200	15	40.5	
3	175	15	25.5	−70.1°
4	150	15	21.5	−76.8°
5	125	15	12	−77.2

Table 6. Recrystallization of the (+)-β-phenyl*iso*propylamine salt of N,N-dimethyldithiocarbamyllactic acid recovered from cryst. No. 1 above. ($[\alpha]_D$ = +15°).

Recryst. No.	Solvent (ml)		Yield of salt (%)	$[\alpha]_D$ of the acid
	EtAc	MeOH		
1	160	40	44	50°
2	100	20	35	59.1°
3	75	20	30	71.7°
4	50	20	25	76.2°
5	50	20	22	75.0°
6	30	15	19.5	76.3°

and it was found to contain an almost pure (+)-acid ($[\alpha]_D$ = + 74.5°). The salt was recrystallized twice from ethyl acetate containing 2−5 % water. The rotatory power of the acid was + 81.3° and + 80.3°. Crystallization at −10°C gave a semi-solid salt but at room temperature the product was crystalline. The pure salts were analyzed, as may be seen from Table 7.

Table 7. Analyses of the pure salts.

Lactic acid derivative	Base	Formula	Calc. (%)			Found (%)		
			C	H	S	C	H	S
(+)-N,N-dimethyl-thiocarbamyl-	(−)-β-Phenyl*iso*-propylamine	$C_{15}H_{24}O_3N_2S$	57.66	7.74	10.26	57.8	7.88	10.8
(−)- —»—	Cinchonidine	$C_{25}H_{33}O_4N_3S$	63.67	7.05	6.80	63.6	7.07	6.89
(−)-N,N-Dimethyl-dithiocarbamyl-	Strychnine	$C_{27}H_{33}O_4N_3S_2$	61.45	6.30	12.15	61.2	6.51	11.6
(+)- —»—	(+)-β-Phenyl*iso*-propylamine	$C_{15}H_{24}O_2N_2S_2$	54.84	7.36	19.52	55.0	7.44	19.4
(+)-N-Penta-methylene-thiocarbamyl-	Brucine	$C_{32}H_{41}O_7N_3S$	62.83	6.76	5.24	62.6	6.90	5.07
(−)- —»—	Brucine	$C_{32}H_{41}O_7N_3S$	62.83	6.76	5.24	62.6	6.80	5.14

Thermal racemization. All melting points were determined with a hot stage microscope according to Kofler and Kofler [11]. On melting the optically active acids new crystals were usually formed in the melt. The recrystallization tendency increased in the following order: Pentamethylenethiocarbamyl $-<$Dimethylthiocarbamyl$-<$Dimethyldithiocarbamyllactic acid. Recrystallization of the last one was so rapid that the primary melting point could not be determined accurately.

After complete crystallization of the melt, the melting point of the new crystals was determined and found to be the same as the melting point of the corresponding racemic acid within 1°C. The optical activity had also disappeared and the melting point depression for a mixture of the racemate and the crystals from the melt was less than 1°C.

Acknowledgements. The author is much indebted to Dr S. Lindenfors for syntheses of the racemic acids and to Professor N. Hellström for all facilities put at the author's disposal at the Royal Agricultural College, Uppsala, where this work was started. The completion of this investigation was made possible by the benevolent support of Mo och Domsjö AB, which is gratefully acknowledged. Part of the expenses involved has been defrayed by a grant from *Jordbrukets Forskningsråd.*

REFERENCES

1. van der Kerk, G. J. M., van Raalte, M. H., Sijpesteijn, A. K. and van der Veen, R. *Nature* **176** (1955) 308.
2. Veldstra, H. *Ann. Rev. Plant Physiol* **4** (1954) 151.
3. Matell, M. *Ann. Agr. Coll. Swed.* **20**, (1953) 205.
4. Åberg, B. *Ann. Agr. Coll. Swed.* **20** (1953) 241.
5. Fredga, A. *Festschrift Arthur Stoll*, Basel 1957, p. 795.
6. Åberg, B. *Kgl. Lantbruks-högskol. Ann.* **26** (1960). *In press.*
7. Chatt, J., Duncanson, L. A. and Venanzi, L. M. *Nature* **177** (1956) 1042.
8. Fawcett, C. H., Wain, R. L. and Wightman, F. *Nature* **178** (1956) 972.
9. van der Kerk, G. J. M. *Private communication.*
10. Matell, M. *Acta Chem. Scand.* **7** (1953) 698.
11. Kofler, L. and Kofler, A. *Thermo-Mikro-Methoden*, Insbruck 1954.
12. Pluijgers, C. W. *Direct and Systemic Antifungal Action of Dithiocarbamic Acid Derivatives.* (Diss). Utrecht 1959.

Received November 5, 1959.

ACTA CHEMICA SCANDINAVICA 14 (1960) 683–688

X-Ray Investigations on Cellulose II and Mixtures of Cellulose I and II

1. A Method for Characterizing and Determining the Relative Contents of the two Modifications

JON GJØNNES and NICO NORMAN

Central Institute for Industrial Research, Oslo, Norway

The previously reported method for characterizing samples of cellulose I by width and position of the peaks in the X-ray diffractograms is extended to include cellulose II and mixtures of cellulose I and II. Procedures for determination of the ratio between the two modifications as well as an estimate of their crystalline order is described. The methods are based on measurements of intensity and width of the $(10\bar{1})$ and (002) diffraction lines of cellulose II and the (002) line of cellulose I.

In a previous paper [1] it was shown that for the same crystalline modification of cellulose, variations in the state of order is clearly reflected in a corresponding change in width of the peaks in X-ray diffractograms of the samples. This suggests the width of the predominating lines in the diffractograms to be the most convenient X-ray parameters describing the state of order in the specimens, as previously utilized [2] for samples of cellulose I. However, the height and the shape of a peak will be strongly influenced by the presence of other modifications, since in this case a superposition of peaks takes place. Mixtures of the most common cellulose modifications, I (native) and II (regenerated), frequently occur both in commercially dissolving pulps [3] and after treatment of native cellulose with swelling reagents. In the hitherto reported X-ray methods for determining the relative contents of the different cellulose modifications no attention has been paid to the state of order in the sample [3–5]. It is the purpose of the present paper to demonstrate how an estimate of crystalline order and a determination of the ratio between the two modifications may be obtained from X-ray diffractograms of the samples, where in the ratio determination the degree of order is taken into account.

The main goal has been to establish a procedure based on parameters which lend themselves readily to measurements. It has been found most practical

to employ the intensity distribution in the region $2\Theta = 18°$ to $24°$ (referred to Cu$K\alpha$ radiation) which usually displays two peaks. The one at $2\Theta = 20°$, consists of the $(10\bar{1})$-line of cellulose II and the (021)-line of cellulose I, the other at $2\Theta = 22°-22.7°$ receives contributions from the (002)-lines of both modifications. For simplicity we shall designate the two peaks $(10\bar{1})$ and (002).

As parameters sensitive to composition both the centre of gravity of the two peaks and the ratio between the peak intensities ($I_{10\bar{1}}/I_{002}$) have been tried. These two parameters display, however, essensially the same features. In the following we shall restrict ourselves to the peak intensity ratio, as this quantity is the one which is most readily measured.

The peak intensity ratio as well as the centre of gravity will to some extend depend on the degree of orientation in the specimens, particularly due to the (021)-reflection of cellulose I. Hence measurements have been carried out both on unoriented samples and pressed sheets. The latter type of specimens has been found most convenient in practice, especially for pulp samples which usually are presented as sheets. Pressed specimens have therefore mainly been used in the experiments.

EXPERIMENTAL PROCEDURE

Transmission diffractograms of the samples were prepared in the manner described previously [2]. For the pressed samples the applied pressure was about 2 500 kg/cm^2. A microphotometer curve for a mixture of cellulose I and II is reproduced in Fig. 1, displaying the cellulose II $(10\bar{1})$-peak and the composite (002)-peak. The sharp peak at 20.88° is the quartz (100) reference line. The parameters used for characterization of the samples are indicated in the figure. The angles refer to Cu$K\alpha$ radiation.

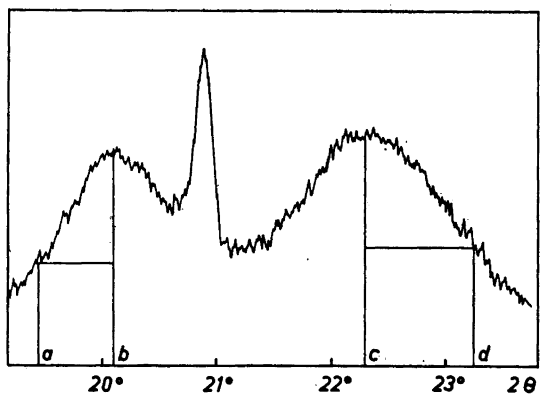

Fig. 1. Microphotometer curve for a sample consisting of a mixture of cellulose I and II. The letters a, b, c, and d indicate the $(10\bar{1})$ inner half value intersection, the $(10\bar{1})$ peak position, the (002) peak position, and the (002) outer half value intersection respectively.

RESULTS

The investigations included two different qualities of each of the two modifications I and II, a number of laboratory mixtures prepared from these samples in known ratios, and finally a series of cotton samples treated with hydrochloric acid for 1 to 4 h. The results are given in Table 1.

Table 1. Peak angles, half value intersections and peak intensity ratio $I_{10\bar{1}}/I_{002}$. Cu$K\alpha$ radiation.

Specimen	No. of samples	($10\bar{1}$), cellulose II		(002), cellulose I & II		$I_{10\bar{1}}/I_{002}$	
Cellulose II		peak angle (degrees)	half value intersection (degrees)	peak angle (degrees)	half value intersection (degrees)	pressed sheets	unoriented sample
1. Mercerized cotton treated with 39 % HCl for 3 h	4	20.08	19.46	22.16	22.72	1.20	1.16
2. Mercerized acetate grade wood pulp	4	20.16	18.73	21.59	23.14	1.26	1.23
Cellulose I							
3. Surgical cotton treated with H_2SO_4	6			22.71	23.42	0.41	0.31
4. Acetate grade wood pulp	5			22.55	23.63	0.64	0.55
Laboratory mixtures							
5. 20 % 1. 80 % 3	3	20.06	19.40	22.16	22.97	1.09	1.055
6. 40 % 1. 60 % 3	3	20.08	19.44	22.23	23.26	0.95	0.905
7. 60 % 1. 40 % 3	4	20.15	19.43	22.47	23.41	0.795	0.67
8. 80 % 1. 20 % 3	3	20.26	19.39	22.67	23.42	0.575	0.495
9. 20 % 2. 80 % 4	4	20.22	18.63	21.74	23.42	1.165	1.14
10. 40 % 2. 60 % 4	4	20.29	18.52	22.04	23.54	1.055	1.00
11. 60 % 2. 40 % 4	4	20.39	18.1	22.36	23.70	0.90	0.87
12. 80 % 2. 20 % 4	3	20.58		22.48	23.62	0.73	0.695
Surgical cotton treated with 39 % HCl							
13. for ½ h	3	20.26		22.58	23.65	0.87	0.79
14. » 1 »	3	20.14	18.6	22.37	23.59	0.97	0.93
15. » 2 »	2	20.07	19.32	22.18	23.23	1.10	1.03
16. » 3 »	2	20.06	19.49	22.19	23.07	1.10	1.08
17. » 4 »	2	20.04	19.43	22.17	23.16	1.06	1.01

From the 47 samples of specimen 1—12 the following mean standard deviations were found: Peak angles 0.035°, half value intersections: 0.03°, intensity ratio: 0.02.

DISCUSSION

The composition-sensitive parameter $I_{10\bar{1}}/I_{002}$ is seen to depend not only on the contents of cellulose I and II but also on the crystalline order in the two modifications. Corrections for the dependence on crystalline order must therefore be applied in order that the peak intensity ratio can be used for composition determination. Such a correction may apparently be based on the half widths of the peaks. For reasons which will be explained below, the angular position of the half value intersections (see Fig. 1) was preferred.

In Fig. 2 the (002) outer intersection is plotted *versus* the peak intensity ratio. As an approximation straight lines through points corresponding to the same composition with respect to crystalline modification may be considered representative for the specific composition. The plot clearly illustrates the magnitude of the corrections which have to be applied to the measured intensity ratio in order to obtain the correct value for the contents of the two cellulose modifications. For samples containing a high percentage of cellulose II the ($10\bar{1}$) half value intersection can be used as ordinate in the calibration chart. It has to be emphasized that the measurements used for constructing the calibration chart in Fig. 2 refer to samples with comparable crystalline order in the two modifications. Measurements on mixtures where the two components differ widely in crystalline order indicate that the correction method applies as well when cellulose I is the most crystalline fraction. When the cellulose II fraction is much more ordered than the cellulose I-fraction, the correction parameter appears to be measured too low, leading to an overestimation of the cellulose II-contents.

Fig. 2 has been used as a calibration chart to determine the cellulose II-contents of the acid-treated samples 13—17, leading to the values given in the first line of Table 2.

Table 2. Contents of cellulose II and estimated half widths for the samples 13—17.

Sample	13	14	15	16	17
per cent cellulose II, pressed sheets	38	50	76	79	73
per cent cellulose II, unoriented samples	39	50	72	81	72
Half width ($10\bar{1}$), degrees	>2.5	2.5	1.5	1.20	1.35
» » (002), »	<1.75	<1.75			

A plot very similar to Fig. 2 except for a translation to the left of the straight lines was obtained from peak intensity ratios measured for unoriented specimens. Cellulose II-contents for samples 13—17 determined by means of this plot and peak intensity ratios for unoriented specimens of these samples are given in the second line of Table 2.

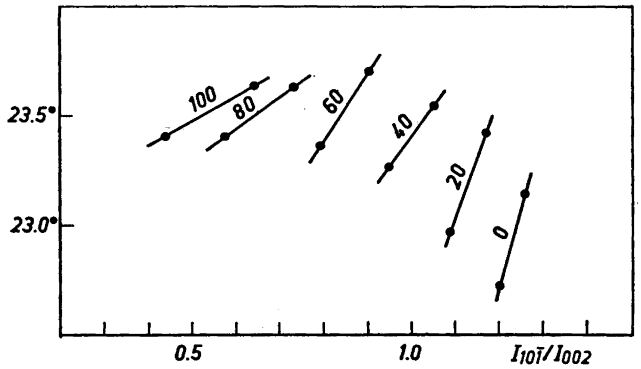

Fig. 2. The (002) outer half value intersection plotted as a function of the peak intensity ratio $I_{10\bar{1}}/I_{002}$ for series of mechanical mixtures of cellulose I and II (See Table 1). The numbers in the figure indicate the percentage of cellulose I in the samples.

An estimation of the half width of the diffraction lines for the major constituent in the mixture may also be done. From Fig. 2 it is seen that the (002) half value intersection for samples of cellulose with the same degree of crystalline order vary very slowly with composition when cellulose I is the main fraction. A similar feature is displayed by the ($10\bar{1}$) half value intersection for samples with cellulose II as the greater part. The position of the peaks, on the other hand, is very sensitive to composition. Thus it appears most reasonable to calculate half widths from the measured intersections and the peak angles corresponding to pure samples of cellulose I and II. This idea is also supported from studies of composite theoretical profiles. It is found that a neighbouring peak will produce a rather small displacement on the half value intersection at the side furtherst away from the interfering peak. For instance will the displacement vanish for the outher half value intersection of two Cauchy peaks separated through a distance equal to their half widths. This corresponds fairly to the influence of the cellulose II ($10\bar{1}$)-peak on the (002)-peak of cellulose I for samples 9—12. The influence of neighbouring peaks on the same side as the intersection may, however, be considerable. Thus it is seen that measurement of cellulose II ($10\bar{1}$) half value intersection may be worthless and in some cases even impossible due to the influence of the neighbouring (101) and ($10\bar{1}$) peaks for cellulose I (samples 11 and 12).

From such considerations the half widths given in Table 2 for samples 13—17 have been estimated, taking the cellulose II ($10\bar{1}$) and cellulose I (002) reflection angles to be 20.08° and 22.70° respectively. Due to great difference in line width between the two components in samples 13 and 14 the (002) line width for cellulose I is probably overestimated, the correct value may not be greater than the value 1.54° found for native cellulose [2]. The half widths of the ($10\bar{1}$) and (002) lines for pure cellulose II samples can be obtained in a similar way, leading to the values 1.18° and 1.13° for the acid treated samples, and 2.78° and 2.70° for the mercerized sample.

CONCLUSION

In the present paper the previously reported method [2] for characterizing samples of cellulose I by width and position of the lines in their X-ray diffractograms is extended to include cellulose II and mixtures of cellulose I and II. The application so far indicate that the method is well suited to detect and to describe structural differences between samples within the same modification as well as the ratio between cellulose I and cellulose II in mixtures. When mixtures of the two modifications are considered, a reliable line width parameter indicating the state of order in the sample can only be ascribed to the major constituent, and there will be some ambiguity for mixtures close to 50—50 %.

The interpretation of the measured widths must take into account both the lateral dimensions and crystalline order of the microfibril. At least for the mercerized samples the crystalline order seems to be the more important factor. The lateral order in cellulose II will be dealt with in a subsequent paper [6]. A thorough discussion of the hydrolysis experiments is given elsewhere [7].

The authors wish to express their thanks to Mrs. L. Bryn and Mrs. T. L. Rolfsen for their help in preparing the diffractograms. This investigation is part of a research program on the structure of cellulose carried out at the Central Institute for Industrial Research and The Norwegian Pulp and Paper Research Institute. Financial support from the *Royal Norwegian Council* for *Scientific and Industrial Research* is gratefully acknowledged. One of the authors (J.G.) is indebted to the *Norwegian Research Council* for *Science* and the *Humanities* for financial support.

REFERENCES

1. Gjønnes, J., Norman, N. and Viervoll, H. *Acta Chem. Scand.* **12** (1958) 489.
2. Gjønnes, J. and Norman, N. *Acta Chem. Scand.* **12** (1958) 2028.
3. Ellefsen, Ø., Tønnesen, B. A., Wang Lund, E and Øien, K. *Norsk Skogind.* **11** (1957) 284.
4. Rånby, B. G. *Acta Chem. Scand.* **6** (1952) 101, 116.
5. Rasch, O. A. and McCarthy, J. L. *Norsk Skogind.* **8** (1954) 329.
6. Gjønnes, J. and Norman, N. *Acta Chem. Scand.* **14** (1960) 689.
7. Ellefsen, Ø., Gjønnes, J. and Norman, N. *Norsk Skogind.* **13** (1959) 411.

Received November 11, 1959.

ACTA CHEMICA SCANDINAVICA 14 (1960) 689–691

X-Ray Investigations on Cellulose II and Mixtures of Cellulose I and II

2. Lateral Order in Cellulose II

JON GJØNNES and NICO NORMAN

Central Institute for Industrial Research, Oslo, Norway

The origin of broadening and displacement of the lines of cellulose II is discussed and related to the lateral order in the micelles.

In the preceding paper [1] a method is devised for characterizing samples of cellulose II and mixtures of cellulose I and II by suitable parameters measured from their X-ray diffractograms. It is the purpose of this paper to discuss the interpretation of the parameters describing the cellulose II-fraction, in particular their relation to the structure and lateral order of the micelles.

Table 1. Peak angles and half widths for samples of cellulose II. Cu$K\alpha$-radiation.

Specimen	($10\bar{1}$) reflection		(002) reflection	
	Peak angle (degree)	Half width (degree)	Peak angle (degree)	Half width (degree)
1. Mercerized cotton treated with 39 % HCl for 3 h	20.08	1.24	22.16	1.12
2. Mercerized acetate grade wood pulp	20.16	2.86	21.59	3.10

The half widths of the reflection ($10\bar{1}$) and (002) obtained from the measurements described in the preceding article are presented in Table 1. As is well known, the X-ray line widths depend both on the size and lattice perfection of the reflecting crystallites. It is seen, however, that the data presented in Table 1 display no differences in line width of the reflections ($10\bar{1}$) and (002)

for the same sample. This is quite remarkable, as the crystallites of cellulose II are commonly accepted to be ribbon shaped with the largest surface parallel to the (101) planes. If the particle size was the most predominant factor in determining the line widths, one would expect considerable differences in widths of the different reflections (*h0l*) from planes parallel to the chain axis, the (10$\bar{1}$)-line being by far the narrowest. We are thus led to the conclusion that at least the width of the (10$\bar{1}$) line to a great extent is determined by other factors, in particular lattice disorder. From the measured half widths *lower limits* for the particle size may be computed, leading to the values 30 Å for the mercerized pulp and 85 Å for the hydrolyzed sample.

There is additional evidence that the actual dimensions of the crystallites may be appreciably greater than the above mentioned values. Thus the line widths obtained for the mercerized pulp also seem to apply to mercerized samples prepared from cotton, which in the native state is reported to have lateral dimensions [2] of 50—80 Å. A particularly illustrative example of the alterations in line width of the cellulose II reflections resulting from chemical treatment is offered when cotton is treated with hydrochloric acid [1,3]. At first when cellulose II is formed there is a pronounced increase in line width, whereas prolonged acid treatment results in a gradual sharpening of the lines leading to a half width still lower than for the original native sample. It seems highly improbable that these variations in line width reflect changes in the lateral dimensions of the micelles. It can therefore be concluded that transformation of native cellulose into cellulose II by mercerization or acid treatment increases lattice disorder, whereas prolonged acid treatment leads to an improvement of the lattice order. This increase in lateral order is far more pronounced than what has been found in the cellulose I fraction after chemical treatments [3,4].

To obtain the best possible interplanar spacings for the investigated pure cellulose II-samples, the peak positions of the (10$\bar{1}$) and (002) reflections were corrected for the effect of overlapping peaks. The correction assumed Cauchy profile for the contribution from the neighbouring peaks and was based upon the half widths given in Table 1. The resulting interplanar spacings are tabulated in Table 2 together with (101)-spacings obtained from peak angles measured above an oblique linear background in the angular region $2\Theta = 10°-15°$.

These results which display considerable anisotropy in the variation of cell dimensions normal to the chain axis is in conformity with other measure-

Table 2. Interplanar spacings for samples of cellulose II.

Specimen	d_{101}(Å)	$d_{10\bar{1}}$(Å)	d_{002}(Å)
1. Mercerized cotton treated with 39 % HCl for 3 h	7.22	4.42	4.01
2. Mercerized acetate grade wood pulp	7.27	4.42	4.05

ments of interplanar spacing of cellulose II [6-8]. It is a general feature that the (10$\bar{1}$) spacing is found to be almost constant, even when cellulose is swelled to form hydrates. The other equatorial reflections, particularly (101) show pronounced variations. According to the currently accepted structure of cellulose II the intermolecular hydrogen bonds are mainly pointing in the direction of the [101] cell diagonal, and the structure can be described as a packing of hydrogen bonded sheets of cellulose chains parallel to the (10$\bar{1}$) planes [9].

It is thus seen that the best ordered cellulose II-samples display a shorter interchain distance within the sheets than the less ordered one, and one may tentatively suggest these differences to reveal variations in the strength and ordering of the hydrogen bonds. Another explanation is to assume the least ordered samples to possess somewhat more inter-crystalline water than the best ordered ones, leading to a greater average interchain distance.

If the above considerations hold true, it is evident that the lateral order concept outlined by Howsmon and others [10,11] and related to the strength and distribution of hydrogen bonds will be most intimately connected with the lattice disorder in the [101] direction. The (10$\bar{1}$) line width will, on the other hand, depend on disorder in the packing of the hydrogen bonded sheets. The nature of this disorder can not be stated from our present knowledge. A tempting explanation may be to assume some of the sheets to be incomplete, implying edge dislocations to be contained in the micelles and taking (101) as the slip plane. Assuming cellulose II to occur in a swollen state in the strong hydrochloric acid [3] this model can apparently account for the ordering resulting from acid treatment.

It should be pointed out, however, that the X-ray measurements within rather narrow limits give the same line width for all reflections from planes containing the chain axis, indicating the combined effect of disorder or distortion and possible particle size on the line width to be of the same magnitude in all directions normal to the chain axis.

REFERENCES

1. Gjønnes, J. and Norman, N. *Acta Chem. Scand.* **14** (1960) 683.
2. Treiber, E. *Die Chemie der Pflanzenzellwand*, Springer, Berlin, 1957, p. 164.
3. Ellefsen, Ø., Gjønnes, J. and Norman, N. *Norsk Skogind.* **13** (1959) 411.
4. Gjønnes, J. and Norman, N. *Acta Chem. Scand.* **12** (1958) 2028.
5. Immergut, E. A. and Rånby, B. G. *Ind. Eng. Chem.* **48** (1956) 1183.
6. Wellard, H. J. *J. Polymer Sci.* **13** (1954) 471.
7. Kast, W. and Schwarz, R. *Z. Elektrochem.* **56** (1952) 220.
8. Kratky, O. and Treiber, E. *Z. Elektrochem.* **55** (1951) 716.
9. Honeyman, J. *Recent Advances in the Chemistry of Cellulose and Starch*, Heywood & Company LTD, London, 1959, p. 165.
10. Ott, E. and Spurling, M. *Cellulose and Cellulose Derivatives*, Interscience, New York, 1954, p. 251.
11. Marchessault, R. H. and Howsmon, J. A. *Textile Research J.* **27** (1957) 30.

Received November 11, 1959.

ACTA CHEMICA SCANDINAVICA 14 (1960) 692–696

Estimation of the Activity Coefficients in a Liquid Mixture of Na_2CO_3 and Na_2S

ERIK ROSÉN and LARS GUNNAR SILLÉN

Department of Inorganic Chemistry, Royal Institute of Technology, Stockholm 70, Sweden

Activity coefficients for the components in Na_2CO_3—Na_2S liquid mixtures are calculated from the freezing point data of Courtois [2], assuming the solutions to be "regular solutions".

We have recently studied [1] the thermodynamics of equilibria on gasification of sodium-base pulping liquors. We then showed that under certain conditions, the condensed phase at equilibrium would be likely to consist mainly of a liquid mixture of Na_2CO_3 and Na_2S. For an accurate calculation of the equilibrium composition of the gas phase and condensed phase obtained, it was desirable to have an estimate of the activity coefficients of the two components, Na_2CO_3 (= 1) and Na_2S (= 2).

The experimental data on the system Na_2CO_3—Na_2S are rather meagre. Courtois [2] has given the temperature of solidification for various mixtures (circles in Fig. 3). He found no intermediate phase, and a simple eutectic equilibrium at 1 068°K. There is no evidence for solid solutions. From his work we may take the melting points to be 1 125°K for Na_2CO_3 and 1 453°K for Na_2S. These values are in good agreement (± 2°) with the work of other investigators [3–5].

Tammann and Oelsen [10] have also measured the freezing point curve. They give fewer points which agree well at low x_2 but deviate seriously at high x_2. We have decided to use Courtois' values; an experimental reinvestigation is however desirable.

The heat of fusion of Na_2CO_3, $L_{f1} = 7.3$ kcal mole^{-1}, has been determined calorimetrically by Ginzburg [3]. The heat of fusion for Na_2S, $L_{f2} \approx 1.6$ kcal mole^{-1}, has been estimated by Kubaschewski and Evans [6]. We have not been able to find any other data, such as heats of mixing, that could be used in the calculation of the activity coefficients of Na_2S and Na_2CO_3.

The two components Na_2S and Na_2CO_3 have the cation in common, and anions of the same charge and roughly the same "ionic radius". It seems likely that the Temkin [7] model can be used for such a mixture, as a good approximation; in this case, it means that the anions are randomly mixed. Then

$$s_1 - s_1^0 = -R \ln x_1; \qquad s_2 - s_2^0 = -R \ln x_2 \tag{1}$$

Let us now assume that the melts behave as "regular solutions" according to Hildebrand [8], which means that eqn (1) is valid and also that the molar heat of mixing is

$$\Delta H = bx_1x_2 \tag{2}$$

Then we can derive, from the definitions of partial molar quantities

$$h_1 - h_1^0 = bx_2^2; \qquad h_2 - h_2^0 = bx_1^2 \tag{3}$$

From the definitions of the thermodynamic quantities, with eqns (1) and (3) we may prove

$$RT \ln f_1 = bx_2^2; \qquad RT \ln f_2 = bx_1^2 \tag{4}$$

These are the well-known relationships for regular solutions [8]; the symbols have their usual significance: s_1, s_2 partial molar entropies; h_1, h_2 partial molar enthalpies; x_1, x_2 molar fractions ($x_1 + x_2 = 1$);

$$f_1 = a_1/x_1; \qquad f_2 = a_2/x_2 \tag{4a}$$

are activity coefficients, and the superscript "0" refers to the standard state, which is the pure liquid in our case.

The constant b is assumed to be independent of temperature, so that a knowledge of this constant makes it possible to calculate f_1 and f_2 for all temperatures. We shall now set out to calculate the constant b, using the available experimental data.

In those parts of the phase diagram where a liquid is in equilibrium with the solid substance 1, we have

$$1 \text{ (solid)} \rightleftharpoons 1 \text{ (liquid, activity } a_1); \; K = a_1; \; \Delta H = L_{f1} \tag{5}$$

where K is the equilibrium constant. By integrating van't Hoff's equation

$$\int_K^{K=1} \mathrm{d} \ln K = R^{-1} \int_T^{T_{f1}} L_{f1} \frac{\mathrm{d}T}{T^2}$$

and assuming L_{f1} to be approximately constant over the interval studied, we obtain

$$RT \ln K = -L_{f1}(1 - TT_{f1}^{-1}) \tag{6}$$

Here, T_{f1} is the melting point for pure Na_2CO_3. From eqns (4), (4a), (5), and (6) we find

$$bx_2^2 + RT \ln x_1 = -L_{f1}(1 - TT_{f1}^{-1}) \tag{7}$$

which may be rewritten in the form

$$T = (L_{f1} + bx_2^2)[L_{f1}T_{f1}^{-1} - R \ln (1 - x_2)]^{-1} \tag{8}$$

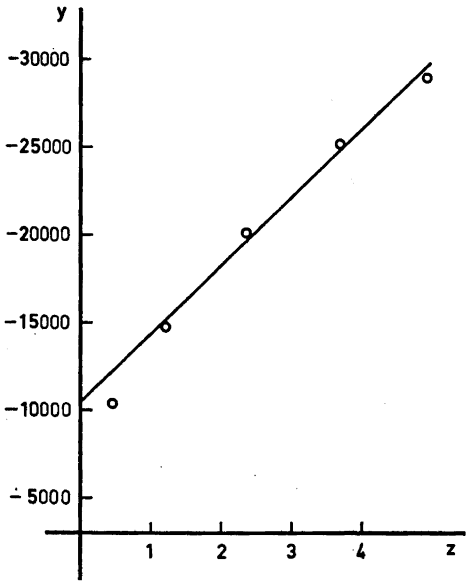

Fig. 1. Plot according to eqn (9). Circles calculated from data of Courtois [2]. Straight line calculated with $L_{fl} = 10.50$ kcal mole^{-1}, $b = 3.84$ kcal mole^{-1}.

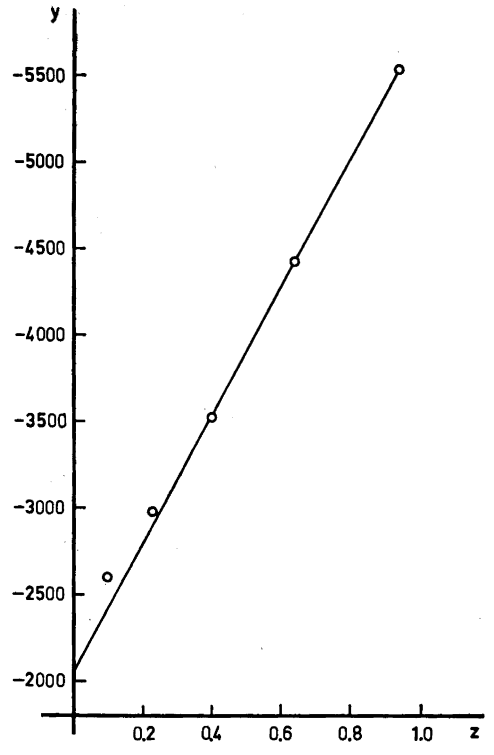

Fig. 2. Plot according to eqn (9) with indices 1 and 2 exchanged. Points calculated from data of Courtois [2]. Straight line calculated assuming $b = 3.69$ kcal mole^{-1} and $L_{f_2} = 2.05$ kcal mole^{-1}.

If b, L_{fl} and T_{fl} are known, we may thus give T as a function of x_2. In the present case, this function is approximately known[2]; in order to calculate the unknown constants b and L_{fl} we may transform eqn (7) to the form

$$L_{fl} + y + bz = 0 \qquad (9)$$

where

$$y = RTT_{fl}(T_{fl} - T)^{-1} \ln (1 - x_2)$$

$$z = T_{fl}(T_{fl} - T)^{-1} x_2^2$$

Eqn (9) has been used by Flood, Förland and Roald [9] for calculating the heat of fusion of $CaCO_3$, from the melting diagram. If y is plotted as a function of z, one will obtain b and L_{fl} from the slope and intercept of the straight line. — One may easily derive equations that are symmetrical to eqns (8) and (9), with 1 and 2 exchanged.

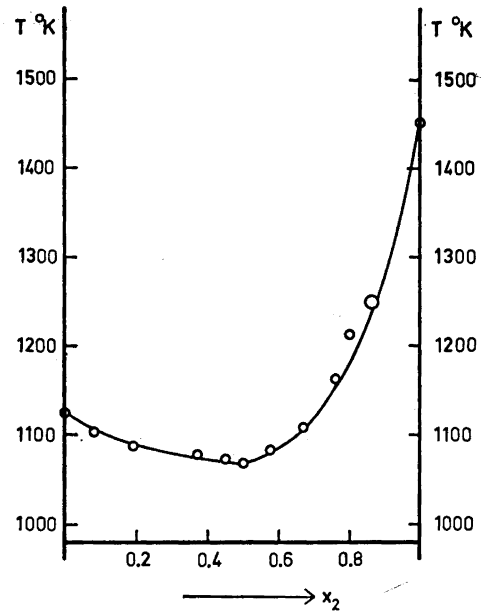

Fig. 3. Freezing point diagram $T(x_2)$ for system Na_2CO_3—Na_2S. Points: data of Courtois [2]. For the larger circle, Courtois gives a higher uncertainty than for the rest. Curve calculated from eqn (8) and its symmetrical form with 1 and 2 reversed, assuming $b = 3.75$ kcal mole^{-1}, $L_{f1} = 10.50$ kcal mole^{-1} and $L_{f2} = 2.00$ kcal mole^{-1}.

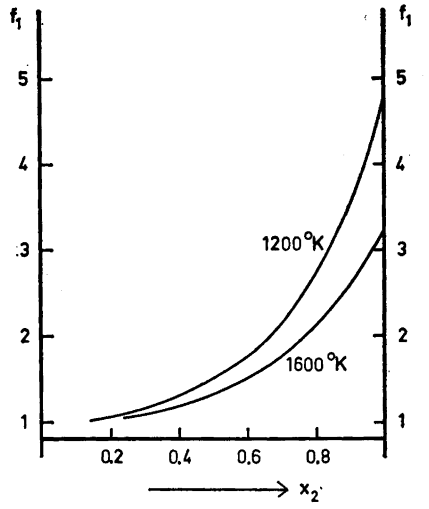

Fig. 4. Activity coefficient f_1 of Na_2CO_3 in melts Na_2CO_3—Na_2S, calculated by means of eqn (4), assuming $b = 3.75$ kcal mole^{-1}.

Fig. 1 gives a linear plot of Courtois' data according to eqn (9); it leads to the values $L_{f1} = 10.50$ kcal mole^{-1} and $b = 3.84$ kcal mole^{-1}. A plot of the symmetrical function is given in Fig. 2; it leads to $L_{f2} = 2.05$ kcal mole^{-1} and $b = 3.69$ kcal mole^{-1}.

Fig. 3 gives the diagram $T(x_2)$ calculated using eqn (8) and its symmetrical analog, with the average value of $b = 3.75$, and the value $L_{f1} = 10.50$ kcal mole^{-1}, and $L_{f2} = 2.00$ kcal mole^{-1}. Here, L_{f2} has been slightly adjusted to give a somewhat better agreement with the (anyway somewhat crude) experimental data.

The good agreement of the values for b obtained from the two independent diagrams (Figs. 1 and 2), and the good agreement of $T(x_2)$ with the experimental data indicate that the "Temkin regular solution" may be used as an approximate model for the melts of $Na_2CO_3 + Na_2S$.

Finally, Fig. 4 gives the activity coefficient, f_1, as a function of x_2, calculated by means of eqn (4), for temperatures 1 200°K and 1 600°K. For 1 200°K, values for f_1, when $x_2 > 0.8$ cannot be obtained experimentally since Na_2S(s) crystallizes.

This is part of a program supported by *Statens Tekniska Forskningsråd (Swedish Technical Research Council)*.

REFERENCES

1. Rosén, E. *Trans. Roy. Inst. Technol. Stockholm. To be published.*
2. Courtois, G. *Compt. rend.* **208** (1939) 277.
3. Ginzburg, D. M. *Zhur. Obshchei Khim.* **26** (1956) 968.
4. May, N. N. *Tappi* **35** (1952) 511.
5. Kohlmeyer, E. J. and Lohrke, G. *Z. anorg. Chem.* **281** (1955) 54.
6. Kubaschewski, O. and Evans, E. LL. *Metallurgical thermochemistry*, 3rd ed. Pergamon Press, London 1958.
7. Temkin, M. *Acta physicochim. URSS* **20** (1945) 411.
8. Hildebrand, J. *Proc. Natl. Acad. Sci. US* **13** (1927) 267; *J. Am. Chem. Soc.* **51** (1929) 66.
9. Flood, M., Förland, T. and Roald, B. *J. Am. Chem. Soc.* **71** (1949) 572.
10. Tammann, G. and Oelsen, W. *Z. anorg. Chem.* **193** (1930) 245.

Received November 17, 1959.

ACTA CHEMICA SCANDINAVICA 14 (1960) 697–710

Studies on Cobaltammines

III. Some Evidence on the Association of Thiocyanate and Perchlorate Ions with the *trans*-Dithiocyanatobis(ethylenediamine) Cobalt(III) Ion

RAGNAR LARSSON

Department of Inorganic and Physical Chemistry, Chemical Institute, University of Lund, Lund, Sweden

The extraction of *trans*-[Co $en_2(SCN)_2$]SCN from aqueous solutions of varying NH_4SCN concentration into a SCN^--saturated anion-exchange resin and also into a mixture of *cyclo*hexanone and 2-octanol has been recorded. In both cases a maximum of the extraction quotient was found at about $C_{NH_4SCN} = 1$ M. This is interpreted as an indication of outer-sphere complex formation.

By a conventional solubility method the first association constant for the reaction between the SCN^- and *trans*-Co $en_2(SCN)_2^+$ ions has been determined at an ionic strength of 3 M ($NaClO_4$). $\beta_1 = 0.3_0$ M^{-1} This result is discussed in relation to a hypothesis of competing associa- of SCN^- and ClO_4^- ions with the complex ion.

Some extraction experiments from solutions of varying concentrations of $NaClO_4$ into two different ketonic solvents are also recorded. These results are not conclusive in regard to the question of perchlorate outer-sphere complexes.

Several reports on the formation of "outer-sphere complexes" have recently been compiled [1,2]. However, some authors seem to regard this kind of association as an "ion-pairing" in the sense of Bjerrum [3]. This point of view is rather trivial in that effects thus described could equally well be accounted for by a calculation of the coefficients of activity of the reacting ions from the equation deduced by Gronwall, LaMer and Sandved [4] or by any still more elaborated treatment.

Therefore it was considered important to demonstrate the existence or non-existence of association in water between some univalent and rather large ions, where "ion-pairs" are not likely to be formed, *i.e.*, where the high order terms in the equation of Gronwall *et al.*[4] can be ignored. Such ions are even less expected to form "triple ions" in the sense of Fuoss and Kraus [5].

As such a system *trans*-Co $en_2(SCN)_2^+$ and SCN^- has been chosen.

The investigation has been pursued along two different lines. The first one has been to decide whether anionic complexes are formed or not. The second one has been an attempt to determine at least the first association constant at a constant ionic strength.

DETECTION OF ANIONIC THIOCYANATO COMPLEXES

Methods and Notations

It has been shown by Fronæus [6,7] that anionic complexes can be detected with the help of anionic exchange resins. If the distrubution of metal between the resin, saturated with the ligand, and the aqueous phase is determined as a function of the ligand concentration in the aqueous phase, then a maximum of that function will indicate the formation of at least one anionic complex.

The detailed deductions are found in the papers referred to. We emply the following symbols:

M	=	*trans*-Co $en_2(SCN)_2^+$
B	=	SCN-
C_M	=	total concn. of M in the aqueous phase
C_{MR}	=	» » » M » » resin »
C_B	=	» » » B » » aqueous »

What we intend to measure is thus $\varphi_R = \frac{C_{MR}}{C_M}$ as a function of C_B.

Likewise, if the distribution of metal between an organic solvent and the aqueous phase is determined at various C_B, then a maximum might be obtained. If it is assumed that only the neutral complex is extracted, this maximum may be taken as an indication of the existence of anionic complexes in the aqueous phase. Activity changes in the organic phase may, however, make the interpretation uncertain. It was found that a mixture of equal volumes of *cyclo*hexanone and 2-octanol was a good extracting solvent for *trans*-Co $en_2(SCN)_2$ SCN. If C_{MS} is the concentration of M extracted into this solvent mixture we will measure $\varphi_S = \frac{C_{MS}}{C_M}$ as a function of C_B.

Measurements

Chemicals used. *Trans*-Co $en_2(SCN)_2ClO_4$ was prepared from analytical grade chemicals following Werner and Bräunlich [8], with the modification that the perchlorate was precipitated by concentrated perchloric acid from the mixture of *cis*- and *trans*-isomers. It was found rather unexpectedly that the *cis*-isomer was precipitated with very great difficulty, so that an apparently pure *trans*-Co $en_2(SCN)_2ClO_4$ was obtained after two reprecipitations. The crystal mass was washed acid-free with ethanol and ether and air-dried. The absorption spectrum of the product compares rather well with the data of Shimura[9,10]. ($\lambda_{max_1} = 510$ mμ, $\varepsilon_{max_1} = 2.82 \times 10^2$; $\lambda_{max_2} = 315.5$ mμ, $\varepsilon_{max_2} = 3.08 \times 10^3$). The equivalent weight was determined alkalimetrically *via* an acid-saturated cation exchange resin; calc. 395; found 392. Cobalt content [11]: calc. 14.93 %; found 14.89 %.

Ammonium thiocyanate solutions were prepared as before [12].

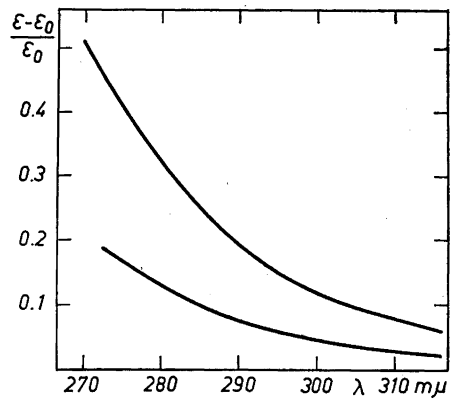

Fig. 1. The relative change of the extinction coefficients in UV. Upper curve: 0.1 mM $MClO_4$ + 1.5 M NaSCN (ε) compared to 0.1 mM $MClO_4$ + 1.5 M $NaClO_4$ (ε_0). Lower curve: 0.15 mM $MClO_4$ + 0.5 M NH_4SCN + 0.5 M NH_4ClO_4 (ε) compared to 0.15 mM $MClO_4$ + 1.0 M NH_4ClO_4 (ε_0).

The *anionc exchange resin* was Dowex 1, with 4 % cross-linking. It was converted into the thiocyanate form by percolating a concentrated solution of potassium thiocyanate, corresponding to ten times the exchange capacity, through a column of the resin, which was afterwards well rinsed with distilled water and air-dried.

*The extracting solvent. Cyclo*hexanone only cannot be used as an extracting solvent because of its tendency to dissolve large quantities of water and ammonium thiocyanate whereby the two-phase character of the system vanishes at rather low thiocyanate concentrations. Therefore an equal volume of 2-octanol was added to the *cyclo*hexanone.

Cyclohexanone (Riedel-de Haën A.-G., *rein*) was purified by distillation at 153.5—7°C and *2-octanol* (Eastman P 66) was distilled at 176—178°C.

Procedure. Ten milliliters of a solution of the composition C_B M NH_4SCN and C'_M M Co $en_2(SCN)_2ClO_4$ were shaken in glass-stoppered bottles together with w g of the resin (where w was kept about 1.5 g) or 10 ml of the extracting solvent. The shaking was performed in a water-thermostat at 20.0°C. The shaking was carried out for two days in the ion-exchange experiments and for about 15 h in the extraction experiments. In order to prevent any photochemical decomposition of the complex the bottles were coated with black paint on the outside. (The photolysis was found to be strongly dependent on the thiocyanate concentration; *cf.* Adamson and Sporer [13].) When equilibrium was reached, which was ascertained by prolonged shaking, the phases were rapidly separated — after centrifugation in the extraction case.

In the ion-exchange experiments the aqueous phase was sucked off as completely as possible with a filter-stick of large porosity. Thereafter the resin was rinsed rapidly in the shaking bottle with two 15 ml portions of distilled water, whereafter 20 ml of water were added and the bottles were subjected to renewed shaking. Then, as the thiocyanate concentration in the aqueous phase must be very low, the cobalt complex sorbed by the resin was almost quantitatively re-extracted. — This procedure was justified by preliminary experiments, that showed the elution process to be a slow one.

Determination of C_M. A photometric determination of C_M was deemed expedient in view of the intense colour of the complex. It was then necessary to investigate the influence of the thiocyanate concentration on the light absorption spectrum of the complex.

It was to be expected [14], that — regardless of the degree of outersphere complex formation — this influence would be small, especially in the region of long wave lengths. This was also found to be the case. There was no variation at constant ionic strength at the 510 mμ maximum within the limits of the experimental error. (The variation recorded in column 3 of Table 3 must be an "ionic strength effect".) Fig. 1 gives the relative change of the extinction coefficient in the ultraviolet wave length region.

The measurements of the absorption spectra and the C_M determinations in the ion-exchange experiments were made with a Beckman Model DK-1 Recording Spectrophotometer.

In the extraction experiments C_M was determined (at 510 mμ) with a Hilger Uvispek H 700 Spectrophotometer. In these experiments the aqueous phase only was examined; C_{MS} was determined by difference. In order to free the solutions from an eventual opalescence caused by small drops of the organic solvents separating at a possible temperature fall, one fifth of the solutions' volume of ethanol was added immediately after phase separation. This ethanol addition was found to cause an increase in the extinction coefficient of 3.7 %.

Determination of φ_R.

E' = optical density at the position of the 510 mμ maximum of a solution of composition C'_M M Co $en_2(SCN)_2ClO_4$ and C_B M NH_4SCN.

E_1 = optical density (at the 510 mμ maximum) of the same solution when 10 ml of it had been shaken with w g of the resin.

E_2 = optical density at the position of 316 mμ maximum of the solution obtained from the re-extraction from the resin (d = 1 cm).

We can now calculate φ_R in two different ways:

1.
$$C_{MR} = \text{const.} \frac{E'-E_1}{w} \times 10^{-2} \text{ mole/g} \quad (1)$$

$$C_M = \text{const. } E_1 \text{ mole/l} \quad (2)$$

$$\therefore \varphi_{R1} = \left(\frac{E'}{E_1} - 1\right) \times \frac{10^{-2}}{w} \text{ l g}^{-1} \quad (3)$$

2.
$$C_{MR} = \frac{10^{-2} \times 2\ E_2}{3.08 \times 10^3 \times w} \text{ mole/g} \quad (4)$$

$$C_M = C'_M - \frac{2\ E_2}{3.08 \times 10^3} \text{ mole/l} \quad (5)$$

$$\varphi_{R2} = \frac{10^{-5} \times 2\ E_2}{3.08\ w \left(C'_M - \dfrac{10^{-3} \times 2\ E_2}{3.08}\right)} \text{ l/g} \quad (6)$$

The factor 2 in eqn (4) originates from the fact that the volume of the solution which was used to extract the complex from the resin was 20 ml compared to the original solution of 10 ml. 3.08×10^3 is, as previously stated, the extinction coefficient of the complex at the second absorption maximum.

Determination of φ_S.

E_3 = optical density of the aqueous phase with an additional one fifth of ethanol measured at 510 mμ.

We easily obtain

$$C_M = \frac{6}{5} \cdot \frac{E_3}{d \times 1.037 \times \varepsilon} \quad (7)$$

where ε is the extinction coefficient at 510 mμ (2.82×10^2) and d is the thickness of the cell (2 cm).

C_{MS} is, however, not so easily obtained as there is still, in spite of the addition of 2-octanol to the *cyclo*hexanone, a tendency for the organic solvent to extract water and NH_4SCN, whereby the volume of the organic phase (V_S) increases and the volume of the aqueous phase (V) decreases. For $C_B > 1$ M it was necessary to make a correction for this effect. Defining $q = V_S/V$ and assuming that the total volume of the two phases is constant, which was apparently true, it is easily deduced

$$C_{MS} = \frac{0.5\ C'_M(1 + q) - C_M}{q} \quad (8)$$

Hence with a knowledge of q, we obtain $\varphi_S = \dfrac{C_{MS}}{C_M}$.

Determination of q. The quantity q was determined simply by shaking equal volumes of the organic solvent mixture and NH_4SCN-solutions in a stoppered, graduated centri-

Table 1. The variation of the volume quotient q with C'_B.

C'_B M	V	Vs	q	log $(q-1)$	log C'_B
2.730	4.20	5.7_9	1.38	-0.42_0	0.436
3.00	3.9_1	6.0_9	1.56	-0.25_2	0.477
3.60	2.7_6	7.2_4	2.62	0.20_0	0.556

fuge tube and reading the volumes. If C'_B means the thiocyanate concentration before equilibration, it was found (Table 1) that q could be related to C'_B by the relation

$$\log(q-1) = -2.7_4 + 5.2_5 \log C'_B \quad (9)$$

Results

The measurements are recorded in Tables 3 and 4. The values of φ_R as well as those of φ_S were reproducible within 1—2 %.

The value of C_B, the ligand concentration after equilibration, was determined as a function of C'_B, the original ligand concentration, by Volhard titration of the aqueous phase.

In the ion-exchange experiments the difference was found to be negligible; for the extraction system $C'_B - C_B$ is given in Table 2.

Table 2. The variation of C_B with C'_B.

C'_B M	C_B M	$\frac{C'_B - C_B}{V C'_B}$
0.2000	0.1916	0.0188
1.000	0.882	0.118
1.800	1.516	0.212
3.000	2.376	0.360

The values obtained in Table 2 were rationalized to the relation

$$C_B = C'_B - 0.119\ (C'_B)^{3/2} \quad (10)$$

which was used for calculation of C_B in Table 4.

From Fig. 2 it follows that the two curves describing φ_{R_1} and φ_{R_2} do not coincide, but that the former one lies always above the latter. This might be explained by assuming that part of the complex sorbed by the resin is adsorbed

Table 3. The ion-exchange measurements.

C'_M = 2.520 mM						
C_B M	w g	E' 510 mμ	E_1 510 mμ	$\varphi_{R1} \times 10^3$ l/g (eqn 3)	E_2 316 mμ	$\varphi_{R2} \times 10^3$ l/g (eqn 6)
0.400	1.49_5	0.726	0.530	2.47	0.847	1.87
1.200	1.44_5	0.732	0.533	2.58	0.778	1.74
1.500	1.51_0	0.735	0.533	2.51	0.773	1.65
2.400	1.44_5	0.739	0.579	1.91	0.640	1.37
4.80	1.58_1	0.748	0.657	0.88	0.423	0.77

C'_M = 2.111 mM						
C_B	w	E'	E_1	$\varphi_{R1} \times 10^3$	E_2	$\varphi_{R2} \times 10^3$
0.200	1.49_7	0.603	0.465	1.98	0.596	1.50
0.400	1.42_1	0.603	0.440	2.61	0.681	1.86
0.800	1.46_5	0.608	0.434	2.74	0.696	1.86
1.200	1.40_8	0.607	0.442	2.65	0.668	1.83
1.500	1.52_3	0.611	0.440	2.55	0.656	1.67
2.400	1.46_7	0.613	0.478	1.93	0.534	1.34
4.80	1.45_0	0.623	0.548	0.94	0.358	0.85

C'_M = 2.030 mM						
C_B	w	E'	E_1	$\varphi_{R1} \times 10^3$	E_2	$\varphi_{R2} \times 10^3$
0.050	1.55_4	0.582	0.519	0.78	0.360	0.84
0.100	1.51_3	0.580	0.480	1.38	0.460	1.14
0.800	1.43_1	0.585	0.420	2.75	0.657	1.86
3.60	1.47_2	0.592	0.499	1.27	0.370	0.91

on its surface only, and that this part is easily washed away and does not enter into the calculation of φ_{R_2}. The adsorption seems to be more pronounced at those ligand concentrations where the neutral complex is formed to a large part.

It is of interest to note that the φ_{R_1}-values determined for C'_M = 2.52 mM are all smaller than those corresponding to C'_M = 2.11 mM.

Although the effect is small it is concordant with the surface adsorption analogue of the criterion on complex formation by the resin put forward by Fronæus [7], *i.e.*, the smaller C'_M is the higher will φ be.

It is also observed that the functions φ_R and φ_S exhibit maxima at almost the same value of C_B. This may, however, be fortuitous; the ion-exchange measurements should be regarded as the significant ones. The position of the

Table 4. The *cyclo*hexanone-2-octanol extractions.

$C'_M = 2.111$ mM; $d = 2$ cm; $\varepsilon_{510} = 2.82 \times 10^2$						
C'_B M	C_B M	E_3	C_M mM	q	C_{MS} mM	φ_S
0.050	0.049	0.568	1.17	1	0.95	0.81
0.100	0.096	0.504	1.03	1	1.08	1.04
0.400	0.370	0.435	0.89	1	1.22	1.37
0.800	0.715	0.466	0.80	1	1.31	1.65
1.200	1.04	0.369	0.76	1.01	1.35	1.79
1.500	1.28	0.403	0.83	1.02	1.28	1.55
1.800	1.51	0.445	0.91	1.04	1.19	1.31
2.400	1.96	0.496	1.02	1.18	1.09	1.07
3.60	2.79	0.596	1.22	2.51	0.99	0.81

maximum in the extraction case may depend on factors such as the mutual solubility of the solvents and the extraction of NH_4SCN into the organic phase.

MEASUREMENTS AT CONSTANT IONIC STRENGTH

Method and Formulae

In 3 M $NaClO_4$ the solubility of Co $en_2(SCN)_2ClO_4$ is rather low (0.6 mM). Hence there is a possibility of studying the complex formation by solubility measurements.

The following notations are used

$$\beta_n = \frac{[MB_n]}{[M][B]^n} \tag{11}$$

$$X = \sum_{n=1}^{n} \beta_n [B]^n \tag{12}$$

$$L = [M][C] \tag{13}$$

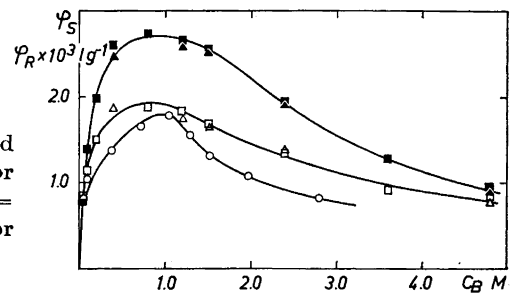

Fig. 2. The distribution quotients φ_R and φ_S. φ_{R1} for $C'_M = 2.52$ mM (▲); φ_{R1} for $C'_M = 2.11$ or 2.03 mM (■); φ_{R2} for $C'_M = 2.52$ mM (△) and φ_{R2} for $C'_M = 2.11$ or 2.03 mM (□). φ_S is marked by (○).

In eqn (13) the abbreviation C stands for ClO_4^-. This notation will be used throughout this paper. We then have

$$C_M = [M](1 + X) \tag{14}$$

From eqns (13) and (14) we obtain

$$1 + X = C_M \cdot [C]/L \tag{15}$$

Now

$$L = [M]_o[C]_o = (C_M)_o[C]_o \tag{16}$$

where indices mean $C_B = 0$. Thus

$$1 + X = \frac{C_M \cdot [C]}{(C_M)_o[C]_o} \tag{17}$$

In the following the approximations $[B] = C_B$ and $[C] = C_C$ will be used, because of the small value of C_M. Hence, by measuring C_M, we can obtain X as a function of C_B. If the coefficients of activity of the ionic species concerned could have been regarded as constant we might have been able to calculate β_1, β_2, ... by conventional methods. However, as the complexity is very weak it was necessary to use large ligand concentrations and thus the salt medium is changed to such a degree as to invalidate the supposition of constant activity coefficients.

The best we can hope for then is to be able to calcuate β_1 from

$$\beta_1 = \lim_{C_B \to 0} \left(\frac{C_M \cdot C_C}{(C_M)_o \cdot (C_C)_o} - 1 \right) \cdot \frac{1}{C_B} \tag{18}$$

Measurements

Procedure. Solutions of the composition

C_B M NaSCN
$3.00 - C_B$ M $NaClO_4$
C'_M M $Coen_2(SCN)_2ClO_4$

were shaken in the same black-painted bottles as before. After some time a precipitation of Co $en_2(SCN)_2ClO_4$ was formed. From time to time samples of the solutions were withdrawn with a filterstick of fine porosity and were analyzed as before by measurement of the optical density at 510 mμ using the Hilger instrument and 2 cm quartz cells.

Chemicals used. Sodium perchlorate was prepared from analytical grade sodium carbonate and perchloric acid. *Sodium thiocyanate* was of analytical grade. The stock solutions were checked by ion-exchange-alkalimetric titration and Volhard titration, respectively.

Results

Unfortunately, equilibrium was very slowly reached. Experiments where solid Co $en_2(SCN)_2ClO_4$ was added in excess to solutions of the above composition did not give reproducible results. The probable explanation may be slow rearrangements in the solid phase.

Table 5. Solubility measurements: Optical densities of the saturated solutions (d = 2 cm; λ = 510 mμ). Calculation of X/C_B.

C_B M	E					$1+X$	X/C_B
	259 h	427 h	619 h	788 h	Mean		
0	0.354	0.345	0.340	0.339	0.345		*0.30*
0.3	0.428	0.419	0.418	0.411	0.419	1.093	0.31
0.43	0.472	0.459	0.456	0.451	0.459	1.140	0.33
0.60	0.520	0.511	0.510	0.507	0.512	1.187	0.31
0.90	0.645	0.637	0.639	0.635	0.639	1.297	0.33
1.20	0.835	0.822	0.819	0.815	0.823	1.431	0.36
$\beta_1 = 0.30 \pm 0.03$ M^{-1}							

In Table 5 are given the results of a representative set of experiments, the precipitation formed from the supersaturated solutions with C'_M = 3.00 mM.

The calculations have been performed on the mean of the determinations at the four different times reported. If the shaking had been further prolonged, the hydration of the complex might have caused undesirable effects. It must be observed, however, that this hydration, the velocity of which is very low at 20°C [15], would cause an *increase* of solubility. Also a *cis-trans* isomerization [15] would have the same effect. Furthermore, if X is calculated from any of the separate sets of solubilities we obtain, within the experimental errors, the same value of $\lim_{C_B \to 0} X/C_B$ as that reported here, *i.e.*, 0.30 M^{-1}.

SEARCH FOR PERCHLORATE COMPLEXES

For reasons put forward in the following discussion it was deemed necessary to investigate also the eventual formation of perchlorate complexes of Co $en_2(SCN)_2^+$. As the sorption of Co $en_2(SCN)_2ClO_4$ on a perchlorate-saturated anion exchange resin was too small to permit a reliable analysis, only the solvent extraction technique was used. In order not to base judgment on one set of measurements only, two different extracting solvents were used, *viz.*, the *cyclo*hexanone-2-octanol mixture and in the second case acetophenone.

Measurements

The measurements were performed as in the thiocyanate extractions.

The *acetophenone* used was a Merck preparation of the "wasserhell" quality. It was used without further purification.

The $NaClO_4$ concentration of the aqueous phase was determined alkalimetrically *via* a cation exchange resin in the acid form.

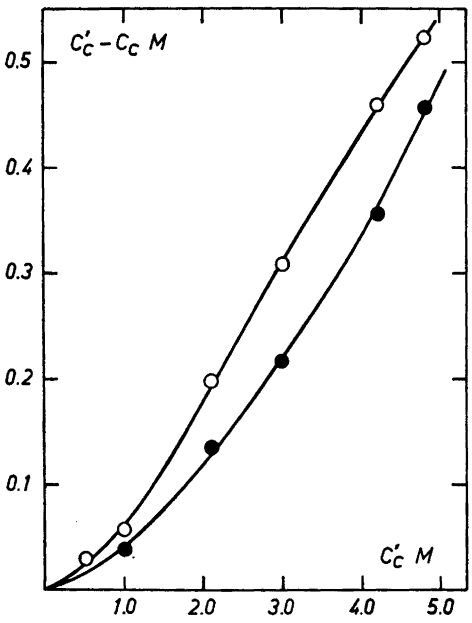

Fig. 3. Change of C_{NaClO_4} due to extraction. *Cyclo*hexanone—2-octanol mixture (O); acetophenone (●).

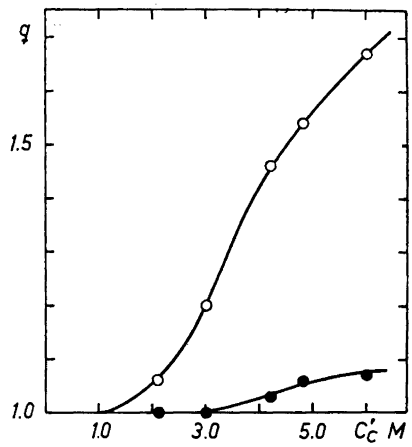

Fig. 4. Change of volume quotient q. *Cyclo*hexanone—2-octanol mixture (O); acetophenone (●).

Results

The results are reported graphically only, as the calculations were very similar to those of the thiocyanate extractions. In Fig. 3 is given the decrease of sodium perchlorate concentration due to extraction into the organic phase. Fig. 4 shows the change in the volume quotient as the electrolyte concentration increases. Fig. 5 gives the final result. The quotient φ was reproducible to within about 1 %. C'_M was kept low to avoid precipitation at the highest perchlorate concentrations.

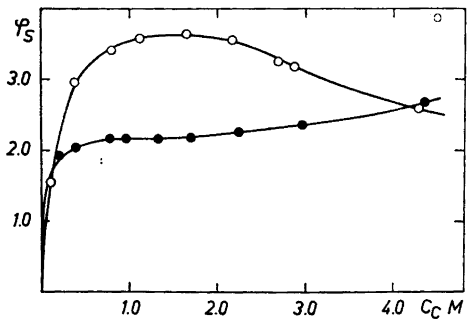

Fig. 5. Distribution quotient φ_S. *Cyclo*hexanone—2-octanol mixture (O); acetophenone (●).

C'_M = 0.5 and 2 mM (*cyclo*hexanone-2-octanol)
C'_M = 2 and 3 mM (acetophenone).

Only at C'_C = 4.8 M, C'_M = 3 mM was precipitation encountered. This point was then omitted.

DISCUSSION

If it is true, as infra-red data [16,17] suggest, that hydrogen-bonding makes an important contribution to the effects causing outer-sphere complexity, then the relation between the complexity constants will depend almost exclusively on electrostatic and statistical factors. Thus if we start from the experimental value of β_1, we can calculate the successive constants $\beta_2 \ldots \beta_n$ from the statistical relation

$$\frac{b_{n+1}}{b_n} = \frac{(N-n)n}{(N-n+1)(n+1)} \tag{19}$$

where

$$b_n = \frac{\beta_n}{\beta_{n-1}} \; ; \quad b_1 = \beta_1 \tag{20}$$

given by Bjerrum (Ref.[18], p. 24). These values must be maximum values, because of the neglect of the increasing electrostatic repulsion of negatively charged entities. In the present case, this neglect is certainly forgivable because we have chosen the large ions so as to minimize the electrical work.

In order to make use of eqn (19), we must make some assumption on the maximum coordination number N. It seems reasonable to assume that in this case $N = 8$, corresponding to the eight faces of an octahedron.

The calculation based on $\beta_1 = 0.3$ M^{-1} gave as result

$$\beta_2 = 0.04 \text{ } M^{-2}; \qquad \beta_3 = 0.003 \text{ } M^{-3}; \qquad \beta_4 = 0.0001 \text{ } M^{-4};$$

Then, from the well-known formula for $\bar{n}$ (Ref.[18], p. 21) we obtain for [B] = 1 M $\bar{n} = 0.28$, $\bar{n} = 0.29$ and $\bar{n} = 0.29$ if only the two, three and four first complexes are considered, respectively.

This result is in obvious variance with the result of the extraction experiments, which indicate, that $\bar{n} \approx 1$ when [B] = 1 M.

Some of this disagreement certainly arises from the fact that we compare measurements made at different ionic strengths and in solutions of ammonium and sodium salts, respectively.

However, it seems to the present author that a rather probable explanation is that there might be a perchlorate complexity too, which is of a strength comparable in magnitude to the thiocyanate complexity.

If this is the case, it must be entirely wrong to compare results from measurements in a perchlorate-rich medium with such obtained in a perchlorate-free one.

In consequence of this assumption we must re-formulate the treatment of the solubility measurements.

The following notations are introduced:

$$\beta_{nB} = \frac{[MB_n]}{[M][B]^n} \tag{21a}$$

$$\beta_{nC} = \frac{[MC_n]}{[M][C]^n} \tag{21b}$$

meaning the "true" complexity constants in the sense of Leden (Ref.[19], p. 40). We will assume in the following calculation that only the first two perchlorate complexes are formed in appreciable amounts. Then the only mixed complex to be considered is MBC, the complexity constant of which is defined as

$$\beta_{2BC} = \frac{[MBC]}{[M][B][C]} \tag{21c}$$

It may be assumed from energetical considerations that

$$2 \log \beta_{2BC} = \log \beta_{2B} + \log \beta_{2C} \tag{22}$$

or

$$\beta_{2BC} = \sqrt{\beta_{2B} \cdot \beta_{2C}} \tag{22a}$$

Hence eqn (14) turns into

$$C_M = [M](1 + X_B + X_C + \sqrt{\beta_{2B} \cdot \beta_{2C}} \cdot [B][C]) \tag{23}$$

Remembering that, in the actual case, $[B] + [C] = 3$, and combining eqn (23) with eqns (21) and (13) we obtain after trivial calculations

$$\frac{C_M \cdot [C]}{C_{M_0} \cdot [C]_0} = 1 + \frac{\beta_{1B} - \beta_{1C} - 6\beta_{2C} + 3\sqrt{\beta_{2B} \cdot \beta_{2C}}}{1 + 3\beta_{1C} + 9\beta_{2C}}[B] +$$

$$+ \frac{\beta_{2B} + \beta_{2C} - \sqrt{\beta_{2B} \cdot \beta_{2C}}}{1 + 3\beta_{1C} + 9\beta_{2C}}[B]^2 + \frac{\beta_{3B}}{1 + 3\beta_{1C} + 9\beta_{2C}}[B]^3 + \ldots . \tag{24}$$

Now the coefficient of the linear term of this expression must correspond to β_1 of eqn (18), *i.e.*, the experimentally determined quantity $\beta_1 = 0.3\ M^{-1}$. Thus we have

$$0.3(1 + 3\beta_{1C} + 9\beta_{2C}) = \beta_{1B} + 3\sqrt{\beta_{2C}} \cdot \sqrt{\beta_{2B}} - \beta_{1C} - 6\beta_{2C} \tag{25}$$

However,

$$\sqrt{\beta_{2B}} = \sqrt{\frac{b_2}{b_1}} \cdot \beta_{1B} \tag{26}$$

where $\frac{b_2}{b_1}$ is given by eqn (19).

Combining eqns (25) and (26) we finally obtain

$$\beta_{1B} = \frac{\beta_{1C} + 6\beta_{2C} + 0.3(1 + 3\beta_{1C} + 9\beta_{2C})}{1 + \frac{\sqrt{7}}{4}\sqrt{\beta_{2C}}} \tag{27}$$

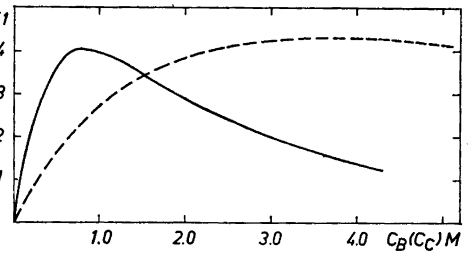

Fig. 6. Solid curve: α_1 of the thiocyanate system, calculated from the constants $\beta_{1B} = 1.4_2$ M^{-1}, $\beta_{2B} = 0.8_8$ M^{-2} and $\beta_{3B} = 0.3_1$ M^{-3}. Broken curve: α_1 of the perchlorate system, calculated from the constants $\beta_{1C} = 0.4$ M^{-1} and $\beta_{2C} = 0.07$ M^{-2}.

From a value of β_{1B} one can calculate β_{2B} *etc.*, from eqns (19) and (20).

We can then *illustrate* the interrelation of the thiocyanate and perchlorate complexity constants with a *numerical example:*

If we *assume* $\beta_{1C} = 0.4$ M^{-1}, eqns (19) and (20) give $\beta_{2C} = 0.07$ M^{-2}. Introducing these quantities in eqn (27) we obtain $\beta_{1B} = 1.4_2$ M^{-1}. Hence $\beta_{2B} = 0.8_8$ M^{-2} and $\beta_{3B} = 0.3_1$ M^{-3}. From these we may calculate $\bar{n}$ for [B] = 1 M.

Then we obtain $\bar{n} = 1.1_4$ if all three complexes are taken into account. Furthermore, a close examination of the φ_R-curves of Fig. 2 indicates that the maximum occurs at $C_B \approx 0.85$ M. For this ligand concentration and the constants calculated above we obtain $\bar{n} = 1.0_1$.

Indeed, we can calculate α_1 for any concentration (Fig. 6). This quantity [7] is directly related to φ_R, and the agreement between the two quantities is very good. (At low concentrations the constants derived here are no longer valid, but should be greater so as to give a steeper rise of φ_R, which is actually found.)

As the curves of activity coefficients for $NaClO_4$ and NaSCN (Ref.[20]) have rather broad minima in the region 1—3 M the variation of the value of the complexity constants with ionic strength may be negligible, which has been assumed above.

It is certainly not neccessary to stress the arbitrary points in the above calculations. The purpose has been only to illustrate the composite problems encountered in the investigations of systems of such an elusively weak complexity.

The extraction experiments in perchlorate solutions were undertaken in an effort to prove the existence of perchlorate complexes. The results are, however, disappointing in this respect.

As these experiments are not a major part of the present investigation only the following may be said:

With systems where the mutual solubility of the two phases is as great as here one might expect large changes in the activity coefficients. These changes make any interpretation of the results very difficult. Reference might be made to the findings of Johnson and Brubaker [21] that *cyclo*hexanone seems to enhance any tendency of anionic complex formation that may exist in the aqueous phase.

Comparison of Figs. 3 and 4 shows that it is not so much the extraction of $NaClO_4$ as the difference in mutual solubility (represented by different q) that causes the different shapes of the φ-curves.

It is interesting to note that if we calculate α_1 from the values of the complexity constants used above, $\beta_{1C} = 0.4\ M^{-1}$ and $\beta_{2C} = 0.07\ M^{-2}$, a very flat maximum is obtained at $C_C = 3.8$ M; *cf.* Fig. 6. (Apart from activity effects causing changes in the parameters involved, α_1 should be related to φ_S in the same way [7] as it is to φ_R.)

Summing up, we may state that there seems to be a definite tendency of thiocyanate ions associating with the *trans*-Co $en_2(SCN)_2^+$ ion, and that the measurements can be correlated semi-quantatively on the basis of the hypothesis of a slight perchlorate complexity of this ion.

The author is indebted to Professor S. Fronæus for a stimulating criticism of this work.

REFERENCES

1. Basolo, F. and Pearson, R. G. *Mechanisms of inorganic reactions. A study of metal complexes in solution.* John Wiley & Sons, Inc., New York; Chapman & Hall Ltd, London 1958. Chapter 9.
2. Larsson, R. *Acta Chem. Scand.* **12** (1958) 708.
3. Bjerrum, N. *Kgl. Danske Videnskab. Selskab, Mat.-fys. Medd.* **7** (1926) No 9.
4. Gronwall, T. H., LaMer, V. K. and Sandved, K. *Physik. Z.* **29** (1928) 358.
5. Fuoss, R. M. and Kraus, C. A. *J. Am. Chem. Soc.* **55** (1933) 2387.
6. Fronæus, S. *Svensk Kem. Tidskr.* **65** (1953) 1.
7. Fronæus, S. *Acta Chem. Scand.* **8** (1954) 1174.
8. Werner, A. and Bräunlich, F. *Z. anorg. Chem.* **22** (1899) 123.
9. Shimura, Y. *J. Am. Chem. Soc.* **73** (1951) 5079.
10. Shimura, Y. and Tsuchida, R. *Bull. Chem. Soc. Japan* **29** (1956) 311.
11. Tomula, E. S. *Z. anal. Chem.* **83** (1931) 6.
12. Larsson, R. *Acta Chem. Scand.* **11** (1957) 1405.
13. Adamson, A. W. and Sporer, H. H. *J. Am. Chem. Soc.* **80** (1958) 3685.
14. Smithson, J. M. and Williams, R. J. P. *J. Chem. Soc.* **1958** 457.
15. Adamson, A. W. and Wilkins, R. G. *J. Am. Chem. Soc.* **76** (1954) 3379.
16. Fujita, J., Nakamoto, K. and Kobayashi, M. *J. Am. Chem. Soc.* **78** (1956) 3295.
17. Block, H. *Trans. Faraday Soc.* **55** (1959) 867.
18. Bjerrum, J. *Metal Ammine Formation in Aqueous Solution,* (Diss.) University, Copenhagen 1941.
19. Leden, I. *Potentiometrisk undersökning av några kadmiumsalters komplexitet,* (Diss.) Lund 1943.
20. Robinson, R. A. and Stokes, R. H. *Trans. Faraday Soc.* **45** (1949) 612.
21. Brubaker, Jr. C. H. and Johnson, C. E. *J. Inorg. & Nuclear Chem.* **9** (1959) 184.

Received November 24, 1959.

ACTA CHEMICA SCANDINAVICA 14 (1960) 711–716

Studies on the Hydrolysis of Metal ions

Part 29. The Hydrolysis of the Silver Ion, Ag^+, in Acid Self-medium *

GEORGE BIEDERMANN and SIRKKA HIETANEN

Department of Inorganic Chemistry, Royal Institute of Technology, Stockholm 70, Sweden

The hydrolysis of the Ag^+ ion has been investigated at 25°C by measuring the hydrogen ion concentration in the self-medium [3] 1 M $Ag^+(NO_3^-)$ with a glass electrode. The data, which indicate an extremely slight hydrolysis at log $[H^+] \geqq -6.3$, can be explained by the equilibrium $Ag^+ + H_2O \rightleftharpoons AgOH + H^+$ with log $*K_1 \leqq -11.1$; the effect may also be due to polynuclear complexes. No evidence was found for the presence of appreciable amounts of polynuclear hydrolysis products proposed previously [1].

Little data can be found in the literature which throw light on the hydrolysis equilibria of the Ag^+ ion. In 1933 Johnston, Čuta and Garrett [1] concluded that about 40 % of the dissolved silver in a saturated solution of Ag_2O is present as positively charged polynuclear ions such as Ag_2OH^+. Their argument is based on a comparison of the analytically determined total silver concentration with the conductometrically measured ionic concentration. Evidence was found by these authors that the concentration of the uncharged species AgOH cannot exceed 0.01 $[Ag(I)]_{total}$.

In 1954 Faucherre [2] studied the hydrogen ion concentration of $AgNO_3$ solutions in the ionic medium 0.2 M NO_3^- with a glass electrode. He explained the increase of log $[H^+]$ from −6 to −5, as log [Ag(I)] varied from −2 to −1, by assuming the equilibrium

$$Ag^+ + H_2O \rightleftharpoons AgOH + H^+ \; ; \; *K_1 = [AgOH]h[Ag^+]^{-1}$$

with log $*K_1 = -9.7$.

The hydrolysis equilibrium of Ag^+ is not easy to investigate because the Ag^+ ion is a very weak acid and the solubility product of Ag_2O is low (pK_s is about 7.7). As a result the acidity range where appreciable hydrolysis occurs but no precipitate is formed is narrow. If solutions dilute in $[Ag^+]$ are investigated, the useful acidity range can be made wider. This was attempted several years ago in this laboratory, but due to the low buffer capacity of dilute silver

* This work is dedicated to the sixtieth birthday of Professor W. Feitknecht, Bern, Switzerland.

solution and to the premature precipitation of Ag_2O no conclusive results could be obtained. In any case the study of dilute solutions can only yield information on mononuclear products.

METHOD OF INVESTIGATION

Recently a method has been proposed by Hietanen and Sillén [3] — the self-medium method — which is particularly suitable for studying the hydrolysis equilibria of such a weak acid as the Ag^+ ion. In the self-medium method the equilibrium concentration of hydrogen ions is measured in solutions containing, at a high and constant concentration, one of the reacting ions and a counter ion which does not take part in the reaction to be studied. The solutions may also contain a small amount of an inert (*i.e.* non protolyzing) cation or anion in order to keep the counter ion concentration constant when the acidity is varied.

In a series of measurements, which may be carried out conveniently as a potentiometric titration, the acidity is changed by replacing the inert ion with H^+ or OH^- ions. If the acidity changes are small and therefore only a small part of the reacting ions is transformed to the hydrolysis products, the composition of the solution is altered only slightly, so that the activity factors may be considered as constants. The advantage of the self-medium method is that the presence of hydrolysis products $Me_q(OH)_p$ (Me = metal ion) with high q/p can easily be detected under conditions when the solutions have an appreciable buffer capacity.

This paper summarizes our hydrogen ion concentration measurements using a glass electrode in a series of 1 M $AgNO_3$ solutions of varying acidity. $AgNO_3$ was chosen because it can be easily purified by recrystallization, in contrast to $AgClO_4$. It is essential to use as pure reagents as possible when the hydrolysis of weak acids is to be studied.

The solutions were prepared by mixing one ("S_0") of low acidity with another one ("T") containing about 0.02 M HNO_3. The results obtained in this work, as well as those found in solutions of 3 M ClO_4^-, show that the hydrolysis of Ag^+ is negligible for $\log [H^+] > -4$, consequently in the 0.02 M HNO_3 + 1.00 M $AgNO_3$ solution, "T", the hydrogen ion concentration h is equal to the analytical excess of hydrogen ions $H = [NO_3^-] - [Ag^+]$.

The starting solution S_0 of low acidity had to be prepared in a special way because addition of dilute NaOH to 1 M $AgNO_3$ always caused a precipitation of Ag_2O, which redissolved very slowly, whatever precautions were taken to avoid a local excess of OH^-. The CO_2-free 1 M $AgNO_3$ solution to be used as the starting solution was passed through a tube containing about 20 g Ag_2O to remove the minute amounts of excess hydrogen ions. This procedure ensures that the solution comes into intimate contact with the Ag_2O particles so that excess hydrogen ions are removed without the introduction of foreign ions. The solubility of Ag_2O is so low that the total silver concentration remains practically unchanged.

In all experiments we have found the analytical excess of hydrogen ions in the starting solution, H_0, to be negative, which indicates that the method used to prepare partially hydrolyzed solutions is an effective one. It is common

experience in this laboratory that equilibrium is established much more rapidly between a solid and a liquid by passing the liquid through a column of the solid than by shaking.

The hydrogen ion concentration at equilibrium was measured by using the cell

$$- \text{ GE} \mid \text{solution S} \mid \text{SE} +$$

where GE denotes the glass electrode, SE is the reference half-cell

$$\mid 1.000 \text{ M } KNO_3 \mid 0.990 \text{ M } KNO_3, \; 0.0100 \text{ M } AgNO_3 \mid AgCl, \; Ag.$$

Solution S had the general composition (neglecting the very small correction for H_o, see below)

$$H \text{ M } H^+, \; 1.000 \text{ M } Ag^+_{aq}, \; (1.000 + H) \text{ M } NO_3^-;$$

In all experiments H was kept below 0.01 M.

The emf of this cell can be written at 25°C

$$E = E_o - 59.15 \log h + E_j \qquad (1)$$

where E_o is a constant and E_j is the liquid junction potential between solution S and 1 M KNO_3. E_j was determined by measuring E in the h range 0.01 to 0.1 M where the hydrolysis is quite negligible. The equation $E_j = 52\ h$ mV was found to describe the data to a good approximation.

The liquid junction potential of the junction h M H^+, $(1.000-h)$ M Na^+, 1.000 M ClO_4^- | 1 M $NaClO_4$ has been previously measured in this laboratory (G. Biedermann unpublished work); up to $h = 0.1$ M the data could be represented by the equation $E_j = 64\ h$ mV, which is reasonably close to the E_j values found for the junction studied in this work.

A series of measurements ("titration") was started with a known volume, V_o ml, of a partially hydrolysed solution with an initially unknown deficit of H^+ ($- H_o$). To this solution an increasing amount V_T ml of an acid solution T (1 M $AgNO_3$, H_T M HNO_3) was added.

For each point H is given by the equation

$$H = \frac{V_T H_T + V_o H_o}{V_T + V_o} \qquad (2)$$

In a first approximation we neglected H_o, obtaining the approximate value

$$H_1 = \frac{V_T H_T}{V_o + V_T} = H - \frac{H_o V_o}{V_o + V_T} \qquad (3)$$

As H_1 increases, $(H_1 - H)/H_1$ decreases and

$$E + 59.15 \log H_1 - E_j(H_1) \qquad (4)$$

tends to E_o.

For each point of a series of measurements (4) was calculated and for $H_1 > 0.005$ M was found to be constant within $\pm$ 0.1 mV; this constant value for (4) was accepted as the correct E_o. We could then calculate h from (1) for each point.

The difference between the free and analytical hydrogen ion concentration is

$$h - H = BZ \tag{5}$$

where B is the total silver concentration and Z is the average number of OH bound per silver ion.

From (2), (3), and (5) we find

$$\left(\frac{V_o + V_T}{V_o}\right)(h - H_1) = BZ\left(\frac{V_o + V_T}{V_o}\right) + H_o \tag{6}$$

The left hand side can now be calculated from known quantities; it tends to H_o as the hydrolysis is suppressed. Indeed, a constant value was obtained within the limits of experimental uncertainty in our experiments in the log h range -5 to -3.5 indicating that hydrolysis is negligible for log $h > -5$. This value was taken to be equal to H_o. For a log h higher than about -3.5 $(h - H_1)$ could not be obtained with sufficient accuracy because the absolute uncertainty increases both for h and H_1. On the other hand, the relative uncertainty is constant, we have estimated a maximal error $\Delta h/h = 0.01$ and $\Delta H_1/H_1 = 0.001$.

EXPERIMENTAL DETAILS

$AgNO_3$ solutions were prepared from $AgNO_3$ p.a., Merck, which was purified by recrystallization and then dried at 140°C. Care was taken to avoid contamination with dust. *Ag_2O* was made by adding 0.1 M $Ba(OH)_2$ dropwise to 0.1 M $AgNO_3$ at 60–70°C; both solutions were prepared by dissolving the purified substances in CO_2-free water. The precipitated Ag_2O was washed with hot CO_2-free water until the washings gave no reaction for Ba^{2+}. The precipitation, washing and the transfer of Ag_2O to the column were made in a specially constructed apparatus in a purified nitrogen atmosphere.

HNO_3 solutions were made from 65 % HNO_3 p.a. Merck. They were standardized to an accuracy of 0.1 % against $KHCO_3$, and *via* NaOH solution against hydrazinium sulfate. *$Ba(OH)_2$* solutions were prepared from $Ba(OH)_2(H_2O)_8$ p.a. Merck, which was made carbonate- and chloride-free by double recrystallization. A 0.25 M $Ba(OH)_2$ solution had a scarcely perceptible turbidity, indicating that the carbonate content was very low. *Nitrogen* from a cylinder was purified by passing through 1 M H_2SO_4 and 1 M NaOH. Doubly distilled water, made CO_2-free by passing N_2 through it for several hours, was used to prepare all the solutions, which were stored and transferred in a nitrogen atmosphere.

The measurements were carried out employing the technique usual in this laboratory [4]. E was determined with a valve potentiometer PHM 4, Copenhagen, which was calibrated against a Leeds & Northrup compensator of the type K3; the reading accuracy of the valve potentiometer was 0.1 mV. A Beckman glass electrode of type No. 1190–80 was employed, which attained a constant potential within about 10 min and which remained constant within ± 0.1 mV for several hours.

All measurements were made in a paraffin-oil thermostat at 25.0 ± 0.1 °C.

RESULTS

Three series of measurements were made, and each time a fresh Ag_2O preparation was used to react with the starting solution. A typical series is shown in Table 1; the additions below 3 ml were made with a weight burette. It may be inferred from the table that the experimental conditions were chosen adequately to obtain the constants E_o and H_o with a satisfactory accuracy.

Table 1. Starting solution So: 49.98 ml $AgNO_3$ 1.000 M passed through a column filled with Ag_2O. Acid solution T: V_T ml $AgNO_3$ 1.000 M, HNO_3 0.01983 M.

	V_T ml	E mV	H_1 M	E_j mV	$E+59.15\times\log H_1-E_j(H_1)$ mV	h M	$Z\left(\frac{V_T}{V_o}+1\right)+H_o$ M	Z
1	—	334.2	.—	—	—	5.06×10^{-7}	5.06×10^{-7}	1.6×10^{-5}
2	0.0764	245.1	$3.02_6\times10^{-5}$	—	155.2	1.62×10^{-5}	$(-1.41\pm0.02)\times10^{-5}$	2×10^{-6}
3	0.1395	221.9	5.52	—	147.5	4.00	(-1.52 ± 0.04)	
4	0.2285	206.0	9.02	—	144.2	7.43	(-1.6 ± 0.1)	
5	0.3190	195.9	$1.25_8\times10^{-4}$	—	142.6	1.10×10^{-4}	(-1.6 ± 0.1)	
6	0.4122	188.7	1.62_2	—	141.9	1.46	(-1.6 ± 0.1)	
7	0.5013	183.1	1.96_9	—	141.3	1.81	(-1.6 ± 0.2)	
8	0.7256	173.0	2.83_7	—	140.6	2.68	(-1.6 ± 0.3)	
9	1.1818	159.9	4.58	—	139.8	4.47	(-1.1 ± 0.5)	
10	3.19	135.2	$1.19_0\times10^{-3}$	0.1	139.6	1.17×10^{-3}	(-2 ± 1)	
11	5.19	123.4	1.86_5	0.1	139.3	1.86		
12	7.19	116.0	2.49_4	0.1	139.4	2.48		
13	11.20	106.3	3.63_0	0.2	139.2			
14	21.21	93.8	5.90_8	0.3	139.1			
15	31.23	87.4	7.62_6	0.4	139.2			
16	41.25	83.2	8.96_6	0.5	139.1			

$E_o = 139.2 \pm 0.1$ mV $\qquad H_o = (-1.6 \pm 0.1) \times 10^{-5}$ M

Table 2 summarizes the results of our measurements.

Table 2.

No. of series	$H_o \times 10^5$	$\log h$	$Z \times 10^5$	$\log {}^*K_1$	$\log {}^*\beta_{12}$	$\log {}^*\beta_{22}$
(1)	(-1.0 ± 0.1)	(-5.82)	(1.15 ± 0.1)	(-10.8)	(-10.8)	(-16.9)
(2)	-1.7 ± 0.1	-6.33	1.7 ± 0.1	-11.10	-11.10	-17.73
(3)	-1.6 ± 0.1	-6.30	1.6 ± 0.1	-11.10	-11.10	-17.70

The H_o and Z values obtained in series (1) — which are set in brackets — are somewhat less accurate than those determined in the two others because at first no weight burette was used for the small additions.

In each series only the first point could be utilized to calculate Z because Z values less than 10^{-5} could not be obtained with satisfactory accuracy.

To explain the $Z(\log h)$ data we shall try what seems to be the three simplest assumptions on the main reaction

$$Ag^+ + H_2O \rightleftharpoons AgOH + H^+ \qquad {}^*K_1 = [AgOH]h[Ag^+]^{-1} \approx Zh$$
$$2\,Ag^+ + H_2O \rightleftharpoons Ag_2OH^+ + H^+ \qquad {}^*\beta_{12} = [Ag_2OH^+]h[Ag^+]^{-2} \approx ZhB^{-1}$$
$$2\,Ag^+ + 2\,H_2O \rightleftharpoons Ag_2(OH)_2 + 2\,H^+ \qquad {}^*\beta_{22} = [Ag_2(OH)_2]h^2[Ag^+]^{-2} \approx \tfrac{1}{2}Zh^2B^{-1}$$

Although great pains were taken to avoid contamination of the solutions we do not feel justified to claim that the extremely small Z values are not partly due to the presence of some impurity. We can therefore only conclude

$$\log {}^*K_1 \leqq -11.1; \log {}^*\beta_{12} \leqq -11.1; \log {}^*\beta_{22} \leqq -17.7$$

In the light of the present results it does not seem likely as suggested by Johnston, Čůta and Garrett [1] that the difference claimed between the analytically and conductometrically determined silver concentrations in a saturated solution of Ag_2O is due to the presence of Ag_2OH^+. If the saturated solution of Johnston *et al.* had contained 5.8×10^{-5} M Ag^+, 1.39×10^{-4} M OH^- and 8.1×10^{-5} M Ag_2OH^+, as they seem to suggest, one would calculate $\log {}^*\beta_{12} = -5.76$ and for the equilibrium

$$\tfrac{1}{2}Ag_2O(s) + \tfrac{1}{2}H_2O + Ag^+ \rightleftharpoons Ag_2OH^+$$

$\log K = 0.15$*. If these values were correct in our solution with $[Ag(I)]_{tot} = 1$ M, $\log h = -6.3$ we would calculate $Z \sim 0.35$ whereas we find 1.7×10^{-5}. It would moreover have been possible to dissolve Ag_2O in 1 M $AgNO_3$ to a value $Z \sim 0.37$.

In a following paper [6] a critical survey of the data on the solubility equilibria of Ag_2O will be given. On the basis of this survey we believe that the inconsistency between the analytical and conductance data of Johnston, Čůta and Garrett [1] is to be ascribed to the presence of minute amounts of impurities, *e.g.* CO_2, which may seriously influence the composition of a solution of such a low buffer capacity as a saturated solution of Ag_2O.

The $\log {}^*K_1$ value obtained in this work is considerably lower than that found by Faucherre [2]. This author assumed the analytical excess of hydrogen ions to be negligible in a CO_2-free solution of $AgNO_3$. However, according to our experience a minute amount of HNO_3 is inevitably occluded in the crystal; the HNO_3 impurity cannot be removed below the melting point of $AgNO_3$.

We are indebted to Professor Lars Gunnar Sillén for his great interest in this work and for his valuable criticism.

This investigation was financially supported by *Statens Naturvetenskapliga Forskningsråd (Swedish Natural Science Research Council)* and by the *Air Force Office of Scientific Research of the ARDC, USAF* through its European Office on contract No AF 61 (052)—162.

REFERENCES

1. Johnston, H. L., Čůta, F. and Garrett, A. B. *J. Am. Chem. Soc.* **55** (1933) 2311.
2. Faucherre, J. *Bull. soc. chim. France* **1954** 253.
3. Hietanen, S. and Sillén, L. G. *Acta Chem. Scand.* **13** (1959) 533.
4. see *e.g.* Biedermann, G. *Arkiv Kemi* **9** (1956) 277.
5. Näsänen, R. *Suomen Kemistilehti* **B 16** (1943) 1.
6. Biedermann, G. and Sillén, L. G. *Acta Chem. Scand.* **14** (1960) 717.

* On different assumptions Näsänen [5] has calculated $\log \beta^*_{12} = -6.61$. Näsänen has assumed that the mobility of Ag_2OH^+ is negligible, whereas we set it equal to the mobility of Ag^+.

Received December 1, 1959.

ACTA CHEMICA SCANDINAVICA 14 (1960) 717–725

Studies on the Hydrolysis of Metal Ions

Part 30. A Critical Survey of the Solubility Equilibria of Ag_2O

GEORGE BIEDERMANN and LARS GUNNAR SILLÉN

Department of Inorganic Chemistry, Royal Institute of Technology, Stockholm 70, Sweden

On the basis of recalculation of the data available in the literature (Table 1) the most probable values of the constants of the following equilibria have been estimated at 25°C:

$\frac{1}{2}\,Ag_2O(s) + \frac{1}{2}\,H_2O \rightleftharpoons Ag^+ + OH^-$ $\quad \log K_{s0} = -7.71 \pm 0.03$
$\frac{1}{2}\,Ag_2O(s) + \frac{1}{2}\,H_2O \rightleftharpoons AgOH$ $\quad \log K_{s1} = -5.75 \pm 0.25$
$\frac{1}{2}\,Ag_2O(s) + \frac{1}{2}\,H_2O + OH^- \rightleftharpoons Ag(OH)_2^-$ $\quad \log K_{s2} = -3.72 \pm 0.03$

For the complex formation OH^--Ag^+ these data give

$\log K_1 = \log [AgOH][Ag^+]^{-1}[OH^-]^{-1} = 2.0 \pm 0.3$;
$\log \beta_2 = \log [Ag(OH)_2^-][Ag^+]^{-1}[OH^-]^{-2} = 3.99 \pm 0.05$

The different experimental methods which were employed to study these equilibria have been discussed in some detail.

In three preceding papers the hydrolysis equilibria of the Ag^+ ion were studied in acid [1], moderately alkaline [2] and highly alkaline [3] solutions by a group of workers in this laboratory. The data obtained by these investigators could be explained by assuming the formation of the species AgOH and $Ag(OH)_2^-$, and no evidence was found for the presence of appreciable amounts of polynuclear products which were claimed by several previous authors [4,5].

As a consequence of these results the solubility equilibria of Ag_2O may be written

$\frac{1}{2}\,Ag_2O(s) + \frac{1}{2}\,H_2O \rightleftharpoons Ag^+ + OH^-$ $\quad K_{s0} = \{Ag^+\}\{OH^-\}\{H_2O\}^{-\frac{1}{2}}$ (1)
$\frac{1}{2}\,Ag_2O(s) + \frac{1}{2}\,H_2O \rightleftharpoons AgOH$ $\quad K_{s1} = \{AgOH\}\{H_2O\}^{-\frac{1}{2}}$ (2)
$\frac{1}{2}\,Ag_2O(s) + OH^- + \frac{1}{2}\,H_2O \rightleftharpoons Ag(OH)_2^-$ $\quad K_{s2} = \{Ag(OH)_2^-\}\{OH^-\}^{-1}\{H_2O\}^{-\frac{1}{2}}$ (3)

where the symbol {} denotes activity. The present paper is devoted to a discussion of the available data concerning equilibria (1), (2) and (3). On the basis of the discussion an attempt has been made to estimate the most probable values at 25°C of K_{s0}, K_{s1} and K_{s2}, which are collected in the Synopsis.

It is believed that the conclusions reached in this work might find a general interest for the study of equilibria involving slightly soluble metal oxides and hydroxides.

ON THE SOLUBILITY PRODUCT OF Ag_2O, K_{s0}

Four methods have been applied to determine K_{s0}: (A) emf measurements (B) study of the equilibrium

$$AgCl(s) + OH^- \rightleftharpoons \tfrac{1}{2}Ag_2O(s) + \tfrac{1}{2}H_2O + Cl^-; K_4 = \{Cl^-\}\{H_2O\}^{1/2}\{OH^-\}^{-1} = \frac{K_{s0}(AgCl)}{K_{s0}(Ag_2O)} \quad (4)$$

(C) conductance measurements and (D) chemical analysis of the saturated solution.

As will be clear from the following discussion K_{s0} may be determined in a straightforward manner by methods (A) and (B), when the measurements are made in solutions of $[OH^-] \geq 0.01$ M which have an appreciable buffer capacity. Methods (C) and (D) require on the other hand the study of a saturated solution of Ag_2O containing no added electrolyte. Since the solubility product of Ag_2O is rather low ($\log K_{s0}$ is about -7.7) the composition of the saturated solution is influenced considerably by the presence of slight amounts of protolyzing impurities, *e.g.* CO_2 or substances dissolved from glass.

Using methods (C) and (D) therefore the nature and concentration of the impurities must be known and their effect on the data must be taken into account. By a correct treatment of the conductance and the analytical data the uncertainty caused by the presence of impurities may become unappreciable, as it is shown by the fact that the results derived from the experiments of the most careful workers are in agreement with those found by the methods (A) and (B), (see Table 1).

(A) Emf measurements with the half-cell $OH^-/Ag_2O(s),Ag$

Previous workers [6-8] had difficulty in obtaining constant and reproducible emf values with Ag_2O,Ag electrodes. More recently, however, Makolkin [9] and Hamer and Craig [10] were able to find the experimental conditions in which the Ag_2O,Ag electrodes function reversibly.

The cell studied by Makolkin had the composition

$$H_2/Ba(OH)_2\ I\ M/Ba(OH)_2\ I\ M/Ag_2O,Ag\ (25°C) \quad (I)$$
$$E(p_{H_2} = 1\ atm) = e°(H^+/Ag_2O,Ag) - 29.58 \log \{H_2O\} \quad (5)$$

and he found

$$E = 1\ 171.9 \pm 0.8\ mV_{int} = 1\ 172.3 \pm 0.8\ mV_{abs}*$$

The cell of Hamer and Craig was

$$Hg,HgO/NaOH\ I\ M/NaOH\ I\ M/Ag_2O,Ag\ (25°C) \quad (II)$$
$$E = e°(H^+/Ag_2O,Ag) - e°(H^+/HgO,Hg) \quad (6)$$

and they obtained

$$E = 244.0 \pm 0.5\ mV_{abs}$$

* The conversion to mV_{abs} was made by the present authors.

Here e° denotes the standard potential referred to the hydrogen scale.

Cells I and II may be expected to yield highly accurate values for K_{s0}. The solubilities of Ag_2O and HgO are so low that the liquid junction potential is quite negligible for $I \geq 0.01$ M. Both these investigators used solutions of $I \geq 0.1$ M, therefore small amounts of CO_2 and substances dissolved from glass, which can hardly be avoided, do not influence appreciably the composition of the solutions. Moreover since the $[OH^-]$ is practically the same in both half-cells the effect of the impurities on the emf will be cancelled out.

The correctness of the assumed cell reaction may be tested, *e.g.* by changing I. Hamer and Craig have found that the emf of cell II remains constant within $\pm$ 0.5 mV as $[OH^-]$ is varied from 1.3 to 10 M.

Since

$$e^\circ(H^+/Ag_2O,Ag) = e^\circ(Ag^+/Ag) + 59.15 \log \frac{K_{s0}}{K_w} \qquad (7)$$

where K_w is the ionic product of water, we need in order to calculate K_{s0} the values of the constants K_w, $e^\circ(Ag^+/Ag)$ and with cell II also $e^\circ(H^+/HgO, Hg)$. We shall use $pK_w = 13.997$; the most probable values for the standard potentials will be taken from a critical survey [11] made in this laboratory: $e^\circ(Ag^+/Ag) = 799.4 \pm 0.2$ mV_{abs} and $e^\circ(H^+/HgO, Hg) = 926.1 \pm 0.3$ mV_{abs}. The term containing $\{H_2O\}$ in (5) has been neglected, since Harned and Mason [12] have shown that in 0.1 M $Ba(OH)_2$ (the concentration presumably used by Makolkin) it is less than 0.05 mV.

With the constants selected Makolkin's data give $-\log K_{s0} = 7.70 \pm 0.02$ and those of Hamer and Craig 7.73 ± 0.02; the difference does not exceed significantly the experimental uncertainty.

(B) Determination of $K_4 = \dfrac{K_{s0}(AgCl)}{K_{s0}(Ag_2O)}$

Since at 25°C the solubility product of AgCl, $K_{s0}(AgCl)$, is about $0.01 \times K_{s0}(Ag_2O)$ the analytical determination of the ratio $[Cl^-]\,[OH^-]^{-1}$ in a solution which is in equilibrium with solid Ag_2O and AgCl may be carried out with a fair degree of accuracy. Two sets of data are available — the measurements of Noyes and Kohr [13] and those of Newton [14], which are in a satisfactory agreement. These investigators have found that equilibrium is established at 25°C within a few hours, so that the attack of OH^- on the glass surface may not introduce an appreciable error.

No systematic trend can be detected in the $[Cl^-]\,[OH^-]^{-1}$ values as $[OH^-]$ varies from 0.05 to 0.35 M. This fact indicates that in these solutions $f(Cl^-)\,f^{-1}(OH^-)$ is equal to unity within the narrow limits of experimental uncertainty. The deviation of $\{H_2O\}$ from unity is certainly negligible. We can thus set $K_4 = [Cl^-][OH^-]^{-1}$.

From the data of Newton [14] the average value of pK_4 is calculated to be 2.045 ± 0.015 and from those of Noyes and Kohr [13] 2.02 ± 0.02. On the basis of a critical examination of the available data Sillén [15] gave as the most probable value of $pK_s(AgCl)$ 9.752 ± 0.005. Introducing this value into (4) we find $pK_{s0} = 7.71 \pm 0.03$ from Newton's results, and 7.73 ± 0.05 from those of Noyes and Kohr; the agreement with the figures deduced from the emf measurements is satisfactory.

(C) Conductance measurements

The conductance of a saturated solution of Ag_2O was determined at 25°C with a high accuracy by Böttger [16] and Laue [17]. Both these investigators employed a Ag_2O preparation of high purity and used as solvent "conductivity water" which denotes pure water kept in contact with air. Böttger evaluated K_{s0} by the classical method; he set $10^3(\varkappa - \varkappa_w) = \sqrt{K_{s0}}\,(\lambda_{Ag^+} + \lambda_{OH^-})$ where $\varkappa$ is the conductance of the saturated solution, $\varkappa_w$ is that of the conductance water and λ denotes ionic conductance.

Laue [17] realized that the chief impurity in conductance water is carbon dioxide at such a high concentration (about 10^{-5} M) that a considerable error is made when in the saturated solution $[Ag^+]$ is set equal to $[OH^-]$. Laue has given a correct treatment of his data and obtained $pK_{s0} = 7.71$. The general principles used by this author form the basis of our approach which is somewhat more simple.

The computation of K_{s0} consists of two steps. First α) the total carbon dioxide content, $[CO_2]_{tot}$, of the conductance water is calculated from $\varkappa_w$, then β) the composition of the saturated solution is obtained from $[CO_2]_{tot}$ and $\varkappa$.

Since the ionic strength of a saturated solution is about 10^{-4} M we have assumed the activity factors of all species present to be unity and we have neglected the variation of the ionic conductances with concentration.

α) $[CO_2]_{tot}$ was calculated from $\varkappa_w$ by combining

$$10^3\varkappa_w = h\lambda_{H^+} + [HCO_3^-]\lambda_{HCO_3^-} = h(\lambda_{H^+} + \lambda_{HCO_3^-}) \tag{8}$$

with

$$K_{a1} = \frac{h[HCO_3^-]}{[H_2CO_3 + CO_2]} \tag{9}$$

and $$[CO_2]_{tot} = [H_2CO_3 + CO_2] + [HCO_3^-] \tag{10}$$

Kolthoff and Elmquist [18] have found that $\varkappa_w$ is decreased by no more than about 90 % if CO_2 is removed by purified air from a conductance water. These experiments indicate that it can be regarded only as a rough approximation if we ascribe $\varkappa_w$ entirely to $[CO_2]_{tot}$ because conductance water contains also non-volatile impurities. However the error introduced by calculating $[CO_2]_{tot}$ with (8) does not exceed the uncertainty of the $\varkappa$ measurement.

β) In a saturated solution of Ag_2O the concentrations of the ionic species present are related by the equation

$$[Ag^+] = [OH^-] + [HCO_3^-] + 2[CO_3^{2-}], \tag{11}$$

the specific conductance is given by

$$10^3\varkappa = [Ag^+]\lambda_{Ag^+} + [OH^-]\lambda_{OH^-} + [HCO_3^-]\lambda_{HCO_3^-} + 2[CO_3^{2-}]\lambda_{CO_3^{2-}} \tag{12}$$

and since $\log h$ is about -10

$$[CO_2]_{tot} \cong [HCO_3^-] + [CO_3^{2-}] \tag{13}$$

By taking into account the equilibrium

$$OH^- + HCO_3^- \rightleftharpoons CO_3^{2-} + H_2O; \frac{K_{a2}}{K_w} = \frac{[CO_3^{2-}]}{[OH^-][HCO_3^-]} = K' \qquad (14)$$

insertion of (11) and (13) into (12) yields

$$10^3\varkappa = x(\lambda_{OH^-} + \lambda_{Ag^+}) + \frac{[CO_2]_{tot}}{1 + K'x}[\lambda_{Ag^+} + \lambda_{HCO_3^-} + 2K'x(\lambda_{CO_3^{2-}} + \lambda_{Ag^+})] \qquad (15)$$

where $[OH^-]$ is denoted by x for convenience. The unknown $[OH^-]$ is obtained by a short series of successive approximations from (15) and the known, $[CO_2]_{tot}$, K' and the λ's, then $[HCO_3^-]$ and $[CO_3^{2-}]$ are calculated using (14) and (13). $[Ag^+]$ is found from (11).

The following numerical values were used: $pK_{a1} = 6.352$ [19], $pK_{a2} = 10.329$ [20]; $\lambda_{H^+} = 349.8$, $\lambda_{Ag^+} = 61.92$, $\lambda_{OH^-} = 197.6$, $\lambda_{HCO_3^-} = 44.5$ [21] and $\lambda_{CO_3^{2-}} = 74.0$ [22].

Application of this calculation to the $\varkappa_w$ and $\varkappa$ data of Böttger has given $pK_{s0} = 7.69 \pm 0.02$ while Laue's figures give 7.71 ± 0.02.

The agreement with the pK_{s0} values found in sections (A) and (B) shows that conductance measurement is also capable of giving accurate results in such an unfavorable system as that discussed.

(D) Chemical analysis

The attempts of workers prior to Laue to determine $[Ag(I)]_{tot}$ in a saturated solution of Ag_2O had the purpose of getting only approximate values. Laue [17] and Johnston *et al.*[4] were able to work out electroanalytical and potentiometric methods suitable for determining a silver concentration of about 10^{-4} M with an accuracy of a few percent. The results of these very careful workers differ considerably. Laue found that in paraffinized flasks the solubility equilibrium is established at 25°C within an hour and he obtained $[Ag(I)]_{tot} = (1.51 \pm 0.10) \times 10^{-4}$ M. According to Johnston *et al.* at least ten days were required to attain equilibrium and they found $[Ag(I)]_{tot} = (2.22 \pm 0.04) \times 10^{-4}$ M.

We have reason to assume that Johnston's value for $[Ag(I)]_{tot}$ was high, because some OH^- reacted with small amounts of carbon dioxide in the conductance water ($\varkappa_w \sim 1.2-2 \times 10^{-5}$) and with the surface of the pyrex flask (which was in contact with an alkaline solution for many days) forming silicates, aluminates and borates.

Assuming that $[Ag(I)]_{tot} = [Ag^+]$ we may give a rough estimate of the amount of OH^- ions which by reacting with glass might have caused the high results of Johnston *et al.* These authors used a water of $\varkappa_w = 1.2 \times 10^{-6}$ corresponding to $[CO_2]_{tot} = 2.4 \times 10^{-5}$ M. With this value and with $pK_{s0} = 7.70$ we estimate that their solution with $[Ag^+] = 2.22 \times 10^{-4}$ M contained also $[OH^-] = 9 \times 10^{-5}$, $[HCO_3^-] = 1.7 \times 10^{-5}$, $[CO_3^{2-}] = 7 \times 10^{-6}$ and $[SiO(OH)_3^-] + [Al(OH)_4^-] + [B(OH)_4^-] = 1 \times 10^{-4}$ M. According to experiences in this laboratory such a value for $[SiO(OH)_3^-] + [Al(OH)_4^-] + [B(OH)_4^-]$ does not seem to be unreasonable.

The apparently slow attainment of the solubility equilibrium may also be explained by reaction of OH^- with glass. As the $[OH^-]$ is decreased more Ag_2O

Table 1. Survey of the calculated pK_{s0} values.

Author	Method	Auxiliary data	pK_{s0}
1. Makolkin [9]	emf of the cell $H_2/Ba(OH)_2$ *I* M/Ag_2O, Ag	$e^o(Ag^+/Ag) = 799.4 \pm 0.2$ mV_{abs}	7.70 ± 0.02
2. Hamer and Craig [10]	emf of the cell Hg, HgO/NaOH *I* M/Ag_2O, Ag	$e^o(Ag^+/Ag) = 799.4 \pm 0.2$ mV_{abs} $e^o(H^+/HgO,Hg) = 926.1 \pm 0.3$ mV_{abs}	7.73 ± 0.02
3. Noyes and Kohr [13]	*K* for $\frac{1}{2}Ag_2O + \frac{1}{2}H_2O + Cl^- \rightleftharpoons AgCl + OH^-$	$pK_s(AgCl) = 9.75_2 \pm 0.005$	7.73 ± 0.06
4. Newton [14]	as 3.	as 3.	7.71 ± 0.03
5. Böttger [16]	conductance	$\varkappa_{H_2O} = 1.15 \times 10^{-6}$	7.69 ± 0.02
6. Laue [17]	conductance	$\varkappa_{H_2O} = (1.35$ and $1.53) \times 10^{-6}$	7.71 ± 0.02
7. Laue [17]	chemical analysis	$\varkappa_{H_2O} = 1.2 \times 10^{-6}$	7.75 ± 0.05

will dissolve until $[Ag^+]\,[OH^-]$ becomes again equal to K_{s0}. Dissolution of glass in alkaline solutions is known to be rapid at first, but after prolonged contact the reaction becomes very slow. Thus after a period the increase of the $[Ag^+]$ is expected to be unappreciable.

Recent experimental results on the hydrolysis of the Ag^+ ion [1] have given no support to the hypothesis of Johnston *et al.* that the high solubility is to be explained by the formation of the species Ag_2OH^+.

Laue's data may be used to get an approximate value of K_{s0}. We have assumed $[Ag(I)]_{tot}$ to be equal to $[Ag^+]$. The discussion presented in the next section indicates that the error so made is less than the experimental uncertainty. First $[CO_2]_{tot}$ was calculated from (8) using $\varkappa_w = 1.2 \times 10^{-5}$ as given by Laue, then $[OH^-]$ was obtained from (14) and (11) by successive approximation. This treatment gave $pK_{s0} = 7.75 \pm 0.05$.

The results of our calculations are summarized in Table 1; this indicates a substantial agreement between the pK_{s0} values based on different assumptions and experimental procedures. As the most probable value we would propose the weighted average $\log K_{s0} = -7.71 \pm 0.03$.

ON THE SOLUBILITY OF Ag_2O IN ALKALINE SOLUTIONS

Johnston *et al.*[4] made an extensive and highly accurate study on the solubility of Ag_2O in NaOH, KOH and $Ba(OH)_2$ solutions at 25°C. A few data in NaOH solutions have also been obtained by Laue [17]. It should be pointed out that as $[OH^-]$ exceeds about 0.01 M the solutions attain such a high buffer

capacity that the carbon dioxide content of the conductance water and the dissolution of oxides from the glass surface have a negligible influence on the solubility equilibrium.

Both authors explained their data by equilibrium (3); Laue obtained log $K_{s2} = -3.70$ and Johnston *et al.* found log $K_{s2} = -3.71$. The latter authors gave moreover log $K_{s1} = -5.60$. The validity of the assumption that exclusively mononuclear hydrolysis products are formed was verified only recently by distribution [2] and emf [3] studies carried out in this laboratory.

We have recalculated both sets of data by a more exact method than was done previously, and we have employed the curve fitting technique [23] which may yield a more reliable estimate of the uncertainties of the computed constants. No attention was paid to the results found in solutions of $[OH^-] \leq 0.01$ M because these may be expected to be not quite reliable.

The water activity and the ratio of the activity factors of OH^- and $Ag(OH)_2^-$ were assumed to be unity; the error made seems to be negligible compared with the experimental uncertainty. We calculated from the vapor pressure measurements of Robinson and Stokes [24] $\frac{1}{2}$ log $\{H_2O\}$ to be -0.0075 at [NaOH] = 1 M; this was the highest $[OH^-]$ considered.

We have also assumed in the following calculation that $f(Ag^+)\ f\ (OH^-) = f_\pm^2 = 1$; this seems to be permissible because, at the $[OH^-]$ values where $f_\pm$ is expected to deviate appreciably from unity, $[Ag^+] = \dfrac{K_{s0}}{f_\pm^2[OH^-]}$ becomes much less than the uncertainty in the $[Ag(I)]_{tot}$ determination.

We started from the equation

$$[Ag]_{tot} = [Ag^+] + [AgOH] + [Ag(OH)_2] = \frac{10^{-7.71}}{[OH^-]} + K_{s1} + K_{s2}[OH^-] \qquad (16)$$

(16) can be rearranged to

$$\log\left([Ag]_{tot} - \frac{10^{-7.71}}{[OH^-]}\right) = \log K_{s1} + \log\ (1 + \frac{K_{s2}}{K_{s1}}\ [OH^-]) \qquad (17)$$

If the data $\log\left([Ag]_{tot} - \dfrac{10^{-7.71}}{[OH^-]}\right) = f(\log\ [OH^-])$ are superimposed on the calculated curve $\log(1 + X) = f(\log X)$ the vertical displacement required to make them coincide yields log K_{s1} and the horisontal one log $\dfrac{K_{s2}}{K_{s1}}$. We have found in this way

$$\log K_{s1} = -5.75 \pm 0.25$$

and

$$\log K_{s2} = -3.72 \pm 0.03,$$

which agree well with the previously determined values.

The solubility equilibria of Ag_2O are visualized in Fig. 1; the curve was calculated with the constants given in the Synopsis. The deviations of the data at log $[OH^-] < -2$ illustrate the great difficulties encountered when poorly buffered solutions are studied.

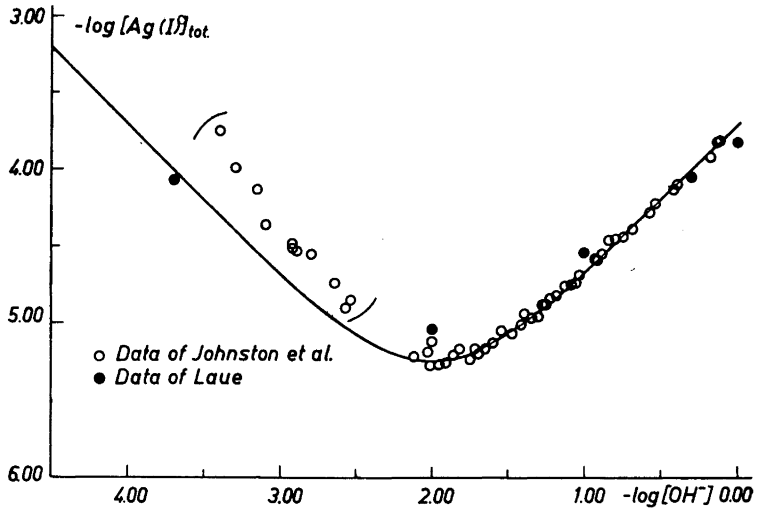

Fig. 1. The solubility equilibria of Ag_2O. log $[Ag(I)]_{tot}$ as a function of log $[OH^-]$. O measurements of Johnston *et al.*[4], ●: measurements of Laue [17]. The curve represents the equation $\log [Ag(I)]_{tot} = \log ([Ag^+] + [AgOH] + [Ag(OH)_2^-] = \log \left(\frac{1.95 \times 10^{-8}}{[OH^-]} + \right.$ $\left. + 1.8 \times 10^{-6} + 1.90 \times 10^{-4}[OH^-] \right)$

For the complex formation $OH^- - Ag^+$ these data give $\log K_1 = \log \{[AgOH]\,[Ag^+]^{-1}\,[OH^-]^{-1}\} = 2.0 \pm 0.3$ and $\log \beta_2 = \log\{[Ag(OH)_2^-]\,[Ag^+]^{-1}\,[OH^-]^{-2}\} = 3.99 \pm 0.05$, which means that $K_1 \sim K_2$.

The corresponding acidity constants of Ag^+ are then both around $10^{-12.0}$ (since $\log K_w = 14.00$ at 25°C), thus Ag^+ is another of the aquo ions with first and second acidity constant of the same order of magnitude.[25]

Note added in proof. After this work was submitted to publication Professor Reino Näsänen has kindly informed us on an investigation recently carried out in his laboratory. Näsänen and Meriläinen has determined K_{s0} at 25°C by emf measurements using a glass electrode, and they obtained $pK_{s0} = 7.74$. This value is in excellent agreement with those calculated by the present authors.

This investigation was financially supported by *Statens Naturvetenskapliga Forskningsråd (Swedish Natural Science Research Council)*.

REFERENCES

1. Biedermann, G. and Hietanen, S. *Acta Chem. Scand.* **14** (1960) 711.
2. Antikainen, P. J. and Dyrssen, D. *Acta Chem. Scand.* **14** (1960) 86.
3. Antikainen, P. J., Hietanen, S. and Sillén, L. G. *Acta Chem. Scand.* **14** (1960) 95.
4. Johnston, H. L., Cuta, F. and Garrett, A. B. *J. Am. Chem. Soc.* **55** (1933) 2311.
5. Pleskov, Yu. V. and Kabanov, B. N. *Zhur. neorg. Khim.* **2** (1957) 1807.
6. Luther, R. and Pokorny, F. *Z. anorg. Chem.* **57** (1908) 290.

7. Lewis, G. N. and Randall, M. *Thermodynamics and the Free Energy of Chemical Substances*, McGraw-Hill Book Company Inc. New York 1923, p. 483.
8. Fried, F. *Z. physik. Chem.* **123** (1926) 406.
9. Makolkin, I. A. *Zhur. Fiz. Khim.* **16** (1942) 13.
10. Hamer, W. J. and Craig, N. D. *J. Electrochem. Soc.* **104** (1957) 206.
11. Berecki-Biedermann, C., Biedermann, G. and Sillén, L. G. *Copper, silver and gold potentials* and *Zinc, cadmium and mercury potentials*, Preliminary report to the Analytical Section of IUPAC, July 1953 (mimeographed).
12. Harned, H. S. and Mason, M. C. *J. Am. Chem. Soc.* **54** (1932) 1439.
13. Noyes, A. A. and Kohr, D. A. *Z. physik. Chem.* **42** (1903) 336.
14. Newton, R. F. *J. Am. Chem. Soc.* **50** (1928) 3258.
15. Sillén, L. G. *Solubility of silver halogenides*, Preliminary report to the Analytical Section of IUPAC, July 1953 (mimeographed).
16. Böttger, W. *Z. physik. Chem.* **46** (1903) 521.
17. Laue, E. *Z. anorg. Chem.* **165** (1927) 325.
18. Kolthoff, I. M. and Elmquist, R. *J. Am. Chem. Soc.* **53** (1931) 1217.
19. Harned, H. S. and Davis, R. Jr. *J. Am. Chem. Soc.* **65** (1943) 2030.
20. Harned, H. S. and Scholes, S. R. Jr. *J. Am. Chem. Soc.* **63** (1941) 1706.
21. Mac Innes, D. A. *Principles of Electrochemistry*, Reinhold Publishing Corporation, New York 1939.
22. Lange, J. *Z. physik. Chem.* **A188** (1941) 284.
23. Sillén, L. G. *Acta Chem. Scand.* **10** (1956) 186.
24. Robinson, R. A. and Stokes, R. H. *Electrolyte solutions*, Butterworths Scientific Publications, London 1959.
25. Sillén, L. G. *Quart. Revs. London.* **13** (1959) 146.

Received December 1, 1959.

ACTA CHEMICA SCANDINAVICA 14 (1960) 726–732

The Crystal Structure of $(TiCl_4 . POCl_3)_2$

CARL-IVAR BRÄNDÉN and INGVAR LINDQVIST

Institute of Chemistry, University of Uppsala, Uppsala, Sweden

The crystal structure of $(TiCl_4 \cdot POCl_3)_2$ has been determined from three-dimensional X-ray data. The structure is built up of dimeric molecules $(TiCl_4 \cdot POCl_3)_2$ with double chlorine bridges between the two titanium atoms of the dimer. The coordination around the titanium atom is octahedral. The oxygen atom in $POCl_3$ functions as donor atom. The approximately tetrahedral structure of $POCl_3$ is preserved.

Titanium tetrachloride is a strong Lewis acid and forms a great number of addition compounds with different donor molecules (Lewis bases). The mole ratio acceptor molecule to donor molecule is 1:1 or 1:2. The phase diagram $TiCl_4$—$POCl_3$ shows the existence of both types of compounds between $TiCl_4$ and $POCl_3$.[1] Sheldon and Tyree [2] have concluded from the shifts in the phosphoryl bond stretching frequency (measured in infrared) that phosphoryl chloride functions as a donor molecule through the oxygen atom. The present study was undertaken as a part of our investigations of the coordination and of the chemical bonds in addition compounds of different oxychlorides.

PREPARATIONS

Single crystals of the very hygroscopic compound were prepared in sealed capillary tubes by a method of zone melting. In most preparations the compound studied in this paper was obtained. Two other compounds appeared, however, in some cases. The unit cell volumes of those two crystals show simple ratios to the unit cell volume of the crystals usually prepared *(vide infra)*. They therefore probably represent other modifications. Preparations from carbon tetrachloride solutions give only the most common modification. We have not further studied the conditions of preparation of the two less common modifications.

CRYSTAL DATA

The unit cell dimensions of the orthorhombic crystals were determined by an extrapolation method used earlier by Hermodsson and Strandberg [3]. The values are $a = 12.42 \pm 0.02$ Å, $b = 12.76 \pm 0.05$ Å and $c = 13.51 \pm 0.02$ Å. The extinctions $h0l$ for l odd, $0kl$ for k odd and $hk0$ for h odd lead to the spacegroup *Pbca*.

This is in agreement with the data published earlier [1,4] except for some small corrections and improvements in accuracy. They also showed that there are eight units of $TiCl_4 \cdot POCl_3$ in the unit cell.

The other two modifications are monoclinic with the following approximate unit cell dimensions:

$a = 9.9$ Å, $b = 8.7$ Å, $c = 12.3$ Å and $\beta = 98°$
$a = 13.9$ Å, $b = 12.1$ Å, $c = 19.1$ Å and $\beta = 105°$

The cell volumes are very nearly one and three halves respectively of the orthorhombic unit cell volume (0.48 and 1.43).

The single crystal was rotated around the *b*-axis and Weissenberg photographs were taken. Nine zones (0—8) were recorded with Ni-filtered Cu-*K* radiation using multiple-film technique. Connection between the zones was obtained using a method described by Magnéli [5].

The 785 independent intensities were estimated visually. The relative $|F|^2$ values were obtained after correction using the chart of Lu [6]. No correction was made for absorption errors. The capillary tube used had an inner diameter of 0.10 mm. The linear absorption coefficient is 236.0 cm^{-1} for Cu-$K\alpha$ radiation.

DETERMINATION OF THE ATOMIC POSITIONS

After some unsuccessful attempts to solve the structure by means of Harker sections a three-dimensional Pattersson synthesis was calculated on the Hägg-Laurent machine [7]. Most of the maxima in this function were rather broad due to overlapping of several peaks of almost equal height. A method suggested by Lindqvist [8] was used to interpret the Pattersson function.

All atoms of the formula unit $TiCl_4 \cdot POCl_3$ are in the general position 8 (*c*) of space group *P b c a*. Between two crystallographically different atoms there are 8 vectors within the asymmetric unit of the cell, related by the following coordinates for the vectors in Pattersson space.

x_1,y_1,z_1; $\frac{1}{2}-x_1$, $\frac{1}{2}-y_2,z_2$; x_2, $\frac{1}{2}-y_1$, $\frac{1}{2}-z_2$;
$\frac{1}{2}-x_2,y_2$, $\frac{1}{2}-z_1$; x_2,y_2,z_2; $\frac{1}{2}-x_2$, $\frac{1}{2}-y_1,z_1$;
x_1, $\frac{1}{2}-y_2$, $\frac{1}{2}-z_1$; $\frac{1}{2}-x_1$, y_1, $\frac{1}{2}-z_2$.

By combining the maxima in the Pattersson function in groups according to this relation, it proved possible to determine approximate coordinates for seven atoms, Ti, O and 5 Cl.

Using these coordinates, signs were determined for F $(0,k,l,)$, F $(h,0,l,)$ and F $(h,k,0)$. The corresponding Fourier projections were calculated and from these the remaining three atoms could be located. Three successive sets of Fourier projections along all three axes were calculated. From the parameters thus obtained the signs were determined for 550 observed F (h,k,l). This and the following calculations were made on the electronic computer BESK in Stockholm. The atomic scattering factors were evaluated by a two-term expansion of Gaussian functions with constants given by Vand *et al.*[9]

Table 1. Final atomic parameters and their standard deviations.

Atom	x	y	z	$\sigma(x)$ Å	$\sigma(y)$ Å	$\sigma(z)$ Å
Ti	0.0629	0.3616	0.4986	0.005	0.006	0.005
P	0.1875	0.4353	0.2819	0.008	0.009	0.008
O	0.1075	0.4124	0.3564	0.020	0.020	0.016
Cl_1	0.1062	0.5507	0.5424	0.007	0.009	0.007
Cl_2	0.2364	0.3205	0.5231	0.008	0.009	0.008
Cl_3	0.0098	0.2107	0.4306	0.008	0.010	0.008
Cl_4	0.0092	0.3285	0.6506	0.008	0.010	0.007
Cl_5	0.2852	0.5483	0.3130	0.010	0.011	0.011
Cl_6	0.2769	0.3103	0.2522	0.009	0.010	0.008
Cl_7	0.1207	0.4706	0.1548	0.009	0.011	0.008

Two successive three-dimensional Fourier synthesis were carried out, the last one giving a broad and miss-shaped maximum for one of the chlorine atoms, indicating an errouneous assumed position for this atom. All other maxima were sharp and well-defined.

In order to get a better position for this atom signs were determined for F (h,k,l) using the other nine atomic positions. Bounded Fourier projections along the a-axis between the planes $x = 0$ and $x = \frac{1}{2}$ as well as along the c = axis with boundaries $z = 0$ and $z = \frac{1}{2}$ were calculated. These projections gave only one extra well-defined maximum besides maxima at the assumed atomic positions.

At this stage the structure was tested against the three-dimensional Pattersson synthesis. The overlap was very large but all maxima were explained.

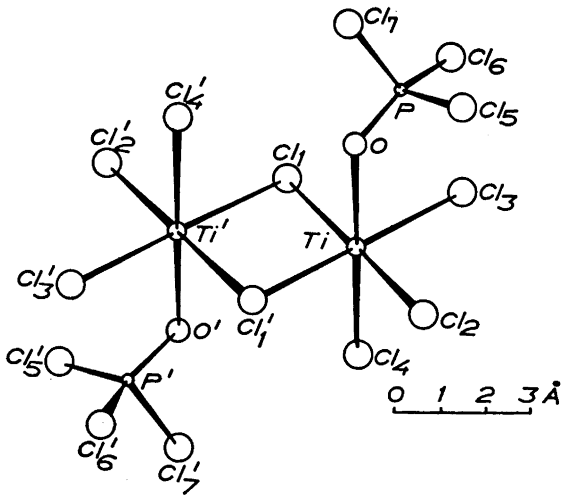

Fig. 1. The molecule of the addition compound $(TiCl_4 \cdot POCl_3)_2$.

REFINEMENT AND ASSESSMENT OF ACCURACY

Two successive three-dimensional Fourier synthesis were computed, in the last one the signs were determined for all F (h,k,l).

Two three-dimensional back-shift corrections were then carried out. To obtain an estimate of the standard deviations in the atomic coordinates Cruickshank's method [10] was used. The second back-shift correction gave smaller shifts than the standard deviation.

The standard deviations obtained with the calculated structure-factors after the back-shift corrections are given in Table 1 together with the final parameters. Using a temperature factor of 4.30 Å^2, the reliability index $R = \Sigma \mid |F_o| - |F_c| \mid / \Sigma |F_o|$ for all observed reflexions is 0.18.

A copy of the observed and calculated F-values can be obtained from this Institute by request.

DESCRIPTION AND DISCUSSION OF THE STRUCTURE

The structure of one adduct molecule is shown in Fig. 1 and the bond lengths and bond angles are given in Table 2 together with their standard deviations.

The molecule is a dimer and the compound should be written $(TiCl_4 \cdot POCl_3)_2$ and named di-μ-chloro-hexachlorobis(phosphorylchloride) dititanium (IV). The double chlorine bridge has not been found earlier in addition compounds of titanium tetrachloride but it has been recognized as a common feature in the adducts of many other acceptor molecules studied by Mann and his school [11]. One example is $(PdBr_2 \cdot Me_3As)_2$. No accurate structure determination has been made of such compounds however.

Table 2. Bond distances and bond angles in $(TiCl_4 \cdot POCl_3)_2$ and their standard deviations.

Distance	(Å)	S.D. (Å)	Angle	(°)	S.D. (°)
Ti — Cl_1	2.44	0.01	Cl_1 — Ti — Cl_1'	78.5	0.3
Ti — Cl_1'	2.54	0.01	Cl_1 — Ti — Cl_3	92.8	0.4
Ti — Cl_2	2.24	0.01	Cl_3 — Ti — Cl_2	98.2	0.4
Ti — Cl_3	2.23	0.01	Cl_2 — Ti — Cl_1'	89.1	0.4
Ti — Cl_4	2.20	0.01	Cl_1' — Ti — Cl_4	91.7	0.4
Ti — O	2.10	0.02	Cl_2 — Ti — Cl_4	96.2	0.4
P — O	1.44	0.02	Cl_3 — Ti — Cl_4	97.4	0.4
P — Cl_5	1.93	0.01	Cl_1 — Ti — Cl_4	92.2	0.4
P — Cl_6	1.98	0.01	Cl_1 — Ti — O	83.0	0.6
P — Cl_7	1.96	0.01	Cl_1' — Ti — O	82.2	0.6
			Cl_2 — Ti — O	87.4	0.6
			Cl_3 — Ti — O	88.1	0.6
			Cl_4 — Ti — O	173.0	0.6
			Cl_3 — Ti — Cl_1'	167.5	0.4
			Cl_2 — Ti — Cl_1	165.0	0.4
			Ti — O — P	151.8	1.3
			O — P — Cl_5	115.6	0.9
			O — P — Cl_6	111.3	0.9
			O — P — Cl_7	111.5	0.9
			Cl_5 — P — Cl_6	107.0	0.6
			Cl_5 — P — Cl_7	106.6	0.6
			Cl_6 — P — Cl_7	104.1	0.5

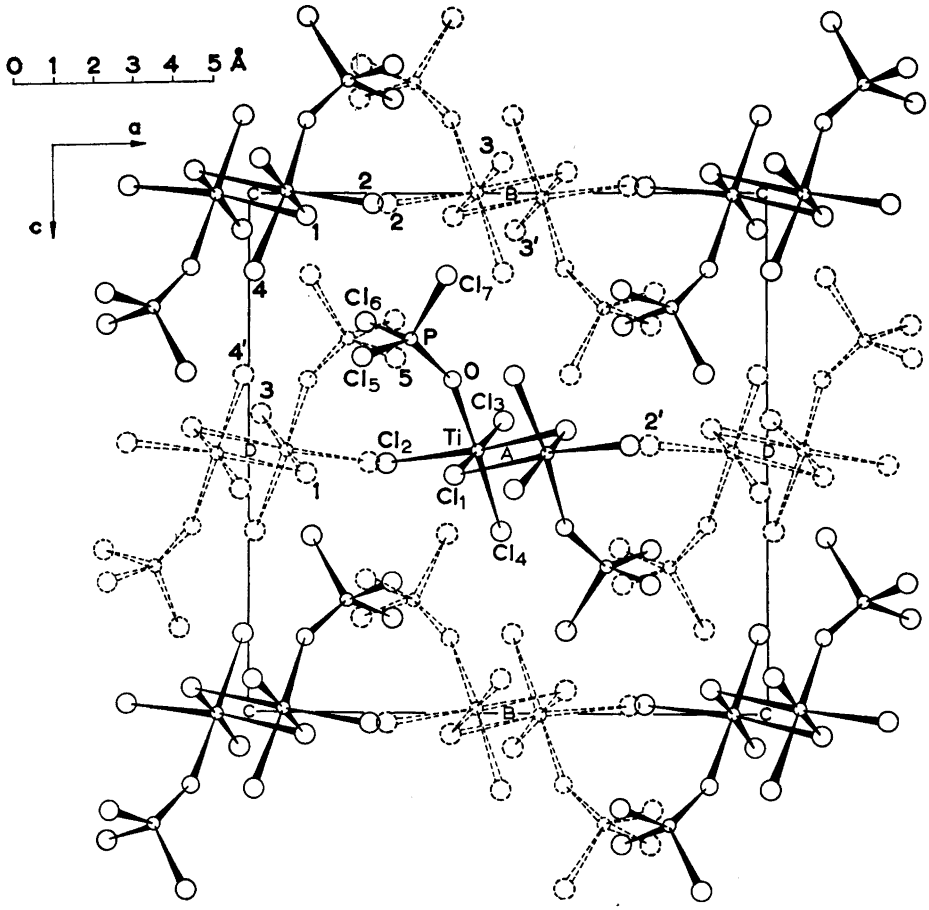

Fig. 2. Projection of the structure along [010], showing different Cl—Cl contacts. The dotted molecules have their centre of symmetry at $y = 1/2$, the other molecules at $y = 0$.

The possible existence of different geometrical isomers in such dimeric molecules was also discussed by Mann and Wells [11]. The present compound has a symmetrical *trans* configuration but the other two modifications found by us may represent other possible geometrical isomers.

The $POCl_3$ molecule has not changed much by the adduct formation and has a structure very similar to free $POCl_3$ [12] and to $POCl_3$ in $SbCl_5 \cdot POCl_3$ [13] (averaged values): P—O 1.44, 1.45 and 1.46 Å; P—Cl 1.96, 1.995 and 1.96 Å; O—P—Cl 112.8°, 114.9° and 112.0°; Cl—P—Cl 105.9°, 103.5° and 106.4°.

The acceptor molecule $TiCl_4$ has changed its co-ordination from tetrahedral to octahedral. The Ti—Cl bond lengths have increased from 2.18 ± 0.04 Å in free $TiCl_4$ [14] to 2.20—2.24 Å ± 0.02 Å for the non-bridging chlorine atoms and the significantly larger values 2.44 and 2.54 ± 0.02 Å for the bridging

Table 3. Packing distances in $(TiCl_4 \cdot POCl_3)_2$.
(*Cf.* Fig. 2.)

	Distance (Å)
$Cl_7(A) - Cl_1$ (C)	3.73
$Cl_7(A) - Cl_2$ (C)	3.66
$Cl_7(A) - Cl_3'$ (B)	3.65
$Cl_6(A) - Cl_1$ (C)	3.65
$Cl_6(A) - Cl_2$ (B)	3.55
$Cl_6(A) - Cl_4'$ (D)	3.63
$Cl_6(A) - Cl_5$ (D)	3.53
$Cl_5(A) - Cl_3$ (D)	3.65
$Cl_5(A) - Cl_4$ (C)	3.72
$Cl_4(A) - Cl_3$ (B)	3.81
$Cl_3(A) - Cl_2'$ (D)	3.48
$Cl_2(A) - Cl_1$ (D)	3.96

chlorine atoms. Such an increase in bond length by bridge formation is to be expected but is easily obscured because of lacking accuracy in the structure determination. Even quite weak bridge interaction is reflected in a bond length increment [15].

The Ti—O bond length of 2.10 Å is almost the same as the Sn—O bond length of 2.12 Å found in $SnCl_4 \cdot 2SeOCl_2$,[16] while the short Ti—Cl bond lengths are appreciably shorter than the corresponding Sn—Cl bond lengths: 2.20—2.24 Å compared with 2.36—2.41 Å. These results will be discussed in a following paper.

Gillespie and Nyholm [17] have suggested that the electronegativity difference between oxygen and the neighbour atoms will determine the bond angle at a bridging oxygen atom. The two known structures of $POCl_3$ addition compounds are in agreement with this idea. Titanium is less electronegative than antimony and the bond angle Ti—O—P is accordingly larger than Sb—O—P: 151.8° compared with 143.7°.

The packing of the molecules is indicated in Fig. 2. All packing distances less than 4.0 Å between different molecules are collected in Table 3.

In the discussion of the structure of another adduct molecule $SeOCl_2 \cdot 2NC_5H_5$[15] it was pointed out that the generally used concepts of covalent and ionic bonds cannot profitably be applied to compounds of this type. A detailed discussion of the conditions will be given in a following paper [18].

We wish to thank Professor G. Hägg for all facilities put at our disposal and Mr Y. Hermodsson for stimulating discussions. These investigations have been sponsored by a grant from the *Air Force Office of Scientific Research and Development Command, United States Air Forces*, through its European Office under Contract No. AF 61 (052)-43. This grant is greatfully acknowledged.

REFERENCES

1. Groeneveld, W. L., van Spronsen, J. W. and Kouwenhoven, H. W. *Rec. trav. chim.* **72** (1953) 950.
2. Sheldon, J. C. and Tyree, S. Y. *J. Am. Chem. Soc.* **80** (1958) 2290.
3. Hermodsson, Y. and Strandberg, B. *Acta Cryst.* **10** (1957) 434.

4. Sørum, H. *Kgl. Norske Videnskab. Selskab, Forh.* **17** (1944) (No 5) 17.
5. Magnéli, A. *Acta Chem. Scand.* **2** (1948) 501.
6. Lu, C.-S. *Rev. Sci. Instr.* **14** (1943) 331.
7. Hägg, G. and Laurent, T. *J. Sci. Instr.* **23** (1946) 155.
8. Lindqvist, I. *Arkiv Mineral. Geol.* (1959), **2** (1960) 505.
9. Vand, V., Eiland, P. F. and Pepinsky, R. *Acta Cryst.* **10** (1957) 303.
10. Cruickshank, D. W. J. *Acta Cryst.* **2** (1949) 65.
11. Mann, F. C. and Wells, A. F. *J. Chem. Soc.* **1938** 702.
12. Badgley, G. R. and Livingston, R. L. *J. Am. Chem. Soc.* **76** (1954) 261.
13. Lindqvist, I. and Brändén, C.-I. *Acta Cryst.* **12** (1959) 642.
14. Lister, M. W. and Sutton, L. E. *Trans. Faraday Soc.* **37** (1941) 393.
15. Lindqvist, I. and Nahringbauer, G. *Acta Cryst.* **12** (1959) 638.
16. Hermodsson, Y. *Acta Cryst.* **13** (1960). *In press.*
17. Gillespie, R. J. and Nyholm, R. S. *Quart. Revs. London* **11** (1957) 339.
18. Lindqvist, I. *Acta Chem. Scand.* **14** (1960). *In press.*

Received December 15, 1959.

ACTA CHEMICA SCANDINAVICA 14 (1960) 733–741

Borides of Rhenium and the Platinum Metals

The Crystal Structure of Re_7B_3, ReB_3, Rh_7B_3, $RhB_{\sim 1.1}$, $IrB_{\sim 1.1}$ and PtB

B. ARONSSON and (in part) E. STENBERG and J. ÅSELIUS*

Institute of Chemistry, University of Uppsala, Uppsala, Sweden

Some features of the binary systems of boron with rhenium and the platinum metals are reported. Re_7B_3 and Rh_7B_3 are isomorphous with Ru_7B_3 (Th_7Fe_3 ($D10_3$)-type). The structure of ReB_3 is closely related to those of Mo_2B_5 and W_2B_5. $RhB_{\sim 1.1}$ and PtB crystallize in the anti-NiAs structure, and a phase with the approximate composition $IrB_{\sim 1.1}$ is isomorphous with $ThSi_2$ (C_c-type).

As mentioned in an earlier communication [1] studies on the borides of the platinum metals are in progress at this Institute. In the previous paper the crystal structure of Ru_7B_3 was dealt with. In this paper we shall discuss some general features of the binary systems of boron with rhenium and the platinum metals and also described the crystal structures of Re_7B_3, ReB_3, Rh_7B_3, $RhB_{\sim 1.1}$, $IrB_{\sim 1.1}$ and PtB.

EXPERIMENTAL

Rhenium, ruthenium, rhodium and osmium (powder) were obtained from Heraeus (Hanau, Germany) and iridium and platinum from Johnson, Matthey & Co (London). Crystalline boron powder was kindly donated by Borax Consolidated (London). The manufactures have given the following information about their products:

Re : ca. 99.8 %
Ru : ca. 99.9 % – 99.95 %, traces of Cu, Fe, Ca, Mg and Si
Rh : ca. 99.95 %, traces of Ru, Fe, Ca and Mg
Os : ca. 99.5 %, main impurity: oxygen, traces of alkali and Fe
Ir : min. 99.8 %
Pt : min. 99.9 %
B : 99.0–99.7 %, main impurities: Fe, Si, O.

All phases reported in this paper were prepared by arc melting weighed amounts of metal and boron powders. Some borides of ruthenium, rhodium, and platinum were also synthesized by sintering in crucibles of recrystallized alumina (Degussit Al 23 from Degussa, Frankfurt).

* *Note on authorship.* E. Stenberg and J. Åselius have collaborated with the main author in the crystal structure determinations of Rh_7B_3, $RhB_{\sim 1.1}$, $IrB_{\sim 1.1}$ and PtB.

No chemical analyses were made. Since the vapour pressures of boron and the metals involved are not very different, we believe that the compositions are not changed much when the samples are melted.

Powder photographs were taken in cameras of the Guinier type (Cu$K\alpha$-radiation) with CaF_2 (a = 5.4630 Å) and NaCl (a = 5.6401 Å) as internal standards. Since the expression for the intensities of powder lines is somewhat different for cameras of the Guinier type than for the ordinary Debye-Scherrer cameras we have also given the calculated $p|F|^2$ values. Single crystals of the phases $RhB_{\sim 1.1}$, $IrB_{\sim 1.1}$ and PtB were examined in Weissenberg cameras. We used Mo$K\alpha$ radiation and the multiple film technique with thin iron foils between the films. The intensities were visually estimated by comparison with an intensity scale. The structure factors of Re_7B_3 and Rh_7B_3 were computed on the digital electronic computer BESK with a program devised by Åsbrink *et al.* [2]. The scattering factors were computed with the formula:

$$f_i = A_i \exp\left(-\frac{a_i}{\lambda^2}\sin^2\Theta\right) + B_i\exp\left(-\frac{b_i}{\lambda^2}\sin^2\Theta\right) + C_i \exp\left(-\frac{c_i}{\lambda^2}\sin^2\Theta\right) + D_i$$

The following constants A_i, B_i, C_i, a_i, b_i and c_i were calculated by Dr. K. Appel at the Quantum Chemistry Group of this University on basis of the scattering factor tables by Tomas and Umeda [3] (rhenium, rhodium) and Ibers [4] (boron):

	A	B	C	a	b	c
Re	25.854	28.303	19.925	0.170	1.885	15.175
Rh	15.520	16.977	12.024	0.237	2.600	20.057
B	1.644	0.406	2.878	0.6069	4.5832	33.019

In the calculations of the structure factors of ReB_3, $RhB_{\sim 1.1}$ and $IrB_{\sim 1.1}$ we used the mentioned scattering factor tables [3,4].

No corrections for dispersion (D_i) absorption or thermal movement were made.

RESULTS

A great number of intermediate phases were observed in the arcmelted alloys. We could characterize some phases by determining their crystal structures or unit cells (Table 1). We have confirmed the observation of Buddery and Welch [5] that many borides of the platinum metals are also easily prepared by sintering in silica tubes. Thus, Ru_7B_3, $RuB_{\sim 1.0}$, Rh_7B_3, $RhB_{\sim 1.1}$, and PtB

Table 1. Crystallographic constants of borides of rhenium and the platinum metals.

	Structure type	Lattice parameters in Å	Unit cell volume in Å^3
Re_3B	(orthorhombic)	$a = 2.89_4$ $b = 9.31_7$ $c = 7.26_4$	
Re_7B_3	Th_7Fe_3	$a = 7.50_4$ $c = 4.77_2$ $c/a = 0.6506$	238.1
ReB_3	ReB_3	$a = 2.900$ $c = 7.475$ $c/a = 2.578$	54.44
Ru_7B_3	Th_7Fe_3	$a = 7.46_9$ $c = 4.71_4$ $c/a = 0.631_1$	227.6
$RuB_{\sim 1.0}$	(cubic?)	$a = 6.98$	
Rh_7B_3	Th_7Fe_3	$a = 7.47_1$ $c = 4.77_7$ $c/a = 0.639_4$	230.9
$RhB_{\sim 1.1}$	anti-NiAs	$a = 3.30_9$ $c = 4.22_4$ $c/a = 1.27_7$	40.0$_5$
$OsB_{\sim 1.0}$	(cubic ?)	$a = 7.04$	
$IrB_{\sim 1.1}$	$ThSi_2$	$a = 2.81_0$ $c = 10.26_3$ $c/a = 3.65_2$	81.0$_4$
PtB	anti-NiAs	$a = 3.35_8$ $c = 4.05_8$ $c/a = 1.20_8$	39.6$_3$

were successfully synthesized in alumina crucibles which had been inserted in evacuated and sealed silica tubes. As pointed out by Rundqvist and Jellinek [6] and also ourselves [7] borides prepared in this way may be contaminated through reactions with the silica tubes. It seems as if the risk of contamination is

Table 2. Powder photograph of an arcmelted alloy with the nominal composition Re_2B-(Cu$K\alpha$ radiation).

$h\ k\ l$ for Re_7B_3	$\sin^2\Theta_{obs}$	$\sin^2\Theta_{calc}$ for Re_7B_3	I_{obs}	I_{calc} for Re_7B_3	$pF^2_{calc} \times 10^{-4}$ for Re_7B_3
101	0.0392	0.0390	m	4	2.0
110	0.0425	0.0422	w+	2	0.8
?	0.0531		w+		
200	0.0563	0.0563	w	7	4.8
201	0.0814	0.0812	st	49	53.0
(ReB_3)	0.0942		vw		
210	0.0987	0.0985	st	69	90.0
002	0.0998	0.0998	m	20	26.9
(ReB_3)	0.1049		m+		
?	0.1090		vw		
102	0.1137	0.1138	st+	93	138.8
211	0.1234	0.1234	vst	241	382.0
300	0.1268	0.1266	m+	19	31.1
(ReB_3)	0.1369		vw		
112	0.1421	0.1420	m	8	14.1
301	0.1517	0.1516	st+	64	121.1
202	0.1560	0.1560	st	48	93.6
220	0.1689	0.1689	st−	27	57.5
310	0.1830	0.1829	vw	1	2.0
(ReB_3)	0.1902		w		
212	0.1983	0.1983	m	11	27.8
311	0.2079	0.2079	m	13	33.8
400	0.2255	0.2251	w+	4	10.3
302		0.2264		8	2.1
103	0.2384	0.2385	vw	2	4.6
401	0.2500	0.2500	m+	19	52.6
222	0.2684	0.2686	w+	8	24.4
203	0.2808	0.2807	st−	29	86.2
321	0.2921	0.2923	m−	10	31.6
410	0.2953	0.2955	w−	4	13.4
411	0.3205	0.3204	w+	7	21.9
213	0.3229	0.3229	(m−) *	11	33.2
402	0.3257	0.3249	(w+) *	3	9.9
303	0.3512	0.3511	vst	92	274.0
500		0.3518		18	54.0
322	0.3673	0.3674	vst	109	310.0
501	0.3768	0.3767	st+	84	235.8
330	0.3800	0.3799	st+	76	212.4
412	0.3956	0.3953	w+	8	22.6
004	0.3990	0.3990	m−	15	39.9
313	0.4074	0.4074	m+	19	50.2
104	0.4127	0.4131	m−	22	55.7

* A powder line of ReB_3 overlaps 213 and 402.

Table 3. Powder photograph of an arcmelted alloy with the nominal composition Rh_7B_3. (Cu$K\alpha$ radiation.)

$h\ k\ l$ Rh_7B_3	$\sin^2\Theta_{obs}$	$\sin^2\Theta_{calc}$ for Rh_7B_3	I_{obs}	I_{calc} for Rh_7B_3	$pF^2_{calc} \times 10^{-4}$ for Rh_7B_3
200	0.0568	0.0568	vw	2.0	1.4
201	0.0829	0.0829	st	14.4	16.0
210	0.0995	0.0995	st+	21.8	28.6
002	0.1042	0.1043	st−	6.0	8.3
102	0.1185	0.1185	st+	29.0	44.7
(Rh)	0.1234		st		
211	0.1256	0.1255	vst	76.2	122.9
300	0.1279	0.1279	m	6.6	10.8
112	0.1471	0.1469	w	2.5	4.7
301	0.1539	0.1540	st	20.7	39.8
202	0.1613	0.1611	st−	15.4	30.7
(Rh)	0.1644		m		
220	0.1706	0.1705	m+	9.0	19.2
212	0.2034	0.2038	w	3.7	9.2
311	0.2107	0.2108	w−	4.3	11.0
400	0.2272	0.2274	vw	1.3	3.4
302	0.2323	0.2322	w−	2.4	6.6
401	0.2532	0.2534	w+	6.0	16.6
222	0.2749	0.2748	w−	2.4	6.9
203	0.2913	0.2915	m	8.8	26.6
(Rh)	0.3286		m		
500	0.3553	0.3553	w	5.4	15.9
303	0.3623	0.3626	st+	28.4	83.5
322	0.3742	0.3743	st+	31.3	89.5
501	0.3820	0.3813	vst	26.1	72.6
330		0.3837		23.6	65.5
004	0.4180	0.4172	w	5.1	12.3
313		0.4194		6.5	15.2
104	0.4311	0.4314	w+	6.9	16.8

reduced when direct contact between sample and silica is avoided, but without complete chemical analyses we can make no quantitative statements on this point.

The lattice parameters (l.p.) of rhenium, ruthenium, rhodium, osmium, iridium and platinum in two-phase metal-boron alloys were not significantly (that is not more than 0.05 %) different from those reported for the pure metals. This indicates that the solubility of boron is small in the solid phases of the metals mentioned.

In arc-melted rhenium-boron alloys only three rhenium borides were observed. Their unit cells are given in Table 1. We could not detect the tetragonal phase Re_2B which Neshpor *et al.*[8] reported to exist in sintered alloys. The other binary systems certainly contain several more intermediate phases than those in Table 1. We have confirmed the observation [5] that the powder photographs of $RuB_{\sim 1.0}$ and $OsB_{\sim 1.0}$ could be indexed with a cubic unit cell. As far as we are aware the other phases of Table I have not been properly characterized before.

The formulæ of Re_7B_3, ReB_3, Ru_7B_3, Rh_7B_3 and PtB are based on the structures of these phases but seem to agree well with their real compositions. The ideal structural formulae of $RhB_{\sim 1.1}$ and $IrB_{\sim 1.1}$ are RhB (or possibly RhB_2) and IrB_2 respectively. In both cases, other phases not yet characterized may have the same ideal composition. It is suggested that the notations $RhB_{\sim 1.1}$ and $IrB_{\sim 1.1}$ be used until the Rh-B and Ir-B systems have been clarified.

The l.p. variations of the phases of Table 1 are small. The largest variations (0.1—0.2 %) were observed for $RhB_{\sim 1.1}$ and PtB. Thus, the reported phases probably have narrow ranges of homogeneity.

The crystal structures of Re_7B_3, ReB_3, Rh_7B_3, $RhB_{\sim 1.1}$, $IrB_{\sim 1.1}$ and PtB: The powder photographs of Re_7B_3 and Rh_7B_3 were very similar to that of Ru_7B_3. When we assumed the atomic parameters to be the same in Re_7B_3 and Rh_7B_3 as in Ru_7B_3 we obtained good agreement between observed and calculated intensities (Tables 2 and 3). Thus, Re_7B_3 and Rh_7B_3 are isomorphous with Ru_7B_3.

The powder photograph of ReB_3 (Table 4) could be indexed with a hexagonal cell. From the size of the unit cell we concluded that it contained two rhenium atoms. The only systematic extinction was observed for $hh\bar{2}hl$ reflexions which only appeared for l even. Thus, the possible space groups are: $P6_3/mmc$ $P\bar{6}2c$, $P6_3mc$, $P\bar{3}1c$ and $P31c$. Assuming the rhenium atoms to occupy two-fold positions 1/3, 2/3, 1/4 (or 1/3, 2/3, z) excellent agreement between observed and calculated intensities is obtained (Table 4). Because of the

Table 4. Powder photograph of an arcmelted alloy with the nominal composition ReB_3. (Cu$K\alpha$ radiation.)

$h\ k\ l$ for ReB_3	$\sin^2\Theta_{obs}$	$\sin^2\Theta_{calc}$ for ReB_3	I_{obs}	I_{calc}* for ReB_3	$pF^2_{calc} \times 10^{-4}$ for ReB_3
002	0.0425	0.0426	st+	6.6	3.26
?	0.0530	—	vw	—	
100	0.0942	0.0942	m—	1.9	2.34
101	0.1048	0.1049	vst	10.0	13.7
102	0.1367	0.1368	m	2.4	4.20
004	0.1702	0.1702	m—	1.2	2.73
103	0.1898	0.1900	st+	4.8	11.3
104	0.2644	0.2644	w+	1.1	3.30
110	0.2827	0.2827	m	2.1	6.42
112	0.3251	0.3252	st	3.9	12.0
105	0.3602	0.3602	m+	2.9	8.62
200	0.3770	0.3769	w—	0.5	1.41
006	0.3830	0.3829	w	0.7	1.87
201	0.3876	0.3876	m+	3.0	8.34
202	0.4197	0.4195	w	1.1	2.66
114	0.4530	0.4529	st	4.6	10.2
203	0.4731	0.4727	st—	3.6	7.54
106	0.4775	0.4773	w+	1.2	2.49

* Only the rhenium contributions have been accounted for in the calculations of pF^2_{calc} and I_{calc}.

Table 5. Interatomic distances in ReB_2 (in Å).

Re	— 6 Re	: 2.90 (6).
	— 8 B_I	: 2.24 (2); 2.24 (6).
	— 6 B_{II}	: 2.51 (6).
B_I	— 4 Re	: 2.24, 2.24 (3).
	— 3 B_I	: 1.83 (3).
	— 3 B_{II}	: 1.71 (3).
B_{II}	— 6 Re	: 2.51 (6).
	— 6 B_I	: 1.71 (6).

great differences in scattering power of rhenium and boron, the boron atoms have to be located from space considerations. If we make the plausible assumptions that Re-B distances are > 2.2 Å and B-B distances > 1.6 Å, six boron atoms can be situated in one four-fold position 1/3, 2/3, z and one two-fold position 0,0,0 (or 0,0,z). The only other boron arrangement which does not seem very improbable is to place the boron atoms in one six-fold position x,0,0 ($x \sim 1/3$). In this second alternative the shortest B—B distances have the normal value of 1.68 Å but the shortest Re—B distance is only 2.10 Å. Therefore, the first proposed structure is considered to be the most probable one. This structure has the symmetry of space group $P6_3/mmc$ with the following atomic positions:

2 Re in 2(c)
4 B_I in 4(f) with $z = 0.55$
2 B_{II} in 2(a)

Interatomic distances are given in Table 5. [The second, less probable structure has the symmetry of space group $P\bar{6}2c$ with two rhenium atoms in 2(c) and six boron atoms in 6(g) with $x \sim 1/3$].

Table 6. Power photographs of arcmelted alloys with the nominal compositions $RhB_{1.5}$ and PtB, respectively. (Cu$K\alpha$ radiation.) Since the relative values of I_{calc} are very similar for $RhB_{\sim 1.1}$ and PtB, they have only been computed for $RhB_{\sim 1.1}$.

$h\ k\ l$ for NiAs-type	$RhB_{1.5}$					PtB		
	$\sin^2\Theta_{obs}$	$\sin^2\Theta_{calc}$ for $RhB_{\sim 1.1}$	I_{obs}	I_{calc} for $RhB_{\sim 1.1}$	$pF^2 \times 10^{-3}$ for $RhB_{\sim 1.1}$	$\sin^2\Theta_{obs}$	$\sin^2\Theta_{calc.}$ for PtB	I_{obs}
?			—			0.0531	—	vw
100	0.0723	0.0723	st—	6.3	5.88	0.0703	0.0703	st
101	0.1057	0.1056	vvst	32.6	44.9	0.1064	0.1064	vst
?			—			0.1158	—	w
002	0.1332	0.1332	m	5.0	7.98	0.1445	0.1444	m
102	0.2058	0.2056	m+	6.0	14.9	0.2143	0.2146	st
110	0.2169	0.2170	st	9.8	25.8	0.2110	0.2108	st
200	0.2896	0.2894	w	1.3	3.80	0.2806	0.2810	w
201	0.3226	0.3227	st	9.3	28.2	0.3168	0.3171	st
112	0.3501	0.3502	st+	10.6	31.6	0.3551	0.3551	st+
103	0.3720	0.3721	st—	9.2	26.3	0.3950	0.3951	m+
202	0.4224	0.4226	m	4.2	10.3	0.4254	0.4254	m

Table 7. Interatomic distances in $RhB_{\sim 1.1}$ and PtB (in Å).

Rh — 12 Rh : 2,85 (6); 3.31 (6).		Pt — 12 Pt : 2.81 (6); 3.36 (6)	
— 6 B : 2.18 (6).		— 6 B : 2.19 (6).	
B — 6 Rh : 2.18 (6).		B — 6 Pt : 2.19 (6).	
— 2 B : 2.21 (2).		— 2 B : 2.03 (2).	

The powder photographs of $RhB_{\sim 1.1}$ and PtB were very similar indicating that these phases were isomorphous. From the systematic extinction of $h\,h\,\bar{2}\bar{h}l$ reflexions with l odd and the unit cell dimension we suspected that the structure of these phases was of the anti-NiAs ($B8$) type. With this assumption (space group $P\bar{6}_3/mmc$, two metal atoms in 2(c) and two boron atoms in 2(a)), good agreement between observed and calculated intensities was obtained (Table 6). A single crystal of each of $RhB_{\sim 1.1}$ and PtB was also studied. The agreement between observed and calculated structure factors for $h\,0\,\bar{h}\,l$ reflexions is satisfactory — the R value was 9.4 % (45 observed reflexions) for $RhB_{\sim 1.1}$ and 10.0 % (29 observed reflexions) for PtB. Interatomic distances are given in Table 7. (In a preliminary communication [5] we described the structure of $RhB_{\sim 1.1}$ and PtB using the orthorhombic space-group $C\,m\,c\,m$. We have found, however, that there are no significant deviations from hexagonal symmetry.)

The single crystal and powder photographs of $IrB_{\sim 1.1}$, finally, could be indexed with a tetragonal unit cell. Since $h\,k\,l$ reflexions were only observed when $h + k + l = 2n$ and $2k + l = 2n + 1$ or $4n$, the only possible space group was $I4_1/amd$. In order to adhere to convention we have chosen the

Table 8. Powder photograph of an arc-melted alloy with the nominal composition $IrB_{1.15}$ (Cu$K\alpha$ radiation).

$h\,k\,l$ for $IrB_{\sim 1.1}$	$\sin^2\Theta_{obs}$	$\sin^2\Theta_{calc}$ for $IrB_{\sim 1.1}$	I_{obs}	I_{calc}** $IrB_{\sim 1.1}$	$pF^2 \times 10^{-4}$ ** for $IrB_{\sim 1.1}$
* 101	0.0809	0.0809	vst	23.0	25.2
004	0.0903	0.0903	m	10.6	12.7
103	0.1260	0.1260	st	15.0	24.4
112	0.1732	0.1731	st +	21.4	45.6
105	0.2165	0.2163	m —	8.0	21.1
* 200	0.3011	0.3010	st	6.2	18.9
107	0.3539	0.3517	st	5.9	17.4
116		0.3536		10.2	30.6
008	0.3609	0.3611	w	2.7	7.8
* 211	0.3824	0.3819	st	10.7	29.8
204	0.3915	0.3913	m	11.2	30.4
213	0.4267	0.4270	m +	12.3	30.1

* The strongest lines of a neigbouring phase, traces of which are present in this alloy coincide with 101, 200 and 211. Therefore, the observed intensities of these lines are stronger than expected.

** In the computations of I_{calc} and pF^2 it has been assumed that the 8(e) positions are statistically occupied by four boron atoms.

Table 9. Interatomic distances in $IrB_{\sim 1.1}$ (in Å).

Ir	— 8 Ir	: 2.81 (4);	2.92 (4).
	— 12 B *	: 2.16 (8);	2.22 (4).
B*	— 6 Ir	: 2.16 (4);	2.22 (2).
	— 3 B*	: 1.66 (2);	1.68 (1).

* The boron positions are occupied to only about 50 %.

origin at $\bar{4}m2$. From the size of the unit cell we concluded that it contained four iridium atoms which were placed in 4(*a*). As in the case of ReB_3 the boron atoms had to be located from space considerations. It seems unlikely that the boron atoms occupy the positions 4(*b*), 8(*c*) or 8(*d*) since with boron in any of these positions Ir—B distances of about 2.0 Å or shorter would be formed. The most probable boron position is in 8(*e*) with $z = 0.41_8$. The agreement between observed and calculated intensities for the proposed structure is good (Table 8). With the boron atoms in 8(*e*), $IrB_{\sim 1.1}$ is isomorphous with $ThSi_2$[9] (C_c type according to the handbooks of Smithells [10] and Pearson [11]). Interatomic distances are shown in Table 9.

DESCRIPTIONS OF THE STRUCTURES AND COMMENTS

The Ru_7B_3 structure was discussed at some length in the previous paper [1]. Somewhat unexpectedly the Me_7B_3 borides are isomorphous with Th_7Fe_3[12] (*D* 10_2-type [10,11]). (In this connection we wish to point out that the structure [12] of ThCo is also isomorphous with a common boride structure, namely the CrB structure).

The rhenium skeleton of ReB_3 is built up of close packed layers arranged in a close packed hexagonal structure (*ABAB* . . .). The shortest intermetallic distance within the layers is 2.90 Å whereas atoms of neighbouring layers only have a remote contact (4.10 Å) with each other. Between the metal layers there are slightly puckered hexagonal sheets of boron atoms with the shortest B—B distances 1.71 Å and 1.83 Å. The distances between atoms of neighbouring boron layers are also quite large (> 3.0 Å). Thus the cohesion in the *c*-direction must be mainly due to metal-boron bonds.

The structures which Kiessling [13] has suggested for W_2B_5 and Mo_2B_5 contain the same building elements as ReB_3. In addition to the puckered boron sheets there are also plane boron layers in W_2B_5 and Mo_2B_5. With the usual notations the sequences of close packed hexagonal metal layers in ReB_3, W_2B_5 and Mo_2B_5 are: *ABAB* . . ., *AABBAABB* . . ., and *AABBCCAABBCC*..., respectively. If, following Kiessling, we denote the puckered boron sheets with *K* and the plane boron sheets in W_2B_5 and Mo_2B_5 with *H*, the complete stacking sequences along the *c* direction of the three structures are as follows:

ReB_3 : *AKBK* . . .
W_2B_5 : *AHAKBHBK* . . .
Mo_2B_5 : *AHAKBHBKCHCK* . . .

Thus, these structures are very closely related.

$IrB_{\sim 1.1}$ is of interest because of its apparent deviation from the ideal formula IrB_2. It should be noted that other compounds with structures closely related to that of $ThSi_2$ also show deviations from the ideal formula. Thus, Perri *et al.*[14] found that a gadolinium silicide with the ideal formula $GdSi_2$ had the composition $GdSi_{1.4}$.

Acknowledgements. We wish to thank professor Hägg for his kind interest. The research described in this paper has been sponsored by *Air Force Office of Scientific Research of the Air Research and Development Command, United States Air Force*, through its European Office under Contract No. AF 61(052)-40 and by the *Swedish Technical Science Research Council*. The financial support from these authorities is gratefully acknowledged.

REFERENCES

1. Aronsson, B. *Acta Chem. Scand.* **13** (1959) 109.
2. Åsbrink, S., Blomqvist, G. and Westman, S. *Arkiv Kemi* **14** (1959) 50.
3. Tomas, L. H. and Umeda, K. *J. Chem. Phys.* **26** (1957) 293.
4. Ibers, J. A. *Acta Cryst.* **10** (1957) 86.
5. Buddery, J. H. and Welch, A. J. E. *Nature* **167** (1951) 362.
6. Rundqvist, S. and Jellinek, F. *Acta Chem. Scand.* **13** (1959) 425.
7. Aronsson, B., Stenberg, E. and Åselius, J. *Nature* **183** (1959) 318.
8. Neshpor, V. S., Paderna, Ya. B. and Samsonov, G. V. *Doklady Akad. Nauk. SSSR* **118** (1958) 515.
9. Brauer, G. and Mitius, A. *Z. anorg. allgem. Chem.* **249** (1942) 325.
10. Smithells, C. H. *Metal reference book*, Butterworth, London 1955.
11. Pearson, W. B. *A handbook of lattice spacings and structures of metals and alloys*, Pergamon Press, London-New York-Paris-Los Angeles 1958.
12. Florio, J. V., Baenziger, N. C. and Rundle, R. E. *Acta Cryst.* **9** (1956) 367.
13. Kiessling, R. *Acta Chem. Scand.* **1** (1947) 893.
14. Perri, J. A., Binder, I. and Post, B. *J. Phys. Chem.* **63** (1959) 616.

Received December 7, 1959.

ACTA CHEMICA SCANDINAVICA 14 (1960) 742–748

Position of the *O*-Acetyl Groups in Birch Xylan *

HANS O. BOUVENG, PER J. GAREGG and BENGT LINDBERG

Svenska Träforskningsinstitutet, Träkemiska avdelningen, Stockholm Ö, Sweden

A xylan containing 11.8 % uronic acid and 16.9 % *O*-acetyl has been isolated from birch holocellulose by extraction with dimethyl sulphoxide. Methylation studies of the acetyl xylan itself and of a deacetylated sample have shown that the *O*-acetyl groups are attached to the xylose residues mainly in the 3-position and only to a lesser extent in the 2-position.

Birch wood xylan, the predominating hemicellulose in birch wood, has been shown to consist of a chain of 1,4-linked β-D-xylose residues, with every tenth to fifteenth residue substituted in the 2-position with a 4-*O*-methyl-α-D-glucopyranosyluronic acid residue [1-3]. Acetic and formic acids have been isolated from several woods [4] but Timell in an examination of birch wood found only acetic acid [5]. The isolation from birch wood of a partly acetylated xylan [6] localised at least part of the acetic acid in the wood.

In the present investigation the acetylated xylan was isolated by extraction with dimethyl sulphoxide (DMSO) from birch wood holocellulose which had been prepared by chlorination and treatment with ethanolic ethanolamine from a mixture of *Betula verrucosa* Ehrh. and *B. pubescens* Ehrh. The holocellulose was subsequently extracted with hot water and 12 % potassium hydroxide. The yield and composition of the different fractions are given in Table 1. The DMSO extract represented about 50 % of the xylan in the wood and xylose formed about 96 % of the aldose residues of the extract. The present results are thus substiantially different from those obtained with birch chlorite holocellulose [6] from which only about 15 % of the acetylated xylan could be extracted by this method. By osmometry according to Pals and Hermans [7] the $\overline{DP}_n$ of the acetylated xylan was estimated as 200 ± 10.

The positions of the *O*-acetyl groups in the acetylated xylan were investigated by two series of methylations. In the first series the acetylated xylan was fully methylated by a slightly modified version [8] of the method described by Kuhn *et al.*[9] The product (*O*-acetyl, 10.1 %; methoxyl, 28.1 %) was reduced with lithium aluminium hydride to yield a partially methylated glucoxylan

* Preliminary results of this investigation have been published in *Chem. and Ind., 1958*, 1727; the results were presented at the 136th meeting of the American Chemical Society, Atlantic City, New Jersey, September 1959. Abstract 3 E.

Table 1. Yield and composition of extracts from birch holocellulose (%).

	Yield	Lignin	CH_3CO	Uronic acid	OCH_3 %	Aldose residues				
						Galactose	Glucose	Mannose	Arabinose	Xylose
Birch holocellulose	—	7.2				0.9	61.0	2.9	1.1	33.9
DMSO extract	15.0	2	16.9	11.8	1.77	0.8	3.1	—	—	96.2
Hot water extract	0.55	5	4.0	42.7	2.58	19.1	18.2	3.5	8.0	49.6
12 % KOH extract	15.6	3	—	14.6	1.57	1.1	3.2	1.6	1.6	92.0
Residue			—			0.9	88.9	3.5	0.7	6.0

(AMX; $\overline{DP}_n$, 60). In the second series the xylan was methylated with simultaneous deacetylation and then after reduction was converted to a fully methylated glucoxylan (MX; $\overline{DP}_n$, 43) by further methylation. The low $\overline{DP}_n$ values for the two methylated xylans indicate that considerable depolymerisation occurred during the methylations.

The two methylated polysaccharides were hydrolysed and the monomeric sugars obtained were separated on a carbon-Celite column and estimated quantatively. 2-*O*- and 3-*O*-methyl-D-xylose were incompletely separated on the column and were separated for quantitative estimation by paper electrophoresis in borate buffer;[10] fractionation on a preparative scale was done on a carbon-Celite column by gradient elution in the presence of borate buffer [11]. The results of the fractionations are summarised in Table 2.

The presence of 2-*O*-methyl-D-xylose in the hydrolysed MX cannot be unequivocally accounted for. It is known from studies on cellulose [10,12] that hydroxyl groups in different positions show considerable differences in reactivity on methylation. It is also known from investigations at this Institute (unpublished results) that 2,3-di-*O*-methyl-D-xylose is demethylated to a small extent under the conditions employed for the hydrolysis of AMX and MX, but without

Table 2. Methyl ethers (in mole %) obtained from methylated xylans from birch wood.

Methyl ether	Acetylated methylated xylan (28.1 % OMe)	Deacetylated methylated xylan (37.4 % OMe)
Xylose	5.4	0.1
2-*O*-Methylxylose	17.5	2.5
3-*O*-Methylxylose	9.1	6.3
2,3-Di-*O*-methylxylose	58.1	78.3
2,3,4-Tri-*O*-methylxylose	—	5.2
2,3,4-Tri-*O*-methylglucose	9.8	4.0
2,3,4,6-Tetra-*O*-methylglucose	—	3.7

any preferential demethylation at either the 2- or the 3-position. Thus the presence in the hydrolysate from MX of 2-*O*-methyl-D-xylose which is often found in hydrolysates from methylated xylans (*cf. e.g.* Ref.[2]) might be explained either by incomplete methylation or by demethylation during hydrolysis. Another possibility is the occurrence of some branching points in the original polysaccharide, which might be correlated with the proportion of 2,3,4-tri-*O*-methyl-D-xylose (5.2 mole %) which is higher than that required by a straight chain of about 40 xylose residues (2.3 mole %). This matter however requires further investigation. Aspinall and Das Gupta have recently obtained evidence for a branched xylose chain in a similar xylan from jute.[13] The 2-*O*-methyl-D-xylose in the hydrolysed MX could also be accounted for by the presence of 3-*O*-(4-*O*-methyl-D-glucuronopyranosyl)-D-xylose residues which have been found in *Pinus radiata* D. Don [14] and various grasses.[15] However, a paper chromatographic investigation of a partial hydrolysate did not reveal the presence of this aldobiouronic acid.

The virtual absence of 2,3,4-tri-*O*-methyl-D-xylose from hydrolysed AMX indicates that most of the terminal non-reducing xylose residues carry *O*-acetyl groups.

The results show that the *O*-acetyl groups in the methylated acetylated xylan are attached to the xylose residues mainly at the 3-position and only to a lesser degree at the 2-position. However, the 30 % of the *O*-acetyl groups that is replaced by methoxyl groups is not accounted for. No indications were found of *O*-acetyl groups on the uronic acid residues. As the conditions during methylation [16] and possibly also in the isolation of the polysaccharide favour the migration of acetyl groups it is not possible to extrapolate the results obtained back to the native polysaccharide. In naturally occurring 1-*O*-acetyl-D-mannitol [17] and 6-*O*-acetyl-D-glucose [18] the *O*-acyl groups occupy the most readily acetylated position. No conclusion can be drawn from the present investigation as to whether this is also the case for the acetylated xylan.

EXPERIMENTAL

All melting points are corrected. Evaporations were done under reduced pressure at a bath temperature below 40°.

Chromatography. Papers: Whatman No. 1 and 3MM. Solvents: A. Ethyl acetate-acetic acid-water, 3:1:3. B. Butanol-ethanol-water 10:3:5. C. *Iso*propyl ether-light petroleum (40–60°), 1:1 (on DMSO-impregnated paper [19]).

Paper electrophoresis. Papers: Whatman No. 1, Schleicher and Schüll 602 hP. Buffers: 0.1 M borate buffer at pH 10, 0.1 M acetate buffer at pH 4. Spray reagents: Aniline hydrogen phthalate, anisidine hydrochloride.

Preparation of birch wood holocellulose. Acetone-extracted birch wood (a technical mixture of *Betula verrucosa* Ehrh. and *B. pubescens* Ehrh.) of particle size 1–2 mm (462 g) was treated with chlorine in ice-water and extracted with 3 % ethanolic ethanolamine according to Timell and Jahn [20], yielding birch holocellulose (373 g). Yields and analytical data for the holocellulose and the extracts described below are given in Table 1.

Extraction of the holocellulose. The holocellulose (300 g) was extracted twice with redistilled dimethyl sulphoxide (3 l) at room temperature. After filtration the combined solutions were acidified with acetic acid and the hemicellulose was precipitated by adding two volumes of ethanol and removed by centrifugation. It was obtained as a powder after reprecipitation from aqueous solution with ethanol, washing with ethanol and ether and drying in a vacuum. The hemicellulose had $\overline{DP}_n$ 200 ± 10 and $[\alpha]_D^{20}$ −69° (*c*, 1.0 in water).

Table 3. Distillation at constant volume of the volatile acid from birch wood xylan and of some known acids.

Distillate ml	Formic acid %	Acetic acid %	Propionic acid %	Acid from xylan
25	17	27	46	28
50	31	46	70	46
75	41	60	82	59
100	50	69	89	68
125	56	76	93	75
150	62	81		80
175	66	85		84
200	70	88		87
225	74	90		90

The residual holocellulose was extracted twice with boiling water for 2 h and then twice with 12 % aqueous potassium hydroxide under nitrogen overnight at room temperature. The extracts were worked up as described above. The lignin in the holocellulose was estimated as Klason lignin, that in the hemicellulose fractions by measuring the absorption at 280 mμ [21]. Uronic acid contents were determined according to Johansson *et al.* [22], and quantitative paper chromatography on aldoses in the hemicellulose hydrolysates was done according to Saeman *et al* [23].

Identification of the O-*acetyl groups.* The acetic acid was identified by Dyers method [24]. The xylan (0.25 g) was heated in N sodium hydroxide at 100° for 15 min. The solution was acidified and the volatile acid was removed by distillation. After neutralisation with sodium hydroxide and concentration the solution containing the acetate was passed through Amberlite IR-120 (H^+), made up to 50 ml and distilled at constant volume. The distillate was collected in 25 ml fractions which were titrated with 0.01 N sodium hydroxide. Solutions with comparable concentrations of authentic formic, acetic and propionic acid were distilled in a similar manner. The results are summarised in Table 3 which shows that only acetic acid was obtained from the xylan.

Methylation of acetylated birch wood xylan. DMSO-extracted xylan (4 g) was dissolved in dry dimethyl formamide (150 ml). Methyl iodide (10 ml) and silver oxide (9 g) were added in small portions over 5 h and the solution was stirred vigorously and cooled externally. The reaction was allowed to proceed for a further 20 h and the product was then isolated as previously described [8]. The product was methylated in the same way a further three times. Yield 1.55 g, OCH_3 28.1 %, CH_3CO 10.1 %. (The calculated methoxyl content for a fully substituted xylan with 10.1 % *O*-acetyl is 28.4 %). This material is referred to as AMX.

Methylation with deacetylation of birch xylan. The xylan (4 g) was first methylated with simultaneous deacetylation using methyl sulphate in aqueous sodium hydroxide and then methylated three times with methyl iodide and silver oxide in dimethyl formamide. Yield 3.32 g, OCH_3 37.4 % (theoretical value 38.3 %). This material is referred to as MX.

Reduction of AMX and MX. AMX (1.5 g) was reduced with lithium aluminium hydride (2 g) in boiling, anhydrous tetrahydrofuran (100 ml) for 4 h. After addition of water to destroy excess reducing agent and neutralisation with sulphuric acid, the reaction mixture was filtered and concentrated to dryness. The product was extracted with chloroform and precipitated in light petroleum from benzene solution. Yield 1.4 g. MX (1.3 g) was reduced similarly to yield 1.2 g of product. This was then methylated twice with methyl iodide and silver oxide in the usual manner. Yield 1.1 g, OCH_3 37.9 %.

Hydrolysis of reduced AMX and MX. Reduced AMX (1 g) was treated with formic acid at 100° for 8 h and then with 0.5 N hydrochloric acid at 100° overnight. The solution was passed through Amberlite IR 4B (free base) and concentrated to a syrup. Yield 0.85 g.

Reduced MX (0.80 g) was hydrolysed in a mixture of 20 ml acetic acid and 40 ml 0.5 N sulphuric acid at 100° overnight. The hydrolysate was treated with barium hydroxide, filtered and concentrated to a small volume. After extraction with ethanol and concentration the mixture of monomeric sugars was obtained as a syrup (0.81 g).

Table 4. Fractionation of hydrolysed AMX. *Gradients:* 0 → 12 % aqueous ethanol (3 l), 12 → 35 % aqueous ethanol (3 l). 20-ml fractions were collected.

Tube No.	Component	Millimole	Mole %
21—38	Xylose	0.198	5.4
41—44	3-*O*-Methylxylose	0.112	3.0
45—88	2-*O*- + 3-*O*-Methylxylose	0.870	23.6
108—166	2,3-Di-*O*-methylxylose	2.14	58.1
Residue	2,3,4-Tri-*O*-methylglucose	0.360	9.8

Ratio: 2-*O*-: 3-*O*-methylxylose in fraction 45—88 was 2.9:1.

Fractionation of hydrolysed AMX and MX. The hydrolysates were fractionated on a carbon-Celite column (4 × 46 cm) by gradient elution with aqueous ethanol [25]. The column was subsequently washed with 50 % acetone. The amount of reducing sugar in each of the combined fractions was determined by hypoiodite oxidation [26]. The fractions containing both 2-*O*- and 3-*O*-methyl-D-xylose were analysed for each component by quantitative paper electrophoresis in borate [10] while fractionation on a preparative scale was done on a carbon-Celite column (2.8 × 30 cm) by gradient elution (2 l 0—6 % aqueous ethanol) in the presence of borate (0.1 M, pH 10); 3-*O*-methyl-D-xylose was eluted first. The results of the fractionations are summarised in Tables 4 and 5.

Characterisation of components

D-*Xylose.* Table 4: Crystallised from ethanol-water, m. p. and mixed m. p. 143—145°. Table 5: Characterised by paper chromatography.

2-O-*Methyl*-D-*xylose.* Table 4: Crystallised from acetone, m. p. 131—133°. Table 5: The ether was indistinguishable by paper electrophoresis from an authentic specimen, kindly supplied by Dr. T. E. Timell, Montreal.

Table 5. Fractionation of hydrolysed MX. *Gradients:* 0 → 12 % aqueous ethanol (3 l), 12 → 30 % aqueous ethanol (2 l), 30 % aqueous ethanol → 30 % aqueous acetone (3 l), 30 % → 50 % aqueous acetone (2 l). 25 ml fractions were collected.

Tube No.	Component	Millimole	Mole %
24— 42	Xylose	0.031	0.1
54— 71	3-*O*-Methylxylose	0.203	4.9
72—120	2-*O*- + 3-*O*-Methylxylose	0.163	3.9
134—224	2,3-Di-*O*-methylxylose	3.25	78.1
230—254	2,3,4-Tri-*O*-methylglucose	0.166	4.0
255—284	2,3,4-Tri-*O*-methylxylose	0.216	5.2
Residue	2,3,4,6-Tetra-*O*-methylglucose	0.154	3.7

Ratio: 2-*O*- : 3-*O*-methylxylose in fraction 72—120 was 1.8:1.

3-O-Methyl-D-xylose. Tables 4 and 5: Crystallised from acetone and methyl ethyl ketone, m. p. and mixed m. p. 96—98°. The ether was indistinguishable from authentic material on paper electrophoresis.

2,3-Di-O-methyl-D-xylose. Table 4: $[\alpha]_D^{20}$ +23° (*c*, 1.5 in water). The anilide had m. p. 124—126°. Table 5: $[\alpha]_D^{20}$ +23.5° (*c*, 1.5 in water). The anilide had m. p. 126—128°. These values are in good agreement with those previously reported [27].

2,3,4-Tri-O-methyl-D-xylose. $[\alpha]_D^{20}$ +18° (*c*, 1.1 in water). The anilide after crystallisation from ligroin had m. p. and mixed m. p. 99—101°. The ether was indistinguishable from authentic material by paper chromatography on DMSO-impregnated paper in solvent C.

2,3,4-Tri-O-methyl-D-glucose. The ether was in both cases indistinguishable from an authentic sample on paper chromatography in solvents A, B and C. Attempts to crystallise the aniline derivative failed; on paper chromatography in solvent C it gave two spots corresponding to the α and β forms, both of which were indistinguishable from the spots given by 2,3,4-tri-*O*-methyl-D-glucopyranosyl-N-phenylamine.

2,3,4,6-Tetra-O-methyl-D-glucose. Demethylation gave glucose only. The ether was indistinguishable from an authentic sample on paper chromatography in solvent A, B and C.

Partial hydrolysis of birch wood xylan. Xylan (5 g) from the 12 % potassium hydroxide extract was dispersed in water (300 ml) and 2 N sulphuric acid (100 ml) was added. The mixture after keeping at 100° for 3 h gave a clear solution. After neutralisation with barium hydroxide and filtration, the solution was concentrated to a small volume. Paper chromatography in the ethyl acetate-pyridine-water, 2:1:2 solvent indicated the presence of at least two acidic components together with xylose and small amounts of other sugars. The barium salts of the acids were precipitated with ethanol. From the supernatant liquid further amounts of barium salts of acids were obtained after concentration and repeated precipitation. The precipitates were washed with ethanol and reprecipitated. The free acids (0.76 g) were obtained after removal of the cations with Amberlite IR-120 (H^+) and concentration to dryness.

Fractionation of the acidic components. The acidic fraction (0.76 g) was adsorbed on a cellulose column, 2.5 × 35 cm, and eluted with ethyl acetate-acetic acid-formic acid-water 19:3:1:4 (3 l). 25 ml fractions were collected. Suitable fractions were combined, evaporated to dryness and examined by paper chromatography in ethyl acetate-acetic acid-water 3:1:1, in ethyl acetate-acetic acid-formic acid-water 19:3:1:4 and by paper electrophoresis in borate and acetate buffer.

Fraction 1 (75 mg) contained mainly 4-*O*-methyl-D-glucuronic acid together with a smaller amount of 2-*O*-(4-*O*-methyl-α-D-glucuronopyranosyl)-D-xylose, both indistinguishable from authentic specimens.

Fraction 2 (250 mg) contained 2-*O*-(4-*O*-methyl-D-glucuronopyranosyl)-D-xylose and a trace of a component of lower R_F-value on paper chromatography. The aldobiouronic acid was indistinguishable from authentic material on chromatography and on electrophoresis.

Fraction 3 (320 mg) consisted of a mixture of higher acids and oligosaccharides and was not examined further. No aldobiouronic acid was observed corresponding to 3-*O*-(4-*O*-methyl-D-glucuronopyranosyl)-D-xylose, which is reported to move faster than 2-*O*-(4-*O*-methyl-D-glucuronopyranosyl)-D-xylose on paper chromatography in ethyl acetate: acetic acid:formic acid-water, 19:3:1:4 [14].

Osmometric DP_n determinations. Osmometric determinations were made on the sodium salt of the acetylated xylan in 0.1 N sodium chloride [7] using "Ultrafein allerfeinst" membranes, supplied by Membranfiltergesellschaft Göttingen. Determinations of the DP_n of AMX and MX were carried out in chloroform and butyl acetate, respectively, using "Ultracellafilter allerfeinst" membranes supplied by the same firm.

One of the authors (PJG) is indebted to *Papirindustriens Forskningsinstitutt*, Oslo, Norway, for a fellowship.

REFERENCES

1. Saarnio, J., Wathén, K. and Gustafsson, C. *Acta Chem. Scand.* **8** (1954) 825.
2. Glaudemans, C. P. J. and Timell, T. E. *J. Am. Chem. Soc.* **80** (1958) 1209.
3. Gorin, P. A. J. and Perlin, A. S. *Can. J. Chem.* **36** (1958) 999.
4. Bird, C. D. and Ritter, G. J. *J. Am. Chem. Soc.* **59** (1937) 802.
5. Timell, T. E. *Svensk Papperstidn.* **60** (1957) 762.
6. Hägglund, E., Lindberg, B. and McPherson, J. *Acta Chem. Scand.* **10** (1956) 1160.
7. Pals, D. T. F. and Hermans, J. J. *Rec. trav. chim.* **71** (1952) 458.
8. Bouveng, H. O. *Acta Chem. Scand.* **12** (1958) 1877.
9. Kuhn, R., Trischmann, H. and Löw, I. *Angew. Chem.* **67** (1955) 32.
10. Croon, I. and Lindberg, B. *Svensk Papperstidn.* **60** (1957) 843.
11. Barker, S. A., Bourne, E. J. and Theander, O. *J. Chem. Soc.* **1955** 4276.
12. Croon, I., *Svensk Papperstidn.* **61** (1958) 919.
13. Aspinall, G. O. and Das Gupta, P. C. *J. Chem. Soc.* **1958** 3627.
14. Brash, D. J. and Wise, L. E. *Tappi* **38** (1956) 581.
15. Roudier, A. *Compt. rend.* **237** (1953) 840.
16. Bouveng, H. O., Lindberg, B. and Theander, O. *Acta Chem. Scand.* **11** (1957) 1788.
17. Lindberg, B. *Acta Chem. Scand.* **7** (1953) 1119.
18. Duff, R. B. and Foumer, V. C. *Nature* **179** (1957) 103.
19. Wickberg, B. *Acta Chem. Scand.* **12** (1958) 615.
20. Timell, T. E. and Jahn, E. C. *Svensk Papperstidn.* **54** (1951) 831.
21. Meier, H. *Acta Chem. Scand.* **12** (1958) 1911.
22. Johansson, A., Lindberg, B. and Theander, O. *Svensk Papperstidn.* **57** (1954) 41.
23. Saeman, J. F., Moore, W. E., Mitchell, R. L. and Millet, M. A. *Tappi* **37** (1954) 336.
24. Clark, E. P. *Semimicro Quantitative Analysis*, New York 1943 p. 85.
25. Lindberg, B. and Wickberg, B. *Acta Chem. Scand.* **8** (1954) 569.
26. Hirst, E. L., Hough, L. and Jones, J. K. N. *J. Chem. Soc.* **1949** 57.
27. Maher, G. G.. *Advances in Carbohydrate Chem.* **10** (1955) 258.

Received November 3, 1959.

ACTA CHEMICA SCANDINAVICA 14 (1960) 749–756

Studies on Glucomannans from Norwegian Spruce

III *. Partial Hydrolysis

HANS MEIER

Träkemiska avdelningen, Svenska Träforskningsinstitutet, Stockholm, Sweden

An easily extractable polysaccharide fraction from Norwegian spruce, containing galactose, glucose and mannose residues, was subjected to partial hydrolysis. A number of oligosaccharides were isolated from the hydrolysate; among them were the four disaccharides and five of the eight trisaccharides that should be formed from a linear glucomannan with β-1,4-linkages and a random distribution of the hexose residues. In addition to these compounds, 6-O-α-D-galactopyranosyl-D-mannose (Ga $\xrightarrow[\alpha]{1\ 6}$ M) and a trisaccharide (Ga $\xrightarrow[\alpha]{1\ 6}$ M $\xrightarrow[\beta]{1\ 4}$ M) were also isolated, indicating that, in addition to the glucomannan, there was also present either a galactomannan of the type found in legume seeds or a galactoglucomannan.

Glucomannans containing glucose and mannose residues in proportions of between 1:3 and 1:4 have been isolated from several coniferous woods. Methylation studies have shown that these polysaccharides are essentially linear with β-1,4-linked hexose residues [1–7], though some indications of branching have been found [3,7,8]. In agreement with this type of structure partial hydrolyses of the glucomannans or of pulps enriched in them [1,5,6,9–12] have afforded 4-*O*-β-D-mannopyranosyl-D-mannose (M $\xrightarrow[\beta]{1\ 4}$ M), 4-*O*-β-D-glucopyranosyl-D-mannose (*G* $\xrightarrow[\beta]{1\ 4}$ M), 4-*O*-β-D-mannopyranosyl-D-glucose (M $\xrightarrow[\beta]{1\ 4}$ G), cellobiose (G $\xrightarrow[\beta]{1\ 4}$ G) and mannotriose (M $\xrightarrow[\beta]{1\ 4}$ M $\xrightarrow[\beta]{1\ 4}$ M).

Some authors [1,4,6,13,14] have obtained polysaccharide fractions which in addition to glucose and mannose residues also contained a high percentage of galactose residues, indicating the presence of a galactomannan or a galactoglucomannan. It was observed in this laboratory that quite high galactose contents in some glucomannan fractions could be reduced to a low value (1 %

* Part II, *Acta Chem. Scand.* **12** (1958) 453.

Table 1. Carbohydrate analyses.

	Galactose %	Glucose %	Mannose %	Arabinose %	Xylose %
Norwegian spruce, extracted with acetone	2.1	70.7	17.2	1.3	8.7
Holocellulose (yield 71.8 %, Klason-lignin 1.4 %)	0.6	77.3	12.8	2.2	7.2
Crude polysaccharide fraction *A*	18.3	15.5	51.1	4.4	10.7
Purified polysaccharide fraction *B*	15.0	10.1	74.2	traces	0.7

or lower) if the polysaccharide material was delignified and precipitated with Fehling's solution [7]. It therefore seems probable that pine and spruce contain galactose-free glucomannans but that linkages between lignin and the polysaccharides make it impossible to separate material that has not been completely delignified, into its components. The most easily extracted, mannose-containing polysaccharide fraction has, however, not been dealt with in previous studies at this laboratory. The present paper describes an investigation of this fraction from Norwegian spruce (*Picea abies* Karst.).

Delignification of spruce wood by the chlorite method dissolves a large part of non-cellulose polysaccharides. This fraction (*A*, Table 1) was recovered by dialysis and was shown to consist mainly of polysaccharides containing mannose residues. To remove contaminating araboxylans, arabogalactans and galactans, *A* was purified by precipitation first with barium hydroxide [15] and then with Fehling's solution, giving fraction *B*. Galactans of the type recently isolated from compression wood [16] are precipitated by barium hydroxide but with Fehling's solution give little or no precipitate. Araboxylans and arabogalactans are not precipitated by either barium hydroxide or Fehling's solution. The material precipitated by barium hydroxide but not precipitated by Fehling's solution therefore contained a large proportion of galactose residues with lesser amounts of xylose and arabinose residues. The material precipitated by both barium hydroxide and Fehling's solution (fraction *B*, Table 1) was not free from lignin, so that contamination with other polysaccharides, *e.g.* a galactan, cannot be excluded, but it should consist essentially only of mannose-containing polysaccharides. *B* differed from other spruce polysaccharides containing mannose residues that have been studied in this laboratory [3,17], not only in its high content of galactose but also in the low ratio of glucose to mannose (1:7.4). *B* on electrophoresis on glass fibre sheets in borate buffer gave a single spot with considerable trailing.

Fraction *B* was subjected to partial hydrolysis, the yield of lower polysaccharides being improved by separation and further hydrolysis of the higher oligosaccharides. The oligosaccharides were then fractionated by carbon column chromatography, by chromatography and electrophoresis on thick filter paper and by chromatography on cellulose and carbon columns. Fifteen oligosaccharides (Table 2) were obtained in a state of purity. As can be seen from Table 2, the R_F values of some of these substances are very close, and separa-

Table 2. Oligosaccharides from the partially hydrolysed, mannose-rich fraction *B*.

	Oligosaccharide[a]	Number of combined[b] fractions	Yield in mg[c]	R_{Gl}[d]	M_G[e]	m. p.	$[\alpha]_D$	Ref.
a	M→M	49–59 (60–86)	810 + (155)	0.65	0.66	204–206°	− 8°	5, 12
b	M→G	60–86	17	0.48	0.43	201–203°	+19°	10, 11, 28
c	Ga→M	60–86	14	0.59	0.66	198–202°		30
d	Ga→Ga	87–95 (60–86)	30	0.57	0.50	208–210°		16
e	G→G	102–109	60	0.66	0.27	235–242° (dec.)		
f	G→M	110–134 (135–146)	650	0.87	0.58	140° (monohydrate) 179–182° (water free)	+ 6°	5, 12, 27–29
g	M→M→M	87–95 (60–86, 96–101)	216 + (189)	0.33	0.53			21
h	Ga→M→M	96–101 (102–109)	16	0.32	0.58			
i	M→M→G	96–101 (102–109)	29	0.28	0.38			
j	G→M→M	135–146 (147–156)	68	0.45	0.50			16
k	Ga→Ga→Ga	147–156	11	0.38	0.39			
l	M→G→M	50 % EtOH (181–186)	77 + (21)	0.39	0.54			
m	G→G→M	50 % EtOH	86	0.53	0.43			
n	M→M→M→M	102–109 (110–134)	227	0.15	0.50	235–250° (dec.)	−28°	
o	G→M→M→M (?)	157–163	19	0.21	0.45			

[a] All linkages are β-1,4, except Ga → in *c* and *h*, which are α-1,6.
[b] Numbers of fractions combined from the first carbon column fractionation. Numbers in brackets indicate that a substance was present in more than one of the combined fractions.
[c] As the separation and purification of the compounds was often tedious and involved considerable losses, the yields are not representative of the amounts present in the hydrolysate. The yields given in brackets are those for the combined fractions given in brackets, in the cases where the substance was isolated from these.
[d] Paper chromatographic mobility relative to glucose in solvent ii.
[e] Paper electrophoretic mobility in 0.1 M borate buffer, pH 10.0, relative to glucose.

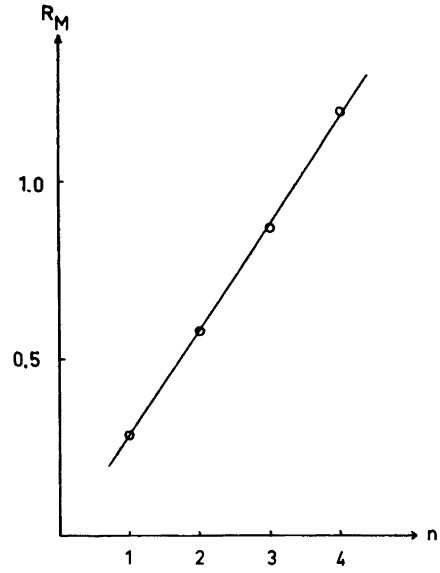

Fig. 1. Relation between R_M-values $[R_M = \log\left(\frac{1}{R_F} - 1\right)]$ and chain length.

tion could hardly have been effected without the aid of all of these methods. The results of the carbon column chromatography are rather surprising, some disaccharides being eluted after some of the trisaccharides and even after mannotetraose.

Definite structures could be assigned to all exept one (*o*, Table 2) of the fifteen oligosaccharides isolated. Total hydrolysis before and after reduction with sodium borohydride, and chromatography of the hydrolysate gave information on the component sugars and the reducing end group. Partial hydrolysis was carried out on the tri- and tetrasaccharides and the components obtained were identified by paper chromatography and paper electrophoresis. The degree of polymerisation of the tri- and tetrasaccharides was determined by the metod of Peat *et al.* [18].

The disaccharides (*a-f*, Table 2) were all known, crystalline compounds.

The mannobiose, mannotriose and mannotetraose which were obtained, belong to a homologous series, as is shown by the linear relationships between R_M and n [19] (Fig. 1) and between $[M]_D/n$ and $\frac{n-1}{n}$ [20] (Fig. 2). The mannotriose was obtained in an amorphous state in the present investigation but has been obtained crystalline by Whistler and Smith [21]; the value for $[M]_D$ in Fig. 2 is calculated from their value for the specific rotation. Fig. 2 gave the specific rotation of a β-1,4-linked mannan by extrapolation as $-48°$ (in water), in good agreement with the value $-46°$ (in N sodium hydroxide), found for ivory nut mannan A, which is known to contain principally these linkages [22].

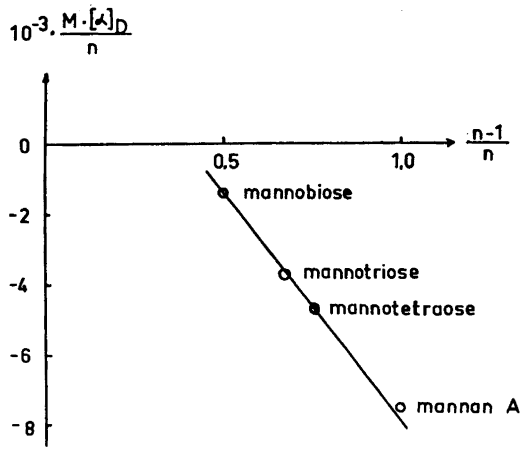

Fig. 2. Application of the Freudenberg-Blomquist relationship to mannose oligosaccharides (M = molecular weight, n = degree of polymerisation).

The galactobiose and galactotriose were obtained only in low yield and probably derive from a galactan of the type recently isolated from spruce compression wood [16].

The oligosaccharides containing both mannose and glucose residues obviously derive from a glucomannan of the ordinary type. The cellobiose may derive from contaminating cellulose, though this is less likely, especially as $G\xrightarrow[\beta]{1\quad 4}G\xrightarrow[\beta]{1\quad 4}M$ was also isolated. All of the disaccharides expected from a glucomannan and five of the eight theoretically possible trisaccharides were isolated. For statistical reasons, elements yielding cellotriose and to a lesser extent the trisaccharides with two glucose residues should be rare, but as glucosidic linkages are more resistant to acid hydrolysis than mannosidic, $G\xrightarrow[\beta]{1\quad 4}G\xrightarrow[\beta]{1\quad 4}M$ should be enriched compared to $M\xrightarrow[\beta]{1\quad 4}G\xrightarrow[\beta]{1\quad 4}G$ and $G\xrightarrow[\beta]{1\quad 4}M\xrightarrow[\beta]{1\quad 4}G$. Thus $G\xrightarrow[\beta]{1\quad 4}G\xrightarrow[\beta]{1\quad 4}M$ was the only trisaccharide with two glucose residues which was obtained in the present investigation. Oligosaccharides, derived from potential branching points in the glucomannan were looked for specially but were not observed. They would be present, however, only in small amounts and might easily have been overlooked.

Two oligosaccharides ($Ga\xrightarrow[\alpha]{1\quad 6}M$ and $Ga\xrightarrow[\alpha]{1\quad 6}M\xrightarrow[\beta]{1\quad 4}M$), containing an α-galactopyranosidic residue, linked to the 6-position in a mannose residue, were also obtained. Partical hydrolysis of the latter after reduction with sodium borohydride and identification of $Ga\xrightarrow[\alpha]{1\quad 6}M$ in the hydrolysate, eliminated the structure $Ga\xrightarrow[\alpha]{1\quad 6}M\xleftarrow[\beta]{4\quad 1}M$. The$Ga\xrightarrow[\alpha]{1\quad 6}M$ residue is known

as a structural element of the galactomannans from legume seeds, *e.g.* in locust bean gum and guaran[23]. These polysaccharides contain a linear chain of β-1,4-linked mannose residues, some of which are substituted in the 6-position by α-galactopyranosidic residues. It is therefore possible that the same type of polysaccharide occurs in spruce wood. These oligosaccharides could also be derived from a galactoglucomannan but the first possibility seems more attractive. If a more or less constant ratio of glucose to mannose of between 1:3.5 and 1:4 is assumed for the spruce glucomannans, then the carbohydrate composition of the present fraction (*B*) implies that it should contain about equal parts of glucomannan and galactomannan. The galactose to mannose ratio in the latter should be lower than 1:2.5, as there are indications that galactans are also present in fraction *B*. The isolation of the two polysaccharides in a state of purity should of course definitely prove this hypothesis, but the separation of a glucomannan and a galactomannan by present methods seems to be a most difficult task. The isolation of $G\xrightarrow[\beta]{1\quad 4}G$ and $G\xrightarrow[\beta]{1\quad 4}G\xrightarrow[\beta]{1\quad 4}M$ from the hydrolysate gives some support to the presence of a glucomannan (glucose:mannose, 1:4), since structural elements giving these oligosaccharides should be even more rare in a galactoglucomannan, in which the proportions of glucose to mannose are 1:7.4.

In methylation studies of mannose-rich polysaccharide fractions from Loblolly pine and Sitka spruce Ball *et al.*[1] and Dutton and Hunt [4] isolated 2,3,4,6-tetra-*O*-methyl-D-galactose and a di-*O*-methyl-D-mannose, believed to be the 2,3-dimethyl-ether. This is in good agreement with our results, which show the presence of galactose residues that are linked to 6-positions in mannose residues and are most probably terminal.

In a recent paper [24] Hamilton and Thompson have reported the isolation and a structural investigation of a polysaccharide, believed to be a galactoglucomannan, from southern pine.

EXPERIMENTAL

Melting points are corrected. Concentration of solutions was done under reduced pressure at a bath temperature of 40°.

Paper chromatography and paper electrophoresis. Whatman No. 1 and No. 3 MM papers were used. The chromatograms were run in the solvent systems (v/v):

i. ethyl acetate-acetic acid-water, 3:1:3 (upper layer)
ii. ethyl acetate-pyridine-water, 2:1:2 (upper layer)
iii. acetone-butan-1-ol-water, 7:2:1.

The method of Saeman *et al.*[25] was used for quantitative determination of monosaccharides. Paper electrophoreses were run in 0.1 M borate buffer of pH 10.

Isolation and fractionation of the polysaccharides. Norwegian spruce wood meal (1 000 g, 0.5—2.0 mm) was extracted with acetone and the residue was delignified by the chlorite method at 60° and pH 4.7. The product remaining after delignification was 71.8 % of the acetone-extracted wood. The combined chlorite solutions (30 l) were dialysed against tap water for five days and then concentrated to about 5 l. After acidification with acetic acid the hemicelluloses were precipitated with 20 l ethanol. The precipitate (*A*, Table 1) was washed with aqueous ethanol, ethanol and then ether and dried (yield 94 g, containing 16 % lignin, determined spectrophotometrically [26]). A sample of this material (70 g) was dissolved in water and saturated barium hydroxide solution was added until precipitation was complete. The precipitate was centrifuged, washed, dis-

solved in dilute acetic acid and the polysaccharides were reprecipitated with ethanol and washed. The product was dissolved in water, Fehling's solution was added, the precipitate formed was centrifuged, washed, dissolved in dilute acetic acid, and the polysaccharides (*B*, Table 1) were recovered by precipitation with ethanol (yield 25 g). The centrifugate, after addition of Fehling's solution, was acidified and dialysed, and the polysaccharides were precipitated with ethanol (yield 8 g). This fraction yielded, after hydrolysis, mainly galactose, with smaller amounts of arabinose, xylose and uronic acids.

Partial hydrolysis of B. A sample of *B* (15 g) dissolved in N sulphuric acid (1 000 ml) was heated on the steam bath for 30 min and then was cooled and neutralised with barium hydroxide. Barium sulphate was removed by centrifuging and the solution was shaken with activated carbon (400 g) and then filtered. The aqueous phase contained only monosaccharides and was discarded. The carbon was eluted first with 15 % and then with 50 % aqueous ethanol. The 15 % ethanol eluate contained monosaccharides and lower oligosaccharides. The second eluate contained higher oligosaccharides, which were subjected to further partial hydrolysis; the whole procedure was repeated twice. The 15 % ethanol eluates and the final 50 % ethanol eluate were combined, concentrated and added to the top of a carbon-Celite column (4 × 45 cm). Gradient elution with aqueous ethanol (6 l, 0—20 %) effected a partial separation of the components (Table 2). In addition to the substances listed in Table 2, some higher, unidentified oligosaccharides were observed in fraction 110 and later fractions. Similar fractions from the carbon column were combined giving eleven main fractions. A twelfth fraction was obtained by elution of the column with 50 % ethanol. Most of the main fractions were fractionated further by chromatography on cellulose columns or on thick filter paper. Sometimes a single separation was sufficient, but for some of the mixtures two successive fractionations in different solvent systems were necessary. For some mixture, *e. g.* substances *c* and *d*, electrophoresis on thick filter paper was also used for separation. The purification of *h* from contaminating *g*, was done by carbon column chromatography.

Identification of the oligosaccharides. The oligosaccharides were identified as described above.

Ga $\overset{1}{\underset{\alpha}{\longrightarrow}}\overset{6}{}$ M was compared with an authentic sample, kindly supplied by Professor Roy L. Whistler. The two samples were chromatographically and electrophoretically indistinguishable, gave an undepressed mixed m. p. and also gave identical X-ray powder diagrams. The lattice spacings in Å were: 6.57 (m), 6.33 (s), 5.22 (vs), 5.06 (m), 4.55 (m), 4.42 (vs), 4.28 (m), 4.18 (m), 4.05 (m-s), 3.69 (s), 3.52 (s).

Substance *f*, (G $\overset{1}{\underset{\beta}{\longrightarrow}}\overset{4}{}$ M) had a specific rotation +6° (in water). Similar values [5,27,28] and some higher values, +12° and +15° [11,29] have been reported for this substance.

Component *o* on hydrolysis yielded one part of glucose to three parts of mannose. After borohydride reduction and hydrolysis the proportions were one to two. A paper chromatographic and electrophoretic examination of a partial hydrolysate of *o* indicated the presence of G, M, G $\overset{1}{\underset{\beta}{\longrightarrow}}\overset{4}{}$ M, M $\overset{1}{\underset{\beta}{\longrightarrow}}\overset{4}{}$ M and G $\overset{1}{\underset{\beta}{\longrightarrow}}\overset{4}{}$ M $\overset{1}{\underset{\beta}{\longrightarrow}}\overset{4}{}$ M. Even though M $\overset{1}{\underset{\beta}{\longrightarrow}}\overset{4}{}$ M $\overset{1}{\underset{\beta}{\longrightarrow}}\overset{4}{}$ M was not detected, the structure G $\overset{1}{\underset{\beta}{\longrightarrow}}\overset{4}{}$ M $\overset{1}{\underset{\beta}{\longrightarrow}}\overset{4}{}$ M $\overset{1}{\underset{\beta}{\longrightarrow}}\overset{4}{}$ M appears to be the most probable for this substance.

Acknowledgement. The author is much indebted to Professor Bengt Lindberg for his interest in this investigation.

REFERENCES

1. Ball, D. H., Jones, J. K. N., Nicholson, W. H. and Painter, T. J. *Tappi* **39** (1956) 438.
2. Aspinall, G. O., Laidlaw, R. A. and Rashbrook, R. B. *J. Chem. Soc.* **1957** 4444.
3. Croon, I. and Lindberg, B. *Acta Chem. Scand.* **12** (1958) 453.
4. Dutton, C. G. S. and Hunt, K. *J. Am. Chem. Soc.* **80** (1958) 5697.
5. Hamilton, J. K. and Kircher, H. W. *J. Am. Chem. Soc.* **80** (1958) 4703.
6. Hamilton, J. K. and Partlow, E. V. *J. Am. Chem. Soc.* **80** (1958) 4880.

7. Croon, I., Lindberg, B. and Meier, H. *Acta Chem. Scand.* **13** (1959) 1299.
8. Hamilton, J. K., Kircher, H. W. and Thompson, N. S. *J. Am. Chem. Soc.* **78** (1956) 2508.
9. Leech, J. G. *Tappi* **35** (1952) 249.
10. Anthis, A. *Tappi* **39** (1956) 401.
11. Jones, J. K. N. and Painter, T. J. *J. Chem. Soc.* **1957** 669.
12. Merler, E. and Wise, L. E. *Tappi* **41** (1958) 80.
13. Adams, G. A. *Tappi* **40** (1957) 721.
14. Hamilton, J. K., Partlow, E. V. and Thompson, N. S. *Tappi* **41** (1958) 803.
15. Meier, H. *Acta Chem. Scand.* **12** (1958) 144.
16. Bouveng, H. O. and Meier, H. *Acta Chem. Scand.* **13** (1959) 1884.
17. Lindberg, B. and Meier, H. *Svensk Papperstidn.* **60** (1957) 785.
18. Peat, S., Whelan, W. J. and Roberts, J. G. *J. Chem. Soc.* **1956** 2258.
19. French, D. and Wild, G. M. *J. Am. Chem. Soc.* **75** (1953) 2612.
20. Freudenberg, K. and Blomquist, G. *Ber.* **68** (1935) 2070.
21. Whistler, R. L. and Smith, C. G. *J. Am. Chem. Soc.* **74** (1952) 3795.
22. Aspinall, G. O., Hirst, E. L., Percival, E. G. V. and Williamson, I. R. *J. Chem. Soc.* **1953** 3184.
23. Whistler, R. L. and Smart, C. L. *Polysaccharide Chemistry*, New York 1953.
24. Hamilton, J. K. and Thompson, N. S. *Tappi* **42** (1959) 752.
25. Saeman, J. F., Moore, W. E., Mitchell, R. L. and Millet, M. A. *Tappi* **37** (1954) 336.
26. Meier, H. *Acta Chem. Scand.* **12** (1958) 1911.
27. Isbell, H. S. *Bur. Standards J. Research* **5** (1930) 1179.
28. Smith, F. and Srivastava, H. C. *J. Am. Chem. Soc.* **78** (1956) 1404.
29. Bergmann, M. and Schotte, H. *Ber.* **54** (1921) 1564.
30. Whistler, R. L. and Durso, D. F. *J. Am. Chem. Soc.* **73** (1951) 4189.

Received December 8, 1959.

ACTA CHEMICA SCANDINAVICA 14 (1960) 757–764

An Electrophoretic Investigation of the Degradation of β-Casein by Crystalline Rennin

BÖRJE LINDQVIST and TORSTEN STORGÅRDS

The Central Laboratory of Mjölkcentralen, Stockholm, Sweden

An attempt was made to chart the primary course of the degradation of β-casein by crystalline rennet. The degradation follows distinctly different paths depending on the temperature, pH and other factors. Under conditions different from those under which the main experiments were made, the electrophoresis diagram shows that substances with mobilities in the range $u \times 10^5 = 0.5-11.5$ can be formed. In some cases only 2 or 3 of these substances with apparently arbitrary u-values may represent almost all of the degradation product.

In the profusion of degradation products derived from it and in the wide differences in the mobility of these products, β-casein differs considerably from α-casein. NPN formation during the degradation proceeds at only a third of the rate at which it is formed from α-casein and can almost be disregarded.

The enzymatic degradation of β-casein has been studied by Christensen[1], using trypsin, chymotrypsin and plasmin for the proteolysis and following the degradation by viscosimetry and NPN determinations. Lillevik *et al.*[2] have continued these investigations using chymotrypsin and following the degradation by alcohol titration. Peterson *et al.*[3] and Groves *et al.*[4] have studied the more or less stable degradation products that can be isolated after proteolysis. They used trypsin and followed the degradation with free electrophoresis, and pepsin together with paper electrophoresis, respectively.

The present investigation was carried out in order to obtain a picture of the earliest stages of the degradation of the β-casein by rennin as shown by changes in the electrophoretic curves. Some experiments were also made using other proteolytic enzymes under conditions that would produce the maximum variation in the appearance of the electrophoresis curves. The investigation followed more or less the same lines as the corresponding investigation on α-casein described previously (Lindqvist and Storgårds [5]).

METHODS

Preparation of β-casein. β-Casein was prepared according to Hipp *et al.*[6] by fractional precipitation from urea solution. The starting material used for the fractionation was the mother liquor left after precipitation of α-casein from a solution of whole casein.

The progress of the fractional precipitation of the β-casein was followed by electrophoresis and the precipitation procedure was adjusted as required to give a β-casein as free as possible from both α-casein and γ-casein. By adding greater or lesser amounts ammonium sulphate to the solution used to precipitate the β-casein the process can be varied to give the best conditions and only three or four reprecipitations are needed to give pure β-casein. When ammonium sulphate was not added, that is, using the original procedure of Hipp *et al.*, this could not be done nearly as readily.

The β-casein thus obtained was free from fat and other opalescent impurities and also from the proteolytic enzymes present in the milk. After freeze-drying the β-casein was stored in a tightly closed jar containing silica gel as a drying agent.

Two different preparations of β-casein were used in this investigation. One of these contained small amounts of degradation products from the β-casein. The other, much smaller batch was completely pure. The batch used in a certain experiment is indicated on the diagrams and electrophoresis curves given below. The presence of these impurities does not interfere with the evaluation of the results obtained or the conclusions drawn.

Enzymes. Rennin was prepared in a crystalline state as described in the preceding paper[5]. *Pepsin* was crystallised according to Northrop[7] from a commercial preparation with an activity of 1:10 000. *Pancreatin* corresponded to the standards of B.P. 1932. Partially *heatinactivated crystalline rennin* was obtained by the following procedure:

A concentrated solution of crystalline rennin (4 000 Ru/ml) * was mixed with an equal volume of 3 % β-casein solution containing 2 % NaCl and 1/15 M NaH_2PO_4 at pH 6.7. Within a few seconds after mixing 0.2 ml was introduced into 2 ml of the same β-casein solution as above. This 2 ml of solution was already placed in a water bath at the inactivation temperature required (60° or 65°). Through this procedure momentaneous heating of the rennin solution was obtained. After the required inactivation time (5 min to 1 h) the temperature was rapidly reduced by injection of a mixture of cold 3 % β-casein solution (20 ml) having a pH of 5.3. This solution was then kept at a temperature of 17° like the other reaction mixtures. It is at present not clear whether the proteolytic action of the partially inactivated material is due to undestroyed rennin, or whether the rennin contains some heat stable modification or whether some completely different enzyme is present in traces in the rennin crystals. Whatever the case the content as measured by the activity was only about 1 %.

The proteolyses with rennin, pepsin, and pancreatin were carried out in exactly the same way as described for the α-casein investigations. The amounts of acid used to obtain a given pH in the reaction mixtures were, however, different from those used in the previous experiments because of the different buffer capacities of the α- and β-caseins. The amount of acid added varied between 0 and 33 ml of N HCl per 125 ml of buffer solutions. When the buffer was mixed with three volumes of 4 % β-casein in water adjusted to pH 9.0 with NaOH the resultant buffered solutions had a pH between 2.4 and 6.1. In the solutions a loose coagulum was formed instead of the sticky precipitate formed in the α-casein experiments. This made it easier to dissolve the samples for analysis.

Analyses. The analyses were done in the same way as in the previous investigation. The non-protein nitrogen (NPN) was determined on a filtrate obtained after the addition of trichloroacetic acid (TCA) to a concentration of 2 %. Because of the limited amounts of β-casein available the determinations of total N och soluble N had to be restricted in order to allow a full electrophoretic investigation. The electrophoresis were run with phosphate buffer of pH 7.3 and ionic strength 0.1 for 120 min at 12 mA. Standard Spinco cells were used.

The β-casein was broken down quite rapidly compared with the α-casein and as a rule the length of the experiments could be limited to 1 week.

RESULTS

A. The formation of soluble nitrogen. The amount on non-protein nitrogen liberated ($NPN_{2\%TCA}$) was low throughout and in no case was greater then

* Ru = rennin units according to Berridge, see Ref.

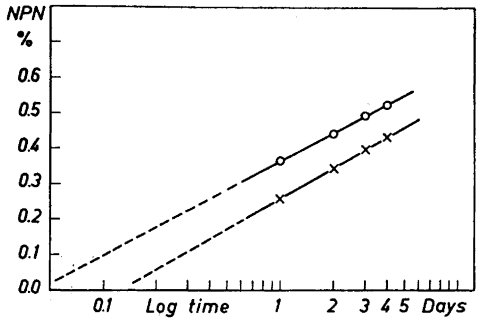

Fig. 1. Formation of NPN from β-casein in proteolysis with rennin. Mean reaction rate for the pH range 2.4—6.10.
O = β-casein containing 5 % of β-casein degradation products
× = pure β-casein

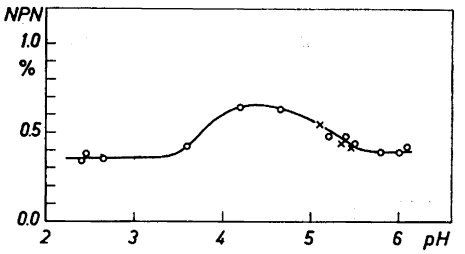

Fig. 2. Amount of NPN released from β-casein by rennin after 4 days at different pH values.

0.7 %. The values obtained showed a greater spread than the corresponding values obtained for α-casein but the tendency was the same — the NPN values plotted against log time gave straight lines starting from about 0.1 days on the time axis. This is shown in the curves in Fig. 1 for the two β-caseins preparations. The curve for the impure preparation showed a parallel displacement upwards caused by the more rapid formation of NPN from the impurities.

The points on the curves are mean values of results obtained in different experiments. Since the NPN formation was relatively independent of the pH, as is shown by Fig. 2, this should be not unreasonable. The pH optimum for NPN formation from β-casein by the action of rennin was the same as for the degradation of α-casein, pH 4.5.

B. Electrophoreses. The first stages of the β-casein degradation proceed very rapidly. It was necessary to take samples about an hour after adding the rennin but in spite of this it was not possible to obtain consecutive pictures demonstrating the details of the degradation. This would require samples to be taken perhaps every 10 min during the first few hours which was not technically feasible.

Fig. 3 gives an indication of the main lines of the degradation. The rule formulated for the degradation of α-casein also applies in this case — the primary cleavage gives only a few simple components with migration rates both higher and lower than that of the parent substance. On of these substances (βb in Fig. 6) had a migration rate of $u \times 10^5 = 0.5$ under the conditions used. Another substance with $u \times 10^5 = 6.8$ (βc) had a very short life and vanished completely within 24 h. A third main component (βa) was broken down fairly rapidly into two new parts (βa_1 and βa_2). One or both of these then underwent further degradation. The rates of degradation were very strongly dependent on the pH.

Table 1. Quantitative analysis of the electrophoresis diagrams shown in Fig. 3. Mean percentage distribution of the components of the reaction mixtures.

pH	βa_1	βa_2	βb	βc	βd	Notes
5.10	37.9	15.4	35.4	27.6	0	The values for βc are for a reaction time of 0.05 days; the values for βb are means for 0.05—4 days less the value for 0 days; other components are given as means for 1—4 days
5.35	42.0	22.5	26.8	30.6	8.6	
5.45	47.3	30.8	21.9	37.3	11.3	

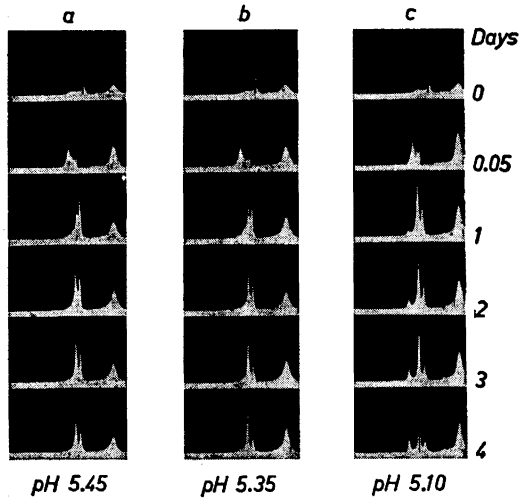

Fig. 3. Electrophoresis curves showing the course of the degradation of β-casein by rennin at three different pH values. The rate of formation and further degradation of the various components can vary widely for pH differences as small as 0.1 units. The purest β-casein was used.

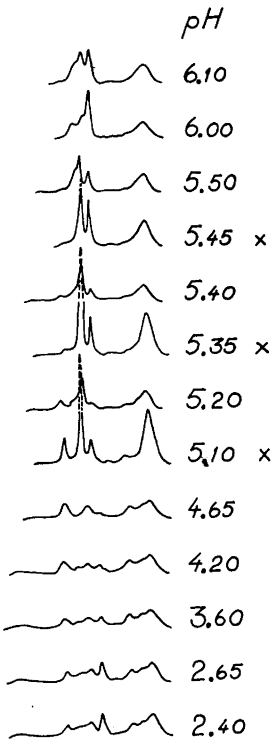

Fig. 4. Electrophoresis curves showing the final result (4 days) of the degradation of β-casein by rennin in the pH range 2.40—6.10. The maximum number of degradation products is shown at pH 4. Degradations using the pure β-casein are marked with ×.

The difficulties of quantitative estimation of the reaction products from the electrophoresis diagrams are considerable and an evaluation was possible in only a limited number of cases. Table 1 gives some measurements made on the components of the mixtures shown in Figs. 3 and 6. The values obtained confirm the subjective impression of the course of the degradation obtained by inspection of Fig. 3.

The final results of degradation varied considerably with the pH. At pH 4 and lower a large number of components are formed; at pH values above 5.4 there were only a few components. This is shown in Fig. 4. There was a certain amount of distortion of the curves when the less pure β-casein was used but this was not so large that it had to be taken into account when comparing the curves.

At pH 4.20 there were about 7—8 components, spread over the mobility range 0.5—11.5. A corresponding large spread of the components of the mixture of degradation products was also obtained at higher pH values when other enzymes were used. This is shown by a number of extreme cases given in Fig. 5. As is clear from this figure the main part of the degradation product may occur at any part of the mobility range and two or more principal components can also occur in apparently arbitrary combinations as shown in Fig. 5 B—G.

DISCUSSION

The tendency of β-casein on enzymatic degradation to give rise to substances with widely varying electrophoretic properties makes much more difficult

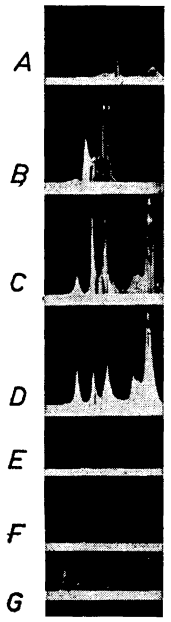

Fig. 5. Degradation of β-casein under different conditions. The electrophoresis curves shown here have been selected to show extreme variations in the distribution of the components.

A. Unaffected β-casein (starting material)
B. Degradation by partially inactivated rennin (heat-treated for 20 min at 65°. Incubated at pH 5.3 and 37° for 8 days)
C. As for B but inactivated for 20 min at 60°
D. As for B but inactivated for 5 min at 65°
E. Degradation by pepsin at pH 5.5 for 11 days at 17°
F. As for E but degradation continued for 18 days
G. Degradation by pancreatin at pH 5.5 for 8 days at 17°

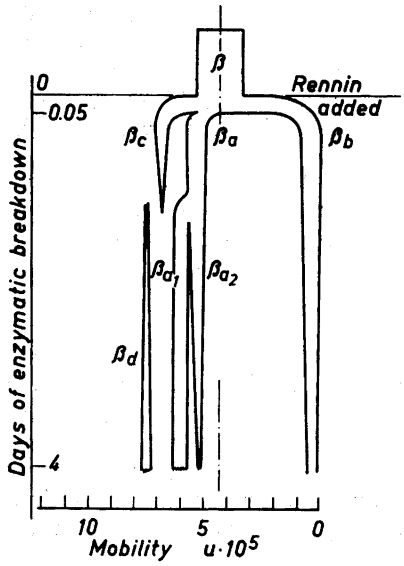

Fig. 6. Diagram of the course of the degradation of β-casein by rennin at pH 5.10 and 17°

the elucidations of the various paths of degradation under different conditions. It is not possible to give any generalised degradation curves covering the whole pH range. Fig. 6 gives a diagrammatic representation of the course of degradation as shown by the electrophoresis curves in Fig. 3 for pH 5.10. Corresponding diagrams are somewhat similar at higher pH values and during the early stages at low pH values.

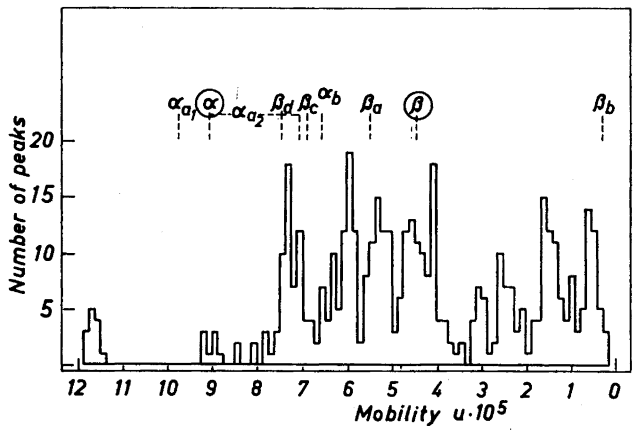

Fig. 7. Frequency of mobilities of approx. 470 peaks measured on electrophoresies from 90 degradation experiments. For comparison the mobilities of β-casein and of the degradation products observed previously för α-casein have also been marked. In this figure as in the preceding, the mobility scale has been placed with the zero point on the right so that the histogram agrees with the electrophoresis curves.

Table 2. The amino acid composition of α- and β-casein [8].

	Amino acid in g/100 g protein	
	α-casein	β-casein
Aspartic acid	8.4	4.9
Alanine	3.7	1.7
Tyrosine	8.1	3.2
Lysine	8.9	6.5
Arginine	4.3	3.4
Valine	6.3	10.2
Methionine	2.5	3.4
Leucine	7.9	11.6
Proline	8.2	16.0
Others	same within 10—15 %	

Fig. 7 gives another picture of the possible paths followed by the degradation in the form of a histogram showing the distribution of 470 peaks of various mobilities that were measured. The β-casein has a mobility in the middle of the mobilities of the group of degradation products. There was a surprisingly high content of substances that migrated very slowly at pH 7.3 and as in the case of α-casein the splitting off of a given substance usually gave a reduction in the mobility.

For comparison the positions of β-casein and its degradation products have been marked on Fig. 7. When a mixture of α- and β-casein is degraded the two sets of components partly overlap which could easily lead to misinterpretations of their origin.

The considerable differences between α- and β-casein in their reaction with proteolytic enzymes depends of course on the amino acid sequence in the two molecules. A comparison between the amino acid sequences of α- and β-casein should therefore give better information on the points of attack of the proteolytic enzymes than in proteolytic experiments with other proteins.

No investigations of this sort have as yet been published. However, a comparison of the amino acid compositions of α- and β-casein shows some points of difference. Some of the most marked of these are shown by the data in Table. 2 (Gordon *et al.*[8]).

Apart from the differences in the amino acid sequences, the major differences between α- and β-casein in potential paths of degradation on enzymatic proteolysis should be due for instance to the low content of aspartic acid and other acidic components and to the high content of proline, leucine, methionine and valine in β-casein.

In the degradation of β-casein as in that of α-casein, the formation of NPN and the cleavage of the β-casein molecule into a few simple parts have no direct connection. The formation of NPN is reasonably independent of pH and other factors but the electrophoresis curve is extremely dependent on the conditions used.

Acknowledgement. The authors wish to express their gratitude to the Scientific Council of Swedish Dairies' Association which made the investigation possible by placing the ultracentrifuge at their disposal.

REFERENCES

1. Christensen, L. R. *Arch. Biochem. Biophys.* **52** (1954) 128.
2. Lillevik, H. A. and Anwar, R. A. *J. Dairy Science* **40** (1957) 597.
3. Peterson, R. F., Naumann, L. W. and McMeekin, T. L. *J. Am. Chem. Soc.* **80** (1958) 95.
4. Groves, M. L., Hipp, N. J. and McMeekin, T. L. *J. Am. Chem. Soc.* **80** (1958) 716.
5. Lindqvist, B. and Storgårds, T. *Acta Chem. Scand.* **13** (1959) 1839.
6. Hipp, N. J., Groves, M. L., Custer, J. H. and McMeekin, T. L. *J. Dairy Sci.* **35** (1952) 272.
7. Northrop, J. H. *J. Gen. Physiol.* **30** (1946) 177.
8. Gordon, W. G., Semmet, F., Cable, R. S. and Morris, M. *J. Am. Chem. Soc.* **71** (1949) 3293.

Received December 14, 1959.

ACTA CHEMICA SCANDINAVICA 14 (1960) 765–784

Short Communications

The Structure of Some Salts of 2:6-Dimethyl-γ-pyrone (2:6-Dimethyl-4H-pyran-4-one)

HÅKON HOPE

Universitetets kjemiske institutt, Blindern-Oslo, Norway

It was first shown by Collie and Tickle [1] that 2:6-dimethyl-γ-pyrone (DMγP) has the property of uniting with various acids to form stable crystalline salts. Since this discovery a considerable amount of work has been done to determine the mechanism of the salt formation (for references see [2]). It is now a widely accepted theory that the proton from the acid is added to the carbonyl oxygen, and that at the same time the pyrone ring acquires an aromatic character. From X-ray data [3] it is known that the free DMγP ring may be described roughly as a system containing two C—C double bonds (C_2-C_3 and C_5-C_6) and two C—C single bonds.

Determination of the crystal structures of some of the DMγP salts will probably give the information which is needed to decide whether these ideas are correct or not. Structure analyses of some of the salts have therefore been started. Up to this time the salts DMγPHBr, DMγPHBr.H_2O, DMγPHBr.$2H_2O$, and DMγPHCl.H_2O have been investigated by X-ray methods.

The salts were prepared by adding dry HBr (HCl) to a solution of DMγP in benzene or ether [4]. The precipitate was collected on a glass filter and dried *in vacuo*. The anhydrous salts were found to be hygroscopic and had to be kept in a desiccator over a drying agent.

Anhydrous DMγPHBr was crystallized by cooling a solution in a mixture of ether and methanol (1:1). The description given by Collie and Tickle [1] is somewhat ambiguous, as the crystals prepared according to their method contain water of crystallization. The crystals are monoclinic, with a marked tendency towards twin formation.

Space group: $P2_1/c$
Cell dimensions: $a = 6.89$ Å; $b = 15.52$ Å;
$c = 15.51$ Å
$\beta = 94.9°$
$Z = 8$ gives $\varrho_{calc} = 1.65$ g/cm³
$\varrho_{obs} = 1.64$ g/cm³

The monohydrate DMγPHBr.H_2O was prepared by exposing anhydrous DMγPHBr to air until one mole of H_2O per mole of the salt had been taken up. It was crystallized in the same manner as the anhydrous salt. The crystals are triclinic plates, also with a tendency to twin formation.

Space group: $P\bar{1}$ (assumed)
Cell dimensions: $a = 7.00$ Å; $b = 8.33$ Å;
$c = 9.47$ Å
$\alpha = 109.9°$; $\beta = 92.9°$;
$\gamma = 106.0°$
$Z = 2$ gives $\varrho_{calc} = 1.50$ g/cm³
$\varrho_{obs} = 1.50$ g/cm³

A Fourier projection along the a axis has been completed, which confirms the assumed space group.

The dihydrate DMγPHBr.$2H_2O$ was prepared by evaporating a solution of the salt in methanol, to which a little water had been added. The crystals are orthorhombic plates. The chloride DMγPHCl.H_2O is isomorphous with the corresponding HBr salt, and was prepared in a similar manner.

More detailed structure determinations of the substances mentioned are under way.

This investigation has been sponsored partly by Alf Bjerckes legat, and partly by the United States Air Force Development Command under contract AF 61 (052) -71.

1. Collie, J. N. and Tickle, T. *J. Chem. Soc.* **75** (1899) 710.
2. Cavalieri, L. *Chem. Revs.* **41** (1947) 525.
3. Brown, G. M., Norment, H. G. and Levy, H. A. *Acta Cryst.* **10** (1957) 806.
4. Gomberg, M. and Cone, L. H. *Ann.* **376** (1910) 228.

Received March 14, 1960.

Detailed ESR Spectra of the Free Radicals of FMN and FAD

ANDERS EHRENBERG

Department of Biochemistry, Nobel Medical Institute, Karolinska Institutet, Stockolm, Sweden

In the last years considerable attention has been paid to the properties of flavin radicals because of their possible role in enzymatic activity. Spectrophotometry [1-3] and electron spin resonance, esr, [4,5] have been used for the study of the free and protein bound flavin radicals. In the latter investigations it was not possible to detect any hyperfine structure of the esr spectra. Commoner *et al.*[6] claimed recently that there is a hyperfine splitting that consists of thirteen lines in the flavin radicals. By improved sensitivity and technique it has now been possible to study these spectra in more detail.

FAD and FMN were half reduced by $Na_2S_2O_4$ or Pd-H_2 and studied at room temperature in an X-band spectrometer equipped with a 100 kc field modulation.

The two coenzyme radicals gave identical spectra but the shape of the hyperfine splitting varied with pH as can be seen from Fig. 1. At both pH 0 and 7 the hyperfine spectrum consists of at least 32 symmetrically arranged lines. The spacing between consecutive resolved lines is not constant and varies at pH 0 from 1.3 to 2.1 gauss and at pH 7 from 1.2 to 1.7 gauss. The total splitting between the uttermost observable hyperfine lines increases with the acidity, being 46 gauss at pH 7 and 50 gauss at pH 0. The accompanying colour change from yellow-green to reddishbrown indicates that a proton dissociation is operable with a pK between these values. The attachment of the proton hence seems to influence the distribution of the odd electron in a way so that its absolute spin density is somewhat increased near the nuclei giving rise to the hyperfine splitting. The theoretical calculations available [7,8] suggest that all the four nitrogens in the *iso*alloxazine nucleus has to be accounted for in this interaction, possibly also the two unsubstituted hydrogens of the benzene part [7]. No direct influence can at present be ascribed to the nuclear magnetic moment of the dissociable proton.

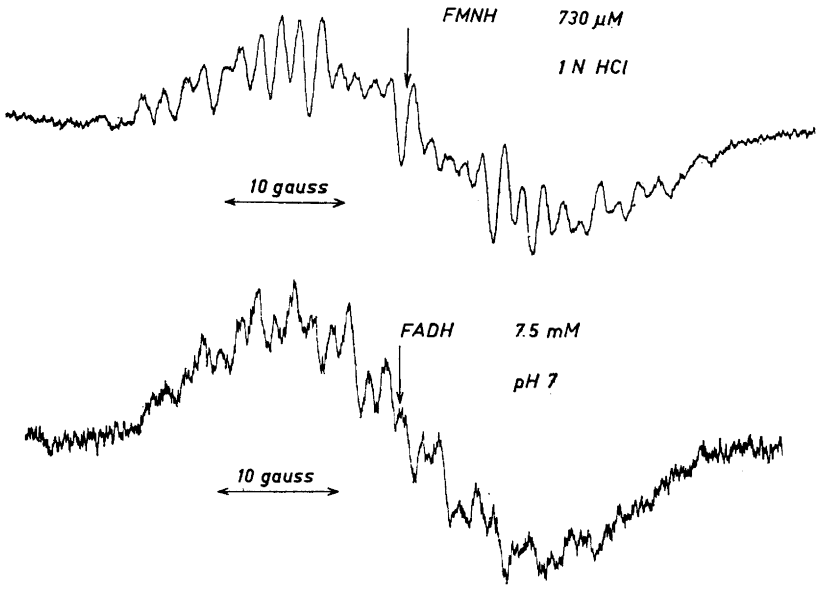

Fig. 1. Derivative records of the esr absorption of the free radicals of FMN at pH 0 (above) and of FAD at pH 7 (below).

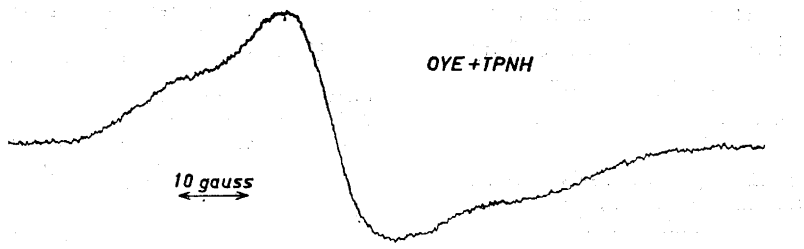

Fig. 2. Derivative record of the esr absorption of the free radicals formed in OYE upon reaction with TPNH.

The hyperfine spectra of Fig. 1 are superposed on broader lines with a width of about 21 gauss between the inflexion points Neither solution contained only radical molecules but were mixtures also containing radical dimers, oxidized and reduced molecules and possibly further complexes of these molecular species. An explanation for the broad underlying absorption might be that the lifetime of the radicals is shortened enough by the dynamic equilibrium established between the solute constituents, in analogy with the explanation forwarded by Ward and Weissman for the equilibrium between naphthalene and its negative ion [9]. The possibility to determine the mean lifetime of the radicals as well as the rate constant of the electron or hydrogen transfer process is now being investigated.

In the previous investigation on old yellow enzyme, OYE, Ehrenberg and Ludwig [4] could not detect any difference between the esr spectra of the FMN free radical and the radical formed in the reaction between OYE and TPNH. In order to achieve enough sensitivity for the detection of the radicals in the latter reaction it was at that time necessary to use a very wide field modulation, that made any search for hyperfine structure impossible, and only the g-values and mean widths of the signals could be compared. With the present technique there is still no hyperfine structure to be seen in the esr absorption of these radicals; see Fig. 2. The spectrum is unsymmetrical and shows only a weak structure consisting of a relatively sharp central peak with broader wings. This observation confirms that the free radicals formed in the reaction between OYE and TPNH really are bound to the protein. The rotational motion of the big protein molecule will be too slow to make the averaging of the anisotropic terms of the interaction between the electron and the magnetic nuclei effective, as it is for the more rapidly tumbling smaller molecules like FMN and FAD. As would be expected the coenzyme radicals give under certain conditions in frozen solutions esr spectra that are rather similar to that of the enzyme radical.

A more detailed report will be published later in this journal.

Acknowledgements: The author is indebted to Miss Jutta Schliack for skilled technical assistance. The work has been supported by grants from the *Magn. Bergvall Foundation* and the *Swedish Natural Science Research Council.*

1. Beinert, H. *J. Am. Chem. Soc.* **78** (1956) 5323.
2. Beinert, H. *Biochim. et Biophys. Acta* **20** (1956) 588.
3. Beinert, H. *J. Biol. Chem.* **225** (1957) 465.
4. Ehrenberg, A. *Acta Chem. Scand.* **11** (1957) 205.
5. Ehrenberg, A. and Ludwig, G. D. *Science* **127** (1958) 1177.
6. Commoner, B. and Lippincott, B. B. *Proc. Natl. Acad. Sci. u.s.* **44** (1958) 1110.
7. Pullman, B. and Pullman, A. *Proc. Natl. Acad. Sci. u.s.* **45** (1959) 136.
8. Grabe, B. *Arkiv Fysik* **17** (1960) 97.
9. Ward, R. L. and Weissman, S. I. *J. Am. Chem. Soc.* **76** (1954) 3612.

Received March 18, 1960.

Über die Addition von Thioglykolsäure an S-Allyl-thioglykolsäure

ERIK LARSSON und BERNDT-OTTO OSBERG

Abteilung für organische Chemie, Chemisches Institut, Universität, Lund, Schweden

Etwa 90 % von allen in der Literatur beschriebenen Additionen von Mercaptoverbindungen RSH an Äthylenverbindungen $R'-CH = CH_2$ verlaufen in Gegenwart von Peroxyden unter Bildung von $R'-CH_2-CH_2-SR$. Dieses gilt für Mercaptoverbindungen wie Alkyl- und Arylmercaptane, Thioglykolsäure, Thioglykolsäureester und Thioessigsäure und für Äthylenverbindungen mit z.B. R' gleich Kohlenwasserstoffreste, CH_3OCH-, $Cl-$, $CN-$, $HOCH_2-$, $CN\cdot CH_2-$, C_2H_5O-, $n-C_4H_9O-$, $n-C_{12}H_{25}-S-CH_2-$, $CHO-$, $HOCO(CH_2)_n-$ mit n = 0, 1, 2, 8.

Wir sind seit einiger Zeit damit beschäftigt, Säuren von der allgemeinen Zusammensetzung $CH_2 = CH(CH_2)_n\cdot S\cdot(CH_2)_m\cdot COOH$ darzustellen und ihr Verhalten gegenüber verschiedenen Mercaptoverbindungen und anderen Addenden zu untersuchen. Im folgenden werden einige Resultate mit S-Allyl-thioglykolsäure und Thioglykolsäure beschrieben. Die S-Allyl-thioglykolsäure wird leicht aus Allylchlorid und Dinatriumthioglykolat in Wasser dargestellt. Sie reagiert nicht mit Thioglykolsäure in Gegenwart von Hydrochinon (ohne Lösungsmittel). Molare Mengen von Thioglykolsäure und S-Allyl-thioglykolsäure ergeben beim Zusatz von etwas Peroxyd (Benzoylperoxyd, Ascaridol) Trimethylen-*bis*-thioglykolsäure. Diese Säure stellt man aber leichter aus Trimethylenbromid und Thioglykolsäure dar [1]. Von präparativem Interesse ist dagegen, dass man aus S-Allyl-thioglykolsäure solche Verbindungen wie

$HOCO\cdot CH_2\cdot S\cdot CH_2\cdot CH_2\cdot CH_2\cdot S\cdot CH_2\cdot CH_2\cdot COOH$ und
$HOCO\cdot CH_2\cdot S\cdot CH_2\cdot CH_2\cdot CH_2\cdot S\cdot R$

darstellen kann, was in einer folgenden Arbeit gezeigt wird.

S-Allyl-thioglykolsäure [2]. 76,5 g (1 Mol) Allylchlorid wurden mit 92,0 g (1 Mol) Thioglykolsäure in 1 Liter 2,0 N Natronlauge geschüttelt, bis die Thioglykolsäure verbraucht war. Das Reaktionsgemisch wurde mit Äther ausgeschüttelt und dann mit Schwefelsäure im Überschuss versetzt. Die erneute Extraktion mit Äther ergab eine Ätherlösung, die bei Destillation 70–80 g (ber. 132 g) S-Allyl-thioglykolsäure vom Sdp 136–138° (15 mm) ergab. (Gef. C 45,7; H 6,1; S 24,4; Äquiv. Gew. 131,4. Ber. C 45,5; H 6,1; S 24,3; Äquiv. Gew. 132,1). d_4^{25} 1,137; n_D^{25} 1,5054; MR_D 34,4 (gef.), 34,4 (ber.).

Trimethylen-bis-thioglykolsäure. 6,6 g (0,05 Mol) S-Allyl-thioglykolsäure und 4,6 g (0,05 Mol) Thioglykolsäure wurden vermischt und mit 0,2 g Ascaridol versetzt. Das Gemisch wurde bei Zimmertemperatur aufbewahrt. Am nächsten Tage war es zu einer festen Krystallmasse erstarrt, die in Essigäther aufgelöst wurde. Mit Benzol wurde aus der Lösung 8,8 g Substanz ausgefällt, die beim Umkrystallisieren aus Essigäther + Petroläther 7,8 g Trimethylen-*bis*-thioglykolsäure vom Schmp. 69,5–70° und Äquiv.-Gew. 112,2 (gef.), 112,1 (ber.) ergab. Mischschmp. mit nach *Rothstein* [2] hergestellter Säure 69,5°. – Um eine gute Ausbeute an Trimethylen-*bis*-thioglykolsäure zu erhalten, muss man eine sorgfältig destillierte S-Allyl-thioglykolsäure verwenden.

1. Rothstein, K. *Ber*, **58** (1925) 53.
2. Vgl. Soper, Q. F., Whitehead, C. W., Behrens, O. K., Corse, J. J. und Jones, R. G. *J. Am. Chem. Soc.* **70** (1948) 2849.

Eingegangen am 28. März, 1960.

On the Crystal Structure of a Basic Aluminium Sulfate and the Corresponding Selenate

GEORG JOHANSSON, GEORG LUNDGREN, LARS GUNNAR SILLÉN and RUNE SÖDERQUIST

Department of Inorganic Chemistry, Royal Institute of Technology, Stockholm 70, and Research Institute of National Defence, Dept. 4, Solna 8, Sweden

Solutions of aluminium chloride can be hydrolyzed by the addition of about 2.5 equivalents of alkali before a permanent precipitate of aluminium hydroxide is formed. The pH of the solution is then still < 7. Measurements of diffusion and freezing point depression seemed to indicate that such hydrolyzed solutions contain polynuclear complexes which may be built up from about six aluminium atoms [1]. Similar conclusions have been drawn from results of pH-measurements in hydrolyzed aluminium perchlorate solutions [2].

Now, the addition of sulfate ions to aged solutions having an Al:OH ratio of about 1:2.5 results in a precipitation of basic aluminium sulfates [3-5] which, under suitable conditions, can be obtained in a well-crystallized form [6]. Since the atomic arrangement in the crystals might give some information about the polynuclear complexes in the solution, an X-ray investigation on the structure of the crystals was initiated. This paper contains some preliminary results on the compounds

$$Na_2O \cdot 13Al_2O_3 \cdot 8SO_3 \cdot xH_2O \text{ and}$$
$$Na_2O \cdot 13\ Al_2O_3 \cdot 8SeO_3 \cdot xH_2O$$

with x apparently varying between 76 and 68. The sulfate has previously been described by formulae which can be written as "$(Al_2(OH)_5)_2SO_4$" [3,4,6] but the present investigation has shown that alkali metal ions are an essential constituent of the salts.

The crystals were prepared in the following way: An aluminium chloride solution was heated to 80°C and hydrolyzed by adding about 2.5 equivalents of sodium hydroxide. The solution was then kept at 80°C for about 30 min, after which the basic salts could be precipitated by the addition of sodium sulfate or selenate solutions. If the aluminium concentration was low (approximately 0.01—0.1 M) and the sulfate or selenate was added in excess, then the crystallization was slow and tetrahedral crystals, large enough for single crystal X-ray work, were formed after a few days.

For the analyses, crystalline samples dried in air were dissolved in dilute hydrochloric acid. *Aluminium* was determined by precipitation with 8-hydroxyquinoline. *Sodium* was precipitated and weighed as sodium magnesium uranyl acetate. The amount of sodium was also determined independently with a flame spectrophotometer using solutions containing known amounts of sodium, aluminium and sulfate as standards. *Sulfate* was precipitated and weighed as $BaSO_4$ or titrated with standard sodium hydroxide after passing the solution through a hydrogen-saturated cation exchange column. The *selenate* ions were reduced with sulfur dioxide and weighed as Se. In the sulfate compound, the *water* was determined by Hartwig-Bendig's modification of Brush and Penfield's method as described by Kolthoff and Sandell [7] but no independent analysis of the water content was made for the selenate compound.

A test for *chloride* in the crystals was negative (<0.01 %).

The *densities* of the crystals were determined by a flotation method (for the sulfate) and by the displacement of benzene (for the sulfate) or of carbon tetrachloride (for the selenate).

The results of the analysis were as follows:

	$Na_2O \cdot 13Al_2O_3 \cdot 8SO_3 \cdot xH_2O$			$Na_2O \cdot 13Al_2O_3 \cdot 8SeO_3 \cdot xH_2O$		
		$x = 76$	$x = 68$		$x = 76$	$x = 68$
	obs. %	calc. %	calc. %	obs. %	calc. %	calc. %
Al_2O_3:	38.7	39.02	40.75	35.8	35.14	36.53
$SO_3(SeO_3)$:	18.5	18.86	19.69	27.1	26.92	27.99
Na_2O:	1.6	1.82	1.90	1.5	1.64	1.71
H_2O:	40.5	40.30	37.66	35.6 (diff).	36.30	33.77
	1.97	1.97	1.88	2.11	2.15	2.07 g/ml

The water content of the sulfate crystals has been found to vary. When the crystals were dried in air at 25°C, the analyses (given above) indicated $x = 76$ but, when the crystals were dried, also at 25°C, in a desiccator over silica gel for a week, they gradually lost weight and attained a water content of 37.5 % corresponding to an x-value of 68 at the end of the drying period. Single crystals picked out from both products all gave apparently identical rotation (around [001]) and Weissenberg photographs ($hk0$, $hk1$). The crystal structure should consequently be the same for both products and some of the water molecules in the air-dried crystals must be zeolitic. When standing in moist air, the desiccator-dried product slowly took up water reversibly. The same phenomenon was also observed for the selenate.

When the preparations were dried over silica gel for a long period the water content continued to decrease slowly. After six weeks' drying, it corresponded to $x \approx 52$. However, the crystals broke and became opaque. The lines in the powder photographs were also broadened and indicated the formation of an X-ray amorphous product. This process seems to start in the neighbourhood of $x = 68$.

Crystals were set with [001] and [110] as rotation axes and rotation and Weissenberg photographs ($hk0-hk7$ (sulfate), $hk0-hk8$ (selenate) and $hhl-h,h+6,l$ (selenate)) were taken with CuK radiation. The crystals were found to be cubic with $a = 17.9 \pm 0.1$ Å (sulfate) and $a = 18.0 \pm 0.1$ Å (selenate). There are two formula weights in the unit cell, *i.e.* 4 Na, 52 Al, 16 S(Se) and about 264 to 280 O (as O, OH and H_2O).

Piezo-electric tests on the crystals were positive, indicating that the atomic arrangement lacks a centre of symmetry. This is also suggested by the tetrahedral shape of the crystals.

The crystals were found to be optically isotropic with a refractive index n_D^{20} of 1.495 (sulfate) and 1.514 (selenate).

The Laue symmetry is $m3m$. For the sulfate crystals, the reflections systematically absent are $h00$ with h odd which is characteristic [8] only for the space group No. 208—$P4_232$. Moreover, all reflections with $h + k$, $h + l$, and $k + l$ = odd are weak. For the selenate crystals, these weak reflections could not be detected even on heavily exposed photographs and may be systematically absent. The selenate compound would then belong to one of the space groups No. 209—$F432$, No. 216—$F\bar{4}3m$ or No. 225—$Fm3m$.[8]

Of these, No. 225 is not in accordance with the piezo-electric tests and No. 216 is the only one offering point positions that would allow the aluminium and selenium atoms to be situated in completely occupied, definite point positions.

The Patterson projections along [001] have been calculated and a survey of possible arrangements of AlO_6-octahedra in accordance both with the Patterson projections and the space groups $P4_232$ (for the sulfate) and $F\bar{4}3m$ (for the selenate) has been made. However, using this information alone, the number of possible Al—O— frameworks is quite large. On the other hand, if we assume that the structure contains only one kind of discrete Al—O—OH—H_2O group, which the solution data seem to suggest, the number of possibilities can be reduced considerably. Thus, there are 52 aluminium atoms in the unit cell and the symmetry (pseudo-symmetry for the sulfate) of the atomic arrangement corresponds to a face-centered cubic cell. Since there are at least four crystallographically equivalent groups in an F-centered cell, there are at most $52/4 = 13$ aluminium atoms in each Al—O—OH—H_2O complex in the structure. But, with the assumption made, the number of aluminium atoms per complex ion could not be less than 13 since this is a prime number. The complexes with six aluminium atoms which have been proposed for perchlorate solutions [1,2] do not thus seem to be present in these crystals which, instead, should contain $Al_{13}O_x(OH)_y(H_2O)_z$ groups.

A complete structure determination of one of the compounds thus seemed to be of interest and a determination of the structure of the selenate has been carried out by one of us (G.J.). The results of that investigation confirm our assumption of discrete groups with 13 aluminium atoms. The groups are, however, built up from twelve AlO_6 octahedra and one AlO_4 tetrahedron instead of 13 AlO_6 octahedra as was at first expected. The formula of the complex ions in the crystals seems to be $Al_{13}O_{40}H_{48}^{7+}$ or $[Al_{13}O_4(OH)_{24}(H_2O)_{12}]^{7+}$.

A detailed account of the results of the structure determination of the selenate will be published later [9]. Further studies on the sulfate are in progress (R.S.).

The authors wish to thank Dr Staffan Tengnér, Department of Analytical Chemistry, Royal Institute of Technology, for his help

with the flame spectrophotometric analyses for sodium, and Dr Torsten Lundström, Department of Chemistry, University of Uppsala, who made the piezo-electric tests. This work has been sponsored in part by the *Air Force Office of Scientific Research of the ARDC, USAF*, through its European Office on contract number AF 61(052)—162. The English text has been revised by Mr Donald Gillam.

1. Kohlschütter, H. W. and Hantelmann, P. *Z. anorg. allgem. Chem.* **248** (1941) 319.
2. Brosset, C., Biedermann, G. and Sillén, L. G. *Acta Chem. Scand.* **8** (1954) 1917.
3. Shishniashvili, M. E., Kargin, V. A. and Batsanadze, A. L. *Zhur. fiz. Khim.* **21** (1947) 391.
4. Denk, G. and Bauer, L. *Z. anorg. allgem. Chem.* **267** (1951) 89.
5. Bassett, H. and Goodwin, T. H. *J. Chem. Soc.* **1949** 2239.
6. Denk, G. and Alt, J. *Z. anorg. allgem. Chem.* **269** (1952) 244.
7. Kolthoff, I. M. and Sandell, E. B. *Textbook of Quantitative Inorganic Analysis*, 3rd ed., Macmillan, New York 1952, p. 717.
8. *International Tables for X-ray Crystallography*, Vol. 1, The Kynoch Press, Birmingham 1952.
9. Johansson, G. *Acta Chem. Scand.* **14** (1960) 771.

Received March 28, 1960.

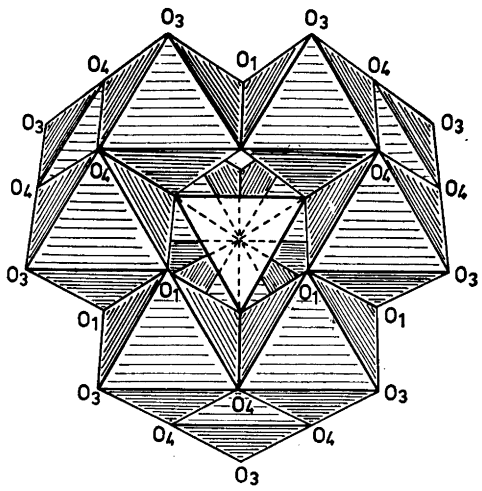

Fig. 1. The $Al_{13}O_4(OH)_{24}(H_2O)_{12}]^{7+}$-ion. The drawing shows how the twelve AlO_6-octahedra are joined together by means of common edges. The tetrahedron of oxygen (O_4) atoms in the center of the group contains the 4-coordinated Al-atom.

On the Crystal Structures of Some Basic Aluminium Salts

GEORG JOHANSSON

Gates and Crellin Laboratories of Chemistry, California Institute of Technology, Pasadena, California, U.S.A., Department of Inorganic Chemistry, The Royal Institute of Technology, Stockholm 70, Sweden

An aluminium chloride solution can be hydrolyzed by the addition of about 2.5 equivalents of alkali without the formation of a permanent precipitate of aluminium hydroxide. The addition of a suitable anion to this hydrolyzed solution precipitates basic salts, the structures of which are of a special interest since they might give some information about the polynuclear complexes that seem to exist in hydrolyzed aluminium salt solutions [1,2]. The structures of a number of them are being investigated and preliminary results of some of the structure determinations are given in this paper.

If the aluminium chloride solution is hydrolyzed by sodium hydroxide and sodium selenate is added, tetrahedral crystals can be obtained, which, when dried in air, have the composition $Na_2O{\cdot}13Al_2O_3{\cdot}8SeO_3{\cdot}xH_2O$ (with x in this case equal to about 74, *cf.* Ref.[3]. The crystals are cubic, with a_o = 18.0 Å and with two formula weights in the unit cell. The space group is $T_d^2-F\bar{4}3m$. Three-dimensional intensity data have been collected with Cu$K\alpha$-radiation. The structure has been solved from the tree-dimensional Patterson function and refined by means of three-dimensional Fourier maps *. At the present stage of the refinement the reliability index, R, is 0.11 for the 245 observed reflections, but the positions of the sodium atoms are still uncertain. The parameters are:

* All calculations were carried out on a Burroughs 205 computer at the California Institute of Technology.

with the flame spectrophotometric analyses for sodium, and Dr Torsten Lundström, Department of Chemistry, University of Uppsala, who made the piezo-electric tests. This work has been sponsored in part by the *Air Force Office of Scientific Research of the ARDC, USAF*, through its European Office on contract number AF 61(052)—162. The English text has been revised by Mr Donald Gillam.

1. Kohlschütter, H. W. and Hantelmann, P. *Z. anorg. allgem. Chem.* **248** (1941) 319.
2. Brosset, C., Biedermann, G. and Sillén, L. G. *Acta Chem. Scand.* **8** (1954) 1917.
3. Shishniashvili, M. E., Kargin, V. A. and Batsanadze, A. L. *Zhur. fiz. Khim.* **21** (1947) 391.
4. Denk, G. and Bauer, L. *Z. anorg. allgem. Chem.* **267** (1951) 89.
5. Bassett, H. and Goodwin, T. H. *J. Chem. Soc.* **1949** 2239.
6. Denk, G. and Alt, J. *Z. anorg. allgem. Chem.* **269** (1952) 244.
7. Kolthoff, I. M. and Sandell, E. B. *Textbook of Quantitative Inorganic Analysis*, 3rd ed., Macmillan, New York 1952, p. 717.
8. *International Tables for X-ray Crystallography*, Vol. 1, The Kynoch Press, Birmingham 1952.
9. Johansson, G. *Acta Chem. Scand.* **14** (1960) 771.

Received March 28, 1960.

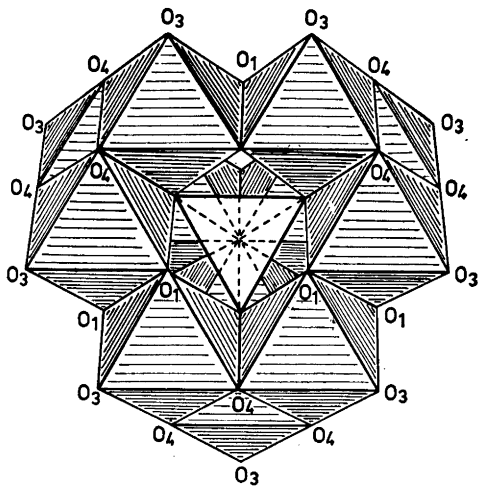

Fig. 1. The $Al_{13}O_4(OH)_{24}(H_2O)_{12}]^{7+}$-ion. The drawing shows how the twelve AlO_6-octahedra are joined together by means of common edges. The tetrahedron of oxygen (O_4) atoms in the center of the group contains the 4-coordinated Al-atom.

On the Crystal Structures of Some Basic Aluminium Salts

GEORG JOHANSSON

Gates and Crellin Laboratories of Chemistry, California Institute of Technology, Pasadena, California, U.S.A., Department of Inorganic Chemistry, The Royal Institute of Technology, Stockholm 70, Sweden

An aluminium chloride solution can be hydrolyzed by the addition of about 2.5 equivalents of alkali without the formation of a permanent precipitate of aluminium hydroxide. The addition of a suitable anion to this hydrolyzed solution precipitates basic salts, the structures of which are of a special interest since they might give some information about the polynuclear complexes that seem to exist in hydrolyzed aluminium salt solutions [1,2]. The structures of a number of them are being investigated and preliminary results of some of the structure determinations are given in this paper.

If the aluminium chloride solution is hydrolyzed by sodium hydroxide and sodium selenate is added, tetrahedral crystals can be obtained, which, when dried in air, have the composition $Na_2O{\cdot}13Al_2O_3{\cdot}8SeO_3{\cdot}xH_2O$ (with x in this case equal to about 74, *cf.* Ref.[3]. The crystals are cubic, with a_o = 18.0 Å and with two formula weights in the unit cell. The space group is $T_d^2-F\bar{4}3m$. Three-dimensional intensity data have been collected with Cu$K\alpha$-radiation. The structure has been solved from the tree-dimensional Patterson function and refined by means of three-dimensional Fourier maps *. At the present stage of the refinement the reliability index, R, is 0.11 for the 245 observed reflections, but the positions of the sodium atoms are still uncertain. The parameters are:

* All calculations were carried out on a Burroughs 205 computer at the California Institute of Technology.

Atom	Position	Positional parameters	Atom	Position	Positional parameters
48 Al_1	48(h)	$x = 0.057$	16 Se	16(e)	$x = 0.882$
		$z = 0.328$	48 O_5	48(h)	$x = 0.138$
4 Al_2	4(b)	—			$z = 0.968$
48 O_1	48(h)	$x = 0.047$	16 O_6	16(e)	$x = 0.828$
		$z = 0.677$	16 O_7	16(e)	$x = 0.663$
16 O_2	16(e)	$x = 0.441$	12 O_8	16(e)	$x = 0.190$
48 O_3	48(h)	$x = 0.069$	24 O_9	24(g)	$z = 0.960$
		$z = 0.223$			
48 O_4	48(h)	$x = 0.158$			
		$z = 0.447$			

The structure is built up from discrete aluminium-oxygen groups (Fig. 1) each containing 12 AlO_6 octahedra sharing O_1-O_1 and O_2-O_4 edges, and with an additional aluminium atom in the center of a tetrahedron of O_2 atoms. These large groups, which have the composition $Al_{13}O_{40}$, are not directly connected but are joined to the selenate groups by means of hydrogen bonds between O_3 of an aluminium-oxygen group and O_5 of a SeO_4 group. If the hydrogen atoms are located from the positions of hydrogen bonds and from Pauling's rule for the sum of the electrostatic bond strengths, the formula for the discrete aluminium-oxygen complexes seems to be $[Al_{13}O_4(OH)_{24}(H_2O)_{12}]^{7+}$. The formula for the basic salt now being considered should then be written $Na[Al_{13}O_4(OH)_{24}(H_2O)_{12}](SeO_4)_4 \cdot 13H_2O$. It is interesting to note that both the rings of six AlO_6 octahedra, that can be distinguished in the hydrargillite structure, and the groups of three octahedra which, linked together by common edges and corners, build up the diaspore and boehmite structures, can also be seen in the $[Al_{13}O_4(OH)_{24}(H_2O)_{12}]^{7+}$-groups (Fig. 1).

If the aluminium chloride solution is hydrolyzed with ammonia and ammonium sulfate is added to a high concentration, tetrahedral crystals of another kind can be obtained. They were first described by Bassett and Goodwin [4] who gave them the formula $6(NH_4)_2SO_4 \cdot 11Al_2O_3 \cdot 6SO_3 \cdot xH_2O$ (x = ca 72). The crystals are tetragonal with Laue symmetry $4/m$ and have the same kind of reflections systematically absent as the basic selenate. If a face centered unit cell is chosen the cell dimensions are $a = b = 19.8$ Å and $c = 19.6$ Å as determined from precession and Weissenberg photographs. The density is 1.86 g/cm³. According to these results and the analysis data given by Bassett and Goodwin [4] the following number of atoms should be present in the unit cell: Al: 52 (51.4), S: 28 (27.9), NH_4^+: 28 (28.0). The formula may therefore be written $(NH_4)_7[Al_{13}O_4(OH)_{24}(H_2O)_{12}](SO_4)_7 \cdot xH_2O$. The similarities to the basic selenate seem to be an indication that the same kind of discrete aluminium-oxygen groups are present in both compounds.

A monoclinic basic aluminium sulfate forming plate-like crystals also seems to be built up from the same kind of aluminium-oxygen complexes. It can be obtained from dilute hydrolyzed aluminium chloride solutions by the addition of sodium sulfate (for example from solutions that are about 0.01 M in Al^{3+} and 0.03 M in SO_4^{2-}). The composition is $13Al_2O_3 \cdot 6SO_3 \cdot xH_2O$ (x = ca 79) and the crystals seem to be identical with the compound $13Al_2O_3 \cdot 6SO_3 \cdot xH_2O$ described by Bassett and Goodwin [4]. The space group is C_{2h}^4 or C_s^2, with the intensity distribution favouring the centrosymmetric C_{2h}^4. The unit cell dimensions are: $a = 20.2$ Å, $b = 11.5$ Å, $c = 25.0$ Å, $\beta = 103°$ (symmetry $P2/a$ or Pa) but the crystals can also occur in a form with a unit cell of only half this size, with $a = 14.2$ Å, $b = 11.5$ Å, $c = 17.7$ Å, $\beta = 102.3°$ (symmetry $P2/n$ or Pn). This, however, can spontaneously switch over to the larger unit cell without any noticeable changes in the appearance of the crystal or of the sharpness of the spots on the Weissenberg photographs. Three-dimensional intensity data have been collected with Cu$K\alpha$ radiation from the crystals containing the smaller unit cell. About 3 200 reflections were observed. The three-dimensional Patterson function could be interpreted by assuming two aluminium-oxygen com-

plexes similar to those in the basic selenate to be present in the unit cell according to the symmetry $P2/n$. Three dimensional Fourier maps seem to confirm this assumption and also reveal the positions of four of the sulfate groups in a fourfold position; the remaining two sulfate groups, however, are apparently statistically distributed over two positions close to a center of symmetry in the unit cell. This result in connection with the fact that for some of the zonal data, for example the $h3l$-reflections, the intensity distribution is closer to one expected for a noncentrosymmetric space group seems to indicate the presence of small deviations from a centrosymmetric arrangement. The space group should then be Pn rather than $P2/n$. The refinement of the structure will be continued according to this space group.

The reliability index, R, assuming the space group to be $P2/n$, is at the present stage of the refinement 0.24 for all observed reflections. The parameters for the aluminium atoms in the aluminium-oxygen complexes are:

Atom	Parameters		
	x	y	z
4 Al_1:	0.338	0.980	0.220
4 Al_2:	0.482	0.796	0.267
4 Al_3:	0.137	0.795	0.390
4 Al_4:	0.307	0.437	0.329
4 Al_5:	0.276	0.620	0.437
4 Al_6:	0.453	0.619	0.375
2 Al_7:	1/4	0.705	1/4

Fellowships from the *Corning Glass Works Foundation* and from the *Sweden-America Foundation* in support of part of this work is gratefully acknowledged.

1. Brosset, C., Biedermann, G. and Sillén, L. G. *Acta Chem. Scand.* **8** (1954) 1917.
2. Kohlschütter, H. W. and Hantelmann, P. *Z. anorg. allgem. Chem.* **248** (1941) 319.
3. Johansson, G., Lundgren, G., Sillén, L. G. and Söderquist, R. *Acta Chem. Scand.* **14** (1960) 769.
4. Bassett, H. and Goodwin, T. H. *J. Chem. Soc.* **1949** 2239.

Received March 28, 1960.

On Observable Discontinuities and Coherence in the Kinetics of Enzymically Reacting Systems. A Misprint

J. A. CHRISTIANSEN

Sundvœnget 9, Hellerup, Denmark

The following misprint in my paper in this volume p. 107 should be corrected: The sequence (A) should read

$$\begin{array}{lll} B_1 + X_1 \rightleftharpoons X_2 + A_2 & (\pm 1) & \\ B_2 + X_2 \rightleftharpoons X_3 + A_3 & (\pm 2) & (A) \\ B_3 + X_3 \rightleftharpoons X_1 + A_1 & (\pm 3) & \end{array}$$

X_1, X_2 and X_3 being three different forms, or compounds with the substrates (B_i, A_i), of the enzyme. The plus signs mean the reactions in the direction from left to right, the minus signs indicating reactions in the opposite direction.

Received March 30, 1960.

Free Butyric Acid as a Possible Source of Off-Flavour of the Cow's Milk After Administration of Oestrogens

TORLEIV LUNAAS

Department of Sexual Physiology and Sexual Pathology, Veterinary College of Norway, Oslo, Norway

During investigations on the metabolism of oestrogens in the cow undertaken at this department[1] peculiar alterations of the milk after parenteral administration of the hormones were repeatedly observed[2]. To further explore the nature of these alterations 10 mg oestradiol-17β in 5 ml propyleneglycol was injected intramusculary to a non-pregnant cow producing 8 liters milk a day. Daily milk samples were frozen on the day of drawing and analysed in series immediately after thawing.

On the week after injection the milk produced per day gradually decreased to

plexes similar to those in the basic selenate to be present in the unit cell according to the symmetry $P2/n$. Three dimensional Fourier maps seem to confirm this assumption and also reveal the positions of four of the sulfate groups in a fourfold position; the remaining two sulfate groups, however, are apparently statistically distributed over two positions close to a center of symmetry in the unit cell. This result in connection with the fact that for some of the zonal data, for example the $h3l$-reflections, the intensity distribution is closer to one expected for a noncentrosymmetric space group seems to indicate the presence of small deviations from a centrosymmetric arrangement. The space group should then be Pn rather than $P2/n$. The refinement of the structure will be continued according to this space group.

The reliability index, R, assuming the space group to be $P2/n$, is at the present stage of the refinement 0.24 for all observed reflections. The parameters for the aluminium atoms in the aluminium-oxygen complexes are:

Atom	Parameters		
	x	y	z
4 Al_1:	0.338	0.980	0.220
4 Al_2:	0.482	0.796	0.267
4 Al_3:	0.137	0.795	0.390
4 Al_4:	0.307	0.437	0.329
4 Al_5:	0.276	0.620	0.437
4 Al_6:	0.453	0.619	0.375
2 Al_7:	1/4	0.705	1/4

Fellowships from the *Corning Glass Works Foundation* and from the *Sweden-America Foundation* in support of part of this work is gratefully acknowledged.

1. Brosset, C., Biedermann, G. and Sillén, L. G. *Acta Chem. Scand.* **8** (1954) 1917.
2. Kohlschütter, H. W. and Hantelmann, P. *Z. anorg. allgem. Chem.* **248** (1941) 319.
3. Johansson, G., Lundgren, G., Sillén, L. G. and Söderquist, R. *Acta Chem. Scand.* **14** (1960) 769.
4. Bassett, H. and Goodwin, T. H. *J. Chem. Soc.* **1949** 2239.

Received March 28, 1960.

On Observable Discontinuities and Coherence in the Kinetics of Enzymically Reacting Systems. A Misprint

J. A. CHRISTIANSEN

Sundvœnget 9, Hellerup, Denmark

The following misprint in my paper in this volume p. 107 should be corrected: The sequence (A) should read

$$\begin{array}{lll} B_1 + X_1 \rightleftharpoons X_2 + A_2 & (\pm 1) & \\ B_2 + X_2 \rightleftharpoons X_3 + A_3 & (\pm 2) & (A) \\ B_3 + X_3 \rightleftharpoons X_1 + A_1 & (\pm 3) & \end{array}$$

X_1, X_2 and X_3 being three different forms, or compounds with the substrates (B_i, A_i), of the enzyme. The plus signs mean the reactions in the direction from left to right, the minus signs indicating reactions in the opposite direction.

Received March 30, 1960.

Free Butyric Acid as a Possible Source of Off-Flavour of the Cow's Milk After Administration of Oestrogens

TORLEIV LUNAAS

Department of Sexual Physiology and Sexual Pathology, Veterinary College of Norway, Oslo, Norway

During investigations on the metabolism of oestrogens in the cow undertaken at this department[1] peculiar alterations of the milk after parenteral administration of the hormones were repeatedly observed[2]. To further explore the nature of these alterations 10 mg oestradiol-17β in 5 ml propyleneglycol was injected intramusculary to a non-pregnant cow producing 8 liters milk a day. Daily milk samples were frozen on the day of drawing and analysed in series immediately after thawing.

On the week after injection the milk produced per day gradually decreased to

5 liters and showed a strong ability to foam when stirred. The most striking change in the milk was the development of an acrid, nauseous taste.

The following milk constituents were determined: sodium and potassium (flame photometry of trichloroacetic filtrates), calcium and magnesium (flame photometry after resp. oxalate and ammoniumphosphate precipitation), chloride (flame photometry after silver precipitation), lactose (polarimetry), fat (Gerber), citric acid (heating with acetic anhydride and pyridine) and free fatty acids (titration of ether-petroleum ether extracts [3]).

The maximal deviations were found to occur on the third day after injection when sodium had increased to 22 mequiv/l (from 15 mequiv/l), chloride to 42 mequiv/l (from 27 mequiv/l) and potassium decreased to 27 mequiv/l (from 38 mequiv/l) indicating a decreased diluting resp. concentrating ability of the mammary gland. At this time calcium had increased to 63 mequiv/l (from 40 mequiv/l), and fat to 5.5 % (from 3.8 %). A few determinations (biuret method) indicated increased protein content. The other constituents analysed showed minor variations in concentration except the extractable fatty acids which had increased 30-fold (see Table 1).

A sample of the milk drawn on the third day after injection was acidified with concentrated phosphoric acid, extracted 3 times with its equal volume of ether and the extracts titrated. After re-acidification the samples were submitted to gas liquid partition chromatography [4] for identification and titration of volatile fatty acids. In each of the three extracts butyric acid corresponding to about 10 % of the titre of the extracted acids was found and the total amount of butyric acid in the milk sample was roughly estimated to 1 g/l. No other volatile acids could be found.

It was therefore suspected that the butyric acid could be responsible for the off-flavour of the milk. This was substantiated by the strong aggravation of the off-flavour following acidification of the milk with mineral acids and by organoleptic comparison with normal milk to which butyric acid had been added.

Small increments of the free fatty acids were also found in connection with the two following natural heats and after an injection of 10 mg oestrone, but no corresponding off-flavour of the milk was perceptible. Injections of various oestrogens to 8 cows

Table 1. Titrable acidity in ether-petroleum ether extracts of milk [3] after administration of oestrogens and during heats. Consecutive days.

ml 0.01 N NaOH per 10 ml milk.	Remarks.
1.0	
1.4	
0.9	10 mg oestradiol−17 β.
10.0	
26.0	
30.2	
18.2	
10.5	
5.3	
2.2	
0.8	Heat.
0.8	
2.0	
1.3	
0.7	
0.7	
0.7	
0.5	10 mg oestrone.
0.7	
1.9	
2.5	
2.5	
—	Sample lost.
1.5	
1.2	
1.0	
0.6	
0.6	
0.7	
1.0	
1.5	
2.5	Heat.
5.2	
4.0	
2.5	
1.5	
1.2	

in high yield (between 1 and 2 months after parturition) did not alter the concentration of free fatty acids of the milk.

It is a clinical experience that cows suffering from cystic ovaries may secrete an off-flavoured milk with a salty and bitter taste [5]. From the above described findings in the milk following parenteral administration of oestrogens and in connection with heat it seems justified to ascribe this milk abnormality to an altered oestrogen status of the cows. The stage of the lactation period seems, however, to be of importance. Milk of this kind, presumably with a high

lipase activity [6], may render large amounts of normal milk inpalatable when admixed prior to processing for consumption.

More systematic investigations are in progress.

For the permission to use the gas liquid chromatography apparatus at the Department of Physiology I wish to thank Karl Halse M.S.

This investigation was supported financially by the *Norwegian Milk Producers National Association* and the *Norwegian Agricultural Research Council.*

1. Velle, W. *Undersökelser over naturlig forekommende östrogener hos drövtyggere og gris,* Thesis, Oslo 1958.
2. Velle, W. *Personal communication.*
3. Frankel, E. N. and Tarassuk, N. P. *J. Dairy Sci.* **38** (1955) 751.
4. James, A. T. and Martin, A. J. P. *Biochem. J.* **50** (1952) 679.
5. Garm, O. *A Study of Bovine Nymphomania.* Thesis. Acta endocr. (Kbh.) (1949) Suppl. 3.
6. Anonymus, *Md. Agr. Expt. Sta. Sixty-fifth Ann. Rpt.* (1951–1952) **43**; Cit. from Herrington, B. L. *J. Dairy Sci.* **37** (1954) 775.

Received February 22, 1960.

The Fatty Acid Composition of Cerebrospinal Fluid Lipids

ROLF BLOMSTRAND

Swedish Medical Research Council, Unit for Biochemical Research Related to Atherosclerosis, University of Lund, Lund, Sweden

The study of the fatty acid composition of the different lipids of human cerebrospinal fluid (CSF) has not previously been possible due to the lack of suitable analytical methods which could be applied to the small amounts of lipid available. The CSF contains only 1–1.5 mg of total lipids [1] per 100 ml and ultramicrochemical techniques have to be applied to normal and abnormal fluids if neurochemical correlations are to be made. Through the use of the technique described below it has been possible to identify the fatty acid pattern of cholesterol esters, glycerides and phospholipids of normal human CSF.

Pooled normal CSF (140 ml) obtained from individuals without neurological symptoms was used for the analysis. The CSF was immediately centrifuged after lumbar puncture, the cell-free supernate was carefully removed and aliquots taken for determination of total protein. The rest of it was kept at −20°C until analyzed. All specimens used had normal white cell count and normal protein concentrations. The pooled CSF was concentrated by dialysis in a collodium bag under reduced pressure according to Mies [2] and extracted with 20 volumes of chloroform:methanol 2:1 and washed with water [3]. The total lipids (1.8 mg) were separated on a silicic acid column [4] (0.2 g) into cholesterol esters, glycerides + free fatty acids and phospholipids. The different lipid fractions were hydrolyzed and the fatty acids were isolated after saponification and acidification. The fatty acid composition was defined by gas-liquid chromatography according to James and Martin [5] using an Argon Pye chromatograph with an ionization chamber as detector. Because of the complexity of the fatty acid pattern, it was necessary to chromatograph the mixed methyl esters on two different stationary phases, a polar polyester (LHC–R–296) [6] and silicone oil. In addition chromatograms were obtained on the mixed esters after complete hydrogenation in order to obtain an accurate chain-length analysis. The analytical procedures used otherwise have been described earlier.[7]

The determination of the fatty acid composition of the different lipid components of human CSF is summarized in Table 1. For comparison the fatty acid composition of the different lipid classes of normal serum is also included in the table. Three characteristic fatty acid patterns are found in the cholesterol esters, glycerides + free fatty acids and phospholipids of human CSF. The fatty acid composition of the CSF resembles the serum lipids, but there are certain differences. Especially remarkable is the very low concentration of linoleic acid in the cholesterol esters of CSF compared with that of the serum cholesterol esters. Another interesting finding is the rather high concentration of palmitoleic acid in the glycerides + free fatty acid fraction and in the cholesterol esters. In the group C_{20-22}? several peaks were found among the phospholipid fatty acids. Significant amounts of a fatty acid with 24 carbon atoms were also found in the phospholipids of the CSF. Work is in progress to identify these fatty

lipase activity [6], may render large amounts of normal milk inpalatable when admixed prior to processing for consumption.

More systematic investigations are in progress.

For the permission to use the gas liquid chromatography apparatus at the Department of Physiology I wish to thank Karl Halse M.S.

This investigation was supported financially by the *Norwegian Milk Producers National Association* and the *Norwegian Agricultural Research Council.*

1. Velle, W. *Undersökelser over naturlig forekommende östrogener hos drövtyggere og gris,* Thesis, Oslo 1958.
2. Velle, W. *Personal communication.*
3. Frankel, E. N. and Tarassuk, N. P. *J. Dairy Sci.* **38** (1955) 751.
4. James, A. T. and Martin, A. J. P. *Biochem. J.* **50** (1952) 679.
5. Garm, O. *A Study of Bovine Nymphomania.* Thesis. Acta endocr. (Kbh.) (1949) Suppl. 3.
6. Anonymus, *Md. Agr. Expt. Sta. Sixty-fifth Ann. Rpt.* (1951–1952) **43**; Cit. from Herrington, B. L. *J. Dairy Sci.* **37** (1954) 775.

Received February 22, 1960.

The Fatty Acid Composition of Cerebrospinal Fluid Lipids

ROLF BLOMSTRAND

Swedish Medical Research Council, Unit for Biochemical Research Related to Atherosclerosis, University of Lund, Lund, Sweden

The study of the fatty acid composition of the different lipids of human cerebrospinal fluid (CSF) has not previously been possible due to the lack of suitable analytical methods which could be applied to the small amounts of lipid available. The CSF contains only 1–1.5 mg of total lipids [1] per 100 ml and ultramicrochemical techniques have to be applied to normal and abnormal fluids if neurochemical correlations are to be made. Through the use of the technique described below it has been possible to identify the fatty acid pattern of cholesterol esters, glycerides and phospholipids of normal human CSF.

Pooled normal CSF (140 ml) obtained from individuals without neurological symptoms was used for the analysis. The CSF was immediately centrifuged after lumbar puncture, the cell-free supernate was carefully removed and aliquots taken for determination of total protein. The rest of it was kept at −20°C until analyzed. All specimens used had normal white cell count and normal protein concentrations. The pooled CSF was concentrated by dialysis in a collodium bag under reduced pressure according to Mies [2] and extracted with 20 volumes of chloroform:methanol 2:1 and washed with water [3]. The total lipids (1.8 mg) were separated on a silicic acid column [4] (0.2 g) into cholesterol esters, glycerides + free fatty acids and phospholipids. The different lipid fractions were hydrolyzed and the fatty acids were isolated after saponification and acidification. The fatty acid composition was defined by gas-liquid chromatography according to James and Martin [5] using an Argon Pye chromatograph with an ionization chamber as detector. Because of the complexity of the fatty acid pattern, it was necessary to chromatograph the mixed methyl esters on two different stationary phases, a polar polyester (LHC–R–296) [6] and silicone oil. In addition chromatograms were obtained on the mixed esters after complete hydrogenation in order to obtain an accurate chain-length analysis. The analytical procedures used otherwise have been described earlier.[7]

The determination of the fatty acid composition of the different lipid components of human CSF is summarized in Table 1. For comparison the fatty acid composition of the different lipid classes of normal serum is also included in the table. Three characteristic fatty acid patterns are found in the cholesterol esters, glycerides + free fatty acids and phospholipids of human CSF. The fatty acid composition of the CSF resembles the serum lipids, but there are certain differences. Especially remarkable is the very low concentration of linoleic acid in the cholesterol esters of CSF compared with that of the serum cholesterol esters. Another interesting finding is the rather high concentration of palmitoleic acid in the glycerides + free fatty acid fraction and in the cholesterol esters. In the group C_{20-22}? several peaks were found among the phospholipid fatty acids. Significant amounts of a fatty acid with 24 carbon atoms were also found in the phospholipids of the CSF. Work is in progress to identify these fatty

Table 1. The fatty acid composition of the different lipid classes of human cerebrospinal fluid (CSF) compared with those of serum. The total lipids were fractionated on silicic acid and the fatty acids were determined with the aid of gas-liquid chromatography. Values are expressed as percentage of total fatty acid methyl esters.

Fatty acid		Percentage of total fatty acids in respective lipids classes					
		Cholesterol ester F.A.		Glyceride + free F.A.		Phospholipid F.A.	
		C.S.F.	Serum	C.S.F.	Serum	C.S.F.	Serum
Saturated							
Myristic	14:0	9.7	1.7	8.2	3.5	6.1	1.5
Pentadecanoic	15:0	7.1	1.5	4.9	1.6	4.7	1.2
Palmitic	16:0	22.1	14.8	33.8	24.1	32.5	29.3
Heptadecanoic	17:0	1.6	—	0.9		1.6	—
Stearic	18:0	5.3	2.3	10.6	6.4	11.0	16.8
Monounsaturated							
Palmitoleic	16:1	18.1	5.2	9.7	7.4	—	4.0
Oleic	18:1	15.4	24.2	20.9	36.4	20.1	16.2
Diunsaturated							
Linoleic	18:2	6.2	44.7	3.3	7.8	12.5	18.8
Polyunsaturated							
Linolenic	18:3	—	0.3	2.1	2.1	1.3	0.5
Arachidonic	20:4	1.6	2.3	—	—	2.3	5.7
	20—22?	2.8	1.2	2.8	1.9	3.4	3.6
	24?					1.6	—

The fatty acids are also designated by a dual symbol giving chain length and number of double bonds. The sum of each column is less than 100 % because traces of unusual fatty acids detected were omitted from the final tabulation. — indicates trace amounts.

acids. Preliminary investigations on the composition of the total fatty acids of CSF with neurologic disease indicate that abnormal fatty acid patterns may be obtained [8].

This work is part of investigations supported by the *Swedish Medical Research Council.*

1. Tourtelotte, W. W., *Neurology* **9** (1959) 375.
2. Mies, H. J. *Klin Wochschr.* **31** (1953) 159.
3. Folch, J. and Lee, J. *J. Biol. Chem.* **191** (1951) 833.
4. Borgström, B. *Acta Physiol. Scand.* **25** (1952) 101.
5. James, A. T. and Martin, A. J. P. *Biochem. J.* **63** (1956) 144.
6. Orr, C. and Callen, J. E. *J. Am. Chem. Soc.* **80** (1958) 249.
7. Blomstrand, R. and Dahlbäck, O. *Acta Soc. Med. Upsaliensis* **114** (1959) 177.
8. Blomstrand, R., Dencker, S. J. and Swahn, B. *Kungl. Fysiogr. Sällsk., Lund. Förh. To be published.*

Received April 9, 1960.

The Preparation and the Kinetics of Solvolysis of Some Derivatives of β,β,β-Trichloroethanol

PENTTI SALOMAA and RAILI LINNANTIE

Department of Chemistry, University of Turku, Turku, Finland

In continuation of earlier investigations on the kinetics of alkoxy-substituted compounds [1-4], a number of compounds of the type $XCH_2OCH_2CCl_3$, where X is a chlorine atom, an alkoxyl group or an acyloxy group, were prepared from β,β,β-trichloroethanol. These compounds were of interest from the kinetic standpoint because they contain three electron-attracting chlorine atoms bound to one carbon atom, which combination was expected to lower greatly the rates of solvolysis (*cf.* Ref.[4]).

Experimental. β,β,β-Trichloroethanol (I) was prepared by reducing chloral according to the directions of Chalmers [5]. Derivatives of this alcohol, which have not been described previously, were synthesized by methods described below. The yields of the pure compounds varied from 30 to 70 %. The compounds and their physical constants are shown in Table 1. The values of the molecular refractivity in the last column were calculated using values of the group refractivities reported by Vogel [6] and the refractivity value 18.078 for three chlorine atoms attached to the same carbon atom. The purities of most of the compounds were also checked by volumetric analysis of formaldehyde liberated on their hydrolysis in 80 % sulphuric acid or, in the case of α-chloromethyl β,β,β-trichloroethyl ether, the formaldehyde and hydrogen chloride formed on hydrolysis of the compound by water, and by determining the molecular weights by cryoscopy in benzene solution. The results of the analyses were in satisfactory agreement with the theoretical values. Thus, for example, the molecular weight determinations of (III) gave the mean value 316 ± 8, whereas the true molecular weight is 311.

α-Chloromethyl β,β,β-trichloroethyl ether (II) was prepared from the trichloroethanol, paraformaldehyde and hydrogen chloride. Although the method of preparation was similar in principle to that employed when preparing other α-chloroethers (for references, see Ref.[1]), poor yields were obtained when the cooled mixture of alcohol and formaldehyde was saturated with hydrogen chloride. The reason for this was that the formal that is produced in a concurrent or intermediate reaction reacts very slowly with hydrogen chloride to form the α-chloroether. In addition, the stream of hydrogen chloride removes from the reaction mixture appreciable amounts of formaldehyde derived from paraformaldehyde evidently owing to the lower solubility of formaldehyde in trichloroethanol than in unsubstituted aliphatic alcohols. The influence of these factors was avoided by saturating the reaction mixture with hydrogen chloride and allowing it to stand about one week at −2°C with intermittent shaking and then resaturating it with hydrogen chloride. The volatilization of formaldehyde was prevented by covering the reaction mixture with concentrated hydrochloric acid before passing hydrogen chloride into the mixture.

Details of a typical synthesis are presented in the following. About 20 ml of concentrated hydrochloric acid was added to form a layer over a mixture of 47 g (0.31 mole) of trichloroethanol and 13 g (0.43 mole) of paraformaldehyde and the whole was cooled in an ice-water mixture and then saturated with hydrogen chloride gas over a period of 5 h. The reaction

Table 1. Boiling points, densities and refractive indexes of the compounds $XCH_2OCH_2CCl_3$.

	X	B.p. °C/mm Hg	d_4^{20}	n_D^{20}	R_D obs.	R_D calc.
(II)	Cl	80– 84/24	1.5113	1.4833	37.41	37.57
(III)	CCl_3CH_2O	125–128/ 7	1.5482	1.4942	58.47	58.49
(IV)	$n-C_3H_7O$	76– 78/ 6	1.2379	1.4510	48.19	48.14
(V)	$sec.-C_3H_7O$	69– 70/ 7	1.2349	1.4486	48.08	48.15
(VI)	HCOO	90– 92/ 7	1.4722	1.4670	38.10	38.96
(VII)	C_3HCOO	104–106/ 7	1.3784	1.4568	43.74	43.58

mixture was stored eight days at −2°C, during which the phases were mixed from time to time by shaking the flask. After the mixture had again been saturated with hydrogen chloride, the upper layer was removed and the lower layer containing the chloroether dried with anhydrous calcium chloride; the hydrogen chloride was removed with a current of carbon dioxide. The layer was then fractionally distilled under reduced pressure. After about 10 % of the distillate had passed over, the main fraction (about 60 %) distilled at 80−84°C and 24 mm Hg; then the temperature rose abruptly owing to the distillation of formal (III) formed as a side product.

Di-(β,β,β-trichloroethoxy)methane (III) was prepared by two different methods. In the first method, an equimolar mixture of (I) and (II) was kept at a temperature of 50°C for 10 h, during which carbon dioxide was passed through the mixture to expel the hydrogen chloride formed. The crude product was washed with sodium bicarbonate solution and water, dried with anhydrous sodium sulphate, and purified by fractional distillation under reduced pressure. In the second method, (I), formaldehyde (added as paraformaldehyde) and anhydrous zinc chloride in the molar ratio of 2:1:0.1 were allowed to react 24 h at 50−60°C. The formal (III) formed in the reaction was isolated by shaking the reaction product with a mixture containing one volume of water and 5 volumes of petroleum ether. The petroleum ether layer containing the formal was dried with sodium sulphate and distilled under reduced pressure. The former method gave the higher yield (about 60 % of theory) of pure product. An attempt was also made to synthesize the formal (III) by distilling a a mixture of di-*sec.*-propyl formal and trichloroethanol acidified with *p*-toluenesulphonic acid to remove the *sec.*-propanol formed in the reaction, but it was found that the replacement of the second alkyl group of di-*sec.*-propyl formal (the same was the case with di-*n*-propyl formal) by a β,β,β-trichloroethyl group took place so slowly that the method can be employed only to prepare asymmetric formals (see below).

Normal and secondary propyl-β,β,β-trichloroethyl formals, (IV) and (V), were prepared from the respective dipropyl formals and trichloroethanol. Equimolar amounts of the reactants were heated together in the presence of *p*-toluenesulphonic acid and the mixture was subjected to fractional distillation to remove the most volatile component, the propanol. Nearly quantitative yields of (IV) and (V) were obtained. When twice the amount of trichloroethanol relative to the dialkyl formal was employed in the first reaction (to prepare IV), only the asymmetric formal was produced. When an equimolar amount of trichloroethanol was added to (IV) or (V), no reaction was observed to take place when the mixture was heated, although the catalyst concentration was greatly increased, as no propanol distilled over during a period of several hours.

The β,β,β-trichloroethoxymethyl esters of formic and acetic acids, (VI) and (VII), were prepared from the chloroether (II) and anhydrous potassium formate or potassium acetate by a procedure similar to that previously employed to prepare alkoxymethyl esters [2-4].

The method of performing the kinetic measurements was the same as described previously [1].

The intention was to obtain kinetic data for a direct comparison with previously reported data on the solvolysis of alkoxymethyl compounds [4]. It was, however, possible to study only the ethanolysis of chloromethyl β,β,β-trichloroethyl ether (II) in ethanol and a 53.3 wt. % ethanol-dioxan mixture. All the compounds prepared in this work were so sparingly soluble in water that their hydrolysis reactions in this solvent could not be studied by customary methods.

The first-order rate coefficients measured for the ethanolysis of the chloroether (II) and the respective parameters of the Arrhenius equation are the following:

		15°	25°	35°	E (kcal/mole)	log A
Ethanol	10^5k(s^{-1})	6.19	17.6	47.7	18.44	9.77
53.3 wt.% ethanol-dioxan	»	1.56	3.95	9.62	16.43	7.64

A comparison of the values with previous data for α-chloroethers [4], $ROCH_2Cl$, reveals that the rate of ethanolysis diminishes rapidly (by a factor of 12−14 for each

chlorine substitution) in the sequence R = CH_3CH_2-, CH_2ClCH_2-, CCl_3CH_2- owing to a large increase in the activation energy. The activation energies in the ethanolysis of the first two compounds in 53.3 wt.% ethanol-dioxan are, respectively, 11.13 and 13.55 kcal per mole [1,4]. The logarithms of the frequency factor for the three compounds have values varying from 7.04 to 7.66 and hence the entropies of activation differ only insignificantly. The structural effects are thus consistent with the unimolecular carbonium ion mechanism of ethanolysis.

On the basis of the data presented it is possible to estimate the effect of the β,β,β-trichloroethyl group on the hydrolysis mechanism of the corresponding alkoxymethyl esters in dilute acid solutions. The polar substituent constant $\bar{\sigma}$ *, as defined in Ref.[4], for this group is + 2.87. From this value it can be estimated that the rate coefficient for the hydrolysis of β,β,β-trichloroethoxymethyl acetate (VII) by the unimolecular $A_{AL}1$ mechanism in dilute aqueous acid at 25°C should be about 7×10^{-7} l mole^{-1}s^{-1}. As this latter value is of a much lower order of magnitude than the rate coefficients relating to the normal type of acid-catalysed hydrolysis reactions of alkyl acetates (about 10^{-4} l mole^{-1}s^{-1}), *i.e.* reactions taking place by the bimolecular $A_{AC}2$ mechanism, it can be assumed that also the ester (VII) hydrolyses almost exclusively by the latter mechanism. In the case of the corresponding formate, (VI), the conditions for the unimolecular hydrolysis mechanism are even less favourable.

1. Salomaa, P. *Ann. Univ. Turkuensis, Ser.* **A XIV** (1953) No. 1.
2. Salomaa, P. *Acta Chem. Scand.* **11** (1957) 132, 141, 235, 239.
3. Salomaa, P. and Linnantie, R. *Acta Chem. Scand.* **12** (1958) 2051; **14** (1960) 586.
4. Salomaa, P. *Suomen Kemistilehti B* **33** (1960) 11.
5. Chalmers, W. *Org. Syntheses* **15** (1935) 80.
6. Vogel, A. J. *J. Chem. Soc.* **1948** 1833.

Received April 5, 1960.

The Effect of Acetone Treatment on Vitamin A_1-Aldehyde Extracts from Herring Roe

OLAF R. BRÆKKAN, HAKON MYKLESTAD and LEIF REIN NJAA

Governmental Vitamin Laboratory, Norwegian Fisheries Research Institute, Bergen, Norway

Plack *et al.*[1] have demonstrated the presence of vitamin A_1 aldehyde in herring ova *(Clupea harengus)* and some other marine teleosts. They investigated several extraction methods, but found that extraction of the eggs with light petroleum followed by addition of ethanol to the blended mixture gave the best results. Pollard and Bieri [2] confirmed some of these findings, but reported that all their samples of herring roe contained only vitamin A_2 aldehyde. They extracted the ova several times with ethanol and isolated the vitamins by hexane extraction of the alcohol extracts.

During studies of the occurrence of vitamin A aldehydes in fish in our laboratory, we applied both the proposed extraction methods on the herring roe *(Clupea harengus)*, and found only vitamin A_1 aldehyde to be present. We were further only able to demonstrate the presence of vitamin A alcohol in these extracts but not the ester. Plack *et al.*[1] estimated the vitamin concentrations by the Carr-Price test, and reported for herring ova 2.4—5.7 μg vitamin A_1 aldehyde per g and 0.3—0.9 μg vitamin A_1 ester and alcohol per g. We have carried out the estimations by spectrophotometric measurements in the ultraviolet and found only 1 μg vitamin A_1 aldehyde and 0.3 μg vitamin A_1 alcohol per g herring roe. The absorption curves of the fractions were plotted, thus establishing the identity of the compounds.

Plack *et al.*[1] studied the effect of acetone treatment of the light-petroleum extracts. They found in liver storage tests in rats that only the acetone-soluble fraction contained biological activity, while the acetone-insoluble fraction showed no activity. In repeated experiments they could only recover about 40 % of the activity originally present in the extracts. This suggested a further investigation of the soluble portion, and the present communication reports some of the findings.

chlorine substitution) in the sequence R = CH_3CH_2-, CH_2ClCH_2-, CCl_3CH_2- owing to a large increase in the activation energy. The activation energies in the ethanolysis of the first two compounds in 53.3 wt.% ethanol-dioxan are, respectively, 11.13 and 13.55 kcal per mole [1,4]. The logarithms of the frequency factor for the three compounds have values varying from 7.04 to 7.66 and hence the entropies of activation differ only insignificantly. The structural effects are thus consistent with the unimolecular carbonium ion mechanism of ethanolysis.

On the basis of the data presented it is possible to estimate the effect of the β,β,β-trichloroethyl group on the hydrolysis mechanism of the corresponding alkoxymethyl esters in dilute acid solutions. The polar substituent constant $\bar{\sigma}$ *, as defined in Ref.[4], for this group is + 2.87. From this value it can be estimated that the rate coefficient for the hydrolysis of β,β,β-trichloroethoxymethyl acetate (VII) by the unimolecular $A_{AL}1$ mechanism in dilute aqueous acid at 25°C should be about 7×10^{-7} l mole^{-1}s^{-1}. As this latter value is of a much lower order of magnitude than the rate coefficients relating to the normal type of acid-catalysed hydrolysis reactions of alkyl acetates (about 10^{-4} l mole^{-1}s^{-1}), *i.e.* reactions taking place by the bimolecular $A_{AC}2$ mechanism, it can be assumed that also the ester (VII) hydrolyses almost exclusively by the latter mechanism. In the case of the corresponding formate, (VI), the conditions for the unimolecular hydrolysis mechanism are even less favourable.

1. Salomaa, P. *Ann. Univ. Turkuensis, Ser.* **A XIV** (1953) No. 1.
2. Salomaa, P. *Acta Chem. Scand.* **11** (1957) 132, 141, 235, 239.
3. Salomaa, P. and Linnantie, R. *Acta Chem. Scand.* **12** (1958) 2051; **14** (1960) 586.
4. Salomaa, P. *Suomen Kemistilehti B* **33** (1960) 11.
5. Chalmers, W. *Org. Syntheses* **15** (1935) 80.
6. Vogel, A. J. *J. Chem. Soc.* **1948** 1833.

Received April 5, 1960.

The Effect of Acetone Treatment on Vitamin A_1-Aldehyde Extracts from Herring Roe

OLAF R. BRÆKKAN, HAKON MYKLESTAD and LEIF REIN NJAA

Governmental Vitamin Laboratory, Norwegian Fisheries Research Institute, Bergen, Norway

Plack *et al.*[1] have demonstrated the presence of vitamin A_1 aldehyde in herring ova *(Clupea harengus)* and some other marine teleosts. They investigated several extraction methods, but found that extraction of the eggs with light petroleum followed by addition of ethanol to the blended mixture gave the best results. Pollard and Bieri [2] confirmed some of these findings, but reported that all their samples of herring roe contained only vitamin A_2 aldehyde. They extracted the ova several times with ethanol and isolated the vitamins by hexane extraction of the alcohol extracts.

During studies of the occurrence of vitamin A aldehydes in fish in our laboratory, we applied both the proposed extraction methods on the herring roe *(Clupea harengus)*, and found only vitamin A_1 aldehyde to be present. We were further only able to demonstrate the presence of vitamin A alcohol in these extracts but not the ester. Plack *et al.*[1] estimated the vitamin concentrations by the Carr-Price test, and reported for herring ova 2.4—5.7 μg vitamin A_1 aldehyde per g and 0.3—0.9 μg vitamin A_1 ester and alcohol per g. We have carried out the estimations by spectrophotometric measurements in the ultraviolet and found only 1 μg vitamin A_1 aldehyde and 0.3 μg vitamin A_1 alcohol per g herring roe. The absorption curves of the fractions were plotted, thus establishing the identity of the compounds.

Plack *et al.*[1] studied the effect of acetone treatment of the light-petroleum extracts. They found in liver storage tests in rats that only the acetone-soluble fraction contained biological activity, while the acetone-insoluble fraction showed no activity. In repeated experiments they could only recover about 40 % of the activity originally present in the extracts. This suggested a further investigation of the soluble portion, and the present communication reports some of the findings.

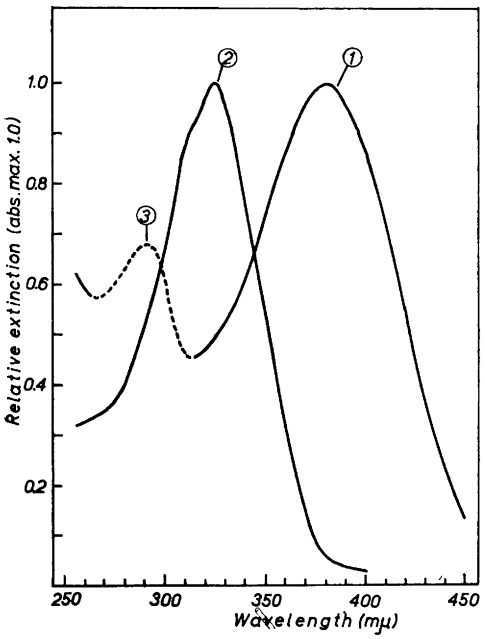

Fig. 1. Absorption curves of vitamin A_1-aldehyde extracted from herring ova (1), and its reduction product vitamin A_1 (2). The dotted band (3) is caused by the presence of α-tocopherol.

Extracts obtained by both the reported methods [1,2] were evaporated to dryness under reduced pressure. The residues were extracted with acetone as described by Plack *et al.*[1] or with the following modification: The residue was dissolved by heating with acetone, and then cooled by partial evaporation in vacuum, whereby a precipitate formed which was insoluble at room temperature. This precipitate was washed several times with cold acetone. The acetone extracts were combined and evaporated to dryness, dissolved in hexane and chromatographed on a soft Al_2O_3-column. The elution was carried out with 2 % (v/v) ethyl ether in hexane. As the aldehyde band approached the end of the column, 10 ml fractions were collected. These fractions were evaporated to dryness, dissolved in ethanol and measured in a Beckman DU spectrophotometer. The "aldehyde" fractions showed absorption curves with maxima between 390—400 mμ. The later fractions had absorption maxima at the highest wavelengths. By the normal procedure (without acetone treatment of the residue), a curve with absorption maximum at 380 mμ, corresponding to vitamin A_1-aldehyde, was observed. Unfortunately vitamin A_1-aldehyde and α-tocopherol present in the extracts move together on this type of column. Thus a band corresponding to α-tocopherol may be observed on the "aldehyde" absorption curves (Fig. 1).

When the different alcohol-solutions were reduced with sodium borohydride [1], the absorption maxima were shifted towards lower wavelengths. The reduction products were readily freed from α-tocopherol by chromatography on soft Al_2O_3. It may be mentioned that the reduction procedure employed did not influence the absorption maximum of α-tocopherol. Vitamin A_1 aldehyde gave a compound with absorption maximum at 325 mμ (vitamin A_1). For all the acetone treated extracts reduction resulted in compounds with absorption maxima at 340—360 mμ. Again the later frac-

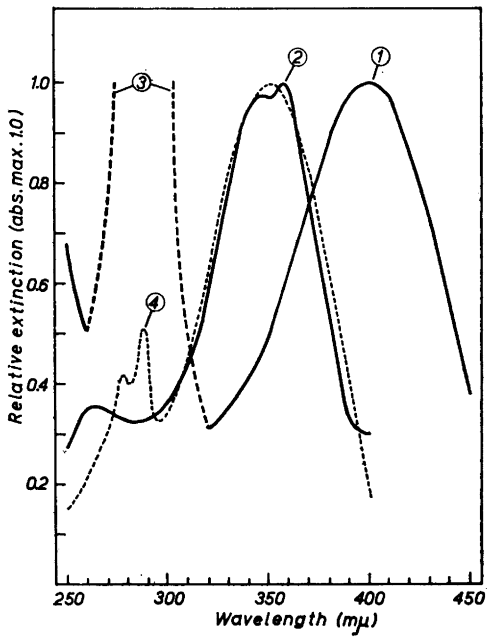

Fig. 2. Absorption curves of compound(s) isolated from acetone treated extracts from herring ova (1), and its reduction product(s) (2). The dotted band (3) is caused by the presence of α-tocopherol. For comparison is plotted vitamin A_2 after Lambertsen & Brækkan[10] (4).

tions showed absorption maxima at the higher wavelengths. A comparison of the fractions indicated the presence of a mixture of two compounds with similar chromatographic properties on the column used. The spectrophotometric data are summarized in Figs. 1 and 2.

The spectrophotometric properties of the fractions obtained were very similar to those reported for oxidation-products obtained by the Oppenauer reaction in the presence of acetone or diethyl ketone [3-5]. Apparently the compounds observed by us are axerophthylidene-acetone [3] and the so-called "C_{20}-aldehyde" [4,5], and their reduction products. In Table 1 are summarized data reported in the literature on the spectrophotometric properties of these compounds in ethanol and their reaction products with $SbCl_3$ in chloroform. The absorption maxima obtained for our compounds (Fig. 2) agree generally well with those reported in the literature, thus indicating the presence of both axerophthylidene-acetone and the C_{20}-aldehyde in our reaction. The possibility, however, of the presence of isomers of only one compound cannot be overlooked.

The treatment with acetone of pure vitamin A_1-aldehyde prepared from vitamin A_1-alcohol [1] caused no change in the retinine$_1$-molecule as judged by the U.V.-absorption curve. This is in agreement with the findings of Plack *et al.*[1]. When, however, vitamin A_1 aldehyde in concentrations equal to those present in herring roe was added to the acetone-treated residue, from which all retinine-like compounds had been removed, storage at room temperature over night resulted in it being transformed to a compound, with absorption maximum at 395 mμ. Reduction of this compound resulted in a substance with absorption maximum at 342 mμ. It thus seems that substances present in the hexane extracts from herring roe, but insoluble in acetone, are necessary for the reactions to take place which result in the formation of axerophthylidene-acetone and the C_{20}-aldehyde.

The absorption maxima for the reduction products, 340—360 mμ, suggested the presence of vitamin A_2 as one of these compounds. Haworth *et al.*[4] thus proposed a reduction of the C_{20}-aldehyde to an alcohol with a formula corresponding to the one at present accepted for vitamin A_2 [8]. Cama *et al.*[7] have discussed this possibility and pointed out that hydrogenation of the β-ionone ring in the second stage of the Oppenauer oxidation seems improbable. They discussed the possible structure for the C_{20}-compound, and suggested as one of the possibilities a *cis*-isomer of vitamin A_2 aldehyde. A reduction of this compound would result in an isomer of vitamin A_2. In this connection it should be born in mind that Haworth *et al.*[4] found the C_{20}-aldehyde to be biologically active, and Plack *et al.*[1] found approx. 40 % of the original activity of the hexane extracts in the acetone-soluble fraction, and no activity in the residue. The lack of the typical absorption maxima at 277 and 286 mμ [9,10]

Table 1. Spectrophotometric data from the literature for the Oppenauer oxidation products of vitamin A and their corresponding reduction products.

Compound	U.V. abs.max.	$SbCl_3$ abs.max.	Reference
Axerophthylidene-acetone	401	646	Batty *et al.*[3]
	395	735	Hawkins & Hunter [5]
» » reduced	354.5	712	Heilbron *et al.*[6]
	351	713	Hawkins & Hunter [5]
The C_{20}-aldehyde	401	740	Haworth *et al.*[4]
	385—395	725—735	Hawkins & Hunter [5]
» » , reduced	359		Haworth *et al.*[4]
	350—370	722	Hawkins & Hunter [5]

weighed against the possibility of the presence of vitamin A_2 after reduction of our acetone extracts. The absorption maximum for the $SbCl_3$-reaction was at 700–720 mμ, compared with 693 mμ for vitamin A_2. We may, however, emphasize that very little is known with regard to all the possible isomers of vitamin A_2 and their spectrophotometric properties. The $SbCl_3$ colour of our "aldehyde"-fraction had a maximum slightly higher than that of the reduced compound.

The present investigation has thus confirmed the findings of Plack *et al.*[1] with regard to the presence of vitamin A_1 aldehyde in herring roe. We could not find vitamin A_2 aldehyde as reported by Pollard and Bieri [2]. The effect of the acetone treatment on vitamin A_1 aldehyde when the acetone-insoluble fraction of hexane extracts of herring roe was present, establishes a case where a natural product catalyses or takes part in the reaction between vitamin A_1 aldehyde and ketone-bodies. The reactions reported, when seen in relation to the chemical studies recorded [3-5], suggest as a possible pathway for the formation *in vivo* of vitamin A_2, that it is derived from vitamin A_1 *via* the retinenes.

1. Plack, P. A., Kon, S. K. and Thompson, S. Y. *Biochem. J.* **71** (1959) 467.
2. Pollard, C. J. and Bieri, J. G. *Biochim. et Biophys. Acta* **31** (1959) 558.
3. Batty, J. W., Burravoy, A., Harper, S. H., Heilbron, I. M. and Jones, W. E. *J. Chem. Soc.* **1938** 175.
4. Haworth, E., Heilbron, I. M., Jones, W. E., Morrison, A. L. and Polya, J. B. *J. Chem. Soc.* **1939** 128.
5. Hawkins, E. G. E. and Hunter, R. F. *Biochem. J.* **38** (1944) 34.
6. Heilbron, I. M., Johnson, A. W. and Jones, W. E. *J. Chem. Soc.* **1939** 1560.
7. Cama, H. R., Field, A. C., Glover, J., Morton, R. A. and Salah, M. K. *Biochem. J.* **52** (1952) 548.
8. Morton, R. A., Salah, M. K. and Stubbs, A. L. *Nature* **159** (1947) 744.
9. Cama, H. R. and Morton, R. A. *Analyst* **78** (1953) 74.
10. Lambertsen, G. and Brækkan, O. R. *Acta Chem. Scand.* **11** (1957) 575.

Received April 12, 1960.

Crystal Data of Nickel(II) dithiosemicarbazide-Sulphate

RITA GRØNBÆK and SVEND ERIK RASMUSSEN*

Chemistry Department A. Technical University of Denmark, Copenhagen, Denmark

K. A. Jensen [1] has described two forms of nickel(II)dithiosemicarbazide sulphate $(Ni(ThiO)_2SO_4$ which he proposed to be *cis-trans* isomers.

As very few examples of stereoismerism of nickel complexes have been definitely proved we have started an X-ray investigation in order to establish the complete structures of the two forms.

The *a* form crystallizes from water when mixing cold aqueous solutions of nickel sulphate and thiosemicarbazide. The product contains water of crystallization and the chemical analysis is consistent with the formula: $Ni(ThiO)_2SO_4$, 3 H_2O. The water is removed by heating the product to 110°C and is slowly taken up again at room temperature.

Oscillation, rotation and Weissenberg diagrams were taken of crystals of $Ni(ThiO)_2SO_4$, 3 H_2O using Cu-radiation.

The crystals are monoclinic with the following dimensions of the unit cell, unique axis b:

$$a = 6.91 \text{ Å}$$
$$b = 16.41 \text{ Å}$$
$$c = 6.32 \text{ Å}$$
$$\beta = 97°.7$$

The density of the crystal is approximately 1.84. Consequently there are two units of $Ni(ThiO)_2SO_4$, $3H_2O$ per unit cell.

The only systematic extinctions are $h\,k\,0$ when k is odd. The possible space groups are $P2_1/m$ and $P2_1$. A Patterson projektion $P(u, v)$ showed a large concentration of peaks at $v = \frac{1}{2}$. No other line exhibited extraordinary concentrations of peaks. Hence the space group $P2_1$ is established.

The β form is precipitated from hot aqueous solutions of nickel sulphate and thiosemicarbazide. It contains no water of crystallization. Its powder diagram is different from that of the *a* form. It was

* Present address: Chemical Institute, University of Aarhus, Aarhus, Denmark.

weighed against the possibility of the presence of vitamin A_2 after reduction of our acetone extracts. The absorption maximum for the $SbCl_3$-reaction was at 700–720 mμ, compared with 693 mμ for vitamin A_2. We may, however, emphasize that very little is known with regard to all the possible isomers of vitamin A_2 and their spectrophotometric properties. The $SbCl_3$ colour of our "aldehyde"-fraction had a maximum slightly higher than that of the reduced compound.

The present investigation has thus confirmed the findings of Plack *et al.*[1] with regard to the presence of vitamin A_1 aldehyde in herring roe. We could not find vitamin A_2 aldehyde as reported by Pollard and Bieri [2]. The effect of the acetone treatment on vitamin A_1 aldehyde when the acetone-insoluble fraction of hexane extracts of herring roe was present, establishes a case where a natural product catalyses or takes part in the reaction between vitamin A_1 aldehyde and ketone-bodies. The reactions reported, when seen in relation to the chemical studies recorded [3-5], suggest as a possible pathway for the formation *in vivo* of vitamin A_2, that it is derived from vitamin A_1 *via* the retinenes.

1. Plack, P. A., Kon, S. K. and Thompson, S. Y. *Biochem. J.* **71** (1959) 467.
2. Pollard, C. J. and Bieri, J. G. *Biochim. et Biophys. Acta* **31** (1959) 558.
3. Batty, J. W., Burravoy, A., Harper, S. H., Heilbron, I. M. and Jones, W. E. *J. Chem. Soc.* **1938** 175.
4. Haworth, E., Heilbron, I. M., Jones, W. E., Morrison, A. L. and Polya, J. B. *J. Chem. Soc.* **1939** 128.
5. Hawkins, E. G. E. and Hunter, R. F. *Biochem. J.* **38** (1944) 34.
6. Heilbron, I. M., Johnson, A. W. and Jones, W. E. *J. Chem. Soc.* **1939** 1560.
7. Cama, H. R., Field, A. C., Glover, J., Morton, R. A. and Salah, M. K. *Biochem. J.* **52** (1952) 548.
8. Morton, R. A., Salah, M. K. and Stubbs, A. L. *Nature* **159** (1947) 744.
9. Cama, H. R. and Morton, R. A. *Analyst* **78** (1953) 74.
10. Lambertsen, G. and Brækkan, O. R. *Acta Chem. Scand.* **11** (1957) 575.

Received April 12, 1960.

Crystal Data of Nickel(II) dithiosemicarbazide-Sulphate

RITA GRØNBÆK and SVEND ERIK RASMUSSEN*

Chemistry Department A. Technical University of Denmark, Copenhagen, Denmark

K. A. Jensen [1] has described two forms of nickel(II)dithiosemicarbazide sulphate $(Ni(ThiO)_2SO_4$ which he proposed to be *cis-trans* isomers.

As very few examples of stereoismerism of nickel complexes have been definitely proved we have started an X-ray investigation in order to establish the complete structures of the two forms.

The *a* form crystallizes from water when mixing cold aqueous solutions of nickel sulphate and thiosemicarbazide. The product contains water of crystallization and the chemical analysis is consistent with the formula: $Ni(ThiO)_2SO_4$, 3 H_2O. The water is removed by heating the product to 110°C and is slowly taken up again at room temperature.

Oscillation, rotation and Weissenberg diagrams were taken of crystals of $Ni(ThiO)_2SO_4$, 3 H_2O using Cu-radiation.

The crystals are monoclinic with the following dimensions of the unit cell, unique axis b:

$$a = 6.91 \text{ Å}$$
$$b = 16.41 \text{ Å}$$
$$c = 6.32 \text{ Å}$$
$$\beta = 97°.7$$

The density of the crystal is approximately 1.84. Consequently there are two units of $Ni(ThiO)_2SO_4$, $3H_2O$ per unit cell.

The only systematic extinctions are $h\,k\,0$ when k is odd. The possible space groups are $P2_1/m$ and $P2_1$. A Patterson projektion $P(u, v)$ showed a large concentration of peaks at $v = \frac{1}{2}$. No other line exhibited extraordinary concentrations of peaks. Hence the space group $P2_1$ is established.

The β form is precipitated from hot aqueous solutions of nickel sulphate and thiosemicarbazide. It contains no water of crystallization. Its powder diagram is different from that of the *a* form. It was

* Present address: Chemical Institute, University of Aarhus, Aarhus, Denmark.

rather difficult to obtain suitable crystals of the β form for single crystal work and its space group has not yet been established.

The solution of the structures will be pursued.

1. Jensen, K. A. and Rancke Madsen, E. *Z. anorg. Chem.* **219** (1934) 243; **221** (1934) 11; **229** (1936) 277.

Received April 20, 1960.

Preliminary Note on the Configuration at C_{22} of *Solanum* Alkaloids

PER M. BOLL

Royal Danish School of Pharmacy, Chemical Laboratory B, Copenhagen, Denmark

Tomatidine and 5α-solasodanol-(3β) are generally believed to represent two types of *Solanum* alkaloids (aminoketal alkaloids) related to each other in the same manner as the "neo" and "iso" steroid sapogenins, *i. e.* they differ in configuration at C_{25} by having an axial C_{25}-methyl group (structure II) and an equatorial C_{25}-methyl group (structure I), respectively.

Recently, Schreiber [1] and later Toldy [2] have suggested, however, that the two compounds differ in configuration at C_{22}. According to their formulation, tomatidine is a 22β-compound (structure III) and 5α-solasodanol-(3β) a 22α-compound (structure I). This difference in configuration at C_{22} will cause the methyl groups at C_{25} in both compounds to be equatorial.

The work submitted in this preliminary note supports the idea that tomatidine and 5α-solasodanol-(3β) in fact differ in configuration at C_{22}. It was found that tomatidine forms an N-bromo as well as an N-chloro derivative, whereas 5α-solasodanol-(3β) only forms an N-chloro derivative.

With the object of estimating the space requirements for binding a halogen atom to the nitrogen atom of ring F the hydrogen:halogen separation distances were measured on Dreiding molecular models. These measurements indicate that the distance between the N-halogen atom and two of the hydrogen atoms of the C_{20}-methyl group in structure I is 2.4 Å. In

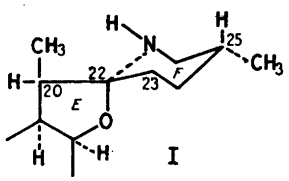

I

22α-iso

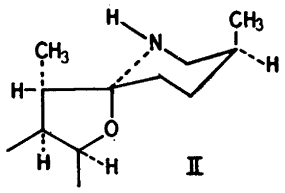

II

22α-neo

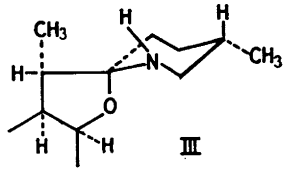

III

22β-iso

structure III the distance between the N-halogen and the hydrogen atom at C_{20} is 2.6 Å.

Assigning a van der Waals radius of 1.0 Å to hydrogen and radii of chlorine and bromine of 1.8 Å and 1.95 Å, respectively, the distances H ⟷ Cl and H ⟷ Br can be estimated to 2.8 Å and 2.95 Å, respectively. Although the measured distances H ⟷ Hlg in structure I and III only are 2.4 Å and 2.6 Å, respectively, one can easily see, remembering the experimental facts, that the difference in the measured distances is of an order of magnitude allowing the formation of an N-chloro derivative, but not the formation of an N-bromo derivative in the case of 5α-solasodanol-(3β). Furthermore, small distortions of the bond angles in rings E and F may increase the H ⟷ Hlg separation distances to values estimated using the van der Waals radii. Such distortions of bond angles are quite common [3].

rather difficult to obtain suitable crystals of the β form for single crystal work and its space group has not yet been established.

The solution of the structures will be pursued.

1. Jensen, K. A. and Rancke Madsen, E. *Z. anorg. Chem.* **219** (1934) 243; **221** (1934) 11; **229** (1936) 277.

Received April 20, 1960.

Preliminary Note on the Configuration at C_{22} of *Solanum* Alkaloids

PER M. BOLL

Royal Danish School of Pharmacy, Chemical Laboratory B, Copenhagen, Denmark

Tomatidine and 5α-solasodanol-(3β) are generally believed to represent two types of *Solanum* alkaloids (aminoketal alkaloids) related to each other in the same manner as the "neo" and "iso" steroid sapogenins, *i. e.* they differ in configuration at C_{25} by having an axial C_{25}-methyl group (structure II) and an equatorial C_{25}-methyl group (structure I), respectively.

Recently, Schreiber [1] and later Toldy [2] have suggested, however, that the two compounds differ in configuration at C_{22}. According to their formulation, tomatidine is a 22β-compound (structure III) and 5α-solasodanol-(3β) a 22α-compound (structure I). This difference in configuration at C_{22} will cause the methyl groups at C_{25} in both compounds to be equatorial.

The work submitted in this preliminary note supports the idea that tomatidine and 5α-solasodanol-(3β) in fact differ in configuration at C_{22}. It was found that tomatidine forms an N-bromo as well as an N-chloro derivative, whereas 5α-solasodanol-(3β) only forms an N-chloro derivative.

With the object of estimating the space requirements for binding a halogen atom to the nitrogen atom of ring F the hydrogen:halogen separation distances were measured on Dreiding molecular models. These measurements indicate that the distance between the N-halogen atom and two of the hydrogen atoms of the C_{20}-methyl group in structure I is 2.4 Å. In

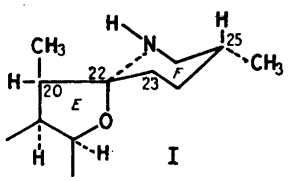

I

22α-iso

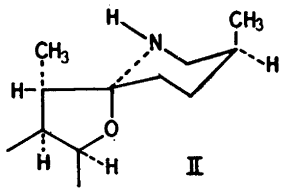

II

22α-neo

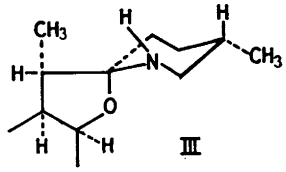

III

22β-iso

structure III the distance between the N-halogen and the hydrogen atom at C_{20} is 2.6 Å.

Assigning a van der Waals radius of 1.0 Å to hydrogen and radii of chlorine and bromine of 1.8 Å and 1.95 Å, respectively, the distances H ⟷ Cl and H ⟷ Br can be estimated to 2.8 Å and 2.95 Å, respectively. Although the measured distances H ⟷ Hlg in structure I and III only are 2.4 Å and 2.6 Å, respectively, one can easily see, remembering the experimental facts, that the difference in the measured distances is of an order of magnitude allowing the formation of an N-chloro derivative, but not the formation of an N-bromo derivative in the case of 5α-solasodanol-(3β). Furthermore, small distortions of the bond angles in rings E and F may increase the H ⟷ Hlg separation distances to values estimated using the van der Waals radii. Such distortions of bond angles are quite common [3].

Table 1. Halogen derivatives of *Solanum* alkaloids.

Derivative	Halogen content * Calc.	Found	M. p., °C **	$[\alpha]_D^{24}$ ($CHCl_3$)
N-Chlorosolasodine	7.92	7.89	153	−114°
N-Chloro-5α-solasodanol-(3β)	7.89	7.97	183	− 59°
N-Chlorotomatidine	7.89	8.06	175	+ 35°
N-Bromotomatidine	16.17	16.18	208 ***	+ 51 ***

* The halogen content determined by iodometric titration.

** The m. p. reported are corrected. All four compounds melt under decomposition.

*** Toldy reports the m. p. 202–205°C and $[\alpha]_D^{20}$ −8.6 (dimethylformamide). However, N-bromotomatidine is quite unstable and decomposes to tomatidine hydrobromide ($[\alpha]_D^{24}$ −8.0 (CH_3OH)).

Fieser and Fieser [4] have suggested that 22β-steroid sapogenins are destabilized by steric interference between the two hydrogens at C_{22} and the hydrogens of the C_{20}-methyl group, these being only 1.8 Å apart. However, similar model considerations by the present author on a 22β-steroid sapogenin and a 22β-aminoketal alkaloid indicate that the above mentioned hydrogens are in fact 2.0 Å apart. This last distance is a permissable hydrogen:hydrogen separation distance.

Further details of this work will be submitted shortly.

1. Schreiber, K. *Abhandl. Deutsch. Akad. Wiss. Berlin, Kl. Chem., Geol. u. Biol.* **1957** 143.
2. Toldy, L. *Acta Chim. Acad. Sci. Hung.* **16** (1958) 403.
3. *Table of Interatomic Distances and Configuration in Molecules and Ions*, The Chemical Society, London 1958.
4. Fieser, L. F. and Fieser, M. *Steroids*, Reinhold Publishing Corporation, New York 1959, p. 824.

Received April 19, 1960.

Den kgl. Veterinær- og

ACTA CHEMICA SCANDINAVICA 14 (1960) 785–788

Structure of the *o*-Formylbenzoate Ion

ERLING BERNATEK

Universitetets Kjemiske Institutt, Blindern, Oslo, Norway

Phthalaldehydic acid exists in aqueous solutions as 3-hydroxyphthalide. This formula has an asymmetric carbon atom, but the acid is not optically resolvable by means of alkaloid salts since its anion only exists in the open (*o*-formylbenzoate) form where no asymmetry occurs. Infra-red absorption shows that this is the case in solid salts as well as in aqueous solution.

Phthalaldehydic acid (*o*-formylbenzoic acid) has been represented as having both an aldehyde group and a carboxyl group (I), but also the ring-tautomeric hydroxyphthalide form (II) has been considered.

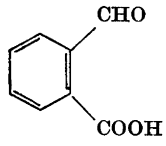

I

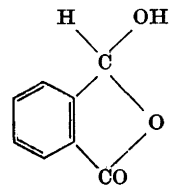

II

Grove and Willis [2] using infra-red absorption spectroscopy concluded that phthalaldehydic acid in the solid state existed exclusively in the cyclic lactol form (II). This was inferred from the single C=O absorption band at 1 738 cm^{-1}, which is much closer to the five-ring lactone frequency of phthalide (1 750 cm^{-1}) than to the aromatic carboxylic acid (1 690 cm^{-1}) frequency of benzoic acid, and from the characteristic alcoholic OH absorption at 3 250 cm^{-1}. Some years later Wheeler, Young and Erley [3] reexamined phthalaldehydic acid and a long series of its functional derivatives. One of their main findings was that the cyclic lactol structure persisted also in aqueous solution. A water solution spectrum clearly indicated the presence of a lactol carbonyl absorption at 1 748 cm^{-1} and the antisymmetric C—O—C stretch of the ring was observed at about 1 090 cm^{-1}. Derivatives were prepared with alcohols, thiols, primary and secondary amines, acid amides, acid anhydrides, urea

and substituted ureas and carbamates. All of these substances existed in the solid state as phthalide derivatives. Esters of phthalaldehydic acid are of two types, normal and *pseudo*-esters (cyclic). These are readily distinguished by chemical methods, *e.g.*, the normal esters undergo a facile reaction with carbonyl reagents, a reaction which is absent in the *pseudo*-esters. Grove and Willis [2] investigated the infra-red absorption of the liquid normal methyl ester and the *pseudo*-ester (m.p. 46—47°) and could corroborate the chemical evidence.

From the cyclic formula (II) is seen that the carbon atom to which the hydroxyl group is linked is asymmetric. The question therefore arises whether a compound of this type is resolvable and in that case if the enantiomers have any degree of optical stability. Preliminary experiments were carried out where the strychnine and brucine salts of phthalaldehydic acid were subjected to fractional crystallisation. The salts were decomposed cautiously with mineral acid and the organic acid isolated, but in no case could any optical activity be observed. This negative result could have one or several causes. The active bases could have been ill-chosen if the diastereomers formed were of similar solubility, the acid itself or the *o*-formylbenzoate ion could have no optical stability, or the mentioned ion could exist entirely in the open non-cyclic form where the asymmetry of the carbon atom would disappear. To test the latter possibility solid state spectra of the strychnine and brucine salts were recorded. A main characteristic of these spectra was that no absorption band occurred between 1 700 and 1 800 cm^{-1}. This fact alone is decisive in ruling out a cyclic form of the *o*-formylbenzoate ion in the solid alkaloid salts. At 1 682 and 1 676 cm^{-1} strong carbonyl absorptions occurred, most likely due to the lactam grouping in strychnine and brucine, respectively. A shoulder on the latter absorption band at 1 690 cm^{-1} is probably due to the free aldehyde group in the *o*-formylbenzoate ion. Carboxylate ion absorption was observed at 1 575 and 1 555 cm^{-1}, but the other expected bands between 1 300 and 1 400 cm^{-1} could not be identified due to several skeletal vibrations in this region.

As a consequence of these observations it became desirable to investigate the infra-red absorption of aqueous solutions of phthalaldehydic acid at different pH (see Fig. 1).

In the spectrum of the free acid (A) is seen the ring carbonyl absorption at 1 756 cm^{-1} (Wheeler *et al.*[3] reported, as mentioned before, the value 1 748 cm^{-1}. Evidently due to less accurate matching of their cell pair this band occurred only as a minor excrescence on a broad water-absorption band. From curve A it is evident that the matching in our case is very good. Further the spectrometer was calibrated in connection with this work and we therefore place more faith in the higher value). At 1 082 cm^{-1} is observed a band, which is due to the C—O—C antisymmetric stretch of the ring. In this region, however, the cell material (calcium fluoride) begins to absorb strongly and the sensitivity of the apparatus is therefore somewhat diminished. In the curve B where the acid is half-way neutralised with sodium hydroxide the ring carbonyl and C—O—C stretch frequencies are still observed, but in addition there has emerged two conspicious bands at 1 565 and 1 392 cm^{-1} characteristic for the carboxylate ion. At about 1 695 cm^{-1} there is a smaller peak probably due to a free aldehyde group, but here the sensitivity of the spectrometer is

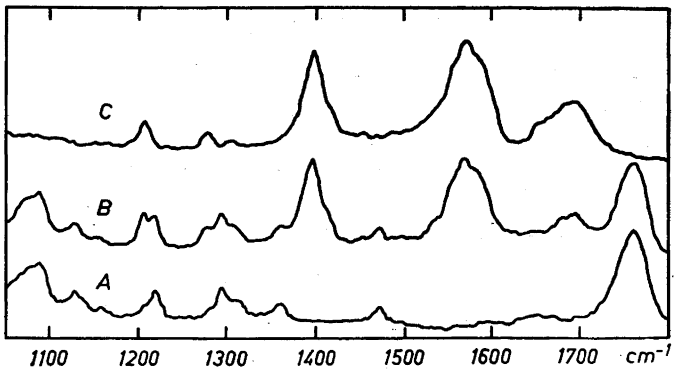

Fig. 1. Infra-red absorption in water of
A: Phthalaldehydic acid
B: Phthalaldehydic acid + half an equivalent of sodium hydroxide
C: Fully neutralised phthalaldehydic acid.

diminished due to strong water absorption. The fully neutralised acid (C) shows no ring carbonyl or ring C—O—C stretch frequencies, while the carboxylate ion and aldehyde group bands are conspicious. It must therefore be concluded that salts of phthalaldehydic acid in the solid state as well as in solution exist in the open form and hence no optical resolution of the acid can be effected through diastereomeric salts.

Phthalaldehydic acid undergoes the Cannizzaro reaction [4], reduces ammoniacal silver solution and forms an oxime. This has been taken as an indication that phthalaldehydic acid has some of the properties which would be expected of the open form [3]. From the present experiments it is clear that the two former reactions deal with the non-cyclic *o*-formylbenzoate ion and throw therefore no light on the structure of the acid itself. Oxime formation can take place in alkaline solution as is by now to be expected (see exptl. part), but also under the slightly acid conditions obtained where phthalaldehydic acid and hydroxylamine hydrochloride are dissolved in water. This may mean that in aqueous solution the acid exists as an equilibrium between the open and the cyclic form, strongly displaced towards the cyclic form. Very small amounts of the open form cannot be detected in the spectra due to the slight solubility of phthalaldehydic acid in water. The solid-state spectrum of the oxime has been recorded and it clearly indicates an open form of the derivative *viz.* benzaldoxime-*o*-carboxylic acid. No ring carbonyl band is observed between 1 700 and 1 800 cm^{-1} and in the region 1 000—1 100 cm^{-1} only one minor band is found, the intensity being far too low for an antisymmetric C—O—C ring stretch band. Carboxyl C=O absorption is found at 1 679 cm^{-1}, which is in the lower part of the region for aryl conjugated acids. There may exist a weak chelation between the carboxyl group and the oxime moiety, but at higher temperatures there must be stronger interaction as the oxime at 100° gradually loses water and is transformed into phthalimide probably through 2,3,1-benzoxaz-1-one and *o*-cyanobenzoic acid [5].

EXPERIMENTAL

Phthalaldehydic acid was prepared by oxidation of naphthalene and recrystallised from water. M. p. 99°.

Strychnine and brucine salts. These salts were prepared in the usual way by heating an aqueous solution of phthalaldehydic acid with an equimolecular amount of the finely ground alkaloid until a clear solution remained. The salts which separated from the filtered solution on cooling were subjected to repeated fractional crystallisations from water.

Phthalaldehydic acid oxime. Phthalaldehydic acid (1.5 g) was dissolved in aqueous sodium carbonate and hydroxylamine hydrochloride (0.7 g) added. The solution was left for 2 h and acidified with hydrochloric acid whereupon the oxime separated immediately (1.4 g). Recrystallised from water. M. p. ca. 125° (rapid increase of temperature).

Infra-red spectra. The spectrometer was a Perkin-Elmer double beam apparatus (Model 21).

Solid compounds were first dried *in vacuo* over phosphorus pentoxide, and the spectra were obtained in Nujol mulls between rock-salt plates. Spectra of the aqueous solutions were obtained in a matched pair of calcium fluoride cells (0.025 mm) compensated with water.

The solutions whose infra-red absorption is recorded in Fig. 1 were made up as follows:
A: 15 mg (0.1 mmole) phthalaldehydic acid per ml of water.
B: 30 mg (0.2 mmole) acid and 4 mg sodium hydroxide (0.1 m equiv.) per ml of water.
C: 15 mg (0.1 mmole) acid and 4 mg sodium hydroxide (0.1 m equiv.) per ml of water.

The author's thanks are due to mag. scient. Else Augdahl for the determination of the infra-red spectra.

REFERENCES

1. Racine, S. *Ber.* **19** (1886) 778.
2. Grove, J. F. and Willis, H. A. *J. Chem. Soc.* **1951** 877.
3. Wheeler, D. D., Young, D. C. and Erley, D. S. *J. Org. Chem.* **22** (1957) 547.
4. Hamburger, A. *Monatsh.* **19** (1898) 430.
5. Allendorff, O. *Ber.* **24** (1891) 2346, 3264.

Received December 12, 1959.

ACTA CHEMICA SCANDINAVICA 14 (1960) 789–796

Reactions between Benzylhydrazine and Dithioesters

BJÖRN FORSGREN and JAN SANDSTRÖM

Department of Organic Chemistry, University of Lund, Lund, Sweden

The formation of pairs of isomeric thiohydrazides in reactions between benzylhydrazine and four different dithiocarboxylic esters has been investigated. The neutral isomers give thiohydrazones, and the acidic isomers thiadiazolines, in reactions with benzaldehyde. pK_a-values for the acidic thiohydrazides in aqueous ethanol are given. Separation of pairs of isomers by paper chromatography is described.

In the course of a current investigation of heterocyclic compounds derived from thiocarbohydrazide, it was considered desirable to prepare methyl 2-benzyldithiocarbazate (Ia). The reaction between benzylhydrazine and dimethyl trithiocarbonate was expected to provide a suitable route. However, the reaction product was found to consist of a mixture of only 20 % of the desired compound and 80 % of the 3-isomer (IIa).

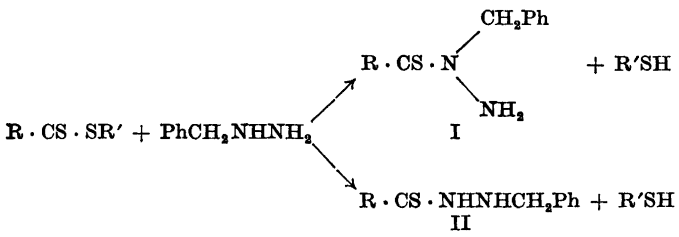

a, R=CH_3S; b, R=Ph; c, R=CH_3O; d, R=$PhCH_2O$.

This result at first seemed somewhat surprising, since monosubstituted aliphatic hydrazines, and also benzylhydrazine, react with cyanic acid [1,2] and thiocyanic acid [3,4] and with their *iso*esters [2,5] as if the —NH-group were more nucleophilic than the NH_2-group, *i.e.* the products are 2-substituted semicarbazides and thiosemicarbazides. As has been pointed out by Greer and Smith [6], this is explained by the electron-donating properties of the alkyl group.

On the other hand, arylhydrazines give 1-arylsemicarbazides and 1-arylthiosemicarbazides [7] as stable products. This is explained by the interaction between the aromatic nucleus and the —NH-group, which makes the latter less nucleophilic than the NH_2-group. The same effects are taken into account to explain why methylamine is more basic and aniline less basic than ammonia [8]. The same difference in orientation is found when methylhydrazine and phenylhydrazine react with carboxylic acid chlorides [9] and with dithioesters such as carboxymethyl dithiobenzoate [10,11] and alkyl trithiocarbonates [12,13]. With methylhydrazine, 1-methyl-1-acyl(thioacyl)-hydrazines (III), and with phenylhydrazine, 1-phenyl-2-acyl(thioacyl)-hydrazines (IV) are formed.

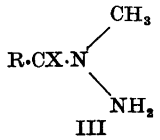

III

a, X=S; b, X=O

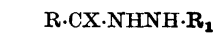

IV

a, X=S b, X=O

R_1=Ph R_1=CH_3

However, there is evidence for the operation of a steric effect in the reactions between methylhydrazine and carboxylic esters. Von Brüning [14] has shown, that methylhydrazine and diethyl oxalate react readily to give 1,1'-oxalyl-bis-2,2'-methylhydrazine, $(CO{\cdot}NHNHCH_3)_2$ (V).

In a recent investigation, Hinman and Fulton [15] have shown, that methyl acetate, propionate, *iso*butyrate, and benzoate, react with methylhydrazine to give mixtures of 1-acylated (IIIb), and 2-acylated (IVb) methylhydrazine, where the latter isomer predominated. With the aliphatic esters both the yield of (IIIb) and the reaction rate fell off with increasing size of the acyl group. On the other hand, reactions between methylhydrazine and carboxylic acid anhydrides gave high yields of the 1-acyl-methylhydrazines (IIIb).

It seems as if dithioesters should occupy a position intermediate between, on the one hand carboxylic esters, and on the other hand cyanic acid and thiocyanic acid and their derivatives, with regard to sensitivity to steric effects in reactions with aliphatic hydrazines. Therefore, it was considered desirable to investigate the reactions of benzylhydrazine with a selection of dithioesters. Carboxymethyl dithiobenzoate, O,S-dimethyl xanthate, O-benzyl-S-carboxymethyl xanthate, and carboxymethyl dithiocarbamate were chosen, together with dimethyl trithiocarbonate. The carboxymethyl dithiocarbamate did not give definable products with benzylhydrazine, but the other esters reacted rapidly and gave mixtures of the possible isomers (I) and (II). The yields and ultra-violet absorption data are recorded in Table 1.

For separation of the isomers the reaction mixtures were dissolved in ether, and the solutions were extracted with a quantity of N NaOH equivalent to the total amount of thiohydrazide present. With the dithiocarbazate and thiobenzhydrazide mixtures one extraction was enough to transfer practically all of the acidic isomer (II) into the alkaline solution, but when the thioncarbazate mixtures were so treated, appreciable quantities of the acid forms

Table 1. Yields and ultraviolet absorption data for the compounds I and II.

Starting material	Yield %	λ_{max} mμ	ε_{max}
$CH_3S \cdot CS \cdot SCH_3$	Ia: 20	255	10 300
		276	11 100
	IIa: 74	277	10 800
$Ph \cdot CS \cdot SCH_2CO_2H$	Ib: 23	288	11 200
	IIb: 72	245	12 400
		298	6 500
$CH_3O \cdot CS \cdot SCH_3$	Ic: 25	—	—
	IIc: 70	250	12 000
$PhCH_2O \cdot CS \cdot SCH_2CO_2H$	Id: 76	252	15 000
	IId: 22	252	11 600

All spectra were taken in absolute ethanol, c, 5×10^{-5}, with a Beckman DU spectrophotometer.

(IIc) and (IId) remained in the ether solution after the first extraction. The progress of the extraction could be followed by paper chromatographic examination of the ether solution after each extraction. For this purpose ordinary paper chromatography with water as the stationary phase was found unsuitable. In the solvents used by Hinman [16] these hydrazides travelled with the solvent front, and the same result was obtained with chloroform saturated with water, a system used with success by Kjær and Rubinstein [17] for substituted thioureas and thiosemicarbazides. Instead, the system developed by Wickberg [18], with dimethyl sulphoxide as the stationary phase and ethers or aliphatic hydrocarbons as the mobile phase, was found very useful. In all the four isomer mixtures obtained in this investigation the acidic isomer travelled slower than the neutral one, which is to be expected, since dimethyl sulphoxide has weakly basic properties [19].

By this method it could be shown that methyl 3-benzylthioncarbazate (IIc) was extracted by two succesive extractions with N NaOH beyond the limit of detection in the ether solution, but that the benzyl analogue (IId) could still be detected after six successive extractions. The partition of an acid between ether and aqueous alkali is governed by the partition coefficient, C, of the undissociated acid between ether and water, by the dissociation constant of the acid, and by the activities of the hydrogen ions and the anions of the acid in the aqueous phase. The partition observed, $P = \frac{[HA]_{ether}}{[HA]_{aq} + [A^-]_{aq}}$ can be expressed in the above quantities by inserting $\frac{K_a \times [HA]_{aq}}{a_{H^+} \times f_{A^-}}$ for $[A^-]_{aq}$ and C for $\frac{[HA]_{ether}}{[HA]_{aq}}$. In this way we obtain $P = \frac{C \times a_{H^+} \times f_{A^-}}{a_{H^+} \times f_{A^-} + K_a}$

The values of the dissociation constants, K_a (Table 2) were determined by electrometric titration with a glass electrode in 20 % and in 3 % aqueous ethanol (w/w). For reasons of solubility no determinations were made in pure water, but approximate values can easily be obtained by extrapolation. However, these can not be the same as in water saturated with ether. The coefficients of partition, C, of the acids between ether and pure water were determined

spectrophotometrically. This method could not be used in alkaline medium because of the rapid oxidation mentioned below. Instead, known quantities of the thioncarbazates were equilibrated between ether and aqueous NaOH, and P was determined by evaporating the ether solutions and weighing the dry residues. For a_{H^+} was inserted the expression $\frac{K_w}{([OH^-] - [A^-]) \times f_{OH^-}}$, where $[OH^-]$ is the concentration of hydroxyl ions in the aqueous phase before equilibration. The activity coefficients f_{A^-} and f_{OH^-} are not known with certainty, but their ratio should not differ much from unity. In solutions with $a_{H^+} < 10^{-12}$, the first term in the denominator of P can be neglected. The value of K_w is probably not the same in water as in water saturated with ether, but the ratio K_w/K_a should not be very much different in the two solvents. The values of C obtained from determinations of P with aqueous alkali were found to rise with pH. For the methyl thioncarbazate (IIc) the increase of C was moderate, but for the benzyl analogue (IId), which is much less soluble in water, the value of C rose steeply with pH (Table 2). This change of C with pH can be correlated with the diminishing mutual solubility of ether and water with increasing alkalinity [20]. Much more clear-cut conditions can be expected by using organic solvents, which are practically insoluble in water, but with benzene and *iso*propyl ether the partition coefficient C has so high values that the extraction from these solvents becomes much more tedious than from ether. Instead, ethanol was added to the aqueous phase in order to increase the mutual solubility of ether and water and to reduce the partition coefficient, and thereby the extraction was considerably facilitated. When the N NaOH used for extraction was diluted with ethanol to about 30 % (v/v), only three successive portions were neccessary for a complete extraction of the benzyl thioncarbazate (IId). From the expression for P and the values in Table 2 it is obvious that the extraction of the thiohydrazides (IIa) and (IIb) is favoured both by dissociation constants and by partition coefficients. The extraction of (IIc) is somewhat impeded by a low dissociation constant, and the extraction of (IId) is highly impeded by low dissociation constant and high partition coefficient.

Both types of thiohydrazides react with benzaldehyde. The neutral isomers (I) with free amino group give hydrazones (VI) and the acidic isomers (II) give thiadiazolines (VII).

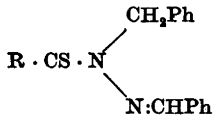

VI

a — d as in (I)

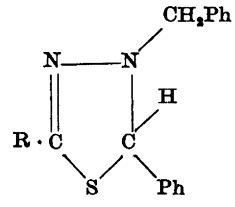

VII

The recording of the ultra-violet absorption spectra of the acidic isomers (II) is complicated by a reaction in very dilute solution with formation of benzaldehyde hydrazones:

$$R \cdot CS \cdot NHNH \cdot CH_2Ph \xrightarrow{-2H} R \cdot CS \cdot NHN{:}CHPh$$

Table 2. pK_a-Values (thermodynamic) and partition coefficients (C) between ether and water for the thiohydrazides, R·CS·NHNHCH$_2$Ph.

	pK_a			C	
R	20 % ethanol	3 % ethanol (w/w)	water	0.1 N NaOH	0.5 N NaOH
CH_3S	7.66	7.56	35		
Ph	7.82	7.63	310		
CH_3O	9.38	9.24	260	330	800
$PhCH_2O$	9.26	9.16	2 400	17 000	39 000

The ether and water used for the partition experiments were saturated with respect to one another prior to measurements. Because of the uncertainties in Ka and Kw and the activity coefficients the values of C must be regarded as very approximate.

The oxidation products have been identified by paper chromatography and UV-spectrum. The change is particularly rapid in alkaline medium. The reaction can be illustrated by the spectra in Fig. 1.

The thiadiazoline (VIIb) is rather unstable and is oxidized by air to a compound $C_{21}H_{18}N_2OS$, probably the 2-hydroxy derivative of the thiadiazoline. Holmberg [10] has found a similar facile oxidation of the 3-methyl analogue.

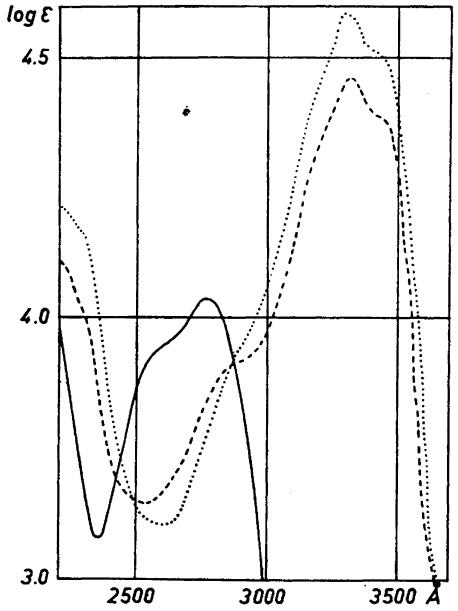

Fig. 1. Ultraviolet absorption curves of:

———————— CH_3S·CS·NHNHCH$_2$Ph, fresh 5 × 10^{-5} M solution in absolute ethanol.
— — — — — — — — The same solution after two days.
..... CH_3S·CS·NHN:CHPh [21], 5 × 10^{-5} M solution in absolute ethanol.

The present investigation shows that different types of dithiocarboxylic esters react with benzylhydrazine to give mixtures of the two possible thiohydrazides. The discussion of a possible steric effect must await the results of an investigation of a wider selection of other closely related esters.

EXPERIMENTAL *

Benzylhydrazine and dimethyl trithiocarbonate. Dimethyl trithiocarbonate (2.8 g) was dissolved in a mixture of ethanol (25 ml) and ether (25 ml), and the solution was added to a solution of benzylhydrazine sulphate (4.6 g) in N NaOH (40 ml) and ethanol (50 ml). On the following day the crystals of sodium sulphate were removed by filtration, and the solvents were taken off *in vacuo*. The remaining oil was dissolved in ether (50 ml), and the solution was extracted with N NaOH (20 ml). The ethereal solution on evaporation gave a solid residue (0.7 g), which crystallized from a mixture of benzene and light petroleum (b.p. 40—60°) as colourless plates with m. p. 91—92°, consisting of *methyl 2-benzyldithiocarbazate* ** (Ia). (Found: C 51.0; H 5.70; N 13.0; S 30.0. Calc. for $C_9H_{12}N_2S_2$: C 50.9; H 5.70; N 13.2; S 30.2.)

Acidification of the alkaline extract from the crude reaction mixture gave a crystalline deposit (2.9 g), which crystallized from a mixture of benzene and light petroleum (40—60°) as colourless prisms, m. p. 58—59°, of *methyl 3-benzyldithiocarbazate* (IIa). (Found: C 50.8; H 5.64; N 13.1; S 30.1. Calc. for $C_9H_{12}N_2S_2$: C 50.9; H 5.70; N 13.2; S 30.2.)

The benzaldehyde hydrazones (VI) and the thiadiazolines (VII) were prepared by reacting the appropriate thiohydrazides with the calculated amount of benzaldehyde in ethanol with a catalytic amount of hydrochloric acid. When necessary, the products were precipitated by the addition of water and purified by recrystallization.

Methyl 2-benzyl-3-benzylidene-dithiocarbazate (VIa) crystallized from ethanol as colourless needles, m. p. 134—135°. (Found: C 63.9; H 5.47; N 9.37; S 21.4. Calc. for $C_{16}H_{16}N_2S_2$: C 64.0; H 5.37; N 9.33; S 21.3.)

2-Phenyl-3-benzyl-5-methylthio-Δ^4-1,3,4-thiadiazoline (VIIa) was too unstable to be recrystallized, but according to analysis the crude product, m. p. 60—62°, was fairly pure. (Found: C 64.2; H 5.47; N 9.27; S 21.2. Calc. for $C_{16}H_{16}N_2S_2$: C 64.0; H 5.37; N 9.33; S 21.3.)

Benzylhydrazine and carboxymethyl dithiobenzoate. Carboxymethyl dithiobenzoate [22] (2.1 g) in N NaOH (10 ml) was added to a solution of benzylhydrazine sulphate (2.2 g) in N NaOH (20.2 ml). The red colour rapidly disappeared, and a crystalline product (2.4 g) was deposited. It was dissolved in ether (50 ml) and the solution was extracted with N NaOH (10 ml). The ethereal solution on evaporation gave a solid residue (0.56 g), which crystallized from a mixture of toluene and light petroleum (80—100°) as colourless plates of *1-benzylthiobenzhydrazide* *** (Ib), m. p. 92—93°. (Found: C 69.8; H 5.93; N 11.5; S 13.1. Calc. for $C_{14}H_{14}N_2S$: C 69.4; H 5.82; N 11.6; S 13.2.)

The acidic isomer, *2-benzylthiobenzhydrazide*, (IIb), separated as pale yellow needles (1.75 g) when the alkaline extract from the crude reaction product was acidified with acetic acid. It crystallized from toluene as pale yellow needles, m. p. 146—147°. (Found: C 69.8; H 5.78; N 11.4; S 13.1. Calc. for $C_{14}H_{14}N_2S$: C 69.4; H 5.82; N 11.6; S 13.2.)

The correctness of structure (Ib) for the neutral thiohydrazide was further demonstrated by its deamination with nitrous acid to N-benzyl-thiobenzamide. The thiohydrazide (Ib) (0.25 g) was dissolved in a mixture of ethanol (5 ml) and N HCl (2 ml), and a solution of sodium nitrite (0.2 g) in water (5 ml) was added. Gas was evolved and an oil was deposited, which solidified to a crystalline material (0.19 g). This crystallized from light petroleum (80—100°) as pale yellow needles of *N-benzylthiobenzamide*, m. p. 86—87°. (Found: N 6.11; S 14.1. Calc. for $C_{14}H_{13}NS$: N 6.16; S 14.1.)

---

* All melting points are uncorrected and taken in capillary tubes in an electrically heated block.

** Numbering according to Chemical Abstracts (see Subject Index, Carbazic acid).

*** Numbering according to Holmberg [19].

This compound was also prepared by reaction between benzylamine and the sodium salt of carboxymethyl dithiobenzoate and was found to be identical with the compound described above. Levi [23] has described the preparation of N-benzylthiobenzamide by reaction between benzylamine and sulphur at 180°, and he reports m. p. 86°.

Benzaldehyde 1-benzylthiobenzhydrazone (VIb) crystallized from toluene-light petroleum (80—100°) as yellow, rhombic prisms, m. p. 116—117°. (Found: C 76.2; H 5.34; N 8.42; S 9.80. Calc. for $C_{21}H_{18}N_2S$: C 76.3; H 5.49; N 8.48; S 9.70.)

2,5-Diphenyl-3-benzyl-Δ^4-1,3,4-thiadiazoline (VIIb) was too unstable to be recrystallized, but according to analysis the crude product, m. p 65—67°, was fairly pure. (Found: C 76.4; H 5.38; N 8.48; S 9.82. Calc. for $C_{21}H_{18}N_2S$: C 76.3; H 5.49; N 8.48; S 9.70.)

The crude thiadiazoline (0.4 g) was dissolved in hot ethanol (8 ml). On cooling, pale yellow needles separated, m. p. 161—162°. (Found: C 72.7; H 5.30; N 7.97; S 9.10. Calc. for $C_{21}H_{18}N_2OS$: C 72.8; H 5.24; N 8.09; S 9.25.)

Benzylhydrazine and dimethyl xanthate. Dimethyl xanthate (6.2 g) in ethanol (150 ml) was added to a solution of benzylhydrazine sulphate (11 g) in 2 N NaOH (50 ml). On the following day the crystals of sodium sulphate were removed by filtration, and then the solvents were removed *in vacuo* at room temperature. The oily residue was dissolved in ether (50 ml), and the solution was extracted twice with N NaOH (each portion 50 ml). After the second extraction only one spot, corresponding to the neutral isomer, could be observed when the ethereal phase was examined with paper chromatography. The ethereal solution was evaporated and gave a non-crystallizing residue (2.5 g) of *methyl 2-benzylthioncarbazate* (Ic). It was not analyzed but only used for preparation of the benzylidene derivative (VIc).

The acidic isomer, *methyl 3-benzylthioncarbazate* (IIc), separated as a crystallizing oil, when the alkaline extract from the crude reaction mixture was acidified with acetic acid. The compound (6.9 g) crystallized from benzene-light petroleum (40—60°) as colourless rods, m. p. 45—46°. (Found: C 55.0; H 6.14; N 14.3; S 16.3. Calc. for $C_9H_{12}N_2OS$: C 55.1; H 6.16; N 14.3; S 16.3.)

Methyl 2-benzyl-3-benzylidene-thioncarbazate (VIc) crystallized from light petroleum (80—100°) as colourless prisms, m. p. 99—100°. (Found: C 67.5; H 5.77; N 9.74; S 11.2. Calc. for $C_{16}H_{16}N_2OS$: C 67.6; H 5.67; N 9.85; S 11.3.)

2-Phenyl-3-benzyl-5-methoxy-Δ^4-1,3,4-thiadiazoline (VIIc) crystallized from ethanol as colourless rods, m. p. 63—66°. (Found: C 67.5; H 5.62; N 9.93; S 11.2. Calc. for $C_{16}H_{16}N_2OS$: C 67.6; H 5.67; N 9.85; S 11.3.)

Benzylhydrazine and O-benzyl-S-carboxymethyl xanthate. O-Benzyl-S-carboxymethyl xanthate [24] (6.0 g) was dissolved in N NaOH (25 ml) and added to a solution of benzylhydrazine sulphate (5.5 g) in N NaOH (50 ml). A non-crystallizing reaction product separated rapidly, and it was dissolved in ether (100 ml) and extracted three times with aqueous ethanolic NaOH (each portion 25 ml N NaOH and 10 ml of ethanol). Then the ether solution on paper chromatography showed only one spot, corresponding to the neutral isomer (Id). The ether solution was evaporated to dryness, and the crystalline residue (5.1 g) crystallized from ethanol as colourless rods of *benzyl 2-benzylthioncarbazate* (Id), m. p. 47—48°. (Found: C 66.0; H 5.97; N 10.4; S 11.8. Calc. for $C_{15}H_{16}N_2OS$: C 66.1; H 5.92; N 10.3; S 11.8.)

The acidic isomer, *benzyl 3-benzylthioncarbazate* (IId), was obtained as a crystallizing oil, when the alkaline extract from the crude reaction mixture was acidified with acetic acid. The yield was increased when the ethanol was removed *in vacuo*. The product (1.5 g) crystallized from benzene-light petroleum (40—60°) at −30° as colourless rods, m. p. 51—52°. (Found: C 66.1; H 5.90; N 10.3; S 11.7. Calc. for $C_{15}H_{16}N_2OS$: C 66.1; H 5.92; N 10.3; S 11.8.)

Benzyl 2-benzyl-3-benzylidene-thioncarbazate (VId) crystallized from light petroleum (80—100°) as colourless rods, m. p. 92—93°. (Found: C 73.0; H 5.78; N 7.98; S 9.09. Calc. for $C_{22}H_{20}N_2OS$: C 73.3; H 5.59; N 7.77; S 8.89.)

2-Phenyl-3-benzyl-5-benzyloxy-Δ^4-1,3,4-thiadiazoline (VIId) crystallized from ethanol as colourless rods, m. p. 96—98°. (Found: C 72.9; H 5.79; N 7.90; S 9.05. Calc. for $C_{22}H_{20}N_2OS$: C 73.3; H 5.59; N 7.77; S 8.89.)

Paper chromatography. The impregnation of the papers with dimethyl sulphoxide was performed as described by Wickberg [18]. Before use the papers were stored in a desiccator over dimethyl sulphoxide and silica for at least 24 h to attain equilibrium. Mixtures of di-*n*-butyl ether and *n*-heptane were used as the mobile phase, and generally the R_F-

values rose with increasing proportion of ether in the solvent. The ascending technique was used, and 20 cm length of paper was in most cases enough to obtain a satisfactory separation of the isomeric pairs (I) and (II). The spots could be made visible by spraying the papers with an aqueous solution 0.1 N in $AgNO_3$ and $CuSO_4$ and 2 N in ammonia. The neutral isomers gave grey spots and the acidic ones brown spots. A more general spray reagent is the iodine-azide reagent [25], but it gave less distinct spots. The different compounds could also conveniently be localized by photographing the papers in UV-light.

Dissociation constants. Titration graphs were recorded with a glass electrode, Radiometer 202 B, against a calomel electrode in saturated KCl, when 0.05 N NaOH in 20 % and 3 % (w/w) aqueous ethanol was added to $3 \times 10^{-3} - 3 \times 10^{-4}$ M solutions of the thiohydrazides (II) in aqueous ethanol of the same composition. Before use the glass electrode was stored over night in the appropriate aqueous ethanol, and then it was calibrated with a standard buffer in water. From 6–9 points around the value for half-neutralization the dissociation constants were calculated and corrected for the activity of the anion.

Acknowledgments. The technical assistance of fil.kand. Lars Andersson, Miss Karin Göransson and Miss Ingeborg Leutiger is acknowledged. The investigation has been supported by grants from the *Swedish Natural Science Research Council*, from *Stiftelsen Lars Hiertas Minne*, and from *Kungliga Fysiografiska Sällskapet.*

REFERENCES

1. Michaelis, A. and Hadanck, E. *Ber.* **41** (1908) 3285.
2. Busch, M., Opfermann, E. and Walter, H. *Ber.* **37** (1904) 2318.
3. Cattelain, E. *Compt. rend.* **209** (1939) 799.
4. Cattelain, E. *Bull. soc. chim. France* **7** (1940) 791.
5. Busch, M. and Schmidt, R. *J. prakt. Chem.* [2] **130** (1931) 342.
6. Greer, A. H. and Smith, G. B. L. *J. Am. Chem. Soc.* **72** (1950) 874.
7. Fischer, E. *Ann.* **190** (1878) 67.
8. Brown, H. C., Mc Daniel, D. H. and Häfliger, O. in Braude, E. A. and Nachod, F. C. *The determination of organic structures by physical methods.* Academic Press, Inc. New York 1955, p. 573.
9. Folpmers, T. *Rec. trav. chim.* **34** (1915) 34.
10. Holmberg, B. *Arkiv Kemi* **9** (1956) 47.
11. Holmberg, B. *Arkiv Kemi* **7** (1954) 517.
12. Sandström, J. *Arkiv Kemi* **9** (1956) 255.
13. Holmberg, B. *Private communication.*
14. von Brüning, G. *Ann.* **253** (1889) 5.
15. Hinman, R. L., and Fulton, D. *J. Am. Chem. Soc.* **80** (1958) 1895.
16. Hinman, R. L. *Anal. Chim. Acta* **15** (1956) 125.
17. Kjær, A. and Rubinstein, K. *Acta Chem. Scand.* **7** (1953) 528.
18. Wickberg, B. *Acta Chem. Scand.* **12** (1958) 615.
19. Nylén, P. *Z. anorg. und allgem. Chem.* **246** (1941) 227.
20. Linde, E. *Arkiv Kemi, Mineral. Geol.* **6** (1917) No. 20.
21. Busch, M. and Starke, M. *J. prakt. Chem.* [2] **93** (1916) 59.
22. Holmberg, B. *Arkiv Kemi, Mineral. Geol.* **17A** (1944) No. 23.
23. Levi, T. G. *Gazz. chim. ital.* **59** (1929) 548. — *Chem. Abstracts* **24** (1930) 353.
24. Lenander, K.-J. *Om aromatiska xantogenatsyror och deras spjälkningsprodukter. (Diss.)* University, Lund 1920.
25. Feigl, F. *Qualitative analysis by spot tests*, 5th Ed. Elseviers Publ. Co., Inc. Amsterdam-New York 1956, p. 258.

Received January 13, 1960.

ACTA CHEMICA SCANDINAVICA 14 (1960) 797–804

The Chemistry of the Natural Order Cupressales

XXVII *. Heartwood Constituents of *Juniperus utahensis* Lemm.

JARL RUNEBERG

Organisk-kemiska institutionen, Kungl. Tekniska Högskolan, Stockholm 70, Sweden

From the heartwood of *Juniperus utahensis* there were isolated: thujopsene, cuparene, widdrol, "Widdringtonia diol", a yellow compound $C_{20}H_{20}O_5$, carvacrol, nootkatin, hinokiic acid as well as a hydroxy acid and a carbonyl containing compound, both probably of a sesquiterpene nature. The presence of β-thujaplicin was indicated by paper chromatography and that of α-cedrene by gas chromatography.

The available literature on juniper wood constituents deals mainly with the isolation and fractionation of essential oils and describes their physical constants. Only in a few cases have the various constituents present been identified. In a previous paper [1] in this series, however, an account was given of a more detailed chemical investigation of the Far Eastern species *Juniperus chinensis* in which a dozen of the heartwood constituents were identified. This paper deals with the constituents of the American desert juniper, *J. utahensis*.

The only previous investigation of this species that has been published was carried out by Adams and Billinghurst [2] who described an oil obtained by steam distillation of leaves and small twigs. They gave the physical constants of the oil but did not isolate or identify any of its constituents.

The wood used in the present investigation came from a tree grown at Grand Canyon, Arizona, U.S.A. It had been cut at least three years before it was worked up and was therefore rather dry.

The wood was extracted with acetone. The ether-soluble portion of the acetone extract was poured into a large volume of light petroleum giving a yellow crystalline precipitate.

On recrystallisation the compound melted with decomposition at 313° and analysed for $C_{20}H_{20}O_5$. The mass spectrum confirmed the molecular weight as 340. The compound contained no methoxyl group; the C-methyl determination gave 1.4 moles of acetic acid. The infrared spectrum (see Fig. 1) indicated

* Part XXVI. *Tetrahedron*. In the press.

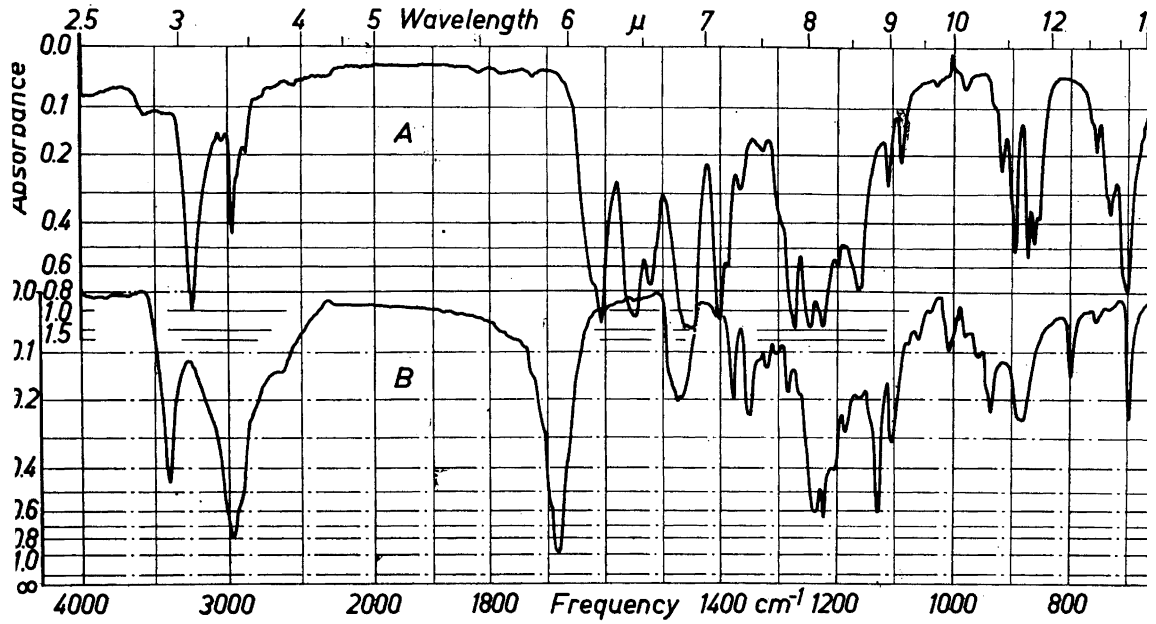

Fig. 1. Infrared spectra of utahin (A) and of hydroxy acid m. p. 181—187° (B) in potassium bromide.

the presence of at least one phenolic hydroxyl group (3 250 cm^{-1}). The absorption at 1 615—1 650 cm^{-1} and the broad, weak OH-absorption near 2 500 cm^{-1} may indicate the presence of a strongly hydrogen-bonded keto function in the molecule. The ultraviolet spectrum of the compound is given in Fig. 2.

Zinc dust distillation afforded a semi-solid product with ultraviolet absorption maxima at 245, 253 and 282 mμ. Selenium dehydrogenation gave a very small yield of a product with maxima at 274 and 277 mμ. Catalytic hydrogenation afforded only unidentifiable products. The compound gave a negative magnesium-hydrochloric acid test.

The name utahin is proposed for the above compound which to our knowledge has not previously been isolated.

Acetylation of utahin afforded a pale yellow di-acetate, $C_{24}H_{24}O_7$, m.p. 205° (decomp.), which was not found to be optically active. Its infrared spectrum showed no absorption band at 3 250 cm^{-1} but the absorption in the 1 615—1 650 cm^{-1} and 2 500 cm^{-1} regions was unchanged. The ultraviolet spectrum of utahin diacetate is given in Fig. 2.

Since the wood used in this investigation had been stored for several years it is possible that utahin may be an artefact formed by oxidation during storage. To check this possibility a large sample of fresh wood (grown near Ogden, Utah, U.S.A.) was obtained. This material also afforded utahin but in considerably lower yield (0.001 %, see below). It therefore seems likely that utahin

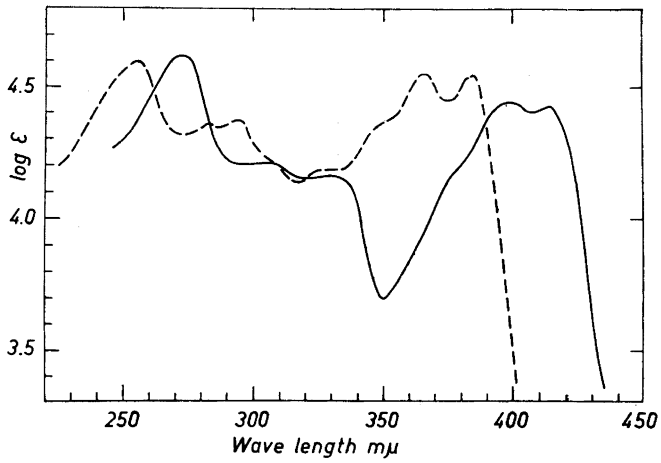

Fig. 2. Ultraviolet spectra of utahin (————) in chloroform and of utahin diacetate (- - - - - -) in ethanol (95 %).

is present in the fresh wood although the possibility that it may have been formed during working up cannot be excluded.

The diterpenes ferruginol, sugiol and xanthoperol have recently been isolated from *J. communis* [3-5]. The empirical formula and the C-methyl content of utahin suggest that it could be related to these diterpenes. Further work on utahin is in progress.

The light petroleum-soluble part of the acetone extract, on standing, gave a yellowish crystalline precipitate (C, see experimental part). The infrared spectrum of this material, except for additional carbonyl absorption (1 745 cm^{-1}) showed great resemblance to that of utahin but it has not yet been investigated.

The remaining light petroleum-soluble acetone extract was separated into neutral and acid fractions by extraction with alkali. The acidic material afforded two sesquiterpene acids.

One of these was hinokiic acid [6] which has also been found in *J. chinensis* [1] as well as in several other trees of the Cupressaceae.

The other acid was a new sesquiterpene hydroxy acid $C_{15}H_{24}O_3$, m.p. 181—187°; unchanged by further recrystallisation or sublimation. Since the acid could not be catalytically hydrogenated, the analysis suggests that the compound may be tricyclic. Except for a very weak maximum at 206 mμ ($\varepsilon = 63$), the ultraviolet spectrum showed no significant absorption in the 195—350 mμ region.

Although the compound itself melted over a wide range, it gave a sharp-melting methyl ester (m.p. 98.0—98.5°) with diazomethane. The ester was reduced to a diol which was dehydrogenated with selenium giving a product that, according to the ultraviolet spectrum, was mainly benzenoid in nature. The dehydrogenation product was chromatographed on alumina but

none of the fractions gave a crystalline picrate. The hydroxy acid was stable to chromic acid in pyridine at room temperature indicating that the alcoholic hydroxyl group is tertiary. Dehydration with formic acid yielded a product which gave a satisfactory analysis but had no sharp melting point and was probably a mixture of isomers. The ultraviolet spectrum showed only a maximum at 205 mμ indicating that the product did not contain an α-β-unsaturated acid. Further work on the structure of this hydroxy acid is in progress.

The remaining acidic material from the light petroleum-soluble acetone extract gave carvacrol on distillation. The tropolones were concentrated by precipitation with copper acetate and decomposition of the crude copper salts with hydrochloric acid. Chromatography of the product obtained gave nootkatin and paper chromatography indicated the presence of β-thujaplicin.

The neutral oil was distilled. Fraction 1 (Table 1) corresponded to a wide boiling point range and according to its infrared spectrum appeared to be a complex mixture of carbonyl compounds, hydrocarbons and alcohols. Fraction 2 consisted almost entirely of hydrocarbons and fraction 3 again showed hydroxyl absorption. Gas chromatography of the first three fractions indicated the following compositions (in percent), assuming complete resolution: Fraction 1 (Table 1), thujopsene [6] 55; α-cedrene 31; two unknowns 7 and 7. Fraction 2, thujopsene 62; α-cedrene 13; four unknowns 10, 8, 6 and 1. Fraction 3, thujopsene 16; cuparene [7] 34; two unknowns 34 and 16.

The major component of fraction 2 (Table 1) was shown to be thujopsene by conversion to the corresponding aldehyde (widdrenal) [6,8]. Fraction 3 (Table 1) was ozonised at low temperature and the material unaffected by ozone was identified as cuparene.

The next higher boiling fraction gave widdrol [8] but no cedrol was detected. However since α-cedrene is present it is not improbable that cedrol might also occur in the wood although in very small amount. The same fraction, on ozonolysis followed by chromatography, afforded a sesquiterpene diol, m.p 154°, previously isolated from *Widdringtonia juniperoides* [8].

Fraction 5 (Table 1) contained a crystalline carbonyl compound which is probably a sesquiterpene but gave a poor analysis.

The compounds isolated are listed below with very approximate estimates of the amounts present (as percentages of the air-dried wood). Total acetone extract 9.3, ether-soluble acetone extract 6.3, light petroleum-soluble acetone extract 1.8, sodium bicarbonate-soluble 0.084, sodium hydroxide-soluble 0.67, neutral 1.1, utahin 0.030, nootkatin 0.0002, β-thujaplicin 0.0001, carvacrol 0.0072, hinokiic acid 0.013, sesquiterpene hydroxy acid 0.070, α-cedrene 0.048, thujopsene 0.18, cuparene 0.047, widdrol 0.051, "Widdringtonia diol" m.p. 154°, 0.0003, high boiling carbonyl compounds 0.020.

EXPERIMENTAL

Rotations were measured in chloroform; melting points, taken on a hot stage, are corrected; boiling points are uncorrected. Light petroleum refers to the fraction b.p. 40–60°.

Isolation of the oils: The ground, air-dried heartwood (9.7 kg) was continuously extracted with acetone for 24 h. The acetone was evaporated and the remaining oil poured with stirring into ten volumes of ether. The ether solution was filtered (precipitate A, 312 g), evaporated and the residue was poured into ten volumes of light petroleum. After filtration (precipitate B, 437 g) the solution was evaporated almost to dryness. On standing for about one month a yellow crystalline precipitate formed (C, 0.373 g). This was removed by filtration. The filtrate was diluted with two volumes of light petroleum and extracted successively with a saturated solution of sodium bicarbonate and 2 N sodium hydroxide. On acidification and extraction with ether the sodium bicarbonate solution yielded a viscous oil (D, 8.1 g) which was not further investigated. The sodium hydroxide-soluble material (E, 65.3 g) was isolated in the same way by acidification and extraction with ether. The light petroleum solution was washed with water, dried and evaporated yielding neutral material (F, 104.0 g).

Precipitate B

Isolation of utahin. Precipitate B was dissolved in an equal amount of acetone. On standing a yellow precipitate (2.8 g) formed. It was separated by filtration, washed with acetone, recrystallised from a large volume of ethyl acetate and sublimed in a high vacuum, m.p. 313° (decomp.) (Found: C 70.6; H 6.2; CH_3O 0.1. $C_{20}H_{20}O_5$ requires C 70.6; H 5.9.) The melting point did not change on further recrystallisation and sublimation. (Found: C 70.9; H 6.0; O 23.3; CH_3-(C) 6.2. $C_{20}H_{20}O_5$ requires O 23.5; CH_3-(C) (one) 4.4.)

The mass-spectrum was recorded on an instrument with an all-glass, heated inlet system [9]. Only major peaks are given. The figures in brackets are intensities given as *per cent* of the strongest peak (m/e = 43). 340 (21), 312 (17), 284 (18), 270 (8), 269 (40), 253 (8), 128 (9), 127 (24), 115 (20), 105 (9), 91 (13), 77 (13), 69 (10), 67 (11), 63 (9), 57 (13), 55 (29), 53 (17), 51 (10), 45 (9), 44 (21), 42 (13), 41 (61), 39 (25), 29 (25), 28 (23), 27 (29), 18 (95), 17 (17) and 15 (10).

Utahin sublimed easily in a high vacuum and had a low solubility in most organic solvents except chloroform. It dissolved in concentrated sulphuric acid giving a pale greenish solution from which it could be recovered by addition of water. A solution in 95 % ethanol gave a brownish colour with aqueous iron (III) chloride. The compound does not dissolve in aqueous sodium hydroxide (2 N) but affords a bright orange salt with alkali. Utahin does not react with carbonyl reagents or with *o*-phenylene diamine in acetic acid.

Because of its very low solubility in ether, utahin was expected also to occur in the precipitate A. This was therefore extracted with chloroform, the extract was evaporated and the residue was dissolved in acetone (50 ml). Only a small amount of utahin (130 mg) precipitated on standing.

The wood remaining after acetone extraction was dried and extracted exhaustively with chloroform. Only a very small amount of utahin was obtained from the chloroform extract.

Utahin diacetate. Utahin (70 mg) in acetic anhydride (2 ml) was treated with perchloric acid (1 drop), the mixture was heated on a boiling water bath for 1 h and poured on to ice. The pale yellow crystalline material formed was separated and recrystallised from 95 % ethanol, m. p. 207° (decomp.), $[\alpha]_D$ 0. (Found: C 68.0; H 5.6; CH_3-CO- 19.7. $C_{24}H_{24}O_7$ requires C 67.9; H 5.7; CH_3-CO- (one) 10.6.)

Alkali-soluble fraction

Hinokiic acid. The alkali-soluble oil E on standing deposited a crystalline material (1.23 g). This was filtered off and recrystallised from light petroleum, m. p. 166.0–167.5° $[\alpha]_D$ −87° (*c* 1.6). It was identified as hinokiic acid [6] (mixed m. p., I.R.).

Hydroxy acid. The material remaining after separation of hinokiic acid from the oil E was dissolved in ether and extracted with aqueous sodium carbonate (2 N). The ether solution on evaporation gave an oil (G). The sodium carbonate solution on acidification and extraction with ether gave a product (36.4 g) which was mixed with light petroleum

and partly crystallised on standing for several months. The crystals (6.76 g) were separated by filtration (filtrate, oil [H], recrystallised several times from ligroin (b. p. 100—125°) and from ethanol-water and were then sublimed in a high vacuum, m. p. 181—187°, $[\alpha]_D$ −47° (*c*, 3.2). (Found: C 71.9; H 9.7; M (Rast) 250; M (titr.) 207; CH_3—(C) 7.4. $C_{15}H_{24}O_3$ requires C 71.4; H 9.6; M 252; CH_3—(C) (one) 6.0.) Further recrystallisation from these solvents and sublimation did not change the melting point (181—187°), (C 71.1; H 9.2).

Hydroxy acid methyl ester. The hydroxy acid (400 mg) was methylated with diazomethane. The ester was recrystallised from ethanol-water and sublimed in a high vacuum, m. p. 98.0—98.5, $[\alpha]_D$ −25° (*c*, 1.0). (Found: C 72.1; H 9.5; M (Rast) 252. $C_{16}H_{26}O_3$ requires C 72.1; H 9.8; M 266.)

Diol. A solution of the hydroxy acid methyl ester (595 mg) in absolute ether was added dropwise with stirring at 0° to a solution of lithium aluminium hydride (455 mg) in absolute ether. After 3 h at room temperature the excess reagent was destroyed with ethyl acetate. Hydrochloric acid (2 N) was added and the solution was extracted with ether. On evaporation the ether solution afforded a substance (518 mg) which was recrystallised from *cyclo*hexane and sublimed in a high vacuum, m. p. 130.0—131.0°, $[\alpha]_D$ +6° (*c*, 2.0). (Found: C 75.4; H 10.9. $C_{15}H_{26}O_2$ requires C 75.6; H 11.0.)

Attempts to hydrogenate the hydroxy acid. Hydroxy acid (60 mg) in 95 % ethanol (10 ml) or in acetic acid was shaken with a platinum oxide catalyst (6 mg) in a hydrogen atmosphere for 6 h. No hydrogen was absorbed and the starting material was recovered unchanged.

Attempted oxidation with chromic acid. Hydroxy acid (21 mg) was added to a solution of chromic acid (32 mg) in glacial acetic acid (2 ml) and dry pyridine (1 drop). After 15 h at room temperature methanol (0.3 ml) was added and the mixture left to stand for another 15 h. It was then acidified with sulfuric acid (2 N) and extracted with ether; the ether solution was washed with water, dried and evaporated. The residue, after recrystallisation from ethanol, afforded unchanged starting material.

Dehydration of the hydroxy acid. A mixture of the hydroxy acid (355 mg) and formic acid (90 %, 7 ml) was heated on a water bath for 2 h. Ether was added and the solution was extracted with aqueous sodium bicarbonate. The ether solution was evaporated affording a residue which was recrystallised from 95 % ethanol and sublimed in a high vacuum, m. p. 87—93°. (Found: C 77.1; H 9.2; CH_3—(C) 11.7. $C_{15}H_{22}O_2$ requires C 76.9; H 9.5; CH_3—(C) (one) 6.4.)

Carvacrol. A sample (17.8 g) of the sodium carbonate insoluble oil (G) was distilled through a spinning band column. The material distilled over a range of 108—170°/20 mm without giving any definite fraction of constant boiling point. The material boiling at 113—122°/20 mm was mainly carvacrol. This fraction was converted into carvacroxy acetic acid, m. p. 151—152°, undepressed by an authentic sample.

The sodium carbonate insoluble oil (G, 10.0 g) was dissolved in ligroin (b.p. 100—125°) and shaken with aqueous copper acetate (saturated). The liquid phases were removed by filtration and the copper salts remaining were washed with ligroin and water, decomposed with hydrochloric acid (2 N) and the product was extracted with ether. On evaporation of the ether solution a viscous oil (I, 481 mg) was obtained. This was chromatographed on silica gel. The silica gel was made iron-free by treatment with aqueous oxalic acid (saturated) and washing with water. It was then treated with a solution of the disodium salt of ethylene diamine tetra-acetic acid (0.002 M), washed with water and dried. The *iso*propyl ether-soluble part of the oil I (232 mg) was chromatographed on this pretreated silica gel (40 g) using *iso*propyl ether as eluent. 200 ml fractions were collected. Each fraction was evaporated and analysed by paper chromatography [10]. Fraction 1 consisted mainly of a yellow compound which was not further investigated, fraction 2 of a mixture of this compound and nootkatin, fraction 3 of nootkatin and a small amount of β-thujaplicin. The crystalline part of this fraction (4 mg) was recrystallised from light petroleum, m. p. 96.0, and identified as *nootkatin* (mixed m. p., I.R.). Fraction 4 consisted of β-thujaplicin, nootkatin and three further compounds with lower R_F values than the first two, fraction 5 mainly of *β-thujaplicin* which however could not be crystallised.

Neutral fraction

The neutral oil F was fractionally distilled through a one metre, vacuum-jacketed, packed column, giving the fractions listed in Table 1.

Table 1. Distillation of fraction F. Total distillate 81.7 g or 80 %.

Fraction	Weight (g)	B.p. (°C)	Pressure (mm Hg)	Rotation ($[\alpha]_D$)	Refractive index (n_D^{25})
1	11.3	101.0–126.5	14	−44.4	1.4933
2	14.9	126.5–135.0	14	−66.4	1.5040
3	12.8	135.0–155.5	14	+27.4	1.5094
4	12.0	155.5–156.0	14	+42.9	1.5079
5	17.8	156.0–160.5	14	+12.6	1.5117
6	12.9	up to 230°	2	+ 3.9	1.5202

Gas chromatographic examination of the sesquiterpene hydrocarbon fractions. A Pye Argon Chromatograph, Cat. No. 12 000, was used together with a Philips Automatic Compensator PR 2210 A/21. (Column length 1.20 m, internal column diameter 5 mm, stationary phase 100–115 mesh Silocel C 22 brick powder impregnated with 2,4-dinitrophenyl-2-naphthyl ether (15 %) and dibenzylpyridine (a mixture of 2,4- and 2,6-isomers, 0.75 %) [11], temperature 150°, charge 0.025 µl, argon flow rate 0.32 ml/sec.

The following peaks were obtained. Recorder deflection (mV) given as a function of time (min). Fractions refer to those in Table 1.

Fraction 1, 9 (17.8); 23 (24.9); 60 (27.2); 9 (29.6).

Fraction 2, 2 (17.8); 12 (24.9); 66 (27.2); 4 (34.7); 4 (39.2); 5 (42.7).

Fraction 3, 7 (27.2); 11 (42.4); 9 (48.9); 8 (60.0).

The peak at 24.9 min corresponded to synthetic *α-cedrene* prepared from cedrol, the peak at 27.2 min to pure thujopsene and the peak at 60.0 min to cuparene.

Thujopsene. Fraction 2 (Table 1, 2.1 g) in 95 % ethanol (40 ml) was refluxed with selenium dioxide (1.2 g) for 4 h. The product was filtered, evaporated to dryness and the residue distilled in a high vacuum. On standing a crystalline precipitate (372 mg) was formed; this was collected by filtration, recrystallised from light petroleum, m. p. 73.5–74.5° and identified as widdrenal [6,8] (mixed m. p., I.R.).

Cuparene. Fraction 3 (Table 1) was redistilled through a spinning band column. The fraction (1.36 g) showing the strongest absorption at 1 525 cm^{-1} was ozonised in methylene chloride at −70°C until an excess of ozone was indicated by the appearance of a blue colour. When the reaction mixture had reached room temperature, hydrogen peroxide (30 %, 4 ml) in potassium hydroxide (10 %, 1.5 ml) was added dropwise. A large quantity of ether was added, the organic phase was separated, washed with water and evaporated giving a viscous oil. This was chromatographed on basic alumina (40 g). The first 100 ml of light petroleum eluted a hydrocarbon (191 mg) which was distilled under reduced pressure. The fraction boiling at 115°/7 mm, n_D^{25} 1.5215, $[\alpha]_D$ +65° (*c*, 1.9) was identified with *cuparene* [7] by comparing its physical constants and infrared spectrum with those of an authentic sample.

Widdrol. Fraction 4 (Table 1) crystallised partly on standing. A sample of this fraction (7.0 g) was filtered, the crystals (684 mg) were washed with light petroleum and recrystallised from acetonitrile, m.p. 95.0–96.0°, $[\alpha]_D$ +103° (*c*, 2.1) identified as widdrol [8] (mixed m. p., I.R.).

Attempts to isolate cedrol. Crude widdrol obtained from fraction 4 (Table 1, 204 mg) was chromatographed on basic alumina. Light petroleum eluted a small quantity of hydrocarbon; 2 % ether in benzene gave an oil with an infrared spectrum different from that of cedrol; ether-benzene (1:1) eluted widdrol.

A sample (1.52 g) of the mother liquor obtained when widdrol was separated from fraction 4 (Table 1) was ozonised as described for cuparene (see above) and the product separated into acidic and neutral fractions with sodium carbonate (2 N). The neutral fraction was chromatographed on basic alumina but no cedrol could be detected. Crude widdrol (204 mg) obtained from fraction 4 (Table 1) was ozonised and chromatographed in the same way but no cedrol was obtained in this case either.

"*Widdringtonia diol.*" In the chromatography of the neutral part of the ozonisation product obtained from crude widdrol, elution of the column with methanol gave a crystalline compound (4 mg). This was recrystallised from light petroleum, m. p. 153—154° and identified (mixed m. p., I.R.) as a "diol" previously isolated from *Widdringtonia juniperoides* [8].

High boiling carbonyl compounds. A sample of fraction 5 (Table 1, 10.0 g) in 95 % ethanol containing 10 % acetic acid (30 ml) was refluxed with Girard D reagent (3.0 g) for 30 min. The reaction mixture was diluted with about five volumes of ice-water and extracted with ether. The aqueous phase was acidified with an equal volume of hydrochloric acid (4 N) and extracted with ether. The ether solution, on evaporation, afforded an oil (1.09 g) which partly crystallised on standing. The crystals (183 mg) were separated by filtration, washed with light petroleum, recrystallised from the same solvent and sublimed in a high vacuum, m. p. 107.5—108.0°, $[\alpha]_D$ +75 (*c*, 1.4). (Found: C 81.5, 81.1; H 10.5, 10.2; $C_{15}H_{24}O$ requires C 81.8; H 11.0.) 2,4-dinitrophenyl-hydrazone, m. p. 198—199°.

Acknowledgements. My thanks are due to Professor H. Erdtman for collecting the initial wood sample used and for his interest in this work, to Dr. Edward G. Locke, United States Department of Agriculture, Forest Service, Forest Products Laboratory, Madison, Wisconsin, for further gifts of material and to Ing. R. Ryhage, Karolinska Institutet, Stockholm, for determination of the mass spectrum of utahin.

I also wish to thank Miss G. Hammarberg for the infrared and ultraviolet spectra and the *Swedish Natural Science Research Council* for financial support.

REFERENCES

1. Pilo, C. and Runeberg, J. *Acta Chem. Scand.* **14** (1960) 353.
2. Adams, M. and Billinghurst, R. *J. Am. Chem. Soc.* **49** (1927) 2896.
3. Bredenberg, J. B. and Gripenberg, J. *Acta Chem. Scand.* **8** (1954) 1728.
4. Bredenberg, J. B. *Acta Chem. Scand.* **11** (1957) 927.
5. Bredenberg, J. B. *Acta Chem. Scand.* **11** (1957) 932.
6. Erdtman, H. and Norin, T. *Acta Chem. Scand.* **13** (1959) 1124.
7. Enzell, C. and Erdtman, H. *Tetrahedron* **4** (1958) 361.
8. Erdtman, H. and Thomas, B. R. *Acta Chem. Scand.* **12** (1958) 267.
9. Ryhage, R. *Arkiv Kemi* **13** (1959) 475.
10. Wachtmeister, C. A. and Wickberg, B. *Acta Chem. Scand.* **12** (1958) 1335.
11. Groth, A. B. *Svensk Papperstidn.* **61** (1958) 10, 315.

Received December 23, 1959.

ACTA CHEMICA SCANDINAVICA 14 (1960) 805–813

Chromatographic Determination of Ascorbic Acid

INGOLF CROSSLAND

Statens Vitamin Laboratorium, Copenhagen, Denmark

A description is given of a quantitative, chromatographic method for the determination of ascorbic acid. According to this method ascorbic acid is separated from interfering substances by chromatography on a cellulose column and determined in the eluate by means of diazotised nitroanisidine. Determinations of ascorbic acid contents down to 1 mg per 100 g in various materials have been tabulated to show the applicability of the method.

A survey of the literature on chemical assay of ascorbic acid in biological materials shows that the specificity of most of the methods used is not very satisfactory.

Thus the method most widely used, *i.e.* titration with an oxidizing reagent, as for instance dichlorophenol-indophenol [1,2], depends solely on the power of reduction of ascorbic acid, and this has certainly proved to give reliable results in the assay of, for instance, most fresh vegetables and fruits, but too high results in the assay of many other materials, for instance dried foods, which contain foreign, reducing substances. Descriptions of methods endeavouring to overcome this difficulty, thereby improving the specificity of the method, abound in the literature (*cf.* review by Sebrell and Harris [3]), but since the chemical nature of the reducing substances concerned are often unknown, it will generally be impossible with absolute certainty to eliminate the process of reduction resulting from their presence.

Another method is to oxidize ascorbic acid to form dehydroascorbic acid and determine the resulting carbonyl function by means of 2,4-dinitrophenylhydrazine [4]. There is a risk, however, that other aldehydes and ketones, partly resulting from the process of oxidation, may react with the reagent, leading to falsely high ascorbic acid values.

A third method for chemical assay of ascorbic acid, devised by Schmall *et al.*[5], depends on the condensation of ascorbic acid with a diazotised *o*-nitroaniline derivative in acid solution and spectrophotometric measurement in alkaline solution of the resulting hydrazide of oxalic acid. Moor [6] has modified the method, adapting it for the determination of ascorbic acid in foods. In this laboratory it has been found, however, that Moor's method may fail when the extract is low in ascorbic acid while at the same time containing substances

which produce high blank values. In a few cases the extinction determined for the blank was found to be higher than the extinction determined for the analytical sample.

A generally applicable way of improving the specificity of the assay involves chromatographic purification of the ascorbic acid prior to the chemical assay. The literature contains many examples of paper-chromatographic separation of ascorbic acid from interfering substances [7-9], but it appears to be difficult to avoid loss of ascorbic acid during the fairly protracted chromatographic separations. Moreover, it is possible to use a limited volume of extract only for this chromatographic separation, since the paper cannot "carry" any large amount of accompanying substances or of the metaphosphoric acid required for the extraction. As a consequence the sensitivity obtained is not satisfactory.

According to the method described in the following these difficulties have been overcome. The method depends on the purification of the ascorbic acid by chromatography on a column, and this has made possible the determination of ascorbic acid contents as low as 0.4 mg ascorbic acid per 100 ml extract. The content of the ascorbic acid in the purified solution is determined according to a modified version of the method devised by Schmall *et al.*[5] mentioned above.

EXPERIMENTAL

Principle of method. The procedure consists in:

(1) extraction of ascorbic acid with metaphosphoric acid,

(2) preliminary treatment of the extract, enabling it to be transferred to a cellulose column,

(3) chromatography of the extract, elution with a mixture of butanol-water-acetic acid,

(4) determination of ascorbic acid in the eluate by means of diazotised 2-nitro-4-methoxyaniline, which interacts with ascorbic acid to form — after shaking with a sodium hydroxide solution — the disodium salt of oxalic acid 4-methoxy-2-nitro-phenylhydrazide, the extinction of which at 570 mμ is proportional to the content of ascorbic acid.

Reagents

(1) *Metaphosphoric acid, 5 %.* Dissolve 5 g "metaphosphoric acid", analytical grade (HPO_3 containing 50—60 % $NaPO_3$), in 100 ml water. Prepare fresh solution on the day of using.

(2) *Acetone,* pure grade.

(3) *Acetone, aqueous solution, 50 % v/v.*

(4) *Acetic acid,* analytical grade.

(5) *n-Butanol,* analytical grade.

(6) *Ethylenediamine-NNN'N'-tetraacetic acid, disodium salt, 10 %.* Dissolve 10 g ethylenediamine-NNN'N'-tetraacetic acid, disodium salt ($C_{10}H_{14}O_8N_2Na_2$, $2H_2O$) in 100 ml water.

(7) *Ethylenediamine-NNN'N'-tetraacetic acid, 0.2 %.* Mix 2 ml 10 % ethylenediamine-NNN'N'-tetraacetic acid (reagent 4) with 2 ml acetic acid and dilute to 100 ml with water. This solution is supersaturated with regard to the free ethylenediamine-NNN'N'-tetraacetic acid, but is good for one week.

(8) *Eluant.* Mix 5 ml ethylenediamine-NNN'N'-tetraacetic acid, 0.2 %, (reagent 7) with 14 ml water, 1 ml acetic acid and 100 ml *n*-butanol by shaking vigorously until the mixture is (apparently) homogeneous. Prepare on the day of using.

(9) *Ascorbic acid,* reference standard, 100 μg/ml. Dissolve 50.0 mg ascorbic acid in 0.2 % ethylenediamine-NNN'N'-tetraacetic acid (reagent 7) and dilute to 50 ml with

this reagent. To a 2 ml portion of this solution add 1 ml acetic acid and dilute with *n*-butanol to 20 ml. This may cause some ethylenediamine-NNN'N'-tetraacetic acid to precipitate.

(10) *Diazotised nitroanisidine.* Mix 1 ml of a solution of 4-amino-3-nitroanisole ($C_7H_8N_2O_3$; dissolve 190 mg in 6 ml acetic acid and dilute to 100 ml with 1 N hydrochloric acid) and 0.1 ml sodium nitrite solution (dissolve 800 mg $NaNO_2$ in 100 ml water). Dilute the colourless solution with 1 ml 96 % ethanol and 2 ml *n*-butanol with stirring. The reagent is now ready for use and will keep for about one hour.

(11) *Cellulose powder.* Whatmann Cellulose Powder, standard grade.

(12) *Sodium hydroxide, 2 %.*

PROCEDURE

Cellulose column for chromatography. The chromatographic tube (*cf.* Bro-Rasmussen and Hjarde [10]) is about 40 cm long (internal diameter 12 mm) with a widening at the top holding 20—30 ml eluant and at the bottom terminating in a capillary tube, about 1 cm long (internal diameter 1 mm, external diameter about 7 mm).

Suspend 10 g cellulose powder in about 100 ml acetone, transfer directly to the chromatographic tube and force through the latter by means of carbon dioxide (at about 0.5 atm). Whenever the capillary tube gets choked with cellulose powder, and a little powder has collected at the bottom, clean the capillary tube with a piece of wire, providing free passage for the acetone. When all the powder has been transferred to the column — using as much acetone as required for this purpose — and the acetone has been forced out without allowing air to enter the cellulose, force the following liquids through the column in the order stated: 2 ml 50 % acetone (reagent 3), 2 ml 10 % ethylenediamine-NNN'N'-tetraacetic acid (reagent 6), 2 ml 50 % acetone (reagent 3), and, finally, 25 ml eluant (reagent 8), each liquid being pressed down to the surface of the column before the next is transferred to the column.

Extraction. Accurately weigh out a sample of not more than 30 g, if necessary under a 5 % solution of metaphosphoric acid, transfer to a Waring blendor with 100 ml 5 % metaphosphoric acid, bubble carbon dioxide through the solution and homogenize. Fill up to 250 ml with water and centrifuge.

From this stage it is necessary to protect the ascorbic acid from daylight, the effect of which is to decompose ascorbic acid. This decomposition causes most trouble in highly diluted solutions.

Preliminary treatment of extract. For the chromatography use, preferably, a volume of extract that contains about 20 μg ascorbic acid. If 0.5 ml extract (or an even smaller volume) is sufficient, add 1 ml acetic acid and a little cellulose powder (up to 0.5 g) to the sample drawn, stir and dilute with 5 ml *n*-butanol.

If more than 0.5 ml extract is used for the analysis, evaporate to a volume which is less than 0.5 ml by means of a stream of electrically heated carbon dioxide, and continue as described above.

In case the volume of the extract sample is more than 0.5 ml, it may be necessary to add hydrochloric acid. As regards this, *cf.* comments on the method.

Chromatography. Stir the suspension carefully and transfer quantitatively to the column by means of a pipette. Begin measuring the volume of the collected eluate from the moment the sample is transferred to the column. Force the sample through the column by means of carbon dioxide (at about 0.5 atm) and wash with three to four 1—2 ml portions of eluant, the liquid being pressed down to the surface of the column following each transference of eluant. Any lumps of cellulose from the sample left in the column should immediately be disintegrated with a spatula. Following the quantitative transference of ascorbic acid material to the column, pour eluant directly into the chromatographic tube and collect the following fractions:

(a) 34 ml, which contains the liquid front and is discarded.
(b) 10 ml, which should not contain any ascorbic acid.
(c) 13 ml, main fraction, which should contain all the ascorbic acid present.
(d) 10 ml, which should not contain any ascorbic acid.

Transfer fractions b, c and d to 50 ml separatory funnels, washing down with 5, 2 and 5 ml eluant, respectively, the volume of liquid in the separatory funnels being thus, in all cases, 15 ml.

Determination of ascorbic acid. To each of the samples b, c and d and to a reference sample (15 ml eluant to which has been added 0.200 ml ascorbic acid standard solution (reagent 9)) in separatory funnels add 0.200 ml diazotized nitroanisidine (reagent 10) and mix by swirling the separatory funnels for 0.5 min following each addition. The period of reaction should not be less than 5 min. Then carefully add 10 ml 2 % sodium hydroxide solution from a pipette, running the solution along the wall of the separatory funnel so as to prevent the two phases from mixing before the subsequent shaking. Now, as quickly as possible, shake vigorously for about one minute. Run out the aqueous solution and centrifuge for 5 minutes. Measure the extinction in the spectrophotometer in a 5 cm cell at 570 mμ.

Since the content of ascorbic acid in the sample is proportional to the extinction measured, the content of ascorbic acid can be calculated from the extinctions of the reference standard and the main fraction, the mean value of the extinctions of the fractions immediately before and after the main fraction being used as blank, *cf.* Discussion.

COMMENTS

re extract. The problems connected with the extraction does not differ from those met with in other methods for ascorbic acid analysis. Metaphosphoric acid solution is now generally acknowledged to be the best extraction agent, oxalic acid, which is otherwise frequently applied, having proved to be unsuitable [11].

To ensure reproducibility of the chromatography, the pH of the extract must be adjusted at about 1, too high pH values resulting in too high retention volumes, while too low pH values (caused for instance by excess of strong acids as trichloroacetic acid) result in too small retention volumes, *i. e.* ascorbic acid will be present in the fractions immediately after or immediately before the main fraction. When the above procedure is followed for the preparation of the extract, the acidity of the latter will in most cases be as required, and the chromatography will proceed satisfactorily without ascorbic acid in the fractions before and after the main fraction. This applies to all the vegetables mentioned in Table 1. It has been found, however, that in the chromatography of a product as cod roe some ascorbic acid will be present in the fractions immediately after the main fraction (5 ml extract was reduced by evaporation before being chromatographed), which is presumably due to a too high pH value of the extract. For this reason 0.1 ml hydrochloric acid (about 3 N) was added per 5 ml extract. This addition is based on qualitative experiments which have shown that chromatography of pure ascorbic acid solutions to which had been added 100 mg "HPO_3" (an analytical preparation containing about 60 % $NaPO_3$) — which corresponds to the quantity of "HPO_3" present in 5 ml extract — results in complete separation, *i. e.* no ascorbic acid in the fractions before and after the main fraction. If about half of the $NaPO_3$ present is neutralized by means of 0.1 ml hydrochloric acid (about 3 N), the ascorbic acid will still be retained quantitatively in the main fraction. This means that whenever the pH of the extract is expected to be too high, it is possible to ensure complete separation by adding hydrochloric acid in the above quantities. Only in the case of extracts which required evaporation did it prove necessary to add hydrochloric acid.

A reasonable accuracy is ensured by transferring a quantity of extract which contains 10—30 μg ascorbic acid to the column. If less than this amount of ascorbic acid is present in 0.5 ml of the extract, a suitable volume must be withdrawn and evaporated to a volume which is less than 0.5 ml. Such evaporation is conveniently performed in a 10 ml sample tube by means of a slight stream of electrically heated carbon dioxide. Temperature and rate of flow must be adjusted so that the tube with the sample is just tepid to the touch. The quantity of extract which may be transferred to the column depends on the nature of the extract, as excessive quantities of extracted substances may in the first place impede the quantitative transference of the sample to the column, because after the butanol addition the cellulose powder may become very tacky, and, in the second place, delay the passage of the ascorbic acid so that traces of ascorbic acid may be present in the fractions following the main fraction. The aim of the abovementioned addition of

cellulose powder to the sample is to enable this cellulose powder to adsorb the components of the extract which are precipitated by the 5 ml *n*-butanol added. Qualitative experiments show that when using 100 mg glucose with 0.3 ml water, 100 mg "HPO_3" and 0.1 ml 3 N hydrochloric acid, the fractions before and after the main fraction will be free from ascorbic acid, while when 250 mg glucose is used instead of 100 mg, the fraction after the main fraction will contain traces of ascorbic acid. The sensitivity of the method depends on these factors. As it appears from Table 1, the volume of the largest sample withdrawn for evaporation and chromatography in the course of the present work was 5 ml.

re chromatographic column. The presence of ascorbic acid in the different fractions collected depends, of course, on the dimensions of the chromatographic tube. Experience has shown that the reproducibility is very good from chromatogram to chromatogram using the same chromatographic column. Whether the dimensions of the column are correct may be checked by measuring the length of the column of cellulose powder, which should be between 31 cm and 33 cm, and by test chromatography as described in the following.

Chromatograph 200 μl of the "strong" standard solution (reagent 9), which contains 200 μg ascorbic acid (adding 1 ml acetic acid, a little cellulose powder, and 5 ml *n*-butanol and pouring this mixture into the tube). Collect the following fractions: 1 (34 ml), 2 and 3 (2 × 5 ml), 4 (2 ml), 5 (5 ml), 6 (4 ml), 7 (2 ml), and 8 (5 ml). Discard fraction 1, and to each of the following add 200 μl diazotised nitroanisidine (reagent 10). Extract the dye by shaking with 1 ml 5 % sodium hydroxide solution. Fractions 5 and 6 should contain the ascorbic acid, while fractions 4 and 7 must show only faint traces of blue colour. If tubes of other dimensions are to be used, the procedure of this qualitative chromatographic separation should be modified to indicate the fractions in which the ascorbic acid occurs in this case.

When acetone is used for charging the tube with cellulose powder, a tightly packed and readily reproducible column will be obtained. Treatment with 2 ml of 10 % aqueous solution of the disodium salt of ethylenediamine-NNN'N'-tetraacetic acid prevents oxidation of the ascorbic acid in the column due to catalytic action of copper and, more-

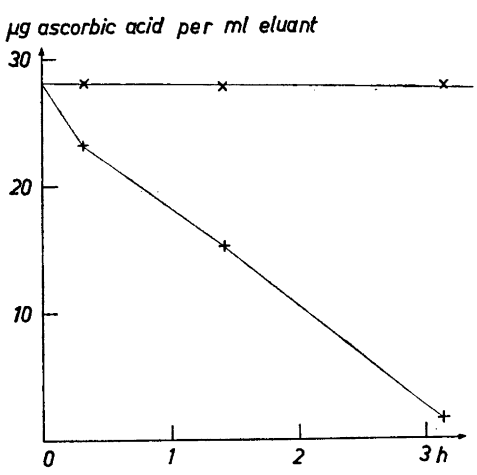

Fig. 1. The stability of ascorbic acid in the eluant (×), compared with the stability in the same medium without ethylenediamine-tetraacetic acid (+). Both solutions were kept at room temperature in artificial light.

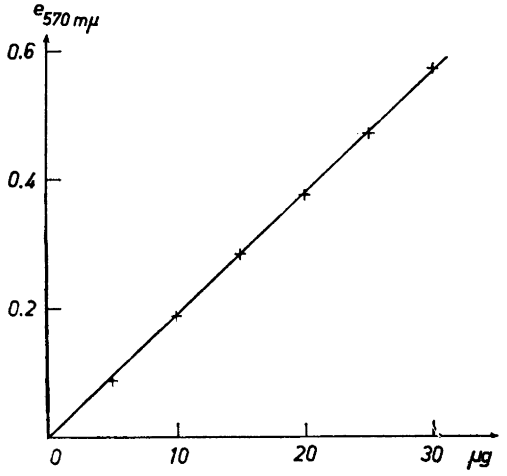

Fig. 2. Standard curve. Abscissa: μg ascorbic acid per 15 ml eluant. Ordinate: extinction at 570 mμ in a 5 cm cell.

over, due to its content of water, ensures that the cellulose powder is saturated with water, which is essential to obtain a reliable chromatographic separation.

re eluant. The eluant should be stabilized by means of ethylenediamine-NNN'N'-tetraacetic acid. The solubility of this substance in the butanol phase is very low, but the stabilizing effect appears clearly from the curve in Fig. 1. Ethylenediamine-NNN'N'-tetraacetic acid does not protect ascorbic acid against the action of light, and artificial illumination should therefore be used throughout. The eluant should be freshly prepared. All distilled water used in these experiments has been condensed in metal equipment and has not been redistilled.

The chromatographic separation is performed rapidly, only 30 min passing from the moment when the sample is transferred to the column and until the final fractions have passed out of the column.

re ascorbic acid determination. The reagent has been chosen with a view to ensure maximum specificity. Experience shows that the extinction of the interfering substances accompanying ascorbic acid in the chromatographic separation generally decreases with increasing wavelength in the range 400 mμ to 600 mμ, consequently a reagent should be chosen which forms a hydrazide of oxalic acid with absorption maximum at the greatest possible wavelength. From this point of view 2-nitro-4-methoxyaniline was the best reagent available.

The interaction of diazotised nitroaniline and ascorbic acid is not instantaneous, maximum yield is obtained by allowing 5—20 min for the reaction.

It is important to follow closely the instructions given with regard to the extraction of the reaction products by means of sodium hydroxide solution. If the mixing of the phases is effected by a slow and cautious shaking, the yield of hydrazide will be reduced.

The colour will not persist for an unlimited period. Following the procedure described, the reduction will be about 1 % per hour at an extinction of 0.400 (corresponding approximately to the 20 μg standard).

In the above description of the procedure the use of only one reference standard sample is prescribed. This has been shown to be justified, as the standard curve (see Fig. 2) has been found to be linear within the range 0—30 μg.

RESULTS AND DISCUSSION

Table 1 summarizes the results of determinations of ascorbic acid obtained by the chromatographic method and by titration with dichlorophenol-indophenol in various biological materials. The following discussion of the specificity and accuracy of the method is based on these measurements taken together with recovery experiments and chromatographic determinations of substances of special nature.

One of the requirements which must be fulfilled to obtain a correct determination of an ascorbic acid content by the chromatographic method is that the extinction determined at 570 mμ in the main fraction derives exclusively from the interaction between the reagent and ascorbic acid. Without a more thorough examination it is not possible to determine whether this is the case. There may be coloured substances in the extract which pass out together with ascorbic acid in the main fraction and is transferred from here to the sodium hydroxide phase, and there may be ascorbic acid analogs which are not separated by chromatography and which react with the reagent in the same way as ascorbic acid.

As it appears from the table illustrating the chromatographic separations performed (Table 1), experience shows, however, that the extinctions measured in the fractions before and after the main fraction are small in the case of nearly all materials. It has been assumed, therefore, that coloured substances

Table 1. Content of ascorbic acid in some natural products and foodstuffs.

Sample	ml extract for chrom-ato-graphy	Extinction at 570 mμ in 5 cm cell			mg ascorbic acid per 100 g determined by	
		Fraction before main fraction	Main fraction	Fraction after main fraction	chrom-ato-graphy	titration
Strawberries	0.2	0.005	0.506	0.001	89.5	88.5
Cauliflower (white head)	0.2	0.002	0.520	0.002	90.5	88.0
Parsley	0.1	0.002	0.547	0.001	192	186
Dill	1	0.039	0.421	0.001	33.5	35.0
Gooseberries (green)	0.2	0.006	0.319	0.000	54.0	51.5
Peas (green)	0.4	0.011	0.445	0.010	47.0	52.0
Potatoes (new)	0.4	0.007	0.375	0.002	27.5	30.0
Oranges	0.2	0.006	0.399	0.005	49.5	47.5
Orange juice (canned)	0.5	0.007	0.318	0.006	31.0	33.5
Broccoli	0.2	0.006	0.309	0.004	145	148
Tomatoes	1	0.010	0.460	0.006	12.5	12.6
Black currant syrup	0.5	0.011	0.354	0.016	55.0	59.0
Beetroot	2	0.005	0.200	0.223	3.6 (max.)	8.9
Milk	4	0.022	0.388	0.017	0.97	1.12
Liver, calf	0.5	0.013	0.357	0.011	22.5	27.5
Kidney, calf	2	0.007	0.565	0.006	9.6	11.2
Rat skin	5	0.012	0.337	0.009	2.8	3.5
Cod roe 1	5	0.001	0.332	0.011	2.9	4.4
» » 2	5	0.025	0.446	0.013	3.9	6.4
Cauliflower (a)	0.5	−0.006	0.231	0.015	19.6	36.2
Tomatoes (a)	1	0.004	0.219	0.020	8.9	22.1
Vegetables, unspecified (a)	1	0.015	0.083	0.009	6.1	35

(a) Dehydrated products, commercial

do not generally cause interference and that the blank value of the main fraction may therefore with reasonable accuracy be determined as the mean value of the extinctions of the fractions immediately before and after the main

Table 2. Recovery of ascorbic acid after chromatography.

Ascorbic acid chromatographed μg	Extract ml	Ascorbic acid recovered μg	Ascorbic acid recovered %
20.0	0.2	20.1	100
20.0	0.2	20.4	102
20.0	0.2	19.9	100
20.0	5 [a]	20.4	102
20.1	5 [b]	20.0	100

a. 5 ml extract of cod roe in 2 % metaphosphoric acid + 0.1 ml appr. 3 N hydrochloric acid + a solution of dichlorophenolindophenol until total oxidation of ascorbic acid. Excess of oxidizing agent is destroyed by allowing the acid solution to stand overnight. 20.0 μg of ascorbic acid is added and the solution is reduced by evaporation to a volume of less than 0.5 ml.

b. 5 ml of a solution of 2 % metaphosphoric acid to which 20.2 μg ascorbic acid is added, is evaporated till the volume is less than 0.5 ml.

fraction. As an exception may be mentioned the highly coloured beet root extract, in the case of which the extinction of the fraction after the main fraction is too high to be used as a blank, and that the ascorbic acid value found therefore must be considered merely to represent a maximum value. Incidentally, this very low value as compared to the titration value tends to confirm the results obtained by Somer *et al.*[12]

*Iso*ascorbic acid and glucoascorbic acid interact with the diazonium reagent and with sodium hydroxide to form the same hydrazide as ascorbic acid. It is impossible by chromatography to separate *iso*ascorbic acid and ascorbic acid, while glucoascorbic acid will follow immediately after ascorbic acid in the chromatogram, *i.e.* in the fraction after the main fraction. Consequently it is not possible according to this method to distinguish between ascorbic acid and *iso*ascorbic acid. Other substances, related to ascorbic acid, which might be expected to interfere in the analysis in this way have not been studied.

In addition to the condition mentioned in the above, which must be fulfilled to ensure correct results, the main fraction must not contain substances the presence of which results in a reduction of the yield obtained from the reaction.

Sulphur dioxide may interfere in this way, since it passes the chromatographic column together with ascorbic acid, resulting in too low ascorbic acid values. If thus the molar ratio of sulphur dioxide to ascorbic acid is as 1:1, the yield of hydrazide will be 5 % too low. However, sulphur dioxide may be removed from the acid extract by bubbling carbon dioxide through the solution.

The reliability of the method in general may be judged by comparing the results obtained when applying the titration method and the chromatographic

method to vegetables and fruits and also by the results of recovery experiments, as those represented in Table 2.

All ascorbic aid determinations hitherto made according to the described method have been included in Table 1. Agreement between the results obtained according to the two methods are seen to be fairly good with regard to most of the vegetables, while considerably lower values are found in the case of products of animal origin and dehydrated vegetables. It should be mentioned that the titrations have been performed by means of dichlorophenol-indophenol, if necessary after extraction with chloroform (a modification of the xylene method [13] generally used with coloured or turbid extracts), without any attempt at improvement of the specificity.

It will be seen that in the case of nearly all the samples the extinction values obtained from fractions before and after the main fraction are small; this applies also to the samples with regard to which chromatography of 5 ml extract was necessary.

It appears from the recovery experiments (Table 2) that the losses resulting both from chromatography and evaporation are very small. An experiment with cod roe extract, in which the ascorbic acid was first oxidized with dichlorophenol-indophenol before the addition of the 20 μg ascorbic acid, also shows that the content of ascorbic acid is maintained quantitatively throughout the procedure.

The sensitivity of the method depends on the nature of the sample and on the demands made as to accuracy. It appears from Table 1 that in protein-containing materials, as for instance cod roe, it is possible to determine ascorbic acid contents down to a concentration of about 3 mg per 100 g without reducing the demands as to a reasonably large deflection of the measuring instrument.

Note added in proof. Apples contain a colourless substance (or several substances) which very nearly follows ascorbic acid on the column and gives a reddish colour with the reagent, thereby interfering with the determination. The chemical nature of the substance has not been investigated.

The author wishes to thank Dr. phil. Willy Hjarde for his very kind interest in this study.

REFERENCES

1. Tillmans, J. *Z. Untersuch. Lebensm.* **60** (1930) 34.
2. Harris, L. J. and Olliver, M. *Biochem. J.* **36** (1942) 155.
3. Sebrell, W. H. and Harris, R. S. (Eds.) *The Vitamins*, Academic Press inc., New York 1954, Vol. I, p. 253.
4. Roe, J. H. and Kuether, C. A. *J. Biol. Chem.* **147** (1943) 399.
5. Schmall, M., Pifer, C. W. and Wallish, E. G. *Anal. Chem.* **25** 1486.
6. Moor, H. *Mitt. Gebiete Lebensm. u. Hyg.* **47** (1956) 20.
7. Ulmann, M. *Pharmazie* **9** [6] (1954) 523.
8. Chen, Y. T., Isherwood, F. A. and Mapson, L. W. *Biochem. J.* **55** (1953) 821.
9. Kadin, K. and Osadca, M. *Agr. Food. Chem.* **7** (1959) 358.
10. Bro-Rasmussen, F. and Hjarde, W. *Acta Chem. Scand.* **11** (1957) 34. (Fig. 1.)
11. Baker, L. C., Lampitt, L. H. and Wittenberg, E. *J. Sci. Food Agr.* **6** (1955) 682.
12. Somers, G. F., Kelly, W. C., Thacker, E. J. and Redder, A. M. *Food Research* **16** (1951) 62.
13. Pepkowitz, L. P. *J. Biol. Chem.* **151** (1943) 405.

Received December 21, 1959.

ACTA CHEMICA SCANDINAVICA 14 (1960) 814–822

Studies on the Hydrolysis of Metal Ions

28. Application of the Self-medium Method to the Hydrolysis of Lead(II) perchlorate Solution

ÅKE OLIN

Department of Inorganic Chemistry, Royal Institute of Technology, Stockholm 70, Sweden

The hydrolysis of Pb(II) has been studied at high Pb^{2+} concentrations, B, in order to enhance the relative amounts of species with a OH^-/Pb(II) ratio < 1. The equilibrium solutions measured had the general composition

B M Pb(II), H M H^+, $(3-2B-H)$ M Na^+, 3 M ClO_4^-

and the hydrolysis was followed to $Z = 0.15$ for $B = 1.490$, 0.990 and 0.500 M. Z is the average number of OH^- groups bound to each Pb(II). If it is assumed that the activity factors stay constant at low Z, the data up to $Z = 0.10$ may be interpreted by the following reactions and equilibrium constants

$4\,Pb^{2+} + 4H_2O \rightleftharpoons Pb_4(OH)_4^{4+} + 4H^+$; $\log \beta_{4,4} = -19.25$ ($B = 0.50$ M), -19.23 ($B = 0.99$ M), -19.28 ($B = 1.49$ M).

$2Pb^{2+} + H_2O \rightleftharpoons Pb_2OH^{3+} + H^+$; $\log \beta_{1,2} = -6.45$ ($B = 0.50$ M), -6.45 ($B = 0.99$ M), -6.34 ($B = 1.49$ M)

For higher values of Z deviations appear which may be due either to complexes other than Pb_2OH^{3+} and $Pb_4(OH)^{4+}$ or to variations in the activity factors.

In a previous study [1], where the hydrogen ion concentration and the concentration of Pb^{2+} in hydrolysed lead(II) perchlorate solutions were measured, evidence was presented for the formation of the species $Pb_4(OH)_4^{4+}$, $Pb_3(OH)_4^{2+}$, $Pb_6(OH)_8^{4+}$ and $PbOH^+$. At the highest Pb(II) concentrations then studied (0.080 M and 0.040 M) there were indications of complexes with a OH^-/Pb(II) ratio < 1 at small degrees of hydrolysis. However the concentrations of these complexes were so small that their formulas could not be found. The self-medium method recently used by Hietanen and Sillén [2] in studies on the hydrolysis of Th^{4+} and UO_2^{2+} seemed to be useful for solving the present problem. The concentration of the unknown species could be expected to be favored by a high metal ion concentration.

When we are dealing with complicated equilibria in solution it is desirable to keep the activity factors constant so that concentrations can be used instead of activities in the law of mass action. Usually this is brought about by the addition of a large amount of a neutral salt. This method has been termed the inert medium method. However if only a minor part of the ions in for example a concentrated metal salt solution is converted to other species by complex formation one might hope that the ionic invironment would be but slightly changed and that therefore as a good approximation concentrations could be used instead of activities. Future experience with the method will show how far this approximation can be used. In the following we shall assume that the activity factors stay constant in the Z range studied here.

The more common symbols used are listed below for reference.

B total concentration of Pb(II)
b concentration of Pb^{2+}
H analytical hydrogen ion concentration (often negative)
h actual hydrogen ion concentration
Z average number of OH^- groups bound per Pb(II) atom
$\beta_{p,q}$ equilibrium constant for the reaction $qPb^{2+} + pH_2O \rightleftharpoons Pb_q(OH)_p^{(2q-p)+} + pH^+$

$y(x)_v$ y as a function of x at constant v
All concentrations are expressed in mole/l (M).

EXPERIMENTAL

Method and apparatus. In the present study we have made a minor alteration in the original method and decided to add $NaClO_4$ to our solutions so that they were always 3 M in ClO_4^-. At the highest total lead(II) concentration studied, 1.490 M, the compositions of the solutions corresponded to the self-medium idea but for the lower values of B the compositions of the solutions approached the inert medium method, but with the restriction that Z was allowed to reach a value of *ca* 0.1 only. The limit set for Z is quite arbitrary. The highest value of Z for which the approximation of constant activity factors may be used, is probably dependent on what species are formed. It may also be dependent on B.

The general composition of the solutions, S, investigated was

B M Pb(II), H M H^+, $(3-2B-H)$ M Na^+, 3 M ClO_4^-

The values of B used were 1.490, 0.990 and 0.500 M. B was kept constant in each run and H was varied by the addition of NaOH. The experiments were carried out as potentiometric titrations in an oil thermostat at 25.0°C. Log h was measured with a calibrated glass electrode using the cell

$$(-) \text{ ref / S / glass } (+) \quad \text{(I)}; \; E = E^0 + 59.15 \log h + E_j \qquad (1)$$

The reference half-cell used was

$$\text{ref} = 3 \text{ M } ClO_4^-, \; (3-2B) \text{ M } Na^+, \; B \text{ M Pb(II) / Pb–Hg}$$

The emf of cell (I) was registered on a Radiometer valve potentiometer (PHM4) to ± 0.2 mV.

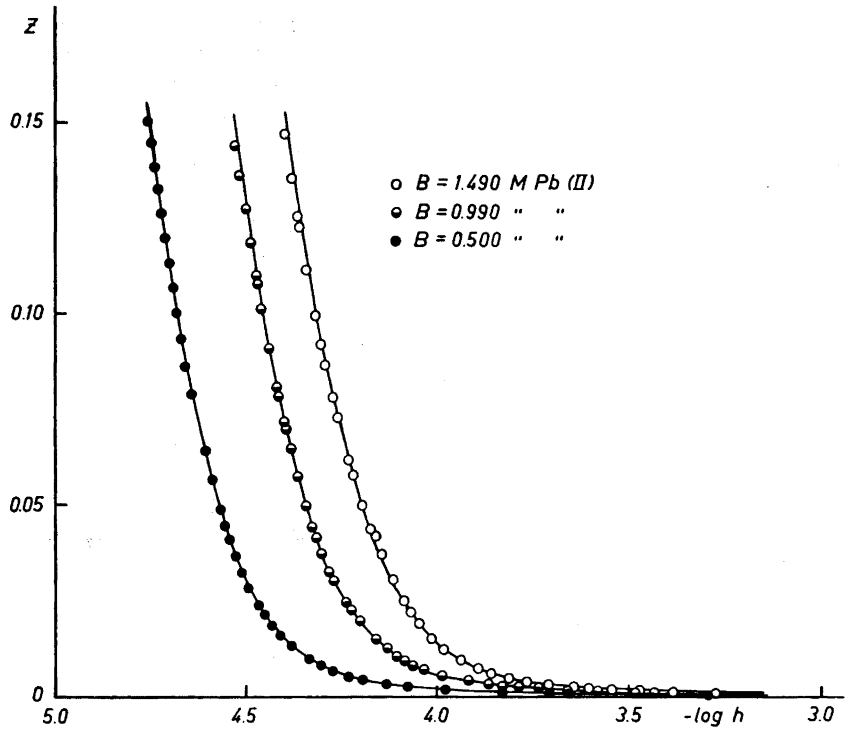

Fig. 1. Z, average number of OH^- bound per Pb(II) atom as a function of log h. Drawn curves have been calculated with the equilibrium constants given in the text.

Experimental details. The liquid junction potential, E_j, in cell (I) was determined in acid solution for $0.005 < h < 0.025$ M by replacing the glass electrode by a lead amalgam electrode. E_j was calculated from the emf's by the procedure described by Biedermann and Sillén [3]. The values thus found could be represented by $E_j = -(18 \pm 3)\,h$. The experimental accuracy did not allow us to determine the coefficient more accurately than this. For the calculations of our experimental quantities, E°, log h and Z this uncertainty was without importance. The numerical value of the coefficient is reasonable considering the value -16.7 found with 3 M $(Na)ClO_4$.

The starting solution contained B M Pb(II) and *ca.* 0.025 M $HClO_4$ in 3 M $(Na)ClO_4$. Equal volumes of NaOH solution and a solution of $Pb(ClO_4)_2$ of concentration $2B$ in 6 M $(Na)ClO_4$ were added from two burets thus keeping $[Pb(II)] = B$ and $[ClO_4^-] = 3$ M during a run. The first few points for $H > 0.01$ M were used to determine E° and the analytical hydrogen ion concentration of the starting solution by a Gran extrapolation [4]. This provided us with a check, since this concentration was also known from the analysis of the stock solutions used to prepare the starting solution.

Two NaOH solutions of different strengths were employed in each titration. The first solution (*ca* 0.15 M) was used to determine E° and to study the hydrolysis for $Z < 0.02$. The second base solution (at least 0.75 M) was then introduced and Z followed to 0.15. We had to use such a strong base in order to limit the volume of solution to a reasonable amount. When the strong base was added a large amount of precipitate was formed. On shaking the precipitate immediately dissolved without leaving any residue. At least three titrations were made for each value of B.

Table 1. Corresponding values of $-\log h$ and Z.

○ $B = 1.490$ M. Run I. $-\log h, Z$ 2.736, 0.0002; 3.274, 0.0009; 3.600, 0.0022; 3.739, 0.0035; 3.808, 0.0048; 3.854, 0.0060; 3.888, 0.0072; 3.933, 0.0094; 3.977, 0.0122; 4.008, 0.0147; 4.050, 0.0194; 4.075, 0.0240; 4.112, 0.0300; 4.158, 0.0416; 4.217, 0.0577; 4.263, 0.0726; 4.290, 0.0864; 4.305, 0.0927; 4.315, 0.0993; 4.341, 0.1095; 4.341, 0.1113; 4.359, 0.1224; 4.364, 0.1254; 4.380. 0.1354; 4.400, 0.1472.

Run II. $-\log h, Z$ 3.382, 0.0012; 3.470, 0.0015; 3.539, 0.0018; 3.637, 0.0025; 3.678, 0.0029; 3.705, 0.0032; 3.771, 0.0042; 3.972, 0.0118; 3.996, 0.0139; 4.010, 0.0154; 4.028, 0.0168; 4.040, 0.0187; 4.057, 0.0204; 4.063, 0.0220; 4.075, 0.0238; 4.079, 0.0253; 4.112, 0.0305; 4.143, 0.0371; 4.172, 0.0435; 4.195, 0.0500; 4.227, 0.0615; 4.256, 0.0721; 4.271, 0.0780.

◒ $B = 0.990$ M. Run I. $-\log h, Z$ 3.431, 0.0010; 3.654, 0.0017; 3.783, 0.0024; 3.862, 0.0032; 3.915, 0.0039; 3.982, 0.0054; 4.026, 0.0067; 4.060, 0.0080; 4.082, 0.0093; 4.102, 0.0104; 4.126, 0.0126; 4.151, 0.0146; 4.219, 0.0225; 4.268, 0.0300; 4.298, 0.0372; 4.324, 0.0442; 4.364, 0.0573; 4.393, 0.0694; 4.418, 0.0807; 4.440, 0.0910; 4.459, 0.1009; 4.474, 0.1099; 4.488, 0.1183; 4.501, 0.1264.

Run II. $-\log h, Z$ 3.480, 0.0011; 3.578, 0.0014; 3.729, 0.0021; 3.825, 0.0028; 3.952, 0.0046; 3.982, 0.0054; 4.101, 0.0103; 4.156, 0.0151; 4.197, 0.0198; 4.234, 0.0244; 4.282, 0.0332; 4.314, 0.0416; 4.341, 0.0496; 4.363, 0.0572; 4.381, 0.0646; 4.398, 0.0715; 4.413, 0.0782; 4.440, 0.0905; 4.469, 0.1077; 4.496, 0.1273; 4.520, 0.1360; 4.532, 0.1440.

● $B = 0.500$ M. Run I. $-\log h, Z$ 3.292, 0.0002; 4.129, 0.0030; 4.270, 0.0065; 4.332, 0.0097; 4.380, 0.0128; 4.408, 0.0157; 4.430, 0.0184; 4.449, 0.0211; 4.464, 0.0235; 4.491, 0.0282; 4.510, 0.0324; 4.525, 0.0365; 4.542, 0.0406; 4.566, 0.0485; 4.589, 0.0563; 4.608, 0.0640; 4.642, 0.0788; 4.667, 0.0930; 4.691, 0.1066; 4.711, 0.1197; 4.730, 0.1323; 4.746, 0.1445.

Run II. $-\log h, Z$ 3.653, 0.0006; 3.705, 0.0007; 3.828, 0.0010; 3.977, 0.0016; 4.074, 0.0023; 4.190, 0.0041; 4.229, 0.0051; 4.302, 0.0081; 4.555, 0.0446; 4.659, 0.0859; 4.682, 0.0998; 4.701, 0.1132; 4.721, 0.1260; 4.740, 0.1383; 4.758, 0.1502.

The equilibria were rapidly established. Within 10 min after each addition of base the emf of the glass electrode showed a constant value.

The $NaClO_4$, $HClO_4$ and NaOH solutions used in the present investigation were prepared and analysed as described previously [1].

The $Pb(ClO_4)_2$ solution was prepared by dissolving PbO (Baker, p.a.) in $HClO_4$ (Kebo, p.a.). The following procedure was used. The oxide was first repeatedly washed with distilled water and then dissolved in acid using an excess of the oxide. This gave us a slightly alkaline solution which was left standing for a week in order to precipitate foreign metal ions as the hydroxides. After filtration the solution was analysed to determine the deficit of hydrogen ions, and a calculated amount of $HClO_4$ was added in order to give the solution the analytical composition $Pb(ClO_4)_2$. Upon addition of the acid the solution turned light brown from the presence of tetravalent lead. The PbO_2 was destroyed by adding platinum black and bubbling with H_2 gas for a few hours. The solution so prepared was optically blank (reference H_2O) for $\lambda > 2\,800$ Å. At $\lambda \sim 2\,800$ Å Pb(II) started to absorb light as indicated by a very rapid increase in the optical density of the solution.

The analysis of the solution was done as described previously [1].

RESULTS AND CONCLUSIONS

The data are presented giving Z as a function of $\log h$ in Fig. 1 and Table 1. Z is the average number of OH^- groups bound per lead(II) atom.

The hydrolysis was followed till Z reached *ca* 0.15. Our basic assumption will be that the activity factors stay constant at low values of Z. However we do not know the value of Z above which this ceases to be true.

We shall start our attempt to interpret the data by comparing the experimental $Z(\log h)_B$ with theoretical curves calculated on the assumption that only one of the complexes $(PbOH^+)_n$ with $n = 1, 2, \ldots$ is formed. From such a comparison we get an idea of how many OH^- groups are present in the complexes formed. The choice of a ratio $OH^-/Pb(II) = 1$ in the complexes is quite arbitrary, but since the number of metal atoms in the complex is less important than the number of OH^- groups in fixing the shape of the $Z(\log h)_B$ curve, a not too large change in this ratio would not alter our conclusions.

The 0.500 M titration fits well the theoretical $Z(\log h)$ curve for $Pb_4(OH)_4^{4+}$ at high values of Z. At lower values of Z the experimental curve is less steep than the theoretical curve. Complexes with $n = 4$ are thus indicated at high Z. At low Z complexes with < 4 OH^- must also be present.

The 0.990 M titration for high values of Z showed agreement with the theoretical $Z(\log h)$ curve for $Pb_3(OH)_3^{3+}$. However if the theoretical and experimental curves were made to fit at high Z values, the experimental curve became steeper than the theoretical curve at intermediate values of Z; this is an impossible result. At low Z the reverse is true. The same statements hold for the 1.490 M titration. From these two titrations we may draw the conclusion that at low Z complexes with < 3 OH^- are formed. It would appear unlikely that both $Pb_3(OH)_3^{3+}$ and $Pb_4(OH)_4^{4+}$ are present simultaneously in comparable amounts. If such were the case the deviations from the theoretical $Z(\log h)_B$ curve for $Pb_4(OH)_4^{4+}$ would have been most pronounced for $B = 0.500$ M, since a lower value fo B favors the formation of $Pb_3(OH)_3^{3+}$ relative to $Pb_4(OH)_4^{4+}$. No evidence for $Pb_3(OH)_3^{3+}$ was found in the previous work with 3 M $(Na)ClO_4$ medium.

It would be very reasonable if $Pb_4(OH)_4^{4+}$ it the main complex formed at high Z. This complex has been shown in a previous work [1] to predominate for lower B values in the Z region now investigated. The position of the $Z(\log h)_B$ curves on the log h axis is also in agreement with the value of $\log \beta_{4,4} = -21.25$ found earlier.

Now we turn to the data for very low Z. Whereas at low Z practically no information can be obtained from a single $Z(\log h)_B$ curve about the number of metal atoms in a complex, we can group the complexes with regard to the number of OH^- groups they contain. Also we are allowed to put $b \simeq B$. Thus we get

$$Z = \Sigma\, \beta_{1,q}\, B^{q-1}h^{-1} + 2\,\Sigma\, \beta_{2,q}B^{q-1}h^{-2} + \ldots p\,\Sigma\, \beta_{p,q}B^{q-1}h^{-p} \qquad (2)$$

If complexes with a certain value of p predominate we find

$$(\partial \log Z/\partial \log h)_B = -p \qquad (3)$$

A plot of log Z *versus* log h should then yield a straight line and p is found from the slope of this line. The presence of complexes with different values of p would give a curved line.

Provided that the changes of the activity factors are not too large on going from one value of B to another, information on the value of q can be found

from $(\partial \log Z/\partial \log B)_h$. For the case that complexes with one value only for q are present the difference quotient is equal to $(q-1)$.

Owing to the large value of the formation constant for $Pb_4(OH)_4^{4+}$, as estimated from the upper parts of the $Z(\log h)_B$ curves, the term for this complex in eqn. (2) is small only if $Z < 0.003$. Therefore it is necessary to substract the term for this complex in order to get a reasonably broad range in Z and $\log h$ from which to determine p.

The term for $Pb_4(OH)_4^{4+}$ was calculated with $b = B$ and assuming $\log \beta_{4,4} = -19.25$ which is the value found from the measurements with 3 M (Na)ClO_4. The choice is somewhat arbitrary but from the 0.500 M titration a value close to -19.25 was indicated by "curve fitting" against a normalized $Z(\log h)$ curve. The Z corrected for $[Pb_4(OH)_4^{4+}]$ will be denoted by Z_c. The calculations were performed only for $Z < 0.01$. The correction at this value of Z is *ca.* 0.005.

The $\log Z_c(\log h)_B$ plots did not deviate much from linearity, and the best straight lines were drawn through the points. The values of the slopes of these lines $(= -p)$ were, $B = 0.500$ M, $p = 1.1$; $B = 0.990$ M, $p = 1.0$; $B = 1.490$, $p = 1.1$. Since p must be a whole number we may conclude $p = 1$. The average value of $(\Delta \log Z_c/\Delta \log B)_h$ was 1.2. This would indicate $q = 2$.

From the above considerations it seems likely that the complex Pb_2OH^{3+} is formed at low Z. This complex has a ratio $OH^-/Pb(II) = 0.5$ whereas the ratio $OH^-/Pb(II) = 1$ in $Pb_4(OH)_4^{4+}$. The quotient $[Pb_2OH^{3+}]/[Pb_4(OH)_4^{4+}]$ would thus be expected to increase with B keeping Z constant. This is in agreement with the experimental results. The deviation of the experimental curves from the calculated $Z(\log h)_B$ curve for $Pb_4(OH)_4^{4+}$ is most pronounced for $B = 1.490$ M. Since the value of q is uncertain we shall briefly discuss other possibilities. For $q = 1$ we would have $PbOH^+$. This complex cannot predominate at low Z because the deviations from the theoretical curve should then be most pronounced for $B = 0.500$ M. From the value of $\log \beta_{1,1} = -7.9$ obtained with 3 M (Na)ClO_4 medium one would also expect the concentration of $PbOH^+$ to be very small. Values of $q > 2$ seem increasingly less likely from the geometry of the complexes. We will thus try to explain our data on the assumption that $Pb_4(OH)_4^{4+}$ and Pb_2OH^{3+} are the only important complexes formed.

Hietanen and Sillén [2] have outlined a method by which two equilibrium constants can be determined by fitting the experimental $Z(\log h)_B$ curves to a family of normalized curves. The shape of each normalized curve is determined by a parameter containing the two equilibrium constants. When the normalized curve has been found which fits the experimental curve best one equilibrium constant is found from the difference between the coordinates on the $\log h$ axes and the other from the parameter. This method has the advantage that it is based on a direct comparison of the experimental $Z(\log h)_B$ with the normalized curves. Therefore its is easier to judge if differences observed between the experimental and normalized curves are reasonable or not.

Now we shall derive the expression for our set of complexes Pb_2OH^{3+} and $Pb_4(OH)_4^{4+}$.

$$B = b + 2\beta_{1,2}b^2h^{-1} + 4\beta_{4,4}b^4h^{-4} \quad (4)$$

$$BZ = \beta_{1,2}b^2h^{-1} + 4\beta_{4,4}b^4h^{-4} \quad (5)$$

It will prove convenient to introduce

$$v = 4B\beta_{1,2}h^{-1} \text{ and } l = \beta_{4,4}/(4B\beta_{1,2}^4) \quad (6), (7)$$

Eliminating b we find

$$Z = v^{-1}(\sqrt{1 + v(1-Z)} - 1)^2 + l(\sqrt{1 + v(1-Z)} - 1)^4 \quad (8)$$

We were not able to express Z as a function of v explicitly. The $Z(-\log v)_l$ curves had to be calculated by successive approximations for each value of l tested. These calculations proved to be very timeconsuming. Therefore it was decided to determine preliminary values of $\beta_{1,1}$ and $\beta_{4,4}$ first. It may be noted, as can be seen directly from eqn. (8), that $Z(\log [h(1-Z)^{-1}])_B$ curves can be normalized explicitly. However we preferred a direct comparison with the experimental $Z(\log h)_B$ data.

Determination of preliminary values of $\beta_{1,2}$ and $\beta_{4,4}$. If approximate values of the equlibrium constants are known we can calculate l from eqn. (7). Then we know beforehand for what values of l our family of normalized curves can be expected to fit the experimental curves thus reducing the number of $Z(-\log v)_l$ curves which need to be calculated.

We shall determine the preliminary values of $\beta_{1,2}$ and $\beta_{4,4}$ from a projection map described by Biedermann and Sillén [5] (See also Ref.[6]). The formulas derived in Ref. [5] were used for calculations on systems where a transition from mononuclear to polynuclear complexes takes place. However analogous formulas can be derived for the case in which one polynuclear complex changes to another complex which is also polynuclear. In the present study we have a transition from Pb_2OH^{3+} to $Pb_4(OH)_4^{4+}$.

$$Z = \frac{\beta_{1,2}bh^{-1} + 4\beta_{4,4}b^3h^{-4}}{1 + 2\beta_{1,2}bh^{-1} + 4\beta_{4,4}b^3h^{-4}} \quad (9)$$

The following substitutions are introduced

$$k^3 = 4\beta_{4,4}; \quad u = kbh^{-4/3}; \quad v = \beta_{1,2}bh^{-1} \quad (10), (11), (12)$$

As the coordinates for the experimental data we shall use

$$x = \log B - \log h \quad (13)$$

$$y = \log B - 4/3 \log h \quad (14)$$

and as the corresponding coordinates for the projection map we shall use

$$X = x + \log \beta_{1,2} \quad (13a)$$

$$Y = y + \log k \quad (14a)$$

It is easily verified that

$$X = \log v + \log (1 + 2v + u^3) \quad (15)$$

$$Y = \log u + \log (1 + 2v + u^3) \quad (16)$$

$$Z = \frac{v + u^3}{1 + 2v + u^3} \quad (17)$$

Thus we can calculate $Y(X)_Z$ curves for different values of Z as the parameter. These curves are then fitted to the experimental $y(x)_Z$ curves and the equilibrium constants found from the differences between the coordinates on the axes. Cuts were made at $Z = 0.01$, 0.02, 0.03, 0.04 and 0.05. Since each $Z(\log h)_B$ curve has to be treated independently the $y(x)_Z$ curve degenerates to a single point. The method, in fact, is closely related to that given in Ref [7].

Final adjustment of $\beta_{1,2}$ *and* $\beta_{4,4}$. With l found from the values of $\beta_{1,2}$ and $\beta_{4,4}$ determined by means of the projection map, normalized curves were calculated. In addition curves were constructed also for values of l somewhat smaller and higher than those obtained from the preliminary $\beta_{1,2}$ and $\beta_{4,4}$.

It was not possible to find constants which could reproduce the data up to $Z = 0.15$ for the two highest values of B. The equilibrium constants given in the table account for the data to 0.001 Z unit or better in the Z range given in the fourth column.

B	$\log \beta_{1,2}$	$\log \beta_{4,4}$	Z
0.500 M	-6.45 ± 0.1	-19.25 ± 0.1	<0.15
0.990 M	-6.45 ± 0.1	-19.23 ± 0.1	<0.12
1.490 M	-6.34 ± 0.1	-19.28 ± 0.1	<0.10

We do not know the reason for the bad agreement at high Z for the two largest values of B. Beside experimental errors as an explanation it may be suggested either that complexes other than Pb_2OH^{3+} and $Pb_4(OH)_4^{4+}$ are also present or that the change in the ionic medium is too large for the activity factors to remain constant. The change of the ionic medium is larger the larger B is and one would expect the variations of the activity factors to show up for $B = 1.490$ M first. On the other hand the relative concentrations of complexes with a OH^-/Pb(II) ratio < 1 increase with B. We have not tried to achieve a better fit by introducing more complexes than those already considered because of the uncertainty of the activity factors.

The values of E^o obtained by putting $h = H$ in eqn. (1) for $0.010 < H < 0.025$ M may be slightly in error. Actually $h = H + [Pb_2OH^{3+}] + 4[Pb_4(OH)_4^{4+}]$. From the equilibrium constants we find that $[Pb_2OH^{3+}]$ would make h somewhat larger than H. $[Pb_4(OH)_4^{4+}]$ is very small and can be neglected. The error in E^o thus introduced is 0.2 mV at most. Practically this error is without importance for our conclusions and would only mean that the $Z(\log h)_B$ curves are slightly displaced along the log h axis.

Another error is caused by the neglect of the liquid junction potential between the hydrolysed solution and the solution in the reference half-cell. Using Henderson's equation and unpublished conductance data by G. Biedermann E_j was calculated to be *ca* 0.2 mV for the solutions of highest Z. Thus the error introduced by neglecting E_j is small.

The close agreement between the numerical values of the equilibrium constants for the different lead(II) concentrations is intriguing considering the differences in the cat-ionic part of the medium. The reason might be that the ratios of the activity factors in the law of mass action expression for the formation of these complexes stay constant, even though the individual activity factors vary. Hietanen and Sillén [2] have observed that the differences

between the numerical values of equilibrium constants which have been determined both with the inert medium method and with the self-medium method are of the order of 0.1 logarithmic unit. This appears to hold also for the formation constant of $Pb_4(OH)_4^{4+}$.

As was mentioned in the introduction previous measurements [1] with 3 M $(Na)ClO_4$ medium indicated the presence of complexes with a $OH^-/Pb(II)$ ratio < 1 at low Z and $B = 0.080$ M and 0.040 M from the fact that the experimental $OH^-/Pb(II)$ ratio was somewhat smaller than 1. The main complex in these solutions was identified as $Pb_4(OH)_4^{4+}$ but the concentrations of the other complexes with a $OH^-/Pb(II)$ ratio < 1 were so small that their formulas could not be found. Assuming $\beta_{1,2}$ to have the same value in 3 M $(Na)ClO_4$ medium as found here the concentration of Pb_2OH^{3+} was calculated from the previously published data. Except for the 0.080 M and 0.040 M titrations at low Z, $[Pb_2OH^{3+}]$ was found to be very small and, for these concentrations, to be consistent with the experimentally found $OH^-/Pb(II)$ ratios.

The formation of complexes of the general composition Me_2OH appears to be quite common. From measurements on hydrolysed $Pb(NO_3)_2$ solutions Pedersen [9] has earlier found evidence for Pb_2OH^{3+}. The value of log $\beta_{1,2}$ (extrapolated to zero ionic strength) found by him was -7.3. Other metal ions for which hydrolysis data have indicated such complexes include Be^{2+} (Ref.[8]), Cu^{2+} (Ref.[10]), UO_2^{2+} (Ref. [11]), and Th^{4+} (Ref. [2]). For the last three ions the complex only is present in appreciable concentrations for high values of B.

Acknowledgements. The author wishes to thank Professor Lars Gunnar Sillén for suggesting this work and for his continual interest in it. He also wishes to thank Professor Robert E. Connick, Univ. of Calif., for helpful comments on the manuscript. Thanks are due also to Dr. Georg Biedermann for helpful suggestions on various problems connected with this work and to Mr. György Patzauer for skilful help with the calculations. The apparatus used was constructed by Mr. F. Ericson. The English of this paper has been corrected by Dr. F. Holmes. This work has been supported by *Statens Tekniska Forskningsråd (Swedish Technical Research Council)* and by the *Air Force Office of Scientific Research of the Air Research and Development Command, United States Air Force,* through its European Office.

REFERENCES

1. Olin, Å. *Acta Chem. Scand.* **14** (1960) 126.
2. Hietanen, S. and Sillén, L. G. *Acta Chem. Scand.* **13** (1959) 533.
3. Biedermann, G. and Sillén, L. G. *Arkiv Kemi* **5** (1953) 425.
4. Gran, G. *Analyst* **77** (1952) 661.
5. Biedermann, G. and Sillén, L. G. *Acta Chem. Scand.* **10** (1956) 1011.
6. Sillén, L. G. *Acta Chem. Scand.* **10** (1956) 803.
7. Rossotti, F. J. C., Rossotti, H. and Sillén, L. G. *Acta Chem. Scand.* **10** (1956) 203.
8. Kakihana, H. and Sillén, L. G. *Acta Chem. Scand.* **10** (1956) 985.
9. Pedersen, K. J. *Kgl. Danske Videnskab Selskab Mat.-fys. Medd.* **22** (1945) No. 10.
10. Pedersen, K. J. *Kgl. Danske Videnskab Selskab Mat.-fys. Medd.* **20** (1943) No. 7.
11. Hietanen, S. and Sillén, L. G. *Acta Chem. Scand.* **13** (1959) 1828.

Received December 23, 1959.

ACTA CHEMICA SCANDINAVICA 14 (1960) 823–828

A New Method of Investigating the Enzymatic Inversion of Sucrose

BJØRN ANDERSEN and THOR A. BAK

Universitetets Fysisk-Kemiske Institut, Copenhagen

A new way of investigating the enzymatic inversion of sucrose is described. The reaction is followed by measuring the optical rotation of the solution, but instead of taking out samples in which the reaction can be stopped and measuring the optical rotation after the mutarotation of glucose and fructose has stopped, the measurements are performed directly on the reacting solution and a correction for the mutarotation is applied. The expression for the correction term is derived as a second order differential equation which is solved numerically by a step by step integration. The mutarotation constants for glucose and fructose have been determined and using these values and an assumed value for the optical rotation of β-fructofuranose it is shown that the correction term is in accord with experiments.

It is well known that sucrose is hydrolyzed in the presence of acids or the enzyme invertase. During the process the optical rotation (sodium light, 589 mμ) of the solution changes sign and the process is therefore known as the inversion of sucrose.

The classical investigation of the acid catalyzed inversion is due to Wilhelmy [1] who showed it to be a first order reaction or rather deduced the mathematical expression for a first order reaction from the experiments. Since then this reaction has been investigated several times and the mechanism is well known. Contrary to this the mechanism for the enzymatic hydrolysis which takes place at pH 4—7 is not known with certainty, although the reaction has often been investigated.

The results of the many experiments on the enzymatic inversion described in the literature are not all consistent with each other. This is probably due to the fact that the conventional method of following the reaction consists of taking out samples in which the reaction can be stopped and then measuring the optical rotation after the mutarotation has ceased If one does not add base which catalyses the mutarotation it is necessary to wait a long time before the measurements are performed. If on the other hand base is added the measurement must be performed very rapidly since fructose decomposes in alkaline solution.

The first of these possibilities (*i.e.*, stopping the reaction without catalysing the mutarotation) was used by Kjeldahl [2], who investigated the influence of temperature on the enzymatic inversion. He stopped the reaction by adding mercuric chloride which does not affect the mutarotation. In his papers he does not mention how long time he waited before he measured the optical rotation of the samples. The necessary time turns out to be in this case approximately 5 hours [3].

Among the other classical investigations we mention the work of Henri [4]. He used direct measurements of the reaction in the polarimeter tube and obtained in this way a perfectly reproducible curve for the apparent degree of reaction as a function of time, which he took to be an expression for the rate of inversion of sucrose alone. He furthermore found that a first order reaction constant calculated from the experimental data increased rapidly with time and concluded that the reaction is not a first order reaction in contrast to the result found earlier by O'Sullivan and Tompson [5]. The last mentioned authors incidentally were the first to use the above described technique in which mutarotation is catalyzed by the addition of base.

Hudson has discussed the work of O'Sullivan and Tompson critically as well as that of Henri [6,7]. Furthermore he repeated the measurements using the technique of O'Sullivan and Tompson (with Na_2CO_3 instead of KOH) and obtained results which were in agreement with their work.

This technique for measuring the reaction, *i.e.* taking out samples in which the reaction is stopped and the mutarotation is catalyzed, has been used in all subsequent papers such as those by Michaelis and Menten [8], Nelson and Hitchcock [9] and Christiansen and Bergthorsson [12]. It is clear that in this method there are a number of possibilities for making errors for instance in measuring the time when the reaction is stopped or in the dilution of the sample which takes place when the reaction is stopped and during which CO_2 is evolved. Apart from this the method is rather tedious and requires large amounts of enzyme since each sample is about 20 ml. It should be said, however, that the results of Nelson and Hitchcock and those of Christiansen and Bergthorsson are in excellent agreement.

A direct method in which the degree of reaction can be found without stopping the reaction is much to be preferred, but in that case one must take into account that the optical rotation of the solutions is not only a function of the degree of advancement for the reaction

$$S \rightarrow F_\beta + G_\alpha \tag{1}$$

but also depends on how far the reactions

$$F_\beta \rightleftharpoons F_\alpha \tag{2}$$

$$G_\alpha \rightleftharpoons G_\beta \tag{3}$$

have progressed. In these expressions S stands for sucrose G_α means α-glucose and G_β means β-glucose. F_β stands for β-fructofuranose and F_α for the form of fructose which is formed from F_β in solution. The following argument is completely independent of whether F_α is a sixmembered ring or just an optical isomer of F_β.

Below we shall derive an expression for the correction one must apply in order to convert the apparent degree of advancement φ defined as

$$\varphi = (a(t) - a(0))/(a(\infty) - a(0))$$

where $a(t)$ is the optical rotation of the solution at time t, to the true degree of advancement

$$\xi = (S(t) - S(0))/(S(\infty) - S(0))$$

where $S(t)$ denotes the concentration of sucrose at time t. The corrected curve will thereafter be compared with experiments made in the classical way.

EXPERIMENTAL

All polarimetric measurements were performed at 25.0°C in a Zeiss "Kreis-polarimeter 0.01°" using a 40 cm polarimeter tube in a thermostated jacket. The kinetic experiments were made in solutions which contained 10 g of sucrose * in 100 ml of solution. The solution was 0.005 M with respect to sodium acetate and 0.005 M with respect to acetic acid. In two experiments samples were taken out and the reaction was stopped by means of 2 ml 0.2 M Na_2CO_3; in two experiments the reaction was followed directly in the polarimeter tube. Fig. 1 shows a curve for the average of the last two experiments and the average points obtained by the first method.

The rate constants for mutarotation of glucose and fructose were also determined by dissolving the two sugars in the same buffer as above and measuring the optical rotation as a function of time. The slope of the line which is obtained by plotting the natural logarithm of the rotation minus final rotation *versus* the time is the sum of the rate constants for the forward and backward first order reactions. For these sums which are the so called mutarotation constants we obtained

(Fructose) $k_F = 0.2750$ min^{-1}

(Glucose) $k_G = 0.02473$ min^{-1}

as an average of two determinations which deviated less than one in thousand.

THE CORRECTION FORMULA

In order to derive the relation between the two degrees of advancement discussed above, we use that instead of considering the reactions

$$F_\beta \rightleftharpoons F_\alpha \qquad \text{and} \qquad G_\alpha \rightleftharpoons G_\beta$$

we may consider the reactions

$$F_1 \rightarrow F_2 \qquad \text{and} \qquad G_1 \rightarrow G_2$$

in which F_1 denotes F_β and F_2 the equilibrium mixture of F_β and F_α. Similarly G_1 denotes α-glucose and G_2 the equilibrium mixture of α and β-glucose. The last equation simply expresses that instead of considering the approach to equilibrium as the net result of two opposing first order reactions we may (formally) consider it as an irreversible transformation of a pure compound to an equilibrium mixture. The first order rate constants for the latter processes are the sums of the rate constants for the opposing reactions $\alpha \rightleftharpoons \beta$. The rate constants for the reactions $F_1 \rightarrow F_2$ and $G_1 \rightarrow G_2$ are therefore the first order mutarotation constants k_F and k_G which we have determined experimentally.

* The sucrose was a high grade product kindly given to us by "De Danske Sukkerfabrikker".

We have therefore the equations

$$S \rightarrow F_1 + G_1$$
$$F_1 \rightarrow F_2$$
$$G_1 \rightarrow G_2$$

and using the same symbols for concentration we have the differential equations

$$\dot{F}_1 + k_F F_1 = -\dot{S}$$
$$\dot{G}_1 + k_G G_1 = -\dot{S}$$

with the initial values $S(0) = S_0$, $G_1(0) = G_2(0) = F_1(0) = F_2(0) = 0$. These equations are first order linear equations with the formal solution

$$F_1 = -S + S_0 e^{-k_F t} + k_F e^{-k_F t} \int_0^t S e^{k_F t} dt$$

$$F_2 = S_0(1 - e^{-k_G t}) - k_G e^{-k_G t} \int_0^t S e^{k_G t} dt$$

and analogous expressions for G_1 and G_2.

The total optical rotation of the reaction mixture is

$$\alpha(t) = \alpha_S S + \alpha_1 F_1 + \alpha_2 F_2 + \beta_1 G_1 + \beta_2 G_2$$

where the α's and β's are the optical rotations of the different species in arbitrary units. Using that $\alpha(0) = S_0 \alpha_S$ and $\alpha(\infty) = (\alpha_2 + \beta_2) S_0$ we can form the expression for the apparent degree of advancement defined as

$$\varphi = (\alpha(t) - \alpha(0))/(\alpha(\infty) - \alpha(0))$$

We obtain

$$\varphi = (1-a_1-a_2)\xi + a_1 k_1 e^{-k_1 t} \int_0^t \xi e^{k_1 t} dt + a_2 k_2 e^{-k_2 t} \int_0^t \xi e^{k_2 t} dt$$

where $\xi = 1 - S/S_0$ is the true degree of advancement and

$$a_1 = (\alpha_1 - \alpha_2)/(\alpha_S - \alpha_2 - \beta_2)$$
$$a_2 = (\beta_1 - \beta_2)/(\alpha_S - \alpha_2 - \beta_2)$$

The value of a_2 ($a_2 = 0.544$) can be calculated from data in the literature about the specific rotation of the sugars, but a_1 cannot be calculated *a priori* since the specific rotation of the form of fructose which is liberated from sucrose is not known.

The above integral equation giving φ in terms of ξ is not useful since φ is the quantity which is easy to measure. Differentiating the equation once and twice with respect to time and eliminating the remaining integrals between the three equations we can, however, obtain a differential equation expressing ξ in terms of φ. It is

$$(1-a_1-a_2)\ddot{\xi} + (k_1+k_2-a_1k_2-a_2k_1)\dot{\xi} + k_1k_2\xi = \ddot{\varphi} + (k_1 + k_2)\dot{\varphi} + k_1k_2\varphi$$

Table 1. The table shows the agreement between the experimental values of ξ (t) and the calculated values. The figures in brackets have been used to determine the initial slope of $\xi_{expt}(t)$.

t (min)	5	10	15	20	40	70
ξ_{expt}	0.065	0.127	0.188	0.242	0.453	0.682
ξ_{theor}	(0.065)	(0.127)	(0.188)	0.238	0.461	0.670

When φ is known as a function of t this equation can be integrated numerically to give ξ. Since φ is found experimentally it will be necessary to use smoothed out values of it to get reasonable values for its derivatives. In the actual experiment φ was measured every minute in the larger part of the experiment and we used smoothing by fives to get a table of φ with five minute intervals. Even then the second derivative was rather erratic and we therefore introduced the new variable $z = \varphi - (1-a_1-a_2)\xi$ obtaining the equation

$$\ddot{z} + \frac{k_1+k_2-a_1k_2-a_2k_1}{1-a_1-a_2}\dot{z} + \frac{k_1k_2}{1-a_1-a_2}z = \frac{k_1a_1+k_2a_2}{1-a_1-a_2}\dot{\varphi} + \frac{k_1k_2(a_1+a_2)}{1-a_1-a_2}\varphi$$

in which the second derivative is absent on the right hand side. Using the smoothed out values for φ the derivative was calculated using a five point differentiation formula.

Had a_1 been known the procedure would now have been to use a power series expansion for φ in the neighbourhood of $t = 0$ obtained by least square curve fitting to obtain a power series expansion for ξ near $t = 0$. From this a sufficient number of ξ values could be obtained to start a step by step integration of the equation for z. Such an integration could for instance follow the method of Milne [10,11] which we used in the calculations described below.

As it is, a_1 is not known and we have therefore used the initial slope of the curve $\xi = \xi(t)$ to determine a_1. Using this value $a_1 = 0.228$ the corrected curve

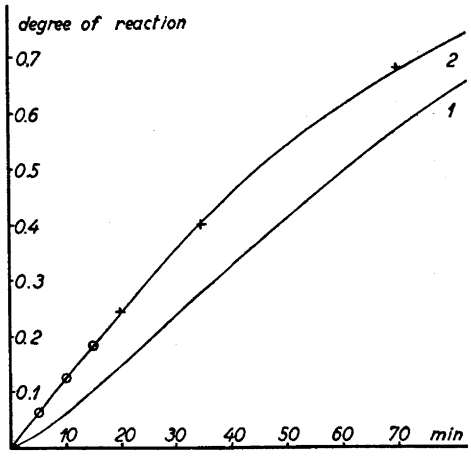

Fig. 1. Curve No. 1 shows the experimental values of $\varphi(t)$, curve No. 2 shows $\xi_{theor}(t)$ calculated using curve No. 1. O are the values of ξ_{expt} which have been used in determining the initial slope of $\xi_{expt}(t)$, + are the other values of ξ_{expt}.

on Fig. 1 has been calculated. Since this curve has been fitted to the experimental data near the origin it is not surprising that it gives a good fit there, but even for $\xi \simeq 0.7$ the disagreement between the calculated values as given in Table 1 and the experimental points is only about 2 % which is only slightly more than the experimental uncertainty. By using a_2 as a parameter which is fitted to give the best agreement on the average the disagreement could be made even smaller and furthermore this would lead to a more precise determination of a_2 and thereby of the optical rotation of fructose as it is formed from sucrose. Such calculations would require calculating facilities which are not at our disposal at the present time but we hope to return to the problem later. Here our primary aim has been to show that a correction of this type is possible but as a byproduct we have obtained a possibly not very accurate value for the optical rotation of β-fructofuranose which from the value of $a_1 = 0.228$ is found to be $-70.8°$ in contrast to the rotation $-95.75°$ found for the equilibrium mixture.

In using this method it is of the utmost importance that φ is known with great accuracy so that its derivatives can be determined with reasonable accuracy. When this is achieved on the other hand, our method presents several advantages. Firstly it is more accurate than the classical method since all errors due to stopping the reaction and diluting the samples are avoided, and more experimental points can be obtained. Secondly the experimental part of it is much quicker so that the method will be faster, provided calculating facilities are available. Finally the method is far less enzyme-consuming than the previous methods. Since earlier experiments always were carried out using enzyme mixtures which were easily obtained the problem of enzyme consumption was not serious. When one wants to use highly purified invertase as we plan to do later the problem becomes important, however, and this has indeed been one of the reasons for developing this method.

We are indebted to Professor J. A. Christiansen for encouragement and advice. B. A. gratefully acknowledges economic support from the *Carlsberg Foundation* and from *Statens Almindelige Videnskabsfond.*

REFERENCES

1. Wilhelmy, L. *Pogg. Ann.* **81** (1850) 413.
2. Kjeldahl, J. *Medd. Carlsberg. Lab.* **1** (1876–82) 331.
3. Nelson, J. M. and Beegle, F. *J. Am. Chem. Soc.* **41** (1919) 572.
4. Henri, V. *Lois générales de l'action des diastases.* Paris 1903.
5. O'Sullivan, C. and Tompson, F. W. *J. Chem. Soc.* **57** (1890) 834.
6. Hudson, C. S. *J. Am. Chem. Soc.* **30** (1908) 1160.
7. Hudson, C. S. *J. Am. Chem. Soc.* **30** (1908) 1664.
8. Michaelis, L. and Menten, M. L. *Biochem. Z.* **49** (1913) 333.
9. Nelson, J. M. and Hitchcock, D. I. *J. Am. Chem. Soc.* **43** (1921) 2632.
10. Milne, E. W. *Am. Math. Mo.* **33** (1926) 455.
11. Bennett, A. A., Milne, E. W. and Bateman, H. *Numerical Integration of Differential Equations.* Dover 1956.
12. Christiansen, J. A. and Bergthorsson, B. *Beretning fra 8. Nordiske Kemikermøde.* (1953) 203.

Received December 21, 1959.

ACTA CHEMICA SCANDINAVICA 14 (1960) 829–835

Crystal Structure of *Cyclo*hexane-1a,3a,5a-thiophosphoric Acid Ester

PER ANDERSEN and K. E. HJORTAAS

Universitetets Kjemiske Institutt, Blindern-Oslo, Norway

An X-ray investigation of the thiophosphoric acid α-floroglucitol ester has been carried out. The space group is $Pna2_1$ and the cell dimensions are a 11.45 ± 0.05 Å; b 7.28 ± 0.04 Å; c 9.47 ± 0.05 Å, with 4 molecules in the unit cell. The structure shows that the three ester oxygen atoms are in axial positions in the *cyclo*hexane ring. The space group of the corresponding phosphoric acid ester is Cc with cell dimensions a 11.37 Å; b 6.25 Å; c 11.74 Å; β 118°, and 4 molecules in the cell.

The esters formed by α-floroglucitol and phosphoric acid and thiophosphoric acid, respectively, were synthesised by Stetter and Steinacker in 1951 [1] and the reactions were shown to be:

$$C_6H_9(OH)_3 + OPCl_3 = C_6H_9O_3PO + 3HCl$$

and

$$C_6H_9(OH)_3 + SPCl_3 = C_6H_9O_3PS + 3HCl$$

They assumed configurations as shown in Fig. 1 and could conclude that α-floroglucitol was the *cis* form of *cyclo*-hexane-1,3,5-triol. This had been proved earlier by an X-ray investigation of the dihydrate of α-floroglucitol [2]. The hydroxygroups were in equatorial rather than in axial positions in this crystal structure, however.

The 1,3-carbon-carbon distance in *cyclo*hexane is 2.51 Å and the Cl—Cl distance in both $OPCl_3$ and $SPCl_3$ is 3.23 Å. Even if these distances are somewhat unfavourable the proposed structure is reasonable when compared with the hydroxy-oxygen distances in phosphoric acid [3] which are 2.50—2.52 Å. The proposed structure should therefore be expected to exhibit undistorted axial bonds.

CRYSTALLOGRAPHIC DATA

The X-ray data were obtained from oscillation and Weissenberg photographs using unfiltered Cu$K\alpha$ radiation. Multiple film technique was employed with visual estimation of the intensities using an experimental intensity scale

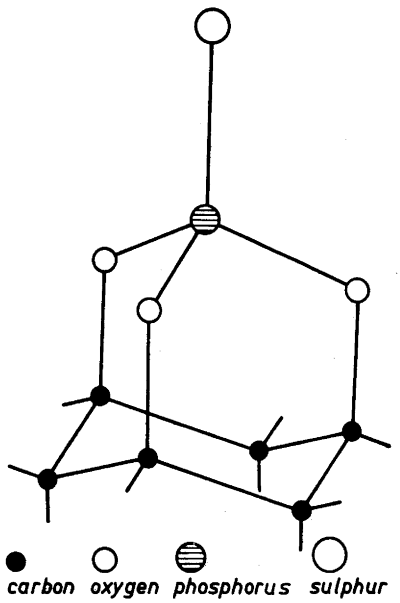

Fig. 1. A model of the molecule.

for comparison. The intensities were corrected in the ordinary way to obtain $|F_o|$ values. The space groups were determined both for the sulphur and oxygen compound, but a structure determination was only carried out for the former.

The thiophosphoric acid ester is orthorhombic with the following unit cell dimensions:

$$a\ 11.45 \pm 0.05\ \text{Å};\quad b\ 7.28 \pm 0.04\ \text{Å};\quad c\ 9.47 \pm 0.05\ \text{Å}$$

The experimental density was found equal to 1.64 g cm^{-3} which gives four molecules in the cell. The systematic extinctions show that reflexions in the $(0kl)$ zone are present only when $k + l = 2n$ and in the $(h0l)$ zone when $h = 2n$. The possible space group could therefore be either $Pnam$ or $Pna2_1$. Both space groups are equally acceptable as the fourfold positions in $Pnam$ require the point symmetry m and the proposed model has the symmetry $3m$. Patterson projections combined with the trial and error computations showed that $Pna2_1$ was the correct space group.

The phosphoric acid ester is monoclinic and has the cell dimensions:

$$a\ 11.37\ \text{Å};\quad b\ 6.25\ \text{Å};\quad c\ 11.74\ \text{Å};\quad \beta\ 118°$$

The density was found to be 1.60 g cm^{-3} which gives four molecules per unit cell. The systematic extictions show that (hkl) reflexions are present when $h + k = 2n$ and $(h0l)$ reflexions for $l = 2n$. This leads to two possible space groups $C2/c$ and Cc. As the fourfold positions in $C2/c$ has the point symmetry 2 or $\bar{1}$ it must be assumed that Cc is the correct space group.

Table 1. Co-ordinates and temperature factors for the [001] and [010] projection, respectively.

	x	*y*	*B*	*x*	*z*	*B*
S	0.227	0.670	3.8	0.226	−0.005	4.1
P	0.341	0.481	3.0	0.341	0	3.1
O_1	0.308	0.310	3.0	0.310	−0.099	3.3
O_2	0.364	0.395	3.0	0.360	0.152	3.3
O_3	0.467	0.540	3.0	0.461	−0.054	3.3
C_1	0.397	0.158	4.0	0.389	−0.090	3.6
C_2	0.406	0.091	4.0	0.410	0.064	3.6
C_3	0.450	0.247	4.0	0.449	0.150	3.6
C_4	0.564	0.324	4.0	0.570	0.095	3.6
C_5	0.560	0.390	4.0	0.552	−0.045	3.6
C_6	0.508	0.239	4.0	0.512	−0.148	3.6
H_1	0.33	0.01	4.0	0.33	0.10	4.0
H_2	0.37	0.05	4.0	0.37	−0.16	4.0
H_3	0.49	−0.02	4.0	0.49	0.06	4.0
H_4	0.46	0.18	4.0	0.46	0.26	4.0
H_5	0.57	0.13	4.0	0.57	−0.16	4.0
H_6	0.50	0.30	4.0	0.50	−0.26	4.0
H_7	0.64	0.23	4.0	0.64	0.09	4.0
H_8	0.59	0.46	4.0	0.59	0.16	4.0
H_9	0.64	0.46	4.0	0.64	−0.09	4.0

It was decided to carry out a structure determination of the sulphur compound because of the higher symmetry in the space group, as in *Cc* not even one projection has a center of symmetry.

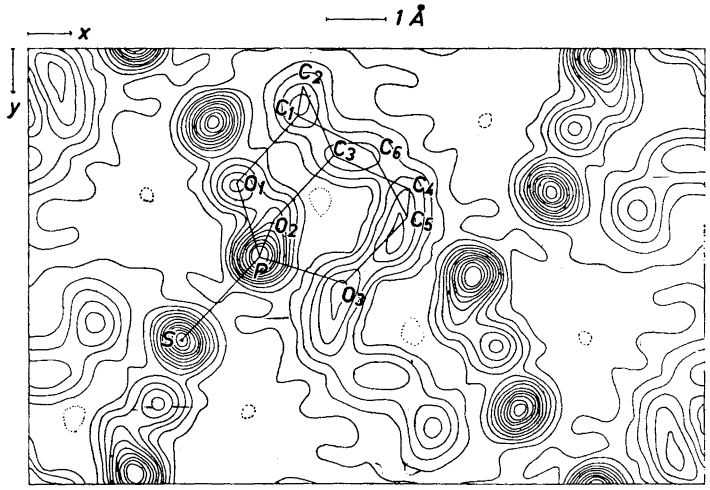

Fig. 2. Projection along [001]. Interval of contour lines 2e Å^{-2}. Zero line dotted.

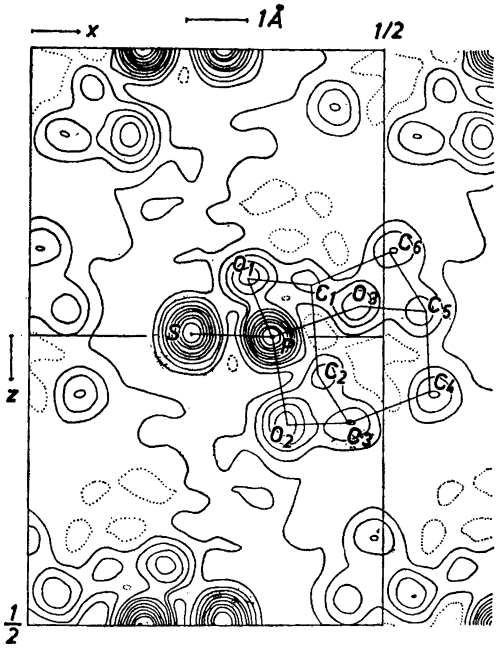

Fig. 3. Projection along [010]. Interval of contour lines 2e Å^{-2}. Zero line dotted.

STRUCTURE DETERMINATION

The Patterson projections $P(u, v)$ and $P(u, w)$ did not give any conclusive indications as to the position or orientation of the molecule. The assumption that the molecule as a whole is roughly spherical (except for the sulphur atom) combined with trial and error computations and informations from the Patterson projections finally lead to a structure which could be refined. One could thus unequivocally exclude the more symmetrical space group *Pnam*.

Table 2. Standard deviation of co-ordinates expressed in Å for the [001] and [010] projection, respectively.

	σ (x)	σ (y)	σ (x)	σ (z)
S	0.005	0.006	0.007	0.013
P	0.005	0.005	0.006	0.007
O	0.015	0.017	0.022	0.027
C			0.026	0.032

Table 3. Bond lengths (Å), bond angles and standard deviations.

						S.d.
S—P	1.90					0.01
P—O_1	1.60	P—O_2	1.59	P—O_3	1.56	0.02
O_1—C_1	1.47	O_2—C_3	1.48	O_3—C_5	1.52	0.04
C_1—C_2	1.55	C_2—C_3	1.48	C_3—C_4	1.54	
C_4—C_5	1.42	C_5—C_6	1.56	C_6—C_1	1.56	0.04
S—P—O_1	113°	S—P—O_2	114°	S—P—O_3	114°	0.9°
O_1—P—O_2	105°	O_2—P—O_3	106°	O_3—P—O_1	103°	1.1°
P—O_1—C_1	114°	P—O_2—C_3	112°	P—O_3—C_5	114°	1.7°

The structure was refined in the [001] and the [010] projection using $(F_o - F_c)$ difference syntheses. The hydrogens were introduced in the final stage for reflexions with ξ values less than about 0.6 and by assuming the C—H bond to be 1.09 Å. In the [001] projection the R factor in the end was 0.13 with an isotropic temperature factor $B = 3.2$ Å^2 for all atoms. The corresponding values for the [010] projection were $R = 0.14$ and $B = 3.6$ Å^2. In calculating R the (002) and (201) reflections are omitted because of extinction. In calculating $\Sigma||F_o|-|F_c||$ unobserved reflections are given the minimum observable value $|F'_o|$ when $|F_c| > |F'_o|$, but are omitted when $|F_c| < |F'_o|$. In either case they are excluded from $\Sigma\,|F_o|$. The difference syntheses in both projec-

Table 4. Shortest intermolecular distances (Å).

O—CH_2	3.40	4.18	4.85
O—S	3.78	4.00	
CH_2—CH_2	3.75	5.21	
S—CH_2	3.89	4.16	4.40

Table 5. Observed and calculated structure factors and phase angles.

h k l	F_{calc}	$\|F_{obs}\|$	*h k l*	F_{calc}	$\|F_{obs}\|$	*h k l*	F_{calc}	$\|F_{obs}\|$
0 2 0	−8	9	3	−18	20	4	−6	4
4	7	7	4	4	6	5	13	15
6	24	25	5	3	4	6	2	<2
8	0	<2	6	4	4	7	−4	2
1 1 0	64	58	7	−20	20	9 1 0	−35	32
2	−28	30	8	−7	8	2	4	4
3	22	24	5 1 0	15	14	3	7	8
4	24	24	2	−62	62	4	8	8
5	8	8	3	15	14	5	−15	12
6	9	10	4	0	<2	6	−6	6
7	4	5	5	4	6	7	−6	7
8	−3	3	6	−11	12	10 0 0	−15	16
9	2	4	7	1	<2	1	12	11
2 0 0	17	14	8	−9	10	2	−17	14
1	59	55	6 0 0	10	10	3	0	<3
2	4	5	1	8	9	4	−8	9
3	17	17	2	29	31	5	−15	14
4	11	11	3	−33	33	6	3	<2
5	2	<2	4	34	32	11 1 0	−5	4
6	−28	28	5	−11	12	2	−1	<3
7	7	8	6	1	<3	3	−9	8
8	6	7	7	5	4	4	−9	9
9	3	4	8	6	9	5	10	10
3 1 0	−25	24	7 1 0	31	31	12 0 0	2	<2
2	−17	16	2	16	14	1	−4	4
3	−20	22	3	5	6	2	7	7
4	−12	14	4	−14	16	3	−1	<2
5	−13	16	5	6	7	4	6	7
6	−2	<3	6	5	7	5	−3	2
7	−3	4	7	7	8	13 1 0	2	<2
8	4	4	8 0 0	−4	6	2	−1	<2
4 0 0	0	<1	1	−21	19	3	11	11
1	−47	51	2	1	<2	14 0 0	3	2
2	−46	48	3	1	<2	1	2	2

Table 5. Continued.

h k l	$\|F_{calc}\|$	$\|F_{obs}\|$	α°	h k l	$\|F_{calc}\|$	$\|F_{obs}\|$	α°
0 0 2	151	72	354	6 0 5	22	22	95
4	44	42	278	6	16	19	18
6	36	36	334	7	18	16	76
8	24	24	5	8	12	11	22
10	12	6	342	9	10	9	63
2 0 0	14	14	0	10	4	6	45
1	84	54	277	8 0 0	8	8	180
2	40	38	174	1	42	43	283
3	18	18	174	2	8	8	180
4	42	42	180	3	30	32	266
5	16	18	192	4	6	4	63
6	30	30	200	5	34	34	242
7	22	24	325	6	12	12	18
8	28	27	197	7	24	24	261
9	14	13	342	8	4	<3	11
10	22	18	180	9	12	10	270
11	8	10	233	10 0 0	18	20	180
4 0 0	3	<2	180	1	18	21	73
1	22	23	52	2	18	18	221
2	34	35	283	3	20	22	85
3	8	7	304	4	16	16	150
4	18	18	354	5	18	20	114
5	8	6	225	6	20	18	139
6	6	6	315	7	12	12	99
7	6	8	104	8	6	4	180
8	14	14	270	12 0 0	2	<3	0
9	12	12	81	1	10	12	239
10	4	6	225	2	6	7	34
11	6	8	104	3	10	9	243
6 0 0	12	12	0	4	12	12	59
1	30	31	101	5	4	6	90
2	16	16	270	6	6	6	45
3	22	23	121	14 0 0	2	<2	0
4	8	8	297	1	2	3	315
				2	6	6	90

tions indicated that individual damping should be used. The phosphorus atom should be damped less and the sulphur atom more. This is also what one should expect from an inspection of the structure.

A least squares refinement carried out on a Ferranti Mercury computer for the two projections in question gave the correlation factors $R = 0.09$ and $R = 0.07$, respectively, for the [001] and [010] projection. The contribution from the hydrogen atoms is here included in all structure factors. The coordinates and the individual isotropic temperature factors are listed in Table 1. Figs. 2 and 3 show the two Fourier projections based on the phases calculated from these parameters. The standard deviations calculated from the equation derived by Cruickshank [4] are listed in Table 2, the values are doubled in the non-centrosymmetrical projection [5]. The interatomic distances and valency angles within the molecule and their standard deviations are listed in Table 3.

DISCUSSION

Orientation of the molecule in the cell is such that the S—P bond lies approximately in the *xy* plane and the axial bonds of the *cyclo*hexane ring are roughly parallel to this plane which is not far from being a plane of symmetry. The closest intermolecular approaches are listed in Table 4. They have all values which are compatible with accepted van der Waals radii.

The structure determination shows that the configuration proposed by Stetter and Steinacker is the correct one, and all distances and angles are within the limits of error those to be expected from an ideal model. The three oxygen atoms are in axial positions and the O—O distances are in good agreement with those computed for axial positions. Both the P—O distance and the O—P—O angle are in good agreement with those found in phosphoric acid [3].

Thanks are due to Dr. H. Stetter for placing samples of the two substances mentioned in this paper at the disposal of the Physical Chemistry Department.

REFERENCES

1. Stetter, H. and Steinacker, K. H. *Chem. Ber.* **85** (1952) 451.
2. Andersen, P. and Hassel, O. *Acta Chem. Scand.* **2** (1948) 527.
3. Furberg, S. *Acta Chem. Scand.* **9** (1955) 1557.
4. Cruickshank, D. W. I. *Acta Cryst.* **2** (1949) 65.
5. Cruickshank, D. W. I. *Acta Cryst.* **3** (1950) 72.

Received December 7, 1959.

ACTA CHEMICA SCANDINAVICA 14 (1960) 836–840

On the Stability of Ozonides

ERLING BERNATEK and METTE HVATUM

Universitetets Kjemiske Institutt, Blindern-Oslo, Norway

Thermal decomposition in benzene of three ozonides has been followed iodometrically. The first half of the reaction is strictly first-order with no induced decomposition. Activation energies have been calculated. The rate-controlling step is probably a homolytic cleavage of the O—O bond. It seems probable that an ozonide can transfer active oxygen to a suitable substrate.

For some time we have been concerned with the ozonolysis of certain benzofurans and benzodifurans [1,2], during which work the formation of stable ozonides has been a matter of great interest.

Isolation of the ozonides in a pure crystalline state has been achieved with varying ease in the different cases chiefly due to great variations in their stability. One of the structural factors guiding the stability is the nature of the substituents at both ends of the double bond. Criegee has made a statement at variance with this[3], but had perhaps only hydrocarbon substituents in mind.

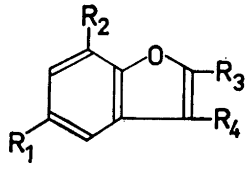

I:	$R_1 = CH_3COO$;	$R_2 = H$;	$R_3 = CH_3$;	$R_4 = COOH$
II:	$R_1 = CH_3COO$;	$R_2 = H$;	$R_3 = CH_3$;	$R_4 = COOCH_3$
III:	$R_1 = CH_3COO$;	$R_2 = H$;	$R_3 = CH_3$;	$R_4 = COOC_2H_5$
IV:	$R_1 = CH_3COO$;	$R_2 = H$;	$R_3 = CH_3$;	$R_4 = COOC_3H_7$
V:	$R_1 = CH_3COO$;	$R_2 = H$;	$R_3 = CH_3$;	$R_4 = COCH_3$
VI:	$R_1 = CH_3COO$;	$R_2 = R_3 = CH_3$;		$R_4 = COOC_2H_5$
VII:	$R_1 = CH_3COO$;	$R_2 = R_3 = CH_3$;		$R_4 = COCH_3$
VIII:	$R_1 = R_2 = H$;		$R_3 = COOCH_3$;	$R_4 = H$

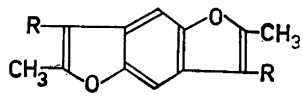

IX: R = $COOC_2H_5$
X: R = $COCH_3$
XI: R = H

Stable ozonides have on previous occasions been prepared in this laboratory from the substances III, VI and IX. An isolable, but rather unstable ozonide was obtained from X, while ozonides from V, VII and XI were too unstable to be isolated. In the experimental section of this work is described the preparation of two new benzofuran derivatives (II and IV) and their stable, monomeric ozonides. Attempts to prepare isolable ozonides from I and VIII met with no success.

Summarising these results it is seen that if only one end of the double bond in the furan ring is substituted, no ozonide can be isolated. This is in agreement with the findings that only 2,3-disubstituted indoles form stable ozonides. Furthermore, a free carboxyl group is evidently detrimental to the stability of an ozonide while an ester group enhances the stability more than does an acetyl group.

Small changes in the substituents therefore bring about great differences in stability. To get a clearer picture of their (thermal) stabilities, absolutely as well as relatively to each other, we have investigated the degradation of three closely related and easily accessible ozonides, *viz.* those of II, III and IV, at elevated temperatures.

The kinetic runs were performed in benzene solution, but some degradation experiments in xylene and decalin will be discussed later in this paper. Analytically the reactions were followed by determining iodometrically the decreasing content of active oxygen. The validity of our kinetic results (*i.e.* that they truly represent the decomposition of the ozonide) is therefore based on the assumption that the rupture of the O—O bond is a rate-controlling step and that no transfer of active oxygen to the solvent or to reaction products take place. Justification of these assumptions is found in the strict adherence of the degradation to first order kinetics (however, see below), and in the rather high activation energies. The relevant kinetic results are summarised in Table 1.

The first-order rate-constants are all calculated from the first half of the reactions. From that point onwards serious deviation from first-order kinetics began to develop in the form of distinct retardation of the reaction. This may be a true kinetic effect, *i.e.* the reaction products exert a negative catalysis or it may be an analytical artefact in the sense that we are no longer measuring the real content of ozonide in solution. Such a situation could arise if the ozonide was able to transfer its active oxygen to any of the reaction products, supposing that the new peroxidic products were more stable that the ozonide itself.

Table 1. First-order rate-constants for the thermal decomposition of benzofuran ozonides in benzene.

Ozonide from	Temperature °C	$C_o \times 10^3$ in mole/l	k in h^{-1}
II	100.0	0.633	0.140
II	100.0	1.962	0.131
II	100.0	3.217	0.142
II	79.65	1.962	0.0147
III	100.0	0.633	0.132
III	100.0	1.962	0.126
III	100.0	3.217	0.122
III	90.0	1.962	0.0436
III	79.15	1.962	0.0127
IV	100.0	0.633	0.134
IV	100.0	1.962	0.124
IV	100.0	3.217	0.130
IV	79.15	1.962	0.0124

No significant changes in the rate-constants at 100° were observed on increasing the concentration of the reactant about five times. First-order kinetics is thus further vindicated and induced decomposition ruled out. We believe that the rate-determining step in the thermal decomposition is a homolytic splitting of the O—O bond producing a diradical like XII. Due to the special

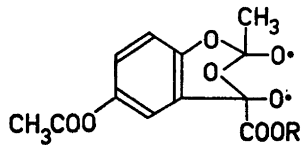

XII

steric situation in this diradical recombination must be frequent. The further reactions are probably of the usual radical type transformations, *viz.* decomposition, rearrangements and attack on substrates. The complexity and partly polymeric nature of the reaction products from our experiments substantiate the belief that several modes of reaction are operative. If the concept of active oxygen transfer is true, even the initial homolytic cleavage may not be entirely homogeneous but mixed with small amounts of another reaction where the O—O bond is preserved. From our kinetic data the following activation energies are calculated: Ozonide of II 28.2 kcal/mole; ozonide of III 28.7 kcal/mole; ozonide of IV 28.8 kcal/mole. These figures are well within the range of activation energies for thermal decompositions of peroxides and therefore compatible with a homolytic cleavage of an O—O bond.

In the initial search for a suitable inert solvent for the decomposition experiments xylene (*o*, *m*-, *p*-mixture) was tried. Surprisingly the content of active oxygen increased when a solution of ozonide in xylene was heated at 100° for some hours. Xylene is known to have a slight tendency to autoxidation and the amount of oxygen in the air in the ampoules was sufficient to explain the

increase in active oxygen. Controls with xylene alone, however, showed only a weak autoxidation under the experimental conditions, so the presence of an ozonide or its immediate decomposition products must be able to catalyse this process. According to our figures the reaction is accelerated at least ten times. Direct transfer of active oxygen from ozonide to the solvent can not be inferred with certainty from these experiments. Decalin has far greater tendency to formation of peroxides than xylene and some runs were made in this solvent under an oxygen-free nitrogen atmosphere. The rate of decomposition at 100° was in this case only about one third of the measured in benzene. This difference is far to large to be explained by general solvent effect, but must be due to the formation of decalin peroxides by the action of the ozonide.

EXPERIMENTAL

Methyl 2-methyl-5-acetoxybenzofuran-3-carboxylate (II). To a continuously agitated solution of anhydrous zinc chloride (35 g) in dry acetone (50 ml) and glacial acetic acid (3 ml) kept at 75°, was added during 8 h a solution of *p*-benzoquinone (27 g) in methyl acetoacetate (100 ml) and acetone (100 ml). The reaction mixture was concentrated in a stream of warm air and placed in a refrigerator when a greyish crystalline product separated which was washed with small amounts of ice-cold methanol. Yield 24.2 g (47 %). Recryst. four times from aqueous acetone (charcoal), m.p. 146.5°. (Found: C 64.1; H 5.2; OCH_3 15.4. Calc. for $C_{11}H_{10}O_4$: C 64.1; H 4.9; OCH_3 15.1.) The product (10 g) was dissolved in acetyl chloride (50 ml), boiled for 15 min and poured into ice-water (2 l) when a dark oil separated. After about 0.5 h this solidified, was broken up and washed thoroughly with water. Recrystallised from aqueous acetone, m.p. 83°. (Found: C 63.1; H 5.0; OCH_3 12.1. Calc. for $C_{13}H_{12}O_5$: C 62.9; H 4.9; OCH_3 12.5.)

n-Propyl 2-methyl-5-acetoxybenzofuran-3-carboxylate (IV). The ethyl ester I (R_1 = OH) (17.5 g) was dissolved in dry propanol-1 (300 ml), saturated at room temperature with hydrogen chloride, and refluxed for 8 h. The main part of the propanol (250 ml) was distilled off and the residue poured into ice-water (1 l) when a crystalline substance separated (18.3 g, 98 %). Recrystallised twice from aqueous acetone and four times from benzene, m.p. 105°. (Found: C 66.6; H 6.2. Calc. for $C_{13}H_{14}O_4$: C 66.7; H 6.0.) Acetylation as for the methyl ester. Recrystallised thrice from aqueous acetone (charcoal), m.p. 45—46°. (Found: C 65.4; H 5.9. Calc for $C_{15}H_{16}O_5$: C 65.2; H 5.8.)

Ozonisation. The ozone generator produced at an oxygen flow of 30 l/h, 2.4 g O_3/h. Methyl ester (II) (9 g) was dissolved in ethyl acetate (250 ml) and ozonised at 0° for 52 min. Most of the ethyl acetate was removed in a stream of air and the remainder *in vacuo*. The residue consisted of yellow, somewhat sticky crystals which were washed with aqueous acetic acid (1:1). Yield 8.7 g (81 %). Recrystallised twice from aqueous acetic acid (8:2) and twice from alcohol. White crystals, m.p. 88—89°. (Found: C 52.7; H 3.9; act. O 5.4; M 294 (benzene). Calc. for $C_{13}H_{12}O_8$: C 52.7; H 4.1; act. O 5.4; M 296). The propyl ester was ozonised in the same way, but at a lower temperature (solid carbon dioxide — acetone). The ozonide had m.p. 68°. (Found: C 55.1; H 4.7; act. O 5.0; M 317 (benzene). Calc. for $C_{15}H_{16}O_8$: C 55.6; H 5.0; act.O 4.9; M 324).

Ozonolysis of 2-methyl-5-acetoxybenzofuran-3-carboxylic acid (I). The acid (5 g) was dissolved in ethyl acetate (200 ml) and ozonised at low temperature (solid carbon dioxide — acetone) for 30 min. To the reaction mixture was added light petroleum until turbidity occurred and a yellow oil which contained active oxygen separated. The solvent mixture was decanted and the last traces removed *in vacuo*. As soon as the oil reached about room temperature it began to decompose with evolution of gas. The residue soon solidified to a yellow crystalline mass which did not contain any active oxygen. Recrystallised from an ether-ligroin mixture (charcoal), m.p. 117—122°, white crystals. Hydrolysis with 2 N hydrochloric acid afforded white needles, recrystallised from water (charcoal), m.p. 198—200°. Blue colour with ferric chloride. Mixed m.p. with an authentic sample of gentisic acid showed no depression.

Kinetics. The purified ozonides were dissolved in reagent grade benzene at room temperature and 10 ml aliquots transferred to glass ampoules which were sealed and placed in a thermostat bath at the appropriate temperature. For analysis the ampoules were rapidly cooled and broken in a tall beaker whereupon glacial acetic acid (15 ml) was added. Pieces of solid carbon dioxide were placed in the mixture and sodium iodide (1 g) added. The beaker was closed with a lid and kept in a dark cupboard for 0.5 h. Recently boiled water (100 ml) was added and the heterogeneous mixture titrated under vigorous stirring with standard (0.01 N) thiosulphate. Controls with samples of the ozonide of III gave results better than 99.5 % of the theoretical value. The starting point in the runs was always a titration value of an actual sample rather than a figure calculated from the weighed amount of ozonide.

Decomposition in xylene and decalin. Ozonide of III was dissolved in pure xylene (free from active oxygen) and 10 ml aliquots were transferred to ampoules and sealed as before. In a typical run the titration value increased from 9.03 ml 0.01316 N sodium thiosulphate to 13.33 ml in 2 h 20 min. Roughly estimated the volume of air in the ampoules was 10 ml, *i.e.* 2 ml of oxygen. This is 0.18 mequiv. (calculated as routed through a hydroperoxide and determined iodometrically) corresponding to a consumption of 13.5 ml 0.01316 N sodium thiosulphate. Ampoules with xylene only were heated 2 h 20 min. Air volume approximately as before. Mean titration value: 0.37 ml of the usual thiosulphate.

The runs in decalin were performed in a reflux apparatus kept in a thermostat at 100° through which a stream of dry oxygen-free nitrogen (washed with alkaline pyrogallol solution) was led. Decalin is a rather poor solvent for the ozonide (of III) and the reaction mixture was therefore made up by saturating the decalin with ozonide at room temperature. Samples of ca 25 ml were withdrawn and cooled to room temperature and from this 20 ml samples were pipetted and analysed. The reaction was not pure first order, but if calculated as such, the average rate-constant was 0.05 h^{-1}.

REFERENCES

1. Bernatek, E. and Thoresen, F. *Acta Chem. Scand.* **9** (1955) 743.
2. Bernatek, E. and Bö, I. *Acta Chem. Scand.* **13** (1959) 337.
3. Criegee, R., Kerckow, A. and Zinke, H. *Chem. Ber.* **88** (1955) 1878.
4. Bailey, P. S. *Chem. Revs.* **58** (1958) 973.

Received December 17, 1959.

ACTA CHEMICA SCANDINAVICA 14 (1960) 841–845

Thiamine and Thiamine Diphosphate in Liver and Brain from Rats Treated with CCl_4

KARL-HEINZ KIESSLING and KARIN TILANDER

Institute of Zoophysiology, University of Uppsala, Sweden

The amount of thiamine and thiamine diphosphate in liver and brain of rats and their distribution in liver cytoplasm fractions has been studied.

The supernatant (including the microsomal fraction) contains nearly twice as much thiamine diphosphate as the mitochondria, while thiamine is present almost exclusively in the supernatant.

In rat livers with fatty infiltration, obtained by injections of CCl_4, the amount of thiamine diphosphate is slightly reduced. The decrease happens mainly in the mitochondria. An increased decomposition of thiamine diphosphate is found in fatty infiltrated liver homogenates as compared with normal ones.

No significant difference is found in thiamine diphosphate concentration between brains from normal and CCl_4-treated rats. The amount of thiamine is very low in either case.

Fatty infiltration of the liver is easily obtained in rats by injections of CCl_4 or white phosphorus, or by feeding them with a diet deficient in choline. Fatty liver may be obtained also by giving rats alcohol for a long time. In rats suffering from fatty liver caused by CCl_4 or white phosphorus, or by feeding on a choline deficient diet the liver mitochondria are morphologically changed in the same way as when treated with hypotonic medium [1]. They also contain less than normal amounts of thiamine diphosphate [2], cytochrome c, pyridine nucleotides, and adenylnucleotides [3-5].

In the present communication the content of thiamine diphosphate and thiamine in liver and brain are analysed and evidence is put forward for an increased decomposition of thiamine diphosphate * in fatty liver produced by CCl_4 treatment as compared with normal conditions.

* Abbreviations used: TDP thiamine diphosphate, T thiamine, P_i inorganic phosphate.

EXPERIMENTAL

Male rats from the same litter and weighing about 200 g were used for the experiments. In each experiment two rats were used parallelly, one with fatty infiltration obtained by CCl_4 treatment and the other a control rat. Fatty infiltration was obtained by daily intraperitoneal injection of CCl_4 (0.2 ml of a 20 % solution in olive oil).

The rats were killed by decapitation, the livers immediately removed and chilled on ice, weighed, minced with a pair of scissors in cold isotonic sucrose, washed twice, and homogenized in a Potter-Elvehjem homogenizer in five volumes of cold 0.25 M sucrose. The homogenisations of the tissues from all animals were performed as uniform as possible, *i.e.* the same homogenizer was used, the pistel was moved with the same rapidity, and the time was always the same. From the homogenate samples were taken for incubation with TD^{32}P or T and $^{32}P_i$ in order to study the decomposition and synthesis of TDP as described elsewhere [6]. From the remaining part of the homogenate mitochondria and supernatant (soluble and microsomal fraction being taken together) were prepared.

Free thiamine was determined as thiochrome according to Hjarde [7], TDP manometrically as described by Westenbrink and Steyn-Parvé [8], and with the thiochrome method as the difference between total and free thiamine. TDP isolated by paper chromatography (*iso*butyric acid—versene—NH_3 [9] followed by propanol — HAc—H_2O [10]) was used as standard in the manometric method. Generally the values for TDP obtained with the thiochrome method were slightly lower than with the manometric method. In the tables the values for TDP obtained with the latter method are given. For determination of protein the Biuret method of Cleland and Slater [11] was used.

RESULTS

Table 1 gives figures about the content and distribution of TDP and T in the liver cells from normal and fatty infiltrated rat livers. The figures are mean values from six experiments, all determinations having been performed in duplicate. To avoid leakage of T and TDP from mitochondria to supernatant during the preparation of the cell fractions the tissues were homogenized very cautiously in a Potter-Elvehjem homogenizer. Our figures for the TDP concentration in mitochondria and supernatant are therefore very low as compared with those for liver given by Goethart [12] and Dianzani and Dianzani Mor [2]. In our experiments about 50 % of the TDP was recovered in the fraction removed by low speed centrifugation, and which contains mainly intact liver cells, blood corpuscles, and nuclei.

When, however, nuclei from rat liver were isolated according to Logan, Ficq, and Errera [13], the content of TDP in this purified fraction was found to be only 0.03 μg TDP per gram of normal liver.

Thus our figures in Table 1 for TDP and T in mitochondria and supernatant (soluble and microsome fraction) only intend to supply an idea about the relative distribution of the two compounds in the cell fractions, and to show the ratio between them. The latter agrees with that obtained by Goethart and Dianzani and Dianzani Mor, *i.e.*, in normal liver the TDP content of mitochondria is about half that of the supernatant. In fatty infiltered liver the mitochondrial TDP is reduced.

Compared with TDP the amount of T in the liver cells is low (Table 1), and is found mainly in the supernatant. In fatty infiltrated liver T is reduced, but since also TDP is reduced, the ratio between T and TDP is nevertheless the same as in normal liver.

Table 1. Content and distribution of thiamine and thiamine diphosphate in normal and fatty infiltered rat liver (T and TDP are mean values from 6 expts., total lipids from 4).

		TDP		T		$\frac{T}{TDP}$	Total lipids mg/g wet weight
		μg/g liver	μg/10 mg prot.	μg/g liver	μg/10 mg prot.		
Normal liver	Homogenate	8.96 ±0.55	0.38 ±0.03	0.59 ±0.01	0.026 ±0.001	$\frac{1}{16}$	41
	Supernatant	3.08 ±0.23	0.23 ±0.02	0.51 ±0.04	0.049 ±0.02	$\frac{1}{6.2}$	
	Mito-chondria	1.64 ±0.18	0.76 ±0.05	0.03 ±0.007	0.012 ±0.001	$\frac{1}{63}$	
Fatty liver	Homogenate	7.17 ±0.34	0.36 ±0.02	0.36 ±0.01	0.019 ±0.002	$\frac{1}{20}$	77
	Supernatant	2.43 ±0.31	0.27 ±0.02	0.38 ±0.03	0.044 ±0.004	$\frac{1}{6.8}$	
	Mito-chondria	0.98 ±0.16	0.48 ±0.06	0.03 ±0.005	0.012 ±0.002	$\frac{1}{42}$	

Table 2 gives figures for the amount of TDP and T in the brain from normal and CCl_4-treated animals. With regard to TDP no obvious differences are found. The amount of T in normal brain is only 1/20 of that in liver, and is still lower in CCl_4-treated animals.

The decomposition of TDP in homogenates from normal and fatty infiltrated rat livers has been investigated by means of radioactive TDP added to the homogenates. The amount of TDP decomposed after 60 min at 37°C is signi-

Table 2. Thiamine and thiamine diphosphate in brain from normal and CCl_4 treated rats (mean value from 6 expts.).

	TDP		T		$\frac{T}{TDP}$
	μg/g liver	μg/10 mg protein	μg/g liver	μg/10 mg protein	
Normal rat	3.68 ± 0.36	0.23 ± 0.04	0.03	0.0025	$\frac{1}{77}$
CCl_4 treated rat	3.61 ± 0.22	0.27 ± 0.02	<0.03	<0.0025	$< \frac{1}{77}$

Table 3. Synthesis and decomposition of thiamine diphosphate in homogenates from normal and fatty infiltered rat livers. Homogenate from 1/5 of a gram of liver has been used. (The values represent the mean of 6 expts.)

	Synthesis (per cent of added ^{32}P)	Decomposition (per cent of added $TD^{32}P$)
Normal liver	2.06 ± 0.25	5.92 ± 0.55
Fatty liver	2.25 ± 0.30	17.14 ± 1.61

ficantly higher in fatty infiltrated liver homogenates than in normal ones (Table 3). The same table shows that the ability to synthesize TDP from added T is uninfluenced by CCl_4 treatment.

DISCUSSION

The figures for TDP in rat liver homogenates (Table 1) are rather low as compared with those given by Goethart [12] and by Dianzani and Dianzani Mor [2], but are more in agreement with those obtained by Siliprandi and Siliprandi [14] and by Ochoa [15]. Possibly the differences can be ascribed to different rat strains.

The total amount of TDP in fatty infiltrated rat livers, produced by injections of CCl_4, is only slightly less than in normal livers (Dianzani and Dianzani Mor [2] and Table 1 in the present paper). The decrease is mainly localized to the mitochondria. Christie and Judah [16], in a study of the mechanism of action of CCl_4, advanced the opinion that the primary locus of action were the membranes of the liver mitochondria. This action is, according to Dianzani and Dianzani Mor, comparable with the displacement of TDP from swollen mitochondria as a consequence of hypotonic treatment.

However, no corresponding increase of the TDP concentration in the supernatant occurs (Table 1). Our results even show a slight decrease also in the supernatant from fatty liver (calculated as μg TDP/g liver).

Table 3 shows that in liver homogenates from CCl_4-treated rats, as compared with normal ones, the decomposition of TDP is increased. This increase of the phosphatase acting on TDP may explain the decrease of TDP in the supernatant and in the mitochondria. In this connection it may be of interest to point to an increased mitochondrial ATP-ase activity observed recently by Recknagel and Anthony [17] in CCl_4-treated rat liver.

On the other hand, an increased decomposition of TDP to thiamine, should result in an increased thiamine level. This is, however, not the case (Table 1). This can be explained by the assumption that tissues are capable of retaining only a limited amount of free thiamine. Thus when the amount is enhanced by increased dephosphorylation of TDP, the excess of thiamine is eliminated by excretion or decomposition.

As CCl_4 is thought to be a hepatotoxin only, no differences in TDP should occur in tissues other than liver. The only tissue, apart from liver, studied by us is brain, where CCl_4 is found to be without effect on the TDP level.

Acknowledgement. This work is part of investigations made possible by support from the *Swedish Medical Research Council.*

REFERENCES

1. Dianzani, M. U. *Giorn. biochim.* **2** (1953) 180.
2. Dianzani, M. U. and Dianzani Mor, M. A. *Biochim. et Biophys. Acta* **24** (1957) 564.
3. Dianzani, M. U. and Viti, I. *Biochem. J.* **59** (1955) 141.
4. Dianzani, M. U. *Biochim. et Biophys. Acta* **17** (1955) 391.
5. Dianzani, M. U. *Biochem. J.* **65** (1957) 116.
6. Kiessling, K.-H. *Biochim. et Biophys. Acta.* **39** (1960) 412.
7. Hjarde, W. *Nogle undersøgelser over B_1-vitaminet in vitro og in vivo.* Diss. Copenhagen 1950.
8. Westenbrink, H. G. K. and Steyn-Parvé, E. P. *Intern. Rev. Vitamin Research 21* (1950) 4.
9. Kiessling, K.-H. *Acta Chem. Scand.* **10** (1956) 1356.
10. Siliprandi, D. and Siliprandi, N. *Biochim. et Biophys. Acta* **14** (1954) 52.
11. Cleland, K. W. and Slater, E. C. *Biochem. J.* **53** (1953) 547.
12. Goethart, G. *Biochim. et Biophys. Acta* **4** (1952) 479.
13. Logan, R., Ficq, A. and Errera, M. *Biochim. et Biophys. Acta* **31** (1959) 402.
14. Siliprandi, D. and Siliprandi, N. *Nature* **168** (1951) 422.
15. Ochoa, S. and Peters, R. A. *Biochem. J.* **32** (1938) 1501.
16. Christie, G. S. and Judah, J. D. *Proc. Roy. Soc. London,* **B 142** (1954) 241.
17. Recknagel, R. O. and Anthony, D. D. *J. Biol. Chem.* **234** (1959) 1052.

Received December 2, 1959.

ACTA CHEMICA SCANDINAVICA 14 (1960) 846–860

On the Oxidation of Cholesterol in Liver Mitochondrial Preparations

Bile Acids and Steroids 99

HENRY DANIELSSON

Department of Chemistry, Karolinska Institutet, Stockholm, Sweden

The oxidation of 4-^{14}C- and 26-^{14}C-cholesterol has been studied in mitochondrial preparations of mouse and rat liver. The simultaneous occurrence of autoxidation and enzymatic oxidation of the added labeled cholesterol, indicated by experiments on the metabolism of cholesterol in different cellfractions of liver and in mitochondria of heart and kidney, has been ascertained by analyses of the labeled products formed under non-enzymatic and "enzymatic" conditions. Among autoxidatively formed products 3β, 5α, 6β-trihydroxycholestane, 7α-hydroxycholesterol, 7β-hydroxycholesterol and 7-ketocholesterol have been identified. Two major enzymically formed compounds both retaining the C_{27}-side-chain, have been isolated. One is less polar than 7α-hydroxycholesterol but more polar than 7-ketocholesterol, while the other shows chromatographic properties similar to a neutral trihydroxy-C_{27}-sterol. This latter compound is metabolized to chenodeoxycholic but not cholic acid in the bile-fistula rat.

Cholesterol is catabolized by the liver *in vivo* to bile acids, which represent the major end-products of cholesterol metabolism in the animal body. The individual steps in this chain of reactions, which entail elimination of the terminal *iso*propyl-group and modifications of the nucleus by saturation of the Δ^5-double bond, reversal of the configuration of the hydroxyl-group at C_3 and introduction of hydroxyls in C_7 and C_{12} or C_6, have not been fully established. The work of Bergström and Lindstedt [1-4] on the metabolism in the bile-fistula rat of possible intermediates between cholesterol and cholic acid has yielded important informations on the likely sequence in this process. Thus, all available evidence makes it probable that the nucleus is hydroxylated, first at C_7 and then, at least in this species, at C_{12} prior to the completion of the side-chain degradation, and that one of the early steps is the introduction of the 7α-hydroxyl-group.

Studies of the metabolism of cholesterol *in vitro* appear a promising approach to further investigations on the individual steps in the degradation

of cholesterol to bile acids. Such investigations have also been undertaken by several groups of workers. Meier *et al.*[5] reported in 1952 on the formation of labeled CO_2 from 26-^{14}C-cholesterol in rat liver slices. Anfinsen and Horning [6,7] demonstrated the same reaction in mouse liver mitochondria in presence of AMP *, DPN and boiled liver juice. Gurin and coworkers [8,9] have reported similar findings and also the formation of labeled 25-dehydrocholesterol, a labeled C_{27}-acid and aldehyde from 26-^{14}C-cholesterol in a solubilized rat liver mitochondrial system.

Fredrickson and Ono [10,11] analyzed the products formed from 4-^{14}-C-cholesterol in the mouse liver mitochondrial system of Anfinsen and Horning and found that of the 25 % of cholesterol metabolized 15 % was present as acidic compounds not identical with cholic or deoxycholic acid, 7 % as 25- and 26-hydroxycholesterol and the remainder as cholesterol esters. In a preliminary communication Danielsson and Horning [12] have reported on the formation of an unknown compound both from 4-^{14}C- and 26-^{14}C-cholesterol in essentially the same mouse liver mitochondrial system. This compound, which had chromatographic properties similar to a trihydroxylated neutral C_{27}-sterol, was metabolized in the bile-fistula rat to chenodeoxycholic acid and to two acids with chromatographic mobilities identical with those of the 6β-hydroxylated acids formed from chenodeoxycholic acid.

Such *in vitro* studies of the oxidation of cholesterol might conceivably be complicated by the well-known fact that cholesterol is easily autoxidized in colloidal solutions in the presence of air. The products of autoxidation are formed by introduction of oxygen functions in the 5,6,7-positions of the cholesterol molecule.

In a thourough study of the autoxidation of cholesterol in aqueous colloidal solutions Bergström and Wintersteiner[13–15] demonstrated the formation of 7-ketocholesterol and the two epimeric 7-hydroxycholesterols. The oxidation proceeded equally well at 37° as at 85°, although slower, reaching completion after 24 h at 37° compared to 3 h at 85°. After this period of time about 60 % of the cholesterol had been transformed into the 7-oxygenated compounds. Later, Mosbach *et al.*[16] could isolate in low yield 3β, 5α, 6β-trihydroxycholestane from samples of autoxidized cholesterol and Schwenk *et al.*[17] detected small amounts of 3β-, 5α-dihydroxy, 6-ketocholestane in samples of cholesterol-extracts from liver.

In the present work the products formed from labeled cholesterol in presence of rat and mouse liver mitochondria have been isolated and partly identified and the conditions under which the products are formed have been investigated.

EXPERIMENTAL

Labeled compounds. 4-^{14}C-cholesterol (60 μC/mg) was obtained from the Radiochemical Centre, Amersham, England. 26-^{14}C-cholesterol (250 μC/mg) was purchased from New England Nuclear Corp., Boston, Mass., USA. Prior to use the labeled cholesterol was checked for absence of autoxidation products by chromatography [18].

* Abbreviations used are: AMP = adenosine-monophosphate: DPN = diphosphopyridine nucleotide; Tris = tris (hydroxymethyl)aminomethane: EDTA = ethylenediaminetetraacetic acid.

Reference compounds. *7-Ketocholesterol* (m.p. 169—170°; reported [15] 170°—172°) was prepared from cholesteryl acetate by oxidation with *t*-butyl chromate according to Heusler and Wettstein [19], followed by hydrolysis with potassium carbonate [20]. *7β-Hydroxycholesterol* (m.p. 172—173°, $[\alpha]_D^{25}$ +5°; reported [24] m.p. 178°, $[\alpha]_D$ +7°) was obtained by lithium aluminum hydride reduction of 7-ketocholesteryl acetate and purified by formation of the dibenzoate [21]. *7α-Hydroxycholesterol* was prepared according to Henbest and Jones [22,23]. Cholesteryl benzoate was treated with N-Br-succinimide in boiling carbon tetrachloride for 5—6 min. The resulting 7α-Br-cholesteryl benzoate was treated with sodium formate to yield 7α-formoxycholesteryl benzoate, purified by chromatography on aluminum oxide (Merck, Darmstadt, Germany) and the free sterol was then obtained by saponification. The resulting 7α-hydroxycholesterol had a m.p. of 184—85°, $[\alpha]_D^{25}$ —92°; reported [23,24] 185° $[\alpha]_D$ —86.6° and 91.6°. *3β, 5α, 6β-Trihydroxycholestane* (m.p. 228—231°; reported [25,26] 229—233° and 237—239°) was prepared according to Fieser *et al.*[26] by treatment of cholesterol with hydrogen peroxide in formic acid. 3β, 5α-Dihydroxy, 6-ketocholestane (m.p. 230—233°; reported [26] 231—232°) was obtained by treatment of cholesterol in methanol with N-Br-succinimide, as described by Fieser *et al.*[26].

Preparation of homogenates. White male mice of the Danish State Serum Institute strain weighing approx. 25 g and white male rats of the Sprague-Dawley strain weighing approx. 150 g were used. 10 or 33 % (liver wet weight/volume) homogenates were prepared in 0.25 M sucrose containing 3.6 mg nicotinamide/ml with a tight-fitting Teflon Potter-Elvehjem homogenizer. Mitochondria were isolated by centrifugation for 10 min at 10 000 × *g* and then washed once with the homogenizing medium. Microsomes were spun down in the Spinco preparative ultracentrifuge at 100 000 × *g*, 60 min. Boiled liver juice was prepared from the supernatant of the 10 000 × *g* centrifugation of mouse liver homogenates by heating for 10 min at 85—95° followed by centrifugation for 20 min at 20 000 × *g* to remove denatured protein. In some cases boiled liver juice was prepared according to Horning *et al.*[7] The boiled liver juice was kept at —15° for not more than 4—6 weeks prior to use.

Mitochondria and microsomes were resuspended in a few ml of the nicotinamide-sucrose medium by homogenization with a loose-fitting pestle 10—20 sec and then diluted to suitable volumes. The composition of the incubations, in which mitochondria, AMP, DPN (purchased from the Sigma Chemical Co., St. Louis, USA and Boehringer, Mannheim, W-Germany, respectively) and boiled liver juice were used simultaneously, was as follows:

Mitochondria from 15 g of liver in 10 ml nicotinamide-sucrose medium
Boiled liver juice 9 ml
0.01 M DPN 1.5 ml
0.04 M AMP 1.5 ml
0.05 M Tris buffer, pH 7.8, 5 ml
Serum albumin suspension of labeled cholesterol 1—2 ml

When less or more mitochondria were used the amounts were proportionally changed. When boiled liver juice was omitted no change in the concentrations of the other components was made. In incubations with microsomes, these were suspended in the amount of solution used for suspending mitochondria.

The labeled cholesterol was added to the incubation mixtures as an emulsion with serum albumin, prepared by dissolving the sterol in 0.1—0.2 ml ethanol and adding 0.9—1.8 ml of a 1 % solution of bovine serum albumin (Armour Lab., Kankakee, Ill. USA) in distilled water. In some instances the cholesterol emulsion was prepared with Tween 20 (Atlas Powder Co., Wilmington, Delaware, USA) as described by Meier *et al.*[5]

Incubations were conducted aerobically at 38° for 4 h with shaking in 50 ml Erlenmeyer-flasks containing each not more than 5—7 ml of the incubation mixture. The incubations were terminated by addition of 3—4 volumes of ethanol.

Analyses of the incubation mixtures. The precipitate formed by the addition of ethanol was removed through filtration and the ethanol was evaporated. The aqueous residue was acidified with hydrochloric acid and then extracted twice with water-saturated *n*-butanol. The combined butanol-extracts were washed with water until neutral and

then taken to dryness. The residue was chromatographed in the reversed phase partition systems earlier described. Phase systems I and III [17] were employed for separation of neutral steroids and systems C1 and F1 [27] for acidic steroids. Hyflo Supercel or Hostalene, prepared as earlier described [18,28], were used as supporting material for the stationary phase.

Phase systems:

	Moving phase	ml	Stationary phase	ml
I	*Iso*propanol:water	165:135	chloroform:heptane	10:40
III	» »	150:150	» »	15:60
C1	Methanol:water	150:150	chloroform:*iso*octanol	15:15
F1	» »	165:135	chloroform:heptane	45:5

Chromatograms were run at constant temperature of 23°. Radioactivity was determined in infinitely thin layers with an automatic end-window counter or in a window-less methane gas-flow counter (Frieseke and Hoepfner, Erlangen, Germany, FH 49 and FH 51, respectively). $^{14}CO_2$ was trapped in 2 N KOH, precipitated with 1.5 M $BaCl_2$ and counted in an infinitely thick layer of $BaCO_3$.

RESULTS

Fractionation of homogenates and optimal conditions for oxidation of 4-^{14}C-cholesterol

In this section experiments are described where the conversion of cholesterol to more polar products was analyzed by chromatography first on phase system I to separate cholesterol from the more polar products (Fig. 1) and then on phase system III (Fig. 2) to separate the more polar products into three fractions, one "acidic" (A Fig. 2), one "trioxy neutral" (B Fig. 2) and one "dioxy neutral" (C Fig. 2).

Fractionation of liver homogenates, which were prepared either as 10 or 33 % homogenates, by differential centrifugation in the usual manner, demonstrated (Table 1) that the oxidation of cholesterol to more polar products

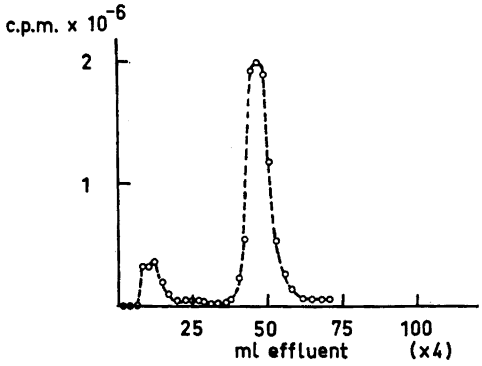

Fig. 1. Chromatogram of the butanol-extract from an incubation of 4-^{14}C-cholesterol with mouse liver mitochondria + boiled juice, AMP and DPN, 18 g Hostalene. Phase system I.

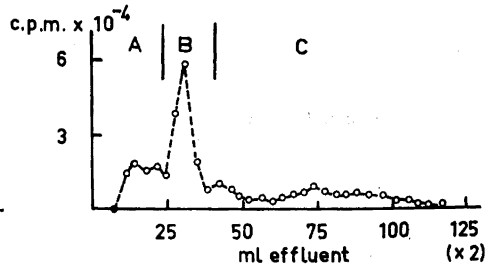

Fig. 2. Rechromatography of first peak in the chromatogram shown in Fig. 1. A = "acidic" fraction; B = "trioxy neutral" fraction; C = "dioxy neutral" fraction. 9 g Hostalene. Phase system III.

Table 1. Oxidation of cholesterol in different cellfractions of mouse and rat liver. 33 % homogenate.

	% conversion to more polar products	
	Rat	Mouse
Mitochondria	3	4.7
Microsomes	0.7	2.5
Supernatant	0.7	2
Mitochondria + supernatant	5	10
Mitochondria + microsomes + supernatant		5.5
Microsomes + supernatant	0.5	3.3

occurred most easily in presence of mitochondria isolated from mouse as well as rat liver. The addition of 100 000 × *g* supernatant (hereafter called supernatant) to mitochondria doubled the conversion. The oxidation was considerably slower in presence of microsomes and the addition of microsomes to mitochondria plus supernatant depressed the oxidation. Supernatant alone was capable of a small transformation of added cholesterol to more polar products. Use of boiled liver juice (prepared in either of the two ways described in the experimental part) instead of fresh supernatant in combination with mouse liver mitochondria resulted in the highest conversion of cholesterol to more polar products (10—15 %) and it was found that this magnitude of conversion could easily be reproduced from experiment to experiment. The extent of conversion was examined at various intervals during a 4 h incubation with this system (Fig. 3) and the oxidation was found to proceed in two phases, one rapid with leveling off after 1 h of incubation and afterwards one linear phase.

This system, mouse liver mitochondria plus boiled liver juice, is the same as the one described for achieving maximal $^{14}CO_2$-production from 26-^{14}C-cholesterol except that in the latter case there is a requirement for DPN and AMP. Using the amount of more polar products formed from 4-^{14}C-cholesterol as index of oxidation, as has been done in this investigation, the addition of DPN and/or AMP to the system had no influence on the magnitude of the oxidation nor could any effect be observed, when these cofactors, alone or in combination, were added to mitochondria alone (Table 2).

Incubation with boiled liver juice only resulted in 2—3 % oxidation of the added 4-^{14}C-cholesterol, easily reproduced in a number of experiments.

Table 2. The effect of cofactors on the oxidation of cholesterol in mouse liver mitochondria. 33 % homogenate.

	% conversion to more polar products
Mitochondria	6
» + DPN	5
» + AMP	5
+ DPN and AMP	6.5
+ boiled juice	11
» + boiled juice and DPN	11.5
» + boiled juice + AMP	9
» + boiled juice + DPN + AMP	11

Table 3. Oxidation of cholesterol in mitochondria isolated from different organs. 33 % homogenate.

	% conversion to more polar products	
	Rat	Mouse
Mitochondria (liver)	6.5	5.5
» + boiled juice	8.6	10
Boiled juice	3.3	3
Mitochondria (kidney)	0.7	1
» + boiled juice	2	
Mitochondria (heart)	2	1

Oxidation of cholesterol in presence of a deproteinized liver extract must be attributed to autoxidation. This finding is not entirely surprising in view of the long recognized sensitivity of cholesterol to autoxidation in colloidal solutions. Considering the appreciable autoxidation occurring in presence of boiled liver juice it was conceivable that at least part of the oxidation taking place in the optimal system (mouse liver mitochondria plus boiled liver juice) or even in mitochondria alone was due to autoxidation. One possible way of establishing if autoxidation occurred in presence of mitochondria alone was thought to be a study of the oxidation, if any, of cholesterol in mitochondria isolated from other organs, *e.g.* heart or kidney, which in the present state of knowledge can be regarded as unlikely sites of cholesterol catabolism *in vivo*. The extent of oxidation in heart or kidney mitochondria isolated from rat or mouse varied from 0.7 to 2 % (Table 3). Judging from the chromatographic behaviour of the polar products formed, these consisted of autoxidation products. It appears likely, therefore, that a certain degree of autoxidation of cholesterol occurs in mitochondrial systems.

Using the analytical procedure outlined at the beginning of this section, a consistent difference in the ratio "trioxy neutral" to "dioxy neutral" fraction was obtained when experiments using the complete system were compared with experiments using boiled liver juice only. Thus, under "enzymatic" conditions, *i.e.* using the full system, this ratio in the isolated products was 1.5—1.8, while non-enzymatic incubations, *i.e.* using boiled liver juice, yielded much less "trioxy neutral" steroids, resulting in a ratio of about 0.5—0.7. After incubations with mouse liver mitochondria alone roughly equal amounts of "trioxy neutral" and "dioxy neutral" steroids were isolated, and with rat liver mitochondria somewhat more of the "dioxy neutral" fraction was formed.

As it seemed apparent that part of the more polar products was formed by autoxidation of the added labeled cholesterol, to be described in more detail in the following section, it was conceivable that the mode of suspending the cholesterol could be a factor to be taken into account. Accordingly several experiments were performed using Tween 20 emulsions, a method that has been widely used for dispersing water-insoluble steroids in aqueous media. However, it was found, that the general pattern of polar products formed in the full system from Tween-emulsified cholesterol did not differ from that obtained when albumin-suspensions of cholesterol were used.

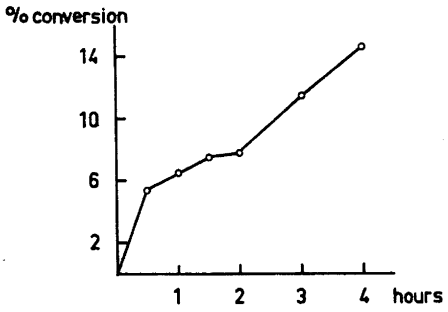

Fig. 3. Time curve of oxidation of cholesterol in mouse liver mitochondria + cofactors.

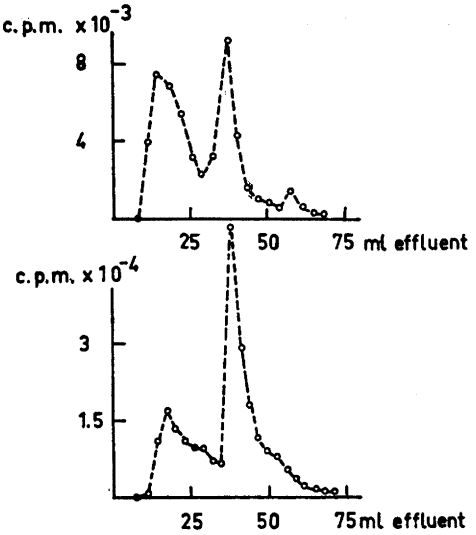

Fig. 4. Rechromatography of "acidic" and "trioxy neutral" fractions from incubation A (upper curve) and C (lower curve). 4.5 g hydrophobic Hyflo Supercel. Phase system III.

In view of the stability of cholesterol towards autoxidation *in vivo*, it appeared possible that the observed occurrence of autoxidation in the mitochondrial system might be due to incomplete penetration of the mitochondrial membrane by the extramitochondrially added cholesterol. As circumstantial evidence for such a concept could be taken the fact that efforts of procuring weighable amounts of the different more polar products by incubating mitochondria from several hundred rat livers did not yield the amounts that could be calculated from the magnitude of conversion of the labeled cholesterol added in these incubations and the amount of endogenous cholesterol present in the mitochondria. Experiments on the distribution of the added cholesterol between the mitochondria and the suspending medium would appear at first sight a more direct approach to this problem. After the termination of a usual 4 h incubation, the mitochondria were isolated again by centrifugation and the amounts of labeled cholesterol and conversion products were assayed both in the mitochondria and in the supernatant fluid. About 75—80 % of the total activity was found associated with the mitochondria. The percentage of more polar products of the total radioactivity was approximately the same in the mitochondria as in the supernatant fluid. Experiments on the rate of association of the added labeled cholesterol with the mitochondria demonstrated that after 15 min incubation 25 %, after 1 h 50 % and, as stated above, after 4 h 75—80 % of the originally added radioactivity was recovered from the mitochondria. That so much of the label was associated with the mitochondria when isolated after a 4 h incubation is by no means any proof, that the label

actually is present inside the mitochondria, as it might just as well be partly or wholly on the surface of the mitochondria. At this time no comparatively simple means of differentiating between these two possibilities could be visualized.

The presence of cupric ions has been shown to be an absolute requirement for the autoxidation of cholesterol in aqueous colloidal solutions [15] and the use of heavy metal complex formers in the incubation mixtures could conceivably reduce the autoxidation occurring in the mitochondrial system. Attempts to achieve a reduction of autoxidation merely by preparing the homogenate and cofactors in redistilled water and carrying out the incubations in flasks carefully rinsed with redistilled water were unsucessful. This is not unexpected since heavy metal ions already occur in the liver. However, in the presence of 10^{-3} M EDTA in the incubation mixture, a considerable reduction of the autoxidation occurred. The conversion to more polar products was in this case 6.4 % compared to 10.8 % in a parallel incubation without EDTA. The distribution of the more polar products between the "acidic", "trioxy neutral" and "dioxy neutral" fractions were in both instances approximately the same, but when the "trioxy neutral" fractions were further analyzed a marked difference was observed. This fraction, as described in detail below, contains 3β, 5α, 6β-trihydroxycholestane, which is the major autoxidation product formed in the present experiments. The content of the cholestanetriol in the "trioxy neutral" fraction from the incubation with EDTA present was only a third (16 %) of that (44 %) found when no EDTA had been added. The used of 10^{-3} M CN^- or 10^{-3} M phenanthroline did not result in the same reduction of autoxidation as the use of EDTA.

Isolation and partial identification of the products of oxidation of cholesterol under non-enzymatic and "enzymatic" conditions

Before undertaking the experiments described below, and the analyses of the products formed in these, a number of testruns and testanalyses were performed. The same chromatographic pattern of products was obtained, whether mitochondria isolated from a 10 % or a 33 % homogenate were employed in incubations with 4-^{14}C-cholesterol together with boiled juice prepared from a water extract of whole liver or from the supernatant fluid obtained after removal of mitochondria. As it was found more practicable to use a 33 % homogenate and boiled juice isolated after spinning down the mitochondria, this method was employed in experiments aiming at isolation of products. When this system was tested in a few experiments for $^{14}CO_2$-production from 26-^{14}C-cholesterol, negligible amounts of labeled CO_2 could be recovered. Chromatography of such incubations demonstrated the presence of the same products found in 4-^{14}C-cholesterol incubations. Two incubations, kindly performed by Dr. M. G. Horning, were run with 26-^{14}C-cholesterol with the aim of also analyzing for $^{14}CO_2$ using a 10 % homogenate and boiled juice from a water extract of whole liver. The yield of labeled CO_2 was 2.5 and 0.4 %, respectively. Due to the use of too small an amount of 26-^{14}C-cholesterol in the first experiment, the conversion products could not be isola-

ted. In the second experiment the conversion to polar products was 10 %. Chromatography of this material did not demonstrate any noticeable difference in the pattern of products compared to, *e.g.*, the ones isolated in the experiments described below.

Isolation and partial identification of products formed from 4-^{14}C-cholesterol under non-enzymatic and "enzymatic" conditions were performed on four separate incubations using: A, cofactors only (boiled juice, AMP and DPN); B, mouse liver mitochondria; C, mouse liver mitochondria plus cofactors; D, rat liver mitochondria. Analyses were performed in the same manner for all four incubations unless otherwise stated.

Chromatography of the butanol-extracts on phase system I allowed calculations of the amount of the more polar products and of cholesteryl esters formed, which latter are retained in the stationary phase. The conversions are given at the top of Table 4. The amount of cholesteryl esters in incubation B was 0.2 %, in C 1.6 % and in D 0.7 %. The more polar products were saponified with 10 % methanolic potassium hydroxide for 1 h. This procedure, which facilitates the further isolation of the products, does not appear to change the chromatographic properties of these. After saponification the polar material was chromatographed on phase system III to separate it into the three fractions earlier discussed. Some 20 % of the radioactivity was retained in the stationary phase and was found to consist of cholesterol as shown by rechromatography on phase system I. An explanation for the presence of cholesterol in this eluate could be that a small part of the cholesterol in the original

Table 4. Fractionation of oxidation products of cholesterol formed under non-enzymatic and "enzymatic" conditions. 33 % homogenate. Amounts of mitochondria and cofactors as given in Experimental. 100 μC of 4-^{14}C-cholesterol was added to each incubation.

	A (Boiled juice, AMP, DPN)	B (Mousemitochondria)	C (Mousemitochondria + boiled juice, AMP, DPN)	D (Rat mitochondria)
Conversion to more polar products in % (before saponification)	4.4	8	15.5	5
Conversion to more polar products in % (after saponification)	3.2	6.7	13.1	3.6
% of total more polar products (after saponification) as Acids	22	20	17	21
3β, 5α, 6β-trihydroxycholestane	14	18	24	13
Ia	6	14	19	12
Ib		3	5	5
7α-Hydroxycholesterol	12	5	5	20
7β-Hydroxycholesterol	26	8	6	
Unidentified material in "dioxy"-fraction (cf. text)	9	7	4	
III	0	18	14	25
7-Ketocholesterol	11	7	6	4

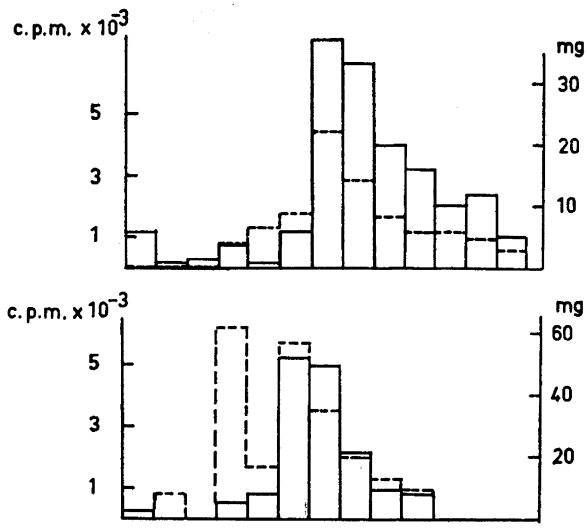

Fig. 5. Chromatography of acetylated "trioxy neutral" fractions of A and C together with unlabeled 3β, 5α, 6β-trihydroxycholestane. *Cf.* Fig. 4. 100 ml fractions. Each bar represents one fraction. 20 g Woelm I. Broken line: radioactivity. Solid line: weight.

butanol-extract was in the form of a complex with lipid material of such a polarity, that it is eluted early with phase system I. After saponification this complex would dissociate and the free cholesterol formed is retained in the stationary phase of the chromatogram with phase system III.

The "acidic" and the "trioxy neutral" fractions were combined and rerun to obtain a more distinct separation of these fractions. This chromatogram is shown in Fig. 4. The upper curve is the one obtained from incubation A (cofactors only) and the lower from incubation C (full system). All subsequent figures will also each show chromatograms from incubation A (upper curves) and C (lower curves).

"*Acidic*" *fraction.* The acidic material was chromatographed together with unlabeled cholic acid with phase system C1. In all cases there was a front peak. In material from incubations B, C and D there was also obtained a peak appearing shortly after cholic acid. The eluates of these columns containing any dihydroxy- and monohydroxy acids were chromatographed together with unlabeled chenodeoxycholic acid on phase system F1. In all four chromatograms two radioactive bands appeared after the titration curve of the added carrier.

"*Trioxy neutral*" *fraction.* The "trioxy neutral" fractions were acetylated together with 200 mg 3β, 5α, 6β-cholestanetriol each and chromatographed on aluminium oxide (Woelm, Eschwege, W-Germany, grade 1) using increasing concentrations of ethyl acetate (from 0 to 5 %) in benzene as eluant. In the chromatograms of this fraction from incubation C, as shown in Fig. 5, a large radioactive peak, designated in Table 4 as Ia, appears before the 3,6-diacetate

of the carrier is eluted. Comparatively small amounts of activity is eluted at this place in the chromatogram of the same fraction from incubation A, *cf.* Fig. 4. The same early radioactive peak, although smaller, was observed in chromatograms of B and D. Radioactivity was in all cases eluted together with the carrier. At the end of the peak of the carrier the specific activity per mg carrier rose, and to find out if this represented another radioactive compound than the cholestanetriol, the carrier peaks were divided into two fractions, that were crystallized separately to constant specific activity (four crystallizations from methanol/water, acetone/water, hexane and methanol/water). It was found that the late increase in specific activity of the carrier observed in the chromatogram represented radioactive material, designated in Table 4 as Ib, not identical with the 3,6-diacetate of the cholestanetriol. As this occurred also in A, it was thought that this material might be the 3-acetate of 3β-, 5α-dihydroxy-6-ketocholestane, but cocrystallization of the radioactive material with this compound failed to establish any such identity. As Ib represented only a small amount of the total "trioxy neutral" fraction any further characterization was not pursued.

Some information on the structure of compound Ia was obtained by its metabolism in the bile-fistula rat. When injected intraperitoneally it was rapidly excreted, 60—70 % the first 24 h, and had been transformed into chenodeoxycholic acid, the identity of which was established by cocrystallization with unlabeled chenodeoxycholic acid, and into two other acids with chromatographic properties identical to those of the 6β-hydroxylated acids formed from chenodeoxycholic acid.

"Dioxy neutral" fraction. The "dioxy neutral" fraction was subjected to additional chromatography on Hyflo Supercel columns using phase system III. By this method of chromatography this fraction could be separated into two distinct peaks in the case of B, C and D, while A yielded only one main peak, *cf.* Fig. 6. The material in the first peak, present in A, B, C and D, had the same elution volume as 7α- and 7β-hydroxycholesterol, which are difficult to separate with this phase system. The method of choice for achieving a separation of these epimers appears to be to form the dibenzoates, which are reported to be separable by chromatography on aluminium oxide [21] and which in addition are easier to crystallize than the free sterols, anyway in the case of the β-epimer. Accordingly the radioactive material was diluted with 100 mg of unlabeled 7β-hydroxycholesterol and benzoylated in the usual manner. The ether extract of the benzoylation mixture was distributed between hexane and 70 % aqueous methanol, a procedure that was found to remove byproducts, which seriously interfered with the chromatography. The hexane-phase containing the hydroxycholesterol dibenzoates was evaporated to dryness and the residue chromatographed on aluminium oxide. In spite of considerable efforts to separate the epimers by careful chromatography on both Woelm, grade I, and Merck aluminium oxide, no such separation could be obtained. However, it was found that in B and C, but not in A (D was lost in an earlier chromatogram), a radioactive peak appeared in the chromatogram just before the elution of the hydroxycholesterol dibenzoates, but whether this early peak represented some unknown compound or just by chance a partial separation of the α-epimer from the β-epimer cannot be stated at present. All material

eluted in respective columns was combined and crystallized to constant specific activity (from methanol once and acetone/water twice) and the amount of 7β-hydroxycholesterol could thus be calculated. The first mother liquor containing the α-epimer, was then diluted with 80 mg unlabeled 7α-hydroxycholesterol dibenzoate and crystallized to constant specific activity (from methanol once and acetone/water twice) giving the amount of this epimer in the original mixture. Isotope dilution as analysis for the two hydroxycholesterol dibenzoates in a mixture of both has been used earlier by Dauben and Payot [25]. In the case of A there remained 20 %, in B 36 % and in C 30 %, of the original radioactivity not accounted for as the 7-hydroxycholesterol dibenzoates. During the course of the attempts to separate the epimeric dibenzoates, it was observed that limited hydrolysis of the dibenzoates occurred, especially when the chromatograms had to be run over several days. Whether the radioactivity not identified as 7α- and 7β-hydroxycholesterol dibenzoate could be accounted for as partly or wholly saponified dibenzoate or represented a new compound(s) was not further investigated with this material.

In the chromatograms of the "dioxy neutral" fraction (*cf.* Fig. 6), as mentioned earlier, another compound, designated as III in Table 4, was eluted after the 7α- and 7β-hydroxycholesterol in B, C and D. The formation of this unknown metabolite has been observed only in "enzymatic" incubations and its nature and further metabolism is presently being studied.

In all four chromatograms of the "dioxy neutral" fraction on Hyflo Supercel columns (Fig. 6) part of the radioactivity was retained in the stationary

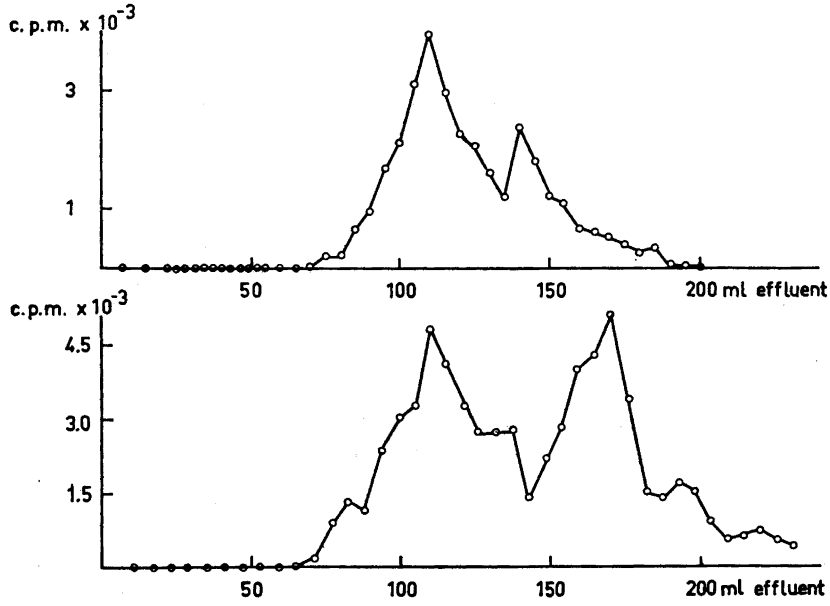

Fig. 6. Chromatograms of "dioxy neutral" fractions of A and C. *Cf.* Fig. 4. 4.5 g hydrophobic Hyflo Supercel. Phase system III.

phase. This material was rechromatographed on phase system I and found to have the same elution volume as 7-ketocholesterol. The identity of the labeled material with 7-ketocholesterol was established by isotope dilution.

DISCUSSION

Prior to the present work only one investigation, that by Fredrickson [10], on the oxidation of 4-^{14}C-cholesterol in a fortified mouse liver mitochondrial system has been published. The results obtained in the two studies are entirely at variance with each other and no explanation can be offered. While Fredrickson found products that appeared to have arisen by enzymatic oxidation only, the results now presented, corroborated by further analyses of the experiments reported by Danielsson and Horning [12], emphasize first of all that a considerable degree of autoxidation of the added 4-^{14}C-cholesterol indubitably occurs. Thus, there appears to be no reason to invoke enzymatic action as an explanation for the formation of such compounds as 3β, 5α, 6β-cholestanetriol, 7β-hydroxycholesterol and 7-ketocholesterol, which were formed in all incubations examined. These compounds are all typical autoxidation products and would be illogical and improbable intermediates in the catabolism of cholesterol to bile acids, which latter have normally a 7α-hydroxyl-group and invariably lack a hydroxyl at position 5. The possibility that 7α-hydroxycholesterol in part was formed enzymatically should not be excluded expecially as the evidence so far available makes it a highly probable early intermediate in the formation of bile acids from cholesterol [3]. On the other hand, it must also have been formed by autoxidation, which yields both epimers. Any possibility of establishing if 7α-hydroxycholesterol was formed partly by enzymatic action on cholesterol in the present experiments appears remote.

Based on the nature of the polar products and the respective amounts of these the extent of autoxidation in the fortified mouse liver mitochondrial system amounted to approximately 50 % of the total amount of labeled cholesterol oxidized.

Although the occurrence of autoxidation in the mitochondrial system cannot be regarded as unexpected in view of the well-documented instability of cholesterol in polar solvents upon exposure to oxygen *, it would seem possible that the mode of solubilizing the cholesterol could be of importance. Attempts to reduce autoxidation by emulsifying with Tween instead of serum albumin were not successful. Recently Avigan [29] published a method for preparing cholesterol solutions with the aid of serum lipoproteins and this method merits to be tested as a possible means of reducing autoxidation in the mitochondrial system. Another possibility could be to run short time incubations. The shape of the time curve was such (Fig. 3) that it had some resemblance to that of an enzymatic process in mitochondria or microsomes during the first 2 h of incuba-

* The radiation of ^{14}C in ^{14}C-labeled cholesterol stored in the dry state in presence of air for long periods of time, 1 month—2 years, has been shown [25] to induce autoxidation proceeding in a manner identical with that of unlabeled cholesterol in colloidal suspensions. The contribution, if any, of the radiation of ^{14}C in the labeled cholesterol to the magnitude of autoxidation in the present experiments was not investigated.

tion. However, some preliminary analyses of polar products formed during this early phase of the incubation did not reveal any striking differences.

A more direct approach to the problem of reducing autoxidation seems to be to incubate in the presence of heavy metal complex formers, as the autoxidation of cholesterol in aqueous colloidal solutions has been shown to require the presence of cupric ions [15]. The use of 10^{-3} M EDTA in the incubation mixture resulted in a considerable but not total reduction of the autoxidation. Further work is needed in order to be able to closer evaluate the possibilities in this method.

The emphasis should, however, not be put only on the occurrence of autoxidation of the added labeled cholesterol in the mitochondrial preparations. Approximately half of the products isolated must have been formed by the action of enzymes. As basis for this conclusion is taken that products formed only in the presence of mitochondria are enzymatic products. The two main enzymatically formed products were Ia, which is identical with the compound earlier reported on by Danielsson and Horning [12], and III (*cf.* Table 4). As earlier stated both compound Ia and III must have a C_{27}-side-chain, as they were formed also from 26-^{14}C-cholesterol, but the detailed structures of these have not been established. Ia had chromatographic properties similar to those of a trihydroxylated neutral C_{27}-sterol both on reversed phase and as acetylated on aluminium oxide columns. It forms probably a triacetate. as it had the same mobility on aluminium oxide as the triacetate of 3α, 7α, 27-trihydroxycoprostane. The manner it was metabolized in the bile-fistula rat, yielding chenodeoxycholic but not cholic acid, indicated that the hydroxyls could be in positions 3, 7 and 27, as 3α, 7α-dihydroxycoprostane is metabolized to both cholic and chenodeoxycholic acid, while 3α, 7α-dihydroxycoprostanic acid gives chenodeoxycholic but not cholic acid [30], *i.e.* the presence of oxygen functions in the side-chain of a steroid with a 3,7-hydroxylated nucleus makes a 12-hydroxylation in the rat impossible.

Compound III showed chromatographic properties similar to those of a saturated dihydroxy neutral C_{27}-sterol or of an unsaturated hydroxyketone with considerably greater polarity than 7-ketocholesterol. Work on the structure and further metabolism of this compound is in progress and will be the subject of a future communication.

Among the acidic products at least one acid, the one which was eluted shortly after cholic acid with phase system C1, was an enzymatic product, but no further characterization of this acid has been carried out. The presence of labeled acidic compounds in the non-enzymatic incubations was unexpected, as such products have not been demonstrated earlier in autoxidized cholesterol. Further work on the nature of these must be done before their chromatographic counterparts in the "enzymatic" incubations can be studied.

In discussing the labeled enzymatic products formed from labeled cholesterol in the mitochondrial preparations, it must be stressed that there is no evidence, either for or against, that these compounds are formed *directly* from cholesterol, as they just as well could be enzymatically transformed autoxidation products, in the case of Ia and III most probably from 7α-hydroxycholesterol and in the case of the acidic compound(s) from any of the autoxidation products.

Whether or not any $^{14}CO_2$ was formed from 26-^{14}C-cholesterol, the same general pattern of polar products was obtained. The results presented therefore have the same bearing on incubations performed with 26-^{12}C-cholesterol as with 4-^{14}C-cholesterol. There can be no doubt that the formation of $^{14}CO_2$ from 26-^{14}C-cholesterol is an enzymatic process but the nature of the substrate in this oxidation is in more doubt, anyway as judged from the results of this investigation. Using only $^{14}CO_2$-formation from 26-^{14}C-cholesterol as an assay it appears that results of studies of the *quantitative* aspects on the conversion of cholesterol to bile acids should be interpreted with caution, especially in incubations of long duration.

Acknowledgments. The skillful technical assistance of Miss Birgitta Holmberg and Miss Electra Pascalides is gratefully acknowledged.

This work is part of investigations supported by *Statens Medicinska Forskningsråd, Knut och Alice Wallenbergs Stiftelse, Karolinska Institutets Reservationsanslag* and *The National Institutes of Health*, Bethesda, Md, USA (H 2842).

REFERENCES

1. Bergström, S. *Record. Chem. Progr. Kresge-Hooker Sci. Lib.* **16** (1955) 63.
2. Bergström, S. and Lindstedt, S. *Biochim. et Biophys. Acta* **19** (1956) 556.
3. Lindstedt, S. *Acta Chem. Scand.* **11** (1957) 417.
4. Lindstedt, S. *Diss.* Lund, 1957.
5. Meier, J. R., Siperstein, M. D. and Chaikoff, I. L. *J. Biol. Chem.* **198** (1952) 105.
6. Anfinsen, C. B. and Horning, M. G. *J. Am. Chem. Soc.* **75** (1953) 1511.
7. Horning, M. G., Fredrickson, D. S. and Anfinsen, C. B. *Arch. Biochem. Biophys.* **71** (1957) 266.
8. Lynn, W. S., Staple, E. and Gurin, S. *Federation. Proc.* **14** (1955) 783.
9. Whitehouse, M. W., Staple, E. and Gurin, S. *J. Biol. Chem.* **234** (1959) 276.
10. Fredrickson, D. S. *J. Biol. Chem.* **222** (1956) 109.
11. Fredrickson, D. S. and Ono, K. *Biochim. et Biophys. Acta* **22** (1956) 183.
12. Danielsson, H. and Horning, M. G. *Biochim. et Biophys. Acta* **34** (1959) 596.
13. Bergström, S. and Wintersteiner, O. *J. Biol. Chem.* **141** (1941) 597.
14. Bergström, S. and Wintersteiner, O. *J. Biol. Chem.* **143** (1942) 503.
15. Bergström, S. *Arkiv Kemi* **16 A** (1942) No. 10.
16. Mosbach, E. H., Nierenberg, M. and Kendall, F. E. *J. Am. Chem. Soc.* **75** (1953) 2358.
17. Schwenk, E., Werthessen, N. T. and Rosenberg, H. *Arch. Biochem. Biophys.* **37** (1952) 247.
18. Danielsson, H. *Biochim. et Biophys. Acta* **27** (1958) 401.
19. Heusler, K. and Wettstein, A. *Helv. Chim. Acta* **35** (1952) 284.
20. Barnett, J., Ryman, B. E. and Smith, F. *J. Chem. Soc.* **1946** 526.
21. Fieser, L. F., Fieser, M. and Chakravarti, R. N. *J. Am. Chem. Soc.* **71** (1949) 2229.
22. Bide, A. E., Henbest, H. B., Jones, E. R. H., Peevers, R. W. and Wilkinson, P. A. *J. Chem. Soc.* **1948** 1783.
23. Henbest, H. B. and Jones, E. R. H. *J. Chem. Soc.* **1948** 1792.
24. Wintersteiner, O. and Ruigh, W. L. *J. Am. Chem. Soc.* **64** (1942) 2453.
25. Dauben, W. G. and Payot, P. H. *J. Am. Chem. Soc.* **78** (1956) 5657.
26. Fieser, L. F. and Rajagopalan, S. *J. Am. Chem. Soc.* **71** (1949) 3938.
27. Norman, A. and Sjövall, J. *J. Biol. Chem.* **233** (1958) 872.
28. Bergström, S., Danielsson, H. and Göransson, Å. *Acta Chem. Scand.* **13** (1959) 776.
29. Avigan, J. *J. Biol. Chem.* **234** (1959) 787.
30. Bridgwater, R. J. and Lindstedt, S. *To be published.*

Received December 17, 1959.

ACTA CHEMICA SCANDINAVICA 14 (1960) 861–870

Substituted 1,3-Diamino-2-propanols

RICHARD DAHLBOM* and ALFONS MISIORNY

Research Laboratories, AB Astra, Södertälje, Sweden

A series of 1,3-diamino-2-propanols of the general formula $R-CH_2 \cdot CHOH \cdot CH_2-Am$ where R is a 2,6-disubstituted anilino residue and Am is an alkylamino group were synthesised. Some compounds were also made with R a benzhydrylamino or 10-phenothiazinyl group.

1,3-Diamino-2-propanols of the general formula $R-CH_2 \cdot CHOH \cdot CH_2-Am$, where R is an unsubstituted or monosubstituted anilino residue and Am is a lower mono- or dialkylamino group were first prepared by Fourneau *et al.*[1,2] in connection with their investigations on antimalarial drugs. Further compounds of this type have been described by Ludwig, West and Farnsworth [3], who stated that these compounds possessed striking convulsant properties.

In connection with work on local anesthetics it was of interest to prepare and study compounds of this type containing a 2,6-disubstituted anilino residue. A number of compounds were synthesised with the general formula

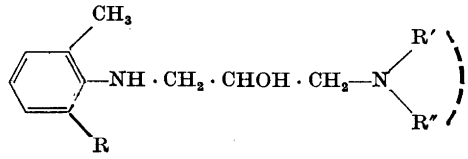

in which R is methyl or chlorine and R′ and R″ are hydrogen, alkyl groups or two connected alkyl groups forming a heterocyclic ring. These compounds were prepared by two methods:

(*A*) Condensation of a 2,6-disubstituted aniline with an N-(2,3-epoxypropyl)-dialkylamine in the presence of lithium amide. Attempts to effect this condensation without a condensing agent gave very poor yields even at elevated temperatures.

---

* Present address: Royal Institute of Pharmacy, Stockholm, Sweden.

(*B*) Treatment of a 2,6-disubstituted aniline with epichlorohydrin giving a 1-anilino-3-chloro-2-propanol, followed by treatment of the product, without isolation, with a large excess of alkali in order to reform an epoxide ring and reaction of the N-(2,3-epoxypropyl)-aniline obtained with a primary or secondary amine.

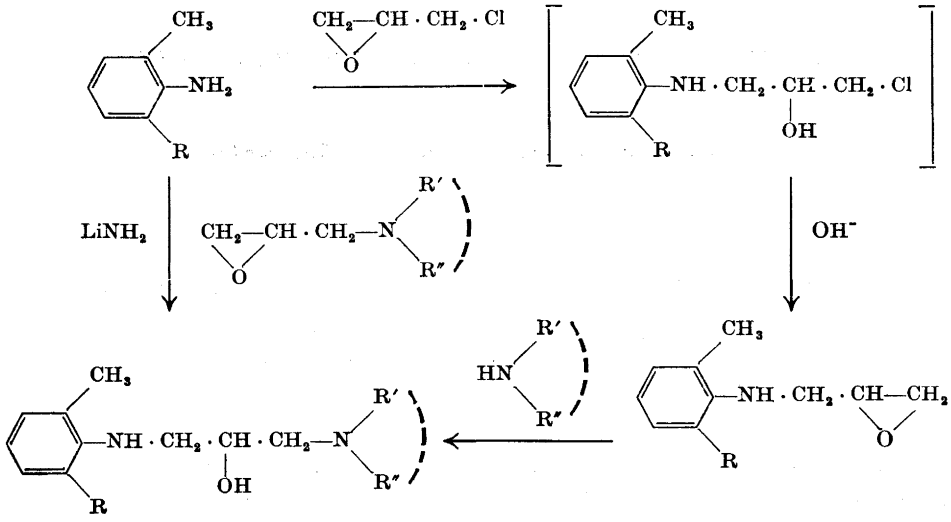

Theoretically the opening of an unsymmetrically substituted epoxide ring can give rise to two structural isomers:

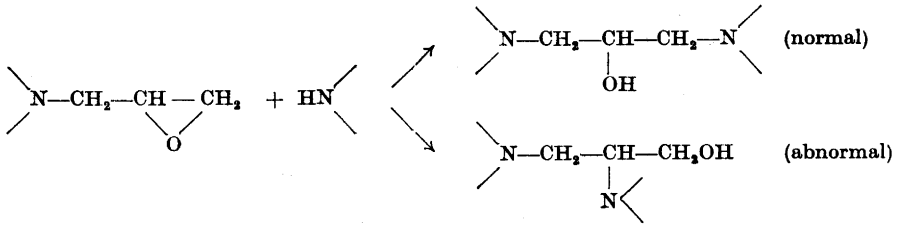

However, there is considerable evidence [4-6] that if the reaction as in this case is a nucleophilic displacement on carbon, the nucleophilic reagent entirely or predominantly attacks the least substituted carbon atom ("normal" ring-opening). We have therefore presumed that the compounds described in this paper are 1,3-diamino-2-propanols and not the isomeric 2,3-diamino-1-propanols which would be the products, if the ring-opening were "abnormal". The compounds (1—20) and their properties are listed in Table 1.

The new compounds were tested for local anesthetic action on rabbit cornea, using Xylocaine as standard. They all had a marked anesthetic effect (usually 1—5 times that of Xylocaine). The *cyclo*hexylamino compounds 7 and 15 were about 15—20 times as active as Xylocaine. The lowest activity

was shown by the compounds containing a morpholino or piperazine residue as amino component. The compounds were usually somewhat more toxic than Xylocaine and moreover had convulsant properties. Some of them had a favourable therapeutic index, but their usefulness as local anesthetics was precluded by the strong irritating properties displayed by all compounds in this series.

Several of the compounds had hypnotic or sedative effects. Attempts were therefore made to enhance this effect by replacing the anilino group by a benzhydrylamino, *p*-chlorobenzhydrylamino or a 10-phenothiazinyl residue (compounds 21—27 in Table 1). Compounds 23 and 27 are of special interest as these compounds bear a certain structural resemblance to hydroxyzine, N-(*p*-chlorobenzhydryl)-N'-[2-(2-hydroxyethoxy)-ethyl]-piperazine, and perphenazine, N-[3-(2-chloro-10-phenothiazinyl)-propyl]-N'-(2-hydroxyethyl)-piperazine, respectively, which are used clinically as ataraxic agents. However, compounds 21—27 had very little or no ataraxic properties in pharmacological tests.

EXPERIMENTAL

2,3-Epoxypropylamines

N-(2,3-Epoxypropyl)-diethylamine and *N-(2,3-epoxypropyl)-piperidine* were prepared from diethylamine and piperidine, respectively, by reaction with epichlorohydrin according to the method of Gilman *et al.*[7]

N-(2,3-Epoxypropyl)-morpholine was prepared in the same way but with some small modifications owing to the greater solubility of the morpholino compound in water. Yield 50 %. B. p. 89—90°/10 mm; n_D^{25} 1.4670. (Found: C 58.8; H 9.07; N 9.86. Calc. for $C_7H_{13}NO_2$: C 58.7; H 9.15; N 9.78.)

N-Methyl-N'-(2,3-epoxypropyl)-piperazine was prepared by the same method from N-methylpiperazine and epichlorohydrin. Yield 22 %. B. p. 95—96°/12 mm; n_D^{25} 1.4727. (Found: C 61.5; H 10.3; N 17.9. Calc. for $C_8H_{16}N_2O$: C 61.3; H 10.4; N 18.1.)

N-(2,3-Epoxypropyl)-2,6-dimethylaniline. A solution of 2,6-dimethylaniline (121 g, 1.0 mole) and epichlorohydrin (102 g, 1.1 mole) in toluene (150 ml) was refluxed for 6 h. After cooling to room temperature, powdered sodium hydroxide (75 g) was added in small portions with stirring and external cooling. After half an hour water (300 ml) was added, the stirring was continued for a further half hour. The toluene layer was separated, washed with water and dried over sodium sulphate. The solvent was evaporated *in vacuo* and the residue distilled giving a colourless oil (76 g, 43 %), b. p. 90—92°/0.3 mm; n_D^{20} 1.5415. (Found: C 74.2; H 8.43; N 8.20. Calc. for $C_{11}H_{15}NO$: C 74.5; H 8.53; N 7.90.)

N-(2,3-Epoxypropyl)-2-chloro-6-methylaniline was prepared in the same way. However, 2-chloro-6-methylaniline reacted rather sluggishly with epichlorohydrin and the reaction was therefore carried out by heating the components in diethylbenzene (mixture of isomers of b.p. 175—181°) at 160—170° for 6 h. Yield 38 %. B. p. 109—111°/1.0 mm; n_D^{20} 1.5562. (Found: C 61.3; H 6.24; N 6.89. Calc. for $C_{10}H_{12}ClNO$: C 60.8; H 6.12; N 7.09.)

N-(2,3-Epoxypropyl)-benzhydrylamine. Benzhydrylamine (216 g, 1.18 mole) was added with stirring in small portions during one hour to epichlorohydrin (111.2 g, 1.20 mole) to which had been added some water (3.6 ml). During the addition the temperature rose to 28°. Stirring was continued for 8 h, during which time the temperature rose slowly to 35° and then decreased.

The reaction product separated gradually as a thick oil. The reaction mixture was allowed to stand overnight and then benzene (150 ml) was added followed by a solution of sodium hydroxide (56 g) in water (90 ml) added with stirring over half an hour. Stirring

Table 1. 1,3-Diamino-2-propanols.

No.	R	Am	Method	Yield %	Derivative	Recryst. solvent[a]
1	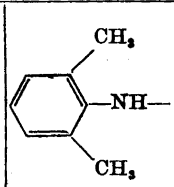	$-N(C_2H_5)_2$	A B	69 58	Base $2\,HClO_4$	— E
2	»	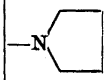	B	73	Base	—
3	»	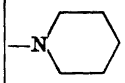	A	70	Base 2 HCl	— E
4	»	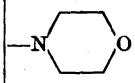	A	73	Base 2 HCl	— E
5	»	$-NH-CH_2\cdot CH_2\cdot CH_3$	B	63	Base	—
6	»	$-NH-CH(CH_3)_2$	B	37	Base	L
7	»	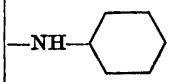	B	78	Base	L
8	»	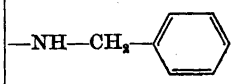	B	50	2 HCl	E—Et
9	»	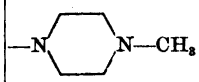	B	86	Base	—
10	»	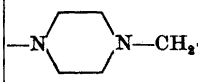	B	82	3 HCl	E—Aq

$R-CH_2-CHOH-CH_2-Am$

M. p. °C	B. p. °C/mm Hg	n_D^{20}	Formula	Calc. %			Found %		
				C	H	N	C	H	N
—	138—140/0.6	1.5194	$C_{15}H_{26}N_2O$	71.95	10.5	11.2	71.7	10.3	11.1
05—206	—	—	$C_{15}H_{26}N_2O \cdot 2HClO_4$	39.9	6.25	—	40.0	6.51	—
44— 45 [b]	141—143/0.3	1.5424	$C_{15}H_{24}N_2O$	72.5	9.74	11.3	72.8	9.69	11.1
—	161—162/0.8	1.5371	$C_{16}H_{26}N_2O$	73.2	9.99	10.7	72.6	9.77	10.4
48—250 (dec.)	—	—	$C_{16}H_{26}N_2O \cdot 2HCl$	—	—	21.2[c]	—	—	21.2[c]
—	175—178/0.8	1.5415	$C_{15}H_{24}N_2O_2$	68.15	9.15	10.6	68.3	9.02	10.6
37—239	—	—	$C_{15}H_{24}N_2O_2 \cdot 2HCl$	—	—	21.1[c]	—	—	21.3[c]
51— 52 [b]	134—136/0.3	—	$C_{14}H_{24}N_2O$	71.1	10.2	11.85	70.6	10.0	11.8
78— 80	146—147/0.7	—	$C_{14}H_{24}N_2O$	71.1	10.2	11.85	71.0	10.3	11.8
39— 70	—	—	$C_{17}H_{28}N_2O$	73.8	10.2	10.1	73.3	10.0	10.4
20—222	—	—	$C_{18}H_{24}N_2O \cdot 2HCl$	60.5	7.34	7.84	60.6	7.36	7.90
—	149—150/0.1	1.5412	$C_{16}H_{27}N_3O$	69.3	9.81	15.15	68.8	9.82	14.9
17—219 (dec.)	—	—	$C_{17}H_{29}N_3O_2 \cdot 3HCl$	49.0	7.74	10.1	48.4	7.99	10.0

Table 1, (continued).

No.	R	Am	Method	Yield %	Derivative	Recryst. solvent[a]
11	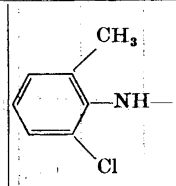	$-N(C_2H_2)_5$	A	62	Base	—
12	»	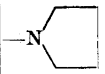	B	75	Base	—
13	»	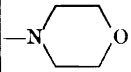	A	67	Base	—
14	»	$-NH\text{-}CH_2\cdot CH_2\cdot CH_3$	B	71	Base	—
15	»	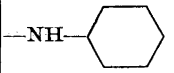	B	74	Base	L
16	»	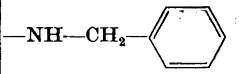	B	81	2 HCl	E—Et
17	»	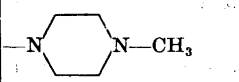	B	93	Base	—
					2 HCl	E—Aq
18	»	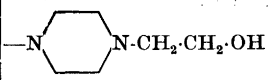	B	79	Base	—
19	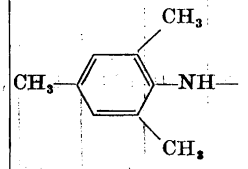	$-N(C_2H_5)_2$	A	43	Base	—
20	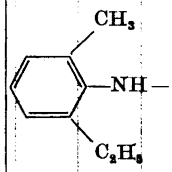	»	A	62	Base	—

M. p. °C	B. p. °C/mm Hg	n_D^{20}	Formula	Calc. %			Found %		
				C	H	N	C	H	N
—	153–154/0.5	1.5311	$C_{14}H_{23}ClN_2O$	62.2	8.55	10.3	62.0	8.35	10.3
—	143–145/0.1	1.5558	$C_{14}H_{21}ClN_2O$	62.55	7.88	10.4	62.1	8.02	10.6
—	173–174/0.5	1.5534	$C_{14}H_{21}ClN_2O_2$	59.0	7.43	9.84	59.4	7.36	9.85
53– 54 [b]	141–142/0.15	—	$C_{13}H_{21}ClN_2O$	60.8	8.24	10.9	60.9	8.21	10.8
52– 53	168–170/0.1	—	$C_{16}H_{25}ClN_2O$	64.7	8.49	9.44	64.4	8.44	9.62
184–186	—	—	$C_{17}H_{21}ClN_2O \cdot 2HCl$	54.05	6.14	7.42	53.8	6.01	7.71
—	160–163/0.3	—	$C_{15}H_{24}ClN_3O$	60.5	8.12	14.1	60.5	8.19	13.8
239–240	—	—	$C_{15}H_{24}ClN_3O \cdot 2HCl$	48.6	7.07	11.2	48.8	7.21	10.9
—	220–223/0.2	—	$C_{16}H_{26}ClN_3O_2$	58.6	7.99	12.8	58.7	8.04	12.7
—	133–135/0.2	1.5169	$C_{16}H_{28}N_2O$	72.7	10.7	10.6	72.4	10.3	10.9
—	146–148/0.4	1.5174	$C_{16}H_{28}N_2O$	72.7	10.7	10.6	72.5	10.3	10.9

Table 1, (continued).

No.	R	Am	Method	Yield %	Derivative	Recryst. solvent[a]
21	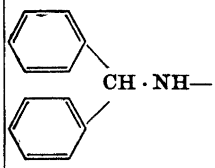	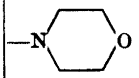	B	68	2 HCl	E—Et
22	»	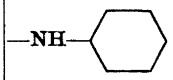	B	69	2 HCl · H_2O	E—Aq
23	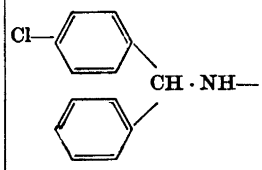	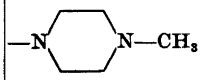	A	64	3 HCl	E
24	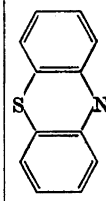	$-N(C_2H_5)_2$	A	86	Base	E
25	»	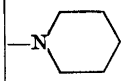	A	94	Base	E
26	»	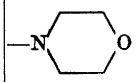	A	86	Base	Et
					HCl	E
27	»	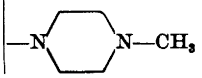	A	64	2 HCl	E—Et

a E, ethanol; Et, ether; Aq, water; L, ligroin.
b M. p. of solidified distillate.
c Chlorine analysis.

M.p. °C	B. p. °C/mm Hg	n_D^{20}	Formula	Calc. %			Found %		
				C	H	N	C	H	N
224–226	–	–	$C_{20}H_{26}N_2O_2 \cdot 2HCl$	60.1	7.07	7.02	59.9	7.12	7.01
268–270	–	–	$C_{22}H_{28}N_2O \cdot 2HCl \cdot H_2O$	61.5	7.98	6.53	61.4	7.95	6.59
262–264 (dec.)	–	–	$C_{21}H_{28}ClN_3O \cdot 3HCl$	52.2	6.47	8.69	51.7	6.43	8.44
139–140	–	–	$C_{19}H_{24}N_2OS$	69.5	7.36	8.53	69.4	7.28	8.58
153–154	–	–	$C_{20}H_{24}N_2OS$	70.5	7.10	8.23	70.6	7.23	7.83
95– 97	–	–	$C_{19}H_{22}N_2O_2S$	66.6	6.48	8.18	66.5	6.41	8.12
206–207	–	–	$C_{19}H_{22}N_2O_2S \cdot HCl$	60.2	6.12	7.39	60.7	6.31	7.63
242–244 (dec.)	–	–	$C_{20}H_{25}N_3OS \cdot 2HCl$	56.1	6.35	9.81	56.4	6.70	9.51

was continued for one hour. Ether (100 ml) was then added and the organic layer was separated and dried over sodium sulphate. The solvent was evaporated under reduced pressure and the residue, a viscous oil (280 g) which did not crystallise was used as starting material for syntheses without further purification. Attempts to distill the oil led to decomposition.

1,3-Diamino-2-propanols

Method A. Lithium amide (0.11 mole) was added to a solution of the aromatic amine (0.1 mole of 2,6-dimethylaniline, 2-chloro-6-methylaniline, phenothiazine, *etc.*) in benzene (150 ml) and the reaction mixture was refluxed with stirring for 1.5 h. After cooling the appropriate N-(2,3-epoxypropyl)-dialkylamine (0.1 mole) was added, and the mixture was refluxed with stirring for a further 2.5 h. After cooling the benzene solution was washed with water and extracted with 2 N hydrochloric acid. The acid extract was then made alkaline with conc. ammonium hydroxide. The reaction product usually separated as an oil that soon crystallised and was purified by recrystallisation. When it was impossible to obtain the product in crystalline form, it was extracted with ether, the ether was evaporated and the residue distilled *in vacuo*. Some of the compounds were converted to a salt and purified by recrystallisation.

In the preparation of the phenothiazine compounds 24—27 the reaction time after the addition of the epoxide was prolonged to 5 h.

Compound 23 was prepared by condensation of *p*-chlorobenzhydrylamine and N-methyl-N′-(2,3-epoxypropyl)-piperazine in boiling xylene for 6 h and it was therefore not necessary to use lithium amide as condensing agent in this case. Compound 23 contains two asymmetric carbon atoms and should be able to give two racemates. No attempts were made to separate these racemates. Method *A* was used for compounds 1, 3, 4, 11, 13, 19, 20 and 23—27.

Method B. A solution of the appropriate N-(2,3-epoxypropyl)-aniline (0.1 mole) and a mono- or dialkylamine (0.2 mole of diethylamine, *n*-propylamine, pyrrolidine, *etc.*) in xylene (50 ml, mixture of isomers of b.p. 138—142°) was refluxed for 6 h. The xylene was washed with water and extracted with 2 N hydrochloric acid. The reaction product was then isolated as described for method A. Method *B* was used for compounds 1, 2, 5—10, 12, 14—18, 21 and 22.

Physical constants and analytical data are collected in Table 1.

REFERENCES

1. Fourneau, E. and Ranedo, J. *An. Soc. Espan.* **18** (1920) 133.
2. Fourneau, E., Tréfouel, J. and Benoit, G. *Ann. Inst. Pasteur* **44** (1930) 719.
3. Ludwig, B. J., West, W. A. and Farnsworth, D. W. *J. Am. Chem. Soc.* **76** (1954) 2891.
4. Winstein, S. and Henderson, R. B. in Elderfield, R. C. *Heterocyclic Compounds*, J. Wiley and Sons, Inc., New York 1950, Vol. I, p. 32.
5. Andersson, S. *The reaction between ethylene oxides and ammonia* (Diss.) Lund 1955, p. 61.
6. Chapman, N. B., Isaacs, N. S. and Parker, R. E. *J. Chem. Soc.* **1959** 1925.
7. Gilman, H., Sherman, C. S., Price, C. C., Elderfield, R. C., Maynard, J. T., Reitsema, R. R., Tolman, L., Massie, S. P., Marshall, F. J. and Goldman, L. *J. Am. Chem. Soc.* **68** (1946) 1291.

Received December 30, 1959.

ACTA CHEMICA SCANDINAVICA 14 (1960) 871–876

The Constitution of an Araboxylan from Scots Pine (*Pinus silvestris* L.)

PER J. GAREGG and BENGT LINDBERG

Svenska Träforskningsinstitutet, Träkemiska avdelningen, Stockholm Ö, Sweden

Pine (*Pinus silvestris* L.) chlorite holocellulose after extraction first with dimethyl sulphoxide and water gives an araboxylan on extraction with 14 % potassium hydroxide. From the results of methylation studies it is concluded that this araboxylan has a backbone of 1,4-linked β-D-xylopyranose residues and that every fifth to sixth xylose residue is substituted in the 2-position with 4-*O*-methyl-D-glucopyranosyluronic acid residues, while every seventh to eighth xylose residue is substituted in the 3-position with L-arabofuranose residues.

The isolation of an araboxylan from Scots pine (*Pinus silvestris L.*) has been described in a previous communication from this Institute [1]. Pine chlorite holocellulose [2] was extracted successively with dimethyl sulphoxide, hot water, 14 % aqueous potassium hydroxide, 14 % aqueous potassium hydroxide containing 3 % boric acid and finally with 24 % aqueous potassium hydroxide containing 3 % boric acid. The hemicellulose extracted with 14 % potassium hydroxide on fractionation first with Fehling's solution and then with aqueous barium hydroxide [3] yielded an araboxylan substantially free from other polysaccharides.

The present paper deals with the results of methylation studies on the araboxylan. The molar ratio arabinose: xylose: 4-*O*-methylglucuronic acid was 1 : 7.7 : 1.5, and the $\overline{DP}_n$ estimated by osmometry in aqueous solution [4] was 133.

The araboxylan was methylated with dimethyl sulphate in sodium hydroxide solution and then treated five times with methyl iodide and silver oxide in dimethyl formamide [5]. The product (methoxyl 38.1 %, $\overline{DP}_n$ 115) was subjected to acid hydrolysis and the acidic and neutral fragments were separated on an anion exchange resin. The acidic portion containing the methylated aldobiouronic acid together with a smaller amount of the methylated uronic acid, after esterification and glycosidation, was reduced with lithium aluminium hydride and then hydrolysed.

The monomeric sugars in the two hydrolysates were fractionated on carbon-Celite columns and estimated quantitatively. The 2-*O*- and 3-*O*-methyl-D-xyloses in the neutral fraction of the hydrolysate from the methylated polysaccharide were incompletely separated on the column; their relative proportion was determined by quantitative paper electrophoresis in borate buffer [6] and a preparative fractionation was done on a carbon-Celite column

Table 1. Methyl ethers (mole %) obtained from methylated araboxylan from pine wood.

Component	Mole %
Xylose	0.4
2-*O*-Methylxylose	9.9
3-*O*-Methylxylose	13.7
"Dimethylarabinose"	0.9
2,3-Di-*O*-methylxylose	49.8
2,3,4-Tri-*O*-methylxylose	1.3
2,3,5-Tri-*O*-methylarabinose	9.7
2,3,4-Tri-*O*-methylglucose	14.3

Table 2. Fractionation of neutral monosaccharides from a hydrolysate of methylated araboxylan. Gradients: 0—12 % aqueous ethanol (3 l), 12—35 % aqueous ethanol (3 l), 35 % aqueous ethanol-35 % aqueous *n*-propanol. Fractions collected: 25 ml.

Tube No.	Component	Millimoles	Mole %
42— 50	Xylose	0.0212	0.5
70— 75	3-*O*-Methylxylose	0.0622	1.5
76—116	2-*O*- and 3-*O*-Methylxylose	0.655	16.0
117—132	"Dimethylarabinose"	0.0596	1.5
133—220	2,3-Di-*O*-methylxylose	2.70	66.0
250—274	2,3,5-Tri-*O*-methylarabinose	0.524	12.8
275—298	2,3,4-Tri-*O*-methylxylose	0.0685	1.7

The ratio 2-*O*- : 3-*O*-methylxylose in fraction 76—116 was 4.5:1.

Table 3. Fractionation of the hydrolysate from the acidic part of the methylated araboxylan hydrolysate. Gradient: 0—50 % aqueous ethanol (5 l). Eluted with 50 % aqueous ethanol. Fractions collected: 25 ml.

Tube no.	Component	Millimole	Mole %
24—80	3-*O*-Methylxylose	0.434	42.0
Remainder	2,3,4-Tri-*O*-methylglucose	0.600	58.0

by gradient elution with borate buffer [7]. The results of the fractionations are summarised in Table 1. In correlating the proportions obtained in the two fractionations (see Tables 2 and 3) to get the values given in Table 1, the ratio of the total amount of monomers in each of the two fractionations was adjusted to give the same uronic acid content as that present in the original araboxylan.

The hydrolysate obtained from the acidic fragments of the methylated polysaccharide hydrolysate contained only 3-*O*-methyl-D-xylose and 2,3,4-tri-*O*-methyl-D-glucose. The aldobiouronic acid from the pine wood thus clearly is 2-*O*-(4-*O*-methyl-D-glucuronopyranosyl)-D-xylose which is the usual aldobiouronic acid fragment found in wood xylans [8–15]. There were no indications of 3-*O*-(4-*O*-methyl-D-glucuronopyranosyl)-D-xylose residues the presence of which has been reported in hydrolysates from *Pinus radiata* D. Don [16] and various grasses [17]. The aldobiouronic acid was isolated from a partial hydrolysate of the araboxylan and was converted to the crystalline methyl-2-*O*-(methyl 2,3-di-*O*-acetyl-4-*O*-methyl-α-D-glucuronopyranosyl)-3,4-di-*O*-acetyl-D-xylopyranoside according to Timell [18]. Some 3-*O*-methyl-D-xylose was found in the hydrolysate from the neutral portion of the methylated polysaccharide. This probably arises from partial hydrolysis of the methylated aldobiouronic acid fragment, as the yield agreed well with the excess of 2,3,4-tri-*O*-methyl-D-glucose from the acid portion. The L-arabofuranose residues therefore appear to be attached exclusively to the 3-positions of the anhydroxylose residues. This is substantiated by the relative proportions of 2-*O*-methyl-D-xylose and 2,3,5-tri-*O*-methyl-L-arabinose. The results give no indication whether the L-arabofuranose residues are linked directly to the anhydroxylose back-bone or are the terminal residues of side-chains of β-1,4-linked xylose units. From the results of previous investigations [19,20], however, it seems likely that the L-arabofuranose residues are linked directly to the anhydroxylose back-bone. The amount of the fraction containing 2,3,4-tri-*O*-methyl-D-xylose (1.3 mole %) appears somewhat higher than that required by a $\overline{DP}_n$ of 115 (0.9 mole %). This fraction did, however, contain a smaller amount of 2,3,5-*O*-tri-methyl-arabinose, and there is therefore little indication of any branching in the β-1,4-linked anhydroxylose back-bone.

Previous studies of the hemicelluloses of coniferous wood have indicated the presence of a xylan composed only of 4-*O*-methyl-glucuronic acid and xylose [9,11,14,15]. This arabinose-free xylan has been extracted directly with alkali from finely ground wood and the hemicelluloses have been fractionated to yield the xylans [9,15]. Fractionation of alkaline holocellulose extracts has also yielded arabinose-free xylans [11,14]. The yields have usually been of the order of 1 % or less of the wood. Xylans containing arabinose residues have been isolated from Norway spruce [21], Western hemlock [10,22] European larch [23] and Sitka spruce [12]; the constitutions of those from Western hemlock [22] and European larch [23] have been investigated and found similar to that of the araboxylan examined in the present work. Structural investigation of the xylans present in Southern pine pulps [24] has indicated a similar structure for the native araboxylan in this case also. The xylan in the present investigation represents 80 % of the total xylan in the wood which amounted to 9—10 % of the dry extractive-free wood. In view of the results of previous investigations, the

presence in the pine wood of an arabinose-free xylan cannot be excluded, but it seems however probable that if present it constitutes only a minor part of the xylan in the wood.

EXPERIMENTAL

All melting points are corrected. Evaporations were done under reduced pressure at a bath temperature below 40°.

Chromatography. Papers: Whatman No. 1. Solvents: A. Ethyl acetate-acetic acid-water 3:1:3. B. Butanol-ethanol-water 10:3:5. C. *Iso*propyl ether-light petroleum (40—60°) 1:1 (on dimethyl sulphoxide-impregnated paper [25]).

Paper electrophoresis. Papers: Whatman No. 1, Schleicher and Schüll 602hP. Buffers: 0.1 M borate buffer at pH 10, 0.1 M acetate buffer at pH 4. Spray reagents: Aniline hydrogen phthalate, anisidine hydrochloride.

Isolation of the araboxylan. The araboxylan was extracted from Scots pine (*Pinus silvestris* L.) chlorite holocellulose. It was obtained in a substantially pure form by the fractionation techniques previously described [1]. OCH_3 2.6 %; 4-*O*-methylglucuronic acid 20.7 %; the ratio galactose:glucose:mannose:arabinose-xylose was trace:trace:nil:12.7:87.3; $\overline{DP}_n$ 133 (in aqueous solution [4]), $[\alpha]_D^{20}$ −59° (*c*, 1.2 in water).

Methylation of the araboxylan. The araboxylan (5 g) was first methylated with methyl sulphate in aqueous sodium hydroxide and then treated five times with methyl iodide and silver oxide in dimethyl formamide [5,26]. Yield 4.4 g, $[\alpha]_D^{20}$ −50°. (*c*, 1 in chloroform), OCH_3 38.1 %, (calculated methoxyl content for a fully substituted araboxylan with 20.7 % methyluronic acid is 38.1), $\overline{DP}_n$ 115.

Hydrolysis of the methylated araboxylan and separation of acid and neutral components. The methylated araboxylan (1.3 g) was hydrolysed first with 72 % sulphuric acid (10 ml) at room temperature for 0.5 h and then with 8 % sulphuric acid (90 ml) at 100° for 2 h. The hydrolysate was neutralised with barium carbonate, filtered and passed through Amberlite IR 120 (H^+ form). The acidic components were absorbed on Dowex 2 (acetate form), 1.5 × 12 cm, the column was eluted with water (1.5 l) and the eluate concentrated to give the neutral fraction (950 mg). The acids were displaced from the column with 3 N acetic acid (500 ml); the eluate was concentrated to give the acidic fraction (275 mg). Paper chromatograms of the two fractions using solvent B indicated a complete separation of neutral and acidic material; the neutral fraction contained methylxylose, dimethylxylose, trimethylarabinose and probably some trimethylxylose; the acid fraction contained two components, probably methylated uronic acid (minor component) and methylated aldobiouronic acid (major component). Paper electrophoresis in the acetate buffer gave two spots with slightly lower mobilities than those of 4-*O*-methyl-D-glucuronic acid and 2-*O*-(4-0-methyl-D-glucuronopyranosyl)-D-xylose, respectively.

Glycosidation, esterification and reduction of the acidic components. The acidic fraction (275 mg) was refluxed with 2.1 % dry methanolic hydrogen chloride for 8 h and the solution was then neutralised with silver carbonate, filtered and concentrated to dryness. The product was reduced with lithium aluminium hydride (1 g) in refluxing ethyl ether (50 ml) for 4 h. Excess hydride was destroyed with anhydrous ethanol and the alcoholates were decomposed with water. Aluminium hydroxide was removed by centrifuging and the supernatant solution was neutralised with sulphuric acid. Lithium sulphate was removed by filtration of the product in ethanolic solution and the filtrate was concentrated to a syrup (260 mg).

Hydrolysis of the reduced acidic fraction. The reduced acidic components (260 mg) were hydrolysed overnight at 100° with 0.5 N sulphuric acid (20 ml), neutralised with barium hydroxide, filtered and concentrated to dryness. Paper chromatography in solvent B and paper electrophoresis in the borate buffer indicated the presence of 3-*O*-methyl-xylose and 2,3,4-tri-*O*-methyl-glucose.

Fractionation of the hydrolysates from the neutral and acidic components. The neutral components (950 mg) from the hydrolysate of the methylated araboxylan were fractionated on a carbon-Celite (1:1) column (4 × 46 cm) by gradient elution [27]; the hydrolysate from the acidic components (260 mg) was fractionated on a carbon-Celite column (3.3 × 25 cm) in the same way. The amount of reducing sugar in each of the combined

fractions was determined by hypoiodite oxidation [28]. 2-*O*- and 3-*O*-methyl-D-xylose were incompletely separated and the relative proportions of these components in the combined mixed fraction were determined by quantitative paper electrophoresis in borate buffer [6]. A preparative fractionation was done on a carbon-Celite (1:1) column (3.3 × 25 cm) using borate buffer [7] (0.1 M; pH 10) and gradient elution (3 l 0—10 % aqueous ethanol). 3-*O*-methyl-D-xylose was eluted first. The results of the fractionations are summarised in Tables 2 and 3.

Characterisation of components

D-*Xylose.* Characterised only by paper chromatography. Indistinguishable from D-xylose in solvents A and B.

2-O-*Methyl*-D-*xylose.* Crystallised from acetone, m. p. 130—132°, undepressed on admixture with authentic material. Indistinguishable from authentic material on paper electrophoresis in borate buffer and on paper chromatography in solvent B.

3-O-*Methyl*-D-*xylose.* Crystallised from acetone and methyl ethyl ketone, m. p. 95—97°, undepressed on admixture with authentic material. Indistinguishable from authentic material on paper electrophoresis in borate and on paper chromatography in solvent B.

"*Dimethylarabinose*" (Table 2). Only examined by paper chromatography. This fraction contained a main component with a mobility slightly lower than that of 2,3-di-*O*-methylxylose, as well as some methylxylose and 2,3-di-*O*-methylxylose. Demethylation indicated arabinose and a smaller amount of xylose.

2,3-*Di*-O-*methyl*-D-*xylose.* The anilide had m. p. 133—135°, undepressed on admixture with authentic material.

2,3,4-*Tri*-O-*methyl*-D-*xylose.* Demethylation indicated xylose and a small amount of arabinose. The methyl sugar and its anilide failed to crystallise. The methyl sugar was indistinguishable from authentic material on paper chromatography in solvent C.

2,3,5-*Tri*-O-*methyl*-D-*arabinose.* Demethylation gave arabinose only. The 2,3,5-tri-*O*-methyl-L-arabonamide had m. p. 135—137°, undepressed on admixture with authentic material.

2,3,4-*Tri*-O-*methyl*-D-*glucose.* The 1,6-diazobenzoate crystallised from ligroin-chloroform (25:1) m. p. 162—164, undepressed on admixture with authentic material.

A crystalline derivative of the aldobiouronic acid. The araboxylan (2 g) was hydrolysed with 0.5 N sulphuric acid (160 ml) at 100° for 3 h and the hydrolysate was neutralised with 0.5 N barium hydroxide, filtered and concentrated to a small volume. Barium ions were removed by passage through Amberlite IR 120 (H^+ form) and the uronic acids were absorbed on Dowex 2 (acetate form). Neutral sugars were eluted with water (2 l), the acids with 3 N acetic acid (500 ml) and then with water until the eluate was neutral. Concentration yielded the acid fraction (0.45 g). Paper chromatography in ethyl acetate-formic acid-acetic acid-water 19:1:3:4 and ethyl acetate-pyridine-water 2:1:2 indicated that the acid fraction contained the aldobiouronic acid slightly contaminated with aldotri- and tetrauronic acids but no spots corresponding to 4-*O*-methylglucuronic acid were observed. The aldobiouronic acid was indistinguishable from 2-*O*-(4-*O*-methyl-D-glucuronopyranosyl)-D-xylopyranose. The crystalline methyl-2-*O*-(methyl 2,3-di-*O*-acetyl-4-*O*-methyl-α-D-glucuronopyranosyl)-3,4-di-*O*-acetyl-D-xylopyranoside prepared according to Timell [18] crystallised from ethyl ether and was recrystallised from ethyl ether-ethanol 1:1, $[\alpha]_D^{20}$ +103° (*c*, 0.5 in chloroform), m. p. 202—203° undepressed on admixture with authentic material kindly supplied by Dr. T. E. Timell, Montreal.

Osmometric $\overline{DP}_n$ *determinations.* Osmometric $\overline{DP}_n$ determinations on the araboxylan were done on the sodium salt in 0.1 N aqueous sodium chloride [4] using "Ultrafein feinst" membranes supplied by Membranfiltergesellschaft, Göttingen. The $\overline{DP}_n$ of the methylated araboxylan was determined in butyl acetate solution using "Ultrazellafilter allerfeinst" membranes supplied by the same firm.

REFERENCES

1. Meier, H. *Acta Chem. Scand.* **12** (1958) 1911.
2. Wise, L. E., Murphy, M. and D'Addieco, A. A. *Paper Trade J.* **122** (1946) No. 2, p. 35.
3. Meier, H. *Acta Chem. Scand.* **12** (1958) 144.
4. Pals, D. T. F. and Hermans, J. J. *Rec. trav. chim.* **71** (1952) 458.
5. Kuhn, R., Trischmann, H. and Löw, I. *Angew. Chem.* **67** (1955) 32.
6. Croon, I. and Lindberg, B. *Svensk Papperstidn.* **61** (1958) 35.
7. Barker, S. A., Bourne, E. J. and Theander, O. *J. Chem. Soc.* **1955** 4276.
8. Gorrod, A. R. N. and Jones, J. K. N. *J. Chem. Soc.* **1954** 2522.
9. Ball, D. H., Jones, J. K. N., Nicholson, W. H. and Painter, T. J. *Tappi* **39** (1956) 438.
10. Dutton, C. G. S. and Smith, F. *J. Am. Chem. Soc.* **76** (1956) 2505.
11. Aspinall, G. O. and Carter, M. *J. Chem. Soc.* **1956** 3744.
12. Dutton, C. G. S. and Hunt, K. *J. Am. Chem. Soc.* **80** (1958) 4420.
13. Whistler, R. L. and Richards, G. N. *J. Am. Chem. Soc.* **80** (1958) 4888.
14. Jones, J. K. N. and Painter, T. J. *J. Chem. Soc.* **1957** 669.
15. Jones, J. K. N. and Painter, T. J. *J. Chem. Soc.* **1959** 573.
16. Brash, D. J. and Wise, L. E. *Tappi* **39** (1956) 581, 768.
17. Roudier, A. and Eberhard, L. *Tappi* **38** (1955) No. 9, 156A.
18. Timell, T. E. *Can. J. Chem.* **37** (1959) 827.
19. Bishop, C. T. *J. Am. Chem. Soc.* **78** (1956) 2840.
20. Aspinall, G. O. and Ferrier, R. J. *J. Chem. Soc.* **1957** 4188.
21. Saarnio, J. *Suomen Kemistilehti* **29B** (1956) No. 2, 35.
22. Dutton, C. G. S. and Smith, F. *J. Am. Chem. Soc.* **78** (1956) 3744.
23. Aspinall, G. O. and McKay, J. E. *J. Chem. Soc.* **1958** 1059.
24. Hamilton, J. K., Partlow, E. V. and Thompson, N. S. *Tappi* **41** (1958) 811.
25. Wickberg, B. *Acta Chem. Scand.* **12** (1958) 615.
26. Bouveng, H. O. *Acta Chem. Scand.* **12** (1958) 1977.
27. Lindberg, B. and Wickberg, B. *Acta Chem. Scand.* **8** (1954) 569.
28. Hirst, E. L., Hough, L. and Jones, J. K. N. *J. Chem. Soc.* **1949** 928.

Received January 13, 1960.

ACTA CHEMICA SCANDINAVICA 14 (1960) 877–881

Action of Strong Acids on Acetylated Glycosides

XIII *. Studies on the Mechanism of the Anomerisation Reaction **

JAN JANSON and BENGT LINDBERG

Institutionen för träkemi, Kungl. Tekniska Högskolan, Stockholm Ö, Sweden

The anomerisation of some acetylated glycosides in sulphuric acid-acetic anhydride-acetic acid has been studied. Replacement of the 2-*O*-acetyl group of *iso*propyl-tetra-*O*-acetyl-β-D-glucopyranoside with a methyl group results in a higher rate of reaction. Thus participation of the 2-*O*-acetyl group does not seem to facilitate the reaction. For a 2-deoxy-glucopyranoside and a galactofuranoside the acetolysis was so fast that no anomerisation could be observed.

The anomerisation of acetylated glycosides, a reaction of considerable preparative interest, is known to be catalysed by strong acids in the generalised sense, *e.g.* titanium tetrachloride and boron trifluoride. The mechanisms of this and similar reactions have recently been discussed by Lemieux [1]. The anomerisation is known to be intramolecular [2,3] and two alternative mechanisms have been suggested. Lindberg [2] assumed that the acid (A) coordinates with

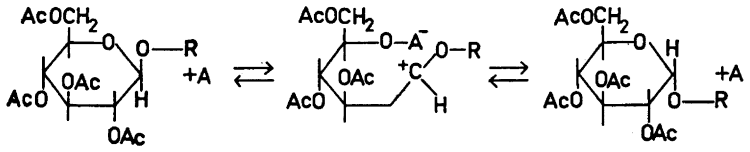

I II III

the ring oxygen in (I) and that the open chain intermediate (II) could reclose to give either of the anomeric glycosides (I or III) while Lemieux on the other hand has assumed that the acid coordinates with the oxygen of the aglycone group (IV). In this case the bond between $C_{(1)}$ and OR is further weakened by participation of the *O*-acetyl group at $C_{(2)}$ (V). When it is finally broken

* Part XII. *Acta Chem. Scand.* 6 (1952) 949.

** Presented at Tionde Nordiska Kemistmötet, Stockholm, 1959.

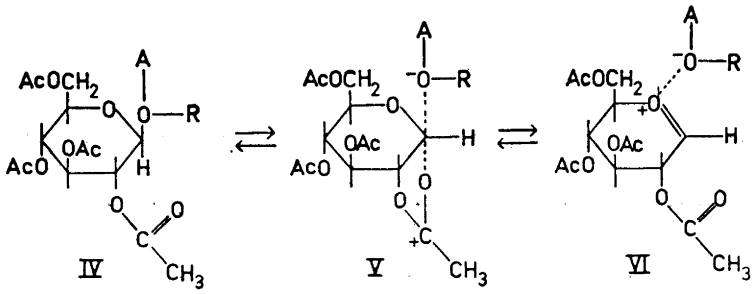

the two ions are not dissociated but exist as an ion pair, formulated as VI. This ion pair can then collapse, giving either the *α*-or the *β*-anomer.

The postulated participation of the neighbouring *O*-acetyl group could be studied by investigating the anomerisation of glycosides in which there is no such group. The anomerisation of *iso*propyl-tetra-*O*-acetyl-*β*-D-glucopyranoside in acetic anhydride-acetic acid (10:3), catalysed by sulphuric acid, is known to proceed 50—60 times faster than the anomerisation of penta-*O*-acetyl-*β*-D-glycopyranose. The corresponding glycoside of 2-*O*-methyl-D-glucose was prepared and its anomerisation studied under the same conditions. The velocity constant for the reaction was about twice that of the glucoside indicating that participation of the 2-*O*-acetyl group does not facilitate the reaction. The acetylated 2-*O*-methyl-*α*-D-glucopyranoside was isolated from the reaction mixture.

There is a remote possibility that the methoxyl group at $C_{(2)}$ might also participate. In a 2-deoxy-glycoside however, participation from a $C_{(2)}$ substituent is eliminated, and *iso*propyl-tri-*O*-acetyl-2-deoxy-*β*-D-glucopyranoside was therefore prepared and investigated in the acetic anhydride-acetic acid-sulphuric acid system. However, the acetolysis of this substance was too fast to allow a study of its anomerisation. A substance, m.p. 111—112°, $[\alpha]_D$ + 104° (chloroform) was isolated from the reaction mixture. It analysed for a tetra-acetate of 2-deoxy-D-glucose, and gave 2-deoxy-D-glucose on deacetylation. The same acetate was also obtained by treating tetra-*O*-acetyl-2-deoxy-*β*-D-glucopyranose with sulphuric acid in acetic anhydride-acetic acid. Overend *et al.*[4] have reported the preparation of two acetates of 2-deoxy-D-glucose. One, m.p. 91°, $[\alpha]_D$ + 12° (ethanol), claimed to be the *α*-acetate, was prepared by acetylation of 2-deoxy-D-glucose with acetic anhydride in pyridine. The other, m.p. 75—78°, $[\alpha]_D$ + 30° (ethanol), claimed to be the *β*-acetate, was prepared by acetylation with acetic anhydride and sodium acetate. On repeating these acetylations using the conditions described by Overend *et al.* the same substance m.p. 91—93°, $[\alpha]_D$ −2° (chloroform) was obtained with both acetylating agents. This substance is apparently tetra-*O*-acetyl-2-deoxy-*β*-D-glucopyranose while the compound with the high optical rotation, + 104°, is the corresponding *α*-acetate, and the product, m.p. 75—78°, reported by Overend *et al.*[4], is a mixture. On these assumptions,there is good agreement between the optical rotations of the anomeric acetates of D-glucose and 2-deoxy-D-glucose (Table 1) and between the methods of preparation.

Table 1. Optical rotations of acetylated pyranosidic D-glucose and 2-deoxy-D-glucose.

Parent sugar	Anomeric form	$[\alpha]_D$ in chloroform
D-Glucose	α	+ 101°
D-Glucose	β	+ 4°
2-Deoxy-D-glucose	α	+ 104° a) + 12° b)
2-Deoxy-D-glucose	β	− 2° a) + 30° b)

a) Present investigation.
b) Ref.[4], optical rotation in ethanol.

If $CH_3\overset{+}{C}O$ is the catalyst in the acetic anhydride-acetic acid-sulphuric acid system, which seems plausible (*cf. e.g.* Refs.[5,6]) then the mechanism proposed by Lemieux becomes less probable. When the acetyl ion is added to the glycosidic oxygen and the linkage between this oxygen and $C_{(1)}$ is broken, the product would be not an ion pair but an ion (VII) and an alkyl acetate, the recombination of which seems most improbable. If the acetyl ion adds to the

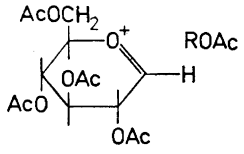

VII

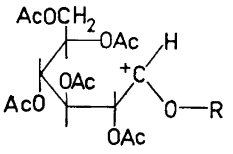

VIII

ring oxygen, the opening of the ring to VIII and the re-formation of either of the forms is possible. As previously suggested [2,7] this theory also acounts for the formation of the open chain acetates that are known to be formed during these reactions. According to this mechanism a furanoside would give the same intermediate as a pyranoside, and it should therefore be possible to convert an acetylated furanoside into the pyranoside by treating it with sulphuric acid in acetic anhydride-acetic acid. When this experiment was done with ethyl-tetra-*O*-acetyl-β-D-galactofuranoside, acetolysis was very rapid and the furanosidic β-acetate of galactose was the only product isolated from the reaction mixture. In contradistinction to the behaviour of the galactopyranosides the β-form thus seems to be the most stable furanosidic acetate. Bearing in mind the ease with which 2-deoxyglycosides and furanosides are hydrolysed in acids, the fast acetolysis of these products is not surprising.

Acid-catalysed hydrolysis, the formation of glycosides and the interconversion of pyranosides and furanosides, recently discussed by Shafizadeh [8], involve protonation of the sugar and the rate determining step should involve the formation of a carbonium ion. These reactions are thus similar to the anomerisations of acetylated glycosides with acids in the generalised sense,

and in neither case has it been possible to decide between the cyclic or the acyclic route. The interconversion of pyranosides and furanosides however is best interpreted by a mechanism involving an acyclic intermediate though it may well be that for all these reactions both pathways are possible and that one or the other predominates, depending on the substances in question and the conditions of the reaction.

EXPERIMENTAL

All melting points are corrected. Concentrations were done under reduced pressure at a bath temperature of 50° or less.

Isopropyl-tri-O-*acetyl-2*-O-*methyl-β*-D-*glucopyranoside.* Tri-*O*-acetyl-2-*O*-methyl-α-D-glucopyranosyl bromide [9] (6.5 g) was dissolved in benzene (20 ml) and *iso*propyl alcohol (15 ml), silver carbonate (8 g) and Drierite (4 g) were added. The mixture was shaken for 3 h at room temperature and allowed to stand overnight. After filtration and concentration a syrup was obtained, which was dissolved in ether and extracted with water. The ether solution was concentrated and the residue was crystallised from aqueous ethanol. The crystals (2.2 g) melted at 64–69°. Further crystallisation raised the m. p. to 67–69°, $[\alpha]_D^{26}$ +1° (*c*, 2.0, chloroform). (Found C 53.2; H 7.2. Calc. for $C_{16}H_{26}O_9$: C 53.0; H 7.2.)

Isopropyl-tri-O-*benzoyl-2-deoxy-β*-D-*glucopyranoside.* Tri-*O*-benzoyl-2-deoxy-α-D-glucopyranosyl bromide [10] (10.4 g) was dissolved in toluene (100 ml) and *iso*propyl alcohol (75 ml), silver carbonate (9 g) and Drierite (10 g) were added. The mixture was shaken for 3 h and left overnight. After filtration the solution was concentrated and crystallised from ether-light petroleum yielding the pure substance (6.0 g), m. p. 107–108°. Further crystallisation raised the m. p. to 108–109°, $[\alpha]_D^{23}$ −57° (*c*, 2.4, chloroform). (Found: C 70.0; H 5.7. Calc. for $C_{30}H_{30}O_8$: C 69.5; H 5.8.)

Isopropyl-2-deoxy-β-D-*glucopyranoside.* The benzoylated glycoside (5.0 g) was debenzoylated with alkali in the usual way and the product (1.4 g) was crystallised twice from butanone. M. p. 120–122°, $[\alpha]_D^{20}$ −51° (*c*, 2.4, water). (Found: C 52.7; H 8.6. Calc. for $C_9H_{18}O_5$: C 52.4; H 8.8.)

Isopropyl-tri-O-*acetyl-2-deoxy-β*-D-*glucopyranoside.* The debenzoylated product (1.3 g) was treated with acetic anhydride and pyridine and then worked up in the usual way. The product (1.9 g), was crystallised from ether-light petroleum. M. p. 67–68°, $[\alpha]_D^{23}$ −37° (*c*, 2.7, chloroform). (Found: C 54.8; H 7.2. Calc. for $C_{15}H_{24}O_8$: C 54.2; H 7.2.)

Ethyl-tetra-O-*acetyl-β*-D-*galactofuranoside* was prepared by acetylation of ethyl-β-D-galactofuranoside [11] with acetic anhydride and pyridine. Its m. p. 55–57° and optical rotation, −52° in chloroform, agreed with the values previously reported [12].

Kinetic experiments. The measurements were made as previously described [2]. Velocity constants were calculated for first order reactions (time in minutes) and expressed in Brigg's logarithms. The values obtained are summarised in Table 2.

Table 2.

Acetylated sugar	M. H_2SO_4	$\alpha_{initial}$	$\alpha_{max.}$	10^3 k	$K_{rel.}$
*Iso*propyl-β-D-glucopyranoside	0.037	−1.24	5.79	52.2	52
β-D-Glucopyranose	0.037	−0.37	4.93	1.00	—
*Iso*propyl-2-*O*-methyl-β-D-glucopyranoside	0.037	−0.14	5.48	103	110
β-D-Glucopyranose	0.037	−0.37	4.93	0.94	—
*Iso*propyl-2-deoxy-glucopyranoside	0.018	−1.50	7.05	—	—
Ethyl-β-D-galactofuranoside	0.018	−1.27	0.58	—	—

Isopropyl-tri-O-*acetyl-2*-O-*methyl-α*-D-*glucopyranoside*. The reaction mixture from the anomerisation of *iso*propyl-tri-*O*-acetyl-2-*O*-methyl-*β*-D-glucopyranoside (0.50 g) yielded a product (0.20 g), m. p. 152—154°, $[\alpha]_D^{25}$ +151° (*c*, 1.0, chloroform) which was obviously *iso*propyl-tri-*O*-acetyl-2-*O*-methyl-α-D-glucopyranoside. (Found: C 53.4; H 7.1. Calc. for $C_{16}H_{26}O_9$: C 53.0, H 7.2.)

Tetra-O-*acetyl-2-deoxy-α*-D-*glucopyranose*. The reaction mixture from attempted anomerisation of *iso*propyl-tri-*O*-acetyl-2-deoxy-*β*-D-glucopyranoside (0.20 g) yielded a product (0.034 g), m. p. 111—112°, $[\alpha]_D^{24}$ +104° (*c*, 1.6, chloroform). (Found: C 50.6; H. 5.8 Calc. for $C_{14}H_{20}O_9$: C 50.6; H 6.1.)

Penta-O-*acetyl-β*-D-*galactofuranose*. The reaction mixture from attempted anomerisation of ethyl-tetra-*O*-acetyl-*β*-D-galactofuranoside (0.25 g) yielded penta-*O*-acetyl-*β*-D-galactofuranose (0.03 g), with m. p. 97—98°, $[\alpha]_D^{24}$ —40° (*c*, 2.3, chloroform) in good agreement with the values reported for that substance [13].

REFERENCES

1. Lemieux, R. U. *Advances in Carbohydrate Chem.* **9** (1954) 1.
2. Lindberg, B. *Acta Chem. Scand.* **3** (1949) 1153.
3. Lemieux, R. U. and Shyluk, W. P. *Can. J. Chem.* **33** (1955) 120.
4. Overend, W. G., Stacey, M. and Staněk, J. *J. Chem. Soc.* **1949** 2841.
5. Russell, J. and Cameron, A. E. *J. Am. Chem. Soc.* **60** (1938) 1345.
6. Burton, H. and Praill, P. G. F. *J. Chem. Soc.* **1950** 1203.
7. Lindberg, B. *Acta Chem. Scand.* **6** (1952) 949.
8. Shafizadeh, F. *Advances in Carbohydrate Chem.* **13** (1958) 9.
9. Micheel, F., Klemer, A. and Flitsch, R. *Ber.* **91** (1958) 663.
10. Bergmann, M., Schotte, H. and Lechinsky, W. *Ber.* **56** (1923) 1052.
11. Green, J. W. and Pacsu, E. *J. Am. Chem. Soc.* **60** (1938) 2056.
12. Schlubach, H. H. and Meisenheimer, K. *Ber.* **67** (1934) 492.

Received December 23, 1959.

ACTA CHEMICA SCANDINAVICA 14 (1960) 882–884

Rapid Paper Chromatography of Carboxylic Acids

GURLI HAMMARBERG and BÖRJE WICKBERG

Organisk-kemiska Institutionen, Kungl. Tekniska Högskolan, Stockholm, Sweden

C_1 to C_{14} straight chain fatty acids have been separated by chromatography on dimethyl sulphoxide impregnated paper. The acids migrated as almost round spots and a complete separation was obtained within less than 2 hours. The method was also found to be useful with alicyclic and higher dicarboxylic acids.

In the course of an investigation on the paper chromatography of sugar acetates, using dimethyl sulphoxide (DMS) as the polar, stationary phase [1], it was found that the normal fatty acids in the range formic to myristic acid could be separated in a similar way. The present investigation includes the separation of normal fatty acids and some alicyclic and dicarboxylic acids (Table 1). When compared to other solvent systems used for the paper chromatography of these acids, those containing DMS seem to give a good resolution in quite a short time.

The papers were usually first impregnated with DMS, the samples were then added as solutions of the free acids and the chromatograms developed with light petroleum, *iso*propyl ether or a solution of DMS in ethyl ether. The spots were detected by spraying with an indicator solution. The total time required for the separation of fatty acids was about 45 min to 2 h.

As is to be expected, the R_F values increase with the number of carbon atoms in an homologous series, with the polarity of the eluant and with the moisture content of the paper. Of monocarboxylic acids having the same number of carbon atoms, those with a straight chain carbon skeleton seem to move faster than those having a cyclic structure. There is a significant difference between normal and *iso*butyric acid (Table 1), but not between the isomeric valeric acids.

To obtain predictable results it is essential to control the moisture content of the papers (see experimental part); it is usually most convenient to run the chromatograms under dry conditions, but slightly moist conditions will sometimes improve the separation (*e.g.* of (+)camphonanic and hinokiic acid, Table 1). The spots are generally almost circular or only very slightly tailing. A conceivable explanation is that the acids in DMS solution are not appreciably dissociated or dimerised. If tailing occurs, this may be caused by too high a

Table 1. R_F values of carboxylic acids on DMS impregnated paper.

Solvents	Light petroleum Dry [a,c]	Light petroleum Moist [b]	*Iso*propyl ether	Ethyl ether — DMS 24:1 v/v [c]
Acids:				
Formic			0.06	0.18
Acetic			0.12	0.27
Propionic			0.21	0.38
n-Butyric	0.03	0.06	0.29	0.48
iso-Butyric	0.04	0.07		
n-Valeric	0.06	0.10	0.38	0.55
Hexanoic	0.09	0.18	0.47	0.61
Heptanoic	0.14	0.29	0.57	
Octanoic	0.20	0.42	0.64	
Nonanoic	0.28	0.55	0.71	
Decanoic	0.35	0.67	0.77	
Hendecanoic	0.42	0.75	0.83	
Lauric	0.49	0.82		
Myristic	0.59			
Palmitic	0.66			
Stearic	0.68			
(+)Camphonanic [d]	0.21	0.45		
Cuparenic [e]	0.16	0.42		
Cedrenic [f]	0.31	0.66		
Hinokiic [g,4]	0.21	0.50		
Glutaric				0.04
Adipic				0.05
a,a-Dimethyladipic				0.15
Sebacic				0.21

[a] Conditioning with silica gel impregnated with DMS
[b] Conditioning with silica gel impregnated with DMS containing 10 % v/v of water.
[c] Diffuse solvent front

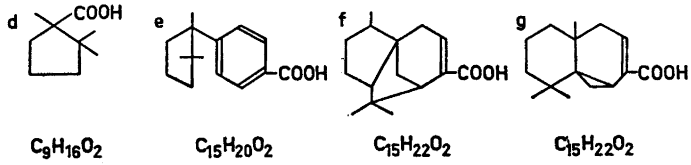

$C_9H_{16}O_2$ $C_{15}H_{20}O_2$ $C_{15}H_{22}O_2$ $C_{15}H_{22}O_2$

water content in the solvents, by insufficient impregnation with DMS, by the application of too large amounts of samples or by crystallisation of the samples on the paper. Evaporation of volatile acids from the chromatograms becomes apparent only on prolonged development. Thus formic, acetic, butyric and valeric acids (*ca* 20 μg of each) could still be detected on chromatograms after 5 h development with light petroleum.

Preparative separations of sesquiterpenic acids have been made on thick filter paper or silica gel columns impregnated with DMS [2]. With silica gel — DMS, adsorption effects may occur as has been indicated by current work at this institute on the resolution of a tropolone—phenol mixture from plant material.

EXPERIMENTAL

Paper. Whatman No. 1 filter paper was cut into strips 23 or 46 cm long, with the starting line 5 or 7 cm, respectively, from the upper end.

Solvents. DMS was of a technical quality * (99.5 % purity) with less than 0.3 % of water. Other solvents were of reagent grade.

Impregnation of papers. The papers were passed at an even rate through a 25 % v/v solution of DMS in toluene, uniformly blotted between layers of filter paper and dried at 60° for 1 min to remove the toluene. This process was repeated once and the papers were then immediately placed between glass plates leaving only the starting line and the paper above it uncovered. (After application of the samples, the papers were transferred to the chromatogram tanks in such a manner that absorption of moisture was avoided.)

When the reproducibility is unimportant, the impregnation may be simplified, *e. g.* by blowing off the toluene with hot air.

Application of samples. Usually 1—2 μl of 2 % solutions of the acids in ethyl ether were applied on the paper, placing the spots at least 1.5 cm from the paper edges and 1 cm from each other on short papers; on long papers the corresponding distances were 2 and 1.5 cm, respectively. 5—100 μl samples of acetic acid have been run on short papers using the ethyl ether — DMS eluant. Normal chromatograms of acetic acid have also been obtained by applying 1—2 μl of aqueous sodium acetate to the starting line before the impregnation with DMS. After impregnation acetic acid was liberated by adding enough of a saturated solution of oxalic acid in acetone-ethyl ether (1:1) to cover the acetate spot.

Development. All chromatograms were developed by the descending technique. The following solvents were used:

Light petroleum, b. p. 60—71° (Skellysolve B), not purified.

*Iso*propyl ether, sodium dried.

Ethyl ether (sodium dried) containing 4 % v/v of DMS.

When light petroleum was used as the eluant, the papers were 46 cm long and the chromatogram tanks were equipped with wire gauze bags containing silica gel impregnated with DMS or DMS-water to obtained standardised moisture conditions. With silica gel impregnated with DMS-water (9:1) there was only a little tailing, but this became very pronounced with DMS-water (8:2).

For safety reasons all experiments with ethyl or *iso*propyl ether were done in small chromatogram tanks using papers 23 cm long. The tanks contained no drying agent but were frequently cleaned and filled with fresh solvent.

Detection of spots. The spots were detected by spraying with the mixed indicator of Duncan and Porteous [3]: Methyl red (200 mg) and bromothymol blue (200 mg) dissolved in formalin (100 ml) and ethanol (400 ml). The pH is adjusted as required below by adding dilute sodium hydroxide solution. Without drying, the chromatograms were briefly exposed to ammonia vapours, then evenly sprayed with indicator solution, treated with ammonia as before and finally sprayed with more indicator till red or orange spots were obtained against a stable green background. The spots were usually stable for more than an hour. If the indicator is too acid, the background colour will not be stable, and if it is too alkaline trace amounts of acids will not be detected. (Duncan and Porteous recommend pH 5.2 and several ammonia treatments after spraying only once with indicator.) It is advisable to mark faint spots as soon as they appear. Strong, blurred spots become sharper if more indicator is applied or if the indicator is more alkaline.

Acknowledgement. One of us (B.W.) would like to thank W. Roos' fund for a grant.

REFERENCES

1. Wickberg, B. *Acta Chem. Scand.* **12** (1958) 615.
2. Enzell, C. *Acta Chem. Scand.* **14** (1960). 81.
3. Duncan, R. E. B. and Porteous, J. W. *Analyst* **78** (1953) 641.
4. Norin, T. *Private communication. To be published in this journal.*

Received January 7, 1960.

* Purchased from Nitroglycerin AB, Gyttorp, Sweden.

ACTA CHEMICA SCANDINAVICA 14 (1960) 885–892

Esters of Aminoacylamido Substituted Methylphenylcarbamic Acids I

CLAËS TEGNÉR and NILS-ERIK WILLMAN

Research Laboratories, AB Astra, Södertälje, Sweden

A series of new aliphatic and alicyclic 4-diethylaminoacetamido-3,5-dimethylphenylcarbamates have been prepared and tested for local anesthetic activity. Some of these compounds showed a high surface anesthetic effect.

In the search for new local anesthetics several variations of the structure of α-diethylamino-2,6-dimethylacetanilide (Xylocaine®) have been tried [1]. Amongst others, investigations on changes in the local anesthetic activity by the introduction of different groups into the *para* position of the aromatic nucleus have been carried out. Thus Büchi *et al.*[2] have examined the effect of a butoxy group and Löfgren and Tegnér[3] have evaluated the influence of hydroxy, methoxy, butoxy and butyryloxy groups. The anesthetic properties of the *p*-hydroxy derivative of Xylocaine has also been reported by Krantz, Lu and O'Malley[4]. Recently Dahlbom, Tegnér and Willman[5] have described the preparation and the local anesthetic activity of some acyl and alkyl derivatives of Xylocaine while a series of *p*-alkoxycarbonyl derivatives has been investigated by Löfgren, Tegnér, Willman and Dahlbom[6].

Since some alkoxycarbonylamino substituted local anesthetics * have been described [8,9] and reported to show favourable anesthetic properties, a study of the influence of inserting an imino group between the alkoxycarbonyl group and the aromatic nucleus in the alkoxycarbonyl derivatives of Xylocaine seemed to be of interest, *i.e.* the preparation of alkyl 4-diethylaminoacetamido-3,5-dimethylphenylcarbamates.

The present paper describes the synthesis of esters of 4-diethylaminoacetamido-3,5-dimethylphenylcarbamic acid of the following general formula

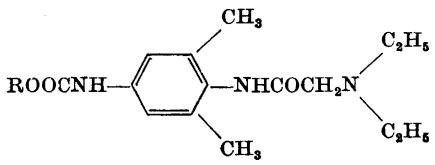

* For a review of earlier investigations on local anesthetics containing the carbamate grouping, see Soehring and Rautmann [7].

Table 1. Chemical data of bases of the general formula

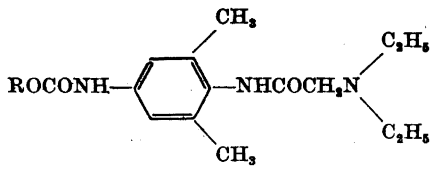

Compound	R	Method [a]	Yield %	Solvent [b] for recryst.	M. p.°C corr.
II	n-C_2H_5–	A	67	A–Aq	124–126
		C	92		
III	n-C_3H_7–	B	87	A–Aq	101–103
IV	n-C_4H_9–	B	77	E–P	87–89
V	n-C_5H_{11}	B	89	A–Aq	95–97
VI	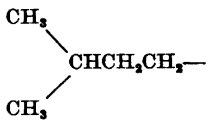	C	88	I	96–98
VII	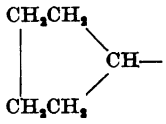	B	92	I	128–129
VIII	n-C_6H_{13}–	B	70	E	90–91
IX	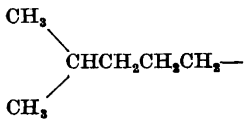	A	71	I	104–105
X	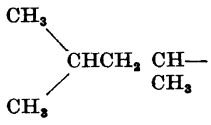	C	86	I	117–119
XI	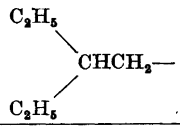	C	82	I	98–100

Empirical formula	Analyses %					
	Found			Calc.		
	C	H	N	C	H	N
$C_{17}H_{27}N_3O_3$	63.7	8.57	13.1	63.5	8.47	13.1
$C_{18}H_{29}N_3O_3$	63.8	8.73	12.8	64.5	8.71	12.5
$C_{19}H_{31}N_3O_3$	65.3	9.12	12.0	65.3	8.94	12.0
$C_{20}H_{33}N_3O_3$	66.2	9.05	11.6	66.1	9.15	11.6
$C_{20}H_{33}N_3O_3$	66.5	9.33	11.3	66.1	9.15	11.6
$C_{20}H_{31}N_3O_3$	66.3	8.56	11.5	66.5	8.64	11.6
$C_{21}H_{35}N_3O_3$	66.9	9.24	10.9	66.8	9.35	11.1
$C_{21}H_{35}N_3O_3$	66.6	9.26	11.4	66.8	9.35	11.1
$C_{21}H_{35}N_3O_3$	66.7	9.38	11.1	66.8	9.35	11.1
$C_{21}H_{35}N_3O_3$	66.8	9.20	11.0	66.8	9.35	11.1

Table 1, continued.

Compound	R	Method [a]	Yield %	Solvent [b] for recryst.	M. p.°C corr.
XII	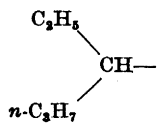	C	94	I	128–129
XIII	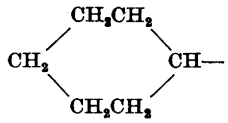	C	88	B	143–146
XIV	n-C_7H_{15}–	B	73	A–Aq	76–78
XV	n-C_8H_{17}–	B	74	E	80–81

[a] *cf.* p. 889.
[b] A = ethanol; Aq = water; B = benzene; E = ether; I = *iso*propyl ether; P = petroleum ether b.p. 40–60°.

where R is a *cyclo*pentyl, *cyclo*hexyl or an alkyl radical containing from two to eight carbon atoms (compounds II–XV, Table 1).

The compounds II and IX were prepared by the reaction of an alkyl chloroformate with α-diethylamino-4-amino-2,6-dimethylacetanilide [5]. Compounds III–V, VII, VIII, XIV and XV were synthesised by transesterification of ethyl 4-diethylaminoacetamido-3,5-dimethylphenylcarbamate (II) by heating under slightly reduced pressure with the appropriate alcohol, using sodium as catalyst.

During the isolation of compound V, a high-melting base, only slightly soluble in ether, was obtained in low yield. The infrared spectrum of this base did not show any urethane band at 1 725 cm^{-1} (KBr disc). It was identified as 1,3-bis(4-diethylaminoacetamido-3,5-dimethylphenyl) urea by comparison of its infrared spectrum and melting point with that of synthetic material [10]. A mixed melting point showed no depression.

Compounds VI and X–XIII were synthesised by reaction of α-diethylamino-4-amino-2,6-dimethylacetanilide with phosgene in toluene solution, and treatment of the precipitate formed, without purification, with the appropriate alcohol to give the desired carbamate.

The chlorine content of the precipitate formed in the reaction between the 4-amino derivative and phosgene indicated the formation of the hydrochloride of the chlorocarbonylamino compound. Attempts to purify this compound and to convert it into the *iso*cyanato derivative failed.

Empirical formula	Analyses %					
	Found			Calc.		
	C	H	N	C	H	N
$C_{21}H_{35}N_3O_3$	67.0	9.26	11.3	66.8	9.35	11.1
$C_{21}H_{33}N_3O_3$	67.5	8.80	11.3	67.2	8.86	11.2
$C_{22}H_{37}N_3O_3$	67.7	9.51	10.7	67.5	9.53	10.7
$C_{23}H_{39}N_3O_3$	68.0	9.56	10.5	68.1	9.69	10.4

The local anesthetic activity of the compounds II—XV was tested on rabbit cornea, by the method of Wiedling [11]. The toxicity (LD50 value) of each compound was determined by subcutaneous injection in white mice. The results of these tests are given in Table 2. Irritation tests [12] carried out with most of the compounds showed that those containing a carbon chain more than five carbon atoms long in the alkoxycarbonylamino group were strongly irritant while those with five carbon atoms or less gave only slight or no irritation *.

EXPERIMENTAL

Iso*hexyl chloroformate (I)*. For the synthesis of compound IX *iso*hexyl chloroformate was prepared from *iso*hexanol [13] as described for benzyl chloroformate [14]. The ester was fractionated in a Vigreux column and the fraction b.p. 57—58°/8 mm was collected. Yield 82 %. (Found: C 51.1; H 7.77. Calc. for $C_7H_{13}ClO_2$: C 51.1; H 7.96.)

4-Diethylaminoacetamido-3,5-dimethylphenylcarbamates. The following three general methods were used for the preparation of compounds II—XV (see Table 1). A typical example is given of each method.

Method A. A solution of α-diethylamino-4-amino-2,6-dimethylacetanilide [5] (15 g, 0.060 mole) in benzene (250 ml) was treated with ethyl chloroformate (6.5 g, 0.060 mole) added dropwise with stirring and the reaction mixture was kept at 40—50° for 1 h. It was then extracted with water and the aqueous extract was made alkaline by the addition of ammonia. The oil that separated soon crystallised and was filtered off. Recrystallisation from aqueous ethanol (1:1) gave colourless crystals, m. p. 124—126° (13 g, 67 %).

* Thanks are due to Dr. S. Wiedling for performing the biological tests.

Table 2. Local anesthetic activity and toxicity of compounds II-XV.

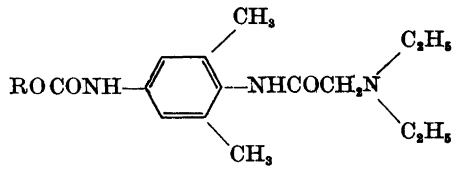

Compound	R	Toxicity * LD50 g base/kg	Anesthetic activity * Xylocaine = 1.0
II	C_2H_5—	0.34	1.2
III	n-C_3H_7—	0.35	1.6
IV	n-C_4H_9—	0.32	10
V	n-C_5H_{11}—	0.38	35
VI	$(CH_3)_2CHCH_2CH_2$—	0.49	20
VII	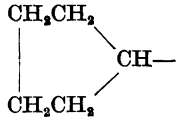	0.48	2.8
VIII	n-C_6H_{13}—	0.84	60
IX	$(CH_3)_2CHCH_2CH_2CH_2$—	0.93	12
X	$(CH_3)_2CHCH_2CH(CH_3)$—	0.84	11
XI	$(C_2H_5)_2CHCH_2$—	0.86	12

Table 2, continued.

Compound	R	Toxicity * LD50 g base/kg	Anesthetic activity * Xylocaine = 1.0
XII	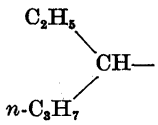	0.69	4.5
XIII	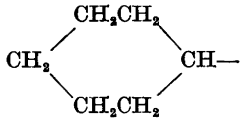	0.85	12
XIV	n-C_7H_{15}—	1.5	50
XV	n-C_8H_{17}—	1.8	70

* *cf.* p. 889 for explanation.

Method B. A small piece of sodium (0.3 g) was dissolved in n-pentanol * (30 g, 0.34 mole) by heating. Ethyl 4-diethylaminoacetamido-3,5-dimethylphenylcarbamate (II) (20 g, 0.062 mole) was added to this solution and the mixture was heated on a water bath at 80° under slightly reduced pressure (~135 mm). After 3 h the excess pentanol was removed under vacuum (8 mm) and the residue was washed with water. The residual crystalline mass was dissolved in benzene and the solution was filtered, dried over sodium sulphate and then passed through an Al_2O_3 column. The base separated on evaporation and was recrystallised from ethanol-water (3:1), colourless needles, m. p. 95—97° (20 g, 89 %).

The filtration of the benzene solution gave a rather insoluble product (~1 g) which was crystallised from chloroform-ethanol, m. p. 261—264°. It was insoluble in water, and bases but soluble in acids. Infrared spectra ** were recorded of this compound and, for comparison, of n-pentyl 4-diethylaminoacetamido-3,5-dimethylphenylcarbamate and 1,3-bis(4-diethylaminoacetamido-3,5-dimethylphenyl) urea[10]. The following strong bands were observed:

Compound m. p. 261—264°: 3 250, 1 665, 1 605, 1 540, 1 495, 1 405, 1 315 and 1 205 cm^{-1}.

n-Pentyl 4-diethylaminoacetamido-3,5-dimethylphenylcarbamate: 3 210, 2 830, 1 725, 1 670, 1 610, 1 550, 1 495, 1 225 and 1 088 cm^{-1}.

1,3-Bis(4-diethylaminoacetamido-3,5- dimethylphenyl) urea: 3 250, 1 665, 1 605, 1 540, 1 495, 1 405, 1 315 and 1 205 cm^{-1}.

As can be seen the compound showed no band at 1 725 cm^{-1} (urethane); comparison with the urea derivative showed that they were identical. A mixed melting point of the two compounds showed no depression.

Method C. α-Diethylamino-4-amino-2,6-dimethylacetanilide [5] (25 g, 0.10 mole) dissolved in dry toluene (400 ml) was added dropwise with stirring to a 10 % (v/v) solution

* As carbamates prepared from the commercial n-pentanol showed a broad melting point interval the alcohol was purified by fractional distillation and the fraction b. p. 138.5—139°, $n_D^{20} = 1.4097$ was collected for use.

** The infrared spectra were recorded with a Perkin-Elmer model 21 spectrophotometer. All compounds were run in KBr discs.

of phosgene (30 g, 0.30 mole) in toluene. The temperature of the reaction mixture was held at 40° by external heating. After standing overnight at this temperature, the precipitate formed was collected and dried in a desiccator. Attempts to purify this compound by recrystallisation caused discolouration and evolution of hydrogen chloride. No *iso*cyanate could be obtained by heating under reflux in an inert solvent (toluene). The chlorine content of the precipitate was determined by titration (Mohr) as 19.8 % indicating the formation to a large extent of the chlorocarbonylamino compound (calc. for $C_{15}H_{23}Cl_2N_3O_2$: Cl 20.4). When heated with 2 moles of ethanol in benzene solution a 92 % yield of the ethyl carbamate derivative was obtained. The precipitate was therefore used for synthesis without purification.

A suspension of the above precipitate in a mixture of dry toluene (150 ml) and *cyclo*hexanol (20 g, 0.20 mole) was heated on a water bath for 2 h. The solution was then diluted with absolute ether and the precipitate formed was filtered off and dissolved in water. The solution was extracted once with ether and then made alkaline by the addition of ammonia. The base liberated was collected and recrystallised from benzene, m. p. 143—146° (33 g, 88 %).

Methods of preparation, yields, solvents for recrystallisation, melting points and analytical data of the bases thus prepared are given in Table 2.

REFERENCES

1. Killian, H. *Lokalanästesie und Lokalanästetika*, Georg Thieme Verlag, Stuttgart 1959, p. 68.
2. Büchi, J., Launer, G., Ragaz, L., Böniger, H. and Lieberherr, R. *Helv. Chim. Acta* **34** (1951) 278.
3. Löfgren, N. and Tegnér, C. *Acta Chem. Scand.* **8** (1954) 1806.
4. Krantz Jr, J. C., Lu, G. and O'Malley, W. E. *J. Pharmacol. Exptl Therap.* **111** (1954) 224.
5. Dahlbom, R., Tegnér, C. and Willman, N.-E. *Acta Chem. Scand.* **13** (1959) 1145.
6. Löfgren, N., Tegnér, C., Willman, N.-E. and Dahlbom, R. *Acta Chem. Scand. To be published.*
7. Soehring, K. and Rautmann, H. D. *Arzneimittel-Forsch.* **2** (1952) 551.
8. Rabjohn, N., Hopkins, T. R. and Nagler, R. C. *J. Am. Chem. Soc.* **74** (1952) 3215.
9. a) Najer, H., Chabrier, P. and Giudicelli, R. *Bull. soc. chim. France* **1955** 1189.
   b) Chabrier, P., Najer, H. and Giudicelli, R. *Bull. soc. chim. France* **1955** 1353.
   c) Najer, H., Chabrier, P. and Giudicelli, R. *Bull. soc. chim. France* **1956** 106.
   d) Chabrier, P., Najer, H., Giudicelli, R. and Voisinet, E. *Bull. soc. chim. France* **1956** 1134.
   e) Chabrier, P., Najer, H. and Giudicelli, R. *Bull. soc. chim. France* **1956** 1669.
   f) Giudicelli, R., Najer, H., Chabrier, P. and Joannic, M. *Ann. pharm. franc.* **14** (1956) 376.
   g) Najer, H., Chabrier, P., Giudicelli, R. and Mabille, P. *Bull. soc. chim. France* **1957** 471.
10. Tegnér, C. and Domeij, K.-E. *Acta Chem. Scand.* **14** (1960) 916.
11. Wiedling, S. *Acta Pharmacol. Toxicol.* **8** (1952) 117.
12. Wiedling, S. *Acta Pharmacol. Toxicol.* **4** (1948) 351.
13. Huston, R. C. and Langham, C. C. *J. Org. Chem.* **12** (1947) 90.
14. Horning, E. C. *Organic Syntheses* Coll. Vol. III, New York 1955, p. 167.

Received December 2, 1959.

ACTA CHEMICA SCANDINAVICA 14 (1960) 893–902

X-Ray Investigation on Rhodium Phosphides. The Crystal Structure of Rh_4P_3

STIG RUNDQVIST and ALLAN HEDE

Institute of Chemistry, University of Uppsala, Uppsala, Sweden

The rhodium-phosphorus system has been investigated in the range 0–75 atom per cent phosphorus using X-ray and chemical analytical methods. Four intermediate phases have been found, *viz.* Rh_2P, Rh_4P_3, RhP_2 and RhP_3. The structure of Rh_2P is of the anti-fluorite (*C* 1) type, $a = 5.498$ Å, and RhP_3 of the skutterudite (*D* 2) type, $a = 7.996$ Å. The crystal structure of Rh_4P_3 has been determined and refined by single-crystal X-ray methods. The space group is *Pnma*; $a = 11.662$ Å; $b = 3.317$ Å; $c = 9.994$ Å, and the unit cell contains sixteen rhodium atoms and twelwe phosphorus atoms on seven 4(*c*) positions. The structure is related to the Fe_2P (*C* 22) and Co_2P (*C* 23) structures.

The binary system rhodium-phosphorus has been earlier investigated using tensimetric and X-ray powder methods by Faller, Strotzer, and Biltz [1]. They reported four intermediate phases with the following compositions: Rh_2P, $RhP_{0.8}$, RhP_2 and RhP_3. Zumbusch [2] found that the structure of Rh_2P was of the anti-fluorite type. One of the present authors (S.R.) earlier [3] reported the structure of RhP_3 (*D* 2 type), and confirmed the anti-fluorite structure of Rh_2P.

The present paper gives an account of phase-analytical observations on the Rh-P system, and in addition describes the crystal structure determination of the phase Rh_4P_3, which has not been previously characterized properly.

EXPERIMENTAL

The alloys were prepared by heating rhodium metal powder (Heraeus, purity 99.95 %) and red phosphorus (purity 99 % or higher) in evacuated and sealed silica tubes at temperatures between 900°C and 1 100°C. The alloys were prevented from contacting the silica tube walls by placing them in small crucibles of pure aluminium oxide.

Chemical analyses were made at the Department of Analytical Chemistry of this Institute. The analytical work, directed by the head of the department, Dr. F. Nydahl, was performed in the following manner.

The samples were dissolved in hydrochloric acid-chlorine by heating in sealed glass tubes at 300°C for 24—48 h [4-7] (*cf* Ref. [8]). Perchloric acid was used as oxidant for the evolution of chlorine. 1—2 g of sodium chloride was added to the solution, which was evaporated to dryness in order to remove traces of silicic acid. The residue was taken up in hydrochloric acid and filtered. Rhodium was precipitated as sulphide, fired and reduced to metal in hydrogen [8]. In the filtrate from the rhodium sulphide, the phosphoric acid was precipitated after evaporation as ammonium molybdophosphate and weighed as $P_2O_5.24MoO_3$ according to Nydahl [9].

X-Ray powder photographs were taken with Guinier-type focussing cameras using Cu$K\alpha$ and Cr$K\alpha_1$ radiation ($\lambda_{CuK\alpha} = 1.5418$ Å; $\lambda_{CrK\alpha_1} = 2.2896$ Å). Each powder film used for lattice parameter measurements was calibrated with either silicon ($a = 5.4306$ Å) or calcium fluoride ($a = 5.4630$ Å) as an internal standard. The accuracy of the lattice parameter determinations is greater than 0.05 %.

Single crystal intensity data were obtained with an ordinary Weissenberg camera and niobium-filtered MoK radiation. The multiple-film technique was used with thin iron foils between successive films, and the intensities were estimated visually with the aid of a standard intensity scale. The single-crystal specimen of Rh_4P_3, picked from a crushed, arc-melted alloy, was roughly cylindrical and of radius 0.025 mm. An intensity correction for the absorption was applied, the single-crystal being regarded as a perfect cylinder.

Fourier series summations, structure factor calculations, and calculations of interatomic distances were made with the electronic digital computer BESK, using programs developed by M. Edstrand and S. Åsbrink, G. Blomqvist and S. Westman [10]. Atomic scattering factors f_i were introduced as analytical expressions of the type;

$$f_i = A_i \exp\left(-\frac{a_i}{\lambda^2}\sin^2\Theta\right) + B_i \exp\left(-\frac{b_i}{\lambda^2}\sin^2\Theta\right) + C_i \exp\left(-\frac{c_i}{\lambda^2}\sin^2\Theta\right).$$

The constants A_i, B_i, C_i, a_i, b_i and c_i, are based on the atomic scattering factor tables given by Thomas and Umeda [11] for Rh and by Tomiie and Stam [12] for P, and were calculated by Appel [13]. No corrections for dispersion were made. The following constants were used:

	A	B	C	a	b	c
Rh	15.520	16.977	12.024	0.237	2.600	20.057
P	1.447	7.971	5.588	0.001	1.528	37.194

PHASE ANALYSIS AND X-RAY POWDER DATA

The phase-analytical investigation showed that there are four intermediate phases with compositions close to Rh_2P, Rh_4P_3, RhP_2 and RhP_3. Within

Table 1. Phase-analytical data of alloys containing Rh_4P_3.

Alloy	Chemical analysis (weight per cent) Rh	P	Phases detected in powder photographs
$RhP_{0.746}$	81.5	18.29	Rh_4P_3 Traces of Rh_2P
$RhP_{0.753}$	81.4	18.45	Rh_4P_3 Traces of RhP_2

Table 2. Powder data for Rh_4P_3 ($CrK\alpha_1$ radiation).

hkl	$\sin^2\Theta_{obs} \times 10^4$	$\sin^2\Theta_{calc} \times 10^4$	$p \cdot F^2 \times 10^{-3}$	I_{calc}	I_{obs}
101	228	228	2	8	w−
200	385	385	2	5	w−
201	516	517	6	10	w−
002	525	525	4	7	w−
102	—	621	0	0	—
202	911	910	21	16	w
301	—	999	2	2	—
103	1 277	1 277	22	13	w
011	1 322	1 323	209	126	m+
302	1 391	1 392	59	34	w
111	1 418	1 419	172	98	m
400	1 541	1 542	62	32	w
203	1 566	1 566	51	25	w
210	—	1 577	0	0	—
401	1 672	1 673	247	118	m+
211	1 708	1 708	61	29	w
112	—	1 812	3	2	—
303	—	2 048	1	0	—
402	—	2 067	4	2	—
004	2 100	2 099	75	30	m
212		2 102	129	52	
311	2 194	2 190	144	56	m+
104		2 196	213	81	
013	—	2 372	11	4	—
113	—	2 468	19	7	—
204	2 484	2 485	217	78	m
501	2 539	2 541	209	75	m
312	2 583	2 583	96	34	w
404	—	2 723	11	4	—
410	2 733	2 733	685	233	st
213	2 757	2 758	1 306	444	st+
411	2 864	2 864	101	34	w
502	—	2 934	14	5	—
304	2 965	2 967	285	91	m
313	—	3 239	19	6	—
412	—	3 258	0	0	—
105	—	3 377	2	1	—
114	3 386	3 387	203	68	m−
600	—	3 469	22	8	—
503	3 591	3 590	76	30	w
601	—	3 600	5	2	—
404	—	3 641	28	10	—
205	—	3 666	0	0	—
214	3 674	3 676	226	78	m
511	3 732	3 732	233	82	m
413	3 917	3 914	91	34	w
602	3 998	3 994	33	13	w−
512	4 125	4 125	225	88	m
305	—	4 148	43	17	—
314	4 157	4 158	233	86	m
015	4 475	4 472	80	35	w
504	—	4 509	9	4	—
115	—	4 568	16	7	—

(*Table 2. cont.*)

hkl	$\sin^2\Theta_{obs} \times 10^4$	$\sin^2\Theta_{calc} \times 10^4$	$p \cdot F^2 \times 10^{-3}$	I_{calc}	I_{obs}
603	4 651	4 650	739	340	st
610	—	4 661	0	0	—
006	4 724	4 724	244	115	m
020	4 765	4 765	679	319	st
513	—	4 781	11	4	—
611	—	4 791	14	7	—
106	—	4 820	20	10	—
405	—	4 822	4	2	—
414	4 830	4 833	111	58	w
701	—	4 853	0	0	—
215	—	4 857	4	2	—
121	—	4 993	2	1	—

experimental error, (0.05 %), the phases did not show any lattice parameter variations. Some phase-analytical data are given in Table 1 for alloys containing Rh_4P_3. These data show that the composition of the pure phase is $RhP_{0.75}$ rather than $RhP_{0.80}$ as reported by Faller, Strotzer and Biltz [1].

No signs of transitions in the solid state at temperatures between 800°C and 1 100°C were observed in quenched alloys. Some alloys were subjected to higher temperatures by heating in an argon-filled arc furnace. Alloys with a phosphorus content higher than about 50 atom per cent evolved phosphorus vapour on heating, but alloys having phosphorus contents lower than about 40 atom per cent could be melted without serious phosphorus losses. Single-crystals of Rh_4P_3 were obtained from such melts.

The anti-fluorite structure [2] of Rh_2P was confirmed by inspection of the X-ray powder photographs. Measurements of the unit cell edge gave the value 5.498 Å, corresponding to the following interatomic distances: Rh—6 Rh 2.749 Å; Rh—12Rh 3.888 Å; Rh—4P 2.381 Å.

The structure of $Rh_4P_3$was determined by employing single-crystal methods (*vide infra*). Powder data for Rh_4P_3 are presented in Table 2. The unit cell is orthorhombic with the dimensions $a = 11.662$ Å; $b = 3.317$ Å; $c = 9.994$ Å.

Attempts to prepare single-crystals of RhP_2 and RhP_3 were unsuccessful and the powder pattern of RhP_2 could not be interpreted. The powder photographs of RhP_3 could be indexed with the cubic unit cell $a = 7.996$ Å. It seems very probable that RhP_3 is isostructural with $CoAs_3$ (*D* 2 type), the structure of which was determined by Oftedal [14]. According to this author, the structure of $CoAs_3$ is based on the space group $Im3$ (No. 204) with eight cobalt atoms in the 8(*c*) position, and twentyfour arsenic atoms in the 24(*g*) position, having the parameters $y = 0.35$; $z = 0.15$. Assuming that RhP_3 has the *D* 2 structure, a satisfactory agreement between observed and calculated intensities was reached with the parameter values $y = 0.34_7$; $z = 0.13_7$ for the phosphorus atoms. Intensity data are given in Table 3. These parameter

Table 3. Powder data for RhP_3 (Cu*Ka* radiation).

hkl	$\sin^2\Theta_{obs} \times 10^4$	$\sin^2\Theta_{calc} \times 10^4$	$p \cdot F^2 \times 10^{-3}$	I_{calc}	I_{obs}
110	186	186	8	3	w
200	372	372	314	74	st+
211	558	558	29	4	w
220	744	744	480	49	st
310	930	929	29	19	m+
301			204		
222	1 116	1 115	306	21	m+
321	1 302	1 301	1	5	w+
312			81		
400	1 488	1 487	131	7	w+
411	1 673	1 673	7	1	w−
330			17		
420	1 860	1 859	663	51	st
402			500		
332	2 045	2 045	27	1	w−
422	2 230	2 231	839	31	st
510	2 417	2 417	27	9	m
501			16		
431			169		
413			44		
521	—	2 788	0	0	—
512			1		
440	2 974	2 974	134	4	w+
530	3 162	3 160	8	3	w
503			34		
433			46		
600	3 347	3 346	16	8	w+
442			215		
611	—	3 532	0	0	—
532			0		
523			0		
620	3 719	3 718	211	18	m
602			286		
541	*	3 904	1	1	w−
514			18		
622	4 090	4 090	447	18	m
631	4 275	4 275	3	3	w
613			55		
444	4 462	4 462	298	13	m
710	*	4 647	7	1	w−
701			1		
550			2		
640	4 832	4 832	285	24	m+
604			210		

* Too weak for accurate measurement of the diffraction angle.

values for the phosphorus atoms cannot be considered very accurate, but the following approximate interatomic distances may be given:

shortest Rh—P distance 2.33 Å,

shortest P—P distances 2.19 and 2.45 Å.

DETERMINATION OF THE STRUCTURE OF Rh_4P_3

Weissenberg photographs of Rh_4P_3 crystals showed that the symmetry is orthorhombic. The unit cell volume is 386.6 Å^3, indicating a unit cell content of sixteen rhodium atoms and twelve phosphorus atoms. The calculated density is 8.67 g.cm^{-3}. An inspection of the intensity data from the layer lines 0 through 3 around the *b*-axis, showed that the reflexions $hk0$ with $h = 2n + 1$ and $0kl$ with $k + l = 2n + 1$ were absent. The space groups *Pnma* and $Pn2_1a$ were thus probable. Due to the short *b*-axis, the position 8(*d*) in space group *Pnma* must be eliminated. Further inspection of the intensity data showed that the intensity sequences in the 0 and 2 layer lines were equal (allowing for the normal intensity decrease), and the same was true for the 1 and 3 layer lines.

The Patterson sections $P(x0z)$ and $P(x\frac{1}{2}z)$ were calculated. It was possible to explain all maxima in these sections with a structure model based on the space group *Pnma* with sixteen rhodium atoms in four 4(*c*) positions, and twelwe phosphorus atoms in three 4(*c*) positions. Due to extensive overlapping it was difficult to obtain accurate atomic parameters from the Harker peaks alone. However, an analysis of the whole Patterson function using the method

Table 4. Interatomic distances in Rh_4P_3 (Å). (Only distances 3.80 Å or shorter listed.)

	Rh_I	Rh_{II}	Rh_{III}	Rh_{IV}	P_I	P_{II}	P_{III}
Rh_I	2.93_8 (2) 3.31_7 (2)	2.91_3 (2) 3.51_3	2.91_7	2.86_2 3.57_0	2.47 (2)	2.28 2.48 (2)	3.54
Rh_{II}	2.91_3 (2) 3.51_3	3.31_7 (2)	2.91_6	2.79_6 2.87_1 (2)	2.27	2.52 (2)	2.35 (2)
Rh_{III}	2.91_8	2.91_6	2.92_5 (2) 3.31_7 (2)	2.91_5 3.71_5	2.30 (2)	—	2.27 2.52 (2)
Rh_{IV}	2.86_2 3.57_0	2.79_6 2.87_1 (2)	2.91_5 3.71_5	3.31_7 (2)	2.61 (2)	2.30 (2)	2.30
P_I	2.47 (2)	2.27	2.30 (2)	2.61 (2)	3.32 (2)	3.32 3.45 3.78 (2)	3.18 3.74 (2) 3.79 (2)
P_{II}	2.28 2.48 (2)	2.52 (2)	—	2.30 (2)	3.31 3.45 3.79 (2)	3.32 (2) 3.75 (2)	3.25 3.80 (2)
P_{III}	3.54	2.35 (2)	2.27 2.51 (2)	2.30	3.18 3.74 (2) 3.79 (2)	3.25 3.80 (2)	3.32 (2) 3.80 (2)

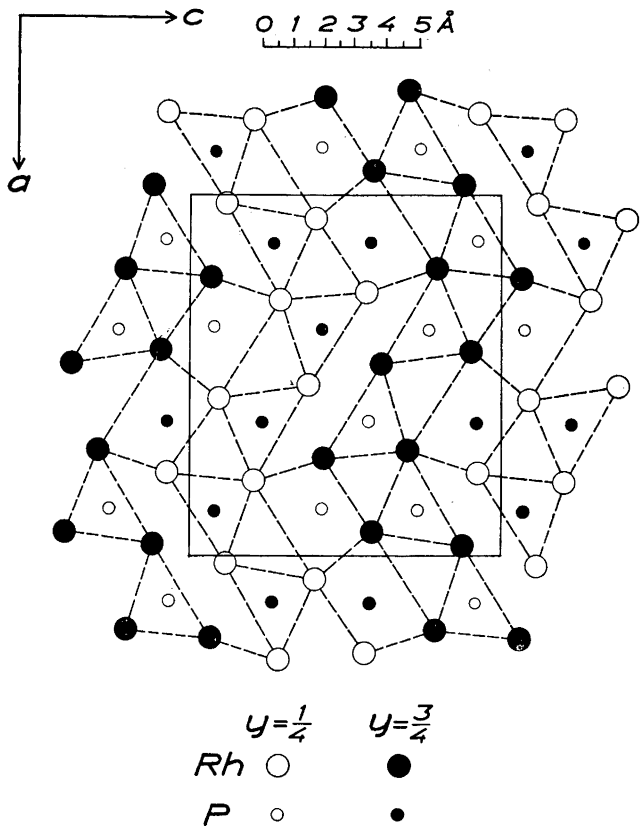

Fig. 1. The structure of Rh_4P_3 projected on (010).

described by Lindqvist [15], provided atomic parameters sufficiently accurate for the determination of a satisfactory number of structure factor signs.

The atomic parameters were refined from electron density projections and difference syntheses in the *ac*-plane. After the last refinement, the *R*-value was found to be 0.105 for the 229 observed $|F(h0l)|$-values. An isotropic, overall temperature factor with $B = 0.20$ Å^2 was applied *. The final structure of Rh_4P_3 is as follows:

Space group *Pnma* — (D_{2h}^{16}), No. 62.
$a = 11.662$ Å; $b = 3.317$ Å; $c = 9.994$ Å; $U = 386.6$ Å^3; $Z = 4$. All atoms on 4(*c*) positions:

* A list of observed and calculated $F(h0l)$-values can be obtained from this Institute on request.

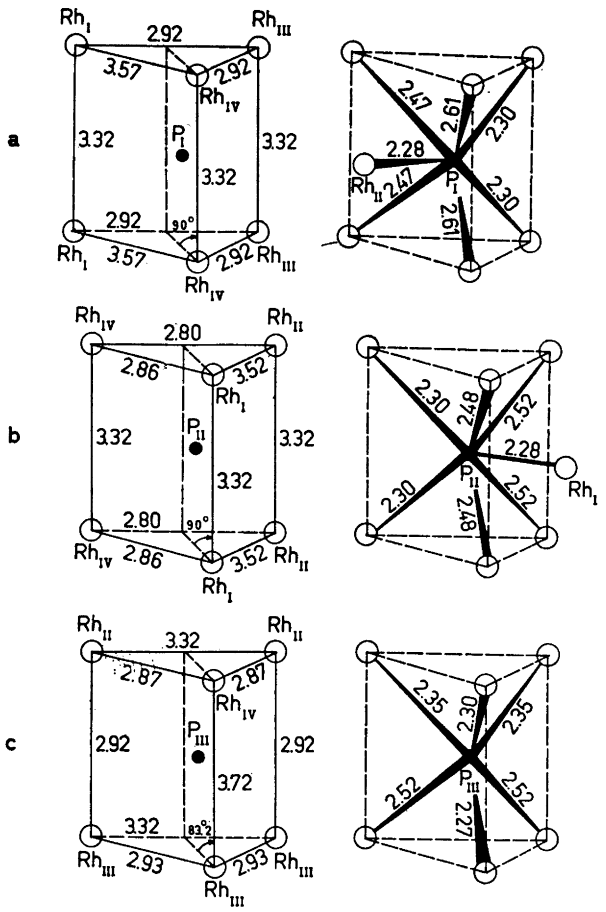

Fig. 2. The environment of the phosphorus atoms in Rh_4P_3.

a. the environment of the P_I atoms
b. the environment of the P_{II} atoms
c. the environment of the P_{III} atoms

	x	*z*
Rh_I	0.0270	0.1172
Rh_{II}	0.2717	0.5696
Rh_{III}	0.0647	0.4059
Rh_{IV}	0.2945	0.2911
P_I	0.3763	0.7616
P_{II}	0.1273	0.9212
P_{III}	0.3704	0.0792

The standard deviation for the rhodium positions, calculated from Cruickshanks [16] formula, is 0.001_9 Å, and for the phosphorus positions 0.007_3 Å. Interatomic distances are listed in Table 4.

DESCRIPTION AND DISCUSSION OF THE Rh_4P_3 STRUCTURE

A projection of the structure onto the *ac*-plane is shown in Fig. 1. The coordination of the phosphorus atoms is shown in greater detail in Fig. 2 a, b and c. The phosphorus atoms are situated at the centres of triangular prisms with rhodium atoms at the corners. This type of nonmetal atom coordination is common with transition metal phosphides, *e.g.* in the (revised) *C* 22 (Fe_2P), and *C* 23 (Co_2P) structures, as well as in transition metal borides and silicides. Each rhodium atom is surrounded by five close phosphorus neighbours, with an average Rh—P distance of 2.41 Å. In the Fe_2P [17] and Co_2P [18] structures, half of the metal atoms are surrounded by four phosphorus atoms in a distorted tetrahedral configuration, and the other half of the metal atoms have five phosphorus neighbours. The rhodium atoms in Rh_4P_3 have on average nine close rhodium contacts with a mean Rh—Rh distance of 3.11 Å.

In transition metal phosphides with a metal content larger than 50 atom per cent, there is no tendency for P—P bond formation [19]. The difference between transition metal phosphides and borides, with respect to the nonmetal-nonmetal bond formation, is clearly illustrated by a comparison of the Rh_4P_3 structure with the orthorhombic Ni_4B_3 structure [20]. The structure of orthorhombic Ni_4B_3 is based on the same space group as Rh_4P_3, the unit cell containing sixteen nickel atoms and twelwe boron atoms distributed on seven 4(*c*) positions. The coordination of the nickel atoms at the corners of triangular prisms around the boron atoms, resembles the coordination of rhodium atoms around the phosphorus atoms in Rh_4B_3; (compare Figs. 1 and 2 in the present paper with Figs. 1 and 3 in Ref.[20]). However, whereas there are no P—P contacts closer than 3.18 Å in Rh_4P_3 two thirds of the boron atoms in Ni_4B_3 are connected in infinite chains with B—B distances of approximately 1.9 Å. Furthermore, each nickel atom in Ni_4B_3 is surrounded by ten or eleven nickel neighbours at an average distance of 2.71 Å, compared with the average coordination of nine rhodium atom neighbours around each rhodium atom in Rh_4P_3 at an average distance of 3.11 Å.

Acknowledgements. This work has been financially supported by the *Swedish State Council of Technical Research* and by the *Air Force Office of Scientific Research of the Air Research and Development Command, United States Air Force,* through its European Office under Contract No. AF 61(052)-40. Facilities for use of the electronic digital computer BESK were given by the *Swedish Board for Computing Machinery.* One of the authors (S.R.) is indebted to the *Swedish State Council of Technical Research* for a generous scholarship.

We wish to thank Professor G. Hägg for his kind interest. Thanks are also due Dr. B. Aronsson for valuable discussions. Finally, we wish to express our gratitude to Dr. F. Nydahl for his great interest in our analytical problems and his work on the analyses.

REFERENCES

1. Faller, F. E., Strotzer, E. F. and Biltz, W. *Z. anorg. Chem.* **244** (1940) 317.
2. Zumbusch, M. *Ibid.* **243** (1940) 322.
3. Rundqvist, S. *Nature* **185** (1960) 31.
4. Gordon, C. L. *J. Research NBS* **30** (1943) 107.
5. Wickers, E., Schlecht, W. G. and Gordon, C. L. *Ibid.* **33** (1944) 363.
6. Wickers, E., Schlecht, W. G. and Gordon, C. L. *Ibid.* **33** (1944) 451.

7. Gordon, C. L., Schlecht, W. G. and Wickers, E. *Ibid.* **33** (1944) 457.
8. Hillebrand, W. F., Lundell, G. E. F., Bright, H. A. and Hoffman, J. I. *Applied Inorganic Analysis*, 2nd ed. N.Y. 1953.
9. Nydahl, F. *Lantbrukshögskol. Ann.* **10** (1942) 110.
10. Åsbrink, S., Blomqvist, G. and Westman, S. *Arkiv Kemi* **14** (1959) 545.
11. Thomas, L. H. and Umeda, K. *J. Chem. Phys.* **26** (1957) 293.
12. Tomiie, Y. and Stam, C. H. *Acta Cryst.* **11** (1958) 126.
13. Appel, K. *Technical Note from the Quantum Chemistry Group, University of Uppsala.*
14. Oftedal, I. *Z. Krist.* **66** (1928) 517.
15. Lindqvist, I. *Arkiv Mineral. Geol.* **2** (1960) 505.
16. Cruickshank, D. W. J. *Acta Cryst.* **2** (1949) 65.
17. Rundqvist, S. and Jellinek, F. *Acta Chem. Scand.* **13** (1959) 425.
18. Nowotny, H. *Z. anorg. Chem.* **254** (1947) 31.
19. Schönberg, N. *Acta Chem. Scand.* **8** (1954) 226.
20. Rundqvist, S. *Ibid.* **13** (1959) 1193.

Received January 11, 1960.

ACTA CHEMICA SCANDINAVICA 14 (1960) 903–908

Heats of Hydrolysis of N-Acetylated Imidazole, 1,2,4-Triazole and Tetrazole

INGEMAR WADSÖ

*Thermochemistry Laboratory *, University of Lund, Sweden*

The heats of hydrolysis of N-acetylated imidazole, 1,2,4-triazole and tetrazole have been determined calorimetrically at 25°C. For the idealized hydrolysis reaction

$$RNAc(s) + H_2O(l) \rightarrow RNH(s) + HOAc(l)$$

the enthalpy changes were found to be: -4.83 ± 0.05 kcal/mole for RNH = imidazole, -7.29 ± 0.06 kcal/mole for RNH = 1,2,4-triazole and -10.31 ± 0.09 kcal/mole for RNH = tetrazole.

Heats of solution in acetone have been determined for the compounds participating in the hydrolysis reaction. From the heats of solution obtained, heats of hydrolysis referring to the reaction RNAc(acetone) + H_2O(acetone) → RNH(acetone) + HOAc(acetone) have been calculated to be: -7.52 ± 0.07 kcal/mole for R = imidazole, -9.03 ± 0.07 kcal/mole for R = 1,2,4-triazole and -12.35 ± 0.10 kcal/mole for R = tetrazole.

Free energy changes in transacetylation from tetrazole → 1,2,4-triazole → imidazole, have been briefly discussed.

During recent years a considerable amount of evidence has accumulated, that the imidazole ring of histidine forms an essential part of the active centre of some hydrolytic enzymes **. These hydrolysis processes in which esters or amides are involved, have been considered as two-step reactions. In the first step an imidazole group in the enzyme is believed to be acylated, after which follows a rapid hydrolysis. The kinetics of these reactions as studied on model substances have been extensively investigated. However, very little attention has been paid to the energetic relationships between substrate, enzyme intermediate, and the products. Therefore, in connection with earlier calorimetric work on acetylated compounds [2-5], it was felt desirable to determine the heat of hydrolysis of N-acetyl imidazole as well as that of N-acetyl 1,2,4-triazole and N-acetyl tetrazole.

* Sponsored by *The Swedish Natural Science Research Council* and by *The Swedish Technical Research Council.*

** See, *e.g.*, the reference list given in Ref.[1]

The compounds participating in the idealized hydrolysis reaction V are in condensed states, being solids and liquids. The derived standard heats of hydrolysis, therefore, are not closely comparable. As heats of vaporisation data are not available, heats of solution in acetone, which is believed to be an inert solvent for these compounds have been determined.

Some years ago the kinetics of the hydrolysis of these N-acetyl compounds were studied by Staab [6], which investigations will be supplemented by some enthalpy data given in this paper.

EXPERIMENTAL

Materials. Imidazole was prepared from D-tartaric acid and hexamethylenetetramine[7], and the crude product was recrystallized from benzene. After sublimation colourless crystals, melting at 88.7—89.4°C, were obtained. Imidazole was acetylated by acetyl chloride in benzene solution [6]. After removing the solvent in vacuum, the colourless crystalline residue was recrystallised from a benzene-ligroin mixture (1:1) and the product obtained was washed with petrol ether (boiling range 40—60°C) and dried in vacuum. After sublimation the melting point of the ester was 103.0—104.0°C. Potentiometric titration on the acetic acid formed by hydrolysis, gave an equivalent weight corresponding to a purity of 99.7 %.

1,2,4-Triazole was prepared from formamide and hydrazine hydrochloride [8], and the crude product was recrystallized from ethyl acetate. After sublimation colourless crystals melting at 120.2—120.9°C were obtained.

Acetylation of the triazole by acetyl chloride was performed in benzene solution [6]. After removing the solvent in vacuum, a white crystalline residue melting at about 37°C was obtained. In the further purification use was made of the exceptionally high vapour pressure of N-acetyl 1,2,4-triazole. The crystalline mass was put in a glass bulb fitted with a 30 cm tube. The tube was connected to a vacuum system for *ca* 10 min, after which it was sealed off. The bulb was placed on a sand bath maintained at a temperature slightly below the melting point of the substance, with the tube in a vertical position and after a week, most of the substance had sublimed into the tube, where it formed big colourless crystals. The process was repeated, after which the melting point was 39.7—40.7°C. Potentiometric titration indicated an equivalent weight equal to the theoretical.

Tetrazole was prepared from cyanogen and hydrazoic acid [9] and the crude product was sublimed to give white crystals melting at 153.5—155.0°C. Potentiometric titration indicated the purity to be 99.5 %.

N-Acetyl-tetrazole was prepared from the silver salt of tetrazole by reaction with acetyl chloride in benzene solution [6]. The light yellow product was recrystallised from a benzene-ligroin (8:2) solution, to give colourless needles. After sublimation the substance melted at 58.0—59.0°C. Equivalent weight, obtained by potentiometric titration with sodium hydroxide in aqueous solution, corresponded to a purity of 99.6 %.

Acetone used in the solution experiments was treated with potassium permanganate [10], dried with Drierite and distilled through a 10-plate column.

The heterocyclic acetates are rapidly hydrolyzed in the air and thus special precautions had to be taken. After the final sublimation, all handling of them, including the filling into ampoules for the calorimetric experiments, was carried out in a "dry air box" fitted with rubber gloves.

Apparatus. The reactions were carried out in a metal "isothermal" calorimeter, which has been described in detail elsewhere (Type D in Ref.[11]).

Calibration. The heat equivalent of the calorimeter, including its content, was determined electrically by passing a known current for a given time (300 sec) through the heating element. The calibrations were performed on the system after the reaction had taken place. The result of each calibration experiment was adjusted to give the heat equivalent of a "standard system", ε°, in which the calorimetric liquid contained the reaction products from a certain amount of substance. The actual heat equivalent values, ε, were obtained from ε°, by applying a small correction for the variations in the amount of substance used.

Calorimetric procedure. The calorimeter was charged with 100 ml of liquid, either 0.8 N aqueous sodium hydroxide solution or acetone. The heats of hydrolysis measurements were supplemented by determination of heats of solution in order to obtain the standard enthalpy changes of the hydrolysis reactions.

All reactions were very rapid, the reaction period was 5 min, and the initial and final thermistor resistance values could therefore be graphically evaluated.

Corrections to the standard states: The idealized, isothermal hydrolysis reaction V is obtained from eqns I—IV, which correspond to the reactions taking place under experimental conditions.

I	$RNAc(s) + H_2O(soln) \rightarrow RNH(soln) + HOAc(soln)$	ΔH_1
II	$RNH(s) \rightarrow RNH(soln)$	ΔH_2
III	$HOAc(l) \rightarrow HOAc(soln)$	ΔH_3
IV	$H_2O(l) \rightarrow H_2O(soln)$	ΔH_4
V	$RNAc(s) + H_2O(l) \rightarrow RNH(s) + HOAc(l)$	ΔH^0

$$\Delta H^\circ = \Delta H_1 - \Delta H_2 - \Delta H_3 + \Delta H_4$$

Units of measurements. The results of the calorimetric experiments are expressed in terms of the defined calorie, equal to 4.1840 abs. joules, and refer to the isothermal process at 25°C, and to the true mass. The molecular weights were computed from the 1951 table of international atomic weights [12].

RESULTS

The experimental results are summarised in Tables 1—4. In the tables the following symbols have been used:

$\log R_i/R_f$ the expression proportional to the temperature change: R_i and R_f are the corrected thermistor resistance values at the start and the end, respectively, of the main period.

ε the heat equivalent of the actual system in calories per unit of $\log R_i/R_f$.

Heats of hydrolysis

From five calibration experiments the standard heat equivalent (referring to 200 mg of substance) was calculated to be 9 071 $\pm$ 5 * cal/unit of $\log R_i/R_f$. Results from heats of hydrolysis measurements are given in Table 1. The amount of N-acetyl imidazole and -tetrazole participating in the reactions was corrected with regard to the analysis performed.

Results from the heats of solution measurements performed in 0.8 N aqueous solution of sodium hydroxide are given in Table 2.

Table 3 contains a summary of data connected with eqns I—V. The uncertainties given in Table 3 do not include possible systematic errors. As the accuracy of the titrations, by which the purity of the N-acetyl compounds and acetic acid was tested, cannot be considered to be better than $\pm$ 0.2 %, the true uncertainties are somewhat greater. Taking this into consideration, the standard enthalpy changes will be taken as $-$ 4.83 $\pm$ 0.05, $-$7.29 $\pm$ 0.06 and $-$10.31 $\pm$ 0.09 kcal/mole for the hydrolysis of N-acetylated imidazole, 1,2,4-triazole and tetrazole, respectively.

* When five or more determinations are performed, the uncertainties are given as the standard deviation of the mean. Otherwise they are the average deviation of the mean.

Table 1.

RNAc	mmoles	ε	$10^4 \times \log R_i/R_f$	$-\Delta H$, kcal/mole
N-Acetyl imidazole	2.748	9 075	45.47	15.02
	2.982	9 076	49.29	15.00
	2.318	9 073	38.27	14.98
	2.148	9 073	35.49	14.99
				Mean 15.00 ± 0.01
N-Acetyl 1,2,4-triazole	2.826	9 075	67.65	21.72
	2.742	9 075	65.68	21.74
	3.267	9 076	78.27	21.74
	3.215	9 076	76.86	21.70
				Mean 21.73 ± 0.02
N-Acetyl tetrazole	2.724	9 071	87.52	29.14
	2.151	9 073	69.14	29.16
	2.202	9 073	70.99	29.25
	2.371	9 074	76.19	29.16
				Mean 29.18 ± 0.04

Table 2.

Substance	mmoles	ε	$10^4 \times \log R_i/R_f$	$-\Delta H$, kcal/mole
Imidazole	3.012	9 071	−11.44	−3.45
	2.557	9 070	− 9.73	−3.45
	2.654	9 070	−10.06	−3.44
				Mean −3.45 ± 0.01
1,2,4-Triazole	3.034	9 071	2.81	0.84
	2.909	9 071	2.62	0.82
	2.713	9 071	2.43	0.81
				Mean 0.82 ± 0.01
Tetrazole	2.149	9 069	12.54	5.29
	2.315	9 069	13.38	5.24
	2.822	9 071	16.28	5.23
				Mean 5.25 ± 0.02
Acetic acid	2.988	9 074	44.83	13.61
	3.173	9 071	47.55	13.59
	2.233	9 068	33.80	13.73
	2.650	9 069	39.86	13.64
	3.744	9 072	56.41	13.67
	3.222	9 071	48.33	13.61
				Mean 13.64 ± 0.02
Water	2.733	9 067	0.07	0.02
	3.695	9 067	0.10	0.02
				Mean 0.02 ± 0.00

Table 3.

RNH	$-\Delta H_1$	$-\Delta H_2$	$-\Delta H_3$	$-\Delta H_4$	$-\Delta H°$
Imidazole	15.00	−3.45	13.64	0.02	4.83 ± 0.03
1,2,4-Triazole	21.73	0.82	13.64	0.02	7.29 ± 0.03
Tetrazole	29.18	5.25	13.64	0.02	10.31 ± 0.05

Heats of hydrolysis in acetone

From three calibration experiments the heat equivalent (variations in the heat capacity of the system were insignificant for the results) was calculated to be 4 268 ± 11 cal/unit of log R_i/R_f. The heats of solution measurements are summarised in Table 4. By combining these heats of solution data with

Table 4

Substance	mmoles	$10^4 \times \log R_i/R_f$	$-\Delta H$, kcal/mole
Imidazole	2.618	−24.59	−4.01
	1.980	−18.82	−4.06
	1.867	−17.72	−4.05
			Mean −4.04 ± 0.02
1,2,4-Triazole	1.979	−18.24	−3.93
	2.349	−21.56	−3.92
			Mean −3.93 ± 0.01
Tetrazole	2.304	−16.28	−3.02
	1.492	−10.64	−3.04
	1.805	−12.89	−3.05
			Mean −3.04 ± 0.01
N-Acetyl imidazole	2.528	−32.67	−5.51
	0.909	−11.90	−5.59
	3.123	−40.10	−5.48
			Mean −5.53 ± 0.04
N-Acetyl 1,2,4-triazole	2.398	−25.02	−4.45
	2.634	−27.65	−4.48
			Mean −4.47 ± 0.02
N-Acetyl tetrazole	1.520	−13.75	−3.86
	1.250	−11.39	−3.89
			Mean −3.88 ± 0.02
Acetic acid	3.252	1.77	0.23
	1.788	0.66	0.16
	2.833	1.03	0.16
			Mean 0.18 ± 0.03
Water	3.331	− 7.96	−1.02
	3.423	− 8.13	−1.01
			Mean −1.02 ± 0.01

the given standard heat of hydrolysis, enthalpy changes referring to reaction VI were obtained.

VI RNAc(acetone) + H_2O(acetone) → RNH(acetone) + HOAc(acetone) ΔH_6

ΔH_6 was calculated to be −7.52 ± 0.07 kal/mole, −9.03 ± 0.07 kcal/mole and −12.35 ± 0.10 kcal/mole for RNH = imidazole, 1,2,4-triazole and tetrazole, respectively.

DISCUSSION

From the heats of hydrolysis data referring to reaction VI, the heats of transacetylation, in acetone solution, from N-acetyl-tetrazole to 1,2,4-triazole, and from N-acetyl 1,2,4-triazole to imidazole, are calculated to be -3.32 ± 0.12 kcal/mole and -1.51 ± 0.10 kcal/mole, respectively. Considering the symmetry of these transacetylation reactions and the absence of phase changes, the entropy changes must be very small. The standard free energy changes, therefore, should be almost the same as the corresponding enthalpy changes. The given data thus indicate, that from an energetic point of view, the transacetylation reactions are favourable only in the direction N-acetyl-tetrazole → 1,2,4-triazole → imidazole. This conclusion is in agreement with the observations made by Staab [6]. Some heats of aminolysis of the N-acetylated compounds investigated here have also been determined. They will be presented in connection with other aminolysis data in a forthcoming paper.

Acknowledgement. This work has been supported by a grant from the *University of Lund.*

REFERENCES

1. Bruice, T. C. and Sturtevant, J. M. *J. Am. Chem. Soc.* **81** (1959) 2860.
2. Wadsö, I. *Acta Chem. Scand.* **11** (1957) 1745.
3. Wadsö, I. *Ibid.* **12** (1958) 630.
4. Wadsö, I. *Ibid.* **12** (1958) 635.
5. Wadsö, I. *Ibid. In press.*
6. Staab, H. A. *Chem. Ber.* **89** (1956) 1927.
7. Snyder, H. R., Handrick, R. G. and Brooks, L. A. *Org. Syntheses* **22** (1942) 65.
8. Strain, H. H. *J. Am. Chem. Soc.* **49** (1927) 1996.
9. Oliveri-Mandalá, E. and Passalacqua, T. *Gazz. chim. ital.* **41** : II (1911) 430.
10. Vogel, A. I. *Practical Organic Chemistry.* Longmans, Green and Co. London 1948.
11. Sunner, S. and Wadsö, I. *Acta Chem. Scand.* **13** (1959) 97.
12. Wichers, E. *J. Am. Chem. Soc.* **74** (1952) 2447.

Received January 15, 1960.

ACTA CHEMICA SCANDINAVICA 14 (1960) 909–915

A Contribution to the Study of the Configuration of Anomeric Sugars

ENDRE BERNER and OVE KJØLBERG

Universitetets Kjemiske Institutt, Blindern-Oslo, Norway

The following methyl aldopentofuranosides have been oxidized by means of periodic acid: α-D-arabofuranoside, α- and β-L-arabofuranosides, α-D-xylofuranoside, and β-D-ribofuranoside. The oxidation of an α-D-pentofuranoside gave the same product as obtained by Jackson and Hudson on oxidation of an α-D-hexopyranoside and corresponding results were arrived at when the β-D- as well as the α-L- and the β-L-forms of the two ring-types of glycosides were oxidized. The correlation between the configuration at carbon atom 1 in the anomeric forms of these types of glycosides is thus established. Reduction of the primarily obtained oxidation products led to enantiomeric diglycols because the asymmetry at carbon atom 4 in this way was eliminated. On discussing the configuration the importance of the use of X-ray methods for determination of the absolute configuration of the anomeric forms is underlined. It is further emphasized that a rational nomenclature for anomeric sugars and their derivatives ought to be worked out and eventually accepted by international agreement.

Jackson and Hudson [1] introduced the method of periodate oxidation in determining the ring structure and alpha-beta configuration of methyl glycosides. By the oxidation of an α-methyl-D-aldohexopyranoside (I) two moles of periodic acid were consumed resulting in the formation of one mole formic acid and a substance III designated D'-methoxy-D-hydroxymethyl-diglycolaldehyde and having the specific rotation +121°. It was found that all the four α-D-aldohexopyranosides which were investigated gave the same diglycolaldehyde with rotation +121°. The dialdehyde could be oxidized to a dibasic acid with the rotation +26° which was transformed into a strontium salt (IV) with rotation −53°. As the configuration at carbon atoms 1 and 5 of the glycoside were retained during these processes, it could be inferred that the configuration also at carbon atom 1 must be the same in all α-D-aldohexopyranosides.

As could be expected the β-methyl-D-aldohexopyranosides gave a dialdehyde different from that obtained from the anomeric α-forms. On the other

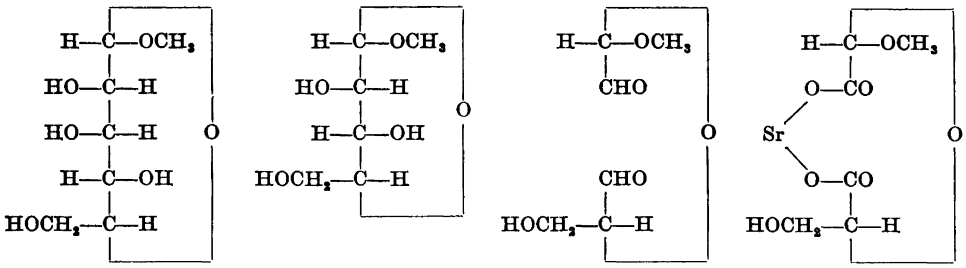

I II III IV

hand Jackson and Hudson found that periodate oxidation of the anomeric forms of methyl aldopentopyranosides led to enantiomeric dialdehydes, a result which is in accordance with the fact that carbon atom 5 in this case is not asymmetric. The mentioned authors also showed that α-methyl-D-arabofuranoside (II) gave an oxidation product identical with that obtained from the α-methyl-D-aldohexopyranosides and that therefore the configuration at carbon atom 1 in this furanoside must be the same as in the α-D-hexopyranosides. We have found that this holds also for other aldopentofuranosides as will be described below.

Smith and co-workers [2] showed that the dialdehydes could be reduced to diglycols either by hydrogenation in the presence of Raney nickel catalyst or by the action of sodium borohydride in aqueous solution. Because the asymmetry of carbon atom 5 in this way is eliminated, enantiomeric diglycols are obtained and consequently also in the case of the aldohexopyranosides the anomers of the D-series can be correlated to those of the L-series.

On the whole the application of the periodate oxidation method to the glycosides has demonstrated a definite correlation between anomers within the series of the aldohexopyranosides, the aldopentopyranosides, and the aldopentofuranosides, and also correlated the anomers of the aldopentofuranosides with those of the aldohexopyranosides. It has, however, not established a correlation between anomers of the aldohexopyranosides and those of the aldopentopyranosides and it does not, of course, give any proof of the absolute configuration at carbon atom 1.

The question of the configuration at carbon atom 1 is of considerable interest and has been the object of many papers. Especially interesting are those of Sørensen and Trumpy [3] and of Riiber and Sørensen [4]. The tentative configuration at C_1 which has in fact been generally accepted as correct is based mainly upon the application of Hudson's rules of isorotation and the displacement rules of Freudenberg and Kuhn, but partly also upon some chemical evidences such as the electric conductivity of glucose solutions to which boric acid has been added, the molecular refraction and the rate of hydrolysis of anomeric glycosides as compared with those of *cis-trans* isomeric diols investigated by Vavon, and further the predominant occurrence of certain glycosides by the addition of methanol to 1,2-oxides of sugars. For sugars belonging to the glucose and galactose series the application of these methods are mostly in agreement with the tentatively accepted configuration. On the other hand,

as especially shown by Riiber [5], molecular refractions and rates of hydrolysis in the case of sugars belonging to the mannose series (mannose, rhamnose, and lyxose) lead to an opposite configuration of that obtained by means of the rules of isorotation and displacement. This anomaly in the mannose series has not yet found an explanation. It would, however, seem reasonable to believe that it has bearing on the various conformations in which the pyranoses and pyranosides can occur. It has been shown in this institute [6] that in the case of the furanosides in which the molecules are supposed to be more or less plane no anomaly is found in the rates of hydrolysis of those of mannose as compared with those of sugars belonging to the glucose and galactose series.

Even if the periodate oxidation method and the other physical and chemical methods mentioned above would indicate a certain configuration at carbon atom 1 in the anomeric sugars and their derivatives this would not represent a strict proof of the configuration. It is therefore of considerable importance that the application of X-ray methods during the later years seems to prove conclusively the correctness of the tentatively accepted configuration at carbon atom 1. Thus Furberg [7] in 1950 showed that the β-D-ribofuranoside which is built into the cytidine molecule has *trans*-position of the groups bound to carbon atoms 1 and 2. The same author [8] has later shown that β-D-arabopyranose contains the hydroxyl groups at C_1 and C_2 in *cis*-position. (It should be remarked that the nomenclature used is based upon the application of the rules of isorotation and displacement mentioned above.) McDonald and Beevers [9] established the *cis*-position of the hydroxyl groups at C_1 and C_2 in α-D-glucopyranose and McGeachin and Beevers [10] the *trans*-position of the same groups in α-L-rhamnopyranose monohydrate.

Although the absolute configuration of the anomeric forms of the sugars and their derivatives can be established by means of X-ray investigations the question of a rational nomenclature is still open. As already emphasized by Riiber and Sørensen [4] it must be hoped that this will be taken up and settled by international agreement.

By means of column chromatography several crystalline methyl aldofuranosides have been prepared in this institute [6], amongst them the one used by Jackson and Hudson: α-methyl-D-arabofuranoside. Our sample of the latter which had the specific rotation +128° on oxidation with periodate gave a dialdehyde with rotation + 120° in good agreement with the values 120—121° obtained by the oxidation of the α-methyl-D-aldohexopyranosides. Jackson and Hudson starting from a slightly impure arabofuranoside (rotation + 123°) found the rotation of the dialdehyde to be + 117.3°. The other aldopentofuranosides which we have oxidized are the α- and β-methyl-L-arabofuranosides, the α-methyl-D-xylofuranoside, and the β-methyl-D-ribofuranoside. (The results of the oxidation of some aldohexofuranosides will be given in another paper.) The present results are collected in Table 1 from which it will be seen that the configuration at carbon atom 1 is the same in the α-D- and β-D-forms, respectively, as in the corresponding froms of the D-aldohexopyranosides and that there accordingly is the same relationship in the case of the L-methylosides.

Owing to the small quantities of furanosides at our disposal only the dialdehyde from α-methyl-D-xylofuranoside was oxidized further. This dialdehyde, according to Jackson and Hudson called D'-methoxy-D-hydroxymethyl-

Table 1. Oxidation of some methyl-aldopentofuranosides.

Substance	Methyl-furanoside $[\alpha]_D^{20}$	Dialdehyde $[\alpha]_D^{20}$	Sr-salt of dibasic acid $[\alpha]_D^{20}$	Diglycol $[\alpha]_D^{20}$
α-Methyl-D-arabofuranoside	+128°	+120.1°		−13.3°
α-Methyl-L- »	−128°	−121.2°		+12.5°
β-Methyl-L- »	+118°	+150.6°		−11.1°
α-Methyl-D-xylofuranoside	+182°	+119.7°	−53.3°	−10.5°
β-Methyl-D-ribofuranoside	− 49.8°	−152.5°		+15.0°

diglycolaldehyde, on oxidation with strontium hypobromite gave the crystalline strontium salt of D′-methoxy-D-hydroxymethyl-diglycolic acid. The composition of the salt was controlled by analysis and it had a specific rotation of −53.3° in good agreement with that of the strontium salt obtained from the α-D-aldohexopyranosides.

As will be seen from the formulae below reduction of the dialdehydes should lead to enantiomeric diglycols because the asymmetry at carbon atom 4 is eliminated. The specific rotations of the diglycols given in Table 1 show that within the limit of the experimental error, unavoidable by the small quantities used, this is the case. Sodium borohydride was found to be most suitable for the reduction of small quantities of the dialdehydes. The process was carried out in aqueous solution at room temperature and took place very rapidly. The reduction product, a methoxy-hydroxymethyldiglycol, was easily hydrolyzed in mineral acid to glycerol, glycolaldehyde, and methanol. After removing the methanol by evaporation, glycerol was identified as the tris-O-*p*-nitrobenzoate, m.p. 197−98°. From the hydrolysate the glycolaldehyde could not be isolated as a hydrazone as it would directly give the osazone. We therefore proceeded in this way that the trihydric alcohols (VI, IX) were

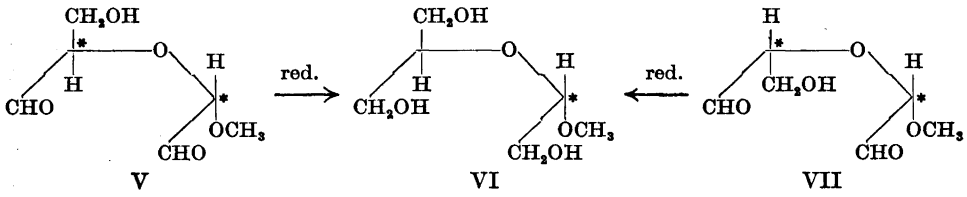

V VI VII

D′-Methoxy-D-hydroxymethyl-diglycolaldehyde — D′-Methoxy-hydroxymethyl-diglycol — D′-Methoxy-L-hydroxymethyl-diglycolaldehyde

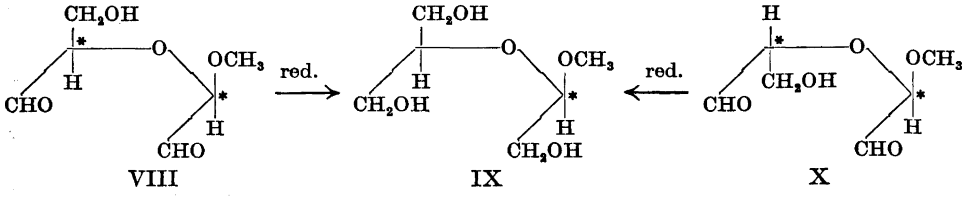

VIII IX X

L′-Methoxy-D-hydroxymethyl-diglycolaldehyde — L′-Methoxy-hydroxymethyl-diglycol — L′-Methoxy-L-hydroxymethyl-diglycolaldehyde

transformed into the tris-O-benzoates in which the acetal linkings could be opened by treatment with N hydrochloric acid in acetic acid without remowing the benzoyl groups. On addition of 2,4-dinitrophenylhydrazine the crystalline hydrazone of glycolaldehyde-O-benzoate separated which was identified by analysis and comparison with an authentic specimen. Keeping the hydrazone in contact with the hydrazine solution for some time resulted in the formation of the osazone of glyoxal.

EXPERIMENTAL

α-Methyl-D-xylofuranoside

Oxidation with periodic acid. To a solution of 0.1649 g (1.01 mmole) of the furanoside in 2.1 ml water 6.6 ml 0.3524 M H_5IO_6 (2.32 mmole) were added. After 100 min the optical rotation became constant $a_D^{20} = +2.18°$ in a 10 cm tube. The concentration of the dialdehyde was calculated to be 1.83 % and the specific rotation accordingly +119.7°. The consumption of periodic acid was determined in samples of 1 ml solution. After dilution with water (10 ml) sodium bicarbonate was added to basic reaction and then 5 ml 0.2016 N sodium arsenite and 0.1 g potassium iodide. After 15 min the solution was retitrated with 7.30 ml 0.1011 N KI_3. This corresponds to 1.10 mole H_5IO_6 per mole xyloside. The dialdehyde was isolated as described by Jackson and Hudson.

Oxidation of the dialdehyde. A quantity of 0.35 g dialdehyde collected from several experiments was oxidized with 1 ml bromine in the presence of 6 g strontium carbonate. The crystalline strontium salt obtained was recrystallized three times by dissolving in hot water and adding hot ethanol until precipitation began. Yield 0.3 g strontium D'-methoxy-D-hydroxymethyl-diglycolate dihydrate. After drying in a vacuum until constant weight the rotation was $[\alpha]_D^{20} = -53.3°$ (*c* 2.5 w). The dihydrate was used for analysis. (Found: C 22.54; H 3.67. Calc. for $C_6H_8O_7Sr \cdot 2H_2O$: C 22.81; H 3.80; Sr 27.76.) For determination of Sr 0.0836 g strontium diglycolate was dissolved in water till 50 ml. To parallels of 10 ml were added 2 ml conc. ammonia, 5 drops 0.1 % phthalein purpur, 10 ml 0.00955 M EDTA and 10 ml ethanol. Retitrated until light blue colour with 4.20 and 4.23 ml 0.00199 N strontium nitrate. Found 28.06, 27.90 % Sr.

Reduction of the dialdehyde. To 0.103 g of the dialdehyde dissolved in 10 ml water 0.1 g sodium borohydride was added in the course of one hour. After standing for another hour excess of borohydride was destroyed by bubling carbon dioxide through the solution until pH 7. The solution was then treated with active carbon after which the rotation in a 10 cm tube was $a_D^{20} = -0.11°$. As the concentration was calculated to be 1.05 % diglycol the specific rotation was −10.5°. In order to isolate the reduction product the solution was evaporated at reduced pressure (bath 35°) and the last trace of water removed in a vacuum desiccator above calcium chloride. The residue was extracted three times with 20 and three times with 10 ml cold anhydrous ethanol. After treatment with active carbon the ethanolic solution was concentrated *in vacuo* (bath 30°) giving about 0.07 g of a not quite pure syrup.

Determination of the glycolaldehyde. The syrup (0.07 g) was dissolved in 5 ml pyridine, benzoyl chloride (0.05 ml) added and the solution heated on the steam bath 40 min. After cooling the solution was poured on 15 ml ice-water saturated with sodium bicarbonate and then extracted three times with chloroform. The chloroform solution was washed thouroughly with water, dried with calcium chloride and the chloroform evaporated *in vacuo*. In order to remove the pyridine the temperature of the bath was in the end raised to 50−60°. The resulting syrup did not crystallize. Dissolved in 5.5 ml glacial acetic acid the rotation in a 10 cm tube was −0.16°. On addition of 0.5 ml conc. hydrochloric acid the optical rotation disappeared in the course of 10 min. After 20 min 2,4-dinitrophenylhydrazine (0.05 g) was added and dissolved easily on stirring. Shortly afterwards a crystalline orange-coloured substance separated which after washing with ethanol was

recrystallized by adding light petroleum (60—70°) to a warm solution of the hydrazone in chloroform. M. p. 187—88° and no depression on mixing with 2,4-dinitrophenylhydrazone of glycolaldehyde-O-benzoate prepared from erythritol [11]. (Found: C 52.46; H 3.55; N 16.07. Calc. for $C_{15}H_{12}O_6N_4$: C 52.32; H 3.51; N 16.27.)

If the hydrazone were left in the mother liquor for some days (or heated with it) the colour changed to dark red indicating that the hydrazone had been transformed into the osazone. Recrystallized from nitrobenzene, m. p. 310—315° (d). (An osazone prepared from glyoxal had the same appearance and melting point.) (Found: C 40.06; H 2.50; N 26.46. Calc. for $C_{14}H_{10}O_8N_4$: C 40.20; H 2.41; N 26.79.)

α-Methyl-D-arabofuranoside

To a solution of 0.2636 g (1.61 mmole) furanoside 5 ml 0.430 M H_5IO_6 (2.15 mmole) was added. After 100 min the optical rotation became constant, $\alpha_D^{20} = +1.93°$ in a 10 cm tube. As the concentration of dialdehyde was calculated to be 1.61 % the specific rotation was +120.1°. Analysis carried out as described for the xylofuranoside showed that 1.01 mole periodic acid had been consumed per mole arabofuranodide. The dialdehyde isolated (0.12 g) was dissolved in 10 ml water and reduced with 0.1 g sodium borohydride. After reduction the rotation of the solution was $\alpha_D^{20} = -0.16°$ and as the concentration of diglycol was calculated to be 1.2 % the specific rotation was −13.3°. The 2,4-dinitrophenylhydrazone of glycolaldehyde-O-benzoate prepared in the same way as described above had m. p. 184—86°.

α-Methyl-L-arabofuranoside

α-L-Arabofuranoside: 0.1607 g (0.98 mmole) in 7 ml water; added 3.0 ml 0.430 M H_5IO_6 (1.29 mmole). After 90 min $\alpha_D^{20} = -1.90°$. Concentration of dialdehyde calculated to 1.57 % and the specific rotation accordingly −121.2°. Analysis showed that 1 mole furanoside had consumed 0.97 mole periodic acid. The dialdehyde (0.088 g) reduced as above gave a solution with $\alpha_D^{20} = +0.11°$. As the concentration of diglycol was 0.88 % the specific rotation was +12.5°. The 2,4-dinitrophenylhydrazone of glycolaldehyde-O-benzoate had m. p. 185—87°.

β-Methyl-L-arabofuranoside

β-L-Arabofuranoside: 0.1219 g (0.74 mmole) in 4.8 ml water; added 2.2 ml 0.408 M H_5IO_6 (0.898 mmole). After 180 min rotation constant $\alpha_D^{20} = +2.56°$. Concentration of dialdehyde 1.70 % and specific rotation accordingly +150.6°. Analysis showed that 1 mole furanoside had consumed 1.04 mole periodic acid. Two experiments gave in all 0.072 g dialdehyde which dissolved i 8 ml water was reduced with 0.05 g sodium borohydride in the course of 10 min. The solution which contained 0.90 % diglycol had $\alpha_D^{20} = -0.10°$ and the specific rotation was accordingly −11.1°. The quantity of the hydrazone of glycolaldehyde-O-benzoate was in this case to small to be recrystallized. It had m. p. 179—181°.

β-Methyl-D-ribofuranoside

β-D-Ribofuranoside: 0.1307 g (0.80 mmole) in 5 ml water; added 3 ml 0.430 M H_5IO_6 (1.29 mmole). After 20 min the rotation became constant $\alpha_D^{20} = -2.44°$. Concentration of dialdehyde 1.60 % and specific rotation −152.5°. One mole of ribofuranoside consumed 1.02 mole periodic acid. The dialdehyde from two experiments (0.16 g) was dissolved in 10 ml water and reduced in 90 min with 0.1 g borohydride. The solution containing 1.60 % of diglycol had $\alpha_D^{20} = +0.24°$ and the specific rotation +15.0°. The diglycol isolated (0.12 g) was transformed into a 2,4-dinitrophenylhydrazone with m. p. 187—88°.

REFERENCES

1. Jackson, E. L. and Hudson, C. S. *J. Am. Chem. Soc.* **59** (1937) 994.
2. Abdel-Akher, M., Cadotte, J. E., Lewis, Bertha, Montgomery, R., Smith, F. and Van Cleve, J. W. *Nature* **171** (1953) 474.
3. Sørensen, N. A. and Trumpy, B. *Kgl. Norske Videnskab. Selskabs Skrifter* **1934** No 6.
4. Riiber, C. N. and Sørensen, N. A. *Kgl. Norske Videnskab. Selskabs Skrifter* **1938** No 1.
5. Riiber, C. N. and Minsaas, J. *Ber.* **60** (1927) 2402; Riiber, C. N. *Kgl. Norske Videnskab. Selskabs Forh. IV* (1931) 157.
6. Augestad, I. and Berner, E. *Acta Chem. Scand.* **8** (1954) 251; **10** (1956) 911.
7. Furberg, S. *Acta Cryst.* **3** (1950) 325.
8. Furberg, S. and Hordvik, A. *Acta Chem. Scand.* **11** (1957) 1594.
9. McDonald, T. R. R. and Beevers, C. A. *Acta Cryst.* **5** (1952) 654.
10. McGeachin, H. Mc. and Beevers, C. A. *Acta Cryst.* **10** (1957) 227.
11. Ohle, H. and Melkonian, G. A. *Ber.* **74** (1941) 291.

Received December 29, 1959.

ACTA CHEMICA SCANDINAVICA 14 (1960) 916–918

Amides of 4-Diethylaminoacetamido-3,5-dimethylphenylcarbamic Acid

CLAËS TEGNÉR and KARL-ERIK DOMEIJ

Research Laboratories, AB Astra, Södertälje, Sweden

Five new amides of 4-diethylaminoacetamido-3,5-dimethylphenylcarbamic acid have been prepared and tested for local anesthetic activity.

Only a few derivatives of urea have been tested for local anesthetic activity. Thus Chabrier, Najer and Giudicelli [1] have described the properties of some ureas and others have been reported by Koelzer and Wehr [2], who also give a review of earlier investigations. The results of the investigations are, however, contradictory with regard to the value of the urea grouping in local anesthetics.

Some esters of 4-diethylaminoacetamido-3,5-dimethylphenylcarbamic acid have been shown to have a high local anesthetic activity when tested on rabbit cornea [3]. Because of the close similarity of the imino group to an oxygen atom it was of interest to study the effect of replacing one of the oxygen atoms in these carbamates by an imino group, *i.e.* to study amides of the general formula

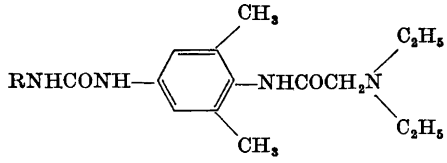

In the present investigation a series of compounds of this formula has been synthesised with R = *n*-C_4H_9— (I), *n*-C_5H_{11}— (II), *n*-C_6H_{13}— (III), C_6H_5— (IV) and 4-[$(C_2H_5)_2N{\cdot}CH_2{\cdot}CO{\cdot}NH$] -3,5-$(CH_3)_2{\cdot}C_6H_2$— (V). The compounds I—IV were prepared by reaction of the appropriate *iso*cyanate with α-diethylamino-4-amino-2,6-dimethylacetanilide [4] in benzene solution. Two of the *iso*cyanates required (*n*-pentyl and *n*-hexyl) were prepared *via* their corresponding azides and Curtius degradation. This method yielded pure compounds but attempts to prepare the *iso*-cyanates by other methods gave impure products.

Table 1.

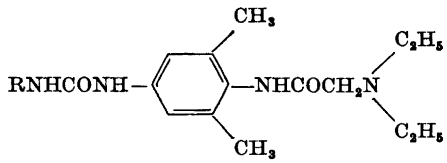

Compd.	R	Yield %	Solvent[a] for recryst.	M. p. °C	Empirical formula	Analyses %					
						Found			Calc.		
						C	H	N	C	H	N
I	*n*-C_4H_9—	84	Me—Aq	141—143	$C_{19}H_{32}N_4O_2$	65.6	9.33	15.9	65.5	9.26	16.1
II	*n*-C_5H_{11}—	95	Me—Aq	131—132	$C_{20}H_{34}N_4O_2$	66.4	9.56	15.7	66.3	9.45	15.5
III	*n*-C_6H_{13}—	89.5	Me—Aq	126—127	$C_{21}H_{36}N_4O_2$	66.9	9.82	15.1	67.0	9.64	14.9
IV	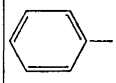	99	Bu	222—224	$C_{21}H_{28}N_4O_2$	68.1	7.78	15.2	68.4	7.66	15.2
V	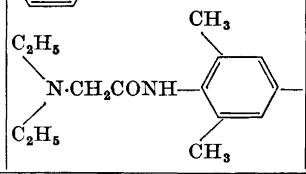	65	Chl—A	261—264	$C_{29}H_{44}N_6O_3$	66.1	8.20	15.7	66.4	8.45	16.0

[a] A = ethanol; Aq = water; Bu = *n*-butanol; Chl = chloroform; Me = methanol.

For the preparation of compound V 1 mole of α-diethylamino-4-amino-2,6-dimethylacetanilide was reacted with 0.5 mole of phosgene. The hydrochloride of the α-diethylamino-4-chlorocarbonylamino-2,6-dimethylacetanilide is formed as an intermediate.

The compounds I—V were tested * for local anesthetic activity on rabbit cornea using xylocaine as a standard [5]. Compounds I, II and III were respectively 1.6, 3 and 9 times more active than xylocaine and IV showed the same activity as xylocaine but V was inactive. The subcutaneous toxicities of the compounds I—V, determined as LD50 values in white mice were 0.45, 0.57, > 1.0 **, > 1.0 ** and and > 0.5 *** g base/kg bodyweight. Compared with the corresponding esters [3] I—III had a lower anesthetic activity. As the amides were all found to be irritants no further tests were carried out.

* Thanks are due to Drs. S. Wiedling and A. Åström for carrying out the biological tests.

** LD50 values of more than 1.0 g/kg were not determined.

*** Owing to the low solubility of the compound higher dosages could not be tested.

EXPERIMENTAL *

n-Butyl and phenyl *iso*cyanates, which are commercially available, were purified by fractional distillation and the fractions b.p. 114—115° and 165—166°, respectively, were used for synthesis. The *n*-pentyl [6] and *n*-hexyl [7] *iso*cyanates were both prepared *via* their azides as described for the preparation of undecyl *iso*cyanate [8]. An *n*-pentyl *iso*cyanate fraction b.p. 138—139.5° and an *n*-hexyl *iso*cyanate fraction b.p. 162—163° were used.

The compounds I—IV (see Table 1) were prepared as described for the following example:

α-Diethylamino-4-amino-2,6-dimethylacetanilide [4] (5.6 g, 0.020 mole) was dissolved in dry benzene (50 ml), a solution of *n*-butyl *iso*cyanate (2.2 g, 0.022 mole) in dry benzene (15 ml) was added and the mixture was heated on a water bath for 1.5 h. The solvent was then evaporated and the residue was recrystallised from methanol-water (3:1) giving colourless crystals, m. p. 141—143°.

For the yields, solvents used for recrystallisation, melting points and analytical data for the individual compounds I—IV, see Table 1.

1,3-Bis(4-diethylaminoacetamido-3,5-dimethylphenyl)urea (V). α-Diethylamino-4-amino-2,6-dimethylacetanilide [4] (12.5 g, 0.050 mole) was added to a 10 % (v/v) solution of phosgene (25 g, 0.025 mole) in toluene and the solution was boiled under reflux for 8 h. After standing over night the mixture was shaken with 2 N sodium hydroxide and the precipitate was collected and dried in a desiccator. It was then treated with hot chloroform (50 ml) and filtered. Recrystallisation of the residue from chloroform-ethanol (3:1) gave colourless crystals, m. p. 261—264° (8.5 g, 65 %). (For analyses, see Table 1.)

* All melting points are corrected.

REFERENCES

1. Chabrier, P., Najer, H. and Giudicelli, P. *Bull. soc. chim. France* **1955** 1603.
2. Koelzer, P. and Wehr, K. H. *Arzneimittel-Forsch.* **8** (1958) 664.
3. Tegnér, C. and Willman, N.-E. *Acta Chem. Scand.* **14** (1960) 885.
4. Dahlbom, R., Tegnér, C. and Willman, N.-E. *Acta Chem. Scand.* **13** (1959) 1145.
5. Wiedling, S. *Acta Pharmacol. Toxicol.* **8** (1952) 117.
6. Siefken, W. *Ann.* **562** (1949) 75.
7. Schröter, G. *Ber.* **42** (1909) 3356.
8. Horning, E. C. *Organic Syntheses* Coll. Vol. III, New York 1955, p. 846.

Received January 20, 1960.

ACTA CHEMICA SCANDINAVICA 14 (1960) 919–926

Magnetic Phase Transitions in Stoichiometric FeS Studied by Means of Neutron Diffraction *

ARNE F. ANDRESEN

Institutt for Atomenergi, Kjeller, Norway

Stoichiometric FeS has been examined by means of neutron diffraction in order to study the phase transitions and the orientation of the magnetic moments in the two antiferromagnetic phases. The magnetic moments are found to point along the c-axis below T_α and perpendicular to the c-axis above T_α. The superstructure derived by Bertaut for the low temperature antiferromagnetic phase has been confirmed only with a larger displacement of the Fe atoms.

According to susceptibility measurements by Haraldsen [1] two phase transitions are taking place in stoichiometric FeS. The α-transition occurring at $T_\alpha \approx 140°C$ is a transition between two antiferromagnetic phases, while the β-transition at $T_N = 325°C$ is a transition between an antiferromagnetic and a paramagnetic phase. Despite continuous efforts the nature of the first transition is not yet fully understood. However, several significant contributions have been made.

X-Ray investigations by Hägg and Sucksdorff [2] revealed slight structural changes at the transition. Above T_α the structure is of the regular NiAs-type with a hexagonal unit cell of dimensions $a_o = 3.44$ Å and $c_o = 5.88$ Å. Below this temperature weak superstructure reflections appear indicating a larger unit cell. Bertaut [3] succeeded in deriving an atomic arrangement to account for this superstructure. However, the small atomic displacements derived by him can not explain the large anomaly in the specific heat, 550 cal/mole, observed by Hirone *et al.*[4]

Recently electrical and magnetic measurements on single crystals of FeS by Kamigaichi *et al.*[5] and Hirahara *et al.*[6] showed a marked anisotropy in the electrical and magnetic properties with abrupt changes at the transition temperature. They interpret their results as indicating a change in the spin direction at the transition. Below T_α the spin is assumed to be parallel to and above T_α perpendicular to the c-axis. In the last case their data are consistent

* Sponsored jointly by *Reactor Centrum Nederland* and *Institutt for Atomenergi*.

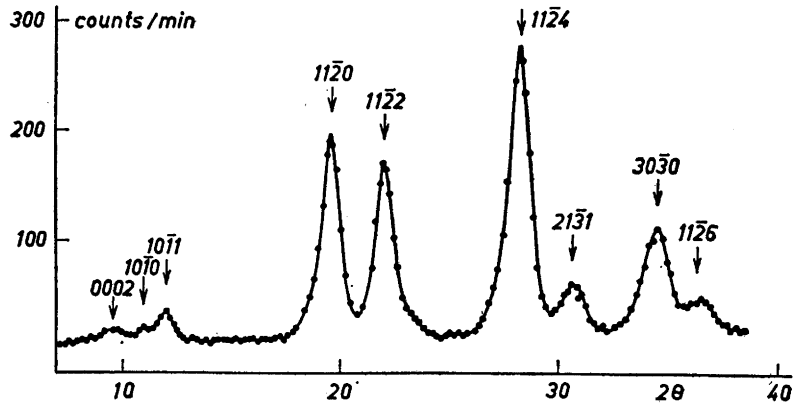

Fig. 1. Room temperature neutron diffraction diagram of $FeS_{1.0}$, instrumental background subtracted (λ = 1.03 Å).

with a model in which the moments take up two or more fixed directions in the *c*-plane.

By neutron diffraction it is possible to determine directly the orientation of the magnetic moments on the individual lattice sites. This was utilized by Sidhu [7] in determining the direction of the magnetic moments in pyrrhotite (FeS_{1+x}). He found here the magnetic moments to be perpendicular to the *c*-axis. Being unaware of the work of Kamigaichi *et al.* and Hirahara *et al.*, but anticipating some change in the spin system at the α-transition of the stoichiometric compound, we undertook a neutron powder diffraction investigation of $FeS_{1.0}$.

Low Temperature Antiferromagnetic Phase

A room temperature diffraction diagram of FeS obtained with the automatic diffractometer at the Kjeller reactor JEEP is shown in Fig. 1. The peaks observed can be well accounted for on the basis of the hexagonal super cell derived by Hägg and Sucksdorff [2]. The axes of this cell are related to those of the small NiAs-type cell mentioned above by $a = a_0\sqrt{3} = 5.97$ Å and $c = 2c_0 = 11.74$ Å.

In Fig. 2 is given the *c*-axis projection of this unit cell, the dotted lines indicating a NiAs-type cell. To account for the observed superstructure Bertaut [3] has suggested small displacements of the atoms from the NiAs positions. The directions of the displacements of the Fe atoms are indicated by the small arrows in the figure. The Fe atoms are displaced only in the *x* and *y* directions while the sulphur atoms are displaced along the *c*-axis. One can visualize the Fe atoms forming triangles of which some are contracted and some dilated. The sulphur atoms situated above or below the center of these triangles are displaced away from contracted triangles and in towards dilated triangles. The atomic positions are given in Table 1.

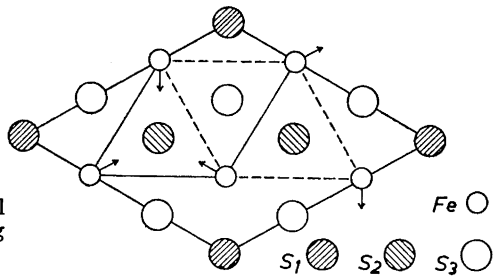

Fig. 2. c-Axis projection of the super cell derived by Bertaut; dotted lines indicating the NiAs-type unit.

From this model nuclear intensities were calculated using the coherent nuclear scattering amplitudes $b_{Fe} = 0.96 \times 10^{-12}$ cm and $b_S = 0.31 \times 10^{-12}$ cm taken from the compilation by Shull and Wollan [8]. By normalizing the observed intensities to the calculated ones for the outer reflections where the magnetic contribution is negligible due to the form factor fall-off, the amount of the inner reflections due to magnetic scattering could be estimated.

The only strong magnetic contribution was found for the reflection $(11\bar{2}2)$ corresponding to the $(10\bar{1}1)$ reflection from the NiAs-type cell (Table 2). This is compatible with an antiferromagnetic alignment of the magnetic moments in which the moments are parallel within each (0001) plane and antiparallel in neighbouring planes, provided the moments point along the c-axis.

Table 1. Atomic positions. Space group: $D_{3h}^4 - P\,\bar{6}2c$.

2 S_1 in	2 *a*:	(0,0,0); (0,0,1/2)
4 S_2 in	4 *f*:	$\pm$ (1/3, 2/3, *z*); $\pm$ (1/3, 2/3, 1/2−*z*); with $z = 0.016$
6 S_3 in	6 *h*:	(*x*, *y*, 1/4); ($\bar{y}$, *x*−*y*, 1/4); (*y*−*x*, $\bar{x}$, *z*); (*y*, *x*, 3/4); ($\bar{x}$, *y*−*x*, 3/4); (*x*−*y*, $\bar{y}$, 3/4); with $x = 2/3$; $y = 0$
12 Fe in	12 *i*:	(*x*, *y*, *z*); ($\bar{y}$, *x*−*y*, *z*); (*y*−*x*, $\bar{x}$, *z*); (*x*, *y*, 1/2−*z*); ($\bar{y}$, *x*−*y*, 1/2−*z*); (*y*−*x*, $\bar{x}$, 1/2−*z*); (*y*, *x*, 1/2+*z*); ($\bar{x}$, *y*−*x*, 1/2+*z*); (*x*−*y*, $\bar{y}$, 1/2+*z*); (*y*, *x*, $\bar{z}$); ($\bar{x}$, *y*−*x*, $\bar{z}$); (*x*−*y*, $\bar{y}$, $\bar{z}$); with $x = 1/3 + \varepsilon$; $y = \varepsilon$; $z = 1/8$; Betaut's value: $\varepsilon = 0.035$ Author's value: $\varepsilon = 0.050 \pm 0.005$

The magnetic intensities were calculated from the expression

$$I_{magn} = v\ Lp^2\ |F|^2\ B_S^2\ q^2 \qquad (1)$$

where v is the multiplicity of the reflection (not necessarily equal to the multiplicity of the corresponding nuclear reflection). L is the Lorentz factor.

$$p = \frac{e^2 \gamma}{m c^2} S f \qquad (2)$$

Table 2.

hkil NiAs-type	*hkil* super cell	Calculated intensities I_{nucl} $\times 10^{-2}$	I_{magn} $\times 10^{-2}$	I_{tot} $\times 10^{-2}$		Obs. intensities I_{obs} norm.	Δ
	0001	0	0	0			
0001	0002	0	0	0		3.74	
	$10\bar{1}0$	3.84	0	3.84		2.57	1.27
	$10\bar{1}1$	8.06	5.94	14.0		9.34	4.66
	0003	0	0	0			
	$10\bar{1}2$	0	1.57	1.57			
	$10\bar{1}3$	2.43	0.81	3.24			
$10\bar{1}0$	$11\bar{2}0$	71.40	0	71.40	94.44	96.02	1.58
0002	0004	19.80	0	19.80			
	$11\bar{2}1$	0	0	0			
$10\bar{1}1$	$11\bar{2}2$	15.87	57.77	73.64			
	$20\bar{2}0$	1.84	0	1.84			
	$10\bar{1}4$	1.99	0	1.99	85.50	85.97	0.47
	$20\bar{2}1$	5.98	2.05	8.03			
	$11\bar{2}3$	0	0	0			
	$20\bar{2}2$	0	0.91	0.91			
	0005	0	0	0			
	$20\bar{2}3$	5.18	0.79	5.97			
	$10\bar{1}5$	3.57	0.09	3.66	149.52	149.06	0.46
$10\bar{1}2$	$11\bar{2}4$	139.89	0	139.89			
0003	0006	0.06	0	0.06			
	$21\bar{3}0$	6.68	0	6.68			
	$20\bar{2}4$	1.90	0	1.90	32.67	32.24	0.43
	$21\bar{3}1$	19.94	4.09	24.03			
	$21\bar{3}2$	0	2.04	2.04			
	$11\bar{2}5$	0	0	0			
	$10\bar{1}6$	0	0.03	0.03			
	$21\bar{3}3$	16.98	1.99	18.97	65.79	68.69	2.90
	$20\bar{2}5$	1.32	0.17	1.49			
$11\bar{2}0$	$30\bar{3}0$	45.30	0	45.30			
	$30\bar{3}1$	0	0	0			
	0007	0	0	0			
$11\bar{2}1$	$30\bar{3}2$	0	0	0			
$10\bar{1}3$	$11\bar{2}6$	5.16	2.22	7.38			
	$21\bar{3}4$	8.99	0	8.99	18.90	20.79	1.89
	$10\bar{1}7$	2.52	0.01	2.53			

where γ is the neutron magnetic moment, $S = 2$ the spin of the iron atoms and f the magnetic form factor. As this we have used the values from the curve for Mn^{2+} derived by Corliss *et al.*[9] F is the geometric structure factor, B_S the Brillouin function for spin S, and $q = \sin a$ where a is the angle between the scattering vector and the direction of the magnetic moment. A Debye-Waller temperature factor with $B = 0.7$ Å^2 was applied. This value was obtained assuming a Debye temperature of approximately $\Theta \approx 344$°K derived from the specific heat measurements of Grønvold *et al.*[10]

Using the parameters given by Bertaut the calculated intensities of the superstructure reflections came out much too low indicating larger displacements. The best fit was obtained with a displacement of the iron atoms of

magnitude $\varepsilon = 0.050 \pm 0.005$ compared to Bertaut's value $\varepsilon = 0.035$. As for the sulphur atoms, their contribution was too small to decide anything about their displacements.

The calculated intensities are given in Table 2 together with the normalized observed values. The fit is seen to be very good leading to a percentage mean error in the integrated peaks of 2.9 %. The (0001) reflection has been omitted. It is calculated zero, but a small peak still exists. This is possibly due to slight impurities or incomplete transition from the high temperature phase. The size of the peak varied from sample to sample and also completely vanished.

High Temperature Investigation

For high temperature runs the sample was placed in an evacuated quartz tube surrounded by a heating coil. A thermocouple protruding from the bottom of the cylinder had its junction near the center just below the irradiated part. A diagram obtained at 177°C, well above the α-transition, is shown in Fig. 3, instrumental background subtracted. Here no superstructure peak is visible and all the reflections can be indexed on the small NiAs-type cell previously described.

The most striking difference from the room temperature diagram is the appearance of a strong (0001) reflection. This must be of magnetic origin since the nuclear reflection is extinguished. However, with an antiferromagnetic alignment of the moments along the c-axis, a magnetic contribution may still occur. At room temperature it was negligible due to the q factor which is zero when the moments point along the scattering vector. Since the reflection now appears, the magnetic moments must have turned away from the c-direction. According to formula (1) the intensity of this reflection varies as $\sin^2\alpha$ with the angle α which the moments make with the c-direction.

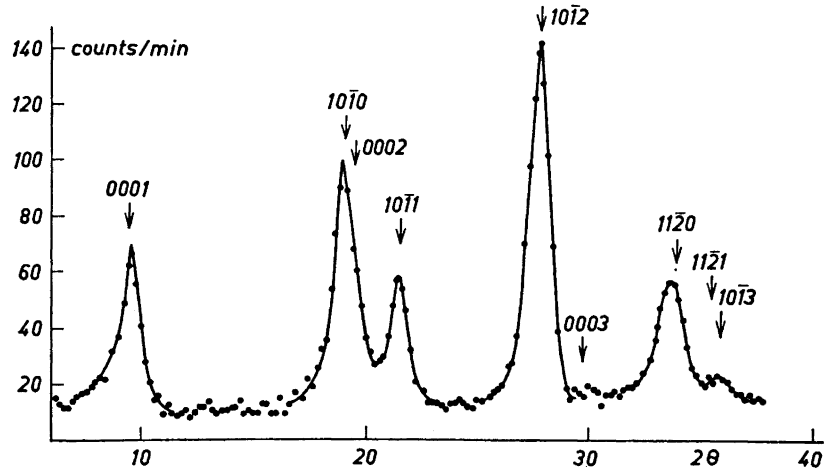

Fig. 3. Neutron diffraction diagram of $FeS_{1.0}$ at 177°C, instrumental background subtracted ($\lambda = 1.03$ Å).

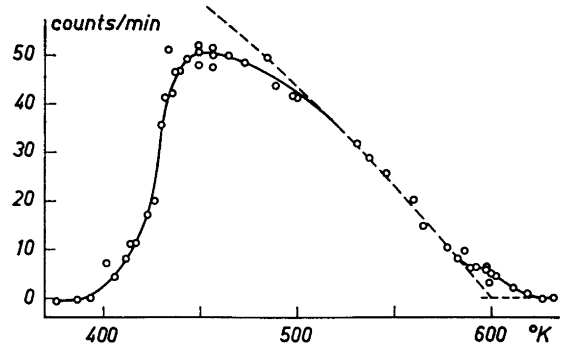

Fig. 4. Peak height of the (0001) reflection as a function of temperature. Dotted line derived from Brillouin function with $S = 2$.

As the (0001) reflection is also completely magnetic, it lends itself remarkably well to a study of the magnetic phase transitions. We have therefore recorded the intensity of this reflection as a function of temperature from room temperature up to 632°K. A close examination of the peaks did not reveal any change in their width with temperature which could be detected with our experimental conditions. We therefore take the peak value as representative of the intensity and this is plotted in Fig. 4 as a function of temperature.

We see that the α-transition starts already at 390°K (117°C) and a maximum is reached at 450°K (177°C). From here on the intensity starts to fall due to the temperature motion of the atoms and reaches zero at 627°K (354°C). Assuming a Néel temperature of $T_N = 600$°K (327°C) the larger part of the slope can be fitted to the Brillouin function with $S = 2$ (dotted line in the figure). The heel on the curve can be ascribed to the critical magnetic scattering which peaks at the Néel point as demonstrated by McReynolds and Riste [11]. Here some broadening of the peaks is expected, but this was not detected due to the low intensity compared to the background scattering.

High Temperature Antiferromagnetic Phase

The diagram shown in Fig. 3 was obtained at the temperature (450°K) corresponding to the maximum of the transition curve (Fig. 4). Still the magnetic intensity has clearly not reached its full value, but is reduced because of the broadness of the α-transition and its close proximity to the Néel point. Extrapolating back from the Brillouin curve, the magnetic intensities at 450°K were found to be reduced by the factor 0.41.

Utilizing this factor and assuming the antiferromagnetically aligned moments to point perpendicular to the c-axis, we find the calculated intensities given in Table 3. A Debye-Waller temperature factor with $B = 1.0$ Å^2 deduced from the Debye temperature $\Theta \approx 344$°K has been applied. The fit to the normalized observed values is seen to be good leading to a percentage

mean error in the integrated peaks of 8 %. The direction of the moments within the c plane can as pointed out by Shirane [12] not be determined from neutron powder diffraction data alone.

Table 3.

	$FeS_{1.0}$ Calculated intensities			Obs. intensities	
hkil	I_{nucl}	I_{magn}	I_{tot}	I_{obs} norm.	Δ
0001	0	198.0	198.0	197.9	0.1
$10\bar{1}0$	251.0				
0002	52.6		303.6	339.0	35.4
$10\bar{1}1$	44.0	74.0	118.0	137.6	19.6
$10\bar{1}2$	451.4		451.4	418.0	33.4
0003	0	5.3	5.3	—	
$11\bar{2}0$	192.8		192.8	180.0	12.8
$11\bar{2}1$	0	6.8			
$10\bar{1}3$	15.4	10.2	32.4	28.9	3.5

DISCUSSION

The results of this investigation is largely in agreement with those derived by other methods. At the α-transition the direction of the magnetic moments change from pointing along the c-axis to pointing perpendicular to it. In the low temperature phase the superstructure is well explained by the arrangement proposed by Bertaut if the displacements of the iron atoms are made somewhat larger. While the β-transition at 327°C is rather well defined and corresponds well with the temperature given by Haraldsen, 325°C, the α-transition is rather broad and varies somewhat from sample to sample both with respect to sharpness and position. This might be due to slight variations in the composition and differences in preparation.

It is interesting to note the close similarity between FeS and α-Fe_2O_3. In the last case there is a transition between two antiferromagnetic states at approximately −20°C, and also here the magnetic moments are found to point along the trigonal axis below the transition and perpendicular to it above the transition (Shull *et al.*[13]). The iron atoms are in both cases surrounded by nearly regular octahedra of sulphur and oxygen atoms, respectively. No attempt will be made here to correlate the slight structural changes observed with the change in the orientation of the magnetic moments.*

Acknowledgements. The author would like to acknowledge the kind cooperation of F. Grønvold and P. Thurmann Moe of the University of Oslo in supplying the samples and much valuable information. He is also indebted to J. A. Goedkoop and T. Riste for illuminating discussions.

* After this investigation was completed the author has become aware of a more extensive investigation of the FeS_{1+x} system by neutron diffraction being carried out at Lawrence Radiatoin Laboratory, University of California, by J. T. Sparks, W. Mead, A. J. Kirschbaum and W. Marshall.

REFERENCES

1. Haraldsen, H. *Z. anorg. allgem. Chem.* **231** (1937) 78.
2. Hägg, G. and Sucksdorff, I. *Z. physik. Chem.* **B 22** (1933) 444.
3. Bertaut, E. F. *J. Bull. Soc. franc. Minér. Crist.* **79** (1956) 276.
4. Hirone, T. Maida, S. and Tsuya, N. *J. Phys. Soc. Japan* **9** (1954) 503.
5. Kamigaichi, T., Hihara, T., Tazaki, M. and Hirahara, E. *J. Phys. Soc. Japan* **11** (1956) 606.
6. Hirahara, E. and Murakami, M. *J. Phys. Chem. Solids* **7** (1958) 281.
7. Sidhu, S. S. Pittsburgh, Diffraction Conference (1954).
8. Shull, C. G. and Wollan, E. O. *Solid State Physics* **2** (1956) 137.
9. Corliss, L. M., Elliott, N. and Hastings, J. M. *Phys. Rev.* **104** (1956) 924.
10. Grønvold, F., Westrum, E. F., Jr. and Chien Chou. *J. Chem. Phys.* **30** (1959) 528.
11. McReynolds, A. W. and Riste, T. *J. phys. radium* **20** (1959) 175.
12. Shirane, G. *Acta Cryst.* **12** (1958) 282.
13. Shull, C. G., Strauser, W. A. and Wollan, E. O. *Phys. Rev.* **83** (1951) 333.

Received December 23, 1959.

ACTA CHEMICA SCANDINAVICA 14 (1960) 927–932

1-(2′-Thiazolylazo)-2-Oxyaryl Compounds as Complexometric Metal Indicators

BROR SKYTTE JENSEN

Danish Atomic Energy Commission, Risø, Denmark

By the coupling of diazotized 2-aminothiazole with β-naphthol β-naphthol-6-sulphonic acid, *p*-cresol, resorcinol, orcinol and *m*-dimethylaminophenol a series of 1-(2′-thiazolylazo)-2-oxyaryl compounds have been prepared. Their properties as metal-indicators for Th^{4+}, La^{3+}, UO_2^{2+}, Pb^{2+}, Hg^{2+}, Cu^{2+}, Co^{2+}, Ni^{2+}, Zn^{2+}, Cd^{2+}, Mg^{2+} and Ca^{2+} ions have been investigated. The compounds seem to be especially suited for the direct titration of Cu^{2+}, Co^{2+} and Ni^{2+} ions with ethylenediaminetetraacetic acid (EDTA) in acid solutions.

The complexometric metal-indicator PAN (1-(2′-pyridylazo)-β-naphthol) was introduced by Cheng and Bray [1] who applied the dye to a few complexometric metal determinations. Later its great versatility as a metal-indicator was confirmed by works of Flaschka *et al.*[2,3] and Cheng *et al.*[4,5] Recently a number of new pyridylazo-dyes have been prepared which also show promise as metal-indicators and colorimetric reagents [6-10].

PAN acts as a tridentate ligand which accounts for the rather high stabilities of its metal-complexes.

By the replacement of the pyridine nucleus in PAN by a thiazole nucleus it should be possible to obtain a chelating agent with similar chelating properties. Hence the dye 1-(2′-thiazolylazo)-β-naphthol (TAN) has been prepared and investigated as a metal-indicator in complexometric titrations (Fig. 1).

By the coupling of diazotized 2-aminothiazole with β-naphthol-6-sulphonic acid, *p*-cresol, resorcinol, orcinol and *m*-dimethylaminophenol the following compounds were also prepared for further investigations.

1-(2′-thiazolylazo)-β-naphthol-6-sulphonic acid	TAN-6-S
2-(2′-thiazolylazo)-*p*-cresol	TAC
6-(2′-thiazolylazo)-resorcinol	TAR
6-(2′-thiazolylazo)-orcinol	TAO
6-(2′-thiazolylazo)-1-oxy-3-dimethylaminobenzene	TAM

The diazotization of 2-aminothiazole took place at 0 C° in *ca.* 6 N hydrochloric acid. The diazotate is so reactive that the couplings with the phenols

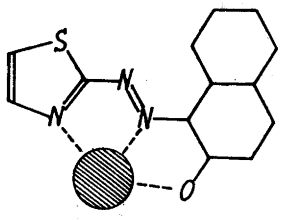

Fig. 1. Shows how 1-(2′-thiazolylazo)-β-naphthol may act as a tridentate ligand.

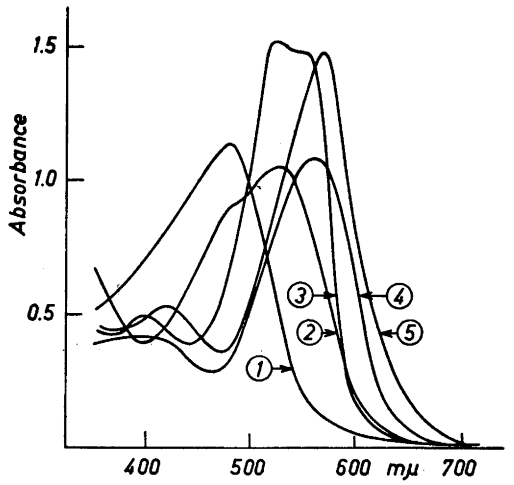

Fig. 2. Spectra of *ca.* 10^{-4} M solutions of TAN-6-S in acid (1) and in basic (2) solutions together with the spectra of its chelates of Zn (3), Pb (4) and Cu (5) in slightly acid solution.

had to be performed in cold acetic acid solutions or in 4 N hydrochloric acid solutions producing the dyes in crystalline form immediately.

Coupling of the diazotate with the phenols under alkaline conditions as is the normal case, produced large amounts of dark coloured by-products and only very low yields of the pure compounds could be obtained.

The pure compounds were obtained be recrystallizations from methanol or ethanol. The dye TAN-6-S was isolated as its sodium salt which was easily salted out from water by sodium chloride.

Previously only TAN and TAR seem to have been prepared.[11]

All the compounds form intensively coloured metal chelates in neutral or slightly acid solutions with Th^{4+}, La^{3+}, UO_2^{2+}, Hg^{2+}, Pb^{2+}, Cu^{2+}, Co^{2+}, Ni^{2+}, Zn^{2+} and Cd^{2+} ions.

The spectra of TAN-6-S alone and in combination with some metal ions are shown in Fig. 2. The effect of complex-formation seems to be a shift towards longer wave-lengths.

The dyes are also pH indicators. Only TAR and TAO do not change colour in an ammonia-buffer (pH = 10) indicating that their pK_a values are larger than 10. For TAN-6-S the pK_a value has been determined to 7.9 [12].

With the exeption of TAN-6-S the compounds are only slightly soluble in water but show appreciable solubility in water-ethanol or water-dioxane mixtures.

The dyes were tested as metal-indicators in complexometric titrations of several metal ions with 0.1 M EDTA solutions. Acetate-acetic acid, pyridine pyridinium chloride and ammonia-ammonium chloride buffers were used. The

changes of their colour at satisfactory endpoints were noted and are listed in Table 1. The amount of indicator used in the titrations was 4—5 drops of a 0.1 % solutions of the dye in methanol.

With all the compounds sharp end-points were obtained in direct titrations of Cu^{2+}, Co^{2+} and Ni^{2+} ions in acetate and in pyridine buffers. The Co^{2+} and Ni^{2+} ions, however, reacted satisfactorily only in hot solutions. The addition of methanol or ethanol often improved the colour changes with TAN, TAC, TAR, TAO and TAM because of the increased solubility of the indicators in the mixed solvents.

No direct complexometric titrations of Co^{2+} and Ni^{2+} ions in acid solutions seem to have been reported in the literature until now.

The direct titrations of Zn^{2+} and Pb^{2+} ions were easily performed in the pyridine buffer but not in the acetate buffer. The direct titration of the Cd^{2+} ion in those two buffers was unsatisfactory.

In pyridine buffer the Th^{4+}, Zr^{4+} and UO_2^{2+} ions formed intensively coloured chelates with all the compounds. However they could not be titrated with EDTA as larger amounts of the titrant were needed to change the colour of the indicator than that corresponding to equivalence.

With TAN, TAN-6-S and TAR the colour changes at the endpoints of the titrations were easily observed with all the metal ions mentioned. With TAO and TAC especially the endpoints in the Cu^{2+} ion titrations were good. When TAM was used as an indicator the colour changes were difficult to observe as the changes usually were from red-violet to pink.

It was found possible to increase the number of metal ions which could be titrated directly by the use of a Cu^{2+} ion-EDTA-dye combination as an indicator. A similar Cu^{2+} ion-EDTA-PAN indicator combination has been described by Flaschka.[3]

One drop of a Cu-salt solution was added to the buffer-indicator mixture and then so much EDTA solution that the indicator just changed colour. The metal ion solution to be determined was pipetted into the mixture where the Cu^{2+} ion was displaced from its EDTA complex in amounts large enough to reverse the colour change of the indicator. Depending on the buffer system used and the metal ion added the accurate determination of the latter was often possible by titration with EDTA to a new colour change.

In Table 2 some succesful titrations are shown which have been made in this way with TAN-6-S, TAR and TAO.

Owing to the small pK_a value of TAN-6-S (7.9 [12]) this indicator could not be used in the ammonia buffer (pH = 10) and therefore it could not be used in the determination of Mg^{2+}, Ca^{2+} and Cd^{2+} ions. With TAR and TAO these ions were succesfully titrated in an ammonia buffer.

The 1-(2′-thiazolylazo)-2-oxyaryl compounds are also useful as colorimetric reagents. A detailed procedure for the determination of uranium with TAN and TAM will be published in the near future [13].

Recently the synthesis of 2-(2′methylthiazolylazo)-*p*-methoxyphenol and its colour reactions with several metal ions have been described [14].

Table 1.

Compound	Metal ion	Buffer	Colour-change
TAN	Cu	Acetate	blue to orange to yellow
	Co	or	violet to orange to yellow
	Ni	pyridine	violet to orange to yellow
TAR	Cu		violet to yellow-green
	Co		violet to dirty yellow
	Ni		red-violet to yellow
TAO	Cu		red to yellow
	Co		red to yellow
	Ni		red to yellow
TAC	Cu		Blue-green to yellow
	Co		smoke to yellow
	Ni		blue-green to yellow
TAM	Cu		red-violet to pink
	Co		red-violet to pink
	Ni		red-violet to pink
TAN-6-S	Cu		blue to yellow-green
	Co		violet to dirty yellow
	Ni		violet to yellow
TAN	Zn	Pyridine	pink to yellow
	Pb		violet to yellow
TAR	Zn		pink to yellow
	Pb		violet to yellow
TAO	Zn		smoke to yellow
	Pb		blue-green to yellow
TAM	Zn		
	Pb		
TAN-6-S	Zn		red-violet to yellow
	Pb		blue-violet to yellow

Table 2.

Compound	Metal ion	Buffer
TAN-6-S	Hg, Zn, Pb La	Acetate or pyridine
TAR	Mg, Ca, Mn Cd	Ammonia
TAO	Mg, Ca, Mn Cd	

EXPERIMENTAL

All the compounds were prepared by essentially the same method. The synthesis of TAM will serve as an example. Owing to the possibility of coupling in positions 2 and 4 with *m*-dimethylaminophenol only a rather low yield of TAM was obtained.

6-(2'-Thiazolylazo)-3-dimethylaminophenol (TAM). 5 g of 2-aminothiazole were dissolved in 40 ml of 6 N hydrochloric acid and cooled in ice. 3.5 g of sodium nitrite were dissolved in a small amount of water. After the addition of crushed ice to both solutions the nitrite solution was slowly poured into the other solution while stirring with a glass spatula. The mixture was left in an icebath for 10 min. The solution of the diazotate was then poured slowly while stirring into a well cooled solution of 7 g of *m*-dimethylaminophenol in 100 ml of 4 N hydrochloric acid (or in acetic acid). An intense colour immediately developed in the mixture and soon yellow-brown crystals of the hydrochloride of TAM were formed.

After 1/2 h in the refrigerator 100 g of sodium acetate in 300 ml of water were added. The colour changed into intense red-violet and after 2—3 h the precipitate formed was filtered with suction on a Büchner-funnel. The filtrate which was almost pure red in colour was discarded. The filter cake was recrystallized from an acetic acid-water mixture yielding the pure product as dark violet needles. Yield 6.3 g (53 %), m. p. 216°C. (Found: C 53.22; H 4.87. Calc. for $C_{11}H_{12}N_4OS$: C 53.45; H 5.09.)

1-(2'-Thiazolylazo)-β-naphthol (TAN). Yield 75 %, m. p. 140°C. (Found: C 61.17; H 3.55. Calc. for $C_{13}H_9N_3OS$: C 61.30; H 3.57.)

1-(2'-Thiazolylazo)-β-naphthol-6-sulphonic acid, sodium (TAN-6-S). Yield 50 %, m. p. (decomp.). (Found: C 41.55; H 2.83. Calc. for $C_{13}H_8N_3O_4S_2Na$, H_2O: C 41.65; H 2.68.)

6-(2'-Thiazolylazo)-resorcinol (TAR). Yield 35 %, m. p. 235°C (decomp.). (Found: C 48.87; H 3.19. Calc. for $C_9H_7N_3O_2S$: C 49.00; H 3.38.)

6-(2'-Thiazolylazo)-orcinol (TAO). Yield 47 %, m. p. 250°C (decomp.). (Found: C 51.06; H 3.85. Calc. for $C_{10}H_9N_3O_2S$: C 51.00; H 3.93.)

2-(2'-Thiazolylazo)-p-cresol (TAC). Yield 57 %, m. p. 129°C. (Found: C 54.79; H 4.13. Calc. for $C_{10}H_9N_3OS$: C 54.70; H 4.18.)

Titrations. The 0.1 M solutions of the metal salts were prepared by dissolving calculated amounts of analytical grade metal nitrates or chlorides in water. The 0.1 M EDTA solution was prepared according to standard procedures [7]. The buffers were made by mixing 1 M solutions of the acids and bases in the proper ratios.

In the titration experiments 5—10 ml of the metal salt solution were pipetted into 30—40 ml of a buffer solution and diluted to ca. 100 ml distilled water. 4—5 drops of a 0.1 % solution of the indicator in methanol were added.

The titrant was added from a 10 ml burette, rapidly at first but dropwise near the expected end-point.

The end-point was taken as the point where further addition of titrant did not change the colour.

A titration was regarded as satisfactory when the experimental endpoint did not deviate more than 1 % from the calculated.

All melting-points were measured on a Kofler hot-bench. The spectra were taken with a Perkin-Elmer Spectracord 4 000 recording spectrophotometer.

Acknowledgements. The author wishes to thank Mr. P. Hansen at the Chemical Laboratory at the University of Copenhagen for performing the microanalyses and Mr. O. Jørgensen for valuable technical assistance.

REFERENCES

1. Cheng, K. L. and Bray, R. H. *Anal. Chem.* **27** (1955) 782.
2. Flaschka, H. and Abdine, H. *Microchim. Acta (Wien)* (1956) 778.
3. Flaschka, H. *Chemist Analyst* **45** (1956) 58.
4. Cheng, K. L. *Anal. Chem.* **27** (1955) 1582.

5. Cheng, K. L. and Williams, T. R., Jr. *Chemist Analyst* **44** (1955) 96.
6. Sommer, L. and Hviličová, M. *Naturwiss.* **46** (1958) 544.
7. *Komplexometrische Bestimmungsmethoden mit Titriplex*, p. 13, E. Merck A/G. Darmstadt.
8. Pollard, F. H., Hansson, P. and Geary, W. J. *Anal. Chim. Acta* **20** (1959) 26.
9. Langmyhr, F. J. and Kristiansen, H. *Anal. Chim. Acta* **20** (1959) 524.
10. Wehber, P. *Z. anal. Chem.* **158** (1957) 10.
11. Traumann *Ann.* **249** (1888) 40.
12. Skytte Jensen, B. *To be published.*
13. Sørensen, E. *To be published.*
14. Yanagihara, T., Matano, N. and Kawase, A. *Z. anal. Chem.* **168** (1959) 359.

Received December 14, 1960.

ACTA CHEMICA SCANDINAVICA 14 (1960) 933–964

Short Communications

Fluorometric Observations of Binary and Ternary Complexes Formed with Malic Dehydrogenase, Coenzyme, and D-Malic Acid

HUGO THEORELL and THOMAS A. LANGAN *

Nobel Medical Institute, Biochemical Department, Stockholm, Sweden

Following the observation by Boyer and Theorell [1] of a change in the fluorescence spectrum of DPNH ** on binding to horse liver alcohol dehydrogenase, enzyme-reduced pyridine nucleotide complexes have been detected fluorometrically with yeast alcohol dehydrogenase[2], lactic[3], glutamic[4], and *iso*citric dehydrogenase [5]. With several of these enzymes fluorometric changes also occur on formation of ternary complexes of enzyme, reduced coenzyme, and substrate analogues. These phemomena have now been observed with malic dehydrogenase by Pfleiderer *et al.*[6,7] and independently in this laboratory. This communication is a report of the changes which occur in the fluorescence spectrum of DPNH on binding to malic dehydrogenase, and on formation of ternary complexes of malic dehydrogenase, DPNH, and D-malic acid. The binding of coenzyme and malic acid in binary and ternary complexes has been studied quantitatively by means of these changes.

Experimental. The fluorometric observations were carried out in the spectrofluorometer previously described [8], and calculations were made using equations based on those employed earlier in this laboratory [8,9]. All measurements were made at 23.5°C in 0.1 μ phosphate buffer containing 10^{-3} M EDTA. The pH was 7.15 unless otherwise noted. Titrations were followed using a measuring wavelength of 420 mμ and an activation wavelength of 352 mμ. Emission and excitation maxima are uncorrected for variations with wavelength in the intensity of the exciting light and sensitivity of the photocell. The correction would move the maxima about 15 mμ towards shorter wavelengths on this apparatus. Pig heart malic dehydrogenase was the product of C. F. Boehringer and Soehne, G.m.b.H. * and was assayed according to Ochoa [10]. DPN and DPNH were obtained from Sigma Chemical Co. and D- and L-malic acid from the California Corp. for Biochemical Research.

Results and discussion. Fig. 1 shows the changes in the fluorescence spectrum of DPNH on binding to malic dehydrogenase, and the further change in the spectrum on the addition of D-malic acid. In the presence of enzyme the observed emission maximum of DPNH shifts from 478 mμ to 470 mμ and doubles in intensity. On addition of 50 mM D-malate the maximum shifts further to 440 mμ and is increased an additional three fold. Changes in the fluorescence of enzyme-bound DPNH produced by substrate analogues or reduced substrates were originally observed with

* Postdoctoral Fellow of the (U.S.) National Science Foundation.

** Abbreviations: DPN and DPNH, oxidized and reduced forms, respectively, of diphosphopyridine nucleotide; EDTA, ethylenediamine tetra-acetic acid. The constants, K, are the dissociation constants of the species whose abbreviations are separated by commas in the subscript. Subscript abbreviations: E, enzyme; R, DPNH; O, DPN; I, D-malate; ER, EO, and EI, binary complexes of enzyme with DPNH, DPN, or D-malate; *e. g.* $K_{EI,R}$ is the dissociation constant for the reaction $EI + R \rightleftharpoons EIR$.

* We would like to thank C. F. Boehringer and Soehne, G.m.b.H. for generous gifts of malic dehydrogenase which were used in these studies.

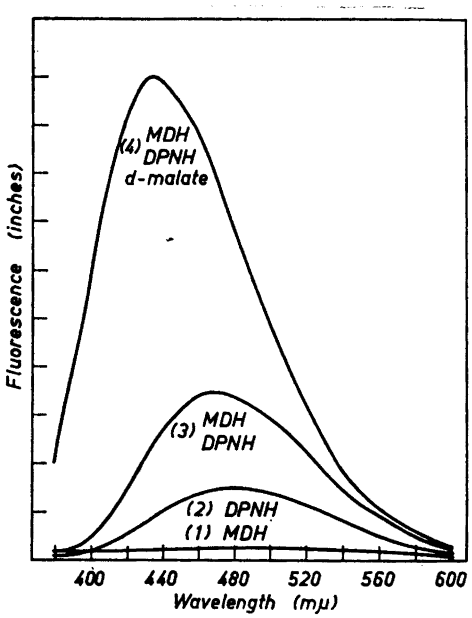

Fig. 1. Fluorescence emission spectrum of DPNH-malic dehydrogenase complex, and the ternary complex of malic dehydrogenase, DPNH, and D-malic acid. Curve (1): 3.6×10^{-4} units of malic dehydrogenase. Curve (2): 3.3×10^{-6} M DPNH. Curve (3): 3.3×10^{-6} M DPNH plus 3.6×10^{-4} units of malic dehydrogenase. Curve (4): 3.3×10^{-6} M DPNH, 3.6×10^{-4} units of malic dehydrogenase, and 5×10^{-2} M D-malate. Activating wavelength 352 mμ. Buffer, 0.1 μ phosphate, pH 7.15, containing 10^{-3} M EDTA. Final volume, 2 ml. Temp., 23.5°C.

lactic dehydrogenase [3], and have since been detected with a number of other dehydrogenases [3,4,11,12]. Kinetic and equilibrium data [9,12] have supported the view that the fluorescence changes result from the formation of ternary complexes of enzyme, coenzyme and substrate analogue.

Addition of L-malate to the malic dehydrogenase-DPNH complex produced no change in fluorescence. However, L-malate competitively displaced D-malate from the ternary complex, producing a return to the original DPNH-enzyme spectrum when added in large excess. Small changes in the fluorescence of the enzyme-DPNH complex were produced by succinate and malonate.

The activation spectra for the fluorescence of the DPNH and D-malate complexes are shown in Fig. 2. The excitation maximum for DPNH fluorescence is seen to increase from 352 mμ to 362 mμ on combination with the enzyme. This is in contrast to the changes which have been observed with other complexes, in which the activation maximum decreases [4,5,14] or is unchanged [12]. On the addition of D-malic acid, there is a decrease in the excitation maximum to 345 mμ, a value below that of free DPNH.

Previous studies on horse liver alcohol dehydrogenase by Theorell and Winer [8,9] have utilized fluorescence changes for the quantitative study of coenzyme binding and ternary complex formation. This technique now has been applied to malic dehydrogenase. The enzyme was found to bind 4.4 moles of DPNH per mole, based on the turnover number of 38 000 moles of DPNH per mole enzyme per min reported by Wolfe and Neilands [15] for the conditions of the assay used in this work *. The binding of DPNH and DPN was competitive. No significant deviations from simple monovalent dissociation were observed, indicating that the binding sites act independently and equally. At pH 7.15, $K_{E,R}$ was 1.0 μM and $K_{E,O}$ 280 μM. From titrations in the presence of D-malate, $K_{EI,R}$ was found to be 0.4 μM, $K_{ER,I}$ 6 000 μM and $K_{E,I}$ 15 000 μM. At high concentrations of D-malate, 80 to 160 mM, $K_{EI,R}$ increased 30 to 50 %, apparently due to the effect of ionic strength. The mutual stabilizing effect of DPNH and D-malate on the binding of one another, shown by the fact that $K_{EI,R} < K_{E,R}$ and $K_{ER,I} < K_{E,I}$, indicates that a ternary complex, in which the bound molecules interact, is formed. D-Malate interacted specifically with DPNH. DPN and D-malate were bound to the enzyme without interaction, since the values found for $K_{EI,O}$, 299 μM, and $K_{EO,I}$, 14 900 μM, are in close agreement with $K_{E,O}$ and $K_{E,I}$. L-Malate apparently has the opposite specificity. It was without effect on the dissociation of DPNH, although it presumably interacts in the binding of DPN in the enzymatically active complex.

Preliminary measurements have been carried out at pH 6.0 and 8.0. The changes in the dissociation constants of the binary

* Pfleiderer has reported [6,7] that his malic dehydrogenase preparations bind one mole of DPNH per 40 000 g of protein, the molecular weight according to Neilands [15].

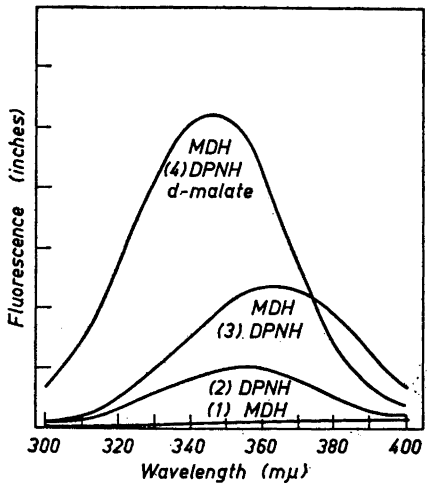

Fig. 2. Activation spectrum for fluorescence of DPNH, DPNH-malic dehydrogenase complex, and the ternary complex of malic dehydrogenase, DPNH, and D-malic acid. Curve (1): 3.6×10^4 units of malic dehydrogenase. Curve (2): 3.3×10^{-6} M DPNH. Curve (3): 3.3×10^{-6} M DPNH plus 3.6×10^4 units of malic dehydrogenase. Curve (4): 3.3×10^{-6} M DPNH, 3.6×10^4 units of malic dehydrogenase, and 5×10^{-2} M D-malate. Fluorescence was measured at the appropriate emission maximum for each system. Buffer, 0.1 μ phosphate, pH 7.15, containing 10^{-3} M EDTA. Final volume, 2 ml. Temp., 23.5°C.

coenzyme complexes are qualitatively similar to those observed with liver alcohol dehydrogenase [8]. The ratio $K_{E,O}/K_{E,R}$ decreases from about 1 400 at pH 6.0 to 100 at pH 8.0. $K_{E,O}$ decreases sharply from pH 6.0 to 7.15, indicating that a group with a pK in this region is involved in the binding of DPN. The mutual stabilization in the binding of D-malate and DPNH is also observed at pH 6 and 8, although $K_{EI,R}$, $K_{E,R}$, $K_{ER,I}$ and $K_{E,I}$ each increase with increasing pH. These studies are being completed and extended and a detailed report will be published.

1. Boyer, P. D. and Theorell, H. *Acta Chem. Scand.* **10** (1956) 447.
2. Duysens, L. N. M. and Kronenberg, G. H. M. *Biochim. et Biophys. Acta* **26** (1957) 437.
3. Winer, A. D., Novoa, W. B. and Schwert, G. W. *J. Am. Chem. Soc.* **79** (1957) 6571.
4. Winer, A. D. and Schwert, G. W. *Biochim. et Biophys. Acta* **29** (1958) 424.
5. Langan, T. A. *Acta Chem. Scand.* **14** (1960) 936.
6. Pfleiderer, G. and Hohnholz, E. *Biochem. Z.* **331** (1959) 245.
7. Pfleiderer, G. *Angew. Chem.* **72** (1960) 160.
8. Theorell, H. and Winer, A. D. *Arch. Biochem. Biophys.* **83** (1959) 291.
9. Winer, A. D. and Theorell, H. *Acta Chem. Scand.* **14** (1960). *In press.*
10. Ochoa, S. in Colowick, S. P. and Kaplan, N. O. *Methods in Enzymology* Vol. 1., Academic Press, Inc., New York 1955, p. 735.
11. Winer, A. D. and Theorell, H. *Acta Chem. Scand.* **13** (1959) 1038.
12. Langan, T. A. *Unpublished observations on yeast alcohol dehydrogenase.*
13. Winer, A. D. and Schwert, G. W. *J. Biol. Chem.* **234** (1959) 1155.
14. Winer, A. D. and Schwert, G. W. *Science* **128** (1958) 660.
15. Wolfe, R. G. and Neilands, J. B. *J. Biol. Chem.* **221** (1956) 61.

Received April 26, 1960.

Changes in the Fluorescence Spectrum of Reduced Triphosphopyridine Nucleotide on Binding to *Iso*-citric Dehydrogenase

THOMAS A. LANGAN*

Nobel Medical Institute, Biochemical Department, Stockholm, Sweden

In 1956, Boyer and Theorell [1] reported a shift to shorter wavelengths and an intensification in the fluorescence spectrum of DPNH ** on binding to horse liver alcohol dehydrogenase. Subsequently, similar changes in DPNH fluorescence have been observed when DPNH combines with yeast alcohol dehydrogenase [2], lactic [3], glutamic [4] and malic dehydrogenase [5,6]. A fluorescence change of the type originally observed with liver alcohol dehydrogenase thus appears to be a general phenomenon in the binding of DPNH to the "alcohol" type [7] of dehydrogenase, and has proved valuable in the quantitative study of coenzyme binding [8-11]. Whether this phenomenon extends also to the case of TPN dependent dehydrogenases of this type has not been previously investigated. The present communication is a report of a change in the fluorescence spectrum of TPNH on combination with *iso*citric dehydrogenase which is similar in essential respects to the changes which have been observed on formation of the DPNH complexes. The fluorescence change is being utilized in a study of coenzyme, substrate and metal binding to the enzyme.

Experimental. The fluorometric observations were carried out in the spectrofluorometer previously described [8], and calculations were made using equations based on those employed earlier in this laboratory [8,9]. All measurements were made at 23.5°C in 0.1 μ Tris-chloride buffer, pH 7.1. Emission and excitation maxima are uncorrected for variations with wavelength in the intensity of the exciting light and sensitivity of the photocell. The correction would move the maxima about 15 mμ towards shorter wavelengths on this apparatus. Pig heart *iso*citric dehydrogenase was prepared and assayed according to the method of Moyle and Dixon [12]. Small amounts of flavin present in this material were removed by adding sufficient calcium phosphate gel in the last step to absorb most of the activity and eluting the enzyme with 0.05 M Tris, pH 7.3, 20 % saturated with ammonium sulfate. EDTA, 10^{-3} M, was included in all solutions from step 3 on. Preparations free of flavin fluorescence with a specific activity of up to 2 100 units/mg were obtained in this way. For the fluorometric experiments the following series of dialyses was employed to remove sulfate ions from the enzyme solution to the point where no cloudiness was visible on addition of $BaCl_2$: 18 h *vs.* 0.1 μ Tris pH 7.1, containing 1 M NaCl and 10^{-3} M EDTA; 24 h *vs.* 0.1 μ Tris pH 7.1; three 3 h periods *vs.* 0.1 μ Tris pH 7.1. These dialyses caused up to 70 % loss of activity. Shorter periods of dialysis gave material of higher specific activity but did not completely remove ammonium sulfate, which had a marked dissociating effect on the binding of coenzymes.

TPN and TPNH were products of Sigma Chemical Co. DL-isocitric acid lactone was obtained from Sigma and from the California Corp. for Biochemical Research. These products assayed enzymatically 47 to 48 % D-isocitric acid after hydrolysis at 60 to 100° in the presence of excess NaOH.

Results and discussion. The changes in the fluorescence spectrum of TPNH on binding to *iso*citric dehydrogenase are shown in Fig. 1. The emission maximum of TPNH is 478 mμ as observed in the apparatus used. In the presence of a stoichiometric amount of *iso*citric dehydrogenase the maximum is shifted towards the ultraviolet to 455 mμ and increased in intensity approximately three fold. Shifts of fluorescence to shorter wavelengths accompanied by an intensification are characteristic of the changes which have been observed on formation of DPNH complexes with "alcohol" dehydrogenases. The close similarity of the fluorescence changes which occur on binding of reduced pyridine nucleotides to this group of enzymes may be an indication of common structures in the region of the binding sites.

Fig. 2 shows the changes in the excitation spectrum for TPNH fluorescence on binding to *iso*citric dehydrogenase. The 352 mμ excitation maximum observed for

* Postdoctoral Fellow of the (U.S.) National Science Foundation.

** Abbreviations: DPN and DPNH, oxidized and reduced forms, respectively, of diphosphopyridine nucleotide; TPN and TPNH, oxidized and reduced forms of triphosphopyridine nucleotide; Tris, tris(hydroxymethyl) aminomethane; EDTA, ethylenediamine tetraacetic acid.

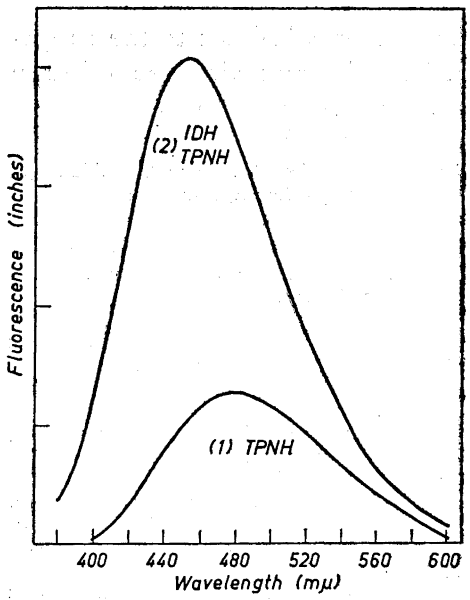

Fig. 1. Fluorescence emission spectrum of TPNH and TPNH-*iso*citric dehydrogenase complex. Curve (1): 2×10^{-6} M TPNH. Curve (2): 2×10^{-6} M TPNH plus 1 500 units of *iso*-citric dehydrogenase. Activating wavelength, 352 mμ. Buffer, 0.1 μ Tris pH 7.1. Final volume, 2 ml. Temp., 23.5°C. The curves are corrected for fluorescence due to buffer and enzyme.

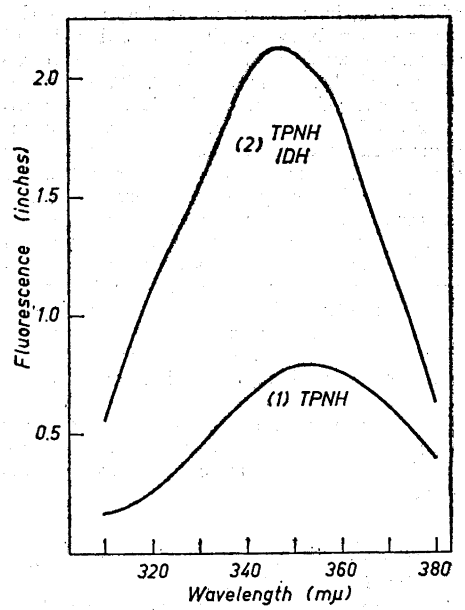

Fig. 2. Activation spectrum for fluorescence of TPNH and TPNH-*iso*citric dehydrogenase complex. Curve (1): 1×10^{-6} M TPNH. Curve (2): 1×10^{-6} M TPNH plus 615 units of *iso*citric dehydrogenase. Measuring wavelength. 460 mμ. Buffer, 0.1 μ Tris, pH 7.1. Final volume, 2 ml. Temp., 23.5°C. Curves corrected for fluorescence of buffer and enzyme.

TPNH fluorescence is seen to shift to 347 mμ in the presence of enzyme. In DPN dependent enzymes, no consistent pattern is evident in the effect of enzyme on the excitation maximum. Shifts to shorter wavelengths have been observed with liver alcohol dehydrogenase [4] and lactic dehydrogenase [13], and to longer wavelengths with malic dehydrogenase [5], while yeast alcohol dehydrogenase has no effect [14].

No difference between the fluorescence properties of unbound TPNH and DPNH has been observed.

The coenzyme binding capacity of *iso*citric dehydrogenase preparations, determined by following fluorescence changes at 410 mμ during titration with TPNH, was found to be 1 mole of coenzyme per 3.8×10^{11} units of enzyme, corresponding to a turnover number of 1 850 moles of TPN per min per mole of coenzyme binding sites. This value was constant over a three fold range of purity of the *iso*citric dehydrogenase. Assuming a molecular weight of 60 000 [15] the specific activity of the material obtained by Siebert *et al.*[15] indicates that the *iso*citric dehydrogenase molecule binds at least two molecules of TPNH. Since there is some evidence of inhomogeneity in this material [15], the binding capacity may be higher than two.

The titrations indicate an extremely tight binding of TPNH, the dissociation constant being on the order of 10^{-8} M. The binding of TPN was competitive with TPNH, with a dissociation constant approximately 200 times larger. A looser binding of the oxidized form of the coenzyme has been observed with other pyridine nucleotide dependent dehydrogenases [10,11,16]. DL-*Iso*citric acid was also found to block competitively the binding

of TPNH, in a manner analogous to the competition between DPNH and reduced substrate analogues in binding to horse liver alcohol dehydrogenase [9]. The competition is a reflection of the fact that complexes of the type *enzyme-reduced coenzyme-reduced substrate* are not formed by *iso*citric dehydrogenase, and emphasizes the role of coenzyme in determining the substrate binding properties of the enzyme. The effectiveness of DL-*iso*citric acid in displacing TPNH was markedly increased in the presence of 10^{-4} M Mn++ ions indicating that Mn++ is involved in the binding of *iso*citric acid. Further studies of this system are being carried out and will be reported in a detailed publication.

The author would like to thank Professor Hugo Theorell for his interest and for many helpful discussions during the course of this work.

1. Boyer, P. D. and Theorell, H. *Acta Chem. Scand.* **10** (1956) 447.
2. Duysens, L. N. M. and Kronenberg, G. H. M. *Biochim. et Biophys. Acta* **26** (1957) 437.
3. Winer, A. D., Novoa, W. B. and Schwert, G. W. *J. Am. Chem. Soc.* **79** (1957) 6571.
4. Winer, A. D. and Schwert, G. W. *Biochim. et Biophys. Acta* **29** (1958) 424.
5. Theorell, H. and Langan, T. A. *Acta Chem. Scand.* **14** (1960) 933.
6. Pfleiderer, G. and Hohnholz, E. *Biochem. Z.* **331** (1959) 245.
7. van Eys, J., San Pietro, A. and Kaplan, N. O. *Science* **127** (1958) 1443.
8. Theorell, H. and Winer, A. D. *Arch. Biochem. Biophys.* **83** (1959) 291.
9. Winer, A. D. and Theorell, H. *Acta Chem. Scand.* **14** (1960) *In press.*
10. Winer, A. D., Schwert, G. W. and Millar, D. B. S. *J. Biol. Chem.* **234** (1959) 1149.
11. Velick, S. F. *J. Biol. Chem.* **233** (1958) 1455.
12. Moyle, J. and Dixon, M. *Biochem. J.* **63** (1956) 548.
13. Winer, A. D. and Schwert, G. W. *Science* **128** (1958) 660.
14. Langan, T. A. *Unpublished experiments.*
15. Siebert, G., Dubuc, J., Warner, R. C. and Plaut, G. W. E. *J. Biol. Chem.* **226** (1957) 965.
16. Hayes, J. E., Jr. and Velick, S. F. *J. Biol. Chem.* **207** (1954) 225.

Received April 26, 1960.

Experiments Related to the Preparation of Pyridoxine from Furan

JØRGEN TORMOD NIELSEN*, NIELS ELMING** and NIELS CLAUSON-KAAS

Centrallaboratoriet, Sadolin & Holmblad A/S, Copenhagen, Denmark

Pyridoxine (X) has previously been prepared from furan by a six-step reaction [1]. A number of variations of this method have been tried by us (*cf.* Ref. [2]), but have so far not lead to any appreciable improvements of the method. However, in the course of the work eight new compounds were prepared, and it was found worth while to publish directions for their preparation, since they at any time may become of use for synthetic work in this field. The reactions in question are summarized below. Compounds II—VIII and XI are new. Their structures follows from the syntheses and from analyses.

Since 2-(α-acetamidoethyl)-furan (I) is obtained from furan in a 44 % yield [3-5], the overall yield of pyridoxine from furan along the route described here is 10 %, as compared to 23 % of the route published previously.

Experimental. Microanalyses by E. Boss and K. Glens.

2-(α-Acetamidoethyl)-3, 4-dicarbethoxyfuran (IV). 2-(α-Acetamidoethyl)-furan [3] (17.2 g, 0.112 mole) and diethyl acetylenedicarboxylate (20.1 g, 0.118 mole) were mixed and heated to 100° for 3.5 h. After cooling, the reaction mixture was dissolved in acetone (120 ml) and shaken with 10 % palladium on carbon catalyst (0.62 g) at room temperature under 1 atm. of hydrogen until about 2 500 ml of hydrogen had been taken up. After filtration the solvent was removed by distillation and the light-brown residue decomposed in an oil bath (190—200°) under 13 mm during 1 h. The reaction mixture was crystallized from ether. Hereby 19.4 g of IV [white crystals, m. p. 51—53° (Hershberg apparatus, corr.)] was obtained (Found: C 56.9; H 6.4; N 4.7; OC_2H_5 30.5; $COCH_3$ 14.8. Calc. for $C_8H_6O_3N(OC_2H_5)_2(COCH_3)$ (297.3): C 56.6; H 6.4; N 4.7; OC_2H_5

* Present address: Chemical Laboratory of the University of Copenhagen, Copenhagen, Denmark.

** Present address: A/S Pharmacia, Copenhagen, Denmark.

of TPNH, in a manner analogous to the competition between DPNH and reduced substrate analogues in binding to horse liver alcohol dehydrogenase [9]. The competition is a reflection of the fact that complexes of the type *enzyme-reduced coenzyme-reduced substrate* are not formed by *iso*citric dehydrogenase, and emphasizes the role of coenzyme in determining the substrate binding properties of the enzyme. The effectiveness of DL-*iso*citric acid in displacing TPNH was markedly increased in the presence of 10^{-4} M Mn++ ions indicating that Mn++ is involved in the binding of *iso*citric acid. Further studies of this system are being carried out and will be reported in a detailed publication.

The author would like to thank Professor Hugo Theorell for his interest and for many helpful discussions during the course of this work.

1. Boyer, P. D. and Theorell, H. *Acta Chem. Scand.* **10** (1956) 447.
2. Duysens, L. N. M. and Kronenberg, G. H. M. *Biochim. et Biophys. Acta* **26** (1957) 437.
3. Winer, A. D., Novoa, W. B. and Schwert, G. W. *J. Am. Chem. Soc.* **79** (1957) 6571.
4. Winer, A. D. and Schwert, G. W. *Biochim. et Biophys. Acta* **29** (1958) 424.
5. Theorell, H. and Langan, T. A. *Acta Chem. Scand.* **14** (1960) 933.
6. Pfleiderer, G. and Hohnholz, E. *Biochem. Z.* **331** (1959) 245.
7. van Eys, J., San Pietro, A. and Kaplan, N. O. *Science* **127** (1958) 1443.
8. Theorell, H. and Winer, A. D. *Arch. Biochem. Biophys.* **83** (1959) 291.
9. Winer, A. D. and Theorell, H. *Acta Chem. Scand.* **14** (1960) *In press.*
10. Winer, A. D., Schwert, G. W. and Millar, D. B. S. *J. Biol. Chem.* **234** (1959) 1149.
11. Velick, S. F. *J. Biol. Chem.* **233** (1958) 1455.
12. Moyle, J. and Dixon, M. *Biochem. J.* **63** (1956) 548.
13. Winer, A. D. and Schwert, G. W. *Science* **128** (1958) 660.
14. Langan, T. A. *Unpublished experiments.*
15. Siebert, G., Dubuc, J., Warner, R. C. and Plaut, G. W. E. *J. Biol. Chem.* **226** (1957) 965.
16. Hayes, J. E., Jr. and Velick, S. F. *J. Biol. Chem.* **207** (1954) 225.

Received April 26, 1960.

Experiments Related to the Preparation of Pyridoxine from Furan

JØRGEN TORMOD NIELSEN*, NIELS ELMING** and NIELS CLAUSON-KAAS

Centrallaboratoriet, Sadolin & Holmblad A/S, Copenhagen, Denmark

Pyridoxine (X) has previously been prepared from furan by a six-step reaction [1]. A number of variations of this method have been tried by us (*cf.* Ref. [2]), but have so far not lead to any appreciable improvements of the method. However, in the course of the work eight new compounds were prepared, and it was found worth while to publish directions for their preparation, since they at any time may become of use for synthetic work in this field. The reactions in question are summarized below. Compounds II—VIII and XI are new. Their structures follows from the syntheses and from analyses.

Since 2-(α-acetamidoethyl)-furan (I) is obtained from furan in a 44 % yield [3-5], the overall yield of pyridoxine from furan along the route described here is 10 %, as compared to 23 % of the route published previously.

Experimental. Microanalyses by E. Boss and K. Glens.

2-(α-Acetamidoethyl)-3, 4-dicarbethoxyfuran (IV). 2-(α-Acetamidoethyl)-furan [3] (17.2 g, 0.112 mole) and diethyl acetylenedicarboxylate (20.1 g, 0.118 mole) were mixed and heated to 100° for 3.5 h. After cooling, the reaction mixture was dissolved in acetone (120 ml) and shaken with 10 % palladium on carbon catalyst (0.62 g) at room temperature under 1 atm. of hydrogen until about 2 500 ml of hydrogen had been taken up. After filtration the solvent was removed by distillation and the light-brown residue decomposed in an oil bath (190—200°) under 13 mm during 1 h. The reaction mixture was crystallized from ether. Hereby 19.4 g of IV [white crystals, m. p. 51—53° (Hershberg apparatus, corr.)] was obtained (Found: C 56.9; H 6.4; N 4.7; OC_2H_5 30.5; $COCH_3$ 14.8. Calc. for $C_8H_6O_3N(OC_2H_5)_2(COCH_3)$ (297.3): C 56.6; H 6.4; N 4.7; OC_2H_5

* Present address: Chemical Laboratory of the University of Copenhagen, Copenhagen, Denmark.

** Present address: A/S Pharmacia, Copenhagen, Denmark.

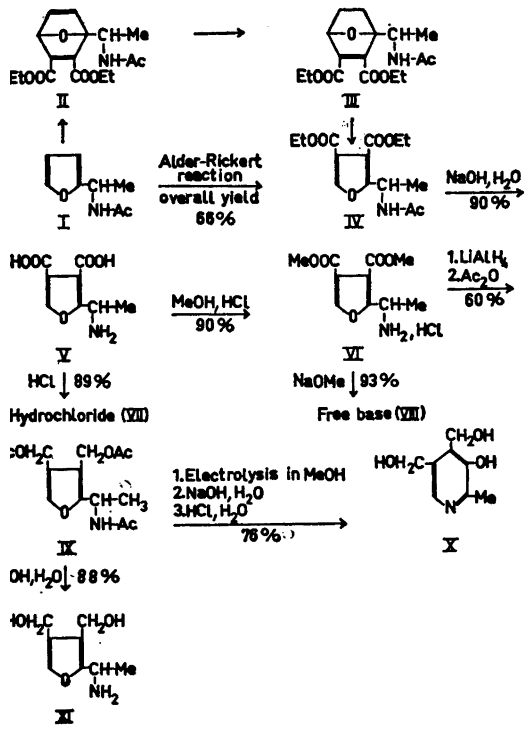

30.3; $COCH_3$ 14.5.) Another 2.6 g of analytically pure IV was isolated by distillation of the mother liquor (b.p. $_{0.1}$ 178—186°) followed by crystallization from ether (m. p. 49—51°), thus bringing the total yield of IV up to 22.0 g (66 %).

In a separate experiment the intermediate compound II was isolated in a 45 % yield; white crystals from ether, m. p. 129—130° (Found: C 59.5; H 6.3; N 4.7; OC_2H_5 27.8; $COCH_3$ 13.8. Calc. for $C_{10}H_9O_3N(OC_2H_5)_2(COCH_3)$ (323.3): C 59.4; H 6.6; N 4.3; OC_2H_5 27.9; $COCH_3$ 13.3.)

In another separate experiment the other intermediate compound (III) was isolated from pure II in a 89 % yield; white crystals from ether, m. p. 109—110°. (Found: C 58.9; H 7.1; N 4.7; OC_2H_5 27.6; $COCH_3$ 13.2. Calc. for $C_{10}H_{10}O_3N(OC_2H_5)_2(COCH_3)$ (325.4): C 59.1; H 7.1; N 4.3; OC_2H_5 27.7; $COCH_3$ 13.2).

2-(α-Aminoethyl)-3,4-dicarboxyfuran (V). IV (10.0 g, 0.034 mole) and sodium hydroxide (3 N, 115 ml, 0.34 mole) were heated under reflux (24 h). After cooling the mixture was brought to pH 8.7 by addition of concentrated hydrochloric acid. A small amount of a voluminous white precipitate was removed by filtration. The filtrate was brought to pH 5.0 by further addition of hydrochloric acid. Hereby 5.42 g of white crystals of V separated. Another 0.56 g of V was obtained by evaporation of the mother liquor to 60 ml. The total yield of V (5.98 g) corresponds to 90 %; m. p. 292—296° after darkening at about 280° (Kofler stage, corr.). (Found: C 48.3; H 4.6; N 7.0. Calc. for $C_8H_9O_5N$ (199.2): C 48.2; H 4.6; N 7.0.)

The hydrochloride of V (VII) was prepared in a 89 % yield in the usual way; white crystals, m. p. 195—200° (decomp.). (Found: C 40.7; H 4.4; N 6.2; Cl 14.5. Calc. for $C_8H_{10}O_5NCl$ (235.6): C 40.8; H 4.3; N 5.9; Cl 15.0.)

2-(α-Aminoethyl)-3,4-dicarbomethoxyfuran hydrochloride (VI). V (5.93 g) and anhydrous methanol (95 ml) were mixed and treated with hydrogen chloride until 4.5 g was absorbed. The pale yellow solution was heated under reflux (10 h). After cooling Drierite was added, the mixture shaken (2 h) and the Drierite removed by filtration. Methanol and excess hydrogen chloride were removed by distillation under vacuum and the residue dried under vacuum in a dessicator over potassium hydroxide. Dissolution in anhydrous methanol (15 ml) and precipitation with anhydrous ether gave 7.10 g (90 %) of VI; white crystals, m. p. 167—169° (decomp.). (Found: C 45.8; H 5.7; N 5.5; Cl 13.6; OCH_3 23.5. Calc. for $C_8H_8O_3NCl(OCH_3)_2$ (263.7): C 45.5; H 5.4; N 5.3; Cl 13.4; OCH_3 23.5.)

The free base of VI (VIII) was prepared from VI and sodium methoxide in methanol in a 93 % yield in the usual way; colorless oil, n_D^{25} 1.4952. (Found: C 52.9; H 5.7; N 6.5; OCH_3 27.1. Calc. for $C_8H_7O_3N(OCH_3)_2$ (227.2): C 52.9; H 5.8; N 6.2; OCH_3 27.3.)

2-(α-Acetamidoethyl)-3,4-bis(acetoxymethyl)-furan (IX). VI (3.27 g, 0.0124 mole) dissolved in anhydrous methanol (12 ml) was transformed into the free base (VIII) as described above. The base was dissolved in anhydrous ether (25 ml) and the solution added with stirring to a mixture of lithium aluminum hydride (0.94 g, 0.025 mole) in ether (40 ml) during 15 min. Stirring was continued for 1 h and the mixture heated under reflux for another hour. After cooling acetic anhydride (40 ml) was added dropwise with stirring at —20°. The ether was evaporated and the residue heated under reflux (30 min). After cooling ether (150 ml) was added, the mixture filtered and distilled from an oil bath. The yield was 2.21 g (60 %) of IX; pale yellow liquid, b. p. $_{0.1}$ 180—190°, n_D^{25} 1.4914; previously found b. p. $_{0.05}$

175–187°, n_D^{25} 1.4905. (Found: C 56.6; H 6.7; N 4.9; $COCH_3$ 42.7. Calc. for $C_8H_{10}O_3N(COCH_3)_3$ (297.3): C 56.6; H 6.4; N 4.7; $COCH_3$ 43.4.) Crystallization from ether gave white crystals, m. p. 89–92°; previously found 95–96° [1].

The transformation of IX into pyridoxine hydrochloride in a 76 % yield has been described previously [1].

2-(α-Aminoethyl) - 3,4-bis(hydroxymethyl)-furan (XI). IX (5.95 g, 0.020 mole) and sodium hydroxide (3 N, 67 ml, 0.20 mole) were mixed and heated under reflux (24 h). After cooling the light brown mixture was continuously extracted with ether (3 days). The etheral extract was distilled from an oil bath. Hereby 3.02 g (88 %) of XI was obtained as a pale yellow oil; b. p. $_{0.05}$ 165–171°, n_D^{25} 1.5304. (Found: C 56.3; H 7.9; N 8.5. Calc. for $C_8H_{13}O_3N$ (171.2): C 56.1; H 7.7; N 8.2.)

1. Elming, N. and Clauson-Kaas, N. *Acta Chem. Scand.* **9** (1955) 23.
2. Elming, N., Nielsen, J. T. and Clauson-Kaas, N. U.S. 2.839.539 (June 17, 1958) (to A/S Sadolin & Holmblad).
3. Clauson-Kaas, N., Elming, N. and Tyle, Z. *Acta Chem. Scand.* **9** (1955) 1.
4. Vargha, L., Ramonczai, J. and Bite, P. *J. Am. Chem. Soc.* **70** (1948) 371.
5. Heid, J. V. and Levine, R. *J. Org. Chem.* **13** (1948) 409.

Received April 19, 1960.

Two Fractions of Melanocyte Stimulating Hormone in Urine

BRUNO DAHLBERG

Womens' Clinic, General Hospital, Malmö, Sweden

One of the hormones secreted from the pituitary is the Melanocyte Stimulating Hormone (MSH). Two different melanocyte stimulating substances have been isolated from porcine pituitary (Lerner and Lee [1]; Lee and Lerner [2]), one is alpha-MSH which has an isoelectric point at pH 10.5–11.0, the other is beta-MSH which has an isoelectric point at pH 5.5.

Other investigators found similar substances with isoelectric points around pH 5 but could not find any activity at pH 11. (Porath *et al*[3]; Benfey and Purvis [4]; Geschwind and Li [5]).

MSH is excreted in the urine of normal men and women (Shizume and Lerner [6]; Dahlberg [7]), as well as during pregnancy (Shizume and Lerner [6]; Dahlberg [8]).

Owing to the inadequate methods for extraction of MSH from urine it has previously been difficult to estimate the excretion in the urine of normal subjects.

As MSH is a pituitary hormone a method for determination of the excretion in urine was thought to give information on certain pituitary functions. A biological assay has therefore been elaborated.

For the determination of the hormone hypophysectomized frogs, *Rana Esculenta*, were used. In the method of extraction used an active melanocyte stimulating substance was found at pH 4.0. In recovery experiments 45.4 % ± 6.4 of a known amount of added MSH could be retrieved.

As the degree of accuracy thus seemed rather low it was thought that part of the hormone might remain in solution. In order to investigate this problem extractions were carried out at both pH 4.0 and pH 11.5 on the urine of normal women. The usual activity was found at pH 4.0, *but in the fraction at pH 11.5 activity was also found.* There are thus *two fractions of melanocyte stimulating hormone in the urine of homo.*

Recovery experiments with a known amount of added MSH yielded the following results:

At pH 4.0 = 40–45 %,
at pH 11.5 = 55–60 %

1. Lerner, A. B. and Lee, T. H. *J. Am. Chem. Soc.* **77** (1955) 1066.
2. Lee, T. H. and Lerner, A. B. *J. Biol. Chem.* **221** (1956) 943.
3. Porath, J., Landgrebe, F. W. and Mitchell, G. M. *Biochim. et Biophys. Acta* **17** (1955) 598.
4. Benfey, B. G. and Purvis, J. L. *J. Am. Chem. Soc.* **77** (1955) 5167.
5. Geschwind, I. I. and Li, C. H. *J. Am. Chem. Soc.* **79** (1957) 615.
6. Shizume, K. & Lerner, A. B. *J. Clin. Endocrinol. & Metabol.* **14** (1954) 1491.
7. Dahlberg, B. *Unpublished results*, 1960.
8. Dahlberg, B. *3rd Acta Endocrinol. congr.* 1958.

Received May 2, 1960.

175–187°, n_D^{25} 1.4905. (Found: C 56.6; H 6.7; N 4.9; $COCH_3$ 42.7. Calc. for $C_8H_{10}O_3N(COCH_3)_3$ (297.3): C 56.6; H 6.4; N 4.7; $COCH_3$ 43.4.) Crystallization from ether gave white crystals, m. p. 89–92°; previously found 95–96° [1].

The transformation of IX into pyridoxine hydrochloride in a 76 % yield has been described previously [1].

2-(α-Aminoethyl) - 3,4-bis(hydroxymethyl)-furan (XI). IX (5.95 g, 0.020 mole) and sodium hydroxide (3 N, 67 ml, 0.20 mole) were mixed and heated under reflux (24 h). After cooling the light brown mixture was continuously extracted with ether (3 days). The etheral extract was distilled from an oil bath. Hereby 3.02 g (88 %) of XI was obtained as a pale yellow oil; b. p. $_{0.05}$ 165–171°, n_D^{25} 1.5304. (Found: C 56.3; H 7.9; N 8.5. Calc. for $C_8H_{13}O_3N$ (171.2): C 56.1; H 7.7; N 8.2.)

1. Elming, N. and Clauson-Kaas, N. *Acta Chem. Scand.* **9** (1955) 23.
2. Elming, N., Nielsen, J. T. and Clauson-Kaas, N. U.S. 2.839.539 (June 17, 1958) (to A/S Sadolin & Holmblad).
3. Clauson-Kaas, N., Elming, N. and Tyle, Z. *Acta Chem. Scand.* **9** (1955) 1.
4. Vargha, L., Ramonczai, J. and Bite, P. *J. Am. Chem. Soc.* **70** (1948) 371.
5. Heid, J. V. and Levine, R. *J. Org. Chem.* **13** (1948) 409.

Received April 19, 1960.

Two Fractions of Melanocyte Stimulating Hormone in Urine

BRUNO DAHLBERG

Womens' Clinic, General Hospital, Malmö, Sweden

One of the hormones secreted from the pituitary is the Melanocyte Stimulating Hormone (MSH). Two different melanocyte stimulating substances have been isolated from porcine pituitary (Lerner and Lee [1]; Lee and Lerner [2]), one is alpha-MSH which has an isoelectric point at pH 10.5–11.0, the other is beta-MSH which has an isoelectric point at pH 5.5.

Other investigators found similar substances with isoelectric points around pH 5 but could not find any activity at pH 11. (Porath *et al*[3]; Benfey and Purvis [4]; Geschwind and Li [5]).

MSH is excreted in the urine of normal men and women (Shizume and Lerner [6]; Dahlberg [7]), as well as during pregnancy (Shizume and Lerner [6]; Dahlberg [8]).

Owing to the inadequate methods for extraction of MSH from urine it has previously been difficult to estimate the excretion in the urine of normal subjects.

As MSH is a pituitary hormone a method for determination of the excretion in urine was thought to give information on certain pituitary functions. A biological assay has therefore been elaborated.

For the determination of the hormone hypophysectomized frogs, *Rana Esculenta*, were used. In the method of extraction used an active melanocyte stimulating substance was found at pH 4.0. In recovery experiments 45.4 % ± 6.4 of a known amount of added MSH could be retrieved.

As the degree of accuracy thus seemed rather low it was thought that part of the hormone might remain in solution. In order to investigate this problem extractions were carried out at both pH 4.0 and pH 11.5 on the urine of normal women. The usual activity was found at pH 4.0, *but in the fraction at pH 11.5 activity was also found.* There are thus *two fractions of melanocyte stimulating hormone in the urine of homo.*

Recovery experiments with a known amount of added MSH yielded the following results:

At pH 4.0 = 40–45 %,
at pH 11.5 = 55–60 %

1. Lerner, A. B. and Lee, T. H. *J. Am. Chem. Soc.* **77** (1955) 1066.
2. Lee, T. H. and Lerner, A. B. *J. Biol. Chem.* **221** (1956) 943.
3. Porath, J., Landgrebe, F. W. and Mitchell, G. M. *Biochim. et Biophys. Acta* **17** (1955) 598.
4. Benfey, B. G. and Purvis, J. L. *J. Am. Chem. Soc.* **77** (1955) 5167.
5. Geschwind, I. I. and Li, C. H. *J. Am. Chem. Soc.* **79** (1957) 615.
6. Shizume, K. & Lerner, A. B. *J. Clin. Endocrinol. & Metabol.* **14** (1954) 1491.
7. Dahlberg, B. *Unpublished results*, 1960.
8. Dahlberg, B. *3rd Acta Endocrinol. congr.* 1958.

Received May 2, 1960.

On the Transfer of Thiocyanate from Fodder to Milk

ARTTURI I. VIRTANEN and ROLF GMELIN

Laboratory of the Foundation for Chemical Research, Biochemical Institute, Helsinki, Finland

In connection with our studies on goitrogenic factors in crucifers, especially those belonging to the *Brassica* species and varieties, the enzymatic formation of the thiocyanate ion SCN^- from some mustard oil glucosides was found [1]. It has been known that SCN^- inhibits iodine uptake by the thyroid gland, and there is reason to assume that SCN^- is one member of the *Brassica* factor which causes goitre in experimental animals.

An important question is to what extent the SCN^- which is formed when the cows chew the fodder is transferred from the rumen to the milk. In order to elucidate this problem we have performed feeding experiments with cows by giving them different amounts of potassium- and ammonium thiocyanate mixtures.

According to our determinations about 0.2 mg % of SCN^- is generally found in the mixed milk during the indoor freeding from the big dairies in Southern Finland. In this area stable feeding commonly consists of hay (mostly timothy, often mixed with red clover), oats, silage (AIV) made of red clover-grass mixtures or sugar beet tops, and sugar beet pulp. If beets are used in the feeding, they are mainly mangels or fodder sugar beets. Marrow kale is still grown to a comparatively small extent. The growing of swedes is also slight.

If the daily feeding of the cows contains about 30 kg of marrow kale or the same amount of swedes, the SCN^- content of the milk is about 0.5 to 0.8 mg % according to our determinations. As already mentioned, the feeding of marrow kale is not general in Finland, and on the farms which grow it, it is restricted to October—November. Swedes again may be fed all the winter, but the daily rations are small on those relatively few farms on which they are grown. It is probable that the growing of marrow kale will increase in Finland. In Northern Finland, up to the polar circle and even beyond it, winter rape and turnip rape will probably become important raw material for silage on the basis of experiments and the experience obtained during the last years. The thiocyanate content of the milk will thus increase in this large area.

Determination of SCN^- in milk and in urine. A modification of Barker's method [2], essentially as described by Michajlovskij and Langer [3], was used for the determination: 10 ml of 20 % trichloroacetic acid was added to 10 ml of milk. 5 ml of the clear filtrate was treated with Fe^{3+}-reagent. The red brown coloration was measured in a Klett-Summerson photometer with filter 50 and compared with a standard SCN^- curve. 5 ml of milk filtrate + 1 ml of water, and 1 ml of Fe-reagent + 5 ml of water was used for background correction.

In the case of urine, exact determinations of SCN^- values were not possible since phenolic substances disturb the Barker method as well as the Aldridge method. The excretion of SCN^- was followed by subtraction of the colorimetric values in parallel experiments, *i. e.* in urines of cows fed with SCN^-, and cows which had received identical feeding but without addition of SCN^-. The found values can therefore be regarded only as approximative values.

First feeding experiment. On January 16, 1960, a mixture of 2 g of NH_4SCN and 2 g of KSCN was fed to the Ayrshire cow Häyri (calved on March 17, 1959) at 7.20 and 17.20; total amount of SCN^-, 5.46 g. The first milk sample was taken just before the feeding of thiocyanate. 0.24 mg % of SCN^- was found in it. The milking times were regularly at 6.30 and 17.10, and a milk sample was taken each time for the determination of SCN^-. Twelve days after the feeding of thiocyanate, a milk sample was taken only once a day for analysis, and after fifteen days only now and then. During the whole test period, the milk production of the cow was mostly 6.5 to 7.5 kg in the morning and 5.0 to 6.0 kg in the evening. The daily production ranged from 11 to 13 kg of milk with 3.5 % of fat. The SCN^- content of the milk is shown in Fig. 1.

The results show that 10 h after the first portion of thiocyanate, the SCN^- content of the milk has risen from the initial value of 0.24 mg % to 0.9 mg %. The feeding of the second portion in the same evening raised the SCN^- content of the following morning milk to 1.4 mg %, after which the content decreased in 24 h to about 0.7 mg %, where it remained for over ten days. The original SCN^- content of the milk was reached only after about four weeks after the feeding of thiocyanate. The total milk

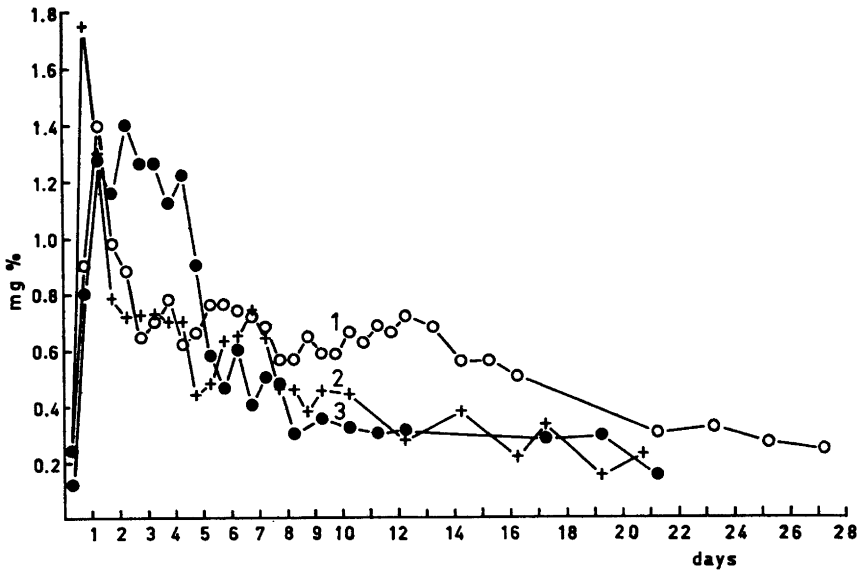

Fig. 1. SCN^- content of milk from cows fed different doses of thiocyanate. 1, Cow Häyri, fed 5.46 g of SCN^- in two doses on January 16, 1960; 2, Cow Häyri, fed 6 g of SCN^- in one dose on February 29, 1960; 3, Cow Mila, fed 24 g of SCN^- during four days in eight doses.

yield was about 315 kg during this time. About 1 000 mg or some 18 % of the 5.46 g of SCN^- fed was excreted in the milk. No SCN^- determinations were performed on the urine.

Second feeding experiment. A mixture of 1.95 g of NH_4SCN and 2.5 g of KSCN, corresponding to 3.0 g of SCN^-, was fed twice a day at 7.00 and 17.00, in total 8 × 3 g = 24 g of SCN^-, to the Ayrshire cow Mila (calved on September 26, 1958). The first milk sample was taken just before the feeding of thiocyanate was begun. 0.12 mg % of SCN^- was then found in the milk, *i. e.* half of Häyri's initial value, although the feeding of both cows was the same: 4 kg of oats, 4 kg of hay, 20 kg of AIV silage made of a red clover-grass mixture, and 2 kg of oat straw. The SCN^- content of the milk yields are shown in Fig.1.

The SCN^- content of Mila's milk also rose to 1.4 mg %, remaining at about this level during the four days in which the thiocyanate preparation was fed. A decreasing tendency appeared, however, already at the fourth day of the feeding. In spite of the fact that Mila got altogether well four times more SCN^- than Häyri, the SCN^- content of Mila's milk decreased more rapidly, reaching 0.3 mg % already after eight days from the beginning of the feeding experiment. Obviously SCN^- was more rapidly oxidized in Mila's organism than in Häyri's. The extremely low initial value of 0.12 mg % of SCN^- in Mila's milk was possibly due to this fact. The daily milk production ranged from 10 to 11.5 kg with 4.7 % of fat. About 900 mg of SCN^-, or less than 4 %, of the 24 g of SCN^- fed was excreted in the milk. The total milk yield was about 220 kg during the three weeks in which the SCN^- content exceeded the initial value. Also in this case no SCN^- determinations were performed on the urine.

The amounts of thiocyanate fed to the cows in the experiments related above were so high that cattle can hardly get larger or even as large ones when plenty of crucifers are used in the feeding. We have found that about 10 mg % of SCN^- is formed in crushed marrow kale, and hence a daily dose of 6 g of SCN^- would theoretically presuppose a ration of 60 kg of marrow kale a day, which is hardly eaten by a cow. Daily rations of more than 30 kg a day are usually not recommended because of the danger of diarrhea.

Table 1. Excretion of SCN^- in urine. On February 2, at 7.00 the cow Häyri was given 6 g of SCN^- (as KSCN + NH_4SCN) in one dose.

date	time	amount of urine/l	SCN^- mg/100 ml of urine	total SCN^- in urine/mg
29.II	10.55	2.0	7.8 (−6)	156 (36)
29.II	15.50	1.5	23.2 (−6)	348 (258)
29.II	22.30	1.5	58.0 (−6)	870 (780)
29.II	23.55	2.2	12.2 (−6)	268 (136)
1.III	01.16	2.7	8.0 (−6)	216 (54)
1.III	02.56	3.0	9.2 (−6)	276 (96)
1.III	04.24	2.1	8.6 (−6)	181 (55)
1.III	05.45	0.8	13.8 (−6)	110 (62)
		15.8 1/24 h		2 425 mg

(1 477 mg SCN^-/15.8 l of urine)

Third feeding experiment. The cow Häyri, the test animal in the first experiment, was given 3.9 g of NH_4SCN and 5 g of KSCN, corresponding to 6 g of SCN^-, in one dose on February 29, 1960 at 7.00. In this experiment the SCN^- content of the urine was also determined during 24 h after the feeding of thiocyanate. The SCN^- content of the milk before the start of the experiment was 0.24 mg %, *i. e.* the same as at the beginning of the first experiment. Ten hours after the feeding of thiocyanate, the SCN^- content of the milk had risen to 1.75 mg %. The SCN^- content of the milk is shown in Fig. 1, and that of the urine in Table 1.

Before the feeding of thiocyanate, the SCN^- content of the cows' urine was on the average about 6 mg of SCN^- per 100 ml. When this amount was subtracted from the SCN^- found in Häyri's urine after the feeding of thiocyanate, it was established that about 1.5 g of SCN^- was excreted in the urine during 24 h. The urine was not collected after this, but the SCN^- content of it had decreased so rapidly during the first day that an excretion of SCN^- in urine over 2 g, *i. e.* one third of the thiocyanate fed, is not probable. Since about 800 mg of the SCN^- fed was excreted in the milk, about half the amount fed has obviously been oxidized in the organism. This is of course only a rough estimation. In experiments with dogs Boxer and Rickards [4] found that about 30 % of SCN^- are metabolized in the body to CO_2.

On the basis of the above results, it does not seem probable that the SCN^- content of cow's milk could rise much above 1 mg % in practice, even when large amounts of crucifers are included in the feeding of cattle. This is in agreement with the results of Wokes *et al.*[5] who found SCN^- values between 0.01 and 1 mg % in a large number of milk samples. The feeding of the cows was probably unknown to the authors (it is not mentioned in the paper), but obviously the samples analysed also included milk from herds fed with marrow kale which is a relatively common fodder plant on farms in England.

With normal feeding Wright [6] found 0.8 mg % of SCN^- and with kale feeding 4.6 mg % in goat's milk. Obviously goat's milk contains about four times more SCN^- than cow's milk, even if its chemical composition is very similar to that of cow's milk.

This investigation is a part of a research project under U. S. Public Law No. 480, 83rd Congress.

1. Gmelin, R. and Virtanen, A. I. *Acta Chem. Scand.* **14** (1960) 507.
2. Barker, H. *J. Am. Med. Assoc.* **106** (1936) 762.
3. Michajlovskij, N. and Langer, P. *Z. physiol. Chem. Hoppe-Seyler* **312** (1958) 26.
4. Boxer, G. E. and Rickards, J. C. *Arch. Biochem. Biophys.* **39** (1952) 7.
5. Wokes, F., Wedgwood, P. and Wyatt, J. *Biochem. J.* **50** (1952) xix.
6. Wright, E. *Nature* **181** (1958) 1602.

Received April 22, 1960.

Studies on Peroxy Compounds

V. The Introduction of the *t*-Butoxy Group into Tetrahydrofuran

SVEN-OLOV LAWESSON, CURT BERGLUND and SUSANNE GRÖNWALL

Department of Organic Chemistry, Chemical Institute, University of Uppsala, Uppsala, Sweden

The benzoyloxy group may be introduced into olefins by the copper salt catalyzed decomposition of *t*-butyl perbenzoate, according to the Kharasch-Sosnovsky [1,2] method whereby the benzoyloxy group enters exclusively the allylic position without the occurrence of isomerisation. Denney *et al.* have proposed a mechanism based on studies with *t*-butyl perbenzoate (carbonyl ^{18}O) and Lawesson and Berglund have found that the benzoyloxy group is introduced into benzyl ethers [4,5] and benzyl sulphides [6] without fragmentation or dimerisation of the respective substrates. In our further studies of the Kharasch-Sosnovsky reaction with various types of ethers we have found that under suitable conditions tetrahydrofuran gives 2-*t*-butoxy tetrahydrofuran. (Found: C 66.57; H 10.93. Calc. C 66.63; H 11.18), b. p. 127°C, $n_D^{20} = 1.4194$. That the *t*-butoxy group enters mainly (possibly exclusively) the 2-position is inferred by the chemical and physical evidence, details of which will be given in a subsequent publication. Contrary to tetrahydrofuran, 1,4-dioxane gives 2-benzoyloxy-1,4-dioxane. (Found: C 63.57; H 5.84. Calc. C 63.45; H 5.81), m. p. 51–52°C and di-*n*-butyl ether gives 2-benzoyloxy-di-*n*-butyl ether. (Found: C 72.25; H 8.91. Calc. C 71.97; H 8.86), b. p. 97–98°C/0.3 mm Hg, $n_D^{20} = 1.4837$. Although there are indications that the benzoyloxy group is first introduced also into tetrahydrofuran, the main product isolated is the *t*-butoxy compound.

At this juncture, we do not want to discuss any theoretical or other aspects of this reaction; however, by extending this work, we are exploring the Kharasch-Sosnovsky reaction more fully and any detailed discussion will be postponed until further experimental work has been completed.

A grant from *Magnus Bergwalls Stiftelse* is acknowledged.

1. Kharasch, M. S. and Sosnovsky, G. *J. Am. Chem. Soc.* **80** (1958) 756.
2. Kharasch, M. S., Sosnovsky, G. and Yang, N. C. *J. Am. Chem. Soc.* **81** (1959) 5819.
3. Denney, D. B., Denney, D. Z. and Feig, G. *Tetrahedron Letters* **15** (1959) 19.
4. Lawesson, S-O. and Berglund, C. *Tetrahedron Letters* **2** (1960) 4.
5. Lawesson, S-O. and Berglund, C. *Arkiv Kemi* **15** (1960). *In press.*
6. Lawesson, S-O. and Berglund, C. *To be published.*

Received May 6, 1960.

On the Crystal Structures of $(BiO)_2SeO_4 \cdot H_2O$, $(BiO)_2SO_4 \cdot H_2O$, $BiOHCrO_4$ and $BiOHSeO_4 \cdot \frac{1}{2}H_2O$

BENGT AURIVILLIUS, OLOV von HEIDENSTAM and INGRID JONSSON

Institute of Inorganic and Physical Chemistry, University of Stockholm, Stockholm, Sweden

In the bismuth oxide salts whose structures have hitherto been reported, a characteristic structural element is frequently present, *viz.* infinite two-dimensional layers of the composition Bi_2O_2. The layers consist of sheets of oxygen atoms which are arranged to form squares. The bismuth atoms are situated alternately above and below the centres of the latter as illustrated in Fig. 1. Each oxygen atom of the sheets is thus tetrahedrically surrounded by four bismuth atoms. The arrangement can also be described geometrically as built up of OBi_4 tetrahedra linked together to form the Bi_2O_2 layers by sharing four edges.

The bismuth oxide compounds reported to contain Bi_2O_2 layers include several bismuth oxide halides [1], some bismuth oxide salts of fatty acids [2], several mixed oxides of bismuth and titanium, niobium or tantalum [3] and one oxide carbonate of bismuth [4].

The present study was undertaken in order to find out whether the Bi_2O_2 layers are also present in compounds containing tetrahedral anions.

Since only preliminary determinations have been made of the positions of the

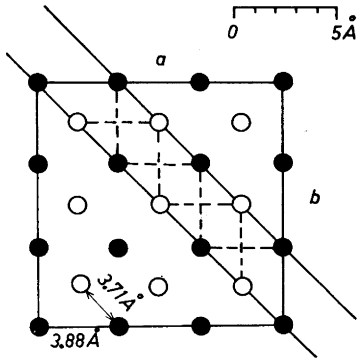

Fig. 1. Projection of the bismuth atom positions in a Bi_2O_2 layer on the *ab* plane. Circles and filled circles mark Bi atoms at the heights zero and 2.50 Å respectively. The Bi-Bi distances are given for BiOCl.

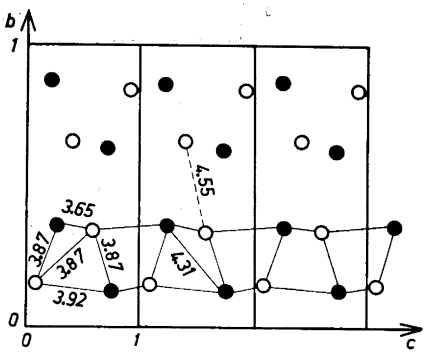

Fig. 2. Projections of the bismuth atom positions in $(BiO)_2SeO_4 \cdot H_2O$ on the *bc* plane. Circles and filled circles denote the positions of the atoms Bi_1 and Bi_2.

oxygen atoms, the formulae given in the title must as yet be regarded as empirical. However, from the positions found for the Bi atoms, the following conclusions can be drawn:

1. The arrangement of the bismuth atoms in $(BiO)_2SO_4 \cdot H_2O$ and $(BiO)_2SeO_4 \cdot H_2O$ have features in common with their arrangement in Bi_2O_2 layers. In fact, in these compounds, idealized bismuth atom positions can be deduced from their arrangement in these layers.

2. The arrangements of the bismuth atoms in $BiOHCrO_4$ and $BiOHSeO_4 \cdot \frac{1}{2} H_2O$ are not compatible with that in Bi_2O_2 layers.

$(BiO)_2SeO_4 \cdot H_2O$ and $(BiO)_2SO_4 \cdot H_2O$

The compounds $(BiO)_2SeO_4 \cdot H_2O$ and $(BiO)_2SO_4 \cdot H_2O$ are isostructural. Space group: $P2_1/c$ (No. 14). The unit cells contain four formula units. The following point positions and parameters were derived:

$(BiO)_2SeO_4 \cdot H_2O$;

4 Bi_1 in 4(*e*):
$\pm(x,y,z)$; $\pm(x,\frac{1}{2}-y,\frac{1}{2}+z)$;
$x = \overline{0.034}$, $y = 0.156$, $z = 0.087$
4 Bi_2 in 4(*e*):
$x = 0.299$, $y = 0.134$, $z = \overline{0.235}$
4 Se in 4(*e*):
$x = 0.366$, $y = 0.634$, $z = 0.087$

$(BiO)_2SO_4 \cdot H_2O$;

4 Bi_1 in 4(*e*):
$x = \overline{0.037}$, $y = 0.155$, $z = 0.088$
4 Bi_2 in 4(*e*):
$x = 0.310$, $y = 0.135$, $z = \overline{0.218}$

Cell dimensions:

$(BiO)_2SeO_4 \cdot H_2O$;
$a = 7.92$ Å, $b = 14.04$ Å, $c = 5.64$ Å, $\beta = 108.8°$
$(BiO)_2SO_4 \cdot H_2O$;
$a = 7.67$ Å, $b = 14{,}00$ Å, $c = 5.70$ Å, $\beta = 109.2°$

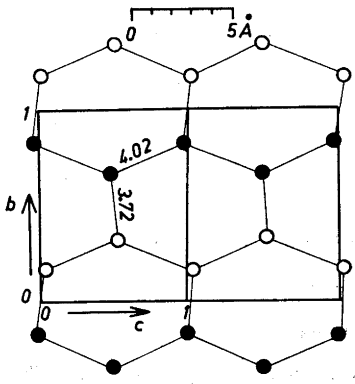

Fig. 3. Projection of the bismuth atom positions in $BiOHCrO_4$ on the *bc* plane. Circles and filled circles mark Bi atoms at $x = 0.16$ and $x = \overline{0.16}$, respectively.

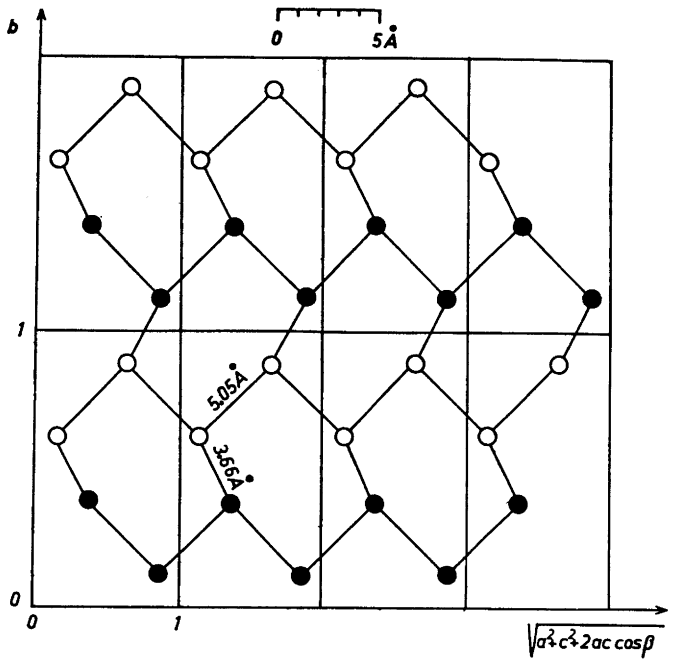

Fig. 4. Projection of the bismuth atom positions of one layer in $BiOHSeO_4 \cdot \frac{1}{2}H_2O$ on the plane (101) along the line [10$\bar{1}$]. The bismuth atoms occur at two heights along [10$\bar{1}$], the difference in the heights being 0.68 Å. Circles and filled circles representent bismuth atoms at different levels.

The bismuth atom positions projected on the *bc* plane are shown in Fig. 2. As seen, the bismuth atoms form double chains along the *c* axis of the unit cell. These chains can be described as being formed by linked tetrahedra, each sharing two opposite edges. A corresponding chain of Bi atoms occurs in the Bi_2O_2 layers and is marked in Fig. 1. Thus the arrangements of the bismuth atoms in $(BiO)_2SeO_4 \cdot H_2O$, $(BiO)_2SO_4 \cdot H_2O$ and in Bi_2O_2 layers are quite similar. In the structures of this selenate and sulphate, OBi_4 tetrahedra with reasonable distances O—Bi are geometrically possible.

$BiOHCrO_4$

Space group: $P2_1/c$ (No. 14). The unit cell contains four formula units. The following point positions and parameters were arrived at for the bismuth and chromium atoms:

4 Bi in 4(*e*):

$\pm(x,y,z)$; $\pm(x,\frac{1}{2}-y,\frac{1}{2}+z)$;
$x = 0.162$, $y = 0.170$, $z = 0.014$

4 Cr in 4(*e*):

$x = 0.270$, $y = 0.580$, $z = 0.177$

Cell dimensions:

$a = 5.61$ Å, $b = 9.54$ Å, $c = 7.44$ Å, $\beta = 93.15°$

The projection of the bismuth atom positions on the *bc* plane is given in Fig. 3. As seen, the bismuth atoms form puckered sheets made up of hexagons along the *bc* planes. The shortest distance between bismuth atoms belonging to different sheets is 5.61 Å. A tetrahedral arrangement OBi_4 with reasonable distances O—Bi is not possible in this structure and the arrangement of the bismuth atoms does not seem to have any relation to the bismuth arrangement occuring in Bi_2O_2 layers.

Judging from the Bi—Bi distances, there seems to exist a weak tendency for the bismuth atoms to form pairs in this structure.

$BiOHSeO_4 \cdot \frac{1}{2} H_2O$

Space group: $P2_1/n$ (No. 14). The unit cell contains four formula units. The following point positions and parameters were derived for the bismuth and selenium atoms:

4 Bi in 4(*e*):
$\pm(x,y,z)$; $\pm(\frac{1}{2}+x,\frac{1}{2}-y,\frac{1}{2}+z)$;
$x = 0.586$, $y = 0.118$, $z = 0.151$
4 Se in 4(*e*):
$x = 0.094$, $y = 0.165$, $z = 0.165$
Cell dimensions:
$a=6.64$ Å, $b=13.60$ Å, $c=6.08$ Å, $\beta=112.2°$

The bismuth atoms form nearly planar sheets parallel to the plane (101). The sheets are made up of hexagons with the edges 3.66 Å and 5.05 Å (Fig. 4). The shortest distances between bismuth atoms in adjacent layers is 5.77 Å. The arrangement of the bismuth atoms in $BiOHSeO_4 \cdot \frac{1}{2}H_2O$ does not bear any resemblance to the quadratic layers of bismuth atoms in the Bi_2O_2 sheets. The tendency of pair formation for the bismuth atoms is more pronounced in this structure than in $BiOHCrO_4$.

These investigations will be continued in order to refine the parameters and to determine the positions of the oxygen atoms. A full account will be published later.

These studies form part of a research program on bismuth oxide salts financially supported by the *Swedish Natural Science Research Council.*

1. Sillén, L. G. *Diss.*, Stockholm 1940.
2. Aurivillius, B. *Acta Chem. Scand.* **9** (1955) 1213.
3. Aurivillius, B. *Diss.*, Stockholm 1951.
4. Lagercrantz, Å. and Sillén, L. G. *Arkiv Kemi, Mineral. Geol.* **25A** (1948) No. 20.

Received May 16, 1960.

Electrophilic Replacement of Bromine by Hydrogen

Debromination of 2,4,6-Tri-*t*-butylbromobenzene

PHILIP C. MYHRE*

Nobel Institute of Chemistry, Stockholm 50, Sweden

When 2,4,6-tri-*t*-butylbromobenzene (*I*) is heated in the presence of a strong acid a mixture of products including 1,3,5-tri-*t*-butylbenzene (*II*) and 3,5-di-*t*-butylbromobenzene is formed. If an acceptor for Br+ such as bromide ion is present in the acid and the resulting bromine is entrained from the solution, *II* is the chief product. In principle, any compound which formally serves as a reducing agent for Br+ and is otherwise inert is suitable for use as an acceptor. Reactive aromatic hydrocarbons prove to be very efficient for this purpose. Trifluoroacetic acid has been used in most experiments because of its high acidity and relatively good solvent properties; however, the reaction occurs with a variety of acids.

The debromination of *I* is viewed as an electrophilic replacement of bromine by hydrogen or the reverse of aromatic bromination. That *I* should undergo electrophilic debromination was by no means unexpected. The observed strong isotope effect in the "positive" bromination [1] of *II* coupled with the known facts about other electrophilic substitutions by hydrogen [2] led us to investigate this reaction possibility. The isotope effect in the bromination of *II* has been explained in terms of steric effects which cause the velocity of step 2 to become less than that of step -1. It is apparent that steric repulsion energy increases as this reaction proceeds towards products. As a result, the energy differ-

* U.S. National Science Foundation Postdoctoral Fellow, 1958—1960.

Studies on Peroxy Compounds

V. The Introduction of the *t*-Butoxy Group into Tetrahydrofuran

SVEN-OLOV LAWESSON, CURT BERGLUND and SUSANNE GRÖNWALL

Department of Organic Chemistry, Chemical Institute, University of Uppsala, Uppsala, Sweden

The benzoyloxy group may be introduced into olefins by the copper salt catalyzed decomposition of *t*-butyl perbenzoate, according to the Kharasch-Sosnovsky [1,2] method whereby the benzoyloxy group enters exclusively the allylic position without the occurrence of isomerisation. Denney *et al.* have proposed a mechanism based on studies with *t*-butyl perbenzoate (carbonyl ^{18}O) and Lawesson and Berglund have found that the benzoyloxy group is introduced into benzyl ethers [4,5] and benzyl sulphides [6] without fragmentation or dimerisation of the respective substrates. In our further studies of the Kharasch-Sosnovsky reaction with various types of ethers we have found that under suitable conditions tetrahydrofuran gives 2-*t*-butoxy tetrahydrofuran. (Found: C 66.57; H 10.93. Calc. C 66.63; H 11.18), b. p. 127°C, $n_D^{20} = 1.4194$. That the *t*-butoxy group enters mainly (possibly exclusively) the 2-position is inferred by the chemical and physical evidence, details of which will be given in a subsequent publication. Contrary to tetrahydrofuran, 1,4-dioxane gives 2-benzoyloxy-1,4-dioxane. (Found: C 63.57; H 5.84. Calc. C 63.45; H 5.81), m. p. 51–52°C and di-*n*-butyl ether gives 2-benzoyloxy-di-*n*-butyl ether. (Found: C 72.25; H 8.91. Calc. C 71.97; H 8.86), b. p. 97–98°C/0.3 mm Hg, $n_D^{20} = 1.4837$. Although there are indications that the benzoyloxy group is first introduced also into tetrahydrofuran, the main product isolated is the *t*-butoxy compound.

At this juncture, we do not want to discuss any theoretical or other aspects of this reaction; however, by extending this work, we are exploring the Kharasch-Sosnovsky reaction more fully and any detailed discussion will be postponed until further experimental work has been completed.

A grant from *Magnus Bergwalls Stiftelse* is acknowledged.

1. Kharasch, M. S. and Sosnovsky, G. *J. Am. Chem. Soc.* **80** (1958) 756.
2. Kharasch, M. S., Sosnovsky, G. and Yang, N. C. *J. Am. Chem. Soc.* **81** (1959) 5819.
3. Denney, D. B., Denney, D. Z. and Feig, G. *Tetrahedron Letters* **15** (1959) 19.
4. Lawesson, S-O. and Berglund, C. *Tetrahedron Letters* **2** (1960) 4.
5. Lawesson, S-O. and Berglund, C. *Arkiv Kemi* **15** (1960). *In press.*
6. Lawesson, S-O. and Berglund, C. *To be published.*

Received May 6, 1960.

On the Crystal Structures of $(BiO)_2SeO_4 \cdot H_2O$, $(BiO)_2SO_4 \cdot H_2O$, $BiOHCrO_4$ and $BiOHSeO_4 \cdot \frac{1}{2}H_2O$

BENGT AURIVILLIUS, OLOV von HEIDENSTAM and INGRID JONSSON

Institute of Inorganic and Physical Chemistry, University of Stockholm, Stockholm, Sweden

In the bismuth oxide salts whose structures have hitherto been reported, a characteristic structural element is frequently present, *viz.* infinite two-dimensional layers of the composition Bi_2O_2. The layers consist of sheets of oxygen atoms which are arranged to form squares. The bismuth atoms are situated alternately above and below the centres of the latter as illustrated in Fig. 1. Each oxygen atom of the sheets is thus tetrahedrically surrounded by four bismuth atoms. The arrangement can also be described geometrically as built up of OBi_4 tetrahedra linked together to form the Bi_2O_2 layers by sharing four edges.

The bismuth oxide compounds reported to contain Bi_2O_2 layers include several bismuth oxide halides [1], some bismuth oxide salts of fatty acids [2], several mixed oxides of bismuth and titanium, niobium or tantalum [3] and one oxide carbonate of bismuth [4].

The present study was undertaken in order to find out whether the Bi_2O_2 layers are also present in compounds containing tetrahedral anions.

Since only preliminary determinations have been made of the positions of the

Judging from the Bi—Bi distances, there seems to exist a weak tendency for the bismuth atoms to form pairs in this structure.

$BiOHSeO_4 \cdot \frac{1}{2} H_2O$

Space group: $P2_1/n$ (No. 14). The unit cell contains four formula units. The following point positions and parameters were derived for the bismuth and selenium atoms:

4 Bi in 4(*e*):
$\pm(x,y,z)$; $\pm(\frac{1}{2}+x,\frac{1}{2}-y,\frac{1}{2}+z)$;
$x = 0.586$, $y = 0.118$, $z = 0.151$
4 Se in 4(*e*):
$x = 0.094$, $y = 0.165$, $z = 0.165$
Cell dimensions:
$a=6.64$ Å, $b=13.60$ Å, $c=6.08$ Å, $\beta=112.2°$

The bismuth atoms form nearly planar sheets parallel to the plane (101). The sheets are made up of hexagons with the edges 3.66 Å and 5.05 Å (Fig. 4). The shortest distances between bismuth atoms in adjacent layers is 5.77 Å. The arrangement of the bismuth atoms in $BiOHSeO_4 \cdot \frac{1}{2}H_2O$ does not bear any resemblance to the quadratic layers of bismuth atoms in the Bi_2O_2 sheets. The tendency of pair formation for the bismuth atoms is more pronounced in this structure than in $BiOHCrO_4$.

These investigations will be continued in order to refine the parameters and to determine the positions of the oxygen atoms. A full account will be published later.

These studies form part of a research program on bismuth oxide salts financially supported by the *Swedish Natural Science Research Council.*

1. Sillén, L. G. *Diss.*, Stockholm 1940.
2. Aurivillius, B. *Acta Chem. Scand.* **9** (1955) 1213.
3. Aurivillius, B. *Diss.*, Stockholm 1951.
4. Lagercrantz, Å. and Sillén, L. G. *Arkiv Kemi, Mineral. Geol.* **25A** (1948) No. 20.

Received May 16, 1960.

Electrophilic Replacement of Bromine by Hydrogen

Debromination of 2,4,6-Tri-*t*-butylbromobenzene

PHILIP C. MYHRE*

Nobel Institute of Chemistry, Stockholm 50, Sweden

When 2,4,6-tri-*t*-butylbromobenzene (*I*) is heated in the presence of a strong acid a mixture of products including 1,3,5-tri-*t*-butylbenzene (*II*) and 3,5-di-*t*-butylbromobenzene is formed. If an acceptor for Br+ such as bromide ion is present in the acid and the resulting bromine is entrained from the solution, *II* is the chief product. In principle, any compound which formally serves as a reducing agent for Br+ and is otherwise inert is suitable for use as an acceptor. Reactive aromatic hydrocarbons prove to be very efficient for this purpose. Trifluoroacetic acid has been used in most experiments because of its high acidity and relatively good solvent properties; however, the reaction occurs with a variety of acids.

The debromination of *I* is viewed as an electrophilic replacement of bromine by hydrogen or the reverse of aromatic bromination. That *I* should undergo electrophilic debromination was by no means unexpected. The observed strong isotope effect in the "positive" bromination [1] of *II* coupled with the known facts about other electrophilic substitutions by hydrogen [2] led us to investigate this reaction possibility. The isotope effect in the bromination of *II* has been explained in terms of steric effects which cause the velocity of step 2 to become less than that of step -1. It is apparent that steric repulsion energy increases as this reaction proceeds towards products. As a result, the energy differ-

* U.S. National Science Foundation Postdoctoral Fellow, 1958—1960.

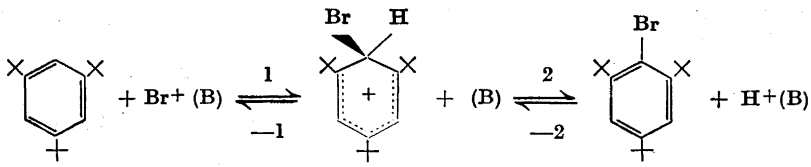

ence between the products and the transition state would be expected to be less for a highly hindered compound such as *I* than for a less hindered alkylbromobenzene. Consequently, one would predict that the reverse reaction, debromination, would become energetically more favorable in highly hindered systems. It should be stressed that the existence of an isotope effect in the bromination of *II* does not imply that the reaction is reversible. However, steric effects serve to explain both the isotope effect and the facile debromination.

Since there are numerous examples in the literature of acid-induced dehalogenations of highly reactive unhindered aromatic compounds such as amines and phenols [3,4], it is important to establish that the lowering of the free energy of activation for the debromination of *I* is in a large measure due to the above mentioned steric effects and not simply to a general activation of the aromatic ring by the alkyl group substituents. Consequently, the possible debromination of 2-bromomesitylene (*III*), a compound whose substituents have as a first approximation similar electron releasing properties but greatly reduced steric hindrance, was investigated. No debromination could be detected when *III* was subjected to conditions which caused extensive debromination of *I* (refluxing trifluoroacetic acid and excess bromide ion). In the course of this work it has been shown that mesitylene is a far better acceptor of Br+ than bromide ion. Therefore, it could be argued that debromination of mesitylene would be difficult to detect because of the rapid back reaction (bromination). A more conclusive test was devised. An equimolar mixture of mesitylene-α-H_1^3, specific activity 228, and inactive 2-bromomesitylene was heated at reflux in trifluoroacetic acid for one hour; this is approximately one half-life for the debromination of *I*. The specific activities of the isolated mesitylene and bromomesitylene were 226 and 3, respectively. From these results it is concluded that *III* does not appreciably debrominate under conditions which lead to extensive debromination of *I*. The results also preclude the exchange of hydrogen in the methyl groups of mesitylene under the reaction conditions.

The facile debromination of *I* led us to investigate the possibility that the reported [5] failure of the iron catalyzed bromination of *II* to yield *I* (only 3,5-di-*t*-butylbromobenzene has been isolated) was due to two competing reactions: the first, a readily reversible bromination at an aromatic carbon bearing a hydrogen; the second, an irreversible bromination at an aromatic carbon bearing a *t*-butyl group. A necessary condition of this proposed scheme is that *I* be converted to 3,5-di-*t*-butylbromobenzene under iron catalyzed bromination conditions. This conversion has been shown to take place. It remains to be shown that *I* is transiently formed in this bromination reaction.

1. Myhre, P. C. *Acta Chem. Scand.* **14** (1960) 219.
2. Schubert, W. M. and Myhre, P. C. *J. Am. Chem. Soc.* **80** (1958) 1755.
3. Nicolet, B. H. *et al. J. Am. Chem. Soc.* **43** (1921) 1796; **49** (1927) 1796, 1801, 1806.
4. Meerwein, H. J., Hofmann, P. and Schill, F. *J. prakt. Chem.* **154** (1940) 266.
5. Bartlett, P. D., Roha, M. and Stiles, R. M. *J. Am. Chem. Soc.* **76** (1954) 2349.

Received May 19, 1960.

The Ternary Compound $SbCl_5 \cdot TiCl_4 \cdot 3POCl_3$

GÖRAN ADOLFSSON, RAGNAR BRYNTSE and INGVAR LINDQVIST

Institute of Chemistry, University of Uppsala, Uppsala, Sweden

In the system $SbCl_5-TiCl_4-POCl_3$ a compound is formed which has a higher melting point than any of the compounds $SbCl_5 \cdot POCl_3$, $TiCl_4 \cdot POCl_3$ or $TiCl_4 \cdot 2POCl_3$. It is rather difficult to obtain the compound pure from excess $SbCl_5$, $TiCl_4$ or $POCl_3$ (depending upon the mole ratios of the original mixture), but all such experiments indicate a composition $SbCl_5 \cdot TiCl_4 \cdot 3POCl_3$. (The high melting point shows that it cannot be a mixture of $SbCl_5 \cdot POCl_3$ and $TiCl_4 \cdot 2POCl_3$). We therefore tried to prepare a pure specimen by dissolving $SbCl_5$ and $TiCl_4$, in the mole ratio 1:1, in ethylene chloride and adding an excess of $POCl_3$. The volatile components were then removed by evacuation, the solid residue was further purified by sublimation and the resulting crystals were analyzed. (Found: Cl 67.5; Ti 5.00; P 10.0. Calc. Cl 67.3; Ti 5.05; P 9.8.)

Titanium was determined spectrophotometrically by the peroxide method with an excess of phosphoric acid in order to make the determination insensitive to the amount of phosphoric acid in the dissolved sample.

Phosphorus was determined by precipitation as $MgNH_4PO_4 \cdot 6H_2O$ in the presence of EDTA and hydrogen peroxide (to keep titanium in solution) and titration by EDTA of the magnesium content in the washed precipitate.

Antimony did not interfere in these determinations.

The crystals sublime before melting at about +200°C.

The high melting point indicates that the ternary compound cannot be a loose addition compound between $SbCl_5 \cdot POCl_3$ and $TiCl_4 \cdot 2POCl_3$. Since co-ordination around Sb and Ti is already as large as possible in those two addition compounds, however no halogen bridged compound of the same type as in $[TiCl_4(OPCl_3)]_2^1$, containing Sb as well as Ti, can therefore have formed. A more probable alternative would be the formation of $SbCl_6^-$ and $[TiCl_3(OPCl_3)_3]^+$ ions.

The latter suggestion has been tested by measurements of the specific conductances of 0.9 M solutions of $SbCl_5 \cdot POCl_3$, $TiCl_4 \cdot 2POCl_3$ and $SbCl_5 \cdot TiCl_4 \cdot 3POCl_3$ in ethylene chloride. The values are approximately (at +21°C):

2.4×10^{-5} ohm^{-1} cm^{-1} ($SbCl_5 \cdot POCl_3$)
3.7×10^{-4} ohm^{-1} cm^{-1} ($TiCl_4 \cdot 2POCl_3$)
6.3×10^{-3} ohm^{-1} cm^{-1} ($SbCl_5 \cdot TiCl_4 \cdot 3POCl_3$)

The evidence so far is thus in accord with the idea that the ternary compound is actually $[TiCl_3(OPCl_3)_3](SbCl_6)$. Conclusive proof is, however, still lacking.

In the systems $SbCl_5-SnCl_4-POCl_3$ and $SbCl_5-AsCl_3-POCl_3$ no ternary compound could be found. The increase in specific conductance is obtained, however, but the magnitude of the conductances is smaller than with $TiCl_4 \cdot 2POCl_3$:

3.6×10^{-5} ohm^{-1}cm^{-1} ($SnCl_4 \cdot 2POCl_3$)
6.1×10^{-4} ohm^{-1}cm^{-1} ($SbCl_5 \cdot POCl_3 + SnCl_4 \cdot 2POCl_3$)

The greater tendency of $TiCl_4$ to act as a chloride ion donor in these systems is in agreement with the active base strength of $TiCl_4$ as determined by potentiometric measurements [2].

This work has been supported by a grant from the *Air Force Office of Scientific Research of the Air Research and Development Command*, United States Air Force, through its European Office under Contract No. AF 61(052)-43. This grant is gratefully acknowledged.

1. Brändén, C.-I. and Lindqvist, I. *Acta Chem. Scand.* **14** (1960). *In the press.*
2. Gutmann, V. and Mairinger, F. *Monatsh.* **89** (1958) 724.

Received May 6, 1960.

Bacterial Carotenoids

VI. A Note on the Constitution of Bacterioruberine *α*

SYNNÖVE LIAAEN JENSEN

Institutt for Organisk Kjemi, Norges Tekniske Högskole, Trondheim, Norway

This paper gives a preliminary report on the chemical constitution of bacterioruberine *α* — the main carotenoid pigment of certain red, rod-shaped, obligate and extremely halophilic bacteria for which Volcani [1] have suggested the genus name *Halobacterium*.

In 1932 Petter [2] isolated two crystalline carotenoids named bacterioruberine *α* (abs. max. 460, 490, 528 mμ in methanol) and bacterioruberine *β* (abs.max. 452, 482, 522 mμ in methanol) from a bacterium which she named *Bacterium halobium*, and which undoubtedly belongs to the genus *Halobacterium* (Volcani). From the same source Lederer [3] could isolate only crystalline bacterioruberine *α* (abs.max. 460, 495, 528 mμ in methanol). The absorption spectrum was found to be similar to that of rhodoviolascin [4], later shown to be identical with spirilloxanthin [5]. Bacterioruberine *α*, however, had a pronounced hypophasic character, and Lederer suggested that this carotenoid possibly was a di-demethylated spirilloxanthin.

A carotenoid with absorption spectrum similar to that of bacterioruberine *α* was present also in cells of an obligate, halophilic bacterium studied by Spruit and Pijper [6]. An interesting chromatographic survey of the carotenoids of a number of halophilic bacteria has recently been given by Baxter [7], again stating that bacterioruberine *α* is the main carotenoid of several red *Halobacterium* species. A sample of bacterioruberine *α* of unreported purity gave a zero methoxyl value.

According to the old formulation of 1940 of the structure of spirilloxanthin (I) [8],

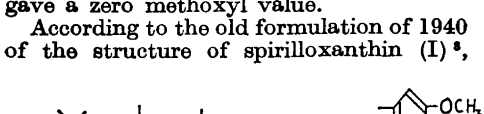

(I)

Lederer's suggestion of 1938 that bacterioruberine *α* was a di-demethylated spirilloxanthin would imply the structure (II) for this carotenoid with two enolic

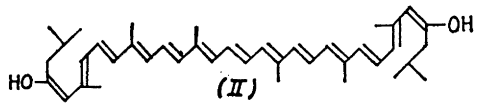

(II)

hydroxyl groups. This has not been confirmed by the present investigation.

In the present investigation bacterioruberine *α* was isolated as the major carotenoid from a *Halobacterium* sp. (Strain No. 1, from the Department of Biochemistry, this University). The carotenoid was extracted with acetone and purified by chromatography of the unsaponifiable matter on deactivated alumina.

Bacterioruberine *α* crystallised with difficulty as the all-*trans* isomer from acetone-petroleum ether solution in mauve-violet, shiny, needles, m. p. 182°C (evacuated tube). Consistent micro combustion analyses could not be obtained. The crystalline carotenoid was readily soluble in pyridine and acetone, fairly readily soluble in methanol, chloroform and carbon disulphide, fairly soluble in benzene and diethyl ether and nearly insoluble in petroleum ether. Absorption maxima in various solvents as recorded immediately after dissolution with a Zeiss PMQ2 calibrated spectrophotometer is presented in Table 1 together with similar data reported for spirilloxanthin [5]. The agreement in absorption maxima for the two carotenoids falls within the experimental errors for different samples and instruments. The shape of the absorption spectra in the utilised solvents was further identical and showed pronounced fine-structure. It appears therefore that bacterioruberine *α* and spirilloxanthin have identical chromophores, that is 13 conjugated carbon-carbon double bonds in an aliphatic chain.

Quantitative extinction coefficient determinations carried out in acetone gave as a maximum value $E^{1\%}_{1\,cm} = 2\,620$ at 499 mμ, a value within the expected range for a di-demethylated spirilloxanthin. Spirilloxanthin in hexane has $E^{1\%}_{1\,cm} = 2\,540$ at 493 mμ [5].

A stereochemical investigation of bacterioruberine *α* was performed by means of a paper-chromatographical method previously reported [9]. Bacterioruberine *α* was found to exhibit a greater stereochemical lability than any other carotenoid so far reported. It might be mentioned that after 24 h in darkness at room temperature the all-*trans* isomer had isomerized spontaneously to Neo U to an extent of 42 % as colorimetrically determined after ra-

Table 1. Absorption maxima in various solvents for all-*trans* bacterioruberine *a* and spirilloxanthin [5].

Carotenoid	Abs.max. in mμ in				
	Pet.ether *	Benzene	Acetone	$CHCl_3$	CS_2
Bacterioruberine *a*	369	378	374	380	
	385	398	389	397	418
	461	481	466	475	500.5
	494	511	499	506	533.5
	528	549	533.5	544	572
Spirilloxanthin	368	378			
	384	395			(418)
	461	479		(475)	495
	493	510		505	532
	528	548.5		543	571.5

* b.p. 60—70°C.

pid chromatographic separation. After 24 h exposure to indirect daylight at room temperature of a solution of the pure *trans* isomer, only 37 % *trans* remained, whereas gross stereoisomerisation to Neo U, Neo A and Neo B had occurred. The composition of the iodine catalyzed equilibrium mixture is presented in Table 2.

The two first maxima give the position of the *cis*-peak, which is very weak for the *trans* isomer and strongest for the Neo U isomer. R_F-values for the different stereoisomers have been published previously [9].

Quantitative partition tests according to the method of Zechmeister and Petracek [10] gave the following partition ratios:

Pet.ether/95 % methanol	1:99
Pet.ether/85 % methanol	3:99

Bacterioruberine *a* is seen to be strongly hypophasic even with 85 % methanol, thus indicating the presence of two or more hydroxy groups in the molecule.

Upon prolonged treatment with acetic anhydride in pyridine bacterioruberine *a* was completely recovered; whereas bacterioruberine *a* was very unstable towards freshly distilled acetyl chloride in pyridine, yielding only decomposition products. The failure of bacterioruberine *a* to yield an acetate indicated that all hydroxyl groups present were tertiary. This was confirmed by the IR-spectrum (KBr) which showed a strong absorption band for the hydroxyl stretching frequency at 3 320 cm^{-1}, no absorption band around 1 030 cm^{-1} characteristic of secondary hydroxyl groups [11], but a fairly strong band typical of tertiary hydroxyl groups at 1 142 cm^{-1} as in chloroxanthin [11], rhodopin [11] and rhodovibrin [12].

$HCl—CHCl_3$-treatment [13] gave no product with extended conjugated chain. Allylic hydroxyl groups are therefore not likely to be present.

Table 2. Composition of the iodine catalyzed equilibrium mixture of bacteriorubine *a*.

Member of the stereoisomeric set	Abs.max. in mμ in		% of total colorimetr. determined *
	pet.eth. bp. 60—70°C	acetone	
Neo B	369, 385, 463, 492, 522	374, 389, 470, 498, 526	1
Neo A	369, 385, 454, 483, 516	374, 389, 460, 489, 522	20
all-*trans*	369, 385, 461, 494, 528	374, 389, 466, 499, 533.5	37
Neo U	369, 385, 460, 490, 522	374, 389, 466, 496, 527	42

* The same extinction coefficient was used for calculating the actual amount of each stereoisomer.

The stability of the chromophore of bacterioruberine *a* in neutral as well as in basic media further refuted the presence of enolic hydroxyl groups [14]. The absence of enolic hydroxyl groups was supported also by the lack of a relatively intense IR-absorption band around 1 660 cm^{-1} attributed by Rosenkrantz and Gut [15] to the grouping $-CH=C-O-$.

The IR-spectrum further showed that no methoxyl groups or carbonyl functions were present in bacterioruberine *a*.

Combining the evidence of a chromophore of 13 conjugated carbon-carbon double bonds in an aliphatic system with the presence of at least two non-allylic, non-enolic, tertiary hydroxyl groups, it seems that only one structure (III) is probable for bacterioruberine *a*.

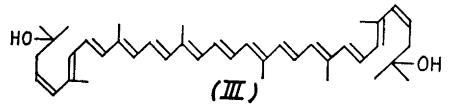

(III)

The presence of no more than two hydroxyl groups was further confirmed by quantitative determination of active hydrogen. (Found: Active H 0.39 %. Calc. for $C_{40}H_{54}(OH)_2$: 0.35 %; for $C_{40}H_{52}(OH)_3$: 0.51 %.)

From the new spirilloxanthin structure (IV) [14, 16] it is thus seen that bacterioruberine *a* should be a di-demethylated spirilloxanthin in agreement with Lederer's [3] original suggestion.

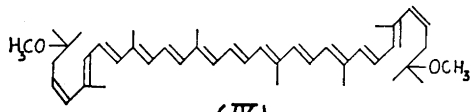

(IV)

Bacterioruberine *a* is another example of a bacterial carotenoid with tertiary hydroxyl groups in addition to chloroxanthin [17, 11], rhodopin [11], rhodovibrin [12] and OH-spirilloxanthin [18] from photosynthetic bacteria. This appears to be a characteristic feature so far not reported for carotenoids from higher organisms. The position of the hydroxyl group in chloroxanthin has not yet been established, but is for the rest of the carotenoids mentioned above invariably located in 1-positions.

This work will be published in more detail elsewhere.

The author is deeply indebted to Siv.ing. Ian Dundas at the Department of Biochemistry for the cultivation of the *Halobacterium* sp., to Professor N. A. Sörensen for his inspiring interest in this work and to Norges Tekniske Högskole for a maintenance grant.

1. Elazari-Volcani, B. *Studies on the Microflora of the Dead Sea, Thesis*, Hebrew University, Jerusalem 1940.
2. Petter, H. F. M. *Over roode en andere bacteriën van gezouten vish, Thesis*, Utrecht 1932.
3. Lederer, E. *Bull. soc. chim. biol.* **20** (1938) 611.
4. Karrer, P. and Solmssen, U. *Helv. Chim. Acta* **19** (1935) 219.
5. Polgàr, A., van Niel, C. B. and Zechmeister, L. *Arch. Biochem.* **5** (1944) 243.
6. Spruit, C. J. P. and Pijper, A. *Antonie van Leeuwenhoek* **18** (1952) 190.
7. Baxter, R. M. *Can. J. Microbiol. In press.*
8. Karrer, P. and Koenig, H. *Helv. Chim. Acta* **23** (1940) 460.
9. Jensen, A. and Liaaen Jensen, S. *Acta Chem. Scand.* **13** (1959) 1863.
10. Zechmeister, L. and Petracek, F. J. *Anal. Chem.* **28** (1956) 1484.
11. Liaaen Jensen, S. *Acta Chem. Scand.* **13** (1959) 842.
12. Liaaen Jensen, S. *Acta Chem. Scand.* **13** (1959) 2143.
13. Wallcave, L. and Zechmeister, L. *J. Am. Chem. Soc.* **75** (1953) 4495.
14. Liaaen Jensen, S. *Acta Chem. Scand.* **13** (1959) 381.
15. Rosenkrantz, H. and Gut, M. *Helv. Chim. Acta* **36** (1953) 1000.
16. Barber, M. S., Jackman, L. M. and Weedon, B. C. L. *Proc. Chem. Soc.* **1959** 96.
17. Nakayama, T. O. M. *Arch. Biochem. Biophys.* **75** (1958) 352.
18. Liaaen Jensen, S. *Acta Chem. Scand.* **14** (1960) 953.

Received May 5, 1960.

Bacterial Carotenoids

VII. A Partial Synthesis of Spirilloxanthin and OH-Spirilloxanthin

SYNNÖVE LIAAEN JENSEN

Institutt for Organisk Kjemi, Norges Tekniske Högskole, Trondheim, Norway

From the structure (I) ascribed to bacterioruberine *a* in the previous paper[1] it

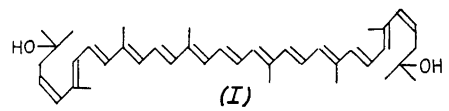

(I)

is seen that bacterioruberine *a* represents a di-demethylated derivative of spirilloxanthin (II)[2,3].

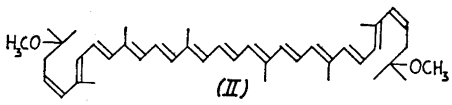

(II)

It is obvious that a mutual support for these structures could be obtained if dimethylated bacterioruberine *a* and spirilloxanthin were shown to be identical.

Bacterioruberine *a* was isolated from a *Halobacterium* sp. (Strain No. 1, from the Department of Biochemistry, this University) as previously described[1]. Several procedures were tried to methylate this carotenoid. The instability of bacterioruberine *a* towards heat and acid catalysts restricted the number of useful methods. Treatment with diazomethane in methanol-ether[4], dimethylsulphate and potassium carbonate in dry acetone[5] or the usual method with potassium *t*-amyloxylate and methyl iodide[6] failed to give any methylation products. This was to be expected in view of the non-enolic, tertiary character of the hydroxyl groups of bacterioruberine *a*.

The careful method reported by Kuhn *et al.*[7] for the methylation of N-acetylglucosamine derivatives with methyl iodide and silver oxide in dimethylformamide proved, however, to be successful also in this case. Following this method mono- and dimethyl-derivatives of bacterioruberine *a* were obtained in maximum yields of 12 % and 2.4 %, respectively, in fourteen different methylation experiments besides unchanged starting material. The reaction was carried out at room temperature, in darkness, under nitrogen and with magnetic stirring. The methylation process was followed paper chromatographically[8] and usually interrupted after about 70 h. The carotenoids were transferred to benzene and separated by chromatography on deactivated alumina. The yields could not be significantly increased by lowering or increasing the reaction temperature, by using dry dimethylformamide or by exchanging the silver oxide for barium oxide[9], and were in any case not well reproducible.

The methylation products could only be isolated in amounts insufficient for crystallization and were characterized by means of absorption spectra in visible light, column and paper[8] chromatography of the main stereoisomers and quantitative partition tests according to Zechmeister and Petracek[10].

The properties of mono-methoxy-bacterioruberine *a* are presented in Tables 1 and 2 together with the corresponding properties of the so-called OH-spirilloxanthin, a minor pigment

Table 1. Absorption maxima for the main stereoisomers of mono-methoxy-bacterioruberine *a* and OH-spirilloxanthin.

Carotenoid	Member of the stereoisomeric set	Abs.max. in mμ in acetone					Abs.max. in mμ in pet.eth.bp. 60–70°C				
Mono-methoxy-bacterioruberine *a*	*trans*	373	389	469	499	533	369	385	462	494	528
	Neo A	373	388	461	490	522					
OH-spirilloxanthin	*trans*	373	389	467	499	533	369	385	462	494	528
	Neo A	373	389	462	491	523					

Table 2. Properties of mono-methoxy-bacterioruberine *a* and OH-spirilloxanthin.

Carotenoid	Member of the stereo-isomeric set	R_F-value *		Quant. partition ratio [10]	
		10 % **	20 % **	Pet.eth. / 95 % methanol	Pet.eth. / 85 % methanol
Mono-methoxy-bacterioruberine *a*	*trans*	0.39	0.80	42:58	95:5
	Neo A	0.59	0.88		
OH-spirillo-xanthin	*trans*	0.40	0.80	44:56	95:5
	Neo A	0.58	0.87		

* on Schleicher and Schüll No. 2 87 paper.
** acetone in pet.ether b.p. 60— 70°C.

present in cells of *Rhodospirillum rubrum* [11, 12] in the exponential growth stage and in *Rhodopseudomonas palustris* [13]. These bacteria were used as sources for the isolation of chromatographically pure fractions of OH-spirilloxanthin.

The absorption spectra of the corresponding stereoisomers of mono-methoxy-bacterioruberine *a* and OH-spirilloxanthin further had analogous shapes. Co-chromatography of the *trans* isomers of the two pigments gave one zone which could not be resolved on kiselguhr paper. The solvents required for elution from deactivated alumina also were similar. The partition tests indicate the presence of one hydroxyl group in both pigments. Both pigments gave the same products upon HCl—$CHCl_3$ treatment [14].

The data presented for mono-methoxy-bacterioruberine *a* and OH-spirilloxanthin strongly suggest that these pigments are identical, leading to a structural formula (III) for OH-spirilloxanthin

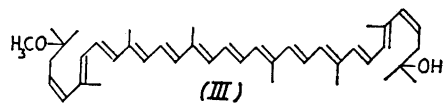

(III)

as a mono-demethylated spirilloxanthin — in good agreement with the previous tentative assumption [11] and the kinetic data for its biosynthesis in *Rhodospirillum rubrum* [12] from rhodovibrin (OH—P481) [15] and as a spirilloxanthin precursor.

Table 3. Absorption maxima for the main stereoisomers of di-methoxy-bacterioruberine *a* and spirilloxanthin.

Carotenoid	Member of the stereo-isomeric set	Abs.max. in mμ in acetone					Abs.max. in mμ in pet.eth. b.p. 60—70°C				
Di-methoxy-bacterio-ruberine *a*	*trans*	373	389	468	498	533	369	385	462	494	527
	Neo A	372	389	468	496	529					
	Neo B	372	389	464	489	523					
Spirillo-xanthin	*trans*	373	389	468	498	533	369	385	462	494	528
	Neo a[8]	372	389	467	495	529					
	Neo b[8]	372	389	462	489	523					

Table 4. Properties of di-methoxy-bacterioruberine *a* and spirilloxanthin.

Carotenoid	Member of the stereo-isomeric set	R_F-value * 5 % *	R_F-value * 10 % **	Quant.partition ratio [10] Pet.eth./95 % methanol
Di-methoxy-bacterio-ruberine *a*	*trans*	0.40	0.76	84:16
	Neo A	0.54		
	Neo B	0.71		
Spirillo-xanthin	*trans*	0.40	0.76	88:14
	Neo a[8]	0.54		
	Neo b[8]	0.73		

* on Schleicher and Schüll No. 287 paper.
** acetone in pet.ether b.p. 60—70°C.

Similar properties for di-methoxy-bacterio-ruberine *a* and spirilloxanthin are presented in Tables 3 and 4. Spirilloxanthin was isolated from the same source as OH-spirillo-xanthin as previously described[8]. The shape of the absorption spectra of the corresponding stereoisomers of the two carotenoids were very similar.

Co-chromatography of the *trans* isomers on kiselguhr paper gave one zone which could not be resolved. Di-methoxy-bacterioruberine *a* and spirilloxanthin further required similar solvents for elution from deactivated alumina.

The data presented are greatly in favour of identity of di-methoxy-bacterioruberine *a* and spirilloxanthin, a fact that strengthens the suggested structures for bacterio-ruberine *a* (I) and spirilloxanthin (II).

This work will be published in more detail elsewhere.

The author is greatly indebted to Prof. C. B. van Niel, Hopkins Marine Station, Pacific Grove, California, for a generous supply of dried cells of *Rhodopseudomonas palustris*, to Siv.ing. Ian Dundas, Dept. of Biochemistry, for the cultivation of the *Halobacterium* sp., to Professor N. A. Sörensen for his inspiring interest and advice in this work and to Norges Tekniske Högskole for a maintenance grant.

1. Liaaen Jensen, S. *Acta Chem. Scand.* **14** (1960) 950.
2. Liaaen Jensen, S. *Acta Chem. Scand.* **13** (1959) 381.
3. Barber, M. S., Jackman, L. M. and Weedon, B. C. L. *Proc. Chem. Soc.* **1959** 96.
4. Eistert, B. *Neuere Meth. der Präp. Org. Chem.* **1**, Verlag Chemie, Berlin 1943, p. 364.
5. *cf.* Seshadri, T. R. and Subramanian, S. S. *Proc. Indian Acad. Sci.* **30A** (1949) 67.
6. Karrer, P. and Takahashi, T. *Helv. Chim. Acta* **16** (1933) 1163.
7. Kuhn, R., Trischmann, H. and Löw, I. T. *Angew. Chem.* **67** (1955) 32.
8. Jensen, A. and Liaaen Jensen, S. *Acta Chem. Scand.* **13** (1959) 1863.
9. Kuhn, R., Baer, H. H. and Seeliger, A. *Ann.* **611** (1958) 236.
10. Zechmeister, L. and Petracek, F. J. *Anal. Chem.* **28** (1956) 1484.
11. van Niel, C. B., Goodwin, T. W. and Sissins, M. E. *Biochem. J.* **63** (1956) 408.
12. Liaaen Jensen, S., Cohen-Bazire, G., Nakayama, T. O. M. and Stanier, R. Y. *Biochem. et Biophys. Acta* **29** (1958) 477.
13. Goodwin, T. W. *Soc. Biol. Chemists, India. Silver Jubilee Souvenir* **1955** 698.
14. Wallcave, L. and Zechmeister, L. *J. Am. Chem. Soc.* **75** (1953) 4495.
15. Liaaen Jensen, S. *Acta Chem. Scand.* **13** (1959) 2143.

Received May 5, 1960.

The Crystal Structures of Zr_5Sn_3 and Zr_3Sn

GUNNAR GRAN AND STEN ANDERSSON

Institute of Inorganic and Physical Chemistry, University of Stockholm, Stockholm, Sweden

In the zirconium-tin system, four intermediate phases have been reported to exist, *viz.* Zr_4Sn, Zr_5Sn_3, ZrSn and $ZrSn_2$ (Refs. [1,2]). Crystal structures have been given only for $ZrSn_2$ (of $C54$ type) and for Zr_5Sn_3 (Ref. [2]). The latter is described as being of the $D8_8$ type but no structural details have hitherto been given.

In the present study, which was undertaken in order to complement the existing knowledge concerning this system, metallic zirconium and tin of 99.95 % purity were used as starting materials. Alloys of several compositions were prepared by melting pressed tablets of the metals in an electric arc furnace under argon atmosphere. The samples were then sealed in evacuated silica tubes and annealed for about two months at 900°C. Tantalum foils protected the alloys from reacting with the silica.

X-Ray powder patterns were registered in a Guinier focusing camera with strictly monochromatized CuKa_1 radiation. Single crystal data were obtained with a Weissenberg camera using CuK radiation.

Rod-formed single crystals were obtained from a sample of a composition close to $ZrSn_{0.5}$. Complete single-crystal data were registered while rotating the crystal around the rod axis, the unit length of which was found to be 5.8 Å. The symmetry proved to be hexagonal and the unit cell dimensions as obtained from the powder pattern were found to be:

$$a = 8.46 \text{ Å}, \qquad c = 5.78 \text{ Å}$$

It was confirmed that the structure was of the $D8_8$ type, as had previously been observed. The space group is thus $P6_3/mcm$ (No. 193) and all the atoms occupy positions 6 (g) (x, 0, ½ etc.). From the electron density projection (x, y, p), the following atomic parameters were obtained:

	Zr	Sn
x	0.245	0.609

Table 1. Powder pattern of the sample $ZrSn_{0.6}$ containing two phases of Zr_5Sn_3 type.

		$\sin^2\Theta$	
hkl	*I*	calc.	obs.
111	w	0.05042	0.05050
		0.05079	0.05077
002	m	0.07029	0.07020
		0.07093	0.07084
210	m	0.07633	0.07660
		0.07713	0.07710
012	w	0.08124	0.08122
		0.08195	0.08187
121	st	0.09420	0.09421
		0.09486	0.09494
030	m	0.09852	0.09857
		0.09916	0.09924
112	m	0.10314	0.10309
		0.10398	0.10397
022	w	0.11408	0.11419
		0.11500	0.11495
130	w	0.14231	0.14228
		0.14324	0.14328
221	w	0.14894	0.14886
		0.14995	0.15020

Table 2.

Composition	X-Ray evidence
$ZrSn_{0.4}$	$Zr_3Sn + Zr_5Sn'_3$
$ZrSn_{0.5}$	$Zr_5Sn'_3$
$ZrSn_{0.6}$	$Zr_5Sn'_3 + Zr_5Sn''_3$
$ZrSn_{0.7}$	$Zr_5Sn''_3 + ZrSn$

However, it was evident that this phase was not of the ideal composition Zr_5Sn_3. When the tin content was increased, extra lines appeared close to the original lines. The sample remained two-phasic after additional heat treatment. The new lines could be indexed in the same way as the former with the following unit cell parameters:

$$a = 8.50 \text{ Å}, \qquad c = 5.81 \text{ Å}$$

An indexed powder pattern of the sample $ZrSn_{0.6}$ is given in Table 1. The existence of two phases of Zr_5Sn_3 type has thus been found.

The symbols $Zr_5Sn'_3$ and $Zr_5Sn''_3$ used in Table 2 designate the ones low and high in tin, respectively. Further studies at the critical compositions of the two phases and concerning the type of defect are contemplated.

At a composition $ZrSn_{0.4}$, the Guinier powder pattern photograph showed, in addition to the pattern of the defective Zr_5Sn_3, a number of strong, extra lines. Assuming a cubic unit cell, these extra lines could be indexed with $a = 5.634$ Å. The structure was found to be of the well-known β-wolfram structure type and should thus be given the formula Zr_3Sn.

Acknowledgements. The authors are much indebted to Dr. Arne Magnéli for valuable discussion and his continuing interest in this work.

1. Mc Phersson, D. J. and Hansen, M. *Trans. Am. Soc. Metals* **45** (1953) 915.
2. Nowotny, H. and Schachner, H. *Monatsh.* **84** (1953) 169.

Received May 16, 1960.

Synthesis of Benzyl 4-*O*-Methyl-β-D-Xylopyranoside

PER J. GAREGG

Svenska Träforskningsinstitutet, Träkemiska avdelningen, Stockholm Ö, Sweden

Previous studies of a naturally occurring acetylated xylan [1] in birch wood have raised the question of whether the *O*-acetyl groups are attached to the most readily acetylated free hydroxyl groups in the β-1,4-linked anhydroxylose chains. In an attempt to investigate which of the two free hydroxyl groups at the 2- and 3-position is the most readily acetylated, benzyl 4-*O*-methyl-β-D-xylopyranoside was selected as a suitable model for partial acetylation. The synthesis of this substance, by a sequence of reactions given below is analogous to that described by Hough and Jones [2] for the synthesis of the corresponding methyl glycoside, is reported in the present paper. The final product and all the intermediates were obtained in a crystalline form and the overall yield from D-arabinose was 10 % of the theoretical.

Experimental. All melting points are corrected. Evaporations were done under reduced pressure at a bath temperature below 40°.

Benzyl 3,4-isopropylidene-2-tosyl-β-D-arabinopyranoside, II. Benzyl-3,4-*iso*propylidene-β-D-arabinopyranoside (81 g, m. p. 55—57°, $[\alpha]_D^{20}$ —195°), prepared from 100 g D-arabinose according to Ballou [3] was dissolved in pyridine (500 ml) and treated with *p*-toluenesulphonyl chloride (112 g). The solution was allowed to stand at room temperature during 48 h and then poured on ice. The mixture was extracted with chloroform and the chloroform solution was dried over anhydrous sodium sulphate, filtered and concentrated to dryness. The syrup obtained was used directly in the next step; a small quantity which was set aside crystallised from 96 % aqueous ethanol, m.p. 62—64° unchanged on further recrystallisation, $[\alpha]_D^{20}$ —194° (*c* 1.0 in chloroform). (Found: C 61.14; H 5.96; O 26.20; S 6.84. Calc. for $C_{22}H_{26}O_7S$: C 60.81, H 6.03; O 26.78; S 7.38.)

Benzyl 2-tosyl-β-D-arabinopyranoside, III. The above product was dissolved in boiling acetone (900 ml) and 0.1 N formic acid (1 800 ml) was added over a period of 20 h under reflux. Concentration yielded a syrup which crystallised from aqueous ethanol. Recrystallisation from ethanol/*iso*propyl ether yielded benzyl 2-tosyl-β-D-arabinopyranoside (70 g) with m. p. 120—123°. The pure substance had m. p. 123.5—124.5°, $[\alpha]_D^{20}$ —156° (*c* 0.8 in chloroform). (Found: C 57.40; H 5.52; O 27.94; S 7.88. Calc. for $C_{19}H_{22}O_7S$: C 57.86; H 5.62; O 28.39: S 8.13.)

Benzyl 2,3-anhydro-β-D-ribopyranoside, IV. Benzyl 2-tosyl-β-D-arabinopyranoside (70 g) was dissolved in methanolic sodium methoxide (1 l, made from 13 g sodium) and allowed to stand overnight. The solution was diluted with water (500 ml) and neutralised with sulphuric acid, the methanol was removed by vacuum distillation and the aqueous solution was extracted with chloroform. The combined chloroform solutions were dried over anhydrous sodium sulphate, filtered and the filtrate was concentrated to dryness. Spontaneous crystallisation occurred giving benzyl 2,3-anhydro-β-D-ribopyranoside (29 g) with m. p. 64—76°. Recrystallisation from *iso*propyl ether gave 25 g with m. p. 74—76°. The pure substance had m. p. 76—77°, $[\alpha]_D^{20}$ —67° (*c* 0.8 in chloroform). (Found: C 64.60; H 6.13; O 29.04. Calc. for $C_{12}H_{14}O_4$: C 64.85; H 6.35; O 28.80.)

Benzyl 4-O-methyl-2,3-anhydro-β-D-ribopyranoside, V. Benzyl 2,3-anhydro-β-D-ribopyranoside (25 g) was methylated with methyl iodide (38 ml) and silver oxide

At a composition $ZrSn_{0.4}$, the Guinier powder pattern photograph showed, in addition to the pattern of the defective Zr_5Sn_3, a number of strong, extra lines. Assuming a cubic unit cell, these extra lines could be indexed with $a = 5.634$ Å. The structure was found to be of the well-known β-wolfram structure type and should thus be given the formula Zr_3Sn.

Acknowledgements. The authors are much indebted to Dr. Arne Magnéli for valuable discussion and his continuing interest in this work.

1. Mc Phersson, D. J. and Hansen, M. *Trans. Am. Soc. Metals* **45** (1953) 915.
2. Nowotny, H. and Schachner, H. *Monatsh.* **84** (1953) 169.

Received May 16, 1960.

Synthesis of Benzyl 4-*O*-Methyl-β-D-Xylopyranoside

PER J. GAREGG

Svenska Träforskningsinstitutet, Träkemiska avdelningen, Stockholm Ö, Sweden

Previous studies of a naturally occurring acetylated xylan [1] in birch wood have raised the question of whether the *O*-acetyl groups are attached to the most readily acetylated free hydroxyl groups in the β-1,4-linked anhydroxylose chains. In an attempt to investigate which of the two free hydroxyl groups at the 2- and 3-position is the most readily acetylated, benzyl 4-*O*-methyl-β-D-xylopyranoside was selected as a suitable model for partial acetylation. The synthesis of this substance, by a sequence of reactions given below is analogous to that described by Hough and Jones [2] for the synthesis of the corresponding methyl glycoside, is reported in the present paper. The final product and all the intermediates were obtained in a crystalline form and the overall yield from D-arabinose was 10 % of the theoretical.

Experimental. All melting points are corrected. Evaporations were done under reduced pressure at a bath temperature below 40°.

Benzyl 3,4-isopropylidene-2-tosyl-β-D-arabinopyranoside, II. Benzyl-3,4-*iso*propylidene-β-D-arabinopyranoside (81 g, m. p. 55—57°, $[\alpha]_D^{20}$ —195°), prepared from 100 g D-arabinose according to Ballou [3] was dissolved in pyridine (500 ml) and treated with *p*-toluenesulphonyl chloride (112 g). The solution was allowed to stand at room temperature during 48 h and then poured on ice. The mixture was extracted with chloroform and the chloroform solution was dried over anhydrous sodium sulphate, filtered and concentrated to dryness. The syrup obtained was used directly in the next step; a small quantity which was set aside crystallised from 96 % aqueous ethanol, m.p. 62—64° unchanged on further recrystallisation, $[\alpha]_D^{20}$ —194° (*c* 1.0 in chloroform). (Found: C 61.14; H 5.96; O 26.20; S 6.84. Calc. for $C_{22}H_{26}O_7S$: C 60.81, H 6.03; O 26.78; S 7.38.)

Benzyl 2-tosyl-β-D-arabinopyranoside, III. The above product was dissolved in boiling acetone (900 ml) and 0.1 N formic acid (1 800 ml) was added over a period of 20 h under reflux. Concentration yielded a syrup which crystallised from aqueous ethanol. Recrystallisation from ethanol/*iso*propyl ether yielded benzyl 2-tosyl-β-D-arabinopyranoside (70 g) with m. p. 120—123°. The pure substance had m. p. 123.5—124.5°, $[\alpha]_D^{20}$ —156° (*c* 0.8 in chloroform). (Found: C 57.40; H 5.52; O 27.94; S 7.88. Calc. for $C_{19}H_{22}O_7S$: C 57.86; H 5.62; O 28.39: S 8.13.)

Benzyl 2,3-anhydro-β-D-ribopyranoside, IV. Benzyl 2-tosyl-β-D-arabinopyranoside (70 g) was dissolved in methanolic sodium methoxide (1 l, made from 13 g sodium) and allowed to stand overnight. The solution was diluted with water (500 ml) and neutralised with sulphuric acid, the methanol was removed by vacuum distillation and the aqueous solution was extracted with chloroform. The combined chloroform solutions were dried over anhydrous sodium sulphate, filtered and the filtrate was concentrated to dryness. Spontaneous crystallisation occurred giving benzyl 2,3-anhydro-β-D-ribopyranoside (29 g) with m. p. 64—76°. Recrystallisation from *iso*propyl ether gave 25 g with m. p. 74—76°. The pure substance had m. p. 76—77°, $[\alpha]_D^{20}$ —67° (*c* 0.8 in chloroform). (Found: C 64.60; H 6.13; O 29.04. Calc. for $C_{12}H_{14}O_4$: C 64.85; H 6.35; O 28.80.)

Benzyl 4-O-methyl-2,3-anhydro-β-D-ribopyranoside, V. Benzyl 2,3-anhydro-β-D-ribopyranoside (25 g) was methylated with methyl iodide (38 ml) and silver oxide

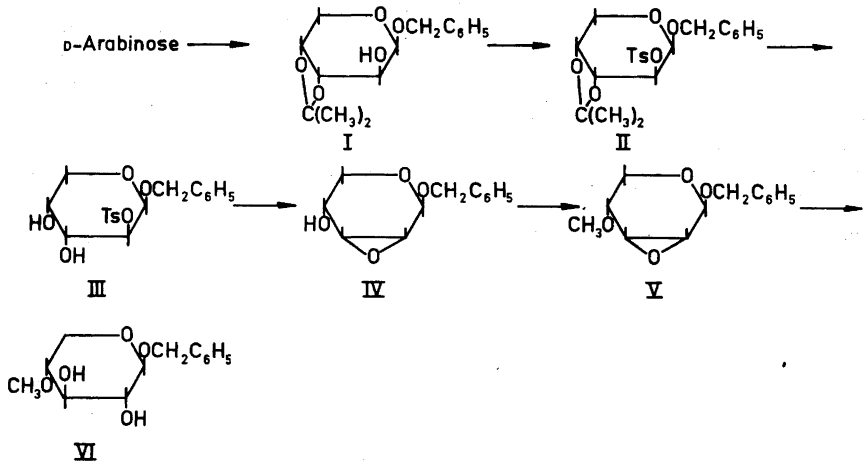

(30 g) in dimethyl formamide (500 ml) according to the method described by Kuhn *et al.*[4] and worked up as described by Bouveng [5]. The product crystallised spontaneously on concentrating a chloroform solution. Recrystallisation from ligroin yielded benzyl 4-*O*-methyl-2,3-anhydro-β-D-ribopyranoside (23 g), m. p. 84—100° and a further recrystallisation yielded 21 g, m. p. 97—99°. The pure substance had m. p. 98—100°, $[\alpha]_D^{20}$ −19° (*c* 1.0 in chloroform). (Found: C 65.73; H 6.86; O 27.76. Calc. for $C_{13}H_{16}O_4$: C 66.08; H 6.83; O 27.09.)

Benzyl 4-O-methyl-β-D-xylopyranoside, VI. Benzyl 4-*O*-methyl-2,3-anhydro-β-D-ribopyranoside (21 g) was heated in 5 % aqueous sodium hydroxide (1.5 l) in a boiling water bath for 60 h, cooled and neutralised with sulphuric acid. The aqueous solution was extracted exhaustively with chloroform, the combined chloroform solutions were dried over sodium sulphate, filtered and concentrated to dryness when spontaneous crystallisation occurred yielding crude benzyl 4-*O*-methyl-β-D-xylopyranoside (21 g) with m. p. 69—77°. Recrystallisation from *iso*propyl ether gave 17 g, m. p. 74—77°. The pure substance had m. p. 77.5—78°, $[\alpha]_D^{20}$ −106° (*c* 0.9 in chloroform). (Found: 61.13; H 7.22; O 31.59. Calc. for $C_{13}H_{18}O_5$: C 61.40; H 7.13; O 31.46.)

Acknowledgement. The author wishes to express his gratitude to Professor Bengt Lindberg for his interest and helpful advice.

1. Bouveng, H. O., Garegg, P. J. and Lindberg, B. *Acta Chem. Scand.* **14** (1960) 742.
2. Hough, L. and Jones, J. K. N. *J. Chem. Soc* **1952** 4349.
3. Ballou, C. E. *J. Am. Chem. Soc.* **78** (1957) 165.
4. Kuhn, R., Trischmann, H. and Löw, I. *Angew. Chem.* **67** (1955) 32.
5. Bouveng, H. O. *Acta Chem. Scand.* **12** (1958) 1977.

Received May 18, 1960.

Mean Amplitudes of Vibration of *Cyclo*propane from Electron Diffraction and Spectroscopic Calculations

A. ALMENNINGEN, O. BASTIANSEN, S. J. CYVIN and P. N. SKANCKE

Universitetets kjemiske institutt, Blindern; Institutt for teoretisk kjemi, Norges tekniske høgskole, Trondheim, Norway

In a previous work [1] values for the mean amplitudes of vibration (u) for the bond distances of *cyclo*propane were reported. The values were obtained a) from electron diffraction studies of the molecule in the gaseous state and b) from theoretical computations based upon spectroscopic data. The values reported were obtained using approximation calculations. In the present work a more rigorous calculation has been carried out using the same two methods.

Electron diffraction calculations. New u values for the bond distances and for the non-bonded C—H distance have been calculated. The following procedures were used: 1. Approximating the radial distribution curves with sums of Gaussian peaks. 2. Using least squares calculations on the intensity curve. 3. Studying the areas under the sinusoidal curve for the outer part of the intensity curve. The last procedure leads to the determination of the u value for the C—C distance. It was found advisable to study the u value for the C—H distances after the subtraction of the contribution from the C—C distance. Attempts were made to determine the error limits of the u value determination. The results of these studies are presented in the last column of Table 1. The resulting u value for C—C is a trifle larger than that obtained earlier. The error estimations indicate that the earlier rough evaluation of the accuracy of the u value for the C—H bond was a little too optimistic.

Spectroscopic calculations. While an electron diffraction study is unable to determine the u values of the H—H distances with any reasonable accuracy, calculations from spectroscopic data yield useful values for all six amplitudes of vibration associated with the various interatomic distances of the *cyclo*propane molecule. The results of the spectroscopic calculations are given in Table 1 computed both for the zero point and for 298°K.

Table 1. Mean amplitudes of vibration (u) in Å units.

Atom pair	u spectroscopic $T = 0$	298°K	u electr. diff.
C—H	0.0750	0.0750	0.0753 ±0.0030
C...H	0.1082	0.1090	0.108 ±0.0030
C—C	0.0510	0.0514	0.0497 ±0.0015
$H_1...H_1'$	0.1180	0.1181	
$H_1...H_2$	0.1758	0.1783	
$H_1...H_2'$	0.1316	0.1320	

The spectroscopic computation is summarized in the following: (For further details of the theory, see *e. g.* Morino *et al.*[2] and Cyvin [3].)

Let Δr_i represent the interatomic displacements for the six types of (bonded and non-bonded) atom pairs ($i = 1, 2, ..., 6$). If the matrix P is formed according to $P_{ij} = \langle \Delta r_i \Delta r_j \rangle$, the mean-square amplitudes of vibration (u^2) will appear on its main diagonal. One has

$$P = K \langle Q^2 \rangle \widetilde{K} \qquad (1)$$

where $\langle Q^2 \rangle$ is a diagonal matrix with the elements $\langle Q^2 \rangle_k = (h/8\pi^2\nu_k) \coth (h\nu_k/2kT)$,[2] and K is the transformation matrix given by $r = KQ$. Here r represents the Δr_i coordinates and Q the vibrational normal coordinates. The K matrix may be computed according to

$$K = VL \qquad (2)$$

The L matrix ($S = LQ$, where S denotes a set of symmetry coordinates) is obtainable by a normal coordinate analysis [4] if the force constants and the equilibrium parameters are known. The V matrix is defined by $r = VS$ and may be obtained from geometrical considerations.

The mean-square amplitude matrix Σ is defined by $\Sigma_{ij} = \langle S_i S_j \rangle$, where S_i and S_j are symmetry coordinates. For this matrix one has

$$\Sigma = L \langle Q^2 \rangle \widetilde{L} \qquad (3)$$

An alternative method of computing the u^2 values may be applied, according to the relation

$$P = V \Sigma \widetilde{V} \qquad (4)$$

from which the u^2 quantities may be expressed in terms of the a matrix elements. The relation (4) is deducible from eqns. (1)–(3).

In the present case a set of force constants for *cyclo*propane has been established [5] by means of vibrational frequencies taken from literature [6] for both C_3H_6 and C_3D_6. For the numerical L matrix elements, see Ref.[5] One of the writers (S. J. Cyvin) intends to give some details of the theory of mean-square amplitude matrices applied to the *cyclo*propane molecule in a coming publication.

1. Bastiansen, O. and Cyvin, S. J. *Acta Chem. Scand.* **11** (1957) 1789.
2. Morino, Y., Kuchitsu, K. and Shimanouchi, T. *J. Chem. Phys.* **20** (1952) 726; Morino, Y., Kuchitsu, K., Takahashi, A. and Maeda, K. *J. Chem. Phys.* **21** (1953) 1927.
3. Cyvin, S. J. *Acta Chem. Scand.* **11** (1957) 1499; *J. Chem. Phys.* **29** (1958) 583; *Spectrochim. Acta* **15** (1959) 828.
4. Wilson, E. B., Jr. *J. Chem. Phys.* **7** (1939) 1047; *J. Chem. Phys.* **9** (1941) 76.
5. Cyvin, S. J. *Spectrochim. Acta. In press.*
6. Baker, A. W. and Lord, R. C. *J. Chem. Phys.* **23** (1955) 1636; Mathai, P. M., Shepherd, G. G. and Welsh, H. L. *Can. J. Phys.* **34** (1956) 1448.

Received May 16, 1956.

A Note on the Crystal Structure of Sodium Dimolybdate

INGVAR LINDQVIST

Institute of Chemistry, University of Uppsala, Uppsala, Sweden

About ten years ago the present author carried out a series of structure determinations of polymolybdates, polytungstates, polyniobates and polytantalates. In most cases the proposed oxygen co-ordination around the heavy atoms was supported by some evidence of vectors in the three-dimensional Patterson functions. There were, however, two exceptional cases with very weak or no evidence at all for the oxygen positions which were assumed from spatial discussions. In one of these cases, $MoO_3 \cdot 2\ H_2O$, the presence of a complicated superstructure has later been shown [1].

The other case is sodium dimolybdate [2]. The molybdenum positions were conclusively derived but the oxygen co-ordination proposed was based on the assumption that the co-ordination around the molybdenum atoms should be either tetrahedral or octahedral. As the resulting structure exhibited an interesting mixed co-ordination an attempt has been made to derive the oxygen positions directly from the three-dimensional Patterson function using the Buerger minimum function [3].

This derivation has confirmed the structural suggestion of the earlier paper. The positions of the oxygen and sodium atoms are, however, shifted to some extent. The old data do not permit a refinement with modern methods and the atomic positions are therefore still very uncertain. The following rough parameters give a R value of 0.17 (the old parameters within brackets):

8 Mo_I	in	8 (*e*)	: $x = 0.25$		
8 Mo_{II}	in	8 (*f*)	: $x = 0.00$		
8 Na_I	in	8 (*d*)	: $x = 0.25$		
8 Na_{II}	in	8 (*f*)	: $x = 0.00$		
16 O_I	in	16 (*g*)	: $x = 0.18$	(0.21)	
16 O_{II}	in	16 (*g*)	: $x = 0.18$	(0.21)	
8 O_{III}	in	8 (*f*)	: $x = 0.00$		
8 O_{IV}	in	8 (*f*)	: $x = 0.00$		
8 O_V	in	8 (*f*)	: $x = 0.00$		

$y = 0.08$		$z = 0.25$	
$y = 0.25$		$z = 0.08$	
$y = 0.00$		$z = 0.00$	
$y = 0.31$	(0.36)	$z = 0.36$	(0.30)
$y = 0.22$	(0.21)	$z = 0.17$	(0.16)
$y = 0.48$	(0.49)	$z = 0.33$	(0.34)
$y = 0.11$	(0.08)	$z = 0.28$	(0.27)
$y = 0.38$	(0.41)	$z = 0.02$	(0.13)
$y = 0.37$	(0.35)	$z = 0.52$	(0.49)

The proposed mixed tetrahedral and octahedral co-ordination around the molybdenum atoms can be considered as strongly supported by this result. The relatively low R value by no means proves, however, that the atomic positions are well determined, as the contributions from the Mo atoms are too dominating. A further discussion of the bond lengths on the basis of these rough parameters therefore cannot be recommended.

1. Lindqvist, I. *Acta Chem. Scand.* **10** (1956) 1362.
2. Lindqvist, I. *Acta Chem. Scand.* **4** (1950) 1066.
3. Buerger, M. J. *Vector Space*, Wiley, New York 1959.

Received May 30, 1960.

from which the u^2 quantities may be expressed in terms of the a matrix elements. The relation (4) is deducible from eqns. (1)–(3).

In the present case a set of force constants for *cyclo*propane has been established [5] by means of vibrational frequencies taken from literature [6] for both C_3H_6 and C_3D_6. For the numerical L matrix elements, see Ref.[5] One of the writers (S. J. Cyvin) intends to give some details of the theory of mean-square amplitude matrices applied to the *cyclo*propane molecule in a coming publication.

1. Bastiansen, O. and Cyvin, S. J. *Acta Chem. Scand.* **11** (1957) 1789.
2. Morino, Y., Kuchitsu, K. and Shimanouchi, T. *J. Chem. Phys.* **20** (1952) 726; Morino, Y., Kuchitsu, K., Takahashi, A. and Maeda, K. *J. Chem. Phys.* **21** (1953) 1927.
3. Cyvin, S. J. *Acta Chem. Scand.* **11** (1957) 1499; *J. Chem. Phys.* **29** (1958) 583; *Spectrochim. Acta* **15** (1959) 828.
4. Wilson, E. B., Jr. *J. Chem. Phys.* **7** (1939) 1047; *J. Chem. Phys.* **9** (1941) 76.
5. Cyvin, S. J. *Spectrochim. Acta. In press.*
6. Baker, A. W. and Lord, R. C. *J. Chem. Phys.* **23** (1955) 1636; Mathai, P. M., Shepherd, G. G. and Welsh, H. L. *Can. J. Phys.* **34** (1956) 1448.

Received May 16, 1956.

A Note on the Crystal Structure of Sodium Dimolybdate

INGVAR LINDQVIST

Institute of Chemistry, University of Uppsala, Uppsala, Sweden

About ten years ago the present author carried out a series of structure determinations of polymolybdates, polytungstates, polyniobates and polytantalates. In most cases the proposed oxygen co-ordination around the heavy atoms was supported by some evidence of vectors in the three-dimensional Patterson functions. There were, however, two exceptional cases with very weak or no evidence at all for the oxygen positions which were assumed from spatial discussions. In one of these cases, $MoO_3 \cdot 2\ H_2O$, the presence of a complicated superstructure has later been shown [1].

The other case is sodium dimolybdate [2]. The molybdenum positions were conclusively derived but the oxygen co-ordination proposed was based on the assumption that the co-ordination around the molybdenum atoms should be either tetrahedral or octahedral. As the resulting structure exhibited an interesting mixed co-ordination an attempt has been made to derive the oxygen positions directly from the three-dimensional Patterson function using the Buerger minimum function [3].

This derivation has confirmed the structural suggestion of the earlier paper. The positions of the oxygen and sodium atoms are, however, shifted to some extent. The old data do not permit a refinement with modern methods and the atomic positions are therefore still very uncertain. The following rough parameters give a R value of 0.17 (the old parameters within brackets):

8 Mo_I	in	8 (*e*)	: $x = 0.25$		
8 Mo_{II}	in	8 (*f*)	: $x = 0.00$		
8 Na_I	in	8 (*d*)	: $x = 0.25$		
8 Na_{II}	in	8 (*f*)	: $x = 0.00$		
16 O_I	in	16 (*g*)	: $x = 0.18$	(0.21)	
16 O_{II}	in	16 (*g*)	: $x = 0.18$	(0.21)	
8 O_{III}	in	8 (*f*)	: $x = 0.00$		
8 O_{IV}	in	8 (*f*)	: $x = 0.00$		
8 O_V	in	8 (*f*)	: $x = 0.00$		

$y = 0.08$		$z = 0.25$	
$y = 0.25$		$z = 0.08$	
$y = 0.00$		$z = 0.00$	
$y = 0.31$	(0.36)	$z = 0.36$	(0.30)
$y = 0.22$	(0.21)	$z = 0.17$	(0.16)
$y = 0.48$	(0.49)	$z = 0.33$	(0.34)
$y = 0.11$	(0.08)	$z = 0.28$	(0.27)
$y = 0.38$	(0.41)	$z = 0.02$	(0.13)
$y = 0.37$	(0.35)	$z = 0.52$	(0.49)

The proposed mixed tetrahedral and octahedral co-ordination around the molybdenum atoms can be considered as strongly supported by this result. The relatively low R value by no means proves, however, that the atomic positions are well determined, as the contributions from the Mo atoms are too dominating. A further discussion of the bond lengths on the basis of these rough parameters therefore cannot be recommended.

1. Lindqvist, I. *Acta Chem. Scand.* **10** (1956) 1362.
2. Lindqvist, I. *Acta Chem. Scand.* **4** (1950) 1066.
3. Buerger, M. J. *Vector Space*, Wiley, New York 1959.

Received May 30, 1960.

Amino Acid Studies. Part III *. Synthesis and Properties of some Isomerides of Albizziine

ANDERS KJÆR AND ELSE VESTERAGER

Organic Chemical Laboratory, Royal Veterinary and Agricultural College, Copenhagen V, Denmark

In a previous paper of this series [1], syntheses were described of L- and DL-albizziine (2-amino-3-ureidopropionic acid), as well as of L-2-ureido-3-aminopropionic acid (L-*iso*albizziine). It is the purpose of the present communication to report on the preparation and physical data of the isomeric compounds: D-albizziine, D-*iso*albizziine and DL-*iso*albizziine.

D-Asparagine was transformed into N-(*p*-toluenesulphonyl)-D-asparagine (I, Ts = *p*-$CH_3C_6H_4SO_2$) by a modification of the procedure employed in the L-series by Zaoral and Rudinger [2]. Hofmann-degradation of the latter compound, conducted according to Rudinger *et al.*[3], afforded D-2-(*p*-toluenesulphonamido)-3-aminopropionic acid (II) which was further converted into D-2-(*p*-toluenesulphonamido)-3-ureidopropionic acid (III) and thence to D-albizziine (IV) as described for the enantiomeric series by the same authors [3].

Detosylation of (II) afforded optically pure D-2,3-diaminopropionic acid, (V), which was converted into D-*iso*albizziine, (VIII), through the steps (VI) and (VII), according to the procedure utilized in this laboratory for the preparation of L-*iso*albizziine [1]. A similar sequence of reactions, starting from DL-2,3-diaminopropionic acid, yielded racemic *iso*albizziine. Synthetic D-albizziine, (IV), and D-*iso*albizziine, (VIII), as well as all intermediate products, possessed specific rotations similar in magnitude but opposite in sign to those of the L-series. Likewise, the infra-red spectra determined in the solid state coincided for the individual enantiomers throughout the two series, whereas the corresponding racemic modifications showed considerable deviations in their IR-patterns.

Results of some microbiological studies of the synthetic amino acids will be presented elsewhere.

Experimental. N-(p-Toluenesulphonyl)-D-asparagine (I). Several trial runs indicated that the tosylation of asparagine proceeded more satisfactorily than formerly described [2], when the following conditions were employed. In the course of 3 h, a total of 9.5 g of *p*-toluenesulphonyl chloride was added portionwise to a vigorously stirred and ice-cooled suspension of D-asparagine * (5.0 g) and magnesium oxide (5.0 g) in water (100 ml). The suspension was stirred overnight at room temperature, cooled in ice, and then acidified with conc. hydrochloric acid. The precipitate was filtered off and thoroughly extracted with ether. Practically pure N-(*p*-toluenesulphonyl)-D-asparagine (I) remained in a yield of 91 % (8.6 g). The product was recrystallized from methanol (175 ml) to give 6.5 g of pure material, m.p. 182° **, $[\alpha]_D^{22}$ −10.7° (*c* 2, H_2O, containing 1 equiv. of NaOH, pH 6.6) ***.

(Found: C 46.20; H 5.03; N 9.63. Calc. for $C_{11}H_{14}N_2O_5S$: C 46.14; H 4.93; N 9.79.) Reported for the enanti-omeric L-compound: m. p. 175°[4], 191°[2]; $[\alpha]_D^{20}$ +6.8° (K-salt in H_2O)[4]; $[\alpha]_D^{20}$ +9.7° ± 0.5° (*c* 5.4, H_2O + 1 equiv.KOH).

D-2-(p-Toluenesulphonamido)-3-aminopropionic acid (II). The Hofmann-degradation of N-tosyl-D-asparagine was performed essentially as described for the L-enantiomer [3], yet in somewhat smaller yields (*ca.* 50 %) than reported [3] (60 %). A pure specimen of D-2-(*p*-toluenesulphonamido)-3-aminopropionic acid hemihydrate (*cf.* Ref.[3]) was obtained on repeated recrystallizations from water, m. p. 200°, $[\alpha]_D^{22}$ −19.6° (*c* 2.5, 5 N HCl). (Found: C 44.85; H 5.60; N 10.38. Calc. for $C_{10}H_{14}N_2O_4S$, 0.5 H_2O: C 44.93; H 5.66;

* Part II: *Acta Chem. Scand.* **13** (1959) 1565.

* Purchased through *California Corporation for Biochemical Research*, Los Angeles, U.S.A.

** All melting points are uncorrected and determined in capillary tubes in an Anschütz-Hershberg apparatus, with a rate of heating of about 1° per minute near the melting points. For most compounds in the present series these are decomposition temperatures, highly dependent on the rate of heating, as has been pointed out also by other authors [2,3].

*** This rotation is quite dependent on pH-values. Thus, for the L-isomeride we found the following $[\alpha]_D^{25}$- values at *c* = 1.7; + 9.3° to + 9.8° at pH 5.3 to 9.3, + 5.5° at pH 10.3, and −3.2° at pH 11.2.

N 10.48.) A specimen of the corresponding L-isomeride, prepared in this laboratory by exactly the same procedure, had m. p. 200° and $[\alpha]_D^{22}$ +19.9° (*c* 2.5, 5 N HCl). Reported for the L-compound [3]: m. p. 225–226° (capillary, corr.) and 214–216° (decomp. Kofler-block) *, $[\alpha]_D^{22}$ +16.5° ± 0.8° (*c* 2.4, 5 N HCl) (anhydrous specimen).

D-*2-(p-Toluenesulphonamido)-3-ureidopropionic acid* (III). This compound was prepared as described for the L-isomer [3], yet in slightly lower yield. An analytical specimen (from water) had m. p. 169–170°, and $[\alpha]_D^{22}$ −15.8° (*c* 1, 96 % EtOH). (Found: C 43.70; H 5.12; N 13.80. Calc. for $C_{11}H_{15}N_3O_5S$: C 43.84; H 5.02; N 13.95.) Reported value for the enantiomer: m. p. 174–179° (decomp. Kofler-block), (no rotation reported).

D-*Albizziine* (IV). Again, the procedure employed in the L-series for detosylation [3] was followed, except that 6 h in stead of 36 h was found sufficient for complete reaction. A specimen for analysis was obtained by three recrystallizations of the crude product from aqueous ethanol, m. p. 202–205°, the same as that of natural L-albizziine when determined in the same bath. $[\alpha]_D^{24}$ +65.5° (*c* 1.7, H_2O), (Found: C 32.55; H 6.17; N 28.72. Calc. for $C_4H_9N_3O_3$: C 32.65; H 6.17; N 28.56.)

D-*2,3-Diaminopropionic acid* (V). In order to remove the tosyl-grouping from 2-N-tosyl-D-diaminopropionic acid (II), the latter (3.75 g) was heated at 70° for 6 h in a 35 % solution of anhydrous hydrogen bromide in glacial acetic acid (70 ml) containing phenol (4 g), conditions similar to those employed by Poduška *et al.*[5] in the detosylation of glycyl-peptides of diaminopropionic acid. Addition of anhydrous ether to the reaction mixture caused the hydrobromide of (V) (3.5 g) to separate as colourless crystals. The salt was purified by dissolving in water and addition of alcohol, to give a pure product (1.70 g), m. p. *ca.* 240°, $[\alpha]_D^{21}$ −17.3° (*c* 2, 1 N HCl). Reported rotation for D-2,3-diaminopropionic acid hydrochloride: $[\alpha]_D^{25}$ −25.2° (*c* 2, 1 N HCl) [6]. With due corrections for the different anions, this value suggested that partial racemization had occurred during the detosylation reaction, conceivably analogous to the recently demonstrated hydrogen bromide-induced racemization of L-diaminopropionic acid in aqueous solution [1]. That this was not the case, however, was proved by transforming an optically pure sample of L-diaminopropionic acid hydrochloride, $[\alpha]_D^{24}$ +25.0° (*c* 4.7, 1 N HCl or 1 N HBr), by means of an ion exchange column, into the corresponding hydrobromide with the rotation $[\alpha]_D^{21}$ +17.4° (*c* 2, 1 N HCl or 1 N HBr), comparable to that of the antipode described above. Reconversion of the hydrobromide into the hydrochloride afforded material with unchanged rotation (+25.3°).

D-*2-Amino-3-benzyloxycarbamidopropionic acid* (VI). D-2,3-Diaminopropionic acid hydrobromide was subjected to carbobenzoxylation in 84 % yield (crude product) as described for the L-acid [1], with the sole modification that four times as much water was used in order to bring the less soluble hydrobromide into solution. A specimen for analysis was produced by two recrystallizations from hot water, m. p. 225°, $[\alpha]_D^{24}$ +15.9° (*c* 1, 1 N HCl). (Found: C 55.65; H 6.00; N 11.82. Calc. for $C_{11}H_{12}N_2O_4$: C 55.45; H 5.92; N 11.76). Reported for the L-enantiomer [1]: m. p. 227–229°, $[\alpha]_D^{21}$ −18.7° (*c* 1, 1 N HCl).

D-*2-Ureido-3-benzyloxycarbamidopropionic acid* (VII). This compound was synthesized according to the directions previously given for the L-isomer [1]. An analytical specimen separated from water in colourless needles, m. p. 190–191°, $[\alpha]_D^{22}$ −4.7° (*c* 1, dimethylformamide). (Found: C 51.10; H 5.34; N 14.79. Calc. for $C_{12}H_{15}N_3O_5$: C 51.24; H 5.38; N 14.94). The formerly described L-isomeride [1], m. p. 188–190°, had the rotation $[\alpha]_D^{22}$ +5.2° (*c* 1, dimethylformamide).

D-*Isoalbizziin* (VIII). Hydrogenolysis of (VII), performed as described in the L-series [1], yielded D-*iso*albizziin, m. p. 204°, $[\alpha]_D^{22}$ +44.6° (*c* 1, 0.1 N HCl). (Found: C 32.30; H 6.09; N 28.48. Calc. for $C_4H_9N_3O_3$: C 32.65; H 6.17; N 28.56.) Reported values for the L-isomeride[1]: m. p. 204–210°, $[\alpha]_D^{25}$ −43° (*c* 1, 1 N HCl.)

DL-*2,3-Diaminopropionic acid.* This racemic amino acid was conveniently synthesized by the method of Hellmann and Haas [7] with a few modifications. Thus, *diethyl benzamidomethyl-acetamidomalonate*, synthesized from

* For a specimen of this hemihydrate, kindly furnished by Dr. Rudinger, we found the m. p. 200°, when determined in the same bath as our D-isomer. The two compounds furthermore had identical IR-spectra.

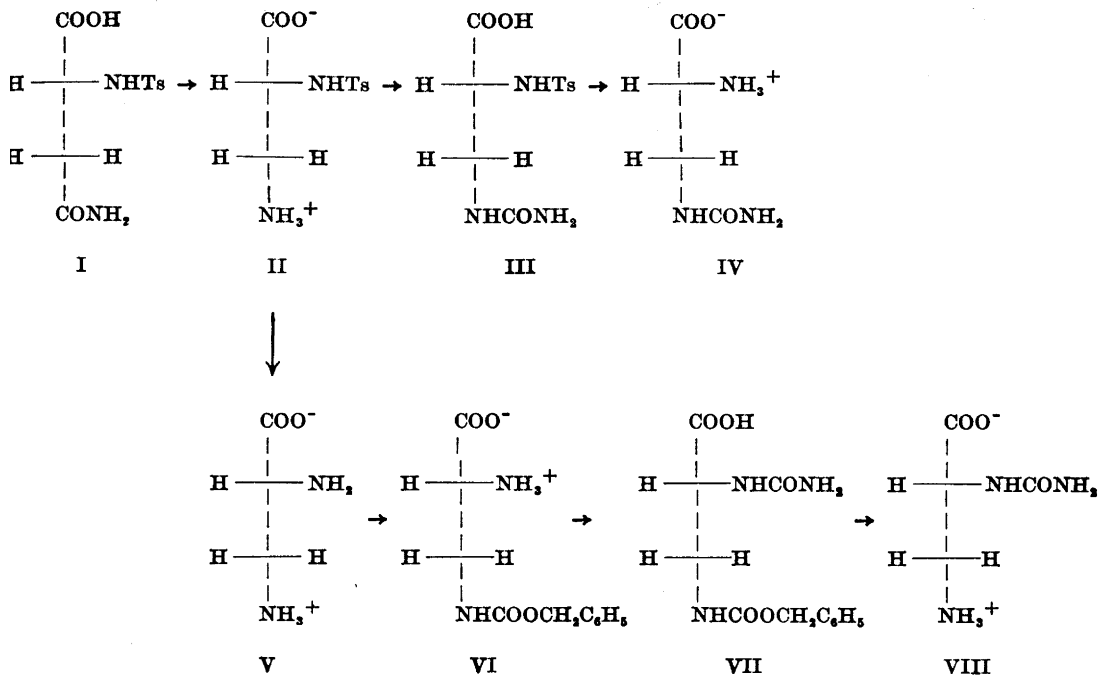

N,N-dimethylaminomethylbenzamide[7] and ethyl acetamidomalonate[8], (m. p. 149—150°, from toluene). (Found: C 57.85; H 6.13; N 7.84. Calc. for $C_{17}H_{22}N_2O_6$: C 58.27; H 6.33; N 8.00), was used in stead of the dimethyl ester formerly employed[7]. Furthermore, boiling xylene was found preferable to toluene as a solvent for the condensation reaction. Racemic diaminopropionic acid hydrobromide was obtained from the ester upon hydrolysis with hydrogen bromide (83 % yield), m. p. 240° (decomp.).

DL - *2 - Amino - 3 - benzyloxycarbamidopropionic acid.* Upon carbobenzoxylation under the same conditions as employed in the optically active series, DL-2,3-diaminopropionic acid afforded DL-2-amino-3-benzyloxycarbamidopropionic acid in 70 % yield. An analytical sample (from water) had the m. p. 241° (Found: C 55.20; H 5.87; N 11.86).

DL - *2 Ureido - 3 - benzyloxycarbamidopropionic acid.* Again, conversion of the above acid into the ureidoacid was performed as described in the L-series [1] to give a 70 % yield of crude reaction product, which was recrystallized twice from water before analysis, m. p. 186°. (Found: C 51.20; H 5.35; N 14.70).

DL-*Isoalbizziin.* Decarbobenzoxylation of the foregoing acid in the customary way [1] afforded racemic *iso*albizziin which was recrystallized twice from water before analysis, m. p. 201°; the racemate was considerably less soluble in water than the optically active forms. (Found: C 32.25; H 6.05; N 28.32).

The authors are grateful to Dr. Rudinger for advance information on the synthesis of L-albizziine. The technical assistance of Mrs. E. Kläning is acknowledged. Microanalyses were performed by Mr. P. Hansen at the Chemical Laboratory of the University of Copenhagen.

Grants from *The Research Council of The Technical Sciences. (Det Teknisk-Videnskabelige Forskningsråd)* and *The Carlsberg Foundation Stipendium for The Royal Veterinary and Agricultural College (Carlsbergfondets Legat for Den. Kgl. Veterinær- og Landbohøjskole)* for the acquisition of infra-red and potentiometric equipment, respectively, are gratefully acknowledged.

1. Kjær, A. and Olesen Larsen, P. *Acta Chem. Scand.* **13** (1959) 1565.
2. Zaoral, M. and Rudinger, J. *Collection Czechoslov. Chem. Communs.* **24** (1959) 1993.
3. Rudinger, J., Poduška, K. and Zaoral, M. *Collection Czechoslov. Chem. Communs.* **25** (1960) 2022.
4. Berlingozzi, S. *Gazz. chim. ital.* **57** (1927) 814.
5. Poduška, K., Rudinger, J. and Šorm, F. *Collection Czechoslov. Chem. Communs.* **20** (1955) 1174.
6. Birnbaum, S. M., Koegel, R. J., Fu, S-C. J. and Greenstein, J. P. *J. Biol. Chem.* **198** (1952) 335.
7. Hellmann, H. and Haas, G. *Chem. Ber.* **90** (1957) 1357.
8. Shaw, K. N. F. and Nolan, C. *J. Org. Chem.* **22** (1957) 1668.

Received May 25, 1960.

ACTA CHEMICA SCANDINAVICA 14 (1960) 965–968

A New Sensitive Reagent for Uranium

1-(2-Thiazolylazo)-*m*-dimethylaminophenol (TAM). Application to the Assay of Rocks and Solutions Low in Uranium

EMIL SØRENSEN

Danish Atomic Energy Commission, Research Establishment, Risø, Denmark

A simple analytical method for uranium is presented. It is based on the extraction of uranyl nitrate with methyl *iso*butyl ketone from a sample solution saturated with aluminium nitrate. An intensely coloured complex is formed *in situ* by addition of the reagent 1-(2-thiazolylazo)-*m*-dimethylaminophenol. The uranium content can be determined spectrophotometrically with a sensitivity of about 0.1 μg.

During the investigation of uranium-bearing rocks from southern Greenland the search for easy-handled, sensitive analytical methods was a major point.

A considerable work has been done with a modification of the dibenzoylmethane method by Booman, Maeck, Elliott and Rein [1]. Its principle is that uranyl nitrate is extracted into methyl *iso*butyl ketone (hexone) from a solution saturated with aluminium nitrate. Colour development is made *in situ* by the addition of dibenzoylmethane in pyridine. The lower level of detection is 0.5 μg of uranium. The new method takes its origin in a paper by Spinner and Miller [2]. These authors have determined uranium in thorium process solutions by means of 1-(2-pyridylazo)-2-naphthol (PAN) which forms an intensely coloured uranium complex.

In this laboratory Skytte Jensen has for other purposes prepared a series of dyes on the basis of 2-aminothiazol [3]. Among these the compound 1-(2-thiazolylazo)-2-naphthol (TAN) has been tried as a reagent for uranium and proved useful. However, previous experience suggested that the introduction of a dimethylamino-group in the molecule would intensify the colour. This led to the synthesis of 1-(2-thiazolylazo)-*m*-dimethylaminophenol (TAM). As shown in Fig. 1, the TAM-uranium chelate has an optical density about 100 % higher than that of the corresponding TAN-compound. Therefore TAM was chosen for the further development of this method.

CHELATE FORMATION

The three dyes mentioned have the formulas

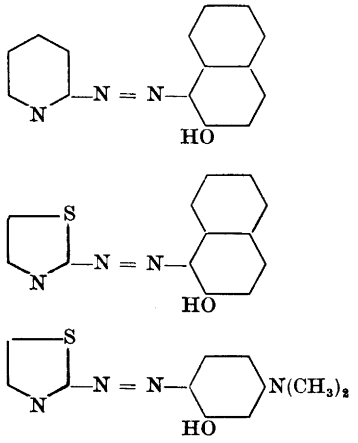

The chelate of TAM with the uranyl ion may be written

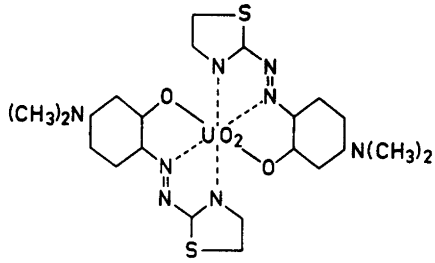

The dye is slightly soluble in water, the uncharged chelate, however, is nearly insoluble. Both are readily dissolved in a variety of organic solvents, *e.g.* hexone.

The colour depends on the composition of the solvent used. To obtain reproduceable results it is recommended to equilibrate the hexone solution with an aqueous buffer. At low pH the chelate will dissociate, and at high pH the uncomplexed dye assumes a colour much like that of the uranium chelate. Thus a pH optimum must exist for the colorimetric measurement of the chelate against a reagent blank. This optimum has been experimentally obtained by using a buffer containing pyridine — pyridinium chloride in the proportion 7 : 1.

EXPERIMENTAL

Reagents: Ammonium hydroxide 12 M. $Al(NO_3)_3$, $9H_2O$, salting agent. $Al(NO_3)_3$-KIO_3 scrub solution. Methyl *iso*butyl ketone (Shell Chemicals). Dye solution: 0.5×10^{-3} M TAM, 4 M pyridine, 0.5 M HCl in H_2O.

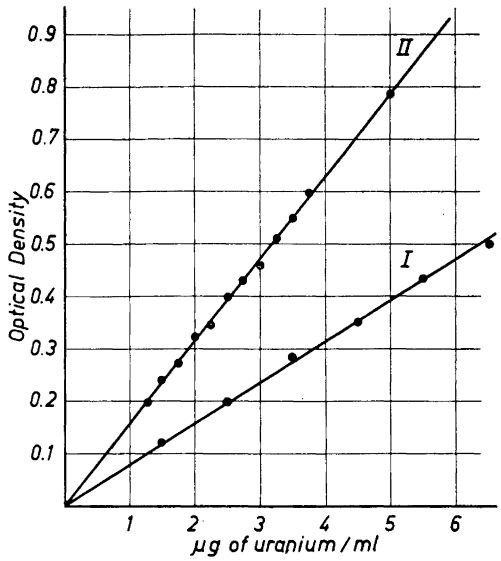

Fig. 1. Standard uranium-optical density curve.

I TAN complex, λ — 585 mμ
II TAM complex, λ — 575 mμ

Aluminium nitrate salting agent: 1 kg of $Al(NO_3)_3$, 9 H_2O (Merck, purum) + 100 ml of H_2O is molten in a beaker and stored in a 1 l two-necked flask. The flask is kept heated on an infrared bath at a temperature just sufficient to prevent crystallization (*ca.* 100°C). One neck is provided with a reflux condenser. The other, allowing for pipetting, is closed with a glass stopper.

$Al(NO_3)_3$-KIO_3-scrub solution. 5.4 g of KIO_3 and 350 g of $Al(NO_3)_3$, $9H_2O$ are dissolved in 250 ml of H_2O. After cooling the specific mass is adjusted to 1.33 g/ml by addition of H_2O or $Al(NO_3)_3$.

Dye solution: 31 mg of TAM are dissolved in 80 ml of pyridine in a 250 ml volumetric flask. About 150 ml of water are added. The mixture is allowed to cool. Then 10.4 ml of conc. HCl are added and the volume is adjusted to the mark with H_2O.

Where not specified, the chemicals used are analytical grade.

Method

Uraniferous rock. In most cases fuming with HF and $HClO_4$ is sufficient to bring the sample in solution. If necessary the fuming may be followed by melting with $NaHSO_4$ without interfering with the extraction procedure. The dissolved sample is oxidized with 2 drops of 6 % H_2O_2 and is neutralized with NH_3 to incipient hydroxide precipitation. Further 0.025 ml of 12 M ammonium hydroxide and 2 ml of salting agent are added per ml of sample solution. After being homogenized by gentle agitation the sample is ready for extraction with hexone of which an amount is taken corresponding to 0.3—1 ml per μg of uranium expected.

It is preferable to carry out the extraction in two stages, proceeding in the following manner: Add exactly half of the hexone to be used, and shake vigorously for 2 min. Centrifuge. Separate in a funnel taking care that the aqueous phase is free from hexone drops. Repeat the operation using the other half of the hexone. Equal volumes from the two extracts are combined and shaken with the scrub solution for 2 min. After complete separation of the phases about 2.5 ml of the organic layer and exactly the same volume of the dye solution are transferred to a small tube with a special pipet arrangement (Fig. 2). They are mixed by gentle agitation for 5 min. (Glass stoppers are used in all

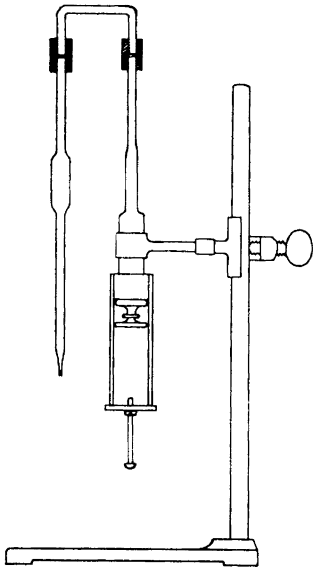

Fig. 2. Syringe with exchangeable pipet.

operations where hexone is involved.) After centrifuging the organic layer is transferred to a 1 cm colorimetric cell and the absorbance is measured at 575 mμ against a reagent blank. The uranium content is read from a standard calibration curve (Fig. 1).

Uranium pregnant liquor. In case of a uranium pregnant liquor the method will be especially applicable for routine work, as the extraction may be carried out in one stage and the scrubbing omitted.

DISCUSSION

The hexone extraction as described here is rather selective for uranium. The most common interfering ions are Ce^{+4}, Fe^{+++} and Th^{+4}. Ce^{+4} is reduced by the H_2O_2-treatment to Ce^{+++}, which is not extracted. Fe^{+++} has a low distribution coefficient but is often present in large concentrations. It is effectively removed by the scrubbing procedure. $Th(NO_3)_4$ is extracted to a considerable extent. However the IO_3^--scrubbing ensures a sufficient low level given by the solubility product of thorium iodate.

Further the two-phase system of chelate formation has an inherent selectivity, as it has been found that only chelates of dipositive metal ions show a definite tendency to be extracted by organic solvents. The calibration curve is a straight line all over the range covered by the spectrophotometer.

The standard deviation of a reading has been estimated to 0.025 μg of uranium per ml.

REFERENCES

1. Booman, G. L., Maeck, W. I., Elliott, M. C. and Rein, I. E. *IDO-14437.*
2. Spinner, I. H. and Miller, F. C. *AECL-789.*
3. Skytte Jensen, B. *Acta Chem. Scand.* **14** (1960) 927.

Received January 29, 1960.

ACTA CHEMICA SCANDINAVICA 14 (1960) 969–978

Outlines of an Optical Method of Measuring Thermal Conductivities of Fluids

OLE LAMM

Institutionen för fysikalisk kemi, Kungl. Tekniska Högskolan, Stockholm 70, Sweden

The relative lack of data on the thermal conductivity of liquids may be ascribed to a certain inconvenience of the methods of measurement in this field. An optical hot wire arrangement is shown to be expedient to an extent, which would hardly have been anticipated. It is necessary to know the change of refractive index with temperature. Many methods, not discussed in this paper, present themselves for this determination.

The analogy between the transport of heat and of matter by diffusion is not limited to the fundamental laws, but also exists in the possibilities of measuring by optical methods. This was very early realized in connection with interference and schlieren observations. Whereas in the field of diffusion and sedimentation [1], electrophoresis [2], and thermodiffusion [3] the practical importance of the optical principles in modern experimental technique is settled, the same cannot, as far as known, be said of thermal conductivity. There is a pronounced need for developments in this latter field, and optical procedures should be investigated besides the electric, thermometric, and calorimetric methods in vogue. The electric arrangement referred to, is especially the "hot wire resistance thermometer" method of Eucken and Englert and of Pfriem [4], which has been the object of a complementary, very careful study in this Institute [5-7]. This is, in part, identical with the Piranie pressure gauge, which is used also for thermal conductivity measurements (von Ubisch[8]). Through all these works, a considerable experience has been won regarding *the state of a liquid or a gas around a vertical hot wire*, characterized by a telescopic symmetry of the convections within certain limits of experimental conditions. In the ideal case, the thermal and optical properties in the horisontal direction around the wire are unaffected by these convections. We will be solely concerned with this "convection free" situation. An elaborate study, among other things of the necessary length of the wire and the permissible output of heat from the wire as a function of viscosity and thermal dilatation, is still lacking.

The curvature of light which propagates in a horisontal plane and passes the region of heat flow around the wire will be the optical basis for the measurement. The phenomenon will be seen from the standpoint of geometrical optics. A refinement according to wave optics can be performed along well known principles. As shown below, the theory and the measurements give a surprisingly simple result. One distinct angle of deflection is observed on each side of the wire. In order to resolve this simple phenomenon in its finer details, if requisite, a wave optical theory will be required; the technically important case of *a hot wall in air* was investigated by optical interferometry well 25 years ago [9,10].

As far as a constant deviation is concerned, there is no need for using methods like the scale or the schlieren arrangements. These methods have been criticized by Gosting; scale method [11], schlieren method [12]. In the *former* case, the criticism is based upon a creditable but incomplete theoretical attempt by Adler and Blanchard, which evidently cannot rival in conclusive evidence with the severe experimental test [13], compare Ref. [14]. (A somewhat modified experimental procedure has been proposed for greater convenience [15].) In the *latter* case, the criticism is limited to the region of maximum deviation of light, in which nobody uses the schlieren method for to some extent exact purposes, owing to the lack of definition of the image which is immediately evident to the experimenter. Hence, the self-warning property [13] is a common characteristic of these methods.

THE THERMAL CONDITIONS

A very thin metal wire is extended in an electrically isolating stationary fluid of thermal conductivity λ and diffusivity $a = \lambda/c\varrho$ (c specific heat at constant pressure, ϱ density). The wire is electrically heated, and represents a linear heat source Q_0 per unit of length and of time (t). Counted from a zero time $t = 0$ ($t < 0$, $Q_0 = 0$), the time derivative of temperature (T) at a radial distance r from the source is [4]

$$\frac{\partial T}{\partial t} = \frac{Q_0}{4\pi\ \lambda t} \exp(-r^2/4at) \tag{1}$$

The heat passing one cm^2 of a coaxial cylindrical surface element at a distance r is, in time dt

$$\mathrm{d}Q = \frac{Q_0}{2\pi r} [\exp(-r^2/4at)]\mathrm{d}t \tag{2}$$

The thermal conductivity is defined according to

$$\mathrm{d}Q = -\ \lambda \frac{\partial T}{\partial r}\ \mathrm{d}t \tag{3}$$

(2) and (3) yield

$$\frac{\partial T}{\partial r} = -\ \frac{Q_0}{2\pi\ \lambda r} \exp\ (-r^2/4at) \tag{4}$$

This gradient corresponds to a refractive index gradient of

$$\frac{\partial n}{\partial r} = -\left(\frac{\partial n}{\partial T}\right)_p \frac{Q_0}{2\pi\ \lambda r} \exp(-\ r^2/4at) \tag{5}$$

In a practical measuring device, the temperature gradient should be as low as possible, and $(\partial n/\partial T)_p$ may be regarded as constant (or nearly constant) and approximated to the value at the temperature of the medium in bulk at the beginning of an experiment (or at the average temperature within the gradient, if needed). This derivative has to be determined in a separate experiment. — For less accurate purposes, it is noted that the equation of Dale and Gladstone, $(n-1)/\varrho$ = const., gives

$$\frac{\mathrm{d}n}{\mathrm{d}T} = -\ (n-1)\gamma \tag{6}$$

and that of Lorenz and Lorentz $(n^2-1)/\varrho\ (n^2 + 2)$ = const.

$$\frac{\mathrm{d}n}{\mathrm{d}T} = -\frac{(n^2-1)(n^2 + 2)}{6n}\ \gamma \tag{7}$$

γ being the coefficient of cubic expansion.

A direct determination of $\partial n/\partial r$, eqn (5), it not easy; it would be measured by the light curvature of rays of incidence *parallel* to the wire. Terminal anomalies make such a procedure seem less advantageous than an incidence transversal to the thread.

THE OPTICAL CONDITIONS

The curvature of light [16] is, according to Snellius' law, always towards regions of higher refractive index. Fig. 1 shows a horizontal section with two cylindrical surfaces S_1 and S_2 of radius $r_1 = r + \mathrm{d}r$ and $r_2 = r$. An incident light ray from the left is deviated at these surfaces in the direction which removes it from the vertical wire at O *. A parallel beam is thus split up in two parts deviated each to its side of the wire. — A ray passing near O is strongly bent in this region; a ray passing at a longer distance from O has a more moderate curvature, but along a greater section of its path. It will appear that this tends to make the resulting deviation independent of the condition of incidence (y_0).

The indices of refraction are, on the two sides of S_1, n and $n' = n + \mathrm{d}n$. By the construction (Fig. 1) is seen that $\mathrm{OA} = r_1 \sin b_1 = r_2 \sin i_2$. Further, by Snellius' law we obtain $n \sin i_1 = n' \sin b_1$. These two relations yield $nr_1 \sin i_1 = n'r_2 \sin i_2$; more generally, C being a constant along the ray,

$$nr \sin i = C \tag{8}$$

We are interested in the differential deviation $\delta = b_1 - i_1$ at the surface S_1. Writing Snellius' law $n \sin i_1 = (n + \mathrm{d}n) \sin (i_1 + \delta)$ and omitting vanishing

* The only ray which would be undeviated is one originally directed towards O. — In practice, the interference phenomenon caused by the wire is considered to be of vanishing intensity.

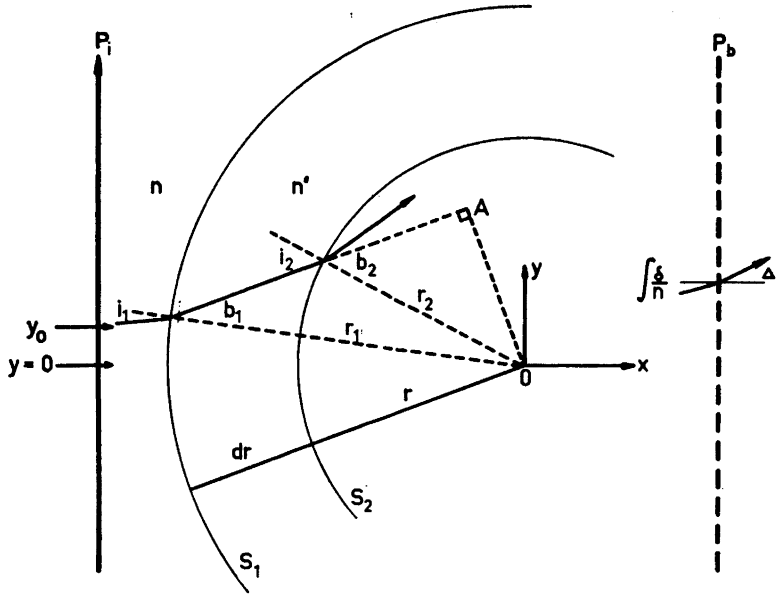

Fig. 1. Horizontal section of the cell, showing the liquid enclosed between P_i and P_b, with the linear source at O, and the direction of light from left to right.

terms, $\sin \delta = -(\mathrm{d}n/n)\ \mathrm{tg}\ i_1$. Approximating $\sin \delta$ by δ, and omitting index 1, yields

$$\delta = -\frac{1}{n}\frac{\partial n}{\partial r}\ \mathrm{tg}\ i\ \mathrm{d}r \tag{9}$$

We introduce i from eqn (8):

$$\delta = -\frac{1}{n}\frac{\partial n}{\partial r}\frac{C\ \mathrm{d}r}{\sqrt{n^2r^2 - C^2}} \tag{10}$$

$\partial n/\partial r$ is given by eqn (5), so we have obtained $\delta = f(r)\mathrm{d}r$ which shall be integrated for different ordinates of incidence y_0 of the cartesian system (x, y of Fig. 1). We will assume

1) a parallel beam of light with an incidence at right angles to the plane P_i and issuing at the plane P_b

2) a temperature gradient which does not reach the planes P_i and P_b, ensuring an integration from $x = -\infty$ to $x = +\infty$

3) refractive indices outside the region between P_i and P_b to be unity

4) that in eqn (8), r and i change significantly along the path of a light ray but neither n nor y. (Owing to $r^2 = x^2 + y^2$, y is of interest in this connection.)

From the approximations 1) and 4) is seen that, along the ray, $y = y_0 = r \sin i$. With this approximation eqn (8) gives $C = ny_0$. Hence, eqn (10) becomes

$$\delta = -\frac{1}{n}\frac{\partial n}{\partial r}\frac{y_0\,\mathrm{d}r}{\sqrt{r^2-y_0^2}} \tag{11}$$

The approximations made, all imply that the total angle of deviation between P_i and P_b, Δ, is supposed to be very small, that is the refractive index gradient is feeble. We will eventually have to demand this from other reasons too, in order to avoid disturbing convections. — It is seen that the argument of eqn (11) becomes infinite at $r = y_0$. This is the point at which the ray passes as near the wire as possible, that is where r is a minimum and $\mathrm{d}r = 0$.

Introducing $\partial n/\partial r$ by eqn (5), and x as independent variable by $r^2 = x^2 + y_0^2$

$$\delta = \frac{1}{n}\left(\frac{\partial n}{\partial T}\right)_p \frac{y_0 Q_0}{2\pi\lambda}\,\frac{\mathrm{d}x}{x^2+y_0^2}\,\exp[-(x^2+y_0^2)/4at] \tag{12}$$

We will integrate this expression in order to obtain the total angle of deviation Δ. The angle in question shall represent the total deviation of the ray, counted from before entering the cell at P_i and after leaving it at P_b, that is in air of refractive index approximately equal to unity. Strictly speaking, all the small angles of Fig. 1 would have to be divided by n (as indicated at the plane P_b), in order to be referred to a specified angle of incidence *in air*. Hence, we obtain Δ directly from eqn (12), as if there were no refraction at P_b

$$\delta = \frac{1}{n}\left(\frac{\partial n}{\partial T}\right)_p \frac{y_0 Q_0}{2\,\pi\lambda}\int_{-\infty}^{+\infty}\frac{\mathrm{d}x}{x^2+y_0^2}\,\exp\,[-(x^2+y_0^2)/4at] \tag{13}$$

The integral reduces to a simple from by assuming $x^2 + y_0^2 = r^2 \ll 4\,at$, an assumption which is strongly supported by the experimental results *. Hence

$$\Delta = \frac{1}{n}\left(\frac{\partial n}{\partial T}\right)_p \frac{y_0 Q_0}{2\pi\lambda}\left|\frac{1}{y_0}\sin^{-1}\frac{x}{\sqrt{x^2+y_0^2}}\right|_{-\infty}^{+\infty}$$

from which

$$2\Delta = -\frac{Q_0}{\lambda n}\left(\frac{\partial n}{\partial T}\right)_p \tag{14}$$

EXPERIMENTAL CONDITIONS

The total angle of deflection, 2Δ may be measured either by photography, see Fig. 5, or with a screw micrometer eyepiece as used in our observations,

* In eqn (5), this approximation leads to a logarithmic decrease of temperature within the region nearest to the wire.

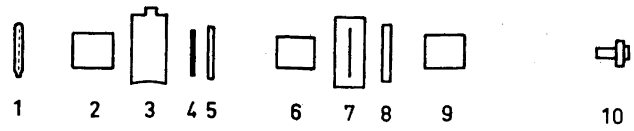

Fig. 2. 1. straight wire lamp, 2. condenser lens, 3. water cell, 4. light filter, 5. fine vertical slit, 6. lens with focal plane at 5, 7. trough with the vertical wire suspended in the liquid to be measured, 8. broad vertical diaphgram, 9. lens, 10. micrometer screw eyepiece adjusted to the slit 5.

see Fig. 2. The arrangement is an Abbe schlieren or Gouy interference device with parallel light passing the cell 7. The eyepiece 10 is adjusted to the focal plane of the lens 9 *.

The diaphragm 8 was 3—4 mm broad. The slit 5 is seen as a central line at the beginning of the experiment, which disappears altogether after in induction time of less than 10 seconds. Instead of this, two distinct lines appear (Fig. 5), the distance of which was read off by the eyepiece micrometer 10 ×. It corresponds to $2\,\Delta$ of eqn (14). The real angle was obtained by comparison with the deviation caused by a glass prism with a *double* deviation angle of 0.01208 radians (red light).

The readings were independent of a diminished breadth of the diaphragm 8. Of course, the lines are finally getting unsharp.

The electric circuit and measurement was the simplest possible, see Fig. 3.

The proportionality of $2\,\Delta$ to Q_0 (eqn 14) has been tested, see Fig. 4. The good linearity observed, and the excellent stability of the eyepiece readings with time is very advantageous for the purpose of determining the coefficient of heat conduction. — An estimation of the systematic error is not possible for the present.

In our experiments, the angle of deviation $2\,\Delta$ varied from 2′ to 10′. — It is interesting to compare $2\,\Delta/Q_0$ of eqn (14) for some substances at 20°C, see Table 1. For the measurement, a high value of $2\,\Delta/Q_0$ is desirable. The step from glycerine to water is, in this respect, greater than that from water to a gas like air. The method might eventually be extended to gases of ordinary or elevated pressures, although the optically useful region around the wire is very narrow in such a case. Hence, the optical requirements become very special, and no test has been made.

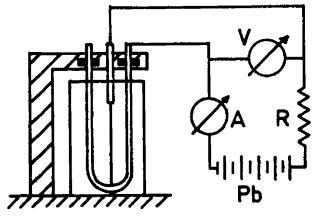

Fig. 3. The vertical wire (0.1 mm Pt) is shown at the left, immersed in the liquid container, a plane parallel glass cuve. The electrical circuit is the simplest possible, by application of a big battery (Pb) of variable voltage, and a high resistance mVVmeter.

* With this adjustment, a screening diaphragm 8 is needed in order to get a clear double line in the eyepiece. However, a re-focusing according to the actual value of Q_0 shows that a double line can be obtained *in absence of the screen.* This gives an insight into the optical properties of the wire surroundings which is not covered by the simple treatment given in this article.

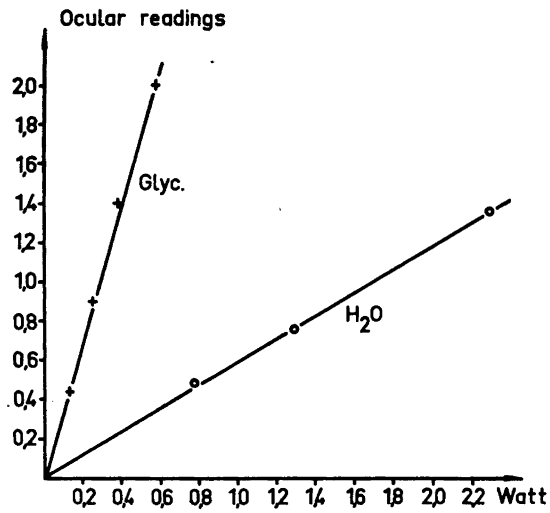

Fig. 4. The proportionality between the ocular readings (line distance in the ocular) and the total energy output from the wire is shown for water and glycerine.

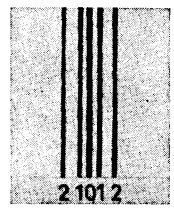

Fig. 5. From photographic exposures of the central line (0) and two double lines (1,1 and 2,2) on an Ilford H.P.S. Plate. Line O: exposure time 7.5 sec., $Q_0 = 0$. Lines 1,1: 15 sec., $Q_0 = 0.00657$ watt/cm. Lines 2,2: 15 sec., $Q_0 = 0.0183$ watt/cm. Voltage of accumulator: 0, 6 and 10, respectively. Substance: colourless liquid paraffin. Light source: straight wire lamp without filter.

A higher energy output Q_0 in the case of water was necessary in order to ensure a sufficient resolving power for this substance, with its exceptionally small $\partial n/\partial T$ and great λ. A refinement of the method of observation is, of course, possible; this would be necessary for an application to water around 4°C (where the risk for convection is specially small), owing to the small value of $\partial n/\partial T$. — The stability in the case of water at 20°C was much better than expected; convections have been observed only when the wire was quite evidently non vertical.

Available experimental data for the calculation of $(dn/dT)_p$ are, even for water, not quite satisfactory. The uncertainty is at least $\pm$ 2 % if estimated without a critical examination of the values of different authors.

Table 2 illuminates further our conditions and presents result on λ as compared with the exact data obtained by Gillam [6].

Additionally, the following data are of interest:

1) The liquid column had the dimensions 4 × 4 × 14 cm, the exact length of the wire was 12.70 cm. The highest effect used for water, 2.28 watt on the whole wire, corresponds to a temperature rise of 10°C/h if no loss of heat occurred to the surroundings.

2) The final reading is normally obtained in 20—30 sec. A high Q_0 and a low λ may increase the induction period considerably. A test of the stability

Table 1.

	$10\lambda^3$ cal/cgs	n		$-10^4\ (dn/dT)_p$ ~D-line	$(-1/\lambda n)(dn/dT)_p = 2\Delta/Q_0$
n-Octanol	0.40	1.429	4.0	(average 18–80°C)	0.70
Glycerine	0.675	1.473	2.79?	(from eqn 7)	0.28
Water	1.44	1.333	0.92	(average from lit.)	0.048
Air (1 at)	0.057	1.00027	0.0100		0.017

Table 2.

21°C	Q_0 watt/cm	$2\Delta/Q_0$ (exp.) cgs/cal	$-10^4\ (1/n)(dn/dT)_p$	$10^3\ \lambda$(opt.) cal/cm sec degree	$10^3\ \lambda$(Gillam [6])
Glycerine	0–0.045	0.269	(1.89)	(0.70)	0.675
Water	0–0.180	0.0460	0.69 ± 2 %	(1.50)	1.44

of the ocular reading over a long period of time was made with glycerine. 0.56 watt was used over the wire, corresponding to the upper limit of Q_0 in Table 2. The line distance was constant over the measured period of 1 ½ h. The lowest value of 5.02 was obtained after 3 and 90 min; the highest value measured was 5.05. The difference is within the accidental errors of the readings. — In the case of mixtures, effects of thermodiffusion may be obtained, and the readings should be made as early as possible.

3) When the current is switched off, the double line disappears and the central line is restored in a time of the order of 5 seconds to several minutes. A new measurement may be started immediately, without stirring of the liquid.

4) With a suitable form of the terminal connections of the wire, a correction for a *low* electrical conductivity of the liquid should be easy to perform.

5) A cylindrical lens may be used in order to decrease the magnification in the direction of the wire, so that an average deviation may be observed in the ocular. However, it is advantageous to use only a narrow middle section of the wire region, where the terminal anomalies are as small as possible.

ELECTROLYTES

Although no experiments on conducting solutions have hitherto been made, there is no doubt as to the possibility of covering the field of most ordinary electrolytes by the use of an electrically isolated wire.

Another possibility is interesting: to use the wire as an electrode and a cylindrical second electrode at a distance around it, and to feed the system with alternating current. It is easily seen that the joule heat evolved per unit of volume of the liquid is inversely proportional to the square of the distance from the wire. This should be compared to the much slower, logarithmic decrease of temperature in the neighbourhood of the heated wire according to our equations. Hence, by electrolytic heating, only the nearest surrounding

of the wire will become appreciably heated directly by the current. — The detailed optical properties of this system, with thermal conduction, has not yet been calculated. However, a simple consideration convinces of that the conductivity even of a thin wire (preferably made of silver) is so much greater than the conductivity of the solution, that hardly any difficulties can arise in obtaining an *even distribution* of the heat effect along the wire. The procedure might be of special interest in cases of very corrosive liquids, molten salts *etc.*, for which an isolating coating of the wire would be difficult to procure. — The optical observations must be made through apertures in the outer electrode.

The arrangement outlined would eventually be another technique for a variety of experiments on the transports of ions and heat.

CONCLUSIONS

In connection with the hot wire arrangement (Schleiermacher and others) an *optical* method has been examined which enables a simple and rapid measuring of coefficients of heat conduction of transparent liquids with considerable exactitude. The experimental test and fundamental theory given, do not allow a final judgement of the attainable accuracy. A separate determination of the change of refractive index with temperature is needed.

The hot wire *resistance thermometer* method, used previously for precision determinations, utilizes the resistance change during the first 20—60 seconds after switching on the current. This valuable method is a typically non stationary procedure. It has many advantages, *e.g.* that of being sufficiently independent of a temperature jump at the wire surface (Eucken). A condition for this seems to be that such a jump does not appreciably depend upon temperature. The optical method described is thermally (quasi-) stationary and *optically stationary*. This greatly simplifies the measuring device. The temperature jump is eliminated, as the method is based on a constant heat source, and not upon the heat flow between surfaces of fixed temperatures. This is especially pronounced in our case, owing to the stationarity mentioned.

The magnitude of the necessary joule heat supply (given the optical arrangement), increases with increasing thermal conductivity and decreasing thermal expansion of the liquid. This did not prevent measurements to be performed with water, using an output of 0.18 watt/cm without disturbances detectable by the method itself. Nevertheless, the procedure may be refined in different directions. Electrolytes can be included.

The method is unsuitable for solids in general. Already the frequent lack of transparency is preventive. By the great simplicity of the method, it may be valuable in improving the evident lack of data in the field of liquids and molten salts, in which essential informations are to be expected.*

* *Note added in proof:* Extended experimental work, and theoretical considerations by O. Bryngdahl, have disclosed fallacies in this work which will become corrected in further publications. Essential for the method is that the stability of the liquid has been established, the disturbances being slower than the restoring by thermal conduction.

REFERENCES

1. Lamm, O. *Z. physik. Chem.* **A 138** (1928) 313.
2. Tiselius, A. *Trans. Faraday Soc.* **33** (1937) 524.
3. Longsworth, L. G. *J. Phys. Chem.* **61** (1957) 1557.
4. Pfriem, H. *VDI Zeitschrift.* **82** (1938) 71.
5. Gillam, D. G., Rombén, L., Nissen, H.-E. and Lamm, O. *Acta Chem. Scand.* **9** (1955) 641.
6. Gillam, D. G. and Lamm, O. *Acta Chem. Scand.* **9** (1955) 657.
7. Lamm, O. *Acta Chem. Scand.* **13** (1959) 1471.
8. von Ubisch, H. *Arkiv Fysik* **16** (1959) No.7.
9. Hansen, G. *Z. tech. Physik* **12** (1931) 436.
10. Kennard, R. B. *J. Research Natl. Bur. Standards* **8** (1932) 787.
11. Gosting, L. J. *Advances. in Protein Chem.* **11** (1956) 429.
12. Kegeles, G. and Gosting, L. J. *J. Am. Chem. Soc.* **69** (1947) 2516.
13. Lamm, O. *Diss.* Upsala 1937 (*Nova Acta Reg. Soc. Sci. Upsaliensis.* IV, **10** (1937) No. 6).
14. Lamm, O. *Trans. Roy. Inst. Technol. Stockholm* **1959,** No. 134.
15. Lamm, O. *Acta Chem. Scand.* **9** (1955) 546.
16. Winkelmann, A. (Ed.) *Handbuch der Physik*, Breslau 1894, Vol. 2, 1, Optik, p. 344.

Received January 13, 1960.

ACTA CHEMICA SCANDINAVICA 14 (1960) 979–993

The Influence of Temperature on the Protolytic Equilibriums and Reaction-Rate Constants of Basic Triphenylmethane Dyes

RUNE CIGÉN

Department of Inorganic and Physical Chemistry, Chemical Institute, University of Lund, Lund, Sweden

The protolytic reaction scheme that was earlier proposed for basic triphenylmethane dyes on the basis of measurements at 20°C in water solutions has now been examined for Methyl Green at 40°C and 60°C. The reaction scheme has proved to be valid at these higher temperatures as well. The dissociation, hydration, and reaction-rate constants have been determined at 20°, 40°, and 60°C. The apparent energies of activation for the slow reactions and the temperature coefficients of the dissociation and hydration constants have been calculated.

The measurements have been carried out spectrophotometrically in water solutions of constant composition and constant ionic strength (0.5 M).

As a continuation of our earlier investigations [1-3] of the protolytic reactions and reaction velocities in water solutions of basic triphenylmethane dyes, we have examined the temperature dependence of the dissociation, hydration, and reaction-rate constants.

The earlier investigations concerning the influence of the temperature on these dyes have only treated the temperature dependence of the reaction rates. They have above all been concerned with the reaction

$$\text{dye ion} + OH^- \rightleftharpoons \text{carbinol}$$

in alkaline solutions. Biddle and Porter [4], it is true, also examined the corresponding reactions in acid solutions, but they did not take into consideration the complicated protolytic scheme and therefore their rate-constants are complex constants for several simultaneous time-reactions. Furthermore, they were not able to take into account the fact that the temperature influences not only the complex rate-constants but the dissociation and hydration constants as well. A determination of all constants in the protolytic scheme was not published until 1956 by Cigén [1].

For Crystal Violet, Langvad [5] made an attempt in 1950 to determine from the Arrhenius equation the energy of activation for the formation of carbinol in alkaline solutions according to the reaction

$$\text{—}\overset{\diagdown}{\underset{\diagup}{}}\text{C}^+ + \text{OH}^- \rightleftharpoons \text{—}\overset{\diagdown}{\underset{\diagup}{}}\text{COH}$$

This led Turgeon and LaMer [6] to a careful reinvestigation of the carbinol formation of Crystal Violet as a complement to Hochberg and LaMer's [7] reaction-rate and equilibrium studies of the carbinol formation of triphenylmethane and sulfonphthalein dyes. In order to determine the true energies and entropies of activation Turgeon and LaMer carried out measurements in isocomposition and isodielectric solutions. Unfortunately specific solvent effects turned up in the measurements in isodielectric solutions (mixtures of water — ethanol and water — acetone) which explains why they were not able to verify the relations, deduced by LaMer and Amis [8], between the dielectric constants of solvents and the reaction rates.

A theoretical treatment of the kinetics of solutions necessitates an extrapolation of the measurements to the ionic strength $\mu = 0$ and the dielectric constant $D = \infty$, as has been shown by Brönsted [9], Christiansen [10], Scatchard [11], LaMer [12] and others, if we want to determine the true energies and entropies of activation and the reaction-rate constants. This leads to experimental difficulties even for quite simple reactions, and for complicated reaction systems it seems at present impossible to determine true thermodynamic quantities in detail.

Owing to the above mentioned difficulties the present investigation has been carried out with solutions of constant composition. The ionic strength was kept constant (0.5 M) in order to keep the activity coefficients of the reacting ions and molecules as constant as possible.

Methyl Green $[[(CH_3)_2NC_6H_4]_2\overset{+}{C}C_6H_4\overset{+}{N}(CH_3)_3](ClO_4^-)_2$ was chosen as a representative of the types of dyes investigated. This dye was earlier investigated in detail at 20°C within the pH-range 0—9 [1]. Other investigations of dyes of the same type have led us to feel that Methyl Green could be investigated in detail also at 40° and 60°C even if the pH-range were extended to include the carbinol formation in strong alkaline solutions. If, for the sake of brevity, we write Methyl Green as $\begin{matrix} R \\ R \end{matrix}\!\!\diagdown\!\overset{+}{C}\!\!\diagup\!\!-R'$, where $R = (CH_3)_2NC_6H_4$ and $R' = (CH_3)_3\overset{+}{N}C_6H_4$, we can schematically indicate the reactions that take place when we change the pH of a solution of Methyl Green in the following manner (*cf.* Refs.[1–3]).

Whole arrows indicate that the reactions proceed with a non-measurable velocity — that is, instantaneously — whereas dashed arrows indicate that the reactions take place with a measurable velocity.

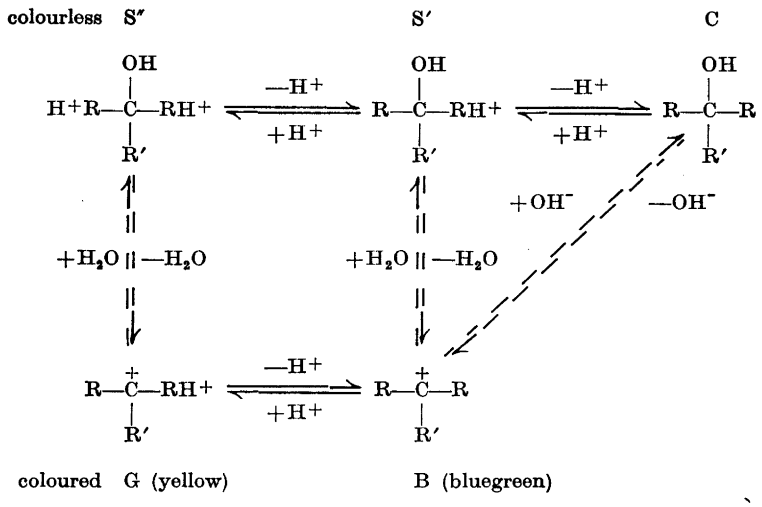

The following constants are defined:

$$K_1 = \frac{[G]}{[B][H^+]},\ K_2 = \frac{[S'']_\infty}{[G]_\infty},\ K_3 = \frac{[S'][H^+]}{[S'']},\ K_4 = \frac{[C][H^+]}{[S']},$$

$$K_6 = \frac{[B]_\infty}{[S']_\infty}$$

k_1 = rate constant for the reaction $G + H_2O \rightarrow S''$
k_2 = » » » » » $S'' \rightarrow H_2O + G$
k_3 = » » » » » $B + H_2O \rightarrow S'$
k_4 = » » » » » $S' \rightarrow B + H_2O$
k_5 = » » » » » $B + OH^- \rightarrow C$
k_6 = » » » » » $C \rightarrow B + OH^-$

The investigations were carried out spectrophotometrically and therefore the concentrations of the dye are given in most cases in the form of specific extinctions. The following symbols are used:

ε_B, ε_G = the molar extinction coefficient of B and G.
e_0, e_t, e_∞ = the specific extinction of a solution at the times 0 and t and at equilibrium (thickness of absorbing layer: $d = 1$ cm).
E_0, E_t, E_∞ = the extinctions for $d \neq 1$ cm.
e_B, e_G = the specific extinction of a solution containing only B resp. G.
C_M = the total concentration of dyestuff.

We can derive the following equation for K_1 (*cf.* Refs.[1-2]):

$$K_1 = \frac{e_B - e_0}{(e_0 - e_G)[H^+]} \qquad (1)$$

which can be transformed to

$$\frac{[H^+]}{e_B - e_0} = [H^+] \frac{1}{e_B - e_G} + \frac{1}{K_1(e_B - e_G)} \tag{2}$$

A plot of $[H^+]/(e_B - e_0)$ against $[H^+]$ gives a straight line. The intercept, y, of this line on the Y-axis and its slope, l, give $e_B - e_G = 1/l$ and $K_1 = l/y$, respectively.

At equilibrium we get the extinction

$$e_\infty = \frac{e_B + K_1[H^+] \cdot e_G}{1 + 1/K_6 + K_4/K_6[H^+] + K_1[H^+](1 + K_2)} \tag{3}$$

For acid solutions, pH ≤ 2, (3) gives

$$K_2 = \frac{e_G}{e_\infty} + \frac{e_B - e_\infty(1 + K_1[H^+] + 1/K_6)}{e_\infty \cdot K_1[H^+]} \tag{4}$$

and for weakly alkaline solutions (3) can be written in the approximate form

$$\frac{[H^+]}{e_\infty} = [H^+] \cdot \frac{1 + K_6}{K_6 \cdot e_B} + \frac{K_4}{K_6 \cdot e_B} \tag{5}$$

We get K_4/K_6 from (5) and, under certain circumstances, K_6 as well if we plot $[H^+]/e_\infty$ against $[H^+]$.

We can derive an expression for K_3K_4 in the following way:

$$e_\infty = [B]_\infty \cdot \varepsilon_B + [G]_\infty \cdot \varepsilon_G = [B]_\infty(\varepsilon_B + K_1[H^+] \cdot \varepsilon_G) \tag{6}$$

$$C_M = [B]_\infty + [G]_\infty + [S'']_\infty + [S']_\infty + [C]_\infty$$

$$= [B]_\infty(1 + K_1[H^+] + 1/K_6 + [H^+]/K_3K_6 + K_4/K_6[H^+]) \tag{7}$$

From (6) and (7) we get

$$e_\infty = \frac{e_B + K_1[H^+] \cdot e_G}{1 + 1/K_6 + K_1[H]^+ + [H^+]/K_3K_6 + K_4/K_6[H^+]} \tag{8}$$

since $C_M \cdot \varepsilon_B = e_B$ and $C_M \cdot \varepsilon_G = e_G$. In very weakly acid solutions, pH ~ 5, we can neglect $K_1[H^+]$ in the denominator and $K_1[H^+] \cdot e_G$ in the numerator if we carry out the measurements at a wavelength where $e_G \leq e_B$. After these approximations we differentiate e_∞ with respect to $[H^+]$ and find that e_∞ has a maximum when $[H^+] = \sqrt{K_3K_4}$.

We can deduce the following rate expression for the reactions if we assume that the individual rate constants k_1 to k_4 in the reaction scheme are independent of pH, which was the case for the dyestuffs investigated earlier. Since the total concentrations, C_M, of the dyestuff is very low as compared with the concentrations of the buffer solutions used during the measurements, the reactions are pseudo-unimolecular reactions.

$$k = \frac{1}{t} \ln \frac{e_0 - e_\infty}{e_t - e_\infty} =$$

$$= \frac{k_2[H^+]^2 + k_4K_3[H^+] + k_6K_3K_4}{[H^+]^2 + K_3[H^+] + K_3K_4} + \frac{k_1K_1[H^+] + k_3 + k_5[OH^-]}{K_1[H^+] + 1} \quad (9)$$

where k is the rate constant of the total reactions.

In strong acid solutions, pH $\leq$ 1, it is possible to approximate (9) to

$$k = \frac{1}{t} \ln \frac{e_0 - e_\infty}{e_t - e_\infty} = k_1 \cdot \frac{K_1[H^+]}{1 + K_1(H^+]} + k_2 \quad (10)$$

In strong alkaline solutions we can aproximate (9) to

$$k = k_3 + k_6 + k_5[OH^-] \quad (11)$$

Between these two extreme approximations we can make a smaller approximation of (9) in the pH-range 4—8.

$$k = \frac{k_4K_3[H^+]}{[H^+]^2 + K_3[H^+] + K_3K_4} + k_3 \quad (12)$$

If we differentiate k with respect to $[H^+]$, we find that k has a maximum when $[H^+] = \sqrt{K_1K_4}$ — that is, the same expression as was deduced above.

If we measure the extinctions at the time $t = 0$ and at equilibrium and determine the total rate-constants for the slow reactions of a great number of solutions — obtained by mixing a dye stock solution with appropriate buffer solutions — we can determine the constants in the reaction scheme from the equations given above.

The above aproximations depend, of course, on the relative sizes of the constants; in some cases it may be necessary to carry out successive approximations.

EXPERIMENTAL

Chemicals und solutions. A commercial preparations of *Methyl Green* ("Methylgrün" from Merck) was converted into the corresponding perchlorate, which was recrystallized in water to optical constancy; beautiful green needles with a metallic lustre were obtained. Stock solutions were prepared by weighing and dissolving the perchlorate in distilled water. In the stock solutions C_M was = 4×10^{-5} M. Owing to the fact that the walls of glass vessels strongly adsorb the dyestuff, a stock solution should be stored for a weck before use. The concentration of the dye in the stock solutions then becomes constant for a few months.

Hydrochloric acid, sodium acetate, disodium hydrogen phosphate, potassium dihydrogen phosphate, boric acid, and *sodium hydroxide,* all of analytical grade, were used in the buffer solutions. *Potassium chloride* of analytical grade was added to keep the ionic strength constant (0.5 M).

Apparatus. For the spectrophotometric measurements a modified Beckman DU spectrophotometer was used. It was furnished with double, heatisolated, thermostatic systems. The internal system contained the absorbtion cells and was kept at the experimental temperature by pumping water from a thermostat through its walls. The external system was kept at 30°C in the same way. The solutions for measurement were carried

from flasks in a thermostat to the absorption cells either with pipettes, furnished with double mantles through which water from a thermostat was pumped, or with special syringes. These syringes were furnished with mechanical stoppers, making it possible to regulate and reproduce the volume of the syringes to within 0.1 %. Furthermore the syringes were furnished with diverse, heat-isolating covers and were thermostated in a special air thermostat. Separate experiments were carried out to determine the loss of heat that might occur during the few seconds taken to carry the solutions for measurement from a thermostated flask to a thermostated absorption cell. The loss was compensated for by temperating the syringes used to a temperature somewhat above that of the actual investigation. All solutions were thermostated with an accuracy of ± 0.01°C, and the temperature inside the absorption-cell house was held constant to within 0.05°C.

The determinations of $[H^+]$ were carried out titrimetrically and potentiometrically. For the potentiometric measurements a reference solution (pH = 2) having the composition 0.01 M HCl + 0.49 M KCl was used. In the present paper pH always means $-\log[H^+]$ and not $-\log a_{H^+}$. As electrodes chinhydron and platinum-plate were used for pH < 6 and platinum-black and hydrogen gas for pH > 6. The electrolytically produced hydrogen gas was led through a wash-flask with 0.5 M KCl, which was held at the same temperature as the solutions for measurement.

MEASUREMENTS AND RESULTS

In a water solution of Methyl Green the dye can only be present, for pH > 9, as a single component of those given in the protolytic scheme. At pH > 9 we only need to consider the almost insoluble carbinol. At lower pH-values we get mixtures of three or four components. This gives rise to some complications when we determine the constants as we can not determine ε_B, ε_G or e_B, e_G directly from the measured absorption curves.

We start with a very weakly buffered stock solution (pH ≈ 4.5) of the dyestuff. In such a solution the concentration of the blue form, B, is 80—90 % of the total dye concentration. The remaining constitutents are distributed among S″, S′, and C. We can neglect [G] as compared with [B], [S′], and [S″]. In such a solution we denote the molar extinction coefficient by ε'_B and the specific extinction by e'_B. From $e'_G/e_G = e'_B/e_B$ and eqn. (2) we can determine K_1 by replacing e_B by e'_B and e_G by e'_G.

Determination of K_1. A series of solutions having the composition x M HCl + $(0.5 - x)$ M KCl were quickly mixed with an equivalent volume of a dye stock-solution containing 0.5 M KCl. In most cases the mixing was carried out by injecting the thermostated buffer directly into the thermostated absorption cell in the absorption-cell house. The equilibrium $B + H^+ \rightleftharpoons G$ is reached instantaneously during the mixing, where upon the solution fades owing to the reaction $G + H_2O \rightleftharpoons S''$. By determining the fading rate and extrapolating the extinction to $t = 0$, e_0 was obtained. The measurements were carried out, as in the following, at the wavelength $\lambda = 633$ mμ, where the absorption curve for the blue component, B, has a sharp maximum and where G has very little extinction, $\varepsilon_G \ll \varepsilon_B$.

In Fig. 1 $[H^+]/(e'_B - e_0)$ is plotted against $[H^+]$. A linear relation is indicated, and from the slopes, l, and the intercepts, y, on the y-axis we can calculate K_1 according to eqn. (2). e'_B was determined from measurements on the dye stock-solution. The following results were obtained ($C_M = 1 \times 10^{-5}$ M):

Table 1. Determination of e_0, e_∞, K_2, k, and k_1 at 40° and 60°C in (HCl + KCl) solutions. $\lambda = 633$ mμ.

	40°C					60°C				
[H+] M	e_0	e_∞	K_2	k min^{-1}	k_1 min^{-1}	e_0	e_∞	K_2	k min^{-1}	k_1 min^{-1}
0.10	0.276	0.0081	66.8	0.394	0.624	0.308	0.0191	32.7	1.882	3.116
0.08	0.310	0.0101	66.6	0.364	0.629	0.344	0.0238	32.5	1.713	3.100
0.06	0.355	0.0134	66.3	0.322	0.629	0.391	0.0315	32.3	1.518	3.118
0.05	0.384	0.0159	66.5	0.297	0.636	0.418	0.0368	32.9	1.389	3.116
0.04	0.418	0.0198	66.6	0.272	0.647	0.453	0.0458	32.6	1.239	3.109
		Mean	66.6		0.633			32.6		3.11

40°C: $e'_B = 0.650$, $y = 0.1092$ M, $l = 1.576$, $e_G = 0.015$, $K_1 = \mathbf{14.43 \pm 0.15\ M^{-1}}$.
60°C: $e'_B = 0.665$, $y = 0.1273$ M, $l = 1.526$, $e_G = 0.010$, $K_1 = \mathbf{11.99 \pm 0.10\ M^{-1}}$.

Determination of K_2. The dye stock-solution was mixed with suitable HCl + KCl buffers. The solutions were thermostated and the equilibrium extinction, E_∞, was determined in 5 cm absorption cells. From eqn. (4) we can determine K_2 only if we know e_B (ε_B). According to later measurements ε_B was 7.75×10^4 at 40° and 7.80×10^4 at 60° in the stock solutions used. C_M was $= 1 \times 10^{-5}$ M and this gives $e_B = 0.775$ at 40° (in this case C_M was

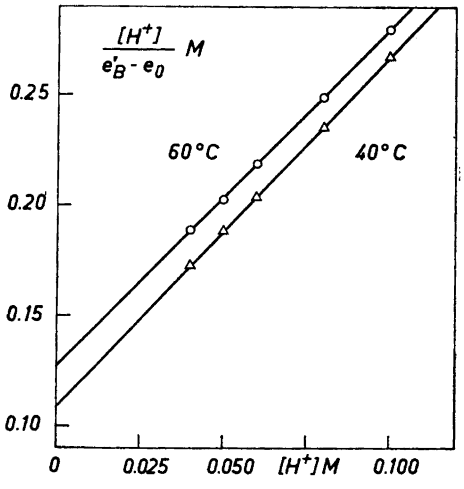

Fig. 1. [H+]/($e'_B - e_0$) as a function of [H+] for the determination of K_1 at 40° (△) and 60° (○). $\lambda = 633$ mμ, $C_M = 1 \times 10^{-5}$ M, $d = 1-2$ cm.

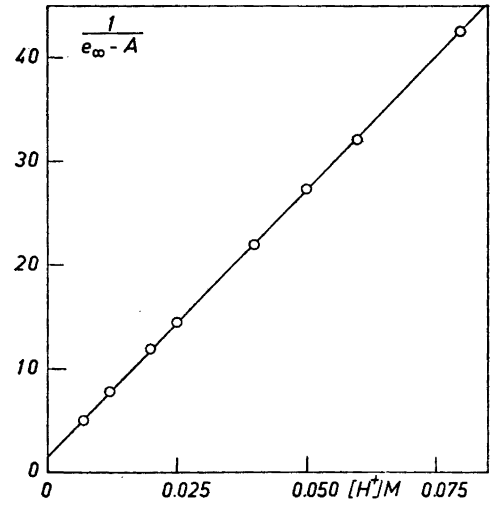

Fig. 2. $1/(e_\infty - A)$ as a function of [H+] for the determination of $K_1 + K_1K_2$ at 60°. $\lambda = 633$ mμ, $C_M = 1 \times 10^{-5}$ M, $d = 2-5$ cm.

$= 0.96 \times 10^{-5}$ M) and $e_B = 0.780$ at 60°. Table 1 gives the e_∞ obtained as well as the calculated K_2-values We get the following mean values: $K_2 = \mathbf{66.6 \pm 0.6}$ at 40° and $K_2 = \mathbf{32.6 \pm 0.3}$ at 60°C.

Because of the high reaction-rates at 60°C the value of K_1 may be uncertain For example, at this temperature the reaction $G + H_2O \rightleftharpoons S''$ has a »half-life period» of 22 seconds when $[H^+] = 0.1$ M. In order to get a further check on K_1 we have proceeded as follows. We can write eqn. (4) as

$$\frac{1}{e_\infty - A} = \frac{1 + 1/K_6}{e_B} + [H^+] \cdot \frac{K_1 + K_1K_2}{e_B} \qquad (13)$$

where $$A = \frac{K_1[H^+] \cdot e_G}{1 + 1/K_6 + [H^+](K_1 + K_1K_2)}$$

In acid solutions with $[H^+] \leq K_1$, A is a correction term which at most reaches one per cent of e_∞. In this correction term we can therefore use the values obtained for K_1 and K_2, even if K_1 is a bit uncertain. In Fig. 2 $1/(e_\infty - A)$ is plotted against $[H^+]$ for $[H^+] = 0.007-0.080$ M. A linear relation is indicated and the slope of the straight line, l, gives us $(K_1 + K_1K_2)/e_B$. From the figure we get $l = 514$ M^{-1} and as $e_B = 0.780$, we get $K_1 + K_1K_2 = 402$ M^{-1}. The above determined K-values ($K_1 = 12.0$, $K_2 = 32.6$) give $K_1 + K_1K_2 = 403$. $K_1 = 12.0$ is therefore correct.

Determination of $K_4/(K_6 + 1)$. A dye stock-solution was mixed with a series of phosphate buffers and the equilibrium extinctions were determined. In Fig. 3 $[H^+]/e_\infty$ is plotted as a function of $[H^+]$. According to eqn. (5)

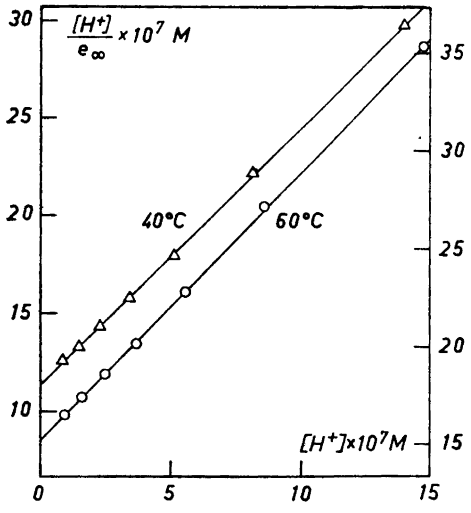

Fig. 3. $[H^+]/e_\infty$ as a function of $[H^+]$ for the determination of $K_4/(1 + K_6)$ at 40° (△, ordinate left) and 60° (○, ordinate right). $\lambda = 633$ mμ, $C_M = 1 \times 10^{-5}$ M, $d = 1$ cm.

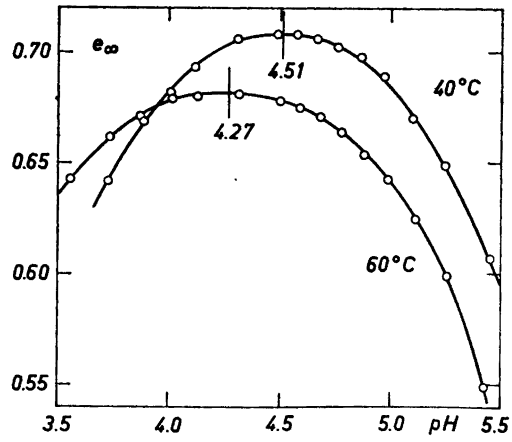

Fig. 4. e_∞ as a function of pH for the determination of K_3K_4 at 40° (upper curve) and 60°. $\lambda = 633$ mμ, $C_M = 1 \times 10^{-5}$ M, $d = 1$ cm.

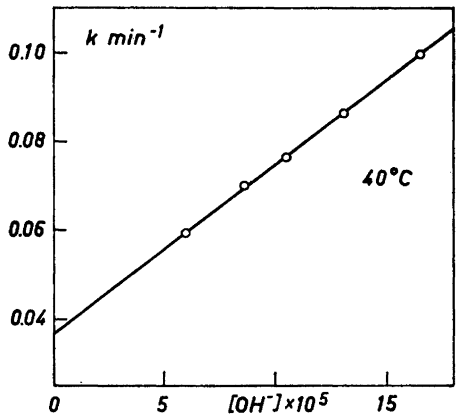

Fig. 5. k as a function of [OH⁻] for the determination of k_5 and $k_3 + k_6$ at 40°. Borate buffers. $\lambda = 633$ mμ, $C_M = 1 \times 10^{-5}$ M, $d = 1$ cm.

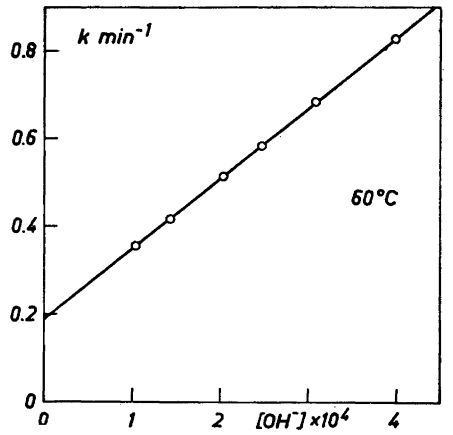

Fig. 6. k as a function of [OH⁻] for the determination of k_5 and $k_3 + k_6$ at 60°. Borate buffers. $\lambda = 633$ mμ. $C_M = 1 \times 10^{-5}$ M, $d = 1$ cm.

we get linear relations; the slopes, l, and intercepts, y, on the y-axis give $K_4/(K_6 + 1) = y/l$ or $K_4/K_6 = y \cdot e_B$. From Fig. 3 we obtain at 40°: $y = 1.130 \times 10^{-6}$ M, $l = 1.314$ and at 60°: $y = 1.517 \times 10^{-6}$ M, $l = 1.367$.

We can determine K_4/K_6 only when we know e_B or K_6. We get $\boldsymbol{K_4/(K_6 + 1) = 8.60 \times 10^{-7}}$ **M** at 40° and $\mathbf{1.110 \times 10^{-6}}$ **M** at 60°C. In these cases the dye sock-solutions used gave, according to later determinations, $e_B = 0.809$ at 40° and $e_B = 0.759$ at 60°C.

Determination of K_3K_4. The equilibrium extinctions were measured for a series of solutions with Methyl Green in acetate buffers. In Fig. 4 e_∞ is plotted as a function of pH. The maxima of the curve in this figure can bee determined (*cf.* p. 982) and we have

$$e_{\infty max} \text{ for } [H^+] = \sqrt{K_3K_4} \qquad (14)$$

From Fig. 4 we obtain $e_{\infty max}$ for pH = 4.51, $\boldsymbol{K_3K_4 = 9.55 \times 10^{-10}}$ **M²** at 40° and pH = 4.27, $\boldsymbol{K_3K_4 = 2.88 \times 10^{-9}}$ **M²** at 60°.

The remaining constants in the protolytic scheme can be determined by means of kinetic measurements and eqn. (9).

Determination of k_3, k_5, *and* k_6. In alkaline solutions eqn. (9) is approximated as $k = k_3 + k_6 + k_5[OH^-]$ (11). The fading rate of Methyl Green in borate buffers was determined for different pH-values and in Figs. 5 and 6 k is plotted against [OH⁻]. We get linear relations that, according to eqn. (11), give at 40°C (Fig. 5): $\boldsymbol{k_5 = 382 \pm 3}$ **min⁻¹ M⁻¹**, $k_3 + k_6 = 0.0367 \pm 0.0003$ min⁻¹ and at 60°C (Fig. 6): $\boldsymbol{k_5 = 1\,500 \pm 10}$ **min⁻¹ M⁻¹**, $k_3 + k_6 = 0.189 \pm 0.002$ min⁻¹. A check on k_5 at 40°C was carried out by kinetic measurement in 0.005

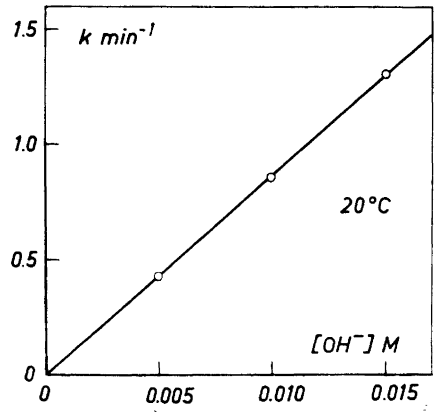

Fig. 7. k as a function of $[OH^-]$ for the determination of k_5 at 20° in NaOH + KCl. λ = 633 mμ, $C_M = 2 \times 10^{-6}$ M, d = 5 cm.

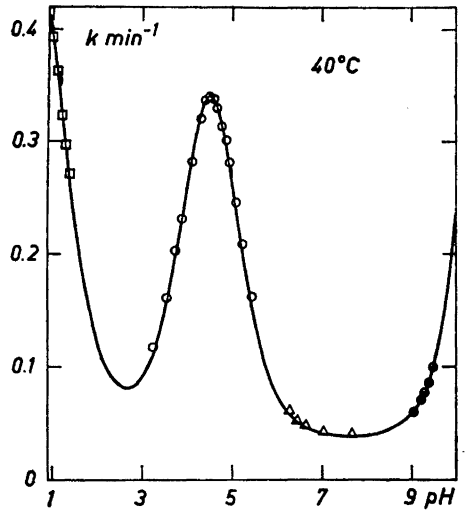

Fig. 8. k as a function of pH at 40°. The solid curve has been calculated from eqn (9). The symbols have been determined experimentally by kinetic measurements in HCl+KCl (□), acetate buffers, (○), phosphate buffers (△), and borate buffers (◒).

M NaOH + 0.495 M KCl. The experimental value for k (1.97 min^{-1}) is in good agreement with the calculated value (1.95 min^{-1}).

In previous investigations on Methyl Green (Ref.[1]) all constants in the protolytic scheme except k_5 and k_6 were determined at 20°C. Those measurements have now been completed with kinetic measurements in NaOH + KCl at 20°C. In Fig. 7, k is plotted against $[OH^-]$ and we get $k_5 = \mathbf{86.8 \pm 0.8\ min^{-1}\ M^{-1}}$ at 20°C. We can not determine $k_3 + k_6$ from the diagram as the straight line passes almost through the origin. However, k_3 has previously been determined to be 0.00621 min^{-1} (in Ref.[1], k_3 = 0.00270 since it was calculated by using ^{10}log). k_6 can be calculated in the following way. At equilibrium we have

$$k_5[OH^-][B]_\infty = k_6[C]_\infty \tag{15}$$

But $[H^+][C]_\infty = K_4[S']_\infty$ and $K_6[S']_\infty = [B]_\infty$ and therefore

$$k_6 = k_5 K_w K_6 / K_4 \tag{16}$$

From Ref.[1] we have $K_w = 1.24 \times 10^{-14}$ M^2 and $K_6/K_4 = 1.43 \times 10^6$ M^{-1} at 20°C and from (16) we get $k_6 = \mathbf{(1.54 \pm 0.06) \times 10^{-6}\ min^{-1}}$. Thus $k_6 \ll k_5$ at 20° and the same is true also at 40° and 60°C. Therefore from Fig. 5 we get $k_3 = \mathbf{0.0367 \pm 0.0003\ min^{-1}}$ at 40° and from Fig. 6, $k_3 = \mathbf{0.189 \pm 0.002\ min^{-1}}$ at 60°C.

Determination of K_3, K_4, K_6 and k_4. These constants can be calculated from eqn. (12), which may be written in the form

$$k = \left(\frac{K_3 K_6 [H^+]}{[H^+]^2 + K_3[H^+] + K_3 K_4} + 1 \right) \cdot k_3 \qquad (17)$$

as $k_3[B]_\infty = k_4[S']_\infty$ and $[B]_\infty = K_6[S']_\infty$, giving $k_4 = k_3 K_6$. We already know $K_3 K_4$, k_3, and $K_4/(K_6 + 1)$. From kinetic measurements in acetate buffers we can determine k for a series of different pH-values.

A stock solution of Methyl Green was almost decoloured by dissolving the dyestuff in 0.01 M HCl + 0.49 M KCl. The greater part of the dye was then transformed into colourless S″ owing to the reactions $B + H^+ + H_2O \rightleftharpoons G + H_2O \rightleftharpoons S''$. This partially decoloured solution was quickly mixed with suitable acetate buffers and the rate, k, was determined. k is the rate at which the blue colour is restored owing to the reactions $S'' \rightleftharpoons S' + H^+ \rightleftharpoons B + H^+ + H_2O$. k was plotted against pH, and then different values of K_6 were tried in eqn. (17).

If we fix K_6 we can determine K_3 and K_4. For every value of K_6 we get a curve from eqn. (17). The value of K_6 was chosen so that the curve calculated from eqn. (17) coincides best with the experimentally found k-values.

In Fig. 8 the k-values, obtained from measurements in acetate buffers at 40°C (circles), are plotted against pH. The solid curve was calculated from eqn. (9). By magnification of the central part of Fig. 8 we find that a curve drawn through the experimental points has a maximum at pH = 4.51, where $[H^+] = \sqrt{K_3 K_4}$. Thus we get the same value of $K_3 K_4$ from the kinetic measurements as from the extinction equilibrium measurements (Fig. 4). The same agreement was also obtained at 60°C. The results were:

at 40°C: $k_{max} = 0.340$ min^{-1} for pH = 4.51, $K_6 = \mathbf{16.0 \pm 0.2}$, $K_3 = \mathbf{(6.54 \pm 0.10) \times 10^{-5}}$ M, $K_4 = \mathbf{(1.46 \pm 0.02) \times 10^{-5}}$ M, $k_4 = \mathbf{0.587 + 0.015}$ min^{-1}.
at 60°C: $k_{max} = 1.118$ min^{-1} for pH = 4.27, $K_6 = \mathbf{27.5 \pm 0.3}$, $K_3 = \mathbf{(9.13 \pm 0.15) \times 10^{-5}}$ M, $K_4 = \mathbf{(3.16 \pm 0.05) \times 10^{-5}}$ M, $k_4 = \mathbf{5.20 \pm 0.10}$ min^{-1}.

Determination of k_6. The ionic product of water, K_w, was determined by measurements with a platinum-hydrogen gas electrode in solutions of the type x M NaOH + $(0.5 - x)$ M KCl, where $x = 0.01$ and 0.02. K_w was found to be 5.21×10^{-14} M^2 at 40° and 1.83×10^{-13} M^2 at 60°C. Then k_6 was obtained from $k_6 = k_5 K_w K_6 / K_4$. $k_6 = \mathbf{(2.18 \pm 0.06) \times 10^{-5}}$ min^{-1} at 40° and $k_6 = \mathbf{(2.39 \pm 0.06) \times 10^{-4}}$ min^{-1} at 60°C.

Determination of k_1 and k_2. The fading rates of the solutions were measured in the experiments giving the K_1-values. In Figs. 9 and 10, $2 + \log(e_t - e_\infty)$ is plotted against the time t. From the intercepts on the ordinate axes the e_0-values were calculated. The e_0-values are tabulated in Table 1, which also contains the complex rate-constants, k, and the k_1-values calculated from eqn. (9). k_2 is obtained from the equations $k_1[G]_\infty = k_2[S'']_\infty$ and $K_2[G]_\infty = [S'']_\infty$, which give $k_2 = k_1/K_2$. The following k-values were obtained: $k_1 = \mathbf{0.633 \pm 0.010}$ min^{-1}, $k_2 = \mathbf{0.00950 \pm 0.00020}$ min^{-1} at 40° and $k_1 = \mathbf{3.11 \pm 0.02}$ min^{-1}, $k_2 = \mathbf{0.0954 \pm 0.0015}$ min^{-1} at 60°C.

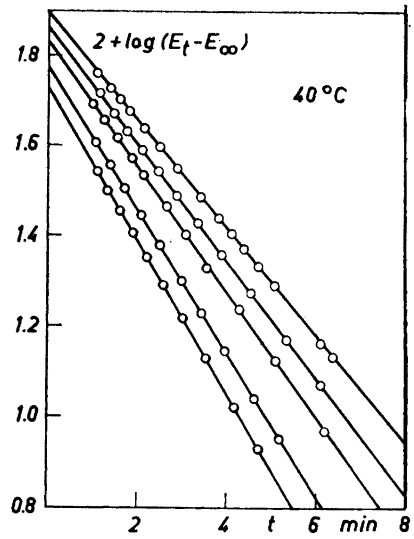

Fig. 9. $2 + \log(E_t - E_\infty)$ as a function of t for the determination of e_0, k_1, and k_2 at 40°. From above [H+] = 0.10, 0.08, 0.06, 0.05, and 0.04 M. λ = 633 mμ, $C_M = 1 \times 10^{-5}$ M, d = 2 cm.

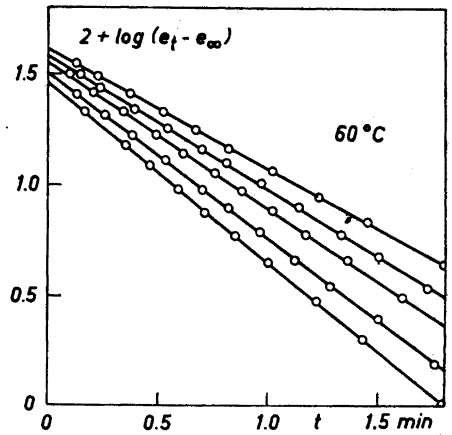

Fig. 10. $2 + \log(e_t - e_\infty)$ as a function of t for the determination of e_0, k_1, and k_2 at 60°. From above [H+] = 0.10, 0.08, 0.06, 0.05, and 0.04 M. λ = 633 mμ. $C_M = 1 \times 10^{-5}$ M, d = 1 cm.

From Fig. 10 we see that it is possible to carry out careful kinetic measurements by means of a manual recording of the extinctions and times even when the "half-life periods" of the reactions are as short as 20 seconds.

In Fig. 8 the experimentally obtained k-values at 40°C are plotted against pH in the pH-interval 1—10. The solid curve was calculated from eqn. (9) by using the values of the constants given above.

Thus all of the constants in the protolytic scheme have been determined. As a check we can use the relation $K_1K_2K_3K_6 = 1$ (by definition). Experimentally we get $K_1K_2K_3K_6 = 0.98$ at 40° and $K_1K_2K_3K_6 = 1.00$ at 60°C. The previous measurements at 20°C gave $K_1K_2K_3K_6 = 1.06$, but the measuring methods and precision have been improved since that time.

At higher temperatures we do not have the same difficulties with the adsorption on the walls of flasks and absorption cells or the precipitation of the almost insoluble carbinol as at 20°C. The most exact measurements were probably carried out at 60°C as the precautions to keep the solutions at the correct temperature in all operations were most rigorous. The reproducibility was very good at 60°C and the greatest uncertainly probably lies in the absolute determination of the temperature inside the absorption-cell house.

A strict, objective error calculation can hardly be performed on such complicated systems as those of the present investigation. The error limits given are therefore based partly on the writer's subjective view gained through many years of work with the same apparatus. The reproducibility of a single

Table 2. The temperature influence on the dissociation and hydration constants. A_K = mean temp.coeff./degree.

Temp.	K_1	A_{K_1}	K_2	A_{K_2}	$K_3 \times 10^5$	A_{K_3}	$K_4 \times 10^6$	A_{K_4}	K_6	A_{K_6}
20°C	16.7		132		5.2		6.5		9.3	
40°C	14.4	0.992	66.6	0.965	6.5	1.014	14.6	1.040	16.0	1.027
60°C	12.0		32.6		9.1		31.6		27.5	

Table 3. Reaction-rate constants at 20°, 40°, and 60°C and "apparent" energies of activation.

	20°C	40°C	60°C	ΔE 40°-20° kcal	ΔE 60°-40° kcal
k_1 min^{-1}	0.124	0.633	3.11	14.9	16.5
$k_2 \times 10^3$ min^{-1}	0.943	9.50	95.4	21.1	23.9
$k_3 \times 10^2$ min^{-1}	0.621	3.67	18.9	16.2	17.0
$k_4 \times 10^1$ min^{-1}	0.575	5.87	52.0	21.2	22.6
k_5 M^{-1} min^{-1}	86.8	382	1 500	13.5	14.2
$k_6 \times 10^5$ min^{-1}	0.154	2.18	23.9	24.2	24.8

measurement is in certain cases greater than the absolute accuracy we can obtain through a whole series of measurements.

DISCUSSION

The protolytic scheme that was previously formulated for basic triphenylmethane dyes on the basis of measurements at 20°C thus proves to be valid even if the temperature is raised up to 60°C. Raising the temperature has the effect of displacing the equilibriums towards the coloured, dehydrated forms. Consequently the values of the rate constants k_2, k_4, and k_6 increase with the temperature considerably more than k_1, k_3, and k_5. The dissociation constants increase with the temperature if they are defined as acid constants — that is, as K_3, K_4, and $1/K_1$.

In Tables 2 and 3 are given all of the constants obtained at 20°, 40°, and 60°C. We can not calculate true reaction heats, nor can we say how specific solvent effects influence the different constants. The dielectric constant, viscosity, and association of water change with temperature and influence the activity factors in a way that is difficult to calculate for undiluted solutions. We may note that the effect of the temperature on the acid dissociation constants K_3 and $1/K_1$ is small — that is, on the average, 0.8 % and 1.4 % per degree, respectively, and somewhat greater for K_4, namely 4.0 % per degree, on the average. For the hydration constants K_2 and K_6 the temperature coefficients are, on the average, 3.6 % and 2 % per degree, respectively, in the interval 20°—60°C. The temperature coefficients A in Table 2 are calculated from $K_{60°} = K_{20°} \cdot A^{40}$. The accuracy of the constants determined hardly permits

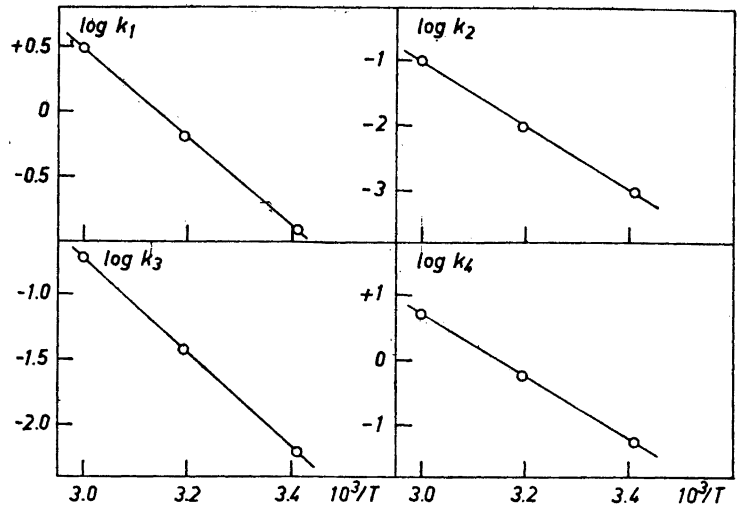

Fig. 11. log k_1, log k_2, log k_3, and log k_6 plotted against $1/T$.

us to decide whether the temperature coefficients are constant or not within the temperature interval investigated.

The rate constants for 20°, 40°, and 60°C are given in Table 3. We can not determine, in the present investigation, the different contributions to the energy of activation and thereby the true energies and entropies of activation. Therefore, the "apparent" energy of activation, ΔE, was only calculated from the Arrhenius equation

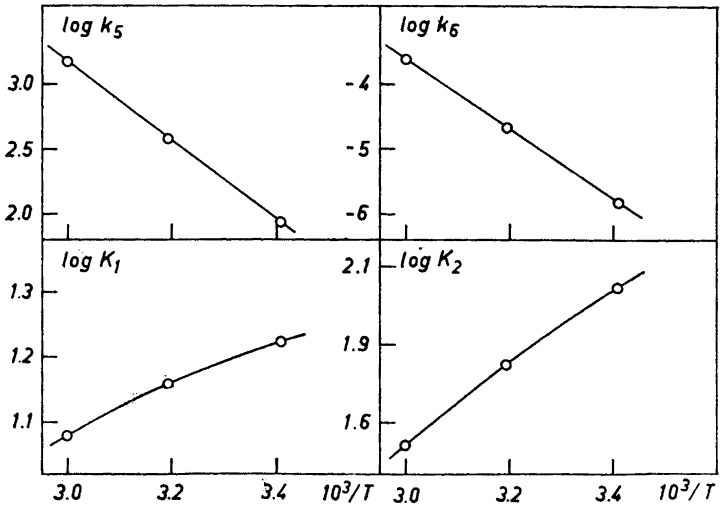

Fig. 12. log k_5, log k_6, log K_1, and log K_2 plotted against $1/T$.

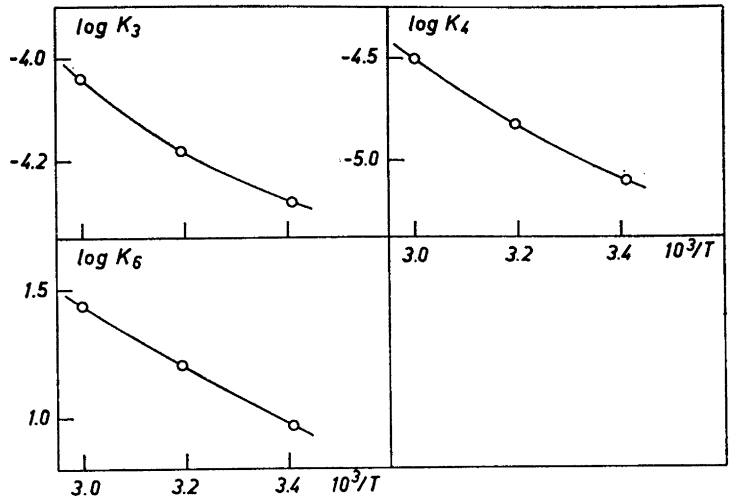

Fig. 13. log K_3, log K_4, and log K_6 plotted against $1/T$.

$$\ln \frac{k_{T''}}{k_{T'}} = \frac{\Delta E}{R} \left(\frac{T'' - T'}{T'T''} \right)$$

ΔE is not constant in the interval 20°—60°C. Table 3 contains the ΔE obtained for the intervals 20°—40°C and 40°—60°C, if it is assumed that ΔE is constant within each of these intervals.

From the table we see that ΔE is 0.7—2.7 kcal higher at 50°C than at 30°C.

In Figs. 11—13 log K; or log k; are plotted against $1/T$. For the rate constants k_1 to k_6 we get almost straight lines, but in each of the small diagrams the middle point lies somewhat below the indicated straight line. This also shows the difference in ΔE at 50° and 30°C. For the remaining constants the small diagrams show curved lines.

REFERENCES

1. Cigén, R. *Protolysengleichgewichte und Reaktionsgeschwindigkeiten einiger basischer Triphenylmethanfarbstoffe (Diss.)*, University, Lund 1956.
2. Cigén, R. *Acta Chem. Scand.* **12** (1958) 1456.
3. Cigén, R. *Acta Chem. Scand.* **13** (1959) 1113.
4. Biddle, H. C. and Porter, C. W. *J. Chem. Soc.* **37** (1915) 1571.
5. Langvad, T. *Acta Chem. Scand.* **4** (1950) 300.
6. Turgeon, J. C. and LaMer, V. K. *J. Am. Chem. Soc.* **74** (1952) 5988.
7. Hochberg, S. and LaMer, V. K. *J. Am. Chem. Soc.* **63** (1941) 3110.
8. Amis, E. S. and LaMer, V. K. *J. Am. Chem. Soc.* **61** (1939) 905.
9. Brönsted, J. N. *Z. physik. Chem.* **102** (1922) 169, **115** (1925) 337.
10. Christiansen, J. A. *Z. physik. Chem.* **113** (1924) 35.
11. Scatchard, G. *Chem. Revs.* **10** (1932) 229.
12. LaMer, V. K. and Kamner, M. E. *J. Am. Chem. Soc.* **57** (1935) 2662.

Received January 11, 1960.

ACTA CHEMICA SCANDINAVICA 14 (1960) 994–1000

A Spectroscopic Study of Some Acceptor-Donor Systems

MARGARETA ZACKRISSON and KARL INGE ALDÉN

Institute of Chemistry, University of Uppsala, Uppsala, Sweden

The liquidus curves have been studied for the systems $BiCl_3$—$POCl_3$, $AsCl_3$—$(CH_3)_2CO$ and $SbCl_3$—$(CH_3)_2CO$. One compound has been found in each system: $BiCl_3 \cdot 2POCl_3$, $AsCl_3 \cdot (CH_3)_2CO$ and $SbCl_3 \cdot 2(CH_3)_2CO$.

Infrared and Raman spectra of the three systems have been investigated. The infrared spectra of the following compounds have been studied: $SbCl_3 \cdot (CH_3)_3PO$, $SbCl_3 \cdot 2(CH_3)_3PO$, $SbCl_5 \cdot (CH_3)_3PO$, $5HgCl_2 \cdot 2(CH_3)_3PO$, $HgCl_2 \cdot (CH_3)_3PO$ and $2HgCl_2 \cdot (C_2H_5)_2S$.

The relative acceptor strengths of the acceptor molecules $SbCl_3$, $SbCl_5$ and $HgCl_2$ with $(CH_3)_3PO$ as donor molecule have been measured. The results are briefly discussed.

A preceding paper [1] dealt with a study of molecular interaction with phosphoryl chloride. It was there suggested that the interaction in the systems $AsCl_3$—$POCl_3$ and $SbCl_3$—$POCl_3$ was a dipole-dipole interaction, caused by favourable charge distribution. Phosphoryl chloride is however known to function as a donor molecule [2] and $AsCl_3$ and $SbCl_3$ are possible acceptor molecules.

$SnCl_4$ and $SbCl_5$ were given as examples of acceptor molecules which give adduct formation with $POCl_3$ by acceptor-donor reactions. In those cases the acceptor molecules change their spectra as can be expected from the change in their coordination and symmetry. It was suggested that intermediate cases could possibly also exist.

It was also assumed that the magnitude of the shift of the symmetrical phosphoryl bond vibration frequency could be a rough measure of the acceptor strength if the acceptor molecules compared are under similar conditions.

In order to obtain a better foundation for a discussion of those problems we decided to study some more acceptor-donor systems.

For systems with melting points lower than room temperature it was possible to obtain Raman spectra at every composition. The systems containing compounds with higher melting points have been studied by infrared spectroscopy in the spectral range 2—35 μ. Unfortunately the lower frequencies of the acceptor molecules are not situated in this range.

As it is difficult to avoid moisture during infrared absorption measurements it was preferred to study compounds stable in air.

EXPERIMENTAL

Chemicals. $AsCl_3$, $POCl_3$, $(CH_3)_2CO$ and $(C_2H_5)_2S$ were purified by distillation (B. p. 129°, 105°, 92° and 57°C). $SbCl_5$ was distilled at reduced pressure. $SbCl_3$ was purified by sublimation. $HgCl_2$, Merck *pro analysi*, was not further purified. $(CH_3)_3PO$ and its addition compounds were prepared as described earlier [3]. Anhydrous $BiCl_3$ was prepared from $BiCl_3 \cdot H_2O$, Mallinkrodt analytical reagent, according to Inorganic Syntheses [4]. $2HgCl_2 \cdot (C_2H_5)_2S$ was precipitated from alcoholic solutions of the components.

Spectroscopic measurements. The Raman spectra were obtained photographically as described earlier [1] (in the institute of Physical Chemistry). The infrared spectra were recorded on a Perkin-Elmer Model 21 Spectrophotometer equipped with NaCl and CsBr prisms (in the institute of Biochemistry). The spectra were run with the solutions in thin layers and the solids dispersed in Nujol between NaCl plates in the range 2—15 μ and between TlBr—TlI plates in the range 15—35 μ.

Phase diagrams. The liquidus curves were obtained by the same methods as described earlier [5].

Thermochemical measurements. The method used for measuring relative enthalpy changes has been described very recently [6].

THE SYSTEM $BiCl_3$—$POCl_3$

The liquidus curve (Fig. 1) has a maximum at the composition $BiCl_3 \cdot 2POCl_3$ with the melting point 37°C. The system can not be studied at higher $BiCl_3$ concentrations than 50 mole per cent by this method, because of the distillation of $POCl_3$ at the high temperature required to dissolve $BiCl_3$.

The Raman spectra are given in Fig. 2. The mixture $BiCl_3 \cdot POCl_3$ 1:2 is studied as supercooled liquid. The spectrum of $BiCl_3$ has earlier only been studied in solid state (*cf.* Kohlrausch, *Hand- und Jahrbuch der Chemischen Physik*, 9:IV, Leipzig 1943) and can therefore not be used for comparison. It differs appreciably from the spectrum of $BiCl_3$ dissolved in $POCl_3$.

The shifts of the phosphoryl chloride spectrum are very similar to those caused by $SbCl_3$ except for a splitting of the symmetrical P—Cl bond vibration frequency, 486 cm^{-1}, not observed with $SbCl_3$.

The lowest frequency of $BiCl_3$ shows an obvious continuous shift.

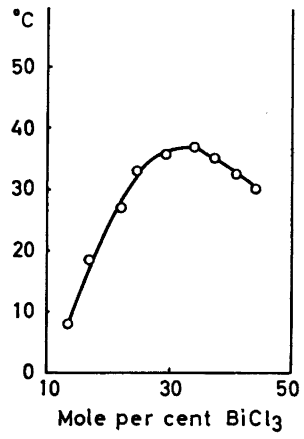

Fig. 1. Liquidus curve for the system $BiCl_3$—$POCl_3$.

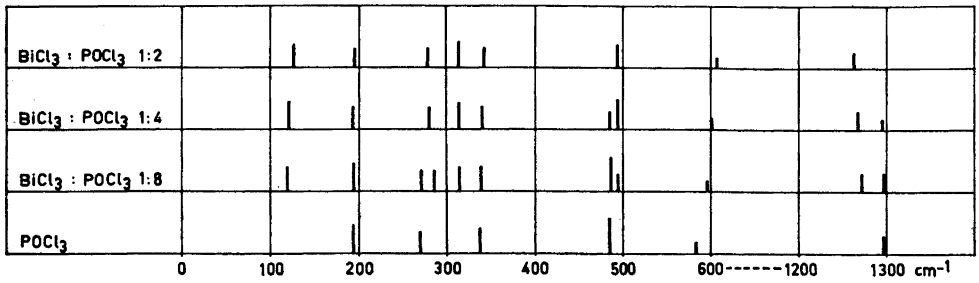

Fig. 2. Raman spectra of the system $BiCl_3-POCl_3$.

THE SYSTEMS $AsCl_3-(CH_3)_2CO$ AND $SbCl_3-(CH_3)_2CO$

The liquidus curves (Figs. 3 a and b) have maxima at the compositions $AsCl_3\cdot(CH_3)_2CO$ and $SbCl_3\cdot 2(CH_3)_2CO$ with melting points $-35°$ and $-24°C$. The tendency of $AsCl_3$ to form 1:1 compounds and of $SbCl_3$ to form 1:2 compounds has been observed before [7]. Studies in the whole range were prevented by supercooling. The reaction vessels were cooled during the measurements. At room temperature a reaction begins in both cases and the liquids darken. (The reaction is probably a condensation of acetone molecules catalysed by the metal halides.)

As the reaction is more rapid in solutions of $AsCl_3$, Raman spectra could not be obtained but the infrared spectra could be recorded.

The solutions of $SbCl_3$ gave a rather dark background in the Raman spectra. The spectrum of the composition 1:1 could not be measured with sufficient accuracy.

The only detectable shifts referred to the spectrum of pure acetone are a decrease of the carbonyl bond stretching frequency and an increase of the antisymmetrical C—C chain vibration frequency. (Only these two frequencies of the acetone spectrum have been listed in Table 1 a.) The same effects were found earlier in addition compounds with acetone as donor and BF_3[8] and $AlBr_3$[9] as acceptors. They are also comparable with the decrease of the phosphoryl band and the increase of the P—Cl bands in the mixtures studied with $POCl_3$.

The infrared spectrum of $AsCl_3$ does not change appreciably.

For comparison the Raman spectra of $SbCl_3$ are tabulated together with the Raman spectra of $SbCl_3$ in $POCl_3$ (Table 1 b).

THE SYSTEM $SbCl_3-(CH_3)_3PO$

The liquidus curve [3] shows maxima at the compositions $SbCl_3\cdot(CH_3)_3PO$ and $SbCl_3\cdot 2(CH_3)_3PO$.

The infrared spectrum of $(CH_3)_3PO$ was investigated by Daasch *et al.*[10] (2—22 μ). We have taken the infrared spectra in the range 2—35 μ and our results are in fairly good agreement with the earlier ones. We have not found

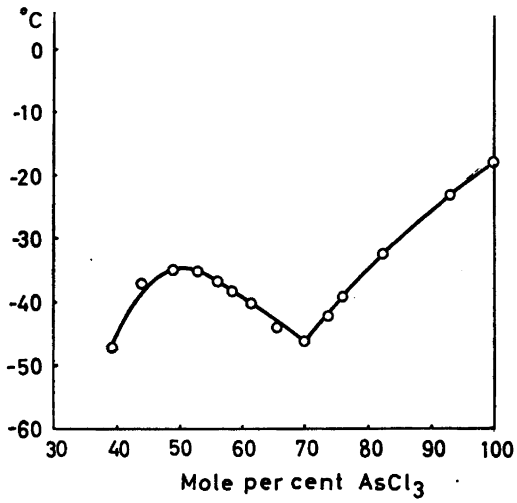

Fig. 3a. Liquidus curve for the system $AsCl_3-(CH_3)_2CO$.

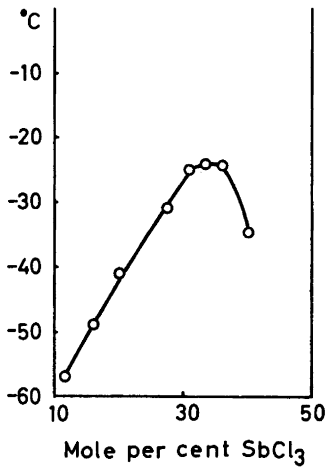

Fig. 3b. Liquidus curve for the system $SbCl_3-(CH_3)_2CO$.

the weak peak at 671 cm^{-1} in the pure substance but it appears in some of the addition compounds. Two new peaks were found in the range 15—35 μ.

(The previous investigators found peaks at 3 410 and 1 672 cm^{-1} and explained the former as arising from reaction with moisture because the substance was very hygroscopic. The latter peak could have the same cause or be a combination frequency. We have also found peaks in those regions but these

Table 1 a.

		I R							Raman		
	$(CH_3)_2CO$	$AsCl_3$:$(CH_3)_2CO$				$SbCl_3$:$(CH_3)_2CO$			$(CH_3)_2CO$	$SbCl_3$:$(CH_3)_2CO$	
		1:4	1:2	1:1	2:1	1:4	1:2	1:1		1:4	1:2
ν (C=O)	1 728	1 712	1 710	1 706	1 700	1 720 1 702	1 718 1 698	1 718 1 695	1 712	1 693	1 691
ν_a(C—C)	1 222	1 228	1 227	1 229	1 228	1 232	1 232	1 234	1 223	1 232	1 230

Table 1 b. Raman.

$SbCl_3$ in $(CH_3)_2CO$		$SbCl_3$ in $POCl_3$	
1:4	1:2	1:4	1:2
134	131	133	133
154	155	156	157
314	319	323	321
351	353	362	363

Table 2.

$(CH_3)_3PO$	$SbCl_3$ in $POCl_3$	$SbCl_3$: $(CH_3)_3PO$ 1:2	$SbCl_3$: $(CH_3)_3PO$ 1:1	$SbCl_5$: $(CH_3)_3PO$ 1:1	$HgCl_2$	$HgCl_2$: $(CH_3)_3PO$ 1:1	$HgCl_2$: $(CH_3)_3PO$ 5:2
(3 325 w)							
(1 640 vw)							
1 425 vw		1 428 vw	1 420 vw	1 420 vw			1 425 vw
1 410 vw			1 410 vw	1 408 vw		1 415 vw	1 415 vw
1 333 vw		1 342 vw				1 333 vw	1 336 vw
1 298 w		1 310 w	1 310 w	1 310 w		1 307 vw	1 308 vw
1 280 w		1 298 w	1 298 w	1 300 w		1 292 w	1 292 w
			1 098 w				
1 158 vs		1 063 vs	1 045 ms	1 037 vs		1 093 vs	1 082 vs
			1 025 s				
945 vs		950 s	948 s	953 s		940 s	943 s
869 ms							
862 ms		868 ms	865 ms	863 ms		860 ms	858 ms
778 vw							755 w
740 s		758 ms	758 w	763 w		749 w	
		670 vw	684 vw	678 vw			749 w
			673 vw				
		596 vw	520 vw				
			438 ms	446 s			
364 vs	363 w	394 vs	403 ms	363 ms	371 s	388 s	397 s
318 ms	333 ms	363 s	359 w	347 ms		359 s	377 ms
		326 ms	338 w	323 w		314 vw	345 s
		317 w	308 vw	296 vw			314 vw
			296 vw				

disappeared completely after adduct formation. This certainly should be the result if the absorption arose from hydrate formation.)

Antimony trichloride has not been investigated by infrared spectroscopy earlier and an attempt failed because the substance reacted with the TlBr—TlI plates. For comparison, the spectrum of $SbCl_3 \cdot 2POCl_3$ was taken. When the peaks from $POCl_3$ were excluded, two peaks remained.

The results from the infrared study are given in Table 2. The phosphoryl bond vibration frequency 1 158 cm^{-1} is split and shows a larger shift in the 1:1 compound than in the 1:2 compound. (The largest shift is 131 cm^{-1}.) In the range 15—35 μ the two addition compounds show great diversities. The spectra of the components seem not to be very much changed in the 1:2 compound but the 1:1 compound shows new absorption peaks.

THE SYSTEM $SbCl_5$—$(CH_3)_3PO$

Relative enthalpy measurements (carried out in 0.4 M ethylene chloride solutions in mole ratio 1:1) show that $SbCl_5$ is a much stronger acceptor than $SbCl_3$ with $(CH_3)_3PO$ as donor molecule.

The results in Table 2 show that the phosphoryl bond frequency has decreased 126 cm^{-1}. The shift is thus in the same order of magnitude as in the compound $SbCl_3 \cdot (CH_3)_3PO$ in spite of the large difference between enthalpy changes of the two reactions.

The infrared spectrum of $SbCl_5$ has not been investigated, which prevents any comparisons.

THE SYSTEM $HgCl_2-(CH_3)_3PO$

Thermochemical measurements carried out in 0.4 M alcoholic solutions show that $SbCl_3$ gives larger enthalpy change than $HgCl_2$ in reacting with $(CH_3)_3PO$ in the mole ratio 1:1.

Two addition compounds are found in this system: $5HgCl_2 \cdot 2(CH_3)_3PO$ and $HgCl_2 \cdot (CH_3)_3PO$.[3] The symmetrical phosphoryl bond vibration frequency has the largest shift in the 5:2 compound but not as large as in the compounds with $SbCl_3$.

$HgCl_2$ has only one infrared active band in the range studied, the antisymmetrical Hg—Cl bond stretching frequency at 371 cm^{-1}. This frequency decreases at adduct formation (*e.g.* with 1,4-dioxane [11] and $(C_6H_5)_3PO$[3]). One of the two compounds gives a more complicated spectrum in this case too.

THE SYSTEM $HgCl_2-(C_2H_5)_2S$

Two compounds in this system have been described earlier [12]: $2HgCl_2 \cdot (C_2H_5)_2S$ and $HgCl_2 \cdot (C_2H_5)_2S$. The 1:1 compound, however, loses ethyl sulfide on grinding [13] and the infrared spectra could not be taken. The ethyl sulfide has no frequency lower than 640 cm^{-1} but the 1:1 adduct has two low frequencies, 343 and 311 cm^{-1} (*cf.* $HgCl_2$, 371 cm^{-1}).

DISCUSSION

1. The spectra of the systems $BiCl_3-POCl_3$, $AsCl_3-(CH_3)_2CO$ and $SbCl_3-(CH_3)_2CO$ show a similar type of interaction, as found earlier [1] in the systems $AsCl_3-POCl_3$ and $SbCl_3-POCl_3$ but the changes in the spectra of the acceptor molecules are larger.

2. In the systems $SbCl_3-(CH_3)_3PO$ and $HgCl_2-(CH_3)_3PO$, where two compounds have been studied in each system, one of the compounds does not change its spectrum very much but the other shows new peaks in the region where the acceptor molecules absorb.

According to the introduction, the spectra of $SbCl_3 \cdot 2(CH_3)_3PO$ and $HgCl_2 \cdot (CH_3)_3PO$ indicate weak dipole-dipole interaction and $SbCl_3 \cdot (CH_3)_3PO$ and $5HgCl_2 \cdot 2(CH_3)_3PO$ strong interaction caused by acceptor-donor reactions. It is however hard to understand how the acceptor-donor bonds could be of different nature in the same acceptor-donor systems.

The present results do not seem to supply evidence for the suggestion that two different types of interaction exist. They indicate rather that the acceptor-donor bond strengths change continuously from weak to strong interaction.

3. The fact that the spectrum of $2HgCl_2 \cdot (C_2H_5)_2S$ has two low frequencies is in agreement with the structure of this compound, very recently determined by X-ray work at this institute [13]. This structure determination shows that the two $HgCl_2$ molecules are bonded in different ways. One of them has changed its coordination and structure by the adduct formation, the other is rather unchanged.

The new peaks in the spectra of the compounds $5HgCl_2 \cdot 2(CH_3)_3PO$ and $SbCl_3 \cdot (CH_3)_3PO$ may also indicate that the acceptor molecules are bonded in different ways or that the chlorine atoms of the same acceptor molecule are not equivalent after the adduct formation. Such structures have already been found: $3HgBr_2 \cdot 2Bu_3As$[14] and $(TiCl_4 \cdot POCl_3)_2$[15].

4. Sheldon and Tyree [16] have interpreted the shifts obtained in the P—O stretching frequency by adduct formation as due to a weakening of the P—O bond. It must be assumed that the magnitude of these shifts is a measure of the weakening if the donor molecule is the same. It might naturally be supposed that this weakening is closely related to the bond strength between the donor and the acceptor atom.

The two adducts $SbCl_3 \cdot (CH_3)_3PO$ and $SbCl_5 \cdot (CH_3)_3PO$ give about the same shifts of the P—O bond frequency but very large difference between the enthalpy changes of the reactions.

If the above assumptions are correct, these results show that the enthalpy changes at the acceptor-donor reactions are not only dependent on the acceptor-donor bond formation but also very much on the gain or loss of energy involved in the structural changes of the acceptor molecules. The reservation in the earlier paper [1], that the magnitude of the shift as a measure of relative acceptor strengths can only be used "if the acceptor molecules to be compared are under very similar conditions" is thus shown to be well justified.

A grant from the *Swedish Natural Science Research Council* is gratefully acknowledged.

We wish to thank Prof. S. Claesson, Prof. G. Hägg and Prof. A. Tiselius for all the facilities put at our disposal and Dr. I. Lindqvist for suggesting the problem and his stimulating interest during the work.

We also wish to thank Dr. P. O. Kinell for valuable discussions and Mr. S. Johansson for helpful assistance.

REFERENCES

1. Kinell, P.-O., Lindqvist, I. and Zackrisson, M. *Acta Chem. Scand.* **13** (1959) 1159.
2. Lindqvist, I. and Brändén, C. I. *Acta Cryst.* **12** (1959) 642.
3. Lindqvist, I. and Olofsson, G. *Acta Chem. Scand.* **13** (1959) 1753.
4. Inorganic Syntheses **5** (1957) 153.
5. Agerman, M., Andersson, L.-H., Lindqvist, I. and Zackrisson, M. *Acta Chem. Scand.* **12** (1958) 477.
6. Lindqvist, I. and Zackrisson, M. *Acta Chem. Scand.* **14** (1960) 453.
7. Lindqvist, I. and Einarsson, P. *Acta Chem. Scand.* **13** (1959) 420.
8. Susz, B. P. and Chalandon, P. *Helv. Chim. Acta* **41** (1958) 1332.
9. Terenin, A., Filimonov, W. and Bystrov, D. *Z. Elektrochem.* **62** (1958) 181.
10. Daasch, L. W. and Smith, D. C. *J. Chem. Phys.* **19** (1951) 22; *Anal. Chem.* **23** (1951) 853.
11. Tarte, P. and Laurent, P. A. *Bull. soc. chim. France* **1957** 403.
12. Faragher, W. F., Morrell, J. C. and Comay, S. *J. Am. Chem. Soc.* **51** (1929) 2774.
13. Brändén, C. I. *Private communication.*
14. Evans, R. C., Mann, F. G., Peiser, H. S. and Purdie, D. *J. Chem. Soc.* **1940** 1209.
15. Brändén, C. I. and Lindqvist, I. *Acta Chem. Scand.* **14** (1960) 726.
16. Sheldon, J. C. and Tyree, S. Y. *J. Am. Chem. Soc.* **80** (1958) 4775.

Received January 30, 1960

ACTA CHEMICA SCANDINAVICA 14 (1960) 1001–1005

The Crystal Structure of Re_3B

B. ARONSSON, (Miss) MAGGIE BÄCKMAN and S. RUNDQVIST

Institute of Chemistry, University of Uppsala, Uppsala, Sweden

The crystal structure of Re_3B has been determined by powder and single crystal methods. The dimensions of the orthorhombic unit cell are $a = 2.890$ Å, $b = 9.313$ Å and $c = 7.258$ Å ($\pm$ 0.05 %). There are four formula units in the elementary cell, and the space-group is *Cmcm*. The twelve rhenium atoms are situated in an eightfold position 8 (*f*) ($y = 0.1345$, $z = 0.0620$) and a fourfold position 4 (*c*) ($y = 0.4262$). From space considerations it has been concluded that the boron atoms are also situated in a 4 (*c*) position ($y \simeq 0.744$).

It was reported in an earlier communication [1] that three intermediate phases had been identified in arcmelted rhenium-boron alloys. Two of the phases, Re_7B_3 and ReB_3, were characterized by crystal structure data and the lattice parameters (l.p.) of the third phase, having the approximate composition Re_3B, were also given. As it was possible to obtain single crystals of Re_3B we decided to try to solve its structure with the principal aim of determining interatomic distances with moderate accuracy.

EXPERIMENTAL

Alloys were prepared by arcmelting rhenium (claimed purity *ca.* 99.8 %, obtained from Heraeus, Hanau, Germany) and boron (claimed purity 99.0–99.7 %, kindly donated by Borax Consolidated, London). No chemical analyses were carried out and all reported compositions are nominal.

Powder photographs using Cu$K\alpha$- and Cr$K\alpha_1$-radiation were taken with cameras of the Guinier type (the internal standard was silicon, $a = 5.4306$ Å) and single crystal photographs around the *a*-axis with an ordinary Weissenberg camera using Mo$K\alpha$ radiation. The multiple film technique was employed with thin iron foil between the films. Intensities were estimated by comparison with an intensity scale. Fourier series and structure factor calculations were made on the electronic digital computer BESK with programs (available at BESK) devised by M. Edstrand and Åsbrink *et al.*[2] In the structure factor calculations the atomic scattering factors were approximated to the following expression:

$$f_i = A_i.\exp\left(-\frac{a_i}{\lambda^2}\sin^2\Theta\right) + B_i.\exp\left(-\frac{b_i}{\lambda^2}\sin^2\Theta\right) + C_i.\exp\left(-\frac{c_i}{\lambda^2}\sin^2\Theta\right) + D_i$$

Appel [3] has calculated the following constants on the basis of the scattering factor tables by Tomas and Umeda [4] (rhenium) and Ibers [5] (boron)

	A	B	C	a	b	c
Rhenium	25.854	28.303	19.925	0.170	1.885	15.175
Boron	1.644	0.406	2.878	0.6069	4.5832	33.019

The real part of the dispersion correction, (D_i in the above expression), for rhenium was taken from the table of Dauben and Templeton[6].

RESULTS

The powder photographs of alloys in the composition range $ReB_{0.2}$—$ReB_{0.4}$ indicated the existence of the two-phase regions Re + Re_3B and Re_3B + Re_7B_3. The powder photograph of an alloy with the nominal composition Re_3B is given in Table 1. It may be seen in the table that nearly all lines can be indexed with a centred orthorhombic cell (a = 2.890 Å, b = 9.313 Å, c = 7.258 Å, ± 0.05 %). The origin of the three non-indexed weak lines is unknown. No l.p. variations greater than 0.1 % for Re_3B have been observed indicating that its range of homogeneity is narrow. It is concluded from the unit cell dimensions that there are twelve rhenium atoms in the elementary cell. The calculated X-ray density of Re_3B is 19.4 g/cm³.

Single crystal photographs confirmed that Re_3B is orthorhombic and since *hkl* reflexions only appeared for $h + k = 2n$ and *h0l* reflexions for $l = 2n$, the most probable space groups are *Cmcm*, *C2cm* and $Cmc2_1$. Apart from the normal decrease the distribution of intensities in the 0*kl* and 2*kl* zones was

Table 1. X-ray powder data of an arcmelted alloy with the nominal composition Re_3B ($CrKa_1$ radiation, λ = 2.2896 Å, internal standard: silicon, a = 5.4306 Å).

h k l for Re_3B	$\sin^2\Theta_{obs}$	$\sin^2\Theta_{calc}$ for Re_3B	I_{obs}	I_{calc} for Re_3B	$p\|F\|^2 \cdot 10^{-3}$ for Re_3B
?	0.0464		w		
020	0.0605	0.0604	w	27	19.8
002	0.0994	0.0995	w	19	25.4
?	0.1079		w		
?	0.1174		w		
022	0.1601	0.1600	m	76	152.9
110	0.1719	0.1720	w	22	47.6
111	0.1968	0.1969	st	207	504.8
040	0.2418	0.2418	st	205	569.0
041	0.2665	0.2667	m	101	289.4
112	0.2714	0.2715	vst	510	1499.2
023	0.2844	0.2844	vst	497	1505.5
130	0.2930	0.2929	st	237	716.7
131	0.3177	0.3178	st	277	840.8
042	0.3413	0.3413	w	82	247.8
132	0.3924	0.3924	m	140	378.4
113	0.3959	0.3959	m	123	331.9
004	0.3982	0.3981	w	38	100.7
024	0.4585	0.4585	vw	29	64.3

similar indicating that the rhenium atoms are situated in planes perpendicular to the a-axis with a spacing of $a/2$. With this distribution of atoms the $|F|^2$ values for $0kl$ and $1kl$ reflexions were sufficient for the evaluation of the Patterson section $P(0yz)$. The position and heights of all peaks in $P(0yz)$ could be explained if the rhenium atoms were assumed to occupy one 8(f) and one 4(c) position in the space group *Cmcm*. This space-group was thus chosen and during the refinement of the structure nothing was found to contradict this choice.

The y and z coordinates of the rhenium atoms were refined from successive $\varrho_o(yz)$ and $\varrho_c(yz)$ electron density projections. In the final stages of refinement the F_o values of the four strongest reflexions, which were obviously weakened because of extinction, were replaced by the corresponding F_c values. Using an empirical isotropic temperature factor ($B = 0.07_8$ Å^2) the final R value of 96 observed $0kl$ reflexions (omitting the four strongest reflexions) was 12.4 % *. This relatively high value for the discrepancy index results from no corrections having been made for absorption, and that extinction has been only partly, and extremely crudely, corrected for. It should be noted that because of these errors the uncertainty of the atomic parameters is probably greater than as indicated by the standard deviations calculated from Cruickshank's [7] formula and given below.

From space considerations it is evident that the boron atoms must be located in a 4(c) position with $y \simeq 0.744$. As no boron parameter can be obtained from the experimental data we have chosen it so that the six shortest rhenium-boron atomic distances are equal.

The resulting atomic parameters are:

8 Re_I in 8(f) : $y = 0.1345 \pm 0.0003$, $z = 0.0620 \pm 0.0003$
4 Re_{II} in 4(c) : $y = 0.4262 \pm 0.0003$
4 B in 4(c) : $y = 0.744$

A projection of the structure on the bc-plane is shown in Fig. 1. The structure is very simple and may be described as being built up of triangular prisms of rhenium atoms at the centres of which are boron atoms. The rhenium skeleton is densely packed and the average values of the shortest rhenium-rhenium distances (see Table 2) are only just greater than the shortest rhenium-rhenium distance in elementary rhenium, *i.e.* 2.74 Å. Parallel to {023} the rhenium atoms form slightly corrugated densely packed planes which consist of interconnected triangles and squares.

The boron atoms have the same environment as in a number of other borides [8]: *i.e.* six neighbours at the corners of a triangular prism and three more remote neighbours outside the rectangular faces of the prism. (The two boron neighbours outside the triangular faces of the prism are probably too distant (2.89 Å) for consideration). The average of the six shortest metal-boron distances is 2.23 Å in good agreement with the value of 2.24 Å which is the sum of the normal atomic radius of boron (0.87 Å according to Kiessling [9]) and the atomic radius of rhenium for coordination number 12 (1.37 Å). In Re_3B, as

* A list of calculated and observed structure factors can be obtained from this Institute on request.

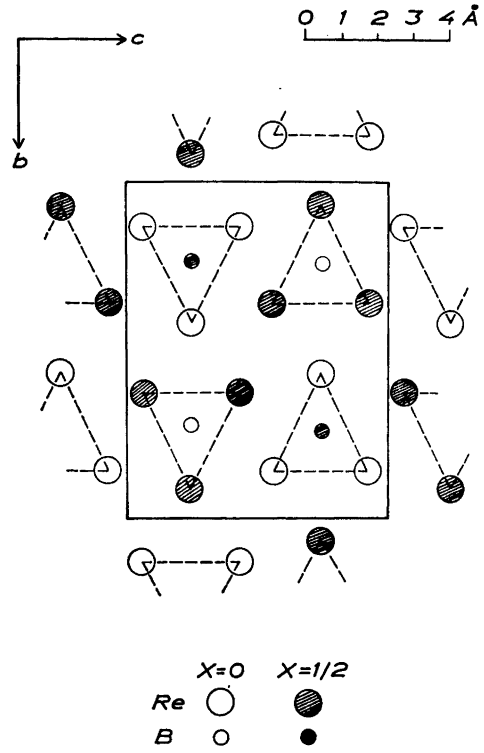

Fig. 1. The structure of Re_3B projected on (100).

in the borides of the Th_7Fe_3 and cementite structures [1,9], all the nine neighbours of boron are metal atoms. The coordinations around the metal atoms are also similar in these three closely related structures.

Table 2. Interatomic distances in Re_3B (in Å).

			Average
Re_I in 8 (*f*)	— 6 Re_I :	2.66, 2.73, 2.74 (2), 2.89 (2)	2.79
	— 5 Re_{II}:	2.74 (2), 2.78 (2), 3.04.	
	— 3 B :	2.23 (2), 2.54.	
Re_{II} in 4 (*c*)	— 10 Re_I :	2.74 (4), 2.78 (4), 3.04 (2)	2.83
	— 2 Re_{II}:	2.89 (2).	
	— 3 B :	2.23 (2), 2.95.	
B 4 (*c*)	— 6 Re_I :	2.23 (4), 2.54 (2)	2.23
	— 3 Re_{II}:	2.23 (2), 2.95	(six first)
	(— 2 B :	2.89 (2)).	

Acknowledgements. The authors wish to thank Professor G. Hägg for his encouraging interest and many valuable comments on the manuscript. Financial support is gratefully

acknowledged from the *Air Force Office of Scientific Research of the Air Research and Development Command, United States Air Force,* through its European Office under Contract No. AF 61(052)-40 and from the *Swedish Technical Science Research Council.*

REFERENCES

1. Aronsson, B., Stenberg, E. and Åselius, J. *Acta Chem. Scand.* **14** (1960) 733.
2. Åsbrink, S., Blomqvist, G. and Westman, S. *Arkiv Kemi* **14** (1959) 545.
3. Appel, K. "*Technical Note from the Quantum Chemistry Group, University of Uppsala*".
4. Tomas, L. H. and Umeda, K. *J. Chem. Phys.* **26** (1957) 293.
5. Ibers, J. A. *Acta Cryst.* **10** (1957) 86.
6. Dauben, C. H. and Templeton, D. H. *Ibid.* **8** (1955) 841.
7. Cruickshank, D. W. J. *Ibid.* **2** (1949) 65.
8. Kiessling, R. *Acta Chem. Scand.* **4** (1950) 209.
9. Rundqvist, S. *Ibid.* **12** (1958) 658.

Received January 25, 1960.

ACTA CHEMICA SCANDINAVICA 14 (1960) 1006–1010

Analysis of Human Bile Lipids by Gas-Liquid Chromatography

ROLF BLOMSTRAND

From the Swedish Medical Research Council, Unit for Biochemical Research Related to Atherosclerosis, University of Lund, Sweden

The lipids of human gall-bladder bile have been fractionated by silicic acid chromatography and the fatty acid composition of the different lipid classes determined with gas-liquid chromatography.

Small amounts of cholesterol ester was found to be present in human bile. Lecithin is the predominating phospholipid.

Palmitic, stearic, oleic and linoleic acid were the major fatty acids in the bile lecithin indicating the presence of several different lecithins in human bile.

An asymmetric or specific positioning of the long chain fatty acids in the bile lecithin is described.

Relatively little is known about the composition of the fatty acids of human bile [1,2]. The major reason for this has been the lack of adequate methods for fatty acid analysis especially on a microscale. From preliminary studies with gas-liquid chromatography (GLC) of the total fatty acids of human bile, it appeared that the fatty acids constituted a complex mixture of several components. The studies were extended with separation of the total bile lipids of human gall-bladder on silicic acid and determination of the fatty acids of the different lipids by GLC.

Furthermore the lecithin of human gall-bladder bile was purified and the fatty acid distribution determined after enzymatic degradation. The results indicate the presence of several different lecithins in the human bile.

METHODS

Bile was collected by aspiration into methanol from the gall-bladder of patients without hepatobiliary disease and also from patients with gall-stones and biliary tract disease (to be published [3]). The bile was extracted with chloroform: methanol 2:1 according to Folch-Lee [4] as modified by Borgström [5]. The total lipids of the bile was subjected to chromatography on silicic acid in order to obtain a neutral fat nonesterified fatty acid fraction and a phospholipid fraction. Then the nonesterified fatty acids were removed from the neutral fat by extraction with alkaline 50 % ethanol. The neutral fat fraction (glycerides, cholesterol and cholesterol esters) were subjected to chromatography on silicic

Table 1. Composition of human gall-bladder bile lipids after separation on silicic acid. The bile was collected from subjects without known biliary disease.

Subject	Total Fat mg/100 ml	Cholesterol mg/100 ml		Fatty acids as percentage of total fatty acids			
		Free	Total	Cholesterol ester FA	Non-esterified FA	Glyceride FA	Phospholipid FA
1	700	110	116	0.7	3.3	4.0	92.0
2	852	120	128	0.4	5.1	3.1	91.4
3	902	125	135	0.9	6.1	7.0	86.0

acid for separation of cholesterol esters and a triglyceride-cholesterol fraction [6]. The phospholipids were fractionated by the procedure described by Hanahan *et al.*[5]

The progress of the chromatographic separation was followed by phosphorus assay and paper chromatography. Lecithin constituted the predominating phospholipid but small amounts of unidentified phospholipids were also found. The lecithins were rechromatographed on aluminium oxide [8]. Enzymatic degradation was performed with phospholipase A *(Crotalus adamanteus* [9]). The hydrolysis products were fractionated on silicic acid in order to separate free fatty acids and unchanged lecithin and lysolecithin. The fatty acids of the lysolecithin were obtained after hydrolysis, acidification and extraction with light petroleum.

GLC was carried out essentially as described by James and Martin [10] using an Argon Pye Chromatograph with an ionization chamber as detector. As stationary phase a polar polyester (LHC–R–296) [11] was used in the ratio Celite: stationary phase 4:1. For identification the samples were also chromatographed at 240°C with silicone oil (Dow Corning High vacuum grease) as stationary phase in the ratio Celite: stationary phase 4:1. The experimental procedures used otherwise have been described earlier [12].

Fatty acids are numbered as suggested by Insull *et al.*[13] The category 20–22? refers to a group of unsaturated fatty acids whose structure has yet to be determined.

RESULTS

The determination of the different lipid components of human gallbladder bile are summarized in Table 1. The phospholipid fatty acids constitute the major components of the total fatty acids of human bile. Small amounts of triglyceride and cholesterol ester fatty acids are also present, as well as small amounts of non-esterified fatty acids. Similar results have been obtained by Nakayama and Johnston [14].

Results of determinations of several components of human biliary fatty acids are summarized in Table 2. Three characteristic fatty acid patterns are found in the phospholipids, triglycerides and cholesterol esters of the human bile. Palmitic, oleic and linoleic acids are the major constituents in all of these lipid classes. Arachidonic acid is also found in significant amounts in the triglycerides, non-esterified fatty acids and the phospholipid fatty acids.

Palmitic acid represents approximately 13 % of the total fatty acids of bile glycerides, 57 % of the cholesterol ester fatty acids and 28 % of the phospholipid total fatty acids. Stearic acid occurs to the extent of 1.8, 9.8 and 3.0 % of the triglyceride, cholesterol ester and phospholipid fatty acids, respectively.

Table 2. The fatty acid composition of the different lipid classes of human gall-bladder bile. The fatty acids were determined with gas-liquid chromatography and the values given are the percentage of the fatty acid methyl esters. The component fatty acids are also designated by a dual symbol giving chain length and number of double bonds. The sum of each column is less than 100 % because of trace amounts of unusual fatty acids detected were omitted from the final tabulation.

Fatty acid		Tri-glyceride FA %	Non-esterified FA %	Cholesterol FA %	Phospho-lipid FA %
Saturated					
Lauric	12:0				1.0
Myristic	14:0	0.9	0.5	0.9	3.2
Pentadecanoic	15:0	0.7	0.7	1.0	1.4
Palmitic	16:0	12.8	22.3	37.2	28.1
Heptadecanoic	17:0	0.4	0.4	0.7	0.7
Stearic	18:0	1.8	8.3	9.8	18.3
Mono-unsaturated					
Palmitoleic	16:1	5.8	7.4	6.1	3.1
Oleic	18:1	6.9	18.6	26.3	14.1
Di-unsaturated					
Linoleic	18:2	39.9	26.8	15.1	12.7
Poly-unsaturated					
Linolenic	18:3	2.3	1.0		2.4
Arachidonic	20·4	14.4	6.2		2.4
	20—22 ?	9.5	5.3	0.7	8.0

The results of this study indicate that palmitic acid occurred as a predominating fatty acid component in the lysolecithin formed from bile lecithin by phospholipase A (Table 3). As with palmitic acid stearic acid was also found predominantly in the lysolecithin formed. Small amounts of lauric, myristic, pentadecanoic, palmitoleic, oleic and linoleic acid were also found in the lysolecithin, together with some unidentified fatty acids with 13 carbon atoms. In the fatty acids released by phospholipase A from the bile lecithin the polyunsaturated fatty acid predominated together with oleic acid. Palmitic acid was also present together with trace amounts of myristic and stearic acid. Linoleic acid was the major polyunsaturated fatty acid but linolenic and arachidonic acid were also found in significant amounts. There were two C_{20-22} fatty acids occurring on the gas-chromatogram of this fraction of the lecithin. The exact nature of these fatty acids has not yet been determined.

From the results of this investigation it is evident that there are several lecithins present in the human bile. Recently new evidence has been provided on the position of saturated and unsaturated fatty acid esters in purified egg lecithin [19]. For this reason a brief discussion on the distribution of the fatty acids of the bile lecithin will be given.

It has been known for several years [15] that snake venom phospholipase A liberates mainly unsaturated fatty acids from lecithins containing saturated and unsaturated fatty acids. In recent years it has also been shown that

Table 3. The fatty acid composition of human gall-bladder bile lecithin. The lecithin was purified by silicic acid column chromatography and hydrolysed with phospholipase A. The fatty acids released by the action of phospholipase A and the fatty acids of the lycolecithin were determined by gas-liquid chromatography.

Fatty acid		Percentage of total fatty acids in respective positions of human bile lecithin	
		Fatty acids freed from bile lecithin by phospholipase A	Fatty acids obtained after hydrolysis of lysolecithin
Saturated			
Lauric	12:0		0.9
	13: ?		5.3
Myristic	14:0	0.6	5.3
Pentadecanoic	15:0	0.7	5.4
Palmitic	16:0	17.1	53.8
Heptadecanoic	17:0	0.7	
Stearic	18:0	1.5	6.5
Mono-unsaturated			
Palmitoleic	16:1	6.4	7.9
Oleic	18:1	25.9	6.6
Di-unsaturated			
Linoleic	18:2	32.1	1.7
Poly-unsaturated			
Linolenic	18:3	1.5	
Arachidonic	20:4	5.1	
	20—22 ?	6.0	

both di-saturated and di-unsaturated lecithins are equally well hydrolysed to yield one mole of fatty acid and the corresponding lysolecithin [8]. It was therefore concluded [16] that the action of the enzyme was directed toward one particular ester group C-1 (α) or C-2 (β) in the lecithin molecule. Hanahan [17] using permanganate oxidation procedures, concluded that the snake venom phospholipase A specifically hydrolyzed the ester linkage in the C-1 (α) position. Several investigators [9] have confirmed this finding, but conflicting results [18] have also been obtained, suggesting the lack of specificity of phospholipase A. Tattrie [19] has with a new approach investigated the position of the fatty acids on lecithin. Purified egg lecithin was enzymatically hydrolysed to the corresponding mixture of α-β-diglycerides with lecithinase D. Myristic acid was incorporated into the α position of the diglyceride and the resulting triglycerides were hydrolysed with pancreatic lipase, which specifically cleaves fatty acids from the α and α' positions. Only saturated fatty acids were freed by the pancreatic lipase, proving that the saturated fatty acids occupy the α position of egg lecithin. Since snake venom phospholipase removes only unsaturated fatty acid from egg lecithin the site of hydrolysis must be at the β position of the lecithin according to Tattrie [19]. The specificity of phospholipase A therefore seems well established, although further work is necessary to definitely settle the question about the site of attack of the enzyme.

From the analysis shown in Table 3 it is apparent that there is an asymmetric distribution of the fatty acids in the human bile lecithin. According to the discussion above the predominant ester pattern should be saturated fatty acids in the C-1 (α) ester position and unsaturated fatty acids in the C-2 (β) ester position. However, both C-1 and C-2 position contained saturated and unsaturated fatty acids.

COMMENTS

Bile contains lecithins and small amounts of soaps to which an accessory function in emulsification has been ascribed [20]. The complex picture of the fatty acid composition of the different lipid classes of the bile and especially the complex composition of the fatty acids of the lecithins makes further studies on the metabolism of the biliary fatty acids necessary. There are very little information available on the influence of the dietary fat on the fatty acid pattern of the bile. Furthermore it will be of interest to investigate how the fatty acid pattern of bile might vary in biliary disease.

Recently Borgström [5] has analysed the fatty acid composition of human bile lecithin with the aid of paper chromatography. He found only oleic acid released form the lecithin by phospholipase A and palmitic acid in the lysolecithin. The difference in results has to be found in the different material and methods used for the analyses.

This work is part of investigations supported by the *Swedish Medical Research Council.*

REFERENCES

1. Sobotka, H. *Physiological Chemistry of the Bile*, Williams and Wilkins, Baltimore; Bailiere, Tindal and Cox, London, 1937.
2. Isaksson, B. *Acta Soc. Med. Upsaliensis* **56** (1951) 177.
3. Blomstrand, R. and Ekdahl, P. *Proc. Soc. Exp. Biol. and Med.* **104** (1960) 205.
4. Folch, J. and Lee, J. *J. Biol. Chem.* **191** (1951) 833.
5. Borgström, B. *Acta Chem. Scand.* **11** (1957) 749.
6. Borgström, B. *Acta Physiol. Scand.* **25** (1952) 101.
7. Hanahan, D. J., Dittmer, J. C. and Warashina, E. *J. Biol. Chem.* **228** (1957) 685.
8. Hanahan, D. J., Rodbell, M. and Turner, L. D. *J. Biol. Chem.* **206** (1954) 431.
9. Long, C. and Penney, I. F. *Biochem. J.* **68** (1957) 382.
10. James, A. T. and Martin, A. J. P. *Biochem. J.* **63** (1956) 144.
11. Orr, C. and Callen, J. E. *J. Am. Chem. Soc.* **80** (1958) 249.
12. Blomstrand, R. and Dahlbäck, O. *Acta Soc. Med. Upsaliensis* **114** (1959) 177.
13. Insull, W. Jr., James, A. T. and Ahrens, E. H. Jr. *J. Clin. Invest.* **38** (1959) 892.
14. Nakayama, F. and Johnston, c.q. Personal communication.
15. Wittcoff, H. *The Phosphatides*, Reinhold Publishing Corp, New York 1951, p. 105.
16. Zeller, E. A. *Federation Proc.* **11** (1952) 316.
17. Hanahan, D. J. *J. Biol. Chem.* **207** (1954), 879.
18. Marinetti, G. V., Erbland, J. and Stotz, E. *J. Am. Chem. Soc.* **81** (1959) 861.
19. Tattrie, N. H. *J. Lipid Research* **1** (1959) 60.
20. Fürth, O. and Minibeck, H. *Biochem. Z.* **237** (1931) 139.

Received January 27, 1960.

ACTA CHEMICA SCANDINAVICA 14 (1960) 1011–1018

The Crystal Structure of Pd_3Si

B. ARONSSON and (Miss) ANNA NYLUND

Institute of Chemistry, University of Uppsala, Uppsala, Sweden

The crystal structure of Pd_3Si has been established from single crystal data. The space-group is *Pnma*, and there are four formula units in the elementary cell which has the dimensions $a = 5.735$ Å, $b = 7.555$ Å, and $c = 5.260$ Å. The twelve palladium atoms are situated in 8 (*d*) ($x = 0.1810$, $y = 0.0508$, $z = 0.3217$) and 4 (*c*) ($x = 0.0053$, $z = 0.9036$) positions, and the silicon atoms occupy a 4 (*c*) position ($x = 0.897_6$, $z = 0.469_6$). Pd_3Si, thus, crystallizes in the cementite ($D0_{11}$) structure. The atomic arrangement in Pd_3Si is compared with those in isomorphous phases.

The crystal structures of some platinum metal silicides are being investigated at this Institute principally to elucidate the coordination around the silicon atom. In this paper we present the results of the structure determination of Pd_3Si and also comment on the Pd–Si system. The crystal structures of Ru_2Si and Rh_2Si have been reported in a preliminary note [1] and will be dealt with more comprehensively in a future paper.

EXPERIMENTAL

Palladium powder, (claimed purity 99.9 %, containing traces of Fe, Cu, and Ag), was obtained from Heraeus (Hanau, Germany), and silicon powder (claimed purity 99.9 %) from Pechiney (Paris). Because of the comparatively low melting points of Pd–Si alloys the samples were easily prepared by sintering (or melting) mixtures of the elements in evacuated and sealed silica tubes. No chemical analyses were made.

Powder photographs were taken in cameras of the Guinier type with CaF_2 ($a = 5.4630$ Å) as an internal standard. Two small single crystals ($\sim 0.3 \times 0.04 \times 0.04$ mm) were picked out of an alloy which had the nominal composition $PdSi_{0.3}$ and had been annealed for two days at 900°C. (This temperature is slightly below the reported peritectic temperature [2,3] of 950°C.) Weissenberg photographs were taken around the *b*- and *c*-axes using Mo$K\alpha$ radiation and the multiple film technique with thin iron foil between the films. Fourier projections were calculated with Beevers-Lipson strips and on the digital electronic computer BESK with a program (available at BESK) devised by M. Edstrand. The structure factors were also computed on BESK with a program devised by Åsbrink *et al.*[4] The following expression was used for the scattering factors:

$$f_i = A_i \cdot \exp(-\frac{a_i}{\lambda^2}\sin^2\Theta) + B_i \cdot \exp(-\frac{b_i}{\lambda^2}\sin^2\Theta) + C_i \cdot \exp(-\frac{c_i}{\lambda^2}\sin^2\Theta)$$

Table 1. Crystallographic constants of the well established silicides of palladium.

	Structure type	Lattice parameters (in Å)	References
Pd_3Si	$D0_{11}$	$a = 5.735$, $b = 7.555$, $c = 5.260$	(This work)
Pd_2Si	$C22$	$a = 6.497$, $c = 3.432$ (silicon-poor) *	» »
	(revised)	$a = 6.528$, $c = 3.437$ (silicon-rich) *	» »
PdSi	B 31	$a = 5.599$, $b = 3.381$, $c = 6.133$	10

* These values refer to alloys sintered at 800°C.

Appel [7] has calculated the following constants on the basis of the scattering factor tables by Tomas and Umeda [5] (palladium) and Tomiie and Stam [6] (silicon).

	A	B	C	a	b	c
Pd	15.865	17.354	12.288	0.233	2.565	19.828
Si	2.8315	6.8065	4.3870	0.3235	2.2965	51.770

RESULTS

The Pd—Si system: We confirmed the existence of the earlier reported phases Pd_3Si[2,8], Pd_2Si[9,2,8], and PdSi [10,8]. In alloys containing more than 75 atom per cent palladium and annealed at 600—700°C, two additional intermediate phases were observed. The thermal effects observed by Lebeau and Jolibois [11] around 600°C in palladium alloys may have been caused by the formation of one of these phases, rather than by the supercooling of the peritectic formation of Pd_3Si as suggested in the handbook by Hansen [3]. The phase Pd_9Si_4 reported by Rao and Winterhager [8] could not be detected in our alloys.

The structures and unit cells of Pd_3Si, Pd_2Si and PdSi are given in Table 1. Schubert and Pfisterer [10] found the structure of PdSi to be of the B 31 type. Schubert and Anderko [2] found that Pd_2Si and Fe_2P were isomorphous and, as pointed out by Rundqvist and Jellinek [12], it is very probable that Pd_2Si, similarly to Fe_2P crystallizes in the revised C 22 structure. The lattice parameters (1. p.) of Pd_3Si, (the existence of this phase was first established by Schubert and Anderko[2]), were determined by the present authors. A typical powder photograph of an alloy with the nominal composition $PdSi_{0.3}$ is given in Table 2. We could not detect any significant (*i.e.* > 0.05 %) l.p. variations for Pd_3Si. The l.p's of Pd_2Si, however, were considerably larger in silicon-rich alloys than in silicon-poor — indicating that Pd_2Si has an appreciable range of homogeneity.

The structure of Pd_3Si: The single crystal photographs showed that Pd_3Si is orthorhombic. Since $0kl$ reflexions were only observed for $k + l = 2n$ and $hk0$ reflexions only for $h = 2n$, the possible space-groups are $Pnma$ and $Pn2_1a$. From the unit cell dimensions of Pd_3Si it was thought likely that it had the cementite structure [13-15] (space group $Pnma$). With this assumption the

Table 2. Powder photograph with Cr$K\alpha$ radiation of an alloy with the nominal composition $PdSi_{0.3}$. (The alloy was sintered at 780°C for five days.)

$h\,k\,l$	$\sin^2\Theta_{obs}$	$\sin^2\Theta_{calc}$ for Pd_3Si	I_{obs}
101	0.0872	0.0873	w
020	~0.0918	0.0919	vw
200	~0.1592	0.1596	vw
121	0.1792	0.1793	st
002	0.1899	0.1897	w−
?	0.2037		vw
201	0.2069	02070	m
102	0.2298	{0.2296	st+
211		{0.2300	
?	0.2253		m−
220	0.2515	0.2515	st
112	0.2526	0.2526	st
031	0.2544	0.2543	st
?	0.2778		w
022	0.2816	0.2816	m
131	0.2940	0.2942	m−
221	0.2989	0.2989	st−
122	0.3216	0.3215	m
202	~0.3495	0.3495	vw
230	0.3666	0.3664	w+
040	0.3676	0.3678	w+
301	~0.407	0.4065	w
231	~0.413	0.4139	vw

$\varrho(xz)$ and $\varrho(xy)$ projections were found to contain the expected number of maxima on an even background. We concluded that Pd_3Si was isomorphous with cementite ($D0_{11}$-type).

The atomic parameters were refined from successive difference syntheses until the backshift corrections were less than half the estimated standard deviations.

In both projections the observed intensities of the strongest reflexions were weaker than the calculated values, probably mainly due to secondary extinction. In the last stages of refinement the F_o-values of these reflexions, (which are marked with an asterisk in Table 3), were replaced by the corresponding F_c-values. Empirical isotropic temperature factors with $B = 0.55_9$ Å^2 ($h0l$-zone), and $B = 0.44_7$ Å^2 ($hk0$-zone) were applied. No corrections were made for absorption or dispersion.

The final parameters and standard deviations estimated using Cruickshank's formula [16] are as follows (space-group *Pnma*):

8 Pd_I in 8 (d) : $x = 0.1810 \pm 0.0002$, $y = 0.0508 \pm 0.0003$, $z = 0.3217 \pm 0.0002$
4 Pd_{II} in 4 (c) : $x = 0.0053 \pm 0.0005$, $z = 0.9036 \pm 0.0005$
4 Si in 4 (c) : $x = 0.897_6 \pm 0.002_0$, $z = 0.469_6 \pm 0.002_0$

Observed and calculated structure factors are given in Table 3. The final R values are 6.1 % for the 94 observed $h0l$ reflexions, and 8.2 % for the 66

Table 3. Observed and calculated structure factors for Pd_3Si.

hkl	F_c	$\|F_o\|$	*hkl*	F_c	$\|F_o\|$
0 0 2	−95.6	82.9 *	4 0 4	−68.1	69.1
0 0 4	−104.9	96.2 *	4 0 5	−80.0	78.4
0 0 6	76.9	75.7	4 0 6	−77.4	71.9
0 0 8	−84.9	87.7	4 0 7	103.8	95.0
0 0 10	46.0	43.3	4 0 8	18.4	—
0 0 12	40.8	42.8	4 0 9	−44.3	43.1
0 0 14	−43.6	37.0	4 0 10	29.6	—
			4 0 11	8.8	—
1 0 1	39.6	—	4 0 12	9.3	—
1 0 2	198.3	162.2 *	4 0 13	34.9	33.2
1 0 3	47.7	47.4	4 0 14	−2.0	—
1 0 4	−188.7	150.2 *			
1 0 5	−153.3	144.6 *	5 0 1	32.8	29.3
1 0 6	45.0	50.2	5 0 2	−63.1	56.6
1 0 7	−31.4	35.1	5 0 3	129.4	108.0 *
1 0 8	32.5	38.7	5 0 4	89.0	80.7
1 0 9	57.6	62.0	5 0 5	−136.9	120.3 *
1 0 10	−66.6	72.5	5 0 6	−30.2	28.9
1 0 11	5.5	—	5 0 7	−20.0	—
1 0 12	31.8	35.7	5 0 8	−26.5	24.4
1 0 13	8.4	—	5 0 9	66.9	66.3
1 0 14	0.4	—	5 0 10	31.2	35.4
			5 0 11	−18.9	—
2 0 0	−33.8	32.8	5 0 12	−14.4	—
2 0 1	−186.6	136.6 *	5 0 13	4.5	—
2 0 2	158.0	130.9 *	5 0 14	1.5	—
2 0 3	60.1	56.8			
2 0 4	−38.7	37.8	6 0 0	201.7	161.0 *
2 0 5	97.9	94.6	6 0 1	−67.3	66.4
2 0 6	−143.0	127.6 *	6 0 2	−68.7	67.8
2 0 7	−80.6	79.9	6 0 3	23.0	24.0
2 0 8	64.1	67.8	6 0 4	−81.5	81.2
2 0 9	44.7	48.4	6 0 5	31.0	31.0
2 0 10	23.4	—	6 0 6	31.0	34.4
2 0 11	15.4	—	6 0 7	−58.4	63.0
2 0 12	−7.2	—	6 0 8	−52.5	55.4
2 0 13	−23.3	21.5	6 0 9	11.2	—
2 0 14	10.3	—	6 0 10	36.2	37.6
			6 0 11	5.0	—
3 0 1	217.3	153.8 *	6 0 12	32.2	34.0
3 0 2	−47.8	47.6	6 0 13	−12.5	—
3 0 3	−208.8	156.1 *			
3 0 4	37.0	37.3	7 0 1	64.2	59.2
3 0 5	43.8	48.1	7 0 2	121.9	107.5
3 0 6	−32.7	36.8	7 0 3	−24.6	—
3 0 7	−23.1	21.3	7 0 4	−90.7	84.9
3 0 8	−25.9	23.0	7 0 5	−38.8	43.1
3 0 9	−34.1	44.8	7 0 6	41.4	40.9
3 0 10	10.6	—	7 0 7	−16.6	—
3 0 11	74.9	79.3	7 0 8	28.6	30.9
3 0 12	−10.1	—	7 0 9	13.8	—
3 0 13	−15.9	—	7 0 10	−44.7	43.3
3 0 14	0.0	—	7 0 11	22.5	—
			7 0 12	31.7	30.8
4 0 0	47.9	46.1	7 0 13	− 1.9	—
4 0 1	200.8	146.6 *			
4 0 2	34.0	31.8	8 0 0	−48.3	52.5
4 0 3	−20.3	—	8 0 1	−27.1	25.7

Table 3. Cont.

h k l	F_c	$\|F_o\|$
8 0 2	89.3	85.5
8 0 3	14.6	—
8 0 4	−10.7	—
8 0 5	11.8	—
8 0 6	−98.2	97.4
8 0 7	−36.3	34.1
8 0 8	54.4	59.8
8 0 9	0.9	—
8 0 10	11.6	—
8 0 11	2.3	—
8 0 12	−11.4	—
9 0 1	57.7	54.3
9 0 2	−38.5	42.2
9 0 3	−77.4	77.2
9 0 4	69.1	68.3
9 0 5	0.5	—
9 0 6	−22.5	—
9 0 7	−13.7	—
9 0 8	−22.4	—
9 0 9	−9.7	—
9 0 10	28.0	31.4
9 0 11	38.4	38.2
9 0 12	−11.4	
10 0 0	78.1	75.3
10 0 1	76.1	81.8
10 0 2	2.8	—
10 0 3	− 2.6	—
10 0 4	−25.1	—
10 0 5	−35.8	41.2
10 0 6	− 2.6	—
10 0 7	41.6	42.2
10 0 8	−12.1	—
10 0 9	−27.2	27.1
10 0 10	17.7	—
10 0 11	− 4.5	—
11 0 1	− 8.4	—
11 0 2	6.4	—
11 0 3	51.0	58.2
11 0 4	7.5	—
11 0 5	−70.4	72.9
11 0 6	− 8.4	—
11 0 7	−10.8	—
11 0 8	−10.5	—
11 0 9	39.1	39.2
11 0 10	− 1.2	—
12 0 0	54.6	61.3
12 0 1	−38.2	36.8
12 0 2	− 6.6	—
12 0 3	23.0	—
12 0 4	−22.5	—
12 0 5	30.4	28.5
12 0 6	1.1	—
12 0 7	−37.7	40.5
12 0 8	−12.4	—
12 0 9	14.4	—
13 0 1	32.6	33.4
13 0 2	37.1	41.5
13 0 3	−29.8	29.2
13 0 4	−29.4	29.7
13 0 5	1.6	—
13 0 6	6.3	—
13 0 7	− 5.9	—
13 0 8	2.3	—
14 0 0	−24.5	25.6
14 0 1	13.0	—
14 0 2	27.1	25.0
14 0 3	7.1	—
14 0 4	− 5.9	—
14 0 5	− 0.7	—
14 0 6	−40.1	34.7
14 0 7	1.2	—
15 0 1	22.5	—
15 0 2	−17.2	16.1
15 0 3	− 7.9	—
15 0 4	33.2	27.9
15 0 5	− 6.2	—
0 2 0	54.7	50.6
0 4 0	236.8	157.1 *
0 6 0	−198.9	145.3 *
0 8 0	−33.0	—
0 10 0	213.1	176.8 *
0 12 0	−16.3	—
0 14 0	−79.7	85.5
0 16 0	62.6	79.7
0 18 0	13.7	—
0 20 0	62.9	—
2 0 0	−33.9	35.7
2 1 0	−44.0	49.0
2 2 0	−295.6	189.5 *
2 3 0	−184.2	145.2 *
2 4 0	81.6	79.5
2 5 0	−141.3	121.8 *
2 6 0	−61.3	56.6
2 7 0	−121.3	106.1
2 8 0	169.0	145.4 *
2 9 0	−16.1	—
2 10 0	14.3	—
2 11 0	22.0	—
2 12 0	102.9	106.5
2 13 0	63.4	68.8
2 14 0	−29.9	—
2 15 0	49.0	55.0
2 16 0	17.2	—
2 17 0	34.8	39.0
2 18 0	−53.0	58.0
2 19 0	5.2	—
2 20 0	− 4.6	—

Table 3. Cont.

h k l	F_c	$\|F_o\|$	*h k l*	F_c	$\|F_o\|$
4 0 0	48.6	53.0	8 11 0	23.6	—
4 1 0	69.2	75.5	8 12 0	80.4	86.5
4 2 0	−108.9	104.7	8 13 0	3.3	—
4 3 0	162.5	137.8 *	8 14 0	−15.5	—
4 4 0	64.0	59.9	8 15 0	25.5	—
4 5 0	177.1	148.3 *	8 16 0	6.7	—
4 6 0	−54.4	52.0	8 17 0	0.5	—
4 7 0	117.3	102.1	8 18 0	−46.7	—
4 8 0	72.4	67.4			
4 9 0	32.6	31.0	10 0 0	85.0	88.3
4 10 0	−26.3	31.0	10 1 0	12.9	—
4 11 0	−35.4	36.6	10 2 0	−24.9	—
4 12 0	47.9	49.8	10 3 0	78.2	79.5
4 13 0	−63.4	73.6	10 4 0	57.0	55.3
4 14 0	−27.0	—	10 5 0	63.7	61.0
4 15 0	−62.7	73.6	10 6 0	−54.0	53.3
4 16 0	20.6	—	10 7 0	−64.1	65.4
4 17 0	−39.4	46.2	10 8 0	18.0	—
4 18 0	−25.9	—	10 9 0	− 6.3	—
4 19 0	− 7.8	—	10 10 0	−55.8	54.6
4 20 0	9.6	—	10 11 0	−10.3	—
			10 12 0	14.1	—
6 0 0	208.0	177.6 *	10 13 0	−44.3	45.3
6 1 0	−57.5	61.5	10 14 0	−27.8	26.5
6 2 0	48.2	49.8	10 15 0	−30.8	29.2
6 3 0	−37.0	37.7	10 16 0	24.7	—
6 4 0	96.2	94.0			
6 5 0	−98.7	100.9	12 0 0	61.7	57.4
6 6 0	−90.9	83.5	12 1 0	−24.6	—
6 7 0	−27.8	25.6	12 2 0	− 6.1	—
6 8 0	−35.3	36.2	12 3 0	−39.2	—
6 9 0	−32.2	36.2	12 4 0	37.5	37.0
6 10 0	−119.4	115.0	12 5 0	−58.8	54.5
6 11 0	30.4	—	12 6 0	−36.2	—
6 12 0	−20.1	—	12 7 0	−32.2	—
6 13 0	19.1	—	12 8 0	4.2	—
6 14 0	−39.7	46.5	12 9 0	−16.9	—
6 15 0	38.3	50.6	12 10 0	−43.4	40.6
6 16 0	38.6	45.9	12 11 0	18.6	—
6 17 0	10.7	—	12 12 0	4.9	—
6 18 0	12.6	—	12 13 0	23.3	—
6 19 0	9.6	24.4	12 14 0	−19.9	—
8 0 0	−51.0	60.8	14 0 0	−29.0	27.8
8 1 0	−41.9	48.0	14 1 0	− 5.9	—
8 2 0	−155.9	150.2	14 2 0	−54.2	45.3
8 3 0	− 2.7	—	14 3 0	16.8	—
8 4 0	29.1	29.1	14 4 0	3.9	—
8 5 0	−60.0	61.5	14 5 0	0.9	—
8 6 0	−21.4	—	14 6 0	− 1.8	—
8 7 0	− 2.0	—	14 7 0	14.6	—
8 8 0	117.2	109.3	14 8 0	45.6	34.0
8 9 0	−25.7	—	14 9 0	− 5.0	—
8 10 0	31.9	39.7	14 10 0	20.8	—

* F_o values with an asterisk have been omitted in the last stages of refinement and are not included in the final R-values.

Table 4. Interatomic distances (< 3.6 Å) in Pd_3Si (in Å units).

		Average
Pd_I in 8 (*d*)	— 6 Pd_I : 2.85 (2), 2.90, 2.97 (2), 3.01	2.95
	— 5 Pd_{II}: 2.78, 2.80, 2.85, 2.93, 3.56	
	— 3 Si : 2.35, 2.48, 2:56	
Pd_{II} in 4 (*c*)	— 10 Pd_I : 2.78 (2), 2.80 (2), 2.85 (2), 2.93 (2), 3.56 (2)	3.03
	— 2 Pd_{II}: 3.29 (2)	
	— 3 Si : 2.35, 2.37, 3.04	
Si in 4 (*c*)	— 6 Pd_I : 2.35 (2), 2.48 (2), 2.56 (2)	2.44
	— 3 Pd_{II}: 2.35, 2.37, 3.04	(8 closest)

observed *hk*0 reflexions (excluding the reflexions marked with an asterisk in Table 3).

Interatomic distances are given in Table 4. The standard deviations of Pd—Pd distances are less than 0.01 Å, whereas the standard deviations of Pd—Si distances vary between 0.00_8 Å and 0.01_4 Å.

COMPARISON WITH ISOMORPHOUS PHASES

The cementite structure, that has been comprehensively described in earlier papers [14,15,17–19], consists of a rather densely packed framework of the larger atoms, (*A* atoms in the following), which each coordinate 11 or 12 similar atoms. The smaller atoms (*X* atoms) are situated in holes in the *A* atom skeleton; the *X* atoms have nine *A* neighbours, but no contact with atoms of their own kind. As seen from Table 5, the environment of the *X* atom is somewhat different in the four cementite-type phases which have been studied in detail, namely Fe_3C [15], Ni_3B[19], Pd_3Si and $NiAl_3$[17]. In Fe_3C and Ni_3B, six *A* neighbours of the *X* atom are much closer than the other three, and form a triangular prism around the *X* atom. In Pd_3Si two of the *A* neighbours outside the 'prism' are brought nearer to the *X* atom whereas the ninth neighbour is still so remote

Table 5. Interatomic distances between unlike atoms in cementite phases (A_3X).

	Distances between the *X* atom and *A* atoms at the corners of the prism			Distances between the *X* atom and *A* atoms outside the prism		Ref.
	A atoms in 4 (*c*)	*A* atoms in 8 (*d*)	Average	A atoms in 8 (*d*)	*A* atom in 4 (*c*)	
Fe_3C	1.85, 1.89	2.06 (2), 2.15 (2)	2.03	2.31 (2)	3.02	15
Ni_3B	2.02, 2.09	1.99 (2), 2.07 (2)	2.04	2.30 (2)	2.59	19
Pd_3Si	2.35, 2.37	2.35 (2), 2.48 (2)	2.39	2.56 (2)	3.05	this work
$NiAl_3$	2.44, 2.46	2.42 (2), 2.44 (2)	2.44	2.52 (2)	2.72	17

that it probably need not be taken into consideration when discussing the environment of the X atom. The eight shortest Pd—Si distances in Pd_3Si are not very different and the polyhedron of palladium atoms around the silicon atom seems to be best described as distorted archimedian antiprism. Finally, in $NiAl_3$, the nine Ni—Al distances do not differ by more than 12 % and probably all represent bonding contacts.

It is also evident from Table 5 that a contraction of the $A-X$ distances takes place in the series Fe_3C, Ni_3B, Pd_3Si and $NiAl_3$. The difference (in Å) between the average of the six shortest $A-X$ distances and the A radii for coordination number 12, ($r_{Fe} = 1.27$, $r_{Ni} = 1.24$, $r_{Pd} = 1.37$ and $r_{Al} = 1.43$) are 0.76, 0.80, 1.02, and 1.01 in Fe_3C, Ni_3B, Pd_3Si, and $NiAl_3$, respectively. Thus, whereas the figures for Fe_3C and Ni_3B agree well with those found in other carbides and borides, the figure for Pd_3Si is considerably smaller than in previously studied silicides. In $NiAl_3$, as in a number of phases between aluminium and transition metals [18], the distances between unlike atoms are very short.

Acknowledgements. We wish to thank professor G. Hägg for his kind interest and valuable comments on the manuscript. Thanks are also due to Dr. S. Rundqvist for helpful discussions. Financial support from the *Air Force Office of Scientific Research of the Air Research and Development Command, United States Air Force*, through its European Office under Contract No. AF 61(052)-40 and from the *Swedish Technical Science Research Council* is gratefully acknowledged.

REFERENCES

1. Aronsson, B., Stenberg, E. and Åselius, J. *Nature* **183** (1959) 318.
2. Anderko, K. and Schubert, K. *Z. Metallkunde* **44** (1953) 307.
3. Hansen, M. *The Constitution of binary alloys*, Mc Graw Hill, New York-Toronto-London 1958.
4. Åsbrink, S., Blomqvist, G. and Westman, S. *Arkiv Kemi* **14** (1959) 545.
5. Tomas, L. H. and Umeda, K. *J. Chem. Phys.* **26** (1957) 293.
6. Tomiie, Y. and Stam, C. H. *Acta Cryst.* **11** (1958) 126.
7. Appel, K. "*Technical Note from the Quantum Chemistry Group, University of Uppsala*".
8. Rao, R. and Winterhager, H. *Trans. Indian Inst. Metals* **10** (1956—57) 139.
9. Buddery, J. H. and Welch, A. J. E. *Nature* **167** (1951) 362.
10. Pfisterer, H. and Schubert, K. *Z. Metallkunde* **41** (1950) 358.
11. Lebeau, P. and Jolibois, P. *Compt. rend.* **146** (1908) 1028.
12. Rundqvist, S. and Jellinek, F. *Acta Chem. Scand.* **13** (1959) 425.
13. Hendricks, S. B. *Z. Krist.* **74** (1930) 534.
14. Westgren, A. *Jernkontorets Ann.* **87** (1932) 457.
15. Lipson, H. and Petch, N. J. *J. Iron Steel Inst.* **142** (1940) 95.
16. Cruickshank, D. W. J. *Acta Cryst.* **2** (1949) 65.
17. Bradley, A. J. and Taylor, A. *Phil. Mag.* **23** (1937) 1049.
18. Black, P. J. *Acta Met.* **4** (1956) 172.
19. Rundqvist, S. *Acta Chem. Scand.* **12** (1958) 658.

Received January 25, 1960.

ACTA CHEMICA SCANDINAVICA 14 (1960) 1019–1024

Enzymic Hydrolysis of Cysteamine S-Phosphate by Human Erythrocytes

STIG ÅKERFELDT

Biochemistry Section, Eastern Pennsylvania Psychiatric Institute, Philadelphia, Pennsylvania, U.S.A.

Human erythrocytes are shown to contain an enzyme that hydrolyzes cysteamine S-phosphate into cysteamine and *ortho*-phosphate. The enzyme activity, which is absent from serum and practically absent from isolated stromata, is optimal at pH 5.7 (5.5—6.0). Some kinetic data are presented.

In addition to the wellknown biological significance of several compounds containing phosphorylated amino and hydroxyl groups, some recently published reports support the possibility that also compounds containing phosphorylated thiol groups may take part in cellular processes.

The first demonstration of an enzymic S-phosphorylation of a biologically important thiol seems to have been performed by Feuer and Wollemann [1–5] in a study of the formation of "active acetate". Using an enzyme system of brain these authors could show that a phosphate group from adenosine-5'-triphosphate is enzymically transferred to the thiol group of coenzyme A forming coenzyme A S-phosphate *. Smith *et al.* have recently obtained evidence for the formation of this compound in *E. coli* [7,8].

An earlier suggestion by Lynen *et al.*[9,10] and by Lipmann and collaborators [11] that coenzyme A S-phosphate or coenzyme A S-diphosphate should be formed as an intermediary step in the formation of "active acetate" in yeast, was later abandoned [12] (*cf.* Refs. [13–15]).

Reports by other workers indicated that coenzyme A might possibly be S-phosphorylated by enzymes in rabbit liver [16] and spinach [17].

Recent studies by Brahms and Kakol [18] give support to the view that thiol groups of myosin are phosphorylated during the action of this protein on adenosine-5'-triphosphate (*cf.* Ref.[19]).

A study of the properties and possible biological significance of S-phosphorylated thiols of a small molecular size is subject to investigations by the present author. As a part of this program a method was recently developed for

* Regarding the nomenclature applied to these compounds see footnote in Ref.[6]

the preparation of various substances belonging to this category [6,20]. A sodium salt of a compound with some structural relationship to coenzyme A S-phosphate, cysteamine S-phosphoric acid (S-(2-aminoethyl) phosphorothioic acid), was thus prepared [6], and the present paper deals with the enzymic hydrolysis of this compound.

Enzymes capable of hydrolyzing cysteine S-phosphate (prepared from cysteine and $POCl_3$) and the phosphorothioate ion have been demonstrated to be present in rat kidney extracts [21,22]. Forrest *et al.*[23] have desribed a "thionophosphatase", present in *Aspergillus oryzae*, which is capable of hydrolyzing certain aromatic esters of phosphorothioic acid. Feuer and Wollemann [4] have demonstrated the enzymic hydrolysis of coenzyme A S-phosphate by a brain extract.

RESULTS AND DISCUSSION

Preliminary investigations showed that when cysteamine S-phosphate is incubated with RBC * at pH 5—6 it is rapidly converted into *ortho*-phosphate and a nitroprussiate positive substance, which was eventually identified as cysteamine (2-aminoethanethiol).

The factor in RBC responsible for the observed hydrolysis was heat sensitive. Complete inactivation occurred in 5 min at 50°C, pH 5.6, or in 5 min 60°C, pH 6.3. About 50% of the activity remained after exposure to 50°C for 5 min at pH 6.3. (The heating took place in the presence of EDTA (25 mM) and remaining activities were determined at the pH's indicated).

Two obvious possibilities present themselves for a quantitative study of the hydrolysis of cysteamine S-phosphate: a) determination of the thiol released, or b) determination of the *ortho*-phosphate formed. Pilot experiments indicated that the thiol group of cysteamine is rapidly oxidized by RBC (even under nitrogen). The reaction could therefore not be followed quantitatively by the appearence of the thiol without special precautions beeing taken.

On the other hand, the acid lability of the remaining cysteamine S-phosphate (*cf.* Fig. 2) made a determination of liberated *ortho*-phosphate impractical.

It was found, however, that added cysteamine could be quantitatively recovered after incubation with RBC if the incubation took place in the presence of EDTA and the pH was simultaneously kept below *ca.* 8. The enzyme responsible for hydrolysis of cysteamine S-phosphate was not inhibited by EDTA in the concentrations necessary for quantitative recovery of cysteamine. This fact made a determination of the liberated thiol convenient for a quantitative study of the reaction, and this method was therefore adopted.

An investigation of the effect of pH (Fig. 1) showed activity maximum at about pH 5.7 (5.5—6.0). Consequently all subsequent experiments were performed at this pH. It is evident from Fig. 1 that the enzyme is only moderately active at physiological pH. Although recovery of liberated cysteamine is not quite quantitative after incubation at pH's above *ca.* 8, it could be concluded from the experiments performed, that only negligible activity remains between pH 8 and 9.

* Abbreviations used: RBC = human erythrocytes; EDTA = (ethylenedinitrilo)tetraacetic acid.

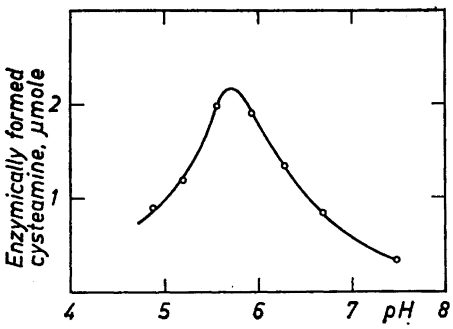

Fig. 1. Effect of pH on the enzymic hydrolysis of cysteamine S-phosphate. Test system (2 ml final volume): cysteamine S-phosphate 9.0 µmole, EDTA 100 µmole, citrate buffer 170 µmole, hemolyzed RBC corresponding to 0.25 ml of packed cells. pH of the complete system as indicated. Blanks contained water instead of RBC. Incubation: 30 min at 37°C. The presented curve constitutes of the average result from 6 different blood samples (individual variations were found to be small).

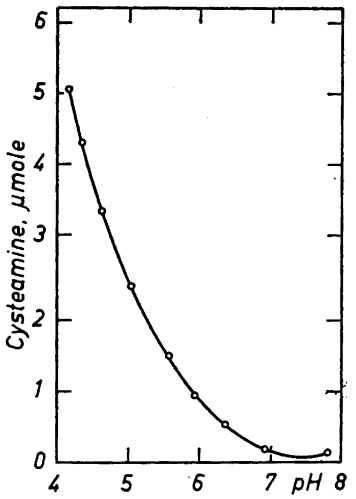

Fig. 2. The spontaneous hydrolysis of cysteamine S-phosphate at 37°C and 30 min as a function of pH. Test system (2 ml final volume): cysteamine S-phosphate 9.0 µmole, EDTA 100 µmole and citrate buffer 170 µmole. pH of the complete system as indicated.

For comparison, the spontaneous hydrolysis of cysteamine S-phosphate in the pH range in question is represented in Fig. 2. As was demonstrated earlier [6] acid hydrolysis of the compound yields the same products as the enzymic hydrolysis. This is in contrast to the behaviour of cysteine S-phosphate as prepared by Binkley [21]. Acid hydrolysis of this compound was reported to give phosphorothioate, ammonia and (presumably) pyruvate. Hydrolysis by rat kidney extract, however, gave cysteine and *ortho*-phosphate. On the other hand, acid hydrolysis of coenzyme A S-phosphate yields coenzyme A and *ortho*-phosphate [4,8].

The enzymic hydrolysis of cysteamine S-phosphate by erythrocytes follows zero order kinetics during the time of the experiments described. The enzyme activity, which seems to be primarily present in the interior of the cells *, is completely absent in serum (Table 1). Substrate saturation of the enzyme is reached at a concentration close to 5 mM (Fig. 3). Higher substrate concentrations are slightly inhibitory.

The effect of enzyme concentration is described in Fig. 4.

* The small activity found in stromata can possibly be attributed to coprecipitation by proteins from the interior of the cells during the preparation of stromata.

Table 1. Enzyme activity of various blood fractions. Test system (2 ml final volume): cysteamine S-phosphate 9.0 μmole, EDTA 100 μmole, citrate buffer 170 μmole. Furthermore the respective solutions contained: hemolyzed RBC corresponding to 0.25 ml of packed cells; stromata corresponding to 0.25 ml of packed cells and serum 0.25 ml. Blanks contained water instead of blood fraction. Final pH 5.6. Incubation: 30 min at 37°C.

Blood fraction	Enzymically formed cysteamine, μmole
Hemolyzed RBC	2.0
Stromata	0.1
Serum	0.0

A phosphomonoesterase having the same optimal pH range as the enzyme described in this paper is known to be present in human erythrocytes (see, *e.g.* Ref.[24]). The previously studied enzyme is only slightly inhibited by fluoride (6—10 % inhibition observed in 10 mM fluoride as determined in RBC hemolysate [25,26]; nor is the purified enzyme markedly inhibited by fluoride [27]), and appears not to be inhibited by small concentrations of EDTA [28].

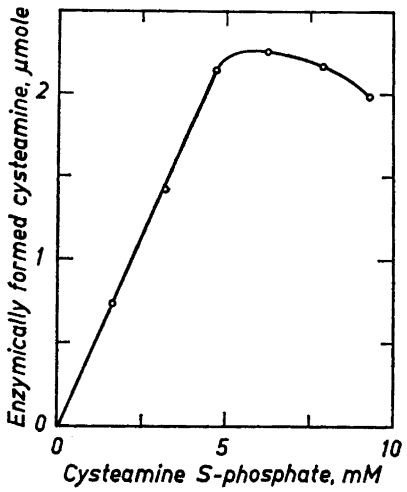

Fig. 3. Effect of cysteamine S-phosphate concentration. Test system (2 ml final volume): EDTA 100 μmole, citrate buffer 170 μmole, cysteamine S-phosphate as indicated and hemolyzed RBC corresponding to 0.25 ml of packed cells. Final pH 5.6. Blanks contained water instead of RBC. Incubation: 30 min at 37°C.

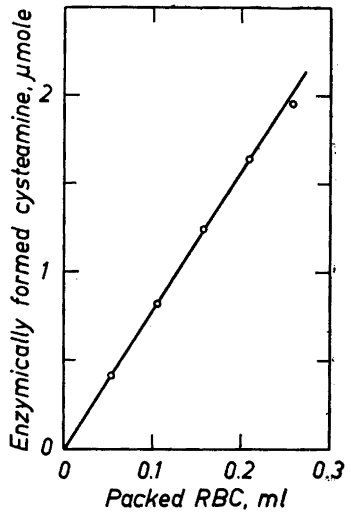

Fig. 4. Effect of enzyme concentration. Test system (2 ml final volume): cysteamine S-phosphate 9.0 μmole, EDTA 100 μmole, citrate buffer 170 μmole and hemolyzed RBC as indicated. Final pH 5.6. Incubation: 30 min at 37°C.

The enzyme hydrolyzing cysteamine S-phosphate shows similar properties, namely: a) the effect of fluoride is small (5 % inhibited by 10 mM NaF and 34 % inhibited by 30 mM NaF); b) it is not inhibited by EDTA (tested up to 75 mM).

Further comparative studies have not been carried out.

EXPERIMENTAL

Materials. Cysteamine S-phosphate was prepared as previously described [6]. RBC were washed several times with 0.9 % NaCl and stored at −20°C. They were used within seven days. The RBC were hemolyzed by thawing and subsequent addition of an equal volume of distilled water immediately before use.

Stromata were prepared at 0°C according to Herbert [29] and were suspended in 0.9 % NaCl before use.

Recovery experiments with cysteamine incubated for 30 min at 37°C with RBC showed that the thiol was quantitatively recovered when the incubation took place in the presence of 50 mM EDTA at pH's between 3 and *ca.* 8 (pH's below 3 were not tested). At pH 3−6 25 mM EDTA was generally sufficient for quantitative recovery, but since the enzyme subject to study, as mentioned, was practically unaffected by the EDTA concentration, 50 mM EDTA was used throughout the experiments.

Determination of cysteamine in the presence of cysteamine S-phosphate. To the incubation tube, containing up to 0.25 ml of hemolyzed RBC in 50 mM EDTA in a total volume of 2.0 ml, was added 1.5 ml of 10 % HPO_3. The mixture was rapidly stirred for 10 sec and 4.0 ml of a 1 M phosphate buffer of pH 7.0 was immediately added. (In order to prevent excessive hydrolysis of cysteamine S-phosphate present, the time allowed for protein precipitation by HPO_3 was kept as short as possible). After stirring the mixture was centrifuged. In the resulting solution of pH *ca.* 6, remaining cysteamine S-phosphate was found to be hydrolyzed at a rate of less than 0.05 % per min at 25°C. The over-all hydrolysis of cysteamine S-phosphate during this procedure was less than 2 %.

Cysteamine was finally determined colorimetrically at 520 mμ with nitroprussiate according to Grunert and Phillips [30], and the results were corrected for the nitroprussiate positive substances already present in the RBC. (The recently developed method [31] employing 2-chloromercuri-6-nitrophenol * as a thiol reagent could not be utilized since this reagent catalyzes the hydrolysis of cysteamine S-phosphate [6].)

Usually the deproteinized solution was slightly colored (owing to the solubilization of some proteins by the change in pH by the addition of the buffer of pH 7.0). Thus a correction was made for the absorption of the test solution at 520 mμ without added nitroprussiate.

In each experiment, where enzyme activity was determined, a correction was made for the spontaneous hydrolysis of cysteamine S-phosphate at the pH in question.

Standardization of the colorimetric method was carried out by the use of: a) commercially available cysteamine hydrochloride, and b) cysteamine solutions obtained by acid hydrolysis of cysteamine S-phosphate. Because of the highly hygroscopic properties of commercial cysteamine and cysteamine hydrochloride, method b) gave more consistent results. However, the two methods agreed within ± 1 %.

Identification of cysteamine as a product of the enzymic hydrolysis of cysteamine S-phosphate. 50 μmole of cysteamine S-phosphate, 1 ml of hemolyzed RBC and 5 ml of 0.15 M citrate buffer, pH 5.6, were incubated at 37°C under nitrogen. A blank sample, carried through the same procedures as the test sample, contained only RBC and buffer. The reaction was stopped after 3 h by the addition of 3.5 ml 10 % trichloroacetic acid. Hydrogen sulfide or ammonia were not detected as products of the hydrolysis. After centrifugation the supernatant solution was divided into two equal parts.

* This numbering follows more closely the system adopted by *Chemical Abstracts*, than the one used previously [31].

One part was treated with iodine in methanol until no more iodine was reduced. Paper chromatography * of the resulting solution was carried out in 1-butanol:acetic acid:water, 4:1:1, and in ethanol:pyridine:water, 2:1:1. Subsequent spraying with ninhydrin and nitroprussiate-cyanide gave, as the only difference between the test and the blank, spots with positions identical with those of cystamine (2,2'-dithiobisethylamine). The spots from the blank sample were faint and did not coincide with the R_F's of cystamine. (Iodine oxidation of the samples was carried out since chromatography of cysteamine in the above solvents gives less satisfactory results than chromatography of cystamine).

The second part of the supernatant solution was made alkaline with KOH and 25 μmole of 2-chloromercuri-6-nitrophenol in 1 ml of 0.1 M NaOH were added. The resulting solution was chromatographed according to Ref.[31] using solvents No. 1 and 3. Only one thiol spot, identical in position with that of MNP-cysteamine [31], was found in this way. (Since EDTA forms a complex with 2-cloromercuri-6-nitrophenol at neutral or alkaline pH's[31], EDTA was omitted from the incubation mixture in this experiment.)

The author is indebted to Mrs. M. Gale for valuable technical assistance.

REFERENCES

1. Feuer, G. and Wollemann, M. *Acta Physiol. Acad. Sci. Hung.* **5** (1954) 553.
2. Wollemann, M. and Feuer, G. *Acta Physiol. Acad. Sci. Hung.* **7** (1955) 329.
3. Feuer, G. and Wollemann, M. *Acta Physiol. Acad. Sci. Hung.* **7** (1955) 343.
4. Feuer, G. and Wollemann, M. *Acta Physiol. Acad. Sci. Hung.* **10** (1956) 1.
5. Wollemann, M. *Acta Physiol. Acad. Sci. Hung.* **10** (1956) 171.
6. Åkerfeldt, S. *Acta Chem. Scand.* **13** (1959) 1479.
7. Smith, R. A., Frank, I. F. and Gunsalus, I. C. *Federation Proc.* **16** (1957) 251.
8. Smith, R. A. *Univ. Microfilms* No. 25286.
9. Lynen, F. and Reichert, E. *Angew. Chem.* **63** (1951) 47.
10. Lynen, F., Reichert, E. and Rueff, L. *Ann.* **574** (1951) 1.
11. Lipmann, F., Jones, M. E., Black, S. and Flynn, R. M. *J. Am. Chem. Soc.* **74** (1952) 2384.
12. Jones, M. E., Lipmann, F., Hilz, H. and Lynen, F. *J. Am. Chem. Soc.* **75** (1953) 3285.
13. Welsh, O' F. E. *Nature* **169** (1952) 546.
14. Green, D. E. *Science* **115** (1952) 661.
15. Nisman, B. *Bacteriol. Revs.* **18** (1954) 16.
16. Rabinowitz, J. C., Jacobs, G., Teply, L. J., Cheldelin, V. H., Dimant, E., Mahler, H. R. and Huennekens, F. M. *Biochim. et Biophys. Acta* **13** (1954) 413.
17. Kaufman, S. *J. Biol. Chem.* **216** (1955) 153.
18. Brahms, J. and Kakol, I. *Acta Biol. Exptl. (Lodz)* **18** (1958) 195.
19. Levy, H. M. and Koshland, D. E. *J. Biol. Chem.* **234** (1959) 1102.
20. Åkerfeldt, S. *Acta Chem. Scand.* **13** (1959) 1897.
21. Binkley, F. *J. Biol. Chem.* **195** (1952) 283.
22. Binkley, F. *J. Biol. Chem.* **181** (1949) 317.
23. Forrest, I. S., Grauer, A. and Neuberg, C. *Enzymologia* **16** (1954) 305.
24. Behrendt, H. *Chemistry of Erythrocytes*, Charles C. Thomas Publisher, Springfield 1957, p. 207.
25. Abul-Fadl, M. A. M. and King, E. J. *Biochem. J.* **45** (1949) 51.
26. Behrendt, H. *Proc. Soc. Exptl. Biol. Med.* **54** (1943) 268.
27. Tsuboi, K. K. and Hudson, P. B. *Arch. Biochem. Biophys.* **61** (1956) 197.
28. Tsuboi, K. K. and Hudson, P. B. *Arch. Biochem. Biophys.* **55** (1955) 206.
29. Herbert, E. *J. Cellular Comp. Physiol.* **47** (1956) 11.
30. Grunert, R. R. and Phillips, P. H. *Arch. Biochem. Biophys.* **30** (1951) 217.
31. Åkerfeldt, S. *Acta Chem. Scand.* **13** (1959) 627.

* Before chromatography most of the trichloroacetic acid was removed by drying the spotted papers in a stream of hot air.

Received January 28, 1960.

ACTA CHEMICA SCANDINAVICA 14 (1960) 1025–1030

Potential Chemotherapeutics

I. Hydrazine Derivatives, Structurally Related to 1-Benzoxythiocarbo-2-salicylidene Hydrazine

KURT SKAGIUS

Research Laboratories, A.B. Pharmacia, Uppsala, Sweden

Structural analogues (fortyone in all), of 1-benzoxythiocarbo-2-salicylidene hydrazine were prepared for antibacterial screening. The substances prepared are aldo- and ketohydrazones of oxycarbo-, oxythiocarbo- and dithiocarbohydrazines and their S- or N-alkylated derivatives.

In 1949 Wangel [1] published a study of some oxythiocarbohydrazides and their hydrazone derivatives. Since these compounds by analogy to the thiosemicarbazones were of interest as potential tuberculostatics, they were subjected to a bacteriologic screening procedure [2]. It was found, in continuation of this work, that the salicylaldehyde hydrazone of benzoxythiocarbohydrazide (I) showed a powerful activity against staphylococci and streptococci *in vitro*. In order to elucidate the structure-activity relation, a series of related substances were synthesized and tested against a number of microorganisms *in vitro*. The results of this investigation will be published elsewhere.

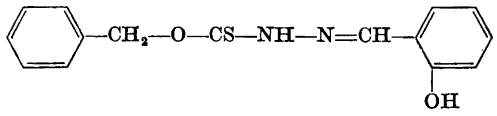

(I)

Firstly, the salicylidene residue of compound (I) was replaced by a number of aromatic aldehyde and ketone residues (Table 1), containing

a) a hydroxyl group in the 2-position of the benzene nucleus and various substituents in other positions
b) a substituted hydroxyl group in the 2-position
c) a hydroxyl group in the 4-position
d) other substituents than hydroxyl in the 2-position.

Table 1. Benzoxythiocarbohydrazones of aromatic aldehydes and ketones.

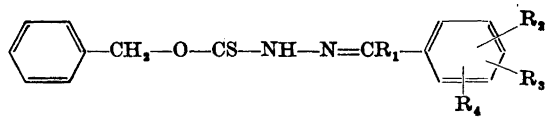

Compound No.	Code No. Ph 762/x	R_1	R_2	R_3	R_4	M. p.
1	38	H	2—OH	5—CH_3	H	179 —180
2	48	H	2—OH	5—$C(CH_3)_2CH_2—C—(CH_3)_3$	H	148 —149
3	12	H	2—OH	4—OH	H	
4	28	H	2—OH	5—Br	H	187.5 decomp.
5	50	H	2—OH	3—OCH_3	H	146 —148.5
6	21	H	2—OCH_3	H	H	119 —120.5
7	15	H	2—$OCOCH_3$	H	H	116 —118.5
8	55	CH_3	2—OH	H	H	133 —134
9	80	CH_3	2—OH	4—CH_3	H	155.5—157
10	75	CH_3	2—OH	4—CH_3	5—Cl	179 —180.5
11	81	C_2H_5	2—OH	H	H	119.5—121
12	84	C_2H_5	2—OH	5—CH_3	H	169.5—170.5
13	79	*n*-C_4H_9	2—OH	H	H	156 —157
14	83	*n*-C_4H_9	2—OH	5—CH_3	H	96.5— 98
15	73	*n*-C_5H_{11}	2—OH	5—CH_3	H	114 —115.5
16	78	C_6H_5	2—OH	5—Cl	H	161.5—163
17	76	C_6H_5	2—OH	5—CH_3	H	115 —117
18	77	$C_6H_5CH_2$	2—OH	5—CH_3	H	145 —147
19	9	H	4—OH	H	H	156 —157 decomp.
20	1	H	4—OH	3—OCH_3	H	146 —147 decomp.
21	49	H	2—NH_2	H	H	149 —151
22	41	H	2—NO_2	H	H	117 —119

Since a hydroxyl group in the 2-position of the benzal residue seemed to be essential for the antistaphylococcal action, some benzoxythiocarbo- and benzyldithiocarbohydrazones of aldehydes and ketones, containing an aromatic hydroxyl group, an enolizable carbonyl group or an aliphatic hydroxyl group in the critical position were also prepared (Table 2).

The possible arrangements around the central carbon atom of the oxythiocarbamide group (II) is of special interest, since the action of many antibacterial agents is referred to their ability for chelate or complex formation with metal ions [3]. Substitution of the hydrogen atom in (II) with alkyl groups effectively blocks the possibility of salt formation, which would be the main contribution of the oxythiocarbohydrazide group to a chelate. Also, substitution of the sulfur atom by oxygen and the oxygen atom by sulfur or nitrogen would influence the enolizability of the hydrogen atom and the ability of chelate formation.

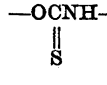

(II)

Table 2. Benzoxythiocarbo- and benzyldithiocarbohydrazones of various aldehydes and ketones.

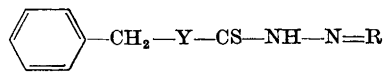

Compound No.	Code No. Ph 762/X	Carbonyl compound, corresponding to R	Y	M.p.
23	34	2-Hydroxy-1-napthaldehyde	O	151 –155
24	35	1-Hydroxy-2-napthaldehyde	O	170 –171
25	92	3-Hydroxypicolinealdehyde	O	168 decomp.
26	36	Dehydroacetic acid	O	125 –127
27	52	Dehydroacetic acid	S	138 –140
28	85	2-Acetyl-3-hydroxy-5-methyl-benzofurane	O	104 –105
29	94	3-Hydroxy-3-methylbutanone-2	O	136.5–138
30	40	Quinoline-2-aldehyde	O	147 –149
31	39	4-Pyridinealdehyde	O	144 decomp.
32	8	2-Thiophenealdehyde	O	107 –108

The N-methylated derivative of (I) was easily obtained from the sodium salt of benzoxythiocarbothioglycolic acid and salicylaldehyde methylhydrazone hydrochloride according to the method described by Wangel [1]. The S-methyl derivative was obtained by methylation of sodium benzoxythiocarbohydrazide with methyl iodide followed by hydrazone formation with salicylaldehyde. The oxycarbo- and dithiocarbohydrazides were prepared according to general principles [4,5], and the S-benzylthiocarbohydrazone from salicylidene hydrazine and S-benzylthiocarbonyl chloride, prepared from toluenethiol and phosgene.

Finally, some variations of the ester residue of the thiocarbonic acid ester grouping of (I) were carried out. These variations included the esters of 2-

Table 3. Acyl substituted salicylidenehydrazines.

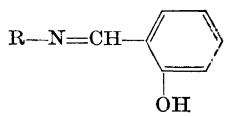

Compound No.	Code No. Ph 762/X	R	M.p.
33	13	$C_2H_5OSCNH-$	167.5–169.5
34	31	$C_6H_5CH_2CH_2OCSNH-$	144 –145
35	45	$4-C_5H_4NCH_2OCSNH-$	176.5–177
36	37	$C_6H_5CH_2NHCSNH-$	195 –196
37	51	$C_6H_5CH_2SCSNH-$	179.5–180.5
38	29	$C_2H_5OCONH-$	126 –128
39	99	$C_6H_5CH_2SCONH-$	181.5–183
40	22	$C_6H_5CH_2OC(SCH_3)=N-$	87 – 89
41	97	$C_6H_5CH_2OCSN(CH_3)-$	139 –141.5

phenylethanol, ethanol, and 4-pyridylmethanol. The hydrazides were prepared from hydrazine hydrate and the potassium xanthates, obtained from potassium hydroxide, carbon disulphide and the alcohol in the usual way.

EXPERIMENTAL *

Hydrazones of the various acylhydrazides were prepared by heating the acylhydrazide and the carbonyl compound in a suitable solvent (ethanol, dioxane, or acetic acid) for a few minutes (if necessary, a few drops of HCl-MeOH were added), and the mixture was left to crystallize. The precipitate formed was recrystallized from dioxane, ethanol or acetic acid. The yields were usually satisfactory (70—90 %). The procedure is illustrated by the following two examples:

3-Hydroxypicolinealdehyde benzoxythiocarbohydrazone. 310 mg (2.5 mmole) of 3-hydroxypicolinealdehyde [6] and 460 mg (2.5 mmole) of benzoxythiocarbohydrazide were dissolved in 5 ml of hot ethanol. After a few minutes crystals appeared. About 15 ml of ethanol was then added and the mixture boiled until the precipitate dissolved. The solution was treated with charcoal, filtered and allowed to cool. The crystals were filtered off and dried. After recrystallization from ethanol, 0.6 g (80 %) of colourless crystals was obtained. The colour changes to yellow-brown in sunlight. The substance begins to melt at 168°C, after which it slowly solidifies and does not melt again below 200°C.

Benzoxythiocarbohydrazone of 3-methyl-3-hydroxybutanone-2. 9.1 g (50 mmole) of benzoxythiocarbohydrazide and 5.1 g (50 mmole) of the ketone were dissolved in about 50 ml of ethanol. The hot solution was treated with charcoal, filtered and the filtrate allowed to cool. After scratching, a slightly cream-coloured precipitate appeared. The crystals were filtered off and dried. After recrystallization from ethanol they melted at 136.5—138°C. Yield 9.8 g (74 %).

Benzylthiocarbonyl chloride. Under external cooling, 50 ml of a 12.5 % solution of phosgene in toluene was stirred in a three-necked flask and a mixture of 5 ml of pyridine and 7.5 ml of toluenethiol in about 50 ml of toluene was added. After one hour the pyridinium chloride was filtered off and the filtrate fractionated *in vacuo*. 8.0 g (70 %) of benzylthiocarbonyl chloride was obtained as an oil, which boiled at 122—123°/10 mm Hg.

1-(S-Benzylthiocarbonyl)-2-salicylidenehydrazine. 5 g (37 mmole) of salicylidenehydrazine were dissolved in dioxane and a solution of 7 g (37 mmole) of benzylthiocarbonyl chloride in ether was added. A colourless precipitate was immediately formed. A solution of 3 ml of pyridine in ether was added and the mixture heated on a steam bath for a few minutes. After cooling, the mixture was poured into water and the ether was allowed to escape. The precipitate was filtered off and dried. 9.2 g (87 %) of a colourless substance was obtained which, after several recrystallizations from ethanol and benzene, melted at 181.5—183°C.

1-Benzoxythiocarbo-1-methyl-2-salicylidenehydrazine. 10 g methylhydrazine sulphate were dissolved in 100 ml of 2 N acetic acid and 40 ml of 5 N sodium hydroxide was added. The solution was heated on a water bath and 11 ml of salicylaldehyde was added with stirring. After half an hour the oily layer was separated and the water layer extracted with ether. The combined organic layers were dried with anhydrous sodium sulphate and methanolic hydrogen chloride was added. Salicylidenemethylhydrazone hydrochloride was obtained as a pale yellow precipitate, which weighed 8.4 g after drying.

5.7 g (30 mmole) of the yellow salt was mixed with 15 ml of 2 N sodium hydroxide and 50 ml of ethanol and a solution of 7.5 g of benzoxythiocarbothioglycolic acid in 15 ml of 2 N sodium hydroxide and 50 ml of water was added. The yellow solution was left at room temperature for three days. The precipitate formed was filtered off and dried. Weight 7.4 g. After repeated recrystallizations from ethanol-dioxane and dioxane-water 4.6 g of 1-benzoxythiocarbo-1-methyl-2-salicylidenehydrazine was obtained. Mp 139—141.5°C.

Potassium 4-pyridylmethylxanthate. 32.7 g (330 mmole) of 4-pyridylmethanol was dissolved in a solution of 22 g of potassium hydroxide in 120 ml of water. 20 ml of carbon

* Microanalyses by Dr. Wolfgang Kirsten.

Table 4. Analytical data.

Compound No.	Formula	% C calc.	% C found	% H calc.	% H found	% N calc.	% N found	% S calc.	% S found
1	$C_{16}H_{16}N_2O_2S$	64.0	63.9	5.4	5.4	9.3	9.5	10.7	10.4
2	$C_{23}H_{30}N_2O_2S$	69.3	69.5	7.6	7.5	7.0	7.0	8.2	8.2
3	$C_{15}H_{14}N_2O_3S$	59.6	59.5	4.7	4.7	9.3	9.3	10.6	10.6
4	$C_{15}H_{13}N_2O_2SBr$	49.3	49.5	3.6	3.6	7.7	7.7	8.8	8.7
5	$C_{16}H_{16}N_2O_3S$	60.7	60.9	5.1	5.1	8.9	9.0	10.1	9.8
6	$C_{16}H_{16}N_2O_2S$	64.0	64.0	5.4	5.5	9.3	9.4	10.7	10.5
7	$C_{17}H_{16}N_2O_3S$	62.2	62.3	4.9	4.9	8.5	8.5	9.8	9.6
8	$C_{16}H_{16}N_2O_2S$	64.0	63.6	5.4	5.4	9.3	9.2	10.7	10.2
9	$C_{17}H_{18}N_2O_2S$	64.9	65.1	5.8	5.9	8.9	8.9	10.2	9.9
10	$C_{17}H_{17}N_2O_2SCl$	58.5	58.4	4.9	4.9	8.0	8.0	9.2	9.3
11	$C_{17}H_{18}N_2O_2S$	64.9	65.2	5.8	5.9	8.9	8.9	10.2	9.8
12	$C_{18}H_{20}N_2O_2S$	65.8	66.1	6.1	6.3	8.5	8.6	9.8	9.7
13	$C_{19}H_{22}N_2O_2S$	66.6	66.8	6.5	6.5	8.2	8.2	9.4	9.4
14	$C_{20}H_{24}N_2O_2S$	67.4	67.3	6.8	6.8	7.9	8.0	9.0	9.2
15	$C_{22}H_{28}N_2O_2S$	68.7	68.8	7.3	7.4	7.3	7.4	8.3	8.0
16	$C_{21}H_{17}N_2O_2SCl$	63.6	63.3	4.3	4.3	7.1	7.1	8.1	8.0
17	$C_{22}H_{20}N_2O_2S$	70.2	70.5	5.4	5.4	7.4	7.5	8.5	8.6
18	$C_{23}H_{22}N_2O_2S$	70.7	70.9	5.7	5.7	7.2	7.2	8.2	8.3
19	$C_{15}H_{14}N_2O_2S$	62.9	63.0	4.9	4.9	9.8	9.9	11.2	10.9
20	$C_{16}H_{16}N_2O_3S$	60.7	60.9	5.1	5.2	8.9	9.0	10.1	10.0
21	$C_{15}H_{15}N_3OS$	63.1	63.2	5.3	5.3	14.7	14.7	11.2	—
22	$C_{15}H_{13}N_3O_3S$	57.1	57.2	4.2	4.2	13.3	13.3	10.2	10.2
23	$C_{19}H_{16}N_2O_2S$	67.8	67.9	4.8	4.9	8.3	8.3	9.5	9.5
24	$C_{19}H_{16}N_2O_2S$	67.8	67.9	4.8	4.8	8.3	8.3	9.5	9.5
25	$C_{14}H_{13}N_3O_2S$	58.5	58.8	4.6	4.7	14.6	14.6	10.7	10.4
26	$C_{16}H_{16}N_2O_4S$	57.8	57.9	4.9	4.9	8.4	8.7	9.7	9.7
27	$C_{16}H_{16}N_2O_3S_2$	55.1	55.0	4.6	4.7	8.0	8.0	18.4	18.6
28	$C_{20}H_{20}N_2O_3S$	65.2	65.2	5.5	5.4	7.6	7.8	8.7	8.4
29	$C_{13}H_{18}N_2O_2S$	58.6	58.6	6.8	6.9	10.5	10.7	12.0	11.5
30	$C_{18}H_{15}N_3OS$	67.3	67.4	4.7	4.7	13.1	13.1	10.0	10.0
31	$C_{14}H_{13}N_3OS$	62.0	61.8	4.8	4.8	15.5	15.4	11.8	11.4
32	$C_{13}H_{12}N_2OS_2$	56.5	56.5	4.4	4.4	10.1	10.1	23.2	23.3
33	$C_{10}H_{12}N_2O_2S$	53.6	53.9	5.4	5.4	12.5	12.5	14.3	
34	$C_{16}H_{16}N_2O_2S$	64.0	63.9	5.4	5.4	9.3	9.3	10.7	10.4
35	$C_{14}H_{12}N_3O_2S$	58.7	58.3	4.2	4.6	14.7	14.7	11.2	10.8
36	$C_{15}H_{15}N_3OS$	63.1	63.4	5.3	5.2	14.7	14.8	11.2	11.2
37	$C_{15}H_{14}N_2OS_2$	59.6	59.5	4.7	4.7	9.3	9.4	21.2	21.3
38	$C_{10}H_{12}N_2O_3$	57.7	57.9	5.8	5.8	13.5	13.5	—	—
39	$C_{15}H_{14}N_2O_2S$	62.9	63.0	4.9	5.0	9.8	9.8	11.2	11.2
40	$C_{16}H_{16}N_2O_2S$	64.0	63.9	5.4	5.4	9.3	9.4	10.7	10.6
41	$C_{16}H_{16}N_2O_2S$	64.0	64.0	5.4	5.4	9.3	9.2	10.7	10.7

disulphide was added and the mixture was stirred at room temperature for 5 h. During the reaction the potassium salt of 4-pyridyl-methylxanthic acid precipitated. The salt was filtered off and dried. Weight 17 g. The mother liquor was concentrated *in vacuo* to about 1/5 of its original volume and chilled strongly. A further 17 g of the salt was obtained, washed with acetone and dried.

4-Pyridylmethoxythiocarbohydrazide. 17.8 g (80 mmole) of potassium pyridylmethyl-xanthate were dissolved in 30 ml of water and 5 ml of hydrazine hydrate was added. The mixture was left at room temperature for 18 h. The crystalline precipitate was filtered off, washed with water and recrystallized from ethanol. 10 g (67 %) of the hydrazide was obtained as colourless shells, which turned slightly reddish in the air. Mp 142.5—143°C. (Found: C 45.9; H 5.0; N 22.9. Calc. C 45.8; H 5.0; N 23.0.)

Acknowledgements. The author is deeply indebted to Mr. Niels Elming of A/S Pharmacia, Copenhagen, Denmark, who kindly supplied a sample of 3-hydroxypicolinealdehyde, and to Mr. S. O. Hall of this laboratory for help with the experimental work.

REFERENCES

1. Wangel, J. *Arkiv Kemi* **1** (1949) 431.
2. Wangel, J. *Kemisk maanedsblad* **39** (1958) 73.
3. Weinberg, E. D. *Bacteriol Rev.* **21** (1957) 46.
4. Stollé, R. and Benrath, A. *J. prakt. Chem.* (2) **70** (1904) 276.
5. Busch, M. and Starke, M. *J. prakt. Chem.* (2) **93** (1916) 59.
6. Elming, N. *Acta Chem. Scand.* **11** (1957) 1496.

Received February 13, 1960.

ACTA CHEMICA SCANDINAVICA 14 (1960) 1031–1036

A Differential Oxygen Analyser

C. U. LINDERSTRØM-LANG

Danish Atomic Energy Commission, Risø, Denmark

For the determination of very small differences in oxygen content of air samples, a method based on the well known absorption of oxygen by pyrogallol was developed.

Principle: Two vessels, connected through a manometer, are filled with the two samples to be compared; the pressure difference is adjusted to zero. The oxygen is absorbed by the pyrogallol and the pressures are again compared, the pressure difference being proportional to the difference in oxygen content.

Apparatus: Fig. 1 shows a diagram of the apparatus used: The manometer M is connected on each side to a ground joint socket. The vessels carry ground joint cones that fit into the sockets. The vessels have only a 1 cm hole which gives free passage between the vessel and the manometer connection when the vessel is turned to the appropriate position. Opposite the manometer connection another glass tube is fitted to the socket. When the vessels are turned through 180°, the air samples may be introduced through these tubes (B' and B''). The manometer liquid is silicone oil (DC 200/10, d 0.94). The reading is carried out with a cathetometer. In this way pressure differences of up to *ca.* 1 cm silicone oil (—○—1 mm Hg) can be read with an accuracy of 0.01 mm silicone oil (—○— 10^{-3} mm Hg), *i.e.* 10^{-4} % of the total pressure (1 atm.).

The volume of each vessel is approximately 200 ml.

Procedure: Small double walled paper bags are made from lens paper (*ca.* 5 cm long and 0.8 cm diameter); each is filled with 1 g of ground pyrogallol. They are closed at both ends by twisting the paper and attached to a small polyethylene covered magnet (stirrer) by means of a cotton thread.

The cones are greased with Apiezon L. A magnet (stirrer) is placed in the larger section (a) of the vessel. The bag with pyrogallol is placed in the front section (b) of the vessel; ca. 15 ml 50 % (w/w) potassium hydroxide are added through a suitably bent pipette to the a-section of the vessels (see Fig. 1). These are then fitted into the sockets and the whole assembly is lowered into a temperature controlled bath.

The air samples are introduced through the outer tubes B' and B'' after evacuation of the vessels.

The vessels are turned through 180° and connected through the valves A' and A''. In order to remove carbon dioxide and to reach water vapour equilibrium the air in the vessels is stirred now and again during one hour by means of the magnet from section a of the vessel, care being taken that no drops of potassium hydroxide touch the pyrogallol bag.

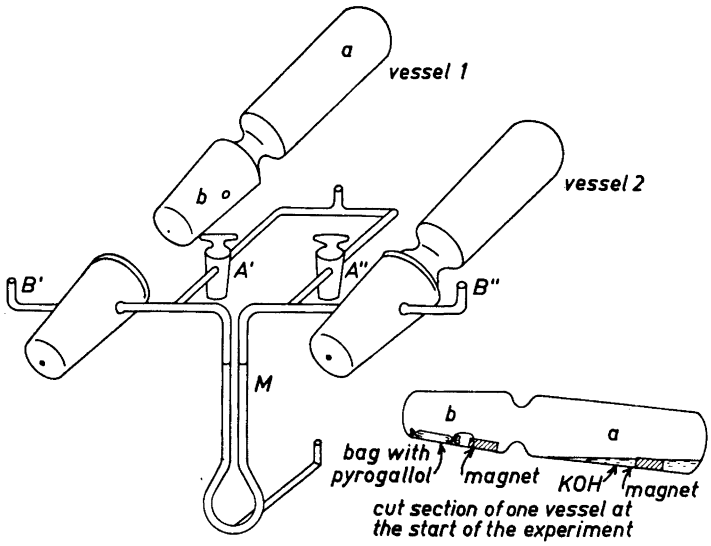

Fig. 1.

A' and A'' are closed and the apparatus is left for at least half an hour during which a small change in manometer reading usually 0—0.05 mm silicone oil may take place.

The vessels are cautiously closed by rotating them until the holes are at the top (tongs are used in order not to heat the samples).

The pyrogallol bags are pulled into the potassium hydroxide solution by the magnet attached; after a couple of minutes of magnetic stirring the bags disintegrate and the pyrogallol dissolves.

Mechanical stirring is effectuated by rocking the apparatus about a horizontal axis until the system approaches equilibrium.

In the meantime the air in the manometer tubes above the silicone oil has been replaced by nitrogen at 0.79 × atmospheric pressure by evacuating and filling through the valves A' and A''. Some time must elapse before the nitrogen is in sufficient equilibrium with the silicone oil in the manometer (after one hour the change may be about 0.01 mm silicone oil per hour). The equilibrium pressure difference is recorded.

The vessels are then opened towards the manometer. Reading and stirring are continued until the manometer is stable, usually after 20 min.

The bulk of each sample is sucked out of the vessel and passed through a carbon monoxide tester under standard conditions. The difference in percentage carbon monoxide is recorded.

Although the principle is very simple, the procedure is never the less a fairly lengthy one. At present only one set of samples can be analysed in a full working day the actual performance of the determination taking 4 h but many improvements can be envisaged which will reduce the labour and shorten the time required to make one determination.

In view of the accuracy obtained this may not compare unfavourably with the best Orsat gas analysis methods.

Calculations: A first approximation: The mole fractions of oxygen in the samples are called $(1-a_1)$ and $(1-a_2)$; total number of gram molecules are n_1° and n_2°. The volumes v_1 and v_2 are assumed to be constant. p_1° and p_2° are the initial pressures, p_1' and p_2' are the final pressures.

According to the gas laws we have at the start of the experiment

$$p_1^\circ v_1 = n_1^\circ RT \qquad \text{and} \qquad p_2^\circ v_2 = n_2^\circ RT$$

At the end

$$p_1' v_1 = a_1 n_1^\circ RT \qquad \text{and} \qquad p_2' v_2 = a_2 n_2^\circ RT$$

or

$$\frac{p_1'}{p_1^\circ} = a_1 \qquad \frac{p_2'}{p_2^\circ} = a_2$$

By subtraction

$$a_1 - a_2 = \frac{p_1'}{p_1^\circ} - \frac{p_2'}{p_2^\circ} = (p_1' - p_2')\frac{1}{p_1^\circ} + (p_2^\circ - p_1^\circ)\frac{p_2'}{p_1^\circ p_2^\circ}$$

$$\frac{}{} \frac{1}{p^\circ}(p_1' - p_2' - \frac{p'}{p^\circ}(p_1^\circ - p_2^\circ)) \quad [(p_1^\circ - p_2^\circ) \text{ is kept as low as possible}];$$

where, when air is tested,

$$p^\circ = 1 \text{ atm and } \frac{p'}{p^\circ} = \frac{4}{5} \text{ (with sufficient accuracy).}$$

For an accurate calculation it is necessary to take the following factors into account:

1. The volumes change when the manometer reading changes.
2. The nitrogen atmosphere that replaces the air in the manometer does not have pressures exactly equal to the pressures inside the vessels after absorption of oxygen.
3. The temperature of the system may change and so may the temperature difference between the vessels.
4. A volume change may take place when potassium hydroxide solution and pyrogallol is mixed.
5. The water vapour pressure will change a) when potassium hydroxide solution and pyrogallol is mixed, b) when the temperature changes.
6. The volumes may change if grease is forced into the vessels from the ground joints.
7. The pyrogallol powder and the bag should have a vapour pressure equivalent to that of the potassium hydroxide solution. In order to obtain this the bags are dried at 80°C and stored in a desiccator over a 50 % potassium hydroxide solution.
8. Deviations from the ideal gas laws may effect the results.
9. Carbon monoxide is produced.

If the conditions listed below are fulfilled then it can be shown by fairly

simple, but rather lengthy, calculations * that the only factors of any importance (*i.e.* factors which give a contribution to the result which approaches the value of the standard deviation) are 1 and 9:

List of conditions:

a. $\frac{\varphi_1}{v_1} - \frac{\varphi_2}{v_2} < 10^{-3}$ and $\frac{\varphi_1}{v_1} \backsimeq \frac{\varphi_2}{v_2} < 10^{-2}$

where φ_1 and φ_2 are the volumes of the manometer tubing above the silicone oil.

b. $p_1 - p_1^* \backsimeq p_2 - p_2^* < 3$ cm silicone oil and $(p_1 - p_2) - p_1^* - p_2^*$ < 0.1 cm silicone oil. p_1^* and p_2^* are the pressures in the manometer after it has been filled with nitrogen but before the vessels are opened (*cf.* p. 1032). p_1 and p_2 are the pressures at the end of the experiment.

c. The one gramme of pyrogallol should be weighed out with an accuracy of a few mg.

d. The 15 ml potassium hydroxide should be measured accurately with a pipette.

e. Variations of bath temperature at any particular point should be less than 0.01°C.

f. The difference between the temperature of vessel 1 and vessel 2 should be less than 0.01°C.

g. The variation of this difference should be less than 0.001°C.

The result of the calculations can be shown to be

$$a_1 - a_2 \backsimeq \frac{1}{p^\circ}\left[(p_1 - p_2) - \frac{4}{5}(p_1^\circ - p_2^\circ) + \left(\frac{p_1}{v_1} + \frac{p_2}{v_2}\right)\frac{A}{2}((p_1-p_2)-(p_1^*-p_2^*))\right] - (co_1 - co_2).$$

Here $p_1^\circ - p_2^\circ$ is the initial pressure difference in cm silicone oil;

$p_1 - p_2$ is the final pressure difference in cm silicone oil;

$p_1^* - p_2^*$ is the pressure difference in cm silicone oil between the manometer tubes after they have been filled with nitrogen but before the vessels are opened;

A is the area (in cm^2) of the cross section of the manometer tubing;

v_1 and v_2 are in cm^3;

co_1 and co_2 are the mole fractions of carbon monoxide in the vessels after the experiment.

A has been found to be 0.048 cm^2. $v_1 \backsimeq v_2 \backsimeq 200$ cm^3,

$$p_1 \backsimeq p_2 \backsimeq \frac{4}{5}p^\circ \backsimeq \frac{4}{5} \times 1.1 \times 10^3 \text{ cm silicone oil,}$$

i.e. $$a_1 - a_2 \backsimeq \frac{1}{p^\circ}((p_1-p_2) - \frac{4}{5}(p_1^\circ - p_2^\circ) + 0.20\,((p_1-p_2) - (p_1^*-p_2^*))) - (co_1 - co_2)$$

* These calculations are available, to anyone interested, by contacting the author.

Table 1. Difference in mole fraction of oxygen in the two vessels: $(1-a_2)-(1-a_1) = a_1-a_2$.

	Series 1	Series 2 A	Series 2 B
	No. a_1-a_2 mole fraction	No. a_1-a_2 mole fraction	No. a_1-a_2 mole fraction
	1 2.0×10^{-5} 2 0.0×10^{-5} 3 2.5×10^{-5} 4 0.0×10^{-5} 5 1.0×10^{-5} 6 1.0×10^{-5} 7 2.0×10^{-5} 8 2.0×10^{-5} 9 0.5×10^{-5} 10 $1.0\ W\ 10^{-5}$	1 -2.5×10^{-5} 4 -1.5×10^{-5} 6 -2.0×10^{-5} 7 -2.5×10^{-5} 10 -2.0×10^{-5} 12 -2.5×10^{-5}	2 0.0×10^{-5} 3 4.5×10^{-5} 5 3.0×10^{-5} 8 4.0×10^{-5} 9 4.5×10^{-5} 11 3.0×10^{-5} 13 4.0×10^{-5}
Average	$(1.2 \pm 0.3) \times 10^{-5}$	$(-2.2 \pm 0.2) \times 10^{-5}$	$(+3.3 \pm 0.6) \times 10^{-5}$
Standard deviation	1×10^{-5}	0.4×10^{-5}	1.6×10^{-5}
Average standard deviation	1×10^{-5}		
Zero of apparatus	$(1.2 \pm 0.3) \times 10^{-5}$	$\frac{-2.2 + 3.3}{2} \times 10^{-5} = (0.6 \pm 0.3) \times 10^{-5}$	
Average zero	1×10^{-5}		
Difference in oxygen content (mole fraction) of the two samples		$\frac{3.3 + 2.2}{2} \times 10^{-5} = (2.8 \pm 0.3) \times 10^{-5}$ *i. e.* $(1.4 \pm 0.15) \times 10^{-2}$ % of the oxygen content	

Table 2. The difference in carbon monoxide production in relation to order of mixing (in cm silicone oil).

Series 1				Series 2			
No.	Vessel 1 first	No.	Vessel 2 first	No.	Vessel 1 first	No.	Vessel 2 first
1	$+1.5 \times 10^{-2}$	6	$+0.5 \times 10^{-2}$	1	—	4	-1.0×10^{-2}
2	$+1.0 \times 10^{-2}$	7	-1.0×10^{-2}	2	$+1.5 \times 10^{-2}$	5	-0.5×10^{-2}
3	$+1.0 \times 10^{-2}$	8	-1.0×10^{-2}	3	$+1.5 \times 10^{-2}$	7	-1.0×10^{-2}
4	$+1.5 \times 10^{-2}$	9	-1.0×10^{-2}	6	$+1.5 \times 10^{-2}$	8	-0.5×10^{-2}
5	$+1.0 \times 10^{-2}$	10	0.0×10^{-2}	9	$+1.0 \times 10^{-2}$	12	-1.5×10^{-2}
				10	$+1.0 \times 10^{-2}$	13	0.0×10^{-2}
				11	$+1.0 \times 10^{-2}$		

Carbon monoxide determination: It was found that using the procedure described on p. 1032 for preparing a pyrogallol solution the amount of carbon monoxide liberated is about 0.008 to 0.01 % of total pressure, which agrees well with Kilday's findings [1].

A Carbon Monoxide Gas Detector, Mines Safety Appliances Co., Ltd. (Glasgow) was used for the determination of carbon monoxide. Small differences can be estimated with an accuracy of about 50 % of the difference. Most differences found were about 0.001 ± 0.0005 %.

Difficulties with the grease add to the fairly high standard deviation found in the actual experiment. For instance when the pressure inside the vessel is changed from 1 atm to 0.8 atm the vessels will be pressed against the wall where the hole is and some grease (an uncontrollable amount) may be forced into the vessels. This is an established source of error but its magnitude is difficult to assess. Its importance can of course be diminished by reducing the amount of grease in the ground joint to a minimum.

Results: Two series of experiments have been performed (Table 1): In the first series the samples were known to be identical and in the second there was a constant well defined difference between the two samples. The oxygen content was close to that of normal air (mole fraction 0.209).

In series 2 the results can be divided into two groups:

A. sample I in vessel 2 and sample II in vessel 1 and
B. » I » » 1 » » II » » 2.

Discussion: It is not quite certain why series 2 in general seems better than 1, nor is it known why No. 2 ser. 2 is out. It is in fact a borderline case and could have been left out.

It may seem rather surprising that the zero of the apparatus lies at + 0.01 cm silicone oil and the reason is in fact not known but a fairly plausible explanation seems to be that due to differences in the quality of the ground joints of the vessels the difference between the volumes of grease forced out during the experiment will on an average show a definite value (10^{-2} cm silicone oil is equivalent to 2 μl).

Conclusion: Small differences in the oxygen content ($<$ 0.1 % of total pressure) of air can be determined with a standard deviation of 0.01 cm silicone oil = 10^{-3} % of total pressure (1 atm) or 0.005 % of the oxygen content.

For comparison it should be noted that the very best Orsat gas analysis apparatus may give results reproducible within 0.003 % of total volume or 0.015 % of the oxygen content.

The value of the carbon monoxide correction: It was found impracticable to mix pyrogallol and potassium hydroxide solution in both vessels simultaneously and it turned out that the vessel which is mixed first would always show the highest carbon monoxide value, see Table 2. This finding is in agreement with that of Kilday [1], who states that contact between a fairly high oxygen concentration and pyrogallol with no proper agitation is unfavourable.

The author is indebted to Dr. C. F. Jacobsen, Mr. Th. Rosenberg and Mr. P. Solgaard for helpful discussions.

REFERENCE

1. Kilday, M. V. *J. Research, NBS* **45** (1950) RP 2112.

Received January 22, 1960.

ACTA CHEMICA SCANDINAVICA 14 (1960) 1037–1042

Cyclizations of Thiocarbohydrazide and its Mono-hydrazones

Part I. Reactions with Orthoesters

JAN SANDSTRÖM

Department of Organic Chemistry, University of Lund, Lund, Sweden

Free thiocarbohydrazide is cyclized by orthoesters to 3-mercapto-4-amino-4,1,2-triazoles, whereas mono-thiocarbohydrazones with the same reagents give the weakly acidic 1,3,4-thiadiazolylhydrazones.

The present investigation was undertaken to find the possibilities of preparing 1,3,4-thiadiazolylhydrazines (I) by cyclization of thiocarbohydrazide (II) with derivatives of carboxylic acids.

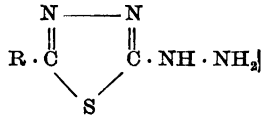

I

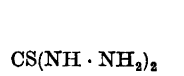

II

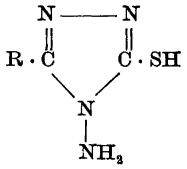

III

However, a direct cyclization of the unsubstituted thiocarbohydrazide was not expected to lead to success, since Stollé and Bowles [1] have shown that this compound reacts with triethyl orthoformate in a closed tube to give 3-mercapto-4-amino-4,1,2-triazole (III, R = H). In the present work, the same compound was obtained when thiocarbohydrazide reacted with formic acid and with formamide. A series of reactions was performed to establish the structure of the triazole, but when the investigation was finished, the author was informed about a more extensive investigation on the same subject by Beyer and Kröger, the results of which were already published [2]. Therefore, the results of the cyclization of the free thiocarbohydrazide are omitted in the present publication.

Thiadiazolylhydrazines (I) have previously been prepared by Stollé and Fehrenbach [3], by Fujii *et al.*[4], and by Kanaoka [5,6] by reduction of 2-nitrosamino-thiadiazoles. Fujii has also used hydrazinolysis of 2-alkylsulphonyl-

thiadiazoles, and Kanaoka has used hydrazinolysis of 2-bromo-thiadiazoles. Goerdeler and Galinke [7] have prepared 1,3,4-thiadiazolylhydrazine (isolated as benzaldehyde hydrazone) by reduction of 2-nitramino-thiadiazole.

In a previous communication [8], attention has been directed to the property of a benzylidene group of inhibiting cyclization of carboxymethyl 3-benzylidene-dithiocarbazate to benzylidenamino-rhodanine. It was now expected that a similar effect might prevent the 2-nitrogen atom of mono-thiocarbohydrazones from taking part in the cyclization with orthoesters, and thus lead the cyclization to hydrazones of (I), rather than to Schiff bases of the carbonyl compounds and 3-mercapto-4-amino-4,1,2-triazole (III). This expectation has been partly fulfilled, not only with monobenzaldehyde thiocarbohydrazone, but also with monoacetone, mono*cyclo*hexanone, and monoacetophenone thiocarbohydrazone. However, the mechanism proposed in Ref.[8] cannot be responsible for the course of the cyclization of the acetone and *cyclo*hexanone derivatives. Possibly a steric effect is also at work to make the 2-nitrogen atom less available for cyclization than the sulphur atom. However, Hünig [9] has recently found a directing effect, which probably has a bearing on the present problem. He found, that 4-phenylthiosemicarbazide condenses with chloroacetone to give 3-amino-4-methyl-thiazol-2(3)-one phenylimine, whereas acetone 4-phenylthiosemicarbazone with chloroacetone gives acetone 3-phenyl-4-methylthiazol-2(3)-one azine. In the first case the 2-nitrogen atom of the thiosemicarbazide is preferred in the cyclization, whereas in the second case the 4-nitrogen atom seems to be the more available one. Obviously the 1-*iso*-propylidene group has some influence on the availability of the 2-nitrogen atom, and in this case a steric effect seems less likely. Instead, the following proposal is made. Thiohydrazides are resonance hybrids with, among others, the limiting structures (IV a) and (IV b).

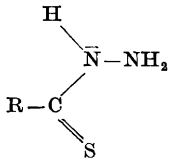

IV a

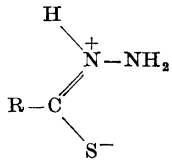

IV b

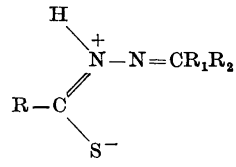

V

In a thiohydrazone the polar structure, (V), becomes relatively more important, because of the conjugation. Therefore, the 2-nitrogen atom is less basic in thiohydrazones than in thiohydrazides. A similar argumentation can be performed for the amidine structures in Hünig's example. Evidence for the existence of such a conjugation is given by the UV-spectra of the thiohydrazides and thiohydrazones. As an example, methyl dithiocarbazate has its maximum at 2 690 Å, with $\varepsilon = 10\,100$, in absolute ethanol, whereas methyl 3-ethylidene-dithiocarbazate has its maximum at 2 970 Å, with $\varepsilon = 21\,200$ in the same solvent. This bathochromic shift obviously calls for some kind of conjugation between the azomethine group and the thioamide group. The yields have been far from quantitative, and as dibenzaldehyde thiocarbohydrazone and 3-

mercapto-4-benzylidenamino-4,1,2-triazole were found among the products of the reaction between monobenzaldehyde thiocarbohydrazone and triethyl orthoformate, the side reaction (A) may be at least partly responsible.

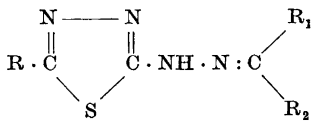

VI

However, a direct formation of 3-mercapto-4-benzylidenamino-4,1,2-triazole cannot be excluded, and the occurrence of dibenzaldehyde thiocarbohydrazone can be explained by the reaction (B), which has been found to occur in boiling toluene.

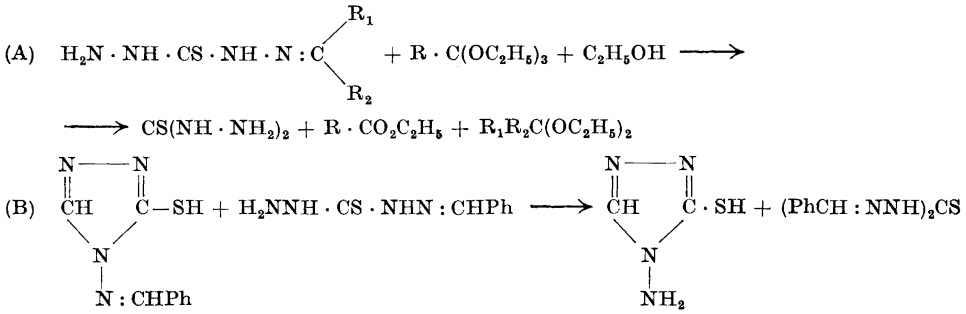

For starting materials, a series of mono-thiocarbohydrazones were prepared by reaction between thiocarbohydrazide and the appropriate carbonyl compound in weakly acidic medium. There is a striking difference between the ease with which the first and the second hydrazine group in thiocarbohydrazide reacts with ketones [10]. The mono-thiocarbohydrazones were refluxed with triethyl orthoformate and triethyl orthoacetate in toluene and without solvent, and the corresponding thiadiazolylhydrazones (VI, R = H and CH_3) were formed in varying yields. Attempts to prepare the free thiadiazolylhydrazines (I) by acid hydrolysis of the acetone hydrazones have failed because the simple thiadiazolylhydrazines are rearranged in acid medium to derivatives of aminotriazole, as will be described in a later publication.

The thiadiazolylhydrazones (VI) are weak acids, and they dissolve readily in aqueous N NaOH but not in N potassium carbonate solution. With benzoyl chloride in pyridine, benzaldehyde thiadiazolylhydrazone (VI, R = R_1 = H, R_2 = Ph) gives two benzoyl derivatives, (VII), and (VIII).

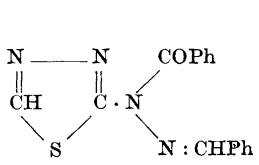

VII

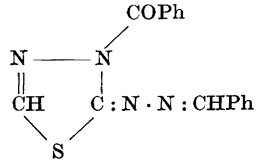

VIII

EXPERIMENTAL

Mono-thiocarbohydrazones

The preparation of monobenzaldehyde thiocarbohydrazone has been described by Stollé and Gaertner [11]. Three new mono-ketone thiocarbohydrazones have been prepared by adding a 50 % excess of the ketone in ethanol to a hot solution of thiocarbohydrazide in N acetic acid. The *monoacetone thiocarbohydrazone* separated as colourless, pointed prisms, m. p. 194—195° (decomp.), in 93 % yield. The product is very slightly soluble in the common organic solvents and in water, and it dissolves with partial decomposition in acidic and alkaline solvents. According to analysis, the crude product is sufficiently pure for all practical purposes. (Found: C 32.9; H 6.99; N 38.2; S 21.9. $C_4H_{10}N_4S$ (146.21) requires C 32.9; H 6.89; N 38.3; S 21.9.)

Monocyclohexanone thiocarbohydrazone was obtained in 83 % yield and crystallized as colourless flakes, m. p. 166—167° (decomp.), from a mixture of absolute ethanol and glacial acetic acid. (Found: C 45.1; H 7.43; N 29.9; S 17.3. $C_7H_{14}N_4S$ (186.27) requires C 45.1; H 7.58; N 30.1; S 17.2.) λ_{max}: 2 500 Å with ε = 12 600.

Monoacetophenone thiocarbohydrazone was obtained in 98 % yield and crystallized from 80 % aqueous ethanol as colourless flakes, m. p. 170—171°. (Found: C 52.1; H 5.95; N 26.9; S 15.3. $C_9H_{12}N_4S$ (208.28) requires C 51.9; H 5.81; N 26.9; S 15.4.) λ_{max}: 3 020 Å with ε = 13 400, λ_{max}: 2 350 Å with ε = 12 000.

1,3,4-Thiadiazolylhydrazones

Acetone thiadiazolylhydrazone (VI, R = H, $R_1 = R_2 = CH_3$). Monoacetone thiocarbohydrazone (9.0 g) and triethyl orthoformate (15 ml) were refluxed for 45 min, and then the volatile material was removed *in vacuo*. The sticky residue was shaken for two days with water (100 ml), and the undissolved material (6.1 g, 63 % yield) crystallized from *n*-butanol as colourless, pointed prisms, m. p. 173—174°. (Found: C 38.6; H 5.26; N 35.8; S 20.6, mol. wt. 160 (Rast). $C_5H_8N_4S$ (156.20) requires C 38.4; H 5.16; N 35.9; S 20.5.) λ_{max}: 2 790 Å with ε = 13 500.

Cyclohexanone thiadiazolylhydrazone (VI, R = H, $R_1R_2 = (CH_2)_5$). Monocyclohexanone thiocarbohydrazone (7.2 g) and triethyl orthoformate (15 ml) were refluxed for 30 min, and then the volatile material was removed *in vacuo*. The sticky residue was dissolved in hot toluene (10 ml), and on cooling, colourless needles separated (1.5 g, 20 % yield), m. p. 168—169° after a further recrystallization from toluene. (Found: C 49.3; H 6.26; N 27.5; S 16.3. $C_8H_{12}N_4S$ (196.27) requires C 49.0; H 6.16; N 28.5; S 16.3.) λ_{max}: 2 790 Å with ε = 14 000.

Benzaldehyde thiadiazolylhydrazone (VI, $R = R_1 = H$, R_2 = Ph). Monobenzaldehyde thiocarbohydrazone (10.0 g) and triethyl orthoformate (10 ml) were refluxed in toluene (100 ml) for one hour. The solution was filtered hot, and on cooling, a colourless crystalline product separated (8.2 g), melting between 165° and 190°. The product was rubbed with a solution of potassium carbonate (10 g) in water (50 ml). The undissolved material was removed by filtration, and the filtrate was acidified with glacial acetic acid. A colourless precipitate was formed (0.9 g, 9 % yield), m. p. 171—172°, identified by mixed m. p. and formation of benzyl derivative [2], as 3-mercapto-4-benzylidenamino-4,1,2-triazole.

The material which did not dissolve in the potassium carbonate solution (6.9 g) was shaken with N NaOH (50 ml) and methanol (50 ml) for 12 h. The undissolved material (1.4 g, 10 % yield) was filtered, and crystallized from glacial acetic acid as colourless needles, m. p. 194—195°, not depressed on admixture with authentic dibenzaldehyde thiocarbohydrazone [1]. (Found: C 63.6; H 4.94. $C_{15}H_{14}N_4S$ (282.37) requires C 63.8; H 5.00.)

Glacial acetic acid (6 ml) was added to the alkaline filtrate, and a pale brown crystalline powder separated (4.8 g, 47 % yield), which crystallized from *n*-butanol as colourless needles of benzaldehyde thiadiazolylhydrazone, m. p. 226—227°. (Found: C 52.9; H 3.94; N 27.5; S 15.7. $C_9H_8N_4S$ (204.24) requires C 52.9; H 3.95; N 27.4; S 15.7.) λ_{max}: 3 210 Å with ε = 24 500, λ_{max}: 2 280 Å with ε = 12 900.

Reaction B: Monobenzaldehyde thiocarbohydrazone (0.5 g) and 3-mercapto-4-benzylidenamino-4,1,2-triazole (0.5 g) were refluxed in toluene for one hour. After cooling, the undissolved material was isolated and extracted with hot water (20 ml). The aqueous

extract was found to be acidic and was neutralized against phenolphthalein with 3.9 ml of 0.1 N NaOH, which corresponds to about 15 % conversion. The aqueous solution was acidified with N HCl (0.5 ml) and a solution of benzaldehyde (0.2 g) in ethanol (10 ml) was added. On the following day the solution had deposited long, colourless needles of 3-mercapto-4-benzylidenamino-4,1,2-triazole (0.09 g), m. p. and mixed m. p. 172—173°.

Benzaldehyde thiadiazolylhydrazone (2.1 g) was dissolved in pyridine (15 ml), and benzoyl chloride (2 ml) was added. On the following day, the brown solution was poured into water (100 ml), and a brownish yellow crystalline product (3.1 g) was precipitated. It was dissolved in 250 ml of boiling ethanol, and on cooling, colourless plates separated (0.5 g, 16 % yield), m. p. 184—186° after recrystallization from toluene. The product was a benzoyl derivative of benzaldehyde thiadiazolylhydrazone. (Found: C 62.5; H 4.00; N 18.0; S 10.3. $C_{16}H_{12}N_4OS$ (308.35) requires C 62.3; H 3.92; N 18.2; S 10.4). λ_{max}: 3 350 Å with ε = 22 000.

An isomer of this compound was obtained by evaporating the mother liquor to one tenth of the original volume. First, unchanged starting material was deposited (0.6 g) and in the filtrate a further amount of crystalline material (0.5 g, 16 % yield) was deposited, m. p. 95—96° after recrystallization from 70 % aqueous ethanol. (Found: C 62.5; H 4.00; N 18.0; S 10.3.) λ_{max}: 2 780 Å with ε = 19 500.

Acetophenone thiadiazolylhydrazone (VI, R = H, R_1 = CH_3, R_2 = Ph). Monoacetophenone thiocarbohydrazone (4.2 g) and triethyl orthoformate (5 ml) were refluxed for 30 min, and then the ethanol and ester were taken off *in vacuo*. The slightly sticky residue was stirred with ethanol (10 ml), and the undissolved material (2.6 g, 60 % yield) crystallized from absolute ethanol as colourless needles, m. p. 198—199°. (Found: C 54.8; H 4.61; N 25.7; S 14.7. $C_{10}H_{10}N_4S$ (218.27) requires C 55.0; H 4.62; N 25.7; S 14.7.) λ_{max}: 3 110 Å with ε = 20 000, λ_{max}: 2 260 Å with ε = 13 000.

5-Methyl-1,3,4-thiadiazol-2-yl-hydrazones (VI, R = CH_3)

By refluxing monoacetone and monobenzaldehyde thiocarbhydrazones with triethyl orthoacetate and working up the solutions as above, low yields of the methyl analogues of the compounds just described were obtained.

Acetone 5-methyl-1,3,4-thiadiazol-2-yl-hydrazone (VI, R = R_1 = R_2 = CH_3) was obtained in 27 % yield and crystallized from absolute ethanol as colourless prisms, m. p. 176—177°. (Found: C 42.4; H 5.92; N 32.9; S 18.8. $C_6H_{10}N_4S$ (170.23) requires C 42.3; H 5.92; N 32.9; S 18.8.) λ_{max}: 2 800 Å with ε = 15 000.

When the mother liquor was made alkaline, and benzyl chloride was added, a 19 % yield of 3-benzylthio-4-amino-5-methyl-4,1,2-triazole [2] was obtained.

Benzaldehyde 5 methyl-1,3,4-thiadiazol-2-yl-hydrazone (VI, R = CH_3, R_1 = H, R_2 = Ph) was obtained in 8 % yield and crystallized from absolute ethanol as colourless needles, m. p. 212—213°. (Found: C 55.2; H 4.71; N 25.6; S 14.6. $C_{10}H_{10}N_4S$ (218.27) requires C 55.0; H 4.62; N 25.7; S 14.7.) λ_{max}: 3 240 Å with ε = 23 800, λ_{max}: 2 300 Å with ε = 12 700.

In the extraction with potassium carbonate solution, a 55 % yield of 3-mercapto-4-benzylidenamino-5-methyl-4,1,2-triazole [12] was obtained.

This investigation has been supported by grants from the *Swedish Natural Science Research Council*, from *Hierta-Retzius Stipendiefond*, and from *Stiftelsen Lars Hiertas Minne*. Experimental assistance from Miss Monica Linders is acknowledged. My thanks are due to Dr. C.-F. Kröger for helpful comments on the manuscript.

REFERENCES

1. Stollé, R., and Bowles, P. E. *Ber.* **41** (1908) 1099.
2. Kröger, C.-F. *Über die Synthese des 1,5-Bis-thiocarbaminyl-thiocarbohydrazids und die Reaktion von Thiocarbohydrazid mit aliphatischen Carbonsäuren und Carbonsäurederivaten.* (Diss.) University, Greifswald 1957.
3. Stollé, R. and Fehrenbach, K. *J. prakt. Chem.* [2] **122** (1929) 289.

4. Fujii, K., Yoshikawa, H. and Yuasu, M. *J. Pharm. Soc. Japan* **74** (1954) 1056. — *Chem. Abstr.* **49** (1955) 11592.
5. Kanaoka, M. *Pharm. Bull.* **5** (1957) 385.
6. Kanaoka, M. *J. Pharm. Soc. Japan* **75** (1955) 1149. — *Chem. Abstr.* **50** (1956) 5647.
7. Galinke, J. *Untersuchungen auf dem Gebiet der 5-Aminothiodiazole mit besonderer Berücksichtigung der Nitrosierung, Diazotierung und Nitrierung dieser Verbindungen.* (Diss.) University, Bonn 1957.
8. Sandström, J. *Svensk Kem. Tidskr.* **68** (1956) 135.
9. Hünig, S. *J. prakt. Chem.* [4] **8** (1959) 264.
10. Stephen, H. W. and Wilson, F. J. *J. Chem. Soc.* **1926** 2531.
11. Stollé, R. and Gaertner, E. *J. prakt. Chem.* [2] **132** (1931) 225.
12. Hoggarth, E. *J. Chem. Soc.* **1952** 4811.

Received January 30, 1960.

ACTA CHEMICA SCANDINAVICA 14 (1960) 1043—1050

Paper Electrophoresis of Carbohydrates in Germanate Buffer

BENGT LINDBERG and BRITA SWAN

Institutionen för träkemi, Kungl. Tekn. Högskolan, Stockholm, Sweden

The paper electrophoretic mobility of some carbohydrates in germanate buffer has been studied. The method seems to be a useful complement to other methods for the separation of these substances. Information of structural significance can be obtained from the mobilities of unknown carbohydrates.

Paper electrophoresis of neutral substances requires the presence of a complexing agent that will give charged complexes with the substances under investigation. Defined spots are obtained either when there is a rapid interconversion between complex and substance or when the equilibrium is displaced strongly towards the complex. The former is preferable as it permits greater differences in mobility between individual substances. Paper electrophoresis of neutral carbohydrates is usually done in borate buffer [1] but hydrogen sulphite [2], arsenite [3], basic lead acetate [3], molybdate [4] and sodium hydroxide [3] have also been used.

Germanate is known to give complexes with polyalcohols, and the reaction has recently been studied by Antikainen [5]. In the present investigation a study has been made of the electrophoretic mobility of some carbohydrates in germanate buffer. After some preliminary experiments the electrophoreses were run in 0.05 M sodium germanate buffer of pH 10.7 at 40° and 1 500 V (25—30 V/cm). The mobilities are given as M_G-values, that is relative to the mobility of glucose. Under these conditions glucose moves about 11 cm in 90 min. The mobilities of the various carbohydrates investigated are given in Tables 1—7. For some substances the M_G-values in borate buffer have also been given. These values are taken from Foster [1] or Frahn and Mills [3] or were determined in separate experiments. The conditions used by Foster [1] and by Frahn and Mills [3] are slighty different, but their M_G-values are very similar and could be compared directly.

As can be seen from Table 1 there are large differences between the mobilities of the monosaccharides in borate and in germanate. In borate, glucose is the fastest sugar and pairs of pentose and hexose sugars with the same configuration, *e. g.* xylose and glucose, have almost the same mobility. In germanate, glucose is the slowest sugar and pentoses move considerably faster than the corresponding hexoses. As discussed below, furanosidic 1,2-*cis*-diols seem

to contribute more to the mobility in germanate than the corresponding pyranosidic groupings, and an M_G-value in this buffer may reflect the conformational stability of the most stable pyranosidic chair form of the sugar. The individual differences between the ketoses is rather small in both buffers, but their mobilities relative to glucose are considerably higher in the germanate buffer.

A study of the mobilities of various partially methylated sugars has enabled some conclusions to be drawn about the structures of the borate complexes [1]. The mobilities in germanate and borate of some sugar derivatives, chiefly methyl ethers, are given in Table 2. Some special effects in germanate buffer can be seen. Firstly, the glucose and xylose derivatives, in which the hydroxyl group at $C_{(2)}$ is replaced by a methoxyl or amino group or by a hydrogen atom, show no mobility at all. This result strongly indicates that germanate complexes with reducing sugars are formed exclusively by 1,2-*cis*-diols in a cyclic form of the sugar. Since sugar alcohols, *e. g.* 2-*O*-methyl-D-glucitol (Table 6), have rather high mobilities, the contributions from complexes with the open chain form of the sugar must be negligible. In the light of these results is seems probable that the same is also true for borate complexes with the sugars. 2-*O*-Methyl-D-galactose, which has a 3,4-*cis*-diol grouping in its pyranose forms, gives a charged complex with germanate.

The high mobilities in germanate of glucose and xylose derivatives in which the $C_{(3)}$-hydroxyl group is etherified or replaced by hydrogen is difficult to understand. A possible explanation may be that, in the parent sugar, this hydroxyl takes part in the formation of an uncharged complex, competing with the charged complex of the α-pyranose or α-furanose form. When the 3-hydroxyl is absent, the uncharged complex cannot be formed and the mobility is therefore higher. The same effect also occurs in the galactose series, where the contribution from the 3,4-*cis*-diol is restricted to the pyranose forms and is probably not very important. In 3-*O*-methyl-D-mannose however the mobility relative to mannose is considerably reduced. In mannose both furanose and pyranose forms can give 2,3-*cis*-diol complexes. The 1,2-complexes are given by the β-forms only and may be less significant than the 2,3-complexes.

Table 1. Monosaccharides.

Substance	M_G in germanate	M_G in borate
D-Glucose	1	1
D-Mannose	1.4	0.72
D-Allose	1.8	0.83
D-Galactose	1.3	0.93
D-Xylose	1.4	1.00
D-Lyxose	1.9	0.71
D-Ribose	2.1	0.77
L-Arabinose	1.5	0.96
L-Rhamnose	1.3	0.52
D-Fructose	2.1	0.90
L-Sorbose	2.0	0.95
D-Tagatose	2.4	0.95

Table 2. Sugar derivatives.

Substance	M_G in germanate	M_G in borate
2-*O*-Methyl-D-glucose	0.0	0.23
2-Deoxy-D-glucose	0.0	0.29
2-Amino-2-deoxy-D-glucose	0.1	—
3-*O*-Methyl-D-glucose	1.4	0.80
3-*O*-Benzyl-D-glucose	1.2	—
3-Deoxy-D-glucose	1.6	0.85
4-*O*-Methyl-D-glucose	0.3	0.24
4-*O*-Benzyl-D-glucose	0.2	0.17
5-*O*-Methyl-D-glucose	1.6	0.65
6-*O*-Methyl-D-glucose	0.96	0.80
2,3-Di-*O*-methyl-D-glucose	0.0	0.12
3-*O*-Methyl-D-mannose	0.8	—
2-*O*-Methyl-D-galactose	0.6	0.43
3-*O*-Methyl-D-galactose	1.4	0.63
4-*O*-Methyl-D-galactose	0.4	0.30
6-*O*-Methyl-D-galactose	1.2	0.86
2,3-Di-*O*-methyl-D-galactose	0.1	—
2,4-Di-*O*-methyl-D-galactose	0.0	—
2,6-Di-*O*-methyl-D-galactose	0.5	—
2-*O*-Methyl-D-xylose	0.0	0.39
3-*O*-Methyl-D-xylose	1.7	0.66
4-*O*-Methyl-D-xylose	0.3	0.21

The low mobilities of 4-*O*-methyl-sugars in borate has been attributed to their inability to give a furanose structure [1]. The mobilities of these sugars are also low in germanate, and this explanation is supported by the very high mobility of 5-*O*-methyl-D-glucose, which can only assume this form. The results also show that the greater complex-forming ability of 1,2-*cis*-diols in a furanose ring relative to that of 1,2-*cis*-diols in a pyranose ring is more pronounced in germanate than in borate.

Table 3. Pyranosides and related substances.

Substance	M_G in germanate	M_G in borate
Methyl-β-D-glucopyranoside	0.0	0.19
Methyl-α-D-glucopyranoside	0.0	0.11
1,5-Anhydro-D-glucitol	0.05	0.20
Methyl-β-D-mannopyranoside	0.4	0.31
Methyl-α-D-mannopyranoside	0.5	0.42
1,5-Anhydro-D-mannitol	0.6	0.40
Methyl-β-D-galactopyranoside	0.5	0.38
Methyl-α-D-galactopyranoside	0.6	0.38
Methyl-β-D-xylopyranoside	0.0	0.0
Methyl-α-D-xylopyranoside	0.0	0.0
Methyl-β-L-arabinopyranoside	0.6	0.38
Methyl-α-L-arabinopyranoside	0.7	0.38
1,6-Anhydro-β-D-glucopyranose	0.0	—

Table 4. Furanosides and related substances.

Substance	M_G in germanate	M_G in borate
1,4-Anhydro-D-glucitol	0.4	—
Methyl-α-D-mannofuranoside	1.4	—
Ethyl-β-D-galactofuranoside	0.2	0.31
Methyl-α-L-arabinofuranoside	0.0	0.035
Methyl-β-D-xylofuranoside	0.05	0.33
1,6-Anhydro-α-D-galactofuranose	0.0	—

Methylation of glucose or galactose in the 6-position gives a slight reduction in the M_G-value in germanate. This is probably due to the elimination of the interaction with the 5,6-diol in the furanose form. With borate, complexes may also be formed at 4,6-positions in the glucopyranoses.

Of the glycopyranosides and the related 1,5-anhydrides of the glycitols (Table 3), only those with a 1,2-*cis*-diol grouping show significant mobility in germanate. There are rather small differences between the individual substances containing one such grouping. For an anomeric pair of glycosides, the anomer with the aglyconic group in an axial position in the most stable chair form has a somewhat higher mobility. Interactions with the 4,6-position, which contribute to the mobility in borate, *e. g.* in the glucosides, seem to be of no importance in germanate. One of the furanosides, which has a 1,2-*cis*-diol grouping, shows a high mobility in germanate but the others (Table 4), without such a grouping, show low mobilities. The xylofuranoside gives a complex with borate, probably due to interaction with the 3,5-hydroxyls [1], but no complex of this type seems to be formed with germanate. Methyl-α-D-glucofuranoside has a high mobility in borate ($M_G = 0.73$), which can be attributed to a tridentate complex involving the 3,5,6-hydroxyls [1]; 1,4-anhydro-D-glucitol would be expected to have a similar mobility in borate. It is questionable whether a tridentate complex is also formed with germanate and the relatively low mobility can also be due, at least to some extent, to complex formation with the 5,6-hydroxyls.

The M_G-values for a number of oligosaccharides that are given in Table 5 can easily be rationalised in terms of contributions from the reducing and non-reducing monomer residues, based on M_G-values for the analogous sugar ethers and glycosides. The effect of a 3-substituent in the glucose and galactose series is also clearly marked in the disaccharides.

A number of glycitols and glycitol methyl ethers were studied; their M_G-values are listed in Table 6. As these substances have less fixed conformations and a variety of competing complexes may be formed, it is rather difficult to interpret the results. An analysis of the M_G-values obtained show , however, that charged complexes are preferentially formed with 1,2-*trans*-diols (*threo*-configuration) and 1,2-diols in which one of the hydroxyls is primary. 1,2-*cis*-Diols (*erythro*-configuration) and 1,3-diols may also contribute, but to a much lesser extent. The same difference between 1,2-*cis*- and 1,2 *trans*-diols can be observed in borate buffer [1]. It seems to be difficult to draw any conclusions of

Table 5. Oligosaccharides.

Substance	Component * sugars	Linkage **	M_G in germanate	M_G in borate
Nigerose	G→G	α(1→3)	1.3	0.69
Laminarobiose	»	β(1→3)	1.1	0.69
Maltose	»	α(1→4)	0.4	0.32
Cellobiose	»	β(1→4)	0.3	0.23
Isomaltose	»	α(1→6)	0.9	0.69
Gentiobiose	»	β(1→6)	1.0	0.75
Lactose	Ga→G	β(1→4)	0.7	0.38
Melibiose	»	α(1→6)	1.4	—
Galactosido-galactose	Ga→Ga	β(1→3)	1.4	0.69
» »	»	β(1→4)	0.7	0.50
» »	»	β(1→6)	1.4	0.83
Mannosido-mannose	M→M	β(1→4)	1.1	0.66
Mannosido-glucose	M→G	β(1→4)	0.7	0.43
Glucosido-mannose	G→M	β(1→4)	0.8	0.58
Sucrose	G↔F	—	0.1	—
Raffinose	Ga→G↔F	—	0.4	—

* G = Glucose, Ga = Galactose, M = Mannose and F = Fructose.
** All linkages pyranosidic, except in the last two oligosaccharides.

Table 6. Glycitols.

Substance	M_G in germanate	M_G in borate
Glycol	0.0	—
Glyceritol	0.4	0.44
Erythritol	1.0	0.75
D-Ribitol	1.2	—
L-Arabinitol	1.8	0.90
D-Xylitol	1.7	—
D-Glucitol	1.9	0.89
D-Mannitol	1.9	0.90
Galactitol	2.1	0.98
Lactitol	1.5	—
Cellobiitol	1.2	—
Melibiitol	1.5	—
2-*O*-Methyl-D-xylitol	1.2	—
3-*O*-Methyl-D-xylitol	0.5	—
2-*O*-Methyl-D-glucitol	1.5	—
3-*O*-Methyl-D-glucitol	0.8	—
4-*O*-Methyl-D-glucitol	1.4	—
2-*O*-Methyl-D-galactitol	1.7	—
3-*O*-Methyl-D-galactitol	1.4	—
6-*O*-Methyl-D-galactitol	1.6	—

Table 7. Cyclitols.

Substance	M_G in germanate	M_G in borate
scyllo-Inositol	0.2	0.05
myo-Inositol	0.7	0.53
D-Inositol	1.0	0.63
epi-Inositol	1.8	0.73
Sequoitol	0.5	0.18
Pinitol	1.0	0.66
Mytilitol	0.2	0.20

structural significance from the electrophoretic mobilities of open chain polyhydroxy compounds in germanate buffer. It does however appear to be a useful method for the separation of for instance the pairs ribitol and arabitol or 2- and 3-*O*-methyl-D-glucitol. Electrophoresis in molybdate [4] seems to be more suitable for the separation of substituted glycitols.

The mobilities of some cyclitols in germanate (Table 7) are rather similar to the corresponding values in borate. It has been demonstrated that tridentate complexes are formed in borate [6] and it is possible that similar complexes are formed with germanate, especially as *scyllo*-inositol shows a definite mobility in this buffer.

DISCUSSION

In a germanate ion with the coordination number six, the distance between two oxygen atoms is 2.64 Å. This is rather close to the distance between the oxygen atoms in tetrahedrally coordinated borate, 2.72 Å (Values for the atomic distances are taken from Pauling [7]). The results described above indicate that germanate gives complexes with 1,2-*cis*-diols in furanosides (O—O = 2.51) and pyranosides (O—O = 2.86) and with open chain 1,2-diols with a *threo*-configuration (the O—O distances are taken from Reeves [8]). The same type of complex is formed with borate but the complexes between germanate and furanosidic 1,2 *cis*-diols seem to be especially strong. The same seems to be true for the complexes with arsenite [3]. Borate also gives complexes with 1,3-diols but this possibility seems to be very limited with germanate. Thus methyl-β-D-glucopyranoside and methyl-β-D-xylofuranoside, although they have low mobilities in germanate (almost nil) show significant mobilities in borate, almost certainly due to the formation of complexes at the 4,6- and 3,5 positions, respectively.

The possibility of the formation of tridentate complexes especially with the cyclitols, can not be excluded, but the mobilities of this substances may also be due to complexes with 1,2-*cis*-diols. *Scyllo*-Inositol, however, has no such groupings but may give an 1,3-*cis*-complex in a boat conformation. With open chain sugars, complexes with 1,3-diols seem to be of lesser importance. As in the case of borate complexes and cyclic acetals, there is little sign of the formation of germanate complexes with 1,2-*trans*-diols in a pyran ring or with open chain 1,2-diols with an *erythro*-configuration.

Germanium has also the coordination number four. For tetrahedrally coordinated germanate the distance between two oxygen atoms is 3.32 Å and any complex formed with this should be uncharged. In furanose rings, the distance between the oxygen atoms in a 1,2-*trans*-diol is 3.45 Å, and such a diol might therefore give uncharged complexe with germanate. There are also other diols, in which the distance between the oxygen atoms can assume values close to 3.32 Å. As mentioned above, derivatives of glucose and xylose, in which the 3-hydroxyl group is replaced by another group, rather unexpectedly have higher mobilities than the parent sugars; this can be explained by the formation of uncharged complexes which will compete with the charged complexes *. It must be admitted, however, that this effect is not perfectly understood.

As can be seen from the Tables, paper electrophoresis in germanate buffer is a useful complement to electrophoresis in borate [1] and other buffers [2-4]. Many separation problems can be dealt with better by electrophoresis in germanate instead of borate and other buffers. For instance, this is probably the only method by which all five mono-*O*-methyl-D-glucoses can be separated in one operation. It should also be possible to obtain information on the structures of unknown carbohydrates from their electrophoretic mobilities in germanate. This is true especially for partially etherified sugars and for reducing oligosaccharides, in which rather few groupings contribute to the mobility and the effect of substitution is often considerable.

Germanate is non-toxic and requires no special precautions. Non-reducing sugars are sometimes difficult to detect on germanate impregnated paper. The same difficulty is observed in borate electrophoresis and may be overcome by increasing the amount of the component or by modifying the method used for localisation. The same spray reagents can be used with both buffer systems.

EXPERIMENTAL

Buffer. An 0.05 M solution of germanate was prepared by adding 50 % aqueous sodium hydroxide to a suspension of germanium dioxide in water until a clear solution of pH 10.7 was obtained. This solution turns milky on keeping but is still quite suitable for use. The milkiness depends on the formation of polygermanates and is accelerated if the solution is heated. After each run, the solutions at the cathode and the anode should be mixed, as the pH increases in the former and decreases in the latter. The pH of the buffer should be checked regularly.

Procedure. The apparatus, of the Kunkel and Tiselius type [9], and the technique were essentially the same as described by Foster [1]. Whatman No. 1 filter paper was used. The electroendosmotic flow is rather high, and the starting line was placed 20 cm from the cathode end of the cooling plate. 2,3,4,6-Tetra-*O*-methyl-D-glucose and D-glucose were run on all papers, the first in order to make a correction for the electroendosmosis, the latter as an internal standard. The electrophoreses were run for 90 min. at 1 500 V, equivalent to 25—30 V/cm. Water at 40° was circulated through the cooling-plate. Under these conditions the migration of D-glucose was about 11 cm.

---

* *Added in proof.* This explanation is probably not valid as we have recently observed that 3-*O*-methyl-D-glucose and 3-*O*-methyl-D-xylose have higher mobilities than their parent sugars also on electrophoresis in sulphonated phenylboronic acid buffers of low pH-values (6—7). In these buffers all complexes must be charged. (P. Garegg and B. Lindberg. *Unpublished results.*)

Localisation of spots. The reducing sugars were localised by spraying with anisidine hydrochloride [10]. Non-reducing sugars were localised either with the silver nitrate — sodium ethoxide reagent [11] or with periodate-benzidine [12], after neutralisation of the paper by spraying with acetic acid. Some spots could not be detected with the former reagent, but the latter, although somewhat more complicated, was more reliable. Distinct, circular spots were usually obtained. The migration distance was measured from the centre of the spots.

Substances. Most of the substances studied were available in this laboratory or at the wood chemistry department of the Swedish Forest Products Research Laboratory. 5-*O*-Methyl-D-glucose and 3-*O*-methyl-D-mannose were kindly supplied by Professor O. Th. Schmidt, Heidelberg, and Dr. G. O. Aspinall, Edinburgh, respectively. The partially methylated glycitols were prepared, in small quantities, by reduction of the corresponding methylated sugars with Raney nickel according to Karabinos and Ballun [13]. These substances, most of which are not described in the literature, were not characterised.

REFERENCES

1. Foster, A. B. *Advances in Carbohydrate Chem.* **12** (1957) 81.
2. Theander, O. *Acta Chem. Scand.* **11** (1957) 717.
3. Frahn, J. L. and Mills, J. A. *Australian J. Chem.* **12** (1959) 65.
4. Bourne, E. F. Hutson, D. H. and Weigel, H. *Chem & Ind. London*, **1959** 1047.
5. Antikainen, P. J. *Acta Chem. Scand.* **13** (1959) 312, and previous papers.
6. Angyal, S. J. and McHugh, D. J. *J. Chem. Soc.* **1957** 1423.
7. Pauling, L. The *Nature of the Chemical Bond*, Cornell University Press 1940.
8. Reeves, R. E. *Advances in Carbohydrate Chem.* **6** (1951) 111.
9. Kunkel, H. G. and Tiselius, A. *J. Gen. Physiol.* **35** (1951) 89.
10. Hough, L., Jones, J. K. N. and Wadman, W. H. *J. Chem. Soc.* **1950** 1702.
11. Trevelyan, W. E., Procter, D. P. and Harrison, J. S. *Nature* **166** (1950) 444.
12. Cifonelli, J. A. and Smith, F. *Anal. Chem.* **26** (1954) 1132.
13. Karabinos, J. V. and Ballun, A. T. *J. Am. Chem. Soc.* **75** (1953) 4501.

Received February 22, 1960.

ACTA CHEMICA SCANDINAVICA 14 (1960) 1051—1053

Synthesis of Cellobiouronic Acid

BENGT LINDBERG and LARS SELLEBY

Institutionen för träkemi, Kungl. Tekniska Högskolan, Stockholm, Sweden

4-*O*-(β-Glucopyranosyluronic acid)-D-glucose or cellobiouronic acid (I) was synthesised starting from 1,6-anhydrocellobiose (IV).

4-*O*-(β-D-Glucopyranosyluronic acid)-D-glucose or cellobiouronic acid has been isolated from hydrolysates of the specific polysaccharides of *Pneumococcus* Types III [1] and VIII [2,3] and its structure has been determined by Hotchkiss and Goebel.[4] The similar serological activity of these and some other bacterial polysaccharides and of oxidised cellulose is apparently related to the presence of cellobiouronic acid residues.

In a recent paper, Marchessault and Rånby [5] have discussed the nature of certain linkages in cellulose, which have an increased sensitivity to acid hydrolysis and have attributed them to the presence of glucuronic acid residues in the cellulose chain. It is known that a biouronic acid linkage, as in cellobiouronic acid (I), is considerably more resistant to acid hydrolysis than an ordinary glycosidic linkage, as in cellobiose (II). Rånby and Marchessault now suggest that the pseudo-biouronic acid linkage, as in pseudo-cellobiouronic acid (III), must be considerably more sensitive to acid hydrolysis than the other linkages.

They also suggest that inductive effects, due to the electrophilic carboxyl groups, are responsible for the known resistance of the biouronic linkage (I) and for the postulated weakness of the pseudo-biouronic linkage (III). A comparison of the rates of acid hydrolysis of the three model substances (I, II and III) is therefore a matter of some interest. The present paper describes the synthesis of cellobiouronic acid (I).

1,6-Anhydro-cellobiose (IV) was prepared by treatment of phenyl-β-cellobioside with alkali.[6] Tritylation and acetylation yielded the pentaacetate trityl ether (V) and detritylation of V gave the pentaacetate (VI), in which all the hydroxyls of cellobiose (II) except the primary hydroxyl in the non-reducing glucose residue are protected. Oxidation of VI with permanganate in acetic acid, as previously used in a similar syntheses of glucuronic acid by Stacey [7], yielded the pentaacetate of 1,6-anhydro-cellobiouronic acid, VIII. This substance was not isolated but was deacetylated and subjected to acid hydrolysis. The 1,6-anhydride linkage was preferentially hydrolysed and the cellobiouronic acid (I) formed was purified from small amounts of contaminating

glucose and glucuronic acid by ion exchange chromatography. The amorphous product was chromatographically and electrophoretically pure and gave the α-heptaacetate methyl ester with m.p. 251—252 °, $[\alpha]_D^{20}$ + 44° (in chloroform), in good agreement with previously recorded values for this substance.[2,3] *

EXPERIMENTAL

Melting points are corrected. Concentrations were done under reduced pressure.

1,6-Anhydro-cellobiose (IV) was prepared according to Montgomery *et al.*[6] An attempt to prepare the intermediate phenyl-hepta-*O*-acetyl-β-cellobioside from octa-*O*-acetyl-α-cellobiose, phenol and *p*-toluene-sulphonic acid by the method of Helferich and Schmitz-Hillebrecht [8], failed, probably because of the difficulty of separating the mixture of α- and β-glycosides formed.

2,3,2',3',4'-Penta-O-*acetyl-6'*-O-*trityl-1,6-anhydrocellobiose.* (V) 1,6-Anhydrocellobiose (5 g) was dissolved in anhydrous pyridine (100 ml) and trityl chloride (6.6 g) was added.

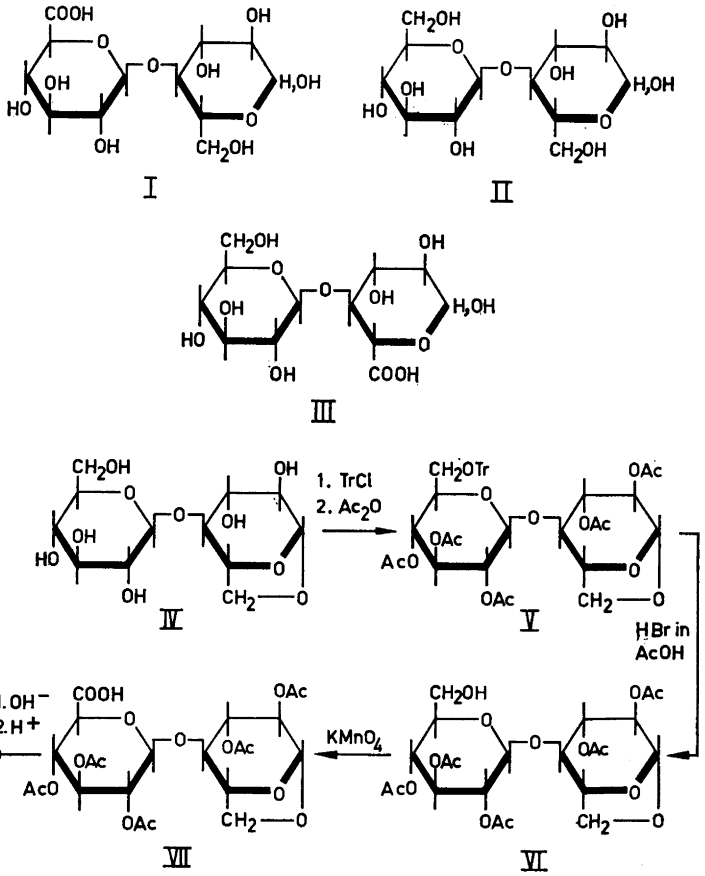

* *Added in proof.* In a recent paper [*Chem. Ber.* **95** (1960) 356] Jayme and Werner report the synthesis of cellobiuronic acid by a different route.

The solution was kept overnight, acetic anhydride (20 ml) was then added and after two days the mixture was poured into ice-water (1 000 ml) containing acetic acid (50 ml). The precipitate was collected and crystallised from ethanol, yielding the pure substance (8.0 g), m. p. 119—120°, $[\alpha]_D^{20}$ —50° (chloroform *c*, 1.1). (Found: C 63.3, H 5.71. Calc. for $C_{41}H_{44}O_{15}$: C 63.5; H 5.58.)

*2,3,2',3',4'-Penta-*O*-acetyl-1,6-anhydro-cellobiose* (VI). The trityl derivative (V) (8.0 g) was dissolved in acetic acid (60 ml) and a saturated solution of hydrogen bromide in acetic acid (15 ml) was added. The mixture was shaken for 45 sec. and the trityl bromide was removed by filtration. The solution was immediately poured into ice-water (500 ml) and extracted with chloroform (3 × 100 ml). The chloroform solution was washed with ice-water (5 × 100 ml), dried over calcium chloride and concentrated to a sirup. The sirup crystallised on addition of ether and scratching and was recrystallised from chloroform-ether. The crystals (2.7 g) had m. p. 156—157° and $[\alpha]_D^{20}$ —133°, (chloroform, *c*, 2.0). (Found: 49.4; H 5.75. Calc. for $C_{22}H_{30}O_{15}$: C 49.4; H 5.66.)

*4-*O*-(β-*D*-Glucopyranosyluronic acid)-*D*-glucose (I).* The pentaacetate (VI) (1.0 g) was dissolved in analytically pure, homologue-free acetic acid (10 ml) and finely powdered potassium permanganate (500 mg, 20 % excess) was added. The mixture was stirred at room temperature, and the reaction was followed by chromatography on dimethyl sulphoxide-impregnated paper [9], using benzene as the mobile phase. The starting material and the reaction product had R_F-values of 0.9 and 0.65, resp. The spots were developed with silver nitrate-sodium ethoxide [10].

After two days, when the reaction was complete, the mixture was concentrated to dryness, dissolved in 0.1 N aqueous potassium hydroxide (50 ml) and kept overnight. The precipitate of manganese dioxide was filtered off and the clear, colourless solution obtained was filtered through a column of cation exchange resin, Amberlite IR 120 (H^+).

The solution was concentrated by freeze-drying, dissolved in 0.5 N sulphuric acid and then kept at 100°. The hydrolysis was followed by paper chromatography (ethyl acetate-acetic acid-water, 3:1:1) and paper electrophoresis (0.1 M borate buffer, pH 10). After 12 h the starting material had disappeared. The solution was neutralised with barium carbonate, barium sulphate was removed by filtration and the salts were converted to acids by filtering through a column of Amberlite IR 120 (H^+). The solution which in addition to cellobiouronic acid contained traces of glucose and glucuronic acid (chiefly as glucurone) was added to the top of a column (23 × 2 cm) of anion exchange resin, Dowex 2, in the acetate form. The column was eluted, first with water (3 000 ml) and then with 3 N aqueous acetic acid (500 ml). The latter eluate, which contained chromatographically and electrophoretically pure cellobiouronic acid was concentrated to dryness, dissolved in water and freeze-dried, yielding the compound as a white, amorphous powder (415 mg).

Methyl ester α-heptaacetate of cellobiouronic acid. Cellobiouronic acid (100 mg) was dissolved in methanol (7 ml) and an excess of diazomethane in ether was added. After a few minutes the solution was concentrated to a sirup, and this was then dissolved in acetic anhydride (10 ml) containing zinc chloride (0.5 g) and kept at 60° for 90 min.

The solution was concentrated and the residue was crystallised from ethanol, yielding the methyl ester acetate (60 mg), m. p. 251—252°, $[\alpha]_D^{20}$ +44° (chloroform, *c* 1.2).

REFERENCES

1. Heidelberger, M. and Goebel, W. F. *J. Biol. Chem.* **74** (1927) 613.
2. Goebel, W. F. *J. Biol. Chem.* **110** (1935) 391.
3. Jones, J. K. N. and Perry, M. B. *J. Am. Chem. Soc.* **79** (1957) 2787.
4. Hotchkiss, R. D. and Goebel, W. F. *J. Biol. Chem.* **121** (1937) 195.
5. Marchessault, R. H. and Rånby, B. G. *Svensk Papperstidn.* **62** (1959) 230.
6. Montgomery, E. M., Richtmeyer, N. K. and Hudson, C. S. *J. Am. Chem. Soc.* **64** (1942) 690.
7. Stacey, M. *J. Chem. Soc.* **1939** 1529.
8. Helferich, B. and Schmitz-Hillebrecht, E. *Ber.* **66** (1933) 378.
9. Wickberg, B. *Acta Chem. Scand.* **12** (1958) 615.
10. Trevelyan, W. E., Procter, D. P. and Harrison, J. S. *Nature* **166** (1950) 444.

Received February 22, 1960.

ACTA CHEMICA SCANDINAVICA 14 (1960) 1054—1058

Potential Chemotherapeutics

II. 2-(5-Nitro-2-furyl)-5-amino-1,3,4-thiadiazoles *

KURT SKAGIUS

Research Laboratories, A. B. Pharmacia, Uppsala, Sweden

KURT RUBINSTEIN and ELSE IFVERSEN †

Research Division, Aktieselskabet Pharmacia, Copenhagen-Vanlöse, Denmark

Seventeen 2-(5-nitro-2-furyl)-5-amino-1,3,4-thiadiazoles were prepared by oxidation of the corresponding thiosemicarbazones with ferric salts according to Young and Eyre or electrolytically in the presence of ferric salts.

In 1944 Dodd and Stillman discovered the antibacterial activity of the nitrofurans [1]. Since then a great number of nitrofuryl derivatives have been synthesized and tested. Several of these compounds are hydrazone-type derivatives of 5-nitrofurfural such as nitrofurazone, nitrofurantoin and furazolidone, all possessing a broad antibacterial spectrum [2]. It is also known, that 5-nitrofurfural thiosemicarbazone, in analogy to many other thiosemicarbazones, has a strong tuberculostatic activity [3].

Since the nitrofurans mentioned have a structure, which could be expected to be relatively easily destroyed, for example by acid hydrolysis, it was of interest to synthesize compounds with a more stable structure. This is readily accomplished for example by oxidative ring closure of nitrofurfural thiosemicarbazone to the corresponding aminothiadiazole. As it became clear that this compound had promising antibacterial properties, a series of derivatives were prepared for antibacterial screening.

All substances prepared are 5-(nitrofuryl)-thiadiazoles with an unsubstituted or a monosubstituted amino group in the 2-position of the thiadiazole ring system. They were prepared from nitrofurfural (or its diacetate) and the corresponding 4-substituted thiosemicarbazide as follows (Nf stands for 5-nitro-2-furyl):

* During the preparation of this manuscript the authors were informed that Dr. W. Sherman at Abbott Labs. during the September Meeting of A.C.S. Division of Medicinal Chemistry lectured on nitrofuryl compounds, comprising some of the compounds mentioned in this paper.

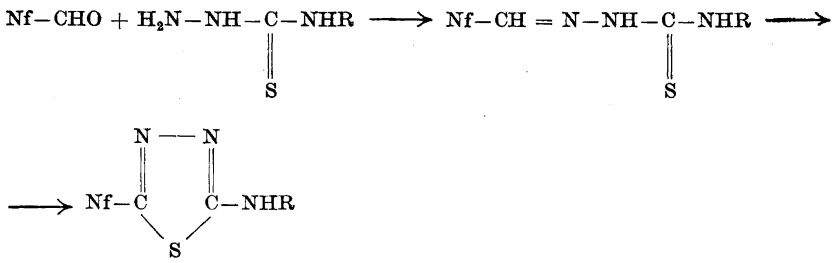

The thiosemicarbazides were prepared from the corresponding *iso*thiocyanates and hydrazine hydrate, with the exception of 4-(2-pyridyl)-thiosemicarbazide. When 2-pyridyl-*iso*thiocyanate was allowed to react with hydrazine hydrate in ethanol under various conditions, only 1,6-dipyridyl-2,5-dithiobiurea was obtained. Therefore, 4-pyridylthiosemicarbazide was prepared from the triethylammonium salt of 2-pyridyldithiocarbamic acid.

The oxidation of thiosemicarbazones of aromatic aldehydes is readily performed with ferric chloride [4]. However, when applied to heterocyclic derivatives the method does not always seem to be convenient. Thus, Erlenmeyer *et al.*[5] obtained only a small yield on ferric chloride oxidation of 2-pyridylaldehyde thiosemicarbazone, and Maffii *et al.*[6] obtained 41.6 % yield on oxida-

Table 1. Substituted 2-(5-nitro-2-furyl)-5-amino-1,3,4-thiadiazoles.

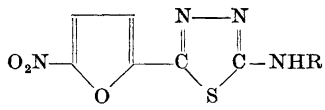

Compd No.	Ph 778/ X	R	M. p.	M.p. of Thiosemicarb.	Yield %	Recrystallization solvent
1	1	H	272 — 3	250	87	DMSO; DMF; HOAc
2	6	CH_3	219 —21	216 —18	63	Ethanol-dioxane
3	8	C_2H_5	219 —21.5	181 — 3	71	Ethanol-dioxane
4	10	*n*-C_3H_7	190 — 1	170 — 1.5	87	Ethanol
5	7	*i*-C_3H_7	213 —15	188 — 9	75	Ethanol-dioxane
6	9	*n*-C_4H_9	186 — 7	152.5— 4	74	Ethanol-dioxane
7	14	*i*-C_4H_9	183.5— 4.5	173.5— 5	80	Ethanol
8	55	*n*-C_6H_{13}	162.5— 3.5	128.5—9.5	50	Ethanol
9	22	C_6H_{11}	214 —15	194 — 5	76	Ethanol-dioxane
10	21	$-CH_2-CH=CH_2$	172.5— 5.5	177 — 8	71	Ethanol
11	12	$-CH_2-C_6H_5$	190 — 1.5	211 —12	50	Ethanol-dioxane
12	43	$-CH_2-CH_2-C_6H_5$	160 — 9	188 — 9	50	Ethanol
13	41	$-CH_2-CH_2-O-CH_3$	169 —71	169 —70	60	Ethanol
14	16	$-CH_2-CO_2-Et$	172.5— 4	178.5— 9.5	77	Ethanol
15	18	$-CH_2-COOH$	243.5— 4	—	—	Ethanol-dioxane
16	19	$-C_6H_5$	253 — 4.5	196.5— 7	62	Ethanol-dioxane
17	24	$-2-C_5H_4N$	dec.	dec.	58	DMF

tion of 2-furfural thiosemicarbazone. In the present work, however, oxidation of 5-nitrofurfural thiosemicarbazone yields about 84 % of the aminothiadiazole. The difference in yield between the furyl and 5-nitrofuryl derivative might be attributed to the inhibitory influence of the nitro group on the acid cleavage of the furyl group.

Attempts were made to use other oxidation agents such as cerium sulphate, lead tetraacetate, chromium trioxide, selenium dioxide, potassium permanganate and hydrogen peroxide. However, either no reaction occurred or unidentified substances were formed (*cf.* Ref.[7]). On the other hand, it was possible to perform an electrolytic oxidation in the presence of small amounts of ferric salts. Probably, the ferrous ions formed by the ring closure were oxidized, thus allowing the reaction to proceed. However, attempts to replace the electric current with potassium permanganate failed, and the yield of aminothiadiazole formed in this case corresponded to the amount of ferric ions originally present in the reaction.

Under alkaline conditions the nitrofuryl group is fairly labile and extensive decomposition may occur. It was found, however, that the oxidation could be performed with potassium ferricyanide in the presence of sodium acetate [8], but the time of reaction was considerably increased.

Compound No. 12 in Table 1 (the 2-phenylethyl derivative) has a very unsharp melting-point in spite of several consecutive recrystallizations. Melting-point depression is obtained when the substance is mixed with the thiosemicarbazone used as starting material. It seems probable, that the broad melting-point interval is due to polymorfism. A similar behaviour is shown by the substance No. 10 (allyl derivative). On recrystallization of the latter compound two kinds of crystals are obtained — brown rods and yellow flakes. At about 150°C the shells turn brown, and a sharp melting point is obtained.

The thiadiazoles prepared are yellow substances with slightly alkaline properties. In contrast to the corresponding thiosemicarbazones, they are readily soluble in cold formic acid, which could be used to separate the substances, when mixtures were obtained. Compound No. 1 (unsubstituted amino group), which is the most promising as a potential chemotherapeutic, is slightly soluble in most common solvents but comparatively soluble in formic acid, dimethyl formamide and dimethyl sulfoxide.

In serial dilution tests *in vitro* Compound No. 1 inhibits growth of a series of strains of *Staphylococcus aureus* in a concentration of 3.2—25 μg/ml, of *Salmonella*, *Shigella* and *Coli* in concentrations of 0.4—6.3 μg/ml and of *Streptococcus* in concentrations of 12.5—200 μg/ml. Further details of the antibacterial screening will be published separately.

Table 2. Analytical results.

Compd No.	Summary formula	% C calc.	% C found	% H calc.	% H found	% N calc.	% N found	% S calc.	% S found
1	$C_6H_4N_4O_3S$	34.0	33.8	1.9	1.9	26.4	26.5	15.1	15.0
2	$C_7H_6N_4O_3S$	37.2	37.0	2.7	3.0	24.8	24.7	14.2	14.0
3	$C_8H_8N_4O_3S$	40.0	40.2	3.4	3.4	23.3	23.3	13.4	13.3
4	$C_9H_{10}N_4O_3S$	42.5	42.4	4.0	4.1	22.0	21.8	12.6	12.8
5	$C_9H_{10}N_4O_3S$	42.5	42.5	4.0	4.1	22.0	21.9	12.6	12.7
6	$C_{10}H_{12}N_4O_3S$	44.8	45.0	4.5	4.6	20.9	20.7	12.0	11.9
7	$C_{10}H_{12}N_4O_3S$	44.8	44.9	4.5	4.6	20.9	20.4	12.0	11.8
8	$C_{12}H_{16}N_4O_3S$	48.6	48.7	5.4	5.6	18.9	18.9	10.8	10.8
9	$C_{12}H_{14}N_4O_3S$	49.0	49.0	4.8	4.9	19.0	19.0	10.9	11.0
10	$C_9H_8N_4O_3S$	43.0	43.0	3.2	3.2	22.3	22.2	12.8	12.8
11	$C_{13}H_{10}N_4O_3S$	51.7	52.0	3.3	3.4	18.5	18.2	10.6	10.2
12	$C_{14}H_{12}N_4O_3S$	53.2	53.3	3.8	3.9	17.7	17.6	10.1	10.4
13	$C_9H_{10}N_4O_4S$	40.0	40.0	3.7	4.0	20.7	20.6	11.9	11.2
14	$C_{10}H_{10}N_4O_5S$	40.3	40.4	3.4	3.4	18.8	18.4	10.8	10.7
16	$C_{12}H_8N_4O_3S$	50.0	49.9	2.8	2.9	19.4	19.2	11.1	11.1
17	$C_{11}H_7N_5O_3S$	45.7	45.9	2.4	2.6	24.2	24.4	11.1	11.0

EXPERIMENTAL *

5-Nitro-2-furyl thiosemicarbazones. The thiosemicarbazones were prepared by refluxing 5-nitro-furfural diacetate and the corresponding thiosemicarbazide in a mixture of ethanol and dilute sulfuric acid, or by heating 5-nitrofurfural and the thiosemicarbazide in ethanol. The product obtained, usually orange-coloured, was recrystallized from dimethyl formamide, dimethyl sulfoxide, dioxane or ethanol. The products decompose on heating at temperatures given in Table 1.

2-(5-Nitro-2-furyl)-5-amino-1,3,4-thiadiazole. a) 125 g (0.58 mole) of 5-nitro-2-furfural thiosemicarbazone and 1 160 g of a 25 % solution of ferric chloride (490 g of $FeCl_3 \cdot 6\ H_2O$) in water are placed in a 1.5 l beaker, fitted with a stirrer and a thermometer. The mixture is stirred on a water bath at 80°C for 90 min and then chilled to room temperature. The precipitate is filtered off and washed with 800 ml of hot water, followed by 800 ml of cold water, and dried at 60°C. Weight 118 g. The substance is dissolved in 360 g of dimethyl sulfoxide, treated with Norite and filtered. 30 ml of distilled water is added to the hot solution and the mixture is chilled in a refrigerator. The yellow crystals are filtered off, washed with 140 ml of ethanol, 180 ml of water and dried. Yield 108 g (87 %). M. p. 270–271° (decomp.). If the substance is heated slowly it darkens gradually without melting.

b) A porcelain cell with a volume of about 200 ml is placed in a 500 ml vessel, used for electrolysis. A mixture of 21.4 g (0.1 mole) of 5-nitro-2-furfural thiosemicarbazone and 125 ml of 15 % potassium ferrisulfate in water is poured in the cell. The mixture is stirred thoroughly with a perforated platinum anode about 5 × 4 cm^2 in size. A cylinder-shaped copper cathode is placed in the cathode-room outside the cell, which is filled with dilute sulfuric acid.

The electrolysis is performed at about 70°C with about 2 A for 4 h. The solid in the anode-cell is filtered off, washed with hot water and recrystallized from DMF-water as described in method a). Yield 14 g. M. p. 270–272°C.

c) 8.5 g (0.04 mole) of nitrofurfural thiosemicarbazone and a solution of 29 g (0.09 mole) of potassium ferricyanide and 25 g of sodium acetate in 200 ml of water were stirred for 8 h on a water bath. The precipitate obtained on cooling was filtered off, washed and dried. 6.3 g (75 %) of yellow crystals were obtained, which decomposed at 272°C. A reaction time of 2 h and 5 h yielded, respectively, 20–30 % and 50 %.

* Microanalyses by Dr. Wolfgang Kirsten.

The 2-(5-nitro-2-furyl)-5-amino-1,3,4-thiadiazoles, listed in Table 1, were prepared in analogy to method a) above. A few examples further illustrate the procedure:

2-(5-Nitro-2-furyl)-5-allylamino-1,3,4-thiadiazole. 25.4 g (0.1 mole) of 1-(nitrofurfural)-4-allylthiosemicarbazone is stirred on a water bath for 2 h with a solution of 50 ml of 50 % $FeCl_3$ and 70 ml of water. The dark product obtained was dissolved in hot ethanol, carbon added, the hot solution filtered and allowed to crystallize. 12.5 g of yellow-brown needles and 5.8 g of yellow flakes were obtained. The needles melt at 172.5–173.5°C. The flakes rearrange to the brown needles at about 150°C and melt at 172.5–173.5°C.

2-(5-Nitro-2-furyl)-5-carboxymethylamino-1,3,4-thiadiazole. 2.5 g of 1-(nitrofurfural)-4-carbethoxymethylthiosemicarbazone is stirred with 15 ml of 15 % $FeCl_3$ and 20 ml of H_2O on a water-bath for one hour. The dark precipitate was dissolved in ethanol, carbon added, and the hot mixture was filtered. After cooling, 1.95 g of 2-(nitrofuryl)-5-carbethoxymethylaminothiadiazole was obtained as yellow flakes melting at 172.5–174°C.

0.9 g of the ester was heated on a water bath for 3 h with 20 ml of 5 N sulfuric acid. The yellow precipitate was filtered off, and washed with ethanol. 0.8 g of needles were obtained which decomposed at 246–248°C. 0.5 g of the substance was dissolved in 50 ml of ethanol-dioxane 1:1 and filtered. After cooling, 0.4 g of yellow crystals was obtained. M.p. 243.5–244°C (decomp.). Equiv. wt: Found 269. Calc. 270.

REFERENCES

1. Dodd, M. C. and Stillman, W. B. *J. Pharmacol. Exptl. Therap.* **82** (1944) 11.
2. *Introduction to the Nitrofurans.* Eaton Laboratories 1958.
3. Freedlander, B. L. and Furst, A. *Wasmann* J. Biol. **9** (1951) 355.
4. Young, G. and Eyre, W. *J. Chem. Soc.* **79** (1901) 54.
5. Hemmerich, P., Prijs, B. and Erlenmeyer, H. *Helv. Chim. Acta* **41** (1958) 2058.
6. Maffii, G., Testa, E. and Ettorre, E. *Il Farmaco* **13** (1958) 187.
7. Hoggarth, E. *J. Chem. Soc.* **1951** 2202.
8. Brown, E. V. *Iowa State Coll. J. Sci.* **11** (1937) 227. *Chem. Abstr.* **31** (1937) 8528.

Received February 13, 1960.

ACTA CHEMICA SCANDINAVICA 14 (1960) 1059—1076

The Ion Exchange Properties of Silica Gel

I. The Sorption of Na^+, Ca^{2+}, Ba^{2+}, UO_2^{2+}, Gd^{3+}, Zr(IV) + Nb, U(IV) and Pu(IV)

STEN AHRLAND, INGMAR GRENTHE and BERTIL NORÉN

Department of Inorganic and Physical Chemistry, Chemical Institute, University of Lund, Lund, Sweden

In the present work the metal ion sorption on silica gel has been investigated. The silica gel acts in this respect as an ion exchanger of the weakly acid type and in the case of a monovalent cation the exhange reaction can be written schematically in the following way

$$\begin{array}{c} | \\ -\mathrm{Si}- \\ | \end{array} \mathrm{OH} + \mathrm{Me}^+ \rightleftharpoons \begin{array}{c} | \\ -\mathrm{Si}- \\ | \end{array} \mathrm{OMe} + \mathrm{H}^+$$

For this equilibrium the law of mass action seems to be valid. Moreover an amount of hydrogen ions equivalent to the amount of metal ions sorbed are set free at the sorption on silica gel which has been saturated with hydrogen ions. The amount of metal ion sorbed depends strongly on the pH of the solution. At the sorption of strongly hydrolysed (presumably high molecular) ions the equilibrium is reached slowly, while the sorption of non-hydrolysed (low molecular) ions is quite rapid, the equilibrium usually being reached within five minutes.

Numerous silicon compounds with good sorption properties have long been known. Such compounds are the zeolites, of natural as well as synthetic origin, which are extensively used for the sorption of metal ions from water solutions. Silica gel has also been used previously as a sorbent, particularly for organic compounds and gases.

This investigation was performed in order to investigate more closely the ability of the silica gel to sorb metal ions from water solutions. The aim was especially to find out how this sorption depends on the previous treatment and grain size of the gel as well as on the hydrogen ion concentration of the solution. The sorption to and the affinity for the gel of different metal ions were also studied. Since all the results obtained can be interpreted on the basis of an ion exchange between gel and solution, a short account will first be given of these properties of the gel which makes such an exchange possible.

An ion exchanger consists primarily of an insoluble network containing charged groups. To these groups counter ions are bound in order to preserve the electroneutrality. As these ions do not belong to the structure, they are easily exchangeable. Cation or anion exchangers are obtained depending upon whether the network has a negative or positive charge, respectively. In the organic ion exchangers the network is produced by polymerization of suitable compounds, *e.g.* divinylbenzene and styrene, where the divinylbenzene forms crosslinkages between the chains of polymerized styrene. The charged groups are obtained by substitution in the carbon chain of acid or basic groups.

Hydroxides and hydrous oxides often have a structure where a network is formed by oxygen bridges between the metal atoms. These compounds show ion exchange properties which have recently been extensively investigated by Kraus *et al.*[1]. Depending upon the pH, they act as anion exchangers (at sufficiently low pH) or as cation exchangers (at higher pH).

The anion exchange can take place in two different ways. In acid solution, the basic group $-\overset{|}{\underset{|}{M}}-OH$ takes up hydrogen ions and $-\overset{|}{\underset{|}{M}}-OH_2^+$ is formed. At the same time an equivalent amount of anions are bound as counter ions. For the sake of simplicity, these anions could be assumed to be the monovalent A^- but the reasoning applies as well to the general case A^{n-}. Then the exchange with another anion, B^-, proceeds according to

$$-\overset{|}{\underset{|}{M}}-OH_2A + B^- \rightleftharpoons -\overset{|}{\underset{|}{M}}-OH_2B + A^- \qquad (1)$$

The ion exchange can also take place by direct substitution of the OH-group with B^-

$$-\overset{|}{\underset{|}{M}}-OH + B^- + H^+ \rightleftharpoons -\overset{|}{\underset{|}{M}}-B + H_2O \qquad (2)$$

In the latter case a bond is formed between B and M.

At higher pH, where cation exchange takes place, the reaction could for the simple case of a monovalent cation be written according to

$$-\overset{|}{\underset{|}{M}}-OH + Me^+ \rightleftharpoons -\overset{|}{\underset{|}{M}}-OMe + H^+ \qquad (3)$$

The position of these exchange equilibria depends, of course, on the basicity of the group $-\overset{|}{\underset{|}{M}}-O^-$. The stronger the ability of this group to bind H^+, the higher the pH at which the transition from anion to cation exchange takes place. As the hydroxide is not strictly monofunctional, but contains groups of different basicity, it exhibits in a transition region both anion and cation exchange properties.

The structure of silica gel seems to be analogous to the structure of the hydroxides described above. It consists of a network of joined SiO_4-tetrahedrons, where however the oxygen atoms are only partially required to make up the Si-O-Si bridges [2,3]. The rest of the oxygen atoms are free to bind ions from the solution out of which the gel is precipitated. Thus the silica gel consists of structural groups of the following type:

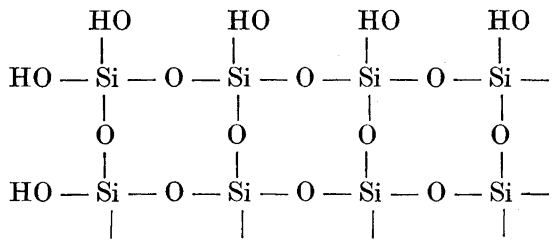

Here the central ion consists of Si^{4+}, which has a rather high electron affinity. This implies that the electron density around an oxygen atom bound to silicon is lower than around one bound to, say, a metal atom. Thus the free electron pairs on the oxygen atoms are comparatively inactive and therefore the basicity relatively low. Hydrogen ions bound to a $-\overset{|}{\underset{|}{Si}}-O^-$ group can therefore be replaced rather easily by other positive ions. The basicity is in fact so low that even if one proton is bound with fair strength (the silica gel is a weak acid), a second proton will not be taken up. Hence cation exchange according to (3) is possible even at comparatively low pH, while anion exchange is not at all possible. So the silica gel will function solely as a weakly acid ion exchanger, for which the exchange reaction can be written schematically as

$$n\ HG + M^{n+} \rightleftharpoons MG_n + nH^+ \qquad (4)$$

In this formula G stands for the unreactive gel framework with its attached functional groups.

The position of this equilibrium depends not only on the basicity of the gel framework but also on its affinity for the metal ion in question. It is reasonable to suppose that those metal ions which have a strong tendency to form complexes with oxygen containing anions can also compete successfully with H^+ in quite acid solutions. This expectation has received full experimental confirmation for such metal ions, *i.e.*, those combining a high charge with a small ionic radius.

EXPERIMENTAL

Chemicals. All chemicals were, if not otherwise stated, of analytical grade and used without further purification.

Two different makes of *silica gel* were used, *viz.* Kebo and Merck 'silica gel for chromatographic use'. The Kebo gel was used in two grain sizes, *viz.* 50—100 mesh and 100—200 mesh. The Merck product had a grain size finer than 300 mesh. Considerable quantities of hydrogen ions were sorbed by all the gels when treated with neutral or acid solutions.

Silica gel, saturated with hydrogen ions, was prepared by repeated washing of these gels with 5 M HNO_3 and/or 5 M HCl at 80–90°C. The gel was then freed from mechanically bound acid by washing with distilled water and dried for 20 h at 100°C. The product sorbed neither hydrogen ions nor water.

Uranyl perchlorate solution was prepared and analysed as described in Ref.[4]

Uranium (IV) perchlorate solution was prepared by electrolytic reduction of uranyl perchlorate solution and analysed according to Ref[5]

Plutonium (A.B. Atomenergi, Stockholm), was obtained as the isotope ^{239}Pu ($T_{1/2}$ = 24 360 years), isolated from neutron irradiated uranium. It was supplied as a nitrate solution of Pu(IV), with $C_{HNO_3} = 0.1$ M and containing about 1 mg Pu/ml ($C_{Pu} \approx 4$ mM). In this solution, however, there exist also appreciable amounts of Pu(III) and Pu(VI). These ions have been formed by the disproportionation of Pu(IV) which can be written as follows, if the nitrate complexes existing in the solution are temporarily neglected

$$3\ Pu^{4+} + 2\ H_2O \rightleftharpoons 2\ Pu^{3+} + PuO_2^{2+} + 4\ H^+$$

If the acidity is increased, the equilibrium is evidently forced strongly to the left, H^+ being present in the fourth power in the equilibrium expression. If nitric acid is used to increase the acidity, a stabilization of Pu(IV) of equal importance will however result from the addition of nitrate ions, as these form complexes preferably with Pu(IV). Thus the equilibrium constant for the plutonium(IV) disproportionation in 1 M perchloric acid [6] is 0.0089 as compared with 4×10^{-7} in 1 M nitric acid [7].

The value of the equilibrium constant also increases rapidly with raising temperature [8]. This is also the case with the tendency of nitric acid to *oxidize* Pu(IV) to Pu(VI)[9,7 p. 270]. It is therefore impossible to convert the plutonium completely into Pu(IV) by heating with only moderately concentrated acid. On the other hand, evaporation with *strong* nitric acid works as a rule (*cf.* Ref.[9]). In those cases where this treatment failed, reduction with hydrogen peroxide has been performed as follows (*cf.* Ref.[10]).

To 5 ml 4 M HNO_3, 0.3 ml of the initial plutonium solution and some drops of 10 % H_2O_2 were added. Then this solution was evaporated nearly to dryness and a new addition of 4 M HNO_3 and 10 % H_2O_2 was made. After 20 h the evaporation was repeated. Then conc. HNO_3 was added and evaporated nearly to dryness. This operation was repeated twice, the solution having a final volume of 0.1 ml of conc. HNO_3. When the evaporation vessel had cooled down to room temperature the content was transferred to a receptable with 10 ml 1 M HNO_3. In this way a stock solution with $C_{Pu(IV)} = 1.2 \times 10^{-4}$ and $C_{HNO_3} \approx 1$ M was obtained, in which Pu(IV) is stable at room temperature.

The amount of plutonium(IV) was determined by investigation of the distribution of the plutonium between 1 M HNO_3 and 0.3 M thenoyltrifluoroacetone in benzene (only plutonium(IV) is extracted into the benzene phase at this acidity) [10,11]. The stock solution contained less than 1 % of the plutonium as Pu(III) + Pu(VI).

All the work with plutonium was carried out either in a glove box or in well-ventilated fumehoods.

Radioactive *zirconium(IV)* solution was prepared by dissolving a known amount of neutron irradiated $ZrO(NO_3)_2 \cdot 2H_2O$ in perchloric acid. The zirconium(IV) concentration of the stock solution was 91.7 mM and its acidity 4 M. By the irradiation (15 g was irradiated for 11 days at a flux of 10^{12} neutrons $\cdot$ cm^{-2} $\cdot$ sec^{-1}) the isotopes ^{93}Zr ($T_{1/2} = 9.5 \times 10^5$ years) and ^{95}Zr ($T_{1/2}$ = 65 days) are preferentially produced. Besides these zirconium isotopes, the preparation also contains two other active nuclides, *viz.* ^{95}Nb ($T_{1/2}$ = 35 days) and to some extent also ^{181}Hf ($T_{1/2}$ = 46 days). ^{95}Nb is an inevitable constituent, as it is the result of the disintegration of ^{95}Zr. Hafnium occurs as a slight impurity in the zirconyl nitrate, but as it has a large thermal neutron cross section relative to zirconium, the formation of the active ^{181}Hf is fairly considerable.

Radioactive *gadolinium (III)* solution was prepared by dissolving neutron irradiated Gd_2O_3 in perchloric acid. The excess of acid was evaporated and the residue dissolved in water. A solution with C_{Gd} = 9.19 mM and pH $\approx$ 3.5 was obtained. The irradiated oxide had been allowed to cool for 3 months and the activity was thus due mainly to ^{153}Gd ($T_{1/2}$ = 236 days).

0.1 M radioactive *sodium chloride* solution was prepared by neutralization of a known amount of neutron irradiated $NaHCO_3$. The CO_2 formed was carefully removed. By

neutron irradiation of $NaHCO_3$ a product was obtained in which the activity comes mainly from ^{24}Na ($T_{1/2}$ = 15 h).

Procedure. The metal ion sorption on the silica gel was established by shaking metal salt solutions of varying pH with a suitable amount of gel. The acidity was adjusted by additions of perchloric acid (for metal ions sorbed at low pH), acetate buffer (for Gd^{3+}), ammonia (for Ba^{2+} and Ca^{2+}) and sodium hydroxide (for Na^+). In principle, the solutions were then shaken until equilibrium was reached. As seen in Tables 3—5 below, this was achieved in quite a short time for ions of charge up to three, while four-valent ions needed several days. In the case of Zr, equilibrium was certainly not reached for $C_H \leq 400$ mM when the experiments were interrupted after three days, and possibly not even completely for values of $C_H \geq 800$ mM which are the ones used for the calculation of D_{Zr} in Fig. 6. The experiments were all performed at 20 ± 0.1°C except one especially mentioned below. The ratio between the volume of solution, v, and the amount of silica gel, m, was as a rule 10^{-2} l/g. The sorbed quantity of metal was obtained by determination of the metal ion concentration in the solution before and after the experiment. For this purpose different analytical methods were used.

The *uranyl* concentration was determined spectrophotometrically by Ahrland's method [13]. Since the solutions contained perchlorate ions, $Na_4Fe(CN)_6$ was used instead of $K_4Fe(CN)_6$ for developing the "uranylhexacyanoferrat colloid". As a suitable wave length 4 900 Å was selected. The acidity and the concentration of cyanoferrate were 0.05 M and 0.2 M respectively. The colloid prepared in this manner has at λ = 4 900 Å a molar extinction coefficient which is only about half as large as that found when the potassium salt is used. Beer's law is however much better fulfilled when the sodium salt is used, especially at the lowest uranyl concentrations measured. In fact concentrations as low as 0.01 mM can be determined in this way with a fair accuracy (≈ 2 %).

Uranium (IV) was determined by cerimetric titration using ferroin (tris-*o*-phenanthroline iron(II) sulfate) as an indicator.

Plutonium was determined radiometrically. Its α-activity was measured with a gas-flow (90 % A, 10 % CH_4) proportional counter (Tracerlab SC-16 P). The samples were measured inside its ionization chamber in a well defined geometry (2 π). Absolute determinations of the concentration of the plutonium solutions were thus feasible. Owing to the short range of the α-particles, dry and very thin samples were prepared, so that the self-absorption of α-particles could be neglected. The α-samples were prepared by evaporation of 0.10 ml of solution to dryness on stainless steel or platinum dishes. The micropipette used for sampling was rinsed once with 1 M HNO_3 and the washing acid was evaporated on the same dish as the main portion of the sample.

Sodium, zirconium and *gadolinium* were also determined radiometrically. The γ-activities of the samples were measured with a scintillation counter (Tracerlab P 20) provided with a thallium activated sodium iodide crystal.

For each radiometrical measurement more than 10 000 counts were registered. Thus the error of counting was always <1 %.

Calcium and *barium* were determined volumetrically with EDTA according to Schwarzenbach [14].

The *hydrogen ion concentrations* of the UO_2^{2+}-solutions were determined by measuring the emf of cells of the type

Au	9.34 mM $HClO_4$ 1 M $NaClO_4$ quinhydrone(s)	1 M $NaClO_4$	C_H mM 1 M $NaClO_4$ quinhydrone(s)	Au

In the rest of the experiments the hydrogen ion concentrations were measured by a glass electrode in connexion with a vacuum-tube potentiometer (Radiometer PHM 3h).

RESULTS

Urunyl sorption isotherms. The description of the sorption properties of the silica gel given here is based upon sorption isotherms obtained for UO_2^{2+}. These were determined at varying pH with three different gels. The results are given

Table 1. The sorption of UO_2^{2+} on silica gel saturated with hydrogen ions. $v/m = 10^{-3}$ l/g. Shaking time 24 h.

1 a. Kebo 50—100 mesh.

C_M mM	C_H mM	C_{MS} mM	$C_{MG} \times 10^3$ mmole/g	$[H^+]_S$ mM	$\frac{1}{2}([H^+]_S - C_H) \times 10^3$ mmole/g
0.20	1	0.073	1.27	1.11	0.55
0.50	1	0.264	2.36	1.30	1.5
0.70	1	0.419	2.81	1.45	2.3
1.00	1	0.655	3.45	1.50	2.5
1.50	1	1.09	4.10	1.65	3.3
2.00	1	1.51	4.86	1.77	3.9
3.00	1	3.12	—	2.15	5.8
4.00	1	3.36	6.40	2.15	5.8
0.20	2	0.111	0.89	2.10	0.5
0.50	2	0.340	1.60	2.51	2.6
1.00	2	0.764	2.36	2.54	2.7
1.50	2	1.20	3.0	2.46	2.3
2.00	2	1.64	3.6	2.71	3.6
3.00	2	2.59	4.1	2.67	3.4
4.00	2	3.52	4.8	3.15	5.8
6.00	2	5.38	6.2	2.99	5.0
0.20	5	0.162	0.38	5.01	
0.50	5	0.420	0.80	5.10	
1.00	5	0.869	1.31	5.21	
1.50	5	1.32	1.8	5.20	
2.00	5	1.80	2.0	5.42	
3.00	5	2.72	2.8	5.40	
4.00	5	3.68	3.2	5.44	
6.00	5	5.51	4.9	5.20	
0.20	10	0.186	0.14	10.05	
0.50	10	0.466	0.34	10.09	
1.00	10	0.93	0.7	10.28	
2.00	10	1.89	1.1	10.20	
3.00	10	2.84	1.6	10.50	
4.00	10	3.80	2.0	10.24	
6.00	10	5.80	2.0	10.45	

in Table 1 and Figs. 1 and 2. C_{MG} (mmoles UO_2^{2+} sorbed per gram silica gel) is plotted against C_{MS} (the concentration of UO_2^{2+} in the water solution expressed in mM) for various C_H (the initial concentration of hydrogen ions).

In the experiments reported in Fig. 1, where silica gels washed only with water have been used the most different behaviour is found for the different gels though the initial concentrations of hydrogen ions were the same. At a given C_H Kebo 50—100 mesh sorbs only about half as much as Kebo 100—200 mesh. The Merck gel, not presented in the figure, sorbs 100 % in the whole range of concentration investigated. It is also evident however, that C_{MG} in-

1 b. Kebo 100—200 mesh.

C_M mM	C_H mM	C_{MS} mM	$C_{MG} \times 10^3$ mmole/g	$[H^+]_S$ mM	$\frac{1}{2}([H^+]_S - C_H) \times 10^3$ mmole/g
0.20	1	0.130	0.70	1.12	0.6
0.50	1	0.265	2.35	1.25	1.3
0.70	1	0.419	2.81	1.31	1.6
1.00	1	0.664	3.36	1.46	2.3
1.50	1	1.09	4.1	1.58	2.9
2.00	1	1.54	4.6	1.70	3.5
3.00	1	2.43	5.7	1.85	4.3
4.00	1	3.35	6.5	2.05	5.3
0.20	2	0.113	0.87	2.02	0.1
0.50	2	0.336	1.64	2.09	0.5
1.00	2	0.763	2.37	2.24	1.2
1.50	2	1.22	2.8	2.43	2.2
2.00	2	1.66	3.4	2.48	2.4
3.00	2	2.56	4.4	2.71	3.6
4.00	2	3.49	5.1	2.71	3.6
6.00	2	5.35	6.5	2.92	4.6
0.20	5	0.163	0.37	4.94	
0.50	5	0.422	0.78	—	
1.00	5	0.867	1.33	5.17	
1.50	5	1.33	1.7	4.03	
2.00	5	1.81	1.9	5.31	
4.00	5	3.66	3.4	5.31	
6.00	5	5.56	4.4	5.05	
0.20	10	0.187	0.13	9.89	
0.50	10	0.465	0.35	10.05	
1.00	10	0.930	0.70	9.85	
1.50	10	1.40	1.0	10.05	
2.00	10	1.89	1.1	10.17	
3.00	10	2.83	1.7	10.01	
4.00	10	3.78	2.2	10.29	
6.00	10	5.71	2.9	10.34	

creases when the hydrogen ion concentration decreases at constant C_{MS}, as could be expected (*cf.* p. 1060).

When the experiments were repeated, using silica gel saturated with hydrogen ions, the results given in Fig. 2 were obtained. At a given pH, the different gels obviously given the same sorption isotherms, within experimental error.

In the series performed with water-washed gels, $[H^+]_S$, the hydrogen ion concentration after the sorption, has dropped considerably below the original hydrogen ion concentration C_H. If the initial concentration of UO_2^{2+} is 0.20 mM and C_H = 1 mM, $[H^+]_S$ is 0.61 mM for the Kebo 50—100 mesh, 0.30 mM for

1 c. Merck.

C_M mM	C_H mM	C_{MS} mM	$C_{MG} \times 10^3$ mmole/g	$[H^+]_S$ mM	$\frac{1}{2}([H^+]_S - C_H) \times 10^3$ mmole/g
0.20	1	0.138	0.62	1.04	0.2
0.50	1	0.275	2.25	1.09	0.5
0.70	1	0.428	2.72	1.19	1.0
1.00	1	0.692	3.08	1.27	1.4
1.50	1	1.10	4.0	1.40	2.0
2.00	1	1.54	4.6	1.51	2.6
3.00	1	2.43	5.7	1.69	3.5
4.00	1	3.41	5.9	1.88	4.4
0.20	2	0.127	0.73	1.88	
0.50	2	0.358	1.42	2.04	0.2
1.00	2	0.779	2.21	2.18	0.9
1.50	2	1.23	2.70	2.29	1.5
2.00	2	1.67	3.30	2.36	1.8
3.00	2	2.55	4.5	2.48	2.4
4.00	2	3.49	5.1	2.60	3.0
6.00	2	5.39	6.1	2.81	4.1
0.20	5	0.170	0.30	4.71	
0.50	5	0.435	0.65	4.83	
1.00	5	0.890	1.10	4.92	
1.50	5	1.36	1.40	5.02	
2.00	5	1.83	1.7	4.96	
3.00	5	2.77	2.3	4.83	
4.00	5	3.70	3.0	5.18	
6.00	5	5.54	4.6	5.00	
0.20	10	0.190	0.10	9.89	
0.50	10	0.474	0.26	10.09	
1.00	10	0.950	0.50	9.96	
1.50	10	1.43	0.7	9.96	
2.00	10	1.91	0.9	10.04	
3.00	10	2.84	1.6	10.16	
4.00	10	3.80	2.0	10.16	
6.00	10	5.72	2.8	10.26	

the Kebo 100—200 mesh and 0.002 mM for the Merck. The decrease in hydrogen ion concentration in the outer solution causes in its turn an increased sorption of UO_2^{2+}.

In the second series on the other hand, $[H^+]_S$ is even somewhat greater than C_H, Table 1. This behaviour is expected, as hydrogen ions must be released from a gel already saturated with these ions, when other cations are sorbed. $[H^+]_S - C_H$ ought to be equivalent to C_{MG}. Bearing in mind the great error inherent in the calculation of $[H^+]_S - C_H$, due to the fact that $[H^+]_S \approx C_H$, it might be considered that this equivalence has been proved, Table 1. A more careful investigation of this point is described later.

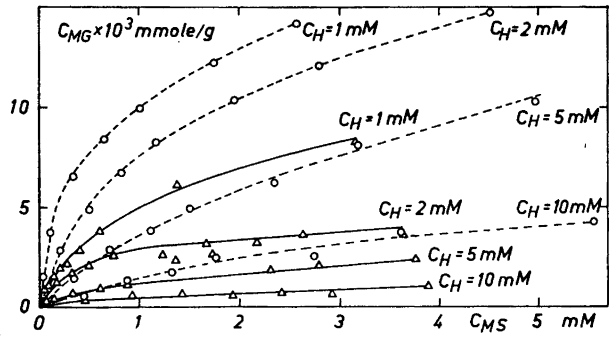

Fig. 1. The sorption of UO_2^{2+} on silica gel washed only with water, $v/m = 10^{-2}$ l/g. Kebo 50—100 mesh △, Kebo 100—200 mesh O.

From the experiments above, it seems reasonable to assume, that the difference between the water-washed gels is due to different counter ions having been sorbed in varying amounts during the preparation of the gel. Hence the more or less pronouced uptake of hydrogen ions from the solution and the lack of reproducibility between different preparations. In order to achieve reproducible conditions only gels saturated with hydrogen ions were used in the subsequent experimental work. These do not alter the pH of the solutions by any irrelevant process.

Alkalimetric titration of H^+-saturated gel. The weakly acid properties of the silica gel are also apparent from an alkalimetric titration of the H^+-saturated gel. The titration was performed by shaking 5 g gel at 20°C with 50 ml sodium hydroxide solution of varying concentration, containing neutral salt to a constant initial concentration of $Na^+ = 100$ mM. The solution and the gel were separated and the pH was determined with a glass electrode or if a substantial part of the base was left by titration. In this case the pH was computed from the relation $pH = 14 - p[OH^-]$. Experiments were performed with Kebo

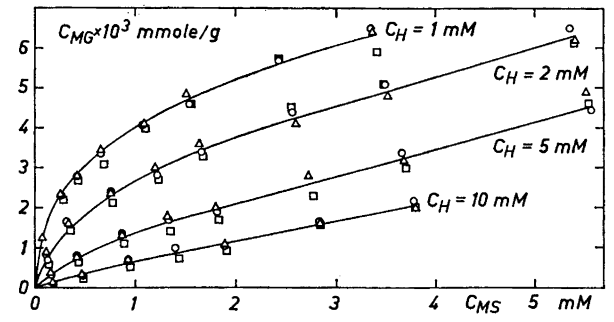

Fig. 2. The sorption of UO_2^{2+} on silica gel washed with acid, $v/m = 10^{-2}$ l/g. Kebo 50—100 mesh △, Kebo 100—200 mesh O, Merck □.

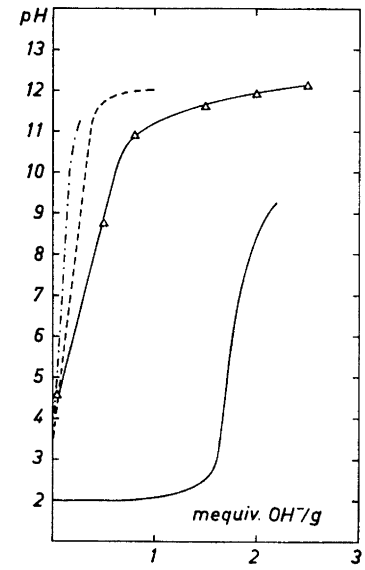

Fig. 3. pH of the outer solution as a function of the total amount of sodium hydroxide added to the solution per g dried ion exchanger. Silica gel △ and ————, sulfonated resin ————, phenolic resin — — — — —, glauconite —.—.—.

50—100 mesh and Kebo 100—200 mesh, both of which gave the same results. Mean values of these are plotted in Fig. 3. Here the titration curves are also drawn for two organic ion exchangers (phenol resin and sulfonated resin) as well as for the ion exchanging mineral glauconite (in greensand) [15]. The titration curve of the silica gel is similar to those of the weakly acid ion exchangers.

Verification of the equivalence between the amount of metal ions sorbed and the amount of hydrogen ions set free. In order to prove more strictly that the silica gel acts as an ion exchanger, a closer investigation than the one previously mentioned has been performed of the relation between the metal ions sorbed and the hydrogen ions set free.

By choosing an ion, *e.g.* Na^+, that is not hydrolysed, it is possible to work with alkaline solutions, thereby obtaining a high sorption. Consequently amounts of H^+ large enough to be accurately determined are set free. This could not be realized for the sorption of UO_2^{2+}.

As in the titration just described the gel was shaken with solution of varying $[OH^-]$, containing a constant initial concentration of $Na^+ = 100$ mM. In this case the neutral salt was however NaCl, labelled wish ^{24}Na. By the determination of the sorbed Na^+ it is necessary to correct for the error caused by the decay of ^{24}Na. This was done by measuring several times during a series the activity of an identical solution with no silica gel added. The amount of H^+ set free was determined by acidimetric titration of the alkali left after the shaking. The results from two series are given in Table 2. In one of the series where as much as 5 g gel was used, it was necessary to correct for the amount of H^+ adhering to the gel on account of incomplete preparatory washing of the gel sample used in these experiments. The correction, which amounted to 0.011 mequiv./g of silica gel, was determined in a special experiment, where silica gel was shaken only with water.

Table 2. The equivalence between the amount of Na^+ sorbed and the amount of H^+ set free. $v = 50$ ml, $m = 0.5$ g and 5 g. Experiments performed with 5 g silica gel are indicated by *. In these cases the amount of H^+ set free is corrected by the amount of acid liberated when the gel is washed only with water (0.011 mequiv./g).

OH^- added mequiv./g	OH^- at equilibrium mequiv./g	H^+ set free mequiv./g	Na^+ sorbed mequiv./g
0.025	0.000	0.014 *	0.019
0.050	0.000	0.039 *	0.043
0.075	0.000	0.064 *	0.064
0.100	0.000	0.089 *	0.090
0.125	0.000	0.114 *	0.115
0.150	0.000	0.139 *	0.140
0.200	0.000	0.189 *	0.188
0.250	0.020	0.230	0.224
0.500	0.050	0.450	0.435
0.750	0.130	0.620	0.597
1.00	0.25	0.75	0.72
1.25	0.41	0.84	0.81
1.50	0.60	0.90	0.88
2.00	1.02	0.98	0.94
3.00	1.65	1.35	1.28
3.50	2.16	1.34	1.27
4.00	2.66	1.33	1.35
5.00	3.77	1.23	1.24

The complete agreement between the amount of sorbed Na^+ and the amount of H^+ set free, fully confirms that the sorption is an ion exchange, as had already appeared probable from the UO_2^{2+}-measurements. This equivalence has also been proved by other workers [16].

The possibility of applying the law of mass action to the exchange reaction (4), was tried on the UO_2^{2+}—H^+ measurements previously mentioned. In this case the reaction could be written as follows

$$2\ HG + UO_2^{2+} \rightleftharpoons UO_2G_2 + 2\ H^+ \qquad (5)$$

Thus from the law of mass action

$$K = \frac{[H^+]^2[UO_2G_2]}{[HG]^2[UO_2^{2+}]} \cdot \frac{\gamma_{H^+}^2 \cdot \gamma_{UO_2G_2}}{\gamma_{HG}^2 \cdot \gamma_{UO_2^{2+}}} \qquad (6)$$

The distribution coefficient D for uranium is defined as the ratio between the concentration of uranium in gel and solution, *viz.* $D = C_{MG}/C_{MS}$ C_{MG} is expressed in mmole/g of silica gel and C_{MS} in mmole/litre. Thus the dimension of D is $l \cdot g^{-1}$. As UO_2^{2+}, under the present conditions, neither forms complexes nor is hydrolysed, the distribution coefficient becomes $= [UO_2G_2]/[UO_2^{2+}]$.

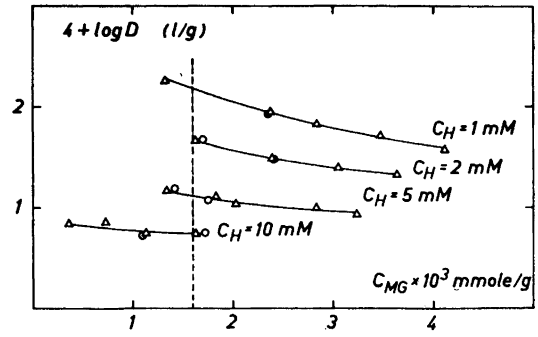

Fig. 4. Log D as a function of C_{MG} for the sorption of UO_2^{2+} on H^+ — saturated silica gel, $v/m = 10^{-2}$ l/g. Kebo 50—100 mesh △, Kebo 100—200 mesh ○.

In Fig. 4, log D is plotted as a function of C_{MG} with C_H as a parameter. The curves are intersected at $C_{MG} = 1.6 \times 10^{-3}$ mmole/g. Thus log D is obtained at a constant and low load. Under these conditions the activity coefficients $\gamma_{UO_2G_2}$ and γ_{HG} as well as [HG] can be considered as fixed.

By taking the logarithms of eqn (6) we obtain

$$\log D = -2 \cdot \log[H^+] \cdot \frac{\gamma_{H^+}}{\sqrt{\gamma_{UO_2^{2+}}}} + \log K \cdot [HG]^2 \frac{\gamma_{HG}^2}{\gamma_{UO_2G_2}} \qquad (7)$$

The last term is a constant and the activity coefficients γ_{H^+} and $\gamma_{UO_2^{2+}}$ could be computed from the equations of Debye-Hückel. $[H^+]$ is obtained by interpolation of the measured $[H^+]_S$ for the points situated on each side of the intersection. If the assumptions made are true, log D plotted as a function of log $[H^+]\,\gamma_{H^+}/\sqrt{\gamma_{UO_2^{2+}}}$ should give a straight line of slope −2.

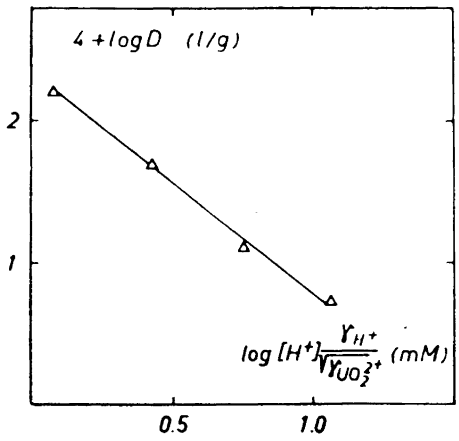

Fig. 5. Log D as a function of log $[H^+]\frac{\gamma_{H^+}}{\sqrt{\gamma_{UO_2^{2+}}}}$ at constant load $C_{MG} = 1.6 \times 10^{-3}$ mmole/g.

From Fig. 5 it is evident that a straight line is obtained, but its slope is only $-(1.6 \pm 0.1)$. This discrepancy can partly be accounted for by the ion invasion into the gel which takes place according to the Donnan equilibrium. The concentration of free hydrogen ions thus established within the gel will strongly influence γ_{HG} which therefore might vary considerably in spite of the load being constant.

Thus, in summing up, the following points are valid for the metal ion sorption on the silica gel:

I. For gel not saturated with hydrogen ions the sorption depends on the manner in which the gel is prepared.

II. If the gel is saturated with hydrogen ions the same sorption isotherms are obtained even with different gel makes.

III. The H^+-saturated gel gives a titration curve similar to those found for weakly acid ion exchangers.

IV. At the sorption of metal ions on a H^+-saturated gel, the amount of hydrogen ions set free is equivalent to the amount of metal ions sorbed.

V. The law of mass action is approximately valid for the exchange reaction.

The affinity of different metal ions to the gel. As previously stated, the sorption of metal ions depends strongly on the pH of the solution. This is true for all of the investigated ions, *viz.* Na^+, Ca^{2+}, Ba^{2+}, UO_2^{2+}, Gd^{3+}, Zr(IV) + Nb, U(IV) and Pu(IV), as is evident from Fig. 6 where log D for the different metal ions is plotted as a function of pH. It is also clear that the log D-curves are displaced to more acid solutions with increasing ratio between the charge and the size of the metal ion. This means that the affinity for the gel follows the

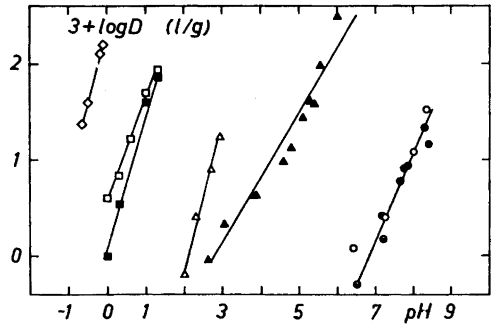

Fig. 6. Log D for some metal ions as a function of pH. Kebo 50—100 mesh, $v/m = 10^{-2}$ l/g.

Element (state)	Zr + Nb	U(IV)	Pu(IV)	U(VI)	Gd	Ca	Ba	Na
Sign	◇	□	■	△	▲	○	◒	●
C_M mM	1.1	2.0	10^{-2}	1.0	0.092	25	25	30

same order which has also been found for the sorption on organic cation exchangers. The position of the UO_2^{2+}-curve about six pH units to the left of the curves of the other ions with charge + 2 is noteworthy. But even though the uranyl ion formally has a charge of only + 2, it often behaves as if its charge is considerably higher [17], *e.g.* on hydrolysis and complex formation.

Obviously the sorption is important only when the pH has passed a definite value. To the left of the log D-curve very little of the metal ion is sorbed, whereas to the right complete sorption occurs. Therefore ions with curves sufficiently apart could, by a suitable choice of pH, be separated from each other.

For practical separations, the sorption capacity, C_{MG}, is of great interest. According to Table 2 the total capacity at saturation is 1.2—1.4 mequiv/g gel. If the total capacity is required the pH must be relatively high at least for ions with a low charge. The sorption capacities for some ions as a function of pH are reported in part II of this work.

The sorption rate is both of theoretical and practical interest. In this respect the different ions can be placed in two groups. Ions like Na^+, Ca^{2+}, Gd^{3+} and UO_2^{2+} are sorbed very fast (in general more than 95 % of the final amount is sorbed within 5 min), whereas ions formed by Zr(IV) + Nb, U(IV) and Pu(IV) are taken up more slowly, see Tables 3, 4 and 5 as well as Fig. 7. The latter group contains those ions which are strongly hydrolysed even in rather acid solution. Moreover large and polynuclear species are formed on the hydrolysis of these ions [18–20].

In order to investigate whether the low reaction rate in the second group is caused by a slow hydrolysis or by a slow sorption, the following experiment was performed.

From the stock solution of Pu(IV), solutions with $C_{Pu} \approx 2 \times 10^{-6}$M and C_{HNO_3} varying between 0.02 and 1 M were prepared. Within the range of $[H^+]$ where the hydrolysis is considerable, *viz.* at $[H^+] \leq 0.5$ M, the sorption rate of both freshly prepared and aged solutions was investigated by analysis of samples taken at different times. When this technique is used the original relations between v and m is admittedly somewhat changed during the experi-

Table 3. The sorption rate of UO_2^{2+}, Gd^{3+}, Ca^{2+} and Na^+. Kebo 50—100 mesh, $v/m = 10^{-2}$ l/g. The initial concentrations and acidities were: $C_U = 0.20$ mM at $C_H = 2$ mM, $C_{Gd} = 0.092$ mM at pH = 5.0, $C_{Ca} = 25.3$ mM at $C_{NH_3} = 140$ mM, $C_{Na} = 100$ mM at $C_{OH} = 50$ mM.

Time min	% sorbed			
	UO_2^{2+}	Gd^{3+}	Ca^{2+}	Na^+
5	37.5	68.0	94.7	48.0
15	39.5	67.7	95.4	48.0
30	41.0	—	95.0	48.0
60	39.5	67.8	95.4	48.0
90	40.0	—	95.4	—
120	40.0	67.7	95.4	—
1 200	40.5	68.0	95.5	46.6

Table 4. The sorption rate of Pu(IV) at different concentrations of nitric acid. Kebo 50—100 mesh, $v/m = 10^{-2}$ l/g. $C_{Pu} = 1.7 \times 10^{-3}$ mM.

	Aged 8 days				Freshly prepared				
C_H mM	20	50	100	500	20	50	100	500	946
Time, h	% sorbed								
1/2	32	43	55	24	74	66	66	23	11
3	44	47	57	26	77	68	67	25	9
7.5	53	56	62	28	80	71	71	28	10
24	70	77	78	27	85	80	80	28	—
48	84	87	79	25	88	86	84	26	—
96	88	88	80	31	92	90	84	30	11
150	89	89	82	27	94	89	84	27	—

ment. In the actual case the change was however slight (≈ 5 %) and could not possibly influence the results very much. The results are given in Table 4.

It is evident, from a comparison between fresh and aged solutions, that both require about the same time to be equilibrated with the gel. A pronounced difference appears, however, in the beginning of the sorption. From the aged solutions with $C_{HNO_3} = 0.02$, 0.05 and 0.1 M, about half the final amount is sorbed in 30 min, whereas the freshly prepared solutions have sorbed as much as 80 % of this amount in this time. A probable explanation of this behaviour is that Pu^{4+} and other low molecular species are preferentially sorbed by the gel. In freshly prepared solutions the polynuclear hydrolysis is not yet finished and therefore the concentration of low molecular easily sorbable species is much higher than in aged ones. Thus the slow sorption of the aged solutions is presumably due to the slow breaking up of the polymerized species dominating there. No difference could be detected at $C_{HNO_3} = 0.5$ M. In this case, as well as for $C_{HNO_3} > 0.5$ M, the equilibrium is also quickly attained. At this acidity Pu(IV) is in fact mainly present (> 95 %) as Pu^{4+} and monomer nitrate complexes [21,22] and the sorption is therefore of the same nature as for Na^+, Ca^{2+}, Gd^{3+} and UO_2^{2+}.

Similar behaviour was found for Zr(IV) + Nb, where only aged solutions were investigated, Table 5. Although the γ-activity used for the analysis

Table 5. The sorption rate of Zr(IV) + Nb at different concentrations of nitric acid. Aged solutions. Kebo 50—100 mesh, $v/m = 10^{-2}$ l/g. $C_{Zr} = 1.1$ mM.

C_H mM	50	100	200	400	800	1 500	3 000	4 500
Time, h	% sorbed							
0.5	23.2	23.7	31.0	31.2	44.4	49.4	52.3	48.4
3	33.2	29.6	39.2	44.3	60.5	63.9	59.1	58.6
18	56.5	59.0	60.5	65.2	74.7	81.1	72.5	63.5
43	68.0	69.3	70.2	79.4	86.2	87.3	75.1	66.4
74	91.5	86.1	81.0	81.1	94.1	92.8	79.9	70.1

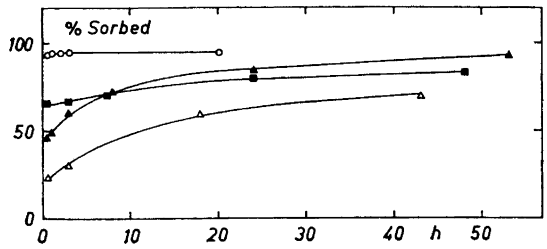

Fig. 7. The sorption rate of Zr + Nb, U(IV), Pu(IV) and Ca. Kebo 50—100 mesh, $v/m = 10^{-2}$ l/g.

Element (state)	Zr + Nb	U(IV)	Pu(IV)	Ca
Sign	△	▲	■	○
C_M mM	1.1	4.2	1.7×10^{-3}	25.3
pH	1	1	1	10.9

of the solutions partly comes from ^{181}Hf, the results obtained should nevertheless represent the sorption properties of Zr(IV) + Nb, as ^{181}Hf occurs only in tracer concentrations and has such a great chemical resemblance to Zr. This is moreover conclusively proved by the fact that the γ-spectrum of the solution indicates the same ratio Hf to Zr + Nb before and after the sorption. As seen from Table 5, the sorption after 74 h for 0.8 M $\leq C_{HNO_3} \leq$ 4.5 M is increasing with decreasing hydrogen ion concentration as is normally the case. The decrease found for $C_{HNO_3} <$ 0.8 M must be due to the fact that equilibrium had not yet been established for these low acidities, in spite of the long shaking time. As is also seen from Table 5, the time necessary for the sorption to reach half the final value decreases with increasing C_{HNO_3}. This is also true for aged

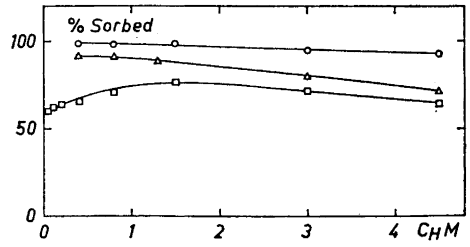

Fig. 8. The sorption rate of Zr + Nb on Kebo 50—100 mesh in hydrochloric (○), perchloric (△) and nitric (□) acid. Shaking time 21 h, $v/m = 10^{-2}$ l/g, $C_{Zr} = 1.1$ mM.

Table 6. The sorption rate of Pu(IV) at 49°C and different concentrations of nitric acid. Freshly prepared solutions. Kebo 50—100 mesh, $v/m = 10^{-3}$ l/g. $C_{Pu} = 2.2 \times 10^{-3}$ mM.

C_H mM	20	50	100	500
Time, h	% sorbed			
1/4	74	66	34	29
1/2	75	50	34	34
1	77	38	38	36
4	81	70	67	41
7	84	84	76	43
24	95	91	88	41
72	96	92	88	41

Pu(IV)-solutions (Table 4). A. comparison was also performed of the sorption of Zr(IV) + Nb from nitric, hydrochloric and perchloric acid, Fig. 8. The shaking time was fixed at 21 h. In the figure one notices particularly, that the curves separate widely at small C_H. In perchloric and hydrochloric acid equilibrium is evidently attained faster than in nitric acid, which is rather remarkable.

In order to investigate the influence of the temperature on the sorption rate, a series with Pu(IV) at 49°C was also performed, Table 6. No significant differences in the rate, compared with the series obtained at 20°C, could be observed. The equilibrium sorption, however, was somewhat higher.

These investigations have been performed under a contract with *AB. Atomenergi* (The Swedish Atomic Energy Company), Stockholm. We would like to express our appreciation of this valuable co-operation which has made the present work possible.

Much technical information has also been received from *Försvarets Forskningsanstalt* (The Research Institute of National Defence), *Avd.* 4, Sundbyberg. The γ-spectrometric measurements have been carried out at the Radiophysical Institute, Lund. We are much indebted to the Head of the Institute, Dr Kurt Lidén, for his aid in this respect.

The lanthanide solutions have been put to our disposal by Dr Arthur Sonesson, Lund. We also want to acknowledge a careful linguistic revision of our manuscripts by Dr George Gamlen, Manchester.

Finally, our most sincere thanks are due to Professor Sture Fronœus, Lund, for many fruitful proposals and valuable comments.

REFERENCES

1. Kraus, K. A., Phillips, H. O., Carlson, T. A. and Johnson, J. S. *Proc. 2. Intern. Conf. Peaceful Uses Atomic Energy Geneva 1958* **28** (1958) 3 (P/1832).
2. Weyl, W. A. and Hauser, E. A. *Kolloid Z.* **124** (1951) 72.
3. Alexander, A. E. and Johnson, P. *Colloid Science*, Oxford University Press, London 1949, Vol. II. p. 608.
4. Ahrland, S., Larsson, R. and Rosengren, K. *Acta Chem. Scand.* **10** (1956) 705.
5. Ahrland, S. and Larsson, R. *Acta Chem. Scand.* **8** (1954) 137.
6. Rabideau, S. W. *J. Am. Chem. Soc.* **75** (1953) 798.
7. Connick, R. E. *The Actinide Elements, Natl. Nuclear Energy Ser.* Div. IV, **14 A** (1954) 241.
8. Rabideau, S. W. and Cowan, H. D. *J. Am. Chem. Soc.* **77** (1955) 6145.

9. Kraus, K. A. *The Transuranium Elements, Natl. Nuclear Energy Ser.* Div. IV, **14 B** (1949) 264.
10. Cuninghame, J. G. and Miles, G. L. *J. Inorg & Nuclear Chem.* **3** (1956/1957) 54.
11. Rydberg, J. *Arkiv Kemi* **9** (1955) 109.
12. Connick, R. E. *The Actinide Elements, Natl. Nuclear Energy Ser.* Div. IV, **14 A** (1954) 276.
13. Ahrland, S. *Svensk Kem. Tidskr.* **61** (1949) 197 and **72** (1960). *In press.*
14. Schwarzenbach, G. *Complexometric Titrations*, Methuen and Co. Ltd London, pp. 66 and 69.
15. Bauman, W. C. *Ind. Eng. Chem.* **38** (1946) 46.
16. French, C. M. and Howard, J. P. *Chem. & Ind. London* **1956** 572.
17. Katz, J. and Seaborg, G. *The Chemistry of the Actinide Elements*, Methuen and Co. Ltd, London 1957, p. 172.
18. Johnson, J. S. and Kraus, K. A. *J. Am. Chem. Soc.* **78** (1956) 3937.
19. Kraus, K. A. *Proc. Intern. Conf. Peaceful Uses Atomic Energy, Geneva 1955*, **7** (1956) 245 (P/731).
20. Hietanen, S. *Acta Chem. Scand.* **10** (1956) 1531.
21. Rabideau, S. W. and Lemons, J. F. *J. Am. Chem. Soc.* **73** (1951) 2895.
22. Hindman, J. C. *The Transuranium Elements, Natl. Nuclear Energy Ser.* Div. IV **14 B** (1949) 388.

Received January 30, 1960.

ACTA CHEMICA SCANDINAVICA 14 (1960) 1077—1090

The Ion Exchange Properties of Silica Gel

II. Separation of Plutonium and Fission Products from Irradiated Uranium

STEN AHRLAND, INGMAR GRENTHE and BERTIL NORÉN

Department of Inorganic and Physical Chemistry, Chemical Institute, University of Lund, Lund, Sweden

A procedure, based on selective sorption on silica gel, has been worked out for the separation of plutonium and fission products from uranium which has been irradiated with thermal neutrons

In part I of this investigation [1], it has been shown that metal ion sorption on silica gel can be described by an ion exchange mechanism, with silica gel acting as an ion exchanger of the weakly acid type.

The distribution coefficient between gel and solution for the different metal ions accordingly increases strongly with increasing pH. The distribution coefficient is also larger for high-valent ions than for low-valent ones at a given acidity of the solution. A graphical comparison of the metal ions investigated is given in Ref.[1], Fig. 6. It can be seen that the affinity for the ion exchanger is given by the order

$$Zr(IV) > U(IV) \approx Pu(IV) > U(VI) > Gd > Ca \approx Ba \approx Na$$

In the same investigation it was also found that some species are sorbed very fast and other more slowly. UO_2^{2+}, Gd^{3+}, Ca^{2+}, Ba^{2+} and Na^{+} belong to the first group while the second contains Zr(IV), U(IV) and Pu(IV). The ions of the second group are all strongly hydrolysed in the actual solutions and occur mainly as polynuclear aggregates. For Pu(IV) it was found that at higher pH the sorption rate is dependent on the age of the solution.

From these results it is clear that it should be possible to separate Zr(IV), U(VI) and Pu(IV) both from one another and from Gd^{3+}, Ca^{2+}, Ba^{2+} and Na^{+} by suitably varying the pH of the solution.

The aim of this investigation has been to use this selective sorption on silica gel for a separation of uranium, plutonium and fission products from a nitric acid solution of neutron irradiated uranium.

After a cooling period of 100 days rather few elements contribute appreciably to the activity still remaining with the irradiated uranium. Apart from plutonium these are, in order of decreasing activity, zirconium + niobium, yttrium and several lanthanides, ruthenium + rhodium, strontium, barium and cesium (see *e.g.* the compilation of Rydberg[2]). A cooling period shorter than 100 days is not used as a rule because most reprocessing methods presuppose that ^{239}Np, ^{237}U, ^{133}Xe and ^{131}I have decayed before the treatment is started [3].

On the dissolution of uranium metal in nitric acid, uranium is oxidized to U(VI), while most of the plutonium is present as Pu(IV). The standard potentials for the different redox steps between Pu(III), Pu(IV), Pu(V) and Pu(VI) are so close to each other [4] that there is always a certain disproportionation in a solution of the mean oxidation state + 4. There are always finite concentrations of at least Pu(III) and Pu(VI) and at lower acidities also Pu(V). Zirconium is found as Zr(IV) and niobium probably as Nb(V), both more or less hydrolysed. Ruthenium occurs mainly as various nitrosyl-nitrato complexes of Ru(III) [5]. The actual state is highly dependent on the conditions at dissolution [6]. The other fission products have a less complicated chemistry and occur as hydrated metal ion. These of higher charge especially exist to a considerable part as nitrate complexes in the solution.

The ions to be found in a solution of neutron irradiated uranium metal are thus the same or in any case analogous to those ions, the sorption properties of which have been investigated in I. The behaviour of ruthenium, which cannot be anticipated from the experiments already performed, remains obscure. Another serious difficulty is that the separation of uranium and plutonium requires that they are in the oxidation states + 6 and + 4, respectively. Pu(VI), as plutonyl ion, has the same sorption properties as the analogous uranyl ion, while tervalent plutonium as Pu^{3+} shows a close resemblance to the lanthanide group. By a suitable choise of pH and total concentration of plutonium, C_{Pu}, the disproportionation can however be greatly suppressed [7-9]. At low pH, the position of the equilibrium which is independent of C_{Pu} strongly favours Pu(IV). As the pH is raised, a considerable disproportionation will exist in equilibrium, but the rate of the disproportionation reaction is quite slow at low values of C_{Pu}. Thus at pH = 1 in perchlorate medium the rate is less than 1 % an hour for $C_{Pu} < 10^{-4}$ M. The rather strong complex formation between Pu^{4+} and NO_3^- [10,11] also stabilises Pu^{4+} relative to Pu^{3+} and PuO_2^{2+} if a nitrate medium is used.

By treating a disproportionated solution of plutonium with nitrite it is possible to transfer all the plutonium to the oxidation state +4. The reaction is complicated and is certainly not yet fully understood [12].

CHEMICALS USED, ANALYTICAL

The preparations of neodymium, cerium, gadolinium and ytterbium salts were the same as used by Sonesson [13].

Neodymium and ytterbium were analyzed spectrophotometrically using aurinetricarboxylic acid [14]. Cerium(III) was oxidized to Ce(IV) by persulfate and then determined by reduction with Fe(II). The gadolinium solutions contained the isotope ^{153}Gd and were analyzed radiometrically.

The other chemicals were the same as used in I, and were analyzed in the same way as described there.

RESULTS

The investigation consists of the following three parts:

1. Investigation of the sorption properties of separate ions using chromatographic methods.

2. Sorption at continuous passage of solution through the column followed by a determination of the sorption capacity for the metal ions in question.

3. Test separations of solutions of known composition.

Chromatographic experiments. Two different columns have been used, one of 100 cm length and 1.0 cm inner diameter and one of 43 cm length and 1.1 cm diameter. The longer column takes a solution volume of 50 ml, the shorter one a volume of 25 ml. By varying the length of the column and the flow rate, the contact time between solution and gel can be widely varied.

When used, the column is first saturated with nitric acid of desired concentration. Then a given volume of metal ion solution is placed on top of the column. This volume is small compared with the total volume of solution in the column. By means of an acid flow from a vessel on higher level the sample is transported down the column. Fractions of the outflowing solution are collected with a fraction collector and analyzed.

The sorption of *U(VI)* from solutions containing 0.1 and 0.5 M nitric acid was investigated. In both cases, U(VI) passed the column in the solution front. No sorption thus occurred at these acidities, a result consistent with the equilibrium experiments reported in Ref.[1], Fig. 6.

In the *Pu* experiments, the contact time is a variable of about the same importance as the acidity. The following experiments, performed at $C_H = 0.5$ and 0.1 M using different flow rates and column lengths are typical for the influence of each of these variables. For $C_H = 0.5$ M, the results are in Figs. 1 and 2 where C_{Pu} of each fraction, expressed in disintegrations·min^{-1}·ml^{-1}, is given as a function of the volume of solution which has passed down the column. The position of U(VI) for each column, as determined by the experiments mentioned above, is also indicated. Obviously, the plutonium is separated into two peaks. The first of these is found in the same position on the volume axis as U(VI). It contains about 2 % of the total amount of plutonium, *i.e.*

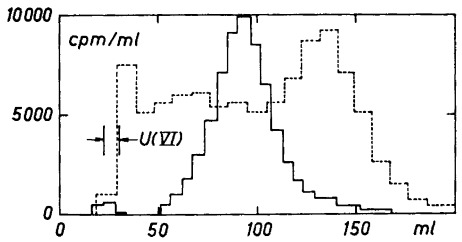

Fig. 1. Sorption of plutonium from 0.5 M nitric acid. Column length 43 cm. Flow rates:
30 ml · h^{-1} · cm^{-2} ————
60 » » » – – – – –
Silica gel: Kebo 100—200 mesh.

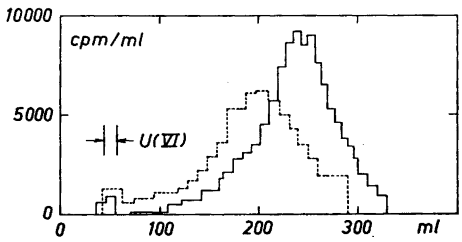

Fig. 2. Sorption of plutonium from 0.5 M nitric acid. Column length 100 cm. Flow rates:
10 ml · h^{-1} · cm^{-2} ————
50 » » » – – – – –
Silica gel: Kebo 50—100 mesh.

Table 1. Plutonium sorption on silica gel from 0.1 M nitric acid, with subsequent elution of Pu(IV) by 4.5 M nitric acid. In the first series, the fractionation was started immediately, in the second after that the plutonium had been sorbed on the column for four days. Flow rate 76 ml · hour^{-1} · cm^{-2}.

Immediate fractionation		Fractionation after 4 days	
0.1 M acid ml	% Pu/fraction	0.1 M acid ml	% Pu/fraction
17.2	0	12.5	0
34.6	0	26.5	0
51.5	3.4	39.9	0
68.5	1.3	52.9	2.9
85.5	0.8	65.9	0.2
438.2	15.4	—	—
4.5 M acid ml		4.5 M acid ml	
25.0	1.2	18.7	0
39.0	0.7	28.8	0
52.5	0.5	39.7	0
66.5	1.1	50.2	0.2
79.5	19.2	60.5	59.6
93.3	55.6	71.0	36.1
106.5	0.8	81.7	0.9
120.3	0	92.2	0.2
133.3	0	103.1	0

just the fraction found by analysis to exist as Pu(III) and Pu(VI). In the second peak the remaining plutonium is found as Pu(IV).

The above conclusions are further strengthened by the fact that the plutonium of the first peak is not extracted at pH = 0 by a 0.1 M solution of thenoyltrifluoroacetone (TTA) in benzene, while the plutonium in the second peak is completely extracted into the organic phase under the same conditions [15].

At the low flow rates a complete separation into two peaks is achieved. If the flowrate is increased, the separation is not so good (as was expected), but the existence of two peaks is nevertheless quite clear.

At $C_H = 0.1$ M, the distribution coefficient for plutonium is much larger than at $C_H = 0.5$ M. An experiment with the long column and a flow rate of 76 ml·hour^{-1}·cm^{-2} is reproduced in Table 1. From this table it can be seen that Pu(IV) is very strongly sorbed and that there is only a small plutonium leakage, less than 1 % of the total amount per fraction of 17 ml, during the continued passage of 0.1 M nitric acid. Pu(III) and Pu(VI) are found as before in the solution front.

By passing 4.5 M nitric acid through the column the plutonium is quantitatively eluted in the strong acid front, as its distribution coefficient at this acidity is very low. In Table 1 another experiment analogous to the previous one is also to be found. The only difference is that in the latter case the plutonium solution has remained for four days on the column before washing

with 0.1 M nitric acid. Pu(III) and Pu(VI) are found as before in the solution front but no Pu(IV) leakage could be detected. On elution with 4.5 M nitric acid, all the Pu(IV) came out as before in the strong acid front.

These column experiments confirm that the plutonium sorption is a fairly slow process. This is also evident from a determination of the *plutonium distribution on the column.* Sorption and subsequent washing with 0.1 M HNO_3 were made in the same way as in earlier experiments. The solution phase was then removed by blowing compressed air through the column. After drying, the silica gel column was removed in sections of fixed length. These were eluted with 4.5 M nitric acid and the amount of plutonium was determined. The resulting distribution curve is reproduced in Fig. 3 and shows that the plutonium penetrates rather deeply into the column before the sorption is complete.

The plutonium(IV) sorption is not entirely reproducible. A large number of experiments have been performed which show a leakage varying between zero and an upper limit given by the first of the experiments reproduced in Table 1. Furthermore the Pu(IV) leakage always decreases with decreasing flow rate.

As is evident from earlier equilibrium experiments [1] the sorption behaviour of *zirconium* is very complicated. The variation in sorption rate with pH is more pronounced than for plutonium(IV). The results from the equilibrium

Table 2. Zirconium sorption on silica gel from nitric acid of different concentrations, with subsequent elution by 0.1 M oxalic acid. Flow rate 38 ml · $hour^{-1}$ · cm^{-2}.

0.1 M acid ml	% Zr/fraction	1.5 M acid ml	% Zr/fraction	5 M acid ml	% Zr/fraction
17.6	0	10.0	0	12.1	0
36.6	6.0	29.0	0.2	35.4	0
53.4	39.2	41.7	2.5	49.0	0.9
72.0	1.2	54.2	0.9	64.5	0.1
89.8	0.5	65.1	0.1	80.8	0
109.2	0.3	76.1	0	94.8	0
126.7	0.1	—	—	—	—
144.5	0.2	—	—	—	—
161.5	1.1	—	—	—	—
179.3	0.6	—	—	—	—
195.8	0.3	—	—	—	—
213.3	0.4	—	—	—	—
226.8	0.3	—	—	—	—
0.1 M oxalic acid ml		0.1 M oxalic acid ml		0.1 M oxalic acid ml	
17.0	0.4	12.5	0	14.8	0
34.7	0.3	28.6	0	28.9	0
51.7	44.7	44.2	9.8	42.0	0
70.3	3.4	60.3	86.0	56.1	90.7
86.7	0.6	71.8	0.4	69.4	7.6
104.0	0.4	—	—	83.7	0.6

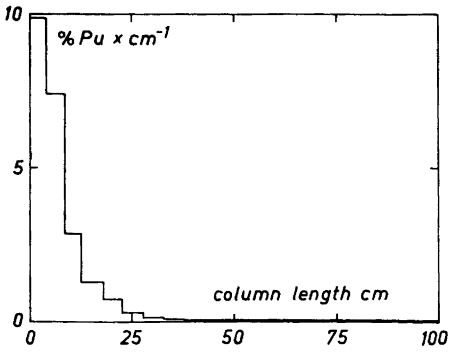

Fig. 3. The distribution of plutonium on the silica gel column when sorbed from 0.1 M nitric acid at a flow rate of 60 ml · h^{-1} · cm^{-2}.

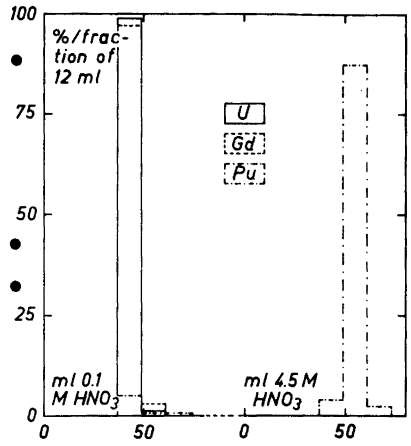

Fig. 4. Separation of Pu(IV) from U(VI), Pu(VI), Pu(III) and Gd(III) by sorption on silica gel from 0.1 M nitric acid, with subsequent elution of Pu(IV) by means of 4.5 M nitric acid. Column length 100 cm, flow rate 60 ml · h^{-1} · cm^{-2}.

measurements have been confirmed qualitatively by column experiments. The long column has been used for all the experiments and the amount of zirconium added has always been 1 ml of 11 mM zirconium(IV) solution.

The results from three runs at C_H = 0.1, 1.5 and 5 M nitric acid and a constant flow rate of about 38 ml·$hour^{-1}$·cm^{-1}, are given in Table 2. The Zr(IV) leakage is very large at the lowest acidity, but rather slight at the higher ones. This behaviour is expected as a result of the very low sorption rate at higher pH-values (*cf.* part I). If the flow rate is increased the leakage also increases rapidly. Thus a doubling of the flow rate at C_H = 1.5 M gives a leakage of the same magnitude as found for C_H = 0.1 M at the lower flow rate.

After a nitric acid wash, the column was eluted with 0.1 M oxalic acid. Because of the high distribution coefficient for Zr(IV) a strong complexing agent is needed for the elution. 1 M sulfuric acid and 0.1 M oxalic acid were both tried, but 0.1 M oxalic acid was the better of the two.

The above is in qualitative accordance with results obtained by Rydberg [2] for sorption of tracer amounts of zirconium on silica gel. According to Rydberg, the leakage is very large even at C_H = 1.5 M. The reason for this difference might be differences in flow rate (not specified in Rydberg's work) or zirconium concentration.

As representatives of yttrium and the lanthanides, neodymium, gadolinium and ytterbium have been studied. The experiments have been performed separately for each ion, using the long column. The result was that no sorption could be proved in 0.1 M nitric acid. Like U(VI), all the lanthanides passed down the column in the solution front.

The results of the chromatographic experiments indicate that Pu(IV) and Zr(IV) might be separated from one another and from U(VI) + lanthanides by a suitable variation of pH. In order to get a good separation the flow rate must not be too high.

The following experiment was performed to confirm this. A solution of U(VI) (0.1 ml 285 mM uranyl perchlorate solution), Pu(IV) (0.1 ml 0.51 mM nitrate solution containing 94.5 % Pu(IV)) and Gd(III) (0.1 ml 4.4 mM perchlorate solution) was chromatographed on the long column at a nitric acid concentration of 0.1 M.

The result, given in Fig. 4 is in complete accord with the previous experiments. U(VI), Gd(III), Pu(III) and Pu(VI) travel down the column in the solution front. Pu(IV) is nearly quantitatively sorbed, the leakage is less than 0.2 % of the total amount of plutonium per fraction of 12 ml. By passing 4.5 M nitric acid, all plutonium sorbed can be quantitatively eluted. The total yield of plutonium is 93.5 %, compared with the initial amount of 94.5 % Pu(IV).

Sorption behaviour on continuous passage of solution. For work with larger amounts of material it is desirable to be able to use a continuous sorption process. In this case it is of interest to know the sorption capacity $S \equiv C_{MG}$ for the column. By applying the law of mass action to the exchange reaction (Ref.[1], eqn. (4)) the following expression is obtained

$$S \equiv [MG_n] = K \frac{[M^{n+}]\ [HG]^n}{[H^+]^n}$$

where K is the concentration constant of the exchange equilibrium. From this expression it can be seen that S increases with increasing $[M^{n+}]$, *i.e.* with increasing C_{MS} and decreasing $[H^+]$. For very high C_{MS}, S will of course finally reach an upper limit when practically all sorption places are occupied by M^{n+} instead of the original H^+. For the sorption of Pu(IV) or fission products where C_{MS} is fairly low as a rule, this saturation value will not, however, be approached in practice.

The sorption capacity, S, has been determined as a function of C_{MS} and pH for a number of metal ions. A solution of fixed metal ion concentration, C_M, and pH is passed down the column and the effluent solution analyzed on the ion in question. The column capacity for a solution of the value of C_M used has been reached when the solutions entering and leaving the column have the same concentration $= C_M$ which is then identical with C_{MS} as defined above. From the break-through curve the sorption capacity is then easily calculated. The value thus obtained was then checked in the following way: The column was rinsed free from mechanically adherent solution by washing with pure solvent of the same pH as was used at the sorption. In order not to disturb the equilibrium in the column appreciably, the volume of the washing liquid was only one to two column volumes. After washing the column was eluted with strong acid and the eluate analyzed. The sorption capacity has been determined in this way as a function of pH for Zr, U(IV), U(VI), Ce(III), Gd, Ca and Ba.

Table 3. The sorption capacities for U(IV) and U(VI) as functions of pH and the total concentration of metal ion, C_M.

U(VI)						U(IV)		
C_M mM	pH	S mequiv/g	C_M mM	pH	S mequiv/g	C_M mM	C_H mM	S mequiv/g
11.4	2.00	0.005	22.8	2.70	0.041	10	25	0.18
11.4	2.30	0.011	22.8	2.86	0.070	10	50	0.12
11.4	2.50	0.016	22.8	3.44	0.296	10	100	0.10
11.4	2.70	0.023	22.8	3.75	0.473	10	500	0.008
11.4	3.10	0.106	22.8	4.21	1.595	25	50	0.13
11.4	3.40	0.176	45.6	2.40	0.023	25	100	0.16
11.4	3.60	0.240	45.6	3.31	0.320	25	500	0.011
11.4	3.80	0.336	45.6	3.58	0.493	50	50	0.25
						50	100	0.16

Table 4. The sorption capacities for Gd(III), Ce(III) and Zr(IV) as functions of pH.

Gd(III) C_M = 2.8 mM		Ce(III) C_M = 25 mM		Zr(IV) C_M = 9.2 mM	
pH	S mequiv/g	pH	S mequiv/g	C_H M	S mequiv/g
1.0	0.000	3.2	0.001	1.5	0.56
2.0	0.003	4.2	0.003	5.0	0.40
3.0	0.006	5.2	0.007		
4.0	0.009				

Table 5. The sorption capacities of Ca^{2+} and Ba^{2+} as functions of pH.

Ca C_M = 25 mM		Ba C_M = 25 mM	
pH	S mequiv/g	pH	S mequiv/g
9.25	0.093	10.30	0.92
9.66	0.378	10.51	1.90
10.25	1.86	10.85	2.52
10.44	2.84	10.94	3.46
10.50	3.97	11.20	3.46
10.61	4.50	11.28	3.76
11.10	4.37		

Because of the very low affinity of the ion exchanger for calcium and barium ion experiments with these ions have been done in ammoniacal solution, all the others in nitric acid solution. The results are given in Tables 3—5.

From these tables it can be seen that the sorption capacities for the trivalent lanthanide ions examined are very small within the pH range investigated.

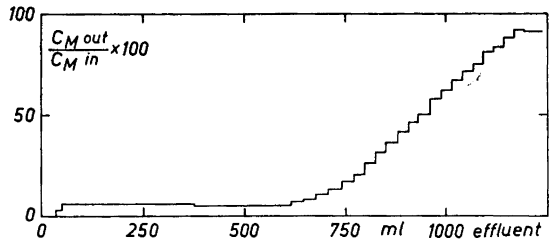

Fig. 5. Break through curve for Zr(IV) on a column filled with 60 g silica gel. Column length 100 cm, corresponding to a solution volume of 50 ml. Flow rate 60 ml · h^{-1} · cm^{-2}. C_M = 0.92 mM, C_H = 5 M.

On the other hand, the capacities for U(VI), U(IV) and Zr(IV) are large even at rather low pH-values. A determination of the sorption capacity for plutonium is not possible because of the small amount of material available. A sorption capacity of the same order of magnitude as for other four-valent ions is a plausible estimate.

Calcium and barium ions are not measurably sorbed at pH-values below 7. At higher pH-values there is a strong increase in sorption, a fact also confirmed by other authors [16-18]. For some reason which is still unknown, saturation capacities much higher than those observed for sodium ions (Ref.[1], Table 2) seem to be reached.

The distribution coefficients $D = C_{MG}/C_{MS}$ which can be calculated from these column experiments as the ratio S/C_M agree fairly well with those obtained in the equilibrium experiments of Ref.[1], even for the four-valent ions.

The slow Zr(IV) sorption gives rise to a leakage of between 5 and 10 % of the total amount Zr on continous passage of solution. A typical break through curve is reproduced in Fig. 5. The rise at about 750 ml is caused by saturation of the column.

Analogous experiments have also been performed on plutonium solutions at concentrations about 10^{-5} M. The flow rate was, however, slower, only 2.3—4.6 ml·$hour^{-1}$·cm^{-2}. The results showed a quantitative sorption of plutonium(IV) and, as before, no retention of plutonium(III) and (VI).

These experiments proved that a selective sorption is possible even with a continuous column process. In the next section some test separations on solutions of known composition are described.

ForU(IV), the found increase of S with C_{MS} is somewhat irregular (*cf.* Table 3) which is certainly due to the fact that solutions of different age were used for the experiments. U(IV) solutions of low C_H alter their properties markedly with time, due to slow hydrolytic reactions [19].

Test separations on solutions of known composition. The first solution had the following composition: C_{Zr} = 9.17 mM, $C_{Pu} = 2.39 \times 10^{-3}$ mM, $C_{U(VI)}$ = 199 mM, C_H = 4 M and a total volume of 100 ml. The γ-activities of the components were measured separately before mixing. For 5 ml samples the U(VI) solution gave 1 525 cpm and the Zr solution 9 663 cpm. The latter

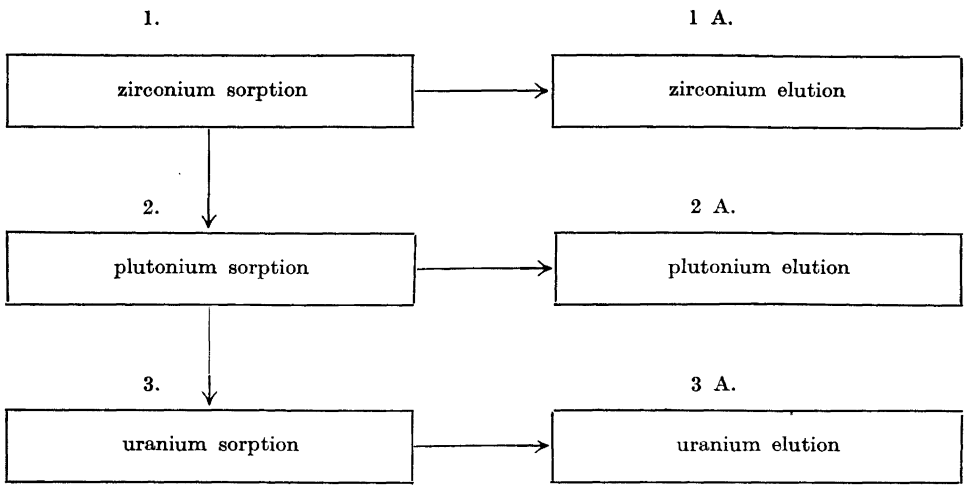

Fig. 6. Block scheme for the separation of uranium, plutonium and zirconium.

solution contained activities from ^{95}Zr, ^{95}Nb and ^{181}Hf, as discussed in Ref.[1] The separation procedure can be illustrated by the block scheme, Fig. 6.

The different steps in the above scheme will now be separately described.

1. The zirconium sorption step is made at $C_H = 4$ M, and a flow rate of about 3.5 ml·hour^{-1}·cm^{-2}.

1 A. After sorption the column is first washed with 4 M nitric acid and then eluted with 0.1 M oxalic acid which quantitatively removes the zirconium.

2. The solution which has passed down the column in step 1 is evaporated to dryness to remove excess nitric acid and is then restored to the initial volume with 100 ml 0.1 M nitric acid. The heating with 4 M nitric acid caused a strong disproportionation and possibly also oxidation of the plutonium. A TTA-extraction proved that only about 12 % of the total amount remained as plutonium (IV). All this amount plus zirconium leakage from step 1 was quantitatively sorbed.

2 A. After washing with 0.1 M HNO_3, plutonium was eluted with 4.5 M HNO_3. Zirconium remained sorbed.

3 and 3 A. After step 2 the solution was partially neutralized with sodium hydroxide, to a pH of about 3. When this solution was passed down the column the uranium was quantitatively sorbed. Sorbed uranium is then removed by a strong acid.

The other solution of known composition which has been separated was a nitric acid solution of neutron irradiated uranium. After irradiation the uranium had cooled for three years. The solution was obtained from A. B. Atomenergi, Stockholm, which gave its composition as: $C_{U(VI)} = 1.075$ M, $C_{Pu} = 1.45 \times 10^{-5}$ M, $C_H = 0.95$ M. The solution also contained long-lived fission products, mainly ^{106}Ru—^{106}Rh, ^{144}Ce—^{144}Pr, ^{90}Sr—^{90}Y and ^{137}Cs—^{137}Ba.

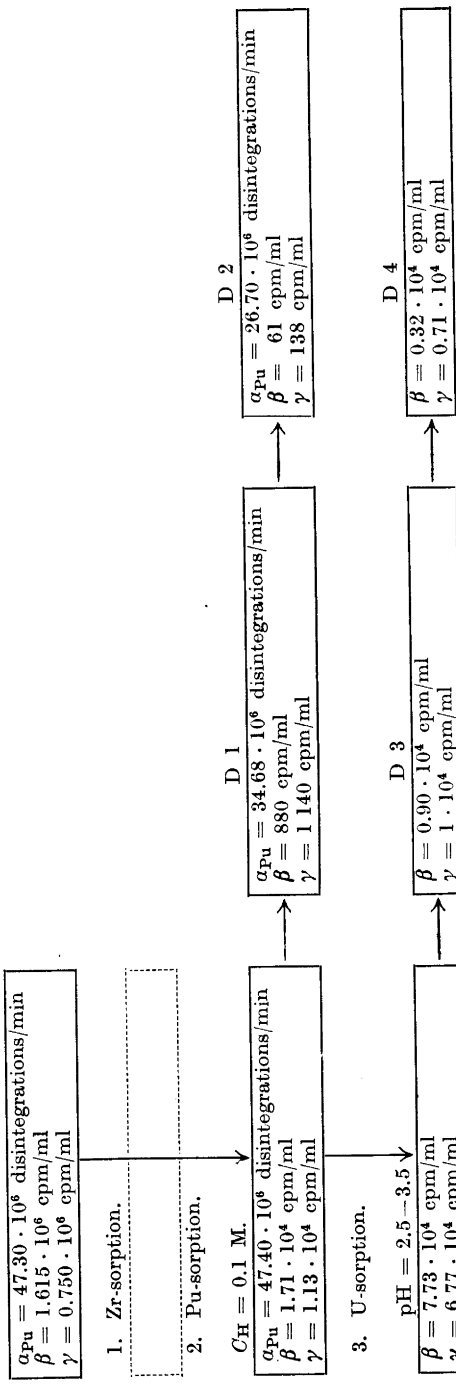

Fig. 7. Block scheme for the separation of the components of a solution of irradiated uranium.

β and γ activities were determined by scintillation counting. The β detector was a Tracerlab P-20 C with a stilbene crystal, the γ detector was the same as used in Ref[1]. The initial activities were $\gamma = 7.500 \times 10^5$ cpm/ml and $\beta = 1.615 \times 10^6$ cpm/ml.

As the amount of plutonium was known (the volume of solution being 100 ml) the total number of plutonium α- decays per minute could be calculated and was $\alpha_{Pu} = 47.30 \times 10^6$. The separation process can be described with the block scheme, Fig. 7, where the different activities at different stages in the separation have also been inserted. The activities are everywhere related to an initial volume of 100 ml and are measured in constant geometry.

1. Because of the short half life ($T_{1/2} = 65$ days) for ^{95}Zr, all $^{95}Zr-^{95}Nb$ has disappeared during the cooling period. The first stage of the process was therefore omitted.

2. The acid excess was removed by evaporationg to dryness and the solid residue dissolved in 100 ml 0.1 M nitric acid. The evaporation also caused in this case a strong plutonium disproportionation but by treating the solution with sodium nitrite the oxidation state was restored to + 4. At a nitrite concentration of 50 mM, this was achieved in a few hours at 80°C. The high concentration of nitrate ions in the rather concentrated uranyl nitrate solution also stabilized the plutonium very much as Pu(IV).

After cooling the solution was passed down the column at a rate of about 3.5 ml·hour^{-1}·cm^{-2}. After washing with 0.1 M nitric acid plutonium was quantitatively eluted with strong nitric acid. The result (Fig. 7) shows that the all plutonium was sorbed and that most of the fission porducts were removed from the plutonium fraction. A further decontamination was obtained by sorbing the plutonium twice more onto the column.

D 1. The eluate from 2 was evaporated to dryness, dissolved in 100 ml 0.1 M nitric acid and treated as before with sodium nitrite. As no uranium was present the nitrate concentration was rather small, 0.1 M compared with 2.3 M at the first reduction. In this solution Pu(IV) disproportionates and in fact only 73.5 % of the plutonium remained fourvalent. On passage down the column a small Pu(IV) leakage, about 0.5 % of the total amount plutonium, was observed. The activity measurements showed a further decontamination from fission products and the plutonium(IV) yield is greater than 99.5 % (Fig. 7).

D 2. The eluate from D 1 is evaporated to dryness and then treated as in the previous decontamination step. About 77 % plutonium was found in the oxidation state + 4. After elution α, β and γ-activities were measured as before (Fig. 7).

The plutonium solution finally obtained was completely separated from uranium and partially decontaminated from fission products. The decontamination factors were for γ-activity 5.4×10^3 and for β-activity 2.65×10^4. On the assumption that plutonium is kept in oxidation state + 4 the separation can be made with a yield larger than 99.5 %. Plutonium missing in D 2 is found as Pu(III) and Pu(VI) leakage from D 1 and D 2. To collect the plutonium in the leakage from D 1, this portion was treated with sodium nitrite. After sorption and elution an amount of plutonium = 9.6×10^6 disintegrations · min^{-1} was recovered.

3. From the solution which hade been passed down the column at 2 the uranium was recovered. By adding sodium hydroxide the pH was increased to between 2.5 and 3.5 and from this solution uranium was sorbed on the column. The column was washed with water and eluted with strong acid. The β and γ activities of this fraction were then measured. After subtracting the activies due to daughter products of uranium (determined separately by measuring a pure uranium solution) the activities of the fission products were obtained.

As seen from Fig. 7 (U-sorption), a small decontamination from fission products was achieved. To get a larger total decontamination the above treatment was repeated twice, decontamination steps D 3 and D 4. The uranium yield was always 100 % and the decontamination factors for the final uranium solution were for β activity 505 and for γ activity 106.

In order to trace the behaviour of the different fission products present, γ-spectra have been recorded for the original solution, the plutonium fraction 2 and the uranium fraction 3. The spectrum of the original solution showed that the γ-activity almost completely came from ^{137}Cs. A small peak from ^{144}Ce, only a few percent of the cesium peak, could also be seen. Spectra from fractions 2 and 3 also showed the presence of ^{137}Cs, while ^{144}Ce had disappeared.

The long cooling period is of course the reason why the γ-activity comes almost exclusively from ^{137}Cs and the uranium decay series and the β-activity from ^{90}Sr and the uranium series.

According to Ref.[1], Fig. 6, Cs^+ and Sr^{2+}, which are very similar to Na^+ and Ca^{2+}, Ba^{2+}, ought not to be sorbed at the pH in question and the decontamination factors are consequently unexpectedly small. For a further study of the pH influence a new decontamination was performed on a part of the original solution. Uranium was sorbed as before but the column was washed with 0.1 mM nitric acid instead of water. After elution and measurements of the activities the decontamination factors were calculated as 75 for γ-activity and 20 for β-activity compared with 8.6 and 6.8 for the corresponding factors in D 3. It is evident that the distribution curve for Cs^+ and Sr^{2+} which ought to be the same as the curves in Ref.[1], Fig. 6, for Na^+ and Ca^{2+}, Ba^{2+} have been shifted towards lower pH-values at the low Cs^+, Sr^{2+} concentrations used here.

REFERENCES

1. Ahrland, S., Grenthe, I. and Norén, B. *Acta Chem. Scand.* **14** (1960) 1059.
2. Rydberg, J. *Acta Chem. Scand.* **9** (1955) 1252.
3. Culler, F. L. *Proc. Intern. Conf. Peaceful Uses Atomic Energy, Geneva 1955*, **9** (1956) 464 (P/822).
4. Connick, R. E. *The Actinide Elements, Natl. Nuclear Energy Ser.* Div. IV, **14 A** (1954) 229.
5. Fletcher, J. M. and Martin, F. S. *Proc. Intern. Conf. Peaceful Uses Atomic Energy, Geneva 1955*, **7** (1956) 141 (P/437).
6. Rudstam, G. *Acta Chem. Scand.* **13** (1959) 1481.
7. Connick, R. E. and McVey, W. H. *J. Am. Chem. Soc.* **75** (1953) 474.
8. Rabideau, S. W. *J. Am. Chem. Soc.* **75** (1953) 798.
9. Rabideau, S. W. and Cowan, H. D. *J. Am. Chem. Soc.* **77** (1955) 6145.
10. Bjerrum, J., Schwarzenbach, G. and Sillén, L. G. *Stability Constants, Part II*, The Chemical Society, London 1958, p. 55.

11. Grenthe, I. and Norén, B. *Acta Chem. Scand.* **14** (1960). *In press.*
12. Connick, R. E. *The Actinide Elements, Natl. Nuclear Energy Ser.* Div. IV, **14 A** (1954) 269.
13. Sonesson, A. *Acta Chem. Scand.* **12** (1958) 165, 1937.
14. Holleck, L., Eckardt, D. and Hartinger, L. *Z. anal. Chem.* **146** (1955) 103.
15. Hyde, E. K. *Proc. Intern. Conf. Peaceful Uses Atomic Energy, Geneva 1955*, **7** (1956) 281 (P/728).
16. Berestnewa, Z. and Kargin, V. *Acta Physicochim. U.R.S.S.* **4** (1936) 675.
17. Bruns, B., Burshtein, R., Feodotov, N., Livshitz, M. *Zhur. Fiz. Khim.* **11** (1938) 7.
18. Nikol'skii, B. P. and Grigorov, O. N. *Doklady Akad. Nauk. S.S.S.R.* **50** (1945) 325.
19. Kraus, K. A. and Nelson, F. *J. Am. Chem. Soc.* **72** (1950) 3901.

Received January 30, 1960.

ACTA CHEMICA SCANDINAVICA 14 (1960) 1091—1099

The Distribution and Dimerization of Di-*n*-butyl Phosphate (DBP) in Different Solvents

DAVID DYRSSEN and LIEM DJIET HAY

Department of Inorganic Chemistry, Royal Institute of Technology, Stockholm 70, Sweden

The distribution of DBP between a number of organic solvents and 0.1 M HNO_3 has been measured at 25°C using ^{32}P-labelled DBP. From the variation of the net distribution ratio, q, with the total concentration of DBP the distribution and the dimerization constants have been determined for the following solvents (log K_d and log K_2 given for each solvent): *n*-hexane (−2.34; +6.87), carbon tetrachloride (−1.44; +6.49), chloroform (+0.24; +4.61), *iso*propyl ether (+0.52; +2.29), tri-*n*-butyl phosphate (+1.97; −0.12), methyl*iso*-butyl carbinol (+2.21, <-1).

An increase in K_d is combined with a decrease in K_2. The explanation given is based on the assumption that complex formation between DBP and the organic solvent molecules competes with the dimerization in the solvent and the solvation of DBP in the aqueous phase. The complex formation constant between DBP (= HA) and TBP (= B), $K_B = [HAB]_{org}\,[HA]_{org}^{-1}\,[B]_{org}^{-1}$, has been determined in carbon tetrachloride as log $K_B = 2.84$.

The results are discussed in relation to some recent work on DBP by Dyrssen [1] and by Hardy and Scargill [2].

It has been shown in previous work by Dyrssen [1] and by Hardy and Scargill [2] that the choice of solvent has great influence on the distribution of DBP (= HA) between an organic solvent and acid aqueous solutions. This is partly due to the fact that the solvent may greatly influence the very pronounced tendency for dialkyl phosphates to dimerize. The purpose of this work was to study the distribution and dimerization of DBP in solvents of different types. The equilibrium constants determined in this work will be used in a study [3] of the extraction of Eu^{3+} and Am^{3+} with DBP in the same set of solvents. A more complete understanding of the reactions between the metal ions and DBP in the organic phase may thus be possible when the concentrations of H_2A_2 (org), HA (org and aq) and A^-(aq) can be calculated. This approach was shown to be fruitful in a study [4] of the extraction of UO_2^{2+} with DBP using chloroform and hexone as solvents.

The same symbols as previously [1] are used in this work except that in accordance with IUPAC K is used instead of k for equilibrium constants.

EXPERIMENTAL

The general procedure has been described earlier [1]. DBP has, however, been purified according to the following new technique (*cf.* Baes [5] *et al.* note 7): 10 ml of DBP was dissolved in 30 ml of petroleum ether (analytical grade). This layer was washed three times with water, and DBP was thereafter extracted with the equivalent amount of 1 M NaOH at 5°C, the cooling being done with ice. The aqueous layer containing the sodium salt of DBP was washed three times with petroleum ether, acidified with HCl and shaken with 30 ml of petroleum ether. The ether phase was washed three times with water and the ether distilled off. The final product, which was pale yellow, was dried at 130°C under reduced pressure (10 mm Hg, N_2 atmosphere) for half an hour. Potentiometric titrations evaluated by the Gran II method [6] for the detection of end-points indicated that the product was free from MBP and at least 99 % pure.

The chloroform (Merck-Darmstadt analytical grade) was washed three times with twice its volume of water to remove the 1 % alcohol. The carbon tetrachloride was of analytical grade (Merck-Darmstadt) and was not further purified. The hexone (methyl *iso*butyl ketone) was washed with $NaHCO_3$ solution, dilute perchloric acid and finally with water. The initial hexone (Kebo) had a boiling range of 114—117°C. The isopropyl ether, boiling range 65—70°C, and *n*-hexane (68—69°C) have a purity of at least 99 % (Kebo). These solvents were not further purified. The hexol (methyl *iso*butyl carbinol), of 99 % purity (Kebo) and boiling range 130—133°C, was treated as hexone. The tri-*n*-

Table 1. Distribution of DBP at 25°C between various solvents and 0.1 M HNO_3 for different initial concentrations of DBP in the organic layer (C_A). $V_{org} = V_{aq} = 15$ ml.

n-Hexane, log C_A (log q): −0.295(+1.119), −0.690(+0.690), −0.976(+0.492), −1.214 (+0.222), −1.690(−0.071), −1.976(−0.260), −2.301(−0.495), −2.580 (−0.796), −2.881(−1.046), −3.580(−1.637), −3.881(−1.947), −4.295(−2.108), −4.580(−2.154), −4.880(−2.546), −4.941(−2.520), −5.098(−2.520), −5.243 (−2.686), −5.465(−2.644), −5.641(−2.710), −5.941(−2.375), −5.941(−2.512).

Carbon tetrachloride, log C_A(log q): −0.304(+1.547), −0.691(+1.335), −0.991(+1.112), −2.311(+0.384), −2.696(+0.204), −2.996(−0.004), −3.696(−0.509), −3.996(−0.745), −4.270(−1.000), −4.627(−1.191), −4.750(−1.514), −4.771(−1.322), −5.149(−1.462), −5.273(−1.536), −5.403(−1.494), −5.432(−1.438), −5.593(−1.698), −5.750(−1.772).

Chloroform, log C_A(log q): −2.016(+1.368), −2.345(+1.204), −2.673(+1.060), −2.980 (+0.895), −3.294(+0.689), −3.692(+0.580), −3.972(+0.433), −4.914 (+0.076), −4.993(+0.080), −5.216(−0.018), −5.295(+0.008), −5.692(−0.036).

Isopropylether, log C_A(log q): −0.358(+1.354), −0.719(+1.168), −1.021(+1.015), −1.321(+0.858), −1.708(+0.549), −2.021(+0.669), −2.359(+0.433), −2.715(+0.318), −3.015(+0.305), −3.345(+0.259), −3.956(+0.256), −4.307(+0.238), −4.686(+0.253), −4.914(+0.212), −4.956(+0.238), −4.993(+0.215), −5.091(+0.210), −5.216(+0.212), −5.391(+0.162), −5.692(+0.188).

Mean value of log $K_d\varphi = 0.218 \pm 0.031$

Tri-n-butyl phosphate, log C_A(log q): −0.383(+1.830), −0.718(+1.754), −0.989(+1.731), −1.718(+1.664), −2.020(+1.680), −4.181(+1.676), −4.305(+1.678), −4.481(+1.638).

Mean value of log $K_d\varphi = 1.672 \pm 0.020$

Isobutyl methyl carbinol, log C_A(log q): −0.340(+1.845), −0.692(+1.917), 0.992(+1.896), −1.340(+1.915), −2.334(+2.005), −2.996(+1.937), −3.243(+1.903), −3.290(+1.906), −3.411(+1.916), −3.720(+1.891), −4.022(+1.958), −5.243(+1.842).

Mean value of log $K_d\varphi = 1.911 \pm 0.050$

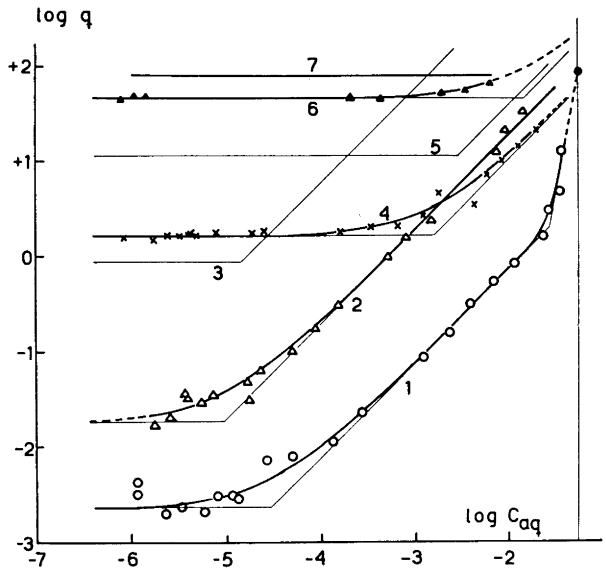

Fig. 1. Distribution of DBP between various solvents and 0.1 M HNO_3 as a function of the total concn. of DBP in the aqueous phase. The maximum value of C_{aq} is determined by the solubility of undiluted DBP in water. Solvents: 1 hexane, 2 carbontetrachloride, 3 chloroform (*cf.* Fig. 2), 4 *iso*propyl ether, 5 hexone (*cf.* Ref.[1]), 6 tributyl phosphate, 7 hexol (*cf.* Table 1). Normalized curve log Y = log $(X + 1)$ is fitted to the data.

butylphosphate (Kebo) was purified by washing it first with an equal volume of 1 M NaOH solution, then with 0.1 M HNO_3 and finally with water.

The radioactive DBP was purchased as previously [1] from Radiochemical Centre, Amersham, England. The aqueous phase was always 0.1 M HNO_3 and the volumes of the two phases were equal.

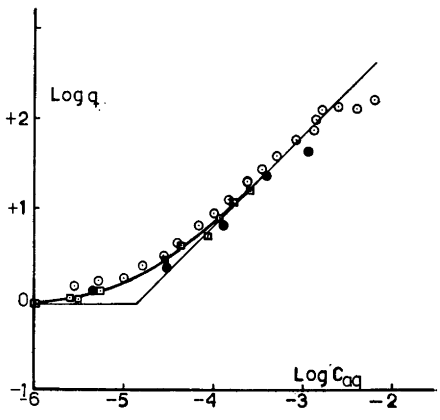

Fig. 2. Distribution of DBP between chloroform and 0.1 M HNO_3 as a function of the total concentration of DBP in the aqueous phase (open squares). Open circles: data from Ref.[1] (aq. phase 0.1 M $HClO_4$). Filled circles: data from Ref.[2] (aq. phase 0.1 M $HClO_4$).

RESULTS

The data are given in Table 1 as log C_A (initial conc. of DBP in the organic layer) and log q (net distribution ratio of DBP). The data, except those for methyl *iso*butyl carbinol where q is independent of C_A, are plotted in Figs. 1 and 2 as log q against log C_{aq} (equilibrium conc. of DBP in the aqueous phase).

C_{aq} was calculated from the following relationship:

$$C_{aq} = C_A(1 + q)^{-1}$$

Assuming that $C_{org} = qC_{aq} = [HA]_{org} + 2[H_2A_2]_{org}$ and

$$C_{aq} = [HA] + [A^-] = [HA] + K_a[HA][H^+]^{-1}$$

the distribution constants, $K_d = [HA]_{org}[HA]^{-1}$, and dimerization constants, $K_2 = [H_2A_2]_{org}[HA]_{org}^{-2}$, were calculated as before [1] by fitting the normalized curve log Y = log $(X + 1)$ to the data $x = \log C_{aq}$, $y = \log q$.

The horizontal asymptote (log $Y = 0$) gives

$$\log K_d\varphi^{-1} = \log Y_0$$

where $\varphi = 1 + K_a[H^+]^{-1} = 2.00$ is kept constant in these experiments and the point of intersection (log X_0, log Y_0) between the two asymptotes gives

$$\log 2\,K_2K_d\varphi^{-1} = -\log X_0;\ \log K_2 = -\log 2\,X_0Y_0$$

The values of K_d and K_2 determined in this manner are collected in Table 2 together with the constants for methyl *iso*butyl ketone (hexone) from earlier work [1] and some constants determined by Hardy and Scargill [2].

The complex formation between DBP and TBP (tri-*n*-butyl phosphate) was determined in a study of the distribution of DBP as a function of the TBP concentration in carbon tetrachloride (= $[B]_{org}$). The aqueous phase was

Table 2. Summary of distribution and dimerization constants for DBP in various two-phase systems.

System	log K_d	log K_2	Reference
Methyl-*iso*butyl carbinol/0.1 M HNO_3	+2.21 ± 0.05	< −1	this work
Tri-*n*-butyl phosphate/0.1 M HNO_3	+1.97 ± 0.02	(−0.12) [1]	this work
Methyl-*iso*butyl ketone/0.1 M $HClO_4$	+1.36	+1.19	1
*Iso*propyl ether/0.1 M HNO_3	+0.52 ± 0.03	+2.29	this work
Chloroform/0.1 M HNO_3	+0.24	+4.61	this work
Carbon tetrachloride/0.1 M HNO_3	−1.44	+6.49	this work
n-Hexane/0.1 M HNO_3	−2.34	+6.87	this work
Nitrobenzene/1 M HNO_3	−0.14	+3.55	2
Benzene/1 N HNO_3	−0.42	+4.88	2
Carbon tetrachloride/1 M HNO_3	−0.91	+5.33	2
Kerosene/1 M HNO_3	−1.96	+5.78	2
n-Butyl ether/0.1 M $HClO_4$	−0.14	+2.84	9

[1] Uncertain, H_2A_2B complex may be formed [7].

Table 3. Distribution of DBP between carbon tetrachloride and 0.1 M HNO_3 for different concentrations of TBP in the organic layer. $[DBP]_{org} < 10^{-4}$ M $\ll [TBP]_{org}$.

$[TBP]_{org}$ M	log q	log $q\,[TBP]_{org}^{-1}$
3.43 (no CCl_4)	+1.672	1.137
2.86	+1.658	1.201
2.06	+1.432	1.118
1.145	+1.139	1.079
0.916	+1.064	1.103
0.686	+0.929	1.094
0.571	+0.904	1.147
0.229	+0.361	1.001
0.103	+0.048	1.034
0.0458	−0.345	0.994
0.0229	−0.513	1.127
0.01145	−0.770	1.170

Mean value of log $K_dK_B\varphi^1 = 1.100 \pm 0.064$

0.1 M HNO_3.* With $[DBP]_{org} < 10^{-4}$ M and $[TBP]_{org} \gg [DBP]_{org}$ it is possible to neglect $[HA]_{org}$ and $[H_2A_2]_{org}$ (cf. Dyrssen [1], eqns (11) and (13)). The principal reaction studied is then

$$HA\ (aq) + B\ (org) = HAB\ (org)$$

$$q = \frac{[HAB]_{org}}{[HA] + [A^-]} = [HAB]_{org}\,[HA]^{-1}\,\varphi^{-1}$$

or if $K_BK_d = [HAB][B]_{org}^{-1}[HA]$ and $\varphi = 2.00$ is introduced

$$q = 0.50\ K_BK_d[B]_{org}$$

It may be seen from Table 3 that log $q[B]_{org}^{-1}$ is constant not only in dilute solutions of TBP in carbon tetrachloride, but also in highly concentrated solutions and undiluted TBP (3.43 M). This demonstrates the validity of the assumptions which lead to the expression for q above. Further evidence of a molecular interaction of this type is supplied by Baker and Baes [7], who studied the system dioctyl phosphate — trioctyl phosphine oxide, $(RO)_2PO(OH)$ — R_3PO, in octane by means of infrared spectroscopy and isopiestic measurements. The value of K_BK_d calculated from the data in Table 3 is

$$\log K_BK_d = 1.40 \pm 0.06;\ \log K_B = 2.84 \pm 0.08$$

The value is very close to the value of log $K_B = 2.83$ for TBP in kerosene obtained by Hardy and Scargill [2] but considerably higher than the value for TBP in chloroform [1] (log $K_B = 1.60$). This is probably due to association of DBP and TBP [1] with $CHCl_3$.

* It has been pointed out by Hardy and Scargill [2] that the nitric acid concentration in the aqueous phase must be kept low or else one has to consider the complex formation between TBP or DBP and HNO_3 also.

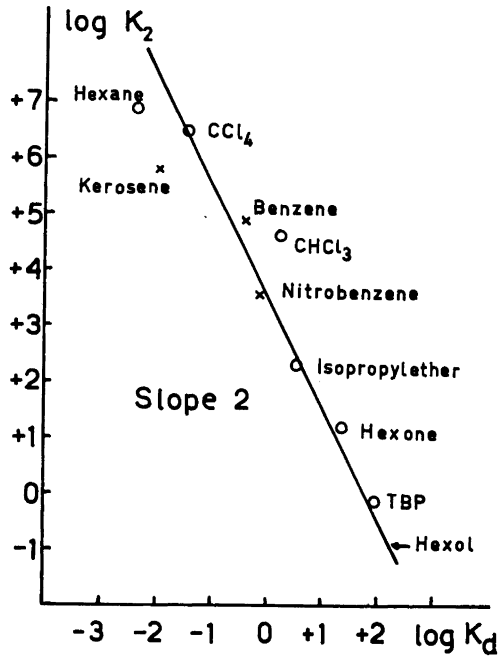

Fig. 3. The dimerization constant, K_2, of DBP in various solvents as function of the distribution constant, K_d. The data are taken from Table 2.

DISCUSSION

It is obvious from Table 2 that an increase in the distribution constant, K_d, is combined with a decrease in the dimerization constant, K_2. If log K_2 is plotted against log K_d as in Fig. 3 the data seem to fall fairly well on a line with a slope of —2. To explain this let us assume a complex formation between the DBP monomer, HA, and the solvent molecule B.

$$\text{HA (org)} + \text{B (org)} = \text{HAB (org)} \qquad \text{(eq. const. } K_B\text{)}$$

The expression for K_d and K_2 may then be written

$$K_d = \frac{[HA]_{org} + [HAB]_{org}}{[HA]} = \frac{[HA]_{org}}{[HA]} (1 + K_B[B]_{org})$$

or $K_d = K_d^\circ(1 + K_B[B]_{org})$

$$K_2 = \frac{[H_2A_2]_{org}}{([HA]_{org} + [HAB]_{org})^2} = K_2^\circ (1 + K_B[B]_{org})^{-2}$$

Combining these equations one obtains

$$K_2 = K_2^\circ K_d^{-2} (K_d^\circ)^2$$

which satisfies the straight line in Fig. 3 (log $K_2^\circ(K_d^\circ)^2 = 3.7$).

The rather good fit of available data to this line means that, apart from the specific interaction due to complex formation between DBP and the solvent, the influence of the solvent on the distribution constant of the dimer ($K_D = [H_2A_2]_{org}[H_2A_2]^{-1}$)is rather independent of organic phase. The solvents have about the same molarity and the picture should therefore not change considerably in going over to mole fraction constants. However, two types of solvents do not fit to the straight line in Fig 3, namely the hydrocarbons, *n*-hexane and kerosene, and chloroform. In the first case it may be explained by assuming that the interaction between the solvent molecule and H_2A_2 is very weak giving a low value of $K_2K_d^2$. In the case of chloroform the reason might be that the interaction between $CHCl_3$ and the dimer is rather much stronger than for the other solvents due to hydrogen bonding with the phosphoryl groups.

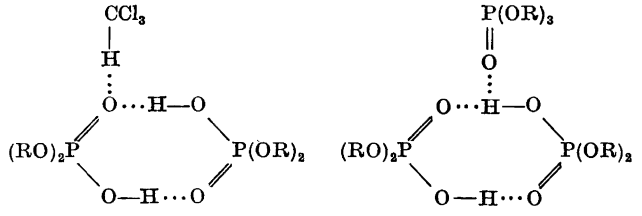

$CHCl_3(DBP)_2$ complex TBP$(DBP)_2$ complex

That a 1 : 1 complex is formed between solvents, which may act as acceptors for hydrogen bonds, and DBP, which is a donor of hydrogen, was proved in the case of TBP in CCl_4. Further support of a molecular interaction between DBP and solvents with phosphoryl groups has been supplied by Baker and Baes [7], who studied the system dioctyl phosphate — trioctyl phophine oxide, $(RO)_2PO(OH)$ — R_3PO, in octane by means of infrared spectroscopy and isopiestic measurements. — They also found some evidence of H_2A_2B complex at higher concentrations of HA. — Assuming that no complex formation occurs between CCl_4 and DBP ($K_B = 0$) we calculate approximately

$$\log K_d^\circ = -1.4 \text{ and } \log K_2^\circ = 6.5$$

The acceptor tendency of the solvents for hydrogen bonds may thus be expressed by the value of K_B calculated from

$$\log K_d = -1.4 + \log (1 + K_B[B]_{org})$$

These values are collected in Table 4 together with values of the molarity of the solvent, $[B]_{org}$, and data for the solubility of water in the solvents. It may be seen from Table 4 that there is a close correlation between K_B and the solubility of water in g/l per mole of solvent. In Fig. 4 one may see that the solubility of water in the solvent is also related to K_d. It may thus be said that the acceptor tendency of the solvents for hydrogen bonds governs the solubility of water in the solvents as well. This fact can be used in choosing a suitable solvent for the extraction of metal ions with dialkyl phosphates. It will be shown in the following paper that the choice of the solvent has great

Table 4. Summary of values of $[B]_{org}$, K_B and the solubility of water (L_{H_2O}) for various solvents.

	$[B]_{org}$ [a] M	K_B	L_{H_2O} g/l	$L_{H_2O}\,[B]_{org}^{-1}$
Hexol $(CH_3)_2CHCH_2CH(OH)CH_3$	7.39	550	58	7.85
TBP $(n\text{-}C_4H_9O)_3PO$	3.43	680 (690)	50.8 [b] (61.8)	14.8
Hexone $(CH_3)_2CHCH_2COCH_3$	7.82	73	19	2.43
*Iso*propyl ether $(CH_3)_2CHOCH(CH_3)_2$	7.03	11.6	5.7	0.81
Nitrobenzene $C_6H_5NO_2$	9.74	1.8	2.4	0.25
Chloroform $CHCl_3$	12.53	3.4	1.46	0.12
Benzene C_6H_6	11.25	0.76	0.6	0.053
Carbon tetrachloride CCl_4	10.37	~0	0.154	0.015
Hexane $n\text{-}C_6H_{12}$	7.66	~0	0.0732	0.0096

[a] Calculated for the solvent saturated with water at 20°C.
[b] Approx. corrected for the amount of water dissolved due to the three ester groups.

influence on the extraction of Eu^{3+} and Am^{3+} with DBP. This can be explained by complex formation reactions between DBP and the solvent molecules as discussed here.

The results with hexane show a marked increase in log q (Fig. 1) for values of log C_{aq} higher than —1.80 (which corresponds to $C_{org} > 0.05$ M). This very

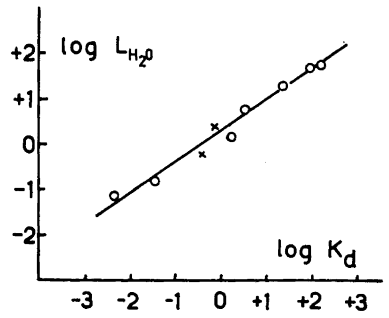

Fig. 4. Correlation between the solubility of water in the organic solvent and the distribution constant, K_d, of DBP between each solvent and 0.1 M HNO_3. The data are summarized in Table 4.

sharp increase of the slope indicates a conversion of the dimer in the form of a eight-membered ring to a polymer possibly in the form of an extended chain:

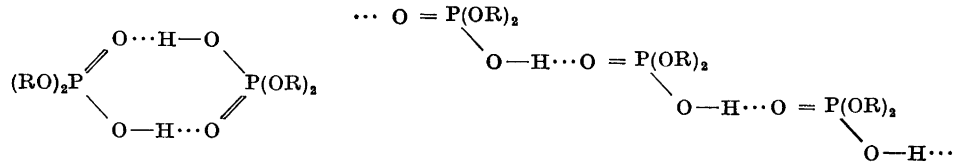

This proposal for the change in structure is supported by the fact the dibenzyl phosphate crystallizes with a structure [8] which is composed of spirals with the chain

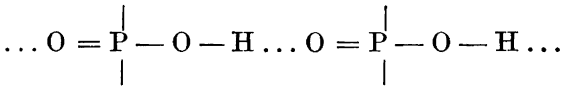

The distance between the two oxygen atoms in the link is very short, 2.494 Å, corresponding to a very strong hydrogen bond.

The transition of DBP in hexane from a dimer to a polymer may also explain the PMR-data and viscosity measurements of solutions of DBP in *n*-hexane. The same type of concentration shift in the proton magnetic resonance and viscosity was also found with carbon tetrachloride as a diluent. This emphasizes the need for great caution in drawing any conclusions about the DBP-species from distribution data where the concentration of DBP in the organic solvent is above 0.05 M. The PMR measurements and viscosity measurements will be extended to the other solvents in the near future and will be published separately.

We wish to thank Professor Lars Gunnar Sillén for his critical examination of our work and Teknologie licentiat Sture Forsén for valuable discussions in connection with his PMR measurements of some of our solutions. The work is part of a program, which is supported by *Statens råd för atomforskning (Swedish Council for Atomic Research)*. The English has been revised by Dr Helen S. Dunsmore.

REFERENCES

1. Dyrssen, D. *Acta Chem. Scand.* **11** (1957) 1771.
2. Hardy, C. J. and Scargill, D. *A.E.R.E. C/R* 2830, Harwell 1959; *J. Inorg. & Nuclear Chem.* **11** (1959) 128.
3. Dyrssen, D. and Liem Djiet Hay *Acta Chem. Scand.* **14** (1960) 1100.
4. Dyrssen, D. and Krašovec, F. *Acta Chem. Scand.* **13** (1959) 561.
5. Baes, C. F., Zingaro, R. A. and Coleman, C. F. *J. Phys. Chem.* **62** (1958) 129.
6. Gran, G. *Analyst* **77** (1952) 661.
7. Baker, H. T. and Baes, C. F. *ORNL-CF*-58-5-93, Oak Ridge, 1958.
8. Dunitz, J. D. and Rollett, J. S. *Acta Cryst.* **9** (1956) 327.
9. Dreze, Ph. *Bull. Soc. Chim. Belg.* **68** (1959) 674.

Received February 2, 1960.

ACTA CHEMICA SCANDINAVICA 14 (1960) 1100—1111

Solvent Extraction of $^{152, 154}$Eu and ^{241}Am by Di-*n*-butyl Phosphate (DBP) in Different Organic Solvents

DAVID DYRSSEN and LIEM DJIET HAY

Department of Inorganic Chemistry, Royal Institute of Technology, Stockholm 70, Sweden

The distribution of ^{241}Am and ^{152,154}Eu between aqueous nitric acid and solutions of di-*n*-butyl phosphate (= HA) has been studied in seven organic solvents. The data indicated that in five systems, M is extracted into the organic phase predominately as $MA_3(HA)_3$. The following values were found for log K for the reaction M^{3+} (aq) + 3 A^-(aq) + 3 HA(aq) $\rightleftharpoons$ $MA_3(HA)_3$(org): in *n*-hexane 13.66 (Eu), 12.38 (Am); in CCl_4 16.80 (Eu), 15.33 (Am); in $CHCl_3$ 19.33 (Eu), 17.98 (Am); in *iso*-propyl ether 14.94 (Eu), 13.72 (Am); in hexone 15.22 (Eu), 14.25 (Am); in hexol 14.15 (Eu), 14.02 (Am). In *n*-hexane, deviations at [HA] $>10^{-1.8}$ M indicate the formation of other complexes, perhaps $MA_3(HA)_6$(org). — In hexol, complexes with less HA appear for [HA] $< 10^{-3}$ M. The data may be accounted for by the additional reaction M^{3+} + 3 A^- $\rightleftharpoons$ MA_3(org), log K = 5.76 (Eu), 5.36 (Am). In tri-*n*-butyl phosphate (TBP), the reaction M^{+3} + $3NO_3^-$ + 3TBP (org) $\rightleftharpoons$ $M(NO_3)_3(TBP)_3$(org) predominates for [HA] $< 10^{-3}$ M; for [HA] $> 10^{-4}$ M, the data indicate M^{3+} + 3 A^- $\rightleftharpoons$ MA_3 (org), log K = 7.49 (Eu), 6.98 (Am).

Parallels are drawn between the effect of the solvent on metal extraction equilibria and on the dimerization and distribution of HA (DBP) itself.

For practical separation of Eu and Am, *n*-hexane, CCl_4 and $CHCl_3$ are the best of the solvents studied; for given concentrations of HA and H^+, *n*-hexane and CCl_4 give the highest distribution ratio.

The use of dialkyl phosphates $(RO)_2P_2OH$ in solvent extraction for trivalent lanthanide and actinide ions has been reported by Peppard *et al.* [1-4], Dyrssen [5], Scadden and Ballou [6].

The aim of the present investigation was to study the influence of various organic solvents on the extraction of Am^{3+} and Eu^{3+} ions from a 0.1 M HNO_3 solution with DBP as complexing agent. The following organic solvents have been used: *n*-hexane, $CH_3(CH_2)_4CH_3$, carbon tetrachloride, CCl_4, chloroform, $CHCl_3$, *iso*propyl ether, $(CH_3)_2CHOCH(CH_3)_2$; methyl *iso*butyl ketone (hexone), $(CH_3)_2CHCH_2COCH_3$, tri-*n*-butyl phosphate, $(n\text{-}C_4H_9O)_3PO$, and methyl *iso*butyl carbinol (hexol), $(CH_3)_4CHCH_2CH(OH)CH_3$.

To explain the results one must take into account the extent of dimerization of DBP in the organic solvents. A separate investigation was carried out to study the distribution behaviour of DBP between the above mentioned organic solvents and an aqueous 0.1 M HNO_3 solution, the results of which are reported in the previous article [7].

EXPERIMENTAL

Reagents: The DBP, $(n\text{-}C_4H_9O)_2PO_2H$, kindly supplied by Albright and Wilson Ltd., London, was purified as described in the previous paper [7].

The β-active nuclide (13 and 16 years) $^{152, 154}$Eu and the α-active 458 years ^{241}Am were obtained from Harwell, England. No carrier was added to the solutions; but the initial concentration of Eu in the 0.1 M HNO_3 solution was about 2×10^{-5} M; the initial concentration of ^{241}Am was calculated as 8×10^{-7} M.

The 0.1 M HNO_3 solution was prepared from analytical grade reagent. The NH_3 solution, used for increasing the pH of the solution in the experiments with hexol, was also of analytical grade.

Distribution measurements: Equal volumes (5 ml) of a solution of DBP in an organic solvent and a 0.1 M HNO_3 solution containing Am and Eu were shaken for 24 h. The two liquid phases were separated by means of centrifugation. All experiments were carried out in a thermostated room at 25.0 ± 0.3°C. From each phase a 0.1 ml volume was pipetted, evaporated to dryness and then heated at 250°C to decompose the remaining organic substances. The activity measurements were carried out in a Tracerlab SC-16 windowless proportional counter. The α-activity was measured at 1 450 V and 10 mV sensitivity and the β-activity at 1 700 V, 1 mV sensitivity and using an Al absorber of 6.2 mg/cm² thickness. Corrections were made for background; in β-activity measurements correction was also made for γ-activity background from Am.

Measurements of the hydrogen ion concentration, when NH_3 was added, were carried out with a Radiometer pHM3i valve potentiometer, equipped with a Radiometer glass electrode G 100 and a calomel electrode K 100. The electrodes were standardized against 0.01 M $HClO_4$ + 0.09 M $NaClO_4$ (-log $[H^+]$ = 2.00). The constants used for the calculations of $[H_2A_2]_{org}$, $[HA]_{org}$, [HA] and $[A^-]$ (ionic medium = 0.1 M HNO_3) are given in the previous article [7].

Symbols and formulas

[ ]	concentrations in the aqueous phase
$[\ ]_{org}$	concentrations in the organic phase
C_A	initial total concentration of DBP in the organic phase
C_{org}; C_{aq}	equilibrium total concentrations of DBP in each phase
HA	di-*n*-butylphosphate (DBP), $(n\text{-}C_4H_9O)_2PO_2H$
K_a (eqn. 3)	stoichiometric acid dissociation constant
K_d (eqn. 1)	distribution constant for HA
K_2 (eqn. 2)	dimerization constant in the organic phase
M	Am or Eu
q_M	net distribution ratio of M (org/aq)

RESULTS AND DISCUSSION

Conclusions about the extractable species

The experimental data obtained with our seven solvents are listed in Tables 1 and 2. The primary data are C_A, the total (analytical) concentration

Table 1. The distribution of Eu and Am between solutions of DBP in different organic diluents and 0.1 M HNO_3 at 25°C.

	log C_A	log [HA]	log q_{Eu}	log q_{Am}
n-Hexane	−0.283	−1.67	> +2.4	+2.351
	−0.313	−1.74	> +2.4	+2.921
	−0.494	−1.76	> +2.4	+2.442
	−0.505	−1.70	> +2.4	+1.901
	−0.711	−1.79	> +2.4	+2.178
	−1.012	−1.88	+2.327	+1.373
	−1.313	−2.01	+1.425	+0.394
	−1.535	−2.16	+0.677	−0.590
	−1.710	−2.27	+0.058	−1.301
	−2.013	−2.49	−1.173	−2.499
	−2.284	−2.62	< −2.5	−3.316
Carbon tetrachloride	−0.301	−2.10	> +2.5	+2.108
	−0.699	−2.31	> +2.5	+1.341
	−1.000	−2.48	+1.806	+0.462
	−1.301	−2.64	+0.818	−0.619
	−1.523	−2.76	+0.188	−1.178
	−1.724	−2.87	−0.421	−1.851
	−2.000	−3.02	−1.205	−2.292
	−2.301	−3.18	−2.203	−3.367
	−2.523	−3.31	< −3.2	< −3.5
	−3.000	−3.61	< −3.5	< −3.5
Chloroform				
	−0.317	−2.86	+2.075	+0.745
	−0.714	−3.06	+0.902	−0.372
	−1.016	−3.22	+0.044	−1.369
	−1.317	−3.37	−0.866	−2.254
	−1.547	−3.49	−1.508	−2.771
	−1.724	−3.57	−2.080	−3.264
*Iso*propyl ether	−0.307	−2.00	+2.541	+1.598
	−0.705	−2.19	+1.616	+0.548
	−1.006	−2.35	+0.661	−0.441
	−1.307	−2.54	−0.250	−1.449
	−1.705	−2.79	−1.589	−2.819
	−2.006	−2.99	−2.577	−3.485
Hexone (methyl *iso*butyl ketone)	−0.304	−2.30	+1.267	+0.284
	−0.401	−2.35	+0.989	+0.097
	−0.577	−2.46	+0.481	−0.470
	−0.702	−2.53	+0.047	−1.054
	−0.799	−2.59	−0.143	−1.102
	−0.906	−2.67	−0.991	−1.988
	−1.100	−2.79	−1.000	−2.000
Tri-*n*-butyl phosphate (TBP)	−0.301	−2.45	+0.143	−0.338
	−0.321	−2.47	+0.125	−0.481
	−0.418	−2.54	−0.158	−0.562
	−0.542	−2.64	−0.554	−1.068
	−0.719	−2.78	−0.782	−1.059
	−1.301	−3.30	−2.025	−2.079
	−1.398	−3.39	−2.353	−2.230
	−1.699	−3.68	−2.312	−2.473
	−2.000	−3.98	−2.299	−2.486

Table 2. The distribution of Eu and Am between solutions of DBP in hexol (methyl *iso*butyl carbinol) and 0.1 M $(H,NH_4)NO_3$ at 25°C.

log C_A	-log [H+]	log [HA]	log q_{Eu}	log q_{Am}
−0.306	1.895	−2.530	+1.630	+1.093
−0.481	1.000	−2.686	−1.700	−1.891
−0.514	1.000	−2.719	−1.636	−2.076
−0.560	1.376	−2.769	−1.110	−1.436
−0.657	1.000	−2.862	−2.636	−2.698
−0.704	2.107	−2.940	+0.473	−0.096
−0.958	1.376	−3.167	−2.575	−2.744
−1.007	2.206	−3.246	−0.378	−0.866
−1.306	2.262	−3.556	−1.058	−1.554
−1.536	2.359	−3.799	−1.616	−2.043
−1.703	2.362	−3.964	−2.042	−2.392

of HA in the organic phase at the start, and q_M, the distribution ratio of the metal between organic and aqueous phase. From previous work [7], the following equilibrium constants are known:

$$K_d = [HA]_{org}[HA]^{-1}; K_2 = [H_2A_2]_{org}[HA]_{org}^{-2}; K_a = [H^+][A^-][HA]^{-1} \quad (1—3)$$

The total concentration of M is so low that the amount of A bound by M can always be neglected and since the volumes of the aqueous and organic phases are equal, we have

$$C_A = 2[H_2A_2]_{org} + [HA]_{org} + [HA] + [A^-] \quad (4)$$

Inserting $[H^+]$ and the equilibrium constants from the previous paper [7], we may then find the concentrations of the various species for each C_A. At $C_A > 0.06$ M for hexane eqn (4) cannot be used since HA is further polymerized; [HA] and $[A^-]$ can, however, be determined from the distribution curve of DBP [7].

We can now proceed to discuss the formulas of the M-containing species. For the five solvents, *hexane*, *carbon tetrachloride*, *chloroform*, *isopropyl ether* and *hexone*, practically rectilinear plots are obtained if log $q_M [A^-]^{-3}$ is plotted as a function of log [HA] (Figs 1—5). In all cases, the slope is practically equal to 3 (straight lines in Figs 1—5). It thus seems likely that the same reaction predominates in all these solvents. At these low concentrations it seems practically certain that the metal atoms exist as a mononuclear species; it should be noticed that the metal concentration in each phase has been varied by a factor of at least 100 which would be expected to cause deviations from linearity if polynuclear complexes had been important.

Moreover, we may assume that the species in aqueous solution is M^{3+}, *i.e.* Eu^{3+} or Am^{3+}. In the various equilibrium mixtures, the concentration [HA] in the aqueous phase has varied from $10^{-2.0}$ to $10^{-3.6}$, and one would have expected bent curves, if several species had been present in the aqueous phase.

Granted that the metals exist as M^{3+} in the aqueous phase, and that q_M is proportional to $[A^-]^3$ and $[HA]^3$, the following reaction is indicated:

$$M^{3+} + 3A^- + 3\ HA \rightleftharpoons MA_3(HA)_3(org) \quad (5)$$

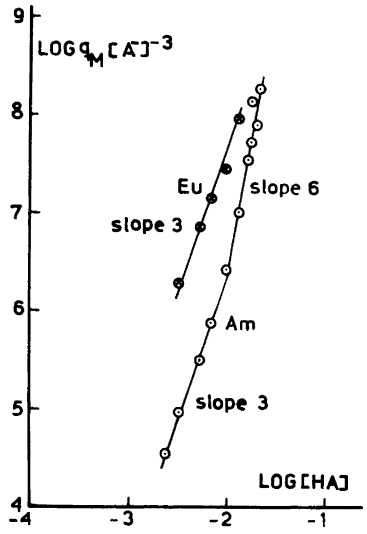

Fig. 1. DBP-hexane: Variation of q_M $[A^-]^{-3}$ with [HA] for the extraction of Eu and Am from 0.1 M HNO_3. The distribution data are given in Table 1. The slope of the straight lines is 3.

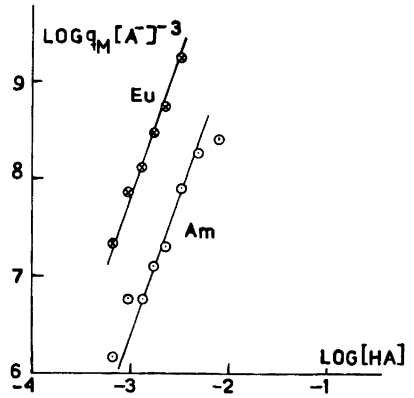

Fig. 2. DBP—CCl_4: Variation of q_M $[A^-]^{-3}$ with [HA] for the extraction of Eu and Am from 0.1 M HNO_3. The distribution data are given in Table 1. The slope of the straight lines is 3.

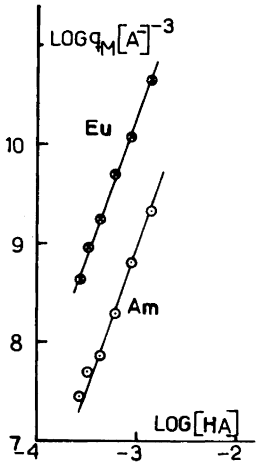

Fig. 3. DBP—$CHCl_3$: Variation of q_M $[A^-]^{-3}$ with [HA] for the extraction of Eu and Am from 0.1 M HNO_3. The distribution data are given in Table 1. The slope of the straight lines is 3.

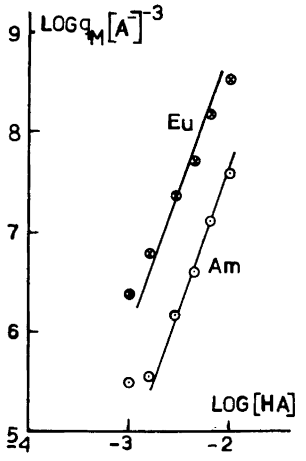

Fig. 4. DBP-*iso*propyl ether: Variation of q_M $[A^-]^{-3}$ with [HA] for the extraction of Eu and Am from 0.1 M HNO_3. The distribution data are given in Table 1. The slope of the straight lines is 3.

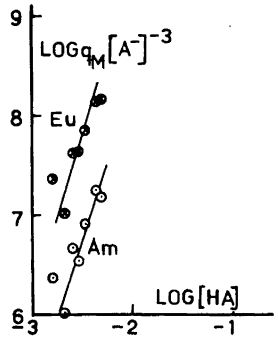

Fig. 5. DBP-hexone: Variation of $q_M\,[A^-]^{-3}$ with [HA] for the extraction of Eu and Am from 0.1 M HNO_3. The distribution data are given in Table 1. The slope of the straight lines is 3.

Since the concentration of HNO_3 is kept constant it is not possible to preclude the possibility that M^{3+} is extracted as a complex also containing HNO_3, *e.g.* $M(NO_3)_3(H_2A_2)_3$. However, since the concentration of HNO_3 is fairly low (0.1 M) it seems probable that nitrate complexes of M may be neglected in the organic phase except when TBP is used as a diluent (see below).

The equilibrium constant for this reaction is easily obtained from the plots:

$$\log K = \log [MA_3(HA)_3]_{org} - \log [M^{3+}] - 3 \log [A^-] - 3 \log [HA] = \\ = \log q_M - 3 \log [A^-] - 3 \log [HA] \qquad (6)$$

The following values for log K were found from Figs 1—5:

In hexane: 13.66 (Eu), 12.38 (Am); in CCl_4: 16.80 (Eu), 15.33 (Am); in $CHCl_3$: 19.33 (Eu), 17.98 (Am); in *iso*propyl ether: 14.94 (Eu), 13.72 (Am); in hexone: 15.22 (Eu), 14.25 (Am).

The large values of K for chloroform suggest that this solvent is more active than the other solvents which might possibly be due to hydrogen bond formation between the H atom in $CHCl_3$ and the PO groups in DBP (*cf.* Ref.[7]).

For *hexane*, the distribution experiments [7] with pure DBP indicated polymers higher than dimers at $C_A > 0.06$ M. It seems as if this polymerization

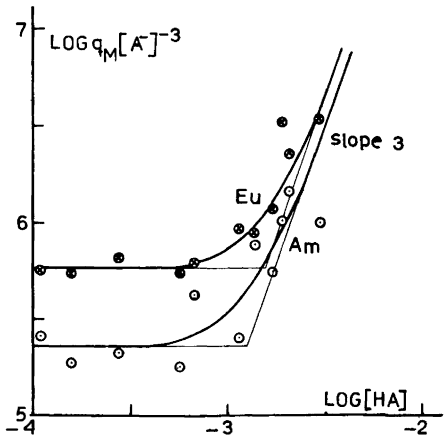

Fig. 6. DBP-hexol: Variation of $q_M\,[A^-]^{-3}$ with [HA] for the extraction of Eu and Am from 0.1 M HNO_3. The distribution data are given in Table 2. The curves are drawn assuming the complexes MA_3 and $MA_3(HA)_3$ in the organic phase (normalized curve: log $(1 + x^3)$ *versus* log x).

affects the distribution of Am; a complex $MA_3(HA)_{\sim 6}$ is indicated in Fig. 1. For Eu, log q is too high to be measured in the region where the corresponding complex could be formed.

For *hexol*, DBP is practically not dimerized in the organic phase. The value of K_d is also fairly large (= 162) and thus $C_A \simeq [HA]_{org}$. The extraction from $[H^+] = 0.1$ was rather low, so experiments were also performed with lower $[H^+]$, see Table 2. Assuming that MA_3 reacts with a certain number of HA's in the organic phase to form an uncharged complex $MA_3(HA)_n$ it is reasonable to plot log $q_M[A^-]^{-3}$ as a function of log [HA] (or log $[HA]_{org}$) as before. The experimental points in Fig. 6 are seen to fall roughly on single curves; there is no indication of a dependence on $[H^+]$ as would be the case if there were complexes other than $MA_3(HA)_n$, *e.g.* $M(NO_3)_3(HA)_3$. The approximate constancy at low C_M indicates that the complex MA_3(org) is formed at low [HA]; one might expect HA to be added stepwise, but the accuracy certainly is insufficient for a detail treatment. Since the slopes tend towards 3, and the species $MA_3(HA)_3$ are indicated by work in other solvents, an attempt was made to describe the data as an approximation, neglecting all reactions except

$M^{3+} + 3\,A^- \rightleftharpoons MA_3$(org) and
$M^{3+} + 3\,A^- + 3\,HA \rightleftharpoons MA_3(HA)_3$(org)

By the usual technique of curve-fitting [8] the equilibrium constants (log K) were found from Fig. 6 to be: for the first reaction + 5.76 (Eu) and + 5.36 (Am); for the second reaction + 14.15 (Eu), + 14.02 (Am).

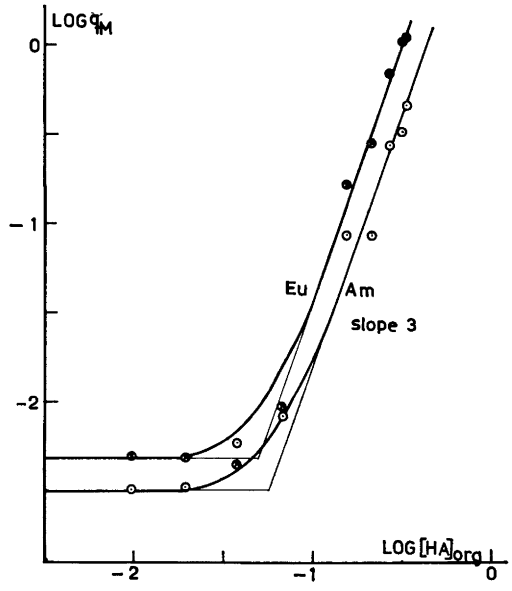

Fig. 7. DBP—TBP: Variation of the net distribution ratio with [HA] org for the extraction of Eu and Am from 0.1 M HNO_3. The distribution data are given in Table 1. The curves are drawn assuming the presence of $M(NO_3)_3$ and MA_3 in the TBP phase (normalized curve: log $(1 + x^3)$ *versus* log x).

Whereas the first values seem to be reliable within $\pm$ 0.1, the second constant is only intended as a very crude approximation, which may be used for approximate calculations but does not satisfactorily describe the real process, which is probably stepwise. A similar curve was previously obtained for the UO_2^{2+}-DBP-hexone system [12].

In *tributyl phosphate* (TBP) also, HA mostly exists as single molecules, HA(org), which are, however, associated with TBP [7]. A plot of log q_M *versus* log $[HA]_{org}$ indicated that q_M approaches a limiting value as $[HA]_{org}$ decreases (Fig. 7). This should correspond to the reaction already studied by McKay *et al.*[9–11]

$$M^{3+} + 3\,NO_3^- + 3\,TBP(org) \rightleftharpoons M(NO_3)_3(TBP)_3(org)$$

The present experiments, where $[TBP]_{org}$ and $[NO]_3^-$ were kept constant, do not give the composition of the complex.

For $[HA]_{org} > 10^{-1.7}$ M, q_M increases with $[HA]_{org}$, which indicates that complexes with A are formed. The limiting slope would correspond to MA_3 (org). The process is probably stepwise but the data suffice only to get approximate values for the total reaction. These were also found by curve-fitting:

$$M^+ + 3\,HA(org) \rightleftharpoons MA_3(org) + 3\,H^+;\ \log K = -1.44\ (Eu),\ -1.81\ (Am)$$

or

$$M^{3+} + 3\,A^- \rightleftharpoons MA_3(org);\ \log K = 7.49\ (Eu),\ 6.98\ (Am)$$

These values are those obtained from the plot of log q_M versus log $[HA]_{org}$. The normalized curves are of the type log $(1 + x^3)$ *versus* log x. The extracted complex may be $MA_3(TBP)_3$, but this can only be proved by variation of the TBP concentration.

Conclusions about the effect of the solvent on the net distribution of Eu and Am

It may be seen from Table 3 and Fig. 8 that for a given total concentration, of DBP ($C_A = 0.1$ M) and acidity ($[H^+] = 0.1$ M) the highest value of q_{Eu} is obtained with *n*-hexane and carbon tetrachloride. The extraction is very poor

Table 3. Summary of the results derived from Tables 1 and 2 for $C_A = 0.1$ M and $[H^+] = 0.1$ M. The net distribution ratio of DBP is derived from data reported in the previous paper [7].

Solvent	log q_{Eu}	log q_{Am}	Δlog q_{Eu-Am}	log q_A
n-Hexane	+2.60	+1.40	1.23	+0.48
CCl_4	+1.81	+0.46	1.30	+1.11
$CHCl_3$	+0.09	−1.27	1.36	+1.87
*Iso*propyl ether	+0.66	−0.44	1.10	+1.02
Hexone	−0.75	−1.81	1.05	+1.42
TBP	−1.78	−2.08	0.46	+1.73
Hexol	−3.34	−3.64	0.33	+1.91

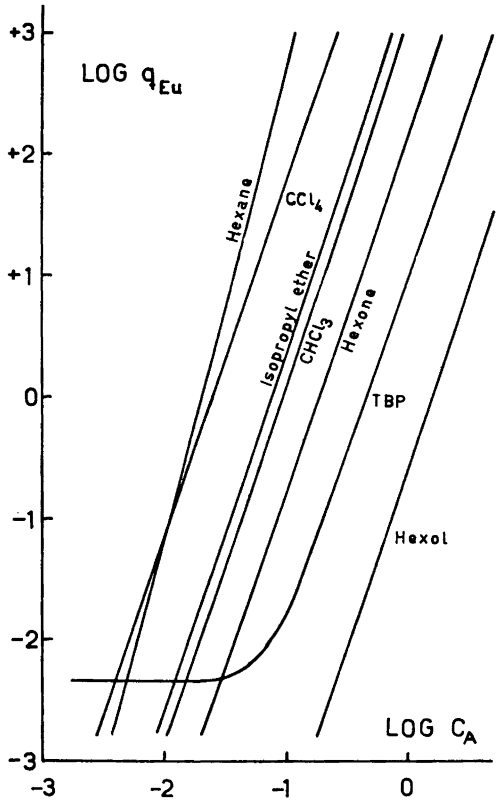

Fig. 8. The distribution of Eu for various organic solvents as a function of the initial concentration of DBP in the organic phase. The aqueous phase was 0.1 M HNO_3 and the volumes of the two phases were equal. Data are given in Tables 1 and 2.

with TBP and hexol. Similar experience has been made with the UO_2^{2+}-dioctyl phosphate and Ca^{2+}-dibutyl phosphate systems (*cf.* Table 4).

In general the order of increasing capacity to extract Eu^{3+} (and Am^{3+}) is that of decreasing value of K_d (*cf.* Table 2 in the previous paper [7]), the distribution constant of DBP monomer, or decreasing solubility of water in the organic solvent (*cf*, Table 4, Ref.[7]). It was pointed out in the previous paper [7] that an increase in K_d was probably due to the formation of a 1 : 1 complex between the DBP monomer, HA, and the solvent molecule. Such a reaction therefore seems to repress the metal extraction. In the case where the metal ion has been extracted from an aqueous phase with DBP in an inert solvent, *e.g.* CCl_4, back extraction into an aqueous layer should then be considerably facilitated by addition of *e.g.*, hexol to the organic layer. This has in fact been utilized by Dyrssen and Ekberg [13] for the preparation of carrier-free ^{90}Y. With the uranyl ion, however, neutral phosphorylated reagents might enter into the coordination sphere, and thus enhance the extraction in spite of any complex formation with the dialkyl phosphate.[17]

Table 4. Influence of the diluent for the UO_2^{2+}-dioctyl phosphate system [14] (initial aq.phase: 0.004 M U(VI) in 0.5 M SO_4^{2-}, pH 1.1) and the Ca^{2+}-dibutyl phosphate system [15] (initial aq.phase: trace quantities of $CaCl_2$ labelled with ^{45}Ca).

Diluent	Distribution ratio	
	UO_2^{2+} — DOP	Ca^{2+} — DBP
Kerosene	135	0.49
Hexane	110	1.13
*Cyclo*hexane	—	1.16
Carbon tetrachloride	20	0.28
*Iso*propyl ether	17	0.121
Benzene	13	0.074
Chloroform	3	0.071
Hexone	—	0.037
*Cyclo*hexanone	—	0.015
*Iso*amyl acetate	—	0.030
2-Ethyl hexanol	0.1	—
Octanol-2	0.08	—
Hexol	—	0.0039

Another factor to consider in choosing a suitable solvent is the distribution of DBP itself. As pointed cut in the previous paper [7], q_A varies considerably with the total concentration of DBP (*cf.* Fig. 1 in Ref.[7]); the values in Table 3 show, however, that for hexane, CCl_4 and *iso*propyl ether considerable amounts of DBP are "lost" in aqueous phase. This could be reduced by using a compound with more carbon atoms, *e.g.* dioctyl phosphate.

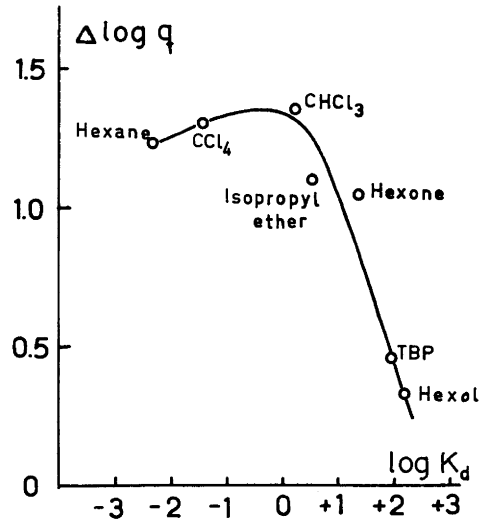

Fig. 9. The difference in distribution ratio q between Eu and Am at $C_A = 0.1$ M for various organic solvents as a function of the distribution constant K_d for the DBP monomer. Aq. phase: 0.1 M HNO_3.

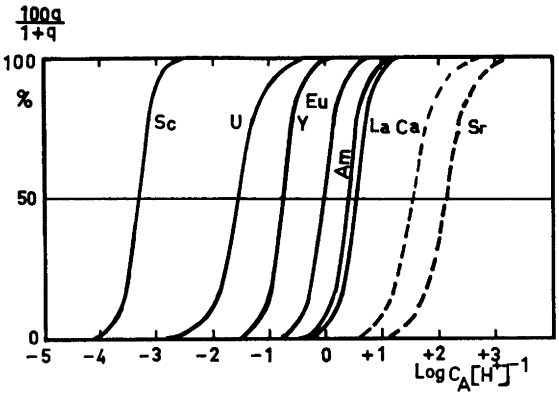

Fig. 10. Curves showing the percentage extraction with DBP—$CHCl_3$ of Sc(III), U(VI), Y(III), Eu(III), Am(III), La(III), Ca(II), and Sr(II) as a function of log $C_A[H^+]^{-1}$. The curves for Ca and Sr are based on very few data.

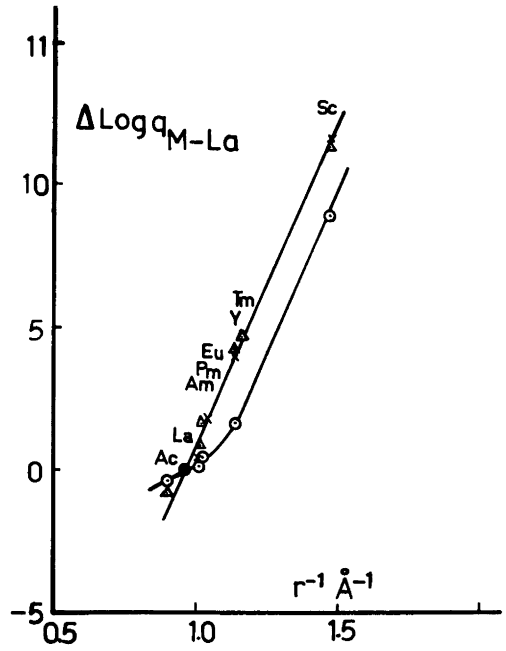

Fig. 11. The difference in distribution ratio, q, between trivalent metal ions and La(III) as a function of the inverted value of the ionic crystal ratio r, according to Zachriasen. Solvent extraction systems: × DBP—$CHCl_3$ reported here, △ Dioctyl phosphate-toluene and O dioctylphenyl phosphate-toluene by Peppard *et al.*[4]

The separation of Eu^{3+} and Am^{3+} may be expressed as $\Delta \log q$. In Table 3 values of $-\log q$ at $C_A = 0.1$ M are given for the various solvents. These data are plotted in Fig. 9 against $\log K_d$. It may be seen that the inert solvents, hexane, CCl_4 and $CHCl_3$ give the best separation.

Throughout our experiments with DBP Eu^{3+} is better extracted than Am^{3+}. This is the order that could be expected from the values of the crystal ionic radii, $r = 0.96$ Å (Eu^{3+}) and $r = 0.99$ Å (Am^{3+}). Fig. 10 summarizes data for other metal ions taken from a FOA-report (not available) by Carlsson, Dyrssen, and Johansson. The order of extraction is generally the same as the order of ionic potential, Nr^{-1}. For three-valent ions there seems to be a straight line relationship between $\Delta \log q_{M-La}$ and $1/r$ (Fig. 11). Similar values of $\Delta \log q$ were found by Peppard *et al.*[4] for dioctyl phosphate in toluene. However, with a dioctylphenyl derivative a different relationship is obtained; it seems as if this rather large complexing agent cannot differentiate very well between the larger tri-valent ions; this might be due to micelle formation. It has been shown by Dyrssen [16] that such a straight line relationship as with DBP and DOP is not obtained with the chelating agent *β-iso*propyl tropolone. Furthermore, with this compound Eu^{3+} is not better extracted than Am^{3+} into chloroform.

The authors wish to thank the head of the institution, Professor Lars Gunnar Sillén, for valuable discussions. The investigation has been supported by *Statens råd för atomforskning (Swedish Council for Atomic Research)*. The English has been revised by Dr. Helen S. Dunsmore.

REFERENCES

1. Peppard, D. F., Mason, G. W., Maier, J. C. and Driscoll, W. *J. Inorg. & Nuclear Chem.* **4** (1957) 344.
2. Peppard, D. F., Mason, G. W. and Moline, S. W. *J. Inorg. & Nuclear Chem.* **5** (1957) 141.
3. Peppard, D. F., Ferraro, J. R. and Mason, G. W. *J. Inorg. & Nuclear Chem.* **4** (1957) 371.
4. Peppard, D. F., Mason, G. W., Driscoll, W. J. and Sironen, R. J. *J. Inorg. & Nuclear Chem.* **7** (1958) 276.
5. Dyrssen, D. *Acta Chem. Scand.* **11** (1957) 1277.
6. Scadden, E. M. and Ballou, N. E. *Anal. Chem.* **25** (1953) 1602.
7. Dyrssen, D. and Liem, D. H. *Acta Chem. Scand.* **14** (1960) 1091.
8. Sillén, L. G. *Acta Chem. Scand.* **10** (1956) 186.
9. Healy, T. V. and McKay, H. A. C. *Rec. trav. chim.* **75** (1956) 730.
10. McKay, H. A. C. and Healy, T. V. *Progress in Nuclear Energy* — series III, vol. 2, Process Chemistry, Pergamon Press, 1958, p. 546.
11. Hesford, E. and McKay, H. A. C. *Trans. Faraday Soc. 54* (1958) 573; *J. Inorg. & Nuclear Chem.* **9** (1959) 279.
12. Dyrssen, D. and Krašovec, F. *Acta Chem. Scand.* **13** (1959) 561.
13. Dyrssen, D. and Ekberg, S. *Acta Chem. Scand.* **13** (1959) 1909.
14. Blake, C. A., Brown, K. B. and Coleman, C. F. *ORNL-1903*, Oak Ridge, 1958.
15. Dahlberg, V. and Dyrssen, D. *Unpublished work.*
16. Dyrssen, D. *Intern. Conf. on Coordination Chem.*, London 1959, *To be published.*
17. Dyrssen, D. and Kuča, L. *Acta Chem. Scand* **14** (1960) *In the press.*

Received February 2, 1960.

ACTA CHEMICA SCANDINAVICA 14 (1960) 1112—1117

Oxide Chlorides and Organometalloid Oxides as Donor Molecules

INGVAR LINDQVIST

Institute of Chemistry, University of Uppsala, Uppsala, Sweden

A model of an idealized structure has been suggested, which can be used for the discussion of adducts of oxide chlorides and organometalloid oxides. No safe distinction between single and double bond structures can be made with the experimental data available at present. The results show, however, the importance of inductive effects in donor-acceptor reactions, and some predictions can be made about other adducts than those studied.

In an earlier paper [1] it was pointed out that the semipolar formulation of the donor-acceptor bond is misleading in most addition compounds. In the compounds which in the preceding paper [1] were formally described as addition compounds with oxygen atoms, the formulation is more appropriate, although not at all necessary. The typical example is amine oxide R_3NO, which is written $R_3N^+O^-$ in the semipolar formulation. In this case, the formal charges on the atoms really indicate a strongly increased heteropolar interaction in the N—O bond (while the R—N bond is weakened). There is no possibility of double bond formation in the amine oxides, and the picture of the bond as a covalent bond with strong additional ionic attraction is obvious. In phosphine oxides on the other hand, the possibility of double bond formation cannot be excluded, and the formulation $R_3P{=}O$ has been advanced as more accurate than $R_3P^+O^-$.

In this paper, this question will be discussed together with the inductive effects of donor-acceptor reactions involving the above-mentioned donors. The available structural information will be used, and the compound $SbCl_5$ ($OPCl_3$) will be taken as an example for the discussion.

THE IDEALIZED STRUCTURE

First it is assumed that the single bond structure is correct; the P—O bond is considered as a donor-acceptor bond. The bond picture of the adduct will then be Cl_3P—O—$SbCl_5$ with strong primary inductive effects due to the formation of the donor-acceptor bonds P—O and Sb—O.

Because of the difficulty of making direct comparisons of the measured bond lengths with predicted values, an idealized charge distribution must first be assumed, for which at least some predictions can be made. The deviations of the actual charge distribution from the idealized one are then estimated and the inductive effects on the bond lengths are predicted in a way suggested in the preceding paper [1]. Finally a comparison is made with the experimental results.

The idealized charge distribution selected for this purpose is the following: The *charge distribution in the bond system Cl—P—O* is assumed to be *the same as if the adduct molecule had a perfectly symmetrical distribution around the oxygen atom* (the fictive ion $Cl_3POPCl_3^{2+}$). A similar assumption is made for the O—Sb—Cl bond system (the fictive ion $Cl_5SbOSbCl_5^{2-}$). The bond lengths P—Cl and P—O are then only influenced by the effective electronegativity differences between P and Cl and O, respectively, and the bond lengths Sb—Cl and Sb—O only by the electronegativity differences between Sb and Cl and O.

The difference between the bond lengths to the chlorine and oxygen atoms: $|P—Cl| - |P—O|$ and $|Sb—Cl| - |Sb—O|$ can rather safely be assumed to have almost equal values because the difference in electronegativity between P and Sb is not very large. If the Shomaker-Stevenson formula $r_{AB} = r_A + r_B + 0.09\,|x_A - x_B|$ were valid, the differences should always have a constant value independant of the atoms bonded to Cl and O, but this is probably too far-going a simplification.

The value of this "reference difference" must be larger than the difference between the atomic radii of chlorine and oxygen, 0.25 Å. The Shomaker-Stevenson formula predicts a value of 0.30 Å, but it generally underestimates the bond contraction as shown by comparison with the difference between the recommended [2] C—Cl and C—O bond lengths which is 0.34 Å. The slightly arbitrary assumption is here introduced that the *reference difference* in adduct molecules with symmetrical arrangement around the central atoms (tetrahedron around P and octahedron around Sb in the example) is independent of the nature of the central atoms and has a value of 0.32 ± 0.02 Å.

This is the most arbitrary assumption introduced so far in these discussions and its limitations must be kept in mind.

THE ACTUAL STRUCTURE

The deviations from the idealized charge distribution in the actual molecule can be discussed as a substitution effect. The P—Cl and P—O bonds are influenced by the fictive substitution of $SbCl_5$ for PCl_3^{2+}. As the electronegativity of P is higher than of Sb, and furthermore a positive charge is placed on the PCl_3 group, it can safely be assumed that the effective electronegativity of the PCl_3^{2+} group is larger than that of $SbCl_5$. Electrons are thus released to the bridging oxygen atom at the substitution. This is the primary effect. As the net charge on P in $POCl_3$ is positive and the heteropolarity is P → O the electron addition will lead to an increased P—O bond energy (an electron withdrawal would lead to loss of bond energy according to the discussion in Ref. [1]). The secondary effect is a transfer of electrons from oxygen to phospho-

rus and to a smaller extent to chlorine. As the net charge on chlorine is negative and the heteropolarity is P → Cl, the electron addition will decrease the P—Cl bond energy. The P—Cl bond will thus be longer and the P—O bond shorter than in the idealized structure, and the difference | P—Cl | — | P—O | should have a larger value than 0.32 Å.

The Sb—Cl and Sb—O bonds are in the same way influenced by the fictive substitution of PCl_3^{2+} for $SbCl_5$. This corresponds to a transfer of electrons away from oxygen (compared with in the idealized structure): the Sb—O bond will be weaker and longer. The secondary effect is a withdrawal of electrons from Sb and to some extent from chlorine: the Sb—Cl bond will be stronger and shorter. The difference | Sb—Cl | — | Sb—O | should thus be smaller than 0.32 Å.

Because of the mutual character of the fictive substitutions, the effects on the P—O and Sb—O bonds should be very similar, while the effect on Sb—Cl should be slightly smaller than on P—Cl because the secondary inductive effect is transmitted to five atoms from Sb and to only three from P. (Variations in polarizability might also be of importance.) If the secondary effect is low, the deviations from the reference difference, 0.32 Å, should, however, be very similar in magnitude, the deviation being possibly somewhat larger on the donor side ($POCl_3$). The values found [3] in $SbCl_5$ ($OPCl_3$) are (averaged values):

$$|\text{P—Cl}| - |\text{P—O}| - 0.32 \text{ Å} = 0.18 \text{ Å}$$
$$|\text{Sb—Cl}| - |\text{Sb—O}| - 0.32 \text{ Å} = -0.17 \text{ Å}$$

Considering the uncertainty in the reference difference and the experimental bond lengths, the agreement is striking.

An equal or slightly larger effect would be expected in the compound $TiCl_4(OPCl_3)$ (the electronegativity of Ti is a little lower than that of Sb). This is actually a dimeric molecule [4], but the chlorine bridge formation will influence the Ti—Cl bonds (to nonbridging Cl) and the Ti—O bond to the same extent (*cf.* the discussion of halogen bridges in Ref.[1]) and the relation should still be valid. The averaged values in $[TiCl_4(OPCl_3)]_2$ are:

$$|\text{P—Cl}| - |\text{P—O}| - 0.32 = 0.20 \text{ Å}$$
$$|\text{Ti—Cl}| - |\text{Ti—O}| - 0.32 = -0.20 \text{ Å}$$

The assumption of a single bond structure is thus in complete accordance with the experimental evidence available at present. In the next section the consequences of the assumption of a double bond structure will be discussed.

THE DOUBLE BOND PICTURE

The introduction of a double bond giving the bond system Cl—P=O—Sb—Cl is tantamount to an electron tranfer from the oxygen towards the phosphorus atom compared with in the bond system Cl—P—O—Sb—Cl discussed above.

If the double bond exists, the P=O bond must be stronger than the P—O bond: the new homopolar bond energy must be larger than the loss of heteropolar bond energy (or there would not be any double bond). The P—Cl will be weakened, and the difference | P—Cl | — | P—O | will increase further. Likewise the Sb—O bond energy will decrease and the Sb—Cl bond energy increase. The difference | Sb—Cl | — | Sb—O | will be reduced accordingly.

The effect of a double bond will thus run parallel with the inductive effect of the donor-acceptor reaction, and no distinction can be made between the two bond pictures only from these data.

ADDUCTS OF SELENIUM OXYCHLORIDE

The discussion of $SbCl_5(OPCl_3)$ can easily be extended to adducts of $SeOCl_2$. The only structure known at present is that of $SnCl_4(OSeCl_2)_2$. The experimental data for this compound are [5] (averaged values):

$$|\,Se—Cl\,| - |\,Se—O\,| - 0.32 = 0.09 \text{ Å}$$
$$|\,Sn—Cl\,| - |\,Sn—O\,| - 0.32 = -0.06 \text{ Å}$$

This structure is complicated by weak chloride bridge formation between Se and Sn, and the agreement with the predicted effect must be considered as good.

The smaller effect of the donor-acceptor reaction with $SeOCl_2$ is not only reflected in the smaller value of the deviations from the reference differences but also directly in the Sn—O and Sb—O distances. The Sn—O bond length is actually shorter than the Sb—O bond lengths (in the two compounds discussed earlier) although the radius of antimony should be smaller than that of tin. (In all periods the same trend is found near the inert gas end, that the covalent radius decreases with increasing atomic number.)

The reason why the effect is larger for $POCl_3$ than for $SeOCl_2$ will not be discussed in this paper.

EXTENSION TO OTHER ADDUCTS

If the ideas advanced here are correct, some predictions can be made about the effect in other adducts.

Adducts of phosphine oxides might first be compared with adducts of $POCl_3$. The only difference is that the positive net charge on the PCl_3^{2+} group must be larger than on PR_3^{2+}, and the effective electronegativity accordingly higher. The deviations from the reference differences should therefore be larger in the $POCl_3$ than in the POR_3 adducts. The structure of $SbCl_5[OP(CH_3)_3]$ is at present being investigated in order to test this conclusion.

A comparison between adducts of amine and phosphine oxides would be quite different. It is true that the inductive effect must be largest for the amine oxide if only single bond structures are compared, but two complicating factors must be considered. One is the fact that the heteropolarities of the bonds to carbon are different, N ← C and P → C. The net charge on carbon

is therefore positive in the amine oxide and negative in the phosphine oxide. The secondary effect of the electron addition (compared with in the idealized structure) will thus be a weakening of the P—C bond while the N—C bond energy will be augmented. (Electron addition gives opposite effects to electron withdrawal.) The difference |N—C| — |N—O| is therefore not increased by the effect on the N—C bond and the deviation from the reference difference can be expected to be reduced to some extent. On the other hand there might be a double bond P=O in the phosphine oxides which cannot have a correspondence in the amine oxide. This would increase the deviation from the reference difference for the phosphine oxide adduct.

Both these factors thus work against the larger inductive effect in the single bond structure of the amine oxide adducts and the deviations from the reference difference might very well be larger for the phosphine oxide adducts than for the amine oxide adducts. Part of these difficulties might also be encountered in a comparison of sulfur and selenium compounds such as sulfoxides and selenium oxides. Structure determinations are in progress which probably will give information about these problems.

THE FREE DONOR MOLECULES

The idealized structure can also be used for a discussion of the free donor molecules. The inductive effect of subtracting of PCl_3^{2+} from the idealized structure $Cl_3POPCl_3^{2+}$ must be even larger than at the fictive substitution discussed for donor-acceptor interaction. The difference |P—Cl| — |P—O| — 0.32 Å is actually + 0.23 Å in $POCl_3$, of the order of 0.05 Å larger than in the adducts studied. A corresponding comparison cannot be made for $SeOCl_2$ because its structure is not known, but a study is in progress.

The discussion of the adducts of amine and phosphine oxides in the preceding section can obviously be directly applied to the free donor molecules. The reference differences |N—C| — |N—O| and |P—C| — |P—O| are 0.12 Å (obtained as described earlier). The assumption that the differences should be equal is doubtful in this case with different heteropolarities in the bonds to carbon, but no other reasonable proposal can be made at present.

The values are:

$$|N—C| — |N—O| — 0.12 = 0.06 \text{ Å (alternative value } -0.07 \text{ Å)}$$
$$|P—C| — |P—O| — 0.12 = 0.21 \text{ Å (Ref. [6])}$$

The larger deviation in the phosphine oxide is not unexpected in view of the preceding discussion. The quite different magnitudes of the two deviations indicates, however, that the phosphine oxide probably contains a double bond P=O: the difference between the single bond structures would be expected to be smaller. This is in agreement with the interpretation of the dipole moment measurements [7]. More structural information is necessary, however, before it can be safely stated that the structural evidence can distinguish between the single and double bond pictures. It would be particularly interesting to

know the S—O bond lengths in adducts of sulfones. A number of such adducts have recently been prepared [8] and the crystal structure determinations have shown that only one of the oxygen atoms functions as a donor atom [9].

CONCLUSION

The preceding discussions indicate that the donor action of oxide halides and organometalloid oxides can be explained, or at least rationalized in a rather simple fashion, if the inductive effects are fully considered in the way proposed. The limitations of the approach must be kept in mind until the experimental evidence is more complete. The arbitrariness of the present paper is obviously greater than in the general discussion of inductive effects in the preceding paper [1], but no other approach seems at present to offer similar possibilities to compare bond length differences in a rather exact way. The future experimental results will show how far this is correct and in which respects the treatment must be modified or amended.

This work has been supported by grants from the *Swedish Natural Science Research Council* and from the *Air Force Office of Scientific Research of the Air Research and Development Command, United States Air Force*, through its European Office under Contract No. AF 61 (052)-43. These grants are gratefully acknowledged.

Finally I wish to thank Professor Hägg for his friendly and encouraging interest and my research students for their active collaboration in the development of these ideas.

REFERENCES

1. Lindqvist, I. *Nova Acta Regiæ Soc. Sci. Upsaliensis (IV)* **17** (1960) No. 11.
2. *Tables of Interatomic Distances*, The Chemical Society, London 1958.
3. Lindqvist, I. and Brändén, C. I. *Acta Cryst.* **12** (1959) 642.
4. Brändén, C. I. and Lindqvist, I. *Acta Chem. Scand.* **14** (1960) 726.
5. Hermodsson, Y. *Acta Cryst.* **13** (1960) 656.
6. Wang, H. K. Forsvarets Forskningsinstitutt, Norge, Intern Rapport IR-K-225.
7. Philips, G. M., Hunter, J. S. and Sutton, L. E. *J. Chem. Soc.* **1945** 154.
8. Lindqvist, I. and Einarsson, P. *Acta Chem. Scand.* **13** (1959) 420.
9. Hansson, A. *Private communication.*

Received February 22, 1960.

ACTA CHEMICA SCANDINAVICA 14 (1960) 1118—1123

A New Method of Degrading Glucose to Xylose and Galactose to Arabinose

OVE KJØLBERG

Universitetets Kjemiske Institutt, Blindern-Oslo, Norway

It has been found that by treatment with periodic acid of such aldohexofuranosides in which the hydroxyl groups at C_2 and C_3 are in *trans*-position, experimental conditions can be established so that the oxidation is restricted to the glycol grouping outside the ring. Formaldehyde is therefore formed, and besides this a monoaldehyde is obtained which by reduction gives an aldopentofuranoside. The method makes it possible to correlate the anomers of the aldohexofuranosides with those of the aldopentofuranosides.

Oxidation of methyl aldohexopyranosides and methyl aldopentofuranosides with periodic acid leads to structurally identical dialdehydes, the optical rotations of which make it possible to correlate the configuration at carbon 1 in the two types of methylosides [1,2]. A marked difference in the oxidation of the two types of methylosides is that the hexopyranosides give formic acid beside the dialdehyde.

On oxidizing a methyl aldohexofuranoside (I) with periodic acid under the same conditions, one would expect the formation of a trialdehyde (II) beside one mole of formaldehyde.

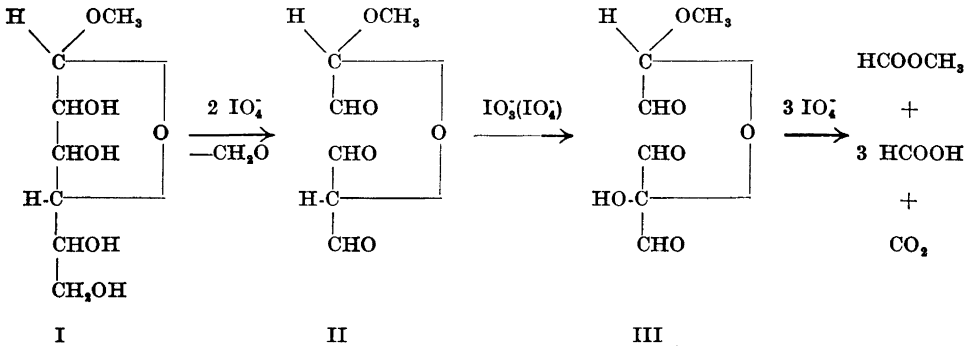

I II III

Experience has, however, shown that the oxidation goes further, and it has been suggested that this is due in the first place to the oxidation of the activated hydrogen atom at C_4 to a hydroxyl group (III). As vicinal hydroxyaldehydes also are easily oxidized by periodic acid [3], the result will be that the whole molecule is disintegrated. Accordingly Hirst *et al.*[4] found that α-methyl-D-mannofuranoside on oxidation gave formaldehyde, formic acid, methyl formate and carbon dioxide. It is therefore not possible to determine the configuration at carbon atom 1 in the aldohexofuranosides in the same way as with the other types of methylosides. On oxidation of α-methyl-D-mannofuranoside and β-ethyl-D-galactofuranoside with lead tetraacetate, Criegee [5] found that in the mannofuranoside the link between C_2 and C_3 was split up first, while in the galactofuranoside the link between C_5 and C_6 was cleaved more easily than that between C_2 and C_3. He meant that the reason for this was that with *cis*-configuration a ring-glycol is attacked more easily by lead tetraacetate than a glycol in which there is free rotation between the carbon atoms, and that the latter glycol is attacked easier than a ring-glycol with *trans*-configuration. Later Price and Knell [6] and Hudson [7] have found that the same is the case on oxidation with periodic acid.

In the present investigation these experiences have been verified. It was further found that starting with galacto- or glucofuranosides in which the configuration at C_2—C_3 is *trans*, the oxidation by lowering the temperature could be localized mainly to the C_5—C_6 position. The oxidation accordingly proceeded as shown in formulae IV—V and VII—VIII. When the temperature during the oxidation was kept at about + 5° each mole of furanoside on consuming one mole of periodic acid gave one mole formaldehyde. After removing iodate and periodate with lead dithionate as described by O'Dea and Gibbons [8], the formaldehyde was determined colorimetrically by means of chromotropic acid according to Eergiwe [9]. During the oxidation the rotation at first changed rapidly, but after one mole periodic acid had been consumed it became practically constant. The oxidation could therefore be followed in a polarimeter. At the appropriate time the oxidation was stopped by addition of barium hydroxide and the C_5-aldehyde isolated as a colourless syrup. Reduction of the aldehyde group would lead to methyl pentofuranoside as shown in the formulae VI and IX. This method therefore represents a degradation of glucose and galactose to xylose and arabinose, respectively.

Sodium borohydride was used as a reducing agent. Experimentally it was found that the α- and β-methyl-D-glucofuranosides gave α- and β-methyl-D-xylofuranosides and that the α- and β-methyl-D-galactofuranosides gave β- and α-methyl-L-arabofuranosides, respectively. The four pentofuranosides were identified by means of paper chromatography. Xylose was also identified by preparing the dibenzylidene derivatives of the dimethyl acetal and comparing it with a sample prepared from authentic xylose. As the glucofuranosides used were slightly impure, the specific rotation of the xylofuranosides prepared from them would not give any proof of their identity and they were not subjected to a more detailed investigation. In the case of the galactofuranosides the specific rotation of the arabofuranosides obtained by degradation (Table 1) agree fairly well with those of the pure substances (—125° and + 118°). The β- and α-methyl-L-arabofuranosides were therefore oxidized

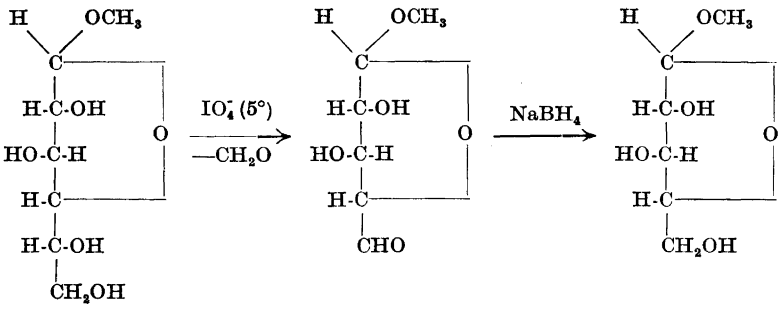

IV α-Methyl-D-glucofuranoside

V

VI α-Methyl-D-xylofuranoside

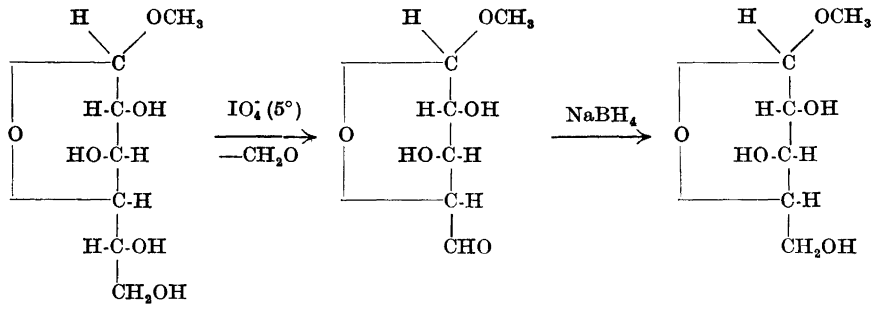

VII α-Methyl-D-galactofuranoside

VIII

IX β-Methyl-L-arabofuranoside

further with periodic acid, giving D'- and L'-methyl-L-hydroxymethyldiglycolaldehyde, respectively. After reduction of these the specific rotation of the enantiomeric diglycols formed were found (Table 1) to be in agreement with the values found before [2,10].

On hydrolyzing the diglycols with mineral acid, methanol, glycerol and glycolaldehyde were obtained. The glycolaldehyde was determined as 2,4-dinitrophenylhydrazone of the *O*-benzoate.

As will be seen this new method of degradation makes it possible to correlate the anomeric aldohexofuranosides to the anomers of the pentofuranosides.

EXPERIMENTAL

β-Methyl-D-galactofuranoside

To a solution of 0.7264 g (3.75 mmole) of the furanoside in water (20 ml) periodic acid (10 ml of 0.430 M solution) was added and the temperature kept at 5°. The optical rotation in a 10 cm tube which was −2.48° after 3 min changed to −2.10° after 25 min and then became constant. The concentration of the monoaldehyde was calculated as 2.00 g in 100 ml and the specific rotation accordingly −105.0°. After 30 min excess of

Table 1. Oxidation of methyl-D-galactofuranosides and methyl-D-glucofuranosides.

Substance	Meth.fur. $[\alpha]_D^{20}$	mole H_5IO_6 per mole furano-side	mole CH_2O per mole furano-side	mono-alde-hyde $[\alpha]_D^{5}$	pento-side $[\alpha]_D^{20}$	mole H_5IO_6 per mole furano-side	dialde-hyde $[\alpha]_D^{20}$	Diglycol $[\alpha]_D^{20}$
β-Meth.-D-galactofur.	−112°	1.06 1.06	1.05 1.02	−105.0° −107.8°	−116.1° −119.7°	1.01 1.01	−116.9° −118.3°	+10°
α-Meth.-D-galactofur.	+104°	1.08	0.99	+102.3°	+114.6°	1.05	+148.8°	−11.1°
β-Meth.-D-glucofur.	−60°	1.11	1.02	−78.5°	−80.3°	—	—	—
α-Meth.-D-glucofur.	+112.5°	1.04	—	+116.2°	+168.2°	—	—	—

periodic acid and the amount of formaldehyde were determined, and after 35 min further oxidation was prevented by adding a hot solution of barium hydroxide until pH 9.5.

Determination of periodic acid: The solution (2 ml) was diluted with water (10 ml) and sodium bicarbonate added until basic reaction. After adding 0.1 g potassium iodide and 5 ml 0.2016 N sodium arsenite the solution was left for 15 min and then titrated with 9.50 ml 0.1015 N KI_3. These data correspond to a consumption of 1.06 mole periodic acid per mole galactoside.

Determination of formaldehyde: The solution (0.3 ml) was neutralized with sodium bicarbonate and diluted with water to 100 ml. To 1 ml of this solution was added 1 ml lead dithionate (2 % in water). After centrifugating, 1 ml of the clear solution was diluted with 9 ml of a solution of 0.25 g chromotropic acid in 250 ml 60 % sulphuric acid. After 30 min the solution was centrifuged and then heated on steam-bath for 40 min. All operations were carried out in darkness. After cooling the absorption at 570 mμ, measured on a Beckmann DU spectrophotometer, was 0.345. As standards of 4.7, 7.1, and 11.8 μg formaldehyde in the same volum showed the absorptions 0.248, 0.413, and 0.680. The absorption 0.345 corresponds to 5.90 μg formaldehyde or 1.05 mole per mole galactofuranoside oxidized.

The isolation of the monoaldehyde was carried out in the same way as described for the dialdehyde by Jackson and Hudson [1]. The monoaldehyde was obtained as a syrup (0.424 g) which was dissolved in water (10 ml) and reduced in the course of one hour by adding 0.1 g sodium borohydride. Excess borohydride was destroyed by bubbling carbon dioxide through the solution until pH 7. After treatment with active carbon α_D in a 10 cm tube was −4.84° and as the concentration of the pentofuranoside was calculated as 4.17 g in 100 ml the specific rotation was −116.1°. In a parallel experiment 0.291 g of β-methyl-D-galactofuranoside gave a monoaldehyde and a pentofuranoside with the specific rotations −107.8° and −119.7°, respectively.

In order to isolate the reduction product, the solution was concentrated at reduced pressure (bath-temperature 35−40°) and the residue dried in a vacuum desiccator above calcium chloride. The residue was shaken with cold anhydrous ethanol (4 times with 10 ml and 3 times with 5 ml) and the ethanolic extract then concentrated *in vacuo*. The resulting syrup was dissolved in water (200 ml) and the solution passed successively through 100 g of Amberlite IR-45 (weak anion exchange type) and 100 g of Amberlite IR-120 (strong cation exchange type). On concentrating the eluate under reduced pressure a pale yellow syrup was obtained which was chromatographed on Whatman paper No. 1 using methyl ethyl ketone as moving phase and *m*-phenylenediamine hydrochloride

(0.6 g in 100 ml 70 % ethanol) as developer. The dominating spot had the same R_F-value as α-methyl-L-arabofuranoside while a smaller spot had the same R_F-value as arabinose.

Oxidation of the pentofuranoside: A solution of the syrupy pentofuranoside in water (10 ml) after treatment with active carbon had $\alpha_D^{20} = -3.34°$ in a 10 cm tube showing that it contained 0.270 g (1.65 mmole) α-methyl-L-arabofuranoside. The solution was mixed with 5 ml 0.430 M periodic acid (2.15 mmole). After 3 h at room temperature α_D^{20} became constant at $-2.12°$ and $[\alpha]_D^{20}$ accordingly $-116.9°$ ($c = 1.77$). In a second experiment was found $-118.3°$. An analysis carried out as described above showed that each mole furanoside had consumed 0.98 mole periodic acid. The dialdehyde was isolated as described for the monoaldehyde and was obtained as a slightly impure syrup (0.140 g) which after dissolving in water (10 ml) was reduced with 0.1 g sodium borohydride. The optical rotation in a 10 cm tube was now found to be $+0.15°$ and as the concentration of the diglycol was calculated as 1.41 g/100 ml the optical rotation was $+10.6°$.

The diglycol was benzoylated and after hydrolyzing the acetal group, the 2,4-dinitrophenylhydrazone of glycolaldehyde-*O*-benzoate was prepared. Recrystallized three times from chloroform-light petroleum, m. p. 187—188°; no depression on mixing with authentic sample. (Found: C 52.24; H 3.68; N 16.41. Calc. for $C_{15}H_{12}O_6N_4$: C 52.38; H 3.55; N 16.20.)

α-Methyl-D-galactofuranoside

The oxidation of this furanoside was performed in the same way as described for β-methyl-D-galactofuranoside. The optical rotation became practically constant in 30 min when $[\alpha]_D$ was $+102.3°$. Analysis showed that each mole furanoside consumed 1.08 mole periodic acid and led to the formation of 0.99 mole formaldehyde. Starting with 0.3188 g of α-methyl-D-galactofuranoside 0.143 g monoaldehyde was obtained which after dissolving in water was reduced by adding 50 mg sodium borohydride. Excess of borohydride was quenched with carbon dioxide and the solution treated with active carbon when it was found that the specific rotation of the pentofuranoside was $+114.6°$. The furanoside was isolated as described above. On a paper chromatogram the main spot had the same R_F-value as β-methyl-L-arabofuranoside. Also in this case a smaller spot with the same R_F-value as arabinose showed that some hydrolysis of the furanoside had taken place.

As a further control the furanoside (0.106 g) was oxidized with periodic acid. Per mole it consumed 1.05 mole periodic acid and the specific rotation of the dialdehyde formed was found to be $+148.8°$. Reduction of the dialdehyde with sodium borohydride led to a diglycol with the specific rotation $-11.1°$.

β-Methyl-D-glucofuranoside

To a solution of 0.3901 g (2.01 mmole) of the slightly impure furanoside (syrup) 10 ml 0.272 M periodic acid was added and the temperature kept at 5°. In 15 min the rotation became practically constant and the specific rotation of the monoaldehyde found to be $-78.5°$. Analysis showed that each mole of the glucofuranoside had consumed 1.11 mole of periodic acid and formed 1.03 mole formaldehyde.

The monoaldehyde (0.195 g) isolated in the usual way was reduced with 0.15 g sodium borohydride and the specific rotation of the reduction product determined to be $-80.3°$. The pentofuranoside was isolated as described for the arabofuranoside, but with the exception that in this case the solution was treated first with the cation exchanger and thereafter with the anion exchanger (Amberlite IR-4B). The result was that more of the furanoside was hydrolyzed and the paper chromatogram showed two spots of nearly equal strength, one with the same R_F-value as β-methyl-D-xylofuranoside and the other with that of xylose. A mixture of ethyl acetate-propanol-water (5:3:2) was used as moving phase.

The presence of xylose was verified in the following way. The pentofuranoside was hydrolyzed in 1 N hydrochloric acid by heating to 100° for 2 h. After removing the acid

by treatment with an ion exchange resin (IR-4B) the solution was concentrated *in vacuo* and the last trace of water removed in a vacuum desiccator above calcium chloride. The residue was dissolved in 4 ml anhydrous methanol containing 0.5 N hydrogen chloride, and 1 ml freshly distilled benzaldehyde was added. After 8 days the dibenzylidene derivative formed was filtered and washed thoroughly first with water and then with cold methanol. Recrystallized from ethyl acetate, m. p. 213.5—214°; no depression on mixing with the dibenzylidene dimethylacetal prepared from D-xylose. (Found: C 67.84; H 6.45; MeO 16.38. Calc. for $C_{21}H_{24}O_6$: C 67.73; H 6.50; MeO 16.65.)

α-Methyl-D-glucofuranoside

The crystalline furanoside, m. p. 61—62° (0.1576 g = 0.81 mmole) dissolved in water (5 ml) was oxidized by adding 3.5 ml 0.272 M periodic acid (0.95 mmole). At 5° the rotation became approximately constant in 20 min when the specific rotation of the monoaldehyde was found to be +116.2°. Analysis showed that each mole furanoside had consumed 1.04 mole periodic acid.

The monoaldehyde (87 mg isolated as above) was reduced with 50 mg sodium borohydride and the specific rotation of the reduction product was found to be +168.2°. Isolated in the usual way the reduction product gave on a paper chromatogram one main spot with the same R_F-value as α-methyl-D-xylofuranoside and a smaller spot showing the presence of xylose.

The author wishes to express his gratitude to Professor Dr. Endre Berner for his kind interest in the work and for many valuable discussions.

REFERENCES

1. Jackson, E. L. and Hudson, C. S. *J. Am. Chem. Soc.* **59** (1937) 994.
2. Berner, E. and Kjølberg, O. *Acta Chem. Scand.* **14** (1960) 909.
3. Clutterbuck, P. W. and Reuter, F. *J. Chem. Soc.* **1935** 1467.
4. Halsall, T. G., Hirst, E. L. and Jones, J. K. N. *J. Chem. Soc.* **1947** 1427.
5. Criegee, R. *Ann.* **495** (1932) 211.
6. Price, C. C. and Knell, M. *J. Am. Chem. Soc.* **64** (1942) 552.
7. Pratt, J. W. Richtmeyer, N. K. and Hudson, C. S. *J. Am. Chem. Soc.* **74** (1952) 2200.
8. O'Dea, J. F. and Gibbons, R. A. *Biochem. J.* **55** (1953) 580.
9. Eergiwe, E. *Z. anal. Chem.* **110** (1937) 22.
10. Smith, F. and Van Cleve, J. W. *J. Am. Chem. Soc.* **77** (1955) 3091.

Received February 1, 1960.

ACTA CHEMICA SCANDINAVICA 14 (1960) 1124—1128

The Solubility of Methane in Hydrocarbons, Alcohols, Water and Other Solvents

AXEL LANNUNG* and J. CHR. GJALDBÆK

The Royal Danish School of Pharmacy, Chem. Laboratory A, Copenhagen, Denmark

The solubility of methane in a series of solvents has been determined. For each solvent used, the values found for the Bunsen absorption coefficients at 18°, 25° and 37°C are, respectively, as follows: *n*-hexane 0.885, 0.869, 0.816; *cyclo*hexane 0.701, 0.675, 0.643; acetone 0.594, 0.564, 0.547; benzene 0.535, 0.523, 0.510; ethanol 0.512, 0.489, 0.455; methanol 0.500, 0.479, 0.446; water 0.0352, 0.0313, 0.0260 and *cyclo*hexanol 0.266 at 25°C and 0.252 at 37°C.

The experimental values obtained are in agreement with values calculated from equations derived on a semiempirical basis, and are compared with values found by other authors.

The experiments presented in this paper have previously been carried out by the first author in the *Chemical Laboratory of the Royal Veterinary and Agricultural College*, Copenhagen.

MATERIALS AND PROCEDURE

Methane was generated from magnesium methyl iodide in a gasometer with airfree water and ethyl ether as blocking liquid; the methane was led slowly through a trap cooled with solid carbon dioxide, dried over concentrated sulphuric acid and phosphorus pentoxide, and condensed in a container cooled with liquid air. The methane was freed from atmospheric air by repeated distillations at a pressure of about 35 mm Hg, the air being pumped out after each distillation. It was finally purified by fractional distillation. The fraction used in the experiments showed by determination of the specific gravity an apparent molecular weight of 16.08 (22.40 l 0°C) in accordance with the corresponding value of the literature.

The solvents used were of the same origin and purity as described in a previous paper [1]. *Normal hexane* was fractionated by distillation of "*n*-Hexan aus Petroleum, Kahlbaum"; the fractions used in the experiments showed boiling point 68.85°C (760 mm) and vapour pressure 154 mm Hg at 25°C. The solubility determinations were carried out as previously described [1].

* Present address: Gentofte Apotek, Copenhagen.

RESULTS

The results of the solubility determinations are shown in Table 1; the calculated mean is considered to be reliable to within 1 %.

Table 2 shows that most of the present solubility determinations are higher than found by other authors; exceptions are the solubility determinations in acetone and benzene. In these solvents the present results are in strict accordance with Horiuti's results.

Table 1. Solubilities of methane expressed as Bunsen absorption coefficients. Experimental values.

Solvent	18°C			25°C			37°C		
	Single determination		Mean	Single determination		Mean	Single determination		Mean
n-Hexane	0.884	0.886	0.885	0.865	0.872	0.869	0.813	0.818	0.816
*Cyclo*hexane	0.702	0.699	0.701	0.677	0.673	0.675	0.645	0.641	0.643
Acetone	0.593	0.594	0.594	0.566	0.562	0.564	0.548	0.546	0.547
Benzene	0.537	0.533	0.535	0.523	0.523	0.523	0.506	0.514	0.510
Ethanol	0.511	0.512	0.512	0.487	0.490	0.489	0.454	0.456	0.455
Methanol	0.500	0.500	0.500	(0.467)	0.479	0.479	0.440	0.451	0.446
*Cyclo*hexanol				0.263	0.268	0.266	0.251	0.253	0.252
Water	0.0350	0.0354	0.0352	0.0315	0.0310	0.0313	0.0259	0.0261	0.0260

Table 2. Solubilities of methane expressed as Ostwald absorption coefficients at 25°C. Comparison with other measurements.

Solvent			Present investigation
n-Hexane	0.584 d)	0.794 g)	0.949
*Cyclo*hexane	0.640 g)		0.737
Acetone	0.409 b)	0.615 f)	0.616
Benzene	0.483 d)	0.568 f)	0.571
Ethanol	0.477 a)	0.458 d)	0.534
Methanol	0.423 b)	0.438 d)	0.523
*Cyclo*hexanol	0.132 (26°) e)		0.290
Water	0.0328 c)	0.0336 h)	0.0342

a) Bunsen, R. *Z. physik. Chem.* **9** (1892) 439.
b) Levi, M. G. *Z. physik. Chem.* **41** (1902) 110.
c) Winkler, L. W. *Ber.* **34** (1901) 1409, 1421.
d) McDaniel, A. S. *J. Phys. Chem.* **15** (1911) 587.
e) Cauquill, G. *J. chim. phys.* **24** (1927) 53.
f) Horiuti, J., see Ref.[4], p. 125.
g) Guerry, D. *Thesis*, Vanderbilt Univ. Nashville Tennessee 1944.
h) Morrison, T. and Billett, F. *J. Chem. Soc.* **1952** 3819.

CORRELATION WITH THEORY

In a previous paper, [2,p.54] it was shown that eqn (1) can account for the solubility of methane in non-polar solvents.

$$\log x_2 = \log x_2^i - \frac{\overline{V}_2}{2.303\ RT}(\delta_1 - \delta_2)^2 - \left[\log \frac{\overline{V}_2}{V_1} + 0.4343\left(1 - \frac{\overline{V}_2}{V_1}\right)\right] \quad (1)$$

In this equation x_2 denotes the solubility in mole fraction, x_2^i the "ideal" solubility, $\overline{V}_2$ the partial molal volume of the gas in the saturated solution, V_1 the molal volume of the solvent, δ_1 the "solubility parameter" of the solvent defined as the square root of the energy of vaporization (ΔE_1) per ml, *i.e.*

$$\delta_1 = \sqrt{\frac{\Delta E_1}{V_1}}$$

δ_2 the "solubility parameter" of the gas (see below) and T the absolute temperature. With regard to the derivation of eqn (1) reference should be made to Hildebrand and Scott [3].

The ideal solubility at 25°C was calculated by means of the equation

$$\log x_2^i = \frac{\Delta H}{2.303\ R}\left(\frac{1}{T} - \frac{1}{T_b}\right)$$

where ΔH is the heat of vaporization of methane (1 955 cal/mole) at the boiling point T_b = 112°K. The value for the ideal solubility was calculated to be 39.8×10^{-4}.

When a gas is dissolved in a liquid the volume of the solution is always greater than the volume of the solvent. From this expansion — which is only to a slight degree dependent on the solvent — one can calculate the partial molal volume of the gas in the solvent. Using the measurements of Horiuti [4] we get the value 52 ml for methane in benzene. The solubility parameter for methane, δ_2, was calculated from eqn (1) to be 6.20, using Horiuti's values for the solubility of methane in benzene and in carbon tetrachloride.

In Table 3 the experimental values of the solubility have been compared with values calculated by means of eqn (1).

In Table 3 we have included the calculated values for the solubility of methane in some polar solvents, listed in the order of their increasing dielectric constant. It can be seen that the experimental values are higher than the values calculated from eqn (1). It should be emphasized that this equation is derived on the assumption that the molecules are non-polar and that chemical reactions are absent. Deviations of the same order of magnitude have previously been found for the calculated solubility of carbon dioxide, oxygen, carbon monoxide and nitrogen in polar solvents [5].

In a recent paper [6] it is shown that eqn (1) can account for the solubility at 25°C of nitrogen, argon and ethane in alcohols, if δ_1 is substituted by δ_1^* calculated from

$$\delta_1^* = \delta_1 - (\varepsilon - 1)(0.165 - 0.00143\alpha \times 10^{25}) \quad (2)$$

In this equation, δ_1 is calculated from

$$\delta_1 = \sqrt{\frac{\Delta E_1}{V_1}} = \sqrt{\frac{\Delta H_1 - RT}{V_1}}$$

where ΔH_1 is the heat of vaporization of the solvent at the absolute temperature T and V_1 the molal volume of the solvent. In eqn (2) ε is the dielectric constant of the solvent and α the polarizability of the gas.

Table 4 shows that the solubilities of methane in ethanol, methanol and in *cyclo*hexanol can also be calculated by the same procedure. For methane we have used $\alpha \times 10^{25} = 26.0$. Included in Table 4 is a calculation of the solubility of methane in water; such a calculation gives only a rough estimate [6], and the fair agreement with the experimental value for this solvent is regarded to be casual.

If we use the δ_1^* values in the calculation of the solubility in the solvents mentioned in Table 3, we get no improvement. The deviations between calculated and experimental values turn out to be nearly the same. For acetone on the contrary we get a much greater deviation; using for this solvent a value

Table 3. Solubilities of methane at 25°C expressed in mole fractions x_2. Comparison of experimental and calculated values.

Solvent	V_1	δ_1	$x_2 \times 10^4$ exptl.	calc.	per cent deviation
n-Hexane	132	7.27	50.8	49.7	+ 2.2
*Cyclo*hexane	109	8.20	32.7	34.8	− 6.4
Carbon tetrachloride	97.1	8.60	28.6	28.2	+ 1.4
Benzene	89.3	9.15	20.9	21.0	− 0.5
Dioxane	86.1	10.0	12.9 g)	12.6	+ 0.2
Diethyl ether	105	7.42	45.4 f)	42.6	+ 6.5
Chlorobenzene	102	9.6	20.0 f)	17.4	+ 15
Methyl acetate	79.9	9.5	19.5 f)	16.6	+ 17
Acetone	74.0	9.65	18.6	14.4	+ 29

g) Guerry, D., see Ref. in Table 2.
f) Horiuti, J., see Ref.[4]

Table 4. Solubilities of methane at 25°C in some alcohols and in water. Comparison of experimental and calculated values.

Solvent	V_1	δ_1	ε	$x_2 \times 10^4$ exptl.	calc.	per cent deviation
Ethanol	58.7	12.8	24.3	12.8	12.7	+ 0.8
*Cyclo*hexanol	106	11.7	15.0	12.6	14.5	−13
Methanol	40.7	14.35	32.8	8.71	9.31	− 6
Water	18.1	23.4	78.0	0.253	0.292	−13

for the dielectric constant of 20.9, we obtain $x_2 = 39 \times 10,^{-4}$ a value much higher than the experimental one, $x_2 = 18.6 \times 10.^{-4}$ It should be mentioned that eqn (2) has been evaluated for alcohols all having nearly equal dipole moments.

REFERENCES

1. Lannung, A. *J. Am. Chem. Soc.* **52** (1930) 68.
2. Gjaldbæk, J. Chr. *Thesis*, Copenhagen 1954.
3. Hildebrand, J. H. and Scott, R. L. *Solubility of Non-electrolytes, 3rd Ed.* Reinhold Publ. Co., New York 1950.
4. Horiuti, J. *Sci. Papers Inst. Phys. Chem. Research (Tokyo)* (1931) No. 341.
5. Gjaldbæk, J. Chr. and Krogh Andersen, E. *Acta Chem. Scand.* **8** (1954) 1398.
6. Gjaldbæk, J. Chr. and Niemann, H. *Acta Chem. Scand.* **12** (1958) 1015.

Received February 17, 1960.

ACTA CHEMICA SCANDINAVICA 14 (1960) 1129—1150

On the Alkylation Type Substitution and Ester Condensation at the α-Position of N,N-disubstituted Amides of Arylacetic Acids

O. MÄRTENSSON and E. NILSSON

Pharmacia, Research Laboratories, Uppsala, Sweden

A simple method for substitution of alkylation type at the α-carbon atom of N,N-disubstituted arylacetic acid amides is described and discussed. Sodamide has been used as basic agent and toluene or benzene as reaction medium. Many compounds have been prepared according to the method and the result can be surveyed in tabular form. The aryl groups used in the investigation are phenyl, 1-naphthyl and 3-phenanthryl. No remarkable changes in reactivity as to sodium salt formation could be observed by these alternations of the aryl group, nor do variations in the substituents on the amide nitrogen change the activation of the α-hydrogen appreciably. The groups introduced are mainly of alkyl type but some heteroaromatic halogenides react in the same way. Condensations of esters (Claisen condensations) with the N,N-disubstituted amides have also been carried out with sodium methoxide or sodium ethoxide as condensing agents in the presence of an inert solvent (toluene or xylene), but this method seems to be less general than the substitution procedure, and somewhat unpredictable as to the results. However, cases including condensation under ring closure seem to form a subgroup in which the method is general.

In contrast to ester and nitrile groups, the activation by an amide group of the hydrogen at the adjacent carbon atom (the α-hydrogen) has been given comparatively little attention. The alkylation of esters and nitriles and ester (Claisen) condensation belong to the basic synthetic methods and have recently been reviewed [1,2]. As to the amides, unless the amide group is disubstituted, reactions generally occur under replacement of amide hydrogen. The main interest has therefore been connected to such reactions and not so much to the secondary effects caused by the amide group as a whole on the adjacent atoms and α-hydrogen in particular. (Since the reactions in the α-position can be studied mainly on N,N-disubstituted amides, for brevity, we omit this epithet unless otherwise stated.) It is also well known that an aryl group (*e.g.* phenyl) definitely activates the hydrogen at an adjacent carbon atom, an effect which

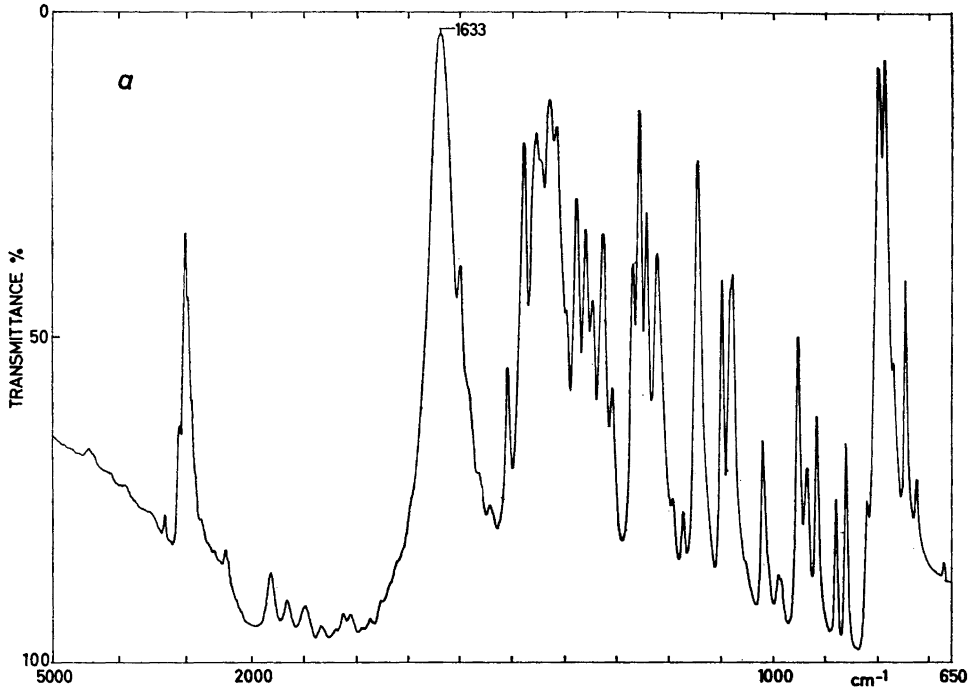

Fig. 1. Infrared spectrum of the parent amide 1-naphthylacetic acid N,N-diethylamide (a) and of its α-(2′-dimethylaminoethyl) derivative (b), showing that the frequency and intensity of the C=O bond of the amide group remain almost unchanged after substitu-

may be exemplified by the increasing mobility of α-hydrogen in the series toluene, diphenylmethane and triphenylmethane. The combined activation of α-hydrogen by an aryl group and nitrile and/or ester groups occurs in well known compounds such as phenylacetonitrile, phenylmalonic esters and phenylcyanoacetic esters. As to arylacetic acid amides, the mobility of the α-hydrogen of the amides of phenylacetic acid was expected to be between that of phenylacetonitrile and that of alkyl phenylacetate. The former compound easily forms a salt with sodamide in toluene in contrast to ethyl phenylacetate, which cannot be alkylated in the presence of sodamide in boiling toluene. It should be pointed out that the ability of salt formation and of alkylation depends very much on the basic agent used and the reaction conditions. The situation is quite different when such a strong agent as phenylsodium is used or when the salt formation is carried out with liquid ammonia as solvent. Thus, ethyl phenylacetate has recently been phenylated, too, in a yield of 63 % by bromobenzene in liquid ammonia and excess of sodamide [3]. In this paper we therefore intend merely to collect our experience and the results of a fairly extensive investigation in this laboratory [4,5] of introducing groups in the α-position of arylacetic acid amides. For completeness some

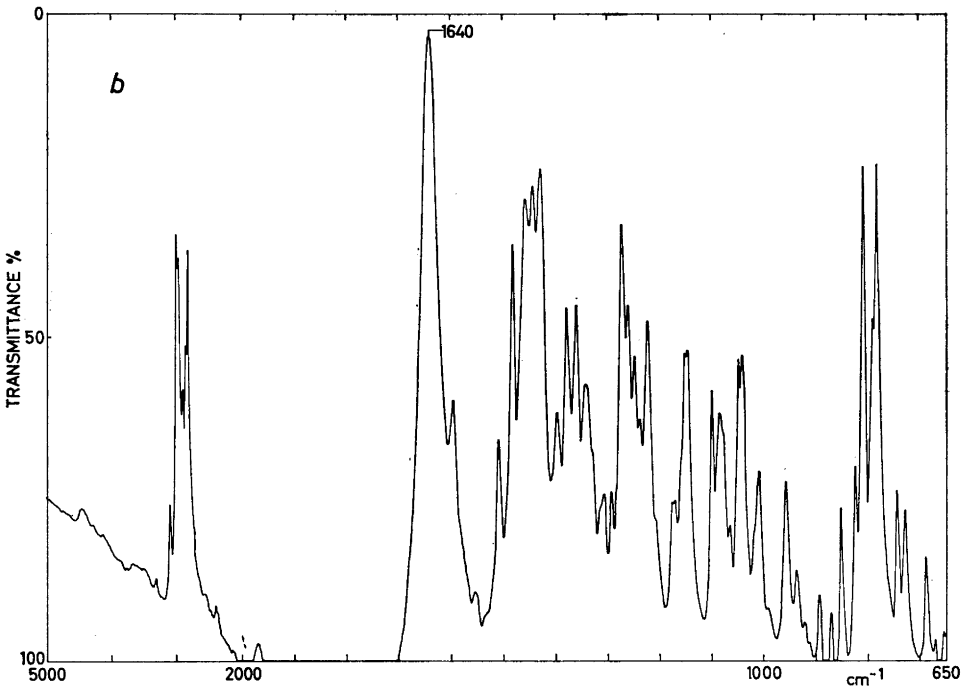

tion. The frequency of ten another compounds investigated proved to be within the range 1 633—1 648 cm^{-1}. — All spectra are drawn with KBr pellet technique on a Unicam SP 100 IR instrument. The experimental error is ± 2 cm^{-1}.

comments have also been given to a patent by Cusic [6] which turned up some years ago. He reports ten basically substituted cyclic amides of phenylacetic acids (they are included in Table 1). With the exception of one case in which sodamide has been used, lithium amide has been preferred as basic agent. The conventional method applied by us consists in substituting the amides in the presence of sodamide in an inert solvent, generally toluene. The reaction, which will be commented on below as to some practical details, can be written:

$$ArCH_2COY + RX \xrightarrow[\text{solvent}]{NaNH_2} \underset{\displaystyle R}{\overset{\displaystyle |}{ArCHCOY}} + NaX$$

Ar = phenyl, substit. phenyl, 1-naphthyl or 3-phenanthryl,
Y = secondary amido group of various types
R = alkyl (mainly tertiary aminoalkyl), *cyclo*alkyl, aralkyl and heteroaromatic radicals,
X = halogen

It is obvious that the reaction leads to substitution at the α-carbon atom and not to O-substitution. Thus the reaction product expected to be 2-phenyl-

(1,4)-butanedioic acid 1-(N,N-diethylamide)-4-(N-methylanilide) is converted by acid hydrolysis to phenylsuccinic acid in a yield of 90 %. Reduction of the amides with lithium aluminium hydride gives tertiary amines in very good yields (Table 2). Moreover, infrared spectra indicate that the carbonyl frequency remains almost unaltered after introduction of R (Fig. 1).

In the case of diphenylacetic acid amides the activation of the α-hydrogen is increased more by the second phenyl group and they form sodium salts more easily than when only one phenyl group is present. Indeed, substitution at the α-carbon atom by conventional methods has been applied [7,9] or probably applied [10] for synthetic purposes several times during the last years. In connection with the diphenylacetic acid amides it may also be pointed out that xanthene-9-carboxylic acid amides can be substituted at the 9-position by almost the same procedure ($LiNH_2$ or NaH in boiling toluene) as Cusic [11] has shown. However, this is easily expected since the corresponding esters can already be substituted at this position under fairly simple conditions: the salt has been formed by boiling the ester solution in toluene with potassium [12]. Further, it may be noted that phenyl-2-pyridyl-acetic acid amides have been alkylated by the conventional method in this laboratory [4].

In addition to this substitution method, which may be interpreted as an alkylation in *sensu lati*, we have also tried to carry out ester (Claisen) condensations with some of the parent acid amides. This reaction which leads to β-ketoamides under liberation of alcohol from the ester with which the amide is condensed, seems to be much more limited as to its application. We now intend to treat these two cases separately in somewhat greater detail.

A. SUBSTITUTION OF ALKYLATION TYPE

According to our standard method for substitution (several examples are given in the experimental part) the amide is dissolved in benzene or toluene (generally 0.1 mole amide per 100 ml solvent), a slight excess of the theoretical amount of sodamide (commercial ground quality has been used) is added, and the mixture warmed to reflux under stirring. A strong evolution of ammonia generally begins before the mixture boils — at least when toluene is used as solvent. After refluxing during 1—2 h the strong evolution of ammonia ceases. (The strength of the ammonia evolution is easily followed by putting dry strips of indicator paper at the mouth of the reflux condensor.) At this time the sodium salt of the amide has formed a precipitate in the flask in most cases. The mixture is then cooled somewhat before the compound RX is added — the extent of cooling, of course, and the rate of adding the alkylating compound must be adapted to the reactivity of the latter. When the agent is added, the salt of the amide generally disappears, the temperature increases, and a second strong evolution of ammonia starts. This second "ammonia peak" probably originates from sodamide which has been enclosed in the sodium salt formed and now can react. When the salt of the amide (*e.g.* N-benzyl-N-propylamide of phenylacetic acid) is soluble the salt formation is more complete and the second "ammonia peak" less pronounced. The reaction is never violent. After the second ammonia evolution has decreased further boiling for 1—2 h is

generally enough to ensure a complete or almost complete reaction. Of course, to be certain, one ought to prolongate the reaction time when, for example, chlorides are used, as they are known to react slowly. In this case the sodium salt formed disappears slowly and the second "ammonia peak" is not pronoucend.

As to the salt formation in toluene or benzene, in no case has this proved to occur at room temperature. Warming to above 50°C is necessary. Heating up to the boiling point of the reaction mixture is to be preferred in most cases. Thus phenylacetonitrile is much more reactive under the same conditions. On the whole the power of forming salts under our conditions varies very little with the substituents at the amide nitrogen. Heavy groups seem merely to increase the solubility of the sodium salt.

On the whole it is of fairly little importance how the substitution reaction is carried out. The procedure described above is of particular interest when the alkylating agent may react with the sodamide itself and one can hardly demand a higher yield than that corresponding to the sodium salt formed during the first reflux. Otherwise, at least on a small laboratory scale, one only has to mix the reacting compounds and the solvent and boil the mixture. Alternatively, one may add the sodamide in portions to the boiling mixture. Since the reaction time is fairly short, a loose cotton plug at the top of the reflux condensor is sufficient for exclusion of moisture. It may be removed during the periods of strong evolution of ammonia. The conditions are not rigorous. However, as in all cases when sodamide is used, its quality is very important for the success of the reaction. Too large an excess of sodamide should be avoided, since some of the alkylation products may be unstable under prolonged reflux with sodamide as has been proved by our attempts to carry out a second alkylation of these monoalkylated compounds.

We have chosen the easily available sodamide as basic agent with benzene or toluene as reaction media. In all the listed examples except one, Cusic [6] has used lithium amide. Since no yields are given, it is difficult to say whether it is to be preferred to the less expensive sodamide. However, the yields obtained by using sodamide are generally so good, that there seems to be no reason to use other alkali amides.

Sodium hydride reacts very slowly in forming salts in benzene or toluene and we have not been able to use it with success. Phenylsodium in toluene has also been used as an agent in forming salts, but it is generally not necessary to use such a reactive compound. As far as we have tried it, it gives no advantages.

A single trial with phenylacetic acid pyrrolidide and di-*iso*butylacetal suggests that the alkylation method of esters and nitriles by Weizmann *et al.* [13] which uses potassium hydroxide in solvents of acetal type, is not applicable with success to our amides.

Other polar solvents such as diglyme (ethylene glycol dimethyl ether) and dioxane have also been tried. With sodium hydride and diglyme the reaction is very slow and the yield almost none. Dioxane and sodium hydride give somewhat better yields. When sodamide has been tried in combination with these solvents, we have not been able to isolate any substitution product from the reaction mixture. On the whole these attempts to replace toluene and

benzene with other "polar" solvents and/or to replace the sodamide with sodium hydride have not been encouraging enough to justify further work in order to improve these modifications.

The compounds RX used for the introduction of R are halogenides. Chlorides and bromides have mainly been used. Alkyl *p*-toluenesulfonates have been tried in a few cases without appreciable success. They seem to react too easily with the sodamide to be recommended. Epoxides (ethylene oxide has been used in a very few trials) do not seem to give unique reaction products. There are reasons to believe that some polymerisation occurs on the hydroxyl groups formed. When R contains one or more ester groups one must expect low yields, since competition reactions occur. However, R containing a N,N-disubstituted amide group (*e.g.* RX = chloroacetyl-N-methylaniline) behave better in this respect. Of course, R is not allowed to bear groups containing a hydrogen atom more active than that in the α-position of the amide, nor groups which may rearrange so that such structures are formed.

As mentioned in the introduction the aryl groups used are phenyl, 1-naphthyl and 3-phenanthryl. No appreciable differences in reactivity as to salt formation have been observed in this series during the synthetic work. Only in the phenyl case syntheses have been carried out with substituents in the aryl group, and then only when the substituent is a halogen atom. Even in this case we have not been able to establish definite differences in reactivity between the *o*-, *m*- and *p*-compounds and the unsubstituted amides which are of interest for the application of the general method used by us. The case where the phenyl group bears one lower alkyl group has also been reported [4,6]. The method is limited as to the substituents of the aryl group and does not allow substituents which contain a hydrogen atom more mobile than that in α-position, such as hydroxy or acetamino groups, nor groups which can rearrange to give such a hydrogen.

A disadvantage of the method is that compounds with small substituents (R) often may be difficult to separate from the parent compound. If R bears a basic group, or is a heavy one, the separation from the parent amide is easy. On the other hand disubstitution seems to be of little importance. On the whole, side reactions are rare. The introduction of a second group in the α-position by this method is generally not so easy as that of the first one. Longer reaction time and sometimes also a stronger salt-forming agent than sodamide are necessary. In some cases proximity effects may also make the introduction of a second group difficult.

Most of the compounds with aryl equal to phenyl or substituted phenyl are viscous, colourless or faintly yellowish oils. When solid, their melting points are generally lower than that of the parent amides. They are very soluble in most organic solvents — often also in petroleum ether — and are difficult to recrystallize in good yields. The group consisting of the α-pyridyl derivatives is an exception to these characteristics.

As to the practical use of the compounds prepared according to this substitution method, those with a tertiary amino group (*e.g.* R = dialkylaminoalkyl) have pronounced and interesting pharmacological properties. Some of the α-substituted amides are also valuable as intermediates for further synthetic work. At least for some compounds a further substitution in the α-position

can be carried out. That this is the case for the phenyl-(2-pyridyl)-acetic acid amides has been shown in this laboratory. Moreover, as far as we have tried, the amide group has been easily reduced to a tertiary amino group by the conventional lithium aluminium hydride method [14] in excellent yield. We have included some amines (see Table 2) prepared according to this method and which do not seem to have been reported previously. Since a necessary condition for success in using this method in the reduction of N,N-disubstituted amides seems to be that there remains at least one hydrogen atom at the α-carbon, and this condition is fulfilled within the series, the reduction method can be expected to be generally applicable.

Finally, it may be noted that we have tried to apply the method to some thiocarbonamides without success. Thus, gentle heating of a mixture of sodamide, phenylthioacetylmorpholine and 2-morpholinoethylchloride in toluene in addition to ammonia causes evolution of hydrogen sulphide. No compound corresponding to a substitution product could be isolated from the refluxed mixture. Some phenylthioacetylmorpholine could be recovered.

B. ESTER (CLAISEN) CONDENSATION

As mentioned above, in contrast to the substitution of alkylation type in the α-position, the condensation of amides with esters need more care, and special conditions in each case, to insure the success of our method (sodium methoxide or sodium ethoxide as condensing agent with an inert solvent, generally toluene or xylene, as reaction medium). Several cases which lead to ring closure, under formation of 1-substituted 3-phenylpyrrolidine-2,4-diones and 1-substituted 3-phenylpiperidine-2,4-diones, have been investigated and they give fairly good to excellent yields, indicating that the method can be expected to be general in these cases. The success is more unpredictable when the condensation does not involve ring closure. At least some of the condensation products (*e.g.* α-methoxalyl-phenylacetic acid dimethylamide) seem to be very sensitive to alkali, thereby undergoing acid cleavage since fairly large amounts of acid corresponding to the ester (from oxalic acid diesters we obtain the monoesters) used can be isolated from the reaction mixture. This sensitivity to alkali is also characteristic for the purified condensation product. The reaction product must therefore be poured into a mixture of ice and dilute acid when worked up. In some cases we have been able to distil off only half the stoichiometric amount of alcohol. From these reaction mixtures we have not yet been able to isolate any condensation product but only the acid and the parent amide. The temperature sensitivity is also pronounced. When too high temperature is used during the reaction — for example when the alcohol formed is distilled off — no desired reaction product can be isolated, but a waxy or highly viscous, yellowish brown product remains after the solvent is removed. At this time we therefore report only those cases in which we have been successful.*

* Stronger condensing agents, such as phenylsodium have not yet been tried.

Table 1. Compounds prepared by substitution of alkylation type at the α-carbon of N,N-disubstituted arylacetic acid amides
Aryl—CHR—CO—Y

Aryl	Y	R	Yield	B.p. °C/mmHg M.p. °C	Formula	Analyses %					
						Calc.			Found		
						C	H	N	C	H	N
henyl	$-N(CH_3)_2$	$-CH_2CH_2C(CH_3)_3$	84	108 —10/0.1							
			71	42 —46 [b]	$C_{16}H_{25}NO$	77.68	10.19	5.66	77.15	10.05	5.82
»	»	$-CH_2CH(OC_2H_5)_2$ [i]	45	185 —87/8	$C_{16}H_{25}NO_3$	68.78	9.02	5.01	68.44	8.84	5.17
»	»	$-CH_2-C_6H_5$	93	135 —38/0.1							
			75	85 —86 [ab]	$C_{17}H_{19}NO$	80.59	7.56	5.53	80.62	7.74	5.43
»	»	$-CH_2CH_2N(C_2H_5)_2$	53	135 —38/0.4	$C_{16}H_{26}N_2O$	73.24	9.99	10.68	73.30	10.18	10.60
»	»	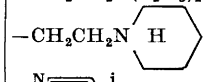	82	151 —53/0.2	$C_{17}H_{26}N_2O$	74.41	9.55	10.21	73.80	9.28	10.36
»	»	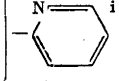	57	92 —93.5 [ab]	$C_{15}H_{16}N_2O$	74.97	6.71	11.66	74.85	6.75	11.59
»	»	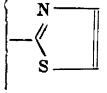	30	121 —22 [c]	$C_{13}H_{14}N_2OS$	63.39	5.73	11.38	63.55	5.85	11.16

otes: In order to make this table complete we have included also about ten compounds for which detailed data are not available. Most of these derivatives are taken from the patent by Cusic mentioned in the text, and they differ from the other compounds listed in so much as generally lithium amide has been used in their syntheses. The yields are the total ones and refer to the parent amide, unless the compounds listed are ammonium salts, in which case the figures refer to the corresponding tertiary base. When more than one yield figure is given, the compound in question has been further purified by redistillation or recrystallization. Melting points and boiling points are uncorrected. The former have been read from short normal thermometers covering intervals of 50°. Unless otherwise stated, X in the compound RX is chlorine. With a few exceptions the substitutions have been carried out with 0.05—0.4 mole of parent amide.

a—g: Recrystallization from a) benzene; b) petroleum ether; ab) a mixture of benzene and petroleum ether; c) *cyclo*hexane;
bc) a mixture of *cyclo*hexane and petroleum ether; d) nysolvin; e) a mixture of ethanol and ether; f) acetone; g) methanol
h) The analytical data refer to halogen (not to nitrogen) of the salt
i) The bromo compound has been used
k) The iodo » » » »

Table 1. Continued.

Aryl	Y	R	Yield	B.p.°C/mmHg M.p.°C	Formula	Analyses %					
						Calc.			Found		
						C	H	N	C	H	N
phenyl	$-N(C_2H_5)_2$	$-CH_2CH_2CH(CH_3)_2$ [i]	76	125 −26/0.6	$C_{17}H_{27}NO$	78.11	10.41	5.36	77.61	10.35	5.42
»	»	$-CH_2CH_2C(CH_3)_3$	90	120 −22/0.1	$C_{18}H_{29}NO$	78.49	10.61	5.09	78.00	10.45	5.24
»	»	$-CH_2CH_2OC_2H_5$ [i]	78	130 −31/0.2	$C_{16}H_{25}NO$	72.96	9.57	5.32	72.89	9.48	5.28
»	»		68	135 −45/0.3							
			52	87 −88 [b]	$C_{18}H_{27}NO$	79.07	9.96	5.12	78.71	9.94	5.23
»	»	$-CH_2-C_6H_5$	72	135 −38/0.2	$C_{19}H_{23}NO$	81.10	8.24	4.98	80.60	8.23	5.03
»	»	$-CH_2-C_6H_4Cl(p)$	60	62 −63 [b]	$C_{19}H_{22}ClNO$	72.25	7.02	4.43	72.75	7.09	4.45
»	»		71	136 −40/0.1	$C_{17}H_{21}NOS$	71.04	7.36	4.86	70.86	7.40	5.20
»	»	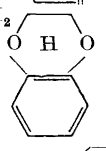	53	200 glass −03/0.2	$C_{21}H_{25}NO_3$	74.31	7.42	4.13	73.75	7.56	4.28
»	»	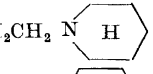	60	143 −45/0.1	$C_{19}H_{30}N_2O$	75.45	10.00	9.26	75.21	9.92	9.02
»	»		68	167 − 68/0.3	$C_{18}H_{28}N_2O_2$	71.01	9.27	9.21	70.71	9.29	9.29
»	»	—»—, CH_3Br	89	~100 (hygrosc.)	$C_{19}H_{31}BrN_2O_2$			20.01 [h]			19.00 [h]
»	»	$-CH_2CON(CH_3)C_6H_5$	50	91 − 93 [c]	$C_{21}H_{26}N_2O_2$	74.52	7.74	8.28	74.38	7.70	8.27

Table 1. Continued.

Aryl	Y	R	Yield	B.p.°C/mmHg M.p.°C	Formula	Analyses %					
						Calc.			Found		
						C	H	N	C	H	N
phenyl	$-N(C_2H_5)_2$	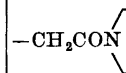	52	95 –96.5 [c]	$C_{18}H_{26}N_2O_3$	67.89	8.23	8.80	68.05	8.27	8.82
»	»	$-CH_2CH_2CH_2N(C_2H_5)_2$	86	137 –41/0.1	$C_{19}H_{32}N_2O$	74.95	10.60	9.20	74.51	10.55	9.28
»	»	—»—, CH_3Br	75	132.5– 34.5 [f]	$C_{20}H_{35}BrN_2O$			20.01[h]			19.4[h]
»	»	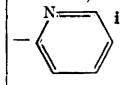	77	185 – 90/1							
			50	63 – 64.5 [ab]	$C_{17}H_{20}N_2O$	76.08	7.51	10.44	76.03	7.47	10.39
»	»	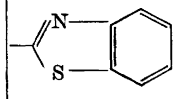	30	215 –20/0.2							
			23	105 –107 [c]	$C_{19}H_{20}NOS$	70.34	6.21	8.64	70.37	6.31	8.65
»	$-[CH(CH_3)_2]_2$	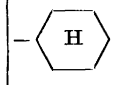	57	128 – 32/0.2							
			40	81– 82.5 [b] and 88.5– 89	$C_{20}H_{31}NO$	79.68	10.37	4.65	79.20	10.44	4.68
»	»	$-CH_2CH_2N(CH_3)_2$	50	113 –15/0.2							
			46	35.5– 37.5 [b]	$C_{18}H_{30}N_2O$	74.43	10.41	9.65	74.36	10.51	9.43
»	»	$-CH_2CH_2N(C_2H_5)_2$	81	115 – 16/0.1	$C_{20}H_{34}N_2O$	75.42	10.76	8.80	74.59	10.64	8.78
»	»	—»—, HCl	90	143.5– 44 [e]	$C_{20}H_{35}ClN_2O$			9.99[h]			9.80[h]
»	»	—»—, CH_3I	55	144 – 46.5 [e]	$C_{21}H_{37}IN_2O$						
»	»	$-CH_2CH_2CH_2N(C_2H_5)_2$	78	130 – 35/0.2	$C_{21}H_{36}N_2O$	75.85	10.91	8.43	75.34	10.95	8.56

able 1. Continued.

Aryl	Y	R	Yield	B.p.°C/mm Hg M.p.°C	Formula	Analyses %					
						Calc.			Found		
						C	H	N	C	H	N
henyl	$-[CH(CH_3)_2]_2$	$-CH_2CH_2CH_2N(C_2H_5)_2$,HCl	95	129 — 30 [e]	$C_{21}H_{37}ClN_2O$			9.88 [h]			9.51 [h]
»	»	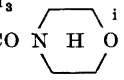	20	100 — 05	$C_{21}H_{32}N_2O_3$						
			15	108 — 11 [b]		69.96	8.95	7.77	70.03	9.07	7.86
»	»	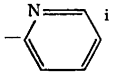	55	brown solid							
			45	104 —106 [bc]	$C_{19}H_{24}N_2O$	76.99	8.16	9.45	77.09	8.15	9.47
»	»	—»—, CH_3Br	50	deliq.				22.0 [h]			20.0 [h]
»	$-N(CH_2CH_2CH_2CH_3)_2$	$-CH_2CH_2N(C_2H_5)_2$	83	135 — 37/0.1	$C_{22}H_{38}N_2O$	76.25	11.06	8.09	76.40	11.19	8.31
»	$-N[CH_2CH(CH_3)_2]_2$	$-CH_2CH_2N(C_2H_5)_2$	45	135 — 40/0.2	$C_{22}H_{38}N_2O$	76.25	11.06	8.09	76.00	11.01	8.30
»		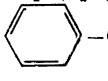	77	205 — 10/0.8							
			71	96 — 97 [c]	$C_{19}H_{20}ClNO$	72.71	6.42	4.46	72.47	6.46	4.45
»	»	$-CH_2CH_2CH_2Cl$ [6]									
»	»	$-CH_2CH_2N_2(C_2H_5)$	81	152 — 57/0.4	$C_{18}H_{28}N_2O$	74.95	9.78	9.71	74.50	9.73	9.60
				176— 80/2 [6]							
		—»—, HCl	95	177 — 79 [c]							
				175 — 77 [6]							
»	»	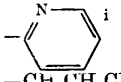	55	108.5—110 [ab]	$C_{17}H_{18}N_2O$	76.66	6.81	10.52	76.69	6.81	10.31
»	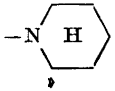	$-CH_2CH_2CH_2CH_3$ [i]	84	138 — 42/0.5	$C_{17}H_{25}NO$	78.71	9.72	5.40	78.23	9.51	5.39
»	»	$-CH_2CH_2C(CH_3)_3$	65	100 —102 [bc]	$C_{19}H_{29}NO$	79.39	10.17	4.87	79.12	10.15	4.82

able 1. Continued.

Aryl	Y	R	Yield	B.p.°C/mmHg M.p.°C	Formula	Analyses %					
						Calc.			Found		
						C	H	N	C	H	N
henyl		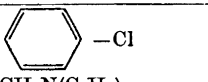	31	82 — 83 [bc]	$C_{20}H_{22}ClNO$	73.27	6.77	4.27	73.25	6.48	4.31
»	»	$-CH_2CH_2N(C_2H_5)_2$		177 — 79/2 [e]							
»	»	—»—, HCl		174 — 75 [e]							
»	»	$-CH_2CH_2N[CH(CH_3)_2]_2$		213 — 18/2 [e]							
»	»	—»—, HCl		188 — 90 [e]							
»	»	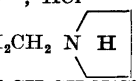		216 — 19/2 [e]							
»	»	$-CH_2CH_2CH_2N(CH_3)_2$	46	160 — 64/0.4	$C_{18}H_{28}N_2O$	74.95	9.79	9.71	75.00	9.60	9.74
»	»	$-CH_2CH_2CH_2N(C_2H_5)_2$	55	159 — 66/0.2	$C_{20}H_{32}N_2O$	75.90	10.19	8.85	75.95	10.14	8.96
»	»	—»—, CH_3Br	72	157 — 59 [f]	$C_{21}H_{35}BrN_2O$			19.4 [h]			19.3 [h]
»	»	$-CH_2CH_2CH_2N[CH(CH_2)_3]_2$	65	182 — 83/0.4	$C_{22}H_{36}N_2O$	76.69	10.53	8.13	76.50	10.40	8.08
»	»	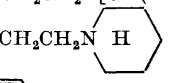	68	175 — 78/0.1	$C_{21}H_{32}N_2O$	76.78	9.82	8.53	76.71	9.57	8.59
»	»	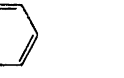	71	195 — 97/0.4							
			66	72.5— 3.5 [bc]	$C_{16}H_{20}N_2O$	77.11	7.19	9.99	77.25	6.95	9.95
»		$-CH_2(CH_2)_5CH_3$ [k]	45	172— 75/0.6	$C_{19}H_{29}NO_2$	75.20	9.64	4.62	75.20	9.65	4.69
»	»	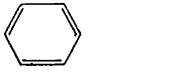	63	171 — 73/0.1							
			50	80.5— 82 [ab]	$C_{19}H_{21}NO_2$	77.26	7.17	4.74	77.20	7.20	5.05

able 1. Continued.

Aryl	Y	R	Yield	B.p.°C/mm Hg M.p.°C	Formula	Analyses %					
						Calc.			Found		
						C	H	N	C	H	N
henyl		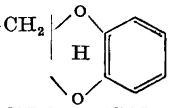	34	219 – 24/0.3	$C_{21}H_{23}NO_4$	71.37	6.56	3.96	71.51	6.73	4.10
»	»	$-CH_2CH_2N(C_2H_5)_2$	77	156 – 60/0.3	$C_{18}H_{28}N_2O_2$	71.01	8.95	9.27	71.11	8.96	9.00
				207 – 15/2 [6]							
		–»–, HCl		185 – 86 [6]							
»	»	$-CH_2CH_2CH_2N(CH_3)_2$	52	187 – 90/1	$C_{17}H_{26}N_2O_2$	70.31	9.03	9.65	69.72	9.06	9.70
»	»	$-CH_2CH_2CH_2N(C_2H_5)_2$	69	156 – 58/0.1	$C_{19}H_{30}N_2O_2$	71.66	9.50	8.80	71.20	9.57	8.83
»	»	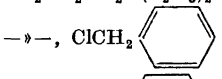	58	189 – 91 [g]	$C_{26}H_{37}ClN_2O_2$			7.97[h]			7.80[h]
»	»	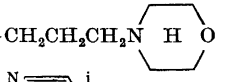		"oil" [6]							
»	»		65	195 – 98/0.4							
	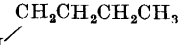		51	84 – 85.5 [ab]	$C_{17}H_{18}N_2O_2$	72.32	6.43	9.92	72.60	6.50	9.92
»	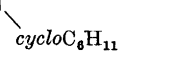	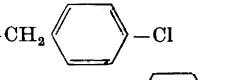	63	195 – 97/0.1	$C_{25}H_{32}ClNO$	75.44	8.11	3.52	75.73	8.18	3.66
»	»	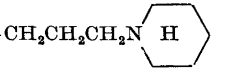	59	202 – 04/0.2	$C_{26}H_{42}N_2O$	78.34	10.62	7.03	78.50	10.60	7.14
:	$-N(cyclo C_6H_{11})_2$	$-CH_2-C_6H_4Cl(p)$	50	225 – 30/0.2 glass-like	$C_{27}H_{34}ClNO$	76.48	8.08	3.30	76.39	8.12	3.39

ɔble 1. Continued.

Aryl	Y	R	Yield	B.p.°C/mm Hg M.p.°C	Formula	Analyses %					
						Calc.			Found		
						C	H	N	C	H	N
ıenyl	$-N(cyclo C_6H_{11})_2$	$-CH_2CH_2N(C_2H_5)_2$, HCl	37	204 – 07	$C_{26}H_{43}ClN_2O$	71.77	9.73	6.44	71.84	10.10	6.34
»	$-N(CH_2CH_2CH_3)(CH_2-C_6H_5)$	$-CH_2-C_6H_5$	90	200 –203/0.2	$C_{25}H_{27}NO$	83.99	7.61	3.92	83.98	7.62	3.94
»	»	$-CH_2CH_2N(CH_3)_2$	64	168 – 72/0.4	$C_{22}H_{30}N_2O$	78.06	8.93	8.28	77.65	8.88	8.20
»	»	$-CH_2CH_2N(C_2H_5)_2$	51	175 – 80/0.2	$C_{24}H_{34}N_2O$	78.64	9.35	7.64	78.33	9.35	7.50
»	»	—»—, HCl		123 – 24.5 [c]	$C_{24}H_{35}ClN_2O$			8.80[h]			8.72[h]
»	$-N(CH_3)(C_6H_5)$	$-CH_2CH_2N(C_2H_5)_2$	62	156 – 58/0.3	$C_{21}H_{28}N_2O$	77.73	8.70	8.63	77.54	8.66	8.39
»	»	$-CH_2CH_2CH_2N(C_2H_5)_2$	77	170 – 74/0.3	$C_{22}H_{30}N_2O$	78.06	8.93	8.28	77.70	8.97	8.13
»	»	—»—, CH_3Br	98	157 – 59	$C_{23}H_{33}BrN_2O$			18.44[h]			18.30[h]
»	»		50	89 – 93							
			41	97 – 98.5 [c]	$C_{20}H_{18}N_2O$	79.44	6.00	9.27	79.14	6.03	9.18
»	$-N(C_6H_5)_2$	$-CH_2CH_2N(C_2H_5)_2$	65	225 – 26/0.8	$C_{26}H_{30}N_2O$	80.79	7.82	7.25	80.30	7.93	7.29
»	»	—»—, CH_3Br	82	191 – 93 [f]	$C_{27}H_{33}BrN_2O$			16.60[h]			16.40[h]
ɔhloro-ıenyl	$-N(CH_3)_2$	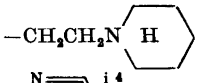	85	145 – 50/0.2	$C_{17}H_{25}ClN_2O$	66.11	8.16	9.07	65.85	8.07	9.01
»	»	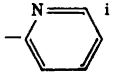									

'able 1. Continued.

Aryl	Y	R	Yield	B.p.°C/mm Hg M.p.°C	Formula	Analyses %					
						Calc.			Found		
						C	H	N	C	H	N
m-chloro-phenyl	$-N(CH_3)_2$	$-CH_2CH_2CH_2N(C_2H_5)_2$	54	152 – 54/0.2	$C_{17}H_{27}ClN_2O$	65.68	8.76	9.01	65.84	8.84	9.14
o-chloro-phenyl	$-N(CH_3)_2$	$-CH_2CH_2CH_2N(C_2H_5)_2$, HCl		113 – 16	$C_{17}H_{28}Cl_2N_2O$			10.18[h]			10.2[h]
»	»	—»—, CH_3Br	71	glass-like	$C_{18}H_{30}BrClN_2O$			19.7[h]			18.6[h]
p-chloro-phenyl	$-N(CH_3)_2$	$-CH_2CH_2CH_2N(C_2H_5)_2$	86	165 – 70/0.3	$C_{17}H_{27}ClN_2O$	65.68	8.76	9.01	65.80	8.85	8.74
»	»	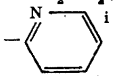	90	180 –205/0.2							
			80	75 – 76.5 [c]	$C_{15}H_{15}ClN_2O$	65.57	5.50	10.20	65.95	5.55	10.15
»	$-N(C_2H_5)_2$		70	69.5– 70 [c]	$C_{17}H_{19}ClN_2O$	67.43	6.33	9.25	67.30	6.38	9.09
»	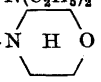	$-CH_2CH_2CH(CH_3)_2$	70	154– 56/0.15							
			45	87.5– 89 [c]	$C_{17}H_{24}ClNO_2$	65.90	7.81	4.52	65.71	7.68	4.70
p-bromo-phenyl	$-N(C_2H_5)_2$	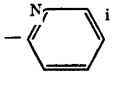		190 –200/1 [d]							
»		» [i]		210 – 20/1 [d]							
p-tolyl		$-CH_2CH_2CH_2CH_2N(CH_3)_2$		210 – 20/1 – 1.5 [e]							
p-tolyl	$-N(CH_3)_2$	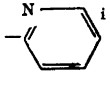		180 – 85/1 [d]							
p-iso-propyl-phenyl		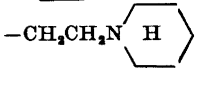		220 – 30/1 [e]							

able 1. Continued.

Aryl	Y	R	Yield	B.p.°C/mm Hg M.p.°C	Formula	Analyses %					
						Calc.			Found		
						C	H	N	C	H	N
·naphthyl	$-N(C_2H_5)_2$	$-CH_2CH_2N(CH_3)_2$	76	66 – 67 [b]	$C_{20}H_{28}N_2O$	76.88	9.04	8.97	76.70	9.03	9.15
»	»	—»—, CH_2Br		186 – 87	$C_{21}H_{31}BrN_2O$			19.64[h]			19.2[h]
»	»	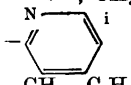	59	165.5 – 66 [ab]	$C_{21}H_{22}N_2O$	79.21	6.97	8.80	79.30	6.95	8.74
»	$-N[CH(CH_3)_2]_2$	$-CH_2-C_6H_5$	71	175 – 78/0.15	$C_{25}H_{29}NO$	83.52	8.13	3.90	83.25	8.29	4.25
»	»	$-CH_2CH_2N(C_2H_5)_2$	77	180 – 82/0.4							
			50	69.5 – 70 [b]	$C_{24}H_{36}N_2O$	78.21	9.85	7.60	78.25	9.85	7.74
»	»	$-CH_2CH_2CH_2N(C_2H_5)_2$	69	185 – 87/0.2	$C_{25}H_{35}N_2O$	78.48	10.01	7.32	78.11	9.96	7.34
			50	143 – 47 [a]							
·phenan-ıryl	$-N(C_2H_5)_2$	$-CH_2-C_6H_5$	67	123 – 24 [d]	$C_{27}H_{27}NO$	85.00	7.13	3.67	84.52	7.15	3.77
»	»	$-CH_2CH_2N(CH_3)_2$	58	58 – 60 [b]	$C_{24}H_{30}N_2O$	79.51	8.34	7.73	79.64	8.29	8.07

Table 2. Tertiary amines prepared from α-substituted N,N-disubstituted arylacetic acid amides by reduction with $LiAlH_4$.

Aryl—CH(R)—CH_2—Y

Aryl	Y	R	Yield	B.p.°C/mm Hg M.p.°C	Formula	Analyses %					
						Calc.			Found		
						C	H	N	C	H	N
)henyl	$-N(C_2H_5)_2$	$-CH_2CH_2C(CH_3)_3$	92	142–44/8	$C_{18}H_{31}N$						
	—»—, HCl	—»—	83	162–63 (methanol + petr. ether)	$C_{18}H_{32}ClN$	72.57	10.83	4.70	72.88	11.12	4.74
»	$-N(C_2H_5)_2$	$-CH_2CH_2N$ (H)	84	120–24/0.5	$C_{19}H_{32}N_2$	79.10	11.18	9.71	78.80	11.22	9.84
»	$-N$ (H) O	$-CH_2CH_2CH_2N(C_2H_5)_2$	82	150–58/1	$C_{19}H_{32}N_2O$	74.95	10.60	9.20	74.93	10.69	9.06
l-naphthyl	$-N(C_2H_5)_2$	$-CH_2CH_2N(CH_3)_2$	88	140–42/0.4	$C_{20}H_{30}N_2$	80.48	10.13	9.39	80.28	9.66	9.16

EXPERIMENTAL

The amides used as starting materials have generally been prepared from the appropriate secondary amines and acid chlorides with benzene as solvent. In fairly few cases the Schotten-Baumann reaction has been applied. The yields are generally excellent or at least good. Several of these amides have been prepared earlier but some do not seem to have been reported previously. Since we find it practical, we have collected the boiling points and/or melting points of all amides used by us (however, the boiling points of the amide esters used in cyclic condensation have been listed in Table 3):

Phenylacetic acid: dimethylamide, b. p. 125—29°/0.7 mm, m. p. 40°; diethylamide, b. p. 111—13°/0.3 mm; di*iso*propylamide, m. p. 50—53°; di-*n*-butylamide, b. p. 122—24°/0.1 mm; di*iso*butylamide, b. p. 113—16°/0.1 mm; di*cyclo*hexylamide, m. p. 83—85°; *cyclo*hexyl-*n*-butylamide, b. p. 148—50°/0.2 mm; benzyl-*n*-propylamide, b. p. 176—78°/0.8 mm; dibenzylamide, m. p. 60.5—62.5°; diphenylamide, m. p. 74—75°; pyrrolidide, m. p. 47—48.5°; piperidide, b. p. 174—79°/8 mm; morpholide, m. p. 65.5—67°.

o-Chlorophenylacetic acid: dimethylamide, m. p. 54—54.5°.

m-Chlorophenylacetic acid: dimethylamide, b. p. 124—25°/0.2 mm.

p-Chlorophenylacetic acid: dimethylamide, b. p. 144—45°/0.4 mm; diethylamide, b. p. 120—25°/0.2 mm; morpholide, m. p. 103—05°.

α-Naphthylacetic acid: diethylamide, m. p. 77.5—79°; di*iso*propylamide, m. p. 84—85°.

Phenanthrene-3-acetic acid: diethylamide, m. p. 94—95°.

A. Examples of substitution of alkylation type

α-(p-Chlorobenzyl)-phenylacetic acid pyrrolidide. In a three-necked 500 ml flask, equipped with a reflux condensor, a mechanical stirrer and a dropping funnel, a mixture of 37.9 g (0.2 mole) phenylacetic acid pyrrolidide (m. p. 47—48.5°), 8.2 g (0.21 mole) commercial, ground sodamide and 200 ml of dry toluene is warmed. At about 80° a strong evolution of ammonia begins. After boiling for about 2 h the strong evolution of ammonia has ceased, and a white precipitate of the sodium salt of the pyrrolidide has been formed. The mixture is now cooled to room temperature. A solution of 33.6 g (0.21 mole) *p*-chlorobenzylchloride in 50 ml of dry toluene is added during a period of about 15 min. by means of the dropping funnel. The temperature in the flask increases to about 60° and the salt disappears. The solution becomes rose-coloured but this colour soon becomes pale as the sodium chloride is formed. The flask is warmed again to reflux. At this point a further strong evolution of ammonia begins but decreases after a boiling time of about 30 min. After further reflux for 2 h the evolution of ammonia has ceased almost completely. The mixture is now cooled to room temperature and cold water added carefully. After one further washing with water the toluene layer is dried with fused magnesium sulphate. The toluene is distilled off under diminished pressure. The remaining oil is distilled and the fraction 205—210°/0.8 mm is collected. Yield 48 g (76.5 %). The oil crystallizes almost immediately, m. p. 92—95°. Recrystallization from 100 ml *cyclo*hexane gives 43.5 g (70.5 %) of white crystals, m. p. 96—97°. For analysis see Table 4.

α-Cyclohexyl-phenylacetic acid diisopropylamide. 109.7 g (0.5 mole) of phenylacetic acid di*iso*propylamide are dissolved in 400 ml of dry toluene, 21 g of sodium amide are added and the mixture refluxed for about 2 h or until the rapid evolution of ammonia has decreased and a large precipitate is obtained in the flask. 65 g (theoret. 59.3 g) of *cyclo*hexylchloride are added gradually to the boiling mixture. During this procedure the salt reacts and disappears and evolution of ammonia takes place. The refluxing is then continued for about 5 h. After cooling to room temperature and twice shaking the reaction mixture with water, the toluene layer is dried with anhydrous sodium sulphate and the solvent distilled off. The main part of the remaining oil distils at 128—132°C/0.1 mm Hg. It solidifies to a mass of crystals. Yield 85 g (57 %). 5.0 g recrystallized from petroleum ether gives 3.5 g (total yield 40 %) of *α-cyclo*hexyl-phenylacetic acid di*iso*propylamide, m. p. 81—82.5° and 88.5—89°C. For analytical data see Table 1.

Table 3. Ester condensations.

Reactant(s)	Product	Yield %	M.p.°C (solvent)	Analyses					
				Calc.			Found		
				C	H	N	C	H	N
$C_6H_5CH_2CON(CH_3)_2$ + + dimethyloxalate	$C_6H_5CHCON(CH_3)_2$ | $COCOOCH_3$	62 52	92–96 94–96 (benzene + + petroleum ether)	62.64	6.07	5.62	62.62	6.10	5.63
$C_6H_5CH_2CON(CH_3)_2$ + diethyl oxalate	$C_6H_5CHCON(CH_3)_2$ | $COCOOC_2H_5$	65 45	~ 100 98–100 (benzene + petroleum ether)	63.86	6.51	5.41	64.09	6.54	5.41
$C_6H_5CH_2CON(C_2H_5)_2$+ethyl nicotinate	$C_6H_5CHCON(C_2H_5)_2$ | $CO-C_5H_4N$	80 68.5	129–133 136–138 (benzene + petroleum ether)	72.95	6.80	9.45	73.36	6.94	9.49
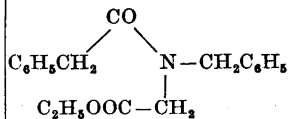 $C_2H_5OOC-CH_2$ B.p. 198–202°/0.5 mm		theor. 58	210–212 (butanol)	76.95	5.70	5.28	76.66	5.70	5.24
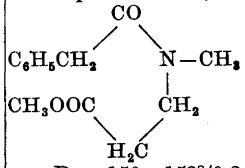 B.p. 150–153°/0.2 mm	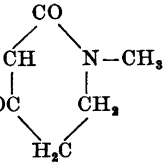	60	135–137 (acetone)	70.91	6.45	6.89	70.80	6.50	6.86
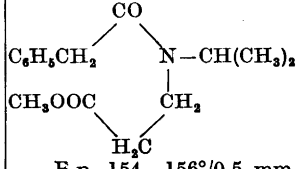 B.p. 154–156°/0.5 mm	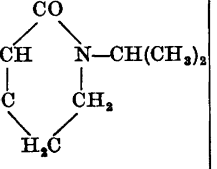	81 67	124–127.5 128–130 (ether + petroleum ether)	72.30	7.41	6.06	72.66	7.45	6.10

[a] This compound is listed by Petersen & Weidemann [15] but no data and references at all are given.

Table 3. Continued.

Reactant(s)	Product	Yield %	M.p.°C (solvent)	Analyses					
				Calc.			Found		
				C	H	N	C	H	N
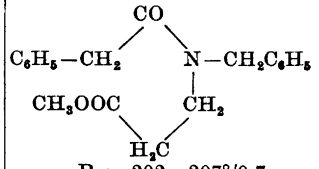 B.p. 202–207°/0.7 mm	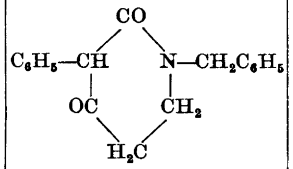	72	138.5–140 (ether + petroleum ether)	77.39	6.14	5.01	73.69	6.17	5.10
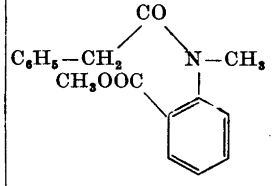 B.p. 175–177°/0.3 mm	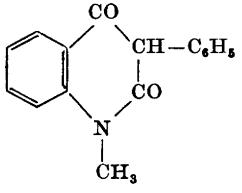	theor. 86	220–225° 222–226 (ethanol)	76.47	5.22	5.58	76.51	5.21	5.60

α-(2-Diethylaminoethyl)-phenylacetic acid diisopropylamide. 109.7 g (0.5 mole) of phenylacetic acid di*iso*propylamide, dissolved in 450 ml of dry toluene is boiled while stirring with 21 g of sodium amide for about 2 h. After that time the strong evolution of ammonia has ceased and a yellow precipitate has been formed in the flask. After cooling to about 50°C, a dried solution of 2-(diethylamino)-ethylchloride (liberated from 98 g of the hydrochloride) in ca. 200 ml of toluene is added. The reaction mixture is gently warmed until the reaction begins, *i. e*, the sodium salt dissolves and evolution of ammonia increases. The reaction mixture is then refluxed for about 3 h. The mixture is cooled to room temperature and water is added carefully. The toluene layer is then washed two times with water and then extracted two times with dilute hydrochloric acid. The base is liberated from the acid solution with dilute sodium hydroxide. The precipitated oil is dissolved in ether and the water phase extracted once more with ether. The united ether solutions are dried with anhydrous sodium sulphate and the ether evaporated. The main part of the remaining oil distils at 115—20°C/0.1 mm and consists of the α-diethylaminoethyl compound. Yield 128 g (81 %).

The hydrochloride precipitates as an oil when ethanolic hydrochloric acid is added to an ether solution of the base. When the acid containing ether is decanted and, to secure basic reactions ether with further base is added the hydrochloride solidifies, m.p. 142—4°C.

To 9.6 g (0.02 mole) of the α-(2-diethylaminoethyl)-phenylacetic acid di*iso*propylamide, dissolved in 100 ml of dry ether, is added 5.5 g of methyl iodide, dissolved in 50 ml of dry ether. After two days 8.4 g of methylammonium compound is filtered off. After recrystallization from a mixture of ethanol and ether 7.7 g (57 %) is collected, m. p. 144—6°C. For analytical data see Table 1.

α-(2-Dimethylaminoethyl)-α-(α'-naphthyl)-acetic acid diethylamide. To 48.3 g (0.2 mole) of α-naphthylacetic acid diethylamide dissolved in 200 ml of dry toluene are added 8.2 g of sodium amide and the mixture is boiled for about 2 h while stirring until the rapid evolution of ammonia has ceased and a yellowish precipitate has been formed. After cooling down to about 50°C, an amount of 2-(dimethylamino)-ethyl chloride, prepared from 35 g of the hydrochloride, dissolved in about 150 ml toluene is added. The mixture is slowly heated, whereby the precipitate is dissolved and ammonia is evolved. The mixture is then refluxed for about 4 h. After cooling, the mixture is shaken two times with water and then extracted two times with dilute hydrochloric acid. The base is liberated from the acid solution by means of dilute sodium hydroxide and dissolved in benzene. The benzene layer is separated and the water phase extracted one time with benzene. The benzene solutions are united and the benzene is driven off. A solidifying oil is obtained. After recrystallization from petroleum ether (cooling with dry ice and ethanol) the α-(2-dimethylaminoethyl) compound is obtained in a yield of 76 % (47 g), m. p. 62—63°C. For analytical data see Table 1.

α-(3-Diethylaminopropyl)-phenylacetic acid morpholide. A mixture of 82.1 g (0.4 mole) of phenylacetic acid morpholide, 350 ml of dry toluene and 16.4 g of sodium amide is refluxed for about 3 h until the strong evolution of ammonia has ceased. The mixture is cooled to about 70°C and 63 g (theoret. 60.0 g) of 3-(diethylamino)-propyl chloride is added gradually. Thereafter the mixture is warmed and refluxed for about 3 h. After cooling to room temperature the reaction mixture is worked up as described in the previous example. After a fore-run of about 20 g the substituted morpholide distils at 156—158°C/0.1 mm. Yield 88 g (69 %). The remainder in the distilling flask is insignificant. For analysis see Table 1.

B. Examples of ester (Claisen) condensation

α-Methoxalyl- and *α-ethoxalyl-phenylacetic acid dimethylamide.* Sodium ethoxide is prepared from 4.8 g (0.21 mole) of sodium and 15 ml of absolute ethanol in 100 ml of dry xylene and the excess of alcohol is distilled off. At room temperature a solution consisting of 32.6 g (0.2 mole) of phenylacetic acid dimethylamide, 30 g (29.2 g = 0.2 mole) of diethyl oxalate and 50 ml of xylene is added to this mixture. The reaction mixture is warmed gently to 85° and kept at this temperature for about 45 min. The reaction mixture is cooled to room temperature and put into a mixture of 75 ml 5 N HCl and ice. Crystals begin to separate from the xylene layer and further precipitate is formed when 200 ml

of petroleum ether is added. The crude product is filtered off, yielding 27 g of the ethoxalyl compound. From the mother liquor another 7.5 g can be obtained with approximately the same melting point, 97—100°. Total yield 65.5 %. Recrystallization from a mixture of benzene and petroleum ether gives 23.5 g (total yield 45 %) with melting point 98—100°. For analytical data see Table 3.

When dimethyl oxalate and sodium methoxide are used, almost the theoretical amount of methanol can be distilled off. The crude yield is 32 g (62 %). After two recrystallizations from a mixture of benzene and petroleum ether the yield is 20 g (40 %). See also Table 3.

α-Nicotinoyl-phenylacetic acid diethylamide. Sodium ethoxide is prepared from 4.8 g of sodium and 15 ml of absolute ethanol, in 100 ml of dry xylene and the excess of ethanol is distilled off. At room temperature a mixture of 38.2 g (0.2 mole) of N,N-diethylphenylacetamide, 30.2 g (0.2 mole) of ethylnicotinate and 100 ml dry xylene is added to the sodium ethoxide suspension during stirring. The mixture is now warmed gently, and in the course of about 2.5 h about the theoretical amount of ethanol (ca. 27 ml) is distilled off. The mixture is then cooled to room temperature and cold water is added. The sodium salt dissolves. The xylene phase is separated and the water phase washed with ether. To the water phase is now added 5 N hydrochloric acid until pH is about 4. The precipitate is collected on a funnel and washed with water. The dried, slightly yellow crude product (47.5 g, 80 %) melts at 129—133°. Recrystallization from a mixture of benzene (100 ml) and petroleum ether (100 ml) raises the m. p. to 136—138°. A further recrystallization from a mixture of benzene and *cyclo*hexane gives 40.5 g (68.5 %), m. p. 136—138°. For analytical data see Table 3.

1-Methyl-3-phenyl-quinoline-2,4-(1H,3H)-dione. 28.2 g (0.1 mole) methyl N-methyl-N-phenacetylanthranilate, dissolved in 50 ml dry toluene is added to sodium methoxide (from 2.7 g sodium) in ca. 50 ml dry toluene at room temperature while stirring. A precipitate is formed. The mixture is warmed and the theoretical amount of methyl alcohol is distilled off. After cooling to room temperature the precipitate is dissolved by adding cold water, and the separated water solution washed with ether. The solution is acidified with 5 N hydrochloric acid, and the precipitate filtered off and washed with water. Yield 24.8 g (99 %), m. p. 220—224°. Recrystallization from 700 ml of ethanol gives 21.5 g (86 %), m. p. 222—226°. For analytical data see Table 3.

The authors are indebted to Mr. W. Kirsten and his assistants for elementary analyses and to Dr. B. Nygård for infrared analyses.

REFERENCES

1. Cope, A. C., Holmes, H. L. and House, H. D. *Org. Reactions* **9** (1957) 107.
2. Hauser, C. R. and Hudson, Jr, B. E. *Org. Reactions* **1** (1942) 266.
3. Leake, W. W. and Levine, R. *J. Am. Chem. Soc.* **81** (1959) 1627.
4. Brändström, A. E., Hjelte, N. S. and Mårtensson, O. Brit. P. 771, 814; U.S.P. 2, 841, 589; Can. P. 573, 771.
5. Mårtensson, O. Brit. P. 796, 839; *Chem. Abstr.* **53** (1959) 11314.
6. Cusic, J. W. U.S.P. 2, 776, 282; *Chem. Abstr.* **51** (1957) 8813.
7. Bockmuhl, M. und Ehrhardt, G. Germ. P. 731 560; Danish P. 61 654.
8. Cheney, I. C., Wheatley, W. R., Speeter, M. E. *et al. J. Org. Chem.* **17** (1952) 770.
9. Moffett, R. B. and Aspegren, B. D. *J. Am. Chem. Soc.* **79** (1957) 4462.
10. Janssen, P. *J. Am. Chem. Soc.* **78** (1956) 3862.
11. Cusic, J. W. U.S.P. 2, 838, 509; *Chem. Abstr.* **53** (1959) 5288.
12. Acheson, R. M., MacPhee, K. E., Philpott, P. G. and Barltrop, J. A. *J. Chem. Soc.* **1956** 698.
13. Weizmann, C. H., Bergman, E. and Sulzbacker, M. *J. Org. Chem.* **15** (1950) 918.
14. Brown, W. G., *Org. Reactions* **6** (1951) 469.
15. Petersen, P. W. and Weidmann, H. *Acta Pharmacol. Toxicol.* **11** (1955) 108.

Received February 13, 1960.

ACTA CHEMICA SCANDINAVICA 14 (1960) 1151—1160

On the Alkylation at the α-Position of Some N,N-disubstituted Toluene(α)sulphonamides and Diphenylmethane-(α)sulphonamides

O. MÄRTENSSON and E. NILSSON

Research Laboratories, A.B. Pharmacia, Uppsala, Sweden

Some N,N-disubstituted toluene(α)sulphonamides and diphenylmethane(α)sulphonamides have been alkylated at the α-position by using sodamide as basic agent and benzene or toluene as solvents. It is shown, that this method is less general and requires more selected reaction conditions than when applied to the corresponding N,N-disubstituted carbonamides. The yields of α-substitution products often are lower. Some of the sulphonamides react very slowly with sodamide. In most of these cases the difficulties can be overcome by using a stronger basic agent, phenylsodium. A survey of the results is given in tabular form.

In a previous paper [1] we have given an account of alkylation at the α-position of N,N-disubstituted arylacetic acid amides. In this context we found it to be of interest to investigate to what extent an exchange of the carbonamide group against a sulphonamide group altered the situation. As expected the activation of the α-hydrogen in many cases proved to be great enough to allow an alkylation by the method applied by us earlier in the carbonamide case, *i.e.* using sodamide as basic agent and benzene or toluene as inert solvent. The reaction can be written

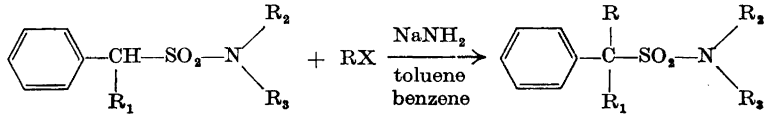

R_1 = H or phenyl,

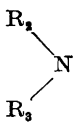

= dialkylamino, benzyl-*n*-propylamino, dibenzylamino, N-methylanilino, pyrrolidino, piperidino and morpholino groups.

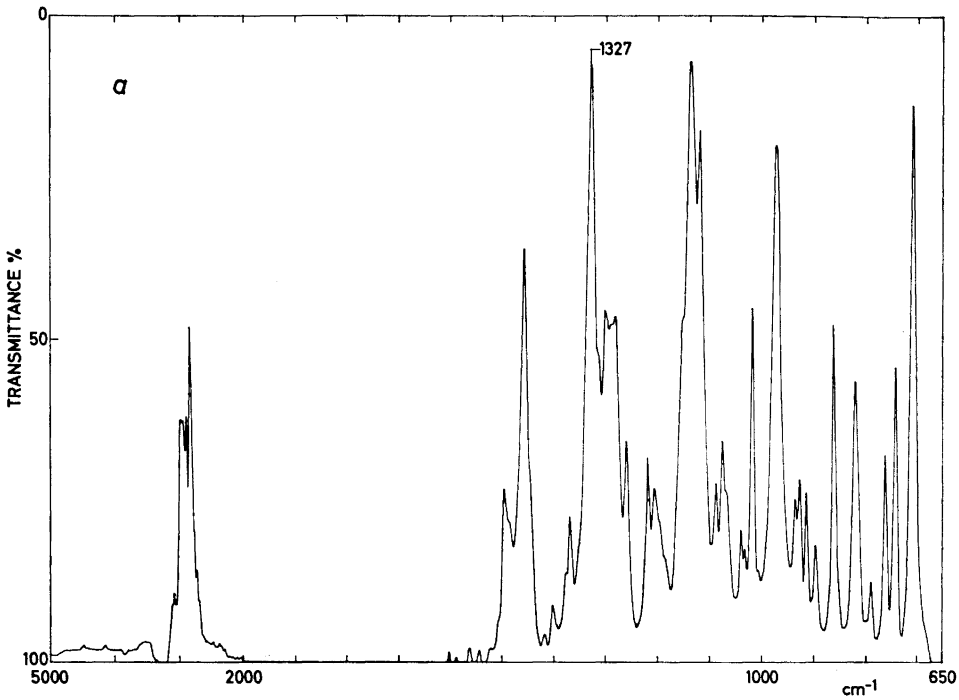

Fig. 1. Infrared spectrum of (a) α-(2-morpholinoethyl)-toluene(α)sulphonic acid N,N-dimethylamide and (b) α-(2-morpholinoethyl)-diphenylmethane(α)sulphonic acid N,N-diethylamide. The significant frequency (at 1 327 cm^{-1} and 1 316 cm^{-1}, respectively)

In most cases we have used 2-morpholinoethyl chloride as RX in order to get substitution products which are easily isolated from the reaction mixture, but some further examples are given in Table 1 in which the results have been compiled.

It is true, that most of the parent toluene(α)sulphonamides and at least some of their α-substituted derivatives can be distilled in vacuum at a pressure of some tenths of a mm Hg. However, this procedure provides that the reaction mixture to be worked up is fairly free from by-products which are still more temperature sensitive, hence would disintegrate and make it difficult to keep the pressure low enough. That is not always the case.

In contrast to the N,N-disubstituted arylacetamides, the N,N-disubstituted toluene(α)sulphonamides and diphenylmethane(α)sulphonamides behave very different as to a variation of the substituents of the amide group when treated with sodamide in an inert solvent such as benzene or toluene. Thus, toluene (α)sulphonylmorpholine reacts fairly slowly with sodamide in boiling toluene under salt formation, while the corresponding dimethylamine compound is rapidly destroyed by sodamide in boiling benzene. From the reaction mixture of this last reaction which proceeds under evolution of sulphur dioxide and

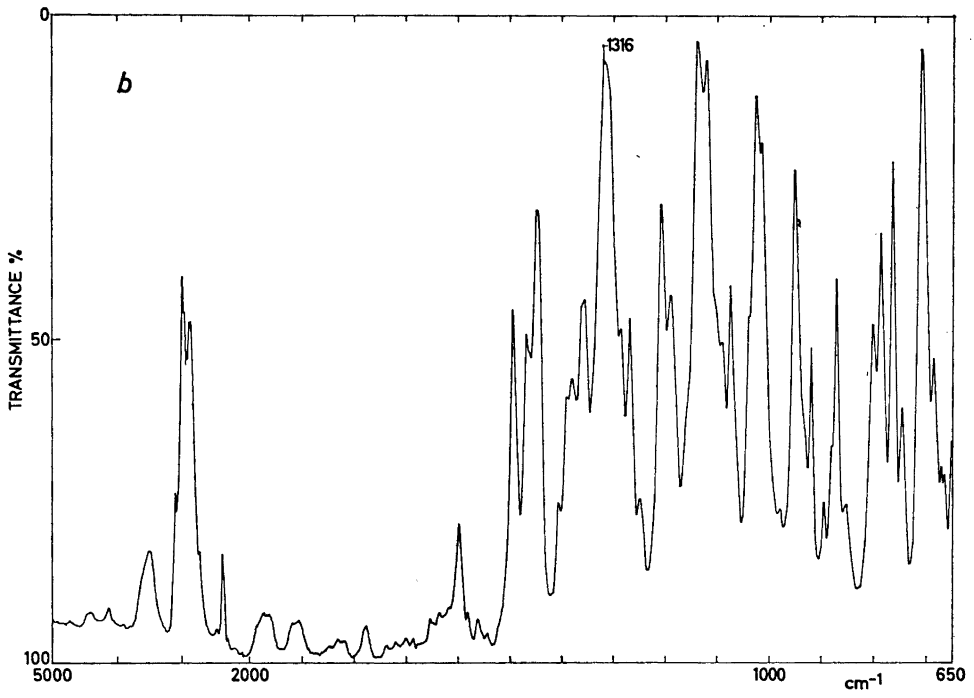

has been indicated by its numerical value. — All spectra are drawn with KBr pellet technique on a Unicam SP 100 IR instrument. The experimental error is 2 cm^{-1}.

dimethylamine, stilbene has been isolated. Tentatively, we suggest the reaction can be explained as including a first benzylation step whereafter the benzylated compound disintegrates according to formula (6) given by Hauser and Harris [2]. However, the dimethylamide can be alkylated in fairly good yield with morpholinoethyl chloride at a temperature of about 70° when the chloride is added to the reaction mixture before warming. The difference between the various N,N-disubstituted sulphonamides is sometimes so pronounced that the sodamide procedure seems to be of limited practical importance for the substitution of some of the sulphonamides. In these cases we have tried phenylsodium as basic agent, and generally with success. N,N-Dibenzyl-toluene(α)sulphonamide, for example, reacts very slowly in boiling toluene. After boiling for about 6 h, 60 % of the parent sulphonamide could be recovered, but no substitution product could be isolated from the reaction mixture. When phenylsodium was used, the yield of recrystallized α-(2-morpholinoethyl) compound was about 70 %.

The optimal reaction conditions are not always easy to find. In some cases of slowly reacting sulphonamides an increase in reaction time and/or reaction temperature does not increase the yield appreciably. To what extent

this result depends on a competitive destruction of the parent sulphonamide and/or the final substitution product, is difficult to say.

The limitation of the alkylation methods applied here are presumably the same as those of the carbonamide case. Some of the sulphonamides are also definitely less soluble in toluene and benzene than the corresponding carbonamides and therefore require more solvent. It should also be pointed out that several of the parent sulphonamides are not easily prepared by conventional methods. Thus, according to our experience to-date, the diphenylmethane(α) sulphonamides can be prepared only *via* diphenyldiazomethane (see also under Experimental). Some of the toluene(α)sulphonamides which otherwise are easily synthetized from toluene(α)sulphonyl chloride and the appropriate secondary amine, may be difficult to prepare or cannot be obtained by this route. Thus, toluene(α)sulphonyl chloride in benzene reacts with di-*iso*propylamine under formation of considerable amounts of a compound with high melting point (240—241.5°C after recrystallization from chloroform), almost insoluble in benzene and most other conventional solvents, including water. Judging from the composition and the fact that not the entire expected amount of amine is consumed during the reaction, we presume this compound to be α-[(toluene(α')sulphonyl)]-toluene(α)sulphonyldi*iso*propylamine, $C_6H_5CH(SO_2CH_2C_6H_5)SO_2N(C_3H_7)_2$.

The results are collected in Table 1. From the above it follows that the alkylations have been carried out by applying three procedures. The first one (1:b) includes more or less incomplete salt formation by boiling the parent sulphonamide with sodamide in toluene for some hours, followed by adding the alkyl halide and further refluxing. It is this procedure which was applied by us as standard method for alkylation of N,N-disubstituted arylacetic acid amides. When it has failed or has not given satisfactory results for the sulphonamides, we have tried a procedure (I:a) which is a slightly modified version of the preceding one. All the reaction components have been mixed together in toluene, and the mixture gently heated until a distinct evolution of ammonia begins and is kept at this temperature until the ammonia evolution has definitely decreased. The third procedure (II) includes the use of phenylsodium as basic agent and has been applied in some cases where the sodamide procedures have not given the desired results. For practical examples of the three procedures see under Experimental.

In order to show that the substituted compounds actually contain the sulphonamide group after alkylation, we have checked the infrared spectra of four of the compounds with reference to the SO_2 frequencies of the sulphonamide group. In Fig. 1 the most significant frequency of the sulphonamide group in the 1 320 cm^{-1} range has been indicated on the curves for two of the compounds investigated.

Some tentative efforts have also been made to condense esters with N,N-disubstituted sulphonamides in the presence of sodium methoxide as condensing agent and with xylene as medium, but these trials have not been encouraging. From a mixture of dimethyl oxalate and N,N-dimethyltoluene(α)sulphonamide only approximately half the theoretical amount of methanol could be distilled off when the temperature was raised to 90°C, and 75 % of the parent sulphonamide could be isolated from the reaction mixture. In order to try

whether a condensation including ring closure would be more easy to carry out or not, we applied the same method to methyl N-(*p*-chlorotoluene(*a*) sulphonyl)-N-*iso*propyl-2- aminopropionate. In this case not less than 87.5 % of N-*iso*propyl-p-chlorotoluene(*a*)sulphonamide (m.p. 137—139°C) could be isolated from the acrylate smelling reaction mixture, indicating that a fission of the amide bond had taken place.

EXPERIMENTAL

As mentioned above the N,N-disubstituted toluene(*a*)sulphonamides have been prepared from toluene(*a*)sulphonyl chloride and the appropriate secondary amines according to known methods and generally with benzene as solvent. Rather few compounds of this type have been reported previously [3,4]. Of course the sulphonamides have considerably higher melting point and boiling point than the corresponding carbonamides and are less soluble than these. That is also the case with the *a*-substitution products. As to the N,N-disubstituted diphenylmethane(*a*)sulphonamides, only the piperidide seems to have been reported earlier [5]. With some minor modifications, which to some extent have been inspired by a recent short communication by Miller [6], we have used the method given by these authors. We have therefore merely collected the melting and/or boiling points of the N,N-disubstituted sulphonamides mentioned in this paper or otherwise known.

Toluene(*a*)sulphonic acid: dimethylamide m. p. 100—101°; diethylamide m. p. ca 30°, b.p. 135—140°/0.3 mm; di-*n*-butylamide b.p. 136—138°/0.1 mm; N-methylanilide m. p. 102—104°; N-ethylanilide m. p. 118—119°; *n*-propyl-benzylamide b.p. 183—188°/0.3 mm; pyrrolidide m. p. 93—94°; piperidide m. p. 136—138°; morpholide m. p. 174—176°.

p-Chlorotoluene(*a*)sulphonic acid: piperidide m. p. 160—162°C; *iso*propyl(*β*-carbomethoxyethyl)-amide m. p. 64.5—66°.

Diphenylmethane(*a*)sulphonic acid: diethylamide m. p. 135—136°; pyrrolidide 175—177°; piperidide m. p. 167—168°.

N,N-Dimethyl-a-(2-morpholinoethyl)-toluene(a)sulphonamide (Method I:a). In a 250 ml flask, equipped with a reflux condenser, stirrer and thermometer, 19.9 g (0.1 mole) of N,N-dimethyltoluene(*a*)sulphonamide, 150 ml of dry toluene, 15.5 g (14.9 g = 0.1 mole) of 2-morpholinoethyl chloride and 4.2 g of commercial, ground sodamide are mixed together. The mixture is warmed gently while stirring. At a temperature of 60—65° a strong evolution of ammonia begins. The reaction mixture is now kept at a temperature of ca 70° for 6 h (a reaction time which perhaps may be shortened). The contents of the flask are cooled to room temperature, water is added and the toluene layer washed with water. The toluene layer is extracted with dilute hydrochloric acid. The united acid solutions are washed with ether, and the base is liberated by adding 5 N sodium hydroxide. When the stirred mixture is inoculated, the oil crystallizes fairly rapidly. The precipitate is filtered off and washed with water and petroleum ether. Yield 22.0 g (70.5 %) m. p. 75.5—77°. After two recrystallizations, the last one including treatment with active carbon, the yield is 17.1 g (55 %) m. p. 76—77°. For analytical data see Table 1.

The hydrochloride can be precipitated in excellent yield from an ether solution of the base by means of alcoholic hydrochloric acid. After recrystallization from methanol and ether the melting point is 203—205°. Yield 83 % (from 5.0 g of the base).

a-(2-Morpholinoethyl)-diphenylmethane(a)sulphonylpyrrolidine (Method I:b). A mixture of 15.1 g (0.05 mole) of diphenylmethane(*a*)sulphonylpyrrolidine, 2.1 g of commercial, ground sodamide and 100 ml of dry toluene is refluxed while stirring for one hour. During this time ammonia is evolved and some precipitate is formed in the flask. The mixture is cooled to about 60° and 8.5 g (theoret. 7.5 g) of 2-morpholinoethyl chloride is added. The mixture is heated again and refluxed for 5 h. After cooling to room temperature, water is added and the mixture washed with water. When excess of 2 N hydrochloric acid is added to the toluene layer under continuous stirring a viscous oil separates, form-

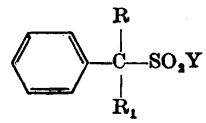

Table 1. Compounds prepared by alkylation at the α-position of some N,N-

R	R_1	Y	Method	React. time, h. Temp.°C	Yield %
H	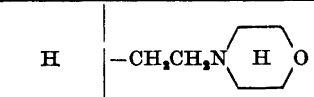	$-N(CH_3)_2$	I:a	8; 70	70 55 83
H	»	$-N(C_2H_5)_2$	I:a	1; 80	32 23
	»	»	II I:a	1; 110 3; 100	35 10
H	»	$-N(n-C_4H_9)_2$	II I:a	1; 105 8; 110	26 0
H	$-CH_2CH_2N(C_2H_5)_2$	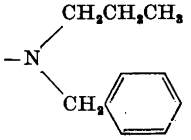	I:b	1; 110	70 38
H	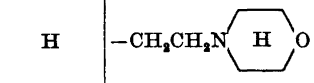	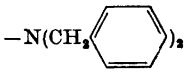	II I:a	1; 110 6; 110	69 63 0
H	»	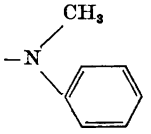	II I:a	0.5; 105 5; 110	32 0
H	»	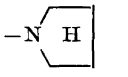	I:a	6; 90	68
	»	»	II I:b	2; 110 5; 110	47 28 53 31

disubstituted toluene(α)-sulphonamides and diphenylmethane(α)sulphonamides.

M.p., °C B = base S = hydrochloride	Formula	Analyses							
		Calc.				Found			
		C	H	N	S	C	H	N	S
B 75.5–77 76–77 [a] S 203–205 [g]	$C_{15}H_{24}N_2O_3S$	57.66	7.74	8.97		58.19	7.84	9.11	
B 50– 54 56.5–58 [a]	$C_{17}H_{28}N_2O_3S$	59.97	8.29	8.23		60.07	8.36	8.27	
B 98–99 [a]	$C_{23}H_{32}N_2O_3S$	66.31	7.74	6.73		66.69	7.74	6.81	
B 97– 99 [a]									
B 59.5–61 [b]	$C_{21}H_{36}N_2O_3S$	63.60	9.15	7.07	8.08	63.80	9.27	7.18	8.06
B oil S 128–132 [c]	$C_{23}H_{35}ClN_2O_2S$	62.91	8.04	6.38		62.88	8.14	6.47	
S 168–170 [c] B 121–122 [a]	$C_{27}H_{32}N_2O_3S$	69.80	6.94	6.03	6.90	70.23	7.19	6.10	6.61
S 173–180 183–185 [d]	$C_{20}H_{27}ClN_2O_3S$	58.45	6.62		7.80	57.86	6.60		7.51
B 85.5–87 [a] S 203–206 [ce]	$C_{17}H_{26}N_2O_3S$	60.32	7.74	8.28		60.66	7.87	8.25	
S dec. 165 [c] B 110–112 [a] S dec. 165 [c] B 110–112 [a]	$C_{23}H_{31}ClN_2O_3S$	61.25	6.93	6.21	7.11	60.80	7.01	6.23	7.21

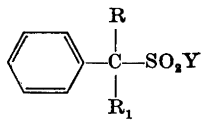

Table 1. Continued.

R	R_1	Y	Method	React. time, h. Temp.°C	Yield %
	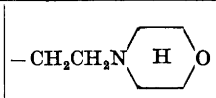	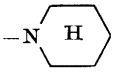	I:a	5; 105	75 61
H[h]	$-CH_2CH_2CH_2N(C_2H_5)_2$	»	I:b	1; 110	63 45
H	$-CH_2CH_2C(CH_3)_3$	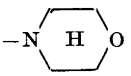	I:a	13; 110	65 30
H	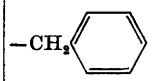	»	I:b	3; 110	60 15
H	$-CH_2CH_2N(C_2H_5)_2$	»	I:b	4; 110	33 24
H	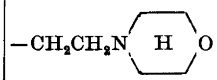	»	I:a II	10; 100 1.5; 110	50 48
H	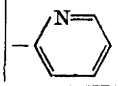	»	I:b	6; 110	12

Notes: It should be observed that one of the parent sulphonamides, *p*-chlorotoluene(*a*)sulphonylpiperidine (and the corresponding substitution product) has a chlorine atom in *para* position (see note h) which is not indicated in the general formula in the heading. — With the exception of 2-bromopyridine, chlorides have been used as alkylating agents. — For methods I:a, I:b and II see the introductory text and under Experimental. — When the substitution products are tertiary amines, B indicates base and S hydrochloride. — The yields are the total ones and refer to the parent sulphonamide. When more than one yield figure is given under a certain method, the compound prepared according to this method has been further purified by recrystall-

ing a third phase. It crystallizes on scratching. The precipitate is filtered off, washed with water and ether. The yield of this almost pure hydrochloride of the substitution compound is 12.0 g (53.5 %) m. p. 163.5—165°. For analytical data see Table 1.

The base can be precipitated from a dilute aqueous solution of the hydrochloride by dilute sodium hydroxide. After recrystallization from *cyclo*hexane the m. p. is 110—112°.

M. p., °C B = base S = hydro-chloride	Formula	Analyses							
		Calc.				Found			
		C	H	N	S	C	H	N	S
B 70–72.5 72–73.5[a]	$C_{18}H_{28}N_2O_3S$	61.33	8.01	7.95		61.45	8.05	8.04	
B oil S 169–172.5[c]	$C_{19}H_{32}Cl_2N_2O_3S$	53.89	7.62		7.57	53.97	7.62		7.44
B 123 –129 128.5–131[a]	$C_{17}H_{27}NO_3S$	62.74	8.36	4.30		62.37	8.34	4.46	
B 134 –141 155.5–157[e]	$C_{18}H_{21}NO_3S$	65.23	6.39	4.23		65.16	6.43	4.20	
B 48–53 54 – 56[b]	$C_{17}H_{23}N_2O_3S$	59.97	8.29	8.23	9.42	60.25	8.39	8.26	9.31
B 84.5–86 B 83–84.5[a]	$C_{17}H_{26}N_2O_4S$	57.60	7.39	7.90		57.74	7.47	7.95	
B 154–156[f]	$C_{16}H_{18}N_2O_3S$	60.35	5.70	8.80	10.07	60.55	5.72	8.96	9.89

ization. — Melting points and boiling points are uncorrected. The former have been read from short normal thermometers covering intervals of 50°. — The alkylations have been carried out with 0.1–0.05 mole of parent sulphonamide.

a–g): Recrystallization from a) *cyclo*hexane; b) petroleum ether; c) acetone; d) ethylene chloride; e) methanol; ce) a mixture of acetone and methanol; f) benzene; g) a mixture of methanol and ether;

h): The parent amide is *p*-chlorotoluene(*α*)sulphonylpiperidine.

N,N-Dibenzyl-α-(2-morpholinoethyl)-toluene(α)sulphonamide (Method II). 50 ml of sodium dispersion (prepared from 12.5 g of sodium, 250 ml of dry toluene and 0.3 ml of oleic acid under nitrogen, by means of an "Ultra-Turrax" dispergator and cooled to room temperature) is pipetted into a 0.5 l flask equipped with reflux condensor, thermometer, stirrer and a dropping funnel. A slow flux of nitrogen is allowed to pass through this

equipment About 10 ml of a solution of 5.7 g (about 0.05 mole) of chlorobenzene in 25 ml of dry toluene is added to the dispersion *via* the dropping funnel in order to start the formation of phenylsodium. When the reaction has started, the remaining chlorobenzene solution is added to the sodium dispersion, while stirring, at such a rate that under intermittent cooling with a dry ice-alcohol bath the reaction temperature is kept at about 25°. When all the chlorobenzene solution has been added, the cooling bath is removed and the black reaction mixture is allowed to stand while stirring for about 15 min. If the temperature increases again during this period, the mixture should be cooled again. A solution of 17.5 g (0.05 mole) of N,N-dibenzyl-toluene (*a*)sulphonamide in about 120 ml of warm, dry toluene (this sulphonamide like some others, *e. g.* the morpholino compound, is only slightly soluble in cold toluene) is added *via* the funnel while stirring, and the flask is warmed to 55° for about 10 min. During this procedure the black colour of phenylsodium disappears and the contents of the flask become grayish. The flask contents are cooled to about 40° and a solution of 8.0 g (7.5 g = 0.05 mole) of 2-morpholinoethyl chloride in 25 ml of dry toluene is added while stirring *via* the funnel. The reaction mixture is now heated. At about 90° the grayish precipitate disappears and the reaction mixture becomes almost clear. The temperature is kept at about 110° for one hour. The flask contents are now cooled to room temperature and water is added carefully. The toluene layer is washed with water. When 2 N hydrochloric acid is added to the toluene phase the hydrochloride of the morpholinoethyl derivative precipitates as a third oily phase, which crystallizes on scratching. The precipitate is filtered off and washed with water and ether. Yield 18.3 g (78.5 %) m. p. about 140°. Recrystallization from a mixture of toluene and acetone gives 14.2 g with m. p. 168—170°. From the mother liquor another 1.5 g can be obtained with the same m. p. Total yield 69 %.

The base was liberated from 5.0 g of the hydrochloride and taken up in ether. When the ether is evaporated, 4.6 g of the base is obtained. After recrystallization from 50 ml of *cyclo*hexane, the yield is 4.3 g (91 %). For analytical data see Table 1.

The authors are indebted to Mr. W. Kirsten and his assistants for elementary analyses and to Dr. B. Nygård for infrared analyses.

REFERENCES

1. Mårtensson, O. and Nilsson, E. *Acta Chem. Scand.* **14** (1960) 1129.
2. Hauser, C. R. and Harris, Th. M. *J. Am. Chem. Soc.* **81** (1959) 1157.
3. Marvel, C. S. and Gillespie, H. B. *J. Am. Chem. Soc.* **48** (1926) 2943.
4. Ingold, C. K. and Wilson, J. S. *J. Chem. Soc.* **1927** 813.
5. Kloosterziel, H., Deinema, M. H. and Backer, H. J. *Rec. trav. chim.* **71** (1952) 1228.
6. Miller, J. B. *J. Org. Chem.* **24** (1959) 560.

Received February 13, 1960.

ACTA CHEMICA SCANDINAVICA 14 (1960) 1161—1172

The Crystal Structure of Ti_5O_9

STEN ANDERSSON

Institute of Inorganic and Physical Chemistry, University of Stockholm, Stockholm, Sweden

The crystal structure of Ti_5O_9, the second member of the homologous series Ti_nO_{2n-1}, has been determined. It is triclinic, spacegroup $P\bar{1}$, with a cell content of 2 Ti_5O_9 and with unit cell dimensions $a = 5.569$ Å, $b = 7.120$ Å, $c = 8.865$ Å, $\alpha = 97.55°$, $\beta = 112.34°$ and $\gamma = 108.50°$. It may be described in terms of TiO_6-octahedra, which are joined by sharing edges and corners to form slabs of rutile structure, extending infinitely in two dimensions and possessing a finite width corresponding to five TiO_6 octahedra. The slabs are mutually connected by octahedra sharing faces.

The Ti_5O_9 structure provides the clue to the problem of finding the crystal structure of any member of the homologous series Ti_nO_{2n-1}, $Ti_{n-2}Cr_2O_{2n-1}$ and V_nO_{2n-1}.

The existence of a considerable number of discrete phases in the composition region $MO_{1.75-1.90}$ has been demonstrated for the titaniumoxygen system[1-3], for the titanium-chromium-oxygen system[4] and for the vanadium-oxygen systems[5]. The related and regularly changing appearance of the powder patterns of all these phases, the compositions of which are in close agreement with the general formula M_nO_{2n-1} (n integer), suggested that the various structures are all based on a common structural principle, in analogy with the case[6-8] for the molybdenum and the molybdenum wolfram oxides of the homologous series $(Mo,W)_nO_{3n-1}$.

It was thus thought possible to derive the structure of any member of the series M_nO_{2n-1} provided that the detailed structure of one homologue were known. This article gives an account of the structure determination of the phase Ti_5O_9. General structural data for the series will be given elsewhere[9].

EXPERIMENTAL

Details about the preparation and some other data concerning the $TiO_{1.80}$ sample have been given in previous communications[1,2]. Crystals of Ti_5O_9 were obtained by heating this sample at 1 150°C for three days in evacuated silica tubes. The crystals formed minute rods always found to be twinned. A fragment obtained by crushing a crystal was, however, found to have only a relatively small twin parasite, and was thus suitable for single-crystal studies.

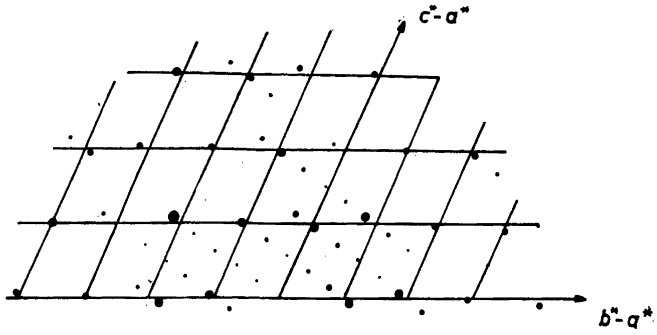

Fig. 1. The reciprocal lattice plane $h0l$ of Ti_5O_9. The networks represent the reciprocal lattice of the subcell (rutile).

Weissenberg photographs of the layer lines $(0-3, k, l)$ and $(h, 0-4, l)$ were registered with CuK radiation using multiple film techniques. The intensities of the reflexions were estimated visually.

A remarkable feature of the photographs was the extremely low number of reflexions hkl with k odd. Thus, the $(h1l)$ layer line contained only three strong, one medium and two weak reflexions.

Accurate unit cell dimensions were obtained from photographs taken in a Guinier focusing camera using strictly monochromatized Cu$K\alpha_1$ radiation and applying a procedure described in a previous communication from this Institute [10].

DERIVATION OF THE STRUCTURE

The single crystal data showed the structure to be triclinic, *i.e.* the symmetry should be $P1$ (No. 1) or $P\bar{1}$ (No. 2).

The Guinier powder photograph gave the following unit cell dimensions, referred to the lattice parameter of potassium chloride $a = 6.2919$ Å at 20 C:

$$a = 5.569 \text{ Å}, \quad b = 7.120 \text{ Å}, \quad c = 8.865 \text{ Å},$$
$$\alpha = 97.55°, \quad \beta = 112.34°, \quad \gamma = 108.50°.$$

The observed density of 4.29 indicated that the unit cell contains 2 formula units of Ti_5O_9, the calculated density being 4.31. The powder pattern has been published in a previous report [11].

The reciprocal lattice plane $h0l$, which is illustrated in Fig. 1, shows the presence of a pronounced substructure in real space. By considering the three-dimensional data, it was found that the substructure unit coincides with the structure of the rutile type, as was already suggested by the appearance of the powder pattern [1-3]. The [010]-direction of Ti_5O_9 was found to correspond to [111] of rutile. The structure determination could thus be started along the lines developed by Magnéli [7,8,12,13] when studying several molybdenum and wolfram oxides and especially $W_{20}O_{58}$.

The substructure character in this case implies that the strong reflexions of Ti_5O_9 occur close to the reciprocal lattice points of rutile. Assuming the structure to possess a centre of symmetry, the various strong reflexions were

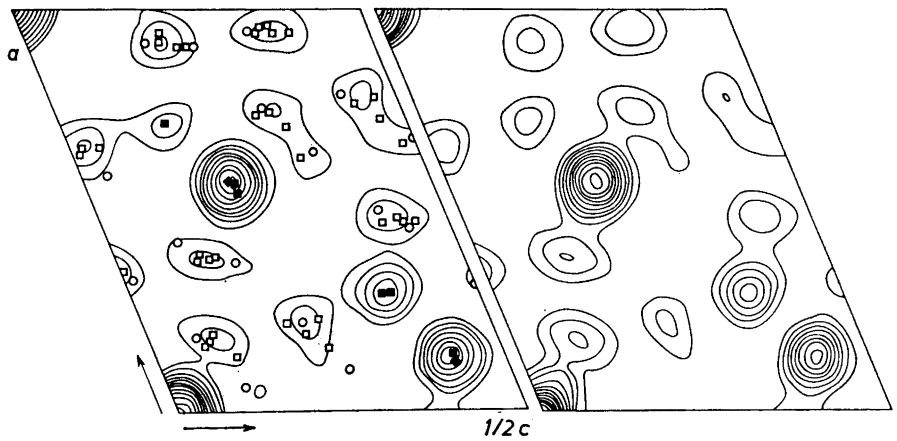

Fig. 2. Patterson projections along [010]. 1) Calculated from $|F|^2_{obs}$. 2) Calculated from $|F|^2_{calc}$. ◆ : Ti-Ti vectors (Multiplicity 8); ■ : Ti-Ti vectors (Multiplicity 4); □ : Ti-O vectors (Multiplicity 4); O : Ti-O vectors (Multiplicity 2).

assigned the signs of the corresponding rutile reflexions. This was done for two alternatives, *viz.* with a metal atom in or not in the origin position.

The two-dimensional Fourier sum* calculated over the strong reflexions *h0l*, which should correspond to a projection parallel to [010] of the "electron density function" for both alternatives, showed heavy maxima which could be attributed to titanium atoms and also minor ones which might be interpreted as due to oxygen atoms. Both alternatives were in fair agreement with the Patterson projection along [010] illustrated in Fig. 2 : 1. By including more reflexions in the Fourier sum, it was found possible to arrive at an index of agreement

$$\frac{\sum || F(h0l_{obs}| - |F(h0l)_{calc} ||}{\sum |F(h0l)_{obs}|}$$

as low as 0.20. It was thus thought that this structure proposal should not be very different from the actual structure, which, however, might lack the centre of symmetry.

In order to find the *y* coordinates corresponding to the approximate structure, the [100] projection of the Patterson function was studied (*cf.* Fig. 3 : 1). In this way it was possible to find the metal atom coordinates. However, when calculating the *F(hkl)* values, it was observed that the agreement was rather poor for the weak layer lines with *k* odd.

* During the later stages of the investigation the computational work was highly facilitated by the employment of the electronic digital computer BESK of the Swedish Board of Computing Machinery. Programmes for automatic Patterson and electron density syntheses and for automatic calculation of structure factors have been prepared by members of this research group [14,15].

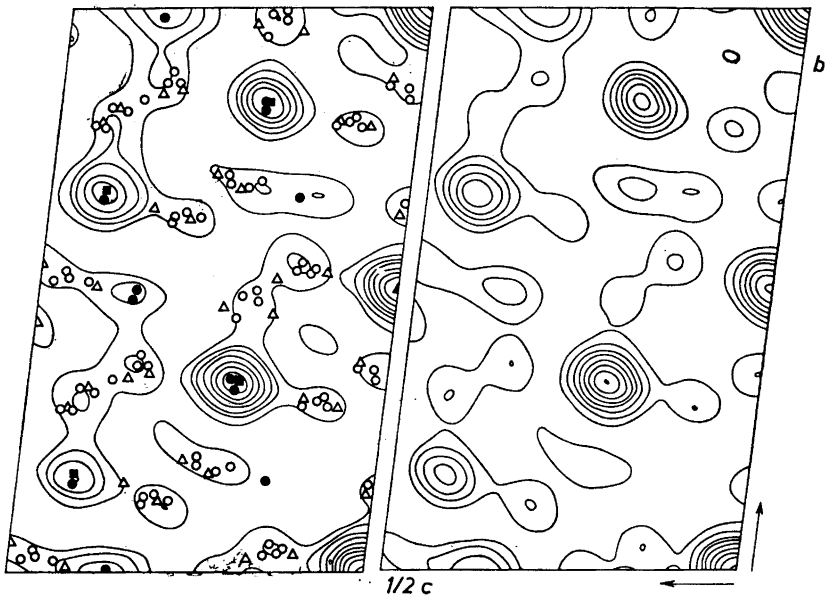

Fig. 3. Patterson projections along [100]. 1) Calculated from $|F|^2_{obs}$. 2) Calculated from $|F|^2_{calc}$. ▲ : Ti-Ti vectors (Multiplicity 10); ■ : Ti-Ti vectors (Multiplicity 4]; ● : Ti-Ti vectors (Multiplicity 2); O: Ti-O vectors (Multiplicity 2); △: Ti-O vectors (Multiplicity 1).

Starting from the approximate centrosymmetric structure thus derived, the metal atom positions were modified to improve the agreement with the Patterson function. The changes of the coordinates were considerable only for one of the ten titanium atoms and implies that the symmetry of the structure was lowered to $P1$. The electron density projections parallel to [010] and [100] calculated on the basis of the modified structure showed maxima interpretable as due to all the titanium and oxygen atoms of the unit cell.

The agreement between the Patterson functions calculated from the observed and the corresponding calculated $|F|^2$ values and the interatomic vector sets required by the structure is demonstrated in Figs. 2 and 3 and Table 1.

In Fig. 3 : 1 it can be seen that there is no maximum in the Patterson projection corresponding to the titanium-titanium vector of the lowest multiplicity required by the structure. Such a phenomenon has been demonstrated by Magnéli [13] to be due to the large number of non-observed reflexions. Thus the Patterson projection calculated from $|F|^2_{calc}$ omitting all reflexions below "the limit of visibility" (Fig. 3 : 2) does not show a maximum corresponding to this titanium-titanium vector. The two weak maxima in Fig. 3 : 1, which are not required by the metal atom structure correspond to the oxygen-oxygen vectors of highest multiplicity.

Table 1. Patterson projections along [010] and [100]. Comparison between observed and calculated coordinates and the heights of the corresponding maxima.

x_{obs} / x_{calc}	z_{obs} / z_{calc}	height$_{obs}$ / height$_{calc}$	y_{obs} / y_{calc}	z_{obs} / z_{calc}	height$_{obs}$ / height$_{calc}$
0.182	0.097	6	0.355	0.004	3
0.178	0.093	9	0.346	0.002	4
0.379	0.124	5	0.500	0.000	29
0.383	0.127	8	0.500	0.000	28
0.657	0.020	9	0.469	0.203	3
0.655	0.015	8	0.482	0.208	3
0.706	0.150	6	0.548	0.140	5
0.713	0.150	6	0.547	0.137	5
0.919	0.196	9	0.665	0.123	4
0.917	0.201	9	0.668	0.130	4
0.571	0.211	37	0.677	0.200	4
0.572	0.215	41	0.676	0.206	5
0.223	0.235	7	0.626	0.302	2
0.220	0.231	5	0.623	0.303	4
0.135	0.421	26	0.789	0.420	5
0.136	0.423	29	0.806	0.425	4
0.294	0.368	16	0.995	0.366	11
0.293	0.365	18	0.997	0.359	12
0.489	0.415	7	0.786	0.080	3
0.485	0.422	8	0.785	0.081	5
0.749	0.314	5	0.834	0.212	21
0.747	0.310	6	0.833	0.212	22
0.786	0.449	6	0.865	0.012	2
0.783	0.446	4	0.852	0.007	3
0.948	0.357	6	0.917	0.094	3
0.950	0.351	8	0.916	0.093	0
0.039	0.133	4	0.980	0.207	4
0.039	0.133	4	0.987	0.214	5
0.187	0.217	2	0.117	0.295	3
0.182	0.216	4	0.115	0.297	5
0.293	0.086	3	0.171	0.422	12
0.291	0.086	4	0.169	0.425	14
0.334	0.213	28	0.305	0.426	4
0.333	0.214	28	0.314	0.429	4

(Table 1 (contd.)

x_{obs} / x_{calc}	z_{obs} / z_{calc}	height$_{obs}$ / height$_{calc}$	x_{obs} / x_{calc}	z_{obs} / z_{cac}	height$_{obs}$ / height$_{calc}$
0.372	0.358	4	0.887	0.363	5
0.366	0.354	4	0.875	0.358	4
0.496	0.377	5	0.550	0.491	2
0.500	0.367	6	0.548	0.485	3
0.672	0.425	18			
0.669	0.427	19			

The index of agreement, R, for the two projections [010] and [100] was found to be 0.13 and 0.15, respectively. For all the 272 registered reflexions, the R-value is 0.18. The 19 observed reflexions hkl with k odd, which are due only to the oxygen atom contributions have $R = 0.10$, which indicates that the oxygen atom positions should be fairly accurate. Table 2 gives the observed and calculated F values for reflexions $h0l$, $0kl$ and hll.

DESCRIPTION OF THE STRUCTURE

The structure is built up of TiO_6 octahedra which are joined by sharing corners, edges and faces. All the interatomic distances are of reasonable lengths, *viz.* 2.81—3.19 Å for the Ti-Ti distances, 1.75—2.35 Å for the Ti-O and 2.4—3.15 Å for the O—O distances. The shortest Ti-Ti distance connects the metal atoms of TiO_6 octahedra with a face in common.

The oxygen atom packing is roughly a deformed hexagonal close packing and similar to that of rutile. The structure may be described as being built up of rutile-type elements, with a complicated arrangement of the metal atoms in the interstitial positions of the lattice formed by the anion packing.

The metal atom positions in the projections along [010] and [100] are shown in Figs. 4 and 5. The dotted lines refer to an alternative origin, which apparently is a centre of symmetry for the metal atom arrangement. However, this is not true since it has a significant deviation from centrosymmetry. The origin chosen was preferred because it emphasizes the true centrosymmetry found to be present in the arrangement of the oxygen atoms.

In both projections the metal atoms form chains of five TiO_6-octahedra (if these chains were of infinite length, the structure would be rutile). The chains are connected to form rutile-type slabs possessing an infinite extension in two dimensions and a characteristic finite width (five TiO_6-octahedra) *i.e.* the length of the chain in a third direction, indicated by arrows in Fig. 5. The mutual connection of the slabs takes place by means of TiO_6-octahedra sharing faces.

Table 2. Observed and calculated structure factors *h0l*, *0kl* and *h1l* for Ti_5O_9. The values of the phase angle, α are expressed as fractions of one cycle.

h 0 l	$\|F\|_{obs}$	$\|F\|_{calc}$	α	*h 0 l*	$\|F\|_{abs}$	$\|F\|_{calc}$	α
2 0 $\bar{11}$	<18	4	0.427	4 0 $\bar{3}$	<35	19	0.366
3 0 $\bar{11}$	<20	8	0.389	5 0 $\bar{3}$	<38	4	0.748
4 0 $\bar{11}$	65	59	0.969	6 0 $\bar{3}$	<30	22	0.969
0 0 $\bar{10}$	56	45	0.947	0 0 $\bar{2}$	26	14	0.742
1 0 $\bar{10}$	<25	13	0.176	1 0 $\bar{2}$	62	72	0.064
2 0 $\bar{10}$	77	82	0.510	2 0 $\bar{2}$	52	38	0.851
3 0 $\bar{10}$	<30	7	0.566	3 0 $\bar{2}$	25	31	0.153
4 0 $\bar{10}$	<27	14	0.128	4 0 $\bar{2}$	<35	22	0.859
5 0 $\bar{10}$	<22	27	0.911	5 0 $\bar{2}$	<37	17	0.078
0 0 $\bar{9}$	67	74	0.037	6 0 $\bar{2}$	111	105	0.498
1 0 $\bar{9}$	<34	18	0.839	0 0 $\bar{1}$	13	11	0.374
2 0 $\bar{9}$	<36	18	0.086	0 0 $\bar{1}$	13	11	0.374
3 0 $\bar{9}$	<36	5	0.518	1 0 $\bar{1}$	25	27	0.683
4 0 $\bar{9}$	<35	13	0.895	2 0 $\bar{1}$	110	104	0.455
5 0 $\bar{9}$	80	81	0.473	3 0 $\bar{1}$	31	27	0.697
6 0 $\bar{9}$	<17	17	0.682	4 0 $\bar{1}$	48	52	0.061
0 0 $\bar{8}$	<36	25	0.641	5 0 $\bar{1}$	<36	17	0.888
1 0 $\bar{8}$	60	43	0.429	6 0 $\bar{1}$	<23	10	0.468
2 0 $\bar{8}$	<38	21	0.606	0 0 0	–	364	0.000
3 0 $\bar{8}$	101	117	0.006	1 0 0	22	18	0.259
4 0 $\bar{8}$	<35	10	0.081	2 0 0	60	50	0.581
5 0 $\bar{8}$	49	51	0.538	3 0 0	55	38	0.391
6 0 $\bar{8}$	36	33	0.425	4 0 0	<38	20	0.734
0 0 $\bar{7}$	<38	20	0.228	5 0 0	<34	24	0.408
1 0 $\bar{7}$	<37	34	0.608	6 0 0	<17	6	0.649
2 0 $\bar{7}$	<36	20	0.340	1 0 1	34	21	0.079
3 0 $\bar{7}$	<37	9	0.777	2 0 1	<26	19	0.725
4 0 $\bar{7}$	<38	10	0.979	3 0 1	85	92	0.038
5 0 $\bar{7}$	<36	10	0.256	4 0 1	<38	20	0.760
6 0 $\bar{7}$	58	66	0.965	5 0 1	78	90	0.474
0 0 $\bar{6}$	<35	27	0.866	1 0 2	97	103	0.505
1 0 $\bar{6}$	33	25	0.196	2 0 2	<29	14	0.229
2 0 $\bar{6}$	62	53	0.936	3 0 2	59	59	0.948
3 0 $\bar{6}$	<36	14	0.173	4 0 2	44	33	0.099
4 0 $\bar{6}$	80	94	0.505	5 0 2	<26	17	0.827
5 0 $\bar{6}$	<37	16	0.568	1 0 3	<26	4	0.619
6 0 $\bar{6}$	<28	23	0.094	2 0 3	<32	21	0.567
0 0 $\bar{5}$	116	113	0.472	3 0 3	<37	18	0.325
1 0 $\bar{5}$	32	26	0.741	4 0 3	70	72	0.540
2 0 $\bar{5}$	114	133	0.029	1 0 4	<31	7	0.313
3 0 $\bar{5}$	30	33	0.914	2 0 4	80	82	0.008
4 0 $\bar{5}$	<36	8	0.157	3 0 4	<36	12	0.772
5 0 $\bar{5}$	<38	10	0.447	4 0 4	54	45	0.444
6 0 $\bar{5}$	<30	13	0.853	1 0 5	<35	12	0.657
0 0 $\bar{4}$	38	35	0.589	2 0 5	<38	5	0.000
1 0 $\bar{4}$	42	39	0.375	3 0 5	<33	15	0.097
2 0 $\bar{4}$	25	34	0.651	4 0 5	<16	13	0.779
3 0 $\bar{4}$	58	55	0.438	1 0 6	<38	25	0.087
4 0 $\bar{4}$	<35	17	0.613	2 0 6	<36	4	0.729
5 0 $\bar{4}$	87	83	0.001	3 0 6	96	112	0.507
6 0 $\bar{4}$	<30	11	0.125	1 0 7	87	89	0.974
0 0 $\bar{3}$	24	17	0.217	2 0 7	<30	7	0.187
1 0 $\bar{3}$	105	142	0.968	1 0 8	<30	20	0.361
2 0 $\bar{3}$	32	33	0.180	2 0 8	<18	15	0.599
3 0 $\bar{3}$	116	139	0.527	1 0 9	<20	16	0.691

Table 2 (cont.)

0 *k l*	$\lvert F\rvert_{obs}$	$\lvert F\rvert_{calc}$	α	0 *k l*	$\lvert F\rvert_{obs}$	$\lvert F\rvert_{calc}$	α
0 0 $\bar{10}$	56	45	0.946	0 0 $\bar{5}$	24	17	0.278
0 1 $\bar{10}$	<22	4	0.997	0 1 $\bar{3}$	<22	8	0.000
0 2 $\bar{10}$	<23	13	0.212	0 2 $\bar{3}$	81	97	0.021
0 3 $\bar{10}$	<23	3	0.006	0 3 $\bar{3}$	<26	3	0.478
0 4 10	28	16	0.016	0 4 $\bar{3}$	<30	26	0.804
0 5 $\bar{10}$	<16	3	0.483	0 5 $\bar{3}$	<35	3	0.967
0 0 $\bar{9}$	67	74	0.038	0 6 $\bar{3}$	<38	14	0.212
0 1 $\bar{9}$	<31	10	0.002	0 7 $\bar{3}$	<36	1	0.478
0 2 $\bar{9}$	<32	12	0.733	0 8 $\bar{3}$	103	91	0.008
0 3 $\bar{9}$	26	29	0.000	0 0 $\bar{2}$	26	14	0.749
0 4 $\bar{9}$	<30	5	0.765	0 1 $\bar{2}$	<17	2	0.498
0 5 $\bar{9}$	<27	8	0.508	0 2 $\bar{2}$	49	35	0.594
0 6 $\bar{9}$	59	73	0.034	0 3 $\bar{2}$	<25	7	0.511
0 0 $\bar{8}$	<36	25	0.657	0 4 $\bar{2}$	88	100	0.459
0 1 $\bar{8}$	<38	2	0.510	0 5 $\bar{2}$	<35	4	0.475
0 2 $\bar{8}$	82	97	0.484	0 6 $\bar{2}$	<38	16	0.621
0 3 $\bar{8}$	<37	3	0.500	0 7 $\bar{2}$	<36	1	0.994
0 4 $\bar{8}$	<35	11	0.362	0 8 $\bar{2}$	37	32	0.537
0 5 $\bar{8}$	<33	5	0.015	0 0 $\bar{1}$	13	11	0.375
0 6 $\bar{8}$	<28	27	0.609	0 1 $\bar{1}$	<15	3	0.504
0 7 $\bar{8}$	<19	1	0.571	0 2 $\bar{1}$	34	28	0.179
0 0 $\bar{7}$	<38	20	0.203	0 3 $\bar{1}$	<24	6	0.014
0 1 $\bar{7}$	<38	1	0.489	0 4 $\bar{1}$	47	62	0.565
0 2 $\bar{7}$	<38	7	0.685	0 5 $\bar{1}$	<35	5	0.983
0 3 $\bar{7}$	<38	5	0.002	0 6 $\bar{1}$	<38	17	0.067
0 4 $\bar{7}$	51	38	0.947	0 7 $\bar{1}$	<35	2	0.509
0 5 $\bar{7}$	<37	1	0.921	0 8 $\bar{1}$	<24	19	0.088
0 6 $\bar{7}$	<33	25	0.129	0 0 0	—	364	0.000
0 7 $\bar{7}$	<26	5	0.478	0 1 0	<14	1	0.511
0 0 $\bar{6}$	<35	27	0.839	0 2 0	42	33	0.170
0 1 $\bar{6}$	<34	2	0.507	0 3 0	85	80	0.001
0 2 $\bar{6}$	<34	8	0.439	0 4 0	18	28	0.850
0 3 $\bar{6}$	<35	2	0.986	0 5 0	<36	2	0.969
0 4 $\bar{6}$	46	60	0.043	0 6 0	113	117	0.004
0 5 $\bar{6}$	<38	5	0.479	0 7 0	<34	2	0.980
0 6 $\bar{6}$	<36	19	0.780	0 8 0	<21	12	0.263
0 7 $\bar{6}$	<30	28	0.503	0 1 1	<16	0	0.134
0 8 $\bar{6}$	<19	10	0.425	0 2 1	86	77	0.564
0 0 $\bar{5}$	116	113	0.470	0 3 1	<26	1	0.590
0 1 $\bar{5}$	<30	3	0.496	0 4 1	<32	20	0.238
0 2 $\bar{5}$	<30	1	0.158	0 5 1	<37	10	0.005
0 3 $\bar{5}$	<32	2	0.025	0 6 1	<38	16	0.495
0 4 $\bar{5}$	34	31	0.607	0 7 1	<31	6	0.011
0 5 $\bar{5}$	<38	6	0.084	0 1 2	<20	4	0.994
0 6 $\bar{5}$	82	93	0.470	0 2 2	87	90	0.448
0 7 $\bar{5}$	<33	4	0.020	0 3 2	<29	1	0.428
0 8 $\bar{5}$	<24	3	0.901	0 4 2	<34	16	0.720
0 0 $\bar{4}$	38	35	0.575	0 5 2	<38	9	0.997
0 1 $\bar{4}$	<25	2	0.503	0 6 2	<36	5	0.863
2 0 $\bar{4}$	33	18	0.943	0 7 2	<27	1	0.614
0 3 $\bar{4}$	<29	0	0.621	0 1 3	81	82	0.500
0 4 $\bar{4}$	23	23	0.206	0 2 3	41	44	0.898
0 5 $\bar{4}$	<36	3	0.462	0 3 3	<32	10	0.506
0 6 $\bar{4}$	<38	23	0.626	0 4 3	64	58	0.033
0 7 $\bar{4}$	<35	4	0.513	0 5 3	<38	7	0.001
0 8 $\bar{4}$	37	24	0.992	0 6 3	<33	9	0.366

Table 2 (cont.)

0 k l	$\|F\|_{obs}$	$\|F\|_{calc}$	a	0 k l	$\|F\|_{obs}$	$\|F\|_{calc}$	a
0 7 3	<20	23	0.496	0 2 6	104	108	0.026
0 1 4	<28	1	0.981	0 3 6	<37	8	0.496
0 2 4	<31	24	0.246	0 4 6	<32	5	0.986
0 3 4	<36	7	0.493	0 5 6	<22	23	0.002
0 4 4	<38	9	0.832	0 1 7	<38	1	0.466
0 5 4	<36	3	0.497	0 2 7	<36	26	0.918
0 6 4	43	41	0.537	0 3 7	<32	1	0.529
0 1 5	<33	1	0.039	0 4 7	<23	10	0.544
0 2 5	<35	28	0.633	0 1 8	<34	3	0.506
0 3 5	<38	6	0.507	0 2 8	<29	13	0.351
0 4 5	<37	4	0.312	0 3 8	<22	4	0.002
0 5 5	<30	4	0.506	0 1 9	<25	1	0.488
0 6 5	61	72	0.476	0 2 9	<17	7	0.752
0 1 6	<37	2	0.991				

In the rutile structure there are channels of empty interstitial positions along the *c* axis ($\frac{1}{2}00$ or $\frac{1}{2}0\frac{1}{2}$). In the Ti_5O_9 structure the end atoms of the chains (*cf.* Figs. 4 and 5) occupy such positions of the neighbouring rutile slabs. The latter are thus mutually "out of phase" by $\frac{1}{2}(b_r + c_r)$ (*cf.* Fig. 6), which gives rise to a so called" shear structure". A term introduced by Wadsley [17].

The structure of the shear plane (the border region of the two "out of phase" rutile-type blocks) is closely related to the corundum-structure type. Thus, parallel to the *b* axis of Ti_5O_9, infinite chains of double-octahedra are found, the doublets being formed by two single TiO_6-octahedra sharing a face. The double octahedra are coupled together within the chains by having edges in common (*cf.* Fig. 7 : 1). These chains are included in the rutile-typs slabs, the connection taking place by octahedra sharing edges and corners (Fig. 7 : 2).

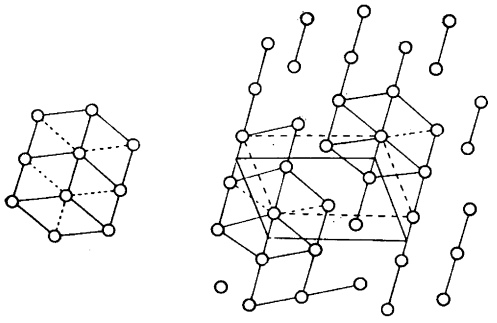

Fig. 4. The metal atom arrangement of Ti_5O_9 viewed along [010] and of rutile parallel to [111].

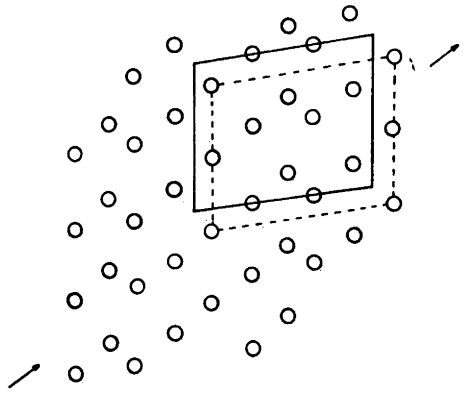

Fig. 5. The metal atom arrangement of Ti_5O_9 viewed along [100]. The arrows show the direction of the finite extension of the rutile slabs.

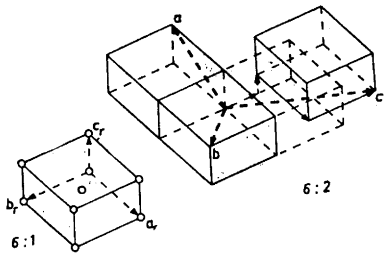

Fig. 6. 1) Unit cell of rutile with positions of metal atoms indicated. 2) Interrelation of basic rutile-type structure of adjacent slabs of Ti_5O_9. Unit cell axes of the latter indicated by dashed heavily-drawn arrows.

The metal-metal distance over the common face is 2.81 Å, while the distance between metal atoms over the common edge is 3.19 Å. The corresponding distance [16] for Ti_2O_3 are 2.56 and 2.99 Å.

The shearing mechanism can be described by means of a translation matrix. Fig. 6 demonstrates the interrelation of the basic rutile-type structure of adjacent slabs of Ti_5O_9. If the axes of the rutile-type subunit cell $\boldsymbol{a}_r$, $\boldsymbol{b}_r$ and $\boldsymbol{c}_r$ are used to define the coordinate system, then the axes of the ideal Ti_5O_9 unit cell will be:

$$\begin{aligned} \boldsymbol{a} &= \boldsymbol{c}_r - \boldsymbol{a}_r \\ \boldsymbol{b} &= \boldsymbol{a}_r + \boldsymbol{b}_r + \boldsymbol{c}_r \\ \boldsymbol{c} &= \boldsymbol{a}_r - \tfrac{3}{2}\,\boldsymbol{b}_r - \tfrac{1}{2}\,\boldsymbol{c}_r \end{aligned}$$

The matrix

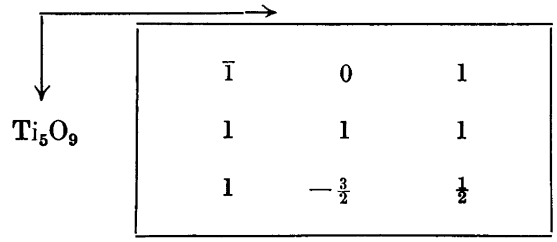

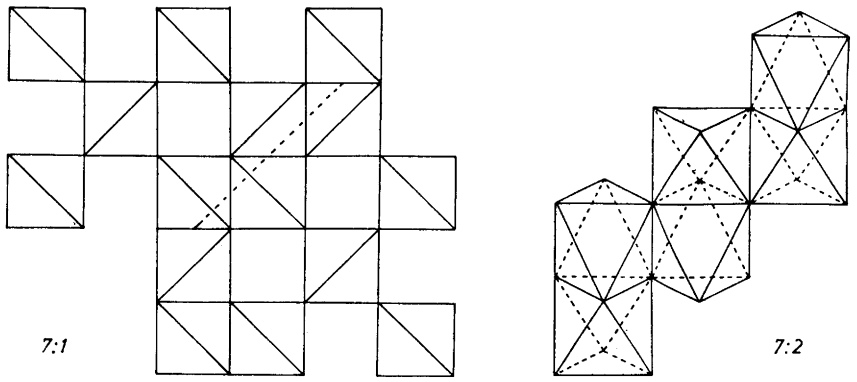

Fig. 7. 1) Projection of part of the Ti_5O_9 structure along the subcell c-axis showing the shear mechanism. The dotted line is parallel to the b-axis and the shear chain of the corundum structure. 2) The shear chain of the corundum structure.

thus makes it possible to obtain the relation between the indices of Ti_5O_9 and rutile.

If the vectorial equations given above are solved for a_r, b_r and c_r, the following expressions are obtained:

$$a_r = \tfrac{1}{9}(-4a + 3b + 2c)$$
$$b_r = \tfrac{1}{9}(-a + 3b - 4c)$$
$$c_r = \tfrac{1}{9}(5a + 3b + 2c)$$

The matrix

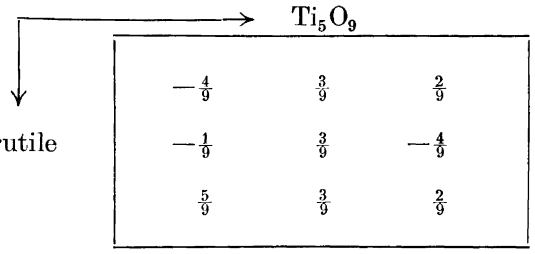

thus interrelates the atomic positions x, y, and z of Ti_5O_9 with those in the coordinate system difined by the rutile-type subcell ($x_r y_r$ and z_r).

By means of the latter matrix it has thus been possible to calculate the "ideal" atomic positions of the structure of Ti_5O_9 (Table 3). The deviation for some atoms from the coordinates of the actual structure should be due to the repulsion between the close metal atoms of octahedra sharing faces.

DISCUSSION OF THE STRUCTURE

It is of considerable interest to compare the structures of Ti_5O_9 and the homologues Ti_nO_{2n-1} with the structures previously found by Magnéli [6] for the series M_nO_{3n-1} and M_nO_{3n-2}. There are, of course, no obvious geometrical rela-

Table 3. Comparison between observed and ideal atomic coordinates for Ti_5O_9.

Atom	Observed coordinates			Ideal coordinates			Atom	Observed coordinates			Ideal coordinates		
	x	y	z	x	y	z		x	y	z	x	y	z
Ti_1	0.276	0.170	0.107	0.278	0.167	0.111	O_5	0.67	0.70	0.23	0.66	0.70	0.27
Ti_2	0.276	0.670	0.107	0.278	0.667	0.111	O_6	0.20	0.65	0.30	0.18	0.67	0.32
Ti_3	0.852	0.008	0.316	0.833	0.000	0.333	O_7	0.51	0.37	0.36	0.49	0.33	0.35
Ti_4	0.852	0.502	0.316	0.833	0.500	0.333	O_8	0.99	0.30	0.43	0.00	0.30	0.40
Ti_5	0.575	0.170	0.470	0.611	0.167	0.444	O_9	0.24	0.04	0.46	0.22	0.04	0.49
Ti_6	0.575	0.670	0.470	0.611	0.667	0.444	O_{10}	0.76	0.96	0.54	0.78	0.96	0.51
Ti_7	0.148	0.992	0.684	0.167	0.000	0.667	O_{11}	0.01	0.70	0.57	0.00	0.70	0.60
Ti_8	0.148	0.492	0.684	0.167	0.500	0.667	O_{12}	0.49	0.63	0.64	0.51	0.67	0.65
Ti_9	0.724	0.330	0.893	0.722	0.333	0.889	O_{13}	0.80	0.35	0.70	0.82	0.33	0.69
Ti_{10}	0.724	0.830	0.893	0.722	0.833	0.889	O_{14}	0.33	0.30	0.77	0.34	0.30	0.74
							O_{15}	0.53	0.03	0.80	0.55	0.04	0.82
O_1	0.63	0.32	0.11	0.62	0.33	0.09	O_{16}	0.08	0.99	0.88	0.07	0.00	0.87
O_2	0.11	0.38	0.03	0.11	0.37	0.04	O_{17}	0.89	0.62	0.97	0.89	0.63	0.96
O_3	0.92	0.01	0.12	0.94	0.00	0.13	O_{18}	0.37	0.68	0.89	0.38	0.67	0.91
O_4	0.47	0.97	0.20	0.45	0.96	0.18							

tions, because the subcells of rutile and of ReO_3-type are quite different. However, the principles for deriving the geometrical relations in each series are exactly the same. For example, in Mo_8O_{23} the major structural elements of the ReO_3-type structure are characterized by a finite width of 8 MoO_6 octahedra. In Mo_9O_{26}, the width of the slabs is extended to comprise one more MoO_6 octahedron. In any member of the series M_nO_{3n-1} there are two constant axes, a and b, parallel to the shear plane, while the c axis is determined by the thickness of the ReO_3-blocks and thus increases with n.

In the series Ti_nO_{2n-1}, V_nO_{2n-1} and $Ti_{n-2}Cr_2O_{2n-1}$ the same characteristics have been observed. The a and b axes and the angle γ all remain constant irrespective of the value of n, while the length and direction of the c axis are determined by the finite width of the rutile-type slabs and are thus functions of n. General structural data for the three series M_nO_{2n-1} have been derived from the matrices given above and will be reported elsewhere.

Acknowledgements. The author wishes to express his sincere gratitude to Professor A. Ölander for his kind interest and to the principal investigator of this research programme, Dr. Arne Magnéli, for having suggested this investigation, for his never-failing interest and for many valuable discussions. I also want to thank Miss Lena Jahnberg for her valuable assistance in the calculations.

The investigation has been sponsored in part by the *Office, Chief of Research and Development, U.S. Department of Army,* through its European Research Office and in part by the *Swedish Natural Science Research Council.*

REFERENCES

1. Andersson, S. and Magnéli, A. *Naturwiss.* **43** (1956) 495.
2. Andersson, S., Collén, B., Kuylenstierna, U. and Magnéli, A. *Acta Chem. Scand.* **11** (1957) 1641.
3. Andersson, S. *XVI^e Congrès International de Chimie Pure et Appliquée,* Paris 1957. Memoires présentés à la Section de Chimie Minérale 53.
4. Andersson, S., Sundholm, A. and Magnéli, A. *Acta Chem. Scand.* **13** (1959) 989.
5. Andersson, G. *Acta Chem. Scand.* **8** (1954) 1599.
6. Magnéli, A. *Acta Cryst.* **6** (1953) 495.
7. Blomberg, B., Kihlborg, L. and Magnéli, A. *Arkiv Kemi* **6** (1953) 133.
8. Magnéli, A., Blomberg-Hansson, B., Kihlborg, L. and Sundkvist, G. *Acta Chem. Scand.* **9** (1955) 1382.
9. Andersson, S. and Jahnberg, L. *To be published.*
10. Westman, S. and Magnéli, A. *Acta Chem. Scand.* **11** (1957) 1587.
11. Andersson, S., Collén, B., Kruuse, G., Kuylenstierna, U., Magnéli, A., Pestmalis, H. and Åsbrink, S. *Acta Chem. Scand.* **11** (1957) 165.
12. Magnéli, A. *Arkiv Kemi* **1** (1950) 513.
13. Magnéli, A. *Acta Cryst.* **4** (1951) 447.
14. Westman, S., Blomqvist, G. and Åsbrink, S. *Arkiv Kemi* **14** (1959) 535.
15. Åsbrink, S., Blomqvist, G. and Westman, S. *Arkiv Kemi* **14** (1959) 545.
16. Nordmark, Claes. *To be published.*
17. Wadsley, A. D. *Revs. Pure Appl. Chem.* **5** (1955) 165.

Received February 19, 1960.

ACTA CHEMICA SCANDINAVICA 14 (1960) 1173—1184

Studies on the Folic Acid, Pyrimidine and Purine Requirements of Four Lactobacilli

ARNE E. BOLINDER and WOLFGANG G. KURZ

Division of Food Chemistry, Royal Institute of Technology, Stockholm 70, Sweden

The specificity of the folic acid *, pyrimidine and purine requirements of four lactobacilli obtained from Moore and Rainbow [1] and isolated from the contaminant flora of English top fermentation brewer's yeast was investigated. The previous findings of these authors that the four strains designated L3, L4, L5, and L6 required pteroylmonoglutamic acid (PGA) **, a pyrimidine and purine(s) were confirmed. Further studies revealed that each of these requirements was non-specific and could be met using a range of related substances. The results obtained can be summarized as follows:

1. PGA could be replaced by N^5-formyltetrahydro-PGA, N^{10}-formyl-PGA, thymidine and TMP.
2. PABA was not essential in the presence of PGA or any compound replacing PGA.
3. The pyrimidine requirement of all four strains could be met using either uracil, uridine, 2′(3′)-UMP, deoxyuridine, cytosine, cytidine, 2′(3′)-CMP, deoxycytidine or deoxy-CMP.
4. The purine requirement of strain L4 could be met using either adenine, adenosine, 2′(3′)-AMP, deoxyadenosine, deoxy-AMP, hypoxanthine, inosine or deoxyinosine.
5. Strains L3, L5, and L6 could utilize as a sole purine source all the purine compounds active for strain L4 as well as guanine, guanosine, 2′(3′)-GMP, deoxyguanosine, deoxy-GMP, xanthine or xanthosine which were all inactive for strain L4.
6. Extracts of barley, kilned malt (without rootlets) and kilned malt rootlets, wort and beer were found to be active for replacing the folic acid, pyrimidine and purine requirements of all four lactobacilli.

Certain lactic acid bacteria have long been known to occur in association with brewery materials, *e.g.* malt, beer and yeast, but few studies have been carried out on their nutritional requirements. Recently, Russel, Bhandari and Walker

* "Folic acid" (factors) refers generally to the group of compounds chemically related to PGA which are capable of stimulating the growth of *Streptococcus faecalis* ATCC 8043 and *Lactobacillus casei* ATCC 7469; individual compounds will be specifically named.

** The following abbreviations are used in this paper: PGA for pteroylmonoglutamic acid; PABA for p-aminobenzoic acid; deoxy-CMP, TMP, deoxy-AMP, and deoxy-GMP for the 5′-monophosphates of deoxycytidine, thymidine, deoxyadenosine and deoxyguanosine; 2′(3′)-UMP, 2′(3′)-CMP, 2′(3′)-AMP and 2′(3′)-GMP for mixtures of the 2′- and 3′-monophosphates of uridine, cytidine, adenosine and guanosine, respectively.

studied the vitamin [2] and amino acid [3] requirements, and the interrelationships affecting the need for purines, PGA, and PABA [4] of 34 lactic acid bacteria isolated from the contaminant flora of English top fermentation beers and yeasts [5]. Moore and Rainbow [1] have studied the nutritional requirements of four strains of lactobacilli isolated from the contaminant flora of English top fermentation brewer's yeasts with respect to growth factors of the vitamin B-complex, purines, pyrimidines, amino acids and major sources of energy, and some biochemical activities. The strains were designated L3, L4, L5, and L6. Strains L3 and L4 were tentatively identified as strains of *Lactobacillus brevis*. According to Moore and Rainbow, all the strains required PGA, uracil and purines. [1] Through the courtesy of Dr. C. Rainbow, Department of Applied Biochemistry, University of Birmingham, we obtained cultures of the strains L3, L4, L5, and L6 for investigations on the replaceability of each of these growth requirements by a range of related substances. [6] In the present investigation, further studies of these and related problems have been made.

EXPERIMENTAL

Organisms. Since receiving the strains L3, L4, L5, and L6 from Dr. Rainbow in January 1956, stab cultures of these lactobacilli were maintained on Bacto micro assay culture agar (Difco) * and transferred at least once every two months. The cultures after incubation overnight at 30°C were stored in the refrigerator. Good growth also occurred in stab cultures on Bacto malt agar (Difco) but Bacto micro assay culture agar was superior.

Strain L6 was the slowest growing organism of the four brewery lactobacilli. The complete semisynthetic medium (see below) used in the tube tests did not give a good early growth with strain L6 and maximum growth did not occur until after 72 h of incubation at 28°C. Only 48 h or an even shorter time of incubation was required by strains L3, L4, and L5 in the tube tests. Sometimes broth subcultures of sufficient growth density were difficult to obtain with strain L6 and, in some tube test series, L6 unexpectedly failed to grow. These difficulties were also encountered to a certain degree with strain L4 whereas strains L3 and L5 were easy to work with.

Inocula. The inoculum medium consisted of equal volumes of single strength complete basal medium (see below) and Micro inoculum broth (Difco). Centrifuge tubes were filled with 5 ml portions of inoculum medium and a glass bead and were sterilized for 15 min at 120°C. Broth subcultures were incubated at 30°C for 18—24 h. For the preparation of inocula the subcultures were centrifuged, washed three times with 5 ml portions of sterile 0.9 % sodium chloride solution, resuspended and diluted in sterile sodium chloride solution to a turbidity of 65 % light transmittance read at 6 400 Å with a Coleman Model 11 Universal spectrophotometer. One ml of this suspension, corresponding to about 0.05 mg dry weight of cell material, was mixed with 50 ml sterile sodium chloride solution and, after thorough shaking, two drops of this dilute suspension was used to inoculate each tube.

Media. The complete medium used in these investigations was that of Moore and Rainbow [1] in a slightly modified form, having the following composition per 500 ml double strength medium: Bacto vitamin-free casamino acids (Difco), 10 g; L-cystine and L-cysteine hydrochloride, 100 mg each; DL-tryptophan, 200 mg; glucose and L-arabinose, 10 g each; sodium acetate (3 H_2O), 20 g; K_2HPO_4, $(NH_4)_2SO_4$, and NaCl, 1 g each; $MgSO_4 . 7H_2O$, 100 mg; $MnSO_4 . 4H_2O$, 30 mg; $FeSO_4 . 7H_2O$, 10 mg; adenine sulfate, guanine hydrochloride, and uracil, 10 mg each; thiamine hydrochloride, riboflavin, nicotinic acid, calcium pantothenate, and pyridoxine, 1 mg each; biotin, 10 μg; PABA, 500 μg; and PGA, 100 μg. The pH was adjusted to 6.5.

* Difco Laboratories, Inc., Detroit, Michigan, U.S.A.

As well as the complete medium, incomplete media lacking one or several essential factors were also used, *e. g.* purine deficient medium, (see below). All media were made up from stock solutions of each constituent as desired and the pH was adjusted to 6.5. The unsterilized double strength media were stored at −20°C. Media stored for 3−4 months have been successfully used.

Tube tests. Tube tests using a final volume of 10 ml were made in optically calibrated tubes (19 × 180 mm). A 5 ml amount of the factors or extracts to be tested was added to the test tubes, followed by 5 ml of double strength medium and a glass bead and the tubes were covered with aluminium caps. The tubes were sterilized by autoclaving at 120°C for 5 min. After cooling to room temperature in running tap water and inoculating (see above), the tubes were incubated at 28°C in a thermostated water bath. After 48, 72 and 96 h of incubation, growth was measured turbidimetrically as % light transmittance against uninoculated blanks set at 100 % light transmittance at 6 400 Å with a Coleman Model 11 Universal spectrophotometer. Since in most cases very little further growth occurred after 72 h of incubation, only the readings after 48 and 72 h of incubation are given in the tables. Each value in the tables is the mean of at least two separate tube tests. In each tube test two duplicate tubes were employed. The readings of identical tube tests made on separate occasions usually agreed very well. When there was poor agreement the tube test was repeated until consistent results were obtained.

Biochemicals. PGA (Folvite), N^5-formyltetrahydro-PGA (synthetic folinic acid, leucovorin), pteroic acid and N^{10}-formylpteroic acid (rhizopterin) were gifts from Lederle Laboratories; N^{10}-formyl-PGA (rhizopterin glutamate) was a gift from Hoffman-La Roche. The pyrimidine and purine derivatives were obtained from the California Corporation for Biochemical Research, Los Angeles, California. The deoxyribonucleotides are the 5′-phosphate esters while the ribonucleotides are mixtures of the 2′- and 3′-phosphate esters. Adenine and cytidine were supplied as hemisulfates, guanine and deoxycytidine as hydrochlorides, deoxy-AMP and deoxy-GMP as the monoammonium salts, TMP as dihydrate of the calciumsalt, 2′(3′)-GMP as dihydrate of the trisodium salt, 2′(3′)-AMP and 2′(3′)-UMP as the dihydrates, and uridine as the monohydrate; all other nucleic acid derivatives were supplied as pure compounds without water of crystallisation etc.

Purity of deoxyuridine, deoxycytidine, thymidine, and TMP. The purity of these deoxyribose compounds was checked by bioautography of paper chromatograms. Two solvent systems were used: (I) *sec.* butanol-water-conc. ammonia (80:20:3 v/v) and (II) *sec.* butanol-water-conc. acetic acid (75:25:3 v/v). The following R_F values were found in solvent system (I): folinic acid factors * and deoxyribonucleotides 0, deoxycytidine and deoxyuridine 0.35, thymidine 0.56; and in solvent system (II): deoxyribonucleotides 0.04−0.10, deoxycytidine 0.38, deoxyuridine 0.53, thymidine 0.65 and folinic acid factors 0.20−0.55. For bioautography, agar plates inoculated with either *Pediococcus cerevisiae (Leuconostoc citrovorum)* ATCC 8081 or *Lactobacillus leichmannii* 313 ATCC 7830 were used. The plates were made according to the procedure reported earlier for the plate assay of folinic acid factors with *P. cerevisiae* [7]. For both test organisms, the *P. cerevisiae* agar medium was used but the amounts of glucose and sodium acetate were doubled. After incubation overnight at 37°C, the plates were read. *P. cerevisiae* responds to thymidine and folinic acid factors whereas *Lb. leichmannii* responds to vitamin B_{12} (and factors), deoxyribonucleosides and deoxyribonucleotides.

Bioautography of moderate amounts (about 10 μg) of deoxyuridine revealed that it was contaminated by a small amount of thymidine. Quantitative work (quantitative paper chromatography combined with microbiological tube assays with *P. cerevisiae* and/or *Lb. leichmannii*) showed that deoxyuridine was contaminated by 0.15 % of thymidine (the mean value obtained from three separate determinations). On the other hand, thymidine was found to be contaminated by 1.5 % of deoxyuridine (only one determination was made). Furthermore, bioautography of large amounts (about 40 μg) of deoxycytidine and TMP revealed that these compounds were contaminated by faint traces (less than 0.02 %) of deoxyuridine and traces (about 0.05 %) of thymidine, respectively. According to the suppliers, these four deoxyribose compounds were guaranteed to have a purity of 100 ± 2 % as tested spectrophotometrically.

---

* "Folinic acid factors" designates those folic acid factors that are closely related to N^5-formyltetrahydro-PGA and are capable of stimulating the growth of *P. cerevisiae*.

Extracts of brewery products. The same brewery products were used as previously investigated [6]. Water extracts of kilned malt (without rootlets) and kilned malt rootlets were made by mixing 5 g of the finely ground (Wiley mill) material with 40 ml 0.1 M phosphate buffer at pH 6.5. After heating at 100°C for 10 min, the volumes were made up to 100 ml with distilled water and centrifuged. Water extracts of barley were made by mixing 5 g of barley with 40 ml 0.1 M phosphate buffer at pH 5.8. The mixture was first homogenized (MSE-homogenizer) and then heated at 100°C for 10 min. After cooling, the starchy mixture was liquefied by treatment for 4 h at 37°C with a bacterial amylase preparation (50 mg of Rapidase). The enzyme action was terminated by steaming for 10 min. The pH was then adjusted to 6.5 and the volume made up to 100 ml with distilled water and centrifuged. Samples of wort (12.5 % extract) and beer (made from this wort) from a top yeast fermentation were treated as follows: to 80 ml of sample were added 5 ml 1 M phosphate buffer, the pH adjusted to 6.5 and the volume made up to 100 ml. After heating at 100°C for 10 min and then cooling, the mixtures were filtered if necessary.

Table 1. Response of lactobacilli strains L3, L4, L5, and L6 in a PGA deficient medium to some folic acid factors and pyrimidine derivatives and extracts of brewery materials [a].

Addition to deficient medium	Amount per tube of 10 ml	L3 Incubation 48 h	L3 Incubation 72 h	L4 Incubation 48 h	L4 Incubation 72 h	L5 Incubation 48 h	L5 Incubation 72 h	L6 Incubation 48 h	L6 Incubation 72 h
None		100	100	100	100	100	100	100	100
PGA	0.001 μg	30	7	100	90	70	70	100	100
	0.01 μg	6	4	80	8	8	8	100	97
	1 μg[b]	3	2	5	3	5	4	15	6
N^5-Formyltetra-hydro-PGA	0.01 μg	8	4	100	30	10	9	100	32
	1 μg	5	3	20	4	6	6	50	5
N^{10}-Formyl-PGA	0.01 μg	5	4	70	7	11	11	100	70
	1 μg	4	3	15	4	7	5	80	13
Thymidine	1 μg	44	25	75	58	46	51	83	65
	10 μg	29	5	42	6	20	12	83	22
	100 μg	22	4	23	4	13	4	73	19
TMP	100 μg	43	10	40	9	60	22	80	30
Extract of barley	50 mg[c]	4	3	77	76	54	54	50	5
Extract of kilned malt (without rootlets)	50 mg[c]	3	3	35	14	6	5	85	30
Extract of kilned malt rootlets	10 mg[c]	3	3	9	8	4	4	65	45
Wort	0.1 ml[d]	4	3	9	8	5	5	27	26
Beer	0.1 ml[d]	3	2	4	3	4	4	24	26

[a] Turbidity readings: % light transmittance; no growth = 100 % transmittance; maximum growth = 2 % transmittance.
[b] Represents composition of complete medium.
[c] Dry weight of original sample.
[d] Original sample.

RESULTS AND DISCUSSION

Folic acid requirement. Moore and Rainbow [1] showed that all four strains required PGA but did not investigate the specificity of this requirement. We found that the PGA requirement of all four strains was quite nonspecific and could be met by any one of N^5-formyltetrahydro-PGA, N^{10}-formyl-PGA, thymidine, TMP or extracts of brewery materials. The growth promoting effects of these compounds and extracts after 48 and 72 h of incubation in a PGA deficient medium are given in Table 1. Omission of PABA from the PGA deficient medium gave the same growth for all compounds and extracts tested in Table 1. PABA was therefore not essential in the presence of PGA or any of the compounds and extracts that were able to replace PGA in the nutrition of these four lactobacilli.

Of the folic acid factors tested, PGA, N^5-formyltetrahydro-PGA, and N^{10}-formyl-PGA were about equally active for all four strains whereas pteroic acid and N^{10}-formylpteroic acid were inactive (see below). Strains L3 and L5 had the smallest folic acid requirement and the complete medium contained over a 100-fold excess of the amount of PGA required for optimum growth for these two strains. Strain L4 and particularly strain L6 had a much higher folic acid requirement than strains L3 and L5. Thymidine and TMP, which also promoted growth for all four strains in a PGA deficient medium, were required in much larger amounts than PGA for obtaining similar growth levels. These two compounds were about equally active on a molar basis.

The following compounds were unable to promote growth in a PGA deficient medium (containing PABA) for all four lactobacilli after 96 h of incubation when tested in the amount per tube given in brackets: pteroic acid (10 μg), N^{10}-formylpteroic acid (1 and 10 μg), thymine (100 and 1 000 μg), uridine (100 and 1 000 μg), 2′(3′)-UMP (100 and 1 000 μg), cytosine (100 and 1 000 μg), cytidine (100 μg), 2′(3′)-CMP (100 μg), deoxycytidine (100 and 500 μg), deoxy-CMP (100 μg), orotic acid (500 μg), deoxyadenosine (100 μg), deoxyguanosine (100 μg), Tween 80 (5 mg) and vitamin B_{12} (0.1 μg).

Somewhat irregular results were obtained when testing the growth promoting effect of deoxyuridine (not tabulated). We reported earlier that 100 μg of deoxyuridine per tube was inactive for all four lactobacilli in PGA deficient medium [6]. Repeated tube tests showed that strain L5 occasionally responded to 100 μg of deoxyuridine and that all four strains responded to 500 μg of deoxyuridine. However, the turbidity readings of repeated experiments were not sufficiently uniform to merit inclusion in Table 1. In all these cases, the growth promoting effect of deoxyuridine was too high to account for the low trace contamination by 0.15 % thymidine. A possible explanation of the irregular growth promoting effect of large amounts of deoxyuridine could be that an uneven carry-over of PGA occurred when inoculating the tubes and that this resulted in a varying degree of formation of thymidine (or TMP) from deoxyuridine. Separate experiments showed that resting cells of strain L5 were able to convert about 1 % of added deoxyuridine to thymidine (mean value of four resting cell experiments) when incubated in buffered glucose-arabinose solution at 28°C for 4 h.

Growth experiments were also made with strain L5 in an attempt to demonstrate the presence of trans-N-deoxyribosylase [8,9] but these tests were negative. No growth of strain L5 after 72 h of incubation was found in a PGA deficient medium with thymine (1 000 μg) + deoxyuridine (100 μg) or thymine (1 000 μg) + deoxycytidine (100 μg).

All the extracts of brewery materials tested were found to be active in replacing the folic requirement for all four lactobacilli. This finding was expected since earlier investigations from this laboratory had shown that these brewery materials contained folic acid factors and thymidine [6,10]. In particular, kilned malt rootlets were found to be rich in both folic acid factors and thymidine. As seen from Table 1, the extract of kilned malt rootlets was more active on a dry weight basis than the extract of kilned malt (without rootlets) and the extract of barley for strains L3, L4, and L5. The reverse order of activity of these extracts was, however, found for strain L6. Wort and beer were very active and both had almost the same growth promoting effect in a PGA deficient medium for all four lactobacilli.

The specificity of the folic acid requirement of lactobacilli varies from organism to organism. The folic acid requirement of these four brewery lactobacilli resembled that of *Lactobacillus casei* ATCC 7469 in many respects [11,12]. Thus, *Lb. casei* as well as the four brewery lactobacilli require the complete folic acid molecule with the glutamic acid group for growth; pteroic acid and N^{10}-formylpteroic acid are completely or almost completely inactive. Thymine is inactive for the four brewery lactobacilli but is active in replacing PGA for *Lb. casei* [11,13]. Thymidine, on the other hand, promotes growth in a PGA deficient medium for all five of these organisms [11,13]. However, none of the thirty-four brewery lactobacilli investigated by Russell *et al.* [2] had any requirement for PGA but one organism required PABA. The method used by Russel *et al.* [2] for determining the vitamin requirements of lactobacilli, which depended upon the evidence of a single transfer into the deficient media, has been critisized by Ford *et al.* [14] who recommend at least two or three transfers when assessing the vitamin requirements of bacteria, particularly when requirements for vitamin B_6, folic acid and biotin are being studied.

Pyrimidine requirement. Moore and Rainbow [1] showed that the pyrimidine requirement of all four lactobacilli could be met by uracil or cytosine but not by thymine. Strains L3, L5, and L6 could utilize orotic acid for growth in a pyrimidine deficient medium. These findings were confirmed. We further found that the pyrimidine requirement of all four strains could be met by any one of uridine, 2′(3′)-UMP, deoxyuridine, cytidine, 2′(3′)-CMP, deoxycytidine, deoxy-CMP or extracts of brewery materials. The growth promoting effects of these compounds and extracts after 48 and 72 h of incubation are given in Table 2. Uracil and cytosine were the most active of these compounds, whereas the ribonucleotides had the lowest activity. Orotic acid had the same growth promoting activity as uracil or cytosine for strains L3, L5, and L6 whereas strain L4 could not utilize orotic acid.

The following compounds were unable to promote growth in a pyrimidine deficient medium for all four lactobacilli after 96 h of incubation when tested in the amounts per tube given in brackets: N^5-formyltetrahydro-PGA (10 μg), N^{10}-formyl-PGA (10 μg) thymine (100 and 1 000 μg), thymidine (100 μg),

Table 2. Response of lactobacilli strains L3, L4, L5, and L6 in a pyrimidine deficient medium to pyrimidine derivatives and extracts of brewery materials.[a]

Addition to deficient medium	Amount per tube of 10 ml	L3 Incubation 48 h	L3 Incubation 72 h	L4 Incubation 48 h	L4 Incubation 72 h	L5 Incubation 48 h	L5 Incubation 72 h	L6 Incubation 48 h	L6 Incubation 72 h
None		100	100	100	100	100	100	100	100
Uracil	10 μg[b]	68	64	80	62	54	44	64	59
	100 μg	3	2	5	3	5	4	15	6
Uridine	100 μg	15	10	88	9	11	10	66	12
2′(3′)-UMP	100 μg	28	20	70	33	19	14	80	27
Deoxyuridine	100 μg	8	5	13	9	9	7	20	7
Orotic acid	100 μg	4	3	100	100	4	3	60	7
Cytosine	100 μg	3	2	68	11	5	4	14	4
Cytidine	100 μg	23	16	80	23	10	8	23	13
2′(3′)-CMP	100 μg	40	33	61	33	26	16	39	28
Deoxycytidine	100 μg	16	10	25	17	14	9	23	11
Deoxy-CMP	100 μg	12	8	17	11	13	9	19	12
Extract of barley	50 mg[c]	85	85	87	84	82	82	82	78
Extract of kilned malt (without rootlets)	50 mg[c]	71	66	68	53	46	36	77	58
Extract of kilned malt rootlets	10 mg[c]	67	63	41	38	33	25	60	38
Wort	0.1 ml[d]	64	60	65	58	57	48	65	64
Beer	0.1 ml[d]	63	59	67	63	54	48	60	60

[a] Turbidity readings: % light transmittance; no growth = 100 % transmittance; maximum growth 2 % transmittance.
[b] Represents composition of complete medium.
[c] Dry weight of original sample.
[d] Original sample.

TMP (100 and 500 μg), Tween 80 (5 mg), and vitamin B_{12} (0.1 μg). When testing 1 000 μg of thymidine per tube, a growth response was obtained for all four strains. However, the contamination of thymidine by 1.5 % of deoxyuridine could completely account for this growth promoting effect of thymidine in the pyrimidine deficient medium.

All the extracts of brewery materials tested were found to be active in replacing the pyrimidine requirement for the four lactobacilli. Extract of kilned malt rootlets was found to be more active on dry weight basis than either of kilned malt (without rootlets) or barley for all four strains. Wort and beer each had the same activity for all four strains. We have shown earlier [6,10] that kilned malt rootlets, wort and beer contained a growth factor for *Lb. leichmannii* 313 ATCC 7830 and *Lb. acidophilus* R-26 ATCC 11506 with the same R_F-value as deoxyuridine in several chromatographic solvent systems.

Russell *et al.* [4] investigated the uracil requirement of thirty-four brewery lactobacilli and found that uracil was essential for seventeen organisms and

stimulatory to four others. The specificity of the uracil requirement of these brewery lactobacilli was not investigated. For pyrimidine requiring lactobacilli the specificity of the requirement for pyrimidine varies greatly from organism to organism. In several instances, it has been shown that lactobacilli can meet their pyrimidine requirement by means of several closely related pyrimidines or pyrimidine derivatives. [15-18]

Purine requirement. Moore and Rainbow [1] showed that the purine requirement of strains L3, L5, and L6 could be met by adenine, guanine, xanthine or hypoxanthine. Strain L4 required hypoxanthine alone or adenine together with either guanine or xanthine [1]. However, the purine requirement of strain L4 has changed somewhat with time. This strain will now also grow on adenine alone (private communication from Dr. Rainbow). We confirmed these findings. Further investigations revealed that the purine requirement of all four lactobacilli could also be met by any one of several purine derivatives or extracts of brewery materials. The growth promoting effects of these compounds and extracts after 48 and 72 h of incubation are given in Table 3.

As seen from Table 3, strains L3, L5, and L6 could utilize any one of the purine derivatives tested as a sole purine source. Strain L4, on the other hand, could only utilize adenine, adenosine, 2′(3′)-AMP, deoxyadenosine, deoxy-AMP, hypoxanthine, inosine or deoxyinosine as a sole purine source. Extracts of brewery materials were active for all four strains.

For all four strains, the highest growth levels (2—10 % light transmittance) were obtained with adenine + guanine (100 μg of each) or deoxyadenosine + deoxyguanosine (100 μg of each) after 72 h of incubation. Strains L3 and L5 were similar in the utilization of individual purine compounds. For both strains, the highest growth levels were also obtained with 100 μg of any one of the purines or adenosine whereas the remaining purine nucleosides had the highest growth levels for strain L3 and good growth (10—20 % light transmittance) for strain L5. The purine nucleotides were less active on a molar basis for both strains.

For strain L4, no single purine compound could duplicate the high growth promoting effect of adenine + guanine or deoxyadenosine + deoxyguanosine. The compounds most active in promoting the growth of strain L4 in a purine deficient medium were adenosine, hypoxanthine, inosine and deoxyinosine followed by deoxyadenosine and deoxy-AMP. Considerably less active for strain L4 on a molar basis were adenine and 2′(3′)-AMP whereas guanine, xanthine and their derivatives were completely inactive. Although guanine alone was inactive, it greatly enhanced the growth promoting effect of adenine. Deoxyguanosine, which was also inactive alone, enhanced the growth promoting effect of deoxyadenosine.

For strain L6, the highest growth levels (after 72 h of incubation) were also obtained with hypoxanthine, inosine or deoxyinosine. Of the remaining purine bases, only guanine gave good growth whereas adenine and xanthine had low growth promoting effects. However, adenine had a synergistic growth effect together with guanine. For all four strains, purine nucleosides were more active growth promotors than purine nucleotides.

The following compounds were unable to promote growth in a purine deficient medium for all four strains after 96 h of incubation when tested in the

Table 3. Response of lactobacilli strains L3, L4, L5, and L6 in a purine deficient medium to purine derivatives and extracts of brewery materials [a].

Addition to deficient medium	Amount per tube of 10 ml	L3 Incubation 48 h	L3 Incubation 72 h	L4 Incubation 48 h	L4 Incubation 72 h	L5 Incubation 48 h	L5 Incubation 72 h	L6 Incubation 48 h	L6 Incubation 72 h
None		100	100	100	100	100	100	100	100
Adenine	10 μg	67	58	96	94	87	71	98	95
	100 μg	6	4	85	40	7	7	85	70
Adenosine	100 μg	9	5	65	7	7	6	90	11
2′(3′)-AMP	100 μg	24	14	82	36	38	20	89	50
Deoxyadenosine	100 μg	17	8	22	14	16	16	39	16
Deoxy-AMP	100 μg	54	36	43	16	22	22	44	22
Guanine	10 μg	60	56	100	100	76	74	90	70
	100 μg	6	4	100	100	11	10	27	13
Guanosine	100 μg	9	7	100	100	19	19	90	24
2′(3′)-GMP	100 μg	25	14	100	100	40	36	90	44
Deoxyguanosine	100 μg	10	7	100	100	17	17	40	15
Deoxy-GMP	100 μg	14	9	100	100	24	24	44	18
Adenine + Guanine	100 μg + 100 μg [b]	3	2	5	3	5	4	15	6
Deoxyadenosine + + Deoxyguanosine	100 μg + 100 μg	5	4	14	5	5	5	75	10
Hypoxanthine	100 μg	5	3	30	9	7	7	92	9
Inosine	100 μg	7	5	35	11	15	15	15	5
Deoxyinosine	100 μg	8	5	26	12	13	13	17	7
Xanthine	100 μg	5	3	100	100	7	6	96	65
Xanthosine	100 μg	9	9	100	100	20	20	88	28
Extract of barley	50 mg [c]	74	74	78	65	75	73	81	69
Extract of kilned malt (without rootlets)	50 mg [c]	46	35	60	33	41	32	94	42
Extract of kilned malt rootlets	10 mg [c]	30	23	32	23	30	24	60	32
Wort	0.1 ml [d]	47	42	82	76	65	59	70	58
Beer	0.1 ml [d]	49	45	84	80	65	60	60	58

[a] Turbidity readings: % light transmittance; no growth = 100 % transmittance; maximum growth 2 % transmittance.
[b] Represents composition of complete medium.
[c] Dry weight of original sample.
[d] Original sample.

amounts per tube given in brackets: thymidine (1 000 μg), deoxyuridine (500 μg) and vitamin B_{12} (0.1 μg).

All extracts of brewery materials tested were found to be active in replacing the purine requirement for all four strains. Extract of kilned malt rootlets was

found to be more active on dry weight basis than either of kilned malt (without rootlets) or barley, just as was the case when these extracts replaced the pyrimidine requirement for all four strains. Wort and beer each had the same activity. Extracts of brewery materials are known to contain purines and purine derivatives. We have shown earlier [6,10] that kilned malt rootlets, wort, and beer contain an acid labile growth factor for *Lb. leichmannii* 313 and *Lb. acidophilus* R-26 with the same R_F-value as deoxyguanosine in several solvent systems. Harris and Parsons [19,20] investigated the purine derivatives present in wort and found that the greater part of these compounds consists of adenosine and guanosine. Deoxyadenosine and deoxyguanosine as well as the free purines adenine and guanine were also identified.

The specificity of the purine requirement of lactobacilli varies greatly from organism to organism and is intimately related to their pyrimidine, folic acid, and vitamin B_{12} requirements [16,21,22]. It should be pointed out that the four strains of brewery lactobacilli investigated here had absolute requirements for folic acid, a pyrimidine and a purine. In no instance, could these requirements be met using vitamin B_{12}.

Russell *et al.*[4] investigated the purine requirements of several brewery lactobacilli by omitting in turn each of the purines, adenine, guanine and xanthine, from the complete medium which contained PGA, PABA, and uracil. Of the thirty-four organisms investigated, twenty-six were unaffected by the omissions of any one of the purines. Adenine was found to be essential to seven organisms. Guanine was essential to one organism and stimulatory to two whereas xanthine was not required by any strain and stimulated the growth of only one strain. The interrelationships in the requirements for purines, PGA, PABA, and uracil were investigated for some of the strains. However, the specificity of the purine requirement of these lactobacilli, found in the presence of PGA, PABA, and uracil, was not investigated.

Combined folic acid, pyrimidine, and purine requirements. The four strains of lactobacilli under investigation had absolute requirements for folic acid, a pyrimidine and a purine. As shown above, each of these requirements could be met by an appropriate deoxyribonucleoside. It was therefore considered of interest to measure the growth promoting effects of various combinations of deoxyribonucleosides in a medium deficient in PGA, PABA, pyrimidines and purines. Extracts of brewery materials were also tested. The turbidity readings after 48 and 72 h of incubation are given in Table 4.

The combination of the four deoxyribonucleosides, deoxyadenosine + deoxyguanosine + deoxyuridine + thymidine (100 μg of each), gave nearly optimum growth for all four strains. Only certain combinations of two or three deoxyribonucleosides gave good growth for some of the strains: for strain L5, the combination of deoxyguanosine + deoxyuridine (100 μg + 500 μg) and, for strains L3 and L5, the two combinations of deoxyadenosine + deoxyuridine + thymidine (100 μg of each) and deoxyguanosine + deoxyuridine + thymidine (100 μg of each). The response of strain L4 to the various combinations of deoxyribonucleosides was in accordance with the previous finding that deoxyguanosine alone could not meet the purine requirement of this strain. As seen from Table 4, the combination of deoxyadenosine + deoxyguanosine + deoxyuridine (100 μg of each) was inactive or almost

Table 4. Response of lactobacilli strains L3, L4, L5, and L6 in a medium deficient in PGA, PABA, pyrimidines and purines to combinations of deoxyribonucleosides and to extracts of brewery materials [a].

Addition to deficient medium	Amount per tube of 10 ml	L3 Incubation 48 h	L3 Incubation 72 h	L4 Incubation 48 h	L4 Incubation 72 h	L5 Incubation 48 h	L5 Incubation 72 h	L6 Incubation 48 h	L6 Incubation 72 h
Deoxyadenosine + + thymidine	100 μg + 500 μg	86	76	100	96	77	62	91	76
Deoxyguanosine + + thymidine	100 μg + 500 μg	75	64	100	100	78	70	95	85
Deoxyguanosine + + deoxyuridine	100 μg + 500 μg	92	80	100	100	36	18	97	96
Deoxyadenosine + + deoxyuridine + + thymidine	100 μg each	62	28	97	75	24	16	90	44
Deoxyguanosine + + deoxyuridine + + thymidine	100 μg each	52	16	100	100	35	20	85	41
Deoxyadenosine + +deoxyguanosine +deoxyuridine	100 μg each	95	95	100	100	98	90	100	100
Deoxyadenosine + +deoxyguanosine + +deoxyuridine + +thymidine	100 μg each	23	5	27	6	10	5	78	18
Extract of barley	50 mg[b]	82	82	91	80	78	75	90	80
	100 mg	81	81	80	74	70	62	90	80
Extract of kilned malt (without rootlets)	50 mg[b]	67	68	69	50	54	31	72	43
	100 mg	62	61	43	20	25	16	57	25
Extract of kilned malt rootlets	10 mg[b]	65	65	65	30	24	19	47	26
	50 mg	8	5	10	5	4	4	5	5
Wort	0.1 ml[c]	52	50	82	70	76	65	69	59
	1.2 ml	3	2	8	4	3	3	5	3
Beer	0.1 ml[c]	55	53	86	56	76	71	68	60
	1.2 ml	3	3	14	6	4	4	6	4

[a] Turbidity readings: % light transmittance; no growth = 100 % transmittance; maximum growth ? % transmittance.
[b] Dry weight of original sample.
[c] Original sample.

inactive for all four strains. This showed that PGA or a compound active in replacing PGA was still required when the purine and pyrimidine requirements were met using suitable deoxyribonucleosides.

Extract of kilned malt rootlets (50 mg), wort (1.2 ml), and beer (1.2 ml) gave optimum growth for all four strains. For strain L6, the turbidity readings after 48 h of incubation with these extracts exceeded those obtained with the complete semisynthetic medium. This difference was more pronounced when the turbidities were compared at shorter incubation times than 48 h. This showed that these extracts contained factors that promoted the early growth of strain L6. For all four strains, extract of barley (100 mg) gave poor growth whereas extract of kilned malt (100 mg) gave good or quite good growth. This indicates that to a certain extent there was a formation of important growth factors for these four lactobacilli during the malting process. A comparison of the growth promoting effects of extract of kilned malt (50 and 100 mg) and of wort (0.1 and 1.2 ml) reveals that, during the mashing process, there was a much greater formation of these growth factors than during the malting process [6] (0.1 and 1.2 ml of wort correspond to about 17 and 200 mg of malt, respectively, since in the brewing process about 6 ml of wort is obtained per gram of malt).

Acknowledgements. The authors are very grateful to Professor H. Lundin, Head of the Division, for his encouraging interest in this work. They are also grateful to Dr. C. Rainbow, Dept. of Applied Biochemistry, University of Birmingham, for providing cultures of the brewery lactobacilli, to Lederle Laboratories Division, American Cyanamide Co., Pearl River, New York, for samples of the different folic acid factors, and to A. B. Stockholms Bryggerier for samples of the brewery materials.

REFERENCES

1. Moore, W. B. and Rainbow, C. *J. Gen. Microbiol.* **13** (1955) 190.
2. Russel, C., Bhandari, R. R. and Walker, T. K. *J. Gen. Microbiol.* **10** (1954) 371.
3. Bhandari, R. R., Russel, C. and Walker, T. K. *J. Sci. Food Agr.* **6** (1955) 133.
4. Russel, C., Bhandari, R. R. and Walker, T. K. *J. Sci. Food Agr.* **6** (1955) 633.
5. Bhandari, R. R., Russel, C. and Walker, T. K. *J. Sci. Food Agr.* **5** (1954) 27.
6. Bolinder, A. E., Kurz, W. G. and Lundin, H. *J. Inst. Brewing* **62** (1956) 497.
7. Bolinder, A. E., Widoff, E. and Ericson, L.-E. *Arkiv Kemi* **6** (1953) 487.
8. MacNutt, W. S. *Biochem. J.* **50** (1951) 384.
9. Roush, A. H. and Betz, R. F. *J. Biol. Chem.* **233** (1958) 261.
10. Lundin, H. *European Brewery Conv. Proc. 4th Congr. Nice,* **1953** 9.
11. Snell, E. E. In György, P. (Ed.) *Vitamin Methods*, Academic Press, New York, 1950, Vol. I, 327, p. 398.
12. Williams, R. J., Eakin, R. E., Beerstecher, E., Jr. and Shive, W. *The Biochemistry of the B-vitamins*, Reinhold Publishing Co., New York, 1950, p. 565.
13. Stokes, J. L. *J. Bacteriol.* **48** (1944) 201.
14. Ford, J. E., Perry, K. D. and Briggs, C. A. E. *J. Gen. Microbiol.* **18** (1958) 273.
15. Merrifield, R. B. and Dunn, M. S. *J. Biol. Chem.* **186** (1950) 331.
16. Skeggs, H. R., Driscoll, C. A., Taylor, H. N. and Wright, L. D. *J. Bacteriol.* **65** (1953) 733.
17. Rose, I. A. and Carter, C. E. *J. Biol. Chem.* **207** (1954) 701.
18. Siedler, A. J., Nayder, F. A. and Schweigert, B. S. *J. Bacteriol.* **73** (1957) 670.
19. Harris, G. and Parsons, R. *J. Inst. Brewing* **61** (1955) 29.
20. Harris, G. and Parsons, R. *J. Inst. Brewing* **63** (1957) 227.
21. Shive, W., Ravel, J. M. and Harding, W. M. *J. Biol. Chem.* **176** (1948) 991.
22. Elion, G. B. and Hitchings, G. H. *J. Biol. Chem.* **185** (1950) 651.

Received February 23, 1960.

ACTA CHEMICA SCANDINAVICA 14 (1960) 1185—1202

On Osmotic Pressure of Macromolecules

J. A. CHRISTIANSEN

Sundvænget 9, Hellerup, Denmark

Elementary considerations show that the osmotic pressure of a solution containing non permeating molecules in a solvent consisting of permeating molecules can be calculated *as if* the former constituted a gas at the same temperature and concentration, *provided* that the form and magnitude of and the forces between them be maintained. The abridged van der Waals equation $p(V-B) = RT$ is derived by introducing in the equation $V\,\mathrm{d}p = n\,\mathrm{d}\mu$ (J. W. Gibbs, 1897) local concentrations and local activity-coefficients.

It is shown anew that if $2b$ be the unavailable volume for a pair of congruent hard molecules and N be the number of molecules in the volume V, the available volume is $V-Nb$ as shown by van der Waals 1899. A short history of this statement is given. It is emphasized that two different definitions of the unavailable volume $2b$ of the pair exist. In the case of hard, spherical molecules they yield the same result, $2b = 8v_m$, where v_m is the volume of one sphere. In all other cases they yield different results. The two definitions are:

I. $2b$ is the volume inside which the centre of one molecule must be if it be required that the one has points in common with the other one, supposed fixed.

II. $2b$ is the volume inside which the center of one molecule can not come without expenditure of work by the surroundings, the other molecule supposed fixed.

Def. I is used by B. H. Zimm and A. Isihara. Def. II is a consequence of the present author's derivation of the abridged van der Waals equation.

It is shown that for long rods Def. II agrees with experiments on long chain-molecules. The condition for this agreement is $b\varrho \geq 8$, where b is in cm^3/g and ϱ is the density in $\mathrm{g/cm}^3$ of the solid solute or is the reciprocal of its partial specific volume in the solution.

The discussion of experimental values yields suggestions regarding the constitution of some chainlike macromolecules. The suggestions seem to be confirmed by knowledge from other sources.

Two corrections mentioned in a paper by the author and the late Dr. C. E. Jensen are withdrawn. The first one relates to the difference in density between the inner and the outer liquid, the other one to the difference in surface-tension between the same two liquids.

Both corrections relate to measurements with the "inverted osmometer". A third correction, subtraction of one third of the diameter of the capillary from the height measured, is introduced.

PART I. THEORY

In the following we shall understand by the osmotic pressure (O.P.) of a solution of macromolecules that measured by means of a membrane which is impermeable and only impermeable to macromolecules, say molecules of molecular weights from some ten thousand and upwards.

It seems to be desirable to survey the basic ideas underlying our present knowledge of O.P. because in the rapidly expanding literature more or less controversial interpretations of the same phenomena have turned up so that the reader sometimes finds himself caught in a maze. The following is an attempt to illustrate different aspects of O.P. Not all of the author's views agree with views expressed by recent authors and his sincere hope is that this presentation should induce readers to meditate themselves on the problems involved.

The thermodynamic definition of osmotic pressure and its realisation by experiments

Fortunately, there are no controversies regarding the thermodynamic definition of O.P. It may be expressed as follows: The osmotic pressure is that excess pressure which must be exerted on the inner liquid, the solution, in an osmometer to prevent flow of the outer liquid, containing only permeating solvent molecules, through the membrane. This is the same as to say, that at equilibrium the chemical potentials of the permeating components of the inner liquid must be equal on both sides of the membrane.

The aim of all direct methods of determination of the O.P. is to realize this definition by experiment. As one example the reader may be referred to the method described by Christiansen and Jensen [1] in which the buoyancy of an air column in a vertical capillary produces the excess pressure on the inner liquid. If that pressure does not equal the O.P. there will be a flow of liquid through the membrane. The rate of flow (positive outwards, negative inwards) is measured by means of a horizontal microscope provided with an ocular micrometer scale. Experiment shows, that it depends linearly on the height of the air column, the resistance of the membrane against flow of the permeating liquid thus being independent of the direction of movement.

In exceptional cases the resistance proved to be greater for outward motions than for inward ones. Such experiments were discarded. In most cases the effect could be eliminated by removal and rinsing of the membrane. It is therefore probable that this valve effect is due to a layer of macromolecules, partly blocking the outward, but not the inward flow.

By means of a graph it is easy to find by interpolation the length of the column which corresponds to zero flow and from this by calculation the O.P.

Even at the largest rates of flow the linear velocity of the permeating liquid through the membrane (a collodion membrane) is extremely small, so small that, if the outer liquid be a mixture, diffusion-equilibrium is extremely nearly maintained in the displaced elements of the permeating liquid.

This follows from the following rough estimate: An exceptionally high rate of movement of the meniscus in the capillary is 20 divisions in the ocular micrometer in 10 min, which corresponds to 0.4 mm^3/10 min. The surface of the membrane is about 200 mm^2 and consequently the linear velocity across the membrane is about 0.002 mm/10 min. As now diffusion coefficients in gels like the water containing collodion membranes used are known not to be much smaller than those in water, we arrive at the result mentioned.

The permeation is therefore very nearly reversible. From this follows, that the liquid which permeates the membrane from the outside must have very nearly the same composition as that which permeates from the inside. In other words, the solvent, the permeating part, of the inner liquid is (very nearly) identical in composition with that of the outer liquid, or we may say that the outer liquid is the solvent of the inner liquid even if the former is a mixture.

Calculation of the osmotic pressure

The thermodynamic definition does not tell us whether or how the O.P. may be calculated from the concentration of the (non permeating) solute. Let us therefore consider the equilibrium situation more closely. It is a fact that at equilibrium there is a pressure-difference between the inner and the outer liquid. It is also a fact, that at equilibrium there is no flow of solvent through the membrane. Furthermore the (permeating) solvent can only contribute to the pressure difference by flowing through the membrane. Consequently its contribution to the pressure difference must be zero at equilibrium. Therefore we should get the same pressure difference if we removed the solvent from both sides of the membrane, *provided* that we maintain not only the temperature and the concentration of the solute molecules, but also their form and magnitude and the forces between them. In other words we may calculate the excess pressure at equilibrium, the osmotic pressure, as if it were the pressure of a gas with the prescribed properties.

From this follows immediately, that the limiting law of van't Hoff must tend to be valid at such dilutions where the effects of the finite volume of the solute molecules and of the forces between them have vanished. Whether we may say, that the pressure difference at equilibrium be "due to" the bombardment of the (non permeating) solute molecules against the semipermeable membrane remains a matter of taste, the essential thing being that it can be calculated as described.

To treat the problem in more detail we shall use a method proposed by Gibbs [2]:

At constant temperature we have generally for a solution containing k + 1 components

$$V\mathrm{d}p = n\mathrm{d}\mu + \sum n_i d\,\mu_i \;(i = 1, 2, ...k) \qquad (1)$$

where V is the volume, and n and μ are, respectively, the number of moles and the chemical potential per mole of the non permeating solute and n_i and μ_i the corresponding quantities for the k permeating molecules. If now this solution is contained in an osmometer surrounded by the semipermeable

membrane and is in equilibrium with an outer liquid containing only the solvent substances at constant temperature, pressure and composition all $d\mu_i$'s are zero and we get

$$Vdp = nd\mu \tag{2}$$

exactly the same equation which is valid for a one component system. It is eqn (2) which we owe to Gibbs. The responsibility for the following must remain with the present author.

Let us now assume as usual that

$$d\mu = RT \, d\ln (cf) \tag{3}$$

where c is the concentration of the solute and f its activity coefficient. Now, if c means the overall concentration it is evident that

$$dn/n = dc/c \tag{4}$$

But (4) is also true if c means a local concentration, which may be different in different volume elements. This follows from the consideration that a small relative increase in the number of molecules of solute in the volume V cannot alter their distribution on the different volume elements.

It should be added that if we let c mean the local concentration it must be understood as the number of centers of gravity of solute molecules in a certain volume-element divided by the volume of that element.

Let us now assume that the solution is so dilute that f equals the same constant everywhere in the solution. Without loss of generality we may put this constant equal to one. Combining (2), (3) and (4) we then get by integration

$$Vp = RTn \tag{5}$$

because V at the small pressures in question is certainly independent of p. We thus arrive at van't Hoff's limiting law, or the gas-law. But evidently this is no proof of that law, because (3) has been chosen so as to lead in the limit to (5). The real proof of (5) rests of course on the validity of Maxwell's law of equipartition.

Let us now proceed one step further. Using again (3) and (4) we get by integration of (2)

$$Vp = RTn + RT\int n d\ln f \tag{6}$$

f is assumed to be defined by

$$f = \exp(g/RT) \tag{7}$$

where g is a molar potential energy depending on the space coordinates of the center of gravity of a solute molecule. In accordance with the Boltzmann principle we shall assume that the activity a of the solute is constant everywhere inside the osmometer, *i.e.*

$$a = cf \qquad (a \text{ constant}) \tag{8}$$

We shall only treat the case in which the solute molecules at a distance do not exert forces on each other, but that to force them nearer to each other, when they are already in contact, requires expenditure by the surroundings of an amount of work (per mole) which is several times as large as RT even for very small displacements. In other words, we consider the molecules to be hard bodies having well defined finite volumes. In that case g is either zero (when the molecules are out of contact) or g/RT is so large that f to all intents and purposes can be considered as infinitely large, the interval between these two cases being so small that it can be neglected. Therefore we have everywhere inside the osmometer

$$c \ln f = a \ln f/f = 0 \tag{9}$$

because if one factor is different from zero the other one is zero. Therefore

$$c \, \mathrm{d}\ln f + \ln f \, \mathrm{d}c = \mathrm{d}(c \ln f) = 0 \tag{10}$$

We have seen before that $\mathrm{d}c/c = \mathrm{d}n/n$ so that (10) can also be written

$$n \, \mathrm{d}\ln f + \ln f \, \mathrm{d}n = 0 \tag{11}$$

As now $n = \int c \mathrm{d}V$, (6) can be rewritten

$$\int (p/RT - c(1 - \ln f))\mathrm{d}V = 0 \tag{12}$$

If in (8) f equals one we have $a = c'$, where c' is the concentration in volume elements where the solute molecules are "free". Therefore

$$\int (p/RT - c'(1 - \ln f)/f)\mathrm{d}V = 0 \tag{13}$$

Now for those parts of the volume, where $\ln f$ is different from zero we get

$$c' \int ((1 - \ln f)/f)\mathrm{d}V = 0 \tag{14}$$

For those parts of the volume, where the centers of the solute molecules are "free", *i.e.* where f equals one

$$\int (p/RT - c')\mathrm{d}V = 0 \tag{15}$$

which means that $p/RT = c'$.
Now

$$n = \int c \, \mathrm{d}V = c' \int \mathrm{d}V/f \tag{16}$$

The contributions to the latter integral evidently comes only from those volume-elements in which f equals one. Denoting that part of the volume, where f is different from one (the unavailable volume) by B, we evidently get

$$c' = n/(V - B) \tag{17}$$

or

$$p(V—B) = nRT \tag{18}$$

That this equation agrees exactly in form with van der Waals's equation for the case where intermolecular forces are absent is no wonder as it has been derived from exactly the same assumptions as the latter.

The unavailable volume

As emphasized by all authors on the subject there are two kinds of unavailable volumes. The first kind is due to the fact, that the centers of the solute molecules cannot approach the inner surfaces of the osmometer beyond a certain distance. The second kind arises from the circumstance that the centers of two solute molecules cannot approach each other beyond a certain distance. A rough estimate shows at once, that if the osmometer be not microscopically small we may completely neglect the first kind. We shall now try to survey the situation concerning the unavailable volume of the second kind.

Statistics. Let us consider at first one pair of molecules identical in magnitude and shape, and let it be assumed that we have somehow succeeded in determining the unavailable volume $2b$ for the pair. Let us further assume that the volume V contains N single molecules of the solute. If we number these and take out, *e.g.*, number one it is evident that we may combine this with the $N—1$ others to $N—1$ pairs with the total unavailable volume $2b(N—1)$. However, as all the $N—1$ pairs contain molecule number one, only half of this volume belongs to the $N—1$ second partners, those with the numbers 2,3.....N. Consequently we must ascribe to each of these partners the part b of the unavailable volume. If furthermore we ascribe the same part b to molecule number one, this paired with any one of the other molecules will form a pair with the unavailable volume $2b$ as it should. It follows from this argument that the space available to the center of molecule number one or to any other of the N molecules is $V—(N—1)b—b = V—Nb$. Thus Nb equals B, the unavailable volume introduced before. B evidently means the same whether we let b mean the unavailable volume for one molecule and N the number of molecules or we let b mean the unavailable volume for one mole and replace N by n, meaning the number of moles. Using the latter convention (18) can be rewritten in the form

$$1—bc = RTc/p \tag{19}$$

where $c = n/V$ is the overall molar concentration of solute molecules. We may also let c mean the concentration in g/litre in which case (19) becomes

$$M(1—bc)/RT = c/p \tag{20}$$

where M is the molecular weight of the solute. In that case b becomes the unavailable volume of the solute in litre/g.

The expression $V—Nb$ for the available volume has a rather complicated history. J. D. van der Waals has it in the second edition of his book: *Die Continuität des Gasförmigen und Flüssigen Zustandes* (1899) **I**, p. 45. His argument, in which he corrects an error committed by R. Clausius, is different from that given above.

L. Boltzmann in his: *Vorlesungen über Gastheorie*, 1st Ed. 1898, reprinted 1912, part II, p. 7, has (our notation) $V-2(N-1)\,b$ for the same quantity. In his argument, which is similar to ours, he counts, however, the contribution to the unavailable volume from what we have denoted as molecule number one $N-1$ times in stead of only once. Then in his last work (with J. Nabl) in *Encyclopädie der Mathematischen Wissenschaften* V (1907) p. 551, Boltzmann quotes, without remarks, from the above mentioned book of van der Waals the latter's value $V-Nb$. It seems evident, therefore, that Bolzmann accepted this value before he died.

Finally, in his *Dynamical Theory of Gases*, 2nd Ed. (1916) p. 138, J. H. Jeans quotes Boltzmann's value from 1898, $V-2(N-1)b$ without mentioning the error.

We shall therefore stick to the value for the unavailable volume $B = Nb$ and not use $B = 2(N-1)b$. It must be added that the expression "an unavailable volume of the second kind" has only a meaning if N is at least two.

Geometry. The magnitude of the unavailable volume, depends on the geometrical form of the solute molecules. Van der Waals and his first successors calculated $2b$, the unavailable volume for a pair of molecules, only for the case of hard spherical bodies which is by far the easiest one to treat. It is easy to see that the volume around a sphere A inside which the centre of another sphere B cannot come without the expenditure of work is a sphere whose radius is d, where d is the diameter of one of the spheres. In other words, the unavailable volume $2b$ for the pair is eight times v_m where v_m is the volume of one of the molecules forming the pair if they are both spherical. For the following it is of interest to note that in this case and only in this case two different definitions of the unavailable volume $2b$ lead to the same result, *viz.*

Def. I: $2b$ is the volume inside which the centre of molecule B must be if molecule A be fixed and it be required, that they shall have points in common.

Def. II: $2b$ is the volume inside which the centre of one molecule cannot come if the other one be fixed, unless work is performed by the surroundings.

For non spherical molecules definitions I and II lead to different results, the more so the more the form of the molecules deviate from a sphere. Def. II evidently is the one required by our derivation of the abridged van der Waals equation.

As examples of approximately spherical molecules certain globular macromolecules, *e.g.* certain proteins might be mentioned, but we shall focus our attention on a quite different type, molecules of the pearl-string type. Most or at least many of them are not at all stiff. If they were they might reasonably be considered as cylindrical rods, a case which seems next to the sphere in simplicity. However they must often be expected to perform not only intermolecular Brownian motions but also intramolecular motions of a similar irregular kind, resulting in incessant changes in "curliness" and end to end length. To take this accurately into account in an attempt to calculate the unavailable volume for a pair of such molecules seems nearly hopeless. The only problem one may reasonably expect to be able to solve is the tremendously simplified problem of determining $2b$ for a pair of stiff circular cylinders with given height and length. Isihara [3] has suggested that for the solution of the corresponding problem for flexible molecules one might use information concerning average dimensions of such molecules obtained by means of light-scattering experiments. To the present author this seems doubtful because it seems to him that the lengths measured by optical methods may be quite

different from those which are decisive for the magnitude of the unavailable volumes. Actually, just because of the flexibility of the pearl-string model one would expect the decisive length for this to be the length of the string, while the average lengths measured by optical methods may be much shorter. Anyhow, we may not commit gross errors by replacing the pearl string by the same in its stretched form and then replace this by a cylinder of the appropriate dimensions, diameter d and height h.

The unavailable volume for a pair of solid cylinders

B. H. Zimm [4] and A. Isihara [5,6] have solved, the former approximately, the latter exactly, the following problem: Given two congruent cylinders, A and B, A being fixed in space and B movable. Find the volume inside which B must move if it be required that the common volume of A and B does not vanish. Zimm and Isihara consider the volume so defined to be the unavailable volume $2b$ for a pair of cylinders, in other words they use Def. I. Isihara's result [3,6] is

$$2b/v_m = \pi + 3 + \pi d/2h + 2h/d \qquad (21)$$

Now b can be determined by measurements of the osmotic pressure p at several concentrations c. We then plot c/p against c. According to (20) the graph obtained should be a straight line and seems to be so when only reliable experiments are taken into account. For details of the experiments and evaluation of the sources of error in osmotic experiments the reader is referred to Part II of this paper. From the intercept of the line with the axis of ordinates we may calculate the molecular weight and from its slope we get b in cm^3/g if c is in g/cm^3. Furthermore v_m might be taken as the partial specific volume in cm^3/g in the solvent in question or failing that, as the reciprocal density (ϱ) of the solid substance. However, measured in this way v_m may very probably be low because evidently the solute molecule may be covered with a sheath of solvent or it may be wound up in a "helix" whose effective volume at collisions may be several times larger than that of the densely packed molecules. Values of $b\varrho$ therefore represent an upper limit to the value of b/v_m. The former values usually lie in the range from about ten to less than one hundred. On the other hand the number of "pearls" on the "string" can be estimated from our knowledge of the chemical composition of the substance in question and its molecular weight. This number cannot be very different from the ratio h/d. A low estimate of this ratio is 100. From (21) it is seen that for this value of h/d, b/v_m becomes 100, and by actual calculations in the particular examples it is found to be much greater. This disagreement between values of $b\varrho$ determined experimentally and b/v_m predicted by the calculation of Isihara [5,6] is so large, that serious doubt arises whether the definition (I) of the unavailable volume be the right one. What can be said at the present stage is that it is certainly different from Def. II adopted by the present author. This definition may be repeated here as follows: Let cylinder A be fixed and B be movable. The volume unavailable to B is then that volume inside which the center of B cannot be brought unless work is performed on the system.

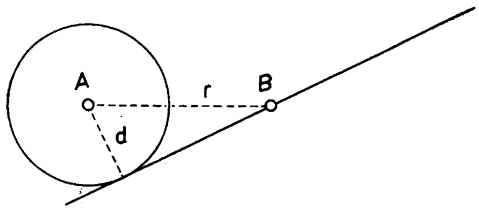

Fig. 1.

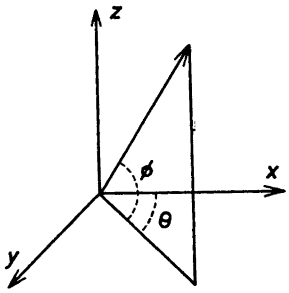

Fig. 2.

To illustrate the difference between the two definitions let us proceed in the following manner: We replace cylinder A by one of the same height but with diameter $2d$ and replace simultaneously B by its axis of lenght h. Furthermore we consider the particular case that the axes of A and B are perpendicular to each other. The projection on a plane perpendicular to the axis of A is shown in Fig. 1. In this plane we may evidently speak of an unavailable area instead of an unavailable volume. Now according to Def. I the middle point of B certainly belongs to the unavailable area if the situation is as illustrated. According to Def. II, however, the same point does not belong to the unavailable area because we may shorten the radius vector r from the center of A to the middle point of B without performing work. Of course the line B will then slide or roll on the circle A but this does not require work as no forces resists a motion of that kind. But the radius vector cannot be decreased to a value less than d, the radius of the circle, unless work is performed on the system. Therefore, according to Def. II, the area unavailable to the centre of B is the area of circle A, which is certainly less than the unavailable area defined according to Def. I.

In this argument we have neglected the fact that both A and B are endowed with kinetic energy, translatory and rotatory. Strictly speaking we should therefore consider the probability of finding the two centers in between distances r and $r + dr$ from each other. This probability depends partly on the kinetic and partly on the potential energy, both corresponding to the distance r. We know, however, from general theory that the average kinetic energy at a given temperature does not depend on r. Consequently our result must remain the same as that obtained under the assumption that the two cylinders are at rest. It seems therefore that both experimental results and theoretical considerations indicate that Def. II and not Def. I. must be the right one.

Calculation of the unavailable volume for a pair of cylindrical molecules.

The unavailable volume evidently depends on the orientation in space of the axes of the cylinders. Let the axis of A be parallel to the x-axis in a system of rectangular space coordinates as in Fig. 2 and let its centre be placed in the

origin. We want now to determine the volume which is unavailable to the centre of B. On account of the cylindrical shape of A and B the unavailable area is for all orientations of the axis of B equal to $\pi\, d^2$. The unavailable length however depends on the orientation of the B-axis. If this be parallel to the x-axis the length is evidently $2h$, beginning at $x = -h$ and ending at $x = +h$. The vectors indicating the possible directions of the B-axis must always be positive and must therefore lie inside the corner limited by the three positive half-axes of coordinates. Denoting geographical longitude by Θ and geographical latitude by φ, the surface element on a sphere with radius unity is $\mathrm{d}S = (\cos\varphi\ \mathrm{d}\Theta)\ (\mathrm{d}\varphi)$. As we shall assume that all orientations (inside the octant) are equally probable the element of probability $\mathrm{d}w$ is $A\mathrm{d}S$. As the vector in question ($\mathrm{d}w$) must have its endpoint somewhere inside the equilateral spherical triangle whose sides are $\pi/2$ we have

$$\int \mathrm{d}w = 1 = A\int \mathrm{d}S = A\ 4\pi/8 \tag{22}$$

Consequently

$$\mathrm{d}w = 2\cos\varphi\ \mathrm{d}\varphi\ \mathrm{d}\Theta/\pi \tag{23}$$

The components of the unavailable length multiplied by the element of probability thus becomes for the axes indicated

$$\begin{aligned} &(x)\colon\ 4h\cos^2\varphi\ \mathrm{d}\varphi\ \cos\Theta\ \mathrm{d}\Theta/\pi \\ &(y)\colon\ 2h\cos^2\varphi\ \mathrm{d}\varphi\ \sin\Theta\ \mathrm{d}\Theta/\pi \\ &(z)\colon\ 2h\sin\varphi\ \cos\varphi\ \mathrm{d}\varphi\ \mathrm{d}\Theta/\pi \end{aligned} \tag{24}$$

where it be remembered that when the B-axis is parallel to either the y or to the z-axis the unavailable length is h, the end correction being already included in the contribution from the (x) position.
Performing now all the integrations from zero to $\pi/2$ we get as contributions to the average length unavailable to the center of B

$$(x)\colon\ h;\ (y)\colon\ h/2;\ (z)\colon\ h/2.$$

Thus the volume unavailable to the center of B, when A is fixed becomes $2h \cdot \pi d^2$. To get the volume unavailable to the center of A when B is fixed we must fix the axis of B perpendicularly to the x-axis. It is immaterial whether we choose the y- or the z-axis. Let us choose the latter and let furthermore the fixed B-axis extend from the origin along the two branches of the z-axis. The calculation need not be repeated as we evidently get the same result as before. We cannot, however, simply add the two results to get $2b$. Each of the two volumes $2\pi hd^2$ represents the volume of a cylinder with height $2h$ and radius d, but their axes intersect at right angles and divide each other in the ratio one to one. In the case of cylindrical bodies this ratio is of course immaterial so long as the two cylinders intersect but if the bodies were *e.g.*, prolate ellipsoids this would not be so. Now the total volume of two cylinders intersecting each other as described is equal to $2b$ and we get

$$2b = 4\pi hd^2(1 - 4d/3\pi h) \text{ if } d \leq h \tag{25}$$

For $d>h$, that is if the molecules are coin-shaped, $2b$ is represented by two "coins" each of radius d and thickness $2h$ intersecting each other symmetrically at right angles. The volume of such a body is

$$2b = 4\pi hd^2 - 16(d^3 - (d^2 - h^2)^{3/2})/3 \quad (26)$$

For small values of h/d this converges against

$$2b = 4\pi hd^2 - 8dh^2 = 4\pi hd^2(1-2h/\pi d) \quad (27)$$

Thus for very long "rods" and for very thin "coins" we get

$$2b = 16v_m \quad (28)$$

while for spherical molecules

$$2b = 8v_m \quad (29)$$

PART II. COMPARISON WITH EXPERIMENTS

In the last two or three decades an immense number of determinations of O.P. particularly such of the filament or the rod type have been carried out. It would take too much time and space to review them all and the following examples are therefore chosen more or less at random. Peculiarly enough many of the results quoted were obtained by the time-consuming and not always quite reliable static method, although the principle of the dynamic method had been known for many years. Even when the present author at the Carlsberg Laboratory constructed an osmometer [7] according to the latter, the principle had been used more than twenty years before. [8,9]

The apparatus constructed by Fuoss and Mead [10] (1943) has since been used by several authors in U.S.A. It works according to the static principle, but with the important improvement, that the osmotic equlibrium is reached in a relatively short time and from both sides.

Some years ago the late Dr. Jensen and the present author [1] constructed, as mentioned before, a new type of a dynamic osmometer, an inverted osmometer, so called because the membrane is at the upper end of the observation capillary. This has since been used by different persons for different purposes and on a number of different solutes, but hitherto only with water or aqueous solutions as solvents. It is believed to have several advantages as compared to older models, particularly also to the Carlsberg model described by Sørensen [7] in 1917. First of all its volume is only about 400 mm^3, its active surface being about 200 mm^2. The Carlsberg model contained about 15 cm^3, including about 4 cm^3 dead space, and had an active surface of about 30 cm^2. The diameters of the cylindrical parts were, respectively, about 7 and about 14 mm. In the new model therefore in which there is practically no dead space the time necessary to reach diffusion equilibrium has been reduced by a factor of about four. Also the mechanical properties have been improved: On changing the hydrostatic pressure on the inner liquid the strain in the membrane is changed. This would be harmless if there were no elastic aftereffects in the collodion membranes used. Sørensen [7] showed that actually such effects seem to be present, but he showed also that the errors they produce were insignificant.

It can be estimated from experiments quoted in detail by Sørensen [7], that his results are reliable to within one in about three hundred. In the new model the small membranes are about as thick as those in the Carlsberg model which are much larger and the resulting strains are therefore smaller. Accordingly elastic after-effects were not observed in experiments with the new model. To avoid these effects some recent osmometers [10] have a plane membrane supported by one or two perforated discs. This, however, has the drawback that the active surface becomes much reduced, or the volume strongly increased, because evidently, even if the whole surface of the disc were active it would be, for the same overall dimensions of the apparatus, less by a factor about two than the test tube shaped membrane.

Experience with the new apparatus has shown that osmotic pressure may be determined with an accuracy better than 0.1 mm water pressure for pressures below 5 mm, the range of the ocular micrometer. Above 5 mm the accuracy is limited to 0.1 mm, the heights being measured by means of a millimeter scale with Vernier on the vertical stem of the microscope. In any case the accuracy obtained can be read from the graph connecting the rate of movement of the air column with its height.

In most other, particularly older apparatuses, including those of both types, static and dynamic, the accuracy seems not to be much better than 1 mm, and sometimes to be worse. Furthermore, at some measurements performed according to the static method and with one-sided approach to equilibrium, complete equilibrium may not always be reached. For these reasons many measurements of O.P. lower than about 10^{-3} atm, reported in the literature, may be off by 10 % or more.

Some earlier authors have used the abridged van der Waals equation to represent their results, *i.e.* they have plotted c/p against c, where c usually is the concentration in g/litre and p the pressure in some arbitrary unit. When points relating to the lowest pressures (less than 10^{-3} atm) are neglected reasonably straight lines are usually obtained. More recent authors often calculate and plot p/c against c, thereby obtaining curves with an upward bend. Some such experiments have been recalculated by the present author who, again omitting low and therefore doubtful pressures, got nearly straight lines.

Fortunately earlier authors gave their numerical results in tables. More recent authors seem to have abandoned this useful habit and give their results in graphs, from which it is difficult to read their numerical results accurately enough for recalculations. In all the following examples the present author has performed a recalculation and redrawn the corresponding graphs, thereby obtaining the values indicated for the molecular weight, M, and the values of b in cm^3/g.

According to theory $b = 8v_m$ if the molecules are (nearly) cylindrical. If v_m were the specific volume of the substance in question we should expect to get $b\varrho = 8$ if ϱ be the density in g/cm^3 of the substance in question. In stead of that one finds in most cases that $b\varrho$ is two to five or even ten times as large as that. The explanation is evident: v_m is the volume of a cylinder, which cannot penetrate a similar one. If now the principal chain in the molecule has many short branches, or if it be wound up in a helix, two such molecules can only penetrate each other to a distance which may be two or three times

that calculated from the densest possible packing of the constituents, as in the corresponding solid. This means that the factor in question may easily be four or even nine. It should of course be more correct to use the partial specific volume of the solute in the solvent in question instead of the reciprocal density of the solid substance, but even the volume measured that way may easily be less than v_m because the small solvent molecules can accomodate themselves in the structure of the solute macromolecules while other solute molecules can not. Therefore, the only thing we can state with some certainty is that the product $b\varrho$ must be equal to or greater than eight, provided that attractions between the rod-molecules can be neglected.

Example 1

Experiments by Kroepelin and Brumshagen [11]. Recalculated by J. A. Chr.
Solute: Caoutchouk. Solvent: Benzene.

Temp.	M	ϱ	b	$b\varrho$
11°C	210 000	0.91 g/cm³	about 40 cm³/g	about 36
40°C	210 000	0.91 »	about 70 »	about 62

Remarks: As mentioned by the authors themselves, the b values are rather inaccurate, but it seems certain that b at 40°C is essentially larger than b at 11°C.

As an explanation it may be suggested that different rubber-molecules be curled into helixes of different diameters, those with the larger diameters having the greater energy-contents.

Example 2

Experiments by Schultz [12]. Recalculated by J. A. Chr.
Solute: Cellulose-nitrate. Solvent: Acetone.
Temp. 27°C. Density, ϱ : 1.35 g/cm³

Specimen	M	b	$b\varrho$
N66	about 54 700	about 25 cm³/g	about 34
N65	about 36 700	about 21 »	about 28

Remarks: Polysaccharide chains are probably straight, but the nitro-groups substituted for hydrogen in the hydroxy-groups may act as short side-chains.

Example 3

Experiments by Schultz [12]. Recalculated by J. A. Chr.
Solute: Polystyrene. Solvent: Toluene.
Temp. 27°C. Density, ϱ : 1.06 g/cm³

Specimen	M	b	$b\varrho$
P.S. 20°	about 141 000	about 30 cm³/g	about 32
P.S. 135°	» 160 000	» 29 »	» 31
P.S. 200°	» 57 500	» 23 »	» 24

Remark: The aromatic side-chains must increase the effective diameter of the principal chain but may prevent its curling up.

Example 4

Experiments by Schultz [12]. Recalculated by J. A. Chr.
Solute: Polyethylene oxide. Solvent: Water.
Temp. 27°C. Density, ϱ : 1.12 g/cm³.

Specimen	M	b	$b\varrho$
II	about 64 400	about 54 cm³/g	about 60
III	» 26 600	» 26 »	» 29
IV	» 17 700	» 26 »	» 29

Remark: In the book by H. Staudinger, *Die hochpolymeren organischen Verbindungen* (1932) p. 293, one author, H. Lohmann, gives arguments for zigzag formulae of the polyethylene oxides illustrated in a plane. This illustration may very naturally be taken as the projection formula of a helix.

Example 5

Experiments by Jensen and Marcker [13]. Recalculated by J. A. Chr.
Solute: Dextrane, fractionated. Solvent: 0.2 M KCl in Water.
Temp. 20°C. Density taken to be 1.588 g/cm³ (sucrose), (starch about 1.5)

Specimen	M	b	$b\varrho$
Dextrane	about 140 000	4.93 cm³/g	7.84

Remarks: Unfortunately no determinations of the density of the solid or of its specific volume in the solution were performed. Assuming that different polysaccharides have the same specific weights the value of ϱ for sucrose has been taken. The value for starch, 1.5, is probably low, because it refers to granules of native starch which may include some air.

It is said in the paper [13] that the (commercial) specimen was very polydisperse and had to be freed from the low molecular fraction by dissolution and reprecipitation, but even so it became certainly not monodisperse. As, by experience, unavailable volumes are usually independent of the molecular weights for rod-molecules derived from the same structural unit, the degree of polymerisation is probably irrelevant for the value of $b\varrho$.

The deviation of $b\varrho$ from 8 is certainly less than the probable error. The result therefore suggests that the polysaccharide chain be not coiled up. Because of the cyclic constitution of the units this seems intrinsically probable.

Addendum to Example 5, and amendments to a paper on the inverted osmometer

In Table 2 in the paper by Jensen and Marcker [13] there is one misprint (19.40 for 10.94) and one line is missing. The complete table shall therefore be reprinted below. Furthermore, the heights of the air-column had not been

corrected for curvature at its ends. This has now been done by subtracting one third of the diameter of the capillary (0.07 cm) from the heights (p) in the table. The corrected values of c/p are under the heading (c/p). Values of c/p have been calculated from the formula $c/p = A—Abc$ with $A = 5.68$, $Ab = 0.0280$. They are under the heading $(c/p)_{calc}$. Finally, values of the difference $(c/p)—(c/p)_{calc}$ are in the last column.

Table 2 by Jensen and Marcker [13], revised and enlarged by J. A. Chr.

c mg/ml	p cm	c/p	(c/p)	$(c/p)_{calc}$	
0				5.68	
5.19	1.05	4.94	5.05	5.54	−0.49
10.94	2.07	5.31	5.37	5.37	0.00
19.40	3.90	4.98	5.01	5.14	−0.13
31.51	6.45	4.89	4.91	4.83	+0.08
40.00	8.80	4.55	4.56	4.56	0.00

The deviations in the last column are such that if caused by errors in the determination of p three of them would correspond to errors of about 1 mm. Such errors are, however, nearly impossible and it is therefore much more probable that they have arisen from lack of homogeneity in the fraction investigated. It should be recalled in this connection, that it was certainly not monodisperse. If this be the cause of the deviations it is quite natural that it is the determination in which the smallest amount of substance (5 mg) was weighed in, which shows the largest deviation.

Amendments to the paper by Christiansen and Jensen[1]

On p. 1252 the authors mention three corrections which should be applied:

1. A correction for the finite density of air (saturated with water vapour at 20°C). This correction varies with the varying total pressure in the apparatus, but it is so small that its value at one atmosphere, 0.0011 g/cm^3, can safely be used in all cases. Therefore the significant figures in the value of q on p. 1254, 246.8, should be replaced by 247.1.

2. A correction for the difference in density between the outer and the inner liquids. This correction is at any rate very small, and if complete equilibrium in the gravity-field has been established, not only across the membrane but also in the column of inner liquid extending from the upper end of the capillary to the upper end of the air-column, only the density of the outer liquid is relevant. This item be therefore withdrawn.

3. A correction for the difference in surface-tension between the solution at the upper end of the air-column and the solvent at the lower end. This be also withdrawn for the following reason: Water adheres strongly to glass. We must therefore assume that the cylindrical part of the air-column is surrounded by a liquid film, which, as known from the works of M. Vollmer, most probably is easily movable along the glass wall. The capillary forces at the ends of this cylindrical film must tend to drag it in opposite directions, and at osmotic equilibrium the forces must counterbalance each other exactly.

Example 6

Experiments by Jensen and Marcker [13]. Recalculated by J. A. Chr.
Solute: Potassium hyaluronate. Solvent: 0.2 M KCl in water.
Temp. 20°C. Density, : 1.16 g/cm³ (spec. vol. det. by Jensen)

Specimen	M	b	$b\varrho$
Prep. I	122 000	35.8 cm³/g	41.6
Prep. II	144 000	35.8 »	41.6
Prep. III	144 000	35.8 »	41.6
Prep. IV	1 066 000	43.0 »	50.0

Remarks: At a former occasion Jensen [14] determined the specific volume of another specimen of potassium hyaluronate by pycnometric determinations in 0.2 M KCl in water. Result: 0.86 cm³/g. It is evident from the table that b depends only slightly on the molecular weight of the preparation. It is also evident that the product $b\varrho$ is 5—6 times larger for the hyaluronate than for dextran, although the former is a derivative of a polysaccharide and the latter is a polysaccharide. This may partly be due to the circumstance that the former contains carboxyl-groups as side-chains, but the effect of this may be masked by the property of its being a polyelectrolyte. In a forthcoming paper, Graae and Marcker point out that the large unavailable volume of the hyaluronate may be due to electrical forces from the ionic atmosphere surrounding the negatively charged "backbone" of the polyion. The effective diameter of the cylinder may be expected to be not very different from the Debyelength $1/\varkappa$ and b should therefore increase with decreasing ionic strength of the solvent. Graae and Marcker have found experimental evidence in the literature that this be true for another chain-like polyelectrolyte.

Addendum to Example 6

The values for c/p in Table 3 of the paper in question have not been corrected for curvature at the ends of the air column. Table 3 has therefore been recalculated by the present author (see below) and the values for M and b in the table above are the results of this recalculation. It should be noted that in the columns marked p in the original table 3 the number of significant figures should have been increased by one in some cases. The figures in the column marked c/p, however, have in all cases been calculated from the orginal data and have sufficient numbers of significant figures. The recalculation, therefore, is based on the figures in that column. One misprint in the original p-column, 1.00 in stead of 1.06, has been found. As in the addendum to Example 5 c/p is the original value, (c/p) the corrected one and $(c/p)_{calc}$ that calculated according to the formula $p/c = A—Abc$. The differences (exp) — (calc) are in the last column.

Table 3 by Jensen and Marcker [13], revised and enlarged by J. A. Chr.

Prep. I. $A = 4.92$; $b = 0.0358$ litre/g.

c mg/ml	p cm	c/p	(c/p)	$(c/p)_{calc}$	
0				4.92	
16.00	7.89	2.03	2.03	2.10	−0.07
13.00	4.91	2.65	2.66	2.63	+0.03
11.00	3.70	2.97	2.99	2.98	+0.01
7.00	1.85	3.78	3 83	3.69	+0.14
5.00	1.292	3.87	3.94	4.04	−0.10

Prep. II. $A = 5.85$; $b = 0.0358$ litre/g.

0				5.85	
16.00	6.50	2.46	2.47	2.50	−0.03
13.00	4.19	3.10	3.12	3.13	−0.01
11.18	3.21	3.49	3.52	3.51	+0.01
5.00	1.059	4.72	4.83	4.80	+0.03

Prep. III. $A = 5.85$; $b = 0.0358$ litre/g.

0				5.85	
7.51	1.85	4.06	4.12	4.27	−0.15
5.10	1.10	4.64	4.74	4.78	−0.04
3.53	0.710	4.97	5.14	5.11	+0.03
2.56	0.490	5.22	5.49	5.31	+0.18

Prep. IV. $A = 43.0$; $b = 0.0432$ litre/g.

0				43.0	
19.99	3.49	5.72	5.76	5.80	−0.04
16.00	1.20	13.33	13.59	13.22	+0.37
13.78	0.85	16.21	16.68	17.38	−0.70
10.21	0.450	22.69	23.90	23.98	−0.08
7.48	0.280	26.71	29.15	29.10	+0.05

It should be noted how surprisingly accurately the van der Waals abridged formula holds, even in cases where the available volume is less than half of the total volume, in the case of Prep. IV even less than one seventh.

It should be added, that in recalculating the tables for Prepns. I—III the present author has taken advantage of the fact found by Jensen and Marcker that the b-values are, inside the experimental errors, the same for these preparations.

It is seen that in all the examples quoted bQ is equal to or greater than eight. On the other hand it is less than one hundred. Now according to the formula of Zimm [4] and Isihara [3,6] the lower limit for the product should be, for long molecules, the height of the cylinder divided by its diameter. The lowest value of this ratio occurring among the examples is probably the one in Example 4, specimen IV, and even here it can hardly be below 150. In the other examples rough estimates yields much larger values for the same ratio. This confirms the suggestion that Def. II and not Def. I be the right one to use.

The authors sincere thanks are due to Dr. Thor A. Bak for his drawing the authors attention to A. Isihara's calculations and to professor Dr. W. Fenchel for his highly instructive explanations and discussions of the same.

Finally the author should like to express his sincere gratitude to his former coworkers, the late Dr. C. E. Jensen, J. Graae and K. Marcker for their careful and intelligent work with the problems of osmotic pressure and its measurement, without which the present paper had had to remain unwritten. Particularly, thanks are due to Mr. Marcker for information regarding technical and other details from his work in cooperation with C. E. Jensen.

REFERENCES

1. Christiansen, J. A. and Jensen, C. E. *Acta Chem. Scand.* **7** (1953) 1247.
2. Gibbs, J. W. *Nature* **55** (1897) 461.
3. Isihara, A. and Hayashida, T. *J. Phys. Soc. Japan* **6** (1951) 40.
4. Zimm, B. H. *J. Chem. Phys.* **14** (1946) 164.
5. Isihara, A. *J. Chem. Phys.* **18** (1950) 1446.
6. Hirschfelder, Curtiss, Bird (Book). *Molecular Theory of Gases and Liquids* (1954) p. 184.
7. Sørensen, S. P. L., Christiansen, J. A., Høyrup, M., Goldschmidt, S. and Palitzsch, S., *Compt. rend. trav. lab. Carlsberg* **12** (1915–1917) 262.
8. Tammann, G. *Z. physik. Chem.* **9** (1890) 97.
9. Berkeley, Earl of and Hartley, E. G. J. *Phil. Trans. (London)* **A 206** (1906) 481.
10. Fuoss, R. M. and Mead, D. J. *J. Phys. Chem.* **47** (1943) 59.
11. Kroepelin, H. and Brumshagen, W. *Ber.* **61** (1928) 2441.
12. Schultz, G. V. *Z. physik. Chem.* **A 176** (1936) 317.
13. Jensen, C. E. and Marcker, K. *Acta Chem. Scand.* **12** (1958) 855.
14. Jensen, C. E. and Djurtoft, R. *Acta Chem. Scand.* **8** (1954) 1659.

Received February 8, 1960.

ACTA CHEMICA SCANDINAVICA 14 (1960) 1203—1210

Dehydrogenation of Phenols

I. Dehydrogenation of 2,6-Dimethylphenol with Silver Oxide

BENGT O. LINDGREN

Wood Chemistry Department, Swedish Forest Products Research Laboratory, Stockholm, Sweden

The dimeric and polymeric products obtained by oxidation of 2,6-dimethylphenol with silver oxide were investigated. The results show that the phenoxyl radicals probably formed as intermediates mainly react to give diphenyl ether groups (Path A in Scheme 1).

One electron oxidation of phenols (reviews [1,2]) affords phenoxyl radicals. Due to their different mesomeric forms they can pair to form stable products in various ways. They may react to form ether linkages (Path A in Scheme 1) or they may form carbon-carbon bonds (Path B). In the first case, quinol ethers and diphenyl ethers are obtained, in the second, bis-(*cyclo*hexadienone) derivatives, diphenyls and diphenoquinones.

Several examples of both types of oxidation products are known. The commonest types of dimers actually obtained are the diphenyls and diphenoquinones. The yields of these products are usually however rather low, the main products often being polymeric materials. It is therefore also necessary to study these polymers before deciding whether A or B represents the preferred reaction path.

These oxidation polymers have been studied only in the case of *o*-cresol. Pummerer [3] has briefly mentioned, without giving experimental details, that potassium ferricyanide oxidation gives a polymer with ether-linked phenolic units. According to Goldschmidt [4] *o*-cresol reacts with lead dioxide in acidified ether to give a trimer of the same type. His arguments are, however, not conclusive.

In some cases, high yields of diphenyls and diphenoquinones have been obtained by oxidation of phenols. For example, both benzoyl peroxide [5] and chromium trioxide in acetic acid [6] convert 2,6-dimethylphenol in high yield into the corresponding diphenoquinone. It is probable, however, that these reactions do not involve one electron mechanisms [7,8] but pass through cationic intermediates, as in the reactions of periodate [9] and lead tetracetate [10] with phenols.

On the other hand, reduction of ferric chloride and potassium ferricyanide involves only one electron and it seems likely therefore that their reactions with phenols involve

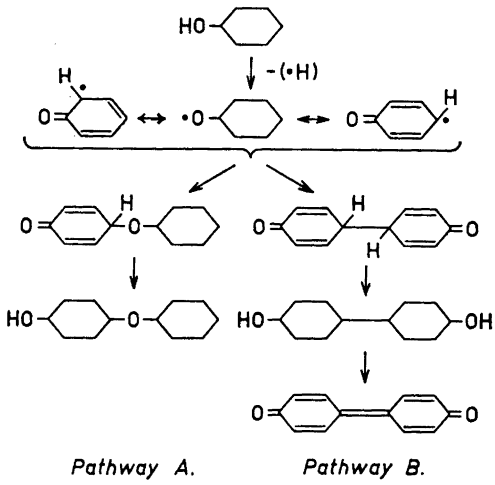

Scheme 1. The reaction pathways at dehydrogenation of phenols.

phenoxyl radicals. These reagents have also been used to prepare relatively stable phenoxyl radicals from sterically hindered phenols. It is of interest that in their reaction with 2,6-dimethylphenol the yields of the diphenyl and the diphenoquinone are much smaller than in the above mentioned cases [6].

Recently Ley, Müller and co-workers [11] have shown that labile quinol ethers are the initial products formed when phenols react with 2,4,6-tri-*tert.* butylphenoxyl-(1) and similar stable radicals. These may then split into radicals, which slowly form bis-(*cyclo*hexadienone) derivatives and diphenyls.

In the present investigation a study has been made of the oxidation of 2,6-dimethylphenol with silver oxide. The polymeric materials formed were examined as well as the dimeric products. This oxidation must be of the one electron type because the reduction of silver oxide, like that of ferric chloride and potassium ferricyanide, involves only one electron. Silver oxide was actually used by Pummerer [12] in some of his pioneer works to prepare stable phenoxyl radicals.

The oxidation was carried out by shaking a benzene solution of the phenol with silver oxide at room temperature. In some experiments sufficient silver oxide was added to abstract one hydrogen atom from each phenol molecule, in others, enough was used to abstract two hydrogen atoms (mole ratio silver oxide/phenol = 0.5 and 1, respectively).

In the first case a compound (I), the composition of which corresponded to $C_{16}H_{18}O_2$, was isolated in a yield of 15 %. The other substances obtained were 3,3′,5,5′-tetramethyl-4,4′-diphenoquinone (yield 11 %) and small amounts of 3,3′,5,5′-tetramethyl-4,4′-dihydroxy-diphenyl. The greater part of the residue was unreacted 2,6-dimethylphenol (yield 31 %) and undistillable, polymeric material.

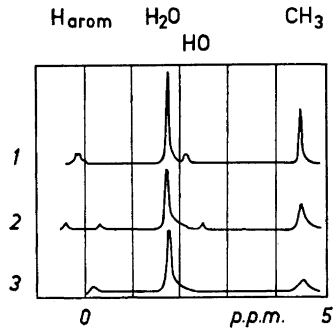

Fig. 1. NMR spectra of 1) 2,6-dimethylphenol, 2) compound (I), and 3) the solid polymer. Carbon tetrachloride solution. External standard: water.

The UV spectrum indicated that substance (I) was aromatic (λ_{max} 288 mμ, ε 7 400 in methanol). Acetylation showed that it contained one hydroxyl group which was found to be phenolic by the bathochromic shift [13] of the 288 mμ maximum in alkaline solution (λ_{max} 310 mμ, ε 9 000 in N methanolic KOH). The IR spectrum of the compound indicated the presence of both 1,2,3-trisubstituted (maxima at 715 and 780 cm^{-1}) [14] and 1,2,3,5-tetrasubstituted (maximum at 850 cm^{-1}) [15] benzene nuclei. (2,6-Dimethylphenol as a trisubstituted benzene derivative has peaks at 722 and 755 cm^{-1}). No carbonyl band was present. From this it was probable that the compound was 3,5,2′,6′-tetramethyl-4-hydroxydiphenyl ether (formula I), which can be obtained from the phenol by Pathway A, Scheme 1.

The NMR spectrum showed a single strong resonance peak at a chemical shift of 4.45 p.p.m. relative to benzene hydrogen (Fig. 1). This must be due to methyl groups in α-position to a benzene nucleus (reported values for methyl substituted benzenes about 4.7 p.p.m.) [16]. 2,6-Dimethylphenol has a strong peak at the same point. The 2.40 p.p.m. peak is probably caused by hydroxylic hydrogen (2.15 for 2,6-dimethylphenol) as it shifted to 2.20 p.p.m. on addition of dimethyl sulphoxide, which would form hydrogen bonds with the hydroxyl groups.

Two single resonance bands were obtained for aromatic hydrogen, one on each side of the peak for benzene hydrogen (—0.40 and 0.24 p.p.m., respectively). They may correspond to the coupled magnetic resonance for the hydrogen atoms in the phenolic benzene nucleus (—0.40 p.p.m.) and in the non-phenolic nucleus (0.24 p.p.m.).

The NMR showed the absence of aliphatic (except CH_3) and olefinic hydrogen. It is thus in agreement with the formula (I):

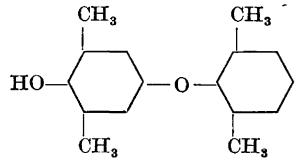

I

Structure (I) was confirmed by periodate degradation which gave 2,6-dimethyl-*p*-quinone. This reaction is analogous to the formation of phenol and *p*-quinone by periodate oxidation of *p*-hydroxy-diphenyl ether [9]. That 2,6-dimethyl-phenol was not obtained from (I) may be due to the fact that it reacts rapidly with periodate [17]. Unsubstituted phenol, on the other hand reacts very slowly with periodate [9].

When 2,6-dimethylphenol was treated with sufficient silver oxide to abstract two hydrogen atoms the diphenyl ether (I) was obtained in very low yield. A white amorphous material was isolated which had the elemental composition $C_8H_{8.12}O_{0.94}$ and must therefore have been formed from dimethyl-phenol by elimination of two hydrogen atoms.

Determination of the molecular weight of this material from the melting point depression of benzene solutions gave values of 1 300 and 1 900 (two samples), corresponding to 10—16 dimethylphenol units, respectively.

Heating with acetic anhydride and pyridine did not introduce any acetyl groups into the product and it therefore contained few or no hydroxyl groups. In agreement its IR spectrum (Fig. 2) showed only weak absorption in the vicinity of 3 500 cm^{-1}. There were two peaks in the carbonyl range, at 1 700 and 1 740 cm^{-1}. The extinction coefficients of these carbonyl peaks were, however, rather low and the occurrence of carbonyl groups was therefore regarded as small in the polymer. These groups have not been further examined.

The product did not oxidise potassium iodide and therefore did not contain any peroxide groups. Thus, the bulk of the oxygen atoms in the polymer must be present in ether groups.

The UV spectrum of the polymer (Fig. 3) showed that it was made up largely of aromatic units. (Maxima at 238 mμ, ε 9 150; 278 mμ, ε 1 670; and 285 mμ, ε 1 640. Dioxan solution; ε-values calculated on a C_8-basis.) Its NMR spectrum (Fig. 1) supported this as it did not contain any resonance peak for aliphatic (except the CH_3 peak at 4.45 p.p.m.) or olefinic hydrogen. The aromatic hydrogen peak (0.22 p.p.m.) was above the benzene hydrogen peak.

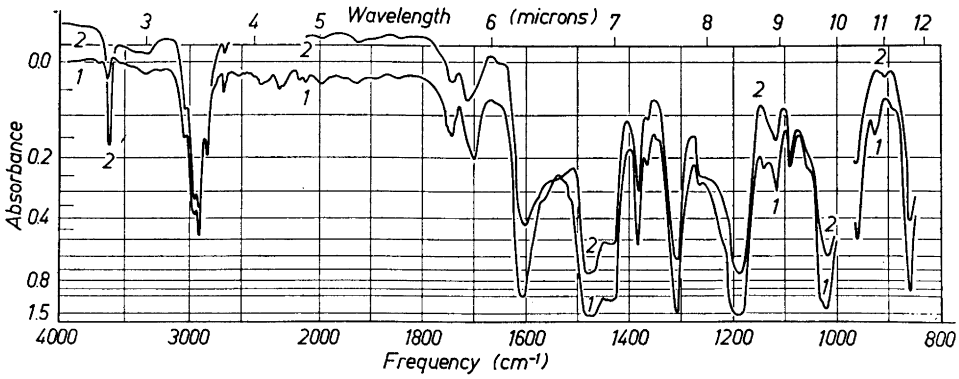

Fig. 2. IR spectra of 1) the solid polymer, and 2) the sirupy material from the mother liqour. Curve 2 displaced to lower absorbance for its separating from curve 1. Carbon tetrachloride solution.

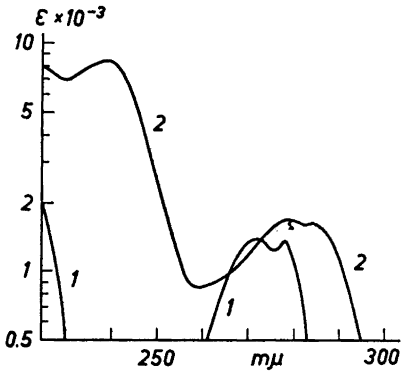

Fig. 3. UV spectra of 1) 2,6-dimethylphenol, and 2) the solid polymer. Methanol solution.

The IR spectrum gave an indication of the substitution in the benzene nucleus since it had a maximum at 850 cm^{-1} characteristic for 1,2,3,5-tetra-substituted benzene derivatives.

No trace of a maximum was present in the UV curve at 250—270 mμ, where diphenyl derivatives show strong absorption. (3,3′,5,5′-Tetramethyl-4,4′-dihydroxy-diphenyl: λ_{max} 267 mμ, ε 17 500 in methanol.)

These findings strongly indicated that the polymer is built up mainly according to formula (II). It also contained other structural features including a small percentage of carbonyl groups.

The polymeric material was obtained in a yield of about 40 %. From the mother liquor a semi-solid material was obtained, which gave essentially the same IR spectrum as the solid polymeric material (Fig. 2) but with the significant difference that the semi-solid material had a strong hydroxyl absorption peak. Its molecular weight was about 390, corresponding to 3.2 dimethylphenol units. These findings indicated that the material was of the same

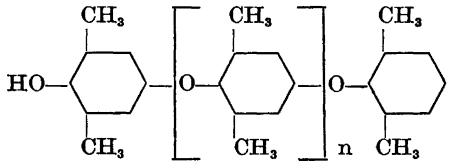

II

type as the solid polymer, but had a lower molecular weight. Distillation of the syrup gave a small amount of the diphenyl ether (I).

The yield of the syrup was about the same as the yield of the solid material (about 40 %). These experiments show therefore that on silver oxide oxidation in benzene the intermediate phenoxyl radicals mostly react according to Path A forming diphenyl ether groups.

The diphenyl ether (I) was obtained only in relatively low yield in these oxidations. Even when a theoretical amount of silver oxide was used the main products isolated were the starting material and the polymer. It is therefore

probable that the dimer (I) is oxidised more easily than the dimethylphenol. This may be due to activation of the phenolic hydroxyl group of (I) by the phenoxy group in the *para*position.

When the oxidation was carried out in the more polar solvent dimethylformamide, the polymeric material was again obtained together with tetramethyl-diphenoquinone. The yield of the polymer was, however, low, at least in part due to difficulties in isolating the material. The similarity of the polymeric materials was shown by the IR spectra.

Kuhn [18] has recently elaborated a new methylation technique for carbohydrates. The sugar, dissolved in dimethylformamide, is treated with silver oxide and methyl iodide. When 2,6-dimethylphenol is methylated in a corresponding way there is competition between the oxidation and the methylation reactions. From the reaction mixture a polymeric material was isolated the IR spectrum of which was identical with those of the above mentioned polymers. Analysis gave the empirical formula $C_8H_{8.03}O_{0.97}(OCH_3)_{0.065}$. The product thus contained one methoxyl group to 15 dimethylphenol units. Cryoscopic molecular weight determination gave a value corresponding to 14 units in the molecule. Probably the methoxyl groups were present as end groups (III) in the polymer.

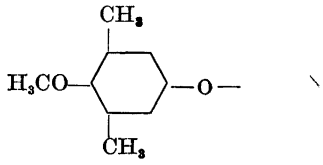

III

EXPERIMENTAL

Oxidation of 2,6-dimethylphenol in benzene solution, mole ratio silver oxide/phenol = 0.5. Silver oxide (25 g) was added in portions to a solution of 2,6-dimethylphenol (25 g) in benzene (500 ml). The mixture was then shaken for 17 h at about 20° in the dark. Undissolved material was collected and extracted with boiling acetic acid. On cooling, red crystals (2.7 g) m.p. 208–210° (undepressed by admixture with 3,3′,5,5′-tetramethyl-4,4′-diphenoquinone) were obtained.

The benzene filtrate was evaporated and the residue was dissolved in a small amount of benzene. Undissolved dark green crystals (0.2 g) were removed. These had m.p. 186–187°, undepressed on admixture with the quinhydrone from 3,3′,5,5′-tetramethyl-4,4′-dihydroxy-diphenyl and 3,3′,5,5′-tetramethyl-4,4′-diphenoquinone. The benzene solution was again evaporated and the residue was distilled. The following fractions were collected: 1) b.p. 60–70° 0.3 mm Hg, 7.7 g of 2,6-dimethylphenol, m.p. 41.5–42°. 2) b.p. 140–150° 0.4 mm Hg, 3.9 g of substance (I), m.p. 101–105°.

The m.p. of substance (I) was raised to 105–108° by repeated recrystallisation from methanol – water. A small amount of crystalline material m.p. 223–225° (undepressed by admixture with 3,3′,5,5′-tetramethyl-4,4′-dihydroxy-diphenyl) was obtained from the mother liquor.

Compound (I). Found: C 78.9; H 7.3; O 14.0; OH 6.3. Calc. for $C_{16}H_{18}O_2$ (242): C 79.3; H 7.4; O 13.2; OH 7.0.

Oxidation with periodate. Sodium *para*periodate (3 g) dissolved in acetic acid – water (1:2 v/v, 100 ml) was added to a solution of substance (I) (0.6 g) in acetic acid (10 ml). The solution turned yellow. It was allowed to stand at room temperature for half an hour. The solution was then extracted with benzene, and the benzene solution was shaken with 5 % sodium hydroxide solution, dried (sodium sulphate) and evaporated. The residue (0.2 g) was sublimed at about 80° (bath temperature) and a pressure of 15 mm Hg to give yellow needles (0.11 g, yield 33 %) m.p. 55–58°. Recrystallisation from light petroleum increased the m.p. to 67–67.5°, undepressed by admixture with 2,6-dimethyl-*p*-quinone.

No 2,6-dimethylphenol was isolated from the sodium hydroxide solution. Similarly, no phenol was obtained when one mole of periodate was added to one mole of substance (I).

Oxidation of 2,6-dimethylphenol in benzene solution, mole ratio silver oxide/phenol = 1. Silver oxide (23 g) was added in portions to a solution of 2,6-dimethylphenol (12 g) in benzene (250 ml). The mixture was then shaken overnight at about 20°. Undissolved material was collected and extracted several times with boiling acetic acid. On cooling, 3,3′,5,5′-tetramethyl-4,4′-diphenoquinone (1.0 g) crystallised from the acetic acid.

The benzene filtrate was extracted with 5 % sodium hydroxide solution (from which 0.17 g of 2,6-dimethylphenol could be recovered) and dried (sodium sulphate). The addition of light petroleum (b.p. 60—70°) to the benzene solution precipitated a white, amorphous material which was collected by centrifuging and washed with light petroleum. Weight after drying in a vacuum at room temperature, 2.1 g. Preparation A. (Found: C 80.4; H 6.7; O 12.6; mol. wt. 1 300). The IR and UV spectra are shown in Fig. 1 and Fig. 2, respectively.

The filtrate from material A was evaporated to dryness and the residue was dissolved in *iso*propyl ether. Ethanol was added to this solution and the white precipitate obtained was collected and washed with light petroleum. Weight 2.6 g. Preparation B. The IR and UV spectra were very similar to those of preparation A. (Found: C 80.5; H 6.8; O 12.5; mol. wt. 1 900).

The *iso*propyl ether — ethanol solution was evaporated to dryness, giving a semi-solid residue (4.7 g). Preparation C. Mol. wt. 390. IR spectrum in Fig. 2.

Acetylation of preparations A and B. Samples of A and B (300 mg each) were heated with pyridine (3 ml) and acetic anhydride (3 ml) for 1 h at 100°. Water was added and the mixture was then extracted with benzene. The benzene solution was shaken with sodium bicarbonate solution and dried. Dissolved material was precipitated by adding methanol, filtered and washed with methanol. Both products gave 0 % acetyl.

Oxidation of 2,6-dimethylphenol in dimethyl formamide solution, mole ratio phenol/silver oxide = 1. Silver oxide (4 g) was added in portions to a solution of 2,6-dimethylphenol (2 g) dissolved in dimethylformamide (40 ml). The mixture was shaken overnight at room temperature. The solid material was then filtered off and extracted with boiling acetic acid. From the acetic acid solution 3,3′,4,4′-tetramethyl-4,4′-diphenoquinone (0.15 g) crystallised during cooling.

Chloroform and water were added to the dimethylformamide filtrate to give two phases. The upper layer was extracted several times with chloroform. The chloroform solutions were combined, shaken with water 6 times, dried and evaporated to dryness. The residue (0.67 g) was dissolved in benzene, and methanol added to the solution. The white precipitate obtained was collected (72 mg). The IR spectrum of this material agreed with those of preparations A and B above.

Oxidation of 2,6-dimethylphenol in dimethylformamide — methyl iodide solution. Silver oxide (7.5 g) was added in portions to a solution of 2,6-dimethylphenol (3 g) in dimethylformamide (15 ml) and methyl iodide (9 ml), and the mixture shaken overnight at room temperature. Undissolved material was removed and the filtrate was shaken with sodium thiosulphate solution and then with water. After drying, the solution was evaporated and the residue (1.35 g) was dissolved in *iso*propyl ether. Crystals of undissolved 3,3′,4,4′-tetramethyl-4,4′-diphenoquinone were removed (a few mg), the solution was poured into ethanol and the white precipitate (0.35 g) obtained was collected by centrifuging. (Found: C 79.5; H 6.8; O 13.6; OCH_3 1.66). The UV and IR spectra were identical with those of preparations A and B.

Acknowledgement. The author wishes to thank Miss Marit Goliath and Mr Sigurd Söderberg for valuable experimental assistance. The IR spectra were recorded at the department of Organic Chemistry, Royal Institute of Technology by Miss Gurli Hammarberg, and the NMR spectra were determined in the department of Physical Chemistry of the Royal Institute of Technology by Dr. Sture Forsén and Mr Jan-Christer Eriksson. I am greatly indebted to them for their co-operation.

REFERENCES

1. Barton, D. H. R. and Cohen, T. *Festschrift Arthur Stoll*, Basel 1957, p. 117.
2. Erdtman, H. and Wachtmeister, C. A. *Festschrift Arthur Stoll*, Basel 1957, p. 144.
3. Pummerer, R., Melamed, D. and Puttfarcken, H. *Ber.* **55** (1922) 3116.
4. Goldschmidt, S., Schultz, E. and Bernard, H. *Ann.* **478** (1930) 1.
5. Cosgrove, S. L. and Waters, W. A. *J. Chem. Soc.* **1951** 388.
6. Auwers, K. and v. Markovits, Th. *Ber.* **38** (1950) 226; **41** (1908) 2332; v. Auwers, K. and Wittig, G. *Ber.* **57** (1924) 1270.
7. Walling, C. and Hodgdon, R. B. Jr. *J. Am. Chem. Soc.* **80** (1958) 228.
8. Lewitt, L. *J. Org. Chem.* **20** (1955) 1297.
9. Adler, E. and Magnusson, R. *Acta Chem. Scand.* **13** (1959) 505.
10. Criegee, R. *Angew. Chem.* **70** (1958) 173.
11. Ley, K., Müller, E., Mayer, R. and Scheffler, K. *Chem. Ber.* **91** (1958) 2670.
12. Pummerer, R. and Frankfurter, F. *Ber.* **47** (1914); 1472; Pummerer, R. and Cherbuliez, E. *Ber.* **47** (1914) 2957.
13. Aulin-Erdtman, G. and Hegbom, L. *Svensk Papperstidn.* **60** (1957) 671.
14. McMurry, H. L. and Thornton, V. *Anal. Chem.* **24** (1952) 318; Colthup, N. B. *J. Optical Soc. Am.* **40** (1950) 397.
15. Connon, C. G. and Sutherland, G. B. B. M. *Spectrochim. Acta* **4** (1951) 373.
16. Chamberlain, N. F. *Anal. Chem.* **31** (1959) 56.
17. Adler, E. *Personal communication.*
18. Kuhn, R., Trischmann, H. and Löw, I. *Angew. Chem.* **67** (1955) 32.

Received February 5, 1960.

ACTA CHEMICA SCANDINAVICA 14 (1960) 1211—1230

Short Communications

The Occurrence of Cephalin, Sphingomyelin, and Lysolecithin in Bile

FUMIO NAKAYAMA and
ROLF BLOMSTRAND

The Swedish Medical Research Council, Unit for Biochemical Research related to Atherosclerosis, University of Lund, Sweden

Since Thudichum studied the phospholipids in bile as early as 1862[1], lecithin has been believed to be the only phospholipid present in bile [2,3]. However, in 1958 Nakayama and Johnston [4] fractionated biliary phospholipids with silicic acid column chromatography and presented data showing the constant presence of several phospholipid peaks other than that corresponding to lecithin. Furthermore, the complicated pattern of fatty acids of biliary phospholipids obtained by gas chromatography suggests the complexity of phospholipids composition in bile [5]. These findings prompted us to identify the phospholipid components in bile.

The bile from rat and rabbit given ^{32}P-orthophosphate intraperitoneally was extracted with chloroform-methanol 2:1 mixture followed by partition with physiological saline solution essentially based on the technique of Folch *et al* [6]. The labelled biliary phospholipids were purified by silicic acid column chromatography [7]. The methanol fraction containing the phospholipids was concentrated and subjected to paper chromatography together with ^{32}P-labelled liver phospholipids using the solvent system of di*iso*butylketone, acetic acid, and water (40:25:5) [8] followed by autoradiography (Fig. 1). The autoradiogram of rat liver phospholipids (Ia) indicated the presence of six phospholipid components which were earlier identified by Marinetti *et al.*[9] as A-unidentified phospholipid, B-lysolecithin, C-sphingomyelin, D-lecithin, E-cephalin, F-unidentified phospholipid, as shown in Fig. 1. The autoradiogram of biliary phospholipids from rabbit (IIa) and from rat revealed the presence of lysolecithin, sphingomyelin, lecithin and cephalin in bile of the two species studied.

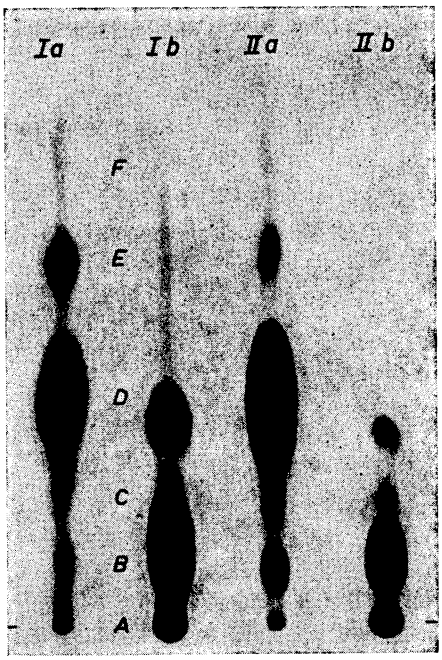

Fig. 1. Autoradiogram of ^{32}P-labelled rabbit liver and bile phospholipids. Ia-liver phospholipids, Ib-liver lecithin hydrolysate with snake venom *(Crotalus adamanteus)*, IIa-bile phospholipids, IIb-its hydrolysate with snake venom. Silicic acid impregnated Whatman No. 3 paper, ascending, solvent system-di*iso*-butylketone: acetic acid:water 40:25:5. A-unidentified phospholipid, B-lysolecithin, C-sphingomyelin, D-lecithin, E-cephalin, and F-unidentified phospholipid.

The further evidence for the presence of lysolecithin in bile was provided using the combination of snake venom and autoradiography. A part of the labelled phospholipids was hydrolyzed with snake venom *(Crotalus adamanteus)* [10] and subjected to paper chromatography together with the original phospholipids. After hydrolysis with snake venom of the pure liver lecithin obtained by preparative paper chromatography, the lecithin spot was diminished greatly and transformed into a lysolecithin spot (Ib). The lecithin spot of biliary phospholipids (IIa) was diminished greatly after similar hydrolysis and transformed into a lysolecithin spot, thus confirming the presence of lysolecithin in bile (IIb).

This work is part of investigations supported by *The Swedish Medical Research Council.*

1. Thudichum, J. L. W. *A treatise on gallstones*, John Churchill and Sons, London 1863.
2. Johnston, C. G., Irvin, J. L. and Walton C. *J. Biol. Chem.* **131** (1939) 425.
3. Polonovski, M. and Bourillon, R. *Bull. soc. chim. biol.* **34** (1952) 720.
4. Nakayama, F. and Johnston, C. G. *Surg. Forum, Am. College Surgeons* **9** (1958) 518.
5. Blomstrand, R. *Acta Chem. Scand. In press.*
6. Folch, J., Ascoli, I., Lees, M., Meath, J. A. and LeBaron, F. N. *J. Biol. Chem.* **191** (1951) 833.
7. Borgström, B. *Acta Physiol. Scand.* **28** (1952) 101.
8. Marinetti, G. V., Albrecht, M., Ford, T. and Stotz, E. *Biochim. et Biophys. Acta* **36** (1959) 4.
9. Marinetti, G. V., Witter, R. F. and Stotz, E. *J. Biol. Chem.* **226** (1957) 475.
10. Dittmer, G. C. and Hanahan, D. J. *J. Biol. Chem.* **234** (1959) 1976.

Received May 31, 1960.

Separation of Nucleic Acids and Protein by Electrophoresis Combined with Counter Flow

R. ELIASSON, E. HAMMARSTEN and H. PALMSTIERNA

Department of Bacteriology Karolinska Institutet, Stockholm 60, Sweden

A good separation of proteins and nucleic acids from cell extracts could be achieved by electrophoresis in long columns stabilised with ethanolised cellulose [1]. The length of the path needed to affect such a separation was 300—320 cm. The diameters of the columns was 3.5 cm, and in a few cases 8.0 cm (unpublished). It became apparent that some material contained in the protein fractions was lost in the large amounts of cellulose (*e. g.* the neurotoxin from *Bordetella pertussis*).

The experiments to be described aim at a separation of the nucleic acids from the proteins in small columns as a preliminary to a further separation of these compound groups by means of chromatography. It was also desirable to let the proteins be in contact with as little cellulose as possible. Very small columns are also desirable for the separation of the components in biologically active nucleoproteins.

From these considerations we have tried to replace the length of the migration path by a steady flow of buffer against the direction of the electrophoretically migrating compounds. For this purpose we have used jacketed and cooled columns, with a length and diameter of 45 and 3.5 cm, respectively. We have also been working with 35 × 1 cm columns, about which will be reported later on. The packing, cooling, continuous buffer exchange and the buffer composition were exactly the same as described before [1]. The end of the side tube was, as usual, closed by a tightly fitting, thick dialysis membrane. Micropumps were constructed with capacities suitable for pumping the buffer in the direction opposite to the electrophoretic migration of the polyelectrolytes to be separated.

In the present paper we report experiments (*cf.* Table 1) where suction was simply applied to the buffer above the stabilised part of the column, with the purpose of finding the rate of flow that would permit the nucleic acid to migrate towards the anode at reduced speed, and drive the

The further evidence for the presence of lysolecithin in bile was provided using the combination of snake venom and autoradiography. A part of the labelled phospholipids was hydrolyzed with snake venom *(Crotalus adamanteus)* [10] and subjected to paper chromatography together with the original phospholipids. After hydrolysis with snake venom of the pure liver lecithin obtained by preparative paper chromatography, the lecithin spot was diminished greatly and transformed into a lysolecithin spot (Ib). The lecithin spot of biliary phospholipids (IIa) was diminished greatly after similar hydrolysis and transformed into a lysolecithin spot, thus confirming the presence of lysolecithin in bile (IIb).

This work is part of investigations supported by *The Swedish Medical Research Council.*

1. Thudichum, J. L. W. *A treatise on gallstones*, John Churchill and Sons, London 1863.
2. Johnston, C. G., Irvin, J. L. and Walton C. *J. Biol. Chem.* **131** (1939) 425.
3. Polonovski, M. and Bourillon, R. *Bull. soc. chim. biol.* **34** (1952) 720.
4. Nakayama, F. and Johnston, C. G. *Surg. Forum, Am. College Surgeons* **9** (1958) 518.
5. Blomstrand, R. *Acta Chem. Scand. In press.*
6. Folch, J., Ascoli, I., Lees, M., Meath, J. A. and LeBaron, F. N. *J. Biol. Chem.* **191** (1951) 833.
7. Borgström, B. *Acta Physiol. Scand.* **28** (1952) 101.
8. Marinetti, G. V., Albrecht, M., Ford, T. and Stotz, E. *Biochim. et Biophys. Acta* **36** (1959) 4.
9. Marinetti, G. V., Witter, R. F. and Stotz, E. *J. Biol. Chem.* **226** (1957) 475.
10. Dittmer, G. C. and Hanahan, D. J. *J. Biol. Chem.* **234** (1959) 1976.

Received May 31, 1960.

Separation of Nucleic Acids and Protein by Electrophoresis Combined with Counter Flow

R. ELIASSON, E. HAMMARSTEN and H. PALMSTIERNA

Department of Bacteriology Karolinska Institutet, Stockholm 60, Sweden

A good separation of proteins and nucleic acids from cell extracts could be achieved by electrophoresis in long columns stabilised with ethanolised cellulose [1]. The length of the path needed to affect such a separation was 300—320 cm. The diameters of the columns was 3.5 cm, and in a few cases 8.0 cm (unpublished). It became apparent that some material contained in the protein fractions was lost in the large amounts of cellulose (*e. g.* the neurotoxin from *Bordetella pertussis*).

The experiments to be described aim at a separation of the nucleic acids from the proteins in small columns as a preliminary to a further separation of these compound groups by means of chromatography. It was also desirable to let the proteins be in contact with as little cellulose as possible. Very small columns are also desirable for the separation of the components in biologically active nucleoproteins.

From these considerations we have tried to replace the length of the migration path by a steady flow of buffer against the direction of the electrophoretically migrating compounds. For this purpose we have used jacketed and cooled columns, with a length and diameter of 45 and 3.5 cm, respectively. We have also been working with 35 × 1 cm columns, about which will be reported later on. The packing, cooling, continuous buffer exchange and the buffer composition were exactly the same as described before [1]. The end of the side tube was, as usual, closed by a tightly fitting, thick dialysis membrane. Micropumps were constructed with capacities suitable for pumping the buffer in the direction opposite to the electrophoretic migration of the polyelectrolytes to be separated.

In the present paper we report experiments (*cf.* Table 1) where suction was simply applied to the buffer above the stabilised part of the column, with the purpose of finding the rate of flow that would permit the nucleic acid to migrate towards the anode at reduced speed, and drive the

Table 1.

Number of expt.	Sample mg		Electrophoresis time, h	Counter flow cm/h	Migration velocities cm/h	
	Protein	DNA			Protein	DNA
1	200	—	7	0	1,4 [e]	—
2	200 [c]	10 [a]	9	0	1,9	3,1
3	200 [c]	—	12	0	1.1 [e]	—
4	200 [c]	—	18	0	1.1 [e]	—
5	200 [c]	10 [a]	19.3	1.95	f	1.1
6	d	18 [b]	6	2.27	f	1.5
7	d	17.5 [b]	17.5	2.23	f	0.8

a) DNA prepared from calf thymus.
b) DNA prepared from *B. pertussis*.
c) Protein: Serum albumin containing praealbumun and some globulin.
d) Protein: Unknown amount of cell proteins from *B. pertussis*.
e) Not corrected for the path passed during the application of the sample before the electro phoresis was started.
f) The protein was driven out of the column by the counter flow. Measured by the photometer mentioned in the text.
g) The migration is measured from the front of the substances, when appearing after elution. The effective volume of the stabilised part of the column was measured by using phenol red.

proteins the opposite way or reduce their mobility to zero. In experiments to be published later suction has been applied with the view of isolating all protein. In Table 1 the mobilities are expressed as the position of the fronts of nucleic acids and proteins, as found after elution of the column following the electrophoresis either they have been performed with or without counter flow of the buffer solution. In cases were the proteins were driven against their electrophoretic mobility by the counter flow, the elution of the proteins was followed during the electrophoresis by a LKB Uvicord continuous photometer at 254 mμ (Svensson [2]). The nucleic acids recovered by elution after electrophoresis contained no protein as judged by the ninhydrin reaction (Moore and Stein [3]) after acid hydrolysis of solutions with 0.2 mg NA/100 ml and sublimation of the ammonium chloride *in vacuo*. Some dilution of the nucleic acid and protein fractions occurred, but the volumes could easily be reduced by a recently developed ultrafiltration method [4].

The authors are grateful to engineer E. Meyer for skilful technical assistance and the construction of the micropumps.

This work has been supported in part by the *Office, Chief of Research and Development, U.S. Department of Army*, through its European Office.

1. Hammarsten, E., Palmstierna, H. and Meyer, E. *J. Biochem. Microbiol. Technol. Eng.* **1** (1959) 273.
2. Svensson, H. *Science Tools* **6** (1960) 21.
3. Moore, S. and Stein, W. *J. Biol. Chem.* **211** (1954) 907.
4. Palmstierna, H. *Biochem. Biophys. Res. Comm.* **2** (1960) 53.

Received June 2, 1960.

Synthesis of Some 1,4-Benzoxazine Derivatives and their Antimicrobial Activity

ERKKI HONKANEN and
ARTTURI I. VIRTANEN

Laboratory of the Foundation for Chemical Research, Biochemical Institute, Helsinki, Finland

After the natural aglucone was isolated from crushed plants, and it was found to possess antimicrobial properties, the activity of different derivatives of this compound arose attention. In an earlier paper the synthesis of 2,4-dihydroxy-1,4-benzoxazin-3-one (I) and 2-hydroxy-1,4-benzoxazin-3-one (II) are described [1]. Another method for preparing 4-hydroxy-1,4-benzoxazine derivatives is also developed. When the reduction of *o*-nitrophenoxy acetic (or *o*-nitrophenoxy malonic) acid ester (III or IV) is performed in neutral medium with zinc dust, the hydroxylamino group in the first formed intermediate product (V) immediately reacts with the carboethoxy group, and ring closure to compounds VI and VII occurs. The compound VII can be readily hydrolyzed to the corresponding acid (VIII) with dilute sodium hydroxide solution.

4 - Hydroxy - 1,4 - benzoxazine - 2,3 - dione (XIII) was prepared by a similar method as 2,4-dihydroxy-1,4-benzoxazin-3-one [1]. The starting material was also now *o*-methoxymethoxyphenyl hydroxylamine (XI). By allowing this compound to react with oxalic acid ethyl ester chloride and hydrolyzing the intermediate product (XII) with methanolic hydrochloric acid, 4 - hydroxy - 1,4 - benzoxazine - 2,3 - dione (XIII) is formed. The rearrangement of 2,4 - dihydroxy - 1,4-benzoxazin - 3-one to benzoxazolinone [3] is obtained also by 4-hydroxy-1,4-benzoxazine-2,3-dione. Benzoxazolinone (XIV) could be detected in the water solution of XIII after heating for half an hour at 100°C.

The syntheses of 1,4-benzoxazine-2,3-dione [8] (XV) and 3,4-dihydro-2H-1,4-benzoxazine [9] (XVI) are described earlier in the literature.

The growth-inhibiting effect of these compounds (I, II, VI, VIII, IX, XIII, and XVI) on *Fusarium nivale* was investigated. The results are given in Fig. 1. The antibacterial activity of the 4-hydroxy-1,4-benzoxazine derivatives (I, VI, VIII, and XIII) was determined with *St. aureus*, *Ps. fluorescens*, and *E. coli*. The results are shown in Fig. 2.

It can be seen in Fig. 1 that the strongest antifungal effect of the 1,4-benzoxazine derivatives was exerted by compound XVI in which the heterocyclic ring is completely hydrogenated. The difference in

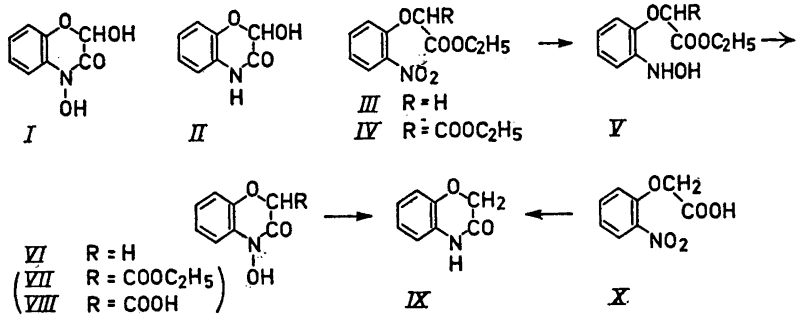

If the reduction of *o*-nitrophenoxy acetic acid (X) is carried out with sodium hydrogen sulphite the lactam, 2H-1,4-benzoxazin-3(4H)-one, is obtained [2]. This compound (IX) is also formed when 4-hydroxy-1,4-benzoxazin-3-one (VI) is reduced with zinc dust in boiling acetic acid.

effectivity between compounds VI and IX on the one hand and XIII and XV on the other shows that the compounds with the NOH group are about twice as effective as the corresponding compounds with the NH group. On this basis the NOH compound corresponding to com-

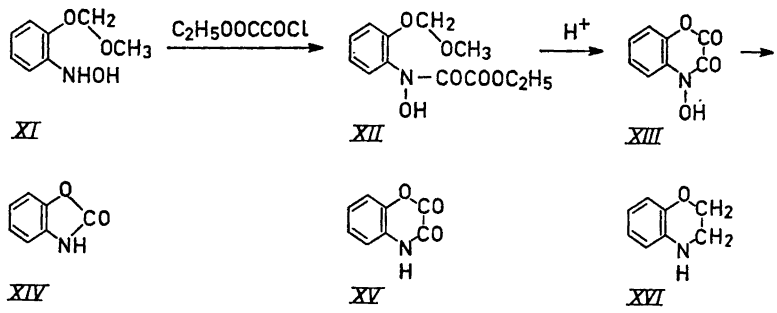

XI XII XIII XIV XV XVI

pound XVI would be the most effective one of the substances in this group. The compound has not, however, been synthesized. The oxidation of 2 as well as 3 carbon atoms lowers the effectivity. The effect of 4-hydroxy-1,4-benzoxazine on bacteria is almost the same as its effect on *Fusarium*. In a concentration of 1 mg/ml compound VI inhibited the growth of *St. aureus*, *Ps. fluorescens*, and *E. coli* (Fig. 2).

All melting points are corrected.

o-*Nitrophenoxy acetic acid ethyl ester* was prepared according to the method of Duparc [4].

4-Hydroxy-1,4-benzoxazin-3-one. A mixture of 225 mg of o-nitrophenoxy acetic acid ethyl ester, 200 mg of ammonium chloride and 200 mg of zinc dust in 10 ml of 60 % ethanol was shaken for 2 h at room temperature. The solution was filtered, and the filter washed first quickly with 2 % acetic acid (to decompose the sparingly soluble zinc salt of the formed hydroxamic acid) and then with alcohol. Water was added to the filtrate, and the solution was extracted with ether. The ether solution was washed with dilute sodium hydroxide. Upon neutralisation of the aqueous layer with hydrochloric acid, the hydroxamic acid was extracted with ether. After drying with sodium sulphate the solvent was evaporated and the residue crystallized from water. Yield 100 mg (60 %); m. p. 168–169°C. (Found: N 8.28. Calc. for $C_8H_7NO_3$: N 8.48.) The compound gave an intensely blue-violet colour with aqueous ferric chloride. UV-Spectrum (in ethanol): max. 258 mμ, ε = 6 300; max. 286

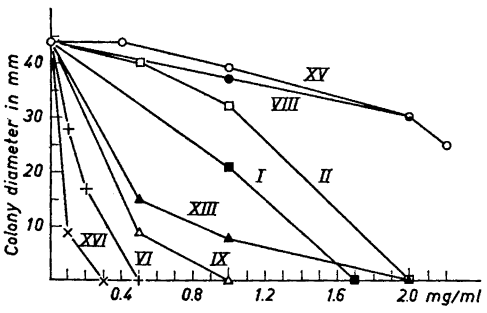

Fig. 1. Growth-inhibiting effect of 1,4-benzoxazine derivatives on *Fusarium nivale*. Oat-glycerol-agar nutrient solution, pH 6.4.

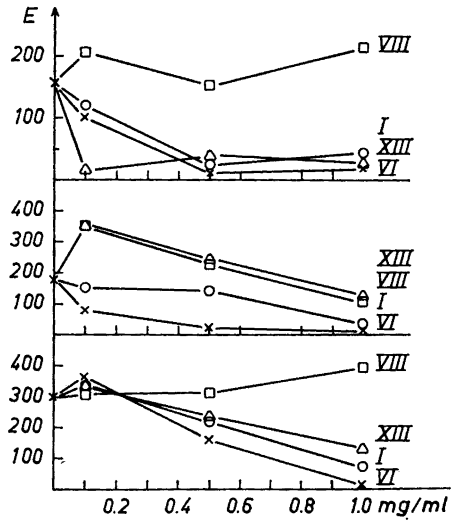

Fig. 2. Growth-inhibiting effect of 4-hydroxy-1,4-benzoxazine derivatives on *St. aureus* (topmost), *Ps. fluorescens* (middlemost), and *E. coli* (undermost). Broth nutrient solution, pH 6.5. Extinction (E) read at 622 mμ.

mμ, ε = 5 100. R_F-Value (Whatman No. 4 paper, solvent *i*-PrOH:NH_4OH:H_2O, 8:1:1) 0.39 (desc.).

Reduction of 4-hydroxy-1,4-benzoxazin-3-one. The reduction was carried out with zinc dust by a similar procedure as in the case of 2,4-dihydroxy-1,4-benzoxazin-3-one [1]. The reduction product melts at 171—172°C, mixed m.p. 171—172°C with 2H-1,4-benzoxazin-3(4H)-one [2].

o-*Nitrophenoxy malonic acid diethyl ester* has been prepared previously from the potassium salt of *o*-nitrophenol and bromomalonic acid diethyl ester by Bischoff [5] who obtained this compound as a crystalline solid (m. p. 116—118°C). When this procedure was repeated, a small amount of crystals were obtained which melted at 115—118°C. On the basis of the molecular weight determination and analysis, this compound should be the bis-(*o*-nitrophenoxy)-malonic acid diethyl ester, for which Bischoff [6] reports the m. p. 119°C. To obtain the *o*-nitrophenoxy malonic acid the uncrystallized part of the reaction mixture was hydrolyzed with aqueous sodium hydroxide at room temperature. Hydrochloric acid was then added to pH 6, and the unreacted *o*-nitrophenol was extracted with ether. The water solution was then made strongly acid and extracted several times with ether. The ether solution was dried, and the solvent evaporated. The residue was dissolved in a few ml of conc. ammonium hydroxide solution, and ethanol was added until separation of crystals occurred. The ammonium salt was filtered off and washed with cold ethanol. After recrystallization from aqueous alcohol the crystals were dissolved in water. The solution was made acid by hydrochloric acid and extracted with ether. After drying the solvent was evaporated, and the residue crystallized from a mixture of ether-benzene. M. p. 128—130°C. (Found: N 5.87. Calc. for $C_9H_7NO_7$: N 5.81.)

The *o*-nitrophenoxy malonic acid was then esterified by refluxing for 4 h with 1 % hydrogen chloride in absolute ethanol. The solvent was evaporated, and the residue dissolved in ether and washed with sodium hydrogen carbonate solution. After drying the ether was evaporated and the residue distilled *in vacuo*. The *o*-nitrophenoxy malonic acid diethyl ester was obtained as a pale yellow oil, which did not crystallize on standing for several weeks at room temperature or in a refrigerator. B. p. 145—150°/0.05 mm. (Found: N 4.77. Calc. for $C_{13}H_{15}NO_7$: N 4.71.)

4-Hydroxy-2-carbethoxy-1,4-benzoxazin-3-one. A mixture of 297 mg of *o*-nitrophenoxy malonic acid diethyl ester, 200 mg of ammonium chloride, and 200 mg of zinc dust in 10 ml of 60 % alcohol was shaken for 2 h at room temperature. The solution was filtered, and water was added to the filtrate. After extraction with ether and drying, the solvent was evaporated, and the residue crystallized from benzene. Yield 120 mg (50 %); m. p. 133—134°C. (Found: N 5.98. Calc. for $C_{11}H_{11}NO_5$: N 5.90.) Violet colour reaction with ferric chloride in alcohol. UV-Spectrum (in ethanol) max. 266 mμ, ε = 5 100; max. 288 mμ, ε = 5 100.

4-Hydroxy-2-carboxy-1,4-benzoxazin - 3 - one. 24 mg of 4-hydroxy-2-carbethoxy-1,4-benzoxazin-3-one were dissolved in 1 ml of 1 N sodium hydroxide solution and allowed to stand overnight. The solution was made slightly acid by hydrochloric acid and extracted several times with ether. After drying the solvent was evaporated and the residue crystallized from an ether-benzene mixture. Yield 15 mg (71 %); m. p. 144—146°C. (Found: N 6.70. Calc. for $C_9H_7NO_5$: N 6.65.) Blue colour reaction with ferric chloride. UV-Spectrum (in ethanol) max. 265 mμ, ε = 5 350; max. 289 mμ, ε = 5 300. R_F-Value (Whatman No. 4 paper, solvent *i*-PrOH:NH_4OH:H_2O, 8:1:1) 0.11 (desc.).

4-Hydroxy-1,4-benzoxazine-2,3-dione. 1.5 g of oxalic acid ethyl ester chloride [7] in 20 ml of ether were gradually added to a solution of 3.3 g of crude *o*-(methoxymethoxy)phenyl hydroxylamine [1] in 50 ml of dry ether under cooling (0°C). The ether solution was decanted from the dark brown oil and evaporated to dryness. The residue was dissolved in 20 ml of methanol and 2 ml of 2 N hydrochloric acid and refluxed for 15 min. The solvent was evaporated under reduced pressure. Water was added, and the mixture was extracted several times with ether. The solvent was evaporated after drying, and the residue crystallized from a mixture of alcohol-benzene. Yield 380 mg (21 %); m. p. 230—233°C (decomp.). (Found: N 7.98. Calc. for $C_8H_5NO_4$: N 7.82.) Red-violet colour reaction with ferric chloride. UV-Spectrum in ethanol max. 303 mμ, ε = 5 900; in water max. 280 mμ, ε = 2 900. R_F-Value (Whatman No. 4 paper, solvent *i*-PrOH:NH_4OH:H_2O, 8:1:1) 0.08 (desc.).

Conversion of 4-hydroxy-1,4-benzoxazine-2,3-dione to benzoxazolinone. A dilute water solution (20 μg/ml) of 4-hydroxy-1,4-benzoxazine-2,3-dione was heated for half an hour on a water bath. The UV-spectrum was then measured. The maximum by 280 mμ was shifted to 270 mμ (ε = 4 200) which is characteristic for benzoxazolinone (max. 270 mμ, ε = 4 200).

1,4-Benzoxazine-2,3-dione was prepared according to the method of Puxeddu and Sanna [8]. UV-Spectrum (in ethanol) max. 303 mμ, ε = 5 800.

3,4-Dihydro-2H-1,4-benzoxazine was prepared from 2H-1,4-benzoxazin-3(4H)-one by reduction with lithium aluminium hydride [2]. UV-Spectrum (in ethanol) max. 274 mμ, $\varepsilon = 5\,350$, max. 296, $\varepsilon = 3\,150$.

This investigation belongs to a research project under U.S. Public Law No. 480, 83rd Congress.

1. Honkanen, E. and Virtanen, A. I. *Acta Chem. Scand.* **14** (1960) 504.
2. Cymerman-Craig, J., Rogers, W. and Tate, M. *Australian J. Chem.* **9** (1956) 397; *Chem. Abstr.* **51** (1957) 1963.
3. Virtanen, A. I. and Hietala, P. K. *Suomen Kemistilehti B* **32** (1959) 138.
4. Duparc, L. *Ber.* **20** (1887) 1942.
5. Bischoff, C. *Ber.* **40** (1907) 3134.
6. Bischoff, C. *Ber.* **40** (1907) 3150.
7. Anschütz, R. *Ber.* **19** (1886) 2158.
8. Puxeddu, E. and Sanna, G. *Gazz. chim. ital.* **61** (1931) 158; **62** (1932) 558.

Received May 23, 1960.

Amino Acid Composition of Seal Myoglobin I

NEVENKA M. RUMEN*

Medicinska Nobelinstitutet, Biokemiska Avdelningen, Stockholm, Sweden

The isolation and purification of seal myoglobin I has been described recently [1]. The quantitative composition of amino acids has been determined by the method of Moore and Stein [3] using Amberlite IR-120 columns. For each analysis, 20 mg of salt-free myoglobin I was dissolved in 6 N HCl, the solution was cooled in an ice bath and the tubes were evacuated with a water pump and sealed. The hydrolyses were conducted in pairs in an oven at 110°C for 20 and 70 h. The cooled tubes were opened and the contents centrifuged and evaporated to dryness over NaOH pellets in a vacuum desiccator at room temperature. The dry material was dissolved in a small amount of water and dried. Each, nearly colorless, residue was dissolved in 0.2 N sodium citrate buffer, pH 3.25 just before putting it on the column. A sample containing 0.0949 μmole of amino acids, calculated on the basis of protein, was used in each run.

The calculations are based on Moore and Stein's [3] values for color yields, and residues/mole are based on a molecular weight of 18 600 deduced from the iron content [1]. It has been possible to detect small peaks for methionine sulfoxide in 20 and 70 h hydrolysates. Table 1 shows the values obtained.

The amide ammonia values are not included in the summation of amino acid residues.

In order to provide a check on the amide NH_3 values calculated from the chromatographic results, the amide nitrogen was determined by two different methods, micro Kjeldahl and Nessler. For the Nessler nitrogen a solution of 3 mg of protein in 2 ml N H_2SO_4 was heated for 4, 6 and 8 h in a sealed tube at 105°C[4]. An ammonium sulfate solution was used as a standard. In the micro-Kjeldahl technique 22 mg of protein was heated with 0.9 ml of 6 N HCl for 20 h in a sealed tube at 110°C. The resulting ammonia was titrated with 0.5 N H_2SO_4 using an "Agla" micrometer

Table 1. Amino acid composition of hydrolysates of seal myoglobin I.

Amino acid	Time of hydrolysis 20 h	70 h	Number of residues to nearest integer
	Residues/mole		
Aspartic acid	10.5	10.4	11
Threonine	4.7	4.7	5
Serine	6.8	5.8	7
Glutamic acid	15.8	15.7	16
Proline	4.2	3.9	4
Glycine	11.8	11.5	12
Alanine	13.9	13.8	14
Valine	5.3	5.9	6
Methionine	1.6	1.3	2
*Iso*leucine	6.3	7.2	7
Leucine	17.9	18.0	18
Tyrosine	1.8	1.6	2
Phenylalanine	6.7	6.6	7
Lysine	17.9	17.9	18
Histidine	12.3	12.0	12
Arginine	4.6	4.9	5
Amide NH_2	6.7	8.1	7
Total			146

* Present address: Laboratoire de Morphologie Animale, Université Libre de Bruxelles, Belgium.

3,4-Dihydro-2H-1,4-benzoxazine was prepared from 2H-1,4-benzoxazin-3(4H)-one by reduction with lithium aluminium hydride [2]. UV-Spectrum (in ethanol) max. 274 mμ, $\varepsilon = 5\,350$, max. 296, $\varepsilon = 3\,150$.

This investigation belongs to a research project under U.S. Public Law No. 480, 83rd Congress.

1. Honkanen, E. and Virtanen, A. I. *Acta Chem. Scand.* **14** (1960) 504.
2. Cymerman-Craig, J., Rogers, W. and Tate, M. *Australian J. Chem.* **9** (1956) 397; *Chem. Abstr.* **51** (1957) 1963.
3. Virtanen, A. I. and Hietala, P. K. *Suomen Kemistilehti B* **32** (1959) 138.
4. Duparc, L. *Ber.* **20** (1887) 1942.
5. Bischoff, C. *Ber.* **40** (1907) 3134.
6. Bischoff, C. *Ber.* **40** (1907) 3150.
7. Anschütz, R. *Ber.* **19** (1886) 2158.
8. Puxeddu, E. and Sanna, G. *Gazz. chim. ital.* **61** (1931) 158; **62** (1932) 558.

Received May 23, 1960.

Amino Acid Composition of Seal Myoglobin I

NEVENKA M. RUMEN*

Medicinska Nobelinstitutet, Biokemiska Avdelningen, Stockholm, Sweden

The isolation and purification of seal myoglobin I has been described recently [1]. The quantitative composition of amino acids has been determined by the method of Moore and Stein [3] using Amberlite IR-120 columns. For each analysis, 20 mg of salt-free myoglobin I was dissolved in 6 N HCl, the solution was cooled in an ice bath and the tubes were evacuated with a water pump and sealed. The hydrolyses were conducted in pairs in an oven at 110°C for 20 and 70 h. The cooled tubes were opened and the contents centrifuged and evaporated to dryness over NaOH pellets in a vacuum desiccator at room temperature. The dry material was dissolved in a small amount of water and dried. Each, nearly colorless, residue was dissolved in 0.2 N sodium citrate buffer, pH 3.25 just before putting it on the column. A sample containing 0.0949 μmole of amino acids, calculated on the basis of protein, was used in each run.

The calculations are based on Moore and Stein's [3] values for color yields, and residues/mole are based on a molecular weight of 18 600 deduced from the iron content [1]. It has been possible to detect small peaks for methionine sulfoxide in 20 and 70 h hydrolysates. Table 1 shows the values obtained.

The amide ammonia values are not included in the summation of amino acid residues.

In order to provide a check on the amide NH_3 values calculated from the chromatographic results, the amide nitrogen was determined by two different methods, micro Kjeldahl and Nessler. For the Nessler nitrogen a solution of 3 mg of protein in 2 ml N H_2SO_4 was heated for 4, 6 and 8 h in a sealed tube at 105°C[4]. An ammonium sulfate solution was used as a standard. In the micro-Kjeldahl technique 22 mg of protein was heated with 0.9 ml of 6 N HCl for 20 h in a sealed tube at 110°C. The resulting ammonia was titrated with 0.5 N H_2SO_4 using an "Agla" micrometer

Table 1. Amino acid composition of hydrolysates of seal myoglobin I.

Amino acid	Time of hydrolysis 20 h	70 h	Number of residues to nearest integer
	Residues/mole		
Aspartic acid	10.5	10.4	11
Threonine	4.7	4.7	5
Serine	6.8	5.8	7
Glutamic acid	15.8	15.7	16
Proline	4.2	3.9	4
Glycine	11.8	11.5	12
Alanine	13.9	13.8	14
Valine	5.3	5.9	6
Methionine	1.6	1.3	2
*Iso*leucine	6.3	7.2	7
Leucine	17.9	18.0	18
Tyrosine	1.8	1.6	2
Phenylalanine	6.7	6.6	7
Lysine	17.9	17.9	18
Histidine	12.3	12.0	12
Arginine	4.6	4.9	5
Amide NH_2	6.7	8.1	7
Total			146

* Present address: Laboratoire de Morphologie Animale, Université Libre de Bruxelles, Belgium.

syringe. The Nessler results after 8 h hydrolyses were the same as the 20 h micro-Kjeldahl.

As Kendrew [5] has mentioned in *Structure and function in myoglobins and other proteins*, "myoglobins from different species have amino acid compositions which are broadly similar, but differ in detail". We may only confirm his statement by comparing the compositions of the purified myoglobins which are presently available, namely sperm whale [6], seal and horse [7] myoglobin. The results show that these myoglobins differ only in details.

The amino acid analysis of Mb II, Mb III, Mb IV and Mb V are in progress using the procedure of Moore and Stein.

I wish to thank Professor Hugo Theorell for his advice and Miss Ann-Marie Fridén for her able technical assistance.

1. Rumen, N. M. *Acta Chem. Scand.* **13** (1959) 1542.
2. Moore, S., Spackman, D. H. and Stein, W. H. *Anal. Chem.* **30** (1958) 1185.
3. Moore, S. and Stein, W. H. *J. Biol. Chem.* **211** (1954) 907.
4. Laki, K., Kominz, D. R., Symonds, P., Lorand, L. and Seegers, W. H. *Arch. Biochem. Biophys.* **49** (1954) 276.
5. Kendrew, J. C. *Federation Proc.* **18** (1959) 740.
6. Edmundson, A. B. *Personal communication* to Benson, E. E. and Linderstrøm-Lang, K. *Biochim. et Biophys. Acta* **32** (1959) 579.
7. Theorell, H. and Åkeson, Å. *In press.*

Received June 3, 1960.

Structure of Rhodan Hydrate

ASBJÖRN HORDVIK

Chemical Institute, University of Bergen, Bergen, Norway

So far X-ray structure determinations of two unsaturated five-membered cyclic disulphides have been reported [1,2]. Observed bond lengths in the thiuret ion [1] and in 4 - methyl - 1,2 - dithia - 4 - *cyclo*pentene - 3 - thione [2] indicate that the five-membered ring has some aromatic character. This seems to explain the relatively high stability of unsaturated five-membered cyclic disulphides as contrasted with saturated ones. It is hoped that a determination of the molecular structure of rhodan hydrate will give further information that can be used to test this idea. The rhodan hydrate molecule has, according to Söderbäck [3], the following structure:

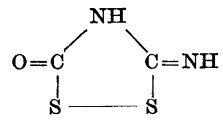

The preparation of rhodan hydrate has been described by Söderbäck [3,4], and the unit cell and space group have been reported by Foss [5]. The crystals are monoclinic, $a = 12.50$ Å, $b = 5.24$ Å, $c = 14.67$ Å,

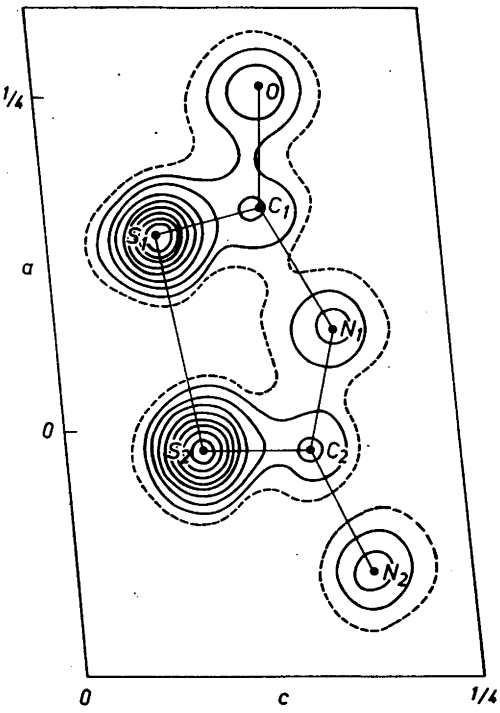

Fig. 1. Electron density projection of rhodan hydrate along the *b*-axis showing one asymmetric unit. Plane group *p*2 and origin in center of symmetry in the projection. Contours at arbitrary but equal intervals.

syringe. The Nessler results after 8 h hydrolyses were the same as the 20 h micro-Kjeldahl.

As Kendrew [5] has mentioned in *Structure and function in myoglobins and other proteins*, "myoglobins from different species have amino acid compositions which are broadly similar, but differ in detail". We may only confirm his statement by comparing the compositions of the purified myoglobins which are presently available, namely sperm whale [6], seal and horse [7] myoglobin. The results show that these myoglobins differ only in details.

The amino acid analysis of Mb II, Mb III, Mb IV and Mb V are in progress using the procedure of Moore and Stein.

I wish to thank Professor Hugo Theorell for his advice and Miss Ann-Marie Fridén for her able technical assistance.

1. Rumen, N. M. *Acta Chem. Scand.* **13** (1959) 1542.
2. Moore, S., Spackman, D. H. and Stein, W. H. *Anal. Chem.* **30** (1958) 1185.
3. Moore, S. and Stein, W. H. *J. Biol. Chem.* **211** (1954) 907.
4. Laki, K., Kominz, D. R., Symonds, P., Lorand, L. and Seegers, W. H. *Arch. Biochem. Biophys.* **49** (1954) 276.
5. Kendrew, J. C. *Federation Proc.* **18** (1959) 740.
6. Edmundson, A. B. *Personal communication* to Benson, E. E. and Linderstrøm-Lang, K. *Biochim. et Biophys. Acta* **32** (1959) 579.
7. Theorell, H. and Åkeson, Å. *In press.*

Received June 3, 1960.

Structure of Rhodan Hydrate

ASBJÖRN HORDVIK

Chemical Institute, University of Bergen, Bergen, Norway

So far X-ray structure determinations of two unsaturated five-membered cyclic disulphides have been reported [1,2]. Observed bond lengths in the thiuret ion [1] and in 4 - methyl - 1,2 - dithia - 4 - *cyclo*pentene - 3 - thione [2] indicate that the five-membered ring has some aromatic character. This seems to explain the relatively high stability of unsaturated five-membered cyclic disulphides as contrasted with saturated ones. It is hoped that a determination of the molecular structure of rhodan hydrate will give further information that can be used to test this idea. The rhodan hydrate molecule has, according to Söderbäck [3], the following structure:

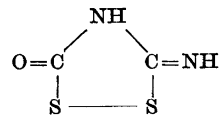

The preparation of rhodan hydrate has been described by Söderbäck [3,4], and the unit cell and space group have been reported by Foss [5]. The crystals are monoclinic, $a = 12.50$ Å, $b = 5.24$ Å, $c = 14.67$ Å,

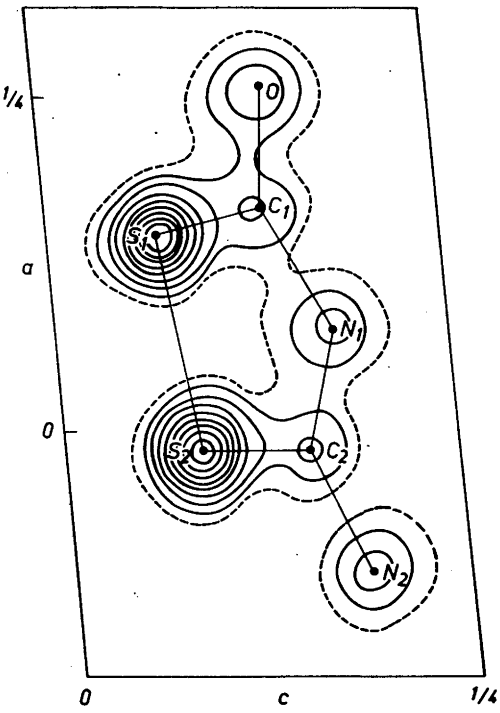

Fig. 1. Electron density projection of rhodan hydrate along the *b*-axis showing one asymmetric unit. Plane group *p*2 and origin in center of symmetry in the projection. Contours at arbitrary but equal intervals.

Table 1. Atomic coordinates, in fractions of corresponding cell edges.

	x	z
S_1	0.1470	0.0695
S_2	−0.0150	0.0865
C_1	0.1635	0.1365
C_2	−0.0135	0.1550
N_1	0.0760	0.1750
N_2	−0.1060	0.1885
O	0.2585	0.1450

$\beta = 95\ 1/2°$. Preliminary results of a complete crystal structure determination of rhodan hydrate are given here.

The space group of rhodan hydrate was found to be either $C2/c$ or C/c. The morphology of the crystals indicates [5] the presence of a twofold axis and thus the correctness of the centrosymmetric space group. The "average test" and "zero moment test" [6] also indicated centrosymmetry.

Attempts to solve the structure from Patterson projections did not succeed, and the solution was then sought by means of Harker Kasper inequalities and the "multiplication rule" [7]. This led to three possible sets of signs for the 35 strongest reflections in the b-axis projection. The molecule was recognised in one of the corresponding Fourier maps, and after three Fourier-refinements the reliability factor R was 0.115. The electron density map is reproduced in Fig. 1. The map shows that the cyclic form of rhodan hydrate, anticipated by Söderbäck [3], is correct. Further refinement will be carried out by means of $(F_o - F_c)$-technique.

1. Foss, O. and Tjomsland, O. *Acta Chem. Scand.* **12** (1958) 1799.
2. Kehl, W. L. and Jeffrey, G. A. *Acta Cryst.* **11** (1958) 813.
3. Söderbäck, E. *Ann.* **419** (1919) 217.
4. Söderbäck, E. *Ann.* **465** (1928) 184.
5. Foss, O. *Acta Chem. Scand.* **10** (1956) 868.
6. *International Tables for X-Ray Crystallography.* The Kynoch Press, Birmingham, England, 1959, Vol. II, p. 356.
7. Zachariasen, W. H. *Acta Cryst.* **5** (1952) 68.

Received June 1, 1960.

The σ-Phase Ta_2Al

LARS-ERIK EDSHAMMAR and BO HOLMBERG

Institute of Inorganic and Physical Chemistry, University of Stockholm, Stockholm, Sweden

In the course of a study of the tantalum-aluminium system recently started at this Institute, the existens of a σ-type phase has been observed in samples of the approximate composition Ta_2Al prepared by arc-melting in an argon atmosphere.

The dimensions of the tetragonal unit cell obtained from a Guinier powder pattern were found to be:

$a = 9.828$ Å $\qquad c = 5.232$ Å

The axial ratio $c/a = 0.532$ is similar to that found for other σ-phases such as the one occurring in the nickel-vanadium system studied by Kasper and Waterstrat [1] using neutron diffraction techniques. Since the ratios of the atomic radii r_{Ta}/r_{Al} and r_V/r_{Ni} are comparable, the atomic distribution reported for the nickel-vanadinium phase was tentatively adopted for Ta_2Al:

Space-group: $D_{4h}^{14}-P4/mnm$.

Unit cell content: 10 Ta_2Al.

Table 1. The Guinier powder pattern of Ta_2Al ($CuK\alpha_1$ radiation).

hkl	$\sin^2\Theta_{obs}$	$\sin^2\Theta_{calc}$	I_{obs}	I_{calc}
110	0.01228	0.01228	vw	0.5
200	—	0.02457	—	0.0
101	0.02782	0.02781	st	5.5
210	0.03068	0.03071	st *	2.5
111	0.03396	0.03396	w	2.0
220	0.04911	0.04914	vw	0.8
211	0.05238	0.05238	vw	0.8
310	0.06142	0.06142	vw	1.0
221	—	0.07081	—	0.0
301	0.07696	0.07695	w	2.2
320	0.07982	0.07985	vw	1.1
311	0.08311	0.08310	m	4.5
002	0.08670	0.08668	vw	0.7
400	0.09831	0.09828	vw	1.5
112	0.09898	0.09897	vw	1.3
321	0.10153	0.10152	vvw	0.6
410	0.10443	0.10442	vst	10.7
330	0.11059	0.11057	st	5.8
202	0.11130	0.11125	st	6.8
212	0.11739	0.11739	vst	10.0
420	0.12285	0.12285	vvw	0.5
411	0.12603	0.12609	vst	9.5
331	0.13224	0.13224	m	4.0

* Line overlaps line of neighbouring phase.

Table 1. Atomic coordinates, in fractions of corresponding cell edges.

	x	z
S_1	0.1470	0.0695
S_2	−0.0150	0.0865
C_1	0.1635	0.1365
C_2	−0.0135	0.1550
N_1	0.0760	0.1750
N_2	−0.1060	0.1885
O	0.2585	0.1450

$\beta = 95\ 1/2°$. Preliminary results of a complete crystal structure determination of rhodan hydrate are given here.

The space group of rhodan hydrate was found to be either $C2/c$ or C/c. The morphology of the crystals indicates [5] the presence of a twofold axis and thus the correctness of the centrosymmetric space group. The "average test" and "zero moment test" [6] also indicated centrosymmetry.

Attempts to solve the structure from Patterson projections did not succeed, and the solution was then sought by means of Harker Kasper inequalities and the "multiplication rule" [7]. This led to three possible sets of signs for the 35 strongest reflections in the b-axis projection. The molecule was recognised in one of the corresponding Fourier maps, and after three Fourier-refinements the reliability factor R was 0.115. The electron density map is reproduced in Fig. 1. The map shows that the cyclic form of rhodan hydrate, anticipated by Söderbäck [3], is correct. Further refinement will be carried out by means of $(F_o - F_c)$-technique.

1. Foss, O. and Tjomsland, O. *Acta Chem. Scand.* **12** (1958) 1799.
2. Kehl, W. L. and Jeffrey, G. A. *Acta Cryst.* **11** (1958) 813.
3. Söderbäck, E. *Ann.* **419** (1919) 217.
4. Söderbäck, E. *Ann.* **465** (1928) 184.
5. Foss, O. *Acta Chem. Scand.* **10** (1956) 868.
6. *International Tables for X-Ray Crystallography.* The Kynoch Press, Birmingham, England, 1959, Vol. II, p. 356.
7. Zachariasen, W. H. *Acta Cryst.* **5** (1952) 68.

Received June 1, 1960.

The σ-Phase Ta_2Al

LARS-ERIK EDSHAMMAR and BO HOLMBERG

Institute of Inorganic and Physical Chemistry, University of Stockholm, Stockholm, Sweden

In the course of a study of the tantalum-aluminium system recently started at this Institute, the existens of a σ-type phase has been observed in samples of the approximate composition Ta_2Al prepared by arc-melting in an argon atmosphere.

The dimensions of the tetragonal unit cell obtained from a Guinier powder pattern were found to be:

$a = 9.828$ Å $\qquad c = 5.232$ Å

The axial ratio $c/a = 0.532$ is similar to that found for other σ-phases such as the one occurring in the nickel-vanadium system studied by Kasper and Waterstrat [1] using neutron diffraction techniques. Since the ratios of the atomic radii r_{Ta}/r_{Al} and r_V/r_{Ni} are comparable, the atomic distribution reported for the nickel-vanadinium phase was tentatively adopted for Ta_2Al:

Space-group: $D_{4h}^{14}-P4/mnm$.

Unit cell content: 10 Ta_2Al.

Table 1. The Guinier powder pattern of Ta_2Al ($CuK\alpha_1$ radiation).

hkl	$\sin^2\Theta_{obs}$	$\sin^2\Theta_{calc}$	I_{obs}	I_{calc}
110	0.01228	0.01228	vw	0.5
200	—	0.02457	—	0.0
101	0.02782	0.02781	st	5.5
210	0.03068	0.03071	st *	2.5
111	0.03396	0.03396	w	2.0
220	0.04911	0.04914	vw	0.8
211	0.05238	0.05238	vw	0.8
310	0.06142	0.06142	vw	1.0
221	—	0.07081	—	0.0
301	0.07696	0.07695	w	2.2
320	0.07982	0.07985	vw	1.1
311	0.08311	0.08310	m	4.5
002	0.08670	0.08668	vw	0.7
400	0.09831	0.09828	vw	1.5
112	0.09898	0.09897	vw	1.3
321	0.10153	0.10152	vvw	0.6
410	0.10443	0.10442	vst	10.7
330	0.11059	0.11057	st	5.8
202	0.11130	0.11125	st	6.8
212	0.11739	0.11739	vst	10.0
420	0.12285	0.12285	vvw	0.5
411	0.12603	0.12609	vst	9.5
331	0.13224	0.13224	m	4.0

* Line overlaps line of neighbouring phase.

(I) 2 Al in 2(*b*).
(II) 4 Ta in 4(*f*) with $x=0.103$.
(III) 8 Ta in 8(*i*) with $x=0.371$, $y=0.037$.
(IV) 8 Al in 8(*i*) with $x=0.566$, $y=0.240$.
(V) 8 Ta in 8(*j*) with $x=0.316$, $z=0.250$.

The powder diffraction pattern required by this atomic arrangement was found to be in satisfactory agreement with the observed data (*cf.* Table 1) which evidently shows that the $\sigma(Ta_2Al)$ phase is essentially ordered.

The existence of a σ-phase in the niobium-aluminium system was recently reported by McKinsey and Faulring [2]. The composition (Nb_2Al) and powder diffraction data suggest that this phase is analogous in structure to Ta_2Al.

Further studies on the tantalum-aluminium system are in progress.

The authors wish to express their sincere gratitude to Dr. Arne Magnéli for his never-failing interest and many valuable discussions. Thanks are due to Mr. A. Eriksson for his skilful experimental assistance.

1. Kasper, J. S. and Waterstrat, R. M. *Acta Cryst.* **9** (1956) 289.
2. McKinsey, C. R. and Faulring, G. M. *Acta Cryst.* **12** (1959) 701.

Received June 21, 1960.

The Crystal Structures of Hf_3Al_2 and of $Hf_5Al_3O_x$

LARS-ERIK EDSHAMMAR

Institute of Inorganic and Physical Chemistry, University of Stockholm, Stockholm, Sweden

The existence of the phases Hf_3Al_2, $HfAl_2$, and $HfAl_3$ in the hafnium-aluminium system was reported in a previous note [1] which also gave the structure types of the two latter phases. Further studies on this system carried out on specimens obtained by arc-melting in an argon atmosphere followed by quenching to room temperature has revealed the existence of two further phases having the compositions Hf_3Al_2 and HfAl.

It was also observed that samples of compositions $HfAl_{0.5-0.7}$ gave a few very weak extra lines which could not be attributed to any of the phases mentioned above but were found to be greatly reminiscent of the strong reflexions [1] given by the oxygen-stabilized phase $Zr_5Al_3O_x$. The isomorphism thus suggested between the hafnium and the zirconium alloy phases was confirmed by gradually adding oxygen (as HfO_2) to the samples. Attempts to prepare a hafnium analogue of the oxygen-free phase Zr_5Al_3 of $D8_m$ type were unsuccessful.

The unit cell of Hf_3Al_2 was found to be tetragonal with the following dimensions:

$a = 7.535$ Å $\qquad c = 6.906$ Å

The powder pattern of the phase demonstrates clearly that it is isomorphous with the corresponding phase in the zirconium-aluminium system. The space group is $D_{4h}^{14}-P4_2/mnm$ and the atomic positions are the same as given by Wilson [2] for Zr_3Al_2:

8 Al in 8(*j*) with $x=\frac{1}{8}$, $z=0.21$.
4 Hf in 4(*f*) with $x=0.34$.
4 Hf in 4(*g*) with $x=0.20$.
4 Hf in 4(*d*).

The agreement between observed and calculated powder patterns is satisfactory.

The powder pattern of $Hf_5Al_3O_x$ could be indexed assuming a hexagonal unit cell with the dimensions:

$a = 8.066$ Å $\qquad c = 5.678$ Å

The following structure of $Hf_5Al_3O_x$ was derived from the powder data:

Cell content: 2 $Hf_5Al_3O_x$.

Space-group: $D_{6h}^3-P6_3/mcm$.

4 Hf in 4(*d*).
6 Hf in 6(*g*) with $x=0.23$.
6 Al in 6(*g*) with $x=0.59$.

The oxygen atoms have been neglected and no attempt was made to estimate the oxygen contents. It seems likely, however, that the oxygen atoms are located in interstitial positions 000 or $00\frac{1}{2}$ as suggested by Aronsson [3] for various $D8_8$ phases stabilized by small non-metal atoms.

The author wishes to express his gratitude to Dr. A. Magnéli for his kind encouragement and many helpful discussions.

1. Edshammar, L.-E. and Andersson, S. *Acta Chem. Scand.* **14** (1960) 223.
2. Wilson, C. G. and Spooner, F. J. *Acta Cryst.* **13** (1960) 358.
3. Aronsson, B. *Acta Chem. Scand.* **12** (1958) 31.

Received June 21, 1960.

Infrared Spectrophotometry: A Semi-Micro Die for Oblong KBr-pellets

FREDRIK MÖHL

Institute of Medical Chemistry, University of Uppsala, Uppsala, Sweden; Institute of Medical Biochemistry, University of Gothenburg, Gothenburg, Sweden

A macro-die for oblong pellets has been described by Kirkland [1]. His pellet was pressed in a rather complicated tool, which was afterwards inserted in the spectrophotometer.

We needed a similar device, but as we wanted to store the samples afterwards and also wanted a smaller pellet (we had earlier made a beam-condensing microscope for our Perkin-Elmer model 21) [2], Kirkland's die was not suitable for our purpose. We therefore constructed a die to press 2.5 × 0.3 mm² pellets in simple plate disks. Semi-micro and micro dies pressing pellets in plate disks have been described [3] and are also commercially available, but these make cylindrical pellets, which obviously means either a waste of substance or a pellet much too small to fill the image of the monochromator's entrance slit. Manufacturing difficulties seem to have prevented the constructions of semi-micro dies for oblong pellets.

Fig. 1 shows our die. The plunger slides in a guide made in two parts forming a cylinder, with the plane of intersection longitudinal but slightly off axis. Into the plane intersection surface of the larger part is milled a space for the plunger and pusher.

Straight through the guide an evacuating hole is bored (across the plunger-space), terminating at each end in a circular groove around the guide. The heavy-duty contact-surface between plunger and pusher is cylindrical. This is to avoid any tilting moment on the plunger.

The power is transmitted to the pusher by a cylindrical piston. Two O-rings ensure tightness, and their compressibility allows a sufficient stroke for the piston.

The disk is punched from an 0.3 mm stainless steel plate. It is kept in position in the die by 3 pins protruding from the guide. One of the pins is slimmer than the others and does not fit in its hole in the disk, it serves only to prevent the disk being turned wrongly. A jig is used when the pin-holes are bored in the disk.

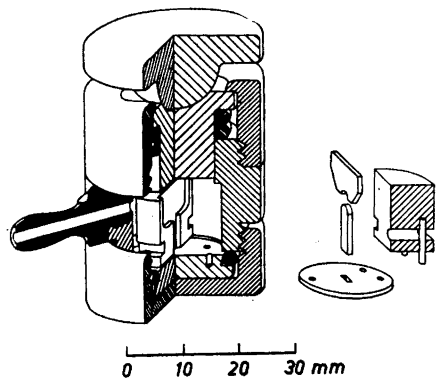

Fig. 1. Die in section. Disk, plunger, pusher and one of the guide halves (in section) lifted out and shown beside the die.

Beneath the disk is a polished bottom-plate kept firmly in position by a screw cap and sealed by an O-ring.

The guide should be made of stainless steel and the plunger, pusher and bottom-plate of hardened alloyed steel.

It proved difficult to make the oblong pellet-hole in the right place in the disk. We finally solved the problem by using the die as a punching tool. Before the punching, the plunger is exchanged for a punch and the bottom-plate for a bolster made in two halves in the same way as the guide.

To make a pellet one turns the die upside down, removes the cap and bottom-plate and pushes down the plunger with a clean plate-strip. Then a mixture of about 35 μg of substance and 1 mg of KBr is filled into the plunger-space. (The operator should wear a mask while handling the tiny amount of powder, to protect it against his breath). The disk, bottom-plate and cap are placed in position (cap tightened firmly) and the pellet can be pressed in the usual way. The force on the piston should be 820 newtons.

The best results are obtained with 30—40 μg of substance, but even less will do (if some loss of detail may be tolerated), as shown in Fig. 2.

To make the pellet 20 μg of 2DL-methyltetracosanoic acid and 1 mg of KBr were

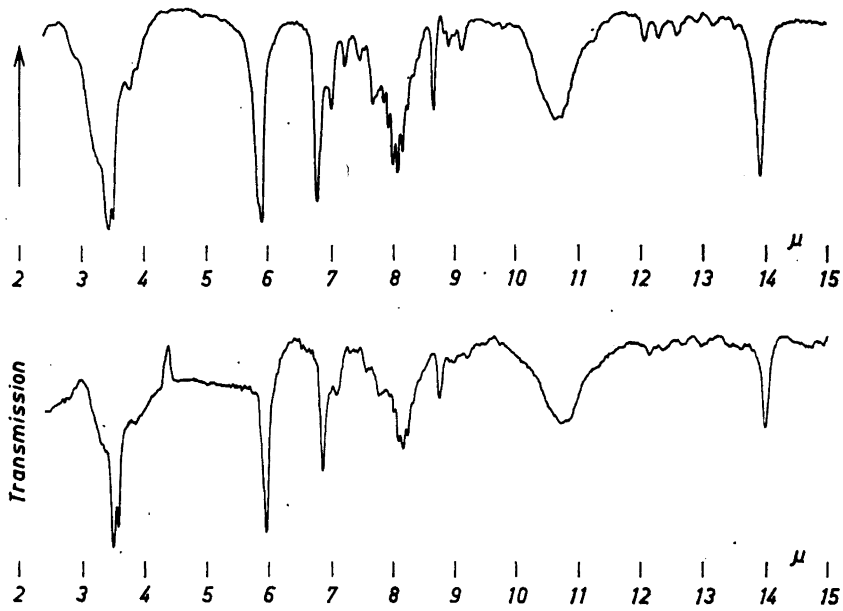

Fig. 2. Spectra of 2 DL-methyltetracosanoic acid. The macro spectrum (top) was made from a circular pellet measuring 13 mm in diameter and containing 3 mg of substance in 300 mg of KBr. The semi-micro spectrum (bottom) was made from a 2.5 × 0.3 mm^2 pellet containing 20 μg of substance in 1 mg of KBr. Spectra scanned at 4 and 6 min/micron, respectively. Slit program was 927 for both.

weighed out and mixed thoroughly with a small spatula (not ground in a mortar, as this would entail considerable loss of material). The slow scanning (6 min/micron) is due not so much to the sample as to the microscope, which transmits only a fraction of the available energy, most of it being masked off by the Schwarzschild condenser. (The construction with elliptic mirrors developed simultaneously by Perkin-Elmer is much better in this respect. But unfortunately it is not a twin device and cannot be used for the comparison of two samples.)

The oblong pellet transmits as much energy as a circular pellet of 6.5 times its area. This of course applies also to a macro pellet, provided it can be brought sufficiently close to focus. The construction described here seems also to be well suited for macro dies.

In a future version of the die we are planning to make the guide conical instead of cylindrical, so that it can be easily lifted out and taken apart for cleaning.

Acknowledgements. The author wants to thank Mr Per Olsson, Uppsala, for making the die, and Mr Donald Burton, Stockholm, for idiomatic corrections of the English text.

1. Kirkland, J. J. *Anal. Chem.* **29** (1957) 1127.
2. Möhl, F. *Acta Chem. Scand.* **12** (1958) 1356.
3. Mason, W. B. *Infrared Microsampling in Bio-Medical Investigations.* The Pittsburgh Conference on Analytical Chemistry and Applid Spectroscopy, March 1958.

A Simple Device for Automatic Equilibration of Paper Chromatograms

LENNART KRABISCH and JAN SJÖVALL

Department of Chemistry, Karolinska Institutet, Stockholm, Sweden

In paper chromatography, it is often necessary to equilibrate the papers with the vapours of the solvents in the chromatographic chamber before they are brought into contact with the mobile phase. Much time would be saved if this contact could be achieved automatically so that the chromatography could start at any time during the night. Delivery of mobile phase from reservoirs by the automatic turning of a stopcock has been described [1-3]. For the chromatography of bile acids [4] we have used a simple and inexpensive device which can be applied to ascending as well as descending chromatography and which can be adapted to suit most sizes of chromatographic vessels.

Since the completion of this work an automatic solvent addition funnel based on a siphon principle has been described [5].

Description of the apparatus. The figures refer to the diagram.

Ascending chromatography. The papers are suspended in the vessel from a bent glass rod (1) inserted into and emerging from a piece of glass tubing which is fixed in a cork (2) placed in a hole in the covering glass plate. The diameter of the glass tubing should be just large enough to permit free vertical movement of the glass rod. With the aid of a clothespin the glass rod is attached to the timer unit with a piece of bent brass wire (3) so that the lower ends of the chromatograms are about one cm above the mobile phase on the bottom of the chromatographic chamber. The timer unit consists of a brass tubing fitted with small spin (4) on which the glass rods with the papers are hung. One end of the brass tubing is connected with the winding screw for the alarm (5) of an alarm clock, the other end is loosely supported in a bearing. The connection between the brass tubing and the clock should be made so that it is easy to take the pieces apart. The clock is adjusted to a predetermined time and when the alarm rings the papers are lowered into the solvent. By a proper adjustment of the clothespin their fall is stopped when they have descended into the mobile phase.

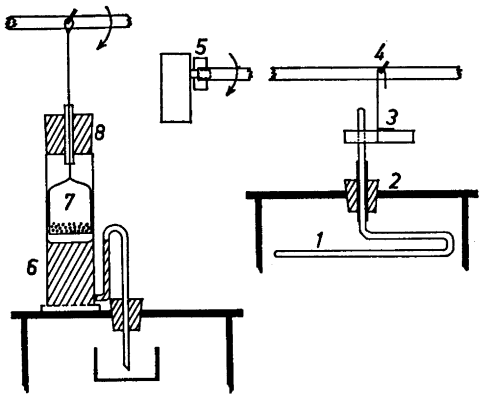

Descending chromatography. The same timer unit is used as for the ascending technique. A siphon made of a measuring cylinder (6) is placed on the glass cover of the tank. The glass tubing is introduced through a cork in a hole in the covering plate, the tip being in position just above the chromatograms in the trough. The desired amount of mobile phase is introduced into the cylinder (maximum just below the bend of the siphon) and a cylindrical glass bulb containing leadshot (7) is cautiously introduced and suspended above the solvent surface in the cylinder. The bulb has a diameter about 3 mm less than the inner diameter of the cylinder. It is attached to the timer unit with a thin silver wire hung on one of the pins of the brass tubing. The measuring cylinder is stoppered with a cork and the silver wire passes through a capillary tube in the cork (8). When the alarm rings the glass bulb hanging above the solvent surface falls and the mobile phase is emptied into the trough. The larger the volume of the bulb, the smaller is the minimum volume that can be drained from the cylinder.

The device described has been in constant use in our laboratory for a year. As judged from the chromatograms, the entrance hole for the glass rod in ascending chromatography and the hole for the silver wire in descending chromatography do not cause changes in the vapour equilibration with our phase systems. The timer unit has the advantage that it can be used for several chromatographies at the same time,

irrespectively of whether the ascending or the descending technique is used. The use of an ordinary alarm clock makes the apparatus inexpensive but if the equilibration time must exceed eleven hours another type of timer is required.

This work has been supported by grants from *Statens Medicinska Forskningsråd.*

1. Martin, S. M. *Anal. Chem.* **30** (1958) 1890.
2. Abelson, D. M. and Fox, J. G. C. *J. Clin. Pathol.* **12** (1959) 375.
3. Decker, J. L. *J. Lab. Clin. Med.* **54** (1959) 476.
4. Sjövall, J. *Clin. Chim. Acta* **4** (1960) 652.
5. Van Duren, B. L. *Anal. Chem.* **32** (1960) 732.

Received June 16, 1960.

A Note on the Action of Firefly-Extracts on ATP

B. O. HANSEN* and JOHN GRAAE

Institute of Biological Chemistry, University of Copenhagen, Denmark

Use of the enzyme system from *Photinus pyralis* for the determination of minor amounts of ATP has been suggested and further a method implying it has been described by Strehler and Totter [1]. In order to study the extent of the postulated linear dependence of light intensity on ATP concentration experiments were carried out with different amounts of firefly-extracts and of ATP.

The experiments were carried out in small test tubes closed with a rubber stopper. ATP solution, enzyme extract and either arsenate buffer or water was mixed by rapid shaking. Light intensity was then determined by a photometer. If we suppose that light intensity is a direct measure of the reaction velocity and accept that the phototube (type RCA 1-P-21) is linear in the spectral area in question [2], then the photometer readings directly express reaction velocity in arbitrary units. It is known that oxygen is required for the reaction but this is supposed to be present in a concentration that is sufficient for the reaction, for two reasons: First it

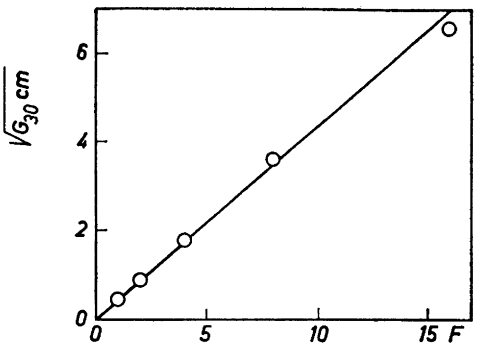

Fig. 1. Abscissa: Concentration of firefly-extract in arbitrary units. Ordinate: Square root of galvanometer deflection measured 30 sec. after start of experiment. Each experiment was made with a mixture of 500 μl water, 100 μl ATP solution (34 μg/100 μl) and 200 μl firefly-extract. t = 25.1°C.

is demonstrated by Hastings *et al.*[3] that only decreasing oxygen pressure to a very minute fraction of the normal has any influence on the reaction and secondly, we have demonstrated that bubbling of atmospheric air through the test tubes did not restore activity when the light intensity had fallen to approximately zero. Yet activity could be restored by the addition of either ATP or firefly extract de-

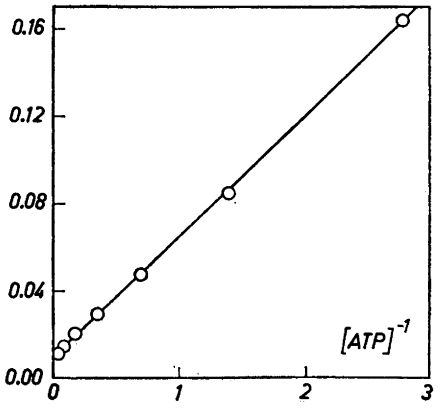

Fig. 2. Abscissa: Reciprocal of ATP concentration in ml · μg^{-1}. Ordinate: Reciprocal of galvanometer deflection. Experiments performed with 500 μl water, 250 μl enzyme solution and 250 μl ATP solution. t = 22.5°C.

* Present address: Centrallaboratoriet, Kommunehospitalet, Copenhagen, Denmark.

irrespectively of whether the ascending or the descending technique is used. The use of an ordinary alarm clock makes the apparatus inexpensive but if the equilibration time must exceed eleven hours another type of timer is required.

This work has been supported by grants from *Statens Medicinska Forskningsråd.*

1. Martin, S. M. *Anal. Chem.* **30** (1958) 1890.
2. Abelson, D. M. and Fox, J. G. C. *J. Clin. Pathol.* **12** (1959) 375.
3. Decker, J. L. *J. Lab. Clin. Med.* **54** (1959) 476.
4. Sjövall, J. *Clin. Chim. Acta* **4** (1960) 652.
5. Van Duren, B. L. *Anal. Chem.* **32** (1960) 732.

Received June 16, 1960.

A Note on the Action of Firefly-Extracts on ATP

B. O. HANSEN* and JOHN GRAAE

Institute of Biological Chemistry, University of Copenhagen, Denmark

Use of the enzyme system from *Photinus pyralis* for the determination of minor amounts of ATP has been suggested and further a method implying it has been described by Strehler and Totter [1]. In order to study the extent of the postulated linear dependence of light intensity on ATP concentration experiments were carried out with different amounts of firefly-extracts and of ATP.

The experiments were carried out in small test tubes closed with a rubber stopper. ATP solution, enzyme extract and either arsenate buffer or water was mixed by rapid shaking. Light intensity was then determined by a photometer. If we suppose that light intensity is a direct measure of the reaction velocity and accept that the phototube (type RCA 1-P-21) is linear in the spectral area in question [2], then the photometer readings directly express reaction velocity in arbitrary units. It is known that oxygen is required for the reaction but this is supposed to be present in a concentration that is sufficient for the reaction, for two reasons: First it

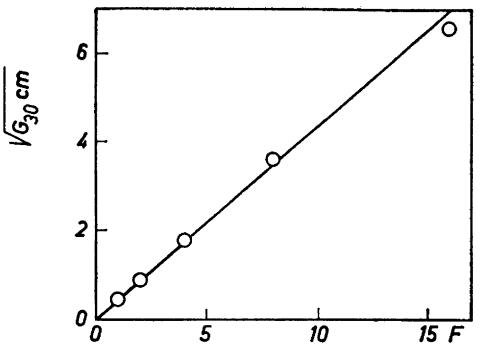

Fig. 1. Abscissa: Concentration of firefly-extract in arbitrary units. Ordinate: Square root of galvanometer deflection measured 30 sec. after start of experiment. Each experiment was made with a mixture of 500 μl water, 100 μl ATP solution (34 μg/100 μl) and 200 μl firefly-extract. t = 25.1°C.

is demonstrated by Hastings *et al.*[3] that only decreasing oxygen pressure to a very minute fraction of the normal has any influence on the reaction and secondly, we have demonstrated that bubbling of atmospheric air through the test tubes did not restore activity when the light intensity had fallen to approximately zero. Yet activity could be restored by the addition of either ATP or firefly extract de-

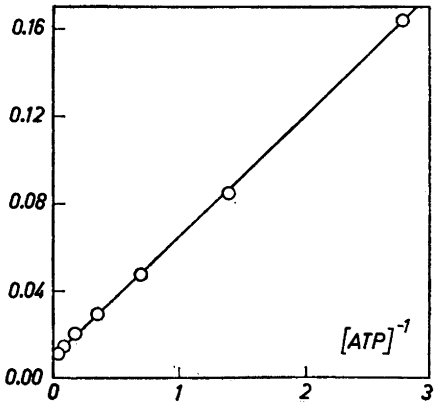

Fig. 2. Abscissa: Reciprocal of ATP concentration in ml · μg^{-1}. Ordinate: Reciprocal of galvanometer deflection. Experiments performed with 500 μl water, 250 μl enzyme solution and 250 μl ATP solution. t = 22.5°C.

* Present address: Centrallaboratoriet, Kommunehospitalet, Copenhagen, Denmark.

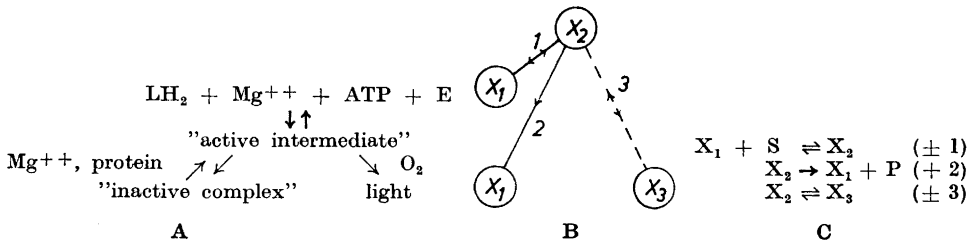

Fig. 3. A. Reaction scheme suggested by McElroy *et al.*[5] for the luciferase reaction. (E = enzyme;LH_2 = reduced luciferin). *B.* Reaction scheme suggested by Christiansen [6] to be the general scheme for a reaction following the Henri-Michaelis chronometric integral. (X_1, X_2 and X_3 are different forms of the enzyme or combinations of enzyme and substrate.) *C.* The same as *B*, written as ordinary equations. (S = substrate and P = products.)

pending on the initial ratio between these two components.

The effect of varying the amount of firefly extract is shown in Fig. 1. It is seen that light intensity measured 30 sec. after mixing the reagents is proportional to the square of the concentration of firefly extract. This is in good agreement with the commonly accepted fact that the extract contains two components that are important for the reaction, the enzyme luciferase and another component, luciferin [3,4].

The dependence of reaction velocity on ATP concentration was studied too. It is seen from Fig. 2 that the reaction kinetics is in accordance with the Henri-Michaelis scheme, when initial velocity is measured 30 sec. after mixing. Frequent readings during initial few minutes do, however, not show reaction kinetics in accordance with a normal Henri-Michaelis reaction, as the extremely rapid initial fall in light intensity is not caused by a decrease in the concentrations of the reactants [3]. To explain this it has been suggested by McElroy *et al.*[5] that part of the luciferase in one way or another is reversibly inactivated (Fig. 3). The scheme suggested for this particular reaction is then identical with the one proposed by Christiansen to be the general scheme for the simplest enzymatic reaction. It is reasonable to suggest that the luciferase reaction differs from the simple enzymatic reactions by approaching steady state with respect to reaction ± 3 (Fig. 3) after a few minutes instead of immediately.

A similar reaction mechanism is described by Andersen [7] in the case with arylsulphatase A, only in this case steady state with respect to the inactivating reaction was reached about 60 min. after the initiation.

1. Strehler, B. L. and Totter, J. R. *Methods of Biochemical Analysis* **I** (1954) 341.
2. McElroy, W. D. *Harvey Lectures* **51** (1955/56) 240.
3. Hastings, J. W., McElroy, W. D. and Coulombre, J. *J. Cellular Comp. Physiol.* **42** (1953) 137.
4. McElroy, W. D. and Strehler, B. L. *Arch. Biochem.* **22** (1949) 420.
5. McElroy, W. D., Hastings, J. W., Coulombre, J. and Sonnenfeld, V. *Arch. Biochem. Biophys.* **46** (1953) 399.
6. Christiansen, J. A. *Acta Chem. Scand.* **11** (1957) 660.
7. Andersen, S. O. *Acta Chem. Scand.* **13** (1959) 120.

Received July 7, 1960.

*iso*Thiocyanates XXXVIII *. Glucocapangulin, a Novel *iso*Thiocyanate-Producing Glucoside

ANDERS KJÆR, HELENE THOMSEN and (in part) S. E. HANSEN

Organic Chemical Laboratory, Royal Veterinary and Agricultural College, Copenhagen, Denmark

Capparis angulata Ruiz et Pav. *(Capparidaceae)* is a shrubby xerophyte indigenous to the coastal regions of Northern Peru. A seed specimen of this plant, made available to us **, possessed a pungent taste, suggestive of the presence of *iso*thiocyanate-producing glycosides. In fact, paper chromatography of an aqueous-methanolic extract of the seed embryos revealed the presence of a single glycoside with an R_B-value [1] of 1.05 in *n*-butanol: acetic acid:water (4:1:5). Enzymic fission with myrosinase produced an ether-soluble *iso*thiocyanate, convertible by methanolic ammonia into a thiourea derivative which on paper chromatography in water-saturated chloroform, migrated at a rate corresponding to an R_{ph}-value [2] of 1.04.

When a crude glycoside fraction, prepared in the usual way from defatted seed embryos (30 g) by extraction with 70 % methanol and subsequent purification on acid-washed alumina [3], was subjected to acetylation [4,5], a water-soluble, crystalline glycoside acetate monohydrate (3 g) was obtained in form of the potassium salt. A pure specimen (from 96 % ethanol), m. p. 168–169° (3°/min.)***, $[\alpha]_D^{22}$ −16.5° (*c* 0.85, CH_3OH), −19.0° (*c* 1.2, H_2O), gave analytical data concordant with the composition $C_{23}H_{32}O_{14}NS_2K,H_2O$. (Found: C 40.46; H 5.27; N 2.10; S 10.08; K 5.99; H_2O 3.0 (Karl Fischer). Calc.: C 40.30; H 5.23; N 2.13; S 9.78; K 5.96; H_2O 2.8), differing from that of all heretofore isolated *iso*thiocyanate glucosides [6]. Upon hydrolysis with conc. HCl at room temperature, the glycoside acetate afforded *hydroxylamine*, identified by paper chromatography [7]. Treatment of the acetate with methanolic ammonia resulted in formation of the free glucoside as a colourless, glassy product. Enzymic fission of the latter in phosphate buffer at pH 6.7 with a sulphate-free myrosinase preparation resulted in liberation of *sulphate* and formation of an ether-extractable mustard oil. In the aqueous phase, enzymically liberated *glucose* could be identified by paper chromatography in several solvent systems. Hence, the new glycoside is of the usual type [7] and accordingly has been named *glucocapangulin*.

On the likely assumption that acetylated glucocapangulin is a tetraacetate, its composition allows for a side-chain of $C_7H_{13}O$. The clue to its identification was found in a conspicuous band at 1 705 cm^{-1} (KBr) in the otherwise orthodox IR-spectrum of acetyl-glucocapangulin, indicative of a carbonyl function in its side-chain. This suspicion was confirmed by a positive qualitative test with 2,4-dinitrophenylhydrazine. Aldehyde or methyl ketone structures were ruled out by standard tests. Since the enzymic hydrolysis of glucocapangulin did not proceed entirely satisfactory, recourse was taken to hydrolytic degradation of the crystalline acetate with 20 % HCl at 50° for 2.5 h. As expected from acid formation in analogous cases [7], a colourless crystalline keto-acid, m. p. 32° (from hexane), was isolated in about 50 % yield. The partial structure, $C_6H_{13}(CO)(COOH)$, was established for this acid by analysis of its *S-benzylthiuronium salt*, m. p. 132°. (Found: C 58.90; H 7.58; N 8.54; S 10.07. Calc. for $C_{16}H_{24}O_3N_2S$: C 59.26; H 7.46; N 8.64; S 9.88), *p-bromophenacyl ester*, m. p. 89°, (Found: C 54.21; H 5.48; Br 22.36. Calc. for $C_{16}H_{19}O_4Br$: C 54.11; H 5.39; Br 22.51), and *semicarbazone*, m. p. 186°. (Found: C 50.22; H 7.97; N 19.52. Calc. for $C_9H_{17}O_3N_3$: C 50.22; H 7.96; N 19.52).

Wolff-Kishner reduction [8] of the keto-acid (88 mg) afforded a reduced acid, characterized as its S-benzylthiuronium salt (40 mg), m. p. 147°, and identical with *octanoic acid*, as apparent from undepressed mixed melting point and coinciding infrared spectra and X-ray diffraction patterns

* Part XXXVII: *Acta Chem. Scand.* **14** (1960) 215.

** The authors are very grateful to their botanical colleagues, Professor T. Böcher, Mr. P. K. Hjerting, Dr. M. Køie and Mr. K. Rahn, of the University of Copenhagen, who all took great efforts in collecting seed material in Peru for our use.

*** All melting points are determined in capillary tubes on immersed thermometers in an Anschütz-Hershberg apparatus. When not otherwise indicated, the rate of heating near the melting points has been less than 1°/min.

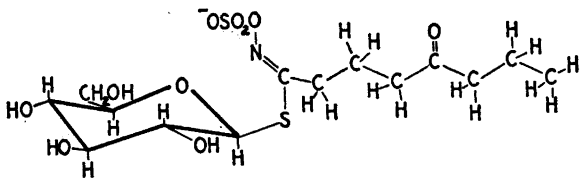

II

of the above salt and one prepared from authentic octanoic acid.

Assignment of the keto-grouping to the 5-position of the unbranched C_8-acid was indirectly rendered possible on basis of the following data. 2-Oxooctanoic acid was ruled out when its S-benzylthiuronium salt was prepared and found to melt at 156°. (Found: C 59.32; H 7.43; N 8.62), the 3-oxo-isomeride is incompatible with the stability properties of the present acid, 4-oxooctanoic acid semicarbazone melts at 153° [9], 6-oxooctanoic acid has the m. p. 52° [10] and, furthermore, is disqualified by the fact that the IR-spectrum of the 'natural' acid is devoid of the skeletal vibration at 720 – 750 cm^{-1} diagnostic of the $(CH_2)_4$-grouping. Finally, negative haloform reaction of the naturally derived acid excludes 7-oxooctanoic acid as a possibility.

$$CH_3CH_2CH_2COCH_2CH_2CH_2COOH$$

I

Confirmation of structure (I) for the acid hydrolysis product of acetylated glucocapangulin was eventually obtained by synthesis of authentic 5-oxooctanoic acid (m. p. 32.8°) according to Yoho and Levine [11]. Comparison of the S-benzylthiuronium salts, *p*-bromophenacyl esters and semicarbazones of the naturally derived and synthetic keto-acid by means of mixed melting points and infra-red spectra left no doubt as to their identity.

From the above experimental data, it follows that the glucocapangulin ion most likely possesses the traditional structure (II) and thus represents the first example of a glucoside of this type containing a carbonyl function. Biogenetically, it may arise from intermediates formed in the fatty acid cycle.

A full account of the present work will be presented in a forthcoming communication in this journal.

The assistance of Miss E. Vesterager in the synthetic work is acknowledged. The authors are thankful to Dr. E. Krogh Andersen for the X-ray diffraction patterns. Microanalyses have been performed by Messrs. G. Cornali and W. Egger. The work is part of investigations supported by *Statens Almindelige Videnskabsfond (The Danish State Research Foundation)*, *Carlsbergfondet (The Carlsberg Foundation)*, and *Kai Hansen's Fond.*

1. Schultz, O.-E. and Wagner, W. *Z. Naturforsch.* **11b** (1956) 73.
2. Kjær, A. and Rubinstein, K. *Acta Chem. Scand.* **7** (1953) 528.
3. Schultz, O.-E. and Gmelin, R. *Arch. Pharm.* **287/59** (1954) 342.
4. Schultz, O.-E. and Wagner, W. *Arch. Pharm.* **288/60** (1955) 525.
5. Kjær, A., Gmelin, R. and Boe Jensen, R. *Acta Chem. Scand.* **10** (1956) 432.
6. Kjær, A. *Fortschr. Chem. org. Naturstoffe* **18** (1960) 122.
7. Ettlinger, M. G. and Lundeen, A. J. *J. Am. Chem. Soc.* **78** (1956) 4172.
8. Stetter, H. and Dierichs, W. *Chem. Ber.* **85** (1952) 61.
9. Clutterbuck, P. W. and Raper, H. S. *Biochem. J.* **19** (1925) 385.
10. Blaise, E. E. and Koehler, A. *Compt. rend.* **148** (1909) 490.
11. Yoho, C. W. and Levine, R. *J. Am. Chem. Soc.* **74** (1952) 5597.

Received June 20, 1960.

The Crystal Structure of Iron(II) Sulphate Pentahydrate Glycine

INGVAR LINDQVIST and ROBERT ROSENSTEIN

Institute of Chemistry, University of Uppsala, Uppsala, Sweden

The bonding between iron and glycine in this compound has never been elucidated, and because of the clinical interest of the compound, AB Pharmacia, Uppsala, has suggested to us to determine the crystal structure so far that the coordination in the compound could be considered as definitely established.

Experimental. Crystals were prepared from a hot concentrated solution of the salt plus an excess of sulphuric acid. The crystallization is best done in an inert atmosphere to prevent oxidation. The carefully dried crystals, which have a pale greenish-blue colour are, however, stable in air.

Roughly prismatic crystals with a cross-section of about 0.02 × 0.02 mm² were used for the X-ray work. Weissenberg photographs were taken of three such crystals around the three almost perpendicular triclinic axes. Lattice parameters were obtained from high-order reflections in the equatorial zones. $a = 6.86$ Å, $b = 13.6$ Å, $c = 6.07$ Å, $\alpha = 96.1°$ $\beta = 96.8°$, $\gamma = 92.5°$. Probable space-group is $P\bar{1}$. Assuming two formula units per cell, the calculated density is 1.92 gcm^{-3}, obs. 1.87 gcm^{-3}, measured by a pycnometric method.

Cu-K radiation could be employed, in spite of the iron content. The intensities were estimated visually by comparison with a standard scale.

Crystal structure. The Patterson projections $P(xy)$ and $P(yz)$ were calculated and the Fe and S positions were derived from these projections. The positions of the light atoms were determined by successive electron density and difference maps. The approximate parameters determined in this way are:

O_1	(0.178, 0.055, 0.708)
O_2	(0.104, 0.133, 0.205)
O_3	(0.759, 0.085, 0.958)
O_4	(0.488, 0.123, 0.287)
O_5	(0.770, 0.140, 0.560)
O_6	(0.655, 0.285, 0.403)
O_7	(0.460, 0.205, 0.670)
O_8	(0.169, 0.383, 0.535)
O_9	(0.633, 0.463, 0.681)
O_{10}	(0.169, 0.343, 0.067)
O_{11}	(0.663, 0.472, 0.869)
C_1	(0.023, 0.322, 0.858)
C_2	(0.149, 0.398, 0.737)
N	(0.003, 0.345, 0.100)
S	(0.588, 0.1885, 0.487)
Fe_1	(0,0,0)
Fe_2	($\frac{1}{2}$,$\frac{1}{2}$,0)

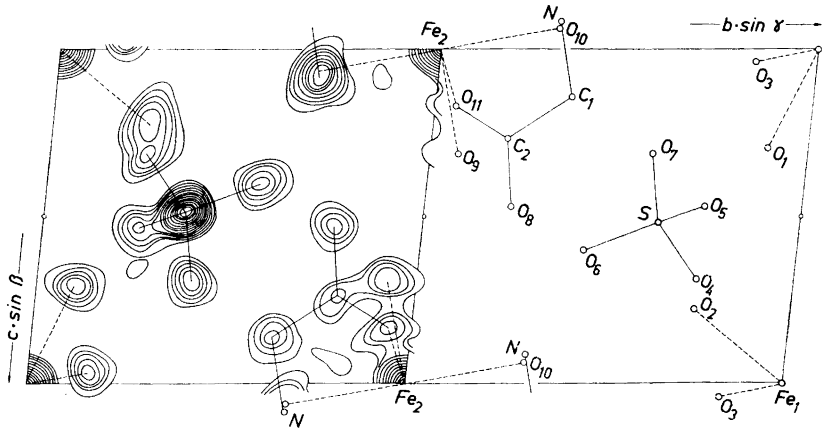

Fig. 1a. Iron (II) sulfate pentahydrate glycine: a axis projection, showing the complete unit cell. Electron density contours are drawn for the unique portion to the left and the corresponding atomic positions are indicated to the right across the center of symmetry.

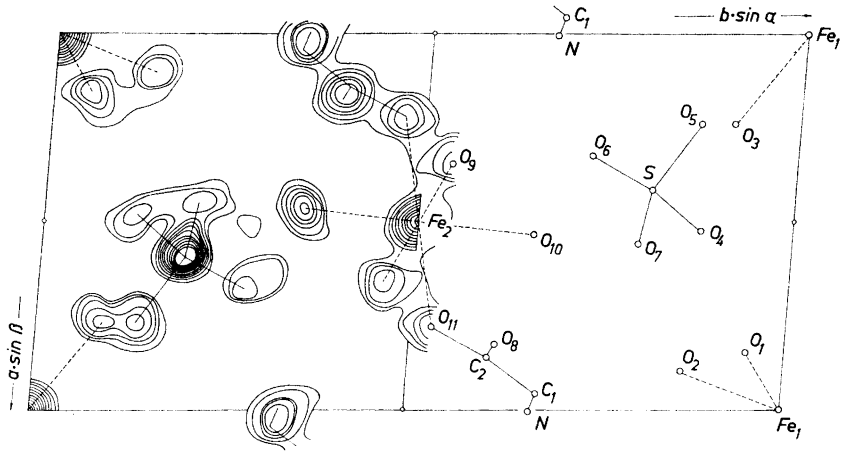

Fig. 1b Iron (II) sulfate pentahydrate glycine: *c* axis projection, showing the complete unit cell. Electron density contours are drawn for the unique portion to the left and the corresponding atomic positions are indicated to the right across the center of symmetry.

Average temperature factors for the two projections, (B *hk*0) : oxygen 3.0, carbon 3.8, nitrogen 3.4, sulfur 1.51, iron 1.62 Å², B (0*kl*): oxygen 2.5, carbon 3.3, nitrogen 2.9, sulfur 0.89, iron 1.00 Å². The residual error indices are R (*kh*0) = 0.14, R (0*kl*) = 0.18.

The structure is shown together with two electron density maps in Fig. 1*a* and *b*. It is built up of two different kinds of complex cations: $Fe(H_2O)_6^{2+}$ and $Fe(H_2O)_4(^-OOCCH_2NH_3^+)_2^{2+}$. In the latter ion one of the oxygen atoms of the carboxyl group in the glycine »Zwitterion» is bonded to the central Fe^{2+} ion. The two glycine molecules are in trans positions. These complex cations obviously can build up a structure, together with the sulphate ions, with more favorable lattice energy than one containing only one type of cation $Fe(H_2O)_5(^-OOCCH_2NH_3^+)^{2+}$. The accuracy of the structure determination does not permit a detailed discussion of the bond lengths but it is quite clear that a complicated hydrogen bridge system joins the different parts of the structure. The aim with this structure determination has, however, only been to establish the co-ordination around the Fe^{2+} ions and this problem has been definitely solved. Every suggestion about chelate bonding with the amino group can thus be rejected.

This work has been supported by a grant from *AB Pharmacia* which is gratefully acknowledged.

Finally we wish to thank Professor Hägg for all facilities put at our disposal.

1. H. Flood and V. Lorås, *Tidskr. Kjemi, Bergvesen Met.* **4** (1944) 35.

Received July 7, 1960.

A Note on the Structure of Barium Tetraborate

J. KROGH-MOE

Svenska Silikatforskningsinstitutet, Göteborg, Sweden

Crystalline barium tetraborate, $BaO \cdot 4B_2O_3$, was obtained by Levin and McMurdie as a congruently melting phase in the system barium oxide — boron oxide[1]. Single crystals of this phase were prepared during the present study by fusing barium carbonate with the calculated amount of boric acid in a platinum

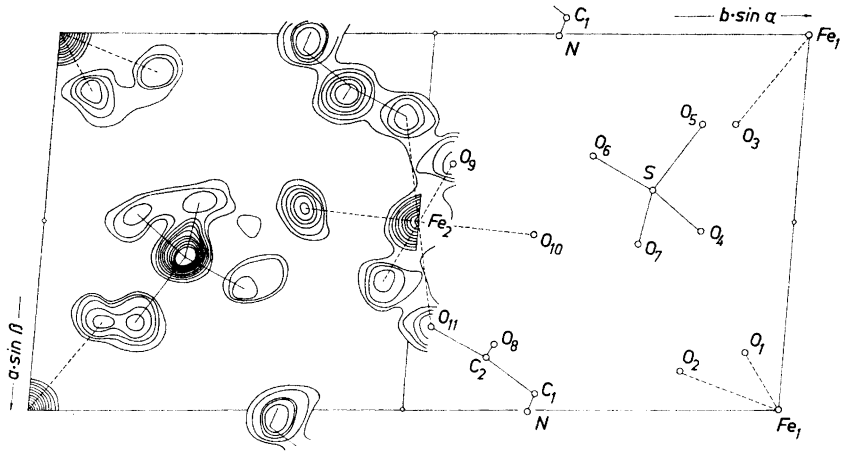

Fig. 1b Iron (II) sulfate pentahydrate glycine: *c* axis projection, showing the complete unit cell. Electron density contours are drawn for the unique portion to the left and the corresponding atomic positions are indicated to the right across the center of symmetry.

Average temperature factors for the two projections, (B *hk*0) : oxygen 3.0, carbon 3.8, nitrogen 3.4, sulfur 1.51, iron 1.62 Å², B (0*kl*): oxygen 2.5, carbon 3.3, nitrogen 2.9, sulfur 0.89, iron 1.00 Å². The residual error indices are R (*kh*0) = 0.14, R (0*kl*) = 0.18.

The structure is shown together with two electron density maps in Fig. 1*a* and *b*. It is built up of two different kinds of complex cations: $Fe(H_2O)_6^{2+}$ and $Fe(H_2O)_4(^-OOCCH_2NH_3^+)_2^{2+}$. In the latter ion one of the oxygen atoms of the carboxyl group in the glycine »Zwitterion» is bonded to the central Fe^{2+} ion. The two glycine molecules are in trans positions. These complex cations obviously can build up a structure, together with the sulphate ions, with more favorable lattice energy than one containing only one type of cation $Fe(H_2O)_5(^-OOCCH_2NH_3^+)^{2+}$. The accuracy of the structure determination does not permit a detailed discussion of the bond lengths but it is quite clear that a complicated hydrogen bridge system joins the different parts of the structure. The aim with this structure determination has, however, only been to establish the co-ordination around the Fe^{2+} ions and this problem has been definitely solved. Every suggestion about chelate bonding with the amino group can thus be rejected.

This work has been supported by a grant from *AB Pharmacia* which is gratefully acknowledged.

Finally we wish to thank Professor Hägg for all facilities put at our disposal.

1. H. Flood and V. Lorås, *Tidskr. Kjemi, Bergvesen Met.* **4** (1944) 35.

Received July 7, 1960.

A Note on the Structure of Barium Tetraborate

J. KROGH-MOE

Svenska Silikatforskningsinstitutet, Göteborg, Sweden

Crystalline barium tetraborate, $BaO \cdot 4B_2O_3$, was obtained by Levin and McMurdie as a congruently melting phase in the system barium oxide — boron oxide[1]. Single crystals of this phase were prepared during the present study by fusing barium carbonate with the calculated amount of boric acid in a platinum

crucible at 1 000°C, and crystallizing the melt at 800°C. Weissenberg and oscillation X-ray photographs, taken about three axes of these crystals, showed an orthorhombic symmetry with the following unit cell dimensions:

$$a = 8.56 \text{ Å}$$
$$b = 2 \times 8.69 \text{ Å}$$
$$c = 13.20 \text{ Å}$$

A very weak doubling along the b axes was observed and is indicated in the above figures by writing 2×8.69 Å instead of 17.38 Å. The calculated density is 2.91 g/cm³ with 8 formula units of $BaO \cdot 4B_2O_3$ in the cell.

The Weissenberg diagrams disclose a pronounced pseudo tetragonal symmetry of barium tetraborate. This agrees with the optical properties of the compound. Thus Levin and McMurdie were unable to decide whether the crystals were uniaxial or biaxial negative [1]. The same authors also noted that the crystals exhibit polysynthetic twinning. Some of the present X-ray diagrams show twinning, in which the twins have paralell c-axes with the 010 plane facing the 100 plane.

Approximate barium positions can be determined by inspecting the X-ray diagrams. From the rotation diagram around the c-axes it is seen that the general hkl reflections are on average considerably stronger for even values of l than for odd. Therefore, as a first approximation, a reduced cell with halved b and c axes may be considered for the heavy barium atoms. This pseudo cell contains two barium atoms. Further information is obtained from equatorial and non-equatorial Weissenberg photograms. It is found that reflections are often weak or missing whenever $h + k' + l' = 2n + 1$. Here the indices k' and l' ($= l/2$) refer to the pseudo cell with halved b and c axes. This partially fulfilled condition of systematic extinctions suggests an approximately body-centered arrangement of the barium atoms in the pseudo cell, where the barium atoms thus can be given the preliminary parameter values 0,0,0 and $\frac{1}{2},\frac{1}{2},\frac{1}{2}$. The shortest distance between two barium atoms is 6.94 Å with these parameter values.

The correct space group of barium tetraborate is difficult to decide because of the pseudo symmetries. The final space group determination will therefore have to await further work.

1. Levin, E. M. and McMurdie, H. F. *J. Am. Ceram. Soc.* **32** (1949) 99.

Received August 10, 1960.

ACTA CHEMICA SCANDINAVICA 14 (1960) 1231—1242

The Bacteriostatic Action of Benzoic and Salicylic Acids

III. The Effect on Pyruvate and Acetate Oxidation by Different Organisms

INGMAR BOSUND

State Dairy Research Station, Alnarp, Sweden

The influence of benzoic and salicylic acids on pyruvate and acetate oxidation by resting cells of different organisms was investigated.

Both inhibitors blocked pyruvate oxidation at the acetate level in experiments with washed cells of *Proteus vulgaris* and *Escherichia coli* harvested from a medium containing amino acids and additional carbon sources. A similar but less marked effect was observed with cells pre-grown without added amino acids, but not in experiments with cells cultivated in a medium with acetate as the sole carbon source.

Benzoic and salicylic acids did not produce a corresponding effect on pyruvate oxidation by *Pseudomonas fluorescens* or baker's yeast in a similar investigation with these organisms. In the presence of benzoic acid washed cells of *Ps. fluorescens* oxidized acetate completely to CO_2 and H_2O, if the cells were pre-grown in a medium with acetate as the sole carbon source.

The experiments with baker's yeast were performed at three different pH-values and included an investigation of the influence of benzoic and salicylic acids on growth and on endogenous respiration. It was shown that all effects could be ascribed solely to the undissociated molecules of the acids. With both inhibitors there was close correspondence between inhibition of acetate oxidation and inhibition of growth at all pH-values.

Previously in this investigation [1,2] the influence of benzoic and salicylic acids on the oxidation of glucose, pyruvate and acetate by washed cells of *Proteus vulgaris* was studied. It was observed that both inhibitors specifically blocked glucose and pyruvate oxidation at the acetate level in experiments with cells grown in a medium containing glucose and amino acids. When the cells were grown with acetate as the sole carbon source no such inhibition was noticed — on the contrary, in such experiments, both benzoic and salicylic acids caused an increase in the total CO_2-output, especially from pyruvate.

These results clearly indicate that the influence of benzoic and salicylic acids on the metabolism of resting cells is largely determined by the prehistory of the cells. It seemed important to investigate this relationship somewhat further and at the same time include other organisms in the study. For this purpose *Escherichia coli*, *Pseudomonas fluorescens* and baker's yeast were selected.

It was suggested previously in this work that the results obtained with *P. vulgaris* might be associated with the presence of a special type of pyruvate oxidase in this organism. This enzyme, which transforms pyruvate directly into acetate without intermediate formation of any metabolically active C_2-compound (Moyed and O'Kane[3]), has also been shown to occur in *E. coli* (Razzell and Gunsalus [4]). It was therefore considered of interest to compare the effects of benzoic and salicylic acids on pyruvate oxidation by these organisms.

Ps. fluorescens and baker's yeast were selected as test organisms for essentially two reasons. Firstly, it was considered of importance to study the effects of the inhibitors under investigation on organisms essentially different from *P. vulgaris* and *E. coli*. Secondly, it was desirable to choose organisms capable of growing with acetate as the sole carbon source and with fairly known pyruvate metabolism.

EXPERIMENTAL

Organisms. The strain of *P. vulgaris* used in this investigation was the same as before. *E. coli* (NCTC 8196) and *Ps. fluorescens* (NCTC 950) were obtained from the National Collection of Type Cultures, London. Baker's yeast was supplied by Svenska Jästfabriks AB.

Media and growth conditions. The liquid media employed for cultivation of *P. vulgaris* and *E. coli* in this investigation were essentially the same as those previously [2] described (medium A containing glucose and casein hydrolysate and medium B with acetate as the sole source of carbon). In some experiments, however, medium A was modified by replacing glucose by sodium pyruvate and sodium succinate (final concentration, 0.5 g per liter of each), and in others casein hydrolysate was omitted.

In all experiments using liquid culture media, the inoculations were made with heavy amounts of washed cells (generally grown in the same media), and the cultures were adequately aerated during growth. The cells were harvested early in the logarithmic growth phase (generally 3—4 h after inoculation), which was ascertained by turbidity measurements. This procedure made it unnecessary to sterilize the growth medium.

Ps. fluorescens was grown for 24—48 h on Petri dishes containing substrates with the same composition as above (nicotinamide omitted) and solidified by addition of 1.5 % agar. In experiments where *Ps. fluorescens* was inoculated in liquid media, aerated or non-aerated, the growth rate was generally low, and the total amount of cell mass obtained was small.

Preparation of cell suspensions. *P. vulgaris* and *E. coli* were harvested from the liquid media by centrifugation, washed and suspended in phosphate buffer at appropriate pH as described previously [1].

Ps. fluorescens was harvested by washing off the colonies from the agar surface with 1/15 M phosphate buffer. The resulting cell suspension was centrifuged, and the cells were washed twice in 1/15 M phosphate buffer. In the work with baker's yeast, the yeast cells were suspended in buffer and aerated for 1 h prior to the experiments in order to reduce endogenous respiration. Some of the studies were performed at pH-values, where phosphate was unsuitable as buffer substance. In these cases 1/15 M potassium biphthalate or a mixture of 1/15 M potassium biphthalate and 1/15 M potassium phosphate was used. It was ascertained by experiments that the biphthalate ion had no influence on the rates of oxygen consumption recorded in the respiration studies.

Respiration studies. The procedure followed was essentially the same as that previously described[1]. The values recorded in figures and tables are, as before, in appropriate cases corrected for endogenous respiration.

RESULTS

Experiments with Proteus vulgaris. Respiration studies described in the first two parts of this series show, that the influence of benzoic and salicylic acids on the metabolism of resting cells varies considerably with conditions prevailing during cultivation of the cells. Especially the composition of the growth medium seems to be of importance. This is demonstrated by the fact that these inhibitors block glucose and pyruvate oxidation by resting cells of *P. vulgaris* at the acetate level, if the cells are pre-grown in glucose-casein hydrolysate medium, but not if the cells are grown in acetate medium. In this work some additional experiments were performed in order to emphasize the validity of these results.

The glucose-casein hydrolysate medium previously employed (medium A) was modified by exchanging glucose for pyruvate and succinate. This supplied the growth medium with an excess of two easily utilizable carbon sources, which as well could give rise to large amounts of starting material for the operation of the TCA cycle. The medium was inoculated with a large amount of cells, which were harvested as soon as the logarithmic growth phase was established. This procedure, besides insuring reproducible conditions of growth, was thought to give rise to cells with a high ability to oxidize acetate. It is evident from Fig. 1 A, however, that benzoic acid, even with such cells, completely inhibited pyruvate oxidation at the acetate level (similar results were obtained with salicylic acid). This inhibition was not affected by simultaneous oxidation of succinate added together with the pyruvate. Previously in this work [2] small amounts of succinate were shown markedly to reduce inhibition of acetate oxidation by benzoic acid.

Fig. 1 B illustrates an experiment with washed cells pre-grown in medium A with omission of casein hydrolysate leaving NH_4^+ ions as the sole source of nitrogen. The presence of benzoic acid during pyruvate oxidation by such cells neither inhibits the oxygen consumption at the acetate level nor increases the total amount of oxygen consumed per mole of pyruvate (as in experiments with cells grown with acetate as the sole carbon source) but seems to produce some intermediary form of effect.

Experiments with E. coli. Figs. 2 A and 2 B illustrate the influence of benzoic acid on pyruvate oxidation by washed *E. coli* cells. The cells were pre-grown in medium A with pyruvate and succinate instead of glucose (Fig 2 A) or in medium B (Fig 2 B) and harvested in the logarithmic growth phase. It is evident, that the results are very similar to those obtained with *P. vulgaris*. Even with *E. coli* pyruvate oxidation is blocked at the acetate level by benzoic acid, when the cells have been cultivated in a fairly rich medium, whereas no such inhibition is observed in studies with cells grown in the simple acetate medium. Corresponding experiments with salicylic acid gave essentially the same results (not shown here). Benzoic and salicylic acids were required at concentrations of about 7 and 1.5 mM, respectively, in order completely to

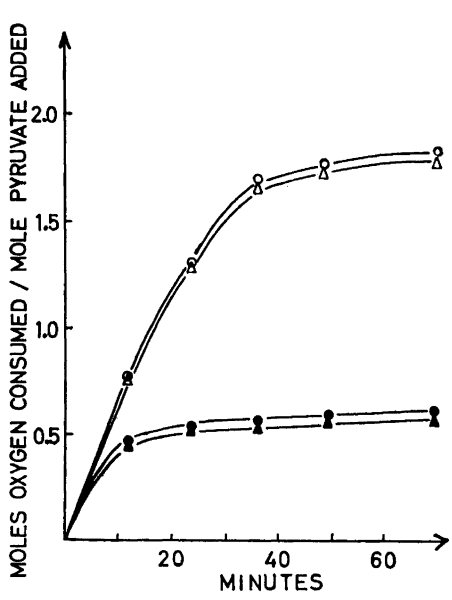

Fig. 1 A. Effect of benzoic acid on pyruvate oxidation by washed *P. vulgaris* cells. The cells were previously grown with aeration in a medium containing pyruvate, succinate and casein hydrolysate and harvested in the logarithmic growth phase. The vessels contained besides 4.5 mg dry wt. of cells, 133 μmoles of potassium phosphate and 7 μmoles of sodium pyruvate: △ no further additions; ○ 0.2 μmoles of sodium succinate; ▲ 8.3 mM benzoic acid; ● 0.2 μmoles of sodium succinate and 8.3 mM benzoic acid. Final volume, 2.4 ml. Experimental conditions: gas phase, air; pH 6.0; temp. 37°C.

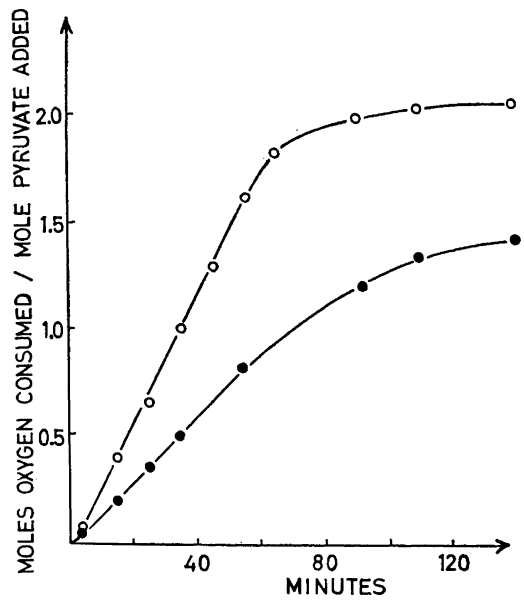

Fig. 1 B. Effect of benzoic acid on pyruvate oxidation by washed *P. vulgaris* cells. The cells were previously grown with aeration in a medium containing glucose and ammonium chloride as carbon and nitrogen sources and harvested in logarithmic growth phase. The vessels contained besides 2.0 mg dry wt. of cells and 133 μmoles of potassium phosphate: ○ 7 μmoles of sodium pyruvate; ● 7 μmoles of sodium pyruvate and 9.7 mM benzoic acid. Final volume, 2.4 ml. Experimental conditions: gas phase, air; pH 6.0; temp. 37°C.

inhibit pyruvate oxidation at the acetate level. In the experiment with acetate grown cells shown in Fig. 2 B benzoic acid did not increase the total amount of oxygen consumed per mole of substrate in contrast to what was observed in corresponding experiments with *P. vulgaris*. Such an increase was, however, occasionally obtained even in respiration studies with *E. coli* in the presence of slightly lower concentrations of benzoic acid.

Experiments with Pseudomonas fluorescens. In another series of experiments the effect of benzoic and salicylic acids on the pyruvate and acetate oxidation by washed *Ps. fluorescens* cells was investigated. The cells were grown on agar plates, as described in the experimental part. The solid media were either pyruvate-succinate-casein hydrolysate agar or acetate agar. In a few experiments the cells were grown on succinate agar (acetate agar with acetate

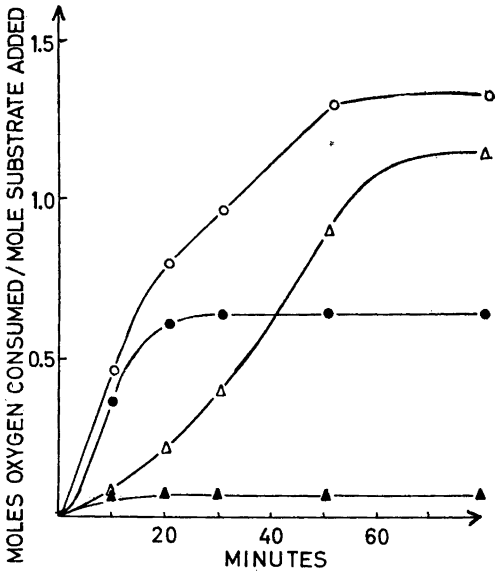

Fig. 2 A. Effect of benzoic acid on pyruvate and acetate oxidation by washed *E. coli* cells. The cells were previously grown with aeration in a medium containing pyruvate, succinate and casein hydrolysate and harvested in the logarithmic growth phase. The vessels contained besides 4.0 mg dry wt. of cells and 133 μmoles of potassium phosphate: O 7 μmoles of sodium pyruvate; ● 7 μmoles of sodium pyruvate and 7.5 mM benzoic acid; △ 7 μmoles of sodium acetate; ▲ 7 μmoles of sodium acetate and 7.5 mM benzoic acid. Final volume, 2.4 ml. Experimental conditions: gas phase, air; pH, 6.0; temp., 37°C.

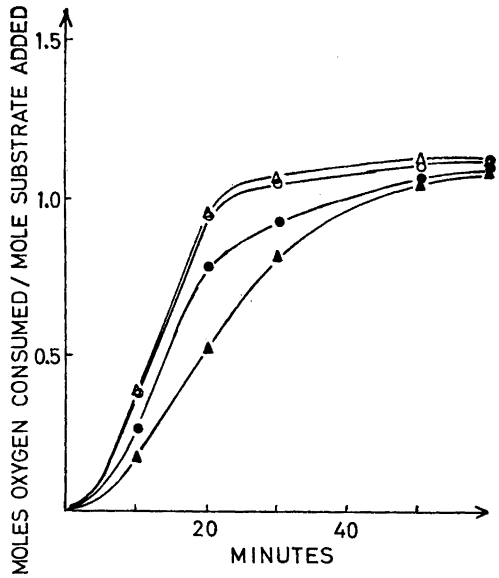

Fig. 2 B. Effect of benzoic acid on pyruvate and acetate oxidation by washed *E. coli* cells. The cells were previously grown with aeration in a medium containing acetate as the sole carbon source and harvested in the logarithmic growth phase. The vessels contained besides 2.5 mg dry wt. of cells and 133 μmoles of potassium phosphate: O 7 μmoles of sodium pyruvate; ● 7 μmoles of sodium pyruvate and 7.5 mM benzoic acid; △ 7 μmoles of sodium acetate; ▲ 7 μmoles of sodium acetate and 7.5 mM benzoic acid. Final volume, 2.4 ml. Experimental conditions: gas phase, air; pH 6.0; temp. 37°C.

replaced with an equal amount of succinate). The results of these studies can be summarized as follows:

1. The rate of oxygen consumption during oxidation of acetate was greatest with cells pre-grown on acetate agar, intermediate with cells pre-grown on succinate agar and smallest with cells pre-grown on pyruvate-succinate-casein hydrolysate agar. The Q_{O_2}-values recorded with such differently grown cells were roughly the same as those obtained in experiments with *P. vulgaris* and *E. coli* pre-grown in liquid media of analogous composition.

2. The inhibiting effect of benzoic acid on the rate of acetate oxidation was strongest in experiments with cells oxidizing acetate at a low rate. Accordingly inhibition was greatest in experiments with cells pre-grown on pyruvate-

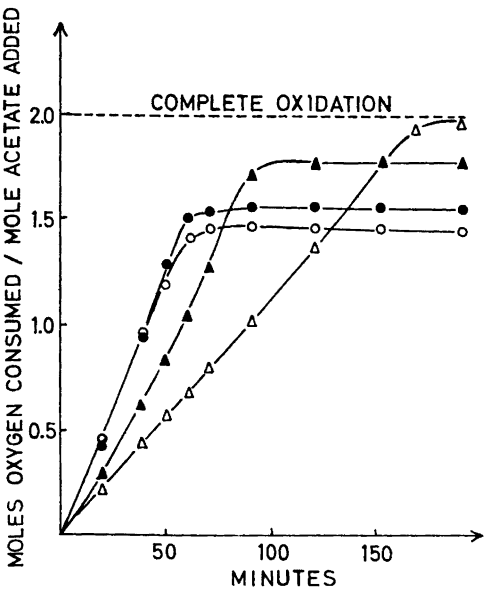

Fig. 3. Effect of benzoic acid on acetate oxidation by washed *Ps. fluorescens* cells. The cells were previously grown on acetate agar. The vessels contained besides 1.2 mg dry wt. of cells, 133 μmoles of potassium phosphate and 7 μmoles of sodium acetate: ○ no further additions; ● 2 mM benzoic acid; ▲ 4 mM benzoic acid; △ 6 mM benzoic acid. Final volume, 2.2 ml. Experimental conditions: gas phase, air; pH 6.0; temp. 25°C.

succinate-casein hydrolysate agar (50 % inhibition at about 2 mM benzoic acid) and smallest in experiments with cells pre-grown on acetate agar and harvested in the logarithmic growth phase (50 % inhibition at about 15 mM benzoic acid). These results are analogous to those previously obtained with *P. vulgaris.*

3. No sign of a specific inhibiting effect on pyruvate oxidation at the oxidation level of acetate in presence of benzoic or salicylic acid was observed in any experiment with washed cells regardless of the composition of the medium on which the cells had been grown. In this respect there exists a clear difference between *Ps. fluorescens* on one hand and *P. vulgaris* and *E. coli* on the other.

4. As with *P. vulgaris,* benzoic acid increased the total amount of oxygen consumed per mole of acetate in experiments with cells previously grown with acetate as the sole carbon source. This increase was most significant if the cells had passed the logarithmic growth phase at the time of harvesting. In respiration studies with such cells the acetate oxidation — in presence of 4—6 mM benzoic acid — proceeded, until the theoretical amount of oxygen required for complete oxidation of the acetate to CO_2 and H_2O had been consumed. At these concentrations the rate of oxygen consumption was inhibited to about 50 % by benzoic acid (Fig. 3). If the cells were grown on succinate agar, a similar but smaller increase was observed in presence of benzoic acid. A corresponding increase in oxygen consumption was recorded in respiration studies with pyruvate as substrate.

Some remarks concerning these experiments may be added to the above summary. Washed cells of *Ps. fluorescens* prepared from cultures grown on yeast extract agar can be adapted to oxidize benzoic acid by incubating them in the

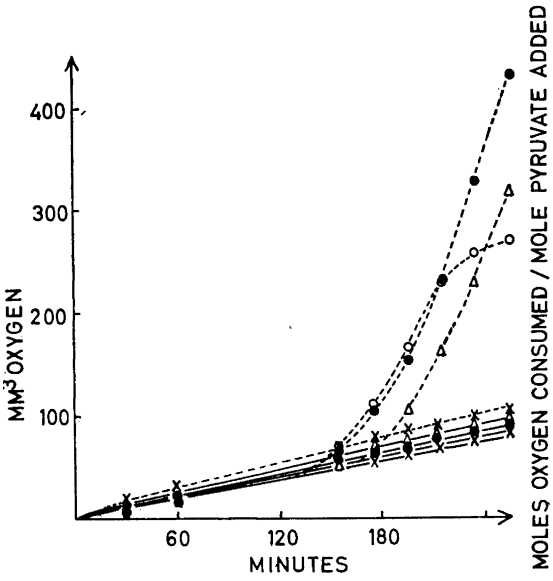

Fig. 4. Adaptation by washed *Ps. fluorescens* cells to oxidation of benzoic acid. The cells were previously grown on yeast extract agar. The vessels contained besides 1.0 mg dry wt. of cells and 33 μmoles of potassium phosphate: × no further additions; O 1.75 μmoles of sodium benzoate; ● 2.50 μmoles of sodium benzoate; △ 4.78 μmoles of sodium benzoate. Dashed lines, pH 7.0; solid lines, pH 6.0; gas phase, air; temp. 25°C.

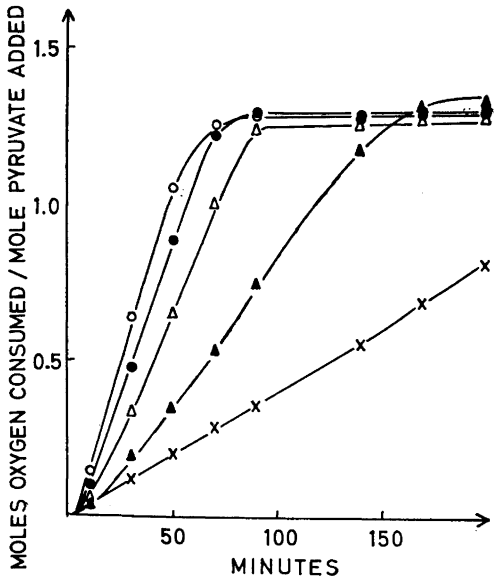

Fig. 5. Effect of benzoic acid on pyruvate oxidation by baker's yeast. The vessels contained 40 mg wet wt. of yeast, 7 μmoles of sodium pyruvate and benzoic acid at the following concentrations: O no benzoic acid; ● 1.4 mM; △ 2.8 mM; ▲ 4.2 mM; × 8.4 mM. Final volume, 2.4 ml. Experimental conditions: gas phase, air; pH 6.0; temp. 25°C.

presence of this substance, as shown by Stanier [5]. It may be argued that some of the oxygen consumed in experiments where benzoic acid is added can be ascribed to such oxidation. This possibility can, however, be ruled out in the present investigation by the following facts: a) in all experiments an aliquot of the cells was incubated with benzoic acid as the sole substrate in a separate vessel, and in no case was any increase of the oxygen consumption observed in these vessels during the experimental time; b) the exponential increase of the rate of oxygen consumption during the adaptation process (Fig. 4) should be clearly revealed, even during simultaneous acetate oxidation, if it actually occurred. The adaptation experiment shown in Fig. 4 was made at pH 7.0 with washed cells grown on yeast extract agar as described by Stanier. It is noteworthy that no adaptation occurred at pH 6.0 — the pH value maintained in the actual experiments in this study; c) the uptake in presence of benzoic acid of almost exactly the amount of oxygen required for complete oxidation of the acetate to CO_2 and H_2O was obtained irrespectively of the amount of acetate added or the length of the experiment.

Table 1. Effect of benzoic acid on pyruvate oxidation by baker's yeast. Each vessel contained 40 mg wet wt. of yeast in 1/15 M biphthalate-phosphate buffer and 7 μmoles of sodium pyruvate. Final volume 2.2 ml. Experimental conditions: gas phase, air; temp. 30°C; pH 5.0.

Time, min.	Without inhibitor			With 0.5 mM benzoic acid		
	O_2consumed, μl	CO_2 evolved, μl	*R.Q.*	O_2consumed, μl	CO_2 evolved, μl	*R.Q.*
10	52	58	1.12	37	42	1.14
20	131	150	1.15	95	107	1.13
30	200	232	1.16	152	177	1.17
50	266	312	1.17	255	302	1.18
70	288	338	1.17	298	351	1.18

Table 2. Effect of benzoic and salicylic acids on oxidative processes and growth in experiments with baker's yeast.

Effect studied	Inhibitor concentration required for the effect studied											
	Benzoic acid						Salicylic acid					
	Total concn., mM			Calculated * concn. of undissociated acid, mM			Total concn., mM			Calculated * concn. of undissociated acid, mM		
	pH 4.1	pH 5.1	pH 6.0	pH 4.1	pH 5.1	pH 6.0	pH 4.1	pH 5.1	pH 6.0	pH 4.1	pH 5.1	pH 6.0
50 % inhibition of the rate of acetate oxidation	1.1	4.0	35	0.62	0.45	0.55	0.6	5.0	45	0.044	0.039	0.045
50 % inhibition of the rate of pyruvate oxidation	0.4	0.6	5.0	0.22	0.067	0.078	0.2	1.5	15	0.015	0.012	0.015
Complete inhibition of growth in glucose-casein hydrolysate medium	—	5.0	60	—	0.56	0.94	—	12	70	—	0.095	0.070
Maximal increase in endogenous respiration	—	—	—	—	—	—	0.55	6.1	43	0.040	0.048	0.043

* In this calculation $10^{-4.20}$ was used as dissociation constant for benzoic acid and $10^{-3.00}$ for salicylic acid.

In studies on cell respiration, where the amount of oxygen consumed per mole of exogenous substrate (substrate added to the medium) is determined, it is of importance that the simultaneous endogenous respiration (oxygen consumption due to oxidation of cell material) is low, since it is a matter of controversy whether this latter oxygen consumption is suppressed during oxidation of exogenous substrate or not. If it is suppressed, it is clearly not correct to substract the value of the endogenous respiration from the experi-

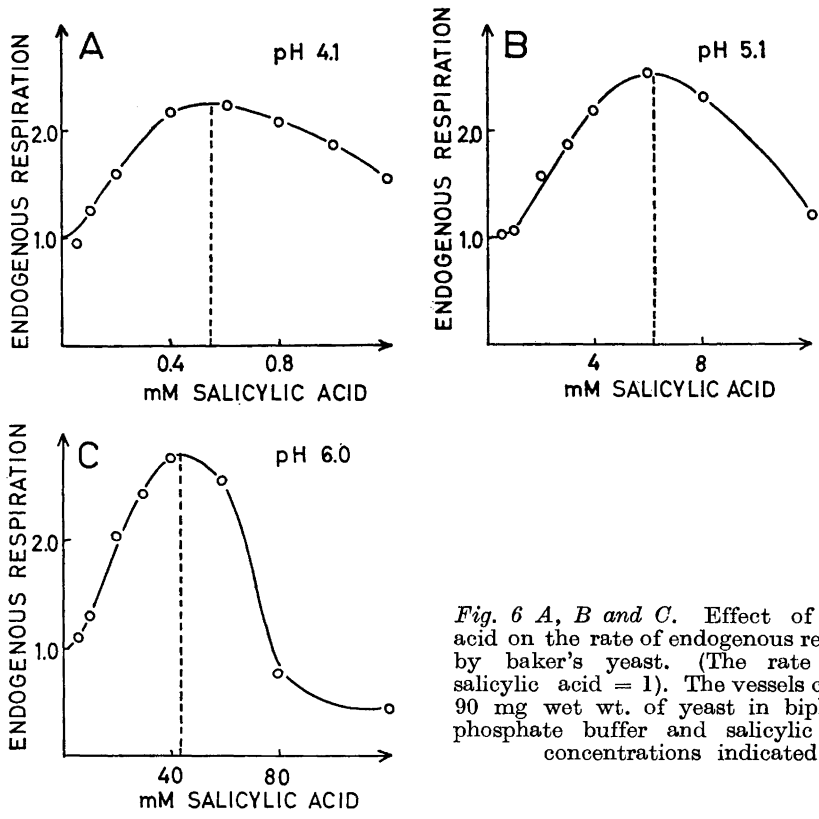

Fig. 6 A, B and C. Effect of salicylic acid on the rate of endogenous respiration by baker's yeast. (The rate without salicylic acid = 1). The vessels contained 90 mg wet wt. of yeast in biphthalate-phosphate buffer and salicylic acid at concentrations indicated.

mentally determined oxygen consumption when calculating the oxygen uptake per mole of exogenous substrate. In the present investigation this problem was of minor importance, since endogenous respiration in *Ps. fluorescens* cells, grown and washed as described, is practically zero.

Experiments with baker's yeast. In this study the effect of benzoic and salicylic acids on pyruvate and acetate oxidation and on endogenous respiration was investigated at three different pH-values. In addition the growth inhibiting effect in glucose-casein hydrolysate medium was determined at the same pH-values. Fig. 5 shows the influence of various concentrations of benzoic acid on pyruvate oxidation by baker's yeast at pH 6.0. It is evident, that there is no sign of a specific inhibiting effect in the presence of benzoic acid at the oxidation level of acetate. This is also apparent from Table 1, which shows the *R.Q.*-values during oxidation of pyruvate in the presence and absence of benzoic acid. Similar results were obtained with salicylic acid. In no case there was any significant increase found in the amount of oxygen consumed per mole of pyruvate or acetate in presence of the inhibitors studied. The results of respiration studies at pH 4.1, 5.1 and 6.0 are shown in Table 2,

which gives the concentrations of benzoic and salicylic acids required for 50 % inhibition of the rates of pyruvate and acetate oxidation. The results can be summarized in the following way:

1. Irrespective of the experimental pH-values, the same concentration of undissociated inhibitor is required for a certain effect.

2. The oxidation of pyruvate and glucose (not shown here for the latter substance) is more sensitive, especially to benzoic acid, than the oxidation of acetate. This is contrary to the results obtained in experiments with *P. vulgaris* and *E. coli* previously reported.

3. There is good agreement between inhibition of acetate oxidation and growth with both benzoic and salicylic acids. The concentrations necessary for complete suppression of acetate oxidation is approximately twice those required for 50 % inhibition and thus closely corresponding to those preventing growth at pH 6.0 and 5.1. At pH 4.1 no growth occurred, not even in the absence of inhibitor.

During this investigation it was noticed that salicylic acid significantly stimulated the endogenous respiration of the yeast cells. The appearance of such an effect generally indicates that the stimulating substance affects the energy conservation process in the cells. Since interference with this process and inhibition of acetate oxidation previously in this work have been placed in relation to each other, the increase in endogenous respiration in the presence of salicylic acid was determined at pH 4.1, 5.1, and 6.0. The result of this study is shown in Fig. 6 A, B, and C. Maximal increase in the rate of endogenous oxygen consumption occurred at 0.55, 6.1 and 43 mM salicylic acid at the three pH-values investigated. These figures correspond to a constant value of undissociated salicylic acid in the three experiments, as calculated in Table 2.

No similar stimulation of endogenous respiration was caused by benzoic acid.

DISCUSSION

The role of pyruvate as a key intermediate in the metabolism of microorganisms has been recognized and studied for a long time. Special attention has been paid to the mechanism by which it is converted to acetyl-CoA, a metabolically active compound, which can be used by the cell as a building stone in the synthesis of cell material or as an energy source. The latter function is fulfilled by its oxidation to CO_2 and H_2O through the TCA cycle. This cycle is now accepted as the chief pathway of terminal respiration in most aerobic organisms. The oxidative decarboxylation of pyruvate may, however, occur by other pathways without the intermediate formation of acetyl-CoA, *e.g.* the direct formation of free acetate from pyruvate by the pyruvate oxidase system in *P. vulgaris*.

The presence of benzoic and salicylic acids during pyruvate oxidation by resting cells of *P. vulgaris* leads to an accumulation of large amounts of acetate in the medium as previously [1] reported. These results were tentatively explained by assuming that some step in the pathway leading from pyruvate to acetyl-CoA was inhibited, while the acetate producing pyruvate oxidase system

was insensitive to the inhibitors investigated. This interpretation was supported by further experiments [2] with *P. vulgaris* grown under different conditions.

The results reported in this work are principally concerned with the effect of benzoic and salicylic acids on pyruvate and acetate metabolism in *Escherichia coli*, *Pseudomonas fluorescens* and baker's yeast. The similarity of the pyruvate metabolism in *P. vulgaris* and *E. coli* was pointed out by Razzell and Gunsalus [4]. They reported that extracts from *E. coli* yield one particulate and one soluble fraction, which combine to generate acetate from pyruvate with oxygen consumption. The two fractions are mutually replaceable with analogous fractions obtained from *P. vulgaris*. Likewise, *P. vulgaris* was shown to possess an acetyl-CoA generating system apparently identical with that in *E. coli*. It is consistent with these findings that benzoic and salicylic acids affect pyruvate oxidation by these two organisms in the same way.

The terminal respiration of *Ps. fluorescens* and baker's yeast has been studied extensively, and no oxidase system analogous to that present in *P. vulgaris* and *E. coli* producing acetate directly from pyruvate has been reported. This may explain the absence of a specific inhibiting effect of benzoic and salicylic acids on the acetate level during pyruvate oxidation by *Ps. fluorescens* and baker's yeast (Fig. 5).

Irrespective of the inhibition pattern, however, the terminal respiration of all the organisms investigated is inhibited by benzoic and salicylic acids at concentrations which suppress the growth rate in a medium containing glucose and amino acids. The close correspondence between these effects is especially apparent in the experiments with baker's yeast (Table 2).

Previously in this work results have been reported indicating that under certain conditions benzoic and salicylic acids may increase both the rate and the extent of substrate breakdown. In particular it was shown in experiments with acetate grown cells of *P. vulgaris* that the assimilation of acetate was more sensitive to benzoic acid than its oxidation. This finding is confirmed by the respiration studies with acetate grown cells of *Ps. fluorescens* reported in this paper (Fig. 3). It is evident that benzoic acid may cause a complete oxidation of acetate to CO_2 and H_2O and thereby prevent utilization of this substance in synthesis of cell material. The effect of benzoic acid in these experiments is quite analogous to that obtained by Clifton [6] in his early investigation of the prevention of acetate assimilation in *Pseudomonas calcoacetica* by 2,4-dinitrophenol, sodium azide and iodoacetate. The two first mentioned substances are now well known as specific inhibitors of oxidative phosphorylation.

It is evident that benzoic and salicylic acids may inhibit both respiration and assimilation at concentrations affecting growth. Inhibition of terminal respiration may well be the primary cause of the growth inhibiting effect in a medium containing large amounts of readily utilized substrates such as glucose and amino acids. Both inhibitors are, however, more effective in a poor medium and it is possible that interference with the synthesis of cell material is a more important factor in this case. This question is now under investigation.

This work is part of an investigation supported by the *Swedish Natural Science Research Council* and the *Swedish Technical Research Council*.

REFERENCES

1. Bosund, I. *Acta Chem. Scand.* **13** (1959) 803.
2. Bosund, I. *Acta Chem. Scand.* **14** (1960) 111.
3. Moyed, H. S. and O'Kane, D. J. *J. Biol. Chem.* **218** (1956) 831.
4. Razzell, W. E. and Gunsalus, I. C. *Bacteriol. Proc.* **1954** 97.
5. Stanier, R. Y. *J. Bacteriol.* **54** (1947) 339.
6. Clifton, C. E. *Enzymologia* **4** (1937) 246.

Received March 9, 1960.

ACTA CHEMICA SCANDINAVICA 14 (1960) 1243—1252

The Bacteriostatic Action of Benzoic and Salicylic Acids

IV. The Effect on Oxidation of TCA Cycle Intermediates, Lactate and Gluconate

INGMAR BOSUND

State Dairy Research Station, Alnarp, Sweden

Resting cells of *Proteus vulgaris* oxidize succinate, fumarate, malate and oxalacetate at similar rates, whereas α-ketoglutarate is attacked more slowly. Exogenous citrate is not metabolized at pH 6.0 by resting cells.

The rate of oxidation of the dicarboxylic acids involved in the TCA cycle is inhibited to a varying extent by benzoic and salicylic acids according to the conditions prevailing during growth of the cells. The total amount of oxygen consumed per mole of substrate is mostly somewhat increased by the inhibitors studied.

The oxidation of lactate (in contrast to the oxidation of pyruvate) is not blocked at the acetate level by benzoic and salicylic acids.

Streptomycin, at concentrations arresting growth, does not affect the oxidation of pyruvate by resting cells of *P. vulgaris*.

Most of the experiments reported in this series have been concerned with the influence of benzoic and salicylic acids on the oxidation of glucose, pyruvate and acetate. Interest has been focused primarily on the effect of these inhibitors on the metabolism of the acetyl group, especially its entrance into the TCA cycle.

Conclusive proof of the occurrence of the TCA cycle in *Proteus vulgaris* has as yet not been produced, in contrast to what has been shown for the other organisms used in this work (*Escherichia coli*, *Pseudomonas fluorescens* and baker's yeast). From a general point of view, however, this metabolic cycle most likely occurs also in *P. vulgaris*. This is indicated by the fact that this organism can be adapted to growth on acetate as the sole carbon source and can oxidize acetate at least almost completely to CO_2 and H_2O.

The present investigation is concerned with the ability of resting cells of *P. vulgaris* to oxidize members of the TCA cycle and the effect of benzoic and salicylic acids on these oxidations. In addition, the effects of benzoic acid on pyruvate and lactate oxidation were compared in respiration studies with labelled substrates. Some experiments with streptomycin were included in these studies owing to certain similarities between the influence of this inhibitor and that of benzoic acid on resting cell metabolism.

EXPERIMENTAL

Organism. The same strain of *Proteus vulgaris* was used as before. The ability of this strain to grow in simple media, especially with acetate as the sole source of carbon, seems to have diminished somewhat in the course of this investigation. No change affecting the results obtained with the inhibitors studied has, however, occurred.

Medium and growth conditions. The cells were cultured at 35 – 37°C with aeration either with glucose as carbon source or with pyruvate and succinate. In the former case the cells were harvested in the stationary phase, in the latter case early in the logarithmic phase. The growth conditions have been described in detail previously [1].

Methods. The procedure adapted in the preparation of cell suspensions and in respiration measurements was essentially the same as previously outlined. In the studies with labelled substrates the respiratory CO_2, absorbed in KOH during the experiment, was precipitated as $BaCO_3$ after dilution with a known amount of K_2CO_3. The precipitate was washed and dried and the radioactivity determined in a Geiger-Müller counter after plating the carbonate on aluminium dishes. The total amount of radioactivity supplied to the cells was determined in the same way after conversion of an aliquot of the substrate into CO_2 by the wet decomposition method of van Slyke and Folch [2].

Reagents. All reagents used were commercial preparations. The pyruvic acid was redistilled before use. Samples of sodium pyruvate-2-^{14}C and sodium DL-lactate-2-^{14}C were supplied by The Radiochemical Centre, Amersham, England. Streptomycin was obtained as the sulfate from AB Kabi, Stockholm, Sweden.

RESULTS

The effect of benzoic and salicylic acids on the oxidation of TCA cycle intermediates. The capacity of washed *Proteus vulgaris* cells to oxidize citrate and the dicarboxylic acids of the TCA cycle is shown in Table 1. Somewhat lower Q_{O_2}-values were generally observed in experiments with cells pre-grown without aeration. In no case was citrate metabolized at the pH in question (6.0). The dicarboxylic acids were oxidized at nearly identical rates with the exception of α-ketoglutaric acid.

Table 1. Rate of oxygen consumption during oxidation of TCA cycle intermediates by washed cells of *P. vulgaris*.

Substrate	A *	B *
	μl oxygen consumed per mg dry wt. and hour	μl oxygen consumed per mg dry wt. and hour
Citrate	0	0
α-Ketoglutarate	20	20
Succinate	60	100
Fumarate	60	100
Malate	50	100
Oxalacetate	50	80

* A. Cells pre-grown in glucose-casein hydrolysate medium, aerated during growth and harvested in the stationary growth phase.
B. Cells pre-grown in pyruvate-succinate-casein hydrolysate medium, aerated during growth and harvested in the logarithmic growth phase.

Benzoic acid at concentrations lower than 8 mM did not appreciably suppress the oxidation of succinate, fumarate, malate or oxalacetate in experiments with resting cells grown as in B, Table 1. The degree of inhibition increased rapidly with increasing concentration of inhibitor and was total at 12—15 mM of benzoic acid. When the cells were cultured as in A, benzoic acid was somewhat more effective as an inhibitor. With both types of cells α-ketoglutarate oxidation was the most sensitive.

The dicarboxylic acids of the TCA cycle can easily be converted to pyruvate in most cells *via* oxidation to oxalacetate followed by decarboxylation of this substance. Such a transformation is, in fact, necessary if these acids are to be oxidized by way of the TCA cycle. Since the oxidation of pyruvate is blocked at the acetate level by benzoic and salicylic acids, these inhibitors might be expected to affect the oxidation of the TCA cycle intermediates in a corresponding way. This would imply that benzoic and salicylic acids would block the oxidation of succinate, fumarate, malate and oxalacetate at the acetate level, *e.g.* after consumption of 1.5, 1.0, 1.0 and 0.5 moles of oxygen per mole of substrate, respectively (Fig. 4). It was thus of considerable interest to investigate the effect of these inhibitors on the total amount of oxygen consumed per mole of acid. Fig. 1 shows an experiment with succinate, fumarate, malate and pyruvate. It is evident that benzoic acid did not affect the oxidation of the dicarboxylic acids in the predicted way. On the contrary, the amount of oxygen consumed was increased in the presence of benzoic acid. Similar results were obtained in experiments with cells pre-grown in glucose-casein hydrolysate medium and in studies with salicylic acid.

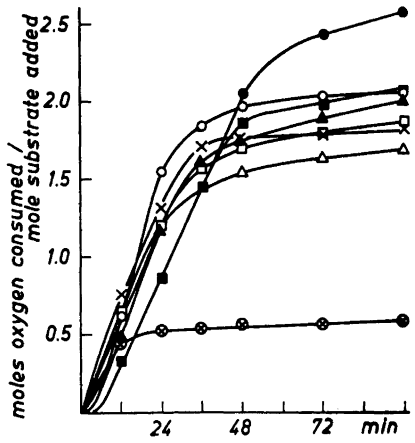

Fig. 1. Effect of benzoic acid on oxidation of succinate, fumarate, malate and pyruvate by washed *P. vulgaris* cells grown as in B, Table 1. Each vessel contained 4.5 mg dry wt. of cells and 133 μmoles of potassium phosphate. ×——× 5 μmoles of sodium pyruvate, ⊗——⊗ 5 μmoles of sodium pyruvate and 8 mM benzoic acid, O——O 5 μmoles of sodium succinate, ●——● 5 μmoles of sodium succinate and 8 mM benzoic acid, □——□ 5 μmoles of sodium fumarate, ■——■ 5 μmoles of sodium fumarate and 8 mM benzoic acid, △——△ 5 μmoles of sodium malate, ▲——▲ 5 μmoles of sodium malate and 8 mM benzoic acid. Temp. 37°C; pH 6.0; final volume 2.4 ml.

Table 2. Effect of benzoic acid on the total amount of oxygen consumed during oxidation of pyruvate and fumarate. The oxidation was carried out with washed cells of *P. vulgaris* pre-grown in glucose-casein hydrolysate medium, aerated during growth and harvested in the stationary phase. Each vessel contained 1/15 M phosphate buffer at pH 6.0 and substrate and inhibitor as shown. Gas phase air; temp. 30°C.

Substrate	Total amount of oxygen consumed, µl	
	without inhibitor	with 10 mM benzoic acid
5 µmoles of pyruvate	210	70
5 µmoles of fumarate	275	285
5 µmoles of pyruvate 5 µmoles of fumarate	455	365

These results seem to indicate that pyruvate formed within the cell during oxidation of TCA cycle intermediates is not freely interchangeable with pyruvate entering the cell from the external medium. Table 2 shows another experiment illustrating the same point. The figures recorded in this table show that the effect of benzoic acid on the total amount of oxygen consumed during oxidation of exogenous pyruvate persists even when an equal amount of fumarate is oxidized simultaneously. The amount of oxygen consumed per mole of fumarate was not influenced by benzoic acid in this experiment.

The influence of benzoic acid and streptomycin on the oxidation of pyruvate and lactate. In another series of experiments the effect of benzoic acid on pyruvate oxidation was compared with its effect on lactate oxidation. It is difficult to imagine any other way of oxidizing lactate in a living cell than *via* pyruvate; consequently, one would expect the lactate oxidation to be strongly inhibited by benzoic acid after consumption of 1.0 mole of oxygen per mole of lactate. But as shown in Fig. 2, no such blocking of the lactate oxidation at the acetate level seemed to occur. This result is supported by the experiments with pyruvate-2-^{14}C and lactate-2-^{14}C summarized in Tables 3 and 4. According to Table 3, benzoic acid almost completely inhibits the occurrence of the keto carbon atom of pyruvate in the respiratory CO_2. Table 4 indicates that the extent of oxidation of the corresponding atom in the lactate molecule to CO_2 is only slightly affected. It may be noted that the rate of lactate oxidation in the latter experiment was strongly inhibited by benzoic acid and that in the presence of 8 mM of the inhibitor the oxidation was stopped before the rate of oxygen consumption had decreased to the value of the endogenous respiration.

Some years ago Umbreit *et al.*[3,4] studied the influence of streptomycin on the oxidative metabolism of resting cells of *Escherichia coli* and observed effects somewhat resembling those obtained with benzoic acid in this work. They reported that under certain conditions streptomycin prevented pyruvate from entering the terminal respiration system and suggested that the inhibited reaction might be a "direct condensation" of oxalacetate and

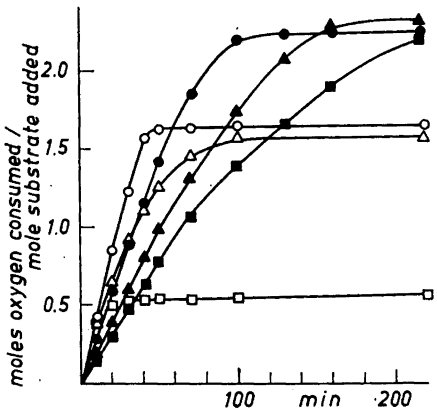

Fig. 2. Effect of benzoic acid on pyruvate and lactate oxidation by washed *P. vulgaris* cells grown as in B, Table 1. Each vessel contained 5.2 mg dry wt. of cells and 133 μmoles of potassium phosphate. O———O 7 μmoles of sodium pyruvate, △———△ 7 μmoles of sodium pyruvate and 4 mM benzoic acid, □———□ 7 μmoles of sodium pyruvate and 8 mM benzoic acid, ●———● 7 μmoles of sodium lactate, ▲———▲ 7 μmoles of sodium lactate and 4 mM benzoic acid, ■———■ 7 μmoles of sodium lactate and 8 mM benzoic acid. Temp. 37°C; pH 6.0; final volume 2.4 ml.

pyruvate to a 7-carbon intermediate. They did not exclude the possibility of formation of a transitory 2-carbon intermediate from pyruvate before the condensation with oxalacetate, but showed later [5] that formation of citrate was not influenced by streptomycin. Since the reaction

$$\text{pyruvate} + 0.5\ O_2 \rightarrow \text{free acetate}$$

Table 3. Effect of streptomycin and benzoic acid on the amount of $^{14}CO_2$ produced during oxidation of $CH_3{}^{14}COCOOH$. The oxidation was carried out with washed cells of *P. vulgaris* pre-grown in pyruvate-succinate-casein hydrolysate medium, aerated during growth and harvested in the logarithmic growth phase. Each vessel contained 1/15 M phosphate buffer, 7 μmoles of sodium pyruvate-2-^{14}C (with a total activity of 11 600 cpm.), 5.5 mg dry wt. of cells, and inhibitor as indicated. Gas phase air; pH 6.0; temp. 30°C.

Inhibitor	Mole O_2 / mole pyruvate	Mole CO_2 / mole pyruvate	*R.Q.*	Fraction of the amount of radioactivity supplied recovered in respiratory CO_2	Fraction of the amount of substrate carbon recovered in respiratory CO_2
—	1.37	1.70	1.24	0.41	0.57
Streptomycin 8 mg/ml	1.36	1.84	1.35	0.40	0.61
Benzoate, 8 mM	0.56	1.02	1.82	0.08	0.34

Table 4. Effect of benzoic acid on the amount of $^{14}CO_2$ produced during oxidation of $CH_3{}^{14}CHOHCOOH$. The oxidation was carried out with washed cells of *P. vulgaris* pre-grown in pyruvate-succinate-casein hydrolysate medium, aerated during growth and harvested in the logarithmic growth phase. Each vessel contained 1/15 M phosphate buffer, 7 μmoles of sodium DL-lactate-2-^{14}C (with a total activity of 12 100 cpm.), 5.5 mg dry wt. of cells, and inhibitor as indicated. Gas phase air; pH 6.0; temp. 30°C.

Inhibitor	$\frac{\text{Mole } O_2}{\text{mole lactate}}$	$\frac{\text{Mole } CO_2}{\text{mole lactate}}$	*R.Q.*	Fraction of the amount of radio-activity supplied recovered in res-piratory CO_2	Fraction of the amount of substrate carbon recovered in respiratory CO_2
—	2.05	2.04	0.99	0.66	0.68
Benzoate, 5 mM	1.83	1.80	0.99	0.56	0.60
Benzoate, 8 mM	1.45	1.40	0.97	0.39	0.47

as well as the subsequent oxidation of acetate seemed to be completely insensitive to streptomycin, the effect of this inhibitor was demonstrable only on cells with a very low capacity to oxidize acetate. In the work of Umbreit *et al.* such cells were obtained by growing the culture in a rich medium without aeration and keeping the washed cells at refrigerator temperatures for some days before the experiments.

According to this study, the effect of streptomycin on the pyruvate oxidation by *P. vulgaris* cells pre-grown with heavy aeration, as in this investigation, should be very small, if any, since the first rapid step in the pyruvate oxidation by such cells is apparently the formation of free acetate from pyruvate. Nevertheless it was of interest to compare the effects of benzoic acid and streptomycin on cells aerated during growth. The data from such an experiment are given in Table 3. It is evident that streptomycin had no influence on the oxidation of pyruvate even in a final concentration of 8 000 μg/ml. The effect was not enhanced by incubation of the cells with streptomycin for one hour before addition of pyruvate. Oxidation of lactate was equally insensitive to streptomycin as was pyruvate oxidation by resting cells grown with acetate as the sole carbon source (resting cells pre-grown in this way apparently [6] have very little tendency to form free acetate during pyruvate oxidation). It may be argued that the experimental pH (6.0) was too low to produce a pronounced streptomycin effect, but growth experiments showed that the strain of *P. vulgaris* used was sensitive to streptomycin at a concentration of 25 μg/ml at this pH.

The effect of benzoic and salicylic acids on the oxidation of gluconate. In recent years it has become increasingly evident that many microorganisms in addition to dissimilating glucose *via* the classical scheme of Embden-Meyerhof may utilize another enzymatic mechanism. This pathway, usually called the hexosemonophosphate pathway, starts with glucose-6-phosphate, which *via* 6-phospho-gluconate is transformed to pentose phosphate in two oxidative

steps (the second accompanied by decarboxylation). From this intermediate glucose-6-phosphate can be regenerated through a series of anaerobic reactions. Consequently glucose can be oxidized completely to CO_2 and H_2O by this pathway without the participation of the TCA cycle.

Since benzoic and salicylic acids block glucose oxidation at the acetate level by inhibiting the function of the TCA cycle, it was considered of interest to investigate the effect of these inhibitors on the oxidation of some intermediate in the hexosemonophosphate pathway. As phosphorylated substances do not readily penetrate the cell membrane of intact cells, these experiments were performed with gluconate. Preliminary studies showed that washed cells of *P. vulgaris* pre-grown in glucose-casein hydrolysate medium and harvested in the logarithmic growth phase oxidized glucose and gluconate at approximately the same rate but in the case of gluconate only after an initial lag phase. The total amount of oxygen consumed per mole of gluconate was generally about 3.5 moles. As is shown in Fig. 3, salicylate inhibited the rate of gluconate oxidation rather strongly, whereas the rate of glucose oxidation was as usual considerably increased at these salicylate concentrations. No clear effect was observed on the oxygen consumption per mole of gluconate. Corresponding results were obtained with benzoic acid.

DISCUSSION

As mentioned above, there is no reason to question the occurrence of the TCA cycle in cells of *Proteus vulgaris* even if, as shown here, citrate (and presumably also the other tricarboxylic acids of the cycle) is oxidized at a

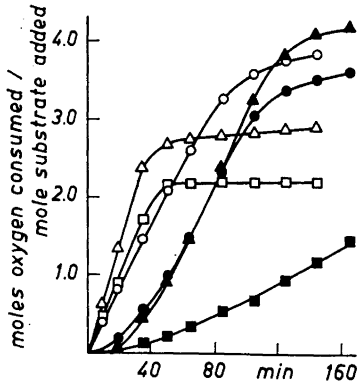

Fig. 3. Effect of salicylic acid on oxidation of glucose and gluconate by washed *P. vulgaris* cells grown in glucose-casein hydrolysate medium, aerated during growth and harvested in the logarithmic growth phase. Each vessel contained 1.6 mg dry wt. of cells and 133 μmoles of potassium phosphate. ○———○ 2.5 μmoles of glucose, △———△ 2.5 μmoles of glucose and 0.75 mM salicylic acid, □———□ 2.5 μmoles of glucose and 3.00 mM salicylic acid, ●———● 2.5 μmoles of sodium gluconate ▲———▲ 2,5 μmoles of sodium gluconate and 0.75 mM salicylic acid, ■———■ 2.5 μmoles of sodium gluconate and 3.00 mM salicylic acid. Temp. 37°C; pH 6.0; final volume 2.4 ml.

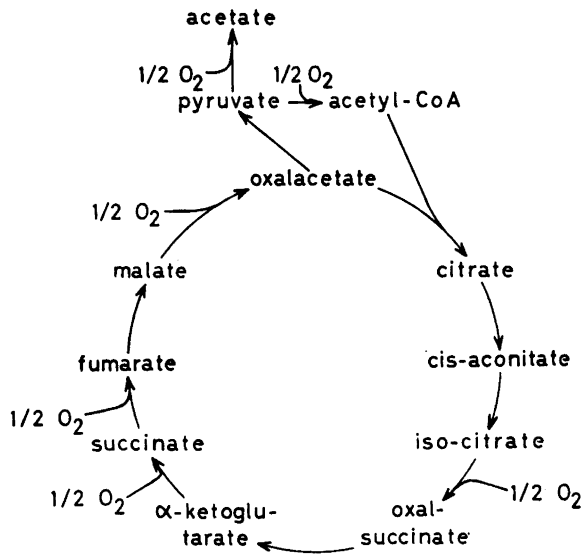

Fig. 4. Oxidative steps in the TCA cycle.

very low rate or not at all when added to suspensions of intact cells. This failure to attack intermediates of the cycle is certainly, as in analogous cases, due to impermeability of the cell membrane.

It was also pointed out that in order to oxidize TCA cycle intermediates beyond the oxalacetate stage, the cell must decarboxylate the oxalacetate to pyruvate (Fig. 4). The further metabolism of this pyruvate is, however, obviously not blocked at the acetate level by benzoic or salicylic acid, since the amount of oxygen consumed during oxidation of TCA cycle intermediates is increased by these inhibitors (Fig. 1). The reason may be that pyruvate formed from oxalacetate does not come into contact with the acetate producing pyruvate oxidase occurring in *P. vulgaris*. Anyhow, the results given in Fig. 1, Fig. 3 and Table 2 suggest that pyruvate originating from TCA cycle intermediates is not freely interchangeable with exogenous pyruvate or pyruvate formed from glucose. Such an interpretation is supported by the general conception that the TCA cycle enzymes, functioning more or less as a unit, are held together by some rigid structure, while the soluble glycolytic enzymes are spread throughout the cell protoplasm. It is a matter of controversy what the rigid structure might be like in a bacterial cell, which can obviously not contain anything as complex as the mitochondria of an animal cell. Evidence seems, however, to be accumulating [7,8] that the function of the TCA cycle in bacteria is closely associated with the cell membrane.

The difference in the action of benzoic acid on pyruvate and lactate oxidation (Fig. 2) is more difficult to interpret. It is possible, however, that better knowledge of the localisation in the cell of the enzymes involved might result

in the same line of reasoning as that set forth above. It may be significant that Mitchell and Moyle [8] reported that 80—95 % of the lactic dehydrogenase in *Staphylococcus aureus* is associated with the cell membrane. Similar results were obtained by Storck and Wachsman [9] in experiments with *Bacillus megaterium*. They showed after carefully controlled disintegration of the cells that the enzymes responsible for lactate oxidation were associated with the cell membrane fraction, while the enzymes responsible for pyruvate and glucose oxidation were localized in the supernatant.

Whatever hypothesis is put forward to account for the experimental data, it is evident that the oxidation of acetate is inhibited more than the oxidation of TCA cycle intermediates by benzoic and salicylic acids. This points to the activation of the acetate molecule as the primary site of action. Among the dicarboxylic acids of the TCA cycle the oxidation of α-ketoglutarate seems to be most sensitive to benzoic acid which agrees with results obtained by Kaplan, Kennedy and Davis [10] in experiments with rat tissue homogenates. It may be significant that the first step of this oxidation is CoA-dependent and the same type of reaction as the transformation of pyruvate to acetyl-CoA. The possibility that benzoic acid (and various other carboxylic acids) affects fatty acid metabolism in liver cells by interfering with the function of CoA has been suggested and investigated by Avigan, Quastel and Scholefield [11]. Their results show that various reactions of acetyl-CoA are specifically inhibited by acyl-CoA compounds such as benzoyl-CoA. The effects were not due to simple removal of free CoA. It is possible but still doubtful whether a similar interference occurs in bacterial cells.

The experiment illustrated in Table 3 shows that streptomycin, at concentrations far exceeding those necessary for inhibition of growth, has no influence on pyruvate oxidation by resting cells of *P. vulgaris* grown in the way described. In this respect, the effects of streptomycin and benzoic acid are clearly different. It is nevertheless true that under certain conditions both inhibitors prevent pyruvate from entering the terminal respiration system and that this effect may be closely associated with the inhibition of growth. As a matter of fact there seems to be other similarities in the action of streptomycin and benzoic and salicylic acids. In 1951 Bernheim and DeTurk [12] reported that streptomycin, benzoic acid and several members of the hydroxy benzoic acid series specifically inhibit the assimilation of ammonia during succinate oxidation by *Pseudomonas aeruginosa*. Fitzgerald and Bernheim [13] have presented data showing that streptomycin inhibits the formation of adaptive enzymes. Results indicating a similar effect by benzoic and salicylic acids have been obtained in this work and will be presented in a future paper. These effects may, of course, be secondary and due to an interference with the formation of high energy compounds, which is very probable in the case of salicylic acid. It may also be mentioned that both salicylic acid [14] and streptomycin [15] have been reported specifically to inhibit the synthesis of pantothenate.

The real significance of these apparent similarities can be made evident only by further research, and it is certainly true that, especially in the case of streptomycin, many facts not mentioned here have to be considered.

Acknowledgements. This work is part of an investigation supported by the *Swedish Natural Science Research Council* and the *Swedish Technical Research Council.*

REFERENCES

1. Bosund, I. *Acta Chem. Scand.* **14** (1960) 1231.
2. van Slyke, D. D. and Folch, J. *J. Biol. Chem.* **136** (1940) 509.
3. Umbreit, W. W. *J. Biol. Chem.* **177** (1949) 703.
4. Oginsky, E. L., Smith, P. H. and Umbreit, W. W. *J. Bacteriol.* **58** (1949) 747.
5. Umbreit, W. W., Smith, P. H. and Oginsky, E. L. *J. Bacteriol.* **61** (1951) 595.
6. Bosund, I. *Acta Chem. Scand.* **14** (1960) 111.
7. Weibull, C. and Bergström, L. *Biochim. et Biophys. Acta* **30** (1958) 340.
8. Mitchell, P. and Moyle, J. *Biochem. J.* **64** (1956) 19P.
9. Storck, R. and Wachsman, J. T. *J. Bacteriol.* **73** (1957) 784.
10. Kaplan, E. H., Kennedy, J. and Davis, J. *Arch. Biochem. Biophys.* **51** (1954) 47.
11. Avigan, J., Quastel, J. H. and Scholefield, P. G. *Biochem. J.* **60** (1955) 329.
12. Bernheim, F. and DeTurk, W. E. *J. Pharmacol. Exptl. Therap.* **103** (1951) 107.
13. Fitzgerald, R. J. and Bernheim, F. *J. Bacteriol.* **55** (1948) 765.
14. Ivanovics, G. *Z. Physiol. Chem. Hoppe-Seyler's* **276** (1942) 33.
15. Lichstein, H. C. and Gilfillan, R. F. *Proc. Soc. Exptl. Biol. Med.* **77** (1951) 459.

Received May 18, 1960.

ACTA CHEMICA SCANDINAVICA 14 (1960) 1253—1260

Pyridine-N-Oxide-Aldoximes

Their Synthesis, and Chemical and Biochemical Properties

KLAS-BERTIL AUGUSTINSSON, HANS HASSELQUIST and LENNART LARSSON

Institute of Organic Chemistry and Biochemistry, University of Stockholm and Research Institute of National Defence, Department 1, Sundbyberg 4, Sweden

The three isomers of pyridine-N-oxide-aldoximes were synthesised and their properties described, including infrared spectra and dissociation constants. The new aldoximes were incapable of reactivating cholinesterases inhibited by tetraethyl pyrophosphate both *in vitro* and *in vivo*.

Successful treatment by certain oximes of poisoning caused by organophosphorus compounds has recently been reported; especially active are pyridine-2-aldoxime-N-methyl iodide (PAM) and its methane sulphonate analogue (P2S)[1]. The present report describes the synthesis and some chemical and biochemical properties of the corresponding pyridine-N-oxide-2-aldoxime and its two isomers (3- and 4-aldoxime).

EXPERIMENTAL

The N-oxides of pyridine-aldoximes were prepared by a general method described previously by Ochiai[2]. Hydrogen peroxide (30 %) is allowed to act upon the pyridine derivative (Schuchardt, Germany) in glacial acetic acid solution at 70—80°C.

Pyridine-N-oxide-2-aldoxime (*POA 2*). To 2 g (16.4 mmole) of pyridine-2-aldoxime, dissolved in 10 ml of glacial acetic acid, was added 2 ml of hydrogen peroxide (30 %). The mixture was heated for 3 h at 80°C. After cooling 40 ml of ethyl acetate was added to the reaction mixture, resulting in the precipitation of the reaction product. The product was collected by filtration after one hour in the refrigerator, and washed with ethyl acetate. Crude product, 0.5 g. A further 0.4 g of crystallized product was obtained from the filtrate after keeping for 48 h in the refrigerator.

The two fractions of crystals were combined and dissolved in a small amount of boiling water, active charcoal was added, and the mixture filtered while still boiling. The pyridine-N-oxide-2-aldoxime crystallized upon cooling. Recrystallization from water gave 0.78 g (34 % yield) of the pure compound as colourless needles; m.p. 221—222°C with slow decomposition and brown-red colourization. Analysis, see Table 1. This aldoxime was synthesised recently by Jerchel and Heider[3] using another method.

The ethyl acetate solution from which the N-oxide aldoxime was isolated was evaporated to dryness under vacuum, leaving a dark-yellow oil, which dissolved on heating in 10 ml of water to give a clear solution. Upon cooling, a colourless substance crystallized out, which was identified as the original pyridine-2-aldoxime (m.p. 111—113°C). Solid sodium carbonate was added to the filtrate to pH 6.5. After 24 h in the refrigerator another portion of pyridine-2-aldoxime was obtained. Altogether 0.85 g of unreacted aldoxime was isolated in this way.

When a longer reaction period or a greater amount of hydrogen peroxide, was employed, approximately the same amount of N-oxide aldoxime was obtained. The remaining solution contained, however, approximately 1 g of picolinic acid (m.p. 138—139°C with rapid decomposition). The latter procedure was therefore not to be preferred because of difficulties in separating the acid from the oxime.

Pyridine-N-oxide-3-aldoxime (*POA 3*). Pyridine-3-aldoxime, 2 g (16.4 mmole), was dissolved in 20 ml of glacial acetic acid, 6 ml of 30 % hydrogen peroxide was added, and the mixture incubated at 35°C for 48 h.; the same yield was obtained on keeping the mixture for ten days at room temperature. Evaporation under vacuum gave a sticky crystalline product, which was dissolved in 10 ml of absolute ethanol with heating. After cooling at room temperature long, light yellow rods crystallized out; m.p. 212—213°C with decomposition. Recrystallization twice from absolute ethanol gave pure pyridine-N-oxide-3-aldoxime; m.p. 217—218°C. Yield, 1.06 g (46 %).

The ethanol filtrate, from which the reaction product was isolated, was evaporated under vacuum to approximately 3 ml. The remaining yellow oil was stirred, and acetone added until no further precipitation occurred. The collected precipitate was washed with acetone and dried, treated with 25 ml of hot *iso*propanol, and the solution filtered hot; the undissolved matter was then washed afterwards with boiling *iso*propanol. The crystallized product was recrystallized twice from small amounts of water; m.p. 256—257°C. Yield, 0.4 g. The product was identified as nicotinic acid-N-oxide with the same m.p.[4]

Pyridine-N-oxide-4-aldoxime (*POA 4*). Pyridine-4-aldoxime, 2 g (16.4 mmole), dissolved in 10 ml of glacial acetic acid, was treated with 2 ml of hydrogen peroxide (30 %) for 48 h at 35°C. The reaction solution was diluted with 10 ml of water and evaporated under vacuum until crystallization began. The crystalline product was dissolved in 10 ml of methanol by gentle heating, and was then left for crystallization. The yellow prisms were recrystallized twice from methanol. The pyridine-N-oxide-4-aldoxime was obtained as colourless prisms, m.p. 228—229°C; yield 720 mg.

The filtrate was evaporated under vacuum to a yellow oil, which was not possible to crystallize from methanol. The oil, probably consisting of the acetate of the reaction product, was dissolved in 5 ml of water and treated with solid sodium carbonate to pH 6.5, when crystals, a mixture of starting material and the N-oxide were formed. The whole mixture was shaken three times with ethyl acetate. The aqueous phase was left for 24 h at room temperature, the precipitated crystals were collected, washed with a small amount of water and recrystallized from methanol. The product was identified as pyridine-N-oxide-4-aldoxime; yield 400 mg. The total yield was 1.12 g (50 %).

From the ethyl acetate filtrate, 0.35 g of unreacted pyridine-4-aldoxime (m.p. 132—133°C) was isolated. No formation of carboxylic acid was observed.

Infra-red spectrophotometric measurements. The infra-red spectra were recorded on a Perkin-Elmer spectrophotometer, Model 21, equipped with a rock-salt prism, and the following settings were used: resolution 927; response 2:1 170; gain 5.9; suppressions 3; speed about 1 μ/min; scale 5 cm/μ. The potassium bromide technique was employed, and 1 mg of sample was ground mechanically with 300 mg of this salt.

Determination of dissociation constants. The dissociation constants of the three aldoximes were determined at 25°C with an automatic recording titrator as described previously by Larsson and Hansen[5]. The compounds were dissolved in 0.100 M potassium chloride solution and the concentration of the compounds was approximately 5.0 mM. Titration was performed with 0.0991 M sodium hydroxide. The pH-meter was standardized against 0.05 M potassium hydrogen *o*-phthalate (pH = 4.01) and 0.01 M borax (pH = 9.18).

Cholinesterase determinations were performed by the Warburg technique at 25°C with acetylcholine chloride (20 mM) as substrate[6]. Purified cholinesterase preparations from human plasma (butyrocholinesterase, BuChE) and *Torpedo* electric organ (acetyl-

cholinesterase, AChE) were employed, and esterase activity was expressed in b_{30}, *i.e.* μl CO_2 evolved in 30 min from a bicarbonate-CO_2 buffer solution (pH 7.4), corrections being made for spontaneous hydrolysis of acetylcholine.

Reactivation experiments. Tetraethyl pyrophosphate (TEPP) was used as »irreversible» cholinesterase inhibitor and appropriate aqueous solutions of it were prepared immediately before use. The enzyme solutions (in bicarbonate buffer, unless otherwise stated) were incubated with the inhibitor for 45 min in the main compartment of the flask; total volume of the incubation mixture, 1.2 ml. The aldoxime (0.4 ml of an aqueous solution) was then added from one of the ampoules, and after various reaction periods (15 to 60 min) the substrate (0.4 ml of a bicarbonate solution) was added to the mixture from the second ampoule. When other techniques were used, this is stated in the legend to the tables.

Pyridine-2-aldoxime-N-methyl methane sulphonate (P2S), known to be a good reactivator of cholinesterases [1], was used as a reference compound.

RESULTS AND DISCUSSION

Properties of the aldoximes. The 2- and 3-aldoximes were readily soluble in water; the 4-aldoxime was less so, but upon heating it dissolved rapidly. All three compounds dissolved readily in boiling methanol, and were sparingly soluble in benzene, acetone and ethyl acetate. Positive oxime reaction according to Feigl and Demant [7] was given by all three aldoximes. The analytical data for the compounds synthesised are listed in Table 1.

Infra-red spectra. The following group frequency assignements can be made from the infra-red spectra (Fig. 1):

The 3 000 cm^{-1} region. The three absorption bands at 3 175—2 958 cm^{-1} can be assigned to CH stretchning frequencies [8], and the unresolved bands at 2 874—2 597 cm^{-1} can probably be ascribed to associated OH stretching frequencies.

The 1 650—1 400 cm^{-1} region. The C=N stretching of the oxime group is expected to occur at about 1 650 cm^{-1}, and the weak absorption band at 1 650—1 639 mc^{-1} has thus been attributed to this group [9]. The remaining five bands in this region may be ascribed to vibrations of the pyridine nucleus [8,10,11]. The origin of the absorption band at 1 508—1 504 cm^{-1} is, however, ambiguous.

The 1 325—1 290 cm^{-1} region. The two absorption bands appearing in this region may be possibly be assigned to the OH bending frequencies [9].

Table 1. Analytical data and thermodynamic dissociation constants of pyridine-N-oxide-X-aldoximes ($C_6H_6N_2O_2$; M = 138.1) and dissociation constants of the corresponding N-methyl-derivatives [13].

X	% C		% H		% N		pK_a	
	Calc.	Found	Calc.	Found	Calc.	Found	N-oxides	N-methyl deriv.
2	52.2	52.0	4.4	4.2	20.3	19.7	9.23	7.82
3	52.2	52.2	4.4	4.3	20.3	19.5	9.68	9.10
4	52.2	52.3	4.4	4.5	20.3	20.1	9.57	8.23

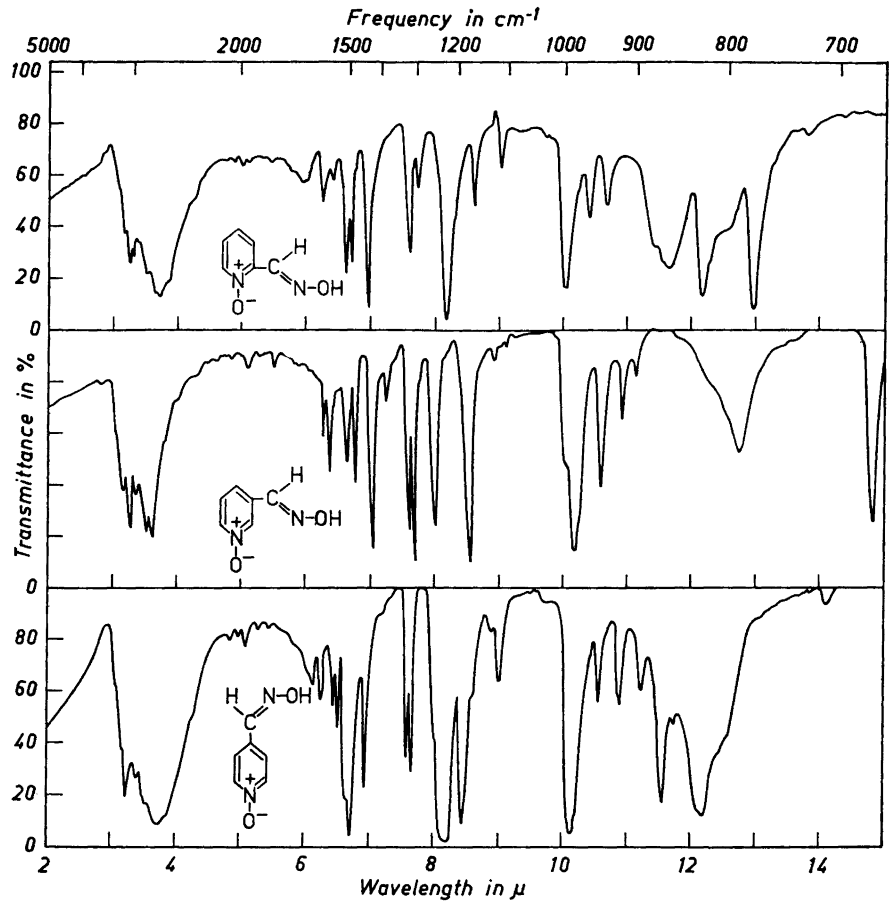

Fig. 1. The infra-red spectra of pyridine-N-oxide-aldoximes.

The 1 255—1 220 cm^{-1} region. The very strong absorption band occurring in this region has been attributed to the $N^+—O^-$ stretching frequency [10,11].

The 1 185—975 cm^{-1} region. The two absorption bands at 1 185—1 159 cm^{-1} and 1 119—1 105 cm^{-1} have been interpreted as CH deformation bands [10,11]. The strong and broad absorption at 996—978 cm^{-1} has been given the same assignment [10,11], but it is probably overlapped by a band caused by stretching of the N-OH linkage [9,12].

The infra-red data obtained are thus in agreement with structures proposed from the synthesis of the compounds, and they indicate that the compounds exist as N-oxides (I) and not in the tautomeric form (II).

An impurity which can be expected to be present in the samples is the carboxylic acid corresponding to the oxime. Owing to the weak overtone

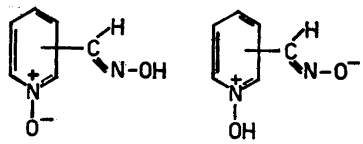

I II

bands of the pyridine nucleus occurring in the region of the carbonyl absorption band (1 700 cm^{-1}) it is, however, not possible to decide from the spectra obtained whether traces of carboxylic acid may be present or not.

From the titration curves of the N-oxide of the pyridine aldoximes it was found that the deviation between the amount of titrand added to the equivalence point, and the amount calculated from the quantity weighed out in no case exceeded 1.1 %.

The thermodynamic dissociation constants of the compounds are given in Table 1, where the constants of the N-methyl pyridine-aldoximes [13] have also been included. A comparison between the constants of the two series shows that the substitution of an oxide group for a methyl group at the nitrogen atom causes an increase in the pK_a-value. Primarily, this increase may be ascribed to the reduction of the strong inductive effect of the positively charged nitrogen atom when the substituent is changed from methyl to oxygen. This increase is expected to be greatest in the 2-aldoxime and least in the 4-aldoxime. As appears from Table 1, the increase is especially pronounced in the 2- and 4-aldoximes which probably depends upon a mesomeric effect. The pyridine-4-aldoxime-N-methyl can be described as a resonance hybrid of structures III and IV, and the N-oxide as a hybrid of the analogous structures V and VI and moreover structure VII [14]. The large difference between the pK_a-value of the N-methyl-derivative and of the oxide indicates that the contribution of structure VII may more or less balance structure VI. This will thus serve as a partial explanation of the lower acidity, *i.e.* higher pK_a-value, of the pyridine-N-oxide-4-aldoxime. Analogous structures and arguments are valid for the 2-aldoxime but not for the 3-aldoxime.

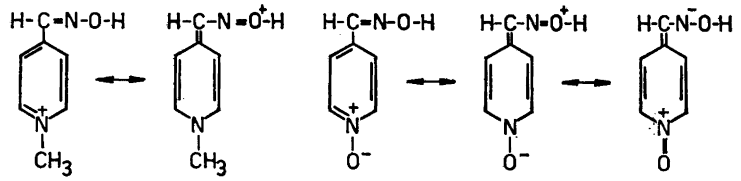

III IV V VI VII

On the presumption that the aldoxime group in the pyridine-N-oxide-2-aldoxime exists in the anti-form, the formation of a weak intramolecular hydrogen bond is conceivable, and such a bond would furthermore increase its pK_a-value. It is, however, not possible to decide from an infra-red spectrum

Table 2. Reactivation of cholinesterases inhibited by tetraethylpyrophosphate (TEPP). The solutions of esterase preparations (E) were incubated with the inhibitor (I) for 45 min before the addition of aldoxime (R). After various periods of time (»reactivation») the substrate (S) was added to the reaction mixture. BuChE, human serum butyrocholinesterase; AChE, electric organ acetylcholinesterase, P2S, pyridine-2-aldoxime-N-methyl methane sulphonate, 0.125 mM; POA 2, POA 3 and POA 4, pyridine-N-oxide-X-aldoximes, 1.25 mM (concentration values for the aldoximes are those during reactivation).

Incubation mixture	Reactivation min	P2S		POA 2		POA 3		POA 4	
		b_{30}	% inhib.	b_{30}	% inhib.	b_{30}	% inhib.	b_{30}	% inhib.
BuChE:									
E		133		135		138		138	
E + I		13	90	71	47	64	54	65	53
E + I + R	0	32	76	71	47	64	54	59	57
—»—	15	32	76	71	47	—	—	59	57
—»—	30	40	70	73	45	64	54	59	57
—»—	60	—	—	81	39	61	56	58	58
AChE:									
E		140		130		112		112	
E + I		34	76	34	74	26	77	26	77
E + I + R	0	139	0	39	70	24	79	25	78
—»—	15	137	2	29	78	19	83	19	83
—»—	30	141	0	23	82	15	87	—	—
—»—	60	137	2	17	87	12	89	11	92

recorded on a solid sample whether there is an intra- or intermolecular hydrogen bond.

Cholinesterase inhibition. None of the three pyridine-N-oxide-aldoximes in 10^{-3}M concentration inhibited acetyl- and butyrocholinesterase. Pyridine-2-aldoxime-N-methyl methane sulphonate, used in the same concentration, inhibited these esterases 12 and 17 % respectively.

Reactivation of cholinesterases inhibited by an organophosphorus compound. In 1.25×10^{-3}M concentration the three pyridine-N-oxide aldoximes were incapable of reactivating both butyro- and acetylcholinesterase inhibited by tetraethyl pyrophosphate (TEPP) (Table 2). For comparison, pyridine-2-aldoxime-N-methyl methane sulphonate used in ten times lower concentration (1.25×10^{-4} M) was tested in the same series of experiments. The results confirmed previous observations [1] that this derivative could reactivate phosphorylated cholinesterases, particularly acetylcholinesterase. It was observed that during incubation of the inhibited acetylcholinesterase with the pyridine-N-oxide-aldoximes, the activity of the partly inhibited esterase was reduced progressively with time. It was concluded that the phosphorylated aldoximes, formed during the incubation with the reaction mixture, containing phosphorylated esterase and unreacted TEPP, are more active esterase inhibitors than TEPP. This further decrease in enzyme activity was not due to TEPP alone, as could be demonstrated in control experiments.

Table 3. Reactivation of inhibited butyrocholinesterase by pyridine-N-oxide-2-aldoxime. Details as in Table 2, except for the concentration of the aldoxime which was seven times higher (8.75 mM). Reactivation period, 60 min.

Incubation mixture	Buffer soln. during incubation with TEPP and reactivations with POA 2			
	Bicarbonate, pH 7.4		Phosphate, pH 8.0	
	b_{30}	% inhib.	b_{30}	% inhib.
E	124		108	
E + I	0	100	0	100
E + I + R	30	75	40	63

It is reasonable to assume that in the reactivation of the phosphorylated enzyme the oximes react in their anionic forms [15]. Owing to the higher pK_a-values of the pyridine-N-oxide-aldoximes it might be expected that they are more nucleophilic and thus better reactivators than the N-methylderivatives, but the higher nucleophility is counteracted by the comparably lower concentration of the anions of the N-oxides at a fixed pH-value. One probable reason of the low reactivation power of the N-oxides may thus be that their pK_a-values are too high to give maximum reactivation at the pH-value in question [16]. According to these hypotheses, the N-oxide-aldoximes are expected to give better reactivation when the pH is increased. Preliminary experiments with pyridine-N-oxide-2-aldoxime used in higher concentration (8.75×10^{-3}M) and in a buffer solution of higher pH (8.0) revealed that butyrocholinesterase inhibited by TEPP could be partly reactivated under such experimental conditions (Table 3). A more decisive reason for the low reactivation power of the N-oxides compared with the N-methyl-derivatives is that the orientating effect of the positively charged nitrogen atom is cancelled by the adjacent, negatively charged oxygen atom [17,18].

Effect in vivo. The pyridine-N-oxide-aldoximes were less toxic ($LD_{50} >$ 200 mg/kg body weight, white mice, i.p.) than P2S. Mice injected intraperitoneally with 200 mg per kg body weight showed no toxic symptoms. Preliminary experiments *in vivo,* revealed that the new aldoximes were inactive in protecting mice from fatal intoxication with ω-dimethylaminoethylthio-*iso*propoxy-methyl-phosphine oxide [19].

Our thanks are due to Prof. Gustaf Ljunggren, Director of Research Institute of National Defence, Department 1, for the kind interest he has shown in this work, to Dr. Anders Sundwall for the toxicological tests, and to Mrs. Gunnel Jonsson for skilled technical assistance.

REFERENCES

1. Davies, D. R. and Green, A. L. *Brit. J. Ind. Med.* **16** (1959) 128.
2. Ochiai, E. *J. Org. Chem.* **18** (1953) 534.
3. Jerchel, D. and Heider, J. *Ann.* **613** (1958) 165.
4. Clemo, G. R. and Koenig, H. *J. Chem. Soc.* **1949** 231.

5. Larsson, L. and Hansen, B. *Svensk Kem. Tidskr.* **68** (1956) 521.
6. Augustinsson, K.-B. *Methods of Biochem. Anal.* **5** (1957) 1.
7. Feigl, F. and Demant, V. *Mikrochim. Acta* **1** (1937) 132.
8. Kline, C. H. and Turkevich, J. *J. Chem. Phys.* **12** (1944) 300.
9. Palm, A. and Werbin, H. *Can. J. Chem.* **31** (1953) 1004.
10. Katritzky, A. R. and Gardner, J. N. *J. Chem. Soc.* **1958** 2192.
11. Katritzky, A. R. and Hands, A. R. *J. Chem. Soc.* **1958** 2195.
12. Hadzi, D. *J. Chem. Soc.* **1956** 2725.
13. Green, A. L. and Saville, B. *J. Chem. Soc.* **1956** 3887.
14. Thomas, K. and Jerchel, D. *Angew. Chem.* **70** (1958) 719.
15. Davies, D. R. and Green, A. L. *Biochem. J.* **63** (1956) 529.
16. Steinberg, G. M., Swidler, R. and Seltzer, S. *Science* **125** (1957) 336.
17. Wilson, I. B. and Ginsburg, S. *Biochim. et Biophys. Acta* **18** (1955) 168.
18. Wilson, I. B. *Federation Proc.* **18** (1959) 752.
19. Tammelin, L.-E. *Acta Chem. Scand.* **11** (1957) 1340.

Received March 30, 1960.

ACTA CHEMICA SCANDINAVICA 14 (1960) 1261—1273

Periodate Oxidation of Phenols

V *. 2,4-Dimethylphenol

ERICH ADLER, LENNART JUNGHAHN, ULF LINDBERG, BRITT BERGGREN and GERTRUD WESTIN

Institutionen för organisk kemi, Chalmers Tekniska Högskola, Göteborg, Sweden

The action of sodium periodate on 2,4-dimethylphenol produces 2,4-dimethyl-*p*-quinol (II), 2,4-dimethyl-*o*-quinol (III) and 3,5-dimethyl-*o*-quinone (XII). However, of these products, only the *p*-quinol (II) remains unchanged and can be separated from the reaction mixture. The *o*-quinol (III) rapidly dimerises by a Diels-Alder addition to give a 1,4-ethenonaphthalene derivative (IV), and as well gives the yellow *o*-quinol-*o*-quinone adduct (XIII) by diene addition to the *o*-quinone (XII). This adduct can also be obtained as the colourless enol XIV.

Although sodium periodate reacts very slowly with unsubstituted phenol [1], it is rapidly consumed by a variety of alkyl-substituted phenols. In several cases, well-defined reaction products can be isolated **. The present paper deals with the action of periodate on 2,4-dimethylphenol (I).

Phenol I when treated in aqueous solution with excess periodate at room temperature consumed slightly more than 1 mole of the oxidant almost instantly; further oxidation after this proceeded very slowly. A methylene chloride extract obtained from the light-red reaction mixture after an oxidation period of a few minutes yielded a crude crystalline product (40 %), from which three substances (A, B, C) were separated.

Substance A, m.p. 73—74°, was obtained in a yield of about 2 %, based on phenol I, by briefly extracting the crude product with ether. It proved to be identical with 2,4-dimethyl-*p*-quinol (II), which has been described by Bamberger and Brady [2].

After removing II, the crude product was treated with dilute aqueous sodium hydroxide giving an alkali-insoluble, white residue (substance B) and a deep-yellow solution, which gave a third solid (substance C) on acidifica-

* Part IV: Adler, E., Magnusson, R. and Berggren, B. *Acta Chem. Scand.* **14** (1960) 539.
** Preliminary communication, see Ref. [16]

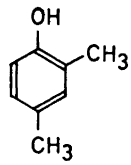

I

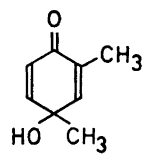

II

tion. These two products were both obtained in about 20 % yield based on phenol I.

Substance B. Analysis and the molecular weight of the alkali-insoluble substance, m.p. 237—238°, indicated the composition $C_{16}H_{20}O_4$, corresponding to a dimeric oxidation product of I with one extra atom of oxygen per molecule of I. The ultraviolet absorption of B (Fig. 1) showed that the aromatic structure of the starting material (I) had been lost. A strong absorption with a shoulder at 225 mμ (log ε, 3.88) ("K-band") and a weaker band at 307 mμ (log ε, 2.48) ("R-band") suggested the presence of an α,β-unsaturated carbonyl grouping. The position of the K-band indicated that the ethylenic bond of this chromophore carried only one substituent (Woodward rules [3], *cf.* also Fieser and Fieser [4]); in the present case this substituent would obviously be the ring carbon atom attached to the β-position of the enone grouping. The presence of the latter grouping was also shown by the infrared absorption spectrum (Fig. 2) which had a strong band at 1 680 cm^{-1} (conjugated CO) as well as a weaker absorption at 1 620 cm^{-1} (C = C conjugated with CO). A strong band at 1 720 cm^{-1} indicated the presence of an isolated carbonyl group, and the occurrence of strong absorption in the hydroxyl band region (3 400 cm^{-1}) and the presence of 2 active hydrogen atoms showed that the substance contained

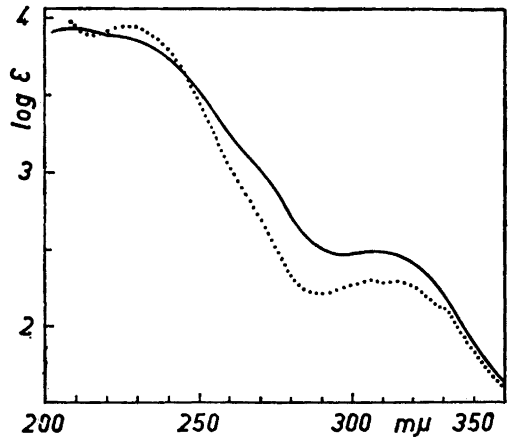

Fig. 1. Ultraviolet absorption spectra. Solvent, 95 % ethanol.
———— Dimeric 2,4-dimethyl-*o*-quinol (IV) (= Substance B)
..... Diacetate (IV, OAc instead of OH).

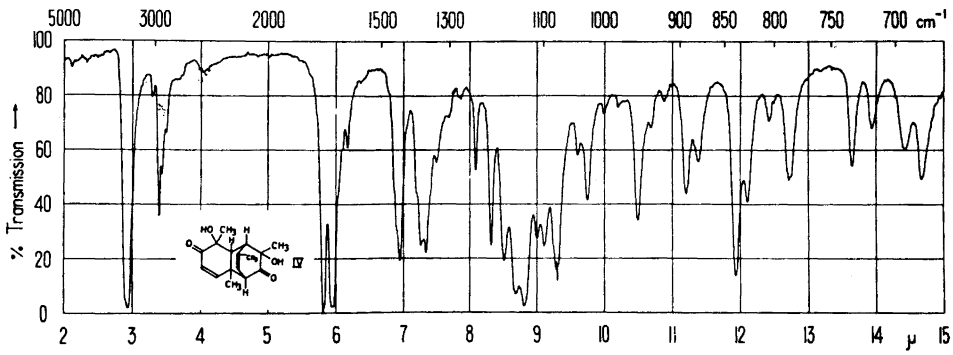

Fig. 2. Infrared spectrum of dimeric 2,4-dimethyl-*o*-quinol (IV) (= Substance B).

two (alcoholic) hydroxyl groups. Although remaining unchanged on refluxing with acetic anhydride-pyridine, substance B gave a diacetate, m.p. 182—184°, in moderate yield when heated with acetic anhydride and sodium acetate, and in good yield when perchloric acid was used as a catalyst. The ultraviolet absorption spectrum of the diacetate (Fig. 1) clearly exhibited the features of an α,β-unsaturated ketone (K-band, λ_{max} 226 mμ, log ε_{max} 3.95). Alkaline hydrolysis of the diacetate regenerated substance B.

The data reported above suggested that substance B was formed by oxidation of phenol I to a quinol, $C_8H_{10}O_2$, followed by dimerisation. Since the *p*-quinol II is stable in the monomeric form, the intermediate quinol undergoing dimerisation should be the 2,4-dimethyl-*o*-quinol III.

Several *o*-quinones have been found [5–10] to undergo dimerisation by diene addition. A similar diene reaction between two molecules of 2,4-dimethyl-*o*-quinol (III) could give rise to four isomeric dimers (IVa-c). Isomer IV would

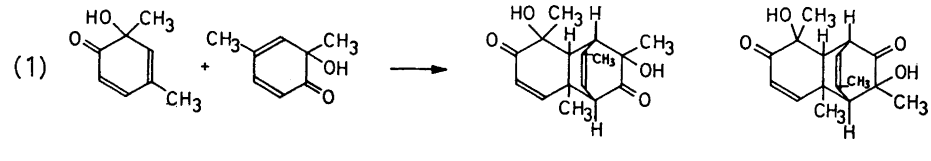

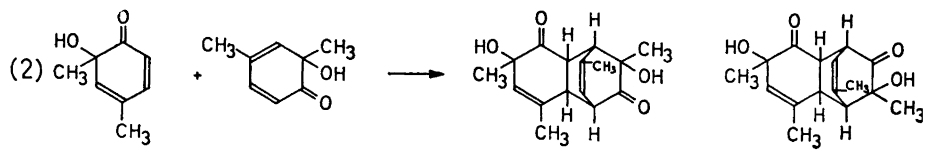

be formed as shown by Scheme (1), the molecule of III acting as a philodiene utilising the γ,δ-double bond of its conjugated carbonyl system. Isomer IVa could be formed in a similar way. The two remaining isomers, IVb and IVc, would be formed by addition of the α,β-ethylenic bond of the philodiene component to the diene system of the second molecule, as shown by Scheme (2). Structures IVb and IVc, however, can be excluded since they do not contain the α,β-unsaturated ketone grouping shown by the ultraviolet and infrared spectra of the substance. Consequently, the neutral dimer, m.p. 237—238° (substance B), could have structures IV or IVa, both of which are in harmony with the experimental data reported above.

No decision between structures IV and IVa has as yet been made, but some evidence in favour of IV is given by a comparison with similar dimeric dienones. Dimerisation by diene addition has recently been found by Metlesics and Wessely [11] in the case of 2-methyl-*o*-quinol acetate (V), obtained by oxidation of *o*-cresol with lead tetraacetate. Unlike 2,4-dimethyl-*o*-quinol (III), the *o*-quinol acetate V was stable in the monomeric state at room temperature; it dimerised, however, on heating to 120° [11]. Hot acid hydrolysis of the result-

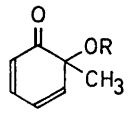

V : R = Ac
VI : R = H

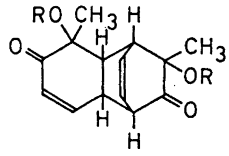

VII : R = Ac
VIII : R = H

ing dimeric *o*-quinol acetate (VII) gave the dimeric *o*-quinol VIII, which was also obtained on similar hydrolysis of V followed by spontaneous dimerisation of the expected monomeric *o*-quinol VI [11]. Metlesics and Wessely [11] have provided unambiguous proof of structure VIII by degrading the dimer to 1,7-dimethylnaphthalene. On the basis of these results, structure IV, which is analogous to VIII, would seem more probable than structure IV a.

Structure IV rather than the isomeric structure IVa would also be analogous to the structure for dimeric 2,6,6-trimethyl-2,4-*cyclo*hexadienone put forward by Brown, Curtin and Fraser [12]. The dimerisation of the latter dienone (and of some other cyclic 2,4-dienones reported in literature [13]) is a diene addition quite similar to that occurring with *o*-quinones and *o*-quinols and is subject to similar possibilities of isomerism. In the following, substance B will be assumed to have structure IV although structure IVa cannot be excluded.

The exclusive formation of only one of four possible dimers of the hypothetical *o*-quinol III is a further example of the frequently encountered selectivity of the Diels-Alder reaction. Reaction at the γ,δ-double bond rather than at the α,β-double bond of an $\alpha,\beta,\gamma,\delta$-unsaturated carbonyl system acting as a philodiene has been previously observed [14,15].

Assuming that the diene reaction of the *o*-quinol III follows the "*endo* rule", dimer IV could be given the following steric representation, which is analogous to those proposed by Brown, Curtin and Frazer [12] for dimeric 2,6,6-trimethyl*cyclo*hexadienone and by Metle-

sics and Wessely [11] for the dimeric *o*-quinol acetate VII; the configuration at the *tert.* carbinol groups is still unknown.

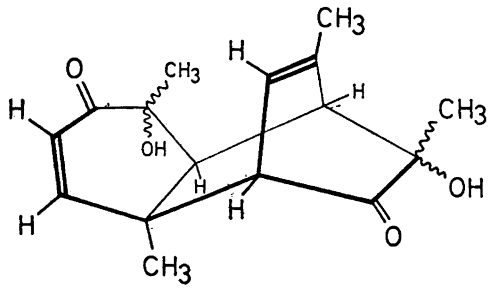

Examination of a Stuart-Briegleb model of IV indicated that the bi*cyclo*octene system present is fairly strained. This may possibly explain the occurrence of the absorption band at 210 mμ (log ε, 3.93) (see Fig. 1), which might be ascribed to the strained ethylenic bridge.

The formation of dimeric *o*-quinols similar to IV has been observed in this laboratory as a result of the periodate oxidation of other alkylated phenols, including 2,5- and 2,6-dimethylphenol, 2,4,6-trimethylphenol (mesitol) and thymol (preliminary communication, see Ref. [16]). In neither case could the expected monomeric *o*-quinol be isolated, since rapid dimerisation took place in the oxidation mixture. Wessely and co-workers [17,18] obtained 2,3-dimethyl-*o*-quinol and 2,3,5-trimethyl-*o*-quinol as monomers. Recently, periodate oxidation of 2,3,5-trimethylphenol was also found [19] to yield monomeric 2,3,5-trimethyl-*o*-quinol, which does not undergo dimerisation at room temperature. Several monomeric and dimeric *o*-benzoquinols carrying an acetonyl residue instead of an alkyl group at the carbinol C-atom of the quinol ring have been obtained in this laboratory by Magnusson [20].

The results of some hydrogenation experiments which were carried out with substance B were in harmony with the proposed structure (IV). Hydrogenation, in ethanolic solution, with a Pd-catalyst gave a dihydro derivative, m.p. 194—5°. It contained two isolated carbonyl groups (infrared absorption bands at 1 723 and 1 710 cm^{-1}), which indicated that the ethylenic double bond of the conjugated enone system had been hydrogenated. Treatment of IV with hydrogen and platinum oxide in 93 % acetic acid resulted in rapid consumption of 1 mole of H_2, followed by slow consumption of a second mole. The tetrahydro derivative thus obtained had m.p. 219—20° and showed only one carbonyl function in its infrared spectrum. The position of this carbonyl absorption band (1 720 cm^{-1}) was similar to that of the unconjugated CO group in the starting material, indicating that, in addition to the ethylenic bond, probably the keto group of the unbridged six-membered ring of IV had been reduced. As a result of the reduction of one of the two keto groups of IV, the infrared spectrum of the tetrahydro compound showed two hydroxyl bands (3 500 and 3 260 cm^{-1}) as well as a band at 1 280 cm^{-1} which can be ascribed to a secondary hydroxyl group. Catalytic hydrogenation of substance B in acetic acid solution over platinum oxide at a pressure of 3.5 atm. produced

a hexahydro derivative, m.p. 201—2°, the infrared spectrum of which was devoid of carbonyl bands but showed strong absorption at 1 280 cm^{-1} (*sec.* OH).

On the basis of these results, structures IX, X and XI are proposed for the dihydro, tetrahydro and hexahydro derivatives of IV.

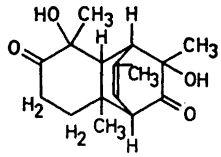

IX

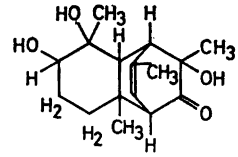

X

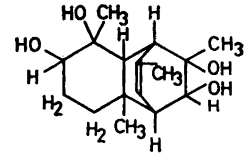

XI

Evidently, hydrogenation of the ethylenic bond of the bridge of the bi*cyclo*octene system did not occur under the experimental conditions used. Another case has recently been reported [21] in which catalytic hydrogenation of a methyl substituted ethylene bridge, similar to that present in IV, was hindered.

An attempt was made to convert the hexahydro derivative (XI), by heating with selenium, into a naphthalene derivative, which would necessarily involve the elimination of the methyl-substituted ethylene bridge as well as migration or loss of the angular methyl group. However, only small amounts of impure oils could be obtained. The oily products formed on Wolff-Kishner or sodium borohydride reduction of IV also failed to give pure reaction products on distillation at atmospheric pressure or on selenium dehydrogenation.

It is striking that when 2,4-dimethylphenol is treated with excess periodate the dimeric *o*-quinol IV is obtained although the postulated monomeric intermediate (*o*-quinol III) as well as the dimer (IV) contain α-ketol groupings which would be expected to be susceptible to periodate cleavage. However, the isolated dimer IV was found to be practically stable even on several hours' treatment with periodate. It was then expected that the α-glycol groupings present in the hydrogenation products X and XI reported above would be more easily oxidised. In fact, the tetrahydro derivative X consumed 1 mole of periodate in 1 h, further oxidation proceeding extremely slowly, and the hexahydro compound XI consumed 2 moles of periodate in 15 min. These results provide further support of structure IV for substance B and of the structures for its hydrogenation products that are given above. They also exclude the possibility that substance B might be a diene adduct of a mol. of *o*-quinol III, acting as a diene, and a mol. of *p*-quinol II, acting as a philodiene, rather than the dimeric *o*-quinol (IV). Neither of the isomers which could possibly arise by *o*-quinol-*p*-quinol addition would be able to give a hexahydro derivative consuming 2 moles of periodate.

Substance C. When the yellow alkaline extract obtained from the crude periodate oxidation product (*cf.* p. 1261) was poured into excess acetic acid, a colourless substance (C), m.p. 192—193°, precipitated. It had the composition $C_{16}H_{18}O_4$ with two hydrogen atoms less than the neutral product B (IV). The acidic character of C is due to the presence of an enolic hydroxyl group; this was indicated by the intense (dark violet-brown) colour reaction with ferric chloride. Absorption at 1 634 and 1 715 cm^{-1} in the infrared spectrum

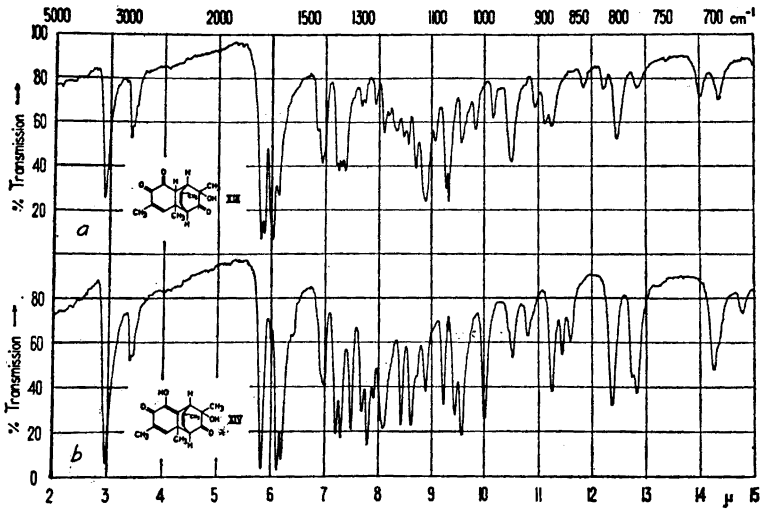

Fig. 3. Infrared spectra of addition product of 2,4-dimethyl-*o*-quinol and 3,5-dimethyl-*o*-quinone (= Substance C); *a*, keto form (XIII) and *b*, enol form (XIV).

of C (Fig. 3b) revealed the presence of one conjugated (and chelated) and one unconjugated carbonyl function. A band at 1 612 cm^{-1} can be ascribed to the ethylenic bond conjugated with the first-mentioned carbonyl group. This data suggested that C might have been formed by Diels-Alder addition of one mol. of *o*-quinol III (diene) and one mol. of 3,5-dimethyl-*o*-quinone (XII) (philodiene), the latter probably also arising on periodate oxidation of the starting phenol I. This *o*-quinol-*o*-quinone addition could give rise to an adduct of structure XIII and enolisation of the latter would yield XIV. (The isomeric structure which would arise if the diene III were inverted, *cf.* the corresponding dimer IVa, p. 1263, cannot be excluded.)

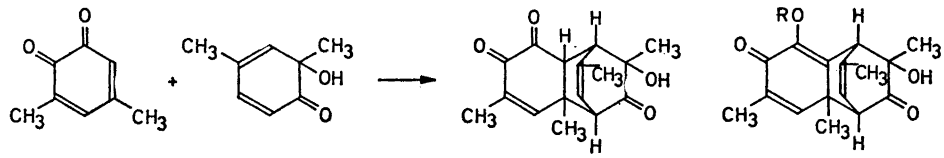

Strong evidence for the correctness of structure XIV for the enol C is provided by the fact that the ultraviolet absorption of the substance (Fig. 4) is very similar to that reported by Horner and Sturm [5] for the dimer of 4,5-dimethyl-*o*-quinone. The latter has been shown [5] to be the enol XVI, containing a 2-hydroxy-2,5-*cyclo*hexadienone chromophore similar to that present

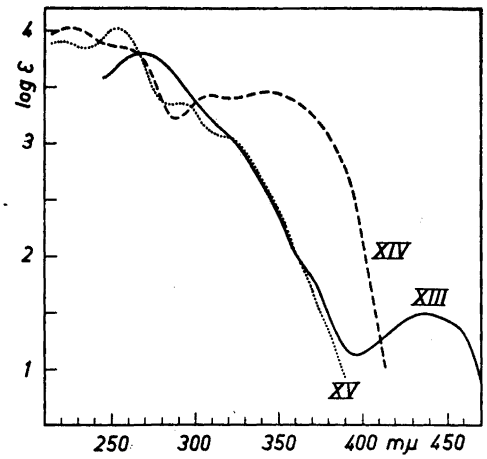

Fig. 4. Ultraviolet absorption spectra. Adduct of 2,4-dimethyl-*o*-quinol and 3,5-dimethyl-*o*-quinone (= Substance C),
———— keto form (XIII); solvent, chloroform
– – – – – enol form (XIV); solvent, 95 % ethanol
..... monoacetate of enol form (XV); solvent, 95 % ethanol.

in the postulated structure XIV. Furthermore, substance C when treated with acetic anhydride-pyridine gave a monoacetate (XV), m.p. 213—214°, the ultraviolet absorption of which (Fig. 4) again was very similar to that of the monoacetate (XVII) of the enol XVI of Horner and Sturm.

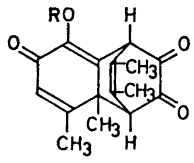

XVI : R = H
XVII : R = Ac

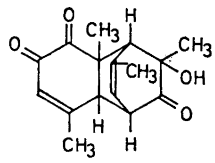

XVIII

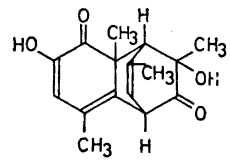

XIX

Since the *o*-quinone XII is unsymmetrically substituted, and either of its two C=C double bonds might be expected to have philodienic properties, a Diels-Alder addition of XII and III could alternatively yield the adduct XVIII, isomeric with XIII. The enol form of XVIII, *i. e.* XIX, however would have a 2-hydroxy-2,4-dienone chromophore rather than the "crossed conjugated" 2-hydroxy-2,5-dienone system present in Horner and Sturm's enol (XVI) and therefore almost certainly would have an ultraviolet absorption markedly different from that of the latter enol. This seems to exclude structure XIX for the enol C.

As mentioned above, the colourless enol XIV is precipitated from its yellow solution in aqueous alkali by pouring the solution into an excess of acetic acid. Slow neutralisation of the alkaline solution with acetic acid, however, produced

a yellow crystalline product, which after recrystallisation from ethyl acetate had a melting point (193—194°) only a few degrees above that of enol XIV; unlike the colourless enol, the yellow product gave no colour reaction with ferric chloride. The infrared spectrum of the yellow substance (Fig. 3a) showed three carbonyl bands (1 724, 1 704 and 1 662 cm^{-1}) instead of the two carbonyl bands for enol XIV; a further band at 1 630 cm^{-1} can be ascribed to an ethylenic bond conjugated with a CO group. The ultraviolet spectrum (Fig. 4) has a maximum at 269 mμ (log ε, 3.80) and in addition, a weak absorption band with a maximum at 437 mμ (log ε, 1.48) which indicates the presence of a 1,2-diketone grouping and is responsible for the yellow colour of the substance. The formation of a quinoxaline derivative (XX), m.p. 161—162°, on treatment with *o*-phenylenediamine confirms the occurrence of a 1,2-diketo grouping. Like enol XIV, the yellow substance dissolves in aqueous alkali yielding an intensely yellow solution (enolate of XIV) from which either the colourless enol XIV or the yellow substance (or mixtures of both) can be recovered depending on the manner, in which neutralisation is carried out (see above). Treatment of the yellow product with acetic anhydride-pyridine gave the enol acetate XV. From these results it is evident that the yellow product is the keto form XIII of substance C, and that the enol form XIV and keto form XIII are interconvertible.

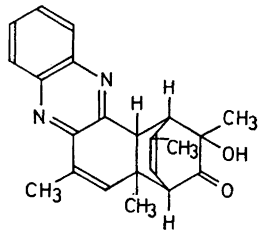

XX

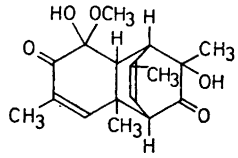

XXI

Recrystallisation of ketone XIII from methanol gave a colourless substance, the m.p. (191—192°) of which was approximately the same as that of XIII and XIV; it gave no colour reaction with ferric chloride. Analysis indicated an addition product of equimolar amounts of XIII and methanol. According to its infrared absorption, the methanol adduct contained a non-conjugated and a conjugated carbonyl group (1 720 and 1 670 cm^{-1}). Structure XXI is therefore ascribed to this compound. A colourless solution of XXI in dioxan when acidified with dilute sulphuric acid turned yellow and deposited yellow crystals of XIII. This behaviour is in harmony with the hemiketal structure XXI.

The fact that the melting points of the enol form XIV, the keto form XIII and also of the hemiketal of the latter (XXI) fall within a very narrow range (190 – 194°) seems to be due to conversion of the enol and the hemiketal into the yellow keto form XIII on heating to temperatures a few degrees below the melting point.

To summarise, the course of the reaction between 2,4-dimethylphenol (I) and periodate, in aqueous solution, can be represented as follows.

Periodate attacks the phenol at the hydroxyl group, producing, possibly by a one-step two-electron transfer [1], the mesomeric aroxyl cation XXII. Addition of water, and loss of a proton, converts XXII competitively into the *p*-quinol II, which is formed in minor amounts, the *o*-quinol III (main

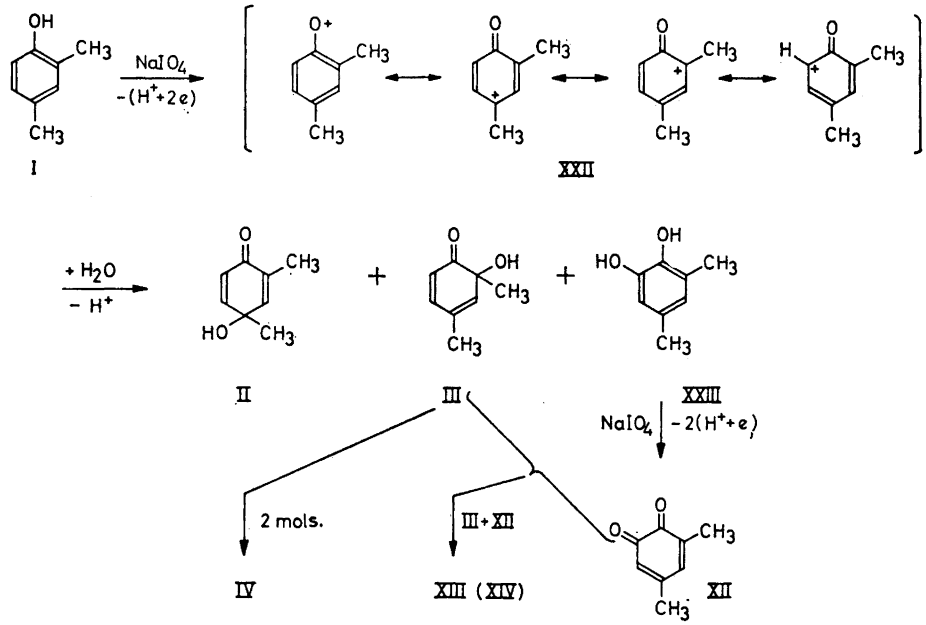

reaction), and the catechol XXIII, the latter being immediately oxidised further to the *o*-quinone XII. While the *p*-quinol (II) is stable, the *o*-quinol III rapidly dimerises by Diels-Alder addition to yield the dimeric *o*-quinol IV, m.p. 237—238°, and simultaneously *o*-quinol III also adds to the *o*-quinone XII with the formation of the *o*-quinol-*o*-quinone adduct XIII, m.p. 193—194°, or its enol form, XIV.

Although *o*-quinones, in dimerisation by a Diels-Alder reaction, act both as diene and as philodiene [5–10], they were found to act as dienes in adding to another 1,3-diene such as butadiene or *cyclo*pentadiene [22,5], while the latter behaved as philodienes. The formation of addition product XIII seems to be the first certain case of an *o*-quinone behaving as a philodiene towards a diene component other than a second molecule of the same *o*-quinone. In the present case, the diene component, *i.e.*, the *o*-quinol III, evidently has more pronounced "diene" properties than the *o*-quinone XII, the latter therefore becoming a philodiene in the addition III + XII. Diene activity of *o*-quinol acetates towards typical dienophilic substances as well as towards 1,3-butadiene and *cyclo*pentadiene has been demonstrated by Wessely and co-workers [23,21]. The formation both of the dimeric *o*-quinol (IV) and of the *o*-quinol-*o*-quinone

adduct XIII seems to proceed much more rapidly than the hitherto unknown self-dimerisation of 3,5-dimethyl-*o*-quinone (XII) which also might have been expected to take place in the periodate reaction mixture. Preliminary experiments showed that the latter *o*-quinone is comparatively stable in aqueous solution and will therefore be available for addition to the highly active diene, *o*-quinol III, present in the periodate oxidation mixture.

The primary steps in the oxidation of 2,4-dimethylphenol with periodate as presented in the scheme above are closely analogous to those observed by Wessely and Sinwel [24] in the oxidation of the same phenol with lead tetraacetate. The latter reaction yielded the acetate of *o*-quinol III and the diacetate of *o*-quinone XII; the acetate of *p*-quinol II was probably formed also. The differences in the final results of the lead tetraacetate and the periodate reactions, respectively, are due to the greater stability of the monomeric *o*-quinol acetates as compared with the marked tendency of free *o*-quinols to undergo diene addition, as demonstrated in the present paper and in unpublished work [16].

EXPERIMENTAL

Ultraviolet and visible absorption spectra were recorded with a Perkin-Elmer Spectracord 4000-A, infrared spectra with a Perkin-Elmer model 21 instrument (KBr-discs). Analyses by A. Bernhardt, Mülheim (Ruhr), Germany. The determinations of active hydrogen have been carried out by Tekn.lic. R. Magnusson.

Oxidation of 2,4-dimethylphenol with periodate. A stirred solution of 2,4-dimethylphenol (20 g) in water (3.5 l) was mixed with 1.2 l of an aqueous solution of sodium metaperiodate (70 g, molar ratio phenol/periodate = 1/2). After 5 min, ethylene glycol (20 g) was added in order to reduce excess periodate. A light-brown amorphous precipitate (0.8 g) was removed by filtration and the orange-red solution was repeatedly extracted with methylene chloride. The combined extracts were dried over anhydrous calcium sulphate and evaporated leaving a reddish-brown, partly crystalline product.

*2,4-Dimethyl-*p*-benzoquinol (II) (= Substance A).* The crude reaction product was treated with ether, in which a minor part of the product dissolved. Concentration of the red ether extract gave a light-red crystalline solid, which was recrystallised several times from benzene-hexane; colourless needles and flat prisms, m. p. 72—73°, identified by infrared absorption (OH, 3 470 cm^{-1}; conjugated CO, 1 670 cm^{-1}) and mixed m. p. with 2,4-dimethyl-*p*-benzoquinol, m. p. 73—73.5° [2]. Yield, about 2 %. Recrystallisation from water gave the hydrate, m. p. 53—54°, reported by Bamberger and Bradey [2].

Dimeric 2,4-dimethyl-o-benzoquinol (IV) (1,2,3,4,4a,7,8,8a-Octahydro-2,8-dihydroxy-2,4a,8,9-tetramethyl-3,7-dioxo-1,4-ethenonaphthalene) (= Substance B). The residue obtained by ether extraction of the crude reaction product was treated with 0.5 N aqueous sodium hydroxide (10 ml per g of the solids). The nearly white insoluble residue was filtered off and washed with water. Recrystallisation from benzene gave colourless prisms, m. p. 237—238°. (Found: C 69.54; H 7.36; active H 0.70; mol. wt. (Rast) 279. Calc. for $C_{16}H_{20}O_4$: C 69.54; H 7.30; active H 0.72; mol. wt. 276.32). UV spectrum, Fig. 1; IR spectrum, Fig. 2.

Diacetate (IV, OAc instead of OH). a) A mixture of IV (0.58 g), acetic anhydride (7 ml) and anhydrous sodium acetate (0.7 g) was refluxed for 2.5 h. The solvent was removed under reduced pressure and the dark-brown oily residue dissolved in ethanol. Addition of water gave colourless prisms (yield, about 25 %), m. p. 183—184° after recrystallisation from ethanol.

b) A 2 M solution of acetic anhydride in ethyl acetate containing 1.15 % of perchloric acid [25] (12 ml) was added to IV (800 mg), which rapidly dissolved. After 10 min at room temperature, water was added, the ethyl acetate layer repeatedly washed with water and dried over anhydrous Na_2SO_4. The solvent was removed under reduced pressure and the residue recrystallised from ethanol, yielding prisms (76 %), identical by m. p. and

mixed m. p. with the product obtained according to a). (Found: C 66.80; H 6.74; CH_3CO 23.04. Calc. for $C_{20}H_{24}O_6$: C 66.65; H 6.71; CH_3CO 23.89.) UV spectrum, Fig. 1.

Treatment of the diacetate with 10 % ethanolic potassium hydroxide for 20 h at room temperature regenerated substance IV, identified by m. p. and mixed m. p. and IR spectrum. Yield, 91 %.

Dihydro derivative of IV (IX) (Decahydro-2,8-dihydroxy-2,4a,8,9-tetramethyl-3,7-dioxo-1,4-ethenonaphthalene). A palladium chloride-barium sulphate catalyst (176 mg), containing 9 % $PdCl_2$, was hydrogenated in abs. ethanol (10 ml). A solution of IV (152 mg) in abs. ethanol (30 ml) was added and shaking in a hydrogen atmosphere was continued. After 10 min. 1 mole of H_2 per mole of IV had been consumed and hydrogen uptake ceased. (In 93 % acetic acid instead of ethanol, similar hydrogenation took place but the time required was 30 min.) Evaporation of the filtered ethanol solution gave a colourless crystalline product, needles from ethyl acetate-hexane, m. p. 194—195°. (Found: C 68.73; H 7.85. Calc. for $C_{16}H_{22}O_4$: C 69.04; H 7.97.) IR maxima (cm^{-1}): 3 410 (OH); 1 723 and 1 710 (CO).

Tetrahydro derivative of IV (X) (Decahydro-2,7(or 3?)8-trihydroxy-2,4a,8,9-tetramethyl-3(or 7?)oxo-1,4-ethenonaphthalene). Platinum oxide (80 mg) was hydrogenated in 93 % aqueous acetic acid (10 ml), and 500 mg IV, dissolved in 10 ml of the same solvent, was added. After 4 min, 1 mole of H_2, and after a further 150 min, a total of 2 moles of H_2, had been consumed. Evaporation and recrystallisation from ethyl acetate-hexane gave needles, m. p. 219—220°. (Found: C 68.68; H 8.56. Calc. for $C_{16}H_{24}O_4$: C 68.54; H 8.63.) IR maxima (cm^{-1}): 3 480 and 3 240 (OH), 1 720 (CO), 1 280 (*sec.* alcohol).

Hexahydro derivative of IV (XI) (Decahydro-2,3,7,8-tetrahydroxy-2,4a,8,9-tetramethyl-1,4-ethenonaphthalene). A solution of IV (1.4 g) in acetic acid (60 ml) was shaken for 24 h, in the presence of 0.17 g PtO_2, with hydrogen at 3.5 atm. pressure. Evaporation of the filtered solution gave a crystalline residue, which was recrystallised from ethyl acetate-hexane. Prisms, m. p. 201—202°. (Found: C 68.07; H 9.07. Calc. for $C_{16}H_{26}O_4$: C 68.05; H 9.28.) IR maximum at 3 330 cm^{-1} (broad), no carbonyl bands.

Adduct of 2,4-dimethyl-o-quinol and 3,5-dimethyl-o-quinone, enol form (XIV) (1,2,3,4,4a,7 - Hexahydro - 2,8 - dihydroxy - 2,4a,6,9 - tetramethyl - 3,7 - dioxo - 1,4 - ethenonaphthalene) (= Substance C). The orange-yellow alkaline solution obtained after filtering off substance B (see above) was allowed to run fairly rapidly into an excess of glacial acetic acid. The almost white precipitate formed was recovered and recrystallised from glacial acetic acid. Colourless prisms, m. p. 191—192°. (Found: C 69.83; H 6.58; active H 0.92. Calc. for $C_{16}H_{18}O_4$: C 70.05; H 6.61; active H 0.73.) IR spectrum, Fig. 3b; UV spectrum, Fig. 4. An alcoholic solution of the substance gave a dark violet-brown colour reaction with alcoholic ferric chloride.

Enol acetate (XV). Acetylation of enol XIV with acetic anhydride in pyridine at room temperature and recrystallisation of the product from ethyl acetate gave the acetate, colourless needles, m.p. 213—214°. No colour reaction with ferric chloride. (Found: C 68.62; H 6.53. Calc. for $C_{18}H_{20}O_5$: C 68.34; H 6.37.) UV spectrum, Fig. 4. IR maxima (cm^{-1}): 3 400 (OH), 1 765 (vinyl ester CO), 1 722 (CO), 1 658 (conj. CO), 1 626 (C=C).

Adduct of 2,4-dimethyl-o-quinol and 3,5-dimethyl-o-quinone, keto form (XIII) (1,2,3,4,4a,7,8,8a-Octahydro-2-hydroxy-2,4a,6,9-tetramethyl-3,7,8-trioxo-1,4 - ethenonaphthalene). A solution of enol XIV (1 g) in 0.5 N aqueous sodium hydroxide (10 ml) was neutralised by dropwise addition of acetic acid. The yellow crystals deposited after cooling were repeatedly recrystallised from ethyl acetate to give yellow prisms, m. p. 194—195°, which gave no colour reaction with alcoholic ferric chloride. (Found: C 70.18; H 6.64; mol. wt. (Rast) 297. Calc. for $C_{16}H_{18}O_4$: C 70.05; H 6.61; mol. wt. 274.30.) UV spectrum, Fig. 4; IR spectrum, Fig. 3a.

Acetylation of XIII with acetic anhydride-pyridine at room temperature gave the enol acetate XV, identical with that obtained from enol XIV. A solution of XIII in acetic anhydride (in the absence of pyridine) was refluxed for 1 h, and the resulting dark-brown solution was poured into water; a dark, amorphous precipitate formed, which was removed by filtration. From the filtrate, unchanged XIII crystallised on cooling.

Quinoxaline derivative from XIII (XX). A solution of XIII (200 mg) and *o*-phenylenediamine (79 mg) in chloroform (50 ml) was kept over anhydrous Na_2SO_4 at room temperature for two weeks. The brown solution was extracted with 0.25 N NaOH, 1 N H_2SO_4 and aqueous $NaHCO_3$, and evaporated. The solid residue (190 mg) was recrystallised

from methanol to give slightly yellow prisms, m. p. 161–162°. (Found: C 75.99; H 6.18; N 8.36. Calc. for $C_{22}H_{22}O_2N_2$: C 76.27; H 6.41; N 8.09.)

Methanol addition product of substance XIII (XXI). A hot methanolic solution of the yellow ketone XIII on cooling deposited colourless needles, m. p. 191–192°, which gave no colour reaction with ferric chloride. IR maxima (cm^{-1}): 3 330–3 280 (OH), 1 720 (CO), 1 670 (conj. CO), 1 635 (C=C). (Found: C 66.65; H 7.61; OCH_3 10.20. Calc. for $C_{17}H_{22}O_5$: C 66.65; H 7.24; OCH_3 10.13.)

A sample of XXI was dissolved in cold dioxane. On addition of a drop of dilute aqueous sulphuric acid the colourless solution became yellow, and, on dilution with water, deposited yellow crystals of XIII.

REFERENCES

1. Adler, E. and Magnusson, R. *Acta Chem. Scand.* **13** (1959) 505.
2. Bamberger, E. and Brady, F. *Ber.* **33** (1900) 3650.
3. Woodward, R. B. *J. Am. Chem. Soc.* **63** (1941) 1123.
4. Fieser, L. F. and Fieser, M. *Natural Products Related to Phenanthrene*, 3rd Ed. *(Am. Chem. Soc. Monogr.* No. **70**), New York, 1949.
5. Horner, L. and Sturm, K. *Ann.* **597** (1955) 1.
6. Teuber, H.-J. *Angew. Chem.* **68** (1956) 420.
7. Patchett, A. A. and Witkop, B. *J. Org. Chem.* **22** (1957) 1477.
8. Harley-Mason, J. and Laird, A. H. *J. Chem. Soc.* **1958** 1718.
9. Horner, L. and Dürckheimer, W. *Chem. Ber.* **91** (1958) 2532.
10. Adler, E., Magnusson, R., Berggren, B. and Thomelius, H. *Acta Chem. Scand.* **14** (1960) 515.
11. Metlesics, W. and Wessely, F. *Monatsh.* **88** (1957) 108.
12. Brown, T. L., Curtin, D. Y. and Fraser, R. R. *J. Am. Chem. Soc.* **80** (1958) 4339.
13. For references see Refs. [11-12].
14. Alder, K. and Vogt, W. *Ann.* **570** (1950) 190.
15. Alder, K., Flock, F. H., Hausweiler, A. and Reeber, R. *Chem. Ber.* **87** (1954) 1752.
16. Adler, E. *Angew. Chem.* **69** (1957) 272.
17. Siegel, A., Wessely, F., Stockhammer, P., Antony, F. and Klezl, P. *Tetrahedron* **4** (1958) 49.
18. Budzikiewicz, H., Schmidt, G., Stockhammer, P. and Wessely, F. *Monatsh.* **90** (1959) 609.
19. Adler, E., Dahlén, J. and Westin, G. *Acta Chem. Scand.* **14** (1960) 512.
20. Magnusson, R. *Acta Chem. Scand. In the press.*
21. Wessely, F., Budzikiewicz, H. and Metlesics, W. *Monatsh.* **90** (1959) 121 (p. 129).
22. Horner, L., Klüpfel, K., Merz, H. and Spietschka, W. *Ann.* **579** (1953) 170.
23. Metlesics, W., Wessely, F. and Budzikiewicz, H. *Monatsh.* **89** (1958) 102.
24. Wessely, F. and Sinwel, F. *Monatsh.* **81** (1950) 1055.
25. Fritz, J. S. and Schenk, G. H. *Anal. Chem.* **31** (1959) 1808.

Received February 23, 1960.

ACTA CHEMICA SCANDINAVICA 14 (1960) 1274—1278

Complex Dibenzofurans

I. Dehydration of Polyhydroxy-*p*-terphenyls

NILS E. STJERNSTRÖM

Organisk-kemiska Institutionen, Kungl. Tekniska Högskolan, Stockholm, Sweden

The synthesis of a series of polymethoxy-*p*-terphenyls, all containing methoxyl groups in the 2,2′,5′,2″-positions, is described. The series was suitable for a study of the structural requirements for facile acid catalysed dehydration of 2,2′-dihydroxydiphenyl derivatives with formation of dibenzofurans. A brief discussion of the dehydration experiments is presented.

During the course of our studies on the acid catalysed polymerisation of quinones crystalline dioxidoterphenyls of still incompletely known structure were obtained in addition to large amounts of amorphous products [1,2], which presumably also contain dibenzofuran units. The mechanism of the formation of the trimeric and polymeric reaction products is not known, but the simplest assumption is that they are formed by dehydration of polyphenolic intermediates.

Several examples of acid catalysed dehydration of hydroxydiphenyls are known. The conversion of *o,o′*-dihydroxydiphenyl to dibenzofuran does not proceed smoothly and heating with zinc chloride is needed [3]. Some substituted *o,o′*-dihydroxylated diphenyls are, however, more easily dehydrated. This dehydration is frequently a source of complication when di- or polyphenol methyl ethers are demethylated with hydrobromic or hydriodic acid. Thus 2,4,2′,4′-tetramethoxydiphenyl [4] easily yields the corresponding dibenzofuran derivative and analogous reactions are reported for 2,4,2′,6′-tetramethoxydiphenyl [5], 4-methyl-2,6,2′,4′-tetramethoxydiphenyl [6], 2,2′-dimethyl-4,6,4′,6′-tetramethoxydiphenyl [7], diphloroglucinol hexamethyl ether [8], 2,4,5,2′,4′,5′-hexamethoxydiphenyl [9] and 2,5,2′,5′-tetrahydroxy-4,4′-dimethoxydiphenyl [10].

Dehydrations, effected under relatively mild conditions, are of obvious interest in relation to the formation of dibenzofuran derivatives in the acid polymerisation of *p*-benzoquinones. Apart from the above mentioned diresorcinol derivatives comparatively little (*cf.* Refs.[2,11] dealing with hydroquinones) is known about the ease with which *o,o′*-hydroxylated di- or polyphenols undergo transformation into dibenzofurans and as a consequence this investigation was undertaken.

An ideal series of compounds for a study of the dehydration reaction would be substituted anisols, containing in the *ortho* position a 2-methoxy-, a 2,3-dimethoxy- or a 2,4-dimethoxyphenyl group, *etc.* Some unsymmetrical polymethoxydiphenyls of this type have been prepared, but they are not easily synthesised.

Our earlier experience in the transformation of trihydroquinone hexamethyl ether (III) to the dioxido-*p*-terphenyl VIIa [2] made the series of 2,5-disubstituted hydroquinone dimethyl ethers I—V attractive for a comparative study, especially because terphenyl derivatives are formed during the polymerisation of *p*-benzoquinones. Compounds of this type are easily prepared by the mixed Ullmann coupling of suitable mono- and diiodophenyl derivatives. The reaction products are readily separated by fractional distillation *in vacuo* followed by recrystallisation.

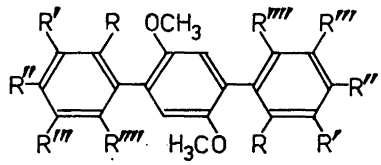

I $R=R'=OCH_3$; $R''=R'''=R''''=H$

II $R=R''=OCH_3$; $R'=R'''=R''''=H$

III $R=R'''=OCH_3$; $R'=R''=R''''=H$

IV $R=R''''=OCH_3$; $R'=R''=R'''=H$

V $R=R'=R''=OCH_3$; $R'''=R''''=H$

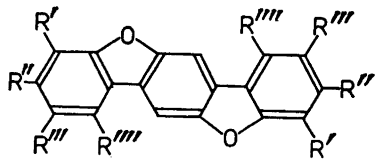

VI $R''=OCH_3$ (VIa: OH instead of OCH_3); $R'=R'''=R''''=H$

VII $R'''=OCH_3$ (VIIa: OH instead of OCH_3); $R'=R''=R''''=H$

VIII $R''''=OCH_3$ (VIIIa: OH instead of OCH_3); $R'=R''=R'''=H$

IX $R'=R''=R'''=R''''=H$

Coupling of 2,5-diiodohydroquinone dimethyl ether with 3-iodoveratrol yielded a mixture containing mainly 2,3,2',3'-tetramethoxydiphenyl and 2,3,2',5',2'',3''-hexamethoxy-*p*-terphenyl (I). Similarly 2,4,2',5',2'',4''-hexamethoxy-*p*-terphenyl (II), 2,6,2',5',2'',6''-hexamethoxy-*p*-terphenyl (IV) and 2,3,4,2',5',2'',3'',4''-octamethoxy-*p*-terphenyl (V) were synthesised employing 4-iodoresorcinol dimethyl ether, 2-iodoresorcinol dimethyl ether and 4-iodopyrogallol trimethyl ether, respectively. A ratio 1:8 of diiodohydroquinone dimethyl ether and monoiodocompound was generally used and the yields were about 40 % based on the diiodocompound. Some dehalogenation of the monoiodocompound with formation of the corresponding phenol ethers always occurred, but this is a common observation in Ullmann reactions.

With one exception the starting materials were prepared according to standard procedures as indicated in the experimental part. Kauffmann and Kieser [12] obtained 4-iodoresorcinol dimethyl ether in a rather poor yield by iodination of resorcinol dimethyl ether in alcoholic solution with iodine and mercuric oxide. Omission of the solvent raised the yield substantially (*cf.* the synthesis of 4-iodopyrogallol trimethyl ether [10]).

Pummerer *et al.*[13] reported the synthesis of the diresorcyl- and dipyrogallylhydroquinones corresponding to II and V by condensing *p*-benzoquinone

with resorcinol and pyrogallol under acid conditions. The present author was, however, unable to confirm the results of Pummerer *et al.* On attempting to synthesise the diresorcyl derivative 2,4,2′,5′,2″,4″-hexahydroxy-*p*-terphenyl (demethylated II), according to Pummerer *et al.* an amorphous product, was obtained. Similar results were reported by Erdtman [1] who after methylation of this amorphous material succeeded in isolating a crystalline substance. This product was assumed to be 2,4,2′,5′,2″,4″-hexamethoxy-*p*-terphenyl (II), but it was not identical with compound II, obtained by the Ullmann reaction. It might perhaps be a diphenyl derivative; this problem, however, requires further investigation.

The formation of 2,4,2′,5′-tetrahydroxydiphenyl by simply heating resorcinol with *p*-benzoquinone has been claimed by Pummerer *et al* [13]. This reaction could not be reproduced either and in an attempt to repeat the synthesis of the dipyrogallylhydroquinone octaacetate (2,3,4,2′,5′,2″,3″,4″-octaacetoxy-*p*-terphenyl, corresponding to V), the present author obtained pyrogallol triacetate as the sole crystalline product. The m.p. of Pummerer's »octaacetate» was surprisingly low (158°). Pyrogallol triacetate melts at 165° and the slightly impure pyrogallol triacetate obtained from the reaction melted at about 160°. These results suggest that Pummerer's »octaacetate» was pyrogallol triacetate.

The dehydrations were studied in the following way. The methoxylated terphenyl was refluxed with an excess of constant boiling hydrobromic acid for three days. The phenol obtained was collected and methylated directly. The methylation product was either identical with the starting material or a substance of dioxidoterphenyl type with a high melting point and exhibiting strong fluorescence in ultra violet light.

In our earlier experiments [2] the trihydroquinone derivative III was converted into the corresponding dioxidoterphenyl VIIa (characterised as the dimethyl ether VII). It has now been found that the diresorcylhydroquinone hexamethyl ethers II and IV are dehydrated to the dihydroxydioxido-*p*-terphenyls VIa and VIIIa (characterised as VI and VIII). The terphenyls I and V, containing veratrol- and pyrogallol trimethyl ether groupings, however, did not undergo ring closure.

The first step in these reactions is of course demethylation and it is interesting to note that the terphenyls II and IV, which show a pronounced aptitude for ring closure, are derivatives of *m*-dihydroxybenzene as are the diresorcinols. The latter also undergo facile dehydration as previously mentioned in this paper. Another interesting feature of these reactions is that a hydroxyl group in the 3 and 3″-positions does not facilitate the dehydration. Other cases of the same type are represented by, *e.g.*, 2,3,4,2′,3′,4′-hexahydroxydiphenyl [14] and a tetrapyrogallol (with the diphenyl linkages in the *o*-positions to hydroxyl groups; Erdtman, unpublished results), both easily prepared by demethylation of the corresponding methyl ethers with hydrogen bromide. This problem will be the subject of a future communication.

Ullmann [15] reported normal demethylation of 2,5,2′,5′-tetramethoxydiphenyl, dihydroquinone dimethyl ether, with hydrobromic acid. According to our experience with trihydroquinone the 2,5,2′,5′-tetrahydroxydiphenyl should undergo dehydration with formation of 2,8-dihydroxydibenzofuran.

A reinvestigation showed that dihydroquinone tetramethyl ether on prolonged refluxing with constant boiling hydrobromic acid gave 2,8-dihydroxydibenzofuran in good yield. This is also in accordance with the early findings of Nietzki *et al.*[11] on the dehydration of a dimethyldihydroquinone dimethyl ether, the structure of which was elucidated by Posternak *et al.*[16], with concentrated hydrochloric acid.

Zinc dust distillation of the dioxido-*p*-terphenyl derivative VIa gave 2,2′,5′,2″-dioxido-*p*-terphenyl (IX) identical with the dioxido-*p*-terphenyl described by Schimmelschmidt [17] (*cf.* Ref.[2]).

EXPERIMENTAL

All melting points are uncorrected

4-Iodoresorcinol dimethyl ether. Finely divided iodine (300 g) followed by freshly precipitated mercuric oxide (240 g) were added in small portions to resorcinol dimethyl ether (150 g) with vigorous stirring. Complete decolouration of the reaction mixture was awaited before each new addition of iodine. The exothermic reaction required about an hour. The hot reaction mixture was filtered with suction and the inorganic material thoroughly washed with ether. The ether was evaporated and the residue, a yellow oil, crystallised on scratching. The crude product (265 g, 92 % yield) was recrystallised from methanol. Yield 215 g, 81 %, m.p. 40—41° (lit.[12] m.p. 40°).

Ullmann reaction. General procedure. 2,5-Diiodohydroquinone dimethylether [18] (3.9 g), copper bronze (35 g) and the monoiodocompound (3-iodoveratrol [19], 4-iodoresorcinol dimethyl ether, 2-iodoresorcinol dimethyl ether [20], 21 g, or 4-iodopyrogallol trimethyl ether [10], 25 g) were thoroughly mixed in a 300 ml flask and heated on a salt bath to 220—240°, when a vigorous reaction started which raised the temperature to about 300°. After some minutes the reaction mixture was allowed to cool and the organic products extracted with chloroform. The solvent was evaporated and the residue subjected to distillation *in vacuo*.

2,3,2′,5′,2″,3″-Hexamethoxy-p-terphenyl (I). The combined extracts from three runs yielded veratrol (3 g), 2,3,2′,3′-tetra methoxydiphenyl (28 g) and a light brown thick syrup (7 g, b.p. about 300°, 0.4 mm), which crystallised on scratching with a few drops of methanol. The substance was recrystallised from *n*-butanol. M.p. 177—179°. (Found: C 69.9; H 6.5. Calc. for $C_{24}H_{26}O_6$: C 70.2; H 6.4.)

2,4,2′,5′,2″,4″-Hexamethoxy-p-terphenyl (II). The distillation *in vacuo* yielded a very small amount of resorcinol dimethyl ether, 2,4,2′,4′-tetramethoxydiphenyl (8.5 g) and an oil (2.5 g, b.p. 215—265°, 1 mm), which crystallised on scratching with a few drops of methanol. The product was recrystallised from acetic anhydride and sublimed *in vacuo*. M.p. 207—209°. (Found: C 69.8; H 6.7. Calc. for $C_{24}H_{26}O_6$: C 70.2; H 6.4.)

2,6,2′,5′,2″,6″-Hexamethoxy-p-terphenyl (IV). The combined products from three runs yielded resorcinol dimethyl ether (5 g), 2,6,2′,6′-tetramethoxydiphenyl (21 g) and a highboiling yellow oil (5,3 g, b.p. 240—300°, 1 mm), which crystallised on cooling. The terphenyl was recrystallised from a mixture of ligroin and benzene and was finally purified by sublimation *in vacuo*. M.p. 227—228°. (Found: C 70.0; H 6.5. Calc. for $C_{24}H_{26}O_6$: C 70.2; H 6.4.)

2,3,4,2′,5′,2″,3″,4″-Octamethoxy-p-terphenyl (V). The combined products from three runs yielded pyrogallol trimethyl ether (5 g), 2,3,4,2′,3′,4′-hexamethoxydiphenyl (31 g) and a dark yellow crystalline material (7 g, b.p. *ca.* 300°, 1 mm), which was recrystallised from ligroin. Colourless crystals, m.p. 171—172°. (Found: C 66.4; H 6.4. Calc. for $C_{26}H_{30}O_8$: C 66.4; H 6.4.)

Demethylation and dehydration. General procedure. The polymethoxy-*p*-terphenyl (*ca.* 500 mg) was refluxed with hydrobromic acid (48 %, 25 ml) in an atmosphere of carbon dioxide or nitrogen for three days. The reaction mixture was allowed to cool, diluted with water (100 ml) and filtered. The crude phenol was directly methylated in methanol suspension with an excess of dimethyl sulphate and sodium hydroxide.

4,4'-Dimethoxy-2,2',5',2''-dioxido-p-terphenyl (VI). 2,4,2',5',2'',4''-Hexamethoxy-*p*-terphenyl (II, 590 mg) yielded a crude blue phenolic precipitate (VIa, 400 mg, m.p. *ca.* 345°, decomp.) which was methylated. The yield of dimethyl ether VI was almost quantitative. It was recrystallised from acetic anhydride. M.p. 290—292°. (Found: C 75.4; H 4.5. Calc. for $C_{20}H_{14}O_4$: C 75.5; H 4.4.)

6,6''-Dimethoxy-2,2',5',2''-dioxido-p-terphenyl (VIII). 2,6,2',5',2'',6''-Hexamethoxy-*p*-terphenyl (IV, 560 mg) yielded a crude brown phenolic precipitate (VIIIa, 330 mg, m.p. *ca.* 330°, decomp.), which was converted into compound VIII in an almost quantitative yield. It was purified by recrystallisation from acetic acid and sublimation *in vacuo*. M.p. 287—289°. (Found: C 75.5; H 4.7. Calc. for $C_{20}H_{14}O_4$: C 75.5; H 4.4.)

Demethylation of 2,3,2',5',2'',3''-hexamethoxy-p-terphenyl (I). This compound (570 mg) yielded a crude blue phenolic precipitate (400 mg, m.p. *ca.* 280°, decomp.) which was quantitatively converted to the starting material by methylation.

Demethylation of 2,3,4,2',5',2'',3'',4''-octamethoxy-p-terphenyl (V). The octamethyl ether (450 mg) yielded a crude blue phenol (350 mg, m.p. *ca.* 260°, decomp.), which on methylation was almost quantitatively converted to the starting material.

Demethylation and dehydration of 2,5,2',5'-tetramethoxydiphenyl. 2,5,2',5'-Tetramethoxydiphenyl [15] (900 mg) was refluxed with constant boiling hydrobromic acid (30 ml) in an atmosphere of carbon dioxide for 80 h. The reaction mixture was then diluted with water (100 ml) and the slightly bluish 2,8-dihydroxydibenzofuran (400 mg) collected. M.p. 233—235°. The phenol was converted to 2,8-dimethoxydibenzofuran, m.p. 89—90°, and 2,8-diacetoxydibenzofuran, m.p. 152—154°, using standard procedures. Swislowsky [21] reports the following melting points for these substances: 242—243°, 88—89° and 150—151°, respectively.

2,2',5',2''-Dioxido-p-terphenyl (IX). 4,4''-Dihydroxy-2,2',5',2''-dioxido-*p*-terphenyl (VIa, 200 mg) was thoroughly mixed with zinc dust (2 g) and heated in a test tube to red heat when a partially phenolic mixture (*ca.* 20 mg) of substances sublimed on the cool walls of the tube. The mixture was treated with dilute sodium hydroxide and the insoluble material sublimed *in vacuo* and recrystallised from chlorobenzene. M.p. 264—266°. Mixed melting point with an authentic sample [2,17], 265—266°.

The author is grateful to Dr. I. Wellings for checking the manuscript.

REFERENCES

1. Erdtman, H. *Proc. Roy. Soc. London.* **A 143** (1933) 228.
2. Erdtman, H. and Stjernström, N. E. *Acta Chem. Scand.* **13** (1959) 653.
3. Kraemer, G. and Weissgerber, R. *Ber.* **34** (1901) 1662.
4. Asahina, Y and Aoki, M. *J. Pharm. Soc. Japan.* **64** (1944) 41.
5. Wachtmeister, C. A. *Acta Chem. Scand.* **8** (1954) 1433.
6. Wachtmeister, C. A. *Acta Chem. Scand.* **10** (1956) 1404.
7. Shibata, S. *Acta Phytochim. Japan.* **14** (1944) 9.
8. Riedl, W. *Ann.* **597** (1953) 148.
9. Schüler, A. *Arch. Pharm.* **245** (1907) 275.
10. Erdtman, H. *Proc. Soc. London.* **A 143** (1933) 191.
11. Nietzki, R. and Bernhard, R. *Ber.* **31** (1898) 1334.
12. Kauffmann, H. and Kieser, F. *Ber.* **45** (1912) 2334.
13. Pummerer, R. and Huppmann, G. *Ber.* **60** (1927) 1442. Huppmann, G. *Über Kondensationen von Chinonen mit Phenolen.* (Diss.) Erlangen 1926.
14. Liebermann, C. and Liebermann, H. *Ber.* **42** (1909) 1922.
15. Ullmann, F. *Ann.* **332** (1904) 38.
16. Posternak, Th., Alcalay, W., Luzzati, R. and Tardent, A. *Helv. Chim. Acta* **31** (1948) 525.
17. Schimmelschmidt, K. *Ann.* **566** (1950) 184.
18. Robinson, G. M. *J. Chem. Soc.* **109** (1916) 1186.
19. Mauthner, F. *J. prakt. Chem.* **149** (1937) 328.
20. Van Arendonk, A. M., Cupery M. E. and Adams, R. *J. Am. Chem. Soc.* **55** (1933) 4226.
21. Swislowsky, I. *Iowa State Coll. J. Sci.* **14** (1939) 92; *cf. Chem. Abstracts* **34** (1940) 6273.

Received March 25, 1960.

ACTA CHEMICA SCANDINAVICA 14 (1960) 1279—1287

Optical Phenomena in Turbidimetric Analysis Applied to Sulfate Determination in Phosphoric Acid

SVEN-ERIC DAHLGREN

Research and Development Dept., AB Förenade Superfosfatfabriker, Landskrona, Sweden

A theory for optimum measuring wavelength at turbidimetric analysis is presented. As the validity of Lambert-Beer's law is limited at short wavelengths the theory has not been satisfactorily verified when applied to barium sulfate dispersions in gelatine solution. The optical properties of such dispersions have been studied and recommendations for measurements are given. A standard deviation of 1.5 % was obtained.

For a rapid and accurate determination of the sulfate content in technical phosphoric acid by wet processes, gravimetric methods are not convenient. Gravimetric methods are time consuming and considerable errors may thereby be introduced. Coprecipitation by cations can be eliminated by an ion-exchange technique, but the fact remains that the phosphate ion is among those anions giving the heaviest coprecipitation with barium sulfate.

A titrimetric method using the sodium salt of rhodizonic acid as an external indicator is rapid and simple but not very accurate, and may in some cases completely fail. Neither is the volumetric estimation of a centrifuged barium sulfate precipitate very accurate.

The two requirements mentioned seem to be most easily obtained by physical methods, primarily by turbidimetric and nephelometric determination of a barium sulfate dispersion. Precipitation in an ethyl alcohol-dipropylene glycol solution [1,2] was considered to be too cumbersome, and a gelatine solution was preferred. A turbidimetric method using gelatine has been presented by Gassner and Friedel [3]. The preparation of the test dispersion described by G. and F. was found to have some disadvantages, which have been eliminated. Further, there was a need for further study of the optical properties of the dispersion based on present knowledge of light-scattering by small particles.

THEORY – OPTIMUM MEASURING CONDITIONS FOR TURBIDIMETRIC ANALYSIS

Light-scattering phenomena by small particles are of a most complicated nature. The light is scattered in different directions and the space distribution of light intensity and polarization is a function of particle size, particle shape, light wavelength and the refractive index of the particles relative to the surrounding medium. In addition to this, the design of the optical geometry of the measuring equipment influences the data obtained. At a turbidimetric measurement part of the scattered light radiation reaches the photoreceiver of the instrument, as it takes a finite space angle. In the following, some fundamentals have been taken from the excellent monograph by van de Hulst [4] and applied to the present problem.

Let the total energy scattered in all directions by a particle be equal to the energy of the incident wave falling on the area C_{sca}, the cross section for scattering. The efficiency factor for scattering, Q_{sca}, is defined by

$$Q_{sca} = \frac{C_{sca}}{G} \tag{1}$$

where G = geometrical cross section of the particle.

Assume a spherical particle and introduce the parameter ϱ

$$\varrho = \frac{4\,\pi\,r \cdot |m - 1|}{\lambda} \tag{2}$$

where r = particle radius

m = relative refractive index, that is the ratio between the refractive index relative to vacuum of the particle, and that of the dispersing medium

λ = light wave length in the medium, that is the the ratio of light wave length in vacuum and the refractive index of the dispersing medium relative to vacuum.

The physical meaning of ϱ is the phase lag suffered by the central ray that passes through the sphere along a full diameter. For non-absorbing spheres m is a real number and for absorbing ones a complex number.

In the case light absorbing particles

$$Q_{ext} = Q_{sca} + Q_{abs} \tag{3}$$

where Q_{ext} = efficiency factor for extinction, Q_{abs} = efficiency factor for absorption.

The efficiency factors for extinction and absorption are analogous to that for scattering. Thus for non-absorbing particles the efficiency factors for scattering and extinction are equal. For the present problem absorption need not to be taken into consideration.

In Fig. 1, the efficiency factor for extinction of non-absorbing spheres is shown as a function of ϱ for different values of the relative refractive index. The wave form of the extinction curves depends on interference between light transmitted through the particles and diffracted light. The "ripple"

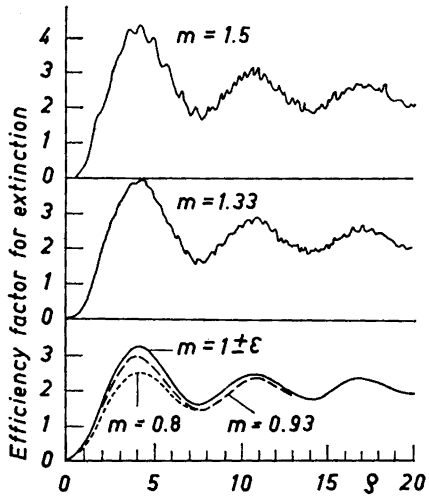

Fig. 1. Extinction curves at different relative refractive indices. After van de Hulst.

which becomes more pronounced when m increases, has no simple explanation. It is of special interest to note that the "ripple" is almost negligible for low values of m and ϱ.

In practice, dispersions of particles of uniform size are seldom found. For mixtures of particles of various sizes we define the effective radius r_{eff} as

$$r_{\text{eff}} = \tfrac{3}{4} \cdot \frac{\text{total particle volume}}{\text{total geometrical cross section}} \tag{4}$$

The corresponding phase lag is denoted by ϱ_{eff} and the effective efficiency factor for extinction by $\overline{Q}$. In Fig. 2 are shown extinction curves for various distributions of radii of dispersed particles when m is close to 1.

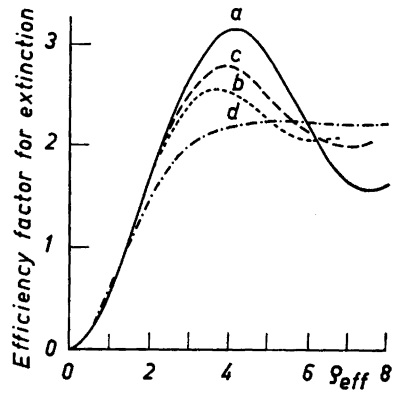

Fig. 2. Extinction curves for mixtures of particles of various sizes, all with m close to 1.

Curve a: uniform size with radius r_1
Curve b: $f(u) = u^{-1}$ for $0 < u \leqslant 1$ $r_{eff} = \frac{2}{3} r_1$
Curve c: $f(u) = 1$ for $0 < u \leqslant 1$ $r_{eff} = \frac{3}{4} r_1$
Curve d: $f(u) = e^{-u}$ for $0 < u < \infty$ $r_{eff} = 3 r_1$
where $u = r/r_1$ and $f(u) =$ the number distribution function.

The curves show how the typical features are washed out if particles of a range of sizes are present. Of interest is that for not too high values of ϱ_{eff} the curves nearly coincide. The transmission T of a dispersion is given by

$$T = \exp(-\overline{Q}\,\pi\, r_{eff}^2 \cdot nl) \tag{5}$$

where $n =$ the number of particles per unit volume of dispersion with size reduced to r_{eff}
$l =$ the path length

On indexing the reference sample with "o" and the test sample with "t" the following expression of the extinction E is obtained

$$E = \log \frac{T_o}{T_t} = \frac{\overline{Q}\,\pi\, r_{eff}^2 \cdot l}{\ln 10} (n_t - n_o) \tag{6}$$

Assume $n_o = 0$, the concentration of the disperged material to be c, and its solubility in the dispersing medium to be s. Thus eqn. 6 changes into

$$E = \frac{k\,\overline{Q}\,l}{r_{eff}} (c - s) \tag{7}$$

where $k =$ a proportionality constant.

Eqn. 7 holds within the region of Lambert-Beer's law. From this equation it is clear that for analytical applications, such a wave length should be chosen that a variation of the effective radius in the preparation is almost completely eliminated by a corresponding change in the effective efficiency factor for extinction. The most favourable wave length can indirectly be obtained from Fig. 2 by determining the tangent point between a straight line through the origin and the extinction curve before the first maximum. Depending on the size distribution, there are different extinction curves and a more or less flat optimum. If the measured extinction of a polydisperse dispersion is plotted against the reciprocal wave length, the curve obtained is equiform to the effective efficiency factor for extinction against ϱ_{eff}. The origin in this case is the point of infinite long wave length. From experimental data the most favourable wave length is thus directly obtained.

A consequence of the above is that the dispersion, if possible, should be prepared under such conditions that in addition to good reproducibility an effective radius is obtained, corresponding to a most favourable wave length within the measuring region of the available equipment.

It is often pointed out that the main drawback of turbidimetric methods of analysis is a lack of reproducibility in preparation of the dispersion. The presented theory shows that the effect of moderate variations in the size distribution can be eliminated. Great care in the preparation work must, however, be maintained.

Investigations by Lewis and Lothian [5] on barium sulfate dispersion with particle radius 4.6 μ gave a refractive index of 1.52 compared with 1.64 on crystalline barium sulfate. This indicates a water content of 60 % by volume of the particles, which is in accordance with specific gravity determination by sedimentation. This is explained by formation of particles through condensation of sub-microscopic units. In a medium with an refractive index close to that of water the relative refractive index will be 1.14. Since this is close to 1 the ripple on the extinction curve may be neglected for not too high values of ϱ.

EXPERIMENTAL

Solutions

Sulfate-free water. The regular distilled water was found to give a weak opalescence on addition of barium chloride. Therefore deionized distilled water has been used. Deionizing was made by Crystalab Deeminizer Model CL-5.

Gelatine solution. For preparing the gelatine solution, sulfate-free gelatine quality 1/241 Special from Deutsche Gelatinfabriken, Göttingen-Würtenberg, is used. Per liter of solution 5 g gelatine and 0.5 g thymol as a preservative are taken. After swelling for 15—30 min in deionized distilled water the mixture is heated under agitation until all gelatine has dissolved and the solution becomes clear. It is then cooled to room temperature. After a day, an increase in viscosity and weak opalescence are apparent. This depends on a transition from sol to gel state, the latter being the stable state at room temperature. On heating to 40—45°C for a few minutes and cooling to room temperature the solution again becomes clear and light-fluid. This should be repeated every day before usage. There is no apparent change in the sol state for several hours after heating. The solution may be used for at least 2 weeks.

Barium chloride — gelatine solution. Except for about 10 ml fill a 1-litre volumetric flask with above described gelatine solution. Add 20 g $BaCl_2 \cdot 2\ H_2O$ and dissolve it completely. The flask is then filled to the mark with gelatine solution.

Standard solution. 0.2718 g K_2SO_4 A R ad 500 ml with deionized distilled water. 1 ml equivalent to 0.1 mg S.

Alternatively: 0.2721 g K_2SO_4 A R ad 500 ml. 1 ml equivalent to 0.3 mg SO_4.

Alternatively: 0.2665 g K_2SO_4 A R ad 500 ml. 1 ml equivalent to 0.3 mg H_2SO_4.

Phosphoric acid solution. 200 g conc. phosphoric acid ad 1 000 ml with deionized distilled water.

Preparation of barium sulfate dispersion with known sulfate content. For work with dispersions with up to 0.35 mg S per 50 ml the standard solution is diluted with deionized distilled water 1:10. From a burette, different amounts of the diluted solution are charged into a series of dry 100 ml Erlenmeyer-flasks. The amount is preferably a multiple of 2.5 or 5 ml, but not greater than 35 ml. To each flask is added 5.0 ml of phosphoric acid solution and deionized distilled water to bring the total volume to 40.0 ml. Then 5.0 ml of gelatine solution is pipetted, and finally 5.0 ml of barium chloride-gelatine solution added drop-wise from a burette under shaking to each flask. After 10 min, extinction measurements can be carried out.

The pH of the solution should be 1—2.5, found by Gassner and Friedel [3] to be optimum.

If some other maximum sulfate content is to be investigated the dilution of the standard solution should be appropriately changed so that no more than 35 ml of the diluted solution need to be taken.

Preparation of the reference sample. In a dry 100 ml Erlenmeyer-flask 35.0 ml of deionized distilled water, 5.0 ml of phosphoric acid solution, 5.0 ml of gelatine solution and 5.0 ml of barium chloride-gelatine solution are taken and the mixture shaken.

Measuring equipment

All measurements in glass cells were made with a Beckman B spectrophotometer and all measurements in quartz cells were made with a Beckman DU spectrophotometer.

RESULTS

Behaviour at very low sulfate concentrations. When measuring at successively decreasing sulfate concentrations, a linear relationship was obtained between extinction and concentration down to a limit where a discontinuous change took place and the extinction was zero (Fig. 3). The reason is that a certain critical supersaturation, a threshold value, must be surpassed to initiate nucleation. From the figure it is clear that there is lower limit for turbidimetric determination in gelatine solution at about 0.05 mg S per 50 ml of final solution, that is about 1 ppm.

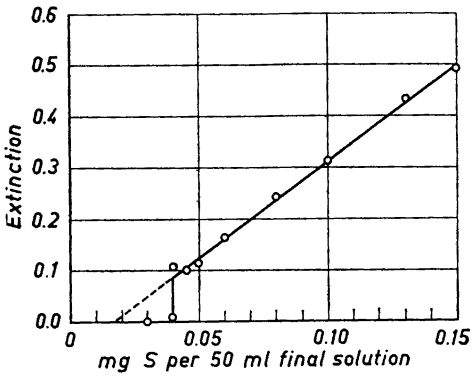

Fig. 3. Behaviour at very low sulfate concentrations. Wave length 420 mμ and 50 mm glass cells.

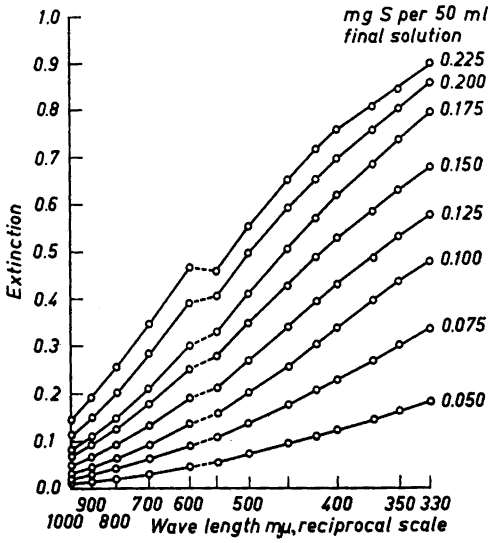

Fig. 4. Influence of light wave length on the extinction at different sulfate concentrations. 50 mm glass cells.

In an ethyl alcohol-dipropylene glycol solution the solubility of barium sulfate is completly different. It is possible in such a solution to determine nephelometrically sulfate concentrations down to 0.01 ppm.[2]

Extinction measurements in glass cells at varying sulfate concentration and light wave length. In a first series of measurements the extinction was determined over the whole wave length range of Backman B for sulfate concentrations from 0.050 to 0.225 mg S per 50 ml final solution at 0.025 intervals in 50 mm glass cells. In Fig. 4 the results are plotted with the sulfate concentration as parameter. When changing over from blue sensitive to red sensitive phototube a kink was obtained on the extinction curves, which was not the case with colorimetric determinations. Since the measurement of scattered light is sensitive to geometrical variations of the optical system in quite another degree than that of directed light, a geometrical dissimilarity between the two tubes may be responsible for the phenomenon. Since there is a reciprocal wave length scale in Fig. 4 a direct comparison with Fig. 1 is possible. This shows that the investigated range must be prior to the first maximum. At still shorter wave lengths an extinction maximum is to be expected.

In Fig. 5 the results are plotted with the wave length as parameter. The curves for 330 and 350 mμ are clearly bent and the points not so well positioned along the curve as for the other wave lengths. At 400 mμ there is a linearity up to 0.15 mg S per 50 ml which is further extended at 420 and 450 mμ. A weak tendency for the 500 and 550 mμ curves to bend in the opposite direction from the other curves is observed.

A similar series of measurements was carried out with 20 mm glass cells within the concentration range 0.05 to 0.30 mg S per 50 ml final solution at 0.05 intervals. The extinction scale in Fig. 6 is enlarged 2.5 times relative to that in Fig. 5 in order to compensate for the difference in light path of the cells. If Lambert-Beer's law is valid, the curves in the two figures should

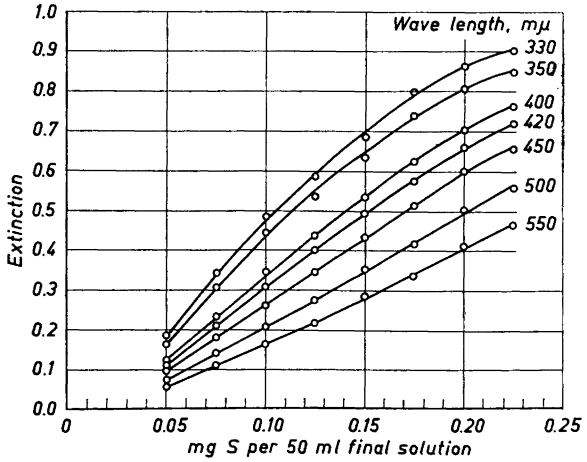

Fig. 5. Influence of sulfate concentration on the extinction at different light wave lengths using 50 mm glass cells.

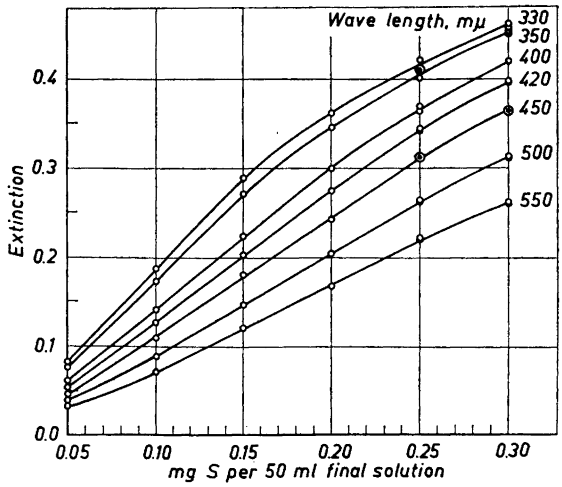

Fig. 6. Influence of sulfate concentration on the extinction at different light wave lengths using 20 mm glass cells.

coincide. After a minute parallel shift it is found that the curves for 330 and 350 mμ do not coincide, but intersect at two points. At 400 mμ they coincide up to 0.15 mg, at 420 mμ up to 0.175 mg, at 450 mμ up to 0.20 mg and at 500 and 550 mμ within the whole range.

The validity limit of Lambert-Beer's law thus varies with the wave length. A series of 11 solutions containing 0.150 mg S per 50 ml final solution were measured in 20 mm glass cells at different wave lengths and standard deviation calculated.

Wave length mμ	Standard deviation %
330	2.2
350	2.3
370	2.6
400	2.6
420	2.5
450	2.9
500	3.5
550	3.6

The relative standard deviation thus increases at increasing wave length in accordance with the theory presented.

Double determinations for the same conditions and lengths were made with a gelatine solution of varying age. When the trial was stopped after 1 month no change had been observed.

Extinction measurements in quartz cells at varying sulfate concentration and light wave length. Since an extinction maximum was expected at a wave length below the Beckman B range, further measurements were made with a Beckman

DU using 10 and 20 mm quartz cells. Owing to light absorption in the suspending medium itself, measurements below 240 mμ were impossible and in fact it has an absorption peak already at 270—280 mμ. This resulted in a marked peak on the extinction curves obtained with 20 mm cells but not on those obtained with 10 mm cells.

At decreasing wave length the linear range of extinction *versus* sulfate concentration diminished considerably, and was too small for practical purposes. Thus since Lambert-Beer's law was not valid here, the theory of optimum measuring wave length could not be satisfactorily verified.

CONCLUSIONS

Some results have been obtained which are in accordance with the presented theory of optimum measuring wave length; however, it could not be satisfactorily verified when applied to barium sulfate dispersions in a gelatine solution. The standard deviation is almost the same in the 330—420 mμ region but increases at longer wave lengths. The sensitivity increases with decreasing wave length. At the same time, however, the validity region of Lambert-Beer's law is decreased. An adequate compromise therefore seems to be a wave length of about 420 mμ, where determinations may be carried out within the range 0.05—0.20 mg S per 50 ml of final solution. Preferably, concentration and cell size is selected so that an extinction of 0.3 to 0.5 is obtained. For that reason a 50 mm cell is well suited. With these specifications 12 equally prepared solutions showed a standard deviation of 1.5 %.

Acknowledgement. Sincere thanks are due to Mr Kornél Horváth, who with great care and interest carried out all the measurements.

REFERENCES

1. Krober, O. A. and Howell, R. W. *J. Agr. Food Chem.* **6** (1958) 591.
2. Toennies, G. and Bakay, B. *Anal. Chem.* **25** (1953) 160.
3. Gassner, K. und Friedel, H. *Z. anal. Chem.* **152** (1956) 420.
4. van de Hulst, H. C. *Light scattering by small particles*, John Wiley & Sons, New York 1957.
5. Lewis, P. C. and Lothian, G. F. *Brit. J. Appl. Phys. Nottingham Conf. Suppl.* 1954, p. 71.

Received February 5, 1960.

ACTA CHEMICA SCANDINAVICA 14 (1960) 1288—1294

The Chemistry of the Natural Order Cupressales XXVIII * Constituents of *Juniperus virginiana* L.

JARL RUNEBERG

Organisk-kemiska Institutionen, Kungl. Tekniska Högskolan, Stockholm, Sweden

Commercial cedarwood oil contains cuparene, cedrol, widdrol, α-cedrene and thujopsene. Evidence was obtained for the presence of a dextrorotatory curcumene containing a vinylidene group and gas chromatography indicated the presence of several other unidentified sesquiterpenes.

Investigations on the heartwood constituents of *Juniperus chinensis* L.[1] and *J. utahensis* Lemm.[2] have been described in two previous papers. Among the compounds identified in these juniper woods were the sesquiterpene hydrocarbons cuparene [3] and thujopsene [4] and the sesquiterpene alcohol widdrol [5]. The structures of the two latter compounds are at present under investigation in this laboratory. Experience gained in the examination of these juniper woods has now been applied to cedarwood oil [6,7]. Commercially this is the most important of the juniper wood oils.

Cedarwood oil is produced by steam distillation of saw mill waste of the American red cedar, *Juniperus virginiana*. The highest yield of oil, about 3.5 % of the wood, is obtained from older trees containing a greater proportion of heartwood. The crude oil is discoloured and the commercial product is obtained by redistillation of the crude material. The boiling point range of cedarwood oil has been given as 264—280° at atmospheric pressure. Several hundred thousand pounds of the oil are produced a year in the United States for use in perfumery and in scenting soaps.

Among the compounds previously reported in cedarwood oil is α-cedrene but although this has been shown to be present it has probably never been isolated in a pure state from the natural oil. Natural cedrene has a lower negative specific rotation (usually about —55°) than the synthetic product (—91°) obtained by dehydration of cedrol [8]. The natural material is considered to be a mixture of α-cedrene and the corresponding exocyclic isomer β-cedrene, but it has not been proved that the exocyclic compound present

* Part XXVII. *Acta Chem. Scand.* **14** (1960) 797.

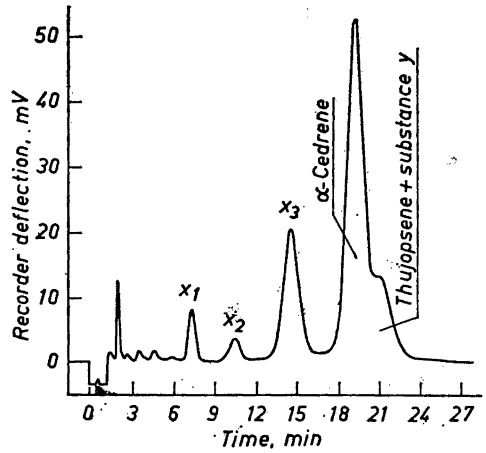

Fig. 1. Gas chromatogram of fraction IIa (Table 2). Argon flow rate 25 ml/min.

actually has the cedrene skeleton. Cedrol has frequently been isolated from *J. virginiana* and cedrenol [9] (*of.* Ref. [10]) and pseudocedrol [11] have also been reported to occur in the wood.

The commercial sample of cedarwood oil used in this investigation was subjected to a preliminary distillation followed by redistillation of some of the fractions obtained. Traces of monoterpenes or compounds with similar boiling points were detected in the lowest boiling fractions by gas chromatography (see Fig. 1, peaks with retention times up to about 11 min.). Only minute amounts of compounds containing hydroxyl groups were present in these fractions. Infrared spectra and gas chromatographic analysis showed that α-cedrene was the main component of the oil. The second largest constituent was thujopsene which has not previously been demonstrated in cedarwood oil. One of the main fractions was oxidised with selenium dioxide to a mixture of aldehydes, and then with silver oxide to yield the corresponding carboxylic acids. Chromatography of this mixture gave α-cedrenic acid [12] and hinokiic acid (thujopsenic acid [4]).

Thujopsene was almost completely separated from α-cedrene by fractional distillation but gas chromatographic analysis showed that both fractions still contained other compounds.

The specific rotations of the distillation fractions listed in Table 2 indicate that in addition to α-cedrene (—91°) and thujopsene (—112°) there are at least two further compounds present, probably with positive rotations. One is concentrated in the first fractions of Table 2 and gives a separate peak on gas chromatography, the other is concentrated in the last fractions and is apparently covered by the thujopsene peak.

Two of the fractions of Table 2 were dehydrogenated and then treated with ozone at low temperature. The material unattacked by ozone was optically inactive and it was identical with a synthetic sample of dihydro-*ar*-curcumene [13]. Neither α-cedrene nor thujopsene gave dihydro-*ar*-curcumene when treated in the same way. *d*-γ-Curcumene [14], which gives dihydro-*ar*-

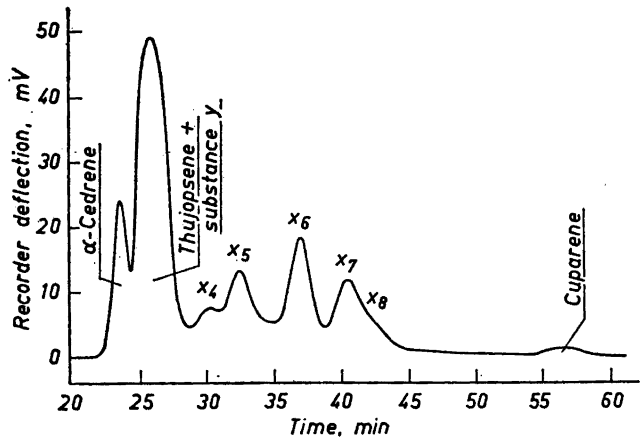

Fig. 2. Gas chromatogram of fraction IIIc (Table 3). Argon flow rate 17 ml/min.

curcumene on selenium dehydrogenation [15] was at first considered a possible precursor of this substance. Since, however, the ultraviolet spectra of the two fractions, before dehydrogenation, show maxima only at 205 and 207 mμ, respectively, they cannot contain any major amounts of *d*-γ-curcumene. However, the infrared spectra of both fractions show comparatively strong bands at 1 645 and 883 cm^{-1} indicating the presence of a compound containing a vinylidene group. It therefore appears likely that the dihydro-*ar*-curcumene precursor (substance *y*, Figs. 1 and 2) is an isomer of curcumene containing a vinylidene group.

An attempt was made to purify the above sesquiterpenes by chromatography on basic alumina. The first fractions eluted by light petroleum were reasonably pure α-cedrene but thujopsene could not be separated from the other components of the mixtures.

Naves has previously reported the presence of dextrorotatory bicyclic sesquiterpenes in *J. virginiana* [16], and one of these has now been identified. The material boiling slightly higher than the main α-cedrene-thujopsene fraction was redistilled and a fraction showing strong aromatic absorption in the infrared and ultraviolet was ozonised at low temperature. The material unattacked by ozone was identified as cuparene [3].

Gas chromatographic analysis of the cuparene containing fractions showed the presence of at least 7 unidentified compounds. The separation of these compounds on a larger scale offers considerable difficulties but could probably be achieved by preparative gas chromatography. No isomerisation of these compounds on the stationary phase used was observed.

The highest boiling part of cedarwood oil was a mixture of sesquiterpene alcohols. The first fractions containing alcohols (fraction IIIh (Table 3) and fractions IVa—IVc (Table 4)) crystallised on standing and were separated into cedrol and widdrol by chromatography on alumina. The highest boiling

alcohol fractions remained liquid and appeared, according to their infrared spectra to consist of a complex mixture of alcohols and carbonyl compounds.

The compounds isolated are listed below with very approximate estimates of the amounts present (as a percentage of dried cedarwood oil): α-Cedrene 35, thujopsene 30, cuparene 2, cedrol 4 and widdrol 2.

EXPERIMENTAL

Rotations were measured in chloroform; melting points, taken on a hot stage, are corrected; boiling points are uncorrected. Light petroleum refers to the fraction b.p. 40–60°.

The cedarwood oil (Ia, Florida, redistilled) used was obtained from the Dragoco Co, Holzminden, Weser, Germany. The oil was dried over sodium sulphate and a sample (2010 g) was then subjected to a preliminary distillation through a 40 cm, packed column. The fractions obtained are listed in Table 1.

Table 1. Distillation of cedarwood oil. Total distillate 1 729 g or 86 %

Fraction	Weight (g)	B.p. (°C)	Pressure (mm Hg)	Rotation ($[\alpha]_D$)	Refractive index ($n_D^{25.0}$)
Ia	181	74–114	11	−57	1.4999
Ib	250	114–118	11	−60	1.5018
Ic	399	82–83	1	−66	1.5007
Id	343	83–84	1	−58	1.5011
Ie	325	84–89	1	−47	1.5024
If	231	89–111	1	+ 4	1.5077
Ig (residue)	271				

Fractions Ia (65 g) and Ib (237 g) were combined and distilled through a 1 m, vacuum jacketed, packed column giving the fractions listed in Table 2.

Table 2. Redistillation of the combined fractions Ia and Ib. Total distillate 283 g or 94 %

Fraction	Weight (g)	B.p./14 mm Hg (°C)	Rotation ($[\alpha]_D$)	Refractive index ($n_D^{25.0}$)
IIa	19.3	76–124	−30	1.4966
IIb	37.8	124	−55	1.4981
IIc	28.8	124–125	−66	1.4983
IId	41.0	125	−74	1.4990
IIe	55.8	125	−80	1.4996
IIf	23.0	125	−81	1.5001
IIg	46.6	125–126	−85	1.5008
IIh	30.4	126–129	−39	1.5053

Dehydrogenations. (a) Dihydro-*ar*-curcumene was obtained from fraction IIb (5 g) by heating with finely powdered selenium (5.0 g) to 200° in a carbon dioxide atmosphere; the temperature was gradually raised to 280° and held there for 48 h. The reaction product was filtered and distilled (b.p. 122–129°/10 mm) and the oil obtained (4.3 g) was ozonised in methylene chloride (20 ml) at −70°C until an excess of ozone was indicated by the appearance of a blue colour. When the reaction mixture had reached room temperature, zinc dust (4.7 g) activated with glacial acetic acid (1 ml) was added with stirring and the mixture was left over-night and filtered. Hydrogen peroxide (30 %, 10 ml) in potassium hydroxide (10 %, 5 ml) was added dropwise to the filtrate and the mixture was refluxed for 5 min. The aqueous phase was separated and the organic phase was extracted with sodium hydroxide (2 N), washed with water, dried and evaporated giving

a viscous oil (3.4 g). This was chromatographed on basic alumina (40 g). The first 100 ml of light petroleum eluted a hydrocarbon fraction which on distillation under reduced pressure gave an oil (0.95 g), b.p. 126°/9 mm, $[\alpha]_D$ 0°, $d_{22.0}$ 0.8767, $n_D^{25.0}$ 1.4862, which was identified as dihydro-*ar*-curcumene [15,17]. The infrared spectra of the dehydrogenation product and of a synthetic sample [18] were superimposable. On treatment with aqueous nitric acid (30 %) in a sealed tube at 170° followed by methylation with diazomethane in ether, the dehydrogenation product gave dimethyl terephthalate, m.p. and mixed m.p. 140.0–140.5°.

(b) Fraction IIh (5.0 g) was dehydrogenated and ozonised in the same way as IIb. The material unattacked by ozone (1.57 g) was identified as dihydro-*ar*-curcumene.

α-Cedrene and thujopsene. Fraction Id (30 g) was dissolved in ethanol (95 %, 500 ml), selenium dioxide (18.0 g) was added and the mixture was refluxed for 5 h. After filtering, the solution was evaporated and the oil obtained was distilled, b.p. 95–115°/1.0 mm (21.8 g). This oil (17.5 g) was added to a suspension of silver oxide (sodium hydroxide 12.9 g, silver nitrate 28.8 g) in water (600 ml). The mixture was refluxed with vigorous stirring for 24 h. Solid material was filtered off and the filtrate was extracted with ether, acidified and again extracted with ether. This second extract, on evaporation gave a crystalline residue (A, 6.4 g).

Silica gel (30 g) suspended in a solution of dimethyl sulphoxide in chloroform (5 %, 100 ml) was poured into a chromatographic column and then washed successively with *iso*propyl ether and light petroleum. The crude acids A (916 mg) were chromatographed on this pretreated silica gel using an *iso*propyl ether-light petroleum mixture (1:2) as mobile phase. The first 250 ml of solvent eluted a crystalline substance (149 mg) which was sublimed three times in a vacuum giving *α*-cedrenic acid [12], m.p. 123.5–125.0°, $[\alpha]_D$ −69° (*c*, 2.0) (identified by mixed m.p. and IR). The next 150 ml of solvent eluted a second compound (240 mg) which was recrystallised from light petroleum, m.p. 166.5–167.5°, $[\alpha]_D$ −85° (*c*, 2.4), identified as hinokiic acid [4] (mixed m.p., IR). The rest of the chromatographed sample appeared to be polymeric material.

Cuparene. Cuparene was concentrated by redistillation of the highest boiling fraction in Table 1 (I f, 210 g).

Table 3. Redistillation of fraction If. Total distillate 192 g or 91 %.

Fraction	Weight (g)	B.p./14 mm Hg (°C)	Rotation ($[\alpha]_D$)	Refractive index ($n_D^{25.0}$)
IIIa	18.4	124–126	−77	1.5000
IIIb	28.7	126–127	−84	1.5012
IIIc	22.0	127–134	−42	1.5050
IIId	27.3	134–136	+32	1.5102
IIIe	24.6	136–138	+43	1.5116
IIIf	25.1	138–139	+42	1.5109
IIIg	11.4	139–147	+42	1.5091
IIIh	34.8	147–153	+31	–

Fraction IIIf (5.0 g) was ozonised and treated in the same way as the dehydrogenation product of fraction IIb. The material unaffected by ozone (810 mg), b.p. 117°/7 mm, $[\alpha]_D$ +65°, $n_D^{25.0}$ 1.5206, was identified as cuparene [3] by comparing its physical constants and infrared spectrum with those of an authentic sample.

Cedrol and widdrol. A sample of the crystalline fraction IIIh (2.5 g) was chromatographed on basic alumina (40 g). Light petroleum eluted an oil (0.17 g) which was not further investigated, 2 % ether in benzene gave cedrol (1.45 g) which was recrystallised from 95 % ethanol, m.p. 85.0–85.5°, $[\alpha]_D$ +11° (identified by mixed m.p. and IR). Elution with benzene-ether (1:1) gave widdrol [5] (0.56 g) which was recrystallised from acetonitrile, m.p. 95.0–96.0°, $[\alpha]_D$ +105° (identified by mixed m.p. and IR).

Main sesquiterpene alcohol fraction. The residue (Ig, 271 g) from the preliminary distillation described in Table 1 was distilled in a 1 m, vacuum-jacketed, packed column, giving the fractions listed in Table 4.

Table 4. Distillation of the main sesquiterpene alcohol fraction. Total distillate 214 g or 79 %.

Fraction	Weight (g)	B.p./14 mm Hg (°C)	Rotation ([α]D)
IVa	19.2	134—154	+30
IVb	26.9	154	+31
IVc	88.6	154—156	+26
IVd	39.5	156—163	+ 4
IVe	40.0	163	+24

Gas chromatographic examination of the sesquiterpene hydrocarbon fractions. A Pye Argon Chromatograph, Cat. No. 12000, was used together with a Philips Automatic Compensator PR 2210 A/21 (Column length 1.20 m, internal column diameter 5 mm, stationary phase 100—115 mesh Silocel C 22 brick powder impregnated with 2,4-dinitrophenyl- 2-naphthyl ether (15 %) and dibenzylpyridine (a mixture of 2,4- and 2,6-isomers, 0.75 %) [19], temperature 150°, charge 0.025 μl).

With an argon flow rate of 25 ml/min the retention times (min) were: α-cedrene 19.1 (reference sample prepared from cedrol), thujopsene 21.0, dihydro-*ar*-curcumene 23.8, cuparene 46.0. In the Tables 5—7 the approximate areas of individual peaks of different retention times are given as percentages of total peak area.

Table 5. Gas chromatographic analysis of the fractions in Table 1. Argon flow rate 25 ml/min.

Fraction	Peak retention time (min)							
	14.6	19.1	21.0	27.0	30.4	33.2	37.6	46.0
Ia	2	55	43					
Ib	2	53	45					
Ic	1	51	48					
Id		49	51					
Ie		44	54			2		
If		18	32	2	7	27	2	12

Table 6. Gas chromatographic analysis of the fractions in Table 2. Argon flow rate 25 ml/min.

Fraction	Peak retention time (min)					
	14.6	19.1	21.0	27.0	30.4	33.2
IIa*	20	56	16			
IIb	9	69	22			
IIc	3	66	31			
IId		65	35			
IIe		59	41			
IIf		48	52			
IIg		29	71			
IIh		11	67	3	8	11

* 8 % of total peak area of this fraction corresponds to several small peaks with retention times similar to those of monoterpenes (*cf.* Fig. 1).

Table 7. Gas chromatographic analysis of the fractions in Table 3. Argon flow rate 17 ml/min.

Fraction	Peak retention time (min)										
	18.4	23.8	26.0	30.1	32.5	36.9	40.3	42.1	46.9	54.9	56.4
IIIa	1	46	50	3							
IIIb		38	57	4		1					
IIIc*		11	41	8	12	13	10	4			1
IIId			1	3	7	21	34	22	4		8
IIIe					1	9	35	27	7	5	16
IIIf						2	23	21	7	20	27
IIIg						1	4	8	8	21	58

* *Cf.* Fig. 2.

With an argon flow rate of 17 ml/min the retention times (min) were: α-cedrene 23.8, thujopsene 26.0 and cuparene 56.4.

Acknowledgements. My thanks are due to Professor H. Erdtman for his interest in this work, to Miss G. Hammarberg for infrared and ultraviolet spectra and to the *Swedish Natural Science Research Council* for financial support.

REFERENCES

1. Runeberg, J. *Acta Chem. Scand.* **14** (1960) 353.
2. Runeberg, J. *Acta Chem. Scand.* **14** (1960) 797.
3. Enzell, C. and Erdtman, H. *Tetrahedron* **4** (1958) 361.
4. Erdtman, H. and Norin, T. *Acta Chem. Scand.* **13** (1959) 1124.
5. Erdtman, H. and Thomas, B. R. *Acta Chem. Scand.* **12** (1958) 267.
6. Guenther, E. *The Essential Oils*, D. van Nostrand, New York 1952, Vol. **VI**, p. 353.
7. Gildemeister, E. and Hoffmann, F. *Die Ätherischen Öle*, Akademie-Verlag, Berlin 1956, Band IV, p. 284.
8. Simonsen, J. and Barton, D. H. R. *The Terpenes*, The University Press, Cambridge 1952, Vol. **III**, p. 75.
9. Semmler, F. W. and Mayer, E. W. *Ber.* **45** (1912) 786.
10. Treibs, W. *Ber.* **70** (1937) 2064.
11. Semmler, F. W. and Mayer, E. W. *Ber.* **45** (1912) 1384.
12. Treibs, W. *Ber.* **70** (1937) 2066.
13. Simonsen, J. and Barton, D. H. R. *The Terpenes*, The University Press, Cambridge 1952, Vol. **III**, p. 25.
14. Simonsen, J. and Barton, D. H. R. *The Terpenes*, The University Press, Cambridge 1957, Vol. **V**, p. 515.
15. Batt, R. D. and Slater, S. N. *J. Chem. Soc.* **1949** 839.
16. Naves, Y. R., Papazian, G. and Perrottet, E. *Helv. Chim. Acta* **26** (1943) 302, 324.
17. Ruzicka, L. and van Veen, A. G. *Ann.* **468** (1929) 143.
18. Enzell, C. *To be published.*
19. Groth, A. B. *Svensk Papperstidn.* **61** (1958) 315.

Received March 19, 1960.

ACTA CHEMICA SCANDINAVICA 14 (1960) 1295—1299

The Beginning Solubilization of 20-Methylcholanthrene in Aqueous Solutions of Conjugated and Unconjugated Bile Acid Salts

Bile Acids and Steroids 79

ARNE NORMAN*

Department of Physiological Chemistry, University of Lund, Lund, Sweden

The first stage of association in aqueous bile salt solutions was studied by measuring the amounts of solubilized 20-methylcholanthrene. It was observed to begin in sodium deoxycholate, chenodeoxycholate and cholate solutions when the concentrations of bile salts rose to approximately 0.005 M, 0.006 M and 0.012 M, respectively. The glycine and taurine conjugates of these bile acid salts were found to undergo initial association in approximately the same concentration ranges as the respective unconjugated bile salts. The sodium and potassium salts of lithocholic and cholanic acids and their taurine and glycine conjugates were found to be only sparingly soluble in water. Even saturated solutions of these compounds were unable to solubilize 20-methylcholanthrene.

Studies carried out using various colloid-chemical methods have shown clearly that association to micelles takes place in aqueous solutions of the sodium salts of conjugated and unconjugated bile acids. The previous work in this field has been reviewed by Ekwall *et al.* [1,2].

The ability to solubilize lipoid substances is a characteristic property of association colloids and the establishment of a beginning solubilization can be taken to indicate the occurrence of association. Ekwall [3] introduced the use of fluorescent polycyclic hydrocarbons in the study of the solubilizing power of association colloids and in the determination of the colloid concentration where solubilization begins. The solubilities of these hydrocarbons can be readily determined by measuring the fluorescence or ultraviolet absorption of their solutions.

* Present address: Department of Chemistry, Karolinska Institutet, Stockholm 60, Sweden.

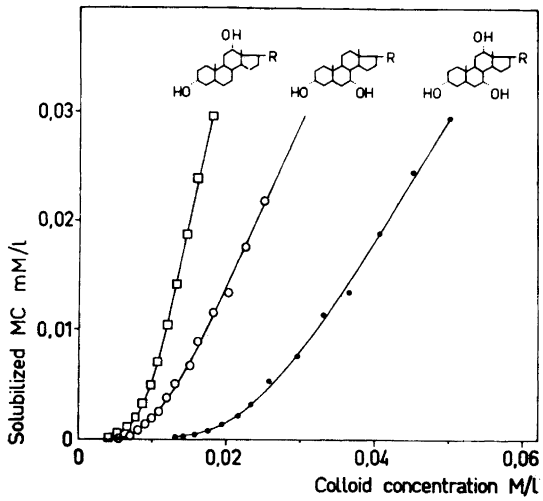

Fig. 1. Solubilization of 20-methylcholanthrene in aqueous solutions of sodium deoxycholate (□—□), sodium chenodeoxycholate (○—○), and sodium cholate (●—●).

The aim of the present study was to compare the first stages of association in solutions of bile acid salts and their taurine and glycine conjugates. The present paper reports the results of fluorometric determinations of the beginning solubilization of 20-methylcholanthrene in solutions of sodium cholate, deoxycholate, chenodeoxycholate, lithocholate and cholanate and their taurine and glycine conjugates.

MATERIALS AND METHODS

20-Methylcholanthrene (MC) was a product of Eastman-Kodak Co., Rochester, N.Y. The synthesis and physical properties of the conjugated and unconjugated bile acid salts were reported in a previous paper of the author [4].

Methylcholanthrene was added in excess to ampoules containing the bile salt solutions. After they had been closed by fusion, the ampoules were shaken at 40°C for 48 h. After this period the undissolved methylcholanthrene was removed from the solutions by filtration and the amounts of methylcholanthrene solubilized by the solutions were determined by measuring the intensity of fluorescence (according to Ekwall *et al.* [5]) or the ultraviolet absorption (according to Klevens [6]). The fluorescence intensities were measured with a Beckman Model DU Quartz Spectrophotometer provided with the fluorescence accessory

Table 1.

Bile acid salt	Solubility mole/litre 20°	40°
Potassium taurolithocholate	0.001	0.0025
Potassium glycolithocholate	0.0004	0.0007
Potassium glycocholanate		0.001
Potassium taurocholanate	0.0006	0.001

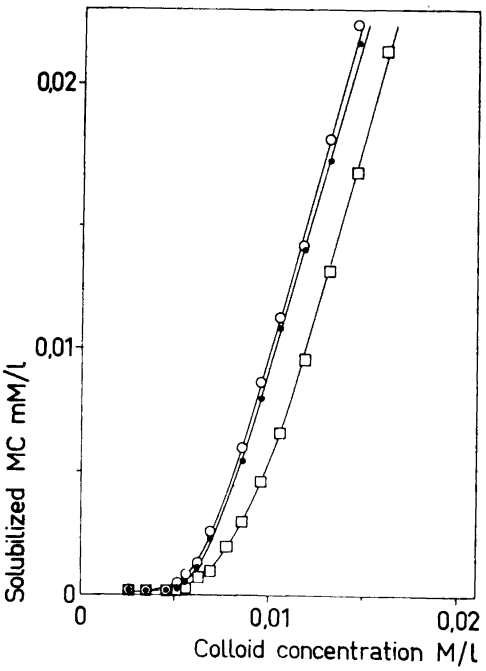

Fig. 2. Solubilization of 20-methylcholanthrene in aqueous solutions of sodium deoxycholate, (□—□) sodium taurodeoxycholate (O—O), and sodium glycodeoxycholate (●—●).

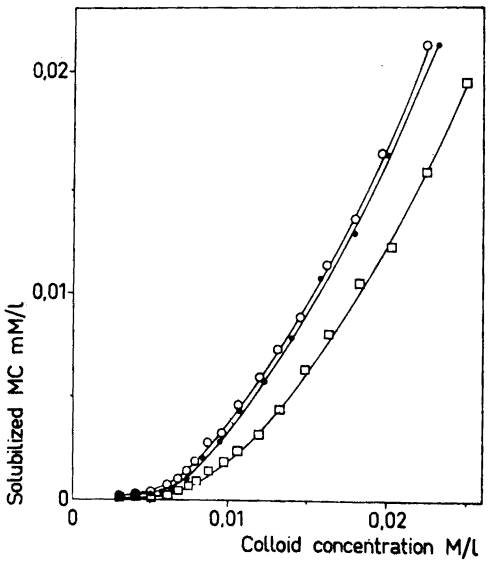

Fig. 3. Solubilization of 20-methylcholanthrene in aqueous solutions of sodium chenodeoxycholate (□—□), sodium taurochenodeoxycholate (O—O), and sodium glycochenodeoxycholate (●—●).

set. The measurements were all made at room temperature. No precipitation was found to occur when the temperature decreased from 40° to 20°C, which is in accordance with the observation of Sjöblom [7] that the solubilizing power of bile acid salts does not diminish with decreasing temperature.

Reference solutions containing different amounts of methylcholanthrene in the same bile salt solution were prepared as follows. A known volume of a standard solution of methylcholanthrene in benzene was added from an Agla micrometer burette to an ampoule and the benzene was evaporated from the ampoule *in vacuo* at room temperature. A measured volume of the bile salt solution was introduced into the ampoule which, after it was closed by fusion, was shaken in a thermostat at 40° for 48 h.

RESULTS

The time necessary to attain maximal solubility of methylcholanthrene in the solutions was studied by determining the amounts of methylcholanthrene solubilized after the ampoules were shaken for different lenghts of time at 40°C. The results obtained with 0.04 M cholate and 0.015 M deoxycholate solutions revealed that equilibrium was attained after 24 h.

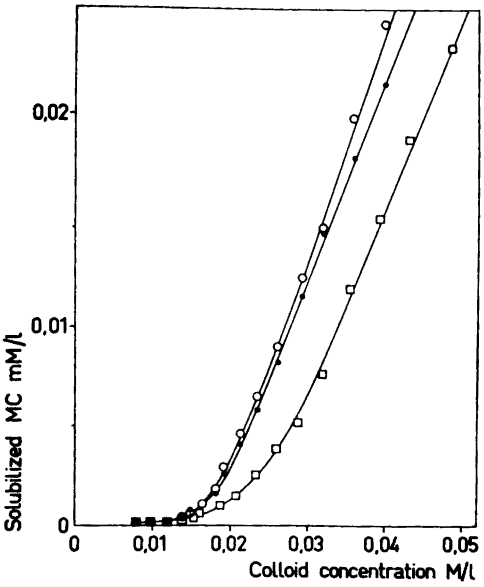

Fig. 4. Solubilization of 20-methylcholanthrene in aqueous solutions of sodium cholate (□—□), sodium taurocholate (○—○), and sodiumglycocholate (●—●).

In a number of cases the amounts of solubilized methylcholanthrene were determined by both fluorescence and ultraviolet absorption methods. Conforming results were obtained by both methods. However, the fluorescence method is appreciably more sensitive and is hence more suitable for the determination of the low solubility when a low degree of association prevails in the colloid solution.

Figs. 1—4 show the results of solubilization determinations by the fluorescence method on solutions of the sodium salts of deoxycholic, chenodeoxycholic and cholic acids and their taurine and glycine conjugates. All these compounds are very soluble in water and the beginning solubilization becomes clearly evident within a narrow concentration range in their solutions. Similar experiments were carried out on solutions of the sodium and potassium salts of lithocholic and cholanic acids and their taurine and glycine conjugates but no solubilization of methylcholanthrene was observed to take place even in their saturated solutions. These compounds are, however, only sparingly soluble in water as shown by the solubilities of the potassium salts of the conjugated acids at 20° and 40° (Table 1). The solubilities of the sodium and potassium salts are approximately equal and the salts of lithocholic and cholanic acids are less soluble than the corresponding salts of the conjugated acids.

DISCUSSION

By determining the solubilities of *p*-xylene, cholic acid, cholesterol and 20-methylcholanthrene in cholate solutions, Ekwall and his collaborators [1,2] found that a beginning solubilization occurs when the cholate concentration

rises to about 0.015 M. The activity of the cholate anion in cholate solutions saturated with cholic acid also changes at the same concentration owing to the beginning association. The corresponding data for sodium deoxycholate show that the first signs of association are observed at a concentration of about 0.005 M. These experiments reveal that the number of hydroxyl groups and their location in the molecule influence the association process. The curves in Fig. 1 show that the solubilizing powers of chenodeoxycholate solutions are weaker than those of deoxycholate solutions. In addition, solubilization begins at a somewhat higher concentration in chenodeoxycholate solutions than in deoxycholate solutions. Hydroxyl groups at carbon atoms 3 and 12 (deoxycholic acid) favour micellar association more than hydroxyl groups at carbon atoms 3 and 7 (chenodeoxycholic acid).

The configurations of the side chains in bile salts apparently have a lesser influence on the association process and the properties of the micelles than the structure of the ring skeleton. Figs. 2, 3 and 4 show that the concentration where beginning association occurs do not differ essentially for the conjugated and unconjugated bile salts with the possible exception that the solubilization begins at a slightly lower concentration in the case of the conjugated salts. The solubilizing powers of the taurine and glycine conjugates are practically equal and slightly greater than those of the corresponding unconjugated bile salts. The solubilizing powers increase more rapidly and become linear, *i.e.*, the ratio of the amount of hydrocarbon solubilized and the concentration of the association colloid becomes constant, at lower concentrations of the conjugated salts.

Acknowledgement. This investigation was begun at the Institute of Physical Chemistry, Åbo Akademi. I wish to express my gratitude to Professor Per Ekwall, the Head of the Institute, for his guidance.

This work has been supported by grants awarded by the *Medical Faculty, University of Lund, Statens Medicinska Forskningsråd,* Stockholm and the *National Heart Institute* (H2842), U.S. Public Health Service, Bethesda, Maryland.

REFERENCES

1. Ekwall, P., Fontell, K. and Sten, A. *Proc. 2nd Intern. Congr. Surface Activity, Gas/Liquid and Liquid/Liquid Interface,* Butterworths, London 1957, p. 357.
2. Ekwall, P. and Ekholm, R. *Proc. 2nd Intern. Congr. Surface Activity, Gas/Liquid and Liquid/Liquid Interface,* Butterworths, London 1957, p. 23.
3. Ekwall, P. *Nord. Kemistmötet. Berättelse och Föredrag. 6th Meeting, Lund* 1947, p. 179.
4. Norman, A. *Arkiv. Kemi* **8** (1955) 331.
5. Ekwall, P., Setälä, K. and Sjöblom, L. *Acta Chem. Scand.* **5** (1951) 175.
6. Klevens, H. B. *J. Phys. & Colloid. Chem.* **54** (1950) 283.
7. Sjöblom, L. *Acta Acad. Aboensis, Math. et Phys.* **XXI** (1958) No. 6.
8. Sjöblom, L. *Acta Acad. Aboensis, Math. et Phys.* **XX** (1956) No. 14.

Received March 1, 1960.

ACTA CHEMICA SCANDINAVICA 14 (1960) 1300—1309

The Conductance of Conjugated and Unconjugated Bile Acid Salts in Aqueous Solutions

Bile Acids and Steroids 80

ARNE NORMAN*

Department of Physiological Chemistry, University of Lund, Lund, Sweden

The equivalent conductances of aqueous solutions of the sodium salts of cholic, taurocholic, glycocholic, deoxycholic, taurodeoxycholic, glycodeoxycholic and dehydrocholic acids in the concentration range from 0.002 to 0.5 M were measured at 40°C. All these bile salts were found to differ from a normal uni-univalent electrolyte in their conductance behaviour. The beginning association leads to a greater than normal increase in the conductance in cholate and deoxycholate solutions. The advancement of the association in more concentrated solutions causes the slope of the curve plotting equivalent conductance against root concentration to decrease. With deoxycholate this results in a maximum which is followed by a minimum, while with cholate only a change in the slope of the curve occurs. The variations in the courses of the conductance curves are less pronounced for bile salts than for paraffin chain salts and therefore an evaluation of the critical concentration from the conductance data is not possible for bile acid salts. The conductance curves for the conjugated bile acid salts do not differ essentially from those for the unconjugated bile acid salts, which may be taken to indicate that the progress of association is similar.

Numerous studies have shown that salts of bile acids are association colloids. From the values of the osmotic coefficients of bile acid solutions Roepke and Mason [2] concluded that an association takes place in solutions of both conjugated and unconjugated bile acid salts. McBain *et al.* [3] studied the solubilization of water-insoluble lipophilic dyes by cholate and deoxycholate solutions and deduced that the hydrotropic properties of bile acid salt solutions are due to the formation of micelles. Micelle formation is not so clearly revealed by conductance data because of the weak influence of association on conductance in bile salt solutions [2]. Mellander and Stenhagen's [4] measurements showed

* Present address: Department of Chemistry, Karolinska Institutet, Stockholm.

that the conductance of sodium taurocholate solutions was normal below 0.01 M but above this concentration the conductance curve suddenly changed its slope. Ekwall and Fontell [5] studied the conductances of sodium cholate solutions over a wide concentration range (0.005 M to 0.4 M) and found that the curve plotting the equivalent conductance against the square root of the concentration resembled the curves obtained for soaps, but was less affected by the association.

Extensive studies of the association in sodium cholate and deoxycholate solutions have been carried out by Ekwall and coworkers [6,7]. A stepwise association was found to take place and three different concentration limits (limits 1, 2 and 3) were shown to exist in the solutions of the bile acid salts studied. Below the first limit, there is no association. Between the limits 1 and 2 the association is of limited scope and leads to the formation of very small aggregates, but already above the limit 2 all the added substance associates to form somewhat larger aggregates. Above the limit 3, the degree of association increases further. Aggregates of colloidal dimensions could be demonstrated to exist down to the limit 3. The concentration limits in deoxycholate solutions were 0.004—0.006 M (limit 1), 0.009—0.010 M (limit 2) and 0.04—0.05 M (limit 3), while those in cholate solutions were 0.013—

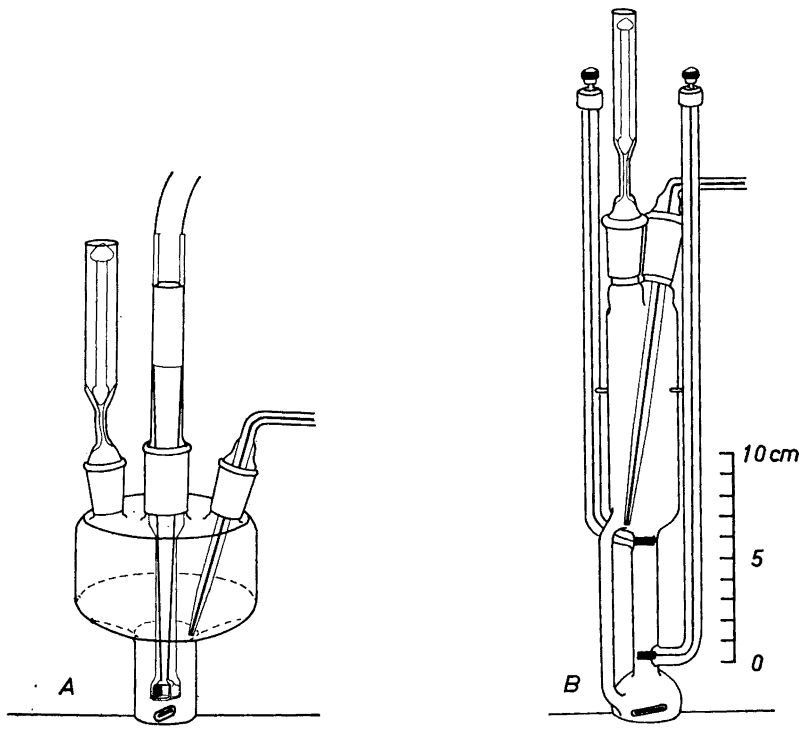

Fig. 1. Conductance cells.

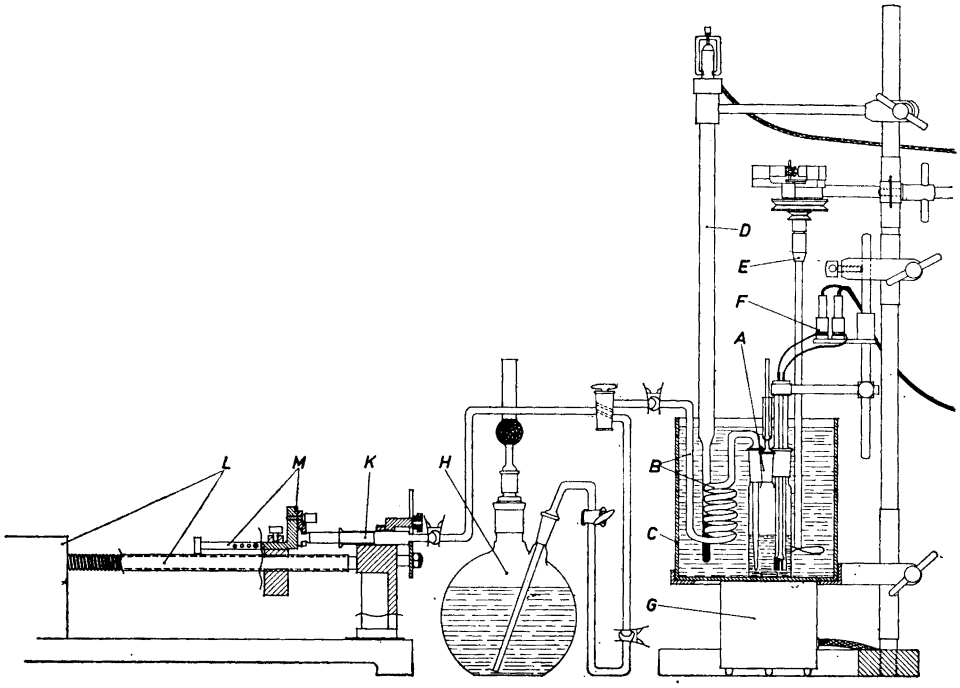

Fig. 2. Apparatus for the continuous introduction of water or solution into a conductance cell at a constant temperature. A: Conductance cell (type C). B: Glass tube through which water or solution enters the cell. C: Thermostat vessel of transparent Lucophlex. D: Contact thermometer. E: Air-driven mixer. F: Leads from platinum electrode to measuring bridge. G: Magnetic mixer. H: Storage vessel. K: All-glass syringe. L: Drive mechanism. M: Bracket moving plunger of syringe.

0.015 M, 0.045—0.050 M and 0.09—0.11 M. If one wishes to define the critical concentration for micelle formation in these solutions of bile acids salts, it lies according to Ekwall at the concentration limit 2 where the association is almost complete.

The aim of the present investigation was to study the influence of association on the conductance of aqueous solutions of sodium cholate, deoxycholate and dehydrocholate. The conductances of aqueous solutions of the glycine and taurine conjugates of cholate and deoxycholate were also measured to permit a comparison of the processes of association in solutions of conjugated and unconjugated bile salts. Automatic recording of resistance according to Andersson, Stenhagen and Mellander [1] was used to determine the resistances of bile acid salt solutions on progressive dilution.

EXPERIMENTAL

Materials. The sodium salts of the conjugated bile acids were synthesized as described previously [8]. All the salts were dried *in vacuo* at 100° for 12 h before use. The water employed had been distilled twice and had a specific conductance not greater than 0.5 $\times 10^{-6}$ ohm^{-1} cm^{-1} at 25°C.

Table 1.

Cell type	Cell constant	Minimum volume (ml)	Total volume (ml)
A	0.87	22	210
B	5.78	29	80
C	0.57	40	120

Conductance cell. The conductance cells were of the types shown is Figs. 1 and 2. It was found that the solutions in these cells could be very effectively mixed with rotating magnetic bars. The cells A and C were made of Pyrex glass and the double electrodes used in them of Jena glass. Cell B was made of Jena glass. Each cell was equipped with a valve that allowed air to escape when liquid was added to the cell. The conductance of the solution determined which cell could be used. The electric field between the electrodes varies with the level of the surface of the solution above the electrodes and the effect of this level on the resistance of the cell was studied. The resistances of the cells were measured after the cells had been filled with 0.01 N potassium chloride so that the electrodes were just covered and then continually as more potassium chloride solution was added. Fig. 3 shows the variation of the cell constant with the height of the electrolyte within the cells. It will be seen that the value of the cell constant no longer changes after a certain level has been exceeded. Characteristic values for the three cells are collected in Table 1. The values of the cell constants were checked from time to time using fresh potassium chloride standard solutions.

Thermostat. To avoid condensation of solvent, the whole conductance cell (A) and the spiral tube (B) through which water was introduced into the cell were immersed in the water of the thermostat to the level indicated in Fig. 2. The thermostat (C) was made of transparent Lucophlex, 4 mm thick, and was fastened to a stand. The heat source was a 250 W infrared lamp which was focussed on the wall of the thermostat. With the lamp connected to the electric mains through an electronic relay operated by a contact thermometer (D), the temperature of the water within the thermostat could be kept constant at 40° ± 0.005°C.

Introduction of solution into the conductance cell. The apparatus employed to effect progressive dilution of the electrolyte solution with water is shown in Fig. 2. An all-glass syringe (K) with a spherical ground surface is fastened to a drive mechanism (L) which moves the plunger at a constant velocity. The syringe is connected by a two-way stopcock and capillary tubes to the inlet tube (B) of the conductance cell and to a storage vessel (H). In this way access of carbon dioxide from the air to the water being introduced into the cell is avoided during an experiment. The rate of flow of water was varied between 1 and 2 ml/min. This rate was determined by the time required for the water to warm up to a constant temperature within the spiral tube.

Procedure. Suitable weights of the bile acid salts were dissolved and the solutions diluted to volume in volumetric flasks at 40°C with water free from carbon dioxide. An amount of each solution was then weighed into the conductance cell. The cell together with the spiral tube was immersed in the thermostat and fastened by a clamp to the stand. The spiral tube was connected to the unit for introducing water into the cell.

The continuous recording of the electrolytic resistance was carried out with an apparatus described by Andersson, Stenhagen and Mellander [1]. A condition that must be fulfilled when this method is employed is that no greater capacitive unbalance develops during the recording. For a discussion of errors in measurement and for a description of a circuit that permits simultaneous compensation and registration of the capacitance, a paper by Andersson, Möhl and Stenhagen may be consulted [9]. On diluting a 0.1 M taurocholate solution to a 0.02 M solution in cell A, the capacitance of the cell increased by only 20 pF while the resistance increased by 335.2 Ω. The null position was re-established eight times by balancing the resistive and capacitive components of the bridge separately while the resistance was being recorded in this experiment. It is thus obvious that the capacitive unbalance developed did not materially affect the recorded resistance values.

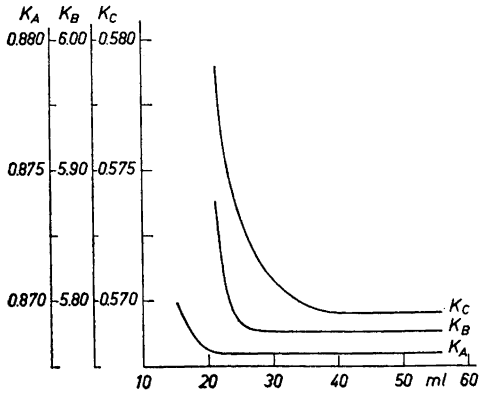

Fig. 3. Variation of cell constants for cells A, B and C as a function of the added volume of 0.01 M potassium chloride solution. Temperature: 40°C. Continuous recording of electrolytic resistance.

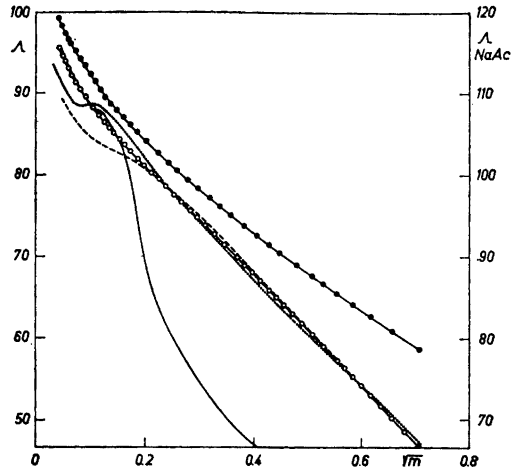

Fig. 4. Equivalent conductance at 40°C. as a function of the square root of the molar concentration for sodium dehydrocholate (O—O), sodium deoxycholate (.....), sodium cholate (— — — —), and sodium acetate (●—●). The values for sodium laurate (———) at 40°C are those reported by Ekwall [14].

RESULTS

The method employed to record the resistance continuously can be applied only to relatively dilute (under 0.05 M) solutions of bile acid salts in which the equilibration of the solution during the addition of water can be effected practically instantaneously. The results of the measurements are plotted in Figs. 5, 7 and 8. When more concentrated solutions are employed, the time that is required before the resistance becomes constant after the addition of a certain quantity of water is so long that a satisfactory accuracy cannot be attained in the measurement of resistance by the continuous recording technique. For example, solutions of the bile salts studied that are between 0.5 and 0.3 M require 10 to 15 min before the value of the resistance becomes constant. Figs. 4, 9 and 10 give the results of the determinations of electrolytic resistance for individual dilution series. Several series of dilutions extending over the same concentration range were prepared from each bile acid salt. Separately recorded curves plotting the equivalent conductance as a function of concentration exhibited satisfactory agreement.

DISCUSSION

The variation of equivalent conductance against root concentration is shown for sodium cholate, deoxycholate, dehydrocholate, acetate and laurate in Fig. 4. The courses of the curves for these compounds in the concentration range 0.002—0.05 M are seen in Fig. 5.

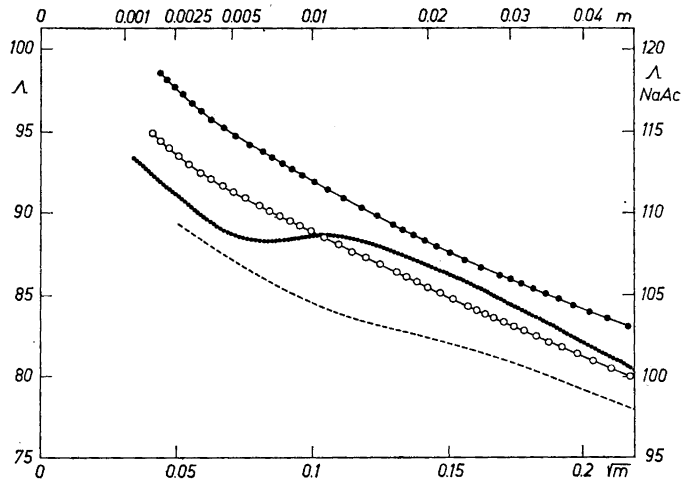

Fig. 5. Equivalent conductance at 40°C as a function of the square root of the molar concentration for sodium dehydrocholate (O—O), sodium deoxycholate (.....), sodium cholate (— — — — —) and sodium acetate (● — ●).

In the concentration range below 0.05 M, the curve for dehydrocholate is similar in form to the curve for a normal uni-univalent electrolyte, *e.g.* sodium acetate. According to McBain [3] the osmotic coefficients of dehydrocholate solutions do not deviate significantly from the values for a normal electrolyte and Ekwall and coworkers [10] were unable to detect any association in dilute solutions of this bile acid salt by solubilization studies. The latter authors found that a low degree of association occurs when the concentration of the salt exceeds 0.15—0.2 M (limit 1) and a higher degree of association at concentrations above 0.7 M (limit 2). Accordingly, no deviation from the normal variation of the conductance was to be expected below 0.15 M.

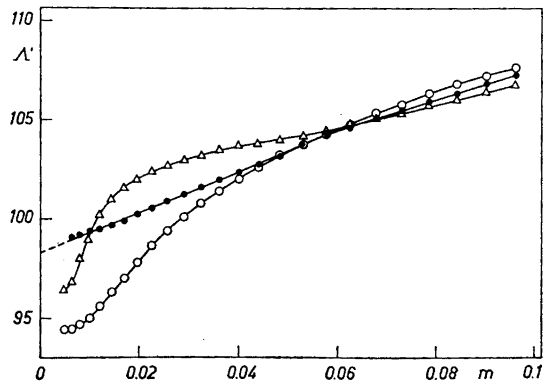

Fig. 6. Plot of Λ' *versus* molar concentration for sodium cholate (O—O), sodium deoxycholate (△—△), and sodium dehydrocholate (● — ●). 40°C.

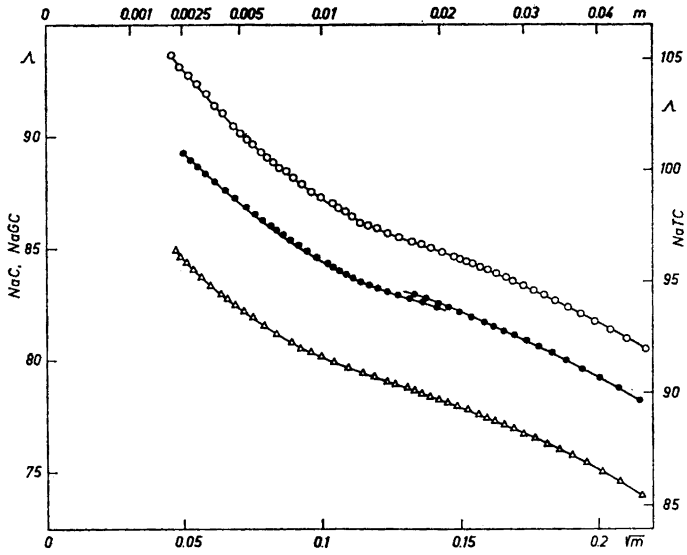

Fig. 7. Equivalent conductance at 40°C as a function of the square root of the molar concentration for sodium cholate (●—●), sodium taurocholate (O—O), and sodium glycocholate (△—△).

Both sodium cholate and sodium deoxycholate exhibit a behaviour that deviates clearly from that of a normal uni-univalent electrolyte. The equivalent conductance of sodium cholate begins to decrease at a slower rate than in the case of a normal electrolyte when the concentration exceeds 0.01 M but when the concentration exceeds 0.04 M the conductance decreases more rapidly. The curve for sodium deoxycholate passes through a minimum at a concentration of 0.005 M and a maximum at a concentration of 0.01 M, while above the latter concentration the equivalent conductance decreases relatively rapidly. The first deviations from the behaviour of a normal electrolyte thus occur with both cholate and deoxycholate at the same concentrations where Ekwall and coworkers [6] detected the first signs of beginning association (limit 1) The second deviations occured at concentrations (limit 2) where the association is, according to Ekwall, of such degree that all the added bile salt anions undergo association.

The deviations from the normal behaviour become more clearly evident when the limiting equivalent conductance Λ_∞ is determined by extrapolating the plot of the function $\Lambda' = \dfrac{\Lambda + A\sqrt{c}}{1 - B\sqrt{c}}$ (where A and B are the constants of the Onsager equation) *versus* concentration (Fig. 6) [11]. The corresponding points for dehydrocholate lie close to a straight line as is the case for a normal electrolyte. The deviations seen at the lowest concentrations are evidently due to hydrolysis and the presence of impurities in the water. The value of the equivalent conductance of sodium dehydrocholate at infinite dilution is

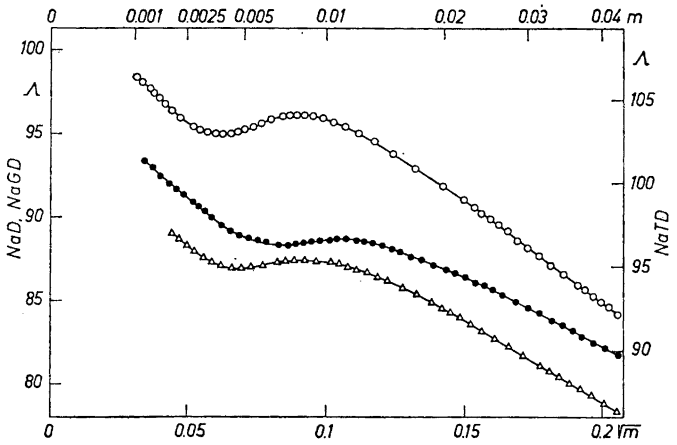

Fig. 8. Equivalent conductance at 40°C as a function of the square root of the molar concentration for sodium deoxycholate (● — ●), sodium taurodeoxycholate (O — O) and sodium glycodeoxycholate (△ — △).

found by extrapolation to be 98.0. The curves plotting Λ' are so abnormal for cholate and, especially, deoxycholate that no value can be obtained for the limiting equivalent conductance by extrapolation.

The equivalent conductance of cholate and deoxycholate solutions between the concentration limits 1 and 2 is higher than the value calculated assuming the existence of single ions only. The increased conductance is possibly due to a higher mobility of the aggregates in accordance with Stokes' law. After the first increase noted in cholate and deoxycholate solutions when association sets in, the conductance decreases more than would be expected for a normal univalent electrolyte as the bile salt concentration increases over the limit 2 (Figs. 4 and 5). The behaviour is similar to that observed in solutions of the sodium salts of higher fatty acids in which a marked decrease in the equivalent conductance occurs above the critical concentration. The decrease in the latter solutions has been mainly ascribed to the binding of gegenions by the micelles. Also the lowering of the conductance with increasing concentration in cholate and deoxycholate solutions above concentration limit 2 may presumably be ascribed to the same factor. Micelle formation in bile salt solutions has only a slight effect on the conductance and hence it is difficult to evaluate the critical micelle concentration of bile salts as in the case of the sodium salts of higher fatty acids.

The curves plotting equivalent conductance against root concentration for solutions of the taurine and glycine conjugates of cholate and deoxycholate (Figs. 7 — 10) all deviate from the corresponding curve for a normal uni--univalent electrolyte but do not differ in this respect essentially from the curves for the unconjugated bile salts. The first deviation from the normal behaviour does, however, occur at a lower concentration (0.003 M) with tauro- and glycodeoxycholate than with unconjugated deoxycholate (0.005 M).

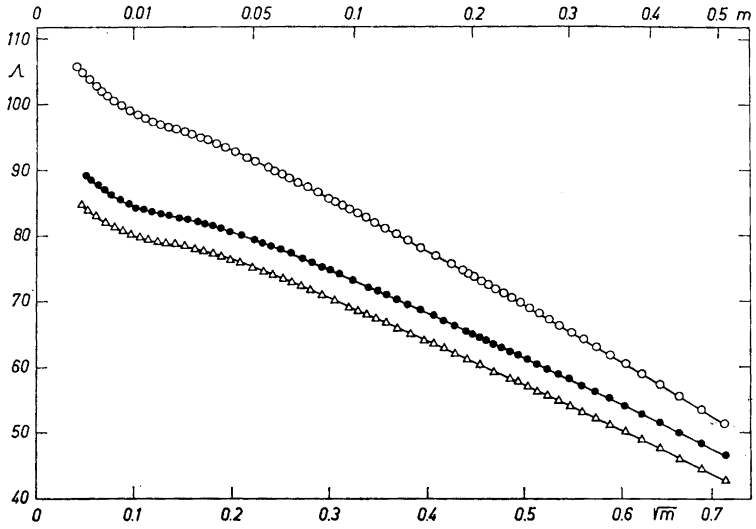

Fig. 9. Equivalent conductance at 40°C as a function of the square root of the molar concentration for sodium cholate (●—●), sodium taurocholate (O—O), and sodium glycocholate (△—△).

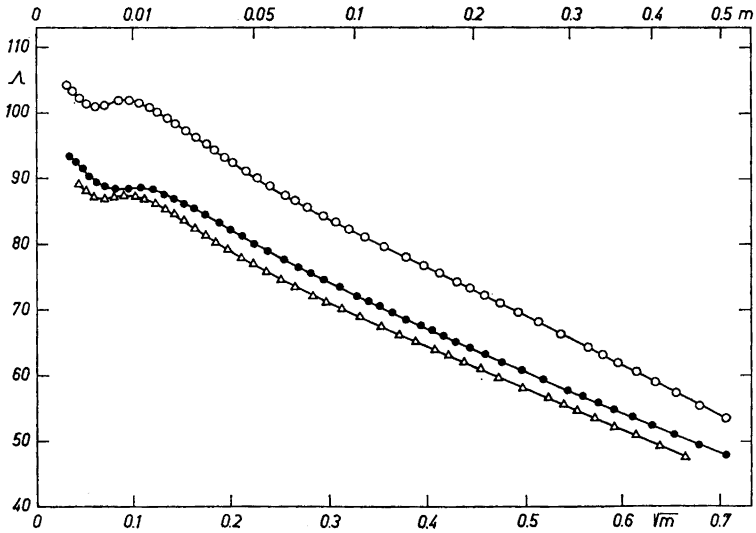

Fig. 10. Equivalent conductance at 40°C as a function of the square root of the molar concentration for sodium deoxycholate (●—●), sodium taurodeoxycholate (O—O), and sodium glycodeoxycholate (△—△).

Judging from the variation of the equivalent conductance with concentration, it seems improbable that there is any greater difference in the nature of the association process between the conjugated and unconjugated compounds. This conclusion is in accord with the results of previous studies of the ability of the taurine and glycine conjugates of cholate and deoxycholate to solubilize xylene [6,12] and 20-methylcholanthrene [13]. These observations suggest that the various phases of the association process, the beginning association and its stepwise development, and the saturation capacities of the aggregates formed are with only minor variations similar for both conjugated and unconjugated bile acid salts.

Acknowledgement. The author wishes to express his gratitude to Professor Einar Stenhagen and Dr. Carl-Ove Andersson for valuable help with construction of the apparatus for conductivity measurements, and to Professor Per Ekwall for helpful discussions. The skilful technical assistance of Mrs. Margret Månsson is gratefully acknowledged. This investigation was supported by grants from *Statens Medicinska Forskningsråd* and the *National Heart Institute* (H2842), U.S. Public Health Service, Bethesda, Maryland.

REFERENCES

1. Andersson, C.-O., Stenhagen, E. and Mellander, O. *Acta Chem. Scand.* **10** (1956) 1317.
2. Roepke, R. R. and Mason, H. L. *J. Biol. Chem.* **133** (1940) 103.
3. McBain, J. W. *Frontiers in Chem.* **7** (1950) 113.
4. Mellander, O. and Stenhagen, E. *Acta Physiol. Scand.* **4** (1942) 349.
5. Ekwall, P. *Acta Acad. Aboensis, Math. Phys.* **XVII** (1951) No. 8.
6. Ekwall, P., Fontell, K. and Sten, *A. Proc. 2nd Intern. Congr. Surface Activity, Gas/Liquid and Liquid/Liquid Interface*, Butlerworths, London 1957, p. 357.
7. Ekwall, P. and Ekholm, R. *Proc. 2nd Intern. Congr. Surface Activity, Gas/Liquid and Liquid/Liquid Interface*, Butterworths, London 1957, p. 23.
8. Norman, A. *Arkiv Kemi* **8** (1955) 331.
9. Andersson, C.-O., Möhl, F. and Stenhagen, E. *Acta Chem. Scand.* **12** (1958) 415.
10. Ekwall, B. and Fontell, M. *To be published.*
11. Shedlovsky, T. *J. Am. Chem. Soc.* **54** (1932) 1405.
12. Ekwall, P. *et al. To be published.*
13. Norman, A. *Acta Chem. Scand.* **14** (1960) 1295.
14. Ekwall, P. *Kolloid-Z.* **101** (1942) 135.

Received March 1, 1960.

ACTA CHEMICA SCANDINAVICA 14 (1960) 1310—1316

A Brownian Motion Theory of Chemical Reactions

THOR A. BAK and IGOR W. PLESNER

Institute for Physical Chemistry, University of Copenhagen, Denmark

A theory for the dissociation of a diatomic molecule in weak interaction with a thermostat is proposed. Exact solutions are given for a harmonic oscillator.

In the classical collision theory of chemical reactions in gases it was generally assumed that dissociation of a molecule occurs by direct transitions from low vibrational states to the dissociated state. In recent years [6] it has however become clear that the energy transfer to the vibrational degrees of freedom during a molecular collision generally is small compared with the dissociation energy. Under these circumstances it is necessary to consider the dissociating molecule as performing a random walk or Brownian motion in "energy space" on its way to the dissociation energy. The small random changes in energy are caused by the collisions between the reacting molecule and the other molecules which act as a thermostat. Although large amounts of translational energy may be transferred during such collisions, only a small part of the collision energy goes into the vibrational degrees of freedom, and we can therefore speak of the reacting molecule as being weakly coupled to a thermostat. For the case of a diatomic molecule imbedded in a crystal lattice it is of course even more so that the molecular oscillator is only loosely coupled to the crystal lattice.

The first one to investigate such an approach to chemical kinetics was Kramers [5] who in 1940 developed a theory of Brownian motion in a field of force and thus was able to make a diffusion model of chemical reactions as suggested many years before by Christiansen [4]. In this theory one visualizes the chemical reaction as the escape of a particle from a potential minimum due to the shuttling action of the thermostat. If $\Phi(E,t)$ denotes the probability that the particle has the energy E at time t, one finds for the case of weak interaction between the particle and the thermostat ("small viscosity" in the language of Kramers)

$$\frac{\partial \Phi}{\partial t} = \eta \frac{\partial}{\partial J} J\left(1 + kT \frac{\partial}{\partial E}\right)\Phi \qquad (1)$$

where $J(E) = \int p dq$ is the action variable, η is the parameter which measures the interaction with the heat bath. In the special case of a parabolic potential minimum this equation reads

$$\frac{\partial \Phi}{\partial t} = \eta \frac{\partial}{\partial x} x \left(1 + \frac{\partial}{\partial x}\right)\Phi \tag{2}$$

where $x = E/kT$.

The coupling parameter (friction coefficient) η is defined by the Langevin equation

$$\dot{p} = -\eta p + K(q) + A(t) \tag{3}$$

in which p is the linear momentum of the particle, $K(q)$ the force whose potential is the potential energy along the reaction coordinate, and $A(t)$ the "random force" which represents the action of the thermostat. It is usually assumed that the friction coefficient is constant (that is, independent of p) but Kramers mentions the possibility that it might be replaced by an arbitrary (even) function of p, although he does not investigate this case further. As we shall see below for the case of Brownian motion in crystals the assumption that η is independent of p is identical with an assumption by Peierls about the interaction between normal modes in a crystal, which can be shown to be valid to the same accuracy as for instance the Debye approximation in the theory of specific heat. It is therefore not inconceivable that one might find physical systems which for their proper description would require a theory in which η is not assumed to be constant.

A quantum mechanical analogue of Kramers' theory was given by Montroll and Shuler [7] for the case of a particle in a parabolic potential minimum, *i.e.* an harmonic oscillator. Let the classical frequency of the oscillator be ω so that the energy levels are $(n + \frac{1}{2})\hbar\omega$ and let Θ denote $\hbar\omega/kT$. Montroll and Shuler then obtain in their random walk model the following equation

$$\frac{dx_n}{dt} = \varkappa \{n e^{-\Theta} x_{n-1} - [n + (n+1) e^{-\Theta}] x_n + (n+1) x_{n+1}\} \tag{4}$$

where x_n is the probability that the oscillator is in a state with energy $n\hbar\omega$ over the zeropoint energy, and $\varkappa$ is a parameter which measures the interaction with the heat bath. A similar equation has been proposed by Nikitin [8].

It is not immediately obvious that an equation of this type is a quantum mechanical analogue of the Kramers equation, but assuming $\Theta << 1$ so that $e^{-\Theta}$ can be replaced by $1-\Theta$ we can write the equation as

$$\frac{dx_n}{dt} = \Theta \varkappa \left\{ n\Theta \frac{x_{n+1} - 2x_n + x_{n-1}}{\Theta^2} + \frac{x_{n+1} - x_n}{\Theta} + n\Theta \frac{x_n - x_{n-1}}{\Theta} + x_n \right\} \tag{5}$$

When we replace $n\Theta$ by x and x_n by Φ and furthermore let $\hbar \to 0$, we get

$$\frac{\partial \Phi}{\partial t} = \eta [x\Phi'' + (1+x)\Phi' + \Phi] = \eta \frac{\partial}{\partial x} x \left(1 + \frac{\partial}{\partial x}\right)\Phi$$

where η is the limit of $\Theta\varkappa$ as $\hbar \to 0$.

In this way we see that the two approaches lead to corresponding equations and that the equation of Montroll and Shuler therefore is the proper generalization of the Kramers equation.

In both theories one uses transition probabilities or random forces, and this gives rise to the parameter η $(= \Theta\varkappa)$ which essentially is a non calculable quantity. It is true that, as stated by Montroll and Shuler, η is in principle calculable from the quantum mechanical theory of collisions, but if one tries to do so eqn. (4) will require additional justification, since there is as yet no simple way of getting such a "master equation" directly from quantum mechanics or classical mechanics. If one can justify the use of the master equation, *i.e.*, essentially explain how irreversibility arises in a mechanical system, then within this framework the calculation of η will be immediate, but within the conceptually much simpler framework of the Kramers theory or Montroll and Shuler theory the coupling constant is, to our minds, best considered as an empirical parameter.

To get a theory for chemical reactions one now assumes that the particle under consideration performs a Brownian motion in the potential hole as long as its energy is smaller than E_{act}, and that it is annihilated when its energy exceeds E_{act}. This is evidently a crude model of a particle passing a potential barrier, and since it is possible to solve eqn. (2) exactly for the boundary condition $\Phi(x^*,t) = 0$ (all t), it is possible in this way to estimate how much the distribution in energy space $\Phi(x,t)$ differs from the equilibrium distribution and how much this influences the rate constant.

BROWNIAN MOTION OF A DIATOMIC MOLECULE

Using the explicit assumption that the oscillating molecule is in weak interaction with the thermostat we can write the energy of the system consisting of a molecule plus the thermostat as

$$\mathcal{H} = H_T + H_M + \lambda V$$

where λ is a small dimensionless parameter.

The energy of the thermostat can be considered as a sum of energies of a large number of subsystems without interaction, that is,

$$H_T = \sum_k H_T^{(k)}$$

and we now introduce angle-action variables for the subsystems of the thermostat and for the molecule and make a Fourier expansion of the interaction potential V on the angle variables. For the special case of a harmonic oscillator imbedded in a lattice, which we have considered previously [1,2,11] we have

$$\mathcal{H} = \sum_{f=1}^{N} \omega_f J_f + \omega J + \lambda \sum_\nu \sum_f \{V_{\nu f}^{+} \, e^{i(a_f + \nu\alpha)} + V_{\nu f}^{-} \, e^{i(-a_f + \nu\alpha)}\}$$

Here f is the wavenumber for the normal modes of the lattice, α and J denote angle-action variables, and $V_{\nu f}{}^{+} = V_f q_f^{\circ}{}_{+} J_\nu(fr_0)$, where $q_f^{\circ}{}_{+}$ is the amplitude of the f'th normal mode, r_0 the amplitude of the molecular oscillator and $J_\nu(fr_0)$ denotes the Bessel function of order ν. V_f is assumed to be independent of the energy of the oscillator. For a derivation of this expression for $\mathcal{H}$ see Ref. [1] or Ref. [2]

Using this Hamiltonian the Liouville equation is set up and solved by the perturbation technique used by Brout and Prigogine [3]. In the limit $\lambda \to 0$, $t \to \infty$, $\lambda^2 t$ finite, $N \to \infty$ this leads to eqn. (2) after an integration over the frequency spectrum of the lattice, provided the so-called Peierls assumption [9]

$$\frac{|V_f|^2}{\omega_f{}^2} = \text{constant}$$

is valid. Since in this derivation of eqn. (2) η is proportional to $|V_f|^2/\omega_f{}^2$ we see that the assumption that this quantity is independent of f and of the energy of the oscillator is tantamount to the assumption of Kramers, that η is independent of the momentum of the particle. The range of validity of the Peierls approximation has been investigated by Plesner [10] who has shown that in a one-dimensional lattice with nearest neighbour interaction it has the same range of validity as the Debye approximation for the frequency spectrum of the lattice. Since the assumption of a Debye spectrum is necessary anyway in integrating over the frequency spectrum of the crystal, the Peierls approximation is a reasonable assumption in this case, but it is quite possible that when considering a system where the thermostat is not a crystal one can get an energy dependent friction coefficient.

CHEMICAL REACTION AS ANNIHILATION OF PARTICLES

To use the equation for Φ in a model of chemical reactions we must have an intramolecular potential which allows a dissociation of the molecule, *i. e.*, a potential for which the particle has one or more "bound states" and a "free state" into which it goes or through which it passes from one bound state to another.

So far we have not been able to treat a potential of this type, and we have therefore used the following model of a chemical reaction. A particle which is weakly coupled to a thermostat moves in potential $V = V(q)$ as long as its energy is smaller that E^*, but when its energy reaches E^*, it ceases to exist. For the special case of a harmonic oscillator eqn. (2) will then apply for $x < x^* = E^*/kT$, but for $x > x^*$ we have $\Phi(x,t) = 0$. The solution of this boundary value problem in the range $0 < x < x^*$ is

$$\Phi = \sum_a c_a e^{-a\eta t} e^{-x} {}_1F_1(-a,1,x)$$

where the summation over a goes over the roots of

$${}_1F_1(-a,1,x^*) = 0$$

Table 1.

x *	α_1	α_2	α_3	α_4	α_5
1.0	10.00000(−1)	71.95819(−1)	18.30293		
1.2	76.97406(−2)	59.41822(−1)	15.19890	28.56591	
1.4	60.82404(−2)	50.50560(−1(	12.98659	24.44412	
1.6	48.96119(−2)	43.86213(−1)	11.33113	21.35661	
1.8	39.96001(−2)	38.72785(−1)	10.04731	18.95957	30.61161
2.0	32.94893(−2)	34.65393(−1)	90.23554(−1)	17.04459	27.53224
2.2	27.38760(−2)	31.34842(−1)	81.88976(−1)	15.48130	25.01535
2.4	22.90635(−2)	28.62121(−1)	74.96262(−1)	14.18098	22.92064
2.6	19.25139(−2)	26.33808(−1)	69.12601(−1)	13.08343	21.15093
2.8	16.24117(−2)	24.40428(−1)	64.14741(−1)	12.14507	19.63642
3.0	13.74233(−2)	22.74995(−1)	59.85461(−1)	11.33406	18.32608
3.2	11.65566(−2)	21.32238(−1)	56.12010(−1)	10.62652	17.18163
3.4	99.02155(−3)	20.08193(−1)	52.84408(−1)	10.00419	16.17379
3.6	84.23423(−3)	18.99773(−1)	49.95132(−1)	94.52907(−1)	15.27981
3.8	71.72192(−3)	18.04421(−1)	47.38103(−1)	89.61433(−1)	14.48182
4.0	61.10610(−3)	17.20256(−1)	45.08492(−1)	85.20806(−1)	13.76510
4.2	52.08030(−3)	16.45650(−1)	43.02396(−1)	81.23801(−1)	13.11836
4.4	44.39394(−3)	15.79309(−1)	41.16610(−1)	77.64445(−1)	12.53196
4.6	37.84039(−3)	15.20119(−1)	39.48498(−1)	74.37784(−1)	11.99804
4.8	32.24797(−3)	14.67208(−1)	37.95862(−1)	71.39850(−1)	11.51003
5.0	27.47317(−3)	14.19805(−1)	36.56844(−1)	68.67103(−1)	11.06244
5.5	18.36738(−3)	13.21352(−1)	33.59200(−1)	62.77588(−1)	10.09137
6.0	12.23186(−3)	12.45678(−1)	31.18660(−1)	57.93720(−1)	92.89385(−1)
6.5	81.09532(−4)	11.87272(−1)	29.22134(−1)	53.91185(−1)	86.17492(−1)
7.0	53.50914(−4)	11.42145(−1)	27.60263(−1)	50.52646(−1)	80.47932(−1)
7.5	35.13758(−4)	11.07323(−1)	26.26165(−1)	47.65390(−1)	75.60263(−1)
8.0	22.96773(−4)	10.80539(−1)	25.14657(−1)	45.19884(−1)	71.39215(−1)
8.5	14.94463(−4)	10.60035(−1)	24.21748(−1)	43.08846(−1)	67.73090(−1)
9.0	96.84116(−5)	10.44433(−1)	23.44301(−1)	41.26605(−1)	64.52799(−1)
9.5	62.51391(−5)	10.32642(−1)	22.79807(−1)	39.68689(−1)	61.71168(−1)
10.0	40.21350(−5)	10.23798(−1)	22.26220(−1)	38.31511(−1)	59.22463(−1)
11.0	16.48616(−5)	10.12366(−1)	21.45267(−1)	36.08260(−1)	55.06124(−1)
12.0	66.87333(−6)	10.06240(−1)	20.90830(−1)	34.39164(−1)	51.75745(−1)
13.0	26.88773(−6)	10.03065(−1)	20.55158(−1)	33.11758(−1)	49.11934(−1)
14.0	10.73105(−6)	10.01469(−1)	20.32486(−1)	32.16846(−1)	47.00818(−1)
15.0	42.56524(−7)	10.00689(−1)	20.18554(−1)	31.47334(−1)	45.32169(−1)
16.0	16.79150(−7)	10.00318(−1)	20.10282(−1)	30.97535(−1)	43.98210(−1)
17.0	65.93358(−8)	10.00144(−1)	20.05540(−1)	30.62793(−1)	42.92842(−1)
18.0	25.78560(−8)	10.00064(−1)	20.02906(−1)	30.39256(−1)	42.11074(−1)
19.0	10.04701(−8)	10.00028(−1)	20.01489(−1)	30.23861(−1)	41.48774(−1)
20.0	39.02197(−9)	10.00012(−1)	20.00747(−1)	30.14040(−1)	41.02246(−1)
∞	0	1	2	3	4

* α_k (k = 1, 2, 3, 4, 5) are the zeros of the function ${}_1F_1(-a, 1, x^*)$ considered as a function of a. The numbers in brackets are the powers of ten by which the values given for α_k should be multiplied.

considered as an equation in a. The first five roots of this equation are tabulated in Table 1 for different values of x^*.

It is seen that when $x^* \sim 10$, α_2 (and *a fortiori* α_3, α_4, ...) will be more than a thousand times larger than α_1, so that to an excellent approximation we can set

$$\Phi = c_1 e^{-\alpha_1 \eta t} e^{-x} {}_1F_1(-\alpha_1, 1, x)$$

where α_1 is the smallest root in the equation ${}_1F_1(-\alpha_1, 1, x^*) = 0$.

Table 2. The table shows the ratio between the "true" rate constant $k = \eta a_1 (x^*)$ and the equilibrium rate constant $k_{eq} = \eta x^* e^{-x^*}$ as function of x^*.

k/k_{eq}	1.21730	0.83407	0.82245	0.85582	0.88576
x^*	2	4	6	8	10
k/k_{eq}	0.90670	0.92180	0.93257	0.94060	0.94661
x^*	12	14	16	18	20

From this we get immediately that the rate constant for escape from the potential minimum is $\alpha_1\eta$ and furthermore we see that while the reaction is going on the change in Φ is so that the relative change in Φ is independent of x. In other words, the distribution function in energy space has a quasi-stationary character.

It is easily verified that as $x^* \to \infty$, α_1 becomes asymptotically equal to $x^* e^{-x^*}$. Since in this limit Φ approaches the equilibrium distribution e^{-x}, we shall denote $k_{eq} = \eta x^* e^{-x^*}$ the equilibrium rate constant. It is well to bear in mind, though, that in deriving this expression we have nowhere used the assumption about equilibrium as is done, for instance, in the transition state method. Table 2 shows how the exact value of $\alpha_1(x^*)$ compares with the "equilibrium value" of α_1, and it is seen that for $x^* > 10$ the error is less than 12 %. It is true, therefore, that for reasonable values of the activation energy the equilibrium hypothesis is a good approximation, but only when the equilibrium result is taken to be the limit of the non-equilibrium result, as the barrier height is increased to infinity. To introduce the equilibrium assumption at an earlier stage would not only lead to a quite different result, but it would also lead to a non-consistent theory.

CONCLUSION

Above we have compared the different Brownian motion approaches to chemical kinetics and shown how they lead to the same result in the case of a dissociating harmonic oscillator. In comparison with earlier derivations of the equation for this case our method which is based on the method of Brout and Prigogine may seem unduly complicated. This is due to the fact that we have not made any assumptions about "random interactions", but only used that the thermostat is large (infinitely many degrees of freedom) and that the interaction is weak ($\lambda \to 0$). Therefore, to our mind, our derivation of the Kramers equation in the weak interaction limit does present some advantage over previous derivations.

Acknowledgements. This work has been sponsored in part by the Aeronautical Research Laboratory, Wright Air Development Center, of the Air Research and Development Command, United States Air Force, through its European Office.

The preparation of the tables was supported by *Carlsberg Fonden* and carried out at Dansk Regnecentral.

REFERENCES

1. Bak, T. A. *Contributions to the Theory of Chemical Reactions*, Wiley, New York 1959.
2. Bak, T. A., Goche, M. and Henin, F. *Molecular Physics* **2** (1959) 181.
3. Brout, R. and Prigogine, I. *Physica* **22** (1956) 35.
4. Christiansen, J. A. *Z. physik. Chem.* **B33** (1936) 145.
5. Kramers, H. A. *Physica* **7** (1940) 284.
6. Mc Coubrey, J. C. and Mc. Grath, W. D. *Quart. Revs. London* **11** (1957) 87.
7. Montroll, E. and Shuler, K. *J. Chem. Phys.* **26** (1957) 454.
8. Nikitin, E. E. *Doklady Akad. Nauk. S.S.S.R.* **121** (1958) 991, translated as *Soviet Phys. Doklady* **3** (1958) 701.
9. Peierls, R. E. *Quantum Theory of Solids*, Oxford University Press 1955, p. 130.
10. Plesner, I. W., Technical Note No. 3, Contract No. AF 61 (052)-133 Air Research and Development Command, United States Air Force.
11. Prigogine, I. and Bak, T. A. *J. Chem. Phys.* **31** (1959) 1368.

Received February 29, 1960.

ACTA CHEMICA SCANDINAVICA 14 (1960) 1317—1324

Hydrogenation as an Aid in the Identification of Unsaturated Hydrocarbons by Gas Chromatography

BENGT SMITH and RAGNAR OHLSON

Institutionen för Organisk Kemi, Chalmers Tekniska Högskola, Göteborg, Sweden

Methods are described for the hydrogenation of unsaturated hydrocarbon fractions obtained by condensation from analytical gas chromatographs. These hydrogenation methods make possible the identification of various unsaturated hydrocarbons on the basis of the retention times of their hydrogenation products.

The identification of unsaturated hydrocarbons by gas chromatography is mainly based on the determination of retention times using various columns (*cf.* Ref[1].). This method is generally successful when applied to alkenes boiling in the range below 100° in which case retention times for the majority of the compounds on a number of columns are well known [1]. However, in the case of higher boiling alkenes and for other types of unsaturated hydrocarbons, *e.g.* alkadienes and alkynes, the situation is less favourable since our knowledge about the retention times of these compounds is not so detailed. To complement the existing identification methods for unsaturated hydrocarbons, we have worked out some micro hydrogenation procedures which are applicable to the hydrogenation of such fractions as are obtained by condensation from analytical gas chromatographs using packed columns. The general principle of the method is to freeze out a compound or a mixture of compounds coming from the gas chromatograph and then hydrogenate the product partly or fully and, finally, re-run the hydrogenated product on a suitable column. From the chromatogram obtained, conclusions may be drawn concerning the nature of the compounds present in the original mixture. The advantage of the method is that compounds, the retention times of which are unknown, can be converted to compounds with known retention times, *e.g.* alkenes to alkanes, alkadienes to alkenes and alkanes, and alkynes to alkenes and alkanes. In addition compounds which cannot be separated on existing stationary phases may be converted by hydrogenation to separable products.

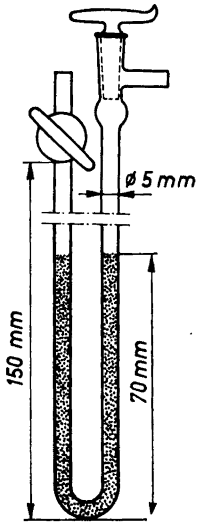

Fig. 1. U-Tube used in the hydrogenation experiments.

HYDROGENATION PROCEDURES

The procedures used in the full and stepwise hydrogenations of unsaturated hydrocarbons will be described in the following.

Procedure for the full hydrogenation of unsaturated hydrocarbons. A mixture of platinum dioxide (Adams catalyst [2]) and iron filings contaning about 1 wt. % of the oxide was used as hydrogenation catalyst. The iron filings acted as carriers for the platinum dioxide but they were also used because of their good heat conduction properties which facilitated the condensation of hydrocarbons from the gas stream coming from the chromatograph*. The iron filings-platinum dioxide mixture was filled into a U-tube (see Fig. 1) and the tube was immersed in a dry ice-acetone cooling bath and connected to the outlet of the chromatograph. In this way, the fraction of interest was condensed in the U-tube.

The tube was disconnected from the chromatograph and removed from the cooling bath. One side of the tube was closed and the other connected to a hydrogen container. Hydrogen was blown into the tube at such a rate that the pressure was raised to 3 kg/cm^2 during about 1 min. The tap on the tube was closed and the tube was removed from the hydrogen container and immersed in hot water (80—90°C) for 10 min. It was then connected to the gas inlet of the chromatograph (Perkin-Elmer Vapor Fractometer Model 154) and the hydrogenated products transferred to the chromatograph. Helium was generally used as the carrier gas. In the case of low boling hydrocarbons, however, it was sometimes necessary to use hydrogen instead since the large peak produced by the hydrogen in the U-tube, using helium as the carrier gas, tended to obscure compounds with short retention times. The same U-tube could be used without repacking for a considerable number of times **.

Procedure for the stepwise hydrogenation of alkadienes. The hydrogenation catalyst and equipment was the same as before but the conditions were changed. Thus, after the condensation of the hydrocarbon fraction in the U-tube, the latter was not removed

* Certain samples of iron filings were found to promote hydrogenation also in the absence of platinum dioxide.

** Care should be exercised in the hydrogenation procedure because of the ignition hazards connected with dry Adam's catalyst. Air must not be allowed to enter the hydrogenation tube.

from the cooling bath but allowed to remain there during the filling of the tube with hydrogen.

The tube was removed from the cooling bath and shaken for a few seconds in order to mix the hydrocarbon fraction with the catalyst and then replaced in the bath. The tube was then connected to the gas inlet of the chromatograph, the cooling bath was exchanged for a beaker containing hot water (80—90°C) and, after 5—10 sec, the contents in the U-tube were blown into the chromatograph. The hydrogenation takes place almost entirely during the short time in the heating bath. It was namely found that, if the hydrogen in the U-tube was exchanged for helium before the heating, almost no hydrogenated products were formed.

Procedures for the stepwise hydrogenation of alkynes. Method 1. This method was identical to that described for the full hydrogenation of unsaturated hydrocarbons with the exception that the hydrogenation was performed at room temperature for 1 min.

Table 1. Hydrogenation of dienes.

Compound	Unchanged (wt %*)	Hydrogenation products (wt %*)	
		Partly hydrogenated	Fully hydrogenated
1,3-Butadiene	82	1-Butene (6) *cis*-2-Butene (1) *trans*-2-Butene (2)	*n*-Butane (9)
1,4-Pentadiene	75	1-Pentene (9)	*n*-Pentane (16)
1, *cis*-3-Pentadiene	21	1-Pentene (4) *cis*-2-Pentene (10) *trans*-2-Pentene (7)	*n*-Pentane (58)
1,*trans*-3-Pentadiene	9	1-Pentene (4) *cis*-2-Pentene (3) *trans*-2-Pentene (6)	*n*-Pentane (78)
1,2-Pentadiene	98	1-Pentene (0.3) *cis*-2-Pentene (0.6) *trans*-2-Pentene (0.1)	*n*-Pentane (1)
1,5-Hexadiene	68	1-Hexene (11)	*n*-Hexane (21)
cis-2,*trans*-4-Hexadiene	22	*cis*-2-Hexene (8) *trans*-2-Hexene (14) *cis*-3-Hexene (3) *trans*-3-Hexene (6)	*n*-Hexane (47)
trans-2, *trans*-4-Hexadiene	15	*cis*-2-Hexene (2) *trans*-2-Hexene (14) *cis*-3-Hexene (3) *trans*-3-Hexene (6)	*n*-Hexane (60)
1,*trans*-3-Hexadiene	70	*cis*-2-Hexene (2) *trans*-2-Hexene (5) *trans*-3-Hexene (3)	*n*-Hexane (20)
1,3-*Cyclo*pentadiene	79	*Cyclo*pentene (8)	*Cyclo*pentane (13)

* These values are only approximate since they were obtained by the internal normalization method putting percentage area equal to the weight per cent.

Method 2 utilized metallic sodium covered by a layer of sodium amide [3,4] as catalyst and source of hydrogen*. A thread of sodium was pressed and transferred to the U-tube in a nitrogen atmosphere. Gaseous ammonia was then passed through the tube in order to form a layer of sodium amide on the surface of the sodium thread. After the condensation of the sample the tube was closed and left for 2 min at room temperature.

Material. The unsaturated hydrocarbons collected in Tables 1 and 2 were prepared in this laboratory. The synthesis of certain of these compounds as well as their retention values on various columns will be published elsewhere.

RESULTS and DISCUSSION

Full hydrogenation of unsaturated hydrocarbons. The hydrogenation procedure previously described was applied to a considerable number of straight chain and cyclic unsaturated hydrocarbons containing double and triple bonds. In all cases, a nearly 100 % conversion to the corresponding saturated hydrocarbons was obtained. No partly hydrogenated products, *e.g.* alkenes from alkadienes and alkynes, were formed. Among the saturated cyclic hydrocarbons, only *cyclo*propanes reacted, yielding paraffins. Aromatic hydrocarbons were converted to *cyclo*hexanes with a yield generally exceeding 90 %.

Stepwise hydrogenation of alkadienes. It turned out to be a difficult task to stop the hydrogenation of an alkadiene at the alkene stage. Several attempts at room temperature, using poisoned platinum dioxide and other less active catalysts, failed. The technique described in the experimental part, however, made possible the conversion of a sufficient amount of a diene to the corresponding monounsaturated hydrocarbons. Some typical results of the hydrogenation of a number of straight chain and cyclic dienes are given in Table 1.

In most instances, the expected hydrogenation products were formed. Thus, there was obtained 1-butene from 1,3-butadiene as the results of 1,2-addition, and *cis*- and *trans*-2-butene as the result of 1,4-addition. Naturally, the fully hydrogenated product, *n*-butane, was also formed. There was a marked difference in reactivity between various dienes, 1, *trans*-3-pentadiene being especially reactive. In this case, it was necessary to shorten the hydrogenation time in order to get enough of the alkenes. The two 1,3-pentadienes gave the same hydrogenation products. It was, however, still possible to distinguish between the two isomers on the basis of the proportions between *cis*- and *trans*-2-pentene. In the case of 1,*cis*-3-pentadiene, more *cis*-2-pentene than *trans*-2-pentene was formed. The *cis* isomer can be formed by 1,2- as well as 1,4-addition but the *trans* isomer only by 1,4-addition**. For 1, *trans*-3-pentadiene, the reverse is true and more *trans*-2-pentene than *cis*-2-pentene was obtained. Although the further hydrogenation to *n*-pentane might change the original proportions between *cis*- and *trans*-2-pentene, the results have in numerous experiments always turned out to be in accordance with the theory.

1,2-Pentadiene was the only diene of allene type investigated here. It was found to be considerably more resistent to hydrogenation than dienes with

---

* Concerning the use of sodium alone as catalyst, *cf.* p. 1322.

** Concerning the possibilities of a *cis-trans* isomerization during the hydrogenation, *cf.* below.

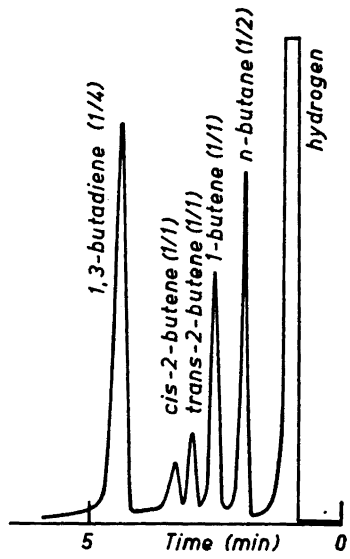

Fig. 2. Hydrogenation of 1,3-butadiene. Column, dimethylsulpholane (20 %) on Chromosorb 30—60 mesh, 3 m. Temperature 25°C. Flow of He 25 ml/min. Recorder attenuation as denoted.

conjugated and isolated double bonds. Thus, only 2 % of it was converted. This difference in reactivity makes it easy to distinguish between 1,2-pentadiene and the two 1,3-pentadienes by partial hydrogenation although the same hydrogenation products are formed.

The results of the hydrogenation of the two 2,4-hexadienes are noteworthy. From *cis*-2,*trans*-4-hexadiene, the expected hydrogenation products were formed. The same hydrogenation products, however, were obtained in the case of *trans*-2,*trans*-4-hexadiene, the formation of *cis*-2-hexene being unexpected. Since we believe that the experimental conditions excluded any contamination from other compounds, we are forced to assume that an isomerization takes place during the hydrogenation. Neither in this case nor in several other cases investigated did any isomerization occur in the absence of hydrogen. Attempts to convert *trans*-2-hexene and *trans*-3-hexene to their *cis* isomers using the method for the partial hydrogenation of alkadienes also failed. Thus, it must be concluded that a *cis-trans* isomerization can take place in certain instances under the experimental conditions used but the phenomenon does not seem to be a general one.

We are not aware of any previous reports on catalytic *cis-trans* conversions of ethylenic hydrocarbons although the corresponding thermal reaction has been studied [5]. Catalytic isomerization of dimethyl maleate on hydrogenation catalysts, however, has been observed [6].

One proposed mechanism [7] for the hydrogenation of ethylenic double bonds on metal catalysts involves a reaction between a chemisorbed alkene molecule and hydrogen to form a chemisorbed alkyl radical which is then further hydrogenated to an alkane during the second step. Since the first step is reversible, the possibility of a *cis-trans* isomerization obviously exists.

Table 2. Hydrogenation of alkynes.

Compound	Catalyst	Unchanged (wt %*)	Hydrogenation products (wt %*)	
			Partly hydrogenated	Fully hydrogenated
3-Hexyne	PtO_2 (method 1)	50	*cis*-3-Hexene (15) *trans*-3-Hexene (3)	*n*-Hexane (32)
	$NaNH_2$ (method 2)	90	*trans*-3-Hexene (10)	0
2-Hexyne	PtO_2 (method 1)	55	*cis*-2-Hexene (10) *trans*-2-Hexene (2)	*n*-Hexane (33)
	$NaNH_2$ (method 2)	60	*trans*-2-Hexene (40)	*n*-Hexane (trace)
1-Hexyne	PtO_2**	96	1-Hexene (3)	*n*-Hexane (1)
	$NaNH_2$ (method 2)	38	1-Hexene (62)	0
	Na (method 2)	37	1-Hexene (63)	0

* *Cf.* note under Table 1.
** The method used for the partial hydrogenation of alkadienes was applied.

It is known that migration of a double bond may occur in the presence of hydrogenation catalysts [8–11]. There are, however, no indications in our experimental material that such a migration takes place under the conditions used for the partial hydrogenation of dienes.

The chromatogram obtained after the hydrogenation of 1,3-butadiene is shown in Fig. 2.

Stepwise hydrogenation of alkynes. Some results from the stepwise hydrogenation of alkynes are given in Table 2. Hydrogenation over platinum dioxide mainly produced alkanes and *cis* alkenes in those instances where two stereoisomeric forms of the alkene were present. This result is in accordance with previous experience [12]. There are no signs of a double bond migration taking place during the hydrogenation (*cf.* above). Hydrogenation in the presence of sodium amide was quite stereospecific, the *trans* alkene being formed only. A possible mechanism for this reaction has been proposed by Raphael [13]. In the hydrogenation of 1-hexyne using method 2, it was found that sodium alone was as effective a catalyst as sodium covered with a layer of sodium amide. In this case hydrogen is furnished in the reaction between 1-hexyne and sodium. No hydrogenation took place when 3-hexyne was treated in the same way, since no hydrogen is formed. It seems possible to identify a triple bond in 1-position by this method.

Sodium amide is said not to promote the hydrogenation of an alkene to the corresponding alkane. We have, however, repeatedly obtained small amounts of *n*-hexane in the hydrogenation of 2-hexyne. It may be that small amounts of impurities in the sodium, *e.g.* traces of metal from the sodium press, are responsible for this conversion.

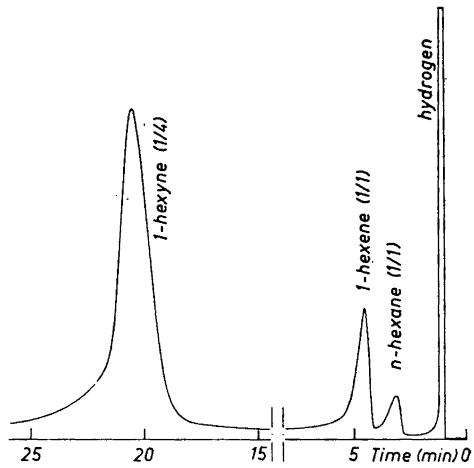

Fig. 3. Hydrogenation of 1-hexyne. Column, β,β'-oxydipropionitrile (20 %) on Chromosorb 30—60 mesh, 2 m. Temperature 25°C. Flow of He 50 ml/min. Recorder attenuation as denoted.

The results of the hydrogenation of 1-hexyne using the method for the partial hydrogenation of alkadienes illustrate the small conversion of an alkyne under these conditions (*cf.* 1,5-hexadiene in Table 1).

It is not possible to hydrogenate dienes to alkenes by any of the methods used for the hydrogenation of alkynes. The first method only produces saturated hydrocarbons and, with the last two, the dienes remain unchanged apart from the possible formation of traces of monounsaturated and saturated products. The chromatogram obtained after the hydrogenation of 1-hexyne over platinum dioxide is shown in Fig. 3.

Use of the hydrogenation methods. The examples given above demonstrate the application of the hydrogenation methods to the identification of unsaturated hydrocarbons. The methods are especially useful in the case of dienes and alkynes and, in many instances, permit a simple and straightforward identification of these hydrocarbons. They are also valuable for deciding whether a band on the chromatogram contains unsaturated hydrocarbons or not and for the conversion of unseparable, unsaturated hydrocarbons to separable, saturated ones. Thus, in the qualitative and quantitative analysis of mixtures of 3- and 4-methyl-1-pentene which until recently[14] could not be separated on any stationary phase known, we hydrogenated the mixture to 2- and 3-methylpentane which could easily be separated on, for example, squalane.

Acknowledgement. This work was supported by grants from the *Swedish Technical Research Council* and the *Town Council of Gothenburg.*

REFERENCES

1. Knight, H. S. *Anal. Chem.* **30** (1958) 9.
2. Voorhees, V. and Adams, R. *J. Am. Chem. Soc.* **44** (1922) 1297. See also *Org. Syntheses*, Coll. Vol. **1**, (1932) 452.
3. Campbell, K. N. and Eby, L. T. *J. Am. Chem. Soc.* **63** (1941) 2684.

4. Henne, A. L. and Greenlee, K. W. *J. Am. Chem. Soc.* **65** (1943) 2022.
5. Kistiakowsky, G. B. and Smith, W. R. *J. Am. Chem. Soc.* **56** (1934) 638; **58** (1936) 766.
6. Freudenberg, K. *Stereochemie*, Franz Deuticke, Leipzig and Wien 1933, p. 918.
7. Twigg, G. H. in *Heterogeneous Catalysis, Discussions of the Faraday Society* **8** (1950) 152.
8. Twigg, G. H. *Proc. Roy. Soc. London*, Ser. **A 178** (1941) 106.
9. Taylor, T. J. and Dibeler, V. H. *J. Phys. & Colloid Chem.* **55** (1951) 1036, 1065.
10. Zelinsky, N. D. and Levina, R. J. *Ber.* **62** (1929) 1861.
11. Richter, F. and Wolf, W. *Ber.* **59** (1926) 1733.
12. Raphael, R. A. *Acetylenic Compounds in Organic Synthesis*, Butterworths Scientific Publications, London 1955, p. 24.
13. Ref. [11], p. 27.
14. Smith, B. and Ohlson, R. *Acta Chem. Scand.* **13** (1959) 1253.

Received March 24, 1960.

ACTA CHEMICA SCANDINAVICA 14 (1960) 1325—1332

The Crystal Structure of Hydrogen Peroxide Dihydrate *

IVAR OLOVSSON** and DAVID H. TEMPLETON

Lawrence Radiation Laboratory and Department of Chemistry, University of California, Berkeley, California, U.S.A.

The crystal structure of hydrogen peroxide dihydrate, $H_2O_2 \cdot 2H_2O$, has been determined from single crystal X-ray data. Exposures at −70° and −190°C indicate the same structure. The crystals are monoclinic (space group $C2/c$) with four molecules in a unit cell of dimensions: $a = 9.400$, $b = 9.479$, $c = 4.51$ Å and $\beta = 121.33°$ at −190°C. The structure contains planar chains of water molecules connected by hydrogen bonds of 2.74 Å. The chains are crosslinked by the hydrogen peroxide molecules into a three-dimensional network by hydrogen bonds of 2.76 and 2.69 Å. Peaks in a difference synthesis suggest the positions of the hydrogen atoms in these bonds, and indicate slight displacements from the lines joining the oxygen atoms. These positions correspond to a dihedral angle of about 130°, in the hydrogen peroxide molecule, between the planes defined by the peroxide link and the hydrogen atoms.

The melting point diagram of the system hydrogen peroxide-water indicates only one intermediary compound, $H_2O_2 \cdot 2H_2O$. The existence of a crystalline phase of this composition has also been confirmed by X-ray powder diffraction data (Natta and Rigamonti [1]). They concluded that the lattice had a low symmetry but were unable to index the photographs. The melting point of the dihydrate has been reported as: —51°C (Maass and Herzberg [2]), —52.10° (Foley and Giguère [3]), —50.2° (Mironov [4]). These investigations also indicate that solid solutions are absent.

The present work involves the determination of the crystal structure of $H_2O_2 \cdot 2H_2O$ from single crystal X-ray diffraction data obtained at —190°C. X-ray photographs taken at —70°C indicate the same structure.

EXPERIMENTAL

The crystals were grown from solutions of hydrogen peroxide and water sealed in glass capillaries (diameter 0.1—0.2 mm. and wall thickness 0.01—0.02 mm.). The hydrogen peroxide (Becco's hydrogen peroxide of 90 %) was distilled in a vacuum system

* This work was performed for the U.S. Atomic Energy Commission.

** Permanent address: Institute of Chemistry, University of Uppsala, Uppsala, Sweden.

and the middle fraction taken out and mixed with distilled water to the desired composition. The analysis was made by titration with permanganate. The sample used had a composition of 48.8 wt. % H_2O_2, corresponding to 1.98 moles per mole of hydrogen peroxide.

The single crystals were grown in the ordinary way in a modified Weissenberg camera (Olovsson and Templeton [5]). As the crystal was grown it was apparent that the melting point was in reasonable agreement with the earlier-published data cited above. It was very difficult to get crystals that were not twinned. The crystal chosen was composed of two twins related by reflexion in the *bc* plane or rotation about *c*, but it was quite easy to get each reflection uniquely indexed. Equi-inclination Weissenberg photographs, layers 0 to 3, were taken with rotation around the *c* axis using Cu-*K* radiation. The results below refer to the data from −190°C but the photographs from −70°C indicate the same structure. The relative intensities were estimated visually by using multiple-film technique (four films) and comparing with an intensity scale. The data were corrected for the Lorentz and polarization effects.

UNIT CELL AND SPACE GROUP

The data showed the diffraction symmetry $2/m$. The systematic absences require an *I*-centered monoclinic cell with almost orthogonal axes ($a' = 8.038$ Å, $b' = 9.479$ Å, $c' = 4.51$ Å, $\beta' = 92.70°$) or a *C*-centered cell with $\beta \sim 120°$. The *C*-centered cell was chosen in order to be in agreement with the International Tables [6]. The unit cell parameters are then*:

$a = 9.400 \pm 0.002$ Å, $b = 9.479 \pm 0.002$ Å,

$c = 4.51 \pm 0.01$ Å, $\beta = 121.33° \pm 0.03°$. ($t = -190°$C)

a, *b* and *c* were determined from rotation and quartz-calibrated zero-layer Weissenberg photographs ($a = 4.913$ Å for *a* -quartz; $\lambda_{\text{Cu-}K\alpha_1} = 1.54051$ Å, $\lambda_{\text{Cu-}K\alpha_2} = 1.54433$ Å), β was obtained by the method of angular lag [7].

Giguère, Knop and Falk [8] report a preliminary value of 1.20 for the density at the melting point. With four molecules per unit cell, the calculated density at −190°C is 1.36. Systematic absences were, in addition to the extinctions due to the *C*-centering: $(h0l)$ for l odd. These data suggest the space groups Cc or $C2/c$, assuming that the absences are space group extinctions. As shown below, the structure is well described in $C2/c$ (C_{2h}^6) with the atoms in the general 8-fold positions: (0,0,0 and $\frac{1}{2},\frac{1}{2},0$) + (x,y,z); $(\bar{x},\bar{y},\bar{z})$; $(\bar{x},y,\frac{1}{2}-z)$; $(x,\bar{y},\frac{1}{2}+z)$.

DETERMINATION OF THE ATOMIC COORDINATES

A comparison of the unit cell dimensions for ice ($a = 4.51$ Å, $c = 7.34$ Å; Megaw [9]), ammonia monohydrate ($a = 4.51$ Å, $b = 5.587$ Å, $c = 9.700$ Å; Olovsson and Templeton [5]), and hydrogen peroxide dihydrate ($a = 9.400$ Å, $b = 9.479$ Å, $c = 4.51$ Å) shows that they all have one axis in common, 4.51 Å. In the first two compounds this corresponds to the unit length of a planar zig-zag chain of tetrahedrally hydrogen bonded water molecules (distance O—H———O = 2.76 Å). This immediately suggests that the present structure also contains such chains, oriented along the *c* axis. The atoms in the chain then must be related to each other by the *c* glide, and the *y* coordinate

* A different choice of *C*-centered cell, gives $a = 9.030$ Å and $\beta = 117.23°$.

of a water oxygen can be estimated to 0.084. The subsequent interpretation of the three-dimensional Patterson maps was based on the four-fold positions in space group *Cc*. In the structure obtained, the oxygen atoms in a H_2O_2 molecule were not symmetry-related to each other and the same refers to the oxygen atoms in the two water molecules. The coordinates of this structure were subjected to about 6 cycles of Fourier and least-squares refinement. After suitable choice of the origin (the x and z coordinates for one atom are arbitrary), these partly refined oxygen coordinates were for H_2O_2: O (1), (−0.009, 0.184, 0.089); O (2), (0.008, −0.181, −0.061) and for H_2O: O (3), (0.299, 0.084, 0.271); O (4), (−0.298, −0.081, −0.299). If the space group were *C*2/*c*, the atoms O (1) and O (2) as well as O (3) and O (4) would be related by the centre of symmetry at (0,0,0), and this is obviously very nearly the case here. The centrosymmetric space group *C*2/*c* was therefore chosen for the further work, which means only two independent oxygen atoms per asymmetric unit. In this structure, according to the interpretation given below, the dihedral angle H-O-O-H of the hydrogen peroxide molecule is about 130°. This seemed somewhat disturbing and other structural solutions were then looked for. However, in a systematic study of the Patterson maps, using both *Cc* and *C*2/*c*, no other structure could be found than the one already obtained.

The coordinates and isotropic temperature factors for oxygen and an over-all scale factor were refined by least-squares methods on the IBM 650 computer (the interlayer scale factor was then based on the relative exposure time). R_3 (see below) was the quantity actually minimized. The weighting factor w in this expression and some other details of the program are described elsewhere (Olovsson and Templeton [5]). For reflections too weak to be observed, the quantity $F_o - F_c$ was set equal to zero in the sums when $F_c < F_{min}$ and equal to $F_{min} - F_c$ when $F_c > F_{min}$. In the »LS II» program, modified for the space group *C*2/*c*, the only crossterms used were those between the x and z coordinates of the same atom. The scattering factors used for oxygen (uncharged) are those published by Berghuis *et al.*[10] The shifts in the coordinates in the final cycles were less than 0.0001. The results, together with the standard deviations, after about 20 cycles of refinements are given in Table 1. The »unreliability factors» at this point were:

$$R_1 = \Sigma \, | \, |F_o| - |F_c| \, | \, / \Sigma \, |F_o| = 0.091$$
$$R_2 = [\Sigma (|F_o| - |F_c|)^2 / \Sigma \, |F_o|^2]^{\frac{1}{2}} = 0.086$$
$$R_3 = \Sigma [w(|F_o| - |F_c|)^2 / \Sigma w \, |F_o|^2]^{\frac{1}{2}} = 0.092$$

The observed and calculated structure factors are compared in Table 2. Hydrogen atoms are omitted from these calculations.

Table 1. Atomic parameters and standard deviations.

Oxygen (O_I) in H_2O_2	Oxygen (O_I) in H_2O
$x = -0.0075 \pm 0.0003$	$x = 0.2980 \pm 0.0003$
$y = 0.1809 \pm 0.0003$	$y = 0.0822 \pm 0.0003$
$z = 0.0785 \pm 0.0009$	$z = 0.2850 \pm 0.0008$
$B = 2.38$ Å^2	$B = 2.08$ Å^2

Table 2. Observed and calculated structure factors

h	k	$\lvert F_o \rvert$	$\lvert F_c \rvert$	h	k	$\lvert F_o \rvert$	$\lvert F_c \rvert$	h	k	$\lvert F_o \rvert$	$\lvert F_c \rvert$	h	k	$\lvert F_o \rvert$	$\lvert F_c \rvert$
	$l = 0$				$l = 1$			4	6	3	2	5	1	11	12
2	0	6	9	− 9	1	6	4	6	6	3	1	7	1	<2	1
4	0	42	45	− 7	1	19	20	− 9	7	7	6	−10	2	6	5
6	0	22	22	− 5	1	3	3	− 7	7	4	2	− 8	2	2	1
8	0	<3	1	− 3	1	40	39	− 5	7	13	14	− 6	2	3	2
10	0	11	12	− 1	1	23	23	− 3	7	5	5	− 4	2	20	19
1	1	8	10	1	1	6	6	− 1	7	9	10	− 2	2	4	7
3	1	49	47	3	1	22	22	1	7	11	11	0	2	27	24
5	1	15	12	5	1	5	5	3	7	<2	1	2	2	3	3
7	1	16	16	7	1	5	5	5	7	7	6	4	2	5	5
9	1	<1	<1	−10	2	11	11	7	7	1	1	6	2	7	6
0	2	6	7	− 8	2	2	<1	− 8	8	6	5	−11	3	<1	<1
2	2	50	50	− 6	2	13	12	− 6	8	4	2	− 9	3	<3	1
4	2	14	14	− 4	2	30	34	− 4	8	5	3	− 7	3	4	4
6	2	8	9	− 2	2	21	18	− 2	8	13	14	− 5	3	8	7
8	2	12	10	0	2	56	56	0	8	9	10	− 3	3	12	13
10	2	<1	<1	2	2	10	10	2	8	9	8	− 1	3	14	14
1	3	44	45	4	2	6	7	4	8	1	<1	1	3	14	12
3	3	30	32	6	2	6	7	6	8	4	2	3	3	11	10
5	3	20	20	8	2	6	5	− 7	9	10	10	5	3	8	6
7	3	9	10	− 9	3	8	8	− 5	9	6	5	7	3	4	4
9	3	6	6	− 7	3	12	12	− 3	9	10	11	−10	4	4	3
0	4	25	25	− 5	3	27	29	− 1	9	5	3	− 8	4	3	3
2	4	9	8	− 3	3	18	18	1	9	3	2	− 6	4	2	3
4	4	6	8	− 1	3	9	9	3	9	11	10	− 4	4	7	7
6	4	3	4	1	3	22	22	5	9	5	6	− 2	4	15	14
8	4	3	2	3	3	21	20	− 6	10	4	4	0	4	9	8
1	5	30	33	5	3	16	16	− 4	10	9	9	2	4	6	6
3	5	4	3	7	3	6	6	− 2	10	<3	3	4	4	3	2
5	5	25	27	−10	4	<1	<1	0	10	12	12	6	4	<2	1
7	5	<1	<1	− 8	4	16	14	2	10	2	2	− 9	5	6	5
9	5	7	7	− 6	4	11	12	4	10	2	3	− 7	5	16	14
0	6	4	4	− 4	4	3	3	− 3	11	3	3	− 5	5	8	9
2	6	37	37	− 2	4	41	47	− 1	11	<1	<1	− 3	5	14	16
4	6	7	8	0	4	13	14	1	11	3	2	− 1	5	10	11
6	6	7	6	2	4	28	26					1	5	4	2
8	6	12	11	4	4	3	3		$l = 2$			3	5	19	17
1	7	3	3	6	4	5	2	−10	0	9	7	5	5	2	2
3	7	14	13	8	4	6	6	− 8	0	8	9	−10	6	5	6
5	7	10	10	− 9	5	7	6	− 6	0	10	12	− 8	6	4	2
7	7	9	7	− 7	5	3	2	− 4	0	11	11	− 6	6	<2	<1
0	8	22	23	− 5	5	17	17	− 2	0	—	—	− 4	6	17	18
2	8	6	6	− 3	5	<1	<1	0	0	12	12	− 2	6	10	11
4	8	14	12	− 1	5	9	9	2	0	22	25	0	6	21	22
6	8	10	8	1	5	12	13	4	0	9	10	2	6	<1	<1
1	9	8	8	3	5	7	6	6	0	<2	<1	4	6	5	4
3	9	8	7	5	5	9	8	−11	1	<2	2	− 9	7	7	5
5	9	5	5	7	5	4	2	− 9	1	8	9	− 7	7	9	9
0	10	10	8	− 8	6	3	3	− 7	1	15	15	− 5	7	11	11
2	10	<1	<1	− 6	6	5	5	− 5	1	26	26	− 3	7	5	5
4	10	6	4	− 4	6	7	6	− 3	1	8	8	− 1	7	<2	1
1	11	6	5	− 2	6	6	5	− 1	1	5	3	1	7	9	8
3	11	12	11	0	6	6	6	1	1	22	23	3	7	9	8
0	12	7	9	2	6	3	3	3	1	10	10	5	7	5	6

Table. 2 (cont.)

h	k	$\lvert F_o \rvert$	$\lvert F_c \rvert$	h	k	$\lvert F_o \rvert$	$\lvert F_c \rvert$	h	k	$\lvert F_o \rvert$	$\lvert F_c \rvert$	h	k	$\lvert F_o \rvert$	$\lvert F_c \rvert$
− 8	8	3	3	− 9	1	15	14	1	3	9	8	− 2	6	6	7
− 6	8	4	4	− 7	1	6	6	3	3	11	12	0	6	6	5
− 4	8	<2	<1	− 5	1	26	26	5	3	2	4	2	6	5	4
− 2	8	13	12	− 3	1	17	17	−10	4	12	12	− 9	7	3	3
0	8	<1	<1	− 1	1	13	14	− 8	4	9	8	− 7	7	14	12
2	8	8	8	1	1	18	19	− 6	4	8	8	− 5	7	6	6
4	8	5	4	3	1	4	3	− 4	4	28	30	− 3	7	12	12
− 7	9	<2	<1	5	1	6	8	− 2	4	3	1	− 1	7	12	11
− 5	9	2	2	−10	2	<1	<1	0	4	22	23	1	7	5	4
− 3	9	3	3	− 8	2	10	11	2	4	8	7	3	7	7	8
− 1	9	4	3	− 6	2	19	19	4	4	4	4	− 8	8	<2	1
1	9	5	4	− 4	2	<1	<1	− 9	5	<1	<1	− 6	8	<1	<1
3	9	4	3	− 2	2	35	33	− 7	5	12	12	− 4	8	10	10
− 6	10	2	1	0	2	1	<1	− 5	5	3	2	− 2	8	6	5
− 4	10	2	2	2	2	9	12	− 3	5	9	10	0	8	8	8
− 2	10	6	5	4	2	7	8	− 1	5	10	10	2	8	<1	<1
0	10	4	2	−11	3	5	5	1	5	<2	1	− 7	9	3	3
2	10	3	3	− 9	3	7	7	3	5	9	8	− 5	9	10	11
− 1	11	2	2	− 7	3	18	18	−10	6	3	3	− 3	9	4	3
				− 5	3	8	9	− 8	6	6	4	− 1	9	2	2
	$l = 3$			− 3	3	9	10	− 6	6	7	6	− 4	10	<1	<1
−11	1	4	4	− 1	3	11	11	− 4	6	7	6	− 2	10	9	11

DISCUSSION OF THE STRUCTURE AND HYDROGEN POSITIONS

The structure is shown in Fig. 1. The bond distances and angles with their standard deviations are given in Table 3 and Fig. 2. The correlations between symmetry-related atoms and the uncertainty of the unit cell dimensions were considered in the calculations of these standard deviations.

The water molecules are hydrogen-bonded to each other into planar chains oriented along the c axis and in the planes $x = 0.20$, 0.30, 0.70 or 0.80, respectively. The chains are cross-linked by the hydrogen peroxide molecules into a three-dimensional network. It appears that the hydrogen peroxide molecules are not bonded to each other; the two-fold axis passes through the centre of the O-O bond. The oxygen-oxygen distance in the water chain (2.741 Å with a standard deviation $\sigma = 0.005$ Å) is slightly different from the corresponding distances in ammonia monohydrate (2.759 Å, $\sigma = 0.005$ Å; Olovsson and Templeton [5]) and ice (2.755 Å, $\sigma = 0.008$ Å; Tables of interatomic distances [11]). One of the oxygen-oxygen distances between water and hydrogen peroxide is 2.761 Å ($\sigma = 0.004$ Å), while the other is significantly shorter, 2.685 Å ($\sigma = 0.004$ Å). When refining the structure, the atomic coordinates were repeatedly changed by hand in trials to make both of these distances equal, but the subsequent least-squares treatment invariably shifted them back again. The O-O distance in hydrogen peroxide, 1.481 Å ($\sigma = 0.009$ Å), is in agreement with the value 1.48 ± 0.01 Å given in Tables of interatomic distances [11].

The bond angle in the water chain is close to the tetrahedral value but the deviations of other angles from their normal values when these water chains and the hydrogen peroxide molecules are linked together (Fig. 2)

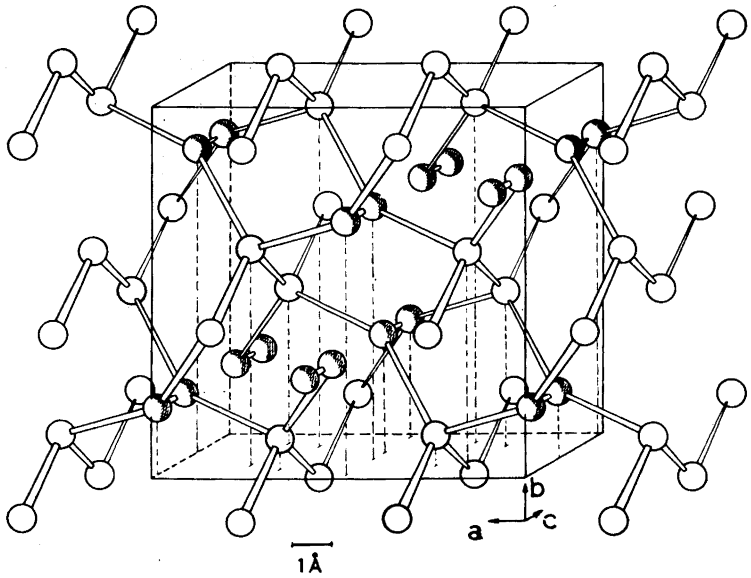

Fig. 1. The crystal structure of hydrogen peroxide dihydrate. The peroxide groups are shaded.

indicate some strain in the structure. The low melting point is another indication of low stability. The following arguments about the locations of the hydrogen atoms are similar to those presented in the case of ammonia monohydrate (Olovsson and Templeton [5]). One of the hydrogen atoms in water

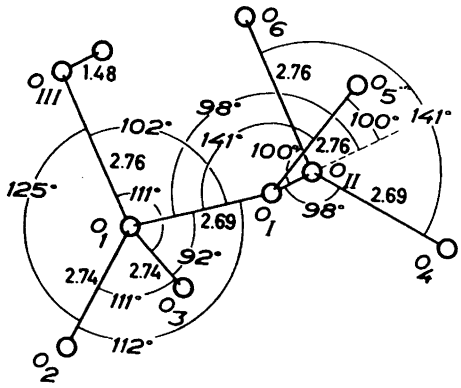

Fig. 2. Bond distances and angles to the neighbors of a water molecule and a hydrogen peroxide molecule (the orientation is the same as in Fig. 1.).

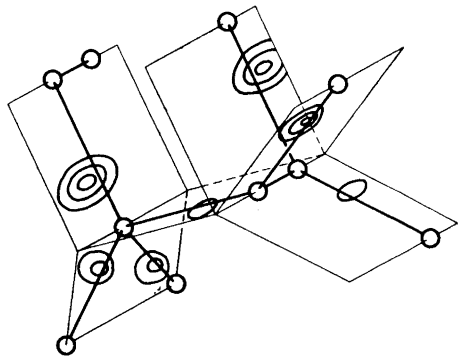

Fig. 3. Schematic representation of the difference synthesis in various sections. The contours are drawn at 0.70, 0.85 and 1.00 e · Å^{-3}. The atoms are the same as in Fig. 2.

Table 3. Bond distances and angles with their standard deviations (*cf.* Fig. 2).

Around O_I:

Bond	Distance (Å)
$O_I - O_{II}$	1.481 ± 0.009
$O_I - O_1$	2.685 ± 0.004
$O_I - O_5$	2.761 ± 0.004

Bonds	Angle (deg.)
$O_{II} - O_I - O_1$	97.7 ± 0.2
$O_{II} - O_I - O_5$	100.4 ± 0.2
$O_1 - O_I - O_5$	140.5 ± 0.2

Around O_1:

Bond	Distance (Å)
$O_1 - O_2$	2.741 ± 0.005
$O_1 - O_3$	2.741 ± 0.005
$O_1 - O_I$	2.685 ± 0.004
$O_1 - O_{III}$	2.761 ± 0.004

Bonds	Angle (deg.)
$O_I - O_1 - O_2$	111.7 ± 0.1
$O_I - O_1 - O_3$	91.5 ± 0.1
$O_I - O_1 - O_{III}$	101.8 ± 0.1
$O_2 - O_1 - O_3$	110.7 ± 0.2
$O_2 - O_1 - O_{III}$	125.0 ± 0.2
$O_3 - O_1 - O_{III}$	110.6 ± 0.2

is obviously involved in the hydrogen bonds of the water chain. The question is then to which one of the two oxygen atoms the hydrogen atom should be pointed. The two directions are not equivalent when regard is paid to the distribution of the other nearest neighbors (in contrast to the situation in ammonia monohydrate). But it is not entirely obvious from a structural point of view which orientation should be preferred. The three-dimensional $F_o - F_c$ synthesis (based on the oxygen coordinates only) seemed to give a definitive answer, as a well resolved »hydrogen peak» appeared in one direction but not in the other. The difference synthesis * is shown schematically in Fig. 3, where all the other hydrogen atoms also seem to be visible. All »hydrogen peaks» in the difference maps are close to the lines connecting the heavier atoms; the approximate coordinates are (0.305, 0.040, 0.105) and (0.385, 0.155, 0.345) for the »hydrogen atoms» bonded to O_1 and (0.105, 0.135, 0.120) for the »hydrogen atom» bonded to O_I. These peaks correspond to O-H

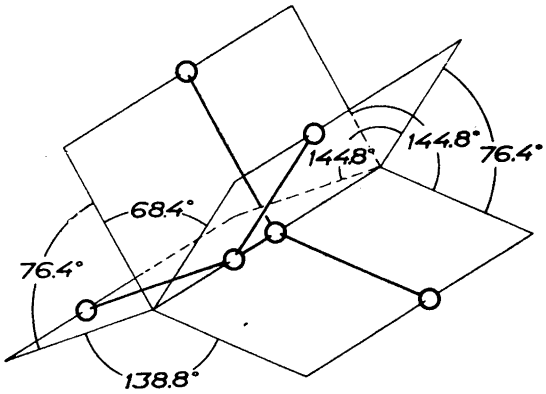

Fig. 4. Dihedral angles with the peroxide group and the nearest oxygen neighbors.

* The Fourier calculations were made on the IBM 701 computer at University of California Computer Center.

bond distances of about 1.0 Å, as expected. The apparent deviations from the connecting lines are such that they make the angles H-O-H in water and O-O-H in hydrogen peroxide closer to the values in the pure compounds ($\wedge$ O-O-H is according to a neutron diffraction investigation by Busing and Levy [12] close to 102°). The dihedral angles between planes defined by the peroxide group and the nearest oxygen neighbors are shown in Fig. 4. If the two-fold symmetry applies to the hydrogen atoms there are obviously only two values possible for the dihedral angle H-O-O-H, namely about 139° or 68° (if hydrogen is on the connecting lines) and the former was definitely indicated by the difference synthesis. The same dihedral angle is about 10° less with the experimental hydrogen positions. The same angle in solid hydrogen peroxide itself is about 90° (Busing and Levy [12]). For the urea-hydrogen peroxide addition compound $CO(NH_2)_2 \cdot H_2O_2$ Lu, Hughes and Giguère [13] report this angle to be 106° (assuming that the hydrogen atoms are on the connecting lines). Spectroscopic evidence indicates that the restoring force for twisting about the O-O bond is rather small (Giguère and Harvey [14]). And infra-red investigation of the crystalline dihydrate at low temperature actually indicates that the peroxide molecule is somewhat distorted in this compound [8].

A travel grant (to I.O.) from the *Swedish Natural Science Research Council* is gratefully acknowledged.

REFERENCES

1. Natta, G. and Rigamonti, R. *Gazz. chim. ital.* **66** (1936) 762.
2. Maass, O. and Herzberg, O. W. *J. Am. Chem. Soc.* **42** (1920) 2569.
3. Foley, W. T. and Giguère, P. A. *Can. J. Chem.* **29** (1951) 123.
4. Mironov, K. E. *Izvest. Sektora Fiz.-Khim. Anal., Inst. Obshcheĭ i Neorg. Khim., Akad. Nauk S.S.S.R.* **26** (1955) 215.
5. Olovsson, I. and Templeton, D. H. *Acta Cryst.* **12** (1959) 827.
6. *International Tables for X-ray Crystallography, Vol. 1,* Kynoch Press, Birmingham 1952.
7. Buerger, M. J. *X-ray Crystallography,* John Wiley & Sons, Inc., New York 1949.
8. Giguère, P. A., Knop, O. and Falk, M. *Can. J. Chem.* **36** (1958) 883.
9. Megaw, H. D. *Nature* **134** (1934) 900.
10. Berghuis, J., Haanappel, I J. M., Potters, M., Loopstra, B. O., MacGillavry, C. H. and Veenendaal, A. L. *Acta Cryst.* **8** (1955) 478.
11. *Tables of interatomic distances and configuration in molecules and ions,* The Chemical Society, Burlington House, W. 1., London 1958.
12. Busing, W. R. and Levy, H. A. *Reports from the meeting of the American Crystallographic Association in Milwaukee,* June 1958.
13. Lu, C. S., Hughes, E. W. and Giguère, P. A. *J. Am. Chem. Soc.* **63** (1941) 1507.
14. Giguère, P. A. and Harvey, K. B. *J. Mol. Spectr.* **3** (1959) 36.

Received March 29, 1960.

ACTA CHEMICA SCANDINAVICA 14 (1960) 1333—1337

Spectroscopic Studies on Enols

II.* Proton Magnetic Resonance and Infrared Spectra of Diacetoacetic and Cinnamoylacetoacetic Esters

STURE FORSÉN and MARTIN NILSSON

Research Group for Nuclear Magnetic Resonance, Division of Physical Chemistry, and Division of Organic Chemistry, Royal Institute of Technology, Stockholm 70, Sweden

Proton magnetic resonance (PMR) data and infrared spectra of methyl and ethyl diacetoacetate confirm the complete enolisation of these compounds and also show that the intramolecular hydrogen bonds are stronger than in the enol of triacetylmethane. The spectra of ethyl cinnamoylacetoacetate and 3-cinnamoylpentane-2,4-dione are also discussed. The PMR spectrum of the latter compound shows the presence of two different chelate enols.

In the first part of these studies the extremely low infrared chelate carbonyl frequency and enol proton resonance field of a complex natural product, ceroptene [1], successively led to the investigation of simple β-triketones. It was found that even the first member of this series, triacetylmethane, was completely enolised in solution. The PMR and IR spectra indicated that the intramolecular hydrogen bond in the enol was very strong.

As β-triketones constitute a special case of α-substituted β-diketones it seemed desirable to investigate the influence of α-substituents other than acyl groups on the properties of the conjugated chelate system.

The esters of diacetoacetic acid are easily prepared and are almost completely enolised, as indicated by bromine titration experiments [2]. Methyl and ethyl diacetoacetate were chosen for comparison with triacetylmethane and cinnamoylacetoacetic ester and 3-cinnamoylpentane-2,4-dione for comparison with the cinnamoyl derivatives investigated in Part I.

---

* Part I. Forsén, S. and Nilsson, M., Proton Magnetic Resonance Studies of Enolised β-Triketones, *Acta Chem. Scand.* **13** (1959) 1383.

EXPERIMENTAL

Methods. The PMR measurements were made on dilute carbon tetrachloride solutions at 40 Mc/s and 22 ± 1°C. The resonance shifts are given in *p.p.m.* against an external water standard and are indicated by δ_{aq}*; a positive sign denotes a shift towards higher field. The infrared spectra were recorded for *ca.* 0.1 M solutions in carbon tetrachloride. For further details the reader is referred to Part I.

Materials. Methyl and ethyl diacetoacetate were prepared according to a standard procedure [3] and were purified *via* the copper salts and distilled through a short Vigreux column. Methyl diacetoacetate,b.p. 84.5–85.0°/12 mm (Lit. b.p. 101–102°/20 mm.[3]) Ethyl diacetoacetate, b.p. 93.0–93.5°/11 mm (Lit. b.p. 95–97°/11 mm [4]).

Ethyl cinnamoylacetoacetate was prepared from sodioacetoacetic ester and cinnamoyl chloride in ether and was recrystallised from methanol and sublimed, m.p. 53–54° (Lit. m.p. 44° [5]). (Found: C 69.0; H 6.4. Calc. for $C_{15}H_{16}O_4$: C 69.2; H 6.2.)

3-Cinnamoylpentane-2,4-dione: Acetylacetone (0.1 mole) in dry ether (100 ml) was treated with powdered sodium or sodium hydride (0.1 mole) at 0° to give the sodium salt. Cinnamoyl chloride (0.1 mole) in ether solution was added with stirring at 0° during 1 h. The colour of the mixture at first became deep yellow but turned to pale yellow towards the end of the addition. The mixture was stirred at room temperature for another hour and water was then added. The ether solution was washed with water and with sodium hydrogen carbonate solution and was then extracted with sodium carbonate (10 %). The extract was acidified and the product recovered by ether extraction. The crude product was recrystallised from *cyclo*hexane to afford 3-cinnamoylpentane-2,4-dione in a 40 % yield. The melting point was, however, unsharp and varied somewhat. The freshly collected material had m.p. 58–62°, but on aging the m.p. range broadened. This as well as the general appearance of the crystals seemed to indicate the presence of two interconvertible forms. A sample was dried at room temperature over paraffin and phosphorus(V)oxide and analysed, m.p. 54–59°. (Found: C 73.2; H 6.1. Calc. for $C_{14}H_{14}O_3$: C 73.0; H 6.1.) 3-Cinnamoylpentane-2,4-dione gave a strong red colour with iron(III)chloride and a green colour with copper(II)acetate.

RESULTS

The PMR spectrum of ethyl diacetoacetate in carbon tetrachloride solution and the chemical shifts are given in Fig. 1. The assignments are obvious. The enol proton signal (1) occurs at δ_{aq}—13.35, markedly lower than for triacetylmethane (δ_{aq}—12.60). The signals from the protons of the acetyl groups (3) coalesce and the ethoxyl group shows up clearly (signal groups 2 and 4). The spectrum of the pure liquid was practically the same as that of the solution and no signals due to the presence of the non-enolised ester were detected.

In methyl diacetoacetate (spectrum not shown) the enol proton gives a signal at even lower field, δ_{aq}—13.43, the acetyl protons absorb at δ_{aq} 2.53 and the methoxyl protons at δ_{aq} 1.07.

The carbonyl region of the infrared spectrum of the ethyl ester is shown in Fig. 2. The peak at 1 710 cm^{-1} was assigned to the ester carbonyl group and the broad band at 1 560 cm^{-1} to the chelate carbonyl group. In the *O-H* region there is a very broad and weak absorption between 3 000 and 2 000 cm^{-1}. The relevant absorptions of the methyl ester are identical with those of the ethyl ester.

---

* For conversion to τ-values [Tiers, G. V. D. *J. Phys. Chem.* **62** (1958) 1151] the following relation is valid at 22°C: $\tau = \delta_{aq} + 5.19$.

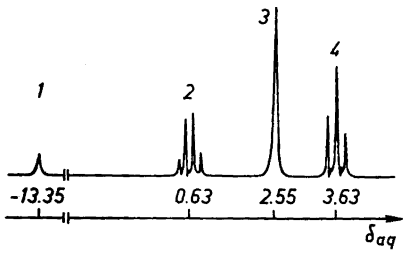

Fig. 1. PMR spectrum of ethyl diacetoacetate (carbon tetrachloride solution, mole fraction, $x = 0.08$).

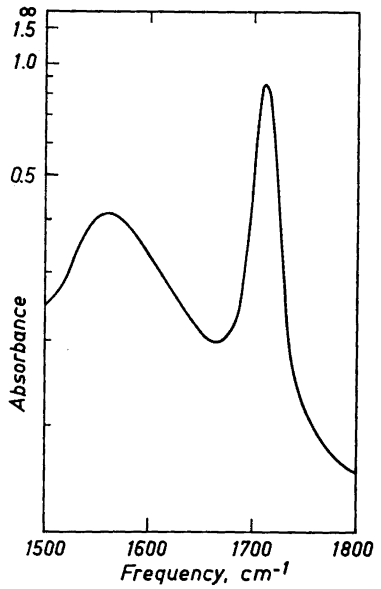

Fig. 2. The carbonyl region of the infrared spectrum of ethyl diacetoacetate (0.1 M solution in carbon tetrachloride, 0.1 mm cell, the absorption of the solvent is compensated)

The PMR spectrum of ethyl cinnamoylacetoacetate, presented in Fig. 3, is more complicated but still easy to interpret. Signal 1 is due to the enol proton and signal group 2 is made up by contributions from the protons of the benzene ring and from the protons at the *trans* ethylenic double bond (conventional coupling constant, $J = 15$ c/s). Signal groups 4 and 6 are due to the ethoxyl protons and signal 5 to the acetyl protons. Signal 3 may be due to the presence of a small amount (less than 5 %) of non-enolised material.

The IR spectrum contains bands due to the ester carbonyl group (1 710 cm^{-1}), to the ethylenic double bond (1 630 cm^{-1}) and to the conjugated benzene ring (1 580 cm^{-1}). A broad band at 1 530 cm^{-1} is tentatively assigned to the chelated carbonyl group.

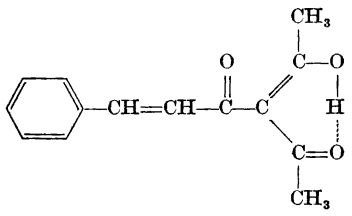

I a

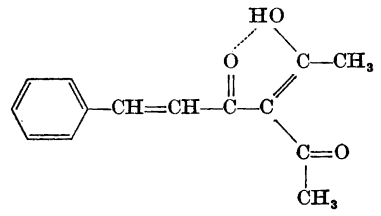

I b

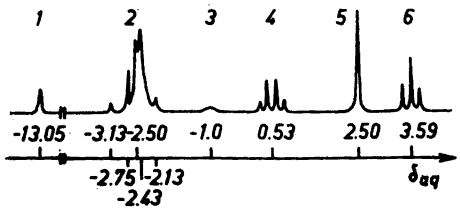

Fig. 3. PMR spectrum of ethyl cinnamoylacetoacetate (carbon tetrachloride solution, $x = 0.08$).

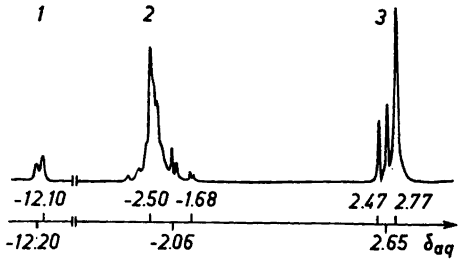

Fig. 4. PMR spectrum of 3-cinnamoylpentane-2,4-dione (carbon tetrachloride solution, $x = 0.08$).

The PMR spectrum of 3-cinnamoylpentane-2,4-dione can be interpreted in terms of the two enol forms I *a* and I *b*.

The spectrum of the enol I *a* should contain a single peak for the acetyl protons, whereas form I *b* should give two different acetyl peaks.

In the PMR spectrum, shown in Fig. 4, there are three peaks in signal group 3, which judged from the chemical shift should be due to acetyl protons. The relative intensities are 4:1:1. Signal group 1 must be due to the enol protons; the intensity ratio is 2:1. Signal group 2 consists of signals from the benzene ring protons and from the protons of the ethylenic double bond. The splitting of the latter indicates *trans* configuration ($J = 15$ c/s) as well as an effect similar to that found in signal groups 1 and 3 (internal intensity ratio 2:1). The spectrum is thus apparently made up by contributions from forms I *a* and I *b* in the proportion 2:1.

In benzene solution the splitting persists approximately unchanged, while the intensity ratio is somewhat lowered (1.8:1).

The infrared spectrum of the solution as well as of the solid compound (recorded on a potassium bromide disc) showed bands at 1 675 cm^{-1} (conjugated carbonyl group), 1 635 cm^{-1} (ethylenic double bond), 1 605 and 1 580 cm^{-1} (benzene ring) and also a broad band with the centre near 1 550 cm^{-1} due to the chelate carbonyl group.

DISCUSSION

The PMR data for the diacetoacetic esters indicate that the protons of the acetyl groups are equivalent. This is analogous to the findings for acetylacetone [6] and triacetylmethane and indicates a rapid transfer of the proton in the hydrogen bond. The equivalence of the acetyl protons and the "normal" infrared absorption of the ester carbonyl group indicates that the ester carbonyl, as expected, is not directly engaged in hydrogen bonding.

The data for the diacetoacetic esters fit well into the correlation of enol proton shifts and chelate carbonyl absorption frequencies for β-triketones in Part I and also indicate that the hydrogen bonds in these esters are stronger

than in the enol of triacetylmethane and similar to that in acetyldimedone (δ_{aq}—13.30).

The carbalkoxy group thus has a larger effect than the acetyl group in increasing the strength of the hydrogen bond and stabilising the conjugated chelate system. As steric factors can be regarded as fairly constant the effect could be described in terms of the greater "inductive, electron-withdrawing power" of the carbalkoxy group.

The data for the cinnamoyl derivatives, however, deviate from this pattern. The comparison of cinnamoylacetoacetic ester and cinnamoylpentanedione indicates that the hydrogen bond is strongest in the former and thus confirms the larger effect of the carbethoxy group on the conjugated chelate system.

The infrared chelate carbonyl absorptions indicate that the hydrogen bond is more marked in the cinnamoyl derivatives than in the simple diacetoacetic esters and unconjugated β-triketones. The PMR enol proton shifts on the other hand indicate the opposite to be the case. For acyl-dimedones both PMR and IR data indicated the hydrogen bonds to be stronger in the conjugated compounds (Part I). The splitting of the enol proton signal from cinnamoylpentanedione also presents the unexpected fact that the isomer, which occurs in the least amount, has the largest negative enol proton shift.

The enol protons of the two forms of cinnamoylpentanedione are situated at different distances from the benzene ring as well as from the ethylenic double bond. Magnetic anisotropy effects from these sources [7,8] may therefore contribute to the observed splitting of the enol proton signal.

When judging the enol proton resonance frequency in cinnamoylacetoacetic ester and cinnamoylpentanedione it is to be noted that the olefinic protons of these compounds absorb around δ_{aq}—2.4, a significantly higher field than that for the corresponding resonance of ceroptene and cinnamoyldimedone (δ_{aq} *ca.*—3.1). For the present no attempt has been made to explain these phenomena, which probably are related to the larger flexibility of the molecules now investigated.

Acknowledgements. We wish to thank Professor H. Erdtman and Dr. E. Forslind for their kind encouragement and interest, Miss Gurli Hammarberg for the infrared measurements, Mr. E. Pettersson for technical assistance and Dr. B. R. Thomas and Dr. I. Wellings for improving the language of the manuscript.

REFERENCES

1. Nilsson, M. *Acta Chem. Scand.* **13** (1959) 750.
2. Böhmne, H. and Fischer, H. *Ber.* **76** (1943) 106.
3. *Org. Synthesis*, **Coll. Vol. III** (1955) 390.
4. Claisen, L. *Ann.* **277** (1893) 162.
5. Bülow, C. and Hailer, E. *Ber.* **35** (1902) 915.
6. Reeves, L. W. *Can. J. Chem.* **35** (1957) 1351.
7. Johnson, C. E., Jr. and Bovey, F. A. *J. Chem. Phys.* **29** (1958) 1012.
8. Jackman, L. M. *Applications of Nuclear Magnetic Resonance Spectroscopy in Organic Chemistry*, Pergamon Press, London 1959, p. 112.

Received March 21, 1960.

ACTA CHEMICA SCANDINAVICA 14 (1960) 1338—1342

Demethylation and Degradation of Sugars in Acid Hydrolysis

INGEMAR CROON, GUNNEL HERRSTRÖM, GÖRAN KULL and BENGT LINDBERG

Institutionen för träkemi, Kungl. Tekniska Högskolan, Stockholm, Sweden

The magnitude of demethylation and degradation of some methylated sugars during conditions of acid hydrolysis has been studied. The conditions were typical for various procedures used for the hydrolysis of methylated polysaccharides. The investigation thus throws some light upon possible sources of error when the structure of a polysaccharide is studied by the methylation technique.

The methylation technique involving the complete methylation of a carbohydrate, hydrolysis and identification and quantitative determination of the methylated sugar obtained is an important method in structural carbohydrate chemistry. A prerequisite for the correct interpretation of the results especially for polysaccharides, which may give mixtures of several methylated sugars, is that the methylation is complete and that the methylated sugars are not degraded or demethylated during the acid hydrolysis of the methylated polysaccharide. Although some polysaccharides are difficult to methylate completely it is usually possible to obtain a product with a methoxyl content rather close to the theoretical value. No systematic studies of the demethylation and degradation of methylated sugars under the conditions used in acid hydrolysis seem to have been made, but some observations have been recorded in the literature.

Freudenberg and Boppel [1] studied the demethylation of 2,3,6-tri-*O*-methyl-D-glucose on treatment with 36 % aqueous hydrochloric acid at +5°, the conditions used for the hydrolysis of methylated starch, and found that 2 % or more of di-*O*-methyl-D-glucoses was formed. They believed that one of these, presumably the 2,6- and definitely not the 2,3-derivative, was formed preferentially. Chanda *et al.*[2] studied the demethylation of 2,3-di-*O*-methyl-D-xylose and 2,3,4-tri-*O*-methyl-D-xylose on treatment with 1 % methanolic hydrogen chloride and found 0.2 and 2 % demethylation, respectively. Croon and Lindberg [3] observed that the treatment of seven partially methylated glucoses, first with 72 % sulphuric acid at 0° and then with 12 % sulphuric acid at 100° did not produce any apparent demethylation but that the sugars showed between 3 and 6 % degradation. In a recent publication, Goldstein

Table 1. Acid hydrolysis conditions.

Conditions	Acid	Temp.	Time
1	2 % HCl in water	100°	13 h
2	a) 2 % HCl in methanol	100°	13 h
	b) 0.5 N HCl in water	100°	8 h
3	a) 72 % sulphuric acid	Room temp.	0.5 h
	b) 12.4 % sulphuric acid	100°	4 h
4	a) 98 % formic acid	100°	6 h
	b) 0.5 N sulphuric acid	100°	14 h

Table 2. Degradation of methylated sugars under hydrolytic conditions.

Conditions used	2,3-Di-*O*-Me-xylose	2,3-Di-*O*-Me-glucose	2,3,6-Tri-*O*-Me-glucose
1	6– 7 %	8 %	7 %
2	1– 3 %	–	7 %
3	2– 4 %	7 %	5 %
4	~ 20 %	23 %	17 %

Table 3. Demethylation during acid hydrolysis, expressed as mole % of ethers formed having a lower degree of methylation.

Substance	Conditions	Demethylation
2,3–X[a]	1	2.1
»	2[b]	1.7
»	3	0.6
»	4	Traces
2,3–G	4 % aq HCl 100, 12 h	2.5
2,3,6–G	2	0.9

a) 2,3-X = 2,3-Di-*O*-methyl-D-xylose, 2,3-G = 2,3-Di-*O*-methyl-D-glucose and so on.
b) The methanolic HCl was heated for 13 h under reflux and not in a sealed tube.

et al.[4] report that 1,4-di-*O*-methylerythritol was demethylated to 1.3 % when refluxed with 3 % methanolic hydrogen chloride for 18 h.

The present paper is a report of studies on the degradation and demethylation of 2,3-di-*O*-methyl-D-xylose, 2,3-di-*O*-methyl-D-glucose and 2,3,6-tri-*O*-methyl-D-glucose under different conditions. The conditions used are listed in Table 1; they were selected as representative of those various procedures used in the hydrolysis of methylated polysaccharides.

The extent of degradation was determined by measuring the decrease in optical rotation after the hydrolytic treatment. This method is subject to serious limitations as some reversion might occur and small mechanical losses

are not excluded. The observed effects were generally rather small and the values in Table 2 should be regarded as highly approximate. They do, however, allow a comparison of the different methods of hydrolysis.

Formolysis in 98 % formic acid involves severe degradation, and the reaction solutions become very dark. The use of 90 % formic acid is often reported and is probably less harmful; Isbell *et al.*[5] report good results with this mixture. In the other treatments the degradation is less, usually of the same order of magnitude as that observed for the free sugars during the total hydrolysis of polysaccharide material.

In order to study the demethylation the products obtained after hydrolytic treatment were fractionated by carbon column chromatography and the lower ethers isolated were characterised by paper chromatography and paper electrophoresis. The percentages of lower methylated products obtained after different treatments are given in Table 3. These values also are probably not very accurate, but they give the correct order of magnitude. Comparable amounts of 2- and 3-*O*-methyl-D-xylose were formed during the demethylation of 2,3-di-*O*-methyl-D-xylose. Similarly, comparable amounts of 2- and 3-*O*-methyl-D-glucose and of 2,3-, 2,6- and 3,6-di-*O*-methyl-D-glucose were formed from 2,3-di-*O*-methyl-D-glucose and 2,3,6-tri-*O*-methyl-D-glucose, respectively.

Methylated polysaccharides are generally insoluble in hot aqueous solutions, and for that reason methanolysis, formolysis or treatment with 72 % sulphuric acid is performed before hydrolysis with dilute, aqueous acid. It is evident from the present investigation that hydrogen chloride, either in water or methanol, causes a significant amount of demethylation and that the use of sulphuric acid is therefore preferable. Formolysis in 98 % formic acid causes almost no demethylation but is accompanied by considerable degradation. Of the methods investigated, the pretreatment with 72 % sulphuric acid followed by hydrolysis with 12 % sulphuric acid offers the best compromise. It is possible, however, that equally good or better results may be obtained by formolysis in 90 % formic acid, followed by acid hydrolysis. Aspinall *et al.*[6] have hydrolysed a methylated polysaccharide that was soluble in cold water, by carrying out the reaction in dilute sulphuric acid and raising the temperature only slowly, so as to keep the material in solution. This method seems to have definite advantages.

The substances studied in the present investigation did not show any selective demethylation and the methoxyl groups in different positions seem to show comparable reactivities. This was to be expected; smaller differences in reactivity are reasonable but a highly selective demethylation seems most improbable.

EXPERIMENTAL

Paper chromatography and *paper electrophoresis* were carried out on Whatman No. 1 filter paper.

Solvent systems: Ethyl acetate-acetic acid-water, 3:1:3.
Butanone, saturated with water.
Buffer: 0.1 M borate buffer at pH 10.

Starting materials. 2,3-Di-*O*-methyl-D-glucose and 2,3,6-tri-*O*-methyl-D-glucose were prepared by conventional methods. 2,3-Di-*O*-methyl-D-xylose was prepared by methylation, detritylation and hydrolysis of methyl-5-*O*-trityl-D-xylofuranosides (α- and β-mixture) analogously to the synthesis by Robertson and Gall [7], of the same substance from methyl-5-*O*-benzoyl-D-xylofuranosides. The substance was purified by carbon column chromatography and distillation under reduced pressure. It did not crystallise but was chromatographically and electrophoretically pure and indistinguishable from 2,3-di-*O*-methyl-D-xylose, obtained as the main product of hydrolysis of fully methylated xylans.

Estimation of the extent of degradation

The optical rotation of an aqueous solution of the methylated sugar (*c* 2.0) was determined, 5.00 ml of this solution was concentrated to dryness in a rotating laboratory evaporator and the residue was treated according to one of the four different alternatives described below.

1. It was dissolved in 2 % aqueous hydrochloric acid (4 ml), refluxed for 13 h, diluted to 5.00 ml and the optical rotation was determined (2 dm tube).
2. It was dissolved in 2 % methanolic hydrogen chloride (5 ml) and heated in a sealed tube to 100° for 13 h. The methanol was replaced with water by distillation under reduced pressure, the volume was adjusted to 4.5 ml and the solution was refluxed for 8 h. The volume was then adjusted to 5.00 ml and the optical rotation was determined.
3. It was dissolved in 72 % sulphuric acid (0.44 ml) and kept at room temperature for 30 min. Water was added (3.52 ml) and the solution was heated to 100° for 4 h, diluted with water to 5.00 ml and the optical rotation was determined.
4. It was dissolved in 98 % formic acid (6 ml) and heated to 100° for 6 h, then concentrated to a syrup under reduced pressure, dissolved in 0.5 N sulphuric acid (4.5 ml) and heated to 100° for 14 h. It was then diluted to 5.00 ml and the optical rotation was determined.

For treatments 1, 2 and 3 the decrease in optical rotation was only between 0.02° and 0.05°, duplicate experiments showing a fairly good agreement. The concentrations during the acid treatments were somewhat too high, and some reversion probably occurred.

The formolysis gave a larger decrease in rotation, about 0.2.°

Estimation of the demethylation

A sample of the methylated sugar (about 1.0 g) was subjected to hydrolytic treatment as described above. The acid was removed by filtration through a column of Amberlite IR 4 B and the aqueous solution was concentrated to a small volume and added to the top of a carbon-Celite column (4 × 40 cm). The sugars were eluted with aqueous ethanol, using gradient elution. For the dimethyl ethers, elution with 5 000 ml, 0 → 25 % ethanol was sufficient. The products from the hydrolytic treatment of 2,3,6-tri-*O*-methyl-D-glucose were eluted with 8 000 ml, 0 → 50 % ethanol. Pure starting material was recovered together with smaller amounts of partially demethylated sugars. The fractionation of the latter was incomplete and they were therefore combined and the total amount present was determined by weighing, hypoiodite titration and determination of the optical rotation. The components of these fractions were characterised by paper chromatography and paper electrophoresis and their proportions were estimated from the intensities of the spots. In the experiments with 2,3-di-*O*-methyl-D-xylose, very small amounts of xylose were observed in the hydrolysate in addition to the mono-*O*-methyl-D-xyloses and starting material.

REFERENCES

1. Freudenberg, K. and Boppel, H., *Ber.* **73** (1940) 609.
2. Chanda, S. K., Hirst, E. L., Jones, J. K. N. and Percival, E. G. V. *J. Chem. Soc.* **1950** 1287.
3. Croon, I. and Lindberg, B. *Svensk Papperstidn.* **60** (1957) 843.
4. Goldstein, I. J., Hamilton, J. K. and Smith, F. *J. Am. Chem. Soc.* **81** (1959) 6252.
5. Isbell, H. S., Frush, H. L., Bruchner, B. H., Kowkabany, G. N. and Wampler, G. *Anal. Chem.* **29** (1957) 1523.
6. Aspinall, G. O., Hirst, E. L. and Ramstad, E. *J. Chem. Soc.* **1958** 593.
7. Robertson, G. J. and Gall, D. *J. Chem. Soc.* **1937** 1600.

Received March 24, 1960.

ACTA CHEMICA SCANDINAVICA 14 (1960) 1343—1348

Kinetics of the Hydrolysis of Acetic Anhydride in Acetone-Water and Dioxane-Water Mixtures

JOUKO KOSKIKALLIO

Department of Chemistry, University of Oulu, Oulu, Finland

From the values obtained for the rate constants and activation entropies and energies of the acid hydrolysis of acetic anhydride in acetone-water and dioxane-water mixtures, it is concluded that the hydrolysis occurs simultaneously by two mechanisms, A-1 and A-2. When the composition of the solvent mixture is altered, one mechanism is favoured over the other. A-2 dominates in mixtures containing approximately 50 % acetone while A-1 dominates in mixtures containing only small amounts of water. An other important factor affecting the rate in solvent mixtures is the variation of the proton availability with solvent composition.

The acid-catalysed solvolysis of acetic anhydride involves, as do many other acid solvolyses, a fast proton transfer pre-equilibrium

$$Ac_2O + SH^+ = Ac_2OH^+ + S \qquad (1)$$

followed by a slow reaction which may be either bimolecular, A-2,

$$Ac_2OH^+ + H_2O \xrightarrow{\text{slow}} AcOH + AcOH_2^+ \qquad (2)$$

or unimolecular, A-1,

$$Ac_2OH^+ \xrightarrow{\text{slow}} AcO^+ + AcOH \qquad (3)$$

The reactions following the step (2) or (3) that lead to the final products are all fast. The equilibrium of reaction (1) is far on the left and therefore the experimental rate constant

$$k_{exp.} = Kk \qquad (4)$$

is equal to the product of the equilibrium constant K of the proton transfer reaction (1) and the rate constant k of the slow reaction, either (2) or (3).

Table 1. Rate constants of the acid-catalysed (k_a) and spontaneous (k_w) hydrolysis reactions of acetic anhydride in acetone-water mixtures.

$t°$	Water wt. %	H_2O mole/l	HCl mole/l	$10^5\ k_a'$ l²/mole² sec	$10^5\ k_w$ l/sec
0°	3.03	1.34	0.0205	12.4	
	5.43	2.47	0.0404	6.85	
	12.8	5.85	0.101	4.85	0.017
	23.7	11.5	0.101	6.07	0.108
	44.6	22.5	0.101	14.6	0.95
	63.8	33.7	0.101	29.6	4.76
	82.1	44.5	0.100	47.2	17.9
	100	55.5	0.199	50.5	47.4
20°	1.14	0.49	0.079	150	
	1.77	0.76	0.0098	167	
	3.03	1.30	0.0198	179	
	5.43	2.40	0.039	81.5	
	12.8	5.70	0.098	43.5	0.083
	12.8	5.70	0.0099	41.1	0.083
	23.7	11.2	0.099	47.7	0.56
	44.6	22.1	0.099	92	4.26
	63.8	33.1	0.099	177	19.6
	82.1	44.0	0.099	333	70.5
	100	55.5	0.199	447	190
40°	3.03	1.26	0.0191	1610	
	5.43	2.34	0.0384	950	0.166
	12.8	5.56	0.096	373	0.34
	23.7	10.9	0.097	371	2.40
	44.6	21.7	0.097	620	15.9
	63.8	32.6	0.097	1155	61.9
	82.1	43.5	0.098	2280	210

Table 2. Second-order (k_a) and third-order ($k_a' = k_a/[H_2O]$) rate constants of acid-catalysed and spontaneous (k_w) hydrolysis reactions of acetic anhydride in dioxane-water mixtures at 20°C.

Water wt. %	H_2O mole/l	HCl mole/l	$10^5\ k_a$ l/mole sec	$10^5\ k_a'$ l²/mole² sec	$10^5\ k_w$ l/sec
0.19	0.107	0.0144		149	
0.19	0.106	0.0456		142	
0.27	0.150	0.0504		261	
0.44	0.249	0.0260		298	
0.49	0.276	0.0400		262	
0.46	0.262	0.0670		272	
0.49	0.274	0.117		241	
0.76	0.431	0.0078		372	
1.10	0.620	0.0101	198	320	
0.98	0.551	0.0574	204	370	
0.99	0.560	0.171	182	325	
2.03	1.17	0.0196	284	243	
3.87	2.21	0.0396	142	64.5	
9.65	5.53	0.099	88	16.0	
19.3	11.0	0.099	80	7.3	0.80
38.5	22.1	0.099	126	5.75	5.57
58.3	33.1	0.099	239	7.22	24.6
78.7	44.0	0.099	369	8.38	79.5
100	55.5	0.199	447	8.05	190

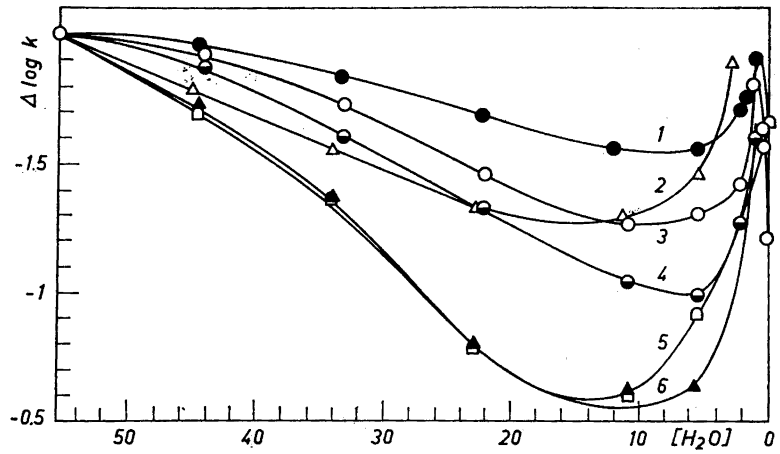

Fig. 1. Plot of log$k$ (solvent mixture) — log$k$ (water) and acidity function H_0 against [H_2O] for the hydrolysis of acetic anhydride in acetone-water and dioxane-water mixtures. 1. ethyl acetate, acetone-water. 2. diethoxymethane, dioxane-water. 3. acetic anhydride, dioxane-water. 4. acetic anhydride, acetone-water. 5. H_0, dioxane-water. 6. H_0, acetone-water.

It was found in a previous study [1] of the acid hydrolysis of acetic anhydride that the rate constant k varies only slightly over the whole range of methanol — water mixtures, whereas K, and therefore also $k_{exp.}$, changes considerably when the composition of the solvent mixture is altered. The change of K could be quantitatively explained by variations in the proton transfer equilibrium between water and methanol. The present investigation was undertaken in order to find out whether similar proton transfer equilibria are important in dioxane — water or acetone — water mixtures.

EXPERIMENTAL

Acetic anhydride (E. Merck AG, pro analysi), aniline (E. Merck AG, pro analysi) and acetone (E. Merck AG, pro analysi) were used as such. The water content of the acetone, 0.21 mole/litre, was determined by the Karl Fischer method. Dioxane (Fluka AG, purified by the method of Hess and Frahm) contained about 0.053 mole/litre of water. In order to remove any remaining hydroxylic compounds the dioxane was purified again by the method of Hess and Frahm [2]. After this treatment the dioxane contained less than 0.002 mole/litre of water. A stock solution of 1 N hydrochloric acid was prepared from a Titrisol ampoule (E. Merck AG). Solutions of hydrochloric acid in dioxane were prepared immediately before use by passing hydrogen chloride produced from sodium chloride and concentrated sulphuric acid into the dioxane. The acetone-water and dioxane-water mixtures were prepared by weighing in volumetric flasks.

Methods previously described [3] were used to determine the rate constants of the hydrolysis of acetic anhydride in the mixtures. The catalytic rate constant was obtained by subtracting the rate constant of the spontaneous reaction in the pure solvent mixture from the rate constant obtained in the same solvent mixture containing added hydrochloric acid. The second-order formula was used to calculate the rate constants when the concentration of water in the solvent mixture was less than 0.5 mole/litre, and the first-

order formula when the other solvent mixtures were employed. A good constancy of the rate constant was obtained in all cases except at the lowest water concentrations of 0.1 – 0.15 mole/litre. In these latter mixtures the second-order rate constant increases about 20 % when the reaction proceeds from 10 to 60 % change. The mean values of the rate constants are given in Tables 1 and 2.

DISCUSSION

In Fig. 1 are shown plots of log$k$ (solvent mixture) — log$k$ (water) against the water concentration of the solvent mixture for the acid hydrolysis of acetic anhydride, diethoxymethane [4], and ethyl acetate [5], and curves plotting values of the acidity function H_0 [6]. All these curves have a similar form and a minimum at a water concentration of about 10 moles/litre. The decrease in the rate at water concentrations below about 1 mole/litre is unexpected. Also the third-order rate constants obtained by dividing the second-order rate constant by the concentration of water vary similarly. The values of H_0 are too few in number to permit a decision as to whether they follow a similar course.

The acid hydrolysis of diethoxymethane is a typical example of the unimolecular reaction (3) with a positive entropy of activation [7] $\Delta S^* = +6.9$ e.u., a zero volume of activation [7] $\Delta V^* = 0$ cm^3 mole^{-1}, and a rate proportional to the acidity function H_0 in mixtures of a strong mineral acid and water [8]. The curve plotting the rate of acid hydrolysis of diethoxymethane is closest to the plot of the acidity function H_0 (Fig. 1). A complete agreement cannot be expected for mixtures of a organic solvent and water [8].

On the other hand, the acid hydrolysis of ethyl acetate is a typical example of a reaction occurring by the bimolecular mechanism (2). It has a negative entropy of activation in water [5]: $\Delta S^* = -22.5$ e.u. For methyl acetate which hydrolyses by the same mechanism as ethyl acetate a negative volume of activation [9] $\Delta V^* = -13.3$ cm^3 mole^{-1} was obtained in 44.1 % w/w acetone-water. The rate of acid hydrolysis of ethyl acetate is not proportional to H_0 in concentrated aqueous mineral acid solutions [10]. The curve for ethyl acetate in Fig. 1 deviates most from the H_0 curve.

The two reactions (2) and (3) probably occur concurrently in the acid hydrolysis of acetic anhydride. The activation entropy in water, $\Delta S^* = -12.3$ e.u. (Table 3), is higher than expected for a bimolecular reaction but

Table 3. Activation energies and entropies of the acid-catalysed hydrolysis of acetic anhydride calculated from the second-order rate constants and of the spontaneous hydrolysis calculated from the first-order rate constants in dioxane-water mixtures. Subscript a refers to acid-catalysed reaction and subscript w to the spontaneous reaction.

H_2O mole/l	E_a kcal/mole	ΔS_a^* e.u.	E_w kcal/mole	ΔS_w^* e.u.
1.30	20.65	— 2.6		
2.4	21.00	— 2.8		
5.7	18.97	—10.7		
11.2	17.44	—16.0	13.34	—39.0
22.1	16.01	—19.6	11.96	—39.7
33.1	15.64	—19.8	10.87	—40.5
44.0	16.52	—15.3	10.40	—39.5
55.5	17.25	—12.3	11.05	—35.1

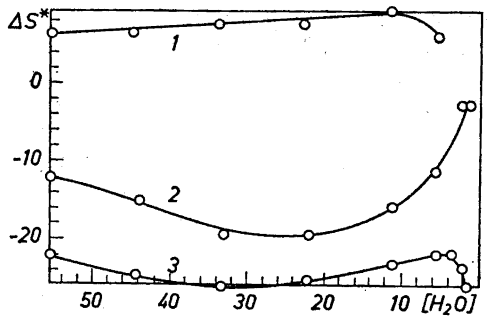

Fig. 2. Plot of ΔS^* against $[H_2O]$. 1. diethoxymethane, dioxane-water. 2. acetic anhydride, acetone-water. 3. ethyl acetate, acetone-water.

lower than expected for a unimolecular reaction (Fig. 2). The rates of unimolecular hydrolyses increase faster than do the rates of bimolecular hydrolyses in aqueous solutions of strong mineral acids when the concentration of the acid is increased. The unimolecular reaction is thus favoured in concentrated mineral acid solutions and this may explain why the rate of acid hydrolysis of acetic anhydride has been found [12] to be proportional to the acidity function H_0.

In a mixture consisting of about half acetone and half water the activation entropy is small and reaches a minimum value $\Delta S^* = -20$ e.u. (Fig. 2). In this range the acid hydrolysis of acetic anhydride is thus mainly a bimolecular reaction. In agreement with this view a small negative volume of activation $\Delta V^* = -17.1$ cm^3 mole^{-1} was obtained [13] for the reaction in 44.1 % acetone-water. At high pressures the bimolecular reaction dominates even more than at low pressures because the rate of a bimolecular reaction is increased by pressure whereas an unimolecular reaction remains almost unaffected. The curve for acetic anhydride lies between those for the ester and the formal in water-rich mixtures (Fig. 1).

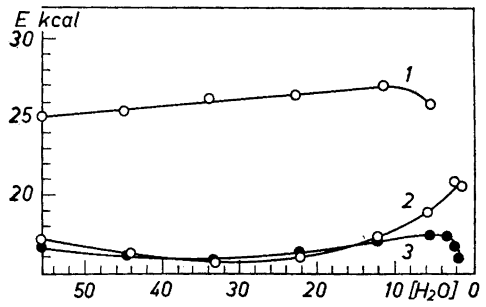

Fig. 3. Plot of E against $[H_2O]$. 1. diethoxymethane, dioxane-water. 2. acetic anhydride, acetone-water. 3. ethyl acetate, acetone-water.

The plots of the activation entropy against water concentration for ethyl acetate and diethoxymethane (Fig. 2) remain fairly horizontal over a wide range of solvent mixtures. The solvent effects in unimolecular and bimolecular reactions are hence small. On the other hand, the activation entropy of the acid hydrolysis of acetic anhydride varies much more when the composition of the solvent mixture is altered. In mixtures containing only small amounts of water the activation entropy ΔS^* reaches a high value of about —2.7 e.u. which is of the order of magnitude typical for unimolecular reactions. If all solvent effects remain insignificant when the concentration of water is decreased, the rate of the bimolecular reaction should be retarded and the unimolecular reaction should remain unaffected because the rate of the former reaction (2) is proportional to the water concentration, whereas the rate of the later (3) is of zero order with respect to water. The solvent effects of a unimolecular and a bimolecular reaction were found to be small. It is then not unexpected that a change occurs in the acid hydrolysis of acetic anhydride from two concurrent reactions in water to a typical unimolecular reaction in acetone containing only small amounts of water. Also the activation energies in Fig. 3 vary in a similar manner as the activation entropies and thus confirm the above conclusions.

REFERENCES

1. Koskikallio, J. *Acta Chem. Scand.* **13** (1959) 671.
2. Hess, K. and Frahm, H. *Ber.* **71** (1938) 2627.
3. Koskikallio, J. *Ann. Acad. Sci. Fennicae Ser.* **A II** (1954) No. 57.
4. Koskikallio, J. *Unpublished work.*
5. Tommila, E. and Hella, A. *Ann. Acad. Sci. Fennicae Ser.* **A II** (1954) No. 53.
6. Braude, E. A. and Stern, E. S. *J. Chem. Soc.* **1948** 1976.
7. Koskikallio, J. and Whalley, E. *Trans. Faraday Soc.* **55** (1959) 809.
8. Long, F. A. and Paul, X. *Chem. Revs.* **57** (1957) 965.
19. Taft, R. W., Deno, N. C. and Skell, P. S. *Ann. Rev. Phys. Chem.* **9** (1955) 287.
10. Bell, R. P., Dowding, A. L., and Noble, J. A. *J. Chem. Soc.* **1955** 3106.
11. Salomaa, P., and Linnantie, R. *Acta Chem. Scand.* **10** (1958) 2051.
12. Gold, V. and Hilton, J. *J. Chem. Soc.* **1955** 843.
13. Koskikallio, J., Pouli, D. and Whalley, E. *Can. J. Chem.* **37** (1959) 1360.

Received March 8, 1960.

ACTA CHEMICA SCANDINAVICA 14 (1960) 1349—1352

Nonaqueous Titration of Phenolic Esters

BENGT SMITH and ÅKE HAGLUND

Institutionen för Organisk Kemi, Chalmers Tekniska Högskola, Göteborg, Sweden

Potentiometric titration of phenolic esters using tetra-*n*-butylammonium hydroxide in acetone has been found suitable for differentiating between various types of phenolic esters. Esters of aliphatic carboxylic acids can be titrated as a rule, provided that strongly electron-repelling groups are absent in the phenolic ring. Unsubstituted esters of aromatic carboxylic acids do not react but replacement of hydrogen atoms in the aromatic nucleus by electron-attracting groups can also render the aromatic esters titratable.

It has been shown by Glenn and Peake [1] that phenolic esters of aliphatic as well as aromatic carboxylic acids can be titrated in ethylenediamine using potassium methoxide in benzene-methanol as titrant. It was assumed that the esters underwent aminolysis with the formation of phenols and amides of ethylenediamine. Attempts in this laboratory to titrate phenolic esters using acetone as solvent and tetra-*n*-butylammonium hydroxide in benzene-methanol as titrant revealed a remarkable difference in reactivity between various types of esters. While certain phenolic esters reacted, consuming about one equivalent of base per ester group, no reaction took place with other esters. In the case of phenyl acetate, which reacted with the tetra-*n*-butylammonium base, the formation of methyl acetate could be proved by gas chromatography. Thus the reaction seems to involve a transesterification of the phenolic ester by methanol under the catalytic influence of base.

$$RCOOAr + CH_3OH \rightleftharpoons RCOOCH_3 + ArOH$$

Methanol is present in the titrant and it has been shown recently [2] that the tetra-*n*-butylammonium base titrant prepared by the Cundiff and Markunas [3] method by reaction of tetra-*n*-butylammonium iodide with silver oxide in anhydrous methanol is an approximately 1 to 1 mixture of methoxide and hydroxide.

The base consumption was generally 10—20 % too high. The reason for this is not clear but it should be pointed out that, if the ester group reacts with a hydroxyl ion, two equivalents of base will be consumed per ester group. Because of the too high base consumption, this method is generally not suited

for the quantitative analysis of phenolic esters. For this purpose, the Glenn and Peake method is superior. However, the structure dependence of the present method makes it useful for differentiating between various types of phenolic esters.

Aryloxysilanes, which have previously been titrated by the Glenn and Peake method [4], were found also to respond to the present method.

The results of the titration of a number of phenolic esters are summarized in Table 1.

EXPERIMENTAL

Materials. Most of the phenolic esters were prepared in this laboratory. Their purity was ascertained by determination of appropriate physical constants.

Titration procedure. The titration was made according to the directions of Fritz and Hammond [5] using 0.1 N tetra-*n*-butylammonium hydroxide in benzene-methanol as titrant and acetone as solvent. Both reagent grade and superdry acetone were used with about the same results. Glass calomel electrodes were used and the titration was followed by means of a Radiometer Titrator model TTT 1.

RESULTS and DISCUSSION

The phenolic esters in Table 1 are arranged in the following order: Unsubstituted phenolic esters of aliphatic acids (Nos. 1—5), phenolic esters of aliphatic acids with various substituents in the phenolic ring (Nos. 6—18), unsubstituted phenolic esters of aromatic acids (No. 19) and phenolic esters of aromatic acids with various substituents in the acid part of the molecule (Nos. 20—25). Compounds Nos. 26 and 27 have been included as examples of lactones and orthoesters. From the material in Table 1, certain conclusions may be drawn concerning the reactivities of various types of phenolic esters.

Phenolic esters of aliphatic carboxylic acids without substituents in the phenolic ring are split (*cf.* Nos. 1—5). Replacement of hydrogen atoms in the phenolic ring by strongly electron-donating groups, *e.g.* hydroxyl and amino groups, however, makes the ester group non-reactive (*cf.* Nos. 6—8). The presence of electron-donating groups of intermediate strength in the phenolic ring like the acetoxy group does not inhibit the splitting of the ester group (*cf.* Nos. 9—11). In diacetates of dihydric phenols, for example, one ester group was split with the formation of a phenoxide ion which then inhibited the splitting of the second ester group. Esters of phenols with weakly activating or deactivating groups can be titrated, as might be expected. An exception to this rule was provided by acetylsalicylic acid which was not split in contrast to its *meta* and *para* isomers (*cf.* Nos. 16—18). The reason for this will be discussed below.

Phenolic esters of aromatic carboxylic acids. For a phenolic ester of this type to be titratable under the conditions used in this work, the presence of electron-attracting groups in the molecule seems to be necessary (*cf.* Nos. 19—25). We have investigated the influence of substituents in the acid part of the molecule only but substituents in the phenolic ring can be expected to exert a similar influence as was found previously for esters of aliphatic carboxylic acids.

Table 1. Titration of phenolic esters in acetone using tetra-*n*-butylammonium hydroxide.

Compound			Base consumption equiv. per mole	Number of phenolic ester groups present	Number of phenolic ester groups split
No.	Name	Formula			
1	Phenyl acetate	$CH_3COOC_6H_5$	1.12	1	1
2	Phenyl *iso*butyrate	$(CH_3)_2CHCOOC_6H_5$	1.30	1	1
3	Diphenyl succinate	$C_6H_5OCOCH_2CH_2COOC_6H_5$	2.30	2	2
4	Phenyl succinate	$C_6H_5OCOCH_2CH_2COOH$	1.87*	1	1
5	β-Naphthyl acetate	$CH_3COOC_{10}H_7$	1.20	1	1
6	*o*-Hydroxyphenyl acetate	$CH_3COOC_6H_4OH$-*o*	1.09	1	0
7	*m*-Hydroxyphenyl acetate	$CH_3COOC_6H_4OH$-*m*	1.09	1	0
8	*p*-Aminophenyl acetate	$CH_3COOC_6H_4NH_2$-*p*	0	1	0
9	Pyrocatechol diacetate	$CH_3COOC_6H_4OCOCH_3$-*o*	1.08	2	1
10	Resorcinol diacetate	$CH_3COOC_6H_4OCOCH_3$-*m*	1.08	2	1
11	Hydroquinone diacetate	$CH_3COOC_6H_4OCOCH_3$-*p*	0.88	2	1
12	*o*-Cresyl acetate	$CH_3COOC_6H_4CH_3$-*o*	1.12	1	1
13	*o*-Chlorophenyl acetate	$CH_3COOC_6H_4Cl$-*o*	1.08	1	1
14	*o*-Nitrophenyl acetate	$CH_3COOC_6H_4NO_2$-*o*	1.11	1	1
15	*p*-Nitrophenyl acetate	$CH_3COOC_6H_4NO_2$-*p*	1.03	1	1
16	Acetylsalicylic acid	$CH_3COOC_6H_4COOH$-*o*	1.00	1	0
17	Acetyl-*m*-hydroxybenzoic acid	$CH_3COOC_6H_4COOH$-*m*	2.02*	1	1
18	Acetyl-*p*-hydroxybenzoic acid	$CH_3COOC_6H_4COOH$-*p*	2.02*	1	1
19	Phenyl benzoate	$C_6H_5COOC_6H_5$	0	1	0
20	Phenyl salicylate	*o*-$HOC_6H_4COOC_6H_5$	2.14	1	1
21	Phenyl *p*-hydroxybenzoate	*p*-$HOC_6H_4COOC_6H_5$	1.08	1	0
22	Phenyl *p*-aminobenzoate	*p*-$NH_2C_6H_4COOC_6H_5$	0	1	0
23	Phenyl *p*-nitrobenzoate	*p*-$NO_2C_6H_4COOC_6H_5$	1.03	1	1
24	Diphenyl phthalate	$C_6H_5OCOC_6H_4COOC_6H_5$-*o*	2.11	2	2
25	Phenyl phthalate	$C_6H_5OCOC_6H_4COOH$-*o*	1.75	1	1
26	Coumarin	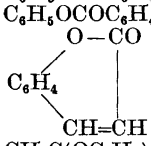	0	1	0
27	Phenyl orthoacetate	$CH_3C(OC_6H_5)_3$	0	3	0

* Two inflexion points were obtained.

Mechanism of the phenolic ester splitting. As previously shown in eqn. 1, the reaction is a re-esterification reaction. The results presented in the previous sections are also compatible with a reaction mechanism involving a nucleophilic attack on the carbonyl carbon atom of the ester group. In accordance with this mechanism, the splitting of esters of aliphatic carboxylic acids is inhibited by the presence of strongly electron-donating groups in the phenolic ring because of the increased electron density at the carbonyl carbon atom. The decreased reactivity of esters of aromatic carboxylic acids in comparison with esters of aliphatic carboxylic acids can be ascribed to the conjugation

of the carbonyl carbon atom with the aromatic nucleus in the former case. Electron-attracting groups once again call the splitting mechanism into play.

In Table 1, there are some exceptions from the general rules. Thus, acetylsalicylic acid (No. 16) was not split unlike its *meta* and *para* isomers. The reason for this might be a steric factor, the bulky carboxyl ion or the corresponding tetra-*n*-butylammonium salt hindering the approach of the nucleophilic reagent. The negative charge on the carboxyl ion is also likely to render the attack more difficult. A similar but less pronounced effect of a "neighbouring" carboxyl group is discernable for phenyl succinate (No. 4) and phenyl phthalate (No. 25) for which the splitting of the ester group is only partial.

The other exception is provided by phenyl salicylate (No. 20) in which the ester group is split in spite of the presence of a hydroxyl group. We believe this to be due to hydrogen bonding which increases the electrophility of the carbonyl carbon atom. It must be assumed that the ester group is split prior to the neutralization of the phenolic hydroxyl group.

Coumarin (No. 26) is the only example of a lactone investigated in this work. No splitting occurred. Although coumarin is to be looked upon as a phenolic ester of an aliphatic carboxylic acid, a reaction is hardly to be expected because of the conjugation of the carbonyl group with the aromatic ring. The fixation of the carbonyl group might also be of some significance for the lack of reactivity. The last compound in Table 1 is phenyl orthoacetate. It did not react with the titrant because of the absence of a carbonyl groop.

Use in identification work. The material collected in Table 1 exemplifies the application of the present titration method for the identification of phenolic esters of various types. While, in the analytical investigation of phenolic esters, hydrolysis of the esters to form the free phenols is often performed, the reverse procedure might sometimes be of value, *i.e.* acetylation of a phenol in order to elucidate its structure by means of the ester splitting method described here.

Acknowledgement. This work was supported by a grant from the *Town Council of Gothenburg.*

REFERENCES

1. Glenn, A. R. and Peake, J. T. *Anal. Chem.* **27** (1955) 205.
2. Cluett, M. L. *Anal. Chem.* **31** (1959) 610.
3. Cundiff, R. H. and Markunas, P. C. *Anal. Chem.* **28** (1956) 792.
4. Smith, B. *Acta Chem. Scand.* **11** (1957) 558.
5. Fritz, J. S. and Hammond, G. S. *Quantitative Organic Analysis*, J. Wiley and Sons, Inc., New York 1957, p. 266.

Received March 24, 1960.

ACTA CHEMICA SCANDINAVICA 14 (1960) 1353—1356

Organophosphorus Analogues of Tropic Acid Esters

1. 2-Phenyl-2-diethoxyphosphoryl Ethanol

L.-E. TAMMELIN and L. FAGERLIND

Research Institute of National Defence, Dept. 1, Sundbyberg 4, Sweden

Phenyl-diethoxyphosphoryl methane, phenyl-diethoxyphosphoryl acetaldehyde and 2-phenyl-2-diethoxyphosphoryl ethanol have been prepared. Infrared spectra, protolytic titration, refractive index, and violet color reaction with iron(III)ions indicate that the aldehyde shows keto-enol tautomerism. The occurrence of tautomerism and the presence of a strong hydrogen bridge in the enol form, support the view that condensation of phenyl-diethoxyphosphoryl methane and methyl formate with sodium results in phenyl-diethoxyphosphoryl acetaldehyde. Catalytic hydrogenation of the aldehyde consequently yields 2-phenyl-2-diethoxyphosphoryl ethanol.

Organophosphorus analogues of acetylcholine have been shown to be of considerable chemical and pharmacological interest [1]. It thus seemed to be of value to prepare phosphoryl analogues to other pharmacodynamically active compounds. This investigation is part of a study on the preparation of organophosphorus analogues of atropine [2,3]. The main purpose with the present part was to show whether phosphoryl compounds react analogously to carbonyl compounds in the ester condensation and hydrogenation reactions used in preparation of tropic acid ester [4]. The following formulae show the sequence of preparations studied.

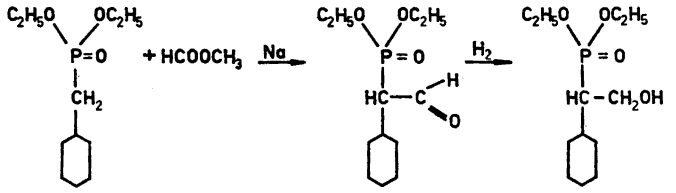

Carbon and hydrogen content of the obtained compounds, and the analogous reactions described in syntheses of tropic acid ester [4] *per se*, suggest that the studied reaction sequence really gives rise to 2-phenyl-2-diethoxy-

phosphoryl ethanol. However, the structure of the parent compound, phenyl-diethoxyphosphoryl acetaldehyde, is of major importance for establishing the structure of the phenyldiethoxyphosphoryl ethanol. Thus the aldehyde was made the subject of the following supplementary determinations: Infrared spectrum, acid properties and reaction with iron chloride. Finally, the infrared spectrum of phenyl-diethoxyphosphoryl ethanol was recorded.

EXPERIMENTAL

Syntheses

Phenyl-diethoxyphosphoryl methane. Two moles of ethanol and two moles of triethylamine were dissolved in 1 l of ether in a round bottomed flask with stirring. One mole of benzyl phosphoryldichloride was added (prepared according to Kinnear and Perren [5]). The triethylammonium chloride formed was filtered off, and the ester separated by fractional distillation, b.p. 115°/0.2 mm Hg. Phenyl-diethoxyphosphoryl methane is a colorless oil with a geranium-like odour. Refractive index $n_D^{25} = 1.4960$. (Found: C 57.8; H 7.52. Calc. for $C_{11}H_{17}O_3P$ (228.2): C 57.8; H 7.52). Yield 80 %.

Phenyl-diethoxyphosphoryl acetaldehyde. 1.0 moles of sodium were allowed to react with 2 moles of methyl formate in 200 ml ether, in a round bottomed flask with reflux condenser. 1 mole of phenyl-diethoxyphosphoryl methane, together with 250 ml of ether, was added when all sodium had been consumed. The mixture was boiled for 4 h and then stirred at room temperature for 24 h, after which the ether solution was extracted with 2 × 200 ml of water. pH of this extract was adjusted to ~10 and the solution extracted with 3 × 100 ml of ether, the ether extracts being discarded. The aqueous solution was acidified with sulfuric acid to pH ~3 and percolated with ether for 12 h. The ether extract thus obtained was evaporated, giving a viscous residue. The residue was dissolved in benzene and the benzene evaporated; this operation was repeated. Finally, the product was distilled at 110°/0.2 mm Hg, the first 5 ml of distillate being discarded. A few brown drops remained in the distillation flask. The phenyl-diethoxyphosphoryl acetaldehyde preparation thus obtained is an oil with a roselike odour. Refractive index is $n_D^{25} = 1.5195$ immediately after distillation, but increases with time and after a week becomes constant at $n_D^{25} = 1.5320$. After a few days of storage at $n_D^{25} = 1.5320$ the compound solidifies to crystals (m.p. 58°C). (Found C 56.3; H 6.61. Calc. for $C_{12}H_{17}O_4P$ (256.2): C 56.3; H 6.68). Yield: 50 %.

2-Phenyl-2-diethoxyphosphoryl ethanol. Phenyl-diethoxyphosphoryl acetaldehyde in ethanol solution was hydrogenated with hydrogen at 50 atm and 70°C for five days, using Adams platinum catalyst. The alcohol was purified by fractional distillation (b.p. 130°C/0.1 mm Hg), and is a liquid with $n_D^{25} = 1.5040$. (Found: C 55.3 H 7.5 Calc. for $C_{12}H_{19}O_4P$ (258.2): C 55.8; H 7.37). Yield 90 %.

Verification of purity and chemical structure

Phenyl-diethoxyphosphoryl acetaldehyde (51 mg + 1 ml C_2H_5OH + 39 ml 0.1 M KCl) was titrated with 0.1 M NaOH. The sodium hydroxide was added in 0.1 ml portions every third minute.

One drop of 5 % $FeCl_3$ solution was added to 5 ml 1 % aqueous solution of the aldehyde.

Infrared spectra of the aldehyde and ethanol were recorded with a Perkin and Elmer Mod 21 spectrophotometer. 0.2 M solutions in carbon tetrachloride were used. The spectrophotometer was used with a sodium chloride prism, resolution 927, response 2 : 1170, gain 5.7, speed 5, suppression 3, and scale 5 cm/μ. The thickness of the cell was about 0.1 mm.

RESULTS

Phenyl-diethoxyphosphoryl methane, phenyl-diethoxyphosphoryl acetaldehyde and phenyl-diethoxyphosphoryl ethanol have been prepared.

Sodium dissolves in phenyl-diethoxyphosphoryl methane in 10 % ether solution under formation of hydrogen and a white precipitate.

Phenyl-diethoxyphosphoryl acetaldehyde in aqueous solution reacts as an acid, and can thus be determined titrimetrically with sodium hydroxide. 95 % of the actual preparation reacted as acid ($pk_a \sim 7$). In aqueous solution, the aldehyde also forms a brilliant violet complex with iron (III) ions. On extraction with chloroform, the chloroform becomes purple.

The infrared spectrum of phenyl-diethoxyphosphoryl acetaldehyde exhibited the following characteristic features: Absorption bands at 2 800—2 600 cm^{-1} indicating a hydrogen bonded hydroxyl group, at 1 725 cm^{-1} indicating a carbonyl group, at 1 630 cm^{-1} indicating a carbon-carbon double bond, and at 1 200 cm^{-1} indicating a strongly hydrogen bonded phosphoryl group.

The infrared spectrum of the 2-phenyl-2-diethoxyphosphoryl ethanol showed the following characteristic features: Absorption bands at 3 500—3 200 cm^{-1} indicating a hydroxyl group with weak hydrogen bond, at 1 250 cm^{-1} indicating a normal phosphoryl group, but no bands at 1 725 cm^{-1} or 1 630 cm^{-1} which indicates that the aldehyde has been hydrogenated. Infrared spectra and a more thorough interpretation of them are given in part 2 of this investigation[2].

DISCUSSION

Phenyl-diethoxyphosphoryl methane apparently contains a reactive hydrogen atom, presumably situated in the methane residue. The structure of the condensation product from phenyl-diethoxyphosphoryl methane and methylformate is of major importance for the confirmation of the structure of the corresponding ethanol.

The first problem was to obtain the phenyl-diethoxyphosphoryl acetaldehyde sufficiently pure for identification. Distillation at 110°C and 0.2 mm Hg is a poor method for fractionation, and the carbon-hydrogen content a poor indicator of purity if, which is reasonable, phenyl-diethoxyphosphoryl methane is the main impurity. However, the protolytic titration method employed solved this problem.

Refractive index of the aldehyde increased with time after distillation. Simultaneously, an increase in the absorption band of hydroxyl in the infrared spectrum was observed [2]. This, together with the other results, strongly suggests that the aldehyde shows keto-enol tautomerism. Moreover, the infrared spectrum indicates a strong hydrogen bond between the enol hydroxyl group and the phosphoryl group, which suggests a sixmembered chelate ring with conjugated double bonds. The only structure which fits all these facts is the following, which is also analogous to the intermediate product in the syntheses of tropic acid.

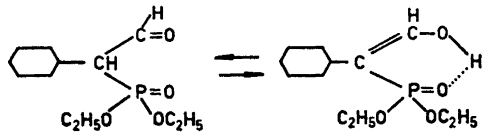

Simpler hydrogenation methods for the aldehyde than the catalytic hydrogenation used in preparation of the phenyl-diethoxyphosphoryl ethanol may exist. However, it was felt that a simple addition of hydrogen is the best way to establish the structure of the ethanol. The infrared spectrum of the ethanol supports the view that in total a hydroxymethylene group has been introduced at the carbon atom between the phenyl and phosphoryl groups.

Our sincere thanks are due to the Director of this Institute, Professor G. Ljunggren, for his kind interest in this work.

REFERENCES

1. Tammelin, L. E. *Svensk Kem. Tidskr.* **70** (1958) 157.
2. Larsson, L. and Tammelin, L. E. *Acta Chem. Scand. In press.*
3. Tammelin, L. E. and Fagerlind, L. *Acta Chem. Scand. In press.*
4. Müller, E. *Ber.* **51** (1918) 254.
5. Kinnear, A. M. and Perren, E. A. *J. Chem. Soc.* **1952** 3437.

Received March 17, 1960.

ACTA CHEMICA SCANDINAVICA 14 (1960) 1357—1363

The Structure of 2-Deoxy-ribose

S. FURBERG

Institute of Chemistry, University of Oslo, Blindern-Norway

The structure of 2-deoxy-ribose in the crystalline state has been determined by X-ray crystallographic methods. The sugar is found to occur in the pyranose form and to belong to the β-series, the conformation being 1*a*3*e*4*a*. This is explained in terms of a general preference for axial substituents on the anomeric carbon atom. The implications of this view are discussed.

The sugar of deoxyribonucleic acid (DNA), 2-deoxy-ribose, has been rather extensively investigated by chemical methods, and a number of reviews on its chemistry have been published [1,2]. However, several features of the stereochemistry of the free sugar are still in some doubt. The ring form does not seem to be definitely established, although a pyranose structure is to be expected, especially in view of recent work on ribose [3]. The methyl glycosides are isolated and assigned to the α- and β-series [4], but the configuration at the anomeric carbon atom in the free sugar does not appear to be known. Finally, the conformation of the sugar has not been determined.

We have now established the structure of 2-deoxyribose in the crystalline state, using the methods of X-ray crystallography. Details of the structure analysis are given below. Projections in two directions of the electron density in the crystal have been calculated (Fig. 1), showing that the molecule has the structure depicted in Fig. 2. It is seen that the molecule occurs in the pyranose structure with the normal staggered "chair" form found in all sugars hitherto studied. The orientation of the anomeric hydroxyl group relative to the two others shows that the sugar belongs to the β-series. The hydroxyl groups on C_4 and C_1 are axial (*a*) whereas that attached to C_3 is equatorial (*e*). The structure may thus be described as 1*a*3*e*4*a*.

As pointed out by Hassel and Ottar [5], there are two possible conformations for each pyranose sugar, the one being derivable from the other by interconversion of the pyranose ring. In the case of β-2-deoxy-ribose the two conformations are 1*a*3*e*4*a* and 1*e*3*a*4*e*. The stabilities of pyranose conformations have been discussed by a number of investigators. Reeves [6] predicts the preferred conformation by means of three instability factors, whereas Barker and Shaw [3] derive the relative stabilities by adding the "overlaps"

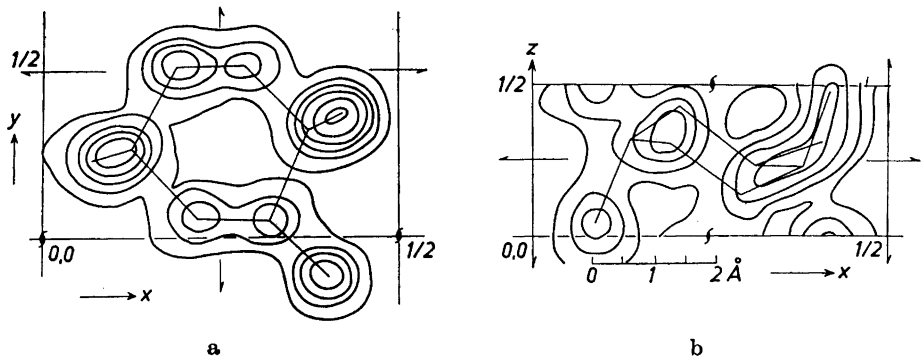

Fig. 1. Electron density projections on the (001) plane (a) and the (100) plane (b). Contours at 2,4,6,. . . e.Å^{-1}.

of non-bonded atoms. These methods have so far not been applied to deoxysugars but as both approaches consist in adding the unfavourable interactions in the molecule, they should be expected to be applicable also to these substances. In fact, the deoxysugars might provide an interesting test of the validity of the principles involved. In the case of 2-deoxy-ribose both methods predict that 1*e*3*a*4*e* is somewhat more stable than the observed form 1*a*3*e*4*a*, equatorial substituents being assumed to be more favourable than axial ones. The difference in stability is not great, and the solid state conformation may be determined by crystal forces. However, it is also possible that the molecular conformation 1*a*3*e*4*a* really is the more stable one, the reason, in case probably being that an equatorial hydroxyl group on the anomeric carbon atom C_1 may be an instability factor of importance in addition to those given by Reeves. This favours 1*a*-conformations, except possibly when there is an axial substituent in positions 3 or 5, in which case the effect is opposed by the repulsion between the two axial groups.

Greater stability of 1*a* substituents has been proposed as a possible explanation of the differences in reaction rates of α- and β-sugars. Thus the methyl β-pyranosides of glucose, mannose and galactose, in which the anomeric methoxyl group is equatorial, are hydrolysed more rapidly than the α-anomers. Edward [7] explained this in terms of electrostatic repulsive forces between the lone-pair electrons on the ring-oxygen atom and the polar group on C_1; this favours axial alkoxyl groups. Similarly, equatorial hydroxyl groups are oxidized more rapidly than axial ones [8]. However, for both types of reactions steric effects may provide an alternative explanation. Recently, the conformations of trans-di-halogeno-dioxanes have been studied in solid state and in solution. The results would seem to be in agreement with the preceding considerations, as the diaxial conformation is found in all cases [9].

The relation between this "1*e*-effect" and the powerful "Δ2-effect" of Reeves [6] should also be noted. The "Δ2-effect" corresponds to the conformation 1*e*2*a*, in other words to the combination of the two unfavourable factors 1*e* and 2*a*. Thus the "1*e*-effect" implies that the Δ2-condition must be unfavourable. Furthermore, it influences the relative importance of the two pyranose chair conformations also in other cases. The most notable deviations from previous stability considerations [3,6] would occur for sugars containing the configuration 1*a*2*a*3*e*⇌1*e*2*e*3*a*. Thus for α-lyxose, 1*a*2*a*3*e*4*e*⇌1*e*2*e*3*a*4*a*,

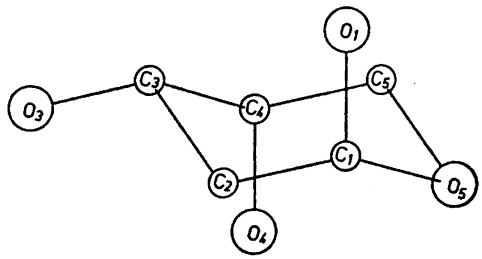

Fig. 2. The molecular structure of 2-deoxy-ribose.

the method of Reeves predicts conformational instability, which was also found in his studies of the cuprammin-complexes of methyl lyxosides. The approach of Barker and Shaw favours 1*e*2*e*3*a*4*a*, whereas the "1*e*-effect" gives preference to 1*a*2*a*3*e*4*e*. Proton magnetic resonance studies [11] have shown that α-lyxose tetra-acetate has the conformation 1*a*2*a*3*e*4*e* in solution.

If a 1*e* hydroxyl group represents an element of instability, the α-anomers of sugars as glucose, galactose and xylose should be more stable than the β-anomers, contrary to the view of Reeves [6]. As heat is evolved during the transformation from α- to β-glucose in aqueous solution, the latter anomer would appear to be the more stable one under these conditions [10]. The composition of the equilibrium mixture, in which the β-anomer predominates, points in the same direction [6]. However, the energy differences are so small that these observations do not represent conclusive evidence as regards the relative stability of the unhydrated molecules.

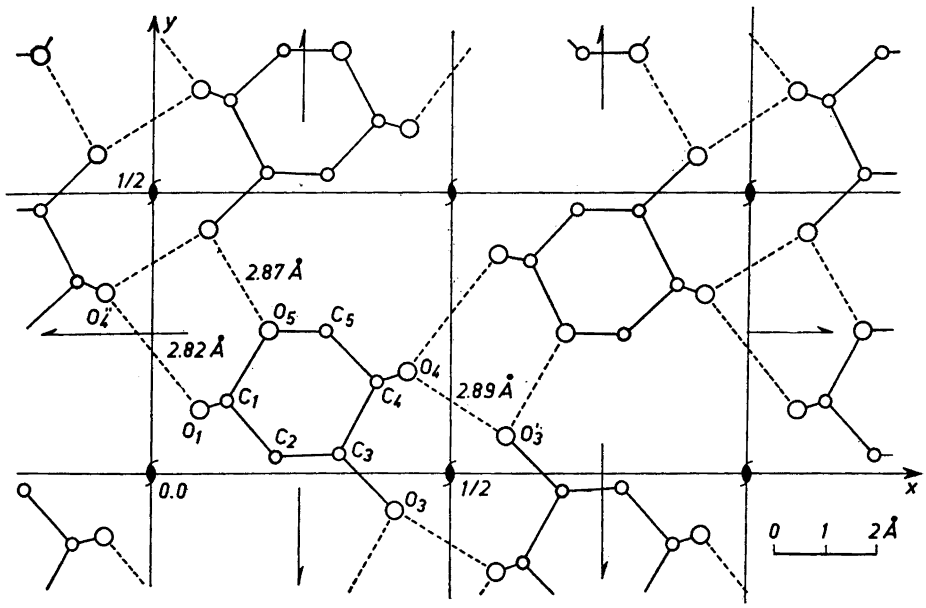

Fig. 3. The c-projection of the structure. Broken lines indicate hydrogen bonds.

Table 1. Atomic coordinates as fractions of the corresponding cell edge.

	x	y	z		x	y	z
C_1	0.130	0.131	0.312	H_1	0.05	0.13	0.45
C_2	0.210	0.030	0.418	H_2	0.23	0.04	0.62
C_3	0.316	0.029	0.239	H_2'	0.15	0.94	0.43
C_4	0.376	0.158	0.233	H_3	0.30	0.00	0.03
C_5	0.286	0.255	0.135	H_4	0.43	0.16	0.05
O_1	0.080	0.155	0.051	H_5	0.34	0.35	0.19
O_3	0.404	0.060	0.324	H_5'	0.27	0.23	0.94
O_4	0.419	0.185	0.496	H_{01}	0.02	0.18	0.01
O_5	0.188	0.252	0.311	H_{03}	0.13	0.38	0.46
				H_{04}	0.48	0.14	0.50

In Table 1 the atomic coordinates deduced from the final difference maps are given. The mean deviation in the x coordinates from the two projections is 0.015 Å and largest discrepancy is 0.04 Å. These figures may be taken as an indication of the accuracy of the coordinates. The corresponding bond lengths and bond angles are given in Table 2.

Table 2. Bond lengths (in Å units) and bond angles.

Bond lengths		Bond angles	
C_1-C_2	1.50	$O_5C_1C_2$	111°
C_2-C_3	1.49	$O_1C_1C_2$	118°
C_3-C_4	1.53	$O_1C_1O_5$	107°
C_4-C_5	1.53	$C_1C_2C_3$	107°
C_5-O_5	1.41	$C_2C_3C_4$	111°
O_5-C_1	1.45	$C_3C_4C_5$	108°
C_1-O_1	1.40	$C_3C_4O_4$	109°
C_3-O_3	1.44	$C_5C_4O_4$	112°
C_4-O_4	1.40	$C_4C_5O_5$	109°
		$C_5O_5C_1$	112.5°
		$C_2C_3O_3$	113.5°
		$C_4C_3O_3$	107°

The bond lengths and bond angles derived in the present investigation are given in Table 2. The bond lengths do not deviate significantly from the normal values of 1.53 Å and 1.42 Å for C-C and C-O distances, respectively. The bond angle at the ring oxygen atom is found to be 112.5°, somewhat greater than the other ring angles, which lie in the range 107° to 111°. The mean value of the external angles is 111°, but some of them show possibly significant variations from the tetrahedral angle, as is found also in other sugar structures [12].

Only three intermolecular distances are shorter than 3.0 Å. As there are three hydroxyl hydrogens in the molecule, these interactions are likely to be hydrogen bonds. It will be seen from Fig. 3 that one of the bonds connect O_3 and the ring oxygen atom O_5. Thus the hydrogen at O_3 is forming this bond. The hydrogen at O_4 must then take part in the hydrogen bond O_4——O_3' and that at O_1 in O_1—O_4''. The lengths of these bonds are 2.87 Å, 2.89 Å and 2.82 Å, respectively.

Table 3. Observed (F_o) and calculated (F_c) structure factors.

hkl	F_o	F_c	*hkl*	F_o	F_c
200	30	−34	940	< 3	− 2
400	51	−47	10 4 0	5	+ 7
600	27	−24	11 4 0	< 3	− 1
800	15	−15	12 4 0	< 2	− 2
10 0 0	17	+17			
12 0 0	< 3	− 1	150	28	−28
110	13	−13	250	19	−19
			350	3	+ 4
210	11	− 8	450	4	− 3
310	6	+ 6	550	14	+15
410	6	+ 7	650	< 3	+ 2
510	14	+14	750	6	+ 5
610	2	0	850	6	+ 6
710	3	− 3	950	< 3	+ 3
810	3	− 4	10 5 0	< 3	+ 2
910	< 3	+ 1	11 5 0	4	− 3
10 1 0	< 3	+ 4	12 5 0	3	− 3
11 1 0	4	− 6			
12 1 0	3	− 3	060	7	− 6
			160	< 3	− 3
020	16	−15	260	9	+10
120	48	−51	360	21	+22
220	< 2	+ 3	460	4	− 6
320	44	−41	560	< 3	− 2
420	< 2	− 2	660	< 3	− 1
520	5	− 4	760	8	−10
620	< 2	− 2	860	3	+ 5
720	5	+ 5	960	< 3	+ 3
820	< 3	+ 3	10 6 0	< 3	− 3
920	< 3	+ 3	11 6 0	< 2	0
10 2 0	< 3	+ 1			
11 2 0	< 3	+ 1	170	14	+11
			270	23	+22
130	< 2	0	370	< 3	0
230	37	−38	470	4	+ 6
330	4	+ 4	570	9	− 9
430	39	−36	670	3	− 3
530	< 2	− 2	770	3	− 4
630	5	+ 5	870	< 3	+ 2
730	4	− 4	970	< 3	+ 1
830	16	+19	10 7 0	6	− 7
930	= 3	+ 4	11 7 0	< 3	+ 2
10 3 0	3	− 3			
11 3 0	= 3	− 2	080	8	+ 8
12 3 0	= 3	+ 3	180	15	−12
			280	13	−12
040	11	+11	380	6	+ 5
140	7	+ 7	480	5	+ 4
240	56	−52	580	5	+ 4
340	49	+46	680	7	+ 7
440	29	+30	780	< 3	− 2
540	2	+ 3	880	< 3	− 2
640	13	+17	980	< 2	0
740	13	−16	10 8 0	< 2	0
840	13	−14	11 8 0	3	− 3

Table 3. Continued.

hkl	F_o	F_c	*hkl*	F_o	F_c
190	14	+14	501	< 6	+ 3
290	5	− 6	601	10	+ 9
390	4	− 4	701	< 6	− 1
490	< 3	− 2	801	< 6	− 8
590	10	−10	901	< 7	+ 5
690	< 3	− 1			
790	< 3	− 3	002	14	−12
890	< 2	+ 1	102	< 5	+ 2
			202	28	−27
0 10 0	10	−10	302	32	−30
1 10 0	4	− 6	402	13	+11
2 10 0	7	+ 7	502	34	−36
3 10 0	< 3	− 1	602	26	+25
4 10 0	< 3	+ 1	702	< 7	0
5 10 0	< 3	+ 1	802	< 7	− 5
6 10 0	3	− 3	902	< 7	− 3
7 10 0	< 2	− 1			
			103	10	+10
1 11 0	< 2	− 2	203	14	+16
2 11 0	< 2	− 1	303	8	− 7
3 11 0	< 2	0	403	< 6	− 3
4 11 0	< 2	0	503	< 7	− 7
			603	< 7	0
0 12 0	< 2	0			
1 12 0	6	− 5	004	9	+ 9
2 12 0	2	− 2	104	< 7	+ 8
3 12 0	< 2	− 2	204	< 7	− 6
			304	9	+ 9
101	19	−22	404	9	−10
201	14	−16	504	< 7	+ 1
301	13	+12	604	< 7	+ 1
401	8	+11			

THE STRUCTURE ANALYSIS

A commercial sample of D-2-deoxyribose from Mann Research Laboratories, New York, was used for the investigation. Single crystals big enough for X-ray work were grown by precipitating the compound from a solution in acetone, the solution being placed in a desiccator containing excess of ethyl acetate. The crystals obtained were elongated along the *c* axis, with (100) as the dominating face.

X-Ray single crystals diagrams of the Weissenberg type were taken around the *c* and *b* axis, using copper radiation. They showed that the crystals are orthorhombic, with unit cell dimensions $a = 11.37$ Å, $b = 10.64$ Å and $c = 4.86$ Å (all ± 0.5 %). The space group is $P2_12_12_1$ as reflexions $h00$, $0k0$ and $00l$ are absent for odd values of the indices. Four molecules in the unit cell correspond to a calculated density of 1.51 g/cm³.

The intensities of the reflexions were estimated visually by comparison with a standard scale. Difficulties were encountered, as the crystals which were big enough to give a satisfactory diagram proved to be aggregates of two or more crystals. The true single crystals found were so small that only the strongest reflexions were recorded. The intensity values derived are therefore probably somewhat less accurate than those usually obtained by this procedure. 69 of the 146 $hk0$ reflexions and 22 of the 63 $h0l$ reflexions obtainable with Cu$K\alpha$ radiation were recorded with measurable intensity.

To determine the *c* projection of the structure, the approximate position of the molecule was first deduced by means of Bragg—Lipson structure factor graphs. These graphs

also indicated the signs of four low-order strong reflexions (240, 400, 120 and 320). Using these signs as a basis, the "multiplication rule" was applied to derive the signs of 16 reflexions expressed by the sign of the 340 reflexion. The two corresponding electron density maps both clearly showed a six-membered ring system, but only one of them indicated a 1,3,4-substituted sugar. The very first set of structure factors based on this structure gave a remarkable agreement with the observed values, the reliability factor $R = \Sigma||F_{obs}| - |F_{calc}||/\Sigma|F_{obs}|$ having the value 0.28. The structure was further refined by a number of difference synthesis. The process was complicated by the fact that in the projection there are hydrogen atoms close to nearly all the heavier atoms. It was found essential for the refinement to include their contribution to the structure factors. The positions of most of them were indicated by the difference maps, but some had to be placed by stereochemical considerations. The final value obtained for R was 0.10. A common isotropic temperature factor $\exp(-4.0 \sin^2\Theta/\lambda^2)$ was used for all the atoms. As the experimental data are rather unsatisfactory, further refinements were not carried out. In Table 3 observed and calculated structure factors are compared. It may be remarked that the 16 signs originally deduced all were correct.

The relative z coordinates of the atoms were calculated from the known c projection and from standard values of the bond lengths. The molecule was then placed so as to give reasonable lengths to the intermolecular hydrogen bonds indicated by the c projection. This postulated structure was refined by difference syntheses, the final value of R being 0.10 also in this case. However, the small number of reflexions and the overlap of atoms make the coordinates less reliable than those derived from the c projection. The electron density projection is shown in Fig.1 b.

The investigation was supported by a grant from *Norsk Hydros Fond.*

REFERENCES

1. Overend, W. G. *Advances in Carbohydrate Chem.* **8** (1953) 45.
2. Overend, W. G. and Stacey M. *The Nucleic Acids*, Academic Press Inc., New York, 1955, Vol. I, p. 48.
3. Barker, G. R. and Shaw, D. F. *J. Chem. Soc.* **1959** 584.
4. Deriaz, R. E., Overend, W. G., Stacey, M. and Wiggins, L. F. *J. Chem. Soc.* **1949** 2836.
5. Hassel, O. and Ottar, B. *Acta Chem. Scand.* **1** (1947) 929.
6. Reeves, R. E. *J. Am. Chem. Soc.* **72** (1950) 1499.
7. Edward, J. T. *Chem. & Ind. (London)* **1955** 1102.
8. Bentley, R. *J. Am. Chem. Soc.* **79** (1957) 1720.
9. Altona, C., Romers, C. and Havinga, E. *Tetrahedron Letters* **1** (1959) 16.
10. Riiber, C. N. *Ber.* **57** (1924) 1599.
11. Lemieux, R. U., Kullnig, R. K., Bernstein, H.J. and Schneider, W.G. *J. Am. Chem. Soc.* **80** (1958) 6098.
12. McGeachin, H. McD., and Beevers, C. A. *Acta Cryst.* **10** (1957) 227.

Received February 10, 1960

ACTA CHEMICA SCANDINAVICA 14 (1960) 1364—1368

Studies on Metal Complexes in Aqueous Solution by Infrared Spectrophotometry

I. A Qualitative Investigation of the Iron(III) and Aluminium Oxalate Systems

STURE FRONÆUS and RAGNAR LARSSON

Department of Inorganic and Physical Chemistry, Chemical Institute, University of Lund, Lund, Sweden

The infrared spectra of the iron(III) and aluminium oxalate systems in aqueous solution have been recorded in the range 1 500—1 200 cm^{-1}. Solutions of compositions corresponding to the first, second, and third mononuclear complexes show absorption peaks of almost the same frequency. The positions of the peaks correspond approximately to those of the third complexes in the solid state reported in the literature. Solutions in which the iron(III) concentration has been greatly increased give spectra showing two new absorption peaks. This fact is thought to indicate the existence of polynuclear complexes.

During the past few years a large amount of data has accumulated concerning the infrared light absorption of coordination compounds. The large majority of these investigations, however, has been confined to the solid state. Only in a few instances have equilibria of complex ions in aqueous solution been investigated. There is no doubt, however, that such measurements can be a valuable complement to conventional methods of investigation. This must be so much more the case when considering strongly coloured solutions of transition metals, where the Raman technique cannot be applied.

Inspired by the interesting achievements of Jones and Penneman [1], we have therefore started a project of infrared absorption investigations on some metal complex systems in aqueous solution.

Owing to the strong absorption of water, measurements must be confined to ions having their characteristic vibration frequencies in those parts of the spectrum where the water absorption is not too strong.

In order to test the possibilities of the method we have made a qualitative investigation of the iron(III) and aluminium oxalate systems by studying the oxalate absorption frequencies in the region 1500—1200 cm^{-1}. Solid state studies

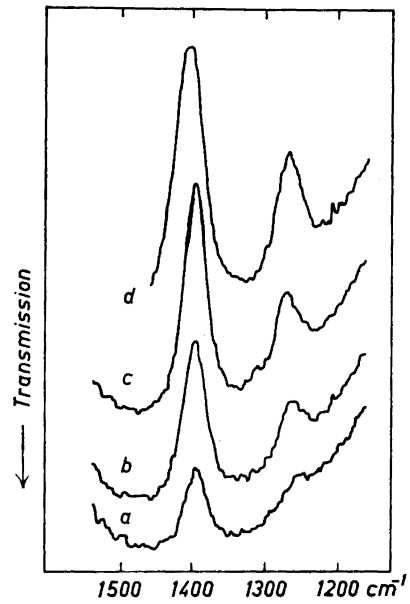

Fig. 1. Spectra of the iron (III)-oxalate system. The compositions of the solutions are found in Table 1. As in all figures of this paper the curves are arbitrarily displaced along the ordinate- (transmission-)axis to increase the readability.

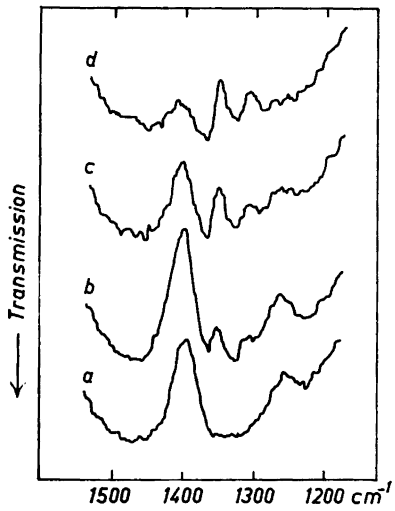

Fig. 2. Spectra of the iron (III-)oxalate system for large metal concentrations. The compositions of the solutions are found in Table 1.

[2,3] of these systems have shown definite shifts of the oxalate ion frequencies to occur as a result of coordination. Conventional investigations have also been reported in the literature [4], the results of which indicate that the complexity is quite strong.

EXPERIMENTAL

General technique. The general procedure was that of Jones and Penneman [1]. The instrument was a Hilger H 800 Infrared Absorption Spectrophotometer fitted with a

Table 1. Wave numbers of the peaks of the iron(III)-oxalate system.

Fig: Curve	C_{FeCl_3} M	$C_{Na_2C_2O_4}$ M	Observed wave numbers, cm^{-1}			
1:a	0.30	0.30		1 393	~1 255	
1:b	0.30	0.60		1 393	1 265	
1:c	0.30	0.90		1 393	1 268	
1:d	1.9	1.9		1 404	1 266	
2:a	1.20	0.60	1 398			1 258
2:b	3.0	1.20	1 403	1 352	1 309	1 265
2:c	3.6	1.20	1 404	1 352	1 309	1 265
2:d	4.1	1.00	1 410	1 351	1 309	?

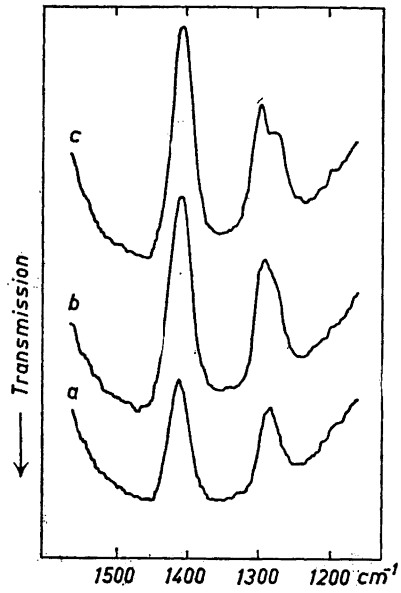

Fig. 3. Spectra of the aluminium-oxalate system. The compositions of the solutions are found in Table 2.

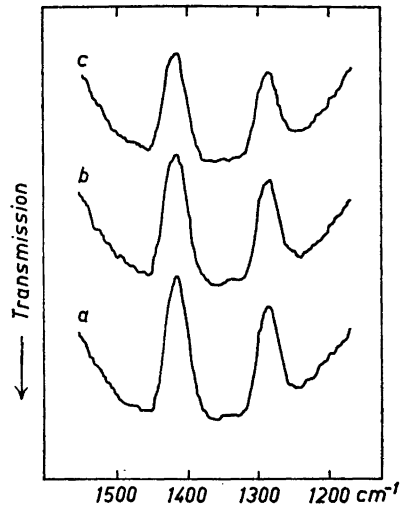

Fig. 4. Spectra of the aluminium-oxalate system for large metal concentrations. The compositions of the solutions are found in Table 2.

rocksalt prism. The window material of the cell was calcium fluoride. Platinum spacers measuring 8.8 and 12.5 μ defined the thickness of the cell. The instrument was used in the double-beam setting but without any compensation cell, The wave number setting was calibrated against benzene and toluene spectra. The reported wave numbers are correct within 2 cm^{-1}.

The solutions to be investigated were made up by dissolving weighed amounts of the salts. The weighing accuracy was limited to about 1 % in view of the qualitative nature of the investigation. For the same reason chlorides were used instead of perchlorates.

Ferric chloride, sodium and *potassium oxalate* were of analytical grade, whereas the *aluminium chloride* was of *purum* quality.

Table 2. Wave numbers of the peaks of the aluminium-oxalate system.

Fig: Curve	C_{AlCl_3} M	$C_{K_2C_2O_4}$ M	Observed wave numbers, cm^{-1}	
3:a	0.50	0.50	1 411	1 283
3:b	0.50	1.00	1 407	1 291
3:c	0.38	1.14	1 406	1 296 1 274
4:a	1.50	0.75	1 415	1 286
4:b	1.87	0.75	1 416	1 285
4:c	1.83	0.61	1 417	1 285

RESULTS

In Fig. 1 are given the absorption curves for some solutions of iron(III) chloride and sodium oxalate in various proportions. Because of the strong complexity we can assume that the curves correspond to the first, second and third complexes, respectively. The wave numbers of the peaks of the third complex agree rather well with those given by Schmelz *et al.*[2] and by Fujita *et al.*[3]

In Fig. 1 is also included the absorption curve of the first complex at a much higher concentration. A shift of the absorption peak at 1 400 cm^{-1} towards a somewhat higher wave number is observed. This fact led us to investigate some solutions in which the ratio between the iron(III) and the oxalate concentration was successively increased. The results given in Fig. 2 indicate the very interesting fact that, in addition to the above-mentioned shift of the 1 400 cm^{-1} peak, two new peaks appear.

Analogous experiments were performed with aluminium in place of iron(III). The results are reported in Figs. 3 and 4. In this case as well (Table 2 and Fig. 3, curve c) the agreement with solid state data [2,3] is fairly good. An examination of Fig. 4 shows that no new peaks appear at high aluminium concentrations, although the shift of the 1 400 cm^{-1} peak towards higher wave numbers is quite obvious.

DISCUSSION

The first point of interest emerging from the presented observations is the very small variation of the position of the absorption peaks as the number of coordinated ligands in increased (Figs. 1 and 3). This fact is quite contrary to the findings of Jones and Penneman [1] for the silver cyanide system. To explain this difference we suggest that a significant wave-number shift will be observed only when the total enthalpy of coordination per ligand is appreciably different for the sequence of complexes with increasing ligand number. For all so-called normally built complex systems the enthalpy of addition of a ligand is almost constant within a given system (*cf.* Bjerrum [5,6]). The total coordination enthalpy per ligand will then also be approximately constant.

For the silver cyanide system, having a "characteristic coordination number" of two and maximum coordination number of four, we can with confidence assume a large difference in the enthalpy of addition of the two last ligands compared to that of the first two. Hence a considerable difference in the positions of the peaks of the second, third and fourth complexes might be expected, as is in fact observed. [1]

The oxalate systems investigated here are most probably quite normally built. The variation in the consecutive formation constants [4] is what might be expected for such a highly charged ligand. The absence of a pronounced shift of the peaks of successive complexes is thus understood.

Hence we conclude that, in general, there is little hope of using infrared spectroscopy as a "finger-print method" to prove the existence of step-wise complex formation.

The second point of interest is the effects produced by increasing the iron(III) concentration. The appearance of two new peaks at 1 352 cm^{-1} and

1 309 cm^{-1} is obviously an indication of a new molecular species (Fig. 2). We assume that this is a polynuclear complex. Whether the displacement of the peak at about 1 400 cm^{-1} is also an indication of polynuclear complex formation or if it is some kind of a "medium effect" is difficult to say. It might be noted, however, that the shift is away from the position of the peak in question for the solid complexes [3,4]. If the first alternative is true, two kinds of polynuclear complexes must be considered. A confirmative correlation between metal — oxalate structure and the infrared spectrum of the oxalate ligand may — in a way — be obtained by a comparison between the solid-state spectra [7,2] of CuC_2O_4 and $Na_2Cu(C_2O_4)_2$. Whereas the first compound shows oxalate peaks that coincide approximately with the peaks ascribed here to polynuclear complexes, the latter one shows a spectrum similar to that of the mononuclear complexes.

The Hilger spectrophotometer used was put at our disposal on loan for a considerable period of time by Messrs. Hilger & Watts, Ltd., London. We wish to express our appreciation of the generosity of this Company as well as of the kind cooperation of its Swedish representatives, Messrs. Bergman & Beving AB, Stockholm.

REFERENCES

1. Jones, L. H. and Penneman, R. A. *J. Chem. Phys.* **22** (1954) 965.
2. Schmelz, M. J., Miyazawa, T., Mizushima, S., Lane, T. J. and Quagliano, J. V. *Spectrochim. Acta* **9** (1957) 51.
3. Fujita, J., Nakamoto, K. and Kobayashi, M. *J. Phys. Chem.* **61** (1957) 1014.
4. *Stability Constants of Metal-ion Complexes. Part I.* The Chemical Society, Burlington House, London, W. 1, 1957.
5. Bjerrum, J. *Chem. Revs.* **46** (1950) 381.
6. Poulsen, I. and Bjerrum, J. *Acta Chem. Scand.* **9** (1955) 1407.
7. Hunt, J. M., Wisherd, M. P. and Bonham, L. C. *Anal. Chem.* **22** (1950) 1478.

Received March 8, 1960.

ACTA CHEMICA SCANDINAVICA 14 (1960) 1369—1373

Studies on Monoalkyl Carbonates

XVII. The Monoalkyl Carbonate of the Glycolate Ion

LEO TOFT

The Royal Danish School of Pharmacy, Copenhagen, Denmark

The velocity constant of the reaction '$^-OOC \cdot CH_2OH + OH^- + CO_2 = {}^-OOC \cdot CH_2CO_3^- + H_2O$' and the equilibrium constant of the reaction '$^-OOC \cdot CH_2 \cdot CO_3^- + H_2O = {}^-OOC \cdot CH_2OH + HCO_3^-$' have been determined. The velocity of the decomposition of the monoalkyl carbonate, $^-OOC \cdot CH_2CO_3^-$, in strongly basic medium is investigated and may be explained by assuming that the decomposition is a twostage reaction *viz.* 1) $^-OOC \cdot CH_2CO_3^- = {}^-OOC \cdot CH_2O^- + CO_2$; 2) $CO_2 + OH^- = HCO_3^-$.

1. The present investigation deals with the equilibrium conditions and the reaction mechanisms for the formation and decomposition of the monoalkyl carbonate of glycolate ion in aqueous medium.

The glycolate ion solution was prepared from glycolic acid and the equivalent amount of sodium hydroxide by gentle boiling, so that anhydrides that might be present were converted into sodium glycolate.

2. The glycolic acid employed was obtained partly from the Riedel-de Haen A. G. as an aqueous solution, and partly from The Fischer Scientific Company as crystals stated to be pure. Upon analysis the solution was found to contain 53.5 % of acid by direct titration with 1 N sodium hydroxide, and 57.3 % of glycolic acid and its anhydrides, determined by boiling with extra sodium hydroxide and titration the excess of sodium hydroxide with hydrochlorid acid. The crystals of glycolic acid — having a rather moist appearance — were dried over phosphorus pentoxide losing about 1.9 % in weight. Thereafter they contained 99.5—100.3 % of glycolic acid. Both samples were free of heavy metals and of halides and gave identical results during the investigations.

3. No attempt was made to prepare the solid monoalkyl carbonate. Solutions were made by dissolving carbon dioxide in solutions which were 0.5—2 M with regard to sodium glycolate and 0.1—0.75 M with regard to sodium hydroxide, thus converting 25—60 % of the carbon dioxide into monoalkyl carbonate and the rest of it into ordinary carbonate.

4. The method of analysis was in principle as in previous investigations [1], *viz.* separation of the monoalkyl carbonate from the ordinary carbonate by precipitating the carbonate with barium chloride and separating the barium carbonate by centrifugation. The supernate was then analysed by means of an apparatus for determination of carbon dioxide introduced by Tovborg Jensen [2]. To the supernate is added a large excess of 2 M hydrochloric acid causing an immediate decomposition of the monoalkyl carbonate. The carbon dioxide evolved is then absorbed in 0.1 N barium hydroxide after which the excess of barium hydroxide is titrated electrometrically with 0.1 N hydrochloric acid to pH = 8.5.

By analogy with the investigations on the monoalkyl carbonate of the lactate ion [3] there has, however, been certain difficulties in separating the barium carbonate from the monoalkyl carbonate. Barium chloride added to the solution containing monoalkyl carbonate and carbonate causes no immediate precipitation of barium carbonate. Only after ½—3 min. a fine-grained precipitate consisting of barium carbonate began to settle, the precipitation of which lasted about 15 min.

In order to accelerate the precipitation a good deal of sodium carbonate solution was set to the solution of barium chloride before the reaction mixture was added. Furthermore the 2 M solutions — due to their rather high viscosity — were diluted with equal parts of water before the centrifugation. After shaking for 2 min. and centrifugating for 3 the precipitation of the barium carbonate succeeded. Due to these difficulties it may be taken in consideration that the data presented may be encumbered with larger errors than usual on analogous investigations.

The data presented are, unless otherwise stated, corrected not only with regard to blank values but also with regard to the decomposition of monoalkyl carbonate taking place during the analysis, see later.

5. The experiments were carried out at 0°C. Velocity constants are expressed on the basis of the Brigg's logarithms, the unit of time being the minute.

On the formation of the monoalkyl carbonate from carbon dioxide and glycolate ion and on the reaction

$$^{-}OOC \cdot CH_2O^{-} + CO_2 \rightleftharpoons {}^{-}OOC \cdot CH_2CO_3^{-}$$

The experiments were carried out in a 0.5 litre flask by vigorously shaking 200 ml of a basic solution of sodium glycolate with atmospheric air of which about 100 ml was substituted by carbon dioxide. The solutions were immediately analysed to determine the percentage of monoalkyl carbonate.

By introduction of the adjusted results in the expression:

$$k' = \frac{\%\ \text{monoalkyl carbonate} \cdot k_{CO_2OH^-}}{\%\ \text{carbonate} \cdot c_{\text{alcohol}}},$$

the k' values presented in Table 1 are calculated, k' being the velocity constant of the overall reaction: $CO_2 + {}^{-}OOC \cdot CH_2OH + OH^- = {}^{-}OOC \cdot CH_2CO_3^- + H_2O$.

Table 1. Carbon dioxide in sodium glycolate + sodium hydroxide. 0°C.

c_{NaOH}	$c_{glycolate}$	Absorbed CO_2 mole/litre	% Alkyl-carbonate	log k'	Mean of log k'
0.25	0.50	0.0233	25.2	4.22	
0.10	0.50	0.0167	25.2	4.22	
0.20	1.00	0.0208	40.5	4.22	4.23
0.50	1.00	0.0208	38.5	4.19	
0.75	2.00	0.0312	59.5	4.26	
0.50	2.00	0.0184	60.8	4.28	

For the value of the velocity constant of the reverse process $k_{-OOC\cdot CH_2CO_3^-}$ we get 0.0079 employing the value of K_{eq} mentioned in Table 2.

The equilibrium of the reaction

$$^-OOC\cdot CH_2CO_3^- + H_2O = HCO_3^- + {}^-OOC\cdot CH_2OH$$

The above equilibrium was established in aqueous solutions of glycolate ion, potassium bicarbonate and sodium carbonate. The content of monoalkyl carbonate has been calculated as a percentage of HCO_3^- initially present; thus no attention was paid to the carbonate.

In Table 2 are presented not only the '% monoalkyl carbonate' corrected for blank values and the decomposition taking place during the analysis but the uncorrected as well. This has been done in order to illustrate the accuracy that may be attached to the values found. From the experimental results the equilibrium constant of the reaction

$$K_{eq} = \frac{c_{-OOC\cdot CH_2OH}\cdot f \cdot c_{HCO_3^-}\cdot f}{c_{-OOC\cdot CH_2CO_3^-}\cdot f^2}$$

may be calculated, the activity constants neutralizing each other as a first approximation.

Table 2. The solutions of carbonate-monoalkyl carbonate in equilibrium, 0°C.

Initial solution			% Alkyl carbonate		log K_{eq}	Mean of log K_{eq}
$c_{glycolate}$	c_{KHCO_3}	$c_{Na_2CO_3}$	uncorr.	corr.		
1.00	0.10	0.05	2.64[a]	1.70	1.78	
1.00	0.20	0.10	1.76[b]	1.24	1.90	1.88
2.00	0.20	0.10	3.65[c]	2.05	1.97	

a) mean of 4 determinations 2.65, 2.74, 2.52, 2.64
b) » » 3 » 1.58, 1.99, 1.72
c) » » 3 » 3.74, 3.53, 3.67

Table 3. Monoalkyl carbonate in sodium hydroxide + glycolate ion, 0°C.

$c_{\text{monoalkyl carbonate}}$	c_{NaOH}	$c_{glycolate}$	Min	% monoalkyl carbonate left	k_{mono}
0.0054	0.25	0.50	0	100	—
			8	75	(0.01540)
			17	76	0.00724
			25	67	0.00762
			40	50	0.00763
			54	45	0.00636
			91	22	0.00727
			126	11	0.00757
			164	6	0.00737
					Mean 0.0073
0.0038	0.10	0.50	0	100	—
			7	91	0.00617
			18	74	0.00717
			27	62	0.00775
			38	54	0.00702
			51	40	0.00781
			81	34	0.00581
			111	19	0.00658
			156	7	0.00742
					Mean 0.0070
0.006	0.20	1.00	0	100	—
			11	90	0.00425
			28	75	0.00454
			55	72	0.00263
			144	29	0.00375
			187	32	0.00268
			277	11	0.00353
			327	7	0.00355
			347	9	0.00296
					Mean 0.0035
0.011	0.50	1.00	0	100	—
			9	93	0.00329
			24	76	0.00501
			54	64	0.00356
			85	50	0.00352
			113	38	0.00373
			160	25	0.00379
			234	18	0.00321
			287	11	0.00330
					Mean 0.0037
0.008	0.20	1.00	0	100	—
			10	98	(0.00096)
			28	87	0.00216
			54	65	0.00353
			99	33	0.00492
			156	25	0.00382
			278	8	0.00396
			288	6	0.00422
					Mean 0.0038
0.016	0.50	2.00	0	100	—
			9	96	0.00172
			17	91	0.00238
			32	87	0.00183
			61	70	0.00252
			103	69	0.00162
			152	53	0.00179
			300	28	0.00183
			425	19	0.00169

On the velocity of the reactions

$$^{-}OOC \cdot CH_2CO_3^{-} + H_2O = {}^{-}OOC \cdot CH_2OH + HCO_3^{-}$$

Determinations have been made from the monoalkyl carbonate side only and in strongly basic medium, the monoalkyl carbonate thus being practically converted into carbonate. The monoalkyl carbonate has been made by shaking the basic solutions with carbon dioxide as stated in the introduction. The solutions, therefore, contain ordinary carbonate, which, however, is of no importance in the present investigations.

In Table 3 are listed the experimental results of the decomposition of the monoalkyl carbonate. k_{mono} stands for $1/t \log a/a—x$.

The experiments are interpreted in a similar way to the one applied to the monoalkyl carbonates previously investigated, the decomposition being a two-stage reaction, *viz.* 1) $^{-}OOC \cdot CH_2CO_3^{-} = {}^{-}OOC \cdot CH_2O^{-} + CO_2$; 2) $CO_2 + OH^{-} = HCO_3^{-}$

k_{mono} may be calculated at $pa_H > 10$ by means of the following expression

$$k_{mono} = \frac{k' \cdot K_{eq} \frac{K_{H_2O}}{K_{CO_2}}}{1 + k' \cdot \frac{c_{^{-}OOC \cdot CH_2OH}}{k_{CO_2OH^{-}}}}$$

the values of K_{H_2O} and K_{CO_2} being $10^{-14.93}$ and $10^{-6.65}$, respectively.

Upon introduction of the constants the equation is

$$k_{mono} = \frac{0.0065}{1 + 0.69\, c_{^{-}OOC \cdot CH_2OH}}$$

and k_{mono} in 0.5 M, 1 M, and 2 M solutions of glycolate ion, $pa_H > 10$, will be calculated to 0.0048, 0.0038, and 0.0027, respectively.

The experimental and calculated values agree fairly good.

The author wishes to express his thanks to Professor Carl Faurholt for his kind interest in the investigation.

REFERENCES

1. Jensen, A., Jørgensen, E. and Faurholt, C. *Acta Chem. Scand.* **6** (1952) 1036.
2. Tovborg-Jensen, S. *Wiss. Arch. Landwirtsch., Abt. A., Arch. Pflanzenbau* **6** (1931) 299.
3. Noiesen, K., Rath, F. and Faurholt, C. *Dansk Tidskr. Farm.* **11** (1937) 268.

Received March 21, 1960.

ACTA CHEMICA SCANDINAVICA 14 (1960) 1374–1380

Studies on Carbamates

XIII. On the Catalytic Action of Zinc Tetrammine on the Process 'Carbon Dioxide ⇌ Carbonic Acid'

MARIANNE GRØNVALD and CARL FAURHOLT

The Royal Danish School of Pharmacy, Copenhagen, Denmark

$Zn(NH_3)_4^{++}$ catalyses the process 'carbamate ⇌ carbonate'. The effect is explained by the catalysis of the $Zn(NH_3)_4^{++}$ on the process '$CO_2 + H_2O \rightleftharpoons H_2CO_3$'.

1. The rate of equilibration of the process '$NH_2COONH_4 + H_2O \rightleftharpoons (NH_4)_2CO_3$' in aqueous medium has previously been studied [1,2]. The decomposition is a two-step reaction, *viz.*

carbamic acid ⇌ ammonia + carbon dioxide
carbon dioxide ⇌ carbonic acid

and for a moderately basic solution the last step will be the rate determining step exclusively.

The zinc-containing enzyme carbonic anhydrase, isolated by Meldrum and Roughton [3], catalyses the process '$CO_2 + H_2O \rightleftharpoons H_2CO_3$'. It was therefore of interest to know if other zinc complexes also could have such an effect. This was examined by means of the process '$NH_2COONH_4 + H_2O \rightleftharpoons (NH_4)_2CO_3$'. We have in the present investigation used zinc tetrammine in NH_4Cl/NH_3 buffers.

2. The method of analysis was in principle that described in previous investigations [4]. The samples were adjusted to 0.1 N with regard to hydroxyl ion. Carbonate but not carbamate was precipitated when barium chloride was added. The barium carbonate was removed by centrifugation. The supernatant was in the previous method heated until the carbamate had been decomposed and precipitated as barium carbonate. The carbonate was then titrated acidimetrically. However, in the presence of zinc tetrammine it appears that the precipitate involves zinc, probably in the form of zinc hydroxide. The supernatant therefore was analysed for carbon dioxide by means of an apparatus introduced by Tovborg-Jensen [5]. The supernatant was acidi-

fied by means of hydrochloric acid and the carbamate decomposes practically instantaneously to carbon dioxide. The carbon dioxide was absorbed in 0.1 N sodium hydroxide. This solution was titrated using a Radiometer-titrigraf, type TTT 1 a. The amount of 0.05 N hydrochloric acid used from pH 8.4 to 4.5 corresponds to the content of carbamate since 1 mole HCl ~ 1 mole CO_2 ~ 1 mole carbamate.

It was necessary to correct all the determinations for blank values since the air in the apparatus at the beginning contains a small amount of carbon dioxide.

The method of analysis was tested by means of solutions containing per litre 0.4 mole NH_4Cl, 0.2 mole NH_3, 0.01 mole $Zn(NH_3)_4(CH_3COO)_2$ and about 0.02 mole carbonate + carbamate. Zinc tetrammine did not interfere with the precision of the method.

3. Ammonium carbamate was prepared from dry ice and liquid ammonia [6]. Anhydrous liquid ammonia was placed in a Dewar flask and powdered dry ice was slowly added. The excess of ammonia was allowed to evaporate, when the mixture had attained a slushy consistency. This material was transferred to a desiccator and kept under slightly reduced pressure for 24 h. The ammonium carbamate was stable when kept in a desiccator over dry calcium chloride. It contained about 5 % carbonate.

The concentrations of zinc acetate and zinc perchlorate were determined by complexometric titrations.

The salts of zinc tetrammine have not been prepared in the solid state. The solutions of zinc tetrammine were prepared by adding zinc acetate or zinc perchlorate to the NH_4^+/NH_3 buffers. In the calculation of the concentrations of ammonia we have taken into account the ammonia used by the process '$Zn^{++} + 4NH_3 = Zn(NH_3)_4^{++}$'.

4. All the experiments were carried out at 0°C. The data presented in the tables were corrected for blank values, *viz.* about 3 units of the percentage. The velocity constants were calculated by means of Brigg's logarithms, the unit of time being the minute. The activity coefficient f was calculated as in earlier investigations from the expression of Bjerrum [7]: $-\log f = 0.3\sqrt[3]{C_{ion.}}$.

The experiments concerning the process 'carbamate ⇌ carbonate'

Two different NH_4^+/NH_3 buffers, 0.40 M NH_4Cl/0.20 M NH_3, and 0.50 M NH_4Cl/0.05 M NH_3 have been used. Experiments were carried out with zinc acetate and zinc perchlorate and, within the experimental error, we attained the same results under the same conditions. Experiments were carried out with and without zinc tetrammine.

Some of the experiments are listed in Tables 1 and 2 and illustrate the precision of the method. The values $k_{amate} + k_{onate}$ are calculated from the expression $k_{amate} + k_{onate} = 1/t \cdot \log \frac{Ka-b}{Ka-b-(1+K)x}$, the expression for a process which is unimolecular from both sides. a and b represent the starting

Table 1. 0.02 M NH_2COONH_4 in 0.4 M NH_4Cl + 0.2 M NH_3

without $Zn(NH_3)_4^{++}$			with 0.04 M $Zn(NH_3)_4^{++}$		
min.	% carbamate left	$k_{amate} + k_{onate}$	min.	% carbamate left	$k_{amate} + k_{onate}$
3	94.8	—	0.5	96.4	—
36	93.4	(0.000285)	7.0	91.3	0.00460
171	86.3	0.000357	36	73.7	0.00432
303	80.2	0.000363	96	53.5	0.00377
463	76.3	0.000310	155	39.8	0.00381
1 420	49.3	0.000361	238	32.5	0.00331
1 860	42.8	0.000365	329	27.2	0.00312
3 230	33.2	0.000367	413	23.0	0.00339
∞	28.9	mean: 0.00035	∞	20.0	mean: 0.0038
k_{amate} = 0.00025; k_{onate} = 0.00010; K = 2.46			k_{amate} = 0.00304; k_{onate} = 0.00076; K = 4.00		

values of carbamate and carbonate, respectively. The constant K signifies the ratio between the equilibrium values of the concentrations of carbonate and carbamate.

It is seen from the tables that the influence of zinc tetrammine is greatest at lower pH values.

It should be pointed out that the value of K is not constant in analogous experiments with and without $Zn(NH_3)_4^{++}$. This may be explained by the fact that the determination of carbamate is relatively inexact in the equilibrium where the percentage of carbamate is rather small. But there is a marked drift, so it is possible that other factors come into play, *e.g.* the formation of zinc carbonato ions.

All experiments are listed in Table 3.

An experiment with $Cu(NH_3)_4^{++}$ is furthermore listed in Table 3, but the effect is small and therefore not reliable. Further experiments are necessary to state a catalytical effect of $Cu(NH_3)_4^{++}$.

Table 2. 0.02 M NH_2COONH_4 in 0.5 M NH_4Cl + 0.05 M NH_3.

without $Zn(NH_3)_4^{++}$			with 0.04 M $Zn(NH_3)_4^{++}$		
min.	% carbamate left	$k_{amate} + k_{onate}$	min.	% carbamate left	$k_{amate} + k_{onate}$
0.75	96.8	—	0.50	84.0	—
8.75	93.3	0.00234	5.10	60.2	0.0357
27.0	89.0	0.00166	9.3	42.2	0.0397
57.0	82.1	0.00153	15.8	33.0	0.0319
107	71.6	0.00151	25.0	21.1	0.0322
172	59.9	0.00152	45.5	12.3	0.0288
284	47.2	0.00200	∞	8.50	
∞	15.0	mean: 0.0018			mean: 0.034
k_{amate} = 0.0015; k_{onate} = 0.00027; K = 5.66			k_{amate} = 0.0308; k_{onate} = 0.0029; K = 10.7		

Table 3.

$c_{Zn(NH_3)_4^{++}}$	$c_{NH_4^{++}}$	c_{NH_3}	c_{CO_2} total	% carbamate in equilibrium	$k_{amate} + k_{onate}$	k_{amate}	k_{onate}
—	0.4	0.2	0.0209	28.9	0.00035	0.00025	0.00010
0.005	0.4	0.2	0.0210	27.1	0.00078	0.00057	0.00021
0.01	0.4	0.2	0.0209	25.7	0.00100	0.00074	0.00026
0.015	0.4	0.2	0.0197	24.0	0.00140	0.00106	0.00034
0.020	0.4	0.2	0.0195	22.4	0.0019	0.00147	0.00043
0.040	0.4	0.2	0.0194	20.0	0.0038	0.00304	0.00076
—	0.5	0.05	0.0205	15.0	0.0018	0.00153	0.00027
0.02	0.5	0.05	0.0191	11.5	0.018	0.0160	0.0020
0.04	0.5	0.05	0.0225	8.5	0.034	0.0308	0.0029
$c_{Cu(NH_3)_4^{++}}$							
0.01	0.4	0.2	0.197	27.3	0.00050	0.00037	0.00013

Calculations on the experiments concerning the process 'carbamate ⇌ carbonate'

Without zinc the conversion of the carbon dioxide into carbonate and the reciprocal conversion take place through the two reactions:

$$CO_2 + H_2O \rightleftharpoons H_2CO_3$$
$$CO_2 + OH^- \rightleftharpoons HCO_3^-$$

and between pH 8 and 10 the velocity of the processes proceeds with the same order of magnitude.

We have the following expression for the conversion of carbamate:

$$\frac{dc_{carbamate}}{dt} = -(k_{CO_2} + k_{CO_2 \cdot OH^-} \cdot c_{OH^-}) \cdot c_{CO_2}$$

$$= -(k_{CO_2} + k_{CO_2 \cdot OH^-} \cdot c_{OH^-}) \cdot a \cdot c_{carbamate} = -k_{amate} \cdot c_{carbamate}$$

where a indicates the part of the carbamate being dissociated into CO_2. a is calculated from:

$$a = \frac{c_{CO_2}}{c_{carbamate}} = \frac{K_{NH_4^+} \cdot K_{Eq}}{K_{CO_2}} \cdot \frac{c_{NH_4^+} \cdot f^2}{c_{NH_3}^2}$$

and then we have

$$k_{amate} = \frac{(k_{CO_2} + k_{CO_2 \cdot OH^-} \cdot c_{OH^-}) \cdot K_{NH_4^+} \cdot K_{Eq} \cdot c_{NH_4^+} \cdot f^2}{K_{CO_2} \cdot c_{NH_3}^2}$$

In the presence of zinc tetrammine the expression must be:

$$\frac{dc_{carbamate}}{dt} = -(k_{CO_2} + k_{CO_2 \cdot OH^-} \cdot c_{OH^-} + k'_{Zn} \cdot c_{Zn(NH_3)_4^{++}}) \cdot c_{CO_2}$$
$$= -k_{amate} \cdot c_{carbamate}$$

This can be transformed to:

$$k_{amate} = \frac{(k_{CO_2} + k_{CO_2 \cdot OH^-} \cdot c_{OH^-} + k'_{Zn} \cdot c_{Zn(NH_3)_4^{++}}) \cdot K_{NH_4^+} \cdot K_{Eq} \cdot c_{NH_4^+} \cdot f^2}{K_{CO_2} \cdot c^2_{NH_3}}$$

For the conversion of carbonate we have:

$$\frac{dc_{carbonate}}{dt} = -k_{H_2CO_3} \cdot c_{H_2CO_3} - k_{HCO_3^-} \cdot c_{HCO_3^-} = -k_{onate} \cdot c_{carbonate}$$

By means of

$$c_{carbonate} = c_{H_2CO_3} + c_{HCO_3^-} + c_{CO_3^{--}}$$

$$a_{H^+} \cdot c_{HCO_3^-} \cdot f = K_{H_2CO_3} \cdot c_{H_2CO_3}$$

$$a_{H^+} \cdot c_{CO_3^{--}} \cdot f^2 = K_{HCO_3^-} \cdot c_{HCO_3^-} \cdot f$$

and

$$a_{H^+} \cdot c_{NH_3} = K_{NH_4^+} \cdot c_{NH_4^+} \cdot f$$

the expression is transformed to

$$k_{onate} = \frac{\dfrac{k_{H_2CO_3} \cdot K_{NH_4^+} \cdot c_{NH_4^+} \cdot f^2}{c_{NH_3}} + k_{HCO_3^-} \cdot K_{H_2CO_3}}{\dfrac{K_{NH_4^+} \cdot c_{NH_4^+} \cdot f^2}{c_{NH_3}} + K_{H_2CO_3} + \dfrac{K_{H_2CO_3} \cdot K_{HCO_3^-} \cdot c_{NH_3}}{K_{NH_4^+} \cdot c_{NH_4^+} \cdot f^2}}$$

In the presence of zinc tetrammine we have:

$$\frac{dc_{carbonate}}{dt} = -(k_{H_2CO_3} \cdot c_{H_2CO_3} + k_{HCO_3^-} \cdot c_{HCO_3^-} + k''_{Zn} \cdot c_{H_2CO_3} \cdot c_{Zn(NH_3)_4^{++}})$$
$$= -k_{onate} \cdot c_{carbonate}$$

which can be transformed into:

$$k_{onate} = \frac{\dfrac{k_{H_2CO_3} \cdot K_{NH_4^+} \cdot c_{NH_4^+} \cdot f^2}{c_{NH_3}} + k_{HCO_3^-} \cdot K_{H_2CO_3} + k''_{Zn} \cdot c_{Zn(NH_3)_4^{++}} \cdot \dfrac{K_{NH_4^+} \cdot c_{NH_4^+} \cdot f^2}{c_{NH_3}}}{\dfrac{K_{NH_4^+} \cdot c_{NH_4^+} \cdot f^2}{c_{NH_3}} + K_{H_2CO_3} + \dfrac{K_{H_2CO_3} \cdot K_{HCO_3^-} \cdot c_{NH_3}}{K_{NH_4^+} \cdot c_{NH_4^+} \cdot f^2}}$$

Table 4.

c_{NH_4Cl}	c_{NH_3}	$c_{Zn(NH_3)_4^{++}}$	k_{amate} exptl.	k_{amate} calc.	k_{onate} exptl.	k_{onate} calc.	k'_{Zn}	$k''_{Zn} \times 10^{-4}$
		—	0.00025	0.00025	0.00010	0.00012	—	—
		0.005	0.00057		0.00021		147	11.5
0.4	0.2	0.010	0.00074		0.00026		115	8.6
		0.015	0.00106		0.00034		127	8.6
		0.020	0.00147		0.00043		146	9.2
		0.040	0.00304		0.00076		171	9.5
		—	0.0015	0.0012	0.00027	0.00022	—	—
0.5	0.05	0.02	0.0160		0.0020		126	8.3
		0.04	0.0308		0.0029		132	6.8

The ratio $c_{NH_4^+}/c_{NH_3}$ is not constant during the experiments with $c_{NH_4Cl}/c_{NH_3} = 0.5/0.05$. The ratio $c_{NH_4^+}/c_{NH_3}$ is in the equilibrium 0.52/0.065, 0.52/0.065 and 0.52/0.068 for $c_{Zn(NH_3)_4^{++}} = 0.00$, 0.02 and 0.04, respectively.

K_{Eq} ($10^{-0.48}$) is the equilibrium constant for the process '$NH_2COO^- + H_2O \rightleftharpoons HCO_3^- + NH_3$', K_{CO_2} ($10^{-6.65}$) is the equilibrium constant for '$CO_2 + H_2O \rightleftharpoons H^+ + HCO_3^-$', $K_{H_2CO_3}$ ($10^{-3.7}$) for '$H_2CO_3 \rightleftharpoons H^+ + HCO_3^-$' and $K_{HCO_3^-}$ ($10^{-10.5}$) for '$HCO_3^- \rightleftharpoons H^+ + CO_3^{--}$'. For K_{H_2O} and $K_{NH_4^+}$ are used $10^{-14.93}$ and $10^{-10.08}$, respectively. k_{CO_2} (0.078) is the velocity constant for '$CO_2 + H_2O \rightleftharpoons H_2CO_3$' from left to right and $k_{H_2CO_3}$ (69.6) from right to left. $k_{CO_2 \cdot OH^-}$ (2.43×10^4) is the velocity constant for '$CO_2 + OH^- \rightleftharpoons HCO_3^-$' from left to right and $k_{HCO_3^-}$ (15.6×10^{-5}) from right to left.

The experimental and calculated values for k_{amate} and k_{onate} are listed in Table 4. Furthermore are listed k'_{Zn} and k''_{Zn} calculated from experimental values of k_{amate} and k_{onate}. The ratio $c_{NH_4^+}/c_{NH_3}$ may be regarded as constant in the experiments with $c_{NH_4Cl}/c_{NH_3} = 2$, but not in the experiments with $c_{NH_4Cl}/c_{NH_3} = 10$. The mean value therefore is used in the calculation.

Table 5.

Metal ammine, M	Initial solution c_{NaOH}	Initial solution c_{NH_3}	Absorbed CO_2 mole/l	% Carbamate	Final solution c_{NaOH}	Final solution c_{NH_3}	Mean c_{NaOH}	Mean c_{NH_3}	log $k_{CO_2 \cdot NH_3}$
	0.2	0.5	0.0191	23.6	0.17	0.5	0.185	0.5	3.45
	0.2	1.0	0.0187	31.9	0.17	1.00	0.185	1.0	3.33
	0.2	1.0	0.0191	31.9	0.17	1.00	0.185	1.0	3.33
0.01 Zn	0.2	0.5	0.0186	26.1	0.17	0.5	0.185	0.5	3.51
0.01 Zn	0.2	1.0	0.0137	33.7	0.18	1.0	0.190	1.0	3.38
0.01 Cu	0.2	1.0	0.0204	32.6	0.17	1.0	0.185	1.0	3.34
0.01 Co	0.2	1.0	0.0209	35.1	0.17	1.0	0.185	1.0	3.39
0.02 Ag	0.2	1.0	0.0194	35.8	0.17	1.0	0.185	1.0	3.40

It is seen that the process '$CO_2 + H_2O \rightleftharpoons H_2CO_3$' in 1 M $Zn(NH_3)_4^{++}$ solution proceeds about 2 000 times faster than in a solution without $Zn(NH_3)_4^{++}$.

Some experiments in strongly basic solution

500 ml of an aqueous solution containing both ammonia and sodium hydroxide were placed in a 2 litre flask. Approximately 225 ml of carbon dioxide were substituted for an equal amount of atmospheric air in the gas phase above this solution, and the flask was shaken vigorously for about 2 min. to obtain absorption of the carbon dioxide.

Other experiments were carried out with the same concentrations of ammonia, sodium hydroxide and carbon dioxide. The solutions furthermore contained 0.01 M $Zn(NH_3)_4(CH_3COO)_2$, 0.01 M $Cu(NH_3)_4Cl_2$, 0.01 M $Co(NH_3)_6Cl_3$ and 0.02 M $Ag(NH_3)_2NO_3$, respectively.

The solutions were immediately analysed in order to determine, how many per cent of the carbon dioxide absorbed had been converted to carbamate and carbonate, respectively. The results are presented in Table 5. It is seen from the table that the influence of the metal ammines is very little. The lack of influence may be due to the predominance of the process '$CO_2 + OH^- \rightleftharpoons HCO_3^-$' in strongly basic solution. Neither the process '$H_2O + CO_2 \rightleftharpoons H_2CO_3$' nor the zinc tetrammine catalysed process can manifest itself appreciably. Furthermore probably all $Zn(NH_3)_4^{++}$ is transformed to $Zn(OH)_4^{--}$.

REFERENCES

1. Faurholt, C. *Kgl. Danske Videnskab. Selskab, Mat.-fys. Medd.* **3** (1921) 20; Abstracts in *Z. anorg. Chem.* **120** (1921) 85 and **122** (1922) 132.
2. Faurholt, C. *Kgl. Veterinær- og Landbohöjskoles Årsskrift* **1** (1924) translated into French in *J. chim. phys.* **21** (1924) 400 and **22** (1925) 1.
3. Meldrum, N. U. and Roughton, F. J. W. *J. Physiol.* **75** (1932) 3 P.
4. Jensen, A. and Faurholt, C. *Acta Chem. Scand.* **6** (1952) 385.
5. Tovberg-Jensen, S. *Wiss. Arch. Landwirtsch., Abt. A. Arch. Pflanzenbau* **6** (1931) 299.
6. *Inorganic Synthesis* **2** (1946) 85.
7. Bjerrum, N. *Z. Elektrochem.* **24** (1918) 321.

Received March 21, 1960.

ACTA CHEMICA SCANDINAVICA 14 (1960) 1381–1388

The Diffusion Process and the Diffusion Potential in Relation to the E.M.F. of Concentration Cells

TORMOD FÖRLAND

N.T.N.F.'s Institute of Silicate Science, N.T.H., Trondheim, Norway

Equations are given for the E.M.F. of a concentration cell with transference and for the electrostatic potential drop over the concentration gradient. The change in electrostatic energy by charge transfer is calculated and found to be very small. It is shown that the diffusion process does not interfere with the cell reaction.

In a previous paper Förland and Krogh-Moe[1] calculated the E. M. F. of a concentration cell with transference. For a cell

$$\mathrm{A;\ (A,B)_I\ Y : (A,B)_{II}\ Y;\ A}$$

with an electrolyte of the two components A^+Y^- and B^+Y^- and with electrodes reversible to A only, the E.M.F. may be expressed by the equation:

$$E \cdot \mathcal{F} = t_{B+(I)}(\Delta\overline{F}_{AY(I)} - \Delta\overline{F}_{BY(I)}) - t_{B+(II)}(\Delta\overline{F}_{AY(II)} - \Delta\overline{F}_{BY(II)} - \int_{N_{A+(I)}}^{N_{A+(II)}} \frac{d\,\Delta F}{d\,N_A^+} \frac{d\,t_A^+}{d\,N_A^+}\, d\,N_A^+ \quad (1)$$

Here E is the E.M.F., $\mathcal{F}$ is Faradays number, the index (I) and (II) refer to the two compartments of the concentration cell, t_A^+ and t_B^+ are transport numbers for the ions A^+ and B^+ referring to the Y^- ions as a reference frame, N_A^+ and N_B^+ are the ionic fractions of the two kinds of ions. $\Delta\overline{F}$ with index is partical molar free energy of mixing and ΔF with index is free energy of mixing per mole mixture. The first and second term of the equation are the free energy changes taking place in the electrolyte close to the two electrodes. The last term is the free energy change over the region of the concentration gradient.

The above equation can be rearranged to the more convenient form:

$$E \cdot \mathcal{F} = \Delta\overline{F}_{AY(I)} - \Delta\overline{F}_{AY(II)} + \int_{\Delta\overline{F}_{AY(I)}}^{\Delta\overline{F}_{AY(II)}} \frac{t_A^+ - N_A^+}{N_B^+} \, d\,\Delta\overline{F}_{AY}$$

From the equation in the differential form:

$$dE \cdot \mathcal{F} = -d\,\Delta\overline{F}_{AY} + \frac{t_A^+ - N_A^+}{N_B^+} \, d\,\Delta\overline{F}_{AY}$$

one can also derive:

$$\Delta\overline{F}_{AY(II)} = \Delta\overline{F}_{AY(I)} - \frac{1}{\mathcal{F}} \int_I^{II} \frac{N_B^+}{t_B^+} \, dE \qquad (2)$$

Thus by plotting corresponding values of N_B^+/t_B^+ and E as coordinates the partial free energy of the component AY is obtained as an area.

In the derivation of eqn. (1) it was assumed that dipol layers in the concentration gradient will not change their electrostatic energy significantly when an electrical charge is transported through the cell. It was further assumed that the diffusion process did not interfere with the cell reaction so the two processes could be treated separately.

It is the object of this paper to show that these assumptions are valid.

First it should be emphasized that an electrostatic potential in the concentration gradient of a concentration cell will in itself not affect the E.M.F. of the cell, since the process taking place is a transport of a neutral component from one side of the cell to the other. Only a change in the electrostatic energy in the concentration gradient may be observed in the outer circuit by the E.M.F. measurement.

THE ELECTROSTATIC POTENTIAL GRADIENT

The electrostatic potential gradient in a concentration gradient has been calculated by Sundheim [2]. As Sundheims reference system seems to be less practical for the present problem, a slightly different derivation of the electrostatic potential gradient (grad φ) will be given below.

We will consider the transports taking place in the gradient of the concentration cell:

$$A;(A^+, B^+)_I \; Y^- : (A^+, B^+)_{II} \; Y^- ; A$$

As a reference for the velocities of the particles in the system we will choose the average velocity of the Y^- ions. We designate by $\vec{J}_A^+$ ($\vec{J}_B^+$) the flux in moles/cm²sec of ions $A^+(B^+)$ and by $\vec{I}$ the electric current density in Faradays/cm²sec, all measured with respect to the average velocity of the Y^- ions. Thus $J_A^+ + \vec{J}_B^+ = \vec{I}$.

The forces corresponding to the above fluxes are grad $\Delta\bar{F}_{AY}(\Delta\bar{F}_{BY})$ and grad φ, respectively. Here $\Delta\bar{F}_{AY}$ ($\Delta\bar{F}_{BY}$) is the partial free energy of the component AY (BY) in cal/moles and φ is the electrostatic potential in cal/Faradays.

The fluxes and forces are connected by the following linear equations:

$$\vec{J}_A+ = -L_{11}\text{grad}\,\Delta\bar{F}_{AY} - L_{12}\text{grad}\,\Delta\bar{F}_{BY} - L_{13}\text{grad}\,\varphi \quad (3)$$

$$\vec{J}_B+ = -L_{21}\text{grad}\,\Delta\bar{F}_{AY} - L_{22}\text{grad}\,\Delta\bar{F}_{BY} - L_{23}\text{grad}\,\varphi \quad (4)$$

$$\vec{I} = -L_{31}\text{grad}\,\Delta\bar{F}_{AY} - L_{32}\text{grad}\,\Delta\bar{F}_{BY} - L_{33}\text{grad}\,\varphi \quad (5)$$

According to Onsager's theory for microscopically reversible processes, we have the following relations between coefficients:

$$L_{12} = L_{21};\ L_{31} = L_{13};\ L_{23} = L_{32}$$

The coefficient L_{33} is the specific elecrical conductance, $\varkappa$, measured in Faradays ^{2}/cal cm sec. By defining $L_{13} = \varkappa t_1$ and $L_{23} = \varkappa t_2$ and further introducing the Gibbs-Duhem equation

$$N_A+\ \text{grad}\,\Delta F_{AY} + N_B+\ \text{grad}\,\Delta F_{BY} = 0 \quad (6)$$

(in which it is assumed that the partial free energy of a neutral component is not changed when the system is electrically charged) we obtain:

$$\vec{J}_A+ = -\left(L_{11} - L_{12}\frac{N_A+}{N_B+}\right)\text{grad}\,\Delta\bar{F}_{AY} - \varkappa t_1\,\text{grad}\,\varphi \quad (7)$$

$$\vec{J}_B+ = -\left(L_{21} - L_{22}\frac{N_A+}{N_B+}\right)\text{grad}\,\Delta\bar{F}_{AY} - \varkappa t_2\,\text{grad}\,\varphi \quad (8)$$

$$\vec{I} = -\varkappa\left(t_1 - t_2\frac{N_A+}{N_B+}\right)\text{grad}\,\Delta\bar{F}_{AY} - \varkappa\,\text{grad}\,\varphi \quad (9)$$

Dividing eqns. (7) and (8) by (9) for the case that the composition is uniform we have:

$$t_1 = \left[\frac{\vec{J}_A+}{\vec{I}}\right]_{\Delta\bar{F}_{AY}} = t_A+ \text{ and } t_2 = \left[\frac{\vec{J}_B+}{\vec{I}}\right]_{\Delta\bar{F}_{AY}} = t_B+$$

where t_A+ and t_B+ are the transport numbers of the cations referring to the anions as a reference frame.

For $\vec{I} = 0$ eqn. (9) gives:

$$\text{grad}\,\varphi = \left(t_B+\frac{N_A+}{N_B+} - t_A+\right)\text{grad}\,\Delta\bar{F}_{AY} \quad (10)$$

To simplify calculations we introduce

$$m = t_B+\frac{N_A+}{N_B+} - t_A+ = -\frac{t_A+ - N_A+}{N_B+}$$

The electrostatic diffusion potential is equal to

$$\Delta\varphi = \int m \operatorname{grad} \Delta\bar{F}_{AY}\, dx = -\int_{\Delta\bar{F}_{AY(I)}}^{\Delta\bar{F}_{AY(II)}} \frac{t_A+ - N_A+}{N_B+}\, d\,\Delta\bar{F}_{AY} \text{ cal/Faraday}$$

where x is the distance from one side of the cell. This integral is finite over the whole concentration interval from $N_A+ = 0$ to $N_A+ = 1$ as long as the $\frac{t_A+}{N_A+}$ or $\frac{t_B+}{N_A+}$ is finite for small values of N_A+ and N_B+, respectively. It appears that the expression for the diffusion potential does not contain the concentration gradient. This also implies that the electrostatic potential is not changed when a small charge is transported through the cell.

If we express the E.M.F. of the cell in cal/Faraday and count it positive from left to right, we see that the E.M.F. can also be expressed by the equation:

$$E' = \Delta F_{AY(II)} - \Delta F_{AY(I)} + \Delta\varphi \tag{12}$$

THE ELECTROSTATIC ENERGY CHANGE

Knowing the gradient of the electrostatic potential, grad φ, the electrostatic energy (U) in the concentration gradient can be calculated

$$U = \tfrac{1}{2}\int_v \varepsilon\, (\operatorname{grad}\varphi)^2\, d\,v \tag{13}$$

where ε is the absolute dielectric constant of the medium measured in Faraday^2/cal cm, and v is a volume covering the concentration gradient. The change in this electrostatic energy by the transport of electrical charge (Q measured in Faradays) through the gradient is given by

$$\frac{\partial U}{\partial Q} = \frac{\partial}{\partial Q}\left(\tfrac{1}{2}\int_v \varepsilon m^2\, (\operatorname{grad}\Delta\bar{F}_{AY})^2\, dv\right) = \frac{q}{2}\frac{\partial}{\partial Q}\int_{\bar{F}_{AY(I)}}^{\bar{F}_{AY(II)}} \varepsilon\, m^2 \operatorname{grad}\Delta\bar{F}_{AY}\, d\,\Delta\bar{F}_{AY} \tag{14}$$

where q is the cross-section of the cell. The only factor of the integral which is changed by the transfer of dQ is grad ΔF_{AY}. We thus have

$$\frac{\partial U}{\partial Q} = \frac{q}{2}\int \varepsilon m^2 \left[\frac{\partial \operatorname{grad}\Delta\bar{F}_{AY}}{\partial Q}\right]_{\Delta\bar{F}_{AY}} d\,\Delta\bar{F}_{AY} \tag{15}$$

Here

$$\left[\frac{\partial \operatorname{grad}\Delta\bar{F}_{AY}}{\partial Q}\right]_{\Delta\bar{F}_{AY}} = \frac{d\,\Delta\bar{F}_{AY}}{d\,N_A+}\left[\frac{\partial}{\partial Q}\left(\frac{\partial N_A+}{\partial x}\right)\right]_{N_A+}$$

$$= \frac{d\,\Delta\bar{F}_{AY}}{d\,N_A+}\left[\frac{\partial}{\partial Q}\left(\frac{1}{\partial x/\partial N_A+}\right)\right]_{N_A+}$$

$$= \frac{\mathrm{d}\,\Delta\overline{F}_{AY}}{\mathrm{d}\,N_{A}+}\left[-\left(\frac{\partial\,N_{A}+}{\partial x}\right)^{2}\frac{\partial}{\partial Q}\left(\frac{\partial\,x}{\partial\,N_{A}-}\right)\right]_{N_{A}+}$$

$$= -\frac{\mathrm{d}\,\Delta\overline{F}_{AY}}{\mathrm{d}\,N_{A}+}\left(\frac{\partial N_{A}+}{\partial\,x}\right)^{2}\frac{\partial}{\partial\,N_{A}+}\left(\frac{\partial x}{\partial Q}\right)_{N_{A}+} \qquad (16)$$

According to derivations (eqn. (8)) in the previous paper [1] (compare the present eqn. (26)), we have

$$\left(\frac{\partial x}{\partial Q}\right)_{N_{A}+} = -\frac{V}{q}\,t'(N_{A}+) \qquad (17)$$

where V is the molar volume of the mixture and $t'(N_{A}+) = \dfrac{\mathrm{d}\,t_{A}+}{\mathrm{d}\,N_{A}+}$.

Introducing eqn. (17) into (16) we have:

$$\left(\frac{\partial\,\mathrm{grad}\,\Delta\overline{F}_{AY}}{\partial\,Q}\right)_{\Delta\overline{F}_{AY}} = \frac{\mathrm{d}\,\Delta\overline{F}_{AY}}{\mathrm{d}\,N_{A}+}\left(\frac{\partial\,N_{A}+}{\partial\,x}\right)^{2}\cdot\frac{V}{q}\,t''(N_{A}+) \qquad (18)$$

neglecting changes in V with changes in composition, and introducing this into eqn. (15) we obtain

$$\frac{\partial\,U}{\partial\,Q} = \frac{V}{2}\int_{N_{A}+_{I}}^{N_{A}+_{II}}\varepsilon\,m^{2}\,t''(N_{A}+)\left(\frac{\mathrm{d}\,\Delta\overline{F}_{AY}}{\mathrm{d}\,N_{A}+}\right)^{2}\left(\frac{\partial\,N_{A}+}{\partial\,x}\right)^{2}\mathrm{d}\,N_{A}+ \quad \text{or}$$

$$\frac{\partial\,U}{\partial\,Q} = \frac{V}{2}\int_{N_{A}+_{I}}^{N_{A}+_{II}}\varepsilon\,m^{2}\,t''(N_{A}+)\,(\mathrm{grad}\,\Delta\overline{F}_{AY})^{2}\,\mathrm{d}\,N_{A}+ \qquad (19)$$

The absolute dielectric constant ε may be expressed by the absolute dielectric constant of vacuum ε_{0} and the relative dielectric constant of the medium ε_{r}:

$$\varepsilon = \varepsilon_{0}\cdot\varepsilon_{r}$$

where $\varepsilon_{0} = \dfrac{1}{\pi\cdot 36}\times 10^{-9}\,(\mathrm{coulomb}^{2}/\mathrm{joule}\cdot\mathrm{m}) = 3.98\times 10^{-23}\left(\dfrac{\mathrm{Faraday}^{2}}{\mathrm{cal}\cdot\mathrm{cm}}\right)$

Due to the small numerical value of ε_{0}, one may expect to find that the change in electrostatic energy in the region of the concentration gradient is negligible compared to the other free energy changes in the cell.

EFFECT OF THE CURRENT DENSITY

In eqn. (14) it is assumed that the current density is zero. However, in a real measurement a small current will generally be drawn. The transport of charge is therefore connected with a loss in electric energy as joule heat. This energy loss will be symmetrical with respect to the sign of the current density, and it will usually not disturb the E.M.F. measurement.

The change in electrostatic energy will, however, have terms in addition to the expression in eqn. (14) when current flows through the cell. According to eqn. (9) the potential gradient is:

$$\text{grad } \varphi = m \text{ grad } \Delta\bar{F}_{AY} - R\vec{I} \qquad \text{where } R = \frac{1}{\varkappa} \tag{20}$$

and $$(\text{grad } \varphi)^2 = m^2 (\text{grad } \Delta\bar{F}_{AY})^2 - 2\, R\vec{I}\, m \text{ grad } \Delta\bar{F}_{AY} + (RI)^2$$

For constant I we have:

$$\frac{\partial}{\partial Q}\left[\frac{1}{2}\int_v \varepsilon\,(2\, R\vec{I}\, m \text{ grad } \Delta\bar{F}_{AY})\, dv\right] = \vec{I}\, q\, \frac{\partial}{\partial Q}\int \varepsilon\, R\, m \text{ grad } \Delta\bar{F}_{AY}\, dx$$

$$= I\, q\, \frac{\partial}{\partial Q}\int_{N_{A^+(I)}}^{N_{A^+(II)}} \varepsilon \cdot R\, m\, \frac{d\, \Delta\bar{F}_{AY}}{d\, N_{A^+}}\, d\, N_{A^+} = 0 \tag{21}$$

As the integral contains only properties of the electrolyte, it is not changed by the transport of a small charge.

The contribution by the term $(RI)^2$ to the change in electrostatic energy for a given current density is equal to:

$$\frac{\partial}{\partial Q}\left(\frac{1}{2}\int_v \varepsilon\,(RI)^2\, dv\right) = \frac{1}{2} I^2 \cdot q \int \varepsilon\, 2\, R \left(\frac{\partial R}{\partial Q}\right)_x dx$$

$$= I^2 \cdot q \int \varepsilon\, R\, \frac{\partial R}{\partial N_{A^+}} \left(\frac{\partial N_{A^+}}{\partial Q}\right)_x dx \tag{22}$$

$$= -I^2\, V \int_{N_{A^+(I)}}^{N_{A^+(II)}} \varepsilon\, R \cdot R'(N_{A^+}) \cdot t'(N_{A^+})\, d\, N_A$$

where eqn. (5) from the previous publication [1]:

$$\frac{\partial\, N_{A^+}}{\partial\, Q} = -\frac{V}{q}\, t'(N_{A^+})\, \frac{\partial\, N_{A^+}}{\partial\, x}$$

has been used (compare the present eqn. (25)). ε is considered constant. One will generally find that this contribution to the measured E.M.F. is negligible. In addition to this the current will cause polarization at the electrodes.

EFFECT OF THE DIFFUSION PROCESS

It may finally be shown that the outer electrical work carried out by the E.M.F. measurement is not influenced by the diffusion process, which is proceeding during the time of the measurement.

At the E.M.F. measurement a small charge ΔQ is transferred through the cell. This transfer is carried out over a short time period Δt. The electrical current is in average

$$I = \frac{1}{q} \frac{\Delta Q}{\Delta t}$$

The number of A^+ ions passing through an unit cross-section of the cell at a distance x from one side of the cell, we denote by $\vec{J}_{A^+(x)}$. The change in content of AY in a volume ranging between two unit cross-sections at the two distances x and $x + dx$ is given by:

$$\Delta\, dn_{A^+} = (\vec{J}_{A^+(x)} - \vec{J}_{A^+(x+dx)})\, \Delta t = -\left(\frac{\partial \vec{J}_{A^+}}{\partial x}\right) dx \cdot \Delta t \qquad (23)$$

From eqns. (7) and (20) we have

$$\vec{J}_{A^+} = -\left(L_{11} - L_{12} \frac{N_{A^+}}{N_{B^+}}\right) \operatorname{grad} \Delta \bar{F}_{AY} - \varkappa t_{A^+} \cdot m \operatorname{grad} \Delta \bar{F}_{AY} + t_{A^+} \cdot \vec{I} \qquad (24)$$

which will be abbreviated to

$$\vec{J}_{A^+} = -\vec{f}(N_{A^+}, \operatorname{grad} N_{A^+}) + t_{A^+} \cdot \vec{I}$$

which combined with eqn. (23) gives

$$\Delta\, d\, n_{A^+} = f'\,(N_{A^+}, \operatorname{grad} N_{A^+})\, dx \cdot \Delta t - t'_{(N_{A^+})} \frac{\partial N_{A^+}}{\partial x}\, dx \frac{\Delta Q}{q}$$

where $f'(N_{A^+}, \operatorname{grad} N_{A^+})$ is the derivative of $\vec{f}(N_{A^+}, \operatorname{grad} N_{A^+})$ with respect to x. As $dn_{A^+} = \frac{dx}{V} \cdot N_{A^+}$, we obtain

$$\Delta\, N_{A^+}{}_{(x = \text{constant})} = V \cdot f'\,(N_{A^+}, \operatorname{grad} N_{A^+}) \cdot \Delta t - \frac{V}{q}\, t'_{(N_{A^+})} \frac{\partial N_{A^+}}{\partial x} \cdot \Delta Q \qquad (25)$$

and $$\Delta x_{(N_{A^+} = \text{const.})} = V \cdot f'\,(N_{A^+}, \operatorname{grad} N_{A^+}) \frac{\partial x}{\partial N_{A^+}} \Delta t - \frac{V}{q}\, t'_{(N_{A^+})} \cdot \Delta Q \qquad (26)$$

The free energy of the electrolyte in the region of the concentration gradient will thus change due to both the charge transfer and the diffusion process. The total free energy change is given by:

$$\Delta F_1 = \int_{\mathrm{I}}^{\mathrm{II}} \frac{q\, dx}{V} \frac{d\, \Delta F}{d\, N_{A^+}}\, \Delta\, N_{A^+}$$

$$= \Delta t \cdot \int_{\mathrm{I}}^{\mathrm{II}} q \cdot \int (N_{A^+}, \operatorname{grad} N_{A^+}) \frac{d\, \Delta F}{d\, N_{A^+}}\, d\, x - \Delta Q \int_{\mathrm{I}}^{\mathrm{II}} \frac{d\, \Delta F}{d\, N_{A^+}}\, t'_{(N_{A^+})}\, d\, N_{A^+} \qquad (27)$$

where the last term is the only term considered in the previous publication [1].

Thus the equations for the change in free energy by the simultaneous diffusion process and charge transfer can be separated into two terms: one containing time and one containing the amount of charge transferred and no term containing both time and charge.

By a similar procedure using eqns. (26) and (14) one can show that the equation for the change in electrostatic energy can be separated in the same way.

It may thus be concluded that there is no interference between the diffusion process and the cell reaction.

The derivation does not contain any assumptions regarding the bonds between the three particles A^+, B^+ and Y^-. The above equation may thus be applied on a concentration cell having, *e.g.*, HCl — H_2O mixtures as electrolyte. This electrolyte can formally be describes as a mixture of the three kinds of particles Cl^-, OH^- and H^+. The fact that the OH^- particles most of the time are associated with H^+ does not affect the derivation of the above equation.

An equation similar to eqn. (1) has been derived by Wagner [3] and later in a modified way by Guggenheim [4]. Wagner's derivation is based on the assumption that the different ions move independent of each other. The more general derivation by Guggenheim is based on the electrochemical potential of a single ion, and the application of the Onsager reciprocal relations to the transfer of single ions. In the present derivation on the other hand unmeasureable quantities like the electrochemical potential of a single ion have been avoided.

Guggenheims equation has been applied to systems of fused salts by Laity [5]. Laity [6,7] has also shown that the derivation by Guggenheim is valid also in cases where the Nernst-Einstein equation connecting diffusion constant and mobility does not hold, and he has extended the treatment of single ion properties to give correlation between coefficients obtained from different kinds of transport measurements.

Acknowledgment. Thanks are expressed to *Norges Teknisk-Naturvitenskapelige Forskningsråd* for financial support.

REFERENCES

1. Førland, T. and Krogh-Moe, J. *Acta Chem. Scand.* **13** (1959) 520.
2. Sundheim, B. R. *J. Phys. Chem.* **61** (1957) 485.
3. Wagner, C. *Z. physik. Chem.* **B21** (1933) 25.
4. Guggenheim, E. A. *Thermodynamics*, North-Holland Publishing Co., Amsterdam 1949.
5. Laity, R. W. *J. Am. Chem. Soc.* **79** (1957) 1849.
6. Laity, R. W. *J. Phys. Chem.* **63** (1959) 80.
7. Laity, R. W. *J. Chem. Phys.* **30** (1959) 682.

Received March 2, 1960.

ACTA CHEMICA SCANDINAVICA 14 (1960) 1389—1402

The Effect of Atabrine and Promazine Derivatives on the Activity of the Old Yellow Enzyme

STEN KISTNER

Medicinska Nobelinstitutet, Biokemiska avd. Stockholm, Sweden

Atabrine, chlorpromazine, and other promazine derivatives inhibited the activity in the aerobic Zwischenferment-OYE * system, but only when preincubated with the apoprotein of the OYE. The inhibition was independent of the FMN concentration. Fluorimetric studies of the apoprotein-FMN association reaction showed that compounds which inhibited the enzyme activity slowed down the reaction rate immediately after being added to the apoprotein, but did not lower the binding capacity for FMN. The mechanism of reaction between inhibitors and enzyme is discussed.

Chlorpromazine potentiated the aerobic OYE activity when added to the apoprotein at the same time as or after the FMN. Other promazine derivatives had the same ability, whereas the corresponding sulphoxides were ineffective. The anaerobic OYE activity was inhibited but not potentiated by chlorpromazine. The potentiating effect could not be explained by the experimental results, although these allowed certain conclusions.

The dissociation constants of complexes, formed between FMN and some promazines, were determined by spectrophotometric measurements.

Certain compounds with chemotherapeutical activity act as flavoprotein inhibitors. The effect of atabrine on respiration in tissue slices [1] and on oxidative phosphorylation in mitochondrial systems [2] has been explained by inhibition of flavin containing enzymes [3,4]. Studying cytochrome c reductase from yeast, Haas [3] found evidence of an irreversible reaction between the apoprotein and atabrine in competition with the coenzyme FMN. Hellerman *et al.*[5] studied the effect of this drug on D-amino acid oxidase and found a competitive inhibition, to which a simple kinetic interpretation could, however, not be applied. They concluded that the reaction between atabrine and apoprotein is complicated and reflects a general effect on proteins by the drug

* Abbreviations: OYE = Old Yellow Enzyme, FMN = flavin mononucleotide, FAD = flavin adenine dinucleotide, TPN = triphosphopyridine nucleotide, TPNH = reduced TPN, DPNH = reduced diphosphopyridine nucleotide, EDTA = ethylene diamine tetraacetic acid.

rather than a specific antagonism with flavin. Other flavoproteins are also inhibited by atabrine [6,7]. Using a fluorimetric technique, Nygaard and Theorell [8] found a reaction between the apoprotein of the OYE and atabrine, similar to that occurring between the apoprotein and FMN. Because of the strong fluorescence of atabrine its influence on the latter reaction was not studied.

Yagi *et al.*[9] showed an inhibition of D-amino acid oxidase by chlorpromazine in competition with the coenzyme FAD and calculated the dissociation constant of the enzyme-inhibitor complex. Inhibition of flavoproteins in the brain was suggested as a possible mechanism of action for the drug. Other investigators [10] found that the inhibition was due to a slow reaction between enzyme and drug and that, once established, it could not be easily reversed even by large excess FAD. The effect upon oxidative phosphorylation in mitochondria by chlorpromazine is similar to that of atabrine [11], and has been suggested to be caused by inhibition of flavoproteins [11,12]. The interaction between chlorpromazine and flavoproteins may also be influenced by the fact that a complex formation occurs between the drug and free flavin [13,14]. Yagi *et al.*[15] determined the dissociation constants for such complexes using a fluorimetric technique and concluded that, due to the high values of these constants, this type of complex formation is not responsible for the inhibition of D-amino acid oxidase by chlorpromazine.

Although many experimental data show that atabrine and chlorpromazine inhibit flavoproteins, the specificity of their activity has not been established. Both of them have also been found to cause inhibition of other isolated enzymes [5,16].

In the present work the effect of atabrine and chlorpromazine upon the activity of the OYE has been studied. Since it was found that chlorpromazine often caused a potentiation of the activity, the investigation was extended to include some other promazine derivatives and compounds of similar structure.

MATERIALS

OYE was prepared from brewer's bottom yeast (kindly supplied by Hamburgerbryggeriet, Stockholm) by the method of Theorell and Åkeson [17], and the *apoprotein* obtained according to Warburg and Christian [18]. Determination of concentration and purity was carried out as described before [19]. All enzyme preparations used in the experiments were of purity 0.75 or more.

Glucose-6-phosphate (di-sodium salt), *glucose-6-phosphate dehydrogenase (Zwischenferment)*, *TPN*, *FMN*, and *cytochrome c* (type III from horse heart) were all commercial preparations (Sigma Chemical Company).

Chlorpromazine [2-chloro-10-(3-dimethylaminopropyl)phenothiazine hydrochloride] was kindly supplied by AB Leo, Hälsingborg. The sulphoxide was obtained by oxidation with H_2O_2 in the presence of peroxidase [20]: To 2 ml of 3×10^{-3} M chlorpromazine solution were added 1 μl 3×10^{-4} M horse radish peroxidase (a gift from Dr. K. G. Paul) and 2μl 8 M H_2O_2 at +4°C. A red colour appeared. The UV-spectrum of the solution was identical with that of chlorpromazine sulphoxide [20], and paper chromatography (see Methods) showed a single spot with R_F value 0.82. *Atabrine* [6-chloro-9-((4-diethylamino-1-methylbutyl)amino)-2-methoxyacridine hydrochloride], *promazine* [10-(3-dimethylaminopropyl)phenothiazine hydrochloride], *promazine sulphoxide* oxalate, *2-methoxypromazine*, *2-methoxypromazine sulphoxide*, and *imipramine* [(3-dimethylaminopropyl)-dibenzyl amine] were all gifts from Dr. H. Löw. *Transergan* [2-diethylaminoethyl phenothiazine-10-carboxylate hydrochloride] was kindly supplied by AB. Astra, Södertälje.

METHODS

Determination of aerobic OYE activity. The same procedure as outlined in a previous publication [21] was used. The total volume of the reaction mixture was always 3.0 ml and contained 0.1 M sodium phosphate buffer pH 6.5. This pH was chosen because of the low solubility of chlorpromazine at higher pH. When not otherwise stated in the section on results, the reaction mixture contained 1.9×10^{-2} M glucose-6-phosphate, 4.5×10^{-4} M TPN, 1 Kornberg Unit Zwischenferment, and 2.7×10^{-3} M KCN. 0.1 mg OYE was added to give a final concentration of 3.2×10^{-7} M. This concentration was rate limiting and gave an oxygen uptake of approximately 100 μl per 30 min, (O_2-atmosphere). When apoprotein was used, an equivalent amount was added, and FMN was added in excess (3×10^{-6} M). All concentrations are given as final concentrations in the reaction mixture. In preincubation experiments drug and enzyme were mixed in the sidearm of the Warburg vessel and allowed to react for 30 min before being added to the other reactants. The volume in the sidearm was 0.2 ml, and thus the concentrations were here 15 times larger than in the final reaction mixture. The reaction velocity was expressed as μl oxygen consumed during a 30 min period. The activity in the vessels, where drug was added, was expressed as per cent of the activity in the control vessels. All experiments were performed at +37.0° C.

Determination of anaerobic OYE activity. The method described by Theorell [22] was used. A Thunberg cuvette contained in a total volume of 3.0 ml 0.1 M sodium phosphate pH 6.5, 9.9×10^{-3} M glucose-6-phosphate, 1 Kornberg Unit Zwischenferment, 4.0×10^{-5} M cytochrome c, and OYE. In the sidearm 0.1 ml 1.3×10^{-2} M TPN was added. The OYE concentration varied in different experiments, and in some experiments chlorpromazine was added in the main compartment. The cytochrome c stock solution was made up in 0.02 N HCl to achieve total oxidation of the cytochrome [22]. The air in the cuvette was replaced by argon, and the cuvette was carefully shaken during 5 min to obtain equilibrium. The cuvette was placed in a Beckman DU spectrophotometer, and the absorption at 550 mμ read against a buffer blank. It was approximately 0.38 in all experiments, and constant during a 10 min period. The cuvette was tilted, and the content of the sidearm mixed with that of the main compartment. The absorption at 550 mμ was measured until a constant value was obtained. The total amount cytochrome c reduced was determined, using the values $\beta = 2.20 \times 10^7$ cm$^2 \cdot$ mole^{-1} for oxidized cytochrome [23] and $\beta = 6.36 \times 10^7$ cm$^2 \cdot$ mole^{-1} for the reduced form [24]. The reaction rate was determined during the early phase of the reaction, when a rectilinear relationship was obtained between the amount of cytochrome reduced and the reaction time. The experiments were run at + 21.0°C.

Fluorimetric study of the apoprotein—FMN association reaction. The apparatus and method described by Theorell and Nygaard [25] was used. This allowed determination of the association velocity constant k_1 and the amount FMN bound by a certain amount of apoprotein. The reactions were performed in 0.1 M sodium phosphate buffer pH 6.5 at + 23.0°C.

Spectrophotometric determination of complex formation with FMN. The change in the absorption spectrum of FMN caused by chlorpromazine [15] and other compounds was used to determine the dissociation constants of the complexes. The solutions were made in 0.1 M sodium phosphate buffer pH 6.5. The experiments were performed at room temperature (+ 21°C).

Paper chromatography of chlorpromazine was carried out as described by Salzman *et al.*[26]

All experiments were done at least twice. Care was always taken to keep out light as much as possible.

RESULTS

The effect of atabrine on the aerobic OYE activity. When atabrine was mixed with FMN and other reactants in the main compartment of the Warburg flask, and the reaction was started by introducing apoprotein from the sidearm, no inhibition occurred even at the highest atabrine concentration tested,

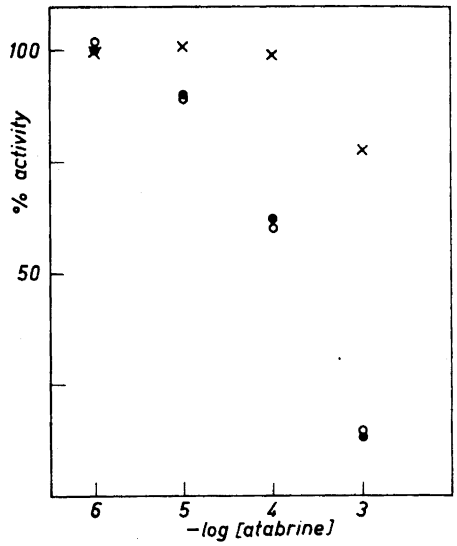

Fig. 1. The effect of atabrine on the aerobic OYE activity. The activity is expressed as per cent of the activity in control experiments, where no drug was added, and marked along the ordinate. Along the abscissa the negative logarithm of the atabrine concentration is marked. Atabrine and enzyme were preincubated in a sidearm of the Warburg flasks, where the volume was 0.2 ml. The total volume of the reaction mixture was 3.0 ml. The concentration of TPN was 4.5×10^{-4} M and of enzyme 3.2×10^{-7} M. All concentrations are expressed as final concentrations in the reaction mixture. Points marked × indicate experiments, where holoenzyme was used. O marks experiments where apoprotein was used, and 3.2×10^{-6} M FMN was added in the main compartment, ● experiments with apoprotein and 3.8×10^{-7} M FMN.

1×10^{-3} M. In different experiments the TPN or FMN concentration was lowered to 1.8×10^{-5} M or 3.8×10^{-7} M, respectively, to become rate limiting in the reaction, other experimental conditions being unchanged. 1×10^{-3} M atabrine was still without effect. However, when atabrine and apoprotein were mixed in the sidearm and thus preincubated during 30 min., inhibition occurred. It was of the same magnitude at low, rate limiting FMN concentrations as when FMN was added in excess. Some effect, although much less pronounced, was noticed also when atabrine was preincubated with the holoenzyme (Fig. 1). The inhibition of the apoprotein after preincubation was reversed by approximately 2/3 when dialysis against buffer was performed overnight at + 4°C immediately after the preincubation.

The effect of chlorpromazine on the aerobic OYE activity. Under various experimental conditions chlorpromazine caused potentiation of the enzymatic activity. This always occurred when the holoenzyme was used. It was of the same magnitude whether preincubation of OYE and chlorpromazine was performed or not. Also in experiments with apoprotein, potentiation occurred if FMN and drug were added simultaneously to the enzyme. On the other hand, if apoprotein and chlorpromazine were preincubated in the sidearm

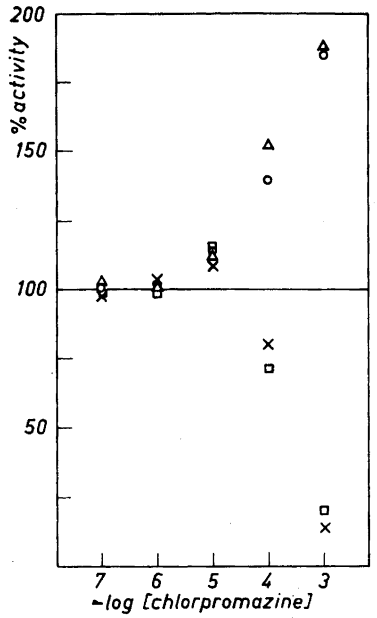

Fig. 2. The effect of chlorpromazine on the aerobic OYE activity. Activity and drug concentrations are marked as in Fig. 1. O marks experiments, where holoenzyme and chlorpromazine were preincubated in the sidearm, △ experiments, where 3.7×10^{-7} M FMN and chlorpromazine were preincubated, and apoprotein kept in the main compartment, × indicates preincubation of apoprotein and drug, when the main compartment contained 3.1×10^{-6} M FMN. □ indicates the same prodedure, but FMN concentration was 4.2×10^{-7} M. Other experimental conditions were as described under Fig. 1.

before being added to the other reactants, high concentrations of chlorpromazine caused inhibition, whereas low concentrations potentiated. Essentially the same effect was obtained at high and low FMN concentrations. In Fig. 2 some experiments are summarized to show the effect of chlorpromazine under various experimental conditions. Higher concentrations of chlorpromazine than those shown in the figure caused precipitation and lowering of the activity.

When the activity in the test system was lowered by diminishing the OYE concentration, the potentiating effect of chlorpromazine remained unchanged. When a lower activity was obtained by diminishing the TPN concentration, the effect of the drug was much less marked. This is shown in Table 1, where the OYE concentration was rate limiting in the first two groups of experiments, and the TPN concentration in the last group.

Paper chromatography was performed on reaction mixtures containing 3.2×10^{-7} M OYE, excess TPN, and 1×10^{-3} M chlorpromazine, which had caused a maximal potentiation of the OYE activity. In different experiments samples containing 10—18 μg chlorpromazine were tested. They all showed the same R_F values as the chlorpromazine blanks, 0.92, and only one spot

Table 1. The effect of chlorpromazine on the aerobic OYE activity. Chlorpromazine and OYE were preincubated in the sidearm for 30 min, then added to TPN and other reactants. In the first two groups of experiments the enzyme concentration was rate limiting in the reaction mixture without drug. In the last group TPN concentration was rate limiting.

OYE concentration	TPN concentration	Chlorpromazine concentration	O_2 uptake during 30 min	Activity in the presence of chlorpromazine
3.2×10^{-7} M	4.5×10^{-4} M	0	100.7	—
3.2×10^{-7} M	4.5×10^{-4} M	5×10^{-4} M	158.3	157.7 %
1.6×10^{-7} M	4.5×10^{-4} M	0	52.4	—
1.6×10^{-7} M	4.5×10^{-4} M	5×10^{-4} M	82.1	156.6 %
3.2×10^{-7} M	1.1×10^{-5} M	0	60.0	—
3.2×10^{-7} M	1.1×10^{-5} M	5×10^{-4} M	66.7	111.1 %

appeared in the chromatograms. Control runs of reaction mixtures without chlorpromazine did not cause any spots.

The effect of other compounds on the aerobic OYE activity. The different compounds tested were preincubated with OYE or apoprotein. The results are summarized in Table 2, where it can be seen that other promazines than the 2-chloro derivative also potentiated the OYE activity, whereas many

Table 2. The effect of various compounds on the aerobic OYE activity. The different compounds and OYE or apoprotein were preincubated for 30 min in the sidearm of the Warburg flask, then added to the other reactants in the main compartment. In experiments with apoprotein this contained also 3.0×10^{-6} M FMN. Other experimental conditions were as described under Fig. 1.

Compound	Concentration M × 10^4	Activity of OYE compared with control %	Activity of apoprotein compared with control %
Chlorpromazine	1	140	80
Daylight exposed chlorpromazine	1	108	77
UV-irradiated chlorpromazine	1	114	
Chlorpromazine sulphoxide	1	100	90
Promazine	1	135	73
Promazine sulphoxide	1	97	99
Methoxypromazine	1	120	94
Methoxypromazine sulphoxide	1	102	84
Imipramine	1	100	93
Transergan	1	98	92
Methylene blue	1	151	154
Adenine	1	98	
Caffeine	10	99	
D-Tryptophan	10	97	
L-Tryptophan	10	101	
EDTA	1	103	

structurally related compounds did not. When chlorpromazine is left in the light, the solution rapidly darkens [27] and becomes strongly fluorescent. Chlorpromazine, which had been left in daylight for 2 days at room temperature had lost most of its potentiating effect. The same change could be accomplished by irradiating the solution for 2 h with the mercury lamp of the fluorimeter.

Most of the promazines and other compounds with a similar structure caused the same degree of inhibition when preincubated with the apoprotein. The irradiated chlorpromazine, which had lost most of its potentiating activity, still caused inhibition.

Methylene blue potentiated the OYE more strongly than chlorpromazine. At 1×10^{-3} M it doubled the activity. When preincubated with the apoprotein, the potentiating effect remained unchanged.

Table 2 shows that adenine, caffeine, and tryptophan did not cause potentiation. These compounds form complexes with FMN of the same type as chlorpromazine [28,29]. EDTA was also without effect.

The effect of chlorpromazine on the anaerobic OYE activity. The results are shown in Table 3. The same amount of cytochrome c was reduced, regardless of the concentration of OYE in the reaction mixture. The variations obtained are explained by experimental error. Without OYE no reduction occurred in the absence or in the presence of chlorpromazine. The reaction rate varied with the amount OYE added, and approximately the same turnover number was obtained. The addition of chlorpromazine caused some inhibition.

Fluorimetric studies of the apoprotein-FMN association reaction. Chlorpromazine showed a slow, constant increase in fluorescence when irradiated by the lamp of the fluorimeter and was therefore excluded from these studies. Promazine, on the other hand, had a low fluorescence that remained unchanged when the solution was illuminated, at least during the period of time necessary for the experiment. Its effect on the fluorescence of FMN at the concentrations used in these experiments was negligible. When promazine was added to apoprotein solutions to give a final concentration of 1×10^{-4} M a few minutes

Table 3. The effect of chlorpromazine on the anaerobic OYE activity. The amount of cytochrome c reduced is calculated from the change in absorption at 550 mμ. The reaction rate is calculated from the beginning of the reaction (10th—30th min) when a constant amount of cytochrome c was reduced per unit time. The last column gives the turnover number of the OYE.

OYE concentration M	Chlorpromazine concentration M	Total change in absorption at 550 mμ	Absorption change at 550 mμ per min	Total amount cytochrome reduced, M	M cytochrome reduced per min	Mole cytochrome reduced per mole OYE per min
1.28×10^{-7}	0	0.719	0.0120	3.97×10^{-5}	6.96×10^{-7}	5.44
2.56×10^{-7}	0	0.760	0.0254	4.21×10^{-5}	14.04×10^{-7}	5.49
2.56×10^{-7}	1.94×10^{-4}	0.756	0.0215	4.18×10^{-5}	11.89×10^{-7}	4.64
1.66×10^{-7}	0	0.720	0.0151	3.98×10^{-5}	8.35×10^{-7}	5.03
1.66×10^{-7}	1.94×10^{-4}	0.734	0.0114	4.05×10^{-5}	6.30×10^{-7}	3.99

Table 4. The effect of promazine on the apoprotein-FMN reaction, studied by fluorimetric technique. The volume of the test solutions was 3.55 ml, containing a constant amount of apoprotein, 0.1 M sodium phosphate buffer pH 6.5 and 1×10^{-4} M promazine when added. To these solutions 2 µl aliquots of 1.17×10^{-4} M FMN were added. The temperature + 23.0°C.

Conditions	Reaction mixture	FMN coupled M	Association velocity constant, k_1 $M^{-1} \cdot sec^{-1}$
FMN added immediately to reaction mixture	Apoprotein	7.08×10^{-7}	11.17×10^4
	Apoprotein + promazine	6.90×10^{-7}	6.41×10^4
Reaction mixture dialyzed before FMN was added	Apoprotein	6.50×10^{-7}	11.97×10^4
	Apoprotein + promazine	6.68×10^{-7}	11.08×10^4

before titration with FMN was undertaken, the association velocity of the apoprotein-FMN reaction was lowered. However, the same amount of FMN was bound on each addition. Incubating promazine and apoprotein for 30 min. at +37°C before adding FMN did not alter the result. When the promazine-apoprotein mixture was dialyzed against buffer at +4°C overnight, the effect of the promazine was completely abolished. Table 4 shows a typical experiment.

Some other compounds structurally related to promazine that had been tested in the Warburg experiments showed the same fluorescence properties as promazine. They were added to apoprotein solutions a few minutes before titration with FMN was undertaken. Results from one experiment are shown in Table 5. Some compounds were much less effective than promazine, but they all influenced the reaction in a similar way.

Although atabrine is strongly fluorescent, attempts were made to study its influence on the apoprotein-FMN reaction with the fluorimetric technique. 5×10^{-6} M atabrine had the same fluorescence as 7×10^{-7} M FMN, which was half of the concentration that began to give self-quenching. Using similar experimental conditions as those, outlined under Table 4, the same increase

Table 5. The effect of various compounds on the apoprotein-FMN reaction. Their concentration was 1×10^{-4} M. FMN was added in 5 µl aliquots of an 1.55×10^{-4} M solution. Other experimental conditions as described under Table 4.

Compound added to apoprotein solution	FMN coupled M	Association velocity constant, k_1 $M^{-1} \cdot sec^{-1}$
None	9.04×10^{-7}	10.55×10^4
Promazine	9.34×10^{-7}	5.72×10^4
Promazine sulphoxide	8.99×10^{-7}	8.96×10^4
Methoxypromazine	8.87×10^{-7}	6.43×10^4
Methoxypromazine sulphoxide	8.95×10^{-7}	7.57×10^4
Imipramine	9.27×10^{-7}	6.70×10^4
Transergan	8.90×10^{-7}	8.26×10^4

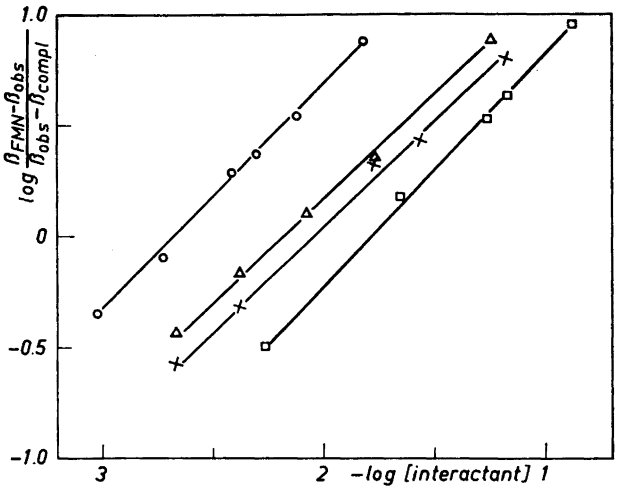

Fig. 3. Graphical determination of dissociation constants of FMN complexes after measuring the absorption at 445 mμ of FMN in the presence of various interactants. β_{FMN} is the absorption of free FMN, β_{obs} the absorption of FMN at different concentrations of interactant, shown on the abscissa, and $\beta_{compl.}$ the absorption of FMN when further addition of interactant did not cause further change in absorption. Readings were made against blanks containing the same amount of interactant as the samples. All solutions contained 0.1 M sodium phosphate pH 6.5. Temperature was + 21°C. O—O chlorpromazine, $K = 2.1 \times 10^{-3}$ M; △—△ promazine sulphoxide, $K = 6.6 \times 10^{-3}$ M; × — × promazine, $K = 9.3 \times 10^{-3}$ M; □—□ transergan, $K = 1.7 \times 10^{-2}$ M. The slopes of all curves equalled 1.

in fluorescence was caused by the FMN additions in samples containing 5×10^{-6} M atabrine as in the controls. The addition of atabrine caused a 20 % decrease of k_1, whereas the amount FMN bound was not affected.

Spectrophotometric studies of flavin complexes. All promazines as well as imipramine and transergan caused a change in the absorption spectrum of FMN, similar to that described for chlorpromazine [15], indicating the formation of a complex. Atabrine was excluded from these studies because of its strong absorption at 445 mμ. The dissociation constants of some of the complexes were determined. The results are shown in Fig. 3.

Spectrophotometric measurements were also made to determine whether complex formation occurred between chlorpromazine and FMN bound to protein in the OYE *. The absorption of 1.95×10^{-5} M OYE and 1×10^{-3} M chlorpromazine, read against a chlorpromazine blank, was compared to that of 1.95×10^{-5} M OYE alone. Certain difficulties were encountered since a slight opalescence occurred when enzyme and chlorpromazine were mixed. After centrifugation the two OYE solutions showed identical spectra in the visible region.

* Experiments concerning the OYE spectra were performed in collaboration with Dr. A. Ehrenberg. The author wishes to thank him for the right to use the results in this connection.

When OYE is reduced with excess TPNH and reoxidized with oxygen, the spectrum is shifted towards the red region [30,31]. The same shift was found in the absence and in the presence of 1×10^{-3} M chlorpromazine.

DISCUSSION

The results of the inhibition studies of the OYE give some support to the idea that atabrine and chlorpromazine, as well as other compounds of similar structure, may act as flavoprotein inhibitors. The potentiation obtained with some of the promazine derivatives is more difficult to explain. Inhibition and potentiation were in some cases caused by the same compound, depending on the experimental conditions, and thus seemed to reflect two different mechanisms of action. The effect of the drugs depended on whether they reacted with the enzyme before or after the coenzyme was bound.

Both atabrine and chlorpromazine caused inhibition of the oxygen uptake in the Zwischenferment-OYE system but, except for atabrine at high concentration, only when preincubated with the apoprotein. This leads to the conclusion that the observed inhibition was due to interference with the activity of the OYE and did not concern any of the other reactants. Also, the inhibitors interferred with the reaction between apoprotein and FMN. The effect was the same at high and low FMN concentrations. These findings bear some resemblance to results obtained with other flavoproteins [3,10], suggesting a little reversible reaction between drug and enzyme that prevents the binding of flavin. That the reaction was reversible to some extent was shown when the effect of atabrine could be partially abolished after dialysis.

Similar results were obtained with promazine and other, structurally related compounds. The formulas of some of the compounds are shown below. They all have a certain structural resemblance to FMN but lack groups of the same type as the special combining groups [8,32] which have been suggested to participate in the binding of the coenzyme to the apoprotein. The binding of the inhibitors to the protein must therefore be supposed to be of a different character, even if they might compete for the same sites as FMN. Considering the great affinity of the apoprotein for FMN [25], one would assume that this could easily replace the inhibitors, even if added later.

Further information was obtained from the fluorimetric studies of the apoprotein-FMN reaction that showed that promazine and structurally related compounds, as well as atabrine in low concentration, slowed down the reaction rate but did not influence the binding capacity of apoprotein for FMN. It did not seem likely that this interferance was due to complex formation with FMN, because of the high values obtained for the dissociation constants of the promazine-FMN and other complexes. Thus it appeared that the inhibitors were bound to the apoprotein without occupying the binding sites of the FMN but making these less accessible. A similar effect on the reaction has been obtained by treating the apoprotein with functional group reagents, which block only some of the binding groups for each FMN molecule [8].

The effect upon the activity of the enzyme by atabrine and promazine derivatives is not explained by a change in the equilibrium between the apopro-

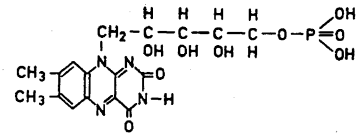

FMN.

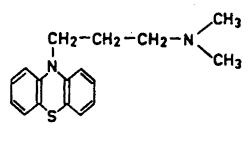

Promazine.

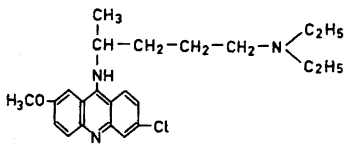

Atabrine.

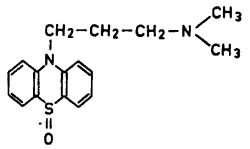

Promazine sulphoxide.

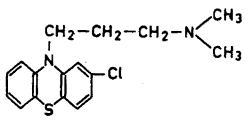

Chlorpromazine.

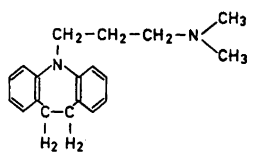

Imipramine.

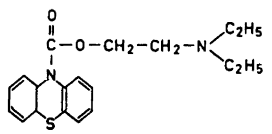

Transergan.

tein and FMN, since the inhibition would then have depended upon the FMN concentration. To offer an explanation of the present results it might be assumed that the apoprotein of the OYE, inhibitor, and FMN form a ternary complex with low or no activity. The presence of the inhibitors disturbs but does not prevent the binding of FMN to the apoprotein. The presence of FMN completely prevents a binding of inhibitors that can reduce the activity. This suggests that FMN and the inhibitors have binding sites located close to each other. No conclusions can be drawn as to whether the inhibitors are also bound to other parts of the enzyme molecule.

The experimental results do not explain the nature of the interaction between enzyme and drug that resulted in increased activity. However, certain conclusions may be drawn that allow a discussion. It is interesting to note that potentiation by chlorpromazine has been observed in other enzyme systems [10,33].

The potentiating effect of the promazines was quite similar to that of methylene blue, which is known to oxidize reduced OYE [34]. This reaction occurs at a faster rate than the oxidation by oxygen in reaction mixtures, where the reducing system (glucose-6-phosphate, Zwischenferment, TPN) is in excess.

In such cases the velocity is determined by the oxidation of the reduced OYE [35]. On the other hand, at low concentrations of the reducing system the velocity depends on the reduction of the OYE, and the enzymatic activity is equally high with oxygen or methylene blue as electron acceptor [35]. In the present experiments it was found that the potentiating effect of chlorpromazine was much less pronounced in reaction mixtures with low concentration of TPN. It appeared that chlorpromazine interfered with the reoxidation of the reduced OYE by oxygen.

It is difficult to believe, however, that chlorpromazine, which has been characterized as an exceptionally good electron donor [14], could act as an oxidant like methylene blue. Metabolites, possibly possessing this property, were not found in paper chromatograms of reaction mixtures, where chlorpromazine had caused potentiation. A comparison between the different compounds tested gives a clue to which parts of the promazine molecule that might be responsible for the effect. Substitution in the 2-position had little influence, whereas oxidation at the sulphur atom abolished the effect. Negative results obtained with imipramine also indicate the importance of the sulphur atom, and those obtained with transergan the importance of the substitution at the nitrogen.

It may be remarked that phenothiazines are considered to form resonance stabilized free radicals [36], where the nitrogen and sulphur atoms hold key positions. Bindings to these atoms may interfere with this activity. The radical formation in chlorpromazine has been suggested as the reason for its antioxidant effect on the formation of lipid peroxides in tissue homogenates [27]. This reaction is also inhibited by methylene blue. It may be postulated that in the OYE system, the promazine radical structure may act as an intermediate in the electron transport system.

The different effect of chlorpromazine on the OYE activity in the aerobic and anaerobic system brings up the question, whether the formation of hydrogen peroxide in the former had any importance. The presence of hydrogen peroxide did not in itself influence the enzymatic activity. Hydrogen peroxide is known to oxidize phenothiazines to sulphoxides under different conditions [37]. In aqueous solutions the oxidation of chlorpromazine requires the presence of catalase or peroxidase to occur at a fast rate [20]. Possibly the nascent peroxide in the Zwischenferment-OYE system, although unable to complete the oxidation, could form a postulated intermediate radical form [38]. This is, however, supposed to appear upon UV irradiation of chlorpromazine solutions. In the present experiments such treatment lead to the disappearance of the potentiation.

Potentiation of aerobic and inhibition of anaerobic activity has also been found in microsomal cytochrome reductase [39] by substituting DPNH with TPNH, or by adding competing nucleotides when DPNH is the substrate. When oxygen is the electron acceptor, the rate limiting step is the oxidation of the reduced enzyme, and this reaction occurs faster when the oxidized pyridine nucleotides dissociate more easily from the enzyme. If the same explanation is applicable to the present experiments, it would mean that the promazines interfered with the binding of TPN, and thus potentiation and inhibition could be attributed to the same type of mechanism. Observations

recently made with horse liver alcohol dehydrogenase [40] give further support to this possibility. Some compounds that do not participate in the enzymatic reaction have been found to form a ternary complex with the enzyme. Depending upon the concentrations of the reactants this sometimes leads to inhibition and sometimes to potentiation of the activity. The potentiation is due to an easier dissociation of the ternary than the binary complex. — Nevertheless, it was possible to form the red intermediate of the OYE [30,31] in the presence of chlorpromazine.

The complex formation that occurs between chlorpromazine and flavin is supposed to involve a transfer of electrons [14]. It did not appear that such a reaction had anything to do with the potentiation. No experimental evidence was found for the formation of a complex between chlorpromazine and protein bound FMN, and other compounds able to form flavin complexes did not potentiate.

Although unexplained, the potentiation of the OYE activity is interesting, considering the exceptionally low turnover number of this enzyme. Whether this type of action has anything to do with the pharmacological properties of the promazines is completely uncertain. It may be remarked, however, that chlorpromazine and its sulphoxide, which behaved differently with regard to the potentiation, also differ to a certain extent in pharmacological activity [41].

Acknowledgements. The author wishes to express his thanks to Professor Hugo Theorell for valuable discussions and criticism during the course of this work. Thanks are also due to Drs. A. Ehrenberg, H. Löw, K. G. Paul and B. Sörbo for helpful suggestions and discussions.

REFERENCES

1. Wright, C. J. and Sabine, J. C. *J. Biol. Chem.* **155** (1944) 315.
2. Hunter, F. E., Jr. in Colowick, S. P. and Kaplan, N. O. *Methods in Enzymology*, Acad. Press Inc. New York, 1955, Vol. II, p. 610.
3. Haas, E. *J. Biol. Chem.* **155** (1944) 321.
4. Löw, H. *Biochim. et Biophys. Acta* **32** (1959) 1.
5. Hellerman, L., Lindsay, A. and Bovarnick, M. R. *J. Biol. Chem.* **163** (1946) 553.
6. Mahler, H. R. in Colowick, S. P. and Kaplan, N. O. *Methods in Enzymology*, Acad. Press Inc., New York, 1955, Vol. II p. 688.
7. Brodie, A. F. in Colowick, S. P. and Kaplan, N. O. *Methods in Enzymology*, Acad. Press Inc., New York, 1955, Vol. II, p. 693.
8. Nygaard, A. P. and Theorell, H. *Acta Chem. Scand.* **9** (1955) 1587.
9. Yagi, K., Nagatsu, T. and Ozawa, T. *Nature* **177** (1956) 891.
10. Lasslo, A. and Meyer, A. L. *Nature* **184** (1959) 1922.
11. Löw, H. *Biochim. et Biophys. Acta* **32** (1959) 11.
12. Dawkins, J. R., Judah, J. D. and Rees, K. R. *Nature* **182** (1958) 875.
13. Szent-Györgyi, A. *Bioenergetics*, Acad. Press Inc. New York, 1957.
14. Karreman, G., Isenberg, I. and Szent-Györgyi, A. *Science* **130** (1959) 1191.
15. Yagi, K., Ozawa, T. and Nagatsu, T. *Nature* **184** (1959) 982.
16. Lip Boen Khuow, Burbridge, T. N. and Simon, A. *Federation. Proc.* **19** (1960) No. 1 Part 1, 280.
17. Theorell, H. and Åkeson, Å. *Arch. Biochem. Biophys.* **65** (1956) 439.
18. Warburg, O. and Christian, W. *Biochem. Z.* **298** (1938) 368.
19. Kistner, S. *Acta Chem. Scand.* **12** (1958) 2034.
20. Cavanaugh, D. J. *Science* **125** (1957) 1040.
21. Kistner, S. *Acta Chem. Scand.* **13** (1959) 1149.
22. Theorell, H. *Biochem. Z.* **288** (1936) 317.

23. Theorell, H. *Biochem.* **285** (1936) 207.
24. Paul, K. G. *Acta Chem. Scand.* **5** (1951) 389.
25. Theorell, H. and Nygaard, A. P. *Acta Chem. Scand.* **8** (1954) 877.
26. Salzman, N. P. and Brodie, B. B. *J. Pharmacol. Exptl. Therap.* **118** (1956) 46.
27. Bernheim, M. L. C. *Proc. Soc. Exptl. Biol. Med.* **102** (1959) 660.
28. Weber, G. *Biochem. J.* **47** (1950) 114.
29. Harbury, H. A. and Foley, K. A. *Proc. Natl. Acad. Sci. U.S.* **44** (1958) 662.
30. Haas, E. *Biochem. Z.* **290** (1937) 291.
31. Ehrenberg, A. and Ludwig, G. *Science* **127** (1958) 1177.
32. Theorell, H. and Nygaard, A. P. *Acta Chem. Scand.* **8** (1954) 1649.
33. McCormick, D. B. and Snell, E. E. *Proc. Natl. Acad. Sci. U.S.* **45** (1959) 1371.
34. Warburg, O. and Christian, W. *Biochem. Z.* **254** (1932) 438.
35. Warburg, O. and Christian, W. *Biochem. Z.* **266** (1933) 377.
36. Murphy, C. M., Ravner, H. and Smith, N. L. *Ind. Eng. Chem.* **42** (1950) 2479.
37. Massie, S. P. *Chem. Revs.* **54** (1954) 797.
38. Forrest, I. S., Forrest, F. M. and Berger, M. *Biochim. et Biophys. Acta* **29** (1958) 441.
39. Strittmatter, P. *J. Biol. Chem.* **234** (1959) 2665.
40. Theorell, H. and McKinley McKee, J. S. *To be published.*
41. Salzman, N. R., Moran, N. C. and Brodie, B. B. *Nature* **176** (1955) 1122.

Received July 1, 1960.

ACTA CHEMICA SCANDINAVICA 14 (1960) 1403—1413

X-Ray Investigations on Me-Si-B Systems (Me = Mn, Fe, Co)

II. Some Features of the Fe-Si-B and Mn-Si-B Systems

BERTIL ARONSSON and INGVAR ENGSTRÖM

Institute of Chemistry, University of Uppsala, Uppsala, Sweden

The main features of the Fe—Si—B system at temperatures around 1 000°C have been determined using X-ray diffraction methods. Four ternary phases exist in the metal-rich part of this system. $Fe_{4.86}Si_2B$ is isomorphous with $Co_{4.7}Si_2B$ but has a more metal-rich composition. Fe_5SiB_2 has the Cr_5B_3 ($D8_l$)-structure, while the structure of a phase with the approximate composition $Fe_2Si_{0.4}B_{0.6}$ has not been solved. There is also a ternary Fe—Si—B phase that crystallizes in the cementite-structure, but the equilibria in which this phase is involved have not been clarified.

In the Mn—Si—B system, which seems to be quite complicated, particularly in the metal-rich part, a phase Mn_5SiB_2 (isomorphous with Fe_5SiB_2) has been identified.

In the previous communication [1] on Me—Si—B systems, the Co—Si—B system was dealt with and, in addition, some crystallographic data on intermediate phases in the Fe—Si—B and Mn—Si—B systems were reported. In this paper we shall present the main features of the Fe—Si—B system at temperatures around 1 000°C and, in particular, discuss the structures and homogeneity ranges of the phases with the composition Fe_5X_3 (X = Si,B). We shall also give some qualitative information on the Mn—Si—B system.

Except for phases with compositions around $MnSi_2$ and in the metal-rich part of the Mn—Si system, intermediate phases in the boundary binary systems Fe—B, Fe—Si, Mn—B and Mn—Si are crystallographically well characterized. Information on these binary phases may be found in a recent review article [2] and, therefore, will not be repeated here. No systematic studies on the ternary systems Fe—Si—B and Mn—Si—B seem to have been made previously.

EXPERIMENTAL

The alloys were prepared from the following chemicals,

Iron rods, from Johnson, Matthey and Co., London, claimed to contain about 0.03 % carbon, 0.01 % oxygen, 0.01 % nitrogen and a few p.p.m. of other elements.

Iron sponge, from Johnson, Matthey and Co., analyzed to contain 95.3 % iron, 2—3 % oxygen (this figure is probably too low), less than 0.001 % nitrogen and about 0.002 % carbon. According to the manufacturer the content of other elements is very low (a few p.p.m.).

Manganese (electrolytic), kindly donated by AB Ferrolegeringar, Stockholm, claimed purity 99.8 %.

Silicon powder, from Pechiney, Paris, claimed purity 99.9 %.

Boron powder, kindly donated by Borax Consolidated, London, claimed purity 99.0—99.7 %.

In some preliminary experiments we also used,

Iron powder, from Baker, Phillipsburg, New Jersey, analyzed to contain 97.8 % iron, ~1.1 % oxygen (this figure is probably too low) less than 0.001 % nitrogen and about 0.004 % carbon).

Carbonyl iron powder, analyzed to contain 98.5 % iron, 0.18 % oxygen, 0.69 % nitrogen and 0.77 % carbon.

Those iron-silicon-boron samples which have been chemically analyzed were prepared from three master alloys:

Fe_2B, analyzed to contain 90.38 % iron and 9.33 % boron, most of the remainder very probably being oxygen, was prepared by repeated sintering and arc-melting mixtures of iron sponge (Johnson, Matthey & Co) and boron, the ferro-magnetic iron boride being magnetically separated after each treatment.

$FeSi_{\sim 0.25}$ was prepared by reacting iron rods with silicon powder in a high-frequency furnace under vacuum so as to obtain a reasonably brittle iron-rich master alloy.

$FeSi_2$, analyzed to contain 46.71 % iron and 52.68 % silicon, most of the remainder very probably being oxygen, was prepared in the same way as $FeSi_{\sim 0.25}$.

The samples were synthesized by arc-melting or sintering mixtures of the master alloys and, depending on the composition of the samples, they were given different heat-treatments as reported in the following paragraph.

In the preliminary studies of the Fe—Si—B system we prepared alloys by sintering mixtures of the elements for 7—10 days at 975 ± 20°C in evacuated and sealed silica tubes which were subsequently quenched in oil. After this time no further changes were observed in the powder photographs of the samples on continued sintering and it was concluded that equilibrium had been attained. Several samples were made in each of the three-phase regions shown in Fig. 1, using the iron sponge, Baker's iron powder and the carbonyl iron powder, and within the experimental error (± 0.05 %) the same l.p. (lattice parameter) of the phases were found. Samples containing α(Fe,Si) were recovered for two hours at 700°C before the exposure in the powder camera.

The Mn—Si—B alloys, which were also prepared by sintering or arc-melting weighed amounts of the elements, were not chemically analyzed.

Powder photographs were taken in cameras of the Guinier type using Cr$K\alpha$- and Cr$K\alpha_1$-radiation with silicon (a = 5.4306 Å) or CaF_2 (a = 5.4630 Å) as internal standards for the l.p. determinations. Because of the low background and the sharp lines on the powder photographs obtained in Guinier cameras, quite small amounts of well-crystallized phases present in a sample can be detected. By mixing small amounts of $Fe_{4.86}Si_2B$ in Fe_5SiB_2, we found that less than 0.5 % of the former phase was sufficient for its identification in Fe_5SiB_2 + $Fe_{4.86}Si_2B$ samples. Since the powder photographs of phases involved in this study have a rather similar complexity, it may be assumed that when the diffraction lines of a well-crystallized phase are not discernable on a powder film, the sample does not contain more than about 0.5 % of that phase.

The chemical analyses of the Fe—Si—B samples were carried out by Dr. Lilly Gustafsson at the analytical department of this Institute. For the determination of iron, a sample was dissolved in HF + HNO_3, the hydrofluoric acid being subsequently removed by evaporation with sulfuric acid. After reduction in a cadmium-reductor, iron was determined through titration with cerium sulphate. The accuracy of this analysis is estimated to be ± 0.1 %.

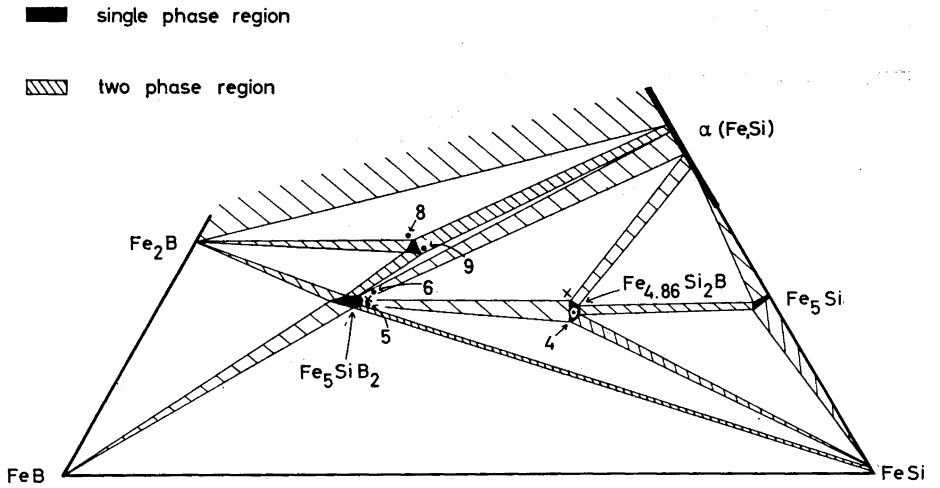

Fig. 1. The Fe—Si—B system in the composition range 50—70 atom per cent iron at temperatures around 1 000°C. The numbers refer to those samples the compositions and heat-treatments of which are given in Table 6. For clarity the narrow α(Fe,Si,B) single phase region is only represented by a line. The compositions Fe_5SiB_2 and Fe_5Si_2B are marked with ×. Error in figure: Fe_5Si should read Fe_5Si_3.

For the determination of silicon and boron, a sample was melted with Na_2CO_3 + KNO_3 in a platinum crucible and the melt was dissolved in diluted hydrochloric acid. Silicon was determined gravimetrically as SiO_2 after the boric acid had been removed by evaporation with methanol. The small amounts of silicon present in the filtrate were determined colorimetrically. For the boron analysis, the acid solution was passed through a hydrogen saturated ion exchanger and, after addition of mannitol, the solution was titrated with sodium hydroxide. The accuracy of the silicon and boron analyses is estimated to be ± 0.5 %.

The oxygen and nitrogen content of the samples was determined by a vacuum fusion technique. These analyses were carried out at the analytical department of Avesta Jernverk, where also the carbon content was determined by standard methods.

RESULTS

The Fe—Si—B system. In Figs. 1 and 2 the Fe—Si—B system at 1 000°C is outlined. (The samples containing less than 50 atomic per cent iron were synthesized by sintering mixtures of the elements at 1 100°C.) The system is characterized by four ternary metal-rich intermediate phases with the approximate compositions $Fe_3(Si,B)$, $Fe_2Si_{0.4}B_{0.6}$, Fe_5SiB_2 and $Fe_{4.86}Si_2B$, respectively. X-Ray powder data of nearly single-phase alloys are presented in Tables 1—4. The powder photographs of all phases, except $Fe_2Si_{0.4}B_{0.6}$, could be indexed. $Fe_3(Si,B)$ has the cementite ($D0_{11}$)-structure, Fe_5SiB_2 is isomorphous with Cr_5B_3 ($D8_l$-type), while $Fe_{4.86}Si_2B$, similar to $Co_{4.7}Si_2B$, crystallizes in the W_5Si_3 ($D8_m$)-structure. The l.p. of the phases in the different three-phase regions (at 975 ± 20°C) are collected in Table 5.

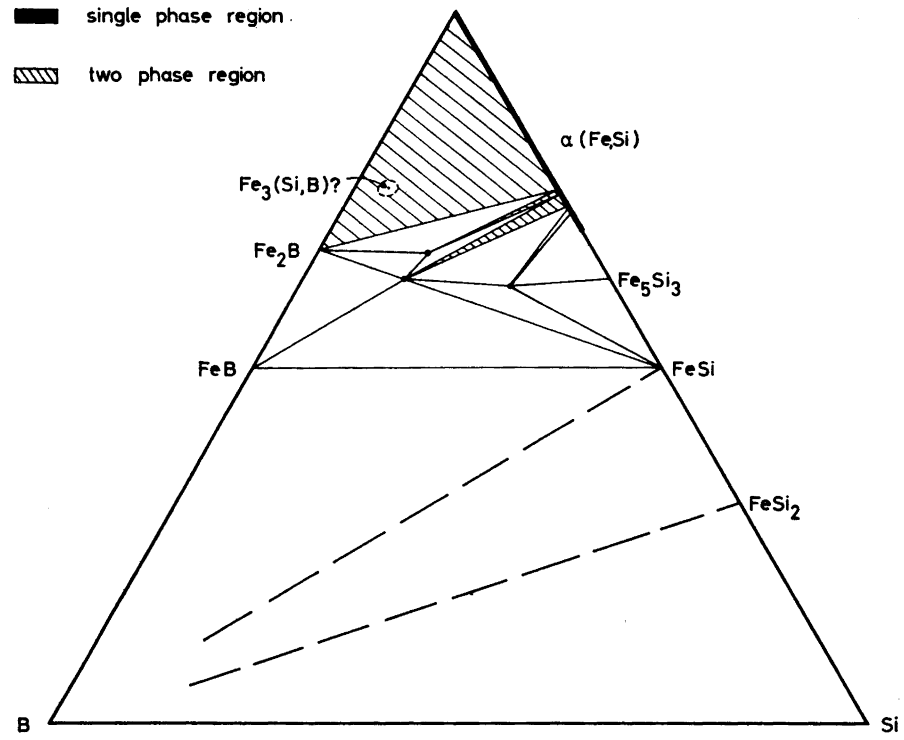

Fig. 2. An outline of the Fe—Si—B system. Most of the two-phase regions are only represented by a line.

Except for Fe_5Si_3 the l.p. of the boundary phases are within 0.1 % equal to those reported for the binary iron-borides and -silicides indicating that the two non-metals do not substitute for each other to any appreciable extent in these phases.

In view of the fact that boron is very little soluble in α- and γ-iron, it seems probable that also its solubility in α(Fe,Si) is very small. This is supported by the observation that Fe_2B is present in metal-rich alloys containing very small amounts of boron. Thus, no great error is likely to be made if the composition of the α(Fe,Si) phase, present in Fe—Si—B alloys, is derived from the l.p. *vs.* composition curve, which Farquhar *et al.*[3] have determined for solid solutions of silicon in α-iron. The composition of α(Fe,Si) in the three-phase equilibria involving this phase are given below

Three phase range	l.p. of α(Fe,Si)	iron content (atom %) of α(Fe,Si)
$Fe_2B + Fe_2Si_{0.4}B_{0.6} + \alpha$(Fe,Si)	$a = 2.826_3$ Å	74.9
$Fe_5SiB_2 + Fe_2Si_{0.4}B_{0.6} + \alpha$(Fe,Si)	$a = 2.826_1$ Å	74.5
$Fe_5SiB_2 + Fe_{4.86}Si_2B + \alpha$(Fe,Si)	$a = 2.821_6$ Å	72.6
$Fe_{4.86}Si_2B + Fe_5Si_3 + \alpha$(Fe,Si)	$a = 2.820_2$ Å	72.0

Table 1. Powder photograph of a sintered alloy, containing Fe_2B and the Fe—Si—B phase isomorphous with cementite. (Cr$K\alpha$-radiation).

hkl	$\sin^2\Theta_{obs}$	$\sin^2\Theta_{calc}$	I_{obs}	$pF^2_{calc} \times 10^{-2}$ for Fe_3C (Ref.[7])
011	—	0.0953	—	0.27
(Fe_2B)	0.1006		st	
101	—	0.1119	—	0.04
020	~0.118	0.1180	vvw	0.16
111	—	0.1414	—	0.16
200	—	0.1845	—	1.2
(Fe_2B)	0.2011		vst	
210	0.2140	0.2140	w+	7.4
121	0.2299	0.2300	st	7.8
201	0.2502	0.2503	m—	6.3
002	0.2630	0.2632	vw	8.2
211	0.2794	0.2798	st	24.8
(Fe_2B)	0.2906		vst	
220	0.3025	0.3025	st+	24.8
102	0.3093	0.3093	st	28.1
(Fe_2B)	0.3240		vvst	
031	0.3313	0.3314	st+	49.0
112	0.3388	0.3388	st	21.1
221	0.3684	0.3683	st	25.9
131	0.3775	0.3775	m	18.3
022	—	0.3812	—	0.92
(Fe_2B)	0.3916		st	
(Fe_2B)	0.4027		m	
122	0.4276	0.4274	st	11.4
202	—	0.4477	—	0.25
230	0.4503	0.4501	w+	7.5
040	0.4721	0.4722	vw	3.4
212	—	0.4772	—	5.9
301	0.4809	0.4809	m	14.6
(Fe_2B)	0.4916		vst	

The l.p. of Fe_5Si_3 are slightly larger in ternary Fe—Si—B alloys than in binary Fe—Si (or ternary Fe—Si—O) alloys, indicating that a small number of boron atoms may be interstitially accomodated in Fe_5Si_3. As pointed out earlier [4], the iron-silicon skeleton of Fe_5Si_3 (Mn_5Si_3 ($D8_8$)-type) contains octahedral holes of convenient size for small non-metal atoms and it seems likely that the boron atom are located in these holes. (It was recently shown [5] that in the isomorphous Mn_5Si_3, the distances from the centre of the "hole" to the surrounding metal atoms is 2.03 Å, which is a short but not unreasonably short Fe—B distance.)

The l.p. variations observed for FeSi and $FeSi_2$ in ternary Fe—Si—B alloys are not greater than those reported for binary FeSi and $FeSi_2$, and thus may be explained as depending on a variation of the Fe/Si ratio in these phases.

As reported in the previous paper [1] a Fe—Si—B phase isomorphous with cementite and tentatively denoted as $Fe_3(Si,B)$ has been identified in metal-rich alloys, sintered at 975°C. A powder photograph of a $Fe_3(Si,B)$ + Fe_2B alloy is given in Table 1. The exact composition of $Fe_3(Si,B)$ and the equilibria

Table 2. Powder photograph of a sintered alloy, containing $Fe_3Si_{0.4}B_{0.6}$, Fe_2B and α(Fe,Si). (Cr$K\alpha$-radiation).

I_{obs}	$\sin^2\Theta_{obs}$	I_{obs}	$\sin^2\Theta_{obs}$	
vw	0.1256	vw	0.3044	
w−	0.1351	vw	0.3058	
vw	0.1626	m+	0.3130	
m	0.1968	w+	0.3242	(Fe_2B)
w	0.2119	st+	0.3287	(α(Fe,Si))
w	0.2147	m−	0.3380	
m	0.2402	st	0.3443	
m	0.2459	st+	0.3592	
m	0.2732	m−	0.3917	
m+	0.2828	m	0.4208	
		w+	0.4424	

in which this phase are involved have not been clarified. The relation between the composition and the l.p. variations displayed by $Fe_3(Si,B)$ is also unknown, although it has been observed [2] that the unit volume increases as the boron content increases.

The composition of the other three ternary phases could be fairly well determined from samples prepared from the master alloys. The compositions

Table 3. Powder photographs of alloys, containing Fe_5SiB_2 and Mn_5SiB_2, respectively *. (Cr$K\alpha$-radiation).

	Fe_5SiB_2			$Mn_5Si_2B_2$			Calculated for Fe_5PB_2 **	
hkl	$\sin^2\Theta_{obs}$	$\sin^2\Theta_{calc}$	I_{obs}	$\sin^2\Theta_{obs}$	$\sin^2\Theta_{calc}$	I_{obs}	I_{calc}	$pF^2 \times 10^{-4}$
002	—	0.0491	—	—	0.0481	—	0.02	0.01
110	0.0850	0.0852	w	0.0833	0.0833	w	0.51	0.61
112	0.1342	0.1342	w+	—	0.1314	—	0.95	1.64
200	0.1703	0.1703	w−	0.1666	0.1667	w−	0.41	0.88
004	0.1963	0.1964	m	0.1926	0.1926	m	1.90	4.66
202	0.2193	0.2194	m−	0.2148	0.2149	m−	1.35	3.68
211	0.2251	0.2252	st	0.2205	0.2204	st	10.2	27.8
114	0.2815	0.2816	st−	0.2759	0.2760	st	7.45	22 0
213	0 3234	0.3234	vst	0.3167	0.3167	vst	21.1	64.4
220	0.3406	0.3406	m+	0.3333	0.3334	m	4.6	13.7
204	0.3669	0.3668	st−	0.3594	0.3593	st	16.0	46.2
222	—	0.3897	—	—	0.3815	—	0.11	0.34
310	0.4423	0.4420	m−	0.4337	0.4334	m−	3.30	7.26

* Only the diffraction lines originating from Fe_5SiB_2 and Mn_5SiB_2 are given in the table. The iron-boron-silicon alloy was a two-phase alloy and contained, besides Fe_5SiB_2, α(Fe,Si) with an observed $\sin^2\Theta$-value for the 110-line of 0.3292. The manganese-boron-silicon alloy was a three-phase alloy, containing Mn_5SiB_2, Mn_5Si_3 and MnB.

** As silicon and phosphorus as well as iron and manganese have very similar scattering factors, we have compared the observed intensities of Fe_5SiB_2 and Mn_5SiB_2 with those calculated for Fe_5PB_2. The structure of the latter phase has been refined from single crystal data by Dr. Rundqvist [6] who was so kind as to put his values at our disposal. In the computations of the $p|F|^2$-values of Fe_5PB_2 the following atomic parameters were used (space-group $I\ 4/mcm$):

16 Fe in 16(l), $x = 0.169_0$, $z = 0.140_5$
4 Fe in 4(c)
8 B in 8(h), $x = 0.37_5$
4 P in 4(a)

and heat-treatments of these samples are given in Table 6. On basis of this information, Fig. 1 has been constructed and the compositions of the ternary phases have been found to be well represented by the formulæ $Fe_2Si_{0.40}B_{0.60}$, $Fe_5Si_{1-x}B_{2+x}$ ($x \sim 0.0$—0.1) and $Fe_{4.86}Si_2B$, respectively.

(Because of the presence of oxygen the amounts of iron, silicon and boron that participate in the Fe—Si—B equilibrium are not likely to be precisely proportional to the total concentration of these elements in a sample as has been assumed in the construction of Fig. 1 and in the determination of the compositions of the ternary phases. The uncertainties in these compositions are larger than the errors in the chemical analyses.)

X-Ray data for $Fe_2Si_{0.4}B_{0.6}$ are given in Table 2. We did not succeed in indexing the powder photograph of this phase and attempts to prepare single crystals were also unsuccessful. $Fe_2Si_{0.4}B_{0.6}$ decomposes at temperatures ~1 100°C and above this temperature there exists a three-phase region $Fe_2B + Fe_5SiB_2 + \alpha$(Fe,Si).

The powder photograph of a $Fe_5SiB_2 + \alpha$(Fe,Si) alloy is given in Table 3 and by assuming Fe_5SiB_2 to possess the Cr_5B_3-structure (as does[6] Fe_5PB_2) good agreement between observed and calculated intensities is obtained. It seems probable that (similar to the situation in Mo_5SiB_2[4] and Fe_5PB_2[6]) the non-metal atoms are ordered in Fe_5SiB_2, the silicon atoms occupying the 4(*a*)-positions and the boron atoms the 8(*h*)-positions. The observed l.p. variations (Table 5) are compatible with the assumption that the homogeneity

Table 4. Powder photograph of an arc-melted alloy with the analyzed composition $Fe_{4.856}Si_{2.043}B_{1.000}$ (sample 4), ($CrK\alpha_1$-radiation).

				I_{calc} (relative) *			$pF^2 \times 10^{-4}$ *		
hkl	$\sin^2\Theta_{obs}$	$\sin^2\Theta_{calc}$	I_{obs}	$Fe_{4.67}Si_2B$	$Fe_{4.86}Si_2B$	Fe_5Si_2B	$Fe_{4.67}Si_2B$	$Fe_{4.86}Si_2B$	Fe_5Si_2B
110	—	0.0339	—	6.1	0.3	0.8	0.23	0.01	0.03
200	—	0.0677	—	0.6	0.1	0.2	0.05	0.01	0.13
220	0.1354	0.1354	m—	15	9	6	2.52	1.63	1.09
211	0.1548	0.1548	w+	6	6	6	1.15	1.15	1.15
310	0.1693	0.1693	st	43	57	63	9.21	12.08	14.45
400	0.2707	0.2709	w	0.9	2.3	3.7	0.28	0.66	1.05
002	0.2808	0.2808	st	65	59	55	19.44	17.71	16.42
321	0.2902	0.2903	vst	141	141	141	42.82	42.82	42.82
330	0.3047	0.3047	st	27	32	36	8.16	9.83	11.16
112	0.3147	0.3146	st—	23	30	36	7.06	9.30	11.10
420	0.3386	0.3386	st+	56	67	76	17.22	20.61	23.26
202	0.3485	0.3485	st	41	50	57	12.22	15.06	17.31
411	0.3579	0.3580	vvst	300	300	300	88.06	88.06	88.06
222	0.4162	0.4162	st+	93	108	120	23.58	27.29	30.20
510	0.4404	0.4402	w—	5.7	2.7	1.1	1.35	0.63	0.28
312	—	0.4501	—	1.4	0.1	0.5	0.31	0.002	0.11
431	0.4937	0.4937	w	16	16	16	3.13	3.13	3.13

* It has been assumed that the metal position in 4(*b*) is occupied to 67, 86 and 100 %, respectively, in $Fe_{4.67}Si_2B$, $Fe_{4.86}Si_2B$ and Fe_5Si_2B, and that the atomic parameters are the same as in $Co_{4.7}Si_2B$ (Ref.[1]).

Table 5. Lattice parameters (in Å) of the various phases in different three-phases regions. The alloys have been prepared by sintering mixtures of the elements at 975°C for 7—10 days.

Three-phase region	Fe_2B	a(Fe,Si)	Fe_5SiB_2	FeB	$Fe_{4.86}Si_2B$	FeSi	Fe_5Si_3	$FeSi_2$	Si
$Fe_2B + Fe_2Si_{0.4}B_{0.6} + a$	$a = 5.109$ $c = 4.249$	$a = 2.826_3$							
$Fe_2B + Fe_2Si_{0.6}B_{0.6} + Fe_5SiB_2$	$a = 5.108$ $c = 4.250$		$a = 5.546$ $c = 10.321$						
$Fe_2B + Fe_5SiB_2 + FeB$	$a = 5.109$ $c = 4.248$		$a = 5.532$ $c = 10.300$	$a = 5.500$ $b = 2.947$ $c = 4.057$					
$Fe_2Si_{0.4}B_{0.6} + a + Fe_5SiB_2$		$a = 2.826_1$	$a = 5.547$ $c = 10.332$						
$Fe_5SiB_2 + Fe_{4.86}Si_2B + a$		$a = 2.821_6$	$a = 5.552$ $c = 10.339$		$a = 8.817$ $c = 4.338$				
$Fe_5SiB_2 + Fe_{4.86}Si_2B + FeSi$			$a = 5.552$ $c = 10.338$		$a = 8.806$ $c = 4.325$	$a = 4.489$			
$Fe_5SiB_2 + FeB + FeSi$			$a = 5.546$ $c = 10.331$	$a = 5.499$ $b = 2.947$ $c = 4.057$		$a = 4.486$			
$Fe_{4.86}Si_2B + Fe_5Si_3 + a$		$a = 2.820_2$			$a = 8.826$ $c = 4.345$		$a = 6.766$ $c = 4.726$		
$Fe_{4.86}Si_2B + Fe_5Si_3 + FeSi$					$a = 8.818$ $c = 4.337$	$a = 4.488$	$a = 6.770$ $c = 4.730$		
$FeSi + FeB + ?$ *				$a = 5.500$ $b = 2.947$ $c = 4.058$		$a = 4.486$			
$FeSi + FeSi_2 + ?$ *						$a = 4.484$		$a = 2.695$ $c = 5.137$	
$FeSi_2 + Si + ?$ *								$a = 2.688$ $c = 5.128$	$a = 5.425$
L.p. of binary phases (ref. 2)	$a = 5.109$ $c = 4.249$			$a = 5.506$ $b = 2.952$ $c = 4.061$		$a = 4.488 - 4.483$	$a = 6.755$ $c = 4.717$	$a = 2.698 - 2.683$ $c = 5.141 - 5.127$	

* Alloys sintered at 1 100°C.

Table 6. Composition and heat-treatment of samples prepared from the master alloys.

Sample	Composition	Heat-treatment	Observed phases
4	% Fe: 79.62 % Si: 16.82 $Fe_{4.856}Si_{2.043}B_{1.060}$ % B: 3.18 Σ *: 99.62	arc-melted	$Fe_{4.86}Si_2B$ (and perhaps a trace of α(Fe,Si))
5	% Fe: 83.60 % Si: 8.54 $Fe_{4.923}Si_{1.001}B_{2.000}$ % B: 6.58 Σ *: 98.72	arc-melted, annealed in evacuated tubes for three days at 1 060°C	Fe_5SiB_2 and a small amount of $Fe_{4.86}Si_2B$. The ratio $Fe_{4.86}Si_2B/Fe_5SiB_2$ is estimated to be not greater than 1/99.
6	% Fe: 84.04 % Si: 8.51 $Fe_{5.152}Si_{1.038}B_{2.000}$ % B: 6.32 Σ *: 98.87	as sample 5	Fe_5SiB_2 + small amounts of α(Fe,Si)
8	% Fe: 85.65 % Si: 8.19 $Fe_{2.000}Si_{0.381}B_{0.607}$ % B: 5.03 Σ *: 98.87	sintered in evacuated silica tubes for 11 days at 1 050°	$Fe_2Si_{0.4}B_{0.6}$ + Fe_2B + + α(Fe,Si)
9	% Fe: 84.90 % Si: 9.27 $Fe_{4.000}Si_{0.435}B_{0.594}$ % B: 4.88 Σ *: 99.05	arc-melted, annealed in evacuated silica tubes for 8 days at 1 040°	$Fe_2Si_{0.4}B_{0.6}$ + α(Fe,Si)

* Samples prepared in exactly the same way as those above were analyzed to contain 0.1 weight % oxygen (arc-melted) to 0.5 weight % oxygen (arc-melted and annealed in silica tubes for 7—10 days), while the carbon content was found to be 0.02—0.03 weight % and the nitrogen content less than 0.001 %. We believe that the figures obtained for the oxygen content are too low (as was also found to be the case when different iron powders were analyzed) and that most of the impurity in the samples is oxygen.

range of Fe_5SiB_2 is associated with a B/Si substitution, the l.p. decreasing with increasing boron content. As the B/Si ratio in silicon-rich Fe_5SiB_2 (as determined from sample 5) is 2.05/1.00, this ratio is greater than 2.00 for all compositions of Fe_5SiB_2. This indicates that the boron atoms may substitute for a fraction of the silicon atoms in the 4(*a*)-positions (which correspond to anti-prismatic holes in the metal atom skeleton) whereas the 8(*h*)-positions (which correspond to smaller triangular prismatic holes in the metal atom skeleton) are only occupied by boron atoms over the whole homogeneity range. The composition of Fe_5SiB_2 may thus be represented by the formula $Fe_5Si_{1-x}B_{2+x}$ ($x \sim 0.0$—0.1).

The arc-melted sample 4 gave a powder photograph on which only the sharp lines originating from $Fe_{4.86}Si_2B$ were observed. As the oxygen content of this sample is very low, it is no doubt that the iron content of $Fe_{4.86}Si_2B$ is lower than that corresponding to the stoichiometric formula Fe_5Si_2B. As pointed out in the previous communication [1], the isomorphous phase $Co_{4.7}Si_2B$

also has a composition deviating from the ideal formula, depending on the fact that the metal position in 4(*b*) is only partially occupied. In Table 4 we have calculated the intensities for the Fe_xSi_2B phase (x = 4.67, 4.86, 5.00) assuming that the 4(*b*) position is occupied by iron atoms to 67, 86 and 100 %, respectively, and that the atomic parameters are the same in $Fe_{4.86}Si_2B$ as in $Co_{4.7}Si_2B$. The marked differences in the observed intensities of 110, 220, 211 and 400 for which $I_{110} << I_{400} < I_{211} < I_{220}$ is in good agreement with the intensities calculated for $Fe_{4.86}Si_2B$ but hardly with those calculated for $Fe_{4.67}Si_2B$ and Fe_5Si_2B. Thus, the X-ray data of $Fe_{4.86}Si_2B$ are not inconsistent with the assumption that the deviation from stoichiometry of this phase depends on the 4(*b*) positions being only partially occupied by iron-atoms. The observed l.p. variations of $Fe_{4.86}Si_2B$ (Table 5) indicates that the homogeneity range of $Fe_{4.86}Si_2B$ may mainly depend on a variation of the number of vacant 4(*b*) positions.

The Fe—Si—B system is of interest since it contains one representative for each of the three common Me_5Si_3 structure types, in which a number of transition metal silicides and silico-borides have been found to crystallize. These structure types are discussed in a recent review article [2] and, therefore, will not be commented on in this paper. It is noteworthy, however, that the variation in composition displayed by $Fe_5Si_3(B)$, Fe_5SiB_2 and $Fe_{4.86}Si_2B$ seems to have quite different causes. In $Fe_5Si_3(B)$ a varying number of boron atoms are interstitially dissolved in the iron-silicon skeleton, in Fe_5SiB_2 the extended homogeneity range is mainly associated with a B/Si substitution, while in $Fe_{4.86}Si_2B$ one of the iron positions is occupied to a varying degree.

The Mn—Si—B system. Our qualitative study of the Mn—Si—B system only aimed at seeing to which extent this system displays similarities to the more comprehensively investigated Fe—Si—B and Co—Si—B systems.

The metal-rich part of the Mn—Si—B system seems to be much more complicated than is the case in the Fe—Si—B and Co—Si—B systems. We found no Mn—Si—B phase isomorphous with $Fe_{4.86}Si_2B$ and $Co_{4.7}Si_2B$, but in alloys sintered at 900—1 000°C, a phase with the Cr_5B_3 structure was identified (Table 3) and this phase is tentatively denoted as Mn_5SiB_2.

The equilibria in the non-metal-rich part of the Mn—Si—B system are also different from those in the Fe—Si—B and Co—Si—B system. Thus, the boron-rich manganese borides Mn_3B_4 and MnB_2 seem to be in equilibrium with silicon, whereas in the other systems no boride is stable in the presence of silicon.

Acknowledgements. We wish to thank Professor G. Hägg for his kind interest in this work and for the facilities put at our disposal. We are also much indebted to the Head of the analytical department of this Institute, Dr. F. Nydahl, and to Dr. Lilly Gustafsson for her courtesy in carrying out the chemical analyses. We want to thank Dr. J. Baecklund and Mr. E. Gunnarsson at Avesta Jernverk for help with the oxygen, nitrogen and carbon analyses.

Many thanks are due to Miss B. Pettersson and Mr. S. Wahlgren for excellent technical assistance.

We sincerely acknowledge financial support from the *Air Force Office of Scientific Research and the Research and Development Command, United States Air Force,* through its European Office under Contract No. AF 61(052)—40 and from the *Swedish State Council of Technical Research.*

REFERENCES

1. Aronsson, B. and Lundgren, G. *Acta Chem. Scand.* **13** (1959) 433.
2. Aronsson, B. *Arkiv Kemi* **16** (1960) 379.
3. Farquhar, M. C., Lipson, H. and Weill, A. R. *J. Iron Steel Inst.* **152** (1945) 457.
4. Aronsson, B. *Acta Chem. Scand.* **12** (1958) 31.
5. Aronsson, B. *Ibid.* **14** (1960) 1414.
6. Rundqvist, S. *Private communication.*
7. Lipson, H. and Petch, N. J. *J. Iron Steel Inst.* **142** (1940) 95.

Received July 1, 1960.

ACTA CHEMICA SCANDINAVICA 14 (1960) 1414–1418

A Note on the Compositions and Crystal Structures of MnB_2, Mn_3Si, Mn_5Si_3 and $FeSi_2$

BERTIL ARONSSON

Institute of Chemistry, University of Uppsala, Uppsala, Sweden

The existence of a manganese diboride, MnB_2, with the AlB_2-structure has been confirmed. Faint super-structure lines on the powder photographs of alloys containing Mn_3Si indicate that in this phase, as in Fe_3Si, some ordering of the silicon and metal atoms takes place at temperatures below 1 000°C. The reported crystal structures of Mn_5Si_3 and $FeSi_2$ have been confirmed and refined with single crystal data.

In connection with investigations on the Mn—Si—B and Fe—Si—B systems [1] some crystallographic studies of the binary phases MnB_2, Mn_3Si, Mn_5Si_3, and $FeSi_2$ were made. It was found appropriate to present the results (which are commented on in a recent review article [2]) in a separate paper.

EXPERIMENTAL

The alloys were prepared by arc-melting or sintering mixtures of the elements. The same chemicals were used as in the study [1] of the Mn—Si—B and Fe—Si—B systems, and the chemical analyses for silicon and boron were also carried out in the same way. Manganese was determined by the bismuthate method after the sample had been dissolved in HF + HNO_3, the hydrofluoric acid removed by evaporating with sulfuric acid, and the solution passed through a cadmium reductor. The accuracy of the manganese analyses is estimated to be ± 0.2 %.

Powder photographs were taken in cameras of the Guinier type with silicon (a = 5.4306 Å) as internal standard for the l.p. (lattice parameter) determinations. Single crystals of Mn_5Si_3 and $FeSi_2$ with cross-sections of about 0.02 mm were examined in a Weissenberg camera. The multiple film technique was used and the intensities were visually estimated. The atomic scattering factors were taken from the tables by Tomas and Umeda [3] (manganese, iron), Tomiie and Stam [4] (silicon) and Ibers [5] (boron). The final structure factors for Mn_5Si_3 were computed on the digital electronic computer BESK with a program devised by Åsbrink *et al.*[6] The scattering factors were approximated with the formula:

$$f_i = A_i \exp(-a_i/\lambda^2\sin^2\Theta) + B_i \exp(-b_i/\lambda^2\sin^2\Theta) + C_i \exp(-c_i/\lambda^2\sin^2\Theta) + D_i$$

On basis of the above mentioned structure factor tables, Appel [7] has calculated the following constants:

	A	B	C	a	b	c
Mn	8.630	9.427	6.744	0.345	3.724	26.541
Si	2.8315	6.8065	4.3870	0.3235	2.2965	51.770

The real part of the dispersion correction, (D_i in the above expression) for manganese was taken from the tables by Dauben and Templeton [8]. No corrections were made for extinction or absorption.

RESULTS

MnB_2. Arc-melted manganese-boron alloys with a boron content higher than 67 atom per cent gave a powder photograph that could be indexed with a small hexagonal cell. From the unit cell dimensions it was evident that the photograph originated from a phase isomorphous with AlB_2, and with this assumption excellent agreement between observed and calculated intensities was obtained (see Table 1). The l.p. of MnB_2, $a = 3.009$ Å, $c = 3.039$ Å, agree very well with those recently reported by Binder and Post [9] who found $a = 3.007$ Å and $c = 3.037$ Å. No variations greater than 0.05 % were observed for the l.p. of MnB_2 in alloys with compositions from $MnB_{1.7}$ to MnB_3, which indicates that the homogeneity range of MnB_2 is narrow. An alloy containing small amounts of Mn_3B_4 was analysed to contain 70.71 (± 0.15) % manganese and 28.12 (± 0.15) % boron most of the remainder very probably being oxygen. Thus, the atomic ratio B/Mn in this sample is 2.019/1.000, indicating that the composition of the manganese diboride is about $MnB_{2.05}$. However, if it is assumed that the oxygen present in the sample is bound to boron as B_2O_3, the composition of the manganese boride is found to correspond to the formula $MnB_{2.01}$, not significantly deviating from the stoichiometric formula $MnB_{2.00}$. Interatomic distances in MnB_2 are collected in Table 2.

Mn_3Si. The simple body-centered cubic structure of Mn_3Si was determined by Laves [10] who found the manganese and silicon atoms to be statistically distributed in the structure. The powder photographs of alloys sintered at 950°C and containing Mn_3Si and Mn_5Si_3 showed some faint lines the positions and intensities of which could be satisfactorily accounted for by assuming the atoms in Mn_3Si to be ordered. Thus, it seems very likely that, similar to the situation in Fe_3Si, the distribution of metal and silicon atoms in Mn_3Si becomes ordered at lower temperatures. The cube-edge of Mn_3Si as determined is this study is 5.722 Å (2 × 2.861) in reasonable agreement with the older values 2.85 Å[10] and 2.857 Å[11].

Mn_5Si_3. The approximate formula of Mn_5Si_3 was determined by Vogel and Bedarff [12] and was confirmed by Åmark *et al.*[11] who also solved the crystal

Table 1. Powder photograph (Cu$K\alpha$) of an arc-melted alloy with the nominal composition MnB_2.

hkl	$\sin^2\Theta_{obs}$	$\sin^2\Theta_{calc}$	I_{obs}	I_{calc}	$pF^2_{calc} \times 10^{-2}$
001	0.0646	0.0644	w	4.7	3.84
100	0.0876	0.0875	st	13.6	16.0
101	0.1519	0.1519	vst	24.1	45.4
002	0.2574	0.2574	vw	2.5	7.16
110	0.2625	0.2625	m	7.3	21.1
111	0.3270	0.3269	vw	4.3	13.4
102	0.3448	0.3449	w	5.9	17.5
200	0.3501	0.3501	vw	2.9	8.70
201	0.4145	0.4144	m	10.3	26.1

Table 2. Interatomic distances in MnB_2 (in Å).

Mn— 8Mn: 3.01(6), 3.04(2)	B—6Mn: 2.31(6)
—12B : 2.31(12)	—3B : 1.74(3)

structure of Mn_5Si_3. The chemical and X-ray analyses of two arc-melted alloys with compositions approximating to Mn_5Si_3 gave the following results

% Mn	% Si	Σ	atomic composition	observed phases	l.p. of Mn_5Si_3
76.61	22.15	98.76	$Mn_5Si_{2.83}$	Mn_5Si_3 and small amounts of Mn_3Si	$a = 6.910$ Å $c = 4.814$ Å
75.94	23.45	99.39	$Mn_5Si_{3.02}$	Mn_5Si_3 and traces (~ 1 %) of MnSi	$a = 6.910$ Å $c = 4.814$ Å

No l.p. variations could be observed for Mn_5Si_3, indicating that its homogeneity range is small. The results of the chemical analyses show that the composition closely corresponds to the stoichiometric formula.

The crystal structure of Mn_5Si_3 was refined from single crystal data. The space-group $P6_3/mcm$ derived by Åmark *et al.*[11] was confirmed and, starting with the atomic parameters given by these authors, the atomic parameters were refined from successive $\varrho_o(xz)$ and $\varrho_o(xz)$—$\varrho_c(xz)$ syntheses until the final back-shift corrections were less than half the standard deviation as estimated with Cruickshank's formula [18]. The final parameters are as follows:

4 Mn in 4(*d*)
6 Mn in 6(*g*) $x = 0.2358 \pm 0.0006$
6 Si in 6(*g*) $x = 0.5992 \pm 0.0015$

The final *R*-value for 51 observed *h*0*l*-reflexions was 8.0 % when an empirical isotropic temperature factor with $B = 0.34_0$ Å^2 had been applied. Observed and calculated structure factors are collected in Table 3 and interatomic distances are given in Table 4. In the last difference synthesis a negative region was observed at the silicon position, indicating that the scattering parameter of the atom in this position is slightly less (about 1 electron) than had been assumed. The experimental data, however, are hardly so accurate that this effect can be regarded as significant.

$FeSi_2$. Phragmén [14] has suggested a very simple structure for this phase, the homogeneity range of which does not include the stoichiometric composition. Phragmén's observations that $FeSi_2$ is tetragonal and that there is one formula unit in the elementary cell were corroborated. There are no systematic extinctions and thus the most symmetrical possible space-group is *P*4/*mmm*. During the refinement no evidence was found indicating that a space-group of lower symmetry should be chosen. The distribution of intensities showed that the structure proposed by Phragmén [13] was approximately correct and starting with his parameter for the silicon atom in 2(*h*) the $\varrho(xz)$ electron density projection was refined by successive F_o and F_o—F_c syntheses. The following atomic and scattering parameters were found for a crystal picked out of an alloy which contained $FeSi_2$ with the l.p. $a = 2.684$ and $c = 5.128$ Å.

	atomic par.	scattering par.
Fe(?) in 1(*a*)		24.0_5
2 Si in 2(*h*)	$z = 0.270_0$	14.0

Table 3. Observed and calculated structure factors for Mn_5Si_3. (A temperature factor with $B = 0.34_0$ Å^2 has been applied to the F_c-values.)

hkl	F_o	F_c	*hkl*	F_o	F_c
1 0 0		— 7.2	8 0 2	— 61.7	— 67.3
2 0 0	— 50.5	— 46.7	9 0 2		— 2.2
3 0 0	107.3	112.9	10 0 2	— 22.4	— 25.1
4 0 0	50.2	46.2	11 0 2		— 0.5
5 0 0	71.7	63.2	12 0 2		— 5.9
6 0 0	26.6	20.6	13 0 2	— 39.2	— 35.3
7 0 0		— 5.1	14 0 2		— 8.3
8 0 0	39.3	37.7	15 0 2		11.8
9 0 0	58.2	59.9	0 0 4	171.3	168.5
10 0 0		2.3	1 0 4		— 4.0
11 0 0	— 18.9	— 21.2	2 0 4	— 29.7	— 25.0
12 0 0	52.6	44.6	3 0 4	74.9	74.8
13 0 0	29.6	20.0	4 0 4	34.5	32.2
14 0 0		— 6.0	5 0 4	42.1	46.1
15 0 0	18.4	13.5	6 0 4		16.2
0 0 2	—107.1	— 93.4	7 0 4		— 5.1
1 0 2	— 80.2	— 67.7	8 0 4	29.9	30.4
2 0 2	— 32.8	— 28.8	9 0 4	51.8	50.7
3 0 2	22.5	21.3	10 0 4		0.0
4 0 2	— 95.8	— 94.1	11 0 4		— 18.4
5 0 2	— 94.7	—104.2	12 0 4	44.1	38.6
6 0 2	56.2	62.0	13 0 4		17.4
7 0 2	— 32.6	— 30.4	14 0 4		— 5.3
15 0 4		11.9	7 0 8		— 4.8
0 0 6	— 36.5	— 44.9	8 0 8	16.3	18.2
1 0 6	— 31.3	— 29.5	9 0 8	36.4	33.3
2 0 6	— 14.9	— 15.1	10 0 8		— 1.0
3 0 6		11.9	11 0 8		— 12.4
4 0 6	— 51.4	— 54.8	12 0 8	25.4	26.9
5 0 6	— 60.8	— 62.0	0 0 10		— 25.6
6 0 6	41.0	39.8	1 0 10	— 16.5	— 17.4
7 0 6	— 15.8	— 19.2	2 0 10		— 8.4
8 0 6	— 46.4	— 45.8	3 0 10		8.0
9 0 6		— 2.1	4 0 10	30.9	— 30.1
10 0 6	— 16.5	— 17.1	5 0 10	— 31.6	— 31.4
11 0 6		— 0.7	6 0 10	21.6	21.8
12 0 6		— 4.2	7 0 10		— 10.1
13 0 6	— 28.9	— 27.9	8 0 10	— 26.9	— 26.6
14 0 6		— 6.5	9 0 10		— 1.5
0 0 8	70.8	80.4	10 0 10		— 9.9
1 0 8		1.2	0 0 12	41.6	39.2
2 0 8		— 15.2	1 0 12		— 0.3
3 0 8	35.7	37.8	2 0 12		— 8.8
4 0 8		18.4	3 0 12		18.8
5 0 8		22.8	4 0 12		9.9
6 0 8		10.3	5 0 12		10.9

The final R-value for the 33 observed $h0l$-reflexions was 7.4 % after an empirical isotropic temperature factor with $B = 0.40_3$ Å^2 had been applied. Interatomic distances are collected in Table 5. The scattering parameter of the atom in 1(a) is (probably significantly) less than 26/14 of that of the atom in 2(h). This indicates that the former position is not completely occupied by

Table 4. Interatomic distances in Mn_5Si_3 (in Å).

			Average
Mn_I in 4(*d*)	— 2 Mn_I	: 2.41 (2)	
	— 6 Mn_{II}	: 2.96 (6)	2.82
	— 6 Si	: 2.43 (6)	
Mn_{II} in 6(*g*)	— 4 Mn_I	: 2.96 (4)	
	— 6 Mn_{II}	: 2.82 (2), 2.91 (4)	2.91
	— 5 Si	: 2.41 (2), 2.51, 2.66 (2)	2.53
Si in 6(*g*)	— 4 Mn_I	: 2.43 (4)	
	— 5 Mn_{II}	: 2.41 (2), 2.51, 2.66 (2)	2.49
	— 2 Si	: 2.77 (2)	

Table 5. Interatomic distances in $FeSi_2$ (in Å).

Fe — 4Fe:	2.68 (4)	Si — 4Fe:	2.35 (4)
— 8Si:	2.35 (8)	— 6Si:	2.36, 2.68(4), 2.77

iron atoms which is consistent with the observation that the iron content of $FeSi_2$ does not attain 33 atom per cent. Siborenko, *et al.*[15] have shovn that the deviation from stoichiometry is very likely associated with a fraction of the iron positions being vacant.

Acknowledgements. I want to express my gratitude to Professor Hägg for his kind interest in this work and for the facilities he has put at my disposal. The chemical analyses were carried out at the analytical department of this Institute and I wish to thank the Head of this department, Dr. F. Nydahl, as well as Dr. L. Gustafsson.

I sincerely acknowledge financial support from the *Air Force Office of Scientific Research and the Research and Development Command, United States Air Force* through its European Office under Contract No. AF 61(052)—40 and from the *Swedish State Council of Technical Research.* Facilities for use of the electronic digital computer BESK were given by the *Swedish Board for Computing Machinery.*

REFERENCES

1. Aronsson, B. and Engström, I. *Acta Chem. Scand.* **14** (1960) 1403.
2. Aronsson, B. *Arkiv Kemi* **16** (1960) 379.
3. Thomas, L. H. and Umeda, K. *J. Chem. Phys.* **26** (1957) 293.
4. Tomiie, Y. and Stam, C. H. *Acta Cryst.* **11** (1958) 126.
5. Ibers, J. A. *Ibid.* **10** (1957) 86.
6. Åsbrink, S., Blomqvist, G. and Westman, S. *Arkiv Kemi* **14** (1959) 545.
7. Appel, K. *Technical Note from the Quantum Chemistry Group,* University of Uppsala.
8. Dauben, C. H. and Templeton, D. H. *Acta Cryst.* **8** (1955) 841.
9. Binder, I. and Post, B. *Ibid.* **13** (1960) 356.
10. Laves, F. *Z. Krist.* **89** (1934) 189.
11. Åmark, K., Borén, B. and Westgren, A. *Svensk Kem. Tidskr.* **48** (1936) 273.
12. Vogel, R. and Bedarff, H. *Arch. Eisenhüttenwes.* **7** (1933—34) 423.
13. Cruickshank, D. W. J. *Acta Cryst.* **2** (1949) 65.
14. Phragmén, G. *Jernkontorets Ann.* **107** (1923) 121.
15. Siborenko, F. A., Gel'd, P. V. and Dubrovskaya, L. B. *Fiz. Metal. i Metalloved.* **8** (1959) 735.

Received July 1, 1960.

ACTA CHEMICA SCANDINAVICA 14 (1960) 1419–1423

Synthetic Aminosugar Derivatives as Potential Antimicrobials; N-Substituted Derivatives of 6-Amino-6-Deoxy-D-glucose Ethylene Dithioacetal

ALF WICKSTRØM and JENS KRISTIAN WOLD

Universitetets Farmasøytiske Institutt, Blindern-Oslo, Norway

A series of N-substituted derivatives of 6-amino-6-deoxy-D-glucose ethylene dithioacetal has been prepared and tested as antimicrobials.

The occurrence of aminosugars is a general characteristic of the structures of several antibiotics [1,2]. Recent developments in the chemistry of antibiotics, therefore, have stimulated the interest in synthetic aminosugar derivatives as potential antimicrobials.

In some of the antibiotics the aminogroup is found in position 3 of the sugar moiety in question. Thus, 3-amino-3-deoxy-D-ribose is the carbohydrate component of puromycin, and rare 3-dimethylamino-hexoses (desosamine, mycaminose) occur in the so-called macrolide antibiotics. Streptomycin is a well-known example of an antibiotic containing a 2-aminosugar (2-methylamino-2-deoxy-L-glucose) and an ω-aminosugar (6-amino-6-deoxy-D-glucose) occurs in the recently described antibiotic kanamycin [3].

Among these aminosugars constituting a part of the specific structure of antibiotics, 6-amino-6-deoxy-D-glucose is of interest because of the possibility of replacing its terminal primary aminogroup by a variety of amine components according to known synthetic methods [4]. The 6-amino-6-deoxy-D-glucose derivatives described in the present work have a tertiary aminogroup linked to carbon 6 and their reducing function blocked in a cyclic dithioacetal group, these features creating a structure which may be expected not to fit into the pattern of the general metabolism of D-glucose. In order to obtain some information about the possible antimicrobial effect of compounds possessing this structure only a short series of derivatives has been prepared, Table 1. One reason for choosing the ethylene dithioacetal group to block the reducing function was that derivatives of 1,3-dithiolane apparently have received some attention as fungicides [5].

Table 1. Analysis of the synthesized N-substituted derivatives of 6-amino-6-deoxy-D-glucose ethylene dithioacetal.

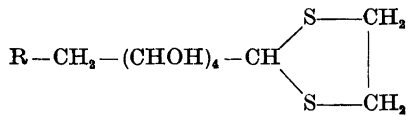

R	m.p. °C	$[\alpha]_D^{23}$ in chloroform	Elementary analysis				
				% C	% H	% N	% S
A. Piperidino-	104–105	−24.1°	found	48.71	7.73	4.40	19.64
		(*c*=2)	calc.	48.27	7.79	4.33	19.83
B. Morpholino-	120–121	− 6.9°	found	44.52	7.13	4.38	20.04
		(*c*=2)	calc.	44.29	7.12	4.31	19.71
C. Pyrrolidino-	113–114	−18.2°	found	46.64	7.51	4.62	20.72
		(*c*=2)	calc.	46.58	7.49	4.53	20.73
D. Dibenzylamino-	137–138	+4.9°	found	60.70	6.68	3.23	14.54
		(*c*=3.8)	calc.	60.68	6.71	3.22	14.72

The compounds listed in Table 1 were tested by the "agar cup" method against a selection of pathogenic bacterium strains (*Pseudomonas aeruginosa, Escherichia coli, Staphylococcus aureus, Streptococcus faecalis*) growing on 10 % peptone-free horse-blood agar, and found to be without antibacterial activity. The same substances were also tested against a selection of pathogenic fungus strains (*Candida albicans, Cryptococcus neoformans, Aspergillus flavus, Aspergillus niger, Trichophyton mentagrophytes*) using the same experimental technique (10 % peptone-free horse-blood agar containing 1 % of D-glucose). The results were in most cases completely negative as to antifungal activity. But two of the compounds of Table 1, A and C, were able at a high concentration (1 %) to inhibit the growth of the highly resistant fungus strains *Cryptococcus neoformans* and *Aspergillus niger*. Since the parent nitrogen-free sugar derivative, D-glucose ethylene dithioacetal [6], was inactive towards all the microorganisms tested, the observed activity of substances A and C (Table 1) should encourage further research on aminosugar derivatives of a structure corresponding to the pattern outlined in the present work.

The synthesis of each of the compounds listed in Table 1 was achieved by classical reactions using 5,6-anhydro-1,2-*iso*-propylidene-D-glucofuranose as starting material: after opening of the epoxide ring by various amines, the *iso*propylidene residue was removed under mild conditions and the resulting aminosugar (without isolation) condensed with ethane-1,2-dithiol. The starting material was prepared from 1,2-*iso*propylidene-D-glucofuranose obtainable either from 1,2-5,6-di-*iso*propylidene-D-glucofuranose or direct from D-glucose. The modification of the direct method [7] described in the experimental section gave in repeated experiments a satisfactory yield of pure 1,2-*iso*propylidene-D-glucofuranose.

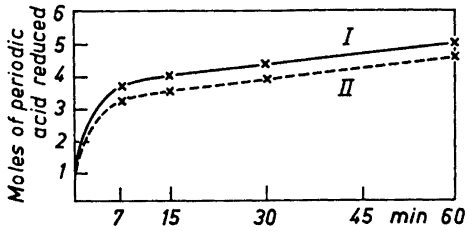

Fig. 1. Periodate uptake in acid solution of D-glucose ethylene dithioacetal, curve I, and of the corresponding 6-amino-6-deoxy-derivatives of Table 1, curve II. Curve II represents the arithmetic mean of the titrations of all four compounds of Table 1, the average deviation of a single measurement at each time interval being 1 % or less. Experimental conditions: 10^{-5} mole of each substance (1 ml) + 10^{-4} mole of sodium metaperiodate (10 ml) + 1 N sulphuric acid (5 ml). Periodate uptake by iodometry.

The opening of the epoxide ring of 5,6-anhydro-1,2-*iso*propylidene-D-glucofuranose by the various amines is, according to the theory [8], expected to proceed as a nucleophilic attack exclusively on carbon 6 and without inversion on carbon 5. Oxidation of the final products (of Table 1) with periodate gave results which tend to confirm that the aminogroup — as predicted by the general reaction mechanism — is located in position 6 of the sugar derivatives prepared.

In strongly acid solution α-amino-alcohols are oxidized by periodate at a considerably slower rate than the corresponding α-glycols [9]. A comparison between the oxidation in acid solution of D-glucose ethylene dithioacetal and the corresponding 6-aminoderivatives (of Table 1) gave results as shown in Fig. 1. The aminosugar derivatives consume about half a molecule of periodate less than the corresponding unsubstituted D-glucose mercaptal and, in contrast to the latter, they do not liberate formaldehyde at the end of one hour's oxidation (colorimetry with chromotropic acid [10]). These results are consistent with the expected effect of the replacement of the hydroxyl group on carbon 6 by an aminogroup, which is to render one carbon to carbon bond (C_6—C_5) more resistant towards periodate in acid solution. The periodate uptake (Fig. 1) is however, always higher than the quantity required to split the α-glycol groups of the compounds studied. A similar over-oxidation of non-cyclic sugar mercaptals has been observed previously [11].

EXPERIMENTAL

All melting points are micro melting points (Kofler's hot-stage microscope).

1. *1,2-Isopropylidene-D-glucofuranose.* D-Glucose (50 g) is shaken for 3—4 h with acetone (1 litre) containing concentrated sulphuric acid (40 ml). After filtration the reaction mixture is neutralized with sodium carbonate monohydrate (100 g) dissolved in water (200 ml). Solid material is removed by filtration and the filtrate concentrated at reduced pressure to 150—200 ml. The solution is heated to 60° and acidified by concentrated hydrochloric acid (about 0.5 ml); the colour of the solution changes from yellowish brown to brown upon acidification. One minute after the acid has been added the solution is cooled and extracted with chloroform (3 × 25 ml), which removes remaining diacetone-glucose and impurities. The colourless aqueous layer is neutralized to pH about 8

by means of a little sodium carbonate solution and then concentrated to dryness at a temperature below 40°. The residue is dried (15 mm Hg, P_2O_5) and then extracted with methanol (30°—40°) which on cooling gives crude, crystalline 1,2-*iso*propylidene-D-glucofuranose, m.p. 150°—160°, yield 50 %. Purification to m.p. 160—161°[7] by recrystallizations from light petroleum (b.p. 60°—80°).

2. *5,6-Anhydro-1,2-iso*propylidene-D-*glucofuranose.* 1,2-*Iso*propylidene-D-glucofuranose was tosylated[12,13] and the 6-tosyl-derivative (m.p. 106°) converted[14,15] into 5,6-anhydro-1,2-*iso*propylidene-D-glucofuranose (m.p. 133°—134°).

3. *Opening of the epoxide ring with amines.* 5,6-Anhydro-1,2-*iso*propylidene-D-glucofuranose (2×10^{-2} mole) dissolved in anhydrous methanol (75 ml) is poured into a solution of 4×10^{-2} mole of the amine in the same solvent (30 ml). Allow to react for half an hour and complete the reaction by smooth reflux for 2 h. The solvent and the majority of the unreacted amine are removed at reduced pressure below 50°. The residual syrups crystallize when kept in a vacuum over P_2O_5. The products were purified by recrystallization from light petroleum (b.p. 60°—80°). Yields 60 to 80 %. Melting points, optical rotations, and the results of potentiometric titration of the various N-substituted 6-amino-6-deoxy-1,2-*iso*propylidene-D-glucofuranoses are enumerated below; the parent amine in brackets: [1: (piperidine) 109—110°; $[\alpha]_D^{20} = +2.8°$ (chloroform, $c = 5$); 98,8 %. [2: (morpholine) 99.5°; $[\alpha]_D^{20} = +7.1°$ (water, $c = 5$); 99.4 %. [3: (pyrrolidine) 92—93°; $[\alpha]_D^{20} = +10.3°$ (water, $c = 5$); 98,0 %. [4. (dibenzylamine) 114—115°; $[\alpha]_D^{20} = +35.6°$ (chloroform, $c = 3.5$); 99.1 %.

The potentiometric titrations were carried out in aqueous solution except for the dibenzylamine derivative which was titrated with perchloric acid in a solution of acetic acid and dioxane.

Two of the four compounds listed above (Nos. 1 and 4) have been described previously by Ohle *et al.*[4]. The melting point (133°) and the optical rotation, $[\alpha]_D^{21} = +1.5°$ (chloroform, $c = 4.41$), attributed to 6-dibenzylamino-6-deoxy-1,2-*iso*propylidene-D-glucofuranose by these authors differ widely from the data recorded in the present work. The substance in question (No. 4) was therefore submitted to a degradation by periodate which gave results in complete agreement with the formula of 6-dibenzylamino-6-deoxy-1,2-*iso*propylidene-D-glucofuranose: In alcaline solution (pH 8) it reduced one molecule of periodate and gave rise to dibenzylamine (detected by paper chromatography) and a reducing compound which on chromatograms (solvent system: acetone, *n*-propanol, water 45:45:10 v/v)) could not be distinguished from 5-aldo-1,2-*iso*propylidene-D-xylofuranose[16] obtained by oxidation of 1,2-*iso*propylidene-D-glucofuranose by periodate (spots, $R_F^{20} = 0.83$, revealed by silver nitrate and ethanolic sodium hydroxide[17]). Further, after removal of the *iso*propylidene residue by mild hydrolysis, our dibenzylamine derivative reduced in acid solution one molecule of periodate less than D-glucose, as expected for an ω-amino-glucose.

4. *Conversion of the N-substituted derivatives of 6-amino-6-deoxy-1,2-iso*propylidene-D-*glucofuranose to the corresponding derivatives of 6-amino-6-deoxy-*D-*glucose ethylene dithioacetal.* Removal of the *iso*propylidene residue is achieved by hydrolysis at room temperature (controlled by paper chromatography): 2×10^{-2} mole of each of the products described above (3) are dissolved in 1 N hydrochloric acid (150 ml) and kept for three days. The hydrolysate is concentrated at reduced pressure (bath temperature below 30°) to 10—15 ml and then completely saturated with HCl gas under cooling in crushed ice. Ethane-1,2-dithiol (equimolecular quantity + 10 % excess) is then added and the mixture is shaken under continuous cooling until it becomes homogeneous. After standing for 2 h in the ice bath the faintly yellow solution is poured into water (100 ml) and left over night. The mixture is made weakly alkaline with 2 N sodium hydroxide and extracted with chloroform (4×200 ml). The combined chloroform extracts are dried (sodium sulphate) and concentrated to dryness at 20°. The partly crystalline residue is (after drying in vacuum over silica gel) recrystallized from benzene. The products are further purified by recrystallization from acetone-ether mixtures. Substance remaining in the mother liquids may be recovered by precipitation with light petroleum (b.p. 60°—80°). Yields are in the range of 50 % of the theoretical. Analysis and properties of the products are summarized in Table 1.

The microbiological tests were carried out at the Department of Bacteriology (head: Dr. Ole G. Clausen) at Universitetets farmasøytiske institutt, Oslo. The authors are indebted to Mr. E. Manser, E.T.H., Zürich, for performing the elementary micro analyses. Gratitude is also expressed to *Norges Almenvitenskapelige Forskningsråd* for the award of a Research Fellowship to one of us (J.K.W.).

REFERENCES

1. Chain, E. B. *Proc. 4th Intern. Congr. Biochem.* 1958, XIV, 170.
2. Brink, N. G. and Harman, R. E. *Quart. Revs.* **12** (1958) 93.
3. Cron, M. J., Farding, O. B., Johnson, D. L., Schmitz, H., Whitehead, D. F., Hooper, I. R. and Lemieux, R. U. *J. Am. Chem. Soc.* **80** (1958) 2342.
4. Ohle, H., Euler, E. and Malerczyk, W. *Ber.* **69** (1936) 1636.
5. Harris, J. F., Jr. *Chem. Abstr.* **52** (1958) 17289; U.S. 2839 445 (1958).
6. Lawrence, W. T. *Ber.* **29** (1896) 547.
7. Mehltretter, C. L., Alexander, B. H., Mellies, R. L. and Rist, C. E. *J. Am. Chem. Soc.* **73** (1951) 2424.
8. Parker, R. E. and Isaacs, N. S. *Chem. Revs.* **59** (1959) 737.
9. Fleury, P., Courtois, J. and Grandchamps, M. *Bull. soc. chim. France* **16** (1949) 88.
10. Mitchell, W. E. A. and Percival, E. *J. Chem. Soc.* **1954** 1423.
11. Hough, L. and Taha, M. I. *J. Chem. Soc.* **1957** 3994.
12. Ohle, H. and Dickhäuser, E. *Ber.* **58** (1925) 2602.
13. Szabolcs, O. and Prey, V. *Monatsh.* **85** (1957) 1112.
14. Ohle, H. and v. Vargha, L. *Ber.* **62** (1929) 2435.
15. Danilov, S. N. and Lishanskii, I. S. *J. Gen. Chem. (U.S.S.R.)* **21** (1951) 366.
16. Iwadare, K. *Bull. Chem. Soc. Japan* **16** (1941) 40.
17. Trevelyan, W. E., Procter, D. P. and Harrison, J. S. *Nature* **166** (1950) 444.

Received March 9, 1960.

ACTA CHEMICA SCANDINAVICA 14 (1960) 1424—1431

Mechanical Losses of Polystyrenes with Different Molecular Weight Distributions

HILDING HÖGBERG,* STUART E. LOVELL, and JOHN D. FERRY

Department of Chemistry, University of Wisconsin, Madison, Wisconsin, U.S.A.

Dynamic mechanical measurements have been made on two polystyrene samples with sharp molecular weight distributions and one with a broad distribution, at temperatures and frequencies corresponding to the plateau zone where the mechanical losses pass through minima. The losses are calculated in terms of the loss compliance J'', loss modulus G'', and loss tangent tan δ. For the sharp distributions, the minima in G'' and tan δ increase in magnitude and shift to higher frequencies with decreasing molecular weight; the frequency dependences of all three loss functions agree approximately with the predictions of a new theory of Marvin, with the molecular weight between entanglement coupling points chosen as 24 000. The results for the broad distribution indicate that molecular weight heterogeneity increases tan δ and J'' but decreases G''.

It is well known that the viscoelastic properties of polymers depend strongly on molecular weight distribution in the terminal zone of the time scale, where transient measurements at long times or dynamic measurements at low frequencies reflect the slowest configurational rearrangements of flexible macromolecules [1,2]. Less attention has been devoted to the effects of molecular weight and molecular weight distribution in the plateau zone, where the mechanical properties of linear polymers are dominated by entanglement coupling and a consequent transient network structure [3–5].

In the plateau zone, so-called because the viscoelastic relaxation spectrum here can be approximated roughly by a plateau or box [6,7] (although in many cases this is a rather crude representation), the dynamic mechanical losses pass through minima. Qualitatively these arise because at lower frequencies large losses occur from the onset of entanglement slippage and flow deformation while at high frequencies large losses occur as the transition from rubberlike to glasslike consistency is approached. At intermediate frequencies, where the entanglements do not slip but between the entanglements the chains

* Telefonaktiebolaget L. M. Ericsson, Stockholm, Sweden.

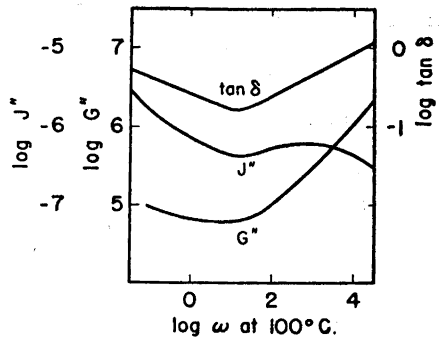

Fig. 1. Mechanical losses of poly-*n*-octyl methacrylate in the plateau zone, plotted logarithmically against radian frequency ω at 100°C. G'', loss modulus (dyne/cm²); J'', loss compliance (cm²/dyne); tan δ, loss tangent.

rearrange freely, the system partakes to a certain extent of the nature of an elastic network with relatively low loss.

The losses (associated with dissipation of heat in oscillating, sinusoidal mechanical deformation) can be described in various ways: [8] the loss modulus G'' or stress 90° out of phase with strain divided by strain; the loss compliance J'' or strain 90° out of phase with stress divided by stress; or the loss tangent tan δ, δ being the phase angle between stress and strain. Typical examples of these functions are shown in Fig. 1, for the plateau region of poly-*n*-octyl methacrylate.[9,10] Each shows a minimum on the frequency scale, though not at exactly the same location.

It is often supposed that mechanical properties in this region are insensitive to the molecular weight. However, the losses, especially tan δ, depend rather considerably on both molecular weight and molecular weight distribution. The present paper cites measurements on certain polystyrene samples and an interpretation in terms of a recent theory of Marvin [11] to illustrate this fact.

MATERIALS AND METHOD

Two polystyrene samples (S8 and S1160) of sharp molecular weight distribution were generously furnished by Dr. H. W. McCormick of Dow Chemical Company [12]. They had been prepared by anionic polymerization followed by terminating the chains with water. A third sample (19F), previously furnished also by Dow, had been prepared by conventional free radical polymerization procedures and presumably had a "most probable" distribution of molecular weights. The initial number and weight average molecular weights are given in Table 1.

For measurements of dynamic mechanical properties at low frequencies with the torsion pendulum apparatus of Plazek, Vrancken, and Berge [13], the samples were molded into discs. Those with the sharp distributions, furnished in finely divided form, were first sintered by heating *in vacuo* a few degrees above the softening point for several hours. Molding was performed in a press at about 100 lbs. per sq. in. at 150°C. Measurements of characteristic frequencies and decrements of free oscillations were made as described elsewhere [13] at temperatures between 125° and 160°C.

After completion of the measurements, borings were taken from the centers of the discs and their intrinsic viscosities were measured in methyl ethyl ketone. Viscosity-average molecular weights calculated therefrom [14] are given in the last column of Table 1, and indicate some but not excessive degradation during the molding and measurements. (Two other samples with sharp distributions and considerably higher molecular weights

Table 1. Initial number and weight-average molecular weights of polystyrene samples, and final viscosity-average molecular weights.

Sample	Initial $\overline{M}_n \times 10^{-3}$	Initial $\overline{M}_w \times 10^{-3}$	Final $\overline{M}_\eta \times 10^{-3}$
S8	159	171	135
S1160 ("60")	279	286	240
19F	190	370	276

were also studied, but experienced more serious degradation, probably because of the longer times necessary for molding; the final $\overline{M}_\eta$ was only about half the initial $\overline{M}_w$. The data from these samples are not reported.)

RESULTS

The measured characteristic frequencies and decrements were converted to the storage and loss moduli and compliances, G', G'', J', and J'', by well-known formulas [8,13]. Although the range of actual frequencies was only from about 0.4 to 7 cycles/sec., the effective range was increased by reducing the measurements at all temperatures to 125°C with the method of reduced variables [15]. The shift factors a_T were calculated from the equation of Williams, Landel, and Ferry [18] in the form

$$\log a_T \frac{9.82(T-T_0)}{91.6 + T-T_0} \tag{1}$$

with $T_0 = 125.0°$. The numerical coefficients here are derived from measurements by Grandine and Ferry [16], and fit quite well also the temperature dependence of stress relaxation data of Ninomiya and Fujita [17]. Logarithmic plots

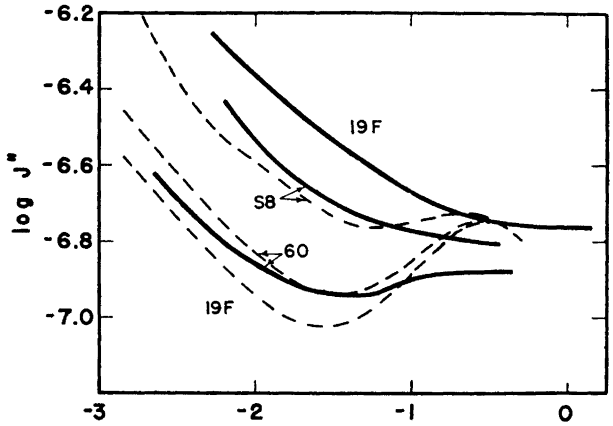

Fig. 2. Log J'' reduced to 125°C., plotted against log ωa_T for three polystyrene samples identified by numbers; "60" is S1160. Solid curves, experimental; dashed curves, calculated from Marvin theory.

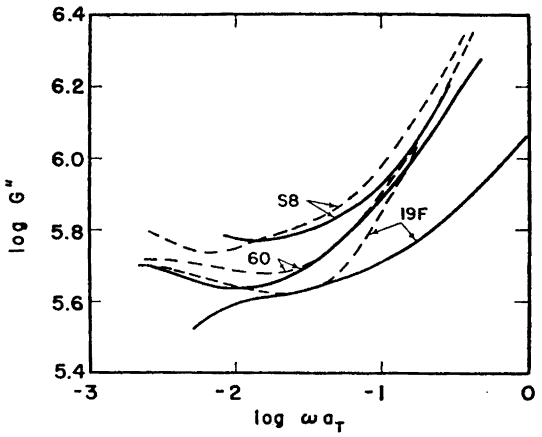

Fig. 3. Log G'' plotted as in Fig. 2.

of J' and J'' (multiplied by the usual temperature and density ratios [15]) against ωa_T gave excellent composite curves for each sample.

The storage compliance, J', ranged from 0.25 to 1 $\times$ 10^{-6}, decreasing monotonically with increasing frequency. To save space, only the loss functions J'', G'', and tan δ are presented here. Logarithmic plots (without points, to avoid confusion) are shown in Figs. 2, 3, and 4. Here ω is the radian frequency per second. The characteristic minima appear, and their dependence on mole-

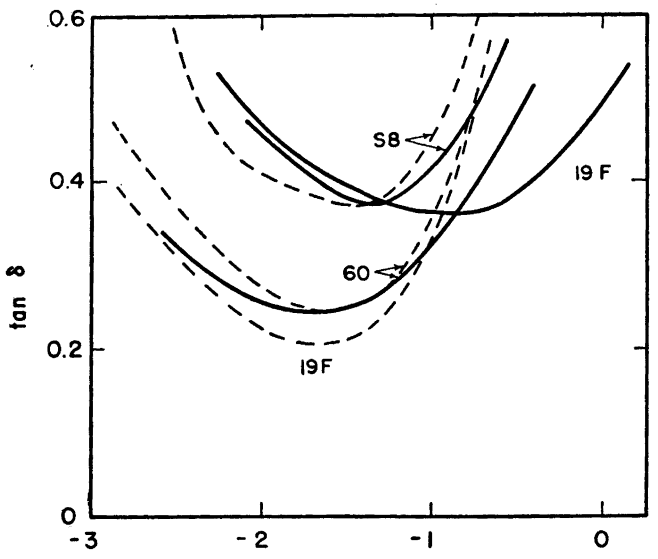

Fig. 4. Tan δ plotted as in Fig. 2.

cular weight and heterogeneity can be summarized as follows. The *loss compliance* increases with decreasing molecular weight and the minimum tends to shift to higher frequencies and disappear. Molecular weight heterogeneity increases the magnitude of J''. The *loss modulus* also increases with decreasing molecular weight, but the effect of heterogeneity is in the opposite direction. The *loss tangent* increases with decreasing molecular weight and the minimum shifts to higher frequencies. Heterogeneity also shifts the minimum to a higher magnitude and a higher frequency.

DISCUSSION

The effects illustrated here can be best interpreted with a very recent theory of Marvin [11], in which viscoelastic properties in the plateau region are described by two ladder network models in series. One ladder represents a mechanical model for the Rouse-Bueche molecular theory of a cross-linked polymer, corresponding to the motions of chain segments between entanglement coupling points as reflected in measurements at high frequencies; the other represents an uncross-linked polymer with a much higher internal friction coefficient, corresponding to long-range motions which are greatly retarded by the entanglements, as reflected in measurements at very low frequencies. The Marvin theory predicts the following frequency dependence for the storage and loss moduli, expressed in slightly modified form: [18]

$$G'_R + iG''_R = P_R^{1/2} \frac{\tanh P_R^{1/2} + Q_e^{1/2} \tanh R_e Q_e^{1/2} P_R^{1/2}}{1 + Q_e^{1/2} \tanh P_R^{1/2} \tanh R_e Q_e^{1/2} P_R^{1/2}} \qquad (2)$$

where $G'_R/G' = G''_R/G'' = 1/K_1$

$P_R = i\omega_R = i\omega K_2$

$Q_e = (M/2M_e)^{2.4}$

$R_e = M/2M_e - 1$

M_e = molecular weight between entanglement coupling points

The molecular interpretation of the parameters K_1 and K_2 will be mentioned later; they are both independent of M, but K_1 is inversely proportional to M_e. Aside from this, the reduced viscoelastic properties G'_R and G''_R (also J'_R and J''_R) are fully determined by the ratio $M/2M_e$, and tan δ as a function of ω_R is determined by this ratio *alone*. An important equalification is that both M and M_e are assumed to be devoid of heterogeneity.

To compare theory with experiment, M_e must be known. Estimates from different kinds of rheological information vary, ranging from 10 000 to 30 000 for polystyrene [19]. For the present purpose, utilization was made of the fact that the level of the minimum in tan δ, a quantity known experimentally with confidence, is a unique function of $M/2M_e$. Calculations of tan δ were made from eqn. (2) with a Bendix G-15D computer for various values of $M/2M_e$; the results near the minima are portrayed in Fig. 5. The level of the minimum

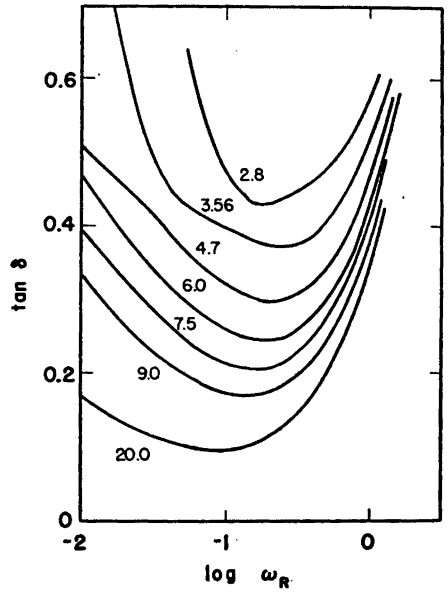

Fig. 5. Tan δ calculated from eqn. (2), plotted against log ω_R, for various values of $M/2M_e$ as indicated by numbers opposite the curves.

increases monotonically with decreasing M_e. In fact, over the range covered it can be represented very well by the following equation:

$$(\tan \delta)_{min} = 1.02(M/2M_e)^{-0.80} \quad (3)$$

Now, by substituting the experimental values for the minimum in eqn. (3), M_e can be calculated. If the weight-average values of M are used, M_e is found to be 24 100 and 23 800 for samples S8 and S1160, respectively. Accordingly, M_e was chosen as 24 000 and the functions G''_R, J''_R, and tan δ were calculated from eqn. (2) for the three experimental samples.

It may be remarked that eqn. (3) provides, in principle, a very simple method for determining molecular weights of any polymer for which M_e is known. The magnitude of tan δ can be easily measured by various experimental methods which do not require absolute calibration [20]. The serious limitation, of course, is the restriction to samples with sharp molecular weight distribution. Heterogeneity causes abnormally high values of tan δ at the minimum, as seen in Fig. 4 and also in the data for the two samples which experienced degradation and consequent heterogeneity, not reported here.

The value of K_2 associated with eqn. (2) was obtained by matching the calculated and experimental minima of tan δ on the logarithmic frequency scale, and was found to be 7.1 sec. To determine the remaining parameter K_1, logarithmic plots of J''_R and G''_R were matched to the corresponding experimental plots of J'' and G'' for the sharp samples S8 and S1160; the best concurrence was obtained for $K_1 = 10^{6.38}$ cm²/dyne. The theoretical predictions for J'', G'', and tan δ as specified by these parameters are drawn in Figs. 2 to 4 as dashed curves.

For the two sharp samples, the respective theoretical and experimental functions agree rather well in shape, supporting the validity of the theory of Marvin as an approximate description of the viscoelastic properties in the plateau zone. For 19F, with a broad molecular weight distribution, the theoretical and experimental functions diverge widely. Of course, the use of $\bar{M}_w$ for M in eqn. (2) for this sample is arbitrary and in a sense meaningless. If $\bar{M}_z$ had been used, the calculated curves would be close to those for S8. In either case, the observed loss compliance is greater than that calculated, while the observed loss modulus is smaller. It appears that viscoelastic measurements in this region could potentially yield information about molecular weight distribution; they have experimental advantages over measurements in the terminal zone, which have previously been explored for this purpose [1,21], but require higher temperatures and/or longer times.

The parameter K_1 has been identified in molecular terms [11,18] as a constant of the order of $\varrho RT/M_e$, where ϱ is the polymer density in g/cc. The value given above corresponds to 1.75 $\varrho RT/M_e$, in reasonable agreement. The parameter K_2 is related to the mobility of short molecular segments. One method of formulating it in molecular terms based on the Rouse theory [18] gives $K_2 = 3a^2 \zeta_0 M_e^2/50 M_0^2 kT$, where a is a characteristic monomeric length, M_0 is the molecular weight of a monomer unit, and ζ_0 is the translational friction coefficient per monomer unit. Substitution of the value of K_2 given above provides $\log \zeta_0 = -1.65$ at 125°C (units dyne-sec/cm.) An independent calculation made from stress relaxation measurements of Fujita and Ninomiya on polystyrene [17] gives $\log \zeta_0 = -2.18$. Considering the widely different sources of information, this represents fair agreement. It may be concluded, therefore, that the Marvin theory provides a semiquantitative description not only of the relative frequency dependence of the viscoelastic losses but also of the parameters which specify their magnitudes and their positions on the frequency scale.

Relaxation (H) and retardation (L) spectra were also calculated from the frequency dependence of G'' and J'', and of the associated storage components G' and J', using customary approximation methods [10]. In each case, the agreement between calculations from the storage and loss components was very satisfactory. The spectra H and L show minima similar to those in G'' and J'' respectively, but shallower; over the limited range of time scale available, they do not provide enough additional information to warrant reproduction here.

Some conclusions qualitatively similar to those presented here were reported very recently by Cox, Isaksen, and Merz.[22]

Acknowledgments. This work was supported in part by a grant from the *National Science Foundation.* One of us (H.H.) is pleased to acknowledge support from *Statens Tekniska Forskningsråd* (*Swedish Technical Research Council*). We are indebted to Dr. R. S. Marvin for communication of his theory before its publication, to Professor J. O. Hirschfelder for use of the Bendix computer, and to Joan Dell and Robert P. Cox for some technical assistance.

REFERENCES

1. Tobolsky, A. V. and Murakami, K. *J. Polymer Sci.* **40** (1959) 443.
2. Ferry, J. D., Williams, M. L. and Stern, D. M. *J. Phys. Chem.* **58** (1954) 987.
3. Mark, H. and Tobolsky, A. V. *Physical Chemistry of High Polymeric Systems,* Interscience Publishers, New York 1950, Chapter X and p. 344.

4. Bueche, F. *J. Chem. Phys.* **20** (1952) 1979.
5. Ferry, J. D., Landel, R. F. and Williams, M. L. *J. Appl. Phys.* **26** (1955) 359.
6. Andrews, R. D., Hofman-Bang, N. and Tobolsky, A. V. *J. Polymer Sci.* **3** (1948) 669.
7. Ferry, J. D., Fitzgerald, E. R., Johnson, M. F. and Grandine, L. D., Jr. *J. Appl. Phys.* **22** (1951) 717.
8. Staverman, A. J. and Schwarzl, F. in Stuart, H. A. *Die Physik der Hochpolymeren*, Springer-Verlag, Berlin 1956, Vol. IV, Chapter I.
9. Dannhauser, W., Child, W. C., Jr. and Ferry, J. D. *J. Colloid Sci.* **13** (1958) 103.
10. Berge, J. W., Saunders, P. R. and Ferry, J. D. *J. Colloid Sci.* **14** (1959) 135.
11. Marvin, R. S., in *Proc. Conf. Symp. Phenomenological Aspects of Viscoelasticity*, Academic Press, New York 1960, p. 27.
12. McCormick, H. W., Brower, F. M. and Kim, L. *J. Polymer Sci.* **39** (1959) 87.
13. Plazek, D. J., Vrancken, M. N. and Berge, J. W. *Trans. Soc. Rheology* **2** (1958) 39.
14. Flory, P. J. *Principles of Polymer Chemistry*, Cornell University Press, Ithaca, N. Y. 1953, p. 312.
15. Ferry, J. D. and Fitzgerald, E. R. *J. Colloid Sci.* **8** (1953) 224.
16. Grandine, L. D., Jr. and Ferry, J. D. *J. Appl. Phys.* **24** (1953) 679.
17. Fujita, H. and Ninomiya, K. *J. Polymer Sci.* **22** (1957) 233.
18. Ferry, J. D. *Viscoelastic Properties of Polymers*, John Wiley and Sons, New York 1961, Chapter 10.
19. Ref. [18], Chapter 13.
20. Ferry, J. D. in Eirich, F. R. *Rheology*, Academic Press, New York 1958, Vol. II; Chapter 11.
21. Watkins, J. M., Spangler, R. D. and McKannan, E. C. *J. Appl. Phys.* **27** (1956) 685.
22. Cox, W. P., Isaksen, R. A. and Merz, E. H., Preprints, *IUPAC Symposium über Makromoleküle*, Wiesbaden, 1959, Vol. 11.

Received April 2, 1960.

ACTA CHEMICA SCANDINAVICA 14 (1960) 1432–1438

An Electrophoretic Investigation of the Degradation of α-Casein by Means of Pepsin and Trypsin

BÖRJE LINDQVIST and TORSTEN STORGÅRDS

The Central Laboratory of Mjölkcentralen, Stockholm, Sweden

Pepsin and trypsin degrade α-casein in completely different ways. If this process (the tertiary phase) is followed by electrophoresis and by the increase of nonprotein nitrogen (NPN), it is then found that pepsin and the previously studied rennin behave similarly in certain respects. Of these three enzymes rennin attacks the α-casein structure more specifically than pepsin and the latter in its turn more specifically than trypsin. The changes in the mobilities of the degradation products which can be observed during the process are different for different pH-values in the reaction mixture. In the pepsin investigations, the changes in the mobilities were proportional to the logarithm of the time. With trypsin, an electrophoresis pattern is obtained, after a few hours, which does not then change character throughout the rest of the experiment. The peaks decrease in height but they do not move or split up into several separate peaks. In the degradation experiments using pepsin, it was found that log NPN is proportional to log time. With trypsin, the process is however more complicated.

In a previous investigation in this series [1] it was shown that the degradation of α-casein by rennin follows completely different paths for different pH-values in the reaction mixture. A similar effect has also been shown for the system β-casein — rennin [7].

In the present investigation, the work has been extended to include in addition α-casein — pepsin and α-casein — trypsin. Pepsin is of interest because of its physiological relationship to rennin. Trypsin was studied because of its ability to break certain known peptide bonds in the protein molecule [4]. For this reason, it may be possible eventually to use the results from the α-casein — trypsin investigations as a standard for judging the specific ability of other enzymes to degrade α-casein.

The action of pepsin on α-casein has been studied by several investigators. Groves and co-workers [2] have, for example, investigated phosphorus peptones which were formed as final products from the attack of pepsin on casein. Zittle and Cerbulius [3] have studied the coagulation of casein with pepsin and inves-

tigated the peptides formed during the so-called primary phase from, amongst other things, α-casein.

The action of trypsin on α-casein has been studied by Christensen [5] by means of viscosity measurements and NPN investigations. Lembke and Kaufmann [6] have investigated the effect of trypsin on total casein by means of electrophoresis. The conclusions which they have drawn concerning the changes in the α- and β-casein peaks upon electrophoresis cannot be considered to be without objection if one takes into account the very large changes in the position of the degradation products relative to the position of the starting substance which has afterwards been observed for β-casein [7].

In all of these investigations, only the degradation process occurring during the primary phase or at the end of the tertiary phase of the casein decomposition was studied while the main process occurring in the tertiary phase has not been touched at all. Just as in the investigation of the effect of rennin on α-casein, the present investigation deals with the process occurring during the whole of the tertiary phase.

EXPERIMENTAL

Casein. The same α-casein sample was used as in the previous investigation. The casein was stored in a tightly closed vessel containing silica gel. A check on the electrophoretic properties of the sample showed that it was completely unchanged at the time at which the investigations were performed.

Enzymes. Pepsin, twice crystallized, was prepared from a commercial product with an activity of 1:10 000 according to Northrop's method [8].

Trypsin, twice crystallized, with 50 % $MgSO_4$ from the Nutritional Biochemicals Corporation was employed.

Procedure and Analyses. In the preparation of the substrate and enzyme solutions as well as in the mixing of these solutions, the same procedure was used as in the previous investigation. This means, in brief, that a 4 % sodium caseinate solution was mixed with a NaCl-phosphate buffer solution containing the enzyme sample in question in such a way that the final solution was 3 % with respect to casein and had at the same time the desired pH-value. The NaCl, phosphate and enzyme concentrations were likewise automatically given the desired values. Upon mixing, the casein coagulates and thus many mixtures containing a suitable amount for one analysis of the type in question must be made. In order to perform the analysis, the whole of the content of the tube was then used.

Certain limits were applied to the experimental conditions, *viz.* the pH interval in the pepsin investigations was 4.6—5.7 and in the trypsin one 5.1—6.3. The enzyme activity of the pepsin was adjusted so that, when measured according to Berridge's method for the determination of rennin activity, it corresponded to 400 Ru/l reaction mixture. The activity of the trypsin could not be determined in this way since a calcium caseinate sol is not coagulated, but rather dissolved, by trypsin. Instead, an amount of pure trypsin was weighed out which corresponded to the amount by weight of rennin which upon solution gave 400 Ru/l, *viz.* 5 mg/l.

The nature and the extent of the analyses were the same as in the previous work, with the exception that the pepsin experiments were allowed to run for 15—36 days and the trypsin experiments for about 12 days.

RESULTS AND DISCUSSION

A. Formation of soluble nitrogen (NPN)

The NPN values of the reaction mixtures after various times are shown in Figs. 1 and 2. A comparison with the previously performed investigations

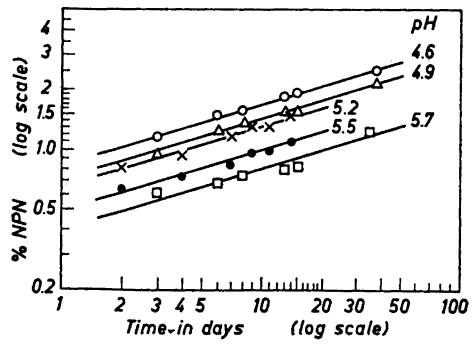

Fig. 1. Release of NPN, as a function of time, from α-casein due to the influence of pepsin. Reaction rate at different pH-values plotted using log NPN and log time scales.

on the properties of rennin shows that the NPN formation occurs in a different way. The reaction for the degradation of both α-casein and β-casein by rennin follows the empirical expression

$$\text{NPN} = k_1 \log \text{time} + C_1$$

For pepsin — α-casein, it was found on the other hand that

$$\log \text{NPN} = k_2 \log \text{time} + C_2$$

where k and C are constants.

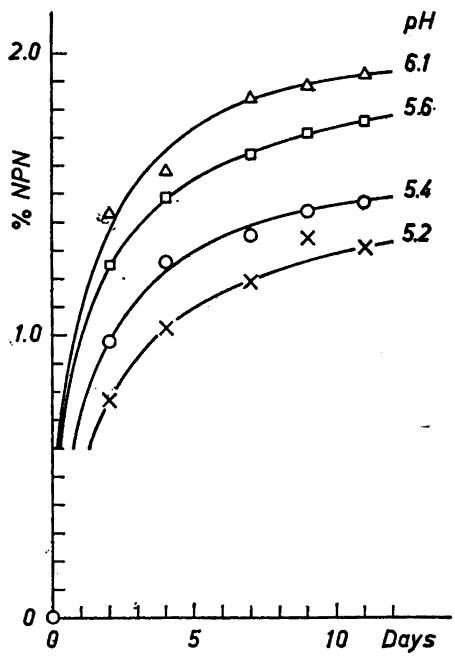

Fig. 2. Release of NPN, as a function of time, from α-casein due to the influence of trypsin. Reaction rate at different pH-values plotted using linear scales.

Table 1. Constants in the equations for the formation of NPN from α-casein.
Rennin: % NPN = k_1 log time + C_1
Pepsin: log % NPN = k_2 log time + C_2

pH	Rennin				Pepsin	
	α-casein		β-casein *		α-casein	
	k_1	C_1	k_1	C_1	k_2	C_2
4.21	1.73	0.42				
4.48	1.84	0.44				
4.6					0.306	−0.07
4.9					0.306	−0.14
5.2					0.306	−0.17
5.21	1.36	0.33	0.29	0.26		
5.45	0.98	0.23				
5.5					0.306	−0.30
5.7					0.306	−0.40
5.75	0.75	0.18				
6.4	0.45	0.11				
6.7	0.36	0.09				
7.0	0.23	0.05				

* The constants apply, approximately, for all pH-values within the interval investigated.

For trypsin — α-casein, the relationship was even more complicated. No simple transformations could be found which could make the experimental values fall on straight lines as in Fig. 1.

In Table 1, the values of the constants have been collected for several cases hitherto investigated for which calculations could be performed. It should be pointed out that the differences in NPN amounts in the cases, α-casein — rennin, α-casein — pepsin, and α-casein — trypsin, are not especially large despite the differences in the respective processes. It is of interest to compare these results with NPN determinations performed on ripening hard cheeses [9]. The casein degradation which occurs in that case is caused by rennin together with different bacterial enzymes that are formed successively. The process leads to higher NPN values and the formation follows the same mathematical expression as given above for the action of pepsin on α-casein.

B. Electrophoretic investigations

A total of about 60 electrophoretic results were obtained from each of the investigations on pepsin and trypsin. The calculation of the results has been performed in such a way that the differences caused by pH and time appear most noticeably. The results from the pepsin experiments resemble in several respects those obtained from the experiments with α-casein — rennin. The trypsin results are quite different.

The main features of the results obtained are as follows:

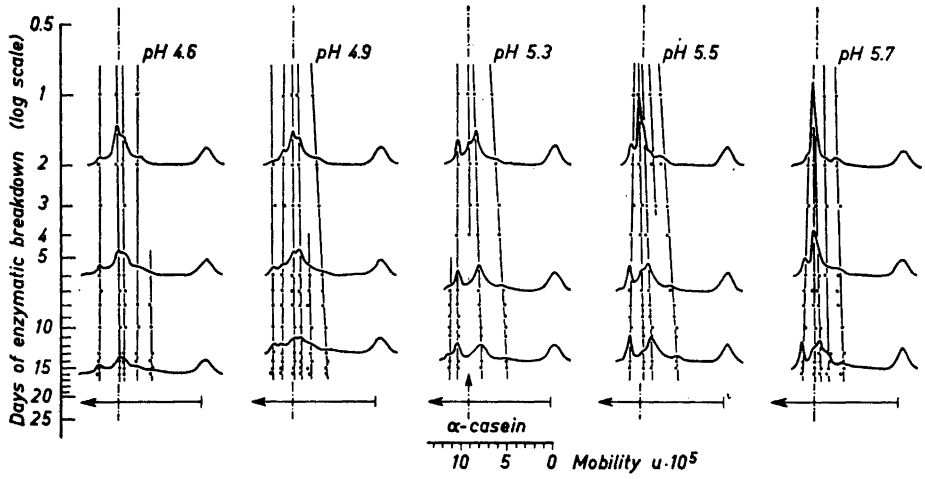

Fig. 3. Summary of the changes in the electrophoresis curves obtained during the degradation of α-casein by pepsin at different pH-values. The changes in mobility are shown by the vertical lines which pass through the points for the mobility of certain peaks in the curves. (To save space, only some of the curves have been drawn in, the positions of peaks in opposite case being marked only with points corresponding to the mobility of the peak). The time scale is logarithmic.

Pepsin experiments. Fig. 3 shows the degradation process occurring in these experiments for different pH-values. The conclusions which can be drawn are:

1) With pepsin, electrophoresis curves of a flatter and more diffuse appearance than with rennin were obtained. This indicates a weakly selective attack on the α-casein molecule.

Instead of getting, as is the case with rennin, a small number of sharp electrophoretic peaks, each of which probably consisting of individual molecules, there is obtained with pepsin a main peptide in each electrophoretic peak together with a large number of other peptides lying close to it.

2) Because of the spreading of these peptides, with respect to their electrophoretic mobilities, around the main substance, the mean mobility of each peak in the electrophoretic diagram will be somewhat different from the corresponding one in the rennin experiments.

3) The difference in mobility of the substances split off from the α-casein was found as previously observed with several corresponding enzyme-substrate systems, *viz.* from a primary component with a certain mobility, various substances with higher and lower mobilities than that of the primary component are obtained. These reaction products are then degraded further, either as just described by cleavage or by a splitting off of dialysable peptides only which outwardly produce a decrease or increase of the mobility as the only effect. Whether a decrease or increase occurs depends on whether mainly

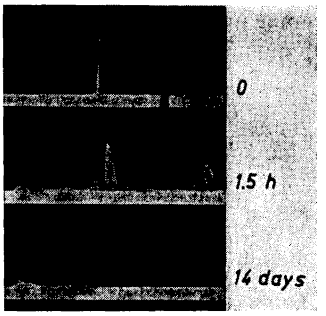

Fig. 4. Electrophoresis diagrams from the degradation of α-casein by trypsin at pH 5.6. Immediately after the start of the experiments, a certain shape for the curve is obtained which remains unchanged throughout the whole of the experiments.

acid or mainly basic amino acids are split off in the form of oligopeptides or as free amino acids.

In the α-casein — pepsin experiments, the mobility changes linearly with log time while, in the α-casein — rennin experiments, the corresponding process was not linear, the various parts of the main processes occurring at different rates, each ebbing out at different times. A process which is linear within a limited time interval should indicate that the degradation process occurs rather independently of the amino acid sequence of the secondary products.

The conclusions which can be drawn from this work is that both the pepsin and the rennin attack α-casein at about the same points in the molecule. While the attack of the rennin is, at least in the beginning, absolutely specific, the pepsin attack occurs rather unspecifically right from the beginning of the process. The tendency towards a more general attack on the molecule increases with increasing degree of degradation of the peptide complex.

The trypsin experiments. A characteristic property for the trypsin is that the degradation products from α-casein are very similar from an electrophoretic point of view, independent of the pH during the reaction. As appears from Fig. 4, the characteristic shape of the curve is obtained within 1.5 h after the start of the experiment and thereafter retains its main features for 14 days, even if the height of the curve has then decreased somewhat. The electrophoresis curve can be described as consisting of one single main peak at the α_{a2} position [1], *i.e.* the mobility of the peak is smaller than that of the α-casein.

Judging by the shape of the curve, there are several components which make up the peak. It is only in exceptional cases that the mobilities of these components have such values that the resulting peak is markedly unsymmetrical or gets a shape differing from the normal distribution curve.

Besides this main peak, there are negligible amounts of components with high and low mobilities. In the electrophoretic diagram, one can observe amongst them a slight majority of very quickly moving substances over those with medium or low mobilities.

The electrophoresis curve does not belie the statement that trypsin splits the protein with a certain selectivity. However, if the attack of rennin on α-casein is compared with the trypsin attack studied here, then it is seen that

the rennin attack is far more specific, expecially in the early stages of the degradation. It is true that the rennin gives eventually rise to several peaks with quite different speeds, in contrast to trypsin's single peak, but on the other hand these more spread-out peaks are much more uniform.

If therefore, when comparing rennin and trypsin, we neglect any possible difference in the total number of components formed, it is nevertheless evident that the following differences in behaviour can be demonstrated:

Rennin gives a few, electrophoretically well-defined substances of about equal amounts with a certain spreading in the mobility values.

Trypsin gives a few, electrophoretically less well-defined substances with a negligible spreading in the mobility values. In addition and in contrast to rennin, trypsin gives small amounts of substances with a considerable spreading in mobility values.

REFERENCES

1. Lindqvist, B. and Storgårds, T. *Acta Chem. Scand.* **13** (1959) 1839.
2. Groves, M. L., Hipp, N. J. and McMeekin, T. L. *J. Am. Chem. Soc.* **80** (1958) 716.
3. Zittle, C. A. and Cerbulius, J. *J. Dairy Sci.* **41** (1958) 241.
4. Sanger, F. and Tuppy, H. *Biochem. J.* **49** (1951) 481.
5. Christensen, L. R. *Arch. Biochem. Biophys.* **53** (1954) 128.
6. Lembke, A. and Kaufmann, W. *Kiel. milchwirtsch. Forschungsber.* **5** (1953) 173.
7. Lindqvist, B. and Storgårds, T. *Acta Chem. Scand.* **14** (1960) 757.
8. Northrop, J. H. *J. Gen. Physiol.* **30** (1946) 177.
9. Lindqvist, B. and Storgårds, T. *XV Intern. Dairy Congr. London 1959, Proc.* Vol. 2, 679.

Received April 6, 1960.

ACTA CHEMICA SCANDINAVICA 14 (1960) 1439–1452

Short Communications

Myrosin-Catalyzed Formation of Turbidity and Hydrogen Sulfide from Sinigrin

SIGMUND SCHWIMMER*

Organic Chemical Laboratory, Royal Veterinary and Agricultural College, Copenhagen, Denmark and Western Regional Research Laboratory Albany, California, USA **

Recent investigations have demonstrated the formation of thiocyanate ion [1,2] and organic thiocyanates from S-glucosyl-thiohydroximyl sulfates (*iso*thiocyanate glucosides), separation of the sulfatase and thioglucosidase functions of myrosin [4], as well as the stimulation of the myrosin action by ascorbic acid [5]. These observations demonstrate that the fate of these thioglucosides can be enzymatically more diverse than that of a simple thioglucosidase action accompanied by Lossen rearrangement with concomitant sulfate displacement and formation of *iso*thiocyanates [6]. The present paper presents hitherto unreported observations which suggest that both the pathway as well as the rate of degradation of these thiohydroximyl sulfates are dependent upon the pH of the medium and upon the presence of foreign protein and ascorbic acid.

A myrosin-sinigrin reaction mixture develops a turbidity at pH 3.0 (glycine-HCl or HCl) (but not at pH 4 or above) which increases with time until a maximum value is reached (Fig. 1). The results

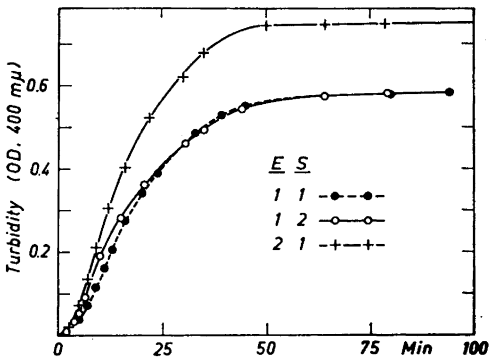

Fig. 1. Development of turbidity in a sinigrin-myrosin reaction mixture at pH 3.0 (0.033 M glycine-HCl). Six ml of reaction mixture at 25° contained 10 μmoles of sinigrin (S = 1) and 1 mg of myrosin (E = 1). Myrosin was prepared by lyophilization of the precipitate obtained from the dialyzed protein fraction (of a water extract of ground black mustard seed) precipitating between 30 and 70 % ethanol. Turbidity measured as optical density at 400 mμ using an Evelyn Colorimeter.

of Fig. 1 show that doubling the enzyme concentration caused an increase in both the rate and the extent of the development of the turbidity, whereas doubling the substrate concentration did not affect these parameters to any appreciable extent. The turbidity did not develop in the absence of substrate at this pH, nor in the presence of glucose, $KHSO_4$ and allyl *iso*thiocyanate added in amounts equivalent to that of the initial substrate. Nor did this turbidity develop when these end-products were added to sinigrin in the absence of enzyme at this pH. Furthermore, when the myrosin was incubated with sinigrin at pH 5.8 (acetate buffer) at 37° for one hour, or at pH 2.1 for 10 min. no turbidity developed after the pH was adjusted to 3.0.

* Senior Post-doctoral Fellow, National Science Foundation, 1958—1959.

** A Laboratory of the Western Utilization Research and Development Division, Agricultural Research Service, U.S. Department of Agriculture.

When centrifuged at 100 000 × *g*, a large proportion but not all of the turbid material sedimented. The precipitate gave a positive biuret test (protein) and a negative Molisch test (carbohydrate) whereas the supernatant fraction gave a strong positive Molisch and a much decreased positive biuret reaction. The UV absorption spectrum of the supernatant liquid exhibited no supplementary absorbency at 280 mμ in the background turbidity absorption as one might expect if residual protein had remained in solution.

In corroboration of the observations of Nagashima and Uchiyama [5], ascorbic acid was found to increase the rate of liberation of glucose and the formation of *iso*thiocyanate at pH 5.8 At pH 3.0, in the presence of ascorbic acid in concentrations equivalent to that of the substrate, immediate evolution of hydrogen sulfide (detected by odor and with lead acetate paper) concomitant with the development of turbidity was observed. Exactly the same conditions which were previously observed to produce turbidity also produced hydrogen sulfide in the presence of ascorbic acid. Additional controls in which ascorbic acid was added after extended reaction time at both pH 5.8 and at pH 3.0, did not evolve hydrogen sulfide. A modification of the test for nitriles of Soloway and Lipschitz [7] showed that nitrile was present in an enzyme reaction mixture containing ascorbic acid at pH 3.0 but not at pH 5.8.

Inasmuch as the turbidity appears to rise as the results of insolubilization of the protein of the myrosin preparation during its action and since the existence of a thiol intermediate as a distinct entity at pH 3.0 appears to be likely in view of the above-mentioned findings of Gaines and Goering , it is suggested that at pH 3.0 this intermediate can react with the protein (P) of the myrosin preparation, possibly *via* a chain type sulfhydryl-disulfide interchange as discussed recently by Jansen [8]:

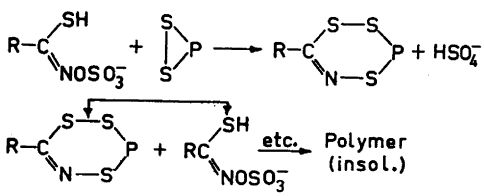

whereas in the presence of ascorbic acid (AH_2), this intermediate decomposes to hydrogen sulfide and nitrile.

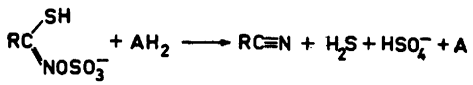

Thus the appearance of nitriles in the myrosin-thioglucoside digests, frequently reported in the literature and outlined, *e.g.*, by Kjær [9], may have arisen as the result of the presence of ascorbic acid in unbuffered crude digests. The interpretation of the results herein obtained may reconcile the apparently contradictory conclusions by Nagashima and Uchiyama [5] and those of Gaines and Goering [4]. The former authors concluded that only one enzyme, a thioglucosidase, is present in myrosin preparations, since application of a variety of fractionation procedures and environmental conditions (including low pH-values) yielded a glucose → sulfate ratio of unity. On the other hand, Gaines and Goering [4] have recently presented convincing evidence that myrosin can indeed be separated into two distinct enzymes, an oxime sulfatase and a thioglucosidase and that only the latter acts appreciably on sinigrin at pH 3.0. According to the postulated mechanism of action of myrosin presented herein, a highly purified preparation containing both enzymes but very little foreign protein would liberate and accumulate only glucose and the above mentioned 3-butenyl thiohydroximyl sulfate at pH 3.0 In relatively crude myrosin preparations, this intermediate reacts with the protein impurities as depicted thus liberating inorganic sulfate non-enzymatically.

Detection of nitrile. Both acrylonitrile (the next lower homologue of the postulated end product, vinylacetonitrile) and sinigrin, but not allyl *iso*thiocyanate, reacted positively in the absence of aqueous solvent as described by Soloway and Lipschitz (Procedure II) [7]. Under conditions of the enzyme reaction, in aqueous solution, a brown color developed after boiling for 4 min. in the presence of hydroxylamine, KOH, and propylene glycol when acrylonitrile was present. No color developed in the presence of sinigrin under the same conditions. Upon the subsequent addition of the $FeCl_3$ reagent, the nitrile containing sample developed a muddy brown color. A

sample from the prolonged digestion of sinigrin by myrosin in the presence of ascorbic acid at pH 3.0 gave a positive modified nitrile test, whereas a positive test for neither nitrile nor sinigrin was observed with a sample from a similar enzyme digestion conducted at pH 5.8.

The author wishes to thank Prof. A. Kjær for his encouragement and advice.

1. Michajlowskij, N. and Langer, P. *Z. physiol. Chem. Hoppe-Seyler's* **317** (1959) 30.
2. Gmelin, R. and Virtanen, A. I. *Acta Chem. Scand.* **14** (1960) 507.
3. Gmelin, R. and Virtanen, A. I. *Suomen Kemistilehti* **B32** (1959) 236; *Acta Chem. Scand.* **13** (1959) 1474.
4. Gaines, R. D. and Goering, K. J. *Biochem. Biophys. Research Comm.* **2** (1960) 207.
5. Nagashima, Z. and Uchiyama, M. *Bull. Agr. Chem. Soc. Japan* **23** (1959) 555.
6. Ettlinger, M. G. and Lundeen, A. J. *J. Am. Chem. Soc.* **78** (1956) 4172.
7. Soloway, S. and Lipschitz, A. *Anal. Chem.* **24** (1952) 898.
8. Jansen, E. V. *Science* **130** (1959) 1319.
9. Kjær, A. *Fortschr. Chem. org. Naturstoffe* **18** (1960) 122.

Received June 20, 1960.

Further Observations on the Immunologic Reactions of the Old Yellow Enzyme

STEN KISTNER

Medicinska Nobelinstitutet, Biokemiska avdelningen, Stockholm, Sweden

The OYE* and its apoprotein were found to react identically with specific antibodies against the enzyme in agar gel diffusion experiments [1]. The antiserum inhibited the enzymatic activity [2], but no influence was noticed upon the association reaction between the apoprotein and the coenzyme FMN which was studied by fluorimetric technique. The inhibition was non-competitive with regard to the substrate TPNH. These results indicate that the antibodies are bound to other parts of the enzyme molecule than the coenzyme or the substrate.

Atabrine and promazines have been found to inhibit the activity of the OYE after preincubation with the apoprotein [3]. Fluorimetric studies showed that the inhibitors did not prevent the binding of FMN to the apoprotein but slowed down the rate of this reaction. It is suggested that the inhibitors are bound to the apoprotein molecule close to the sites of the FMN. The two different types of inhibitors, drugs and antibodies, thus seemed to exert their effect on different parts of the enzyme molecule. The inhibition studies did not allow any conclusions, however, as to whether the drugs are exclusively bound to sites where they interfere with the coupling of the coenzyme, or whether they affect other parts of the enzyme molecule as well.

In the present work the inhibition of the OYE by anti-serum has been studied at different FMN concentrations. The quantitative precipitation reactions of the OYE and its apoprotein with antibodies, and the influence of atabrine upon these reactions, has been investigated. The effect of the promazines could not be studied, since it was found that precipitation occurred upon mixing promazine or chlorpromazine with rabbit serum.

Materials and methods. The OYE used had been recrystallized once, and the apoprotein was obtained from the same preparation. Immunization with OYE and collection of serum was carried out as described before [1]. The manometric technique used for the inhibition studies has already been described in detail [3]. Quantitative precipitin reactions were performed after the serum had been inactivated at +56°C for 20 min. Varying amounts of antigen in 0.3 ml 0.15 M sodium phosphate buffer pH 7.4 were added to 0.25 ml serum and incubation performed at +37°C for 30 min, followed by 24 h at +4°. After being washed several times in buffer and distilled water, the precipitates were dissolved in 0.3 ml 1 N NaOH and the protein content determined according to Lowry *et al.* [4] The absorption values were compared to those of a bovine serum albumin (Armour) standard. In some experiments antigen solutions containing 0.25 mg OYE or apoprotein per ml were incubated with 2×10^{-4} M atabrine at +37°C for 30 min before being added to the serum. The concentration of atabrine in the antigen-serum mixture was 1.1×10^{-4} M.

* Abbreviations: OYE = old yellow enzyme, FMN = flavin mononucleotide, TPNH = reduced triphosphopyridine nucleotide.

sample from the prolonged digestion of sinigrin by myrosin in the presence of ascorbic acid at pH 3.0 gave a positive modified nitrile test, whereas a positive test for neither nitrile nor sinigrin was observed with a sample from a similar enzyme digestion conducted at pH 5.8.

The author wishes to thank Prof. A. Kjær for his encouragement and advice.

1. Michajlowskij, N. and Langer, P. *Z. physiol. Chem. Hoppe-Seyler's* **317** (1959) 30.
2. Gmelin, R. and Virtanen, A. I. *Acta Chem. Scand.* **14** (1960) 507.
3. Gmelin, R. and Virtanen, A. I. *Suomen Kemistilehti* **B32** (1959) 236; *Acta Chem. Scand.* **13** (1959) 1474.
4. Gaines, R. D. and Goering, K. J. *Biochem. Biophys. Research Comm.* **2** (1960) 207.
5. Nagashima, Z. and Uchiyama, M. *Bull. Agr. Chem. Soc. Japan* **23** (1959) 555.
6. Ettlinger, M. G. and Lundeen, A. J. *J. Am. Chem. Soc.* **78** (1956) 4172.
7. Soloway, S. and Lipschitz, A. *Anal. Chem.* **24** (1952) 898.
8. Jansen, E. V. *Science* **130** (1959) 1319.
9. Kjær, A. *Fortschr. Chem. org. Naturstoffe* **18** (1960) 122.

Received June 20, 1960.

Further Observations on the Immunologic Reactions of the Old Yellow Enzyme

STEN KISTNER

Medicinska Nobelinstitutet, Biokemiska avdelningen, Stockholm, Sweden

The OYE* and its apoprotein were found to react identically with specific antibodies against the enzyme in agar gel diffusion experiments [1]. The antiserum inhibited the enzymatic activity [2], but no influence was noticed upon the association reaction between the apoprotein and the coenzyme FMN which was studied by fluorimetric technique. The inhibition was non-competitive with regard to the substrate TPNH. These results indicate that the antibodies are bound to other parts of the enzyme molecule than the coenzyme or the substrate.

Atabrine and promazines have been found to inhibit the activity of the OYE after preincubation with the apoprotein [3]. Fluorimetric studies showed that the inhibitors did not prevent the binding of FMN to the apoprotein but slowed down the rate of this reaction. It is suggested that the inhibitors are bound to the apoprotein molecule close to the sites of the FMN. The two different types of inhibitors, drugs and antibodies, thus seemed to exert their effect on different parts of the enzyme molecule. The inhibition studies did not allow any conclusions, however, as to whether the drugs are exclusively bound to sites where they interfere with the coupling of the coenzyme, or whether they affect other parts of the enzyme molecule as well.

In the present work the inhibition of the OYE by anti-serum has been studied at different FMN concentrations. The quantitative precipitation reactions of the OYE and its apoprotein with antibodies, and the influence of atabrine upon these reactions, has been investigated. The effect of the promazines could not be studied, since it was found that precipitation occurred upon mixing promazine or chlorpromazine with rabbit serum.

Materials and methods. The OYE used had been recrystallized once, and the apoprotein was obtained from the same preparation. Immunization with OYE and collection of serum was carried out as described before [1]. The manometric technique used for the inhibition studies has already been described in detail [3]. Quantitative precipitin reactions were performed after the serum had been inactivated at +56°C for 20 min. Varying amounts of antigen in 0.3 ml 0.15 M sodium phosphate buffer pH 7.4 were added to 0.25 ml serum and incubation performed at +37°C for 30 min, followed by 24 h at +4°. After being washed several times in buffer and distilled water, the precipitates were dissolved in 0.3 ml 1 N NaOH and the protein content determined according to Lowry *et al.* [4] The absorption values were compared to those of a bovine serum albumin (Armour) standard. In some experiments antigen solutions containing 0.25 mg OYE or apoprotein per ml were incubated with 2×10^{-4} M atabrine at +37°C for 30 min before being added to the serum. The concentration of atabrine in the antigen-serum mixture was 1.1×10^{-4} M.

* Abbreviations: OYE = old yellow enzyme, FMN = flavin mononucleotide, TPNH = reduced triphosphopyridine nucleotide.

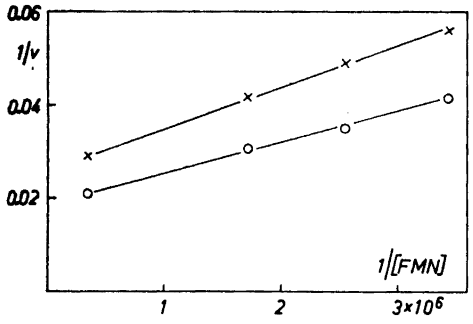

Fig. 1. The inhibition of the OYE activity by antiserum at different concentrations of FMN, measured by Warburg technique. Along the ordinate $1/v$ is marked, where v means the oxygen uptake during 30 min. The total volume of the reaction mixture was 3.0 ml, containing 1.9×10^{-2} M glucose-6-phosphate, 1 Kornberg Unit of Zwischenferment, 4.5×10^{-4} M TPN, 2×10^{-7} M apoprotein, 2.7×10^{-3} M KCN, 0.13 M sodium phosphate buffer pH 7.4, and varying concentrations of FMN, which are marked along the abscissa. Points marked × indicate experiments where the reaction mixture contained 0.5 ml rabbit anti-OYE serum, and points marked O experiments where 0.5 ml normal rabbit serum was added. The reactions were started by introducing the apoprotein from the sidearm.

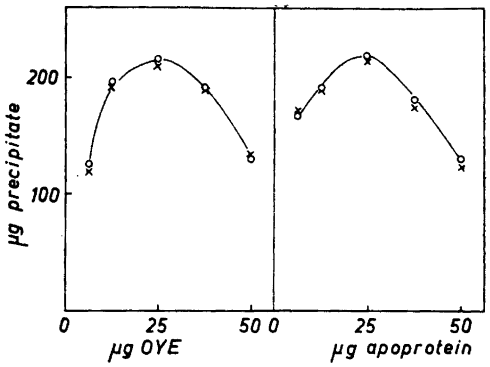

Fig. 2. Two experiments where the influence of atabrine on the quantitative precipitin reaction between the OYE and antiserum was studied. To the left is an experiment where the holoenzyme was used as antigen. O marks results obtained in the absence of atabrine, and × results obtained in the presence of 1.1×10^{-4} M atabrine. To the right is a similar experiment with the same marking, where the antigen used was the apoprotein of the OYE. The same serum, obtained after immunization with OYE, was used in both experiments.

Fig. 1 shows a non-competitive inhibition of the OYE by antiserum, when the concentration of FMN was varied in the reaction system. Essentially identical results were obtained in the quantitative precipitin reactions when either holoenzyme or apoprotein was used as antigen (Fig. 2). These results thus confirm previous conclusions that the antibodies and FMN are bound to different parts of the molecule. Fig. 2 also shows that the presence of atabrine did not disturb the reaction of the enzyme with antibodies. Atabrine was only slightly soluble in the reagent used for the protein analysis, and tests using a saturated solution showed no influence on the readings of the standard. The failure of atabrine to influence the reaction between enzyme and antibody supports the conclusions of the inhibition studies that different binding sites are concerned in the reactions of the drug and the antibodies with the enzyme.

1. Kistner, S. *Acta Chem. Scand.* **12** (1958) 2034.
2. Kistner, S. *Acta Chem. Scand.* **13** (1959) 1149.
3. Kistner, S. *Acta Chem. Scand.* **14** (1960) 1389.
4. Lowry, O. H., Rosebrough, N. J., Farr, A. L. and Randall, R. J. *J. Biol. Chem.* **193** (1951) 265.

Received July 19, 1960.

Crystal Structure of the Perhydroanthracene Isomeride of M.P. 121° C

K. E. HJORTAAS

Universitetets Kjemiske Institutt, Blindern, Oslo, Norway

Structure determinations by physical methods of the isomeric perhydroanthracenes have proved to be far from easy. In the case of the 90° isomer however, an X-ray crystallographic analysis has been carried out [1] which shows the molecule to be of the »*trans-trans*» type with three parallel »chair» *cyclo*hexane rings.

The new isomer (m.p. 123°C) [2] has been investigated by both X-ray crystallographic and electron diffraction [3] (vapour phase) techniques by members of this department. The results show conclusively that in this isomer the six-membered rings have the »chair» form, both outer rings being connected to the central ring in *cis* position.

Some details of the X-ray analysis are given:

The crystals are *monoclinic*, space group $P2_1/c$ with two (centrosymmetrical) molecules in the unit cell.

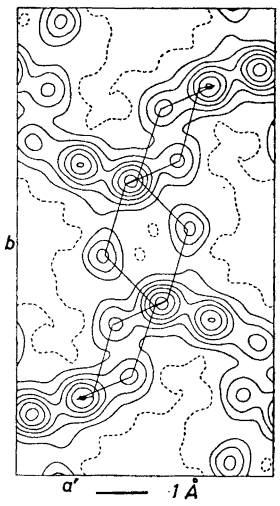

Fig. 2. Projection on the plane normal to [1 0 1]. Contours at 2 (dotted), 4, 6 ··· eÅ^{-3}.

The crystal parameters are: a = 5.36, b = 9.55, c = 12.07 (Å), β = 112.6°. Two-dimensional Fourier maps with projections along [1 0 0] and [1 0 1] are reproduced in Figs. 1 and 2.

The final coordinates of an asymmetrical unit based on least squares refinements

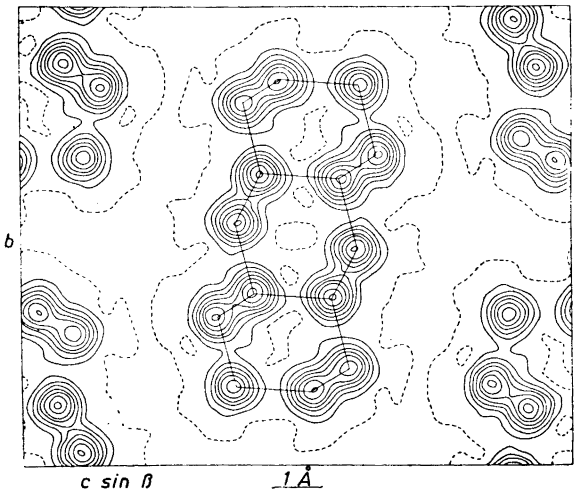

Fig. 1. Projection on the plane normal to [1 0 0]. Contours at 1 (dotted), 2, 3 ··· eÅ^{-3}.

	[1 0 0]		[1 0 1] ($x = x' + z$)		[0 1 0]		Mean values		
	y	z	x'	y	x	z	x	y	z
C_1	0.124	0.076	−0.081	0.124	−0.007	0.076	−0.006	0.124	0.076
C_2	0.175	0.145	0.129	0.177	0.275	0.144	0.274	0.176	0.145
C_3	0.327	0.111	0.206	0.330	0.319	0.114	0.319	0.328	0.112
C_4	0.339	−0.025	0.267	0.337	0.243	−0.024	0.243	0.338	−0.025
C_5	0.289	−0.094	0.056	0.287	−0.040	−0.094	−0.039	0.288	−0.094
C_6	0.136	−0.062	−0.034	0.137	−0.094	−0.064	−0.096	0.136	−0.063
C_7	0.028	−0.109	0.162	0.027	0.055	−0.108	0.054	0.028	−0.109

where the hydrogen atoms were included are as follows:

»Reliability factors» for the three projections are 0.09, 0.06, and 0.08, respectively. The C-C bond distances computed from these coordinates range from 1.49 to 1.56 (Å); mean value 1.54 Å.

The C-C-C bond angles range from 109° to 114°; mean value 112°. Shortest intermolecular C-C distance 3.83 Å.

We thank Professor H. B. Henbest for the substance placed at our disposal in 1958. Thanks are also due to Professor O. Hassel for his interest and advice throughout this work.

1. Bog, S., Hassel, O. and Vihovde, E. H. *Acta Chem. Scand.* **7** (1953) 1308.
2. Hill, R. K. and Martin, J. G. *Proc. Chem. Soc.* **1959** 390.
3. Hassel, O. and Davis, M. *To be published.*

Received July 11, 1960.

Die Umsetzung des Trichlormethylphenylsulfids mit Grignardreagenz

ALEXANDER SENNING und SVEN-OLOV LAWESSON

Laboratorium für Organische Chemie, Chemisches Institut der Universität Uppsala, Uppsala, Schweden

Die von Sanna [1] beschriebene Darstellung von Trichlormethylphenylsulfid durch Umsetzung von Trichlormethansulfenylchlorid mit Phenylmagnesiumbromid ist u.a. von Egen [2] und Böhme [3] widerlegt worden, wird aber andererseits in neueren Übersichten, wie denen von Schöberl und Wagner [4], Sosnovsky [5] und Reid [6] ohne Kritik zitiert. Egen und Böhme bezweifelten die Angaben Sannas auf Grund der physikalischen Eigenschaften seines Produkts (und der von ihm als Trichlormethylphenylsulfon beschriebenen Verbindung), die mit denen des von ihnen auf anderem Wege dargestellten Trichlormethylphenylsulfids (bzw. Trichlormethylphenylsulfons) in keiner Weise übereinstimmten. Dagegen ist Sannas Artikel unseres Wissens noch nicht nachgearbeitet worden. Wir haben diese Nacharbeitung durchgeführt und festgestellt, dass bei dieser Reaktion keine definierten Produkte zu erhalten sind. Interessant ist in diesem Zusammenhang, dass das Trichlormethylphenylsulfid, das 1951 von Egen und 1953 von Böhme dargestellt und als neue Verbindung beschrieben wurde, bereits 1938 in einem amerikanischen [7] und einem gleichlautenden französischen [7] Patent als Ausgangsmaterial für ein technisches Verfahren genannt wird, allerdings ohne nähere Angaben.

Zwei in der Literatur beschriebene Umsetzungen organischer Schwefelverbindungen mit Grignardreagenz liessen vermuten, dass Trichlormethylphenylsulfid mit Grignardreagenz reagiert und es erschien von Interesse zu untersuchen, welcher der beiden denkbaren Reaktionswege beschritten wird. Adams und Mitarbeiter [8] erhielten bei der Umsetzung organischer Rhodanide mit Grignardreagenz Merkaptane und/oder Sulfide in wechselnden Ausbeuten, während Brintzinger [9] aus Chlormethansulfenylchlorid und Phenylmagnesiumbromid in 55 %-iger Ausbeute Phenylbenzylsulfid darstellen konnte.

Wir setzten Trichlormethylphenylsulfid mit Phenyl- bzw. 1-Naphthylmagnesiumbromid um und erhielten Diphenylsulfid bzw. 1-Naphthylphenylsulfid in 47 bzw. 33 % Ausbeute.

	[1 0 0]		[1 0 1] ($x = x' + z$)		[0 1 0]		Mean values		
	y	z	x'	y	x	z	x	y	z
C_1	0.124	0.076	−0.081	0.124	−0.007	0.076	−0.006	0.124	0.076
C_2	0.175	0.145	0.129	0.177	0.275	0.144	0.274	0.176	0.145
C_3	0.327	0.111	0.206	0.330	0.319	0.114	0.319	0.328	0.112
C_4	0.339	−0.025	0.267	0.337	0.243	−0.024	0.243	0.338	−0.025
C_5	0.289	−0.094	0.056	0.287	−0.040	−0.094	−0.039	0.288	−0.094
C_6	0.136	−0.062	−0.034	0.137	−0.094	−0.064	−0.096	0.136	−0.063
C_7	0.028	−0.109	0.162	0.027	0.055	−0.108	0.054	0.028	−0.109

where the hydrogen atoms were included are as follows:

»Reliability factors» for the three projections are 0.09, 0.06, and 0.08, respectively. The C-C bond distances computed from these coordinates range from 1.49 to 1.56 (Å); mean value 1.54 Å.

The C-C-C bond angles range from 109° to 114°; mean value 112°. Shortest intermolecular C-C distance 3.83 Å.

We thank Professor H. B. Henbest for the substance placed at our disposal in 1958. Thanks are also due to Professor O. Hassel for his interest and advice throughout this work.

1. Bog, S., Hassel, O. and Vihovde, E. H. *Acta Chem. Scand.* **7** (1953) 1308.
2. Hill, R. K. and Martin, J. G. *Proc. Chem. Soc.* **1959** 390.
3. Hassel, O. and Davis, M. *To be published.*

Received July 11, 1960.

Die Umsetzung des Trichlormethylphenylsulfids mit Grignardreagenz

ALEXANDER SENNING und SVEN-OLOV LAWESSON

Laboratorium für Organische Chemie, Chemisches Institut der Universität Uppsala, Uppsala, Schweden

Die von Sanna [1] beschriebene Darstellung von Trichlormethylphenylsulfid durch Umsetzung von Trichlormethansulfenylchlorid mit Phenylmagnesiumbromid ist u.a. von Egen [2] und Böhme [3] widerlegt worden, wird aber andererseits in neueren Übersichten, wie denen von Schöberl und Wagner [4], Sosnovsky [5] und Reid [6] ohne Kritik zitiert. Egen und Böhme bezweifelten die Angaben Sannas auf Grund der physikalischen Eigenschaften seines Produkts (und der von ihm als Trichlormethylphenylsulfon beschriebenen Verbindung), die mit denen des von ihnen auf anderem Wege dargestellten Trichlormethylphenylsulfids (bzw. Trichlormethylphenylsulfons) in keiner Weise übereinstimmten. Dagegen ist Sannas Artikel unseres Wissens noch nicht nachgearbeitet worden. Wir haben diese Nacharbeitung durchgeführt und festgestellt, dass bei dieser Reaktion keine definierten Produkte zu erhalten sind. Interessant ist in diesem Zusammenhang, dass das Trichlormethylphenylsulfid, das 1951 von Egen und 1953 von Böhme dargestellt und als neue Verbindung beschrieben wurde, bereits 1938 in einem amerikanischen [7] und einem gleichlautenden französischen [7] Patent als Ausgangsmaterial für ein technisches Verfahren genannt wird, allerdings ohne nähere Angaben.

Zwei in der Literatur beschriebene Umsetzungen organischer Schwefelverbindungen mit Grignardreagenz liessen vermuten, dass Trichlormethylphenylsulfid mit Grignardreagenz reagiert und es erschien von Interesse zu untersuchen, welcher der beiden denkbaren Reaktionswege beschritten wird. Adams und Mitarbeiter [8] erhielten bei der Umsetzung organischer Rhodanide mit Grignardreagenz Merkaptane und/oder Sulfide in wechselnden Ausbeuten, während Brintzinger [9] aus Chlormethansulfenylchlorid und Phenylmagnesiumbromid in 55 %-iger Ausbeute Phenylbenzylsulfid darstellen konnte.

Wir setzten Trichlormethylphenylsulfid mit Phenyl- bzw. 1-Naphthylmagnesiumbromid um und erhielten Diphenylsulfid bzw. 1-Naphthylphenylsulfid in 47 bzw. 33 % Ausbeute.

VERSUCHE

Trichlormethansulfenylchlorid und Phenylmagnesiumbromid. Die beiden Verbindungen wurden in Ätherlösung in wechselnden Mengenverhältnissen bei Temperaturen zwischen −70° und +34° miteinander umgesetzt. Die stark exotherme Reaktion lieferte keine definierten Produkte.

Trichlormethylphenylsulfid und Phenylmagnesiumbromid. Zu einer Lösung von 20,0 g (0,088 Mol) Trichlormethylphenylsulfid in Äther wurden unter Rühren in Stickstoffatmosphäre 148 ml einer 1,78-molaren ätherischen Phenylmagnesiumbromidlösung (0,264 Mol) zugetropft. Anschliessend wurde noch 2 Stunden gekocht, mit Eiswasser und Salzsäure zersetzt und wie üblich aufgearbeitet. Zwischen 80°/0,4 mm und 96°/0,4 mm gingen 7,8 g (47 % der Theorie) Diphenylsulfid über. n_D^{20} = 1,6236 (Literatur 1,6312). Das Sulfon schmolz zwischen 122° und 127° (Literatur 128°), der Mischschmelzpunkt mit authentischem Diphenylsulfon (F: 127°) war 123°—127°. Das Produkt war mit Diphenyl (von der Bereitung des Grignardreagenz) verunreinigt, das sich nicht vollständig abtrennen liess.

Trichlormethylphenylsulfid und 1-Naphthylmagnesiumbromid. Die Umsetzung wurde wie oben durchgeführt, zur besseren Lösung der Grignardverbindung wurde etwas Benzol zugesetzt. Zwischen 211°/11 mm und 225°/11 mm gingen 7,0 g (33 % der Theorie) 1-Naphthylphenylsulfid über. Die Substanz schmolz nach Umkristallisieren aus Alkohol zwischen 37° und 39° (Literatur 41,8°). Das Sulfon schmolz zwischen 97° und 99° (Literatur 99,5°—100,5°). Das Produkt war mit Dinaphthyl-(1,1') verunreinigt.

Wir danken Herrn Professor A. Fredga für das Interesse, das er unserer Arbeit entgegengebracht hat. Wir sind Herrn Professor A. Fredga für die Überlassung des Arbeitsplatzes und *Jordbrukets Forskningsråd* für die finanzielle Unterstützung unserer Arbeit zu Dank verpflichtet.

1. Sanna, G. und Stefano, S. *Gazz. chim. ital.* **72** (1942) 305.
2. Egen, R. *Diss.* Erlangen 1951.
3. Böhme, H. und Gran, H.-J. *Ann.* **581** (1953) 133.
4. Schöberl, A. und Wagner, A. *Houben-Weyl* **9** (1955) 139.
5. Sosnovsky, G. *Chem. Revs.* **58** (1958) 509.
6. Reid, E. *Organic Chemistry of Bivalent Sulfur*, I (1960) 290.
7. US Pat. 2108606, Frz. Pat. 820796, vgl. Scherer, *Angew. Chem.* **52** (1939) 457.
8. Adams, R., Bramlet, H. B. und Tendick, F. H. *J. Am. Chem. Soc.* **42** (1920) 2369.
9. Brintzinger, H. und Schmahl, H. *Ber.* **87** (1954) 314.

Eingegangen am 8. September 1960.

Studies on Peroxy Compounds VI.* A Novel Method for the Preparation of Acyloins

SVEN-OLOV LAWESSON and SUSANNE GRÖNWALL

Department of Organic Chemistry, Chemical Institute, University of Uppsala, Uppsala, Sweden

In connection with our current studies of the reaction between benzoyl peroxide and sodium compounds of so called active methylene compounds [1], we have recently completed a project on ethyl acetoacetate and ethyl benzoylacetate. Inspired by the work of Treibs and Hintermeier [2] we directed our attention to *t*-butyl acetoacetate which is easily prepared in high yields from *t*-butyl alcohol and diketene. First we synthesized a series of *α*-alkyl and *α*-aralkyl substituted homologues of *t*-butyl acetoacetate with sodium ethoxide in ethanol as condensation agent. The benzoyloxy group is then easily introduced into the *α*-position of the ester by reacting its sodium compound with benzoyl peroxide in an inert solvent at 0—4°C. The benzoate, however, decomposes upon distillation. By reacting the crude ester with a catalytic amount of *p*-toluenesulphonic acid (TS) the carbo *t*-butoxy group is eliminated, and a benzoyl derivative of the corresponding acyloin is obtained. Hydrolysis may then give the acyloin according to the following formulas.

With certain limitations, it would be possible to prepare *t*-butyl esters of different *β*-keto acids according to well-known methods, and therefore the synthetic route outlined above appears to be general for the preparations of acyloins. As a full paper will be published at a later date,

* Part V: *Acta Chem. Scand.* **14** (1960) 944.

VERSUCHE

Trichlormethansulfenylchlorid und Phenylmagnesiumbromid. Die beiden Verbindungen wurden in Ätherlösung in wechselnden Mengenverhältnissen bei Temperaturen zwischen −70° und +34° miteinander umgesetzt. Die stark exotherme Reaktion lieferte keine definierten Produkte.

Trichlormethylphenylsulfid und Phenylmagnesiumbromid. Zu einer Lösung von 20,0 g (0,088 Mol) Trichlormethylphenylsulfid in Äther wurden unter Rühren in Stickstoffatmosphäre 148 ml einer 1,78-molaren ätherischen Phenylmagnesiumbromidlösung (0,264 Mol) zugetropft. Anschliessend wurde noch 2 Stunden gekocht, mit Eiswasser und Salzsäure zersetzt und wie üblich aufgearbeitet. Zwischen 80°/0,4 mm und 96°/0,4 mm gingen 7,8 g (47 % der Theorie) Diphenylsulfid über. n_D^{20} = 1,6236 (Literatur 1,6312). Das Sulfon schmolz zwischen 122° und 127° (Literatur 128°), der Mischschmelzpunkt mit authentischem Diphenylsulfon (F: 127°) war 123°—127°. Das Produkt war mit Diphenyl (von der Bereitung des Grignardreagenz) verunreinigt, das sich nicht vollständig abtrennen liess.

Trichlormethylphenylsulfid und 1-Naphthylmagnesiumbromid. Die Umsetzung wurde wie oben durchgeführt, zur besseren Lösung der Grignardverbindung wurde etwas Benzol zugesetzt. Zwischen 211°/11 mm und 225°/11 mm gingen 7,0 g (33 % der Theorie) 1-Naphthylphenylsulfid über. Die Substanz schmolz nach Umkristallisieren aus Alkohol zwischen 37° und 39° (Literatur 41,8°). Das Sulfon schmolz zwischen 97° und 99° (Literatur 99,5°—100,5°). Das Produkt war mit Dinaphthyl-(1,1') verunreinigt.

Wir danken Herrn Professor A. Fredga für das Interesse, das er unserer Arbeit entgegengebracht hat. Wir sind Herrn Professor A. Fredga für die Überlassung des Arbeitsplatzes und *Jordbrukets Forskningsråd* für die finanzielle Unterstützung unserer Arbeit zu Dank verpflichtet.

1. Sanna, G. und Stefano, S. *Gazz. chim. ital.* **72** (1942) 305.
2. Egen, R. *Diss.* Erlangen 1951.
3. Böhme, H. und Gran, H.-J. *Ann.* **581** (1953) 133.
4. Schöberl, A. und Wagner, A. *Houben-Weyl* **9** (1955) 139.
5. Sosnovsky, G. *Chem. Revs.* **58** (1958) 509.
6. Reid, E. *Organic Chemistry of Bivalent Sulfur*, I (1960) 290.
7. US Pat. 2108606, Frz. Pat. 820796, vgl. Scherer, *Angew. Chem.* **52** (1939) 457.
8. Adams, R., Bramlet, H. B. und Tendick, F. H. *J. Am. Chem. Soc.* **42** (1920) 2369.
9. Brintzinger, H. und Schmahl, H. *Ber.* **87** (1954) 314.

Eingegangen am 8. September 1960.

Studies on Peroxy Compounds VI.* A Novel Method for the Preparation of Acyloins

SVEN-OLOV LAWESSON and SUSANNE GRÖNWALL

Department of Organic Chemistry, Chemical Institute, University of Uppsala, Uppsala, Sweden

In connection with our current studies of the reaction between benzoyl peroxide and sodium compounds of so called active methylene compounds [1], we have recently completed a project on ethyl acetoacetate and ethyl benzoylacetate. Inspired by the work of Treibs and Hintermeier [2] we directed our attention to *t*-butyl acetoacetate which is easily prepared in high yields from *t*-butyl alcohol and diketene. First we synthesized a series of *α*-alkyl and *α*-aralkyl substituted homologues of *t*-butyl acetoacetate with sodium ethoxide in ethanol as condensation agent. The benzoyloxy group is then easily introduced into the *α*-position of the ester by reacting its sodium compound with benzoyl peroxide in an inert solvent at 0—4°C. The benzoate, however, decomposes upon distillation. By reacting the crude ester with a catalytic amount of *p*-toluenesulphonic acid (TS) the carbo *t*-butoxy group is eliminated, and a benzoyl derivative of the corresponding acyloin is obtained. Hydrolysis may then give the acyloin according to the following formulas.

With certain limitations, it would be possible to prepare *t*-butyl esters of different *β*-keto acids according to well-known methods, and therefore the synthetic route outlined above appears to be general for the preparations of acyloins. As a full paper will be published at a later date,

* Part V: *Acta Chem. Scand.* **14** (1960) 944.

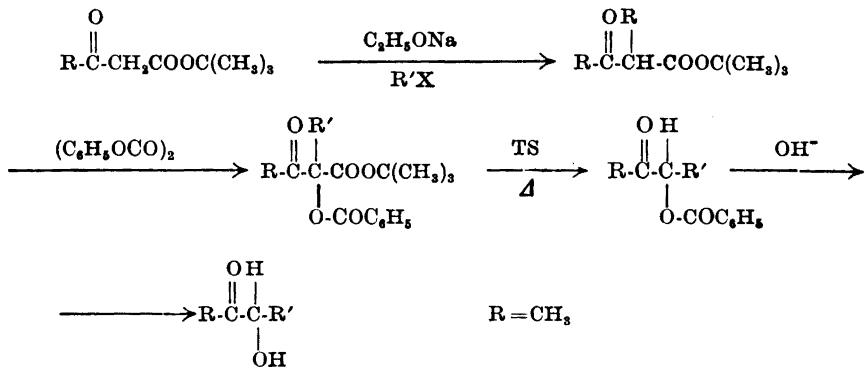

only one series of experiments is described here.

Preparation of t-butyl-α-n-amyl acetoacetate. To a sodium alcoholate solution prepared from 6.9 g of sodium in 150 ml of absolute ethyl alcohol, 47.4 g (0.3 mole) of *t*-butyl acetoacetate is added. After 10 min, 45.3 g (0.3 mole) of redistilled *n*-amyl bromide is added droppwise during 25 min and thereafter the mixture is refluxed for half an hour. The excess of ethanol is then immediately stripped off at reduced pressure, and the remainder poured onto water. The water phase is twice extracted with ether, and the combined ether extracts washed with water until neutral and then dried over sodium sulphate. Distillation gives the main fraction at b.p. 120—122°/10 mm Hg (Found: C 67.85; H. 10.57; Calc. C 68.38; H 10.59) $n_D^{20} = 1.4308$. Weight 46 g, yield 67 %.

The purity of the product has been verified by gas chromatographic analysis. When the *t*-butyl ester is heated, *iso*butylene rapidly splits off, and its incomplete combustion causes the low carbon yield percentage.

Preparation of octan-2-one-O-benzoyl-3-ol. In a 1 l three-necked flask, fitted with a mechanical stirrer, a reflux condenser, and a dropping funnel, is placed 4.8 g of sodium hydride and covered with 200 ml of dry benzene. 45.6 g (0.2 mole) of *t*-butyl-α-*n*-amyl acetoacetate is added dropwise to the sodium hydride, and after 2 h of rapid stirring almost all hydride has reacted, the evolution of hydrogen has ceased and a clear solution is formed. Then the flask is cooled in an ice-water bath to about 0° and 36.3 g (0.15 mole) of benzoyl peroxide in 200 ml of dry benzene is added droppwise through the dropping funnel during 45 min. After another 15 min, the peroxide test is negative and the porridge-like mixture is poured into water. The benzene phase is separated, the water phase extracted once with ether and the combined organic extracts washed neutral with water; 15.2 g of benzoic acid is isolated. From the organic phase, solvents and excess of starting material are distilled off. To the residue, 0.25 g *p*-toluene sulphonic acid is added. The distillation vessel is connected to a water pump and warmed on an oil bath maintained at a temperature of 160°C. When the decomposition is complete (constant pressure), the product is distilled. The main fraction is obtained at b.p. 114—115°/0.1 mm Hg. (Found: C 72.55; H 8.19. Calc. C 72.55; H 8.12). $n_D^{20} = 1.4959$. Weight 31 g, yield 83 %.

Preparation of octan-2-one-3-ol. In a flask fitted with a mechanical stirrer and a reflux condenser is placed 27 g of octan-2-one-O-benzoyl-3-ol and 200 ml of 10 % sodium hydroxide solution. Gentle heat is applied(inner temperature of the flask 60°C); after one hour's violent stirring, the mixture becomes homogeneous and turns a deep yellow colour. It is then extracted three times with ether and the organic layers are poured together, washed neutral with water and dried over sodium sulphate. 13 g of benzoic acid is obtained from the water phase. By vacuum distillation, 8 g of octan-2-one-3-ol at b.p. 93—94°/12 mm Hg is obtained (Found: C 66.57; H 11.03. Calc. 66.63; H 11.18). $n_D^{20} = 1.4340$, yield 51 %.

A grant from *Statens naturvetenskapliga forskningsråd* is gratefully acknowledged.

1. Lawesson, S.-O. and Busch, T. *Acta Chem. Scand.* **13** (1959) 1716.
2. Treibs, A. and Hintermeier, K. *Ber.* **87** (1954) 1163.

Received July 26, 1960.

Surface Tension of Water Solutions of Fluorophosphorus Compounds

GUNNAR AKSNES

Norwegian Defence Research Establishment, Toxicological Group, Kjeller pr Lillestrøm, Norway

In connection with a study of the action of fluorophosphorus compounds as potent inhibitors of cholinesterases it was desirable to investigate whether these compounds possessed surface active properties. Such properties may be expected to exert influence upon biochemical reactions due to the fact that enzymatic processes depend to a great extent upon the presence of lipoid-water interfaces. The observation of the very strong polar character of the phosphoryl group [1] suggests that fluorophosphorus compounds with sufficient large hydrocarbon groups may possess considerable surface activity.

Materials. The preparation of the fluorophosphorus compounds was performed as previously described [1]. The water used for making

Table 1. Surface tension of water solutions of fluorophosphorus compounds (1 %). Temperature: 20°C.

Compound	Observed values	Corrected values, dyn/cm	Distribution coefficients CCl_4/H_2O
Pure water	77.4, 77.2, 77.0	72.6	—
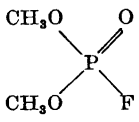	70.0, 70.1, 69.8	65.8	0.9
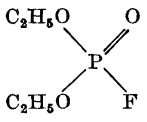	56.7, 56.8, 56.9	53.3	3.46
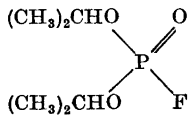	37.2, 38.2, 38.0	35.5	38.3
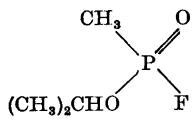	65.7, 66.4, 66.2	62.0	—
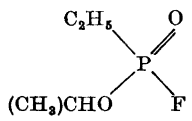	52.3, 52.4, 52.6	49.3	—

the solutions was distilled twice in a glass apparatus.

Apparatus. The measurements of the surface tension of the water solutions were performed with a torsion weight tensiometer (Cenco, Model No. 70540). All the measurements refer to 1 % solutions of fluorophosphorus compounds. The surface tension was measured at 20°C. Three independent measurements of each solution were taken. The correction factor of the instrument was 0.94.

Results and discussion. In Table 1 are collected the data from the present study. In the same table are included also the partition coefficients for the distribution of some of the fluorophosphorus compounds between water and carbon tetrachloride [2]. We recognize a rapid rise in surface activity of the fluorophosphorus compounds with the increase of their hydrocarbon content. The rise of the surface activities of the compounds is accompanied by a corresponding increase of the partition coefficients in the system CCl_4/H_2O.

From analogy with the present results we expect that fluorophosphorus compounds are capable of changing the interfacial tension between lipoids and water to a considerable degree, and in this way may play a role when the whole picture of the phosphorylating process of the enzyme is considered.

Table 1. Rate of decomposition of urethane at 37.0°C.

c	$k \times 10^7$	$-H_0$	a_{H_2O}
Hydrochloric acid:			
1.00	0.60	0.20	0.955
2.00	1.36	0.69	0.900
3.00	2.32	1.05	0.836
4.00	3.56	1.40	0.765
4.00 *	3.67		
5.32	5.81	1.87	0.659
6.03	7.39	2.13	0.598
Sulphuric acid:			
1.00	0.78	0.26	0.960
2.00	1.90	0.84	0.903
3.00	3.55	1.38	0.823
4.00	5.70	1.85	0.721
5.00	8.98	2.28	0.603
6.00	12.86	2.76	0.479
6.96	17.6	3.30	0.366
8.00	22.2	3.87	0.258
8.97	24.9	4.38	0.175
10.00	24.2	4.89	0.108

* The solution contained in addition 0.10 M cupric chloride.

1. Aksnes, G. and Gramstad, T. *Acta Chem. Scand.* **14** (1960). *In press.*
2. Öksne, S. *Acta Chem. Scand.* **13** (1959) 1814.

Received July 12, 1960.

The Rate of Decomposition of Urethane in Acid Solution

KAI JULIUS PEDERSEN

Chemical Laboratory, Royal Veterinary and Agricultural College, Copenhagen, Denmark

The rate of the reaction

$$C_2H_5OCONH_2 + H^+ + H_2O \rightarrow C_2H_5OH + NH_4^+ + CO_2$$

was studied manometrically at 37.0°C in concentrated aqueous solutions of hydrochloric and sulphuric acids (c moles per liter solution). Owing to the slowness of the reaction, the final pressure was not observed but calculated from the pressure increase when, instead of urethane, calcium carbonate was dissolved. In general, only 5 to 30 % of the decomposition was observed, but in one experiment (solvent 10 M sulphuric acid) readings were taken till more than 80 % of the urethane had decomposed, and it was shown that the reaction follows the first-order law. The initial concentrations of urethane varied from 0.02 to 0.1 M. The urethane (m.p. 48.1°C) had been purified by melting and partly crystallising the commercial preparation. Velocity constants k (in sec^{-1}) are given in Table 1 together with values of the Hammett H_0 acidity function [1] and the water activities a_{H_2O} of the solutions computed from vapour-pressure data [2,3]. The velocity constant k increases more rapidly than c, but less rapidly than h_0 (where $H_0 = -\log h_0$). When the three most concentrated solutions are left out of consideration, k is roughly proportional to $h_0 a_{H_2O}^4$ as shown in Fig. 1 where log k has been plotted against $-H_0 + 4 \log a_{H_2O}$. The points fall fairly close to a straight line with the

the solutions was distilled twice in a glass apparatus.

Apparatus. The measurements of the surface tension of the water solutions were performed with a torsion weight tensiometer (Cenco, Model No. 70540). All the measurements refer to 1 % solutions of fluorophosphorus compounds. The surface tension was measured at 20°C. Three independent measurements of each solution were taken. The correction factor of the instrument was 0.94.

Results and discussion. In Table 1 are collected the data from the present study. In the same table are included also the partition coefficients for the distribution of some of the fluorophosphorus compounds between water and carbon tetrachloride [2]. We recognize a rapid rise in surface activity of the fluorophosphorus compounds with the increase of their hydrocarbon content. The rise of the surface activities of the compounds is accompanied by a corresponding increase of the partition coefficients in the system CCl_4/H_2O.

From analogy with the present results we expect that fluorophosphorus compounds are capable of changing the interfacial tension between lipoids and water to a considerable degree, and in this way may play a role when the whole picture of the phosphorylating process of the enzyme is considered.

Table 1. Rate of decomposition of urethane at 37.0°C.

c	$k \times 10^7$	$-H_0$	a_{H_2O}
Hydrochloric acid:			
1.00	0.60	0.20	0.955
2.00	1.36	0.69	0.900
3.00	2.32	1.05	0.836
4.00	3.56	1.40	0.765
4.00 *	3.67		
5.32	5.81	1.87	0.659
6.03	7.39	2.13	0.598
Sulphuric acid:			
1.00	0.78	0.26	0.960
2.00	1.90	0.84	0.903
3.00	3.55	1.38	0.823
4.00	5.70	1.85	0.721
5.00	8.98	2.28	0.603
6.00	12.86	2.76	0.479
6.96	17.6	3.30	0.366
8.00	22.2	3.87	0.258
8.97	24.9	4.38	0.175
10.00	24.2	4.89	0.108

* The solution contained in addition 0.10 M cupric chloride.

1. Aksnes, G. and Gramstad, T. *Acta Chem. Scand.* **14** (1960). *In press.*
2. Öksne, S. *Acta Chem. Scand.* **13** (1959) 1814.

Received July 12, 1960.

The Rate of Decomposition of Urethane in Acid Solution

KAI JULIUS PEDERSEN

Chemical Laboratory, Royal Veterinary and Agricultural College, Copenhagen, Denmark

The rate of the reaction

$$C_2H_5OCONH_2 + H^+ + H_2O \rightarrow C_2H_5OH + NH_4^+ + CO_2$$

was studied manometrically at 37.0°C in concentrated aqueous solutions of hydrochloric and sulphuric acids (c moles per liter solution). Owing to the slowness of the reaction, the final pressure was not observed but calculated from the pressure increase when, instead of urethane, calcium carbonate was dissolved. In general, only 5 to 30 % of the decomposition was observed, but in one experiment (solvent 10 M sulphuric acid) readings were taken till more than 80 % of the urethane had decomposed, and it was shown that the reaction follows the first-order law. The initial concentrations of urethane varied from 0.02 to 0.1 M. The urethane (m.p. 48.1°C) had been purified by melting and partly crystallising the commercial preparation. Velocity constants k (in sec^{-1}) are given in Table 1 together with values of the Hammett H_0 acidity function [1] and the water activities a_{H_2O} of the solutions computed from vapour-pressure data [2,3]. The velocity constant k increases more rapidly than c, but less rapidly than h_0 (where $H_0 = -\log h_0$). When the three most concentrated solutions are left out of consideration, k is roughly proportional to $h_0 a_{H_2O}^4$ as shown in Fig. 1 where log k has been plotted against $-H_0 + 4 \log a_{H_2O}$. The points fall fairly close to a straight line with the

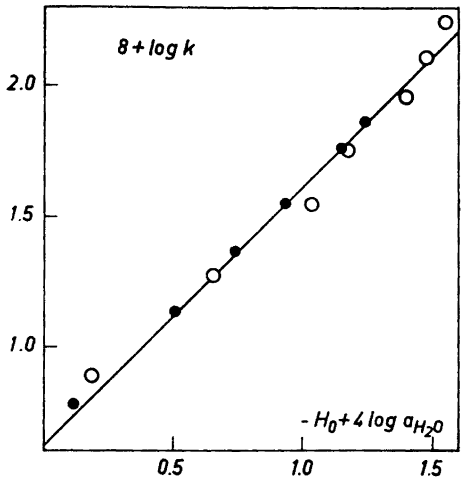

Fig. 1. Plot of log k against $-H_0 + 4 \log a_{H_2O}$ for the decomposition of urethane in solutions of hydrochloric acid (closed circles) and sulphuric acid (open circles). The straight line has the slope unity.

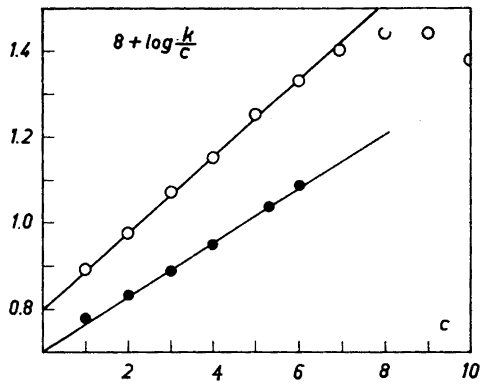

Fig. 2. Plot of $\log \frac{k}{c}$ against c for the decomposition of urethane in solutions of hydrochloric acid (closed circles) and sulphuric acid (open circles).

slope unity. This indicates that a bimolecular reaction between a urethane molecule (U) and the ion $H(H_2O)_4^+$ is rate-determining, since, in this case, the rate will be proportional to

$$a_U a_{H(H_2O)_4^+} / f_{UH(H_2O)_4^+} \quad (1)$$
$$= [U] f_U a_{H^+} a_{H_2O}^4 / f_{UH(H_2O)_4^+}$$
$$\simeq [U] h_0 a_{H_2O}^4$$

It has recently been derived in different ways [4-6] that the hydrogen ion in aqueous solution is hydrated with 4 molecules of water. If it is assumed that $[H(H_2O)_4^+] = c$, we obtain from expression (1) that

$$k = A c f_U / f_{UH(H_2O)_4^+}$$

where A is a constant. Since it may be expected that to a first approximation

$$\log (f_U / f_{UH(H_2O)_4^+}) = Bc$$

where B is a constant, we obtain the following approximate formula

$$\log \frac{k}{c} = \log A + Bc$$

In Fig. 2 it is shown that the experimental data agree well with this formula up to $c = 6$. From the graph is obtained for solutions of hydrochloric acid

$$\log \frac{k}{c} = 0.705 - 8 + 0.063\ c$$

and for solutions of sulphuric acid

$$\log \frac{k}{c} = 0.801 - 8 + 0.0895\ c$$

By extrapolation to $c = 0$ is found for hydrochloric acid $k = 5.07 \times 10^{-8} \times c$, and for sulphuric acid $k = 6.32 \times 10^{-8} \times c$. The larger value for sulphuric acid may possibly be attributed to catalysis by hydrogen sulphate ions in addition to the hydrogen ion catalysis.

1. Paul, M. A. and Long, F. A. *Chem. Revs.* **57** (1957) 1.
2. *International Critical Tables*, Vol. **III** (1928) p. 301.
3. Robinson, R. A. and Stokes, R. H. *Electrolyte Solutions*, Butterworths, London 1955, p. 462.
4. Wicke, E., Eigen, M. and Ackermann, Th. *Z. physik. Chem. (Frankfurt)* **1** (1954) 340.
5. Glueckauf, E. *Trans. Faraday Soc.* **51** (1955) 1235.
6. Bascombe, K. N. and Bell, R. P. *Discussions Faraday Soc.* **24** (1957) 158.

Received August 20, 1960.

Redetermined Lattice Constants of PtP_2, $PtAs_2$, $PtSb_2$, and α-$PtBi_2$

ARNE KJEKSHUS

Kjemisk Institutt A, Universitetet i Oslo, Blindern, Norway

A number of compounds have earlier been prepared and investigated in the binary systems between platinum and elements of group V in the periodic table. Compounds with composition metal : metalloid = 1 : 2 are found in all systems, except the platinum-nitrogen system, where no intermediate compounds are known at present. The compounds PtP_2, $PtAs_2$, $PtSb_2$, and α-$PtBi_2$ have been studied by means of X-ray methods and all of them have structures of the pyrite ($C2$) type.

Platinum diphosphide was first prepared by Davey [1]. The structure was established by Thomassen [2] and later confirmed by Biltz *et al.* [3] and Rundqvist [4].

Platinum diarsenide was first synthesized by Gehlen [5]. It occurs in nature as the mineral sperrylite. The structural identity of sperrylite and artificial $PtAs_2$ was established by Ramsdell [6] and De Jong [7] by means of X-rays. The structure of $PtAs_2$ has later been investigated by Aminoff and Parsons [8] and Thomassen [2].

Platinum diantimonide was first obtained by Roessler [9]. The structure, *i.e.*, its lattice constant and atomic parameter, was determined by Thomassen [10].

Platinum dibismuthide was also first prepared by Roessler [9]. The crystal structure was established by Wallbaum [11] and its correctness later confirmed by Zhuravlev and Kertes [12]. By thermal, metallographic and X-ray studies these authors found the existence of one more $PtBi_2$ phase, β-$PtBi_2$, which was found to be hexagonal.

The *alloys* were prepared by heating accurately weighed quantities of platinum and phosphorus, arsenic, antimony or bismuth, respectively, in evacuated and sealed silica tubes. In each system alloys with 25.00, 33.33 and 40.00 atomic % platinum were made. All samples were heated at 650°C for 30 days and cooled slowly to room temperature over a period of another 30 days.

All samples were crushed and X-ray powder photographs taken in cameras with 114.6 mm effective diameter and asymmetric film mounting. The lattice constants, which were found by extrapolation according to the method of Nelson and Riley [13], are expressed in Ångstrøm units on the basis of λ $CuK\alpha_1$ = 1.54050 Å. Results from earlier investigations expressed in kX-units have been transformed to Å by multiplication by the factor 1.00202.

Table 1. Lattice constants of PtP_2, $PtAs_2$, $PtSb_2$, and α-$PtBi_2$.

Sample	a (Å)	Reference
PtP_2	5.6956 ± 0.0005	Present
	5.694 ± 0.004	Thomassen [2]
	5.694	Rundqvist [4]
$PtAs_2$	5.9665 ± 0.0004	Present
	5.97	Ramsdell [6]
	5.95 (sperrylite)	Ramsdell [6]
	5.93 (sperrylite)	De Jong [7]
	6.01 (sperrylite)	Aminoff and Parsons [8]
	5.969 ± 0.003	Thomassen [2]
$PtSb_2$	6.4400 ± 0.0004	Present
	6.441 ± 0.003	Thomassen [10]
α-$PtBi_2$	6.7022 ± 0.0006	Present
	6.696 ± 0.005	Wallbaum [11]

The lattice constants of the samples with composition PtX_2 are found in Table 1 together with the previous lattice constant values. The lattice constants of the different compounds are found to be independent of the composition of the alloys within the experimental error, indicated by the limits in Table 1. Thus, the homogeneity ranges of the phases are supposedly rather narrow. The earlier data agree well within their limited accuracy except for α-$PtBi_2$.

The redetermination of the atomic parameters in these compounds will be discussed in a forth-coming paper.

Acknowledgements. The author wishes to thank Professor Haakon Haraldsen and Dosent Fredrik Grønvold for their kind interest in this study.

1. Davey, E. *Phil. Mag.* **40** (1812) 28; *Journal f. Chem. u. Phys.* **10** (1814) 382.
2. Thomassen, L. *Z. physik. Chem.* **B4** (1929) 277.

3. Biltz, W., Weibke, F., May, E. and Meisel, K. *Z. anorg. u. allgem. Chem.* **223** (1935) 129.
4. Rundqvist, S. *Nature* **185** (1960) 31.
5. Gehlen, A. F. *Journal f. Chem. u. Phys.* **20** (1817) 353.
6. Ramsdell, L. S. *Am. Mineralogist* **10** (1925) 281; **12** (1927) 79.
7. De Jong, W. F. *Physica* **5** (1925) 292.
8. Aminoff, G. and Parsons, L. *Univ. Toronto Studies. Geol. Ser.* **1928** No. 26.
9. Roessler, F. *Z. anorg. Chem.* **9** (1895) 31.
10. Thomassen, L. *Z. physik. Chem.* **B2** (1929) 349.
11. Wallbaum, H. J. *Z. Metallkunde* **35** (1943) 200.
12. Zhuravlev, N. N. and Kertes, L. *Zhur. Eksp. i Teoret. Fiz.* **32** (1957) 1313; *Soviet Physics JEPT* **5** (1957) 1073.
13. Nelson, J. B. and Riley, D. P. *Proc. Phys. Soc. (London)* **57** (1945) 160.

Received August 23, 1960.

The Alkaline Hydrolysis of Diethyl Acetomalonate

KAI JULIUS PEDERSEN

Chemical Laboratory, Royal Veterinary and Agricultural College, Copenhagen, Denmark

When diethyl acetomalonate is dissolved in an aqueous solution of a strong base it will react with 3 hydroxyl ions according to the scheme

$$CH_3COCH(COOEt)_2 + 3\,HO^- \rightarrow CH_2(COO^-)_2 + CH_3COO^- + 2\,EtOH \quad (1)$$

One hydroxyl ion disappears immediately, while the other two are consumed at a measurable rate which is proportional to the ester concentration but independent of the hydroxyl ion concentration. This experimental result is explained as follows. The keto-form of the diethyl ester is rapidly and nearly completely transformed into enolate ion by the balanced reaction

$$CH_3COCH(COOEt)_2 + HO^- \rightleftharpoons CH_3C\bar{O}{:}C(COOEt)_2 + H_2O \quad (2)$$

The rate-determining reaction is

$$CH_3COCH(COOEt)_2 + HO^- \rightarrow CH_3COCH(COOEt)COO^- + EtOH \quad (3)$$

It is followed by the two rapid reactions

$$CH_3COCH(COOEt)COO^- + HO^- \rightarrow CH_3COCH(COO^-)_2 + EtOH$$

$$CH_3COCH(COO^-)_2 + HO^- \rightarrow CH_3COO^- + CH_2(COO^-)_2$$

The rate of reaction 3 will be proportional to the product of the hydroxyl ion concentration and the concentration of the keto-form of the diethyl ester, but since the latter, according to scheme 2, is inversely proportional to the hydroxyl ion concentration, the rate will be independent of the hydroxyl ion concentration and of first order with respect to the total concentration of diethyl acetomalonate (keto-form and enolate ion).

Diethyl acetomalonate was prepared according to Lund [1] and was distilled twice under reduced pressure in an all-glass apparatus fitted with a Widmer stillhead. The fraction used in the experiments distilled within less than 1°C. It was found that the ester could be titrated as a monobasic acid when thymolphthalein was used as indicator and a rather strongly blue colour was chosen as end-point. The average of several titrations was that 99.7 % of the calculated amount of base was used. When the ester is dissolved in an excess of strong base, it will therefore be rapidly and nearly completely transformed into enolate ion by reaction 2.

To 60 ml of 0.2 N barium hydroxide in a glass-stoppered flask was added 0.8 g of the ester. The clear solution was left at room temperature. After half an hour the first crystals were noticed, and the next day a large crystalline precipitate had been formed. The crystals were isolated by suction, washed with ice-cold water, and air-dried to constant weight. It was shown that they did not contain carbonate, from which it is concluded that no decarboxylation takes place in the reaction. In order to show that the crystals consisted of barium malonate this substance was prepared by mixing solutions of malonic acid and barium acetate. The crystals obtained here were isolated and dried in the same way as before. Weighed amounts of the two preparations were transformed into carbonate by ignition in a platinum crucible, and the residues were weighed. On the assumption that one molecule of both substances gives one molecule of barium carbonate, it was found that the molecular weight of the substance prepared from diethyl acetomalonate was 254.5 while that of the salt prepared from malonic acid was 255.0 (calc.

3. Biltz, W., Weibke, F., May, E. and Meisel, K. *Z. anorg. u. allgem. Chem.* **223** (1935) 129.
4. Rundqvist, S. *Nature* **185** (1960) 31.
5. Gehlen, A. F. *Journal f. Chem. u. Phys.* **20** (1817) 353.
6. Ramsdell, L. S. *Am. Mineralogist* **10** (1925) 281; **12** (1927) 79.
7. De Jong, W. F. *Physica* **5** (1925) 292.
8. Aminoff, G. and Parsons, L. *Univ. Toronto Studies. Geol. Ser.* **1928** No. 26.
9. Roessler, F. *Z. anorg. Chem.* **9** (1895) 31.
10. Thomassen, L. *Z. physik. Chem.* **B2** (1929) 349.
11. Wallbaum, H. J. *Z. Metallkunde* **35** (1943) 200.
12. Zhuravlev, N. N. and Kertes, L. *Zhur. Eksp. i Teoret. Fiz.* **32** (1957) 1313; *Soviet Physics JEPT* **5** (1957) 1073.
13. Nelson, J. B. and Riley, D. P. *Proc. Phys. Soc. (London)* **57** (1945) 160.

Received August 23, 1960.

The Alkaline Hydrolysis of Diethyl Acetomalonate

KAI JULIUS PEDERSEN

Chemical Laboratory, Royal Veterinary and Agricultural College, Copenhagen, Denmark

When diethyl acetomalonate is dissolved in an aqueous solution of a strong base it will react with 3 hydroxyl ions according to the scheme

$$CH_3COCH(COOEt)_2 + 3\,HO^- \rightarrow CH_2(COO^-)_2 + CH_3COO^- + 2\,EtOH \quad (1)$$

One hydroxyl ion disappears immediately, while the other two are consumed at a measurable rate which is proportional to the ester concentration but independent of the hydroxyl ion concentration. This experimental result is explained as follows. The keto-form of the diethyl ester is rapidly and nearly completely transformed into enolate ion by the balanced reaction

$$CH_3COCH(COOEt)_2 + HO^- \rightleftharpoons CH_3C\bar{O}{:}C(COOEt)_2 + H_2O \quad (2)$$

The rate-determining reaction is

$$CH_3COCH(COOEt)_2 + HO^- \rightarrow CH_3COCH(COOEt)COO^- + EtOH \quad (3)$$

It is followed by the two rapid reactions

$$CH_3COCH(COOEt)COO^- + HO^- \rightarrow CH_3COCH(COO^-)_2 + EtOH$$

$$CH_3COCH(COO^-)_2 + HO^- \rightarrow CH_3COO^- + CH_2(COO^-)_2$$

The rate of reaction 3 will be proportional to the product of the hydroxyl ion concentration and the concentration of the keto-form of the diethyl ester, but since the latter, according to scheme 2, is inversely proportional to the hydroxyl ion concentration, the rate will be independent of the hydroxyl ion concentration and of first order with respect to the total concentration of diethyl acetomalonate (keto-form and enolate ion).

Diethyl acetomalonate was prepared according to Lund [1] and was distilled twice under reduced pressure in an all-glass apparatus fitted with a Widmer stillhead. The fraction used in the experiments distilled within less than 1°C. It was found that the ester could be titrated as a monobasic acid when thymolphthalein was used as indicator and a rather strongly blue colour was chosen as end-point. The average of several titrations was that 99.7 % of the calculated amount of base was used. When the ester is dissolved in an excess of strong base, it will therefore be rapidly and nearly completely transformed into enolate ion by reaction 2.

To 60 ml of 0.2 N barium hydroxide in a glass-stoppered flask was added 0.8 g of the ester. The clear solution was left at room temperature. After half an hour the first crystals were noticed, and the next day a large crystalline precipitate had been formed. The crystals were isolated by suction, washed with ice-cold water, and air-dried to constant weight. It was shown that they did not contain carbonate, from which it is concluded that no decarboxylation takes place in the reaction. In order to show that the crystals consisted of barium malonate this substance was prepared by mixing solutions of malonic acid and barium acetate. The crystals obtained here were isolated and dried in the same way as before. Weighed amounts of the two preparations were transformed into carbonate by ignition in a platinum crucible, and the residues were weighed. On the assumption that one molecule of both substances gives one molecule of barium carbonate, it was found that the molecular weight of the substance prepared from diethyl acetomalonate was 254.5 while that of the salt prepared from malonic acid was 255.0 (calc.

for $CH_2(COO)_2Ba,H_2O$: 257.4). From acidimetric titration of the two residues was found 254.2 and 254.8, respectively. It is therefore concluded that the two substances are identical, and that malonate is formed as end-product in the alkaline hydrolysis of diethyl acetomalonate (scheme 1).

Measurements of the rate of hydrolysis of diethyl acetomalonate in solutions of sodium hydroxide were carried out at the two temperatures 25.0 and 37.0°C. A graduated flask filled to a little below the mark with sodium hydroxide solution was placed in a water thermostat. When temperature equilibrium was attained, a weighed-out amount of the ester was dissolved, and the flask was quickly filled to the mark with water of the proper temperature. At suitable time-intervals during the reaction, and after it had come to an end, samples of the solution were pipetted into an excess of 0.1 N hydrochloric acid; thymolphthalein was added, and the solutions were titrated back with 0.03 N sodium hydroxide to a rather strongly blue colour. When x denotes the concentration of titratable base, and c that of diethyl ester in the reacting solution at the time t after the start of the reaction, we have according to our assumptions that $x-x_\infty = 2c$ where subscript ∞ denotes final value. When $\log (x-x_\infty)$ was plotted against t, the points fell in all the experiments very close to straight lines showing that the first-order law holds for the reaction. The composition of the solutions examined, and the rate constants k (in sec^{-1}) found, are given in Table 1. The values of k increase slightly with increasing concentration of strong base in the original solution, and, as shown in one experiment, with addition of sodium chloride. It also appears from the table that the number of hydroxyl ions reacting per molecule of diethyl acetomalonate $(x_0-x_\infty)/c_0$ is always 3 in agreement with scheme 1.

Table 1. Rate of hydrolysis of diethyl acetomalonate (initially c_0 M) in solutions of sodium hydroxide (initially x_0 M). x_∞ is the final concentration of sodium hydroxide and k the rate constant in sec^{-1}.

c_0	x_0	x_∞	$\frac{x_0-x_\infty}{c_0}$	$k \times 10^4$
Temperature 25.0°C:				
0.02012	0.0774	0.0169	3.01	1.070
0.03980	0.1351	0.0153	3.01	1.097
0.03990	0.1549	0.0352	3.00	1.110
0.04000	0.1852	0.0647	3.01	1.132
0.04042	0.1349*	0.0133	3.01	1.161
Temperature 37.0°C:				
0.01979	0.0770	0.0174	3.01	3.57
0.03983	0.1342	0.0145	3.01	3.73
0.03956	0.1539	0.0353	3.00	3.86
0.03952	0.1834	0.0647	3.00	3.93

* The solution contained in addition 0.300 M sodium chloride.

1. Lund, H. *Ber.* **67** (1934) 935.

Received September 10, 1960.

ACTA CHEMICA SCANDINAVICA 14 (1960) 1453–1465

The Crystal Structures of the Triammines of the Ammonium Halides

IVAR OLOVSSON

Institute of Chemistry, University of Uppsala, Uppsala, Sweden

The crystal structures of $NH_4Cl \cdot 3NH_3$, $NH_4Br \cdot 3NH_3$ and $NH_4I \cdot 3NH_3$ have been determined from single-crystal X-ray data. No phase transitions were observed from the melting point down to −140°C. The crystals are orthorhombic with four molecules per unit cell; the space group for the chloride and bromide is $P2_12_12_1$ and for the iodide $P2_1nb$. The cell dimensions at −35°C are for $NH_4Cl \cdot 3NH_3$: $a = 8.795$, $b = 8.68$, $c = 8.989$ Å; for $NH_4Br \cdot 3NH_3$: $a = 8.96$, $b = 8.996$, $c = 9.263$ Å; for $NH_4I \cdot 3NH_3$: $a = 8.32$, $b = 9.91$, $c = 9.96$ Å. The ammonium ion is tetrahedrally surrounded by three ammonia molecules and one halide ion. The hydrogen atoms of ammonium are evidently involved in the hydrogen bonds within this group. The forces between the different groups are relatively weak but may restrict the possible rotation of the ammonia molecules about their threefold axes.

The present investigation is the first in a series of planned structure determinations of some ammines formed with salts of the alkali metals and ammonium.

The systems NH_4X—NH_3 (X = F, Cl, Br, I) have been studied in several earlier works and reported compounds are: $NH_4F \cdot NH_3$; $NH_4Cl \cdot 3$ and $6NH_3$; $NH_4Br \cdot 1$, 3, 4, and $6NH_3$; $NH_4I \cdot 1$, 2, 3, 4, 5, and $6NH_3$. A list of references is given in the work by Watt and McBride [1]. The compounds $NH_4Cl \cdot 3NH_3$, $NH_4Br \cdot 3NH_3$, $NH_4I \cdot 3NH_3$ and $NH_4I \cdot 4NH_3$ seem to be established with certainty in these works. The present investigation involves the determination of the crystal structures of $NH_4Cl \cdot 3NH_3$, $NH_4Br \cdot 3NH_3$ and $NH_4I \cdot 3NH_3$ from single crystal X-ray diffraction data obtained at —35°C. A preliminary report of the work on these compounds has been published earlier [2].

EXPERIMENTAL

The crystals were grown from solutions of ammonia and ammonium halide sealed in glass capillaries. The capillaries were made by drawing out one end of a thin-walled glass tube (diameter about 2 mm) to a diameter of 0.1 to 0.2 mm and a wall

thickness of 0.01 to 0.02 mm. The ammonium halide was weighed into the capillary and carefully dried ammonia condensed over it. Reweighing, after sealing with a microflame, gave the amount of ammonia. The desired composition was easily obtained by trial and error. The melting points of the samples were in reasonable agreement with earlier published data; a sample of the chloride used for the X-ray work with a composition 3.0 moles NH_3/mole NH_4Cl melted at + 10°C (reported values 7°, 7.6°, 9.8°, 10.7°). For $NH_4Br \cdot 3NH_3$ (actual composition 2.9 moles NH_3/mole NH_4Br) the melting point was + 8.5°C (reported 6°, 8.7°, 13.7°), for the iodide (3.1 moles NH_3/mole NH_4I) −9°C (reported −8°, −12°).

The X-ray photographs were taken in a special Weissenberg camera [3], modified to make it even simpler to handle. It was then also possible to use an undivided film which has some obvious advantages. The single crystals were grown in the camera in the usual way by blowing a cooled stream of gas parallel to the capillary and following the growth with a polarizing microscope. The crystals apparently grow with no strongly preferred orientation with respect to the capillary as they were differently oriented in each case. In this case the cooling gas was carefully dried air, passed through copper spirals in solid carbon dioxide or liquid air. The consumption of liquid air was 0.5 l/h when working at −140°C. The other details are similar to those described earlier [4].

Equi-inclination Weissenberg photographs were taken at −35°C by use of Cu-K-radiation; for the chloride with rotation about the a and b axes (layers 0−6 and 0−8, resp.), for the bromide about the a axis (layers 0−7) and for the iodide about the a axis (layers 0−6). In addition, exposures were taken at −10°, −85° and −140°C, but no changes in structure were indicated by these photographs.

A crystal grown from a sample of the composition 4.1 moles NH_3/mole NH_4Cl gave the same X-ray photographs as $NH_4Cl \cdot 3NH_3$.

The relative intensities were estimated visually by using the multiple-film technique (five films) and comparing with an intensity scale. The intensities varied from 1 to 8 000. The data were corrected for the Lorentz and polarization effects.

UNIT CELL

The data showed the diffraction symmetry *mmm*, indicating an orthorhombic unit cell. The approximate cell dimensions were first obtained from rotation and Weissenberg photographs; accurate determination with powder methods was impossible as the crystallites could not be obtained sufficiently small. A single crystal method described by Weisz, Cochran and Cole [5] was therefore applied ("the Θ-method"). The selected reflection was located to half a degree on the scale of rotation by Weissenberg oscillations of $\pm$ 2°. A series of exposures was then made with stationary camera and crystal, using a special collimator of 0.15 mm diameter. The crystal was turned 10′ between successive exposures and by interpolation between the estimated intensities, the crystal orientation for maximum reflection intensity could be determined to better than $\pm$ 5′. Systematic errors in the measurements were eliminated by extrapolation to $\Theta = 90°$. The errors due to eccentricity and graduation on the scale of rotation were negligible.

The method as given only determines the axes occurring in the zero layer and to obtain the dimensions of all three axes the crystal must be remounted. According to a modified method by Löfgren [6], the dimension of the rotation axis is obtained directly from the higher layers without reorientation. As the reflections were relatively more diffuse in the higher layers, there was here a larger uncertainty in the determination of the crystal orientation for maximum reflection intensity. The cell dimensions obtained are:

$NH_4Cl \cdot 3NH_3$: $a = 8.795 \pm 0.002$, $b = 8.68 \pm 0.01$, $c = 8.989 \pm 0.002$ Å
$NH_4Br \cdot 3NH_3$: $a = 8.96 \pm 0.01$, $b = 8.996 \pm 0.002$, $c = 9.263 \pm 0.002$ Å
$NH_4I \cdot 3NH_3$: $a = 8.32 \pm 0.02$, $b = 9.91 \pm 0.01$, $c = 9.96 \pm 0.01$ Å
($t = -35$°C, λCu-$K\alpha_1 = 1.54051$ Å, λCu-$K\alpha_2 = 1.54433$ Å.)

From existing literature data, no definite conclusions can be drawn about the extent of solid solutions in these systems.

The approximate density was obtained from the volume and weight of a completely homogeneous crystal in a cylindrical capillary of uniform thickness. The volume was measured with a microscope, the weight being known from the preparation. The densities thus observed, together with those calculated with four molecules per unit cell are ($t = -35$°C):

$NH_4Cl \cdot 3NH_3$: $d_{obs} = 1.0$, $d_{calc} = 1.01$ g.cm^{-3}
$NH_4Br \cdot 3NH_3$: $d_{obs} = 1.4$, $d_{calc} = 1.33$
$NH_4I \cdot 3NH_3$: $d_{obs} = 1.6$, $d_{calc} = 1.59$

SPACE GROUP

Systematic absences for the chloride and bromide compounds were: ($h00$), ($0k0$), ($00l$) for h, k and l odd, resp. This suggests the space group $P2_12_12_1$ (D_2^4), assuming that the absences are space group extinctions. The subsequent refinement of the structure in this space group gave good agreement with the data indicating that this choice is correct.

For the iodide compound the systematic absences were: ($h0l$) for $h + l$ odd, ($hk0$) for k odd. This suggests $P2_1nb$ or $Pmnb$ (with different choice of axes these correspond to $Pna2_1$ and $Pnma$ of the *International Tables* [7]). As will be shown later, the structure could be refined successfully only in $P2_1nb$ (C_{2v}^9).

In the chloride and bromide structure the atomic arrangement is about the same as in the iodide; the differences are discussed in detail later. However, it was evident from the refinements that the iodide structure could not be brought into sufficiently good agreement with the data by the use of $P2_12_12_1$ (see further below). The original choice of axes was made such that all structures were oriented in the same way. The work on the chloride and bromide was finished before the space group of the iodide was established with certainty, and the original choice of axes was then maintained even though this does not correspond to the standard setting of the *International Tables* [7] for the iodide.

The equivalent positions for $NH_4Cl \cdot 3NH_3$ and $NH_4Br \cdot 3NH_3$ in $P2_12_12_1$ are: (x,y,z); $(\frac{1}{2}+x, \frac{1}{2}-y, z)$; $(\frac{1}{2}-x, \bar{y}, \frac{1}{2}+z)$; $(\bar{x}, \frac{1}{2}+y, \frac{1}{2}-z)$. For $NH_4I \cdot 3NH_3$ in $P2_1nb$: (x,y,z); $(\frac{1}{2}+x, \frac{1}{2}-y, z)$; $(\frac{1}{2}+x, \bar{y}, \frac{1}{2}+z)$; $(x, \frac{1}{2}+y, \frac{1}{2}-z)$. The arrangement of the symmetry elements in $P2_1nb$ with the chosen setting is given in Fig. 1.

DETERMINATION OF THE ATOMIC COORDINATES

The positions of the halogen atoms were obtained independently for each substance from the Harker vectors. From three-dimensional F_o and F_o—F_c syntheses based on these positions, the coordinates of the nitrogen atoms were

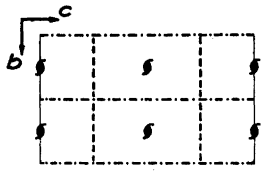

Fig. 1. The arrangement of the symmetry elements in $P2_1nb$.

then determined. The analogue computer by Hägg and Laurent [8] was used for the preliminary Fourier calculations. Subsequent Fourier refinements were made on the IBM 701 computer.

For the chloride and bromide compounds, the refinements gave no indication of deviation from the space group $P2_12_12_1$ suggested by the systematic absences. In the iodide, there was first of all a choice between $P2_1nb$ and $Pmnb$. The latter space group was first tried; the general positions are eightfold and the iodine atom had to be placed in a special fourfold position on a mirror plane. From the F_o—F_c syntheses based on this iodine position, quite acceptable nitrogen peaks could be found for N_0, N_2 and N_3 (N_0 is nitrogen in the ammonium ion; N_1, N_2 and N_3 are the nitrogen atoms in the three ammonia molecules; see further below). N_0 then was in a special fourfold position and N_2 and N_3 together occupied a general eightfold position. Finally, the remaining N_1 had to be placed in a fourfold position on a mirror plane, although the very pronounced elongation of the corresponding Fourier peak rather indicated that it should be about 0.4 Å from this plane. However, the coordinates of this structure were subjected to several cycles of least-squares refinement. It appeared that the temperature factor for N_1 became successively larger, while the other atoms refined rather normally. Soon the temperature factor for N_1 had grown beyond all reasonable limits, thus confirming the indications from the difference synthesis that N_1 should not be placed on the mirror plane. As the structure now discussed was the only one to be considered in $Pmnb$ this space group had to be abandoned and $P2_1nb$ was tried. Here all positions are general fourfold and N_1 could be moved away from the old mirror plane. Also, N_2 and N_3 were of course no longer symmetry-related to each other. Apart from this, no changes were undertaken in the above structure. The subsequent least-squares refinement in $P2_1nb$ now proceeded successfully.

Finally, one possibility that should be considered is that the systematic absences are not real space group extinctions and that the space group of the iodide then might be, for example, the same as for the chloride and bromide, $P2_12_12_1$. The arguments against this alternative are similar to those presented above against $Pmnb$. From the equivalent positions written down earlier, it is evident that if the actual space group is $P2_12_12_1$, but the x coordinates of I, N_0 and N_1 very close to 0.50, the coordinates for N_2 are (x_2,y_2,z_2) and for N_3 very close to $(\bar{x}_2,y_2,z_2)$; the net result is false absences corresponding to those for $P2_1nb$. However, from the difference maps, for example, it was evident that the x coordinate of N_1 should be about 0.45. This is so far from 0.50 that the false space group extinctions would be easily revealed.

The relation between the structures of $NH_4Cl \cdot 3NH_3$ and $NH_4Br \cdot 3NH_3$ on one hand, and $NH_4I \cdot 3NH_3$ on the other, may be described in the following way. The space groups $P2_12_12_1$ and $P2_1nb$ are both subgroups of $Pmnb$ (full symbol $P2_1/m\ 2_1/n\ 2_1/b$) and the two different structures represent two different distortions from that higher symmetry. The practical difference in the two distortions is that in one case the extinction rules change and in the other they do not. The hypothetical structure for $NH_4I \cdot 3NH_3$, discussed in the preceding paragraph, approaches the symmetry $Pmnb$; if the conditions were exact, it would be the ideal structure from which the two actual ones can be considered to be derived.

The coordinates and isotropic temperature factors for the halogen and nitrogen atoms and an over-all scale factor were finally refined by least-squares methods on the IBM 650 computer. R_3, (see below), was the quantity actually minimized. The weighting factor w in this expression and some other details of the program are described elsewhere [4]. In the iodide, the chosen space group ($P2_1nb$) is polar, but with a single heavy atom, the least-squares refinement using only diagonal matrix elements involves no special problems (*cf.* Ref.[9]). The scattering factors for N° and Cl^- were based on *f*-values published by Berghuis *et al.*[10], for Br^- and I^- they were estimated from the *f*-values for Br° and I° published by Thomas and Umeda [11]. The shifts of the atoms in the final cycles were less than about one tenth of the standard deviation for the coordinate in question. The results together with the standard deviations after about 15 cycles of refinement are given in Table 1. (The x coordinate of iodine was arbitrarily set equal to 0.50000. There is no variance for this coordi-

Table 1. Atomic parameters and standard deviations.

	$NH_4Cl \cdot 3NH_3$	$NH_4Br \cdot 3NH_3$	$NH_4I \cdot 3NH_3$
N_0: x =	0.479(9) ± 0.001(2)	0.484(6) ± 0.002(1)	0.487(9) ± 0.006(9)
y =	0.117(2) ± 0.001(2)	0.120(9) ± 0.001(6)	0.114(0) ± 0.002(6)
z =	0.280(1) ± 0.001(1)	0.288(4) ± 0.001(7)	0.298(4) ± 0.002(4)
B =	6.23 Å²	4.18 Å²	5.63 Å²
N_1: x =	0.434(3) ± 0.001(2)	0.442(0) ± 0.002(4)	0.448(2) ± 0.006(1)
y =	−0.111(0) ± 0.001(2)	−0.099(0) ± 0.001(9)	−0.097(0) ± 0.004(5)
z =	0.525(8) ± 0.001(2)	0.521(3) ± 0.002(0)	0.519(9) ± 0.003(9)
B =	6.73 Å²	4.99 Å²	7.84 Å²
N_2: x =	0.772(1) ± 0.001(2)	0.762(4) ± 0.002(2)	0.777(7) ± 0.006(2)
y =	0.266(6) ± 0.001(2)	0.264(6) ± 0.002(1)	0.290(0) ± 0.004(6)
z =	0.315(4) ± 0.001(2)	0.316(7) ± 0.001(9)	0.322(0) ± 0.004(0)
B =	6.19 Å²	5.43 Å²	8.20 Å²
N_3: x =	0.234(7) ± 0.001(1)	0.239(4) ± 0.002(2)	0.243(7) ± 0.005(1)
y =	0.343(6) ± 0.001(2)	0.332(2) ± 0.002(2)	0.284(6) ± 0.004(0)
z =	0.312(3) ± 0.001(1)	0.314(2) ± 0.002(1)	0.323(9) ± 0.003(6)
B =	6.12 Å²	5.50 Å²	7.72 Å²
X x =	0.4578(5) ± 0.0003(3)	0.4628(2) ± 0.0002(3)	0.50000
y =	−0.0039(9) ± 0.0003(9)	−0.0004(9) ± 0.0001(8)	0.0153(0) ± 0.0002(2)
z =	−0.0579(2) ± 0.0003(2)	−0.0575(4) ± 0.0001(7)	−0.0536(3) ± 0.0001(8)
B =	5.85 Å²	3.70 Å²	5.03 Å²

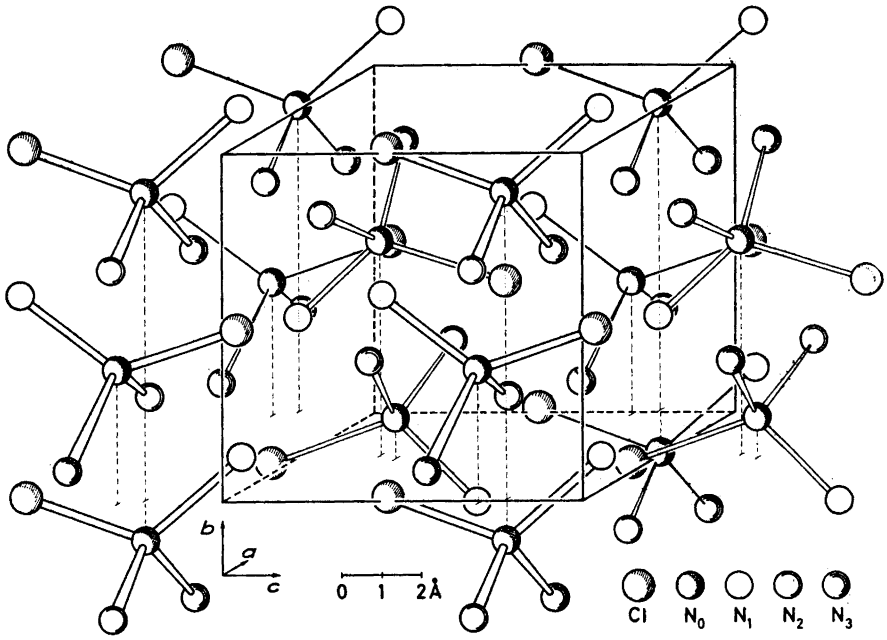

Fig. 2. The crystal structure of $NH_4Cl \cdot 3NH_3$. N_0 is nitrogen in the ammonium ion; N_1, N_2 and N_3 belong to the three ammonia molecules. The hydrogen bonds within the discrete chlorotriammineammonium tetrahedra are indicated.

nate since the iodine atom determines the origin.) The "unreliability factors" at this point were:

For the chloride: $R_1 = \Sigma \| F_o | - | F_c \| / \Sigma | F_o | = 0.117$
$R_2 = [\Sigma (| F_o | - | F_c |)^2 / \Sigma | F_o |^2]^{1/2} = 0.118$
$R_3 = [\Sigma w (| F_o | - | F_c |)^2 / \Sigma w | F_o |^2]^{1/2} = 0.120$
For the bromide $R_1 = 0.115$, $R_2 = 0.138$, $R_3 = 0.142$
For the iodide: $R_1 = 0.101$, $R_2 = 0.121$, $R_3 = 0.138$

The number of reflections recorded (not counting the space group extinctions) was 743 for the chloride, 758 for the bromide and 584 for the iodide *.

DISCUSSION OF THE STRUCTURE

The structure of the chloride and bromide compounds is illustrated in Figs. 2 and 3 (the pictures are based on the parameters of the chloride). The structure of the iodide is shown in Fig. 4. Apart from some shifts in the atomic positions, the main difference between the two structures is that N_2 and N_3 are interchanged in certain cases. In other words, N_2 and N_3 taken together occupy

* Copies of the lists of observed and calculated structure factors may be obtained on request from the Institute of Chemistry, University of Uppsala, Uppsala, Sweden.

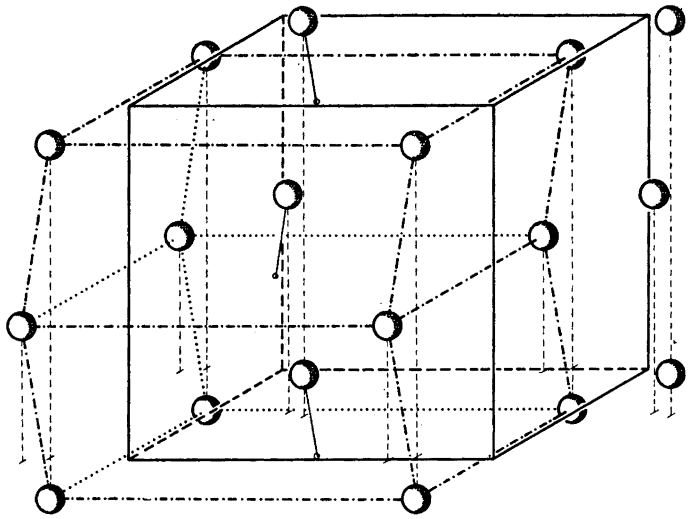

Fig. 3. The arrangement of the central atoms (N_0) in the tetrahedra of Fig. 2 ($NH_4Cl \cdot 3NH_3$). These centers, as indicated by the dotted lines, approximate a body-centered lattice.

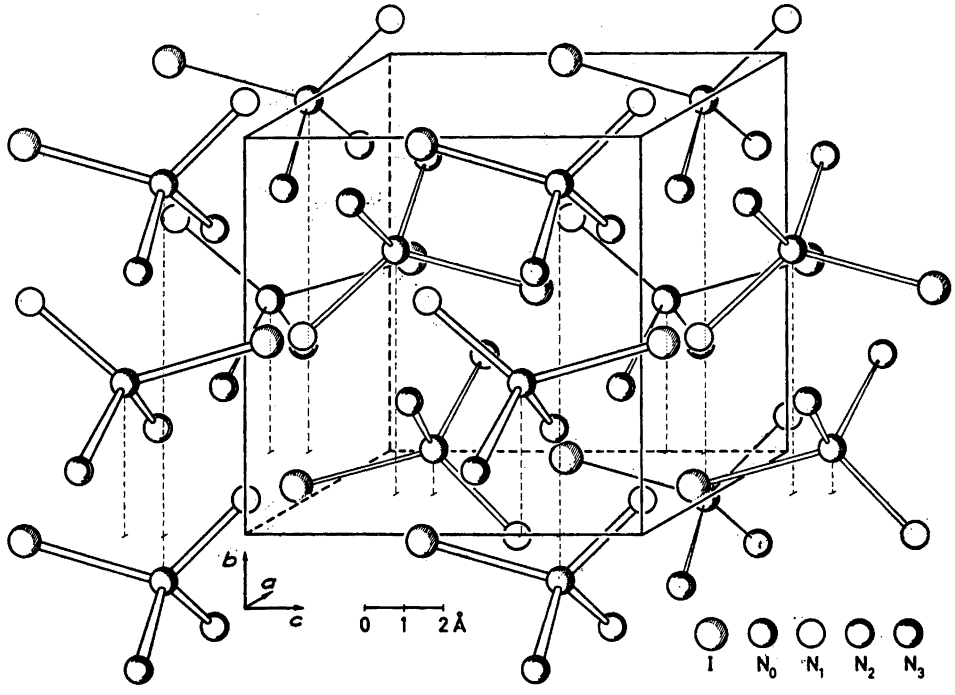

Fig. 4. The crystal structure of $NH_4I \cdot 3NH_3$; *cf.* Fig. 2.

nearly the same positions in the two structures, which is plainly noticeable when all equivalent positions are written down.

It appears that one of the four non-equivalent nitrogen atoms (N_0) is tetrahedrally surrounded by one halogen and three other nitrogen atoms (N_1, N_2 and N_3). These three nitrogen atoms have very similar environments, completely different from that of N_0. These facts give rather definite indication that N_0 belongs to the ammonium ion and N_1, N_2 and N_3 to the ammonia molecules. A detailed discussion of the bonding situation is given below.

1. Ammonium

The bond distances and angles to the four nearest neighbors of ammonium are shown in Figs. 5 and 6 for the chloride compound. The distances and angles, together with their standard deviations for all three compounds, are given in Table 2. The hydrogen atoms of ammonium are obviously used to form hydrogen bonds to the four neighbors. The somewhat distorted tetrahedral arrangement suggests that the hydrogen atoms may be somewhat removed from the bond axes. The difference synthesis for the chloride, shown schematically in Fig. 7, supports this suggestion and also indicates an expected anisotropy of thermal vibration. The distances N——N are within the usual range for hydrogen bonds of this kind [12], except for the short distance N_0—N_3 in the iodide, 2.66 Å. Compare the distances N_0——X with the corresponding distances in the simple ammonium halides: NH_4Cl (*CsCl-type*, 3.35 Å; *NaCl-type* (250°C), 3.26 Å), NH_4Br (3.50 and (250°C) 3.45 Å, resp.), NH_4I (3.79 (—17°C) and 3.62 Å, resp.). Compare also with other N—H——X distances collected in Ref.[12]

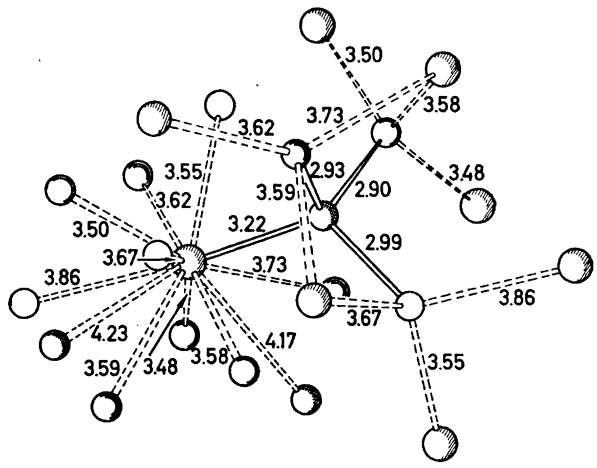

Fig. 5. Bond distances to the neighbors of the different atoms in $NH_4Cl \cdot 3NH_3$. The central atom N_0 is at (0.48, 0.12, 0.28) in Fig. 2. Atoms are designated as in Fig. 2.

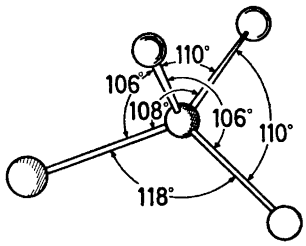

Fig. 6. Bond angles within the tetrahedral groups of Fig. 2 ($NH_4Cl \cdot 3NH_3$). The corresponding distances are shown in Fig. 5.

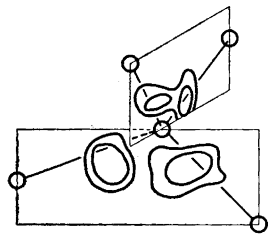

Fig. 7. Schematic representation of the difference synthesis in various sections ($NH_4Cl \cdot 3NH_3$). The atoms are the same as in Fig. 6. The contours are drawn at 0.4 and 0.5 e. Å^{-3}.

2. Ammonia

From the discussion above, it follows that the free electron pairs of the ammonia molecules are involved in hydrogen bonds to the central ammonium ion. Bonding between the ammonia molecules themselves then seems improbable and the large interatomic distances support this (all such distances are larger than 3.5 Å). The other kind of neighbors to be considered are the halogen atoms. Each ammonia molecule forms, together with the three closest halogen neighbors, a fairly symmetric low pyramid; the distances and angles for the chloride are shown in Figs. 5 and 8 and for all three compounds in Table 3. The average distances are: N———Cl = 3.59 Å, N———Br = 3.72 Å, N———I = 3.86 Å (the distances N_1———Cl = 3.86 Å, N_1———Br = 4.01 Å and N_1———I = 4.41 Å are not included in these average values, as they deviate significantly from the rest). The distances to other halogen neighbors are larger than 5 Å.

Table 2. Bond distances and angles with their standard deviations around the ammonium ion (*cf.* Figs. 5 and 6)

Distance	$NH_4Cl \cdot 3NH_3$	$NH_4Br \cdot 3NH_3$	$NH_4I \cdot 3NH_3$
N_0-N_1	2.99(3) ± 0.01(4) Å	2.95(2) ± 0.02(3) Å	3.05(8) ± 0.04(9) Å
N_0-N_2	2.89(6) ± 0.01(5)	2.81(7) ± 0.02(6)	2.98(5) ± 0.07(0)
N_0-N_3	2.93(2) ± 0.01(5)	2.91(5) ± 0.02(5)	2.65(5) ± 0.06(2)
N_0-X	3.22(1) ± 0.01(0)	3.39(1) ± 0.01(5)	3.64(1) ± 0.02(3)
N_0-others	>3.6 Å	>3.7 Å	>4.0 Å
Angle			
$N_1-N_0-N_2$	109.5 ± 0.4°	110.7 ± 0.7°	115.5 ± 1.8°
$N_1-N_0-N_3$	105.8 ± 0.4	106.3 ± 0.7	106.5 ± 1.9
N_1-N_0-X	118.2 ± 0.4	117.9 ± 0.6	120.9 ± 1.1
$N_2-N_0-N_3$	110.0 ± 0.4	111.0 ± 0.7	103.8 ± 1.5
N_2-N_0-X	107.6 ± 0.4	106.6 ± 0.6	102.2 ± 1.4
N_3-N_0-X	105.5 ± 0.4	104.1 ± 0.6	106.5 ± 1.4

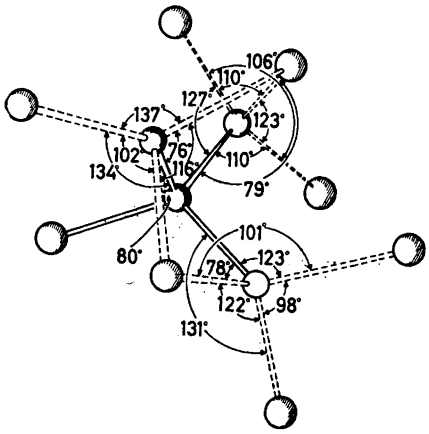

Fig. 8. Angles between the N—N_0 and N—Cl lines of each ammonia molecule. The corresponding distances are shown in Fig. 5.

The interaction of the ammonia molecules with their neighbors is obviously weak and makes it probable that the threefold axis is oriented along the hydrogen bond to the central ammonium ion. An interesting question is then the extent of rotation around the threefold axis. The favorable arrangement of three negatively charged halogen atoms suggests that the hydrogen atoms are preferably oriented towards these atoms; the three-dimensional difference synthesis of the chloride seems to give rather definite support to this suggestion. Two typical sections are illustrated in Fig. 9; the corresponding sections involving the other ammonia molecules are very similar. As expected (if the threefold axis is oriented along N_0—N_2), the "hydrogen atom" appearing in the plane of N_0, N_2 and Cl′ is quite far off the connecting line N_2—Cl′ which gives more reasonable bond angles in the ammonia molecule (the angle N_0—N_2—Cl′ is 79°, see Fig. 8). It seems likely that a phase transition

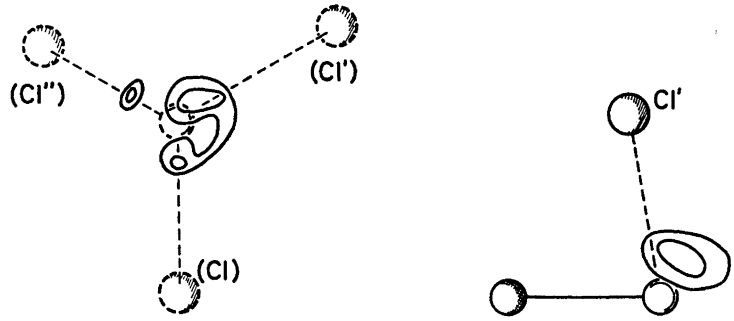

Fig. 9. Difference synthesis in two different sections. In the right picture the section passes through N_0, N_2 and Cl′; in the left it is drawn approximately perpendicular to the N_0—N_2 bond axis and through those places expected for the hydrogen atoms of N_2, as discussed in the text. The contours are drawn at 0.4 and 0.5 e. Å^{-3}.

Table 3. Distances and angles to the neighbors of the ammonia molecules (*cf.* Figs. 5 and 8)

Distance	$NH_4Cl \cdot 3NH_3$	$NH_4Br \cdot 3NH_3$	$NH_4I \cdot 3NH_3$
N_1-N_0	2.99(3) Å	2.95(2) Å	3.05(8) Å
N_1-X	3.86(1)	4.00(5)	4.41(2)
N_1-X'	3.66(9)	3.80(7)	3.88(6)
N_1-X''	3.55(2)	3.72(6)	3.88(1)
N_1-other N	>3.6 Å	>3.7 Å	>3.7 Å
N_2-N_0	2.89(6)	2.81(7)	2.98(5)
N_2-X	3.48(4)	3.61(5)	3.75(6)
N_2-X'	3.57(9)	3.67(6)	3.95(6)
N_2-X''	3.50(3)	3.67(3)	3.78(0)
N_2-other N	>3.5 Å	>3.5 Å	>3.6 Å
N_3-N_0	2.93(2)	2.91(5)	2.65(5)
N_3-X	3.59(4)	3.68(8)	3.79(9)
N_3-X'	3.73(3)	3.80(3)	3.87(4)
N_3-X''	3.61(9)	3.75(3)	3.91(0)
N_3-other N	>3.5 Å	>3.5 Å	>3.6 Å
Angle	$NH_4Cl \cdot 3NH_3$	$NH_4Br \cdot 3NH_3$	$NH_4I \cdot 3NH_3$
N_0-N_1-X	123.3°	123.9°	120.8°
N_0-N_1-X'	78.1	79.9	79.9
N_0-N_1-X''	131.3	133.3	136.7
$X-N_1-X'$	100.6	100.3	102.9
$X-N_1-X''$	97.9	96.7	98.9
$X'-N_1-X''$	121.9	117.6	109.2
N_0-N_2-X	110.3	109.3	87.3
N_0-N_2-X'	79.3	80.5	84.5
N_0-N_2-X''	127.2	129.5	129.6
$X-N_2-X'$	123.4	123.8	123.4
$X-N_2-X''$	106.4	104.9	113.8
$X'-N_2-X''$	109.8	109.4	114.2
N_0-N_3-X	80.1	82.5	86.6
N_0-N_3-X'	76.3	77.2	90.6
N_0-N_3-X''	133.7	135.1	130.8
$X-N_3-X'$	116.1	118.3	124.5
$X-N_3-X''$	101.7	101.9	109.9
$X'-N_3-X''$	136.5	132.8	113.1

should be expected if relatively unrestricted rotation around the threefold axis occurred at higher temperatures. As pointed out earlier, no phase transitions were observed in the X-ray photographs as the crystals were cooled down from the melting point to —140°C. So far no heat capacity measurements have been published.

3. Halogen

The closest neighbors to a halogen atom are three nitrogen atoms of each kind. The distances for the chloride are shown in Fig. 5 and for all three compounds in Table 4. Of the three ammonium neighbors, only one points a

Table 4. Distances to the neighbors of the halogen atoms (*cf.* Fig. 5).

Distance	$NH_4Cl \cdot 3NH_3$	$NH_4Br \cdot 3NH_3$	$NH_4I \cdot 3NH_3$
$X-N_0$	3.22(1) Å	3.39(1) Å	3.64(1) Å
$X-N_0'$	4.23(2)	4.39(1)	4.68(7)
$X-N_0''$	4.16(5)	4.24(7)	4.72(1) *
$X-N_1$	3.86(1)	4.00(5)	4.41(2) **
$X-N_1'$	3.66(9)	3.80(7)	3.88(6)
$X-N_1''$	3.55(2)	3.72(6)	3.88(1)
$X-N_3$	3.48(4)	3.61(5)	3.79(9) ($I-N_3$)
$X-N_2'$	3.57(9)	3.67(6)	3.87(4) ($I-N_3'$)
$X-N_2''$	3.50(3)	3.67(3)	3.78(0)
$X-N_3$	3.59(4)	3.68(8)	3.75(6) ($I-N_2$)
$X-N_3'$	3.73(3)	3.80(3)	3.95(6) ($I-N_2'$)
$X-N_3''$	3.61(9)	3.75(3)	3.91(0)
X-others	>4.9 Å	>5.0 Å	>5.1 Å

* Also: 4.50(5).
** Also: 4.71(9).

hydrogen atom towards this halogen atom as the other two are directly involved in bonds to other halogen atoms. These two ammonium ions are also considerably more distant. If now the hydrogen atoms of the ammonia molecules are also preferably oriented towards halogen as discussed above, this means that altogether ten hydrogen atoms are more or less directed towards halogen. The preceding discussion has to be modified somewhat in the iodide case. From Table 4 it is apparent that the distances $I-N_0'$, $I-N_0''$ and $I-N_1$ are considerably larger than the corresponding distances in the chloride and bromide structure. It is then not too surprising that two extra atoms, other than these twelve, are also situated at comparable distances (see the foot-note in the table). As was pointed out earlier, N_2 and N_3 are interchanged in certain cases when the iodide structure is compared to the chloride and bromide structure, which is also shown in this table.

It may be worth mentioning that the halogen atoms form an approximately face-centered arrangement. If the halogen coordinates were $(\frac{1}{2},0,0)$ instead of those given in Table 1, the face-centering would be perfect.

As a summary, the structures are characterized by rather discrete halidotriammineammonium tetrahedra (Figs. 2 and 4). The forces between these groups are relatively weak; the tetrahedra are arranged in such a way that their centers form a flat (close to) body-centered lattice (Fig. 3). The possible rotation of the ammonia molecules about their threefold axes may be relatively restricted by interaction with the halide neighbors. It must be pointed out that the individuality of the tetrahedral groups is much less pronounced in the iodide than in the other two. Note, for example, that the distance N_0—I within the group is 3.64 Å, while the distance from N_2 to one of the iodine atoms in a neighboring group is not much longer, 3.76 Å.

Acknowledgements. The preliminary work on the bromide and iodide compounds was done in collaboration with Mr Gunnar Larsson and Mr Rune Liminga and I am much indebted to them for their very valuable assistance.

Sincere thanks are due to Professor G. Hägg for his great interest in this work and for all the facilities put at my disposal. The refinements were performed on the IBM 650 and 701 computers during my stay at the Lawrence Radiation Laboratory of the University of California, Berkeley, U.S.A., with support of the U.S. Atomic Energy Commission, and I am much indebted to Professor D. H. Templeton for permission to use these facilities.

This work has been supported by several grants from the *Swedish Natural Science Research Council* which are here gratefully acknowledged.

REFERENCES

1. Watt, G. W. and McBride, W. R. *J. Am. Chem. Soc.* **77** (1955) 1317.
2. Olovsson, I. *Acta Chem. Scand.* **11** (1957) 1273.
3. Kreuger, A. *Acta Cryst.* **8** (1955) 348.
4. Olovsson, I. and Templeton, D. H. *Acta Cryst.* **12** (1959) 827.
5. Weisz, O., Cochran, W. and Cole, W. F. *Acta Cryst* **1** (1948) 83.
6. Löfgren, T. *Acta Cryst.* (1960) *In press.*
7. *International Tables for X-ray Crystallography*, Vol 1, Kynoch Press, Birmingham 1952.
8. Hägg, G., and Laurent, T. *J. Sci. Instr.* **23** (1946) 155.
9. Templeton, D. H. *Z. Krist.* **113** (1960) 234.
10. Berghuis, J., Haanappel, IJ. M., Potters, M., Loopstra, B. O., MacGillavry, C. H. and Veenendaal, A. L. *Acta Cryst.* **8** (1955) 478.
11. Thomas, L. H. and Umeda, K. *J. Chem. Phys.* **26** (1957) 293.
12. Pimentel, G. C., and McClellan, A. L. *The Hydrogen Bond*, Freeman and Co., San Francisco and London 1960.

Received July 1, 1960.

ACTA CHEMICA SCANDINAVICA 14 (1960) 1466–1474

The Crystal Structure of Tetrammineammonium Iodide

IVAR OLOVSSON

Institute of Chemistry, University of Uppsala, Uppsala, Sweden

The crystal structure of $NH_4I \cdot 4NH_3$ has been determined from single crystal X-ray data obtained at −140°C. No phase changes were observed between this temperature and the melting point. There are two formula units in the tetragonal cell of the dimensions: a = 8.94 Å, c = 6.55 Å. The space group is $P4/n$. The four ammonia molecules are hydrogen-bonded to ammonium into tetrahedral tetrammine-ammonium groups. The different groups are relatively isolated from each other and are distributed in such a way that an almost close-packed arrangement of twelve nitrogen neighbors is formed around iodine.

In an earlier report on the structures of the triammines of the ammonium halides [1] a general introduction was given to the system NH_4X—NH_3 (X = F, Cl, Br, I). The tetrammine of ammonium iodide has been reported in several earlier works; the corresponding bromide compound so far only by Watt and McBride [2]. For references to earlier works see this article. The present investigation involves the determination of the crystal structure of $NH_4I \cdot 4NH_3$ from single crystal X-ray diffraction data obtained at —140°C. Some preliminary data have been published earlier [3].

EXPERIMENTAL

The crystals were grown from solutions of ammonia and ammonium iodide sealed in glass capillaries. The samples were prepared in the way described earlier [1]. The sample used for the X-ray work had the ratio 4.0 moles ammonia per mole of ammonium iodide. The melting point of this sample was −6°C (earlier reported value −5.1°C).

The single crystals were grown in the usual way by blowing a cooled stream of gas parallel to the capillary; all crystals prepared preferably oriented their a axes along the axis of the capillary. Equi-inclination Weissenberg photographs were taken around the a axis, layers 0−6, at −140°C by the use of Cu-K-radiation. The experimental set-up was the same as that used earlier [1]. Exposures taken at −25°C indicated no changes in structure.

The relative intensities were estimated visually by the use of multiple-film technique (5 films) and comparison with an intensity scale. The data were corrected for the Lorentz and polarization effects.

UNIT CELL AND SPACE GROUP

The data showed the diffraction symmetry of the tetragonal Laue group $4/m$. Systematic absences were: $(hk0)$ for $h + k$ odd. All reflections (hkl) with $h + k + l$ odd were in general considerably weaker than those with $h + k + l$ even. The systematic absences suggest the space group $P4/n$ (C_{4h}^3) and the refinements indicated no deviation from this choice.

The unit-cell dimensions were first approximately determined from rotation and Weissenberg photographs and then somewhat more accurately by the single crystal method described by Weisz, Cochran and Cole [4] ("the Θ-method"). The practical procedure was described earlier [1]. The following values were obtained: $a = 8.94 \pm 0.01$ Å, $c = 6.55 \pm 0.01$ Å. ($t = -140$°C, λCu-$K\alpha_1 = 1.54051$ Å, λCu-$K\alpha_2 = 1.54433$ Å). The approximate density was obtained from the volume and weight of a homogeneous crystal in a cylindrical capillary (the weight was known from the preparation): $d_{obs} = 1.5$ g/cm^3. With two molecules per unit cell a value of 1.35 is calculated.

The general equivalent positions in $P4/n$ are (origin at $\bar{4}$, *cf. International Tables* [5]): (x,y,z); $(\bar{x},\bar{y},z)$; $(\frac{1}{2}+x,\frac{1}{2}+y,\bar{z})$; $(\frac{1}{2}-x,\frac{1}{2}-y,\bar{z})$; $(\bar{y},x,\bar{z})$; $(y,\bar{x},\bar{z})$; $(\frac{1}{2}-y,\frac{1}{2}+x,z)$; $(\frac{1}{2}+y,\frac{1}{2}-x,z)$.

DETERMINATION OF THE ATOMIC COORDINATES

The intensities of the reflections indicated that, among the twofold positions, only those of the form $(0,\frac{1}{2},z)$; $(\frac{1}{2},0,\bar{z})$ were possible for iodine. The z coordinate could be estimated to be about 0.24. This z coordinate was refined in two cycles of least-squares refinement and a three-dimensional F_o-F_c synthesis, based on iodine only, was calculated. From these difference maps,

Table 1. Atomic parameters and standard deviations.

Nitrogen (N_0) in ammonium:	$x = 0$
	$y = 0$
	$z = \frac{1}{2}$
	$B = 2.75$ Å^2
Nitrogen (N_1) in ammonia:	$x = 0.246(4) \pm 0.002(8)$
	$y = 0.132(6) \pm 0.002(8)$
	$z = 0.259(5) \pm 0.002(1)$
	$B = 4.23$ Å^2
Iodine:	$x = 0$
	$y = \frac{1}{2}$
	$z = 0.2414(9) \pm 0.0001(8)$
	$B = 1.20$ Å^2

Table 2. Observed and calculated structure factors. All F values have been multiplied by 1.25.

k	l	$\|F_o\|$	$\|F_c\|$	k	l	$\|F_o\|$	$\|F_c\|$	k	l	$\|F_o\|$	$\|F_c\|$	k	l	$\|F_o\|$	$\|F_c\|$
	$h = 0$			7	4	<10	11	3	6	55	56	8	3	43	46
0	1	16	13	7	5	41	41	−3	6	50	47	8	4	< 8	10
0	2	119	145	7	6	12	13	3	7	13	13	8	5	33	37
0	3	20	18	8	0	81	69	−3	7	18	15	−8	5	41	38
0	4	104	105	8	1	< 5	<1	4	1	85	85	9	0	42	48
0	5	<10	9	8	2	62	58	−4	1	72	77	9	1	< 9	5
0	6	65	58	8	3	10	9	4	2	11	9	9	2	43	49
0	7	16	17	8	4	49	51	−4	2	< 5	10	9	3	< 8	5
1	1	71	101	8	5	< 8	8	4	3	80	71	9	4	33	38
1	2	14	13	9	1	51	49	−4	3	64	66	−9	4	38	37
1	3	79	82	9	2	<10	5	4	4	16	15				
1	4	22	18	9	3	36	44	−4	4	18	15		$h = 2$		
1	5	66	59	9	4	< 8	9	4	5	63	53	2	0	106	126
1	6	23	18	10	0	37	42	−4	5	58	51	2	1	12	6
1	7	54	41	10	1	< 6	<1	4	6	15	16	2	2	83	90
2	0	73	101	10	2	30	37	−4	6	18	16	2	3	19	20
2	1	12	6	10	3	< 7	8	4	7	42	38	2	4	81	78
2	2	56	69	11	1	31	39	−4	7	44	37	2	5	14	12
2	3	27	25	11	2	< 5	4	5	0	62	57	2	6	48	48
2	4	72	70					5	1	12	12	2	7	19	18
2	5	17	15		$h = 1$			−5	1	15	10	3	1	58	66
2	6	50	45	1	0	80	107	5	2	71	66	−3	1	80	100
2	7	22	20	1	1	23	21	−5	2	82	96	3	2	13	12
3	1	109	118	1	2	98	116	5	3	9	9	−3	2	13	9
3	2	9	8	1	3	< 6	6	−5	3	< 7	4	3	3	57	60
3	3	86	91	1	4	73	70	5	4	50	47	−3	3	78	81
3	4	13	14	1	5	21	21	−5	4	69	64	3	4	20	18
3	5	65	63	1	6	56	55	5	5	15	19	−3	4	18	14
3	6	15	15	1	7	14	15	−5	5	15	15	3	5	57	49
3	7	55	42	2	1	87	102	5	6	41	42	−3	5	71	58
4	0	96	105	−2	1	119	153	−5	6	59	49	3	6	20	18
4	1	< 7	4	2	2	11	11	5	7	16	14	−3	6	14	16
4	2	80	79	−2	2	8	7	−5	7	14	12	3	7	41	36
4	3	19	18	2	3	80	82	6	1	91	84	−3	7	50	40
4	4	77	70	−2	3	104	110	−6	1	59	70	4	0	99	110
4	5	12	12	2	4	17	17	6	2	< 9	6	−4	0	93	113
4	6	51	45	−2	4	13	12	−6	2	< 7	7	4	1	< 6	4
4	7	19	17	2	5	61	59	6	3	76	70	−4	1	< 5	4
5	1	85	90	−2	5	81	71	−6	3	66	60	4	2	81	84
5	2	12	7	2	6	11	17	6	4	<10	10	−4	2	85	86
5	3	84	74	−2	6	11	14	−6	4	<10	12	4	3	16	16
5	4	14	12	2	7	43	41	6	5	50	52	−4	3	17	15
5	5	60	54	−2	7	51	46	−6	5	47	47	4	4	72	72
5	6	16	14	3	0	107	124	6	6	< 8	12	−4	4	73	73
5	7	46	38	−3	0	43	66	−6	6	12	13	4	5	9	11
6	0	81	73	3	1	20	14	7	0	72	63	−4	5	13	11
6	1	< 7	<1	−3	1	16	17	7	1	< 9	7	4	6	46	46
6	2	70	59	3	2	117	124	7	2	71	65	−4	6	54	46
6	3	14	14	−3	2	72	81	7	3	<10	6	4	7	18	16
6	4	60	55	3	3	< 7	4	7	4	41	48	−4	7	20	16
6	5	14	11	−3	3	< 6	9	7	5	12	13	5	1	80	83
6	6	39	37	3	4	83	76	7	6	42	39	−5	1	51	63
7	1	62	57	−3	4	64	55	−7	6	42	38	5	2	< 8	7
7	2	<10	7	3	5	17	17	8	1	57	52	−5	2	9	9
7	3	53	51	−3	5	24	21	8	2	<10	6	5	3	72	69

Table 2 (cont.)

k	l	$\|F_o\|$	$\|F_c\|$	k	l	$\|F_o\|$	$\|F_c\|$	k	l	$\|F_o\|$	$\|F_c\|$	k	l	$\|F_o\|$	$\|F_c\|$
−5	3	63	56	4	3	76	74	9	4	30	34	9	2	< 7	5
5	4	14	12	−4	3	77	76	−9	4	42	39	9	3	31	38
−5	4	14	14	4	4	< 8	12	10	1	34	41	10	0	32	42
5	5	49	52	−4	4	12	12	10	2	< 6	4	10	1	<3	<1
−5	5	52	45	4	5	64	55	10	3	30	36	10	2	31	37
5	6	15	14	−4	5	64	56	11	0	25	35				
−5	6	18	15	4	6	14	14							$h = 5$	
6	0	76	76	−4	6	12	13			$h = 4$		5	0	57	61
−6	0	71	73	4	7	47	38	4	0	57	64	5	1	< 8	7
6	1	< 7	<1	−4	7	49	38	4	1	< 2	<1	5	2	64	64
−6	1	< 5	<1	5	0	73	73	4	2	54	51	5	3	< 9	6
6	2	65	61	−5	0	57	69	4	3	19	17	5	4	49	47
−6	2	55	59	5	1	< 7	9	4	4	55	51	5	5	17	14
6	3	16	13	−5	1	8	9	4	5	14	13	5	6	47	39
−6	3	< 9	13	5	2	81	77	4	6	33	36	6	1	58	60
6	4	61	56	−5	2	69	73	5	1	70	71	−6	1	45	50
−6	4	62	55	5	3	< 8	6	−5	1	67	73	6	2	< 9	5
6	5	10	11	−5	3	10	7	5	2	< 8	7	−6	2	<10	6
−6	5	10	11	5	4	62	54	−5	2	< 8	6	6	3	56	53
6	6	42	38	−5	4	59	52	5	3	62	61	−6	3	44	45
−6	6	44	37	5	5	13	15	−5	3	65	62	6	4	< 8	9
7	1	63	61	−5	5	16	16	5	4	< 8	11	−6	4	14	11
7	2	< 9	6	5	6	46	44	−5	4	< 9	11	6	5	43	41
7	3	56	53	−5	6	47	43	5	5	48	47	−6	5	46	37
7	4	9	10	6	1	53	54	−5	5	58	47	7	0	38	45
7	5	42	42	−6	1	60	68	5	6	11	13	7	1	< 9	6
−7	5	57	47	6	2	< 8	8	−5	6	14	13	7	2	43	47
7	6	14	12	−6	2	< 9	6	6	0	71	74	7	3	< 8	6
−7	6	9	11	6	3	51	49	−6	0	75	75	7	4	35	37
8	0	54	53	−6	3	60	58	6	1	< 6	<1	−7	4	52	42
8	1	< 4	<1	6	4	9	13	−6	1	< 7	<1	7	5	14	12
8	2	46	45	−6	4	<10	11	6	2	64	61	−7	5	12	11
8	3	9	11	6	5	39	40	−6	2	65	62	8	1	40	47
8	4	39	42	−6	5	55	45	6	3	10	11	8	2	< 8	5
9	1	47	52	6	6	16	14	−6	3	<10	10	8	3	41	42
9	2	< 8	4	−6	6	15	12	6	4	54	55	9	0	41	44
9	3	43	46	7	0	63	61	−6	4	67	55	9	1	< 7	4
10	0	40	46	7	1	< 8	6	6	5	< 7	9	9	2	42	45
10	1	< 3	<1	7	2	66	63	−6	5	9	9	9	3	< 5	4
10	2	37	40	7	3	< 8	5	6	6	43	37	10	1	27	35
10	3	< 5	7	7	4	47	47	−6	6	46	37				
11	1	25	34	7	5	8	12	7	1	55	53			$h = 6$	
		$h = 3$		−7	5	15	14	7	2	< 8	6	6	0	50	54
3	0	73	83	8	1	58	57	7	3	46	48	6	1	< 3	<1
3	1	13	13	8	2	< 8	5	7	4	< 8	10	6	2	46	46
3	2	82	89	8	3	46	50	7	5	38	38	6	3	<10	10
3	3	< 7	7	8	4	< 7	8	−7	5	40	37	6	4	44	43
3	4	62	60	−8	4	10	9	8	0	53	53	7	1	54	53
3	5	17	18	8	5	38	39	8	1	< 3	<1	7	2	<10	4
3	6	49	48	−8	5	41	37	8	2	40	45	7	3	45	46
3	7	15	13	9	0	35	41	8	3	< 7	9	8	0	40	44
4	1	82	91	9	1	< 8	5	8	4	37	42	8	1	< 5	<1
−4	1	86	94	9	2	36	43	−8	4	44	41	8	2	38	39
4	2	7	7	9	3	< 7	5	9	1	36	42	9	1	35	38
−4	2	< 6	7												

the nitrogen atoms (N_0) in ammonium could be located in the twofold positions $(0,0,\frac{1}{2})$ and $(\frac{1}{2},\frac{1}{2},\frac{1}{2})$. Finally the nitrogen atoms (N_1) belonging to the four ammonia molecules were found to occupy together the general 8-fold positions written down earlier.

The coordinates and isotropic temperature factors for iodine and nitrogen and an over-all scale factor were finally refined by least-squares methods on the IBM 650 computer. R_3 (see below) was the quantity actually minimized; the weighting factor w and some other details of the program have been described earlier [6]. The scattering factors used in these calculations were those of Berghuis *et al.*[7] for neutral N; for I^- they were estimated from the values for neutral I published by Thomas and Umeda [8]. The shifts in the coordinates in the final cycle were less than 0.00002. The results, together with the standard deviations after 12 cycles of refinement, are given in Table 1. The "unreliability factors" at this point were:

$$R_1 = \Sigma||F_o|-|F_c|| \,/\, \Sigma|F_o| = 0.105.$$
$$R_2 = [\Sigma(|F_o|-|F_c|)^2/\Sigma|F_o|^2]^{\frac{1}{2}} = 0.137$$
$$R_3 = [\Sigma w(|F_o|-|F_c|)^2/\Sigma w|F_o|^2]^{\frac{1}{2}} = 0.140$$

The observed and calculated structure factors are compared in Table 2. Notice that the positions of iodine and nitrogen N_0 (but not nitrogen N_1) are consistent with the space group $P4/nmm$. The deviation of the diffraction symmetry from $4/mmm$ is therefore expected to be quite small (but is nevertheless obviously real) which is noticeable in Table 2.

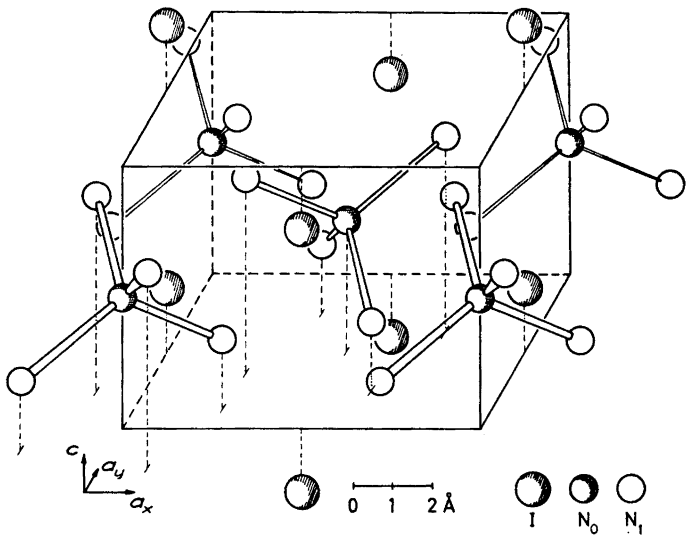

Fig. 1. The crystal structure of $NH_4I \cdot 4NH_3$. N_0 is nitrogen in ammonium, N_1 belongs to ammonia. The hydrogen bonds within the discrete tetrammineammonium tetrahedra are indicated.

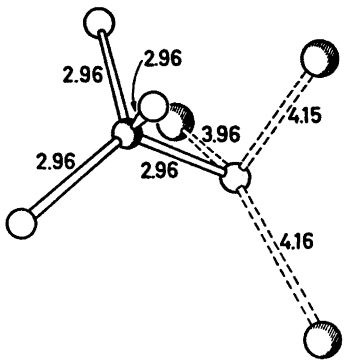

Fig. 2. Bond distances in the tetrammine-ammonium group and the distances between ammonia and its three iodine neighbors.

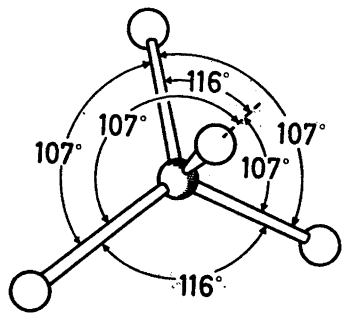

Fig. 3. Bond angles in the tetrammine-ammonium group. The corresponding distances are shown in Fig. 2.

DISCUSSION OF THE STRUCTURE

The structure is shown in Fig. 1. The ammonium ion is tetrahedrally surrounded by the four ammonia molecules, all at 2.96 Å from N_0, see Fig. 2

Table 3. Distances and angles with their standard deviations (compare with Figs. 2—5).

1. Around ammonium

Bond	Distance (Å)	Bonds	Angle (°)
N_0-N_1	2.95(6) ± 0.02(2)	$N_1-N_0-N_1'$	106.5 ± 0.3
N_0-N_1'	—»—	$N_1-N_0-N_1''$	106.5 ± 0.3
N_0-N_1''	—»—	$N_1-N_0-N_1'''$	115.6 ± 0.7
N_0-N_1'''	—»—	$N_1'-N_0-N_1''$	115.6 ± 0.7
		$N_1'-N_0-N_1'''$	106.5 ± 0.3
		$N_1''-N_0-N_1'''$	106.5 ± 0.3

2. Around ammonia

Bond	Distance (Å)	Bonds	Angle (°)
N_1-N_0	2.95(6) ± 0.02(2)	N_0-N_1-I	86.2
N_1-I	3.95(6)	N_0-N_1-I'	82.7
N_1-I'	4.15(1)	N_0-N_1-I''	135.4
N_1-I''	4.16(1)	$I-N_1-I'$	124.4
N_1-other N	>3.6	$I-N_1-I''$	121.1
N_1-other I	>6.1	$I'-N_1-I''$	104.0

3. Around iodine

Four distances $I-N_1$ equal to	3.95(6) Å
» » » » »	4.15(1) Å
» » » » »	4.16(1) Å
Other distances $I-N_1$:	>6.1 Å

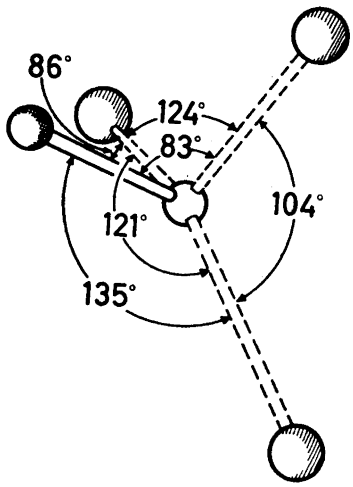

Fig. 4. Angles between the N—N_0 and N—I lines of ammonia. The corresponding distances are shown in Fig. 2.

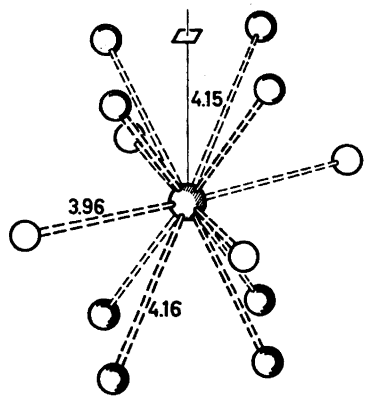

Fig. 5. Distances to the neighbors of iodine. The twelve nitrogen atoms (N_1) form an almost cubic close-packed arrangement around iodine.

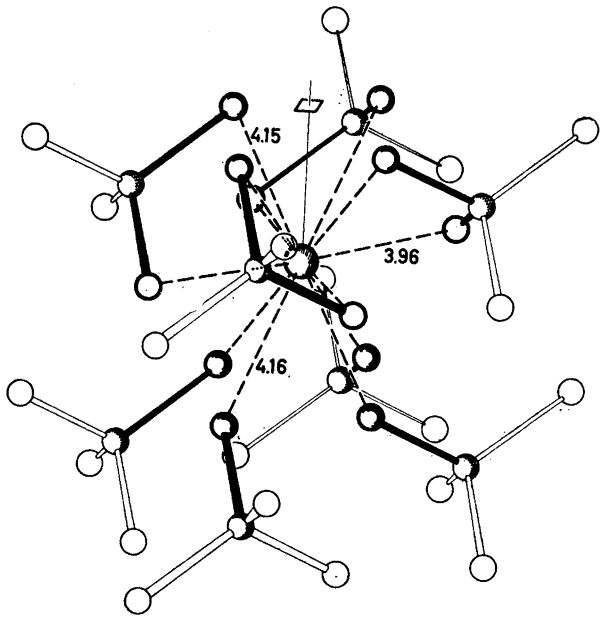

Fig. 6. The distribution of the tetrammineammonium groups around iodine. The twelve closest neighbors (shown separately in Fig. 5) are heavily drawn.

and Table 3. The bond angles are shown in Fig. 3. The central atoms (N_0) are located at $\bar{4}$ and form a *C*-centered arrangement. The hydrogen atoms of ammonium are obviously involved in hydrogen bonds to the ammonia neighbors. The distance $N_0 - - - N_1$, 2.96 Å, is within the usual range for hydrogen bonds of this kind [9]. Compare also with the corresponding distances in $NH_4Cl \cdot 3NH_3$ (2.90, 2.93, and 2.99 Å), $NH_4Br \cdot 3NH_3$ (2.82, 2.92, and 2.95 Å) and $NH_4I \cdot 3NH_3$ (2.66, 2.99, and 3.06 Å) [1].

As the free electron pair of ammonia is obviously involved in the hydrogen bond to ammonium, it seems unlikely that bonding between the different ammonia molecules will occur. All such distances are larger than 3.6 Å. The distances to the iodine neighbors are listed in Table 3. The interaction between ammonia and its neighbors is obviously weak and makes it probable that the threefold axis is oriented along the hydrogen bond to the central ammonium ion. The relatively favorable arrangement of three negatively charged iodine atoms around ammonia (see Figs. 2 and 4) may suggest that the possible rotation around the threefold axis is somewhat restricted and that the molecule is preferably oriented towards these iodide ions. The situation is very similar to that in $NH_4Cl \cdot 3NH_3$, $NH_4Br \cdot 3NH_3$ and $NH_4I \cdot 3NH_3$ [1].

Iodine is located on a fourfold axis and surrounded by twelve nitrogen atoms (N_1) in an almost cubic close-packed arrangement (see Fig. 5). The distribution of the tetrahedral tetrammineammonium groups around iodine is shown in Fig. 6. Compare the distances iodine-ammonia in this compound (3.96, 4.15, and 4.16 Å, *cf.* Table 3) with the corresponding distances in $NH_4I \cdot 3NH_3$ (mean value 3.9 Å)[1]. The iodine atoms form an almost body-centered arrangement (if the *z* coordinate were 1/4 instead of 0.2415, the body-centering would be perfect). This is of course the reason why reflections (*hkl*), with $h+k+l$ odd, are in general considerably weaker than those with $h+k+l$ even.

Acknowledgements. I am much indebted to Prof. G. Hägg for his great interest in this work and for all the facilities put at my disposal. I also wish to thank Mrs E. Hadler Vihovde, Oslo, Mr Rune Liminga and Mr Gunnar Larsson for their valuable assistance during the preliminary work on this compound.

The refinements were performed on the IBM 650 and 701 computers during my stay at the Lawrence Radiation Laboratory of the University of California, Berkeley, U.S.A., with support by the U.S. Atomic Energy Commission, and I am very grateful to Prof. D. H. Templeton for permission to use these facilities.

This work has been supported by grants from the *Swedish Natural Science Research Council* which are here gratefully acknowledged.

REFERENCES

1. Olovsson, I. *Acta Chem. Scand.* **14** (1960) 1453.
2. Watt, G. W. and McBride, W. R. *J. Am. Chem. Soc.* **77** (1955) 1317.
3. Olovsson, I. *Acta Chem. Scand.* **11** (1957) 1273.
4. Weisz, O., Cochran, W. and Cole, W. F. *Acta Cryst.* **1** (1948) 83.
5. *International Tables for X-ray Crystallography, Vol. 1,* Kynoch Press, Birmingham 1952.

6. Olovsson, I and Templeton, D. H. *Acta Cryst* **12** (1959) 827.
7. Berghuis, J., Haanappel, IJ. M., Potters, M., Loopstra, B. O., MacGillavry, C. H. and Veenendaal, A. L. *Acta Cryst.* **8** (1955) 478.
8. Thomas, L. H. and Umeda, K. *J. Chem. Phys.* **26** (1957) 293.
9. Pimentel, G. C. and McClellan, A. L. *The Hydrogen Bond*, Freeman and Co., San Francisco and London 1960.

Received July 1, 1960.

ACTA CHEMICA SCANDINAVICA 14 (1960) 1475–1484

Intermolecular Hydrogen Bond Association between Phenol and Compounds which Contain the Phosphoryl and Carbonyl Groups

GUNNAR AKSNES*

Norwegian Defence Research Establishment, Toxicological Group, Kjeller, pr Lillestrøm, Norway

The intermolecular hydrogen bond association between phenol and triethylphosphate respectively N-diethylacetamide gives 1:1 association complexes, where the P=O respectively the C=O group participates in the hydrogen bond. The association constants and molar extinction coefficients of the hydrogen bond complexes have been determined. The salt-like addition compounds between tertiary amides and strong acids (HCl) give proton transfer bond where the hydrogen is attached to the amide nitrogen. By using triethylphosphate it has been possible to locate 6 bands in the infrared spectrum of phenol which are due to vibrations of the free hydroxyl group. Two of the bands are interpreted as bands due to bending vibrations and four as bands due to combination between stretching and bending of the hydroxyl group. The vibrations of the hydroxyl group in alcohols are also discussed.

It has long been recognized that hydroxylic compounds show a strong tendency for hydrogen bond association. In the infrared spectral region the ground state stretching vibration of the free O—H bond will be displaced towards lower frequencies upon association [1–6]. Alcohols and phenols give rise to both dimeric and polymeric association [7–8]. The degree of association is very sensitive to changes in concentration and temperature [8].

It is known that the hydrogen bond association between compounds which contain the hydroxyl and carbonyl groups gives rise to displacement of the stretching frequencies of both the OH and C=O band. This is explained by assuming hydrogen bond between the two groups: ROH...O=C. Examples are dimeric carboxylic acids [9–13] and intramolecular association in hydroxy keto compounds [14–17], but intermolecular associations between unlike species are also known [8,18–20,24].

* Present address: Chemical Institute, University of Bergen, Bergen, Norway.

THEORETICAL

The strong hydrogen bond association between phenol and N-dialkylacetamide respectively orthophosphate esters makes it possible to study the bond formation with sufficiently low concentration of phenol to avoid dimeric and polymeric phenol association. The hydrogen bond must therefore be due to association between unlike species. If we assume the molar ratio of phenol and substrate in the complex to be 1:1 we have for the equilibrium condition:

$$\mathrm{ROH} + \mathrm{S} \rightleftharpoons \mathrm{RO{-}H \cdots S}$$

When the total concentration of phenol and substrate is constant $= c$, and α and $1 - \alpha$ are the mole fractions of phenol and substrate, respectively, and X = concentration of complex we have:

$$K = \frac{X}{[a \cdot c - x]\,[(1 - a)\,c - X]} \tag{1}$$

where K = association constant.

The solution of the equation gives:

$$X = \frac{(K \cdot c + 1) \pm \sqrt{(K \cdot c + 1)^2 - 4K^2\alpha \cdot c^2\,(1-\alpha)}}{2K} \tag{2}$$

where the sign $-$ is the only valid.

Upon derivation we find:

$$X_{\max} = \frac{(Kc - 1) - \sqrt{2Kc + 1}}{2K} \tag{3}$$

when $\alpha = \frac{1}{2}$.

The concentration of phenol or substrate is $\frac{c}{2} - X_{\max}$ when $\alpha = \frac{1}{2}$. The complex is therefore 1:1 if X has maximum at $\alpha = \frac{1}{2}$. A plot of the concentration of X as function of α is symmetrical on both sides of $\alpha = \frac{1}{2}$.

The concentration of phenol and substrates (N-diethylacetamide and triethylphosphate) can be determined from the optical density of the free O-H stretching band, and from the C=O or P=O bands of the substrates when the molar extinction coefficients are known and as a first approximation we assume the Lambert-Beer's law to be valid. The molar extinction of the complex, $\varepsilon_{\max}$, can be calculated from two different sets of values of phenol and substrate.

If we use equimolecular amounts of phenol and substrate we have:

$$K = \frac{X_1}{(A_1 - X_1)^2} = \frac{X_2}{(A_2 - X_2)^2} \tag{4}$$

where: X_1 and X_2 = concentration of complex
A_1 and A_2 = concentration of phenol and substrate.

If we assume Lambert-Beer's law to be valid we get:

$$K = \frac{f \cdot E_1}{(A_1 - f \cdot E_1)^2} = \frac{f \cdot E_2}{(A_2 - f \cdot E_2)^2} \qquad (5)$$

$$\text{where } f = \frac{1}{\varepsilon_{max} \cdot l} \text{ and } E = \log \frac{I_0}{I}.$$

The equation gives for f:

$$f = \frac{1}{\varepsilon_{max} \cdot l} = \frac{(A_2 - A_1) \pm \sqrt{A_2^2 \frac{E_1}{E_2} + A_1^2 \frac{E_2}{E_1} - 2A_2 \cdot A_1}}{E_2 - E_1} \qquad (6)$$

where the sign — is the only valid when $A_2 - A_1 > 0$.

Table 1. Calculation of the association constant between phenol and triethylphosphate from the hydroxyl stretching vibration band.

Conc. of phenol (moles/l)	Conc. of triethyl-phosphate	Optical density, free OH	Optical density, ass. OH	Conc. of complex	K	Temperature 30°C ε_{max} of ass. OH bond calculated	
						From free OH-bond	From eqn. (6)
0.03	0	0.160	—	—			
0.02625	0.00375	0.122	0.057	0.00340	(431)	167	164
0.0225	0.00775	0.083	0.115	0.00694	550	166	
0.01875	0.01125	0.050	0.153	0.00937	532	163	
0.0150	0.0150	0.025	0.170	0.01031	468	165	
0.01125	0.01875	—	0.153	0.00933	516*	164*	
0.00775	0.0225	—	0.115	0.00700	591*	164*	
0.00375	0.02625	—	0.057	0.00347	544*	164*	
0	0.03	—	—	—			

* Calculated from the associated OH-band.

Table 2. Calculation of the association constant between phenol and N-diethylacetamide from the hydroxyl stretching vibration band.

Temperature 30°C

Conc. of phenol (moles/l)	Conc. of N-diethyl-acetamide	Optical density, free OH	Optical density, ass. OH	Conc. of complex	K	ε_{max} ass. OH
0.03	0	0.160	—	—	—	
0.02625	0.00375	0.123	0.040	0.00319	(246)	122
0.0225	0.00775	0.090	0.075	0.00562	156	134
0.01875	0.01125	0.060	0.095	0.00750	178	127
0.0150	0.0150	0.035	0.102	0.00844	196	121
0.01125	0.01875	0.020	0.098	0.00750	178	131
0.00775	0.0225	—	0.080	—	—	—
0.00375	0.02625	—	0.040	—	—	—
0	0.03	—	—	—	—	—

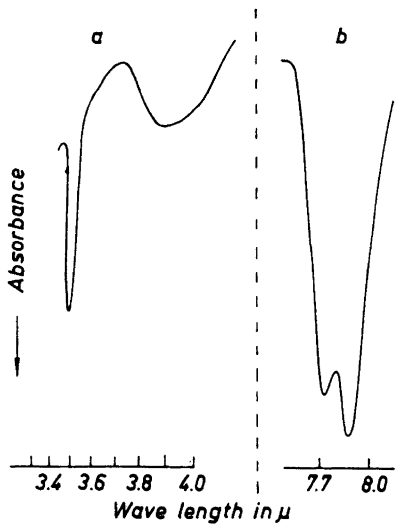

Fig. 1. a). Free and associated stretching bands of HCl (0.03 M) in CCl_4 in the presence of di*iso*propylfluorophosphate (0.03 M). *b*) Free and associated stretching bands of the P=O group of di*iso*propylfluorophosphate (0.03 M) in CCl_4 in the presence of HCl (0.03 M).

RESULTS OF THE MEASUREMENTS

The results of the measurements are collected in Tables 1 and 2. From the approximate constancy of the association constant at different concentrations of phenol and substrate we conclude that the complexes between phenol and diethylacetamide and between phenol and triethylphosphate are 1:1. The same results is also reached by comparing the optical densities of the associated hydroxyl stretching vibration band at different concentrations of phenol and substrate recorded in column 4, Tables 1 and 2. The expected maximum in optical density at $\alpha = \frac{1}{2}$ and the symmetrical distribution of the complex concentration on both sides of $\alpha = \frac{1}{2}$ give a convincing picture of the 1:1 association. In column 7, Tables 1 and 2, are recorded the calculated molar extinction coefficients of the two different complexes. The complex with the highest association constant shows the greatest molar extinction coefficient. A reasonable interpretation of this behaviour is that the complex with the highest association constant gives rise to the strongest change in dipole moment of the hydroxyl group during the vibration and in this way contributes to a greater intensity of absorption.

The stretching vibration band of the free and associated phosphoryl- and carbonyl group at 1 271 cm^{-1} and 1 655 cm^{-1} vary with the mole fraction of phenol in the same manner as the free and associated hydroxyl group. The displacements of the C=O and P=O bands upon hydrogen bonding are approximately 18 cm^{-1} and 30 cm^{-1}, respectively. For quantitative study of the hydrogen bond formation the use of the C=O and P=O bands are less suitable due to the small displacements of the associated bands.

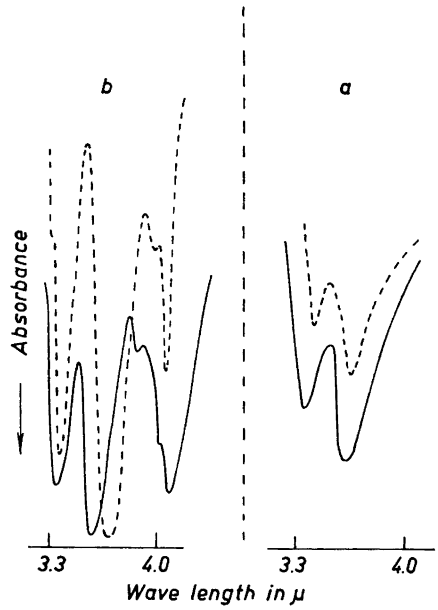

Fig. 2. a). Solid curve: Spectrum of N-dimethylacetamide hydrochloride (0.1 M) in $CHCl_3$; Dotted curve: Spectrum of trimethylamine hydrochloride (0.1 M) in $CHCl_3$. *b*) Solid curve: Spectrum of N-dimethylacetamide (0.5 %) in solid phase (KBr-briquet); Dotted curve: Spectrum of trimethylamine hydrochloride (0.5 %) in solid phase (KBr-briquet).

THE BEHAVIOUR OF ESTERS OF PHOSPHORIC ACID AND TERTIARY AMIDES UPON ASSOCIATION WITH HYDROCHLORIC ACID

Hydrochloric acid gives with esters of phosphoric acid in carbon tetrachloride the normal hydrogen bond association product where the phosphoryl oxygen participates in the hydrogen bond. Fig. 1 shows the free and associated stretching frequencies of the HCl-bond at 2 825 cm^{-1} and 2 440 cm^{-1}. The displacement is practically identical with the displacement of the H—Cl bond which is observed when hydrochloric acid is associated with ethyl ether [22]. The free and the associated P=O stretching frequencies are observed at 1 295 cm^{-1} and 1 268 cm^{-1} (Fig. 1). With tertiary amides the picture is quite different. The salt-like compounds which are formed between hydrochloric acid and tertiary amides were studied both in solid phase (KBr-briquet) and in chloroform solution. The solution showed no free or associated H—Cl stretching vibration and the frequencies of the vibration of the C=O bond were slightly higher than for the vibration of the C=O group in the pure amide solution. The spectrum between 2 300 cm^{-1} and 3 000 cm^{-1} showed the typical character of quaternary ammonium compounds with 3 carbon and 1 hydrogen atom attached to the nitrogen. In Fig. 2 are compared the spectra of trimethylamine hydrochloride with N-dimethyl acetamide hydrochloride in chloroform solution (a) and in solid phase (b). The very similar form of these spectra gives strong support to the quaternary nitrogen structure of the addition compounds between tertiary amides and strong acids. The above observations give evidence that there exist principal differences

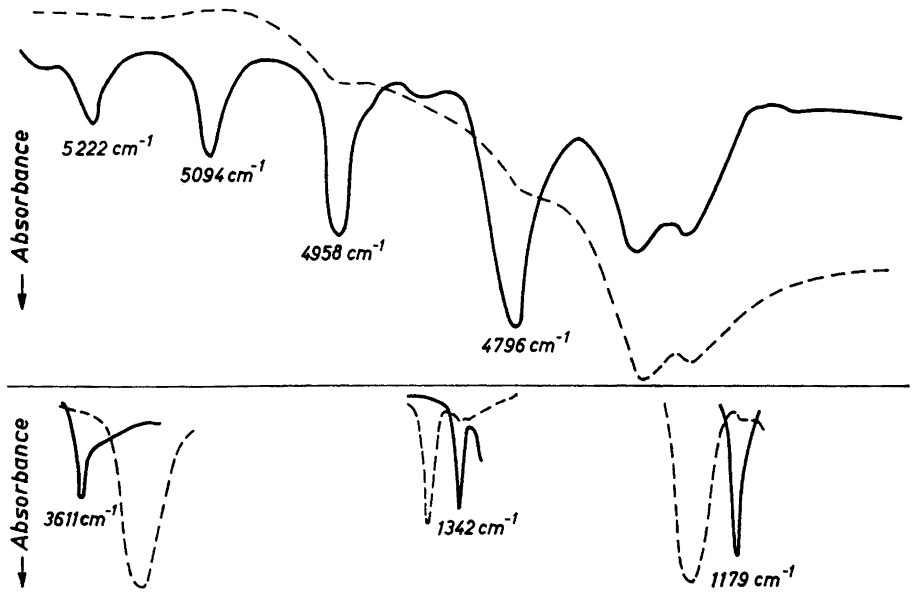

Fig. 3. Solid lines: Absorption bands of the free hydroxyl group of phenol (0.2 M) in CCl_4; Dotted lines: The disappearance of the free hydroxyl group of phenol (0.02 M) in CCl_4 in the presence of triethylphosphate (0.02 M).

between the formation of hydrogen bonds and proton transfer bonds. The explanation may be that the semi-polar oxygen is favoured in hydrogen bonding due to a great polarity of the bond but the nitrogen is favoured in proton transfer due to a greater tendency to share an electron pair with hydrogen.

THE APPLICATION OF TRIETHYLPHOSPHATE FOR THE IDENTIFICATION OF BANDS WHICH ARE DUE TO VIBRATIONS OF THE HYDROXYL GROUP

The very strong hydrogen bond between phenol and triethylphosphate makes the latter compound suitable for identification of the different vibrations of the hydroxyl group. When the hydroxyl group participates in hydrogen bond formation the bands due to the free hydroxyl disappear. The association constant between phenol and triethylphosphate in CCl_4 was found to be approximately 500. By using equimolecular amounts of phenol and triethylphosphate, concentrations of 0.2 M will reduce the concentration of free phenol to about 10 % of its original value. By using a double beam infrared instrument it is easy to compensate for the added triethylphosphate. In this way the disappearance of bands due to vibration of the free hydroxyl group is easily detected. Six hydroxyl bands were found at the following wave numbers: 1 178 cm^{-1}, 1 342 cm^{-1}, 4 796 cm^{-1}, 4 958 cm^{-1}, 5 094 cm^{-1} and 5 222 cm^{-1}. In Fig. 3 are recorded the spectra of the vibrations of the hydroxyl group in the above mentioned regions before and after addition of triethylphosphate.

Table 3. Optical densities of hydroxyl vibration bands of phenol in carbon tetrachloride (Measured at bond maximum).

Conc. of phenol (moles/l)	Optical density (cell length 10 mm)				Optical density (cell length 1 mm)					
	free OH 5 222 cm^{-1}	free OH 5 094 cm^{-1}	free OH 4 958 cm^{-1}	free OH 4 796 cm^{-1}	free OH 3 611 cm^{-1}	ass. OH 3 300 cm^{-1}	free OH 1 342 cm^{-1}	ass. OH 1 358 cm^{-1}	free OH 1 178 cm^{-1}	ass. OH 1 215 cm^{-1}
0.1	0.022	0.032	0.062	0.090	0.03	0.03	0.155	0.02	0.46	0.05
0.2	0.040	0.061	0.108	0.168	0.04	0.08	0.275	0.07	0.81	0.19
0.3	—	—	—	—	0.06	0.17	0.385	0.135	1.15	0.39
0.4	0.060	0.088	0.160	0.256	0.09	0.28	0.455	0.205	1.30	0.62
0.5	—	—	—	—	0.011	0.39	0.535	0.280	1.60	0.89
0.6	0.080	0.120	0.220	0.360	0.014	0.51	0.620	0.365	1.80	1.07

To prove that the six hydroxyl bands which were located with triethylphosphate are free hydroxyl bands their optical densities were studied as function of phenol concentration. The results are recorded in Table 3. Due to the increasing association of phenol the optical densities of the free hydroxyl bands shall increase less than proportional to the concentration of phenol. It is seen that the absorbance of the six hydroxyl bands vary with the concentrations of phenol in exactly the same way. The observed variations are just the same as the variation of the free stretching vibration band at 3 611 cm^{-1}.

It is observed that upon increasing the concentration of phenol two new bands appear displaced to higher frequencies of the free hydroxyl bands. These two association bands are located at 1 358 cm^{-1} and 1 215 cm^{-1}. The optical densities of the bands increase more rapidly than proportional to the concentration of phenol. From Table 3 we observe that the increase in optical densities are exactly parallel to the increase of absorbance of the association band at 3 300 cm^{-1} which is due to the hydroxyl stretching vibration of associated phenol.

INTERPRETATION OF THE LOCATED HYDROXYL BONDS

1. Bending vibrations of the hydroxyl group

There has for a long time been disagreement about the location of the bending vibrations of the hydroxyl group. Of the two bending vibrations, δ-OH (in-plane bending) and γ-OH (out-of-plane bending) one has expected to find the δ-OH in the region 1 300—1 200 cm^{-1} and the γ-OH in the region 1 000—600 cm^{-1} [22]. The present findings suggest that the δ-OH and γ-OH vibration bands of phenol are the absorption bands which are found at 1 342 cm^{-1} and 1 178 cm^{-1}.

The arguments for this interpretation are:

a) The bending vibrations of the hydroxyl group are perpendicular to the hydrogen bond. The hydrogen bond should therefore contribute to a stronger restoring force of the bending vibrations. The frequency of the hydroxyl bending vibrations should therefore be expected to increase upon formation of the hydrogen bond. This is also the situation of the two bands which are located at 1 342 cm^{-1} and 1 178 cm^{-1}. Their association bands are found at 1 358 cm^{-1} and 1 215 cm^{-1}, respectively.

b) The hydrogen bond should be expected to decrease the amplitude of the bending vibration. The change in dipole moment during vibration will therefore be smaller, which is tantamount to a lower intensity of the bending vibration of the associated hydroxyl bond. If we compare the absorbance of the free and the associated vibration bands with the free and the associated stretching bands at corresponding phenol concentrations in Table 3 it is seen that the ratios between the absorbances of the free and the associated vibration bands are opposite to the ratio observed for the stretching band. If the breadth of the bands are also considered which must be done when intensities are to be compared, the inverse relationship is still greater than when only the absorbances are compared.

2. Combination between stretching and bending vibrations

The most reasonable interpretation of the 4 hydroxyl bands located in near infrared at 5 222 cm^{-1}, 5 094 cm^{-1}, 4 958 cm^{-1} and 4 796 cm^{-1} seems to be that the two bands of highest frequencies are bands due to combination between the free stretching vibration and the in-plane bending vibration and the two bands at the lowest frequencies are combination bands between the free stretching vibration and the free out-of-plane bending vibration.

The arguments for this view are:

a) From the experiment with phenol and triethylphosphate it was found that the four bands were all due to free hydroxyl groups. The same result was also found in the study of the concentration dependence of the bands.

b) If the two bending vibrations combine with the same stretching vibration to give combination vibrations it is reasonable to expect that the ratio between the absorbance of the two bending vibrations should be identical with the ratio between the corresponding combination vibrations.

Table 4. Bands due to bending of the hydroxyl group in alcohols.

Compounds	Band maxima (cm^{-1})
Methyl alcohol	1 328
Ethyl alcohol	1 236
Propyl alcohol	1 210
Butyl alcohol	1 202
Amyl alcohol	1 200

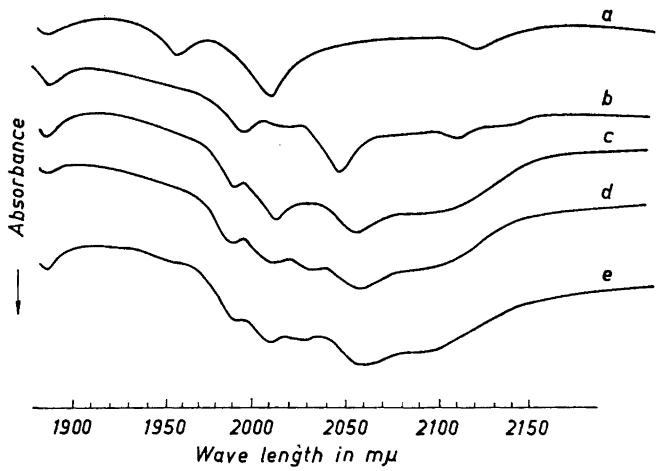

Fig. 4. Combination bands of alcohols in CCl_4 (0.4 M). *a*) Methyl alcohol, *b*) ethyl alcohol, *c*) propyl alcohol, *d*) butyl alcohol, *e*) amyl alcohol.

From Table 3 we calculate that the average ratio between the absorbance of the two bending vibrations at the six different phenol concentrations is 2.9. The average ratio between the absorbances of the bands at 5 222 cm^{-1} and 4 958 cm^{-1} is 2.8, and the average ratio between the absorbances of the bands at 5 094 cm^{-1} and 4 796 cm^{-1} is 2.9. Why the combined vibration of bending and stretching vibrations should give rise to splitting of the combination bands is not known. It seems worthwhile to mention that similar splitting of the overtone bands of the C—H group is also observed [23].

THE BENDING AND COMBINATION BANDS OF ALCOHOLS]

The previous described technique of hydroxyl bands localisation has been used in an attempt to locate the bending and the combination bands of alcoholic hydroxyl groups. In this case we have been able to locate with certainty only one bending vibration band in the region 1 400—1 100 cm^{-1}. The frequencies of the bending vibrations of different alcohols are recorded in Table 4. The observed frequencies correspond with the frequencies of δ-OH vibrations put forward of Stuart and Sutherland [24]. The interesting observation which is also mentioned by Stuart and Sutherland [24] is that the frequency of the bending band of methyl alcohol is abnormally high. This anomaly of the methyl alcohol gives an argument that the combination vibration of the hydroxyl groups of alcohols observed in near infrared are composed of stretching and bending vibrations. The combination vibrations of the hydroxyl in methyl alcohol must in this case show the same strong displacement towards higher frequencies when it is compared with the other alcohols. This is exactly the case as shown in Fig. 4.

Another observation is that in methyl alcohol there are only two free hydroxyl bands in near infrared. In ethyl- and propyl alcohol we can recognize three and in the higher members of alcohols four free hydroxyl bands (Fig. 4.)

The intensities of the combination bands of alcohols are much lower than the intensities of the corresponding phenol bands. The same relation should therefore be expected to hold for the bending vibrations, and this may explain why the bending vibration bands of alcohols are more difficult to locate.

EXPERIMENTAL

The infrared spectra of the compounds studied were recorded on a Perkin-Elmer Spectrometer Model 21. The measurements were performed in carbon tetrachloride in sodium chloride cells of 1 mm thickness compensated against carbon tetrachloride. The temperature was maintained constant within a range of ± 1°C during the measurements.

The spectra in near infrared were recorded on a Beckman instrument, Model DK 2. The measurements were performed in carbon tetrachloride solution in quartz cells of 10 mm thickness compensated against carbon tetrachloride.

The compounds studied were synthesized according to descriptions in the literature [25,26].

REFERENCES

1. Errero, J. and Mollet, P. *Nature* **138** (1936) 882.
2. Fox, J. J. and Martin, A. E. *Nature* **139** (1937) 507.
3. Buswell, A., Deitz, V. and Rodebush, W. H. *J. Chem. Phys.* **5** (1937) 84, 501.
4. Gordy, W. *J. Chem. Phys.* **5** (1937) 399.
5. Errero, J. and Sack, H. *Trans. Faraday Soc.* **34** (1938) 728.
6. Fox, J. J. and Martin, A. E. *Proc. Roy. Soc. London* **A 162** (1937) 419.
7. Kempter, H. and Mecke, R. *Z. Physik. Chem.* **B 46** (1940) 229.
8. Coggeshall, N. L. and Saier, E. L. *J. Am. Chem. Soc.* **73** (1951) 5414.
9. Lord, K. C. and Merrifield, K. E. *J. Chem. Phys.* **21** (1953) 166.
10. Bovner, L. G. and Hofstadter, R. *J. Chem. Phys.* **6** (1938) 531.
11. Davies, N. M. and Sutherland, G. *J. Chem. Phys.* **6** (1938) 755.
12. Bushwell, A. M., Rodebush, W. H. and Roy, M. F. *J. Am. Chem. Soc.* **60** (1938) 2239.
13. Flett, M. *J. Chem. Soc.* **1951** 962.
14. Rasmussen, R. S., Tunnicliff, D. D. and Brattain R. R. *J. Am. Chem. Soc.* **7** (1949) 1068.
15. Le Feure and Welsh, H. *J. Chem. Soc.* **1949** 2230.
16. Koch, H. P. *J. Chem. Soc.* **1951** 512.
17. Grove, J. F. and Wellis, H. A. *J. Chem. Soc.* **1951** 877.
18. Badger, R. M. and Bauer, S. H. *J. Chem. Phys.* **5** (1937) 369.
19. Shigorin, D. N. *Zhur. Fiz. Khim.* **23** (1949) 506.
20. Bagder, R. M. *J. Chem. Phys.* **8** (1940) 288.
21. Sheppard, N. *Hydrogen Bonding*, Papers presented at the Symposium of Hydrogen Bonding held at Ljubljana, 29 July – 3 August 1957, Symposium Publication Division, Pergamon Press, London 1959.
22. Ganthier, G. *Compt. rend.* **231** (1950) 1138.
23. Stuart, A. V. and Sutherland, G. B. B. M. *J. Chem. Phys.* **24** (1956) 556.
24. Larsson, L. *Arkiv Kemi* **13** (1958) 259.
25. Wagner, B. R. *Synthetic Organic Chemistry*, John Wiley and Sons Inc., London 1953, p. 515.
26. Kosolapoff, G. M. *Organophosphorus Compounds*, John Wiley and Sons, Inc., London 1950, p. 211.

Received February 8, 1960.

ACTA CHEMICA SCANDINAVICA 14 (1960) 1485–1494

Intermolecular Hydrogen Bond Association between Phenol and Organophosphorus Compounds

GUNNAR AKSNES* and THOR GRAMSTAD

Norwegian Defence Research Establishment, Toxicological Group, Kjeller, pr Lillestrøm, Norway

The intermolecular hydrogen bond association constants between phenol and eighteen organophosphorus compounds have been determined at 20°C and 50°C.

The ΔF, ΔH and ΔS values of the equilibrium reactions are found to vary linearly with the hydrogen bond shift in such a way that an increase in enthalpy is counteracted by a decrease in entropy.

The strong influence of the substituents in organophosphorus compounds on the hydrogen bond association constants is discussed in terms of the electronic properties of the phosphorus atom and the substituents.

The connection between hydrogen bond formation and proton transfer reaction is commented upon.

In a previous paper the very strong intermolecular hydrogen bond between phenol and triethylphosphate was reported [1]. It was shown that it is the phosphoryl group which participates in hydrogen bonding. When sufficiently low concentrations of phenol and triethylphosphate are used the only association complex formed is the dimeric intermolecular hydrogen bond complex.

This paper is devoted to the study of the influence of different substituents in the phosphorus compounds on the dimeric hydrogen bond complex. Studies of the self-association of phenol made it clear that the phenol concentration range used in the previous study [1] (0—0.03 M) was not quite low enough to exclude self-association of phenol. To avoid any disturbance of self-association of phenol it was found necessary to reduce the concentration range to 0—0.006 M.

We found it of special interest to evaluate the thermodynamic functions of the hydrogen bond equilibrium reaction. It was therefore necessary to determine the association constants at two different temperatures. An accurate temperature control is difficult to obtain in salt cells, and the ground state

* Present address: Chemical Institute, University of Bergen, Bergen, Norway.

Table 1. Determination of the association constant between phenol and methoxyethylphosphoryl fluoride in carbon tetrachloride. Cell length = 10 cm. Temperature 20°C.

Concentration (moles/l)		Optical density, free OH	Conc. (moles/l) of free phenol	Conc. of complex	K_{ass} (l/mole) calc.	K_{ass} mean value
Phenol						
0.00600	0	0.1643	0.00600	—	—	
0.00480	0.00120	0.1308	0.00447	0.000330	84.8	
0.00420	0.00180	0.1107	0.00377	0.000427	82.4	
0.00360	0.00240	0.0915	0.00312	0.000481	80.4	
0.00300	0.00300	0.0731	0.00249	0.000509	82.1	82.5
0.00240	0.00360	0.0560	0.00191	0.000491	82.6	
0.00180	0.00420	0.0405	0.00138	0.000419	80.2	
0.00120	0.00480	0.0255	0.000869	0.000331	85.2	

stretching vibration band of phenol is therefore less suitable to use as measure of free phenol concentration. We therefore decided to employ the first overtone band of the hydroxyl group of phenol at 7 052 cm^{-1}. In this spectral region one can use absorption cells of quartz, and a good temperature control is therefore easily obtained.

EXPERIMENTAL

Materials. The phosphorus esters studied were synthesized from the corresponding chlorides. An equivalent amount of alcohol was added to the organophosphorus chloride in carbon tetrachloride in the presence of pyridine. The pyridine salt was filtered off and the phosphorus ester distilled under reduced pressure. The ester was purified by repeated fractionations. The organophosphorus chlorides were synthesized according to descriptions in the literature. The chlorides of the compounds Nos. 1, 3, 9, 11, 13 and 14 in Table 2 were prepared according to the method of Kinnear and Perren [2], and the chloride of the compound No. 15 according to the method of Michaelis [3]. Compounds Nos. 4, 6, 8 and 10 were prepared according to the method of Nylén [4], and the derivatives of phosphine oxide (compounds Nos. 16, 17 and 18) were synthesized according to the description of Kosolapoff [5].

The fluorine-containing compounds (Nos. 2 and 5) were synthesized from the corresponding chlorides. The chloride (20 g) was added to an excess of sodium fluoride (10 g) in benzene (50 ml). The reaction mixture was rapidly stirred, and the temperature in the mixture was kept at 60°C for one hour. The sodium salts were filtered off and the fluorophosphorus compound distilled under reduced pressure.

The method used for the calculation of the association constants was the same as described previously [1]. The concentration of the free phenol was determined from the first overtone band of the stretching vibration of the phenolic hydroxyl group at 7 052 cm^{-1}.

The absorption curves were recorded on a Beckman DK 2 double beam spectrophotometer. Cylindrical quartz absorption cells of 10 cm path length were used. The absorption cell which contained the mixture of phenol and the phosphorus compound in carbon tetrachloride was jacketed with a polyethylene tube. The tube was welded to the absorption cell approximately 5 mm from the windows. A constant temperature circulating water bath maintained the polyethylene jacketed cell at ± 0.1°C. The reference cell contained carbon tetrachloride.

The frequency shifts of the ground state stretching vibration band of the associated hydroxyl group of phenol in CCl_4 were measured with a Perkin Elmer infrared spectrophotometer Model 21. The same instrument was used for the determination of the stretching frequencies of the P=O group of the phosphorus compounds in CCl_4. The values of the association constants recorded in Table 2 are the mean values of seven separate determinations of each association constant. In Table 1 are recorded the experimental results from the determination of K_{ass} of one of the compounds studied.

The indexes of refraction of the phosphorus compounds were determined with a thermostated Abbe refractometer. The molar refractions (M.R.) recorded in column 5, Table 2, are calculated with the atomic refractivities of phosphorus compounds given by Jones, Davies and Dyke [6], Vogel [7] and Holmstedt [8].

DISCUSSION

Previous findings indicate that there exists a linear relation between the logarithms of the association constants (or ΔF) and the frequency shift of different hydrogen bonded systems [9]. In Fig. 1 are plotted our results of log K as function of the frequency shift of the ground state stretching vibration of the hydrogen bonded hydroxyl group of phenol. The straight lines drawn through the calculated log K values at 20°C and 50°C, respectively, are both within the limits of experimental errors. The slopes of the two lines are different at the two temperatures studied. The free energy, ΔF, of the hydrogen bond equilibrium reaction can thus be fairly accurately described as a linear function of the frequency shift. Since the enthalpy is interconnected with the free energy through the thermodynamic relation $\Delta F = \Delta H - T\Delta S$, it is a necessary consequence of the linear relation between ΔF and $\Delta\vartheta$ at different temperatures that both the enthalpy and the entropy are proportional to the frequency shift. In Figs. 2 and 3 are shown the variation of ΔF, ΔH and ΔS with $\Delta\vartheta$ calculated from the smoothed values of log K found from the two straight lines in Fig. 1. From the frequency shift of the hydroxyl group of phenol with the different phosphoryl compounds studied we find that in the observed series of compounds there is an increase of ΔH from approximately 5 to 8 kcal but a decrease of ΔS from −6 to −11 E.U.

We interpret this observation as due to an increase in the polarity of the hydrogen bond complex as compared with the reactants. Such increase of polarity upon hydrogen bonding has in fact been observed in dipole moment studies of hydrogen bond complexes. Thus Sutton *et al.* [10,11] have shown that in the O—H···N bond in the complex of phenol and trimethylamine, using *cyclo*hexane as solvent, there appears to be an additional moment of 0.8 *D*. Further evidence may be found in the work of Eda and Ito [12] on the dipole moment of salicyl aldehyde. An increase of polarity from the reactants to the hydrogen bond complex will contribute to a negative entropy of reaction due to a greater orientation of the solvent molecules around the complex.

Table 2. Physical data of organophosphorus compounds (columns 1—6). Data of dimeric hydrogen bonding between organophosphorus compounds and phenol in carbon tetrachloride (columns 7—10).

Compound	1	2	3	4	5	6	7	8	9	10
	Bp°C/$\frac{mm}{Hg}$	n_D^{20}	d^{20}	M.R. calc.	M.R. theory	$\vartheta_{P=O}$ cm^{-1}	$\Delta\vartheta_{P=O}$ cm^{-1}	$\Delta\vartheta_{O-H}$ cm^{-1}	K_{ass} 20°C	K_{ass} 50°C
1. $CCl_3-P(=O)(OC_2H_5)(OC_2H_5)$	106°/3.5	1.4597	1.3568	51.54	50.40	1 280	2	260	73.2	44.8
2. $F-P(=O)(C_2H_5)(OCH_3)$	58°/20	1.3858	1.1710	25.25	25.73	1 296	—	270	82.5	37.5
3. $CHCl_2-P(=O)(OC_2H_5)(CO_2H_5)$	89.5°/0.8	1.4537	1.2978	46.09	45.67	1 276	2	275	133.1	60.7
4. $H-P(=O)(OCH_3)(OCH_3)$	53°/10	1.4016	1.1983	22.34	22.74	1 267	41	300	123.1	53.4
5. $F-P(=O)(C_2H_5)(C_2H_5)$	72°/9	1.4134	1.0851	28.45	29.40	1 278	—	305	129.0	61.4
6. $H-P(=O)(OC_2H_5)(OC_2H_5)$	69°/10	1.4076	1.0728	31.73	31.66	1 260	35	310	161.9	76.8
7. $CH_3O-P(=O)(OCH_3)(OCH_3)$	76°/10	1.3954	1.2147	27.67	27.89	1 279	31	315	182.9	78.9
8. $H-P(=O)(OCH_2.CH_2.CH_3)(OCH_2.CH_2.CH_3)$	97°/12	1.4165	1.0188	40.97	40.94	1 262	38	320	199.7	86.9
9. $CH_2Cl-P(=O)(OC_2H_5)(OC_2H_5)$	86°/3.5	1.4385	1.1938	41.07	40.94	1 268	1	325	239.0	84.2
10. $H-P(=O)(OCH(CH_3)_2)(OCH(CH_3)_2)$	79°/13	1.4060	0.9949	40.95	40.94	1 210	34	330	237.3	99.9

Table 2, cont.

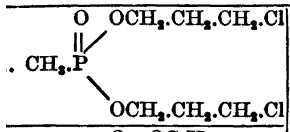	131°/0.6	1.4663	1.2632	54.64	54.87	1 243	28	335	247.0	95.7
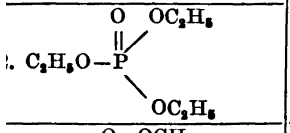	58°/0.5	1.4053	1.0690	41.79	41.83	1 271	30	345	350.5	121.1
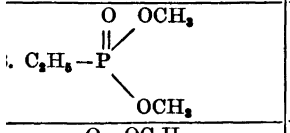	59°/6	1.4170	1.1134	31.19	31.56	1 228	20	355	329.7	126.5
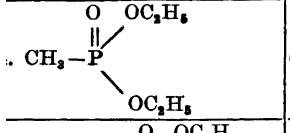	69–70°/8	1.4165	1.0520	36.33	36.20	1 237	23	360	381.0	141.0
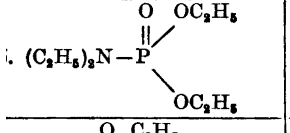	88°/3.5	1.4226	1.0116	52.62	52.86	1 251	28	395	518.2	211.8
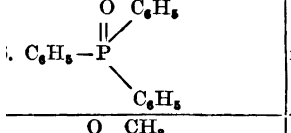	215°/0.6 m.p. 157.5°	–	–	–	–	1 200	21	430	1055.4	365.5
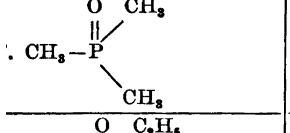	m.p. 141°	–	–	–	–	1 177	9	470	1836.0	639.4
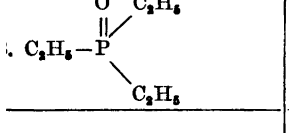	127°/20	–	–	–	–	1 176	23	510	2522.0	858.0
Pyridine	115°/760	–	–	–	–	–	–	465	64.0	19.3

The stronger the dipole in the phosphoryl group, the stronger will be the deformation of the electrons in the hydrogen bond. We find therefore that the contribution of a negative entropy difference between reactants and complex shall be greatest for the strongest hydrogen bond. Evidence for the above interpretation are also found from other hydrogen bond measurements[13]. Some calculated ΔH and ΔS values are collected in Table 3. We recognize also here the same tendency of ΔH and ΔS to counteract each other.

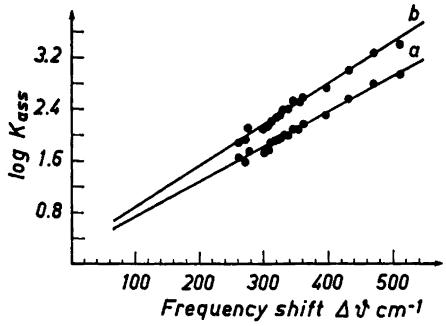

Fig. 1. The relation between the logarithms of the association constants and the frequency shift for the hydrogen bond complexes between phenol and phosphoryl compounds. *a* : 20°C, *b* : 50°C.

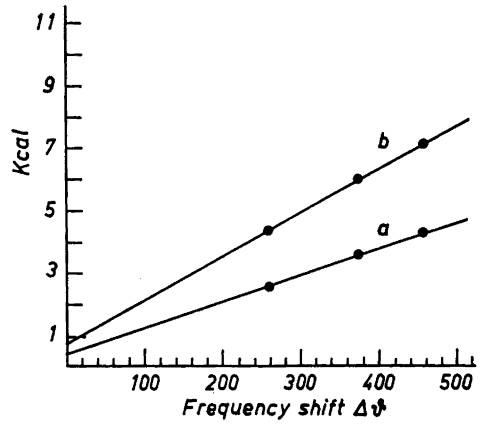

Fig. 2. The relation between ΔF at 20°C (a), respectively, ΔH (b) and the frequency shift for the hydrogen bond complexes between phenol and phosphoryl compounds.

It is of interest that the same opposite operating influence on the activation energy and activation entropy is found in reaction kinetic studies of phosphorus compounds [14].

In Fig. 4 are plotted the observed half bond width $\vartheta\frac{1}{2}$ as function of the frequency shift $\Delta\vartheta$ of the ground state stretching vibration band of phenol when it is hydrogen bonded with different phosphoryl compounds. The straight line drawn through the observed values cuts the $\vartheta\frac{1}{2}$-axis at 35 cm^{-1}. This is

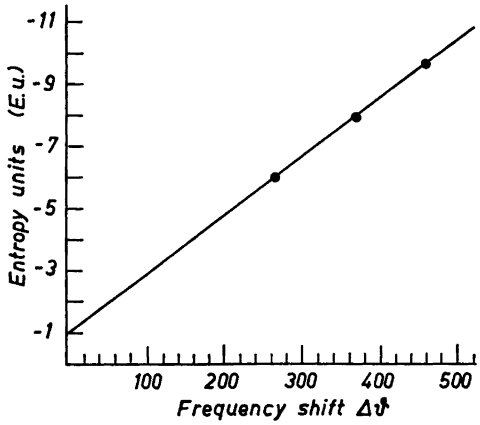

Fig. 3. The relation between ΔS and the frequency shift for the hydrogen bond complexes between phenol and phosphoryl compounds.

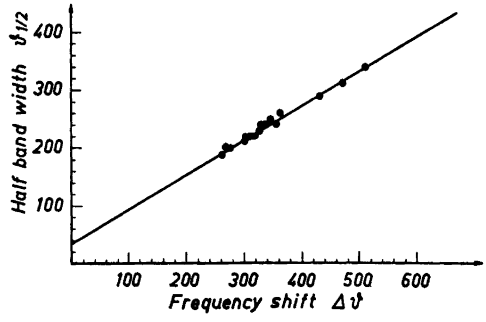

Fig. 4. The relation between the half bond width, $\vartheta_{\frac{1}{2}}$ and the frequency shift $\Delta\vartheta$ for the hydrogen bond complexes between phenol and phosphoryl compounds.

Table 3. ΔH and ΔS of the hydrogen bond reaction between phenolic hydroxyl and different compounds [13]

System	Solvent	ΔH kcal/mole	ΔS E.U.
Phenol-methylacetate [10]	*n*-heptane	$-5.3 \pm (0.1)$	$-12.8 \pm (0.2)$
p-Chlorophenol-methylacetate [10]	*n*-heptane	$-6.7 \pm (0.1)$	-16.9 ± 0.4
m-Chlorophenol-methylacetate [10]	*n*-heptane	$-6.5 \pm (0.3)$	$-15.2 \pm (1.0)$
o-Chlorophenol-methylacetate [10]	*n*-heptane	$-1.4 \pm (0.3)$	$-3.5 \pm (1.0)$
Phenol-pyridine *	carbon tetrachloride	-7.5	-17.4

* Data from this work.

approximately the half band width of the hydroxyl group of phenol in carbon tetrachloride. It is very interesting that the linear relation between $\vartheta_{\frac{1}{2}}$ and $\Delta\vartheta$ seems to be independent of the hydrogen bonded species involved. This conclusion is reached by comparing our results with the observations made by Huggins *et al.*[15]. They find for quite different hydrogen bonding species not only the same linear relation between $\vartheta_{\frac{1}{2}}$ and $\Delta\vartheta$, but also approximately the same slope of the line. The empirical relation seems to be of such general validity that we may suppose that it is connected with some fundamental properties of the hydrogen bond.

To shed further light on this problem we have tried to determine the intensity of the hydrogen bonded hydroxyl groups. Due to the experimental difficulties in the determination of this quantity we have used the product $\vartheta_{\frac{1}{2}} \times \varepsilon_{max}$ (where ε_{max} is the absorption coefficient of the band at the band maximum) as a relative measure of the intensity. The ε_{max} is determined by using so great excess of phosphoryl compound that all of the free phenol has disappeared (0.003 M phenol + 0.2 M phosphoryl compound). The results of the determination of ε_{max} is plotted in Fig. 5. We find in this case a nearly linear relation between ε_{max} and $\Delta\vartheta$ up to frequency shift of approximately 400 cm^{-1}. The ε_{max} of the two last compounds have decreased very markedly. The ε_{max} seems therefore to increase to a maximum value in the neighbourhood of 400 cm^{-1}. The same variation of ε_{max} was also observed by Gordy [16] in his study of hydrogen bond between amines and deuterium oxide. If we consider only the phosphorus compounds which cause frequency shifts of less than 400 cm^{-1} it seems that the intensity as function of the frequency shift can be approximately described by the following equation:

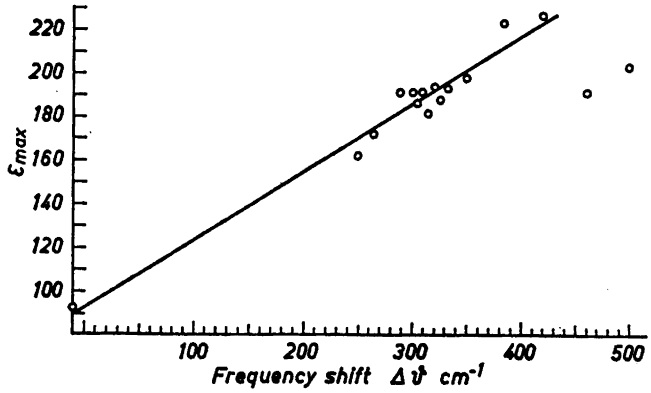

Fig. 5. The relation between ε_{max} and $\Delta\vartheta$ for the hydrogen bond complexes between phenol and phosphoryl compounds.

Intensity $\approx \vartheta_{\frac{1}{2}} \times \varepsilon_{max} \approx$

$(\text{const}_1 + f_1 \Delta\vartheta)\ (\text{const}_2 + f_2\Delta\vartheta) = a + b\ \Delta\vartheta + c(\Delta\vartheta)^2$ where a, b and c are constants.

That the variation of the intensity as function of the frequency shift is better described by a parabolic equation than by a linear one, is also clearly observed from the intensity data collected by Huggins and *et al.* [15].

An interesting result of the present study is the observed strong influence of the substituents in the phosphorus compounds on the equilibrium constants of the hydrogen bonded complexes. This must be connected with an easy deformation of the electronic atmosphere around the phosphorus atom. The influence of the substituents upon the polarity of the P = O bond is shown in Table 2, column 6, where the frequencies of the stretching vibration band of the phosphoryl group in carbon tetrachloride are recorded. The general tendency is that electron withdrawing substituents on the phosphorus atom strongly reduce the polarity of the P=O bond. The displacement of the stretching vibration frequency of the P=O group upon hydrogen bonding will be a measure of the polarisability of the phosphorus compound involved. The observed frequency shifts are seen in Table 2, column 7. We recognize that the most strongly polarisable substituents, amino and alkoxy groups, give rise to the greatest frequency shifts of the P=O bond. The chlorine substituted phosphorus compounds are seen to stabilize the electronic constitution of the compounds to such a degree that the formation of the hydrogen bond complex occurs almost without any electronic deformation of the phosphorus compounds. The present findings provide further evidence for the view that the phosphorus atom has a marked tendency to expand its valence shell by utilization of its 3*d* orbitals in the formation of a double bond [17,18]. It seems reasonable that the main contributing structures of the resonance hybrid of phosphorus compounds are as follows [18]:

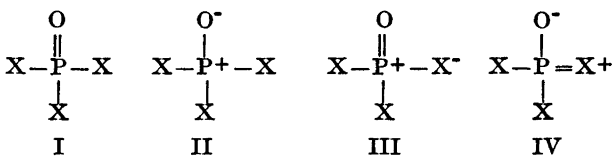

I II III IV

The frequencies of the stretching vibrations of the different phosphorus compounds in carbon tetrachloride summarized in Table 2 indicate that both the inductive and mesomeric effects of the substituents contribute to the observed polarity of the phosphoryl bond. We suppose that the structures I and II will be the main contributing structures of trialkylphosphine oxides. When strongly negative substituents as fluorine and chlorine are present in the molecule, structure III may be expected to contribute to a larger degree due to the strong $-I$ effect. The mesomeric effect ($+M$) of alkoxy and amino substituents should be characterized by an increasing contribution from structure IV. The observed strong frequency shifts of the phosphoryl group in the alkoxy and amino substituted phosphorus compounds upon hydrogen bonding with phenol points to the conclusion that also the electromeric effect of these substituents are considerable. This effect requires a phosphorus π-orbital capable of interacting with the unshared pair of electrons on the oxygen and nitrogen atoms. The above conclusions are in accordance with the interpretation of Larsson summarized in a recent review [18].

In the previous paper [1] it was shown that the carbonyl group of N-diethylacetamide participated in the hydrogen bonding with phenol. When sufficiently strong acid was used (HCl) a proton transfer reaction occurred, but in this case the proton was attached to the nitrogen. It was mentioned that there seems to exist a principal difference between groups which are involved in hydrogen bonding and proton transfer reaction. We have therefore in this paper included the results of the measurements of the association constants of the complex between phenol and pyridine at 20° and 50°C (Table 2). From Table 3 we observe that the calculated ΔH value of 7.5 kcal of the pyridine-phenol reaction is approximately identical with the ΔH value expected from the frequency shift of 465 cm^{-1} (Fig. 5 b). The reason for the low association constant of the phenol-pyridine complex must therefore be found in an unfavorable entropy of reaction.

The calculated value —17.4 E.U. is in fact approximately 7 E.U. lower than the entropy of the phosphoryl complex with the same ΔH. The more unfavorable entropy of the formation of the pyridine-phenol complex as compared with the phosphate-phenol complex may depend on different steric properties of the complexes. Another reasonable explanation may be found in a difference of polarity of the two types of hydrogen bonds.

REFERENCES

1. Aksnes, G. *Acta Chem. Scand.* **14** (1960) 1475.
2. Kinnear, A. M. and Perren, E. A. *J. Chem. Soc.* **1952** 3437.
3. Michaelis, A. *Ann.* **326** (1903) 129.
4. Nylén, P. *Studien über Organische Phosphorverbindungen.* Diss., Uppsala 1930, p. 27.

5. Kosolapoff, G. M. *Organophosphorus Compounds*, John Wiley and Sons, Inc., New York 1950, p. 107.
6. Jones, W. J., Davies, W. C. and Dyke, J. C. *J. Phys. Chem.* **37** (1933) 583.
7. Vogel, A. I. *J. Chem. Soc.* **1948** 1842.
8. Holmstedt, B. *Acta Physiol. Scand.* **25** (1951) Suppl. 90, p. 23.
9. Grundwald, E. and Coburn, Jr., W. C. *J. Am. Chem. Soc.* **80** (1958) 1322.
10. Sutton, L. E. *J. chim. phys.* **46** (1949) 435.
11. Hulett, J. R., Pegg, J. A. and Sutton, L. E. *J. Chem. Soc.* **1955** 3901.
12. Eda, B. and Ito, K. *Bull. Chem. Soc. Japan* **30** (1957) 164.
13. Lippert, E. *Hydrogen Bonding*, Papers presented at the Symposium of Hydrogen Bonding held at Ljubljana, 29 July – 3 August 1957, p. 217. Edited by Hadzi, D. and Thompson, H. W., Pergamon Press, London 1959.
14. Aksnes, G. *Acta Chem. Scand.* **14** (1960) 1515.
15. Huggins, C. M. and Pimentell, G. *J. Phys. Chem.* **60** (1956) 1615.
16. Gordy, W. *J. Chem. Phys.* **9** (1941) 215.
17. Pauling, L. *The Nature of the Chemical Bond*, Cornell University Press, London 1948.
18. Larsson, L. *Svensk Kem. Tidskr.* **71** (1959) 336.

Received February 8, 1960.

ACTA CHEMICA SCANDINAVICA 14 (1960) 1495–1498

On the Complex Chemistry of the Tervalent Rare-Earth Ions

V. The Acetate and Glycolate Systems of Yttrium

ARTUR SONESSON

Department of Inorganic and Physical Chemistry, Chemical Institute, University of Lund, Lund, Sweden

The complex formation of the yttrium acetate system and the yttrium glycolate system has been studied potentiometrically. The measurements were performed at 20°C in perchlorate medium of ionic strength 2.0 M. It was found that both the systems show significant similarities with the correspondent systems in the middle of the lanthanum series.

The complexity constants of the yttrium acetate system are lower than the constants of the dysprosium system, but the ratios b_n/b_{n+1} between the consecutive stability constants coincide rather well for the two systems. The complexity constants of the yttrium glycolate system show a rather good agreement with the complexity constants of the gadolinium glycolate system. The values of the ratios b_n/b_{n+1} place the yttrium system between the samarium and the gadolinium systems.

For the tervalent yttrium ion the electron configuration of the outer shell is $4s^2\ 4p^6$. It is thus similar to the electron configuration of the tervalent ions of the lanthanum series — that is, $5s^2\ 5p^6$. Moreover the yttrium ion has about the same ionic radius (0.90 Å) as the middle rare-earth ions (Dy — 0.91 Å, Ho — 0.89 Å). Therefore the chemical similarity between yttrium and the middle rare-earths is rather great. Schwarzenbach *et al.*[1] have shown that the yttrium ions show the greatest similarity with the rare-earth ions in the middle of the lanthanum series when strong complexes are formed, *e.g.* with ethylenediamine tetra-acetate ions.

CHEMICALS USED

A stock solution of *yttrium perchlorate* was prepared by dissolving a weighed amount of yttrium oxide (99.5 % purity) in somewhat more than the calculated amount of perchloric acid. Most of the acid excess was then removed by evaporation.

The remaining excess of acid in the stock solution was determined by electrometric titration with sodium hydroxide.

The yttrium concentration of the stock solution was calculated from the weighed amount of yttrium oxide. The same value of the yttrium concentration was obtained

by means of a cation exchanger column, after having corrected for the free perchloric acid in the stock solution.

The stock solution was examined spectrographically and it was found that no foreign elements absorbing in the range 250 mμ – 900 mμ were present in detectable amounts.

The other solutions used in this investigation were prepared and analyzed in the way described in the preceding parts [2,3,4].

RESULTS

The investigation of the yttrium acetate and the yttrium glycolate systems was performed potentiometrically by means of quinhydrone electrodes as described in Parts I, II and III. The composition of the galvanic cells is shown in I p. 169 and III p. 999. For the notations and the functions used for the calculations of the complexity constants the reader is referred to II p. 1938.

The yttrium acetate system. It was checked that the hydrolysis of the non-complex yttrium ions did not seriously affect the complex formation. Buffer solutions having the composition 2 M HAc + 1 M NaAc and 4 M HAc + 1 M NaAc gave $\bar{n}/[A^-]$-functions coinciding within the limits of the random errors.

As before, when the rare-earth acetate complexes were investigated, a correction has been applied for the decrease of the ionic strength caused by the complex formation. It was found that the relation between ΔE_A, the increase of E_A, and ΔI, the increase of the ionic strength I, was $\Delta E_A = -4.2 \times \Delta I$, *i.e.* about the same function was obtained as for the other rare-earth acetate systems (*cf.* I p. 171). ΔI was computed by means of approximate ligand numbers. Then, the ligand numbers $\bar{n}$ have been computed from $E_A + \Delta E_A$.

The $\bar{n}/[A^-]$-values at low acetate concentrations seem to increase somewhat with increasing yttrium concentrations in the same way as for the higher rare earths (*cf.* II). Then the system probably has a slight tendency to form polynuclear complexes. If only mono- and dinuclear complexes are assumed, the value of the complexity constant for the first dinuclear complex $\beta_1^2 = [M_2A] \cdot [M]^{-2} \cdot [A]^{-1}$ should be 20–30 M^{-2}.

The results of the measurements on the yttrium acetate system are shown in Fig. 1 and in Tables 1 and 2.

The yttrium glycolate system. The yttrium glycolate proved rather slightly soluble as was also found for the lower rare earths (*cf.* Jantsch and Grünkraut [5]). However, the solution remained supersaturated for several minutes. Therefore the complex formation could be studied also at high glycolate concentrations by performing the measurements rapidly.

For the glycolate system the E_A-values measured must be increased by $\Delta E_A = -2.8 \times \Delta I$. Then the E_A-values varied with the ionic strength in about the same way as for the other rare earth glycolate systems.

No significant signs of polynuclear complexes could be detected.

The results of the measurements on the yttrium glycolate system are collected in Fig. 2 and in Tables 1 and 2.

DISCUSSION

If the complexity constants of the yttrium acetate system are compared with the corresponding constants of the rare-earth acetate systems that have

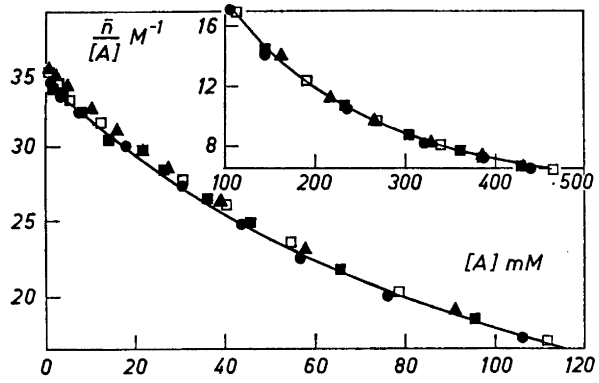

Fig. 1. $\bar{n}/[A^-]$ as a function of $[A^-]$ for the yttrium acetate system. Ionic strength 2.0 M. Open symbols: a buffer solution having the composition 2 M HAc + 1 M NaAc has been added to the yttrium perchlorate solution.
Filled symbols: a buffer solution 4 M HAc + 1 M NaAc has been used.
●: C_M^o (= the initial concentration of yttrium perchlorate) was 20 mM;
■, □: C_M^o = 40 mM; ▲: C_M^o = 80 mM.

been investigated before (I p. 180 and II p. 1952), it is found that the yttrium system has a considerably lower β_1-value than the other rare-earth systems. Also the lanthanum system shows a higher value for β_1. The increase of the complexity constants from β_1 to β_3 is, however, relatively greater for the yttrium system than for the lower rare-earth systems. Therefore the ratios b_n/b_{n+1} indicate a rather significant relationship between the acetate systems of yttrium and of the higher rare earths, especially those of dysprosium and holmium.

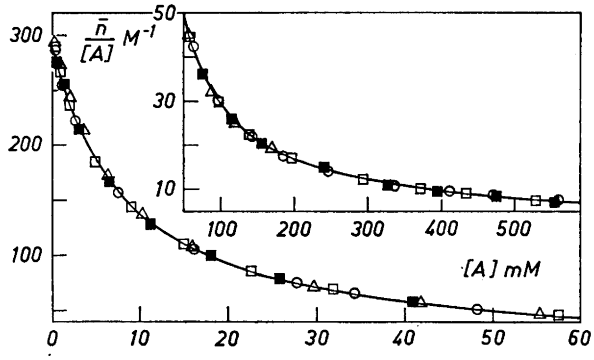

Fig. 2. $\bar{n}/[A^-]$ as a function of $[A^-]$ for the yttrium glycolate system. Ionic strength 2.0 M. Open symbols: a buffer solution 0.5 M HAcOH + 1 M NaAcOH was used.
Filled symbols: a buffer solution 1 M HAcOH + 1 M NaAcOH was used.
○: C_M^o (= the initial concentration of yttrium perchlorate) was 20 mM;
■, □: C_M^o = 40 mM; △: C_M^o = 80 mM.

Table 1. The complexity constants of the yttrium acetate system (Y^{3+} $-Ac^-$) and the yttrium glycolate system (Y^{3+} $-AcOH^-$) with their estimated random errors. $\beta_n = [MA_n] \cdot [M]^{-1} \cdot [A]^{-n}$ means the complexity constants of the mononuclear complexes and $\beta_1' = [M_2A] \cdot [M]^{-2} \cdot [A]^{-1}$ the complexity constant of the first dinuclear complex. The temperature was 20°C and the ionic strength 2.0 M (perchlorate medium).

	$\beta_1 M^{-1}$	$\beta_2 M^{-2}$	$\beta_3 M^{-3}$	$\beta_4 M^{-4}$	$\beta_5 M^{-5}$	$\beta_1' M^{-2}$
Y^{3+} $-Ac^-$	34 ± 2	460 ± 50	2 400 ± 400	~2 000	— — —	~20
Y^{3+} $-AcOH^-$	295 ± 15	$(25 \pm 2) \times 10^2$	$(50 \pm 7) \times 10^4$	$(18 \pm 4) \times 10^5$	$\sim 20 \times 10^5$	— —

Table 2. The stability constants $b_1 = \beta_1$, $b_n = \beta_{n+1}/\beta_n$ and the ratios between the consecutive stability constants for the acetate and the glycolate systems of yttrium.

	b_1	b_2	b_3	b_4	b_1/b_2	b_2/b_3	b_3/b_4
Y^{3+} $-Ac^-$	34	13.5	5.2	0.8	2.5	2.6	6
Y^{3+} $-AcOH^-$	295	85	20	3.6	3.5	4.2	5.5

The complexity constants of the yttrium glycolate system are about the same as those of the gadolinium glycolate system (III p. 1008, 1009). Then there is also a good correspondence between the two glycolate systems concerning the stability constants as well as the ratios b_n/b_{n+1}. The values for b_n/b_{n+1} show possibly a slight tendency towards samarium.

The similarity between yttrium and the other rare earths with about the same ionic radius (especially Ho) is shown also by the ratios between the corresponding complexity constants of the glycolate and the acetate systems, *i.e.* the ratios $\beta_{n,gl}/\beta_{n,ac}$. Thus we find that the ratio $\beta_{1,gl}/\beta_{1,ac}$ is 3—5 for the lighter rare earths, 4.3 for Gd, 7.0 for Dy, 8.2 for Ho, 8.7 for Y, 10.0 for Er, and 11.8 for Yb.

The author is indebted to Professor Sture Fronæus for kind interest and fruitful discussions.

This work is a part of an investigation supported by *Swedish Natural Science Research Council*, which is gratefully acknowledged.

REFERENCES

1. Wheelwright, E. J., Spedding, F. H. and Schwarzenbach, G. *J. Am. Chem. Soc.* **75** (1953) 4196.
2. Sonesson, A. *Acta Chem. Scand.* **12** (1958) 165 (=I).
3. Sonesson, A. *Acta Chem. Scand.* **12** (1958) 1937 (=II).
4. Sonesson, A. *Acta Chem. Scand.* **13** (1959) 998 (=III).
5. Jantsch, G. and Grünkraut, A. *Z. anorg. Chem.* **79** (1913) 305.

Received April 27, 1960.

ACTA CHEMICA SCANDINAVICA 14 (1960) 1499–1502

Effect or Urea and Sodium Chloride on the Colloid Osmotic Pressure of Hyaluronate

J. PIKKARAINEN, T. NIKKARI and E. KULONEN

Department of Medical Chemistry, University of Turku, Finland

Colloid osmotic pressure of hyaluronate was measured in solutions containing varying amounts of sodium chloride or urea.

The effect of salt strength was considered physiologically nonsignificant.

In 6.5 M urea the colloid osmotic pressure of 0.25 % solution of hyaluronate increased 2.5-fold. The apparent molecular weight decreased from 110×10^3 to 46×10^3. On the basis of sedimentation and viscosity data molecular weights of 950×10^3 (original) and 600×10^3 (in 6.5 M urea) were calculated.

The purpose of these measurements was to determine whether physiologically possible changes in the sodium chloride content of extracellular fluid could affect the colloid osmotic pressure of hyaluronate and whether the hydrogen bonds were significant. Because the use of urea revealed an apparent dissociating effect, the sedimentation and viscosity data were determined.

EXPERIMENTAL

The osmometer of Bull [1] (immersed in a water bath at $+25 \pm 0.01$°C) was used and the colloid osmotic pressure could be measured with an accuracy of 0.01 mm H_2O.

The material was prepared from human umbilical cords by extraction with sodium chloride and fractional precipitation with »Cetavlon» according to the principle of Scott [2]. It was ascertained by column chromatography [3] that it did not contain chondrosamine and it was homogeneous in the ultracentrifuge (Fig. 3). The sample contained 3.58 % N and 16.7 % ash. The sample was kept in a desiccator above conc. sulphuric acid. For the measurements 0.5 % or 0.25 % solutions were prepared in 0.0067 M phosphate buffer (pH 7.3) containing 1 mg/100 ml sodium azide as preservative.

The salt effect was studied all the time with the same cellulose membrane bag and same 0.5 % hyaluronate solution (37 ml) but the outer fluid (68 ml, containing increasing amounts of sodium chloride in the phosphate buffer) was changed.

The effect of urea was studied similarly, but with 0.25 % solution of hyaluronate. The fluids contained 0.25 M sodium chloride.

The sedimentation studies were carried out with a »Spinco» analytical ultracentrifuge using wedge cells. The calculations were made according to Ogston [4].

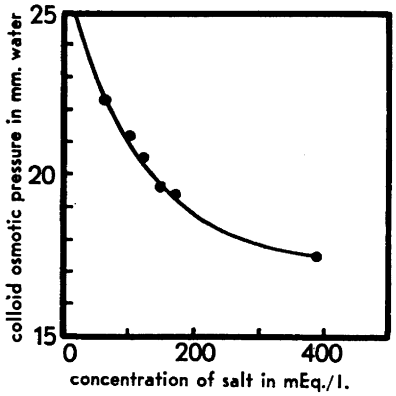

Fig. 1. Colloid osmotic pressure of 0.5 % hyaluronate solution plotted against sodium chloride concentration. (At the zero concentration of salt the colloid osmotic pressure was 66 mm H_2O).

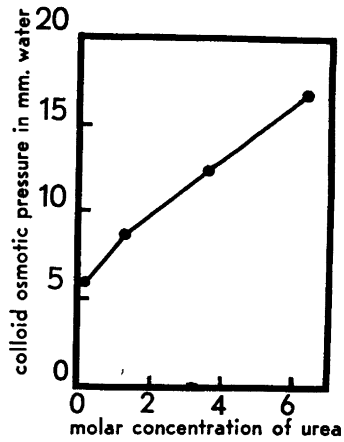

Fig. 2. Colloid osmotic pressure of 0.25 % hyaluronate plotted against urea concentration.

RESULTS

The effect of salt concentration on the colloid osmotic pressure is shown in Fig. 1 and of urea in Fig. 2. At the 140 mequiv./l level of sodium chloride a 10 mequiv./l increase in the salt concentration causes a decrease in the colloid osmotic pressure of only 0.4 mm H_2O at 0.5 % concentration of hyaluronate, which roughly corresponds to that present in tissues. Fig. 3 shows the sedimentation pattern and Table 1 contains the viscosity and sedimentation data with some relevant calculations.

DISCUSSION

The relations between hyaluronate and salt observed earlier [6] seem to be best explained by the different diffusion rates of the electrolytes in solu-

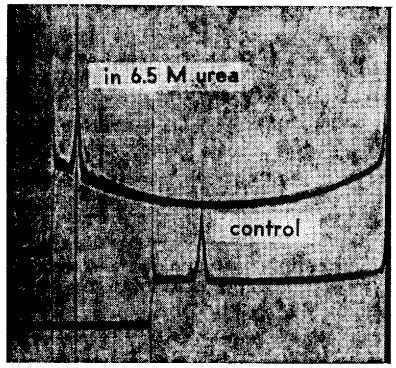

Fig. 3. Sedimentation pattern of hyaluronate (52 min. after reaching the speed of 59 780 rpm., c = 0.25 %, angle 75°). The control cell has leaked.

Table 1. Viscosity and sedimentation data of hyaluronate in urea.

Solvent	0.25 M NaCl in 1/300 M pH 7.3 phosphate buffer	6.5 M urea and 0.25 M NaCl in 1/300 M pH 7.3 phosphate buffer
Solvent density at 20°C	1.0100	1.1045
Solvent viscosity at 20°C (in poises)	0.0107	0.0158
Data for hyaluronate solution:		
Intrinsic viscosity (c = g/100 ml)	8.4	9.3
Sedimentation coefficients (s_0 in Svedberg units)		
uncorrected	4.95	2.19
corrected to $s_{w,20}$	5.65	4.14
$d(1/s)/dc$, $c \rightarrow 0$;		
from uncorrected s-values	2.09	3.04
from corrected s-values	1.97	1.69
Calculated molecular dimensions[4]*:*		
(assumptions[5]: $\overline{V} = 0.69$, $\xi/k = 0.37$)		
J from corrected s_0-values	5	10
V from corrected s_0-values	135	70
M from uncorrected s_0-values	920×10^3	670×10^3
from corrected s_0-values	950×10^3	600×10^3
from osmotic pressure (c = 0.25 %)	110×10^3	46×10^3

tions containing hyaluronate. The significance of the Donnan effect on the colloid osmotic pressure of the extracellular fluid is slight.

Bull and Currie [7] studied the effect of urea on the molecular weight of β-lactoglobulin and Gutter, Sober and Peterson [8] the effect on hemoglobin. In both cases a degradation of the protein molecule was observed. The experiments reported above give an analogous result.

There exist controversial opinions on the necessity of a density correction in the ultracentrifugation due to the presence of urea [8,9]. If in the calculations uncorrected s_0-values are used with the density and viscosity of the urea solution, this difficulty is avoided. In this case the corrected s_0-values with density and viscosity of the phosphate-NaCl-solution gave almost identical results.

There is a large difference between the molecular weights obtained from the osmotic pressure and from the sedimentation data. Blumberg and Ogston [10] pointed out that the osmotic pressure of hyaluronate tends to be unduly high because of the high entropy of dilution consequent to the large volume of the particles (*cf.* discussion by Jensen [11] and by Bull [1]). If true, this concept has a physiological implication in the maintenance of the tissue turgor in spite of the low concentration of the polysaccharide.

Acknowledgement. We thank Professor A. G. Ogston, F.R.S., for advice and acknowledge the financial support from the *Jenny and Antti Wihuri Foundation* and the *Sigrid Jusélius Foundation.*

REFERENCES

1. Bull, H. B. *Physical Biochemistry*, 2nd ed., John Wiley & Sons, 1951.
2. Scott, J. E. *Biochem. J.* **62** (1956) 31P.
3. Gardell, S. *Acta Chem. Scand.* **7** (1953) 207.
4. Ogston, A. G. *Trans. Faraday Soc.* **49** (1953) 1481.
5. Ogston, A. G. and Stanier, J. E. *Biochem. J.* **46** (1950) 364.
6. Kulonen, E. *Acta Physiol. Scand.* **27** (1952) 82.
7. Bull, H. B. and Currie, B. T. *J. Am. Chem. Soc.* **68** (1946) 742.
8. Gutter, F. J., Sober, H. A. and Peterson, E. A. *Arch. Biochem. Biophys.* **62** (1956) 427.
9. Schachman, H. K. and Lauffer, M. A. *J. Am. Chem. Soc.* **72** (1950) 4266.
10. Blumberg, B. S. and Ogston, A. G. in *Chemistry and Biology of Mucopolysaccharides*, Ciba Foundation Symposia, Churchill, London 1958.
11. Jensen, C. E. *Studier over Hyaluronsyre*, Thesis, Nyt Nordisk Forlag Arnold Busck, København 1957.

Received March 30, 1960.

ACTA CHEMICA SCANDINAVICA 14 (1960) 1503–1508

Secretion of Radioactivity in Milk Fat after a Single Oral Dose of (^{3}H)Myristic Acid to a Goat

L. REINIUS and J. HASAN

Department of Physiology and Biochemistry, Veterinary College, Helsinki
and
Institute of Occupational Health, Helsinki, Finland

Tritium-labelled myristic acid was administered orally as free acid to a lactating goat and then the secretion of the radioactivity in the total milk lipids and milk glyceride fatty acids was followed for thirteen days. Measurable activity was found in the milk fat 4 h after administration and the maximum specific activity occurred within 28 h. About 10 % of the radioactivity administered was recovered during the experimental period and about 25 % of the activity collected during 13 days was secreted in the first 28 h. In the beginning the non-volatile fatty acids had a higher specific activity than the volatile fatty acids and there seemed to be a tendency for the specific activities in the short chain acids to increase with time whereas the long-chain acids appeared to be less active later in the experiment.

The relative importance of various lipid constituents in the diet for the formation of characteristic elements of milk fat is a question of great interest both from the quantitative and qualitative points of view. It has been demonstrated that, in the ruminant, acetate is a precursor of short-chain fatty acids of the milk [1]. Of the total acetate present in the body of the goat at any moment, about 80 % is oxidised within 6 h while some 50 % of the remainder will participate in the fat metabolism of the udder [2]. Evidence for the existence in the mammary gland of a system capable of synthetising fatty acids up to $C_{(18)}$ from acetate has been produced by Popják and Tietz [3], Hele and Popjak [4] and Hele, Popjak and Lauryssens [5].

In a study of the role played by dietary long-chain fatty acids in the formation of ruminant milk fat [6] it was shown that after oral administration of (^{3}H)stearic acid, the short-chain acids in the milk fat had a much lower specific activity than the long-chain acids and the tentative conclusion was drawn that the contribution of the long-chain acids of the blood to the short-chain acids of ruminant milk fat was small.

The work quoted above deals with fatty acids of very short ($C_{(2)}$) or extremely long ($C_{(18)}$) chain length. In the experiment to be described, which is

an extension of the work done by Glascook *et al.*[6], (^{3}H)myristic acid — representing a dietary fatty acid of an intermediate chain length — was fed to a lactating goat and the time of appearance, rate of excretion of radioactivity in the milk lipids, and the distribution of radioactivity in various fractions of milk lipid was studied.

Radioactive myristic acid

EXPERIMENTAL

(^{3}H)Myristic acid was prepared by treating inactive myristic acid (Fluka, purum) in an evacuated and sealed ampoule for two days at 98°—100°C with concentrated sulphuric acid (sp.d. 1.84) and tritiated water (200 mC/ml) according to the method of van Heyningen, Rittenberg and Schoenheimer [7]. The reaction product, diluted with water and dissolved in ether, was extracted with a solution of alcoholic potassium hydroxide. The radioactive myristic acid obtained after acidification and extraction with ether was recrystallised from aqueous acetone. The product had a melting point of 57.6°C (published melting point 58°C) and a specific activity of 2.55×10^6 counts/min/mg H_2O as assayed with our apparatus.

To check the radiochemical purity of the product, a sample was run on a paper chromatogram [8] together with chemically pure, inactive myristic acid. After development the strip containing the radioactive sample was cut into bands 1 cm wide which were eluated with toluene and the eluates were assayed for radioactivity in a liquid scintillation counter (Packard Tri-Carb Scintillation Spectrometer). The radioactivity was found to be incorporated into a single, welldefined area on the chromatogram, the location of which was the same as that of the pure inactive myristic acid.

It was expected that as a result of the tritiation process used, the radioactivity would be bound to $C_{(2)}$. This was checked by brominating the (^{3}H)myristic acid (as described by van Heyningen *et al.*[7]) and then reassaying the radioactivity of the product. By this procedure 46 % of the radioactivity was lost, indicating that most (92 %) of the tritium was bound to the $C_{(2)}$ atom.

Animal experiment

The experimental animal was a goat of Finnish breed yielding about 1 l milk/day. The labelled material consisted of 3.82 g (^{3}H)myristic acid prepared as above and containing a total activity of 1.08×10^{10} counts/min/mg. A mixture of the myristic acid, 40 ml arachis oil, 2 g sodium stearate and 0.5 g sodium carbonate was homogenised at 60°C for 65 min. and at a pressure of 2 600—2 700 lbs/sq.in. The mean diameter of the particles in the resultant emulsion was about 1 μ.

After an injection of oxytocin the goat was milked out and the emulsion, warmed to body temperature, was administered in one dose by mouth followed by 50 ml water. Water and hay were provided *ad libitum* and concentrates according to the calculated need. The goat was kept in an isolation pen and milked three times a day for the first two days and then twice daily for the following 11 days of the experiment. The two milkings of the 4th, 5th and 6th experimental days were combined to give three samples and from the 7th day onwards the milkings of two successive days were pooled to one sample. Altogether, 15 samples were obtained for radioactivity measurements of the total milk fat. The fractionation of the milk fat was done on three pooled milk fat samples representing the total milkings of following successive periods of the experiment —1st day; 2nd, 3rd and 4th day; and 5th to 13th days.

Chemical methods

The isolation of milk fat for radioactivity analysis was made following the description given by Glascock *et al.*[6] The fractionation of the milk fat into non-volatile saturated, non-volatile unsaturated, steam-volatile water soluble and steam-volatile water-insoluble

glyceride fatty acids was done by procedures similar to those described by Popják and Beeckmans [9].

Radioactivity measurements

After combustion of the lipid samples in a stream of oxygen, the tritium content of the combustion water was measured in a gas counter with a stainless steel cathode after conversion into butane with the aid of *n*-butyl magnesium bromide [10]. All combustions and measurements were made in duplicate. The specific activities are given as counts/min/mg of combustion water as observed with our equipment.

RESULTS

The specific activities of the total milk lipids in successive samples are plotted semi-logaritmically against time in Fig. 1, the time for each point on the curve being the mid-point of the period during which the milk was secreted. Measurable radioactivity appeared in the total lipids as early as 4 h after administration of the (^{3}H)myristic acid, and the milk fat with the highest specific activity (1.2×10^4 counts/min/mg) was collected 28 h after dosing. The specific activity then declined rapidly, and the specific activities of the milk lipids on the 12th and 13th experimental days were only about 100 c.p.m.

The cumulative secretion as a percentage of the total dose administered is shown in Fig. 2 plotted against time. The radioactivity collected during the whole experimental period of 13 days was about 10 % of the dose administered. It can be seen that of the total activity collected, about 25 % was secreted during the first 28 h. Some secretion, however, was still going on at the end of the experimental period.

The specific activities of the four glyceride fatty acid fractions from milk collected during successive experimental periods are shown in Fig. 3. It can be seen that the specific activity of the non-volatile saturated fatty acids

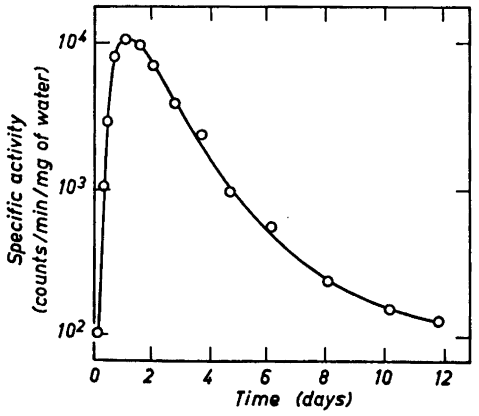

Fig. 1. Specific activity of total lipids in goat milk after ingestion of (^{3}H)myristic acid administered in one dose.

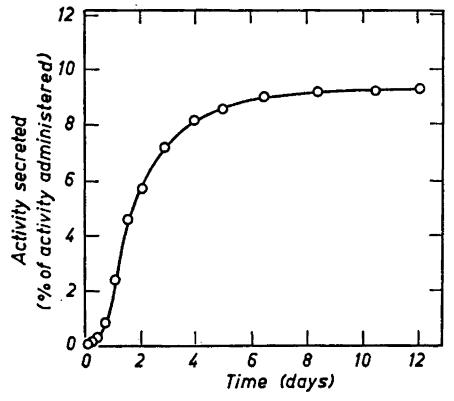

Fig. 2. Cumulative secretion of radioactivity in total milk lipids of goat after ingestion of (^{3}H)myristic acid administered in one dose.

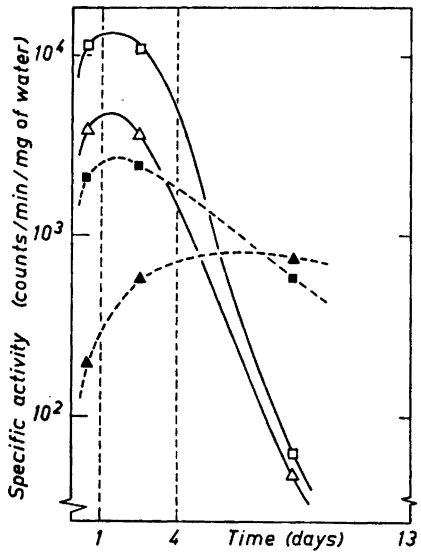

Fig. 3. Mean specific activities of pooled milk glyceride fatty acids on three successive experimental periods after ingestion of (^{3}H)myristic acid administered in one dose. Experimental periods indicated by dotted lines. □ : non-volatile saturated fatty acids; ■ non-volatile unsaturated fatty acids; △ : steamvolatile water-insoluble fatty acids; ▲ : steam-volatile water-soluble fatty acids. A smooth curve drawn arbitrarily through corresponping points.

secreted during the first day is of about the same magnitude as the maximum specific activity of milk fat collected during this period. The radioactivity of this fraction subsequently declined. The other fractions contain considerable less radioactivity, and while the specific activity of long-chain unsaturated fatty acids also declines with time, there seems to be a trend for higher activities in the short-chain fatty acid fractions from samples collected during later periods; the variations, however, are slight and it is difficult to asses their significance. It may be noted that although the short-chain fatty acids contain less radioactivity than the long-chain acids in the beginning, considerable activity is found in these as well.

DISCUSSION

The results described above give information on the role of dietary myristic acid as a precursor of constituents in the milk fat. The appearance, the time curve of secretion, the total amount secreted in the milk lipids, and the distribution of radioactivity between various fractions of the milk fat seem on the whole, to be comparable with corresponding data [6] obtained by using stearic acid in a rather similar experiment. Some divergent points, however, should be noted.

The total amount of secreted radioactivity in the milk was only 10 % of the dose administered. This is a small fraction as compared with the values 25 % and 49 % obtained after 8 and 14 days, respectively, by Glascock *et al.*[3] in the two experiments where free (^{3}H)stearic acid was fed to goats. Since we did not examine the faeces, it is impossible to say whether the results reflect only poor absorption of the (^{3}H)myristic acid or differences in the metabolic

behaviour between myristic and stearic acid of fat in the diet. It seems, however, that in a system including such a multitude of independently variable mechanisms as in the transport of fatty acids from the digestive tract to milk, great differences can exist between different animals as well as considerable short-time variations in the same animal. In both experiments, however, the radioactivity in the milk lipids after administration of the labelled acid was found in the first sample collected 4 h after administration. Maximum activity was reached in the myristic acid experiment after 28 h as compared with 23 h in the stearic acid experiment.

In the experiments of Glascock *et al.*[6] the specific activities of the saturated and unsaturated long-chain fatty acids in the milk were of the same magnitude whereas the unsaturated long-chain acids in our experiment apparently were of significantly lower specific activity than that of the saturated. An explanation for the low specific activity of the unsaturated long-chain fatty acid fraction as compared with the saturated could be the relatively high content of myristic acid in goat milk lipids and the very low content of the corresponding unsaturated acid the myristoleic — 12.3 % for myristic acid (tetradecanoic) and 0.8 % for tetradecenoic. The converse is true for stearic and oleic acids [11]. Our explanation assumes that myristoleic acid is the natural desaturation product of myristic acid in the goat as has been shown [12] to be in the rat and that biological desaturation of myristic acid exclusively labelled at $C_{(2)}$ would not lead to a significant loss of radioactivity. The latter assumption may be valid considering that Hilditch and Longenecker [13] have observed that the double bond in the monoethenoic acids of milk is in the $C_{(9)}$—$C_{(10)}$ position.

Another point of interest in this experiment is the high specific activity in the water-insoluble steam-volatile fraction. From the experiments with (^{3}H)myristic acid, Glascock *et al.*[6] concluded that no significant formation of milk short-chain fatty acids occurred through break-down of dietary long-chain acids. If this also applies for myristic acid, the activity of the short-chain acids in our experiment should originate from radioactive precursors (acetate) formed by degradation of myristic acid. In this case, however, even greater specific activities would be expected in the water-soluble portion of the steam-volatile fatty acids which, in our experiment, actually contain very little activity. Even if small quantities of $C_{(8)}$—$C_{(10)}$ acids are known to pass over into the steam distillate [14,15] it is highly improbable that radioactive contamination from myristic acid $C_{(14)}$ could account for this finding. Considering the specific activity of the long-chain unsaturated fatty acids (highest value about 4 000 counts/min/mg of H_2O), it does not seem possible that the traces of oleic acid, which may also be carried over in the distillation, could cause contamination of the steam-volatile water-insoluble acids (about 2 000 counts/min/mg of H_2O) to the extent observed.

Of interest is the apparent trend for higher specific activities in the short-chain acids during later experimental periods while the radioactivity secreted in the long-chain acids seems to decline with time. This could indicate that a chain-shortening is actually going on in the organism with a fairly slow reaction velocity, but a more probable explanation would be the successively higher radioactivity gained by the metabolic pool of small-molecular entities available for resynthesis from degradation of (^{3}H)myristic acid.

We wish to thank Dr. R. F. Glascock for some complementary ^3H determinations and for helpful advise in presenting the data. Dr. O. Perilä kindly prepared the myristic acid paper chromatogram using his system. We are also most grateful to Prof. L. Paloheimo and Dr. S. Ullberg who offered their help during different phases of the work. This study was aided by a grant from the *State Commission for Natural Sciences (Valtion Luonnontieteellinen Toimikunta)*.

REFERENCES

1. Folley, S. J. *The physiology and biochemistry of lactation*, Oliver & Boyd, Edinburgh 1956.
2. Popják, G., French, T. H. and Folley, S. J. *Biochem. J.* **48** (1951) 411.
3. Popják, G. and Tietz, A. *Biochem. J.* **56** (1954) 46.
4. Hele, P. and Popják, G. *Biochemical problems of lipids*, Butterworths Scientific Publications, London 1956, p. 135.
5. Hele, P., Popják, G. and Lauryssens, M. *Biochem. J.* **65** (1957) 348.
6. Glascock, R. F., Duncombe, W. G. and Reinius, L. R. *Biochem. J.* **62** (1956) 535.
7. van Heyningen, W. E., Rittenberg, D. and Schoenheimer, R. *J. Biol. Chem.* **125** (1938) 495.
8. Perilä, O. *Acta Chem. Scand.* **9** (1955) 864.
9. Popják, G. and Beeckmans, M.-L. *Biochem. J.* **46** (1950) 547.
10. Glascock, R. F. *Isotopic Gas Analysis for Biochemists*, Academic Press, New York 1954.
11. Hilditch, T. P. and Jasperson, H. *Biochem. J.* **38** (1944) 443.
12. Anker, H. S. *J. Biol. Chem.* **194** (1952) 177.
13. Hilditch, T. P. and Longenecker, H. E. *J. Biol. Chem.* **122** (1938) 497.
14. Hilditch, T. P. *The Chemical Constitution of Natural Fats*, Chapman & Hall Ltd., London 1956, p. 574.
15. Gunstone, F. D. *An Introduction to the Chemistry of Fats and Fatty acids*, Chapman & Hall Ltd., London 1958, p. 47.

Received April 12, 1960.

ACTA CHEMICA SCANDINAVICA 14 (1960) 1509–1514

Equilibrium Studies on the Disproportionation Reaction Between Some Dialkyl Disulfides

L. HARALDSON*, C. J. OLANDER, S. SUNNER and E. VARDE**

Thermochemistry Laboratory ***, *University of Lund, Lund, Sweden*

The disproportionation equilibrium between two symmetric disulfides and the corresponding mixed one has been determined at 25° and at 60° by use of vapor phase chromatographic technique. For diethyl disulfide in mixture with dimethyl- and di-*i*-propyl disulfide, respectively, the equilibrium constant is close to the statistically expected value, 4. For the pair diethyl- and di-*t*-butyl disulfide, the constant is 24. Within the uncertainty of the experiments, the equilibrium constant is temperature independent and thus ΔH is equal to zero. The strongly restricted internal rotation in di-*t*-butyl disulfide is responsible for the high value of the equilibrium constant.

It is a well-known fact that disulfides undergo disproportionation reactions according to

$$R_1SSR_1 + R_2SSR_2 \rightleftharpoons 2\ R_1SSR_2 \qquad (1)$$

This reaction has been used particularly for the synthesis of mixed disulfides [1–5].

McAllan *et al.*[5] have shown by distillation of equilibrium mixtures that the position of the equilibrium depends on the nature of R_1 and R_2. When R_1, R_2 were *n*-alkyl groups, the expected statistical distribution $(R_1S)_2$:$R_1R_2S_2$:$(R_2S)_2$ = 1:2:1 was reached, whereas for R_1 = Et and R_2 = *s*-Bu and *t*-Bu, the ratios were found to be close to 1:4.5:1 and 1:6:1, respectively.

During the course of an extended investigation on the energetics of the disulfide bond it was found of importance to determine rather precisely the equilibrium constant for a number of dialkyl disulfides. Calvin *et al.*[6] studied a slightly different system, namely

$$BzSSBz + HS(CH_2)_3SH \rightleftharpoons 2\ BzSH + \overline{\text{S-(CH}_2)_3\text{-S}} \qquad (2)$$

* Dept. of Analytical Chemistry, Lund University.
** Present address: Dept. of Physical Chemistry, University of Zürich, Switzerland.
*** Sponsored by the *Swedish Natural Science Research Council* and by the *Swedish Technical Research Council.*

They were able to determine the equilibrium constant utilizing the fact that the disulfide 1,2-dithiolane has an absorption maximum at 330 mμ, whereas open chain dialkyl disulfides show a peak at 250 mμ. It is evident that this technique does not work in the case of a mixture of dialkyl disulfides.

The distillation method suffers from several disadvantages — it is slow and poorly quantitative, the separation efficiency is rather low, and, most important, it is difficult, if not impossible, to prevent completely the disulfide from further disproportionation during the distillation.

The vapor phase chromatographic technique was chosen as the analytical tool for the separation and quantitative determination of the homologous disulfides. This technique seemed to offer a number of advantages. The method is rapid and the separation is quantitative and of high efficiency. The duration of the sojourn of the unseparated mixture on the column is very short, decreasing the risk for any reaction to take place during the analysis. In a symmetric reaction like the one under investigation where absolute concentration values do not enter into the equilibrium equation, the relative concentrations can easily be determined from the evaluation of the areas under the peaks of the chromatogram and with an error of only a few per cent. By using an appropriate detector, the size of the sample can be kept very small, allowing the study of gas equilibria at low pressures without increasing the volume of the system inconveniently. Finally, the presence of impurities from side reactions will usually be immediately revealed during the analysis and is of no influence upon the desired result, provided the main reaction equilibrium has been attained.

Two conditions must be fulfilled in order to make the vapor phase chromatographic method useful. Reactions of any kind must not occur on the column, and a linear relationship must exist between the area under the peak on the chromatogram and the amount of substance passing the detector. Both conditions could be experimentally tested in our case and shown to be fulfilled.

CALCULATION

For reaction (1), the equilibrium constant K is given by

$$K = \frac{m_{12}^2}{m_{11} \cdot m_{22}} = \frac{n_{12}^2}{n_{11} \cdot n_{22}} \qquad \text{(I)}$$

where m represents molarities and n the total number of moles present in a given sample; index 11 stands for diethyl disulfide, 22 for another symmetrical dialkyl disulfide, and 12 for the mixed disulfide.

The chromatograph is operated under such conditions as to fulfil the relation $n_i = k_i \cdot y_i$, where k_i is a constant and y_i the area under the peak on the chromatogram, related to the component i. In the present case, one of the reaction participants can be used as a reference substance, *e.g.*

$$n_{11} = k_{11} \times y_{11} \qquad \text{(IIa)}$$
$$n_{22} = k_{22} \times y_{22} \qquad \text{(IIb)}$$

which gives

$$\frac{n_{11}}{n_{22}} = k_{11,22} \times \frac{y_{11}}{y_{22}} \qquad \text{(III)}$$

By calibrating the apparatus with known amounts of pairs of disulfides, the constants $k_{11,22}$, $k_{11,12}$ and $k_{12,22}$ can be separately determined and the relation

$$k_{11,22} = k_{11,12} \times k_{12,22} \qquad \text{(IV)}$$

can be checked.

Finally, the equilibrium constant is

$$K = \frac{k_{12,22}}{k_{11,12}} \times \frac{y_{12}^2}{y_{11} \cdot y_{22}} \qquad \text{(V)}$$

EXPERIMENTAL

Materials

Dimethyl disulfide and *diethyl disulfide* (Eastman chemicals) were distilled twice under reduced pressure to give pure fractions as judged from the chromatograms. *Di-i-propyl disulfide* and *di-t-butyl disulfide* were prepared from the corresponding mercaptans by oxidation with iodine, and distilled twice. After a final distillation at room temperature the purity was checked on the chromatograph.

Ethyl methyl disulfide was prepared both from dimethyl disulfide and ethyl mercaptan, as well as from a mixture of the symmetric disulfides with NaSEt as a catalyst. It was not feasible to obtain a completely pure sample by distillation (*cf.* Ref.[5]). The purest fraction contained 4 % of Me_2S_2 and no detectable amount of Et_2S_2. It was used in the experiments and proper correction was applied in the calibration runs.

Ethyl i-propyl disulfide and *t-butyl ethyl disulfide* were prepared according to method I and II, respectively, in Ref.[5]. They did not contain amounts of the symmetrical disulfides detectable on the chromatogram.

Methods

In the present investigation a Pye Argon chromatograph was used with a 5 mm column, 120 cm in length, filled with 100–120 mesh crushed brick stone, containing 5 % by weight of apiezon grease L. In the experiments with R_2 = Me the temperature was kept at *ca.* 105°C, when R_2 = *i*-Pr and *t*-Bu the temperature was *ca.* 115° and 125°C, respectively.

Calibration was carried out with all pairs of disulfides in molar ratios well covering the expected concentration ratios in the equilibrium mixtures. With the set-up given, in no case was the third disulfide formed which could be easily seen on the chromatogram. A possible disproportionation reaction occurring on the column was therefore judged to be completely insignificant *.

The equilibration experiments were carried out in a *cyclo*hexane solution (R_2 = Me, *i*-Pr) and the total concentration of disulfides was in most cases kept close to one mole per liter. The equilibrium was reached from both sides by use of an ionic catalyst (NaOH, method Ia), or by irradiation with light from a low pressure mercury lamp (method Ib). Experiments were carried out at 25° and 60°C. The solutions treated with sodium hydroxide were kept in 7 × 100 mm test tubes with ground glass stoppers. The catalyst was deposited from an ethanol solution as a very thin film on the inner surface of the

* Note: With metal columns and high boiling esters as the stationary phase disproportionation occurred frequently on the column (*cf.* Ref. [7]).

tube before it was filled with the solution. The irradiated solutions were kept in quartz tubes with ground Pyrex glass stoppers.

Neither method Ia, nor method Ib worked very well. The equilibration time was often of considerable length and in many experiments the initial rate of reaction was extremely slow. The results from the experiments with R_1 = Me did indicate that a true equilibrium was not reached either from one or from both sides. For unknown reasons, all attempts to obtain an equilibrium mixture at 60°C with R_1 = *i*-Pr failed. Finally, when R_1 = *t*-Bu, neither method for equilibration was applicable. The reaction rate was extremely slow using the two-phase ionic system and the decomposition during irradiation was much faster than the disproportionation reaction. The equilibration runs were therefore carried out in the following solution (method II).

Freshly cut sodium (40 mg) was dissolved in 0.4 ml of ethanol, 96 % by volume, and 0.03 ml of *t*-BuSH was added together with 0.3 ml each of the symmetrical (or 0.6 ml of the mixed) disulfides. The solution was enclosed in a sealed Pyrex ampoule which was placed in a thermostat. In preparing the sample for the analysis, water was added to the content of the ampoule, the disulfide layer was washed once with water, and *iso*-pentane was added. The organic solution was washed twice with water, dried, and directly used for the analyses.

The same series of runs were performed with R_1 = Me, substituting EtSH for *t*-BuSH.

RESULTS

The results from the calibration experiments are found in Table 1. The concentration ratios between the two disulfides compared in each run were 1:2; 1:1 and 2:1 (R_2 = Me, *i*-Pr all combinations, and R_2 = *t*-Bu in mixtures between the symmetrical compounds). For both mixtures Et_2S_2-*t*-BuEtS_2 and *t*-Bu_2S_2-*t*-BuEtS_2, the ratios tested were 1:1; 1:2; 1:4 and 1:6. The same concentration ratio was measured in three parallel runs and each chromatogram was planimetered at least 6 times. The agreement between the calculated and the found $k_{11,22}$-values is satisfactory.

Table 2 gives a summary of the equilibrium measurements. Although the time for the experiments extended over several months, equilibrium was not reached with method I (R_2 = Me). The experiments according to method II indicate that the true equilibrium is close to the value obtained with method I starting with the unsymmetrical disulfide. Although a number of trials were performed with R_2 = *i*-Pr at 60°C no acceptable values of the equilibrium constant were obtained.

Method II gave much more reproducible results. For R_2 = *t*-Bu, altogether 12 equilibrium experiments were started. In three cases at 25°C, however, equilibrium was not attained within 6 months.

The *K*-values of the disproportionation reaction have been used to calculate the accompanying changes in free energy at 25°C, ΔF_{298}, and in enthalpy at the average temperature 42°, ΔH_{313} (Table 3). Assuming ΔH to be temperature independent within the small interval studied and thus zero at 25°, the corresponding changes in entropy have been calculated and are given in the table.

Table 1. Calibration experiments.

R_1	$k_{11,12}$	$k_{12,22}$	$k_{11,22}$ calc.	$k_{11,22}$ found
Me	1.04 ± 0.02	1.03 ± 0.02	1.07 ± 0.03	1.11 ± 0.02
i-Pr	1.20 ± 0.03	1.18 ± 0.04	1.42 ± 0.05	1.40 ± 0.04
t-Bu	1.11 ± 0.02	1.40 ± 0.04	1.55 ± 0.04	1.60 ± 0.06

Table 2. Equilibration experiments.

Reactants	Method	Temp. °C	K	Mean value
$Et_2S_2 + Me_2S_2$	I a	25	5.2 ± 0.2	
	I b	25	5.0	5.1 ± 0.2
	I a	60	5.1	5.1 ± 0.2
$EtMeS_2$	I a	25	5.4	
	I b	25	5.7	5.55 ± 0.2
	I a	60	5.6	5.6 ± 0.2
$Et_2S_2 + Me_2S_2$	II	25	5.61	5.6 ± 0.1
	II	60	5.56	5.6 ± 0.1
$EtMeS_2$	II	25	5.68	5.7 ± 0.1
	II	60	5.50	5.5 ± 0.1
$Et_2S_2 + i\text{-}Pr_2S_2$	I a	25	4.30	4.15 ± 0.15
	I b	25	4.05	
Et *i*-PrS_2	I a	25	4.05	4.05 ± 0.15
$Et_2S_2 + t\text{-}Bu_2S_2$	II	25	24.6	24.65 ± 0.1
		25	24.7	
		60	24.5	
		60	24.5	24.60 ± 0.1
		60	24.8	
t-BuEtS_2	II	25	24.4	24.4 ± 0.1
		60	24.5	
		60	24.3	24.5 ± 0.1
		60	24.6	

Table 3. Free energy and enthalpy changes for the reaction $R_1SSR_1 + R_2SSR_2 \rightarrow 2\ R_1SSR_2$

R_2	ΔF_{298}	ΔH_{315}	ΔS
Me	−1.020 ± 0.015	0.0 ± 0.15	3.42
i-Pr	−0.840 ± 0.015		2.82 *
t-Bu	−1.895 ± 0.015	0.0 ± 0.05	6.36

DISCUSSION

Provided the statistical distribution is the only factor governing the equilibrium between the two symmetric and the corresponding mixed disulfide, the equilibrium constant should be 4, ΔH should equal zero and ΔS should be R ln 4 = 2.76 e.u. The experimental results clearly lend support to the suggestion that this is principally true for R_2 = *i*-Pr and also almost so for R_2 = Me. When R_2 = *t*-Bu the equilibrium constant is 6 times as large as is

* ΔH assumed to be = 0. The statistical value of K = 4 gives ΔS = 2.76 e.u.

required from statistical grounds. One explanation could be that the di-*t*-butyl disulfide is sterically strained while *t*-butyl ethyl disulfide is not or only to a small extent. However, this should be reflected in the ΔH-value which then must be negative with about 1 kcal·mole^{-1} for the forward reaction. The experimentally found value, $\Delta H \simeq 0$, rules out this possible explanation. The di-*t*-butyl disulfide molecule may be constructed from atomic models without introduction of strain from angle distortions and with a normal value (100°) of the dihedral angle between the C—S—S and S—S—C planes. In this model, however, the two *t*-butyl groups are very close together and any rotation round the C—S bonds seems to be highly hindered. The free independent rotations of the two *t*-butyl groups can be accomplished only when the dihedral angle exceeds *ca.* 135°. On the other hand, the intramolecular freedom in the *t*-butyl ethyl disulfide is much greater. Thus, the increased probability for the formation of the mixed disulfide in this case is caused by the "release" of conformations when the di-*t*-butyl disulfide molecule breaks up.

Acknowledgements. This work has been sponsored by *Air Force Office of Scientific Research* through the European Office of Air Research and Development Command, U.S. Air Force, and by *Knut and Alice Wallenberg's Foundation.*

REFERENCES

1. Kleiman, M. to Velsicol Corp., Chicago, US Pat 2, 474, 849. Appl. 20 Dec. 1946, Pat. 5 July 1949.
2. Kleiman, M. to Velsicol Corp., Chicago, US Pat 2, 510, 893. Appl. 20 Dec. 1946, Pat. 6 June 1950.
3. Proell, W. A. to Standard Oil Co., Chicago. US Pat 2, 521, 870. Appl. 22 Oct. 1946, Pat. 12 Sept. 1950.
4. Proell, W. A. and Adams, C. E. to Standard Oil Co., Chicago. US Pat 2, 577, 312. Appl. 12 Febr. 1949, Pat. 19 June 1951.
5. McAllan, D. T., Cullum, T. V., Dean, R. A. and Fidler, F. A. *J. Am. Chem. Soc.* **73** (1951) 3627.
6. Barltrop, J. A., Hayes, P. M. and Calvin, M. *J. Am. Chem. Soc.* **76** (1954) 4348.
7. Carson, J. F., Woug, F. F. *J. Org. Chem.* **24** (1959) 175.

Received April 24, 1960.

Kgl. Veterinær- og Landbohøjskole
LABORATORIUM

ACTA CHEMICA SCANDINAVICA 14 (1960) 1515–1525

Nucleophilic Displacements on Phosphorus

Reaction of Hydroxyl Ion and *Iso*nitroso Acetone with Organofluorophosphorus Compounds

GUNNAR AKSNES*

Norwegian Defence Research Establishment, Toxicological Group, Kjeller, pr Lillestrøm, Norway

The reactions of hydroxyl ion and of *iso*nitroso acetone with three organofluorophosphorus compounds have been studied. The three compounds are dimethoxyphosphoryl fluoride, methoxyethylphosphoryl fluoride and diethylphosphoryl fluoride. The thermodynamic functions, activation energy and activation entropy have been calculated and discussed in relation to physical and chemical behaviour of substrates and nucleophilic reagents. This study together with observations made by other workers indicate that nucleophilic displacements on phosphorus depend on an intimate cooperation between the polarity and polarisability of the phosphorus compounds and the basicity and polarisability of the nucleophilic reagent.

Many organofluorophosphorus compounds are known to be highly toxic to insect and animal life [1,2]. The main reason for their toxicity is their ability to inhibit the cholinesterase enzymes. The inhibition of the enzymes by these compounds cannot be reversed by dilution or dialysis. Aldridge [3] and later Tammelin [4] have shown that the process of inhibition is due to phosphorylation of the enzyme. It has been observed that several nucleophilic reagents as hydroxylamine and some of its derivatives, in particular hydroxamic acids and oximes, react quickly with the phosphorylated enzyme and in this way restore its original activity [5,6]. Due to their ability to restore the enzyme activity, these groups of compounds have been named reactivators. In the last years it has been found that the reactivators also very quickly react with organofluorophosphorus compounds in nearly neutral water solution [7–9]. In the present work we have been interested in correlating the alkaline hydrolysis of some organofluorophosphorus compounds with the nucleophilic reaction between a reactivator and the same phosphorus compounds. The investigations have been performed by an electrometric titration method. The instrumental set up in very similar to that developed by Larsson and Hansen [10].

* Present address: Chemical Institute, University of Bergen, Bergen, Norway.

KINETICS OF THE REACTION BETWEEN ORGANOFLUOROPHOSPHATES AND *iso*NITROSO ACETONE

The kinetics of the reaction between several organofluorophosphates and different oximes were studied by Green and Saville [8]. When a great excess of oximes was used they found that the decomposition of the organofluorophosphates followed a first order law. The rate was proportional to the ionized form of the oximes. The rate was followed by titration of the total amount of acids formed. For every mole of organofluorophosphate decomposed 3 moles of acid were neutralized. They postulated a two steps reaction mechanism:

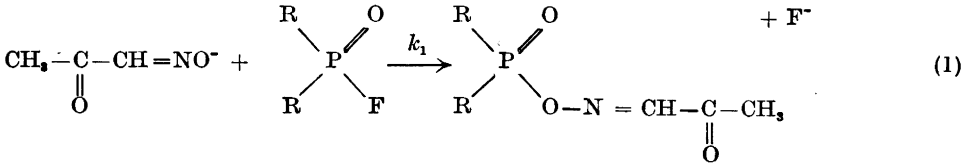

(1)

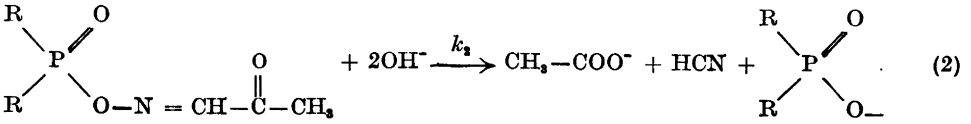

(2)

In the pH region of pH 7.5 Green and Saville [8] found that step (1) was rate determining. The total amount of acid produced as function of time obeyed a first order law. They concluded therefore that the second step in the reaction was immeasurably rapid.

The three organofluorophosphates studied in this paper were very reactive and it was found preferable to study the reaction between the oxime *iso*nitroso acetone and the organofluorophosphates in the pH-interval 6.00—6.70. In this region it was observed that the production of acid during the course of reaction did not follow a first order law. In Fig. 1 is plotted the acid production of the reaction as function of time. The curve shows an inflection in the first minutes of hydrolysis. An analysis of the experimental values showed that the rate of the second step in the above reaction was slow enough to influence on the kinetic of the decomposition reaction.

In the two-step reaction between organofluorophosphates and *iso*nitroso acetone (eqns. (1) and (2)) one mole of hydroxyl ions is consumed in the first step and two moles in the second step. The reaction is studied at so low pH that the dissociation of hydrocyanic acid is negligible. When great excess of *iso*nitroso acetone is used (*i.e.* the concentration of *iso*nitroso acetone remains approx. constant during the reaction) we get for the decomposition of organofluorophosphate:

$$-\frac{dC_N}{dt} = k_1 \cdot C_N \qquad (3)$$

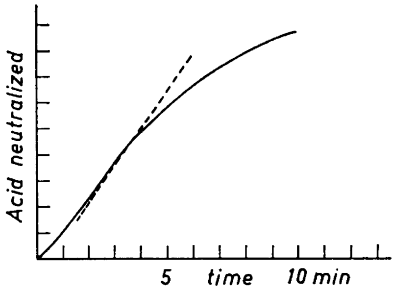

Fig. 1. Acid production in the hydrolysis of methoxyethylphosphoryl fluoride with *iso*nitroso acetone as function of time.

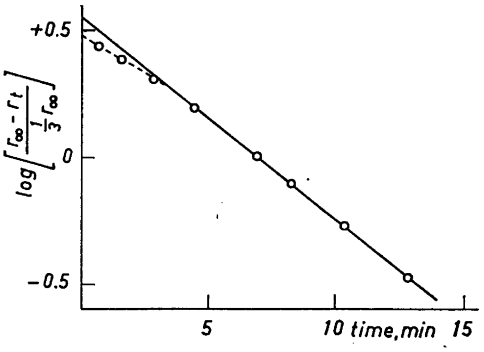

Fig. 2. Determination of the rate constant for the reaction between methoxyethylphosphoryl fluoride and *iso*nitroso acetone at pH = 6.00 according to eqn. (13).

where k_1 = pseudo first order rate constant of the first step. C_N = concentration of organofluorophosphate. The rate of formation and disappearance of the phosphorylated *iso*nitroso acetone is governed by the following equation:

$$\frac{dC_{NR}}{dt} = k_1 \cdot C_N - k_2 \cdot C_{NR} \quad (4)$$

C_{NR} = concentration of the phosphorylated *iso*nitroso acetone,
k_2 = pseudo first order rate constant of the second step.

The amount of hydroxyl ions used during the first step as function of time is:

$$C_{OH^-(1)} = C_{N_0} - C_N \quad (5)$$

where, by integration of eqn. (3)

$$C_N = C_{N_0} \cdot e^{-k_1 t} \quad (6)$$

C_{N_0} = the initial concentration of organofluorophosphate.

Integration of eqn. (4) after inserting the value of C_N from eqn. (6) gives:

$$C_{NR} = \frac{k_1 C_{N_0}}{k_2 - k_1} (e^{-k_1 t} - e^{-k_2 t}) \quad (7)$$

The material balance gives for the amount of hydroxyl ions used during the second step:

$$\tfrac{1}{2} C_{OH^-(2)} = C_{N_0} - C_N - C_{NR} \quad (8)$$

The total amount of hydroxyl ions consumed as function of time is thus:

$$C_{OH^-(total)} = C_{OH^-(1)} + C_{OH^-(2)} = 3(C_{N_0} - C_N) - 2\ C_{NR} \quad (9)$$

which by insertion of eqns. (6) and (7) gives:

$$C_{OH^-(total)} = C_{N_0}\left[3 + \frac{k_1 - k_2}{k_2 - k_1} e^{-k_1 t} + \frac{2k_1}{k_2 - k_1} e^{-k_2 t}\right] \quad (10)$$

An exact solution of k_1 and k_2 from eqn. (10) cannot be found. In this work we have used a graphical extrapolation method. The experimental values showed that $k_2 \gg k_1$, and thus, at high values of t the second exponential term of eqn. (10) goes rapidly towards

zero. Therefore, if we only use the experimental values of $C_{OH^-(total)}$ at relatively high t-values we get a good approximation for k_1 by taking only the first exponential term of eqn. (10):

$$C_{OH^-(total)} = 3\,C_{N_0} + C_{N_0} \cdot \frac{k_1 - 3\,k_2}{k_2 - k_1} \cdot e^{-k_1 t} \tag{11}$$

or in logarithmic form:

$$\log\left(\frac{3\,C_{N_0} - C_{OH^-(total)}}{C_{N_0}}\right) = -\log\left(\frac{k_1 - 3\,k_2}{k_2 - k_1}\right) - \frac{k_1 t}{2.303} \tag{12}$$

We therefore find k_1 by plotting $\log\left(\frac{3\,C_{N_0} - C_{OH^-(total)}}{C_{N_0}}\right)$

as function of t. If the method can be used we shall get a straight line with tangens $-\frac{k_1}{2.303}$. The intercept which the line cuts of the ordinate-axis is $-\log\frac{k_1 - 3\,k_2}{k_2 - k_1}$. Inserting k_1 in the latter equation gives k_2. The automatic recording instrument which is connected with the titrator, plots the number of turns of the micrometer screw as measure of concentration. Eqn. (12) is then transformed to:

$$\log\frac{r_\infty - r_t}{1/3\,r_\infty} = -\log\frac{k_1 - 3\,k_2}{k_2 - k_1} - \frac{k_1}{2.303} \cdot t \tag{13}$$

where r_∞ = number of turns of the micrometer screw when all the organofluorophosphate is transformed to end products (3 moles OH^- are consumed per mole organofluorophosphate). r_t = number of turns at the time t.

Fig. 2 shows the plot of the experimental values for the reaction between methoxyethylphosphoryl fluoride and *iso*nitroso acetone according to eqn. (13).

The second order rate constants, k_{R^-} recorded in Table 1 are found from the formula:

$$k_{R^-} = \frac{k_1}{C_{A^-}} \tag{14}$$

where C_{A^-} is the concentration of the anion of the *iso*nitroso acetone at the pH used. C_{A^-} is calculated from the following equation:

$$C_{A^-} = a_0 \frac{\text{antilog}\,(\text{pH} - \text{p}K - \log\gamma)}{1 + \text{antilog}\,(\text{pH} - \text{p}K - \log\gamma)} \tag{15}$$

where a_0 is the total concentration of *iso*nitroso acetone and γ is the activity coefficient of the hydrogen ions.

The rate constants of the reaction with hydroxyl ion were calculated according to the following equation [11]:

$$k_1 = k_{OH^-} \cdot C_{OH^-} = k_{OH^-} \cdot \frac{a_{OH^-}}{f_{OH^-}} \tag{16}$$

k_1 is the first order rate constant at a fixed pH determined by the extrapolation method of Guggenheim [12]. k_{OH^-} is the second order rate constant for the reaction with hydroxyl ion. a_{OH^-} and f_{OH^-} are the activity and activity coefficients, respectively, of the hydroxyl ions.

Values of the Arrhenius activation energy E_A were obtained in the usual fashion from the gradients of plots of $\log k$ *vs.* $\frac{1}{T}$.

The entropy of activation was calculated according to the formulae of Eyring [13] for reaction in solution:

$$k_r = e \cdot \frac{k\,T}{h} \cdot e^{-E_A/RT} \cdot e^{\Delta S^{\neq}/R} \tag{17}$$

EXPERIMENTAL

Materials. Dimethoxyphosphoryl fluoride, methoxyethylphosphoryl fluoride and diethylphosphoryl fluoride were synthesized in this institute [14]. The compounds were redistilled immediately before use and their equivalent weights were determined by hydrolysis of the compounds with excess of 0.1 N $Ba(OH)_2$ followed by back-titration with 0.1 N HCl.

Dimethoxyphosphoryl fluoride, b.p. 54°/20, equiv. wt, found: 63.9, calc. 64.0. Methoxyethylphosphoryl fluoride, b.p. 58°/20, equiv. wt, found 63.3, calc. 63.0. Diethylphosphoryl fluoride, b.p. 72°/9, equiv. wt, found 61.7, calc. 62.0. *Iso*nitroso acetone was synthesized according to description in the literature [15].

Kinetic measurements. The rates of the hydrolysis were studied by means of an automatic recording titrator. The instrument used was a Radiometer Titrator, type TTTI. The principle of the instrumental set up is that the acid products formed during the hydrolysis of the organofluorophosphates are neutralized by automatic addition of alkali at such a rate that the pH of the reaction solution is maintained constant. The alkali is delivered from a 5 ml syrette driven by a micrometer screw connected with a motor. The motor is started and stopped automatically by the titrator when the pH of the solution drifts below or above the required value. A Radiometer glass electrode, type G 202 A was employed and a saturated calomel electrode type K 300 was used as reference electrode. The fluctuation during the reaction was approximately ± 0.02 pH-units. A constant temperature circulating water bath maintained the jacketed reaction vessel at ± 0.05°C. The capacity of the reaction vessel was 50 ml. An automatic recording device connected with the micrometer screw records the number of turns of the micrometer screw as function of time. The number of turns are used as relative measure of the amount of alkali added. The pH-meter in the titrator was standardized against a known buffer before each run. The procedure for the titration was the following:

The phosphorus compound was immediately before use weighed out and diluted with 50 ml 0.1 N KCl to a concentration of approximately 2×10^{-4} M. When the reaction with hydroxyl ion was studied, the titrator was standardized against a known buffer, the instrument set at the required pH and the automatic titration started. This reaction was studied in the pH-range 7.70—9.00. When the rate of the reaction between *iso*nitroso acetone and the organofluorophosphate was determined the 0.1 N potassium chloride solution contained a hundred fold excess of *iso*nitroso acetone. The drop in concentration of *iso*nitroso acetone during the reaction could therefore be neglected. The reaction was studied in the pH-range 6.00—6.70. The concentration of sodium hydroxide added from the syrette was 0.05 N. The slight dilution of the reaction solution during the hydrolysis due to the added alkali was neglected in the calculation of the rate constants.

The second order rate constants k_{OH^-} and k_{R^-} were calculate according to eqns. (13), (14) and (16). The pK values of *iso*nitroso acetone were determined by potentiometric titration and found to be 8.30 and 8.15 at 25°C and 35°C, respectively. The activity coefficients of hydrogen ions in 0.1 N KCl are 0.782 and 0.778 at 25°C and 35°C [16]. The activity coefficients of the hydroxyl ions in 0.1 N KCl (0.776 and 0.762) at 25°C and 35°C were taken from the paper of Larsson [11]. In Table 1 are recorded the data from the present study. The estimated errors in the rate constants are approximately ± 3 %. This corresponds to the accuracy of the rate constants found by Larsson and Hansen [10], determined by a similar instrumental set up.

DISCUSSION

The reactions between organic chloro- or fluorophosphorus compounds and nucleophilic reagents are generally believed to belong to A-2 mechanisms [11,18]. From theoretical reasons one must assume that during formation of the transition state the collision complex adapts a bipyramidal (sp^3d hybridised) transition state with the reacting groups and the phosphorus atom collinear:

Table 1. Rate constants and thermodynamic functions for nucleophilic reactions of dimethoxy-, methoxyethyl- and diethylphosphoryl fluoride.

Compound	Reaction with hydroxyl ion			
	k_{OH}- l mole^{-1} sec^{-1}		Activation energy kcal/mole	Activation entropy E.U.
	25.1°C	35.1°C		
Dimethoxy phosphoryl fluoride	18.2	34.3	11.6	−16
Methoxyethyl phosphoryl fluoride	49.1	85.3	10.1	−19
Diethyl phosphoryl fluoride	726	1140	8.3	−20
	Reaction with anion of *iso*nitrosoacetone			
	k_R- l mole^{-1} sec^{-1}		Activation energy kcal/mole	Activation entropy E.U.
	25.1°C	35.1°C		
Dimethoxy phosphoryl fluoride	4.01	8.82	14.3	−10
Methoxyethyl phosphoryl fluoride	4.58	9.32	12.9	−14
Diethyl phosphoryl fluoride	3.40	6.35	11.5	−20

Table 2. Stretching frequencies of the P=O and P−F bands of phosphorus compounds and their association constants with phenol in CCl_4[14].

Compound	Stretching frequencies cm^{-1}		Association constants 20°C
	P=O	P−F	
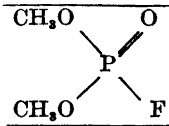	1 308	864	26.3
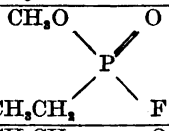	1 295	858	82.5
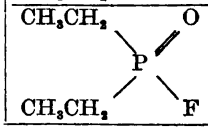	1 278	845	129.9

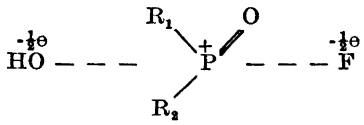

(I)

Displacement reactions of optically active phosphorus compounds give strong evidence for this interpretation [19]. The activation energy necessary to form the transition complex according to (I) should be expected to decrease with increasing residual positive charge on the phosphorus atom. This increase will render the P-atom more susceptible to attack from the nucleophile. The activation energy for the nucleophilic reaction between hydroxyl ion or the anion of *iso*nitroso acetone with the three different fluorophosphorus compounds studied in this paper (Table 1), decreases successively when methoxy groups are replaced by alkyl substituents. This observation is attributed to the mesomeric effect ($+M$) of alkoxy groups. Such an effect will reduce the positive charge on the phosphorus atom and in this way counteract the attack from nucleophilic agents. The observed results are in accordance with the general electronic picture of the phosphorus compounds discussed in the previous paper [14]. In Table 2 are recorded the stretching frequencies of the P=O and P—F bonds of the three fluorophosphorus compounds studied. In the same table are also included the association constants of the dimeric hydrogen bond complexes between phenol and the same compounds in carbon tetrachloride. The increase of the polarity of the P=O and P—F bonds from the dimethoxyphosphoryl fluoride to diethylphosphoryl fluoride is consistent with the above conclusions. The same conclusion can also be drawn from the activation energy of the reaction with hydroxyl ion of the three last phosphorus compounds recorded in Table 3.

Table 3. Thermodynamic function of nucleophilic substitutions on phosphorus.

Substrate	Reagent	Activation energy kcal/mole	Activation entropy E.U.
Diethoxyphosphoryl *p*-nitrophenoxyde ○	OH^-	7.4	−45
	OOH^-	8.3	−33
Methyl *iso*propoxy phosphoryl fluoride	OH^- □	9.1	−24
	OOH^- □	7.7 ± 1.6	−20 ± 5
	OCl^- ■	11.4	−18
Trimethyl phosphate ●	OH^-	16.3	−32
Dimethyl ethylphosphonate ●	OH^-	14.0	−34
Methyl diethylphosphonate ●	OH^-	10.6	−40

● Values calculated from the paper of Hudson and Harper [18].
○ Values calculated from the paper of Epstein, Demek and Rosenblatt [24].
□ Values taken from the papers of Larsson [11,25].
■ Values calculated from the papers of Epstein *et al.*[26].

It has been observed that the reactions between organophosphorus compounds and substituted hydroxamic acids obey a linear relation between the logarithms of the rate constants and the logarithms of the dissociation constants of the corresponding hydroxamic acids [9,17]:

$$\log k = \log G + \beta(\mathrm{p}K\text{—}14) \qquad (16)$$

where G and β are constants. The proportionality factor β decreases when alkyl groups in the phosphorus compounds are substituted with alkoxy groups[9]. The importance of the basicity of the nucleophilic reagent in substitution reactions with the phosphorus compounds must therefore decrease from the alkyl to the alkoxy substituted compounds. According to Hammet [20] we must assume that the thermodynamic reason for the above mentioned linear relationship is that the entropy of reaction remains approximately constant for the reactions between the particular phosphorus compound and the different hydroxamic acids. This assumption is based on the similarity between the above linear relation and the expression of the rate constant according to the transition state theory (eqn. (17)) [20]. It seems therefore reasonable to assume that the importance of the basicity of the nucleophilic reagent in substitution reactions with phosphorus compounds should be reflected largely in the activation energy term. We arrive also to the conclusion that the activation energies of nucleophilic reactions with alkoxy substituted phosphorus compounds as compared with alkyl substituted compounds, should be less susceptible to changes of the basicity of the attacking reagents. The last assumption is supported by the activation energy data in Table 1.

The general tendency of the calculated entropy of activation for the nucleophilic displacement on phosphorus is to oppose the effect of the activation energy (Tables 1 and 3). A favourable activation energy is compensated by an unfavourable activation entropy and *vice versa*. We assume that this effect is connected with the differences in the polarisability of the reacting molecules. In a previous paper [14] where the hydrogen bond formation between phenol and organophosphorus compounds was studied, a similar compensating action between the enthalpy and entropy of the equilibrium reaction was observed. It was postulated that the polarity of the hydrogen bond successively increased with increasing strength of the hydrogen bond. Due to the polarity or the polarisability of the solvent molecules an increase in the polarity of the hydrogen bond will contribute to a stronger orientation of solvent molecules and a corresponding decrease in entropy. At the beginning of this discussion was mentioned that there is strong evidence for the view that the nucleophilic reaction of fluorophosphorus compounds belong to an A-2 mechanism. It appears to be well established that bimolecular reactions of type A-2 are always accompanied by a large negative activation entropy due to the partial valence bonds which are formed in the transition state [21,22]. A considerable part of the reaction entropy is attributed to the difference in the orientation of solvent molecules in the transition state and the reacting molecules [21,22]. If the electronic effects in the reacting molecules are of such character that they are able to decrease the charge concentration in the transition state we should expect an increase in the activation entropy. During the formation

Table 4. The rate constants for the reaction between tetraethylpyrophosphate and different anions.

Anion	k_R l mole^{-1} min^{-1} ●	pK of corresponding acids
OH^-	21	14
$AcC(CH_3) = NO^-$	16	9.3
$(Ac)_2C=NO^-$	35	7.4
$AcCH=NO^-$	59	8.3
$BzNHO^-$	160	8.8
OOH^-	2 180	11.8
ONO^-	high	—
$S_2O_3^{--}$	unmeasurably small	—

● Values taken from the work of Green *et al.*[9]

of the transition state in the reactions between the nucleophiles and the phosphorus compounds recorded in Table 1, the electronic effect of the methoxy groups will be expected to contribute to a delocalization of the charge in the collision complex. We therefore attribute the observed favourable entropies of the reactions of the methoxy substituted compounds to this delocalization effect which correspondingly will decrease the solvent constriction in the transition state.

The strong influence of substituents in phosphorus compounds upon delocalization of the charge in nucleophilic substitution may be attributed to the fact that the available *d*-orbitals of phosphorus are involved in π-bonding and that these orbitals during the formation of the transition state also can enter the σ-bond structure of the activated complex. The character of the partial valence bonds of the activated complex will thus approach the character of true chemical bonds rather than a special orientation of reacting molecules with correspondingly great charge separation.

From Table 1 it is observed that the reactions of *iso*nitroso acetone with the phosphorus compounds proceed with much higher entropies of reaction than the corresponding reactions of the hydroxyl ion. We suggest that in this case the transition state has the possibility to delocalize the charge due to the partial valence bonds by mutual electromeric cooperation between the phosphorus compound and the attacking reagent.

A favourable entropy of reaction seems to be a common feature for all the reagents of low basicity which show abnormally high rate of reaction with the organophosphorus compounds, the reactivators included. In Table 4 are collected some results from the literature [11,23–26]. It is observed that all of the reactive nucleophiles are strongly polarisable molecules. It seems therefore possible that the explanation put forward for the *iso*nitroso acetone will apply to all of the different nucleophilic reagents studied.

Studies of nucleophiles with very high reactivity with phosphorus compounds reveal that it is an oxygen atom in the reagents which participates in

the displacement reaction (Table 4)[9]. The preference of the oxygen atom to participate in the displacement reaction with phosphorus compounds is most likely due to its high negativity and its small size. These qualities will make the oxygen atom favourable for π-bond formation with the *d*-orbitals of phosphorus. Linear polarisable groups as HOO^-, ClO^-, $O=N-O^-$, $-NHO^-$, $-C=N-O^-$ appear to be a common feature of the highly reactive nucleophiles (Table 4). Substitution in the atom adjacent to the reacting oxygen atom with greater groups than hydrogen (*e.g.* methyl) always reduce the reactivity of the nucleophiles with the phosphorus compounds. It seems reasonable to attribute this effect to steric retardation.

Nucleophilic reactions with the phosphorus compounds seems to be strongly dependent on two main factors of the nucleophilic reagent: its basicity and its polarisability[9,27,28]. The above mentioned observations indicate that the basicity effect is chiefly reflected in the activation energy term and the polarisability effect especially in the entropy term. Nucleophilic displacements on phosphorus depend also on the polarity and the polarisability of the phosphorus compounds[9]. The basicity effect of the nucleophilic reagent is most pronounced in reactions with phosphorus compounds of the highest polarity, and the polarisability effect of the reagent is most effective in reactions with the strongest polarisable substrate.

The kinetic studies in this paper together with the previous hydrogen bond studies of phosphorus compounds[14] point to the conclusion that the significance of the mutual polarisability of reactants is much greater in the reactions of phosphorus compounds than in the reactions of carbon compounds. It seems possible that just this property of phosphorus may play an important role in the wide-spread transphosphorylation processes which occur in all living tissues. A kinetic study of the biochemical reaction between cholinesterase and the three organofluorophosphorus compounds which have been studied in this paper (Table 1) has shown that the relative rates of reaction between cholinesterase and the phosphorus compounds correspond to the relative rates between *iso*nitroso acetone and the same phosphorus compounds. In both cases methoxyethylphosphoryl fluoride was found to react most rapidly with cholinesterase resp. *iso*nitroso acetone. This observation points to the conclusion that the rate determining factors in the phosphorylation of cholinesterase and *iso*nitroso acetone appear to be governed by the same fundamental properties of the reactants. In our opinion the relationship in reaction properties of cholinesterase and *iso*nitroso acetone gives reasonable explanation of the effectiveness of the reactivators to regenerate phosphorylated cholinesterase.

The kinetic study of the phosphorylation of cholinesterase will be published elsewhere.

REFERENCES

1. Holmstedt, B. *Acta Physiol. Scand.* **25** (1951) Suppl. 90.
2. Sartori, M. *Chem. Revs.* **48** (1951) 1.
3. Aldridge, W. N. *Biochem. J.* **54** (1953) 442.
4. Tammelin, L. E. *Arkiv Kemi* **12** (1958) 287.
5. Davies, D. R. and Green, A. L. *Biochem. J.* **63** (1956) 529.

6. Wilson, I. B. *J. Biol. Chem.* **190** (1951) 111.
7. Swidler, R. and Steinberg, G. M. *J. Am. Chem. Soc.* **78** (1956) 3594.
8. Green, A. L. and Saville, B. *J. Chem. Soc.* **1956** 3887.
9. Green, A. L., Sainsbury, G. L., Saville, B. and Stansfield, M. *J. Chem. Soc.* **1958** 1583.
10. Larsson, L. and Hansen, B. *Svensk Kem. Tidsskr.* **68** (1956) 521.
11. Larsson, L. *Acta Chem. Scand.* **11** (1957) 1131.
12. Guggenheim, E. A. *Phil. Mag.* **2** (1926) 538.
13. Glasstone, S., Laidler, K. and Eyring, H. *The Theory of Rate Processes*, Mc.Graw-Hill Book Company, Inc., New York 1941, p. 199.
14. Aksnes, G. and Gramstad, T. *Acta Chem. Scand.* **14** (1960) 1485.
15. Freon, P. *Ann. Chim. (Paris)* **11** (1939) 460.
16. Harned, H. S. and Owen, B. B. *The Physical Chemistry of Electrolytic Solutions*, Reinhold Publishing Co., New York 1943, p. 575.
17. Swidler, R. and Steinberg, G. M. *J. Am. Chem. Soc.* **81** (1959) 3721.
18. Dostrovsky, I. and Halmann, M. *J. Chem. Soc.* **1956** 1004.
19. Green, M. and Hudson, R. F. *Proc. Chem. Soc.* **1959** 227.
20. Hammet, L. P. *Physical Organic Chemistry*, Mc.Graw-Hill Book Company, Inc., New York 1940, p. 118.
21. Whally, E. *Trans. Faraday Soc.* **55** (1959) 798.
22. Long, F. A., Pritchard, J. G. and Stafford, F. E. *J. Am. Chem. Soc.* **79** (1957) 2362.
23. Hudson, R. F. and Harper, D. C. *J. Chem. Soc.* **1958** 1356.
24. Epstein, J., Demek, M. M. and Rosenblatt, D. H. *J. Org. Chem.* **21** (1956) 796.
25. Larsson, L. *Acta Chem. Scand.* **12** (1958) 723.
26. Epstein, J., Bauer, V. E., Saxe, M. and Demek, M. M. *J. Am. Chem. Soc.* **78** (1956) 4068.
27. Swain, C. G. and Scott, C. B. *J. Am. Chem. Soc.* **75** (1953) 141.
28. Edwards, J. O. *J. Am. Chem. Soc.* **76** (1954) 1540.

Received February 8, 1960.

ACTA CHEMICA SCANDINAVICA 14 (1960) 1526–1532

A Comparison between Hydrogen Bond Formation and the Acid Hydrolysis of Phosphoryl and Carbonyl Compounds

GUNNAR AKSNES*

Norwegian Defence Research Establishment, Toxicological Group, Kjeller, pr Lillestrøm, Norway

The acid catalysed reactions of trialkylphosphites, di*iso*propyl fluorophosphate and acetamide are discussed in relation to their ability to form hydrogen bonds. Their special behaviour in acid hydrolysis, the decrease of the specific rate constant of the hydrogen ions with increasing concentration of acid, is assumed to be due to hydrogen bonding between the hydroxonium ions and the substrate.

In two previous papers [1,2] we have examined the very strong hydrogen bonds which are formed between phenol and the phosphoryl group in organophosphorus compounds and between phenol and the carbonyl group in N-diethylacetamide. In a third paper [3], nucleophilic displacements on phosphorus are discussed. Evidence has been gathered that the chemical reactivity with regard to nucleophilic substitution on phosphorus depends strongly on both the polarity and the polarisability of the phosphorus compounds. The purpose of this paper is to examine the connection between the ability of hydrogen bond formation of some phosphoryl and carbonyl compounds and their chemical reactivity in acid catalysis.

PREVIOUS FINDINGS CONCERNING THE ACID HYDROLYSIS OF AMIDES AND ORGANOPHOSPHORUS COMPOUNDS

It has been known for a long time that the acid hydrolysis of amides and organophosphorus compounds show exceptional behaviour. Euler [4] showed that in the acid hydrolysis of acetamide the first order rate constant of the hydrogen ion catalysis increased less than directly proportional to the acid concentration. Later it was observed that this behaviour was a common feature of all amides [5]. Nylén [6] found that the acid catalysis of dialkylphosphites depended on the hydrogen ion concentration in the same way as

* Present address: Chemical Institute, University of Bergen, Bergen, Norway.

for the amides. The same observation was made by Kilpatrick and Kilpatrick[7] in their study of the acid catalysis of di*iso*propylfluorophosphate.

Euler explained the results from his ionization theory of catalysis[8]. He considered the substrate (S) and the acid HA to be in equilibrium with the conjugated acid SH^+ of the substrate:

$$S + HA \underset{k_{1-}}{\overset{k_1}{\rightleftharpoons}} A^- + SH^+ \qquad (1)$$

The rate of hydrolysis was then determined by the rate of splitting of SH^+

$$SH^+ \xrightarrow[\text{slow}]{k^*} \text{product} \qquad (2)$$

He assumed than that the base strength of S was of the same order as A^-, *i.e.* $k_1 \sim k_{1-}$. If now $k^* \ll k_{1-}$ it is easily found that the observed rate of hydrolysis (k_{obs}) is satisfied by the following equation

$$k_{obs} = \frac{k^* \cdot H^+ \cdot K_B}{1 + H^+ \cdot K_B} \qquad (3)$$

where k^* is the specific rate constant of the hydrogen ions. H^+ is the concentration of hydrogen ions. K_B is the base constant of the substrate defined as: $K_B = K_1/K_W$, where K_1 is the ionization constant of the base referred to water solution, and K_W is the ion product of water.

When eqn. (3) above is rearranged we get:

$$\frac{k_{obs}}{H^+} = -k_{obs} \cdot K_B + k^* \cdot K_B \qquad (4)$$

We find therefore that k_{obs}/H^+ shall vary linearly with k_{obs}. The slope of the line is equal to K_B.

The experimental data of Euler[4], Nylén[6], Kilpatrick and Kilpatrick[7] obey all a linear relation according to eqn. (4). In Table 1 are recorded the base constants of different substrates calculated according to eqn. (4).

Table 1. K_B-values calculated from reaction kinetic data (eqn. 4).

Compound	Constant ionic strength: 4.00			HCl, ionic strength: 0—0.3
	HCl + NaCl	HBr + NaBr	$HClO_4$ + $NaClO_4$	
Dimethyl-phosphite	~0.5	0.3	0.5	~0.5
Diethylphosphite	1.1	1.3	1.3	~0.7
Di-*n*-propyl phosphite	1.6	1.7	1.7	~0.9
Di*iso*propyl-phosphite	1.9	1.8	1.8	~2.0
Di*iso*propyl-fluorophosphate	—	—	—	2.2
Acetamide	—	—	—	0.7

Table 2. Association constants between phenol and different compounds in CCl_4[1,2].

Compound	Association constant l/mole, 20°C
Dimethylphosphite	123
Diethylphosphite	167
Di-*n*-propylphosphite	200
Di*iso*propylphosphite	237
N-Diethylacetamide	170

HYDROGEN BOND ASSOCIATION CONSTANTS

In Table 2 are recorded the association constants for the hydrogen bond association between phenol and dialkylphosphites and between phenol and N-diethylacetamide in carbon tetrachloride [1,2].

From the presence of the stretching vibration band of the phosphoryl group and its displacement upon hydrogen bonding we conclude that the dialkylphosphites have phosphoryl structure and that it is the P=O bond which participates in hydrogen bonding [2].

THE CONNECTION BETWEEN pK_B OF SOLVENTS AND THE FREQUENCY SHIFT OF THE O–D BAND IN THE SAME SOLVENTS

Gordy [9] has shown that there exist a simple relation between the basicity of solvents and their ability to form hydrogen bonds. He observed that the frequency shifts of the O—D stretching band of deuterium alcohol and deuterium oxide in different basic solvents are proportional to the pK_B of the solvents. In Fig. 1 are reproduced his observations of the frequency shift of the O—D stretching band of deuterium oxide in 19 different solvents. The equation of the line is according to Gordy [9]:

$$\Delta\mu = 0.0175 \log K_B + 0.297 \quad (5)$$

where $\Delta\mu$ is the frequency shift of the O—D band. K_B is defined as: $K_B = K_1/K_W$, where K_1 is the ionization constant of the base referred to water solution and K_W is the ion product of water.

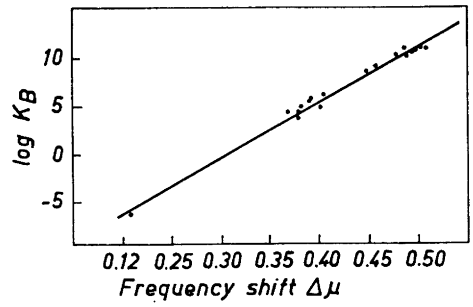

Fig. 1. Relation of basicity constants of solvent to their shifts of the vibrational band of D_2O. (Reproduced from the paper of Gordy [9]). Lowest point in fig.: acetophenone; middle points in fig.: pyridine and aniline derivatives; upper points in fig.: aliphatic and alicyclic amines.

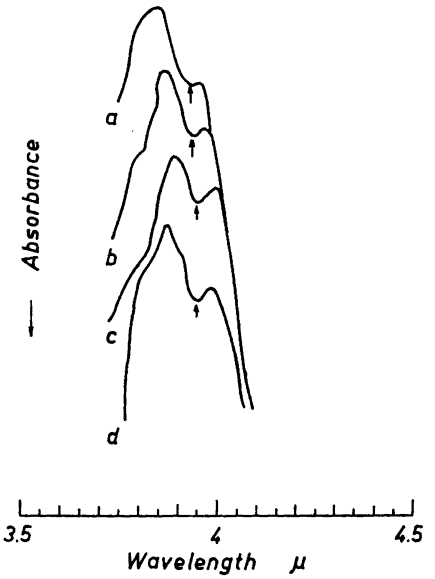

Fig. 2. The vibrational bands of D_2O in dialkylphosphites. a) Dimethylphosphite, b) diethylphosphite, c) dipropylphosphite, d) di*iso*propylphosphite.

We have used this equation to estimate the apparent basicity constants of the trialkylphosphites, di*iso*propylfluorophosphate and acetamide. In Fig. 2 are shown the absorption bands of the O—D stretching vibration of deuterium-oxide when it is dissolved in the different dialkylphosphites. Due to the broadness of the O—D band it is difficult to get a very accurate measure of the O—D displacement, but there is a distinct increase of $\Delta\mu$ of the O—D band from dimethyl to di*iso*propylphosphite. The calculated basicity constants are recorded in Table 3.

DISCUSSION

If we compare the basicity constants calculated from eqn. (4) in Table 1 with the basicity constants of the compounds determined from the frequency shift of the O—D band in Table 3, we find in both cases K_B values of the same order of magnitude. The K_B values calculated from the kinetic data show the ordinary variation with ionic strength. None of the methods can be expected to give very accurate values of K_B. The K_B values of the dialkylphosphites calculated from the kinetic measurements indicate an increase in basicity of the dialkylphosphites from dimethyl- to di*iso*propylphosphite. This is in agreement with the determined association constants between phenol and dialkylphosphites in carbon tetrachloride recorded in Table 2. The same general tendency is shown by the K_B-values of the dialkylphosphites determined by the frequency shift method in Table 3.

The kinetic picture given by Euler [4,8] is apparently in good agreement with the above results. But there is a serious objection to the application of the theory of Euler. If there existed a proton transfer equilibrium between the

Table 3. K_B-values calculated from the frequency shift of the stretching band (eqn. 5).

Compound	$\Delta\mu$ of O—D band	Calculated K_B
Dimethylphosphite	0.282	0.2
Diethylphosphite	0.290	0.4
Di-*n*-propylphosphite	0.295	0.8
Di*iso*propylphosphite	0.300	1.5
Acetamide	0.285	0.3
Di*iso*propylfluoro-phosphate	0.300	1.5

hydrogen ions and the substrate we should expect a measurable change in the pH of the solution when the substrate is dissolved in water.

Nylén [6] was unable to find any significant change in the pH of water solutions of dialkylphosphites. We have repeated the pH-measurements not only for the dialkylphosphites but also for the extremely strong hydrogen bonding substrate trimethylphosphine oxide which, according to the relation found by Gordy [9], should have a K_B value of approximately 10^4. In none of the cases have we been able to demonstrate the expected changes in the pH of their water solutions.

We conclude therefore that the observed reaction kinetics do not deal with proton transfer equilibrium but with hydrogen bond equilibrium. The following kinetic scheme is postulated:

$$S + H_3O^+ \ldots nH_2O \overset{K_{ass}}{\rightleftharpoons} S \ldots H_3O^+ + nH_2O \qquad (6)$$

$$S \ldots H_3O^+ + H_2O \xrightarrow[\text{slow}]{k^*} \text{product} \qquad (7)$$

The reaction (6) shows that the substrate due to its tendency of hydrogen bond formation will compete with water in capturing hydroxonium ions. The kinetics of the reaction will be the same as in theory of Euler [4]. The difference lies in the meaning of the equilibrium constants. K_{ass} in eqn. (6) is not the base constant of the substrate but the hydrogen bond association constant between substrate and hydroxonium ions relative to that of water. But since the hydrogen ions are not lost from the water to the substrate through a proton transfer reaction but are only gathered in the neighbourhood of the substrate due to hydrogen bonding, we cannot expect the same influence on the acidity in the last case as compared with a proton transfer reaction. It seems more correct to speak about a small influence upon the activity of the hydrogen ions due to their hydrogen bonding with the substrate.

The hydrolysis of dialkylphosphites and di*iso*propylfluorophosphate shows general acid catalysis [6,7,10]. This observations are in complete agreement with

the postulated reaction scheme. In this case one will in addition to the equilibrium reaction (6) have to include an eqilibrium reaction of the general type:

$$S + HA \overset{K_{ass}}{\rightleftharpoons} S \ldots HA \qquad (8)$$

where HA means an undissociated acid, and

$$S \ldots HA + H_2O \xrightarrow[\text{slow}]{k_{HA}} \text{product} \qquad (9)$$

where k_{HA} is the rate constant of hydrolysis due to the undissociated acid.

The hydrolysis of amides gives also support to the hydrogen bond mechanism of hydrolysis. It was mentioned in a previous paper [1] that it is the C=O bond in amides which participates in hydrogen bonding, but when a sufficiently strong acid is used to produce a proton transfer reaction the proton is captured by the nitrogen:

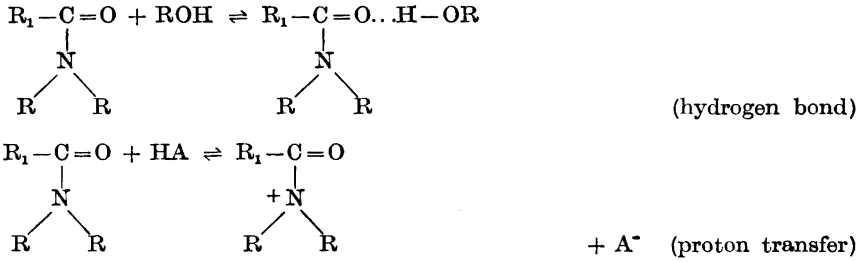

Now it is known that the rate of acid hydrolysis of amides goes through a maximum at about 5—6 M acid [5]. The maximum in rate has been explained as caused by the drop of water concentration (or of its activity) at high acid concentrations [5].

Lately it has been observed that the amides in nearly water-free strong acids are also hydrolysed at a relative high rate and that the rate decreases upon adding small amounts of water [11].

The only reasonable explanation of this behaviour is that there exists two different mechanisms of hydrolysis of the amides. In water-free strong acids all of the amides will exist in the protonised form with the proton attached to the nitrogen. The splitting of the protonised form in concentrated acids will most likely be a unimolecular reaction which is retarded in the presence of too much water. The logical interpretation of the hydrolysis of amides in dilute water solution (which are the measurements referred to in this paper) is therefore that the reaction follows a bimolecular reaction scheme (A-2) according to eqns. (6) and (7) where the C=O group participates in a hydrogen bond equilibrium reaction with the hydroxonium ions.

The phosphoryl and carbonyl compounds discussed in this paper show a common feature in their strong ability of hydrogen bond formation. It seems unlikely that other carbonyl and phosphoryl compounds with less polar C=O or P=O bonds should behave in a different manner. But their hydrogen bond

association constants with hydroxonium ions should be expected to be so small that the measured rate constants will appear to be proportional to the acid concentration. From the paper of Gordy [9] we find that the O—D shift, $\Delta\mu$, of deuterium oxide in ethylacetate is 0.21, which corresponds to an apparent K_B-value of approximately 10^{-5}. Such a low K_B-value incerted in eqn. (3) will not give observable deviation of k_{obs} from proportionality. A consequence of this view is that the acid catalysed reaction of compounds where the C=O or P=O bonds are attacked by the acid previous to the formation of the transition state should be expected to belong to the bimolecular reaction scheme (A-2). This follows from eqn. (7).

In a previous paper [12] where the acid hydrolysis of quaternary ammonium esters were studied, it was found that the carbonyl oxygen was attacked by the hydroxonium ions during the hydrolysis of the esters. There is now convincing evidence that the hydrolysis of aliphatic esters belong to a bimolecular mechanism (A-2) [13]. The hydrolysis of esters will therefore fit into the reaction scheme proposed in this paper.

Direct evidence for an acid catalysed ester hydrolysis by the unimolecular mechanism (A-1) was obtained in the hydrolysis of esters of mesotoic acids [14] (2,4,6-trimethylbenzoic acid). These esters give with concentrated strong acids benzoylium ions. But this observation proves that the proton transfer reaction in this case must have occurred at the ether oxygen of the esters.

REFERENCES

1. Aksnes, G. *Acta Chem. Scand.* **14** (1960) 1475.
2. Aksnes, G. and Gramstad, T. *Acta Chem. Scand.* **14** (1960) 1485.
3. Aksnes, G. *Acta Chem. Scand.* **14** (1960) 1515.
4. Euler, H. and Ölander, A. *Z. physik. Chem.* **131** (1928) 107.
5. Hammet, L. P. *Physical Organic Chemistry*, Mc Graw-Hill Book Company, New York 1940, p. 365.
6. Nylén, P. *Svensk Kem. Tidsskr.* **49** (1937) 29.
7. Kilpatrick, M. and Kilpatrick, M. L. *J. Phys. & Colloid Chem.* **53** (1949) 1371.
8. Bell, R. P. *Acid-Base Catalysis*, Clarendon Press, Oxford 1941, p. 122.
9. Gordy, W. *J. Chem. Phys.* **9** (1941) 204, 215.
10. Ref.[8] p. 48.
11. Dufey, J. A. and Leisten, J. A. *Nature* **178** (1956) 1242.
12. Aksnes, G. and Prue, J. *J. Chem. Soc.* **1959** 103.
13. Whaley, E. *Trans. Faraday Soc.* **55** (1959) 802.
14. Treffers, H. P. and Hammet, L. P. *J. Am. Chem. Soc.* **59** (1937) 1708.

Received February 8, 1960.

ACTA CHEMICA SCANDINAVICA 14 (1960) 1533–1554

Electrochemical Behaviour of Iron

TOR HURLEN

Central Institute for Industrial Research, Blindern, Oslo, Norway

As part of a research programme on the kinetics of metal/metal-ion electrodes in aqueous solutions, investigations have been made on the anodic dissolution and cathodic deposition of iron in acid chloride solutions at 20°C by means of a slow amperostatic technique. The reactions are found to obey the Tafel relationship (except at higher current densities) and to have mutually symmetric Tafel lines with slopes of numerically 0.029 V ($2.303RT/2F$). The rate of either reaction is moreover found to be proportional to the hydroxyl ion activity, and the rate of deposition to be proportional to the square of the ferrous ion activity. This indicates a mechanism covered by the equation:

$$2Fe + OH^- \rightleftharpoons 2Fe^{++} + OH^- + 4e^-$$

This mechanism is discussed, and a possible explanation is suggested.

For the exchange current (i_o) and the standard potential (E_o) of the Fe/Fe^{++}, aq-electrode, it is found:

$$\log i_o\ (A/cm^2) = 3.58 - pOH - pFe$$
$$E_o = -0.467\ V$$

The latter value includes a (probably small) liquid junction potential, and both equations depend somewhat on the validity of the activity data applied.

Some measurements have also been made on the hydrogen evolution reaction at iron cathodes. The results indicate a Tafel slope of -0.116 V ($-2.303 \cdot 2RT/F$) and an exchange current of

$$\log i_o(A/cm^2) = -5.36 - 0.5\ pH$$

for this reaction in acid solutions. It is further found that the hydrogen evolution reaction is positively affected (stimulated) by the iron dissolution reaction and negatively affected (depressed) by the iron deposition reaction, and that it transforms from a pH-dependent to a pH-independent mechanism at a pH quite near to the neutral point. The Tafel slope is not affected by this change in reaction mechanism.

1.0 INTRODUCTION

A most important trend in recent studies of electrochemical kinetics is the development of theoretical equations for the rate of activation controlled electrode reactions [1–3]. These equations enable the identification of the rate

determining step and the determination of stoichiometric factors from suitable polarization measurements. The theory has so far mainly been used in elucidating the mechanism of hydrogen evolution at metal cathodes as this is by far the best known electrode reaction [1,2]. It has in this case apparently met with considerable success, making it a promising basis also for the study of other electrode reactions. On the other hand, such studies may also be of value in providing further data for testing the validity and applicability of the theory (see the criticism given by Horiuti [4] and Rüetschi [5]).

Metal deposition and dissolution constitute an important class of electrode reactions showing strong technological and practical implications (metal production, metal refining, electro-plating, corrosion, *etc.*). In spite of this, little seems to be known concerning their kinetics. This has been clearly demonstrated by Bockris [2] and Hoar [6], who have collected and discussed most of the relevant data available. These authors ascribe this state of affairs partly to experimental difficulties which have prevented many results being expressed in a form which allows theoretical analysis. Several of the results do also indicate that the polarization data to some extent depend on the method by which they have been obtained.

On this basis, it was assumed desirable to make renewed and extended investigations on a series of metal/metalion electrodes, using the same method for polarization measurements on all the metals. The metals which have been included in this programme, are *iron*, *cobalt*, *nickel*, *copper*, and *zinc*. The polarization method adopted, is a "slow" amperostatic method which allows the partial current density of the reactions to be estimated from the weight change of the electrodes. For checking the reliability of the method, parallel measurements have been made on the hydrogen evolution reaction at cathodes of the various metals involved. Other methods have also been applied.

This work will be presented in a series of papers of which this is the first. Experiments on *iron* in de-aerated acid chloride solutions at 20°C are here described and the kinetics of the anodic dissolution and cathodic deposition of this metal is discussed.

2.0 PREVIOUS WORK

Most of our present knowledge of the electrochemical behaviour of iron has come from the study of corrosion and allied processes. General reference may therefore be given to the corrosion monographs by Gatty and Spooner [7], Evans [8], Uhlig [9], Speller [10], Tödt [11], and Klas and Steinrath [12] and to the corrosion review by Grubitsch [13] where further references to original work — except the most recent — will be found. A general reference may also be given to the monograph by Fischer [14] on electrocrystallization of metals.

As already mentioned, most of the few data from this work which allow direct analysis on the basis of modern theory, have been collected and discussed by Bockris [2] and Hoar [6]. A great many of the additional data, however, may be used in testing the validity of the more direct ones by comparison with consequences deduced from these. Important data in this connection are for instance those on the relations between corrosion potential, corrosion rate

and pH. This will be discussed separately in a subsequent paper, and we will here only deal with the more direct results.

A complete analysis of the kinetics of an electrode reaction often requires data also for its reverse reaction [1,2]. This is especially the case for metal dissolution processes, as we here have no means of altering the activity of the main reactant, the solid metal itself. The work of Hoar and Hurlen [15-17] on iron and mild steel in acid sulphate solutions is the only work we are aware of in which the potential/rate relationship for anodic dissolution and cathodic deposition of iron has been studied under equivalent conditions. They found the Fe/Fe^{++}.aq-electrode to behave symmetrically and to have a Tafel slope of numerically 2.303 $RT/2F$ (0.029 V at 25°C) for either of its reactions. The rate of both reactions was moreover found to be proportional to the hydroxyl ion activity, the rate of deposition to be proportional to the square of the ferrous sulphate activity, and the rate of dissolution to be independent of the latter activity. The extrapolated Tafel curves gave reasonable values for the reversible potential and exchange current values directly proportional to both the above mentioned activities, *e.g.* —0.507 V (normal hydrogen scale) and 2.6×10^{-11} A/cm^2 in 0.1 M sodium hydrogen sulphate + 0.05 M ferrous sulphate at 25°C. This work includes experiments at 0, 25, and 50°C, and the method used was the same as in the present work.

Rojter, Juza, and Polujan [18] determined the exchange current of the Fe/Fe^{++}.aq-electrode in 1.25 M ferrous sulphate presumably at room temperature (not specified) from oscillographically determined charging curves and obtained approximately 10^{-8} A/cm^2. This is in reasonable agreement with the results of Hoar and Hurlen when the effect of ferrous ion activity and pH is considered.

Bonhoeffer and Heusler [19-21], from rapid oscillographic potential measurements, found a Tafel slope of 0.030 V for the stationary anodic dissolution of iron in acid sulphate and perchlorate solutions. They further found proportionality between the dissolution rate and the hydroxyl ion activity raised to a power of 1.55. Heusler [21] assumes 2 to be the correct value of this exponent. These results are only partly in accordance with those of Hoar and Hurlen.

Kabanow, Burstein, and Frumkin [22] found an anodic Tafel slope varying from 0.02 to 0.04 V for iron in 2 N sodium hydroxide. By comparing with corresponding results in 1 N hydrochloric acid (obtained by Kusnezov [23]), they further found indications that the dissolution at equal potentials was several orders of magnitude faster in alkaline than in acid solutions. These authors were thereby probably the first to draw attention to the effect of pH on the anodic dissolution of active iron. They also discussed the effect of chloride ions on the anodic dissolution reaction in alkaline solutions.

Values for the Tafel slope of anodic dissolution have been given also by a few other authors. Kaesche [24] found 0.03 V for iron in acid perchlorate solutions at 25°C. Makrides, Komodromos, and Hackerman [25] found 0.04 V for iron in 2 M hydrochlorid acid and Gatos [26] 0.06 V in 1 N sulphuric acid when the dissolution was caused by depolarizers. Hoar and Holliday [27] found 0.051 V for mild steel in 0.5 M sulphuric acid at 40°C, and Hoar and Farrer [28] 0.05 to 0.07 V for mild steel in 0.001 N solutions of various magnesium, calcium, and sodium salts at 25°C. Okamoto, Nagayama, and Sato [29] found about 0.1

V for iron in 0.3 N sulphuric acid when varying the current density be about twice every 0.1 sec. Stern and Roth [30] have moreover given an estimated value of 0.078 V for iron in an acid chloride solution.

According to Bockris [2], little relevant work has been done on the cathodic deposition of iron. A detailed discussion of results obtained up to 1954 has been given by Fischer [14]. A description of modern ideas on the mechanism of metal deposition reactions has more recently also been given by Conway [31]. Lyons [32] has described how the discharge process of cations may be visualized on the basis of electron configurations, and Conway and Bockris [33] have made a theoretical treatment of the mechanism of metal deposition. The most recent work we are aware of as to the deposition of iron, is that of Hoar and Hurlen [15-17] mentioned above.

A detailed description of the hydrogen evolution reaction at iron cathodes is outside the scope of the present work, and a few references will be given for comparison and checking purposes only. The most usual Tafel slope for hydrogen evolution at metal cathodes is 4.606 RT/F (0.117 V at 25°C), a value also easily derivable by theory [1,2]. The results obtained for this reaction on iron in acid sulphate solutions by Hoar and Hurlen [15-17], in acid sulphate and perchlorate solutions by Bonhoeffer and Heusler [19,21], in acid perchlorate solutions by Kaesche [24], in acid chloride solutions by Stern [34,35], and by Fischer and Thoresen [35] (just to mention some of the most recent results) are partly in excellent agreement with this value. It is further to be expected that the rate of hydrogen evolution in this case should be proportional to the hydrogen ion activity provided the pH is not too high and excess indifferent salt is present [1,2]. The results of Hoar and Hurlen [16,17] show an effect of pH in accordance with this, while those of Stern [34,35] and of Bonhoeffer and Heusler [19,21] show a somewhat smaller pH effect. A modern analysis of the effect of the electrode material on the hydrogen evolution reaction is given by Parsons [37].

Stern [35] and Hoar and Hurlen [15-17] have recently studied the effect of impurities in iron on its electrode behaviour (the latter authors by comparing the behaviour of pure iron with that of a relatively clean mild steel). In both these investigations, a distinct stimulating effect especially of non-metallic impurities (as sulphur and phosphor) on the hydrogen evolution reaction was observed. Hoar and Hurlen found no differences in the pure dissolution and deposition characteristics of their iron and mild steel electrodes. Some earlier indications [38-40] that sulphur should promote also the anodic dissolution reaction were thereby not confirmed.

Most of the work on the electrochemical behaviour of iron has been performed with polycrystalline electrodes. Engell [41] and Buck and Leidheiser [42], however, have made some investigations on single crystals of α-iron. Engell found that the dissolution was nearly independent of the orientation of the crystal surfaces at low current densities (less than about 2 mA/cm^2), whereas the (111) and (110) surfaces dissolved faster than the cube faces by a factor of about 2 at higher anodic loads. These investigations were performed in dilute sulphuric, perchloric, and nitric acid. Similarly, Buck and Leidheiser found that the rate of corrosion of the (321) face was approximately twice that of the (100) face in 0.2 M citric acid. The corrosion potential of the latter face was moreover more cathodic than that of the former face. This indicates that,

besides a possible difference in the cathodic hydrogen evolution reaction at these faces there is also a difference in the anodic dissolution reaction.

Buck and Leidheiser [42] further found that the rate of corrosion of the polycrystalline starting material from which the single crystals were prepared was several times greater than those of the single crystals, and that the conversion of the single crystals to polycrystalline material resulted in a considerably increased corrosion. They ascribe this to an effect of grain boundaries on the dissolution reaction. The effect of dislocation steps in the surface on the rate of dissolution and deposition has recently been treated theoretically by Vermilyea [43].

Reviews and dicussions of recent work of general interest to electrochemical kinetics are moreover presented by Grahame [44], Butler [45], Delahay [46,47], Breyer [48], Thirsk [49], Fleischmann and Oldham [50], and Frumkin [51].

The passivity of iron is not considered here as the present work solely deals with the electrochemistry of active iron.

3.0 MATERIALS AND METHODS

Electrodes of iron (0.03 % C, 0.01 % Si, 0.19 % Mn, 0.027 % P, 0.030 % S), presented by Domnarfvets Jernverk (Sweden), were used in the form of circular sheets (about 4.5 cm diameter and 0.5 mm thickness) punched out from cold-rolled strips. Prior to use, the electrodes were vacuum annealed for about one hour at about 700°C, polished with emery paper, etched in dilute nitric acid, washed in running water, distilled water, and acetone, dried, and weighed.

Electrolytes were prepared from A.R. quality ferrous chloride, potassium chloride, and hydrochloric acid in water distilled from a "pure" and soft fresh water. The solutions were presaturated with hydrogen which first was purified by passing a palladium catalyst at about 250°C. For the ferrous chloride solutions, the presaturation was performed in the presence of a large piece of platinized platinum. This reduced the ferric ion content to a very low level (as judged from the red-ox potential). The electrolytes were also stored under hydrogen and were further transferred to the test cell by hydrogen pressure. A sketch of the electrolyte preparation and storage unit is shown in Fig. 1.

The test cell was a cylindrical Pyrex glass cell (about 10 cm^3 internal cross section and about 15 cm long) carrying tubes for the ingress and egress of liquid and gas. Two

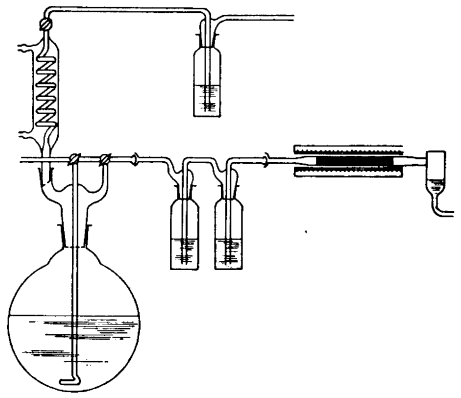

Fig. 1. The unit for preparation, pretreatment, and storage of electrolyte solutions.

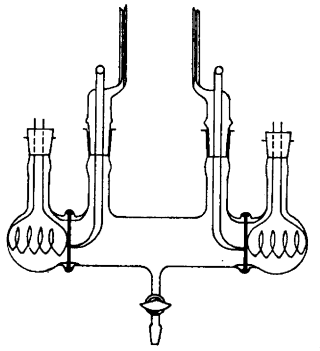

Fig. 2. The experimental cell.

electrodes could here be placed so as to form the two end walls of the cell. After having been clamped in position, the electrodes were covered around their outer edge with polystyrene (dissolved in chloroform) and paraffine wax. The cell further had two Haber-Luggin capillaries for electrolytic connections to two external reference electrodes, and copper wires for metallic connections to the potentiometer and to the current source. A sketch of the test cell, which could hold about 200 ml electrolyte, is shown in Fig. 2. In this cell, the electrolyte is exposed to the atmosphere only in two capillaries of about one millimeter diameter.

The experiments were performed galvanostatically. The current was supplied from an assembly of four 12 V accumulators connected in series. It was read on a calibrated Avo-meter and controlled by a number of variable resistances in series with the cell. The electrode potential of each electrode as a function of time was measured against a saturated calomel electrode by means of a Cambridge pH-meter.

The partial current density of the iron electrode reactions was estimated from the weight change of the electrodes over a considerable time at constant total current density. A Mettler semi-micro balance was used for these weighings. The duration of the runs varied from about one hour to two days, depending on the current applied (10^{-5} — 10^{-2} A/cm^2). The experiments were performed in a thermostated room at 20 ± 0.5°C.

4.0 THE ELECTROLYTE SOLUTIONS

The electrolyte solutions (I—IX) used in the present work, are described in Table 1. Data are there given for the composition and for the "molal ionic strength" defined by:

$$I(m) = \frac{1}{2} \sum_i m_i \cdot z_i^2$$

$I(m)$ is nearly equal to the ionic strength divided by the density of the solution (I/d). Values are moreover given for the mean molal activity coefficient (γ) of the solutes and for the activity (a) of the solvent (water). The dissociation constant of water (K_w) at 20°C is given by [52]

$$-\log K_w = 14.1666$$

The mean molal activity coefficients of hydrochloric acid and of potassium chloride have been calculated from the recent results of Harned and Gancy [53] on mixtures of these two electrolytes. For the ferrous chloride containing solutions, it has been assumed as an approximation that γ_{HCl} and γ_{KCl} have the same values as in corresponding solutions in which the ferrous ions have been substituted by an equivalent amount of potassium ions. The mean molal activity coefficients of ferrous chloride have been estimated graphically, $\log \gamma$ *vs.* $I(m)$, from data tabulated by Robinson and Stokes [52].

The activity of water in the solutions I—IV has been calculated from the data given by Harned and Gancy [53] for the osmotic coefficient of such solutions. For solution V, in which ferrous chloride is the main electrolyte, the water activity has been calculated from the molal osmotic coefficient of 0.5 m ferrous chloride [52]. For the solutions VI—IX, a_{H_2O} has been estimated on the basis of data from the above mentioned sources.

All the data used in these calculations apply to 25°C. It will here be assumed, however, that the values in Table 1 are sufficiently valid also at 20°C.

Table 1. Composition, ionic strength, and thermodynamic activity data for the applied solutions (I—IX).

	Molality			$I(m)$	$-\log \gamma$			$-\log a$
	HCl	KCl	$FeCl_2$	$(\approx I/d)$	HCl	KCl	$FeCl_2$	H_2O
I	1	0	0	1.0	0.0908	0.1502		0.016
II	0.1	0.9	0	1.0	0.1406	0.2119		0.014
III	0.01	0.99	0	1.0	0.1458	0.2176		0.014
IV	0.001	0.999	0	1.0	0.1462	0.2181		0.014
V	0.001	0	0.5	1.5	(0.146)		0.347	0.011
VI	0.001	0.6	0.2	1.2	(0.146)	(0.218)	(0.349)	(0.013)
VII	0.001	0.8	0.1	1.1	(0.146)	(0.218)	(0.348)	(0.013)
VIII	0.001	0.9	0.05	1.05	(0.146)	(0.218)	(0.347)	(0.014)
IX	0.0001	1.8	0.1	2.1	(0.120)	(0.240)	(0.334)	(0.014)

In electrode kinetics, we are interested in knowing single ion activities. These cannot be calculated from thermodynamic data (as those in Table 1) without the introduction of some non-thermodynamic (or extrathermodynamic) assumptions [52,54-57]. For solutions of single univalent chlorides, two approaches have often been used:

a) *The MacInnes assumption*, which states that the chloride ion activity in a solution of any chloride is the same as the mean ionic activity in a solution of potassium chloride at the same total concentration.

b) *The Guggenheim assumption*, which states that the activity of the chloride ion of any univalent chloride is equal to the mean ionic activity.

The first of these assumptions may directly and equally well be applied to mixed electrolytes, and this gives for the ferrous chloride free solutions (I—IV):

$$\log \gamma_H = 2 \log \gamma_{HCl} - \log \gamma_{KCl(o)} \quad (1)$$

where γ_H is the activity coefficient of the hydrogen ions in the mixed electrolyte, and $\gamma_{KCl(o)}$ is the mean activity coefficient of potassium chloride in a pure solution of this salt at the same total concentration. Results of calculations of pH ($= -\log a_H$) on this basis are given in Table 2.

The Guggenheim assumption allows us to calculate the activity coefficent of hydrogen ions in a pure hydrochloric acid solution, $\gamma_{H(o)}$, as well as their limiting activity coefficient, $\gamma_{(o)H}$, in a mixed electrolyte of hydrochloric acid and potassium chloride by the relations:

$$\log \gamma_{H(o)} = \log \gamma_{HCl(o)} \quad (2a)$$

$$\log \gamma_{(o)H} = 2 \log \gamma_{(o)HCl} - \log \gamma_{KCl(o)} \quad (2b)$$

From the Guggenheim theory [52] of mixed electrolytes, one further has:

$$\log \gamma_H = \log \gamma_{(o)H} + x(\log \gamma_{H(o)} - \log \gamma_{(o)H}) \quad (3)$$

where x is the mole fraction of hydrochloric acid in the two component mixed electrolyte. Results of calculations of pH from these equations are also given in Table 2. As the *Guggenheim assumption* seems the thermodynamically most sound, the pH-values obtained on this assumption (together with the a_{H_2O}-values in Table 1) have been used in calculating the pOH-values given in Table 2.

For a pure ferrous chloride solution, the Debye-Hückel theory gives

$$\log \gamma_{Cl(Fe)} = \tfrac{1}{2} \log \gamma_{FeCl_2(o)} \quad (4)$$

when also the definition of the mean ionic activity coefficient is considered. On this basis and on the basis of the Guggenheim theory of mixed electrolytes, one may further assume the activity coefficient of chloride ions in a mixed solution of ferrous chloride and potassium chloride to be given by:

$$\log \gamma_{Cl(K,Fe)} = x_{KCl} \log \gamma_{KCl(o)} + \tfrac{1}{2}\, x_{FeCl_2} \log \gamma_{FeCl_2(o)} \quad (5)$$

where all the activity coefficients apply to the same ionic strength and x means the ionic strength fraction of the salts in the mixed solution. This equation has been used in calculating γ_{Cl} for the solutions V—IX (neglecting the possible effect of the small amount of hydrochloric acid present). γ_H and γ_{Fe} have then been calculated from the relationships:

$$\log \gamma_H = 2 \log \gamma_{HCl} - \log \gamma_{Cl} \quad (6a)$$

$$\log \gamma_{Fe} = 3 \log \gamma_{FeCl_2} - 2 \log \gamma_{Cl} \quad (6b)$$

where all the activity coefficients apply to the same solution. The ion activities thus obtained, are given in Table 2.

The values of γ_{FeCl_2} (see Table 1) needed in the just described calculations of γ_{Fe}, have been obtained on the assumption that the former coefficient is the same in any of the mixed solutions as in a pure ferrous chloride solution of the same $I(m)$-value. The ferrous ion activity coefficient may also be calculated on the assumption that this coefficient (instead of the mean ionic activity coefficient) obeys the above equality. This means, when eqn. 4 is considered, that

$$\log \gamma_{Fe} = 2 \log \gamma_{FeCl_2(o)} \quad (7)$$

where the two activity coefficients apply to solutions of the same ionic strength. The results of such calculations are also given in Table 2, and it will here be assumed that the thereby obtained activity values are the most correct ones.

Ferrous chloride has here been treated as a non-associated electrolyte. This may seem justified by the fact that its mean acitivity coefficient is well described by the Stokes-Robinson two-parameter equation [52] for this type of electrolytes. A possible hydrolysis of the ferrous ion has also been ignored, and this seems justified on the basis of the low value ($10^{-9.5}$) found by Hedström [58] for the hydrolysis constant of this ion.

Table 2. Estimated single ion activities of H^+, OH^-, and Fe^{++} in the applied solutions (I—IX).

	pH(1)	pH(2)	pOH(2)	*Notes:* (1) MacInnes assumption (2) Guggenheim assumption (3) From eqns. 5 and 6 (4) From eqn. 7		
				pFe(3)	pFe(4)	a_{Fe}(4)
I	−0.037	0.091	14.060			
II	1.063	1.076	13.077			
III	2.073	2.074	12.079			
IV	3.074	3.074	11.079			
V		3.118	11.038	0.995	0.995	0.101
VI		3.091	11.063	1.345	1.397	0.040
VII		3.083	11.071	1.625	1.696	0.020
VII	(3.074)	3.081	11.072	1.920	1.995	0.010
IX	(4.000)	4.024	10.129	1.570	1.668	0.021

5.0 RESULTS AND INTERPRETATIONS

Examples of potential-time curves obtained for hydrogen evolution at iron cathodes and for anodic dissolution and cathodic deposition of iron, are given in Figs. 3, 4, and 5, respectively. The applied current density is given in A/cm^2 for the various curves in the diagrams. Due to corrosion and to simultaneously occurring hydrogen evolution and iron deposition, the partial current density of the reactions (as determined by weight change measurements) sometimes was quite different from the applied current density (see below). The former of these current densities and potential data from the potential-time curves have been used in constructing Tafel diagrams for the three reactions studied. The potentials most representative for the hydrogen evolution reaction at the initial pH of the solutions have been assumed to be those obtained by extrapolating the potential-time curves to zero time. For the dissolution and the deposition reaction, the stationary potentials (or in some cases the potential in the beginning of a period of nearly stationary potential) have been assumed the most representative ones. The Tafel diagrams obtained in this way are shown in Figs. 6—10.

In transforming the readings made against the saturated calomel electrode, to potentials on the normal hydrogen scale, a value of + 0.245 V has been used for the calomel electrode at 20°C (Potter [59]). No attempts have been made to correct for the possible liquid junction potentials between the test solutions and the saturated potassium chloride solution. On the basis of data tabulated by Milazzo [60], however, it is believed that these junction potentials are small.

Hydrogen evolution

The hydrogen evolution reaction has mainly been studied in the ferrous ion free solutions (I—IV), but partly (at low current densities) also in the solution of the lowest ferrous chloride content (VIII). The polarization data obtai-

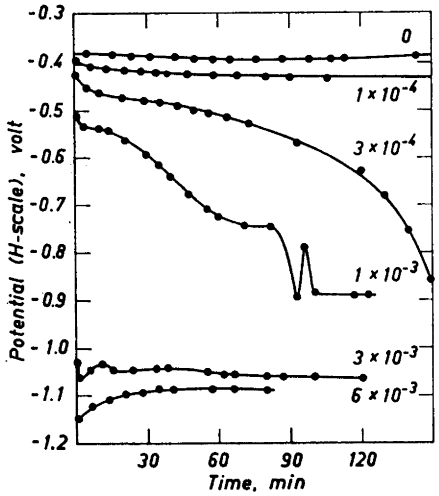

Fig. 3. Potential-time curves for hydrogen evolution at iron cathodes in solution III at various applied current densities (A/cm²).

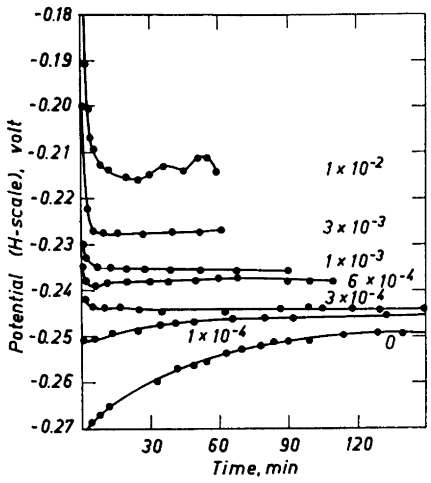

Fig. 4. Potential-time curves for anodic dissolution of iron in solution I at various applied current densities (A/cm²).

ned are given in Fig. 6, where the closed circles apply to cathodically polarized electrodes, the open circles to anodically polarized electrodes, and the centred circles to freely corroding electrodes. The terms *anodic* and *cathodic* are here used in reference to the corrosion potential so as to indicate the direction of the applied current.

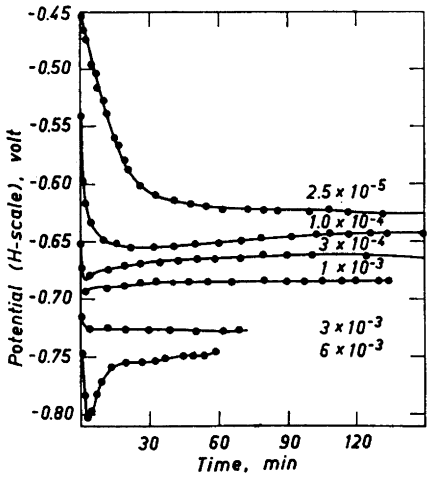

Fig. 5. Potential-time curves for cathodic deposition of iron in solution VII at various applied current densities (A/cm²).

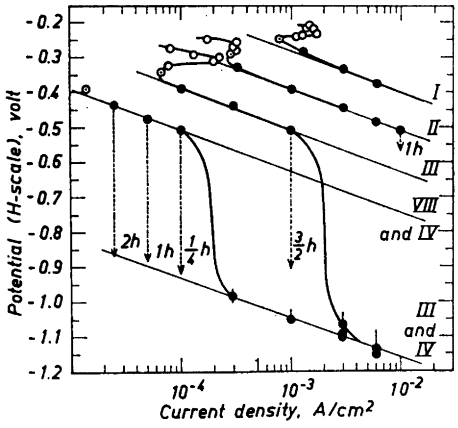

Fig. 6. Tafel diagram for hydrogen evolution at iron cathodes.

The partial current density of hydrogen evolution on anodically polarized electrodes has been estimated by the difference between the gravimetrically determined and the applied current density with corrections for the corrosion occurring prior to and after the application of current. On cathodically polarized electrodes, it has similarly been taken as the sum of the applied and the gravimetrically determined corrosion current. It is only at the lowest current densities in the two most acid solutions that a measurable corrosion occurred on electrodes of this kind, however.

The results (Fig. 6) clearly show that the hydrogen evolution reaction in these cases is strongly stimulated by a simultaneously occurring iron dissolution reaction when the rate of the latter approaches and exceeds that of the former (see the position of the corrosion points and the higher lying points in the diagram). This stimulating effect seems otherwise to be a complex function of the dissolution rate and possibly also of pH. It may here be of interest also to note that there both in the present work and especially in the previous work of Hoar and Hurlen [15,16] are indications that the hydrogen evolution reaction is affected in the opposite way by a simultaneously occurring iron deposition reaction.

The results further show that the hydrogen evolution reaction, when being the main or the only process occurring, follows the Tafel relationship with a Tafel slope (b) of very nearly —0.116 V. This indicates that

$$b = -2.303(2RT/F) \tag{8}$$

which is in agreement with previous results (see above). The data in Fig. 6 and in Table 2 with very good approximation also give the following corresponding relationships for the effect of pH on this reaction in the acid chloride solutions (when the current density is not too high):

$$(\partial \log i/\partial \text{ pH})_V = -1 \tag{9a}$$

$$(\partial V/\partial \text{pH})_i = -2.303(2RT/F) \tag{9b}$$

This is the same as previously found by Hoar and Hurlen [15-17] in acid sulphate solutions.

At the higher current densities in the less acid solutions (III and IV) the polarization points fall on a much lower lying and apparently pH-independent Tafel line with the same slope as the other ones. Also at the lower current densities in the solution of the highest pH (IV) does the potential seem to reach this Tafel line after some time (as indicated in Fig. 6) and then to stabilize there. It may certainly be that the potential at the higher current densities also starts at the pH-dependent Tafel line, but falls so rapidly (in less than half a minute) down to the pH-independent line that this possible happening escapes observation by the technique used.

According to the present results and the data given in Table 2, the pH-independent Tafel line has a position corresponding to that to be expected for the pH-dependent lines at a pH of 6.8. This is not far from the neutral point in these solutions which is near to pH 7.07 at 20°C. It seems thus natural to assume that the pH-dependent and the pH-independent Tafel lines represent

a reduction of hydrogen ions and water molecules, respectively, and that the observed transition from the former to the latter of these lines is due to the pH-change accompanying the hydrogen evolution reaction. Such a transition has also been observed by Stern [34] for hydrogen evolution on iron in acid chloride solutions. The slope of the pH-independent Tafel line was by him found to be — 0.174 V at 25°C, however.

The values obtained for the exchange current (i_o) of the H_2/H^+.aq-electrode on iron by extrapolating the Tafel lines in Fig. 6 to the reversible potential of this electrode in the corresponding solutions are covered by the equation

$$-\log i_o \ (20°C) = 5.36 + 0.5 \ pH \qquad (10)$$

where the exchange current is given in A/cm^2. This equation tells that the exchange current is inversely proportional to the square root of the hydrogen ion activity, and that (at 20°C) it should be $10^{-5.36}$ A/cm^2 when pH = 0. One should be aware of the fact, however, that the above results have been obtained mainly in the presence of excess neutral salt, and that divergences very well may occur in the absence of such salt [2]. On this basis, the results compare well with those tabulated by Parsons [60]: $-\log i_o$ = 5.9, 6.29, and 6.19 in 1 M HCl (16°C), 0.01 M HCl (20°C), and 0.001 M HCl (20°C), respectively. Stern [34], however, found an essentially pH-indenpendent exchange current of the order of 10^{-4} A/cm^2 in acidified 4 % sodium chloride solutions at 25°C. It may also be of interest to compare the present results with those of Hoar and Hurlen [15-17] in acid sulphate solutions at 25°C: $-\log i_o$ = 5.9 and 6.3 at pH = 1.5 and 2.4, respectively. The difference in temperature taken into account, it may thus seem that the rate constant of the hydrogen evolution reaction at iron cathodes is very much the same in sulphate as in chloride solutions. In this respect, iron differs distinctly from nickel as electrode material [61,62]. This will be discussed in a subsequent paper.

Iron dissolution

The anodic dissolution reaction has been studied in all the solutions (I—IX) described above, and the polarization data obtained are given in Figs. 7 and 8. In the least acid solution (IX), the tendency of passivation was more marked and the reproducibility somewhat poorer than in the other solutions, and the anodic data obtained in this solution have therefore been omitted.

The results clearly show that the anodic dissolution reaction follows the Tafel relationship except at the higher current densities in the less acid solutions (IV—IX). The deviation from this relationship in the latter cases may be due to an initiation of passivation. The Tafel lines in Figs. 7 and 8 have been drawn with a slope of 0.029 V, and the reasonable fit of these lines to the experimental points (which apply to 20°C) indicates that the Tafel slope (b) of anodic dissolution of active iron is given by

$$b = 2.303(RT/2F) \qquad (11)$$

This is in agreement with the previous results of Hoar and Hurlen [15-17] in acid sulphate solutions, of Bonhoeffer and Heusler [19-21] in acid perchlorate solutions, and also with some of the other results quoted above.

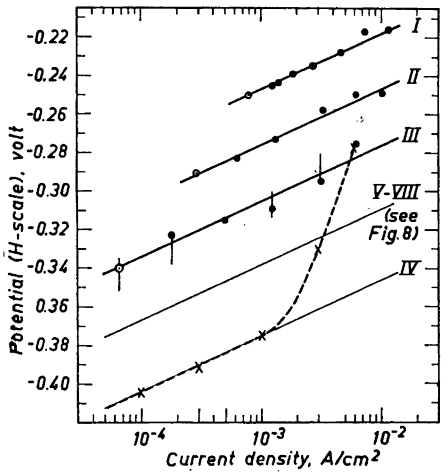

Fig. 7. Tafel diagram for anodic dissolution of iron.

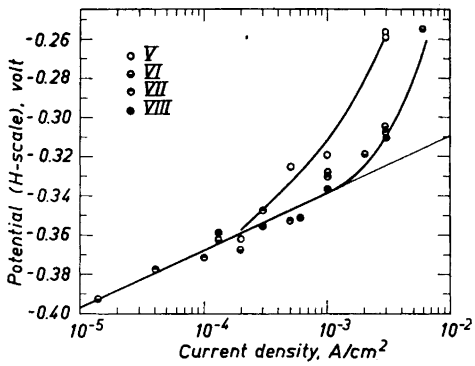

Fig. 8. Tafel diagram for anodic dissolution of iron in the ferrous ion containing solutions V—VIII.

The present data also agree with those of Hoar and Hurlen [15-17] and of Bonhoeffer and Heusler [19-21] in indicating a strong stimulating effect of hydroxyl ions on the dissolution reaction. Fig. 7 shows that the relationships

$$(\partial \log i/\partial \text{ pOH})_V = -1 \tag{12a}$$

$$(\partial V/\partial \text{pOH})_i = 2.303(RT/2F) \tag{12b}$$

with relatively good approximation apply to the results except for those obtained in solution IV. In this solution, the dissolution occurred much faster (by a factor of about twenty) than is to be expected from the above relationships and the results in the other solutions. This exception seemed so strange, especially when compared with the "normal" behaviour of the ferrous chloride containing solutions of very nearly the same pH (V—VIII), that three independent series of experiments were made with solutions of this type. As very nearly idential results were obtained in these series, this matter obviously needs further investigation. It may be that we here have some reason for the somewhat larger pOH-effect found by Bonhoeffer and Heusler [19-21].

The data in Fig. 8 further show that the rate of anodic dissolution reaction on active iron is essentially independent of the ferrous ion activity. Also in this connection, however, solution IV represents an exceptional, although extreme case.

There are no indications that a simultaneously occurring hydrogen evolution reaction does have any effect on the iron dissolution reaction comparable to that found for the opposite case (see above).

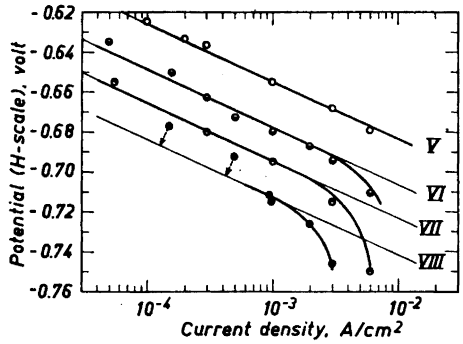

Fig. 9. Tafel diagram for cathodic deposition of iron (effect of ferrous ion activity).

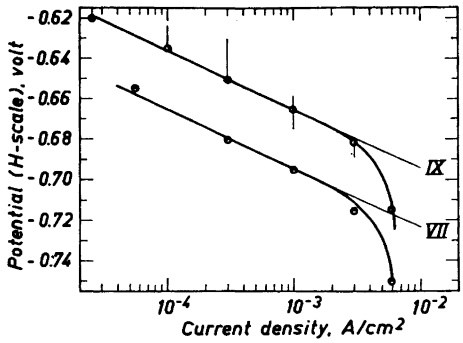

Fig. 10. Tafel diagram for cathodic deposition of iron (effect of pH).

Iron deposition

The polarization data obtained for the iron deposition reaction are given in Figs. 9 and 10. Also this reaction evidently follows the Tafel relationship except at the highest current densities applied. These deviations, however, are easily explained by the transition from activation control to diffusion control when approaching the limiting current. Especially in the solution of the lowest ferrous chloride content (VIII), there also are some distinct deviations at low current densities. In these cases, however, there was a relatively strong simultaneous evolution of hydrogen, and the deviations may very well be due to the pH-change accompanying this process (see below).

The Tafel lines in Figs 9 and 10 have been drawn with a slope of —0.029 V corresponding to

$$b = -2.303(RT/2F) \tag{13}$$

for the iron deposition reaction. This is numerically the same value as for the dissolution reaction, indicating that the Fe/Fe^{++}.aq-electrode behaves symmetrically. Also this is in agreement with the previous results of Hoar and Hurlen [15-17] for iron in acid sulphate solutions.

The results in Fig. 9 further show that the effect of the ferrous ion activity on the rate of the activation controlled deposition reaction is very nearly given by the following corresponding equations:

$$(\partial \log i/\partial \mathrm{pFe})_{V,\ \mathrm{pOH}} = -2 \tag{14a}$$

$$(\partial V/\partial \mathrm{pFe})_{i,\ \mathrm{pOH}} = -2.303(RT/F) \tag{14b}$$

This means that the deposition rate at any given potential and hydroxyl ion activity is proportional to the square of the ferrous ion activity, or, correspondingly, that the variation of the deposition potential with the ferrous ion activity at any given hydroxyl ion activity and deposition rate is twice that of the reversible potential of the Fe/Fe^{++}.aq-electrode. This, which also is in

accordance with the previous results of Hoar and Hurlen [16,17], is simply what thermodynamics requires on the basis of the Tafel slope values and the independence of the anodic Tafel line on the ferrous ion activity.

On the further basis of the pOH-dependence of the anodic Tafel line, thermodynamics also requires that the relationships

$$(\partial \log i/\partial \text{ pOH})_{V,\text{pFe}} = -1 \tag{15a}$$

$$(\partial V/\partial \text{pOH})_{i,\text{pFe}} = -2.303(RT/F) \tag{15b}$$

should apply to the deposition reaction. The results shown in Fig. 10 are in good agreement with these corresponding requirements.

The Fe/Fe^{++}.aq-Electrode

The values obtained for the reversible potential (E) and the exchange current (i_o) of the Fe/Fe^{++}.aq-electrode by extrapolating the Tafel lines for the dissolution and the deposition reaction (Figs. 8—10) to intersection, are covered by the following equations:

$$E(20°C) = -0.467 - 0.029 \text{ pFe} \tag{16a}$$

$$\log i_o(20°C) = 3.58 - \text{pFe} - \text{pOH} \tag{16b}$$

when the activity data in Table 2 are applied, and E and i_o are given in V and A/cm^2, respectively.

Eqn. 16a apparently gives a value of —0.467 V for the standard potential of this electrode at 20°C. However, this value includes both the uncertainties attached to the single ion activities used for the ferrous ion, and the unknown liquid junction potentials between the test solutions and a saturated potassium chloride solution. The observed effects of the ion activities do suggest that these junction potentials are very much the same for all the solutions applied, and the data tabulated by Milazzo [63] for such potentials, do suggest that it should be very small, probably not more than 1—2 mV. The same data also show that the liquid junction in the present cases should be expected to make the experimentally obtained potentials too negative.

The previous work of Hoar and Hurlen [15-17] similarly led to a value of —0.442 V for the standard potential at 25°C. This is close to the so far accepted value [64] of —0.440 V. However, these measurements were made in more acid solutions (pH 1.5—2.4) of relatively low ferrous ion concentration (0.05—0.15 M), and the deposition reaction was accompanied by a much stronger simultaneous hydrogen evolution reaction than in the present work (in which many of the results have been obtained at very nearly 100 % deposition). Even though the sulphate solutions have a better buffer action than the chloride solutions, it may be that the potentials of iron deposition in the previous Hoar-Hurlen work have been affected by a pH-change caused by the hydrogen evolution reaction, and thereby got a too high position in the Tafel diagram (see eqn. 15b).

On this basis, and assuming the applied activity data to represent a fair approximation, the author is inclined to believe that the standard potential of the Fe/Fe^{++}.aq-electrode should be more negative than the at present accepted value of —0.440 V.

Eqn. 16b for the exchange current (as well as eqns. 12 and 15) is written according to the assumption that the observed effect of pH on the iron electrode reactions is caused by the hydroxyl ions and not directly by the hydrogen ions. This assumption is based on the facts

a) that the effect is stoichiometric,
b) that it is positive (stimulating) with regard to hydroxyl ions, but negative (inhibiting) with regard to hydrogen ions,
c) that it is easily explained by a direct interaction of hydroxyl ions in the reactions, and
d) that there seems no reason why a possible inhibiting effect of hydrogen ions should be stoichiometric.

Some evidence for the validity of this assumption is provided by the previous data of Hoar and Hurlen [15,16] on the effect of temperature on the ion electrode reactions in acid sulphate solutions. These results, when treated conventionally, give an unreasonably high value for the virtual heat of activation [2] at the reversible potential. This is most probably due to a relatively strong variation in the activity of some of the reaction participants (what is not accounted for in the conventional treatment). The change in ferrous ion activity and pH with temperature in the applied solutions is relatively small, but pOH changes by more than one and a half unit over the temperature range concerned (0—50°C). This will be more thoroughly discussed in a subsequent paper [65].

Accepting the hydroxyl effect assumption as correct, one may rewrite eqn. 16b in the form:

$$-\log i_o\,(20°C) = 10.59 + \mathrm{pFe} - \mathrm{pH} + \mathrm{pH_2O} \qquad (17)$$

in which the constant is equivalent to "pK_w — 3.58". In the present case, the pH_2O-term is almost negligible. The previous work of Hoar and Hurlen [15–17] in sulphate solutions gave:

$$-\log i_o\,(25°C) = 9.7 + \mathrm{pFe} - \mathrm{pH} \qquad (18)$$

in which equation the negligible pH_2O-term is included in the constant.

The difference between the constants in eqns. 17 and 18 is nearly what is to be expected from the temperature difference on the basis of the heats of activation and the effect of temperature on the dissociation constant of water. This strongly indicates that neither chloride ions nor sulphate ions do have any direct effect on the dissolution and the deposition reaction of an active iron electrode. As there further are distinct differences in the chemical and metallurgical conditions (impurity content, coldwork, annealing) of the electrode materials used in these cases, nor these conditions do seem to have any great effect on these reactions in the pH-range 0 to 4. The hydrogen evolution reaction, however, is strongly influenced by some of these conditions (see the above discussion of previous work).

Thermodynamically, the overall reactions of the $Fe/Fe^{++}.aq$-electrode are undoubtedly represented by:

$$Fe \rightleftharpoons Fe^{++}.aq + 2e^- \tag{19}$$

Kinetically, however, this equation gives a too simplified and partly wrong impression. For characterizing such reactions, the modern theory of electrode kinetics [1,2] introduces the stoichiometric number (ν), which is defined as the number of times the rate determining reaction is represented in the overall electrode reaction considered. The theory further gives the following relationships between ν and other reaction parameters:

$$\nu = b_a b_c nF/2.303RT(b_c - b_a) \tag{20a}$$

$$\partial \log i/\partial pQ = -q/\nu \tag{20b}$$

$$\Delta H^*_{o,a} - \Delta H^*_{o,c} = \Delta H_{o,a}/\nu \tag{20c}$$

in which pQ means the negative logarithm of the activity of a reactant Q with stoichiometric factor q in the overall reaction, and the indexes a and c refer to the anodic and the cathodic reaction, respectively. There are just as many equations of type 20b as there are activity variable components in the overall reaction (only one in the present case), and ν may be determined independently from any of these or from eqn. 20a. To be strictly valid, however, eqn. 20b usually requires that excess inert electrolyte be present. Eqn. 20c can only be used for checking, as a knowledge of ν already is required in the determination of the heats of activation. When ν is known, eqn. 20b can also be applied for determining the stoichiometric factor of a possible interacting component not appearing in the equation for the overall reaction (*e.g.* hydroxyl ions in the present case).

On this basis, the data presented in eqns. 11, 13, 14, and 17 above show that

$$\nu = \tfrac{1}{2} \tag{21}$$

for the $Fe/Fe^{++}.aq$-electrode when its overall reactions are represented by eqn. 19. The data presented in eqns. 12 and 15 further show that the hydroxyl ion effect is accounted for by regarding the hydroxyl ion as a catalytic reactant with the stoichiometric factor

$$q_{OH} = \tfrac{1}{2} \tag{22}$$

in the overall reactions. These results simply mean that the reactions occurring for each act of the rate determining step in either direction of the $Fe/Fe^{++}.aq$-electrode is covered by the equation:

$$2Fe + OH^-.aq \rightleftharpoons 2Fe^{++}.aq + OH^-.aq + 4e^- \tag{23}$$

According to the present results, the above equation represents the smallest repeating reaction unit of the $Fe/Fe^{++}.aq$-electrode. In correspondance with

the terminology used in the crystal structure field, the term *unit reaction* or *kinetic unit reaction* may be proposed for reactions of this type. Just as a unit cell may contain more than one atom, ion, or molecule, a unit reaction may very well comprise more than one reaction step. It may even comprise more than one act of the rate determining step if defined as *the smallest reaction having integral values for all the stoichiometric factors and for the stoichiometric number.*

It is easily seen that the kinetic unit reactions arrived at in the present work (eqn. 23), is thermodynamically in accordance with the previously well established overall reactions of the Fe/Fe^{++}.aq-electrode (eqn. 19).

6.0 DISCUSSION

The hydrogen evolution reaction has been discussed in detail by many authors. As the present results on this reaction at iron cathodes moreover are essentially in agreement with previous data and with what is to be expected from theory [1,2], it will here be refrained from a further discussion of this subject, and the discussion will be confined to the Fe/Fe^{++}.aq-electrode reactions.

The results obtained in eight of the nine electrolyte solutions used in the present work, have been shown to indicate that these reactions are governed by a hydroxyl catalyzed double metal ion mechanism as that covered by eqn. 23. The results in the strange behaving solution (IV) are also in agreement with the double metal ion mechanism, but apparently show a relatively stronger hydroxyl ion interaction than found in the other solutions.

The hydroxyl ion interaction seems to occur stoichiometrically even in solutions in which the activity of this ion is as low as 10^{-14}. However, it is not the bulk activity, but the activity at the electrode surface that counts in such a catalytic interaction as in the present case. Due to the ionic distribution at electrified interfaces, to adsorption and perhaps chemisorption, and to corrosion at anodes and partial hydrogen evolution at cathodes, the latter activity may be much higher than the former. The observed stoichiometry may thus be assumed to indicate an approximately constant proportionality between these two activities, and the above mentioned deviation to be due to a breakdown of this constancy for some reason or another. Further work is needed to clarify this matter.

The Tafel slopes obtained are just what to be expected from a double metal ion mechanism without hydroxyl ion interaction, and this may indicate that the activity of the interacting hydroxyl ions does not change very much with the electrode potential over the regions in which the gradients have been determined. That corresponding Tafel lines intersect somewhat below what to be expected from the ferrous ion activity and the accepted standard potential of this electrode, however, could mean that the effective hydroxyl ion activity is somewhat higher at the anodes than at the cathodes.

According to the results of recent experiments in our laboratory [66], hydroxyl ions do also seem to interact with the Co/Co^{++}.aq-electrode reactions, but not with the reactions of the Ni/Ni^{++}.aq.-, the Cu/Cu^{++}.aq-, and the Zn/Zn^{++}.aq-electrode.

The double metal ion mechanism may be one involving two ferrous ions jointly undergoing a 4-electron process in either direction (Hoar [15]). However, it may just as well be one involving the following two steps:

$$Fe + OH^-.aq \rightleftharpoons Fe^{++}.aq + OH^-.aq + 2e^- \quad (24a)$$

$$Fe \rightleftharpoons Fe^{++}.aq + 2e^- \quad (24b)$$

and the author is inclined to believe more in this than in the former possibility.

The above equations may give the impression that the double metal ion mechanism simply is a consequence of the hydroxyl ion interaction, but this impression obviously is an artificial one only. There must be some more basic reason why just half the iron atoms (or ions) do need the assistance of a hydroxyl ion to make the jump through the electrode interface. That the double metal ion mechanism is not a consequence of the hydroxyl ion interaction, has become even more clear by the recent findings in our laboratory [66] that the pOH-independent reactions of the $Cu/Cu^{++}.aq$-electrode and probably those of the $Ni/Ni^{++}.aq$- and the $Zn/Zn^{++}.aq$-electrode also are governed by such a mechanism, and that this also is the case for the $Co/Co^{++}.aq$-electrode reactions in which there probably is an interaction of one hydroxyl ion for each metal ion reacting in either direction. The double metal ion mechanism may thus seem to be almost a general one for metal/metalion electrodes in aqueous solutions. It is likely, therefore, that it also should have an explanation of equally general character.

As already previously suggested by the author [15–17,62], an explanation may be provided on the basis of the steric conditions at the metal/water interface. In liquid water, the volume per molecule (H_2O) is very nearly 30 Å^3 (see Ref.[52], p. 3). If we as a first approximation regard water as consisting of close-packed spherical molecules, we easily calculate that there should be about 9.54×10^{14} water molecules per cm^2 in a close-packed water plane. In α-iron, the approximate number of atoms per cm^2 is [67]:

1.88×10^{15} in the (111)-plane,
1.73×10^{15} in the (110)-plane,
1.22×10^{15} in the (100)-plane.

The (111)-plane is here the plane of closest packing, and we see that it contains very nearly *twice* the number of iron atoms as there are water molecules in a close-packed water plane. Just as there are more and less closely packed planes in a crystal, one may also imagine the existence of more and less closely packed planes of water molecules. It might further be that the special structure of any surface plane of an iron crystal and the interaction between this plane and the water might favour such a packing of the water molecules at the interface as to give very nearly *one* water molecule for every *two* metal atoms even in those cases where there of purely steric reasons should be space for some more water molecules.

On this basis, the anodic reaction of the $Fe/Fe^{++}.aq$-electrode may be imagined somewhat as follows:

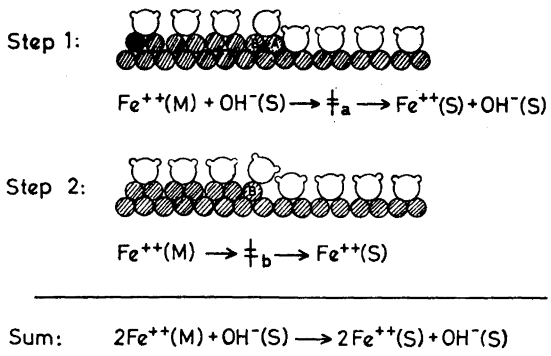

Fig. 11. An illustration to the possible kinetic effect of the steric conditions at an iron/water interface.

Let us consider a "unit" of two iron atoms and one water molecule at the electrode surface. The water molecule interacts with both the iron atoms and is not quite free to "help" only one of them into the solution. The first of these two atoms to dissolve, may therefore need a relatively high energy to make the jump, unless this jump is facilitated by the interaction of a hydroxyl ion. When this atom has left the surface, the water molecule (or another water molecule) may be more free to help the remaining atom to dissolve whereby the energy needed in this case should be smaller. The rate determining step should thus be connected to the removal of the first of these two atoms from the surface. These considerations are illustrated by the sketches in Fig. 11.

Similar considerations could also be given to the cathodic reaction of the Fe/Fe^{++}.aq-electrode and to the reactions of other metal/metalion-electrodes in aqueous solutions.

The hypothesis suggested here could easily be somewhat more elaborated and refined, but it seems unprofitable to do this until more data are available. A more complete discussion will therefore be postponed until the above mentioned work on other metal/metalion-electrodes has been finished.

Acknowledgement. The author is much indebted to Miss T. Tönderum and Miss K. Damm for technical assistance, to various members of the staff at the Central Institute for Industrial Research for valuable discussions, and to the *Royal Norwegian Council for Scientific and Industrial Research* for financial support.

Thanks are also due to Dr. T. P. Hoar and other authorities at the Department of Metallurgy, University of Cambridge, England, for letting me do some previous work on this subject in their laboratories.

REFERENCES

1. Parsons, R. *Trans. Faraday Soc.* **47** (1951) 1332.
2. Bockris, J. O'M. in *Modern Aspects of Electrochemistry* (ed. J. O'M. Bockris), Butterworths, London 1954, Chapter 4.
3. Gerischer, H. *Z. Electrochem.* **55** (1951) 98; **57** (1953) 604; *Z. physik. Chem. (Frankfurt)* **2** (1954) 79; *Angew. Chem.* **68** (1956) 20.
4. Horiuti, J. *J. Research Inst. Catalysis Hokkaido Univ.* **4** (1956) 55.
5. Rüetschi, P. *J. Electrochem. Soc.* **106** (1959) 819.
6. Hoar, T. P. in *Modern Aspects of Electrochemistry No. 2* (ed. J. O'M. Bockris), Butterworths, London 1959, Chapter 4.

7. Gatty, O. and Spooner, E. C. R. *The Electrode Potential Behaviour of Corroding Metals in Aqueous Solutions*, Clarendon Press, Oxford 1938.
8. Evans, U. R. *Metallic Corrosion, Passivity and Protection*, Arnold, London, 2nd ed. 1946; *Introduction to Metallic Corrosion*, Arnold, London 1948; *The Corrosion and Oxidation of Metals*, Arnold, London, 1960.
9. Uhlig, H. H. *Corrosion Handbook*, Wiley, New York 1948.
10. Speller, F. N. *Corrosion, Causes and Prevention*, Mc Graw-Hill, New York and London, 3rd ed. 1951.
11. Tödt, F. *Korrosion und Korrosionsschutz*, de Gruyter, Berlin 1955.
12. Klas, H. and Steinroth, H. *Die Korrosion des Eisens und ihre Verhütung*, Stahleisen, Düsseldorf 1956.
13. Grubitsch, H. *Chem.-Ing.-Tech.* **27** (1955) 287; **28** (1956) 9; **29** (1957) 312.
14. Fischer, H. *Elektrolytische Abscheidung und Elektrokristallisation von Metallen*, Springer, Berlin/Göttingen/Heidelberg 1954.
15. Hoar, T. P. and Hurlen, T. *CITCE VIII (1956)*, Butterworths, London 1958, p. 445; Hurlen, T. *Report (part 1)* to Department of Metallurgy, University of Cambridge, January 1957.
16. Hoar, T. P. and Hurlen, T. *To be published;* Hurlen, T. *Report (part 2)* to Department of Metallurgy, University of Cambridge, January 1957.
17. Hurlen, T. *Tek. Ukeblad* **105** (1958) 101, 119.
18. Rojter, W. A., Juza, W. A. and Polujan, E. S. *Acta Physicochim. URSS* **10** (1939) 389.
19. Bonhoeffer, K. F. and Heusler, K. E. *Z. physik. Chem. (Frankfurt)* **8** (1956) 390.
20. Bonhoeffer, K. F. and Heusler, K. E. *Z. Elektrochem.* **61** (1957) 122.
21. Heusler, K. E. *Z. Elektrochem.* **62** (1958) 582.
22. Kabanov, B., Burstein, R. and Frumkin, A. *Discussions Faraday Soc.* **1** (1947) 259.
23. Kusnezov, J. *Zhur. Fiz. Khim.* **21** (1947) 201.
24. Kaesche, H. *Z. Elektrochem.* **63** (1959) 492.
25. Makrides, A. C., Komodromos, N. M. and Hackerman, N. *J. Electrochem. Soc.* **103** (1955) 363.
26. Gatos, H. C. *J. Electrochem. Soc.* **103** (1956) 286.
27. Hoar, T. P. and Holliday, R. D. *J. Appl. Chem. (London)* **3** (1953) 502.
28. Hoar, T. P. and Farrer, W. T. *To be published;* Farrer, W. T. *Thesis*, Cambridge 1958.
29. Okamoto, G., Nagayama, M. and Sato, N. *CITCE VIII (1956)*, Butterworths, London 1958, p. 72.
30. Stern, M. and Roth, R. M. *J. Electrochem. Soc.* **104** (1957) 390.
31. Conway, B. E. *Chem. in Can.* **9** (1957) 4, 39; **9** (1957) 5, 45.
32. Lyons, E. H. *J. Electrochem. Soc.* **101** (1954) 363, 376.
33. Conway, B. E. and Bockris, J. O'M. *Proc. Roy. Soc. (London)* **A 248** (1958) 394.
34. Stern, M. *J. Electrochem. Soc.* **102** (1955) 609.
35. Stern, M. *J. Electrochem. Soc.* **102** (1955) 663.
36. Fischer, H. and Thoresen, G. *Z. Elektrochem.* **62** (1958) 235.
37. Parsons, R. *Trans. Faraday Soc.* **54** (1958) 1053.
38. Britton, S. C., Hoar, T. P. and Evans, U. R. *J. Iron Steel Inst.* **126** (1932) 365.
39. Hoar, T. P. and Havenhand, D. *J. Iron Steel Inst.* **133** (1936) 239 P.
40. Hoar, T. P. *The Mechanism of Anodic Inhibitors of Corrosion*, paper presented at the Reunion Commune of the Association Belge pour l'Etude, l'Essai et l'Emploi des Materiaux, Corrosion Group, Commission No. IV, June 1954.
41. Engell, H.-J. *Arch. Eisenhüttenw.* **26** (1955) 393.
42. Buck, W. R. and Leidheiser, H. *J. Electrochem. Soc.* **104** (1957) 474.
43. Vermilyea, D. A. *J. Chem. Phys.* **25** (1956) 1254.
44. Grahame, D. C. *Chem. Revs.* **41** (1947) 441; *Ann. Rev. Phys. Chem.* **6** (1955) 337.
45. Butler, J. A. V. *Electrical Phenomena at Interfaces*, Methuen, London 1951.
46. Delahay, P. *New Instrumental Methods in Electrochemistry*, Butterworths, London 1954; Academic Press, New York 1954.
47. Delahay, P. *Ann. Rev. Phys. Chem.* **9** (1958) 229.
48. Breyer, B. *Revs. Pure and Appl. Chem. (Australia)* **6** (1958) 249.
49. Thirsk, H. R., *Ann. Repts. on Progr. Chem. (Chem. Soc. London)* **54** (1957) 17.
50. Fleischmann, M. and Oldham, K. B. *Ann. Repts. on Progr. Chem. (Chem. Soc. London)* **55** (1958) 67.

51. Frumkin, A. N. *Chim. Nauk. Prom.* No. 4, 1958 (translation from Hochschule für Elektrochemie, Ilmenau).
52. Robinson, R. A. and Stokes, R. H. *Electrolyte Solutions*, Butterworths, London 1955, p. 506.
53. Harned, H. S. and Gancy, A. B. *J. Phys. Chem.* **62** (1958) 627.
54. Harned, H. S. and Owen, B. B. *The Physical Chemistry of Electrolytic Solutions*, Reinhold, New York 1943.
55. Guggenheim, E. A. *Thermodynamics*, North-Holland, Amsterdam 1957.
56. MacInnes, D. A. *The Principles of Electrochemistry*, Reinhold, New York 1939.
57. Bjerrum, N. *Acta Chem. Scand.* **12** (1958) 945.
58. Hedström, O. A. *Arkiv Kemi* **5** (1953) 457.
59. Potter, E. C. *Electrochemistry*, Cleaver-Hume, London 1956, p. 112.
60. Parsons, R. *Handbook of Electrochemical Constants*, Butterworths, London 1959, p. 95.
61. Hoare, J. P. and Schuldiner, S. *J. Phys. Chem.* **62** (1958) 229.
62. Hurlen, T. *Paper read at the 10th Meeting of CITCE*, Amsterdam 1958 (to be published).
63. Milazzo, G. *Elektrochemie*, Springer, Wien 1952, p. 98.
64. Latimer, W. M. *Oxidation Potentials*, Prentice-Hall, New York 1952, p. 220.
65. Hurlen, T. *Acta Chem. Scand.* **14** (1960) 1564.
66. Hurlen, T. *To be published.*
67. Smithells, C. J. *Metals Reference Book*, Butterworths, London, 2nd ed. 1955, p. 179.

Received March 25, 1960.

ACTA CHEMICA SCANDINAVICA 14 (1960) 1555–1563

Corrosion of Iron

Effect of pH and Ferrous Ion Activity

TOR HURLEN

Central Institute for Industrial Research, Blindern, Oslo, Norway

The effect of pH and ferrous ion activity on the corrosion potential (E_c) and the corrosion rate (i_c) of iron is considered on the basis of recent data on the kinetics of the $Fe/Fe^{++}aq$- and the $H_2(Fe)/H^+$ aq-electrode. For solutions of negligible ferrous ion content, it is deduced that dE_c/dpH should be $-(4/5)\,(2.303\,RT/F)$ in acid solutions and $-(2/5)\,(2.303\,RT/F)$ in alkaline solutions until the corrosion potential above a certain pH-value (dependent on the hydrogen pressure) becomes nearly equal to the reversible hydrogen potential. It is further deduced that $d\log i_c/dpH$ in these three pH-ranges should be $-3/5$, $+1/5$, and -1, respectively. For solutions of appreciable ferrous ion content, it is shown that the corrosion potential in a certain pH-range (dependent on the ferrous ion activity) should be nearly equal to the reversible iron potential. It is also shown how this will affect the corrosion rate.

The effect of dissolved oxygen and of the ferrous hydroxide precipitation is somewhat discussed, and all the deductions are compared with experimental data.

1.0 INTRODUCTION

It has long been known that the corrosion potential of iron in many acid solutions varies with pH almost (but not quite) parallel to the reversible potential of the hydrogen electrode [1–4]. Some earlier workers apparently believed that the parallelism should be exact, and that the observed deviations were due to experimental faults. However, through the development of *the theory of mixed potentials* [5,6] for corrosion processes, it has become clear that this relationship cannot be more than an accidental one, whereby the observations very well may be correct.

The theory of mixed potentials allows the relationships between corrosion potential (E_c) and corrosion rate (i_c) and pH to be derived from a knowledge of the kinetics of the electrode reactions simultaneously occurring on the corroding metal surface. Such derivations have been attempted by Thomashov [7], Audubert [8], Uhlig [9], Bockris [10], Stern [11], Stern and Geary [12], and Ammar

and Riad [13], but all these derivations suffer from a poor knowledge of the anodic dissolution reaction.

The kinetics of the iron dissolution reaction has recently been studied by the author and others (see Ref.[14]), and some new data are also available on the hydrogen evolution reaction at iron electrodes. On this basis, a theoretical redetermination will here be made of the effect of pH on the corrosion potential and the corrosion rate of iron in air free solutions. The effect of ferrous ions will also be considered, and comparisons will be made with experimental data.

2.0 THEORETICAL DEDUCTIONS

The following symbols shall here be used:

i_c = rate of corrosion
i_{diss} = rate of iron dissolution
i_{dep} = rate of iron deposition
i_H = rate of hydrogen evolution
$i_o(Fe)$ = exhange current of the $Fe/Fe^{++}aq$-electrode
$i_o(H)$ = exchange current of the H_2/H^+aq-electrode
$i_o(OH)$ = exchange current of the H_2/OH^-aq-electrode
E_c = corrosion potential
$E_o(Fe)$ = standard potential of the $Fe/Fe^{++}aq$-electrode
$E_o(H)$ = standard potential of the H_2/H^+aq-electrode
$E_o(OH)$ = standard potential of the H_2/OH^-aq-electrode
V = electrode potential in general

All the rates will be expressed in equivalent units (*e.g.* as partial current densities) and will be regarded positive (regardless of the reactions being anodic or cathodic).

When iron is immersed in a solution, it acquires a corrosion potential and a corrosion rate defined by:

$$E_c = V \tag{1a}$$

$$i_c = i_{diss} - i_{dep} \tag{1b}$$

We shall here mainly consider cases in which hydrogen evolution is the only reaction occurring in addition to the $Fe/Fe^{++}aq$-electrode reactions themselves. For such cases, stationary conditions require

$$i_H = i_{diss} - i_{dep} \tag{2}$$

and the corrosion potential must obviously be that mixed potential at which this equation is satisfied.

In a previous work [14], it has been shown that:

$$\log i_{diss} = J(Fe) - pOH + (2F/2.303\,RT)\,(V - E_o(Fe)) \tag{3a}$$
$$\log i_{dep} = J(Fe) - pOH - 2pFe - (2F/2.303\,RT)\,(V - E_o(Fe)) \tag{3b}$$
$$\log i_{(H)}(a) = J(H) - pH - (F/4.606\,RT)\,(V - E_o(H)) \tag{3c}$$
$$\log i_{(H)}(b) = J(OH) - (F/4.606\,RT)\,(V - E_o(OH)) \tag{3d}$$

where (a) and (b) refer to acid and alkaline solutions, respectively, and

$$J(\mathrm{Fe}) = \log i_o(\mathrm{Fe}) \text{ at } \mathrm{pFe} = \mathrm{pOH} = 0 \quad (4a)$$
$$J(\mathrm{H}) = \log i_o(\mathrm{H}) \text{ at } \mathrm{pH} = 0 \quad (4b)$$
$$J(\mathrm{OH}) = \log i_o(\mathrm{OH}) \text{ at } \mathrm{pOH} = 0 \quad (4c)$$

Strictly, (3c) and (3d) are not always valid at and above the corrosion potential because of a promoting effect of the iron dissolution reaction on the hydrogen evolution reaction [14]. This effect will certainly affect the corrosion, but not necessarily the pH-dependence of the corrosion, and will therefore be neglected in the present treatment.

By the equations (2) and (3), both the mixed potential (V) of the corroding metal and the partial rate of the various reactions (i_{diss}, i_{dep}, i_H) at this potential are completely determined. Through the definitions (1), the corrosion potential (E_c) and the corrosion rate (i_c) are thereby also given as functions of pH, pOH, and pFe at constant temperature.

Solutions of negligible ferrous ion content

Most corrosion cases of practical importance imply aqueous solutions of relatively low ferrous ion content. This content may for the present purpose be regarded negligible when

$$i_{dep} < i_{diss}/100 \quad (5)$$

which, according to (3a) and (3b), means:

$$E_c > E_o(\mathrm{Fe}) - (2.303\, RT/2F)\,(\mathrm{pFe} - 1) \quad (6)$$

In such cases, the corrosion rate is given within an accuracy of 1 % by:

$$i_c = i_H = i_{diss} \quad (7)$$

Remembering $\mathrm{p}K_w = \mathrm{pH} + \mathrm{pOH}$, we easily have from (1a), 3a), (3c), (3d), and (7):

$$E_c(\mathrm{a}) = (2/5)\,(2.303\, RT/F)\,[J(\mathrm{H}) - J\,(\mathrm{Fe}) + \mathrm{p}K_w - 2\mathrm{pH}] + (1/5)\,[E_o(\mathrm{H}) + 4E_o(\mathrm{Fe})] \quad (8a)$$

$$E_c(\mathrm{b}) = (2/5)\,(2.303\, RT/F)\,[J(\mathrm{OH}) - J(\mathrm{Fe}) + \mathrm{p}K_w - \mathrm{pH}]) + (1/5)\,[E_o(\mathrm{OH}) + 4E_o(\mathrm{Fe})] \quad (8b)$$

$$\log i_c(\mathrm{a}) = (1/5)\,[4J(\mathrm{H}) + J(\mathrm{Fe}) - \mathrm{p}K_w - 3\mathrm{pH}] + (2/5)\,(F/2.303\, RT)\,[E_o(\mathrm{H}) - E_o(\mathrm{Fe})] \quad (8c)$$

$$\log i_c(\mathrm{b}) = (1/5)\,[4J(\mathrm{OH}) + J(\mathrm{Fe}) - \mathrm{p}K_w + \mathrm{pH}] + (2/5)\,(F/2.303\, RT)\,(E_o\,(\mathrm{OH}) - E_o\,(\mathrm{Fe})] \quad (8d)$$

For cases in which $\mathrm{p}K_w$, $J(\mathrm{H})$, $J(\mathrm{OH})$, and $J(\mathrm{Fe})$ are independent of pH (this will usually be the case when excess indifferent electrolyte is present), these equations further show:

$$\mathrm{d}E_c(\mathrm{a})/\mathrm{dpH} = -(4/5)(2.303\, RT/F) \quad (9a)$$
$$\mathrm{d}E_c(\mathrm{b})/\mathrm{dpH} = -(2/5)(2.303\, RT/F) \quad (9b)$$
$$\mathrm{dlog}\, i_c(\mathrm{a})/\mathrm{dpH} = -3/5 \quad (9c)$$
$$\mathrm{dlog}\, i_c(\mathrm{b})/\mathrm{dpH} = +1/5 \quad (9d)$$

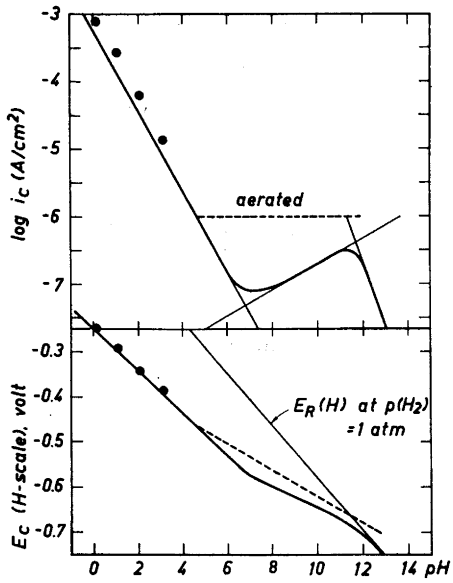

Fig. 1. Calculated effect of pH at a hydrogen pressure of 1 atm. (fully drawn lines) and of dissolved oxygen (stipulated lines) on the corrosion potential and the corrosion rate of iron. The points apply to iron in HCl—KCl—($FeCl_2$) solutions at 20°C (Hurlen[14]).

The deductions represented by eqns. (8) are graphically presented in Fig. 1. The following values have there been used for the various constants [14]:

T = 293° K	pK_w = 14.17		
E_o(H) = 0	E_o(OH) = — 0.82	E_o(Fe) = — 0.46	
J(H) = — 5.36	J(OH) = — 5.07	J(Fe) = 3.58	

By these values, the corrosion rate is given in A/cm² and the corrosion potential in Volt on the normal hydrogen scale.

In Fig. 1 is also indicated what is to be expected when the corrosion potential approaches the reversible potential of the hydrogen electrode, E_R(H). The latter potential can certainly not be exceeded by the former in a completely de-aerated solution, and we have as a limit:

$$(E_c)_{lim} = E_o(H) - (2.303\ RT/F)pH \qquad (10)$$

At this limit, when considering (1a), 3a), (7), and (10), we also have

$$(d\log i_c/dpH)_{lim} = -1 \qquad (11)$$

In all the above calculations, the solutions have been assumed to be in equilibrium with hydrogen of standard atmospheric pressure, and no account has been made of a possible formation of solid corrosion products on the metal surface. Such a formation will certainly affect the corrosion by the resistance barrier it creates for at least some of the part reactions.

The points shown in Fig. 1, represent values experimentally found by the author [14] in HCl—KCl—($FeCl_2$) solutions. These points lie somewhat above the calculated lines because of a promoting effect of the iron dissolution reac-

tion on the hydrogen evolution reaction (see Ref.[14]). The dashed lines in Fig. 1 indicate what is to be expected for the corrosion rate and the corrosion potential when the solution contains dissolved oxygen of an amount giving a limiting oxygen reduction current of 10^{-6} A/cm^2. Also in this case, an upper pH-limit must be reached above which the corrosion potential will be equal to the reversible potential of the oxygen electrode, and the corrosion rate will vary according to (11). This is not shown in Fig. 1. A more detailed discussion of the effect of dissolved oxygen must await further data on the kinetics of the oxygen reduction reaction.

Solutions of appreciable ferrous ion content

Also in ferrous ion containing solutions, we must expect the corrosion rate and the corrosion potential to be in accordance with the above deductions as long as the requirement (6) is obeyed. However, with increasing pH (decreasing E_c) and increasing ferrous ion activity (decreasing pFe) this requirement must subsequently be broken. Under such conditions, we are not allowed to neglect the deposition reaction, and the corrosion rate must be represented by the complete equation (1b). Considering further the equations (2), (3c), (3d), and the obvious limiting condition

$$(E_c)_{lim} = E_o(Fe) - (2.303\, RT/2F)pFe \qquad (12)$$

we easily have:

$$(\log i_c(a))_{lim} = J(H) - pH + \tfrac{1}{4}\, pFe - (F/4.606\, RT)\,[E_o(Fe) - E_o(H)] \qquad (13a)$$

$$(\log i_c(b))_{lim} = J(OH) + \tfrac{1}{4}\, pFe - (F/4.606\, RT)\,[E_o(Fe) - E_o(OH)] \qquad (13b)$$

These deductions are presented graphically in Fig. 2, where they are represented by the curves extending into the dashed lines. These curves represent what is to be expected for the corrosion rate and the corrosion potential if there were no ferrous hydroxide precipitation, and if the solution were in equilibrium with hydrogen of sufficiently low pressure to satisfy the requirement

$$E_R(H) > E_c + (2.303\, RT/F) \qquad (14)$$

all over the pH-range considered.

The completely drawn curves in Fig. 2 represent what is to be expected at a hydrogen pressure of one atmosphere if there were no ferrous hydroxide precipitation. In actual cases, however, precipitation will occur when [15,16]

$$pH = 6.7 + 0.5\, pFe \qquad (15)$$

This equation also gives the minimum pFe (maximum ferrous ion activity) obtainable at any given pH, and it shows how pFe will vary with pH when precipitation occurs.

The curves in Fig. 2 have been crossed at those points at which, from (15), we have to expect the ferrous hydroxide precipitation to start. For any of these curves, that part lying to the right of such a point cannot be realized.

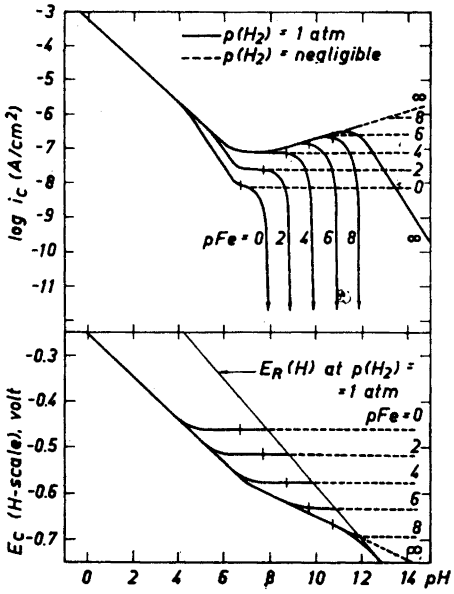

Fig. 2. Calculated effect of pH and ferrous ion activity on the corrosion potential and the corrosion rate of iron at a hydrogen pressure of 1 atm. (fully drawn lines) and at a negligibly small hydrogen pressure (stipulated lines) in the hypothetic absence of ferrous hydroxide precipitation (see the text).

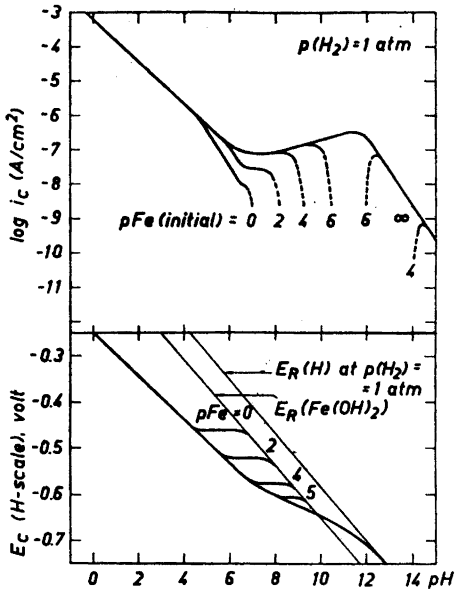

Fig. 3. Effect of pH and ferrous ion activity on the corrosion potential and the corrosion rate of iron at a hydrogen pressure of 1 atm. when regard is made of the ferrous hydroxide precipitation (see the text).

A prediction of how the corrosion potential will behave when precipitation occurs, is given in Fig. 3. It is much more difficult to predict what will happen to the corrosion rate. If the only effect of the precipitation were to decrease the ferrous ion activity, we should expect the corrosion rate to vary along a curve given by the precipitation points (crossed points in Fig. 2) for solutions of lower ferrous ion activity (higher pFe) than the one considered. It is likely, however, that a more marked effect of the precipitation is to give a protective film of ferrous hydroxide on the iron surface. The stability of such a film will probably increase with pH until the ferroate formation begins to destroy it. According to the data given by Pourbaix [15], we should expect that this starts at a pH of about 10.6, and that no precipitate should remain at pH-values above that given by:

$$\mathrm{pH} = 18.3 - \mathrm{pFe\ (initial)} \qquad (16)$$

From (15) and (16), it appears that precipitation should not occur at all in solutions of initial pFe-values above 7.7. In such solutions, therefore, the corrosion of iron is most likely not affected by the ferrous ions whereby the corrosion rate curves should follow the one applying to $\mathrm{pFe} = \infty$. Also in

solutions of initial pFe-values below 7.7, the corrosion must be expected to be independent of the ferrous and the ferroate ions at pH-values above that given by (16). The situation should then be somewhat as shown in Fig. 3.

In this treatment, the homogeneous hydrolysis of the ferrous ion has been ignored, and this seems justified on the basis of the low value ($10^{-9.5}$) found by Hedström [16] for the hydrolysis constant of this ion.

3.0 DISCUSSION

The above deductions have been made without considering the possible effect of impurities in the electrode material and of anions on the reactions of the $Fe/Fe^{++}aq$- and the $H_2(Fe)/H^+aq$-electrode. There are indications [14] that the impurities usually present in mild steel do not affect the iron electrode reations very much, whereas some of them strongly affect the hydrogen evolution reaction. Thereby, the corrosion behaviour will certainly also be affected. However, if the impurity effect is pH-independent, the relative relationship between corrosion and pH may still be as deduced above. There further are indications [14] that neither chloride ions nor sulphate ions do directly affect any of the above reactions. The deductions should therefore apply to both chloride and sulphate solutions. However, it may be a requirement that excess indifferent salt be present. The data used above are namely determined under such conditions, and it is further well known [6] that the effective potential drop at the electrode surface in dilute solutions may be affected by the salt content.

The literature is rich in experimental studies concerning the effect of pH on the corrosion of iron and steel (especially the latter), but only few of these seem to have been carried out under rigorous experimental conditions. Gatty and Spooner [1] have given a general summary of the data obtained up to 1938. They conclude that the variation of the corrosion potential with pH in acid solutions of several types is just that given by (9a) above. It has already been shown (Fig. 1) that this relationship also is in agreement with recent results of the author in acid chloride solutions. It is further in accordance with relatively recent results of Makrides, Komodromos, and Hackerman [17] in acid chloride solutions, of Hoar and Hurlen [18,19] in acid sulphate solutions, and of Bonhoeffer and Heusler [20,21] in acid sulphate and perchlorate solutions. Stern [22,23] and D'Ans and Breckheimer [24] report a variation more parallel to the reversible hydrogen potential.

The relationship (9b) for the corrosion potential in de-aerated alkaline solutions is also in relatively good agreement with the data gathered by Gatty and Spooner [1]. These data further show that the corrosion potential reaches the reversible hydrogen potential at a pH of about 12 and from there on follows this potential. This compares well with the deductions graphically presented in Fig. 1. As (9b) has been deduced partly on the basis of data obtained on the kinetics of the iron dissolution reaction in acid solutions, its good agreement with experimental data may be regarded a strong indication that the dissolution mechanism is the same in alkaline as in acid solutions (see Ref.[14]).

The deductions showing that the corrosion potential in ferrous ion containing solutions should be independent of the ferrous ion activity at low

pH-values and be nearly equal to the reversible potential of the $Fe/Fe^{++}aq$-electrode at somewhat higher pH-values (see eqn. (12) and Figs. 2 and 3) are excellently confirmed by the observations of D'Ans and Breckheimer [24].

The data available on the effect of pH on the corrosion rate of iron are somewhat conflicting. Thus, Stern [22,23] and Bonhoeffer and Heusler [20,21] in their recent work found a nearly pH-independent corrosion rate in solutions of low pH, whereas previous authors mostly have reported a logarithmic relationship to be obeyed under such conditions (see Refs.[1-4]). The recent work of Hoar and Hurlen [18,19] in acid sulphate solutions and of the present author [14] in acid chloride solutions (see Fig. 1) also gave a logarithmic relationship between corrosion rate and pH. Such a relationship is also reported by Novikov [25] and by Balezin and Krasovitskaya [26] as a result of comprehensive investigations on this subject with various types of iron and steel in various types of solutions. The results of the latter authors in acid sulphate solutions moreover agree with those of Hoar and Hurlen in such solutions and with those of the present author in acid chloride solutions in showing a pH-dependence quite near to that given by (9c) above.

The deductions predicting that the corrosion rate should go through a minimum in the vicinity of the neutral point and thereafter increase with pH according to (9d) until it again should fall when the corrosion potential approaches the reversible hydrogen potential (see Fig. 1), may be more difficult to test experimentally. In this pH-region, the measurements may easily be affected by dissolved oxygen (if not adequately removed) and by a possible formation of solid corrosion products on the metal surface (if the ferrous ion content in the solution is not kept low enough). In the vicinity of the neutral point, it is also difficult to have an adequate control of the pH. On this basis, the predicted corrosion-rate/pH relationship shown in Figs. 1 and 3 for iron in alkaline solutions is not in disagreement with the experimental results quoted in the well known corrosion monographs [1-4]. Some authors [27-29] have also experimentally found that the corrosion rate (especially in streaming solutions) goes through a minimum at a pH somewhat below the neutral point and through a maximum at a higher pH (*cf.* Figs. 1 and 3).

The electrode behaviour of corroding iron has been the subject of much study, thought, and speculation. This applies especially to the potential/pH-relationship in acid solutions, which long has been known [1] to be linear with a slope somewhat less than the 58 mV/pH of the reversible hydrogen electrode. Attempts have previously been made to explain this relationship on the assumption either of a hydride film formation on the iron surface [1,30,31] or of a formation of an ideal iron-hydrogen alloy in the surface [24,32-34]. Neither of these explanations have been accepted as satisfactory[20], however. More promising attempts have been made on the basis of the theory of mixed potentials [7-13], but also these have been unsatisfactory, mainly because of a poor knowledge of the kinetics of the iron dissolution reaction.

The present treatment represents a new attempt in solving this classical problem of corrosion science. Also this treatment is based on the theory of mixed potentials, and it applies the improved knowledge which recently has been gained on the iron dissolution reaction [14]. The reasonable fit of the theo-

retical deductions to many experimental data gives rise to the hope that we now are nearer to understand the corrosion behaviour of iron.

Acknowledgement. The author is much indebted to various members of the staff at the Central Institute for Industrial Research for valuable discussions and to the *Royal Norwegian Council for Scientific and Industrial Research* for financial support.

REFERENCES

1. Gatty, O. and Spooner, E. C. R. *Electrode Potential Behaviour of Corroding Metals in Aqueous Solutions*, Clarendon Press, Oxford 1939.
2. Evans, U. R. *Metallic Corrosion, Passivity and Protection*, Arnold, London (2nd ed.) 1946; *The Corrosion and Oxidation of Metals*, Arnold, London, 1960.
3. Tödt, F. *Korrosion und Korrosionsschutz*, de Gruyter, Berlin 1955.
4. Klas, H. and Steinroth, H. *Die Korrosion des Eisens und ihre Verhütung*, Stahleisen, Düsseldorf 1956.
5. Wagner, C. and Traud, W. *Z. Elektrochem.* **44** (1938) 391.
6. Bockris, J. O'M. *Modern Aspects of Electrochemistry*, Butterworths, London 1954, Chapter 4.
7. Tomashov, N. *Compt. Rend. Acad. Sci. U.S.S.R.* **30** (1941) 621.
8. Audubert, R. *J. Chim. Phys.* **49** (1952) C 97.
9. Uhlig, H. H. *Proc. N.A.S.* **40** (1954) 276.
10. Bockris, J. O'M. *Ann. Rev. Phys. Chem.* **5** (1954) 477.
11. Stern, M. *J. Electrochem. Soc.* **102** (1955) 609.
12. Stern, M. and Geary, A. *J. Electrochem. Soc.* **104** (1957) 56.
13. Ammar, I. A. and Riad, S. *J. Phys. Chem.* **62** (1958) 150.
14. Hurlen, T. *Acta Chem. Scand.* **14** (1960) 1533.
15. Pourbaix, M. J. N. *Thermodynamics of Dilute Aqueous Solutions*, Arnold, London 1949.
16. Hedström, O. A. *Arkiv Kemi* **5** (1953) 457.
17. Makrides, A. C., Komodromos, N. M. and Hackerman, N. *J. Electrochem. Soc.* **102** (1955) 363.
18. Hoar, T. P. and Hurlen, T. *To be published;* Hurlen, T. *Report (part 2)* to Department of Metallurgy, University of Cambridge, England. January 1957.
19. Hurlen, T. *Tek. Ukeblad* **105** (1958) 101, 119.
20. Bonhoeffer, K. F. and Heusler, K. E. *Z. physik. Chem. (Frankfurt)* **8** (1956) 390.
21. Heusler, K. E. *Z Elektrochem.* **62** (1958) 582.
22. Stern, M. *J. Electrochem. Soc.* **102** (1955) 609.
23. Stern, M. *J. Electrochem. Soc.* **102** (1955) 663.
24. D'Ans, J. and Breckheimer, W. *Z. Elektrochem.* **56** (1952) 585.
25. Novikov, S. K. *Lenin Moscow State Polytechn. Inst.* **44** (1947) 42 (reviewed in *Corrosion Data Charts, Am. Chem. Soc.* 1952).
26. Balezin, S. A. and Krasovitskaya, T. I. *J. Appl. Chem. U.S.S.R.* **24** (1951) 197 (reviewed in *Corrosion Data Charts, Am. Chem. Soc.* 1952).
27. Larson, T. E. and Skold, R. V. *Corrosion* **14** (1958) 285.
28. Eliassen, R. *J. Am. Water Works Assoc.* **48** (1956) 1005.
29. Fontana, M. G. and Luce, W. A. *Corrosion* **5** (1949) 189.
30. Bodforss, S. *Z. physik. Chem.* **160** (1932) 41.
31. Ergang, R. *Z. Metallk.* **40** (1949) 76.
32. D'Ans, J. and Breckheimer, W. *Naturwiss.* (1951) 282.
33. Hickling, A. and Salt, F. W. *Trans. Faraday Soc.* **38** (1942) 474.
34. Kobosew, N. and Nekrassow, N. J. *Z. Elektrochem.* **36** (1930) 529.

Received March 25, 1960.

ACTA CHEMICA SCANDINAVICA 14 (1960) 1564–1570

Heat of Activation in Electrode Kinetics

The $Fe/Fe^{++}\cdot aq$ Electrode

TOR HURLEN

Central Institute for Industrial Research, Blindern, Oslo, Norway

The treatment of data on the effect of temperature on the rate of electrode reactions is considered, and a way is shown in which the standard heat of activation (ΔH_o^*) of symmetric electrode reactions may be determined. The method is applied to the $Fe/Fe^{++}aq$ electrode reactions, for which the available data indicate:

ΔH_o^* (anodic) = 2 kcal(H-scale)

ΔH_o^* (cathodic) = 44 kcal(H-scale)

The accurary and the meaning of these values are somewhat discussed.

1.0 INTRODUCTION

There seems at present to be some confusion as to the determination of the energy or heat of activation of electrode reactions. The so far most commonly accepted ways of determining such an energy are based on the equations:

$$Q_V = -2.303\, R\, (\mathrm{d}\log i/\mathrm{d}(1/T))_V \qquad (1)$$

$$Q_o = -2.303\, R\, (\mathrm{d}\log i_o/\mathrm{d}(1/T)) \qquad (2)$$

where i_o is the exchange current of the electrode reaction considered, and Q_V and Q_o are called the Arrhenius energy of activation at the potential V and at the reversible potential, respectively.

Bockris [1] has clearly shown that these quantities are not »true» energies or heats of activation, but that they also include other terms, the main of which is proportional to the change in standard heat content for the overall electrode reaction. He therefore has suggested that Q_o be termed »the virtual heat of activation at the reversible potential». This quantity is common for two mutually reverse reactions. The application of (1) and (2) includes moreover the often inadequate assumption that the reactant activities are temperature independent. Eqn. (2) even implies that the activities of the reaction products also are independent of temperature.

Some investigators have improved (2) by putting i_o/T into it instead of merely i_o. This certainly brings the equation in better agreement with the absolute rate theory [2]. However, it does not alter the fact that the quantity determined is not a true heat of activation, and that it therefore is of minor use in revealing the properties of the activated state.

The quantity that would serve best in this respect, is the *standard heat* of activation, as this would give the best basis for comparison with other often well known standard energies connected with the reaction system (*e.g.* heat of reaction, heat of formation, heat of sublimation, *etc.*). Because of the apparent inaccessibility of single electrode potentials, the standard heat of activation of an electrode reaction may at present seem difficult to determine [1]. In the present paper, however, a way is suggested that should be applicable to symmetric reactions. The method is moreover applied to determine the standard heat of activation of the reactions of the $Fe/Fe^{++}aq$ electrode from experimental data previously obtained by Hoar and Hurlen [3].

2.0 THEORETICAL DEDUCTIONS

The standard heat of activation (ΔH_o^*) for any reaction is defined as the change in standard heat content of the reaction system when going from its initial to its activated state:

$$\Delta H_o^* = H_o^* - H_o^{(i)} \tag{3}$$

Quite analogous definitions apply to the standard energy and the standard entropy of activation. All these definitions, however, imply that the initial state should encompass just as many moles of the reactants as there are molecules (or atoms or ions) reacting for each act of the rate determining step. This is not necessarily equal to what is indicated by the equation for the overall reaction considered, but depends on the number of times(ν) the rate determining step occurs when the overall reaction occurs once. Thus, if we choose to define the initial state in the ordinary thermodynamic way (which certainly is the best in order to avoid confusion), (3) must be rewritten in the form:

$$\Delta H_o^* = H_o^* - \frac{1}{\nu} H_o^i \tag{4}$$

From (4), it is further seen that the standard heat of activation of a reaction should be related to that of its reverse reaction and to the ordinary standard heat of reaction by the following equation:

$$\Delta \vec{H}_o^* - \Delta \overleftarrow{H}_o^* = \frac{1}{\nu} \Delta \vec{H}_o \tag{5}$$

In the modern theory of electrode kinetics [1,4], the standard exhange current (J_o) of a reaction system is given by an Arrhenius equation of the following type:

$$\log (J_o/T) = C - \frac{\alpha n F \Delta \emptyset_o}{2.303 \nu RT} - \frac{\Delta H_o^*}{2.303 RT} \tag{6}$$

J_o is defined by

$$J_o = i_o \left[(\Pi a)_r^{1-\alpha} (\Pi a)_p^{\alpha}\right]^{-1/\nu} \tag{7}$$

where i_o is the exchange current at the activity products $(\Pi a)_r$ and $(\Pi a)_p$ of the reactants and the reaction products, respectively, (each activity counting as many times as given by the respective stoichiometric factors in the overall reaction). α is the apparent symmetry factor (equal to $\beta + \gamma$ in Refs.[1,4]) · n is the number of electrons *consumed* during one act of the overall reaction (positive for cathodic and negative for anodic reactions). $\Delta \phi_o$ is the Galvani potential difference between electrode and solution $(\phi_M - \phi_{sl})$ at the standard potential of the reaction system. C consists mainly of temperature independent constants and includes moreover the standard entropy of activation and the activity coefficient of the activated complex (both of which will here be assumed independent of temperature). The presumably small energy term δ introduced by Parsons [4] to represent the possible potential independent part of the electrical contribution to the standard free energy required to transform the system from the two end states (initial and final) to the two states nearest to the activated state (one on each side), may here be regarded either as neglected or as included in the standard heat of activation. It seems so far quite impossible to separate these two energy terms experimentally.

If $\Delta \phi_o$ and its temperature dependence were known, the standard heat of activation of a reaction could have been determined through the relationship (6), but it is well recognized that we so far are unable to determine the Galvani potential difference between two phases. In the case of symmetric reactions, however, we can easily manage without this knowledge. Such reactions are characterized by

$$\alpha = \tfrac{1}{2} \tag{8}$$

For two mutually reverse reactions of this type, the term containing $\Delta \phi_o$ in (6) will be equal in magnitude, but opposite in sign, whereby this term will cancel out in the sum of the heats of activation of these two reactions. We thus have from (6) and (8):

$$2 \log(J_o/T) = \vec{C} + \overleftarrow{C} - \frac{\Delta \vec{H}_o^* + \Delta \overleftarrow{H}_o^*}{2.303\, RT} \tag{9}$$

By differentiating (9) with respect to $1/T$ and combining with (5), we further have:

$$\Delta H_o^* = -2.303\, R \frac{\mathrm{d}\log(J_o/T)}{\mathrm{d}(1/T)} + \frac{1}{2\nu} \Delta H_o \tag{10}$$

From this relationship, we should be able to determine the standard heat of activation of any single electrode reaction for which (8) is valid. However, if hydrogen scale values of ΔH_o are used, ΔH_o^* will also be referred to this arbitrary scale.

3.0 APPLICATION TO THE Fe/Fe^{++}aq ELECTRODE

In a previous work[5], it has been shown that we for the Fe/Fe^{++}aq electrode reactions have:

$$\alpha = \tfrac{1}{2} \tag{11a}$$
$$\nu = \tfrac{1}{2} \tag{11b}$$
$$n_a = -2 \tag{11c}$$
$$n_c = +2 \tag{11d}$$
$$(\Pi a)_a = a_{OH^-}^{1/2} \tag{11e}$$
$$(\Pi a)_c = a_{Fe^{++}} \cdot a_{OH^-}^{1/2} \tag{11f}$$

where the indexes a and c refer to the anodic and the cathodic reaction, respectively. As (11a) is in accordance with (8), the heats of activation of these reactions should be in accordance with (10).

Values obtained by Hoar and Hurlen [3] for the exchange current (i_o) of the Fe/Fe^{++}aq electrode in a solution of 0.05 M $FeSO_4$ + 0.1 M $NaHSO_4$ at 0,25, and 50°C are quoted in Table 1. This table also gives data for the pH of the solutions, for the dissociation constant of water, and for the values thereby obtained for pOH at the three temperatures concerned.

There does not seem to be any direct data available on the effect of temperature on the ferrous ion activity. In this treatment, therefore, we shall assume this effect to be negligible and the ferrous ion activity coefficient to be the same as in a pure ferrous sulphate solution of the same ionic strength. The actual ionic strength is about 0.4 which corresponds to that of 0.1 M $FeSO_4$. From the activity coefficient data given by Robinson and Stokes [7] for similar divalent metal sulphates, we thus have $\gamma_{FeSO_4} = 0.15$. By further assuming the relationship $\gamma_{Fe^{++}} = \gamma_{SO_4^{--}} = \gamma_{FeSO_4}$ to be sufficiently valid, the ferrous ion activity should be as given in Table 1.

From the data in Table 1 and eqns. (11), values have been calculated for the quantity J_o defined by (7). These values are given in Table 2.

In Fig. 1, $\log(J_o/T)$ it plotted against $1/T$, and the line drawn in this diagram, corresponds to:

$$-2.303\,R\frac{d\log(J_o/T)}{d(1/T)} = 23.0 \text{ kcal} \tag{12}$$

Less attention is thereby paid to the data at 50°C than to those at 25 and 0°C. Both the potential measurements and the pH measurements by which the data have been obtained, have namely been carried out with quinhydrone electrodes, and it is well known that such a reference electrode is less reliable at higher temperatures. Strictly, it is not recommended [8] for use at temperatures above 38°C.

The accepted value for the standard heat of reaction of the iron electrode is [9]:

$$\Delta H_{o,a} = -\Delta H_{o,c} = -21.0 \text{ kcal (H-scale)} \tag{13}$$

Table 1. Data for $Fe/Fe^{++}aq$ and activities in 0.05 M $FeSO_4$ + 0.1 M $NaHSO_4$ at various temperatures

Temperature (°C)	0	25	50
Exchange current[3] (A/cm^2)	3.9×10^{-14}	2.5×10^{-11}	1.2×10^{-9}
pH (Ref.[3b])	1.317	1.474	1.615
pK_w (Ref.[6])	14.944	13.997	13.262
pOH (see text)	13.627	12.523	11.647
a_{Fe++} (see text)	(0.0075)	0.0075	(0.0075)

Table 2. Calculated values of J_o (defined by (7)) at various temperatures

T (°C)	0	25	50
log J_o (A/cm^2)	2.343	4.046	4.851
log (J_o/T)	−0.093	1.572	2.342

From (10), (11b), (12), and (13), we then have for the standard heats of activation of the iron electrode reactions:

$$\Delta H^*_{o,a} = 2 \text{ kcal (H-scale)} \tag{14a}$$

$$\Delta H^*_{o,c} = 44 \text{ kcal (H-scale)} \tag{14b}$$

As these values are based on measurements at three different temperatures only, and the data for one of these temperatures probably are less reliable, they cannot be regarded very much accurate. It is not likely, however, that they should be more than 1-2 kcal wrong in either direction. The data obtained at 50°C may further possibly indicate that they are rather too high than too low.

It has previously [5] been shown that the kinetic unit reactions (the reaction occurring for each act of the rate determining step) of the $Fe/Fe^{++}aq$ electrode are represented by:

$$2Fe + OH^- \rightleftharpoons 2Fe^{++} + OH^- + 4e^- \tag{15}$$

This means that the heats of activation refer to the transfer of two gram-atoms iron and one gramatom hydroxyl ions from the initial to the activated state. Thus, if one should like to express these heats as energy per gramatom iron, the values obtained must be divided by two.

Even though the present results are based on rather meager experimental data, it seems justified to conclude that the standard enthalpy of the activated state of the $Fe/Fe^{++}aq$ electrode is not much higher than that of the reduced

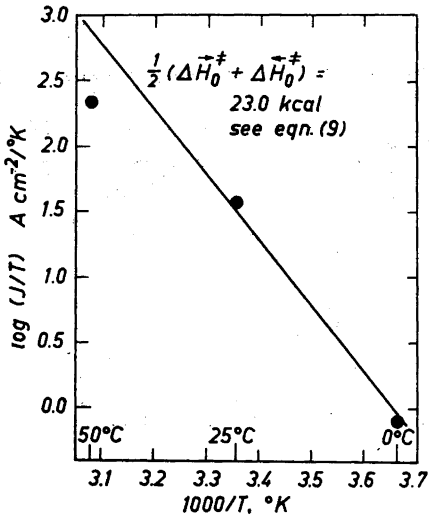

Fig. 1. Arrhenius plot for the standard exchange current of the $Fe/Fe^{++}aq$ electrode.

state (the initial state of the anodic reaction) of this electrode. It should have been interesting to compare the iron electrode with other metal/metal-ion electrodes in this respect. As far as we know, however, this is the very first determination of the standard heat of activation of any such electrode reaction, and further work is therefore needed before a comparison can be made.

4.0 DISCUSSION

In the well known monograph by Bockris [1] on electrode kinetics, it is stated that »little interest attaches to the evaluation of the standard heats of activation of electrode reactions because the potentials to which they refer cannot be experimentally determined». In this connection, Bockris also refers to a work of Temkin[10]. To the author, however, this statement seems rather strange. The standard heat of activation is namely a pure chemical term that is independent of the potential in just the same way as the standard heat of reaction. It should therefore be no more need of referring the one than the other of these quantities to any special potential.

Another problem is that the standard heat of activation may be difficult to determine because of the inaccessibility of single electrode potentials (see eqn. (6)). In the present paper, however, it has been shown that this problem is easily eliminated in the case of symmetric reactions ($\alpha = \frac{1}{2}$). As most electrode systems appear to be symmetric (or nearly symmetric), the way here suggested for the determination of standard heats of activation might have a rather wide applicability.

Acknowledgements. The author is much indebted to various members of the staff at the Central Institute for Industrial Research for valuable discussions and to the *Royal Norwegian Council for Scientific and Industrial Research* for financial support.

REFERENCES

1. Bockris, J. O'M. *Modern Aspects of Electrochemistry*, Butterworths, London 1954, Chapter 4.
2. Glasstone, S., Laidler, K. J. and Eyring, H. *Theory of Rate Processes*, McGraw Hill, New York 1941.
3. Hoar, T. P. and Hurlen, T. *CITCE VIII (1956)*, Butterworths, London 1958, p. 445; Hurlen, T. *Report (Part I)* to the Department of Metallurgy, University of Cambridge, England, January 1957.
4. Parsons, R. *Trans. Faraday Soc.* **47** (1951) 1332.
5. Hurlen, T. *Acta Chem. Scand.* **14** (1960) 1533.
6. Robinson, R. A. and Stokes, R. H. *Electrolyte Solutions*, Butterworths, London 1955, p. 506.
7. See Ref.[6], p. 487.
8. Kolthoff, I. M. and Laitinen, H. A. *pH and Electro-Titrations*, McGraw Hill, New York (2nd Ed.) 1948, pp. 91—96.
9. Latimer, W. M. *Oxidation Potentials*, Prentice-Hall, New York 1952, p. 220.
10. Temkin, M. *Zhur. Fiz. Khim.* **22** (1948) 1081.

Received March 25, 1960.

ACTA CHEMICA SCANDINAVICA 14 (1960) 1571–1579

Studies in the Determination of Silica

III. Interference from Aluminum, Iron and Fluorine in the Spectrophotometric Determination of Silica

LARS HENRIK ANDERSSON

Dept. of Analytical Chemistry, Institute of Chemistry, University of Uppsala, Uppsala, Sweden

Experiments with the effects of aluminum, ferric iron and sodium fluoride on the spectrophotometric silica determination are described. In the presence of aluminum the lower limit for the molybdate concentration is higher than that found for solutions containing only silica, sodium molybdate and acid. Sodium fluoride has qualitatively the same effect as aluminum. In connection with the work of Langmyhr and Graff [1] some experiments with solutions containing aluminum and sodium fluoride have also been made, which show that the pH must sometimes be chosen lower than recommended by them. In the case of iron only small amounts may be present. Iron interference has been eliminated by extraction of the iron-acetylacetone complex with carbon tetrachloride.

Ferric iron and aluminium react in water solutions with molybdate ions to form 2-heteropoly-12-molybdate ions and salts [2]. The presence of Fe(III) and Al(III) in solutions in which silica is to be determined spectrophotometrically as α-silicomolybdate may therefore have the effect of diminishing the amount of molybdate available for silicomolybdate formation. Another source of error which must be investigated is that an iron compound with molybdate may precipitate under certain conditions, removing some silicomolybdate from solution as a coprecipitate. Ferric molybdate solutions are also yellow in color at low pH values, causing high blanks. King *et al.*[3] found that small amounts of iron did not interfere with their molybdenum blue method.

When fluoride is present at least three specific effects should be considered: (1) glass vessels are attacked at low pH, (2) fluoride ions (hydrofluoric acid) may react with molybdate ions and/or (3) with silicic acid. Langmyhr and Graff [1] added aluminium to eliminate interference from fluoride in the determination of silica in hydrofluoric acid.

1. EXPERIMENTAL DETAILS

Extinction measurements were made as earlier described [4]. The temperature was 20.0° in all cases. The wavelength was 400 mμ.

pH measurements were in general carried out using a calomel reference electrode with asbestos fibre in the liquid junction. This electrode could not be used in solutions containing large amounts of aluminum chloride. An electrode with an open, bent up tip was used in such cases.

The chemicals used were of analytical grade. Acetylacetone was distilled once using a small Vigreux column.

Care must be taken that solutions containing fluoride do not remain in contact with glass long enough to dissolve measurable amounts of silica from the glass. At room temperature it is possible to handle solutions 0.1 M in NaF and 0.2 M in HCl in measuring flasks if dilution and mixing is done quickly.

If not otherwise stated, the following procedure was used in the experiments which are described later.

The silica solution was mixed with solutions of the interfering element in a polythene beaker, the pH was adjusted to the desired value and sodium molybdate solution having about the same pH was added. The pH was once more adjusted and the contents of the beaker transferred to a polythene bottle, which was placed on the steam bath. A longer heating time than that recommended earlier [4] was required with solutions containing fluoride or aluminum: 6 hours have always been sufficient. When equilibrium was reached the bottles were placed in a thermostat (20.0°C) and the solutions diluted to volume in measuring flasks before the extinction measurements

2. INTERFERENCE FROM SODIUM FLUORIDE

The ionic and molecular species that exist in aqueous solutions of sodium fluoride are determined by the following equilibria:

$$HF = H^+ + F^-$$
$$HF + F^- = HF_2^-$$

In 0.53 M KNO_3 solutions the equilibrium constants have been reported to be $10^{-2.91}$ and $10^{-0.56}$, respectively [5]. In the pH interval 1.0—4.0 the concentration of the undissociated hydrofluoric acid varies considerably with pH.

Preliminary experiments indicated that the presence of sodium fluoride increased the minimum concentration of molybdate required to obtain the full silicomolybdate color. This is shown in the following experiment, which is quite analogous to the one referred to on page 500, section 3.4 in the first paper in this series [4].

The standard procedure described in section 1 was applied. The final solutions were 0.114×10^{-3} M in Si * and 0.02 M in NaF: pH was adjusted with HCl to 3.5 and 1.5 in the solutions placed on the steam bath. The volume was then about 45 ml and the final volume was 50 ml.

In Fig. 1 the results are shown together with the curve from Fig. 5 in the previous paper [4]. The effect of decreasing the pH is to increase the effective molybdate concentration. If, however, a comparatively large excess of sodium molybdate is used, the pH interval for complete silico-molybdate formation is about the same as that obtained earlier when no fluoride was added. This is demonstrated in the following experiment.

* In the previous paper [4] sections 3.2, 3.3 and 3.4, the silica concentration is incorrectly given as 0.144×10^{-3} M in Si: the correct value is 0.114×10^{-3} M in Si.

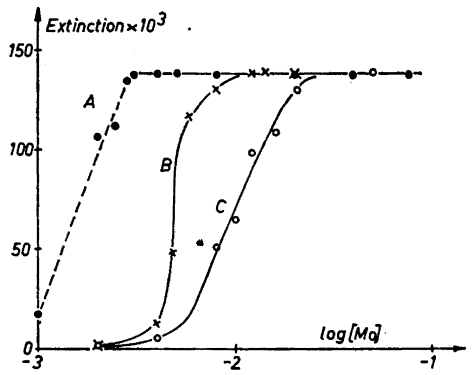

Fig. 1. Extinction as a function of the molybdate concentration for solutions containing sodium fluoride.
Curve A: 0.114×10^{-3} M Si, pH 2.0 with HCl.
Curve B: 0.114×10^{-3} M Si, 0.02 M NaF, pH 1.5 with HCl.
Curve C: » » » » » » » 3.5 » »

The standard procedure was applied. The final solutions were 0.117×10^{-3} M in Si, 0.02 M in NaF and 0.08 M in Na_2MoO_4. pH was varied between 1.0 and 4.0 by adding HCl.

The results of this experiment are given in Table 1. The extinction of blank solutions varies strongly at low pH values. Such a variation is not observed in solutions containing only silica, sodium molybdate and, *e.g.*, hydrochloric acid. Some experiments made at pH 1.0 resulted in the formation of a white precipitate: extinctions of such solutions were too low.

Langmyhr and Graff [1] have studied the behavior of solutions containing more fluoride than in the cases here treated. They show that the interfering action of fluoride can be eliminated if aluminium is added. Some experiments related to their paper are described in section 3.2.

Table 1. Extinction of silicomolybdate solutions containing sodium fluoride as a function of pH.

pH	Extinction of blank solution	Net extinction of silica solution
1.0	0.029	0.122 *
1.5	19	143
2.0	14	142
2.5	7	144
3.0	6	144
3.5	6	142
4.0	6	144

* Remark: Precipitate formed.

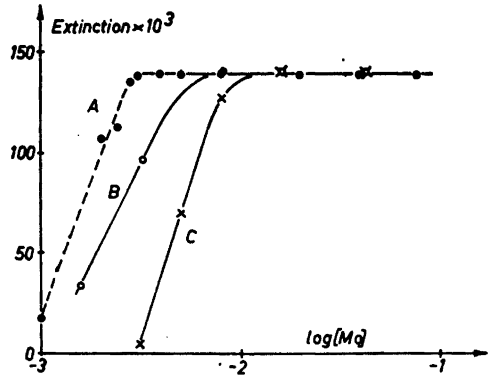

Fig. 2. Extintion as a function of the molybdate concentration for solutions containing aluminum chloride.
Curve A: 0.114 × 10^{-3} M Si, pH 2.0 with HCl.
Curve B: » » » 1.2 × 10^{-3} M Al.
Curve C: » » » 6.0 × 10^{-3} M Al.

3. INTERFERENCE FROM ALUMINUM

3.1. The effect of aluminum on the lower limit of sodium molybdate concentration.

Using the standard procedure solutions with two different aluminum concentrations were prepared. The final solutions were 0.114 × 10^{-3} M in Si, 0.0012 or 0.006 M in $AlCl_3$ and with varying sodium molybdate concentration. The pH was 2.0.

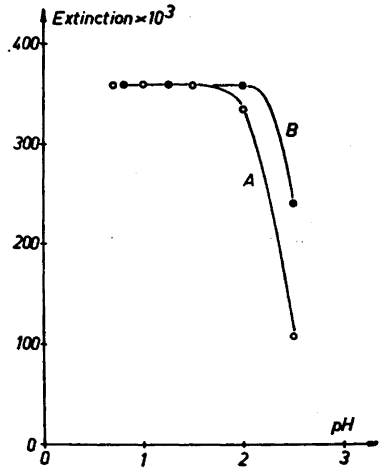

Fig. 3. Extinction as a function of pH for solutions containing aluminum chloride at two different sodium molybdate concentrations.
Curve A: 0.294 × 10^{-3} M Si, 0.1 M $AlCl_3$, 0.04 M Na_2MoO_4.
Curve B: » » » » » » 0.1 » »

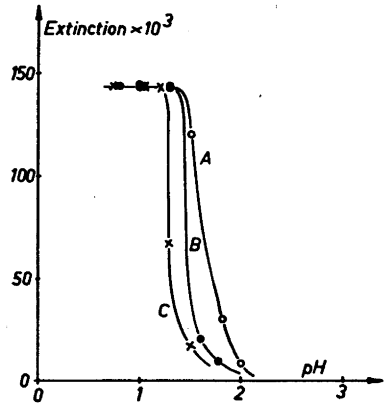

Fig. 4. Extinction as a function of pH for solutions containing sodium fluoride and large amounts of aluminum chloride.
Curve A: 0.114 × 10^{-3} M Si, 0.02 M NaF, 3.2 × 10^{-3} M Na_2MoO_4, 0.15 M Al.
Curve B: » » » » » » » » » 0.3 » »
Curve C: » » » » » » » » » 0.6 » »

Fig. 2 shows the resulting curves: the extinction has been plotted against log [Mo]. The lowest value of sodium molybdate necessary for a full development of the silicomolybdate color is higher than when no aluminum has been added.

3.2. Variation of pH in solutions of silica, sodium molybdate and aluminum chloride.

Using the standard procedure two series of solutions were prepared, which when measured in the spectrophotometer were 0.294 × 10^{-3} M in Si, 0.1 M in $AlCl_3$ and either 0.04 or 0.1 M in Na_2MoO_4. The pH was adjusted to different values with HCl.

In Fig. 3 the extinctions from the last experiments are plotted as functions of pH. The useful pH range is restricted and is a function of the molybdate concentration. It was found that a precipitate was formed when the pH was higher than about 2.5.

3.3. Experiments on the usefulness of aluminum chloride additions as a means of eliminating fluoride interference.

Langmyhr and Graff [1] were able to determine silica in hydrofluoric acid by the silicomolybdate method by adding aluminum chloride, which forms complexes with fluoride ions. They state that when their method is used the pH can be chosen anywhere in the interval 0.5—1.5. It is our experience however that the upper limit should be somewhat lower than 1.5. The following experiment is illuminating.

Using the standard procedure, series of solutions with varying pH were prepared. The aluminum concentration varied from series to series. The final solutions were 0.117 × 10^{-3} M in Si, 0.02 M in NaF and 3.2 × 10^{-3} M in Na_2MoO_4.

The curves from this experiment (Fig. 4) show that in the vicinity of pH 1.5 the extinction is a function of pH and of the aluminum concentration. It must therefore be concluded that a lower pH value than 1.5 must sometimes be chosen.

4. INTERFERENCE FROM FERRIC IRON

4.1. The presence of comparatively large amounts of iron.

If a sodium molybdate solution is mixed with a ferric chloride solution under suitable conditions, a white precipitate is formed. The possibility of determining silica spectrophotometrically in solutions in contact with such precipitates has been investigated.

The standard procedure was applied. pH was adjusted with HCl to 1.5. The final solutions were 0.3×10^{-3} M in Si, 0.05 M in Na_2MoO_4 and up to 12×10^{-3} M in $FeCl_3$. Heating on the steam bath was maintained for 3 h. The solutions were then placed in a thermostat (20.0°C) and the extinctions measured as soon as the supernatant liquids were clear. The extinction measurements were repeated several times during a period of 7 days.

The results of extinction measurements on solutions which have been allowed to stand 24 h in the thermostat are shown in Fig. 5. Measurements earlier and later indicate that the extinction of solutions in contact with precipitates is not constant but a function of time.

4.2. The presence of small amounts of iron. Variation of pH.

The investigations by Baker *et al.*[2] show that colorless complexes between ferric iron and molybdate are formed at pH values lower than about 4. It might therefore be possible to determine silica spectrophotometrically in the presence of small amounts of iron if the pH is chosen high enough.

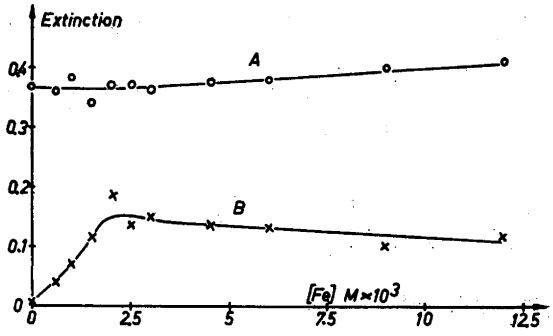

Fig. 5. Extinction in solutions containing large amounts of $FeCl_3$ as a function of the ferric iron concentration.
Curve A: 0.3×10^{-3} M Si, 0.05 M Na_2MoO_4, pH 1.5 with HCl.
Curve B: 0.05 M Na_2MoO_4, pH 1.5 with HCl.

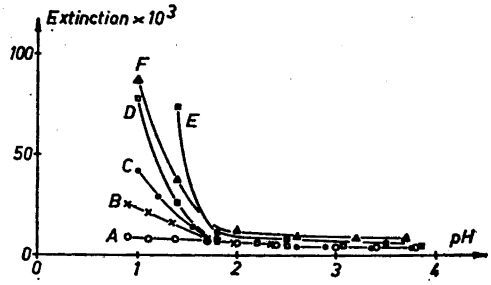

Fig. 6. Extinction of blank solutions as a function of pH at various $FeCl_3$ concentrations.
Curve A: 0.03 M Na_2MoO_4.
Curve B: » » » ,0.036 × 10^{-3} M $FeCl_3$.
Curve C: » » » ,0.09 × 10^{-3} » »
Curve D: » » » ,0.3 × 10^{-3} » »
Curve E: » » » ,0.9 × 10^{-3} » »
Curve F: 0.06 » » ,0.3 × 10^{-3} » »

Clarke [6] gave the average percent composition with respect to silicon and iron of igneous rocks as 59 % SiO_2, 3 % Fe_2O_3 and 4 % FeO. This corresponds to a Si:Fe mole ratio of roughly 10:1. If silicon is to be determined spectrophotometrically in rock analysis an iron concentration of about 0.03 × 10^{-3} M

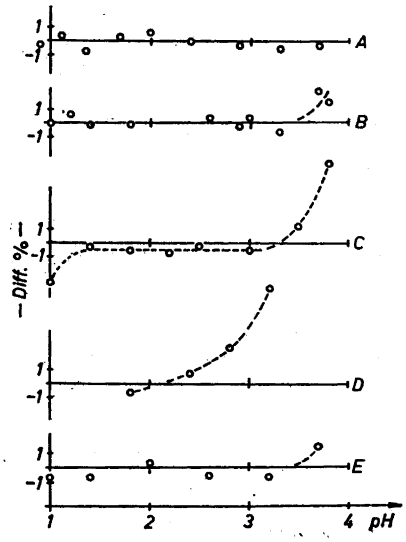

Fig. 7. Difference (in per cent of the total extinction) between measured and calculated extinction as a function of pH at various $FeCl_3$ concentrations.
Curve A: 0.3 × 10^{-3} M Si, 0.03 M Na_2MoO_4, 0.036 × 10^{-3} M $FeCl_3$
Curve B: » » » » » 0.09 × 10^{-3} » »
Curve C: » » » » » 0.3 × 10^{-3} » »
Curve D: » » » » » 0.9 × 10^{-3} » »
Curve E: » » » 0.06 » » 0.3 × 10^{-3} » »

Table 2. Extinction of silicomolybdate solutions from which iron has been removed by extraction with acetylacetone-carbon tetrachloride.

Final silica concentration (molarity)	Extinction of fluoride-free solution	Extinction of fluoride-containing solution	Calculated extinction
0.396×10^{-4}	0.048	0.049	0.048
0.396×10^{-4}	0.047	0.049	0.048
0.396×10^{-4}	0.047	0.050	0.048
0.396×10^{-3}	0.482	0.478	0.482
0.396×10^{-3}	0.484	0.484	0.482
0.396×10^{-3}	0.485	0.483	0.482

is to be expected for a silica concentration chosen to give an extinction of about 0.35.

The standard procedure was used and the final solutions were 0.3×10^{-3} M in Si, 0.03 or 0.06 M in Na_2MoO_4 and 0.036×10^{-3}, 0.09×10^{-3}, 0.3×10^{-3} or 0.9×10^{-3} M in $FeCl_3$. The pH was adjusted with HCl.

The results are shown in Figs. 6 and 7. The blank solutions containing ferric iron show a marked increase in extinction measured against water when the pH sinks below about 2. They are then strongly pH-dependent. For higher pH values the blank extinctions are low and uninfluenced by small changes in pH and ferric iron concentration. However, iron concentrations higher than about 0.3×10^{-3} M should not be used, since the results are then usually too high, especially at high pH values. At low pH values, precipitates may also be formed.

4.3. The effect of anions other than Cl^-.

If the anions SO_4^{2-}, NO_3^- and ClO_4^- are substituted for Cl^- in the experiments described above, results are similar except that precipitates formed more easily in HNO_3 and $HClO_4$ solutions, and the interfering action of small iron concentrations was more pronounced in H_2SO_4 solutions. Attempts to use F^- ions for complexing ferric ions proved unsuccessful.

5. EXTRACTION OF FERRIC IRON PRIOR TO THE SPECTROPHOTOMETRIC SILICA DETERMINATION

Several methods to extract ferric iron from aqueous solutions into organic phases using complexing substances are described in the literature [7]. In connection with the work presented here, it was important that after the extraction had been made, it should be possible to determine accurately the amount of silica in the remaining water phase, and that the amount of silica present before extraction should be the same as that present after extraction. The possibility that fluoride may be present had also to be taken into account.

In the method finally adopted, acetylacetone was used as the complexing agent and carbon tetrachloride as the extracting solvent. If no fluoride was present, extraction was made at pH 4. The separatory funnels were conditioned before extraction by soaking overnight in dilute HCl (pH 4). In this way, interference from dissolved glass was considerably reduced. When fluoride was present the extractions were carried out in platinum dishes at pH 7.5; the phases were mixed by a motordriven aluminum stirring rod. The heavy organic phase was drawn off with pipettes with long capillary tips.

The composition of the solutions which were extracted was about 0.57×10^{-3} M in Si, 8.6×10^{-3} M in $FeCl_3$ and in cases where fluoride had been added 30×10^{-3} M in NaF. 2 ml acetylacetone was added to this solution, pH was adjusted with HCl to the appropriate value and the extractions carried out.

When the iron had been removed with three extractions of the water phase (about 35 ml) using 5 ml portions of CCl_4, 0.50 g sodium carbonate was added to the remaining water phase in a platinum dish. After evaporation to dryness on the steam bath, the remaining organic compounds were destroyed by heating the dish over a Meker burner until a clear melt was formed. The contents of the dish were then dissolved in water and the amount of silica left determined spectrophotometrically.

The results from these experiments are summarized in Table 2.

I wish to thank Dr F. Nydahl, Head of the department of Analytical chemistry, for his interest in this investigation and for the facilities put at my disposal.

REFERENCES

1. Langmyhr, F. J. and Graff, P. R. *Anal. Chim. Acta* **21** (1959) 334.
2. Baker, L. C. W., Foster, G., Tan, W., Scholnick, F. and McCutcheon, T. P. *J. Am. Chem. Soc.* **77** (1955) 2136.
3. King, E. J. *et al.*, *Analyst* **80** (1955) 441.
4. Andersson, L. H. *Acta Chem. Scand.* **12** (1958) 495.
5. Brosset, C. *Svensk Kem. Tidskr.* **54** (1942) 155.
6. Clarke, F. W. *Bull. U.S. Geol. Survey* **No. 770** (1924) 29.
7. Sandell, E. B. *Colorimetric Determination of Traces of Metals*, New York 1959.

Received April 27, 1960.

ACTA CHEMICA SCANDINAVICA 14 (1960) 1580–1596

Perjodatoxydation von Phenolen

VII *. 2,6-Dimethylphenol sowie 2,4,6- und 2,3,5-Trimethylphenol

ERICH ADLER, JOSEF DAHLÉN und GERTRUD WESTIN

Institutionen för organisk kemi, Chalmers Tekniska Högskola, Göteborg, Schweden

2,6-Dimethylphenol und 2,4,6-Trimethylphenol liefern bei der Einwirkung von Perjodat die entsprechenden dimeren *o*-Chinole (VIII bzw. IV) neben 2,6-Dimethyl-*p*-chinon bzw. 2,4,6-Trimethyl-*p*-chinol, während 2,3,5-Trimethylphenol ein Gemisch von monomerem 2,3,5-Trimethyl-*o*-chinol (XI) und 2,3,5-Trimethyl-*p*-chinon gibt.

Die Dimeren VIII und IV lassen sich mit AcOAc–$HClO_4$ in die Diacetylderivate überführen, welche bei 180° Retrodienzerfall zu 2,6-Dimethyl-*o*-chinolacetat bzw. 2,4,6-Trimethyl-*o*-chinolacetat erleiden. Bei 120° geht 2,6-Dimethyl-*o*-chinolacetat wieder in sein Dimeres über. Bei alkalischer Verseifung wird aus dem Diacetat des Dimeren IV letzteres zurückgebildet, während aus dem Diacetat des Dimeren VIII teils das Dimere VIII, teils — unter Abspaltung von 1 Mol HOAc — ein phenolisches Anhydro-dimeres (XXIII) entsteht.

Diese Ergebnisse stehen in Einklang mit den Strukturen VIII bzw. IV für die beiden *o*-Chinoldimeren.

In einer früheren Mitteilung [1] wurde gezeigt, dass der rasch verlaufende Angriff von Natriumperjodat auf 2,4-Dimethylphenol hauptsächlich zu den beiden *ortho*-Oxydationsprodukten, dem 2,4-Dimethyl-*o*-chinol und dem 3,5-Dimethyl-*o*-chinon, führt. In geringem Ausmass entstand das *p*-Oxydationsprodukt, 2,4-Dimethyl-*p*-chinol. Das gebildete *o*-Chinol war in monomerer Form nicht existenzfähig, sondern stabilisierte sich sofort teils durch Dimerisierung, teils durch Addition an das 3,5-Dimethyl-*o*-chinon zu Derivaten des 1,4-Äthenonaphthalins. Beide Stabilisierungsreaktionen sind Diels-Alder-Additionen.

Erwartungsgemäss verbrauchte auch 2,4,6-Trimethylphenol (Mesitol, I) in wässriger Lösung sehr rasch 1 Mol Perjodat. In dem nach einer Oxydationsdauer von 5 Min. mittels Methylenchlorid extrahierbaren Gemisch der Reaktionsprodukte liess sich IR-spektroskopisch kein Mesitol mehr erkennen. Das

* VI. Mitt. (vorläufige Mitteilung zur vorliegenden Arbeit): Adler, E., Dahlén, J. und Westin, G. *Acta Chem. Scand.* **14** (1960) 512.

Rohprodukt konnte leicht aufgetrennt werden in 2,4,6-Trimethyl-*p*-chinol (II) [2] (Ausbeute 28 %) und eine Substanz vom Schmp. 182—183°, welcher nach Analyse und Molekulargewichtsbestimmung die Zusammensetzung $C_{18}H_{24}O_4$ zukam (Ausbeute 53 %). Es war naheliegend, in dieser Substanz ein durch Diels-Alder-Reaktion gebildetes Dimeres des primär zu erwartenden 2,4,6-Trimethyl-*o*-chinols (III) anzunehmen, und nach den beim 2,4-Dimethylphenol gemachten Erfahrungen kamen in erster Linie die Strukturen IV und IVa in Betracht (vorläufige Mitteilung, s. Zitat [3]).

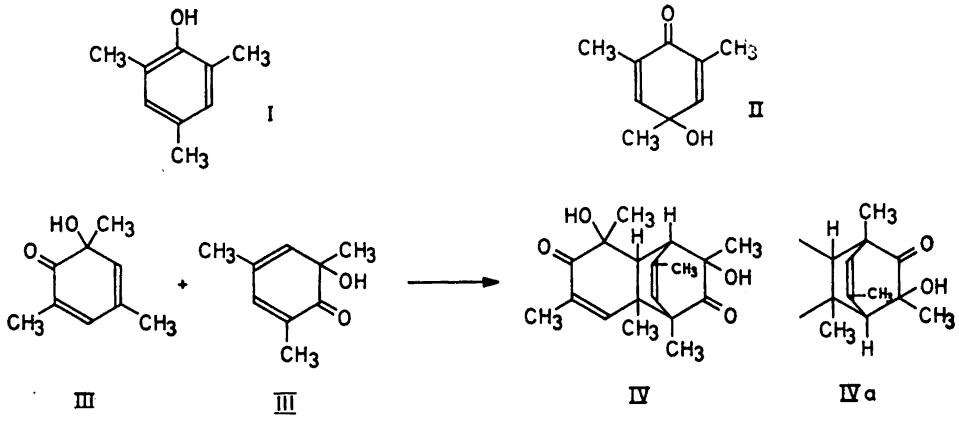

2,6-Dimethylphenol (V) reagierte ebenfalls rasch mit Natriumperjodat und lieferte nach Verbrauch von etwas mehr als 1 Mol des Oxydationsmittels ein Gemisch von 2,6-Dimethyl-*p*-chinon (VI) (Ausbeute 12 %) und einer farblosen, neutralen Substanz $C_{16}H_{20}O_4$ vom Schmp. 194—196° (Ausbeute 64%), in welcher ein Dimerisierungsprodukt des 2,6-Dimethyl-*o*-chinols (VII), und zwar in erster Linie ein Dimeres der Struktur VIII oder VIIIa, vermutet werden konnte.

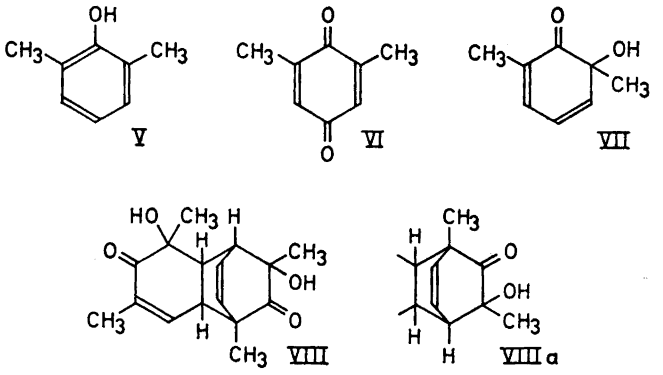

Wenn wir die aus Mesitol bzw. 2,6-Dimethylphenol gewonnenen hochschmelzenden Produkte einstweilen als Dimere der Strukturen IV bzw. VIII betrachten — diese Strukturen werden weiter unten eingehend behandelt —, so finden wir, dass der Verlauf der Perjodatoxydation der beiden genannten Phenole dem früher [1] beim 2,4-Dimethylphenol beobachteten weitgehend ähnlich ist. (Zur Frage des Mechanismus vgl.[1]). In allen drei Fällen überwiegen die *o*-Oxydationsprodukte (hier die *o*-Chinole III bzw. VII) im Vergleich zu den *p*-Oxydationsprodukten (II bzw. VI), und die primär gebildeten *o*-Chinole sind nicht fassbar, da sie sich rasch durch Diels-Alder-Reaktion dimerisieren.

In der vorliegenden Arbeit richtet sich das Hauptinteresse auf die Struktur der aus Mesitol bzw. 2,6-Dimethylphenol erhaltenen Dimeren. Sie seien der Kürze halber im folgenden als "2,4,6-Dimeres" bzw. "2,6-Dimeres" bezeichnet.

Das 2,4,6-Dimere war von uns schon vor einigen Jahren als Dien-Philodienaddukt der Formel IV bzw. IVa aufgefasst worden [3]. Wie uns Herr Prof. F. Wessely, Wien, mitteilte, war man in seinem Arbeitskreis um etwa dieselbe Zeit zu der gleichen Auffassung gekommen. Das Dimere war im Wiener Institut bei der Hydrolyse von monomerem 2,4,6-Trimethyl-*o*-chinolacetat (X) erhalten worden; ein direkter Vergleich des so gebildeten Dimeren mit unserem bei der Perjodatoxydation gewonnenen Produkt vom Schmp. 182—183° bestätigte die Identität der beiden Substanzen (vgl. hierzu auch Zitat [4]). Später gelang es Metlesics und Wessely [5], das einfachste *o*-Chinolacetat, 2-Methyl-*o*-chinolacetat, in das dimere 2-Methyl-*o*-chinol überzuführen und für letzteres die Struktur

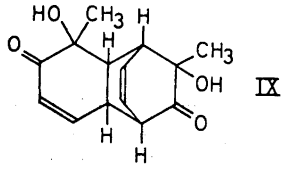

IX

IX eindeutig festzustellen. Dieses Ergebnis stützte auch die für das 2,4,6-Dimere angenommene Struktur (IV oder IVa) *.

Kürzlich veröffentlichten aber Wessely und Mitarbeiter [6] ** Versuche, die sie zu einer Revision der Formel IV (bzw. IVa) veranlassten. Man hatte gefunden, dass kalte alkalische Verseifung von 2,4,6-Trimethyl-*o*-chinolacetat (X) neben dem Dimeren vom Schmp. 182—183° auch ein monomeres Trimethyl-*o*-chinol lieferte. Letzteres war jedoch nicht das erwartete 2,4,6-Trimethyl-*o*-chinol (III), sondern das isomere 2,3,5-Trimethyl-*o*-chinol (XI), das auch bei alkalischer Hydrolyse von 2,3,5-Trimethyl-*o*-chinolacetat (XII) entstand. Wurde das 2,3,5-Trimethyl-*o*-chinol XI auf 130° erhitzt, so ging es in das Dimere vom Schmp. 182—183° über, und letzteres zerfiel beim Erhitzen auf 200° teilweise unter Bildung des monomeren 2,3,5-substituierten *o*-Chinols (XI).

Diese Ergebnisse erklärten Wessely und Mitarbeiter [6] folgendermassen: Das bei der Verseifung von 2,4,6-Trimethyl-*o*-chinolacetat (X) freigelegte *o*-Chinol III unterlag unter der Einwirkung des Alkalis einer Acyloinumlagerung (vgl. Zitat [7]) zu 2,3,5-Trimethyl-*o*-chinol (XI), welches zum Teil dimerisierte. Dem Dimeren vom Schmp. 182—183° sollte demnach nicht die bis dahin angenommene Struktur des dimeren 2,4,6-Trimethyl-

* Im folgenden wird der Einfachheit halber von den beiden möglichen Formeln IV und IVa für das 2,4,6-Dimere die dem Dimeren IX entsprechende Formel IV als die richtige angenommen. Für die übrigen in der vorliegenden Arbeit behandelten *o*-Chinoldimeren wird analog verfahren.

** Herr Professor Wessely machte uns diese Arbeit freundlicherweise vor ihrem Erscheinen als Korrekturabzug zugänglich.

o-chinols (IV), sondern die des dimeren 2,3,5-Trimethyl-*o*-chinols (XIII) zukommen. Damit schien auch die thermische Bildung des Dimeren aus dem Monomeren XI und die Regenerierung des letzteren beim Erhitzen des Dimeren verständlich zu sein.

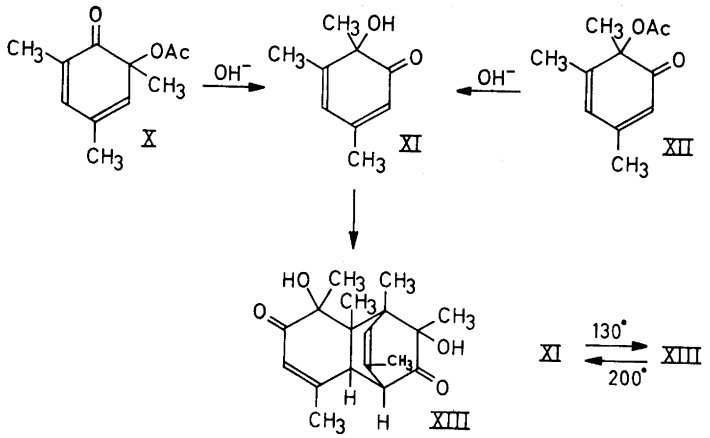

Ähnliche Verhältnisse fanden Wessely und Mitarbeiter[6] beim 2,6-Dimethyl-*o*-chinolacetat (XIV). Dies ging beim alkalischen Verseifen direkt in ein Dimeres vom Schmp. 196° über, welches beim Erhitzen auf 280° 2,3-Dimethyl-*o*-chinol (XVI) lieferte. Diese Ergebnisse deuteten darauf hin, dass bei der alkalischen Verseifung von XIV unter Acyloinumlagerung Isomerisierung zu XVI eintrat, und dass letzteres sich sofort zum dimeren 2,3-Dimethyl-*o*-chinol (XV) stabilisierte. Das gleiche Dimere erhielt man auch bei alkalischer Verseifung von 2,3-Dimethyl-*o*-chinolacetat (XVII).

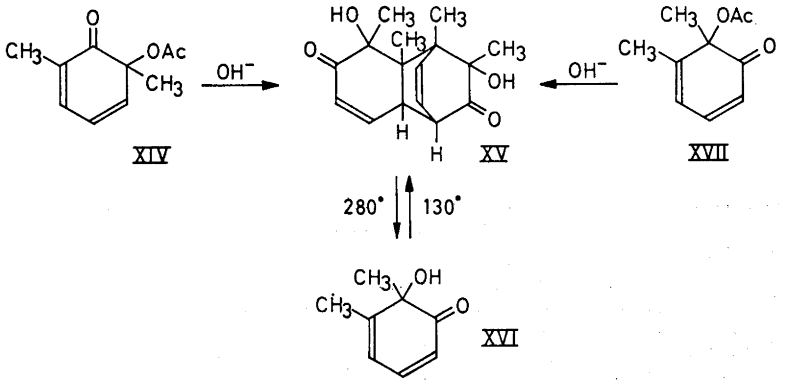

Wie bereits erwähnt, ist das von Wessely c.s.[6] aus 2,4,6- und aus 2,3,5-Trimethyl-*o*-chinolacetat (X, XII) (alkalische Verseifung) sowie aus 2,3,5-Trimethyl-*o*-chinol (bei 130°) erhaltene Dimere (Schmp. 182—183°) identisch mit dem von uns bei der Perjodatoxydation von Mesitol erhaltenen Produkt gleichen Schmelzpunkts. Neuerdings erwies sich auch das in Wien aus 2,6-

und aus 2,3-Dimethyl-*o*-chinolacetat (XIV, XVII) (alkalische Verseifung) erhaltene Dimere (Schmp. 196°) als identisch mit dem im hiesigen Laboratorium durch Perjodatoxydation von 2,6-Dimethylphenol (V) gewonnenen Produkt vom selben Schmelzpunkt *. Wären die von Wessely und Mitarb.[6] gezogenen Schlussfolgerungen richtig, müssten demnach auch den aus Mesitol bzw. 2,6-Dimethylphenol mittels Perjodat erhaltenen Dimeren anstelle der bisher angenommenen Formeln IV bzw. VIII die Formeln XIII (dimeres 2,3,5-Trimethyl-*o*-chinol) bzw. XV (dimeres 2,3-Dimethyl-*o*-chinol) zugeschrieben werden. Es wäre dann notwendig anzunehmen, dass bei der Perjodatoxydation der Phenole I bzw. V die primär zu erwartenden monomeren *o*-Chinole III (2,4,6-Trimethyl-*o*-chinol) bzw. VII (2,6-Dimethyl-*o*-chinol) sich durch Acyloinumlagerung rasch in die Isomeren XI (2,3,5-Trimethyl-*o*-chinol) bzw. XVI (2,3-Dimethyl-*o*-chinol) umwandelten, worauf die letzteren

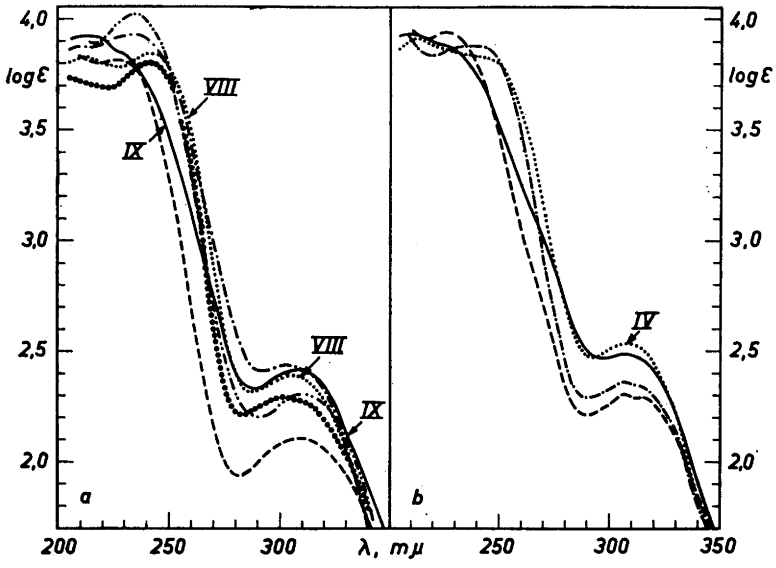

Fig. 1. Ultraviolett-Absorptionsspektren. Lösungsmittel: 96-proz. Äthanol. (Strukturformeln, s. auch Tab. 1).

a. Dimeres 2-Methyl-*o*-chinol (IX) ————
und dessen Diacetat (IX, OAc statt OH) — — — —
Dimeres 2,5-Dimethyl-*o*-chinol — · — · — · und
dessen Diacetat — · · — · · — · ·
Dimeres 2,6-Dimethyl-*o*-chinol (VIII) ..... und
dessen Diacetat (VIII, OAc statt OH) ooooooo
b. Dimeres 2,4-Dimethyl-*o*-chinol ———— und dessen
Diacetat — — — —
Dimeres 2,4,6-Trimethyl-*o*-chinol (IV) ..... und
dessen Diacetat (IV, OAc statt OH) — · — · — · —

* Wir möchten auch an dieser Stelle Herrn Prof. Wessely für die Überlassung einer Probe des Dimethyl-*o*-chinoldimeren sowie für die Untersuchung unseres an ihn übersandten Perjodatproduktes unseren besten Dank aussprechen.

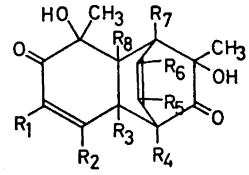

Tabelle 1. Maxima der K-Banden einiger *o*-Chinoldimeren (Lösungsmittel: 96 % Äthanol).

Substanz	R_1	R_2	R_3	R_4	R_5	R_6	R_7	R_8	K-Bande log ε_{max}	K-Bande λ_{max} (mμ) gef.	K-Bande λ_{max} (mμ) ber.
Dimeres 2-Methyl-*o*-chinol (IX)[5]	H	H	H	H	H	H	H	H	3.89	228[a]	227
Diacetat von IX[5]	„	„	„	„	„	„	„	„	3.81	227	227
Dimeres 2,4-Dimethyl-*o*-chinol [1]	H	H	CH_3	H	H	CH_3	H	H	3.88	225[a]	227
Diacetat [1]	„	„	„	„	„	„	„	„	3.95	226	227
Dimeres 2,5-Dimethyl-*o*-chinol [10]	H	CH_3	H	H	CH_3	H	H	H	3.93	236	239
Diacetat [10]	„	„	„	„	„	„	„	„	4.01	235	239
Dimeres 2,6-Dimethyl-*o*-chinol (VIII)	CH_3	H	H	CH_3	H	H	H	H	3.84	242	237
Diacetat von VIII	„	„	„	„	„	„	„	„	3.80	241	237
Dimeres 2,3-Dimethyl-*o*-chinol (XV) (*unbekannt*)	H	H	H	H	H	H	CH_3	CH_3	—	—	227
Dimeres 2,4,6-Trimethyl-*o*-chinol (IV)	CH_3	H	CH_3	CH_3	H	CH_3	H	H	3.83	240[a]	237
Diacetat von IV	„	„	„	„	„	„	„	„	3.88	240	237
Dimeres 2,3,5-Trimethyl-*o*-chinol (XIII) (*unbekannt*)	H	CH_3	H	H	CH_3	H	CH_3	CH_3	—	—	239

[a] Maximum unscharf (Schulter) wegen Überlagung der K-Bande mit einer Bande mit Max. bei 210—212 mμ (gespannte Äthylenbrücke, vgl. S. 1586). In den übrigen Fällen war das K-Maximum von der kürzerwelligen Bande deutlich getrennt (s. Fig. 1).

dimerisierten. Unter den Bedingungen, wie sie von uns bei der Perjodatoxydation verwendet wurden — das pH der wässrigen $NaJO_4$-Lösung ist 4—5 — erschien indessen die Annahme einer Acyloinumlagerung, noch dazu einer rasch verlaufenden, recht unwahrscheinlich.

Im folgenden soll gezeigt werden, dass den beiden Dimeren die Strukturen des dimeren 2,4,6-Trimethyl-*o*-chinols (IV) bzw. des dimeren 2,6-Dimethyl-*o*-chinols (VIII) zukommen; die von Wessely und Mitarbeitern [6] vorgeschlage-

nen isomeren Strukturen XIII (2,3,5-Trimethylstruktur) und XV (2,3-Dimethylstruktur) (s.s. 1583) sind durch IV bzw. VIII zu ersetzen.*

Wertvolle Aufschlüsse lieferte zunächst ein Vergleich der UV-Absorptionsspektren verschiedener dimerer *o*-Chinole. Diese Substanzen zeigen die für α,β-ungesättigte Ketonsysteme charakteristischen Spektren mit einer kurzwelligen Bande hoher Extinktion (K-Bande) und einer längerwelligen Bande niedrigerer Extinktion (R-Bande) (Fig. 1). Die Lage des Maximums der K-Bande wird bekanntlich beeinflusst von der Anzahl und Stellung der Substituenten an der Äthylenbindung des konjugierten Enonsystems und lässt sich nach den von Woodward [8] angegebenen und von Fieser und Fieser [9] besonders in der Sterinreihe weiter geprüften Regeln berechnen. In Tabelle 1 sind die von uns bestimmten K-Maxima für fünf verschiedene Dimere und deren Diacetylderivate zusammengestellt. Es zeigt sich, dass die Werte für die Dimeren des 2-Methyl-[5], 2,4-[1] und 2,5-Dimethyl-*o*-chinols [10] sich gut an die berechneten Werte anschliessen. Was das Trimethylchinoldimere betrifft, lässt sich auf Grund der Lage der K-Bande keine Entscheidung zwischen den Isomeren IV (2,4,6-Struktur mit α,β-Substitution) und XIII (2,3,5-Struktur mit β,β-Substitution) treffen, da der Unterschied zwischen den für die beiden Isomeren berechneten Werten (2 $m\mu$) zu gering ist. Aufschlussreich ist dagegen das Spektrum des 2,6(2,3?)-Dimethyl-*o*-chinol-dimeren. Die Lage seines K-Maximums ist die für ein α,β-disubstituiertes Enon der Struktur VIII (dimeres 2,6-Dimethyl-*o*-chinol) zu erwartende und lässt sich nicht vereinbaren mit der von Wessely c.s.[6] angenommenen Struktur XV eines dimeren 2,3-Dimethyl-*o*-chinols (β-monosubstituiertes Enon).

Die in Fig. 1 wiedergegebenen Spektren der fünf verschiedenen *o*-Chinoldimeren und ihrer Acetate zeigen eine der K-Bande vorgelagerte, mehr oder weniger deutlich ausgeprägte Absorptionsbande im Bereich von 210—215 mμ. Es erscheint möglich, dass es sich hier um die Absorption der Äthylenbrücke handelt, die wegen der beträchtlichen Spannung des Bi*cyclo*octensystems gegenüber der normalen Äthylenabsorption bathochrom verschoben ist. Diese Annahme wird dadurch gestützt, dass die Bande verschwindet, d.h. vermutlich ihre normale Lage unterhalb 200 mμ annimmt, wenn die Ketolgruppierung des Bi*cyclo*octensystems durch Perjodat aufgespalten wird, wobei ein spannungsfreies Naphthalinsystem entsteht. Hierüber soll später berichtet werden.

Für die Richtigkeit der Strukturen IV bzw. VIII für die aus Mesitol bzw. 2,6-Dimethylphenol erhaltenen Dimeren (2,4,6-Dimeres bzw. 2,6-Dimeres) sprechen ferner folgende Ergebnisse:

Das 2,4,6-Dimere lieferte beim kurzen Behandeln mit Essigsäureanhydrid in Äthylacetatlösung und in Gegenwart von Perchlorsäure als Katalysator (eine Methode [11], die sich für die Acetylierung des dimeren 2,4-Dimethyl-*o*-chinols bewährt hatte [1]) ein Diacetat (IV, OAc statt OH) vom Schmp. 162—163°. Sein UV-Spektrum (Fig. 1) zeigte an, dass das konjugierte Enonsystem

* Nach Fertigstellung des vorliegenden Manuskriptes übersandte uns Herr Prof. F. Wessely den Sonderdruck einer soeben erschienenen Arbeit von Zbiral, E., Wessely, F. und Lahrmann, E. *Monatsh.* **91** (1960) 92, in welcher die genannten Autoren gewisse Zweifel an der Richtigkeit der früher [6] angenommenen Dimerstrukturen XIII und XV äussern. Nach gleichzeitiger brieflicher Mitteilung von Herrn Prof. Wessely liegen nun in seinem Arbeitskreis weitere Ergebnisse vor, welche nicht mit Struktur XV sondern nur mit Struktur VIII für das dimere Dimethyl-*o*-chinol in Einklang gebracht werden können.

erhalten geblieben und demnach eine Acyloinumlagerung nicht eingetreten war. Durch milde alkalische Verseifung (äthanolische Kalilauge, Zimmertemp.) wurde aus dem Diacetat das 2,4,6-Dimere IV regeneriert. Auch unter dem Einfluss des Alkalis erfolgte also beim Dimeren keine Acyloinumlagerung. Wurde nun das Diacetat auf 180° erhitzt, so trat Retrodienzerfall unter Bildung von 2,4,6-Trimethyl-*o*-chinolacetat (X), Schmp. 82—84°, ein, das durch Vergleich mit einer nach Wessely und Sinwel [12] aus Mesitol und Bleitetraacetat dargestellten Probe identifiziert wurde.

Die einfachste Schlussfolgerung aus diesen Ergebnissen ist, dass das aus Mesitol mit Perjodat erhaltene Produkt das Dimere des 2,4,6-Trimethyl-*o*-chinols und nicht des 2,3,5-Trimethylisomeren ist. Folgende Versuche über die Perjodatoxydation des 2,3,5-Trimethylphenols (XVIII) bestätigen diese Auffassung.

2,3,5-Trimethylphenol (XVIII) verbrauchte unter den beim Mesitol bzw. 2,6-Dimethylphenol angewandten Bedingungen Perjodat erheblich langsamer als die beiden letztgenannten Phenole. Erst nach mehreren Stunden war XVIII nicht mehr nachweisbar. Aus dem Reaktionsgemisch liess sich in guter Ausbeute ein rotes Öl isolieren, das leicht im Vakuum destillierte. Das Destillat, ein gelbes, bei Temperaturen unter 12° kristallin erstarrendes Öl, erwies sich als ein Gemisch von 2,3,5-Trimethyl-*p*-chinon, Schmp. 34°, (XIX) [13], und monomerem 2,3,5-Trimethyl-*o*-chinol, Schmp. 42°, (XI) [6]. Ein dimeres Produkt war nicht zu entdecken.

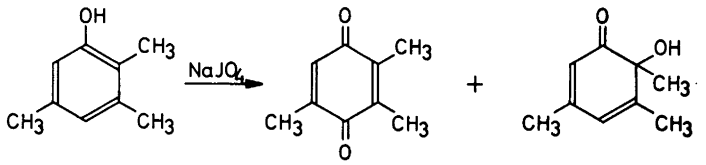

XVIII XIX XI

Die Perjodatoxydation von 2,3,5-Trimethyl-phenol (XVIII) lieferte somit — neben dem *p*-Oxydationsprodukt XIX — monomeres 2,3,5-Trimethyl-*o*-chinol (XI), das unter den Versuchsbedingungen nicht in ein Dimeres überging. Dieses Ergebnis schliesst aus, dass das bei der analogen Oxydation des Mesitols erhaltene Produkt vom Schmp. 182—183° ein Dimeres des 2,3,5-Trimethyl-*o*-chinols (XIII) sein könne, wie von Wessely c.s.[6] angenommen wurde.

Über die unterschiedliche Geschwindigkeit der Perjodatoxydation verschiedener Typen von Alkylphenolen sowie über die verschiedene Neigung der entsprechenden Alkyl-*o*-chinole zur Dimerisierung soll später zusammenhängend berichtet werden.

Ähnliche, bisher nur orientierende, Versuche wurden mit 2,3-Dimethylphenol unternommen. Auch sie gaben kein dimeres Produkt. Dies spricht gegen die Auffassung, dass das aus 2,6-Dimethylphenol mit Perjodat sowie das von Wessely c.s.[6] auf andere Weise erhaltene, damit identische Produkt

vom Schmp. 194—196° ein dimeres 2,3-Dimethyl-*o*-chinol sei. Die Richtigkeit unserer Auffassung, dass dieses Produkt das 2,6-Dimere (VIII) ist, wurde durch die folgenden Versuche gestützt.

Das "2,6-Dimere" gab mit AcOAc—$HClO_4$ glatt ein Diacetat vom Schmp. 159—160° (Formel VIII, OAc statt OH). Sein UV-Spektrum (Fig. 1) zeigt wie das Ausgangsmaterial die für das α,β-substituierte konjugierte Enonsystem charakteristische K-Bande (s. Tab. 1) sowie die R-Bande um 300 mμ. Wurde das Diacetat auf 180° erhitzt, so gab es unter Retrodienzerfall 2,6-Dimethyl-*o*-chinolacetat (XIV), identifiziert mit einer nach Wessely und Mitarb.[6] erhaltenen Probe derselben Substanz. Umgekehrt liess sich das monomere Acetat XIV durch Erhitzen auf 120° wieder in das dimere Dimethyl-*o*-chinolacetat vom Schmp. 159—160° überführen. Diese Ergebnisse sind analog den von Metlesics und Wessely [5] für das Dimere des 2-Methyl-*o*-chinolacetats (IX, OAc statt OH) bzw. das entsprechende Monomere beschriebenen; sie sind im Einklang mit Formel VIII für das Dimethyl-*o*-chinoldimere.

Bei der thermischen Dimerisierung des 2,6-Dimethyl-*o*-chinolacetats (XIV) entstand neben dem acetylierten Dimeren vom Schmp. 159—160° noch ein isomeres Produkt vom Schmp. 182—84°. Es enthält ebenfalls das α,β-substituierte konjugierte Enonsystem (K-band bei 238 mμ, R-band bei 310 mμ) und könnte vielleicht das Diacetat des isomeren 2,6-Dimeren (VIIIa, OAc statt OH) sein.

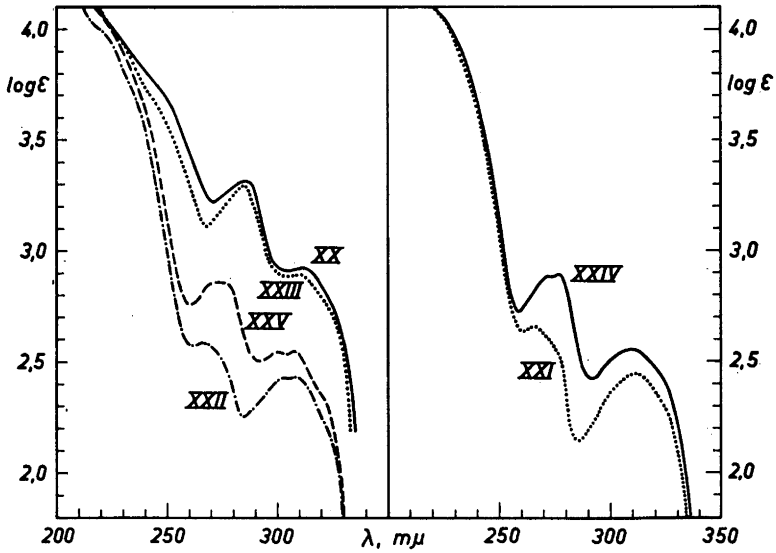

Fig. 2. Ultraviolett-Absorptionsspektren. Lösungsmittel: 96-proz. Äthanol.
2-Methyl-*o*-chinol-anhydrodimeres (XX), dessen
Monoacetat (XXI) und Diacetat (XXII).
2,6-Dimethyl-*o*-chinol-anhydrodimeres (XXIII),
dessen Monoacetat (XXIV) und Diacetat (XXV).

Im Gegensatz zum 2,6-Dimethyl-*o*-chinolacetat blieb das von Wessely und Mitarb.[14] beschriebene 2,3-Dimethyl-*o*-chinolacetat bei 120° unverändert.

Ein weiteres für das vorliegende Strukturproblem wichtiges Ergebnis lieferte die alkalische Hydrolyse des acetylierten 2,6-Dimeren (VIII, OAc statt OH). Es entstanden zwei Produkte in ungefähr gleicher Menge, nämlich ein in wässrigem Alkali unlösliches sowie ein alkalilösliches, das beim Neutralisieren der alkalischen Lösung mit CO_2 ausfiel. Das erstere war das erwartete Ausgangsdimere $C_{16}H_{20}O_4$ (VIII). Das zweite, vom Schmp. 172—174°, hatte die Zusammensetzung $C_{16}H_{18}O_3$, enthielt also 1 Mol. H_2O weniger als VIII; es sei als "Anhydro-2,6-dimeres" bezeichnet. Sein IR-Spektrum zeigte neben der für die dimeren *o*-Chinole typischen Hydroxylbande um 3 460 cm^{-1} eine längerwellige Hydroxylbande (bei 3 290 cm^{-1}). Von den beiden im Spektrum des Ausgangsdimeren VIII vorhandenen CO-Banden (1 672 cm^{-1} für die konjugierte, und 1 712 cm^{-1} für die isolierte Ketogruppe) war im Spektrum des Anhydrodimeren nur noch die Bande der isolierten Ketogruppe zu erkennen. Um 1 600 cm^{-1} gab sich eine, allerdings schwach ausgeprägte, "aromatische" Doppelbande (1 614 und 1 586 cm^{-1}) zu erkennen. Diese Daten legten nahe, dass es sich um ein Phenol handelte. Das UV-Spektrum der Substanz (Fig. 2) wies eine Bande mit Maximum bei 285 $m\mu$ ($\log \varepsilon = 3.29$) auf, sowie eine längerwellige Bande bei 311 $m\mu$ ($\log \varepsilon = 2.89$).

Durch Essigsäureanhydrid-Pyridin wurde die saure Hydroxylgruppe des Anhydrodimeren unter Bildung eines Monoacetats vom Schmp. 150—152° (UV-Spektrum, Fig. 2) verestert, während das tert. alkoholische Hydroxyl intakt blieb. Im IR-Spektrum liess sich das Phenolester-CO bei 1 755 cm^{-1}, das tert. OH bei 3 430 cm^{-1} erkennen. (Auch die tertiären Hydroxylgruppen des 2,6-Dimeren und anderer *o*-Chinoldimeren sind gegen AcOAc-Pyridin, selbst beim Kochen, resistent.) Einwirkung von AcOAc-$HClO_4$ auf das Anhydrodimere oder dessen Monoacetat lieferte dagegen erwartungsgemäss ein Diacetat, Schmp. 176—178°, (UV-Spektrum, Fig. 2), aus welchem durch milde alkalische Verseifung das Anhydro-2,6-dimere vom Schmp. 172—174° regeneriert wurde.

Die Struktur des Anhydro-2,6-dimeren ergab sich aus Vergleichsversuchen mit dem dimeren 2-Methyl-*o*-chinolacetat (IX, OAc statt OH) von Metlesics und Wessely[5]. Wurde die letztgenannte Substanz mit äthanolischer Kalilauge bei Zimmertemperatur behandelt, so entstand das Phenol XX, dessen Diacetat XXII Metlesics und Wessely[5] aus dem Dimeren IX oder seinem Diacetat durch Erhitzen mit Essigsäureanhydrid-Natriumacetat erhalten und zu XX verseift hatten. Die Struktur des Phenols XX ist von den genannten Autoren eindeutig festgelegt worden[5].

XX : R=H; R'=R''=H
XXI : R=H; R'=Ac; R''=H
XXII: R=H; R'=R''=Ac

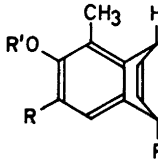

XXIII: R=CH3; R'=R''=H
XXIV: R=CH3; R'=Ac; R''=H
XXV : R=CH3; R'=R''=Ac

Das Phenol XX zeigt weitgehende spektrale Ähnlichkeit mit dem oben beschriebenen Anhydro-2,6-dimeren; im IR-Spektrum des Phenols XX [5] sind die "aromatischen Banden" um 1 600 und 1 500 cm^{-1} jedoch deutlich ausgeprägt. Überzeugend für die strukturelle Analogie ist vor allem die Ähnlichkeit der charakteristischen UV-Spektren der beiden Phenole (Fig. 2). Wie das Anhydro-2,6-dimere gibt auch Phenol XX mit AcOAc-Pyridin ein Monoacetat, Schmp. 127—129° (XXI), und mit AcOAc-$HClO_4$ das bereits von Metlesics und Wessely [5] beschriebene Diacetat (XXII) (UV-Spektren, Fig. 2).

Auf Grund dieser klaren Analogien kann dem Anhydro-2,6-dimeren die Struktur XXIII, seinem Monoacetat Struktur XXIV und seinem Diacetat Struktur XXV zuerteilt werden.

Die Bildung des Phenols XXIII aus dem Acetat des Dimethyl-*o*-chinoldimeren lässt sich aber wieder nur mit der 2,6-Dimethylstruktur (VIII) für das letztere in Einklang bringen. In dieser Struktur sind — wie beim Acetat des dimeren 2-Methyl-*o*-chinols (IX) — die angulären Positionen mit Wasserstoff besetzt. Dies lässt die bei der alkalischen Verseifung eintretende Abspaltung von HOAc und die damit einhergehende Aromatisierung des brückenlosen Sechsrings verstehen. Ein solcher Reaktionsverlauf wäre nicht möglich, wenn dem ursprünglichen Dimeren die von Wessely c.s.[6] vorgeschlagene Struktur des dimeren 2,3-Dimethyl-*o*-chinols XV (mit einer angulären CH_3-Gruppe) zukäme.

Die Mono- und Diacetate der Phenolalkohole XX und XXIII zeigen wie diese selbst in ihren UV-Spektren zwei Banden oder Bandengruppen (Fig. 2). Von diesen ist die kürzerwellige sicher auf den phenolischen Ring zurückzuführen; die längerwellige ist möglicherweise einem Überschneiden der π-Orbitale des aromatischen Rings und der in β,γ-Stellung zu ihm stehenden Ketogruppe (und Äthylengruppe?) zuzuschreiben, wie es von Cookson und Wariyar[15] für β, γ-ungesättigte Ketone von geeignetem sterischem Bau angenommen wird. Für eine Verbindung verwandter Struktur (β-Naphthol-Maleinsäureanhydrid-Addukt, *exo*-Form) hat Wariyar [16] eine Absorptionskurve von recht ähnlichem Typus angegeben.

Wie bereits erwähnt, erhielten Metlesics und Wessely [5] das aromatische Diacetat XXII durch (2-stündiges) Erhitzen des dimeren 2-Methyl-*o*-chinols (IX) mit AcOAc-NaOAc. Auch bei solcher Behandlung verhielt sich das 2,6-Dimere (VIII) im Prinzip analog, denn aus dem Reaktionsgemisch konnte das Diacetat XXV des Anhydro-2,6-dimeren isoliert werden. Daneben entstand noch das Diacetat von VIII, und ausserdem war in beträchtlichem Ausmass Retrodienzerfall zum 2,6-Dimethyl-*o*-chinolacetat (XIV) eingetreten. Erwartungsgemäss lieferte auch das Diacetat von VIII beim Erhitzen mit AcOAc-NaOAc das Diacetat XXV neben monomerem 2,6-Dimethyl-*o*-chinolacetat (XIV).

DISKUSSION

Mit den voranstehenden Ergebnissen dürften die Strukturen des 2,4,6-Dimeren und des 2,6-Dimeren eindeutig im Sinne der Formeln IV bzw. VIII entschieden sein. Es erhebt sich dann die Frage, wie die eingangs kurz besprochenen Versuche von Wessely und Mitarbeitern [6] zu erklären sind, wonach dieselben Dimeren auch aus 2,3,5-Trimethyl-*o*-chinol bzw. 2,3-Dimethyl-*o*-

chinol in Gegenwart von Alkali oder beim Erhitzen auf 130° entstehen. Es seien zunächst die Verhältnisse bei den Trimethyl-*o*-chinolen betrachtet.

Wessely und Mitarb.[4,6] fanden, dass alkalische Verseifung von 2,4,6-Trimethyl-*o*-chinolacetat (X) zur gleichzeitigen Bildung von 2,3,5-Trimethyl-*o*-chinol (XI) und des Dimeren vom Schmp. 182—183° führt und nahmen an, dass letzteres durch Dimerisierung von XI entstand, das seinerseits aus dem eigentlich zu erwartenden 2,4,6-Trimethyl-*o*-chinol (III) durch Acyloinumlagerung gebildet worden war. Wir nehmen nun an, dass ein Teil des primär aus X freigelegten *o*-Chinols III sich zum Dimeren IV dimerisiert, während ein anderer Teil, in Konkurrenz mit der Dimerisierung, durch Acyloinumlagerung in das isomere *o*-Chinol XI übergeführt wird. Dem letzteren geht aber, wie oben gezeigt wurde, die Fähigkeit zur Dimerisierung ab und es kann deshalb als Monomeres isoliert werden.

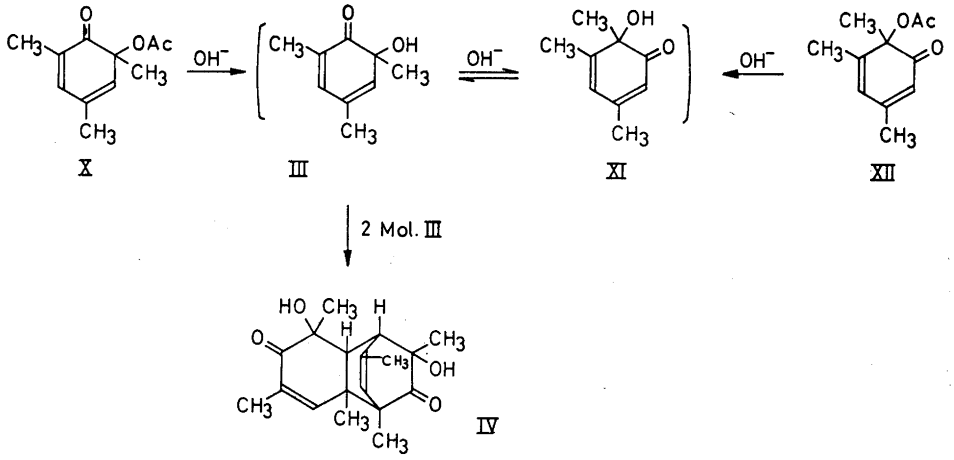

Es ist weiterhin anzunehmen, dass die Acyloinumlagerung III ⇌ XI reversibel ist (vgl. hierzu auch Derkosch und Kaltenegger [17]); man wird deshalb erwarten müssen, dass das 2,4,6-Dimere IV auch bei alkalischer Verseifung von 2,3,5-Trimethyl-*o*-chinolacetat (XII) — neben dem freien 2,3,5-Trimethylchinol XI — entsteht. Wessely c.s. geben allerdings nur die Bildung von XI an. Man würde ferner erwarten, dass aus dem Gleichgewicht III ⇌ XI allmählich alles *o*-Chinol in das Dimere IV übergeht. Dass bei der Verseifung von X die Produkte XI und IV nebeneinander gefunden wurden [4,6], ist wohl auf die Kürze der Versuchsdauer (10 Min.) zurückzuführen.

Bei der Oxydation des Mesitols mit Perjodat entsteht als *o*-Oxydationsprodukt zweifellos das 2,4,6-Trimethyl-*o*-chinol III. Es dimerisiert sich sehr rasch vollständig zum Dimeren IV. Unter den angewandten Versuchsbedingungen (wässerige Lösung, pH 4—5) erfolgt keine Acyloinumlagerung, denn im rohen Reaktionsprodukt liess sich infrarotspektroskopisch kein 2,3,5-Trimethyl-*o*-chinol nachweisen. Bei der Perjodatoxydation von 2,3,5-Trimethylphenol (XVIII) dagegen entstand als *o*-Oxydationsprodukt ausschliess-

lich 2,3,5-Trimethyl-*o*-chinol (XI) — welches nicht dimerisiert —, und da Acyloinumlagerung bei pH 4—5 offenbar nicht stattfindet, trat auch kein 2,4,6-Dimeres (IV) auf.

Die Ergebnisse der thermischen Versuche lassen sich auf ähnlicher Grundlage deuten. Nimmt man an, dass 2,3,5-Trimethyl-*o*-chinol (XI) bei höherer Temperatur einer reversiblen Acyloinumlagerung unterliegt, so versteht man, weshalb es — über 2,4,6-Trimethyl-*o*-chinol (III) — allmählich in das 2,4,6-Dimere (IV) übergeht [6]. Und man versteht auch, warum das Dimere IV beim thermischen Retrodienzerfall [6] — über 2,4,6-Trimethyl-*o*-chinol — das 2,3,5-Trimethyl-*o*-chinol (XI), neben unverändertem Dimeren IV, liefert:

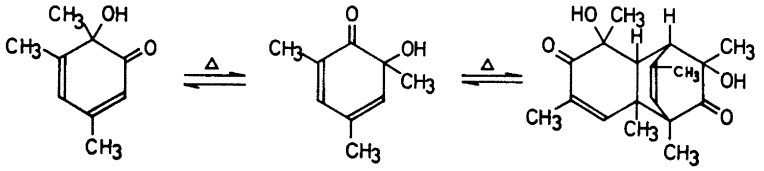

XI III IV

Das Eintreten der Acyloinumlagerung nicht nur in alkalischer Lösung sondern auch bei höherer Temperatur, die Reversibilität dieser Umlagerungen, sowie die Tatsache, dass 2,4,6-Trimethyl-*o*-chinol unter allen bisher untersuchten Bedingungen rasch dimerisiert, während dem 2,3,5-Trimethyl-*o*-chinol die Dimerisierungstendenz abgeht, scheinen somit alle bisher bekannt gewordenen Befunde widerspruchsfrei zu erklären.

Bei den entsprechenden Acetaten liegen etwas andere Verhältnisse vor. Sowohl 2,3,5- wie 2,4,6-Trimethyl-*o*-chinolacetat, welche durch die Bleitetraacetatmethode von Wessely zugänglich sind, sind als Monomere haltbar. Ihre thermische Dimerisierung ist noch nicht untersucht. Bei der thermischen Spaltung des Acetates des Mesitoldimeren erhielten wir in normaler Weise das 2,4,6-Trimethyl-*o*-chinolacetat (X) (s.S. 1587). Im Gegensatz zum freien *o*-Chinol gibt das Acetat keine thermische Acyloinumlagerung, was im Hinblick auf den mutmasslichen Mechanismus dieser Umlagerungsreaktion ganz natürlich erscheint.

Was in der voranstehenden Diskussion am Beispiel des Isomerenpaares 2,4,6- und 2,3,5-Trimethyl-*o*-chinol gesagt wurde, gilt offensichtlich auch für das Paar 2,6- und 2,3-Dimethyl-*o*-chinol. Wir wollen hierauf zurückkommen, wenn begonnene Versuche, insbesondere über das Verhalten des 2,3-Dimethylphenols gegen Perjodat, abgeschlossen sind. Vorläufig lässt sich sagen, dass 2,3-Dimethylphenol — ganz ähnlich wie das 2,3,5-Homologe — verhältnismässig langsam oxydiert wird und dass dabei kein Dimeres entsteht. Dagegen reagiert 2,6-Dimethylphenol, wie oben gezeigt, rasch unter Bildung des dimeren 2,6-Dimethyl-*o*-chinols (VIII). Die von uns gemachte Beobachtung, dass 2,3-Dimethyl-*o*-chinolacetat beim zweistündigen Erhitzen auf 120° unverändert blieb, während das entsprechende 2,6-Isomere dimeri-

sierte (s. S. 1588-9), fügt sich gut in die hier angeführten Zusammenhänge ein. Dies gilt schliesslich auch für den Befund, dass das Diacetat des 2,6-Dimeren thermisch zum monomeren 2,6-Dimethyl-*o*-chinolacetat spaltbar ist (s. S. 1588).

EXPERIMENTELLES

Absorptionsspektren im ultravioletten und sichtbaren Gebiet wurden mit einem registrierenden Spektrophotometer (Perkin-Elmer Spectracord 4 000-A), IR-Spektren mit dem Perkin-Elmer-Instrument, Modell 21, aufgenommen. Die Elementaranalysen wurden im Laboratorium Alfred Bernhardt, Mülheim, ausgeführt.

Perjodatoxydation von Mesitol (I). Zu einer Lösung von 5 g Mesitol in 2.3 l Äthanol-Wasser (15:85) wurden 15.7 g Natriummetaperjodat ($NaJO_4$) (Molverhältnis 1:2), gelöst in 200 ml Wasser, unter Umschütteln zugegeben. Nach 5 Min. wurde unverbrauchtes Perjodat durch Zusatz von 4.55 g Äthylenglykol reduziert. Die schwach grünlichgelb gefärbte Lösung wurde sechsmal mit Methylenchlorid ausgeschüttelt, und die vereinigten Extrakte wurden nach Trocknen mit wasserfreiem Calciumsulfat im Vakuum zur Trockene gebracht. Der teilweise kristalline Rückstand wurde einige Male mit kaltem Hexan ausgezogen, und der ungelöst verbleibende kristalline Anteil aus Benzol umkristallisiert. Farblose Prismen von *dimerem 2,4,6-Trimethyl-o-chinol (IV)* *, Schmp. 182–183°; Ausbeute 53 %. (Gef.: C 71.00; H 7.97; aktiver H ** 0.64; Mol.-Gew., kryoskop. in HOAc **, 318. Ber. für $C_{18}H_{24}O_4$: C 71.03; H 7.95; aktiver H 0.66; Mol.-Gew. 304.37.) UV-Spektrum s. Tab. 1 und Fig. 1. IR-Banden (cm^{-1}): 3 490, 3 400 (aliph. OH), 1 710 (CO), 1 684 (konj. CO).

Aus dem oben erwähnten Hexanextrakt kristallisierte nach dem Einengen noch eine kleine Menge des Dimeren IV. Nach Entfernen des restlichen Lösungsmittels hinterblieb ein schwach gelbes Öl, das beim Abkühlen kristallisierte (Ausbeute 28 %). Umkristallisieren aus *Iso*propyläther gab farbloses *2,4,6-Trimethyl-p-chinol (II)*, Schmp. 45–46° (45.5–46° nach Bamberger und Rising [2]). Das UV-Spektrum der Substanz stimmte mit dem von Derkosch und Kaltenegger [18] angegebenen überein.

Dimeres 2,6-Dimethyl-o-chinol (VIII). Eine Lösung von 8.8 g 2,6-Dimethylphenol in 2.4 l Wasser wurde unter Rühren mit einer Lösung von 36 g $NaJO_4$ in 1.2 l Wasser (Molverhältnis Xylenol: $NaJO_4$ = 1 : 2.34) versetzt. Nach einer Reaktionsdauer von 30 Min. wurde überschüssiges Perjodat durch Zusatz von 8 ml Äthylenglykol entfernt, und die gelbe, etwas trübe Lösung portionsweise mit insgesamt 800 ml Methylenchlorid ausgeschüttelt. Aus dem Extrakt wurde nach Trocknen mit wasserfreiem Gips und Eindampfen i.V. ein uneinheitliches kristallines Rohprodukt erhalten. Letzteres wurde mit 30 ml Hexan ausgekocht, wobei 6.3 g rohes VIII vom Schmp. 187–192° zurückblieben. Ausbeute 64 %. Umkristallisieren aus Benzol-Hexan gab farblose Prismen, Schmp. 194–196°. (Gef.: C 69.33; H 7.27; O 23.15. Ber. für $C_{16}H_{20}O_4$: C 69.54; H 7.30; O 23.16.) UV-Spektrum s. Tab. 1 und Fig. 1. IR-Banden (cm^{-1}): 3 400 (aliph. OH), 1 712 (CO), 1 672 (konj. CO).

Aus dem Hexanextrakt (s. oben) kristallisierten 1.1 g (12 %) *2,6-Dimethyl-p-chinon (VI)*, Schmp. 73°.

Diacetat des dimeren 2,4,6-Trimethyl-o-chinols (IV, OAc statt OH). Dimeres 2,4,6-Trimethyl-*o*-chinol (IV) (1.2 g) wurde in 15 ml einer 2 M Lösung von Essigsäureanhydrid in Äthylacetat, die 1.15 % Perchlorsäure enthielt [11], gelöst. Nach 10 Min. wurde mit etwas Wasser zersetzt, die Äthylacetatschicht einige Male mit Wasser gewaschen, mit Na_2SO_4 getrocknet und i.V. eingedampft. Der feste Rückstand gab beim Umkristallisieren aus Äthanol farblose Prismen vom Schmp. 162–163° (69 %). (Gef.: C 67.87; H 7.31; $COCH_3$ 21.12. Ber. für $C_{22}H_{28}O_6$: C 68.02; H 7.27; $COCH_3$ 22.17.) UV-Spektrum s. Tab. 1 und Fig. 1. IR-Banden (cm^{-1}): 1 738 (Inflexion), 1 730 (Ester-CO und CO), 1 696 (konj. CO).

Verseifung des Diacetats mit 10-proz. äthanolischer Kalilauge (16 Std. bei Zimmertemp.) gab das Ausgangsdimere IV.

---

* Diplomarbeit L. Junghahn, 1954 [3].

** Diese Bestimmungen wurden von Herrn tekn.lic. R. Magnusson ausgeführt.

Thermische Spaltung des dimeren 2,4,6-Trimethyl-o-chinolacetats (IV, OAc statt OH). Das Acetat (650 mg) wurde in einem Knierohr, das an das Vakuum einer Wasserstrahlpumpe angeschlossen war, durch Eintauchen des Rohres in ein auf 180° erwärmtes Ölbad rasch erhitzt. Innerhalb weniger Minuten destillierte ein gelbliches, allmählich kristallin erstarrendes Öl in den gekühlten Teil des Röhrchens über. Umkristallisieren aus *Iso*propyläther gab gelblich-weisse Prismen von *2,4,6-Trimethyl-o-chinolacetat (III)*, (Ausbeute 73 %), Schmp. 82–84°, wie von Wessely und Sinwel [12] angegeben. UV- und IR-Spektrum stimmten mit den von Derkosch und Kaltenegger [17,18] veröffentlichten Spektren überein.

Perjodatoxydation von 2,3,5-Trimethylphenol (XVIII). Eine Lösung von 4 g des Phenols in 1.8 l Äthanol-Wasser (15:85) wurde mit einer Lösung von 18.95 g $NaJO_4$ (Molverhältnis 1:3) in 400 ml Wasser versetzt. Nach 16-stündigem Stehen bei Zimmertemperatur wurde das rote Reaktionsgemisch mit Methylenchlorid ausgeschüttelt. Eindampfen der mit wasserfreiem Na_2SO_4 getrockneten Methylenchloridlösung i.V. gab ein braunrotes Öl (4.3 g), das bei 2 mm Hg bei 70–80° destillierte. Das goldgelbe Destillat erstarrte unterhalb 12° kristallin. (Versuche mit 30- bzw. 45-stündiger Oxydationsdauer gaben dasselbe Resultat.) Das Absorptionsspektrum einer alkoholischen Lösung des Produktes (Max. bei 225, 255 und 313 mμ, Min. bei 213 und 284 mμ) war mit der Annahme eines Gemisches von 2,3,5-Trimethyl-*p*-chinon (XIX) (λ_{max} = 254 mμ) und 2,3,5-Trimethyl-*o*-chinol (XI) (λ_{max} = 312 mμ [18]) vereinbar. Das IR-Spektrum des Gemisches gab dieselbe Information. Versuche, die Komponenten durch fraktionierte Destillation zu trennen, waren erfolglos.

Die Hexanlösung einer Probe des gelben Gemisches wurde auf eine Säule von Aluminiumoxyd (Merck, stand., "sauer") gebracht. Beim Waschen mit Hexan-Benzol (90:10) wurde eine goldgelbe Zone eluiert, während eine heller gelbe Zone im oberen Teil der Säule adsorbiert blieb und auch mit anderen Lösungsmitteln nicht ausgewaschen werden konnte. Das Hexan-Benzol-Eluat hinterliess beim Eindunsten *2,3,5-Trimethyl-p-chinon (XIX)*, identifiziert durch Schmp., Misch-Schmp. und Spektren mit einem nach Teuber und Rau [13] dargestellten Vergleichspräparat.

Eine weitere Probe des gelben Gemisches wurde in 50-proz. Äthanol gelöst und durch 20 Min. langes Einleiten von SO_2 reduziert. Das Reaktionsgemisch färbte sich zunächst dunkel (Chinhydron) und nahm darauf eine blassgelbe Farbe an. Nach Verdünnen mit Wasser wurde mit Methylenchlorid ausgeschüttelt, und der nach dem Eindampfen der Methylenchloridphase verbleibende Rückstand mit Hexan ausgezogen. Aus der eingeengten Hexanlösung kristallisierten beim Abkühlen farblose Nadeln, die nach Umkristallisieren aus Wasser bei 96–97° schmolzen und mit *2,3,5-Trimethylphenol (XVIII)* keine Schmelzpunktsdepression gaben. Da im Gemisch vor der Reduktion UV- und IR-spektroskopisch kein Phenol nachweisbar war, muss dieses aus 2,3,5-Trimethyl-*o*-chinol (XI) bei der Reduktion mit SO_2 enstanden sein. Der in Hexan unlösliche Anteil des Reduktionsproduktes war 2,3,5-Trimethyl-hydrochinon, Schmp. 168-169°.

Diacetat des dimeren 2,6-Dimethyl-o-chinols (VIII, OAc statt OH). Das Dimere VIII (850 mg) wurde in 10 ml des AcOAc–$HClO_4$-Äthylacetat-Reagenses von Fritz und Schenk [11] gelöst. Nach 10 Min. wurde mit 2 ml Wasser zersetzt, die Äthylacetatschicht mit Wasser gewaschen, mit $CaSO_4$ getrocknet und i.V. eingedampft. Der kristalline Rückstand gab nach dem Umkristallisieren aus Äthanol Prismen vom Schmp. 159–160°. Ausbeute 74 %. (Gef.: C 66.88; H 6.79; CH_3CO 20.81. Ber. für $C_{20}H_{24}O_6$: C 66.65; H 6.71; CH_3CO 23.89.) UV-Spektrum s. Tab. 1 und Fig. 1. IR-Banden (cm^{-1}): 1 751, 1 736 (Ester-CO), 1 726 (CO), 1 702 (konj. CO), 1 658 (C=C).

Thermische Spaltung des dimeren 2,6-Dimethyl-o-chinolacetats (VIII, OAc statt OH). Das Dimeracetat (190 mg) wurde in einem Knierohr unter Wasserstrahlvakuum rasch auf 180° erhitzt. Nach etwa 10 Min. hatten sich im gekühlten Teil des Röhrchens 175 mg (92 %) eines hellgelben Öls angesammelt, das im Kühlschrank kristallisierte. Umkristallisieren aus *Iso*propyläther gab fast weisses *2,6-Dimethyl-o-chinolacetat (XIV)*, Schmp. 34–35°, keine Schmelzpunktsdepression mit einem nach Wessely und Mitarb.[6] hergestellten Vergleichspräparat gleichen Schmelzpunkts. Auch die UV- und IR-Spektren waren identisch. (Gef.: C 66.64; H 6.51; CH_3CO 25.86. Ber. für $C_{10}H_{12}O_3$: C 66.65; H 6.71; CH_3CO 23.89.)

Thermische Dimerisierung von 2,6-Dimethyl-o-chinolacetat (XIV). Das monomere Acetat XIV (3.125 g) wurde in einem Kölbchen während 2.5 Std. in N_2-Atmosphäre bei 120° gehalten. Das entstandene Öl wurde in 5 ml warmem Äthanol gelöst; beim Abkühlen

wurden 2.05 g (66 Gew.-%) eines farblosen, kristallinen Produkts vom Schmp. 130—155° erhalten. Durch fraktioniertes Kristallisieren aus Äthanol konnte die Hauptmenge dieses Produktes als reines *dimeres 2,6-Dimethyl-o-chinolacetat (VIII, OAc statt OH)*, Schmp. 159—160° (s.o.), erhalten werden. Identifizierung durch Mischschmelzp. und IR-Spektrum.

Als Nebenprodukt wurde aus den Mutterlaugen ein *isomeres Diacetat* vom Schmp. 182—184° in Form farbloser, zugespitzter Prismen isoliert (Gef.: C 66.70; H 6.84; $COCH_3$ 24.21; Ber. für $C_{20}H_{24}O_6$: C 66.65; H 6.71; $COCH_3$ 23.89). UV-Spektrum: Max. bei 238 mμ (log ε = 3.81) und 310 mμ (log ε = 2.18). Das IR-Spektrum zeigt eine zusammengesetzte Bande mit Max. bei 1 726, und Inflexionen bei ca. 1 748, 1 738 und 1 710 cm^{-1}.

Alkalische Verseifung des dimeren 2,6-Dimethyl-o-chinolacetats (VIII, OAc statt OH). Dimeracetat VIII (OAc statt OH) (2.8 g) wurde in 100 ml 10-proz. äthanolischer Kalilauge (die mittels 2-st. Durchleitens von N_2 von Luft befreit worden war) gelöst. Nach 16-stündigem Stehen unter N_2 bei Zimmertemperatur wurde die nunmehr schwach gelbliche Lösung mit Wasser verdünnt und der Hauptanteil des Alkohols i.V. entfernt. Beim Abkühlen kristallisierten 770 mg farbloser Plättchen, Schmp. 189—194°, nach Mischschmp. und IR-Spektrum identisch mit *dimerem 2,6-Dimethyl-o-chinol (VIII)* (Ausbeute 36 %).

Die Mutterlauge wurde mit CO_2 neutralisiert, worauf 725 mg farbloser Stäbchen vom Schmp. 167—72° ausfielen. Umkristallisieren aus Äthanol-Wasser erhöhte den Schmp. auf 172—174°: *Anhydroprodukt des dimeren 2,6-Dimethyl-o-chinols (XXIII)* (Ausbeute 36 %). (Gef.: C 74.51; H 7.14. Ber. für $C_{16}H_{18}O_3$: C 74.40; H 7.02.) UV-Spektrum s. Fig. 2. IR-Banden (cm^{-1}): 3 460 (aliph. OH), 3 290 (phenol. OH), 1 712 (CO), 1 615, 1 586 (schwach, arom. Ring).

Monoacetat (XXIV) des "Anhydro-2,6-dimethyldimeren". Phenol XXIII (200 mg) wurde in 20 ml eines Gemisches von AcOAc und Pyridin (1:1) gelöst. Nach 16-stündigem Stehen bei Zimmertemp. wurde in Eiswasser gegossen und das ausgefallene Öl in Methylenchlorid aufgenommen. Die Methylenchloridphase wurde mit wässrigem Bikarbonat und Wasser gewaschen, mit $CaSO_4$ getrocknet und i.V. eingedampft. Der feste Rückstand gab nach dem Umkristallisieren aus Benzol-Hexan das Monoacetat XXIV vom Schmp. 150—152°. Ausbeute 82 %. (Gef.: C 71.83; H 6.62. Ber. für $C_{18}H_{20}O_4$: C 71.98; H 6.71.) UV-Spektrum s. Fig. 2. IR-Banden (cm^{-1}): 3 475 (aliph. OH), 1 769 (Enolester-CO), 1 713 (CO), 1 617, 1 593 (schwach, aromat. Ring).

Diacetat (XXV) des "Anhydro-2,6-dimethyldimeren". a) Phenol XXIII (47 mg) wurde in 1 ml des AcOAc—$HClO_4$-Reagenses [11] gelöst. Nach 10 Min. wurde mit Wasser zersetzt und mit Äthylacetat ausgeschüttelt. Aus der Äthylacetatphase wurde das Diacetat XXV erhalten, das nach Umkristallisieren aus Äthanol bei 176—178° schmolz. (Ausbeute 79 %). (Gef.: C 70.13; H 6.48; $COCH_3$ 25.13. Ber. für $C_{20}H_{22}O_6$: C 69.98; H 6.39; $COCH_3$ 27.07.) UV-Spektrum s. Fig. 2. IR-Banden (cm^{-1}): 1 758 (Enolester-CO), 1 738 (Ester-CO), 1 730 (Inflexion, CO), 1 615 (schwach, arom. Ring).

b) Analoge Behandlung des Monoacetats XXIV lieferte ebenfalls das Diacetat XXV.

Verseifung mit 10-proz. alkoholischem KOH in der Kälte regenerierte aus dem Diacetat XXV den Phenolalkohol XXIII.

Alkalische Verseifung des dimeren 2-Methyl-o-chinolacetats (IX, OAc statt OH). Dimeracetat IX (OAc statt OH) [5] (135 mg) wurde in 4 ml luftfreier 10-proz. alkoholischer Kalilauge 16 Std. unter N_2 stehen gelassen. Nach Verdünnen mit Wasser und Neutralisieren mit HOAc wurde ein Teil des Alkohols i.V. entfernt, wobei ein Rohprodukt ausfiel (ca 50 %), das nach Umkristallisieren aus abs. Äthanol-Benzol das *phenolische Anhydroprodukt XX*, Schmp. 184—185°, gab. Es war nach Mischschmp. und Spektren identisch mit einer nach Metlesics und Wessely [5] dargestellten Probe gleichen Schmelzpunkts. UV-Spektrum s. Fig. 2. IR-Banden wie von Metlesics und Wessely [5] angegeben; zusätzlich sei das Vorkommen einer Bande bei 1 497 cm^{-1} (arom. Ring) vermerkt.

Monoacetat XXI. Acetylierung von XX mit AcOAc-Pyridin bei Zimmertemp. gab farblose Kristalle von XXI, Schmp. nach Umkristallisieren aus Benzol-Hexan 127—129°. (Gef.: C 70.42; H 5.66. Ber. für $C_{18}H_{16}O_4$: C 70.57; H 5.92.) UV-Spektrum s. Fig. 2. IR-Banden (cm^{-1}): 3 450 (aliph. OH), 1 754 (Enolester-CO), 1 716 (CO), 1 604 (schwach, arom. Ring).

Zu den bei den entsprechenden Verbindungen angegebenen IR-Daten der *o*-Chinoldimeren sowie der Anhydrodimeren und ihrer Acetylderivate sei hier folgendes bemerkt. Während bei den *o*-Chinoldimeren (vgl. IV und VIII) sowohl die isolierte wie die konju-

gierte CO-Gruppe durch Banden normaler Lage gekennzeichnet sind, liegen die entsprechenden Banden bei den Diacetaten (IV bzw. VIII, OAc statt OH) nach ungewöhnlich hoher Frequenz verschoben; die Banden für das konjugierte CO finden sich bei 1 696 bzw. 1 702 cm^{-1}, und diejenigen des isolierten CO werden teilweise von den Estercarbonylbanden überlagert. Ähnliche Verhältnisse werden bei den Anhydrodimeren beobachtet. Sowohl die freien Verbindungen (XXIII, XX [5]) wie deren Monoacetate (mit verestertem Phenolhydroxyl) geben eine CO-Absorption normaler Lage, während bei den Diacetaten (XXV bzw. dem Diacetat von XX [5]) die entsprechenden Banden bei 1 730 bzw. 1 732 als Inflexionen, überlagert von den Estercarbonylbanden, auftreten.

Erhitzen von dimerem 2,6-Dimethyl-o-chinol (VIII) mit AcOAc—AcONa. Das Dimere VIII (2.0 g) wurde mit 20 ml AcOAc und 2 g AcONa 2 Std. unter Rückfluss erhitzt. Die Hauptmenge des Essigsäureanhydrids wurde i.V abdestilliert, der Rückstand mit Wasser zersetzt und das ausfallende Produkt in Methylenchlorid übergeführt. Der ölige Abdampfrückstand der Methylenchloridlösung wurde in warmem Äthanol gelöst. In der Kälte kristallisierten 160 mg des Anhydrodimer-diacetats XXV, Schmp. 176—178° (s.o.), Ausbeute 6 %.

Die Mutterlauge wurde vom Lösungsmittel befreit und der ölige Rückstand bei 0.005 mm Hg und 60° Badtemp. destilliert. Das Destillat kristallisierte nach nochmaliger Destillation und gab nach Umkristallisieren aus *Iso*propyläther bei —80° 795 mg (31 %) des monomeren *2,6-Dimethyl-o-chinolacetats* (XIV), Schmp. 32—34° (s.o.).

Der feste Destillationsrückstand, der leicht sublimierte, gab beim Umkristallisieren aus wenig Äthanol das *dimere 2,6-Dimethyl-o-chinolacetat (VIII, OAc statt OH)*, Schmp. 157—159° (s.o.). Ausbeute 25 %.

Unter ähnlichen Bedingungen mit AcOAc—AcONa erhitzt, lieferte das Diacetat des 2,6-Dimeren (VIII, OAc statt OH) 57 % des monomeren 2,6-Dimethyl-o-chinolacetats (XIV) und ein Gemisch des Ausgangsmaterials mit dem Anhydrodimer-diacetat XXV.

Herrn Ing. Bo Skarstedt danken wir für wertvolle Hilfe bei der Aufnahme der UV- und IR-Spektren. *Statens Tekniska Forskningsråd* danken wir für die Gewährung eines Forschungsbeitrags.

LITERATUR

1. Adler, E., Junghahn, L., Lindberg, U., Berggren, B. und Westin, G. *Acta Chem. Scand.* **14** (1960) 1261.
2. Bamberger, E. und Rising, A. *Ber.* **33** (1900) 3636.
3. Adler, E. *Angew. Chem.* **69** (1957) 272.
4. Siegel, A., Wessely, F., Stockhammer, P., Antony, F. und Klezl, P. *Tetrahedron* **4** (1958) 49.
5. Metlesics, W. und Wessely, F. *Monatsh.* **88** (1957) 108.
6. Budzikiewicz, H., Schmidt, G., Stockhammer, P. und Wessely, F. *Monatsh.* **90** (1959) 609.
7. Elphimoff-Felkin, I. *Bull. soc. chim. France* **1956** 1845.
8. Woodward, R. B. *J. Am. Chem. Soc.* **63** (1941) 1123.
9. Fieser, L. F. und Fieser, M. *Natural Products Related to Phenanthrene*, 3d Ed. (*Am. Chem. Soc. Monogr.* No. **70**), New York, 1949.
10. Adler, E., Berggren, B. und Jansson, I. *Unveröffentlicht.*
11. Fritz, J. S. und Schenk, G. H. *Anal. Chem.* **31** (1959) 1808.
12. Wessely, F. und Sinwel, F. *Monatsh.* **81** (1950) 1055.
13. Nietzki, R. und Schneider, J. *Ber.* **27** (1894) 1430; Teuber, H.-J. und Rau, W. *Chem. Ber.* **86** (1953) 1036.
14. Wessely, F., Kotlan, J. und Metlesics, W. *Monatsh.* **85** (1954) 69.
15. Cookson, R. C. und Wariyar, N. S. *J. Chem. Soc.* **1956** 2302.
16. Wariyar, N. S. *Pr. Indian Acad.* **43 A** (1956) 231.
17. Derkosch, J. und Kaltenegger, W. *Monatsh.* **90** (1959) 872.
18. Derkosch, J. und Kaltenegger, W. *Monatsh.* **88** (1957) 778.

Eingegangen am 26. April 1960.

ACTA CHEMICA SCANDINAVICA 14 (1960) 1597–1611

On the Thermodynamics of Hydrated Protons Activities, Activity Coefficients and the Average Degree of Hydration

ERIK HÖGFELDT

Department of Inorganic Chemistry, Royal Institute of Technology, Stockholm 70, Sweden

Activities and activity coefficients for hydrated ions in mixtures of acids with water are derived and their properties investigated. It is shown that the activity product $a_{n+} \cdot a_{n-}$ of the ions $H^+(H_2O)_{n+}$ and $A^-(H_2O)_{n-}$ (A^- = anion of the strong acid HA) must have a maximum at $X = \frac{1}{1+n}$ where X is the stoichiometric mole fraction of HA and $n = n_+ + n_-$. The maximum is obtained independent of whether the ions in question predominate or even exist.

Various activity coefficients are studied and it is found that the molarity activity coefficient for $H^+(H_2O)_4$, ClO_4^- passes through a maximum near 8 M (moles · liter^{-1}) $HClO_4$ while the corresponding function for $H^+(H_2O)_4$,NO_3^- is practically constant in the range 9–16 M HNO_3. This difference in behavior can be primarily attributed to differences in dissociation of the two acids. Above 9.5 M $HClO_4$, there is not enough water present to keep all H^+ in the form $H^+(H_2O)_4$ while, on the other hand, there is sufficient water in the HNO_3 mixtures all the way up to 16 M.

By considering hydrated ions as mononuclear complexes, ordinary complex chemistry methods can be employed to derive a function $\bar{n}'$ closely related to the "true" average degree of hydration. It is found that $\bar{n}'$ is practically the same for H^+, ClO_4^- and H^+, HSO_4^- in a large part of the range of overlap while it is smaller for H^+, NO_3^- thus implying a smaller degree of hydration for NO_3^- than for ClO_4^- and HSO_4^-. For the ion pair H^+, HSO_4^- $\bar{n}'$ tends towards unity upon approaching pure acid. It is also shown that a maximum ionic concentration will appear at $X = \frac{1}{1+\bar{n}'}$. For H_2SO_4 and $HClO_4$, the maximum is located in the range $X = 0.4–0.5$ while HNO_3 has its maximum at about $X = 0.2–0.3$ consistent with the view that HNO_3 forms a compound $HNO_3 \cdot H_2O$ before it starts to dissociate.

In dealing with electrolyte solutions, Bjerrum [1] and Scatchard [2,3] made use of a simple model in which ions and molecules are considered to bind part of the solvent giving solvated species that are dissolved in the remaining free solvent. This distinction between two different kinds of water, free water and water bound as water of hydration, has been used in several instances

and recently by Stokes and Robinson [4a] as well as Glueckauf [5] and Miller [6] in their attempts to evaluate hydration numbers. All these treatments were restricted to dilute solutions where the average degree of hydration can be imagined to stay practically constant. However, upon decreasing the water content in the system by increasing the ionic concentration, the amount of water considered as bound as water of hydration must decrease. In case of the proton, it has been suggested that $H^+(H_2O)_4$ should be an especially stable complex in dilute solutions [5,7—10]. In concentrated solutions, most of this water is stripped off until H_3O^+ is finally obtained which seems to be the predominating proton species in these solutions [11a] and so stable that it may be recovered in the crystalline state [12].

In the following, the properties of the activities and activity coefficients of hydrated ions are investigated. Since $H^+(H_2O)_4$ and H_3O^+ seem to be so stable as to be experimentally observable, the thermodynamic functions for these two compositions of the hydrated proton will be evaluated and used as examples. We shall then construct a function approximating the average degree of hydration and investigate its bearing on the maxima in ionic concentration found in mixtures of strong acids with water.

Some of the results below have been given in a preliminary note [11b].

LIST OF SYMBOLS

a_{H^+}, a_{A^-}, a_{HA}	Activities of H^+, A^-, HA *etc.*
a_{n+}, a_{n-}	» » $H^+(H_2O)_{n+}$, $A^-(H_2O)_{n-}$
a_1, a_4	» » H_3O^+ and $H^+(H_2O)_4$
y_+, y_-	"True" molarity activity coefficients of various hydrated ions
y_{n+}, y_{n-}	Stoichiometric molarity activity coefficients of $H^+(H_2O)_{n+}$ and $A^-(H_2O)_{n-}$
y_1, y_4	Stoichiometric molarity activity coefficients of H_3O^+ and $H^+(H_2O)_4$
$y = [y_{H^+} \cdot y_{A^-}]^{\frac{1}{2}}$	Stoichiometric molarity mean activity coefficient of H^+, A^-
γ_{n+}, γ_{n-}	» molarity activity coefficients of $H^+(H_2O)_{n+}$ and $A^-(H_2O)_{n-}$
$\gamma = [\gamma_{H^+} \cdot \gamma_{A^-}]^{\frac{1}{2}}$	Stoichiometric molality mean activity coefficient of H^+, A^-
f_{n+}, f_{n-}	» mole fraction activity coefficients of $H^+(H_2O)_{n+}$ and $A^-(H_2O)_{n-}$
$f = [f_{H^+} \cdot f_{A^-}]^{\frac{1}{2}}$	Stoichiometric mole fraction mean activity coefficient of H^+, A^-
C_{H^+}, C_{A^-}	Molarities of H^+, A^-
C	Stoichiometric molarity of acid
m_{H^+}, m_{A^-}	Molalities of H^+, A^-
m	Stoichiometric molality of acid
X_{H^+}, X_{A^-}	Mole fraction of H^+, A^-
X	Stoichiometric mole fraction of acid
K, K_n	Equilibrium constants
N_{H_2O}, N_{HA}	Number of moles of H_2O and HA mixed together

n	Number of water molecules attached to an ion
$\bar{n}$	Average degree of hydration
$\bar{n}'$	Function approximating $\bar{n}$
S^+, S, S^-	$S = \Sigma K_n a_{H_2O}^n$ Function appearing in the treatment of complex equilibria
α	Degree of dissociation

SELECTION OF EXPERIMENTAL DATA

In the choice of experimental data for the computation of thermodynamic functions involving hydrated ions, the measurements that appear to be the most careful have been used wherever possible.

The data selected will now be discussed for each acid in turn.

a) *Hydrochloric acid.* Densities of HCl solutions at 25°C, necessary for the transformation from the molality to the molarity scale, were computed from the formulas given by Åkerlöf and Teare [13]. Stoichiometric mean activity coefficients were taken from Harned and Owen [14] for dilute solutions and from Robinson and Stokes for concentrated solutions [4b]. The activity coefficients of Harned and Owen are based on emf measurements by Harned and Ehlers [15]. The activities of Robinson and Stokes are calculated from their own isopiestic measurements [16,17] and agree well with those of Åkerlöf and Teare [18] obtained from emf measurements. Water activities were computed from osmotic coefficients given by Robinson and Stokes [4c].

b) *Perchloric acid.* Densities for $HClO_4$ solutions at 25°C have been taken from Markham [19] and water activities together with stoichiometric mean activity ceofficients from Robinson and Baker [20] who used the isopiestic method. These data seem to be accepted as being the best available at present [21]. For estimating the concentration of various species, the results from the NMR (nuclear magnetic resonance) measurements by Hood, Redlich and Reilly [21] have been used, which values show a better consistency than the Raman measurements by Redlich, Holt and Bigeleisen [22].

c) *Nitric acid.* Densities of HNO_3 solutions at 20°C have been taken from Landolt-Börnstein [23a]. Concerning water and nitric acid activities at this temperature, the agreement between different investigations is not as good as could be desired [23b, 24—26]. For this reason, it is difficult to make a choice between the various data. However, those by Potier [26] have been chosen because of the large concentration range studied and the reasonably good internal consistency.

The concentrations of the species present have been determined with the Raman technique by Redlich and Bigeleisen [27] and by Young and Krawetz [28,29a]. Concentrations determined from NMR measurements by Redlich *et al* [21]. are said to agree well with the Raman measurements by Krawetz [29a]. The precision of the NMR measurements is not quite so good as for the Raman method but the NMR data were the only data accessible to the present writer and they have been used in this paper.

d) *Sulfuric acid.* Densities of H_2SO_4 solutions at 25°C have been taken from the International Critical Tables [30]. When the present investigation

was begun, the best available thermodynamic data for sulfuric acid seemed to be the recent isopiestic measurements by Glueckauf and Kitt [31] which agree well with the vapor pressure measurements of Shankman and Gordon [32] and Hornung and Giauque [33]. The measurements of Glueckauf and Kitt stop around 16 M (moles · liter^{-1}). Now Deno and Taft [34] have given water activities up to nearly pure H_2SO_4 using a simple empirical relation between the water activity and the Hammett acidity function, H_0. Both sets of values agree well in the overlapping part of the range. The present writer has used Deno and Taft's water activities to compute the corresponding sulfuric acid activities by graphical integration with the aid of the Gibbs-Duhem equation. The value for pure sulfuric acid obtained by extrapolation, $\log a^2_{H^+} \cdot a_{SO_4^{--}} = 9.55$, differs considerably from the value 8.76 estimated by Abel [35] from literature data available at that time. However, thanks to the courtesy of Professor Giauque, a set of thermodynamic data, unpublished at that time, for sulfuric acid collected during the course of many years in Berkeley [36] were made available to the present writer. The value for pure sulfuric acid at 25°C is $\log a^2_{H^+} \cdot a_{SO_4^{--}} = 9.53$ which is so close to the value found from the data of Deno and Taft that their empirical method for correlating water activities with H_0 must be regarded as essentially correct. The water activity and the stoichiometric activity coefficient of H_2SO_4 obtained by Giauque *et al.* agree within a few per cent with those of Glueckauf and Kitt in the overlapping section of the range. This is such a good agreement that no recalculation using the data of Giauque *et al.* seemed necessary.

For the concentrations of the species present, Raman [29a,37] and NMR [38] measurements are available. The Raman measurements reported by Young *et al.*[29a] are believed to be more accurate than the early measurements reported by Young and Blatz [37,39]. Since the evaluation of the NMR data depends upon the Raman measurements, no decisive information about the correctness of the Raman data can be obtained from them. In the following, the more recent Raman data [29a] will be used.

ACTIVITIES

Definitions. In the Bjerrum treatment of solvation, ions are assumed to bind the solvent to form solvated ions. For the acid HA, we wish to consider the following reaction:

$$HA + n\ H_2O \rightleftharpoons H^+(H_2O)_{n_+} + A^-\ (H_2O)_{n_-} \tag{1}$$

where

$$n = n_+ + n_- \tag{2}$$

Application of the law of mass action to (1) gives:

$$a_{H^+(H_2O)_{n+}} \cdot a_{A^-(H_2O)_{n-}} = K_n \cdot a_{HA} \cdot a^n_{H_2O} \tag{3a}$$

For the sake of simplicity in notation, we write:

$$\begin{aligned} a_{n+} &= a_{H^+(H_2O)_{n+}} \\ a_{n-} &= a_{A^-(H_2O)_{n-}} \end{aligned} \tag{4a, b}$$

and thus

$$a_{n+} \cdot a_{n-} = K_n \cdot a_{HA} \cdot a^n_{H_2O} \tag{3b}$$

For the dissociation into unhydrated ions, we have

$$a_{H^+} \cdot a_{A^-} = K \cdot a_{HA} \tag{5}$$

where K is the thermodynamic dissociation constant of HA. The activities of H_+ and A^- are defined such that they approach the analytical concentrations of these ions in dilute solutions. From (3b) and (5) it is found:

$$a_{n+} \cdot a_{n-} = \frac{K_n}{K} \cdot a_{H^+} \cdot a_{A^-} \cdot a^n_{H_2O}$$

The simplest way of relating the activity scale of hydrated ions to that of the unhydrated ions is to define

$$K_n = K \qquad n = 1, 2 \ldots . \tag{6}$$

for all possible values of n. We thus obtain:

$$a_{n+} \cdot a_{n-} = a_{H^+} \cdot a_{A^-} \cdot a^n_{H_2O} \tag{7}$$

Since $a_{H_2O} \rightarrow 1$ when approaching infinite dilution, the reference state of the hydrated ions is the same as for the unhydrated ions, *i.e.* the activity tends towards the analytical concentration upon dilution. Since the activity product $a_{H^+} \cdot a_{A^-}$ can be obtained from the stoichiometric activity coefficients and water activities which are either tabulated directly or can be computed from osmotic coefficients reported in the literature, the activity products given by (7) can be evaluated for several strong acids and often over considerable concentration ranges.

The maximum. From eqn. (7), it is seen that the activity product of the hydrated ions is composed of two terms, one containing the activity product of the unhydrated ions and the other the activity of water. Since the first term increases monotonically and tends towards a finite limit and the second, the water activity, decreases monotonically towards zero with increasing concentration of acid, there must be a maximum for the activity product of the hydrated ions. In order to investigate this, (5) is substituted in (7), *i.e.*

$$a_{n+} \cdot a_{n-} = K \cdot a_{HA} \cdot a^n_{H_2O} \tag{8}$$

Logarithmic differentiation of (8) gives:

$$\mathrm{d}\ln a_{n+} + \mathrm{d}\ln a_{n-} = \mathrm{d}\ln a_{HA} + n\mathrm{d}\ln a_{H_2O} \tag{9}$$

Application of the Gibbs-Duhem equation to this system gives:

$$N_{HA}\, \mathrm{d}\ln a_{HA} = -N_{H_2O}\, \mathrm{d}\ln a_{H_2O} \tag{10}$$

N_{HA} and N_{H_2O} are the number of moles of HA and H_2O mixed together. By inserting (10) into (9) and using the condition that at the maximum $\mathrm{d}\ln a_{n+} + \mathrm{d}\ln a_{n-} = 0$ we find:

$$\mathrm{d}\ln a_{H_2O} \left(n - \frac{N_{H_2O}}{N_{HA}} \right) = 0$$

Since $\mathrm{d}\ln a_{H_2O} \neq 0$, the maximum must be located at the stoichiometric mole fraction of acid given by:

$$X = \frac{1}{1+n} \tag{11}$$

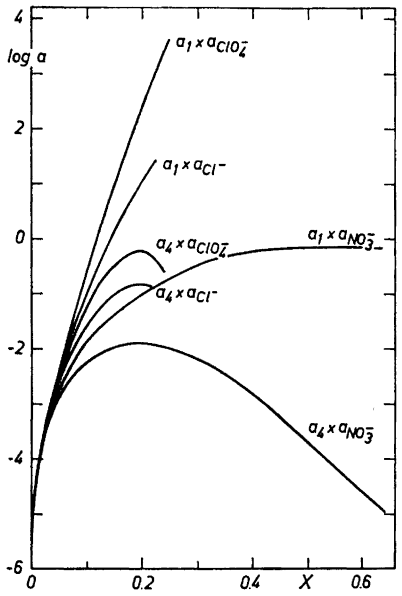

Fig. 1. The logarithms of the mole fraction activity products $a_1 \cdot a_A$- and $a_4 \cdot a_A$- plotted *versus* stoichiometric mole fraction, X, of acid for the three acids: HNO_3, HCl and $HClO_4$.

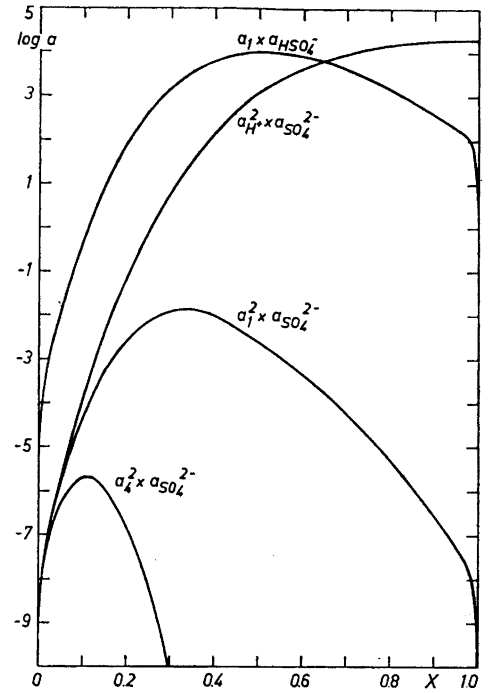

Fig. 2. The logarithms of the mole fraction activity products $(a_{H+})^2 \cdot a_{SO_4^{2-}}$, $a_1 \cdot a_{HSO_4^-}$, $a_1^2 \cdot a_{SO_4^{2-}}$ and $a_4^2 \cdot a_{SO_4^{2-}}$ plotted versus X.

This maximum is a purely thermodynamic consequence and shows that the activity product $a_{n+} \cdot a_{n-}$ has a maximum when the solution has the corresponding composition HA, n H_2O. The maximum is obtained independent of whether the ions in question exist or not.

Comparison of the activity products for two different n*-values.* Since many differently hydrated ions are possible, a large number of activity products $a_{n+} \cdot a_{n-}$ can be constructed. In order to study the properties of these activities, the following two special cases will be considered:

$$a_{H_3O+} \cdot a_{A^-} = a_1 \cdot a_{A^-} = a_{H+} \cdot a_{A^-} \cdot a_{H_2O} \quad (12a)$$

$$a_{H+(H_2O)_4} \cdot a_{A^-} = a_4 \cdot a_{A^-} = a_{H+} \cdot a_{A^-} \cdot a^4_{H_2O} \quad (12b)$$

where a_1 and a_4 are convenient notations. In Fig. 1, the activity products (12) on the mole fraction scale for the two acids HNO_3 and $HClO_4$ are plotted *versus* the stoichiometric mole fraction of acid. As is seen, the maximum of $a_4 \cdot a_{A^-}$ appears, for both acids, at $X = 0.2$. For HNO_3, the maximum for $a_1 \cdot a_{A^-}$ at $X = 0.5$ is hard to locate since the curve is very flat. For $HClO_4$, data are not available up to $X = 0.5$.

The only strong acid which has been studied over the whole concentration range from pure water to pure acid is sulfuric acid. In Fig. 2, the mole fraction activity products, $(a_{H^+})^2 \cdot a_{SO_4^{2-}}$, $a_1 \cdot a_{HSO_4^-}$ $a_1^2 \cdot a_{SO_4^{2-}}$ and $a_4^2 \cdot a_{SO_4^{2-}}$, are plotted on a logarithmic scale against stoichiometric mole fraction of H_2SO_4. The activity product $a_1 \cdot a_{HSO_4^-}$ can be computed from $(a_{H^+})^2 \cdot a_{SO_4^{2-}}$ and a_{H_2O} with knowledge of the second dissociation constant of sulfuric acid. The value $pK_{HSO_4^-} = 2.00$ for 25°C recently suggested by Hamer [29b] from considerations of available literature data has been accepted. This value agrees well with $pK_{HSO_4^-} = 2.01$ calculated by Kerker [40] from transference and conductance data. The activity product $a_1 \cdot a_{HSO_4^-}$ can now be computed from

$$\log a_1 \cdot a_{HSO_4^-} = \log (a_{H^+})^2 \cdot a_{SO_4^{2-}} \cdot a_{H_2O} \cdot K^{-1}_{HSO_4^-} =$$
$$= \log (a_{H^+})^2 \cdot a_{SO_4^{2-}} + \log a_{H_2O} + 2.00 \qquad (13)$$

As seen from Fig. 2, all functions have maxima as requested by (11). The function $(a_{H^+})^2 \cdot a_{SO_4^{2-}}$ can be considered as a special case with $n = 0$ for which (11) gives a maximum for the pure acid.

ACTIVITY COEFFICIENTS

For the acids, $HClO_4$, HNO_3 and H_2SO_4, Raman and NMR methods have been used to distinguish between the undissociated and dissociated parts of acids in concentrated solutions. It is thus possible to compute activity coefficients and study their properties.

a) *Definitions.* For the strong acid HA where the concentrations of the species present have been estimated using one of the methods mentioned above, the ionic activity coefficient products on the molarity scale for $H^+(H_2O)_{n+}$, $A^-(H_2O)_{n-}$ can be computed from

$$y_{n+} \cdot y_{n-} = \frac{a^c_{n+} \cdot a^c_{n-}}{(\alpha C)^2} \qquad (14a)$$

where the superscript c refers to the molarity scale, α is the degree of dissociation and C the stoichiometric molarity of HA.

The analogous expressions on the molality (m) and mole fraction (x) scales are:

$$\gamma_{n+} \cdot \gamma_{n-} = \frac{a^m_{n+} \cdot a^m_{n-}}{m_{H^+} \cdot m_{A^-}}; \quad f_{n+} \cdot f_{n-} = \frac{a^x_{n+} \cdot a^x_{n-}}{x_{H^+} \cdot x_{A^-}} \qquad (14b, c)$$

The activity coefficients in (14) have the same reference state as ordinary activity coefficients, *i.e.* they approach unity at infinite dilution. In the evaluation of these activity coefficients, the total ionic concentration is used because of the difficulty of making a distinction between differently hydrated ions. They are thus stoichiometric activity coefficients which approach the true ones at those concentrations where the corresponding ionic species may predominate.

b) *Properties.* The stoichiometric activity coefficients of the hydrated ions are related to the ordinary stoichiometric activity coefficients in the following way:

$$y_{n+} \cdot y_{n-} = \left(\frac{y}{a}\right)^2 \cdot a^n_{H_2O}$$

$$\gamma_{n+} \cdot \gamma_{n-} = \left(\frac{\gamma}{a}\right)^2 \cdot a^n_{H_2O} \, [1 - a\, n \cdot m \cdot (55.51)^{-1}]^2 \qquad (15a, b, c)$$

$$f_{n+} \cdot f_{n-} = \left(\frac{f}{a}\right)^2 \cdot a^n_{H_2O} \, [1 - a(n-1)X]^2$$

The term $(n\text{-}1)$ appearing in (15c) is due to the convention that, in the evaluation of the mole fractions, the ions of the dissociated acid are counted as separate entities. For $n = 0$, (15b) degenerates into the relation $\gamma_{H^+} \cdot \gamma_{A^-} = \left(\frac{\gamma}{a}\right)^2$ used by Robinson and Stokes [4]. From (15), it is seen that the activity coefficient product of the hydrated ions will always be smaller than that of the unhydrated ions because $a_{H_2O} \leq 1$.

It can be shown from (15) that the ratio of the activity coefficient product of any pair of hydrated ions to that of the unhydrated ions will in pure acid be the same for all three kinds of activity coefficients and equal to $a^n_{H_2O}$, where a_{H_2O} refers to the activity of water in pure acid.

c) *Comparison of activity coefficient products for some different* n*-values.* For the two cases H_3O^+, A^- and $H^+(H_2O)_4$, A^- considered in the discussion of the activities, the activity coefficients on the molarity scale take the form:

$$y_1 \cdot y_{A^-} = \left(\frac{y}{a}\right)^2 \cdot a_{H_2O} \qquad (16a)$$

$$y_4 \cdot y_{A^-} = \left(\frac{y}{a}\right)^2 \cdot a^4_{H_2O} \qquad (16b)$$

As seen from (15), the activity coefficients take the most simple form on the molarity scale because it is not necessary to distinguish between free and bound water when evaluating the molarities of the constituents present.

In Fig. 3, $\log y_1 \cdot y_{A^-}$ and $\log y_4 \cdot y_{A^-}$ are plotted against the stoichiometric molarity of the acid for HNO_3 and $HClO_4$. It is not suitable to plot the activity

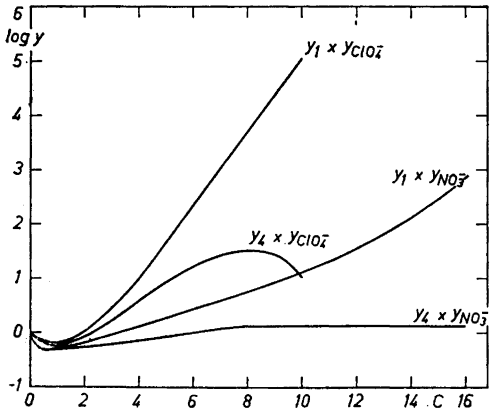

Fig. 3. The molarity activity coefficients $y_1 \cdot y_{A^-}$ and $y_4 \cdot y_{A^-}$ plotted on a logarithmic scale *versus* stoichiometric molarity of acid, C, for HNO_3 and $HClO_4$.

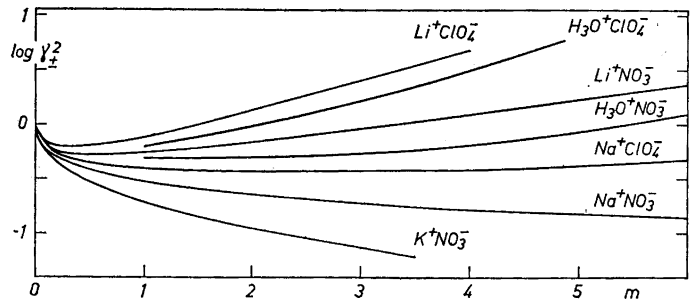

Fig. 4. The logarithms of the stoichiometric molality activity coefficients $\gamma_+ \cdot \gamma_-$ for $LiClO_4$, $LiNO_3$, $NaClO_4$, $NaNO_3$, KNO_3, H_3O^+, ClO_4^-, and H_3O^+, NO_3^- plotted *versus* the stoichiometric molality m.

coefficients *versus* the ionic strength or the total ionic concentration since these quantities go through a maximum and do not lead to single-valued activity coefficient functions.

It should be noted that, while $y_4 \cdot y_{ClO_4^-}$ goes through a maximum near 8 M $HClO_4$, $y_4 \cdot y_{NO_3^-}$ seems to be practically constant in the range 9—16 M HNO_3. On the other hand, both curves $y_1 \cdot y_{A^-}$ rise steeply. The maximum of $y_4 \cdot y_{ClO_4^-}$ can be imagined to be due to overcompensation caused by assuming too high a hydration number. From the data of Redlich *et al.*[21] near 9.5 M $HClO_4$, it appears that the amount of water present has decreased to four times that of H^+. Above this concentration, there is not enough water present to have all protons in the form of $H^+(H_2O)_4$. This may be the main reason for the maximum in $y_4 \cdot y_{ClO_4^-}$.

For HNO_3 on the other hand, the data by Redlich *et al.*[21] show that the amount of water present is at least six times that of H^+ even at 16 M HNO_3. For this acid, there is sufficient water to have a considerable fraction of the

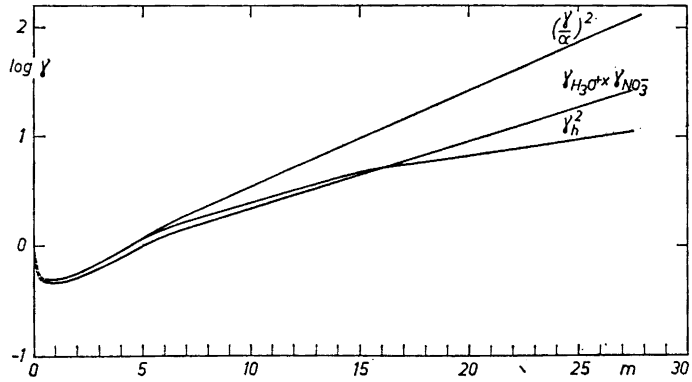

Fig. 5. log $\gamma_{H_3O^+} \cdot \gamma_{NO_3^-}$ compared with log $\left(\frac{\gamma}{a}\right)^2$ and log γ_h^2.

protons as $H^+(H_2O)_4$ or $H^+(H_2O)_3$. The nearly constant value of $y_4 \cdot y_{NO_3^-}$ between 9 and 16 M might thus be due to a practically negligible displacement of the proton equilibria towards less hydrated protons over almost the whole range of dissociation of HNO_3. On the other hand, for stronger acids like $HClO_4$, there is a change from something like $H^+(H_2O)_4$ in dilute solutions towards H_3O^+ in concentrated solutions.

Since free protons do not seem to exist in water solutions in measurable amounts, it is natural to consider H_3O^+ as the primary proton species which like any other ion upon dilution undergoes further hydration. Since H_3O^+ is a singly charged ion of a size comparable to K^+, it might be of interest to compare the molality activity coefficient products of H_3O^+, NO_3^- and H_3O^+, ClO_4^- with those of some related 1:1 electrolytes. This has been done in Fig. 4 where log $\gamma_{X^+} \cdot \gamma_{A^-}$ is plotted *versus* the stoichiometric molality for $LiClO_4$, $LiNO_3$, $NaNO_4$, KNO_3, N_3O^+, ClO_4^- and H_3O^+, NO_3^-. As seen, H_3O^+ falls between Li^+ and Na^+ for both NO_3^- and ClO_4^-. Upon considering only the size effect, one should have expected H_3O^+ to fall closer to K^+. The order of decreasing activity coefficients suggests that the degree of hydration decreases in the order $Li^+ > H_3O^+ > Na^+ > K^+$ in qualitative agreement with recent estimates[4a,5,6] although the different authors do not agree about the magnitude of the hydration numbers.

McKay[41] has recently evaluated an activity coefficient for the ionized part of HNO_3 where the tries to account formally for the influence of undissociated acid on the ions. In Fig. 5, this activity coefficient, γ_h, is compared with those of H^+, NO_3^- and H_3O^+, NO_3^-. Log γ_h^2 was computed from

$$\log(\gamma_h)^2 = \log\left(\frac{\gamma}{a}\right)^2 - 0.048\ (1-a) \cdot m$$

For the derivation of this expression, the reader is referred to the original paper. As seen in Fig. 5, γ_h^2 is close to $\left(\frac{\gamma}{a}\right)^2$ in dilute solutions while in concentrated solutions it falls below $\gamma_{H_3O^+} \cdot \gamma_{NO_3^-}$. Although the construction of γ_h contains an interesting attempt to correct for the influence of undissociated acid on the ionic activity coefficients, it suffers from the defect of referring to unhydrated protons and not to the actual species present.

A FUNCTION APPROXIMATING TO THE AVERAGE DEGREE OF HYDRATION

Considerations of only one kind of hydrated ionic species at a time must necessarily always be very crude. By considering the more realistic case of the simultaneous existence of several differently hydrated ionic constituents and by applying ordinary complex chemistry methods to the ion-water equilibria, a function closely related to the average degree of hydration can be derived as follows:

For the two types of reactions (n may have several values):

$$\left.\begin{aligned} H^+ + n\ H_2O &\rightleftharpoons H^+(H_2O)_n \\ A^- + n\ H_2O &\rightleftharpoons A^-(H_2O)_n \end{aligned}\right\} \qquad (17a, b)$$

the law of mass action gives:

$$\left.\begin{aligned} C_{H^+(aq)} &= \frac{K_n}{y_+} \cdot a_{H^+} \cdot a^n_{H_2O} \\ C_{A^-(aq)} &= \frac{K_n}{y_-}\, a_{A^-} \cdot a^n_{H_2O} \end{aligned}\right\} \qquad (18a, b)$$

We can now sum over all differently hydrated ionic constituents and get

$$\left.\begin{aligned} C_{H^+} = aC = \Sigma\, C_{H^+(aq)} &= \frac{a_{H^+}}{y_+} \Sigma\, K_{n+} \cdot a^n_{H_2O} = \frac{a_{H^+}}{y_+} \cdot S^+ \\ C_{A^-} = aC = \Sigma\, C_{A^-(aq)} &= \frac{a_{A^-}}{y_-} \Sigma\, K_{n-}\, a^n_{H_2O} = \frac{a_{A^-}}{y_-} \cdot S^- \end{aligned}\right\} \qquad (19a, b)$$

In the derivation of (19), it is assumed that the activity coefficients of the differently hydrated protons are the same ($= y_+$) and can be placed outside the summation sign and analogously for the anions.

The sums S^+ and S^- are functions appearing in the mathematical treatment of complex equilibria. They have the property:

$$\frac{\mathrm{d}\log S}{\mathrm{d}\log a_{H_2O}} = \frac{\Sigma\, n\, K_n\, a^n_{H_2O}}{\Sigma\, K_n\, a^n_{H_2O}} = \bar{n} \qquad (20)$$

where $\bar{n}$ is the average number of water molecules attached to the ion under consideration.

By multiplying (19a) with (19b) and inserting the stoichiometric activity coefficient $y = \left[\frac{a^c_{H^+} \cdot a^c_{H}}{C_{H^+} \cdot C_{A^-}}\right]^{\frac{1}{2}} = (y_{H^+} \cdot y_{A^-})^{\frac{1}{2}}$ we get after differentiation and use of equation (20):

$$\mathrm{d}\log(y_+ \cdot y_-)/\mathrm{d}\log a_{H_2O} - \mathrm{d}\log\left(\frac{y}{a}\right)^2 / \mathrm{d}\log a_{H_2O} = \bar{n}_+ + \bar{n}_- = \bar{n} \qquad (21)$$

In (21), all quantities except $y_+ \cdot y_-$ are known from experimental measurements. Various attempts to estimate related activity coefficient products have been made in recent papers on ionic hydration [4a,5,6]. However, these treatments employ the Debye-Hückel expression which is likely to break down in concentrated solutions. Because of our lack of knowledge of how to correct for electrostatic interactions in concentrated solutions of electrolytes, (21) cannot be employed for computing absolute $\bar{n}$-values. It can be used, however, for the computation of relative hydration numbers. When comparing the two acids HA and HB at the same water activity, we get from (21)

$$\mathrm{d}\log\left(\frac{y}{a}\right)^2_{HA} / \mathrm{d}\log a_{H_2O} - \mathrm{d}\log\left(\frac{y}{a}\right)^2_{HB} / \mathrm{d}\log a_{H_2O} = \bar{n}_{B^-} - \bar{n}_{A^-} \qquad (22)$$

if the assumption

$$\frac{\mathrm{d}\log y_{A^-}}{\mathrm{d}\log a_{H_2O}} = \frac{\mathrm{d}\log y_{B^-}}{\mathrm{d}\log a_{H_2O}} \qquad (23)$$

is correct. Even if not strictly valid, (23) might be a good first approximation and thus eqn. (22) may give reasonably good relative hydration numbers.

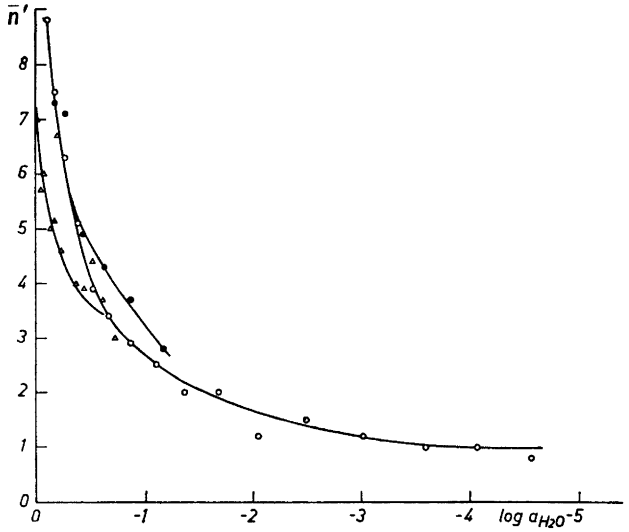

Fig. 6. The function $\bar{n}'$ for various ion pairs plotted *versus* log a_{H_2O}.
○ H^+, HSO_4^-
● H^+, ClO_4^-
△ H^+, NO_3^-

We can also use (21) to define an approximation to $\bar{n}$. From (21) we get

$$\bar{n}' = -\,\mathrm{d}\,\log\left(\frac{y}{a}\right)^2 / \,\mathrm{d}\,\log a_{H_2O} = \bar{n} - \mathrm{d}\log y_+ y_- / \mathrm{d}\log a_{H_2O} \qquad (24)$$

This approximation may be expected to be bad in dilute solutions because the activity coefficients vary very much while a_{H_2O} varies rather little. In concentrated solutions, on the other hand, activity coefficients seem to vary relatively little while the variation of a_{H_2O} is large and the function $\frac{\mathrm{d}\log y_+ \cdot y_-}{\mathrm{d}\log a_{H_2O}}$ therefore close to zero. One might thus expect $\bar{n}'$ to approach $\bar{n}$ in very concentrated solutions.

In order to study the behavior of $\bar{n}'$, this function, calculated according to (24), is plotted in Fig. 6 *versus* log a_{H_2O} for the three ion pairs: H^+, ClO_4^-, H^+, NO_3^- and H^+, HSO_4^-. As seen, the curves for H^+, ClO_4^- and H^+, HSO_4^- prachically coincide at high water activities. On the other hand, the curve for H^+, NO_3^- lies below the two others indicating a smaller degree of hydration for NO_3^- as compared with ClO_4^- and HSO_4^-. Unfortunately, there is a large scattering in the data for H^+, NO_3^- — it seems however that, in dilute solutions, ClO_4^- and HSO_4^- contain 2—3 more H_2O in the hydration shell as compared with NO_3^-. In more concentrated solutions, this difference decreases to ½—1 around log $a_{H_2O} = -0.5$. It should also be noted that, in the range $-0.3 >$ log $a_{H_2O} > -0.9$ corresponding to 9—16 M HMO_3^- $\bar{n}'$ varies rather little in agreement with previous considerations of $y_4 \cdot y_{NO_3^-}$

in the same concentration range. For the pair H^+, HSO_4^-, it is interesting to note that $\bar{n}' \rightarrow 1$ upon approaching pure H_2SO_4. This result seems reasonable since $H^+(H_2O)_n$ can be imagined to tend towards H_3O^+ and HSO_4^- to loose all its water of hydration with decreasing water activity. From the data presented here, it cannot be definitely concluded whether the remaining water molecule in the hydration shell belongs to H^+ or HSO_4^-. However, in a following paper, evidence is given that H^+ is likely to exist as H_3O^+ in concentrated solutions of H_2SO_4[11a]. The fact that $\bar{n}'$ tends towards a plausible limit lends support to the suggestion that $d \log y_+ \cdot y_-/d \log a_{H_2O} \approx 0$ in concentrated solutions and thus $\bar{n}' \approx \bar{n}$.

THE MAXIMUM IN IONIC CONCENTRATION

From Raman and NMR measurements in mixtures of strong acids with water, it has been found that each ionic constituent has a maximum concentration at a certain composition of the mixture. The location of this maximum can be correlated with the hydration of the ions in the following manner.

By multiplying (19a) and (19b) we get

$$C_{H^+} \cdot C_{A^-} = (C_{A^-})^2 = \frac{a^c_{H^+} \cdot a^c_{A^-}}{y_+ \cdot y_-} \cdot S^+ \cdot S^- = \frac{K \cdot a_{HA}}{y_+ \cdot y_-} \cdot S^+ \cdot S^- \qquad (25)$$

Differentiating (25) logarithmically, using the definition of $\bar{n}'$ given by (24) and the condition that at the maximum $d \log C_{A^-} = 0$ gives, after combining with the Gibbs-Duhem equation (10):

$$X = \frac{1}{1 + \bar{n}'} \qquad (26)$$

Eqn. (26) is obviously an extention of (11). In order to estimate which $\bar{n}'$-values correspond to the maxima found experimentally, the locations of the maximum ionic concentration for NO_3^-, ClO_4^- and HSO_4^- are compared with equation (26) in Table 1.

As seen from Table 1, the ions ClO_4^- and HSO_4^- have their maximum concentration in a range where $\bar{n}' \approx 1-2$ while NO_3^- has its maximum in a more

Table 1. Comparison of experimental material with eqn (26).

$\bar{n}'$	X Eqn. (26)	X Exptl. NO_3^-	ClO_4^-	HSO_4^-
1	0.50			
2	0.33		0.40—0.50 (21)	0.42 (29a)
3	0.25	(28, 29a) * (21) 0.21—0.26		
4	0.20			

* Quoted from Ref[41].

dilute solution where $\bar{n}' \approx 3-4$. This might be due to the weaker dissociation of HNO_3. If we consider the reaction:

$$HA + H_2O \rightleftharpoons H_3O^+ + A^- \qquad (27a)$$

an infinitely strong acid will give one H_3O^+ and one A^- for every H_2O added. In such a case, the maximum will be at $X = 0.5$. Weaker acids on the other hand will have their maxima displaced towards lower concentrations. The maxima for $HClO_4$ and H_2SO_4 near $X = 0.5$ imply that these acids should be considered very strong and much stronger than HNO_3. It is surprising that such a difference is not more emphasized in the values of the thermodynamic dissociation constants of HNO_3 (22)[21] and $HClO_4$(38)[21]. If, on the other hand, HNO_3 first reacts with water to form a compound like $HNO_3.H_2O$ before it dissociates, then the reaction might be:

$$HNO_3 \cdot H_2O + H_2O \rightleftharpoons H^+ (H_2O)_{n_+} + NO_3^- (H_2O)_{n_-} \qquad n_+ + n_- = 2 \qquad (27b)$$

and the maximum in ionic concentration would be located somewhere below $X = 0.33$. The dissociation constant could nevertheless be of the same order of magnitude as that of $HClO_4$ in spite of the lower dissociation. Actually there is evidence that HNO_3 forms hydrates before it dissociates and also the Raman measurements show that the dissociation starts near the composition $HNO_3 \cdot H_2O$. These results support the dissociation reaction (27b) rather than (27a) for HNO_3.

For H_2SO_4, $X = 0.42$ gives $\bar{n}' = 1.40$ which implies that at the maximum concentration of HSO_4^- practically all of the free water has become bound as water of hydration. Now, the Raman measurements by Young et al show that measurable amounts of H_2SO_4 start to appear at about the same concentration. It thus seems that molecules of H_2SO_4 cannot appear until nearly all of the free water has been tied up as water of hydration.

Acknowledgements. The author wants to express his sincere thanks to Professors L. G. Sillén and R. E. Connick for valuable discussions and helpful advice, to Professor T. F. Young for comments on equilibria in strong sulfuric acid and to Professor W. F. Giauque for providing access to previously unpublished data for the system $H_2SO_4-H_2O$. Mr D. Gillam corrected the English text. The financial support of the *Swedish Atomic Energy Committee* and the *Swedish Natural Science Research Council* is gratefully acknowledged.

REFERENCES:

1. Bjerrum N. *Medd. Vetenskapsakad. Nobelinst.* **5** (1919) 1.
2. Scatchard G. *J. Am. Chem. Soc.* **43** (1921) 2406.
3. Scatchard G. *Ibid.* **47** (1925) 2098.
4. Robinson, R. A. and Stokes, R. H. *Electrolyte Solutions*, Butterworth, London 1955; a) p 239–253, b) 489, c) 468.
5. Glueckauf, E. *Trans. Faraday Soc.* **51** (1955) 1235.
6. Miller, D. G. *J. Phys. Chem.* **60** (1956) 1296.
7. *Discussions Faraday Soc.* **24** (1957)
   a) Bascombe, R. N. and Bell, R. P. p. 158,
   b) Wyatt, P. A. H. p. 162,
   c) van Panthaleon van Eck, C. L., Mendel, H. and Boog, W. p. 200,
   d) Redlich, O. and Hood, G. C. p. 87.

8. Glueckauf, E. and Kitt, G. P. *Proc. Roy. Soc. London* **A 228** (1955) 322.
9. Wicke, E., Eigen, M. and Ackermann, Th. *Z. physik. Chem.* NF **1** (1954) 340.
10. Tuck, D. G. and Diamond, R. M. *Proc. Chem. Soc.* **1958** 236.
11. a) Högfeldt, E. *Acta Chem. Scand.*, **14** (1960) 1627.
b) Högfeldt, E. *Nature* **185** (1960) 760.
12. Volmer, M. *Ann.* **440** (1924) 200.
13. Åkerlöf, G. and Teare, J. *J. Am. Chem. Soc.* **60** (1938) 1226.
14. Harned, H. S. and Owen, B. B. *The Physical Chemistry of Electrolytic Solutions*, Third Ed., Reinhold, N. Y. 1958, p. 716.
15. Harned, H. S. and Ehlers, R. W. *J. Am. Chem. Soc.* **55** (1933) 2179.
16. Stokes, R. H. *Trans. Faraday Soc.* **44** (1948) 295.
17. Robinson, R. A. and Stokes, R. H. *Trans. Faraday Soc.* **45** (1959) 612.
18. Åkerlöf, G. and Teare, J. W. *J. Am. Chem. Soc.* **59** (1937) 1855.
19. Markham, A. E. *J. Am. Chem. Soc.* **63** (1941) 874.
20. Robinson, R. A. and Baker, O. J. *Trans. Proc. Roy. Soc. New Zealand* **76** (1946) 250, as reported in *Chem. Abstr.* **41** (1947) 5000 d.
21. Hood, G. C., Redlich, O. and Reilly, C. A. *J. Chem. Phys.* **22** (1954) 2067.
22. Redlich, O., Holt, E. K. and Bigeleisen, J. *J. Am. Chem. Soc.* **66** (1944) 13.
23. *Landolt-Börnstein Physikalisch-Chemische Tabellen.* Julius Springer, Berlin.
a) Eg II a, 1931, p. 254;
b) Eg III c, 1936, p. 2145.
24. Forsythe, W. R. and Giauque, W. F. *J. Am. Chem. Soc.* **64** (1942) 48.
25. Vandoni, M. R. and Laudy, M. *J. chim. phys.* **49** (1952) 99.
26. Potier, A. *Ann. fac. sci. univ. Toulouse* **20** (1956) 1.
27. Redlich, O. and Bigeleisen, J. *J. Am. Chem. Soc.* **65** (1943) 1883.
28. Krawetz, A. A. *Thesis*, University of Chicago 1955.
29. Hamer, W. J. *The Structure of Electrolytic Solutions*, John Wiley, New York 1959.
a) Young, T. F., Maranville, L. F. and Smith, M. M. p. 35,
b) Hamer, W. J., p. 236.
30. *International Critical Tables*, Vol 3, McGraw Hill, New York 1928 p. 56—57.
31. Glueckauf, E. and Kitt, G. *Trans. Faraday Soc.* **52** (1956) 1074.
32. Shankman, S. and Gordon, A. R. *J. Am. Chem. Soc.* **61** (1939) 2370.
33. Hornung, E. W. and Giauque, W. F. *J. Am. Chem. Soc.* **77** (1955) 2744.
34. Deno, N. C. and Taft, R. W. Jr. *J. Am. Chem. Soc.* **76** (1954) 244.
35. Abel, E. *J. Phys. Chem.* **52** (1948) 908.
36. Giauque, W. F., Hornung, E. W. Kunzler, J. E. and Rubin, T. R. *J. Am. Chem. Soc.* **82** (1960) 62.
37. Young, T. F. and Blatz, L. A. *Chem. Revs.* **44** (1949) 93.
38. Hood, G. C. and Reilly, C. A. *J. Chem. Phys.* **27** (1957) 1126.
39. Young, T. F. *Private communication.*
40. Kerker, W. *J. Am. Chem. Soc.* **79** (1957) 3664.
41. McKay, H. A. C. *Trans. Faraday Soc.* **52** (1956) 1568.

Received April 2, 1960.

ACTA CHEMICA SCANDINAVICA 14 (1960) 1612–1622

The Crystal Structure of $Mo_{17}O_{47}$

LARS KIHLBORG

Institute of Chemistry, University of Uppsala, Uppsala, Sweden

A crystal structure determination has been carried out on the $\varkappa$-molybdenum oxide, which has confirmed the proposed formula $Mo_{17}O_{47}$ and the orthorhombic space-group *Pba*2 for this phase.

The structure may be considered as built up from MoO_6 octahedra and pentagonal MoO_7 bipyramids. The Mo—O distances within the latter are rather unequal suggesting that the coordination is not so high as sevenfold. Fairly short O—O distances (mean value 2.32 Å) have been observed within the pentagonal rings of the oxygens in these bipyramids.

The polyhedra are connected in one dimension through common corners and in two dimensions by sharing corners and edges. A distance of 2.64 Å between two molybdenum atoms suggests a direct bond between them of the same kind as is known for example in several transition metal dioxides.

The structure is closely related to that of $W_{18}O_{49}$, previously determined by Magnéli, and this relationship is discussed.

The results of a phase analysis study of the MoO_2—MoO_3 region of the molybdenum — oxygen system were recently published in this journal [1]. In the course of these investigations a phase of composition near $MoO_{2.78}$ was observed formed below 560° ± 10°C and was designated the *$\varkappa$-oxide*. From its X-ray powder pattern, obtained with a Guinier focussing camera using Cu$K\alpha$ radiation, the following dimensions were derived for the orthorhombic unit cell:

$a = 21.61_5$ Å, $b = 19.63_2$ Å, $c = 3.951_5$ Å.

The observed density was found to be consistent with the formula $Mo_{17}O_{47}$, having 2 formula units in the unit cell.

A structure determination of this phase has now been carried out on the basis of single crystal data and is presented in this article.

EXPERIMENTAL

Details concerning the preparation of the oxide are given in Ref.[1] The single crystals obtainable were in the form of very thin, fragile needles which were too small to give reflexions with MoK radiation within reasonable time. The crystal investigated had a

length of 0.15 mm and a rectangular cross-section of 0.012 × 0.002 mm². The pronounced needle shape allowed the crystal to be rotated about the needle axis only, this being the *c*-axis of the unit cell. The layer lines *hk*0 to *hk*3 were registered in a Weissenberg camera with Cu*Ka* radiation using the multiple film technique. The intensities were estimated visually and the various layer lines were correlated by exposing parts of each of them on the same pack of films, using carefully controlled exposure times and radiation conditions [2].

A few photographs were also taken with a Buerger precession camera, which allowed 00*l* reflexions to be registered.

Lorentz-polarization corrections were applied by the method given by Löfgren [3]. The *hk*0 reflexions were corrected for the effect of absorption by means of a graphical method developed by Hesse [4]. In this way a set of relative structure amplitudes were obtained which were later brought to an absolute scale by comparison with the calculated structure factors.

Most of the calculations were carried out by means of the digital computers BESK and Facit EDB in Stockholm. A description of some of the programmes used with these machines has recently been published [5,6]. The atomic scattering curves of Thomas and Umeda [7] (for Mo) and Berghuis *et al.*[8] (for O) were used in the form of analytical representations given by Appel [9].

DETERMINATION OF THE STRUCTURE

The reflexions *h*0*l* and 0*kl* are absent for odd *h* and *k* which suggests the space groups *Pba*2 (No. 32) or *Pbam* (No. 55). In *Pbam* there are mirror planes perpendicular to the *c* axis and owing to the shortness of this axis it is unlikely that an atom could be in a general position relative to these symmetry elements. If the atoms were situated on the mirror planes, *i.e.* on one or both of the planes $z = 0$ and $z = \frac{1}{2}$, the observed relative intensities of the 00*l* reflexions could not be explained. It was therefore assumed that the space group is *Pba*2, which has been confirmed by the structure determination.

The projection on (001) is centro-symmetrical in contrast to the space group as a whole, and in the present case is the most important one as it contains the two long axes. The atomic *x* and *y* coordinates were derived exclusively from this projection on the basis of *hk*0 data, and when they had been established the *z* parameters were determined with use of full *hkl* data.

a. Determination of the *x* and *y* coordinates

In the space group *Pba*2 there are 2- and 4-fold positions. As the unit cell was supposed to contain 34 Mo atoms, two of these must be in one of the two 2-fold positions. Starting from this, it was possible to find an arrangement of the metal atoms that fully accounted for the Patterson projection $P(UV)$ shown in Fig. 1a. After two cycles of computation of structure factors $F_c(hk0)$ and electron density projections $\varrho(XY)$, correct signs could be assigned to all the observed structure amplitudes $|F(hk0)|$.

The electron density maps showed minor maxima, which could reasonably be interpreted as being due to 4 × 15 oxygen atoms (O_{10}—O_{24}, *cf.* Fig. 2). In a difference synthesis, where the contribution from all the Mo atoms had been subtracted, the remaining 2 × 1 + 4 × 8 oxygen atoms (O_1—O_9) were clearly revealed as rest maxima close to the positions of the Mo atoms. These maxima were about 20 % lower than the other oxygen peaks, even after the

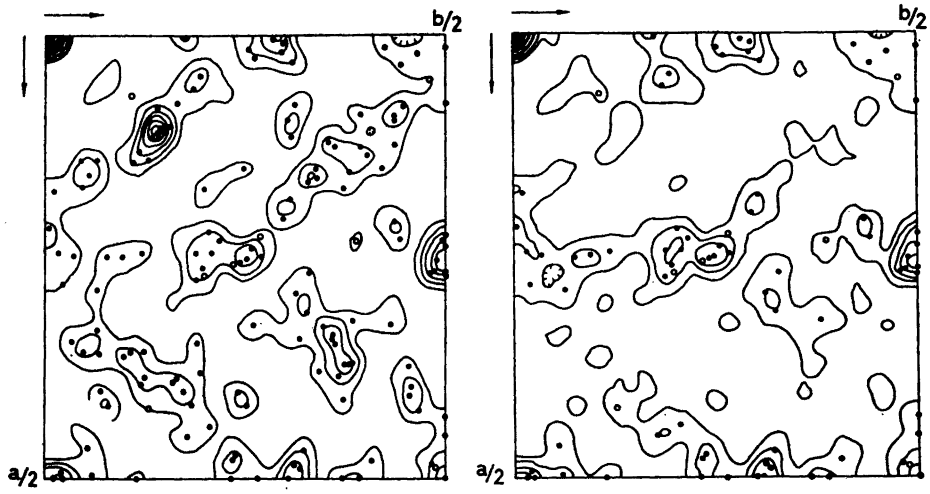

a b

Fig. 1. Patterson function and corresponding Mo—Mo vector set obtained from the final atomic coordinates. Full circles indicate vectors of multiplicity 2, open circles multiplicity 1.
a. Projection on (001), $P(UV)$. *b.* Section at $w = 0$, $P(UV0)$.

refinement. Their heights are, however, very sensitive to the scattering factor used for molybdenum, and the fact that the calculated structure factors were based on the scattering curve of zero-valent molybdenum, can therefore explain the difference.

Structure factors were calculated with the coordinates of the strong peaks in $\varrho_o(XY)$ given to both $Mo_1—Mo_9$ and $O_1—O_9$ and the coordinates of the remaining oxygens obtained from the difference map. The corresponding $\varrho_c(XY)$ function was calculated and the back-shifts of the strong peaks were applied on the Mo positions. New parameters for all the oxygen atoms were obtained from a difference map, and these were used in a second back-shift of the Mo-coordinates. These last shifts did not exceed 0.007 Å. The final oxygen parameters were then derived from a new difference map.

An isotropic, over-all temperature factor with the value $B = 0.81$ Å^2 was used in the calculations. The reliability index obtained after this refinement is given in Table 1.

The x and y coordinates thus obtained are given in Table 2, together with standard deviations calculated according to Cruickshank [10]. For the oxygens $O_1—O_9$ no standard deviations are given, as the parameters derived for them may be systematically influenced by the presence of the Mo atoms. The coordinates of these latter atoms on the other hand are not likely to be seriously in error owing to the overlapping oxygen atoms.

Table 1. The reliability indices R of various layer lines. $R = \Sigma(|F_o|-|F_c|)/\Sigma|F_o|$ calculated from observed reflexions only.

Layer line	Number of independent reflexions	R
$hk0$	259	0.073
$hk1$	219	0.100
$hk2$	201	0.109
$hk3$	90	0.108

b. Determination of the z coordinates

From the appearance of some regions of the three-dimensional Patterson function, the conclusion could be drawn, that all the Mo atoms are situated near to two planes perpendicular to the c axis with a separation of $\Delta z \approx 0.16$. It was possible to distribute these atoms on two planes in such a way that the Patterson section $P(UV0)$ shown in Fig. 1b could be fully explained. The calculated phase angles were assigned to the observed structure factor amplitudes, and electron density sections were computed, from which the coordinates of $O_{10}-O_{24}$, as well as new parameters for Mo_1-Mo_9 were obtained. Maxima corresponding to the oxygens O_1-O_9 were observed around $z = 0$, but they were very broad and less well-shaped due to partly coinciding with the termination of series effects from the heavy atoms. In the calculations they were assigned the parameter values $z(O_n) = z(Mo_n) + \frac{1}{2}$, where $z(Mo_n)$ is the coordinate of the molybdenum atom with approximately the same x and y parameters.

After two more phase angle — electron density cycles a back-shift was performed, which yielded shifts within $\Delta z \leq 0.003$ for Mo and $\Delta z \leq 0.021$ for $O_{10}-O_{24}$. The coordinates thus obtained are listed in Table 2. The final z parameters of O_1-O_9 given in Table 2 have been obtained by consideration of interatomic distances. If these atoms were situated exactly halfway between the two molybdenum neighbours in the c-axis direction, they would in most cases have four oxygen atoms very close on one side and four others rather distant on the other side. The z coordinates have therefore been choosen so as to make the distances $O_{1-9}-O_{10-24}$ greater than 2.52 Å and approximately equal on both sides. This can be attained if Mo—O distances as short as 1.69 Å are allowed.

The reliability indices are given in Table 1.

The standard deviations calculated according to Cruickshank [10] (multiplied by 2 on behalf of the non-centrosymmetry) are $\sigma_{Mo}(z) = \pm 0.03$ ($= \pm 0.12$ Å) and $\sigma_O(z) = \pm 0.16$ ($= \pm 0.64$ Å). The low number of terms in the Fourier synthesis along the z axis and the fact that no absorption correction was applied to the reflexions hkl, $l \neq 0$, contributes to the large $\sigma(z)$ value. As the absorption coefficient is fairly constant for reflexions with the same values of h and k, this effect can not give rise to serious errors in the z parameters. For space reasons the value of $\sigma_O(z)$ seems much too high to have any real meaning. A deviation $\Delta z = 0.6$ Å for an oxygen atom decreases the distances to some

Table 2. The crystal structure of $Mo_{17}O_{47}$

Space-group: *Pba*2 (No. 32)
Unit cell dimensions: $a = 21.61_5$ Å
$b = 19.63_2$ Å
$c = 3.951$ Å

Cell content: 2 $Mo_{17}O_{47}$
2 Mo and 2 O in 2 × 2(*a*): (0,0,*z*; ½,½,*z*)
32 Mo and 92 O in 31 × 4(*c*): (x,y,z; $\bar{x},\bar{y},z$; ½−x, ½+y,z; ½+x, ½−y,z)

Atom	Position	$x \pm \sigma(x)$	$y \pm \sigma(y)$	$z \pm \sigma(z)$
Mo_1	2 (*a*)	0	0	.579 ± .030
Mo_2	4 (*c*)	.0244 ± .0002	.2606 ± .0002	.581 ± .030
Mo_3	4 (*c*)	.1299 ± .0002	.1189 ± .0002	.425 ± .030
Mo_4	4 (*c*)	.1355 ± .0002	.4005 ± .0002	.434 ± .030
Mo_5	4 (*c*)	.2424 ± .0002	.2573 ± .0002	.575 ± .030
Mo_6	4 (*c*)	.2881 ± .0002	.0653 ± .0002	.579 ± .030
Mo_7	4 (*c*)	.3824 ± .0002	.1944 ± .0002	.428 ± .030
Mo_8	4 (*c*)	.3851 ± .0002	.3661 ± .0002	.424 ± .030
Mo_9	4 (*c*)	.4657 ± .0002	.0556 ± .0002	.565 ± .030
O_1	2 (*a*)	0	0	.01
O_2	4 (*c*)	.020	.266	.01
O_3	4 (*c*)	.126	.115	.98
O_4	4 (*c*)	.140	.396	.98
O_5	4 (*c*)	.246	.251	.00
O_6	4 (*c*)	.288	.069	.01
O_7	4 (*c*)	.383	.191	.00
O_8	4 (*c*)	.392	.360	.00
O_9	4 (*c*)	.465	.052	.05
O_{10}	4 (*c*)	.076 ± .002	.045 ± .002	.46
O_{11}	4 (*c*)	.060 ± .002	.181 ± .002	.52
O_{12}	4 (*c*)	.093 ± .002	.324 ± .003	.44
O_{13}	4 (*c*)	.059 ± .002	.462 ± .005	.57
O_{14}	4 (*c*)	.206 ± .002	.067 ± .002	.48
O_{15}	4 (*c*)	.180 ± .002	.195 ± .004	.46
O_{16}	4 (*c*)	.203 ± .002	.335 ± .002	.50
O_{17}	4 (*c*)	.191 ± .002	.475 ± .002	.54
O_{18}	4 (*c*)	.297 ± .002	.165 ± .003	.48
O_{19}	4 (*c*)	.330 ± .002	.280 ± .003	.48
O_{20}	4 (*c*)	.325 ± .002	.427 ± .004	.41
O_{21}	4 (*c*)	.380 ± .002	.091 ± .002	.56
O_{22}	4 (*c*)	.465 ± .002	.160 ± .003	.50
O_{23}	4 (*c*)	.434 ± .002	.275 ± .006	.52
O_{24}	4 (*c*)	.455 ± .002	.411 ± .002	.52

of its oxygen neighbours to generally below 2.30 Å. In Table 3, where interatomic distances *d* are listed, the standard deviations are given only for those distances where $\sigma(z)$ makes only a small contribution to $\sigma(d)$, and the more probable value $\sigma_O(z) = \pm 0.3$ Å was used in these cases.

Copies of a table of observed and calculated $|F(hkl)|$ values may be obtained on request.

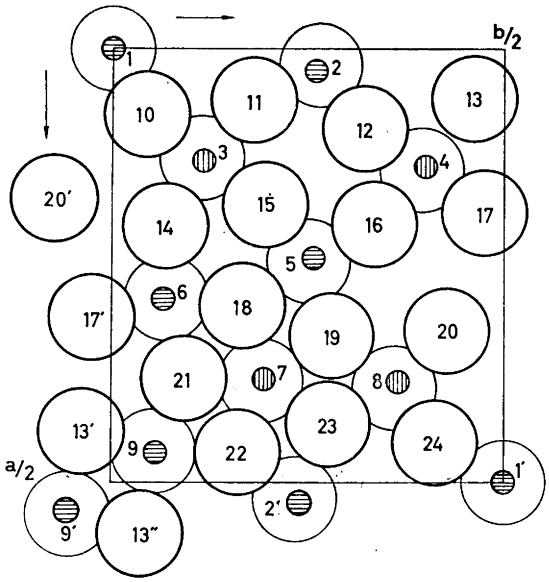

Fig. 2. Numbering of the atoms. Small circles = molybdenum. Large circles = oxygen. The numbers 1 to 9 refer to both molybdenum and oxygen.

DESCRIPTION OF THE STRUCTURE

The structural elements can, with one exception, be considered as distorted MoO_6 octahedra, coupled together by sharing corners or edges. The exception is the coordination polyhedron around Mo_7, which is fairly close to a pentagonal bipyramid.

Along the *c* axis, the extension of the polyhedra is one identity period. The coupling between them in this direction is brought about exclusively through common corners formed by the atoms O_1-O_9, which all lie at about the same height $z \approx 0$. The metal atoms are distorted from the centre of the polyhedra by an amount $\Delta z \approx \pm 0.08$, the distortion being in the same direction for Mo atoms with about the same x coordinates. The metal atoms thus form corrugated layers, as in Fig. 3.

Perpendicular to the *c* axis the polyhedra are linked together in a rather complicated way, which is best illustrated by Fig. 3. Only one fifth of the octahedra are of ReO_3 type, *i.e.* share all six corners with six neighbouring octahedra.

Mo_7 is the centre of an interesting arrangement, which has been found in $W_{18}O_{49}$ [11] (see below under Discussion) but has no counterpart among the other molybdenum oxides whose crystal structures are known at present. It has five Mo neighbours at the corners of a (puckered) pentagon, the projection of which along [001] is fairly regular. The distances to these corner atoms are 3.25—3.37 Å, which is normal for MoO_6 octahedra sharing edges [12]. The

Table 3. Interatomic distances d in Å.

Mo—Mo	d	$\pm\sigma(d)$
1 3	3.70	0.03
2 3	3.65	0.03
2 4	3.69	0.03
3 5	3.69	0.03
3 6	3.63	0.03
4 5	3.68	0.03
5 6	3.90	0.006
5 7	3.32	0.03
5 8	3.80	0.03
6 7	3.31	0.03
6 9	3.84	0.006
6 4′	3.68	0.03
7 8	3.37	0.006
7 9	3.31	0.03
7 2′	3.25	0.03
8 1′	3.67	0.03
8 2′	3.95	0.03
9 4′	3.78	0.03
9 9′	2.639	0.007
9 2′	3.83	0.006
9′ 4′	3.81	0.03
n n' along [001]	3.951	

Mo—O	d	$\pm\sigma(d)$
1 1	1.70	
1 1′	2.25	
1 10	1.92	0.08
1 24′	2.00	0.10
2 2	1.70	
2 2′	2.26	
2 11	1.76	0.08
2 12	2.02	0.12
2 22′	2.04	0.08
2 23′	2.10	0.08
3 3	2.19	
3 3′	1.76	
3 10	1.87	0.06
3 11	1.97	0.10
3 14	1.94	0.08
3 15	1.85	0.06
4 4	2.14	
4 4′	1.81	
4 12	1.77	0.06
4 13	2.12	0.12
4 16	1.97	0.08
4 17	1.94	0.08
5 5	1.70	
5 5′	2.25	
5 15	1.87	0.10
5 16	1.77	0.08
5 18	2.20	0.10
5 19	1.98	0.10
6 6	1.72	
6 6′	2.23	
6 14	1.83	0.10
6 17′	1.83	0.06
6 18	2.00	0.10
6 21	2.06	0.06
7 7	2.25	
7 7′	1.70	
7 18	1.94	0.08
7 19	2.04	0.08
7 21	2.10	0.10
7 22	1.93	0.08
7 23	1.96	0.10
8 8	1.69	
8 8′	2.28	
8 19	2.08	0.08
8 20	1.76	0.08
8 23	2.10	0.08
8 24	1.80	0.08
9 9	2.05	
9 9′	1.90	
9 13′	1.91	0.06
9 13″	2.04	0.06
9 21	1.97	0.06
9 22	2.07	0.08

O—O	d	$\pm\sigma(d)$
12 16	2.40	0.07
18 19	2.37	0.07
18 21	2.33	0.07
19 23	2.24	0.07
21 22	2.30	0.07
22 23	2.36	0.07
all other	≥ 2.53	

distances from Mo_7 to the five oxygen neighbours O_{18}, O_{19}, O_{21}, O_{22}, and O_{23} range from 1.93 to 2.10 Å, with a mean value of 1.99 Å, which is somewhat greater than the mean 1.94 Å for the rest of the $Mo_{1-9}—O_{10-24}$ distances. As the distances to the two remaining oxygens, O_7 and $O_{7'}$, are very unequal,

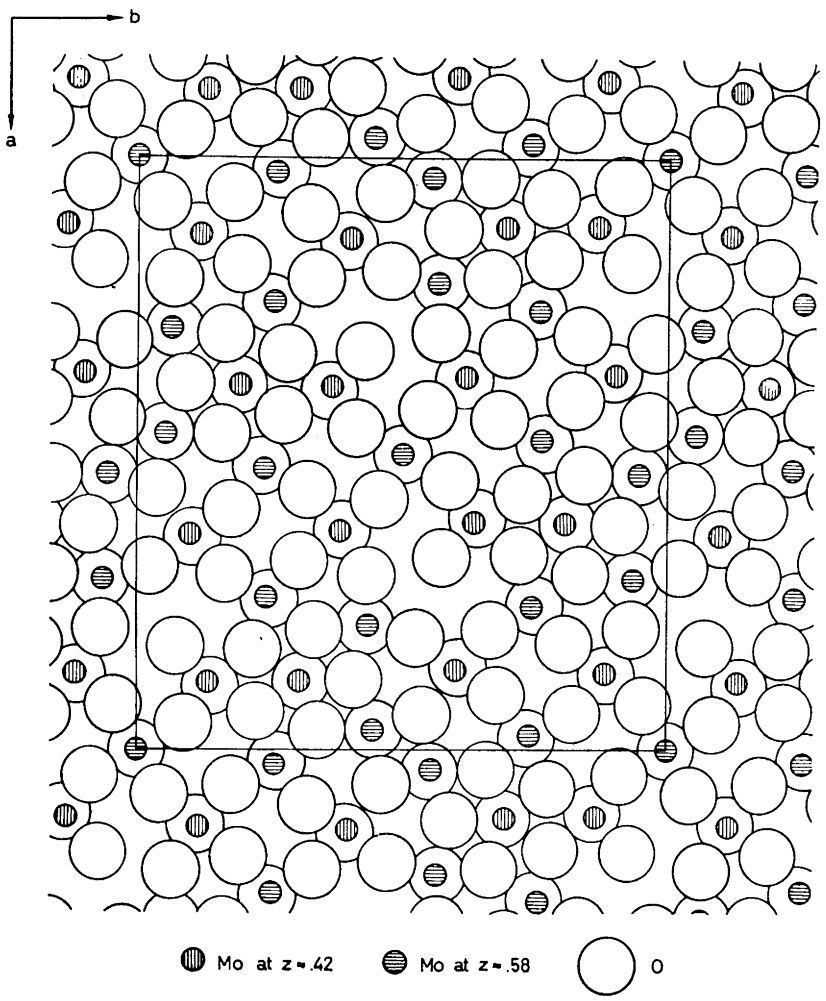

Fig. 3. The structure $Mo_{17}O_{47}$ viewed along [001]. The extension of one unit cell indicated. The oxygen atom above each molybdenum, in a position identical with that below it, has not been shown.

viz. 2.2 and 1.7 Å, the coordination can not be regarded as strictly sevenfold. The oxygens within the pentagon are very close together, the mean O—O distance being 2.32 Å, which is considerably shorter than has been observed for other molybdenum oxides.

The distance between Mo_9 and $Mo_{9'}$, which are related by a 2-fold axis, is only 2.639 Å. This indicates a bond between these atoms of the same kind that has been observed for example in MoO_2[13] and several other dioxides and dioxide systems [14] and recently also in low-Ti_3O_5[15]. In $W_{18}O_{49}$ the correspond-

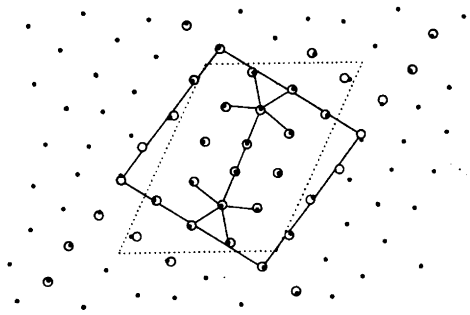

Fig. 4. Comparison between the metal atom patterns of $W_{18}O_{49}$ and $Mo_{17}O_{47}$; projection along the short axes. Dots = W positions in $W_{18}O_{49}$; dotted lines = extension of the unit cell of $W_{18}O_{49}$; circles = corresponding Mo positions in $Mo_{17}O_{47}$. The arrangement in two pentagons is indicated and the rhombic unit building up the structure of $Mo_{17}O_{47}$ also shown.

ing distance is 2.60 Å [11]. A formal treatment, where each oxygen atom is assigned 2 valence electrons taken equally from its molybdenum neighbours [15], yields a number of $2\frac{2}{3}$ valence electrons available for the formation of this bond, which fits well into the diagram of metal-metal bond lengths *versus* available valence electrons given by Marinder and Magnéli [14].

The atom O_{20} is bonded to only one molybdenum *viz.* Mo_8. The distance between them is 1.76 Å, which is among the shortest of the Mo—O distances in this plane. Such singly bonded oxygens exist in MoO_3, where the corresponding bond length is 1.8 Å [16], but has not been found in any other molybdenum or tungsten oxide.

DISCUSSION

The molybdenum oxides, besides $Mo_{17}O_{47}$, whose crystal structures are known at present are: MoO_3 with a layer structure [16-18], Mo_9O_{26} (mon.)[2], Mo_8O_{23} [2] and Mo_4O_{11} (o.-rh.) [19] containing two-dimensionally infinite blocks of the ReO_3 type, MoO_2 of deformed rutile type [13], and the metallic oxide Mo_3O, probably of defective BiF_3 type [20]. Although MoO_6 octahedra can be distinguished as the main structural element in all but the last of these structures, these do not show any strong resemblance to the present structure. In the closely interrelated phases Mo_9O_{26} (mon.) and Mo_8O_{23} the metal atoms form layers which are puckered to about the same degree as in $Mo_{17}O_{47}$, but the arrangement within these layers is quite different.

There is, however, an extremely interesting and close relationship between the present structure and that of γ-tungsten oxide, $W_{18}O_{49}$, determined by Magnéli [11]. This structure is monoclinic with the space group $P2/m$. In Fig. 4 the black dots indicate the positions of the W atoms in a projection along the unique axis, and the extension of one unit cell is marked by dotted lines (the origin has been moved to $(\frac{1}{2}, 0, \frac{1}{2})$ compared with Magnéli's notation). If the 2-fold axis in the centre of this cell is brought into coincidence with the 2-fold axis at $(0, \frac{1}{2}, z)$ or $(\frac{1}{2}, 0, z)$ in $Mo_{17}O_{47}$, there is an almost complete accordance

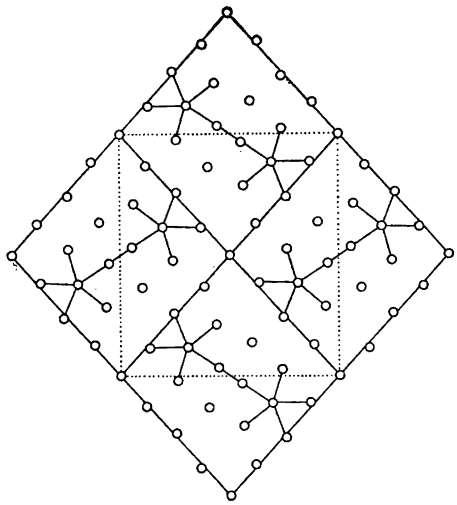

Fig. 5. The manner in which the $Mo_{17}O_{47}$ structure is built up from the rhombic unit of Fig. 4. Only metal atoms are indicated. Dotted lines show the extension of the unit cell.

between the metal atom patterns within an area containing 38 metal atoms. This can be seen in Fig. 4 where the positions of the Mo atoms within this area are marked by small circles. The pattern within the rhomb indicated by full lines builds up the $Mo_{17}O_{47}$ structure in the way shown in Fig. 5.

The oxygen positions in $W_{18}O_{49}$ were not revealed experimentally because of the unfavorable ratio between the scattering factors of oxygen and tungsten, but were derived by Magnéli from spatial considerations. Nevertheless they agree with those of $Mo_{17}O_{47}$ to about the same extent as do the metal positions. Oxygen-oxygen distances as short as 2.32 Å were quite naturally avoided, and this gave rise to a less symmetrical arrangement of oxygens around the tungsten atom equivalent to Mo_7, *i.e.* within the pentagons. It now seems most probable, however, that the arrangement is the same in $W_{18}O_{49}$ as in $Mo_{17}O_{47}$ in this respect too.

Both structures are thus built up from blocks, containing the two centered pentagons of metal atoms joined by a short metal-metal bond, and the essential difference between them is the way in which these blocks are mutually connected.

The wide, empty channels in $W_{18}O_{49}$, bordered by rings of six octahedra and running through the structure along the unique axis, have no counterpart in $Mo_{17}O_{47}$. Also in this structure, six octahedra are connected so as to form a ring, but in one of these octahedra the coupling is across a diagonal, leaving an oxygen atom (O_{20}) in the middle of the ring which fills up most of the available space. In spite of this, the oxygen packing is equally dense on the average in both structures, since the unit cell volume divided by the number of oxygen atoms has the same value 17.8 Å^3.

There is a further difference that becomes clear when the conditions in the third direction are examined. In $Mo_{17}O_{47}$ the metal atoms form layers

which are puckered with an amplitude of $\pm$ 0.3 Å, while in $W_{18}O_{49}$ all tungsten atoms are situated at the same height (on a mirror plane). This is partly reflected in the length of the corresponding axis, which is 3.951 Å in $Mo_{17}O_{47}$ and 3.775 Å in $W_{18}O_{49}$ [21]. The same difference between molybdenum and tungsten has been found in the closely interrelated structures of Mo_8O_{23} [2], Mo_9O_{26} (mon.)[2] and $W_{20}O_{58}$ [22], and has been discussed by Magnéli [23]. An analogous puckering of the layers in the $W_{18}O_{49}$ structure would imply doubling of the unit cell.

Although it can not be excluded that a molybdenum oxide of the $W_{18}O_{49}$ type or a tungsten oxide of the $Mo_{17}O_{47}$ type may form at conditions different from those hitherto used in the phase analysis of the Mo—O [1] and W—O [24] systems, there is no evidence for their existence at present. A study of the extent to which molybdenum and tungsten can replace each other in $Mo_{17}O_{47}$ and $W_{18}O_{49}$ would perhaps throw light on these problems.

Acknowledgements. I wish to express my gratitude to Professor G. Hägg for all the facilities put at my disposal and to Dr. A. Magnéli for stimulating discussions and continued interest in this investigation. Thanks are also due to Mr. S. Åsbrink and Mr. S. Westman for assisting me with the programmes for the digital computers.

The *Royal Swedish Academy of Sciences* is gratefully acknowledged for a grant from *Th. Nordströms testamentsfond.*

This research has been sponsored in part by the *Swedish Natural Science Research Council* and in part by the *Office, Chief of Research and Development, U.S. Department of Army* through its European Office under contract number DA-91-591-EUC-1319.

The computers BESK and FACIT EDB were used by kind permission of the *Swedish Board for Computing Machinery.*

REFERENCES

1. Kihlborg, L. *Acta Chem. Scand.* **13** (1959) 954.
2. Magnéli, A. *Acta Chem. Scand.* **2** (1948) 501.
3. Löfgren, T. *Acta Cryst.* **13** (1960) 156.
4. Hesse, R. *To be published.*
5. Westman, S., Blomqvist, G. and Åsbrink, S. *Arkiv Kemi* **14** (1959) 535.
6. Åsbrink, S., Blomqvist, G. and Westman, S. *Arkiv Kemi* **14** (1959) 545.
7. Thomas, L. H. and Umeda, K. *J. Chem. Phys.* **26** (1957) 293.
8. Berghuis, J., Haanappel, I J. M., Potters, M., Loopstra, B. O., MacGillavry, C. H. and Veenendaal, A. L. *Acta Cryst.* **8** (1955) 478.
9. Appel, K. *Private communication.*
10. Cruickshank, D. W. J. *Acta Cryst.* **2** (1949) 65.
11. Magnéli, A. *Arkiv Kemi* **1** (1949) 223.
12. Magnéli, A. *Nova Acta Regiæ Soc. Sci. Upsaliensis* [IV] **14** (1950) No. 8.
13. Magnéli, A. *Arkiv Kemi, Mineral. Geol.* **A 24** (1946) No. 2.
14. Marinder, B.-O. and Magnéli, A. *Acta Chem. Scand.* **11** (1957) 1635.
15. Åsbrink, S. and Magnéli, A. *Acta Cryst.* **12** (1959) 575.
16. Andersson, G. and Magnéli, A. *Acta Chem. Scand.* **4** (1950) 793.
17. Bräkken, H. *Z. Krist.* **78** (1931) 484.
18. Wooster, N. *Z. Krist.* **80** (1931) 504.
19. Magnéli, A. *Acta Chem. Scand.* **2** (1948) 861.
20. Schönberg, N. *Acta Chem. Scand.* **8** (1954) 617.
21. Magnéli, A., Andersson, G., Blomberg, B. and Kihlborg, L. *Anal. Chem.* **24** (1952) 1998.
22. Magnéli, A. *Arkiv Kemi* **1** (1950) 513.
23. Magnéli, A. *J. Inorg. & Nuclear Chem.* **2** (1956) 330.
24. Hägg, G. and Magnéli, A. *Arkiv Kemi, Mineral. Geol.* **A 19** (1944) No. 2.

Received April 13, 1960.

ACTA CHEMICA SCANDINAVICA 14 (1960) 1623–1626

High Temperature X-Ray Study of the Thermal Expansion of Pd_9Se_8 and Rh_9S_8

ARNE KJEKSHUS

Kjemisk Institutt A, Universitetet i Oslo, Blindern, Norway

Pd_9Se_8 and Rh_9S_8 with cubic crystal symmetry, have been studied by the X-ray powder method at temperatures in the range from 20 to 940°C. The average linear thermal expansion coefficient, β_a, is equal to 9.8×10^{-6} °C^{-1} for Pd_9Se_8 (20–625°C), 9.3×10^{-6} °C^{-1} for Rh_9S_8 (20–300°C) and 7.4×10^{-6} °C^{-1} for Rh_9S_8 (428–866°C). The volume expansion coefficient, a, is 29.5×10^{-6} °C^{-1} for Pd_9Se_8 (20–625°C), 27.8×10^{-6} °C^{-1} for Rh_9S_8 (20–300°C) and 22.2×10^{-6} °C^{-1} for Rh_9S_8 (428–866°C).

In a recent study of the thermal expansion of PtS_2, $PtSe_2$, $PtTe_2$ and $PdTe_2$, all with structures of the $Cd(OH)_2$-type, Kjekshus and Grønvold [1] found a general departure from linearity in the expansion perpendicular to the layers at higher temperatures. Since the reasons for the different modes of thermal expansion at higher temperatures are not fully explained by the existing theories for the perfect lattice, further experimental data might be desirable before a theoretical explanation is proposed.

The present paper is concerned with the thermal expansion of Pd_9Se_8 [2] and Rh_9S_8 [3], which have cubic symmetry and are probably isostructural. These compounds were also chosen in order to check the accuracy of the X-ray method for thermal expansion studies of compounds with relatively long cell edges of about 10 Å. The fact that the positions of the atoms in the unit cell are not known is of secondary importance, since the thermal expansion of the interatomic distances is equal to the expansion of the cell edges.

EXPERIMENTAL

Pd_9Se_8 was prepared [2] by heating a mixture of $PdSe_{1.00}$ and palladium, corresponding to the formula Pd_9Se_8, in an evacuated and sealed silica tube for 10 days at 650°C and 50 days at 450°C. Rh_9S_8 was prepared [3] by heating rhodium and sulfur in the right proportions in an evacuated, sealed silica tube for 14 days at 690°C and another 14 days at 350°C. Both samples were finally slowly cooled to room temperature.

Information about the purity of the elements is given elsewhere [2,3].

Table 1. Lattice constants and unit cell volumes for Pd_9Se_8 at different temperatures.

t(°C)	a(Å)	V(Å^3)
20	10.6060	1193.04
155	10.6200	1197.77
220	10.6268	1200.07
330	10.6382	1203.94
402	10.6457	1206.49
531	10.6595	1211.18
625	10.6694	1214.51
650	10.6725	1215.62

X-Ray powder photographs of the compounds were taken in a 190 mm Unicam high-temperature camera, with the samples sealed in thin-walled quartz capillaries. Pd_9Se_8 was studied at temperatures between 20 and 650°C. The highest temperature is close to the melting point of 665 ± 15°C. Rh_9S_8 was studied at temperatures between 20 and 940°C.

By means of a voltage regulator, the registered temperature of the furnace surrounding the specimen was kept constant within ± 5°C. The Pt/Pt-Rh thermocouples of the furnace had been calibrated with a standard couple located at the position of the specimen. Lattice constants are given i Ångström units ($\lambda_{CuK\alpha_1}$ = 1.54050 Å). Only the high-angle reflections of the diffraction pattern were used in the calculation of the lattice constants. The lattice constants were found by extrapolation according to the method given by Nelson and Riley [4]. The probable error in the lattice constant determinations at temperatures above room temperature was estimated to be about 0.01 %. This included a possible error due to variation in the composition of the sample with temperature. A much better reproducibility of about 0.003 % is found, however, between the results for two different expansion runs. Errors due to specimen contamination can be neglected, since the lattice constants at room temperature before and after the high temperature treatment were equal within the limits of the experimental error.

RESULTS

The results of the lattice constant measurements are listed in Tables 1 and 2. Here are also listed the unit cell volumes. The ratios $\frac{a_t - a_{20}}{a_{20}} = \frac{\Delta a}{a_{20}}$

Table 2. Lattice constants and unit cell volumes for Rh_9S_8 at different temperatures.

t(°C)	a(Å)	V(Å^3)
20	9.9116	973.71
120	9.9204	976.31
208	9.9289	978.82
300	9.9383	981.60
428	9.9495	984.93
538	9.9576	987.33
615	9.9632	989.00
681	9.9683	990.52
766	9.9744	992.34
866	9.9818	994.55
940	9.9894	996.52

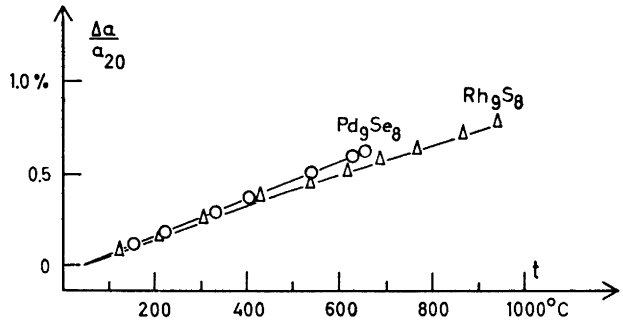

Fig. 1. Relative lattice constant variation as function of temperature.

and $\frac{V_t - V_{20}}{V_{20}} = \frac{\Delta V}{V_{20}}$ are calculated and plotted as $\frac{\Delta a}{a_{20}}$ *versus* t, and $\frac{\Delta V}{V_{20}}$ *versus* t, respectively. The calculations of the expansion coefficients were based upon these data.

The change in the length of the a-axis is similar below about 300°C for both Pd_9Se_8 and Rh_9S_8. As shown in Fig. 1, the a-axis increases linearly with increasing temperature. The expansion coefficient β_a is equal to 9.8×10^{-6} $°C^{-1}$ for Pd_9Se_8 (20—625°C) and 9.3×10^{-6} $°C^{-1}$ for Rh_9S_8 (20—300°C). At temperatures between 428 and 866°C the a-axis of Rh_9S_8 increases more slowly

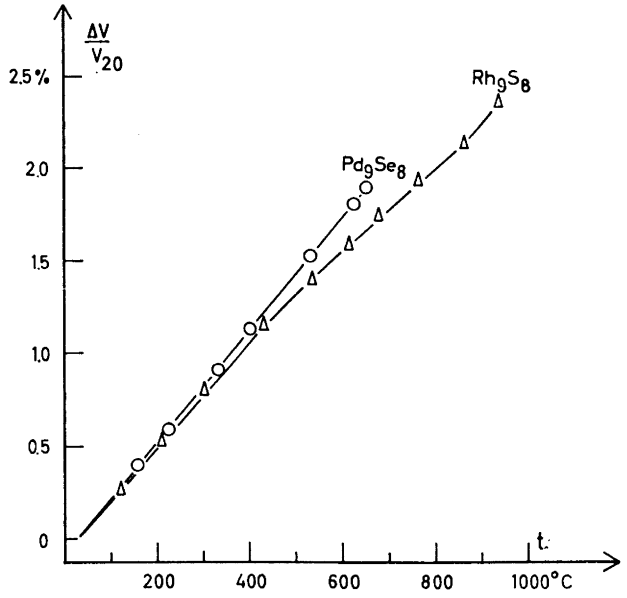

Fig. 2. Relative changes in volume with temperature.

than at lower temperatures. The thermal expansion is approximately linear, with expansion coefficient β_a equal to 7.4×10^{-6} °C^{-1} for Rh_9S_8 (428—866°C).

The volume expansion is plotted as function of the temperature in Fig. 2. For both compounds the volume expansion has a similar temperature dependence as the a-axis. Since β_a is of the order 10^{-5}, the average thermal volume expansion coefficient α is approximately $3\beta_a$. The numerical values for α are 29.5×10^{-6} °C^{-1} for Pd_9Se_8 (20—625°C), 27.8×10^{-6} °C^{-1} for Rh_9S_8 (20—300°C) and 22.2×10^{-6} °C^{-1} for Rh_9S_8 (428—866°C).

The intensities of the reflections on X-ray photographs taken at higher temperatures are almost equal to those of the corresponding photographs taken at room temperature. The parameters must thus be nearly the same. Because of the cubic symmetry the thermal expansion of the interatomic distances is approximately equal to the expansion of the a-axis (*cf.* Fig. 1).

The obtained expansion curves for Pd_9Se_9 deviate little from linearity. The assumed large increase [5,6] in the coefficient of thermal expansion in the temperature region just below melting does not occur. As the a-axis and the volume of Rh_9S_8 increase more slowly above 428°C than at lower temperatures, the relative expansion is still on the upper part of the sigmoidal curve. The values for the a-axis at 940°C (*cf.* Table 1) indicate that a more rapid increase might well take place above this temperature.

Acknowledgements. The author wishes to thank Professor Haakon Haraldsen and Dosent Fredrik Grønvold for their interest in this study. Thanks are due to Mr. Håkon Mohn for skillful technical assistance.

REFERENCES

1. Kjekshus, A. and Grønvold, F. *Acta Chem. Scand.* **13** (1959) 1767.
2. Grønvold, F. and Røst, E. *Acta Chem. Scand.* **10** (1956) 1620.
3. Steen, Ø. *Thesis*, University of Oslo, 1955.
4. Nelson, J. B. and Riley, D. P. *Proc. Phys. Soc. (London)* **57** (1945) 160.
5. Lawson, A. W. *Phys. Rev.* **78** (1950) 185.
6. Fletcher, G. C. *Phil. Mag.* **2** (1957) 639; *Australian J. Phys.* **12** (1959) 237.

Received April 9, 1960.

ACTA CHEMICA SCANDINAVICA 14 (1960) 1627–1642

Relations between the Hammett Acidity Function, H_0, and Ion Activities in Mixtures of strong Acids and Water

ERIK HÖGFELDT

Department of Inorganic Chemistry, Royal Institute of Technology, Stockholm 70, Sweden

By combining of the Hammett acidity function, H_0, with activity data in mixtures of strong acids with water, functions $\varphi^{\nu} \cdot a_{X}{}^{\nu}$ can be constructed. ν is the ionic charge of species X and $\varphi = y_B / y_{BH}+$ *i.e.* the activity coefficient ratio of the basic and acid forms of the indicators used for the determination of H_0. The properties of these functions are investigated. It is found that the plot of log $\varphi \cdot a_{H_3O}+$ *versus* H_0 is the same for the acids, HCl, HBr, HNO_3, $HClO_4$ and H_2SO_4.

The functions $\varphi^{-1} \cdot a_{A^-}$ (A^- = anion of the acid HA) show a more individualistic behavior. The plots of log $\varphi^{-1} \cdot a_{ClO_4^-}$ and log $\varphi^{-1} \cdot a_{HSO_4^-}$ *versus* H_0 practically coincide in the range of overlap, those for Br^- and Cl^- form a different set of almost parallel curves but the curve for NO_3^- differs from all of the others.

From a plot of log $\varphi^{\nu} \cdot a_{X}{}^{\nu}$ *versus* H_0 for several species assumed to be present in H_2SO_4–H_2O mixtures, it is found that, from 10 M H_2SO_4 up to pure H_2SO_4, the curve for H_3O^+ runs parallel with that of HSO_4^-, that for SO_4^{2-} with log a_{H_2O} and the curve for $H_3SO_4^+$ with that of $HS_2O_7^-$. This behavior is found to be the result of the almost complete constancy of the activity coefficient expression $\varphi^2 \cdot y_{H_3O}+ / y_{HSO_4^-}$. Also, the following relation holds in the same concentration range:

$$-2H_0 - \log a_{H}^{2}+ \cdot a_{SO_4^{2-}} + \log a_{H_2O} = 3.95 \pm 0.03$$

A function closely related to the average degree of hydration of the various ions present is introduced. In concentrated solutions of H_2SO_4, this function tends towards unity for H^+ and towards zero for HSO_4^- implying the existence of H^+ as H_3O^+ in these concentrated solutions and that HSO_4^- is practically unhydrated.

From the slope of curves log $\varphi^{\nu} \cdot y_{X}{}^{\nu}$ *versus* H_0 where y symbolizes a kind of a stoichiometric activity coefficient, it is found that protons seem to be hydrated to the same extent in all strong acids when compared at the same water activity. The anions, ClO_4^- and HSO_4^-, seem to be hydrated to approximately the same extent up to about 7 M and much more so than NO_3^-, the slopes indicating a difference of 3 in hydration number.

In a preceding paper[1], activities and activity coefficients of hydrated ions were derived and their properties investigated. In addition a function closely related to the average degree of hydration of the ions was constructed and its bearing on the existence of maxima in ionic concentration demonstrated. Since individual ionic activities cannot be measured separately, the approximate hydration numbers evaluated referred to various combinations of positive and negative ions. In the following it will be shown, however, that for solutions of strong acids in water, combination of acidity function data with water and acid activities will give functions that depend mainly upon the activity of one of the ions.

LIST OF SYMBOLS

a_{X^ν}	Activity on the molarity scale of constituent X^ν
a_n	Activity of $H^+(H_2O)_n$
C	Stoichiometric molarity of acid
C_{X^ν}	Concentration of X^ν on the molarity scale
D	Spacing between the curves log $\varphi \cdot a_{H_3O^+}$ and log $\varphi^{-1} \cdot a_{HSO_4^-}$
d_o	Density of pure water
f_{X^ν}	Activity coefficient on the mole fraction scale of X^ν
K_1, K_n etc	Thermodynamic equilibrium constants
m	Stoichiometric molality of acid
M	Molar = moles · liter^{-1}
$\bar{n}$	Average hydration number
$\bar{n}'$, $\bar{n}''$	Functions closely related to $\bar{n}$, defined by eqns (38) and (40)
pK	$-\log K$
S	$S = \Sigma K_n a^n_{H_2O}$
X_{X^ν}	Mole fraction of X^ν
y_{X^ν}	Stoichiometric activity coefficient on the molarity scale of X^ν
$y = [y_{H^+} \cdot y_{A^-}]^{\frac{1}{2}}$	» mean activity coefficient of H^+, A^-
y_+, y_-	"True" activity coefficients on the molarity scale
$\varphi = y_B/y_{BH^+}$	Ratio of the activity coefficients on the molarity scale of the acid and base forms of the indicator B
α	Degree of dissociation of the strong acid HA
$\gamma = [\gamma_{H^+} \cdot \gamma_{A^-}]^{\frac{1}{2}}$	Stoichiometric mean activity coefficient of H^+, A^- on the molality scale
ν	Ionic charge.

THE IONIC ACTIVITY FUNCTIONS

For the acid-base equilibrium of an uncharged weak base indicator B, we can write:

$$BH^+ \rightleftharpoons B + H^+ \qquad (1)$$

The thermodynamic equilibrium constant of this reaction is defined by

$$K_{BH^+} = a_{H^+} \cdot a_B \cdot a^{-1}_{BH^+} \quad (2)$$

H^+ and a_{H^+} in (1) and (2) refer formally to the bare, unhydrated proton. a_{H^+} is so defined that it approaches C_{H^+} upon dilution.

By taking the logarithm of (2) and rearranging, we get:

$$pK_{BH^+} - \log(C_{BH^+} / C_B) = -\log a_{H^+} - \log(y_B / y_{BH^+}) \equiv H_0 \quad (3)$$

Eqn. (3) defines H_0. The left hand side indicates how it can be determined experimentally, *e.g.* by spectrophotometric measurements of the ratio C_{BH^+} / C_B The right hand side shows the relation of H_0 to the activity of free protons. Activities and concentrations are expressed on the molarity scale. When not otherwise stated this scale is used throughout the paper.

The quotient

$$\varphi = y_B / y_{BH^+} \quad (4)$$

is unknown although it has been suggested [2] that this term becomes nearly independent of electrolyte content over a wide range of concentration, *e.g.* for H_2SO_4 above 4—5 M. It is generally accepted that, at any given concentration of strong acid, φ is independent of indicator used as long as it belongs to the same charge type [3].

With the aid of (4), eqn. (3) rearranges to:

$$\log \varphi \cdot a_{H^+} = -H_0 \quad (5)$$

As stated by Guggenheim [4], single activities like a_{H^+} and activity coefficient ratios like y_B / y_{BH^+} can be neither experimentally determined nor satisfactorily defined within the framework of thermodynamics. Only by using some extra-thermodynamic assumption can ion activities be defined — as exemplified [5] by the definition of pH. As seen from (5), however, the quantity $y_B \cdot y^{-1}_{BH^+} \cdot a_{H^+}$ is experimentally available. It is obvious that H_0 is closely related to the activity of free protons although this activity cannot, of course, be evaluated because of the unknown function φ.

Since free protons do not exist in measurable amounts in water solutions but are known to be hydrated, it may be of interest now to consider the thermodynamic functions of these constituents.

For the reaction:

$$H^+ + n\ H_2O \rightleftharpoons H^+(H_2O)_n \quad (6)$$

the law of mass action yields:

$$K_n = \frac{a_n}{a_{H^+} \cdot a^n_{H_2O}} \quad (7)$$

where a_n is a convenient notation for the activity of $H^+(H_2O)_n$. The activity scale of the hydrated proton is conveniently fixed to that of H^+ by putting $K_n = 1$ as was done by Brönsted [6,7] for $n = 1$.

a_n is thus defined by:

$$a_n = a_{H^+} \cdot a^n_{H_2O} \quad (8)$$

By combining (5) and (8) we get

$$\log \varphi \cdot a_n = -H_o + n \log a_{H_2O} \tag{9}$$

In the following, we shall limit the discussion to H_3O^+, *i.e.*$n = 1$ in (9).

In order to derive the analogous function for A^- (anion of the strong acid HA), we make use of the reaction:

$$HA + H_2O \rightleftharpoons H_3O^+ + A^- \tag{10}$$

with the thermodynamic equilibrium constant, K, defined by:

$$K = \frac{a_{H_3O^+} \cdot a_{A^-}}{a_{H_2O} \cdot a_{HA}} \tag{11}$$

From (9) and (11):

$$\log \varphi^{-1} \cdot a_{A^-} = H_o + \log K \cdot a_{HA} \tag{12}$$

The quantity $K \cdot a_{HA}$ can be obtained from:

$$K \cdot a_{HA} = a_{H^+} \cdot a_{A^-} = (d^o \cdot \gamma \cdot m)^2 \tag{13}$$

Since our activities are given on the molarity scale, it is necessary to transform the activity on the molality scale to that on the molarity scale — this is done using d^o, the density of pure water. The stoichiometric mean molality activity coefficient, γ, is frequently tabulated in the literature together with a_{H_2O} or the osmotic coefficient. The ion activity functions (9) and (13) can thus be computed from such data, and often over considerable concentration ranges.

EXPERIMENTAL DATA SELECTED

In the following, a short survey of the experimental data employed in this investigation will be given. With the exception of HBr, they are more thoroughly discussed in Ref.[1]

a) *HCl.* Densities of HCl solutions at 25°C have been computed from formulas given by Åkerlöf and Teare [8]. Hydrochloric acid activities have been taken from Harned and Owen [9] for dilute solutions and from Robinson and Stokes for concentrated solutions [10a]. Water activities were computed from osmotic coefficients compiled by Robinson and Stokes.[10b].

b) *HBr.* Densities of HBr solutions at 20°C were taken from Landolt-Börnstein [11a]. Water and hydrobromic acid activities are also from the same source [11b] where Redlich has made a compilation of available freezing point, vapor pressure and emf data from several different investigations.

c) *HNO_3.* Densities of HNO_3 solutions at 20°C have been taken from Landolt-Börnstein [11a]. Water and nitric acid activities at the same temperature have been computed from vapor pressure measurements by Potier [12]. The concentrations of dissociated and undissociated acid have been taken from NMR measurements reported by Redlich et al [13].

d) *$HClO_4$.* Densities of $HClO_4$ solutions at 25°C have been taken from Markham [14] and water and perchloric acids activities from the isopiestic measurements of Robinson and Baker [15]. The concentrations of dissociated respectively undissociated acid are from Ref 13.

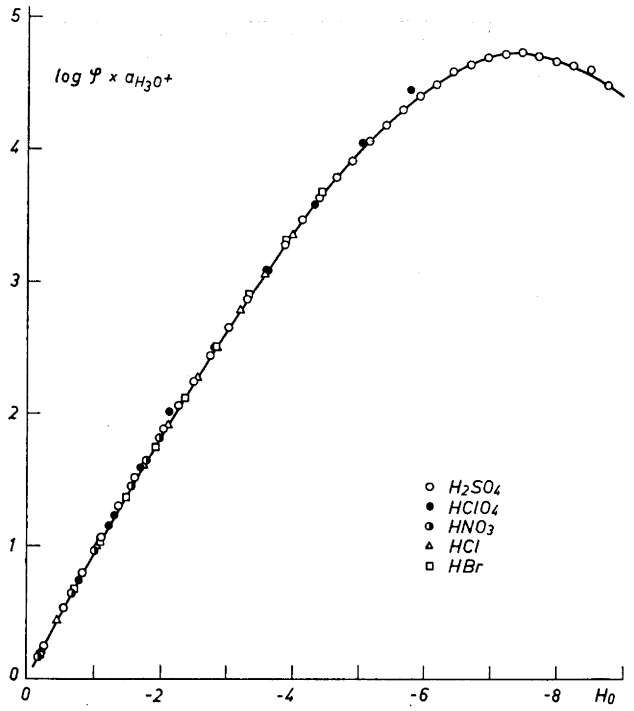

Fig. 1. The function log $\varphi \cdot a_{H_3O^+}$ *versus* H_0 for various strong acids: ○ H_2SO_4; ● $HClO_4$; ◑ HNO_3; △ HCl; □ HBr.

e) *H_2SO_4*. Densities of H_2SO_4 solutions at 25°C have been taken from International Critical Tables [16]. Water and sulfuric acid activities are the recent isopiestic measurements by Glueckauf and Kitt [17] which extended up to about 16 M. Above that concentration, water activities given by Deno and Taft [18] from an empirical relation between H_0 and a_{H_2O} were used and the corresponding water activities computed with the aid of the Gibbs—Duhem equation by the present writer. As discussed in Ref.1, the activities thus computed agree quite well with the vapor and freezing point measurements recently reported by Giauque *et al* [19]. Concentrations of species present have been taken from the Raman measurements reported by Young *et al.*[20a].

f) *H_0-data*. The H_0-data for dilute HCl solutions and H_2SO_4, solutions up to 12 M were taken from the author's own measurements [21] and in other cases from the review by Paul and Long [3]. Where the measurements of the present writer overlap those in the compilation of Paul and Long, the agreement was found to be good.

COMPARISON OF ION ACTIVITY FUNCTIONS IN SOME DIFFERENT ACIDS

Using the experimental data selected above, the ion activity functions $\varphi \cdot a_{H_2O^+}$ and $\varphi^{-1} \cdot a_{A^-}$ have been computed for the five acids in question.

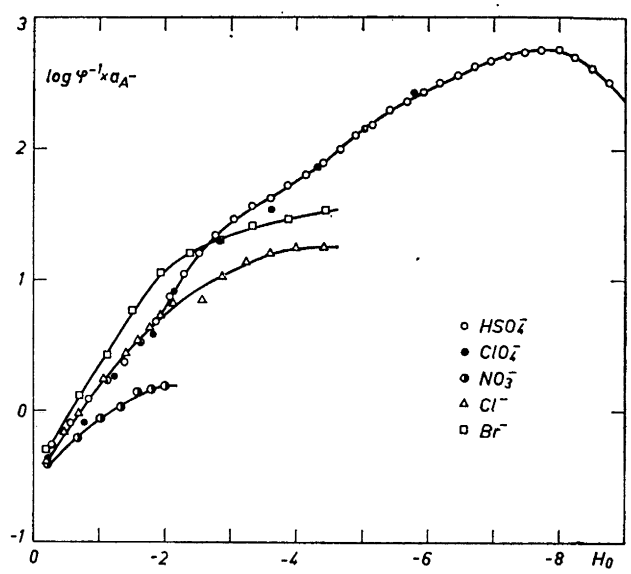

Fig. 2. The function log $\varphi^{-1} \cdot a_{A^-}$ *versus* H_0 for various anions: ○ HSO_4^-; ● ClO_4^-; ◑ NO_3^- △ Cl^-; □ Br^-.

In Fig. 1, log $\varphi \cdot a_{H_3O^+}$ is plotted *versus* H_0 and it can be noted that, within the limits of experimental error and within the range of overlap, they all fall on a single curve. This is equivalent to a finding by Wyatt [22] that, when H_0 was plotted against a_{H_2O} for several acids, all data fell on a single curve. From eqn. (9) it is seen that, if the curve H_0 *vs* a_{H_2O} is the same for all acids, $\varphi \cdot a_{H_3O^+}$ *vs* H_0 must also be the same. This behavior can be imagined to be due to the fact that the hydration equilibria:

$$H^+ + n\,H_2O \rightleftharpoons H^+(H_2O)_n \qquad n = 1,2,3\ldots$$

as well as the φ-values are the same in all acids when the comparison is made at the same water activity.

In Fig. 2, log $\varphi^{-1} \cdot a_{A^-}$ is plotted *versus* H_0 for the five anions: Cl^-, Br^-, NO_3^-, ClO_4^-, HSO_4^-. The anions behave more individually than the common cation, and no coinciding curves are obtained with the exception of the curves for the structurally similar ions HSO_4^- and ClO_4^- which lie quite close to each other. The curves for Br^- and Cl^- are nearly parallel and distinctly different from those for ClO_4^- and HSO_4^- and even more so from the curve for NO_3^- since the latter deviates markedly from all of the other anions already in dilute solutions. The significance of these differences is difficult to grasp with our present knowledge of concentrated electrolytes. That structural similarities should enter into the explanation seems plausible from the way into which the curves divide themselves into different groups with structurally similar ions.

THE PLOT $\log \varphi^{\nu} \cdot a_x{}^{\nu}$ FOR $H_2SO_4 - H_2O$

The only acid where H_0 and activity data are available over the whole concentration range from pure water up to pure acid is sulfuric acid. Since this acid is a dibasic acid, there are several species present and the relations between H_0 and the ionic activities take a slightly different form as compared with the monobasic acids. Consider the reactions:

$$H_2SO_4 + H_2O \rightleftharpoons H_3O^+ + HSO_4^-;\ K_{H_2SO_4} = \frac{a_{H_3O^+} \cdot a_{HSO_4^-}}{a_{H_2O} \cdot a_{H_2SO_4}} \qquad (14, 15)$$

$$HSO_4^- + H_2O \rightleftharpoons H_3O^+ + SO_4^{2-};\ K_{HSO_4^-} = \frac{a_{H_3O^+} \cdot a_{SO_4^{2-}}}{a_{H_2O} \cdot a_{HSO_4^-}} \qquad (16, 17)$$

$$2\ H_2SO_4 \rightleftharpoons H_3SO_4^+ + HSO_4^-;\ K_1 = \frac{a_{H_3SO_4^+} \cdot a_{HSO_4^-}}{a^2_{H_2SO_4}} \qquad (18, 19)$$

$$2\ H_2SO_4 \rightleftharpoons H_3O^+ + HS_2O_7^-;\ K_2 = \frac{a_{H_3O^+} \cdot a_{HS_2O_7^-}}{a^2_{H_2SO_4}} \qquad (20, 21)$$

$$a^2_{H^+} \cdot a_{SO_4^{2-}} = K_{H_2SO_4} \cdot K_{HSO_4^-} \cdot a_{H_2SO_4} \qquad (22)$$

For H_3O^+ we have eqn. (9) and for the other ions we find from (9), (15), (17), (19), (21) and (22)

$$\left.\begin{aligned}
&\log \varphi \cdot a_{H_2SO_4} = -H_0 + \log a_{H^+}{}^2 \cdot a_{SO_4^{2-}} + 2\ pK_{H_2SO_4} + \\
&+ pK_{HSO_4^-} - pK_1 \\
&\log \varphi^{-1} \cdot a_{HSO_4^-} = H_0 + \log a_{H^+}{}^2 \cdot a_{SO_4^{2-}} \cdot + pK_{HSO_4^-} \\
&\log \varphi^{-2} \cdot a_{SO_4^{2-}} = 2\ H_0 + \log a_{H^+}{}^2 \cdot a_{SO_4^{2-}} \\
&\log \varphi^{-1} \cdot a_{HS_2O_7^-} = H_0 + 2 \log a_{H^+}{}^2 \cdot a_{SO_4^{2-}} - \log a_{H_2O} + \\
&+ 2\ pK_{H_2SO_4} + 2\ pK_{HSO_4^-} - pK_2
\end{aligned}\right\} \qquad (23\ a—d)$$

All of the constants except $K_{H_2SO_4}$ are known with some certainty. For $K_{HSO_4^-}$, the recent value 1.00×10^{-2} given by Hamer [20a] from considerations of available literature data has been accepted. For K_1 and K_2, Kirkbride and Wyatt [23] report $K_1 = 3.45 \times 10^{-4}$ (moles per kg H_2SO_4)^2 and $K_2 = 1.8 \times 10^{-4}$ (moles per kg H_2SO_4)^2 in pure H_2SO_4. These values are fairly consistent with those reported by Gillespie and co-workers [24–26]. K_1 and K_2 are given with concentrations in moles per kg H_2SO_4 and with pure sulfuric acid as standard state for $a_{H_2SO_4}$. All other activities are referred to pure water and therefore K_2 and K_4 have to be transformed to the molarity scale and the standard state of H_2SO_4 changed to that in water. Using the density of pure sulfuric acid, 1.83, and the value [1] $\log a_{H^+}{}^2 \cdot a_{SO_4^{2-}} = 9.55$ in pure H_2SO_4, this transformation was performed with the aid of (22) giving:

$$pK_1 = 26.04 - 2\ pK_{H_2SO_4} \qquad (24\ a,b)$$

$$pK_2 = 26.31 - 2\ pK_{H_2SO_4}$$

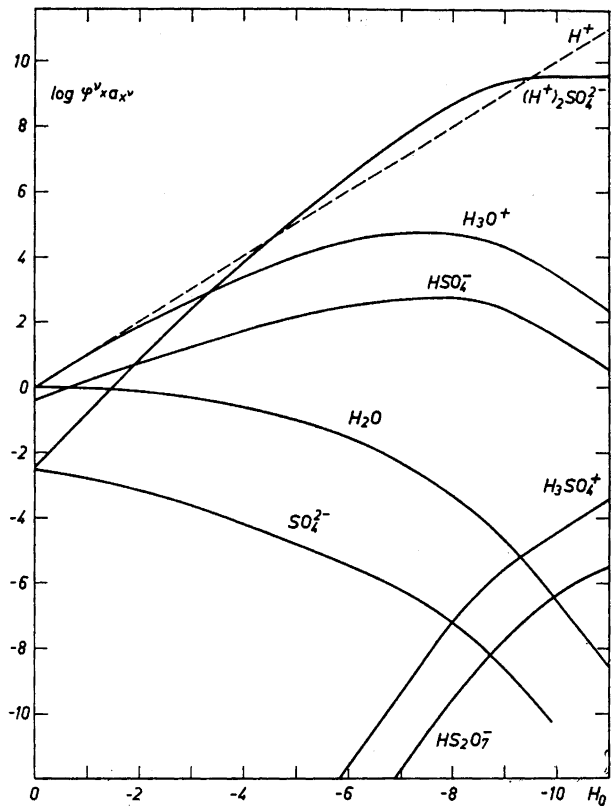

Fig. 3. The functions log $\varphi^{\nu} \cdot a_x{}^{\nu}$ *versus* H_0 for several species assumed to be present in mixtures of water and sulfuric acid.

Inserting the value for $pK_{HSO_4^-}$ and the expression for pK_1 and pK_2 from (24) into (23), we get:

$$\log \varphi \cdot a_{H_2SO_4} = -H_0 + \log a_{H^+}{}^2 \cdot a_{SO_4^{2-}} - 24.04$$

$$\log \varphi^{-1} \cdot a_{HSO_4^-} = H_0 + \log a_{H^+}{}^2 \cdot a_{SO_4^{2-}} + 2.00 \qquad (25\,a,b,c)$$

$$\log \varphi^{-1} \cdot a_{HS_2O_7^-} = H_0 + 2 \log a_{H^+}{}^2 \cdot a_{SO_4^{2-}} - \log a_{H_2O} - 22.31$$

In Fig. 3 the functions log $\varphi^{\nu} \cdot a_x{}^{\nu}$ for H^+, H_3O^+, $H_3SO_4^+$, H_2O, $(H^+)_2SO_4^{2-}$, HSO_4^-, $HS_2O_7^-$ and SO_4^{2-}, are plotted *versus* H_0.

For H_2SO_4 eqn. (22) has been used and the quantity log $a_{H^+}{}^2 \cdot a_{SO_4^{2-}}$, which differs from log $a_{H_2SO_4}$ by the constant log $K_{H_2SO_4} \cdot K_{HSO_4^-}$, is plotted in Fig. 3. Since $K_{H_2SO_4}$ is unknown, log $a_{H_2SO_4}$ itself cannot be evaluated.

The curve for H^+, is dashed because measurable amounts of hydrogen ions do not occur, a_{H^+} being only a formal quantity equal to $a_{H_3O^+}/a_{H_2O}$. It deserves also to be mentioned that there is still some uncertainty about the composition of the main species in concentrated sulfuric acid solutions [26].

SOME RELATIONS BETWEEN ACTIVITIES AND ACTIVITY COEFFICIENTS IN CONCENTRATED SOLUTIONS OF SULFURIC ACID

As seen from Fig. 3, all species with the exception of H_2SO_4 give curves that can be divided into three different sets of parallel or nearly parallel curves. The spacing between the curves for H_3O^+ and HSO_4^- will be denoted by $2\,D$, i.e.

$$\log \varphi \cdot a_{H_3O^+} - \log \varphi^{-1} \cdot a_{HSO_4^-} = 2\,D$$

which can be rearranged to give the following expression for

$$\varphi = \frac{y_B}{y_{BH^+}} = 10^D \left(\frac{a_{HSO_4^-}}{a_{H_3O^+}}\right)^{\frac{1}{2}} \tag{26}$$

Above 12 M, where the concentration of SO_4^{2-} can be neglected in comparison to HSO_4^-, $C_{H_3O^+} = C_{HSO_4^-}$ and we obtain from eqn. (26)

$$\varphi^2 \cdot \frac{y_{H_3O^+}}{y_{HSO_4^-}} = 10^{2D} \tag{27}$$

In order to test how constant D is, we make use of the expression

$$-2H_0 - \log a_{H^+}{}^3 \cdot a_{SO_4^{2-}} + \log a_{H_2O} = 2\,D + pK_{HSO_4^-} = 2(D + 1.00) \tag{28}$$

which can be obtained from (26), (9) and (25b). Since all three quantities, H_0, $a_{H^+}{}^2 \cdot a_{SO_4^{2-}}$ and a_{H_2O} have been measured, we can find the range of validity of a constant D value. In Table 1, values of H_0, $a_{H^+}{}^2 \cdot a_{SO_4^{2-}}$ and a_{H_2O} are listed together with the quantity $2(D + 1.00)$ computed from (28). It is seen that, above about 10 M H_2SO_4, $2(D + 1.00)$ is practically constant. For most of the data, the deviation from the average is less than $\pm$ 0.1. This is about the accurary with which H_0 can be determined in concentrated sulfuric acid [21]. Since the accurary of the water and sulfuric acid activities is higher [19], it can be concluded that, within the uncertainty in H_0, the relation (28) with a constant D-value is valid in the concentration range 10 — 18.61 M H_2SO_4.

Consequently the relation:

$$\varphi^2 \cdot \left(\frac{y_{H_3O^+}}{y_{HSO_4^-}}\right) = 10^{1.95 \pm 0.03} = 89 \pm 6 \tag{29}$$

will hold from 12 to 18.61 M H_2SO_4.

It is tempting to speculate about the physical significance of (29). In any such discussion must enter, however, a knowledge of the electrostatic interactions between the ions. Our lack of knowledge of the variation of the dielectric constant in these concentrated solutions does not permit a comparison with even very naive models for the ion-ion interactions. Until the necessary data and useful theories for concentrated solutions have been obtained, (29) must stand as a surprisingly simple empirical relation covering a large concentration range. Another consequence of the constant D-value is the parallelism of the three sets of curves: H_3O^+ and HSO_4^-, SO_4^{2-} and H_2O, and $H_3SO_4^+$ and $HS_2O_7^-$.

Table 1. Water and sulfuric acid activities and H_0 data for the system $H_2O-H_2SO_4$.

C	log a_{H_2O}	log $a_{H^+}{}^2 \cdot a_{SO_4^{--}}$	H_0	$2(D + 1.00)$ from eqn. (28)
0.10	−0.00	−4.13	+0.83	2.47
0.50	−0.01	−2.74	+0.13	2.47
1.0	−0.02	−2.00	−0.26	2.50
1.5	−0.03	−1.53	−0.56	2.62
2.0	−0.05	−1.07	−0.84	2.70
2.5	−0.06	−0.65	−1.12	2.83
3.0	−0.08	−0.25	−1.38	2.93
3.5	−0.11	+0.14	−1.62	2.99
4.0	−0.14	0.53	−1.85	3.03
4.5	−0.18	0.93	−1.06	3.01
5.0	−0.22	1.32	−2.28	3.02
5.5	−0.27	1.71	−2.51	3.04
6.0	−0.32	2.09	−2.76	3.11
6.5	−0.38	2.49	−3.03	3.19
7.0	−0.45	2.88	−3.32	3.31
7.5	−0.52	3.22	−3.60	3.46
8.0	−0.59	3.59	−3.87	3.56
8.5	−0.67	3.94	−4.14	3.67
9.0	−0.76	4.29	−4.40	3.75
9.5	−0.86	4.64	−4.65	3.80
10.0	−0.97	4.99	−4.89	3.82
10.5	−1.08	5.33	−5.15	3.89
11.0	−1.22	5.70	−5.41	3.91
11.5	−1.36	6.03	−5.67	3.95
12.0	−1.51	6.36	−5.93	3.99
12.5	−1.68	6.68	−6.18	4.00
13.0	−1.84	7.00	−6.44	4.04
13.5	−2.05	7.33	−6.70	4.02
14.0	−2.26	7.63	−6.96	4.03
14.5	−2.49	7.93	−7.22	4.02
15.0	−2.73	8.21	−7.47	4.00
15.5	−3.00	8.48	−7.72	3.95
16.0	−3.31	8.74	−7.98	3.91
16.5	−3.59	8.94	−8.23	3.93
17.0	−3.88	9.11	−8.49	3.99
17.5	−4.26	9.27	−8.75	3.97
18.0	−4.88	9.43	−9.04	3.77
18.1	−5.03	9.46	−9.13	3.77
18.2	−5.20	9.49	−9.22	3.75
18.3	−5.36	9.52	−9.36	3.84
18.4	−5.57	9.53	−9.56	4.02
18.5	−5.82	9.54	−9.89	4.42
18.61	−8.81*	9.55	−11.10	3.84

* From Giauque *et al.*[19]

Average : 3.95±0.03
in the range 10 — 18.61 M

Eqn. (19) can be used for defining single ion activities in the concentration range where D is found to be practically constant. The simplest choice is perhaps to define

$$y_{H_3O^+} = y_{HSO_4^-} \text{ for } 12 \leq C \leq 18.61 \quad (30)$$

Inserting (30) into (29) gives:

$$\varphi = 9.4 \pm 0.3 \text{ for } 12 \leq C \leq 18.61 \quad (31)$$

Expressions for the activities of the other ions are obtained by inserting the φ-value given in (31) into (9), (23 c) and (25). Especially the expression for the activity of SO_4^{2-} takes a very simple form:

$$\log a_{SO_4^{2-}} = \log a_{H_2O} - 2.00 \quad (32)$$

According to (32), the solubility of sulfates should be proportional to the water activity provided that the activity coefficient of the cation stays practically constant. No simultaneous solubility and water activity measurements seem to exist at present so the exact relation between solubility and water activity cannot be obtained. For the solubility of $BaSO_4$ in concentrated sulfuric acid solutions, Hammet and Deyrup [27] noted that the solubility decreased with increasing water content in qualitative agreement with (32).

Finally it may be mentioned that Brand [28] as well as Deno and Taft [18] have found empirical relations between H_0 and the concentrations of various species present in concentrated sulfuric acid solutions. Analogous expressions can be derived from (9), (25b) and (23) using the transformation from the molarity to the mole fraction scale. Using the Raman data of Young et al.[20a] it was found that

$$\log \frac{\varphi^{-1} \cdot f_{HSO_4^-}}{K_{H_2SO_4} \cdot f_{H_2SO_4}} \sim 8.51 = H_0 - \log \frac{X_{HSO_4^-}}{X_{H_2SO_4}} \quad (33)$$

above 16 M H_2SO_4 (90 % H_2SO_4), in excellent agreement with Brand's empirical constant 8.48 (corrected to the H_0-scale adopted by Paul and Long [3]).

Analogously, it was found that the same Raman data [20a] gave

$$\log \frac{f_{H_2O}}{\varphi \cdot f_{H_3O^+}} - 1.74 \sim 7.06 = H_0 - \log \frac{X_{H_2O}}{X_{H_3O^+}} \quad (34)$$

above 15 M H_2SO_4.

This differs by about 0.3 from the value 6.78 used by Deno and Taft (corrected to the H_0-scale adopted by Paul and Long [3]). The range of validity of (34) is the same as that found by Deno and Taft for their empirical relation. The Raman data thus confirm the validity of their equation although there is some uncertainty about the exact value of their empirical constant.

The relations (29), (33) and (34) show that the variations of several activity coefficients must practically cancel each other in concentrated solutions. Deno and Taft suggested that the individual activity coefficients may approach constancy in concentrated sulfuric acid. The ideal behavior of such solutions was suggested to be a result of the high dielectric constant [29]. The similarity to fused salts which are known to behave as practically ideal solutions [30] was also emphasized.

COMPARISON OF ION ACTIVITY COEFFICIENT FUNCTIONS IN SOME DIFFERENT ACIDS

In a preceding paper, stoichiometric activity coefficient products for hydrated ions were investigated [1]. With the aid of the functions (9), (12), (23c) and (25), analogous functions for the single ions can be defined. For H_3O^+ we can write:

$$\varphi \cdot y_{H_3O^+} = \frac{\varphi \cdot a_{H_3O^+}}{C_{H^+}} \tag{35}$$

where $\varphi \cdot a_{H_3O^+}$ is given by eqn. (9) with $n = 1$ and C_{H^+} is the total, *i.e.* the equilibrium concentration of solvated protons in the solution. In Fig. 4, $\log \varphi \cdot y_{H_3O^+}$ is plotted versus H_0 for the three acids, HNO_3, $HClO_4$ and H_2SO_4, for which Raman and NMR data have made possible a distinction between dissociated and undissociated acid. As seen, the three acids give practically parallel straight lines in the range of overlap. It does not seem unreasonable to suppose that, if no systematic experimental errors were present, all three curves would coincide as do the corresponding activities.

In analogy to (35) the function $\varphi^{-1} \cdot y_{A^-}$ is defined by:

$$\varphi^{-1} \cdot y_{A^-} = \frac{\varphi^{-1} \cdot a_{A^-}}{C_{A^-}} \tag{36}$$

where C_{A^-} is the equilibrium amount of A^-. For a monobasic acid HA, we have:

$$C_{H^+} = C_{A^-} = \alpha \cdot C \tag{37}$$

where α is the degree of dissociation of HA.

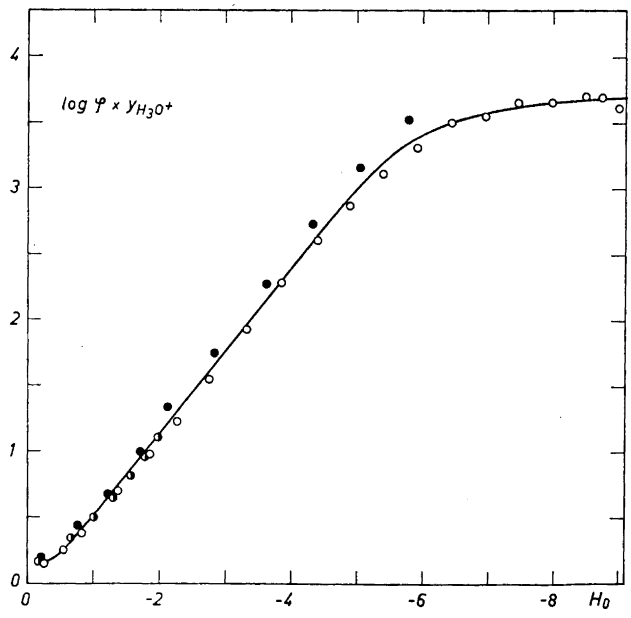

Fig. 4. The function $\log \varphi \cdot y_{H_3O^+}$ *versus* H_0 for the acids: ○ H_2SO_4; ● $HClO_4$; ◑ HNO_3

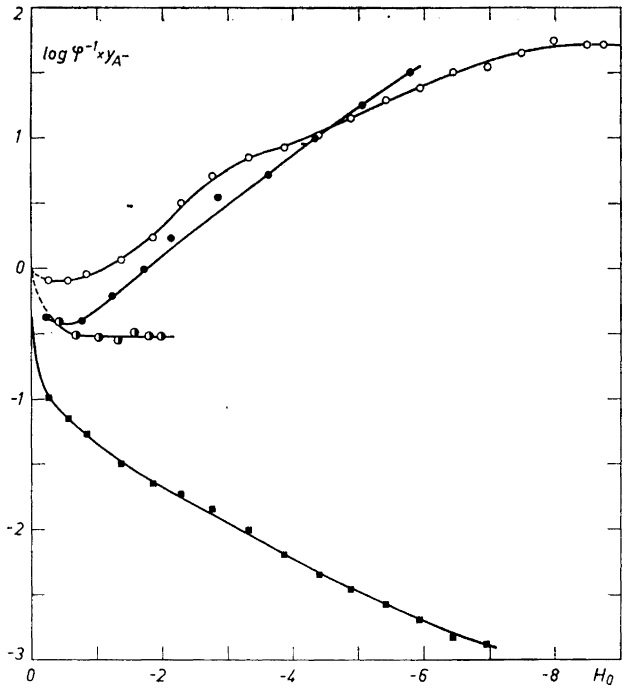

Fig. 5. The function log $\varphi^{-1} \cdot y_{A^-}$ *versus* H_0 for various anions: ○ HSO_4^-; ● ClO_4^- ◑ NO_3^-; ■ SO_4^{2-}.

In Fig. 5, log $\varphi^{-1} \cdot y_{A^-}$ is plotted against H_0 for the anions, NO_3^-, ClO_4^-, HSO_4^- and SO_4^{2-}. As seen, HSO_4^- and ClO_4^- give parallel curves for H_0 down to —3 while the curve for NO_3^- seems to be practically constant and the curve for SO_4^{2-} slopes in the other direction. In the following section, it will be shown how the slopes of the activity coefficient curves are related to the average degree of hydration.

THE AVERAGE DEGREE OF HYDRATION

In a preceding paper[1], it was shown that a function $\bar{n}'$ approximating to the average degree of hydration of the ions H^+, A^- could be computed from

$$\bar{n}' = -\operatorname{dlog}\left(\frac{y}{a}\right)^2 / \operatorname{dlog} a_{H_2O} = -\frac{\operatorname{dlog} y_{H^+} \cdot y_{A^-}}{\operatorname{dlog} a_{H_2O}} \tag{38}$$

where $\bar{n}'$ approaches the true hydration number $\bar{n}$ when

$$\frac{\operatorname{dlog} y_+ \cdot y_-}{\operatorname{dlog} a_{H_2O}} \sim 0 \tag{39}$$

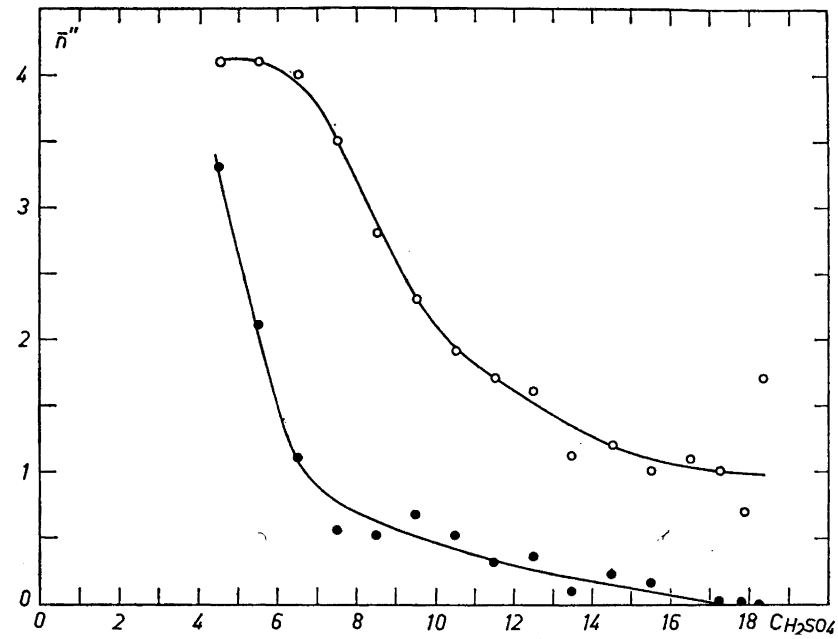

Fig. 6. The function $\bar{n}''$ for H^+ and HSO_4^- in H_2SO_4 *versus* the stoichiometric molarity, C, of the acid: ○ H^+; ● HSO_4^-.

y_+ and y_- are the »true» activity coefficients of the various hydrated ions with the simplifying assumption that y_+ is the same for all differently hydrated protons and y_- the same for all differently hydrated anions at each concentration.

From (38) we obtain by introducing the φ-function:

$$\bar{n}''_{H^+} = \frac{-\text{dlog } \varphi \cdot y_{H^+}}{\text{dlog } a_{H_2O}} \qquad \bar{n}''_{A^-} = \frac{-\text{dlog } \varphi^{-1} y_{A^-}}{\text{dlog } a_{H_2O}} \tag{40 a,b}$$

Using the definition of H_0 (eqn. 3) (40a) can be rearranged to

$$\bar{n}''_{H^+} = \frac{\delta \log C_{H^+} + \delta H_0}{\delta \log a_{H_2O}} \tag{41}$$

$\bar{n}''_{H^+}$ and $\bar{n}''_{A^-}$ approach the true hydration numbers if

$$\frac{\text{dlog } \varphi \cdot y_+}{\text{dlog } a_{H_2O}} \sim 0, \quad \frac{\text{dlog } \varphi^{-1} \cdot y_-}{\text{dlog } a_{H_2O}} \sim 0 \tag{42 a,b}$$

which may happen in concentrated solutions where, as seen in Fig. 3, a_{H_2O} decreases rapidly while the activity coefficients may approach constant values as indicated in Figs. 4 and 5 by the behavior of the stoichiometric coefficients. In Fig. 6, $\bar{n}''_{H^+}$ and $\bar{n}''_{HSO_4^-}$ are plotted versus C from 4 M to pure H_2SO_4. In this concentration range, $\bar{n}''_{H^+}$ decreases from about 4 in dilute solutions

to 1 in concentrated solutions while $\bar{n}''_{HSO_4^-}$ decreases from about 3 to 0. That $H^+(H_2O)_n$ tends towards H_3O^+, and $HSO_4^-(H_2O)_n$ towards HSO_4^- is quite reasonable. It thus seems that the conditions (42) may be valid in concentrated solutions and $\bar{n}''$ close to the real hydration number. Since the curve H_0 *versus* a_{H_2O} is the same for all strong acids, it is seen from eqn. (40) that the slopes of the curves log $\varphi^{\nu} \cdot y_X^{\nu}$ *versus* H_0 are proportional to $\bar{n}''$ and thus closely related to $\bar{n}$. In Fig. 4 the parallelism of the curves log $\varphi \cdot {}_{H_3O^+}$ for different acids implies that when compared at the same water activity (or H_0-value) the protons seem to be hydrated to the same extent in all strong acids.

In Fig. 5 it is seen that, in dilute and moderately concentrated solutions, ClO_4^- and HSO_4^- seem to be hydrated to the same extent. In more concentrated solutions, ClO_4^- seems to be more strongly hydrated than HSO_4^- as indicated by the steeper slope. On the other hand, the practically constant value for log $\varphi^{-1} \cdot y_{NO_3^-}$ implies a much smaller and nearly constant degree of hydration for NO_3^- as compared with ClO_4^- and HSO_4^- in the range of overlap. By adding 3·log a_{H_2O} to log $\varphi^{-1} \cdot y_{NO_3^-}$, a curve parallel to those for ClO_4^- and HSO_4^- is obtained. This implies a difference of 3 in hydration number in moderately concentrated solutions between NO_3^- on the one hand and ClO_4^- and HSO_4^- on the other.

For SO_4^{2-}, the slope of the curve log $\cdot \varphi^{-2} y_{SO_4^{2-}}$ is in the other direction compared with those for ClO_4^- and HSO_4^-. No explanation of this behavior has been found. Solvation by H_2SO_4 instead of H_2O might explain the different slope altough it is difficult to see how this might occur in solutions where SO_4^{2-} exists in measurable amounts only up to 12 M while measurable amount of H_2SO_4 do not seem to appear below 14 M.

Note added in proof. Recently, Young [26] and Wyatt [*Trans. Faraday Soc.* **56** (1960) 490] have suggested the existence of $H_3O^+ \cdot H_2SO_4$ in concentrated solutions of sulfuric acid. That $\bar{n}''_{H_3O^+}$ nevertheless tends towards unity suggssts that to a first approximation the interaction between H_3O^+ and H_2SO_4 can be neglected compared to the strong interaction between H^+ and H_2O.

Acknowledgements. The author wishes to express his sincere thanks to Professor Charles D. Coryell for stimulating discussions and encouraging interest when this work was in its infancy. Much helpful advice from Professor Lars Gunnar Sillén concerning the presentation of the material in this paper is gratefully acknowledged. Professor T. F. Young is thanked for comments on equilibria in concentrated solutions of sulfuric acid and Professor W. F. Giauque for giving access to thermodynamic data unpublished at that time for the system H_2SO_4—H_2O. Mr Don Gillam corrected the English text. Dr Åke Olin is also thanked for some helpful comments. Thanks are due to the *Swedish Atomic Energy Committee* and the *Swedish Natural Science Research Council* for financial support.

REFERENCES

1. Högfeldt, E. *Acta Chem. Scand.*, **14** (1960) 1597.
2. Coryell, C. D. and Fix, R. *J. Inorg. Nuclear Chem.* **1** (1955) 119.
3. Paul, M. A. and Long, F. A. *Chem. Revs.* **57** (1957) 1.
4. Guggenheim, E. A. *J. Phys. Chem.* **33** (1929) 842.
5. Bates, R. G. *Electrometric pH Determinations, Theory and Practice*, John Wiley, New York 1954.

6. Brönsted, J. N. *Rec. trav. chim.* **42** (1923) 718.
7. Brönsted, J. N. *Z. physik. Chem.* **169A** (1934) 52.
8. Åkerlöf, G. and Teare, J. *J. Am. Chem. Soc.* **60** (1938) 1226.
9. Harned, H. S. and Owen, B. B. *The Physical Chemistry of Electrolytic Solutions*, 3rd Ed, Reinhold, N.Y. 1958, p. 716.
10. Robinson, R. A. and Stokes, R. H. *Electrolytic Solutions*, Butterworth, London 1955; a) p. 489, b) p. 468.
11. Landolt-Börnstein, *Physikalisch-Chemische Tabellen*, Julius Springer Berlin, a) Eg II a, 1931, p. 254, b) Eg II b, 1936, p. 1118.
12. Potier, A. *Ann. fac. sci., univ. Toulouse* **20** (1956) 1.
13. Hood, G. C., Redlich, O. and Reilly, C. A. *J. Chem. Phys.* **22** (1954) 2067.
14. Markham, A. E. *J. Am. Chem. Soc.* **63** (1941) 874.
15. Robinson, R. A. and Baker, O. J. *Trans. Proc. Roy. Soc. New Zealand*, **76** (1946) 250 as reported in *Chem. Abstr.* **41** (1947) 5000 d.
16. *International Critical Tables*, Vol 3, McGraw Hill, New York 1928, p. 56—57.
17. Glueckauf, E. and Kitt, G. P. *Trans. Faraday Soc.* **52** (1956) 1074.
18. Deno, N. C. and Taft, R. W. Jr. *J. Am. Chem. Soc.* **76** (1954) 244.
19. Giauque, W. F., Hornung, E. W., Kunzler, J. E. and Rubin, T. R. *J. Am. Chem. Soc.* **82** (1960) 62.
20. Hamer, W. J. *Structure of Electrolytic Solutions*, John Wiley, New York 1959, a) Young, T. F., Maranville, L. F. and Smith, M. M., p. 35, b) Hamer, W. J., p. 236.
21. Högfeldt, E. and Bigeleisen, J. *J. Am. Chem. Soc.* **82** (1960) 15.
22. Wyatt, P. A. H. *Discussions Faraday Soc. No* **24** (1957) 162.
23. Kirkbride, B. T. and Wyatt, P. A. H. *Trans. Faraday Soc.* **54** (1958) 483.
24. Gillespie, R. J., Hughes, E. D. and Ingold, C. K. *J. Chem. Soc.* **1950**, 2473.
25. Gillespie, R. J. and Oubridge, J. V. *J. Chem. Soc.* **1956** 80.
26. Young, T. F. *Private communication*, June 1959.
27. Hammet, L. P. and Deyrup, A. J. *J. Am. Chem. Soc.* **55** (1933) 1900.
28. Brand, J. C. *J. Chem. Soc.* **1950** 997.
29. Gillespie, R. J. and Cole, R. H. *Trans. Faraday Soc.* **52** (1956) 1325.
30. Seward, R. P. *J. Am. Chem. Soc.* **67** (1945) 1189.

Received April 13, 1960.

ACTA CHEMICA SCANDINAVICA 14 (1960) 1643–1653

Reactions between Quinones and Carbonyl Compounds Catalysed by Aluminium Oxide

Part II *. The Addition of Acetone to *o*-Benzoquinones

RUNE MAGNUSSON

Institutionen för organisk kemi, Chalmers Tekniska Högskola, Göteborg, Sweden

o-Benzoquinones react with acetone at room temperature in the presence of aluminium oxide to form 2-acetonyl-*o*-benzoquinols by the addition of one mole of acetone at one of the carbonyls by an aldol type condensation. An investigation was made of this reaction with unsubstituted *o*-benzoquinone and various alkyl and alkoxyl substituted *o*-benzoquinones. In most cases the *o*-benzoquinol could be isolated in a pure form but in two cases the crude *o*-quinol dimerised too rapidly for it to be purified.

In a preceding communication [1] it was briefly reported that 3,8-dimethoxy-1,2-naphthoquinone and 2,6-dimethoxy-1,4-benzoquinone reacted with acetone in the presence of aluminium oxide; one mole of acetone was added with the formation of an acetonyl-quinol. It has now been shown that similar aldol condensations occur with *o*-benzoquinones and the present paper is a report of an investigation of the addition of acetone to a number of *o*-benzoquinones in the presence of aluminium oxide.

The addition of ketones to tetrachloro-*o*-quinone has been investigated by Schenck *et al.*[2] Dry hydrogen chloride was used as a catalyst and the corresponding *o*-quinol was formed.

When an acetone solution of *o*-benzoquinone (I) is shaken with aluminium oxide, pyrocatechol is formed in 11 % yield. The formation of pyrocatechol also occurs spontaneously in an aqueous solution of *o*-benzoquinone and is probably the result of a complicated disproportionation [3]. The expected 2-acetonyl-*o*-benzoquinol (II) has not been isolated but its formation has been shown indirectly by the isolation of a small amount of 2-acetonyl-phenol (III) after treatment of the acetone solution with zinc and acetic acid.

* Part I, See Ref. [1]

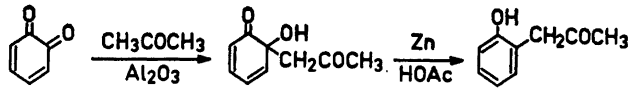

I II III

In the experiments described below the reaction was applied to a number of alkyl and alkoxyl substituted *o*-benzoquinones (IV—XIII) which are more stable than *o*-benzoquinone. When a freshly prepared solution of the substituted *o*-benzoquinone in acetone was shaken with neutral aluminium oxide, the colour of the solution turned from red to yellow. Analysis of the reaction products showed that in all cases they were adducts of quinone and acetone in a 1:1 ratio.

Under these conditions, the aldol condensation between *o*-quinone and acetone was accompanied by competing dimerisation and polymerisation reactions of the *o*-quinones [4-9]. These products however, unlike the acetone adduct, were strongly adsorbed on the aluminium oxide which usually acquired a dark colour. Dimeric *o*-benzoquinone for example was 95 % adsorbed on shaking with aluminium oxide in acetone. Thus the acetone adducts were purified automatically.

Reduction [10] of the *o*-quinone acetone adducts with zinc and acetic acid gave *o*-acetonylphenols, supporting the view that the adducts had an *o*-benzoquinol structure.

The addition of acetone to either of the carbonyl groups in the symmetrically substituted *o*-benzoquinone V would give only a single acetonyl-quinol, XV, but the unsymmetrically substituted *o*-quinones (IV and VI—XIII) could, formally, give two isomers. However in all cases only one isomer was obtained. To decide which was formed of two possible *o*-acetonyl-quinols in the case where one isomer had a free 4-position and the other a free 5-position the following method * was used. The phenol obtained by reduction of the quinol was treated with potassium nitrosodisulphonate[17]. The formation of a *p*-benzoquinone indicated that the phenol had a free *p*-position and therefore that the 4-position was free in the quinol. The quinones IV, VI, VIII, X, XI and XIII gave quinols which were shown in this way to have a free 4-position and could therefore be ascribed the structures XIV, XVI, XVIII, XX, XXI and XXIII, respectively. The quinone XII gave a quinol, the reduction product of which was slowly oxidised by potassium nitrosodisulphonate to an *o*-quinone with simultaneous loss of a tert-butyl group. The quinol must therefore be substituted in both the 4 and 6 positions, as in structure XXII. The quinones VII and IX gave quinols that were shown by spectrophotometric evidence (see below) to have the structures XVII and XIX.

The *o*-acetonylquinols XVI, XVII, XVIII, XIX, XX, XXI and XXII were crystalline while XIV was an oil and was purified by distillation. The *o*-quinols XV and XXIII were oils and could not be obtained in an analytically pure condition. Most of the *o*-quinols dimerised on keeping at room temperature and in the case of the latter two compounds, dimerisation was so

* Further details will be given in a following paper [10].

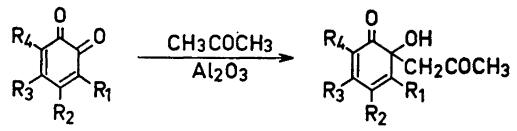

IV–XIII XIV–XXIII

IV, XIV $R_1=R_3=CH_3$; $R_2=R_4=H$
V, XV $R_1=R_4=H$; $R_2=R_3=CH_3$
VI, XVI $R_1=R_3=R_4=CH_3$; $R_2=H$
VII, XVII $R_1=OCH_3$; $R_2=R_3=R_4=H$
VIII, XVIII $R_1=OCH_3$; $R_2=R_4=H$; $R_3=CH_3$
IX, XIX $R_1=OCH_3$; $R_2=R_4=H$; $R_3=CH_2CH_2CH_3$
X, XX $R_1=R_2=R_4=H$; $R_3=OCH_3$
XI, XXI $R_1=R_2=R_4=H$; $R_3=OCH_2C_6H_5$
XII, XXII $R_1=R_3=C(CH_3)_3$; $R_2=R_4=H$
XIII, XXIII $R_1=R_2=R_4=H$; $R_3=C(CH_3)_3$

fast that it was impossible to purify the monomers. The dimeric products will be dealt with in a following paper [11].

The infrared spectra of the acetone adducts, some of which are shown in Fig. 1, were in full accord with the postulated *o*-benzoquinol structures. They showed a strong hydroxyl absorption with maxima varying between 3 194 and 3 472 cm^{-1}. The absorption bands between 1 705 and 1 721 cm^{-1} confirm the presence of the acetonyl groups and the bands between 1 667 and 1 686 cm^{-1} can be explained by the presence of an $\alpha,\beta,\gamma,\delta$-unsaturated carbonyl grouping. The lowest frequency for the conjugated carbonyl band was shown by the substances XVII, XVIII and XIX (1 667, 1 669 and 1 669 cm^{-1}) all of which have a 3-methoxyl substituent (see below). All compounds showed two bands in the intervals 1 616—1 647 and 1 538—1 582 cm^{-1}, which can be ascribed to the two double bonds in the *o*-quinol ring. These absorption bands of the dienone system in the acetone adducts are similar to those reported [12] for the first two *o*-benzoquinols known, 2,3-dimethyl-*o*-benzoquinol and 2,3,5-trimethyl-*o*-benzoquinol.

The ultraviolet spectra of the acetone adducts also confirmed the *o*-benzoquinol structure. This type of conjugated system has been investigated by Derkosch and Kaltenegger [13], who have determined the ultraviolet spectra of a number of 2-methyl-*o*-benzoquinol acetates and of 2,3,5-trimethyl-*o*-benzoquinol *. Ethanol solutions of these compounds give a relatively broad K-band with maxima in the region of 298—312 mμ and an R-band varying between 349 and 369 mμ. The K-band is present in all the spectra shown in Figs. 2 and 3 but the R-band can be seen only in the spectrum of 2-acetonyl-4,6-di-tert-butyl-*o*-benzoquinol (XXII). This band is present as an inflection at 373 mμ while the main absorption peak for this compound is at 313 mμ.

* In the quoted work the substance was erroneously assumed to be 2,4,6-trimethyl-*o*-benzoquinol (cf. Ref. [14]).

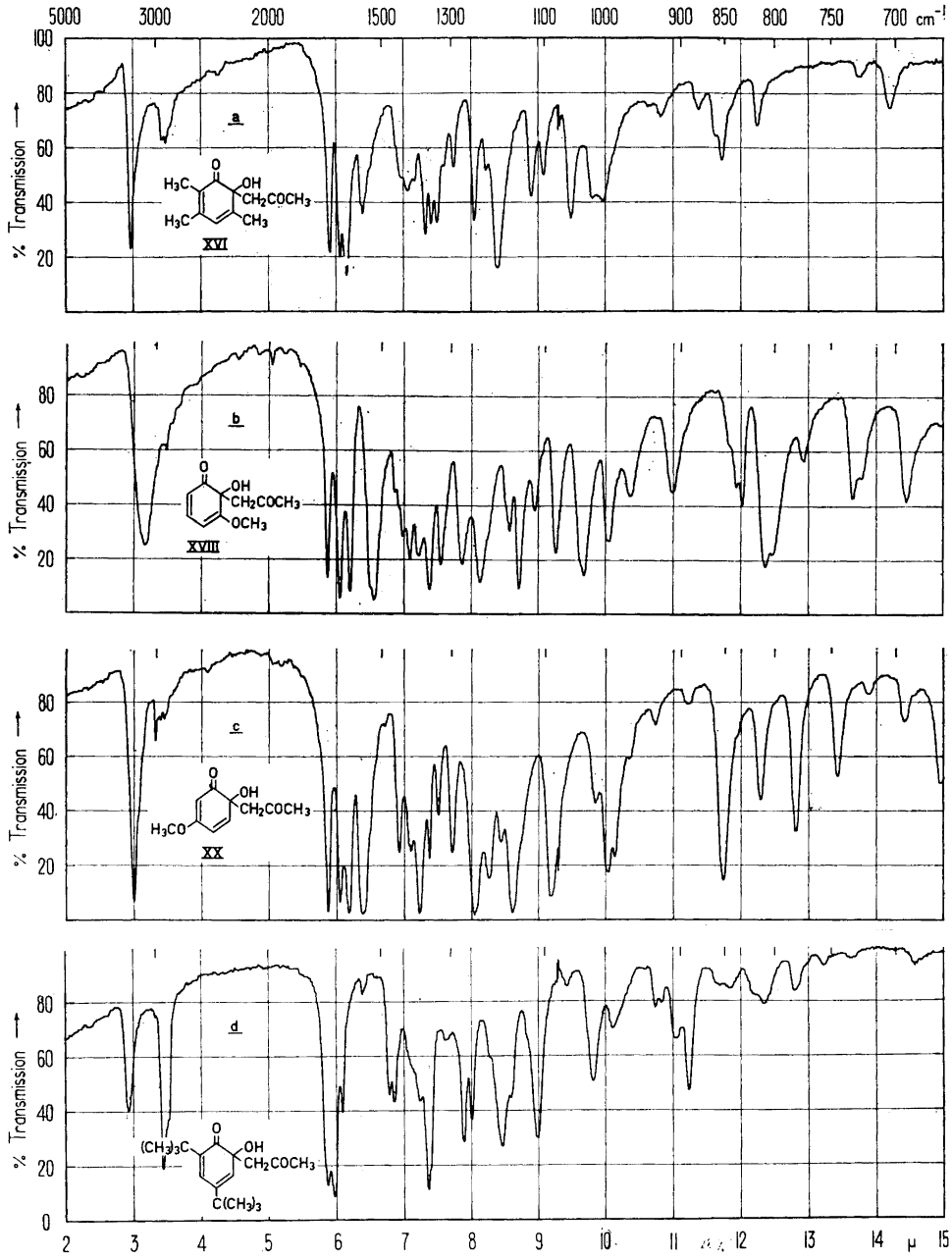

Fig. 1. Infrared absorption spectra (KBr method).

a. 2-Acetonyl-3,5,6-trimethyl-*o*-benzoquinol (XVI)
b. 2-Acetonyl-3-methoxy-*o*-benzoquinol (XVII)
c. 2-Acetonyl-5-methoxy-*o*-benzoquinol (XX)
d. 2-Acetonyl-4,6-di-tert-butyl-*o*-benzoquinol (XXII)

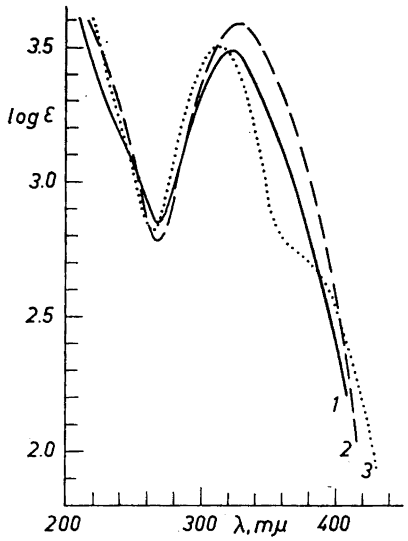

Fig. 2. Absorption spectra.
1. 2-Acetonyl-3,5-dimethyl-*o*-benzoquinol (XIV)
2. 2-Acetonyl-3,5,6-trimethyl-*o*-benzoquinol (XVI)
3. 2-Acetonyl-4,6-di-tert-butyl-*o*-benzoquinol (XXII)

Solvent: 95 % Ethanol.

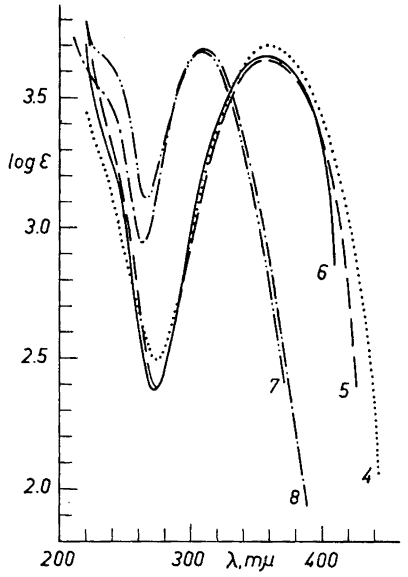

Fig. 3. Absorption spectra.
4. 2-Acetonyl-3-methoxy-*o*-benzoquinol (XVII)
5. 2-Acetonyl-3-methoxy-5-methyl-*o*-benzoquinol (XVIII)
6. 2-Acetonyl-3-methoxy-5-propyl-*o*-benzoquinol (XIX)
7. 2-Acetonyl-5-methoxy-*o*-benzoquinol (XX)
8. 2-Acetonyl-5-benzyloxy-*o*-benzoquinol (XXI)

Solvent: 95 % Ethanol.

The two other alkyl-substituted quinols, 2-acetonyl-3,5-dimethyl- and 2-acetonyl-3,5,6-trimethyl-*o*-benzoquinol (XIV and XVI) have maxima at 321 and 327 mμ, respectively; the K-bands in these two *o*-quinols are thus at a relatively long wavelength and, since they are relatively wide, could possibly cover a smaller R-band.

2-Acetonyl-3-methoxy-5-methyl-*o*-benzoquinol (XVIII) has an ultraviolet spectrum (shown in Fig. 3) with an absorption maximum at a significantly longer wavelength, 356 mμ, than 2-acetonyl-3,5-dimethyl-*o*-benzoquinol (XIV), 321 mμ. This bathochromic shift can be explained by the mesomeric effect of the methoxyl group.

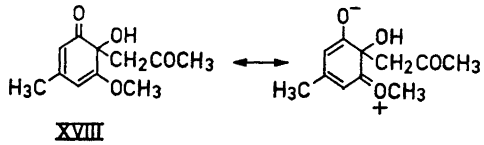

XVIII

The ultraviolet spectra of XVII, XVIII and XIX are almost identical and since structural investigation [10] has shown that XVIII has a 3-methoxyl group it can be assumed that the same is also true for the other two compounds.

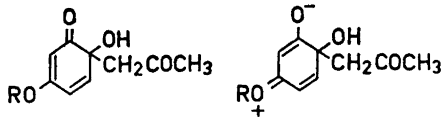

XX R = CH_3 XXI R = $CH_2C_6H_5$

In 2-acetonyl-5-methoxy-*o*-benzoquinol (XX) the methoxyl group makes possible a cross-conjugated resonance structure. This does not however give rise to any bathochromic displacement of the K-band. The spectra of this 5-methoxy-substituted quinol and of 2-acetonyl-5-tert-butyl-*o*-benzoquinol (XXIII) show absorption maxima at the same wavelength (305 mμ) and 2-acetonyl-5-benzyloxy-*o*-benzoquinol (XXI) with a maximum at 310 mμ shows only a very slight shift.

The aluminium oxide-catalysed addition of acetone to *o*-benzoquinones is of an aldol condensation type and therefore should be catalysed by alkali as well. Because of the instability of *o*-benzoquinones, alkali cannot be used as a catalyst in this case. The aluminium oxide may be assumed to act as a Lewis base, and the mechanism of the addition reaction may be presented as follows.

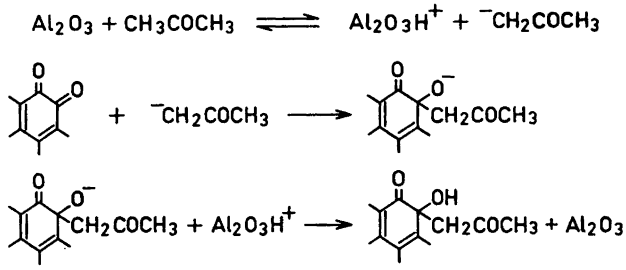

The acetonyl anion, when attacking the *o*-benzoquinone, would be expected to prefer the more positive of the two carbonyl carbon atoms. Which of carbon atoms 1 and 2 of the *o*-quinone ring will be the more strongly positive will depend on the inductive and mesomeric effects of the substituents in the ring. Thus the methyl groups in 3,5-dimethyl-*o*-benzoquinone (IV) by electron

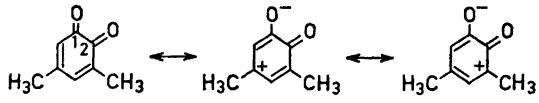

IV a b

release should favour the resonance structures a and b. This will weaken the carbonyl character of the carbonyl group in position 1 and as a result carbon atom 2 will be comparatively more positive. Addition can therefore be expected to occur at 2, which is in agreement with the experimental result. Analogously favoured resonance structures can similarly be postulated for 3,5,6-trimethyl-*o*-benzoquinone (VI). In this case one of the methyl groups (that in the three

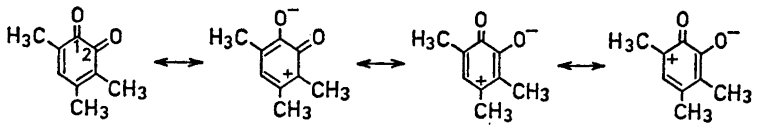

VI

position) will favour reaction at carbonyl group 2 while the two others (in positions 4 and 6) will favour reaction at carbonyl group 1. The product of the reaction of 3,4,6-trimethyl-*o*-benzoquinone was 2-acetonyl-3,5,6-trimethyl-*o*-benzoquinole (XVI) which shows that the two methyl groups acting together exerted the dominant effect.

In 3-methoxy-*o*-benzoquinone (VII), 3-methoxy-5-methyl-*o*-benzoquinone (VIII) and 3-methoxy-5-propyl-*o*-benzoquinone (IX), the methoxyl group

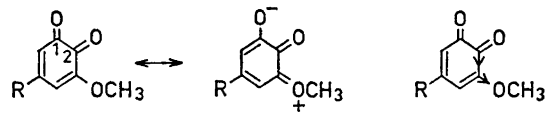

VII R=H, VIII R=CH_3, IX R=$CH_2CH_2CH_3$

weakens the carbonyl character of carbonyl group 1 by a resonance effect and the acetonyl anion will therefore be accepted by carbon atom 2. Electron attraction by the methoxyl group may also contribute to make carbon atom 2 more positive than carbon atom 1. In VIII and IX, the alkyl group will co-operate with the methoxyl group to make carbonyl group 1 less reactive towards acetone than carbonyl group 2.

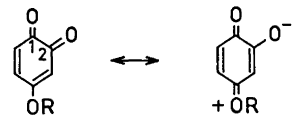

X R=CH_3, XI R=$CH_2C_6H_5$

For both 4-methoxy-*o*-benzoquinone (X) and for 4-benzyloxy-*o*-benzoquinone (XI) *p*-quinonoid resonance structures are possible and as a result carbonyl group 2 will be less receptive to attack than carbonyl group 1.

An exception to the rule that acetone addition will take place at the carbonyl group that can be regarded as having the more strongly positive C-atom was found in the addition of acetone to 3,5-di-tert-butyl-*o*-benzoquinone (XII). This gave 2-acetonyl-4,6-di-tert-butyl-*o*-benzoquinol (XXII), probably

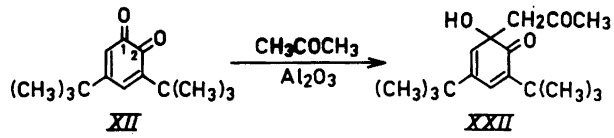

XII XXII

because carbonyl group 2 which should have the more strongly positive C-atom was hindered by the bulky butyl group in the 3-position. A tert-butyl group not present in a sterically hindering position directs the addition in the same way as methyl groups. 4-tert-Butyl-*o*-benzoquinone (XIII) gave 2-acetonyl-5-tert-butyl-*o*-benzoquinol (XXIII) which is in harmony with the expected electron displacement shown in the formula below.

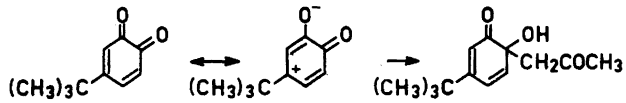

XIII XXIII

EXPERIMENTAL

Melting points are uncorrected. Infrared spectra were recorded on a Perkin Elmer model 21 spectrophotometer using KBr discs in the case of solid substances and films between salt plates in the case of oils. Ultraviolet spectra were measured with a Beckman DU spectrophotometer. Microanalyses were done by Alfred Bernhardt, Mülheim (Ruhr).

Materials. *o*-Benzoquinone and 3-methoxy-*o*-benzoquinone were prepared by dehydrogenation of pyrocatechol and pyrogallol-1-methyl ether, respectively, with tetrachloro-*o*-quinone * according to Horner and Dürckheimer [15]. 3,5-Di-tert-butyl-*o*-benzoquinone was prepared according to Flaig *et al.*[16] and the other quinones with the exception of 4-tert-butyl-*o*-benzoquinone (see below) were prepared according to Teuber and Staiger [17]. Neutral aluminium oxide "Woelm" of activity 1 and acetone purum or p.a. were used. No differences were observed between the two grades.

4-tert-Butyl-o-benzoquinone (XIII). This *o*-quinone was prepared by dehydrogenation of the corresponding pyrocatechol by periodate according to the procedure described by Adler and Magnusson [18]. A solution of 1,2-dihydroxy-4-tert-butylbenzene (7.0 g) in water (1 l) was mixed with sodium metaperiodate (10 g) dissolved in water (150 ml). The red reaction mixture was extracted immediately with methylene chloride. The extract was dried with sodium sulphate and evaporated. The residue was recrystallised from a mixture of ether and light petroleum, giving red needles of 4-tert-butyl-*o*-benzoquinone, m.p. 66—67° [17] (3.8 g, 54 %).

Addition of acetone to *o*-benzoquinones

General procedure. A solution of the *o*-benzoquinone in acetone was shaken with aluminium oxide at room temperature. The end of the reaction was indicated by a colour change from red or red-brown to yellow. The quantities of reactants used and the time of shaking are given below. The solution was decanted and the aluminium oxide, which usually was strongly discoloured, was washed several times with acetone. The combined solutions were centrifuged to remove traces of alumina. The acetone solution was then evaporated in a rotary vacuum evaporator and the reaction product obtained purified as described below.

* *o*-Benzoquinone as well as 3-methoxy-*o*-benzoquinone when prepared in this way on keeping sometimes suddenly decomposed. However if the crude substance was recrystallised immediately from ether it was usually stable.

o-*Benzoquinone* (I) a) *o*-Benzoquinone (0.82 g) in acetone (15 ml) was shaken with aluminium oxide (12.5 g) for 30 min. The reaction solution on evaporation (see above) gave a partially crystalline residue. It was extracted with boiling hexane. On cooling, the extract gave *pyrocatechol* (89 mg, 11 %), identified by m.p. and mixed m.p.

b) *o*-Benzoquinone (8.0 g) in acetone (300 ml) was shaken with aluminium oxide (200 g) for 30 min. The solution was decanted and shaken with zinc dust (20 g) and acetic acid (20 ml) until colourless. The aluminium oxide was washed with acetone and the washings were treated in the same way. The combined solutions were filtered and neutralised with sodium bicarbonate solution. The acetone was distilled off under reduced pressure and the aqueous solution remaining was extracted with ether. The ether solution, which contained 2.0 g of product, was extracted with 20 % aqueous sodium bisulphite (10 × 50 ml). The bisulphite solution was neutralised with sodium bicarbonate and extracted with ether. The ether solution was dried and evaporated giving an oil (0.55 g) which crystallised after a day. Recrystallisation from hexane gave colourless plates of *2-acetonylphenol* (*III*), m.p. 62—64° (0.20 g, 2 %). After sublimation (0.05 mm Hg, bath temperature 70°) and further recrystallisation from hexane it had m.p. 63—64°. (Found: C 71.99; H 6.82. Calc. for $C_9H_{10}O_2$: C 71.98; H 6.71). Infrared bands (cm^{-1}): 3408 (OH), 1712 (C=O), 1616, 1597 and 1504—1513 (benzene ring); ultraviolet maximum at 276 mμ, log ε, 3.12. The substance could be converted into 3-methylcoumarone by boiling with ethanolic hydrochloric acid.

Since this experiment was carried out, the preparation of the compound in another way has been reported [20].

3,5-Dimethyl-o-*benzoquinone* (*IV*) (2.30 g) in acetone (125 ml) was shaken (15 min) with aluminium oxide (50 g). The reaction mixture when worked up gave a yellow oil (1.26 g). Distillation at 10^{-3} mm Hg (bath temp. 110°) gave *2-acetonyl-3,5-dimethyl*-o-*benzoquinol* (*XIV*) as a yellow viscous oil. (Found: C 68.45; H 7.66. Calc. for $C_{11}H_{14}O_3$: C 68.02; H 7.26). Infrared bands (cm^{-1}): 3 401 (OH), 1 715 (C=O), 1 671 (conj. C=O), 1 645 (C=C) and 1 580 (C=C); ultraviolet spectrum, see Fig. 2. The yield was low since a part of the substance decomposed on distillation giving a black tarry residue. The substance dimerises [11] at room temperature but can be stored at —20° for some weeks without change.

4,5-Dimethyl-o-*benzoquinone* (*V*) (3.80 g) in acetone (150 ml) was shaken with aluminium oxide (100 g) for 5 min and the mixture was then cooled to —80°. It was worked up rapidly at low temperature (*ca.* 0°) giving *2-acetonyl-4,5-dimethyl*-o-*benzoquinol* (*XV*) as a yellow viscous oil (1.45 g). Infrared bands (cm^{-1}): 3 448 (OH), 1 712 (C=O), 1 686 (conj. C=O) and 1 647 (C=C). On warming to room temperature the product dimerised rapidly and after 30 min the dimer was crystalline. Recrystallisation twice from acetone gave colurless prisms (0.91 g) of *2-acetonyl-4,5-dimethyl*-o-*benzoquinol dimer* which turned dark at 186° and decomposed at 205° [Found: C 67.89; H 7.16; MW 388 (cryoscopic in acetic acid). Calc. for $C_{22}H_{28}O_6$: C 68.02; H 7.26; MW 388.44].

3,4,6-Trimethyl-o-*benzoquinone* (*VI*) (1.58 g) in acetone (50 ml) was shaken with aluminium oxide (30 g) for 30 min. The reaction solution on evaporation gave a yellow oil (1.22 g) which was distilled at 10^{-3} mm Hg (bath temperature 90°) and after one day crystallised. The product was recrystallised from ethanol giving *2-acetonyl-3,5,6-trimethyl*-o-*benzoquinol* (*XVI*), yellow prisms, m.p. 57—59° (0.28 g) (Found: C 68.91; H 7.64. Calc. for $C_{12}H_{16}O_3$: C 69.20; H 7.55). Infrared spectrum, see Fig 1; ultraviolet spectrum, see Fig. 2. In another experiment the crude undistilled *o*-quinol was seeded with crystalline material. The solid obtained was recrystallised giving 53 % of XVI. The substance is stable at room temperature.

3-Methoxy-o-*benzoquinone* (*VII*) (6.58 g) in acetone (400 ml) was shaken with aluminium oxide (200 g) for 15 min. The reaction mixture when worked up gave a yellow oil (2.61 g) which crystallised on standing for some days. The product was dissolved in ethanol at room temperature and cooled to —20° giving *2-acetonyl-3-methoxy*-o-*benzoquinol* (*XVII*) as a yellow crystalline conglomerate, m.p. 68—69° (2.10 g, 23 %) (Found: C 61.37; H 6.30; OCH_3 16.04. Calc. for $C_{10}H_{12}O_4$: C 61.21; H 6.18; OCH_3 15.81). Infrared spectrum, see Fig. 1; ultraviolet spectrum, see Fig. 3. The substance is stable at room temperature.

3-Methoxy-5-methyl-o-*benzoquinone* (*VIII*) (1.78 g) in acetone (100 ml) was shaken (1 h) with aluminium oxide (50 g). The reaction solution when evaporated gave a yellow oil (1.04 g) which crystallised after some hours. The product was recrystallised from

ethanol giving *2-acetonyl-3-methoxy-5-methyl*-o-*benzoquinol (XVIII)* as a yellow crystalline conglomerate, m.p. 109° (0.64 g, 26 %) (Found: C 62.72; H 7.01; OCH_3 14.74. Calc. for $C_{11}H_{14}O_4$: C 62.84; H 6.71; OCH_3 14.76). Infrared bands (cm^{-1}) 3 344 (OH), 1 718 (C=O), 1 669 (conj. C=O), 1 629 (C=C), 1 558 (C=C); ultraviolet spectrum, see Fig. 3. The substance is stable at room temperature.

3-Methoxy-5-propyl-o-*benzoquinone*[19] *(IX)* (1.67 g) in acetone (30 ml) was shaken with aluminium oxide (25 g) for 1 h. On evaporation the reaction solution gave a yellow oil (0.90 g) which crystallised after several days. The product was recrystallised from ethanol giving *2-acetonyl-3-methoxy-5-propyl*-o-*benzoquinol (XIX)* as a yellow crystalline conglomerate, m.p. 56° (0.65 g, 30 %) (Found: C 65.08; H 7.36; OCH_3 13.17. Calc. for $C_{13}H_{18}O_4$ C 65.43; H 7.61; OCH_3 13.02). Infrared bands (cm^{-1}): 3 425 (OH), 1 718 (C=O), 1 669 (conj. C=O), 1 629 (C=C), 1 553 (C=C); ultraviolet spectrum, see Fig. 3. The substance is stable at room temperature.

4-Methoxy-o-*benzoquinone (X)* (3.0 g) in acetone (200 ml) was shaken with aluminium oxide (90 g) for 20 min and the mixture was then cooled rapidly (*ca.* 0°) and worked up fairly quickly (30 min). The product was an orange-coloured oil (1.06 g) which was kept at −80° and crystallised after some days. It was dissolved in ether at room temperature and cooled to −20° giving *2-acetonyl-5-methoxy*-o-*benzoquinol (XX)* as pale yellow needles, m.p. 66−67° (0.48 g, 11 %) (Found: C 61.52; H 6.12; OCH_3 15.93. Calc. for $C_{10}H_{12}O_4$: C 61.21; H 6.17; OCH_3 15.82). Infrared spectrum, see Fig. 1; ultraviolet spectrum, see Fig. 3. The substance can be kept at −20° without changing but dimerises at room temperature.

4-Benzyloxy-o-*benzoquinone (XI)* (4.40 g) in acetone (220 ml) was shaken with aluminium oxide (110 g) for 20 min. On evaporation the reaction solution gave a yellow oil (1.05 g) which crystallised after several hours. After treatment with charcoal and recrystallisation from ethanol it gave *2-acetonyl-5-benzyloxy*-o-*benzoquinol (XXI)* as almost colourless needles, m.p. 108° (0.77 g, 14 %) (Found: C 70.65; H 6.01. Calc. for $C_{16}H_{16}O_4$: C 70.57; H 5.92). Infrared bands (cm^{-1}): 3 356 (OH), 1 721 (C=O), 1 670 (conj. C=O), 1 634 (C=C), 1 577 (broad, C=C and phenyl ring) and 1 504 (phenyl ring); ultraviolet spectrum, see Fig. 3. This compound could be kept at room temperature for several days. Changes occurring after that have not been investigated.

3,5-Di-tert-butyl-o-*benzoquinone (XII)* (20.0 g) in acetone (600 ml) was shaken with aluminium oxide (400 g) for 1 h. The product obtained on working up was a brown oil which crystallised from light petroleum giving *2-acetonyl-4,6-di-tert-butyl*-o-*benzoquinol (XXII)* as yellow needles, m.p. 64−65° (11.8 g, 47 %) (Found: C 73.53; H 9.26. Calc. for $C_{17}H_{26}O_3$: C 73.34; H 9.42). Infrared spectrum, see Fig. 1; ultraviolet spectrum, see Fig. 2. The substance has been kept for several months at room temperature without change.

4-tert-Butyl-o-*benzoquinone (XIII)* (3.14 g) in acetone (100 ml) was shaken with aluminium oxide (50 g) for 30 min and the mixture was then cooled to −80°. It was worked up rapidly at low temperature (*ca.* 0°) and gave *2-acetonyl-5-tert-butyl*-o-*benzoquinol (XXIII)* as a viscous yellow oil (2.22 g); infrared bands at 3 449 (OH), 1 712 (C=O), 1 670 (conj. C=O), 1 645 (C=C) and 1 577 (C=C) cm^{-1}; ultraviolet maximum at 305 mμ (log ε, 3.50). On warming to room temperature the substance dimerised rapidly and after 30 min the dimer began to crystallise. Recrystallisation from ethanol gave colourless prisms, m.p. 173−175° (Found: C 70.60; H 8.02; MW 472 (cryoscopic in acetic acid). Calc. for $C_{26}H_{36}O_6$: C 70.24; H 8.10; MW 444.52).

Acknowledgements. I am much indebted to Professor Erich Adler for his interest in this work and would also like to acknowledge the technical assistance of Mrs. Ilona Bukowinsky and Miss Gunilla Björkman.

This investigation has been supported financially by *Statens Tekniska Forskningsråd.*

REFERENCES

1. Magnusson, R. *Acta Chem. Scand.* **12** (1958) 791.
2. Schenck, G. O., Brähler, B. and Chiesla, M. *Angew. Chem.* **68** (1956) 247.
3. Hayaishi, O., Patchett, A. A. and Witkop, B. *Ann.* **608** (1957) 158.
4. Horner, L. and Sturm, K. *Ann.* **597** (1955) 1.
5. Teuber, H.-J. *Angew. Chem.* **68** (1956) 420.

6. Patchett, A. A. and Witkop, B. *J. Org. Chem.* **22** (1957) 1477.
7. Harley-Mason, J. and Laird, A. H. *J. Chem. Soc.* **1958** 1718.
8. Horner, L. and Dürckheimer, W. *Chem. Ber.* **91** (1958) 2532.
9. Adler, E., Magnusson, R., Berggren, B. and Thomelius, H. *Acta Chem. Scand.* **14** (1960) 515.
10. Magnusson, R. *To be published.*
11. Magnusson, R. *To be published.*
12. Derkosch, J. and Kaltenegger, W. *Monatsh.* **90** (1959) 872.
13. Derkosch, J. and Kaltenegger, W. *Monatsh.* **88** (1957) 778.
14. Budzikiewicz, H., Schmidt, G., Stockhammer, P. and Wessely, F. *Monatsh.* **90** (1959) 609.
15. Horner, L. and Dürckheimer, W. *Z. Naturforsch.* **14 b** (1959) 741.
16. Flaig, W., Ploetz, T., and Biergans, H. *Ann.* **597** (1955) 196.
17. Teuber, H.-J. and Staiger, G. *Chem. Ber.* **88** (1955) 802.
18. Adler, E. and Magnusson, R. *Acta Chem. Scand.* **13** (1959) 505.
19. Adler, E. and Lindberg, C. B. *To be published.*
20. Finsley, S. W. *J. Org. Chem.* **24** (1959) 1197.

Received April 22, 1960.

ACTA CHEMICA SCANDINAVICA 14 (1960) 1654–1659

The Kinetics of Calcium Oxalate Precipitation

ARNE E. NIELSEN

Universitetets fysisk-kemiske institut, Copenhagen, Denmark.

At concentrations below 1 mM the rate determining step in the precipitation of calcium oxalate is a reaction in the surface of the crystals. It is apparently of an order between 3.0 and 3.5. It is shown that when the incompleteness of the dissociation of calcium oxalate is taken into account the »true» order of the reaction is 4, when the rate is expressed by the ionic concentrations, and 2, when expressed by the concentration of the undissociated calcium oxalate.

At concentrations above 1 mM the rate is determined by diffusion.

In a previous work [1] the kinetics of calcium oxalate precipitation was investigated by means of experiments with the initial concentration c_0 = 0.75 and 0.50 mM. It was found that the rate of formation of the precipitate — measured by the electric conductance of the aqueous solution — was proportional to the total surface area of the precipitate and to a power of the concentration of the unprecipitated calcium oxalate close to 3.5. The power was clearly larger than 3 and less than 4.

The data found in the present work where c_0 = 1 and 5 mM, are treated in the way described in a previous work [2] on barium sulfate and the logarithm of the growth rate, dl/dt, where l is the length of a cube of the same volume as one of the growing crystals, and t is time, is plotted as a function of the logarithm of the concentration of the calcium oxalate in the solution at that time; see Fig. 1. In the region where $c < 1$ mM the points lie close to a straight line of slope 3.3, which means that the rate is proportional to the 3.3-rd power of c. At $c > 1$ mM the rate is proportional to c. Later on we shall see that in this part of the curve the rate is diffusion controlled. But first we shall consider the steeper part of the curve.

THE ORDER OF THE SURFACE REACTION

In interpreting the power or order of the reaction it must be remembered that calcium oxalate may be incompletely dissociated at the concentrations used. When this is taken into account it turns out that the precipitation (or crystal growth) rate follows

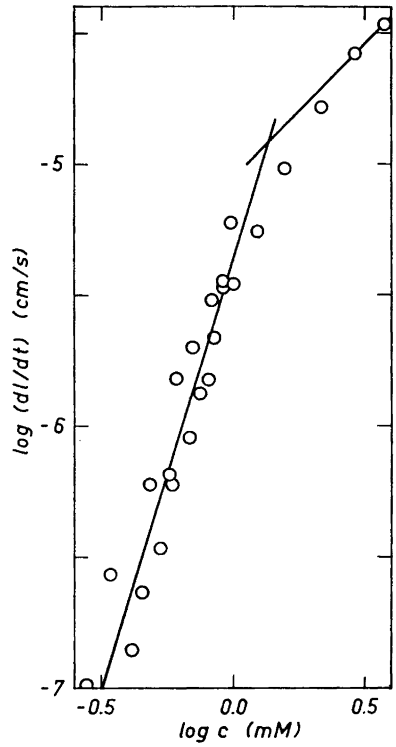

Fig. 1. The linear rate of crystal growth as function of (CaOx) in a logarithmic diagram. Below 1 mM the rate is proportional to the 3.3rd power of the concentration. Above 1 mM the rate is proportional to the concentration.

$$J_1 = k_1\,(\mathrm{CaOx})^2$$
$$J_2 = k_2\,(\mathrm{Ca^{++}})^2\,(\mathrm{Ox^{--}})^2$$
$$J = J_1 + J_2 = k_1\,(\mathrm{CaOx})^2 + k_2\,(\mathrm{Ca^{++}})^2\,(\mathrm{Ox^{--}})^2$$

where J is the total rate of depositing matter per unit area of the crystal surfaces.
From the law of mass action

$$(\mathrm{Ca^{++}})\,(\mathrm{Ox^{--}}) = K \cdot (\mathrm{CaOx})$$

it follows that

$$J = k_{\mathrm{I}}(\mathrm{CaOx})^{\,2} = k_{\mathrm{II}}(\mathrm{Ca^{++}})^{\,2}(\mathrm{Ox^{--}})^{\,2}$$

where $k_{\mathrm{I}} = k_1 + k_2K$

$$k_{\mathrm{II}} = k_1/K + k_2$$

When the ionic species Ca^{++} and Ox^{--} are present in equivalent concentrations we define $c = (\mathrm{CaOx}) + (\mathrm{Ca^{++}}) = (\mathrm{CaOx}) + (\mathrm{Ox^{--}})$.

At *low* concentrations we have $(\mathrm{CaOx}) \ll (\mathrm{Ca^{++}}) = (\mathrm{Ox^{--}})$

$$(\mathrm{Ca^{++}}) = (\mathrm{Ox^{++}}) = c$$

$\therefore J = k_{II}c^4$

At *high* concentrations $(CaOx) \gg (Ca^{++}) = (Ox^{++})$

$c = (CaOx)$

$\therefore J = k_I c^2$

If however (CaOx), (Ca^{++}) and (Ox^{--}) are of the same order of magnitude none of the above mentioned approximations is valid and if one writes

$J = kc^p$

p is only apparently a constant, $2 < p < 4$, in limited concentration ranges. To be more precise we may define p by

$p = d\ln J/d\ln c.$

Putting $(CaOx) = x$, $(Ca^{++}) = (Ox^{--}) = c - x$ we find

$(c - x)^2 = Kx$

$$\therefore \frac{dx}{dc} = \frac{1}{1 + (K/2(c - x))}$$

$J = k_1 x^2$

$$p = \frac{d\ln J}{d\ln c} = \frac{c}{J}\frac{dJ}{dc} = \frac{2c}{x[1 + (K/2(c - x))]}$$

Solving the mass action law with respect to x we find

$$x = c - \frac{K}{2}\left(\sqrt{1 + \frac{4c}{K}} - 1\right)$$

$$\therefore p = \frac{2c}{[c - (K/2)(\sqrt{1 + (4c/K)} - 1)][1 + (1/(\sqrt{1 + (4c/K)} - 1))]}$$

$$= \frac{2}{[1 - (1/2q)(\sqrt{1 + 4q} - 1)][1 + (1/(\sqrt{1 + 4q} - 1))]}$$

Table 1.

q	p
0.001	3.989
0.01	3.961
0.05	3.826
0.1	3.690
0.2	3.491
0.5	3.155
1	2.895
2	2.667
5	2.437
10	2.312
100	2.100
1 000	2.041

where $q = c/K$. Values of p calculated by this formula are in Table 1. It is easily seen that $p \to 2$ for $q \to \infty$ and $p \to 4$ for $q \to 0$.

DETERMINATION OF THE DISSOCIATION CONSTANT

The calibration measurements were performed on solutions of $CaCl_2$, Na_2Ox and NaCl having the same compositions as the reaction mixture at different degrees of advancement during a kinetic run. From these measurements the dissociation constant may be estimated neglecting the dependence of the molar conductivities on the concentration. This is only permissible when the range of ionic strengths used is small. We write

$$10^3 \varkappa = c_0(\Lambda_{CaOx}(1 - \alpha)\delta + 2\Lambda_{NaCl})$$

$$10^3 \varkappa_1 = 2c_0\Lambda_{NaCl}$$

$$K = (Ca^{++})(Ox^{--})/(CaOx) = c_0(1 - \alpha)\delta^2/(1 - \delta)$$

where

$\varkappa$ = specific electric conductance
c_0 = initial concentration of CaOx
Λ_{CaOx} and Λ_{NaCl} = molar conductivities
α = degree of reaction
δ = degree of dissociation of CaOx.

Eliminating δ and Λ_{NaCl} we obtain

$$\frac{c_0(1 - \alpha)}{\varkappa - \varkappa_1} = \frac{\varkappa - \varkappa_1}{K\Lambda_{CaOx}^2} + \frac{1}{\Lambda_{CaOx}}$$

A diagram of $c_0(1 - \alpha)/(\varkappa - \varkappa_1)$ as function of $\varkappa - \varkappa_1$ should thus yield a straigth line intersecting the ordinate axis at $1/\Lambda_{CaOx}$ and having the slope $1/K\Lambda_{CaOx}^2$. From Fig. 2 we see that a straigth line is really found in this way, and that

$$\Lambda_{CaOx} = 192; \quad K = 0.00162 \text{ M}.$$

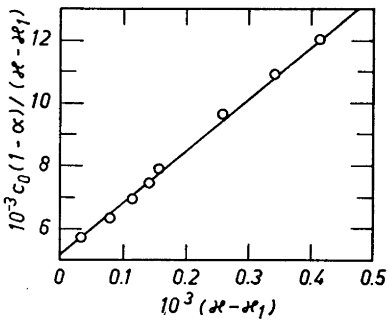

Fig. 2. A plot of $c_0(1 - \alpha)/(\varkappa - \varkappa_1)$ as function of $\varkappa - \varkappa_1$. From the slope of the straight line the dissociation constant of calcium oxalate can be determined (Units: mM, Ω and cm).

This number is, within the uncertainties and errors of approximations, the concentration dissociation constant. The activity dissociation constant K_a (or, the former extrapolated to ionic strength zero) can be estimated in the following way. The ionic strength is

$$I = \frac{1}{2}\Sigma c_i z_i^2 = 2c_0(1 + 2(1 - \alpha)\delta)$$

Assuming values of K, c_0 and α, δ can be calculated from

$$\delta^2/(1 - \delta) = K/c_0(1 - \alpha)$$

With $K = 0.001$ M, $c_0 = 0.001$ M, $\alpha = 0.8$, we find the lowest ionic strength used: $I_{min} = 0.0027$ M; with the same K, $c_0 = 0.005$ M and $\alpha = 0$ we find the highest ionic strenth $I_{max} = 0.017$. Using furthermore the Debye-Hückel equation in the Güntelberg formulation [3]

$$\log f_z = -0.5\, z^2 \sqrt{I}/(1 + \sqrt{I})$$

we find that f_2, the activity coefficient of a doubly charged ion lies between 0.59 and 0.80; now $K_a = Kf_2^2$. Since the mean value of 0.59^2 and 0.80^2 is near to 0.50 we may estimate

$$K_a = 0.0008 \text{ M}$$

This may be compared with the value 0.0010 M reported by Davies [4].

DISCUSSION OF THE KINETICS

In Fig. 1 the range of concentrations corresponding to the steeper part of the curve is $0.0003 < c < 0.001$ M. Since $q = c/K$ where $K = 0.0016$ we have $0.2 < q < 0.6$ and consequently (see Table 1) $3.5 > p > 3.1$. We may therefore conclude from the experimental slope 3.3 that the surface reaction controlling the rate of growth of the calcium oxalate crystals is of the fourth order in the ionic concentration or, which is equivalent, of the second order in the concentration of the undissociated calcium oxalate.

This is similar to the result obtained in experiments on the precipitation of barium sulfate [2,5]. For $BaSO_4$ it has been shown [5] that $K > 0.004$ M, and most probably K is about 0.008 M. The surface reaction is rate determining for the precipitation of barium sulfate when $c < 0.4$ mM. When $q = c/K < 0.05$ Table 1 shows that $3.8 < p < 4.0$ which is just what has been found.

In the high concentration end of the curve on Fig. 1 the slope approaches 1. This is easily explained since at these high concentrations the diffusion of the matter from the bulk of the solution to the surface becomes rate determining — as explained in greater detail in the papers on barium sulfate [4]. From the electric mobilities $l_+ = 5.9 \times 10^{-4}$ and $l_+ = 7.4 \times 10^{-4}$ cm²/s·V we calculate the diffusion coefficient

$$D = 2kTl_+l_-/(l_+ + l_-)q = 8.5 \times 10^{-6} \text{ cm}^2/\text{s}$$

and the diffusional growth rate should consequently follow, in CGS-units:

$$dl/dt = 2.60\ vDc/l = 0.00147\ c/l$$

With the value of l in the highest point on Fig. 1, $l = 3.12 \times 10^{-4}$, cm we find $dl/dt = 4.7\ c$; the experiments give $(dl/dt) = 8.9\ c$. The reason why the growth rate is larger than calculated, is probably that the particles are not — as assumed in the calculations — spheres or cubes, but show the shape of small »stars» when viewed in a microscope. The rate of growth depends — in case of diffusion — rather on the largest corner to corner dimensions of the particles than of the volume. There is no doubt, therefore, that the rate is mainly controlled by diffusion at $c > 1$ mM.

REFERENCES

1. Nielsen, A. E. *J. Colloid Sci.* **10** (1955) 576.
2. Nielsen, A. E. *Acta Chem. Scand.* **12** (1958) 951.
3. Güntelberg, E. *Z. physik. Chem.* **123** (1926) 199, p. 243.
4. Davies, C. W. *Endeavour* **4** (1945) 114.
5. Nielsen, A. E. *Acta Chem. Scand.* **13** (1959) 784, 1680.

Received April 22, 1960.

ACTA CHEMICA SCANDINAVICA 14 (1960) 1660–1666

Physical Properties of Isotopic Forms of Some Inorganic Acid-Water Azeotropes

KARL ERIK HOLMBERG

Division of Chemistry, Section for Nuclear Chemistry, AB Atomenergi, Stockholm, Sweden

The azeotropes of DCl, DBr or DNO_3 with D_2O are more volatile than the corresponding azeotropes containing H. In the $HCl-H_2O$ and $HBr-H_2O$ azeotropes, the difference in volatility of ^{16}O and ^{18}O is larger than in water. Other isotope enrichment effects are small or imperceptible. Differences in other physical properties, such as density, viscosity and refractive index, are similar to those between H_2O and D_2O though less pronounced.

In the maximum boiling point azeotropes formed by various inorganic acids and water, there is a considerable interaction between the components in the liquid phase but not in the vapour phase. Different isotopic forms of the azeotropes may therefore differ with respect to volatility and composition (mole ratio acid : water).

The azeotropes of HCl, HBr or HNO_3 with H_2O and the corresponding fully deuterated azeotropes have been prepared and compared with each other with respect to composition, boiling point and some other physical properties. Separation factors for the various isotopes have been determined by Rayleigh distillation at atmospheric pressure and, in some cases, at reduced pressure. The results are summarized in Tables 1—5. For convenience, the following abbreviations will be used for the azeotropes:
$HClH_2O$, $DClD_2O$, $HBrH_2O$, $DBrD_2O$, HNO_3H_2O and DNO_3D_2O although, of course, they are not composed of equimolecular amounts of acid and water.

Physical properties. The H and D forms of the azeotropes do not differ much in composition and the difference with respect to physical properties between them is a reflection of the difference between the two forms of water. Thus, the D azeotropes have a higher density and viscosity and a lower refractive index and the relative differences are approximately proportional to the water content of the azeotrope.

Volatilities. The D forms of the azeotropes are the more volatile while, for pure water, the opposite holds true. This phenomenon is no doubt the same as what was found by Combs and Smith [1] who investigated the volatility of light and heavy water from salt solutions. They found that the relative vola-

Table 1. Composition and physical properties of the H and D forms of the azeotropes of some inorganic acids and water.

	$HClH_2O$	$DClD_2O$	$HBrH_2O$	$DBrD_2O$	HNO_3H_2O	DNO_3D_2O
Weight % of acid	20.22	17.55	47.9	45.0	67.87	66.22
Mole % of acid	11.14	10.33	16.9	16.6	37.66	38.00
Formula	HCl 7.98 H_2O	DCl 8.68 D_2O	HBr 4.92 H_2O	DBr 5.02 D_2O	HNO_3 1.655 H_2O	DNO_3 1.631 D_2O
Boiling point at 760 mm Hg, °C	108.58	108.45	124.84	124.38	121.0	118.2
Boiling point difference, °C	0.13		0.46		2.8	
$(dp/dt)_{760}$, mm Hg/°C	27.7		27.8		27.2	
d_4^{25}, g/ml	1.10295	1.18915	1.48015	1.56201	1.39815	1.44873
η_{25}, centipoise	1.29	1.49	1.46	1.67	1.85	2.00
n_D^{25}	1.3800	1.3715	1.4370	1.4310		

Table 2. Ratio of the vapour pressures of H and D forms of azeotropes, and separation factors for isotopes upon distillation. Water is included for comparison.

	$HClH_2O$ at 108°C	$HBrH_2O$ at 124°C	HNO_3H_2O at 121°C	H_2O at 100°C
$p(D)/p(H)$	1.0047 ± 0.0007	1.017 ± 0.001	1.100 ± 0.004	0.950
$\frac{(D/H)_{vap}}{(D/H)_{liq}}$	1.0043 ± 0.0014		1.044 ± 0.008	0.978 ± 0.001
$\frac{(^{16}O/^{18}O)_{vap}}{(^{16}O/^{18}O)_{liq}}$	1.0074 ± 0.0009	1.0086 ± 0.0009	1.0009 ± 0.0009	1.0039 ± 0.0009
$\frac{(^{37}Cl/^{35}Cl)_{vap}}{(^{37}Cl/^{35}Cl)_{liq}}$	> 0.995			
$\frac{(^{81}Br/^{79}Br)_{vap}}{^{81}Br/^{79}Br)_{liq}}$		1.000 ± 0.002		
$\frac{(^{14}N/^{15}N)_{vap}}{(^{14}N/^{15}N)_{liq}}$			1.0003 ± 0.0012	

Table 3. Separation factors by Rayleigh distillation of azeotropes at reduced pressure. Water included for comparison.

	$HClH_2O$ about 10°C	$HBrH_2O$ about 10°C	H_2O about 10°C
$\frac{(^{16}O/^{18}O)_{vap}}{(^{16}O/^{18}O)_{liq}}$	1.0143 ± 0.0009	1.0167 ± 0.0009	1.0076 ± 0.0009
$\frac{(^{37}Cl/^{35}Cl)_{vap}}{(^{37}Cl/^{35}Cl)_{liq}}$	1.0008 ± 0.002		
$\frac{(^{81}Br/^{79}Br)_{vap}}{(^{81}Br/^{79}Br)_{liq}}$		1.000 ± 0.002	

Table 4. Boiling points of HNO_3H_2O and DNO_3D_2O azeotropes at various pressures; p and b.p. are not corrected. The values at low pressures are uncertain because of bumping.

p mm Hg	HNO_3H_2O b.p. °C	DNO_3D_2O b.p. °C	difference °C
50.5	57.95	55.87	2.08
105.5	72.12	70.17	1.95
310	96.35	93.93	2.42
776	120.67	117.83	2.84

Table 5. Comparison of separation factors by column distillation of $HClH_2O$ azeotrope containing about 10 % D. The figure in bold type is assumed to be correct and is used for calculating the number of theoretical plates.

Isotope pair	Q	Elementary separation factor α			error in α from error in Q
D/H	1.054	1.0058	**1.0047**	**1.0043**	± 0.0002
$^{16}O/^{18}O$	1.0685	**1.0074**	1.0059	1.0054	± 0.0003
$^{37}Cl/^{35}Cl$	1.003_2	1.0003_6	1.0002_8	1.0002_6	± 0.0002
Number of theoretical plates		9	11.5	12.5	

tility of D_2O increases with the salt concentration and that the effect is more pronounced at higher temperatures.

The ratios of the vapour pressures of the H and D forms of the azeotropes have been calculated from the boiling point differences. The separation factors for H/D have been determined by Rayleigh distillation using $HClH_2O$ and HNO_3H_2O containing a fair amount of D.

Distillation of $HClH_2O$, containing 18.5 % D, gave a separation factor $\alpha = 1.0043$ with an estimated error of ± 0.0014 in close agreement with the

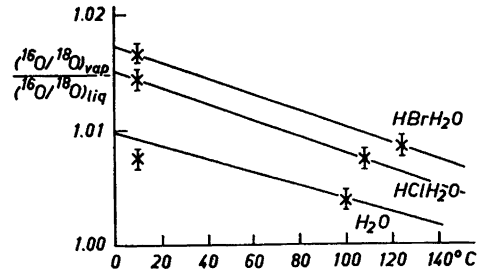

Fig. 1. Separation factors for $^{16}O/^{18}O$ from Rayleigh distillations. The line for H_2O is drawn according to a compilation by Dostrovsky[6].

ratio of the vapour pressures of the D and H systems. In fact, the separation factor α would be expected to be the square root of the vapour pressure ratio (or even smaller) just as the separation factor upon distillation of water is the square root of $p(H_2O)/p(D_2O)$. The reason for the different behaviour may be that the H and D forms of the azeotrope have somewhat different compositions, or it may be partly due to experimental errors.

The ratio of the vapour pressures of the H and D forms of HNO_3H_2O was found to be 1.100. The separation factor upon distillation of a mixture may be predicted tentatively. If differences in the forces between the water molecules are chiefly responsible it may be expected to be $1.100^{1.65/(1+2\times1.65)} = 1.037$ while, if it is due to the differences in the forces between HNO_3 and H_2O, we would get $1.100^{1/(1+2\times1.65)} = 1.022$.

From a Rayleigh distillation of a HNO_3H_2O azeotrope with about 4.5 % D abundance, the separation factor α was found to be 1.052 calculated on the first distillate and 1.037 calculated on the residue. A weighted average was 1.044. This is probably not too large considering the tendency of the Rayleigh distillations to give low values [2].

From boiling point measurements at various pressures (Table 4), it is evident that the separation factor will not be much better at other pressures than atmospheric. In this connection, it may be observed that Dawber and Wyatt [3] have found that at 0°C the vapour pressure of pure DNO_3 is more than 7 % larger than that of HNO_3.

The behaviour of the oxygen isotopes is very interesting. In the $HClH_2O$ and $HBrH_2O$ azeotropes, ^{16}O is enriched in the vapour, just as for water, but with a considerably larger factor, *cf.* Fig. 1. Further, the enrichment increases when the temperature decreases. This is quite in contrast to the H isotopes which are enriched in different directions in water and in the azeotropes.

In the HNO_3H_2O system, there is almost no enrichment of oxygen isotopes possibly because there is an exchange of O between H_2O and HNO_3 [4,5] and because the tendency of ^{18}O enrichment in the H_2O and HNO_3 vapours from the azeotrope may be in opposite directions.

Heavy isotopes of oxygen have been enriched, *e.g.* by Dostrovsky [6], on a rather large scale by the distillation of water. From the point of view of column volume and heat consumption, the $HClH_2O$ and $HBrH_2O$ azeotropes should be more favourable but the corrosion problems will probably be so serious as to offset the advantages.

The possibility of an enrichment of Cl isotopes by distillation of azeotropic hydrochloric acid has been pointed out by London [7]. The actual separation is, however, very small and therefore difficult to ascertain. By Rayleigh distillation, it has now been found that the separation factor is probably less than 1.001, ^{37}Cl enriching in the vapour. According to a column distillation experiment, described below, it is probably about 1.0003. This is a little surprising. It has been found by Johnston and Hutchison [8] that, upon electrolysis of a NaCl solution, ^{37}Cl enriches in the liquid by a factor of 1.0060. If this is an equilibrium process, the separation factor for the exchange between $Cl^-(aq)$ and $Cl_2(gas)$ will be the same ($\alpha = 1.0060$). It has been calculated by Urey [9] that, upon exchange between gaseous HCl and Cl_2, ^{37}Cl will enrich in the Cl_2 by the factor 1.003. From this, it is expected that, on exchange between $Cl^-(aq)$ and HCl (gas), which must occur between the liquid and gaseous $HClH_2O$ azeotrope, ^{37}Cl should be enriched in the liquid by a factor of 1.009 (at 25°C).

The present experimental results, however, agree with those of Urey *et al.*[10] who found a rather small enrichment of ^{37}Cl in the gas upon exchange between HCl (gas) and HCl (aq) at ambient temperature.

Similarly, for $HBrH_2O$, no separation of Br isotopes could be observed.

Considerable difficulties are met with when very small separation factors are to be determined. Ordinary mass spectrometric measurements seldom give the isotope ratio with a better accuracy than 0.1 %. To obtain a better accuracy, the elementary factor must be multiplied. By means of Rayleigh distillation, it is possible to have conveniently an enrichment corresponding to four single steps.

Column distillation would be an excellent multiplication method if the actual number of theoretical plates at equilibrium were known. A given column operates with a different number of theoretical plates for different systems. Therefore, it is not possible to evaluate a column with a known system and then use it to investigate unknown systems (if any accuracy is desired).

It may be thought that an internal comparison of different separation factors within the same system by column distillation would be possible with a good accuracy. It is, however, probable that even in this case the theoretical plate height (H.E.T.P.) may be different for different separations. On the other hand, the results could be expected to be much better than for a comparison of quite different systems by means of separate distillations.

A method of distillation where the number of theoretical plates may be predicted has been suggested by Kuhn *et al.*[11] but it requires an accurate regulation of the reflux ratio.

To have a check on the results of the Rayleigh distillations, a column distillation has been performed with the $HClH_2O$ azeotrope containing about 10 % D. In the top reservoir of the column, the various isotopes were enriched by the factors Q given in Table 5. A certain separation factor, determined above, is assumed to be correct and from it the number of theoretical plates is calculated and from this number the separation factors for the other isotopes are found. The discrepancy between the different calculations may be due to errors in the values from the Rayleigh distillations or, perhaps, to a different efficiency of the column towards the different isotope pairs in the system.

EXPERIMENTAL

Preparations. $HClH_2O$ was prepared by dilution of hydrochloric acid to the proper concentration and distillation at atmospheric pressure through a 1 meter column, with glass helices, to obtain an azeotrope with a narrow boiling point range (0.1°C).

SO_2Cl_2 was reacted with an excess of D_2O and distilled. The distillate was fractionated to give the azeotrope $DClD_2O$ with a narrow b.p. range.

$HBrH_2O$ was prepared by distillation from $KBr + H_2O + H_2SO_4$ and fractionation of the product with the 1 meter column [12].

$DBrD_2O$ was prepared in the same way from $KBr + D_2O + D_2SO_4$. D_2SO_4 had been obtained in the reaction above of $SO_2Cl_2 + D_2O$ or by reaction of SO_3 with D_2O.

HNO_3H_2O azeotrope was obtained by fractionation of common nitric acid.

DNO_3D_2O was prepared by distillation from $KNO_3 + D_2O + D_2SO_4$ and fractionation of the product.

Analyses. Analyses were made by titration with standard alkali.

Physical properties. The measurement of boiling points, densities and viscosities has been described earlier [2].

Rayleigh distillations. The apparatus for Rayleigh distillation at atmospheric pressure has been described earlier [2]. Rayleigh distillations at reduced pressure were performed from one flask to another, the first being heated by the surrounding air or a water bath and the second being cooled to 0°C or lower with alcohol and solid CO_2. The distillation temperature was adjusted to be about 10°C.

Test distillations with water followed by oxygen isotope analyses showed that the Rayleigh distillation gave slightly too low values for the separation factors, just as had been found earlier with H_2O—D_2O mixtures [2].

Column distillations. Azeotropic $HClH_2O$ with about 10 % D abundance was distilled in a column of 1.5 meter length packed with glass helices and with a reservoir at the top. It was refluxed for 9 days which was much more than was estimated to be necessary to reach equilibrium. Samples from the top and the still pot were analysed for the abundance of H, O and Cl isotopes.

Preparations for isotopic analyses

D analysis. The acid sample was neutralized with anhydrous Na_2CO_3 and the water was distilled off quantitatively under vacuum. It was purified by redistillation in vacuum and its density was measured.

^{18}O analysis. The acid sample together with a small amount of CO_2 was sealed in a glass tube and equilibrated at room temperature for a few days. The CO_2 was separated from the sample by freezing out. The dilution error was about 1 %.

Cl isotope analysis. Cl was precipitated as AgCl which was reacted with CH_3I in a sealed tube to give CH_3Cl [13].

Br isotope analysis. $HBrH_2O$ and CH_3OH were heated in a sealed tube to give CH_3Br which was separated and analysed [14].

^{15}N analysis. HNO_3 was reduced to NH_3 with Arnd's alloy [15] and then handled as usual for a N isotope analysis.

Errors

The errors in the ratios of the vapour pressures of the H and D forms of the azetropes are calculated from the estimated errors of the b.p. differences. The errors in the H/D separation factors correspond to the scattering of the experimental values. The other errors given correspond to the estimated errors of the mass spectrometric measurements and do not include accidental or systematic experimental errors.

Acknowledgement. Thanks are due to Mr. R. Cedenholt for assistance with the experimental work and to AB Atomenergi for permission to publish the results. The isotope abundance measurements were performed by the Mass Spectrometer Laboratory, Karolinska Institutet, Stockholm.

REFERENCES

1. Combs, R. L. and Smith, H. A. *J. Phys. Chem.* **61** (1957) 441.
2. Holmberg, K. E. *Acta Chem. Scand.* **13** (1959) 717.
3. Dawber, J. G. and Wyatt, P. A. H. *J. Chem. Soc.* **1958** 3636.
4. Klein, R. and Friedel, R. A. *J. Am. Chem. Soc.* **72** (1950) 3810.
5. Bunton, C. A., Halevi, E. A. and Llewellyn, D. R. *J. Chem. Soc.* **1952** 4913.
6. Dostrovsky, I. and Raviv, A. *Proc. Intern. Symposium Isotope Separation, Amsterdam* **1957**, North Holland Publishing Co., Amsterdam 1958, p. 336.
7. London, H. *Ibid.* Remark p. 203.
8. Johnston, H. L. and Hutchison, D. A. *J. Chem. Phys.* **10** (1942) 469.
9. Urey, H. C. *J. Chem. Soc.* **1947** 562.
10. Urey, H. C., Mills, A., Roberts, I., Thode, H. G. and Huffman, J. R. *J. Chem. Phys.* **7** (1939) 138.
11. Kuhn, W., Thürkauf, M. and Narten, A. *Proc. Second Intern. Conf. Peaceful Uses Atomic Energy*, Geneva 1958, Vol. 4, p. 371.
12. *Inorganic Syntheses*, **1** (1939) 155.
13. Langvad, T. *Acta Chem. Scand.* **8** (1954) 526.
14. Clusius, K. *Z. Naturforsch.* **12 a** (1957) 974.
15. Kolthoff, I. M. and Sandell, E. B. *Textbook of Quantitative Inorganic Analysis*, The MacMillan Co., New York 1938, p. 536.

Received April 8, 1960.

ACTA CHEMICA SCANDINAVICA 14 (1960) 1667–1672

Short Communications

The Acid Soluble Nucleotides of *Vicia Faba* II

M. F. ABDEL-WAHAB and S. A. EL-KINAWI

Radioisotope Centre, A.E.E., Dokki, Cairo, U.A.R.

In a previous work from this department the acid soluble nucleotides, obtained by perchloric acid (PCA) extraction, of *Vicia Faba* plant just before fruiting, were studied [1]. The yield was found to be low at that stage of growth; this urged us to estimate the acid soluble nucleotides in the plant at different stages of germination.

In the last few years some important papers have been published about the metabolism of the acid soluble nucleotides in some plants and yeast [2-4]. Some difficulties arising in the separation from interfering substances of the nucleotides in plants in the pure form were overcome [5]. Previous methods developed primarily for the isolation of nucleotides from animal tissue proved to be unsatisfactory for the isolation of these compounds from plants. An improved method for the isolation of the acid soluble nucleotides from plant tissue has been described by Bergkvist [2]. The application of this method to *Vicia Faba*, seeds, pods, and seedling, has established the occurrence of ten nucleotides, *viz.* cytidine monophosphate, diphosphopyridine nucleotide, adenosine monophosphate, guanosine monophosphate, uridine monophosphate, adenosine diphosphate, a sugar derivative of uridine diphosphate, adenosine triphosphate, uridine triphosphate, and guanosine triphosphate.

Extracts prepared by directly homogenising plant material from any source in ice-cold perchloric acid demonstrated complex ultraviolet absorption spectra and hardly any separation of the acid soluble nucleotides from impurities [2]. Chromatography or ionophoresis at this stage proved also to be impracticable. Bergkvist overcame this difficulty by adsorbing the nucleotides quantitatively on Norite, and recovered them by repeated elution with 25 % aqueous ethanol containing 0.5 % ammonia. Spectrophotometric analysis of the combined eluates showed that the nucleotides were mixed with large quantities of non-nucleotides material [5].

In our laboratories a similar method was used where the whole organ was homogenised in 10 % PCA and reextracted with 5 % PCA in a Waring Blender. The nucleotides were isolated from the acid extract by the method used before [1]. After extraction and purification from the non-nucleotide fractions, the nucleotides were adsorbed on a strong base anion exchanger in the formate form. The individual nucleotides were eluted with formic acid solutions containing increasing concentrations of sodium formate. Elution of the nucleotides was followed by measuring the optical densities of the effluent fractions at 260 mμ and 270 mμ. The optical densities were plotted against the effluent volume. The extinction obtained from the eluate was plotted for the seeds, pods and seedlings, one, two, three and four weeks old. An example is shown in Fig. 1. The investigation was carried out on plants grown out of doors. The radioactivity of the effluent fractions was also determined. At all stages of germination the peaks of the extinction curves and the radioactivity curves coincided. This confirms the previous results that no reduced nucleotides are found in *Vicia Faba* [1]. The fact that in the course of germination ten distinct peaks

Table 1.

Compound	μmoles of nucleotides at different stages					
	seeds	1st week	2nd week	3rd week	4th week	Pods
CMP	2.00	1.00	1.50	1.00	0.32	0.08
DPN	0.30	0.20	0.60	0.20	0.28	0.07
AMP	0.28	0.30	0.50	0.21	0.50	0.10
GMP	0.20	0.22	0.20	0.24	0.26	0.08
UMP	0.32	0.32	0.30	0.22	0.30	0.07
ADP	0.21	0.20	0.20	0.23	0.28	0.08
UDPx	0.08	0.22	0.50	0.24	0.24	0.12
ATP	0.22	0.44	0.72	0.26	0.24	0.08
UTP	0.12	0.45	0.98	0.23	0.08	0.20
GTP	0.13	0.46	0.25	0.24	0.09	0.18

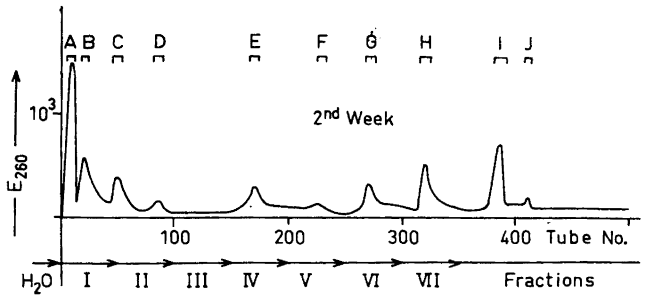

Fig. 1.

were observed, confirmed that no other nucleotides could exist.

Characterisation of the nucleotides was obtained by the following procedures:

1. Paper chromatography identification of the nucleotides and their bases after hydrolysis.
2. The position of the phosphate group on the different nucleotides was confirmed by oxidation with periodate [6].
3. Estimation of phosphorus for the different nucleotides [7].

Table 1 summarises the results obtained by plotting the extinction of the nucleotides at 260 mμ against the effluent fractions at different stages of germination.

Fig. 1 shows the absorption chromatogram at 260 mμ of the effluent fractions, collected by an automatic fraction collector, against the tube number. The material was obtained from 150 g of whole fresh *Vicia Faba* plants (2nd week seedlings) grown out of doors. Extraction by PCA as described above. Adsorption on Dowex 1, X-10, 200—400 mesh, 1 × 20 cm, formate form, flow rate 1 ml per min. The extinction was measured by means of a spectrophometer, Zeiss type PMQ II.

The peaks are identified as follows: A:CMP; B:DPN; C:AMP; D:GMP; E:UMP; F:ADP; G:UDPx; H:ATP; I:UTP; J:GTP. UDPx is a sugar derivative of uridine diphosphate.

The present work establishes the occurrence, in the beans, of all the four ribonucleotides in the form of the acid soluble 5′-nucleotides at different levels of phosphorylation. Nearly 30 % of the acid soluble nucleotides consists of cytidine and adenosine derivatives, the cytidine derivatives predominating. The acid extract of the seeds showed that CMP corresponds to the highest peak in the whole spectrum, next to CMP come UMP, DNP, AMP and ATP. The other five nucleotides are present to lesser extents. The same picture is found in the seedlings which are one week old with the exception that CMP is half its amount in the seeds. Another slightly different picture was observed in the second week but still CMP is present in the highest amount. Next in abundance are UTP, ATP, DNP, UDPx and UMP. GMP, GTP and ADP are present at levels which are nearly equal for the three nucleotides. At the end of the third week the acid extract showed another picture where almost all the nucleotides are present in more or less equal quantities with the exception that the amount of CMP is still high.

In the fourth week chromatogram, before fruiting, the picture was exactly the same as that previously obtained [1]. Experiments carried out with pods revealed a very low nucleotide yield.

From the preceding discussion one can conclude that the best material for obtaining good yield of the different nucleotides is the second week seedlings, see Fig. 1. Not only are the nucleotides present in good amounts, but they can also be well separated.

1. Abdel-Wahab, M. F. and El.Kinawi, S. A. *Acta Chem. Scand.* **13** (1959) 1653.
2. Bergkvist, R. *Acta Chem. Scand.* **10** (1956) 1303; **11** (1957) 1457; **12** (1958) 555.
3. Abdel-Wahab, M. F. *J. Chem. UAR* **3** (1960) 119.
4. Hoffmann-Ostenhoff, O., Kenedy, J., Keck, K. and Gabriel, O. *Biochim. et Biophys. Acta* **14** (1954) 285.
5. Cohn, W. E. *J. Am. Chem. Soc.* **72** (1950) 1471; (1954) 1818.
6. Dixon, J. S. and Lipkin, D. *Anal. Chem.* **76** (1954) 1092.
7. Allen, R. J. L. *Biochem. J.* **34** (1940) 858.

Received August 5, 1960.

Thiamine Phosphatases in Liver, Kidney, and Brain of the Rat

KARL-HEINZ KIESSLING

Institute of Zoophysiology, University of Uppsala, Sweden

In previous papers [1,2] it has been shown that thiamine diphosphate * is hydrolyzed by liver fractions to TMP and TMP to thiamine with different optimal rates, *viz.* at pH 9.3 and 6.0, respectively. This fact together with the findings that the TDP splitting capacity could be separated from that of TMP at the extraction of a liver homogenate in a special way, indicates that the two steps are catalyzed by different enzymes.

In the present communication the occurrence of the enzymes hydrolyzing TDP to TMP (TDPase) and TMP to thiamine (TMPase) are studied for liver, kidney, and brain.

Experimental. Whistar rats were decapitated, brain, liver, and kidneys rapidly removed, and put in icecold 0.02 M $KHCO_3$, cut in pieces with a pair of scissors, washed, and homogenized in a Waring blendor for 2 min in acetone at −15°C. After filtration on a Büchner funnel the powder was suspended in cold acetone, rehomogenized, collected by filtration, weighed, and suspended in 20 vol. of 0.02 M $KHCO_3$ at 0°C. After 25 min. extraction at 0°C with continuous stirring the sample was centrifuged, and the clear supernatant used as source of enzyme.

0.25−0.5 ml of the supernatants was used for incubation together with 1 ml 0.1 M Tris-maleate buffer (pH 5−7.5) or 0.1 M Tris-buffer (pH 7.5−10), 0.2 ml 0.1 M $MgCl_2$, 0.5 $TD^{32}P$, containing 1 μmole TDP and giving about 2×10^3 counts/min, and water to 2.5 ml. To find out if the Tris-maleate and the Tris-buffer acted differently on the enzymes, an incubation at pH 7.5 was made with either of the two buffers. No significant difference was found. After 20 min incubation at 37°C with continuous shaking, the samples were cooled to 0°C, 5 M H_2SO_4 added to a final concentration of 0.5 M, proteins removed by centrifugation, and 1 ml samples taken for determination of inorganic and organic radioactive phosphate according to Ernster *et al.*[3]

$TD^{32}P$ and $TM^{32}P$ were prepared according to Viscontini *et al.*[4] with the addition that radioactive inorganic phosphate was also present during the synthesis. The compounds were then separated by paper chromatography [5].

Results and discussion. A comparison of the TDPase and TMPase activities in the different rat organs at pH 6, 7 and 9 gave the following proportions between liver, brain, and kidney. The figures are mean values of four experiments.

TDPase	pH 7	1.5 : 1 : 3
	pH 9	2.2 : 1 : 4.7
TMPase	pH 6	2.2 : 1 : 1.9
	pH 7	1.6 : 1 : 3.3

Figs. 1 and 2 show the activities of TDPase and TMPase at different pH values. There, the percentages of hydrolyzed TDP are not comparable from one tissue to the other, the tissues being taken from different individuals and also different amounts of enzyme having been used.

Of the tissues investigated kidney is most active in hydrolyzing TDP to TMP. From Fig. 2 it is seen, however, that kidney and brain, but not liver, have two optima for hydrolyzing TMP, one at pH 6 and another at pH about 9, while liver shows one only at pH 6. The figures for TDPase activity in kidney at pH 9, given above, could therefore be expected not only to show TDPase activity but also TMPase activity as the TMP formed by the first enzyme might be further hydrolyzed to thiamine by the second enzyme. This might also be the case with enzymes prepared from brain, although to a smaller extent. Paper chromatographic analysis of the samples after finished incubations, however, shows that a surprisingly small amount of the TMP formed has been further hydrolyzed. This may very truly be ascribed to the short incubation times (20 min) used in these experiments.

In none of the tissues examined TDPase and TMPase are dependent in the same manner upon pH. With the liver enzymes the two substrates TDP and TMP are hydrolyzed with optimal rate at distinctly different pH, with the kidney enzyme one peak is common to the two substrates, while the brain enzyme gives two common

* Abbreviations: TDP: thiamine diphosphate, TMP: thiamine monophosphate, TDPase: Thiamine diphosphatase, TMPase: thiamine monophosphatase.

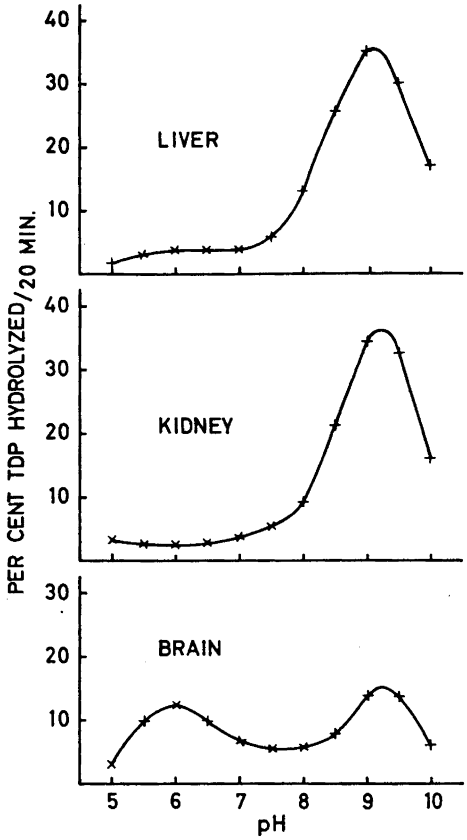

Fig. 1. Enzymatic hydrolysis of thiamine diphosphate to thiamine monophosphate. Incubations were performed as desribed in Experimental.

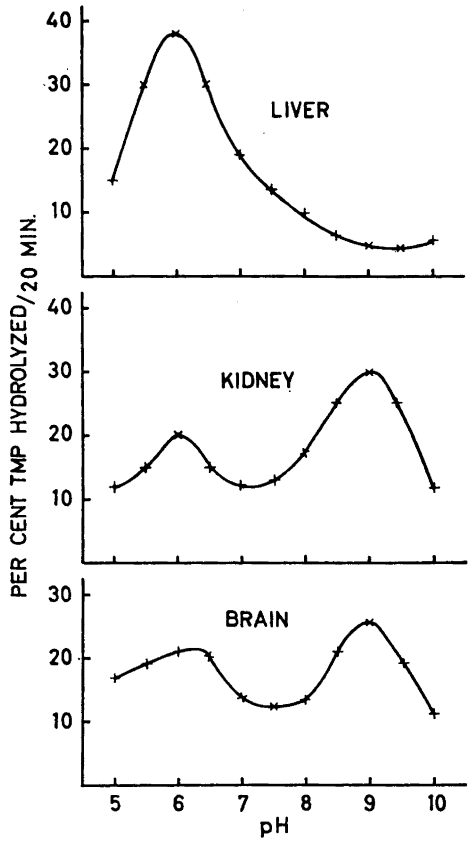

Fig. 2. Enzymatic hydrolysis of thiamine monophosphate to thiamine. Incubations were performed as described in Experimental.

peaks. With the last enzyme the peaks with TDP as a substrate are not very distinct, that is, TDP is hydrolyzed at moderate speed over a broad pH range. This is in agreement with findings by Naidoo and Pratt [6] in their histochemical investigation of a thiamine pyrophosphatase in nervous tissue from chicken.

Acknowledgements. I am indebted to Miss Margareta Schiöld for technical assistance. This work is part of investigations made possible by grants from the *Swedish Natural Science Research Council.*

1. Kiessling, K.-H. and Tilander, K. *Biochim. et Biophys. Acta* **43** (1960) 335.
2. Kiessling, K.-H. and Tilander, K. *Acta Chem. Scand.* **14** (1960) 841.
3. Ernster, L., Zetterström, R. and Lindberg, O. *Acta Chem. Scand.* **4** (1950) 942.
4. Viscontini, M., Bonetti, G. and Karrer, P. *Helv. Chim. Acta* **32** (1949) 1478.
5. Kiessling, K.-H. *Acta Chem. Scand.* **10** (1956) 1356.
6. Naidoo, D. and Pratt, O. E. *Biochim. et Biophys. Acta* **18** (1955) 75.

Received September 20, 1960.

The Synthesis of DL-Hinokione Methyl Ether

YUAN-LANG CHOW

Kungl. Tekniska Högskolan, Organisk-kemiska Institutionen, Stockholm, Sweden

Hinokione has been isolated from the heartwood of several conifers [1] and its structure has recently been shown to be VIII (R = H) [1]. A synthesis of the DL-form of hinokione methyl ether (R = CH_3) has been carried out as indicated in the following scheme:

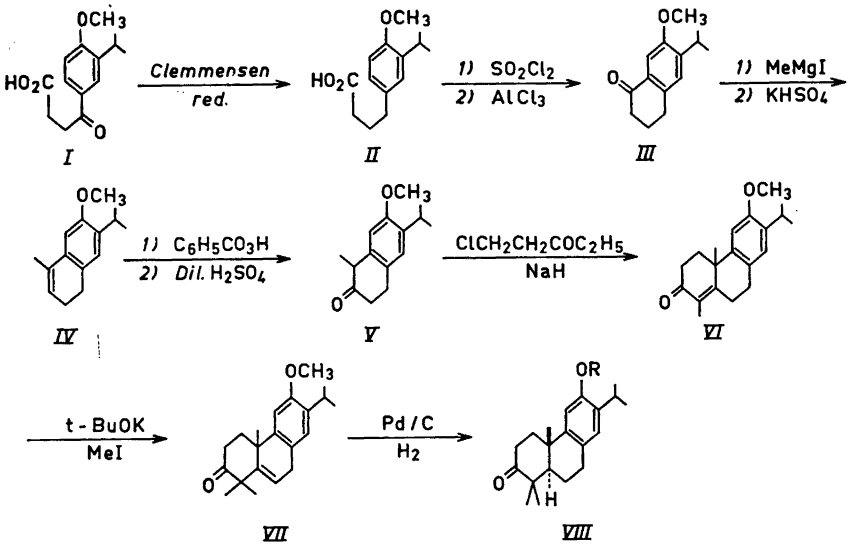

Succinoylation of 2-*iso*propylphenol methyl ether gave the keto-acid I, m.p. 133—135°, which furnished a deep red 2,4-dinitrophenylhydrazone, m.p. 85—88°. The keto-acid was reduced by Clemmensen's method to the acid II, m.p. 31—34°. The corresponding acid chloride when treated with aluminium chloride furnished the α-tetralone III, b.p. 136—138°/1 mm, λ_{max} 263 mμ (ε, 12 700) and 225 (19 700), ν_{CO} 1 675 cm^{-1} (film), further characterised as the deep red dinitrophenylhydrazone, m.p. 198—200°. The α-tetralone III reacted with methyl magnesium iodide giving a product that on treatment with potassium hydrogen sulphate underwent dehydration to yield the dihydronaphthalene IV, b.p. 101—104°/0.3 mm. IV was epoxidised with perbenzoic acid and the product isomerised [2] with dilute sulphuric acid to the β-tetralone V, b.p. 111—116°/0.1 mm, ν_{CO} 1 715 cm^{-1} (film) which gave a crystalline semicarbazone, m.p. 184—187°.

The β-tetralone V was condensed with β-chlorodiethyl ketone in the presence of sodium hydride [2] to give the α,β-unsaturated ketone VI, m.p. 92—94°, ν_{CO} 1 665 and $\nu_{C:C}$ 1 623 cm^{-1}, λ_{max} 287 mμ (ε 4 160), 279 (4 720), 230 (16 000) and 247 (17 100), giving a red 2,4-dinitrophenylhydrazone, m.p. 225—228°. Methylation of VI with methyl iodide and potassium *t*-butoxide led to the ketone VII, m.p. 92—94°, ν_{CO} 1 712 and $\nu_{C:C}$ 1 668 cm^{-1}, (2,4-dinitrophenylhydrazone, m.p. 212—214°), which was hydrogenated in ethanol in the presence of Pd/C to DL-hinokione methyl ether VIII (R = CH_3), m.p. 119—121°, (2,4-dinitrophenylhydrazone, m.p. 215—218°). The I.R. spectra of the synthetic and the natural hinokione methyl ether (in carbon tetrachloride) were superimposable.

The U.V. spectra were taken in 95 % ethanol solution and the I.R. spectra in carbon tetrachloride unless otherwise specified. Satisfactory analyses were obtained for all the compounds described.

The details of this investigation will be published elsewhere. This research was sponsored in part by the *Office of Research and Development, U.S. Department of Army*, through its European Office. The author is indebted to Professor H. Erdtman for his interest in this work.

1. Chow, Y. L. and Erdtman, H. *Proc. Chem. Soc.* **1960** 174; Erdtman, H. and Vorbrüggen, H. (Hinokiol in *Arthrotaxis* species). *Acta Chem. Scand. In the press;* Barreto, H. and Enzell, C. (Hinokione in *Cupressus torulosa*). *To be published shortly.*
2. Howell, F. H. and Taylor, D. A. H. *J. Chem. Soc.* **1958** 248.

Received September 23, 1960.

ACTA CHEMICA SCANDINAVICA 14 (1960) 1673–1676

Chemistry Department of Karolinska Mediko-kirurgiska Institutet in Stockholm 1810—1960

J. ERIK JORPES

Chemistry Department II, Karolinska Institutet, Stockholm, Sweden

Karolinska Institutet, the State Medical School in Stockholm, this year celebrates its 150th Anniversary. With its forty-five professors, twenty-two associate professors, 250 assistant teachers and about 1 000 undergraduates it is at present about twice as large as any of the other medical faculties of Sweden. It is an independent medical school with otherwise the same academic status as the medical faculties of the universities at Uppsala, Lund, Gothenburg and Umeå. Its activities, however, have in the past and in recent times as well extended considerably beyond the grounds of the purely medical sciences, particularly in the field of chemistry.

It is unique among the medical schools of Europe in that, from the beginning, chemistry was taught to the medical students by a full time professor. Furthermore, this professor happened to be *Jöns Jacob Berzelius* (1779—1848). In 1802 he began lecturing on chemistry to the medical profession of Stockholm. In 1807 he was appointed professor of medicine and pharmacy at the Surgical School of the Medical Board and from 1813 professor of chemistry and pharmacy at the new Medical School, Karolinska Institutet, erected in 1810 in Stockholm.

In one respect the teaching system of the medical faculties in Sweden including Karolinska Institutet differs from that prevailing outside of Scandinavia. *Complete medical education is as a rule a prerequisite for an appointment as teacher at a medical school*, a system introduced already in Berzelius' days. He himself, Olof Hammarsten and Torsten Thunberg were physicians like all the present members of the teachers' staff with only one exception amongst 200 chairs, including the chairs of chemistry, physiology, pharmacology, bacteriology, anatomy and histology.

On this occasion it may not be out of place to review shortly the main scientific achievements reached at the Chemistry Department of Karolinska Institutet. It is quite remarkable that before the time of spectral analysis no less than 9 new elements were discovered within a short space of time at one and the same institute.

Few chemists have been as successful in their work as Berzelius. His influence upon events in the field of chemistry rivalled that of Linnaeus in botany. In 1813 he introduced the chemical nomenclature in use today, applying the first letter or letters of the Latin name of the elements as their symbols. He determined the combining weights of 45 of the 49 elements then known. He himself discovered cerium, selenium and thorium, and his pupils *Arfwedson* and *Sefström* lithium and vanadium, respectively. His co-worker and successor, *C. G. Mosander*, discovered lanthanum, didymium, erbium and terbium, the two latter from the famous yttria earth — named after the small village Ytterby in the archipelago of Stockholm. The concepts of *isomerism* and *catalysis* were created by him. His textbook in chemistry was a standard work of its time, the fifth German edition of which appeared in 5 volumes between 1843 and 1848, with no fewer than 4650 pages. His animal chemistry of 1806 and 1830 and his annual reviews of the progress of chemistry, physics and mineralogy for the years 1821—1848 were highly appreciated by the contemporary scientific world. Here only a short reference is made to the literature dealing with Berzelius *. His successor Mosander is presented in a separate paper.

Count Karl Axel Hampus Mörner, professor of chemistry and pharmacy between 1884 and 1917, was a prominent personality. In 1897 he discovered myoglobin, a substance which *Hugo Theorell* crystallized in 1932 in Mörner's old laboratory at Karolinska Institutet. In 1899 Mörner demonstrated that cystine, found by Wollaston in 1810 in a urinary calculus, is an ordinary amino acid, occurring in most proteins, and very abundantly in keratin. As Dean of the faculty 1897—1917 he helped to draw up the Articles of the Nobel Foundation and was head of the Nobel Committee for Physiology and Medicine from 1901 to 1917.

The research activities of the Chemistry Department were greatly expanded under the leadership of *Einar Hammarsten* (associate professor of chemistry and pharmacy 1918—1928; professor 1928—1957). About 1920 he showed that not only guanylic acid but also pyrimidine pentose nucleotides do occur in the pancreas. In his doctor's dissertation of 1924 he demonstrated that the laws of the osmotic pressure do not apply to the salts of thymonucleic acid and similar high molecular acids, the cations being devoid of osmotic effects. This phenomenon enables thymonucleic acid to be stored in high concentration in

* H. G. Söderbaum: Jac Berzelius, *Levnadsteckning* (in Swedish) I and II 1929, III 1931. Edited by the Royal Swedish Academy of Sciences. Almqvist & Wiksell, Uppsala. I—III about 1600 pages.

Arne Holmberg: *Biografi över J. J. Berzelius utgiven av K. Sv. Vetenskapsakademien*; I Printed material written by and about Berzelius 1933; Supplem. 1936 and 1953; II Manuscripts 1936; Supplem. 1953.

Jöns Jacob Berzelius: *Autobiographical notes* (in Swedish), published by the Royal Swedish Academy of Sciences through H. G. Söderbaum 1901. Edit. Norstedt & Söner, Stockholm. *English translation* by Olof Larsell, Professor of Anatomy, University of Oregon, Med. School, Portland. 1934. Edit. Williams & Wilkins, Baltimore.

Harold Hartley: *The place of Berzelius in the history of chemistry.* Lecture delivered at the meeting of the Swedish Academy of Sciences September 22, 1948. *Levnadsteckningar över K. Sv. Vetenskapsakademiens ledamöter*, No. 135. Almqvist & Wiksell, Uppsala 1948.

Arne Fredga: *Jöns Jacob Berzelius.* Minnesteckning föredragen vid minnesfesten över Berzelius i Stockholms Stadshus den 20 september 1948. *Levnadsteckningar över K. Sv. Vetenskapsakademiens ledamöter*, No. 134. Almqvist & Wiksell, 1948.

the cell nuclei, as also the heparin in the granules of the mast cells, without osmotic breakdown of the nuclear or granular membranes due to uptake of water. Hammarsten's institute was at that time one of the few research centres devoted to the study of nucleic acid chemistry. With the advent in later years of the isotope technique for the study of the metabolism of purines and pyrimidines his institute was well equipped to enter the new field.

In the course of the years, under Hammarsten's leadership, several independent research institutes were erected closely connected to his own department: the Biochemistry Department of the Nobel Institute of Medicine under *Hugo Theorell* (professor of biochemistry 1937 —), the Institute of Cell Research under *Torbjörn Caspersson* (professor of cell research 1944—), and the Institute of Medical Physics under Arne Engström (professor of medical physics 1952—).

Theorell's work from 1934 on the isolation of Warburg's yellow respiratory enzyme by means of an electrophoresis apparatus, designed by Theorell himself, his demonstration of phosphoric acid in its prosthetic group and the separation of the co-enzyme and apo-enzyme and their reunion into an active enzyme, and the crystallization of the enzyme, aroused great attention. In 1934 Caspersson introduced ultra-violet microscopy into histology, thus enabling the morphological processes to be studied without fixation or destruction of the tissues.

In the 1930's Hammarsten and *Gunnar Ågren*, in collaboration with *Henrik Lagerlöf* and *Hilding Berglund*, made fundamental studies on the intestinal hormone secretin. A secretin test for the pancreatic function was elaborated.

In 1935 *Erik Jorpes* (associate professor of chemistry and pharmacy 1919—1947; professor of medical chemistry 1947—) found heparin to be a highly esterified sulfo-mucopolysaccharide. A number of Swedish clinicians headed by *Clarence Crafoord* and *Gunnar Bauer* then started to use heparin as a remedy against thrombosis, simultaneously with Charles Best, Gordon Murray and their co-workers of the University of Toronto. In 1937 *Jorpes* and *Olof Wilander* in collaboration with the histologist *Hjalmar Holmgren* discovered that the metachromatic granules of the tissue mast cells of Ehrlich consist of heparin. An overwhelming literature is now dealing with the mast cells as well as with the therapeutic and prophylactic use of anticoagulants against thrombosis.

In recent years *Jorpes* and *Viktor Mutt* purified cholecystokinin and secretin. The latter was found to have an extremely high biological activity.

The extended study of heparin and of its interference in the coagulation mechanism resulted in new findings in the coagulation field. Thus, *Margareta* and *Birger Blombäck* succeeded in 1956 in elaborating a new technique of preparing fibrinogen which made this plasma protein more easily accessible for use in surgery and obstetrics. With the same technique a preparation can be obtained, containing the antihemophilic globilin, coagulation factor VIII, now in use as a specific therapeutic agent in hemophilia A.

Per Edman initiated his studies on proteins at the Chemistry Department with his thesis of 1945 on the purification of hypertensin. During his subsequent stay at the University of Lund they were followed up with his invention of a new ingenious technique for the determination of N-terminal amino acids in proteins and peptides and for the determination of the sequence of the amino acids in a peptide chain.

Likewise *Torsten Teorell*, professor of physiology, Uppsala, got his education under Hammarsten.

Robin Fåhraeus, later professor of pathology at Uppsala, performed at the Chemsistry Department around 1920 the experimental work in connection with his discovery of the erythrocyte suspension stability test, which later became an extremely important diagnostic tool in medicine.

As previously pointed out complete medical education is as a rule a prerequisite for an appointment as teacher at a medical school in Sweden. Along the same line *the chemical laboratories for clinical pathology* are run by medical men, trained in biochemistry at the medical faculties; thus *Greta Hammarsten*, *Kjell Agner*, *Bertil Josephson*, *Bo Norberg*, *Bertil Swedin* and *Ingemar Jungner* in Stockholm, *Olof Wilander* in Örebro, *Carl-Olof Oldfeldt* in Linköping and *Gunnar Jungner* in Gothenburg got their postgraduate training at the Chemistry Department of Karolinska Institutet. During the last 30 years 37 such laboratories attached to larger clinical centres have been erected in Sweden, not less than 7 in the City of Stockholm, a trend in the recent development of our hospital system which pays due attention to the importance of biochemistry for medicine. The head of a clinical laboratory attached to a university clinic has teaching obligations as well. This system enables the doctors to have in their vicinity laboratory people speaking their own language, helping them in interpreting the chemical tests and discussing diagnostic and therapeutic problems.

ACTA CHEMICA SCANDINAVICA 14 (1960) 1677–1680

On Dry Distilled Racemic Acid

J. J. BERZELIUS*

Communication of the Swedish Academy of Sciences 1835 p. 142.

INTRODUCTION

The products resulting from the dry distillation of organic substances have recently been the object of particularly thorough study. Mention may be made of Faraday's investigation of the several forms of carbon-bound nitrogen obtained in this way, Bussy and Lecanu's of the distillation products of fatty oils, Riechenbach's of the products obtained from beech-wood and Pelouze's of the distillates of tannins, pyrogallic acid and malic acid. Despite the fairly important findings that have then been made, it is evident that this subject is still in its cradle, and that the so-called dry distillation of organic substances opens up an entirely new field in chemistry.

It is namely not only by means of the distillation of various substances, or of a mixture of several organic substances, that different products are formed, but the same substances — or mixtures of substances — may give rise to different products, according to temperature and the admixture of different inorganic substances.

It is easily realized that if one would undertake to study the dry distillation of a certain substance — for example, cane sugar — under all these varying conditions, a number of different compounds would be formed, among them perhaps many as yet unknown. If one then undertook the similar treatment of one unmixed substance after the other, it is impossible to predict the number of substances that would be produced in this way. It is nevertheless evident that if one would first study the special distillation of each organic substance, it would then be all the easier to analyze the products of their mixtures, *e.g.* woods, seeds, leaves, *etc.*, that are distilled.

* The Editor presents here a translation of the handwritten original of Berzelius' communication to the Swedish Academy of Science in 1835 concerning his discovery of pyruvic acid and its preparation and properties. The paramount interest taken in this compound by the biochemists of today may justify a reproduction of Berzelius' paper. It may also be of interest to note that he, when he in 1835 created the concept of catalysis, metal catalysis in chemistry and enzyme catalysis in biology, claimed that "the catalytic force ... functions largely in the same manner as heat". Here his experimental skill allowed him to produce at 200°C and to isolate the same labile compound, which much later was shown to be produced by enzymes when sugar and similar substances are burnt at ordinary temperature in the living organisms.

Published by permission of the Swedish Academy of Sciences, Stockholm.

The excellent investigations for which we are indebted to Pelouze, of the dry distillation of pyrogallic acid and malic acid, prompted me to resume an interrupted study of the distillation products of tartaric acid and racemic acid, in particular of the latter. Since, in the course of this work, I found myself forestalled by the same distinguished chemist, I can only hope that the ears I have plucked on the field left by him are not entirely without value.

ON PYRUVIC ACID AND THE CHANGES WHICH OCCUR WHEN RACEMIC ACID IS SUBMITTED TO DRY DISTILLATION AT A TEMPERATURE NOT EXCEEDING + 250°C.

In the report of my investigation of the composition of tartaric acid and racemic acid, which I had the honour to present to the Royal Swedish Academy of Sciences in 1832, I pointed out that racemic acid on dry distillation produces an acid different from the pyrotartaric acid arising from tartaric acid, which has been well known for a long time.

This pyrotartaric acid was intensively studied first by Gruner and then by Pelouze, who showed that the distillation products of tartaric and racemic acids are the same, mainly pyrotartaric acid and acetic acid, the latter in such a high concentration that it almost crystallizes out. Although I have confirmed the findings of Pelouze that tartaric acid and racemic acid give the same distillation products, I did not reach the same conclusion that he did concerning the nature of the main part of the distillate, which he considered, because of its smell, to consist of acetic acid. This acid is the same as that which I orginally thought to be formed from racemic acid alone, which I called pyruvic acid and described as a volatile acid.

I will go on using the name pyruvic acid, *acidum pyruvicum*, as an indication of its origin from the grape. The same acid is also found in the acidic fluid which is formed when solid potassium tartrate is submitted to dry distillation; it consequently occurs in an ancient remedy, *mixtura diatrion* or *m. pyrotartarica* and deserves to be known for this reason as well.

I distilled a sample of tartaric acid in a tubulated glass retort on a sand bath, the temperature of which could be kept almost constant by increasing or reducing the draught. The mass started to give off a water clear distillate of a sharp taste, smelling of acetic acid, whereupon it melted, turned grayish, and began to foam.

When the material showed a tendency to boil over, the cork was removed from the tubular extension and a rigid platinum wire was introduced to break the foaming, which was easily accomplished. It was sometimes necessary to repeat this procedure. Without this precaution the distillation proceeds extremely slowly and the entire foaming mass collects in the upper part of the retort leaving the lower part empty. During the operation carbon dioxide is developed in a continuous stream, necessitating tubulation of the receiver, the end of the tube being submerged in water.

The content of the retort gets very sticky before the end of the operation, mostly due to condensed pyruvic acid. Later on in the operation the distillate gets more and more concentrated, and becomes yellow in colour, but even at the end is no more than pale yellow if the temperature does not exceed + 220°

(Celcius). The residue in the retort becomes more and more sticky, finally changing to a fluid which boils without foaming; the temperature is then about + 200°, and when the boiling is finished and nothing more distils at + 200° the operation is finished. There is then left in the retort a mass which is soft while still hot but after cooling behaves like carbon.

The distilled acid contains no oil although the last fraction becomes slightly cloudy on dilution with water. It has an acetic acid like smell although slightly burned, a burning sharp acid taste, a consistency like sulfuric acid, and a yellow colour. If it is distilled over a water bath, which proceeds very slowly, one gets at first a colourless acid smelling strongly of acetic acid but also slightly of formic acid. The distillate usually turns yellow and assumes a thick consistency. In the last viscous fraction I found a specific gravity of 1.2792 or even slightly more. During the procedure carbon dioxide gas develops continuously, although no gas bubbles can be seen in the liquor, and the carbon dioxide must be given a possibility to escape; the fluid in the retort darkens more and more, finally turns dark brown and leaves a residue of a resinous mass at the end of the distillation. *Sometimes in my experiments the syrupy distillate, on cooling, was completely filled with crystals of pyruvic acid*, but this happened only half the number of times that I repeated the process. Before the distillation this pyrotartaric acid (?) was dissolved in the fluid together with part of the brown sticky material, most of which is formed during the redistillation; new quantities of this material are formed each time the distillation is repeated.

I have tried to redistil the acid in an apparatus from which I had removed the air in order to find out whether the air exerted any influence on its formation; the result, however, was the same, the only difference was that the distillation proceeded much more slowly. When the apparatus was opened carbon dioxide gas escaped with an explosion and showed that an increased pressure of carbon dioxide gas was the reason for slowing up the distillation. A considerable quantity of the resinous mass remains after distillation indicating that the acid after a few redistillations would soon be destroyed. The test with silver carbonate (carbonated silver oxide) indicated that formic acid could be present in the distillate. However, the salts prepared with sodium hydroxide and lead oxide always indicated the presence of acetic acid through their solubility in alcohol in which the lead salt of formic acid is almost insoluble. Also the acid does not become opalescent on boiling.

Since an attempt to obtain *the free acid* from its sodium salt, through distillation with sulfuric acid, failed, while the acid was almost completely destroyed, I had to find another way to obtain pure acid in a fairly strong concentration. This can be achieved in the following way. Freshly precipitated lead carbonate is dissolved in the redistilled acid to full saturation; at first the oxide dissolves but later on it is precipitated as a granular powder increasing in amount during 48 hrs, particularly in the cold. It is collected on a filter paper and washed.

The lead salt is suspended in a minute quantity of water, treated with hydrogen sulphide and strained through cloth. The lead sulphide is pressed and the mother liquor evaporated over sulfuric acid *in vacuo*. A thick syrup results which finally ..... (unreadable). No gas is evolved during this

concentration. A certain amount of the acid disappears, however, because of its volatility.

The properties of the acid are as follows: thick syrup which can be drawn out in threads, weak but sticky acid smell, strongly acid, later bitter taste. Turns fluid in the air. Soluble in alcohol and ether. On heating it partly evaporates and partly disintegrates, as previously described. The composition and the degree of saturation of this acid were elucidated through the analyses of its silver and sodium salts. The analyses were as follows: 0.31546 g acid produced with copper oxide 0.5225 g carbonic acid and 0.0145 g water It gave in per cent:

	Found	Atoms	Calculated
Carbon	45.80	6—458.628	46.042
Hydrogen	3.68	6— 37.488	3.463
Oxygen	50.52	5—500.000	50.195
	100.00	999.116	100.00

Its formula is consequently $C_6H_6O_5$. Upon comparison of this formula with that of tartaric acid and racemic acid, which is $C_4H_4O_5$, one finds that *this acid can be considered to be a lower degree of oxidation of the same radical.* On the same quantity of oxygen it contains one and a half times as much of the radical as do the tartaric and racemic acids, giving a formula for the latter acids 2 CH + 5 O, while the formula for the pyruvic acid is 3 CH + 5 O.

One could say that formic acid, tartaric acid, pyrogallic acid and pyruvic acid are derived from the same radical giving them the following composition:

Pyrogallic	acid	3 CH + 3 O
Pyruvic	»	3 CH + 5 O
Racemic and tartaric	»	2 CH + 5 O
Citric	»	2 CH + 4 O
Formic	»	CH + 3 O

Berzelius goes on to describe in six large pages no less than *20 different metal salts of the new acid,* all prepared and analyzed by himself. It is very typical of this tremendously diligent and ambitious chemist that he did not feel satisfied until he had prepared the potassium, sodium, silver, ammonium, barium, strontium, calcium, aluminium, beryllium, ytterbium, thorium, manganese, iron, cobalt, mercury, lead, basic lead, uranium, copper, platinum, and gold salts of his new acid.

As is evident, Berzelius interpreted the structure of the pyruvic acid in accordance with the ruling concepts of those days. He considered the acid to be an oxide of an organic radical, the ethine radical C_2H_2, here written as CH, assumed to be common to a series of well known organic acids. In spite of the improvement Berzelius made of the quantitative organic analysis by introducing the use of the calcium chloride tube for the collection of the water of combustion, his technique of analysis was by far not so accurate in the organic field as it was in the inorganic. Hence the misleading figures, which allowed him to drawn the wrong conclusions. On another occasion the theory about organic radicals influenced Berzelius' thinking, namely when in 1838 he suggested the name "protein" for a new radical, that the Dutch chemist Mulder claimed that he had found in all kinds of animal and plant material.

ACTA CHEMICA SCANDINAVICA 14 (1960) 1681–1683

Carl Gustaf Mosander

J. ERIK JORPES

Chemistry Department II, Karolinska Institutet, Stockholm, Sweden

Mosander became through his discoveries of the new elements lanthanum (1839), didymium (1842), erbium and terbium (1842) a worthy successor of Berzelius. In 1831 Berzelius decided to withdraw from the professorship of chemistry and pharmacy at the Karolinska Medico-Chirurgical Institute in Stockholm, partly because of his desire as secretary of the Academy of Science to devote himself exclusively to his research work and partly in order to give his co-worker Mosander an opportunity to get a position as full term professor, which the latter then held for 26 years until his death in 1858.

Mosander was born in 1797 in the city of Kalmar. Like Scheele he started his career as a pharmacist. At the age of 15 he enlisted as an apprentice at the Owl's Apothecary in Stockholm and at 22 took up medical studies. In 1824 he was appointed as teacher in chemistry at Karolinska Institutet, the medical school in Stockholm under Berzelius and in 1832 he succeded him as professor of chemistry and pharmacy.

Although Mosander took over Berzelius' teaching at the medical school he did not share his teacher's devotion to physiological chemistry in its broadest sense. Mosander restricted his work mainly to the field of inorganic chemistry and mineralogy. In these fields he became the master's equal. He spent much of his time organizing the Collection of Minerals at the State Museum of Natural History.

Here follows an English translation of the history of Mosander's discoveries, written for the Swedish Academy of Science by A. Erdman in 1873.

"In 1803 Berzelius and Hisinger discovered a new metal in a mineral that had recently been found in the Bastnäs copper mine in the Skinnskatteberg district of the province of Västmanland. They called it *cerium*. The methods of reduction known at that time were not, however, sufficiently effective to enable them to obtain their new substance in a pure metallic state. — After a long interval of time this substance was examined again by Mosander and the success of his efforts is described in a paper in the proceedings of the Swedish Academy of Science for 1826. This paper describes a number of new or previously little known compounds of the metal cerium with other elements.

A few years later in 1829 Mosander made an important contribution to the knowledge of the composition of titanium compounds.

Previous experiments made at the end of the eighteen-twenties had led Mosander to suspect that cerium oxide contained some other substance but

he was unable to separate it. After he had obtained sufficient material, he took up the investigation again in the middle of the eighteen-thirties and in 1839 had the satisfaction of being able to announce to the scientific world that the number of known elements had been increased by one more to which he had given the name *lanthanum* from the Greek work *λανθανειν*, to conceal, because the presence of this substance in cerium oxide had long remained a secret.

Mosander's next task was a study of the properties of the new element or rather of the two separated elements, lanthanum and cerium. These investigations, which he pursued with all the perspicacity and clearsightedness that always marked his scientific activities, took up all the time left over from his official duties for several years. Some of the results he obtained led him to suspect that there was also a third element present, that in some experiments followed the lanthanum oxide and in others was distributed between the lanthanum and cerium oxides. This third substance he called *didymium* from the Greek *διδυμοι*, twins, since it followed cerium or lanthanum in cerium-containing minerals like a twin brother. It took a large number of experiments over a long period before Mosander finally ventured to announce the discovery of the oxide of another previously unknown metal at the second Scandinavian Scientific Meeting in Stockholm in 1842. This was nearly three years after he had first succeeded in separating it from lanthanum oxide — a striking instance of the praiseworthy care and reticence which Mosander always showed in such cases.

The very complex reactions characterizing the recently discovered lanthanum and didymium and the difficulties that arose in trying to prepare them in a completely pure state caused Mosander to make similar studies on the oxide yttria which often accompanies cerium in nature. These experiments soon led to a result that was just as unexpected as it was gratifying. As a consequence at the same time as he announced the discovery of didymium at the 1842 meeting, Mosander was also able to inform the meeting that the earth that hitherto had been named yttria, "ytterjord" in Swedish, was not a pure earth but was mixed with another of previously unknown properties. Continued investigations soon showed that Mosander had in no way allowed himself to announce any hasty conclusions to his scientific audience but was fully able to confirm his statement. He was able to announce before the end of the year that the old *yttria* which is one of the main components of the mineral gadolinite from the Ytterby feldspar works near Vaxholm in the Stockholm archipelago was *a mixture of three different earths*, two of which were new to science. He called the elements from which the two new ones derived *erbium* and *terbium* from parts of the name Ytterby. The element in the third earth was left with the old name *yttrium*.

The inscription on a medal struck by the Swedish Academy of Science in 1869 in honour of Mosander, 'Coacta disjungit semina terrarum' referred to all of these discoveries."

New findings were later added to those of Mosander. Thus Auer von Welsbach resolved in 1885 the earth didymia into two different oxides, *praseodymia* and *neodymia*. The names of the earths erbia and terbia were later interchanged. In 1878 Marignac dissolved the erbia from the gadolinite into *erbia* and

ytterbia, and from the latter Nilsson separated in 1879 a new element, *scandium*, the second newly discovered element which fitted into Mendelejev's periodic system on the place of ekabor. After removal of ytterbia and scandia from the erbia Cleve in Uppsala found in the same year another two new oxides *thulia* and *holmia*. As to the names of these two elements, the last ones in a series of 22 elements discovered between 1730 and 1879 in Sweden, Cleve suggested *thulium*, deriving from Thule, the ancient name of Scandinavia, and *holmium*, from the latinized name of Stockholm in whose vicinity occur so many minerals rich in yttria.

(*Vide* Findlay: A hundred years of chemistry, Duckworth 1948, and Helen Miles Davis: The chemical elements, Science Service, Washington 1952).

ELEMENTS DISCOVERED BY OLD SWEDISH CHEMISTS

Georg Brandt	Cobalt	Co	1735	
Axel Fredrik Cronstedt	Nickel	Ni	1751	
Carl Wilhelm Scheele	Fluorine	F	1771	Isolated by Moissan 1801
	Oxygen	O	1772	Priestley 1774
	Chlorine	Cl	1774	Isolated by S.
	Molybdenum	Mo	1778	Isolated by Peter Jakob Hjelm 1782
	Tungsten	W	1781	
Johan Gottlieb Gahn	Manganese	Mn	1774	Isolated by G., discovered by Bergman and Scheele
Anders Gustaf Ekeberg	Tantalum	Ta	1802	
Jöns Jacob Berzelius	Cerium	Ce	1803	Simult. with Klaproth
	Selenium	Se	1817	
	Thorium	Th	1828	
Johan August Arfwedson	Lithium	Li	1817	
Nils Gabriel Sefström	Vanadium	V	1830	
Carl Gustav Mosander	Lanthanum	La	1839	
	Didymium	—	1842	Divided by Auer v. Welsbach into Praseodymium, Pr and Neodymium, Nd in 1878
	Erbium	Er	1843	
	Terbium	Tb	1843	
	Yttrium	Y	1843	(Gadolin 1794)
Lars Fredrik Nilsson	Scandium	Sc	1879	
Per Teodor Cleve	Holmium	Ho	1879	Isolated by Holmberg 1911
	Thulium	Tm	1879	

ACTA CHEMICA SCANDINAVICA 14 (1960) 1684–1692

Properties and Structure of the Compounds Formed between Cytochrome c and Nitric Oxide *

ANDERS EHRENBERG and TADEUSZ W. SZCZEPKOWSKI**

Medicinska Nobelinstitutet, Biokemiska avdelningen, Stockholm, Sweden

The compound formed between ferricytochrome c and nitric oxide has been found to be diamagnetic. It is proposed to be a ferrocytochrome c nitrosyl compound from which the ferrocytochrome c nitric oxide compound can be obtained by alkalinization. Other haemoproteins behave similarly. The relationship between the optical absorption spectra of the nitrosyl, nitric oxide and carbon monoxide compounds of some ferrohaemoproteins is discussed. The haemlinked group of cytochrome c that is replaced by nitric oxide cannot be detected as a normal histidine imidazole by acid base titration. The possibility of a sterically hindered imidazole group has to be considered.

It is well known that nitric oxide, NO, has the power of combining with iron-porphyrin compounds containing either ferrous or ferric iron [1–3]. Reactions take place with iron-porphyrin bound to proteins [1,2] as well as in haemi- or haemochromogens [2] or with free haem or haematin under certain conditions [3]. While ferricytochrome c combines easily with NO, the reduced form, ferrocytochrome c, seems to be very inert to NO, and attempts to produce a distinct compound have so far failed.

The ferrous NO compounds which are all stable exhibit typical haemochrome spectra not very different from those of the corresponding CO compounds. Magnetic measurements on the NO derivative of haemoglobin have shown that this complex holds only one unpaired electron [4] which means that the ferrous iron here is surrounded by six octahedral d^2sp^3 bonds and has all its d-electrons paired. The odd electron detected, originates from the NO molecule and is supposed still to belong to the same atomic grouping in the complex. A similar state of affairs is very probably valid for the other ferrous NO compounds.

The ferric NO compounds also show two-banded absorption spectra in the visible but the bands are more distinct and shifted 5 to 10 mμ towards shorter wavelengths, as compared with the corresponding reduced form. Most of the ferric compounds are unstable, *e.g.* ferri HbNO[1] and ferri MbNO which are

* Most of the experimental work was made during the stay of T. S. in Stockholm, 1956—57, Fellowship of the Polish Academy of Sciences.

** Present address: Zakad Chemii Fizjologiczbej, ul. Kopernika 7, Krakow, Poland.

gradually autoreduced. In contradistinction to these compounds ferricytochrome-c-NO is stable for a long period of time.

A discussion of the properties of these ferric NO-compounds in terms of the bonds involved in the iron porphyrin complex has not yet been possible, mainly because of lack of magnetic data for the compounds considered. In the present paper it will be shown that these compounds are diamagnetic and contain ferrous iron. The formation of ferrocytochrome-c-NO as a spectroscopically well characterized compound will also be demonstrated.

EXPERIMENTAL

Materials

Nitric oxide was generated from sodium nitrite mixed with ferrous sulphate by addition of dilute sulphuric acid. The gas was passed through two traps filled with dilute potassium hydroxide and collected in a glass gasometer over dilute hydroxide with phenolphthaleine added as an indicator.

Commercial *nitrogen* from a gas tank was made oxygen free by passing through two traps with vanadyl sulphate dissolved in dilute sulphuric acid and in contact with amalgated zinc.

Cytochrome c was prepared from beef heart according to Paléus and Neilands [5] and contained 0.43 % iron. The haemopeptide was purified after degradation of the cytochrome c by pepsin [6]. These preparations were put at our disposal by Dr. S. Paléus.

Myoglobin, prepared from horse muscle was kindly given to us by Mr. Å. Åkeson. We are indebted to Dr. K. G. Paul for a sample of *horseradish-peroxidase*.

Methods

The magnetic measurements were performed in the instrument constructed by Theorell and Ehrenberg [7] and later modified to allow for better temperature control and give better reproducibility in the readings [8]. Since the nitric oxide compound of cytochrome c is more stable at lower temperatures all the measurements were made at + 7°C, the lowest temperature at which it was feasible to operate the instrument.

A weighed amount (about 30 mg) of lyophilized cytochrome c was placed in a small Thunberg tube. Since part of the cytochrome was present in the reduced form the sample was first dissolved in 0.25 ml 0.2 N HCl and left in this solution until a spectroscopic test revealed that all the reduced cytochrome c had been autoxidized. The sample was thereafter adjusted to the desired pH and concentration, either by 6 N NaOH and M/15 phosphate buffer to a final volume of 1 ml and pH 7.2, or by water to a final volume of 0.5 ml containing 0.1 N HCl, which together with the protein, gave a pH of about 3. In every case two more Thunberg tubes were filled in an identical way, except that the cytochrome c was omitted. These solutions served as blanks in the magnetic determinations, one being measured before and the other after the sample. The magnetic susceptibility was determined prior to and after treatment with NO. This treatment and the measurement on the NO–derivative were made as follows.

The three Thunberg tubes were placed in an ice bath in order to minimize evaporation when the tubes were evacuated. They were connected to a common three way outlet through which they could be quickly evacuated and subsequently filled with nitrogen. This procedure was repeated seven times. The connection leading to the NO-gasometer was also flushed with nitrogen. The Thunberg tubes were then filled twice with NO and left after the last filling for at least 10 min in order to assure a complete reaction, a condition that had been spectrophotometrically controlled for similar samples. The tubes were again quickly evacuated and thereafter placed in a jacket connected to the magnet thermostat and allowed to equilibrate for 20 min to the desired temperature of 7°C. Immediately before the measurement nitrogen was let in and care was also taken to flush with nitrogen the magnet tube and the glass pipet used for transferring the liquid.

The results were corrected for the diamagnetism of the protein by means of data obtained by measuring in the magnet the reduced form of similar samples of cytochrome c.

The acid-base titrations were made on 3 ml samples in a small glass beaker with ground neck and a tightly fitting perspex stopper. Holes were drilled in the stopper for one glass and one calomel electrode, two micrometer burets (Agla syringes), and two tubes for inlet and outlet of the gas. A rubber collar was placed in each hole and sealed to the perspex and the inserted glass tube by paraffin. To ensure complete tightness the perspex stopper was provided with a collar and covered with a one cm thick layer of mercury. As an extra precaution the outlet tube was immersed in a vessel filled with mercury to give a constant overpressure in the vessel. Before entering this the gas was freed from traces of acid by passing through a trap filled with dilute potassium hydroxide. Temperature was kept constant by streaming thermostated water in an outer water jacket and stirring was achieved by a magnetic stirrer. 15 to 30 mg cytochrome c was dissolved in 3 ml 0.2 M sodium chloride. 50 μl of this solution was taken for spectrophotometric determination of the concentration after dilution and reduction. The sample was brought to a pH below 3 by addition of 0.4 N HCl and left there in contact with air and with slow stirring for about 1 h to ensure complete autoxidation. A stream of nitrogen was started and the ferricytochrome c was titrated with 0.4 N NaOH up to pH 10 and then titrated back with 0.4 N HCl to a pH just below 5. Nitric oxide was now introduced until the colour of the sample had changed. Most of the nitric oxide was replaced by nitrogen and the titration of the NO-compound was made with just enough nitrogen streaming to maintain the small overpressure.

For the amounts of cytochrome c used in the experiments 2 to 4 μl of the 0.4 N acid or base corresponded to 1 equivalent. The volumes could be read to every 0.2 μl. The pH was measured by a Radiometer pH-meter, model PHM3. The glass electrode was standardised with phthalate and borate buffers before and after each run. In every case the change was less than 0.01 pH unit.

The spectrophotometric absorption curves were made with a Beckman DK 2 recording spectrophotometer. Cuvettes with a side bulb, ground stoppers and stopcocks were used. They could be evacuated and washed with nitrogen or argon before NO was let in and later on reaction with the contents in the side bulb could be started. When desired the excess of NO could be removed by evacuation and flushing with argon. All spectrophotometric analyses were made with a Beckman DU spectrophotometer.

RESULTS AND DISCUSSION

The magnetic susceptibility of the NO-derivative was found to be 490×10^{-6} emu at pH 7.2 and 220×10^{-6} emu at pH 3. In both cases the error of the determination was estimated to be $\pm 100 \times 10^{-6}$ emu. These data prove that the complex is diamagnetic. The small positive susceptibility values obtained can be explained by some dissociation of the NO-compound, a process that gives two paramagnetic molecules out of one diamagnetic. The experimental value at pH 3 is lower than that at pH 7.2 in spite of the increased susceptibility of cytochrome c at the lower pH [9]. This indicates that the NO-compound is stabilized in the more acid solution. Since the compound is thus found to be diamagnetic as compared with another diamagnetic derivative, ferrocytochrome c, and we are here interested in the "spin susceptibility" there was no reason to correct our data for the "orbital susceptibility" estimated by Griffith for this type of complex [10].

The diamagnetism of the compound immediately leads to the conclusion that there must be an odd number of NO molecules that combine with the ferric iron, so that the total number of electrons becomes even and the spins can pair out. Earlier equilibrium data support the view that there is only one NO molecule reacting with each cytochrome c molecule [2]. If NO in this

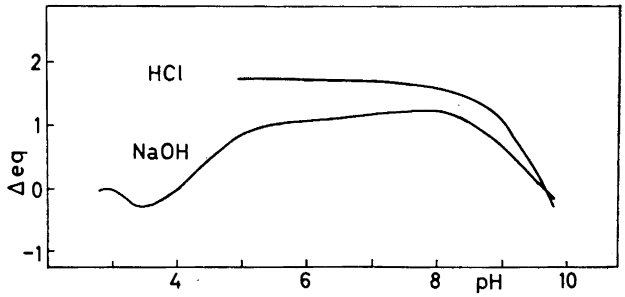

Fig. 1. Difference titration curve of ferricytochrome c after and before reaction with NO.

reaction replaces one of the nonporphyrin ligands and this ligand is a histidine residue it might be possible to identify it by a difference titration. When NO reacts the pH of the solution would rise if the pK of the replaced ligand is equal or higher than the pH of the solution. The pH would be unaffected if the pK of the ligand is low enough. In all the experiments a drop in pH was instead observed upon reaction with NO and in the different experiments a number of equivalents that varied from slightly less than one to more than four were titrated in the range pH 3 to 5 as seen from the difference curve between the titrations of NO-cytochrome c and ferricytochrome c. A typical curve is given in Fig. 1. Apparently the removal of oxygen had not been complete and some nitrous acid with pK = 3.4 had been formed. 4 to 8 μl of oxygen of normal temperature and pressure corresponds to 1 equivalent of cytochrome c in the present experiment. The amount of oxygen dissolved in the standard acid and base used can be neglected, since the solutions were stored under vaccum for some time before the burets were filled. The difference curve also reveals that some groups that are titratable above pH 8 in ferricytochrome c have disappeared in the NO-compound. It is quite reasonable that some of the free amino groups in the protein could react with the nitrous acid and thus be transformed into alcoholic hydroxyls.

In no case more than fractions of one equivalent were titrated in the range between pH 5 and 8. All the equivalents titrated below pH 5 are not necessarily artefacts due to nitrous acid and our experiments are compatible with a pK somewhere between 3 and 5 for the released haemlinked group. This low pK might either correspond to a carboxyl group or a histidine residue with its pK shifted from the normal range. Such a shift might be caused by the histidine being embedded between the protein helices as suggested in the proposed structure of cytochrome c [11]. Also surrounding positively charged groups will operate in the same direction by decreasing the local concentration of the hydrogen ions. The possibility that no haemlinked group is replaced and that the NO is capable of joining to the iron through a new seventh bond of considerable strength must be considered highly improbable, *e.g.* because of the symmetry properties of the bonding orbitals of the porphyrin iron.

When NO reacts with ferricytochrome c to form a diamagnetic compound iron might either donate one electron to NO or accept one electron that is given off by the ligand. In the former case the iron would be oxidized to the

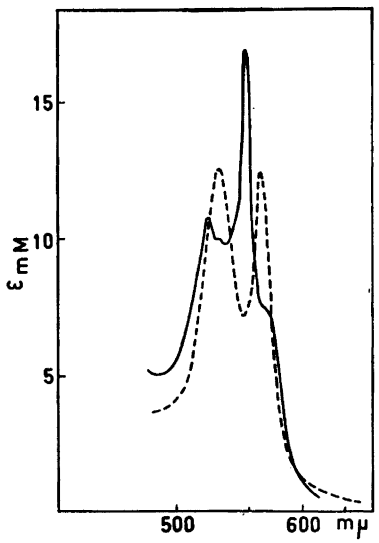

Fig. 2. Broken curve: Spectrum of ferrocytochrome c nitrosyl compound formed in acid or neutral solution from ferricytochrome and nitric oxide. Full drawn curve: Spectrum of the same solution after removal of excess nitric oxide and addition of alkali to obtain pH 12.

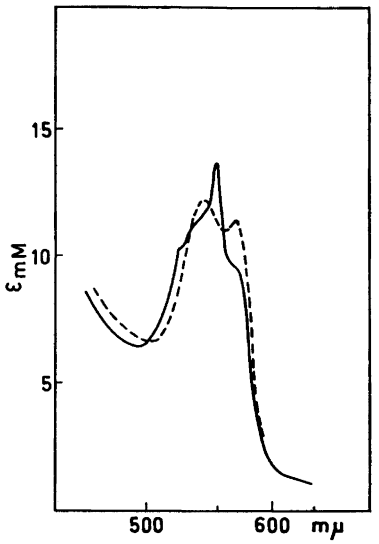

Fig. 3. Full drawn curve: Transient spectrum 2 min after alkalinization of the ferrocytochrome c nitrosyl compound with excess of NO present. Broken curve: Final spectrum 30 min later.

ferryl state and NO reduced to a negative ion that would be isoelectronic with molecular oxygen. A compound of this type is, however, unlikely to be diamagnetic since the third 3 d orbital of the iron would be left empty. The theory predicts electronic configurations of ferryl iron with four unpaired electrons in the high spin state and two, but not zero, unpaired electrons in the low spin state [12]. The secondary peroxide complexes of catalase or horseradish peroxidase and the peroxide compounds of myoglobin are thought to be of this ferryl type [13]. They might be considered to be compounds formed between ferric iron and a free radical representing the rest of the peroxide and have indeed two odd electrons [14,15]. In the second case the iron is reduced to the ferrous state and NO is oxidized to the positive nitrosyl ion, NO^+, that is isoelectronic with carbon monoxide and by analogy is likely to form a stable compound with the reduced haem iron. The compound formed in the reaction between ferricytochrome c and NO would thus be a ferrocytochrome c nitrosyl compound as schematically shown in reaction (1).

$$Fe^{+++} + NO \rightleftharpoons [Fe^{+++} - NO] \rightleftharpoons \underset{I}{Fe^{++} - NO^+} \qquad (1)$$

The intermediary complex put within brackets has not been demonstrated and it must be very shortlived if it exists. The spectrophotometric experiments to

be reported below have supplied considerable support for the correctness of the proposed formation of the ferro-nitrosyl compound (I) to the right in formula (1).

When ferricytochrome c reacts with NO at a neutral or acid pH, compound I is rapidly formed. The spectrum, part of which is shown in Fig. 2, has absorption maxima at 417, 530, and 564 mμ. The dissociation constant for the back reaction is so very small that practically all the excess NO gas can be removed and the compound is still stable at these low pH values. If the formulation of I as a ferro-nitrosyl compound is correct it would, however, be possible for this compound also to dissociate into ferrocytochrome c and the nitrosyl ion:

$$Fe^{++} - NO^{+} \rightleftharpoons Fe^{++} + NO^{+} \quad (2)$$

The nitrosyl ions are in equilibrium with the hydroxyl ions, nitrous acid and nitrite ions:

$$NO^{+} + OH^{-} \rightleftharpoons HNO_2 \quad (3)$$

$$HNO_2 + OH^{-} \rightleftharpoons NO_2^{-} + H_2O \quad (4)$$

A high pH would thus force reaction (2) to the right. Indeed, if the excess NO gas was removed from an acid solution of I, and this solution was brought under anaerobic conditions to pH 12, a new and stable spectrum quickly appeared. As can be seen from Fig. 2 this spectrum is complicated but the main bands in the visible are situated at 520 and 550 mμ thus confirming the formation of reduced cytochrome c in a high yield. Less intense bands are situated at 530, 540 and 567 mμ.

If the alkalinization of I is made in the presence of excess NO-gas the complicated spectrum just described is first rapidly formed. However, it gradually changes into a simpler spectrum with absorption bands in the visible at 540 and 567 mμ, as shown in Fig. 3, and the Soret band at 411 mμ. Very similar intermediary spectra are observed and an identical end product is formed when oxidized or reduced cytochrome c or a mixture of the two is reacted with NO at pH 12. The compound formed in all these reactions has to be formulated as a complex with nitric oxide bound to the iron of ferrocytochrome c, and is here labeled II:

$$Fe^{++} + NO \rightleftharpoons Fe^{++} - NO \quad (5)$$

II

Compound II has also been shown to be stable at lower pH-values. It was first formed from ferrocytochrome c and NO at pH 12 and then in the presence of NO brought to pH 7.5 by addition of a measured amount of primary phosphate. No marked change in the spectrum was observed after 30 min. At still lower pH-values and in the presence of nitrite compound I is formed by reversal of reactions (2)—(5). Enough nitrite for this reaction sequence is easily formed by incomplete anaerobiosis during exposure to NO, especially if compound II has originally been obtained from I, in which reaction one equivalent of nitrite is formed.

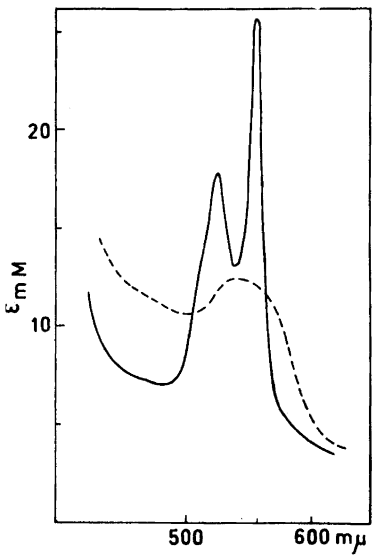

Fig. 4. Spectrum of ferrohaemopeptide at pH 7, full drawn curve, and the products after reaction with NO, broken curve.

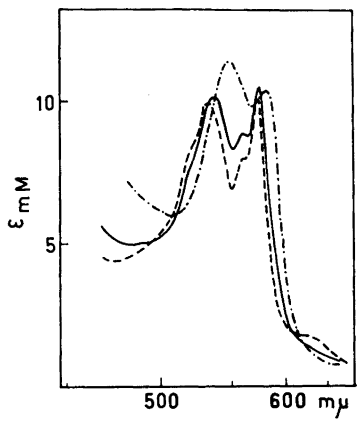

Fig. 5. Transient spectrum of ferrimyoglobin immediately after reaction with NO at pH 7 (— — — —) and the stable spectrum of the ferronitrosyl compound measured 3 hrs later (————). At pH 10 the later spectrum is immediately formed, and with excess NO the stable spectrum of the ferromyoglobin NO-compound could be measured after 2 hrs (— . — .).

From formula (3) it can be seen that the nitrosyl ion concentration would be expected to increase with the concentration of nitric acid and the concentration of hydrogen ions. This dependence is illustrated by the spectral changes of reduced cytochrome c in 10 mM nitrite solutions of different pH. At pH 2 and 4.2 the reduced cytochrome c was immediately transformed into compound I. At pH 5.3 the transformation is slower and at pH 7 or higher no reaction at all takes place.

At pH-values below 2 oxidized cytochrome c is also quantitatively transformed into I by the action of nitrous acid. This shows that NO must be formed from nitrous acid under these conditions, probably by disproportion into nitric acid and nitric oxide. At pH 5.3 the spectrum of oxidized cytochrome c is not affected by added nitrite.

The inability of ferrocytochrome c to react with NO in neutral solution parallells its behaviour towards CO and O_2. These molecules are all small and uncharged but can nevertheless not reach and react with the iron. A very close and tight structure is thus necessary around the haem of cytochrome c. This structure is opened slightly when the cytochrome is oxidized, and the NO molecule can now penetrate and react with the iron. Molecules of similar size but with an electrical charge, *e.g.* CN^-, can still not reach the iron because

Table 1. Comparison of the absorption band positions of some ferrohaemoprotein derivatives. Data on the CO compounds of cytochrome c and catalase are taken from Refs.[17,18], respectively.

Haemoprotein	Derivative	Wavelength of absorption maximum in mμ		
Cytochrome c	NO+	563	530	417
	CO	563	530	—
	NO	567	540	411
Myoglobin	NO+	575	537	420
	CO	578	542	423
	NO	580	548	421
Haemoglobin	NO+	568	532	—
	CO	568	538	419
	NO	576	542	—
Horseradishperoxidase	NO+	570	539.5	423
	CO	573	542	423
	NO	575	545	423.5
Catalase	NO+	576	540	—
	CO	580	545	—
	NO	—	—	—

of a potential barrier due to charge groups in the protein moiety. The same potential barrier helps to stabilize the ferro-nitrosyl complex formed, by protecting the positively charged nitrosyl ion from "leaking" out. This protection is strongest in acid solutions, when positive charges dominate on the protein surface, and will decrease with increasing pH, thus explaining the observed pH dependence of the stability of the ferrocytochrome c nitrosyl complex. The compact structure itself will also be opened at higher pH-values. Ferrocytochrome c can now combine with NO or CO or it can be oxidized by O_2. The stability of the ferro-NO compound when neutralised also demonstrates that an uncharged molecule can be captured inside the closed structure surrounding the haem.

The spectra and reactions of some compounds related to cytochrome c have also been explored. Thus the ferrihaemopeptide gives with NO a compound with α-and β-bands that are indistinguishable from those of I. This is to be expected, since there is the same configuration around the iron whether NO reacts with the ferrihaemopeptide from the opposite side to the single histidine imidazole present, or with ferricytochrome c by replacement of one of the coordinated histidines. As distinct from ferrocytochrome c the ferrohaemopeptide that has no closed structure reacts with NO in neutral solution as is seen in Fig. 4. The spectrum is poorly defined and probably represents a mixture of compounds. Possibly more than one NO molecule could be coordinated.

When NO reacts with ferrimyoglobin at pH 7 a distinct but rather complicated spectrum is immediately formed, see Fig. 5. This spectrum is not stable but in a couple of hours changes into one where the main absorption maxima are at slightly longer wavelengths. The concomitant disappearance of a weak

absorption at 630 mμ indicates that some ferrimyoglobin is slowly transformed into the ferronitrosyl compound, which itself is stable for many hours in the neutral solution. At pH 10 the ferro-nitrosyl compound is formed immediately. but in the presence of excess NO it is completely transformed into the ferro-myoglobin NO-compound in less than two hours. The latter can be formed directly from ferromyoglobin and NO at pH 10 and also at pH 7. All the main features of these reactions of myoglobin are compatible with a structure where the haem is more exposed than in cytochrome c.

It is very interesting to compare the absorption maxima of the compounds listed in Table 1. Changing the ligand to the reduced haem iron from NO^+ to CO and then to NO the general trend is that the wavelengths of the α- and β-bands increase slightly, while the γ-band remains constant or is somewhat shifted towards shorter wavelengths. Both NO^+ and CO have empty orbitals and are capable of forming a weak double bond with the iron, thus pulling electrons away from the iron. The effect of the positively charged NO^+ will be more pronounced than for the neutral CO. NO is not capable of forming a double bond, because there is no empty orbital, and its effect will be even smaller. The pull on the electrons will be transmitted from the iron out through the conjugated bond system of the porphyrin. The excitations corresponding to the α- and β-bands are believed to be associated with a charge-redistribution resulting in a shift of the electrons towards the perifery of the porphyrin disc [16]. The pull on the electrons exerted by a ligand at the iron will make these excitations more difficult and hence will shift the bands towards shorter wavelengths, as observed. The γ-excitation is associated with less pronounced charge-redistribution [16], the direction of which cannot be settled with certainty from the data of the γ-bands in Table 1.

Acknowledgement. The authors wish to thank Professor H. Theorell for his stimulating interest in the work, and one of us (T.S.) wishes to thank Professor Theorell for his kind hospitality.

REFERENCES

1. Keilin, D. and Hartree, E. F. *Nature* **139** (1937) 548.
2. Szczepkowski, T. W. *Acta Biochim. Polon.* **2** (1955) 343.
3. Keilin, J. *Biochem. J.* **59** (1955) 571.
4. Coryell, C. D., Pauling, L. and Dodson, R. W. *J. Phys. Chem.* **43** (1939) 825.
5. Paléus, S. and Neilands, J. B. *Acta Chem. Scand.* **4** (1950) 1024.
6. Tuppy, H. and Paléus, S. *Acta Chem. Scand.* **9** (1955) 353.
7. Theorell, H. and Ehrenberg, A. *Arkiv Fysik* **3** (1951) 299.
8. Ehrenberg, A. *Unpublished.*
9. Boeri, E., Ehrenberg, A., Paul, K. G. and Theorell, H. *Biochim. et Biophys. Acta* **12** (1953) 273.
10. Griffith, J. S. *Biochim. et Biophys. Acta* **28** (1958) 439.
11. Ehrenberg, A. and Theorell, H. *Acta Chem. Scand.* **9** (1955) 1193.
12. Orgel, L. E. *Symposium on Haematin Enzymes*, Canberra (1959).
13. George, P. and Irvine, D. H. *Biochem. J.* **60** (1955) 596.
14. Theorell, H. and Ehrenberg, A. *Arch. Biochem. Biophys.* **41** (1952) 442.
15. Brill, A. S., Ehrenberg, A. and den Hartog, H. *Biochim. et Biophys. Acta* **40** (1960) 313.
16. Falk, J. E. and Perrin, D. D. *Symposium on Haematin Enzymes*, Canberra (1959).
17. Theorell, H. and Åkeson, Å. *J. Am. Chem. Soc.* **63** (1941) 1812.
18. Keilin, D. and Hartree, E. F. *Proc. Roy. Soc. (London)* **B121** (1936) 173.

Received June 8, 1960.

ACTA CHEMICA SCANDINAVICA 14 (1960) 1693–1700

The Isolation of Prostaglandin F from Sheep Prostate Glands

SUNE BERGSTRÖM and JAN SJÖVALL

Department of Chemistry, Karolinska Institutet, Stockholm, Sweden

A smooth muscle stimulating factor present in vacuum-dried sheep prostate glands has been isolated in crystalline form. The formula $C_{20}H_{36}O_5$ has been suggested.

Goldblatt [1] and U. S. von Euler [2,3] described the presence of a smooth muscle stimulating and blood pressure reducing activity in sperm and in extracts of the prostate glands of certain species. The activity was ascribed to a factor named "Prostaglandin" by von Euler, who made studies on the distribution of this type of activity in various organs and species. He also made extensive physiological studies on a concentrate prepared from sheep prostate glands [4–6].

This raw material was used by Bergström [7] for further concentration of the factor. We have continued this work and have succeeded in isolating a crystalline compound, PGF, from vacuum-dried sheep prostate glands. This compound has a stimulating effect on smooth muscles of rabbit intestinal strips but does not show any effect on the blood pressure of rabbits. This paper describes the isolation procedure and some of the properties of the compound. The isolation of a second factor from frozen sheep prostate glands is described in a following paper.

EXPERIMENTAL AND RESULTS

Starting material. The glands (*glandula vesicalis*) located in the area where the urethra leaves the bladder, were removed at slaughter, immediately frozen in dry ice and stored at —20°C. They were then ground through a quarter-inch plate in a semifrozen condition and promptly dried in a vacuum mixer. The dehydrated material was then shipped to our laboratory and stored at —20°C for several years before being processed. Only this type of starting material was used for the work described in this paper.

We are greatly indebted to Dr. Walter Lundberg of the Hormel Institute, to Mr. Murphy, and Hormel & Co., Austin, Minn. U.S.A., for the collection of the sheep prostate glands used in this investigation.

Extraction procedure. During the various stages of the isolation procedure, the physiological activity was determined on duodenal intestinal strips of rabbits in a bath of 30 ml (*cf.* Ref.[5]).

The dried glands were suspended with a mechanical stirrer in 4 liters of tap water per kg of dried glands and 15 min later 12 liters of 95 % ethanol were added. The suspension was stirred mechanically for about one hour and then left to sediment overnight. The supernatant, clear, ethanol solution was siphoned off and the insoluble residue strained through cheese cloth and filtered. The combined extracts were evaporated *in vacuo* to about one twentieth of their original volume.

This crude extract was first extracted once with its own volume of ether. The aqueous phase was then acidified to about pH 3.5 with 6 N hydrochloric acid and extracted once with its own volume and then twice with half the volume of ether. The aqueous phase was discarded and the combined ether extracts were extracted 6 times with half the volume of 0.2 M sodium phosphate buffer of pH 8. During the first extraction, the pH of the buffer had to be adjusted back to pH 8 with 2 M sodium carbonate. The ether phase was discarded and the combined buffer phases were acidified to pH 3 with hydrochloric acid. They were extracted once with one volume of ether and then twice with half the volume of ether. The aqueous phase was discarded. The combined ether extracts were washed until free of chloride ions with small portions of water, each of which passed a second ether phase. The combined ether phases were then evaporated to dryness *in vacuo* leaving a dark, brown paste.

Preliminary purification. The residue obtained as described in the previous section was subjected to a five or ten-stage counter-current distribution between equal volumes (200 ml per 5 g of extract) of ether and 0.5 M sodium phosphate buffer pH 6.4. The buffer phases were acidified and extracted three times with ether. All the phases were evaporated and weighed and the physiological activity of each phase was determined. An example of a five-stage, counter-current distribution is given in Table 1, though a ten-stage procedure is more efficient and has more often been used.

Table 1.

Phase number	Weight (g)	Physiological activity Relative units per phase	per mg
Ether 1	6.40	7 200	1
» 2	0.80	2 200	3
» 3	0.25	1 300	5
» 4	0.15	1 000	7
» 5	0.10	1 200	12
Buffer 5	0.06	1 700	28
» 4	0.05	1 900	38
» 3	0.05	2 400	48
» 2	0.06	2 200	37
» 1	0.80	2 100	3

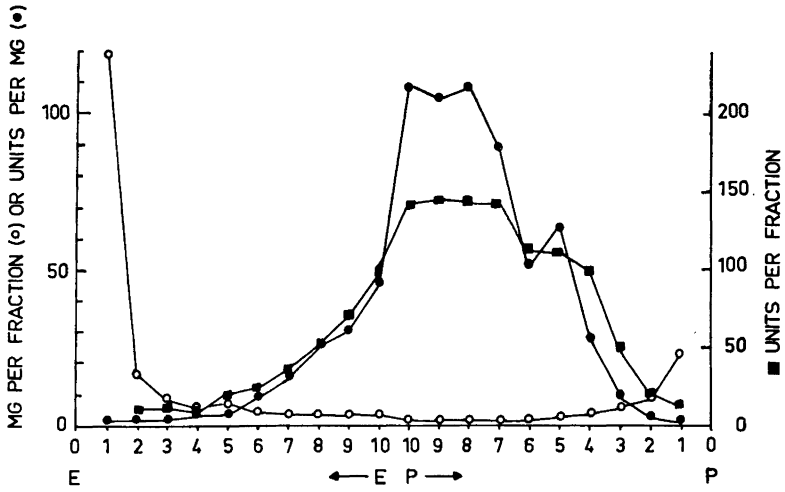

Fig. 1. Purification of PGF with a ten-stage, counter-current distribution of the crude extract of prostate glands. E = ether phases, P = buffer phases.

The material corresponding to that contained in ether 4 to buffer 2 was combined and used for the further purification of PGF. Different lots of prostate glands gave somewhat different distributions of physiological activity in the counter-current distribution procedure. The activity in the earlier ether phases only occurred in certain batches of dried glands apparently due to the handling during collection and drying. In Fig. 1 a ten-stage distribution of material that did not contain any activity in the first ether phases is

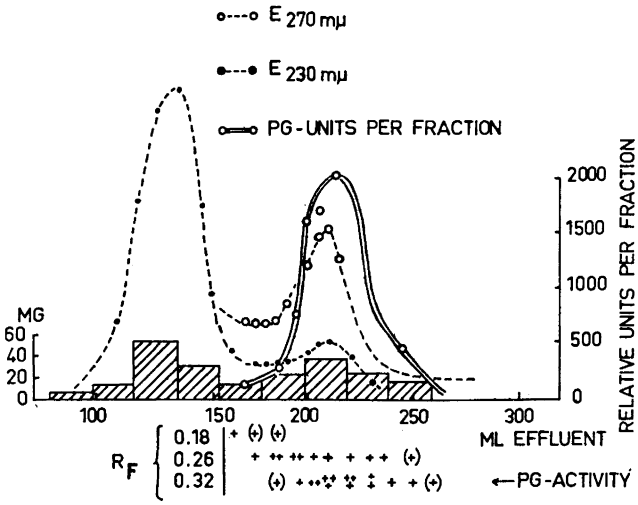

Fig. 2. Reversed phase chromatography of material (prostaglandin concentrate, sheep) from the countercurrent distribution. For explanations see text.

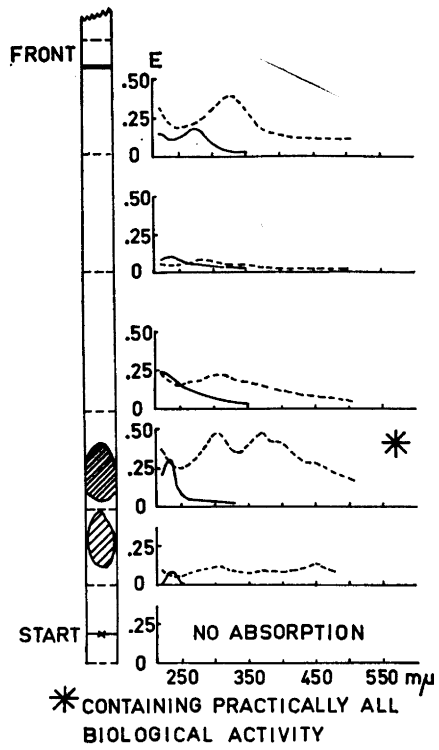

Fig. 3. Paper chromatographic analysis of the active material obtained after the purification with reversed-phase chromatography. For explanations see text.

shown. A study of the more lipophilic factor will be described in a following paper.

First partition chromatography. The material from the phases ether 4 to buffer 2 in a five-stage, counter-current distribution, or the corresponding phases in a ten-stage procedure, was subjected to reversed phase partition chromatography. 300 ml of 50 % (v/v) methanol/water was equilibrated with 30 ml of 50 % (v/v) *iso*octanol/chloroform in a separatory funnel. 4 ml of the less polar phase were supported on 4.5 g of hydrophobic Supercel (silane treated kieselguhr) which was then slurried in the aqueous phase, poured into a chromatography tube and allowed to settle. A one cm layer of sand was put on the top of the column. About 100 mg of the material was then dissolved in the smallest possible amount of moving phase and added onto the top of the column. When larger amounts of material were run, the size of the column was correspondingly increased and it was found that columns with 90 g of Supercel gave good results with 2—3 g of material.

A typical result of a chromatographic separation with an 18 g column is shown in Fig. 2. Besides the distribution of physiological activity (determined in every third fraction) and weight, the light absorption at 270 and 230 mμ of diluted aliquots of the fractions are shown.

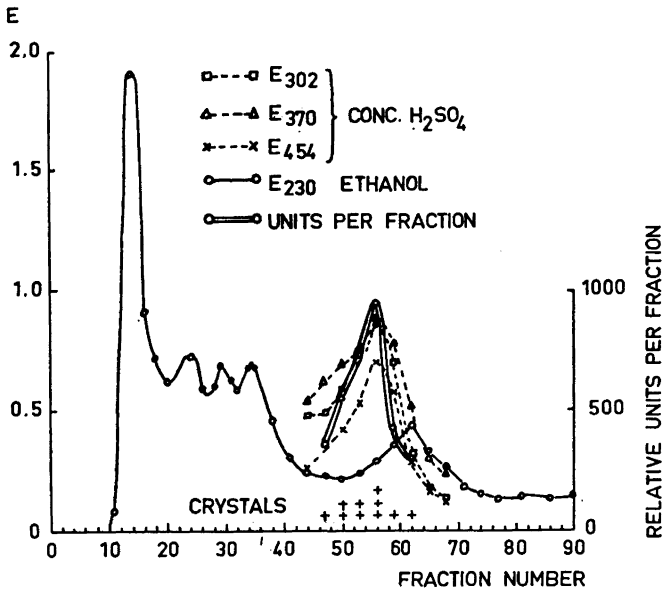

Fig. 4. Chromatography with the acid solvent system of the active material (purified PG) obtained after reversed-phase chromatography. For explanations see text.

Paper chromatography. The phase system used for the paper chromatography of prostaglandin concentrates has been utilized before for the separation of bile acids [8,9]. Ethylene chloride/heptane 50/50 was used as moving phase after equilibration with an equal volume of 70 % (v/v) acetic acid/water. A suitable aliquot of the fractions (usually about 50 μg of material) was put on the starting line of the filter paper (Whatman 3 MM). After equilibration overnight in the chromatographic tank in the vapors of both phases, the papers were brought into contact with the moving phase and developed for 6 h using the ascending technique. After drying, the papers were sprayed with a 15 % ethanolic solution of phosphomolybdic acid. Heating for a few minutes at 80°C revealed blue spots on the chromatograms. Ethanol elution of zones on unsprayed papers, corresponding to these spots, revealed that practically all of the physiological activity was confined to the zone of one of the spots. The results of paper chromatographic analyses of fractions from the chromatography shown in Fig. 2 are shown in the same figure below the chromatogram. The R_F values of the spots varied in different runs, but the relative position of the spots and the physiological activity was unchanged.

The fractions from the reversed-phase partition chromatography that contained the physiological activity were combined. Aliquots of this material were used for a spectrophotometric analysis after paper chromatography, according to the method described by Sjövall [9]. Paper chromatography, with the phase system described above, was performed on washed filter paper strips with purified solvents. After the development of the chromatograms, unsprayed

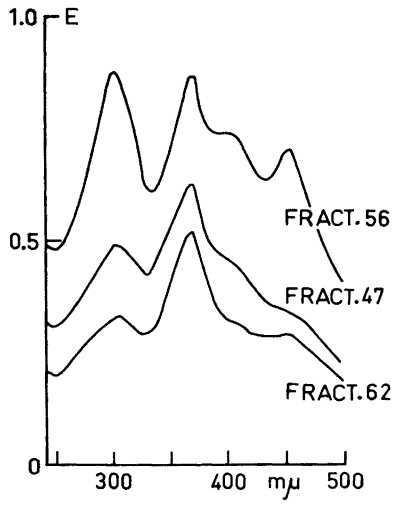

Fig. 5. Sulphuric acid spectra of active material (fractions from K 25) from the chromatography shown in Fig. 4. The fraction numbers refer to this figure.

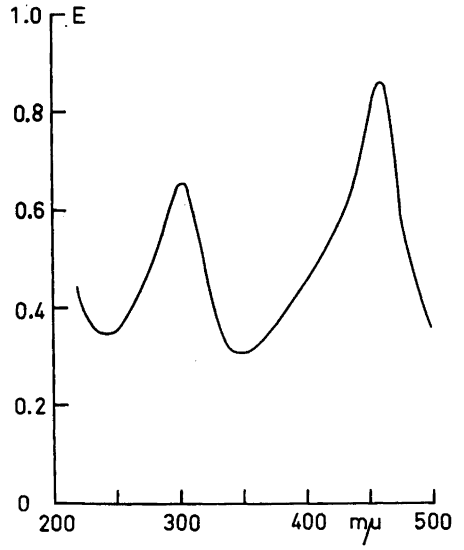

Fig. 6. Sulphuric acid spectrum of crystalline PGF, (31.2 μg after 2 h at room temperature in 1 ml conc. H_2SO_4).

strips were cut into pieces with the guidance of the spots on the sprayed strip. These pieces were eluted with ethanol and the eluates evaporated to dryness *in vacuo*. Light absorption spectra were then recorded in ethanol solution and in 96 % sulphuric acid after 2—3 h at room temperature. An automatic spectrophotometer (Perkin-Elmer, Spectracord 4 000) was used. The physiological activity of the eluates was also determined; the results of a typical analysis are shown in Fig. 3. The area containing the physiological activity had a typical sulphuric acid spectrum, and corresponded to a blue spot obtained with phosphomolybdic acid.

Second partition chromatography. It was evident (Fig. 3) that the material from the reversed-phase partition chromatography was inhomogeneous. A column chromatography with an acid solvent system was therefore developed. Ethylene chloride/heptane 50/50, after equilibration with 1/3 of its volume of acetic acid/water 60/40 was found to be a suitable moving phase. 4 ml of the acetic acid/water phase were supported on 4.5 g of Hyflo Supercel and served as stationary phase. The column was prepared as described for the reversed phase column. 50 mg of the material from the reversed-phase partition chromatography were run on a column of this size. With larger amounts, the column was correspondingly increased. The material was transferred onto the top of the column dissolved in the smallest possible amount of moving phase.

Fig. 4 illustrates a run of about 200 mg of material on a column with 18 g of Supercel. The peak of physiological activity appeared at approximately 280 ml effluent. Suitable aliquots of every third fraction were evaporated to

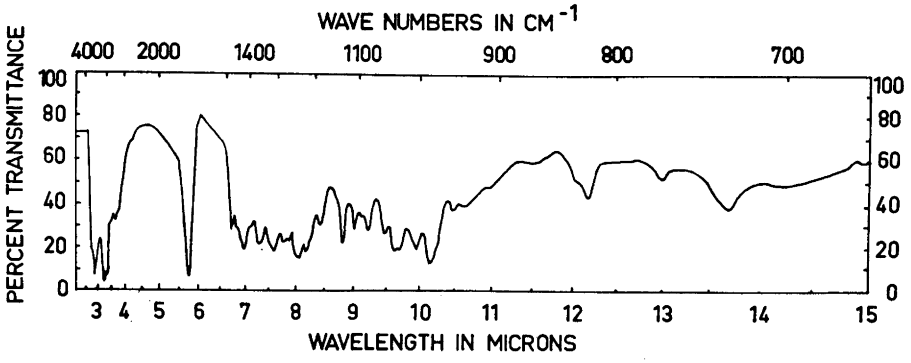

Fig. 7. Infrared spectrum of the methyl ester of PGF (KBr disc).

dryness *in vacuo* and were dissolved in one ml of ethanol. The U.V. spectra were recorded and it was found that most fractions had an absorption maximum at 230 mμ. The extinction of the different fractions at this wavelength is shown in Fig. 4. It is evident that there is no correlation to the physiological activity. One-thirtieth of each of these fractions was then evaporated to dryness and dissolved in 1 ml of 96 % sulphuric acid. After 2—3 h at room temperature, the U.V. spectra were recorded. The spectra of fractions at the beginning, middle and end of the band of physiological activity are shown in Fig. 5. Three absorption maxima are found at 302, 370 and 454 mμ, respectively, and the extinctions at these wavelengths are recorded in Fig. 4. As seen from Fig. 5, the band of physiological activity does not consist of a pure compound since the ratios between the extinctions at the three maxima are different in the beginning, middle and end of the band. The best correlation between activity and light absorption was found for the maxima at 320 and 454 mμ.

Paper chromatography of aliquots of the fractions showed just one spot with the phosphomolybdic acid reagent and physiological activity was confined to the same zone as this spot. By making spot tests with approximately 20 μl of the effluent from the acetic acid columns, the material containing the physiological activity could be detected. This method was sometimes used instead of testing on intestinal strips.

Crystallization. After evaporation in a vacuum oven at 50°C, the fractions containing the main part of the physiological activity crystallized partly in needle-shaped crystals. The relative distribution of crystals is shown in Fig. 3. The amount of crystals in each tube was less than 1 mg in this run.

The crystals were found to be relatively insoluble in ether. Trituration of each fraction with a few drops of ether at 0° dissolved the oily substance, leaving most of the crystals. After pipetting off the ether, the crystalline residues were combined and recrystallized several times from ethyl acetate/light petroleum until a constant m.p. of 102—103°C was reached. The crystals were small, colourless needles. In all, we have had about 20 mg of this material. The sulphuric acid spectrum of pure PGF is shown in Fig. 6.

Elementaly analysis yielded the following results:

		C	H	O	N
Found:		67.2	10.0	22.6	0.0
Calc. for	$C_{20}H_{32}O_5$ (352.45)	68.2	9.2	22.7	
	$C_{20}H_{34}O_5$ (354.47)	67.8	9.7	22.6	
	$C_{20}H_{36}O_5$ (356.49)	67.4	10.2	22.4	

CHN-analysis was done with an ultramicro gasometric technic by Dr. W. Kirsten, Uppsala, and oxygen determinations by Dr. K. J. Karrman, Lund.

A titration of 2.50 mg in 50 % ethanol yielded a curve indicating a pK of 6.3 and an equivalent weight of 357 ($\pm$ 20).

A titration of cholic acid under the same conditions yielded the half equivalent point at 6.3 and an equivalent weight of 412 (calc. 409).

A microhydrogenation in ethanol-acetic acid and Adams-Shriner platinum catalyst at room temperature resulted in the uptake of slightly more than one mole of hydrogen per an assumed molecular weight of 356.

The infrared spectrum of the methylester is shown in Fig. 7.

Dr. Sixten Abrahamsson, Uppsala, has kindly determined the interplanar spacings by X-ray diffraction of crystalline PGF. The values obtained were as follows (Ångström units; intensities put in brackets with the scale *v*ery *s*trong, *s*trong, *m*edium, *w*eak, *v*ery *w*eak): 16.44 (s), 9.46 (w), 8.16 (w), 6.19 (m), 5.46 (m), 5.05 (m), 4.71 (vw), 4.63 (vs), 4.54 (m), 4.46 (m), 4.08 (m), 4.02 (s), 3.74 (w), 3.56 (w), 3.45 (vw), 3.07 (vw), 2.93 (w), 2.80 (w), 2.67 (vw), 2.56 (vw), 2.48 (vw), 2.39 (vw), 2.34 (vw) 2.02 (w), 1.48 (w).

One mg of the compound was treated with diazomethane and the resulting methyl ester subjected to cracking in a mass spectrometer (Dr. R. Ryhage, Stockholm). The masspectrum indicated a molecular weight of 356 for PGF. The details will be discussed in a forthcoming publication.

The results obtained would thus suggest the compound to be an unsaturated acid with the formula $C_{20}H_{36}O_5$.

Acknowledgements. The technical assistance of Mr. L. Krabisch, Miss Anita Ivarsson and Miss Berit Persson is gratefully acknowledged.

REFERENCES

1. Goldblatt, M. W. *Chem. & Ind. London* **52** (1933) 1056.
2. v. Euler, U. S. *Arch. exptl. Pathol. Pharmakol. Naunyn-Schmiedeberg's* **175** (1934) 78.
3. v. Euler, U. S. *J. Physiol.* **84** (1935) 21P.
4. v. Euler, U. S. *J. Physiol.* **88** (1936) 213.
5. v. Euler, U. S. *Skand. Arch. Physiol.* **77** (1937) 96.
6. v. Euler, U. S. *Skand. Arch. Physiol.* **81** (1939) 65.
7. Bergström, S. *Nord. Med.* **42** (1949) 1465.
8. Sjövall, J. *Arkiv. Kemi* **8** (1955) 299.
9. Sjövall, J. *Arkiv Kemi* **8** (1955) 317.

Received June 16, 1960.

ACTA CHEMICA SCANDINAVICA 14 (1960) 1701–1705

The Isolation of Prostaglandin E from Sheep Prostate Glands

SUNE BERGSTRÖM and JAN SJÖVALL

Department of Chemistry, Karolinska Institutet, Stockholm, Sweden

A smooth muscle stimulating and blood pressure depressing factor present in sheep prostate glands — Prostaglandin E — has been isolated in crystalline form. The most likely formula is $C_{20}H_{34}O_5$.

We have described the isolation of prostaglandin F from vacuum dried sheep prostate glands in the preceding paper [1].

In that work it was noticed that a more lipid soluble factor was sometimes present which showed activity both on intestinal strips and on rabbit blood pressure. It has been found that this fraction is responsible for most of the activity of the fresh or frozen glands.

The isolation of this factor, prostaglandin E (PGE) in crystalline form, will be described in this paper.

EXPERIMENTAL AND RESULTS

Starting material. Frozen sheep prostate glands were obtained from various slaughter houses.

Extraction procedure. The frozen glands were minced in a meat grinder. After addition of 4 liters of 95 % ethanol per kg, the suspension was stirred mechanically for one hour and then left to sediment over night. The extract was separated and concentrated as described in the preceding paper [1]. The crude concentrate was then extracted into ether and transferred into phosphate buffer as described in the same paper.

Partition chromatography. In this work, we left out the counter-current distribution procedure for the preliminary purification of the crude extract. Instead, this extract was directly subjected to reversed-phase chromatography with 50 % methanol/water as moving phase and 50 % *iso*octanol/chloroform as stationary phase, supported on Hostalen (Hoechst). In most cases the extract from 12.5 kg of prostate glands weighed 5—7 g and this material was put on a column with 67 ml of stationary phase on 100 g of Hostalen. The result of such a chromatography is shown in Fig. 1. The peak of physiological activity appeared at about 1.5 l effluent. This position varied somewhat depending

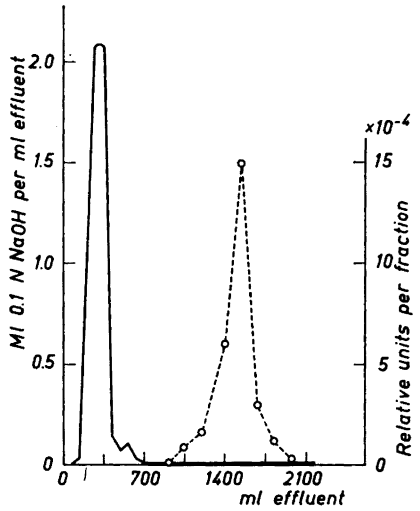

Fig. 1. Reversed phase partition chromatography of the crude extract of prostate glands.

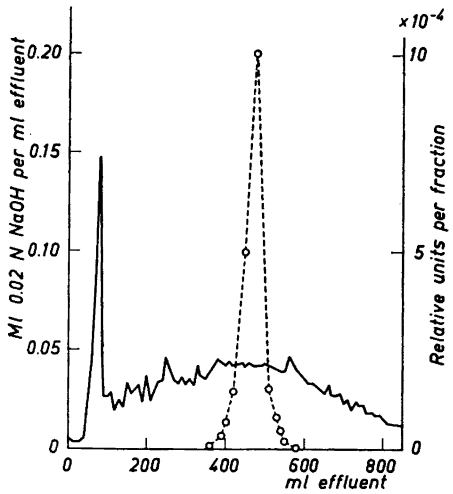

Fig. 2. Reversed phase chromatography of the active material obtained from the chromatography shown in Fig. 1.

upon the amount of material put on the column. Good separations have been obtained with 24 g of extract put on a column with 200 g of Hostalen. A 10 to 30-fold purification of the active material was obtained with the reversed phase chromatography.

The material obtained was found to lower rabbit blood pressure. This effect is not obtained with previously isolated PGF. It was found, however, that PGE, although being eluted somewhat later than PGF, was not separated from this compound. Therefore, a second reversed-phase chromatography was run using 35 % (v/v) methanol/water saturated with 1/10 of its volume of 40 % (v/v) *iso*amyl acetate/chloroform as moving phase. The hydrophobic phase was used as stationary phase, 4 ml being supported on each 4.5 g of silane treated kieselguhr. With this system, PGF is eluted just after the front, separated from PGE which is eluted at about 50 ml effluent from a 4.5 g column. For preparative purposes, 250—500 mg of material from the first chromatography were usually run on a column with 45 g of hydrophobic kieselguhr. Columns with up to 200 g of kieselguhr have been used for separation of larger amounts of material (3 g). Fig. 2 shows the chromatogram of the active material obtained from the chromatography shown in Fig. 1. No activity was found at the place of PGF in this case and an approximate 4-fold purification was obtained.

Paper chromatography. During the chromatographic purifications, paper chromatography was used to test the purity of the fractions eluted from the columns. This method was described in the preceding paper [1]. PGE was found to move somewhat faster than PGF on the chromatograms and clearly separated from this compound. However, attempts to use the column chroma-

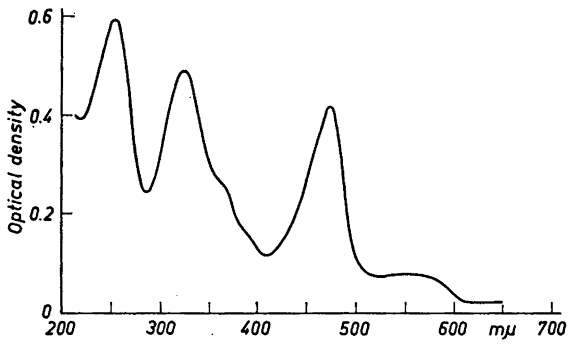

Fig. 3. Absorption spectrum of 40 μg of PGE after 85 min in 96 % sulphuric acid.

tography with acid solvent systems [1] for the preparative separation of PGF and PGE failed; the compounds being eluted together in one peak with a displacement of only a few fractions. Paper chromatograms of the fractions from the second reversed-phase chromatography showed the highest purity of PGE in the last part of the peak of activity. Besides PGE, the first part of the active peak contained a compound giving a spot on the chromatograms between the positions of PGE and PGF.

Crystallization of prostaglandin E. The fractions from the second reversed phase chromatography, containing the last half of the active band, were combined as also were those containing the first half. After evaporation to dryness *in vacuo*, the residues were dissolved in a few ml of ethyl acetate and allowed to stand overnight at room temperature. Needle-shaped crystals were usually obtained from the material contained in the last half of the active band in contrast to the material from the first half of this band. The latter material, from several chromatograms, was therefore again subjected to reversed phase chromatography with 35 % methanol as moving phase and 40 % *iso*amyl acetate/chloroform as stationary phase and crystallization procedure repeated. In some cases, the noncrystalline material was subjected to chromatography with the acid solvent system [1] prior to the second reversed phase chromatography.

The crystalline material was recrystallized several times from ethyl acetate and ethyl acetate/heptane until a constant m.p. of 115—117°C was reached. The sulphuric acid spectrum [1] of the crystalline compound is shown in Fig. 3.

Ultramicro C, H analysis and oxygen determinations yielded the following results:

Found	C 68.0	H 9.7	O 22.9
Calc. for $C_{20}H_{34}O_5$:	67.8	9.7	22.6

C, H analysis was done with an ultramicro gasometric technique by Dr. W. Kirsten, Uppsala, and oxygen determinations by Dr. K. J. Karrman, Lund.

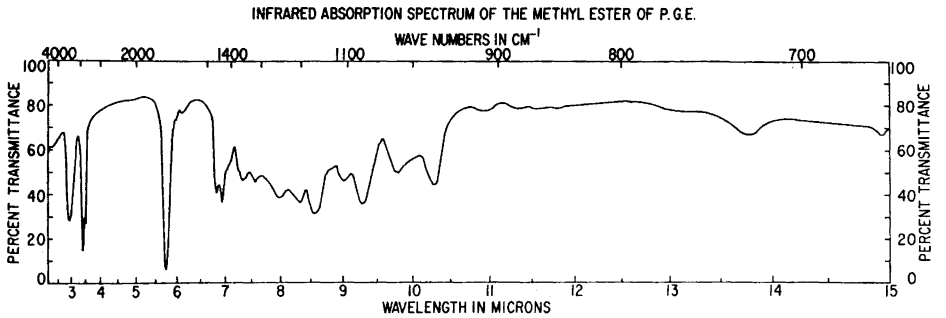

Fig. 4. Infrared spectrum of the methyl ester of PGE (KBr disc).

A microtitration curve obtained in 50 % ethanol indicated a pK of 6.5 and a molecular weight of 350 ± 20.

The methyl ester was prepared from one mg of the compound and subjected to cracking in a mass spectrometer (Dr. R. Ryhage, Stockholm). The results indicated a molecular weight of 354.

In a single crystal X-ray study done for us by Dr. S. Abrahamsson, Uppsala, it was found that there were eight molecules per unit cell. The unit cell dimensions were: $a = 8.23 \pm 0.04$; $b = 19.4 \pm 0.1$; and $c = 25.9 \pm 0.1$ Å. The specific gravity, as determined by flotation in potassium bromide solution, was 1.135 g/cm^3. These results give a molecular weight of 353 ± 5.

The interplanar spacings in Ångström units obtained by X-ray diffraction of crystalline PGE (Dr. S. Abrahamsson, Uppsala), were as follows (the intensities are denoted with *v*ery *s*trong, *s*trong, *m*edium, *w*eak, *v*ery *w*eak): 13.00 (s), 6.45 (vw), 6.13 (vw), 5.80 (w), 5.75 (m), 5.01 (m), 4.26 (vw), 4.20 (vw), 4.14 (vs), 3.97 (s), 3.91 (m), 3.75 (vw), 3.48 (w), 3.25 (w), 3.18 (w), 3.06 (w), 2.87 (vw), 2.75 (w), 2.65 (vw), 2.59 (vw), 2.50 (w), 2.44 (vw), 2.39 (vw), 2.38 (vw), 2.35 (vw).

The infrared spectrum of the methyl ester of PGE is shown in Fig. 4.

In a microhydrogenation of PGE in ethanol-acetic acid and Adams-Shriner platinum catalyst at room temperature, hydrogen was taken up corresponding to approximately one mole of hydrogen per molecule of 354.

The results, taken together, strongly indicate a C_{20} formula. The elementary analysis, the mass spectrometer data, and the X-ray data together support the formula $C_{20}H_{34}O_5$ (354.5). The C values obtained are a little low, but ultramicro analysis of cholic acid also yielded carbon values that were about 0.5 % low.

The mass spectrometer data indicate that the peaks at 332 and 350, differing by 18 units, correspond to fragments of the methyl ester that have lost two and one molecule of water, respectively. The whole ester molecule would then have the weight 368 and the corresponding free acid a molecular weight of 354. This is also made very likely by the mass spectra of the ethyl ester.

Results of investigations of the physiological activity of PGE have been published separately [2,3].

Acknowledgements. The technical assistance of Mr. L. Krabisch, Miss Anita Ivarsson and Miss Berit Persson is gratefully acknowledged.

REFERENCES

1. Bergström, S. and Sjövall, J. *Acta Chem. Scand.* **14** (1960) 1693.
2. Bergström, S., Eliasson, R., v. Euler, U. S. and Sjövall, J. *Acta Physiol. Scand.* **45** (1959) 133.
3. Bergström, S., Dunér, H., v. Euler, U. S., Pernow, B. and Sjövall, J. *Acta Physiol. Scand.* **45** (1959) 145.

Received June 16, 1960.

ACTA CHEMICA SCANDINAVICA 14 (1960) 1706–1710

Smooth Muscle Stimulating Factors in Ram Semen

SUNE BERGSTRÖM, LENNART KRABISCH and JAN SJÖVALL

Department of Chemistry, Karolinska Institutet, Stockholm, Sweden

Extraction and chromatographic separation of lipid soluble, acidic material in ram seminal plasma has shown the presence of at least two different factors with smooth muscle stimulating and blood pressure lowering effects. One of the factors shows certain properties similar to those of the PGE previously isolated from sheep prostate glands.

The pharmacodynamic effects of extracts of seminal fluid and male accessory glands of humans and some animal species were observed independently by Goldblatt [1] and U.S. von Euler [2,3]. The active principle was called prostaglandin.

We have recently described the isolation of two factors, PGE and PGF, from the prostate glands of sheep in crystalline form [4,5]. The compound PGE predominates in the extracts of frozen glands, while roughly equal amounts of the two compounds were found in vacuum-dried glands.

In order to ascertain the nature of the active compounds present in the seminal plasma, we have made a preliminary study of the chemical properties of the physiologically active factors normally present in ram semen plasma.

EXPERIMENTAL AND RESULTS

Ram seminal plasma was obtained through the courtesy of Dr. T. Mann, Molteno Institute, Cambridge, to whom we are greatly indebted for his help. The ram semen had been collected at the A.R.C. Unit of reproductive Physiology and Biochemistry, Cambridge. The seminal plasma was obtained by centrifugation of 23 ejaculates (30 ml). The supernatant seminal plasma (24 ml) was precipitated with two volumes of 96 % ethanol and was sent by air mail to our laboratory.

Extraction and chromatography. The ethanolic solution was filtered and the precipitate washed several times with 96 % ethanol. About 150 ml of clear solution was obtained and evaporated *in vacuo* to a volume of a few ml After dilution to about 10 ml with water, the solution was acidified with hydrochloric acid to pH 3 and extracted three times with equal volumes of ether.

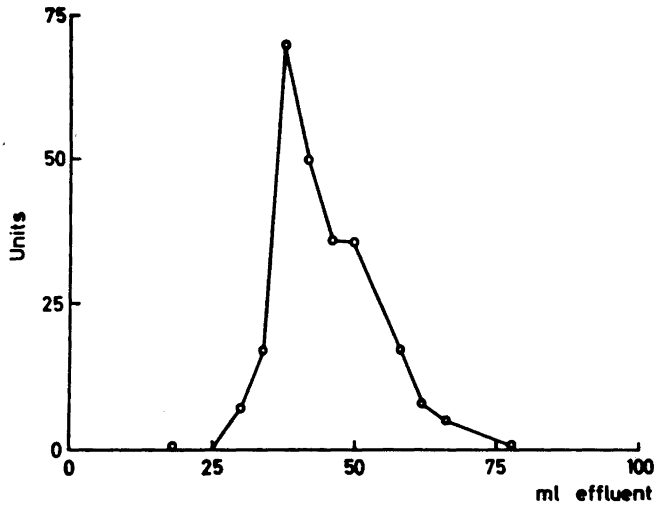

Fig. 1. First chromatography of the physiologically active material in ram seminal plasma.

The combined ether extracts were extracted twice with half the volume of 0.2 M sodium phosphate pH 8, the pH having been corrected to 8 with sodium carbonate during the first extraction.

The buffer solution was acidified to pH 3 with hydrochloric acid and extracted twice with equal volumes of ether. After washing with small portions of water, each of which was passed through a second ether phase, evaporation of the combined ether extracts left about one mg of residue.

This material was subjected to reversed-phase chromatography. 150 ml methanol, 150 ml water, 15 ml chloroform and 15 ml *iso*octanol were shaken in a separatory funnel and left to separate at 23°C. The less polar phase was used as the stationary phase; 3 ml were supported on 4.5 g of Hostalen (Hoechst) that had been purified by continuous ethanol extraction in a Soxhlet apparatus for two days. The column was prepared as described earlier [4]. The residue was dissolved in a few ml of the moving phase and transferred onto the top of the column. 100 ml of the moving phase were allowed to pass through the column and 2 ml fractions were collected. The activity of every third fraction was determined on duodenal intestinal strips; results are shown in Fig. 1. The activity appeared at the same place in the chromatogram as PGE and PGF which move together in this system. The testing was done against a standard of pure PGE, *1 μg being defined as one PGE rabbit intestinal unit.* The total activity corresponded to approximately 500 μg of PGE. The effect of the fractions at 34 and 58 ml effluent was tested on rabbit blood pressure and it was found that 2—4 intestinal units produced a distinct lowering of blood pressure.

The fractions between 25 and 75 ml effluent were combined and subjected to reversed-phase chromatography, using methanol/water/*iso*amylacetate/chlo-

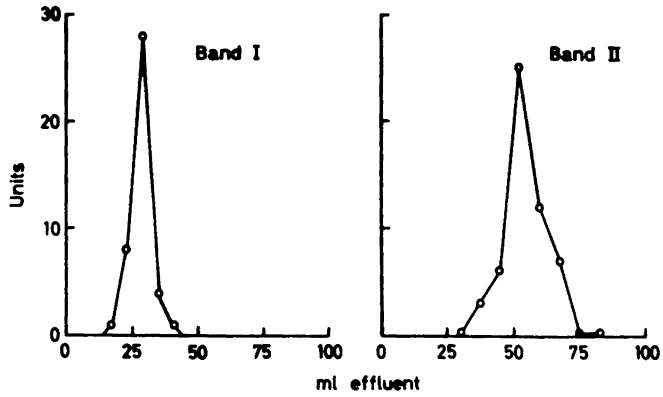

Fig. 2. Chromatography of the two active bands separated by chromatography of the active band shown in Fig. 1. See text.

roform (70/130/8/12/ (v/v)). Four ml of the less polar phase were supported on 4.5 g of silane treated hydrophobic Supercel. On testing the fractions on the intestinal strip, it was found that the activity had been separated into two bands. The peak of the first band appeared at 27 ml effluent and that of the second band at 56 ml effluent. Both bands contained material with a depressing effect on rabbit blood pressure.

The peak fractions of both the bands were used for paper chromatography with ethylene chloride/heptane 5:5 as moving phase and acetic acid/water 7:3 as stationary phase at a constant temperature of 23°C. After the developed chromatograms were sprayed and heated at 80° for a few minutes, one blue spot was revealed which had moved as PGE in the case of the second band and slightly slower in the case of the first one.

The fractions of each peak from the reversed-phase chromatography were then combined and rechromatographed with the same solvent system as that used for their separation (Fig. 2).

Spectroscopic properties. The peak fractions of the chromatograms shown in Fig. 2 were used for a study of the spectroscopic behaviour of the compounds in alkaline and acid solution. After evaporation of the solvents, the residues were dissolved in spectroscopically pure absolute ethanol and the U.V. spectra were recorded with an automatic spectrophotometer (Perkin-Elmer, Spectracord 4 000). The ethanol was then evaporated and the fractions dissolved in 0.01 N sodium hydroxide in 50 % ethanol and heated from 2 h at 100°C in sealed tubes. The U.V. spectra were again recorded against an appropriate solvent blank. After the addition of 50 μl of 0.1 N sodium hydroxide and having been heated for one hour at 100°C in sealed tubes, a third recording of the spectra was made. After addition of 0.5 ml of 4 N hydrochloric acid to each sample and having been heated at 100°C for one hour in sealed tubes, a final recording of the spectra was made.

The results with the peak fraction of band II (Fig. 2) are shown in Fig. 3. The original ethanolic solution of the substance showed a low, noncharacteristic

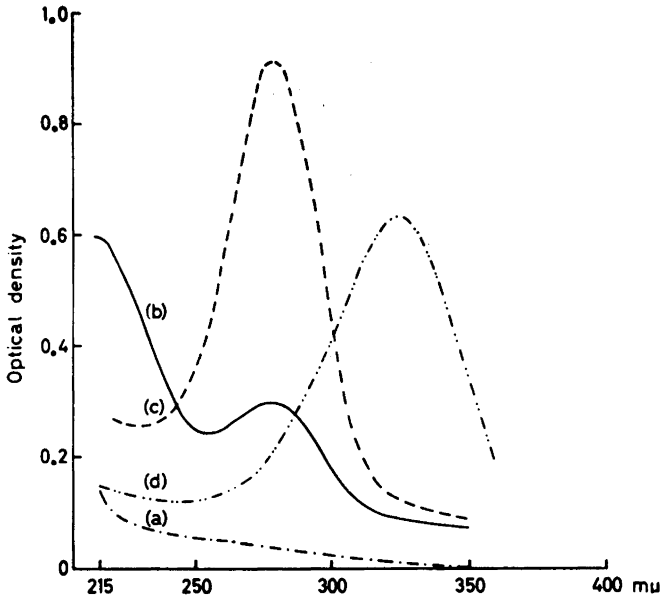

Fig. 3. Absorption spectra of the peak fraction of band II, Fig. 2: (a) in ethanol, (b) after 2 h at 100°C in 0.01 N NaOH, (c) after another hour at 100°C after addition of 50 μl of 0.1 N NaOH, (d) after another hour at 100°C after the addition of 0.5 ml of 4 N HCl. For further explanations see text.

increase of the extinction towards shorter wavelengths (Fig. 3a). After it was heated in 0.01 N sodium hydroxide, a large increase in the absorption at 215 mμ was observed and a lower maximum was present at 280 mμ (Fig. 3b). The latter band increased several times on reheating with more alkali, whereas the absorption at 215 mμ decreased (Fig. 3c). After heating in hydrochloric acid, the maximum at 280 mμ had disappeared and a new maximum at 325 mμ was found (Fig. 3d). All the changes observed are typical for PGE.

In the case of the peak fraction of band I (Fig. 2), no such typical changes in the spectra were found. There was only a noncharacteristic, continuous increase in extinction values towards lower wave-lengths, and heating in alkali and acid increased these values only slightly.

DISCUSSION

The extraction and the chromatographic separation of the lipid soluble, acidic material present in ram seminal plasma has shown that at least two different factors are present in comparable amounts, judging from the activity on intestinal strips from rabbits.

One of these behaves in the column chromatographic separations as well as on paper chromatograms, as the PGE isolated from sheep prostate glands. The purified fractions also show the same typical U.V. spectra on heating with

alkali and acid. The extinctions observed are in rough agreement with those expected from the biological activity.

The observed activity corresponds to a content of about 10 μg of PGE per ml of seminal plasma, *i.e.* the avarage content of prostaglandin E per ejaculate would be slightly higher.

The second active compound is likewise active, both on the intestinal strip on rabbit blood pressure, *i.e.* it is not identical with PGF which shows no activity on the blood pressure. It is furthermore differentiated from PGF by the absence of a maximum at about 225 mμ after being heated with acid. Possibly minor amounts of PGE may be present, but if so, the third physiologically active compound observed in this paper predominates.

This work has been supported by a grant from *Stiftelsen Gustaf och Tyra Svenssons Minne.*

REFERENCES

1. Goldblatt, M. W. *Chem. & Ind. London* **52** (1933) 1056.
2. v. Euler, U. S. *Arch. exptl. Pathol. Pharmakol. Naunyn-Schmiedeberg's* **175** (1934) 78.
3. v. Euler, U. S. *J. Physiol.* **84** (1935) 21 P.
4. Bergström, S. and Sjövall, J. *Acta Chem. Scand.* **14** (1960) 1693.
5. Bergström, S. and Sjövall, J. *Acta Chem. Scand.* **14** (1960) 1701.

Received June 16, 1960.

ACTA CHEMICA SCANDINAVICA 14 (1960) 1711–1716

A Specific Depression of the Reactivity of Peroxidase Complex II towards Donor Molecules by Substitutions in the Haem Group

BRITTON CHANCE and KARL-GUSTAV PAUL

Johnson Research Foundation, University of Pennsylvania, Philadelphia, Penn., U.S.A., and Biokemiska institutionen, Medicinska Nobelinstitutet and Karolinska institutet, Stockholm, Sweden

The substitution of the vinyl groups in the horse radish peroxidase protohaematin by acetyl groups has previously [1] been found to give decreased overall peroxidase activity. It is now demonstrated that the substitution affects the reaction between peroxidase-peroxide complex II and donor (k_4) whereas the rate of formation of complex I remains constant. The substitution has a greater effect upon the reactivity with uric acid than with ascorbic acid. The reason for the change in the complex II-donor reaction is briefly discussed. The experiment suggests a specific control of enzyme reactivity by side chain substitutions in the haematin.

For several reasons it has become of interest to determine the way in which the enzymic activity of horse radish peroxidase is affected by changes in the structure of its haem group. The initial studies of Theorell, Bergström and Åkeson [2] showed that successful recombinations with meso- or deutero-haematins and peroxidase apoprotein can be achieved. The activity with these haematins was found to be about half of that of the intact enzyme; a considerably higher activity with mesohaematin was, however, also reported [3]. Somewhat later monoazahaematin peroxidase was found to be one fifth as active as the intact enzyme [4]. Recently the activities of some of the previously studied artificial peroxidases were redetermined and in some cases also compared with the activities obtained with isomers of the haematins [1]. It is now well established that the propionic acid residues at the positions 6 and 7 are needed for the formation of an enzymatically active peroxidase [1,2,5]. Some 2,4-substitutions cause parallel shifts in peroxidase activity and pyridine haemochromogen spectrum [1]. Deuterohaematin is an exception, but its two free pyrrolic 2-positions may influence the activity. The homologue with three free 2-positions gave one tenth of the activity obtained with deuterohaematin itself [6].

Further studies of the artificial peroxidases are of interest also in view of the knowledge of haemoprotein structures now available through X-ray crystallography [7,8] and of the effect of haematin substitutions on the reactivity of myoglobin [9,10]. The fact that meso-, haemato-, and deuterohaematins but not diacetyldeuterohaematin can be utilized as growth factors by a haem-requiring *Staphylococcus* mutant [11] also will draw attention to the mechanism by which the artificial peroxidases differ.

In most determinations of the activity of reconstituted peroxidases, the purpurogallin test was used. A study of this reaction indicated the possibility of a rate-limiting step between the completion of the enzyme activity and the formation of coloured products [12]. Whereas such a slow step will not necessarily be of great consequence in determinations of protoperoxidase purity the situation may not be identical with substituted peroxidases. The mesidine test, used in some activity determinations, is at present being studied in the same way (B.C. *et al.*). A further complication is introduced by the fact that the over-all assays may measure either k_1 or k_4 according to the following equation [12]:

$$\frac{dx}{dt} = \frac{e}{(1/k_4 a) \times (1/k_1 x)} \qquad (1)$$

where k_1 and k_4 are defined below, a and x are the donor and peroxide concentrations and dx/dt is the rate of disappearance of x.

It is the purpose of this paper to study a reconstituted peroxidase of an activity sufficiently different from that of the protohaematin enzyme to permit the assigning of the decrease in activity to one or more steps in the following reaction mechanism (*cf.* Ref.[13]):

$$HRP + H_2O_2 \underset{k_2}{\overset{k_1}{\rightleftharpoons}} HRP - I + H_2O \qquad (2)$$

$$HRP - I + AH_2 \xrightarrow{k_7} HRP - II + AH^\circ \qquad (3)$$

$$HRP - II + AH_2 \xrightarrow{k_4} HRP + AH^\circ \qquad (4)$$

Diacetyldeuterohaematin peroxidase is such an enzyme [1].

MATERIAL AND METHODS

Horse radish peroxidase was prepared as previously described [14], and Fraction C was crystallized twice from ammonium sulfate solution. The preparation of the apoprotein and the coupling was performed as usual [5], ethanol being added to stabilize the haematin solutions in alkali [15]. After the chromatography on Dowex — 2 the concentrations of the reconstituted enzymes were determined by pyridine haemochromogen measurements [5].

The methyl peroxide solution was standardized by UV absorption as previously described [16]. Tenth molar acetate buffer of pH 4.6 and 26° were used in all experiments.

The stopped-flow apparatus [17] (optical path length 1 cm) was used to record the cycle of formation and disappearance of the enzymesubstrate intermediates. With this, a double-beam spectrophotometer [18] was used to record the absorbancy changes of the reactants, the wavelengths being set to the peak and trough values for the difference between the free enzyme and the secondary peroxidase complex, II. For protoperoxidase the appro-

priate wavelengths were 427 and 395 mμ, and for diacetyldeuteroperoxidase 415 and 388 mμ. The initial rate of the absorbancy change was measured from a mirror oscillograph recording and the full cycle of appearance and disappearance of the intermediate was recorded on a slower time scale (Fig. 1).

The peroxide was added to a solution containing the enzyme and the donor in the stopped-flow apparatus. This procedure was desirable since any trace of peroxide formed by autoxidation of the donor would be removed prior to testing the activity. The final concentration of haematin was 0.5 μM.

The molecular extinction coefficient of the protohaematin peroxidase was $\varepsilon = 108$ cm^{-1} mM^{-1} and that of the diacetyldeuterohaematin peroxidase was 71 cm^{-1} mM^{-1} at 403 and 405 mμ, respectively. The reconstituted protohaematin peroxidase gave this value whereas the unsplit material [14] gave 98 cm^{-1} mM^{-1}, both on the basis of pyridine haemochromogen measurements. $\varepsilon = 108$ has been used for the present calculations.

According to determinations in the split-beam recording spectrophotometer [19] the extinction coefficient of the secondary complex as measured at the pairs of wavelengths 427—395 mμ and 415—388 for proto- and diacetyldeuterhaemin peroxidases, respectively, were 84 and 59 cm^{-1} mM^{-1}. In the flow apparatus, however, where the absorbancy change is measured immediately after the reaction of peroxidase with donor and peroxide, the values were higher, 106 and 74 cm^{-1} mM^{-1}. These were used in calculating k_4 from the cycles of the intermediate compounds.

RESULTS

Typical experimental results are shown on the superimposed tracings of Fig. 1 which represents the formation and disappearance of complex II of protohaematin peroxidase (upper trace) in the presence of 7 μM uric acid and 1.5 μM methyl peroxide. Time proceeds from left to right and illustrates the reaction kinetics which ensue upon mixing peroxide with enzyme plus donor. The upward deflections of the traces indicate increases of absorbancy at 427 and 415 mμ, measured with respect to 395 and 388 mμ, respectively. The intermediate forms abruptly in both cases. In the case of protohaemin peroxidase the concentration of the intermediate falls to zero in a few seconds, the value of $t_{\frac{1}{2}\ off}$ being 4.8 sec. In the case of diacetyldeuterohaemin peroxidase $t_{\frac{1}{2}\ off}$ is 8 times larger (40 sec.).

A quantitative determination of the values of k_4 can be obtained from the formula [20,21]:

$$k_4 = \frac{x_o}{p_{max}\ t_{\frac{1}{2}\ off}\ [AH_2]} \qquad (5)$$

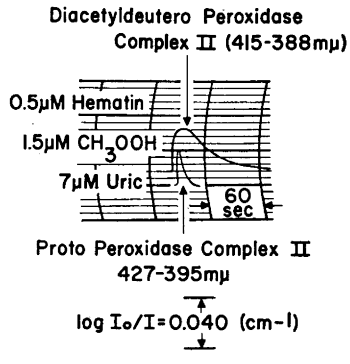

Fig. 1. Superimposed spectrophotometric records showing the kinetics of formation and disappearance of protohemin peroxidase and deuterohemin peroxidase, measured at the appropriate wavelengths indicated on the diagram. Time moves from left to right; an upward deflection of the trace corresponds to increased absorbancy at the longer wavelengths. 0.5 μM peroxidase, 0.1 M acetate buffer, pH 4.6, 26°C. Other conditions indicated on the diagram (Expts. 132 b—6,7).

Table 1. Comparison of the kinetics of proto- and diacetyldeuterohematin peroxidase (Expt. 132 b).

Hematin	Proto-	Diacetyl-deutero-	Proto-	Diacetyl-deutero-
λ(mμ)	427–395	415–388	427–395	415–388
(x_o) CH_3OOH (μM) Donor	1.5 Ascorbic acid	1.5 Ascorbic acid	1.5 Uric acid	1.5 Uric acid
(a_o) Donor concentration (μM)	10	10	7	7
p_{max} (μM)	0.31	0.28	0.26	0.43
$t_{\frac{1}{2}\ off}$ (sec)	5.0	20	5.0	40
$k_4 \times 10^4$ ($M^{-1} \times sec^{-1}$)	0.97	0.26	2.0	0.13
Rate of formation (μM/sec)	0.49	0.42	0.63	0.51

The values of k_4 calculated in Table 1 by eqn. 5 show that the ratio of the activities for proto- and diacetyldeuteroperoxidases is 15 with uric acid as the donor. Experiments carried out with ascorbic acid as the donor give a ratio of 3.7. It should be noted that the values of k_4 for protoperoxidase obtained in the presence of ascorbic acid are significantly less than those obtained with previous preparations [22]. No explanation is put forward for this difference at the present time.

The data of Fig. 1 show qualitatively the cause of the low reactivity of diacetyldeuteroperoxidase, namely that there is a higher steady-state concentration of complex II in this substituted peroxidase than in the natural one. This suggests that the formation of the intermediate is not a ratelimiting factor and that its decomposition is the rate-limiting factor.

Support for the idea that the rate of formation of the intermediates is not greatly affected by the substitution of the haematin is afforded by kinetic data obtained with the stopped flow method. The last row of Table 1 gives the rates of formation of the intermediates in μmoles per liter per second (μM/sec) in the four experiments. It can be seen that the values for diacetyldeuterohaematin peroxidase are between 80 and 85 % of those for the protohaematin enzyme.

Table 2. Values of k_4 as determined in open cuvettes.

	Ascorbic acid	Uric acid
	$k_4 \times 10^{-4}$ M^{-1} s^{-1} (S.D.,n)	
Protohaematin-HRP	0.62 ± 0.04 (6)	1.88 ± 0.52 (5)
Diacetyldeutero-haematin-HRP	0.12 ± 0.02 (3)	0.21 ± 0.01 (7)

In another series of experiments varying amounts of peroxide were added to a solution of peroxidase and donor in an open cuvette (Table 2). In this series the ratio of activities in the presence of ascorbic acid was 5 and in the presence of uric acid 9. Measurements of the overall reaction in terms of the formation of "tetraguaiacol" from guaiacol were also studied. When performed as previously described [23] the guaiacol test gave the values 2.86 and 2.56×10^4 M^{-1} sec^{-1}. Under these conditions the test gives mainly k_1 with some contribution from k_4.

DISCUSSION

In these experiments it has for the first time been possible to assign to a substitution of groups in the haematin of the peroxidase a depression of one of the three reaction velocity constants for the action of this enzyme (see eqns. 2—4). That this is a specific effect is clear from a comparison of the lifetime of complex II of the proto- and diacetyldeuterohaematin enzymes in the presence of equal concentrations of donor and peroxide, as shown by Fig. 1. When suitable corrections have been made for the actual amount of complex II present, these curves show a 15-fold decrease in the rate of reaction with uric acid and an approximately fourfold decrease in the reaction with ascorbic acid.

Several causes for the reduction in reactivity of complex II can be discussed. The possibility that the splitting procedure somehow altered the apoprotein is ruled out by previous investigations [1,2,4] as well as by the present experiments, in which both peroxidases were recombined from the same batch of apoprotein. An alternative explanation is presented by a comparison with kinetic studies on catalase [24] which suggested a limited accessability of complex I to donor molecules of increasing chain length. At that time related effects had not yet been observed with horse radish peroxidase. A consideration of the crystallographic data on metmyoglobin [8] indicates that its haematin might be of limited accessability and, of most importance, that the vinyl groups of the haematin could be a factor in determining the accessibility of the iron porphyrin group to large molecules [10]. Although no noticeable limitation to the accessibility of peroxidase haematin is observed with the native enzyme, the haematin configuration in the diacetyldeuteroperoxidase may represent a less favourable steric situation. However, dipropionyldeuterohaematin peroxidase showed approximately the same activity as the diacetyl enzyme in the quaiacol test. If steric effects account for the decrease in the rate of reaction one would expect an inhibition of the reaction of complex I with the donor molecule to form complex II, provided that the same reactive site is involved in this transformation. Further, an inhibition of the reactivity of the peroxidase to alkyl hydrogen peroxides of increasing chain length to form complex I would also be expected. Experiments on this point will be taken up.

Acknowledgement. This research has been supported by grants from the *National Science Foundation* and *Statens naturvetenskapliga forskningsråd.* K.G.P. is grateful for a grant from *Magn. Bergvalls stiftelse,* which enabled him to visit Philadelphia.

REFERENCES

1. Paul, K. G. *Acta Chem. Scand.* **13** (1959) 1239.
2. Theorell, H., Bergström, S. and Åkeson, A. *Arkiv Kemi* **16 A** (1942) No. 13.
3. Gjessing, E. C. and Summer, J. B. *Arch. Biochem.* **1** (1943) 1.
4. Theorell, H. and Maehly, A. C. *Acta Chem. Scand.* **4** (1950) 422.
5. Paul, K. G. *Acta Chem. Scand.* **12** (1958) 1611.
6. Paul, K. G., Gewitz, H.-S. and Völker, W. *Acta Chem. Scand.* **13** (1959) 1240.
7. Perutz, M. F., Rossman, M. G., Cullis, A. F., Muirhead, H., Will, G. and North, A. C. T. *Nature* **185** (1960) 416.
8. Kendrew, J. C., Dickerson, R. E., Strandberg, B. E., Hart, R. G., Davies, D. R., Phillips, D. C. and Shore, V. C. *Nature* **185** (1960) 422.
9. Rossi-Fanelli, A. and Antonini, E. *Arch. Biochem. Biophys.* **80** (1959) 299.
10. Kendrew, J. C. *Private communication.*
11. Paul, K. G. and Thofern, E. *Acta Chem. Scand.* **14** (1960) 1770.
12. Chance, B. *Arch. Biochem. Biophys.* **24** (1949) 410.
13. Chance, B. *Arch. Biochem. Biophys.* **41** (1952) 416.
14. Paul, K. G. *Acta Chem. Scand.* **12** (1958) 1312.
15. Maehly, A. C. and Åkeson, A. *Acta Chem. Scand.* **12** (1958) 1259.
16. Chance, B. *In Methods in Biochemical Analysis*, vol. 1 (D. Glick, Ed.) Interscience, New York 1954, p. 412.
17. Chance, B. and Legallais, V. *Rev. Scientific Instr.* **22** (1951) 627.
18. Chance, B. *Rev. Scientific Instr.* **22** (1951) 634.
19. Chance, B. *Science* **120** (1954) 767.
20. Chance, B. *J. Biol. Chem.* **151** (1943) 553.
21. Chance, B. *Arch. Biochem. Biophys.* **24** (1949) 389.
22. Chance, B. *Adv. Enzymol.* **12** (1949) 153.
23. Maehly, A. C. *Methods in Biochemical Analysis*, Vol. 1 (D. Glick, Ed.) Interscience, New York 1954, p. 357.
24. Chance, B. *J. Biol. Chem.* **179** (1949) 1341.

Received July 4, 1960.

ACTA CHEMICA SCANDINAVICA 14 (1960) 1717–1728

The Binding of DPNH by Liver Alcohol Dehydrogenase

ALBERT WITTER*

Medicinska Nobelinstitutet, Biokemiska avdelningen, Stockholm, Sweden

1. Pure horse liver alcohol dehydrogenase (LADH) contains 28 —SH groups/mole enzyme as determined spectrophotometrically with PCMB. There is no decrease in —SH groups after addition of DPNH or of DPNH and *n*-butyramide, the reaction with PCMB, however, being somewhat retarded in the latter case.

2. Incubation of LADH and LADH—DPNH with sulfhydryl reagents leads to a protection against inactivation in case of the enzyme-coenzyme complex as compared with enzyme alone.

The number of reacted —SH groups seems to be the same in both cases, however.

3. With PCMB as the sulfhydryl reagent the decrease in enzymatic activity and the decrease in bound coenzyme is about linear with increasing PCMB concentrations.

Only after complete reaction of the LADH with PCMB, the enzymatic activity and the coenzyme binding capacity become zero.

4. The role of the —SH groups in the working mechanism of LADH is discussed. The role of helping in maintaining the requisite ternary structure seems more likely than one of direct binding of coenzyme alone, but a combination of these roles is possible.

5. N(-4-Dimethylamino-3,5-dinitrophenyl)maleimide reacts with only about 30 % of the —SH groups, leading to a corresponding decrease in activity. The partly reacted LADH is precipitated by *iso*propanol (*ca.* 5 % v/v) as a deeply coloured product.

6. The inhibitory effect upon activity of *iso*propanol in higher concentration is probably due to oxidation of *iso*propanol by LADH and DPN.

7. Inactivation of LADH by Cd^{2+} is to a great extent prevented by DPNH and Zn^{2+}. This leads to the conclusion that: a) DPNH is bound directly via Zn to LADH, and b) the inactivation by Cd^{2+} is primarily caused by replacement of Zn by Cd, leading to a less active enzyme and secondarily to reaction with —SH groups.

In 1951 Theorell and Bonnichsen [1] considered the possibility of direct interaction between the —SH groups of LADH ** and its coenzyme. The absorb-

* Present address: Organisch Chemisch Laboratorium der Rijks-Universiteit, Bloemsingel 10, Groningen, Netherlands.

** The following abbreviations will be used: LADH = Horse liver alcohol dehydrogenase; DPN respectively DPNH = oxidized and reduced form, respectively, of diphosphopyridine-nucleotide; PCMB = *p*-chloromercuribenzoic acid; YADH = yeast alcohol dehydrogenase; NEM = N-ethyl maleimide; DDPM = N(-4-dimethylamino-3,5-dinitrophenyl)maleimide; μ = ionic strength.

tion maximum of DPNH at 340 mμ is replaced by a new absorbtion maximum at 325 mμ when LADH was added, because of the formation of an enzyme-coenzyme complex. Addition of PCMB, which inhibits the enzyme, immediately caused the absorbtion maximum to shift back to 340 mμ, the maximum of free DPNH.

This, together with the fact that a dissociable group with $pK' = 10$ was found to be involved in the binding of DPNH by the enzyme, lead to the aforementioned possibility.

Although the —SH groups in LADH definitely play a very important role in the working mechanism of this enzyme, there is no further evidence for its role being one of direct coenzyme binding. The finding that 2 Zn atoms are firmly bound by LADH and the fact that LADH is inhibited by metal binding agents such as 1,10-phenanthroline [2] indicate that Zn has a possible role in coenzyme binding [3]. This was stressed by the fact that both DPN and DPNH compete with 1,10-phenanthroline [4].

Other parts of the protein molecule cannot *a priori* be excluded as possible binding sites for the coenzyme, but the known inhibition of LADH by PCMB and 1,10-phenanthroline draws attention first of all to —SH groups and to Zn atoms.

Regarding the coenzyme, nearly all of the groups present in the coenzyme molecule (the carbonamide group, the pyridine nitrogen, the phosphate group, the adenine part) have been considered, as possible sites for binding to the protein molecule, especially in those papers dealing with speculative mechanisms for the action of the related enzyme YADH [3,8,15].

In this paper some experiments with LADH will be described which show the protective effect of coenzyme against some inhibitory —SH reagents.

EXPERIMENTAL

The LADH was prepared as described by Dalziel [5], and was stored at −15°C as a crystalline suspension in 30 % ethanol. After centrifugation, the crystals were dissolved in pH = 9 buffer [5] and dialysed against phosphate buffer pH = 7.05, $\mu = 0.1$, and a solution about 4.5×10^{-5} M in this buffer was obtained. This solution, when stored at about 4°C, keeps its original activity for a few days. If not stated otherwise the purity of the preparation was about 65−70 % based on enzymatic activity [6] and absorbtion at 280 mμ, assuming that all the material absorbing at this wavelength has the same extinction coefficient as LADH.

The DPNH and DPN used were preparations from Sigma Chemical Company. The purities were 90 % and 92 % for DPN and DPNH, respectively. Fresh solutions containing 1 mg/ml were used.

NEM was a Theodor Schuchardt (Munich) product.

$CuSO_4 \cdot 5H_2O$ and $Zn(OOCCH_3)_2 \cdot 2H_2O$ were p.a. Merck products.

$3CdSO_4 \cdot 8H_2O$ was a Baker Analyzed Reagent, lot no. 3363.

PCMB c.p. was a product from the Amend Drug and Chemical Co., New York.

n-Butyramide was purchased from Eastman Kodak, while the *iso*propanol was an Analar product.

The —SH groups were titrated spectrophotometrically with PCMB at 255 mμ [7]. Usually 20 μl quantities of a 10^{-3} M PCMB solution were added to a 2 to 2.5 μM solution of LADH in phosphate buffer pH = 7.05, $\mu = 0.1$, at 23.5°C.

In the presence of DPNH or DPN, however, smaller concentrations of LADH were used to permit the formation of the enzyme-coenzyme complex without having to add too much DPN(H).

Absorbance was measured with a Beckman DU Spectrophotometer and the end point was estimated graphically. A Beckman Energy Recording Adapter in connection with a Philips Recorder was used to follow the reactions kinetically.

RESULTS

The number of sulfhydryl reagents which also inhibit LADH is rather limited. Compounds such as iodoacetic acid or chloroacetophenone do not inhibit the enzyme and NEM reacts only very slowly. Heavy metal ions inhibit readily [8], but their specificity is questionable. Amperometric titrations have not been carried out, but might give additional information.

I. Interactions with PCMB

98 % pure LADH has 28 SH groups/mole enzyme (mol.wt. 84 000) as was found independently at the Nobel Medical Institute [9] and by the author at the State University's Laboratory for Organic Chemistry in Groningen. The enzyme preparation used in this investigation contained 25.5 ± 0.5 SH groups/mole of active enzyme. Active enzyme means that the enzyme concentration is calculated from the enzymatic activity test. In the case of pure LADH in the presence of enzymatic inactive, no —SH groups containing material, the number of —SH groups/mole of active enzyme, should be 28. The presence of enzymatic inactive, but —SH groups containing material should give a higher value, whereas enzymatic active, but no —SH groups containing material should give a lower value.

In the presence of DPNH or DPN the same number of —SH groups were found [9]. The dissociation constant for LADH-DPN at pH = 7.0 is

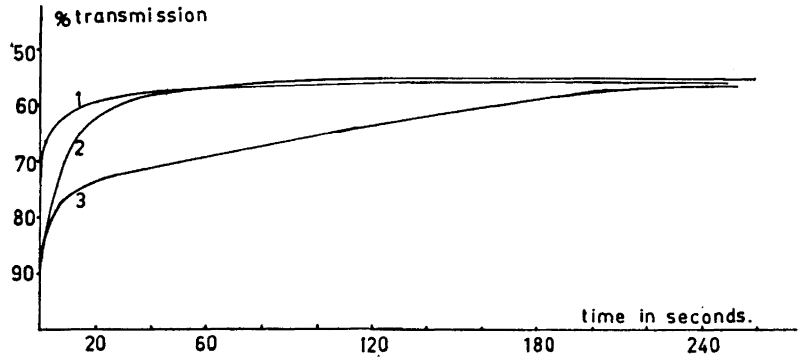

Fig. 1. The reaction of PCMB with LADH, LADH—DPNH—*n*-butyramide and LADH + imidazole *versus* time.
1: [LADH] * = 1 μM, alone, or with [DPNH] = 20 μM or [DPN] = 40 μM.
2: [LADH] = 1 μM, [DPNH] = 20 μM, [*n*-butyramide] = 1 M.
3: [LADH] = 1 μM, [imidazole] = 0.1 M.
In 3.0 ml μ = 0.1 phosphate buffer pH = 7.05. Temperature 23.5°C. In all cases PCMB was added at zero time to a final concentration of 30 μM. λ = 255 mμ.

* Concentrations of LADH in this article are given as molarities of active enzyme.

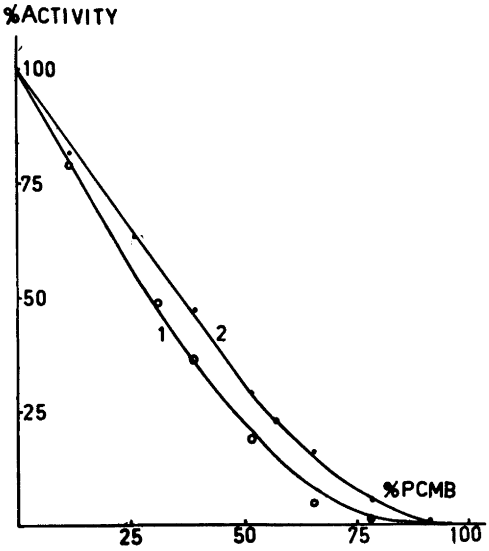

Fig. 2. The decrease in activity of LADH and LADH—DPNH, when increasing amounts of PCMB are added.

1: [LADH] = 2.03 μM.
2: [LADH] = 2.03 μM, [DPNH] = 40 μM.

Total volume = 1.50 ml, μ = 0.1, phosphate buffer p_H = 7.05. Room temperature was used. All the enzyme or coenzyme solutions were incubated 15 min and 10^{-3} M PCMB was added, then, in increasing amounts and after 15 min the activities were measured. 100 % PCMB means conversion of all the —SH groups in LADH.

160×10^{-6} M;* the dissociation constant for LADH—DPNH at pH = 7.0 is 0.31×10^{-6} M [10]. This makes it possible to have at least 95 % association in the case of DPNH, whereas in the case of DPN, under the experimental conditions used, it is difficult to get more than about 40 % association, without causing interference in the PCMB titration because of high absorbtion at 255 mμ. In this case, a difference of 1 or 2 SH groups would be difficult to detect. When the reaction is followed with a recorder there is no detectable difference in the reaction velocities of the two complexes, but, in as much as the reaction is fast, a refinement in the measuring methods might possibly reveal differences (Fig. 1).

Recently Winer and Theorell [11] described very stable ternary complexes of the type LADH—DPNH—fatty acid-amide and LADH—DPN—fatty acid*. The ternary complex LADH—DPNH—*n*-butyramide was further investigated, but showed no difference from LADH alone in —SH groups titrable with PCMB. The —SH groups of the complex, however, react more slowly with PCMB (Fig. 1). There is no evidence from this figure, that some special —SH groups are involved in this retardation of the reaction. In this laboratory it was also found [9] that imidazole forms a complex with LADH—DPNH; in this case the reaction with PCMB was strongly retarded (Fig. 1).

Bovine serum albumin (a commercial sample, titrating 0.42 SH/mole) reacted immediately with PCMB either with or without the presence of imidazole. In both cases the same amount of —SH groups was found, but, when plotting the $\Delta E_{255\ m\mu}$ against the amount of PCMB added, in the case when imidazole was present, it was found that the second part of the curve, representing the addition of PCMB to fully reacted serum albumin, was not straight, but bent downwards. This thus resulted in a smaller $\Delta E_{255\ m\mu}$ when excess

* See the following paper.

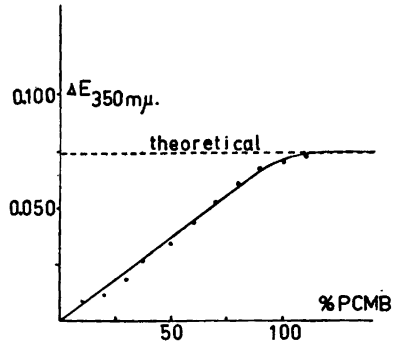

Fig. 3. The liberation of DPNH from LADH—DPNH by PCMB. [LADH] = 16.3 μM, [DPNH] = 50 μM in μ = 0.1 phosphate buffer pH = 7.05. Temperature 23.5°C.
PCMB added every 2 min and measurements made 1 min after each PCMB addition. Corrected for protein absorbtion and oxidation of DPNH in the presence of LADH.

PCMB was added to serum albumin. The same was also found to occur in the case of LADH. Furthermore, it was found that when PCMB was added to imidazole, a small absorption maximum occurred at around 245 mμ.

When the activity of LADH is plotted against increasing amounts of PCMB, a curve as in Fig. 2 is obtained, as was found in this laboratory [9].

The first part of the curves is practically straight and only towards the end is the fall in activity somewhat less than observed at the beginning. An incubation time of 15 min with PCMB ensures practically complete reaction at a temperature of 23°C. It can be seen that with or without DPNH all the —SH groups are necessary for activity. I am much indebted to Dr. J. S. McKinley McKee for letting me know the results of these experiments.

Another interesting feature is the small, but consistent protective effect of DPNH against PCMB inactivation. Although the titration curve is the same with or without DPNH, the inactivation curve is clearly distinct in the two cases.

In order to get somewhat more information about the breakdown of the LADH—DPNH complex by PCMB, it seemed useful to add the PCMB stepwise and to measure the breakdown at 350 mμ [1]. Accurate titration of the LADH—DPNH complex with PCMB was rather difficult, however.

Rather high concentrations of LADH and DPNH must be used in order to follow the breakdown of the complex spectrophotometrically, and at these high concentrations, there is an as yet unexplained oxidation of DPNH, which can be easily followed by the decrease of absorption at 340 mμ with time. This effect had earlier been observed with water purified on ion exchangers and was then explained by the presence of aldehyde which had dissolved from the resin [10]. Here, however, ordinary distilled water was used.

As was described by Theorell and Bonnichsen [1], the greatest difference in extinction between free and enzyme bound DPNH occurs at 350 mμ. The increase in extinction at 350 mμ *versus* added PCMB, corrected for protein absorbtion and DPNH oxidation, and thus representing the breakdown of the complex by PCMB, is shown in Fig. 3.

The curve obtained resembles that of Fig. 2. Again, complete breakdown of the complex seems to be reached only after complete reaction of LADH with PCMB. This breakdown is at first directly proportional to the amount

of PCMB added and deviates from linearity, at higher PCMB concentrations. The most likely conclusion is that most, if not all, of the —SH groups are important for the coenzyme binding.

II. Interactions with NEM

Direct titration of the —SH groups of LADH or LADH—DPNH with NEM at 300 mμ [12] is practically made impossible by turbidity and even the formation of a precipitate after about 8 h incubation. Furthermore, the reaction is very slow. It was observed, however, that in the case of LADH—DPNH the turbidity was much less pronounced than in the case of LADH alone.

LADH and LADH—DPNH were incubated with NEM, and the decrease in activity and —SH groups was followed. The determination of remaining —SH groups was carried out by titrating back with excess PCMB as follows. The incubation mixtures were centrifuged, and 3.0 ml of the supernatant solution was immediately pipetted out, the extinction at 255 mμ measured, and a small excess of PCMB added. The increase in extinction at $\lambda = 255$ mμ was measured after 1, 10, 20 and 30 min and the solution was again centrifuged. The $\Delta E_{255\ m\mu}$ was measured immediately and the percentage of remaining —SH groups was calculated from the last values. The discrepancies between the percentages obtained at the different time intervals indicated that the SH titration was only approximate. The results are given in Fig. 4.

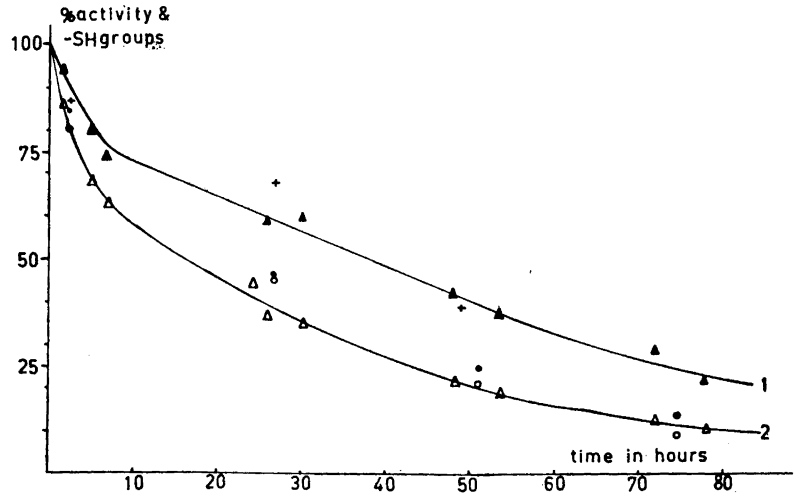

Fig. 4. The effect of excess NEM on activity and —SH titer of LADH and LADH—DPNH with time.
1: [LADH] = 1.00 μM, [DPNH] = 40 μM, [NEM] = 267 μM (▲).
2: [LADH] = 1.00 μM, [NEM] = 267 μM (△).
Total volume 15.0 ml in $\mu = 0.1$ phosphate buffer pH = 7.05. Room temperature.
● = percentage of —SH groups for 1, O = *idem* for 2.
\+ = *idem* for LADH—DPNH without NEM.
Determined by addition of 200 μl 5.15×10^{-4} M PCMB to 3.0 ml solutions, after centrifugation, at 255 mμ.

The activity decreases of LADH and LADH—DPNH without the addition of NEM were comparable.

The loss in activity of the LADH—DPNH without added NEM is similar to that for curve 1. However, in this case the decrease in free —SH groups runs parallel with the decrease in activity. There is a very strong protective effect of DPNH against inactivation, but there seems to be no protection against the decrease in free —SH groups. There is, however, a small difference in —SH groups titrated between LADH—DPNH and LADH at the end of the experiment, where it is most difficult to get clear-cut results with PCMB. Whether this difference is real or not has yet to be ascertained.

In the presence of DPN, a protection against inactivation is also present; no —SH determinations were carried out as relatively high DPN concentrations were used. On the other hand, in the case of the ternary complex LADH—DPNH—*n*-butyramide no activities could be measured because *n*-butyramide completely inhibits the enzyme. The decrease in —SH titre, however, was rather slow, about 60 % of the —SH groups still being present after 75 h.

III. Interaction with DDPM

DDPM, a coloured maleimide derivative used for the identification of cysteinyl peptides (Witter and Tuppy, unpublished results), behaves somewhat differently from NEM. Because of its rather poor solubility in water, the reaction was performed in alcohol-water mixtures.

Reaction in isopropanol. Solutions were made up in the following way: in a total volume of 3.0 ml (phosphate, $\mu = 0.1$, pH = 7.05) containing [LADH] = 0.71 μM, the concentrations of *iso*propanol were, respectively, 0.22 M, 0.44 M, 0.66 M, 0.88 M, 1.10 M, 2.20 M, and the corresponding concentrations of DDPM were, respectively, 4 μM, 8 μM, 12 μM, 16 μM, 20 μM, 40 μM, made by the addition of a 2.42×10^{-4} M solution of DDPM in *iso*propanol. The enzymatic activities of these solutions, and of the corresponding solutions with only

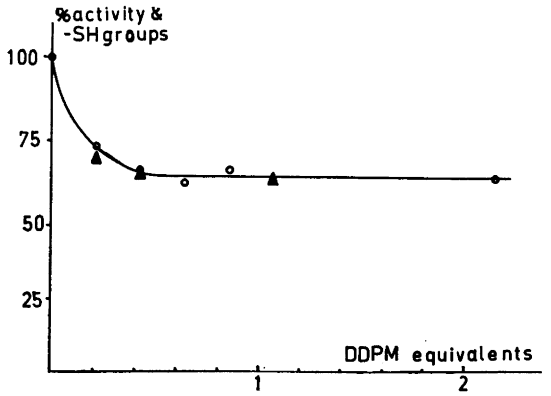

Fig. 5. The effect of DDPM on activity and — SH titer of LADH, corrected for the influence of the solvent, *iso*propanol.
○ = % activity, ▲ = % free —SH groups.

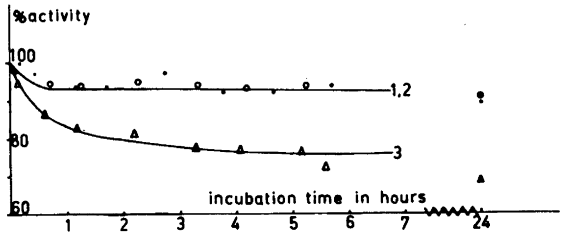

Fig. 6. The effect of excess DDPM on activity of LADH and LADH—DPNH with time.

1: [LADH] = 0.9 μM, [DPNH] = 14 μM, [DDPM] = 52.5 μM (O).
2: [LADH] = 0.9 μM (●).
3: [LADH] = 0.9 μM, [DDPM] = 52.5 μM (△).

All solutions in μ = 0.1 phosphate buffer p_H = 7.05, containing 1 % ethanol, which gives the optimal ethanol concentration in the test, as 150 μl of the incubation mixture was used for activity tests. Incubation at room temperature.

*iso*propanol (and thus no DDPM) were tested after 5 h incubation; after 7 h of incubation, the —SH groups were titrated with PCMB, after centrifugation. The differences in activities and —SH groups for the solutions containing DDPM and those containing only *iso*propanol (*vide infra*) are shown in Fig. 5.

As can be seen from this figure the decrease in activity and —SH titer are about parallel and seem to reach a constant value after about a 30 % decrease.

As in the case of NEM, an excess of DDPM is necessary to get complete reaction of the —SH groups, but a further increase in reagent concentration than used here will lead to difficulties. The enzyme will precipitate at high *iso*propanol concentrations, the absorbtion of DDPM at 255 mμ will make the —SH titrations doubtful, and also the DDPM itself may precipitate. However, as the decrease is constant from about 0.5 to 2 equivalents DDPM, it seems that with the rather weak reagent DDPM, only about 30 % of the —SH groups can react. Also in the case of NEM (Fig. 4), and to a lesser extent in the case of PCMB (Figs. 1 and 2), there seem to be faster and slower-reacting —SH groups.

Two other interesting observations were made. In the solutions containing DDPM, the reacted LADH forms a deep-yellow precipitate (from the solution containing 12 μM DDPM and 0.66 M *iso*propanol onward), which can be easily removed by centrifugation. In the solution containing only *iso*propanol, a small precipitate was observed in the test tube containing 2.20 M *iso*propanol (that is about 13 %), but in all the other solutions no precipitate was formed during the time the experiment lasted.

The second point is the effect of *iso*propanol. This secondary alcohol is reported not to be oxidized [13,14]. However, an inhibitory effect of *iso*propanol on LADH activity was found under the conditions described here (in the case of the solution containing 2.20 M *iso*propanol, there is present in the test solution 73 mM *iso*propanol and 8 mM ethanol). The inhibition might be due to impurities in the *iso*propanol used, but as other secondary alcohols (second-

ary butanol for example) are reported to be oxidized [14], the oxidation of *iso*-propanol itself cannot be excluded.

In a separate experiment the K_m for this *iso*propanol at pH = 10.05 and 23.5°C was found to be 9.2 mM, using [LADH] = 13.3 μg/ml, [DPN] = 0.42 mM and [*iso*propanol] = 1.75 to 44.0 mM.

Acetone (Analar) in a concentration of 900 mM with [DPNH] = 0.2 mM and [LADH] = 13.3 μg/ml at pH = 7.05 (μ = 0.1, phosphate) was found to be very slowly reduced.

It thus seems possible that *iso*propanol also is a substrate for LADH, but highly purified material will be necessary to ascertain this.

The effect of *iso*propanol on the —SH titer is very small, so that the corrections for the solvent made in Fig. 5 are mainly those caused by the reduced enzymatic activity, being about 10, 15 and 45 % for *iso*propanol concentrations of, respectively, 0.88, 1.10 and 2.20 M.

Reaction in ethanol. In this case an excess of DDPM in ethanol was added to LADH and LADH—DPNH and the fall in activity was measured with time. No —SH titrations were carried out. The addition of DDPM (5.25×10^{-3} M, dissolved by heating) is best carried out with the help of a stirring rod, as otherwise the DDPM will precipitate. In the enzymatic activity test, minor corrections were made for the absorbance of the DDPM at 340 mμ. The results and the experimental conditions can be seen in Fig. 6.

Because of the low alcohol concentration (1 %), all solutions remained clear throughout the experiment. Again a decrease of about 30 % in activity was observed. In the presence of DPNH, there was complete protection against this fall in activity.

IV. Interaction with heavy-metal ions

Heavy metals inhibit LADH and this was explained by their interaction with the —SH groups of the enzyme [8]. In order to get more information about the interaction of LADH with heavy metals, the fall in activity of LADH and LADH—DPNH upon incubation with heavy metals was followed, as was the —SH titer. The addition of Ag^+ ions results in a rapid precipitation and inactivation of both LADH and LADH—DPNH. In the case of Cu^{2+}, precipitation started after complete inactivation had occurred, and increased gradually with time. LADH was completely inactivated within 3 min, whereas LADH—DPNH was completely inactivated after 45 min. With Zn^{2+} on the other hand, a very slow inactivation occurred, the enzyme still having about 50 % of its original activity after 48 h. There was a definite protective effect against inactivation in the case of LADH—DPNH. In both cases no precipitation occurs.

The most interesting effects were obtained with Cd^{2+}, and were studied in more detail. The concentrations, which were the same as used for the experiments with Ag^+, Cu^{2+} and Zn^{2+}, were: [LADH] = 2.0 μM, [DPNH] = 40 μM, [$CdSO_4$] = 80 μM. All solutions were made up in μ = 0.1 phosphate buffer pH = 7.05, and incubated at room temperature. The result can be seen in Fig. 7. The protective effect of DPNH against inactivation of LADH

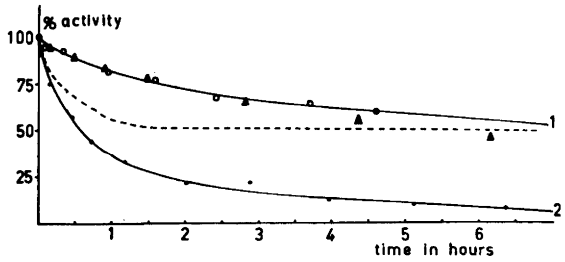

Fig. 7. Inactivation of LADH (2) and LADH—DPNH (1) by Cd^{2+} ions. ▲ represents the fall in activity in the case: [LADH] = 2 μM + [Zn acetate] = 80 μM + after 10 min [$CdSO_4$] = 80 μM. ----- = (1) + 100 % − (2), (see text).

by Cd^{2+} is very large. The same effect was observed when LADH alone was pre-incubated with Zn^{2+} before the addition of Cd^{2+}.

Addition of Zn^{2+} to LADH + Cd^{2+} after 15 min incubation does not lead to reactivation, but the slope of the inactivation curve decreases to become similar to that of the LADH—DPNH + Cd^{2+} curve. The concentration of the added Zn was 400 μM. The results show that the inactivation of LADH by Cd^{2+} is not primarily due to a reaction with —SH groups, but probably to replacement of the Zn by Cd in the active centre, leading to a less active enzyme. As DPNH has the same effect as Zn^{2+}, the coenzyme seems to be bound via Zn^{2+} to the enzyme, thus protecting the Zn atom against the replacement reaction. The very slow inactivation by Zn^{2+} could thus be due entirely to reaction with —SH groups. In the latter case, the DPNH has a smaller protective effect.

Assuming that in the case of LADH—DPNH the inactivation by Cd^{2+} is due entirely to interaction with —SH groups, the sum of curve 1 and 100 % minus curve 2 in Fig. 7 should roughly give the effect due to replacement alone. Equilibrium is reached within 2 h and remains constant for the 6 h of the experiment; the inactivation due to replacement is thus roughly 50 %.

Once replaced by Cd in the concentration used, Zn is unable to replace the Cd again, but can prevent further replacement when added in excess. Further evidence that not the reaction of —SH groups, but rather the replacement of Zn^{2+} plays the primary role in inactivation was obtained by titrating the —SH groups. Solutions containing [LADH] = 2.3 μM with or without [DPNH] = 45 μM were incubated with [$CdSO_4$] = 150 μM at room temperature and in μ = 0.1 phosphate buffer pH 7.05. Three ml samples, immediately after centrifugation, were titrated with excess PCMB (50 μl of a 5×10^{-4} M solution), the $\Delta E_{255\ m\mu}$ measured after 1 min and 30 min and the percentage of titrable —SH groups (which were within 2 % for the two time intervals) calculated. The decrease in —SH titer was roughly parallel to the inactivation curve of LADH—DPNH (curve 1 in Fig. 7), but was about 5—10 % lower, indicating that in the case of LADH—DPNH, the replacement reaction takes place to a very small extent. The decrease of —SH groups was the same for both LADH and for LADH—DPNH, but as in the case of NEM, at the end of the incubation time, the fall was somewhat less in the case of LADH—DPNH.

DISCUSSION

These results, together with the previous results of other investigators, mainly Vallee, Hoch and coworkers [2,4], make it seem highly probable that DPNH is bound to LADH by way of Zn atoms. The way this binding takes place is as yet unknown; the carbonamide group [3], the phosphate groups [15] and the adenine part [8] have all been proposed. Also the mode of binding of the Zn to the enzyme is unknown; it has not been possible to demonstrate the role of sulfhydryl groups in this respect.

It is difficult to understand what role the —SH groups play in the working mechanism. The following possibilities seem to be the most likely ones:

1) *Help in maintaining a requisite ternary structure.* From the experiments, specially those with PCMB, it can be concluded that both activity and DPNH binding depend on the presence of all the —SH groups, about equally for the first 70 % and to a lesser extent for the last 30 % of the —SH groups. To this comes the fact that the protective effect of DPNH against inactivation is very marked, and in the first period of inactivation with NEM or Cd^{2+} or Zn^{2+} this protective effect is not caused by a protection of —SH groups. In the case of Cd^{2+}, this is very probably due to prevention of the Zn-Cd replacement, but this is not so in the case of NEM or Zn^{2+}, nor in the case of PCMB, where the protective effect is small, but the amount of reacted —SH groups the same throughout the PCMB concentration range used. The necessity of all —SH groups for both activity and DPNH binding, and the lack of a convincing demonstration of direct coenzyme binding through —SH groups, could thus indicate that the role of the —SH groups lies in their help in maintaining a requisite ternary structure. This would explain the necessity for all the —SH groups, and the fact that the last remaining —SH groups have a smaller effect. In the case of LADH—DPNH it is possible that bound DPNH, to a certain extenct, takes over the role of the —SH groups in the maintenance of the ternary structure, leading to a partial protection against inactivation by sulfhydryl reagents.

2) *Binding of coenzyme.* When some —SH groups are involved in coenzyme binding, the explanation of the experiments would not be that both activity and DPNH binding depend on the presence of all the —SH groups, but that all —SH groups have the same reactivity towards the sulfhydryl reagents used and that the binding of coenzyme, as far as —SH groups are involved, is rather weak.

Because of the equal reactivity of the —SH groups towards sulfhydryl reagents, the decrease in activity with increasing concentration of sulfhydryl reagent will be linear, independent of the value of the coenzyme and not coenzyme binding —SH groups for enzymatic activity.

Because of the weak bond between coenzyme and binding —SH groups, the relative reactivity of these —SH groups towards sulfhydryl reagents will only be somewhat reduced, the degree depending upon the efficiency of the sulfhydryl reagent.

With an effective reagent for sulfhydryl groups, as for example PCMB, the effect of bound coenzyme will be small. The same number of —SH groups will be found, and only the somewhat higher enzymatic activity of the enzyme-

coenzyme complex as compared with enzyme alone (Fig. 2) results from the bound DPNH because of the suppressed possibility of reaction of the coenzyme binding —SH groups with PCMB.

With NEM, which only reacts very slowly with the —SH groups of LADH, the effect of DPNH in preventing the reaction of the coenzyme binding —SH groups with the sulfhydryl reagent will be more efficient and the resulting protection against enzymatic inactivation is much larger.

When the reaction of these essential —SH groups with NEM would be prevented completely, a difference in remaining —SH groups between LADH and LADH—DPNH after complete reaction with NEM would be found. This was indeed the case, but as outlined, these results were rather unreliable and the reaction with NEM was not complete at the end of the experiment (Fig. 4). It would also implicate that the —SH groups, which don't play a role in coenzyme binding do play a role in enzymatic activity.

It is of course possible that the role of the —SH groups involves both possibilities, but further work will be necessary to ascertain the role of —SH groups in LADH.

Acknowledgments. The author wishes to thank Professor H. Theorell for his generous hospitality and for his interest in this work. Thanks are also due to Dr. J. S. McKinley McKee for helpful discussions, and to Mr. L. G. Falksveden for skilled technical assistance. The stay was made possible by a grant from the *H. J. Backer Fonds.*

REFERENCES

1. Theorell, H. and Bonnichsen, R. *Acta Chem. Scand.* **5** (1951) 1105.
2. Vallee, B. L. and Hoch, F. L. *J. Biol. Chem.* **225** (1957) 185.
3. Theorell, H., Nygaard, A. P. and Bonnichsen, R. *Acta Chem. Scand.* **9** (1955) 1148.
4. Hoch, F. L., Williams, R. J. P. and Vallee, B. L. *J. Biol. Chem.* **232** (1958) 453, 465.
5. Dalziel, K. *Acta Chem. Scand.* **12** (1958) 459.
6. Dalziel, K. *Acta Chem. Scand.* **11** (1957) 397.
7. Boyer, P. D. *J. Am. Chem. Soc.* **76** (1954) 4331.
8. Wallenfels, K., Sund, H., Zarnitz, M. L., Malhotra, O. P. and Fischer, J. in *Sulfur in proteins*, Academic Press, New York and London 1959, p. 215, especially p. 225.
9. Theorell, H. and McKinley McKee, J. S. *Personal communication.*
10. Theorell, H. and Winer, A. D. *Arch. Biochem. Biophys.* **83** (1959) 291.
11. Winer, A. D. and Theorell, H. *Acta Chem. Scand.* **13** (1959) 1038.
12. Roberts, E. and Rouser, G. *Anal. Chem.* **30** (1958) 1291.
13. Winer, A. D. *Acta Chem. Scand.* **12** (1958) 1695.
14. Merrit, A. D. and Tomkins, G. M. *J. Biol. Chem.* **234** (1959) 2778.
15. van Eys, J., Ciotti, M. M. and Kaplan, N. O. *J. Biol. Chem.* **231** (1958) 571.

Received February 11, 1960.

ACTA CHEMICA SCANDINAVICA 14 (1960) 1729–1742

Dissociation Constants of Ternary Complexes of Fatty Acids and Fatty Acid Amides with Horse Liver Alcohol Dehydrogenase-Coenzyme Complexes

ALFRED D. WINER* and HUGO THEORELL

Nobel Medical Institute, Biochemical Department, Stockholm, Sweden

1. Fatty acids form dissociable binary compounds with liver alcohol dehydrogenase (ADH), and ternary compounds with DPN—ADH, but not with DPNH—ADH. The fatty acids compete with alcohols for the same binding site.

2. The amides of fatty acids form binary compounds with ADH, and ternary complexes with DPN—HADH, but not with DPN · ADH. They compete with aldehyde for the same binding site.

3. Spectrophotofluorometric methods were elaborated for determining all the dissociation constants involved: $K_{E,I}$; $K_{E.O}$; $K_{EO,I}$; and $K_{EI,O}$ in the case of fatty acids, $K_{E,I}$; $K_{E,R}$; $K_{ER,I}$; and $K_{EI,R}$ in the case of amides.

4. With increasing C-chain length the complex forming power increases for both acids and amides, in some of the combinations many thousand-fold. For the fatty acids this increase continues up to C_{15}. From C_{16} and upwards the complexing ability practically disappears.

5. In these ternary complexes coenzyme and substrate analog mutually stabilize one another's binding to the enzyme.

6. The high affinity of the long-chain fatty acids and amides for ADH—DPN or ADH—DPNH is parallelled by the high reaction velocities observed with higher alcohols and aldehydes in comparison with ethanol.

7. The significance of these results is discussed.

In 1955 Theorell *et al.*[1] presented data on the effects of anions on the liver-ADH ** system as determined from reaction velocity measurements. Strong effects with anions such as chloride, bromide, nitrate and sulfate were reported as had been previously observed from work on the old yellow enzyme [2]. Surprisingly, however, it was found that formate and acetate, which were inactive

* This investigation was carried out during the tenure of a Postdoctoral Fellowship from the National Institute of Neurological Diseases and Blindness, United States Public Health Service. Present address: Department of Biochemistry, University of Kentucky Medical Center, Lexington, Kentucky.

** Abbreviations, see p. 1730.

in the O.Y.E. system, had strong effects on the liver-ADH system. Formate was found to effect only two of the six velocity constants, *i. e.* DPN · ADH $\xrightarrow{k_2'}$ DPN + ADH and DPN · ADH + alcohol $\xrightarrow{k'}$ DPNH · ADH + + aldehyde + H^+. On this basis it was suggested that formate reacts with the DPN · ADH complex, but not with the reduced complex, DPNH·ADH. Since formate inhibited competitively with alcohol it was presumed that formate enters into the binding site for ethanol in DPN.ADH. The effect of acetate appeared to be weaker than for formate.

More recent work by Theorell and Winer [3] using the fluorometric technique to measure dissociation constants showed that while formate has a small apparent effect on $K_{E,R}$ it exerts a very strong apparent effect on $K_{E,O}$. This again suggested that the effect of formate depends on the formation of a ternary ADH · DPN · formate complex. Since the fluorometric method offers a rapid procedure for the determination of dissociation constants, it was decided to investigate the effects of other saturated fatty acids on the ADH-coenzyme system. The effects of fatty acid amides were also investigated in line with recent substrate specificity studies on liver ADH by one of us (A.D.W.) [4] which indicated that long chain aldehydes were, in some cases, better substrates than acetaldehyde.

It was found that all the fatty acids studied (C_1—C_{20}) form ternary complexes with ADH · DPN and compete with the ethanol binding site while all of the fatty acid amides studied (C_1—C_6) form ternary complexes with ADH · DPNH and compete with the aldehyde binding site. In this way fatty acids and amides act as inhibitors. Remarkably strong effects were found with increasing chain length for both acids and amides. From a suitable choice of experimental conditions it is possible to calculate the dissociation constants describing the effect of the inhibitor on ADH ($K_{E,I}$), on the ADH · coenzyme complex ($K_{ER,I}$ and $K_{EO,I}$) and of the coenzyme on the ADH · inhibitor complex ($K_{EI,O}$ and $K_{EI,R}$). It is suggested that the ADH · DPNH · amide and

---

** ADH—DPN and ADH—DPNH, 1/2 molecule of horse liver alcohol dehydrogenase (E) and oxidized (O) or reduced (R) diphosphopyridine nucleotide, respectively.

E_t = Total conc. of liver alcohol dehydrogenase (ADH) (μN)
E = Conc. of free » » » » »
R_t = Total conc. of reduced diphosphopyridinenucleotide (DPNH)
R = Conc. of free » » (»)
O_t = Total conc. of oxidized » (DPN)
O = Conc. of free » » (»)
I_t = Total conc. of fatty acid or amide
I = Conc. of free » » » »

$$K_{E,R} = \frac{E \times R}{ER}$$

$K_{E,R,app}$ = apparent dissociation constant of ADH · DPNH in presence of I

$$K_{E,O} = \frac{E \times O}{EO}; \qquad K_{EI,R} = \frac{EI \times R}{ERI}$$

$$K_{E,I} = \frac{E \times I}{EI}; \qquad K_{EO,I} = \frac{EO \times I}{EOI}$$

$$K_{ER,I} = \frac{ER \times I}{ERI}; \qquad K_{EI,O} = \frac{EI \times O}{EOI}$$

ADH · DPN · fatty acid complexes, just like the fluorescent lactic dehydrogenase · DPNH · anion complexes recently described by Winer and Schwert [5], are similar in structure to activated complexes formed between ADH, DPNH, aldehyde and ADH, DPN, alcohol.

EXPERIMENTAL

Fluorometric measurements of emission spectra, the calculation of the dissociation constants $K_{E,R}$ and $K_{E,O}$, the buffer salts used and the purity of DPN and DPNH (Sigma) have been previously described [3]. Fatty acids, C_1-C_9, were reagent grade chemicals further purified by distillation under suitable pressures; $C_{10}-C_{20}$ acids were gifts of Professor E. Stenhagen, Uppsala, and had the following melting points in °C: C_{10} 31.2—32.0; C_{11} 28.0—28.5; C_{12} 43.7—43.9; C_{13} 41.5—41.7; C_{14} 54.5—54.9; C_{15} 59.5—59.8; C_{16} 62.5——62.9; C_{17} 61.3—61.4; C_{18} 69.6—69.8; C_{19} 68.4—68.5; C_{20} 75.2—75.3. These acids were solubilized after lyophilization of the potassium salts. The amides were products of the Eastman Kodak Company and recrystallized twice from water prior to use. Heart muscle lactic dehydrogenase and beef liver glutamic dehydrogenase were commercial preparations from C. F. Boehringer and Son, Mannheim.

Enzyme preparation. Crystalline ADH as prepared by the method of Bonnichsen and Brink [6] and treated with DPN to remove traces of endogenous ethanol as previously described [3] was used for all experiments. Liver ADH prepared in this manner is surprisingly stable for long periods of time (2—3 weeks at 2°). The concentration of the enzyme * in the fatty acid experiments was determined by calculations from $C\left(\frac{a''}{b''}-\frac{a'}{b'}\right)Z^2-(a''-a')\,Z+(b''+b')=0$ ** using $Q_{E,R}$*** = 13.5 as determined previously. Calculated values for enzyme concentration were 10—20 % lower than those determined from activity measurements at pH 10 using the assay method of Dalziel [7].

In the amide experiments the concentration of ADH was determined by titration with DPNH in the presence of excess *iso*butyramide. This method of determining enzyme concentration has been found very much superior to activity measurements because of the high Q and the low dissociation constant $K_{EI,R}$ (= 0.02 μM).

The enzyme concentration as determined by the amide procedure was also 10—20 % lower than that determined by activity measurements. The Q for different amides was determined by two methods:

1. Addition of a small amount of DPNH to an excess of ADH and amide (»direct» method).

2. Titration of ~1 μN ADH with 6—10 steps of ~0.5 μM DPNH, and in experiments where appreciable dissociation occurred (for instance with acetamide) calculation of Z ($= Q-1$) from [3]

$$C\left(\frac{a''}{b''}-\frac{a'}{b'}\right)Z^2-(a''-a')\,Z+(b''+b')=0$$

and extrapolation to $I=\infty$ by the aid of eqn. (14) ("calculated" method).

METHODS OF CALCULATION OF DISSOCIATION CONSTANTS

1. I = Fatty Acids

The experimental results were found to agree with the assumption that fatty acids form binary complexes EI with ADH, but not ternary ERI complexes. Thus

* By ADH concentrations the number of binding sites is meant (2 sites/mole from pH 6—9).

** See the previous publication [3] for derivation of this equation.

*** Q is the deflection ratio DPNH · ADH/DPNH as measured with our apparatus at 410 mμ when activated at 325—330 mμ.

$$K_{E,R} = \frac{(E_t - ER - EI)(R_t - ER)}{ER} \quad (1)$$

From the experiments in presence of I we obtain:

$$K_{E,R\ app} = \frac{(E_t - ER)(R_t - ER)}{ER} \quad (2)$$

Only EI is unknown. Therefore

$$EI = (1 - K_{E,R} / K_{E,R\ app})\ (E_t - ER), \text{ and} \quad (3)$$

$$K_{E,I} = \frac{(E_t - ER - EI)(I_t - EI)}{EI} \quad (4)$$

When mixtures of ADH, I and DPN were titrated with DPNH, the experimental results were found to agree with the assumption that besides EI and ER also EO and EOI were formed.

$$K_{E,R} = \frac{(E_t - ER - EO - EI - EOI)(R_t - ER)}{ER} \quad (5)$$

$$K_{E,O} = \frac{(E_t - ER - EO - EI - EOI)(O_t - EO - EOI)}{EO} \quad (6)$$

$$K_{E,I} = \frac{(E_t - ER - EO - EI - EOI)(I_t - EI - EOI)}{EI} \quad (7)$$

ER is determined experimentally, EO, EI and EOI are unknown.

$K_{E,R}$ and $K_{E,O}$ are determined separately in experiments without I [3], $K_{E,I}$ from eqns 3 and 4.

Since O in these experiments was always much larger than EO and EOI, from eqns 5 and 6:

$$EO = \frac{K_{E,R} \times ER \times O}{K_{E,O}\ (R - ER)} \quad (8)$$

From eqns 6 and 7 when $I \gg EI + EOI$, $O \gg EO + EOI$:

$$EI = \frac{EO \times K_{E,O} \times I}{O \times K_{E,I}} \quad (9)$$

$$EOI = E_t - ER - EO - EI - \frac{ER \times K_{E,R}}{R_t - ER} \text{ (where the last term} = E) \quad (10)$$

$$K_{EO,I} = \frac{EO(I_t - EI - EOI)}{EOI} \quad (11)$$

$$K_{EI,O} = \frac{EI(O_t - EO - EOI)}{EOI} \quad (12)$$

2. I = Fatty acid amides

Fatty acid amides, unlike the free acids, were found to form ternary complexes ERI, as indicated by changes in fluorescence intensity (See Table 4)

and by decreased values for the apparent $K_{E,R}$. Binary complexes EI (and ER) are also formed. The mode of calculation is somewhat different in cases where Q_{ERI} differs markedly from Q_{ER}, and in cases where Q_{ERI} is $\approx Q_{ER}$.

$$Q_{ERI} \neq Q_{ER}.$$

In the presence of large excess of I, E and ER are negligible. Titration with R therefore gives the value of $K_{EI,R}$. In addition one obtains the Q-values for ERI (Q_{ERI}) which varies for different amides (See Table 4). In the cases where Q_{ERI} is sufficiently different from Q_{ER} (≈ 13.5), as for example with *iso*butyramide, this offers a possibility of determining the ratio ER/ERI experimentally at intermediate I. When $I >> EI + ERI$, which is mostly the case

$$K_{ER,I} = \frac{ER \times I}{ERI} \tag{13}$$

and the ratio ER/ERI is independent of R and remains constant through the titration, just as the fluorescence increase factor Q_{ER+ERI} for the mixture of ER + ERI. Therefore

$$\frac{ER}{ERI} = \frac{Q_{ERI} - Q_{(ERI+ER)}}{Q_{(ERI+ER)} - Q_{ER}} \tag{14}$$

On the other hand, ER + ERI can be calculated using Q_{ER+ERI} for any point of the titration curve. These values of ER/ERI and ER + ERI give ER and ERI which if inserted in either of the equations

$$K_{EI,R} = \frac{EI(R_t - ER - ERI)}{ERI} \tag{15}$$

or

$$K_{E,R} = \frac{(E_t - EI - ER - ERI)(R_t - ER - ERI)}{ER} \tag{16}$$

give EI, and allow the calculation of $K_{E,I}$.

If now another titration with R is carried out on a solution containing the same amounts of E and I, but in addition a suitable amount of O ($[DPN] \approx K_{E,O}$) it is found that the calculated values of EI, ER and ERI when introduced into (16) give a higher value than $K_{E,R}$ ($= K_{E,R,app}$). This was to be expected since some of the free E is bound to O, but it could not be predicted whether this occurs both as EO and EOI. It was found, however, that under the assumption that *only* EO is formed, the values for EO, calculated from

$$K_{E,R} = \frac{(E_t - EI - ER - ERI - EO)(R_t - ER - ERI)}{ER} \tag{17}$$

and inserted into

$$K_{E,O} = \frac{(E_t - EI - ER - ERI - EO)(O - EO)}{EO} \tag{18}$$

gave values for $K_{E,O}$ which agreed as well as could be expected with the values for $K_{E,O}$ obtained in titrations without inhibitors; see Table 5. *The conclusion is that EO, unlike ER, does not form ternary complexes with fatty acid amides.*

$$Q_{ERI} \approx Q_{ER}.$$

In this case the experiments give values only for $ER' = ER + ERI$. $K_{EI,R}$ is determined directly in experiments with large excess of I. Then from experiments with intermediate I the ratio EI/ERI is obtained from

$$\frac{EI}{ERI} = \frac{K_{EI,R}}{R_t - ER'} \tag{19}$$

which together with the equations

$$ER' = ER + ERI \text{ and} \tag{20}$$

$$K_{ER} = \frac{(E_t - EI - ER')(R_t - ER')}{ER} \tag{21}$$

allows the calculation of the three unknown ER, EI and ERI, and the corresponding dissociation constants. Experiments in the presence of DPN are evaluated as described above.

In the case of high affinity of the inhibitors for the binary complexes, sometimes such small concentrations of I had to be used that corrections for the amount of bound I had to be introduced.

As is easily derived from the above formulae the dissociation constants for the binary and ternary complexes are related by

$$\frac{K_{EI,R}}{K_{E,R}} = \frac{K_{ER,I}}{K_{E,I}} = \frac{EI \times ER}{ERI \times E}, \tag{22}$$

and *vice versa* for the complexes with DPN. When the constants are calculated as described above, eqn. 22 serves as an excellent check on the correctness of the calculations. The data given in Tables 1, 2, 3 and 5 have all been found to fulfil condition (22) within the limits of error.

Table 1. The effect of saturated fatty acids on the dissociation constants at pH 7 23.5°C ($K_{E,O} = 84$).

Chain Length	$K_{EI,O}$	in μM $K_{EO,I}$	$K_{E,I}$
C_1	5.2	2 900	47 000
C_2	7.2	9 500	100 000
C_3	5.7	2 700	40 000
C_4	2.1	1 600	63 000
C_5	4.1	1 400	35 000
C_6	7.0	300	3 100
C_7	2.5	131	4 000
C_8	6.6	84	1 100
C_9	4.2	40	700
C_{10}	1.8	5.0	230
C_{11}	11.0	1.4	10.2
C_{12}	6.4	0.8	10.3
C_{13}	38.0	4.0	9.9
C_{14}	35.0	3.8	9.1
C_{15}	11.0	0.7	5.7
C_{16}		24	$>>58$
C_{17}		22	$>>22$
C_{18}		26	$>>21$
C_{19}		28	$>>18$
C_{20}		22	$>>20$

RESULTS

The dissociation constants $K_{E,I}$, $K_{EI,O}$ and $K_{EO,I}$ (I = Fatty acid)

It is seen from Table 1 that fatty acids exhibit strong ternary complex formation with ADH · DPN complex and that the affinity on the whole increases strongly with the length of the carbon chain of the acid up to C_{15}. The dissociation constant for the ternary complex ADH · DPN · fatty acid, $K_{EO,I}$, decreases from 2 900 μM for formate and 9 500 for acetate to 0.7 μM for C_{15} acid, while the dissociation constant for fatty acid and ADH, $K_{E,I}$, decreases from 47 000 μM for formate and 100 000 for acetate to 6 μM for C_{15} fatty acid. The dissociation constant reflecting the effect of DPN on the ADH · fatty acid complex, $K_{EI,O}$, is rather constant at about 5 μM to the C_{11} acid, and then increases from 2—7 times this value from C_{11}—C_{15}. The ability of the fatty acids to form complexes and the dissociation constant reflecting the formation of a ternary complex between EO and I, $K_{EO,I}$, increasing to a constant level of about 25 μM for the acids C_{16} to C_{20}.

Table 2. Dissociation constants (K) for complexes of liver ADH (E) with DPN (O), DPNH (R) and capric acid (I). 23.5° C, phosphate μ = 0.1.

	pH 6	pH 7	pH 8
$K_{E,R}$	0.26 μM	0.38 μM	0.45 μM
$K_{E,O}$	107 »	84 »	28 »
$K_{E,I}$	31 »	200 »	290 »
$K_{EO,I}$	1.1 »	3.8 »	11.4 »
$K_{EI,O}$	3.7 »	1.6 »	1.1 »

Table 2 shows the effects of capric acid (C_{10}) at different pH-values. The dissociation constants $K_{E,R}$ and $K_{E,O}$ were taken from independent determinations with the same enzyme solution and used to calculate the other constants. It can be seen that both $K_{E,I}$ and $K_{EO,I}$, the constants reflecting the effect on inhibitor on free ADH and on ADH · DPN complex, increase with increasing pH while the constant reflecting the effect of DPN on ADH · inhibitor complex decreases as the pH increases. The presence of fatty acid stabilizes the binding of DPN in the ternary complex, ADH · DPN · fatty acid, particularly at pH 6, and *vice versa*, DPN stabilizes the fatty acid in the ternary complex.

The dissociation constants $K_{I,E}$, $K_{EI,R}$ and $K_{ER,I}$ of fatty acid amide complexes.

Table 3 shows the effects of amides as indicated by the various dissociation constants. The presence of inhibitor lowers the dissociation constant $K_{EI,R}$ from 0.31 to 0.02 μM for the amides C_4—C_6 whereas it is slightly higher for the lower amides. The lowering of the constants, reflecting the effects of inhibitor on free ADH and on ADH · DPNH complex is about 10 000 times from acetamide to hexamide. Column 6 in Table 3 is the calculated $K_{E,O}$ as determined

Table 3. The effect of straight chain amides on the dissociation constants at pH 7, 23.5°C ($K_{E,R} = 0.31$).

Chain Length	$K_{EI,R}$	in μM $K_{ER,I}$	$K_{E,I}$	[DPN]	$K_{E,O}$ (calc.)
C_1	0.11	103 000	360 000	193	84
C_2	0.05	5 000	36 000	306	88
C_3	0.025	505	6 170	109	125
C_4	0.020	64	1 000	218	130
C_5	0.020	25	400	109	89
C_6	0.020	11	165	218	95

from eqn. 15. The amount of DPN used to determine the constants is listed in column 5 of the table. As stated in the experimental section, the determination of the Q_{ERI}-values for the various amides used to determine the constants was made by one of two methods. Table 4 states the values of Q_{ERI} for the amides tested together with the concentration used and the method of determination. The Q_{ERI}-values increase from formamide to propionamide and then decrease from butyramide to hexamide. The value for *iso*butyramide is specially high, about 3 times the value obtained in the absence of inhibitor. Q is independent of pH from 6—9. The fluorescence changes observed with acetamide are shown in Fig. 1. As previously noted [7,8], the shift of wavelength observed when DPNH combines with ADH is about 20 mμ from 472 mμ to 450 mμ (uncorr.). The further shift to 435 mμ is observed in the presence of nearly saturating amounts of acetamide. A similar shift to wave length when the ADH · DPNH ·

Table 4. Q_{ERI} values for amides at pH 7. Emission recorded at 410 mμ. $Q_{ER} = 13.5$ (in absence of inhibitor).

Amide	Concentration mM	Method of determination	Q_{ERI}
Formamide	250	Calculated	11.7
Acetamide	250	Directly	16.5
	10	Calculated	16.6
Propionamide	6.1	Directly	18.9
	30.4	Directly	19.0
	30.4	Calculated	20.3
	3.04	Calculated	18.4
Butyramide	50.5	Directly	15.6
	50.5	Calculated	13.4
	5.05	Calculated	14.5
*Iso*butyramide	40.7	Directly	40
Valeramide	0.244	Calculated	8.9
	0.122	Calculated	8.4
*Iso*valeramide	19.3	Directly	11.7
	0.384	Calculated	11.8
Hexamide	0.0259	Calculated	11.1

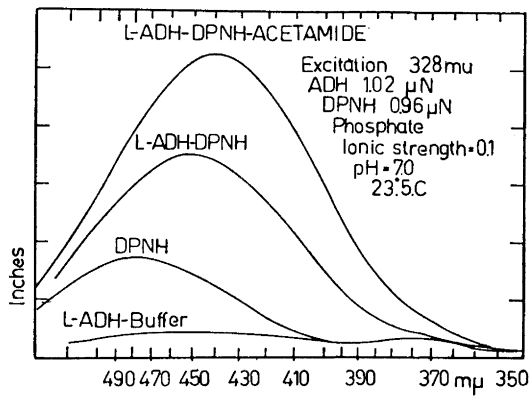

Fig. 1. The effect of adding acetamide to a partly dissociated L-ADH-DPNH complex; the fluorescence increases both because a much less dissociated ternary complex is formed and because the ternary complex has a somewhat higher Q-value than for ER.

amide complex was formed is seen with all amides tested, independent of the fact noted in Table 4 that some amides actually quench, others increase, to varying extents, the fluorescence of ADH · DPNH. Ternary complex formation with ADH—DPNH is specific for carbon chain amides and is not observed with glutamine, nicotinamide or succinimide. Benzamide, if analogous to benzaldehyde (which is a good substrate for liver ADH [4]), would form a ternary complex with ADH—DPNH, but such a complex, if formed, is obscured by the non-specific quenching of this amide. Partly dissociated complexes of lactic and glutamic acid dehydrogenase of the type ER show no observable fluorescence changes at either the protein or DPNH wave lengths upon the addition of acetamide.

Table 5 indicates the changes in the dissociation constants with pH. The constant $K_{E,R}$ was determined from independent experiments without amides, and $K_{E,O}$ was calculated using eqn. 15 from titrations of ADH + DPN + ami-

Table 5. Dissociation constants (K) in μM for complexes of liver ADH (E) with DPN (O); DPNH (R) and *iso*butyramide (I) at 23.5°C.

	pH 6	pH 7	pH 8	pH 9
$K_{E,R}$	0.25	0.31	0.45	0.95
$K_{E,O}$	125	88	22	15
$K_{E,I}$	270	5 750	930	540
$K_{ER,I}$	180	450	210	120
$K_{EI,R}$	0.17	0.02	0.10	0.20

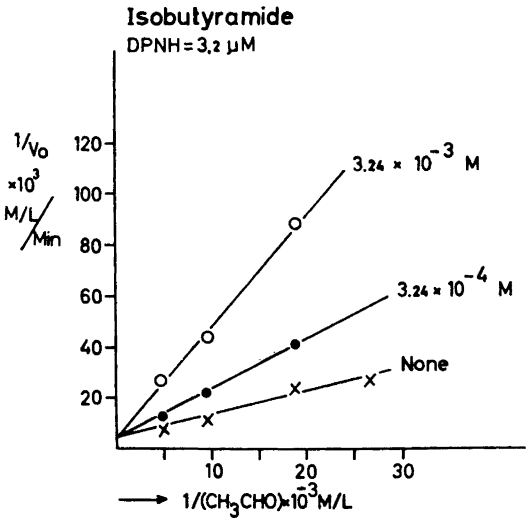

Fig. 2. Lineweaver-Burk plots demonstrating the competitiveness of *iso*butyramide with acetaldehyde. pH = 7.0. Phosphate buffer ionic strength 0.1; temp. 23.5°.

des with DPNH. The agreement of these values for $K_{E,O}$ with the earlier values[3] give strong support to the assumption that ternary complexes between ADH, DPN and amides are not formed.

Competition of amides and fatty acids for the aldehyde and alcohol binding sites respectively.

As noted in the introduction formate was earlier found from reaction velocity constant measurements to compete with ethanol. Fig. 2 shows a typical Lineweaver-Burk plot of the competitiveness of *iso*butyramide with acetaldehyde.

Fluorescence emission data of amide and fatty acid complexes when excited with 289 mμ light.

As Velick [10] has reported with glyceraldehyde phosphate and heart muscle lactic dehydrogenase, the protein fluorescence at 350 mμ when activated at 289 mμ is quenched by either DPN or DPNH. Fig. 3 shows a typical spectrum of the effects observed at 350 mμ when DPNH in a final concentration of 0.70 μM is added to an 0.59 μN ADH solution in phosphate buffer, pH 7. The fluorescence of ADH is quenched somewhat but there is no shift in the wave length when ADH · DPNH complex is formed. The addition of 2.6×10^{-2} M acetamide quenches the fluorescence and shifts the wave length about 10 mμ to 360 mμ. The emission bands in the visible wave lengths when ADH · DPNH and ADH · DPNH · acetamide complexes are formed are similar to those

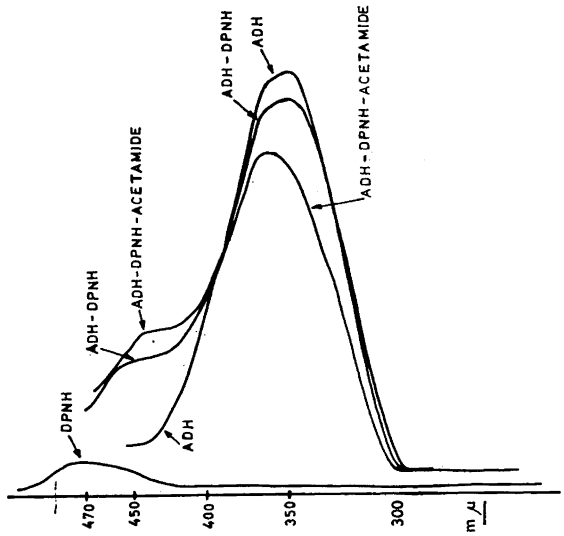

Fig. 3. Emission spectra of ADH, ADH—DPNH and ADH—DPNH-acetamide, when activated by 289 mμ. Complex formation with DPNH causes slight quenching and shift of maximum emission from 350 to 360 mμ. The emission of the complexes in the visible light is presumably caused by energy transfer from the protein moiety to the coenzyme.

shown in Fig. 1. No effect is seen when fatty acids are added to the ADH·DPNH complex nor is any effect observable when an amide is added to the ADH · DPN complex. The latter observations support the conclusion that ternary complexes are not formed in these cases.

DISCUSSION

While the measurements of dissociation constants by the fluorometric technique indicates the existence of complexes of the type ADH · DPNH · fatty acid and ADH · DPNH · amide, it is not immediately apparent that these complexes bear any relation to the enzymatically active complexes. However, the following lines of evidence suggest that such complexes are indeed similar in structure to the activated complexes involved in the interconversion of ADH, DPNH, aldehyde and ADH, DPN, alcohol:

1. The fluorometric results can be fitted to a mathematical treatment which is based upon the postulate that in the case of amides no EOI or OI and in the case of fatty acids no ERI or RI is formed.

2. Fatty acids show competitive behaviour with ethanol, and fatty acid amides with acetaldehyde.

3. The spectroscopic emission data of the amide complexes both at the pyridine nucleotide fluorescence band and at the protein fluorescence band and of the fatty acid complexes at the protein fluorescence band indicate the analogy with true enzyme-coenzyme-substrate complexes.

4. The inhibition effect of acids and amides increase with the length of the C-chain just like the enzymatic activity on alcohols and aldehydes, as indicated from substrate specificity studies.

5. Neither amides nor fatty acids show any observable effects with other pyridine-coenzyme dehydrogenase complexes studied, such as lactic acid dehydrogenase-DPNH and glutamic acid dehydrogenase-DPNH.

6. The observation of ternary complex formation of lactic dehydrogenase · DPNH with anions such as oxamate and oxalate has recently been reported by Winer and Schwert [5]. The values of the dissociation constant of oxamate from the LDH · DPNH · oxamate complex were found to be of the same order of magnitude, and to vary in the same way with pH, irrespective of whether the values were estimated from kinetic inhibition or from quenching experiments.

The effect of saturated fatty acids and fatty acid amides in lowering the dissociation constants indicates that the substrate analogs stabilize the binding of the coenzyme with ADH. *Vice versa*, the coenzyme stabilizes the binding of I on the ternary complexes. In the case of the acids the relative magnitudes of $K_{EI,O}$ and $K_{EO,I}$ indicate that from C_1 to C_{10} I dissociates easier than O from EOI, whereas the reverse is true from C_{11} to C_{15}. The *preferred* * order of the dissociation reaction of EOI is thus from C_1 to C_{10} the same as that assumed for ADH—DPN-alcohol by Theorell and Chance [13], but is reversed for C_{11} to C_{15}. In the case of acetate and formate it appears, as had been indicated earlier from kinetic data [1], that acetate dissociates easier from ADH and from ADH—DPN than does formate. It should be pointed out that the apparently irregular variations in the dissociation constants with stepwise increasing chain length may be largely due to experimental errors. The general trend is, however, very obvious.

The low solubility in water of the potassium salts of the acids from C_{16} upwards prevented the use of higher concentrations, but it is clear from the results that complexes of the type EI for C_{16} to C_{20}, if existent, are much more dissociated than C_{11} to C_{15}, see Table 1. The sudden change between C_{15} and C_{16} may reasonably be attributed to difference in micelle formation, and would in such case be expected to be temperature dependent. Further investigations are needed to solve this problem.

It is evident from Table 2 that changes in pH can invoke changes in the preferred order of reaction, as seen from a comparison between the values for $K_{EO,I}$ and $K_{EI,O}$. At pH 8 I is much more easily dissociated from EOI than is O, as postulated by Theorell and Chance [13] for a ternary ADH · DPN · ethanol complex. But at pH 6 the order is reversed, so that O is more easily dissociated from EOI than is I. This could explain the discrepancies between the values for $K_{E,O}$ found in equilibrium and kinetic measurements [3]. The kinetic values would then be calculated on the basis of a wrong assumption. The differences were by far the greatest in acid solutions, as we indeed would expect if a qualitative analogy can be drawn between the EOI and EO-ethanol complexes. Too high values for $K_{E,O}$ would be found in kinetic experiments in case the presence

* We consider *"preferred"* order rather than *"compulsory"* order more appropriate when speaking of enzyme-coenzyme complexes since the order may change depending on the experimental conditions employed. This has already been pointed out by one of us (H.T.) [12].

of ethanol in the ternary complex would loosen the attachment of DPN, thus increasing the "off" velocity rate constant *.

In the case of *iso*butyramide (see Table 5), $K_{ER,I}$ is $\gg K_{EI,R}$ at all pH values. This indicates that the dissociation of the ADH · DPNH · amide complex preferably leads to ER + I, whereupon the dissociation of ER goes much easier. If we assume, by analogy, that $K_{ER,S}$ is $\gg K_{ES,R}$, where S means acetaldehyde, the dissociation velocity constant (k_2) of ER would most probably be rate limiting in the reaction between ADH and an excess of DPN and alcohol, since the large difference between $K_{ER,S}$ and $K_{ES,R}$ could scarcely depend only on differences between the association velocity constants of ER to S and ES to R. The kinetic experiments should therefore be expected to give the true values of $k_2 \cdot K_{E,R}$ as determined either in equilibrium or in kinetic measurements agreed at all pH values [3], that is $K_{E,R} = k_2/k_1$ (where k_2 is the dissociation, k_1 the association velocity constant). Since $K_{E,R}$ and k_2 are most probably essentially correct we may draw the conclusion that the value found for k_1 in kinetic experiments must be near the true one too. Why is this so? $K_{E,I}$ for *iso*butyramide is certainly much larger than $K_{E,R}$ (See Table 5), which could depend in part on the association velocity constant of E + R being larger than that of E + I. If, by analogy, the same holds true for E + R *versus* E + S (aldehyde) this would imply preferred formation of ER in a mixture E + R + S. However, in the kinetic experiments k_1 becomes rate-limiting only at low [R] and high [S], so that E will nevertheless perhaps combine with S before it combines with R. If this is the case, the kinetic experiments can give true values for k_1, only if the association velocity constants of E + R and of ES + R are about the same.

The formation of ternary complexes with long-chain acids and amides is in line with the substrate specificity studies on the liver ADH system with different aldehydes and alcohols recently reported by one of us (A.D.W.) [4] **. Higher alcohols such as octanol and decanol are good substrates whereas cetyl- and stearyl-alcohols are very poor substrates, and both of the latter alcohols show about the same initial reaction velocities under identical experimental conditions ***. The failure of the fatty acids from C_{16} upwards to form complexes of the type EI may reflect the orientation of the fatty acid on the substrate site. If it is considered, therefore, that aldehydes and amides on one side, and alcohol and acids on the other side function as structural analogs, there is strong suggestion that the ADH · DPNH · amide and ADH · DPN · fatty acid complexes, in which no net reaction occurs, represent complexes analogous with those formed between ADH, DPNH, aldehyde and ADH, DPN · alcohol.

---

* An example of ternary complex formation leading to $K_{EI,R}$ being $> K_{E,R}$ has recently been observed by H. Theorell and J. S. McKinleyMcKee (unpublished) in the highly fluorescent complex ADH · DPNH · imidazole.

** With yeast ADH, ternary complexes of the type ERI with amides and EOI with fatty acids are also formed. However, in this case increasing chain length does not seem to increase the stability of the complexes appreciably (unpublished observations of Thomas Langan Jr.). This is in accord with the very different specificity requirements of the yeast enzyme.

*** A manuscript describing the specificity of higher alcohols on the liver alcohol dehydrogenase system is in preparation.

Thus, from these inhibition studies of substrate analogs, it seems that not only is the coenzyme important for the binding of substrate but also the substrate is important for the binding of coenzyme. One should perhaps speak of enzyme-coenzyme specificity rather than enzyme specificity. In the natural enzymatic reaction involving a simultaneous change of one form of the coenzyme to another and a corresponding change in the substrate, it would appear that the change from one to another requires a coordinated change in molecular shape of both coenzyme and substrate. The fact that the substrate analogs were found to form ternary complexes with ADH and either, but not both, DPN or DPNH, suggests that the reactive ADH · DPN · alcohol and ADH · DPNH · aldehyde complexes can be formed, but not the non-reacting ADH · DPN · aldehyde or ADH · DPNH · alcohol complexes. Such complexes would involve a corresponding inhibition of enzyme activity and Nature has, it seems, found stereochemical means of preventing their formation at least to any disturbing extent.

Remark by H.T., February 10, 1960. The experimental work described here was finished in June 1959. Refinement of the fluorometric technique has afterwards revealed that DPN to some extent lowers the Q-values of ER. As a consequence hereof the values for $K_{E,O}$ given in this paper and in Ref.[14] (84—125 μM) are somewhat too low. A more probable value is 160 μM. This discrepancy does not affect the general conclusions, but the absolute values of the dissociation constants $K_{EO,I}$ and $K_{EI,O}$ may have to be somewhat revised.

Acknowledgements. Thanks are due to Mr. L.-G. Falksveden for skilful technical assistance, and to *Knut och Alice Wallenbergs Stiftelse, The Rockefeller Foundation, Statens naturvetenskapliga forskningsråd* and *Statens medicinska forskningsråd* for financial support.

REFERENCES

1. Theorell, H., Nygaard, A. P. and Bonnichsen, R. *Acta Chem. Scand.* **9** (1955) 1148.
2. Theorell, H. and Nygaard, A. P. *Acta Chem. Scand.* **8** (1954) 1649.
3. Theorell, H. and Winer, A. D. *Arch. Biochem. Biophys.* **83** (1959) 291.
4. Winer, A. D. *Acta Chem. Scand.* **12** (1958) 1695.
5. Winer, A. D. and Schwert, G. W. *J. Biol. Chem.* **234** (1959) 1155.
6. Bonnichsen, R. and Brink, N. G. in Colowick, S. P. and Kaplan, N. O. *Methods in Enzymology*, Vol. I, p. 495. Academic Press, New York 1955.
7. Dalziel, K. *Acta Chem. Scand.* **11** (1957) 397.
8. Boyer, P. D. and Theorell, H. *Acta Chem. Scand.* **10** (1956) 447.
9. Theorell, H. *Scand. J. Clin. Lab. Invest.* **10**, suppl. 31 (1957).
10. Velick, S. *J. Biol. Chem.* **233** (1958) 1455.
11. Winer, A. D. and Schwert, G. W. *Biochim. et Biophys. Acta* **29** (1958) 424.
12. Theorell, H. *Advances in Enzymol.* **20** (1958) 31.
13. Theorell, H. and Chance, B. *Acta Chem. Scand.* **5** (1951) 1127.
14. Theorell, H. *Ciba Foundation Symposium on Significant Trends in Medical Research* 1959, p. 18.

Received February 11, 1960.

ACTA CHEMICA SCANDINAVICA 14 (1960) 1743–1748

Preparation of Crystalline Cytochrome c from Beef Heart Muscle

SVEN PALÉUS

Medicinska Nobelinstitutet, Biokemiska avdelningen, Karolinska Institutet, Stockholm, Sweden

A simple method for the crystallization of beef heart cytochrome c is described. Amino acid analysis together with a number of physico-chemical characteristics of the preparation are reported. An explanation for previous discrepancies in the sulphur content of cytochrome c is given.

For some years we have been concerned with the development of a simple, reproducible method [1] of preparing crystalline mammalian cytochrome c *. As early as 1950 we introduced a new chromatographic procedure [2] in the preparation of cytochrome c. This involved the use of the ion-exchange resin Amberlite IRC-50 and much of the procedure to be described is based on the use of this carboxylic acid type resin. Japanese biochemists [3–6] who have recently carried out a great deal of work with cytochrome c from a variety of sources have taken advantage of this ion exchange treatment during the purification and concentration procedure. The acid extraction of cytochrome c was introduced by Theorell [7] and was also employed in the classical modifications by Keilin and Hartree [8,9]. The latter workers, however, used trichloroacetic acid both for the extraction and the final precipitation of the pigment. There has been some question, however, as to the effect of TCA on cyt.c and as we [10] had already found H_2SO_4 to give a better yield in the extraction of salmon heart cyt.c this acid was accordingly used for the extraction of beef heart cyt.c.

EXPERIMENTAL

Assay method. The concentration of cyt.c was determined spectrophotometrically after reduction with sodium dithionite in 0.065 M phosphate buffer, pH 6.8 using $E_1^{1\ \mathrm{cm}}_{\%}$ 550 mμ = 22.7, corresponding to cytochrome c of 0.435 % iron content.

* The following abbreviations will be used: cyt.c = cytochrome c, TCA = trichloroacetic acid.

Preparation of resin

(*A*) *Amberlite.* 1/2 kg Amberlite XE-64 was suspended in 1 l 2 N NaOH and allowed to stand in a water-bath (50°) for 6 h with occasional stirring. The supernatant was discarded and the resin washed with distilled water until neutral. 5 l of 5 % H_2SO_4 were then added and the mixture after stirring allowed to stand for 1/2 h. The resin was next washed with distilled water until neutral and then suspended in 5 l of 5 % ammonium hydroxide and allowed to stand for 1 h with occasional stirring. Finally the resin was washed with redistilled water until neutral and filtered on a Büchner funnel until nearly dry (20 % moisture content). The resin was stored in this state.

(*B*) *Duolite.* 10 g of Duolite CS-101 was ground by hand using a pestle and mortar and suspended in 200 ml 2.5 % H_2SO_4. It was then washed with distilled water until neutral; at the same time the finest particles were removed by decantation. The ammonium salt of the resin was formed by standing for 1/2 h with occasional stirring in 250 ml of 5 % ammonium hydroxide. It was then washed with distilled water until neutral. The regeneration procedure was repeated once, using redistilled water instead of distilled water as formerly. It was filtered and stored damp as for the Amberlite.

Preparation and purification of cytochrome c

Step 1. 6 kg fresh cow hearts were minced, 15 l of cold distilled water added and the pH adjusted to 4.1 with 1 N H_2SO_4. This and the subsequent steps were carried out at 4°. The mixture was allowed to stand for about 1 h with occasional stirring. After filtration through cheese cloth the mince was extracted further with 6 l of water. The total extract was brought to pH 7 with 4 N ammonia, allowed to stand for 1 ½ h, then centrifuged (2 000 *g*) and the supernatant filtered through Whatman No. 1 paper. This resulted in a volume of 20.7 l, which contained 132 g total protein determined by the biuret reaction as modified by Gornall *et al.*[11]

Step 2. 198 g of Amberlite XE-64 were added and the mixture stirred occasionally over 2 h. The resin which by then had taken up the cyt.c was washed with about 50 l distilled water on a Büchner funnel. The cyt.c. was eluted in a total volume of 3 400 ml 0.15 M phosphate buffer, pH 7. It was then dialyzed against 65 l of 0.002 M ammonium hydroxide and centrifuged. The final volume was 3 425 ml with a total protein content of 6.2 g and a cyt.c. content of 925 mg as determined by spectrophotometric assay.

Step 3. The preparation was next concentrated by adsorption on 10 g of Amberlite XE-64. The resin was washed with about 400 ml 0.002 M ammonium hydroxide and the cyt.c eluted in 475 ml 0.09 M phosphate buffer, pH 7.5.

Step 4. Am_2SO_4 was now added in a concentration of 0.6 g/ml, the preparation allowed to stand overnight and filtered through a Whatman No. 1 filter paper (14 cm diam.). The volume at this stage was 600 ml. The preparation was dialyzed against approx. 50 l 0.002 M ammonium hydroxide, and finally against 18 l of 0.05 M ammonium phosphate buffer, pH 7.

Step 5. The preparation (volume 850 ml) was next concentrated on a column (2 × 20 cm) of Duolite CS-101 and washed with 150 ml 0.05 M ammonium phosphate buffer pH 7 and eluted in 28 ml 0.4 M ammonium phosphate buffer pH 7. The total yield of cyt.c was 436 mg.

Crystallization

346 mg of the above material was dialyzed against a total of 6 l of 0.002 M ammonium hydroxide in 3 changes. Part of this preparation was used for an iron content determination and other analyses; the remainder was dialyzed against 50 % saturated Am_2SO_4, pH 7, and finally against 98 % saturated Am_2SO_4, pH 7. The starting volume for crystallization was 12.5 ml and the concentration of cyt.c was 23.9 mg/ml. 200 µl ammonium hydroxide (25 %) and 10 mg ascorbic acid were added; the pH as measured with the glass electrode was 8.5. After 12 h at room temperature there was a precipitate of rod-like crystals, which after several days were transformed into ball-like aggregates which have earlier been described by Hagihara *et al.*[3] The crystals which were collected by centrifuga-

tion were in the reduced state. The supernatant (10 ml) was also completely reduced, and contained 4.26 mg cyt. c/ml. The yield of crystals was therefore 86 %. The crystals were dissolved in 0.8 ml distilled water, 5 mg ascorbic acid and, 150 µl ammonium hydroxide (25 %) were added, and Am_2SO_4 was then added in solid form to 93 % saturation. Similar crystals were again obtained on standing; in this case the supernatant contained 20 mg cyt. c and the crystal yield here was 92 %. For a third crystallization the crystals were again collected by centrifugation. They were then washed with 5 ml 98 % saturated Am_2SO_4-solution (pH 8) and dissolved to 5 ml with distilled water. 250 µl ammonium hydroxide (25 %) and 5 mg ascorbic acid were added (pH 9.5) and then solid Am_2SO_4 to 80 % saturation whereupon precipitation occurred. Crystals (Fig. 1) formed after 1 ½ days. There was again a tendency of the crystals, especially at first, to come together in ball-like aggregates. On standing, a partial transformation of the crystals into plates occurred as was described by Hagihara *et al.*[4] The crystals were collected by centrifugation (87 % yield), dissolved in the minimum volume of water and dialyzed against distilled water until sulphate free.

Analytical results obtained on thrice crystallized cytochrome c

The iron content as determined by the modified Lorber method [12] was 0.43 %.

The homogeneity of the pigment was tested by electrophoresis in the Spinco model H instrument. The preparation was dissolved in phosphate buffer pH 7.08, ionic strength 0.1, and completely oxidized by careful addition of $K_3Fe(CN)_6$. Only one symmetrical peak was obtained after 4 h running.

The extinction ratios $\frac{E_{550\ m\mu\ red}}{E_{280\ m\mu\ ox}} = 1.20$, $\frac{E_{590\ m\mu\ ox}}{E_{590\ m\mu\ red}} = 5.85$ and $E^{1\ \%}_{1\ cm}$ 550 mμ = 22.6 were obtained.

The nitrogen content (Dumas) was 14.83 %. The sulphur content of the preparation at this stage was determined to be 1.42 %. However, after passage through a column (10 × 2 cm) of Lewatite MIH (a weakly basic anion exchange resin from Farbenfabriken

Table 1. Amino acid composition of crystalline beef cytochrome c (0.43 % Fe; Mol. wt = 12 900; 14.83 % N — Dumas method). 2.5—5.5 mg of cyt.c hydrolyzed 20 and 70 h at 110 °C with 0.5 ml 5.7 N HCl in a sealed, evacuated tube. For a small (< 1 %) residue of black humin substance, correction was made in the 70 h sample.

Amino acid residue	Number per molecule			Amino acid residue	Number per molecule		
	Time of hydrolysis 20 h	70 h	According to Ehrenberg and Theorell [16]		Time of hydrolysis 20 h	70 h	According to Ehrenberg and Theorell [16]
Aspartic acid	7.93	8.11	9.4	Lysine	17.11	18.48	18.3
Serine + Threonine	8.38	7.02	8.5	Histidine	2.83	3.20	3.1
Glutamic acid	11.62	11.9	11.9	Arginine	1.98	2.05	3.4
Glycine	15.13	14.85	15.5	Phenylalanine	4.17	4.06	3.3
α-Alanine	6.04	6.07	6.6	Methionine	1.68	1.01	
Valine	3.06	2.80	3.3	Cysteine	2.0 *		
Proline	4.29	3.83	3.9	Tryptophane	1.0 **		
*Iso*leucine	5.86	5.88	6.2				
Leucine	5.88	6.38	6.2				
Tyrosine	3.63	3.40	3.8				

* According to Paléus [21]

** According to Theorell and Åkesson [18]

Table 2. Summary of purification procedure of cytochrome c.

	Fe content %	Amount of cyt.c.* Volume (ml)	mg/ml	total mg	Yield %	Purity $E^{1\,\%}_{1\,cm}$ 550 mμ
1. Extraction		20 700	—	—	—	—
2. After concentration on XE-64, 1st time	0.17	3 425	0.27	925	100	6.7
3. Concentration on XE-64, 2nd time		475	1.41	670	72	—
4. After Am_2SO_4 treatment	0.38	614	0.99	612	66	19.8
5. After concentration and chromatography on Duolite CS-101	0.41	28	15.57	436	47	21.8
After third crystallization	0.43			284	31	22.6

* Starting weight of minced beef heart —6 kg.

Bayer, Leverkusen) this value was reduced to 1.05 %. An amino acid analysis according to Moore *et al.*[13] is given in Table 1. A portion of the sample dissolved in 0.065 M phosphate buffer, pH 6.8, and reduced with a small excess of ascorbic acid in a loosely capped cuvette was still in the fully reduced state over a period of three days.

DISCUSSION

As already reported [1] the early method of preparing crystalline beef heart cyt.c by Hagihara *et al.*[3] did not give a homogeneous preparation. The homogeneity of the preparation described here was indicted by the electrophoretical result and the yield of crystals calculated on the weight of the starting material has been nearly doubled over that obtained by the above workers. In Table 2 a summary has been given of the purification method. It should be noted how well the iron-content increases up to the value of 0.43 % in the last step and also how the $E^{1\,\%}_{1\,cm}$ 550 mμ-values conform with the iron-values. It was very difficult to obtain the high ratios of $\frac{E_{550\ m\mu\ red}}{E_{280\ m\mu\ ox}}$ as reported by Hagihara *et al.*[3] The values were variable without apparent reason within the range 1.15—1.30. On the other hand the value of 5.85 for the ratio $\frac{E_{590\ m\mu\ ox}}{E_{590\ m\mu\ red}}$ was close to but slightly higher than the values reported by Henderson and Rawlinson [14] and also Margoliash *et al.*[15] for resin-purified but not crystallized material.

The amino acid analysis (Table 1) revealed values which agreed well in most cases with the results of Ehrenberg and Theorell [16]. There is a difference of one amino acid residue in the case of aspartic acid, arginine and phenylalanine; the difference in the case of glycine, serine and threonine is insignificant. Compared with the results of Takahashi *et al.*[17] there are some further small differences, especially in the case of glutamic acid, serine and threonine, tyrosine and α-alanine. On the other hand the phenylalanine content is the

Fig. 1. Crystalline beef cytochrome c (× 430), Crystal size, 2 × 10 μ. Reduced form.

same in both preparations. It should be noted that the three above-mentioned analyses were carried out on samples of cyt.c prepared by different methods.

The nitrogen content (14.83 %) of the crystals was rather low and corresponded to 137 N-atoms per iron atom. This result was in conformity with other analyses carried out by the author on different preparations of cyt.c [10]. On adding the nitrogen-atoms of all the amino acids present (using the highest value from the 20 and 70 h hydrolyses) together with the four porphyrin-nitrogen atoms, 139 nitrogen-atoms (15.08 % N) are obtained. Earlier, Theorell and Åkeson [18] had found 143 and Paul [19] 145 nitrogen atoms per iron atom, but their preparations had been obtained by different methods.

The iron content of 0.43 % corresponds to a minimal molecular weight of 12 900, which value was used in the calculation of the amino acid content of the preparation.

Åkeson [20] showed that two methionine residues were present in cyt. c. Confirmation of this was obtained by the author [21] but at the same time four sulphur atoms only were found to be present. The remaining two S-atoms were accounted for as the two cysteine residues shown by Theorell [22] to be concerned in the prosthetic group linkage. There still remained, however, the discrepancy between the 5—6 sulphur atoms observed by Theorell and Åkeson [18] and Åkeson [20]. This appears now to be explained by the finding that the sulphur content is reduced from 6 to 4 atoms per cyt.c molecule by passage through an anionic resin. As no other significant change in the cytochrome c molecule has been observed by this treatment and as the author's former value

of 4 sulphur atoms per molecule was obtained after exhaustive dialysis it would seem likely that two salt linked sulphate ions are removed by the anionic resin.

Addendum: The sedimentation constant of this thrice crystallized material was $S^\circ_{20} = 1.62 \times 10^{-13}$ *s*, very close to the value found in this laboratory for previous preparations [23]. Determination of the molecular weight of crystalline beef cyt.c by Ehrenberg [24] has given a value of 13 300, which is in agreement with the value obtained above from the iron content (12 900).

Acknowledgements. The author wants to express his sincere gratitude to Professor H. Theorell and Dr. R. W. Henderson for kind criticism in connection with the work.

The work was supported by grants from *Statens naturvetenskapliga forskningsråd* and *Magn. Bergvalls Stiftelse.* It is a pleasure to thank Misses A.-M. Fridén and G. Tietgen for technical assistance.

REFERENCES

1. Paléus, S. and Theorell, H. *Acta Chem. Scand.* **11** (1957) 905.
2. Paléus, S. and Neilands, J. B. *Acta Chem. Scand.* **4** (1950) 1024.
3. Hagihara, B., Morikawa, I., Sekuzu, I., Horio, T. and Okunuki, K. *Nature* **178** (1956) 629.
4. Hagihara, B., Morikawa, I., Sekuzu, I. and Okunuki, K. *J. Biochem. Tokyo* **45** (1958) 551.
5. Hagihara, B., Yoneda, M., Tagawa, K., Morikawa, I. and Okunuki, K. *J. Biochem. Tokyo* **45** (1958) 565.
6. Hagihara, B., Tagawa, K., Morikawa, I., Shin, M. and Okunuki, K. *J. Biochem. Tokyo* **45** (1958) 725.
7. Theorell, H. *Biochem. Z.* **279** (1935) 463.
8. Keilin, D. and Hartree, E. F. *Proc. Roy. Soc. (London)* **B 122** (1937) 298.
9. Keilin, D. and Hartree, E. F. *Biochem. J.* **39** (1945) 289.
10. Paléus, S. *Acta Chem. Scand.* **8** (1954) 971.
11. Gornall, A. G., Bardawill, C. J. and David, M. M. *J. Biol. Chem.* **177** (1949) 751.
12. Paul, K. G. *Acta Chem. Scand.* **2** (1948) 430.
13. Moore, S., Spackman, D. H. and Stein, W. H. *Anal. Chem.* **30** (1958) 1185.
14. Henderson, R. W. and Rawlinson, W. A. *Biochem. J.* **62** (1956) 21.
15. Margoliash, E., Frohwirt, N., and Wiener, E. *Biochem. J.* **71** (1959) 559.
16. Ehrenberg, A. and Theorell, H. *Acta Chem. Scand.* **9** (1955) 1193.
17. Takahaski, K., Titani, K. and Minakami, S. *J. Biochem. Tokyo* **46** (1959) 1323.
18. Theorell, H. and Åkeson, Å. *J. Am. Chem. Soc.* **63** (1941) 1804.
19. Paul, K. G. *Acta Chem. Scand.* **5** (1951) 379.
20. Åkeson, Å. *Acta Physiol. Scand.* **4** (1942) 362.
21. Paléus, S. *Acta Chem. Scand.* **9** (1955) 335.
22. Theorell, H. *Enzymologia* **6** (1939) 88.
23. Ehrenberg, A. and Paléus, S. *Acta Chem. Scand.* **9** (1955) 538.
24. Ehrenberg, A. *Acta Chem. Scand.* **11** (1957) 1257.

Received July 19, 1960.

ACTA CHEMICA SCANDINAVICA 14 (1960) 1749–1762

Application of Edman's Phenyl*iso*thiocyanate Method in the Determination of C-terminal Amino Acids and Peptides after Hydrazinolysis *

PER WALLÉN and INGVAR SJÖHOLM**

Chemistry Department II, Karolinska Institutet, Stockholm, Sweden

Edman's phenyl*iso*thiocyanate method has been used for identification and quantitative determination of the C-terminal amino acids released in hydrazinolysis of fibrinopeptides A and B and of insulin. The method is found to be particularly suitable in cases where relatively large amounts of C-terminal peptides are formed, since it can also be used for sequence determinations of these peptides. For more detailed studies of complicated hydrazinolysates, Edman's method can be preceded by electrophoretic separation. The C-terminal sequences of fibrinopeptides A and B and of insulin as found in the present work are in accordance with the known structure of these substances.

Certain peptide bonds are found to be highly resistant to hydrazine under the conditions used (100°C for 10 h). In hydrazinolysis of fibrinopeptide A, only an inappreciable quantity (5 %) of ornithine is obtained from the C-terminal amino acid arginine, whereas a good yield (about 70 %) is obtained from the di- and tripeptides val-orn and gly-val-orn, respectively, deriving from the C-terminal end. Thus, the peptide bond val-orn (val-arg) seems to be only inappreciably split in hydrazinolysis. The C-terminal peptide bond in fibrinopeptide B, ala-orn (ala-arg), also seems to be relatively resistant, as is the penultimate peptide bond in the B-chain of insulin, pro-lys.

The phenylthiohydantoin (PTH) derivative of ornithine has been synthesized. A solvent system is described for separation of the phenylthiohydantoin derivatives of lysine and ornithine.

After the introduction by Akabori *et al.*[1] of the hydrazinolysis method for determination of C-terminal amino acids in peptides and proteins, this technique has been applied in many investigations. The method elaborated by Ohno [2] for identification and determination of the amino acids obtained after hydrazinolysis as the dinitrophenyl derivatives has subsequently been

* This work has been supported by Research Grant No. H—4295 (R 1) to Professor E. Jorpes from the *National Heart Institute, National Institutes of Health, United States Public Health Service*, and by grants from *Karolinska Institutets Reservationsanslag, Svenska Sällskapet för Medicinsk Forskning* and *Svenska Nationalföreningen mot tuberkulos och andra folksjukdomar.*

** Present address: Pharmacognosy Department, Kungl. Farmaceutiska Institutet, Stockholm, Sweden.

adopted by many workers, particularly in the modification of Niu and Fraenkel-Conrat [3]. In view of the finding of Ohno [2,4] and of Niu and Fraenkel-Conrat [3] that C-terminal peptides are formed both on partial hydrazinolysis and when the C-terminally situated peptide bonds are resistant to hydrazine, the question arose of whether the phenyl*iso*thiocyanate method of Edman [5] could be applied in the analysis of amino acids and peptides obtained on hydrazinolysis. In the determination of the amino acid sequence of peptides, this method is more advantageous than the dinitrophenyl (DNP) method most often used hitherto.

An account is given in the present paper of the application of Edman's method in C-terminal analyses of fibrinopeptides A and B and of insulin by the hydrazinolysis method, as well as of some observations on the resistance of certain peptide bonds to hydrazine. The phenyl*iso*thiocyanate method as modified by Sjöquist [6-8,22] was used.

EXPERIMENTAL

Materials

*Fibrinopeptide A**.

*Fibrinopeptide B**.

Insulin, recrystallized 7 times **.

Hydrazine, anhydrous. Prepared according to Kusama [10]***. 50 g of 99 % $N_2H_4 \cdot H_2O$, 500 g of crushed CaO and 500 g of toluene were allowed to stand overnight. The mixture was then refluxed for 3 h and distilled. An azeotropic mixture was obtained, consisting of toluene and hydrazine, b.p. 89—92°C. The hydrazine content was determined with KIO_3, using the method of Kolthoff [11]. Content: 98.2—99.5 %. Fresh hydrazine was prepared for each hydrazinolysis.

n-*Heptaldehyde*, technical, Hopkin & Williams. Distilled *in vacuo*.

n-*Heptane*, Eastman-Kodak. Distilled, b.p. 98°C.

5-[3-(β-Phenylthioureido)-propyl]-3-phenyl-2-thiohydantoin (Ornithine-PTH). Prepared according to Edman's method for preparation of lysine-PTH [12]. The extinction curve showed a maximum at $\lambda = 268$ mμ ($\varepsilon = 27\,650$). $E^{245}/E^{269} = 0.71$. M.p. 196-7°C (decomp.). (Found: N 14.45 %. Calc. 14.57).

n-*Pentane*, A. R., Kebo, Stockholm.

1,2-Dichloroethane, Hopkin & Williams. Distilled, b.p. 83—84°C.

Ethyl acetate, Hopkin & Williams. Distilled, b.p. 77°C.

Formic acid, A. R., Merck.

Methods

Hydrazinolysis. Before hydrazinolysis, the peptide material was dried *in vacuo* for 8—10 h in a desiccator over phosphorus pentoxide. 100 μl of N_2H_4 were used for 3 mg of peptide, 200 μl for 12 mg, and 500 μl for 55 mg. Four-ml test tubes with groundglass stoppers were used for hydrazinolysis, which was carried out for 10 h at 100°C. The excess N_2H_4 was evaporated *in vacuo* over concentrated sulphuric acid for 2—3 h. After this time, no smell of hydrazine was present.

Aldehyde treatment. The hydrazides formed were removed by shaking with *n*-heptaldehyde, as recommended by Kusama [10]. The preparations were dissolved in 0.5 ml

* Prepared according to Ref.[9] and kindly placed at our disposal by Dr. B. Blombäck, Karolinska Institutet, Stockholm.

** Kindly placed at our disposal by Mr. G. Lindén, Apoteksvarucentralen Vitrum, Stockholm.

*** Hydrazine prepared according to Ståhler [13] or Locker [14] had no advantages, both the relative quantity of C-terminal amino acids obtained and the total yield were smaller.

of water, shaken three times with 0.75 ml of *n*-heptane + *n*-heptaldehyde (1 : 1) for 5, 30 and 30 min, after which the aqueous phase was freed from heptaldehyde by shaking twice with 0.5 ml of heptane. Finally, it was shaken twice with 0.5 ml of *n*-pentane. The aqueous phase was evaporated *in vacuo* over P_2O_5. The dried preparations were kept at −15°C.

The addition of heptane during the aldehyde treatment results in a larger yield of amino acids and peptides in the aqueous phase. In order to minimize the risk of the hydrazides being hydrolyzed, the first treatment with heptane-heptaldehyde should be carried out quickly.

Sequence determination. The amino acid sequence in the peptides was determined with the phenyl*iso*thiocyanate method of Edman, as modified by Sjöquist [6-8,22]. The peptide material was treated with phenyl*iso*thiocyanate in a buffer solution of pH 10 for 1 h at 40°C, resulting in formation of the phenylthiocarbamyl (PTC) derivatives of the peptides. The samples were washed with heptane and dried *in vacuo* (< 0.01 mm Hg). The phenyl*iso*thiocyanate treatment was repeated once. The phenylthiohydantoin (PTH) derivatives of the N-terminal amino acids were obtained from the PTC peptides by treating them with a mixture of acetic acid saturated with hydrogen chloride and water (2 : 1) at 40°C for 2 1/2 h. The samples were then re-dried *in vacuo*.

A mixture of dichloroethane, ethyl acetate and *n*-heptane (2 : 2 : 1.5) with a density slightly lower than that of water, was washed 3 times with an equal volume of water. The last washing water (aqueous phase) was used to dissolve the vacuum-dried samples, after which the PTH derivatives were extracted twice with 0.75 ml and three times with 0.5 ml of the solvent mixture. The organic phase was evaporated by a stream of air, and the aqueous phase *in vacuo* over P_2O_5.

The dried aqueous phase, which contained the remaining part of the peptide, could then be re-treated with phenyl*iso*thiocyanate, after which the procedure already described was repeated. All operations, from hydrazinolysis to extraction of the PTH derivatives inclusively, were performed in the same test tube.

The PTH derivatives were identified and determined quantitatively by paper chromatography, according to Sjöquist [8]. On hydrazinolysis arginine is converted to ornithine. In Sjöquist's system, ornithine-PTH migrates with lysine-PTH and glycine-PTH in solvent II, and with lysine-PTH and alanine-PTH in solvent III. Consequently, ornithine cannot be determined separately from lysine. In order to permit concurrent determination of the two basic amino acids separately in a mixture, we used a solvent system consisting of *n*-heptane, dichloroethane and 75 % formic acid (1 : 1 : 2). The organic phase was used as eluent, and was also sprayed over the strips of filter paper on the short ends of a chromatography tank of the kind described by Sjöquist [8]. The formic acid phase (stationary phase) was sprayed over the strips of filter paper hanging in the tank. Each time the tank was used, the old stationary phase was replaced by a fresh one. One hour was required for equilibration. With this system, the PTH-derivatives of glycine, ornithine, lysine and alanine could be completely separated (see Fig. 1).

Paper electrophoresis. Electrophoresis of the peptide material obtained after hydrazinolysis and heptaldehyde treatment was performed with a water-cooled high-voltage apparatus of Perspex. A buffer consisting of 6 ml of glacial acetic acid and 8 ml of pyridine in 1 liter of water (pH 4.9) was used throughout. Whatman No. 3 MM paper was used for preparative electrophoresis. A potential of 25 V/cm was applied across the paper, resulting in a current intensity of approximately 30 mA. Adequate separation was obtained after about 1 1/2 h.

The preparation was placed on a 5 cm wide strip. In order to identify the fractions, a small quantity of the preparation was applied as a spot beside the main part of it. After electrophoresis and drying at 100°C, a strip corresponding to this spot was cut out, and developed with a ninhydrin reagent (0.25 % ninhydrin + 0.5 % collidine in 95 % ethanol). The fluorescence of the substances in ultraviolet light was also used for identification purposes. The fractions were eluted with water, and the eluates evaporated *in vacuo* over P_2O_5.

Hydrolysis. Hydrolysis of the peptides was carried out in constantly boiling hydrochloric acid at 105°C for 23 h, using evacuated sealed glass tubes.

Two-dimensional paper chromatography. Two-dimensional paper chromatography, performed on both unhydrolyzed and hydrolyzed electrophoretic fractions, was done on Whatman No. 1 paper. Development of the chromatograms took place in the first direc-

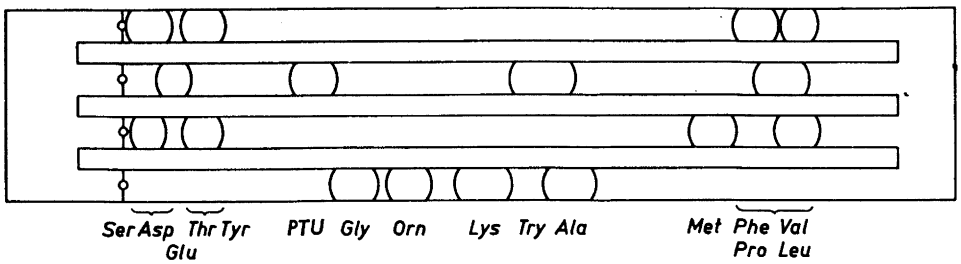

Fig. 1. Separation of PTH derivatives of glycine, ornithine, lysine and alanine. Solvent: *n*-heptane-dichloroethane -75 % formic acid (1 : 1 : 2).

tion (descending) with the upper phase of a mixture of acetic acid, *n*-butanol and water (1 : 4 : 5), and in the second direction (ascending) with 80 % pyridine in water.

Quantitative amino acid analysis. Quantitative analysis of the amino acids in hydrolyzed material was performed according to Sjöquist [8].

RESULTS

Fibrinopeptide A. Hydrazinolysis according to the standard procedure described in the aforegoing was performed on about 1 μmole (1.89 mg) of fibrinopeptide A. After removal of the hydrazides, sequence determination was made on the C-terminal fraction, without previous separation by electrophoresis or paper chromatography. The results are shown in Table 1. In the first step, glycine and valine were obtained as the main components. On the other hand, ornithine — which on hydrazinolysis is formed from arginine — appeared only in extremely small quantities, and was completely lacking in some experiments. This is remarkable, since it has recently been demonstrated that the C-terminal sequence in fibrinopeptide A is gly-val-arg [15,16]. In the second and third steps, on the contrary, ornithine appeared in considerably larger quantities, amounting to 70—80 % of the valine in the preceding step. The valine in the second step corresponded fairly well to the glycine in the first step. In the fourth step, no PTH amino acids could be demonstrated. These experiments seemed to afford definite evidence that hydrazinolysis results in formation chiefly of the C-terminal residues gly-val-orn and val-orn, whereas only extremely small quantities of the C-terminal amino acid are present.

Table 1. Amino acid sequence determination of the heptaldehyde-treated hydrazinolysate of fibrinopeptide A. The values are not corrected for the loss in hydrazinolysis and heptaldehyde treatment.

Amino acid	Mole PTH derivative per mole fibrinopeptide A			
	Step 1	Step 2	Step 3	Step 4
gly	0.35	—	—	Trace
val	0.34	0.22	—	—
orn	0.05	0.27	0.19	—
pro	0.08	—	—	—
asp	0.03	0.04	—	—
glu	0.05	—	—	Trace
ser	0.03	Trace	—	—

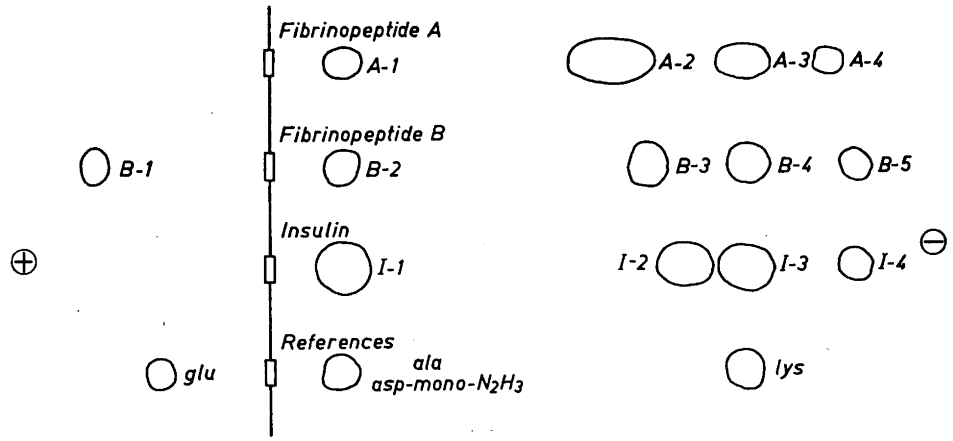

Fig. 2. Electropherograms of hydrazinolyzed and heptaldehyde-treated fibrinopeptides A and B and insulin (pH = 4.9, μ = 0.1 and length of runs 90 min at 25 V/cm in all figures).

For additional verification of these results, attempts were made to separate the components of the hydrazinolysate freed from the hydrazides, by means of electrophoresis and paper chromatography. About 8 μmoles (15 mg) of fibrinopeptide A were hydrazinolyzed with 0.2 ml of hydrazine. The excess hydrazine and the hydrazides were removed as described earlier. In electrophoresis, four fractions could be identified (Fig. 2); they all migrated to the cathode. In the following, they are denoted as A-1, A-2, A-3, and A-4.

A-1, which migrated at the same rate as the neutral amino acids, and A-2, which migrated somewhat more slowly than lysine, were consistently present. A-3, at the site of lysine and ornithine, and A-4, which was strongly basic and could be identified only by its UV fluorescence, were weak and were sometimes lacking altogether.

The fractions were eluted from the paper, divided into two equal parts, and dried. One part of each electrophoretic fraction was used for two-dimensional paper chromatography and for sequence determination (Fig. 3 and Table 2). The other part was hydrolyzed, after which the component amino acids were identified by means of two-dimensional paper chromatography.

In two-dimensional paper chromatography, fraction A-1 showed only two weak components, one of which was probably glycine (Fig. 3). After hydrolysis, on the other hand, several amino acids appeared, *i.e.* proline, as well as traces of serine, aspartic acid, glutamic acid and glycine. Sequence analysis of the unhydrolyzed part of the fraction disclosed that all these amino acids already appeared in the first step, and serine and aspartic acid in the second step as well (Table 2).

Fraction A-2 was shown by two-dimensional paper chromatography to consist of two strong components, which were partly confluent (Fig. 3). Owing to lack of material, no attempt was made to separate and analyze these components individually. After hydrolysis of this fraction, large quan-

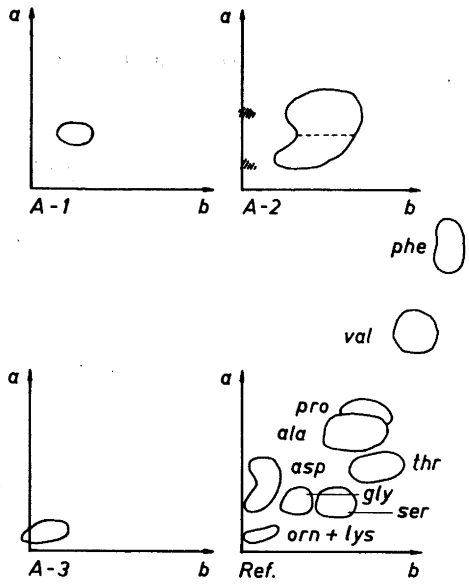

Fig. 3. Two-dimensional paper chromatograms of the electrophoretic fractions A-1, A-2, and A-3, obtained from hydrazinolyzed and heptaldehyde-treated fibrinopeptide A. Solvent a: *n*-butanol-acetic acid-water (4 : 1 : 5). Solvent b: pyridine-water (4 : 1). Traces are indicated by shaded areas.

tities of glycine, valine and ornithine could be demonstrated. In sequence determination, only glycine and valine appeared in the first step (Table 2). In the second step, valine and ornithine appeared in quantities corresponding approximately to the glycine and valine, respectively, in the first step. No glycine appeared in this step. In the third step, ornithine appeared in quantities corresponding to the valine in the second step. No other amino acids could be identified in this step. Fraction A-2 thus seemed to consist of two peptides, val-orn and gly-val-orn.

Table 2. Amino acid sequence determination of electrophoretic fractions from heptaldehyde-treated hydrazinolysate of fibrinopeptide A. The figures denote the number of μmoles obtained from about 4 μmoles (7.6 mg) of fibrinopeptide A. The values are not corrected for the loss in hydrazinolysis, heptaldehyde treatment and electrophoresis.

Fraction	Amino acid	Step 1	Step 2	Step 3
A—1	pro	0.09	—	—
	ser	0.03	0.03	—
	asp	0.03	0.03	—
	glu	0.06	—	—
	gly	Trace	—	—
A—2	gly	0.60	—	—
	val	0.92	0.41	—
	orn	—	0.92	0.47
A—3	orn	0.08	—	—
A—4	—			

Table 3. Amino acid sequence determination of the heptaldehyde-treated hydrazinolysate of fibrinopeptide B. The values are not corrected for the loss in hydrazinolysis and heptaldehyde treatment.

Amino acid	Mole PTH derivative per mole fibrinopeptide B		
	Step 1	Step 2	Step 3
pro	0.03	—	—
ala	0.14	0.02	—
orn	0.18	0.09	Trace
lys	0.03	0.01	—
glu	0.05	—	—
asp	0.16	—	0.02
gly	Trace	Trace	—

In paper chromatography of fraction A-3, only one spot at the site of lysine and ornithine was obtained before hydrolysis (Fig. 3). The result was the same after hydrolysis. Sequence determination gave ornithine alone in the first step, and no amino acids in the two subsequent steps. This fraction thus consisted only of ornithine. Quantitatively, however, it amounted to only a small proportion (6—7 %) of the ornithine in the C-terminal fragments of A-2.

Fraction A-4 gave no ninhydrin-positive spot in direct paper chromatography. After hydrolysis, one weak spot at the site of lysine and ornithine was obtained in two-dimensional chromatography. No PTH derivatives of these amino acids were, however, obtained in determination with Sjöquist's method.

Fibrinopeptide B. Fibrinopeptide B was studied in largely the same way as fibrinopeptide A. Sequence determinations were made on the hydrazinolysate remaining after heptaldehyde treatment. The results of one such test are shown in Table 3. In the first step, ornithine, was obtained which agrees with arginine being the C-terminal amino acid. In addition, alanine and aspartic acid appeared in quantities that could not be neglected. The presence of alanine might indicate that the C-terminal dipeptide was present in the sample. As has been shown recently, the C-terminal sequence in fibrinopeptide B is gly-ala-arg [15,16]. In the second step, it was chiefly ornithine that appeared. This may agree with the sequence ala-arg. However, in view of the high aspartic acid value in the first step, the ornithine might equally well have derived from an asp-arg sequence.

In order to obtain further information, paper electrophoresis was performed on the heptaldehyde-treated hydrazinolysate. The appearance of the electropherograms is shown in Fig. 2. Five fractions were identified; they are denoted in the following as B-1, B-2, B-3, B-4, and B-5. B-1 had a negative charge, and all the other fractions a positive charge.

The fractions were eluted with water. Two-dimensional paper chromatography was performed on a small part of each fraction (Fig. 4). Except for traces of glycine in fraction B-2, and spots corresponding to ornithine or lysine in B-3 and B-4, no spots indicative of free amino acids were present. The spots in fraction B-5 could not have been free amino acids, since in electrophoresis

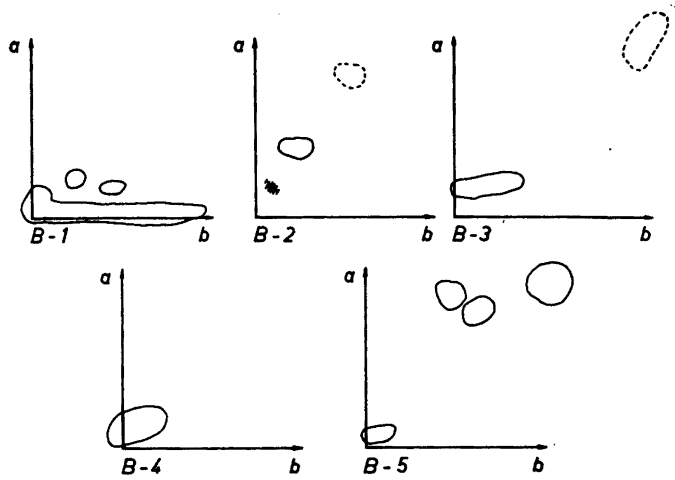

Fig. 4. Two-dimensional paper chromatograms of the electrophoretic fractions B-1, B-2, B-3, B-4, and B-5, obtained from hydrazinolyzed and heptaldehyde-treated fibrinopeptide B. (The solvent system is the same as in Fig. 3.) Faint spots are indicated by dotted lines, traces by shaded areas.

this fraction migrated further than the amino acids conceivably present in the sample.

Part of each electrophoretic fraction was removed and hydrolyzed. Quantitative amino acid analysis according to Sjöquist was then done on the hydrolysate. The results are listed in Table 4. In fractions B-1 and B-2, glutamic acid and aspartic acid predominated. Traces of ornithine and glycine were also demonstrable. Fraction B-3 was found to consist mainly of equally large quantities of alanine and ornithine, in addition to extremely small quantities of lysine, glutamic acid and aspartic acid.

In sequence analysis of the unhydrolyzed fraction B-3, alanine alone appeared in the first step, and ornithine in the second step. It is evident that this fraction consisted chiefly of the dipeptide ala-orn, which must have derived from the C-terminal dipeptide ala-arg. Both before and after hydrolysis, frac-

Table 4. Quantitative determination of the amino acid content of the electrophoretic fractions of hydrazinolyzed and heptaldehyde-treated fibrinopeptide B. The figures denote the number of μmoles obtained from about 3.3 μmoles (8.2 mg) of fibrinopeptide B. The values are not corrected for the loss in hydrazinolysis, heptaldehyde treatment and electrophoresis.

Amino acid	Fraction B—1	B—2	B—3	B—4	B—5
ala	—	—	0.40	Trace	—
orn	0.07	0.06	0.43	0.53	0.14
lys	—	—	0.07	0.08	—
gly	0.13	0.29	—	—	—
glu	0.24	0.47	0.04	0.04	0.04
asp	0.36	0.87	0.03	Trace	Trace

tion B-4 yielded only large quantities of ornithine, in addition to traces of alanine and lysine. This fraction thus consisted mainly of the ornithine derived from the C-terminal amino acid arginine. After hydrolysis of fraction B-5, ornithine appeared, probably derived from the ornithine hydrazide.

In some experiments with fibrinopeptide B, PTH proline appeared in fairly large quantities in the first step of sequence determination of the unfractionated hydrazinolysate. In these cases, approximately equimolar amounts of the PTH derivatives of lysine and valine were obtained in the second and third step, respectively. In the fourth step, glycine could also be traced, but was not determined quantitatively. In qualitative amino acid determinations of the electrophoretic fractions after hydrolysis, fraction B-4 was found to contain proline, lysine, valine and glycine, in addition to the ornithine normally present. Fraction B-3 also contained these amino acids, although in smaller amounts, which made the quantitative determinations unreliable.

In determination of the sequences in these two fractions, proline, lysine, valine, and glycine appeared in the first, second, third, and fourth step, respectively. It is possible that, in these experiments, a peptide hydrazide was formed with the sequence pro-lys-val-gly, which was present in the electrophoretic fraction B-4. In this event, the hydrazide would have been partly hydrolyzed during the procedure, resulting in formation of the corresponding peptide, present in fraction B-3. The reason why this hydrazide was not removed by aldehyde treatment is uncertain. A possible explanation is that, because of its size and charge, this hydrazide had become so hydrophilic that it remained in the aqueous phase on treatment with aldehyde. We did, in fact, also obtain small quantities of ornithine and lysine hydrazides in the electrophoretic fractions B-5 and I-4 (see the following), which indicates that the basic hydrazides are not, as a rule, completely removed by aldehyde treatment.

Insulin. Sequence determination with the procedure described earlier was performed on the heptaldehyde-treated hydrazinolysate from about 2μmoles (11.5 mg) of insulin. The results are summarized in Table 5. Each value is the mean of the values obtained in 14 hydrazinolyses with only small differences between them. As could be expected, alanine appeared in relatively large quantities in step 1, but measurable amounts of proline, lysine and ornithine could also be identified, as well as traces of glycine, glutamic acid and aspartic acid. Since the B-chain of insulin ends with pro-lys-ala [17], it seemed likely that the lysine and proline demonstrable in step 1 comprised the N-terminals of the C-terminal peptides formed in hydrazinolysis. The subsequent analysis did not verify this assumption, since the amount of alanine in steps 2 and 3 by no means corresponded to the quantity of lysine obtained in the preceding step. The results of the sequence determination indicated instead that the hydrazinolysate contained — in addition to small quantities of C-terminal peptides, lys-ala and pro-lys-ala — free lysine and possibly some proline, as well as the peptide pro-lys.

For further elucidation, electrophoretic separation of the heptaldehyde-treated hydrazinolysate was performed, as well as subsequent analysis of the various fractions. In electrophoresis, we obtained four fractions — in one case a fifth as well (Fig. 2); they are denoted in the following as I-1, I-2, I-3, I-4, and I-5. All fractions migrated to the cathode. I-5, which was not invariably

Table 5. Amino acid sequence determination of the heptaldehyde-treated hydrazinolysate of insulin. The values are not corrected for the loss in hydrazinolysis and heptaldehyde treatment.

Amino acid	Mole PTH derivative per mole insulin		
	Step 1	Step 2	Step 3
ala	0.38	Trace	Trace
lys	0.07	0.10	—
pro	0.22	Trace	—
orn	0.04	Trace	—
gly	Trace	—	—
glu	Trace	—	—
asp	Trace	—	—

present, moved further than lysine, and probably consisted of strongly basic hydrazides, which had not been completely removed by aldehyde treatment. No analysis was therefore made of this fraction.

The various electrophoretic fractions were chromatographed both before (Fig. 5) and after hydrolysis in the two-dimensional chromatography system described.

In electrophoresis, fraction I-1 migrated as far as the neutral amino acids and the glutamic and aspartic acid monohydrazides. Chromatographically, it consisted of two fractions. One of them migrated at the site of alanine, and one at the site of glycine. No proline — which, if it had been present in free form, should have appeared in this fraction — was, however, observed. After hydrolysis, a fairly complicated pattern was obtained. In addition to alanine, which gave a strong spot, small quantities of aspartic acid, glycine, serine, lysine and/or ornithine were present, as well as traces of valine, proline and threonine. Thus, in I-1, alanine and possibly glycine migrated, whereas the other amino acids obtained on hydrolysis derived from small quantities of peptide hydrazides with one free carboxyl group, as well as aspartic and glutamic monohydrazides.

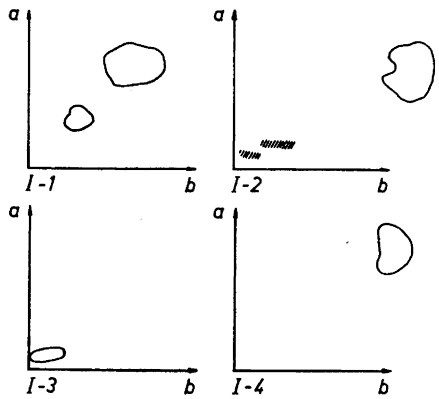

Fig. 5. Two-dimensional paper chromatograms of the electrophoretic fractions I-1, I-2, I-3, and I-4, obtained from hydrazinolyzed and heptaldehyde-treated insulin. (The solvent system is the same as in Fig. 3.) Traces are indicated by shaded areas.

Electrophoretically, fraction I-2 migrated somewhat more slowly than lysine and ornithine. In chromatography of the fraction, we obtained a component which moved like alanine in the butanol direction, but somewhat more slowly than alanine in the pyridine direction. This component reacted strongly to ninhydrin. Two additional fractions, which reacted very weakly to ninhydrin, were present. They migrated close to the site of lysine. After hydrolysis, relatively large quantities of proline and lysine were obtained, as well as extremely small amounts of aspartic acid, glycine and alanine. This fraction thus seemed to consist chiefly of a peptide containing proline and lysine.

Fraction I-3 moved as rapidly in electrophoresis as lysine and ornithine. In our system, the fraction was found chromatographically uniform with a single spot at the site of lysine and ornithine. After hydrolysis, lysine and/or ornithine were demonstrable, as well as traces of aspartic acid and glycine. This fraction thus consisted of free lysine and/or ornithine.

In chromatography, fraction I-4 which yielded a yellow spot in the ninhydrin reaction, moved slightly more rapidly than alanine. After hydrolysis, it proved to consist of lysine and/or ornithine.

The analysis therefore showed that the hydrazinolysate consisted principally of alanine and pro-lys, as well as small amounts of lys-ala, lysine and ornithine. In addition to these peptides and amino acids, it contained small quantities of hydrazides of amino acids and peptides, which had not been removed completely through the aldehyde treatment. The presence of amino acids and peptides that were not C-terminal might imply that undesirable hydrolysis of hydrazides to free amino acids and peptides had occurred in the course of analysis. Previous investigations have, however, shown that if removal of the hydrazides is done rapidly, such hydrolysis takes place only to an inappreciable extent [18]. Another possible explanation is that in preparation of the insulin, it might have been partially split by the traces of trypsin present. Since the action of trypsin has been found to be strictly confined to peptide bonds in which the carboxyl groups of basic amino acids are included, such splitting could have taken place only in the B-chain, between the amino acids 22—23 (arg-gly) and 29—30 (lys-ala) [19]. It is probable that the large fragments thus formed follow the unaltered insulin during the preparation. Those amino acids and peptides obtained in the analysis that can not have been released from the C-terminal sequence in the complete insulin molecule can all have derived from the C-terminal sequence in the fragments formed by the action of trypsin, *i.e.*, glu-arg, which yields orn, and thr-pro-lys, which yields both pro-lys and lys. Evidently the recrystallized insulin used in this work was prepared with a technique in which a certain enzymatic destruction is unavoidable. That such an interaction of trypsin on insulin can occur in the process of manufacturing has since then been demonstrated by Jorpes and Lindén [20]. However heating of the crude alcoholic extract of the pancreatic gland at pH 2.0—4.5 at a temperature of 70°—75°C for 10 min will destroy the trypsin and considerably increase the yield in the large scale manufacture of insulin. The recrystallized insulin used in this work was in fact prepared with a technique in which a certain enzymatic destruction of insulin is unavoidable.

DISCUSSION

When Edman's phenyl*iso*thiocyanate method is applied to a hydrazinolysate of a peptide, the C-terminal amino acid released is determined, as well as the N-terminal amino acids of the C-terminal peptides formed in hydrazinolysis. By utilizing the possibility of sequence determination given by this method, the C-terminal sequence can, in favourable cases, be determined directly on the heptaldehyde-treated hydrazinolysate, without further separation. About 1—2 μmoles of peptide material are required for such an analysis.

A direct sequence determination according to the aforegoing should give sufficiently reliable results in a relatively pure hydrazinolysate from peptides consisting of a single chain. In certain cases, however, it is not possible to obtain a clear picture of the C-terminal constitution of the peptide without further separation of the components of the hydrazinolysate. This applies, for example, in studies of peptides with more than one chain, and those whose structure disposes to the formation of acid peptide hydrazides, which are difficult to remove completely from the hydrazinolysate. By using high-voltage electrophoresis and two-dimensional paper chromatography, we were able to separate from the hydrazinolysate several fractions, which were subsequently analyzed.

Of the analyses performed in the present investigation, those on fibrinopeptide A and insulin gave results that are in agreement with the C-terminal sequence of the peptides. In application of Edman's method to the hydrazinolysate of these peptides, we obtained exceedingly small — in certain cases not measurable — amounts of PTH derivatives, particularly from glycine, aspartic acid and glutamic acid, that could not have been released from the C-terminal parts. The quantities of these amino acids were about as large as those reported by Bradbury [21] in his studies on insulin, *i.e.*, as a rule < 0.05 mole per mole of peptide. After electrophoresis and two-dimensional paper chromatography of the hydrazinolysate it could, in fact, be shown that — with the possible exception of glycine — they did not derive from free amino acids. After hydrolysis of the less basic electrophoretic fractions, we nevertheless obtained small quantities of glutamic and aspartic acid. In view of the rate of migration of the electrophoretic fractions they should have derived from hydrazides. Glutamic and aspartic acid can occur inside a peptide chain with free carboxyl groups. In hydrazinolysis, the free carboxyl group remains intact, whereas a hydrazide group is obtained from the carboxyl group in the peptide bond. It is probable that, at the pH applied in heptaldehyde treatment, the free carboxyl group makes the hydrazone formed slightly hydrophilic, so that in certain cases it is not completely extracted with the organic heptane-heptaldehyde phase. In an attempt to produce more effective removal of the hydrazides, we substituted benzaldehyde for heptaldehyde in some experiments, but this did not prove to have any advantage.

The results obtained in hydrazinolysis of fibrinopeptide B were less clear. The analyses indicated that the hydrazinolysate contained — in addition to ornithine and ala-orn, which may have derived from the C-terminal sequence — aspartic acid and glutamic acid hydrazides and, in some cases, also a tetrapeptide hydrazide with the sequence pro-lys-val-gly. The same sequence has been demonstrated in sequence studies of fibrinopeptide B [22].

Since some of the hydrazides formed in hydrazinolysis contain one or several free carboxyl groups, which make them extremely difficult to remove from the water phase, the value of this method for C-terminal analyses is presumably reduced in some cases. This is because certain difficulties may arise in studies of *e.g.* peptides and proteins containing large quantities of aspartic and glutamic acid. It is, however, possible that the use of solid polyaldehydes — *e.g.* polyacrolein as introduced by Kauffmann and Boettcher [23] — would result in more effective removal of the hydrazides, and thus in a still more reliable method for C-terminal studies.

Our experiments were made on peptides containing basic amino acids in their C-terminal part. After 10 hours' treatment with hydrazine, we were able to demonstrate relatively large quantities of peptides. This might indicate that the peptide bonds in which basic amino acids are present are fairly resistant to hydrazine. Thus, we found, for example, in hydrazinolysis of fibrinopeptide B that the peptide ala-orn was obtained in almost as large a quantity as ornithine (Table 3). The lys-ala bond in the intact insulin molecule seems, on the contrary, to be fairly easily split, since only small amounts of lys-ala were demonstrable. On the other hand, large quantities of the dipeptide pro-lys were present, and small quantities of lys. This implies that the peptide bond pro-lys is also relatively resistant in hydrazinolysis. The resistance of the val-arg (orn) bond, which occurs C-terminally in peptide A, is still more marked. In analysis of fibrinopeptide A we obtained, in fact, in the first step of sequence determination 0.36 mole of gly (from gly-val-orn) and 0.34 mole of val (from val-orn), but only 0.05 mole of orn per mole of peptide A. In this case, the amount of peptide is 14 times the amount of C-terminal amino acid. Our results seem to show that the gly-val bond is also relatively stable.

The number of hydrazinolysis studies is still too small to permit any definite conclusions regarding which peptide bonds are difficult to split, or the reason underlying the difference between the sensitivity of the bonds to hydrazine. No complete investigation has yet been made of the kinetics in hydrazinolysis of peptides, although Bradbury [21] has studied the rate of hydrazinolysis in certain tri- and dipeptides as catalyzed by hydrazonium sulphate. He was able to demonstrate considerable differences between the stability of the peptides. For example, the peptide leu-val was much more stable than leu-gly which, in turn, showed greater stability than gly-gly. Judging by the material hitherto available for analysis, a peptide bond whose amino group derives from a basic amino acid is relatively stable, as are bonds containing amino acids with longer and branched carbon chains.

Our results indicate the existence of certain peptide bonds that are considerably more resistant to hydrazine than was formerly believed. If a peptide or a protein has resistant peptide bonds in its C-terminal part, the hydrazinolysate from them will contain a varying proportion of peptides even after relatively lengthy hydrazine treatment. If the C-terminal peptide bond is almost completely resistant — as, *e.g.* val-arg in fibrinopeptide A — the yield of the free C-terminal amino acid will be extremely small. Naturally, in such cases it is not possible to apply the criteria suggested by Akabori *et al.*[18] for evaluation of whether or not the amino acid is situated C-terminally. According to these criteria, the yield should be at least 20 % of a certain amino acid

for it to be regarded as C-terminal. The value often falls below this figure, and the yield may even be so low that it is difficult to determine exactly. For example, Dixon, Kauffmann and Neurath [24] recently described a peptide obtained by tryptic hydrolysis of oxidized di-*iso*propyl-phosphoryl-trypsin, and denoted as O-Tr-1, in which no C-terminal amino acid could be determined by hydrazinolysis in the modification of Niu and Fraenkel-Conrat. They were, however, able to show by partial hydrolysis that the C-terminal sequence was gly-lys. Like ala-orn (arg) in fibrinopeptide B, this peptide bond is probably relatively stable in hydrazinolysis.

Our knowledge of which amino acids or combinations of them determine the resistance of the peptide bonds to hydrazine is still incomplete. Consequently, a full analysis must be made of the hydrazinolysate obtained in order to get an accurate picture of the C-terminal structure of an unknown peptide. A suitable tool for such an analysis is Edman's phenyl*iso*thiocyanate method, possibly preceded by electrophoretic separation of peptides and amino acids in the aldehyde-treated hydrazinolysate. Edman's method seems to have certain advantages over other techniques hitherto available. This is because it gives a good quantitative picture of the composition of the hydrazinolysate, and also permits a stepwise breakdown of the existing peptides.

Acknowledgements. The authors' thanks are due to Professor Erik Jorpes. We feel much indebted to Docent John Sjöquist, Lund, for valuable advice and discussions.

REFERENCES

1. Akabori, S., Ohno, K. and Narita, K. *Bull. Chem. Soc. Japan* **25** (1952) 214.
2. Ohno, K. *J. Biochem.* **40** (1953) 621.
3. Niu, C. I. and Fraenkel-Conrat, H. *J. Am. Chem. Soc.* **77** (1955) 5882.
4. Ohno, K. *J. Biochem. Tokyo* **42** (1955) 615.
5. Edman, P. *Acta Chem. Scand.* **4** (1950) 283.
6. Sjöquist, J. *Arkiv Kemi* **11** (1957) 129.
7. Sjöquist, J. *Arkiv Kemi* **14** (1959) 291.
8. Sjöquist, J. *Biochim. et Biophys. Acta.* **41** (1960) 20.
9. Blombäck, B. and Vestermark, A. *Arkiv Kemi* **12** (1958) 173.
10. Kusama, K. *J. Biochem. Tokyo* **44** (1957) 375.
11. Kolthoff, I. M. *J. Am. Chem. Soc.* **46** (1924) 2009.
12. Edman, P. *Acta Chem. Scand.* **4** (1950) 277.
13. Stähler, A. *Ber.* **42** (1909) 3018.
14. Locker, R. H. *Biochim. et Biophys. Acta* **14** (1954) 533.
15. Blombäck, B., Sjöquist, J. and Wallén, P. *Acta Chem. Scand.* **13** (1959) 819.
16. Folk, J. E., Gladner, J. A. and Laki, K. *J. Biol. Chem.* **234** (1959) 67.
17. Sanger, F. and Tuppy, H. *Biochem. J.* **49** (1951) 481.
18. Akabori, S., Ohno, K., Ikenaka, T., Okada, Y., Hanafusa, H., Haruna, I., Tsugita, A., Sugoe, K. and Matsushima, T. *Bull. Chem. Soc. Japan* **29** (1956) 507.
19. Sanger, F. and Tuppy, H. *Biochem. J.* **49** (1951) 481.
20. Jorpes, J. E. and Lindén, J. G. B. Canadian patent 594 614, March 22, 1960.
21. Bradbury, J. H. *Biochem. J.* **68** (1958) 482.
22. Sjöquist, J., Blombäck, B. and Wallén, P. *Arkiv Kemi.* **16** (1960) 425.
23. Kauffmann, T. and Boettcher, F.-P. *Ann.* **625** (1959) 123.
24. Dixon, G. H., Kauffmann, D.-L. and Neurath, H. *J. Biol. Chem.* **233** (1958) 1373.

Received June 14, 1960.

ACTA CHEMICA SCANDINAVICA 14 (1960) 1763–1769

Metabolism of Chenodeoxycholic Acid in the Rabbit

Bile Acids and Steroids 104

KJELL HELLSTRÖM and JAN SJÖVALL

Department of Medicine, Serafimerlasarettet, and
Department of Chemistry, Karolinska Institutet, Stockholm, Sweden

Two rabbits, one with a permanent duodenal fistula and the other with a permanent stomach fistula, were given chenodeoxycholic acid-24-^{14}C intravenously. Bile samples were taken intermittently for three days through the fistulas which were closed except during the sampling periods. Unchanged chenodeoxycholic acid could not be positively identified. Lithocholic acid was the main metabolite in the feces and bile of one rabbit. In addition to lithocholic acid, ursodeoxycholic acid and small amounts of 7-ketolithocholic acid were found in both the bile and feces of the other animal. The excretion of isotope in feces indicated a slow turnover of the acids.

Cholic and deoxycholic acids are the main bile acids in rabbit bile (for references see Ref.[1]). Cholic acid is formed from cholesterol in the liver whereas deoxycholic acid is secondarily formed from cholic acid by intestinal microorganisms [1]. Chenodeoxycholic acid has not been found in rabbit bile but lithocholic acid, which can be formed from this acid in the rat intestine [2], has been isolated in minor amounts [3]. The rabbit has been extensively used for studies of atherosclerosis and in connection with an investigation of bile acid production in this animal we found it necessary to acquire more information on the qualitative metabolism of chenodeoxycholic acid in the rabbit. Results obtained with the aid of labelled chenodeoxychclic acid are presented in this paper.

EXPERIMENTAL

Chenodeoxycholic acid-24-^{14}C was synthesized according to Bergström, Rottenberg and Voltz [4]. The specific activity was about 10 μC per mg. Ursodeoxycholic acid (m.p. 202–203°) was prepared according to Samuelsson [5].

Animal experiments. Two rabbits weighing about 2.5 kg were used. One of these was provided with a permanent fistula between the duodenum and the abdominal wall (rabbit DK), the other one was provided with a similar fistula between the distal part of the stomach and the abdominal wall (rabbit VK). The fistula consisted of a plexi-glas tube (length 5 cm) that could be closed with a plexi-glas stopper occupying the whole

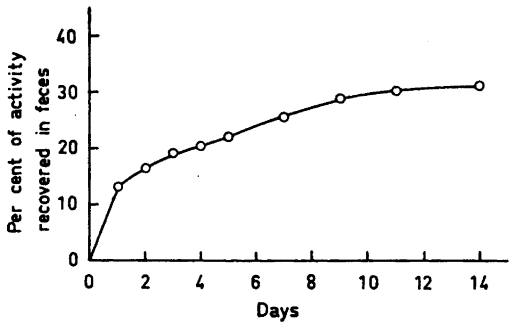

Fig. 1. Cumulative excretion in the feces of rabbit VK of activity not removed through the fistula.

volume of the tube up to the level of the mucosa [6]. Bile samples were taken directly *via* the duodenal fistula by removing the stopper, or by introducing a rubber tube through the stomach fistula into the duodenum. Except when samples were being taken, the plexiglas tubes were stoppered and the animals were allowed to move freely in their cages. This technique was adopted in order to follow specific activities of bile acids *in vivo* and details will be described later. The experiments were started about one month after the operation. The animals had free access to cabbage and carrots, were apparently healthy and increased in weight. Rabbit VK is still in good health 10 months after the operation.

2.8 mg of the sodium salt of the labelled chenodeoxycholic acid was given intravenously in 4 ml of saline. 24 h later duodenal contents was collected after i.v. injection of cholecystokinin-pancreozymin (kindly supplied by Prof. E. Jorpes). Collection was continued for 6 h and the procedure repeated on the following two days. Feces were collected every day.

Extraction and chromatography. About 10 volumes of ethanol was added to the duodenal contents. After filtration, most of the solvent was evaporated on the water bath and the bile acids were extracted with butanol from the acidified aqueous solution. The homogenized daily portions of feces were extracted 4—5 times with ethanol by refluxing for 2 h. Complete extraction of the isotope was ascertained by radioactivity measurements on each extract. After concentration of the combined extracts, the bile acids were extracted with ether from an acidified aqueous solution. Reversed phase chromatography was performed as previously described [7,8]. The following phase systems were used:

Phase system	Moving phase (ml)	Stationary phase (ml)
C 1	Methanol-water 150:150	Chloroform-*iso*octanol 15:15
F 1	Methanol-water 165:135	Chloroform-heptane 45:5
F 2	Methanol-water 180:120	Chloroform-heptane 45:5
F 3	Methanol-water 180:120	Chloroform-heptane 40:10

4.5 g of hydrophobic Supercel or Hostalen (Hoechst) [9] was used to support 4 and 3 ml, respectively, of the stationary phase. When larger columns were needed these amounts were proportionally increased. Radioactivity was determined by the counting of an infinitely thin layer in a Frieseke-Hoepfner (FH 51) methane gas-flow counter.

RESULTS

A total of about 15 % of the isotope injected was recovered by collection of duodenal contents for 6 h during each of the 3 days following the injection of chenodeoxycholic acid-24-^{14}C. The fecal excretion of isotope was extremely

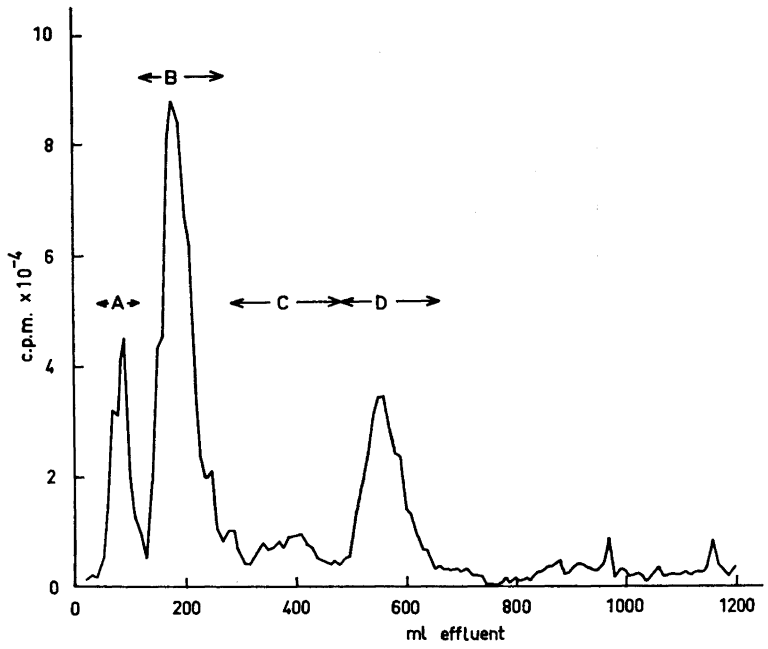

Fig. 2. Chromatogram of labelled compounds in the bile of rabbit VK. Column: 36 g Hostalen, phase system F 1.

slow. Only 22 % of the activity not recovered from the duodenum was excreted during the first 4 days in rabbit DK. Rabbit VK was therefore studied for 14 days and the same result was obtained as shown in Fig. 1.

Radioactive compounds in duodenum. The radioactive compounds extracted from the bile obtained from the duodenum were separated on Hostalen columns with phase system F 1. The result for rabbit VK is shown in Fig. 2. Conjugated bile acids appear with the front in this phase system but, as seen in the figure, only a minor part of the activity is eluted with the front (A, Fig. 2). The main part of the isotope is present in two peaks (B and D, Fig. 2) which appear at places corresponding to ursodeoxycholic and lithocholic acids, respectively. Only about 2 % of the total activity remained in the stationary phase. The active bands A, B, C, D (Fig. 2) were further purified by rechromatography on hydrophobic Supercel.

When peak A was chromatographed with phase system C 1, one main peak was found (Fig. 3, left curve). Chromatography, with inactive cholic acid added as carrier, showed that no radioactive cholic acid was present. The nature of the compounds separated with phase system C 1 has not been further investigated.

The rechromatography of peak B (Fig. 2) on Supercel columns with phase system F 1 is shown in Fig. 3 (middle curve). The isotope appears just before the large titration peak of the deoxycholic acid normally found conjugated in

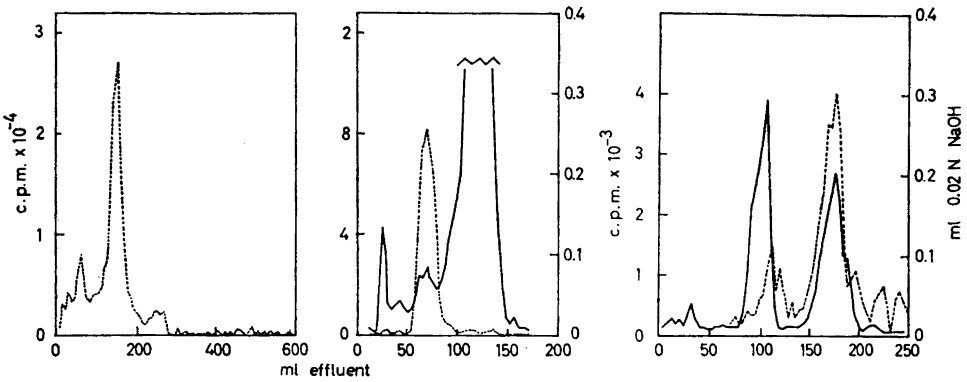

Fig. 3. Left curve: Rechromatography of peak A (Fig. 2) on a 18 g Hostalen column with phase system C 1. Middle curve: Rechromatography of peak B (Fig. 2) on a 9 g Supercel column with phase system F 1. Right curve: Rechromatography of band C (Fig. 2) together with unlabelled 7-ketolithocholic acid. 9 g Supercel, phase system F 1. Solid line: Titration. Broken line: Radioactivity.

rabbit bile. There is a small but definite titration peak coinciding with the radioactive one. No isotope is seen at the place of chenodeoxycholic acid. The radioactive fractions were re-run together with inactive ursodeoxycholic acid and the activity coincided with the titration peak of the added carrier (Fig. 4, left curve). The small titration peak which can be seen after the main peak is due to incomplete removal of the deoxycholic acid originally present in the bile. The identity of the labelled compound with ursodeoxycholic acid was further established by isotope dilution.

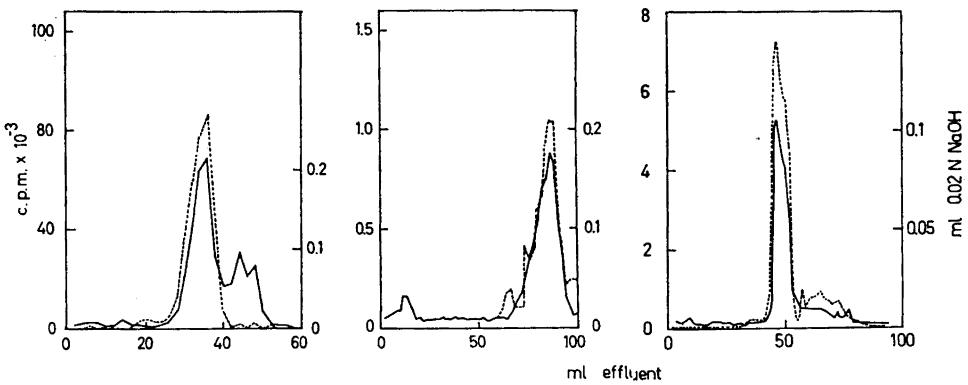

Fig. 4. Left curve: Rechromatography of peak B (Fig. 2) together with inactive ursodeoxycholic acid. 4.5 g Supercel, phase system F 1. Middle curve: Rechromatography of peak C from feces (Fig. 5) together with inactive 7-ketolithocholic acid. 4.5 g Supercel, phase system F 1. Right curve: Rechromatography of part of the "lithocholic acid band" from feces of rabbit DK together with inactive lithocholic acid. Solid line: Titration. Broken line: Radioactivity.

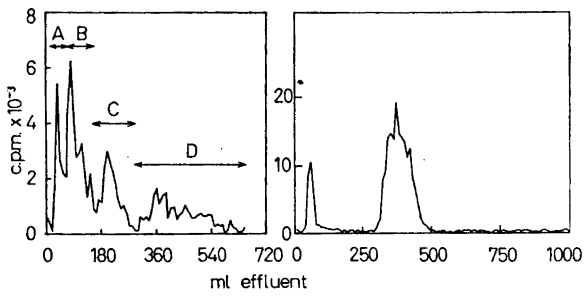

Fig. 5. Chromatograms of labelled fecal acids obtained from rabbit VK (left curve, 18 g Hostalen) and from rabbit DK (right curve, 27 g Hostalen). Phase system F 1 was used in both cases.

After one rechromatography with phase system F 1, band C (Fig. 2) was re-run with unlabelled 7-ketolithocholic acid. Most of the isotope appeared together with the carrier (Fig. 3, right curve) and the identity was established by isotope dilution. As was the case with the rechromatography of ursodeoxycholic acid, not all of the very large amounts of inactive deoxycholic acid had been removed. Therefore, a titration peak of this acid is still seen in Fig. 3 at 100 ml effluent.

The last radioactive band seen in Fig. 2 (peak D,) was rechromatographed with phase system F 2 and a titration peak coincided with the isotope peak. Chromatography with carrier lithocholic acid and determinations of specific activity upon recrystallization with lithocholic acid, showed that the labelled compound (Fig. 2, D) was identical with this acid.

Analysis of the duodenal bile from rabbit DK gave essentially the same result as above but, in this animal, lithocholic acid was by far the dominating metabolite (74 %) whereas only about 10 % of the total activity appeared in the ursodeoxycholic acid band. Furthermore, 7-ketolithocholic acid could not be found but this acid also accounted for only 5—10 % of the total metabolites in rabbit VK.

Radioactive compounds in feces. The analysis of the metabolites in feces was carried out in the same way as described for the duodenal bile. The main bands of radioactivity present in the chromatograms of feces were the same as those of the duodenal bile. The first chromatographies of a fecal sample from both rabbit VK and rabbit DK on Hostalen columns with phase system F 1 are shown in Fig. 5 (left and right curves resp.). Lithocholic acid was even more dominating in the feces of rabbit DK than in the duodenal contents of this animal (Fig. 5, right curve). It was identified by rechromatography with carrier lithocholic acid (Fig. 4, right curve) and by isotope dilution. Chromatograms of fecal extracts from the first, second and third days after the injection of the labelled chenodeoxycholic acid were very similar.

The labelled bands B, C, and D from rabbit VK shown in Fig. 5 (left curve) were rechromatographed with inactive ursodeoxycholic, 7-ketolithocholic and lithocholic acids, respectively. In all cases most of the isotope appeared

together with the reference compounds. This is shown for 7-ketolithocholic acid in Fig. 4 (middle curve). No isotope dilution experiments were made. The small amount of isotope appearing with the front (A, Fig. 5) was not studied further.

DISCUSSION

A striking finding is the very slow excretion of isotope in the feces of both the rabbits. This indicates a much longer half-life time of the chenodeoxycholic acid in the rabbit than in the rat. In this connection it is interesting to note that the amount of bile acids taking part in the enterohepatic circulation seemed to be very large in the rabbits previously studied (about 550 mg) [1]. In view of the sensitivity of the rabbit for hypercholesteremia, these quantitative aspects of the bile acid metabolism are now being studied.

Another finding differing from that found in rat and man is the occurrence of large amounts of unconjugated bile acids in the duodenal contents. In the bile all bile acids are conjugated [1]. This indicates a bacterial hydrolysis of bile acids already in the duodenum. In order to find out whether this was due to the presence of a fistula, four normal rabbits were killed and the duodenal contents was analyzed with paper chromatography. Large but variable amounts of free bile acids were found.

Unpublished findings by S. Lindstedt indicate that minute amounts of chenodeoxycholic acid are formed from cholesterol in bile fistula rabbits. We have now shown that chenodeoxycholic acid is rapidly and almost completely metabolized mainly to lithocholic and ursodeoxycholic acids. It is therefore probable that any chenodeoxycholic acid formed will be transformed and escape detection in normal bile. Lithocholic acid has been isolated from rabbit bile [3] and we have seen titration peaks in the chromatograms coinciding with both the labelled lithocholic acid and the labelled ursodeoxycholic acid.

Although we have not determined whether the transformation of chenodeoxycholic acid takes place in the liver or in the intestine, or in both, it seems most probable that lithocholic acid is formed by microorganisms, as is the case in the rat [3]. The transformation of chenodeoxycholic acid during the enterohepatic circulation is very extensive in the rabbit, which is also true for cholic acid in this animal [1]. The ursodeoxycholic acid found is probably formed *via* the 7-ketolithocholic acid also found. Whether the 7-ketolithocholic acid has been formed both by liver enzymes [10] and in the intestine by the action of *E. coli* [11] is not known.

Acknowledgments. We are greatly indebted to Dr. Lars Olbe for help and advice with the fistula operations. The technical assistance of Miss A. Björkman and Miss M. Frankesten is gratefully acknowledged.

This work is part of investigations supported by *Statens Medicinska Forskningsråd* and the *National Heart Institute (H 2842) U.S. Public Health Service*, Bethesda, Maryland.

REFERENCES

1. Lindstedt, S. and Sjövall, J. *Acta Chem. Scand.* **11** (1957) 421.
2. Norman, A. and Sjövall, J. *Acta Chem. Scand.* **14** (1960) 1815.
3. Kishi, S. *Z. Physiol. Chem. Hoppe Seyler's* **238** (1936) 210.
4. Bergström, S., Rottenberg, M. and Voltz, J. *Acta Chem. Scand.* **7** (1953) 481.
5. Samuelsson, B. *Acta Chem. Scand.* **14** (1960) 17.
6. Emås, S. *Gastroenterology, In press.*
7. Sjövall, J. *Acta Physiol. Scand.* **29** (1953) 232.
8. Norman, A. *Acta Chem. Scand.* **7** (1953) 1413.
9. Wiss, O. and Gloor, U. *Z. physiol. Chem. Heppe-Seyler's* **310** (1958) 260.
10. Samuelsson, B. *Acta Chem. Scand.* **13** (1959) 976.
11. Norman, A. and Bergman, S. *Acta Chem. Scand.* **14** (1960) 1781.

Received June 16, 1960.

ACTA CHEMICA SCANDINAVICA 14 (1960) 1770–1776

Hämine verschiedener Strukturen als Bakterienwuchsstoffe

K. G. PAUL und E. THOFERN

Biokemiska institutionen, Karolinska institutet, Stockholm, Schweden; Hygiene-Institut der Universität Göttingen, Bundesrepublik Deutschland

Eine früher beschriebene häminheterotrophe, streptomycinresistente Mutante von *Micrococcus pyogenes* var. *aureus* SG 511 kann statt Protohämin IX Hämato- und Mesohämin IX, dagegen nicht Mesohämin I und Diacetyldeuterohämin IX, für ihre Hämoproteidesynthese ausnützen.

Jensen und Thofern haben eine streptomycinresistente häminheterotrophe Mutante des *Micrococcus pyogenes* var. *aureus* S. G. 511 isoliert [1,2], die imstande ist, die Apoproteine ihrer Hämoproteide aufzubauen und mit Häminen zu kuppeln. Die Synthese der Holohämoproteide ist aber nur nach der Zugabe von Hämin möglich.

Es ist mit einigen Hämoproteiden gelungen die reversible Spaltung in Hämin und Eiweiss durchzuführen [3–5]. Nicht nur Protohämin sondern auch gewisse andere Hämine können die spezifische Wirkung wiederherstellen [6,7], aber nur solche, die Propionsäuren an den Stellungen 6 und 7 (»Reihe IX») besitzen [8]. Die 6,8-Isomeren (»Reihe I») dagegen geben inaktive, auf Anionenaustauschern spaltbare Verbindungen [9]. Aber nicht alle dikarboxyligen Hämine der Reihe IX geben aktive Verbindungen. Bei Meerettichperoxydase scheint eine Beziehung zwischen Aktivität und Spektrum vorzuliegen, indem die Aktivität geringer wird je langwelliger die α-Bande im Hämochromogenspektrum liegt. Diacetyldeuterohämin IX, z.B., ruft keine Peroxydaseaktivität hervor obwohl es eine feste Verbindung, ein wahres Holohämoproteid, mit Apo-Meerrettichperoxydase bildet [9].

Es war nun von Interesse herauszufinden, ob auch die Mutante eine Isomeriespezifizität aufwiese und ob auch eine Beziehung zwischen Häminspektrum und den Lebensäusserungen der Mutante bestände.

MATERIALIEN UND METHODEN

Die wachsende Mutante gibt auf Nähragar (2 % Agar in 1.5 % Caseinpepton — 1 % Glukose — Na-Phosphatpuffer 67 mM, pH 7.6) einen hauchdünnen Rasen, der ringsum ein Stanzloch mit der zu prüfenden Lösung einen Wachstumshof, einen Hemmhof oder

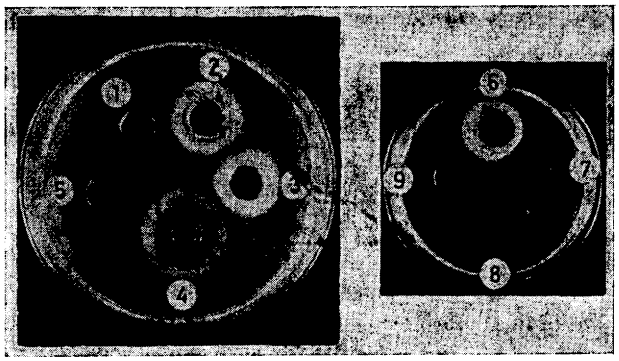

Abb. 1. Wachstumsförderung von verschiedenen Häminen in Stanzlochtest. Die Löcher enthielten:

1. Natriumkarbonat
2. Protohämin IX
3. Hämatohämin IX
4. Mesohämin IX
5. Mesohämin I
6. Protohämin IX
7. Diacetyldeuterohämin IX ($2{,}5 \times 10^{-9}$ Mole)
8. Diacetyldeuterohämin IX (5×10^{-11} Mole)
9. Natriumkarbonat

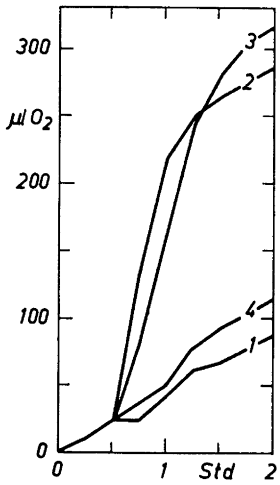

Abb. 2. Sauerstoffverbrauch ruhender Zellen der Mutante nach Zusatz verschiedener Hämine.

1. Ohne Hämin
2. Protohämin IX nach 30 min (6 µM)
3. Mesohämin IX nach 30 min (6 µM)
4. Mesohämin I nach 30 min (9 µM)

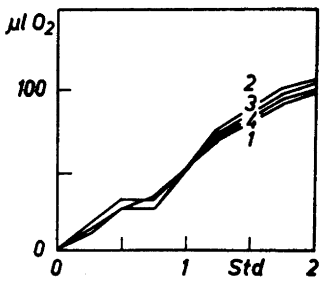

Abb. 3. Sauerstoffverbrauch ruhender Zellen der Mutante nach Zusatz von verschiedenen Häminen.

1. Ohne Hämin
2. Mesohämin I nach 30 min (Endkonzentration im Gefäss 1,8 µM)
3. Wie 2 + Mesohämin IX nach 60 min (1 µM)
4. Wie 2 + Protohämin IX nach 60 min (1,2 µM).

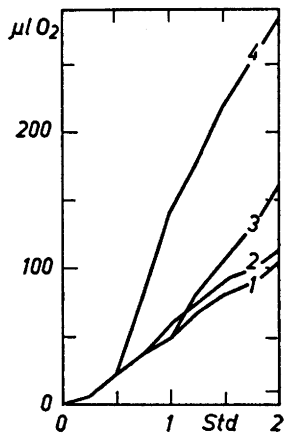

Abb. 4. Sauerstoffverbrauch ruhender Zellen der Mutante nach Zusatz von Diacetyldeuterohämin IX.

1. Ohne Hämin
2. Diacetyldeuterohämin IX nach 30 min (25 µM)
3. Wie 2 + Protohämin IX nach 60 min (5 µM)
4. Protohämin IX nach 30 min.

keine Veränderung zeigt. Von der Häminlösungen (0,05—0,10 mM in 0,1 M Natriumkarbonat) wurden 0,05 ml pro Loch abgemessen. Die Platten wurden nach 20 Std bei 37°C abgelesen.

Die ruhende Mutante, in der obigen Bouillon ohne Agar anaerob vorgezüchtet und mit Kochsalzlösung und Puffer gewaschen, zeigt in Manometerversuchen eine mässige Sauerstoffaufnahme. Sie wurde während 30 min verfolgt ehe die Häminlösung eingekippt wurde. Bei dem Kippen erschien meistens eine CO_2-Freisetzung (siehe z. B. Abb. 3). Für die Messungen wurden verwendet 5 mg von Bakterien, als Trockengewicht

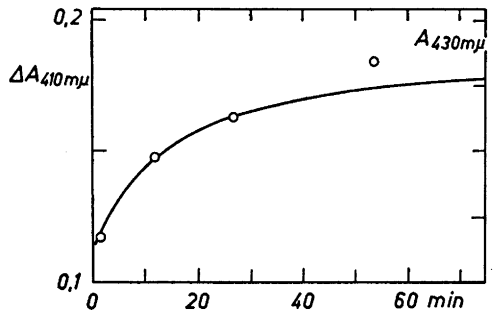

Abb. 5. Lichtabsorption- und Aktivitätszunahme während der Reaktion zwischen Apomeerrettichperoxydase und Hämatohämin. Probeküvette: 0,02 μ Mole Protein + 0,03 μ Mole Hämatohämin in 3,7 ml 0,1 M Na – Phosphat, pH 7,1. Referenzküvette: Dasselbe ohne Protein. Lichtabsorption: Ordinate links und Kurve. In den Aktivitätsmessungen wurden 0,15 ml des Küvetteninhaltes für die Purpurogallinreaktion verwendet, 250 ml Äther. Ordinate rechts und Cirkel (Zusammen mit Y. Avi-Dor, 1952).

berechnet, 67 mM Na-Phosphat von pH 7,6, 100 mM Glukose, Luft als Gasphase, 37°C und 110 Oscillationen pro Minute. Anschliessend an die Atmungsversuche wurde die Katalaseaktivität bei 0–2°C titrimetrisch bestimmt [10] und als ml 10 mN Wasserstoffperoxyd ausgedrückt, die in 12 min zerlegt werden.

Sämtliche Hämine ausser Hämatohämin waren als Porphyrinester chromatographiert, nach Verseifung mittels Äther – HCl gereinigt und in Hämine mittels Ferroacetat in Eisessig überführt.

Die Kuppelung in Abb. 5 geschah wie früher beschrieben [9].

ERGEBNISSE

Die Ergebnisse sind in Abb. 1—5 und in Tabelle 1 gesammelt.

Tabelle 1. Katalaseaktivitäten der Gefässinhalte in Abb. 2–4.

Abbildung	Kurve	Hämine	Katalaseaktivität ml 10 mN H_2O_2/12 min	
2	1	Ohne Zusatz	0,07	
	2	PH IX	1,20	
	3	MH IX	0,85	
	4	MH I	0,01	
3	1	Ohne Zusatz	0,08	
	2	MH I	0,10	
	3	MH I + MH IX	0,13	
	4	MH I + PH IX	0,47	
4	1	Ohne Zusatz	0,00	0,03
	2	DiAcDH IX	0,06	0,19
	3	PH IX	0,46	0,38
	4	DiAcDH IX + PH IX	0,33	0,20

DISKUSSION

Die Beobachtungen in den Agar-Stanzlochtesten und in den Manometerversuchen mit den anschliessenden Katalasebestimmungen stimmen insofern gut überein, dass von den geprüften Häminen nur Proto-, Meso- und Hämatohämin IX positive Reaktionen hervorrufen, Mesohämin I und Diacetyldeuterohämin IX aber nicht. In Vorversuchen zeigte sich auch Deuterohämin IX als wirksam. Es ist unwahrscheinlich, dass die Mutante Enzyme für die Umwandlung der Meso-, Deutero- und Hämatohämine — nicht aber Diacetyldeuterohämin — in Protohämin parat hat. Man könnte deshalb vermuten, dass die zugesetzten Hämine unverändert eingebaut werden. Solche artifizielle Hämoproteide sind in der Natur früher nicht gefunden worden. Hämin a kann aus den Bakterien nach Protohäminzugabe isoliert werden [11], ob die zugegebenen Protohäminmoleküle in Hämin a übergehen ist aber nicht eindeutig beantwortet. Für die Identifizierung der prosthetischen Gruppen müssen die gebildeten Hämoproteide von dem Überschuss an zugesetztem Hämin isoliert werden. Solche Versuche mit Verwendung von $^{14}C/^{59}Fe$-Hämin sind im Gange.

Genau jene Hämine sind für die Mutante nutzbar, die mit Apo-Meerrettichperoxydase aktive Verbindungen geben [8]. Dies ist um so bemerkenswerter da nach Protohäminzugabe mehrere Hämoproteide zu finden sind [12]. Unter den verwendeten Bedingungen wird die steigernde Wirkung des Protohämins auf die Sauerstoffaufnahme durch Diacetyldeuterohämin reduziert, zu 78 und 56 % in Doppelbestimmungen in Abb. 4; die Katalasebestimmungen gaben 72 und 47 %. In Abb. 1 sieht man zwischen den Löchern 6 und 7 eine gerade Begrenzung. Diese Befunde deuten eine Konkurrenz zwischen den beiden Häminen an. In dieser ist es wegen der Spektra zu erwarten, dass Protohämin fester als Diacetyldeuterohämin gebunden wird. Die Hemmung in Abb. 4 wurde mittels einem fünffachen Überschuss an Diacetyldeuterohämin erhalten. Da weiter Mesohämin I die Bakterien gegen die IX-Isomeren vollständig blockiert, muss man das Vorkommen von spezifischen Haftstellen, reaktiven Gruppen, in den Bakterien annehmen. Es ist an sich nicht überraschend, dass Mesohämin I als Wuchsstoff oder Co-Faktor nicht verwendbar ist, da bisher alle in der Natur gefundenen Hämoproteide Hämine der Reihe IX enthalten.

Die Zunahme des Sauerstoffverbrauchs der ruhenden Mutante nach Häminzugabe (Abb. 2) kommt schnell, noch schneller als die Aktivitätszunahme nach dem Vermischen von Hämin mit Apoperoxydase (Abb. 5). Dies könnte mit einer unspezifischen Redoxwirkung vom Hämin erklärt werden. Der Unterschied zwischen den vier untersuchten Häminen der Reihe IX wäre dadurch zu verstehen, nicht aber die Unfähigkeit Mesohämins I Sauerstoffaufnahme und Wachstum zu fördern, auch nicht die oben erwähnte Konkurrenz.

Bei den auf Agar aerob wachsenden Bakterien begrenzt die Diffusion des Hämins den Wachstum, daher werden die Zeitverhältnisse unklarer. In den inneren Teilen des Wachstumshofs verschwand mit allen drei Häminen der Wachstum mehr oder weniger. Da aber diese leere Zone bei Mesohämin am breitesten war, kann Mangel an CoA, das für den bakteriellen Einbau von Protohämin in die Katalase notwendig sein soll [13], oder an anderen Co-Faktoren

kaum die Ursache sein. Von den drei Häminen zeigt Hämatohämin in Wasserlösungen eine hohe Polymerisierung, Mesohämin eine niedrigere. Dementsprechend diffundiert Mesohämin weiter als die beiden anderen, und die Ausdehnung der leeren Zone mag damit verbunden sein. In Stanzlochversuchen mit Kobaltporphyrinen und *Lactobacillus lactis* Dorner bewirkten die Hämato- und Protoverbindungen Wachstum, Meso dagegen Hemmung [14].

Alle bisherigen Ergebnisse wären durch die Annahme, dass die Bakterien spezifische Apoeiweissmoleküle besitzen, die ihre Haftgruppen oberflächlich tragen, erklärt. Sie schliessen aber auch beinahe aus, dass die Zunahme der Sauerstoffaufnahme nach Häminzugabe durch eine Kette von Hämin-Redoxkatalysatoren stattfindet, fastmehr scheint es sich um nur ein Hämoproteid zu handeln. Die Peroxydasewirkung der Katalase könnte hier die Funktion einer terminalen Oxydase einnehmen.

In den hier beschriebenen Versuchen (Abb. 2—4) wurden die Bakterien während der Phase ihres schnellsten Wachstums geerntet. Zu dieser Zeit sollten sie also, nachdem was oben gesagt wurde, Apokatalase enthalten. Aus der Literatur ist zu entnehmen, dass eine Beziehung zwischen Wachstum und Peroxydase- bzw. Katalaseaktivität vorliegen könnte. Es ist schon längst bekannt, dass Kürbiskotyledone an Katalase sehr reich sind [15]; eine nähere Untersuchung [16] ergab das Katalasemaximum zwischen den 6. und 8. Tag bei 15°C in Erbsenpflanzen. Auch in tierischen Geweben sind ähnliche Beobachtungen gemacht worden. Während der Oestradiol-induzierten Uterushyperplasie steigt bei Mäusen die Peroxydaseaktivität stark an [17,18]. Ein eingehender Vergleich zwischen den durch Peroxydase und Zytochrome bedingten Sauerstoffaufnahmen während der verschiedenen Phasen des Wachstums wäre von Interesse. Aus der allgemeinen Verbreitung und der hohen Katalaseaktivität in den Erythrozyten geht aber hervor, dass die Wirkung der Hydroperoxydasen nicht nur mit Wachstum verknüpft sein können.

Die Untersuchung wurde von *Statens naturvetenskapliga forskningsråd*, Schweden (K. G. P.) und die *Deutsche Forschungsgemainschaft* (E. Th.) unterstützt.

REFERENZEN

1. Jensen, J. und Thofern, E. *Z. Naturforsch.* **8 b** (1953) 599.
2. Jensen, J. und Thofern, E. *Z. Naturforsch.* **8 b** (1953) 604.
3. Theorell, H. *Arkiv Kemi, Mineral. Geol.* **14 B** (1940) No. 20.
4. Theorell, H. und Åkeson, Å. *Ann. Acad. Fennicae Ser. A II Chem.* **60** (1955) 303. Vgl. auch Rossi-Fanelli, A. und Antonini, E. *Arch. Biochem. Biophys.* **77** (1958) 478.
5. Rossi-Fanelli, A., Antonini, E. und Caputo, A. *Biochim. et Biophys. Acta* **28** (1958) 221. Vgl. auch Rossi-Fanelli, A. und Antonini, E. *Arch. Biochem. Biophys.* **80** (1959) 299.
6. Theorell, H., Bergström, S. und Åkeson, Å. *Arkiv Kemi, Mineral. Geol.* **16 A** (1942) No. 13.
7. Gjessing, E. C. und Sumner, J. B. *Arch. Biochem.* **1** (1943) 1.
8. Paul, K. G. *Acta Chem. Scand.* **13** (1959) 1239.
9. Paul, K. G. *Acta Chem. Scand.* **12** (1958) 1611.
10. Sumner, J. B. and Somers, G. F. *Chemistry and Methods of Enzymes.* 2nd ed., Academic Press, New York, 1953, p. 27.
11. Jensen, J. und Thofern, E. *Z. Naturforsch.* **9 b** (1954) 596.

12. Kiese, M., Kurz, H. und Thofern, E. *Biochem. Z.* **330** (1958) 541.
13. Jensen, J. *J. Bacteriol.* **73** (1957) 324.
14. Banhidi, Z. G., Sjöström, A. G. M. und Paul, K. G. *Exptl. Cell. Research* **3** (1952) 489.
15. Zeile, K. in Bamann, E. und Myrbäck, K. (Ed.) *Die Methoden der Fermentforschung*, Band 3, 2626. G. Thieme, Leipzig, 1941.
16. Goksöyr, J., Boeri, E. und Bonnichsen, R. K. *Acta Chem. Scand.* **7** (1953) 657.
17. Martin, A. P., Neufeld, H. A., Lucas, F. V. und Stotz, E. *J. Biol. Chem.* **233** (1958) 206.
18. Paul, K. G. und Wiqvist, N. *Experientia* **16** (1960) 421.

Eingegangen am 2. April 1960.

ACTA CHEMICA SCANDINAVICA 14 (1960) 1777–1780

A New Principle for Large Scale Production of Insulin

ERIK JORPES, VIKTOR MUTT and SELAHADDIN RASTGELDI

Chemistry Department II, Karolinska Institutet, Stockholm, Sweden

The conventional method for large scale manufacture of insulin starts with an extraction of the pancreatic glands with acidified ethyl alcohol and subsequent evaporation of the alcohol *in vacuo* at low temperature. The authors present a technique of adsorbing the insulin from the alcoholic extract at pH about 3 on an ion exchanger, alginic acid, with subsequent elution of the insulin by means of 0.2 N HCl. The use of a cumbersome and expensive distilling equipment is thereby made superfluous. Fats are not adsorbed. An increased yield of insulin is obtained if the traces of tryptic enzymes still present in the extract are destroyed by heating the alcoholic extract at pH 3.2 to 70°C before adsorbtion.

Since the very first beginning, when insulin in 1921—1922 became available for clinical use through the endeavours of the University of Toronto group, the manufacturing process has included extraction of the pancreatic glands with alcohol, acidified with hydrochloric or sulphuric acid, evaporation of the alcohol *in vacuo* at low temperature, removal of fats from the aqueous residue and precipitation of proteins with sodium chloride followed by isoelectric precipitation of the insulin from water at pH 5.2 and subsequent crystallization. During all these years, no major changes have been made in this procedure.

Since no information was available on the successful use of ion exchangers for recovery of the insulin from the alcoholic extract, we in 1954 took up experiments along such a line. As a result the Swedish manufacturer of insulin, Vitrum AB, Stockholm, could in 1956 start to apply a new technique, which now has been in use for the last three years. Since no distillation at low temperature is necessary, the large-scale production has been greatly facilitated.

Historical. The technique of adsorbing bases on inorganic ion-exchangers was introduced in biochemistry in 1917 by Otto Folin, who adsorbed ammonia on Permutite. The same reagent was later used extensively for the adsorption of organic bases, basic proteins of low molecular weight and peptides [1].

From 1950 on, the carboxylic acid ion-exchange resin Amberlite IRC-50 was used by different authors to study the homogeneity of basic proteins of low molecular weight, such as cytochrome c [2], ribonuclease [3], lysozyme [4] and chymotrypsinogen [5]. Up to 1953, the ion-exchange resins had been used only

for chromatographic analysis of small quantities of purified proteins, the applicability being limited to low-molecular basic proteins.

When Peterson and Sober [6] in 1956 recommended cellulose ion-exchangers for the chromatography of proteins, they stated that "the application of chromatography to the separation of proteins has not met with the general success obtained with smaller, simpler molecules. The large size of the protein molecule prevents its penetration into the adsorbent particle, therefore only the adsorbing sites located on the exterior can be utilized."

Boardman [7] tried in 1955 to increase the surface of a sulphonated polystyrene ion-exchanger by precipitating the resin on the surface of kieselguhr (Celite 545), and used the product for the study of the purity of crystalline insulin.

The only successful attempt at using ion-exchangers on a technical scale for the reversible adsorption of proteins was that of Astwood, Raben, Payne and Grady [8] of 1951. They adsorbed the basic peptide hormone, corticotropin, on oxycellulose from dilute aqueous acetic acid.

No attempts seem to have been made to take up the insulin from the acidic alcoholic extract on ion-exchangers. As an illustration, it can be mentioned that as late as June 1956, Samsonov and Faddajeva [9] published a study of the possibility of adsorbing insulin on an ion-exchange resin, SBS-1, having a particularly suitable porosity. Elution was performed with 1 **N** ammonia. They applied their technique to the residual aqueous extract after distilling off the alcohol.

Own work. Since the previous discussion dealt with ion-exchange chromatography in aqueous solution and, furthermore, was confined to more or less basic proteins of low molecular weight, removal of the acidic protein insulin from a crude alcoholic extract offered new aspects. The use of ordinary cation-exchangers of the Dowex-50 type was excluded because of the size of the insulin molecule, which does not allow a diffusion into the inner spaces of the resin. Moreover, if adsorption is to be carried out at an acidic reaction, pH below 4, making the insulin a cation, the most commonly used adsorbent, Amberlite, IRC-50, is only sparingly ionized and less efficient as an adsorbent. An ion-exchanger with easily accessible ionizable groups is necessary.

We found alginic acid to be a highly suitable ion exchanger for this purpose *. Insulin is taken up quantitatively by the alginic acid from a 65 % ethanolic solution having an acidity of pH 2.8—3.4. The bulk of fats remains in the alcoholic extract from which the alcohol is recovered in an ordinary rectifying column. The insulin is eluted from the alginic acid with 0.2—0.3 N aqueous hydrochloric acid. The stability of the molecule of the alginic acid, its chain-like structure [19] and the strong ionization of the carboxylic groups of this polyhydroxyacid at pH 3.4 [11] could explain its usefulness in this respect.

Since the previous technique of manufacturing insulin required an elaborate distillation plant with evaporators, condensers, vacuum pumps and a heavy cooling machinery, demanding both manpower, steam and electricity

* Jorpes, J. E., Mutt, V. and Rastgeldi, S. Swedish patent 157, 387 Oct. 18, 1956. Priority date Feb. 9, 1955, Swed. patent 162, 669 Jan. 23, 1958, Britt. patent 797, 959 Oct. 29, 1958, U.S. patent 2, 878, 159 March 17, 1958.

to run it, the possibility of taking up the insulin directly on an ion-exchanger completely altered the large-scale manufacturing process.

EXPERIMENTAL

The minced frozen glands are extracted with the ordinary amount of ethyl alcohol, acidified with oxalic acid (30 g per kg pancreas, dissolved in water), citric acid (70 g per kg) or preferably phosphoric acid (15—20 ml conc. per kg).

In this procedure as in the old one ammonia is added to pH 8.0 and the proteins precipitated are removed. The ammonium ions present would prevent the adsorption on the alginic acid and are therefore to be removed. This is achieved by means of Dowex-50 in the hydrogen form, added step-wise until pH 3.2 is reached. The ion-exchanger is collected for regeneration with acid.

Before use the alginic acid is washed free of metallic ions with 0.3 N hydrochloric acid and then with water. It is usually stored slightly moistened at —15°C. If dry it must be moistened with water before adding it to the alcoholic extract. *The capacity of new lots of alginic acid to adsorb insulin was constantly low, about 50 % of normal, and increased to an optimum level after 2 regenerations.* Per kg pancreas 30 g of alginic acid is taken, to be left in contact with the extract during 4 h at room temperature under constant stirring. The acid is collected through filtration or centrifugation and washed with 95 % and absolute ethanol in order to remove fats, and the alcohol is removed by aeration. Elution of the insulin is performed with 0.2—0.3 N hydrochloric acid at room temperature. The alginic acid is washed with water and used again for at least 10, possibly 15 times.

Elimination of proteolytic enzymes. In using calf pancreas the procedure worked excellently. When it was applied to ordinary frozen ox pancreas the yield of insulin slowly dropped, until on the sixth to eighth time the alginic acid was in use, no insulin at all precipitated on adding sodium chloride to the eluate. The different behaviour of the calf and the ox pancreas could hardly be due to anything else than a destruction of the insulin through enzymes still present in the extract and accumulated on the alginic acid during its repeated use. As most clearly demonstrated by Birgitta Werner [12] in 1948, the enzyme-producing apparatus of the pancreas is, in man, not yet fully developed in the newborn.

We therefore together with Mr Gunnar Lindén of Vitrum AB after removal of the Dowex-50 heated the alcoholic extract of the ox pancreas at pH 3.2 before addition of the alginic acid. The yield of insulin then even exceeded the expected level and the product crystallized readily. This also applies to the hog pancreas. After introducing this procedure of raising the temperature of the alcoholic extract up to 70—75°C in the course of 30 min, and cooling it to 30°C during a further 30 min — a procedure which destroys the proteolytic enzymes — the manufacturing process ran smoothly.

The yield of insulin depends not only upon the manufacturing process, but also upon the gland material available. Old dairy cows, an important source of glands in some countries, may have as low an insulin level in the pancreas as 400—500 units per pound, whereas the corresponding figure for young cattle is about 2 000 units. The collection and the storage of the glands also influence the yield. The heaviest losses are of course made during the concentration of the alcoholic extract, particularly if the distilling equipment is less efficient. The new procedure eliminates this risk, thereby increasing the yield of insulin with at least 20—30 %. The simultaneous gain through the saving of laboratory space, equipment, power consumption and labour add further to the value of the technique.

REFERENCES

1. Nachod, F. C. *Ion exchange.* Acad. Press, New York 1949.
2. Paleus, S. and Neilands, J. B. *Acta Chem. Scand.* **4** (1950) 1024.
3. Hirs, C. H. W., Moore, S. and Stein, W. H. *J. Am. Chem. Soc.* **73** (1951) 1893.

4. Tallan, H. H. and Stein, W. H *J Biol Chem* **200** (1953) 507.
5. Hirs, C. H. W. *J. Biol. Chem.* **205** (1953) 93.
6. Peterson, E. A and Sober, H. A *J. Am. Chem. Soc.* **78** (1956) 751.
7. Boardman, N. K. *Biochim. et Biophys. Acta* **18** (1955) 290.
8. Astwood, E. B., Raben, M. S., Payne, R. W. and Grady, A. B. *J. Am. Chem. Soc.* **73** (1951) 2969.
9. Samsonov, G. V. and Faddajeva, M. D. *Biokhimiya* **21** (1956) 403.
10. Percival, E. G. V. *Structural Carbohydrate Chemsitry*, London 1950.
11. Heming, A. E. and Flanagan, Th. L. *Ann. N. Y. Acad. Sci.* **57** (1953) Art. 3, p. 246.
12. Werner, B. *Acta Paediat.* **35** (1948) Suppl. 6.

Received May 30, 1960.

ACTA CHEMICA SCANDINAVICA 14 (1960) 1781–1789

The Action of Intestinal Microorganisms on Bile Acids

Bile Acids and Steroids 101

ARNE NORMAN* and SVEN BERGMAN

Department of Physiological Chemistry and Department of Bacteriology, University of Lund, Lund, Sweden

The transformation of cholic-24-^{14}C acid by intestinal microorganisms of the rat in aerobic and anaerobic cultures has been studied. 7-Ketodeoxycholic, deoxycholic, 12-ketolithocholic and 3,12-diketocholanic acids were isolated from the cultures and identified. 7-Ketodeoxycholic acid was the main metabolite formed in the aerobic cultures. The removal of the hydroxyl group at C-7 in cholic acid was mainly effected by anaerobic microorganisms. The ability of different intestinal miroorganisms to transform cholic acid was also tested. Certain strains of *Escherichia coli* and *Clostridium perfringens* oxidize cholic acid to 7-ketodeoxycholic acid.

Numerous bacteria and fungi are known to transform bile acids and related steroids into a variety of metabolites both *in vivo* and *in vitro* (see, *e.g.*, the reviews by Haslewood [1] and Talalay [2]). When labelled bile acids are given to rats, their radioactive metabolites occur as a complicated mixture of unconjugated compounds in the feces [3,4]. The products of purely microbial transformation of cholic acid have been isolated from the feces of rats with biliary fistula following the injection of cholic-24-^{14}C acid into the caeca. The main metabolites have been identified as 3α, 12α-dihydroxy-7-ketocholanic, deoxycholic and 3α-hydroxy-12-ketocholanic acids [5,6]. Small amounts of at least four unidentified labelled products were also isolated from the feces specimens.

In the present investigation we have studied the microbial transformation of cholic acid *in vitro*. The metabolites of the acid formed in cultures of both aerobic and anaerobic intestinal microorganisms were isolated and the major metabolites were identified. Also different bacterial strains isolated from the caecum of the rat were tested for their ability to transform cholic acid.

* Present address: Department of Chemistry, Karolinska Institutet, Stockholm, Sweden.

EXPERIMENTAL

Bile acids. 24-^{14}C-Labelled cholic, deoxycholic and chenodeoxycholic acids were prepared by the procedure of Bergström, Rottenberg and Voltz [7].

Taurocholic-24-^{14}C and glycocholic-24-^{14}C acids were synthesized as described by Bergström and Norman [24]. The conjugated bile acids were isolated from the products of the reactions by reversed-phase partition chromatography [8].

7-Ketodeoxycholic acid (3α,12α-dihydroxy-7-ketocholanic acid) was obtained by oxidizing cholic acid with N-bromosuccinimide [9] and was crystallized in the form of its methyl ester from ethyl acetate-light petroleum. The melting point of the methyl ester was 153—155°C.

7-Ketolithocholic acid (3α-hydroxy-7-ketocholanic acid) was synthesized as described by Samuelsson [10] and was kindly supplied by him.

12-Ketolithocholic acid (3α-hydroxy-12-ketocholanic acid) was prepared according to Bergström and Haslewood [11]. Its melting point was 160—161°C.

3,12-Diketocholanic acid was synthesized by chromic acid oxidation of deoxycholic acid. It melted at 183—185°C.

Column chromatography. The technique of reversed-phase partition chromatography developed by Bergström, Sjövall and Norman [12-14] was employed using the following phase systems:

Phase system	Moving phase (ml)	Stationary phase (ml)
C 1	methanol-water 150—150	chloroform-*iso*octanol 15—15
C 2	methanol-water 144—156	chloroform-*iso*octanol 15—15
C 4	methanol-water 165—135	chloroform-*iso*octanol 15—15
F 1	methanol-water 165—135	chloroform-heptane 45— 5
F 3	methanol-water 180—120	chloroform-heptane 45— 5.

Four ml of the stationary phase was supported on 4.5 g of hydrophobic Super Cel.

Paper chromatography. The routine method employed to isolate the metabolites of cholic acid-24-^{14}C produced by different microorganisms was the paper chromatographic method developed by Sjövall [15,16]. Specimens of broth culture media, 0.05 ml in volume, were run on strips of Whatmann 3 MM paper 1.5 cm wide. Cholic acid and 7-ketodeoxycholic acid were separated by descending paper chromatography with *iso*propyl ether-heptane (50:50 v/v) as the moving phase. The more hydrophobic metabolites, including deoxycholic acid, were separated from unchanged cholic acid by ascending paper chromatography with 70 % acetic acid as the stationary phase and *iso*propyl ether-heptane (85:15 v/v) as the moving phase.

Radioassays. ^{14}C was determined with a Tracerlab end-window or a gas-flow counter. The radioactivity on the paper chromatograms was measured with an automatic scanning device with a G.M. tube.

Bacteriological procedures. The culture medium employed was a placenta digest broth prepared according to Erlansson [17] to which 10 μg of labelled bile acid had been added per ml. After autoclaving, the broth media were inoculated with different strains of intestinal microorganisms or fecal suspensions and incubated at 37°C under aerobic or anaerobic conditions. The anaerobic cultures were incubated in an anaerobic jar of the Fildes-McIntosh type.

RESULTS

Transformation of cholic acid by intestinal microorganisms in vitro. A loopful of the caecal content from rats was transferred to broth containing cholic-24-^{14}C acid. After either aerobic or anaerobic incubation for seven days, the labelled compounds in the broth were separated by column chromatography.

Fig. 1 shows chromatograms of the metabolites formed in anaerobic cultures of caecal microorganisms. Chromatographic analysis of the ether extract

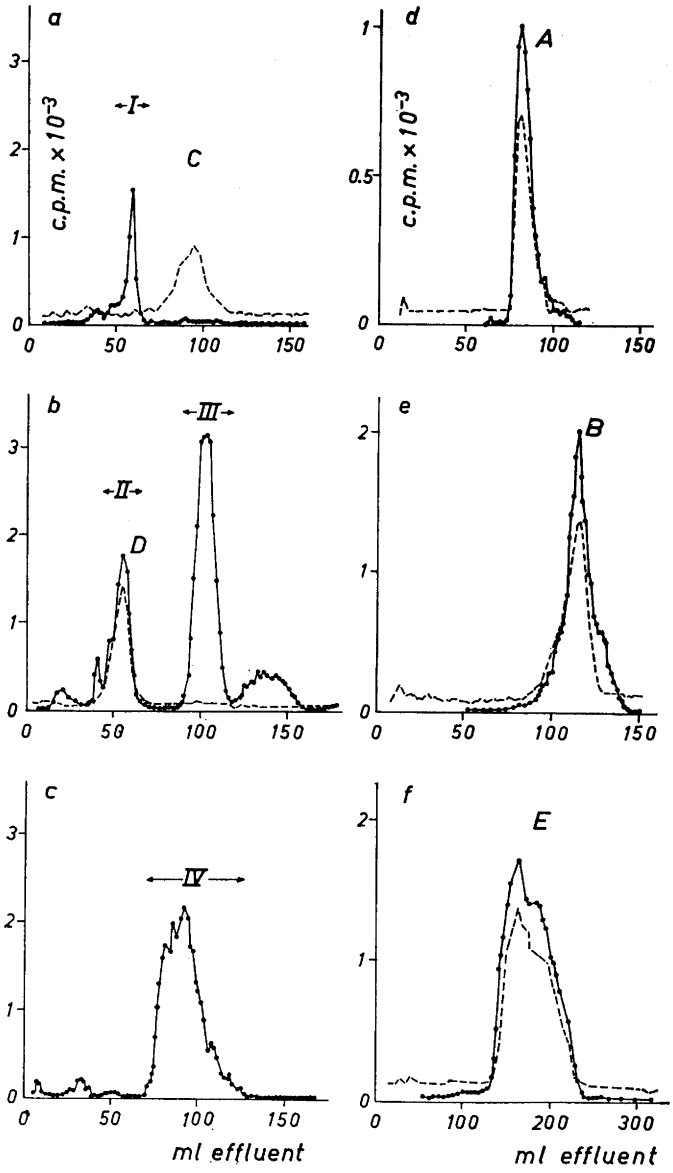

Fig. 1. Separation of metabolites of cholic acid formed in anaerobic cultures of caecal microorganisms. The following fractions were subjected to chromatography. *a*: Ether extract of the broth. Phase system C 1. *b*: Labelled compounds remaining in the stationary phase after the preceding chromatographic elution. Phase system F 1. *c*: Labelled compounds remaining in the stationary phase after the preceding chromatographic elution. Phase system F 3. *d*: Radioactive band I. Phase system C 2. *e*: Radioactive band III. Phase system F 1 *f*: Radioactive band IV. Phase system C 4. Reference substances: cholic (C), deoxycholic (D), 7-ketodeoxycholic (A), 12-ketolithocholic (B), 3, 13-diketocholanic (E) acids. ●—●—●, radioactivity; ————, titration.

of the broth medium with phase system C 1 yielded the chromatogram shown in Fig. 1 a. A separation of 3,12-dihydroxy-7-ketocholanic acid (in effluent fraction 60—70 ml), 3-hydroxy-7,12-diketocholanic acid (80—110 ml) and 3,7,12-triketocholanic acid (110—150 ml) is effected by this phase system. The only labelled compound (I) was found in the effluent fraction where 7-ketodeoxycholic acid is eluted. Most of the radioactive compounds were retained in the stationary phase. When the chromatographic analysis of these metabolites was continued with phase system F 1 (Fig. 1 b) three radioactive bands were eluted; the first two emerged in the effluent fractions where a dihydroxycholanic acid (II) and a monoketomonohydroxycholanic acid (III) were expected. The remaining labelled material in the stationary phase was eluted at 70—100 ml (IV) when phase system F 3 was employed (Fig. 1 c). Lithocholic and 3,12-diketocholanic acids are eluted at about the same rate (70—100 ml) by phase system F 3. To separate these we employ *iso*octanol-chloroform instead of heptane-chloroform as the stationary phase because *iso*octanol retains hydroxy derivatives of cholanic acid more effectively than it retains the keto derivatives of the acid. When phase system C 4 is employed, 3,12-diketocholanic acid is eluted in the effluent fraction 100—210 ml, whereas lithocholic acid stays in the stationary phase. Rechromatography of compound IV with phase system C 4 showed that it behave like 3,12-diketocholanic acid (Fig. 1 f).

The analyses thus showed that no unchanged cholic acid was left in the anaerobic cultures of caecal microorganisms, but instead five metabolites had been formed. Radioactive bands appeared in the effluent fractions where 7-ketodeoxycholic acid (I), 3,12-diketocholanic acid (IV), a dihydroxycholanic acid (II) and a monoketomonohydroxycholanic acid (III) appear. These radioactive metabolites were rechromatographed together with appropriate inactive carriers: fraction I with 7-ketodeoxycholic acid, fraction II with deoxycholic acid, fraction III with 12-ketolithocholic acid, and fraction IV with 3,12-diketocholanic acid. As seen from Fig. 1, the titration peaks coincided with the radioactive peaks. The identities of the metabolites were also confirmed by determining the specific activities after they had been recrystallized together with the inactive reference compounds. The identity of the fifth metabolite (effluent fraction 120—160 ml, Fig. 1 b) was not established.

Chromatographic separations of metabolites formed in aerobic cultures of caecal microorganisms showed that a complete transformation of cholic acid had occurred also in these cultures. The separated metabolites appeared in the same places in the chromatograms as the metabolites produced in the anaerobic cultures. The quantitative distribution, however, was different. More than 80 % of the cholic acid was transformed into deoxycholic, 12-ketolithocholic and 3,12-diketocholanic acids in the anaerobic cultures, whereas only 10 % was transformed into these metabolites in aerobic cultures of the same inocula. It is thus obvious that anaerobic microorganisms are responsible for the removal of the 7α-hydroxyl group. The main metabolite formed in the aerobic cultures was 7-ketodeoxycholic acid. Oxidation of cholic acid to 3-hydroxy-7,12-diketocholanic or 3,7,12-trihydroxycholanic acid was not found to occur.

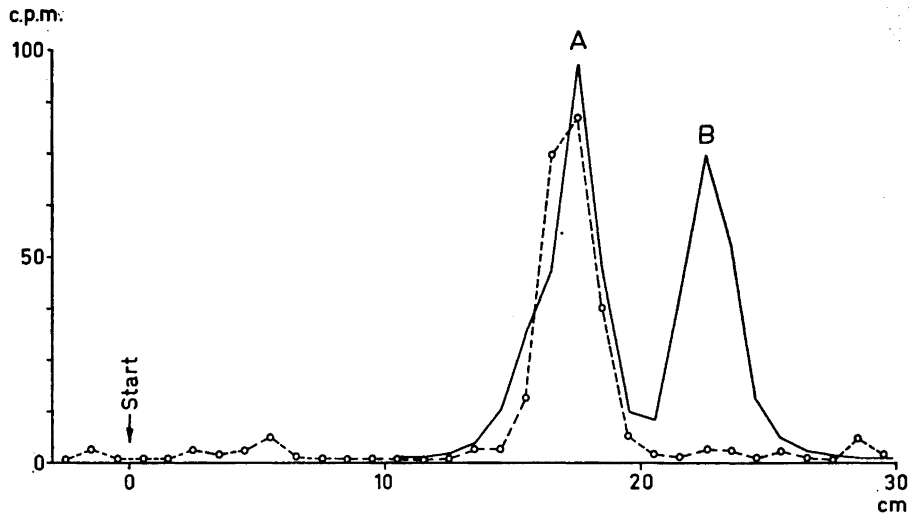

Fig. 2. Descending paper chromatography with *iso*propyl ether-heptane (50—50) as moving phase. ————, 24-^{14}C-labelled 7-ketodeoxycholic (A) and cholic (B) acids. O—O—O, 0.05 ml of a broth originally containing cholic acid-24-^{14}C incubated seven days after inoculation with *E. coli*.

Transformation of cholic acid by microorganisms isolated from the rat caecum. A number of aerobic and anaerobic intestinal microorganisms were isolated from the rat caecum. A loopful or organisms from a blood agar plate was inoculated into the broth and incubated for seven days. The ability of the organisms to transform cholic acid was determined by paper-chromatographic analysis. Of the isolated strains the following were found to be inactive: various strains of aerobic and anaerobic streptococci, *B. proteus*, *Pseudomonas pyocyanea*, *Aerobacter aerogenes*, *Staphylococcus aureus* and *albus*, *B. subtilis*, *diphtheroids* and some *candida* and *streptomyces* strains.

Different strains of *E. coli* transformed cholic acid completely into a labelled compound that appeared in the chromatogram in the same place as 7-ketodeoxycholic acid (Fig. 2). The same transformation was effected by strains of *Clostridium perfringens*. No intestinal microorganisms have yet been isolated that are capable of removing the 7α-hydroxyl group from cholic acid.

Oxidations of bile acids by E. coli and Clostridia. Fig. 3 shows chromatograms of broth specimens containing cholic acid that had been incubated 24 and 72 h after inoculation with *E. coli*. After three days the cholic acid had been completely transformed into a compound with the same chromatographic behaviour as 7-ketodeoxycholic acid (Fig. 4 a). An aliquot of the labelled metabolite was treated with chromic acid under conditions known to oxidize 7-ketodeoxycholic acid to dehydrocholic acid. After rechromatography the radioactivity then moved with dehydrocholic acid added as carrier. After its reduction with sodium borohydride the labelled compound exhibited the same

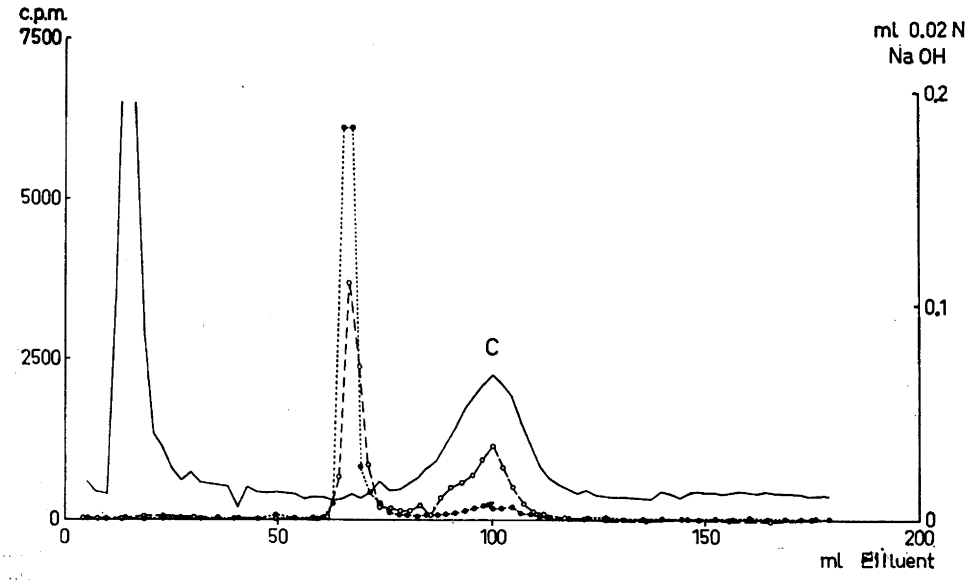

Fig. 3. Separation of labelled products formed in a broth originally containing cholic acid-24-^{14}C and inoculated with a strain of *E. coli* after 24 (O—O—O) and 72 (●—●—●), hours incubation. Phase system C 1. Reference substance: cholic acid (C). ———— titration.

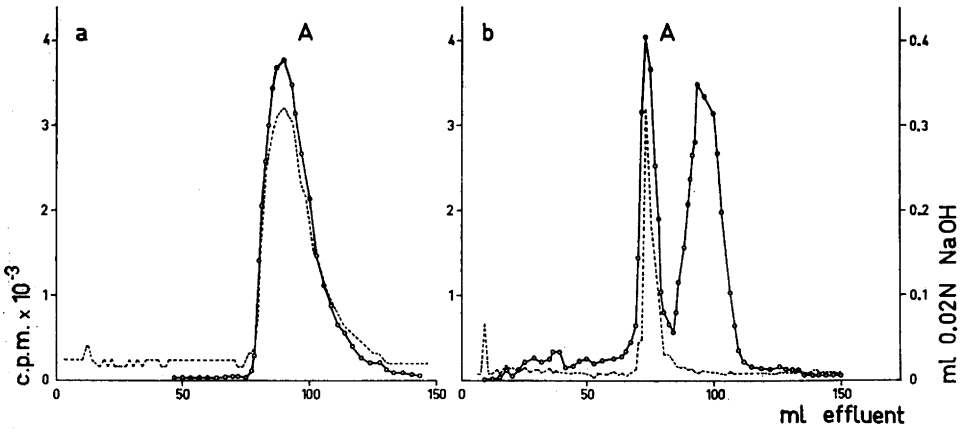

Fig. 4. a: Rechromatography with phase system C 2 of labelled material appearing before cholic acid in the chromatogram shown in Fig. 3.
Fig. 4. b: Chromagraphy of metabolites of cholic acid-24-^{14}C formed by *Clostridium perfringens* type E during seven days' incubation. Phase system C 1. Reference substance: 7-ketodeoxycholic acid (A). ————, radioactivity; — — — — —, titration.

Table 1. Transformation of cholic acid into 3,12-dihydroxy-7-ketocholanic acid by different strains of *E.coli* isolated from human feces. 5 ml of inoculated placenta broth containing 0.1 mg of cholic acid-24-^{14}C were cultured one and seven days. The quantitative estimates were based on paper-chromatographic analyses.

All the *E.coli* strains produced acid from arabinose, glucose, maltose and mannitol (also gas) and also produced indole.

No. of strain	Per cent of cholic acid transformed after 1 day	7 days	Biochemical reactions Sucrose	Dulcitol	Sorbitol	Salicin
I	61	100	−	−	+	−
II	71	100	−	−	+	−
III	79	100	−	−	+	−
V	62	100	−	−	+	−
VI	81	100	−	−	+	−
VII	75	100	−	−	+	−
VIII	79	100	−	−	+	−
IX	71	100	−	−	+	−
X	67	100	−	+	+	−
XI	74	100	+	−	+	+
XII	0	0	−	−	−	−
XIII	69	100	−	−	+	+
XIV	60	100	−	+	+	−
XV	68	100	−	+	+	−
XVI	88	100	−	−	+	−
uninoculated control	0	0				

chromatographic behaviour as cholic acid. The identity of the metabolite was confirmed further by recrystallizing it together with unlabelled 7-ketodeoxycholic acid. The specific activity remained constant through five recrystallizations.

E. coli strains are capable of oxidizing only the hydroxyl group at C-7 as no oxidation to 3-hydroxy-7,12-diketocholanic or 3,7,12-trihydroxycholanic acid was established. Chenodeoxycholic acid was transformed in cultures of *E. coli* into a compound that behaved like 12-ketolithocholic acid (Fig. 5 a) in chromatography and which was further identified by cocrystallization with unlabelled 12-ketolithocholic acid. No oxidation of deoxycholic acid occurred (Fig. 5 b) in similar tests. Experiments with 24-^{14}C-labelled glycocholic and taurocholic acids have shown that these conjugates undergo a similar oxidation by *E. coli*. No splitting of peptide bonds was observed.

Sixteen strains of *E. coli* isolated from human feces were tested for their ability to oxidize cholic acid to 7-ketodeoxycholic acid (Table 1). All the strains except one effected a rapid and complete oxidation of the cholic acid.

In a previous study [18] it was found that different strains of *Clostridium perfringens* quickly hydrolyze conjugated bile acids and transform a minor part of cholic acid into a more polar compound. Fig. 4 b shows a chromatogram of a broth culture of *Clostridium perfringens* type E originally containing cholic-24-^{14}C acid. The metabolite formed was eluted at the same rate as 7-ketodeoxycholic acid. It was identified as 7-ketodeoxycholic acid in the manner described above.

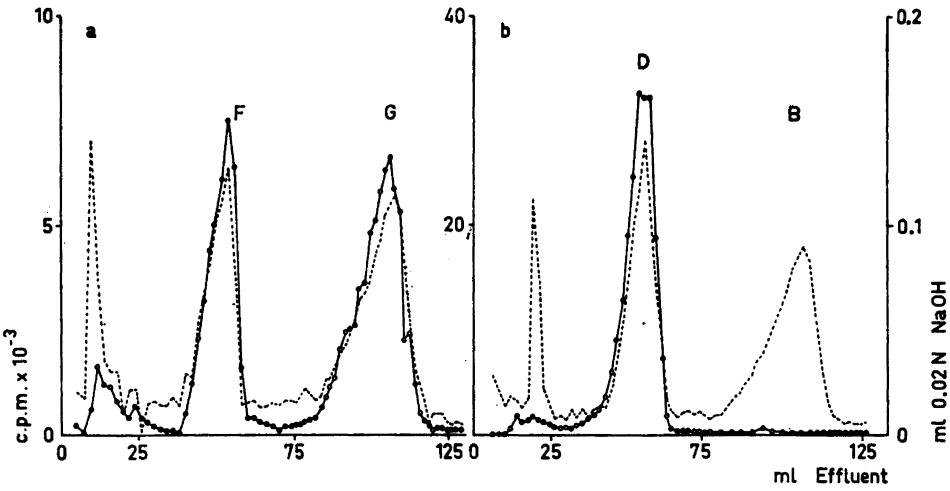

Fig. 5. Chromatographic analyses of three-day-old broth cultures of *E. coli*. *a*: broth originally contained chenodeoxycholic acid 24-^{14}C. *b*: broth originally contained deoxycholic acid-24-^{14}C. Phase system F 1. Reference substances: deoxycholic (D), chenodeoxycholic (F), 12-ketolithocholic (B) and 7-ketolithocholic (G) acids. ————, radioactivity; — — — — —, titration.

DISCUSSION

A transformation of cholic acid similar to that taking place *in vivo* is effected by anaerobic caecal microorganisms *in vitro*. The 7*α*-hydroxyl group is removed for the most part. Whereas the greater part of deoxycholic acid is excreted unchanged by the rat, the acid is for the most part oxidized by caecal microorganisms in vitro to 12-keto-3-hydroxycholanic and 3,12-diketocholanic acids. However, the caecal microorganisms more quickly remove the 7*α*-hydroxyl group than oxidize the hydroxyl groups at C-3 and C-12.

Schmidt and Hughes [19,20] demonstrated that a rapid and extensive decomposition of cholic acid occurs in the caecum of the guinea pig. They assumed this to be mainly due to an oxidative breakdown of the acid by strains of *Alcaligenes faecalis via* 7-keto-3,12-dihydroxycholanic and 7,12-diketo-3-hydroxycholanic acids to 3,7,12-triketocholanic acid. We have found that a rapid oxidation of cholic acid to 7-ketodeoxycholic acid occurs in aerobic cultures of microorganisms isolated from the rat caecum where the removal of the 7-*α*-hydroxyl group takes place only in minor degree. No further oxidation of the hydroxyl groups at C-3 and C-12 in cholic acid has been demonstrated. Neither 7,12-diketo-3-hydroxycholanic nor 3,7,12-triketocholanic acids has been isolated from the rat feces.

Turfitt [21] and Hayakawa *et al.*[22] have reported that the bile acid side chain is degraded by *Proactionomyces* and *Streptomyces gelatinus* 1164, respectively. Our experiments with 24-^{14}C-labelled cholic acid did not provide any evidence showing that a degradation of the bile acid side chain occurs in cultures of

microorganisms isolated from the rat caecum. Several investigators [22,23] have shown that cholic acid is oxidized to derivates of 3-keto-Δ^4-cholanic acid by different microorganisms. The formation of such compounds by intestinal microorganisms of the rat seems to be of minor degree.

Acknowledgements. This work is part of investigations supported by the *Statens Medicinska Forskningsråd* and the *National Heart Institute* (H2842), *U. S. Public Health Service*, Bethesda, Maryland.

The technical assistance of Misses Margret Månsson and Margaretha Persson is gratefully acknowledged.

REFERENCES

1. Haslewood, G. A. D. *Physiol. Revs.* **35** (1955) 178.
2. Talalay, P. *Physiol. Revs.* **37** (1957) 362.
3. Bergström, S. and Norman, A. *Proc. Soc. Exptl. Biol. Med.* **83** (1953) 71.
4. Lindstedt, S. and Norman, A. *Acta Physiol. Scand.* **34** (1955) 1.
5. Norman, A. and Sjövall, J. *Biochim. et Biophys. Acta* **29** (1958) 467.
6. Norman, A. and Sjövall, J. *J. Biol. Chem.* **233** (1958) 872.
7. Bergström, S., Rottenberg, M. and Voltz, J. *Acta Chem. Scand.* **7** (1953) 481.
8. Norman, A. *Arkiv Kemi* **8** (1955) 331.
9. Fieser, L. and Rajagopalan, S. *J. Am. Chem. Soc.* **71** (1949) 3935.
10. Samuelsson, B. *Acta Chem. Scand.* **13** (1959) 236.
11. Bergström, S. and Haslewood, G. A. D. *J. Chem. Soc.* **1939** 540.
12. Bergström, S. and Sjövall, J. *Acta Chem. Scand.* **5** (1951) 1267.
13. Sjövall, J. *Acta Physiol. Scand.* **29** (1953) 232.
14. Norman, A. *Acta Chem. Scand.* **7** (1953) 1413.
15. Sjövall, J. *Acta Chem. Scand.* **6** (1952) 1552.
16. Sjövall, J. *Acta Chem. Scand.* **8** (1954) 339.
17. Erlansson, P. *Acta Pathol. Microbiol. Scand. Suppl.* **85** (1951) 155.
18. Norman, A. and Grubb, R. *Acta Pathol. Microbiol. Scand* **36** (1955) 537.
19. Schmidt, L. H. and Hughes, H. B. *J. Biol. Chem.* **143** (1942) 771.
20. Schmidt, L. H., Hughes, H. B., Green, M. H. and Cooper, E. *J. Biol. Chem.* **145** (1942) 229.
21. Turfitt, G. E. *Biochem. J.* **42** (1948) 376.
22. Hayakawa, S., Fujii, T., Saburi, Y. and Eguchi, T. *Nature* **179** (1957) 537.
23. Halperin, A. H., Quastel, J. H. and Scholefield, P. G. *Arch. Biochem. Biophys.* **52** (1954) 4.
24. Bergström, S. and Norman, A. *Acta Chem. Scand.* **7** (1953) 1126.

Received April 20, 1960.

ACTA CHEMICA SCANDINAVICA 14 (1960) 1790–1796

Isolation of Seromucoids from Human Serum

JOHN GOA

Department of Medical Biochemistry, University of Gothenburg, Sweden *

A mixture of seromucoids has been prepared by means of fractional precipitation with perchloric acid and phosphotungstic acid. The seromucoids were separated into three fractions by means of chromatography on DEAE-cellulose. Each fraction was separated into subfractions by preparative paper electrophoresis, a total of seven fractions being obtained. One fraction was shown to be identical with MP-1 of Winzler or α_1-acid glycoprotein of Schmid. With the unfractionated seromucoid mixture six to eight precipitation lines were obtained immunologically by gel precipitation technique. Some chemical data of the proteins are given, — they are all rich in carbohydrate.

According to Winzler [1] seromucoids means a heterogeneous group of serum proteins left in solution by perchloric acid and precipitated by phosphotungstic acid. These proteins are rich in carbohydrate, which can be split from the protein only by very drastic treatment, and differ from other glycoproteins by their higher solubility.

Zanetti [2], Bywaters [3] and Rimington [4] prepared proteins of this type from the filtrate after heat coagulation of the bulk of the serum proteins. Winzler *et al.*[5] prepared them by ammonium sulphate precipitation of the perchloric acid filtrate of serum, and by means of electrophoresis found three components. The largest component moved like α_1-globulin at pH 8.4, the two other and smaller components moved slower [6]. The first component was subsequently prepared in pure state by ammonium sulphate precipitation of serum [7], and the chemical composition was studied. It was called M-1 or MP-1.

From Cohn-fraction VI, Schmid [8,9] isolated an α_1-acid glycoprotein which was shown to be identical with Winzlers MP-1. Later on Schmid isolated another carbohydrate-rich protein [10,11] which moved like α_2-globulin at pH 8.6. This protein, however, was heterogeneous in acetate buffer at pH 3.5 where it showed three components.

* Present address: Central Laboratory, Rikshospitalet, Oslo, Norway.

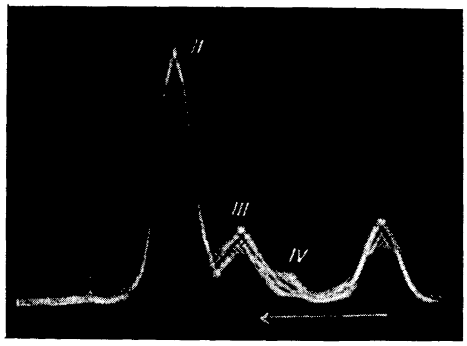

Fig. 1. Moving boundary electrophoresis of seromucoids. Barbital buffer pH 8.6, $\mu = 0.1$. Temp. + 1.5°C. Potential: 7.60 V/cm. Time:115 min. descending.
Mobility: I -8.2×10^{-5} cm²/V sec.
II -5.7×10^{-5} cm²/V sec.
III -3.5×10^{-5} cm²/V sec.
IV -1.9×10^{-5} cm²/V sec.

Of the seromucoids mentioned here, only Winzlers MP-1 or Schmids α_1-acid glycoprotein has been characterized. This protein has also been called orosomucoid [1].

During recent years chromatography on different ion exchangers has been used for isolation and purification of many proteins. Peterson and Sober [12] introduced several derivatives of cellulose, of which diethylaminoethyl-(DEAE)-cellulose has been especially useful. In the present study a combination of fractional precipitation, chromatograhy on DEAE-cellulose and preparative paper electrophoresis has been used for isolation of some carbohydrate-rich serum proteins which are not precipitated by perchloric acid.

METHODS OF PREPARATION

Fractional precipitation

One volume of serum or plasma was diluted with one volume of 0.9 % sodium chloride and precipitated by addition of two volumes of 1 M perchloric acid (final concentration 0.5 M). The precipitate was immediately centrifuged off or filtered. To the filtrate was added 1/20 volume of 2 % phosphotungstic acid in 2 N hydrochloric acid, the precipitated

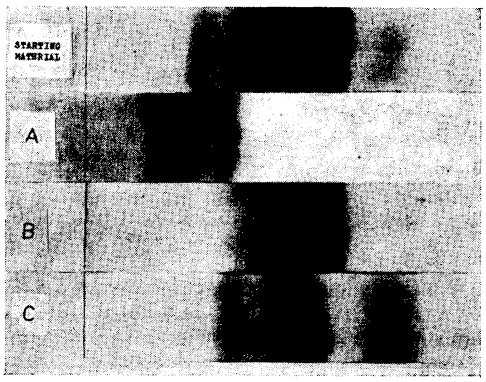

Fig. 2. Paper electrophoresis of seromucoids in barbital buffer pH 8.6. Starting material is the serum proteins left in solution by perchloric acid. A, B, and C are the fractions obtained by chromatography on DEAE-cellulose. The fractions are concentrated before electrophoresis and there is no quantitative relation between the amount of protein on the papers and the proportions in which they are present in the starting material.

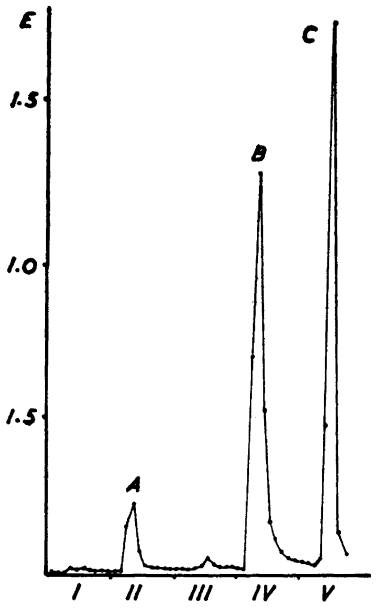

Fig. 3. Elution curve of 110 mg seromucoids. The Roman figures indicate the eluting buffers. I = 0.005 M phosphate, II = 0.005 M phosphate + 0.08 N sodium chloride, III = 0.05 M phosphate, IV = 0.05 M phosphate + 0.1 N sodium chloride and V = 1 N sodium chloride + 0.1 N sodium hydroxide. In all phosphate buffers pH was 6.8–6.9.

seromucoids were centrifuged off and dissolved by dropwise addition of 0.1 N sodium hydroxide to pH 6–7. To the solution obtained was added three times its volume of 95 % ethanol, and centrifuged. The precipitate was dissolved in distilled water and dialyzed. At pH 8.6 it consists electrophoretically of four fractions as shown in Figs. 1 and 2.

Chromatography

DEAE-cellulose was prepared exactly according to Sober *et al.*[13] The nitrogen content of the dried powder was 1.3 %. The cellulose ion exchanger was equilibrated with 0.005 M phosphate buffer pH 6.9 and packed in chromatographic columns (25 × 200 mm, fitted with a G2 sintered glass disk). The length of the cellulose columns were 6–7 cm. The proteins were eluted stepwise by increasing the ionic strength of the eluting buffer.

Step I. About 200 mg seromucoids were applied on each column at room temperature. All the protein was adsorbed to the cellulose, and an addition of 100 ml 0.005 M phosphate buffer resulted in no elution of protein.

Step II. The composition of the eluting buffer was changed to 0.005 M phosphate + 0.08 N sodium chloride, pH 6.9. The protein eluted with this buffer was called fraction A, and a paper electrophoresis strip of this fraction is shown in Fig. 2.

Step III. When no more protein was eluted in step II, some 100 ml 0.05 M phosphate buffer, pH 6.8 was allowed to pass the column, only traces of protein being eluted.

Step IV. The eluting buffer was now changed to 0.05 M phosphate + 0.1 N sodium chloride. The protein eluted was called fraction B and showed electrophoretically one large fraction (about 90 %), followed by a small one (Fig. 2).

Step V. After elution of fraction B about 40 % of the applied protein was left on the column. This protein was eluted with 1 N sodium chloride + 0.1 N sodium hydroxide and called fraction C. Electrophoretically it consists of three components (Fig. 2).

The effluent was collected in 10 ml samples and read in a Beckman DU spectrophotometer at 278 mμ. An elution curve is shown in Fig. 3.

Table 1. The table shows the approximate amounts of the different seromucoids isolated from 1 litre human serum. It also shows the percentage of hexose and hexosamine and the glucosamine/galactosamine ratio in the preparations.

Fraction	mg per litre serum	Hexose in per cent of protein	Hexosamine in per cent of protein	Glucosamine/ galactosamine ratio
A-1	20	6.6	7.1	1 : 0.12
A-2	20	5.1	5.6	1 : 0
B-1	250	16.2	11.3	1 : 0
B-2	25	10.6	10.6	1 : 0.28
C-1	25	7.2	3.5	1 : 1.10
C-2	100	9.3	10.4	1 : 0.35
C-3	75	7.8	8.3	1 : 0.50

Preparative paper electrophoresis

The fractions eluted from the column were dialyzed and concentrated by pervaporation to a concentration of 4—5 % protein. About 0.5 ml of the concentrated solution was placed evenly along a line transversely on 10 × 40 cm Munktell No. 150/20 filter paper strips, and run for 6—7 h with a voltage of 300 V as described previously [14]. The buffer used was barbital pH 8.6, ionic strength 0.05. When the electrophoresis was completed the paper was dried in the air and a strip cut out longitudinally and stained with bromophenol blue. With this strip as reference the protein fractions were cut out, eluted from the paper in 0.9 % sodium chloride, dialyzed and lyophilyzed.

RESULTS

Each of the fractions from the chromatographic column could be separated into subfractions by means of preparative paper electrophoresis. Fraction A was separated into two subfractions, the fastest called A-1, the slowest A-2. Fraction B was also separated into two subfractions, the fastest called B-1, the slowest B-2. Fraction C was separated into three subfractions, which were called C-1, C-2, and C-3, according to their mobilities.

All the isolated subfractions were homogeneous in paper electrophoresis at pH 8.6. The amounts prepared from one litre human serum are given in Table 1.

Table 2. Comparison between analytical data of fraction B-1 and "acid glycoprotein" of Schmid [9].

	Nitrogen per cent of protein	*Hexose* per cent of protein	*Hexosamine* per cent of protein	*Glucosamine/ galactosamine* ratio
Fraction B-1	10.6	16.2	11.3	1 : 0
Acid glycoprotein (own preparation)	11.3	16.4	11.3	1 : 0
Acid glycoprotein (values given by Schmid)	10.7	17.2	11.5	

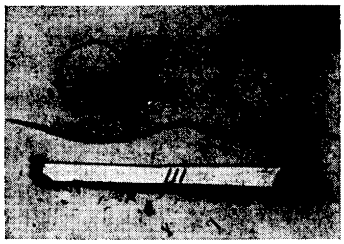

Fig. 4. Immunological identification test of fraction B-1 and "acid glycoprotein". In I 15 µl 5 % fraction B-1, in II 15 µl 5 % "acid glycoprotein" and in III 20 µl antihuman serum from rabbit (Behringwerke). The precipitation lines are stained with Amidoblack.

One of these fractions is well known beforehand, *viz.* fraction B-1, which is also present in largest amount in serum. It is identical with α_1-acid glycoprotein of Schmid or MP-1 of Winzler. To show the identity, α_1-acid glycoprotein was prepared according to the description of Schmid [9]. The protein thus prepared and fraction B-1 were analyzed for nitrogen (micro Kjeldahl), hexose [14], hexosamine [15] and the glucosamine/galactosamine ratio [16]. The values are given in Table 2 together with values given by Schmid [9].

In paper electrophoresis fraction B-1 had the same mobility as α_1-acid glycoprotein, and by moving boundary electrophoresis it moved like α_1-globulin with the mobility -5.7×10^{-5} cm^2/V sec. in barbital buffer pH 8.6 and ionic strength 0.1. In acetate buffer pH 4.5 and ionic strength 0.1 it moved with the mobility -3.2×10^{-5} cm^2/V sec.

Immunological experiments with gel precipitation technique according to the principle of double diffusion as worked out by Ouchterlony [17,18], were carried out with fraction B-1 and α_1-acid glycoprotein. With anti-human serum from rabbit and 2 % agar as diffusion medium, the two preparations gave a common precipitation line indicating identity (Fig. 4).

Fig. 5. The seromucoid preparation (15 µl, 5 %) precipitated in agar against antihuman serum from rabbit (Behringwerke). Four precipitation lines are seen (stained with Amidoblack).

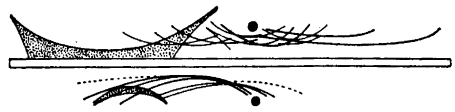

Fig. 6. Immune electrophoresis of normal serum (upper part) and a 10 % solution of the unfractionated seromucoid mixture (lower part).

Of other seromucoids described earlier, *e.g.* MP-2 and MP-3 of Winzler *et al.*[5] or α_2-glycoprotein of Schmid [11] there are no chemical data for comparison.

The content of hexose, hexosamine and the glycosamine/galactosamine ratio for all the fractions are given in Table 1. The values are not corrected for ash and water content except for fraction B-1. It will be seen that they are all rich in carbohydrate.

The possibility exists that some of the fractions described are artefacts or in some way modified proteins. Thus de Vaux St-Cyr *et al.*[19] found a lower mobility of orosomucoid prepared by perchloric acid than with trichloroacetic acid precipitation. However, with the immunological double diffusion gel technique the unfractionated seromucoid mixture showed four precipitation lines (Fig. 5), and by immunoelectrophoresis according to Grabar [20] it showed five distinct lines, one diffuse and two week lines (Fig. 6). When run simultaneously with normal serum the precipitation lines were found in the region of α-globulins (Fig. 6). In a similar preparation de Vaux St-Cyr *et al.*[19] found six precipitation lines.

In a previous paper [21] it has been reported that fraction C-2 and C-3 have antitryptic effect. Work is in progress on preparation and purification of the fractions in a preparative scale.

The author is greatly indebted to Miss Anita Boman for skilful technical assistance.
This investigation has been supported by a grant from *Statens Medicinska Forskningsråd.*

REFERENCES

1. Winzler, R. J. *Methods of Biochem. Analysis,* Interscience Publishers, Inc. New York. **2** (1955) 279.
2. Zanetti, C. V. *Gazz. chim. ital.* **33** (1903) 160.
3. Bywaters, H. W. *Biochem. Z.* **15** (1909) 322.
4. Rimington, C. *Biochem. J.* **34** (1940) 931.
5. Winzler, R. J., Devor, A. W., Mehl, J. W. and Smyth, I. M. *J. Clin. Invest.* **27** (1948) 609.
6. Mehl, J. W., Humphrey, J. and Winzler, R. J. *Proc. Soc. Exptl. Biol. Med.* **72** (1949) 106.
7. Weimer, H. E., Mehl, J. W. and Winzler, R. J. *J. Biol. Chem.* **185** (1950) 561.
8. Schmid, K. *J. Am. Chem. Soc.* **72** (1950) 2816.
9. Schmid, K. *J. Am. Chem. Soc.* **75** (1953) 60.
10. Schmid, K. *J. Am. Chem. Soc.* **75** (1953) 2532.
11. Schmid, K. *J. Am. Chem. Soc.* **77** (1955) 742.
12. Peterson, E. A. and Sober, H. A. *J. Am. Chem. Soc.* **78** (1956) 751.
13. Sober, H. A., Gutter, F. J., Wyckoff, M. M. and Peterson, E. A. *J. Am. Chem. Soc.* **78** (1956) 756.
14. Goa, J. *Scand. J. Clin. & Lab. Invest.* **7**, Suppl. 22 (1955) 13.

15. Svennerholm, L. *Acta Soc. Med. Upsaliensis* **61** (1957) 287.
16. Gardell, S. *Acta Chem. Scand.* **7** (1953) 207.
17. Ouchterlony, Ö. *Arkiv Kemi, Mineral. Geol.* **26** (1948) 1.
18. Ouchterlony, Ö. *Acta Pathol. Microbiol. Scand.* **26** (1949) 507.
19. de Vaux St-Cyr, Ch., Courcon, J. and Grabar, P. *Bull. Soc. Chim. Biol.* **40** (1958) 579.
20. Grabar, P. and Williams, C. A. *Biochim. et Biophys. Acta* **10** (1953) 193.
21. Bennich, H. and Goa, J. *Acta Chem. Scand.* **12** (1958) 781.

Received June 16, 1960.

ACTA CHEMICA SCANDINAVICA 14 (1960) 1797–1808

"Substrate Inhibition" of Intestinal Glycosidases

ARNE DAHLQVIST

Department of Physiological Chemistry, University of Lund, Lund, Sweden

The influence of *substrate concentration* on the initial rate of hydrolysis of different glycosides by hog intestinal glycosidases has been studied.

In some cases marked "substrate inhibition" was observed at 0.139 M substrate concentration, which is the concentration previously used as a standard concentration for the determination of intestinal glycosidase activities. *Transglycosylation* plays an important role in the "substrate inhibition" but it is not the only factor involved.

The use of 0.028 M substrate concentration as a standard concentration for the determination of intestinal glycosidase activities, rather than 0.139 M, is recommended. The influence of this lower substrate concentration on the absolute and relative activities of some purified hog intestinal glycosidases, and of crude hog intestinal glycosidase preparations, on different substrates has been determined.

Methods for determination of intestinal glycosidase activities are described, and units for expressing intestinal glycosidase activities are defined.

For studies of glycosidases, 0.139 M substrate is commonly used as a standard concentration [1], and so was done by the present author in a recent investigation of hog intestinal α-glucosidases [2]. During this investigation it was observed, however, that some intestinal α-glucosidases show marked "substrate inhibition" at 0.139 M substrate concentration and that lowering the concentration of substrate resulted in an *increase* of glycosidase activity with these enzymes [3].

A similiar observation has recently been made with invertase from sheep rumen protozoa [4,5]. In that case the authors found 0.025 M sucrose to give maximal invertase activity.

In the present paper a detailed study on the influence of substrate concentration on hog intestinal glycosidase (α-glucosidase, β-galactosidase and β-glucosidase) activities will be reported and procedures for the quantitative determination of intestinal glycosidase activities will be described. Since the standard substrate concentration now recommended is lower than the concentration used earlier, the absolute and relative activities of crude and purified intestinal glycosidase preparations on different substrates have been determined at this new substrate concentration.

RESULTS AND DISCUSSION

Influence of substrate concentration on the activities of isolated intestinal glycosidases

A) α-Glucosidases

The different α-glucosidase activities exerted by extracts from hog intestinal mucosa are caused by a mixture of at least five separate enzymes with varying specificity [2]. Three of these enzymes have been isolated, namely *invertase* (= maltase I), *maltase III* and *trehalase.** The "substrate inhibition" has been studied with each of these enzymes separately.

1) *Invertase.* Purified hog intestinal invertase hydrolyzes *sucrose*, *maltose* and *turanose* [6]. The influence of substrate concentration upon these activities of purified invertase is seen in Fig. 1. V_{max} in the figure has been calculated from the v_{obs} (observed initial velocity of hydrolysis) at *low* substrate concentrations (below 0.06 M) by the graphical method of Lineweaver and Burk [7] as modified by Dixon [8].

When the substrate concentration exceeded 0.1 M, the initial velocity of hydrolysis of all three substrates was *lower* than could be predicted from the Michaelis-Menten equation [9]. The "substrate inhibition" was more marked with *turanose* than with the other two substrates. At 0.28 M substrate concentration the initial velocity of hydrolysis of turanose was 30 % lower than the value calculated from the Michaelis-Menten equation. With sucrose or maltose as substrates the initial velocity at 0.28 M substrate concentration was 10—

* Maltase II has been isolated too, but only in small amounts [3].

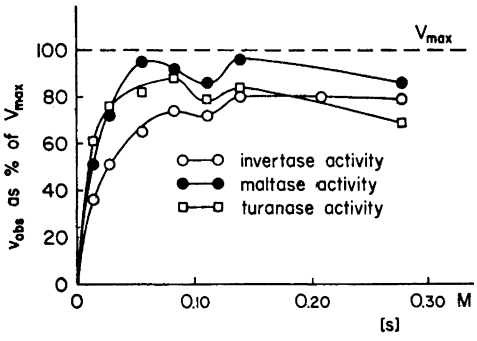

Fig. 1. Influence of substrate concentration, [s], on the invertase, maltase and turanase activities of purified intestinal invertase. Temp. 37°C, pH 6.5 (0.05 M maleate buffer). The observed initial rate of hydrolysis (v_{obs}) is expressed as per cent of V_{max} (calculated from the v_{obs} at low substrate concentrations as described in the text).

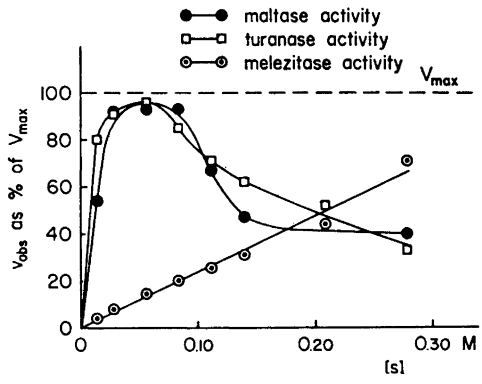

Fig. 2. Influence of substrate concentration on the maltase, turanase and melezitase activities of purified intestinal maltase III. Experimental conditions, see Fig. 1.

15 % too low. These findings suggest that *transglycosylation* may be the cause of the "substrate inhibition", since the invertase and maltase activities were measured with reducing sugar methods, which measure both the glycon and the aglycon liberated, while the turanase activity was measured with a glucose oxidase reagent, which measures only the glycon liberated. If transglycosylation is the cause of the "substrate inhibition" the amount of glycon liberated will be lower than the amount of aglycon liberated.

To elucidate whether transglycosylation was the cause of the "substrate inhibition" the amounts of glucose (glycon) and fructose (aglycon) liberated during the hydrolysis of turanose were measured separately by quantitative paper chromatography [10]. The amount of glucose liberated at 0.28 M substrate concentration was 31 % lower than the amount of fructose liberated. This indicates that transglycosylation is the main factor responsible for the "substrate inhibition" of this enzyme.

An irregularity of the shape of the curve between 0.08 and 0.15 M substrate concentration was observed with all three activities (Fig. 1). The cause of the irregularity is not known. It may indicate that more than one factor is involved in the "substrate inhibition" of intestinal invertase.

2) *Maltase III.* Purified hog intestinal maltase III hydrolyses *maltose, isomaltose, turanose, phenyl-α-D-glucopyranoside* and *melezitose* [2,3,11]. The influence of substrate concentration upon the maltase, turanase and melezitase activities of this enzyme is seen in Fig. 2.

With this enzyme the "substrate inhibition" of the maltase and turanase activities was considerably more marked than with the activities exerted by invertase (= maltase I) (Fig. 1). When the substrate concentration exceeded 0.05 M, the initial velocity of hydrolysis of these substrates was lower than calculated from the Michaelis-Menten equation and at 0.28 M substrate concentration the initial velocity was about 60 % lower.

With the melezitase activity no "substrate inhibition" could be demonstrated. This fact is, however, readily explained by the low affinity of the enzyme for melezitose (see Fig. 2) [11,13].

As was done in the experiments with purified invertase described above, the amounts of glucose and fructose liberated from turanose by maltase III were measured separately. At 0.28 M substrate concentration the amount of glucose liberated was 35 % lower than the amount of fructose liberated. This indicates that the transglycosylase reaction also with maltase III plays an important role in the "substrate inhibition", although it can explain only a part of the inhibition.

3) *Trehalase.* Purified hog intestinal trehalase differs from the two enzymes described above by that it hydrolyzes only one single substrate, namely *α,α-trehalose* [12]. The influence of substrate concentration upon trehalase activity is seen in Fig. 3. No "substrate inhibition" could be demonstrated with this enzyme. In other experiments substrate concentrations as high as 0.8 M (= 30 % trehalose) were used without any decrease of trehalase activity. It is known that intestinal trehalase, in contrast to other intestinal glycosidases, has no transglycosylase activity [12].

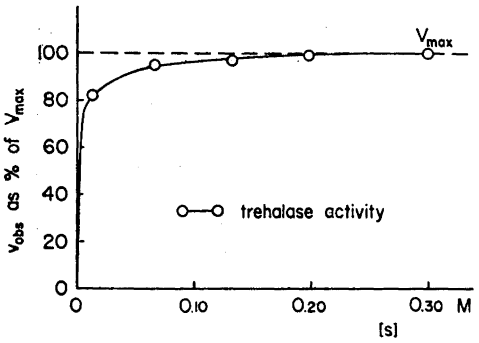

Fig. 3. Influence of substrate concentration on the activity of purified intestinal trehalase. Temp. 37°C, pH 6.0 (0.05 M maleate buffer).

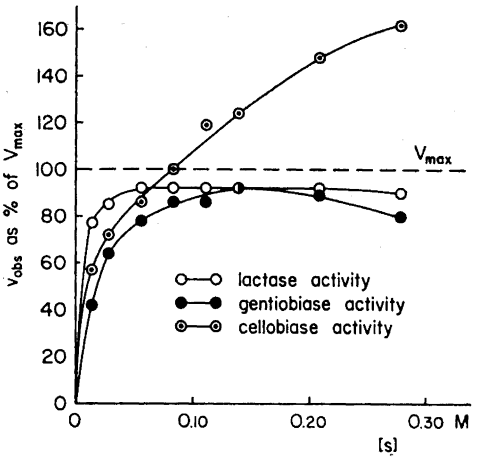

Fig. 4. Influence of substrate concentration on the lactase, cellobiase and gentiobiase activities of a crude hog intestinal glycosidase preparation. Temp. 37°C, pH 6.0 (0.05 M maleate buffer). When the substrate concentration exceeds 0.10 M, the observed initial rate of hydrolysis (v_{obs}) of cellobiose exceeds the V_{max} calculated from the v_{obs} at substrate concentrations below 0.06 M.

B) β-Galactosidase and β-Glucosidase

Hog intestinal mucosa preparations hydrolyze *lactose*, which is a β-galactoside, and a number of β-glucosides as *cellobiose*, *gentiobiose* and *phenyl-β-D-glucopyranoside*. The relation between these activities is under current investigation, but preliminary results indicate that the β-galactosidase and β-glucosidase activities of hog intestinal mucosa are caused by one single enzyme, intestinal lactase. The activities on these substrates therefore were studied with crude hog intestinal glycosidase preparations, obtained as described earlier [2].

The influence of substrate concentration upon the *lactase*, *cellobiase* and *gentiobiase* activities of a crude hog intestinal glycosidase preparation is seen in Fig. 4. The "substrate inhibition" of the lactase and gentiobiase activities is relatively weak. Up to 0.1 M substrate concentration these activities followed the Michaelis-Menten relationship. At 0.28 M substrate concentration the lactase activity was 10 % and the gentiobiase activity 15 % lower than calculated. The velocity of hydrolysis of these substrates was measured with the glucose oxidase reagent, and therefore with lactose as substrate only the *aglycon* (glucose) liberated was measured. The *glycon* (galactose) does not react with this reagent. This means that even if the transglycosylase reaction may contribute to the "substrate inhibition" of lactase, it is not the only factor

involved, for in that case the rate of liberation of the aglycon would not have decreased.

The *cellobiase* activity shows a behaviour quite different from that of the other activities studied in the present paper. It shows "substrate *activation*" rather than "substrate innibition". At low substrate concentration (0.01—0.06 M) the cellobiase activity seemed to follow the Michaelis-Menten equation, but when the substrate concentration was further increased, the velocity of hydrolysis became considerably greater than the V_{max} calculated from the values obtained at low substrate concentrations (Fig. 4). This phenomenon appeared in repeated experiments. At present no explanation can be given for this behaviour of the cellobiase activity.

The choice of a standard substrate concentration

As was pointed out in the introduction of the present paper, 0.139 M is commonly used as a standard substrate concentration for glycosidase activity determinations. From the results described above it appears, however, that some of the intestinal glycosidases show marked "substrate inhibition" at that concentration. In studies of intestinal glycosidases it seems preferable therefore, to use 0.028 M substrate as a standard concentration. At that substrate concentration all the activities hitherto studied (with the exception of melezitase, which has an extremely high K_s value [11]) will yield a velocity of hydrolysis which is more than 50 % of V_{max}.

There is one additional advantage in using the more dilute substrate as a standard concentration. The low solubilities of heteroglycosides (*e.g.* phenylglycosides) make it difficult to prepare reaction mixtures with 0.139 M concentration of these substrates [3]. The preparation of a reaction mixture with 0.028 M substrate will, however, not be difficult in these cases.

If 0.028 M substrate is selected as a standard concentration for the determination of intestinal glycosidase activities, the figures earlier reported [2,3] for the relative activities on different substrates of crude intestinal glycosidase preparations and of purified intestinal glycosidases will have to be recalculated. A comparison therefore was made of the relative activities of intestinal glycosidases on different substrates at 0.139 M and at 0.028 M substrate concentration.

Relative activities at 0.139 M and at 0.028 M substrate concentration

The lowering of the standard substrate concentration for determination of intestinal glycosidase activities to 0.028 M will result in the following alterations of the absolute and relative rates of hydrolysis of different substrates.

A. Isolated enzymes

1) *Invertase* (= *Maltase I*). The *invertase* activity will *decrease* by 40 %, the *maltase* activity by 30 % and the *turanase* activity by about 10 % (Table 1). The *maltase/invertase activity quotient* of purified invertase (maltase I)

Table 1. Relative activity of purified hog intestinal invertase (= maltase I) on different substrates at 0.139 M and 0.028 M substrate concentration in the presence of 0.05 M maleate buffer pH 6.5 and at temperature 37°C. The maltase activity of the enzyme at 0.139 M substrate concentration has been arbitrarily set at 100.

Substrate	Relative activity at 0.139 M substrate concentration	Relative activity at 0.028 M substrate concentration
Maltose	100	75
Sucrose	170	110
Turanose	7.5	7.0

thus will increase from 0.6 to 0.7, and the *turanase/invertase activity quotient* from 0.04 to 0.06.

2) *Maltase II.* The influence of the substrate concentration upon the activities of purified maltase II has not been studied, but from the similiarity of this enzyme with maltase III may be expected that the dilution of the substrate will *increase* the rate of hydrolysis of the different substrates hydrolyzed by maltase II. This theory was confirmed by the alteration of the total maltase activity of a *crude* hog intestinal glycosidase preparation (Table 4).

3) *Maltase III.* The *maltase* activity of this enzyme will increase by 100 % (Table 2). Also the *isomaltase* and *turanase* activities of this enzyme will increase. The *phenyl-α-D-glucopyranosidase* activity will not be measurably affected. The *melezitase* activity, due to the low affinity of the enzyme for this substrate, will be lowered by 75 %.

The *isomaltase/maltase activity quotient* will decrease from 0.05 to 0.04, the *turanase/maltase activity quotient* from 0.06 to 0.05, the *phenyl-α-D-glucopyranosidase/maltase activity quotient* from 0.05 to 0.03 and the *melezitase/maltase activity quotient* from 0.0040 to 0.0005.

4) *Trehalase.* The *trehalse* activity will be lowered by about 10 %.

Table 2. Relative activity of purified hog intestinal maltase III on different substrates at 0.139 M and at 0.028 M substrate concentration in the presence of 0.05 M maleate buffer pH 6.5 and at temperature 37°C. The maltase activity of the enzyme at 0.139 M substrate concentration has been arbitrarily set at 100.

Substrate	Relative activity at 0.139 M substrate concentration	Relative activity at 0.028 M substrate concentration
Maltose	100	200
Isomaltose	5	7
Turanose	6	9
Phenyl-α-D-glucopyranoside	5	5
Melezitose	0.4	0.1

Table 3. Relative activity of intestinal lactase (?) on lactose and some β-glucosides at 0.139 M and at 0.028 M substrate concentration in the presence of 0.05 m maleate buffer pH 6.0 and at temperature 37°C. The lactase activity at 0.139 M substrate concentration has been arbitrarily set at 100.

Substrate	Relative activity at 0.139 M substrate concentration	Relative activity at 0.028 M substrate concentration
Lactose	100	90
Cellobiose	50	30
Gentiobiose	1.5	1
Phenyl-β-D-glucopyranoside	5.0	4.5

5) *"Specific" isomaltase and "specific" phenyl-α-D-glucopyranosidase* *. These enzymes have not been isolated, and the influence of the substrate concentration on their activities is not known.

6) *β-Galactosidase and β-glucosidase.* The *lactase* activity will decrease by 10 % and the *cellobiase* activity by 40 % (Table 3). The *cellobiase/lactase activity quotient* consequently will decrease from 0.5 to 0.3. The absolute and relative rates of hydrolysis of *gentiobiose* and *phenyl-β-D-glucopyranoside* will undergo only small alterations.

B. Crude intestinal glycosidase preparations

The relative activities on different substrates by a crude hog intestinal glycosidase preparation will of course be dependent on the relative amounts of the different intestinal glycosidases present in the preparation. Since many substrates are hydrolyzed by two or three different enzymes in the preparation, the relative activity on each of these substrates at 0.139 M and at 0.028 M substrate concentration will also vary with the composition of the enzyme mixture.

The variations in the relative amounts of the different glycosidases present in hog intestinal glycosidase preparations, obtained on different occasions, are, however, usually not great. It has been reported earlier that the *maltase/invertase activity quotient* of such preparations when measured at *0.139 M* substrate concentration usually is about 2, the *trehalase/invertase activity quotient* 0.5 (provided the preparation is obtained from the *upper* part of the small intestine [12]) and the *lactase/invertase activity quotient* 0.2 [15]. At this substrate concentration the three different maltases present (maltase I—III) account for about *one third each* of the total maltase activity [2,3].

The activities on different substrates at *0.028 M* substrate concentration by a preparation which the composition described above has been investigated, and the results are seen in Table 4. At 0.028 M substrate concentration the *maltase/invertase activity quotient* was 5, the *trehalase/invertase activity quotient*

* "Specific" isomaltase and "specific" phenyl-α-D-glucopyranosidase may be identical [8].

Table 4. Relative activities of a crude hog intestinal glycosidase preparation * on different substrates, measured in the presence of 0.05 M maleate buffer, at pH 6.0 for trehalase, β-galactosidase and β-glucosidase activities, and at pH 6.5 for the other activities, at temperature 37°C. The maltase activity at 0.139 M substrate concentration has been arbitrarily set at 100.

Substrate	Enzymes acting upon each substrate	Relative activity at 0.139 M substrate concentration	Relative activity at 0.028 M substrate concentration
Maltose	{Invertase (= Maltase I) Maltase II Maltase III}	100	150
Sucrose	Invertase (= Maltase I)	50	30
Trehalose	Trehalase	25 **	23 **
Isomaltose	{"Specific" isomaltase? † Maltase II Maltase III}	8—10	8—10
Turanose	{Invertase (= Maltase I) Maltase II Maltase III}	7—8	7—8
Phenyl-α-D-glucopyranoside	{"Specific" phenyl-α-D-glucopyranosidase? † Maltase II Maltase III}	5—6	6—7
Melezitose	{Maltase II Maltase III}	0.20***	0.05***
Lactose	{Lactase?}	10	9
Cellobiose		5	3
Gentiobiose		0.20	0.15
Phenyl-β-D-glucopyranoside		0.50	0.45

* Prepared as described earlier. [2]

** Provided ethanol precipitation (which inactivates trehalase) has been omitted, and that the preparation has been obtained from the upper part of the jejunum. [2,12]

*** Calculated as complete hydrolysis of the trisaccharide. [13]

† "Specific" isomaltase and "specific" phenyl-α-D-glucopyranosidase may be identical.[14]

0.8 and the *lactase/invertase activity quotient* 0.3. Maltase I accounted for 15 % only of the total maltase activity, the remaining 85 % of the total maltase activity was exerted by maltase II and maltase III.

METHODS FOR DETERMINATION OF INTESTINAL GLYCOSIDASE ACTIVITIES

Substrates

Maltose (4-(α-D-glucopyranosyl)-D-glucose) monohydrate was obtained from Merck A.G. (Germany), *sucrose* (2-(α-D-glucopyranosyl)-β-D-fructofuranoside) and *lactose* (4-(β-D-galactopyranosyl)-D-glucose) monohydrate from Baker Co. (U.S.A.), *trehalose* (1-(α-D-glucopyranosyl)-α-D-glucopyranoside) dihydrate, *melezitose* (α-D-glucopyranosyl-

(1→3)-β-D-fructofuranosyl-(2→1)-α-D-glucopyranoside) dihydrate. and *cellobiose* (4-(β-glucopyranosyl)-D-glucose) from Pfanstiehl Chemical Co (U.S.A.), *turanose* (3-(α-D-glucopyranosyl)-D-fructose), *gentiobiose* (6-(β-D-glucopyranosyl)-D-glucose) and *phenyl-β-D-glucopyranoside* dihydrate from Nutritional Biochemicals Co. (U.S.A.). *Isomaltose* (6-(α-D-glucopyranosyl)-D-glucose) and *phenyl-α-D-glucopyranoside* were prepared as described earlier [14,12].

Incubation conditions and units

The *standard conditions* for determination of intestinal glycosidase activities are as follows. The enzyme acts in a 0.028 M solution of substrate in the presence of 0.05 M maleate buffer [16] at optimum pH (*i.e.* pH 6.5 for all α-glucosidase activities except trehalase, pH 6.0 for trehalase, β-galactosidase and β-glucosidase activities) at 37°C. Toluene is used as a preservative. The degree of hydrolysis is not allowed to exceed 15 % (within this limit the reaction follows zero order kinetics and the (initial) velocity of hydrolysis is proportional to the amount of enzyme present).

One unit of glycosidase activity is the activity which causes 5 % of hydrolysis in 2.0 ml of reaction mixture in 60 min under these conditions. 5 % of hydrolysis in 2.0 ml of reaction mixture at 0.028 M substrate concentration is equal to the formation of *1 mg of glucose* with maltose, isomaltose, trehalose, cellobiose or gentiobiose as substrate, *1 mg of invert sugar* (= 0.5 mg of glucose) with sucrose or turanose as substrate, and *0.5 mg of glucose* with phenyl-α-D-glucopyranoside, phenyl-β-D-glucopyranoside or lactose as substrate.

Preparation of the substrate solutions

The reaction mixture is generally obtained by mixing equal volumes of substrate solution and a suitably diluted enzyme solution. Since the reaction mixture shall contain 0.028 M substrate and 0.05 M maleate buffer, the substrate solution shall contain 0.056 M substrate and 0.10 M buffer. The substrate solutions are prepared (according to Table 5) by dissolving the substrates in 0.10 M maleate buffer [16] of suitable pH.

Table 5. Composition of substrate solutions. The solutions also contain 1 ml of toluene per 100 ml and should be stored in a refrigerator.

Substrate	Gram of substrate per 100 ml of substrate solution	pH of maleate buffer
Maltose monohydrate	2.00	6.5
Sucrose	1.90	6.5
Trehalose dihydrate	2.10	6.0
Isomaltose	1.90	6.5
Turanose	1.90	6.5
Phenyl-α-D-glucopyranoside monohydrate	1.52	6.5
Phenyl-α-D-glucopyranoside anhydric	1.42	6.5
Phenyl-β-D-glucopyranoside dihydrate	1.62	6.0
Melezitose dihydrate	3.00	6.5
Lactose monohydrate	2.00	6.0
Cellobiose	1.90	6.0
Gentiobiose	1.90	6.0

Determination of the degree of hydrolysis

The method which is most suitable for the determination of the degree of hydrolysis of the substrate, will vary with the properties of the substrates.

A) *3,5-Dinitrosalicylic acid.* The 3,5-dinitrosalicylate reagent, introduced by Sumner [17] for the determination of reducing sugars, is very suitable for the determination of the degree of hydrolysis of nonreducing substrates as sucrose, trehalose or melezitose. (It is, however, not suited for phenyl-glycosidase activity determinations [2]). The method has the advantage that the presence of proteins does not interfere, and therefore protein precipitation is not necessary.

For glycosidase activity determinations 1.0 ml of substrate solution is mixed with 1.0 ml of enzyme solution (diluted to contain 0.5—3.0 units of glycosidase activity per ml) in a test tube immersed in a water bath at 37°C. After 60 min the reaction is interrupted by the addition of 2.0 ml of 3,5-dinitrosalicylate reagent (most readily prepared as described by Hostettler *et al.*[18]) A blank with the same composition is prepared, in which the 3,5-dinitrosalicylate reagent is added *before* the mixing of the substrate and enzyme solutions. The tubes are then heated in a boiling water bath for 10 min, chilled for a few min in running tap water, and diluted with 20.0 ml of distilled water. The red colour produced is measured in a Beckman B spectrophotometer at 530 mμ using 1 cm cuvettes. The colour is stable for at least 24 h.

The amount of monohexoses produced in each sample is calculated from a standard curve made with known amounts of glucose (0.5—3.0 mg). Glucose and fructose have the same extinction coefficient with the 3,5-dinitrosalicylate reagent.

If the enzyme solution contains 1 unit/ml of *invertase* or *trehalase*, 1 mg of monohexoses will be formed during the procedure described above. If more than 3 mg are formed, the determination has to be repeated with a more dilute enzyme solution.

The amount of reducing sugars produced from a trisaccharide as *melezitose* will depend on whether one or both of the glycosidic links are hydrolyzed.

The 3,5-dinitrosalicylic acid method is not sensitive enough when only a small amount of the substrate or the enzyme is available, or when it is desired to use very dilute substrate solutions. In these cases the amount of monohexoses produced from a non-reducing substrate may be determined with Somogyi-Nelson's copper reduction method [19,20], after the precipitation of the proteins with Somogyi's Zn-Ba-reagents [21].

B) *Glucose oxidase.* When the substrate is a *reducing* disaccharide, the 3,5-dinitrosalicylic acid method is not applicable. The amount of glucose liberated in those cases may be determined specifically with a reagent containing glucose oxidase. This reagent does not react with fructose or galactose. It does, however, react with maltose and isomaltose,[2] and cannot, therefore, be used for the determination of the degree of hydrolysis of these substrates.

The glucose oxidase reagent is used for the determination of turanase, lactase, cellobiase and gentiobiase activity. It cannot be used for phenyl-glucosidase activity determinations, since free phenol interferes with the production of the colour.

The determination of glycosidase activity is performed in the following way. The enzyme solution is diluted with water to contain 0.2—1.0 units/ml of cellobiase or gentiobiase activity or 0.5—2.0 units/ml of any of the other activities. In a 7 × 120 mm test tube 0.1 ml of the diluted enzyme solution is mixed with 0.1 ml of the substrate solution, and the tube is immersed in a water bath at 37°C for 60 min. Then 0.8 ml of water is added, and the enzymatic reaction is interrupted by immersing the tube in a boiling water bath for 2 min. A blank is prepared with the same composition, which immediately after the mixing of enzyme and substrate is immersed in a boiling water bath for 2 min.

When turanose is used as substrate, the water added after incubation is replaced by 0.8 ml of 0.1 M acetate buffer pH 5.0. (Turanose will undergo partial alkaline hydrolysis when boiled at a pH higher than 6.0.) This is not necessary with the other substrates. The addition of acetate buffer does not interfere with the subsequent enzymatic determination of the amount of glucose liberated.

After chilling the tubes, 0.5 ml of the contents of each tube is transferred to a 17 × 180 mm tube, added 3.0 ml of the glucose oxidase reagent (prepared as described by Huggett and Nixon [22]), mixed and placed in a water bath at 37°C for 1 h for development of the colour. After that time the colour produced is measured in a Beckman B spectrophotometer at 420 mμ using 1 cm cuvettes.

A standard curve is made with known solutions of glucose, containing 10, 30 and 50 μg of glucose/0.5 ml (0.5 ml of the standard solution is mixed with 3.0 ml of the glucose oxidase reagent and placed at 37°C for 1 h).

If the enzyme solution contains 1 unit/ml of glycosidase activity, 50 μg of glucose will be formed under these conditions with cellobiose or gentiobiose as substrates, and 25 μg with turanose or lactose as substrates.

C) *Acid copper reagent.* For the determination of the degree of hydrolysis of maltose and isomaltose is used an acid copper reagent, which is reduced to a much smaller extent by reducing disaccharides than by monosaccharides [2].

The enzyme solution is diluted with water to contain 1.0—3.0 units/ml of glycosidase activity. In a 7 × 120 mm test tube 0.1 ml of enzyme solution and 0.1 ml of substrate solution are mixed, and the tube is immersed in a water bath at 37°C for 60 min. Then 1.0 ml of a 0.3 N $Ba(OH)_2$-solution, 1.0 ml of a 0.15 M $ZnSO_4$-solution and 1.8 ml of water are added (the $Ba(OH)_2$- and $ZnSO_4$-solutions are previously titrated against each other and adjusted so as to give an ion-free supernatant [21]) which precipitate the proteins and interrupt the enzymatic reaction. A blank is prepared with the same composition, which is precipitated immediately after mixing the enzyme and the substrate. The content of each tube is transferred to a centrifuge tube and centrifuged for 5 min.

Then 2.0 ml of the clear supernatant is transferred to a Folin tube for sugar determination (with a narrow part to prevent oxidation of the cuprous oxide by air, and graduated at 12.5 and 25.0 ml) and 2.0 ml of acid copper reagent is added (prepared as described by Tauber and Kleiner [22]). The tubes are immersed in a boiling water bath for exactly 10 min, and chilled with tap water for 2 min. 2.0 ml of Benedict's molybdate reagent [23] is added and after a further 2 min water to the 25 ml mark. The blue colour is immediately measured in a Beckman B spectrophotometer at 660 mμ, using 1 cm cuvettes.

When the determination is performed in this way, the Folin tube will contain 0.1 ml of reaction mixture. Even when more dilute substrate solutions are used (*e.g.* for K_s determinations) it is impossible to use a greater amount of the reaction mixture for the sugar determination, since the maleate buffer then will interfere with the reaction [2]. For maltase activity determinations the reagents in such experiments may be replaced by the modified reagents described by Caputto *et al.*[24] which are less sensitive to the interference by the buffer. These reagents are not suitable for isomaltase activity determinations [2].

The degree of hydrolysis is calculated from a series of tubes containing mixtures of maltose (isomaltose) and glucose corresponding to 0, 5, 10 and 15 % hydrolysis of the substrate. One unit of maltase (isomaltase) activity per ml in the enzyme solution used will cause 5 % of hydrolysis of the substrate. If the degree of hydrolysis exceeds 15 %, the determination should be repeated with a more dilute enzyme solution.

In determinations with this reagent it is necessary to include a new standard series in each set of tubes that is boiled.

Maltase III (heat-stable maltase) in the presence of maltase I and maltase II is determined by the same method, but after heating the enzyme solution in 0.01 M phosphate buffer pH 6.0 at 60°C for 45 min as described earlier [25].

D) *Phenol determination reagent.* For the determination of the degree of hydrolysis of phenyl-α-D-glucopyranoside and phenyl-β-D-glucopyranoside the amount of phenol liberated is determined with the commercial Folin-Ciocalteau reagent [26] (obtained from G.T.Gurr Ltd., England).

The procedure is as follows. 0.5 ml of diluted enzyme solution (containing 0.5—2.0 units/ml of glycosidase activity) is mixed with 0.5 ml of substrate solution at 37°C. After 60 min the proteins are precipitated by the addition of 1.0 ml of 0.3 N $Ba(OH)_2$, 1.0 ml of 0.15 M $ZnSO_4$ and 1.0 ml of water (see above). A blank is prepared with the same composition, which is precipitated immediately after mixing the enzyme and the substrate.

After centrifugation for 5 min, 1.0 ml of the clear supernatant is transferred to another test tube. To this tube is added 2.0 ml of Folin-Ciocalteau reagent (the commercial reagent diluted with four volumes of distilled water) and 6.0 ml of 1 N Na_2CO_3. The tube is immersed in a water bath at 37°C for 20 min, and then the blue colour produced is measured in a Beckman B spectrophotometer at 675 mμ using 1 cm cuvettes.

A standard curve is made with solutions of phenol in water (32.5 and 65.0 μg of phenol/ml), treated in the same way as the supernatants of the precipitated reaction mixture.

If the enzyme solution contains 1 unit of glycosidase activity/ml, 32.5 μg of phenol will be formed during these conditions.

Acknowledgment. This work has been supported by grants from the *Medical Faculty of the University of Lund.*

The skillful technical assistance of Mrs. K. Hagebris is gratefully acknowledged.

REFERENCES

1. Hestrin, S., Feingold, D. S. and Schramm, M. in Colowick, S. P. and Kaplan, N. O. (Eds.) *Methods in Enzymology* Vol. I, p. 231 (Academic Press, Inc., New York 1955).
2. Dahlqvist, A. *Hog Intestinal α-Glucosidases, Diss.* Lund 1960.
3. Dahlqvist, A. *Acta Chem. Scand.* **14** (1960) 1.
4. Christie, A. O. and Porteous, J. W. *Biochem. J.* **67** (1957) 19 P.
5. Carnie, J. A. and Porteous, J. W. *Biochem. J.* **73** (1959) 47 P.
6. Dahlqvist, A. *Acta Chem. Scand.* **14** (1960) 63.
7. Lineweaver, H. and Burk, D. *J. Am. Chem. Soc.* **56** (1934) 658.
8. Dixon, M. *Biochem. J.* **55** (1953) 170.
9. Dixon, M. and Webb, E. C. *Enzymes*, Longmans, Green & Co, London 1958.
10. Dahlqvist, A. and Borgström, B. *Acta Chem. Scand.* **13** (1959) 1659.
11. Dahlqvist, A. *Acta Chem. Scand.* **13** (1959) 2156.
12. Dahlqvist, A. *Acta Chem. Scand.* **14** (1960) 9.
13. Dahlqvist, A. *Acta Chem. Scand.* **12** (1958) 2012.
14. Dahlqvist, A. *Acta Chem. Scand.* **14** (1960) 72.
15. Borgström, B. and Dahlqvist, A. *Acta Chem. Scand.* **12** (1958) 1997.
16. Gomori, G., in Colowick, S. P. and Kaplan, N. O. (Eds.) *Methods in Enzymology* Vol. I, p. 142 (Academic Press, Inc., New York 1955).
17. Sumner, J. B. *J. Biol. Chem.* **62** (1924) 287.
18. Hostettler, F., Borel, E. and Deuel, H. *Helv. Chim. Acta* **34** (1951) 2132.
19. Somogyi, M. *J. Biol. Chem.* **195** (1952) 19.
20. Nelson, N. *J. Biol. Chem.* **153** (1944) 375.
21. Somogyi, M. *J. Biol. Chem.* **160** (1945) 69.
22. Huggett, A. St. G. and Nixon, D. A. *Lancet* **1957** 368.
23. Tauber, H. and Kleiner, I. S. *J. Biol. Chem.* **99** (1932) 249.
24. Caputto, R., Leloir, F. and Trucco, R. E. *Enzymologia* **12** (1947) 350.
25. Dahlqvist, A. *Acta Chem. Scand.* **13** (1959) 1817.
26. Kerr, L. M. H., Graham, A. F. and Levvy, G. A. *Biochem. J.* **42** (1948) 191.

Received June 27, 1960.

ACTA CHEMICA SCANDINAVICA 14 (1960) 1809–1814

The Sialic Acids of Bovine and Equine Submaxillary Mucins

GUNNAR BLIX and EWERT LINDBERG

Institute of Medical Chemistry, University of Uppsala, Sweden

The sialic acids of bovine submaxillary mucin (BSM) were separated and isolated by the aid of paper column chromatography. The predominant sialic acids in BSM are an N,O-diacetylneuraminic acid (with the O-acetyl in C-7 position) and an N-acetyl-di-O-acetylneuraminic acid (with one of the O-acetyls at C-7 and the other at C-8 or C-9). Small quantities of N-glycollylneuraminic acid and N-acetylneuraminic acid were also found, the latter possibly formed from the diacetylneuraminic acid during the isolation procedure. In addition there appeared small amounts of a fifth sialic acid which contained O-acetyl and was possibly a labile isomer of the N-acetyl-7-O-acetylneuraminic acid.

The sialic acid of equine submaxillary mucin was isolated in pure crystalline form. It was identified as N-acetyl-4-O-acetylneuraminic acid.

In an earlier investigation [1] it was found that, on paper chromatography, several-times-recrystallized *bovine* submaxillary mucin (BSM) regularly yielded four spots as indicated by the orcinol or Ehrlich reagents. Numbering the fractions I—IV with increasing R_F-values, fraction II was the predominant one. The amounts of fraction II isolated at that time were too small to allow closer analysis. It could hardly be doubted, however, that this fraction was an O,N-diacetylneuraminic acid, the O-acetyl of which, according to the result of periodate oxidation, was at the C-7 position. The R_F of fraction I tallied with that of N-acetylneuraminic acid. The nature of the faint fraction III and of fraction IV remained unelucidated.

The heterogeneity of sialic acid preparations of BSM was also brought out by work of Klenk and Uhlenbruck [2]. Applying a micro-method for the quantitative determination of the glycollyl group they obtained values corresponding to the presence of 21—25 % N-glycollylneuraminic acid in their preparations. We have arrived [3] at somewhat lower values (13—17 %), the difference probably depending on somewhat differing methods of preparation.

The ratio between the different kinds of sialic acid may well be different in the mucin (BSM) from that in the several-times-recrystallized preparation of sialic acid obtained from it. The sialic acids differ in solubility, and the

O-acetyl groups are very easily split off [3]. The preparation method has therefore been modified in the endeavour to minimize the risk of losses in the mother liquors and by decomposition. In preparations obtained by the modified method fractions II and IV clearly predominate, and seem to be present in about equal amounts, perhaps with some preponderance of the latter. Both were isolated and analysed. It was confirmed that fraction II was an O,N-diacetylneuraminic acid. It appeared chromatographically uniform, but contained about 1—2 % glycollyl. Fraction IV proved to be an N-acetyl-di-O-acetylneuraminic acid. It was also found uniform on rechromatographing, and contained no glycollyl.

In the new preparations fraction I could be resolved chromatographically into two spots, one with the same R_F as N-glycollylneuraminic acid, the other moving as N-acetylneuraminic acid. Crystalline matter obtained from total fraction I gave the X-ray powder pattern of N-acetylneuraminic acid, indicating that this substance was the main component of the crystals (concerning mixed sialic acid crystals see Abrahamsson and Svennerholm [6]). Glycollyl determinations of total fraction I gave values corresponding to a content of 7—12 % of N-glycollylneuraminic acid. The N-glycollylneuraminic acid is probably, at least in the main, preformed, since fractions III and IV do not contain any glycollyl and fraction II contains little of it. The N-acetylneuraminic acid present may be preformed, or it may have been formed from the di- and triacetylneuraminic acids during the isolation procedure.

The di- and triacetylneuraminic acids are not stable in aqueous solutions at + 37°. When pure aqueous solutions of the diacetylneuraminic acid are kept for various lengths of time at + 37° and the ensuing changes followed with paper chromatography, there arises at first a new spot which moves with the R_F of fraction III. With longer times a spot with the R_F of N-acetylneuraminic acid appears which increases in size as the two others diminish. Attempts to obtain fraction III in crystalline form were unsuccessful. This fraction gives a positive ester reaction with the $FeCl_3$-hydroxylamine test. It is probably a labile isomerization product of the diacetylneuraminic acid (formed by acetyl migration?). In similar experiments with the triacetylneuraminic acid the product which first formed had the R_F of the bovine diacetylneuraminic acid. Later spots appeared with the R_F-values of fraction III and N-acetylneuraminic acid, respectively. This result seems to indicate that one of the O-acetyl groups of the triacetylneuraminic acid has the same position as the O-acetyl of the bovine diacetylneuraminic acid, that is at C-7. Since the triacetylneuraminic acid is not oxidized by periodate, the second O-acetyl must be at C-8 or C-9.

In the earlier investigation [1] sialic acid from *equine* submaxillary mucin (ESM) was not obtained in a pure state. The analyses of the impure preparations suggested that this substance was an isomer to the bovine diacetylneuraminic acid. The purification procedure has now been improved and the nicely crystallizing substance obtained was chromatographically uniform.

Analysis of the substance has fully confirmed that it is an O,N-diacetylneuraminic acid. Contrary to the bovine diacetylneuraminic acid it consumes two molecules of periodate per molecule. Since the C-2 position is excluded, because this group is bound to hexosamine in the mucin, the result of the

periodate oxidation indicates that the equine sialic acid is N-acetyl-4-O-acetylneuraminic acid.

EXPERIMENTAL

1. Preparation of submaxillary mucins

The method is in principle the same as that used in earlier works from this laboratory [1]. The procedure is now described in more detail, to facilitate its reproduction.

Fresh glands are freed from adherent lymph glands, fat, and connective tissue, and are then frozen. Batches of 3 kg of frozen glands are cut into cubes of about 2 cm^3. The cut glands are then barely covered with distilled water, and kept at + 4° for 24 h, with occasional stirring. The cubes are removed by pouring the mixture through a stainless steel cone perforated with holes about 4 mm in diameter. The "filtrate" is freed from coarse particles by centrifuging. The first extract is usually strongly tinged by haemoglobin, and contains in addition much protein other than mucin, which may disturb the precipitation of the latter. It is therefore best discarded. The glands may be extracted at least 5—7 times in this way.

Dilute hydrochloric acid is added to the extract until the mucin just dissolves on the acid side of its isoelectric zone. The amount of HCl required may vary, and is conveniently determined in a preliminary test on a few ml of the extract. The mucin is precipitated by dilution with a few volumes of water. If the solution is vigorously stirred during and after the process of dilution, the mucin precipitate as a rule coalesces and adheres as an elastic clot to the spatula or rod used for stirring. The mucin is then dehydrated by alcohol, and torn into small pieces during the procedure. It is then ground to a powder, and freed from fatty impurities by extraction with ether.

2. Isolation of the BSM sialic acids

40 g of mucin is placed in a 2-litre flask. Small portions of water are added, and the whole vigorously shaken until a viscid suspension is obtained. The suspension is then made up to 400—500 ml water with gentle warming and constant shaking. The suspension, which has a pH of 3.3—3.4, is heated for 1 h in the boiling water bath. After cooling to room temperature the mixture is centrifuged, and the undissolved residue washed with 200 ml water. The supernatants are combined and freeze-dried.

The residue is repeatedly (6 times) extracted with methanol for 4—5 h at + 4°. Since the tri- and di-acetylneuraminic acids dissolve much more readily in methanol than do the N-acetyl- and N-glycollylneuraminic acids, the first extracts of the residue contain the main part of the two former kinds of sialic acid and nothing or very little of the two latter, which predominate in the last extracts (Fig. 1). In order to minimize methyl ester formation each extract is evaporated below 0° in the freeze-drying apparatus. The residues are dissolved in small quantities of methanol, and the solutions then combined and brought to dryness below 0°. The final residue thus obtained is dissolved in a minimum of water (about 2 ml); 30 ml of methanol is added, followed by 90 ml of ether. An amorphous precipitate formed is immediately filtered off. The filtrate is evaporated in the freeze-drying apparatus. The residue is dissolved in 5 ml of water-*n*-butanol-acetic acid (5:4:1), and then chromatographed on a paper roll (75 × 6 cm) in the same solvent. The LKB Chromax pressurized paper column system * was used. The eluate is collected in fractions of about 20 ml. Of each or each second fraction 0.5 ml is taken for sialic acid analysis (with the Ehrlich reagent). Fractions II, III, and IV are not completely separated in this procedure, but the separation is sufficient for the preparation of fractions II and IV in pure or almost pure state.

The fractions containing the di- and triacetylneuraminic acid are pooled separately, and evaporated to dryness in the freeze-dryer. In order to remove the last traces of butanol the residues are dissolved in about 100 ml of methanol, and the solution evaporated to dryness in the same manner.

* May be obtained from AB LKB-Produkter, Stockholm, Sweden.

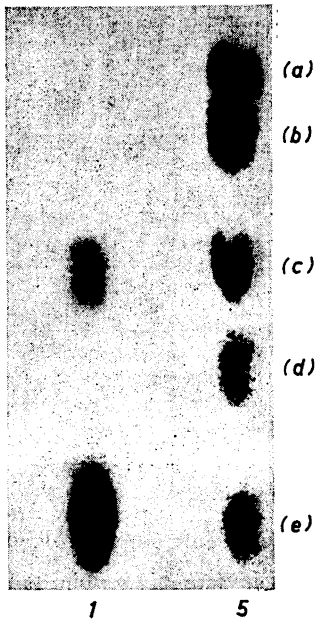

Fig. 1. Paper chromatogram of the first (1) and fifth (5) methanol extract of sialic acids of BSM. Solvent: *n*-butanol-pyridine-water, 6:4:3.
(a) N-glycollylneuraminic acid, (b) N-acetylneuraminic acid, (c) diacetylneuraminic acid,
(d) "fraction III", (e) triacetylneuraminic acid.

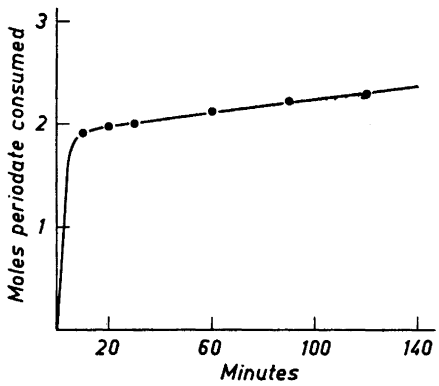

Fig. 2. Periodate oxidation of the sialic acid of equine submaxillary mucin in acetate buffer of pH 4.4 at + 8—10°. Moles periodate consumed per mole of substance oxidized.

For crystallization fraction II is dissolved in 1—2 ml water, fraction IV in at most 1 ml water; 30 ml of methanol is added, followed by 90 ml of ether. Light petroleum is then added drop by drop to the filtrate until faint turbidity appears. Crystallization takes place at room temperature or in the refrigerator. More substance crystallizes on each addition of a few drops of light petroleum during the next few days. The formation of crystals may continue for a week or more. (If too much light petroleum is added at one time the sialic acid comes out as an oil.) Recrystallization is performed in the same way. The yield of the once-recrystallized substances is 150—200 mg of diacetylneuraminic acid and about 500 mg of triacetylneuraminic acid.

3. Analysis of the BSM sialic acids

The *diacetylneuraminic acid* crystallizes with 1 molecule crystal water in rectangular plates, just as the crude substance obtained in the earlier investigation [1]. The substance decomposed with browning at 138—140°. $[\alpha]_D^{22}$ (H_2O) + 6 ± 2°. These values differ slightly from those originally given for this substance [1].

The nitrogen determinations were carried out by Dumas' method, the total acetyl as described by Friedrich and Rapaport [4], and the O-acetyl by Hestrin's method [5]. Two

Nitrogen analyses,			
$C_{13}H_{21}NO_{10}$(351)	Calc.	N	3.99
(dried at 100° *in vacuo*)	Found 1.		3.98
			3.98
	2.		3.84
			3.82
$C_{13}H_{21}NO_{10} \cdot H_2O$(369)	Calc.	N	3.79
(dried in desiccator)	Found		3.74
			3.77
Total acetyl,			
$C_{13}H_{21}NO_{10} \cdot H_2O$	Calc.		23.3
	Found		21.2
			21.4
			22.0
O-acetyl,			
$C_{13}H_{21}NO_{10} \cdot H_2O$	Calc.		11.6
	Found		10.7

glycollyl determinations (method of Klenk and Uhlenbruck [2]) gave values between 1.3 and 2.2 %. The X-ray powder pattern was identical with that of the crude product earlier investigated [1].

The *triacetylneuraminic acid* crystallized in needles or prisms with one molecule of crystal methanol, which did not disappear on heating at + 70° for several hours. It was driven off by heating *in vacuo* at 100° for 10 h. Methoxyl determination on the substance dried at 70° gave 7.4 % (calc. for $C_{15}H_{23}NO_{11} \cdot CH_3OH$ 7.4 %), whereas the substance dried at 100° gave no methoxyl value. It does not consume any periodate at pH 4.4 and + 10°.

The substance is more easily soluble in methanol than the other sialic acids. It melts with gas evolution but without discoloration at 130—131°. $[\alpha]_D^{22}$ (H_2O) + 9 ± 2°. The elementary and acetyl analyses agreed reasonably with the formula $C_{15}H_{23}NO_{11} \cdot CH_3OH$.

$C_{15}H_{23}NO_{11} \cdot CH_3OH$ (425)	Calc.	C	45.17	H 6.40	N 3.29
	Found 1.		44.83	6.53	—
			44.85	6.50	—
	2.		44.60	6.45	3.41
			44.58	6.43	3.42
	3.		44.77	6.43	3.30
			44.66	6.46	3.31

Total acetyl,	Calc. (three acetyls)		30.35
	Found		29.8
			32.9
O-acetyl,	Calc. (two acetyls)		20.21
	Found		20.6
			20.9

3. Isolation of the *equine diacetylneuraminic acid*

40 g of mucin is suspended in 400—500 ml water as described above for BSM. The pH is then adjusted to 2.5, and the suspension heated for 1 h in the boiling water bath with occasional shaking. The pH tends to rise, and should therefore be adjusted to pH 2.5 two or three times during the heating. After cooling to room temperature the mixture is centrifuged, and the undissolved residue washed with 200 ml water. The supernatants are combined and neutralized to pH 3.5 with dilute barium hydroxide. The new mixture is then freeze-dried without previous filtration.

The residue is repeatedly (5—6 times) extracted with methanol for 4—5 h at + 4°. In order to minimize methyl ester formation each extract is evaporated below 0° in the freeze-dryer.

The residues are dissolved in small quantities of methanol. The solutions are combined and brought to dryness in the freeze-dryer. The final residue thus obtained is dissolved in a minimum of water (4—5 ml), 30 ml methanol is added, followed by ether and light petroleum in the same manner as described for the BSM sialic acid. On recrystallization the addition of light petroleum is superfluous. The pure substance may be recrystallized from methanol without addition of ether. They equine sialic acid crystallizes in long needles. 40 g mucin yields 0.4—0.5 g of recrystallized substance.

4. Analyses of the *equine diacetylneuraminic acid*

The substance decomposes with browning at about + 200°. $[\alpha]_D^{22}$ (H_2O) −62 ± 1°. These values are slightly higher than those reported for the impure substance [1].

$C_{13}H_{21}NO_{10}$ (351),			Calc.	C 44.44	H 6.03	N 3.99
			Found	44.34	6.26	4.04
				44.18	6.17	4.07
Total acetyl,	Calc.	(two acetyls)		24.5		
	Found			21.0		
O-acetyl,	Calc.	(one acetyl)		21.5		
	Found			11.6		

The substance contained no appreciable amounts of methoxyl or glycollyl groups. The X-ray powder diagram was identical with that of the impure product given in the earlier report [1]. Periodate oxidation was carried out at pH 4.4 and + 8—10°, as earlier [1] described. The result of one such experiment is given in Fig. 2: 2 moles of periodate are evidently consumed per mole sialic acid.

REFERENCES

1. Blix, G., Lindberg, E., Odin, L. and Werner, I. *Acta Med. Soc. Upsaliensis* **61** (1956) 1.
2. Klenk, E. and Uhlenbruck, G. *Z. physiol. Chem. Hoppe Seyler's* **307** (1957) 266.
3. Blix, G. *Proc. Intern. Congr. Biochem.* 4th Congr. Vienna 1958 (1959). **1**, *Symp. Carbohydrate Chem. Subst. Biol. Interest*, p. 94.
4. Friedrich, A. and Rapaport, S. *Biochem. Z.* **251** (1932) 432.
5. Hestrin, S. *J. Biol. Chem.* **180** (1949) 149.
6. Abrahamsson, S. and Svennerholm, L. *Arkiv Kemi. To be published.*

Received June 27, 1960.

ACTA CHEMICA SCANDINAVICA 14 (1960) 1815–1818

Formation of Lithocholic Acid from Chenodeoxycholic Acid in the Rat

Bile Acids and Steroids 103

ARNE NORMAN and JAN SJÖVALL

Department of Chemistry, Karolinska Institutet, Stockholm 60, Sweden

Chenodeoxycholic acid-24-^{14}C has been injected into the cecum of bile fistula rats. 50–60 % of the isotope was absorbed. Lithocholic acid comprised more than 50 % of the labelled fecal acids but only traces were found in the bile. At least eight other microbial transformation products were present. One of these was probably 3-ketocholanic acid.

Cholic and chenodeoxycholic acids are the primary bile acids formed from cholesterol in the rat liver (*cf.* Ref.[1]). Chenodeoxycholic acid is further tranformed by liver enzymes into 3α, 6β, 7α- and 3α, 6β, 7β-trihydroxycholanic acids and to a small extent into 7-ketolithocholic and ursodeoxycholic (3α, 7β-diol) acids [2–4].

During the enterohepatic circulation, the bile acids are attacked by microbial enzymes in the cecum and colon and the metabolites formed are partly absorbed [5]. By this mechanism deoxycholic acid is formed from cholic acid. The aim of the present investigation was to find out whether a similar removal of the 7-α-hydroxyl group from chenodeoxycholic acid takes place during the enterohepatic circulation. If this were so, labelled lithocholic acid would be found in the bile and feces of rats which had received chenodeoxycholic acid-24-^{14}C. The presence of lithocholic acid in the bile of different animals has been repeatedly shown (*cf.* Sobotka [6]).

EXPERIMENTAL

Chenodeoxycholic acid-24-^{14}C (10 μC per mg) was prepared according to Bergström *et al.*[7]

Animal experiments. Bile duct-cannulated white rats weighing 200–300 g were used [8]. 0.5 mg of labelled sodium chenodeoxycholate in 0.2 ml of saline was injected into the cecal content [5]. Bile and feces were collected for two days.

Analysis of bile and feces. Bile acids were extracted from feces by refluxing three times for 2 h with 80 % aqueous ethanol. After evaporation to dryness the bile acids were extracted with ether from an acidified water solution. The bile was hydrolyzed with N NaOH in a closed steel tube for 6 h at 120° and the bile acids were extracted as described above.

The bile acids were separated with reversed phase column chromatography [9,10] using the following solvent systems:

Phase system	Moving phase (ml)	Stationary phase (ml)
C 1	Methanol-water 150:150	Chloroform-*iso*octanol 15:15
F 1	Methanol-water 165:135	Chloroform-heptane 45:5
F 2	Methanol-water 180:120	Chloroform-heptane 45:5
F 3	Methanol-water 195:105	Chloroform-heptane 25:25

4 ml of stationary phase were supported on 4.5 g of hydrophobic Supercel. The fractions collected from the columns were titrated and isotope determined on aliquots. For the sake of comparison, the effluent volumes of the figures have been corrected to correspond to a 4.5 g column.

RESULTS

After intracecal injection of labelled sodium chenodeoxycholate 40—50 % of the isotope was excreted in the feces. The remaining labelled products were absorbed and excreted in the bile.

Separation of labelled bile acids in feces. The ether extract of the feces was first chromatographed with phase system F 2. The labelled products appearing before lithocholic acid and those remaining in the stationary phase were rechromatographed with phase systems F 1 and F 3, respectively. The front band from the chromatography with phase system F 1 was re-run with phase system C 1.

As shown in Fig. 1 only a few per cent of the chenodeoxycholic acid was unchanged (Fig. 1., Phase system F 1, 45—65 ml). At least nine different metabolites were separated. Most of these were more hydrophobic than chenodeoxycholic acid. More than half of the isotope appeared at the site of lithocholic acid added as carrier (Fig. 1., Phase system F 1, 70 — 100 ml). The identity of the radioactive compound with lithocholic acid was established by isotope dilution. Rechromatography of the metabolites more hydrophobic than lithocholic acid (Fig. 1., Phase system F 3), together with 3-ketocholanic acid, showed that the radioactivity of the fourth band (100—150 ml) coincided with the titration peak of the carrier.

Since *E. coli* oxidizes chenodeoxycholic acid to 7-ketolithocholic acid *in vitro* we expected to find this acid in the feces [11]. A radioactive peak was present in the chromatogram very close to 7-ketolithocholic acid added as carrier (Fig. 1., Phase system F 1, A). Rechromatography showed that only a small fraction of isotope was eluted together with the carrier acid while the main peak appeared immediately afterwards.

The small amount of metabolites more hydrophilic than chenodeoxycholic acid was separated with phase system C 1 (Fig. 1). One band of activity appeared before, and another one just after, cholic acid added as carrier.

Separation of labelled bile acids in bile. As shown in Fig. 2 chromatographic analysis of the bile revealed the presence of at least eight radioactive com-

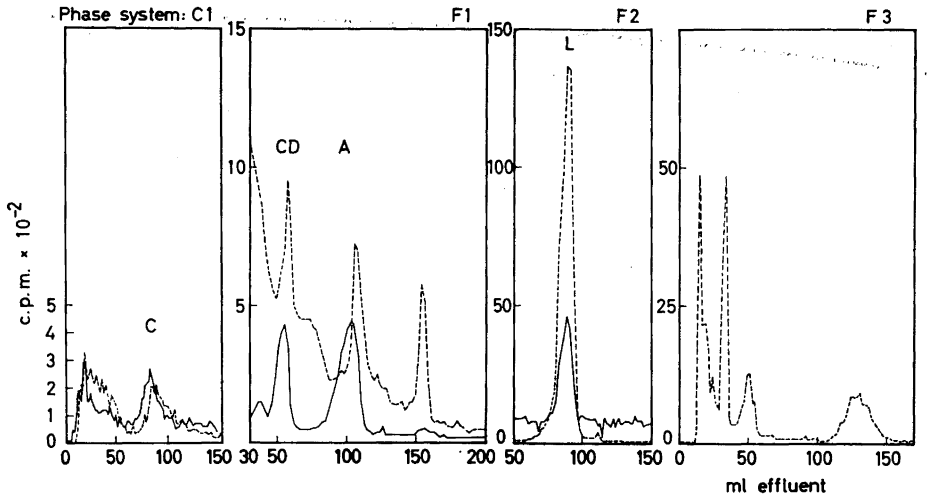

Fig. 1. Chromatographic separations of labelled products in feces after the injection of chenodeoxycholic acid-24-^{14}C into the cecum of a bile fistula rat. Reference substances: cholic (C), chenodeoxycholic (CD), 7-ketolithocholic (A), and lithocholic (L) acids. Solid line: Titration. Broken line: Radioactivity.

pounds. Apart from unchanged chenodeoxycholic acid (Fig. 2., Phase system F 1, 40—60 ml) radioactive peaks appeared at the sites of 3α, 6β, 7α- and 3α, 6β, 7β- trihydrocycholanic acids (Fig. 2., Phase system C 1, 60—80 ml and 100—140 ml, respectively). The metabolite eluted before chenodeoxycholic

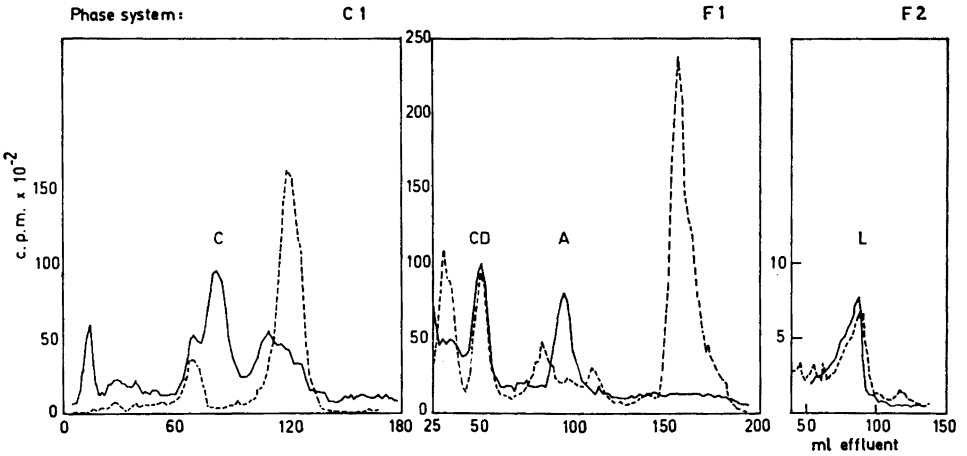

Fig. 2. Chromatographic separations of the labelled products in the bile of the same rat as used for the experiment shown in Fig. 1. The extract was first chromatographed with phase system F 1. The activity in the front band and that remaining in the stationary phase were rechromatographed with phase systems C 1 and F 2, respectively. For reference substances see Fig. 1.

acid (Fig. 2., Phase system F 1, 25—40 ml) was rechromatographed with ursodeoxycholic acid and the radioactivity and the titration peak coincided.

The metabolites described above are also present in the bile after intraperitoneal injection of chenodeoxycholic acid. The other compounds separated are thus microbial transformation products and/or liver metabolites of these substances. Except for lithocholic acid present in very small amounts, the nature of these compounds is unknown.

DISCUSSION

According to Siperstein *et al.*[12] lithocholic acid might be an intermediate in the formation of cholic and chenodeoxycholic acids from cholesterol. This would explain the presence of lithocholic acid in the bile. Their hypothesis has not been generally accepted (*cf.* Ref.[1]). In the present study we have shown that the 7α-hydroxylgroup of chenodeoxycholic acid can be removed by microorganisms in the large intestine. The lithocholic acid thus formed can be absorbed and appears in the bile. At the present time the microbial biogenesis seems to us to be the most plausible mechanism for the formation of lithocholic acid.

The technical assistance of Miss Margret Månsson and Miss Margaretha Persson is gratefully acknowledged. This work has been supported by grants from *Statens Medicinska Forskningsråd* and the *National Heart Institute* (H 2842), U.S. Public Health Service, Bethesda, Maryland, U.S.A.

REFERENCES

1. Bergström, S. and Borgström, B. *Ann. Rev. Biochem.* **25** (1956) 177.
2. Hsia, S. L., Matschiner, J. T., Mahowald, T. A., Elliott, W. H., Doisy, E. A. Jr., Thayer, S. A. and Doisy, E. A. *J. Biol. Chem.* **226** (1957) 667.
3. Hsia, S. L., Matschiner, J. T., Mahowald, T. A., Elliott, W. H., Doisy, E. A. Jr., Thayer, S. A. and Doisy, E. A. *J. Biol. Chem.* **230** (1958) 573.
4. Samuelsson, B. *Acta Chem. Scand.* **13** (1959) 983.
5. Norman, A. and Sjövall, J. *J. Biol. Chem.* **233** (1958) 872.
6. Sobotka, H. *Physiological chemistry of the bile.* Baltimore 1937.
7. Bergström, S., Rottenberg, M. and Voltz, J. *Acta Chem. Scand.* **7** (1953) 481.
8. Bergström, S., Sjövall, J. and Voltz, J. *Acta Physiol. Scand.* **30** (1953) 22.
9. Sjövall, J. *Acta Physiol. Scand.* **29** (1953) 232.
10. Norman, A. *Acta Chem. Scand.* **7** (1953) 1413.
11. Norman, A. and Bergman, S. *Acta Chem. Scand.* **14** (1960) 1781.
12. Siperstein, M. D., Harold, F. M., Chaikoff, I. L. and Dauben, W. G. *J. Biol. Chem.* **210** (1954) 181.

Received June 10, 1960.

ACTA CHEMICA SCANDINAVICA 14 (1960) 1819–1827

Crystalline Leghemoglobin

II. The Molecular Weights and Shapes of the two Main Components

NILS ELLFOLK*

Medicinska Nobelinstitutet, Biokemiska avdelningen, Stockholm, Sweden

The molecular weights of the two main components of leghemoglobin have been determined, on the basis of sedimentation and diffusion studies, to be 16 800 for the electrophoretically faster component, and 15 400 for the slower one. The sedimentation constants, extrapolated to infinite dilution, were 2.01 S for the electrophoretically faster component, and 2.04 S for the slower one, whereas the diffusion constant was 11.18 F for the faster component and 12.35 F for the slower one. The partial specific volume of the unresolved material was 0.740 ml/g. The molar frictional ratio was 1.118 for the electrophoretically faster component and 1.043 for the slower one. The results of this study show that the two main components of leghemoglobin differ slightly from each other in molecular size and shape.

Studies on the molecular weight of leghemoglobin (Lhb) have not been made until quite recently. In 1952 Ellfolk and Virtanen [1], on the basis of their osmotic and sedimentation and diffusion studies, reported that the unresolved chromoprotein had an average molecular weight of 20 000. Difficulties in resolving the chromoprotein into its components in good yield limited the studies of the individual components. The electrophoretically faster component was found to have an iron content of 0.34 % [1]. This caused the authors to assume that the electrophoretically faster component represented pure Lhb and that the electrophoretically slower component was an inhomogeneous protein. After the recent development of a procedure for preparing the two main components in good yield in a crystalline state [2], it was decided to reinvestigate the molecular sizes and shapes of the two individual main components.

EXPERIMENTAL

Material. Pure fractions of the electrophoretically faster and slower components of Lhb were prepared by a chromatographic procedure that was published earlier [2]. For the sedimentation and diffusion measurements, the protein solutions were dialyzed for

* Permanent address: Research laboratories of the State Alcohol Monopoly, Helsinki, Finland

48 h at + 3°C against a 0.283 μ buffer of pH 7 that contained 0.05 M sodium phosphate and 0.171 M sodium chloride.

Sedimentation. The sedimentation analyses were made in a Spinco analytical ultracentrifuge model E. All analyses were performed at 59 780 r.p.m. Because of the low molecular weight of the two chromoproteins studied, only the synthetic boundary cell was used. Inasmuch as the distances moved by the boundaries were rather small, ten photographs of the sedimenting boundary position were obtained in each experiment. The sedimentation coefficients were evaluated from enlarged images of the photographs projected onto millimeter graph paper. By inserting a scale into the rotor in place of the cell, a reference plate, which can be used to combine the magnification of the camera and enlarger into one, is obtained. The sedimentation constants were reduced to pure water at 20°C by applying the usual corrections for the density and viscosity of the medium [3]. The results are given in Svedberg units (1 S = 10^{-13} cm sec^{-1} $dyne^{-1}$).

Diffusion. The diffusion experiments were conducted in a Spinco diffusion and electrophoresis instrument at a temperature of 0.6°C. Boundary sharpening was obtained by withdrawing a small amount of solution from the vicinity of the boundary with a long hypodermic needle, and then allowing the diffusion to occur. By repeating this procedure, a sharp boundary was obtained. The optics were adjusted for studying the Rayleigh-Calvet-Philpot interferogram at 644 mμ. The number of fringes, and the position of the maxima and minima were measured visually by means of the optical system of a Hilger densitometer. The cell magnification was 1.0105. The diffusion constants were evaluated according to the "height-area" method described by Svensson [4].

$$D_A = \frac{(n_1 - n_2)^2}{4\,\pi\,t\,n'^2_{max\,(x)}}$$

where n_1 and n_2 are the refractive indices of the two solutions, t is the time, and $n'_{max(x)}$ is the maximum value for the derivative of the refractive index function with respect to position in the cell. Some exposures were evaluated according to the "moment" method using the equation by Svensson [5] as slightly modified by Ehrenberg and Agner [6]

$$D_m = \frac{\int_{n_o}^{n_c} x^2\,dn}{2(t-t_o)\,(n_c-n_o)} = \frac{a}{t-t_o}$$

where n denotes the refractive index increment measured at a particular fringe number, x is the fringe coordinate measured from the center of the boundary, and t is the length of time of diffusion. The diffusion constants were reduced to pure water at 20°C by applying corrections for the density and viscosity of the medium. The results are given in Fick's units (F = 10^{-7} cm^2 sec^{-1}).

Partial specific volume. The partial specific volume was determined for solutions of Lhb that were extensively dialyzed against distilled water. The densities of the solutions and of the solvent were measured at 24.45°C using a pycnometer of the Sprengel-Ostwald type having a capacity of about 10 ml.

RESULTS

Sedimentation coefficients. The two main components of Lhb, as far as could be judged from the photographs obtained in the ultracentifuge experiments, appeared to be homogeneous throughout the concentration ratios studied (Fig. 1). All the sedimentation patterns consisted of single, symmetrical peaks showing no indications of more than one component. The sedimentation constants for the two components were concentration dependent, increasing in value with dilution. Values of the sedimentation constants at different

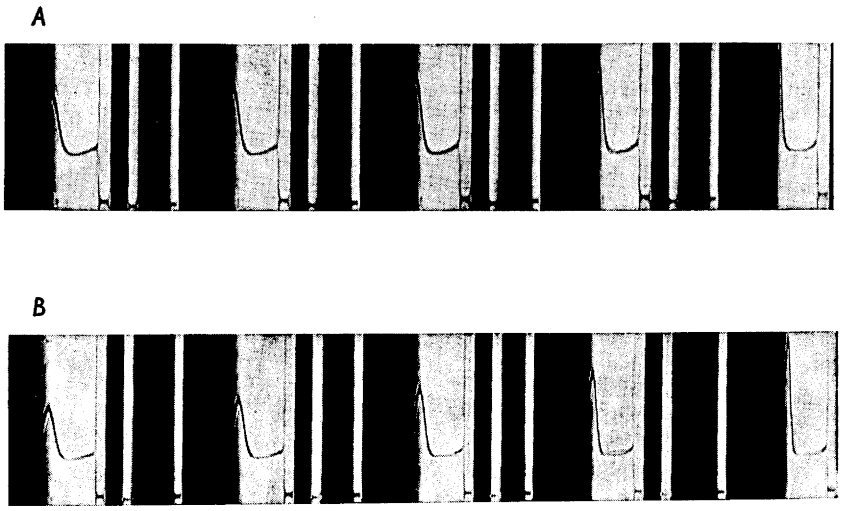

Fig. 1. Representative photographs obtained during the sedimentation analyses of the two main components of leghemoglobin. The pictures at the right represent the beginning of the runs.

A) The electrophoretically faster component at a protein concentration of 8.23 mg/ml (in sodium phosphate-NaCl buffer as described in the text) measured at an average temperature of 19.83°C and at a rotor speed of 59 780 rpm. Photographs were taken at intervals of 8 min. The five first photographs are reproduced.

B) The electrophoretically slower component at a concentration of 6.40 mg/ml measured at an average temperature of 18.78°C. The other conditions are the same as in A.

protein concentrations are shown in Fig. 2. The lines drawn through these data were calculated by the method of least squares, and fit the equation

$$S^{\circ}_{20} = S_{\infty} - \beta a$$

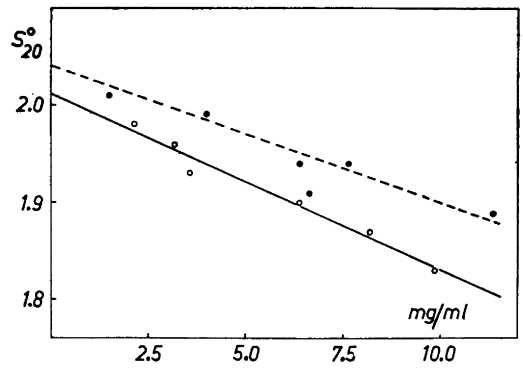

Fig. 2. Concentration dependence of the sedimentation constants of the electrophoretically faster (O) and slower (●) components of leghemoglobin in sodium phosphate-NaCl buffer (pH 7.0, ionic strength 0.283).

where S_∞ is the sedimentation coefficient extrapolated to infinite dilution, and a is the concentration of protein in mg/ml. S_∞ was found to be 2.012 S for the faster component and 2.041 S for the slower one. The equations for the sedimentation coefficients of the two components were:

$$S^\circ_{20} = 2.012 - 0.0180\ a \quad \text{(fast component)}$$
$$S^\circ_{20} = 2.041 - 0.0138\ a \quad \text{(slow component)}$$

The close similarity in the sedimentation data for the two components indicates that these proteins cannot be distinguished from each other by their behavior in the ultracentrifuge.

Diffusion coefficient. Several experiments were performed on each of the two components prepared from different batches. The experiments usually were performed in the standard cell. The protein concentrations for the two

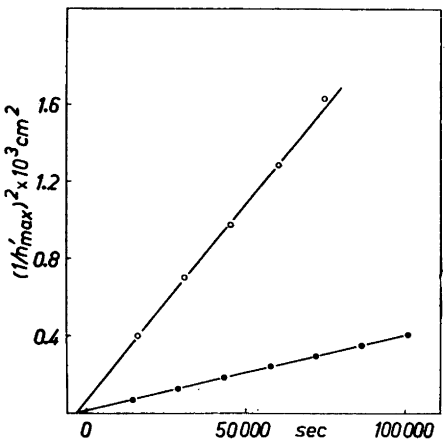

Fig. 3. A plot of inverted squares of the maximum fringe densities *versus* the length of time of diffusion. This plot was used for the calculation of the diffusion constants for the electrophoretically faster component according to the "height-area" method. Protein concentrations were 1.35 mg/ml (O) and 3.20 mg/ml (●) in sodium phosphate-NalC buffer (pH 7.0, ionic strength 0.283).

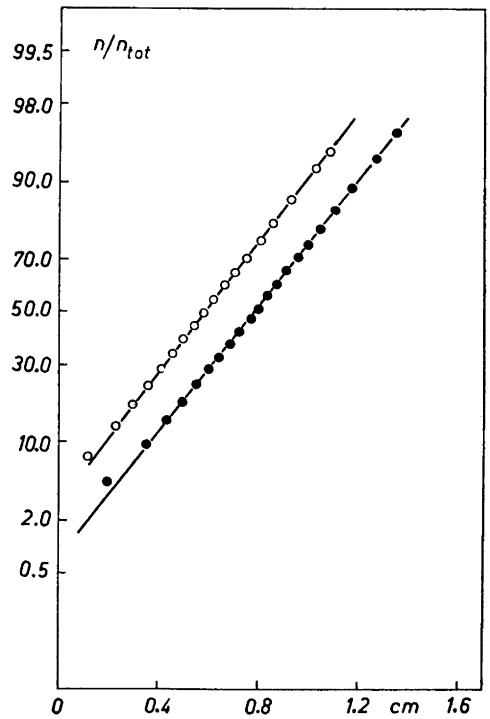

Fig. 4. Plots of relative fringe numbers *versus* fringe coordinates on a normal distribution graph in order to test the fit of the experimental diffusion curve of the electrophoretically faster component. The exposures are for protein concentratoins of 1.35 mg/ml (after 73 980 sec. of diffusion) (O), and for 3.20 mg/ml (after 86 400 sec.) (●).

Table 1. Diffusion data for the two main components of leghemoglobin obtained by the "height-area" method.

Component	Conc. mg/ml	t_o sec.	$D_{0.6}$ F	D^o_{20} F
Fast	1.35	−3 769	5.787	11.29
»	3.20	−3 874	5.620	10.96
		Average value		11.13
Slow	2.40	−3 111	6.174	12.04
»	7.40	−1 491	6.143	11.98
		Average value		12.01

experiments with the faster component were 1.35 mg/ml and 3.20 mg/ml, and the total fringe numbers were 19.10 and 42.62 respectively. Fringe intervals, Δn, of 4 and 9, respectively, were chosen for the calculation of the maximum fringe density, n'_{max}[4]. When applying the "height-area" method, the rate of increase of $(1/n'_{max})^2$ with time was determined. Five and seven exposures were evaluated in the first and second experiments, respectively. The corresponding plots of the data for the two experiments are shown in Fig. 3. The equations of the lines drawn through the points obtained in the two experiments have been calculated by the least squares method. The numerical data are given in Table 1. Four exposures from the higher concentration were evaluated according to the "moment method", and the results are given in Table 2. The zero-time correction, as determined by the "height-area" method, has been used.

The diffusion curve of a homogeneous, ideal-diffusing substance has the form of the normal probability curve, and for such a substance D_A and D_m should have the same value. Curves of mixtures have sharper peaks than the normal curve, and hence $D_m > D_A$. The close agreement between the values obtained

Table 2. Diffusion data for the two main components of leghemoglobin obtained by the "moment" method.

Component	Conc. mg/ml	t sec.	$t-t_o$ sec.	$D_{0.6}$ F	D^o_{20} F
Fast	3.20	43 200	47 074	5.784	11.28
		57 600	61 474	5.769	11.25
		86 400	90 274	5.746	11.20
		100 800	104 674	5.720	11.15
			Average value		11.22
Slow	7.40	66 600	68 091	6.575	12.82
		81 000	82 491	6.488	12.65
		95 400	96 891	6.464	12.61
			Average value		12.69

by the two different methods for the faster component is an indication of the essentially homogeneous character of the protein.

A more sensitive test of the diffusion behaviour, however, is to compare the experimental curve with a normal probability curve drawn on graph paper [6]. In Fig. 4, the relative fringe numbers, n/n_{tot}, have been plotted against the fringe coordinates determined from two exposures, one for each concentration. The line drawn for the lower concentration (19.10 fringes) corresponds to $D^{\circ}_{20} = 11.29$ F, whereas the line for the higher concentration (42.62 fringes) corresponds to $D^{\circ}_{20} = 10.98$ F. The zero-time correction obtained by the "height-area" method was applied in these calculations.

A value of 11.18 F is obtained as an average value for the two methods of calculation in the concentration range studied. This value has been used for the calculations of the molecular weight and the asymmetry of the faster component.

In a preliminary study, a diffusion constant equal to 8.5 F was reported for the slower component [2]. In more recent studies, this value has not been confirmed. If precaution were taken to avoid all possibility of denaturation during

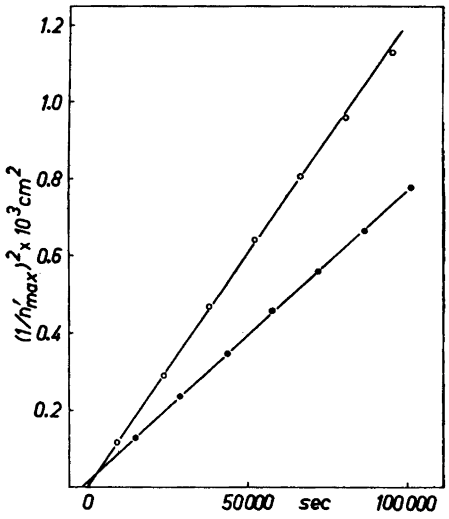

Fig. 5. A plot of inverted squares of the maximum fringe densities *versus* the length of time of diffusion. This plot was used for the calculation of the diffusion constants for the electrophoretically slower component according to the "height-area" method. Protein concentrations were 2.40 mg/ml (O) and 7.40 mg/ml (●) in sodium phosphate-NaCl buffer (pH 7.0, ionic strength 0.283).

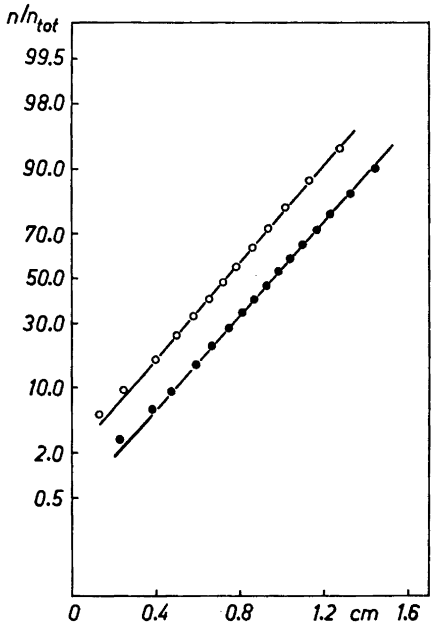

Fig. 6. Plots of relative fringe numbers *versus* fringe coordinates on a normal distribution graph in order to test the fit of the experimental diffusion curve of the electrophoretically slower component. The exposures are for protein concentrations of 2.40 mg/ml (after 95 400 sec. of diffusion) (O) and for 7.40 mg/ml (after 100 800 sec.) (●).

preparation, the value obtained was higher. Several experiments were run, two of which are reported here. One experiment in which the protein concentration was 2.40 mg/ml was conducted in the standard cell, whereas another experiment in which the protein concentration was 7.40 mg/ml was conducted in the micro cell. (The optical path in the micro cell is 1/4 of that in the standard cell). The total fringe numbers were 32.20 for the lower concentration and 25.60 for the higher one. A fringe interval, Δn, of 5 and 7 was used in the calculation of the maximum fringe density, n'_{max}, with 7 exposures evaluated at both concentrations. The corresponding plots of the data for the two experiments as calculated by the "height-area" method are given in Fig. 5, whereas the numerical data are recorded in Table 1.

Three exposures from the higher concentration were evaluated according to the "moment method", and the results are recorded in Table 2. The zero-time correction from the "height-area" method was used.

The closeness of fit to the requirements of ideal diffusion was checked by plotting the data from the two experiments on a normal distribution graph (Fig. 6). The line drawn for the lower concentration (32.60 fringes) corresponds to $D^{\circ}_{20} = 12.21$ F, whereas for the higher concentration, the line corresponds to 12.35 F.

An average value of 12.35 F was obtained by the two methods of calculation. This value has been used for the calculation of the molecular weight and asymmetry of the slower component.

Partial specific volume. The partial specific volume was determined in three experiments. The unresolved material was used because as high a protein concentration as possible was desired. A solution of 5 mg/ml gave the following values: 0.740, 0.740 and 0.739 ml/g. A value of 0.740 ml/g was used for the calculations that follow.

Molecular weight. The values of the molecular weights of the two components were calculated by means of Svedberg's formula [3]

$$M = \frac{RTs}{D(1-V\varrho)}.$$

From the determined values of s, D and V, the electrophoretically faster component was found to have a molecular weight of 16 800, and the electrophoretically slower one a molecular weight of 15 400.

Molecular shape. The molecular frictional ratio f/f was calculated according to the following formula [3]:

$$f/f_o = \left[\frac{1-V}{D^2_{20}s_{20}V}\right]^{1/6} 10^{-8}$$

The molar frictional ratio was found to be 1.118 for the faster component and 1.043 for the slower one. Following the procedure of Oncley [3], f/f_o can be represented as a product of two factors, f/f_e and f_e/f_o. The first factor, f/f_e, represents the effect of hydration, while the second factor, f_e/f_o, represents the influence of the asymmetry of the molecule. Kramer [3] has shown that the hydration factor is related to the grams of water per gram of protein, w, by the formula

$$f/f_e = \left[1 + \frac{w}{V\varrho}\right]^{1/3}$$

in which ϱ is the density of the water solvating one gram of pure solute of the partial specific bolume V. The maximum possible degree of hydration for the electrophoretically faster component would make f/f_e equal to 1.118 and would lead to a value of 0.29 for w. On the other hand, if the entire molar frictional ratio is due to asymmetry, f_e/f_o would be equal to 1.118. In the equations of Perrin [3], this value would represent axial ratios of 3.1 and 3.2 for prolate and oblate ellipsoids, respectively. Assuming an elongated ellipsoid and zero hydration, the faster component would have a minor axis of 23 Å and major axis of 72 Å.

If the molecular frictional ratio, $f/f_o = 1.043$, of the slower component is due entirely to hydration, the value for w would be 0.032. If the frictional ratio is due only to asymmetry, the axial ratios would be equal to 2.0 for both prolate and oblate ellipoids. An unhydrated ellipsoid of the slower component would have a minor axis of 26 Å and a major axis of 52 Å.

DISCUSSION

Both of the main components of leghemoglobin appear to be single, homogeneous proteins in the ultracentrifuge. Earlier ultracentrifugal studies [1] distinguished two components of unequal concentration. The predominant component was slowly sedimenting (1.9 S), whereas the lesser component was a rapidly sedimenting fragment (5 to 6 S). The rapidly sedimenting fraction seemed to form a part of the electrophoretically slower component. The presence of such a small, heavy component could not be confirmed in the present studies of the individual components.

The molecular weight of 20 000 found earlier for the unresolved material [1] deviates considerably from the new molecular weights of 16 800 and 15 400 presently determined for the electrophoretically faster and slower components, respectively. This discrepancy is essentially due to differences in the diffusion constants of the different preparations investigated. The latter difference probably occurs because of the introduction of chromatography in the purification of the individual components [2]. The chromatographic procedure fractionates the unresolved material into at least four different components and removes some denaturated material which was not removed by ammonium sulphate fractionation [2]. The heavy component observed earlier in the unresolved material might consist of this denaturated material. Hence, the former assumption [1] that the electrophoretically slower component is an artefact of a heavy, iron-free protein surrounded by leghemoglobin molecules has no experimental basis.

The two main components are highly symmetrical in shape. The values for the frictional ratios calculated for both of the components are among the lowest that have been described. Our knowledge of the hydration of proteins is not in an advanced state, but undoubtedly water is immobilized on the surfaces of protein molecules. A value of 0.3 g of water per g of dry protein would

seem to be a reasonable figure and would lead to a value of 1.120 for the frictional ratio. This is evidently an upper limit of the possible contribution of hydration to the frictional ratio. If the frictional ratios of the two components were explained only on the basis of hydration a great difference in hydration would exist between the two components. This may be explained as being caused by differences in the amino-acid content of the components.

Leghemoglobin shows similarities to other hemin proteins in respect to molecular weights. The molecular weight of 16 800 for the faster component closely resembles the unit molecular weight of animal hemin proteins. Such a molecular weight has also been found for the hemoglobin of *Lampetra fluviatilis* [3]. The electrophoretically slower component, with its molecular weight of 15 400, falls in a class between the molecular weight of *Lampetra* hemoglobin and that of animal cytochrome c.

Acknowledgements. The author wishes to express his thanks to Professor Hugo Theorell and to Dr Anders Ehrenberg for valuable discussions and advice during the course of this work. Able technical assistance has been given by Miss Bodild von Sobeck in running the ultracentrifuge. The investigation has been supported by a grant from *Finlands State Commission of Natural Sciences* (*Statens Naturvetenskapliga Kommission*) which is gratefully acknowledged.

REFERENCES

1. Ellfolk, N. and Virtanen, A. I. *Acta Chem. Scand.* **6** (1952) 411.
2. Ellfolk, N. *Acta Chem. Scand.* **13** (1959) 596; **14** (1960). 609.
3. Svedberg, T. and Pedersen, K. O. *The Ultraceentrifuge.* Oxford University Press New York, N.Y. 1940.
4. Svensson, H. *Acta Chem. Scand.* **5** (1951) 72.
5. Svensson, H. *Acta Chem. Scand.* **5** (1951) 1410.
6. Ehrenberg, A. and Agner, K. *Acta Chem. Scand.* **12** (1958) 95.

Received June 2, 1960.

ACTA CHEMICA SCANDINAVICA 14 (1960) 1828–1832

Extraction of Mucopolysaccharides from Connective Tissue

ANUND HALLÉN

Chemistry Department II, Karolinska Institutet, Stockholm, Sweden

Human *nucleus pulposus* and umbilical cords were extracted with water, and the extracts and residues obtained on centrifugation were analyzed for mucopolysaccharides. It was found that, in the extract of *nucleus pulposus*, the yield of keratosulphate was smaller than that of chondroitin sulphate. In the umbilical cord extract, the yield of chondroitin sulphate was smaller than that of hyaluronate.

It is a general experience that the chondroitin sulphate of cartilage is so firmly bound that a good yield can be obtained only with the use of drastic methods for preparation, such as extraction with strong alkali [1–4], or disintegration of the tissue by proteolytic digestion [5–7], by autodigestion [8] or by vigorous mechanical treatment [9]. With neutral salt solutions, only small amounts of mucopolysaccharides are extracted [10,4]. Even such a strong solution as 10 % calcium chloride [11] is ineffective [10], whereas 1 % potassium carbonate in 30 % potassium chloride [8] is moderately effective in extracting the chondroitin sulphate of cartilage.

Differences are, however, present between various tissues with respect to the ease with which their mucopolysaccharides can be extracted. For instance, a large part of the hyaluronate can be extracted from umbilical cords with such a mild agent as distilled water [12].

It was considered of interest to investigate in some detail differences in the extractability of individual mucopolysaccharides. An account is given in the following of experiments with adult human *nucleus pulposus*, and with human umbilical cords, freed from vessels. It seems to be well established [13–17] that chondroitin sulphate and keratosulphate are the main polysaccharides in the *nucleus pulposus*. As indicated by the results of infrared spectrum [18] and alcohol fractionation studies [17], the chondroitin sulphate is the 6-isomer. The mucopolysaccharides of the umbilical cord are less well characterized, although hyaluronate is known to be the main polysaccharide [12,19,16]. According to results of Meyer *et al.*[12,19,20] and of Mathews [21], chondroitin-6-sulphate is also present.

EXPERIMENTAL

Prparation of the tissues. Healthy intervertebral discs were taken at autopsy from a 59-year-old man, one day after death. The *nucleus pulposus*, the central part of the disc, was dissected free from the surrounding *annulus fibrosus*.

Human umbilical cords were obtained not more than one day after delivery, and were freed from blood vessels. It was found that the most suitable procedure was to cut the cord into 2 cm pieces, thread a peg through the vein, fix the peg on a stand and dissect out the stroma with a razor-blade. The arteries were then removed by blunt dissection.

The tissues were homogenized by grating and grinding. The doughy material was stored for some weeks at −15°C, and thawed immediately before use.

Extraction of the mucopolysaccharides. About 4 g each of wet *nucleus pulposus* and umbilical cord tissues were extracted with 250 ml of distilled water overnight at 0°C, under gentle stirring. Centrifugation for 20 min at about 15,000 *g* yielded a clear extract and a residue from both tissues. After evaporation of the extract *in vacuo* to a small volume, the material was freeze-dried.

Analysis of the freeze-dried extracts and residues. Hexosamines and disaccharides were analyzed with the chromatographic method described earlier [16], glucosamine and galactosamine after hydrolysis for 8 h in 6 M hydrochloric acid, chondrosin and hyalobiuronic acid after hydrolysis for 2.5 h in 0.6 M hydrochloric acid. Sulphate sulphur was determined gravimetrically as barium sulphate, after hydrolysis for 4 h with 4 M hydrochloric acid. Nitrogen was determined by a micro-Kjeldahl procedure. Collagen was determined by means of hydroxyproline analysis [22,23]. The collagen content was obtained by multiplying the hydroxyproline value by the factor 7.5.

The ratio of galactose/glucuronic acid in the *nucleus pulposus* extract and residue was determined colorimetrically after partial purification of the mucopolysaccharides. Samples of the extract and residue were boiled with water for 30 min, and submitted to digestion with glycerol extracts of pig pancreas and intestinal mucosa [6,13] for 2 months. To ensure complete hydrolysis of the proteins, a second digestion with papain [7] was carried out overnight, after preliminary heat denaturation in a boiling water bath for 15 min. The mucopolysaccharides, together with some impurities, were precipitated by the addition of one volume of 10 % calcium chloride in glacial acetic acid and four volumes of 10 % calcium chloride in ethanol. The mucopolysaccharides were then extracted from the precipitate by stirring vigorously with distilled water. The galactose content of the clear and colourless solutions obtained on centrifugation was determined with the anthrone method of Scott and Melvin [24], and the glucuronic acid content with the carbazole method of Dische [25]. The interference, amounting to some 10 %, of glucuronic acid in the anthrone reaction, and of galactose in the carbazole reaction was neglected. This approximation is possible provided that the galactose/glucuronic acid ratio does not differ greatly from 1. The presence of interfering sugars other than galactose and glucuronic acid is not probable, but has not yet been experimentally excluded.

Table 1. Analyses of freeze-dried extracts and residues of *nucleus pulposus* and umbilical cord *.

Material analyzed	Moisture %	Ash %	Collagen %	Nitrogen %	Sulphur %	Hexosamine %	Hexosamine % of total	Hexosamine / Sulphur molar ratio
Nucleus pulposus								
Extract: 0.42 g	10.1	15.4	0.1	5.9	2.73	9.2	52	0.6
Residue: 1.32 g	9.2	3.2	40.2	14.3	0.52	2.7	48	0.9
Umbilical cord								
Extract: 0.36 g	5.9	22.1	0.1	8.5	0.20	2.0	66	1.8
Residue: 0.93 g	11.3	2.7	50.3	14.8	0.10	0.4	34	0.7

* Hexosamine content of freeze-dried tissues: *nucleus pulposus* 6.5 %; umbilical cord 1.3 %.

RESULTS AND DISCUSSION

Behaviour of nucleus pulposus. As shown in Table 1, the hexosamines, *i.e.* glucosamine + galactosamine, were obtained in about 50 % yield in the extract. The molar ratio of hexosamine/sulphate was close to 1 in the residue, but somewhat less in the extract, probably depending on the presence of sulphate ions. The collagen remained, as expected, quantitatively in the residue. The high nitrogen contents indicate the presence of protein other than collagen. Nitrogen values higher than expected from the collagen and hexosamine contents have proved to be a constant finding, even after careful exclusion of blood contamination and dialysis.

For a more detailed study of the hexosamines in the extract, another water extract was prepared from 13 g of a pooled *nucleus pulposus* sample. The molar ratio of hexosamine/sulphate was found to be 0.79, but after dialysis it rose to 1.04. The ratio of glucosamine/galactosamine was 0.65 before dialysis, and 0.62 after, thus practically the same. The hexosamine losses during dialysis were negligible. These results are well compatible with the presence of keratosulphate and chondroitin sulphate.

Table 2. Molar ratios of sugar components in freeze-dried tissue specimens, extracts and residues of *nucleus pulposus* and umbilical cord *.

Material analyzed	*Nucleus pulposus*			*Umbilical cord*	
	glucosamine / galactosamine	glucosamine / chondrosin	galactose / glucuronate	glucosamine / galactosamine	mucosin / chondrosin
Untreated tissue	0.97	1.05	—	3.5	1.8
Extract	0.82	0.44	0.79	9.5	12.6
Residue	1.68	1.91	1.23	1.5	0.8

* Mucosin synonymous with hyalobiuronic acid. The glucosamine/galactosamine ratio in annulus fibrosus surrounding the *nucleus pulposus* was 0.89.

As shown in Table 2, the ratio of glucosamine/galactosamine was lower in the extract than in the residue. This implies that the ratio of keratosulphate/chondroitin sulphate was lower in the extract than in the residue. Further evidence is afforded by the fact that the ratio of glucosamine/chondrosin was lower in the mild acid hydrolysate of the extract than of the residue, as was the ratio of galactose/glucuronic acid.

In order to study the influence of salt on the extraction, 5—6 g of pooled *nucleus pulposus* were extracted with 500 ml of 1 % sodium chloride. The residue was then extracted twice with 250 ml of 1 % sodium chloride. The ratio of glucosamine/galactosamine, which was 0.89 in the original sample, was 0.57 in the first extract and 0.91 in the second. The third extraction yielded practically no material, the ratio in the residue being 2.00. In another experiment, 10 % calcium chloride was used; the ratio of glucosamine/galactosamine was 0.75 in the first extract, 1.03 in the second, 1.03 in the small amount of material obtained in the third extract, and 1.26 in the residue. In this experiment, as in that with 1 % sodium chloride, all the material had been dialyzed before

freeze-drying. The results indicate that salts do not influence the differences in extractability.

In the experiments with 1 % sodium chloride and 10 % calcium chloride, only some 1—2 %, and 2—3 %, respectively, of the collagen was obtained in the extracts. This is in accordance with findings of Davidson and Woodhall [17]. The yield of hexosamines in the extracts was the same as when distilled water was used, or slightly greater, in conformity with the results of Hass and Garthwaite [10] in the case of cartilage.

Behaviour of umbilical cord. It is evident from Table 1 that the hexosamine/sulphate ratio was fairly high in the extract, as could be expected in view of the predominance of hyaluronate, whereas the very approximate value of this ratio in the residue was lower. As seen in Table 2, the ratio of glucosamine/galactosamine was much higher in the extract than in the residue. These results are in good agreement with those of Meyer and Palmer [12], and indicate a higher hyaluronate/chondroitin sulphate ratio in the extract than in the residue. This is also borne out by the higher ratio of hyalobiuronic acid/chondrosin in mild acid hydrolysates of the extract than of the residue.

Interpretation of the results. The results of this study indicate that differences are present between the mucopolysaccharides with respect to their extractability. Thus, in *nucleus pulposus* keratosulphate is more difficult to extract than chondroitin sulphate, whereas in umbilical cord chondroitin sulphate is more difficult to extract than hyaluronate. Since the experiments were performed with homogeneous tissues, the conditions of extraction of the individual mucopolysaccharides thus being comparable, these differences may reflect differences in the properties of the mucopolysaccharides themselves, of their complexes with non-collagenous protein [26,27], or their attachment to the collagen fibers. Unfortunately, a detailed interpretation is, as yet, difficult, in view of our incomplete knowledge of the mucopolysaccharides and of the proteins in the connective tissue.

It is possible that the extractability of the mucopolysaccharide fraction may influence the physical and morphological properties of the tissue. For instance, the *nucleus pulposus* of a young subject is a viscous fluid, whereas in the old it is somewhat dry and firm and — in the highest age groups — is easily torn. This might be explained, to some degree, by an increase in the ratio of keratosulphate/chondroitin sulphate with age [15,16], which — according to the results of the present investigation — would imply a shift to a less easily extractable mucopolysaccharide component. There are reasons to believe that the deposition of other materials that are difficult to extract, such as collagen and "lipofuscin", may also be of importance for the change in the nature of the tissue with age.

Acknowledgements. I am greatly indebted to Docent Lennart Rodén and Docent Sven Gardell for valuable discussions, as well as to Mrs. Ruth Flagell for skilful technical assistance.

The investigation has been aided by grants from *Karolinska Institutets reservationsanslag.*

REFERENCES

1. Krukenberg, C. F. W. *Z. Biol.* **20** (1884) 307.
2. Mörner, C. T. *Skand. Arch. Physiol.* **1** (1889) 210.
3. Levene, P. A. and LaForge, F. B. *J. Biol. Chem.* **15** (1913) 69.
4. Jorpes, E. *Biochem. Z.* **204** (1929) 354.

5. Schmiedeberg, O. *Arch. exptl. Pathol. Pharmakol. Naunyn-Schmiedeberg's* **28** (1891) **355.**
6. Gardell, S. *Arkiv. Kemi* **4** (1952) 449.
7. Scott, J. E. in Glick, D. *Methods of Biochemical Analysis* **8** (1960) 145.
8. Einbinder, J. and Schubert, M. *J. Biol. Chem.* **185** (1950) 725.
9. Malawista, I. and Schubert, M. *J. Biol. Chem.* **230** (1958) 535.
10. Hass, G. M. and Garthwaite, A. B. *A.M.A. Arch. Pathol.* **33** (1942) 145.
11. Meyer, K. and Smyth, E. M. *J. Biol. Chem.* **119** (1937) 507.
12. Meyer, K. and Palmer, J. W. *J. Biol. Chem.* **114** (1936) 689.
13. Gardell, S. and Rastgeldi, S. *Acta Chem. Scand.* **8** (1954) 362.
14. Gardell, S. *Acta Chem. Scand.* **11** (1957) 668.
15. Hallén, A. *Acta Chem. Scand.* **12** (1958) 1869.
16. Hallén, A. *Acta Chem. Scand.* **13** (1959) 1919.
17. Davidson, E. A. and Woodhall, B. *J. Biol. Chem.* **234** (1959) 2951.
18. Orr, S. F. D. *Biochim. et Biophys. Acta* **14** (1954) 173.
19. Meyer, K., Davidson, E., Linker, A. and Hoffman, P. *Biochim. et Biophys. Acta* **21** (1956) 506.
20. Hoffman, P., Linker, A. and Meyer, K. *Federation Proc.* **17** (1958) 1078.
21. Mathews, M. B. *Nature* **181** (1958) 421.
22. Neuman, R. E. and Logan, M. A. *J. Biol. Chem.* **184** (1950) 299.
23. Martin, C. J. and Axelrod, A. E. *Proc. Soc. Exptl. Biol. Med.* **83** (1953) 461.
24. Scott, T. A. and Melvin, E. H. *Anal. Chem.* **25** (1953) 1656.
25. Dische, Z. *J. Biol. Chem.* **167** (1947) 189.
26. Schubert, M. *Federation Proc.* **17** (1958) 1099.
27. Muir, H. *Biochem. J.* **69** (1958) 195.

Received July 26, 1960.

ACTA CHEMICA SCANDINAVICA 14 (1960) 1833–1851

Proceedings of the Third Scandinavian Summer Meeting of Biochemistry, Medical Chemistry, Pharmacology and Physiology Oslo, Norway, August 22—24, 1960

Papers Read in the Section of Biochemistry

Effect of Arsenate on Oxidative Phosphorylation and Related Reactions

G. F. Azzone* and L. Ernster

Wenner-Grens Institute, University of Stockholm, Stockholm, Sweden

Crane and Lipmann [1] have shown in 1953 that arsenate causes uncoupling of respiration from phosphorylation in washed particles from rat liver, accompanied by a depression of the respiration in the presence of various substrates. The uncoupling occurred in a gradual manner, increasing in extent with the duration of the incubation. We have now been able to confirm these findings using intact rat liver mitochondria and a variety of substrates including glutamate, succinate and β-hydroxybutyrate. We have found, furthermore, that arsenate also induces an adenosine triphosphatase activity in the mitochondria, as well as a release of endogenous inorganic and high-energy phosphates, and that these effects take place prior to the uncoupling of the electron transport coupled phosphorylation. These findings are illustrated in Tables 1 and 2.

Table 1 shows that the arsenate-induced ATP-ase (which has recently also been observed by Azzone *et al.*[2] and by Wadkins [3]) reached a maximal activity at 3 mM arsenate, and that this activity was about 8 times higher than that found in the absence of arsenate; this maximum was about 2-3-fold lower than the ATPase activity induced by 10^{-4} M 2,4-dinitrophenol. Addition of succinate (or other substrates) resulted in an apparent depression of the ATPase activity, due to the phosphate uptake accompanying the oxidation of these substrates which, as could be ascertained in parallel tests, was not seriously impaired by low concentrations of arsenate in these short-term experiments. As expected, this effect of added substrates could be abolished by inhibiting the respiration with antimycin A (and, in the case of DPN-linked substrates, also with amytal).

The depleting effect of arsenate on mitochondrial endogenous phosphates is illustrated in Table 2. For these studies, so-called "^{32}P-labelled mitochondria" were prepared according to Beyer *et al.*[4], *i. e.*, preparations of mitochondria obtained from liver to which a suitable quantity of ^{32}P-orthophosphate was added during the homogenization procedure. These mitochondria, as demonstrated by Beyer *et al.*[4], contain most of the bound ^{32}P in the form of orthophosphate and high-energy phosphates, the ratio of the former to the latter varying between 7:3 and 5:5. When such mitochondria were suspended in a sucrose-KCl medium and incubated at 30°C in the presence of 1—3 mM arsenate, a rapid release of the bound ^{32}P took place, reaching nearly completeness within 5 min. 2 mM amytal, which caused a slight release by itself, greatly protected the mitochondria against the arsenate-induced release; antimycin A and cyanide, in contrast, gave only a weak protection. Of interest is also that 2,4-dinitrophenol, which has earlier been shown by Teply [5] to release the so-called "gel-phosphate" from "cyclophorase" preparations, had only a partial releasing effect under the present

* Fellow of the Consiglio Nazionale delle Ricerche. Permanent address: Istituto di Patologia Generale, Università di Padova, Italy.

Table 1. Stimulation of ATP hydrolysis by arsenate.

Concentration of arsenate mM	Additions none	succinate	succinate + antimycin A
		μmoles P_i liberated	
none	0.22	0	1.12
0.1	0.95	0	1.46
1	1.58	0	1.76
3	1.97	0.10	1.80
10	1.88	0.77	2.07

Each tube contained: 100 μmoles KCl, 50 μmoles TRIS buffer pH 7.5, 10 μmoles ATP, 125 μmoles sucrose, mitochondria from 100 mg rat liver (wet weight) and, when indicated, 10 μmoles succinate and 1 μg antimycin A; final volume 2.0 ml. Temp. 30°C. Time of incubation 20 min.

conditions. However this effect could be markedly enhanced by adenosine-5′-phosphate, presumably due to a conversion of intramitochondrial ATP into extramitochondrial (*cf.*Ref.[6]). Finally, succinate greatly inhibited the releasing effect of arsenate, at the same time as it promoted the effect of dinitrophenol. These effects, the possible mechanisms of which will be discussed in some detail, have recently been of great importance as a basis for demonstrating a requirement of high-energy phosphate for the aerobic oxidation of succinate by intact rat liver mitochondria [7].

The above findings will be discussed in relation to the hypothesis that the arsenate-induced ATPase and release of mitochondrial endogenous phosphate are primary manifestations of the general, gradual uncoupling effect of arsenate, observed by Crane and Lipmann [1]. It is visualized that these primary effects reflect an active uptake of arsenate by the mitochondria, this process possibly involving an electron transport via the amytal-sensitive step of the respiratory chain, accompanied by an oxidative arsenylation.

This work has been supported by grants from the *Swedish Medical Research Council.*

1. Crane, R. K. and Lipmann, F. *J. Biol. Chem.* **201** (1953) 235.
2. Azzone, G. F., Carafoli, E. and Muscatello, U. *Exptl. Cell Research. In press.*
3. Wadkins, G. L. *Federation Proc.* **19** (1960) 39.
4. Beyer, R. E., Glomset, J. and Beyer, T. *Biochim. et Biophys. Acta* **18** (1955) 292.
5. Teply, L. J. *Arch. Biochem. Biophys.* **24** (1949) 383.
6. Siekevitz, P. and Potter, V. R. *J. Biol. Chem.* **215** (1955) 237.
7. Azzone, G. F. and Ernster, L. *Nature* **187** (1960) 65.

Table 2. Depletion of intramitochondrial phosphate.

Addition	no arsenate	10^{-3} M arsenate
none	867	185
2 mM amytal	620	541
2 mM KCN	574	298
1 μg antimycin A	561	286

The incubation medium contained: 150 μmoles KCl, 50 μmoles TRIS buffer pH 7.5, 325 μmoles sucrose and ^{32}P labelled mitochondria from 200 mg rat liver (wet weight); final volume 3 ml. Temp. 30°C. Time of incubation 5 min. Values are given in number of counts/sec.

The Presence of a Phosphodeoxyribomutase Activator in Deoxyribose 1-Phosphate Preparations

E. Christiansen, J. Jonsen, S. Laland and J. McKinley McKee

Department of Biochemistry, University of Oslo, Blindern, Norway

The presence of an enzyme in calf thymus converting deoxyribose 1-phosphate to the 5-phosphate was originally described by Manson and Lampen [1]. In studying this reaction, we have prepared the substrate deoxyribose 1-phosphate enzymatically from thymidine and phosphate using horse liver phosphorylase [2]. The sugar phosphate was isolated as the crystalline di*cyclo*hexylamine salt. When chromatographed in *n*-propanol-conc. NH_3 (6:4) and developed with the diphenylamine spray it was homogeneous and had R_F value different from that of deoxyribose 5-phosphate. Paper electrophoresis in phosphate buffer pH 7.5 gave one band only. Its phosphorus/deoxyribose ratio was 1.01.

The phosphodeoxyribomutase used was extracted from calf thymus with 1 % KCl and purified by ammonium sulphate fractionation, phosphate gel adsorption and gradient elution with Tris-hydrochloric acid, pH 7.4, on a DEAE cellulose column. A fifty-fold purification was usually achieved.

The presence of an activator in the substrate was demonstrated in the following way. 3 μmoles of the di*cyclo*hexylamine salt of deoxyribose 1-phosphate were run electrophoretically in phosphate buffer pH 7.5. Ribose 1-phosphate and ribose 1,5-diphosphate were used as reference substances. Deoxyribose 1-phosphate was located by the diphenylamine test whereas the ribose phosphates were detected by the aniline phthalate spray. In one experiment deoxyribose 1-phosphate and ribose 1-phosphate had a mobility of 9.5 cm compared with 12.5 cm for ribose 1,5-diphosphate. Activation was demonstrated with material eluted from an area of the deoxyribose 1-phosphate run corresponding to the mobility of ribose 1,5-diphosphate. The activating material (A) and the deoxyribose 1-phosphate band (purified deoxyribose 1-phosphate) were freeze-dried after elution from the paper.

The enzymatic test system was set up in 0.004 M Tris-hydrochloric acid buffer, pH 7.4, and contained 0.34 μmoles deoxyribose 1-phosphate, 9.6 μg purified enzyme (60 × purification) in a total volume of 0.85 ml. The mixture was incubated for 30 min at 23°C. The amount of deoxyribose 5-phosphate formed was estimated by a novel procedure [3] utilizing the difference in the diphenylamine colour before and after reduction with sodium borohydride.

It is apparent from the table that purification of the substrate by electrophoresis substantially reduces the enzymic activity. The activity is not restored by the addition of 8-hydroxyquinoline whereas the addition of ribose 1,5-diphosphate in the presence of 8-hydroxyquinoline restores the activity. Addition of part of the material present in area A also restores the activity. Furthermore it was shown that the eluate of a similar blank area of the paper did not restore the activity. Since the mobility of the activating substance is equal to that of ribose 1,5-diphosphate, the presence of a sugar diphosphate in the deoxyribose 1-phosphate employed is suggested. Analysis of the material in area A showed that only traces (<0.4 %) of a deoxyribose 1,5-diphosphate could be present.

Deoxyribose 1-phosphate	8-hydroxy quinoline μmoles	Ribose 1.5-diphosphate μmoles	A[a] μl	% Activity [b]
Not purified	0	0	0	100
Purified	0	0	0	25
»	0.1	0	0	27
»	0.1	0.05	0	114
»	0	0.05	0	88
»	0.1	0.01	0	106
»	0.1	0.001	0	116
»	0.1	0.0001	0	64
»	0.1	0	100	109
»	0.1	0	10	41

[a] The material obtained from 3 μmoles of deoxyribose 1-phosphate was dissolved in 1 ml water.
[b] Activity of enzyme in the presence of not purified deoxyribose 1-phosphate: 100 %.

In connection with the present finding it is interesting to note that biosynthetically prepared ribose 1-phosphate contains an activator, for the phosphoribose mutase reaction. This activator is removed by ion exchange chromatography of the substrate [4].

1. Manson, L. A. and Lampen, J. O. *J. Biol. Chem.* **191** (1951) 95.
2. Friedkin, M. and Roberts, D. *J. Biol. Chem.* **207** (1954) 257.
3. *To be published.*
4. Klenow, H. *Arch. Biochem. Biophys.* **46** (1953) 186.

Enzymic Properties of Human Skeletal Muscle Mitochondria

O. Eeg-Olofsson*, G. F. Azzone**, R. Luft and L. Ernster

Wenner-Gren Institute, University of Stockholm, and Department of Endocrinology, Karolinska Sjukhuset, Stockholm, Sweden

Certain enzymic properties of isolated human skeletal muscle mitochondria have been investigated on the basis of knowledge from, and in comparison with, known properties of mitochondria from animal tissues, in the first place skeletal muscle, heart muscle, and liver. Human skeletal muscle mitochondria catalyze a rapid aerobic oxidation of pyruvate (in the presence of malate) and of α-ketoglutarate, whereas other Krebs-cycle metabolites are oxidized at relatively low rates. However, the oxidation of succinate can be greatly enhanced if the accumulation of oxaloacetate is prevented by the addition of either amytal or cysteine sulfinic acid. Glutamate is oxidized usually at high rate, whereas other amino acids as well as fatty acids give rise only to low rates of respiration. Glycerol-1-phosphate was oxidized at low rate under the experimental conditions used.

The respiration with all substrates was accompanied by a phosphate uptake, and the P/O ratios approached the values generally accepted for intact mitochondria, *i. e.* 3 in the case of DPN-linked substrates, and 2 in the case of succinate. The mitochondria exhibited a high extent of respiratory control, as revealed by a severe lowering of the respiratory rate when the terminal phosphate acceptor system, *i. e.* ATP, hexokinase and glucose, was omitted from the incubating medium. Catalytic amounts of ATP enhanced this "resting" respiration, and this enhancement was a function of the concentration of Mg^{++} present in the medium. This function parallelled the resting ATPase activity of the mitochondria, both reaching maximum at a Mg^{++} concentration of 0.5—1 mM. A relatively high Mg^{++}-activated ATPase activity seems to be a common attribute of intact muscle mitochondria from different sources, which, as will be pointed out, must be taken into account when desiring to obtain an adequate estimate of the respiratory control capacity of these mitochondria; addition of catalytic amounts of ATP to the resting respiratory system may obscure the true extent of respiratory control. It is postulated that this ATPase differs in mechanism from that found in structurally damaged rat liver mitochondria in that it does not involve the primary high-energy intermediate(s) of electron transport coupled phosphorylation.

2,4-Dinitrophenol uncouples respiration from phosphorylation in human skeletal muscle mitochondria and gives rise to an increased ATPase activity, both effects reaching maximal extent at a dinitrophenol concentration of 10^{-4} M. On the other hand a concentration of dinitrophenol as low as 10^{-5} M, which affects phosphorylation and ATPase activity only slightly, completely abolishes respiratory control, *i. e.* gives rise to maximal respiration even in the absence of terminal phosphate acceptor. Possible interpretations of this phenomenon will be discussed. 10^{-4} M dinitriphenol also inhibits to some extent the respiration of human skeletal muscle mitochondria when this is supported by glutamate, but not when it is supported by α-ketoglutarate. Bovine serum albumin partially protects against all effects of dinitrophenol, as well as of other uncouplers such as dicoumarol and gramicidine.

The data will be discussed in relation to some earlier findings [1] made with skeletal muscle mitochondria from patients with elevated basal metabolic rates.

This work has been supported by grants from the *Swedish Medical Research Council*, and from *Vera and Carl J. Michaelsens donationsfond*, Hälsingborg.

1. Ernster, L., Ikkos, D. and Luft, R. *Nature* **184** (1959) 1851.

* Present address: Pediatric Clinic, University of Göteborg, Sweden.

** Fellow of the Consiglio Nazionale delle Ricerche. Permanent address: Istituto di Patologia Generale, University of Padova, Italy.

Selective Extraction of DT Diaphorase from Mitochondria and Microsomes

L. Danielson, L. Ernster and M. Ljunggren

Wenner-Gren Institute, University of Stockholm, Stockholm, Sweden

We recently reported the purification from the soluble fraction of rat liver cytoplasm of a diaphorase oxidizing DPNH and TPNH at equal rates, and reacting with a number of dyestuffs and quinones as electron acceptors [1]. The enzyme, called DT diaphorase, was characterized by a requirement for an activator, in the form of a dispersing agent such as serum-albumin or Tween-20, to exhibit maximal activity, as well as by a high sensitivity to dicoumarol. Although the bulk of the enzyme was found in the soluble fraction of the cytoplasm, portions of the enzyme were consistently recovered in the mitochondrial and microsomal pellets, and could not be removed from these by repeated washing with 0.25 M sucrose. However, when these pellets were suspended in 0.003 M phosphate-buffer, pH 7.5, and the suspensions treated in the cold with a Super-Thurrax blendor for 2 min, the clear supernatant obtained upon recentrifugation of the suspensions at high speed contained DT diaphorase. Moreover, the solutions so obtained were practically free from other diaphorase elements present in the mitochondria and microsomes. Illustrative data are summarized in Tables 1 and 2.

Table 1 shows an experiment with mitochondria. The blendorizing procedure employed here was adapted from that previously used by Kielley and Kielley [2] for the preparation of mitochondrial adenosine triphosphatase. It consisted of a treatment of the mitochondrial suspension with the Super-Thurrax blendor as described above, followed by a centrifugation of the treated suspension at 20 000 *g* for 10 min. The sediment was resuspended in 0.003 M phosphate buffer and the suspension was blendorized once again and recentrifuged as above. The two supernatants were combined and centrifuged at 105 000 *g* for 30 min. Three fractions were thus obtained: a "low-speed pellet", a "high-speed pellet", and a final supernatant. As shown in Table 1, only the final supernatant exhibited an appreciable TPNH diaphorase activity, and this was accompanied by an equally high DPNH diaphorase activity. Moreover, these activities were enhanced by 0.3 % Tween-20 and strongly inhibited by 10^{-6} M dicoumarol. By contrast, the DPNH diaphorase activities found in the low- and high-speed pellets were not stimulated (and even slightly inhibited) by 0.3 % Tween-20, and were completely insensitive to 10^{-6} M dicoumarol. When the supernatant solution was subjected to chromatography on DEAE-cellulose column, the TPNH and

Table 1. Diaphorase activities of mitochondrial subfractions. For fractionation procedure, see text. The test system contained: 0.04 mM 2,6-dichlorophenolindophenol (DCPIP), 0.1 mM DPNH or TPNH, 0.33 mM KCN and 0.05 M potassium phosphate, pH 7.5.

Fraction	Substrate	Diaphorase activity (μmoles DCPIP reduced / min / g liver) no add.	0.3 % Tween-20	10^{-6} M dicoumarol
Mitochondria	DPNH	3.93	3.93	3.57
	TPNH	0.71	1.61	0.36
Final Supernatant	DPNH	0.57	1.18	0.20
	TPNH	0.70	1.25	0.11
High-speed Pellet	DPNH	0.86	0.73	0.86
	TPNH	0.03	—	—
Low-speed Pellet	DPNH	1.34	1.01	1.34
	TPNH	0.04	—	—
Recovery	DPNH	2.77		
	TPNH	0.77		

Table 2. Diaphorase activities of microsomal subfractions. For fractionation procedure, see text. Test system as in Table 1.

Fraction	Substrate	Diaphorase activity μmoles DCPIP reduced / min / g liver: no add.	0.3 % Tween-20	10^{-6} M dicoumarol
Micro-somes	DPNH	3.31	1.95	3.40
	TPNH	0.37	0.70	0.25
1st Supernatant	DPNH	0.17	0.32	0.06
	TPNH	0.15	0.40	0.02
2nd Supernatant	DPNH	0.07		
	TPNH	0.03		
3rd Supernatant	DPNH	0.06		
	TPNH	0.01		
Final Pellet	DPNH	1.03	0.66	1.02
	TPNH	0.15	0.27	0.16
Recovery	DPNH	1.33		
	TPNH	0.34		

DPNH diaphorase activities were recovered in the same fraction.

An experiment with microsomes is shown in Table 2. Here, the treatment with the Super-Thurrax blendor was followed directly by centrifugation at 105 000 *g* for 60 min, after which the pellet was resuspended in 0.003 M phosphate-buffer, retreated with the blendor, and recentrifuged. The procedure was repeated three times altogether, thus resulting in three supernatant fractions and one final pellet. As seen in Table 2, the first supernatant exhibited equally high DPNH and TPNH diaphorase activities, and these were stimulated by 0.3 % Tween-20 and strongly inhibited by 10^{-6} M dicoumarol. The second and third supernatants exhibited only low TPNH diaphorase activities, and definitely higher, though still low, DPNH diaphorase activities. The final pellet revealed a high DPNH diaphorase activity, which was partially inhibited by 0.3 % Tween-20, and completely insensitive to 10^{-6} M dicoumarol. This fraction contained furthermore a definite portion, about half, of the TPNH diaphorase activity of the original microsomes. This TPNH diaphorase was, like the one found in the first supernatant, markedly enhanced by 0.3 % Tween-20, but in contrast, it was completely insensitive to 10^{-6} M dicoumarol.

The data presented above are consistent with the conclusion that DT diaphorase occurs both in mitochondria and microsomes, and can be selectively released from these elements after disruption of their structure by suitable means. Mitochondria seem to contain only one major enzyme with TPNH diaphorase activity and this is entirely accounted for by DT diaphorase. This conclusion is consistent with the previous finding of Stein and Kaplan [3] that column-chromatography of extracts of sonicated mitochondria yielded only one fraction with TPNH diaphorase activity, and that this fraction coincided with one of the two DPNH diaphorase fractions found by these authors. Microsomes, on the other hand, seem according to the present data to contain two types of TPNH diaphorase activity. One of these is accounted for by DT diaphorase, whereas the other seems to be independent of this enzyme as indicated by its resistance to dicoumarol and its firm association with the microsomal structure. The possible relation between this enzyme and the TPNH-neotetrazolium reductase recently found in microsomes by Williams *et al.*[4] is presently being investigated.

This work has been supported by a grant from the *Swedish Cancer Society.*

1. Ernster, L., Ljunggren, M. and Danielson, L. *Biochem. Biophys. Research Commun.* **2** (1960) 88.
2. Kielley, W. W. and Kielley, R. K. *J. Biol. Chem.* **200** (1953) 213.
3. Stein, A. M. and Kaplan, N. O. *Biochim. et Biophys. Acta* **29** (1958) 452.
4. Williams, C. H., Gibbs, R. H. and Kamin, H. *Biochim. et Biophys. Acta* **32** (1959) 568.

A Liver-Microsomal Enzyme System Liberating Orthophosphate from Nucleoside Di- and Triphosphates

Lois C. Jones and Lars Ernster

Wenner-Gren Institute, University of Stockholm, Stockholm, Sweden

Freshly prepared microsomes from 0.25 M sucrose homogenates of rat liver exhibit a high "ATPase" activity. This activity resembles the "latent" ATPase activity [1] appearing in liver mitochondria upon structural damage in the following respects: 1) it requires added Mg^{++} [1]; 2) it is stimulated by $Na_2S_2O_4$ [2,3]; 3) it is inhibited by atebrin [3], chlorpromazine [4], azide [5,6]; 4) the enzyme is not strictly specific (like the dinitrophenol-induced ATPase of intact mitochondria) for ATP, but reacts, in a non-additive manner, with the five nucleoside triphosphates, ATP, GTP, UTP, CTP and ITP [7].

In the course of attempts to more closely characterize this enzyme it was observed that the activities with the different nucleoside triphosphates responded in different ways to the presence of sodium deoxycholate (DOC) in the test system. Thus, at 0.05 % DOC, the GTPase and UTPase activities became markedly stimulated, whereas the activities with the other three triphosphates either decreased or remained unchanged; at higher DOC concentrations, all five activities were strongly inhibited. Simultaneously it was also found that a nucleoside diphosphatase activity, which was relatively low in the absence of DOC, revealed a strong increase at both 0.05 and 0.1 % DOC in the case of GDP, UDP or IDP as substrates, whereas it remained unchanged or became inhibited with ADP or CDP as substrates.

Treatment of microsomes with 0.26 % DOC in the cold, and subsequent centrifugation at 105 000 *g* for 2 h, resulted in a clear supernatant fraction, which exhibited a high activity toward GDP, UDP and IDP as compared with the two remaining diphosphates and the five triphosphates. Table 1 illustrates the nucleoside di- and triphosphatase activities of this fraction as compared with those found in the original microsomes. The activities of the three active diphosphatases recovered in this fraction corresponded to about 90 % of the total activities found in the DOC-treated microsomes. The five triphosphatase activities were concentrated, 2—8 fold on the protein basis, in a loose pellet appearing in this fractionation [8] on the top of the tightly packed ribonucleoprotein particles. This loose pellet has recently been found [9] to contain the microsomal DPNH-cytochrome c reductase and glucose-6-phosphatase activities in a concentrated form. The ribonucleoprotein particle fraction exhibited only marginal di- and triphosphatase activities.

When the clear DOC supernatant was tested with the three active diphosphates in combination the resulting activity did not exceed the maximum found with the individual diphosphates; addition of the two remaining diphosphates lowered this activity slightly. The di-

Table 1. Nucleoside di- and triphosphatase activities of rat liver microsomes, as determined in fresh preparations and in deoxycholate-extracts. The test system contained microsomes or microsomal extract from 40 mg wet weight liver, 2.5 μmoles substrate, 2 μmoles $MgCl_2$, and 25 μmoles TRIS buffer, pH 7.5, in a final volume of 0.5 ml. Incubation at 30°C. The values are expressed in terms of μmoles orthophosphate liberated in 10 min. per gram microsomal protein.

Substrate	Microsomes	Deoxycholate-extract
ATP	846	158
GTP	865	525
UTP	702	420
CTP	747	281
ITP	1 026	368
ADP	387	105
GDP	594	2 370
UDP	576	2 012
CDP	207	123
IDP	640	1 595

phosphatase activities required added Mg++ and were inhibited by atebrine, chlorpromazine and azide to about the same extent as the triphosphatases.

The above findings seem to indicate that freshly prepared rat liver microsomes exhibit a nucleoside triphosphatase activity which resembles that of structurally damaged rat liver mitochondria in regards to behavior toward certain activators and inhibitors, lacking nucleoside specificity, and firm association with the membrane structure. In addition, microsomes seem to contain a "latent" nucleoside diphosphatase activity, which can be rendered manifest by disruption of the microsomal membranes. This enzyme resembles the nucleoside triphosphatase in its behavior toward certain activators and inhibitors, but differs from the latter in possessing a more restricted array of nucleoside specificity, as well as in being more loosely associated with the microsomes.

An enzyme with a similar array of specificity has been known for some time [10-13], but its association with microsomes and its latent character have not been reported.

This work has been supported by a grant from the *Swedish Cancer Society*.

1. Kielley, W. W. and Kielley, R. K. *J. Biol. Chem.* **191** (1951) 485.
2. Myers, D. K. and Slater, E. C. *Biochem. J.* **67** (1957) 572.
3. Löw, H. *Biochim. et Biophys. Acta* **32** (1959) 1.
4. Löw, H. *Biochim. et Biophys. Acta* **32** (1959) 11.
5. Novikoff, A. B., Hecht, L., Podber, E. and Ryan, J. *J. Biol. Chem.* **194** (1952) 153.
6. Siekevitz, P., Löw, H., Ernster, L. and Lindberg, O. *Biochim. et Biophys. Acta* **29** (1958) 378.
7. Cooper, C. and Lehninger, A. L. *J. Biol. Chem.* **224** (1957) 547.
8. Palade, G. E. and Siekevitz, P. *J. Biophys. Biochem. Cytol.* **2** (1956) 171.
9. Ernster, L., Palade, G. E. and Siekevitz, P. *In preparation.*
10. Gibson, D. M., Ayengar, P. and Sanadi, D. R. *Biochim. Biophys. Acta* **16** (1955) 536.
11. Plaut, G. W. E. *J. Biol. Chem.* **217** (1955) 235.
12. Gregory, J. D. *Fed. Proc.* **14** (1955) 221.
13. Heppel, L. A., Strominger, J. L. and Maxwell, E. S. *Biochim. Biophys. Acta* **32** (1959) 422.

By-Pass of the Amytal-Sensitive Site of the Respiratory Chain in Mitochondria by Means of Vitamin K_3

T. E. Conover* and L. Ernster

Wenner-Gren Institute, University of Stockholm, Stockholm, Sweden

A soluble diaphorase (DT diaphorase) from liver has been isolated which can couple the oxidation of extramitochondrial reduced pyridine nucleotide through vitamin K_3 to the respiratory chain of mitochondria [1]. The cellular distribution of this enzyme has been shown[2], and significant amounts can be extracted from isolated mitochondria [3].

The presence of this enzyme in intact mitochondria and its interaction with intramitochondrially-generated reduced pyridine nucleotide is demonstrated in this paper by the bypassing of the point of amytal inhibition in the respiratory chain with the addition of vitamin K_3.

Mitochondria freshly prepared from rat liver as previously described [4] were incubated in a isotonic, buffered medium containing substrate, phosphate, Mg++, adenosine triphosphate, hexokinase and glucose. In these conditions the pyridine nucleotide-linked oxidation of substrates showed the usual high rates and strong sensitivity to amytal as is shown for glutamate in Table 1. The addition of low concentrations of vitamin K_3 (5×10^{-6} M) to the amytal-inhibited system gave a complete recovery of the maximal respiration. It can also be seen from Table 1 that this respiration was highly sensitive to antimycin A, KCN, and dicumarol. The high degree of inhibition obtained by low concentrations of dicumarol strongly implies the role of DT diaphorase, as the high sensitivity of this enzyme to dicumarol is considered to be very characteristic[2].

It was found that the concentration the of vitamin K_3 was important in this reaction as concentrations under 5×10^{-6} M were limiting in the oxidation of glutamate in these conditions, while higher concentrations were often inhibitory. This inhibition seemed to be related to a loss of pyridine nucleotide and could be protected at least partially by added nucleotide or nicotinamide.

* Fellow of the National Foundation, New York, N. Y.

phosphatase activities required added Mg++ and were inhibited by atebrine, chlorpromazine and azide to about the same extent as the triphosphatases.

The above findings seem to indicate that freshly prepared rat liver microsomes exhibit a nucleoside triphosphatase activity which resembles that of structurally damaged rat liver mitochondria in regards to behavior toward certain activators and inhibitors, lacking nucleoside specificity, and firm association with the membrane structure. In addition, microsomes seem to contain a "latent" nucleoside diphosphatase activity, which can be rendered manifest by disruption of the microsomal membranes. This enzyme resembles the nucleoside triphosphatase in its behavior toward certain activators and inhibitors, but differs from the latter in possessing a more restricted array of nucleoside specificity, as well as in being more loosely associated with the microsomes.

An enzyme with a similar array of specificity has been known for some time [10-13], but its association with microsomes and its latent character have not been reported.

This work has been supported by a grant from the *Swedish Cancer Society*.

1. Kielley, W. W. and Kielley, R. K. *J. Biol. Chem.* **191** (1951) 485.
2. Myers, D. K. and Slater, E. C. *Biochem. J.* **67** (1957) 572.
3. Löw, H. *Biochim. et Biophys. Acta* **32** (1959) 1.
4. Löw, H. *Biochim. et Biophys. Acta* **32** (1959) 11.
5. Novikoff, A. B., Hecht, L., Podber, E. and Ryan, J. *J. Biol. Chem.* **194** (1952) 153.
6. Siekevitz, P., Löw, H., Ernster, L. and Lindberg, O. *Biochim. et Biophys. Acta* **29** (1958) 378.
7. Cooper, C. and Lehninger, A. L. *J. Biol. Chem.* **224** (1957) 547.
8. Palade, G. E. and Siekevitz, P. *J. Biophys. Biochem. Cytol.* **2** (1956) 171.
9. Ernster, L., Palade, G. E. and Siekevitz, P. *In preparation.*
10. Gibson, D. M., Ayengar, P. and Sanadi, D. R. *Biochim. Biophys. Acta* **16** (1955) 536.
11. Plaut, G. W. E. *J. Biol. Chem.* **217** (1955) 235.
12. Gregory, J. D. *Fed. Proc.* **14** (1955) 221.
13. Heppel, L. A., Strominger, J. L. and Maxwell, E. S. *Biochim. Biophys. Acta* **32** (1959) 422.

By-Pass of the Amytal-Sensitive Site of the Respiratory Chain in Mitochondria by Means of Vitamin K_3

T. E. Conover* and L. Ernster

Wenner-Gren Institute, University of Stockholm, Stockholm, Sweden

A soluble diaphorase (DT diaphorase) from liver has been isolated which can couple the oxidation of extramitochondrial reduced pyridine nucleotide through vitamin K_3 to the respiratory chain of mitochondria [1]. The cellular distribution of this enzyme has been shown[2], and significant amounts can be extracted from isolated mitochondria [3].

The presence of this enzyme in intact mitochondria and its interaction with intramitochondrially-generated reduced pyridine nucleotide is demonstrated in this paper by the bypassing of the point of amytal inhibition in the respiratory chain with the addition of vitamin K_3.

Mitochondria freshly prepared from rat liver as previously described [4] were incubated in a isotonic, buffered medium containing substrate, phosphate, Mg++, adenosine triphosphate, hexokinase and glucose. In these conditions the pyridine nucleotide-linked oxidation of substrates showed the usual high rates and strong sensitivity to amytal as is shown for glutamate in Table 1. The addition of low concentrations of vitamin K_3 (5×10^{-6} M) to the amytal-inhibited system gave a complete recovery of the maximal respiration. It can also be seen from Table 1 that this respiration was highly sensitive to antimycin A, KCN, and dicumarol. The high degree of inhibition obtained by low concentrations of dicumarol strongly implies the role of DT diaphorase, as the high sensitivity of this enzyme to dicumarol is considered to be very characteristic[2].

It was found that the concentration the of vitamin K_3 was important in this reaction as concentrations under 5×10^{-6} M were limiting in the oxidation of glutamate in these conditions, while higher concentrations were often inhibitory. This inhibition seemed to be related to a loss of pyridine nucleotide and could be protected at least partially by added nucleotide or nicotinamide.

* Fellow of the National Foundation, New York, N. Y.

Table 1. Effect of vitamin K_3 and various inhibitors on the respiration of mitochondria in the presence of amytal.

Additions	μatoms oxygen
none	5.49
vitamin K_3	5.57
dicumarol	5.32
amytal	0.22
amytal + vitamin K_3	5.25
amytal + vitamin K_3 + antimycin A	1.57
amytal + vitamin K_3 + KCN	1.18
amytal + vitamin K_3 + dicumarol	1.13

The complete system contained per Warburg vessel: 10 μmoles glutamate, 20 μmoles Tris buffer (pH 7.4), 20 μmoles orthophosphate (pH 7.4), 4 μmoles $MgCl_2$, 2 μmoles adenosine triphosphate, 24 μmoles glucose, an excess of yeast hexokinase, 50 μmoles sucrose, and mitochondria from 200 mg rat liver. The amounts of the additions were as follows: 5×10^{-3} μmoles vitamin K_3, 10^{-2} μmoles dicumarol, 1.0 μmoles amytal, 1 μg antimycin A, and 1.0 μmoles KCN. Final volume, 1.0 ml. Temperature, 30°C. Reading begun after 6 min. thermoequilibration. Time measured, 20 min.

Table 2. Effect of various oxidation-reduction compounds on the respiration of mitochondria in the presence of amytal.

Additions	μatoms oxygen Expt. 1	Expt. 2	Expt. 3
none	4.47	7.00	5.15
amytal	0.73	0.33	1.12
amytal + 10^{-5} M vitamin K_3	5.75	8.23	6.05
amytal + 10^{-3} M DPN	0.79		
» + 10^{-3} M FAD	0.93		
» + 10^{-3} M FMN	0.89		
» + 6×10^{-5} M cytochrome c	0.55		
amytal + 10^{-5} M ascorbate	0.88		
» + 10^{-5} M ferricyanide		0.38	
» + 10^{-5} M silicomolybdate		0.35	
amytal + 10^{-5} M vitamin K_1		0.46	
» + 10^{-5} M vitamin K_2		0.43	
amytal + 10^{-5} M 1,2-naphthoquinone			1.13
» + 10^{-5} M 1,4-naphthoquinone			1.37
» + 10^{-5} M 2-hydroxy-1,4-naphthoquinone			1.59
» + 10^{-5} M 2-methyl-3-hydroxy-1,4-naphthoquinone			2.80
» + 10^{-5} M p-benzoquinone			0.88
» + 10^{-5} M 2-methylbenzoquinone			0.79
» + 10^{-5} M 2,6-dimethyl-benzoquinone			0.74
» + 10^{-5} M coenzyme Q_0			0.72

Conditions were the same as Table 1. Quinones were added in 10 μl ethanol. Time measured, 20 min.

It was of great interest to observe also that there was a very high degree of specificity with regards to the structure of the quinone. As can be observed in Table 2, not only did other common electron carriers such as DPN, FAD, cytochrome c, and ascorbate fail to give the bypass of the amytal inhibition, but likewise closely related benzoquinones and naphthoquinones were considerably less active. Since it has been shown that these quinones may accept electrons from the DT diaphorase [2] the specificity must be in the interaction of the reduced quinone with the respiratory chain.

This amytal-insensitive system shows the ability to couple respiration to the esterification of phosphate. The P/O ratios observed vary depending upon the substrate used from approximately 0.9 with β-hydroxybutyrate to 1.3 with glutamate. It is difficult to determine from these values whether one or two sites of respiratory chain phosphorylation are involved. However, the low values may be partly due to a slight uncoupling activity of the vitamin K_3 as determined with succinate as substrate. The phosphorylation was completely sensitive to 10^{-4} M DNP.

The question of the antimycin A sensitivity of this respiration has been further investigated. It is felt that it must be due to an unavailability of the cytochromes of the respiratory chain on the oxidizing side of the antimycin A-sensitive site, such as, for instance, cytochrome c, which has been shown [2] to be rapidly reduced in isolated systems by reduced pyridine nucleotide in the presence of DT diaphorase and vitamin K_3. The addition of purified cytochrome c to the mitochondrial system gives a several fold stimulation of the antimycin A-insensitive respiration. This respiration is also sensitive to KCN and dicumarol.

This work has been supported by a grant from the *Swedish Cancer Society*.

1. Conover, T. E. and Ernster, L. *Biochem. Biophys. Research Commun.* **2** (1960) 26.
2. Ernster, L., Ljunggren, M. and Danielson, L. *Biochem. Biophys. Research Commun.* **2** (1960) 88.
3. Danielson, L., Ernster, L. and Ljunggren, M. *Acta Chem. Scand.* **14** (1960) 1837.
4. Ernster, L. and Löw, H. *Exptl. Cell Research*, Suppl. **3** (1955) 133.

Oxidative Phosphorylation with Endogenous Mitochondrial Substrates

Eugene C. Weinbach*

National Institutes of Health, Bethesda, Maryland, U.S.A.

During recent studies of oxidative phosphorylation [1,2], we observed that carefully isolated rat liver mitochondria, when incubated in media containing the usual cofactors of oxidative phosphorylation, catalyzed a substantial uptake of inorganic orthophosphate in the absence of any added exogenous substrate. In Table 1 are shown representative data that illustrate the magnitude of this activity as well as the excellent stoichiometry that was obtained when the endogenous values were subtracted from those observed with added substrate. Independent experiments revealed that the internal substrates were not readily exhausted in short term incubations at 30°. In view of the large endogenous activity found with these preparations, in contrast to what has been observed previously [3-5], it was necessary to establish by anion exchange chromatography, and other tests, that the endogenous phosphate uptake was not an artefact of the assay procedure and that it led to an aerobic synthesis of ATP.

Experiments with inhibitors indicated the following: a) the endogenous phosphate uptake is associated with an *oxidative* phosphorylation since it was completely abolished by anaerobiosis, cyanide, azide, antimycin A, dinitrophenol and other uncoupling agents; b) tricarboxcylic acid cycle intermediates are not sole contributors to the endogenous activity since only partial inhibition was obtained with malonate and fluoroacetate; c) the internal substrates are oxidized *via* pyridine nucleotides. This was demonstrated by the finding that amytal completely prevented the endogenous phosphate uptake (*cf.* Ref.[6]).

Previously we had observed [2] that a high rate of endogenous activity was characteristic of mitochondria which were stable to prolonged storage at 4°. Indeed, when mitochondria from tissues other than liver were assessed both for their endogenous activity and for their stability of oxidative phosphorylation with added substrate, a positive correlation was found; *i. e.* those preparations which exhibited the

* Present address: Wenner-Grens Institute, University of Stockholm, Stockholm, Sweden.

It was of great interest to observe also that there was a very high degree of specificity with regards to the structure of the quinone. As can be observed in Table 2, not only did other common electron carriers such as DPN, FAD, cytochrome c, and ascorbate fail to give the bypass of the amytal inhibition, but likewise closely related benzoquinones and naphthoquinones were considerably less active. Since it has been shown that these quinones may accept electrons from the DT diaphorase [2] the specificity must be in the interaction of the reduced quinone with the respiratory chain.

This amytal-insensitive system shows the ability to couple respiration to the esterification of phosphate. The P/O ratios observed vary depending upon the substrate used from approximately 0.9 with β-hydroxybutyrate to 1.3 with glutamate. It is difficult to determine from these values whether one or two sites of respiratory chain phosphorylation are involved. However, the low values may be partly due to a slight uncoupling activity of the vitamin K_3 as determined with succinate as substrate. The phosphorylation was completely sensitive to 10^{-4} M DNP.

The question of the antimycin A sensitivity of this respiration has been further investigated. It is felt that it must be due to an unavailability of the cytochromes of the respiratory chain on the oxidizing side of the antimycin A-sensitive site, such as, for instance, cytochrome c, which has been shown [2] to be rapidly reduced in isolated systems by reduced pyridine nucleotide in the presence of DT diaphorase and vitamin K_3. The addition of purified cytochrome c to the mitochondrial system gives a several fold stimulation of the antimycin A-insensitive respiration. This respiration is also sensitive to KCN and dicumarol.

This work has been supported by a grant from the *Swedish Cancer Society*.

1. Conover, T. E. and Ernster, L. *Biochem. Biophys. Research Commun.* **2** (1960) 26.
2. Ernster, L., Ljunggren, M. and Danielson, L. *Biochem. Biophys. Research Commun.* **2** (1960) 88.
3. Danielson, L., Ernster, L. and Ljunggren, M. *Acta Chem. Scand.* **14** (1960) 1837.
4. Ernster, L. and Löw, H. *Exptl. Cell Research*, Suppl. **3** (1955) 133.

Oxidative Phosphorylation with Endogenous Mitochondrial Substrates

Eugene C. Weinbach*

National Institutes of Health, Bethesda, Maryland, U.S.A.

During recent studies of oxidative phosphorylation [1,2], we observed that carefully isolated rat liver mitochondria, when incubated in media containing the usual cofactors of oxidative phosphorylation, catalyzed a substantial uptake of inorganic orthophosphate in the absence of any added exogenous substrate. In Table 1 are shown representative data that illustrate the magnitude of this activity as well as the excellent stoichiometry that was obtained when the endogenous values were subtracted from those observed with added substrate. Independent experiments revealed that the internal substrates were not readily exhausted in short term incubations at 30°. In view of the large endogenous activity found with these preparations, in contrast to what has been observed previously [3-5], it was necessary to establish by anion exchange chromatography, and other tests, that the endogenous phosphate uptake was not an artefact of the assay procedure and that it led to an aerobic synthesis of ATP.

Experiments with inhibitors indicated the following: a) the endogenous phosphate uptake is associated with an *oxidative* phosphorylation since it was completely abolished by anaerobiosis, cyanide, azide, antimycin A, dinitrophenol and other uncoupling agents; b) tricarboxcylic acid cycle intermediates are not sole contributors to the endogenous activity since only partial inhibition was obtained with malonate and fluoroacetate; c) the internal substrates are oxidized *via* pyridine nucleotides. This was demonstrated by the finding that amytal completely prevented the endogenous phosphate uptake (*cf.* Ref.[6]).

Previously we had observed [2] that a high rate of endogenous activity was characteristic of mitochondria which were stable to prolonged storage at 4°. Indeed, when mitochondria from tissues other than liver were assessed both for their endogenous activity and for their stability of oxidative phosphorylation with added substrate, a positive correlation was found; *i. e.* those preparations which exhibited the

* Present address: Wenner-Grens Institute, University of Stockholm, Stockholm, Sweden.

Table 1. Endogenous phosphorylation. Each flask contained: 80 μmoles of glycylglycine buffer, pH 7.4; 20 or 30 μmoles of orthophosphate, pH 7.4; 5 μmoles of ADP; 5 μmoles of DPN; 0.03 μmoles of cytochrome c; 50 μmoles of glucose; 0.5 mg of hexokinase; 10 μmoles of $MgCl_2$, and 0.5 ml of mitochondria in a final volume of 2 ml. 50 μmoles of DL-β-hydroxybutyrate were added only where indicated. Incubated in air for 20 min at 30°. Other details given in Ref.[2].

Added substrate	Oxygen uptake μatoms/mg N	Acetoacetate formed μmoles/mg N	Phosphate uptake μmoles/mg N	P/O
None	3.1	0	5.7	1.8
β-Hydroxybutyrate	8.5	5.3	22.0	2.6
Substrate minus endogenous	5.4	5.3	16.3	3.0

highest rate of endogenous phosphorylation were most stable to storage at 4°. Furthermore, certain pretreatments of liver mitochondria, such as freezing and thawing, or preincubation with low concentrations of phosphate which, among other detrimental changes (*cf.* Ref.[7]), abolished the endogenous activity, also decreased the stability of the stored preparations. The implication of these findings with regard to a possible correlation between endogenous phosphorylation and mitochondrial stability will be discussed.

1. Weinbach, E. C. and Garbus, J. *J. Biol. Chem.* **234** (1959) 412.
2. Weinbach, E. C. *J. Biol. Chem.* **234** (1959) 1580.
3. Siekevitz, P. and Potter, V. R. *J. Biol. Chem.* **200** (1953) 187.
4. Borgstrom, B., Sudduth, H. C. and Lehninger, A. L. *J. Biol. Chem.* **215** (1955) 571.
5. Chance, B. and Williams, G. R. *J. Biol. Chem.* **217** (1955) 383.
6. Ernster, L., Jalling, O., Löw, H. and Lindberg, O. *Exptl. Cell Research*, Suppl. 3 (1955) 124.
7. Hunter, F. E. Jr. and Ford, L. *J. Biol. Chem.* **216** (1955) 357.

Particulate and Soluble D-Lactic Cytochrome c Reductase of Yeast

Agnar P. Nygaard

Johan Throne Holst's Institutt for Ernæringsforskning, Blindern, Oslo, Norway

The main fraction of the D-lactic cytochrome c reductase activity (D-LDH) of aerobic yeast was associated with respiratory particles. By means of the extraction of lipids with *n*-butanol, acetone, and ether, 40 % of the enzyme was solubilized. The solubilized enzyme has been purified one thousand fold. The difference spectrum of oxidized/reduced enzyme had absorption maximum at 450 mμ. At pH 3, flavin fluorescence appeared. The flavin concentration, calculated from the spectral difference, agreed well with that obtained from fluorescence intensity. In contrast to the flavohaemoprotein L-lactic cytochrome c reductase (L-LDH), there was no haem associated with the D-enzyme, and the D-enzyme did not reduce the haem of L-LDH. The turnover number of D-LDH was 20 000 min^{-1} $mole^{-1}$, compared with 15 000 for L-LDH.

Particulate as well as solubilized D-LDH were absolutely specific for D-lactate. A preparation of D-LDH, which was obtained directly in a soluble form in the cell homogenate[1], has erroneously been determined to have relative stereospecificity [2]. The apparent Michaelis constant of D-lactate for D-LDH was under certain conditions one thousand fold lower than that of L-lactate for L-LDH.

The oxidation of D-lactate to pyruvate went to completion with excess of cytochrome c. At a relatively high buffer concentration (μ 0.08), the initial rate of reaction has been determined for a series of cytochrome c concentrations, each with a series of D-lactate concentrations. The results can be summarized as follows: The apparent Michaelis constant of D-lactate was proportional to the cytochrome c concentration, and the rate, obtained with excess of lactate, was proportional to the cytochrome c concentration. These criteria, which were the same for soluble and particulate enzyme, are fullfilled in the following reaction scheme (where E = enzyme, SH_2 = lactate, and A = cytochrome c):

$$SH_2 + E \rightleftharpoons SH_2 \cdot E \xrightarrow{k_3} S + EH_2$$

$$EH_2 + A \xrightarrow{k_4} E + AH_2$$

In this scheme, $k_3 \gg k_4 \times A$

Table 1. Endogenous phosphorylation. Each flask contained: 80 μmoles of glycylglycine buffer, pH 7.4; 20 or 30 μmoles of orthophosphate, pH 7.4; 5 μmoles of ADP; 5 μmoles of DPN; 0.03 μmoles of cytochrome c; 50 μmoles of glucose; 0.5 mg of hexokinase; 10 μmoles of $MgCl_2$, and 0.5 ml of mitochondria in a final volume of 2 ml. 50 μmoles of DL-β-hydroxybutyrate were added only where indicated. Incubated in air for 20 min at 30°. Other details given in Ref.[2].

Added substrate	Oxygen uptake μatoms/mg N	Acetoacetate formed μmoles/mg N	Phosphate uptake μmoles/mg N	P/O
None	3.1	0	5.7	1.8
β-Hydroxybutyrate	8.5	5.3	22.0	2.6
Substrate minus endogenous	5.4	5.3	16.3	3.0

highest rate of endogenous phosphorylation were most stable to storage at 4°. Furthermore, certain pretreatments of liver mitochondria, such as freezing and thawing, or preincubation with low concentrations of phosphate which, among other detrimental changes (*cf.* Ref.[7]), abolished the endogenous activity, also decreased the stability of the stored preparations. The implication of these findings with regard to a possible correlation between endogenous phosphorylation and mitochondrial stability will be discussed.

1. Weinbach, E. C. and Garbus, J. *J. Biol. Chem.* **234** (1959) 412.
2. Weinbach, E. C. *J. Biol. Chem.* **234** (1959) 1580.
3. Siekevitz, P. and Potter, V. R. *J. Biol. Chem.* **200** (1953) 187.
4. Borgstrom, B., Sudduth, H. C. and Lehninger, A. L. *J. Biol. Chem.* **215** (1955) 571.
5. Chance, B. and Williams, G. R. *J. Biol. Chem.* **217** (1955) 383.
6. Ernster, L., Jalling, O., Löw, H. and Lindberg, O. *Exptl. Cell Research*, Suppl. 3 (1955) 124.
7. Hunter, F. E. Jr. and Ford, L. *J. Biol. Chem.* **216** (1955) 357.

Particulate and Soluble D-Lactic Cytochrome c Reductase of Yeast

Agnar P. Nygaard

Johan Throne Holst's Institutt for Ernæringsforskning, Blindern, Oslo, Norway

The main fraction of the D-lactic cytochrome c reductase activity (D-LDH) of aerobic yeast was associated with respiratory particles. By means of the extraction of lipids with *n*-butanol, acetone, and ether, 40 % of the enzyme was solubilized. The solubilized enzyme has been purified one thousand fold. The difference spectrum of oxidized/reduced enzyme had absorption maximum at 450 mμ. At pH 3, flavin fluorescence appeared. The flavin concentration, calculated from the spectral difference, agreed well with that obtained from fluorescence intensity. In contrast to the flavohaemoprotein L-lactic cytochrome c reductase (L-LDH), there was no haem associated with the D-enzyme, and the D-enzyme did not reduce the haem of L-LDH. The turnover number of D-LDH was 20 000 min^{-1} $mole^{-1}$, compared with 15 000 for L-LDH.

Particulate as well as solubilized D-LDH were absolutely specific for D-lactate. A preparation of D-LDH, which was obtained directly in a soluble form in the cell homogenate[1], has erroneously been determined to have relative stereospecificity [2]. The apparent Michaelis constant of D-lactate for D-LDH was under certain conditions one thousand fold lower than that of L-lactate for L-LDH.

The oxidation of D-lactate to pyruvate went to completion with excess of cytochrome c. At a relatively high buffer concentration (μ 0.08), the initial rate of reaction has been determined for a series of cytochrome c concentrations, each with a series of D-lactate concentrations. The results can be summarized as follows: The apparent Michaelis constant of D-lactate was proportional to the cytochrome c concentration, and the rate, obtained with excess of lactate, was proportional to the cytochrome c concentration. These criteria, which were the same for soluble and particulate enzyme, are fullfilled in the following reaction scheme (where E = enzyme, SH_2 = lactate, and A = cytochrome c):

$$SH_2 + E \rightleftharpoons SH_2 \cdot E \xrightarrow{k_3} S + EH_2$$

$$EH_2 + A \xrightarrow{k_4} E + AH_2$$

In this scheme, $k_3 \gg k_4 \times A$

The fresh preparations of soluble D-LDH reduced ferricyanide at a rate which was 5 % of that with cytochrome c. On storage, the ferricyanide reduction was lost more rapidly than the cytochrome c reductase activity. This could either be ascribed to a modification of D-LDH, or to the presence of another enzyme. The aerobic "D-lactic ferricyanide reductase" had reaction properties strikingly different from those of the corresponding anaerobic enzyme.

1. Nygaard, A. P. *Biochim. et Biophys. Acta* **40** (1960) 85.
2. Nygaard, A. P. *Arch. Biochem. Biophys.* **88** (1960) 178.

Purification of Yeast Hexokinase by Cellulose Ion Exchanger Chromatography

Gunnar Ågren, Lorentz Engström and Sten Eklund

Institute of Medical Chemistry, University of Uppsala, Sweden

In an earlier communication from this laboratory, it was reported that radioactive phosphorylserine could be isolated from a hydrolysate of a crude yeast hexokinase preparation which had been incubated with its radioactive substrate, AT^{32}P or glucose-6-^{32}P[1]. It seemed necessary to perform further studies with a more purified enzyme. Yeast hexokinase was isolated in a crystalline form several years ago [2,3]. By using cellulose ion exchanger chromatography, it now appears possible to obtain a more active preparation than the crystalline enzyme in an easy way.

As starting material, a commercial preparation (Sigma hexokinase, Type III) was used having a specific activity of 100–150 units per mg of preparation (estimated according to Kunitz *et al.*[3]). The activity was raised by two consecutive chromatographic separations using carboxymethyl cellulose columns (Serva Entwicklungslab., Germany) to between 1 200 and 1 900 units/mg protein, respectively. The elution was performed at pH 5 with a gradient increase in the concentration of the acetate buffer (0.02 N → 0.30 N with regard to sodium acetate). The enzyme was then chromatographed on a column of diethylaminoethyl cellulose (Eastman Org. Chem., U.S.A.). It was eluted with a potassium phosphate buffer of pH 7.0, increasing gradually from 0.05 M to 0.30 M. The enzyme was eluted as a main peak with nearly constant specific activity from fraction to fraction. No inactive protein could be separated from the enzyme activity by similar rechromatography of the main part of the enzyme peak. The specific activity was about 3 000 units/mg protein (as compared to about 1 400 units/mg protein found by Kunitz *et al.*[3]). The average yield in the three step purification was about 10 %.

When a sedimentation analysis was carried out in a Spinco ultracentrifuge, Model E, only one boundary was obtained. A single determination of the molecular weight was performed according to Archibald [4], and it was found to be about 50 000.

1. Ågren, G. and Engström, L. *Acta Chem. Scand.* **10** (1956) 489.
2. Berger, L., Colowick, S. R. and Cori, C. F. *J. Gen. Physiol.* **29** (1946) 379.
3. Kunitz, M. and McDonald, M. R. *J. Gen. Physiol.* **29** (1946). 393.
4. Archibald, W. *J. Phys. & Colloid Chem.* **51** (1947) 1204.

On Electron Transport and Phosphorylation in Plant and Bacterial Light-Induced Phosphorylation

Herrick Baltscheffsky, Margareta Baltscheffsky and Barbro Arwidsson

Wenner-Gren Institute, University of Stockholm, Stockholm, Sweden

The following findings from experiments on light-induced phosphorylation (aerobic conditions, saturating light-intensities) will be discussed:

(1) Coenzyme Q_0 stimulates light-induced phosphorylation in isolated spinach chloroplasts. It is, however, less efficient as stimulatory agent than menadione. At 10^{-4} M concentration, for example, coenzyme Q_0 gives only 70 % of the stimulation obtained with the same concentration of menadione.

(2) Valinomycin, which completely uncouples oxidative phosphorylation in animal mitochondria at low concentrations [1], inhibits light-induced phosphorylation in isolated chromatophores of the photosynthetic bacterium *Rhodospirillum rubrum* to approximately 50 %. This may indicate that two phos-

The fresh preparations of soluble D-LDH reduced ferricyanide at a rate which was 5 % of that with cytochrome c. On storage, the ferricyanide reduction was lost more rapidly than the cytochrome c reductase activity. This could either be ascribed to a modification of D-LDH, or to the presence of another enzyme. The aerobic "D-lactic ferricyanide reductase" had reaction properties strikingly different from those of the corresponding anaerobic enzyme.

1. Nygaard, A. P. *Biochim. et Biophys. Acta* **40** (1960) 85.
2. Nygaard, A. P. *Arch. Biochem. Biophys.* **88** (1960) 178.

Purification of Yeast Hexokinase by Cellulose Ion Exchanger Chromatography

Gunnar Ågren, Lorentz Engström and Sten Eklund

Institute of Medical Chemistry, University of Uppsala, Sweden

In an earlier communication from this laboratory, it was reported that radioactive phosphorylserine could be isolated from a hydrolysate of a crude yeast hexokinase preparation which had been incubated with its radioactive substrate, AT^{32}P or glucose-6-^{32}P[1]. It seemed necessary to perform further studies with a more purified enzyme. Yeast hexokinase was isolated in a crystalline form several years ago [2,3]. By using cellulose ion exchanger chromatography, it now appears possible to obtain a more active preparation than the crystalline enzyme in an easy way.

As starting material, a commercial preparation (Sigma hexokinase, Type III) was used having a specific activity of 100–150 units per mg of preparation (estimated according to Kunitz *et al.*[3]). The activity was raised by two consecutive chromatographic separations using carboxymethyl cellulose columns (Serva Entwicklungslab., Germany) to between 1 200 and 1 900 units/mg protein, respectively. The elution was performed at pH 5 with a gradient increase in the concentration of the acetate buffer (0.02 N → 0.30 N with regard to sodium acetate). The enzyme was then chromatographed on a column of diethylaminoethyl cellulose (Eastman Org. Chem., U.S.A.). It was eluted with a potassium phosphate buffer of pH 7.0, increasing gradually from 0.05 M to 0.30 M. The enzyme was eluted as a main peak with nearly constant specific activity from fraction to fraction. No inactive protein could be separated from the enzyme activity by similar rechromatography of the main part of the enzyme peak. The specific activity was about 3 000 units/mg protein (as compared to about 1 400 units/mg protein found by Kunitz *et al.*[3]). The average yield in the three step purification was about 10 %.

When a sedimentation analysis was carried out in a Spinco ultracentrifuge, Model E, only one boundary was obtained. A single determination of the molecular weight was performed according to Archibald [4], and it was found to be about 50 000.

1. Ågren, G. and Engström, L. *Acta Chem. Scand.* **10** (1956) 489.
2. Berger, L., Colowick, S. R. and Cori, C. F. *J. Gen. Physiol.* **29** (1946) 379.
3. Kunitz, M. and McDonald, M. R. *J. Gen. Physiol.* **29** (1946). 393.
4. Archibald, W. *J. Phys. & Colloid Chem.* **51** (1947) 1204.

On Electron Transport and Phosphorylation in Plant and Bacterial Light-Induced Phosphorylation

Herrick Baltscheffsky, Margareta Baltscheffsky and Barbro Arwidsson

Wenner-Gren Institute, University of Stockholm, Stockholm, Sweden

The following findings from experiments on light-induced phosphorylation (aerobic conditions, saturating light-intensities) will be discussed:

(1) Coenzyme Q_0 stimulates light-induced phosphorylation in isolated spinach chloroplasts. It is, however, less efficient as stimulatory agent than menadione. At 10^{-4} M concentration, for example, coenzyme Q_0 gives only 70 % of the stimulation obtained with the same concentration of menadione.

(2) Valinomycin, which completely uncouples oxidative phosphorylation in animal mitochondria at low concentrations [1], inhibits light-induced phosphorylation in isolated chromatophores of the photosynthetic bacterium *Rhodospirillum rubrum* to approximately 50 %. This may indicate that two phos-

phorylation sites are involved, one of which is affected, whereas the other one remains unaffected. When the rate of light-induced phosphorylation is stimulated several fold by phenazine methosulfate, only a small part of the phosphorylation, which is about equivalent to the sensitive part of the unstimulated system, is inhibited by valinomycin. This supports the conclusion that one of two sites, the "valinomycin-insensitive" one, is activated by addition of phenazine methosulfate. "Cyclic" light-induced phosphorylation in spinach chloroplasts remains unaffected by valinomycin, which may indicate that only a site corresponding to the "valinomycin-insensitive" site in bacterial chromatophores is participating in light-induced phosphorylation of the isolated spinach chloroplasts.

(3) When a preparation of bacterial chromatophores has been aged at 55–57°C, the initially very low stimulation obtained by menadione increases with the aging time, up to 15–25 minutes of preaging, after which a very rapid decrease occurs. In contrast to the stimulation obtained by phenazine methosulfate, that obtained by menadione is very sensitive to low concentrations of the inhibitors antimycin A and 2-*n*-heptyl-4-hydroxyquinoline-N-oxide. Thus a difference has been found between the modes of action of the two stimulatory agents on light-induced phosphorylation.

1. McMurray, W. C. and Begg, R. W. *Arch. Biochem. Biophys.* **84** (1959) 546.

Glycolysis in Human Erythrocytes Studied with ^{14}C-labelled Glucose

C.-H. de Verdier

Department of Clinical Chemistry, University Hospital, Uppsala, Sweden

The energy required for the maintenance of viability of the erythrocytes is obtained through breakdown of glucose mainly to lactate. Some hemolytic anemias and the aging of erythrocytes *in vitro* or *in vivo* have been shown to be accompanied by disorders in the glycolytic system [1-4].

In order to study these disorders more closely a test system has been worked out. The erythrocytes are washed at 4°C and finally suspended in an inorganic buffered salt solution with the following composition: NaCl 108 mM; KCl 3.9 mM; $MgCl_2$ 5 mM; Na-phosphate (pH 7.4) 20 mM. 2 ml of the suspension (holding 15 % hemoglobin) are incubated at 37° in the two media described in Table 1. After 60 min the glycolysis is stopped by adding perchloric acid. Different perchloric acid soluble substances are then separated using stepwise elution through a Dowex 1 column according to Bartlett [4]. Methylene blue stimulates breakdown along the pentose phosphate shunt [5] and the CO_2 formed during incubation is absorbed to NaOH moistened filter paper strips in the center well of the Erlenmeyer

Table 1. Composition of media.

	− methylene blue ml	+ methylene blue ml
Erythrocyte suspension	2.0	2.0
Buffered salt solution	0.6	0.6
0.05 % methylene blue	—	0.2
Distilled water	0.2	—
0.15 M ^{14}C-glucose (uniformly labelled, containing $1.3 \cdot 10^6$ cpm).	0.2	0.2
Total volume	3.0	3.0

Table 2.

	− methylene blue	+ methylene blue
ATP, μmoles per incubation flask	0.38	0.45
2,3-diP-glycerate, μmoles per incubation flask	2.8	2.9
% radioactivity in CO_2	—	3.5
% » » 2,3-diP-glycerate	2.7	4.8
% » » lactate	1.9	2.9

The fresh preparations of soluble D-LDH reduced ferricyanide at a rate which was 5 % of that with cytochrome c. On storage, the ferricyanide reduction was lost more rapidly than the cytochrome c reductase activity. This could either be ascribed to a modification of D-LDH, or to the presence of another enzyme. The aerobic "D-lactic ferricyanide reductase" had reaction properties strikingly different from those of the corresponding anaerobic enzyme.

1. Nygaard, A. P. *Biochim. et Biophys. Acta* **40** (1960) 85.
2. Nygaard, A. P. *Arch. Biochem. Biophys.* **88** (1960) 178.

Purification of Yeast Hexokinase by Cellulose Ion Exchanger Chromatography

Gunnar Ågren, Lorentz Engström and Sten Eklund

Institute of Medical Chemistry, University of Uppsala, Sweden

In an earlier communication from this laboratory, it was reported that radioactive phosphorylserine could be isolated from a hydrolysate of a crude yeast hexokinase preparation which had been incubated with its radioactive substrate, AT^{32}P or glucose-6-^{32}P[1]. It seemed necessary to perform further studies with a more purified enzyme. Yeast hexokinase was isolated in a crystalline form several years ago [2,3]. By using cellulose ion exchanger chromatography, it now appears possible to obtain a more active preparation than the crystalline enzyme in an easy way.

As starting material, a commercial preparation (Sigma hexokinase, Type III) was used having a specific activity of 100–150 units per mg of preparation (estimated according to Kunitz *et al.*[3]). The activity was raised by two consecutive chromatographic separations using carboxymethyl cellulose columns (Serva Entwicklungslab., Germany) to between 1 200 and 1 900 units/mg protein, respectively. The elution was performed at pH 5 with a gradient increase in the concentration of the acetate buffer (0.02 N → 0.30 N with regard to sodium acetate). The enzyme was then chromatographed on a column of diethylaminoethyl cellulose (Eastman Org. Chem., U.S.A.). It was eluted with a potassium phosphate buffer of pH 7.0, increasing gradually from 0.05 M to 0.30 M. The enzyme was eluted as a main peak with nearly constant specific activity from fraction to fraction. No inactive protein could be separated from the enzyme activity by similar rechromatography of the main part of the enzyme peak. The specific activity was about 3 000 units/mg protein (as compared to about 1 400 units/mg protein found by Kunitz *et al.*[3]). The average yield in the three step purification was about 10 %.

When a sedimentation analysis was carried out in a Spinco ultracentrifuge, Model E, only one boundary was obtained. A single determination of the molecular weight was performed according to Archibald [4], and it was found to be about 50 000.

1. Ågren, G. and Engström, L. *Acta Chem. Scand.* **10** (1956) 489.
2. Berger, L., Colowick, S. R. and Cori, C. F. *J. Gen. Physiol.* **29** (1946) 379.
3. Kunitz, M. and McDonald, M. R. *J. Gen. Physiol.* **29** (1946). 393.
4. Archibald, W. *J. Phys. & Colloid Chem.* **51** (1947) 1204.

On Electron Transport and Phosphorylation in Plant and Bacterial Light-Induced Phosphorylation

Herrick Baltscheffsky, Margareta Baltscheffsky and Barbro Arwidsson

Wenner-Gren Institute, University of Stockholm, Stockholm, Sweden

The following findings from experiments on light-induced phosphorylation (aerobic conditions, saturating light-intensities) will be discussed:

(1) Coenzyme Q_0 stimulates light-induced phosphorylation in isolated spinach chloroplasts. It is, however, less efficient as stimulatory agent than menadione. At 10^{-4} M concentration, for example, coenzyme Q_0 gives only 70 % of the stimulation obtained with the same concentration of menadione.

(2) Valinomycin, which completely uncouples oxidative phosphorylation in animal mitochondria at low concentrations [1], inhibits light-induced phosphorylation in isolated chromatophores of the photosynthetic bacterium *Rhodospirillum rubrum* to approximately 50 %. This may indicate that two phos-

phorylation sites are involved, one of which is affected, whereas the other one remains unaffected. When the rate of light-induced phosphorylation is stimulated several fold by phenazine methosulfate, only a small part of the phosphorylation, which is about equivalent to the sensitive part of the unstimulated system, is inhibited by valinomycin. This supports the conclusion that one of two sites, the "valinomycin-insensitive" one, is activated by addition of phenazine methosulfate. "Cyclic" light-induced phosphorylation in spinach chloroplasts remains unaffected by valinomycin, which may indicate that only a site corresponding to the "valinomycin-insensitive" site in bacterial chromatophores is participating in light-induced phosphorylation of the isolated spinach chloroplasts.

(3) When a preparation of bacterial chromatophores has been aged at 55–57°C, the initially very low stimulation obtained by menadione increases with the aging time, up to 15–25 minutes of preaging, after which a very rapid decrease occurs. In contrast to the stimulation obtained by phenazine methosulfate, that obtained by menadione is very sensitive to low concentrations of the inhibitors antimycin A and 2-*n*-heptyl-4-hydroxyquinoline-N-oxide. Thus a difference has been found between the modes of action of the two stimulatory agents on light-induced phosphorylation.

1. McMurray, W. C. and Begg, R. W. *Arch. Biochem. Biophys.* **84** (1959) 546.

Glycolysis in Human Erythrocytes Studied with ^{14}C-labelled Glucose

C.-H. de Verdier

Department of Clinical Chemistry, University Hospital, Uppsala, Sweden

The energy required for the maintenance of viability of the erythrocytes is obtained through breakdown of glucose mainly to lactate. Some hemolytic anemias and the aging of erythrocytes *in vitro* or *in vivo* have been shown to be accompanied by disorders in the glycolytic system [1-4].

In order to study these disorders more closely a test system has been worked out. The erythrocytes are washed at 4°C and finally suspended in an inorganic buffered salt solution with the following composition: NaCl 108 mM; KCl 3.9 mM; $MgCl_2$ 5 mM; Na-phosphate (pH 7.4) 20 mM. 2 ml of the suspension (holding 15 % hemoglobin) are incubated at 37° in the two media described in Table 1. After 60 min the glycolysis is stopped by adding perchloric acid. Different perchloric acid soluble substances are then separated using stepwise elution through a Dowex 1 column according to Bartlett [4]. Methylene blue stimulates breakdown along the pentose phosphate shunt [5] and the CO_2 formed during incubation is absorbed to NaOH moistened filter paper strips in the center well of the Erlenmeyer

Table 1. Composition of media.

	− methylene blue ml	+ methylene blue ml
Erythrocyte suspension	2.0	2.0
Buffered salt solution	0.6	0.6
0.05 % methylene blue	—	0.2
Distilled water	0.2	—
0.15 M ^{14}C-glucose (uniformly labelled, containing $1.3 \cdot 10^6$ cpm).	0.2	0.2
Total volume	3.0	3.0

Table 2.

	− methylene blue	+ methylene blue
ATP, μmoles per incubation flask	0.38	0.45
2,3-diP-glycerate, μmoles per incubation flask	2.8	2.9
% radioactivity in CO_2	—	3.5
% » » 2,3-diP-glycerate	2.7	4.8
% » » lactate	1.9	2.9

flask used for the incubation. Some parameters studied are listed in Table 2 together with the mean values of three different blood samples. Some examples of application will be given.

1. Beutler, E. *Blood* **14** (1959) 103.
2. Prankerd, T. A. J. *Am. J. Med.* **22** (1957) 724.
3. Löhr, G. W. and Waller, H. D. *Klin. Wochschr.* **37** (1959) 833.
4. Bartlett, G. R. *J. Clin. Invest.* **39** (1960) 56.
5. Brin, M. and Yonemoto, R. H. *J. Biol. Chem.* **230** (1958) 307.

Dilatometry in the Study of Acyl Shift in Peptides and Proteins

Lars Josefsson

Department of Physiological Chemistry, University of Lund, Lund, Sweden

The dilatometer technique as described by Linderstrøm-Lang [1] has been introduced in our studies on the formic acid induced reversible inactivation of protein enzymes [2-4] in order to elucidate the mechanism of the reactivation process.

From our previous studies three reactions were thought possible in this process, namely 1. an O,N-acyl shift, 2. deformylation of the formylated amino groups, or 3. deformylation of the formylated hydroxyl groups of the hydroxyamino acid residues.

Therefore the volume changes accompanying some proton transfers as well as the O,N-acyl shift in some model substances have been determined in addition to those accompanying the reactivation of formic acid inactivated protein enzymes.

The volume change accompanying the reactivation of ribonuclease when performed in phosphate buffer, *i. e.* 15.3 ml per equivalent base consumed, is in good agreement with that accompanying the proton transfers in the neutralisation of formic acid with secondary phosphate ions, *i. e.* 15.7 ml. In contrast, the value found for an O,N-acyl shift is 21.1 ml. Thus the data strongly suggest that the reactivation is based on a deformylation process.

Dilatometer experiments on formic acid treated glycyl-DL-serine as well as glycyl-O-formyl-DL-serine further suggest that the deformylating process is a splitting of the formamid bond in the O-acyl formed structure.

1. Linderstrøm-Lang, K. in Myrbäck, K. and Bamann, E., eds., *"Methoden der Enzymforschung"*, Leipzig, 1940.
2. Josefsson, L. and Edman, P. *Biochim. Biophys. Acta* **25** (1957) 614.
3. Josefsson, L. *Arkiv Kemi* **12** (1958) 183.
4. Josefsson, L. *Arkiv Kemi* **12** (1958) 195.

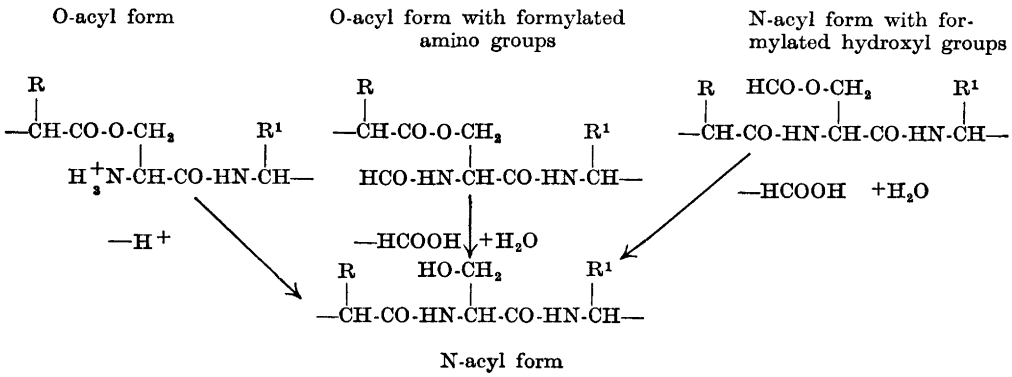

flask used for the incubation. Some parameters studied are listed in Table 2 together with the mean values of three different blood samples. Some examples of application will be given.

1. Beutler, E. *Blood* **14** (1959) 103.
2. Prankerd, T. A. J. *Am. J. Med.* **22** (1957) 724.
3. Löhr, G. W. and Waller, H. D. *Klin. Wochschr.* **37** (1959) 833.
4. Bartlett, G. R. *J. Clin. Invest.* **39** (1960) 56.
5. Brin, M. and Yonemoto, R. H. *J. Biol. Chem.* **230** (1958) 307.

Dilatometry in the Study of Acyl Shift in Peptides and Proteins

Lars Josefsson

Department of Physiological Chemistry, University of Lund, Lund, Sweden

The dilatometer technique as described by Linderstrøm-Lang [1] has been introduced in our studies on the formic acid induced reversible inactivation of protein enzymes [2-4] in order to elucidate the mechanism of the reactivation process.

From our previous studies three reactions were thought possible in this process, namely 1. an O,N-acyl shift, 2. deformylation of the formylated amino groups, or 3. deformylation of the formylated hydroxyl groups of the hydroxyamino acid residues.

Therefore the volume changes accompanying some proton transfers as well as the O,N-acyl shift in some model substances have been determined in addition to those accompanying the reactivation of formic acid inactivated protein enzymes.

The volume change accompanying the reactivation of ribonuclease when performed in phosphate buffer, *i. e.* 15.3 ml per equivalent base consumed, is in good agreement with that accompanying the proton transfers in the neutralisation of formic acid with secondary phosphate ions, *i. e.* 15.7 ml. In contrast, the value found for an O,N-acyl shift is 21.1 ml. Thus the data strongly suggest that the reactivation is based on a deformylation process.

Dilatometer experiments on formic acid treated glycyl-DL-serine as well as glycyl-O-formyl-DL-serine further suggest that the deformylating process is a splitting of the formamid bond in the O-acyl formed structure.

1. Linderstrøm-Lang, K. in Myrbäck, K. and Bamann, E., eds., *"Methoden der Enzymforschung"*, Leipzig, 1940.
2. Josefsson, L. and Edman, P. *Biochim. Biophys. Acta* **25** (1957) 614.
3. Josefsson, L. *Arkiv Kemi* **12** (1958) 183.
4. Josefsson, L. *Arkiv Kemi* **12** (1958) 195.

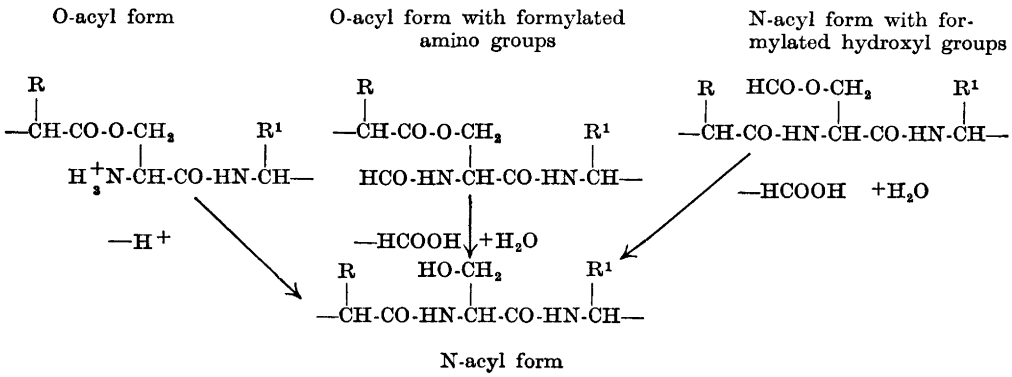

The Mechanism of the Vitamin K_3 Induced Glutathione Instability in Human Red Blood Cells. The Possible Intermediary Role of Methemoglobin

Andrew Sass-Kortsak*, Bertil Thalme, and Lars Ernster

Wenner-Gren Institute, University of Stockholm, Stockholm, Sweden

It has been known for some time that administration of vitamin K_3 to premature newborn infants may lead to the development of kernicterus. The kernicterus is probably the result of an increased rate of destruction of red blood cells, which in turn is brought about by a precipitous drop in the GSH ** content of the erythrocytes, as Zinkham has shown in *in vitro* studies [1]. The exact mechanism whereby vitamin K_3 produces this effect is not known.

It has been noted by others, and recently shown at this laboratory [2] that vitamin K_3, when incubated with red blood cells, hemolysates, or a solution of crystalline Hb, induces a rapid formation of MeHb. Vitamin K_1 does not share this effect of K_3, nor does vitamin K_1 lead to hemolytic disease in the newborn.

* On study leave from the Research Institute of the Hospital for Sick Children, Toronto, Canada.

** Abbreviations: GSH, reduced glutathione; Hb, hemoglobin; MeHb, methemoglobin; TPNH, reduced triphosphopyridine nucleotide.

Table 1. Oxidation of GSH by MeHb. Incubation at 37°C with constant shaking in tubes open to air. Final concentrations: NaCl 0.077 M; phosphate buffer, pH 7.4, 0.05 M, MeHb and GSH indicated. Total volume, 2 ml/tube.

Series No.		Initial concentration mM	MeHb reduced or GSH oxidized, μmoles/2 ml incubate 0 h	1 h	2 h	3 h
1	MeHb	2.0	0	0.40	0.88	1.0
	GSH	1.0	0	1.07	1.62	1.63
2	MeHb	2.0	0	1.32	1.68	—
	GSH	2.0	0	2.23	3.55	—
3	MeHb	2.0	0	1.96	2.72	2.50
	GSH	5.0	0	3.00	4.48	5.76

With this information on hand it seemed of interest to investigate whether MeHb may play an intermediary role in the loss of erythrocyte GHS, brought about by vitamin K_3.

In the first series of experiments red blood cells from freshly obtained and defibrinated adult human blood were used. The red cells were washed three times and incubated in Krebs-Ringer-phosphate solution (approx. 40 % hematocrit) at 37°C in open tubes with constant shaking. At periodic intervals aliquots were removed for the simultaneous determination of GSH and MeHb contents. GSH was determined by the method of Grunert and Phillips [3]. The relative amounts of MeHb were assessed in samples diluted with distilled water, by measuring the optical density at 630 and 700 mμ, before and after

Table 2. Interaction between GSH, Hb and vitamin K_3-bisulfite. Incubation at 37°C with constant shaking in tubes open to air. Final concentrations: NaCl, 0.077 M; phosphate buffer, pH 7.4, 0.05 M; GSH, 1 mM; and when indicated: Hb 3.6 mM = 6.2 gm %, K_3bisulfite, 0.33 mM. Total volume, 2 ml/tube.

Additions	0 h MeHb	0 h GSH	1 h MeHb	1 h GSH	2 h MeHb	2 h GSH	3 h MeHb	3 h GSH
	μmoles/2 ml incubation mixture							
GSH	—	2.0	—	2.0	—	1.6	—	1.4
GSH + Hb	0	1.8	0	1.9	0	1.5	0	1.6
GSH + K_3bisulfite	—	1.8	—	1.8	—	1.5	—	1.4
GSH + Hb + K_3bisulfite	0	1.8	2.9	1.2	4.6	0.8	5.5	0.6

the addition of an excess of potassium ferricyanide.

During 4 h of incubation of the washed cells, without addition of substrate, the GSH levels in the cells remained constant and formation of MeHb was not observed. When vitamin K_3bisulfite (final concentration 0.33 mM) was added, considerable amounts of MeHb were formed and the level of GSH fell to 30 % of the original. Addition of glucose in 6 mM final concentration prevented the fall of GSH level, and lessened, but did not entirely abolish, the formation of MeHb. These findings confirm some of the observations made by Zinkham [1]; moreover they prove that, in addition to its detrimental effect on GSH, vitamin K_3 bisulfite induces the formation of MeHb as well.

It has been found by others that GSH can be oxidized by simple chemical interaction with MeHb [4]. It seemed that this reaction could be one way by which vitamin K_3 could bring about loss of GSH. Experiments were carried out to explore this possibility. These consisted of incubating vitamin K_3bisulfite, GSH, Hb and MeHb in various combinations and concentrations under the conditions specified in Tables 1 and 2. The Hb solution used in these experiments was prepared according to Beutler [5], but the use of toluene was avoided, and hemolysis without undue dilution was effected by rapid freezing and thawing of the washed cells three times. MeHb was prepared by adding to the Hb solution twice the equivalent amount of solid potassium ferricyanide, followed by dialysis against large volumes of distilled water. GSH and MeHb were determined as specified above.

When GSH, in 1 mM concentration, was incubated without any addition, during 3 h the GSH concentration declined only slightly, probably due to oxidation by atmospheric oxygen. The addition of 0.33 or 3.3 mM vitamin K_3bisulfite did not lead to an acceleration of the slow autooxidation of GSH. When MeHb in 2 mM (3.4 mg %) concentration was incubated with three different concentrations of GSH, and without addition of vitamin K_3bisulfite, GSH was rapidly oxidized and MeHb was reduced (Table 1). The expected stoichiometric relation of 2 moles of GSH oxidized by 1 mole of MeHb is supported by these data. The rate of the reaction was found to depend on the concentration of both MeHb and GSH, according to first order kinetics.

Further experiments were carried out to observe the interaction between vitamin K_3bisulfite, Hb and GSH. In Table 2 it can be seen that the addition of either one of Hb or vitamin K_3bisulfite to GSH did not accelerate the slow rate of autoxidation of GSH. Furthermore, when Hb was incubated in the presence of GSH, no MeHb was formed. However, when GSH was incubated in the presence of both Hb and vitamin K_3bisulfite, MeHb formation occurred and simultaneously the rate of oxidation of GSH was definitely increased. During 3 h of incubation, 76 % of the added Hb was oxidized and 66 % of the GSH was lost.

Another possible route by which formation of MeHb induced by vitamin K_3 may lead to glutathione instability in the red blood cell was also investigated. One may suppose that the accumulation of MeHb may lead to drainage of the existing stores of TPNH *via* the TPNH dependent MeHb reductase. Under these conditions it may be difficult for the exclusively TPNH dependent glutathione reductase to maintain glutathione in the reduced state and the GSH levels may decrease as a consequence. To explore this possibility experimental conditions were chosen to observe the effect of active intracellular MeHb reduction on the ability to maintain high levels of GSH in the erythrocyte. By exposing washed adult red blood cells to trace amounts of amylnitrite according to the method of Gibson [6], 40–50 % of the total Hb was oxidized to MeHb. When these cells, after washing, were suspended in physiological saline containing 0.01 M phosphate buffer (pH 7.4) and incubated without the addition of substrate, the amount of preformed MeHb remained constant. The GSH levels, which were reduced somewhat by the pretreatment with amylnitrite, remained also constant during the subsequent 4 h of incubation. Addition of glucose (final concentration 10 mM) led to a gradual reduction of the preformed MeHb in the cells, disposing of about 50 % of the MeHb in 4 h. This process was markedly enhanced by further addition of catalytic amounts of methylene blue (final concentration 0.01 mM), the MeHb virtually disappearing from the cells at the end of merely 1 h of incubation. Under the latter two conditions, however, and especially when glucose and methylene blue were added together, and when there was an extremely rapid reduction of MeHb, the GSH levels did not decrease but remained stable. This suggests that at least under these experimental conditions the drainage of the TPNH stores by the MeHb reductase did not influence the maintenance of the reduced state of glutathione.

The results of these studies suggest that the formation of MeHb may play an intermediary role in the oxidation of GSH in erythrocytes exposed to vitamin K_3bisulfite.

It seems likely that this mechanism consists of direct chemical interaction between MeHb and GSH. In order to reconcile the present tentative conclusions with the often emphasized fact that methemoglobinemia and glutathione instability are not necessarily correlated *in vivo* [7], it will be necessary to investigate more closely the mechanisms which, in the intact cell, may protect GSH from the oxidizing effect of MeHb, or may be able to replenish the losses of GSH effectively. It may well be that ultimately it will depend on the effectiveness or failure of these mechanisms whether an increased rate of formation of MeHb will lead to actual loss of GSH.

1. Zinkham, W. H. *Pediatrics* **22** (1959) 18.
2. Broberger, O., Ernster, L. and Zetterström, R. *Nature* **188** (1960) 316.
3. Grunert, R. R. and Phillips, P. H. *Arch. Biochem.* **30** (1951) 217.
4. Eggleton, P. and Fegler, G. *Quart. J. Exptl. Physiol.* **37** (1952) 163.
5. Beutler, E., Robson, M. and Buttenwieser, E. *J. Clin Invest.* **36** (1957) 617.
6. Gibson, Q. H. *Biochem. J.* **42** (1948) 13.
7. Beutler, E. *Blood* **14** (1959) 103.

Isolation of β-Fructofuranosidase from Yeast by Ion Exchange Chromatography on Diethylaminoethylcellulose

Bjørn Andersen

Universitetets fysisk-kemiske Institut, Copenhagen, Denmark

The mechanism of the splitting of sucrose into α-D-glucopyranose and β-D-fructofuranose by invertase from yeast has been investigated by numerous workers. This has given rise to a great number of papers describing purification procedures of the enzyme. One of the most successful is that of Fischer and Kohtes [1], which using precipitation with picric acid and acetone, followed by adsorption to $Al(OH)_3$ obtained a preparation containing 4–5 % N with an activity of 4 000 units/mg N.

The development of cellulose derivatives for separation of proteins by ion exchange chromatography [2,3] has opened new possibilities for a further purification of the enzyme.

In the present work the β-fructofuranosidase from yeast has been separated on a N,N-diethylaminoethylcellulose (DEAE) column. The starting material was »Invertan.K.B.» (commercial invertase preparation, manufactured by De forenede Bryggerier, Copenhagen.) After dialysis against distilled water at 4°C for 24 h the solution was added to the column, previously equilibrated with 0.005 M phosphate buffer, pH 6.5. Eluation was made with increasing concentrations of sodium chloride (0–0.25 M). A sharp separation was obtained between the active component and the other proteins in the solution. After freeze-drying the nitrogen content was determined to give a value of 11.02 %. The enzyme activity was determined according to a method described in a previous publication [4]. Converted to the units of Fisher and Kohtes the activity was 22 000 units/mg N to be compared with the 4 000 units/mg N obtained by these authors. Electrophoresis, which at the present time has only been carried out at one pH, indicates one single protein component. Determination of the molecular weight at the optimal pH (4.75), using the osmometer designed by Christiansen and Jensen [5] gave the value 116 000. Calculation of the enzyme activity as number of substrate molecules reacting per min per molecule of enzyme gives a value of 260 000.

A more detailed description of the isolation will be given.

1. Fischer, E. H. and Kohtes, L. *Helv. Chim. Acta* **34** (1951) 1123.
2. Sober, H. A. and Petterson, E. A. *J. Am. Chem. Soc.* **76** (1954) 1711.
3. Petterson, E. A. and Sober, H. A. *J. Am. Chem. Soc.* **78** (1956) 751.
4. Andersen, B. and Bak, T. A. *Acta Chem. Scand. In press.*
5. Christiansen, J. A. and Jensen, C. E. *Acta Chem. Scand.* **7** (1953) 1247.

It seems likely that this mechanism consists of direct chemical interaction between MeHb and GSH. In order to reconcile the present tentative conclusions with the often emphasized fact that methemoglobinemia and glutathione instability are not necessarily correlated *in vivo* [7], it will be necessary to investigate more closely the mechanisms which, in the intact cell, may protect GSH from the oxidizing effect of MeHb, or may be able to replenish the losses of GSH effectively. It may well be that ultimately it will depend on the effectiveness or failure of these mechanisms whether an increased rate of formation of MeHb will lead to actual loss of GSH.

1. Zinkham, W. H. *Pediatrics* **22** (1959) 18.
2. Broberger, O., Ernster, L. and Zetterström, R. *Nature* **188** (1960) 316.
3. Grunert, R. R. and Phillips, P. H. *Arch. Biochem.* **30** (1951) 217.
4. Eggleton, P. and Fegler, G. *Quart. J. Exptl. Physiol.* **37** (1952) 163.
5. Beutler, E., Robson, M. and Buttenwieser, E. *J. Clin Invest.* **36** (1957) 617.
6. Gibson, Q. H. *Biochem. J.* **42** (1948) 13.
7. Beutler, E. *Blood* **14** (1959) 103.

Isolation of β-Fructofuranosidase from Yeast by Ion Exchange Chromatography on Diethylaminoethylcellulose

Bjørn Andersen

Universitetets fysisk-kemiske Institut, Copenhagen, Denmark

The mechanism of the splitting of sucrose into α-D-glucopyranose and β-D-fructofuranose by invertase from yeast has been investigated by numerous workers. This has given rise to a great number of papers describing purification procedures of the enzyme. One of the most successful is that of Fischer and Kohtes [1], which using precipitation with picric acid and acetone, followed by adsorption to $Al(OH)_3$ obtained a preparation containing 4–5 % N with an activity of 4 000 units/mg N.

The development of cellulose derivatives for separation of proteins by ion exchange chromatography [2,3] has opened new possibilities for a further purification of the enzyme.

In the present work the β-fructofuranosidase from yeast has been separated on a N,N-diethylaminoethylcellulose (DEAE) column. The starting material was »Invertan.K.B.» (commercial invertase preparation, manufactured by De forenede Bryggerier, Copenhagen.) After dialysis against distilled water at 4°C for 24 h the solution was added to the column, previously equilibrated with 0.005 M phosphate buffer, pH 6.5. Eluation was made with increasing concentrations of sodium chloride (0–0.25 M). A sharp separation was obtained between the active component and the other proteins in the solution. After freeze-drying the nitrogen content was determined to give a value of 11.02 %. The enzyme activity was determined according to a method described in a previous publication [4]. Converted to the units of Fisher and Kohtes the activity was 22 000 units/mg N to be compared with the 4 000 units/mg N obtained by these authors. Electrophoresis, which at the present time has only been carried out at one pH, indicates one single protein component. Determination of the molecular weight at the optimal pH (4.75), using the osmometer designed by Christiansen and Jensen [5] gave the value 116 000. Calculation of the enzyme activity as number of substrate molecules reacting per min per molecule of enzyme gives a value of 260 000.

A more detailed description of the isolation will be given.

1. Fischer, E. H. and Kohtes, L. *Helv. Chim. Acta* **34** (1951) 1123.
2. Sober, H. A. and Petterson, E. A. *J. Am. Chem. Soc.* **76** (1954) 1711.
3. Petterson, E. A. and Sober, H. A. *J. Am. Chem. Soc.* **78** (1956) 751.
4. Andersen, B. and Bak, T. A. *Acta Chem. Scand. In press.*
5. Christiansen, J. A. and Jensen, C. E. *Acta Chem. Scand.* **7** (1953) 1247.

A Study of the Effect of Amytal on the Respiration of Rat Liver Slices

B. Kadenbach*, T. E. Conover** and L. Ernster

Wenner-Gren Institute, University of Stockholm, Stockholm, Sweden

It has been reported [1] that rat liver slices, incubated for 1 h in a Krebs-Ringer solution containing glucose, exhibit an oxygen uptake which is resistant to amytal (5-ethyl-5-*iso*amyl-barbituric acid) to an extent of about 40 %. Closer examination of this amytal-resistant respiration has now revealed that it is characterized by a declining initial phase, lasting about 20—30 min., during which its rate drops from about 60 to 20 % of the control rate, followed by a second stationary phase where the respiration remains constant at about 20 % of the control rate over a period of at least 1 h. Omission of glucose and/or addition of α-ketoglutarate, malate, glutamate, lactate and glycerol-1-phosphate increased the respiration with and without amytal (Table 1). Addition of the glycolytic inhibitors, iodoacetate or fluoride, both of which strongly depressed the control rate, had little effect on the level of the amytal-resistant respiration. Addition of succinate caused, in agreement with earlier literature [2], about a ten fold increase of the respiratory rate, and this respiration was entirely amytal-insensitive. This finding is consistent with the concept [3] that succinate is oxidized by an amytal-insensitive oxidase.

Added DPN or TPN caused about an equal, 50—100 % stimulation of the control respiratory rate both in the absence of added substrate and in the presence of added glucose or the previously mentioned pyridine nucleotide-linked substrates. The two pyridine nucleotides differed, however, with respect to their effect on the amytal-resistant respiration, this being stimulated more by TPN than by DPN. Moreover DPN and TPN added together stimulated the amytal-resistant respiration by more than the sum of the individual stimulations. These effects were apparent only on the stationary, and not the initial, phase of the amytal-resistant respiration. It would therefore seem that while the initial phase of the amytal resistant respiration probably originates from some endogenous substrate which is not continuously formed during incubation, the constant respiration phase is due to substrates which are continuously available, and part of which, at least, appear to be oxidized by way of TPN. The glucose-6-phosphate dehydrogenase shunt would seem to be a likely reaction of this type. That added DPN, in combination with TPN, further increases the amytal-resistant respiratory rate, may be due to the stimulation of a pyridine nucleotide transhydrogenase mechanism, conceivably through the mediation of lactic dehydrogenase [4].

It has been of interest also to establish whether the recently described DT diaphorase [5] is involved in the amytal-resistant respiration. This enzyme can mediate electron transport between both intra- and extramitochondrial [6] DPNH and TPNH and the cytochrome system

Table 1. Effect of added substrates and pyridine nucleotides on the amytal-resistant respiration of rat liver slices. 80 to 120 mg of liver slices (20 mg with succinate) were incubated for 1 h at 37.5°C in Krebs-Ringer-phosphate solution (half Ca^{++} conc.) with 100 % O_2 as gas phase. Final volume, 1 ml; final concentrations of the additions were: glucose, α-ketoglutarate and malate, 0.025 M; glycerol-1-phosphate, lactate, glutamate and succinate, 0.05 M; amytal, 0.002 M.

Expt. No.	Additions	μatoms oxygen/60 min./100 mg wet weight without amytal	with amytal
1	none	4.57	2.39
	glucose	4.11	1.84
2	none	4.51	1.82
	α-ketoglutarate	6.12	4.30
	malate	5.36	2.49
3	none	4.21	1.53
	glutamate	7.15	2.28
	succinate	55.4	60.5
4	none	6.07	7.71
	lactate	8.90	3.71
	glycerol-1-phosph.	7.37	4.48
5	glucose	3.98	2.10
	glucose + DPN	5.58	3.16
	glucose + TPN	5.65	3.70
	gluc. + DPN + TPN	7.85	7.90

* Fellow of the Deutsche Akademie der Wissenschaften zu Berlin, Germany.

** Fellow of the National Foundation, New York, N.Y., U.S.A.

Table 2. Dicoumarol-sensitive respiration of rat liver slices. Conditions as in Table 1. Final concentrations of the additions were: glucose, 0.05 M; iodoacetate, 0.2 mM; amytal 2 mM; vitamin K_3-bisulfite, 0.005 mM; citrate, 0.025 M; TPN, 0.001 M; dicoumarol, 0.005 mM. The system was preincubated for 20 min in the presence of all additions except amytal. The values give the respiration obtained during 48 min following the addition of amytal.

Additions	μatoms oxygen/100 mg wet weight without dicoumarol	with dicoumarol	% inhibition
none	1.79	2.43	−39
vitamin K_3-bisulfite	1.31	1.53	−19
citrate	2.46	1.72	30
citrate + vit. K_3-bis.	4.06	2.46	39
citrate + vit. K_3-bis. + TPN	7.88	4.61	41

of isolated mitochondria in an amytal-insensitive way provided that a catalytic amount of vitamin K_3 is added. To investigate this possibility, the sensitivity of the respiration to dicoumarol was tested, since it has been shown that DT diaphorase is highly sensitive to this agent [7]. It was found that 5×10^{-6}M dicoumarol, which completely inhibits DT diaphorase, had no effect on the respiration under any of the above conditions, either in the absence or in the presence of added vitamin K_3, and occasionally it even caused a slight stimulation probably due to release of the respiratory control. It was found (Table 2), however, that preincubation of the slices for 20 min. in the presence of iodoacetate in order to exhaust glycolytic intermediates, and subsequent incubation with added citrate, resulted in an increased amytal-resistant respiration which now was inhibited by 5×10^{-6}M dicoumarol to about 30 %. Moreover, addition of vitamin K_3 or of vitamin K_3 and TPN both of which further increased the amytal-resistant respiratory rate, also increased its dicoumarol sensitivity in an absolute as well as relative fashion. These findings are preliminarily interpreted to indicate that the DT diaphorase apparently takes no major part in the normal respiration of the liver cell, but may act as an alternative pathway of TPNH (and DPNH) oxidation, which can be made manifest experimentally by suppressing more efficient pathways. The main interest of these findings may lie in the fact that a dicoumarol-sensitive respiration, *i.e.* a DT diaphorase reaction, has been demonstrated in these conditions to function in the intact liver cell even without supplementation with vitamin K_3.

This work has been supported by a grant from the Swedish Cancer Society.

1. Ernster, L. *Biochem. Soc. Symposia, Cambridge, Engl.* **16** (1959) 54.
2. Kidd, J. G., Winzler, R. J. and Burk, D. *Cancer Research* **4** (1944) 547.
3. Ernster, L., Jalling, O., Löw, H. and Lindberg, O. *Exptl. Cell Research Suppl.* **3** (1955) 124.
4. Navazio, F., Ernster, B. B. and Ernster, L. *Biochim. et Biophys. Acta* **26** (1957) 416.
5. Ernster, L., Ljunggren, M. and Danielson, L. *Biochem. Biophys. Research Comm.* **2** (1960) 88.
6. Conover, T. E. and Ernster, L. *Acta Chem. Scand.* **14** (1960) 1840.
7. Conover, T. E. and Ernster, L. *Biochem. Biophys. Research Comm.* **2** (1960) 26.

ACTA CHEMICA SCANDINAVICA 14 (1960) 1852–1866

Short Communications

Totarolone, a New Diterpene Ketophenol from *Tetraclinis articulata* *

YUAN-LANG CHOW and HOLGER ERDTMAN

Organisk-kemiska Institutionen, Kungl. Tekniska Högskolan, Stockholm, Sweden

A mixture of two new ketones, totarolone and totarolenone, has recently been isolated from the heartwood extract of *Tetraclinis articulata* (Vahl, Masters).[1] Hydrogenation of the mixture over Pd/C in ethanol gave pure totarolone, $C_{20}H_{28}O_2$, m.p. 188–189°, $[\alpha]_D$ + 102°. The empirical composition, the U.V. absorption of totarolone [λ_{max}] 208 mμ (ε 37 700), 281 (1 900), and 286 (1 900)] and the I.R. absorption [3 380, 1 685 (1 705 in CCl_4), 1 590, and 810 cm^{-1}] suggests that totarolone is a new diterpene ketophenol containing a keto group that is not conjugated with the aromatic ring. This is supported by the physical properties of totarolone acetate, $C_{22}H_{30}O_3$, m.p. 113–115°, $[\alpha]_D$ + 96.6° ν_{max} at 1 755, 1 704 and 1 210 cm^{-1}, λ_{max} 207 mμ (ε 5 600), 266 (470).

Totarolone, now shown to be Ia, gave on Clemmensen reduction a good yield of totarol [2] (IIIa). Reduction of totarolone with potassium borohydride gave a diol, totaradiol (IIIb), $C_{20}H_{30}O_2$, m.p. 100–102°, $[\alpha]_D$ + 38.5°, ν_{max} 3 610, 1 002 and 3 380 cm^{-1}. Acetylation (pyridine-acetic anhydride) furnished a diacetate (IIIc): $C_{24}H_{34}O_4$, $[\alpha]_D$ + 41°, ν_{max} 1 766 and 1 725 cm^{-1}. The molecular rotation shift between totaradiol and its diacetate, m.p. 120–122°, $\Delta[M]_D$ + 43° is very similar to that between hinokiol (IIa) and its diacetate (IIb) $\Delta[M]_D$ + 47° [3] suggesting that the environments of the assymetric centres are similar in both cases. Confirmation of structure Ia for totarolcne was obtained as follows.

Totarolone benzyl ether, m.p. 169–171°, (Ib) was reduced with lithium aluminium hydride to totaradiol benzyl ether, (IIId) m.p. $C_{27}H_{36}O_2$, 192–193°, ν_{max} 3 420, 1 032, and 1 264 cm^{-1}. The ether (IIId) was treated successively with phosphorus pentachloride, osmium tetroxide and lead tetraacetate as recently described for hinokiol [3]; acetone and the trisnor-ketone (IV), ν_{max} (in CCl_4) at 1 740 and 1 260 cm^{-1}, [2,4-dinitrophenylhydrazone (amorphous), $C_{30}H_{32}O_5N_4$, λ_{max} 363 mμ (ε 20 200)] were obtained. The optical rotatory dispersion curve of IV was very similar to that of a 5β-A-norsteroid [4] indicating that inversion had occurred at C_5 during the reactions [5].

Furthermore the large positive Cotton effect shown by totarolone (and also by hinokione) is similar to that shown by lanost-8-en-3-one [6]. The A/B ring junction in totarolone, and consequently that in totarol, must therefore possess the conventional steroid absolute configuration, namely 5α,10β. The correctness of this assignment was also demonstrated by a direct correlation of totarol with dehydroabietic acid *etc.* in the following manner. Ozonisation, or better chromic acid oxidation, of totarol acetate (IIIe) gave 7-keto-totarol acetate (V), $C_{22}H_{30}O_3$, m.p. 169–170°, λ_{max} at 213 mμ (ε 23 900), 252 (8 100), and 297 (2 600), ν_{max} at 1 758 and 1 676 cm^{-1}, $[\alpha]_D$ + 43.3° (in $CHCl_3$). Successive treatment of V with trifluoroperacetic acid, ozone and alkaline hydrogen peroxide afforded the dicarboxylic acid VI [7], m.p. 160–163° (identified by mixed

* This research was sponsored in part by the *Office of Research and Development, U.S. Army Department*, through its European Office. Part of this investigation was first presented during "Svenska kemistdagarna", Stockholm, June 9–11, 1960. (*Svensk Kem. Tidskr.* **72** (1960) 602).

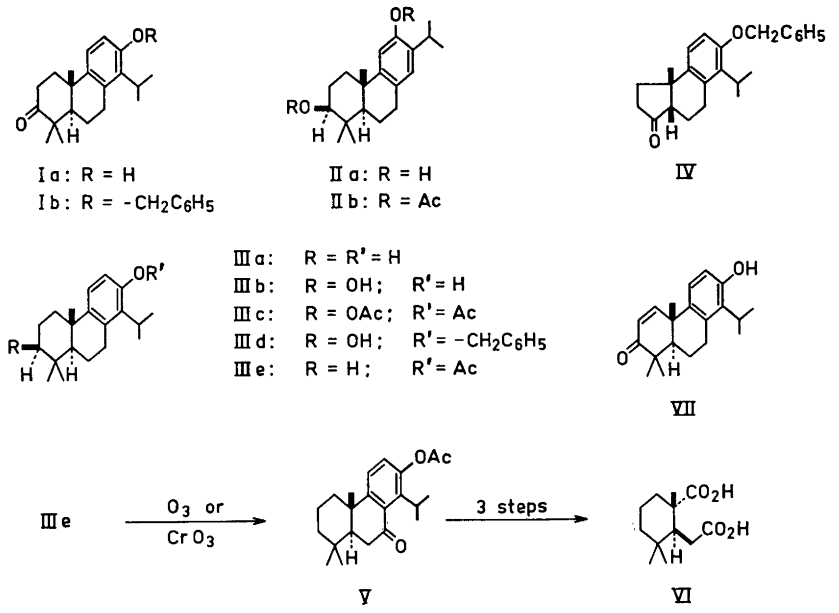

melting point and its I.R. spectrum). A racemic totarolone methyl ether having the structure I (R = CH_3) has recently been synthesised by Taylor [8] and its I.R. spectrum was shown to be identical with that of the methyl ether of the natural product (m.p. 98—100°).

Since the original mixture of totarolone and totarolenone has a U.V. absorption at 223 mμ and an I.R. band at 1 652 cm^{-1} in addition to those of totarolone, it follows that the unisolated totarolenone must be 1,2-di-dehydrototarolone (VII).

Infrared spectra were taken in KBr discs and optical rotations in ethanol unless otherwise specified. All ultraviolet spectra were taken in ethanol solution. Satisfactory analyses were obtained for all the compounds described. We thank Dr. W. Klyne for the rotatory dispersion data and valuable discussions and Professor O. Jeger for an authentic specimen of the dicarboxylic acid VI.

1. Work done in this laboratory. To be published shortly.
2. Simonsen, L. and Barton, D. H. R. *The Terpenes*, Vol. III, p. 358. Cambridge University Press 1952; Barltrop, J. A. and Rogers, N. A. J. *J. Chem. Soc.* **1958** 2566.
3. Chow, Y. L. and Erdtman, H. *Proc. Chem. Soc.* **1960** 174.
4. Djerassi, C., Riniker, R. and Riniker, B. *J. Am. Chem. Soc. 78* (1956) 6362.
5. Baddeley, G. V., Halsall, T. G. and Jones, E. R. H. *J. Chem. Soc.* **1960** 1715.
6. Djerassi, C., Halpern, O., Halpern, V. and Riniker, B. *J. Am. Chem. Soc.* **80** (1958) 4001; Djerassi, C., Osiecki, J. and Closson, W. *Ibid.* **81** (1959) 4587.
7. Shaffner, K., Viterbo, R., Arigoni, B. and Jeger, O. *Helv. Chem. Acta* **39** (1956) 174.
8. Taylor, D. A. H. University College, Ibadan, Nigeria. *Private communication.*

Received October 8, 1960.

Studies on Peroxy Compounds

IX *. The Introduction of Alkoxy Groups into Tetrahydrofuran

SVEN-OLOW LAWESSON and
CURT BERGLUND

Department of Organic Chemistry, Chemical Institute, University of Uppsala, Uppsala, Sweden

When *t*-butyl perbenzoate is decomposed in the presence of various types of substrates such as olefins [1,2], benzyl ethers [3], benzyl sulphides [4], simple ethers and sulphides [5] (catalytic amounts of cuprous salt being present) according to a method first described by Kharasch and Sosnovsky [1], the benzoyloxy group is introduced without rearrangement, fragmentation, dimerization or isomerisation of the substrate. No oxidation occurs when the substrate is a sulphide. In the case of tetrahydrofuran, tetrahydropyran and di-*n*-butyl ether, however, the *α*-*t*-butoxy compounds [6,7] are obtained. It is most probable that the benzoyloxy compounds are first formed, which revert to the *t*-butoxy compound, since we have found [5] that when the benzoyloxy compound I is heated under mild conditions with *t*-butanol, the *t*-butoxy compound II is formed.

The sulphur analogue III, however, gives an *α*,*β*-unsaturated sulphide IV [5] when heated with or without *t*-butanol.

* Part VIII: See Ref.[5]

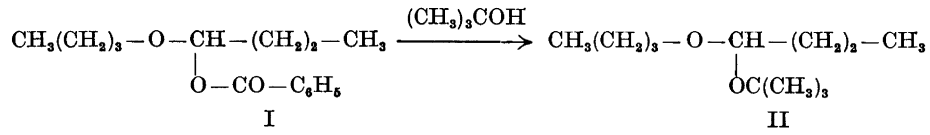

I II

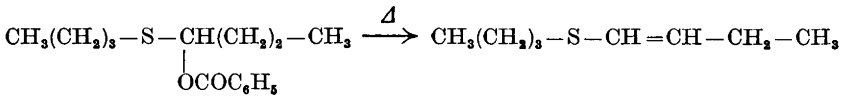

III IV

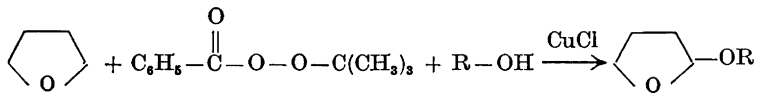

V

V a: C_2H_5
V b: i-C_3H_7
V c: t-C_4H_9
V d: n-C_6H_{13}

Product	Yield %	B.p. (°C)	mm Hg	n_D^{20}	Formula	Carbon, %		Hydrogen, %	
						Calc.	Found	Calc.	Found
V a	31	125	760	1.4149	$C_6H_{12}O_2$	62.04	62.05	10.41	10.50
V b	35	132	760	1.4147	$C_7H_{14}O_2$	64.58	64.37	10.84	10.89
V c	51	140–141*	760	1.4193					
V d	36	87–88	10	1.4330	$C_{10}H_{20}O_2$	69.72	69.59	11.70	11.74

* by a mistake the boiling point was said to be 127°/760 mm Hg in an earlier paper [7].

In further studies of the reaction between *t*-butyl perbenzoate and cyclic ethers and sulphides, we found, that if an alcohol (R—OH) is added to the substrate (tetrahydrofuran) before carrying out the reaction with *t*-butyl perbenzoate in the usual way, the alkoxy compound V is formed.

Yields cited are based on one series of experiment only and are not considered to be the maximum obtainable. A more detailed paper [8] on this subject will be published in the near future.

Financial support from *Magnus Bergwalls stiftelse* is acknowledged.

1. Kharasch, M. S. and Sosnovsky, G. *J. Am. Chem. Soc.* **80** (1958) 756.
2. Kharasch, M. S., Sosnovsky, G. and Yang, N. C. *J. Am. Chem. Soc.* **81** (1959) 5819.
3. Lawesson, S.-O. and Berglund, C. *Arkiv Kemi* **16** (1960) 287.
4. Lawesson, S.-O. and Berglund, C. *Acta Chem. Scand.* **14** (1960) *In press.*
5. Lawesson, S.-O., Berglund, C. and Grönwall, S. *Acta Chem. Scand.* **15** (1961) *In press.*
6. Sosnovsky, G. *J. Org. Chem.* **25** (1960) 874.
7. Lawesson, S.-O., Berglund, C. and Grönwall, S. *Acta Chem. Scand.* **14** (1960) 944.
8. Lawesson, S.-O. and Berglund, C. *To be* published.

Received October 6, 1960.

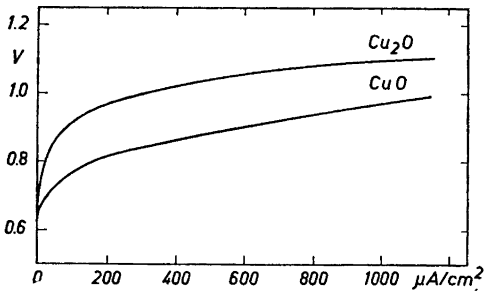

Fig. 1. Reduction potential of the two copper oxides, measured against an Ag—AgCl electrode in 0.1 M KOH, as a function of the current density.

Analysis of Oxide Films on Copper by Coulometric Reduction

A. RÖNNQUIST

Institute of Chemistry, University of Uppsala, Sweden

Several methods have been used for analysing oxide films on copper [1]. The most attractive features of the coulometric method, originally developed by Evans and Bannister [2] and by Miley [3,4], are its high sensitivity and the possibility of determining both cuprous and cupric oxide in the same run. When determining the two oxides the choice of a suitable electrolyte is important. Campbell and Thomas [5] pointed out that since copper oxide will dissolve in ammonium chloride, there is a possibility of error in earlier determinations made with NH_4Cl as electrolyte. KCl does not have this disadvantage, but it usually fails to give separation of the two oxides. Later Mills [6] suggested a phosphate buffer of pH 6.9 as a suitable electrolyte for separate determinations of the two oxides. To improve the coulometric method Lambert and Trevoy [7] recently demonstrated the importance of the complete elimination of dissolved oxygen and also of plateable cations from the electrolyte. This can be achieved by pre-electrolysis. The present paper demonstrates the possibility of using KOH (0.1 M) as electrolyte in the analysis

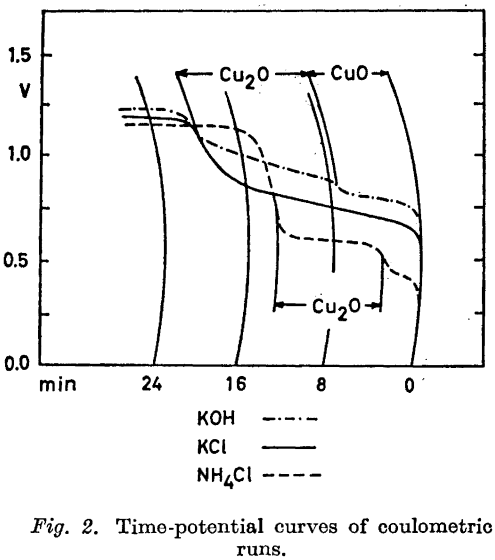

Fig. 2. Time-potential curves of coulometric runs.

In further studies of the reaction between *t*-butyl perbenzoate and cyclic ethers and sulphides, we found, that if an alcohol (R—OH) is added to the substrate (tetrahydrofuran) before carrying out the reaction with *t*-butyl perbenzoate in the usual way, the alkoxy compound V is formed.

Yields cited are based on one series of experiment only and are not considered to be the maximum obtainable. A more detailed paper [8] on this subject will be published in the near future.

Financial support from *Magnus Bergwalls stiftelse* is acknowledged.

1. Kharasch, M. S. and Sosnovsky, G. *J. Am. Chem. Soc.* **80** (1958) 756.
2. Kharasch, M. S., Sosnovsky, G. and Yang, N. C. *J. Am. Chem. Soc.* **81** (1959) 5819.
3. Lawesson, S.-O. and Berglund, C. *Arkiv Kemi* **16** (1960) 287.
4. Lawesson, S.-O. and Berglund, C. *Acta Chem. Scand.* **14** (1960) *In press.*
5. Lawesson, S.-O., Berglund, C. and Grönwall, S. *Acta Chem. Scand.* **15** (1961) *In press.*
6. Sosnovsky, G. *J. Org. Chem.* **25** (1960) 874.
7. Lawesson, S.-O., Berglund, C. and Grönwall, S. *Acta Chem. Scand.* **14** (1960) 944.
8. Lawesson, S.-O. and Berglund, C. *To be* published.

Received October 6, 1960.

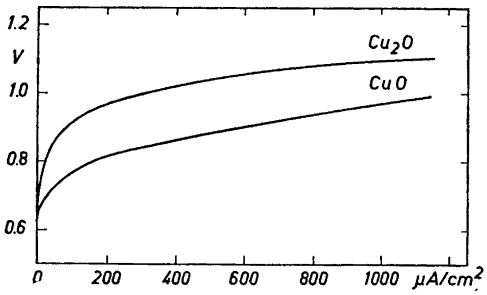

Fig. 1. Reduction potential of the two copper oxides, measured against an Ag—AgCl electrode in 0.1 M KOH, as a function of the current density.

Analysis of Oxide Films on Copper by Coulometric Reduction

A. RÖNNQUIST

Institute of Chemistry, University of Uppsala, Sweden

Several methods have been used for analysing oxide films on copper [1]. The most attractive features of the coulometric method, originally developed by Evans and Bannister [2] and by Miley [3,4], are its high sensitivity and the possibility of determining both cuprous and cupric oxide in the same run. When determining the two oxides the choice of a suitable electrolyte is important. Campbell and Thomas [5] pointed out that since copper oxide will dissolve in ammonium chloride, there is a possibility of error in earlier determinations made with NH_4Cl as electrolyte. KCl does not have this disadvantage, but it usually fails to give separation of the two oxides. Later Mills [6] suggested a phosphate buffer of pH 6.9 as a suitable electrolyte for separate determinations of the two oxides. To improve the coulometric method Lambert and Trevoy [7] recently demonstrated the importance of the complete elimination of dissolved oxygen and also of plateable cations from the electrolyte. This can be achieved by pre-electrolysis. The present paper demonstrates the possibility of using KOH (0.1 M) as electrolyte in the analysis

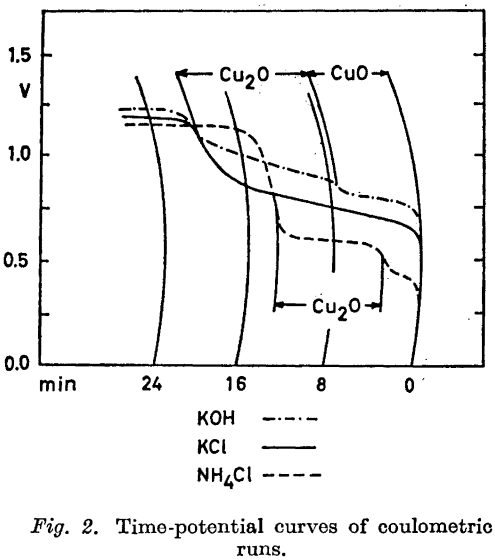

Fig. 2. Time-potential curves of coulometric runs.

Table 1.

Electrolyte	Cu_2O $\mu g/cm^2$	CuO $\mu g/cm^2$	Cu_2O+CuO $\mu g/cm^2$
KCl	—	—	51
NH_4Cl	29	10	39
KOH	37	15	52

of oxide films on copper. The use of this electrolyte has been developed during studies of morphological and kinetic phenomena in the oxidation of copper.

When KCl is used as the electrolyte, the difference between the potentials at which CuO and Cu_2O are reduced is very small and varies with the density of the reducing current. Because of this small difference potassium chloride usually fails to give separation of the two oxides. When KOH is used, the potential difference is independent of the current density and large enough to give separation in a coulometric run. Fig. 1 shows the potential at which the two oxides are reduced in KOH, measured against an Ag—AgCl electrode, as a function of the current density.

To demonstrate the possibility of using KOH as the electrolyte, the following experiment was carried out. A copper wire was mechanically polished and oxidized for one minute at 560°. The wire was then cut into three equal lengths. The amount of oxide on each part was coulometrically determined using NH_4Cl, KCl and KOH, respectively, as the electrolytes. The current density was the same in all three cases (670 $\mu A/cm^2$). The electrolytes were all cleaned by bubbling oxygen-free nitrogen through them. Oxygen was removed from the nitrogen in the usual manner with pyrogallol and a solution of chrome (II) ions. The time-potential curves for the three runs are given in Fig 2.

With KCl only one potential plateau appeared. With KOH and NH_4Cl two plateaus were obtained, indicating the presence of the two oxides. The time for complete reduction is equal in the cases of KCl and KOH, but when using NH_4Cl it becomes shorter because of dissolution of the two oxides. Table 1 gives the amount of oxide determined in the different electrolytes.

A special examination of the dissolution of the two oxides in KOH has been made. Samples of cuprous and cupric oxide powders (supplied by May and Baker Co. Ltd) were left in contact for one month with KOH of molarities 0.05, 0.1, 0.3, and 0.5. A determination of dissolved copper was then made by complexometric titration [8]. The result of the titrations showed that CuO does not dissolve. No dissolution of Cu_2O could be observed in KOH of molarities 0.05 and 0.1. In solutions of molarities 0.3 and 0.5 the amounts of dissolved cuprous oxide were determined to be less than 2.4 and 7.2 mg/100 ml, respectively. It is seen that within the normal duration of a coulometric analysis, no dissolution is to be expected.

Conclusions. The solubility of cuprous and cupric oxide in 0.1 M KOH is small enough to be neglected in this instance. The difference between the potentials at which the two oxides are reduced is nearly constant and independent of the current density. These properties make KOH (0.1 M) a possible electrolyte in the analysis of oxide films on copper.

Acknowledgements. I wish to thank Professor G. Hägg for his interest in this work and for the facilities placed at my disposal. Thanks are also due to Dr. L. H. Andersson for suggesting the method of titration and to Dr. H. Fischmeister and Dr. J. Drott for stimulating discussions. The work has been supported by a grant from the *Swedish Natural Science* and *Technical Research Councils.*

1. Rönnquist, A. and Fischmeister, H. *J. Inst. Metals.* **89** (1960—61) 65.
2. Evans, U. R. and Bannister, L. C. *Proc. Roy. Soc. London* **A125** (1929) 370.
3. Miley, H. A. *Carnegie School. Memoirs (Iron and Steel Inst.)* **25** (1936) 197.
4. Dyess, J. B. and Miley, H. A. *Trans. AIMME* **133** (1939) 239.
5. Campbell, W. E. and Thomas, U. B. *Trans. Electrochem. Soc.* **76** (1939) 303.
6. Mills, T. and Evans, U. R. *J. Chem. Soc.* **1956** 2182.
7. Lambert, R. H. and Trevoy, D. J. *J. Electrochem. Soc.* **105** (1958) 8.
8. Schwarzenbach, G. *Die chemische Analyse* **45** (1955) 68.

Received October 13, 1960.

Sorption of Organic Vapours in Organic Ion Exchanging Substances

TORBJÖRN WESTERMARK

Division of Physical Chemistry, The Royal Institute of Technology, Stockholm 70, Sweden

When it was shown that the transmission properties of beta particles through layers of matter possessing sorption properties (*e.g.* towards vapours) could be used to study these processes [1] (kinetics, equilibria), the author tried to find illustrative examples of how the method might be applied. Some of these examples have been published [1] but some others have not. Some of them concern the sorption properties of ion exchangers. The observations made were not pursued systematically but, as nothing similar has apparently been given in the literature, two short notes will be given. The present note concerns the sorption of organic vapours in ion exchanging materials. Another note will deal with water sorption kinetics.

Ion exchanging substances containing typical functional groups, *e.g.* SO_3^-, COOH, NH_2, *etc.*, can to our present knowledge be considered to react within their whole volume at least for small ions (*cf.* Kunin and Myers [2]) in the liquid phase. It was therefore judged likely that they would have a very high "inner surface" (in about the same sense as is used for, *e.g.*, activated charcoal) and consequently be able to sorb polar molecules to a great extent, for example, when exposed to gases.

Simple experiments to test this idea were made by bubbling dry nitrogen from a tank tube through wash-bottles containing some organic liquids at room temperature. The gas stream (a few ml/sec) thereby becomes saturated (or very nearly so) and thus the sorption figures given correspond to the vapour pressure at room temperature under these conditions. Table 1 summarizes the observed percentage weight increase of the material when apparent equilibrium was reached.

Table 1. Equilbrium sorption of some organic vapours in ion exchangers at 21°C. The ion exchange material was present in a glass tube in grain form (50—100 Mesh) and was nearly dry at the beginning of the experiment.

Ion exchanger	Vapour	Percent weight increase referred to dry material
Wofatite KS—Na	Diethylether	15
» »	Methanol	21
Dowex 50-H	*n*-Butanol	43.1
» »	Benzene	4.7

From these few observations, it is indicated that the hydrophilic substances (*e.g.* the alcohols) are sorbed to a greater extent than a less hydrophilic one (*e.g.* benzene). It might from this evidence be assumed that ion-dipole interaction plays a role in the sorption process.

The sorption rate was interpreted in terms of spherical diffusion which gives as is well known [3]:

$$F = 1 - \frac{6}{\pi^2} \sum_{n=1}^{\infty} \frac{1}{n^2} \exp\left(-\frac{n^2 \pi^2 D}{\gamma_0^2} t\right)$$

where D is the diffusion coefficient of the organic molecule within the ion exchanger grains, t time, γ_0 grain radius and F fractional attainment of equilibrium.

The results are in rough accordance with this formula which is valid if the diffusion is rate-determining. The diffusion coefficient for benzene is about 12×10^{-10} cm²/sec and, for n—C_4H_9OH, 6×10^{-10} cm²/sec according to these estimates in Dowex 50-H. It was demonstrated that the sorption processes mentioned could be easily followed by beta ray transmission.

It might be added that it has been found in this laboratory that molecular iodine (as fission product ^{131}I) is readily sorbed [4] from the gas phase on an anion exchanger Dowex 2.

Obviously it would be of interest to study sorption equilibria and kinetics systematically for different types of ion exchangers. The sorption properties of ion exchangers normally used in liquid systems might find applications in certain cases. It might well be possible to use these pro-

perties for some vapour chromatographic purposes.

1. Westermark, T. *Some Applications of Beta Radiation. Transactions, Instruments and Measurements Conference, Stockholm* 1949, p. 308–314.
2. Kunin, R. and Myers, R. J. *Ion Exchange Resins*, John Wiley 1950 (Ch. 2).
3. *Cf. e.g.* Boyd, G. E., Adamson, A. W. and Myers, L. S. *J. Am. Chem. Soc.* **69** (1947) 2836.
4. Forberg, S., Westermark, T. and Holmquist, C.-E. *Sorption of fission product iodine from air on different materials with applications to nuclear reactor accidents (in course of publication).*

Received October 18, 1960.

Note on the Sorption Rate of Water Vapour in Almost Dry Ion Exchangers

TORBJÖRN WESTERMARK

Division of Physical Chemistry, The Royal Institute of Technology, Stockholm 70, Sweden

This note will draw attention to some aspects of the sorption rate of water vapour in organic cation exchangers. The results were obtained when the beta ray transmission technique was used to follow (*in situ*) the sorption properties of various solids towards vapours [1]. Another note describes the sorption of organic vapours by organic cation exchangers [2]. It was shown that the sorption rate and attainment of equilibrium could be easily followed by measuring the transmission of a pencil of ^{32}P beta rays through a flat cell of the type described (in Ref.[1]) filled with the grainy ion exchange material. Such studies are nowadays facilitated by stable vibration-reed-electrometers and rapid recorders. The data presented below, however, have been obtained using ordinary weighing procedures.

The experiments were performed using several organic cation exchangers but the main efforts were concentrated on Dowex 50, 50–100 mesh grain size. The material was treated according to standard practice with 3 N HCl until every trace of three-valent iron had been eluted. The resin was then transferred to the forms required by eluting with an excess of simple inorganic electrolytes in a pure form and containing the cation wanted, *e.g.* $Ca(NO_3)_2$, $RbNO_3$, *etc.* After complete expulsion of the acidic ions, the resin was treated with distilled water, transferred to weighed glass vessels and then carefully dried by successively heating until constant weight was obtained (highest temperature 105°C). A similar procedure was used with other cations to yield Dowex 50 in the following ionic forms: H^+, Rb^+, Cs^+, H_4N^+, $(CH_3)_4N^+$, Be^{2+}, Mg^{2+}, Sr^{2+}, Ba^{2+}, Cu^{2+}, Zn^{2+}, Cd^{2+}, Pb^{2+}, Ce^{3+}, Fe^{2+}, Fe^{3+} and UO_2^{2+}.

Vessels containing a certain cation form of Dowex 50 were placed in air of a definite humidity. This was accomplished by using standard electrolytic solutions giving, after equilibrium, well-known relative humidities [3].

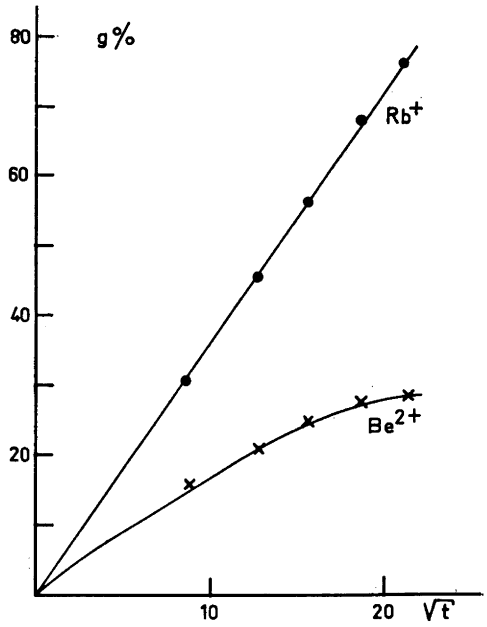

Fig. 1. Fractional attainment of equilibrium (g, in %) for water sorption on Dowex 50-Me as a function of $\sqrt{t}$ (t in min). The two cases of Me = Rb^+ and Be^{2+} are seen to behave somewhat differently.

perties for some vapour chromatographic purposes.

1. Westermark, T. *Some Applications of Beta Radiation. Transactions, Instruments and Measurements Conference, Stockholm* 1949, p. 308–314.
2. Kunin, R. and Myers, R. J. *Ion Exchange Resins*, John Wiley 1950 (Ch. 2).
3. *Cf. e.g.* Boyd, G. E., Adamson, A. W. and Myers, L. S. *J. Am. Chem. Soc.* **69** (1947) 2836.
4. Forberg, S., Westermark, T. and Holmquist, C.-E. *Sorption of fission product iodine from air on different materials with applications to nuclear reactor accidents (in course of publication).*

Received October 18, 1960.

Note on the Sorption Rate of Water Vapour in Almost Dry Ion Exchangers

TORBJÖRN WESTERMARK

Division of Physical Chemistry, The Royal Institute of Technology, Stockholm 70, Sweden

This note will draw attention to some aspects of the sorption rate of water vapour in organic cation exchangers. The results were obtained when the beta ray transmission technique was used to follow (*in situ*) the sorption properties of various solids towards vapours [1]. Another note describes the sorption of organic vapours by organic cation exchangers [2]. It was shown that the sorption rate and attainment of equilibrium could be easily followed by measuring the transmission of a pencil of ^{32}P beta rays through a flat cell of the type described (in Ref.[1]) filled with the grainy ion exchange material. Such studies are nowadays facilitated by stable vibration-reed-electrometers and rapid recorders. The data presented below, however, have been obtained using ordinary weighing procedures.

The experiments were performed using several organic cation exchangers but the main efforts were concentrated on Dowex 50, 50–100 mesh grain size. The material was treated according to standard practice with 3 N HCl until every trace of three-valent iron had been eluted. The resin was then transferred to the forms required by eluting with an excess of simple inorganic electrolytes in a pure form and containing the cation wanted, *e.g.* $Ca(NO_3)_2$, $RbNO_3$, *etc.* After complete expulsion of the acidic ions, the resin was treated with distilled water, transferred to weighed glass vessels and then carefully dried by successively heating until constant weight was obtained (highest temperature 105°C). A similar procedure was used with other cations to yield Dowex 50 in the following ionic forms: H^+, Rb^+, Cs^+, H_4N^+, $(CH_3)_4N^+$, Be^{2+}, Mg^{2+}, Sr^{2+}, Ba^{2+}, Cu^{2+}, Zn^{2+}, Cd^{2+}, Pb^{2+}, Ce^{3+}, Fe^{2+}, Fe^{3+} and UO_2^{2+}.

Vessels containing a certain cation form of Dowex 50 were placed in air of a definite humidity. This was accomplished by using standard electrolytic solutions giving, after equilibrium, well-known relative humidities [3].

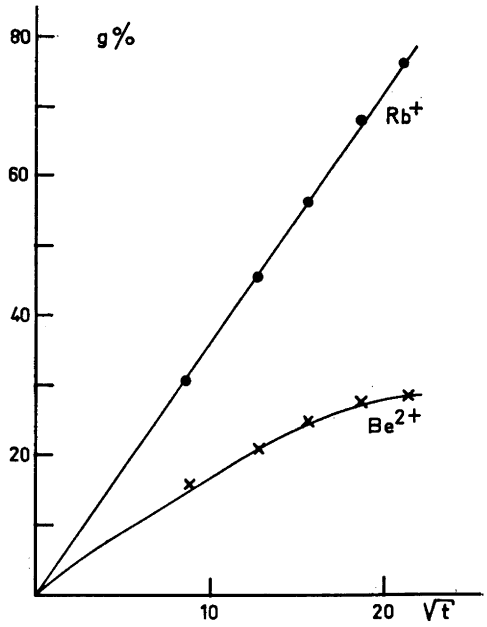

Fig. 1. Fractional attainment of equilibrium (g, in %) for water sorption on Dowex 50-Me as a function of $\sqrt{t}$ (t in min). The two cases of Me = Rb^+ and Be^{2+} are seen to behave somewhat differently.

The increase in weight was found as a function of time at a single temperature (23° ± 1) until apparent equilibrium was reached at a certain relative humidity (RH). Then a new step to a higher RH was taken and the resulting kinetics and equilibrium were studied. RH up to 90 % were studied. Especially at these high RH, equilibrium took a long time — up to two weeks — to become established.

The weight increase at a certain RH was divided by the final equilibrium weight increase under the same conditions in order to yield the "fractional attainment of equilibrium", g[4]. The g-value did not follow any definite function of time. In some cases (especially for the alkali cations) it followed the wellknown $\sqrt{t}$-behaviour. Fig. 1 illustrates this behaviour for Dowex 50—Rb^+. In the same figure, another extreme is represented by Dowex 50—Be^{2+}. The best (but not exact) description was given by the known relation:

$$g = 1 - \frac{6}{\pi^2} \sum_{n=1}^{\infty} \frac{1}{n^2} \exp\left(-\frac{D\pi^2 n^2 t}{r_0^2}\right) \quad (1)$$

This equation was theoretically derived [5] for the case of diffusion controlled sorption into spherical grains of radius, r_0. (D is the diffusion coefficient of water in the material). Various factors seem to cause deviations from the conditions for which (1) was derived. One is certainly that the grain radius, r_0, increases during sorption. Microscopic examination revealed a very rapid increase of r_0 at the beginning of the exposure to water vapour followed by a slower one. (The grain diameter was found to increase with the ionic volume of the cation.) Some of the originally almost spherical grains became cracked (probably during drying) and thus many were only hemispheres.

For the above reasons, the evaluation of a diffusion coefficient from (1) for all the materials investigated would not correspond to reality. Therefore we simply take the g-value after a certain time for all the materials and represent this as a function of some cation property.

The most interesting behaviour is got by studying the kinetics of the step from the dry state to the state corresponding to RH 8.7 %. The sorption of water at equilibrium at this RH does not correspond to more than 10 % (for H^+) of the weight of the ion exchanger material. Usually about 5 % is obtained and so the regain at

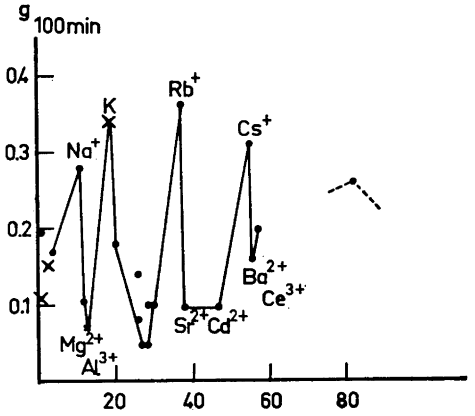

Fig. 2. g-Value for 100 min sorption of water at 8.7 % relative humidity starting from dry material. The g-value, as given as a function of the atomic number of the cation of the Dowex 50, exhibits a periodical character. (Points not explained are H^+ and Li^+ at the left end, and then after K^+, Ca^{2+}, Fe^{3+} (highest), Fe^{2+}, Co^{2+}, Ni^{2+}, Cu^{2+}, Zn^{2+}. Points to the right are Pb^{2+} and UO_2^{2+}).

equilibrium corresponds to a state of less than one water molecule per monomer unit (assumed to be (—CH_2-CH- 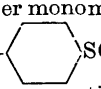 $SO_3Me)_n$.

Thus we are justified in expecting the individuality of the different cations to appear under these conditions.

Fig. 2 shows the fractional attainment (g) figures (for 100 min sorption from the dry state) as a function of the atomic number of the counter ions of the ion exchanger. It is seen that a periodic function is obtained which to some extent resembles the behaviour of, *e.g.*, the atomic volume [6]. If similar studies are made for the steps involving higher RH's, the individuality of the cations disappears almost completely and the kinetics are nearly identical for all materials studied. Adsorption isoterms were obtained for the materials (and for other types of cation exchangers) but resemble those published by Gluechauf [7] and others and will therefore not be presented here.

Although too little systematic material is available, we feel justified in suggesting that the initial hydration is a dipole-ion interaction involving the cation of the ion

exchanger (and also the sulphonic acid anion).

A complete description of the sorption rate might necessarily involve the interaction energy for the process considered as an activation energy for the diffusion coefficient. If so, a larger ion would exhibit a smaller activation energy and hence a larger sorption rate (or diffusion coefficient). The results of Fig. 2 could then be reasonably connected with the periodicity of the atomic volumes. As for the latter, the ion charge must also be taken into account. Among the alkalis, the sorption rate increases with increasing (crystallographic) ion volume in accordance with the above picture. Unfortunately, the result for $Z > 45$, was obtained with a different batch of Dowex 50 and so no conclusions can be drawn from the result for cesium. The complete description might also contain entropy factors. These are apparently not known for the systems studied here. Following the picture given above it is reasonable that, under wetter conditions, the sorbing water molecules would mainly interact with water already sorbed, thus roughly explaining why the individuality of the counter ions disappears in such a case.

A more complete study of these phenomena would seem to be of interest. The temperature dependence of the sorption rate might give a clue for the interpretation of the interaction mechanism suggested.

1. Westermark, T. *Some applications of beta radiation, Transactions of Instruments and Measurements*, Stockholm 1949, p. 308.
2. Westermark, T. *Acta Chem. Scand.* **14** (1960) 0000.
3. *Handbook of Physics and Chemistry*, 41st Ed. 1959–60, Chemical Rubber Publishing Co, p. 2499 ff.
4. Boyd, G. E., Adamson, A. W. and Myers, L. S. *J. Am. Chem. Soc.* **69** (1947) 2836.
5. Barrer, R. M. *Diffusion in and through solids*. Cambridge University Press 1941, Ch. 1.
6. *Cf. e.g.* Moelwyn-Huges, E. A. *Physical Chemistry*, Cambridge University Press 1947, p. 233, Fig. 1.
7. Gluechauf, E. *Endeavour*, **10** (1951) No. 37.

Received October 18, 1960.

Sheet Ion Exchangers as Resistance Gauges for Moisture in Gases

TORBJÖRN WESTERMARK

Division of Physical Chemistry, The Royal Institute of Technology, Stockholm 70, Sweden

The sulphonation of sheets, rods, tubes or any shape of solid polystyrene yields a thin layer of polystyrene sulphonic acid [1], a well-known cation exchange material. Many other ways of forming a sheet ion exchanger are possible [1] or conceivable.

It has been found that the electrical resistance of this material is a good measure of the relative humidity in air. The ion exchange groups may be saturated by Na^+-ions for instance, so that the moisture detector is less likely to be affected by materials sorbed from the gas which may cause precipitation *etc.* The ion exchange layer of course is a hydrophilic substance, the moisture content of which is a function of the water partial pressure in the surrounding gas if equilibrium prevails. The conductance of the sheet ion exchanger will increase with increasing moisture content and so the resistance of an exchanger unit will be an appropriate measure of the moisture content. At constant temperature, it will after calibration with standard salt solutions [2] be a good moisture detector. Changing the temperature of course changes both the equilibrium conditions and conductance and must be corrected for by recalibration.

Practical exchanger units can be made by simply clamping two platinum electrodes on a sulphonated piece of polystyrene or better by winding a double spiral on a sulphonated (sodium ion-saturated) rod or hole cylinder using two wires of platinum (stainless steel was found to corrode in the long run), the wires being separated by about 0.5 mm or so. The wires should be long in order to reduce the resistance.

A typical calibration curve is given in Fig. 1. At decreasing humidities, the resistance increases steadily; at very low figures, the resistance may be impractically high. The resistance is preferably measured at 1 000 Hz to avoid polarization phenomena at the electrodes. Such effects were often obtained when DC was used. Any of the common electrical circuits can be used

exchanger (and also the sulphonic acid anion).

A complete description of the sorption rate might necessarily involve the interaction energy for the process considered as an activation energy for the diffusion coefficient. If so, a larger ion would exhibit a smaller activation energy and hence a larger sorption rate (or diffusion coefficient). The results of Fig. 2 could then be reasonably connected with the periodicity of the atomic volumes. As for the latter, the ion charge must also be taken into account. Among the alkalis, the sorption rate increases with increasing (crystallographic) ion volume in accordance with the above picture. Unfortunately, the result for $Z > 45$, was obtained with a different batch of Dowex 50 and so no conclusions can be drawn from the result for cesium. The complete description might also contain entropy factors. These are apparently not known for the systems studied here. Following the picture given above it is reasonable that, under wetter conditions, the sorbing water molecules would mainly interact with water already sorbed, thus roughly explaining why the individuality of the counter ions disappears in such a case.

A more complete study of these phenomena would seem to be of interest. The temperature dependence of the sorption rate might give a clue for the interpretation of the interaction mechanism suggested.

1. Westermark, T. *Some applications of beta radiation, Transactions of Instruments and Measurements*, Stockholm 1949, p. 308.
2. Westermark, T. *Acta Chem. Scand.* **14** (1960) 0000.
3. *Handbook of Physics and Chemistry*, 41st Ed. 1959–60, Chemical Rubber Publishing Co, p. 2499 ff.
4. Boyd, G. E., Adamson, A. W. and Myers, L. S. *J. Am. Chem. Soc.* **69** (1947) 2836.
5. Barrer, R. M. *Diffusion in and through solids*. Cambridge University Press 1941, Ch. 1.
6. *Cf. e.g.* Moelwyn-Huges, E. A. *Physical Chemistry*, Cambridge University Press 1947, p. 233, Fig. 1.
7. Gluechauf, E. *Endeavour*, **10** (1951) No. 37.

Received October 18, 1960.

Sheet Ion Exchangers as Resistance Gauges for Moisture in Gases

TORBJÖRN WESTERMARK

Division of Physical Chemistry, The Royal Institute of Technology, Stockholm 70, Sweden

The sulphonation of sheets, rods, tubes or any shape of solid polystyrene yields a thin layer of polystyrene sulphonic acid [1], a well-known cation exchange material. Many other ways of forming a sheet ion exchanger are possible [1] or conceivable.

It has been found that the electrical resistance of this material is a good measure of the relative humidity in air. The ion exchange groups may be saturated by Na^+-ions for instance, so that the moisture detector is less likely to be affected by materials sorbed from the gas which may cause precipitation *etc.* The ion exchange layer of course is a hydrophilic substance, the moisture content of which is a function of the water partial pressure in the surrounding gas if equilibrium prevails. The conductance of the sheet ion exchanger will increase with increasing moisture content and so the resistance of an exchanger unit will be an appropriate measure of the moisture content. At constant temperature, it will after calibration with standard salt solutions [2] be a good moisture detector. Changing the temperature of course changes both the equilibrium conditions and conductance and must be corrected for by recalibration.

Practical exchanger units can be made by simply clamping two platinum electrodes on a sulphonated piece of polystyrene or better by winding a double spiral on a sulphonated (sodium ion-saturated) rod or hole cylinder using two wires of platinum (stainless steel was found to corrode in the long run), the wires being separated by about 0.5 mm or so. The wires should be long in order to reduce the resistance.

A typical calibration curve is given in Fig. 1. At decreasing humidities, the resistance increases steadily; at very low figures, the resistance may be impractically high. The resistance is preferably measured at 1 000 Hz to avoid polarization phenomena at the electrodes. Such effects were often obtained when DC was used. Any of the common electrical circuits can be used

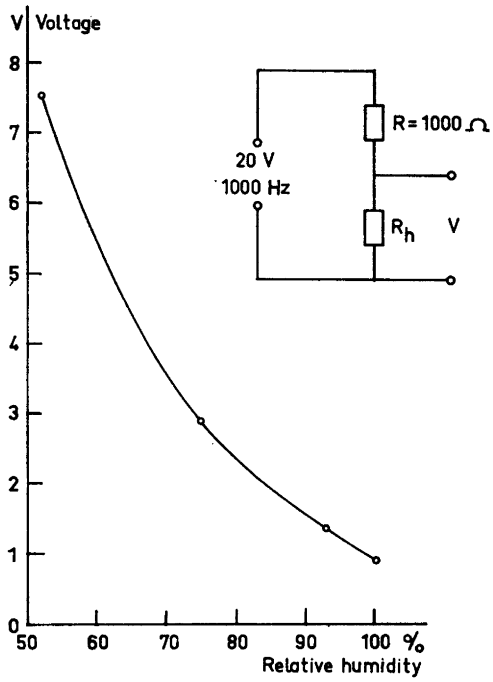

Fig. 1. Typical calibration curve of sheet ion exchanger resistance hygrometer. The voltage, V, is measured (at equilibrium) across the variable hygrometer resistance, R_h, with an electronic voltmeter in the circuit as indicated. The hygrometer is placed in a closed glass vessel, the relative humidity of which is varied by using standard salt solutions. The temperatur was 25° ± 0.1.

including AC bridges, simple volt-ampère coupling, or cross-coil instruments.

The unit responds quickly to changes in humidity. The rate is probably governed by the diffusion of water in the layer and thus the latter should be thin (a few microns). Units responding in a few seconds can be produced.

A special point for the possible use of this method for meteorological purposes is that pure water can be condensed or poured on the unit and the calibration will still be valid after evaporation and subsequent equilibration. This property is hardly provided by such hygrometers that are based on the impregnation of glass with lithium salts or phosphoric acid.

The units can be made very small and might be applicable in cavities difficult to reach with other hygrometers.

Obviously, the calibration curve will change if another cation is used. The study of the resistance properties and water diffusion kinetics would themselves be an interesting field of study.

A draw-back of the method is that some hysteresis effects have been detected when travelling along a resistance-humidity curve. The effect was not found to exceed what corresponds to 2 % RH. Another draw-back is that, if thicker layers of sheet ion exchangers are wanted, they are difficult to prepare from commercial polystyrene apparently due to the very low, or quite absent, cross-linkage and to mechanical cracking of the hydrophilic material formed on the polymer blocks or sheets. ¡It seems that this disadvantage could now be overcome by a moderate dose of ionizing radiation (*e.g.* by ^{60}Co γ-rays) which is known to introduce cross-linking [3]. This would be expected to improve the mechanical stability but might at the same time decrease the swelling of the ion-exchanger and hence somewhat decrease the sensitivity of the hygrometer.

This hygrometer is an example of the application of ion exchangers for quite a different use than the usual one. There is a commercial unit which has properties very similar to the present unit (which has been used since 1953 in this laboratory) but, from the pamphlets [4] supplied, it was not possible to see whether the ideas and the materials are the same or not. The applications should comprise a lot of cases of interest in the laboratory and elsewhere. A special case is the dry-boxes used for radioactive or moisture-sensitive materials. We have not attempted any extended systematic studies of the design of this hygrometer. It is therefore likely that anyone interested can find useful modifications and improvements of the description given above.

Valuable discussions and encouragement of Eng. S. Almberg of AB Billmanregulator, Stockholm, is greatly acknowledged. Eng. L.E. Lundh assisted in taking the data of Fig. 1.

1. Westermark, T. *Acta Chem. Scand.* **6** (1952) 1194.
2. See *e.g., Handbook of Physics and Chemistry*, 41st Ed. 1959–60. Chemical Rubber Publishing Co., p. 2499 f.

3. Bovey, F. A. *The Effects of Ionizing Radiation on Natural and Synthetic High Polymers.* Interscience Publishers, New York 1958, p. 120 f.f.
4. *Electronics Inc., Philadelphia, USA. Technical Bulletins* N:o 2, pp 102, 103 and 201.

Received October 18, 1960.

The Structure of Arsenobenzene

SVEND ERIK RASMUSSEN and JACOB DANIELSEN

Department of Inorganic Chemistry, University of Aarhus, Aarhus, Denmark

Arsenobenzene is generally formulated as: 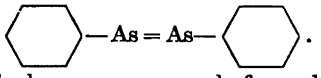 . Double bonds, however, are rarely formed between atoms heavier than oxygen.

Lyon and Mann [1] have previously cast some doubt upon the validity of the classical formula on the basis of molecular weight determinations but no satisfactory structure of the molecule has so far been proposed.

In order to obtain a satisfactory molecular formula we are investigating the crystal structure of arsenobenzene. The compound was obtained by the reduction of phenyl arsonic acid. Two different kinds of crystals can be recognised under the polarizing microscope. One kind forms transparent needle shaped crystals which exhibit parallel extinction and are optically biaxial. The other kind of crystals are a little opaque and show oblique extinction. The transparent ones become opaque between 182°C and 192°C and melt at 196°C. The opaque crystals melt at 196°C. We have not yet proved that the transparent crystals are changed to the opaque form by heating but it appears to be likely. Chemical analysis on the mixture give the following results: C 47.60; H 3.37; calc. for $(AsC_6H_5)_n$: C 47.40; H 3.32.

Weissenberg and precession photographs proved the transparent crystals to be monoclinic. Filtered Cu-radiation was employed. The unit cell has the following dimensions, unique axis *b*, the needle axis:

$$a = 24.04 \text{ Å}$$
$$b = 6.20 \text{ Å}$$
$$c = 12.22 \text{ Å}$$
$$\beta = 111.2°$$

The following extinctions were found: $h0l$ for $h = 2n + 1$ and $0k0$ for $k = 2n + 1$. Hence the space group is $P2_1/a$. The density of the crystal is 1.73. Consequently there are 12 $As-C_6H_5$ groups in the unit cell. As the general point is four fold the $As-C_6H_5$ groups must be linked together in groups of three or of six.

The Patterson projection along the *b*-axis indicated very strongly that the molecular unit contains six arsenic atoms forming a non planar ring with a centre of symmetry. A Fourier projection based upon the As-coordinates reveals the whereabouts of the benzene rings.

On this basis we propose that arsenobenzene is $(AsC_6H_5)_6$. Each As-atom forms two single As—As bonds (approximately 2.4 Å) with its neighbours in the ring and a third As—C bond. Isomers of different conformations are possible. The opaque crystals are triclinic. They will be investigated in more detail later.

A refinement of the structure of the monolinic crystals is in progress.

1. Lyon, D. R. and Mann, F. G. *J. Chem. Soc.* **1945** 30.

Received October 13, 1960.

3. Bovey, F. A. *The Effects of Ionizing Radiation on Natural and Synthetic High Polymers.* Interscience Publishers, New York 1958, p. 120 f.f.
4. *Electronics Inc., Philadelphia, USA. Technical Bulletins* N:o 2, pp 102, 103 and 201.

Received October 18, 1960.

The Structure of Arsenobenzene

SVEND ERIK RASMUSSEN and JACOB DANIELSEN

Department of Inorganic Chemistry, University of Aarhus, Aarhus, Denmark

Arsenobenzene is generally formulated as: 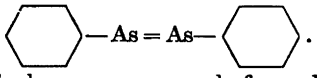 . Double bonds, however, are rarely formed between atoms heavier than oxygen.

Lyon and Mann [1] have previously cast some doubt upon the validity of the classical formula on the basis of molecular weight determinations but no satisfactory structure of the molecule has so far been proposed.

In order to obtain a satisfactory molecular formula we are investigating the crystal structure of arsenobenzene. The compound was obtained by the reduction of phenyl arsonic acid. Two different kinds of crystals can be recognised under the polarizing microscope. One kind forms transparent needle shaped crystals which exhibit parallel extinction and are optically biaxial. The other kind of crystals are a little opaque and show oblique extinction. The transparent ones become opaque between 182°C and 192°C and melt at 196°C. The opaque crystals melt at 196°C. We have not yet proved that the transparent crystals are changed to the opaque form by heating but it appears to be likely. Chemical analysis on the mixture give the following results: C 47.60; H 3.37; calc. for $(AsC_6H_5)_n$: C 47.40; H 3.32.

Weissenberg and precession photographs proved the transparent crystals to be monoclinic. Filtered Cu-radiation was employed. The unit cell has the following dimensions, unique axis *b*, the needle axis:

$$a = 24.04 \text{ Å}$$
$$b = 6.20 \text{ Å}$$
$$c = 12.22 \text{ Å}$$
$$\beta = 111.2°$$

The following extinctions were found: $h0l$ for $h = 2n + 1$ and $0k0$ for $k = 2n + 1$. Hence the space group is $P2_1/a$. The density of the crystal is 1.73. Consequently there are 12 $As-C_6H_5$ groups in the unit cell. As the general point is four fold the $As-C_6H_5$ groups must be linked together in groups of three or of six.

The Patterson projection along the *b*-axis indicated very strongly that the molecular unit contains six arsenic atoms forming a non planar ring with a centre of symmetry. A Fourier projection based upon the As-coordinates reveals the whereabouts of the benzene rings.

On this basis we propose that arsenobenzene is $(AsC_6H_5)_6$. Each As-atom forms two single As—As bonds (approximately 2.4 Å) with its neighbours in the ring and a third As—C bond. Isomers of different conformations are possible. The opaque crystals are triclinic. They will be investigated in more detail later.

A refinement of the structure of the monolinic crystals is in progress.

1. Lyon, D. R. and Mann, F. G. *J. Chem. Soc.* **1945** 30.

Received October 13, 1960.

Note on the Development of Methods for Studying the Polymerisation of Styrene and Acrylonitrile by Positive Gaseous Ions

T. WESTERMARK, L. WESTFELT, H. LINDROTH and N. GHANEM

Division of Physical Chemistry, The Royal Institute of Technology, Stockholm 70, Sweden

It has been argued that positive gaseous ions, due to their very high electron affinity, act radiation-like and are thereby capable of breaking covalent chemical bonds. Accordingly these ions might be assumed to be precursors to reactive entities characteristic for radiation chemistry, *e.g.* free radicals. Thus, upon bringing positive gaseous ions into contact with liquids containing monomers, one would expect polymerisation to occur. It is thought that the polymerisation produced by ionizing radiations proceed in some cases *via* free radicals and in other cases (often at low temperatures) *via* ionic species [2,3].

We have developed methods for studying the polymerisation of styrene and acrylonitrile by positive gaseous ions. For styrene, some postive evidence has been found. It seems, however, that emphasis has to be placed primarily on the design of the apparatuses and the methods by which basic studies can be made. We shall discuss such points by referring to Fig. 1 which shows a modification of an apparatus developed for studies on aqueous solutions [4].

One of the main methodological problems is that the liquid phase has to be sufficiently conductive to allow the passage of unipolar charges through the system. For this purpose, one has to select solutions which contain some electrolyte, but the latter should be chosen so as not to inhibit the polymerisation too much. For styrene it was found possible, after performing the conventional extraction of inhibitors by means of a dilute NaOH solution, to add alcohol (about 25 %), water (about 1.3 %) and $CaCl_2$ (less than 0.1 %) to give a solution of sufficient conductivity. Due to these additions, the radiation chemical G-value is reduced — this can be elucidated by means of γ-ray induced polymerisations of samples of the solution. Using this solution in the apparatus of Fig. 1, it was found possible to achieve corona currents of some μA with helium flushing through the space over the section 1 of the apparatus. It was found possible to maintain stable conditions over a period of many days. The formation of polystyrene was detected by precipitating with methanol after cooling with ice.

For acrylonitrile the conductivity problem is easier since it is soluble in water. A distillation of the monomer under oxygen-free conditions served to remove inhibitors. Samples of the monomer were dissolved in distilled water which had been previously redistilled twice in a quartz apparatus. The solution was made 5 % in acrylonitrile and then 0.1 % in $CaCl_2$ in order to increase the conductivity sufficiently so as to allow currents of the order of some μA to be used. In addition, a radiation polymerisation by means of gamma rays was performed in the same way as that described by Dainton [5].

The helium gas used was 99.99 % pure, the possible impurities stated being N_2 0.01 %, O_2 0.0005 %, H_2 0.0005 %. The gas was purified using a 1 m tube containing granular copper * at 175°C. This removed traces of oxygen from the gas but not nitrogen. It is therefore possible that some charge transfer from helium to nitrogen may have taken place.

Positive evidence has been obtained with styrene but the yield was small. A clear turbidity in the contents from cell 1 was observed upon methanol treatment but nothing occurred in the samples from cells 2, 3 and 4. The yield was 0.2 mg and the total number of μAh was 34 as found by a recorder. The voltage used was $\sim$ 5kV and the current a few μA. The helium flow-rate was about 15 ml/min. The anode light was confined to the tungsten wire and no sparking was detected. Some difficulties due to alcohol evaporation were encountered in the experiments. This caused a

* We are indebted to Mr. F. Ericsson of the Inorganic Division of this Institute for the preparation of this purification column.

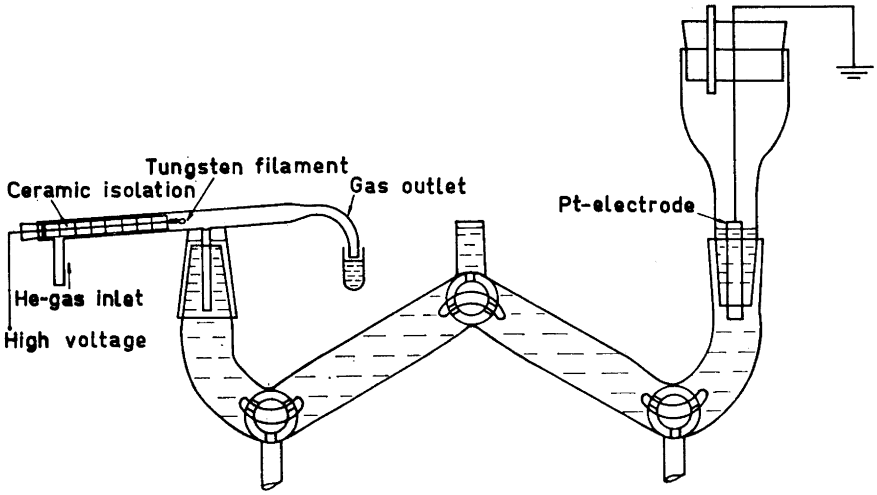

Fig. 1. Glass apparatus for positive gas ion production and performance of radiation-like polymerisation reactions. A series resistor of 100 Mohm is placed between H.T. generator (0—10 keV) and anode filament. The platinum cathode is connected to a current recording device. The left side of the apparatus is denoted cell 1, the next part cell 2 etc. The part on the right containing the platinum electrode is denoted cell 4.

gradual decrease in ion current due to the decrease in level. The molecular weight of the product is not known but, if it is assumed to be 100 000, we arrive at an M/N value (M total number of molecules produced, N total number of ions) of ~ 0.02.

It is hoped that further experiments with the methods described will contribute to an understanding of the initiation process involved in polymerisations of this type. Tye presence of OH groups in the polymers will be investigated using the method of Dainton [5] in order to prove or disprove the formation of OH-radicals by the positive ions.

1. Westermark, T. Gaseous ions as radiomimetic agents and their possible role in the ethiology of lung cancer. Paper presented before the *"Symposium on Chemical and Biological Problems Related to Smoking"*, May 2nd, 1960 in Stockholm.
2. Okamura, S. and Futami, S. *J. Appl. Rad. and Isotopes* **8** (1960) 46.
3. Chapiro, A. and Stannett, V. *J. Chem. Phys.* **57** (1960) 35.
4. Westermark, T. and Lindroth, H. An approach so the study of chemical reactions of gaseous ions in liquids and gels and some notes on their possible biological effects. To be published.
5. Dainton, F. S. *J. Phys. & Colloid. Chem.* **52** (1948) 490.

Received October 26, 1960.

Preparation of Carbon Isotopically Labelled Thiophenes

BØRGE BAK, JØRN CHRISTIANSEN, and JØRGEN TORMOD NIELSEN

Chemical Laboratory of the University of Copenhagen, Copenhagen, Denmark

As a pre-requisite for a complete determination of the structure of thiophene by microwave technique, enriched samples of 2-^{13}C- and 3-^{13}C-thiophene have been prepared. The methods given below were adopted after repeated experiments with non-labelled compounds. The purity of the resulting isotopically labelled samples was satisfactorily checked by controlling the vapor-pressure and by recording the infra-red absorption curves. Microwave lines from the ^{13}C-labelled species appeared with expected intensity. No lines from impurities were observed in the microwave region, but the infra-red spectra showed the presence of about 5 % CS_2.

Experimental. Preparation of 2-^{13}C-thiophene. Ethylene bromide (3.99 g, 0.0212 mole) and 2.90 g (0.0446 mole) of potassium cyanide, 22 % enriched in ^{13}C, were placed in a 50 ml glass ampulla with 5.2 ml of water and 10.5 ml ethanol. The ampulla was sealed-off under a high vacuum and heated for 3 h on a steam bath under occasional shaking, after which the contents were transferred to a small distilling flask. 10 ml of water and 20 ml of conc. hydrochloric acid was added. Water, ethanol and surplus halogen acids were removed by a slow distillation (1—2 h) at atmospheric pressure, the final temperature of the oilbath applied being 180°C. During this distillation the hydrolysis of the dicyanide is completed. The remainder was quantitatively transferred to a 1 l beaker by means of 200 ml water. 24 g crystalline $BaCl_2$ was added and dissolved. Also, 400 ml of ethanol were added. At this stage, minor quantities of solid impurities were filtered off. 6 ml conc. NH_4OH was added to the filtrate, hereby causing barium succinate (I) to precipitate. The yield was 4.46 g (0.0175 mole). Its purity was checked by comparing its infra-red spectrum (1 mg sample to 300 mg KBr, disk technique) with the spectrum of an authentic sample.

4.46 g (I) was transformed to sodium succinate (II) by adding 50 ml of water and 5.58 g of Na_2SO_4,10 H_2O (0.0174 mole). This mixture was shaken vigorously for 18 h, followed by removal of the $BaSO_4$-precipitate by filtering, whereafter the filtrate was evaporated to dryness. 2.84 g of (II) was obtained, its purity being checked as above. A completely dry sample is essential for the final transformation into thiophene.

2.84 g of (II) was thoroughly mixed with 13 g P_4S_6 (from P and S) [1] in a 50 ml reaction flask which could be heated and swept with dry N_2. The flask was immersed in a bath of 110°C and quickly heated to 300°C. At this temperature a gas mixture was evolved, carried off by the stream of N_2, and finally condensed in a liquid-air cooled trap. After 30 min. heating at 300—310°C the trapped, volatile products (*e.g.* H_2S) were removed by distillation *in vacuo*, the liquid-air bath being substituted by a dry-ice bath. The remainder was distilled *in vacuo* at room temperature into a fresh ampulla containing crushed NaOH pellets in order to retain mercaptanes, CS_2, *etc.* After one hour the liquid product was distilled *in vacuo* onto fresh NaOH, this time allowing for a contact period of 24 h. After a new distillation *in vacuo* the final product had the correct vapor-pressure (21.5 ± 0.5 mm at 0°C). The infra-red spectrum indicated about 95 % purity, a 5 % impurity apparently consisting entirely of CS_2. Since microwaves are not absorbed by CS_2 the purity was satisfactory for our purpose. The contents of 2,5-^{13}C-thiophene (4 %) did not interfere with the spectral interpretation. The yield of 2-^{13}C-thiophene (30 % enriched) was 430 mg (0.0051 mole), representing 23 % with respect to applied, enriched potassium cyanide.

As to the reproducibility of the procedure, compare the next section.

Preparation of 3-^{13}C-thiophene. 1.63 g (0.025 mole) K^{13}CN (22 % enriched in ^{13}C) was transformed into 0.93 g enriched $CH_3{}^{13}CH_2OH$ (0.020 mole), following our earlier procedure [2]. This quantity of ethanol was mixed with 25 g P_2O_5 in a 350 ml glas ampulla, evacuated and sealed-off. After 1.5 h heating at 180°—190°C the volatile products were condensed. By distillation *in vacuo* from a dry-ice bath, 0.0175 mole of gaseous ethylene of high purity (~ 98 %) was collected. In a new ampulla, 0.0166 mole of bromine was reacted with all the ethylene at room temperature, admitting small quantities of ethylene at a time. 0.0166 mole of ethylene bromide was formed, the

purity of which was assumed equal to the purity of ethylene bromide, produced in model experiments and checked by its infra-red spectrum. From hereon the procedure given under 2-^{13}C-thiophene was followed. The final yield of 3-^{13}C-thiophene was 0.0061 mole (510 mg), 22 % enriched in ^{13}C and with no carbon isotopic impurities other than thiophene. The over-all yield thus becomes 24 % as compared to 23 % in the previous case.

These syntheses are of value not only to spectroscopists wanting the ^{13}C-species but also to biochemists wanting radioactive labelled ^{14}C-thiophene or one of its derivatives.

Acknowledgment. The research reported in this paper has been sponsored in part by the *Air Force Office of Scientific Research of the Air Research Development Command, United States Air Force*, through its European Office.

1. *Organic Synthesis, Coll. Vol.* **2**, John Wiley and Sons, New York, p. 578.
2. Bak, B., Detoni, S., Hansen-Nygaard, L., Nielsen J. T. and Rastrup-Andersen, J. *Spectrochim. Acta* **16** (1960) 376.

Received October 17, 1960.

ACTA CHEMICA SCANDINAVICA 14 (1960) 1867–1878

The Infrared Absorption Spectra of some Mono-unsaturated and Saturated Fatty Acids and Esters

AAGE JART

Danish Fat Research Institute, Copenhagen, Denmark

Infrared spectra (from 600 to 4 000 cm^{-1}) of 43 different fatty acids and fatty acid esters in carbon disulphide solution have been recorded. Main stress has been laid on the study of the *trans* absorption at 962 cm^{-1}, and extinction coefficients of the pure substances at the *trans* maximum have been calculated. Beer's law has been shown to apply for concentrations upto 200 g substance per liter of solution. Mention is further made of a base line method for the quantitative determination of *trans* monoene fatty acids in mixtures with saturated acids and *cis* forms of unsaturated fatty acids and fatty acid esters. Ten of the recorded infrared spectra are reproduced.

The study of the *cis-trans* isomerism of unsaturated fatty acids is of interest in connection with the industrial production of hydrogenated edible fats as well as the preparation of pure organic compounds in the laboratory. For quantitative determination of a *trans* isomer of the type RCH:CHR [1] occurring together with the corresponding *cis* isomer and the saturated compound the absorption at 960—970 cm^{-1} in the infrared spectrum may be used. The absorption is the result of a deformation vibration of the carbon-hydrogen bond; on account of this origin of the absorption band, the weight of the groups linked to the carbon atoms of the double bond has only a slight influence on the location of the band.

In 1950 the results were published of the first systematic determinations of the extinction coefficients at 965 cm^{-1} of certain fatty acids, fatty acid methyl esters and triglycerides [1,2]. The extinction values determined in these works were mainly those of four systems of "corresponding compounds", *viz.* derived from 9-octadecenoic acid, its methyl ester, the corresponding alcohol and 6-octadecenoic acid (petroselinic acid). For this purpose the term "corresponding compounds" is intended to cover a monounsaturated *cis* compound, the *trans* compound and the corresponding saturated compound; oleic acid, elaidic acid and stearic acid thus form a system of "corresponding acids".

In a work [3] from 1953, which deals exclusively with C_{18}-fatty acids, extinction coefficients are given for the oleic acid system and, in addition, for the

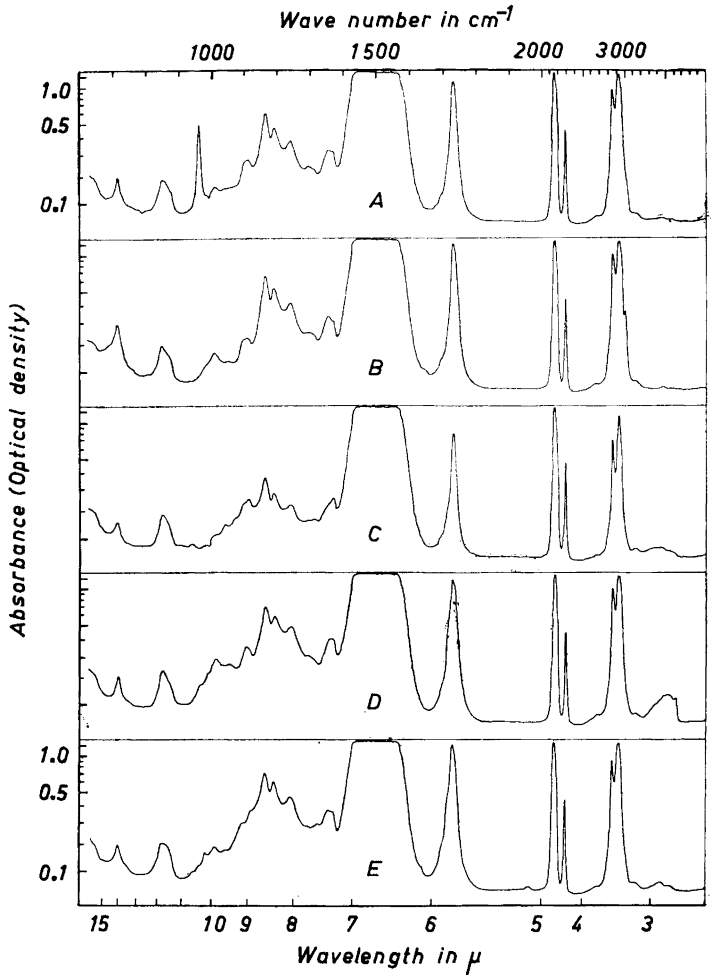

Fig. 1. Infrared spectra. (Carbon disulphide solutions; 0.0110 cm sodium chloride cell). A, Methyl brassidate (98.8 g/l); B, Methyl erucate (108.4 g/l); C, Methyl behenate (57.9 g/l); D, Methyl 12-hydroxy-stearate (102.8 g/l); E, Methyl stearolate (100.6 g/l).

two 12-hydroxy-9-octadecenoic acids (ricinoleic acid and ricinelaidic acid) and for various conjugated and non-conjugated polyene fatty acids.

In a study from 1955 of glycerides [4] mention is made of triolein and trielaidin, various butyro- and aceto-glycerides as well as tributyrin and triacetin.

A work [5] from 1956 gives extinction coefficients of the oleic acid system (in the form of acids, methyl esters and triglycerides) as well as of lauric acid, myristic acid and palmitic acid and the corresponding methyl esters. In another work [6] from 1956 mention is made of the oleic acid system, palmitic acid and linoleic and linolenic acid.

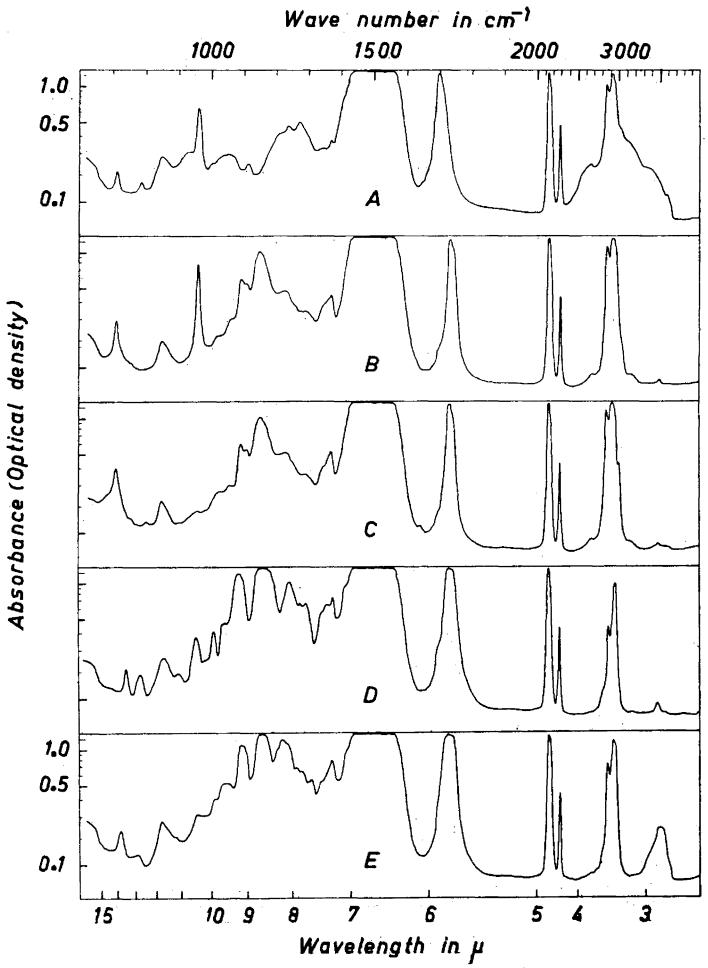

Fig 2 Infrared spectra (Carbon disulphide solutions; 0.0110 cm sodium chloride cell). A, Ricinelaidic acid (99.9 g/l); B, Tribrassidin (152.0 g/l); C, Trierucin (159.7 g/l); D, Tributyrin (116.6 g/l); E, Tricaproin (126.0 g/l).

The determination of ricinelaidic acid and its methyl ester as well as various derivatives of ricinelaidic acid is studied in two works [7,8], published in 1959. Another work [9] dealing with the oleic acid, elaidic acid, erucic acid and brassidic acid, the corresponding methyl esters and barium salts as well as a few glycerides of lower fatty acids appeared also at this time.

The aims of the present work are to perform a systematic determination of extinction coefficients at the *trans* maximum (960—970 cm^{-1}) of a series of monounsaturated and saturated fatty acids and fatty acid esters by means of a widely used spectrophotometer (Perkin-Elmer, Model 21) and to study

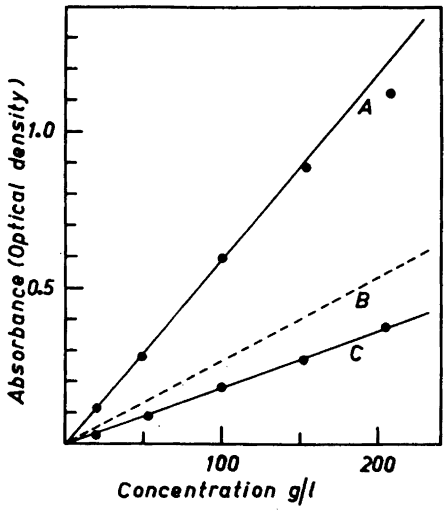

Fig. 3. Relationship between optical density and concentration in the ricinoleic acid system (0.0110 cm sodium chloride cell). A, Ricinelaidic acid; B, 12-hydroxy-stearic acid; C, Ricinoleic acid.

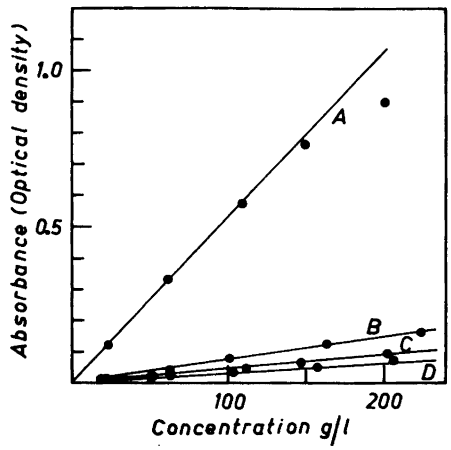

Fig. 4. Relationship between optical density and concentration in the oleic acid methyl ester system (0.0110 cm sodium chloride cell). A, Methyl elaidate; B, Methyl stearolate; C, Methyl oleate; C, Methyl stearate.

conditions in connection with the quantitative determination of *trans* monoene fatty acids with a particular view to the study of the *cis-trans* transformation which may occur during the catalytic hydrogenation of fats.

DETERMINATION OF EXTINCTION COEFFICIENTS AT 962 cm^{-1}

The examination has dealt with eight systems of corresponding compounds (Table 1) based on oleic acid and consisting of acid, methyl ester and triglyceride, on erucic acid in the form of acid, methyl ester and triglyceride, as well as on ricinoleic acid in the form of acid and methyl ester. Furthermore the methyl ester of stearolic acid (which has a triple bond in the 9,10-position) has been investigated; the results are given in connection with the oleic acid methyl ester system.

The twenty-five compounds comprised by this part of the study were examined in carbon disulphide solution. Usually, concentrations of 20, 50, 100, 150, and 200 g of the compound per 1 liter solution were applied. A 0.0110 cm sodium chloride cell was used. As the solubility of the saturated compounds in carbon disulphide is in many cases rather small, a weaker solution in a 0.114 cm sodium chloride cell has been used in these cases.

A comparison of the spectra of the *cis* compounds, *trans* compounds and saturated compounds will disclose the existence of characteristic differences (*cf.* Figs. 1 and 2 *). Unlike the *cis* compounds and the saturated compounds,

* Owing to considerations of space, it will be impossible in this publication to record the spectra of all the compounds examined.

trans compounds display a considerable absorption at 962 cm^{-1} (CH bending about the *trans* C=C group). The *cis* compounds differ from the other two groups in two ways; in the first place the absorption band at 715 cm^{-1} (CH_2 rocking) is wider, and, in the second place, an absorption band may be observed at 3 020 cm^{-1}, forming a shoulder on the broad band (C—H stretching from $CH_3 + CH_2$), which is located between 2 800 and 3 000 cm^{-1}. A further examination of this part of the spectrum should be performed by means of a fluoride prism, and the following will consequently only deal with the absorption at 962 cm^{-1}.

In the absorption spectrum of the free fatty acids there is a very broad and relatively strong band within the range 925—940 cm^{-1}. This band will always be produced by solutions of fatty acids in carbon disulphide, and it is assumed to be due to an OH-deformation vibration in the carboxyl group. As it will appear from the spectra (Fig. 2, A), this band is partially superimposed on the *trans* band at 962 cm^{-1}, and in the case of free *trans* acids the extinction at 962 cm^{-1} consequently receives contributions both from the *trans* extinction and the extinction deriving from the presence of the carboxyl group. In the ricinoleic acid system the extinction is further increased on account of the broad band with maximum at 1 010—1 015 cm^{-1} (C—O stretching).

Fig. 3 shows the optical density in the ricinoleic acid system plotted against the concentration. The relationship is seen to be rectilinear as long as $D < 0.7$. Closely corresponding pictures are obtained in the case of the oleic acid system and the erucic acid system. The corresponding extinction coefficients calculated from

$$a = \frac{\text{optical density at } 962 \text{ cm}^{-1}}{(\text{concentration in g/l}) \times (\text{width of cell in cm})}$$

are given in Table 1.

In the spectra of the methyl esters of the fatty acids (Fig. 1) the band at 925—940 cm^{-1} is seen to have disappeared completely, and in the case of esters of *trans* configuration the extinction at 962 cm^{-1} derives almost exclusively from the *trans* absorption — in the ricinoleic acid system also from the abovementioned band at 1 010—1 015 cm^{-1}. In Fig. 4 the optical density of the methyl esters of the oleic acid system has been plotted against the concentration; the corresponding graphs for the methyl esters of the two other systems have a very much similar appearance. It should again be noted that the relationship is perfectly linear as long as $D < 0.7$. The calculated extinction coefficients appear from the central column of Table 1.

The spectra of the triglycerides (Fig. 2, B and C) resemble those of the methyl esters very much. Also in the case of the *trans* isomers of these esters it applies that the absorption at 962 cm^{-1} derives chiefly from the *trans* band. The dependence of the optical density on the concentration in the case of the triglycerides of the erucic acid system appears from Fig. 5; a corresponding picture is obtained from the triglycerides of the oleic acid system. Conditions are as in the six systems previously mentioned, the relationship being linear for $D < 0.7$. The extinction coefficients are listed in the last column of Table 1;

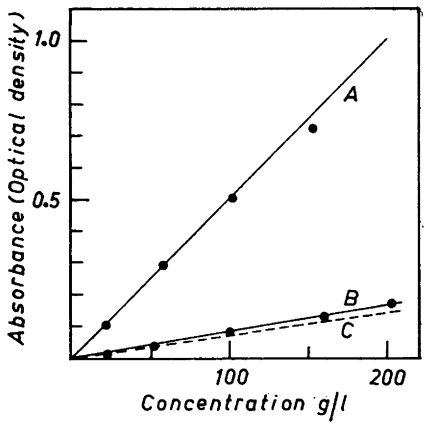

Fig. 5. Relationship between optical density and concentration in the erucic acid triglyceride system (0.0110 cm sodium chloride cell). A, Tribrassidin; B, Trierucin; C, Tribehenin.

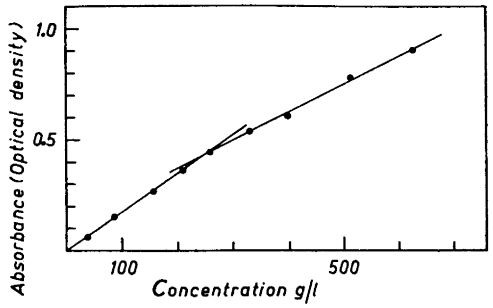

Fig. 6. Relationship between optical density and concentration for methyl elaidate (0.00353 cm potassium bromide cell).

they are somewhat higher than those of the methyl esters, but lower than those of the free fatty acids.

The phenomenon that the optical density is relatively smaller at higher concentrations than at lower concentrations, which is illustrated in Figs. 3—5, may be accounted for in two ways. It may either be the result of a considerable deviation from Beer's law, the extinction coefficient being dependent on the concentration, or the spectrophotometer may exhibit considerable deviation with regard to optical densities higher than 0.7, or both explanations may apply, producing a combined effect. To throw more light on this problem, supplementary investigations were made by means of a thinner cell (0.00353 cm KBr). These experiments showed (Fig. 6) that the relationship is rectilinear up to concentrations of 250 g methyl elaidate per liter solution; the corresponding extinction coefficient was 0.490 — a value which agrees with that found previously. Also in the concentration range 250—650 g per liter solution the relationship seemed to be linear, although the straight line did not coincide with the former, and the dispersion of the points was greater. A corresponding examination was made with respect to trielaidin, and the result corresponds closely to that given for methyl elaidate. Also with respect to ricinelaidic acid it was found that the first part of the curve was a straight line (on account of the lower solubility of this compound in carbon disulphide the shape of the last part of the curve could not be ascertained). For concentrations up to 200—250 g per liter solution no deviations from Beer's law have thus been ascertained.

EXTINCTION COEFFICIENTS OF A NUMBER OF SATURATED FATTY ACID ESTERS

When determining *trans* fatty acids in fatty acid mixtures occurring in practice, it is necessary to make allowance for other saturated acids than those

Table 1. Extinction coefficients at 962 cm^{-1}.

Compound	free acid	methyl ester	glyceride
Oleic acid	0.132	0.041	0.081
Elaidic acid	0.619	0.482	0.538
Stearic acid	0.116	0.028	0.074
Stearolic acid	—	0.066	—
Erucic acid	0.118	0.035	0 077
Brassidic acid	0.537	0.417	0.460
Behenic acid	0.102	0.034	0.067
Ricinoleic acid	0.166	0.094	—
Ricinelaidic acid	0.540	0.460	—
12-Hydroxy-stearic acid	0.242	0.110	—

previously mentioned. Such fatty acids are present in large quantities in a number of natural fats (for instance in coconut oil and consequently in margarine fats) and in certain synthetic triglycerides. A systematic examination of the extinction coefficients at 962 cm^{-1} of the most frequently occurring saturated fatty acid esters was made, and the results are summarized in Table 2. As will be seen from the table, the extinction coefficients of the methyl esters from C_6 decrease with increasing number of carbon atoms in the fatty acid. In the triglyceride series the extinction coefficients decrease steadily with increasing number of carbon atoms, while the molecular extinction coefficient ($= M \times a$, where M is the molecular weight of the triglyceride) is fairly constant (67 ± 9). In the case of triacetin and tributyrin (Fig. 2, D) there are pronounced absorption maxima very near 962 cm^{-1}, *viz.* at 954 cm^{-1} ($a = 0.345$) and at 957 cm^{-1} ($a = 0.260$), while in the case of tricaproin (Fig. 2, E) only an indistinct maximum at 959 cm^{-1} can be observed, and in the case of the higher members of the series the maximum cannot be distinguished from the background.

THE BASE-LINE TECHNIQUE

To be able to determine the content of a *trans* fatty acid in a mixture of fatty acids by means of its extinction coefficient, it is necessary to have a fairly accurate knowledge of the accompanying components of the mixture, which must be determined by gas chromatography or another method. Since the spectra of *cis* fatty acids and of saturated acids resemble each other very much within the range about 962 cm^{-1}, the *trans* absorption may be separated from the "background" absorption by means of a suitable base line. This line may either be drawn in such a way that it approximates the spectrum of the corresponding *cis* isomer, or a straight line may simply be traced as shown in Fig. 7 for a number of *trans* compounds. The distance, D *, from this base line to the peak of the maximum at 962 cm^{-1} corresponds to pure *trans* absorption, and the relationship between this value and the concentration is in principle the same as that found with respect to the total absorption, D, at 962

Table 2. Extinctions at 962 cm^{-1} of methyl esters and triglycerides of saturated acids.

Compound	Methyl ester	triglyceride	
	a	a	ε
Acetic acid	0.036	0.290	63
Butyric acid	0.024	0.246	74
Caproic acid	0.062	0.189	73
Caprylic acid	0.046	0.124	58
Capric acid	0.049	0.116	64
Lauric acid	0.035	0.097	62
Myristic acid	0.037	0.082	59
Palmitic acid	0.031	0.076	61
Stearic acid	0.028	0.074	66
Arachidic acid	0.030	0.078	76
Behenic acid	0.034	0.067	71

cm^{-1}. Fig. 8 shows the curve plotted for tribrassidin; with respect to the remaining seven compounds the curves correspond closely to the *trans* fatty acid curves shown in Figs. 3—5. The curves are straight lines, but also in this case the higher values of the optical density are too small. From the magnitude D^* it is possible to calculate a corresponding *trans* extinction coefficient, a^*, from:

$$a^* = \frac{D^*}{(\text{conc. in g/l}) \times (\text{width of cell in cm})}$$

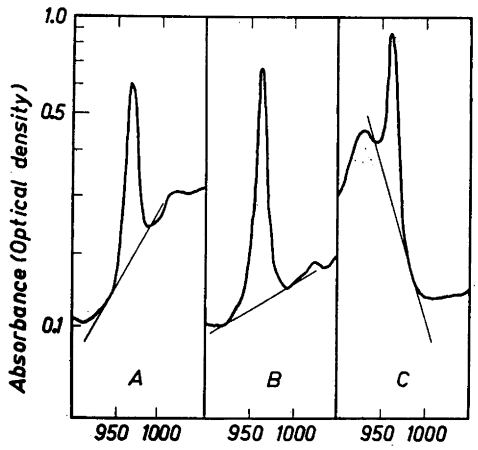

Fig. 7. Tracing of base line for a number of *trans* compounds. A, Methyl ricinoleate (108.6 g/l); B, Trielaidin (105.3 g/l); C, Brassidic acid (147.3 g/l). Abscissas: Wave number in cm^{-1}.

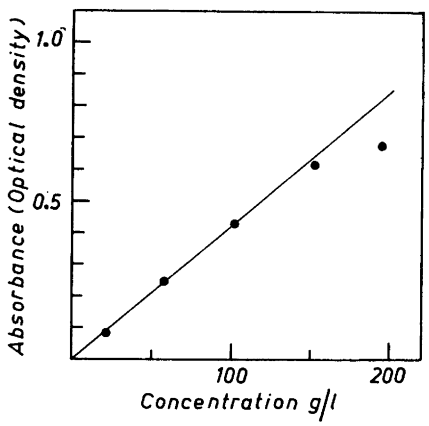

Fig. 8. Relationship between optical density and concentration for brassidic acid triglyceride (base line method, 0.0110 cm sodium chloride cell).

Table 3. Pure *trans* absorptions at 962 cm^{-1}.

Compound	Absorptivity a *	Molar absorptivity ε *
Elaidic acid	0.445	125.9
Brassidic acid	0.376	127.1
Methyl elaidate	0.423	125.4
Methyl brassidate	0.355	125.2
Trielaidin	0.467	413.5 (138)
Tribrassidin	0.387	407.9 (136)
Ricinelaidic acid	0.354	110.6
Methyl ricinelaidate	0.340	101.5

The calculated values are listed in the first column of Table 3. The last column lists the corresponding molecular values, ε *, which are obtained by multiplying values of a * by the corresponding molecular weights. It will be seen that in the case of the simple fatty acids, elaidic acid and brassidic acid and their methyl esters, the molecular value may be taken to be 126. The values for the glycerides are somewhat higher (138 and 136, respectively, calculated per molecule of fatty acid), while those for the hydroxy-substituted compounds are somewhat lower.

In the case that a great precision is not necessary it thus seems favourable to use the base-line technique.

THE PURITY OF THE SUBSTANCES USED

The preparation of the fatty acids and fatty acid esters used in the present investigation is described under the heading Experimental. All *trans* isomers were prepared to such a grade of purity that it was not possible by gas chromatography or other methods to demonstrate the presence of impurities. The purity of the saturated acids is about 99.5 %, which is sufficient for the present purposes as the impurities in this case consist of closely related substances with a corresponding absorption at 962 cm^{-1}. The purity of ricinoleic acid is 99 %, that of oleic acid and erucic acid about 97—98 %, and the same applies to stearolic acid. None of these deviations from 100 % purity should cause any significant alteration of the numerical values of the extinction coefficients. In the case of the triglycerides of some of the lower acids (fats which were originally prepared for feeding experiments) the contents of impurities were determined by gas chromatography, and the extinction coefficients were corrected accordingly. A little content of free hydroxy groups in some of these triglycerides was noticed, but in this connection it does not influence the extinction values.

Direct comparison of extinction values determined by means of different spectrophotometers is not possible, since the individual instruments may differ considerably with regard to scattered radiation, slit width, *etc.* The numerical values found in the present work do, however, agree well with the results of most of the works mentioned in the above. The extinction coefficient values found for the *trans* isomers were, however, about 10 % higher than the results generally given in the literature. The extinction coefficient values given in the following are believed to be in most cases accurate to ± 2 %.

EXPERIMENTAL

Equipment. A Perkin-Elmer spectrophotometer, model 21, with sodium chloride prism was used without any reference cell. The settings used were: speed, 6; automatic suppression, 6; gain, 5.3; intensity, 0.32 A; response, 1; resolution, 927; and slit width at 962 cm^{-1}, 120 μ. Alteration of the speed from 6 to 3 gave no significant alteration of the results.

Cells. The thickness of the 0.0110 cm sodium chloride cell was measured by the interference method. The thickness of the 0.00353 cm potassium bromide cell could not be measured in this way; it was measured by means of pure benzene. The thick cell (0.114 cm, sodium chloride) was measured by means of solutions of fatty acid esters in carbon disulphide.

Determination of extinction coefficients. A sample of the compound under examination was weighed in a calibrated volumetric flask and dissolved in carbon disulphide (Merck, analytical grade). The temperature was 24°C.

I. *Oleic acid.* Olive oil was converted into methyl esters by shaking at 60°C with 1.6 times the theoretical quantity of methanol in which 0.5 % of sodium hydroxide was dissolved; the mixture was set aside for one hour at 60°C and allowed to stand overnight at room temperature. The upper phase was then separated and distilled *in vacuo*. Saturated acids were removed by setting aside the methyl oleate for one week at −40°C in acetone (10 ml per g of methyl ester). Crystallization was effected at −60°C by means of dry ice with gentle stirring; the resulting precipitate was isolated, and oleic acid was recovered by saponifying with 2 N ethanolic potassium hydroxide and acidifying with 50 % sulfuric acid. Linoleic acid was removed from the resulting free acid by recrystallizing three times from acetone at −40°C. The precipitate was evaporated to dryness *in vacuo*. The purity was determined by alkali-isomerization, determination of iodine value and gas chromatography [10].

II. *Elaidic acid.* A commercial product (B.D.H.) was recrystallized three times from three times its volume of 99.9 % ethanol by being allowed to stand at 5°C. Melting point, 43.8−44.0°C.

III *Stearic acid.* A commercial product (B.D.H.), which was found by gas chromatography to contain 96 % stearic acid and 4 % palmitic acid, was fractionated on a 0.6 m packed column (with 1/8 in. Dixon rings). Melting point, 68.6°C.

IV. *Erucic acid.* Rape seed oil was converted into methyl esters as described under I. The esters were carefully fractionated by vacuum distillation, and the C_{22} fraction was allowed to crystallize from acetone at low temperature in a similar manner to that described in the case of methyl oleate under I. The test for purity was performed as in the case of oleic acid.

V. *Brassidic acid.* A commercial product (California Corporation for Biochemical Research) was recrystallized six times from 99.9 % ethanol (at a ratio of 1:1.5) by being allowed to stand at 5°C. Melting point, 59.0−59.2°C.

VI. *Behenic acid.* A technical grade product was converted into methyl esters by means of methanol and sulfuric acid and fractionated on a 0.6 m packed column (Dixon rings). A suitable fraction was recrystallized three times from 96 % ethanol (at a ratio of 1:10) at room temperature. Melting point, 79.8°C.

VII. *Ricinoleic acid.* Castor oil was converted into methyl esters as described under I. The methyl esters were fractionated *in vacuo*, and one fraction which, by gas chromatography, was found to be pure was saponified by means of ethanolic potassium hydroxide

and acidified with 50 % sulfuric acid. Test for purity as described in the case of oleic acid (I).

VIII. *Ricinelaidic acid.* Castor oil was saponified and acidified, and mercury and strong nitric acid were allowed to act on the free fatty acids with stirring. The mixture was washed with water and recrystallized six times from light petroleum at room temperature. Melting point, 50.4°C.

IX. *12-Hydroxy-stearic acid.* Ricinoleic acid methyl ester (*cf.* VII) was hydrogenated with palladium catalyst (10 % Pd on activated carbon) for 8.5 h at 65° in methanol solution; in this way 60 % of the double bonds were hydrogenated. The resulting product was saponified by addition of excess of 2 N aqueous potassium hydroxide and acidified with 50 % sulfuric acid to precipitate the fatty acids. Following two recrystallizations from 96 % ethanol, the melting point of the acids was 76°C. The acids were esterified with methanol and sulfuric acid and fractionated by vacuum distillation. One fraction, with melting point at 49°C, was recrystallized twice from 99.9 % ethanol at 5°C. Melting point, 56.0—56.3°C. The ester was saponified with ethanolic potassium hydroxide and acidified with sulfuric acid. Melting point of the acid, 79.4°C.

X. *Methyl acetate.* A commercial product (B.D.H.) was used.

XI. *Methyl butyrate.* A commercial product was ascertained by gas chromatography to be sufficiently pure.

XII. *Methyl caproate.* Technical grade caproic acid was esterified with methanol and sulfuric acid and fractionated on a 1 m spinning-band column. Tested for purity by gas chromatography.

XIII. *Methyl caprylate.* Prepared in the same way as XII.

XIV. *Methyl caprate.* Prepared in the same way as XII.

XV. *Methyl laurate.* Prepared in the same way as XII.

XVI. *Methyl myristate.* Prepared in the same way as XII.

XVII. *Methyl palmitate.* Prepared in the same way as XII.

XVIII. *Methyl oleate.* Prepared from I by esterification with methanol and sulfuric acid.

XIX. *Methyl elaidate.* A, Prepared from II by esterification with diazomethane [11]. B, Another quantity was prepared by alcoholysis of trielaidin (XXXVIII B) with methanol (according to I) and vacuum distillation of methyl elaidate.

XX. *Methyl stearate.* Prepared from III by esterification with methanol and sulfuric acid.

XXI. *Methyl stearolate.* Prepared according to *Org. Syntheses* [12] by bromination of methyl oleate and treatment of the product obtained with potassium hydroxide and *n*-amyl alcohol. The mixture was acidified with hydrochloric acid to yield the acid which was recrystallized several times from 70 % ethanol, followed by esterification with methanol and sulfuric acid.

XXII. *Methyl arachinate.* Arachidic acid, 95 % pure, war recrystallized three times from 95 % ethanol and esterified with diazomethane [11].

XXIII. *Methyl erucate.* Prepared from IV by esterification with methanol and sulfuric acid.

XXIV. *Methyl brassidate.* Prepared from V by esterification with diazomethane [11].

XXV. *Methyl behenate.* Prepared from VI by esterification with diazomethane [11].

XXVI. *Methyl ricinoleate.* Intermediate from the preparation of VII.

XXVII. *Methyl ricinelaidate.* Prepared from VIII by esterification with diazomethane [11].

XXVIII. *Methyl 12-hydroxy-stearate; cf.* IX. Melting point, 56.0—56.3°C.

XXIX. *Triacetin.* Commercial product (from R de H). Tested for purity by gas chromatography.

XXX. *Tributyrin.* Commercial product (from B.D.H.). Fractionated by vacuum distillation. Tested for purity by gas chromatography.

XXXI. *Tricaproin.* Technical grade caproic acid (R de H) was esterified with methanol and sulfuric acid. After washing with sodium bicarbonate solution and drying with anhydrous sodium sulfate, the methyl ester was fractionated by distillation. Interesterification of methyl caproate and triacetin was effected by heating for 5 h to 80°C with 95 % of the theoretical quantity of neutralized and dried triacetin (R de H) to which had been added 1 % sodium methylate dissolved in methanol; the methyl acetate formed was removed during the process by suction with a water-jet pump. Excess methyl ester

was subsequently removed by passing steam through the triglyceride at 80°C and 20 mm Hg. The resulting triglyceride was treated with 1 % activated carbon and filtered. Composition: 99.5 % C_8; 0.5 % C_8.

XXXII. *Tricaprylin.* Prepared from technical grade caprylic acid (R de H) in the same way as XXXI. Composition: 98.5 % C_8; 1.5 % C_{10}.

XXXIII. *Tricaprin.* Prepared from technical grade capric acid (B D. H) in the same way as XXXI. Composition: 3.1 % C_8; 93.5 % C_{10}; 3.4 % C_{12}.

XXXIV. *Trilaurin.* Prepared from technical grade lauric acid by esterification with 98 % glycerol *in vacuo* at 200°C for 5 h with 0.2 % stannous chloride as catalyst. Washed with aqueous sodium carbonate solution and dried with kieselguhr. Composition: 0.6 % C_8; 10.7 % C_{10}; 86 % C_{12}; 2.7 % C_{14}.

XXXV. *Trimyristin.* Prepared from 98 % myristic acid (B.D.H.) by esterification with 95 % glycerol *in vacuo* at 200°C for 5 h with 1 % stannous chloride as catalyst. Washed with sodium bicarbonate solution and water. Recrystallized three times from benzene. Melting point, 56.8°C.

XXXVI. *Tripalmitin.* Prepared from palmitic acid (B.D.H.) in the same way as XXXV. Recrystallized three times from benzene. Melting point, 65.3°C.

XXXVII. *Triolein.* Prepared from I by esterification with 90—95 % glycerol at 125°C for 8 h, passing nitrogen through the solution and using 1 % *p*-toluene sulfonic acid as catalyst. The mixture was dissolved in two volumes of petroleum ether, washed with two portions of 70 % ethanol, the first containing potassium hydroxide for the purpose of removing free acids, and subsequently with water. Triolein was finally crystallized from acetone (1 g of triglyceride per 10 ml) at −40°C and evaporated to dryness *in vacuo*.

XXXVIII. *Trielaidin.* A, Prepared from II by esterification in the same way as XXXV. Recrystallized several times at 5°C from ethyl ether. Melting point, 42.9—43.2°C. B, Another batch equally pure was prepared from a product obtained from olive oil which was treated with sodium nitrite and nitric acid, the resulting product being washed with water and recrystallized five times at 5°C from ethyl ether.

XXXIX. *Tristearin.* Prepared from III in the same way as XXXV. Melting point, 72.6°C.

XL. *Triarachin.* Prepared from arachidic acid (*cf.* XXII) in the same way as XXXV. Recrystallized three times from benzene. Melting point, 76.9°C.

XLI. *Trierucin.* Prepared from IV by esterification with glycerol as described in the case of XXXVII.

XLII. *Tribrassidin.* Prepared from V by esterification as described in the case of XXXV. Recrystallized five times from ethyl ether at 5°C. Melting point, 58°C.

XLIII. *Tribehenin.* Prepared from VI by esterification as described in the case of XXXV. Recrystallized three times from benzene. Melting point, 81.6°C.

REFERENCES

1. Swern, D., Knight, H. B., Shreve, O. D. and Heether, M. R. *J. Am. Oil Chemist's Soc.* **27** (1950) 17.
2. Shreve, O. D., Heether, M. R., Knight, H. B. and Swern, D. *Anal. Chem.* **22** (1950) 1261.
3. Ahlers, N. H., Brett, R. A. and McTaggart, N. G. *J. Appl. Chem.* **3** (1953) 433.
4. O'Connor, R. T., DuPre, E. F. and Feuge, R. O. *J. Am. Oil Chemist's Soc.* **32** (1955) 88.
5. Malbrouk, A. F. and Brown, J. B. *J. Am. Oil Chemist's Soc.* **33** (1956) 98.
6. Sreenivasan, B. and Brown, J. B. *J. Am. Oil Chemist's Soc.* **33** (1956) 341.
7. McCutchon, M. A., O'Connor, R. T., DuPre, E. F., Goldblatt, L. A. and Bickford, W. G. *J. Am. Oil Chemist's Soc.* **36** (1959) 115.
8. McCutchon, M. A., O'Connor, R. T., DuPre, E. F., Goldblatt, L. A. and Bickford, W. G. *J. Am. Oil Chemist's Soc.* **36** (1959) 450.
9. Kaufmann, H. P., Volbert, F. and Mankel, G. *Fette. Seifen. Anstrichmittel* **61** (1959) 643.
10. Jart, Aa. *Acta Chem. Scand.* **13** (1959) 1723.
11. Jart, Aa. *Oléagineux* **14** (1959) 651.
12. *Org. Syntheses*, Coll. Vol. **3** (1955) 785.

Received June 8, 1960.

ACTA CHEMICA SCANDINAVICA 14 (1960) 1879–1893

On the Sulfides, Selenides and Tellurides of Platinum

FREDRIK GRØNVOLD, HAAKON HARALDSEN and ARNE KJEKSHUS

Kjemisk Institutt A, Universitetet i Oslo, Blindern, Norway

The phase relationships in the systems platinum sulfur, platinum selenium and platinum tellurium have been studied by means of X-rays. Density determinations and magnetic susceptibility measurements have been carried out. Two new, intermediate phases were identified:

1. $PtSe_{0.80}$, with monoclinic structure, $a = 6.5806$ Å, $b = 4.6248$ Å, $c = 11.145$ Å, $\beta = 78.40°$. The pycnometric density is 12.79 g cm^{-3} at 25°C. The unit cell contains ten formula units and the probable space group is Pc or $P2/c$.

2. PtTe, with orthorhombic structure, $a = 6.6144$ Å, $b = 5.6360$ Å, $c = 11.865$ Å. The observed density is 12.01 g cm^{-3}. The unit cell contains ten formula units.

The earlier known phases PtS, PtS_2, $PtSe_2$ and $PtTe_2$ have been reinvestigated. The lattice constants and the observed densities are:

PtS, $a = 3.4700$ Å, $c = 6.1096$ Å
PtS_2, $a = 3.5432$ Å, $c = 5.0388$ Å, density: 7.83 g cm^{-3}
$PtSe_2$, $a = 3.7278$ Å, $c = 5.0813$ Å, density: 9.53 g cm^{-3}
$PtTe_2$, $a = 4.0259$ Å, $c = 5.2209$ Å, density: 10.16 g cm^{-3}

The correctness of the earlier assumed, tetragonal structure of PtS has been confirmed as result of intensity measurements and calculations.

The value $z = 0.250$ of the parameter in the $Cd(OH)_2$-type structures of PtS_2, $PtSe_2$ and $PtTe_2$ gives the best agreement between observed and calculated X-ray intensities.

The magnetic susceptibilities of the different phases have been measured between −183 and 450°C. The compounds show almost zero magnetic susceptibility.

EARLIER RESULTS

Platinum monosulfide was first prepared by Davey [1] by heating platinum sponge and sulfur in a closed tube. Vauquelin [2] prepared it by heating ammonium hexachloroplatinate(IV) with sulfur and sodium carbonate. According to Schneider [3] such products contain more sulfur than corresponding to the formula PtS, and are better described by the formula $4PtS \cdot PtS_2$, *i.e.* Pt_5S_6. At red heat the reported compound looses one sixth of its sulfur and

PtS is formed. Platinum monosulfide occurs in nature as cooperite and its crystal structure was determined by Bannister and Hey [4].

Platinum disulfide was prepared by Davey [1] by heating ammonium hexachloroplatinate(IV) with sulfur at red heat in the absence of air. Berzelius [5] prepared it by treating a solution of hexachloroplatinum(IV) acid with hydrogen disulfide or alkali metal sulfides. Thomassen [6] tried to make PtS_2 by heating stoichiometric amounts of the elements in an evacuated and sealed quartz tube. He obtained a product with composition $PtS_{1.94}$ and found from X-ray powder photographs that it had a hexagonal structure of the $Cd(OH)_2$-type.

In addition to postulating the existence of Pt_5S_6, Schneider [3] also reported a platinum sulfide with composition Pt_2S_3. Neither of these compounds were found by Wöhler, Ewald and Krall [7], who studied the platinum sulfur system by preparative-analytic methods, or by Biltz and Juza [8], who studied the system by tensimetric analysis. The latter authors found no indications of other compounds than PtS and PtS_2. For further references to earlier studies of the platinum-sulfur system, see Gmelin [9].

The reaction between platinum and selenium was observed by Berzelius [10]. The first analyzed compound in this system was platinum monoselenide, prepared from the elements by Roessler [11]. Its existence has not been confirmed by other investigators.

Platinum diselenide has, however, been described by several investigators. Minozzi [12] synthesized $PtSe_2$ from the elements, while Moser and Atynski [13] prepared the compound by precipitation with hydrogen selenide in aqueous solution. Wöhler *et al.*[7] obtained $PtSe_2$ by heating platinum tetrachloride with a large amount of selenium. Thomassen [6] studied $PtSe_2$ by means of X-rays and found that it had a structure of the $Cd(OH)_2$-type.

Minozzi [12] reports also the existence of $PtSe_3$. This compound was prepared by reacting pctassium hexachloroplatinate(IV) with selenium dioxide in an alkaline formaldehyde solution.

Platinum ditelluride was prepared by Roessler [14] by heating platinum and tellurium. Wöhler *et al.*[7] synthesized $PtTe_2$ from platinum tetrachloride and tellurium. In contrast to Tibbals, Jr.[15], who reported that sodium telluride reduced platinum tetrachloride solutions to elemental platinum, Brukl [16] claimed that $PtTe_2$ could be precipitated from aqueous solutions by means of hydrogen telluride. Thomassen [6] determined the crystal structure of $PtTe_2$ and found that it was of the same type as PtS_2 and $PtSe_2$. The lattice constants of $PtTe_2$ were redetermined by Groeneveld Meijer [17].

Experiments to obtain other platinum tellurides have been less successful. Roessler [14] claims that the compounds PtTe and Pt_2Te are formed by decomposing platinum tellurides richer in tellurium. Attempts by Thomassen [6] to make PtTe resulted in heterogeneous products with $PtTe_2$ as the main constituent.

The existence of a platinum telluride mineral with composition $PtTe_3$ was claimed by Scholtz [18]. The reported X-ray data for the mineral, named niggliite, were interpreted by Groeneveld Meijer [19] as mainly caused by a hexagonal NiAs-like structure. On this basis Groeneveld Meijer assigned the composition PtTe to the mineral.

EXPERIMENTAL

Most of the platinum metal used in this study was kindly placed at our disposal by Falconbridge Nikkelverk A/S, Norway. A spectrographic analysis showed presence of the following impurities: about 0.07 % Au, 0.02 % Ir, 0.01 % Pd, 0.01 % Rh, 0.001 % Cu and less than 0.001 % Ag. Some platinum thermocouple wire was also used. A spectrographic analysis of this platinum showed about 0.05 % Au, 0.05 % Cu, 0.02 % Ir, 0.01 % Pd and 0.01 % Rh.

An X-ray powder photograph of the Falconbridge platinum taken at 19 ± 2°C gave a lattice constant of 3.9232 Å, in close agreement with the value 3.9231 Å by Swanson and Tatge [20].

Sulfur from Schering-Kahlbaum A.G. (Sulfur cryst. puriss.) was purified by double distillation in a silica apparatus. Only the middle fractions were used. The highly purified selenium was a gift from Bolidens Gruvaktiebolag, Sweden. It carried the analysis: 0.0002 % Cu, 0.0007 % Fe, 0.003 % Te, 0.01 % S and 0.003 % non volatile matter. Tellurium from The British Drug Houses Ltd. was purified by vacuum distillation in a silica apparatus. According to the spectrographic analysis the distilled product contained less than 0.01 % Fe and only traces of Al, Mg and Pb.

The alloys were prepared by heating accurately weighed quantities of platinum and sulfur, selenium or tellurium, respectively, in evacuated and sealed silica tubes.

In the platinum-sulfur system alloys with 25.00, 33.33, 40.00, 47.37, 48.72, 50.00, 51.22, 52.38, 54.55, 60.00, 66.10, 66.67 and 75.00 atomic % sulfur were made. All samples except those with 25.00, 40.00 and 54.55 atomic % S were heated at 825°C for 30 days and cooled slowly to room temperature over a period of another 30 days. The samples with 66.67 and 75.00 atomic % S were afterwards annealed for 50 days at a temperature of 650°C. The samples with 25.00, 40.00 and 54.55 atomic % S were quenched in ice water from 1 150, 825 and 650°C, respectively.

In the platinum-selenium system alloys with 25.00, 33.33, 37.11, 38.65, 40.00, 41.18, 42.86, 43.50, 44.44, 45.95, 47.61, 50.00, 60.00, 66.67, 75.00 atomic % selenium were made. All samples except those with 25.00, 40.00 and 50.00 atomic % Se were heated at 825°C for 30 days and cooled slowly to room temperature over a period of another 30 days. The samples with 44.44, 50.00, 66.67 and 75.00 atomic % Se were also heated at 1 000 and 600°C for 20 to 30 days. The alloy with 44.44 atomic % Se was furthermore heated at 400°C for 60 days. The samples with 25.00, 40.00, 44.44 and 50.00 atomic % Se were quenched in ice water from 1 200, 825, 1 155 and 825°C, respectively. For density measurements samples with 41.18, 42.28, 44.44 and 45.95 atomic % Se were heated at 1 150°C for 2 days. The melted alloys were afterwards crushed and annealed at 850°C for 10 days and slowly cooled to room temperature over a period of 14 days.

In the platinum-tellurium system alloys with 33.33, 40.00, 47.37, 50.00, 52.24, 60.00, 66.67, 67.74 and 75.00 atomic % tellurium were synthesized. The alloys were heated for 30 days at 825°C and cooled slowly to room temperature over a period of another 30 days. The samples with 40.00 and 50.00 atomic % Te were afterwards annealed at 750°C for 20 and 30 days, respectively. The alloy with 50.00 atomic % Te was also heated at 400°C for 40 days. The samples with 33.33, 50.00 and 60.00 atomic % Te were quenched in ice water from 750, 925 and 825°C, respectively.

During the heat treatments some of the samples were subject to sintering or melting. The alloys with 33.33 atomic % selenium or tellurium had melted at 825 and 750°C, respectively. In both samples a lump of elemental platinum was present, indicating that during cooling platinum was primarily deposited from the melt. The melting point of the alloys with 44.44 atomic % Se and 50.00 atomic % Te was determined to be 1 055 ± 15 and 925 ± 15°C, respectively. Thus, the composition of the eutectic alloy lies between 33.33 and 44.44 atomic % Se in the platinum-selenium system and between 33.33 and 50.00 atomic % Te in the platinum-tellurium system. The alloys were black or grey in colour. When heated to 825°C and above the platinum tellurium alloys showed metallic lustre.

All samples were crushed and X-ray photographs taken in cameras with 114.6 mm effective diameter and asymmetric film mounting. X-Ray photographs were also taken in a Weissenberg camera with 57.3 mm diameter. X-Ray powder data on PtTe were obtained with a Guinier focusing camera of 80 mm diameter and strictly monochroma-

tized Cu$K\alpha_1$ radiation. Guinier photographs of the $PtSe_{0.80}$-phase were taken in a Nonius camera of 114.6 mm diameter. Spectrometer diagrams were taken in a Philips Geiger spectrometer. For the calculation of lattice constants by the Guinier method, potassium chloride (Analar, The British Drug Houses Ltd. $a = 6.2919$ Å[21]) was added to the specimen as an internal standard. The lattice constant of the different samples of platinum was found by extrapolation according to the method of Nelson and Riley [22].

Lattice constants are expressed in Ångström units on the basis of $\lambda_{CuK\alpha_1} = 1.54050$ Å. Results from earlier investigations expressed in kX-units have been transformed to Å by multiplication by the factor 1.00202.

The density of the phases was determined by the pycnometric method at 25°C with kerosene as displacement liquid. To remove gases adsorbed by the sample, the pycnometer was filled under vacuum with kerosene. Each sample weighed from 2 to 3 g. The magnetic susceptibilities of the phases were measured by the Gouy method at three different maximum field strengths at −183, −78, 20, 150, 300 and 450°C. The samples were filled in thin-walled silica tubes of about 2 mm internal diameter and to a height of about 85 mm.

X-RAY RESULTS

A. Platinum sulfides

In agreement with the results by Biltz and Juza [8] only the PtS-phase and PtS_2-phase were found in the platinum sulfur system. The existence of the compounds Pt_2S_3 and Pt_5S_6, claimed by Schneider [3], was thus not confirmed.

The lattice constant of platinum was found to be 3.9234 Å in an alloy with 33.33 atomic % S, containing Pt and PtS in equilibrium. Within the limits of experimental error this value is equal to that of pure platinum, and indicates that sulfur is practically insoluble in solid platinum.

The PtS-phase. Powder photographs of the PtS-phase were indexed on the basis of a tetragonal unit cell, *cf.* Table 1. The lattice constants of the sample with composition $PtS_{1.00}$ are found in Table 2 together with the lattice constants of the PtS-phase in the samples $PtS_{0.90}$ and $PtS_{1.10}$, in which PtS is in equilibrium with Pt and PtS_2, respectively. As the lattice constants do not vary with composition, the homogeneity range of the PtS-phase is not noticeable. The only previous determinations, due to Bannister and Hey [4], are also given in Table 2. The accordance is very satisfactory.

The systematic missing reflections were of the type *(hkl)* absent when $l = 2n + 1$. The highest symmetric space group is thus $P4_2/mmc$ (D^9_{4h}).

Bannister and Hey [4] described the structure of PtS by means of a *C*-centered unit cell to bring out the relationships with the face-centered unit cell of platinum. In Table 1 the *C*-centered indices *(HKL)* are also listed. The corresponding extinctions are of the type *(HKL)* absent when $H + K = 2n + 1$ and $(H0L)$ absent when $H = 2n + 1$ and $L = 2n + 1$. The corresponding space group orientation is $C4/mcm$. By the transformation to the *C*-centered unit cell only the *a*-axis is changed, and

$$A = a\sqrt{2} \quad , \quad C = c$$

with numerical values

$$A = 4.9073 \text{ Å} \quad , \quad C = 6.1096 \text{ Å}$$

for $PtS_{1.00}$.

Table 1. Powder photograph data of PtS taken with CuK-radiation, α_2 and β lines omitted.

$\sin^2\Theta \times 10^4$	HKL	hkl	I_{obs}	I_{calc}
493	110	100	1	0.9
—	002	002	37	1.1
651	111	101		40.2
987	200	110	5	7.9
1131	112	102	1	0.5
1627	202	112	13.5	14.6
1929	113	103	7.5	8.2
1976	220	200	5	5.3
—	221	201	0	0.00
—	310	210	0	0.1
2550	004	004	2	1.8
2612	222	202	13.5	3.5
2627	311	211		9.9
—	114	104	0	0.1
—	312	212	0	0.2
—	223	203	0	0.00
3533	204	114	2.5	2.1
3901	313	213	6	5.2
3947	400	220	2	1.7
—	330	300	0	0.03
4472	115	105	3	2.1
4521	224	204	3.5	2.8
4585	402	222	4	1.5
4599	331	301		2.1
—	420	310	0	0.05
—	314	214	0	0.1
—	332	302	0	0.05
—	421	311	0	0.00
5575	422	312	6	4.6
5727	006	006	0.1	0.3
5873	333	303	2	1.6

$\sin^2\Theta \times 10^4$	HKL	hkl	I_{obs}	I_{calc}
—	225	205	0	0.00
—	116	106	0	0.04
—	423	313	0	0.00
—	510	320	0	0.04
6442	315	215	4.5	3.2
6486	404	224	3.5	2.1
6573	511	321	4	3.2
6713	206	116	3.5	2.2
—	334	304	0	0.04
—	512	322	0	0.08
7473	424	314	3.5	2.5
7697	226	206	1.5	1.3
7840	513	323	4.5	3.7
7883	440	400	1.5	1.3
—	441	401	0	0.00
—	316	216	0	0.1
8284	117	107	3	2.1
—	530	410	0	0.05
8414	335	305	3	2.2
8524	442	402	6	1.6
8540	531	411		4.5
—	514	324	0	0.1
—	425	315	0	0.00
8875	600	330	1	0.9
—	532	412	0	0.1
—	443	403	0	0.00
9505.4	602	332	5	5.2
9664.8	406	226	3.5	3.4
—	227	207	0	0.00
9806.3	533	413	9	12.5
9854.1	620	420	9	11.0

Bannister and Hey based their structure determination on the intensities of a few reflections only. For this reason a new comparison of observed and calculated intensities of the reflections was carried out. In terms of the space group $P4_2/mmc$ (D_{4h}^9) the atomic arrangement in PtS is as follows:

2 Pt in (c) $0,\frac{1}{2},0$; $\frac{1}{2},0,\frac{1}{2}$, and 2 S in ($e$) $0,0,\frac{1}{4}$; $0,0,\frac{3}{4}$.

The intensities of the reflections were calculated using the formula

$$I_{calc} = 10^{-5} \times |F|^2 \times Lp \times \nu$$

No corrections for absorption and temperature factors were thus applied. The observed intensities were obtained from photometer recordings and referred to a relative, absolute scale by making the sums of I_{obs} and I_{calc} equal. As can be seen from Table 1 the agreement between the two sets of values is very good, and leaves no doubt about the correctness of the proposed structure.

Table 2. Lattice constants of the PtS-phase.

Sample	a(Å)	c(Å)	Reference
$PtS_{0.90}$	3.4695	6.1087	Present
$PtS_{1.00}$	3.4700	6.1096	Present
$PtS_{1.10}$	3.4701	6.1089	Present
$PtS_{1.02}$ (Cooperite)	3.48	6.11	Bannister and Hey [4]
$PtS_{1.29}$ (Cooperite)	3.48	6.11	Bannister and Hey [4]
$PtS_{1.10}$ (Synthetic)	3.49	6.13	Bannister and Hey [4]
$PtS_{1.27}$ (Synthetic)	3.49	6.13	Bannister and Hey [4]

Table 3. Powder photograph data of PtS_2 taken with CuK-radiation, α_2 and β lines omitted.

$\sin^2\Theta \times 10^4$	hkl	I_{obs}	I_{calc}	$\sin^2\Theta \times 10^4$	hkl	I_{obs}	I_{calc}
234	001	7	8.7	5682	300	0.5	0.6
632	100	5.5	5.4	—	005	0	0.1
865	101	10.5	11.2	5915	301	1	0.6
934	002	6.5	6.9	6263	204	0.4	0.4
1565	102	5.5	5.8	6476	105	0.5	0.7
1891	110	4.5	5.6	6517	213	1.5	1.3
2124	003	3	0.4	6608	302	0.3	0.3
	111		2.7	7569	220	0.5	0.6
2525	200	1	0.7	7732	115	0.5	0.7
2733	103	4	1.9	7781	303	1	0.7
2759	201		1.9	7802	221	1	0.7
2827	112	1	0.8	8150	214	1	1.1
3463	202	1.5	1.6	8194	310	0.5	0.5
3742	004	0.3	0.3	8364	205	0.5	0.8
3997	113	1	1.3	—	006	0	0.1
4373	104	0.5	0.6	8431	311	2	1.8
4418	210	0.5	0.6	8501	222	0.5	0.4
4636	203	2.5	0.8	9042.1	106	1.5	1.4
4654	211		1.7	9127.1	312	2.5	2.9
5356	212	2	1.8	9410.0	304	2	2.3
5630	114	1	1.1	9664.9	223	1.5	1.8

Table 4. Lattice constants of the PtS_2-phase.

Sample	a(Å)	c(Å)	Reference
$PtS_{1.50}$	3.543	5.040	Present
$PtS_{1.94}$	3.5431	5.0389	Present
$PtS_{2.00}$	3.5432	5.0388	Present
$PtS_{3.00}$	3.5428	5.0415	Present
$PtS_{1.94}$	3.544 ± 0.004	5.029 ± 0.005	Thomassen [6]
$PtS_{2.00}$	3.55	5.03	Bannister and Hey [4]

The interatomic distances are only slightly altered by the new data. Four sulfur atoms are arranged around each platinum atom at the corners of a rectangle (3.040×3.470 Å^2). The shortest interatomic distances are: platinum-sulfur 2.312 Å, sulfur-sulfur 3.040 and 3.470 Å, and platinum-platinum 3.470 and 3.907 Å.

The PtS_2-phase. Powder photographs of the PtS_2-phase were indexed as hexagonal, *cf.* Table 3. The lattice constants of $PtS_{2.00}$ are listed in Table 4 together with the lattice constants of the PtS_2-phase for the samples $PtS_{1.50}$ and $PtS_{3.00}$ in which PtS_2 is in equilibrium with PtS and S, respectively. In addition, a sample with 24.2 weight % sulfur, corresponding to the non-stoichiometric composition $PtS_{1.94}$, found for the PtS_2-phase by Thomassen [6] was prepared and examined. The lattice constants of this sample are listed in Table 4 together with previous lattice constant values by Thomassen [6] and Bannister and Hey [4]. The difference between the values for the *c*-axis in the samples $PtS_{2.00}$ and $PtS_{3.00}$ might indicate a narrow range of homogeneity for the PtS_2-phase.

The pycnometric densities of $PtS_{1.94}$ and $PtS_{2.00}$ at 25°C were found to be 7.80 and 7.83 g cm^{-3}, respectively, in close agreement with the density 7.86 g cm^{-3} calculated for $PtS_{2.00}$ from the X-ray data. Earlier values by Biltz and Juza [8] for samples with composition $PtS_{2.00}$ are about 2 % lower.

According to Thomassen the structure of PtS_2 is of the $Cd(OH)_2$-type. The space group is $P\bar{3}m1$ (D_{3d}^3) with

1 Pt in *(a)* 0,0,0 and 2 S in *(d)* $2/3,1/3,z;1/3,2/3,\bar{z}$.

Thomassen obtained good agreement between I_{obs} and I_{calc} using the parameter value $z = 1/4$. In order to check the parameter value intensities were calculated for $z = 0.240$, 0.245, 0.250, 0.255 and 0.260. The value $z = 0.250$ gives indeed the best agreement between I_{obs} and I_{calc}. The corresponding calculated intensities are listed in Table 3 together with the observed ones.

The interatomic distances are only slightly altered by the new lattice constant values. Each platinum atom is surrounded octahedrally by six sulfur atoms at the distance 2.402 Å. The twelve shortest sulfur-sulfur distances are 3.245 Å and the six shortest platinum-platinum distances are 3.543 Å.

B. Platinum selenides

In the platinum-selenium system two intermediate phases, the $PtSe_{0.80}$-phase and the $PtSe_2$-phase, were identified. This is in accordance with earlier results if the $PtSe_{0.80}$-phase is identified with the monoselenide described by Roessler [11]. The existence of $PtSe_3$, claimed by Minozzi [12], could not be confirmed.

The lattice constant of platinum was found to be 3.9233 Å in an alloy with 33.33 atomic % Se, in which Pt is in equilibrium with $PtSe_{0.80}$. This indicates that selenium is practically insoluble in solid platinum.

The $PtSe_{0.80}$-phase. Powder photographs of different samples of PtSe and $PtSe_{0.909}$ contain some of the strongest reflections from the $PtSe_2$-phase, while powder photographs of $PtS_{0.50}$, $PtSe_{0.667}$ and $PtSe_{0.70}$ contain reflections

from pure platinum. The additional reflections are very weak on photographs of samples with composition $PtSe_{0.75}$ and $PtSe_{0.85}$ and are absent on photographs of samples with composition $PtSe_{0.80}$. Thus the composition of the phase is provisionally designated $PtSe_{0.80}$. As the specific volume turned out to be an approximately linear function of atomic % Se in the whole concentration range from 0 to 66.67 atomic % Se, density determinations alone could not be used for an accurate determination of the composition of the phase.

Since no unit cell fitting all lines on the complex powder photographs could be found, it was tried to isolate crystallites large enough for single crystal work. After several unsuccessful attempts, a fairly useful fragment of a crystal was obtained. Oscillation photographs contained reflections from several crystals and traces of powder lines. By means of Weissenberg photographs the crystal was found to exhibit monoclinic symmetry and these photographs also gave the approximate cell dimensions. The Guinier photographs could then be indexed as shown in Table 5.

The lattice constants of the $PtSe_{0.80}$-phase in the samples $PtSe_{0.70}$, $PtSe_{0.75}$, $PtSe_{0.80}$ and $PtSe_{0.85}$, annealed at 850°C, are listed in Table 6. The slight

Table 5. Guinier powder photograph data of $PtSe_{0.80}$ taken with Cu$K\alpha$-radiation.

I_{obs}	$\sin^2\Theta \times 10^4$ obs	$\sin^2\Theta \times 10^4$ calc	*hkl*
vw	143.2	143.0	100
m	199.1	199.4	002
w	273.9	274.6	$10\bar{2}$
vw	327.3	327.8	011
w	409.5	410.2	102
w	420.7	420.9	110
w	477.2	476.8	012
m	505.1	504.7	111
st	552.5	552.5	$11\bar{2}$
vw	571.1	572.0	200
vw	636.2	635.8	$20\bar{2}$
st	688.1	688.1	112
vw	726.9	726.6	013
st	767.9	767.9	$11\bar{3}$
vw	798.4	797.8	004
vw	806.0	805.2	$10\bar{4}$
st	831.7	832.0	$21\bar{1}$
st	849.4	849.9	210
m	913.2	913.7	$21\bar{2}$
m	968.1	967.6	211
m	972.2	971.3	113
w	1075.9	1075.7	014
		1076.4	104
w	1082.9	1083.1	$11\bar{4}$
vw	1097.1	1095.3	$21\bar{3}$
		1098.7	$20\bar{4}$
vw	1255.2	1254.6	120
w	1283.6	1283.1	$30\bar{2}$
		1287.0	300
w	1355.1	1354.3	$11\bar{4}$
vw	1377.4	1376.6	$21\bar{4}$
vw	1387.5	1386.2	$12\bar{2}$
vw	1497.5	1498.2	$11\bar{5}$
w	1525.6	1524.4	015
w	1562.0	1561.0	$31\bar{2}$
		1564.9	310
w	1602.3	1601.6	$12\bar{3}$
vw	1663.4	1665.7	$22\bar{1}$
st	1679.2	1678.1	$30\bar{4}$
st	1688.5	1683.6	220
		1689.7	302
vw	1714.4	1716.5	311
vw	1755.9	1757.5	$21\bar{5}$
m	1796.1	1795.0	006
m	1803.1	1801.3	221
		1805.0	123
m	1917.1	1916.8	$12\bar{4}$
		1918.8	214
vw	2186.1	2188.0	$12\bar{4}$
w	2212.3	2210.3	$22\bar{4}$
		2216.3	$40\bar{2}$
w	2236.4	2238.2	$21\bar{6}$
vw	2289.3	2288.0	400
vw	2437.8	2435.3	$21\bar{5}$
m	2475.5	2472.0	$30\bar{6}$
m	2492.4	2491.5	304
m	2552.2	2550.2	321

Table 6. Lattice constants of the $PtSe_{0.80}$-phase.

Sample	a(Å)	b(Å)	c(Å)	β (°)
$PtSe_{0.70}$	6.5812	4.6255	11.147	78.39
$PtSe_{0.75}$	6.5812	4.6252	11.148	78.39
$PtSe_{0.80}$	6.5806	4.6248	11.145	78.40
$PtSe_{0.85}$	6.5805	4.6244	11.144	78.41

variations in unit cell dimensions indicate that the homogeneity range of the phase is rather narrow.

The $h0l$ reflections are absent when $l = 2n + 1$. The probable space group is thus Pc (C_s^2) or $P2/c$ (C_{2h}^4).

The density of $PtSe_{0.80}$ was determined to be 12.79 g cm^{-3}. This corresponds to 9.91 Pt and 7.93 Se atoms in the unit cell. If the composition of the phase was assumed to be $PtSe_{0.75}$, the observed density 12.92 g cm^{-3} would give a cell content of 10.18 Pt and 7.64 Se atoms, and for $PtSe_{0.85}$ with observed density of 12.41 g cm^{-3}, 9.47 Pt and 8.05 Se atoms. As the probable space groups Pc and $P2/c$ only have four-fold and two-fold point symmetry, a composition $Pt_{10}Se_8$ seems most reasonable. The calculated density for $Pt_{10}Se_8$ from the X-ray measurements is 12.90 g cm^{-3}.

Samples with composition $PtSe_{0.80}$, heated at 400°C for two months, gave diffuse X-ray photographs indicating some sort of disorder in the structure. The annealing time was probably not sufficiently long to establish equilibrium at that temperature.

Heat treatment at 1 050 and 1 150°C of the samples $PtSe_{0.667}$, $PtSe_{0.70}$, $PtSe_{0.75}$, $PtSe_{0.80}$, $PtSe_{0.85}$ and $PtSe_{0.909}$ indicates that the $PtSe_{0.80}$-phase is formed peritectically, as the X-ray photographs show presence of considerable amounts of Pt and $PtSe_2$.

The $PtSe_2$-phase. Powder photographs of $PtSe_2$ were indexed as hexagonal, *cf.* Table 7. The lattice constants of $PtSe_{2.00}$ are listed in Table 8 together with the lattice constants of $PtSe_{1.50}$ and $PtSe_{3.00}$. From these values the homogeneity range of the $PtSe_2$-phase is not noticeable. In the quenched $PtSe_{1.00}$-sample, however, the c-axis of the $PtSe_2$-phase has a smaller value, indicating a slight change in composition of the $PtSe_2$-phase with temperature. The only previous lattice constant determination of $PtSe_2$, due to Thomassen [6] is also listed in Table 8. The values agree best with those for the quenched sample.

The pycnometric density of $PtSe_2$, 9.53 g cm^{-3}, is in close agreement with the density 9.59 g cm^{-3} calculated on the basis of the X-ray data.

Thomassen found that $PtSe_2$ was isostructural with PtS_2. In order to verify the parameter value, intensities were calculated in the same way as for PtS_2. Also here the parameter value $z = 0.250$ gives the best agreement, I_{obs} and I_{calc}, *cf.* Table 7.

The corresponding interatomic distances are: platinum-selenium 2.499 Å, selenium-selenium 3.330 Å and platinum-platinum 3.728 Å.

Table 7. Powder photograph data of $PtSe_2$ taken with CuK-radiation, α_2 and β lines omitted.

$\sin^2\Theta \times 10^4$	hkl	I_{obs}	I_{calc}	$\sin^2\Theta \times 10^4$	hkl	I_{obs}	I_{calc}
230	001	7	9.0	—	005	0	0.1
570	100	3	3.1	5961	204	0.2	0.2
800	101	17	17.0	6060	213	2	1.7
—	002	0	0.1		302		0.03
1492	102	8.5	8.9	6318	105	1	0.8
1710	110	6	6.1	6836	220	1	0.9
1941	111	3.5	3.0	7064	221	0.5	0.6
2074	003	0.5	0.5	7195	303	1	0.6
2283	200	0.5	0.4	7406	310	0.3	0.3
2510	201	3	2.9	7456	115	0.5	0.7
—	112	0	0.1	7630	311	2	1.9
2643	103	3	2.6	7666	214	0.3	0.5
3200	202	3	2.5	—	222	0	0.1
3682	004	0.5	0.6	8024	205	1	1.0
3780	113	1.5	1.0	—	006	0	0.01
3988	210	0.5	0.4	8323	312	3	3.0
4220	211	2.5	2.4	8800	304	2.5	2.9
4240	104	0.5	0.3	8842	106	1.5	1.8
4353	203	1.5	1.2	8899	223	1.5	1.0
4904	212	3	2.7	9108	400	0.2	0.2
5122	300	1	1.0	9337.8	401	1.5	1.8
5363	301	1	0.7	9468.3	313	3	3.9
5389	114	2.5	2.0	9729.2	215	3.5	5.5

Table 8. Lattice constants of the $PtSe_2$-phase.

Sample	a(Å)	c(Å)	Reference
$PtSe_{1.50}$	3.7279	5.0808	Present
$PtSe_{2.00}$	3.7278	5.0813	Present
$PtSe_{3.00}$	3.7283	5.0812	Present
$PtSe_{1.00}$ (quenched)	3.7279	5.0722	Present
$PtSe_{2.00}$	3.732 ± 0.004	5.072 ± 0.004	Thomassen [6]

C. Platinum tellurides

In the system platinum-tellurium the existence of two of the earlier reported intermediate phases, *i.e.*, the PtTe-phase and the $PtTe_2$-phase, was confirmed. A phase with composition Pt_2Te, described by Roessler [14], was not found.

The lattice constant of platinum was found to be 3.9234 Å in an alloy with 33.33 atomic% Te, in which Pt exists in equilibrium with PtTe. Evidently, platinum does not dissolve any appreciable amounts of tellurium.

The PtTe-phase. Samples with the composition PtTe, heated at 825°C for 30 days, give powder photographs containing very few lines. In order

Table 9. Guinier powder photograph data of PtTe taken with strictly monochromatized CuKa_1-radiation.

I_{obs}	$\sin^2\Theta \times 10^4$ obs	$\sin^2\Theta \times 10^4$ calc	*hkl*
st	135.5	135.6	100
vw	168.2	168.5	002
vw	187.1	186.7	010
vw	305.2	304.0	102
vw	378.0	379.2	003
w	517.9	514.7	103
w	541.8	542.4	200
w	563.2	565.9	013
w	727.8	729.1	210
st	747.1	747.1	020
m	1243.7	1240.7	015
vw	1295.4	1289.5	220
vw	1425.8	1421.4	024
m	1459.8	1458.0	222
vst	1517.2	1517.2	006
m	1649.6	1652.7	106
vw	2010.8	2009.7	321
w	2055.3	2055.0	007
		2059.6	206
		2060.2	033
vw	2080.5	2081.5	314
vw	2169.7	2169.7	400
m	2261.1	2264.3	026
m	2339.0	2338.3	402
st	2986.6	2988.4	040
w	3392.1	3390.2	500
m	3577.7	3575.7	334
vw	3686.4	3686.9	406
st	3773.8	3769.5	503
w	3848.2	3850.6	430
m	4253.5	4251.2	514
m	4507.9	4505.6	046
m	4538.5	4536.8	1,1,10
vw	4672.8	4669.4	050

to grow single crystals, the samples were heated to a temperature just below the melting point, 925 ± 15°C. After many trials some crystals with platy, hexagonal habit were obtained. When slowly cooled to room temperature these crystals disintegrated to a powder after some time. In quenched samples the crystals retained their habit at room temperature. Oscillation photographs of the crystals gave only powder lines, some times with preferred orientation. A possible explanation of these phenomena might be sought in a phase transition.

In order to determine the unit cell dimensions of the unknown structure powder photographs were taken in a Guinier focusing camera of high resolution. Using the Lipson [23] method the unit cell of PtTe could be indexed as orthorhombic, *cf.* Table 9. The lattice constants of PtTe and of the PtTe-phase in the samples $PtTe_{0.90}$ and $PtTe_{1.10}$, in which it exists in equilibrium with Pt or $PtTe_2$, respectively, are listed in Table 10. The slight variations in unit cell dimensions between the three samples indicate that the homogeneity range of the PtTe-phase is rather narrow. The reflections observed in the powder photographs show that the unit cell is primitive.

Table 10. Lattice constants of the PtTe-phase.

Sample	*a*(Å)	*b*(Å)	*c*(Å)
$PtTe_{0.90}$	6.6132	5.6351	11.858
$PtTe_{1.00}$	6.6144	5.6360	11.865
$PtTe_{1.10}$	6.6157	5.6369	11.869

On the basis of the observed density, 12.01 g cm^{-3}, the unit cell contains ten platinum and ten tellurium atoms. The calculated density for $Pt_{10}Te_{10}$ from the X-ray measurements is 12.11 g cm^{-3}.

The pronounced orientation effects observed for the PtTe-phase in form of variable intensities for some of the reflections indicate that it must have a typical layer structure. Thus, the same powder sample as was used for the Guinier photographs gave pronounced enforcements of the (h00) reflections (h = 1, 2, 4 and 5) when using a Geiger spectrometer. In contrast to this, a sample of PtTe that had been melted, formed mica-like flakes, which mounted on a glass plate gave a Geiger-spectrogram with (00l) reflections only (l = 1, 2, 3, 4, 6, 7, and 9). The direction of cleavage therefore seems to change as result of melting.

These preliminary results about the structure of PtTe are not consistent with earlier statements. Both Hume-Rothery [24] and Zhdanov and Gladoleva [25], list PtTe among substances having NiAs-type structure. Apparently, no structure determination of PtTe has been made before 1955 when Groeneveld Meijer [19] interpreted the X-ray photograph of niggliite as due to a phase with NiAs-like structure and composition PtTe. It should, however be remarked, that neither Thomassen [6] nor Groeneveld Meijer [17,19] succeeded in

Table 11. Powder photograph data of $PtTe_2$ taken with CuK-radiation, α_2 and β lines omitted.

$\sin^2\Theta \times 10^4$	hkl	I_{obs}	I_{calc}	$\sin^2\Theta \times 10^4$	hkl	I_{obs}	I_{calc}
218	001	6	9.5	5935	105	2	1.3
488	100	1	1.5	6079	221	1	0.6
708	101	19.5	30.2	—	310	0	0.1
—	002	0	0.1	6356	303	1	0.6
872	200	1	0.7	6567	311	3	2.6
1366	102	13.5	14.2	—	222	0	0.04
1466	110	10	12.3	—	214	0	0.2
1688	111	3.5	3.8	6908	115	1	0.6
1966	003	0.5	0.5	7221	312	4	3.3
2175	201	5.5	5.6	7398	205	2.5	1.4
—	112	0	0.1	—	400	0	0.1
2453	103	5	4.6	7822	223	1	0.7
2829	202	3.5	4.3	—	006	0	0.01
—	210	0	0.2	7879	304	5.5	3.5
3429	113	1.5	1.2	8030	401	2	1.6
3486	004	1.5	1.0	8306	313	6	3.4
3641	211	4.5	4.7	8329	106		2.1
3914	203	3.5	4.2	8684	402	3	2.3
—	104	0	0.1	8862	215	5.5	4.1
4292	212	4	4.4	—	320	0	0.2
4400	300	1.5	2.1	—	116	0	0.1
4620	301	1	0.8	9340.7	224	8	6.2
4956	114	4.5	3.6	9492.8	321	6.5	6.1
—	302	0	0.04	9766.5	403	5	4.4
5382	213	3	2.8	9787.9	206	6.5	5.7
—	204	0	0.1	9834.7	314	3.5	0.8
—	005	0	0.1		305		2.5
5865	220	1.5	1.6				

Table 12. Lattice constants of the $PtTe_2$-phase.

Sample	a(Å)	c(Å)	Reference
$PtTe_{1.50}$	4.0261	5.2212	Present
$PtTe_{2.00}$	4.0259	5.2209	Present
$PtTe_{2.10}$	4.0267	5.2221	Present
$PtTe_{3.00}$	4.0269	5.2224	Present
$PtTe_{2.00}$	4.018 ± 0.004	5.212 ± 0.005	Thomassen [6]
$PtTe_{2.00}$	4.010	5.201	Groeneveld Meijer [17]

synthesizing any other platinum telluride phases than the ditelluride, and that the monotelluride reported here gives a completely different X-ray picture from that of niggliite. Nevertheless, a PtTe-phase with NiAs-like structure might possibly exist at higher temperatures, and thus explain the observed hexagonal habit of the crystals.

The $PtTe_2$-phase. The lattice constants of the hexagonal $PtTe_2$-phase were redetermined. The results of the X-ray measurements are given in Table 11 and the lattice constant values are listed in Table 12 for samples of various compositions. The homogeneity range of the phase is apparently narrow, and slightly on the tellurium-rich side of the composition $PtTe_2$. The previous determinations by Thomassen [6] and Groeneveld Meijer [17], also given in Table 12, differ to some extent from the values found here for the $PtTe_2$-phase.

The observed density, 10.16 g cm^{-3}, is in close agreement with the density 10.20 g cm^{-3} calculated assuming one platinum and two tellurium atoms in the unit cell.

According to Thomassen, $PtTe_2$ is isostructural with PtS_2 and $PtSe_2$. In order to verify the parameter value, intensities were calculated in the same way as for PtS_2 and $PtSe_2$. Here too, the parameter value $z = 0.250$ gives the best agreement betveen I_{obs} and I_{calc}, *cf.* Table 11.

The shortest interatomic distances are: platinum-tellurium 2.666 Å, tellurium-tellurium 3.495 Å and platinum-platinum 4.026 Å.

Table 13. Magnetic susceptibilities of the platinum chalcogenides, $\chi_g \times 10^6$.

Compound	Temperature °C						Induced diamagnetism
	−183	−78	20	150	300	450	
PtS		−0.14	−0.14	−0.13	−0.14	−0.14	−0.26
PtS_2	−0.28	−0.28	−0.28	−0.28	−0.28	−0.28	−0.36
$PtSe_{0.80}$		−0.12	−0.12	−0.11	−0.11	−0.10	−0.25
$PtSe_2$	−0.12	−0.12	−0.13	−0.13	−0.13	−0.13	−0.35
PtTe		−0.13	−0.13	−0.12	−0.12	−0.12	−0.30
$PtTe_2$	−0.05	−0.05	−0.05	−0.05	−0.05	−0.05	−0.37

Table 14. The field strength dependent susceptibilities of PtS, $PtSe_{0.80}$ and PtTe, $\chi_g \times 10^6$, at liquid air temperature.

H_{max} (Ø)	PtS	$PtSe_{0.80}$	PtTe
4 015	0.20	0.10	0.02
4 700	0.16	0.08	0.01
5 110	0.14	0.06	0.01

MAGNETIC PROPERTIES OF THE PLATINUM CHALCOGENIDES

The magnetic susceptibilities of PtS, PtS_2, $PtSe_{0.80}$, PtTe and $PtTe_2$ were measured at six different temperatures between — 183 and 450°C. The results are listed in Table 13. With three exceptions they are mean values of the susceptibilities at three different field strengths (H_{max} = 4 015, 4 700 and 5 110 Ø, respectively).

The measured susceptibilities are all exceedingly low and almost balanced by the diamagnetism induced in the compounds. The diamagnetic corrections are -27.3×10^{-6} per mole Pt° according to Hoare and Matthews [26], -32.6×10^{-6} per mole S^{2-}, -47.6×10^{-6} per mole Se^{2-} and -70.6×10^{-6} per mole Te^{2-} according to Angus [27]. The corrections are listed for one gram of the compounds in the far right column of Table 13. By subtracting these values from the measured susceptibilities, the susceptibilities of the paramagnetic ions are obtained. These corrected susceptibilities increase from sulfide *via* selenide to telluride both for the di- and »mono»-compounds in accordance with the more metallic behavior of the tellurides.

The effective magnetic moments, ranging from 0.11 to 0.91 Bohr magnetons, show that the compounds are of an essentially metallic or covalent type. In case the bonds had been of ionic type, the »spin only» theory demands a magnetic moment of 2.83 μB for compounds containing the Pt^{2+}-ion and 4.90 μB for compounds containing the Pt^{4+}-ion.

The only irregularities observed are that the susceptibilities of all three »mono»-compounds are slightly field strength dependent at liquid air temperature, *cf.* Table 14. Similar effects, but of a much larger magnitude, have earlier been observed for the palladium chalcogenides Pd_4S, Pd_4Se and Pd_4Te[28].

Acknowledgements. The authors wish to thank Falconbridge Nikkelverk A/S for placing platinum metal at their disposal and to thank Bolidens Gruvaktiebolag for the selenium. They also wish to express their thanks to Dr. Arne Magnéli, Stockholms Høgskola, Sweden, for taking Guinier photographs of PtTe, to Siv.ing. Sigurd Rutlin, Sentralinstitutt for Industriell Forskning, for carrying out the spectrographic analysis and to Mr. Håkon Mohn for carrying out some of the magnetic measurements.

REFERENCES

1. Davey, E. *Phil. Mag.* **40** (1812) 28; *Journal f. Chem. u. Phys.* **10** (1814) 382.
2. Vauquelin, L. N. *Ann. chim. et phys.* **5** (1817) 260; *Journal f. Chem. u. Phys.* **20** (1818) 394.
3. Schneider, R. *Ann. Physik* **138** (1869) 604; **148** (1873) 625.
4. Bannister, F. A. and Hey, M. H. *Mineral. Mag.* **23** (1932) 188.

5. Berzelius, J. *Kgl. Svenska Vetenskapsakad. Handl.* **1813** 203.
6. Thomassen, L. *Z. physik. Chem.* **B2** (1929) 349.
7. Wöhler, L., Ewald, K. and Krall, H. G. *Ber.* **66B** (1933) 1638.
8. Biltz, W. and Juza, R. *Z. anorg. u. allgem. Chem.* **190** (1930) 161.
9. Gmelins *Handbuch der anorganischen Chemie*, System-Nummer 68: Platin, Berlin 1939.
10. Berzelius, J. *Journal f. Chem. u. Phys.* **23** (1818) 430.
11. Roessler, F. *Z. anorg. Chem.* **9** (1895) 31.
12. Minozzi, A. *Atti reale accad. Lincei.* **18** (1909) 150.
13. Moser, L. and Atynski, K. *Monatsh.* **45** (1924) 235.
14. Roessler, C. *Z. anorg. Chem.* **15** (1897) 405.
15. Tibbals, C. A., Jr. *J. Am. Chem. Soc.* **31** (1909) 902.
16. Brukl, A. *Monatsh.* **45** (1924) 471.
17. Groeneveld Meijer, W. O. J. *Am. Mineralogist* **40** (1955) 647.
18. Scholtz, D. L. *Trans. Geol. Soc. S. Africa* **39** (1936) 81.
19. Groeneveld Meijer, W. O. J. *Am. Mineralogist* **40** (1955) 693.
20. Swanson, H. E. and Tatge, E. *National Bureau of Standards* Circular 539, Vol. 1 p. 31.
21. Hambling, P. G. *Acta Cryst.* **6** (1953) 98.
22. Nelson, J. B. and Riley, D. P. *Proc. Phys. Soc. (London)* **57** (1945) 160.
23. Lipson, H. *Acta Cryst.* **2** (1949) 43.
24. Hume-Rothery, W. *The structure of metals and alloys.* London 1947, p. 110.
25. Zhdanov, G. S. and Gladoleva, V. P. *Trudy Inst. Krist. Akad. Nauk. S.S.S.R.* **9** (1954) 211.
26. Hoare, F. E. and Matthews, J. C. *Proc. Roy. Soc. (London)* **A212** (1952) 137.
27. Angus, W. R. *Proc. Roy. Soc. (London)* **A136** (1932) 573.
28. Grønvold, F. and Røst, E. *Acta Chem. Scand.* **10** (1956) 1620.

Received April 9, 1960.

ACTA CHEMICA SCANDINAVICA 14 (1960) 1894–1898

An Apparatus for Following Reactions Evolving Gas

E. A. BIRKHIMER, BØRGE NORUP and THOR A. BAK

Institute for Physical Chemistry, University of Copenhagen, Denmark

An apparatus for investigating the kinetics of reactions which evolve a gas is described. Manometer readings are recorded automatically, and the solution in which the reactions occur is stirred magnetically. The apparatus is used to investigate the decomposition of *o*-nitrophenylazide in dibutylphthalate solution. An *ortho*quinoid structure is proposed for the transition state in this reaction.

In 1925 Brønsted and Duus [1] developed a simple apparatus for studying the kinetics of reactions which evolve gas. Its main feature is that the reaction vessel can be shaken continuously. This prevents the reaction solution from becoming supersaturated with the gas formed by the reaction. The reaction vessel is connected to a mercury manometer by means of a glass capillary which allows motion of the reaction vessel relative to the manometer.

Equipment of this general type has been used several times since then for various investigations [2]. Under some types of use certain weaknesses have appeared.

1. The apparatus is fairly fragile because of the glass capillary.

2. Since the manometer is not immersed in the thermostat, variations in room temperature influence its readings by changing the volume of the gas. This is particulary bad for slow reactions where the room temperature may change considerably during a run. Additional complications in this respect arise at higher temperatures.

3. The apparatus requires an observer for reading the manometer. This is especially inconvenient for measuring slow reactions.

Andersen [2] avoided the first two of these difficulties, but since we were primarily interested in studying fairly slow reactions we decided on a different design of the apparatus. First the shaking of the reaction vessel was abandoned in favor of a vigorous magnetic stirring. This eliminates the capillary and made the apparatus both stronger and more compact. Secondly, the manometer was changed so that it can be read electrically. As a result of this the apparatus can be immersed completely in the thermostat. Complete immersion is especially important for reactions occurring at elevated temperatures. Finally, the manometer was connected to a recording potentiometer which allows us to follow the reaction continuously for long periods.

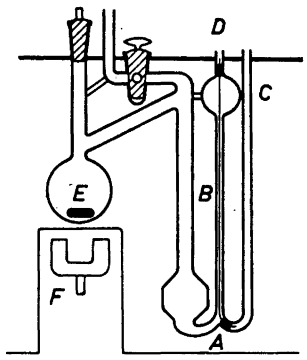

Fig. 1. B is the manometer. A and D are the two points between which the platinum resistance wire is stretched. E is the glasscovered magnet, which is moved by the motor driven magnet F.

2. Fig. 1 shows the construction of the apparatus. A platinum resistance wire is stretched from A to D through the mercury column in the manometer B. The platinum wire is straightened after it has been inserted in the glass [3]. At points A and D the platinum wire passes through the glass and is connected to external leads through pools of mercury. The glass bulb C is inserted to eliminate the effects of traces of air trapped in the manometer when it is filled initially. The reaction solution is stirred by the glass-covered magnet E. The magnet is moved by a motordriven magnet F which is installed under the thermostat as shown in Fig. 1. The entire apparatus is immersed in a suitable thermostat depending on the temperature required.

In order to read the closed manometer B the current from a storage battery is sent through a large constant resistance (about 300 Ω) in series with the platinum wire. The potential across the platinum wire is then a linear function of the height of the mercury in the manometer provided the diameter of the capillary is uniform, and the resistance of the wire is uniform and is much smaller than the constant resistance.

The potential across AD is recorded on a Philips recording potentiometer type PR 3210. In order to check for linearity the reading of the potentiometer was plotted against the height of the mercury read with a kathetometer for various heights of mercury. In the three pieces of apparatus of the above type we have used, the maximum deviation from linearity in the voltage across AD was found to be a few thousandths of the total change in voltage which could be observed as the height of the mercury was increased. As we have constructed it, the apparatus is capable of measuring gas over a 0—100 mm Hg range.

Since we have been interested in investigating first order reactions, we have had no reason to use this linear relationship to obtain the pressure. Instead, we have calculated the rate constant for the reaction from the recorder's curve of voltage *versus* time.

For many of the reactions we have investigated, the change in voltage with time was followed over a period of several days at thermostat temperatures close to 100°C. For such experiments the bath temperature and the voltage across the storage battery were measured continuously by the recording poten-

tiometer. This made it possible to explain most of the irregularities which were occasionally observed in the voltage-time curves and either to apply suitable corrections or reject the data.

3. In order to test the apparatus we have followed the kinetics of the reaction

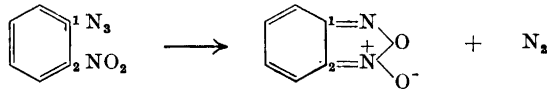

o-nitrophenylazide benzfurazan oxide

which is known to be a first order reaction for which the reverse reaction can be neglected [4]. Dibutylphthalate was used as a solvent since it is stable and has negligible vapor pressure at the moderately high temperatures that were used. Preliminary experiments showed the first order rate constant to be independent of the concentration of *o*-nitrophenylazide. The following technique was employed. 10 ml of the solvent is put into the reaction vessel and stirred for an hour to reach the thermostat temperature. A small platinum bucket containing about 1 mmole of *o*-nitrophenylazide is dropped into the reaction vessel. The reaction is allowed to proceed for 10 min while the system is being evacuated with an oil pump and the reaction solution regains thermostat temperature. Under these circumstances the nitrogen dissolved in the solution may be expected to be in equilibrium with the free nitrogen when the recording of the pressure begins. If stirring is stopped during these 10 min, a supersaturated solution of nitrogen in the diphenylphthalate is generally formed. This completely distorts the voltage-time curve when stirring is resumed. If stirring is not used during a run, the pressure-time curve is more irregular than usual, and the apparent rate constant is about 10 or 15 % too low.

As is well known, it is usally not advisable to use the infinity value method when calculating first order rate constants. This seems to be true for this apparatus to an even higher degree than usual. By using the trick of estimating the asymptotic value of the voltage by the smallest value obtained during the run, the results are improved somewhat. However, repeated runs under indentical conditions still tend to give rather scattered values for the rate constant, since small variations in the infinity value have a relatively large effect on the rate constant.

The rate constants obtained by the method of Guggenheim [5], or even better by an interative least squares method [6,7], are far more consistent. We have generally used the latter method in spite of the additional work it requires. Although to our knowledge there is as yet no sound theoretical basis for using a least squares method for non-linear curve fitting, the method produces remarkably consistent sets of rate constants from repeated measurements. Table 1 shows the results obtained for the first order rate constant for the decomposition of *o*-nitrophenylazide at various temperatures. The temperatures were read with a 1/10°C thermometer, calibrated by comparing it with a 1/10°C thermometer which had been calibrated at the Physikalisch-Technische Reichsanstalt, Charlottenburg, in 1909 and recalibrated at the Fysisk Laboratorium, Danmarks Tekniske Højskole, in 1957. The temperatures given in

Table 1.

Temp., °C	$k \times 10^4$, sec^{-1}
76.22	0.867
76.23	0.893
76.24	0.873
76.27	0.903
81.14	1.492
81.20	1.488
81.22	1.537
81.28	1.488
90.54	3.759
90.54	3.855
90.54	3.717
90.57	3.770
90.57	3.732
90.58	3.843
90.63	3.997
90.85	3.874

Table 1 have been corrected for exposed stem and are believed to be correct to 0.05°C. Internal consistency is somewhat better and should not be in error more than 0.02°C. It was not possible to detect variations in the temperature of the thermostat during a single run. Therefore, it is to be expected that the variations were not more than 0.02°C.

From the data given in Table 1 the activation energy of the reaction is calculated to be 25.7 cal/mole. The entropy of activation, which is derived from the equation [8]

$$k = e \frac{kT}{h} e^{-E/RT} e^{\Delta S^{\neq}/R}$$

is —5.9 cal/mole deg. These values are in reasonable agreement with the results obtained by Fagley *et al.*[4]

5. The structure of *o*-nitrophenylazide is undoubtedly a resonance hybrid of classical structures I, II, and III. Wheland [9] gives evidence for believing that the azide group ordinarily includes contribution from structures such as I and II. It is also reasonable to expect the azide and nitro groups to interact to form a structure such as III because of the favorable charge distribution which it represents. Scale models show that this structure, which is completely planar, is not sterically hindered. We propose that the reaction proceeds through a transition state with the quinoid structure IV. Such a transition state would be expected to have a small negative entropy of activation which is in agreement with the observed one. The alternative cage-type transition state, V, on the other hand would be expected to have a fairly large negative entropy of activation. In addition, while the quinoid transition state is readily formed from the contribution of structure III to the structure of *o*-nitrophenylazide, both charge distribution and the molecule's tendency toward planarity make the formation of the cage transition state difficult.

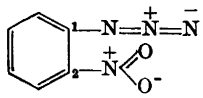

I

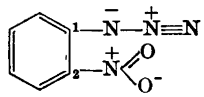

II

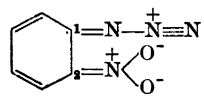

III

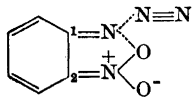

IV

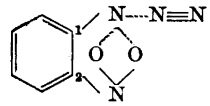

V

However, without the cage model the experimental fact that 4- and 5-substituted *o*-nitrophenylazides give identical products is not easily explained. For an explanation we must assume that the following equilibrium exists:

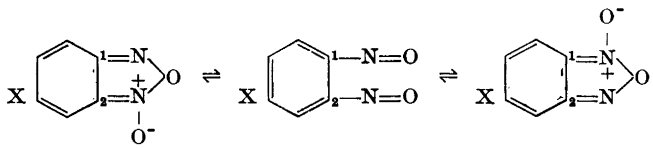

The fact that benzfurazane oxide solutions become colored on heating and lose the color again when cooled tends to support the existence of such an equilibrium. This problem is discussed in more detail by Hammick *et al.*[10]

Acknowledgements. We are indebted to Professor Dr. phil. R. W. Asmussen for the loan of a recording potentiometer with which preliminary experiments were carried out, and to *Statens Almindelige Videnskabsfond* for a grant to buy one. E.A.B. and B.N. acknowledge financial support from a *U.S.government grant* and *Carlsbergfonden*, respectively.

REFERENCES

1. Brønsted, J. N. and Duus, H. C. *Z. physik. Chem.* **117** (1925) 299.
2. Hofman-Bang, N. *Acta Chem. Scand.* **3** (1949) 872; Lund, V. *Acta Chem. Scand.* **5** (1951) 555; Bak, T. *Acta Chem. Scand.* **8** (1954) 1733; Andersen, V. S. and Niemann, H. *Acta Chem. Scand.* **12** (1958) 896.
3. Gillam, D. G., Rombén, L., Nissen, H. and Lamm, O. *Acta Chem. Scand.* **9** (1955) 641.
4. Fagley, T. F., Sutter, J. R. and Oglukian, R. L. *J. Am. Chem. Soc.* **78** (1956) 5567.
5. Guggenheim, E. A. *Phil. Mag.* **2** (1926) 538.
6. Bond, W. N. *Probability and Random Errors*, Arnold and Co., London 1935, p. 112.
7. Guggenheim, E. A. and Wiseman, L. A. *Proc. Royal Soc. London* **203** (1950) 17.
8. Glasstone, S., Laidler, K. J. and Eyring, H. *The Theory of Rate Processes*, Mc. Graw-Hill, New York 1941, p. 199.
9. Wheland, G. W. *The Theory of Resonance*, Wiley, New York 1944, p. 128.
10. Hammick, D. L., Edwardes, W. A. M. and Steiner, E. R. *J. Chem. Soc.* **1931** 3308.

Received June 15, 1960.

ACTA CHEMICA SCANDINAVICA 14 (1960) 1899–1904

An Extension of Hammett's $\sigma - \varrho$ Relation

ELLEN ANDERSEN, E. A. BIRKHIMER and THOR A. BAK

Institute for Physical Chemistry, University of Copenhagen, Denmark

It is proposed that the Hammett $\sigma-\varrho$ relation can be extended to account for the influence of substituents on the rate of reactions in which two groups substituted in a benzene ring react with each other. It is shown experimentally for the reaction of substituted *ortho*nitrophenylazides, in which the azide group reacts with the nitro group, that the more general relation has the form

$$\log_{10}k/k_0 = \sigma_1\varrho_1 + \sigma_2\varrho_2$$

Here σ_1 and σ_2 are the normal substituent coefficients and ϱ_1 and ϱ_2 are partial reaction coefficients. It is argued that they give an indication of the charge distribution in the transition state. The mechanism of the decomposition of *ortho*nitrophenylazide is discussed in terms of the values obtained for ϱ_1 and ϱ_2.

The effect of substituents on the rate of a side chain reaction of benzene derivatives can be described semiquantitatively by means of the Hammett equation [1a]

$$\log_{10}k/k_0 = \sigma\varrho$$

in which k_0 is the rate constant for the reaction of the unsubstituted compound and k is the rate constant for the reaction of a compound which has a substituent *meta* or *para* relative to the reacting group. ϱ is a quantity which depends only on the type of reaction. σ depends only on the substituent one considers and whether it is *meta* or *para* relative to the reacting group.

Since an equilibrium is a balance between two chemical reactions, it is immediately clear that a similar equation will also hold for equilibrium constants of side chain reactions of benzene derivatives.

Clearly the value of a σ-coefficient is only determined relative to some standard reaction for which ϱ is set equal to one. Rather than using a chemical reaction for this, Hammett chose to use the dissociation of benzoic acid. That is, for the equilibrium

$$\varphi^*\mathrm{COOH} \rightleftharpoons \varphi^*\mathrm{COO}^- + \mathrm{H}^+$$

where the star indicates that there is a substituent in the benzene nucleus, one sets arbitrarily

$$\log_{10}K/K_o = \sigma$$

where K and K_o are now equilibrium constants for the dissociation of the substituted and the unsubstituted acid, respectively.

When the σ-values are determined in this way, the ϱ-value for a reaction or an equilibrium is determined by plotting the logarithm of the rate constants of several differently substituted derivatives *versus* the σ-values. Extensive tables of σ- and ϱ-values have been published [2].

Ever since Hammett discovered that the effect of structure on reactivity could be accounted for by this simple relation, attempts have been made to give it some theoretical justification. $\text{Log}_{10}k/k_o$ is proportional to the difference in standard free energy between the reaction of the substituted molecule and the unsubstituted molecule when an equilibrium is considered. For rate constants it is proportional to a similar difference in standard free energies of activation when the transition state theory is assumed. Therefore, the Hammett equation is often called a "linear free energy relationship". Since for many processes of this kind it has been observed that, within the experimental error, the entropy term is independent of the substituent or a linear function of the activation energy it can, however, be restated as a "linear bonding energy relationship". It is therefore reasonable to assume that the σ-values should be correlated with the change caused by the substituents in electron densities at the reaction site.

Corio and Dailey [3] have shown experimentally that there is such a correlation between σ-values and electron densities determined by nuclear magnetic resonance technique. Van Beek [4] has shown that a relation similar to the Hammett equation also holds for dipole moments. This indicates clearly that the σ-values depend on the change of electron density in the benzene ring, produced by the substituent. Jaffe [5] has succeeded in making this statement at least semiquantitative by correlating the σ-values with electron densities obtained from molecular orbital calculations. In spite of all this one must say, however, that the σ-ϱ relationship itself, as well as the ϱ-values, still must be viewed mainly as an empirical result.

This of course limits the use of the σ-ϱ relationship somewhat, but since one can interpret the σ-and the ϱ-values in terms of electron density, albeit somewhat vaguely, the rule can at least be applied to confirm or reject certain reaction mechanisms which involve a specific charge distribution in the transition state. In order to do this is necessary in some cases, to know whether one can extend the Hammett rule to be valid for reactions in which, for instance, two neighbouring groups in a benzene molecule react with each other. To give a specific example in a reaction such as

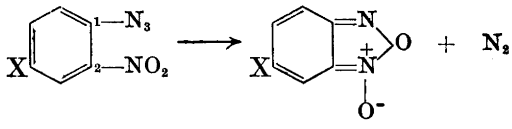

which we have studied previously, one would like to know the validity of the relation

$$\log_{10}k/k_o = \sigma_A\varrho_A + \sigma_N\varrho_N$$

where σ_A and σ_N are the *meta*- and *para*-substituent coefficients for the substituent X, and ϱ_A and ϱ_N are constants. If this relationship is valid, ϱ_A and ϱ_N would naturally be taken as the reaction coefficient for the reaction "at the azide group" and "at the nitro group". Since ϱ is usually negative when a high electron density is favourable for the reaction, this in turn would indicate the charge distribution in the transition state.

To our knowledge a relationship of this kind has never been checked experimentally, although it is a quite obvious extension of Hammett's idea. The purpose of this paper is therefore primarily to verify the extended rule for the reaction mentioned above, and secondly to discuss the values obtained in this case for ϱ_A and ϱ_N in terms of the mechanism which we have previously suggested.

2. The derivatives of *ortho*nitrophenylazide shown in Table 1 were used in this investigation.

In all cases the compounds were prepared from the corresponding derivatives of *ortho*nitroaniline by diazotization and coupling with azide ions. The *ortho*nitroaniline derivatives used were either the purest grade obtainable from Eastman Kodak Organic Chemicals, or compounds prepared at the Laboratories for Organic Chemistry at the University of Copenhagen and at the Technical University of Denmark *. In all cases the melting points of the *ortho*nitroanilines checked with those reported in the literature.

After preparation, the *ortho*nitrophenylazides were stored at 0°C and in most cases the experiments using any compound were completed within two weeks. Under these circumstances only a negligible amount of the azide had reacted in the solid state, except for the case of 2,4-dinitrophenylazide which reacts very fast. In this case, therefore, several preparations were made.

The measurements of the first order rate constant for the decomposition of the azides were measured in an apparatus described previously [6], following the same method. The results obtained are given in Table 1. It is seen that the reproducibility of an experiment is in general better than 2 %. Barring systematic errors, the average of 3—4 experiments may be assumed to be correct to within 1 %. This is probably the best one may hope to obtain by a method of this kind.

Table 2 gives the average values of the rate constants referred to a common temperature. From this table the values of ϱ_A and ϱ_N in the expression

$$\log_{10} k/k_o = \sigma_A \varrho_A + \sigma_N \varrho_N$$

have been calculated by the method of least squares, using values of σ_A and σ_N taken from the literature. σ_A is the substituent coefficient for the influence of the substituent on the azide group, and σ_N the coefficient for its influence on the nitro group. One obtains

$$\varrho_A = 1.353 \quad \varrho_N = -0.676$$

and Table 2 shows the agreement between measured values of k and the values calculated using the above values of ϱ_A and ϱ_N (and the tabulated values of σ_A and σ_N).

* We are indebted to Mrs. Else Plejl and Mr. Børge Nygaard for letting us have these chemicals.

Table 1.

Compound	T, °C	$k \times 10^4$, sec^{-1}	Compound	T, °C	$k \times 10^4$, sec^{-1}
o-$NO_2\varphi N_3$	76.22	0.867	4-φ-$2NO_2\varphi N_3$	80.26	1.599
	76.23	0.893		80.26	1.618
	76.24	0.873		80.44	1.645
	76.27	0.903		80.44	1.671
	81.14	1.492		90.43	4.538
	81.20	1.488		90.44	4.391
	81.22	1.537		90.44	4.478
	81.28	1.488		90.44	4.543
	90.54	3.759		100.11	11.53
	90.54	3.855		100.12	11.75
	90.54	3.717		100.12	12.30
	90.57	3.770		100.15	11.58
	90.57	3.732		100.15	11.07
	90.58	3.843			
	90.63	3.997	5-CH_3-$2NO_2\varphi N_3$	70.76	0.5673
	90.85	3.874		70.76	0.5886
				70.76	0.5866
4-CH_3O-2-$NO_2\varphi N_3$	80.36	0.5000			
	80.36	0.4945		76.25	0.9909
	80.40	0.4970			
				77.18	1.1498
	90.50	1.330		77.18	1.1740
	90.52	1.365			
	90.54	1.324		81.21	1.682
	90.55	1.321		81.24	1.684
	90.56	1.374		81.25	1.707
	90.57	1.343		81.29	1.650
	90.59	1.341			
	90.60	1.374		90.40	3.86
				90.45	4.09
	100.11	3.446		90.46	3.77
	100.12	3.446		90.46	4.06
	100.14	3.521			
	100.15	3.369	4-Cl-$2NO_2\varphi N_3$	81.20	1.758
	100.15	3.509		81.22	1.840
	100.30	3.422			
	100.30	3.442	2,4-$(NO_2)_2\varphi N_3$	40.32	0.1690
	100.34	3.430		40.32	0.1716
				40.32	0.1662
4-CH_3-$2NO_2\varphi N_3$	70.76	0.3171		40.32	0.1669
	70.76	0.3221		40.32	0.1643
	70.76	0.3224			
				50.38	0.6506
	81.21	0.9274		50.38	0.6486
	81.22	0.9298			
	81.23	0.9298			
	90.48	2.450			
	90.52	2.241			
	90.52	2.232			

The σ-values used are those of Hammett [1,7] except for the phenyl group where later work is more accurate. For *m*-phenyl a value of 0.06 was used [8]. For the nitro and phenyl groups *para* to the azide group, the corresponding σ-values for reactions of aniline were used [7,9]. Because of the rather large uncertainty and confusion which still exists in regard to σ-values for the phenyl

Table 2. k_{exp} are the experimental values of the rate constant referred to a common temperature 81.20°C and k_{calc} are the rate constants as calculated from the extended Hammett relation. E are the experimental activation energies and $\Delta S^{\ddagger}$ are the activation entropies.

Compound	$k_{exp} \times 10^4$ sec^{-1}	σ_A[1a]	σ_N[1a]	$k_{calc} \times 10^4$ sec^{-1}	$E_{kcal/mole}$	$\Delta S^{\ddagger}$ cal/mole/deg
o-NO_2-φ-N_3	1.50	—	—	—	25.7	− 5.9
4Cl-2$NO_2\varphi$-N_3	1.80	+0.227	+0.373	1.70	—	—
4CH_3O-2$NO_2\varphi$-N_3	0.535	−0.268	+0.115	0.544	25.6	− 8.1
2,4$(NO_2)_2\varphi$-N_3	25.5	+0.778	+0.710	25.9	27.1	+ 3.9
4CH_3-2$NO_2\varphi$-N_3	0.927	−0.170	−0.069	0.984	24.8	− 9.3
5CH_3-2$NO_2\varphi$-N_3	1.67	−0.069	−0.170	1.58	24.2	−10.1
4φ-2$NO_2\varphi$-N_3	1.78	+0.009	+0.218	1.92	26.0	− 4.6

group, these data were not used in calculating the ϱ-values. However the rate constant has been calculated and correlates moderately well with the experimental one.

From this we may of course only conclude that this extension of the σ-ϱ rule applies to the reaction in question, but it seems most likely that it should be true in general for substituents which are *meta* or *para* to both the reacting groups.

3. It is of some interest to consider the activation energies and activation entropies of the reactions investigated. Table 2 gives the values of the energies and entropies of activation one obtains.

The plot of $\Delta S^{\ddagger}$ *versus* the experimental activation energy in Fig. 1 shows that the activation entropy increases systematically with the activation energy. When the errors in the determination of E and $\Delta S^{\ddagger}$ are taken into account one may almost take this to be a linear relationship. Such a relationship has been observed previously for other reactions and as mentioned above it is the reason that the Hammett equation may hold even when the activation entropy is not independent of the substituents.

It has been stated for instance by Hammett [1b] that there is no reason to expect a correlation between activation entropy and activation energy. Indeed his whole argument for the existence of the σ-ϱ relation was based on the assumption that $\Delta S^{\ddagger}$ is independent of substituents. Contrary to this point

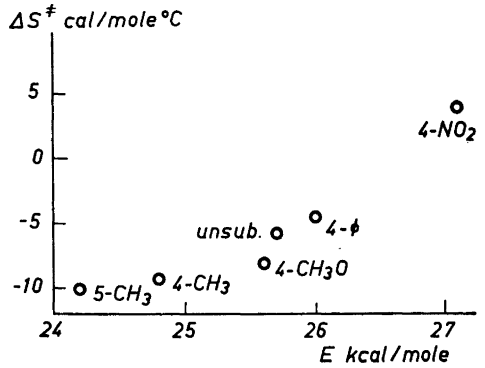

Fig. 1. A plot of $\Delta S^{\ddagger}$ *versus* the experimental activation energy. It shows that the activation entropy increases systematically with the activation energy.

of view, we think that the relation between $\Delta S^{\ddagger}$ and E is perfectly reasonable, at least for unimolecular reactions, and of more general validity than Hammett's assumption. It is clear that if one strengthens the bond which must break by "adding electrons", the molecule must vibrate violently in order to break the bond. This means that the amplitudes of the normal modes in a molecule which is able to break a certain bond when the normal modes get into phase will in general increase as the activation energy increases. This again means that a molecule which can react (*i.e.*, is in the transition state) must have a larger entropy as the activation energy increases. Even though the relationship may not be linear, it will appear almost to be so when used only over a small range of activation energies.

4. We have previously suggested that the reaction of *o*-nitrophenylazides proceeds through the following transition state

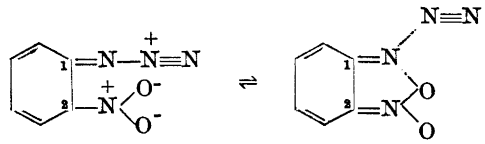

in which there is a low electron density around carbon atom No. 1 and a high electron density around carbon atom No. 2. If this mechanism is correct therefore, ϱ_A should be positive and ϱ_N should be negative, since the favourable effect of high electron density implies a negative value of ϱ. The values found experimentally for the two reaction coefficients therefore support the suggested mechanism.

It is seen from this, however, how careful one should be when correlating negative entropies of activation with cyclic transition states and *vice versa* as is often done. In the reaction we have considered here the activation entropy is generally negative and we believe the transition state to be cyclic. For the 2,4-dinitro compound which reacts very fast and has a high activation energy, $\Delta S^{\ddagger}$ is, however, positive and presumably this does not mean that the mechanism of the reaction has changed.

Acknowledgement. E. A. and E. A. B. gratefully acknowledge financial support from *Teknisk Videnskabelig Forskningsraad* and a *U.S. government grant (Fulbright)*.

REFERENCES

1. Hammett, L. P. *Physical Organic Chemistry.* McGraw-Hill, New York 1940 (a) p. 184 ff (b) p. 121 ff.
2. Jaffe, H. H. *Chem. Revs.* **53** (1953) 191.
3. Corio, P. L. and Dailey, B. P. *J. Am. Chem. Soc.* **78** (1956) 3043.
4. Van Beek, L. K. H. *Rec. trav. chim.* **76** (1957) 729.
5. Jaffe, H. H. *J. Chem. Phys.* **21** (1953) 415.
6. Birkhimer, E. A., Norup, B. and Bak, T. A. *Acta Chem. Scand.* **14** (1960) 1894.
7. Hammett, L. P. *J. Am. Chem. Soc.* **59** (1937) 96.
8. Lichtin, N. N. and Leflin, H. P. *J. Am. Chem. Soc.* **74** (1952) 4207.
9. Berliner, E. and Lin, L. H. *J. Am. Chem. Soc.* **75** (1953) 2417.

Received June 15, 1960.

ACTA CHEMICA SCANDINAVICA 14 (1960) 1905–1912

A Colloidal Water-soluble Double Sulphide Containing Mercury(II) and Tin(IV)

C. E. FOVERSKOV and NIELS HOFMAN-BANG

Chemistry Department A, Technical University of Denmark, Copenhagen, Denmark

If tin(IV), mercury(II) and sodium sulphide are present within certain concentration limits, addition of ammonium chloride yields a red precipitate, which upon washing with water dissolves to a deep red solution. Addition of ethanol to this solution again gives a red precipitate. After the precipitate is completely dried, it becomes almost black, and the compound is no longer water-soluble.

A quantitative analysis of the compound showed a somewhat varying composition, which approximated the formula Hg_2SnS_4 within 10 %.

The red aqueous solution has been the object of different investigations, which all show that a colloidal solution with negatively charged particles is involved. Sedimentation in an ultracentrifuge shows that the particle size varies. The mass of the particles lies in the range 1 300 to 40 000 atomic mass units.

X-Ray investigation of the completely dry double sulphide by the powder method does not show crystallinity.

In inorganic qualitative analysis mercury is often separated from tin, antimony, arsenic and molybdenum by precipitation of mercuric sulphide by the addition of ammonium chloride to a solution containing these metals as thio-ions. When teaching qualitative analysis one of the authors (H-B) has noticed that addition of ammonium chloride to a solution containing thiomercurate, thiostannate and sulphide ions sometimes yields a red precipitate instead of black mercuric sulphide. The red precipitate dissolves readily in water forming a deep red solution.

It is well known that separation of mercury and tin as mentioned above is incomplete. Storch [1] has remarked that mercuric sulphide is soluble to some extent in ammonium thiostannate solution, whereas it is insoluble in ammonium sulphide. He stated that a more detailed investigation would be undertaken, but it evidently has never been published. Wilm [2] has mentioned that mercuric sulphide can be only partly precipitated by ammonium sulphide when tetravalent tin is present. Feigl [3] has observed that mercuric sulphide which is precipitated by the addition of ammonium chloride to a solution of thiomercurate and thiostannate is greatly contaminated with stannic sulphide.

QUALITATIVE EXPERIMENTS

A series of test tube experiments were carried out in order to get an impression of the colour and the amount of impure mercuric sulphide precipitated by the addition of ammonium chloride to a solution containing Sn(IV), Hg(II) and sodium sulphide. The mole ratio of tin to mercury (f), the total molar concentration of tin + mercury (c) and the added amount of ammonium chloride in g/10 ml (m) were varied. The experiments were carried out as follows:

Stock solutions of thiomercurate and thiostannate were made by dissolving mercuric chloride and potassium hexachlorostannate, respectively, in the amount of 2 M sodium sulphide just sufficient to dissolve the primarily formed sulphides, and then diluting with water to the desired concentrations of the metals. In a test tube thiostannate and thiomercurate solutions were carefully mixed so that the total volume was 10 ml; m g ammonium chloride was then added and dissolved by shaking. The progress of the precipitation was observed during the first hour, and after 24 h the colour and amount of the final precipitate and the colour of the clear supernatant solution were judged. Thirty five such experiments were carried out; the values of c were 0.1, 0.2 and 0.5, f varied from 0.4 to 5.7 and m from 0.15 to 2.00.

The results may be summarized as follows:

1. *The progress of the precipitation.* At $f \leq 1.5$ the precipitation takes place immediately upon the addition of ammonium chloride, while at $2.3 \leq f \leq 4.0$ from 2 to 50 min elapse before the precipitation starts. During this period of time the colour of the solution changes from pale yellow to orange. At $f \leq 1$ the precipitate is very dark. At $1.5 \leq f \leq 4.0$ the colour of the precipitate is first yellowish but, as the precipitation is progressing, it gradually changes to orange or orange red. At $m > 1.7$ the precipitate, however, stays yellow.

2. *The amount of the precipitate.* The amounts were only judged visually by comparing the heights of the precipitates in the test tubes after 24 h. The amount of precipitate is not much different at $c = 0.2$ and $c = 0.5$, while it is about half as much at $c = 0.1$. The amount of precipitate rapidly decreases with increasing f; at $f = 4.5$ the amount is negligible, and at $f = 5.7$ no precipitation at all takes place even after 5 days. At $0.5 \leq m \leq 1.5$ the amount of precipitate is fairly constant, but at $m > 1.5$ it increases somewhat and at $m < 0.5$ it decreases; *e.g.* at $m = 0.15$ the amount of precipitate is only 1/5 of the amount at $m = 1$.

3. *The colour of the precipitate.* The colour of the precipitate does not depend upon c, and is fairly independent of f at $1.5 \leq f \leq 4.5$. At $f \leq 1.5$ the precipitate gradually becomes darker with decreasing f, *e.g.* red brown at $f = 1.0$ and very dark brown at $f = 0.4$. However, the colour is strongly dependent upon m; at $0.15 \leq m \leq 0.3$ it is dark red, at $m = 0.5$ bright red, at $m = 1.2$ orange, and at $m > 1.5$ yellow.

4. *The colour of the filtrate.* The colour of the clear supernatant solution is nearly independent of c and f and mostly depends upon m. At $0.15 \leq m \leq 0.3$ the filtrate is red, at $m = 0.7$ orange, and at $m > 1.2$ yellowish. The change of colour is accompanied by decreasing intensity of colour.

PREPARATION OF THE RED DOUBLE SULPHIDES

For the sake of analysis and other investigations several preparations were carried out. After some preliminary investigations the following method was found suitable.

Weighed amounts of potassium hexachlorostannate and mercuric chloride are each dissolved in a slight excess of 2 M sodium sulphide. The two solutions are filtered through a hardened filter paper and the flasks and the filter washed with distilled water. Then the solutions are mixed and diluted with water to 250 ml. Finally the ammonium chloride is added while stirring.

After about 20 h the precipitate formed, 0.6—8 g, is filtered off on a medium filter paper. After as much as possible of the filtrate has run off the filter, the precipitate is transferred to an Erlenmeyer flask containing 50 ml of water at 25—30°C. After complete dissolving (a few of the preparations required somewhat more than 50 ml water) 50 ml ethanol are added. This addition causes reprecipitation of the red double sulphide. After 2 h filtration is carried out and the precipitate is washed first with two 30 ml portions of 50 % ethanol in order to remove ionic impurities, then with three 30 ml portions of ethanol and lastly with three 30 ml portions of dry ether. When especially large precipitates are involved, larger volumes of washing liquid are used.

The precipitate is allowed to dry overnight and is then cautiously pulverized and put into a vacuum desiccator over potassium hydroxide pellets. Drying to constant weight requires nearly a month.

Twelve preparations of the type just described were carried out, *cf.* Table 1. Two of them, Nos. 5 and 8, failed, No. 5 because the yield was negligible, and No. 8 because the precipitate could not be quite redissolved in water for the sake of purification.

ANALYSIS OF THE PREPARED DOUBLE SULPHIDES

The percentages of mercury, tin and sulphur in the completely dried double sulphides were determined by slightly modified standard methods.

Table 1. Preparations of water-soluble double sulphides of tin(IV) and mercury(II). The total volume of sodium thiomercurate and thiostannate solution was 250 ml before addition of ammonium chloride. c is the total molar concentration of tin + mercury, f is the mole ratio tin to mercury, and m is the added amount of ammonium chloride in g/10 ml. The yield is given in g of the totally dried product.

No.	c	f	m	yield
1	0.2	1.0	0.5	5.69
2	0.2	1.5	0.5	3.60
3	0.2	2.2	0.5	1.70
4	0.2	3.0	0.5	0.61
5	0.2	4.0	0.5	nil
6	0.2	2.2	0.25	1.43
7	0.2	2.2	1.0	1.82
8	0.2	2.2	2.0	—
9	0.2	1.8	0.5	2.33
10	0.2	1.8	0.5	1.79
11	0.2	1.8	1.0	1.69
12	0.2	0.5	0.5	7.71

Determination of mercury. The double sulphide is dissolved in 2 M sodium sulphide, after which mercury and tin are separated according to the method of Hiltner and Gittel [4]. Hydrogen peroxide is added dropwise to the sulphide solution with the result that the free sulphide ions and the sulphide in the thiostannate ions are oxidized to sulphate, and mercuric sulphide separates quantitatively. Tartrate ions are present in order to keep the tin in solution. According to our experience no greater excess of 30 % hydrogen peroxide than 0.5 ml should be added. The precipitated mercuric sulphide is filtered off on filter paper, washed and dissolved (both filter and sulphide) in conc. sulphuric acid plus nitric acid. After complete oxidation of the filter the sulphuric acid is diluted with water to twice its volume and boiled again in order to hydrolyze the nitrosyl sulphuric acid formed. After the solution is diluted with water and cooled down to below 15°C the mercury is titrated with standard thiocyanate solution. The thiocyanate solution is standardized against mercuric oxide (Merck, rubrum, p.a.). Experiments show that titration of mercury in sulphuric acid solution yields practically the same results as the usual titration in nitric acid solution. The method has been tested on known mixtures of mercury and tin with good results.

Determination of tin. The determination of tin is simply carried out by roasting the double sulphide, whereby the sulphur is oxidized to sulphur dioxide and the mercury evaporates while the tin is transformed to stannic oxide, which can be weighed. In order to determine the amount of impurities in the stannic oxide, the last compound is volatilized by heating with ammonium iodide according to Caley and Burford [5]. The method has been tested with good results on sulphide precipitates containing known amounts of mercury and tin.

Determination of sulphur. The determination of sulphur is carried out by oxidation of the sulphide to sulphate by means of bromine, the same method as often used for sulphur determination in pyrite [6]. The sulphate formed is precipitated with barium chloride according to Hintz and Weber [7]. The method yields excellent results when no tin is present, but too high results with tin present (coprecipitation of tin). This difficulty can be overcome by allowing the boiling with hydrochloric acid to proceed only to near dryness so that no stannic acid is formed, and further by precipitating the barium sulphate in 0.4 M hydrochloric acid, which at the same time is 0.2 M with respect to sodium chloride.

The results of the analyses carried out are given in Tables 2a and 2b. The estimations of mercury and sulphur were carried out without complications and the results are assumed to be rather accurate. The tin estimations, however, were rather tedious and inaccurate. It appeared that complete volatilization of stannic oxide with ammonium iodide required several heatings with ammonium iodide because of the impurities in the stannic oxide. These impurities turned out to be mainly silica. This silica must come from the

Table 2a. Analysis of the prepared double sulphides. The preparation numbers refer to the nos. in Table 1. The figures marked with * are not measured but calculated from the equation: % HgS + % SnS_2 = 94.0.

Preparation No.	% Hg	% Sn	% S	% Hg + Sn + S
1	58.49	17.70	19.87	96.06
2	57.35	18.43	19.48	95.26
3	57.30	17.92	20.10	95.32
4	56.63	18.5 *	19.67	—
6	57.53	17.46	19.35	94.34
7	56.78	18.84	20.35	95.97
9	57.43	18.74	19.76	95.93
10	57.72	—	19.71	—
11	56.94	18.72	20.48	96.14
12	59.0 *	16.42	—	—

Table 2b. "% S calculated" is calculated from the found (Table 2a) Hg and Sn percentages assuming that Hg is found as HgS and Sn as SnS_2. The atomic ratios are calculated from the analysis given in Table 2a.

Preparation No.	% S calculated	Atomic ratios Sn/Hg	S/Hg	Yields in the preparations % Hg	% Sn
1	18.91	0.511	2.124	66.7	33.2
2	19.12	0.543	2.125	51.6	18.7
3	18.83	0.529	2.195	31.2	7.5
4	—	0.55	2.173	13.8	2.5
6	18.63	0.514	2.104	26.2	6.1
7	19.25	0.560	2.242	34.0	8.6
9	19.30	0.551	2.153	38.1	11.6
10	—	—	2.136	28.9	—
11	19.21	0.555	2.250	26.9	8.3
12	—	0.47	—	68.2	64.1

action of sodium sulphide solution upon the glass containers, and then be coprecipitated when precipitating the double sulphides. We assume the tin determinations to be correct within 2 % and we assume them generally to be too low. The general features shown by Tables 2a and 2b are:

a. The sum of the three principal components is somewhat less than 100 %. The sulphur percentages, which correspond to the amounts found for mercury and tin, are somewhat smaller than the experimentally found percentages. The reason for this is partly that the tin determinations are a little too low and partly a considerable impurity of ammonium sulphide. In four of the preparations ammonia was determined. The content calculated as ammonium hydrogen sulphide was between 0.8 and 1.2 %. As will be evident from investigations later mentioned, the red double sulphides are colloidal and the particles negatively charged. The negative charge is presumably caused by adsorbed sulphide ions, which in the solid double sulphide must be accompanied by positive ions, *viz.* ammonium ions. All the solid double sulphides showed a considerable content of ammonia, while no chloride and no sodium could be detected.

b. The atomic ratios show that the composition of the double sulphides is not far from SnS_2,2HgS. However, the deviations from this formula are so considerable that they can hardly be due to analytical errors, and besides the composition is not constant. The atomic ratios Sn/Hg and S/Hg seem to increase with increasing f (the ratio between tin and mercury concentrations in the solution used for preparation). The atomic ratios Sn/Hg and S/Hg increase with increasing m (quantity of ammonium chloride added when precipitating the double sulphides).

c. The yields of both tin and mercury in the precipitates rapidly decrease with increasing f. In all the preparations the yield of mercury is greater than the yield of tin.

PROPERTIES OF THE DRIED DOUBLE SULPHIDES

After complete drying the double sulphides are black powders, some of them with a red tinge. They are nearly insoluble in water. In order to see

whether the substances are crystalline or not, X-ray powder photographs were taken of two of the preparations. The result was entirely negative, there being no indication at all of lines on the film.

PROPERTIES OF THE RED SOLUTION

Right after precipitation the double sulphides are, as mentioned above, readily soluble in water, and even after reprecipitation with ethanol and washing they are still water-soluble. The solution is deep red and of colloidal character.

A double sulphide was prepared as before (Table 1, expt. No. 2). After the ether used for the final washing had been allowed to evaporate, the double sulphide was dissolved in 100 ml water. This solution had a content of dry double sulphide of 3.6 g (solution A).

1. *Ultracentifuge investigation* *. The measurements were carried out in a Svedberg-type oil-turbine ultracentifuge at a speed of 1 000 r.p.s. at 27°C. A mixture of 1 volume "solution A" and 1 volume 0.2 M sodium chloride was used. The sedimentation was followed by the Schlieren-method. The colloidal particles had sedimentation constants between 2×10^{-13} and 20×10^{-13} c.g.s. units. Assuming that the particles are spherical and introducing Stokes's law, and assuming the density of the particles in water to be the same as that measured pycnometrically on the completely dried solid, namely 4, it is found that the mass of the particles lies in the range 1 300 to 40 000 atomic mass units, and their diameter in the range 10 to 30 Å.

2. *Conductance measurements.* The conductance was measured by a commercial instrument with dipping electrodes. The specific conductance of solution A was found to be 2.20 mohms^{-1} cm^{-1}. After 10 times dilution with water the specific conductance decreased to 295 μohms^{-1} cm^{-1} and after 100 times dilution to 47 μohms^{-1} cm^{-1}. The corresponding conductance per gram-atom mercury per cm^3 is calculated to 21, 29 and 45 ohms^{-1} cm^2, respectively. These values are rather high for a colloidal solution. However, the conductance is not only due to the charged colloidal particles and their "gegenions", but at least two thirds of the measured conductance is due to ionic impurities. Solution A diluted 10 times with water was dialysed 5 days; hereby the conductance decreased from 295 to 70 μohms^{-1} cm^{-1}.

3. *Dialysis.* The red constituent of the solution turned out not to be able to penetrate an ordinary dialysis membrane, (Visking cellulose casing), which fact showed that a colloidal solution was involved.

4. *Coagulation by the addition of electrolytes.* In the recorded experiments solution A was used 10 times diluted with water. To 4 ml of this solution was added 1 ml of a solution of an electrolyte. In Table 3 are recorded the electrolyte concentrations which cause half of the red double sulphide to coagulate. It is seen that the ratio of the concentrations of tri-, bi-, and uni-valent cations is 1:3:600. Magnesium does not seem, for some obscure reason, to fit into the scheme. The coagulating effect of electrolytes shows that the red double

* The authors are much indebted to the Research Laboratory of the Carlsberg Breweries, Copenhagen, for running the sedimentation measurements.

Table 3. Coagulation of the red water-soluble double sulphide by addition of different electrolytes. The given concentrations are the concentrations of electrolyte which are able to coagulate half of the red double sulphide.

Electrolyte	Molar conc.
NaCl	0.6
KCl	0.8
$NaNO_3$	0.8
$MgCl_2$	0.03
$ZnCl_2$	0.004
$BaCl_2$	0.003
$MgSO_4$	0.5
$ZnSO_4$	0.003
$AlCl_3$	0.0009
$CeCl_3$	0.0015

sulphide is a negatively charged colloid. The negative charge of the colloid was confirmed by paper electrophoresis.

5. *The action of acids and bases.* Diluted acid coagulated the colloidal particles. Diluted sodium carbonate solution had no influence on the colloidal solution. On the other hand a black precipitate of mercuric sulphide was formed and the supernatant liquid became colourless when the colloidal solution was made 0.1 M with respect to sodium hydroxide.

6. *Absorption spectrum in visible and ultraviolet light.* The absorption spectrum of solution A was measured by means of a recording spectrophotometer (Cary Model 11). In the range 800—700 mμ the absorption coefficient was very small (order of magnitude 0.1) but with decreasing wavelength it increased continuously in the range down to 200 mμ, *e.g.*, it is 3 at 650 mμ and 530 at 400 mμ. The laws of Lambert and Beer were found to be valid. The absorption spectrum is consistent with assuming the solution to be colloidal.

DISCUSSION

The investigated phenomena are consistent with many complications met when precipitating sulphides.

Some of the properties of the colloidal double sulphide can be explained by assuming a mixture of mercuric and stannic sulphide, *e.g.* the behaviour upon dry heating and the action of strong base, whereas other properties indicate a chemical compound, *e.g.* the colour of the substance and the pronounced tendency to form colloidal solutions.

The X-ray powder photographs of the dried double sulphide show that it is either built up of small colloidal crystallites or has a random or almost random structure.

The precipitation of the colloidal double sulphide proceeds rather slowly, and only part of the mercury is precipitated. The solution changes colour before the precipitation has become visible; this indicates that the first stage involves the mercury becoming bound in some way to the tin, possibly by formation of polynuclear sulphide complexes containing sulphide ions in excess to give a negative charge. These polynuclear complexes grow until they reach colloidal dimensions, and may then be precipitated by electrolytes.

REFERENCES

1. Storch, L. *Ber.* **16** (1883) 2015.
2. Wilm, Th. *Zhur. Russ. Fiz-Khim. Obshchestva* **19** 1 (1887) 60; abstracted in *Ber.* **20** R (1887) 232.
3. Feigl, F. *Z. anal. Chem.* **65** (1924) 25.
4. Hiltner, W. and Gittel, W. *Z. anal. Chem.* **101** (1935) 28.
5. Caley, E. R. and Burford, M. G. *Ind. Eng. Chem., Anal. Ed.* **8** (1936) 114.
6. Pierce, W. C. and Haenisch, E. L. *Quantitative Analysis*, 3rd Ed., John Wiley & Sons, Inc., New York 1948.
7. Hintz, E. and Weber, H. *Z. anal. Chem.* **45** (1906) 31.

Received June 27, 1960.

ACTA CHEMICA SCANDINAVICA 14 (1960) 1913–1918

Cleavage of Alkyl Cysteine Sulphoxides by an Enzyme in Onion (*Allium cepa*)

FLOYD P. KUPIECKI* and ARTTURI I. VIRTANEN

Laboratory of the Foundation for Chemical Research, Biochemical Institute, Helsinki, Finland

An enzyme which is specific for alkyl cysteine sulphoxides has been partially purified from onion. The enzyme appears to require pyridoxal phosphate as a cofactor, but shows no stimulation in activity by various metals. It shows a very low order of inhibition by various sulphydryl group reagents. Electrophoresis shows a single protein peak at two pH levels.

The first report of the enzymatic degradation of an alkyl cysteine sulphoxide was made by Stoll and Seebeck [1]. They have shown that an enzyme in garlic (*Allium sativum*) catalyzed the splitting of alliin (allyl cysteine sulphoxide) to pyruvic acid, ammonia, and allicin according to the following equation:

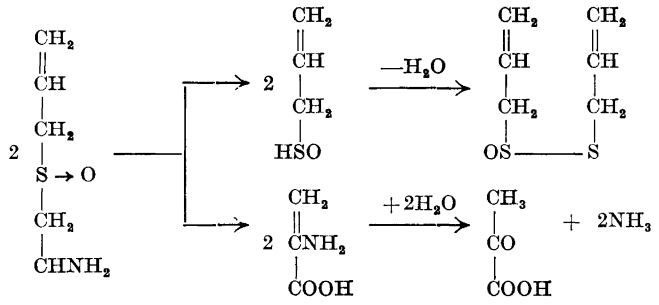

These authors postulated that the enzyme, alliinase, brought about the initial cleavage and that the primary products were split spontaneously to allicin, pyruvic acid, and ammonia.

Of the alkyl cysteine sulphoxides occurring naturally, methyl cysteine sulphoxide appears to have the widest distribution [2]. It occurs in several members of the *Liliaceae* and *Cruciferae* families as well as sporadically in the families *Compositae* (in *Lactuca sativa* L.), *Umbelliferae* (in *Cryptotaenia japonica* Hasskare) and *Leguminosae* (*Phaseolus vulgaris* L.) [3]. Propyl- and allyl

* Fulbright Research Fellow, 1959—1960. Present address: Departement of Biological Chemistry, University of Michigan, Ann Arbor, U.S.A.

cysteine sulphoxides have been reported only in *Liliaceae*, where they are less widely distributed than is the methyl homologue. Ethyl cysteine sulphoxide has thus far been reported only in *Ipheon uniformum*, a member of *Liliaceae*. The reported occurrence of specific alkyl cysteine sulphoxide splitting enzymes is restricted to the *Liliaceae* family.

The known occurrence in appreciable quantities of methyl- and propyl cysteine sulphoxides in onion [4], and the release of pyruvic acid in fresh onion extracts [5,6] has led us to choose this plant for studying the cleavage of alkyl cysteine sulphoxides. The following is a report on the partial purification of the enzyme and some of its properties.

EXPERIMENTAL

Preparation of enzyme. All steps were carried out at 0° unless otherwise indicated. 800 g of mature onions freed of skins, tops, and roots were homogenized in a "Waring type" blendor with 400 ml of 0.10 M potassium phosphate, pH 7.4, for 3 min in four equal portions. The thick suspension was stirred for 30 min and filtered through cheese cloth. The filtrate was centrifuged at 12 000 × *g* for 15 min. 40 mg per ml of charcoal was added to the bright yellow solution. After stirring for 15 min the charcoal was removed by centrifugation. This step removes a large amount of the coloured non-protein material as well as about one-half of the proteins. The resulting supernatant solution is almost colourless.

Calcium phosphate gel [7] (1 mg for each 3 ml of solution) was added and after stirring 15 min the suspension was centrifuged. There is only a small increase in specific activity following this step, but more of the non-protein material is removed and the solution becomes colourless.

The enzyme solution was brought to 0.8 saturation by the addition of solid ammonium sulphate during a 20 min period. After stirring 45 min Hyflo Super Cel (1 g per each 200 g of onion) was added and stirring was continued 15 min longer. The precipitate was removed by centrifugation and the Hyflo was washed twice with 0.05 M potassium phosphate pH 7.4 to give a final protein concentration of 30—35 mg per ml. The enzyme solution was brought to 0.40 saturation with ammonium sulphate, stirred 30 min and centrifuged. The precipitate was dissolved in the same phosphate buffer as above to give a solution containing 40—45 mg protein per ml. This was again treated with ammonium sulphate. The fraction obtained at 0.25 saturation was discarded, the solution was brought to 0.60 saturation and the precipitate was dissolved in 0.05 M potassium phosphate, pH 7.4. The resulting enzyme solution was clear and bright yellow. The enzyme is stable at all stages of purification to storage at −20° for several weeks. All fractions, except the extract, retain almost full activity when stored at 0° for 1 to 2 weeks. Protein concentration of the enzyme solutions was determined spectrophotometrically by light absorption at 280 and 260 mμ [8].

Enzyme assay: The enzyme was assayed by measuring the amount of pyruvic acid liberated according to the method of Friedemann and Haugen [9]. The standard assay system contained 125 μmoles of potassium phosphate buffer, pH 7.4, 2.5 μmoles $MgCl_2$, 25 μg of pyridoxal phosphate, 13 μmoles alliin (or other alkyl cysteine sulphoxide), and enzyme in a final volume of 1.0 ml. All components except the substrate were preincubated 10 min at 20°. Addition of substrate was followed by incubation at 20° for 20 min. A control tube without substrate was included for each sample of enzyme. No pyruvate was generated from the substrate in the absence of enzyme. 0.25 ml of 40 % TCA was added after incubation and 0.40 ml aliquots were used in the determination of pyruvic acid. A unit of enzyme is defined as that amount which yields 1 μmole of pyruvic acid under the assay conditions. The specific activity of the enzyme is expressed as the number of units per mg of protein.

RESULTS

Electrophoresis. The enzyme solution was subjected to electrophoresis at two stages of preparation and at pH 6.8 and 7.8. The apparatus was the Perkin-

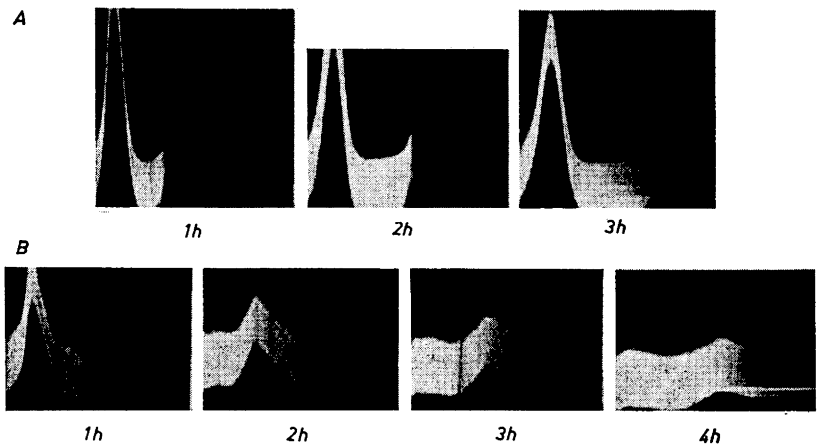

Fig. 1. Electrophoresis patterns. A shows the pattern obtained after calcium phosphate gel treatment (see text), B after 0.25—0.60 ammonium sulphate precipitation.

Elmer Model 38. Fig. 1A shows the pattern given after calcium phosphate gel treatment. To concentrate the protein by a factor of 10 the enzyme was subjected to lyophilization, dialyzed against distilled water and lyophilized again before dialysis against the buffer used for electrophoresis. The fraction obtained at 0.25—0.60 saturation with ammonium sulphate was also subjected to electrophoresis. Both preparations showed similar results at both pH's. The calcium phosphate gel supernate, however, contained a second peak which did not move at either pH. Fig. 1B shows that this peak was removed by precipitation with ammonium sulphate.

Enzyme activity as a function of pH. Fig. 2 shows that the enzyme is active over the range of pH 5.6 to 9.0, with maximal activity at pH 7.4.

Substrate specificity. Table 1 shows the various substrates that have been tested with the enzyme. As can be seen in the table only sulphoxides that are derived from cysteine are cleaved by the enzyme.

Inhibition by carbonyl group reagents. Table 2 gives the results obtained when the enzyme was tested with the three carbonyl group reagents: hydroxyl-

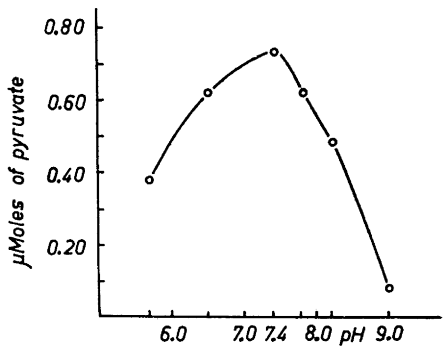

Fig. 2. Enzyme activity as a function of pH. The assay described in the text (with 250 µmoles of buffer) was used with 20 µg of the enzyme after treatment with charcoal. The substrate was synthetic methyl cysteine sulphoxide. Potassium phosphate buffers were used at pH 5.7, 6.5, 7.4, and 7.8. Tris buffer was used at pH 7.4, 8.2, and 9.0.

Table 1. Effect of carbonyl group reagents on enzymatic activity. The standard assay described in the text was used with some modifications. In experiments numbered 1 pyridoxal phosphate was omitted and the appropriate inhibitor was preincubated with all components except alliin for 20 min at 20°. In experiments numbered 2 the inhibitor was preincubated 10 min with the other components, the pyridoxal phosphate was added and preincubation was continued for 10 min. The order of preincubation of pyridoxal phosphate and inhibitor was reversed in experiments numbered 3. Pyridoxal phosphate concentration was 4×10^{-3} M.

No.	Substance added	Molarity of inhibitor	% inhib.	Molar conc. of inhibitor	% inhib.	Molar conc. of inhibitor	% inhib.
1	Hydroxylamine	10^{-6}	38	10^{-5}	75	10^{-4}	93
2	Hydroxylamine + pyridoxal—PO_4	10^{-6}	13	10^{-5}	58	10^{-4}	90
3	Pyridoxal—PO_4 hydroxylamine	10^{-6}	5	10^{-5}	38	10^{-4}	74
1	Hydrazine	10^{-6}	12	10^{-5}	25	10^{-4}	66
2	Hydrazine + pyridoxal—PO_4	10^{-6}	0	10^{-5}	17	10^{-4}	59
3	Hydrazine + pyridoxal—PO_4	10^{-6}	0	10^{-5}	2	10^{-4}	37
1	*Iso*nicotinic hydrazide	10^{-6}	0	10^{-5}	0	10^{-4}	0
2	*Iso*nicotinic hydrazide + pyr.—PO_4	10^{-6}	0	10^{-5}	0	10^{-4}	0
3	*Iso*nicotinic hydrazide + pyr.—PO_4	10^{-6}	0	10^{-5}	0	10^{-4}	0

amine, hydrazine, and *iso*nicotinic acid hydrazide, at three concentrations. At the concentrations used hydroxylamine was the most effective inhibitor. Hydrazine was somewhat less effective, while *iso*nicotinic acid hydrazide failed to show any inhibition at these concentrations.

Stimulation by pyridoxal phosphate. The stimulation due to pyridoxal phosphate is shown in Table 3. As can be seen in the table, very little increase in pyruvate generation is found when pyridoxal phosphate is added to the crude extract. The stimulation shown in other fractions is about 40 %. Dialysis reduces enzymatic activity to less than one-half (Expts. 4 and 5). The stimulation due to pyridoxal phosphate is, however, the same in each case.

The effect of sulphydryl group inhibitors on enzyme activity. The following inhibitors were tested at each of the molar concentrations, 10^{-6}, 10^{-5}, and 10^{-4}: *p*-chloromercuribenzoate, N-ethylmaleimide, iodosobenzoate; none inhibited at these concentrations. The latter two were also tested at a concentration of 10^{-2} M and were found to inhibit 30 % and 25 %, respectively. Iodoacetate and iodoacetamide failed to inhibit at 10^{-2} M but showed an inhibition of 25—30 % at 5×10^{-2} M. When corrected for an observed reaction with pyruvic acid, cyanide showed no inhibition even at 10^{-2} M while sulphide inhibited 30 % at this concentration.

Table 2. Specificity of enzyme. The standard assay described in the text was used except with benzyl cysteine sulphoxide. Because of the low solubility the substrate concentration was only half of the concentration used in the standard assay.

Substrate	μmoles of 2,4-dinitrophenylhydrazone
Alliin	2.49
Methyl cysteine sulphoxide	0.61
Ethyl » »	0.86
Propyl » »	0.53
i-Propyl » »	0.38
Benzyl » »	0.34
*Cyclo*alliin	0
Cysteine	0
Methyl cysteine	0
Ethyl »	0
Propyl »	0
Allyl »	0
S-Methylmethionine sulphonium bromide	0
S-Benzylmethionine » chloride	0
Thiazolidine carboxylic acid	0
Methionine sulphoxide	0
Methionine sulphone	0
Cysteine sulphinic acid	0

DISCUSSION

The experimental data presented here show the results of our attempts to purify the S-alkyl cysteine sulphoxide splitting enzyme. Renis [10] states that all attempts to purify the enzyme from onion were unsuccessful, although active crude extracts could be obtained in his laboratory. We have tried many of the usual procedures for enzyme purification, *e.g.* precipitation with ammonium sulphate, alcohol, or acetone. These procedures, in various combinations, together with gel absorption steps have given about 4—5 fold purification, but with serious losses in enzyme units. Dialysis was tried at various points in the purification and always resulted in a large loss of activity, only a part of

Table 3. The influence of pyridoxal phosphate on enzymatic activity. The standard assay was used except that pyridoxal phosphate was omitted from the experimental tube as well as the control tube (without substrate) where indicated.

Expt. No.	Enzyme fraction	μmoles pyruvate released		% Stimulation
		with pyridoxal—P	without pyridoxal—P	
1	Extract	1.09	0.99	10
2	Calcium PO_4 gel supernate	1.07	0.76	42
3	Extract	1.55	1.44	8
4	Dialyzed 0—0.40 $(NH_4)_2SO_4$ fraction	0.30	0.22	39
5	Undialyzed 0—0.40 $(NH_4)_2SO_4$ fraction	0.69	0.49	41

which could be restored with pyridoxal phosphate. Pretreatment of the extract with the relatively large amount of charcoal, as described, removes most of the interfering materials and makes some further purification possible. The series of steps described here results in preparations which have a specific activity about six times as great as the original extracts. However, the electrophoretic pattern of the most purified fraction and failure to increase the specific activity beyond 6 suggest that the purity of the enzyme may already be fairly high.

In all experiments reported here the Mg^{++} ion was used routinely, although no stimulation by this ion or Al^{+++}, Cu^{++}, Co^{++}, and Mn^{++} could be shown. Furthermore, a several fold excess of Versene failed to inhibit the reaction. The loss in units upon dialysis could be only partly regained by addition of pyridoxal phosphate. Addition of concentrated dialysate, boiled enzyme, or preparations from which protein was removed by alcohol did not further increase the activity.

The sharp pH optimum shown at pH 7.4 is in marked contrast to that reported by Stoll and Seebeck [1] for the alliin cleaving enzyme from garlic. Their enzyme was active between pH 4 and 9, but showed a broad optimum range from pH 5 to 8. Unlike the garlic enzyme, which could be precipitated at pH 4, the onion enzyme lost all its activity after this precipitation.

As shown in Table 2, the enzyme cleaves all the alkyl cysteine sulphoxides that were tested and alliin is the best substrate. This fact is somewhat surprising since alliin appears to be absent from onion. An alkyl cysteine sulphoxide splitting enzyme has recently been purified 200 fold from *Albizzia lophanta* by Schwimmer and Kjaer [11] but it splits the S-alkyl cysteines as well as the sulphoxides.

At the present time it is not possible to state conclusively whether one or more enzymes are involved in cleaving the sulphoxides to pyruvic acid, ammonia, and alkyl thiosulphinates. We have tried recombination of various fractions a number of times and have never found any indications that more than a single enzyme could be involved.

REFERENCES

1. Stoll, A. and Seebeck, E. *Helv. Chim. Acta* **32** (1949) 197.
2. Fujiwara, M., Yoshimura, M., Tsuno, S. and Murakami, F. *J. Biochem. Tokyo* **45** (1958) 141.
3. Morris, C. J., Thompson, J. F. and Zacharius, R. M. *Nature* **178** (1956) 593.
4. Virtanen, A. I. and Matikkala, E. J. *Acta Chem. Scand.* **13** (1959) 623.
5. Morgan, E. J. *Nature* **157** (1946) 512.
6. Vilkki, P. *Suomen Kemistilehti* **B 27** (1954) 21.
7. Keilin, D. and Hartree, E. F. *Proc. Roy. Soc. London* **B 124** (1938) 397.
8. Warburg, O. and Christian, W. *Biochem. Z.* **310** (1941) 402.
9. Friedemann, T. E. and Haugen, G. E. *J. Biol. Chem.* **147** (1943) 415.
10. Renis, H. E. *Dissertation Abstr.* **17** (1956–7) 1456.
11. Schwimmer, S. and Kjaer, A. *Biochim. et Biophys. Acta* **42** (1960) 316.

Received May 28, 1960.

ACTA CHEMICA SCANDINAVICA 14 (1960) 1919–1926

Compounds Formed by Air-dried Insulin Crystals on Uptake of Metal Salts from Ethanolic Solutions

E. JENSEN, A. TOVBORG JENSEN and K. MARCKER*

Den Kgl. Veterinær- og Landbohøjskoles Kemiske Laboratorium, København, Denmark

X-Ray powder diffractometer data from air-dried insulin yield good lattice constants and a surmise of degree of crystallinity. Although the uptake by air-dried insulin of zinc ion and zinc chloride from an ethanolic solution seems to follow an adsorption isotherm, chemical compounds are formed, since lattice constants and reflection intensities in the products vary systematically with increasing zinc content. From X-ray data the uptake is seen to fall in three distinct stages: I, until 2 zinc atoms per Sanger unit are taken up; II, till 4 zinc atoms are taken up; III, when more zinc is taken up. As shown earlier step I is an exchange of zinc ions for hydrogen ions. In steps II and III zinc chloride is taken up. Lattice constants for a few compounds with other metal salts are given.

The shrinking of insulin crystals on drying is not reversed by uptake of water vapour. Air-dried insulin took up 18 % of water, but the lattice constants remained unchanged.

Marcker [1] recently described some new compounds of insulin with metals (metal ions) and metal salts, formed by treating air-dried insulin crystals with ethanolic solutions of metal salts. An X-ray crystallographic study of the compounds was begun at an early stage of this work. It has given a more detailed picture of the compounds than unaided chemical methods. A few experiments of the influence of air-drying and subsequent moistening of insulin crystals on their lattice constants will also be described.

X-RAY TECHNIQUE

Insulin crystals under mother liquor are well ordered, and give X-ray reflections up to glancing angles corresponding to interplanar spacings to about 1 Å. Air-dried insulin crystals, on the other hand, have lost the finer details of their internal order. X-Ray reflections corresponding to interplanar spacings shorter than 5—7 Å have vanished on drying. Since Marckers com-

* Present address: Universitetets Fysisk-Kemiske Institut Copenhagen, Denmark.

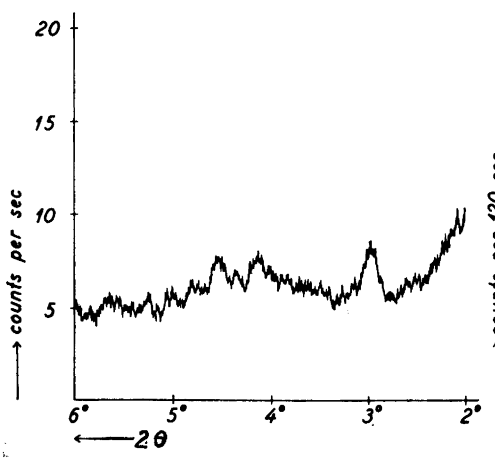

Fig. 1. Powder diagram of air dried insulin crystals. Specimen 1. 6.8 atoms of zinc per Sanger unit. Cu*Kα* radiation, automatic recording. 2Θ from 2 to 6°.

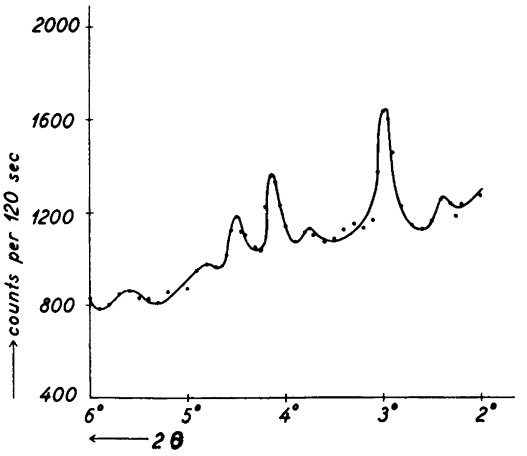

Fig. 2. Powder diagram of air dried insulin crystals. 2Θ from 2° to 6°. Specimen as in Fig. 1. Cu*Kα* radiation. Stationary 120 secs. counting at intervals of 0.05° to 0.10° in 2Θ.

pounds were prepared from air-dried insulin, and because the crystals were small, no attempt was made to apply single crystals methods to them.

The powder method, unpromising at first, was found quite useful. In the early days of protein crystallography, powder methods were used a good deal. However poor the diagrams, they contained lines and gave evidence of internal order, and of the very long interplanar spacings present. But the lines of early powder diagrams of protein crystals were in general »clashings» between several reflections. Only two cases are known to us where the indexing of four or five lines from a protein crystal powder diagram has been claimed: ferritin and apoferritin (Fankuchen [2]).

Fig. 1 shows an automatic recording of the powder diagram of crystalline air-dried insulin from $2\Theta = 2°$ to $2\Theta = 6°$. The diagram was taken with a General Electric X-Ray Diffractometer (XRD-3) fitted with a special linear amplifier, radiation filtered Cu*Kα*. The slit system was very narrow as seen from the low intensity. The diagram shows 3 dubious lines. Fig. 2 shows the improvement obtained when the same diagram is constructed from 120 sec. stationary countings at points 0.05° to 0.10° apart. Seven lines are seen now. The same technique was adopted in all further work, and similar diagrams obtained, except of course for samples whose structure had deteriorated as a result of chemical treatment of the sample. The lines could always be indexed by an adaption of Crowfoots lattice constants for air-dried insulin. An example is given in Table 1, where the results from the diagram, Fig. 2, are given. All lattice constants have been referred to the hexagonal cell whose volume is three times that of the true rhombohedral cell, and contains 18 Sanger units of molecular weight 5 800 plus water *etc.* Since the innermost part of the powder diagram is so easily indexed it is tempting to proceed further out, *inter alia* in

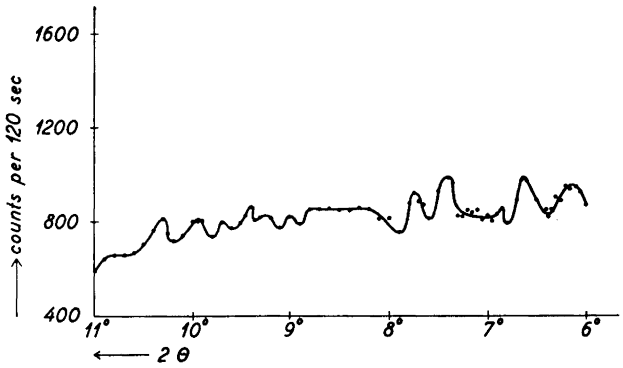

Fig. 3. Powder diagram of air dried insulin crystals. 2Θ from 6° to 11°. Same technique as in Fig. 2.

order to obtain more accurate lattice constants. A glance at Fig. 3 which gives the diagram from $2\,\Theta = 6°$ to $2\,\Theta = 11°$ will show why such attempts at indexing failed. A considerably refined technique or independent knowledge of relative intensities would be necessary, since calculation shows that there are some 30 possible reflections in this part of the diagram.

INSULIN-ZINC AND INSULIN-ZINC-$ZnCl_2$ COMPOUNDS

The following work was done using twice recrystallized pig-insulin *. Table 2 gives lattice constants for 4 chemically untreated samples of insulin crystals, all data obtained as described. The classical data by Crowfoot-Hodgkin [3] and Crowfoot and Riley [4] for dry and wet insulin are also tabulated. In column 4 of Table 2 are given the lattice constants for a specimen of insulin under its mother liquor **. In column 5 is given the lattice constants for the same speci-

Table 1. X-Ray diffractometer data for insulin, 6.8 Zn atoms per Sanger unit (specimen 1). Comparison of observed and calculated $\sin^2\Theta$-values. Cu-$K\alpha$ radiation.

$2\,\Theta$	Indices $h\,k\,i\,l$	$10^4 \times \sin^2\Theta_{obs.}$	$10^2 \times \sin^2\Theta_{calc.}$	Relative intensity obs.
2.36°	$11\bar{2}0$	4.24	4.26	11
2.97°	$10\bar{1}1$	6.72	6.79	100
3.76°	$20\bar{2}1$	10.76	11.05	5
4.13°	$30\bar{3}0$	12.98	12.78	46
4.49°	$21\bar{3}1$	15.34	15.31	23
4.70°	$22\bar{4}0$	16.81	17.04	1
5.60°	$10\bar{1}2$ $13\bar{4}1$	23.86	22.90 23.82	15

Unit cell $a = b = 74.7 \pm 0.4$ Å
$c = 33.3 \pm 0.2$ Å

* kindly placed at our disposal by Roskilde Medical Company, Roskilde.
** a phosphate buffer with pH = 6.7, total phosphate molarity approximately 0.035.

Table 2. Lattice constants for untreated insulin crystals.

No.	1	2	3	4	5	6
Specimen	Crowfoot [3]	R M C	Novo	R M C	No. 4 dried	Crowfoot and Riley [4]
Zinc content	?	0.8 %	2.2 %	0.6 %	0.6 %	?
Humidity	air dried	air dried	air dried	wet	air dried	wet
a, Å	74.8	74.1	75.0	90.4	77.0	83.0
c, Å	30.9	32.8	31.8	32.8	31.7	34.0

men after air drying. The figures in columns 4 and 5 are not as accurate as the other figures in Table 2, but they prove beyond doubt that our wet specimen has been in a higher state of hydration than that of Crowfoot and Riley (column 6). In order to see whether the lattice constants of dry and shrunk insulin crystals varied when the crystals took up humidity from the air — in which case we would have had to work in a controlled atmosphere — we left a specimen overnight in an atmosphere of 95 % relative humidity at room temperature. The weight of the sample increased by 18 %. We registered its powder diagram in the humid state, dried it again and registered the powder diagram a third time. The same glancing angles and reflection intensities were found in the three experiments within experimental error. So the shrinking was not reversed by the uptake of humidity from the air, and controlled atmospheric humidity is unnecessary when working with air-dried crystals. Whether the molecules of the 18 % of water taken up were placed in holes in the insulin crystals proper, or in an amorphous fraction undoubtedly present, is not clear to us.

In Figs. 4 and 5 the lattice constants of one untreated specimen of air-dried insulin crystals and of 7 specimens treated with ethanolic solutions of zinc chloride are plotted against the zinc content of the specimens. For details

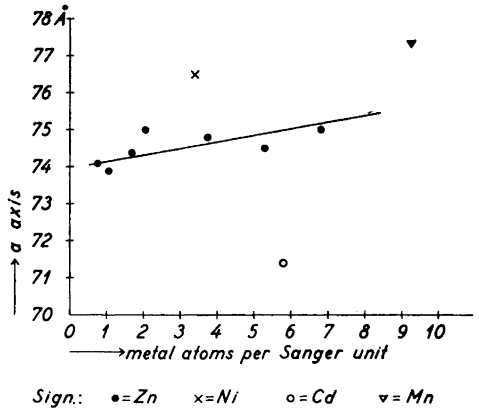

Fig. 4. Variation in *a*-axis length of dry insulin with increasing zinc content.

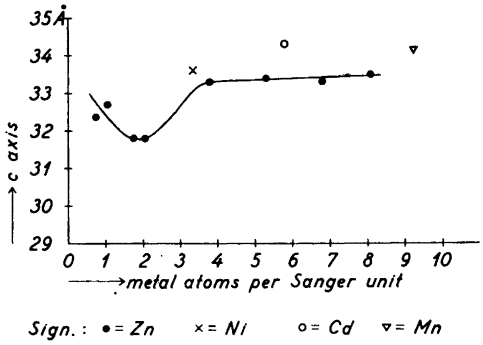

Fig. 5. Variation in *c*-axis length of dry insulin with increasing zinc content.

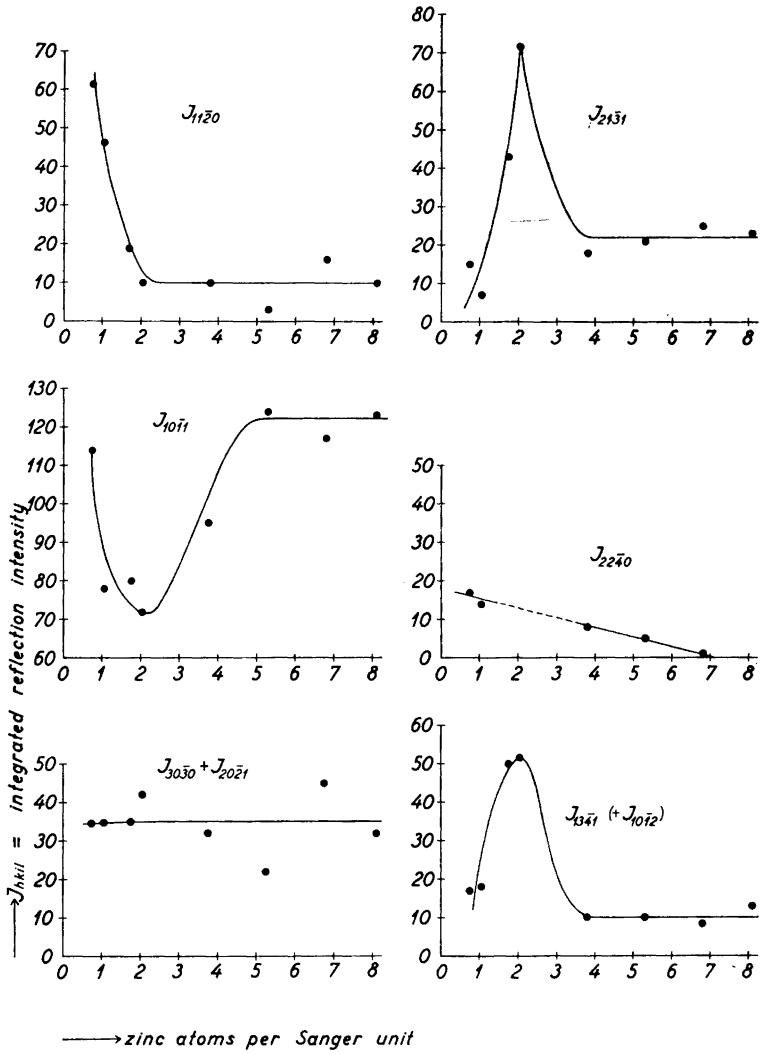

Fig. 6. Variation in integrated reflection intensity with increasing zinc content for the innermost lines in the powder diagram of dry insulin.

of preparation see Ref.[1] When the accuracy of the a-axis values ($\pm$ 0.4 Å) is borne in mind it is difficult to conclude anything from Fig. 4, except that the uptake of zinc brings about a gradual increase in a. On the other hand, it seems legitimate to conclude from Fig. 5 that the c-axis (accuracy $\pm$ 0.2 Å) shrinks when the zinc content increases to 2 atoms per Sanger unit, and expands again as two more atoms are taken up. If the zinc content increases from 4 to the maximal 8 atoms per unit the c-axis remains constant. This indicates

that the reaction is a 3-stage process. Fig. 4 from which nothing definite could be concluded is perhaps not incompatible with a 3-stage process.

Considerably more evidence for a 3-stage process is provided by the variation in reflection intensity with zinc content for 6 lines, as seen from Fig. 6. The intensities are given as integrated intensities measured as peak area over a smoothed background. Four of the curves indicate a break at about 2 zinc atoms per Sanger unit, three curves another break at about 4 atoms of zinc per unit. No significant variation occurs at higher values. The diagram for reflection $30\bar{3}0$ plus $20\bar{2}1$ presents a confused picture. The shape of the combined peaks made a graphical separation impossible. In addition the combined peak area contained in 2 out of 3 diagrams a third peak of an unknown impurity. This peak was the only one found in any diagram which could not be accounted for by the "quadratic form" for insulin. Its area could not be measured and subtracted, and since it varied between zero and a finite value its presence adds to the confusion in reflection intensity.

The break at 2 atoms of zinc was explained later when it was found by chemical analysis that at this point the reaction between insulin crystals and an ethanolic zinc chloride solution changes from an exchange of hydrogen ions in the crystal for zinc ions from the solution to an uptake of zinc and chloride ions [1]. The break at 4 zinc per Sanger unit is so far unexplained chemically. From chemical evidence, especially the remarkable work by Schlichtkrull [5], it seems beyond doubt that the zinc atom per 3 Sanger units which is necessary to obtain insulin in the crystalline state, is placed in a fixed position in the crystal. From our work we think it may be safely concluded that the zinc ions subsequently taken up by ion exchange until two atoms are present, *and* the first two moles of zinc chloride taken up when the ion-exchange capacity is exhausted, are likewise placed in fixed positions. Were they placed at random it would be difficult to understand the gradual but drastic changes in reflection intensity caused by their gradual introduction. So we must conclude that these products are chemical compounds. On the other hand, there seems to be no evidence for a fixed position of the last four molecules of zinc chloride, since they cause no systematic change in reflection intensities.

It is somewhat unexpected that the reaction between insulin crystals and an ethanolic solution of zinc chloride is a three-stage process where first and second stage lead to chemical compounds, since the entire reaction seems to follow an adsorption isotherm; see Fig. 1 in Ref.[1] But there is in fact nothing contradictory in the findings. Stage 3 *is* most probably an adsorption process, stage 2 is the formation of a kind of interstitial compound, and stage 1 an ion exchange process, all of which follow a function similar to an adsorption isotherm. The experiments, the results of which are given in Fig. 1 in Ref. [1] could hardly be expected to distinguish between one adsorption isotherm and three adsorption isotherms pieced together: one from ordinates 0 to 2, another between ordinates 2 and 4 and a third at ordinate values higher than 4.

COMPOUNDS OF ZINC-INSULIN WITH OTHER METAL CHLORIDES

The reaction between dry insulin crystals and ethanolic solutions of $NiCl_2$, $CdCl_2$, $CaCl_2$, $MgCl_2$, $MnCl_2$ and $CoCl_2$, briefly mentioned in Ref.[1] was

Table 3. Chemical composition and X-ray characterisation of compounds formed when crystalline zinc-insulin was suspended in an ethanolic solution of another heavy metal chloride.

Metal chloride	Me atoms/unit	Zn atoms/unit	*a*, Å	*c*, Å	powder diagram
$NiCl_2$	2.8	0.5	76.5	33.6	good
$MnCl_2$	8.8	0.4	77.3	34.1	good
$CdCl_2$	5.4	0.3	71	34	bad
$CoCl_2$	7.8	<0.1			no diagram
[untreated	0	0.7	74.1	32.4	good]

not followed up by a systematic X-ray study as in the case of the reaction with a $ZnCl_2$ solution. Lattice constants and compositions for three compounds of insulin and manganese, nickel and cadmium chlorides are given in Table 3. The compounds are also entered in Figs. 4 and 5. The lattice constants are seen to differ widely from those of compounds in the $ZnCl_2$ series. The partial replacement of zinc ions with other heavy metal ions, and the uptake of additional metal ion and metal chloride apparently cause more drastic changes than the reaction with zinc chloride.

This phenomenon deserves a closer study. Chemical composition of the products and the character of their powder diagrams are also given in Table 3. It is seen that as long as 0.4 atoms of zinc per Sanger unit are left in the crystals their X-ray diagram is good. When only 0.3 atoms are left their structure has deteriorated, and when less than 0.1 atom is left the structure is so deranged that no powder diagram lines are visible, although the appearance of the crystals under the microscope is unchanged. The deterioration sets in between the limits of 0.4 and 0.3 atoms of zinc per Sanger unit. It will be remembered that one metal atom per 3 Sanger units is the minimum number of metal atoms that can produce crystalline insulin. It is tempting to identify the minimum number of zinc atoms (roughly 0.35) that must be left in air-dried insulin if the ordered internal structure shall not break down, with the number of atoms (*i.e.* 0.33) that must be built in, if insulin shall crystallize from an aqueous solution. It is true — as known from Schlichtkrulls tracer experiments [6] with ^{65}Zn — that any zinc atom in wet insulin crystals can be replaced rapidly by any other zinc atom without deterioration of structure. But it is not improbable that the replacement of a zinc atom with another zinc atom be a milder process than the replacement of a zinc atom with a cobalt atom. The cobalt atom might cause a change of coordination, or it might occupy another site than the zinc atom and hereby cause a breakdown of the order still left in insulin crystals after drying.

CONCLUSION

The study of powder diagrams — or as here diffractograms — is not a general method for the investigation of crystalline proteins. Insulin with its small and highly symmetric unit cell is uniquely favourable. There is hardly any other proteins with which experiments similar to those described above could be made. But the method might be of interest in other studies of

that particularly important protein. It is a routine method, it is "non-destructive", and it yields well defined physical constants, *viz.* degree of crystallinity, lattice constants and reflection intensities from known sets of lattice planes, properties whose variations under different circumstances are of some interest.

ADDENDUM

The number (N) of metal atoms per Sanger unit has been calculated from

$$N = \frac{\%\ \text{Me}}{\text{atomic weight of Me}} \Big/ \frac{100 - \%\ \text{Me} - \%\ \text{Cl}}{6\,000} \qquad \text{(A)}$$

In this equation the weight of a Sanger unit of air-dry pig-insulin including 6 % of water has been set equal to 6 000, and it has been assumed that no water is expelled when metal and salt are taken up. In a previous paper [1] the metal contents of the same specimens were calculated from

$$N = \frac{\%\ \text{Me}}{\text{atomic weight of Me}} \Big/ \frac{100}{6\,000} \qquad \text{(B)}$$

which gives the number of metal atoms per Sanger unit, provided the amount of water expelled equals that of the metal plus metal salt taken up. We think (A) is less arbitrary than (B). However, only complete analysis of a specimen can decide which assumption be the better. For specimens containing less than four metal atoms per Sanger unit there will be no significant differences. For the specimens with higher metal contents discussed in Ref.[1] we think the following stoichiometric formulae calculated from (A) are more probable than those given by Marcker (shown in brackets)

Insulin, 2 Zn, 6 $ZnCl_2$	(Insulin, 2 Zn, 5 $ZnCl_2$)
Insulin, $\frac{1}{3}$ Zn, $1\frac{2}{3}$Mn, 7 $MnCl_2$	(Insulin, $\frac{1}{3}$ Zn, $1\frac{2}{3}$ Mn, 6 $MnCl_2$)
Insulin, $\frac{1}{3}$ Zn, $1\frac{2}{3}$ Cd, 4$CdCl_2$	(Insulin, $\frac{2}{3}$Zn, $1\frac{2}{3}$ Cd, 3 $CdCl_2$)
Insulin, 2 Co, 6 $CoCl_2$	(Insulin, 2 Co, 5 $CoCl_2$)

REFERENCES

1. Marcker, K. *Acta Chem. Scand.* **13** (1959) 2036.
2. Fankuchen, I. *J. Biol. Chem.* **150** (1943) 57.
3. Crowfoot, D. *Proc. Roy. Soc. London (A)* **164** (1958) 550.
4. Crowfoot, D. and Riley, D. *Nature* **144** (1939) 1011.
5. Schlichtkrull, J. *Acta Chem. Scand.* **10** (1956) 1455.
6. Schlichtkrull, I. *Insulin Crystals. Diss. København* 1958, p. 66.

Received April 30, 1960.

ACTA CHEMICA SCANDINAVICA 14 (1960) 1927–1938

Electroörganic Preparations

IX *. Polarography and Reduction of Substituted Aryl Alkyl Ketones

HENNING LUND

Leo Pharmaceutical Products, Ballerup, Denmark **

Ketones with the general formula Ar—CO—CRR'X, where R and R' are hydrogen, alkyl or aryl and X is —Cl, —OH, —OCH_3, —OC_6H_5, —OOCR, —SC_6H_5, —SCN, —CN, or —ONO_2, have been investigated polarographically and by means of controlled potential reductions at a macro mercury cathode. In most cases the reduction of the C—X bond occurs at less negative potentials than that of the carbonyl group.

Some types of 2-substituted acetophenones have previously been investigated polarographically. Thus Pasternak and Halban [1] studied 2-bromoacetophenone, Adkins and Cox[2] 2-bromo*iso*butyrophenone, Elving and Leone [3] 2-fluoroacetophenone, and Zuman and Horak [4] investigated a series of N-substituted 2-aminoacetophenones. Methylbenzoylcarbinol has been studied by Fedoronko [5] and benzoin by Pasternak [6] and Santavy [7].

Elving and Leone [3] studied the electrode reaction by means of controlled potential reductions at a macro mercury electrode and Zuman and Horak [4] identified the reduction products from a prolonged electrolysis at the dropping mercury electrode by means of paper chromatography. In both cases the electrode reaction corresponding to the first wave was a reduction to acetophenone.

Benzoin has been investigated by means of controlled potential reductions by Pasternak [6], and it was found that the reduction product at pH 8 was hydrobenzoin, whereas the isolated product from a reduction at pH 1.3 was the higher melting form of deoxybenzoin pinacol, 1,2-diphenyl-1,2-dibenzylethylene glycol.

In the present investigation compounds with the general formula Ar—CO—CRR'—X, where R and R' are hydrogen, alkyl or aryl, X is —OH, —OCH_3, —OC_6H_5, —OOCR, —SC_6H_5, —SCN, —ONO_2, or —CN, have been

* Part VIII: *Collection Czechoslov. Chem. Communs. In press.*

** Present address: Chemical Department, University of Aarhus, Denmark

investigated polarographically and the electrode reactions have been studied by means of controlled potential reductions at a macro mercury electrode. The results obtained at the micro and the macro electrodes are compared and discussed.

RESULTS

In Table 1 are given polarographic data for 2-hydroxyacetophenone (I), 2-acetoxyacetophenone (II), 2-benzoxyacetophenone (III), 2-phenoxyacetophenone (IV), phenacyl phenyl sulfide (V), 2-thiocyanatoacetophenone (VI), and phenacyl nitrate (VII).

2-Hydroxyacetophenone shows in mineral acid solution two waves. The height of the first wave corresponds to a two-electron reduction, whereas the second one is somewhat smaller than corresponding to a one-electron reduction. The half-wave potential of the second wave coincides with that of acetophenone in the same solution. This suggests that the electrode reaction corresponding to the first wave is a reduction of the primary alcohol to a methyl group and the second wave is due to the reduction of the acetophenone thus formed, and this has been confirmed by a controlled potential reduction. The electrode reaction is analogous to that of certain 16-hydroxy-17-ketosteroids [8], in which the hydroxyl group is reduced at less negative potentials than the carbonyl group; the half-wave potentials of the steroids are, however, considerably more negative.

At higher pH-values the waves of 2-hydroxyacetophenone merge; the reduction path is not clear and the low stability of the compound at high pH-

Table 1. Limiting currents in μA and half-wave potentials *vs* S.C.E. of 2-hydroxyacetophenone (I), 2-acetoxyacetophenone (II), 2-benzoxyacetophenone (III), 2-phenoxyacetophenone (IV), phenyl phenacyl sulfide (V), 2-thiocyanatoacetophenone (VI), and phenacyl nitrate (VII). Concentration 10^{-3} M. 0.008 % gelatin added as maximum suppressor.

pH	1.0		3.5		5.3		7.3		9.7		13	
Compound	i_l	$-E_{\frac{1}{2}}$	i_l	$-E_{\frac{1}{2}}$	i_l	$-E_{\frac{1}{2}}$	i_l	$-E_{\frac{1}{2}}$	i_l	$-E_{\frac{1}{2}}$	i_l	$-E_{\frac{1}{2}}$
I	4.8	0.85	4.8	1.10	5.5	1.28	6.1	1.41	6.1	1.49	4.4	1.59
	1.7	1.05	1.0	1.26								
II	4.9	0.75	4.6	1.00	4.7	1.15	4.9	1.30	4.5	1.32	a	
	2.5	1.04	0.8	1.22	0.3	1.35	3.6	1.54	4.3	1.57		
III	4.3	0.75	4.4	0.93	4.4	1.13	4.1	1.27	4.3	1.32	a	
	1.9	1.09	1.3	1.27	1.0	1.38	3.4	1.57	4.3	1.62		
IV	4.5	0.83	4.5	0.96	4.3	1.09	4.3	1.22	4.2	1.32	3.2	1.41
	2.3	1.09	0.8	1.26	0.5	1.4	3.1	1.55	4.1	1.62	1.8[b]	1.73
V	4.5	0.59	4.3	0.82	4.2	1.00	4.0	1.22	3.7	1.30	4.2	1.33
	2.1	1.07	1.0	1.26	0.8	1.4	4.0	1.58	4.0	1.63	1.7[b]	1.73
VI	5.1	0.51	5.2	0.66	4.9	0.68	4.6	0.68	4.6	0.67	a	
	2.5	1.05	1.2	1.22	0.7	1.35	3.5	1.56	3.3	1.59		
VII	5.5	0.45	5.0	0.46	4.6	0.46	a	0.46	—		—	
	10.6	0.91	14.5	1.2	c	1.3						
	9.1	1.05										

a. The compound is hydrolyzed; b. Minimum between the two waves;
c. Poorly defined wave.

values makes the results from the preparative reductions dubious. The results seem to indicate that more than two electrons are involved in the reaction and from a partially reduced reaction mixture a minor amount (10 %) of acetophenone was isolated as the 2,4-dinitrophenylhydrazone.

As in the reduction of tropyl alcohol [9] the first wave in acid solution of 2-hydroxyacetophenone corresponds to the reduction of the protonated compound, but whether the reaction is a direct reduction of the carbon-oxygen bond or the reduction is preceded by formation of a "phenacylium ion" by loss of water from the protonated compound is not known.

The acetylated compound, 2-acetoxyacetophenone, shows both in acid and alkaline solution two polarographic waves and the more negative wave occurs at the same potential as that of acetophenone in the same solution. The polarographic data thus suggest that the electrode reaction corresponding to the first wave is a reduction of the acetoxyacetophenone to acetophenone according to

$$C_6H_5COCH_2OCOCH_3 + 2\ e^- + 2\ H^+ \rightarrow C_6H_5COCH_3 + CH_3COOH$$

and this was confirmed by a controlled potential reduction in acid solution from which acetophenone was isolated in good yield as its 2,4-dinitrophenylhydrazone.

In alkaline solution both waves correspond to two-electron reductions, but no preparative reduction has been made due to the hydrolysis of the compound at high pH-values. The polarographic data, however, strongly suggest a reduction to acetophenone in this case too. The reduction of 2-acetoxyacetophenone thus resembles that of the acetyl derivatives of the above mentioned steroids [8].

The polarographic reduction of phenacyl phenyl ether and phenacyl phenyl sulfide gives at most pH-values rise to two well defined waves. As is found in the polarographic reduction of most of the 2-substituted acetophenones the height of the second wave is from pH about 1 to pH about 6 smaller than the height of the polarographic wave of an equimolar solution of acetophenone. This is believed to be connected with the rate of a reaction between protons and the primarily formed product.

The polarographic data suggest an electrode reaction corresponding to the first wave in which the carbon-oxygen or carbon-sulfur bond is cleaved thus yielding acetophenone and phenol or thiophenol. By controlled potential reduction of phenacyl phenyl ether it was found that acetophenone was formed in good yield both in mineral acid solution and at pH 13.

The polarographic reduction of an aryl alkyl ether is not a frequent polarographic electrode reaction, but has previously been found in the reduction of phenoxyacetamidines [10]. The protection of a phenolic group by transforming it to a benzyl ether followed by a cleavage of the ether bond by hydrogenation is well known; it was attempted to reduce phenyl benzyl ether in buffered media, but no reduction wave was found between 0 and 2.0 V *vs* S.C.E. A protection of a phenolic group by a phenacyl group followed by an electrolytic cleavage of the ether bond might be possible, but whether it would present any advantage in comparison with the known method will be investigated.

The half-wave potential of the first wave of 2-thiocyanatoacetophenone is independent of pH at pH-values higher than about 3, whereas the half-wave potential of the second wave is similar to that of acetophenone in the media employed. The polarographic data thus suggest that acetophenone is formed in the electrode reaction corresponding to the first wave and this was also found by a controlled potential reduction of 2-thiocyanatoacetophenone in an acetate buffer pH 5. The electrode reaction can be formulated as

$$C_6H_5COCH_2SCN + 2\ e^- \rightleftharpoons C_6H_5COCH_2^- + SCN^-$$
$$+ H^+ \rightarrow C_6H_5COCH_3$$

The electrode reaction is thus different from those of aromatic thiocyanates [11,12], which are reduced to the mercapto derivative and cyanide ion.

The half-wave potential of the first wave of phenacyl nitrate is independent of pH. The following waves are consistent with the assumption that 2-hydroxyacetophenone and nitrous acid are formed in the electrode reaction which thus would be similar to that of other organic nitrates [13].

In Table 2 are found polarographic data for 2-acetoxy-4′-chlorobutyrophenone (VIII), 2-thiocyanato-4′-chloro-butyrophenone (IX), and 4′-chlorobutyrophenone (X).

Table 2. Limiting currents in μA and half-wave potentials *vs* S.C.E. of 2-acetoxy-4′-chloro-butyrophenone (VIII), 2-thiocyanato-4′-chlorobutyrophenone (IX), and 4′-chlorobutyrophenone (X). Concentration 10^{-3} M, 0.008 % gelatin added as maximum suppressor.

pH	1.0		3.5		5.3		7.3		9.7		13	
Compound	i_l	$-E_{\frac{1}{2}}$	i_l	$-E_{\frac{1}{2}}$	i_l	$-E_{\frac{1}{2}}$	i_l	$-E_{\frac{1}{2}}$	i_l	$-E_{\frac{1}{2}}$	i_l	$-E_{\frac{1}{2}}$
VIII	4.0	0.78	3.8	1.03	4.1	1.22	4.1	1.34	4.0	1.36	a	
	1.7	1.06							3.6	1.62		
IX	4.4	0.44	4.3	0.44	4.3	0.44	4.1	0.44	a	0.44	a	
	1.3	1.04					1.4	1.53		1.59		
X	2.5	1.03	2.5	1.21	2.5	1.33	4.1	1.53	4.3	1.60	2.6	1.75

a. The compound is hydrolyzed.

The polarographic reduction of the 4′-chlorobutyrophenones resembles that of the corresponding acetophenones. The height of the second wave is, however, in acid solution much smaller than that of an equimolar solution of the parent ketone and from pH about 3 the wave is hardly visible. The region in alkaline solution where the second wave is found begins at a higher pH value than for the corresponding acetophenone derivative. The electrode reactions are similar to those of the corresponding acetophenone derivatives.

In Table 3 are given polarographic data for 2-hydroxy*iso*butyrophenone (XI), 2-acetoxy*iso*butyrophenone (XII), and 2-thiocyanato*iso*butyrophenone (XIII).

Table 3. Limiting currents in μA and half-wave potentials *vs* S.C.E. of 2-hydroxy*iso*butyrophenone (XI), 2-acetoxy*iso*butyrophenone (XII), and 2-thiocyanato*iso*butyrophenone (XIII). Concentration 10^{-3} M. 0.008 % gelatin added as maximum suppressor.

pH	0.3		1.0		3.5		5.3		7.3		9.7		13	
Compound	i_l	$-E_{\frac{1}{2}}$	i_l	$-E_{\frac{1}{2}}$	i_l	$-E_{\frac{1}{2}}$	i_l	$-E_{\frac{1}{2}}$	i_l	$-E_{\frac{1}{2}}$	i_l	$-E_{\frac{1}{2}}$	i_l	$-E_{\frac{1}{2}}$
XI	3.7	0.87	3.6	0.94	a		4.2	1.54	4.2	1.57	4.2	1.63	4.2	1.73
XII	3.3	0.90	3.2	1.00	a		3.7	1.50	3.8	1.54	4.3	1.55	b	1.57
														1.78
XIII	3.8	0.36	4.3	0.38	4.3	0.38	4.2	0.38	4.5	0.38	b		b	b

a. Poorly defined wave.
b. The compound is hydrolyzed.

In the polarographic reduction of derivatives of *iso*butyrophenone a reduction wave of the *iso*butyrophenone formed in the first electrode reaction is hardly visible in acid solution and in alkaline solution the wave can only be seen at high pH-values (pH > 10.5). The compounds here investigated are, however, hydrolyzed at high pH-values which makes measurements difficult.

Controlled potential reductions in mineral acid solution at a cathode potential corresponding to the half-wave potential of the compound in the medium employed showed that the electrode reaction of 2-hydroxy*iso*butyrophenone and 2-thiocyanato*iso*butyrophenone was a two-electron reduction to *iso*butyrophenone. Although it thus is demonstrated that *iso*butyrophenone is formed in the reduction of 2-thiocyanato*iso*butyrophenone no polarographic wave of *iso*butyrophenone is found on the polarographic curve obtained in a solution of 2-thiocyanato*iso*butyrophenone in the medium and concentration here employed.

In the preparative reduction of 2-hydroxy*iso*butyrophenone it is not possible to use a cathode potential corresponding to a potential where the polar-

Table 4. Limiting currents in μA and half-wave potentials *vs* S.C.E. of benzoin (XIV), acetylbenzoin (XV), 2-thiocyanatodeoxybenzoin (XVI), 2-chlorodeoxybenzoin (XVII), and deoxybenzoin (XVIII). Concentration 10^{-3} M. 0.008 % gelatin added as maximum suppressor.

pH	0.3		1.0		3.5		5.3		7.3		9.8		13	
Compound	i_l	$-E_{\frac{1}{2}}$	i_l	$-E_{\frac{1}{2}}$	i_l	$-E_{\frac{1}{2}}$	i_l	$-E_{\frac{1}{2}}$	i_l	$-E_{\frac{1}{2}}$	i_l	$-E_{\frac{1}{2}}$	i_l	$-E_{\frac{1}{2}}$
XIV	4.4	0.79	4.4	0.87	4.9	1.15	4.4	1.32	4.6	1.44	4.7	1.57	4.0	1.65
	0.9	1.01												
XV	3.8	0.73	3.4	0.80	a		4.0	1.27	3.8	1.34	3.8	1.36	b	
	0.8	1.01							1.0	1.5	3.4	1.58		
XVI[c]	3.3	0.22	3.7	0.21	3.5	0.20	3.5	0.20	b	0.20	b		b	
XVII	3.8	0.16	3.6	0.15	3.8	0.13	3.6	0.13	3.9	0.14	3.8	0.21	b	
	1.2	1.01							1.0	1.47	3.2	1.58		
XVIII	2.0	0.98	1.9	1.03	2.0	1.18	2.7[a]	1.33	3.7	1.47	4.2	1.56	2.3	1.65

a. Poorly defined wave.
b. The compound is hydrolyzed.
c. 40 % dioxane.

ographic limiting current is reached as the half-wave potential of the *iso*-butyrophenone formed in the reduction is only 0.2 V more negative than that of 2-hydroxy*iso*butyrophenone. This can not be predicted from the polarographic curve of 2-hydroxy*iso*butyrophenone and the polarographic data are thus in such a case not a reliable guide for the reduction.

The polarographic data of the following derivatives of deoxybenzoin are found in Table 4: benzoin (XIV), acetylbenzoin (XV), 2-thiocyanatodeoxybenzoin (XVI), 2-chlorodeoxybenzoin (XVII), and deoxybenzoin (XVIII).

The polarographic behaviour of derivatives of deoxybenzoin resembles that of the above mentioned compounds. Whereas 2-thiocyanatodeoxybenzoin only yields a single wave acetylbenzoin shows a small second wave in strongly acid solution and a second wave with a height corresponding to a two-electron reduction in alkaline solution. The second wave appears in both cases at the potential at which deoxybenzoin is reduced in the same solution. The assumption that the reduction corresponding to the first wave of acetylbenzoin yielded deoxybenzoin was confirmed by a controlled potential reduction of acetylbenzoin from which deoxybenzoin could be isolated in good yield.

Benzoin yields in alkaline solution quantitatively hydrobenzoin [6] but from a reduction in mineral acid solution Pasternak [6] isolated the highest melting form (α-form) of deoxybenzoinpinacol (1,2-diphenyl-1,2-dibenzyl-ethylene glycol). Wawzonek [14] has interpreted the occurrence of this reduction product as being due to a reduction of the benzoin to hydrobenzoin followed by an acid catalyzed dehydration to deoxybenzoin which on reduction produced among other compounds the isolated pinacol.

A solution of hydrobenzoin in N hydrochloric acid solution containing 40 % alcohol was, however, not dehydrated to deoxybenzoin on standing at room temperature for 18 h as no polarographic wave of deoxybenzoin appeared, and in view of the results from the reduction of acetylbenzoin in mineral acid solution it seems just as plausible that the secondary alcohol group of benzoin is reduced directly to a methylene group and the deoxybenzoin thus formed is reduced further. A polarographic reduction of a secondary alcohol to a methylene group has also been assumed by Wawzonek and Fredrickson [15] in the reduction of α-hydroxy-*p*-methoxy-phenylacetonitrile, and it was shown that α-benzoxy-*p*-methoxy-phenylacetonitrile in good yield formed *p*-methoxyphenylacetonitrile on electrolytic reduction at a mercury cathode.

The reduction of deoxybenzoin is of some interest. It has long been known that two pinacols of deoxybenzoin exist, "α", m.p. 212°, and "β", m.p. 173°; the existence of these two forms is due to two asymmetric carbon atoms in the pinacols. From a controlled potential reduction of deoxybenzoin in mineral acid solution the pinacol with m.p. 212° ("α") precipitated; this is in agreement with Pasternak's results from the reduction of benzoin under similar conditions. Other compounds, probably formed by dehydration and rearrangement of the pinacol, were also formed. In strongly alkaline solution in 60 % dioxane some secondary alcohol was formed but the main product was a mixture of pinacols which consisted mainly of the lower melting isomer; an infrared analysis of the mixture suggested about 80 % "β-pinacol" and 20 % "α-pinacol". In acid solution thus mainly the highest melting and in alkaline solution mainly the lowest melting pinacol is formed. A similar observation

Table 5. Limiting currents in μA and half-wave potentials *vs* S.C.E. of phenylbenzoin (XIX), 2-acetoxy-2,2-diphenylacetophenone (XX), 2-methoxy-2,2-diphenylacetophenone (XXI), and 2,2-diphenylacetophenone (XXII). Concentration 10^{-3} M. 0.008 % gelatin added as maximum suppressor.

pH	0.3		1.0		3.5		5.3		7.3		9.8		13	
Compound	i_l	$-E_{\frac{1}{2}}$	i_l	$-E_{\frac{1}{2}}$	i_l	$-E_{\frac{1}{2}}$	i_l	$-E_{\frac{1}{2}}$	i_l	$-E_{\frac{1}{2}}$	i_l	$-E_{\frac{1}{2}}$	i_l	$-E_{\frac{1}{2}}$
XIX	3.7	0.88	3.4	0.95	3.2[a]	1.23	3.2	1.35	3.4	1.45	3.6	1.56	3.2	1.63
													1.7	1.75
XX	2.9	0.80	2.9	0.88	a		2.9	1.37	3.1	1.38	3.1	1.39	3.2[b]	1.39
													2.0	1.73
XXI	3.3	0.88	3.3	0.96	2.2[a]	1.16	a		3.1	1.48	3.3	1.53	3.1	1.55
													1.7	1.72
XXII	1.7	1.03	1.7	1.05	2.8[a]	1.34	3.3	1.37	3.5	1.53	3.4	1.59	1.8	1.71

a. Poorly defined wave.
b. The compound is hydrolyzed.

has been made by Allen [16] in the reduction of *p*-dimethylaminoacetophenone which in acid solution was reduced to the higher melting pinacol and in alkaline solution to a lower melting pinacol. The reduction of certain α,β-unsaturated 3-ketosteroids [17] also produced a different mixture of pinacols in acid and alkaline solution, and in this connection it is also of interest that the polarographic reduction of α-methyldeoxybenzoin in weakly alkaline solution primarily yielded the *erythro*-alcohol [18].

In Table 5 are found polarographic data for phenylbenzoin (XIX), 2-acetoxy-2,2-diphenylacetophenone (XX), 2-methoxy-2,2-diphenylacetophenone (XXI), and 2,2-diphenylacetophenone (XXII).

The polarographic behaviour of derivatives of diphenylacetophenone resembles that of the derivatives of deoxybenzoin; the second wave of, *e.g.*, 2-acetoxy-2,2-diphenylacetophenone which is due to the reduction of the diphenylacetophenone formed in the first electrode reaction is, however, only visible at pH-values higher than 11, whereas the second wave of acetylbenzoin can be seen from about 7.5.

The reduction of 2-methoxy-2,2-diphenylacetophenone is interesting as only few examples of a polarographic reduction of an alkyl arylalkyl ether bond have been reported. A similar reaction has, however, been found in the reduction of *o*-benzoylbenzoic acid *pseudo*ethylester [19].

Diphenylacetophenone was once believed to exist mainly as triphenylvinyl alcohol; one of the arguments in favour of this formulation was the easy formation of the O-benzoylated derivative, triphenylvinyl benzoate. The polarographic data are consistent with the formulation of 2,2-diphenylacetophenone as a carbonyl compound as the half-wave potentials are close to those of deoxybenzoin, and as it was found that triphenylvinyl benzoate did not yield a polarographic wave in the pH-region in which it is sufficiently stable for a polarographic investigation.

The polarographic behaviour of 2-cyanoacetophenone is quite different from the above mentioned compounds. In acid solution is found one wave with a wave height corresponding to a two-electron reduction, but about

Table 6. Limiting currents in μA and half-wave potentials *vs* S.C.E. of 2-cyanoacetophenone at different pH-values. Concentration 10^{-3} M. 0.008 % gelatin added as maximum suppressor.

pH	i_l μA	$-E_{\frac{1}{2}}$ V	pH	i_l μA	$-E_{\frac{1}{2}}$ V	pH	i_l μA	$-E_{\frac{1}{2}}$ V
3.57	5.30	1.15	7.63	4.55	1.35	8.55	1.60	1.41
5.35	5.10	1.22	7.80	4.30	1.36	9.31	1.05	1.44
6.33	4.95	1.29	8.00	3.65	1.37	9.65	0.70	1.45
7.31	4.85	1.32	8.29	2.40	1.38	10.50	0.25	1.51

pH 7 the height of the wave diminishes and the wave disappears about pH 11 (Table 6).

The reason for this disappearence of the polarographic wave is that the ketone exists in equilibrium with its enol form, and that this enol form in the pH-interval pH 7 to 11 increasingly is found as the enolate-ion according to

$$C_6H_5COCH_2CN \rightleftharpoons C_6H_5C(OH)=CHCN \rightleftharpoons C_6H_5C(O^-)=CHCN + H^+$$

The enolate-ion is not reducible in the potential interval 0—2.0 V *vs* S.C.E.

This explanation was corroborated by a potentiometric titration of 2-cyanoacetophenone in 40 % alcohol which yielded a normal titration curve, the midpoint being at pH 7.8. When the height of the polarographic wave is plotted against pH the pH-value at which the height of the wave has diminished to half of the value in acid solution is 8.2. The curve obtained is not symmetrical as the wave height diminishes too slowly in alkaline solution compared with the decrease about pH 7 to yield a symmetrical curve. This is probably due to a recombination at the electrode surface of the non-reducible enolate anion with a proton to yield the reducible keto form, as the height of the polarographic wave of 2-cyanoacetophenone at pH 10 was not dependent on the height of the mercury reservoir.

The reduction of 2-bromoacetophenone has been investigated previously [1]; the reduction of the carbon-bromine bond occurs at a very positive potential. When the compound is transformed into its ethylene ketal, 2-(bromomethyl)-2-phenyl-1,3-dioxolane, the reduction of the carbon-bromine bond occurs at a much more negative potential. The half-wave potential in a 40 % alcoholic solution containing 4 % tetramethylammonium hydroxide was found to be —1.78 V *vs* S.C.E. This is consistent with the very much lower reactivity of the ketal compared with that of the phenacyl bromide.

DISCUSSION

When the results from the polarographic investigation and from the controlled potential reductions are compared it is seen that the data obtained at the dropping mercury electrode are not always a reliable guide for the preparative reductions. The observed effects are caused by differences in the duration of the experiments and in the concentrations employed at the dropping mercury electrode and at the macro-scale reductions.

A species formed as an intermediate in the electrode reaction will at the dropping mercury electrode behave as the final reduction product if it is stable for more than a few seconds; in that case it is able to diffuse from the electrode to the bulk of the solution before it is transformed to the stable reduction product. The concentration of the stable reduction product will remain low and although the compound might be reducible at the electrode its concentration will be too low to influence the recorded polarographic curve.

Differences between the results obtained at the dropping mercury electrode and at the macro electrode are found, *e.g.*, when the relatively stable intermediate is non-reducible and the stable reduction product can be reduced further.

At the macro-electrode the intermediate also is transformed to the stable reduction product in the bulk of the solution but in the course of the reduction a high concentration of this product is built up; if the cathode potential is sufficiently negative the reduction product is reduced further. According to the polarographic data any potential where the diffusion plateau is reached would be equally satisfactory for a preparative reduction but this does not hold true in the case under discussion. The cathode potential must under such circumstances be held more positive than the foot of the polarographic wave of the partially reduced compound and that means that in some cases it is not advisable to employ a cathode potential more negative than the half-wave potential of the compound reduced, if a selective reduction is to succeed.

In this connection it can be recalled that the half-wave potentials of many irreversibly reduced compounds are dependent on the concentration and that the waves at high concentrations often "cover" a greater potential interval than under normal polarographic conditions. The separation of waves obtained in solutions of high concentrations is often less satisfactory than at low concentrations and this makes it advisable always to employ as positive a cathode potential as possible in preparative reductions.

In the present investigation it is found for most of the compounds that in a certain pH-interval either only one wave is detectable, although the product from the first reduction is reducible, or the second wave is smaller than the wave of an equimolar solution of the partially reduced compound. A typical example is 2-thiocyanato*iso*butyrophenone which shows only one wave in the pH-interval in which this compound can be investigated; the preparative reduction at controlled cathode potential shows that the product from the electrode reaction corresponding to the observed wave is the reducible *iso*-butyrophenone.

A comparatively stable, non-reducible intermediate is thus likely to be formed during the electrode reaction. The half-wave potential of the wave of 2-thiocyanato*iso*butyrophenone is independent of pH and the reaction can thus be formulated

$$C_6H_5COC(CH_3)_2SCN + 2\ e^- \rightarrow C_6H_5COC(CH_3)_2^- + SCN^-$$

$$+ H^+ \rightarrow C_6H_5COCH(CH_3)_2$$

where the species $C_6H_5COC(CH_3)_2^-$ is the non-reducible, relatively stable intermediate. A similar species must be assumed to be formed in the corresponding

electrode reactions of the compounds investigated, and it is probably stabilized in some way at the electrode.

There seems to be a connection between the strength of the acid from which the substituent is derived and the pH-dependence of the first wave. When the substituent is derived from a strong acid as HCl, HBr, HSCN, or HNO_3 the half-wave potential of the first wave is independent of pH above pH 2-3; when the substituent, however, is derived from a weak acid as HF[3], CH_3COOH, C_6H_5OH, C_6H_5SH, or CH_3OH the half-wave potential is in acid solution dependent on pH. Considerations as those used by Elving and Leone to explain the pH-dependence of the reduction of 2-fluoroacetophenone may be applied in those cases.

It is of interest to compare for the same derivative of different ketones the pH-intervals in which only one wave is observed. It is found that the interval grows in the order $C_6H_5COCH_2X < ClC_6H_4COCH(C_2H_5)X < C_6H_5COCH(C_6H_5)X < C_6H_5COC(CH_3)_2X \leqq C_6H_5CO(C_6H_5)_2X$. This sequence is understandable in view of the reduction route indicated above. The postulated primarily formed carbanion is stabilized by substitution by alkyl or aryl at the carbon atom at which the reduction occurs, and the carbanion thus reacts more slowly with protons to form the reduction product, the ketone. Besides stabilizing the carbanion the substituents may produce a shielding effect which lowers the rate of the reaction with protons.

In the acid region the second wave is greater at the lowest pH-values which is understandable if the rate of a reaction between a carbanion and a proton determines the height of the wave. In the alkaline region the formation of the reducible ketone is most rapid at high pH-values, as if the hydroxyl ions catalyzed the reaction between the carbanion and a water molecule to form the ketone and a hydroxyl ion. This is also found in the reduction of benzil which in most buffers yields only a single wave, although a preparative reduction at controlled potential has shown [6] that the reducible benzoin is formed. In 0.1 N sodium hydroxide, however, a wave due to the reduction of the benzoin formed in the first electrode reaction is visible which indicates that the non-reducible intermediate is transformed to benzoin most rapidly in strongly alkaline solution.

EXPERIMENTAL

The polarograph was a recording polarograph Radiometer Type PO 3 a. The capillary delivered 2.27 mg of mercury at a corrected mercury column height of 48.5 cm. The drop time 3.90 sec. (H_2O, open circuit). The capillary constant, $m^{2/3}t^{1/6} = 2.13$ $mg^{2/3}sec^{-\frac{1}{2}}$.

The apparatus used for the controlled potential reductions was an electromechanical potentiostat of the Lingane-Jones type. The buffer solutions employed were from pH 2.5 to 8 a sodium phosphate-citric acid buffer and from pH 8 to 11 a sodium borate buffer. The medium generally used was 40 % aqueous alcohol containing 1 M potassium chloride and 0.008 % gelatin. In a few cases the alcohol was replaced by peroxide-free dioxane.

The following compounds were prepared according to *Organic Syntheses:* 2-Bromoacetophenone, desylchloride, deoxybenzoin, benzoin, and acetylbenzoin. By reaction between a bromoketone and an alkali metal salt in alcohol or acetonitrile were prepared: 2-Acetoxyacetophenone, m.p. 48.5°—49.5°, 2-acetoxy-4′-chlorobutyrophenone, m.p. 73.5°—74°, 2-acetoxy*iso*butyrophenone, m.p. 61°—61.5°, 2-thiocyanatoacetophenone, m.p. 72.5°—73.5°, 2-thiocyanato-4′-chloro-butyrophenone, m.p. 67°—67.5°. (Found: C 55.05; H 4.36; N 6.01; S 13.60. Calc. for $C_{11}H_{10}ClNOS$: C 55.10; H 4.20; N 5.85; S 13.37). 2-Thiocyanato*iso*butyrophenone, m.p. 20°—22°. (Found: C 64.31; H 5.31; N 6.60; S 15.56.

Calc. for $C_{11}H_{11}NOS$: C 64.36; H 5.40; N 6.83; S 15.63). 2-Thiocyanatodeoxybenzoin, m.p. 112.5°—113°. (Found: C 71.06; H 4.14; N 5.46; S 12.71. Calc. for $C_{15}H_{11}NOS$: C 71.12; H 4.38; N 5.53; S 12.66). Phenacyl phenyl ether, m.p. 73°—73.5°, phenacyl phenyl sulfide, m.p. 53°—53.5°, 2-cyanoacetophenone, m.p. 80.5°—81°, phenacyl nitrate, m.p. 53.5°—54° (4°—5° [20]). (Found: C 53.06; H 3.98; N 5.6—7.3. Calc. for $C_8H_7NO_4$: C 53.04; H 3.89; N 7.72). Although the nitrogen determinations were low and variable the compound isolated from the reaction between phenacyl bromide and silver nitrate in acetonitrile is believed to be phenacyl nitrate. The infrared spectrum of the compound contains strong bands at 1 640 cm^{-1} and 1 283 cm^{-1}; covalent nitrates generally absorb in the region 1 650—1 600 cm^{-1} and 1 300—1 250 cm^{-1}.

2-Bromo-2,2-diphenylacetophenone, 2-methoxy-2,2-diphenylacetophenone, and 2-hydroxy-2,2-diphenylacetophenone were made according to Stevens and DeYoung [21], and 2-(bromomethyl)-2-phenyl-1,3-dioxolane according to Kuhn [22].

Reduction of 2-acetoxyacetophenone: 1.00 g of 2-acetoxyacetophenone was reduced in 55 % alcoholic 0.1 N hydrochloric acid at a cathode potential of −0.9 V *vs* S.C.E. The reduction consumed 2.1 electrons per molecule. The odour of the reduction mixture suggested the presence of acetophenone, which was confirmed by polarographic analysis. To the solution were added 2.5 g of 2,4-dinitrophenylhydrazine; the precipitate was filtered off and recrystallized from amyl acetate, 1.05 g, m.p. 246°—248°. It was identified as the 2,4-dinitrophenylhydrazone of acetophenone.

2-Hydroxyacetophenone was reduced in 50 % alcoholic N hydrochloric acid as described above, $n = 2.0$. The product was isolated as described above; 1.55 g of acetophenone 2,4-dinitrophenylhydrazone.

In a similar manner *2-phenoxyacetophenone* was reduced at −0.85 V *vs* S.C.E.; $n = 2.0$. Isolated were 1.1 g of 2,4-dinitrophenylhydrazone of acetophenone.

2-Phenoxyacetophenone was also reduced in 50 % alcoholic 0.1 N sodium hydroxide at −1.5 V *vs* S.C.E., and in this case, too, the only isolated compound was the 2,4-dinitrophenylhydrazone of acetophenone (0.65 g).

2-Thiocyanatoacetophenone (1.00 g) was reduced in an acetate buffer, pH 5, containing 50 % alcohol at −0.85 V *vs* S.C.E., $n = 2.0$. From the reduction were isolated acetophenone as its 2,4-dinitrophenylhydrazone (1.5 g).

Reduction of 2-hydroxyisobutyrophenone: 1.00 g of 2-hydroxy*iso*butyrophenone was reduced in 50 % alcoholic N hydrochloric acid at −0.85 V *vs* S.C.E., $n = 2$. On the polarograms from the reaction medium a high wave followed by a very small one were visible at the beginning of the reduction; the first wave disappeared gradually whereas the second wave grew. After completion of the reduction 2,4-dinitrophenylhydrazine was added and the precipitate recrystallized from *n*-butanol, 1.65 g, m.p. 161°—162.5°. It was identified as the 2,4-dinitrophenylhydrazone of *iso*butyrophenone by the mixed m.p. 160°—162° with an authentic sample of *iso*butyrophenone 2,4-dinitrophenylhydrazone.

In a similar manner *2-thiocyanato*iso*butyrophenone* was reduced at −0.65 V *vs* S.C.E. in 50 % alcoholic N hydrochloric acid; $n = 2.0$. From the reduction mixture *iso*butyrophenone was isolated as its 2,4-dinitrophenylhydrazone (1.50 g) as described above.

Acetylbenzoin was reduced (1.00 g) in N hydrochloric acid containing 50 % dioxane; $n = 2$. The reduction mixture was diluted with water and extracted with ether which was dried and evaporated. The residue, 0.83 g, m.p. 45°—50°, was recrystallized from 4 ml methanol. Isolated were 285 mg deoxybenzoin, m.p. 60°, and from the mother liquor 430 mg of deoxybenzoin 2,4-dinitrophenylhydrazone, m.p. 201°—203°.

REFERENCES

1. Pasternak, R. and von Halban, H. *Helv. Chim. Acta* **29** (1946) 190.
2. Adkins, H. and Cox, F. W. *J. Am. Chem. Soc.* **60** (1938) 1151.
3. Elving, P. J. and Leone, J. T. *J. Am. Chem. Soc.* **79** (1957) 1546.
4. Zuman, P. and Horak, V. *2nd International Congress of Polarography, Cambridge 1959.*
5. Fedoronko, M. *Chem. zvesti* **12** (1958) 17; *Chem. Abstr.* **52** (1958) 10768.
6. Pasternak, R. *Helv. Chim. Acta* **31** (1948) 753.
7. Santavy, F. *Collection Czechoslov. Chem. Communs.* **14** (1949) 145.

8. Kabasakalian, P. and McGlotten, J. *Anal. Chem.* **31** (1959) 1091.
9. Zuman, P., Chodkowski, J., Potesilova, H. and Santavy, F. *Nature* **182** (1958) 1535.
10. Kane, P. O. *Z. anal. Chem.* **173** (1960) 50.
11. Schwabe, K. and Voigt, J. *Z. Elektrochem.* **56** (1952) 44.
12. Lanza, P., Griggio, L. and Semerano, G. *Ricerca sci.* **26** (1956) S 230.
13. Kaufman, F., Cook, H. J. and Davis, S. M. *Anal. Chem.* **24** (1952) 971.
14. Kolthoff, I. M. and Lingane, J. J. *Polarography*, 2nd Ed., Interscience Publishers, New York, London 1952, p. 694.
15. Wawzonek, S. and Fredrickson, J. D. *J. Electrochem. Soc.* **106** (1959) 325.
16. Allen, M. J. *J. Chem. Soc.* **1951** 1598.
17. Lund, H. *Acta Chem. Scand.* **11** (1957) 283.
18. Mandell, L., Powers, R. M. and Day, R. A. *J. Am. Chem. Soc.* **80** (1958) 5284.
19. Lund, H. *Acta Chem. Scand.* **14** (1960) 359.
20. Emmons, W. D. and Freeman, J. P. *J. Am. Chem. Soc.* **77** (1955) 4415.
21. Stevens, C. L. and DeYoung, J. J. *J. Am. Chem. Soc.* **76** (1954) 718.
22. Kuhn, M. *J. prakt. Chem.* **156** (1940) 103.

Received June 4, 1960.

ACTA CHEMICA SCANDINAVICA 14 (1960) 1939–1944

Cyclizations of Thiocarbohydrazide and its Mono-hydrazones Part II *. Reactions with Dialkyl Trithiocarbonates

JAN SANDSTRÖM

Department of Organic Chemistry, University of Lund, Lund, Sweden

Thiocarbohydrazide and mono-thiocarbohydrazones react with trithiocarbonates in strongly alkaline solution to form dithiocarbalkoxy-thiocarbohydrazides and their hydrazones, respectively. When heated in the solid state, these compounds are cyclized, with elimination of hydrogen sulphide, to alkylthio-thiadiazolhydrazines and hydrazones, respectively. In acid medium, the products of decomposition are mercapto-alkylthio-thiadiazoles.

The present investigation was undertaken to test the possibilities of preparing 5-alkylthio-1,3,4-thiadiazol-2-yl-hydrazines (I) by reactions of thiocarbohydrazide or derivatives thereof with dialkyl trithiocarbonates. Thiocarbohydrazide was found to react with dimethyl trithiocarbonate only in strongly alkaline solution, with liberation of methanethiol and formation of 1-dithiocarbomethoxy-thiocarbohydrazide (II, R = CH_3) as alkali salt. The dithiocarbomethoxy-thiocarbohydrazide (II, R = CH_3) could be cyclized by two different methods. When heated above its melting point it eliminated hydrogen sulphide, methanethiol, and hydrazine, and from the reaction mixture could be isolated 5-methylthio-1,3,4-thiadiazol-2-yl-hydrazine (I, R = CH_3, isolated in 55 % yield as acetone hydrazone), 2-mercapto-5-methylthio-1,3,4-thiadiazole [1] (III, R = CH_3, 23 % yield), and 3-mercapto-4-amino-5-hydrazino-4,1,2-triazole [2] (IV, 10 % yield). The triazole (IV) may be formed in a side reaction between dithiocarbomethoxy-thiocarbohydrazide (II) and hydrazine.

The cyclization of (II) in acid medium followed a different course, with exclusive formation of 2-mercapto-5-methylthio-1,3,4-thiadiazole (III, R=CH_3) and hydrazine.

Mono-thiocarbohydrazones were found to react with dialkyl trithiocarbonates under the same conditions as thiocarbohydrazide, and the products were 5-dithiocarbalkoxy-thiocarbohydrazones (V). When heated above their melting points they eliminated hydrogen sulphide and gave alkylthio-thiadiazolylhydrazones (VI). The acetone 5-dithiocarbalkoxy-thiocarbohydrazones

* Part I. *Acta Chem. Scand.* **14** (1960) 1037.

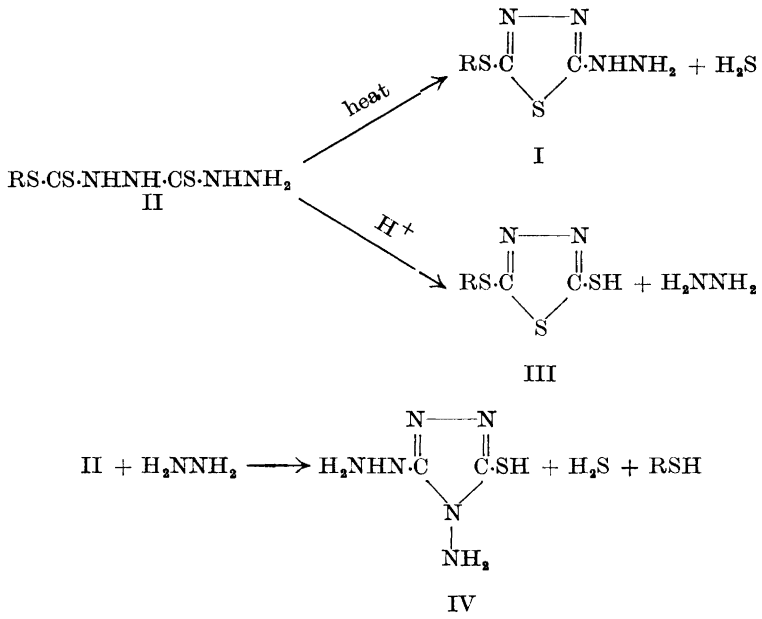

I III IV

(V, $R_1 = R_2 = CH_3$) gave some acetone 5-mercapto-1,3,4-thiadiazol-2-yl-hydrazone (VI, R = H, $R_1 = R_2 = CH_3$) as by-product. The structure of the benzaldehyde 5-methylthio-1,3,4-thiadiazol-2-yl-hydrazone was demonstrated by its formation from benzaldehyde 5-mercapto-1,3,4-thiadiazol-2-yl-hydrazone (prepared according to Stollé and Fehrenbach [3]) and methyl iodide in alkaline solution.

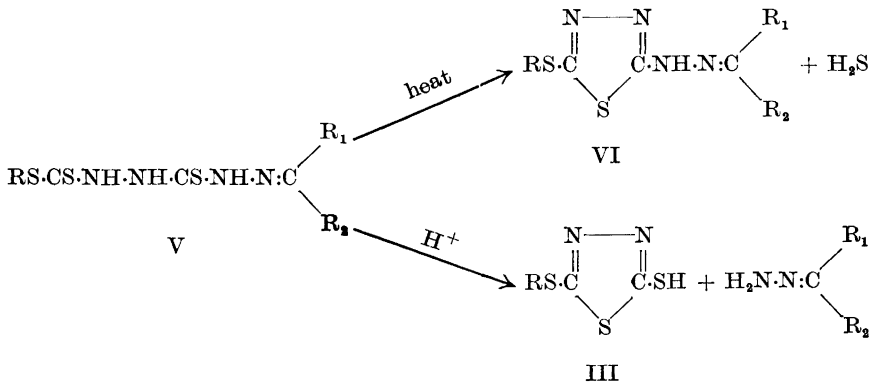

V VI III

When the dithiocarbalkoxy-thiocarbohydrazones (V) were heated in hydrochloric acid solution, mercapto-alkylthio-thiadiazoles (III) were formed with elimination of the corresponding hydrazone, which could then be disproportionated to azine and hydrazine.

Like the analogues described in part I, the alkylthio-thiadiazolylhydrazones (VI) are weak acids. The alkylthio-thiadiazolylhydrazines (I) are quite stable in acid solution, and are conveniently prepared by acid hydrolysis of the corresponding acetone hydrazones.

EXPERIMENTAL

Preparation and decomposition of 1-dithiocarbomethoxy-thiocarbohydrazide (II, R = CH_3)

Thiocarbohydrazide (10.6 g, 0.1 mole) was dissolved in 2 N KOH in 75 % aqueous ethanol (50 ml), and dimethyl trithiocarbonate (7.0 g, 0.05 mole) in ethanol (50 ml) was added. After a few hours, the excess thiocarbohydrazide began to separate, and on the following day the filtrate was acidified with acetic acid, and the ethanol was taken off *in vacuo* at 20°. Then, colourless plates had separated (9.2 g, 93 % yield), m.p. 134—135° (decomp.) after recrystallization from 50 % aqueous ethanol. (Found: C 18.6; H 4.07; N 28.6; S 48.5. $C_3H_8N_4S_3$ (196.30) requires C 18.4; H 4.11; N 28.5; S 49.0).

Thermal decomposition.

Dithiocarbomethoxy-thiocarbohydrazide (II, R = CH_3, 98 g) was heated at 160° until the evolution of gas had ceased. After cooling, the residue was extracted at 50° with N HCl (600 ml). The mixture was cooled to 0°, and the undissolved material was separated (18.5 g). It crystallized from toluene as colourless rods, m.p. 136—137°, consisting of 2-mercapto-5-methylthio-1,3,4-thiadiazole (III, R = CH_3). (Found: C 22.0; H 2.60; N 16.8; S 58.5. $C_3H_4N_2S_3$ (164.25) requires C 21.9; H 2.45; N 17.1; S 58.6).

The acid filtrate was evaporated *in vacuo* to about one fourth of the original volume. A further quantity (0.8 g) of less pure mercapto-methylthio-thiadiazole was separated, and then a solution of crystalline sodium acetate (140 g) in water (100 ml) was added. A pale brown crystalline deposit (68.5 g) was obtained, which was extracted with three portions of boiling ethanol (together 400 ml). The undissolved material was a white, microcrystalline powder (7.2 g), m.p. 226—227° (decomp.), consisting according to analysis of 3-mercapto-4-amino-5-hydrazino-4,1,2-triazole (IV). For this compound Hoggarth [2] reports m.p. 232°. (Found: C 16.5; H 4.23; N 57.9; S 22.3. $C_2H_6N_6S$ (146.18) requires C 16.4; H 4.14; N 57.5; S 21.9).

A dibenzylidene derivative was prepared according to Hoggarth as pale yellow plates, m.p. 242—244° (245—246° according to Ref.[2]) (Found: C 60.2; H 4.62. $C_{16}H_{14}N_6S$ (322.38) requires C 59.6; H 4.38).

To the ethanolic filtrate from the triazole (IV) was added acetone (40 ml) in water (400 ml). Pale yellow rods separated (56.0 g), which crystallized from ethanol as colourless rods, m.p. 162—163°, consisting of acetone 5-methylthio-1,3,4-thiadiazol-2-yl-hydrazone (VI, R = R_1 = R_2 = CH_3). (Found: C 35.4; H 4.92. $C_6H_{10}N_4S_2$ (202.29) requires C 35.6; H 4.98). λ_{max}: 2 980 Å with ε : 14 900. From the filtrate of the acetone thiadiazolylhydrazone no further definable products could be isolated.

Decomposition in acid solution.

Dithiocarbomethoxythiocarbohydrazide (II, 2.0 g) was refluxed for 10 min. in ethanol (10 ml) and 5 N HCl (5 ml). The ethanol was removed *in vacuo*, and the solution was cooled. Colourless rods separated (1.5 g, 90 % yield), m.p. 136—137° after recrystallization from toluene, consisting of 2-mercapto-5-methylthio-1,3,4-thiadiazole (III). (Found: N 16.9; S 58.4. $C_3H_4N_2S_3$ (164.25) requires N 17.1; S 58.6). For this compound Busch [1] reports m.p. 136°.

Benzaldehyde (2.2 g) in ethanol (10 ml) was added to the acid filtrate, and benzalazine (1.9 g, 90 % yield) crystallized at once, m.p. and mixed m.p. 92—93°.

5-Dithiocarbalkoxy-thiocarbohydrazones (V)

The general procedure for the preparation of these compounds was to dissolve the appropriate mono-thiocarbohydrazone (Part I) in 2 equivalents of N sodium ethoxide in absolute ethanol, add the calculated quantity of the dialkyl trithiocarbonate, and leave the solution at room temperature for 24 h. Addition of the calculated volume of N acetic acid was generally sufficient to precipitate most of the product, but often a further quantity could be obtained by evaporating the mother liquor. On recrystallization, prolonged heating must be avoided. As the compounds melt with decomposition, the melting points are not sharp and are of little use for characterization.

Acetone dithiocarbomethoxy-thiocarbohydrazone (V, R = R_1 = R_2 = CH_3) was obtained in 65 % yield and crystallized from ethanol as colourless rods, m.p. 134–139° (decomp.). (Found: C 30.1; H 5.13; N 23.4; S 41.0. $C_6H_{12}N_4S_3$ (236.37) requires C 30.5; H 5.12; N 23.7; S 40.7). λ_{max}: 3 200 Å with ε: 13 300, λ_{max}: 2 690 Å with ε: 22 800.

Acetone dithiocarbobenzoxy-thiocarbohydrazone (V, R = $PhCH_2$, R_1 = R_2 = CH_3) was obtained from acetone mono-thiocarbohydrazone and dibenzyl trithiocarbonate in 55 % yield, and crystallized from absolute ethanol as colourless rods, m.p. 132–138° (decomp.). (Found: C 46.3; H 5.28; N 17.9; S 31.0. $C_{12}H_{16}N_4S_3$ (312.46) requires C 46.1; H 5.16; N 17.9; S 30.8).

Benzaldehyde dithiocarbomethoxy-thiocarbohydrazone (V, R = CH_3, R_1 = H, R_2 = Ph) was obtained in quantitative yield, and crystallized from a mixture of absolute ethanol and toluene as colourless hairs, m.p. 185–195°. (Found: C 42.2; H 4.23; N 19.9; S 33.6. $C_{10}H_{12}N_4S_3$ (284.41) requires C 42.2; H 4.25; N 19.7; S 33.8).

Acetophenone dithiocarbethoxy-thiocarbohydrazone (V, R = C_2H_5, R_1 = CH_3, R_2 = Ph) was obtained in 85 % yield when monoacetophenone thiocarbohydrazone reacted with diethyl trithiocarbonate under the conditions described above. It crystallized from ethanol as colourless plates, m.p. 178–179° after considerable sintering between 130 and 140°. (Found: C 46.4; H 5.16; N 18.0; S 30.8. $C_{12}H_{16}N_4S_3$ (312.46) requires C 46.1; H 5.16; N 17.9; S 30.8).

Monobenzophenone thiocarbohydrazone has not been described before. It was prepared like the mono-thiocarbohydrazones described in Part I, in 45 % yield, and it crystallized from glacial acetic acid as long, pale yellow plates, m.p. 213–214° (decomp.) (Found: C 62.5; H 5.20; N 20.5; S 11.7. $C_{14}H_{14}N_4S$ (270.34) requires C 62.2; H 5.22; N 20.7; S 11.9).

Benzophenone dithiocarbomethoxy-thiocarbohydrazone (V, R = CH_3, R_1 = R_2 = Ph) was obtained in quantitative yield and crystallized from a mixture of absolute ethanol and toluene as colourless rods, m.p. 155–158°. (Found: C 53.7; H 4.60; N 15.6; S 26.8. $C_{16}H_{16}N_4S_3$ (360.50) requires C 53.3; H 4.47; N 15.6; S 26.7).

Alkylthio-thiadiazolylhydrazones (VI)

These were prepared by heating the dithiocarbalkoxy-thiocarbohydrazones above their melting points until the evolution of gas had ceased. The molten residues crystallized on cooling and could in most cases be recrystallized directly, if the comparatively small amounts of by-products did not interfere.

Acetone 5-methylthio- and 5-mercapto-1,3,4-thiadiazol-2-yl-hydrazone (VI, R = R_1 = R_2 = CH_3, and VI, R = H, R_1 = R_2 = CH_3). The residue after melting acetone dithiocarbomethoxythiocarbohydrazone consisted of a mixture of acetone methylthiothiadiazolylhydrazone and its 5-mercapto analogue. Boiling toluene extracted the former, and when the toluene was taken off *in vacuo* the product was obtained in 80 % yield. It crystallized from ethanol as colourless rods, m.p. 162–163°, not depressed on admixture with the hydrazone described on p. 000. (Found: C 35.2; H 4.95; N 27.4; S 32.0. $C_6H_{10}N_4S_2$ (202.29) requires C 35.6; H 4.98; N 27.7; S 31.7). The toluene-insoluble material (VI, R = H, R_1 = R_2 = CH_3, 15 % yield) crystallized from ethanol as colourless rods, m.p. 216–217° (decomp.). (Found: C 31.9; H 4.14; N 29.8; S 34.2; equiv.wt.: 189.6. $C_5H_8N_4S_2$ (188.26) requires C 31.9; H 4.28; N 29.8; S 34.1). λ_{max}: 3 270 Å with ε: 17 500. When this compound was methylated with methyl iodide in alkaline solution, the methylthio derivative described above was formed.

Acetone benzylthio-thiadiazolylhydrazone (VI, R = $PhCH_2$, R_1 = R_2 = CH_3) was obtained in 70 % yield after separation from 15 % of the thiol (VI, R = H, R_1 = R_2 = CH_3).

It crystallized from absolute ethanol as colourless rods, m.p. 139—140°. (Found: C 51.5; H 5.07; N 20.3; S 23.3. $C_{12}H_{14}N_4S_2$ (278.38) requires C 51.8; H 5.07; N 20.1; S 23.0).

Benzaldehyde methylthio-thiadiazolylhydrazone (VI, R = CH_3, R_1 = H, R_2 = Ph) was obtained in 70 % yield after recrystallization from *n*-butanol, colourless rods, m.p. 208—209°. (Found: C 48.3; H 4.08; N 22.4; S 25.6. $C_{10}H_{10}N_4S_2$ (250.33) requires C 48.0; H 4.03; N 22.4; S 25.6). λ_{max}: 3 350 Å with ε: 25 000; λ_{max}: 2 540 Å with ε: 8 300; λ_{max}: 2 260 Å with ε: 13 700.

Benzaldehyde 5-mercapto-1,3,4-thiadiazol-2-yl-hydrazone (V, R = R_1 = H, R_2 = Ph, 0.20 g), prepared according to Stollé and Fehrenbach [3], was dispersed in ethanol (3 ml). Methyl iodide (0.2 g) and N NaOH (1 ml) were added, and the hydrazone rapidly dissolved. Within a few minutes a pale yellow precipitate began to form (0.22 g), which crystallized from *n*-butanol as colourless rods, m.p. and mixed m.p. 208—209°. The UV spectrum of this specimen was found to be identical with that of the benzaldehyde methylthio-thiadiazolylhydrazone described above.

Acetophenone ethylthio-thiadiazolylhydrazone (VI, R = C_2H_5, R_1 = CH_3, R_2 = Ph) was obtained in 80 % yield after recrystallization from ethanol. Colourless rods, m.p. 182—183°. (Found: C 51.9; H 5.04; N 20.2; S 22.9. $C_{12}H_{14}N_4S_2$ (278.38) requires C 51.8; H 5.04; N 20.1; S 23.0). λ_{max}: 3 250 Å with ε: 20 500; λ_{max}: 2 260 Å with ε: 11 700.

Benzophenone methylthio-thiadiazolylhydrazone (VI, R = CH_3, R_1 = R_2 = Ph) was obtained in 87 % yield. It crystallized from toluene as pale yellow, irregular prisms, m.p. 170—171°. (Found: C 58.9; H 4.41; N 17.2; S 19.6. $C_{16}H_{14}N_4S_2$ (326.42) requires C 58.9; H 4.32; N 17.2; S 19.6).

Decomposition of dithiocarbalkoxy-thiocarbohydrazones in acid solution

Acetone dithiocarbomethoxy-thiocarbohydrazone was decomposed exactly as dithiocarbomethoxy-thiocarbohydrazide (II, p. 1941). The same products were obtained in much the same yields.

Benzaldehyde dithiocarbomethoxy-thiocarbohydrazone (2.8 g) was refluxed in ethanol (50 ml) and concentrated hydrochloric acid (1 ml) for 5 min. The mixture was evaporated to dryness on a boiling water bath, and the residue was extracted with water (10 ml), and the extract added to benzaldehyde (1.2 g) in ethanol (10 ml). Benzalazine (0.95 g, 90 % yield) separated, m.p. and mixed m.p. 92—93°. The water-insoluble residue was ground with N NaOH (20 ml), and benzalazine (1.0 g, 96 % yield) remained undissolved. The alkaline solution was acidified with N HCl, and colourless rods were deposited (1.4 g, 87 % yield), m.p. 135—136°, not depressed by addition of mercapto-methylthio-thiadiazole (III, R = CH_3). Obviously the initially formed benzaldehyde hydrazone had disproportionated to benzalazine and hydrazine.

Alkylthio-thiadiazolylhydrazines (I)

Methylthio-thiadiazolylhydrazine (I, R = CH_3). Acetone methylthio-thiadiazolylhydrazone (20.3 g) was refluxed for one hour with ethanol (100 ml) and 5 N HCl (100 ml). The solvents were removed by distillation under reduced pressure, and the flask was immersed in a boiling water bath to prevent the separation of unchanged starting material. The dry residue was dissolved in ethanol (200 ml) and ether (800 ml) was added. A hydrochloride of not very well defined composition separated as colourless prisms (18.3 g). It was dissolved in water (200 ml), and the free thiadiazolylhydrazine was precipitated by the addition of crystalline sodium acetate (30 g). Colourless rods separated at once (13.5 g, 83 % yield), m.p. 117—118° after recrystallization from toluene. (Found: C 22.4; H 3.69; N 34.6; S 39.4. $C_3H_6N_4S_2$ (162.23) requires C 22.2; H 3.73; N 34.5; S 39.5). λ_{max}: 2 820 Å with ε: 8 200.

Benzylthio-thiadiazolylhydrazine (I, R = $PhCH_2$). Acetone benzylthio-thiadiazolylhydrazone was hydrolyzed as above, but the isolation of a crystalline hydrochloride was not attempted. Instead, the residue after evaporation was directly dissolved in water, and the hydrazine was precipitated by the addition of crystalline sodium acetate. The

yield was 76 %, colourless rods with m.p. 111—112° after recrystallization from absolute ethanol. (Found: C 45.4; H 4.30; N 23.5; S 26.7. $C_9H_{10}N_4S_2$ (238.32) requires C 45.4; H 4.32; N 23.5; S 26.9).

The UV-spectra were recorded with a Beckman DU spectrophotometer in absolute ethanol solution.

The technical assistance of Miss Monica Linders is acknowledged. The investigation has been supported by grants from the *Swedish Natural Science Research Council*, from *Stiftelsen Lars Hiertas Minne*, and from *Hierta-Retzius Stipendiefond*.

REFERENCES

1. Busch, M. and Biehler, F. *J. prakt. Chem.* [2] **93** (1916) 354.
2. Hoggarth, E. *J. Chem. Soc.* **1952** 4817.
3. Stollé, R. and Fehrenbach, K. *J. prakt. Chem.* [2] **122** (1929) 289.

Received May 18, 1960.

ACTA CHEMICA SCANDINAVICA 14 (1960) 1945–1956

The Extraction of Uranium(VI) with DBP in the Presence of TBP. The "Synergic" Effect: Substitution or Addition?

DAVID DYRSSEN and LIBOR KUČA*

Department of Inorganic Chemistry, Royal Institute of Technology, Stockholm 70, Sweden

The nature of the mixed complexes, $UO_2A_2(HA)_xB_y$, of the uranyl ion with di-*n*-butyl phosphate (DBP = HA) and tri-*n*-butyl phosphate (TBP = B) in carbon tetrachloride has been investigated at at 25°C by measuring the distribution ratio q of ^{233}U between carbon tetrachloride and 0.1 M sulfuric acid. At concentrations of DBP between 0.0003 and 0.06 M, and of TBP between 0 and 0.1 M, two complexes are formed, namely $UO_2A_2(HA)_2$ at low $[B]_{org}[HA]_{org}^{-1}$, and $UO_2A_2(HA)B$ at high $[B]_{org}[HA]_{org}^{-1}$. The value obtained for the equilibrium constant of the following reaction in carbon tetrachloride

$$UO_2A_2(HA)_2 + B \rightleftharpoons UO_2A_2(HA)B + HA$$

is $\log K_{20}^{-1}K_{11} = -3.0 \pm 0.2$. The concentrations of free HA and B were calculated from data of Dyrssen and Liem [9].

It may thus be stated that in the present case the »synergic» effect is due to substitution rather than addition.

Dialkyl phosphates have proved to be efficient extraction agents for lanthanide and actinide ions. At present, extraction with dialkyl phosphates has been developed by Brown and his co-workers at Oak Ridge to an industrial process for extraction of uranium from acid solutions [1]. In the course of systematic studies of various classes of organic phosphorus compounds as extracting agents for uranium, it was noticed that the addition of non-ionic phosphorylated reagent, X_3PO (X = alkyl group R or alkoxy group RO), to the dialkyl phosphate, $(RO)_2POOH$, increased the distribution ratio considerably. This enhancement of U(VI) extraction has been called a »synergic» (synergistic, synergetic) effect.

Let us denote the dialkyl phosphate, which is an acid, by HA, and the non-ionic phosphorylated compound, *i.e.* TBP, by B. It should be noted that HA, dissolved in an inert organic solvent like CCl_4 or hexane, exists predo-

* Present address: Institute of Nuclear Research, Prague, Czechoslovakia.

minantly in the form of a dimer, H_2A_2. The extraction of uranyl, in the absence of B, may be expressed by the equation [2-4]:

$$UO_2^{2+}(aq) + 2H_2A_2(org) \rightleftharpoons UO_2A_2(HA)_2(org) + 2H^+(aq)$$

Two explanations of the »synergic» effect have been proposed, but neither has had up to now, adequate experimental support.

According to one hypothesis, which has been proposed by Brown *et al.*[1] the non-ionic molecule B is *added* to the previous complex through a hydrogen bond:

$$UO_2A_2(HA) + B \rightleftharpoons UO_2A_2(HA)_2B$$

There is said to be some experimental evidence for this hypothesis [5].

On the other hand, Kennedy [6] suggests that two molecules of B substitute for two molecules of HA:

$$UO_2A_2(HA)_2 + 2B \rightleftharpoons UO_2A_2B_2 + (HA)_2$$

Some indirect evidence [7] for this hypothesis is given by Kennedy's observation that a non-ionic phosphorylated resin absorbs uranium as UO_2A_2 from a solution of uranium di-*n*-butyl phosphate in benzene, and liberates HA.

In two preceding papers from this laboratory [8,9], the reactions of di-*n*-butyl phosphate (DBP = HA) with various solvents — among these tri-*n*-butyl phosphate (TBP = B) — was studied. The data make it possible to calculate the concentrations of individual species in the system DBP-TBP-CCl_4-H_2O, namely, HA and A^- in the aqueous phase, and HA, H_2A_2, B, and HAB in the organic phase.

The present work has aimed at studying the distribution of uranium (VI) between CCl_4 and 0.1 M H_2SO_4. The experiments were so planned that either the concentration of free HA in the organic phase, $[HA]_{org}$ was kept constant, and $[B]_{org}$ was varied, or $[B]_{org}$ was kept constant, and $[HA]_{org}$ was varied.

Our results elucidate the mechanism of the so-called synergic effect for the DBP-TBP-CCl_4 system, and it seems possible in this case to decide between the two mechanisms proposed: addition or substitution.

EXPERIMENTAL

The di-*n*-butyl phosphate (DBP = HA) was supplied by Albright and Wilson Ltd, London. It was purified in the way previously described [9]. Tri-*n*-butyl phosphate (TBP = B), Kebo, Stockholm, was purified as follows: first it was stirred for several hours with the same volume of 4 % NaOH. After that, 4 % $KMnO_4$ was added dropwise to the NaOH, still with vigorous stirring. At first, the solution was decolorized, but after the addition of a certain amount of $KMnO_4$, the color remained constant. The TBP was then washed with 0.1 M HNO_3 and water, and finally dried at 130°C in a slow current of dry N_2 gas at reduced pressure. Carbon tetrachloride (Merck) was of analytical grade and was not further purified.

A solution of $^{233}U(VI)$ in 0.1 M H_2SO_4 was made from sulfuric acid, *pro analysi* (Merck). The α-emitter ^{233}U was purchased in the form of $UO_3(H_2O)_2$ from AERE, Harwell, England. In most experiments, the initial concentration of U(VI) in the aqueous phase was 6.9×10^{-6} M, which is negligible in comparison with the total concentration of HA(B).

In experiments with log $[HA]_{org} = -5.50$, the concentration of uranium(VI) was 3.7×10^{-5} M. Also in this case, the concentration of U in the organic phase was negligible in comparison with the concentration of HA (see below).

All experiments were carried out at 25°C in thermostated rooms. The practical details of the distribution experiments have been described in a previous paper [4]. The α-activity was measured in a Tracerlab SC-16 windowless proportional counter. The distribution ratio q of ^{233}U was calculated as before [4].

In the measurements, the aqueous phase contained 0.1 M H_2SO_4; thus we may calculate $[H^+] = 0.133$ M, using the data of Bray and Liebhafsky [10].

We decided to work with sulfate medium in order to bring the distribution ratio into a suitable range for measurement ($3 > \log q > -3$). A 1 M $HClO_4$ medium might have been used, but extraction of some $HClO_4$ with TBP [11], and of some uranium as $UO_2(ClO_4)_2(TBP)_2$, might occur. Nitrate medium would not be suited for these studies, since uranium would be extracted — in the form of $UO_2(NO_3)_2(TBP)_2$ or $UO_2(NO_3)_2(DBP)_2$ — to an even greater extent than from perchlorate medium [12-15].

CALCULATION OF $[HA]_{org}$ AND $[B]_{org}$

The symbols are in general the same as in our earlier work on similar systems [9]. Let us denote the concentrations of free HA and B in the organic phase as:

$$[HA]_{org} = a;\ [B]_{org} = b$$

Let K_d be the distribution constant for monomer HA between organic and aqueous phase, K_a the acidity constant of HA in the aqueous phase, K_2 the equilibrium constant for dimerization of HA in the organic phase and K the association constant of HA and B. Then we have ([HA] and $[A^-]$ refer to the aqueous phase):

$$[HA] = aK_d^{-1};\ [A^-] = aK_d^{-1}K_a h^{-1};\ [H_2A_2]_{org} = K_2a^2\ ;\ [HAB]_{org} = Kab$$

Since the volumes of the organic and aqueous phases are equal, we may simply add the concentrations in two phases; the »total concentrations» of HA and B are then:

$$A = a(1 + K_d^{-1} + K_d^{-1}K_a h^{-1}) + 2K_2a^2 + Kab$$

$$B = b(1 + Ka)$$

Since K and K_2 refer to reactions in the organic phase only, it seems reasonable that they would be almost the same as in previous studies [9] on the distribution between CCl_4 and 0.1 M HNO_3, namely:

$$\log K_2 = 6.49\ ;\ \log K = 2.84$$

In the first calculation, a value of K_d (determined for the 0.1 M HNO_3 medium), was used: $\log K_d = -1.44$. Due to the difference in ionic strength between 0.1 M $HClO_4$ and 0.1 M H_2SO_4, $\log K_a$ was chosen as -0.98 instead of -1.00 (Ref.[8]). These values were used initially, since no radioactive DBP was available at the time, to measure the distribution of HA between CCl_4 and 0.1 M H_2SO_4 directly. However, as we shall see later, the measurements on uranium distribution will suggest that the constants for the sulfuric acid system are somewhat different from those determined for 0.1 M HNO_3. We

may note that Hardy and Scargill [16] give values of K_2 and K_d with 1 M HNO_3 that differ somewhat from our values [9] with 0.1 M HNO_3.

As already mentioned, the concentration of uranium is always so low in the organic phase that it can be neglected in comparison with A and B.

THE DATA

The Tables 1 and 2 gives the primary experimental data which consist of the total concentrations A and B, the distribution ratio q and the calculated values for $[HA]_{org} = a$ and $[B]_{org} = b$. The values of A and B have been chosen to give the values for a and b, using the known equilibrium constants.

Table 1. Data for the distribution of ^{233}U between equal volumes of CCl_4 and 0.1 H_2SO_4 at different total molar concentrations of DBP (= A) and TBP (= B). These concentrations have been calculated (see text) in such a manner that the concn. of free DBP was kept constant in the organic layer while the concn. of free TBP was varied stepwise. In Fig. 1 the distribution of U(VI) is plotted as log q $[A^-]^2$ against log $[HA]_{org}$ (= log a) for different values of log $[B]_{org}$ (= log b).

log b	log A	log B	log q
log a = −3.5, log $[A^-]$ = −2.16			
0	−0.070	0.086	2.01
−1	−0.184	−0.914	2.10
−2	−0.197	−1.914	2.08
−3	−0.199	−2.914	2.06
−4	−0.199	−3.914	2.05
−5	−0.199	−4.914	2.04
log a = −4, log $[H^+]$ = −2.66			
0	−0.866	0.029	1.96
−1	−1.133	−0.971	1.96
−2	−1.171	−1.971	1.86
−3	−1.175	−2.971	1.90
−4	−1.176	−3.971	1.87
−5	−1.176	−4.971	1.94
log a = −4.25, log $[A^-]$ = −2.91			
0	−1.213	0.017	1.84
−0.5	−1.461	−0.484	1.81
−1	−1.582	−0.983	1.85
−1.5	−1.629	−1.484	1.59
−2	−1.644	−1.983	1.47
−2.5	−1.650	−2.484	1.39
−3	−1.652	−2.983	1.37
−4	−1.652	−3.983	1.36
−5	−1.652	−4.983	1.37
log a = −4.5, log $[A^-]$ = −3.16			
0	−1.529	0.009	1.42
−0.5	−1.836	−0.491	1.33
−1	−2.004	−0.991	1.17
−1.5	−2.075	−1.491	0.79
−2	−2.100	−1.991	0.67
−2.5	−2.108	−2.491	0.39
−3	−2.110	−2.991	0.40
−4	−2.111	−3.991	0.29
−5	−2.112	−4.991	0.31
log a = −4.75, log $[A^-]$ = −3.41			
0	−1.820	0.005	0.87
−0.5	−2.172	−0.495	0.73
−1.0	−2.390	−0.995	0.30
−1.5	−2.492	−1.495	−0.10
−2.0	−2.529	−1.995	−0.45
−2.5	−2.542	−2.495	−0.69
−3	−2.545	−2.995	−0.77
−4	−2.547	−3.995	−0.87
−5	−2.548	−4.995	−0.90
log a = −5, log $[A^-]$ = −3.66			
0	−2.097	0.003	−0.08, +0.03
−0.5	−2.481	−0.498	−0.23
−1	−2.745	−0.997	−0.65
−1.5	−2.876	−1.498	−1.16
−2	−2.928	−1.997	−1.46
−2.5	−2.947	−2.498	−1.60
−3	−2.951	−2.997	−1.90
−4	−2.955	−3.997	−1.92
−5	−2.955	−4.997	−1.94
log a = −5.25, log $[A^-]$ = −3.91			
0	−2.361	0.002	−0.89
−0.5	−2.773	−0.499	−1.13
−1	−3.065	−0.998	−1.58
−1.5	−3.225	−1.499	−2.01
−2	−3.292	−1.998	−2.36
−2.5	−3.314	−2.499	−2.78
log a = −5.5, log $[A^-]$ = −4.16			
0	−2.620	0.001	−1.70
−0.5	−3.040	−0.499	−1.88
−1	−3.360	−0.999	−2.36
−1.5	−3.544	−1.499	−2.87

Table 2. Data for the distribution of ^{233}U between equal volumes of CCl_4 and 0.1 M H_2SO_4 or 0.133 M $HClO_4$ at different total concentrations of DBP (= A): In these experiments no TBP was added. The data are treated in Figs. 1 and 3.

aq medium	log A	log q	log A	log q
0.1 M HS_2O_4	−1.30	+1.74	−2.30	−0.24
	−1.70	+1.22	−2.70	−1.25
	−2.00	+0.48	−3.00	−1.97
			−3.30	−2.75
0.133 M $HClO_4$	−1.30	+1.89	−2.70	−0.48
	−2.00	+1.22	−3.00	−1.12
	−2.30	+0.81	−3.30	−1.71

In Fig. 1, the data are plotted in the form log $q[A^-]^{-2}$ *versus* log $[HA]_{org}$. Points with the same symbol have the same calculated value for b. (The values of a and b were calculated with the set of constants for 0.1 M HNO_3 and may thus have to be slightly corrected later on). The numbers in Fig. 1 denote the slope of the linear parts of the curves.

At the lowest value for b, up to log $b \sim -3$, the experimental points approached the curve obtained for $b = 0$. As shown in earlier papers [2-4] this curve is determined in an inert solvent by the reaction

$$UO_2^{2+}(aq) + 2(HA)_2(org) \rightleftharpoons UO_2A_2(HA)_2(org) + 2H^+(aq)$$

The slope of the limiting curve in Fig. 1 is not exactly 2.0 as one might have expected, but about 2.3. This discrepancy can probably be ascribed to small errors in the equilibrium constants used for the calculation of a and b.

At the highest values for a, the curves bend in the other direction, with a slope of −1.7 instead of +2; moreover, the addition of B now has no influence at all. This effect has not been studied more closely. It may be that UO_2SO_4 is extracted to some extent and, UO_2^{2+} and A^- possibly form complexes in the aqueous phase. It should be noted also that in this region, HA is further polymerized in the organic phase according to physico-chemical experiments made at our institute. Furthermore, there may be minor impurities [12,23] in the sample of ^{233}U, which could influence the measurements at $100 > q < 0.01$.

The fact that the curves spread out as log b increases above −2.5, proves that B in some way enters into complexes with the uranium. (It should be noted that the complex between HA and B has been allowed for and the concentrations used in Fig. 1 are the calculated concentrations of free HA and B).

As may been seen in Fig. 1 the slope of the curves decreases with increasing b. This indicates that some of the complexes, which may in general be written as $UO_2A_2(HA)_xB_y$, contain less than 2 HA. Thus the effect cannot be explained by addition compounds only.

At low $[HA]_{org}$ the same upward bend in the curves is observed as previously [4] with the DBP-hexone system. In this case it was concluded, that in addition to $UO_2A_2(HA)_2$ a complex $UO_2A_2(hexone)_x$ was extracted at low [HA].

Let us start with the simplest assumption that might be consistent with these data, namely that, besides $UO_2A_2(HA)_2$, only the first substitution complex, $UO_2A_2(HA)B$, appears in the organic phase.

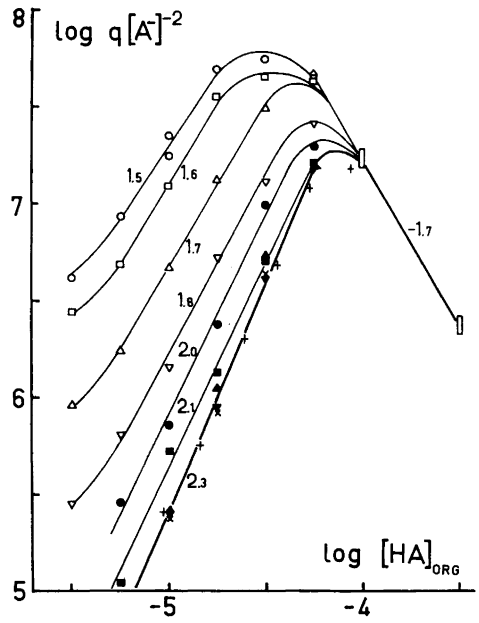

Fig. 1. The distribution of U(VI) between solutions of DBP (= HA) and TBP (= B) in CCl_4 and 0.1 M H_2SO_4. Each curve represents a constant value of the pre-calculated molar concn. of free TBP, $[B]_{org}$. The limiting curve for $[B]_{org} \leq 10^{-3}$ is shown as a thick line. The slopes of linear parts of the curves ars noted in the figure. Symbols (log $[B_{org}]$: ○ (0), □ (−0.5), △ (−1), ▽ (−1.5), ● (−2), ■ (−2.5), ▲ (−3), ▼ (−4), × (−5), and + (−∞, no TBP). The distribution of ^{233}U is independent of $[B]_{org}$ at log $[HA]_{org} = -4$ and −3.5.

For this case, let us define the equilibrium constants

$K_{20} = [UO_2A_2(HA)_2]_{org}\ [UO_2^{2+}]^{-1}[A^-]^{-2}[HA]_{org}^{-2}$

$K_{11} = [UO_2A_2HAB]_{org}\ [UO_2^{2+}]_{org}^{-1}[A^-]^{-2}[HA]_{org}^{-1}[B]_{org}^{-1}$

Moreover we use the conventional notation that $[UO_2^{2+}]$ stands for the sum of all complexes of UO_2^{2+} including those with SO_4^{2-} with the aqueous medium *. Assuming that $UO_2A_2(HA)_2$ and UO_2A_2HAB are the only species formed in the organic layer, the net distribution ratio is then:

$$q = ([UO_2A_2(HA)_2]_{org} + [UO_2A_2HAB]_{org})[UO_2^{2+}]^{-1} = [A^-]^2(K_{20}a^2 + K_{11}ab)$$

and

$$q[A^-]^{-2}a^{-2}K_{20}^{-1} = 1 + K_{11}K_{20}^{-1}ba^{-1}$$

* The amount of UO_2^{2+} bound to SO_4^{2-} can be estimated from separate experiments with 0.133 M $HClO_4$ (*cf.* Fig. 3). These data indicate that $[UO_2^{2+}]_{H_2SO_4}\ [UO_2^{2+}]^{-1}_{HClO_4} = 1 + \beta_1[SO_4^{2-}] + \beta_2[SO_4^{2-}]^2 \sim 10$, which agrees fairly well with the value that can be estimated from values of Davies and Monk [17] for β_1 and β_2.

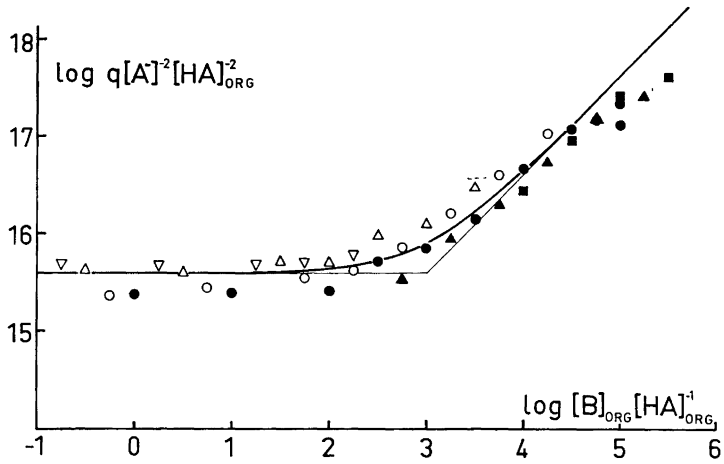

Fig. 2. Plot based on the assumption of the formation of a substitution complex in the CCl_4 phase, $UO_2A_2(HA)B$. The normalized curve log Y = log (1 + X) is fitted to the data. K_{20} and $K_{20}K_{11}^{-1}$ (see text) are obtained from the position of the asymptotes (thin lines) to the curve. Symbols denote different constant values of log [HA]org: ▽(−4.25), △(−4.50), ○ −4.75), ● (−5.00), ▲ (−5.25), and ■ (−5.50). The variables are calculated from data in Table 1.

In Fig. 2, the quantity log $q[A^-]^{-2}a^{-2}$ is plotted as a function of log ba^{-1}. Values on the descending parts of the curves in Fig. 1 are not included in Fig. 2. It can be seen from the figure that the experimental points fall reasonably well on the normalized curve log Y = log (1 + X). From the position of the asymtotes of the normalized curve one may calculate the values log K_{20} = 15.6 ± 0.2 and log K_{20} — log K_{11} = 3.0 ± 0.2. Hence log K_{11} = 12.6 ± 0.2

It thus seems that the data may be rather well explained by assuming that one HA in the original complex is substituted with B. From the present data there is no strong evidence for the second complex, $UO_2A_2B_2$, which, in the diagram, Fig. 2, would have caused a steeper slope of the curve at high ba^{-1}. However, it is quite possible that the second type of substitution complex, which has been proposed by Kennedy [6], may well exist with other more basic substituting substances B, for instance with phosphine oxides, R_3PO.

CONCLUSION

It does not seem possible to explain the data on the increased (synergic) extraction of uranyl by DBP in the presence of TBP by assuming the formation of addition compounds only, since with this assumption, one would have had a constant slope of 2 to the right in Fig. 1. In fact the slope really decreases with increasing b.

On the other hand, the substitution hypotesis seems to explain the data well; the diagram in Fig. 2 gives a good fit of the theoretical curve assuming

only one substitution. Thus, in addition to $UO_2A_2(HA)_2$ we would have $UO_2A_2(HA)B$ in the following concentration ranges: 0.0003 — 0.06 M DBP (= HA) and 0 — 1 M TBP (= B).

ADJUSTMENT OF $K_aK_d^2$

It remains however, to explain why in Fig. 1 the limiting slope for $b \to 0$ is +2.3 rather than +2.0 because the difference is, we feel, outside of the experimental error. There seems to be no reason to doubt the formula $UO_2A_2(HA)_2$ for the predominant complex in the organic phase [2-4] since it has been proved in many other systems. Small amounts [12,23] of the decay products of ^{232}U present in the sample of ^{233}U would rather have decreased the slope, and it is therefore reasonable to suppose that the difference is due to small errors in the values assumed for the equilibrium constants that determine a and b. Let us consider the case of a solution with no B added. The total concentration of A is then

$$A = [HA]_{org} + [HA] + [A^-] + 2[H_2A_2]_{org} = a(1 + K_d^{-1}(1 + K_a h^{-1})) + 2a^2K_2$$

With the previous definition of K_{20} we have

$$[UO_2A_2(HA)_2]_{org} = K_{20}[UO_2^{2+}][A^-]^2a^2 = [UO_2^{2+}]K_{20}a^4h^{-2}K_d^{-2}K_a^2 = q[UO_2^{2+}]$$

In these experiments, the hydrogen ion concentration h is a constant, and we may simplify these equations. Normalizing, we find

$A = \alpha + L_2\alpha^2$ and $q = L_1\alpha^4$, where

$$\alpha = a(1 + K_d^{-1}(1 + K_a h^{-1})) \simeq aK_d^{-1}(1 + K_a h^{-1})$$

$$L_1 = K_{20}h^{-2}K_a^2(1 + K_d^{-1}(1 + K_a h^{-1}))^{-4} \simeq K_{20}h^{-2}K_d^2K_a^2(1 + K_a h^{-1})^4$$

$$L_2 = 2K_2(1 + K_d^{-1}(1 + K_a h^{-1}))^{-2} \simeq 2K_2K_d^2(1 + K_a h^{-1})^{-2}$$

L_2 and L_1 may be obtained by plotting on one axis (Fig. 3)

$$\log A - \tfrac{1}{4}\log q = \log(1 + L_2\alpha) - \tfrac{1}{4}\log L_1$$

and, on the other axis,

$$\tfrac{1}{4}\log q = \log \alpha + \tfrac{1}{4}\log L_1$$

Comparing this plot with the normalized curve, $Y = \log(1 + X)$ we find, from the positions of the coordinates,

$$\tfrac{1}{4}\log L_1 - \log L_2 = 0.35 \text{ and } \tfrac{1}{4}\log L_1 = 2.74$$

Using $K_a h^{-1} = 0.8$ we obtain

$$\log K_2 + 2\log K_d = 3.3_0$$

whereas the value for this sum was 3.61 for nitrate medium. Fig. 3 also gives the corresponding data for 0.133 M $HClO_4$, which can be fitted, within the experimental error, with $\log K_2K_d^2 = 3.61$, the same value as in 0.1 M HNO_3.

For 0.1 M H_2SO_4 we may accept $\log K_2K_d^2 = 3.3_1$ assuming $\log K_2 = 6.49$ as with 0.1 M HNO_3 and thus giving $\log K_d = -1.59$. Using these constants

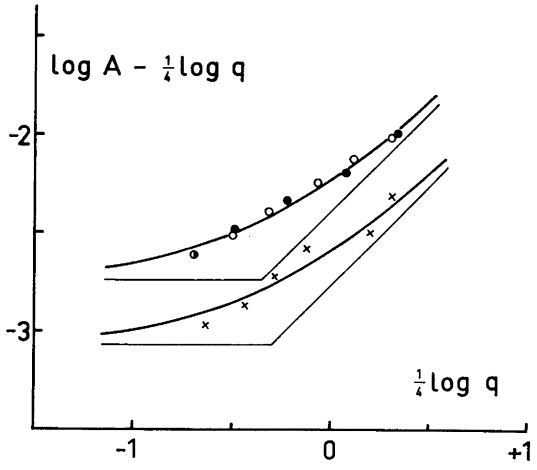

Fig. 3. Determination of $K_2K_d^3$ for the 0.1 M H_2SO_4 medium. The normalized curve log Y = log (1 + X) is fitted to the data: O experiments with no TBP, ● experiments with $[TBP]_{org} \leq 10^{-3}$M, × aq. phase 0.133 M $HClO_4$, no TBP. The point of intersection of the asymptotes to the curves gives the values of ¼ log L_1 − log L_2 and ¼ log L_1 (se text).

the data in Table 1 were recalculated. They are plotted in Fig. 4, and it is seen that the spread is less than in Fig. 2. This gives additional support to the interpretation of the nature of the complexes $UO_2A_2(HA)_xB_y$. The deviation from the theoretical curve at high ba^{-1} is probably due to a decrease in

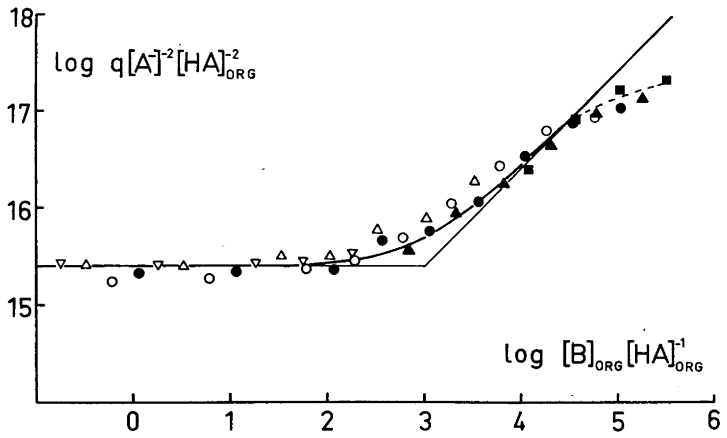

Fig. 4. Plot based on recalculated values of $[HA]_{org}$ (= a) and $[B]_{org}$ (= b) using log K_d = − 1.59 instead of −1.44 (*cf.* Fig. 2). The symbols refer to the same concentrations of DBP as in Fig. 2. The curve log Y = log(1 + X) is fitted to the data; deviation from this curve occurs with b = 0. 0.316 and 1 M. The position of the asymptotes (thin lines) gives log K_{20} = 15.4 ± 0.2 and log $K_{20}K_{11}^{-1}$ = 3.0 ± 0.2.

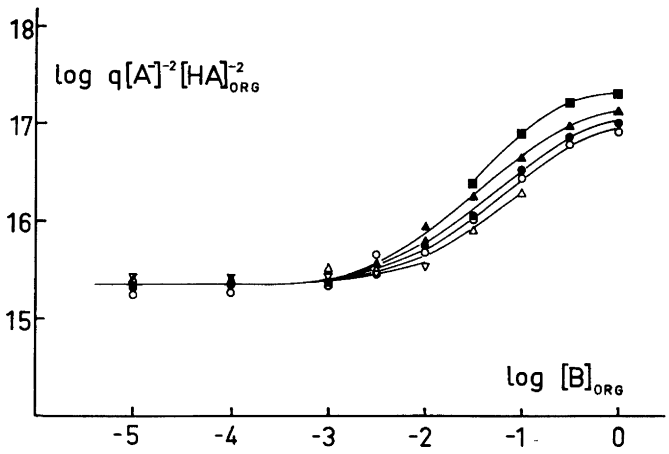

Fig. 5. Attempt to explain the synergic effect with the formation of $UO_2A_2(HA)_2B$. The choice of the variables is explained in the text. The symbols are defined in Fig. 2.

the activity coefficient of TBP in CCl_4 at $b = 0.317$ and 1 M (undiluted TBP is 3.66 M). From Fig. 4 one may calculate $\log K_{20} = 15.4 \pm 0.2$ and $\log K_{11} = 12.4 \pm 0.2$.

It may be worthwile to see whether the data can be explained by a simple addition mechanism, as proposed by Brown *et al.*[1], even if the curves in Fig. 1 are not favorable for such a hypothesis. If this were so, we would, instead of K_{11}, have to consider the equilibrium constant:

$$K_{21} = [UO_2A_2(HA)_2B]_{org}[UO_2^{2+}]^{-1}[A^-]^{-2}[HA]_{org}^{2}[B]_{org}^{-1}$$

As before, we would have obtained the expression

$$q[A^-]^{-2}a^{-2}K_{20}^{-1} = 1 + K_{20}^{-1}K_{21}b$$

Thus, if the experimental data had been plotted as $\log q[A^-]^{-2}a^{-2}$ *versus* $\log b$, a single curve should have resulted, which would have been fitted with a normalized curve $\log Y = \log (1 + X)$. As seen in Fig. 5, the spread is considerable at high b where the complex $UO_2A_2(HA)_2B$ would be formed. As in Fig. 4 the curves fall off at $b = 0.317$ and 1 M.

The calculations we have made in this part support the conclusion that was drawn from the uncorrected data in Figs. 1 and 2.

DISCUSSION

In calculating the economy of using the synergic effect with dialkyl phosphates, one must consider not only the formation of substitution complexes like $UO_2A_2(HA)B$ but also the dimerization of HA and the complex formation between HA and B in the organic phase.

If the cost of organic phosphorus per mole of uranium to be extracted is important, then the economy of a process should gain if the more expensive

dialkyl phosphates (HA) can in part be replaced by the less expensive trialkyl phosphates (B). However, if the constants K_{20} and K_{11} are compared, it may be seen that the replacement of HA with B requires a large value for $[B]_{org}[HA]_{org}^{-1}$ (*cf.* Figs. 2 and 4). The reason may be that the extra HA in $UO_2A_2(HA)_2$ are not only bound with the phosphoryl oxygens to U (which probably has the coordination number of 8 as in $UO_2(CH_3COO)_3^-$, Ref.[18]), but also with strong hydrogen bonds to the oxygen atoms in UO_2^{2+}; the basicity of the PO groups in DBP and TBP should be about the same.

The difference between DBP (= HA) and TBP (= B) as solvate molecules may be further stressed if we compare the two reactions

$UO_2^{2+}(aq) + 2\ NO_3^-(aq) + 2HA\ (toluene) \rightleftharpoons UO_2(NO_3)_2(HA)_2\ (toluene)$

and

$UO_2^{2+}(aq) + 2NO_3^-(aq) + 2B\ (benzene) \rightleftharpoons UO_2(NO_3)_2B_2\ (benzene)$

From data as Hardy [12] and of Healy and Kennedy [19] we may calculate the equilibrium constants of these reactions as log K = 6.76 and 1.44. With the more basic compound tributyl phosphine oxide, Bu_3PO, the value of log K is 4.62 for benzene.

It may be noted that Brown *et al.*[1] have shown that q increases more (using dioctyl phosphate as HA), if the more basic tributyl phosphine oxide (TBPO) is added than if TBP is added. It is possible that B = TBPO can replace two HA = DBP (*cf.* Kennedy [7]) at a value of $[B]_{org}[HA]_{org}^{-1}$ where TBP only replaces one DBP. In the case of hexone [4], which is 8 M, evidence was found of UO_2A_2 at low [HA].

The complex formation between HA and B will diminish the loss of HA to the aqueous phase, but at the same time, this reaction will decrease the amount of free HA and B that can react with UO_2^{2+}. If the total load of organic phosphate per unit volume of the organic diluent, *e.g.* kerosene, needs to be kept low, then it might be more favorable to increase the concn. of HA than to add B. The situation should be different with a chelating agent like TTA, where the acid hydrogen is engaged in an intramolecular hydrogen bond and the tendency for the formation of H_2A_2 and HAB is thereby weak (*cf.* Edgington and Irving [20]).

As the extraction of tri- and tetravalent ions seems to decrease on the addition of neutral esters of phosphoric acid (*cf.* Refs.[21,22]), it may be possible in many cases to increase the separation of di- and tri- or tetravalent ions by adding neutral ligands to the organic layer.

Acknowledgements. The present investigation has been supported by the *Swedish Council of Atomic Research*, and by a grant from the *Institute of Nuclear Research*, Prague. The data have been treated in collaboration with the head of the department, Professor Lars Gunnar Sillén. The English text has been revised by Dr. Valentine Tyrrell. We wish to thank Mr. H.A.C. McKay for valuable comments on the manurcript and for support io obtaining the uranium-233.

REFERENCES

1. Blake, C. A., Baes, C. F., Brown, K. B., Coleman, C. F. and White, J. C. *Second Intern. Conf. Peaceful Uses Atomic Energy*, Paper 1550, Geneva 1958; *ORNL*-2172, Oak Ridge 1956.

2. Baes, C. F., Zingaro, R. A. and Coleman, C. F. *J. Phys Chem.* **62** (1958) 129.
3. Dyrssen, D. *J. Inorg. Nuclear Chem.* **8** (1958) **291**.
4. Dyrssen, D. and Krašovec, F. *Acta Chem. Scand.* **13** (1959) **561**.
5. Blake, C. A., Horner, D.E. and Schmitt, J. M. *ORNL*-2259, Oak Ridge 1959.
6. Kennedy, J. *AERE C/M* 369, Harwell 1958.
7. Kennedy, J., Burford, F. A. and Sammes, P. G. *AERE-R* 3077, Harwell 1959; *J. Inorg. Nuclear Chem.* **14** (1960) 114. Kennedy, J., Sammes, P. G. and Deane, A. M. *Chem. & Ind. London* **1960** 443.
8. Dyrssen, D. *Acta Chem. Scand.* **11** (1957) 1771.
9. Dyrssen, D. and Liem, D. H. *Acta Chem. Scand.* **14** (1960) 1091.
10. Bray, W. C. and Liebhafsky, H. A. *J. Am. Chem. Soc.* **57** (1935) 51.
11. Hardy, C. J. *AERE-R* 3124, Harwell 1959.
12. Hardy, C. J. *AERE-R* 3267, Harwell 1960.
13. Moore, R. L. *AECD*-3196 (1951).
14. Healy, T. V. and McKay, H. A. C. *Rec. trav. chim.* **75** (1956) 730.
15. Hesford, E. and McKay, H. A. C. *Trans. Faraday Soc.* **54** (1958) 573.
16. Hardy, C. J. and Scargill, D. *J. Inorg. Nuclear Chem.* **11** (1959) 128; *AERE C/R* 2830, Harwell 1959.
17. Davies, E. W. and Monk, C. B. *Trans. Faraday Soc.* **53** (1957) 442.
18. Zachariasen, W. H. and Plettinger, H. A. *Acta Cryst.* **12** (1959) 526.
19. Healy, T. V. and Kennedy, J. *AERE C/R* 2686, Harwell, 1958.
20. Irving, H. and Edgington, D. N. *Proc. Chem. Soc. London* **1959** 360.
21. Dyrssen, D. and Liem, D. H. *Acta Chem. Scand.* **14** (1960) 1100.
22. Dyrssen, D. and Ekberg, S. *Acta Chem. Scand.* **13** (1960) 1909.
23. Alcock, H., Best, C. F., Hesford, E. and McKay, H. A. C. *J. Inorg. Nuclear Chem.* **6** (1958) 328.

Received May 9, 1960.

ACTA CHEMICA SCANDINAVICA 14 (1960) 1957–1960

Quantitative Determination of Pentetrazol

EVA ANDERSSON, MILES FORS and JAN-ERIK LINDGREN

Laboratory of the Swedish Pharmacopoeia Commission, Stockholm, Sweden

A method for quantitative determination of pentetrazol has been worked out based on the precipitation of the cadmium chloride complex and subsequent complexometric titration of the cadmium content in the precipitate.

Pentetrazol [Cardiazol ®, Leptazol (Belg. 30, Suppl. 51, B.P. 58), Pentylenetetrazol (U.S.P. 55)] has usually been determined with the help of its more or less insoluble complexes with different inorganic salts [1–8]. Several authors [1,4,5,7] have found the complex with cuprous chloride to be the most convenient for this purpose. Ph. Helv. 33, Add. 55 has admitted the cuprous chloride method of Dister [4], and the British Pharmacopoeia of 1958 a modification of it, worked out by Sharp [5]. We have examined both methods and found none of them to be accurate enough despite rigorous precautions. Since the accuracy of other methods, cited in literature, was judged not to be greater, we have on the suggestion of Dr. T. Canbäck * investigated the possibilities of using the complex proposed by Warren [2] for identification purposes, *i.e.* with cadmium chloride even for quantitative determination. The solubility of the cadmium chloride complex of pentetrazol in water is reported by several authors to be too great for quantitative precipitation. Warren [2] found it to be about 1:95 and Paulsen [7] reports the solubility in 0.1 M cadmium chloride to be 0.25 %. Paulsen [7] moreover reports that there are two different complexes with cadmium chloride, one with a composition of $CdCl_2 \cdot 2C_6H_{10}N_4$, obtained by mixing about equimolecular quantities of pentetrazol and cadmium chloride, and the other with a composition of $CdCl_2 \cdot C_6H_{10}N_4$, obtained by adding cadmium chloride in excess to a solution of pentetrazol, both compositions being determined after drying at 150°C.

As a result of this we have tried to find a suitable medium, where the solubility of the cadmium chloride complex, obtained by excess of the reagent, is small enough for quantitative precipitation. We have found that a mixture of *iso*propanol and water complies with this requirement and have worked out a method for quantitative determination of pentetrazol based on the precipi-

* Chairman of the Swedish Subcommittee on Chemistry.

tation of the cadmium chloride complex and subsequent complexometric titration of the cadmium content in the precipitate.

EXPERIMENTAL

The cadmium chloride complex, $C_6H_{10}N_4 \cdot CdCl_2 \cdot 3H_2O$ was precipitated with an excess of the reagent and isolated. The solubility of the complex was determined in different solutions of alkaline salts, hydrochloric acid and in some organic solvents. The complex was found to be more or less soluble in the solutions of alkaline salts and hydrochloric acid but almost insoluble in *iso*propanol. Cadmium chloride was found to have a solubility of about 1:1 000 in *iso*propanol and by using a mixture of *iso*propanol and water, it is possible to get a relatively strong reagent solution, without any risk of precipitation of the reagent. After some preliminary work we have found the following method suitable.

Mix 0.1500 g, dissolved in 2 ml of a mixture of 3 volume parts of *iso*propanol and 2 volume parts of water, with 10 ml of cadmium chloride-*iso*propanol-R. Filtrate the mixture after 10 min, during which time the bottle from time to time is swirled, through a glass crucible (3 G 4). Transfer the precipitate completely with the aid of the filtrate. Wash the filter twice with 5 ml of a mixture of 9 volume parts of *iso*propanol and 1 volume part of water, and finally 3 times with *iso*propanol, each time with 10 ml. Transfer the filter to another suction flask and dissolve the precipitate in 100 ml of water, heated to boiling-point. Cool the solution, add 10 ml of ammonium chloride-ammonia-R and 5 drops of eriochrome black-I and titrate immediately with 0.1 N tetracemindisodium to a blue colour. Each ml of 0.1 N tetracemindisodium is equivalent to 0.006909 g of $C_6H_{10}N_4$.

Reagents

Iso*propanol*, purum min. 99 %. B.p. 81–83°C.

Cadmium chloride-iso*propanol-R.* Dissolve 15.0 g of cadmium chloride ($CdCl_2 \cdot 2\frac{1}{2} H_2O$) in 40 ml of water by warming. Filter the solution and dilute with *iso*propanol to 100 ml after cooling. The solution must be freshly prepared.

Ammonium chloride-ammonia-R *. Dissolve 6.75 g of ammonium chloride (NH_4Cl) in 57 ml of strong ammonia solution and dilute with water to 100 ml.

Eriochrome black-I *. Dissolve 0.50 g of eriochrome black T and 4.5 g of hydroxylamine hydrochloride in 100 ml of methanol.

*0.1 N Tetracemindisodium 0.05 M**. Tetracemindisodium (EDTA, Komplexon, Titriplex) dissolved in water to contain in 1 000 ml 18.61 g of $C_{10}H_{14}O_8N_2Na_2 \cdot 2H_2O$.

DISCUSSION

The content of cadmium in the precipitate was determined after repeated washings and drying in the air and found to be 34.96 % (calculated for

Table 1. The solubility of $C_6H_{10}N_4 \cdot CdCl_2$ in different solvents, g/100 g.

Ammonium chloride 2 M	0.80	Ether	0
Sodium chloride 10 %	0.55	*Iso*propanol 50 % v/v	0.79
Hydrochloric acid 0.1 M	0.97	*Iso*propanol 60 % v/v	0.61
Hydrochloric acid 0.5 M	0.78	*Iso*propanol 70 % v/v	0.53
Hydrochloric acid 1 M	0.68	*Iso*propanol 80 % v/v	0.24
Hydrochloric acid 2 M	0.76	*Iso*propanol 90 % v/v	0.10
Hydrochloric acid 3 M	1.02	*Iso*propanol 95 % v/v	0.06
Hydrochloric acid 4 M	1.20	*Iso*propanol	0
Acetone	0		

* From prescriptions accepted by the Scandinavian Pharmacopoeia Council for the Nordic Pharmacopoeia.

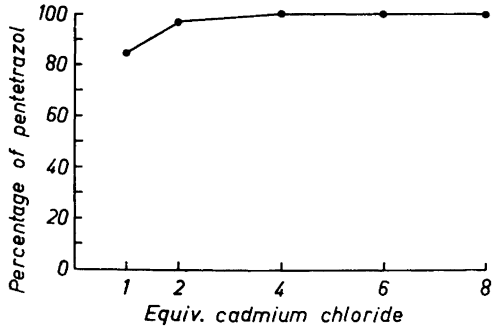

Fig. 1. Relation between results in percentage of pentetrazol and equivalents of cadmium chloride.

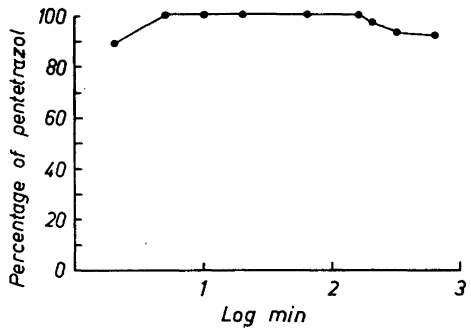

Fig. 2. Relation between results in percentage of pentetrazol and time of precipitation.

$C_6H_{10}N_4 \cdot CdCl_2$: 34.96 %). By heating at 105°C and 150°C for about 20 h it did not lose appreciably in weight. According to Zwikker [1] and Paulsen [7] the complex hydrate $C_6H_{10}N_4 \cdot CdCl_2 \cdot 3H_2O$ (= 29.93 % Cd) loses its water by drying at 150°C and becomes anhydrous. The precipitate obtained in the mixture of *iso*propanol and water is therefore obviously anhydrous and has a composition of $C_6H_{10}N_4 \cdot CdCl_2$.

The solubility of the complex is 0.61 g/100 g (Table 1) in a mixture of 3 parts of *iso*propanol and 2 parts of water but in the presence of cadmium chloride, the solubility decreases so that a quantitative precipitation is possible. The solubility in the wash liquid, 9 parts of *iso*propanol and 1 part of water is 0.10 g/100 ml but the loss in the washing is unnoticeable, owing to the excess of cadmium chloride in the precipitate, which is only gradually washed out, and to the short time of the washing. For that reason correction for solubility is not necessary.

To obtain quantitative precipitation a certain excess of the precipitant is necessary. We have found that under the present conditions a quantity of cadmium chloride is required which is about 4 times that calculated (Fig. 1). We have chosen a somewhat greater excess, about 6 times the quantity calculated.

The precipitate does not appear until about half a minute after the addition of the reagent and it takes some minutes until the precipitation is complete. If the precipitate stands in contact with the mother liquid for a longer time than about 2.5 h, the precipitate is changed and passes easily through the filter, perhaps owing to hydrolysis to basic complexes (Fig. 2).

Table 2. The importance of swirling the bottle during the precipitation. Sample C.

Swirled	Not swirled
99.9—99.8 %	97.4—98.3 %

Table 3. The cadmium content of the precipitate after washing with the number of *iso*propanol-water mixture 9 + 1 noted, followed by 3 × 10 ml of *iso*propanol.

1 × 2 ml	2 × 2 ml	3 × 2 ml	1 × 5 ml	2 × 5 ml	3 × 5 ml	4 × 5 ml
36.47 %	35.60 %	34.82 %	35.25 %	34.96 %	34.98 %	34.98 %

Table 4. Results obtained with commercial samples: I, In original state; II, After one recrystallization from water.

	Sample A	Sample B	Sample C
I.	99.1—99.2—99.3— —99.1—99.2 %	100.2—100.2—100.0— —100.0—100.2—99.9— —100.2—100.0— —100.0—100.1 %	99.9—100.2—99.9— —100.1—99.9—99.8— —99.8—99.9—99.9— —99.8—99.6 %
II.	99.5—99.6 %	— — — — —	100.0—99.8 %

During the precipitation the bottle must be swirled from time to time, as otherwise low results are obtained (Table 2) and the precipitate sometimes becomes fine-grained and passes easily through the filter.

To wash out the great excess of cadmium chloride it is necessary to use a mixture of *iso*propanol and water. The water content of the wash liquid can however be decreased considerably compared with the mixture that is used in the reagent solution, since the precipitation of cadmium chloride of the reagent solution on the addition of more *iso*propanol is markedly delayed. When washed with 2×5 ml of a mixture of 9 volume parts of *iso*propanol and 1 volume part of water, the excess of cadmium chloride is removed from the precipitate (Table 3).

The results obtained with commercial samples are tabulated in Table 4.

The method can also be used for the determination of pentetrazol in plain aqueous solutions by adding *iso*propanol to the solution in the amount required to get the same proportion of *iso*propanol and water as is used for the substance.

REFERENCES

1. Zwikker, J. J. L. *Pharm. Weekblad* **71** (1934) 1170.
2. Warren, L. E. *J. Assoc. Offic. Agr. Chemists* **29** (1946) 296.
3. Horsley, T. E. V. *Analyst* **71** (1946) 308.
4. Dister, A. *J. pharm. Belg.* **3** (1948) 190.
5. Sharp, L. K. *J. Pharm. Pharmacol.* **4** (1952) 52.
6. Winterfeld, K., Bodendorf, K. and Kraft, K. *Pharm. Ztg. ver. Apotheker-Ztg.* **100** (1955) 609.
7. Paulsen, A. *Medd. Norsk Farm. Selskap* **18** (1956) 139.
8. Spacu, P., Albescu, I. and Gheorghiu, C. *Acad. rep. populare Romine, Stud. cercetari Chim.* **6** (1958) 565, from *Anal. Abstr.* **6** (1959) 4577.

Received May 20, 1960.

ACTA CHEMICA SCANDINAVICA 14 (1960) 1961–1979

The Structures of Co_2P, Ru_2P and Related Phases

STIG RUNDQVIST

Institute of Chemistry, University of Uppsala, Uppsala, Sweden

The crystal structures of Co_2P and Ru_2P have been refined using single-crystal methods. Both phosphides crystallize in the *C* 23 structure type. A structural comparison with related phosphides and silicides is given.

Co_2P has an extended homogeneity range at higher temperatures, the phosphorus-rich limit at 1 000°C corresponds to the formula $Co_{1.94}P$. There are evidences that the widening of the homogeneity range is connected with random vacancies on metal atom sites.

The structure of Co_2P was originally determined by Nowotny [1]. According to him, the Co_2P structure belongs to the *C* 23 (anti-$PbCl_2$) type. The structure of Co_2Si was first investigated by Borén [2]. Borén *et al.*[3] also made a structure proposal based on X-ray powder data. This structure was later shown to be incorrect by Geller [4], who determined the Co_2Si structure by X-ray single-crystal methods. It was then recognized by Laves [5] that Co_2P and Co_2Si are isotypic, which was the first known case of isomorphism between a silicide and a phosphide of the same metal. Recently, a second case has been found for Ru_2P[6] and Ru_2Si[7], which are isostructural with Co_2P and Co_2Si.

From the crystal-chemical point of view it seems valuable to possess detailed structural information on the four above-mentioned phases. This paper gives an account of single-crystal structure determinations of Co_2P and Ru_2P. Some phase-analytical data for the binary Co_2P and Ru_2P, and the ternary $Co_2(P, Si)$ phases are also reported and discussed.

EXPERIMENTAL

Preparation. The starting materials for the preparation of the phosphides were cobalt rods (Johnson, Matthey & Co., Ltd., London, spectrographically standardized), ruthenium sponge (Heraeus, Hanau, Germany claimed purity 99.8 %) and red phosphorus (purity higher than 99 %). Master alloys of Co_2P were prepared according to a method, described in principle by Haughton [8] and Hägg [9]. Pellets of red phosphorus were dropped into molten cobalt. The melting was done by induction heating in a closed chamber in a purified argon atmosphere under reduced pressure. Cobalt phosphides of varying compositions were prepared by mixing appropriate quantities of the crushed master

alloys and heating the mixtures in evacuated and sealed silica tubes. Ruthenium phosphides were prepared directly by heating ruthenium sponge and red phosphorus in evacuated silica tubes. The alloys of both cobalt and ruthenium were protected from contacting the silica tube walls by placing them in small crucibles of recrystallized alumina (Degussit Al 23 from Degussa, Frankfurt).

Chemical analyses. Chemical analyses were made at the Department of Analytical Chemistry of this Institute under the direction of the head of the department, Dr. F. Nydahl.

The cobalt phosphides were dissolved in *aqua regia*, and the hydrochloric acid removed by evaporation with nitric acid. The residue was dissolved in dilute nitric acid and made up to volume. Aliquots were analysed for phosphorus and cobalt. Phosphate was precipitated as ammonium molybdophosphate and weighed as $P_2O_5 \cdot 24\ MoO_3$ according to Nydahl [10]. Cobalt was determined by titration with EDTA, standardized against pure cobalt (cobalt rods, Johnson, Matthey & Co., Ltd.). Murexid was used as indicator and the pH adjusted with sodium carbonate in stead of ammonia to avoid formation of ammines [11].

The compositions of the ruthenium phosphides were checked by analyses for phosphorus only. The alloys were dissolved in hydrochloric acid — chlorine by heating in sealed glass tubes at 300°C for 24—48 h [12-15] (*cf.* [16]). Perchloric acid was used as oxidant for the evolution of chlorine. 1—2 g of sodium chloride was added to the solution, which was then evaporated to dryness to remove traces of silicic acid. The residue was taken up in hydrochloric acid and filtered. Ruthenium was removed by precipitation as the sulphide and phosphorus determined in the filtrate according to the method described above.

X-Ray methods. X-Ray powder photographs were taken using Guinier-type focussing cameras and Cr-$K\alpha_1$ and Cu-$K\alpha$ radiation ($\lambda_{Cr\text{-}K\alpha_1} = 2.2896$ Å; $\lambda_{Cu\text{-}K\alpha} = 1.5418$ Å). Calcium fluoride ($a = 5.4630$ Å) or silicon ($a = 5.4306$ Å) was used as the internal calibration standard on each powder film. Differences larger than 0.02 % for lattice parameters of the same phase, measured in different alloys, were estimated to be significant, whereas the absolute accuracy of a single lattice parameter measurement is not claimed to be greater than 0.04 %.

For the structure determinations, single-crystal fragments were picked from crushed alloys. Weissenberg photographs were taken with niobium-filtered Mo-K radiation. The multiple-film technique was used, and thin iron foil was placed between successive films. The intensities were estimated by visual comparison with a standard intensity scale. Since it was only possible to obtain single-crystals of rather irregular shape, absorption corrections could not be readily applied. However, care was taken to use small crystals (maximum thickness not exceeding 0.04 mm) with a fairly uniform cross-section, thus minimizing the influence of absorption as well as secondary extinction.

The refinement of the structures was made with the aid of the electronic digital computer BESK. The programs for Fourier summations and structure factor calculations are designed by Edstrand, Westman *et al.*[17] and Åsbrink *et al.*[18] For the atomic scattering factors f_i, analytical expressions of the type $f_i = A_i \exp\left(-\frac{a_i}{\lambda^2}\sin^2\Theta\right) + B_i \exp\left(-\frac{b_i}{\lambda^2}\sin^2\Theta\right) + C_i \exp\left(-\frac{c_i}{\lambda}\sin^2\Theta\right) + D_i$ were used. The constants A_i, B_i, C_i and a_i b_i, c_i, have been determined by Appel [19] on the basis of atomic scattering factor tables given by Thomas and Umeda [20] for Co and Ru, and by Tomiie and Stam [21] for P. The following constants were used:

	A_i	B_i	C_i	a_i	b_i	c_i
Co	9.319	10.181	7.273	0.328	3.556	25.673
Ru	15.176	16.599	11.760	0.240	2.637	20.292
P	1.447	7.971	5.588	0.001	1.528	37.194

In the case of Ru, a correction for dispersion was made by introducing the real part of the dispersion correction as the constant D_i in the above-mentioned expression for the scattering factors. This was taken as the value calculated by Dauben and Templeton [22].

PHASE-ANALYTICAL INVESTIGATIONS

In the binary system Co—P, three intermediate phases have been reported, *viz.* Co_2P, CoP and CoP_3, [23-25,1,26], and in the binary system Ru—P three phases Ru_2P, RuP and RuP_2 are known [27,6].

Nowotny [1] found that the unit cell dimensions of Co_2P are variable, indicating an extended homogeneity range. The present investigation shows that the unit cell of Co_2P decreases with decreasing cobalt content, which has also been verified by Nowotny [28]. The phase-analytical data are collected in Tables 1 and 2. On account of the difficulties of detecting small amounts of cobalt with the X-ray method, the cobalt-rich limit of the homogeneity range could not be accurately located. Judging from the lattice parameter measurements in Table 2, this limit is probably not far from the ideal composition Co_2P. The X-ray method is more sensitive for the detection of small amounts of CoP. The data in Tables 1 and 2 show that the phosphorus-rich limit at 1 000°C is very close to the composition $Co_{1.94}P$, and furthermore that the homogeneity range of Co_2P becomes larger when the temperature is increased from 900°C to 1 100°C.

No lattice parameter variations were found for Ru_2P in alloys with different compositions quenched from temperatures up to 1 100°C. The composi-

Table 1. Phase-analytical data for alloys containing Co_2P.

Alloy	Chemical analysis		Phases present in alloys quenched from		
	Weight % Co	Weight % P	900°C	1 000°C	1 100°C
$Co_{2.07}P$	79.57	20.20	Co_2P traces of Co	Co_2P traces of Co	Co_2P traces of Co
$Co_{1.94}P$	78.51	21.28	Co_2P traces of CoP	Co_2P	Co_2P
$Co_{1.89}P$	78.20	21.70	Co_2P traces of CoP	Co_2P traces of CoP	Co_2P traces of CoP

Table 2. Unit cell dimensions of Co_2P in Å measured on the alloys specified in Table 1.

Quenching temp. °C	Axis	$Co_{2.07}P$	$Co_{1.94}P$	$Co_{1.89}P$
900	a	5.646	5.640	5.641
	b	3.513	3.509	3.509
	c	6.608	6.605	6.605
1 000	a	5.646	5.638	5.638
	b	3.513	3.507	3.507
	c	6.608	6.603	6.603
1 100	a	5.646	5.638	5.634
	b	3.513	3.507	3.505
	c	6.608	6.603	6.601

tion of Ru_2P at 1 100°C was "bracketed" with two annealed and quenched alloys; one containing (besides Ru_2P) traces of ruthenium, and the other containing (besides Ru_2P) traces of RuP. Chemical analysis of the first alloy gave a phosphorus content of 13.20 wt % and the other 13.34 wt %. The phosphorus content calculated for the ideal composition Ru_2P is 13.29 wt %. Thus, at 1 100°C, the composition of Ru_2P is close to the ideal formula. (There is no reason to believe that the alloys take up any appreciable amount of impurities during the preparations.) The melting point of Ru_2P is much higher than that of Co_2P, and a widening of the homogeneity range of Ru_2P at temperatures above 1 100°C cannot be excluded. In fact, the structure determination made on a single-crystal picked from an arc-melted alloy, indicates such a possibility (*vide infra*).

THE REFINEMENT OF THE Co_2P STRUCTURE

In view of the phase-analytical results it was thought worthwhile to collect intensity data for two Co_2P single-crystals with different compositions. One crystal was selected from a cobalt-rich alloy sintered at 1 100°C. Since it proved very difficult to obtain phosphorus-rich single-crystals from alloys sintered in silica tubes, a very small single-crystal was finally taken from an alloy, melted in an argon-filled arc furnace and rapidly cooled. The composition of the alloy before melting was $Co_{1.89}P$, but some phosphorus was lost during the melting. The powder photograph of the arc-melted alloy gave the following lattice parameter values: $a = 5.638$ Å; $b = 3.507$ Å; $c = 6.603$ Å, corresponding to a composition around $Co_{1.94}P$. Since the diffraction lines were not as sharp as those of carefully annealed alloys, the arc-melted alloy may have been slightly inhomogeneous.

In the following text, the sintered crystal is denoted as Co_2P and the arc-melted crystal $Co_{1.94}P$. Weissenberg diagrams of both crystals were taken about the b axis.

According to Nowotny [1], the structure of Co_2P is based on space-group $Pnma$ — (D_{2h}^{16}), with eight cobalt atoms in two 4(c) positions and four phosphorus atoms in one 4(c) position *. If the space-group is $Pnma$, the reflexions (h00) with $h = 2n + 1$ are extinct. However, a weak (300) reflexion was observed for both crystals (although relatively weaker for the $Co_{1.94}P$ crystal than for the Co_2P crystal), and these spots on the photographic films were not significantly different in shape from the spots of other reflexions. It was nevertheless suspected that (300) might arise from double-reflexion. Calculations showed that the geometrical conditions for double-reflexion from ($\bar{2}1\bar{1}$) and (511) were closely fulfilled. Furthermore, (211) and (511) were observed to be among the very strongest reflexions. It has been pointed out by Jellinek [29] that the effect of double-reflexion can be recognized in single-crystal photographs taken with unfiltered radiation. If the geometrical conditions for

* The C 23 structure has been described with different settings of the unit cell. Nowotny [1] (and *Strukturbericht*) used the space-group $P\,b\,n\,m$, and Geller [4] $P\,n\,a\,m$. In the present paper, the C 23 structure is always described on space-group $P\,n\,m\,a$, following the standard setting (No. 62) in the 1952 edition of *International Tables for X-ray Crystallography*.

double-reflexion are fulfilled for the $K\alpha$ radiation this will not hold for the $K\beta$ radiation. A special exposure with unfiltered MoK radiation was therefore made. β-reflexions corresponding to α-reflexions of equal or even lower intensity than (300), *e.g.* (400), were clearly seen but no β-reflexion corresponding to (300) was discernible. This was taken as definite evidence that (300) arises from double-reflexion.

All the remaining reflexions were consistent with space-group $Pnma$ or $Pn2_1a$. Since the intensity sequences for the ($h0l$) and the ($h2l$) reflexions were equal, and the same was true for the ($h1l$) and ($h3l$) reflexions, it was not considered necessary to take the lower space-group $Pn\ 2_1a$ into account, and it was assumed that Nowotny's structure proposal was essentially correct. The signs of the $F(h0l)$-values were obtained from the atomic parameters given by Nowotny, and the electron density projections $\varrho(xz)$ were computed. All atoms are well resolved in this projection, and maxima appeared at the expected positions. The structures were refined with successive difference syntheses.

In the difference synthesis of the $Co_{1.94}P$ crystal, a distinct negative region of "electron density" was observed at the Co_{II} position, whereas the electron density was not very different from zero in other parts of the difference map, including the regions around the Co_I and P positions. No such phenomenon was observed in the difference maps for the Co_2P crystal. The minimum may originate from various sources. A closer analysis of the electron density maxima in the ϱ_{obs} and ϱ_{calc} projections showed that the effect must be ascribed to an incorrect scale factor for the Co_{II} atoms rather than an incorrect temperature factor. There were no definite indications that the temperature factors for Co_I, Co_{II} and P were very different or anisotropic. It was found that the minimum at the Co_{II} position was removed from the difference map, when an atomic scattering factor $f_{CoII} = 0.96 \cdot f_{CoI}$ was inserted in the structure factor calculations. The introduction of the lower scattering parameter for Co_{II} resulted in a decrease of the R-value for the 87 observed F-values from 0.060 to 0.053. An overall temperature factor with B = 0.40 Å^2 was applied.

$Co_{1.94}P$ presents a favourable case for scattering parameter comparison of the metal atoms from relative intensities only. Since the same kind of "heavy" atoms is compared in the same type of crystallographic position, the choice of scale factor between absolute and observed structure factors is not critical. However, the influence of absorption and extinction may not be negligible, and the question still remains whether the observed difference between the scattering parameters of Co_I and Co_{II} is significant or not. An attempt to study this problem was made in the following way.

A difference synthesis map for $Co_{1.94}P$, based on F_c-values computed with the atomic scattering factors $f_{CoII} = 0.96 \cdot f_{CoI}$, was prepared by calculating $\Delta\varrho$-values for every sixtieth x and z. The standard deviation $\sigma(\Delta\varrho) = \{\overline{(\Delta\varrho)^2}\}^{\frac{1}{2}}$ was calculated for the 900 independent $\Delta\varrho$-values. In the $\varrho_{obs}(xz)$ projection, the area around each cobalt position, in which the electron density values rose appreciably over the background, extended over some 30—40/3 600 of the projection. 35 $\Delta\varrho$-values for adjoining points in the difference map were summed over areas in various positions of the unit cell. The standard deviation of this sum is $\sqrt{35} \cdot \sigma(\Delta\varrho) = \sigma(N)$. The value of the sum in the area around an atomic position, gives a measure of the difference between the observed and calculated scattering parameter of the actual atom, and the sum is not very sensitive to errors in the assigned temperature factors. It was found that the numerical value of the sum never exceeded $4 \cdot \sigma(N)$ wherever the closed area was placed in the difference map.

Another difference map was calculated on the basis of equal scattering parameters for Co_I and Co_{II}. As mentioned before, this map contained a large minimum at the Co_{II} position; this minimum was not removed by omitting $F_o - F_c$ values for the strong reflexions, which shows that it cannot be ascribed to secondary extinction. When the sum over 35 $\Delta\varrho$-values was evaluated in the area around the Co_{II} position the numerical value of the sum was found to be 14 times larger than $\sigma(N)$, whereas the sum did not exceed $4 \cdot \sigma(N)$ in other areas of the difference map. This indicates that the difference between the scattering parameters of Co_I and Co_{II} is a significant effect. It is felt, however, that only a limited confidence can be attached to the actual numerical value of 1.1 electrons.

The interpretation of the difference is not obvious, and several explanations are possible. It will be shown later, however, that the assumption of random vacancies on the Co_{II} position leads to a satisfactory agreement with phase-analytical data and crystal chemical considerations. The final structural data obtained for the two crystals are the following:

Space-group $Pnma - (D_{2h}^{16})$, (No. 62)
All atoms in 4(c) positions.

The Co_2P crystal

$a = 5.646$ Å; $b = 3.513$ Å; $c = 6.608$ Å; $U = 131.1$ Å^3

	Atomic parameters and standard deviations				*Scattering parameters* (electrons)
	x	$\sigma(x)$	z	$\sigma(z)$	
Co_I	0.8560	0.0003_8	0.0647	0.0003_3	27.0
Co_{II}	0.9685	0.0003_8	0.6657	0.0003_3	27.0
P	0.2461	0.0007_8	0.1249	0.0006_7	15.0

The $Co_{1.94}P$ crystal

$a = 5.638$ Å; $b = 3.507$ Å; $c = 6.603$ Å; $U = 130.6$ Å^3

	Atomic parameters and standard deviations				*Scattering parameters* (electrons)
	x	$\sigma(x)$	z	$\sigma(z)$	
Co_I	0.8562	0.0003_3	0.0631	0.0002_8	27.0
Co_{II}	0.9684	0.0003_3	0.6664	0.0002_8	25.9
P	0.2437	0.0006_5	0.1232	0.0005_5	15.0

The standard deviations of the atomic parameters were estimated by Cruickshank's [30] formula. Observed and calculated structure factors for both crystals are collected in Table 3. For the Co_2P crystal (which was larger than the $Co_{1.94}P$ crystal) the R-value for the 104 observed reflexions is 0.088. An overall temperature factor with $B = 0.42$ Å^2 was applied.

Interatomic distances are listed in Table 4a and b. The standard deviations of the Co—Co distances are smaller than 0.004 Å; those of the Co—P distances smaller than 0.005 Å. (Errors in the unit cell dimensions have not been taken into account.) A comparison of corresponding interatomic distances in Co_2P and $Co_{1.94}P$ shows that the differences are very small.

Table 3. Calculated and observed F(*h*0*l*)-values for Co_2P, $Co_{1.94}P$ and Ru_2P.

		Co_2P		$Co_{1.94}P$		Ru_2P	
h	*l*	F_c	F_o	F_c	F_o	F_c	F_o
2	0	15.9	16.7	13.0	17.6	55.8	65.6
4	0	19.4	16.5	17.3	18.7	18.9	21.1
6	0	21.5	16.5	20.9	18.4	71.9	71.7
8	0	33.9	34.8	33.8	34.2	82.7	84.8
10	0	−40.5	41.2	−40.3	40.2	− 42.5	50.0
12	0	− 7.3		− 7.8		− 5.6	
14	0	− 3.6		− 2.3		11.5	
16	0					11.7	
1	1	7.8	10.4	10.9	10.9	10.0	7.2
2	1	− 2.8		− 2.2		− 29.0	31.3
3	1	−88.6	77.4	−88.6	90.8	−152.4	146.1
4	1	44.8	42.8	42.0	45.9	58.7	64.6
5	1	−20.3	16.6	−18.6	19.2	− 53.2	58.6
6	1	49.6	39.6	49.8	48.8	76.5	78.8
7	1	27.6	24.4	26.7	27.1	38.6	47.9
8	1	14.4		12.5		19.0	12.7
9	1	− 2.0		− 0.6		− 12.1	
10	1	16.3	14.9	16.9	16.8	25.6	24.3
11	1	−11.3	12.5	−13.0		− 35.2	38.9
12	1	14.7		13.6		37.4	37.4
13	1	16.1	19.0	16.9		20.0	
14	1	4.3		4.9		20.3	
15	1	13.4		12.6		7.3	
16	1					2.2	
0	2	17.8	13.3	21.2	20.0	38.6	35.6
1	2	−20.7	26.1	−19.2	21.9	− 62.0	61.8
2	2	−46.5	53.9	−46.6	48.0	− 69.2	73.7
3	2	−84.3	77.8	−82.7	83.6	−113.3	112.5
4	2	−53.9	52.4	−53.7	54.0	− 82.7	84.3
5	2	25.1	21.8	25.7	26.3	46.2	46.2
6	2	11.2	13.9	11.2	13.3	3.6	
7	2	−50.7	46.3	−49.0	47.6	− 63.6	65.4
8	2	12.2	9.2	13.1	16.3	16.2	11.6
9	2	−26.9	25.2	−26.5	24.0	− 66.0	70.9
10	2	− 9.8		−10.4		− 27.3	27.9
11	2	−14.9		−14.3		− 30.2	25.3
12	2	4.2		4.1		− 4.1	
13	2	6.1		6.1		4.7	
14	2	13.2	15.5	13.7	14.0	16.8	
15	2	−13.1	10.6	−12.5	13.6	− 30.9	24.2
16	2					3.5	
1	3	87.6	91.4	85.8	82.3	130.4	118.8
2	3	−60.1	64.1	−59.0	59.3	−105.9	98.2
3	3	32.7	33.1	30.1	32.1	73.9	74.8
4	3	21.6	17.9	19.4	20.1	41.4	40.9
5	3	20.2	16.8	17.6	17.6	53.6	54.4
6	3	31.1	32.9	32.1	31.7	70.0	77.2
7	3	20.2	19.3	22.2	23.7	47.8	49.4
8	3	−23.9	23.1	−25.5	25.2	− 36.9	41.0

Table 3. Cont.

9	3	− 9.6		−10.8		11.2	
10	3	− 5.3		− 4.6		− 12.7	
11	3	−14.3	14.0	−14.0		− 3.0	
12	3	13.4	10.6	12.5		31.9	35.1
13	3	− 9.3		− 9.6		− 4.4	
14	3	0.0		0.9		7.6	
15	3	− 7.9		− 6.9		− 5.4	
16	3					− 16.3	
0	4	−70.8	75.6	−65.9	63.0	−135.0	119.3
1	4	−39.5	41.6	−38.5	38.8	− 62.5	58.1
2	4	2.6		4.0		− 27.2	30.5
3	4	3.4		1.3		− 23.2	22.1
4	4	−41.5	38.1	−42.0	40.8	− 50.5	50.7
5	4	72.9	65.0	73.4	69.6	115.1	113.7
6	4	11.5	14.1	12.7	13.2	− 20.4	24.2
7	4	25.4	24.7	24.4	25.2	33.9	37.2
8	4	−14.9	14.8	−13.9		− 39.8	47.2
9	4	− 2.9		− 3.2		− 10.1	
10	4	14.8		13.5		15.1	
11	4	21.3	19.8	20.8	20.0	34.0	32.3
12	4	− 4.8		− 3.9		− 2.3	
13	4	15.3		15.9		41.6	35.8
14	4	8.7		8.7		3.2	
15	4	− 6.8	8.7	− 7.2		− 2.2	
16	4					4.0	
1	5	−42.0	45.3	−40.9	40.8	− 67.5	62.9
2	5	−65.5	65.7	−66.5	62.3	− 92.1	85.5
3	5	2.0		0.9		34.5	33.0
4	5	− 7.9		− 5.5		− 13.7	12.8
5	5	− 8.8	11.1	−10.4		− 4.2	
6	5	− 6.8		− 5.8		− 6.1	
7	5	−14.1		−11.4		− 44.3	46.6
8	5	−40.2	39.7	−38.9	39.1	− 67.6	65.5
9	5	3.4		1.9		− 2.0	
10	5	−23.8	25.0	−24.6	24.9	− 50.3	56.6
11	5	12.5		13.1		23.6	26.5
12	5	5.4		7.0		− 4.9	
13	5	0.0		− 0.2		− 9.8	
14	5	− 5.3		− 5.5		− 17.6	
15	5	2.9		3.8		− 5.5	
16	5					− 23.4	
0	6	11.7	12.1	10.1	9.4	− 13.2	
1	6	−50.9	51.4	−53.1	49.7	− 45.8	42.7
2	6	52.0	52.2	51.6	47.7	101.6	95.4
3	6	12.8	12.0	11.2	10.9	18.5	16.0
4	6	55.0	52.1	51.5	48.1	111.0	103.5
5	6	4.5		5.6		17.1	16.7
6	6	− 4.0		− 2.5		11.8	
7	6	14.5	11.1	13.6		27.9	22.7
8	6	−11.1	10.2	−11.7		− 16.4	
9	6	−22.4	23.1	−23.9	24.1	− 13.8	
10	6	5.8		5.9		39.8	36.5
11	6	12.3		12.1		20.0	19.9
12	6	− 8.5		− 8.7		1.9	
13	6	1.4		2.1		9.7	

Table 3. Cont.

14	6	−16.6	17.0	−16.0	17.0	− 25.0	22.7
15	6	− 1.6		− 2.4		3.1	
1	7	−47.6	45.2	−45.1	42.0	−106.9	101.3
2	7	1.0		− 2.6		18.6	19.9
3	7	15.4	16.0	15.6	15.9	14.4	14.2
4	7	27.5	29.1	29.3	27.5	21.3	21.9
5	7	− 2.2		− 0.6		− 18.1	
6	7	27.2	28.4	27.5	27.2	18.1	19.0
7	7	−28.5	31.2	−28.8	32.3	− 71.3	75.0
8	7	15.2	13.6	14.9		30.0	28.2
9	7	9.0		9.4		− 2.7	
10	7	10.2		8.7		20.1	
11	7	15.3	19.0	14.4		26.9	27.0
12	7	12.5		14.3		15.9	
13	7	− 1.4		− 1.1		− 8.1	
14	7	2.1		1.4		9.8	
15	7					− 6.6	
0	8	−34.3	35.0	−35.3	33.7	− 49.8	51.2
1	8	− 3.4		− 7.2		7.6	
2	8	−26.3	26.8	−26.8	27.2	− 12.9	
3	8	−15.3	12.2	−14.0	15.2	1.2	
4	8	34.5	36.1	34.7	34.9	56.1	59.0
5	8	−24.6	21.9	−22.6	24.4	− 71.5	76.0
6	8	−34.6	34.5	−34.8	35.0	− 41.1	44.8
7	8	−20.1	19.9	−18.4	18.3	− 30.7	33.0
8	8	− 2.1		− 2.7		− 16.6	
9	8	−14.0		−15.5		10.9	
10	8	11.1		11.9		16.7	14.1
11	8	−11.0		− 9.6		− 25.3	22.6
12	8	10.3		10.6		11.5	
13	8	− 5.9		− 5.4		− 33.0	28.1
14	8	− 8.3	7.5	− 8.2		− 18.5	16.8
15	8					− 6.3	
1	9	14.6	12.6	12.9	11.9	34.1	33.6
2	9	16.3	16.5	13.8	15.9	57.4	58.7
3	9	47.4	47.4	47.4	44.2	71.7	72.3
4	9	− 6.2		− 6.5		− 6.5	
5	9	19.4	20.0	20.3	19.4	42.8	47.3
6	9	− 6.3		− 5.4		− 17.0	20.8
7	9	−15.7	19.5	−18.0	20.1	− 3.3	
8	9	7.5		5.0		37.8	37.7
9	9	1.8		2.8		14.2	
10	9	4.8		4.5		26.1	25.7
11	9	1.4		1.5		12.4	
12	9	− 6.0		− 6.0		− 9.3	
13	9	−17.3	12.4	−16.7	16.7	− 8.3	
14	9					5.7	
0	10	−32.7	33.9	−32.0	32.9	− 41.0	44.2
1	10	37.0	39.5	35.9	36.7	58.1	60.5
2	10	−10.1		− 9.8		− 52.8	54.8
3	10	7.4		6.9		22.7	23.6
4	10	3.7		7.9		− 21.9	20.4
5	10	9.2		10.5		− 19.4	23.0
6	10	−12.7		−14.5		− 33.3	35.6

Table 3. Cont.

7	10	7.7		7.8		6.3	
8	10	− 5.8		− 6.0		− 9.5	
9	10	38.0	30.8	36.4	32.7	51.7	57.0
10	10	10.6		11.0		− 7.7	
11	10	− 1.1		− 0.5		0.0	
12	10	5.0		5.4		5.1	
13	10	2.1		2.1		− 3.2	
14	10					2.5	
1	11	−14.4	14.0	−16.9	15.2	12.7	
2	11	14.7	13.3	15.0	14.5	30.8	33.3
3	11	− 2.8		− 0.8		− 13.3	
4	11	−24.3	23.7	−24.0	22.3	− 40.0	43.9
5	11	− 4.8		− 5.1		− 2.8	
6	11	−28.4	29.4	−27.0	29.7	− 54.3	59.6
7	11	− 4.6		− 6.2		13.3	
8	11	− 4.3		− 5.7		− 7.5	
9	11	1.3		1.5		− 1.2	
10	11	− 4.9		− 3.7		− 11.3	
11	11	5.8		7.5		− 7.8	
12	11	−17.7	15.8	−17.9	19.4	− 39.7	34.5
13	11					3.4	
0	12	14.6	14.1	11.5		59.9	66.5
1	12	17.0	17.4	18.6	17.4	34.3	36.6
2	12	28.5	28.3	28.7	28.2	34.3	37.5
3	12	9.0		7.5		13.5	
4	12	1.8		3.5		− 5.2	
5	12	−16.3	21.7	−16.7		− 3.0	
6	12	15.3	14.8	13.8		38.8	40.7
7	12	1.8		− 0.8		8.0	
8	12	− 4.5		− 5.4		17.2	
9	12	12.8	16.8	13.4	18.3	35.8	35.4
10	12	− 2.0		− 0.9		− 8.6	
11	12	− 6.2		− 7.2		4.1	
12	12	− 9.5		− 9.3		− 8.2	
13	12					2.6	
1	13	− 4.3		− 4.6		− 13.1	
2	13	20.5	22.6	22.0	21.7	13.7	
3	13	−16.7	14.0	−13.8		− 60.8	66.3
4	13	3.9		3.7		3.2	
5	13	− 7.2		− 6.9		− 33.0	33.4
6	13	1.1		0.1		2.3	
7	13	6.6		6.0		13.4	
8	13	19.5	20.4	20.9	23.6	14.0	
9	13	− 1.1		− 1.4		− 11.8	
10	12	18.0		18.0		11.3	
11	13	− 0.7		0.4		− 16.9	15.4
12	13					2.3	
0	14	6.6		3.6		32.1	40.0
1	14	− 2.8		− 1.1		− 13.9	
2	14	− 9.4		− 8.8		6.3	
3	14	15.6		15.8		− 11.9	
4	14	−15.5	17.0	−16.3	18.3	− 28.2	31.0
5	14	−24.1	26.5	−25.5	31.1	− 21.1	
6	14	5.1		5.1		24.3	24.7

Table 3. Cont.

7	14	— 5.8		— 5.4		— 18.3	
8	14	5.3		4.4		13.2	
9	14	— 9.4		— 6.6		— 27.2	21.1
10	14	— 5.4		— 4.2		— 12.3	
11	14					— 15.2	
1	15	22.8	22.5	22.6	27.4	37.0	36.9
2	15	2.8		4.4		— 12.0	
3	15	— 1.2		— 1.3		0.5	
4	15	0.1		— 1.1		17.2	
5	15	4.9		4.9		9.8	
6	15	— 1.1		— 3.6		24.2	21.1
7	15	11.9	10.8	11.7	11.4	28.0	25.2
8	15	3.5		4.7		5.5	
9	15	— 3.8		— 3.6		2.3	
10	15					6.5	
0	16	9.9		11.4		— 14.0	
1	16	— 0.2		0.6		— 22.3	25.6
2	16	—14.1	14.6	—13.6	11.9	— 30.6	31.3
3	16	4.4		6.2		— 2.6	
4	16	—10.1		—10.2		— 29.2	26.1
5	16	9.6		7.5		18.9	19.8
6	16	4.0		4.7		— 11.9	
7	16	7.8		8.8		9.1	
8	16	8.0		8.4		— 2.0	
9	16					— 13.8	
1	17	1.1		1.3		8.4	
2	17	— 9.6		— 8.1		— 28.3	27.6
3	17	—11.2	14.3	—11.0		7.3	
4	17	— 5.3		— 5.8		— 3.1	
5	17	— 3.4		— 3.7		6.4	
6	17	— 3.2		— 3.7		0.0	
7	17					3.0	
8	17					— 27.5	
0	18	14.7	19.8	17.1	18.6	9.2	
1	18	— 2.8		— 2.3		— 10.1	
2	18	7.3		6.3		11.3	
3	18	— 5.9		6.1		— 1.6	
4	18					22.4	19.6
5	18					26.1	19.9
6	18					0.6	
1	19					— 29.1	19.5
2	19					— 9.3	
3	19					— 6.6	

THE REFINEMENT OF THE Ru_2P STRUCTURE

Since it was virtually impossible to obtain single-crystals of Ru_2P in alloys sintered in silica tubes, single-crystal fragments were picked from an arc-melted alloy. Within experimental error the lattice parameters of Ru_2P in this alloy were equal to those measured in carefully annealed alloys. How-

Table 4a. Interatomic distances in Co_2P (Å). (Distances shorter than 3.3 Å listed).

	Co_I	Co_{II}	P
Co_I	$2.54_2(2)$	$2.62_4(2)$, 2.66_5 $2.69_1(2)$, 2.71_2	2.14, 2.23(2) 2.24
Co_{II}	$2.62_4(2)$, 2.66_5 $2.69_1(2)$, 2.71_2	$2.83_0(2)$ $3.03_5(2)$	2.29, 2.40(2) 2.54(2)
P	2.14, 2.23(2) 2.24	2.29, 2.40(2) 2.54(2)	3.27(2)

Table 4b. Interatomic distances in $Co_{1.94}P$ (Å). (Distances shorter than 3.3 Å listed).

	Co_I	Co_{II}	P
Co_I	$2.53_0(2)$	$2.62_5(2)$, 2.66_0 $2.69_1(2)$, 2.69_5	2.17, 2.21(2) 2.22
Co_{II}	$2.62_5(2)$, 2.66_0 $2.69_1(2)$, 2.69_5	$2.83_4(2)$ $3.02_7(2)$	2.29, 2.41(2) 2.54(2)
P	2.17, 2.21(2) 2.22	2.29, 2.41(2) 2.54(2)	3.28(2)

ever, the powder diffraction lines of the arc-melted alloy were not very sharp and the experimental error was therefore rather large (about 0.1 %). A widening of the homogeneity range of Ru_2P at higher temperatures (in analogy to Co_2P) cannot be excluded.

The Weissenberg photographs showed that Ru_2P is isostructural with Co_2P. The $\varrho(xz)$ projection was refined in a similar way to that described for Co_2P. It was observed in the difference syntheses of Ru_2P that there was a strong minimum of electron density at the Ru_{II} position as for $Co_{1.94}P$. Furthermore, an anisotropic temperature factor for Ru_{II} was indicated. The axes of the projected vibration ellipsoid for Ru_{II} happened to coincide rather closely to the directions of the crystallographic axes, and therefore, an anisotropic temperature factor of the simple form $\exp -(ah^2 + \gamma l^2)$ was applied.

The absorption was stronger in the Ru_2P crystal than in the Co_2P crystals, but it seems improbable that absorption errors would accumulate in such a way that a strong minimum of electron density is created at the Ru_{II} position, leaving the remaining part of the difference map, especially the vicinity of the Ru_I position, almost unaffected. After lowering the scattering parameter of Ru_{II} by 5.9 %, the resulting difference synthesis was free from large maxima and minima. A significance test, made in the way described earlier, yielded a similar result to that obtained for $Co_{1.94}P$.

The final structural data of the Ru_2P crystal are as follows:

Space-group *Pnma* – (D_{2h}^{16}) No. 62.
All atoms in 4(*c*) positions.

	Atomic parameters and standard deviations				*Scattering parameters* (electrons)
	x	$\sigma(x)$	z	$\sigma(z)$	
Ru_I	0.8585	0.0003_0	0.0736	0.0002_6	44.0
Ru_{II}	0.9780	0.0003_3	0.6586	0.0002_9	41.4
P	0.2455	0.0009_5	0.1135	0.0008_1	15.0

The standard deviations were estimated by Cruickshank's [30] formula. Observed and calculated structure factors are given in Table 3. For Ru_I and P, isotropic temperature factors with $B_{Ru_I} = 0.30$ Å^2 and $B_P = 0.40$ Å^2 were applied, whereas for Ru_{II} the anisotropic temperature factor, exp—(0.00265 h^2 + 0.00120 l^2), was applied. The R-value for the 124 observed reflexions is 0.073.

Table 5. Interatomic distances in Ru_2P (Å). (Distances shorter than 3.5 Å listed).

	Ru_I	Ru_{II}	P
Ru_I	$2.74_6(2)$	2.75_8, $2.83_0(2)$ $2.84_0(2)$, 2.94_7	2.26, 2.30 2.40(2)
Ru_{II}	2.75_8, $2.83_0(2)$ $2.84_0(2)$, 2.94_7	$2.92_8(2)$ $3.20_9(2)$	2.32, 2.55(2) 2.82(2)
P	2.26, 2.30 2.40(2)	2.32, 2.55(2) 2.82(2)	

Interatomic distances calculated on the basis of the unit cell dimensions $a = 5.902$ Å; $b = 3.859$ Å; $c = 6.896$ Å; (obtained from powder photographs of carefully annealed alloys) are given in Table 5. The standard deviations for the Ru—Ru distances are smaller than 0.004 Å; those for the Ru—P distances smaller than 0.006 Å.

DESCRIPTIONS OF THE Co_2P AND Ru_2P STRUCTURES COMPARISONS WITH RELATED STRUCTURES

A projection of the Co_2P structure on the *ac* plane is shown in Fig. 1. The phosphorus atoms are situated in triangular prismatic "holes" in the metal atom lattice, with six metal atoms in the corners of the prism, and three metal atoms outside each rectangular side of the prism forming a triangle around the phosphorus atoms. The environment of the phosphorus atoms is shown for Co_2P in Fig. 2, and for Ru_2P in Fig. 3. These phosphides have their type of non-metal atom coordination in common with many other transition metal phosphides as well as with several transition metal borides, silicides and carbides. A study of the coordination of the phosphorus atoms around the metal

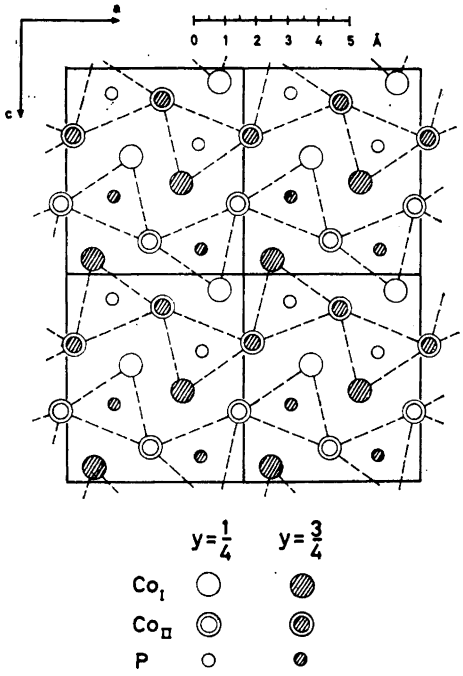

Fig. 1. The structure of Co_2P projected on (010).

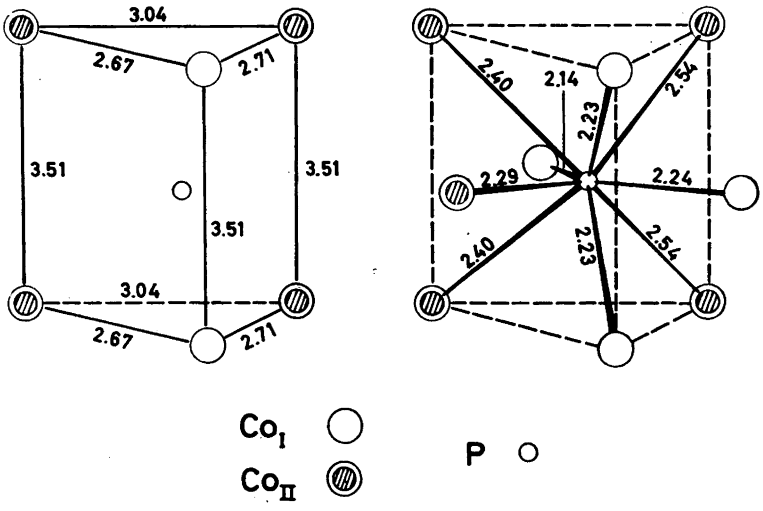

Fig. 2. The environment of the phosphorus atoms in Co_2P.

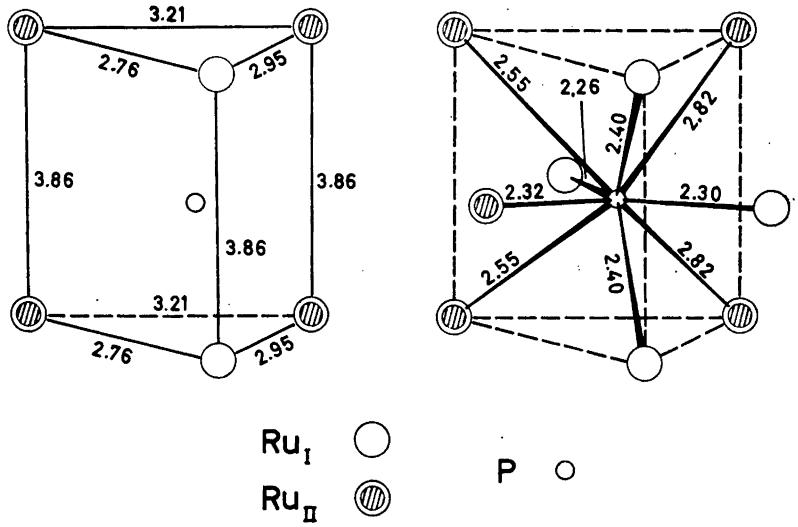

Fig. 3. The environment of the phosphorus atoms in Ru_2P.

atoms shows that Co_I and Ru_I have four phosphorus neighbours arranged in a slightly deformed tetrahedral configuration. The mean value of the Co_I—P distances is 2.21 Å and the mean of the Ru_I—P distances is 2.34 Å. These values are considerably smaller than the average Co_{II}—P and Ru_{II}—P distances. Co_{II} and Ru_{II} have five phosphorus neighbours with a mean Co_{II}—P distance of 2.44 Å and a mean Ru_{II}—P distance of 2.61 Å.

Besides Co_2P and Ru_2P, the structures of the following Me_2P phosphides (Me = transition metal) have been reported; *viz.* Mn_2P, Fe_2P and Ni_2P, which belong to the (revised) *C* 22 structure type [28], and Rh_2P and Ir_2P, which crystallize in the *C* 1 (anti-fluorite) structure [31,6].

The Co_2P and Ru_2P structures bear many resemblances to the *C* 22 type. A projection of the hexagonal Fe_2P structure on the basal plane is shown in Fig. 4. The coordination around the phosphorus atoms in Fe_2P is closely similar to the coordination of the phosphorus atoms in Co_2P. The Fe_I atoms have four phosphorus neighbours in a slightly distorted tetrahedral arrangement (average Fe_I—P distance 2.26 Å) and the Fe_{II} atoms have five phosphorus neighbours (average Fe_{II}—P distance 2.46 Å).

In Rh_2P and Ir_2P, all metal atoms have tetrahedral phosphorus coordination with the Rh—P distance 2.381 Å and the Ir—P distance 2.400 Å.

It was mentioned earlier in this paper that the structures of Co_2P and Co_2Si as well as those of Ru_2P and Ru_2Si are isotypic. A detailed comparison of Co_2P and Co_2Si, however, reveals distinct differences. The situation is quite analogous for Ru_2P and Ru_2Si.

A projection of the Co_2Si structure on the *ac*-plane (according to Geller [4]) is shown in Fig. 5. The near environment of the silicon atoms consists of ten cobalt atoms at distances between 2.32 and 2.57 Å. (An eleventh cobalt atom is

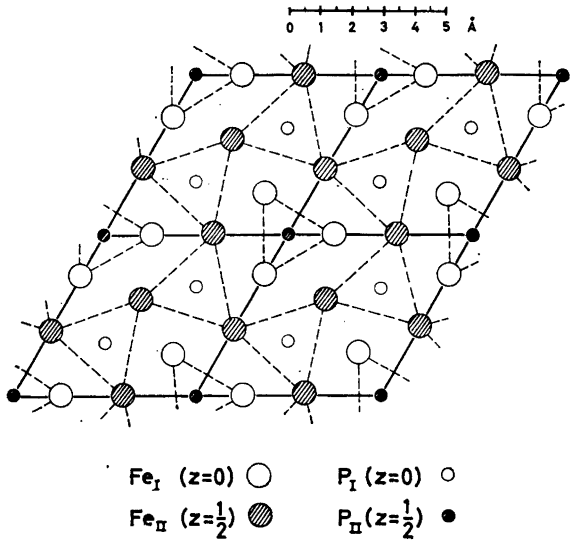

Fig. 4. The structure of Fe_2P projected on (001).

situated at a distance of 3.25 Å and four silicon atoms at a distance of 3.15 Å). In Co_2P, the phosphorus atoms have only nine close cobalt contacts with P—Co distances between 2.14 and 2.55 Å. (Two additional cobalt atoms are situated at distances of 3.42 Å and 3.47 Å, and two phosphorus atoms at a distance of 3.27 Å.) As pointed out before, the coordination of the Co_I atoms in Co_2P is markedly different from that of the Co_{II} atoms. The situation is not analogous in Co_2Si, where the two sets of cobalt atoms each have eight cobalt neighbours and five silicon neighbours:

Co_I —8Co, average distance 2.63 Å; Co_I —5Si, average distance 2.39 Å
Co_{II}—8Co, average distance 2.59 Å; Co_{II}—5Si, average distance 2.46 Å

The unit cell volume of Co_2P is 131.1 Å^3 and the volume of Co_2Si is 130.7 Å^3. The two unit cells are, however, rather different in shape. The *b* and *c* axes in Co_2Si are larger than the corresponding axes in Co_2P, but the reverse is true for the *a* axis. There exists a limited mutual solid solubility between Co_2P and Co_2Si. The changes of the unit cell dimensions of Co_2P and Co_2Si, when these phases dissolve silicon and phosphorus respectively, are seen in Table 6, where lattice parameter measurements have been collected from two-phase Co_2P + Co_2Si alloys, quenched from various temperatures. As seen in Table 6, the mutual solid solubility increases with increasing temperature. Data obtained with the "disappearing phase" method indicated that neither the solid solubility of Co_2P in Co_2Si, nor the solid solubility of Co_2Si in Co_2P exceeds 15 % in the investigated temperature range. In view of the differences between the structures of Co_2P and Co_2Si, it is not surprising that the mutual solid solubility is restricted, although the size-factor is favourable.

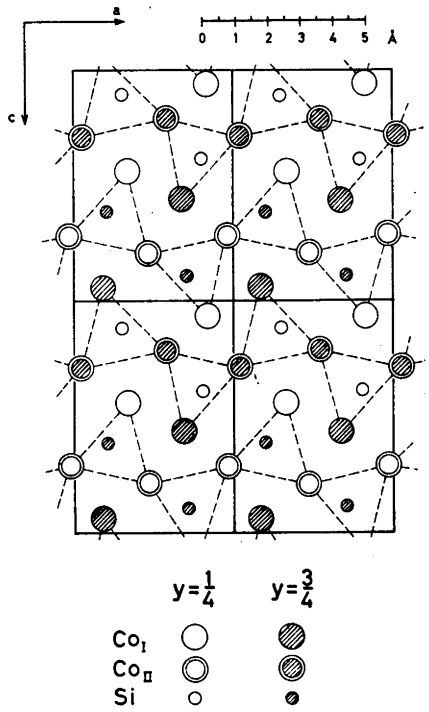

Fig. 5. The structure of Co_2Si projected on (010).

THE HOMOGENEITY RANGE OF Co_2P

The *C* 23 type of structure is rather close-packed, and the "holes" in the structure are not large enough for accomodation of additional atoms without profound distortion of the structure. The extended homogeneity range of Co_2P, (and probably of Ru_2P too), must therefore arise either from metal/phosphorus substitution or from vacant metal atoms sites (or possibly a combination of substitution and vacancies). This is also evident from the decrease of the Co_2P unit cell with increasing P/Co ratio.

The structure determinations on Co_2P and Ru_2P show that there are conspicuous differences between the Co_I and Ru_I atoms on one hand, and the Co_{II} and Ru_{II} atoms on the other. The coordination around the Co_I and Ru_I atoms is different from that of the Co_{II} and Ru_{II} atoms, and furthermore the electron counts indicate a lower scattering parameter for Co_{II} than for Co_I in the $Co_{1.94}P$ crystal (and analogously in the Ru_2P crystal).

The scattering parameter fo Co_{II} in the $Co_{1.94}P$ crystal was observed to be 1.1 electrons less than that of Co_I. If the scattering parameter difference is entirely ascribed to Co_{II}/P substitution, the calculated composition of the crystal is $Co_{1.75}P$, which is not compatible with the phase-analytical results. If the possibility of simultaneous vacancies on the P position is taken into account, the calculated composition of the crystal may be brought to a more

Table 6. Lattice parameters of Co_2P—Co_2Si mixed crystals. (Measurements made on a two-phase alloy with the composition $Co_2P_{0.5}Si_{0.5}$, quenched from various temperatures).

Quenching temp. °C	Phase	Lattice parameters (Å)		
		a	*b*	*c*
—	Co_2P	5.646	3.513	6.608
—	Co_2Si	4.918	3.737	7.109
1 000	$Co_2P(Si)$	5.607	3.537	6.644
	$Co_2Si(P)$	4.954	3.719	7.065
1 075	$Co_2P(Si)$	5.600	3.540	6.650
	$Co_2Si(P)$	4.965	3.715	7.048
1 150	$Co_2P(Si)$	5.595	3.543	6.654
	$Co_2Si(P)$	4.982	3.709	7.039

reasonable value, but this idea seems far-fetched and it is not supported by the data of the structure determination. On the other hand, if the lowering of the Co_{II} scattering parameter is ascribed only to random vacancies among the Co_{II} atoms, the composition of the crystal should be $Co_{1.96}P$, which is in fairly good agreement with the phase-analytical data. This supports the hypothesis of metal atom vacancies. It must be remembered, however, that it is possible to interpret the observed difference between the scattering parameters of Co_I and Co_{II} in other ways than those mentioned here.

Although the existence of metal/phosphorus substitution has been recognized in transition metals, *e.g.* in α-iron [32], the conditions for metal/phosphorus substitution in Co_2P and Ru_2P are probably less favourable. In the structures of transition metal phosphides with phosphorus contents of 50 atom per cent or less, P—P distances shorter than 3.0 Å have not been observed [33,34,26,28,35] Considering that metal/phosphorus substitution in Co_2P or Ru_2P would imply P—P distances shorter than 2.4 Å, the hypothesis of metal/phosphorus substitution in these phases appears less attractive. However, vacancies on transition metal sites has been found in phases similar to Ru_2P and Co_2P, *e.g.* in many phases belonging to the NiAs structure family.

Since strong arguments in favour of the hypothesis of metal/phosphorus substitution are lacking, it seems most reasonable to assume that the extended homogeneity range of Co_2P is connected with vacancies on cobalt atom sites.

One might ask if an analogous phenomenon exists in phosphides of the Fe_2P type. As mentioned earlier, the Fe_2P structure closely resembles the Co_2P structure. Unfortunately, accurate phase-analytical data are not available for any of the Fe_2P type phosphides, but a qualitative observation by Haughton [8] indicates an extended homogeneity range of Fe_2P. In his metallographic investigation of iron phosphides, Haughton found signs of secondary precipitation of FeP in the Fe_2P phase. His equilibrium diagram of the Fe—P system therefore contains a (dotted) line, which extends the Fe_2P single-phase field at higher temperatures towards the phosphorus-rich side of the diagram.

Acknowledgements: This work has been financially supported by the *Swedish State Council of Technical Research* and by the *Air Force Office of Scientific Research of the Air Research and Development Command, United States Air Force*, through its European Office under contract No. AF 61(052)–40. Facilities for use of the electronic digital computer BESK were given by the *Swedish Board for Computing Machinery*.

The author wishes to express his gratitude to Professor G. Hägg for his kind interest and valuable comments on the manuscript. Thanks are also due Dr. F. Nydahl and Dr. L. Gustafsson for their careful work on the chemical analyses. The author is much indebted to Mr. K. Nordgren, who collected the intensity material for the Co_2P crystal and made preliminary lattice parameter measurements on Co–P and Co–P–Si alloys, and also wishes to thank Dr. B. Aronsson and Dr. R. Hesse for many stimulating discussions.

REFERENCES

1. Nowotny, H. *Z. anorg. Chem.* **254** (1947) 31.
2. Borén, B. *Arkiv Kemi, Mineral. Geol.* **11 A** (1933) No. 10.
3. Borén, B., Ståhl, S. and Westgren, A. *Z. physik. Chem.* **B 29** (1935) 231.
4. Geller, S. *Acta Cryst.* **8** (1955) 83.
5. Laves, F. in Smithells, C. J. *Metals Reference Book*, 2nd ed. London 1955, p. 221.
6. Rundqvist, S. *Nature* **185** (1960) 31.
7. Aronsson, B., Åselius, J. and Stenberg, E. *Nature* **183** (1959) 1318.
8. Haughton, J. L. *J. Iron Steel Inst.* **115** (1927) 417.
9. Hägg, G. *Nova Acta Regiae Soc. Sci. Upsaliensis*, Ser. IV, **7** (1929) No. 1.
10. Nydahl, F. *Lantbrukshögsk. Ann.* **10** (1942) 114.
11. Nydahl, F. *Unpublished.*
12. Gordon, C. L. *J. Research NBS* **30** (1943) 107.
13. Wickers, E., Schlecht, W. G. and Gordon, C. L. *Ibid.* **33** (1944) 363.
14. Wickers, E., Schlecht, W. G. and Gordon, C. L. *Ibid.* **33** (1944) 451.
15 Gordon, C L., Schlecht, W. G. and Wickers, E. *Ibid.* **33** (1944) 457.
16. Hillebrand, W. F., Lundell, G. E. F., Bright, H. A. and Hoffman, J. I. *Applied Inorganic Analysis*, 2nd ed. New York 1953.
17. Westman, S., Blomqvist, G. and Åsbrink, S. *Arkiv Kemi* **14** (1959) 535.
18. Åsbrink, S., Blomqvist, G. and Westman, S. *Ibid.* **14** (1959) 545.
19. Appel, K. *Technical Note from the Quantum Chemistry Group, University of Uppsala.*
20. Thomas, L. H. and Umeda, K. *J. Chem. Phys.* **26** (1957) 293.
21. Tomiie, Y. and Stam, C. H. *Acta Cryst.* **11** (1958) 126.
22. Dauben, C. H. and Templeton, D. H. *Ibid.* **8** (1955) 841.
23. Żemczużny, S. and Schepelew, J. *Z. anorg. Chem.* **64** (1909) 245.
24. Biltz, W., Heimbrecht, M. and Meisel, K. *Ibid.* **241** (1939) 349.
25. Fylking, K.-E. *Arkiv Kemi Mineral. Geol.* **11 B** (1935) No. 48.
26. Rundqvist, S. and Larsson, E. *Acta Chem. Scand.* **13** (1959) 551.
27. Biltz, W., Ehrhorn, H. J. and Meisel, K. *Z. anorg. Chem.* **240** (1939) 117.
28. Rundqvist, S. and Jellinek, F. *Acta Chem. Scand.* **13** (1959) 431 (*footnote*).
29. Jellinek, F. *Acta Cryst.* **11** (1958) 677.
30. Cruickshank, D. W. J. *Ibid.* **2** (1949) 65.
31. Zumbusch, M. *Z. anorg. Chem.* **243** (1940) 322.
32. Gale, B. *Acta Met.* **7** (1959) 420.
33. Schönberg, N. *Acta Chem. Scand.* **8** (1954) 226.
34. Aronsson, B. *Ibid.* **9** (1955) 137.
35. Rundqvist, S. and Hede, A. *Ibid.* **14** (1960) 893.

ACTA CHEMICA SCANDINAVICA 14 (1960) 1980–1984

Cysteamine S-Phosphoric Acid

STIG ÅKERFELDT

Biochemistry Section, Eastern Pennsylvania Psychiatric Institute, Philadelphia 29, Pennsylvania, U.S.A.

Free cysteamine S-phosphoric acid has been prepared. The effect of pH on the hydrolysis of the synthesized compound has been studied and a mechanism for its reaction with iodine is suggested. Some solvent systems and spray reagents useful in paper chromatography of cysteamine S-phosphate are described.

A convenient, high yield method for the synthesis of trisodium phosphorothioate, used in the preparation of the title compound, has been worked out.

In two earlier papers [1,2] a method employing trisodium phosphorothioate for the preparation of some S-substituted phosphorothioic acids was reported. Among the compounds thus prepared was the sodiumhydrogen salt of cysteamine S-phosphoric acid (S-(2-aminoethyl) phosphorothioic acid). This compound was later found to be enzymically hydrolyzed to *ortho*-phosphate and cysteamine by human erythrocytes [3].

In the present paper the preparation of free cysteamine S-phosphoric acid is reported and some of its properties are described.

Cysteamine S-phosphoric acid has been prepared by dissolving the sodiumhydrogen salt in glacial acetic acid. Upon standing the free acid crystallizes out, whereas the simultaneously formed sodium acetate remains in solution.

The S-P bond in cysteamine S-phosphoric acid is extremely acid labile. Thus a 2.5 mM solution of the compound in 1 M HCl is completely hydrolyzed in less than one minute at 100°, giving a quantitative yield of cysteamine and *ortho*-phosphate. In neutral or slightly alkaline solutions the compound is relatively stable at room temperature.

The rate of hydrolysis of cysteamine S-phosphate as a function of pH at 37° is described in Fig. 1. The reaction was followed by the appearance of thiol groups [4] and (ethylenedinitrilo) tetraacetic acid was added to prevent heavy metal catalyzed oxidation of the cysteamine formed. Standardization of the colorimetric method was carried out as described previously [3]. A maximum rate of hydrolysis takes place around pH 3, where the compound is primarily in the form of $NH_3^+CH_2CH_2SPO_3H^-$ as concluded from acid-base titrations.

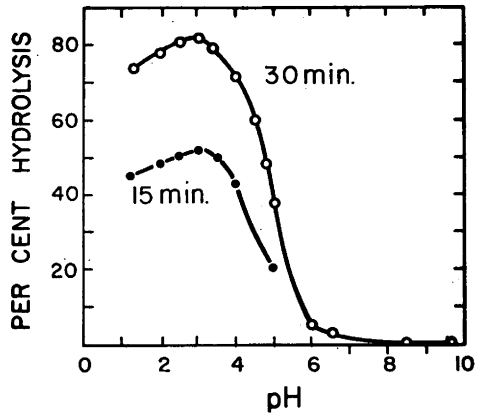

Fig. 1. Effect of pH on the hydrolysis of cysteamine S-phosphate (5 mM) at 37° in the presence of (ethylenedinitrilo)tetraacetic acid (13 mM). Ionic strength close to 0.15.

Such titrations were performed on both the free cysteamine S-phosphoric acid as well as on the sodiumhydrogen salt (10 mM solutions, 25°). Since the formation of some *ortho*-phosphate during the course of the titrations is inevitable in the acid region, other pK_a measurements were performed by adding just enough HCl to solutions of sodiumhydrogen cysteamine S-phosphate to reach the half titration points. The pH was then determined instantly. The apparent pK_a values obtained in this way agreed within ± 0.05 pK_a units with those obtained from rapidly performed acid-base titrations.

The results are reported in Table 1, from which it is evident that the second and third apparent pK_a values of cysteamine S-phosphate are relatively similar to those reported for 2-aminoethanol O-phosphate. The largest deviation in the results is to be found in the first pK_a, which for cysteamine S-phosphate is close to the lowest pK_a of *ortho*-phosphate ($pK_a = 2.1$), whereas the value for 2-aminoethanol O-phosphate is considerably lower.

In comparison with 2-aminoethanol O-phosphate cysteamine S-phosphate melts appreciably lower and is hydrolyzed by 1 M HCl at 100° some 1 000 times faster than the former (Table 1).

The observed rate of hydrolysis of cysteamine S-phosphate as a function of pH is qualitatively similar to that found for S-(*n*-butyl) phosphorothioate

Table 1. Comparison between some properties of cysteamine S-phosphoric acid and 2-aminoethanol O-phosphoric acid.

Property	$NH_2CH_2CH_2SPO_3H_2$	$NH_2CH_2CH_2OPO_3H_2$
Melting point	156°	244° [10]
Half life in 1 M HCl at 100°	<1 min	≈ 17 h [11]
pK_a	2.2; 5.0; 10.3	<1; 5.57; 10.10 [12]
		<1; 5.84; 10.89 [13]

by Herr and Koshland [5]. These authors proposed a mechanism for the observed hydrolysis. Several monoesters of *ortho*-phosphoric acid also give hydrolysis curves similar to those obtained for the S-substituted phosphorothioic acids mentioned here (see, *e.g.*, Ref.[6]).

Above pH≈2 cysteamine S-phosphate reacts momentarily with iodine, one atom of iodine being consumed per molecule of S-phosphate. During this process *ortho*-phosphate is formed together with a ninhydrin and cyanide-nitroprussiate positive substance with the same R_F-value in ethanol : pyridine : water, 2 : 1 : 1, and in *n*-butanol : acetic acid : water, 4 : 1 : 1, as cystamine (2,2′-dithiobisethylamine).

At pH≤1 the reaction between cysteamine S-phosphate and iodine is very slow *. At this pH at least part of the observed decolorization of iodine could be attributed to release of thiol groups by hydrolysis of the S-P bond.

The reaction between cysteamine S-phosphate and iodine in slightly acid and neutral solutions is similar to that described by Wieland and Lambert [7], who found that iodine is momentarily decolorized by a solution of S-(*n*-butyl) phosphorothioate around pH 7. These authors proposed a mechanism for the interaction between iodine and the S-substituted phosphorothioate used. However, this mechanism does not explain the failure of iodine to react rapidly with cysteamine S-phosphate at pH≤1.

A mechanism that explains the experimental results is given in Fig. 2. This is essentially a combination of the Herr and Koshland [5] mechanism with that of Wieland and Lambert [7].

In their suggested mechanism for acid hydrolysis of *S*-(*n*-butyl) phosphorothioate, Herr and Koshland [5] propose that one (and only one) of the OH-groups attached to the phosphate residue should be dissociated for maximum rate of hydrolysis. The dissociated OH-group should serve to activate a hydro-

* For instance, 3 mmole of cysteamine S-phosphate in 50 ml of 2 M HCl required more than 12 h to decolorize an equivalent amount of iodine.

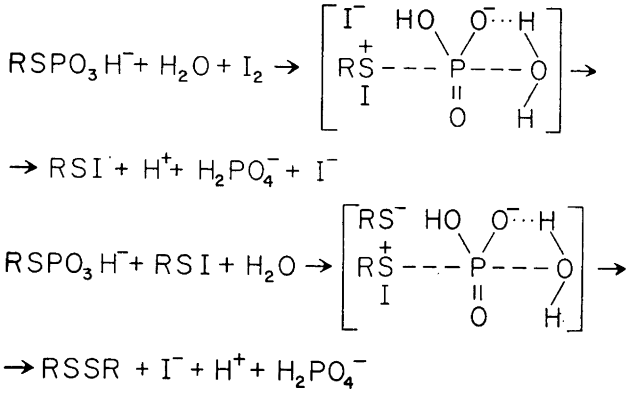

Fig. 2. Suggested mechanism for the reaction between iodine and cysteamine S-phosphate (R = $NH_3^+CH_2CH_2^-$).

gen bonded water molecule attached to the phosphate residue. The second (undissociated) OH-group on the phosphate residue should serve as a proton donor to the sulfur atom. When this OH-group is also dissociated, the molecule is thus stable.

In the scheme in Fig. 2 the dissociated OH-group serves the same purpose as in the Herr and Koshland mechanism as explained above. The presence of an undissociated OH-group, however, is not needed, since the intermediary step, like in the Wieland and Lambert scheme, is suggested to be RSI. This explains the fact that the cysteamine S-phosphate — iodine reaction (in contrast to the hydrolysis) proceeds rapidly also at pH 7.

Cysteamine S-phosphate can be separated from *ortho*-phosphate and from phosphorothioate by paper chromatography. Some solvent systems for this purpose are listed in Table 2. In addition to the commonly used phosphate sprays, the following spray reagents were useful in the identification of the above mentioned substances on the chromatograms:

1. 0.2 % ninhydrin in ethanol : pyridine, 8 : 2. Cysteamine S-phosphate gives a violet spot after heating for 5 min at 100°. (Ninhydrin in ethanol without added pyridine gives only weakly colored spots).
2. 0.1 % iodine in 5 % KI gives decolorized zones for cysteamine S-phosphate and phosphorothioate.
3. 1 % copper(II)chloride in 50 % ethanol containing 5 % NH_3 gives yellow brown spots with trisodium phosphorothioate and black spots with cysteamine S-phosphate.

Trisodium phosphorothioate, which was utilized for the synthesis of cysteamine S-phosphate [1], was previously prepared in about 40 % yield according to Yasuda and Lambert [8]. In this method $PSCl_3$ and a solution of sodium hydroxide in water are refluxed together. However, during this operation much phosphorothioate is hydrolyzed and large amounts of *ortho*-phosphate are formed. Improved experimental conditions for this reaction were therefore worked out. Lowering the reaction temperature to 75—85° gave 85—90 % final yield of anhydrous trisodium phosphorothioate of high purity. The decrease in reaction temperature did not unduly decrease the reaction rate *.

Table 2. Approximate R_F-values in three solvent systems. Solvents: 1, Ethanol:pyridine: water, 10:5:8. 2, 2-Methoxyethanol:NH_3(29 %):water, 3:2:2. 3, Ethanol:NH_3 (29 %): water, 6:1:3. The substances were chromatographed (ascending solvents) on Whatman No. 4 papers.

Substance	Solvent No. 1	2	3
$NH_2CH_2CH_2SPO_3HNa$	0.39	0.71	0.54
K_2HPO_4	0.18	0.54	0.29
Na_3SPO_3	0.30	0.62	0.31

* Yasuda and Lambert have later published a slightly modified procedure, which gives a yield of *ca.* 57 % Na_3SPO_3[14].

Binkley [9] performed the same reaction at 0°. In the present author's experience, however, the reaction rate at this temperature is inconveniently slow.

EXPERIMENTAL

Cysteamine S-phosphoric acid. 5.0 g of freshly prepared sodiumhydrogen cysteamine S-phosphate [1] were stirred at 25° in 100 ml of glacial acetic acid under exclusion of moisture for 30 min. During the process the S-phosphate dissolved completely and after a few minutes of stirring the crude free acid started to separate. The crystalline precipitate was filtered off and washed thoroughly with glacial acetic acid and with dry petroleum ether (b.p. 30–60°). The product was further purified by dissolving it in 50 ml of 10 % acetic acid and reprecipitating with 150 ml of ethanol. This purification process was repeated twice. 2.9 g (66 %) of crystalline substance were thus obtained (average of three prepns.) melting at 156° (corr.). Further reprecipitations did not increase the melting point. (Found: C 15.3; H 5.2; P 19.8. Calc. for $NH_2CH_2CH_2SPO_3H_2$ (157.14): C 15.3; H 5.1; P 19.7.)

Trisodium phosphorothioate. 80 g (2.0 mole) of sodium hydroxide were dissolved in 500 ml of water and 35 ml (0.34 mole) of $PSCl_3$ were added. The reaction flask was equipped with a reflux condenser and the synthesis was carried out on a combined magnetic stirrer-hot plate. After initial heating to about 80°, the reaction was allowed to proceed at 75–85° under constant stirring until all $PSCl_3$ had reacted (about 2 h). The slightly yellow solution was kept in the refrigerator (4°) over night. The precipitated white crystals were filtered off and washed with ethanol (100 ml). They were dissolved in 250 ml of distilled water at 45° and reprecipitated by the slow addition of 200 ml of ethanol under constant, rapid stirring. The solution was cooled under tap water, filtered and the crystals washed with ethanol (100 ml). The substance was dehydrated by stirring in 600 ml of dry methanol for 1.5 h, filtered and finally dried at 105° for 1 h. 52–55 g (85–90 %) of anhydrous trisodium phosphorothioate were thus obtained.

Phosphate determinations [9] and iodine titrations [8] showed the substance to be 99–100 % pure.

The author is indebted to Miss S. Perry and to Mrs. M. Gale for skillful assistance.

REFERENCES

1. Åkerfeldt, S. *Acta Chem. Scand.* **13** (1959) 1479.
2. Åkerfeldt, S. *Acta Chem. Scand.* **13** (1959) 1897.
3. Åkerfeldt, S. *Acta Chem. Scand.* **14** (1960) 1019.
4. Grunert, R. R. and Phillips, P. H. *Arch. Biochem. Biophys.* **30** (1951) 217.
5. Herr, E. B. and Koshland, D. E. *Biochim. et Biophys. Acta* **25** (1957) 219.
6. Vernon, C. A. in Kenner, G. W. and Brown, D. M. *Phosphoric Esters and Related Compounds*, The Chemical Society, London 1957, p. 17.
7. Wieland, T. and Lambert, R. *Chem. Ber.* **89** (1956) 2476.
8. Yasuda, S. K. and Lambert, J. L. *J. Am. Chem. Soc.* **76** (1954) 5356.
9. Binkley, F. *J. Biol. Chem.* **181** (1949) 317
10. Outhouse, E. L. *Biochem. J.* **31** (1937) 1459.
11. Cherbuliez, E. and Bouvier, M. *Helv. Chim. Acta* **36** (1953) 1200.
12. Fölsch, G. and Österberg, R. *J. Biol. Chem.* **234** (1959) 2298.
13. Clarke, H. B., Datta, S. P. and Rabin, B. R. *Biochem. J.* **59** (1955) 209.
14. Yasuda, S. K. and Lambert, J. L. in Moeller, T. *Inorganic Synthesis*, Mc Graw-Hill, New York 1957, Vol. 5, p. 102.

Received July 11, 1960.

ACTA CHEMICA SCANDINAVICA 14 (1960) 1985–1990

The Chemistry of the Natural Order Cupressales

XXIX *. Heartwood Constituents of *Juniperus thurifera* L.

JARL RUNEBERG

Organisk-kemiska Institutionen, Kungl. Tekniska Högskolan, Stockholm, Sweden

The heartwood of *Juniperus thurifera* contains α-cedrene, thujopsene, two apparently new $C_{15}H_{24}$ hydrocarbons, cuparene, cedrol, a compound $C_{20}H_{16}O_6$, a diol $C_{30}H_{54}O_2$, carvacrol, nootkatin, β-thujaplicin, hinokiic acid and "Widdringtonia acid II". Two further sesquiterpene hydrocarbons were present, which contained vinylidene groups; one of these probably has a curcumene skeleton.

In continuation of the studies at present being carried out in this laboratory on the heartwood constituents of the genus *Juniperus* [1-3], an investigation was made of a sample of *Juniperus thurifera* obtained from Spain.

The wood was extracted with acetone and the light petroleum-soluble part of the acetone extract was separated into neutral and acid fractions. Crystallisation of the acidic material gave two sesquiterpene acids, hinokiic acid [4], which has also been found in *J. chinensis* [1] and in *J. utahensis* [2], and the "acid II" previously isolated from *Widdringtonia* [5], from *J. chinensis* [1] and from several other species of the *Cupressaceae*.

The acidic material was treated with copper acetate to precipitate any tropolones present. The product obtained on decomposition of the precipitate with hydrochloric acid gave nootkatin; according to paper chromatography it also contained β-thujaplicin. Paper chromatography showed the presence of carvacrol in the remaining acidic material.

The neutral oil was distilled. The lowest boiling part of the main sesquiterpene fraction was chromatographed on polyvinyl chloride powder impregnated with light petroleum, using a solution of silver fluoborate in aqueous methanol as eluant. This gave five main fractions x, y, z, u and v. Compounds containing vinylidene groups would be expected to form relatively strong silver complexes and therefore to be eluted first. In accordance with this the infrared spectrum of the first fraction x showed strong absorption at 1 635, 1 645 and 883 cm^{-1} indicating the presence of vinylidene groups.

* Part XXVIII. *Acta Chem. Scand.* 14 (1960) 1288.

Gas chromatographic analysis showed that fraction x contained two components (X_1 and X_2) in about equal amounts. The retention time (R_t) of X_1 was close to that of α-cedrene and that of X_2 was close to that of thujopsene. It was thus impossible to detect the compounds X_1 and X_2 by gas chromatography with the system used when α-cedrene and thujopsene were present.

On dehydrogenation with selenium, X_2 gave dihydro-*ar*-curcumene, previously obtained in the same way from "Substance Y" of a crude sesquiterpene hydrocarbon fraction isolated from *Juniperus virginiana* [3]. Gas chromatography showed that X_1 remained almost unchanged after similar treatment with selenium.

Fraction y was pure thujopsene and on ozonolysis gave the corresponding keto-carboxylic acid [4].

Fractions z and u gave two sesquiterpene hydrocarbons Z and U which, apparently, have not been isolated previously. According to elemental analysis and infrared spectra both compounds may be tricyclic with one double bond. On gas chromatography both had almost the same R_t-value but were easily separated from α-cedrene and thujopsene. The R_t-values of Z and U agree well with the R_t-value of peak x_3 on a gas chromatogram of a crude sesquiterpene hydrocarbon fraction from *Juniperus virginiana* [3]. A sample of U was dehydrogenated with selenium and the product was chromatographed but no crystalline picrate could be obtained.

Fraction v was α-cedrene and gave on oxidation α-cedrenic acid [6].

The sesquiterpene hydrocarbon fraction, b.p. 121—123°/10 mm, showed aromatic absorption in the ultraviolet. It was redistilled and ozonised at low temperature. The material unaffected by ozone was identified as cuparene [7].

Chromatography of the sesquiterpene alcohol fraction gave cedrol but no widdrol [5] was detected. This fraction, however, also gave a mixture of carbonyl compounds.

The highest boiling neutral oil afforded a small amount of crystalline material. On chromatography this was separated into three compounds:

The waxy compound I, m.p. 67.5—68.5° was not further investigated.

Compound II, m.p. 156.0—157.5° analysed for $C_{20}H_{16}O_6$ and contained no methoxyl group, its ultraviolet spectrum showed a shoulder at 220 mμ (ε 19 200) and maxima at 237 mμ (ε 19 030), 293 mμ (ε 16 600) and 333 mμ (ε 22 300). The infrared spectrum showed aromatic absorption (1 495, 1 507, 1 606 and 1 625 cm^{-1}) and appeared to indicate the presence of a lactone ring (1 745 cm^{-1}). In addition there was a medium strength absorption peak at 1 644 cm^{-1}. A small amount of a substance now shown to be identical with "compound II" has previously been isolated from *J. communis* [8]. This compound is presently under investigation.

Compound III, m.p. 243.5—244.0° analysed for $C_{30}H_{54}O_2$. It appeared to contain two hydroxyl groups; an acetate was prepared but it gave a poor analysis.

The compounds isolated are listed below with very approximate estimates of the amounts present (as percentages of the air-dried wood). Total acetone extract 9.9, ether-soluble acetone extract 7.3, light petroleum-soluble acetone extract 5.7, sodium bicarbonate-soluble 0.03, potassium hydroxide-soluble 1.0, neutral 4.6, nootkatin 0.01, β-thujaplicin 0.001, carvacrol 0.1, hinokiic acid

0.2, "Widdringtonia acid II" 0.07, sesquiterpene hydrocarbons $X_1 + X_2$ 0.3, sesquiterpene hydrocarbon Z 0.01, sesquiterpene hydrocarbon U 0.05, α-cedrene 0.6, thujopsene 0.4, cuparene 0.1, cedrol 0.7, "compound II" 0.005, "compound III" 0.003, high-boiling carbonyl compounds 0.03.

EXPERIMENTAL

Rotations were measured in chloroform unless otherwise specified; melting points were taken on a hot stage and are corrected; boiling points are uncorrected. Light petroleum refers to the fraction b.p. 40—60°.

Isolation of the oils. Ground, air-dried heartwood (15.2 kg) of *J. thurifera* was extracted with acetone for 24 h. The acetone was evaporated and the oil obtained was poured with stirring into ten volumes of ether. The ether solution was filtered (precipitate A, 388 g), evaporated and the residue was poured into ten volumes of light petroleum. After filtration (precipitate B, 254 g) the solution was evaporated to dryness, diluted with two volumes of light petroleum and extracted successively with sodium bicarbonate (saturated solution) and potassium hydroxide (2 N). Acidification of the alkaline solutions and extraction with ether gave a sodium bicarbonate-soluble fraction C (4.4 g), which was not further investigated, and a potassium hydroxide-soluble fraction D (152 g). The remaining light petroleum solution was washed with water, dried and evaporated giving neutral material E (704 g).

Alkali-soluble fraction. The potassium hydroxide-soluble oil D was diluted with two volumes of ether and extracted with sodium carbonate-solution (2 N). On acidification and extraction with ether an oil F (124 g) was obtained, which partly crystallised on standing. The material insoluble in sodium carbonate was an oil G (24 g).

The crystalline part (41.4 g) of F was filtered off and a sample (3 g) was fractionally recrystallised from ether. The material less soluble in ether (0.9 g) was recrystallised from light petroleum, m.p. 190.0—191.5°, $[\alpha]_D$ —99° (*c*, 1.5), and identified (mixed m.p., IR) as the "acid II", isolated from *Widdringtonia* [5]. The material slightly more soluble in ether, m.p. 166.0—167.5°, was identified as *hinokiic acid* [4].

The oil G (24.0 g) was dissolved in five volumes of ligroin (b.p. 100—125°) and shaken with aqueous copper acetate (saturated solution). The copper salts were filtered off and washed with ligroin and water to give a combined ligroin phase H. The salts were decomposed with hydrochloric acid (2 N) and the resulting product was extracted with ether. The residue obtained on evaporation of the ether solution (2.4 g) was recrystallised from light petroleum and sublimed in a high vacuum, m.p. 93.5—95.0°. It was identified as *nootkatin* (mixed m.p., IR). The presence of *β-thujaplicin* in the mother liquors was demonstrated by paper chromatography [9].

The ligroin phase H was separated, washed with water and evaporated to dryness. The residue was shown by paper chromatography [9] to contain *carvacrol.*

Neutral fraction. The neutral oil E (518 g) was subjected to a quick preliminary distillation up to 150°/2 mm giving a distillate K (476 g) and a high-boiling residue L (43 g). A sample of the neutral oil K was distilled through a one meter, vacuum-jacketed, packed column giving the fractions listed in Table I.

Fraction Ib was redistilled through a 70 cm spinning band column and the first fraction (IIa, 3.0 g), b.p. 136—137°/25 mm, $[\alpha]_D$ —42°, n_D^{25} 1.4975 was chromatographed according to a method developed by B. Wickberg using polyvinylchloride powder impregnated with light petroleum and eluting with a solution of silver fluoborate in aqueous methanol. A detailed account of the separation will be published later in this journal. The main fractions, x, y, z, u and v, were eluted in this order. Fraction x (279 mg) b.p. 121°/10 mm was a mixture of two compounds X_1 and X_2 which both, according to the infrared spectrum, appear to contain vinylidene groups. The ultraviolet spectrum of the fraction (in 95 % ethanolic solution) showed maxima at 205, 206 and 242 mμ.

Thujopsene. Fraction y (314 mg) was redistilled and a sample (200 mg) in ethyl acetate-methanol (4:1, 10 ml) was ozonised at —70° until the blue colour indicating excess ozone appeared. When the reaction mixture had reached room temperature zinc dust (1 g) activated with acetic acid was added. After one hour, ether (50 ml) was added

Table 1. Distillation of neutral fraction K (256 g). Total distillate 212 g or 83 %.

Fraction	Weight (g)	B.p. (°C)	Pressure (mm Hg)	Rotation $[\alpha]_D$	Refractive index (n_D^{25})
Ia	9.5	64—126	14	−39	1.4968
Ib	68.3	126—127	14	−68	1.4993
Ic	47.3	127—149	14	−14	1.5078
Id	10.1	149—158	14	+15	—
Ie	28.0	158	14	+14	—
If	25.1	158—160	14	+16	—
Ig	11.4	160—163	14	+23	—
Ih	12.3	142—145	3	+22	1.5145

followed by aqueous acetic acid (10 %, 50 ml); the reaction mixture was filtered and the organic phase was separated, washed with water, dried and evaporated to dryness. The residue (0.65 g) was recrystallised from ethyl acetate, m.p. 165.0—166.0°, and identified as thujopsene ketocarboxylic acid [4] (mixed m.p., IR).

Fraction z (73 mg, from 6 g of IIa) was redistilled to give *sesquiterpene hydrocarbon Z*, b.p. 122°/10 mm, $[\alpha]_D$ + 75° (*c*, 2.2), n_D^{25} 1.4942. (Found: C 88.2; H 11.8; CH_3-(C) 5.6. $C_{15}H_{24}$ requires C 88.2; H 11.8; CH_3-(C) (one) 7.4.) Infrared spectrum (in carbon tetrachloride solution): 3 010 s, 2 960 vs, 2 870 vs, 2 720 w, 1 640 w, 1 462 vs, 1 450 vs, 1 433 vs, 1 375 vs, 1 364 vs, 1 346 m, 1 327 w, 1 315 m, 1 296 m, 1 279 s, 1 186 s, 1 175 m, 1 154 s, 1 129 s, 1 102 w, 1 062 m, 1 045 w, 1 021 s, 958 w, 945 w, 925 m, 910 cm^{-1} s. The ultraviolet spectrum of this fraction (in 95 % ethanolic solution) showed a maximum at 207 mμ (ε 1 050).

Fraction u (298 mg, from 6 g of IIa) was redistilled to give *sesquiterpene hydrocarbon U*, b.p. 122°/10 mm, $[\alpha]_D$ + 33° (c, 2.2), n_D^{25} 1.4961. (Found: C 88.0; H 11.7; CH_3-(C) 6.5; M 209 (Rast). $C_{15}H_{24}$ requires C 88.2; H 11.8; CH_3-(C) (one) 7.4; M 204.) Infrared spectrum (pure oil): 3 065 s, 2 950 vs, 2 745 w, 1 647 w, 1 485 s, 1 467 vs, 1 448 vs, 1 390 s, 1 378 vs, 1 366 vs, 1 341 m, 1 330 m, 1 320 m, 1 295 w, 1 280 w, 1 223 w, 1 211 w, 1 194 w, 1 175 m, 1 134 w, 1 098 w, 1 083 w, 1 063 w, 1 035 w, 1 023 m, 1 005 m, 983 w, 972 m, 925 s, 909 w, 867 w, 839 m, 794 s, 777 s, 695 cm^{-1} w.

A sample of fraction x (52 mg) was heated with selenium (50 mg) in a carbon dioxide atmosphere for 24 h at 270°. A gas chromatogram showed that the compound X_1 was largely unchanged; no peak corresponding to X_2 could be detected but a new peak was obtained with the same R_f-value as dihydro-*ar*-curcumene [3]. The dehydrogenation product was ozonised as described for cuparene (see below) and the material unattacked by ozone (20 mg), n_D^{25} 1.4865, was identified as dihydro-*ar*-curcumene by comparison of its infrared spectrum with that of a synthetic sample [10,11].

α-Cedrene. Fraction v (1.47 g, from 3 g of IIa) was redistilled, b.p. 113°/11 mm, $[\alpha]_D$-86° (c, 2.8), n_D^{25} 1.4960. A sample (0.78 g) in ethanol (95 %, 15 ml) was refluxed with selenium dioxide (0.47 g) for 3 h. The reaction product was filtered, the alcohol-solution was evaporated to dryness and the residue was distilled under reduced pressure. The distillate (0.54 g) was added to a suspension of silver oxide (sodium hydroxide (0.38 g), silver nitrate (0.79 g)) in water (60 ml) and the mixture was refluxed with vigorous stirring for 9 h. The solution was then filtered, and after extraction with ether to remove neutral material, the alkaline solution was acidified and extracted with ether. This ether extract was evaporated and the product (0.26 g) was sublimed three times in a high vacuum giving a substance, m.p. 123.0—124.5°, which was identified as α-cedrenic acid [6] (mixed m.p., IR).

Cuparene. Fraction Ic was redistilled through a 70 cm spinning band column and the fractions obtained were analysed by gas chromatography (*cf.* below). The material (3.0 g) containing most cuparene was dissolved in methylene chloride (15 ml) and treated at −70° with an excess of ozone. When the reaction mixture had reached room temperature, hydro-

gen peroxide (30 %, 8 ml) in potassium hydroxide (10 %, 3 ml) was added and the organic phase was separated, washed with water and evaporated giving a viscous oil. This was chromatographed on basic alumina (40 g). The first 100 ml of light petroleum eluted a hydrocarbon (0.13 g) which was distilled under reduced pressure, b.p. 117°/7 mm, $[\alpha]_D$ + 63° (*c*, 2.0), n_D^{25} 1.5207, and identified (IR) as cuparene [7].

Gas chromatographic investigation of the sesquiterpene hydrocarbon fractions. Gas chromatograms were run on a Pye Argon Chromatograph using a system described in a previous paper in this series [3]. (Temp. 150°, charge 0.025 µl, argon flow rate 27 ml/min). This gave the following retention times (min): Compound Z 13.2, compound U 13.7, compound X_1 17.3, α-cedrene 17.4, thujopsene 19.1, compound X_2 20.2, dihydro-*ar*-curcumene 21.6 and cuparene 42.8.

Cedrol. The crystalline part (1.36 g) of Ig was separated by filtration (filtrate Ig_2) and a sample (300 mg) was chromatographed on basic alumina (50 g). Ether-benzene (1:5) eluted a substance (210 mg) which was recrystallised from ethanol (95 %), m.p. 88.5—89.5°, $[\alpha]_D$ + 11°, (*c*, 1.9); this was identified as cedrol (mixed m.p., IR). Ether-benzene (1:1) and ether eluted small amounts of an oil with an infrared spectrum different from that of widdrol [5].

High-boiling carbonyl compounds. Fraction Ig_2 (5.5 g) in ethanol (95 %, 20 ml) containing acetic acid (10 %) was refluxed with Girard D reagent (2.0 g) for 30 min and the reaction product was extracted with ether at 0°. The aqueous solution was acidified with an equal volume of hydrochloric acid (4 N) while kept cool and then extracted with ether. The ether solution yielded a liquid mixture of carbonyl compounds (0.88 g); these were not further investigated.

The high-boiling neutral residue L, on standing, deposited a small amount of crystalline material. This was filtered off (1.49 g) and recrystallised from benzene to give compound III (240 mg, see below). The mother liquor was evaporated to dryness and the residue (1.25 g) was chromatographed on silica gel (200 g).

Compound I. Ether-benzene (1:17) eluted a substance (93 mg) which was recrystallised from ethanol (95 %) giving compound I, m.p. 67.5—68.5°, $[\alpha]_D$—2° (*c*, 1.3). (Found: C 78.3; H 12.7.)

Compound II. Ether-benzene (3:7) eluted a yellowish compound, m.p. 141—144°, $[\alpha]_D$—75° (*c*, 1.4). On recrystallisation from benzene and then from ethanol (95 %) followed by sublimation in a high vacuum the compound melted at 146—150°, $[\alpha]_D$ —20° (*c*, 2.9) and two further sublimations gave colourless crystals, m.p. 156.0—157.5°, $[\alpha]_D$ —4° (*c*, 0.7). (Found: C 68.5; H 4.7; CH_3O— 0.0; CH_3—(C) 2.5; M (Rast) 346. $C_{20}H_{16}O_6$ requires C 68.2; H 4.6; CH_3—(C) (one) 4.3; M 352.) Compound II in methanol gave no colour with methanolic ferric chloride. On attempted acetylation with acetic anhydride and pyridine at 100° for 5 h most of the starting material was recovered unchanged. Compound II did not react with 2,4-dinitrophenylhydrazine in dilute hydrochloric acid and was recovered unchanged when treated for 24 h with a mixture of diazomethane in ether and methanol.

Compound III. Ether-benzene (7:3) eluted a compound (143 mg) which was combined with the sample of compound III obtained above. The combined material was recrystallised from benzene and then from ethanol (95 %) and sublimed in a high vacuum, m.p. 243.5—244.0°, $[\alpha]_D$ + 14° (*c*, 2.2). (Found: C 80.3; H 11.9; active H 0.43; CH_3—(C) 9.4. $C_{30}H_{54}O_2$ requires C 80.6; H 12.2; active H (one) 0.22; CH_3—(C) (one) 3.4.) Infrared spectrum (KBr): 3 430 s, 2 935 vs, 2 880 vs, 2 660 w, 1 633 w, 1 465 s, 1 450 s, 1 386 s, 1 370 m, 1 336 m, 1 304 w, 1 285 m, 1 270 m, 1 252 m, 1 235 m, 1 211 w, 1 166 m, 1 140 w, 1 120 w, 1 075 m, 1 050 w, 1 035 m, 1 005 s, 974 s, 963 m, 945 w, 902 w, 880 w, 870 w, 845 w, 826 w, 730 w, 702 cm^{-1}w.

Compound III on acetylation (acetic anhydride/pyridine) afforded an acetate, m.p. 127.0—128.0°. (Found: C 76.1; H 10.8. $C_{34}H_{58}O_4$ requires C 76.9; H 11.0.)

Acknowledgements. My thanks are due to Professor H. Erdtman for his interest in this work, to Ingeniero José Benito Martinez, Instituto Forestal, Madrid, Spain, for his kind assistance in obtaining the wood sample, to Miss G. Hammarberg for infrared and ultraviolet spectra and to the *Swedish Natural Science Research Council* for financial support.

REFERENCES

1. Runeberg, J. *Acta Chem. Scand.* **14** (1960) 353.
2. Runeberg, J. *Acta Chem. Scand.* **14** (1960) 797.
3. Runeberg, J. *Acta Chem. Scand.* **14** (1960) 1288.
4. Erdtman, H. and Norin, T. *Acta Chem. Scand.* **13** (1959) 1124.
5. Erdtman, H. and Thomas, B. R. *Acta Chem. Scand.* **12** (1958) 267.
6. Treibs, W. *Ber.* **70** (1937) 2066.
7. Enzell, C. and Erdtman, H. *Tetrahedron* **4** (1958) 361.
8. Bredenberg, J. B. *Private communication.*
9. Wachtmeister, C. A. and Wickberg, B. *Acta Chem. Scand.* **12** (1958) 1335.
10. Batt, R. D. and Slater, S. N. *J. Chem. Soc.* **1949** 834.
11. Ruzicka, L. and van Veen, A. G. *Ann.* **468** (1929) 143.

Received May 23, 1960.

ACTA CHEMICA SCANDINAVICA 14 (1960) 1991–1994

The Chemistry of the Natural Order Cupressales

XXX *. Heartwood Constituents of *Juniperus cedrus* L.

JARL RUNEBERG

Organisk-kemiska Institutionen, Kungl. Tekniska Högskolan, Stockholm, Sweden

The heartwood of *Juniperus cedrus* contains thymoquinone, thujopsene, cuparene, cedrol, δ-cadinol, widdrol, "Widdringtonia acid II", nootkatin, β-thujaplicin and carvacrol.

The genus *Juniperus*, which comprises about 60 species, is divided into the sections *Oxycedrus* and *Sabina*. Previous papers [1] have dealt with the wood constituents of a number of junipers, all belonging to the section *Sabina*. In order to compare the two sections chemically a sample of *J. cedrus* (*Oxycedrus*) has now been investigated. The wood was obtained from the Canary Islands.

Only a few papers have been published on the wood oils of *Oxycedrus* junipers. From branches of *J. taxifolia* Shinozaki [2] obtained an oil containing 50 % α-pinene, an alcohol $C_{10}H_{18}O$, an unknown sesquiterpene hydrocarbon and a sesquiterpene alcohol. According to Mousseron [3] a wood pyrolysate of *J. oxycedrus* contained a *d*-cadinene and an *l*-cadinol in addition to a sesquiterpene hydrocarbon and a sesquiterpene alcohol which have not been further investigated. From the wood of *J. communis* Bredenberg [4–6] has isolated ferruginol, Δ^9-dehydroferruginol, 9-ketoferruginol and 9,10-diketoferruginol. Cedrene and cedrol have not previously been found in any *Oxycedrus* junipers and Bredenberg [7] has suggested that the presence or absence of cedrene and cedrol can be used to differentiate between the sections *Sabina* and *Oxycedrus*. However, the isolation of cedrol from *J. cedrus* (*Oxycedrus*) described in the present paper makes this suggestion untenable.

In this investigation the wood was extracted with acetone and the acetone extract was evaporated and poured into ten volumes of light petroleum. The light petroleum-soluble oil was separated into neutral and acidic fractions by extraction with alkali. The acidic material afforded the "acid II", m.p. 190.0—191.0°, of *Widdringtonia* [8]. The presence of nootkatin, β-thujaplicin

* Part XXIX. *Acta Chem. Scand.* **14** (1960) 1985.

and carvacrol in the remaining acidic material was indicated by paper chromatography.

The neutral oil was distilled and the fractions analysed by gas chromatography. According to its infrared spectrum the first fraction, which was yellow, appeared to contain thymoquinone. It also contained hydrocarbons and traces of alcohols. A sample was reduced, and from the product hydrothymoquinone was isolated.

The main component of all the hydrocarbon fractions was thujopsene [9] which was oxidised to the corresponding crystalline aldehyde (widdrenal) [8]. The infrared spectra of these fractions indicated the presence of small amounts of two compounds containing a vinylidene group (1 645 cm^{-1}, 883 cm^{-1}). One of these hydrocarbons may be identical with the curcumene isomer which appears to be present in corresponding sesquiterpene hydrocarbon fractions of *J. virginiana* and *J. thurifera* [1]. This has not been separated from thujopsene by the gas chromatographic system used.

The question of the presence or absence of α-cedrene in this wood could not be settled. On gas chromatography several of the hydrocarbon fractions gave a small peak with a retention time very close to that of α-cedrene but the infrared spectra of these fractions did not show any bands typical of α-cedrene; this, however, does not exclude the presence of small amounts.

The highest boiling hydrocarbon fraction was ozonised at low temperature and the material unattacked by ozone was identified as cuparene [10].

Chromatography of the sesquiterpene alcohol fraction gave cedrol, δ-cadinol [11] and widdrol [8]. Carbonyl compounds present in the residue, obtained on distillation of the neutral oil, were isolated using the Girard D reagent and chromatographed on alumina. Several liquid fractions were obtained but these have not been further investigated.

The compounds isolated are listed below with very approximate estimates of the amounts present (as percentages of the air-dried wood). Total acetone extract 6.1, light petroleum-soluble acetone extract 5.4, sodium bicarbonate-soluble 0.02, potassium hydroxide-soluble 0.09, neutral 5.3, nootkatin 0.0003, β-thujaplicin (traces), carvacrol 0.01, thymoquinone 0.04, thujopsene 2.2, cuparene 0.1, cedrol 0.06, δ-cadinol 0.04, widdrol 0.07, high-boiling carbonyl compounds 0.2.

EXPERIMENTAL

Rotations were measured in chloroform unless otherwise specified; melting points, taken on a hot stage, are corrected; boiling points are uncorrected. Light petroleum refers to the fraction b.p. 40 – 60°.

Isolation of the oils. The ground, air-dried, heartwood (3.90 kg) was extracted with acetone for 48 h. The acetone was evaporated and the remaining oil poured with stirring into ten volumes of light petroleum. The solution was filtered (precipitate A, 30.1 g) and evaporated. The remaining oil was diluted with two volumes of light petroleum and extracted successively with solutions of sodium bicarbonate (saturated) and potassium hydroxide (2 N). On acidification and extraction with ether the sodium bicarbonate solution afforded a viscous oil B (0.74 g) which was not further investigated. The potassium hydroxide-soluble material C (3.62 g) was isolated in the same way by acidification and extraction with ether. The remaining light petroleum solution was washed with water, dried and evaporated giving neutral material E (205 g).

Table 1. Distillation of neutral fraction E. Total distillate 149 g or 73 %.

Fraction	Weight (g)	B.p./22 mm Hg (°C)	Rotation ($[\alpha]_D$)	Refractive index (n_D^{25})
Ia	10.0	119–136	−47	1.5018
Ib	19.1	136–137	−78	1.5017
Ic	19.8	137–138	−91	1.5024
Id	16.6	138–139	−87	1.5030
Ie	23.4	139–148	−48	1.5063
If	14.1	148–150	+21	1.5126
Ig	22.5	150–164	+12	1.5131
Ih	14.8	164–166	+ 4	1.5062
Ii	8.7	166–168	+ 5	1.5071
Ik (residue)				

Alkali-soluble fraction. The alkali-soluble oil C was dissolved in ten volumes of ether and extracted with a solution of sodium carbonate (2 N). The ether solution on evaporation afforded an oil F (0.98 g). The sodium carbonate solution was acidified, extracted with ether and the ether solution was evaporated yielding an oil G (2.41 g) which partly crystallised on standing. The crystals (32 mg) were filtered off, recrystallised from light petroleum, m.p. 190.0–191.0°, $[\alpha]_D$ −98° (*c*, 2.1) and identified (mixed m.p., IR) as the *acid II* isolated from *Widdringtonia* [8]. Paper chromatography [12] showed that the non-crystalline part of G contained *nootkatin* and *β-thujaplicin* and the oil F contained *carvacrol.*

Neutral fraction. The neutral oil E was distilled through a one metre, vacuum-jacketed, packed column giving the fractions listed in Table 1.

Gas chromatographic examination of the sesquiterpene hydrocarbon fractions. Gas chromatograms were run on a Pye Argon Chromatograph as described in a previous paper [13] (temperature 150°, charge 0.025 μl).

In Table 2 the approximate areas of individual peaks of different retention times are given as percentages of total peak area.

With an argon flow rate of 25 ml/min the R_t-values (min) of the following known compounds were: α-cedrene (prepared from cedrol) 19.1, thujopsene 21.0 and cuparene 46.0.

Identification of thymoquinone. The yellow fraction Ia (2.0 g) was suspended in water (5 ml), and the mixture was saturated with sulphur dioxide. The reaction flask was stoppered and allowed to stand for three days. The product was then dissolved in ether, extracted with sodium hydroxide (2 N) and the alkaline solution was acidified and extracted with ether. On evaporation the ether solution gave a crystalline product (0.28 g), which was sublimed in a high vacuum, and identified (mixed m.p., IR) as hydrothymoquinone, m.p. 143.5–144.5°.

Table 2. Gas chromatographic analysis of the sesquiterpene hydrocarbon fractions in Table 1. Argon flow rate 25 ml/min.

Fraction	Peak retention time (min)											
	10.1	12.4	14.6	18.9	21.0	22.9	30.4	33.2	34.9	46.0	48.4	49.9
Ia	1	2	6	6	73						12	
Ib		1	3	9	87							
Ic			1	4	95							
Id					100							
Ie					60	9	9	15		5		2
If					1	2	9	42	20	20		6

Identification of thujopsene. Fraction Id (1.0 g) in ethanol (95 %, 20 ml) was refluxed with selenium dioxide (0.6 g) for 4 h and the product was filtered and evaporated to dryness. The residue (0.82 g) was recrystallised from light petroleum, m.p. 73.5—74.5°, and identified as widdrenal [8] (mixed m.p. IR).

Cuparene. Fraction If (3.0 g) in methylene chloride (15 ml) was ozonised at −70° until an excess of ozone was indicated by the appearance of a blue colour. When the reaction mixture had reached room temperature, hydrogen peroxide (30 %, 8 ml) in potassium hydroxide (10 %, 3 ml) was added dropwise and the mixture was heated on a water bath for 5 min. The organic phase was diluted with a large quantity of ether, separated and evaporated to dryness. The remaining viscous oil was chromatographed on basic alumina (40 g). The first fraction of light petroleum (100 ml) eluted a hydrocarbon (460 mg) which was distilled under reduced pressure. The fraction boiling at 118°/8 mm, n_D^{25} 1.5206, $[\alpha]_D$ + 65° (*c*, 2.2) was identified as *cuparene* [10] by comparing its physical constants and infrared spectra with those of an authentic sample.

Sesquiterpene alcohols. Fraction Ii (2.52 g) was chromatographed on basic alumina (100 g). Light petroleum eluted an oil (0.22 g), benzene also eluted oily material (0.39 g) (neither of these have been investigated further). Ether-benzene (1:50) eluted a compound (0.26 g) which was recrystallised from ethanol (95 %), m.p. 88.0—88.5°, and identified as *cedrol.* Ether-benzene (3:7) eluted *δ-cadinol* [11] (0.17 g) which after recrystallisation from acetonitrile had the m.p. 138.0—139.0°. Ether eluted a compound (0.31 g) which was recrystallised from acetonitrile and sublimed in a high vacuum to yield *widdrol* [8], m.p. 95.0—96.0°, $[\alpha]_D$ + 105° (*c*, 2.2). (All identifications were made by mixed m.p. and IR.) Elution of the column with methanol gave a resinous material.

High-boiling carbonyl compounds. A mixture of carbonyl compounds (0.72 g) was separated from a sample of the neutral distillation residue Ik (5.0 g) using Girard D reagent (2.0 g) as described in a previous paper in this series [13].

Acknowledgements. My thanks are due to Professor H. Erdtman for his interest in this work, to Ingeniero José Benito Martinez, Instituto Forestal, Madrid, Spain, for his kind assistance in obtaining the wood sample, to Miss G. Hammarberg for infrared and ultraviolet spectra and to the *Swedish Natural Science Research Council* for financial support.

REFERENCES

1. Runeberg, J. *Acta Chem. Scand.* **14** (1960) 1288 and earlier publications.
2. Shinozaki, Y. *J. Chem. Ind. Japan* **24** (1921) 202; *Chem. Zentr.* **1922** IV 763.
3. Mousseron, M., Granger, R. and Ronayrox, M. *Compt. rend.* **208** (1939) 1411.
4. Brendenberg, J. B. *Acta Chem. Scand.* **11** (1957) 932.
5. Bredenberg, J. B. and Gripenberg, J. *Acta Chem. Scand.* **8** (1954) 1728.
6. Bredenberg, J. B. *Acta Chem. Scand.* **14** (1960) 385.
7. Bredenberg, J. B. *Acta Chem. Scand.* **11** (1957) 98.
8. Erdtman, H. and Thomas, B. R. *Acta Chem. Scand.* **12** (1958) 267.
9. Erdtman, H. and Norin, T. *Chem. & Ind. London* **1960** 622.
10. Enzell, C. and Erdtman, H. *Tetrahedron* **4** (1958) 361.
11. Herout, V. and Sykora, V. *Tetrahedron* **4** (1958) 250.
12. Wachtmeister, C. A. and Wickberg, B. *Acta Chem. Scand.* **12** (1958) 1335.
13. Runeberg, J. *Acta Chem. Scand.* **14** (1960) 797.

Received June 7, 1960.

ACTA CHEMICA SCANDINAVICA 14 (1960) 1995–1998

The Chemistry of the Natural Order Cupressales

XXXI *. Heartwood Constituents of *Juniperus phoenicea* L.

JARL RUNEBERG

Organisk-kemiska Institutionen, Kungl. Tekniska Högskolan, Stockholm, Sweden

The heartwood of *Juniperus phoenicea* contains thujopsene, cuparene, cedrol, widdrol, "Widdringtonia acid II", hinokiic acid, nootkatin, β-thujaplicin and carvacrol.

The phoenicean juniper is widely distributed throughout the Mediterranean region, growing in dry situations on rocky hills. In Algeria it ascends to an altitude of about 6 000 feet. It also occurs in the Canary Islands where it is reported to attain a great age and enormous size [1].

Little has been published on the wood oil of *J. phoenicea*. Umney and Bennett [2] analysed an oil consisting mainly of α-pinene and also containing cadinene and traces of aldehydes. Rodié [3] made a study of an oil obtained from berryless branches. He identified pinene, camphene, phellandrene and cadinene and observed the presence of alcohols, esters and small amounts of aldehydes.

Commercial savin oil, obtained by steam distillation of branches and leaves of *J. sabina* has been adulterated by similar preparations obtained from *J. phoenicea*. Manceau [4] however noticed that while only about 24 % of the former oil distils below 170—175°, 79 % of the oil of *J. phoenicea* distils below 180°. This observation has been used to detect adulteration of savin oil. The oil described in this paper, obtained exclusively from heartwood, contained only about 4 % of monoterpenes or compounds with similar boiling points.

The previous paper [5] in this series described some constituents of *Juniperus cedrus*. This paper deals with the heartwood constituents of a sample of *J. phoenicea* obtained from the island of Cyprus.

The wood was extracted with acetone and the light petroleum-soluble part of the acetone extract was separated into neutral and acid fraction. Crystallisation of the acidic material gave "Widdringtonia acid II" [6], m.p. 190.0—191.5° and hinokiic acid [7]. The presence of nootkatin, β-thujaplicin and carvacrol in the remaining acidic material was shown by paper chromatography.

* Part XXX. *Acta Chem. Scand.* 14 (1960) 1991.

The neutral oil was distilled. The lowest boiling part of the oil, which apparently contains monoterpenes, has not been investigated. The next higher boiling sesquiterpene fraction had a relatively simple composition with thujopsene [7] as the main constituent.

J. phoenicea appears to be the most convenient source of thujopsene so far encountered. In all thujopsene-producing conifers so far investigated in this laboratory thujopsene occurs mixed with comparatively large amounts of compounds with very similar boiling points such as α-cedrene or certain incompletely characterised dextrorotatory sesquiterpene hydrocarbons. Large amounts of pure thujopsene can, however, be obtained by a simple distillation of the oil described in this paper.

The highest boiling part of the sesquiterpene hydrocarbon fraction was ozonised at low temperature and the material unaffected by ozone was identified as cuparene [8].

One of the sesquiterpene alcohol fractions crystallised on standing. The crystalline part was separated by chromatography into cedrol and widdrol [6].

Carbonyl compounds present in the residue obtained on distillation of the neutral oil were isolated using the Girard D reagent.

The compounds isolated are listed below with very approximate estimates of the amounts present (as percentages of the air-dried wood). Total acetone extract 8.9, ether-soluble acetone extract 7.5, light petroleum-soluble acetone extract 6.0, sodium bicarbonate-soluble 0.03, potassium hydroxide-soluble 0.5, neutral 5.5, carvacrol 0.1, "Widdringtonia acid II" 0.1, hinokiic acid 0.04, thujopsene 2.2, cuparene 0.08, cedrol 0.2, widdrol 0.003, high-boiling carbonyl compounds 0.05.

EXPERIMENTAL

Rotations were measured in chloroform unless otherwise specified; melting points, taken on a hot stage, are corrected; boiling points are uncorrected. Light petroleum refers to the fraction b.p. 40–60°.

The air-dried heartwood of *J. phoenicea* (7.0 kg) was extracted with acetone for 24 h and fractionated as described in a previous paper in this series [11] (precipitate A, 96 g, precipitate B 108 g, sodium bicarbonate-soluble oil C 2.3 g, potassium hydroxide-soluble oil D, 35 g, neutral oil E, 384 g).

Alkali-soluble fraction. The oil D crystallised partly on standing. The crystals (F, 6.0 g) were filtered off and the remaining oil was dissolved in ether and separated into a sodium carbonate-soluble fraction (G, 15.1 g) and a sodium carbonate-insoluble oil (H, 11.5 g). A crude tropolone fraction (I, 1.22 g) was separated from this oil *via* the copper complexes.

A sample of fraction F was fractionated by crystallisation from ether. The material less soluble in ether was sublimed in a high vacuum, m.p. 190.0–192.0°, and identified (mixed m.p., I.R.) as the "acid II", isolated from *Widdringtonia* [6]. The material slightly more soluble in ether, m.p. 165.5–167.0°, was identified as *hinokiic acid* [7]. From fraction G an additional amount (2.1 g) of the above mixture of acids crystallised on standing.

On paper chromatography [9] fractions I and G were shown to contain *nootkatin* and *β-thujaplicin*. Paper chromatography also showed the presence of *carvacrol* in the oil H.

By a fast preliminary distillation the neutral oil E was divided into fraction K, b.p. up to 50°/70 mm (16.0 g), fraction L (264 g), b.p. 50°/70 mm–140°/1 mm, and a residue M (100 g). The oil L was distilled through a 1 m, vacuum-jacketed, packed column giving the fractions listed in Table 1.

Table 1. Distillation of neutral fraction L. Total distillate 220 g or 83 %.

Fraction	Weight (g)	B.p./15 mm Hg (°C)	Rotation $[\alpha]_D$	Refractive index (n^{25}_D)
Ia	13.7	123–127	−94	1.5020
Ib	21.2	127	−101	1.5026
Ic	26.5	127	−106	1.5030
Id	22.7	127	−109	1.5031
Ie	23.4	127	−115	1.5031
If	34.0	127–128	−106	1.5030
Ig	21.1	128–138	−12	1.5070
Ih	13.9	138–147	+ 52	1.5093
Ii	10.9	147–154	+ 34	1.5071
Ik	18.5	154–156	+ 37	—
Il	14.4	156–159	+ 25	1.5060

Gas chromatographic analysis of sesquiterpene hydrocarbon fractions. Gas chromatograms were run on a Pye Argon Chromatograph as described in a previous paper in this series [10]. (Temperature 150°, charge 0.025 μl.)

In Table 2 the approximate areas of individual peaks of different retention times are given as percentages of total peak area.

Identification of thujopsene. Fraction Ie (2.0 g) in ethanol (95 %, 40 ml) was refluxed with selenium dioxide (1.2 g) for 4 h and the product was filtered and evaporated to dryness. The crystalline residue (1.8 g) was recrystallised from light petroleum and sublimed in a high vacuum, m.p. 73.5–74.5°, and identified as widdrenal [6,7] (mixed m.p., I.R.).

Cuparene. Fraction Ih (3.0 g) was ozonised and treated as described in a previous paper [10]. The material unaffected by ozone (0.43 g), b.p. 121°/10 mm), $[\alpha]_D$ + 65° (*c*, 2.1), n_D^{25} 1.5200, was identified as cuparene [8] by comparing its physical constants and infrared spectrum with those of an authentic sample.

Sesquiterpene alcohols. Fraction Ik crystallised partly on standing. A sample (5.1 g) was mixed with ethanol (95 %, 10 ml), filtered and the crystalline precipitate (1.8 g) was chromatographed on basic alumina (40 g). Ether-benzene (1:99) eluted *cedrol* (1.60 g), recrystallised from ethanol (95 %), m.p. 85.0–86.0°, $[\alpha]_D$ + 11° (*c*, 1.7) and ether-benzene (1:1) eluted *widdrol* [6] (0.09 g), sublimed twice in a high vacuum, m.p. 95.0–96.0°, $[\alpha]_D$ + 103° (*c*, 2.2) (identifications by mixed m.p. and I.R.).

Table 2. Gas chromatographic analysis of the sesquiterpene hydrocarbon fractions in Table 1. Argon flow rate 25 ml/min.

Fraction	Peak retention time (min)				
	15.1	21.0	29.8	33.2	46.0
Ia	1	99			
Ib–If		100			
Ig		58	12	19	11
Ih			10	47	43

With an argon flow rate of 25 ml/min the retention times of the following known compounds were: thujopsene 21.0, and cuparene 46.0.

High-boiling carbonyl compounds. A liquid mixture of carbonyl compounds (N, 0.16 g) was separated from a sample of the neutral distillation residue M (5.0 g) using Girard D reagent (2.0 g) as described in a previous paper in this series [10].

Acknowledgements. My thanks are due to Professor H. Erdtman for his interest in this work, to the Tropical Products Institute, London, for kind assistance in obtaining the wood sample, to Miss G. Hammarberg for infrared and ultraviolet spectra, and to the *Swedish Natural Science Research Council* for financial support.

REFERENCES

1. Dallimore, W. and Jackson, A. B. *A Hand bookof Coniferae including Ginkgoaceae* Edward Arnold & Co, London 1948, p. 317.
2. Umney, J. C. and Bennett, C. T. *Pharm. J.* **75** (1905) 827; *Chem. Zentr.* **1906** *I* 237.
3. Rodié, J. *Bull. soc. chim. France* (3) **35** (1906) 922; (4) **1** (1907) 492; *Rev. gén. chim.* **9** (1906) 444; **10** (1907) 18; *Chem. Abstr.* **1** (1907) 1042.
4. Manceau, P., Revol, L. and Vernet, A. M. *Bull. sci. pharmacol.* **43** (1936) 14; *Chem. Zentr.* **1936 II**, 1261.
5. Runeberg, J. *Acta Chem. Scand.* **14** (1960) 1991.
6. Erdtman, H. and Thomas, B. R. *Acta Chem. Scand.* **12** (1958) 267.
7. Erdtman, H. and Norin, T. *Chem. & Ind. London* **1960** 622.
8. Enzell, C. and Erdtman, H. *Tetrahedron* **4** (1958) 361.
9. Wachtmeister, C. A. and Wickberg, B. *Acta Chem. Scand.* **12** (1958) 1335.
10. Runeberg, J. *Acta Chem. Scand.* **14** (1960) 803.
11. Runeberg, J. *Acta Chem. Scand.* **14** (1960) 1987.

Received June 21, 1960.

ACTA CHEMICA SCANDINAVICA 14 (1960) 1999–2008

Studies on the Hydrolysis of Metal Ions

31. The Complex Formation between Pb^{2+} and OH^- in Na^+ (OH^-, ClO_4^-) Medium

BIRGITTA CARELL and ÅKE OLIN

Department of Inorganic Chemistry, Royal Institute of Technology, Stockholm 70, Sweden

The complex formation between Pb^{2+} and OH^- has been studied in alkaline solution at 25°C. From measurements on the cell

Pb (in Hg)/ *B* M $Pb(ClO_4)_2$, *A* M NaOH, (*I*−*A*) M $NaClO_4$/ ref.

it is concluded that the mononuclear species $Pb(OH)_2$ and $Pb(OH)_3^-$ are formed. No evidence of the species $Pb(OH)_4^{2-}$ was found in the $[OH^-]$ range ($[OH^-] < 0.5$ M) studied. The following values of the equilibrium constants were obtained.

		3 M $Na(ClO_4)$	0.3 M $Na(ClO_4)$
$Pb^{2+} + 2OH^- \rightleftharpoons Pb(OH)_2$	$\log \beta_2$	10.90 ± 0.1	10.34 ± 0.1
$Pb^{2+} + 3OH^- \rightleftharpoons Pb(OH)_3^-$	$\log \beta_3$	13.66 ± 0.05	13.29 ± 0.05

The solubility of lead oxide in alkali has been studied by a number of authors [1–6] and found to be proportional to the concentration of free alkali. The results have been interpreted in terms of the formation of $Pb(OH)_3^-$ as the main leadbearing species in alkaline solution. $HPbO_2^-$ or $PbOOH^-$ is equivalent to $Pb(OH)_3^-$ and these species cannot be distinguished by this type of measurement. In the following we shall write $Pb(OH)_3^-$. — The interpretation is not unequivocal since any species $Pb_n(OH)_{2n+1}^-$ would be compatible with the experimental facts (Leden [7]).

Polarographic measurements have been carried out by Heyrovský [8], Lingane [9] and Goward [10] and their results indicated that $Pb(OH)_2$ and $Pb(OH)_3^-$ are formed. Also from polarographic measurements, Akselrud [11] has suggested that Pb(II) is present as a trinuclear anionic complex in alkaline solution.

Johnson and Kraus [12] have concluded from ultracentrifugation studies that the system is monodisperse and mononuclear. They ascribed to the ion present the formula PbO_2^{2-}. According to Johnson [13] $Pb(OH)_3^-$ would also be in agreement with the experimental data.

The reversibility of the lead amalgam electrode in alkaline solution as shown by Lingane [9] and Goward [10] suggested that the complex formation

between Pb^{2+} and OH^- could be studied by the titration technique with a stationary lead amalgam electrode as the indicator electrode. This is the aim of the present work.

SYMBOLS

A	total concentration of OH^-.
a	$[OH^-]$, concentration of free OH^-.
B	total concentration of Pb(II).
b	concentration of Pb^{2+}.
Z	average number of OH^- per Pb(II) in complexes.
η	$\log \frac{B}{b}$
β_n	formation constant of $Pb(OH)_n^{(n-2)-}$ from Pb^{2+} and OH^-.
$*K_n$	acidity constant of $Pb(OH)_{n-1}^{(n-3)-}$

All concentrations in tables and figures are expressed in M (moles/l), and equilibrium constants are given on the M scale. In the text, however, the more convenient unit mM will be used frequently.

METHOD

The concentration of Pb^{2+} (b) has been measured electrometrically, using a lead amalgam electrode, in a large number of equilibrium solutions(S) which had the analytical composition

S = B M $Pb(ClO_4)_2$, A M NaOH, $(I-A)$ M $NaClO_4$

Since the Pb(II) in alkaline solution is present almost exclusively as uncharged and anionic species, the cationic composition of the solutions S is constant and equal to I M Na^+. In the following we shall, therefore, assume that the variations of the activity factors are so small that activities can be replaced by concentrations in the equations expressing the chemical equilibria in our solutions.

The cell used was

$$-\text{Pb(in Hg)} \;/\; \text{S} \;/\; \text{ref.} + \qquad \text{(I)}$$

$$E_{Pb} = E^\circ_{Pb} - 29.58 \log b - 29.58 \log f_{Pb^{2+}} - E_j \qquad (1)$$

the reference half-cell was

$$/I \text{ M } NaClO_4/ \; (I - 0.01) \text{ M } Na^+, \; 0.01 \text{ M } Ag^+, \; I \text{ M } ClO^-/ \; Ag, AgCl \qquad \text{(II)}$$

and the salt bridge was of the "Wilhelm" type [14].

Eqn.(1) is the simplest relation between the measured potential and the concentration of one of the lead species in solution. It also offers a simple means of putting the results of the emf measurements on an absolute scale by determining E°_{Pb} in acid solution.

Attempts were made to measure $\log[OH^-]$ in these solutions, but we were unsuccessful in finding a glass electrode which functioned like a hydrogen electrode when $\log [OH^-] > -3$. This failure is not serious since $[OH^-]$ can readily be calculated from the analytical OH^- concentrations and the amalgam data.

The liquid junction potential (E_j) in cell (I) was determined on the assumption that it has the same value as in the cell

$$-\text{Pt/H}_2, \; A \text{ M NaOH}, \; (I-A) \text{ M } NaClO_4/ \text{ ref} + \qquad \text{(III)}$$

$$E_H = E^\circ_H + 59.15 \log A + 59.15 \log f_{OH^-} - E_j \qquad (2)$$

E_j, or rather ($59.15 \log f_{OH^-} - E_j$) was obtained from the measurements by the method described by Biedermann and Sillén [15]. It was found to be 7.8 [OH^-] mV. This agrees well with the result obtained by Ingri *et al.*[16] who got 8 [OH^-] mV.

The amalgam electrode [17], which consisted of a pool on the bottom of the titration vessel, was quite slow in attaining its equilibrium value. We had to wait 0.5 to 1 h after each addition before a constant reading was obtained.

Chemicals. The chemicals used in this work were prepared and analysed as described previously [17].

PRELIMINARY EXPERIMENTS

Since previous work on the behaviour of Pb(II) in alkaline solution indicated that the main lead-bearing species is mononuclear with a charge of —1, some preliminary measurements were carried out in order to verify these results.

Measurements at constant a and varying B. These measurements were carried out at $a = (A—3B) = 0.25$ M and B was varied between 0.1 and 10 mM. The results were plotted as $\log B(\log b)$. The plot was linear with a slope close to unity, which shows that the complexes are mononuclear.

Measurements at constant B and varying a. These measurements were made with the values of $B = 0.2$ and 0.5 mM and $0.1 < [OH^-] < 0.5$ M. The results were plotted as $\eta(\log(A—2B))$. The actual OH^- concentration is unknown, but it is reasonable to assume at least two OH^- groups attached to a Pb(II). The use of a high ligand concentration and low metal ion concentrations makes $(A—2B)$ a good approximation for a. The experimental data when plotted as described fell on a single straight line of slope $\simeq 3$.

The concentration of Pb^{2+} in these solutions is very small and we therefore have

$$B = \Sigma\beta_n b a^n; \quad \eta = \log \Sigma\beta_n a^n \qquad (3)\ (3a)$$

and from (3a)

$$\frac{d\eta}{d \log a} = \frac{\Sigma n\beta_n a^n}{\Sigma\beta_n a^n} = Z \qquad (4)$$

The invariance of the difference quotient $\Delta\eta/\Delta\log a$ with a suggest the presence of only one complex and with $\bar{Z} = 3$. The preliminary measurements thus show that $Pb(OH)_3^-$ is formed as the main species in strongly alkaline solution.

A numerical calculation on the data, however, showed that they were not entirely satisfactory. $\Delta\eta/\Delta\log a$ was found to reach a maximum value of $\simeq 2.97$ and then it started to decrease and reached the value 2.9 at [OH^-] = 0.5 M. This would contradict the law of mass action and we began to search for the cause of this behavior. The measurements had been carried out in unprotected glass vessels and dissolution of silica was therefore suspected to occur. A titration carried out in a vessel covered with paraffin gave, however, the same results. The constancy of the amalgam potential for long periods of time would also indicate that no dissolution occurs (see also Ref.[18]).

Contamination of the alkali from the polyethylene bottles used to store the alkali was next considered. Titrations with alkali which had been stored in bottles covered with paraffin gave the same results. A very large contamination of the alkali by carbonate could also be responsible for the observed effect, but this is unlikely since tests with Ba^{2+} gave no precipitate of $BaCO_3$. A titration with alkali to which Na_2CO_3 has been added to give a OH^-/CO_3^{2-} ratio = 10 gave the same results as the other titrations. We were thus unable to find a simple explanation in terms of faulty experimental technique, for

this apparent contradiction of the law of mass action as applied by us and we have been led to the conclusion that deviations in the activity factors occur when the ionic medium is changed considerably.

FINAL EXPERIMENTS

The equilibrium solutions were prepared by a titration technique. Usually the experiments were started from an acid solution of the following composition

$$B \text{ M } Pb(ClO_4)_2,\ H \text{ M } HClO_4,\ I \text{ M } NaClO_4$$

To the starting solution, 50 ml by volume, equal volumes of solution from two burets were added. One buret contained an A M NaOH solution and the other contained a solution of composition $2B$ M $Pb(ClO_4)_2$, $(2I—A)$ M $NaClO_4$. Thus the concentrations of Pb(II) = B and of $Na^+ = I$ M were maintained constant during a run.

In order to ensure a broad range in $[OH^-]$ we always attempted to start with an OH^- concentration close to the solubility limit of $Pb(OH)_2$, although no particular care was taken to be very close to it. The solubility data by Garrett, Vellenga and Fontana [6] were used as a guidance. No troubles were experienced on passing from the acid to the alkaline range from the intermediate formation of lead hydroxide. The precipitate dissolved rapidly and completely in the excess alkali.

Titrations were frequently made on alkaline starting solutions prepared a couple of days before an experiment was performed in order to see if there was any difference between fresh and aged alkaline solutions. The results from these titrations did not differ from the other titrations. As a further check on the reversibility of the equilibria, back-titrations were made. The initial solution was made strongly alkaline and acid was added. These titrations gave the same results as the preceding ones. It is therefore likely that true equilibria were measured.

RESULTS WITH 3 M $Na(ClO_4)$ AS MEDIUM

With 3 M $Na(ClO_4)$ as medium the following total Pb(II) concentrations were used; B = 10, 5, 2.5, 1, 0.5 and 0.25 mM. Since log $[OH^-]$ was not measured it had to be calculated. Hedström [19] has given formulas which allow the calculation of the free ligand concentration from a knowledge of the total ligand concentration and the free metal ion concentration only. The preliminary measurements had shown that the complexes formed were mononuclear and moreover the concentration of free ligand is large compared to B. In our case, therefore, the method developed by Leden [20] easily leads to the goal. With our notations we have

$$\frac{\partial \eta}{\partial \log a} = Z \tag{4}$$

$$a = A—BZ \tag{5}$$

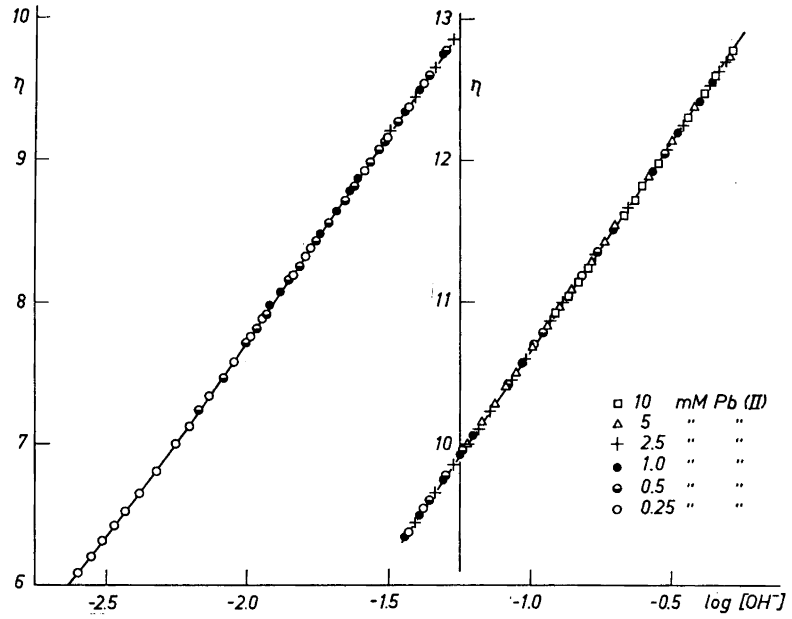

Fig. 1. η = log [Pb(II)]$_{tot}$/[Pb^{2+}] as a function of log[OH$^-$]. The solid line is calculated with log β_2 = 10.9 and log β_3 = 13.66.

Neighbouring points were used to find $\Delta\eta/\Delta\log a$ and as a first estimate of a, $(A—3B)$ was used. The successive approximations were repeated till the third place in log$a$ did not change on a further calculation.

The η values at low B and [OH$^-$] have been corrected for the presence of small amounts of $PbOH^+$ and $Pb_3(OH)_4^{2+}$, which still persist in these solutions [17]. The data plotted as η(log [OH$^-$]) fall on a single curve as can be seen from Fig. 1.

Determination of the equilibrium constants. The mononuclear complexes present are most likely to be only $Pb(OH)_3^-$ and $Pb(OH)_2$, whereas $Pb(OH)_4^{2-}$ and higher complexes cannot be present in larger amounts since Z never exceeds 3. We have

$$B = \beta_2 ba^2 + \beta_3 ba^3 + \beta_4 ba^4 + \text{----------} \quad (6)$$

$$Ba^{-2}b^{-1} = \beta_2 + \beta_3 a + \beta_4 a^2 + \text{----------} \quad (7)$$

By plotting $Ba^{-2}b^{-1}$ as a function of a, β_2 is found from the intercept on the $Ba^{-2}b^{-1}$ axis and β_3 from the slope of the straight line which should be obtained if the hypothesis is valid. The presence of $Pb(OH)_4^{2-}$ *etc.* should make the line bend upwards at high a. The plot is shown in Fig. 2.

It is obvious that the data can not be fitted to a straight line over the whole log[OH$^-$] studied. This leads to a certain ambiguity when fitting the data to

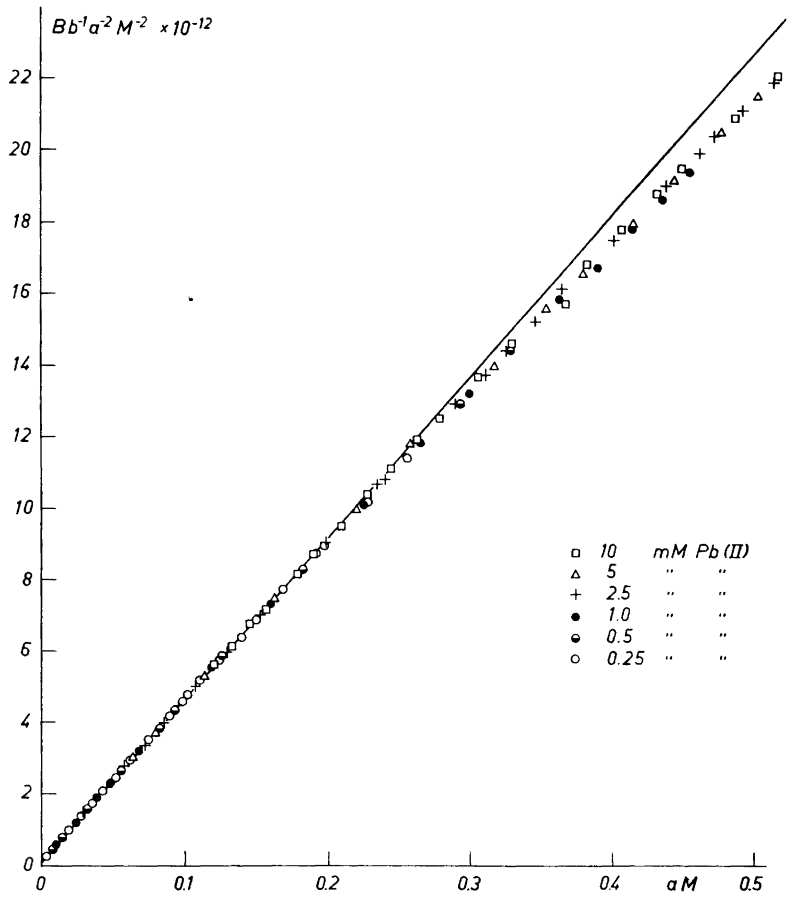

Fig. 2. $[Pb(II)]_{tot}/([Pb^{2+}][OH]^2)$ as a function of $[OH^-]$. The straight line gives $\log \beta_2 = 10.9$ and $\log \beta_3 = 13.65$.

the best straight line. Two such lines have been drawn. The first line was drawn so as to fit all the data for $[OH^-] < 0.2$ M best (Fig. 2). For $[OH^-] > 0.2$ M the deviations from linearity are so large that these data can not be used for the determination of the equilibrium constants. The values of the constants obtained from the line were

$$\log\beta_2 = 10.9 \pm 0.1$$

$$\log\beta_3 = 13.65 \pm 0.05$$

The deviations are in a direction opposite to that expected for the formation of $Pb(OH)_4^{2-}$. A tentative explanation could be variations in the activity factors when the composition of the medium has been changed considerably.

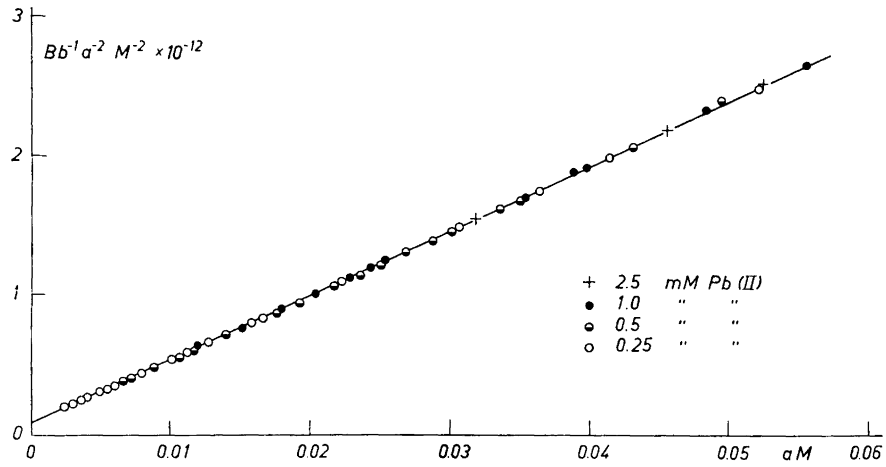

Fig. 3. $[Pb(II)]_{tot}/([Pb^{2+}][OH^-]^2)$ as a function of $[OH^-]$. The straight line gives $\log \beta_2 = 10.9$ and $\log \beta_3 = 13.66$.

This would suggest that the data at low $[OH^-]$ give better values of the equilibrium constants. A straight line drawn through the points for $[OH^-] < 0.05$ M (Fig. 3) gave

$$\log\beta_2 = 10.9 \pm 0.1$$

$$\log\beta_3 = 13.66 \pm 0.05$$

The deviations at large $[OH^-]$ are somewhat surprising in view of the measurements of Garrett, Vellenga and Fontana [6]. They determined the equilibrium constant for the reaction

$$PbO\ (s) + OH^- \rightleftharpoons Pb(OH)_3^-$$

$$K = \frac{[Pb(OH)_3^-]}{[OH^-]} \tag{8}$$

and calculated K by inserting analytical concentrations in (8). For $[OH^-] < 1$ M, K did not vary systematically with $[OH^-]$ and this would indicate that $f_{Pb(OH)_3^-}/f_{OH^-}$ is close to unity. We have calculated the activity factor ratio by combining the measurements from the cells (I) and (III). The variation in the water activity is very small and is neglected.

From eqn. (2) we obtain

$$E_H - E_H^\circ - 59.15 \log a = 59.15 \log f_{OH^-} - E_j = -7.8\,a \tag{2a}$$

and substituting $bf_{Pb^{2+}}$ from

$$\beta_3 = \frac{[Pb(OH)_3^-]}{ba^3} \frac{f_{Pb(OH)_3^-}}{f_{Pb^{2+}} f_{OH^-}^3} \tag{9}$$

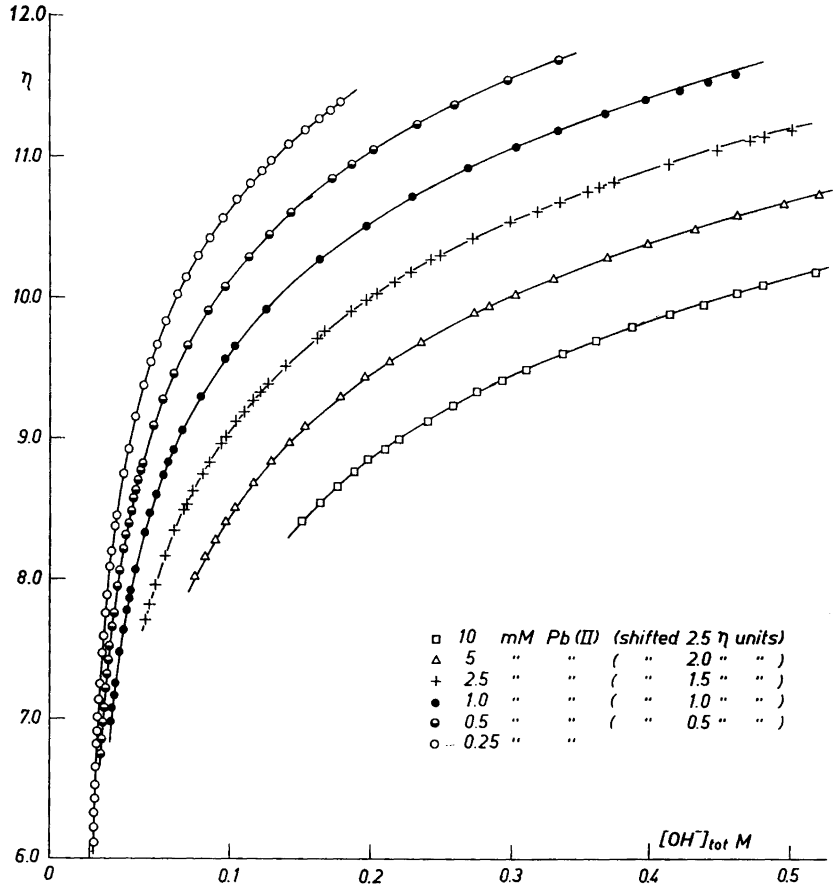

Fig. 4. η as a function of $[OH^-]_{tot}$. The solid lines are calculated using $\log \beta_3 = -10.9$ and $\log \beta_3 = 13.66$.

in eqn. (1) and putting $a = (A—3B)$ and $[Pb(OH)_3^-] = B$ we get

$$\log f_{OH^-}/f_{Pb(OH)_3^-} = (E_{Pb}—E^o_{Pb})/29.58 + \log B—\log\beta_3— \\ — 3 \log (A—3B) + 7.8 (A—3B)/29.58 \quad (10)$$

The expression is valid for $[OH^-] > 0.2$ M where $[Pb(OH)_2]$ can be neglected. $f_{OH^-}/f_{Pb(OH)_3^-}$ was found to decrease from unity to $\simeq 0.93$ at 0.5 M OH^-.

If the assumption of constant activity factors is still upheld the result would have to be explained in terms of incomplete dissociation of NaOH. It would, however, be necessary to assume that "$(OH)_2^{2-}$" complexes are formed. The formation of NaOH although leading to a $f_{OH^-}/f_{Pb(OH)_3^-}$ ratio different from unity, would not give a ratio varying with $[OH^-]$.

The previous measurements [17] on the hydrolysis of Pb(II) in acid and neutral solution had been discontinued at $\log h \simeq —8.5$ when a precipitate of basic

lead perchlorates started to form. Thus there is a gap between the old and the new sets of data of *ca.* 3 log$h$ units. We have tried to fill this gap by measurements with $B = 0.1$, 0.2 and 0.4 mM in 0.3 M Na(ClO_4). We were, however, unsuccessful and could not obtain stable potentials when $\log[OH^-] < -3$. In more alkaline solutions the potentials were stable and yielded the following values of the equilibrium constants.

$$\log\beta_2 = 10.34 \pm 0.1$$
$$\log\beta_3 = 13.29 \pm 0.05$$

In order to show the agreement between the experimental data and the values calculated from the equilibrium constants given, Fig. 4 was constructed. Note that the $\eta(A)_B$ curves have been successively displaced by 0.5 η unit in order to increase the clarity of the figure.

DISCUSSION

With the exception of Akselrud's work, all investigations on the behavior of Pb(II) in alkaline solution point to the formation of $Pb(OH)_2$ and $Pb(OH)_3^-$. The table gives the values of $\log\beta_2$ and $\log\beta_3$ found in the literature.

			$\log\beta_2$	$\log\beta_3$
Heyrovský [8]	var. NaOH		———	12.15
Lingane [9]	var. NaOH	25°C	———	12.9
Goward [10]	1 M KNO_3	25°C	10.77	13.31
This work	3 M $NaClO_4$	25°C	10.90	13.66
This work	0.3 M $NaClO_4$	25°C	10.34	13.29

From solubility measurements we may calculate

$$K_3 = \frac{[Pb(OH)_3^-]}{[Pb(OH)_2]\,[OH^-]} = \frac{\beta_3}{\beta_2} \qquad (11)$$

and find from the data by Garrett, Vellenga and Fontana [6] $\log K_3 = 2.86$ for the yellow oxide and 3.06 for the red oxide. Our value of $\log K_3$ is 2.76 (3 M $NaClO_4$) and 2.95 (0.3 M $NaClO_4$).

Considering that the constants have been obtained under different experimental conditions the agreement between the numerical values may be considered satisfactory.

Published values of the solubility product of lead oxide vary considerably [22]. The highest value of $\log K_{S0}$ is —13.96 and the smallest value is —19.96. From our value of β_2 in 3 M Na(ClO_4) and the solubility of $Pb(OH)_{2(aq)}$ ($1 \cdot 10^{-4}$ M for the yellow oxide and $4 \cdot 10^{-5}$ for the red oxide[6]) we may estimate $\log K_{S0} \simeq$ —14.9 and —15.3. This agrees fairly well with the value of $\log K_{S0} =$ —15.04 and — 15.23 found by Applebey and Reid [3] from measurements of the cell Pb, PbO/1 M NaOH/ HgO, Hg.

From the β values and the ionic product of water ($\lg K_w =$ —14.22 in 3 M $NaClO_4$ (Ingri *et al.*[15]) and $\log K_w =$ —13.76 in 0.3 M $NaClO_4$ (determined by us) we find the following values of the acidity constants of Pb^{2+}.

	3 M $NaClO_4$	0.3 M $NaClO_4$
log $*K_1$	— 7.9	— 7.8
log $*K_2$	— 9.6	— 9.4
log $*K_3$	—11.5	—10.8

The regular sequence of the log$*K_n$ values shows an interesting break after log$*K_3$. The value of log$*K_4$ must be much smaller than expected from the sequence. The ratio between the successive acidity constants of Pb^{2+} ($10^{-1.4}$ to $10^{-1.9}$) is considerably larger than for hydroxide acids (such as H_3PO_4), where the ratio is around 10^{-5}, but smaller than found for other metal ions. For a large number of metal ions log$*K_1$ and log$*K_2$ have about the same value (Sillén [21]).

Acknowledgements. We wish to thank Professor Lars Gunnar Sillén for his continual interest in our work and to Dr. V. Tyrrell for having corrected the English of this paper. Thanks are also due to Mr Frans Ericson for construction of the apparatus. This work has been supported by *Statens Tekniska Forskningsråd* (*Swedish Technical Research Council*).

REFERENCES

1. Berl, E. and Austerweil, G. *Z. Elektrochem.* **13** (1907) 165.
2. Glasstone, S. *J. Chem. Soc.* **119** (1921) 1689.
3. Applebey, M. P. and Reid, R. D. *J. Chem. Soc.* **121** (1922) 2129.
4. Randall, M. and Spencer, H. M. *J. Am. Chem. Soc.* **50** (1928) 1572.
5. Töpelmann, H. *J. prakt. Chem.* **121** (1929) 320.
6. Garrett, A. B., Vellenga, S. and Fontana, C. M. *J. Am. Chem. Soc.* **61** (1939) 367.
7. Leden, I. *Symposium on Coordination Chemistry*, Copenhagen, 1953, p. 77.
8. Heyrovský, J. *Trans. Faraday Soc.* **19** (1924) 692.
9. Lingane, J. J. *Chem. Revs.* **29** (1941) 1.
10. Goward, G. W. *Thesis*, Princeton Univ. 1954, Univ. Microfilms 9414.
11. Akselrud, N. V. *Zhur. neorg. Khim.* **3** (1958) 1738.
12. Johnson, J. S. and Kraus, K. A. *J. Am. Chem. Soc.* **81** (1959) 1569.
13. Johnson, J. S. *Private communication.*
14. Forsling, W., Hietanen, S. and Sillén, L. G. *Acta Chem. Scand.* **6** (1952) 901.
15. Biedermann, G. and Sillén, L. G. *Arkiv Kemi* **5** (1953) 425.
16. Ingri, N., Lagerström, G., Frydman, M. and Sillén, L. G. *Acta Chem. Scand.* **11** (1957) 1034.
17. Olin, Å. *Acta Chem. Scand.* **14** (1960) 126.
18. Lagerström, G. *Acta Chem. Scand.* **13** (1959) 722.
19. Hedström, B. *Acta Chem. Scand.* **9** (1955) 613.
20. Leden, I. *Thesis*, Lund. 1943, p. 14.
21. Sillén, L. G. *Quart. Revs. London* **13** (1959) 146.
22. Bjerrum, J., Schwarzenbach, G. and Sillén, L. G. *Stability Constants*, Part II, The Chemical Society, London, 1958. Chem. Soc. Spec. Publ. No. 7.

Received May 24, 1960.

ACTA CHEMICA SCANDINAVICA 14 (1960) 2009–2020

Radiochemical Determination of Polythionates

NILS-HERMAN SCHÖÖN

Department of Engineering Chemistry, Chalmers Tekniska Högskola, Göteborg, Sweden

Two radiochemical methods have been developed for the determination of polythionates. In the first method, the polythionates are reacted with sulphite and with a mixture of sulphite and sulphide. The thiosulphate formed in these reactions is then determined with ^{110}AgSCN. In the second method, the sulphide contains the radioactive isotope ^{35}S and the amount of radioactive thiosulphate formed is instead determined. A correction must be applied for the amount of radioactive thiosulphate formed by isotopic exchange between the sulphide and thiosulphate.

The common method for determining polythionates in mixtures is based on the fact that these ions, on reaction with sulphite, sulphide, cyanide, and hydroxide, give amongst other compounds thiosulphate [1,2]. The thiosulphate formed can be determined iodometrically in a weakly acid solution after the disturbing influence of sulphite, sulphide and cyanide has been eliminated.

In the present work, two radiochemical methods for the determination of the total amount of polythionate have been developed. Both of the methods are intended for use in the determination of polythionate in spent liquors from the sulphite cellulose process. With the iodometric method, the errors are considerable in this case and with many types of liquors it is impossible to use a method of this sort.

In the first method, the amount of thiosulphate formed in the reaction with sulphite and the amount of thiosulphate formed in the reaction with a mixture of sulphite and sulphide are determined. The thiosulphate determinations are performed by means of the silver thiocyanate method using silver thiocyanate containing the radioactive isotope ^{110}Ag. From these two determinations, it is possible to calculate the amount of polythionate as well as the mean number of sulphur atoms per mole polythionate.

In the second method, the polythionates are first made to react with sulphite and then with sulphide containing the radioactive isotope ^{35}S. After precipitation of sulphide, the amount of radioactive thiosulphate formed is determined. From this determination, it is possible to calculate the original amount of polythionate after correcting for the radioactive thiosulphate which is formed by isotope exchange between thiosulphate and sulphide.

I. THE SILVER(^{110}Ag) THIOCYANATE METHOD

Polythionates with more than three sulphur atoms per molecule react in alkaline solution with sulphite forming thiosulphate and trithionate according to the equation:

$$S_nO_6^{2-} + (n-3)\ SO_3^{2-} \rightarrow S_3O_6^{2-} + (n-3)\ S_2O_3^{2-},\ n > 3 \qquad (1)$$

Even at room temperature, the reaction proceeds very rapidly in the presence of an excess of sulphite. Trithionate does not react with sulphite under the conditions existing in this case. In weakly acid or neutral solutions, the reaction proceeds slowly. Moreover, the reaction does not give a complete yield, a state of equilibrium being instead obtained.

In the reaction between polythionates and a mixture of sulphite and sulphide, it has been found that all of the polythionates give thiosulphate according to the equation:

$$S_nO_6^{2-} + S^{2-} + (n-3)\ SO_3^{2-} \rightarrow (n-1)\ S_2O_3^{2-},\ n \geq 3 \qquad (2)$$

This reaction is carried out at about 100°C since the reaction rate is relatively low at room temperature.

If the amount of thiosulphate formed in these two reactions is determined, it is possible to calculate the total amount of polythionate in the following way:

In a solution containing a_2 mole $S_2O_3^{2-}$, a_3 mole $S_3O_6^{2-}$, a_4 mole $S_4O_6^{2-}$, ... a_n mole $S_nO_6^{2-}$, we obtain after the reaction with sulphite a thiosulphate amount, $A = a_2 + \Sigma(n-3)\ a_n$, and after the reaction with sulphite-sulphide a thiosulphate amount, $B = a_2 + \Sigma(n-1)\ a_n$. From these two quantities, the amount of polythionate is obtained as $\Sigma a_n = \frac{B-A}{2}$ while the average number of sulphur atoms per molecule is

$$\bar{n} = \frac{n\Sigma a_n}{\Sigma a_n} = \frac{B + \frac{B-A}{2} - a_2}{\frac{B-A}{2}}$$

In order to calculate $\bar{n}$, it is evident that the original thiosulphate content of the solution must be determined. As has been previously shown [3], it is also possible to perform this determination with the silver thiocyanate method.

The determination of thiosulphate with the silver thiocyanate method is based on the property of the thiosulphate ion of forming stable silver thiosulphate complexes with silver ions [4]. Thus, if an excess of solid silver thiocyanate is shaken with a thiosulphate solution, the following equilibrium between the solid phase and solution is obtained after only 10 min at 20°C:

$$m\ AgSCN_{(s)} + n\ S_2O_3^{2-} \rightleftharpoons Ag_m(S_2O_3)_n^{(2n-m)-} + m\ SCN^-$$

Since the silver thiocyanate contains the radioactive isotope ^{110}Ag, the total amount of silver in the solution can be determined by measuring the activity of the solution after removal of the solid phase. The thiosulphate content is then calculated by means of a calibration curve between thiosulphate content and silver content.

The determination of the thiosulphate which is formed in the sulphite reaction is complicated by the fact that the sulphite ions like the thiosulphate ions give stable complexes with silver ions. The formation of silver sulphite complexes can, however, be completely avoided if the solution is acidified before the analysis. This is due to the fact that hydrogen sulphite ions in contrast to sulphite ions do not form complexes with silver ions. However, it has been found [3] that hydrogen sulphite has a certain effect on the determination of thiosulphate by the silver thiocyanate method. In the present work, it has therefore been necessary to study how this effect depends on the pH of the solution, in order to determine to what pH the solution should be adjusted after the sulphite reaction.

Before determining the thiosulphate after the sulphite-sulphide reaction, the remaining sulphide is removed by precipitation with zinc carbonate. The solution is thereafter acidified in order to convert the sulphite to hydrogen sulphite. The effect on the thiosulphate determination of any possible remaining traces of sulphide was also studied.

Experimental

Chemicals

Potassium trithionate, $K_2S_3O_6$, has been prepared according to Kurtenacker and Matejka [5] and potassium pentathionate, $K_2S_5O_6 \cdot 1.5\ H_2O$, according to Stamm, Siepold and Goehring [6]. Sodium tetrathionate, $Na_2S_4O_6 \cdot 2\ H_2O$, was prepared by shaking solid sodium thiosulphate with an excess of iodine dissolved in absolute alcohol. The purity of the trithionate and pentathionate was better than 97 % while the impurity content in the tetrathionate was less than 0.5 %. The purity of these substances was determined using the sulphite method and the sulphite-sulphide method as described by Kurtenacker [1] and using the mercury(II) chloride method according to Jay [7].

The sodium sulphide solution was prepared by passing hydrogen sulphide into a sodium hydroxide solution. The surface of the sulphide solution was covered with paraffin oil in order to minimize aerial oxidation. The sulphite solution was freshly prepared for each series of experiments.

The silver isotope, ^{110}Ag, was provided by AB Atomenergi — it had been prepared by neutron irradiation of a piece of silver foil. About 1 g of foil was irradiated to an activity of 1—2 mC. It was then dissolved in 50 ml hot nitric acid (diluted 1:4) and diluted to 500 ml. Of this solution, 100 ml was taken and sufficient inactive silver nitrate added to lower the activity to 800—1 000 c.p.m./10^{-4} M silver (GM-tube for liquids). The solution obtained was diluted and silver thiocyanate was precipitated at about 100°C using an excess of potassium thiocyanate solution. The precipitate was washed with water until the washings no longer produced a colour with iron(III) nitrate. In order to determine the relation between activity and silver content, a weighed amount of silver thiocyanate was dissolved in an excess of 1 M potassium cyanide. After diluting, 10 ml of the solution was taken for activity measurements.

Apparatus

The shaking of the silver thiocyanate suspension was carried out using a "Microid flask shaker" from Griffin and George Ltd. The filtering of the suspension was performed in a Thiessen filtration apparatus provided with a colloid filter (according to Zsigmondy). The pore width of the colloid filter was 200—300 mμ.

The radioactivity was measured with a GM-tube for liquids made by Mullard Ltd. Before each measurement, the GM-tube had to be washed with conc. potassium cyanide solution. The scaler used was a Type 1 000 apparatus from AB Nukleonikinstrument, Göteborg.

Procedure

The sulphite reaction. To 10 ml of the sample, 5 ml 0.4 M sodium sulphite was added after which the solution was allowed to stand for 15 min at room temperature. The solution was acidified with 5 ml 0.5 M formic acid and, to 10 ml of the solution thus obtained, 10 ml silver thiocyanate suspension containing 10—25 mg precipitate was added. The mixture was shaken vigorously for 15 min at 20 ± 1°C after which the solution was filtered. The activity was measured on 10 ml of the filtrate. The activity obtained was corrected for background radiation and radioactive decay.

The sulphite-sulphide reaction. To 25 ml of the sample, 5 ml 0.4 M sodium sulphite and 5 ml 0.25 M sodium sulphide were added and the solution was heated in boiling water for 15 min. Then, 10 ml 0.35 M freshly prepared zinc carbonate suspension was added and the mixture was cooled to room temperature and filtered. After adding 10 ml 1 M formic acid, the filtrate was diluted to 100 ml. A 10 ml sample of this solution was taken and 10 ml silver thiocyanate suspension was added. Shaking and filtration were performed as described above.

Results

Determinations of the thiosulphate formed in the sulphite and sulphite-sulphide reactions are shown in Table 1. In order to be able to compare the

Table 1. Determination of polythionates using the silver(^{110}Ag)thiocyanate method.

Reaction	Polythionate, added			$c_{S_2O_3} \times 10^3$ Calc.	$c_{Ag} \times 10^3$		Deviation %
	$cS_3O_6 \times 10^3$	$cS_4O_6 \times 10^3$	$cS_5O_6 \times 10^3$		Found	Calc.	
sulphite		0.05		0.05	0.036	0.036	0.0
		0.1		0.1	0.068	0.067	+ 1.5
		0.3		0.3	0.181	0.186	−2.7
		0.5		0.5	0.293	0.295	−0.7
		1.0		1.0	0.567	0.560	+ 1.2
			0.05	0.1	0.066	0.067	−1.5
			0.5	1.0	0.553	0.560	−1.2
	0.5	0.5	0.25	1.0	0.561	0.560	+ 0.2
sulphite-sulphide	—	—	—	0.04	0.030	—	—
	0.05			0.14	0.092	0.093	−1.1
	0.5			1.04	0.575	0.570	+ 0.9
		0.033		0.14	0.096	0.093	+ 3.2
		0.1		0.34	0.209	0.205	+ 2.0
		0.167		0.54	0.319	0.317	+ 0.6
		0.33		1.04	0.570	0.570	0.0
			0.025	0.14	0.095	0.093	+ 2.2
			0.25	1.04	0.580	0.570	+ 1.8
	0.2	0.1	0.075	1.04	0.577	0.570	+ 1.2

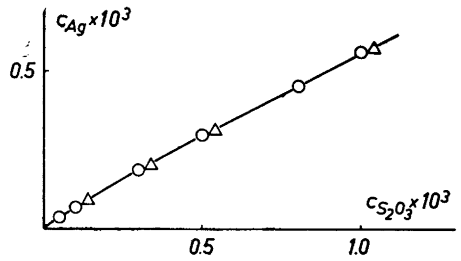

Fig. 1. Standard curve for the determination of thiosulphate by the silver(^{110}Ag) thiocyanate method.
—O— sulphite reaction
—△— sulphite-sulphide reaction.

results in the sulphite series with those in the sulphite-sulphide series, the silver concentrations measured are given in the table instead of the thiosulphate concentrations calculated from the calibration curve. All the concentrations in the table refer to the filtrate obtained after shaking with silver thiocyanate.

The concentrations are given in mole/litre.

Under "calc." are reported the silver contents which were obtained in parallel experiments with thiosulphate.

As may be seen from the table, the agreement between the calibration series with thiosulphate and the actual experiments with polythionates is good. The maximum deviation amounts to 3 %. The results of the sulphite series show, in addition, that the trithionate formed by the reaction does not affect the thiosulphate determination. A comparison of the silver concentrations in the sulphite series and sulphite-sulphide series is not possible in the table since the thiosulphate concentrations in the sulphite-sulphide series are, owing to aerial oxidation of the sulphide, somewhat higher than those in the sulphite series. A comparison between the calibrations with thiosulphate for both of the experimental series has instead been made in Fig. 1. As may be seen from the figure, the agreement between the two series is good which shows that the higher silver content which is obtained in the sulphite-sulphide series can be completely attributed to the amount of thiosulphate which is formed by aerial oxidation of the sulphide.

Influence of hydrogen sulphite at various pH values. In all experiments reported in Table 1, the solution has been acidified with formic acid to pH 4.0 before the determination of thiosulphate. Since the formation of the silver thiosulphate complexes is influenced by the presence of hydrogen sulphite, this effect has been studied as a function of the pH of the solution. The pH interval studied was 2.6—4.9 and the sulphite concentrations were 0.01, 0.05, and 0.1 M. Comparative experiments with thiosulphate solutions in the absence of hydrogen sulphite have also been performed. As is obvious from Table 2, a change in the total sulphite content or in the pH has only a very slight effect on the formation of the silver thiosulphate complexes. The variations in the silver content which have been obtained lie, with exception of the smallest

Table 2. Influence of pH and total sulphite on the determination of thiosulphate.

Temp. °C	c_{SO_3}	$c_{S_2O_3} \times 10^3$ / pH	0.1	0.3	0.5	1.0
			$c_{Ag} \times 10^3$			
24	0.05	2.6	0.070	0.195	0.308	0.575
	0.05	3.5	0.077	0.192	0.320	0.588
	0.10	3.5	0.083	0.198	0.309	0.590
	0.05	4.3	0.068	0.199	0.309	0.573
	0.01	4.3	0.075	0.199	0.310	0.578
	0.05	4.9	0.075	0.199	0.311	0.593
		6.7	0.078	0.214	0.327	0.598
20		2.1	0.075	0.193	0.305	0.550
		4.3	0.075	0.200	0.315	0.580
		6.7	0.078	0.198	0.322	0.575

thiosulphate content, within the experimental error for the method. The acidification after the sulphite reaction can therefore be performed to any pH within the interval 2.6—4.9 without the formation of the silver thiosulphate complexes being thereby appreciably affected. From the comparative experiments performed without the addition of hydrogen sulphite, it is evident that a decrease in the formation of the silver thiosulphate complexes occurs only at a relatively low pH. Whether or not this decrease is due to a decomposition of the thiosulphate added has not been investigated.

Influence of sulphide. For a complete precipitation of sulphide ions as zinc sulphide, it is important to use a freshly prepared zinc carbonate suspension and to filtrate the solution after cooling to room temperature. Otherwise the filtrate will contain a small amount of sulphide ions which give a precipitation of silver sulphide on shaking with solid silver thiocyanate according to

$$2\ AgSCN_{(s)} + S^{2-} \rightarrow Ag_2S_{(s)} + 2\ SCN^-$$

The thiocyanate ions formed in this reaction would then displace the equilibrium between the solid silver thiocyanate and the thiosulphate ions in such a way that the total amount of complex-bound silver would decrease. Some experiments carried out at 24 ± 1°C were performed in order to illustrate how the sulphide and thiocyanate ions affect the formation of the silver thiosulphate complexes. A zinc carbonate suspension was not added in these experiments (*cf.* Table 3). It is seen that the influence of thiocyanate ions is considerable. A corresponding decrease in the total silver content has, however, not been obtained in the presence of sulphide ions. The silver content was found instead to have increased. This is due to the fact that part of the precipitated silver sulphide exists in a colloidal state with such a small particle size that it can pass through even a very fine colloid filter (pore diameter 150 mμ). The presence of silver sulphide in the solution is apparent from its weakly yellow colour.

Table 3. Influence of sulphide and thiocyanate on the determination of thiosulphate.

$c_{S_2O_3} \times 10^3$ / $c_S \times 10^3$	0.3	0.5	1.0
	$c_{Ag} \times 10^3$		
—	0.214	0.327	0.598
—*	0.141	0.220	0.462
0.5	0.322		
0.05	0.287	0.404	

* One μmole KSCN was added per ml solution.

II. THE SULPHIDE(^{35}S) METHOD

In this method, the polythionate solution is first of all allowed to react with an excess of sulphite thus forming thiosulphate as well as one mole of trithionate per mole polythionate (*cf.* eqn. (1) given above). The solution is then made to react at about 100°C with an excess of sulphide containing the radioactive isotope ^{35}S. In this reaction, one mole radioactive thiosulphate is obtained per mole trithionate, *i.e.* one mole radioactive thiosulphate per mole polythionate in the original sample.

The reaction between sulphide and trithionate can be written as follows:

$$S_3O_6^{2-} + {}^*S^{2-} \rightarrow {}^*S_2O_3^{2-} + S_2O_3^{2-}$$

After the remaining sulphide has been precipitated with zinc carbonate, an excess of alkali is added and the thiosulphate and sulphite are oxidized at about 100°C to sulphate by means of hydrogen peroxide. The sulphate is precipitated as barium sulphate and the activity of the precipitate is measured in a proportional counter of the "flow-counter" type. Because the sulphur isotope ^{35}S is a very weak β-emitter ($E_{max} = 0.167$ MeV), the measurements have been performed using the "infinitely thick layer" method. In this method, the thickness of the barium sulphate layer is chosen so that it exceeds the maximum range of the β-radiation. Since the absorption coefficient for β-radiation in barium sulphate is of the order of 0.2 cm^2/mg[8], it can be calculated that the required thickness corresponds to 25 mg $BaSO_4$/cm^2. In this method, the activity measured is proportional to the specific activity of the precipitate. The original amount of polythionate in the sample is, however, proportional to the total activity. A relative measure of the total activity can be obtained by multiplying the measured activity by the total weight of precipitate.

Parallel to the reaction between sulphide and trithionate, radioactive thiosulphate is also formed by isotopic exchange between sulphide and thiosulphate in the following way:

$$*S^{2-} + S{-}SO_3^{2-} \rightarrow *S{-}SO_3^{2-} + S^{2-}$$

This reaction has been studied by Voge [9] who found that the exchange took place very slowly even at 100°C. In the present investigation, it was however found that this exchange is of such a magnitude that it cannot be neglected in the determination of polythionate. Hence, a correction has to be applied if the original sample contains thiosulphate or higher polythionates.

Experimental

Chemicals

Except for the potassium pentathionate, the polythionate preparations have been the same as in the previous section. The pentathionate sample used here contained a relatively large amount of tetrathionate (*cf.* Table 5).

Radioactive sodium sulphide was obtained from the Radiochemical Centre, Amersham, England. The radioactive sulphide solution was prepared by dissolving about 3 mC radioactive sulphide in 1 l 0.25 M inactive sulphide solution containing at most 0.5 mole per cent thiosulphate. In order to determine the relationship between sulphide content and activity, one aliquot of the solution was taken and, after addition of inactive sulphate, oxidized at 90—100°C with hydrogen peroxide. The activity of the precipitated barium sulphate was then measured. Because the sulphide solution contained thiosulphate with a high specific activity, it was necessary to correct the relation between activity and sulphide content for the activity of the thiosulphate. In order to perform this determination, the sulphide was first of all precipitated using zinc carbonate after which the filtrate was treated as above.

Apparatus

In order to obtain reproducible measurements of the activity of the barium sulphate, it is necessary that the precipitate should be spread evenly over a given surface. This has been accomplished by means of a filtration procedure. The suspension of barium sulphate was transferred by means of a slow filtering to a plexiglas crucible provided with a fine filter paper. The inner diameter of the crucible was 3 cm and thus an "infinitely thick layer" could be obtained since the amount of precipitate exceeded 175 mg. When filtering, the plexiglas crucible was mounted between a porcelain muff and a glass sleeve. After filtration and drying, the crucible was placed in a proportional counter in order to measure the activity.

The counter was of the "flow-counter" type. It was equipped with a thin window consisting of a plastic film in order to diminish the comsumption of the gas used for the measurements. This gas was a mixture of 20 % methane and 80 % argon. The counter, amplifier and scaler were manufactured by AB Nukleonikinstrument, Göteborg.

Procedure

To 10—15 ml of the sample, about 5 ml 0.4 M sulphite solution was added after which the liquid was allowed to stand for 15 min at room temperature. Radioactive sulphide solution, 5 ml 0.25 M, was added and the resultant solution was heated in boiling water for 15 min. Then, 10 ml 0.35 M freshly prepared zinc carbonate suspension was added after which the mixture was cooled and filtered. To the filtrate, 5 ml 1 M sodium hydroxide and 10 ml 30 % hydrogen peroxide were added and the solution obtained was heated for 20 min in boiling water. Then, 15 ml 1 M hydrochloric acid was added and, thereafter, an excess of hot 0.2 M barium chloride, dropwise under stirring. After cooling, the solution obtained was filtered in the same way as described above. The precipitate was washed with alcohol and ether and dried at 50°C. The activity and weight of the precipitate were then measured. The activity was corrected for the background radiation. The correction for the radioactive decay was obtained by comparing in each series, the activity

Table 4. Determination of trithionate using the sulphide(^{35}S) method.

Trithionate mmole	Barium sulphate g			Activity, measured c.p.m. × 10^{-3}			Activity × Weight of $BaSO_4$ c.p.m. × g × 10^{-3}			
							Found			Calc.
—	0.458	0.452	0.478	3.30	4.02	4.38	—	—	—	—
0.021	0.473			3.62			0.20			0.20
0.041	0.490			3.85			0.38			0.39
0.103	0.548	0.536	0.565	4.57	5.17	5.40	0.99	0.95	0.96	0.98
0.206	0.632	0.625	0.659	5.48	5.97	6.15	1.95	1.91	1.96	1.96
0.309		0.721	0.752		6.72	6.69		3.03	2.94	2.94
0.412	0.807	0.814	0.847	6.99	7.11	7.18	4.13	3.97	3.99	3.92

obtained with the activity of a standard sample of radioactive barium sulphate. Since it was found to be difficult to transfer the barium sulphate quantitatively to the filter and, at the same time, to obtain a completely even surface, another procedure has also been tried. In it, the barium sulphate suspension was filtered through a glass filter and the weight of the precipitate was obtained. Thereafter, the precipitate was suspended once again in water and then transferred to the plexiglas crucible in order to measure the activity. Hence, in this case, it was not necessary to transfer the precipitate quantitatively to the plexiglas crucible.

Table 5. Influence of thiosulphate upon the determination of polythionates by the sulphide(^{35}S) method.

Polythionate mmole		Thiosulphate mmole	Barium sulphate g	Activity, measured c.p.m. × 10^{-3}	Activity × Weight of $BaSO_4$ c.p.m. × g × 10^{-3}	
		—	0.474	4.44	—	
		0.100	0.516	4.20	0.06	
		0.200	0.563	4.02	0.16	
		0.300	0.610	4.00	0.34	
		0.400	0.656	3.84	0.41	
					Found	*Calc.*
—		—	0.431	3.74	—	—
0.206	$S_3O_6^{2-}$	—	0.633	5.63	1.95	1.96
0.206	$S_3O_6^{2-}$	0.200	0.719	5.20	2.13	2.12
0.206	$S_3O_6^{2-}$	0.400	0.804	4.98	2.39	2.37
—			0.474	4.39	—	—
0.206	$S_3O_6^{2-}$		0.657	6.15	1.96	1.96
0.200	$S_4O_6^{2-}$		0.703	5.80	2.00	2.06
0.2	$S_5O_6^{2-}$ *		0.765	5.87	2.41	2.26
0.041 0.100 0.06	$S_3O_6^{2-}$ + $S_4O_6^{2-}$ + $S_5O_6^{2-}$ *		0.723	5.88	2.17	2.10

* 0.2 mmole of the pentathionate sample contained 0.183 mmole pentathionate and 0.034 mmole tetrathionate.

Results

The radioactive sulphide method has been tried, first of all, for the determination of trithionate. The results are shown in Table 4. The table contains three series which have been performed at intervals of about one month. The values given under "Activity × Weight of $BaSO_4$" have been corrected for the value obtained in the blank measurement. It is seen that a large amount of radioactive thiosulphate is obtained in the blank. This amount of thiosulphate was found already in the original sulphide solution and thus the formation of thiosulphate by aerial oxidation during the heating must be negligible. The more laborious filtration procedure described above (*cf.* under Procedure) has only been used in the third series. It is seen that the difference from the calculated value is least in this series, at most 2 %. In the other two series, it is somewhat larger, *viz.* 5 %.

The mean values obtained for the activity in the three series correspond to a 100 % yield of radioactive thiosulphate which means that the isotope exchange between the radioactive sulphide and the inactive thiosulphate formed by the reaction falls within the experimental error for the method. If, on the other hand, the solution contains thiosulphate at the beginning of the sulphide reaction, the formation of radioactive thiosulphate will be greater. As can be seen from Table 5, this formation of radioactive thiosulphate is proportional to the thiosulphate content and amounts to 10 % of this content. From the experiments with polythionates, it is seen in addition that the isotope exchange between thiosulphate and sulphide occurs independently of the presence of trithionate. This means that, with tetrathionate, a 10 % and, with pentathionate, a 20 % larger amount of radioactive thiosulphate is obtained than in the reaction with trithionate. For a correct determination of the total amount of polythionate, it is therefore necessary to determine, in addition, the total thiosulphate content after the sulphite reaction. This determination can, of course, be performed by means of the ^{110}AgSCN-method but an indirect determination should also be possible by means of the ^{35}S-method. If the latter procedure is used, the solution is oxidized with iodine after the sulphite reaction, and sulphite and radioactive sulphide are thereafter added to the solution as above. The amounts of radioactive thiosulphate formed by means of the original procedure ($*a_2^{I}$) and by means of the modified procedure including oxidation with iodine ($*a_2^{II}$) can be written:

$$*a_2^{I} = \Sigma a_n + 0.1\ [a_2 + \Sigma(n-3)\ a_n]$$
$$*a_2^{II} = \Sigma a_n + 0.55\ [a_2 + \Sigma(n-3)\ a_n]$$

where a_2 and a_n are the amounts of thiosulphate and polythionate $S_nO_6^{2-}$ in the original sample. From these two equations, the amount of polythionate can be calculated as:

$$\Sigma a_n = 1.22\ *a_2^{I} - 0.22\ *a_2^{II}$$

DISCUSSION

In the determination of the total amount of polythionate by the ^{110}AgSCN-method, the uncertainty in the measurement is dependent on the amount of thiosulphate in the original sample and also on $\bar{n}$, the average number of

sulphur atoms per mole polythionate. This is due to the fact that the amount of polythionate is calculated as half the difference between the thiosulphate amounts present in the solution after the sulphite-sulphide and the sulphite reactions. If an excess of thiosulphate is present in the original sample or if $\bar{n}$ is large, the total polythionate content is obtained as a relatively small difference between two large quantities. As appears from the results in Table 1, the largest difference in the determination of thiosulphate amounted to 3 %. From this, it follows that, in a solution which contains only trithionate, the maximum error in the determination of polythionate amounts to 3 %. This error rises to 33 % if the solution also contains, besides trithionate, an amount of thiosulphate which is ten times greater than the amount of the trithionate present. If the solution contains, instead, a higher polythionate, *e.g.* pentathionate, then the maximum error amounts to 9 % if the pentathionate is present alone. In the same way, the error rises to 39 % if the thiosulphate to pentathionate ratio is 10:1.

For a maximum error of 3 % in the thiosulphate determination, the maximum error in $\bar{n}$ can be estimated, according to the conventional calculation of error, to be 10—20 % (for $\bar{n}$ = 3—6) in the case where the sample contains only polythionates. If thiosulphate is present in a ten times larger amount, then the error in $\bar{n}$ is larger.

The determination of polythionates by the ^{35}S-method can be performed with a smaller error than that in the $^{110}AgSCN$-method. The amount of polythionate is obtained in this case as the difference in relative total activity (Weight × Activity of $BaSO_4$; Table 5) between the sample and the blank. Even in the less laborious procedure, the maximum error is less than 5 % despite the relatively high activity in the blank. In the presence of thiosulphate or with higher polythionates, the activity must be corrected for the activity arising from the isotopic exchange between the thiosulphate and sulphide. This correction does not have any appreciable influence on the accuracy of the polythionate determination if the thiosulphate content is determined using the $^{110}AgSCN$-method. The maximum error in the correction will in this case amount to 0.3 % of the thiosulphate content. If the amount of thiosulphate is ten times greater than the amount of trithionate, the maximum error in the polythionates will thus increase from 5 % to 8 %. Due to the greater accuracy in the determination of polythionates by this method, it is clear that the error in $\bar{n}$ will also be smaller. The maximum error in $\bar{n}$ has been calculated to be about 10 %. If, on the other hand, the correction for the isotopic exchange is determined by the ^{35}S-method, the maximum error in the polythionate determination will be much greater. This error increases from 5 % to 19 % if the amount of thiosulphate is ten times greater than the amount of trithionate. The maximum error in $\bar{n}$ also increases in this case.

A further comparison between the two methods shows that, in the ^{35}S-method, the activity is proportional to the amount of polythionate. This is not the case with the $^{110}AgSCN$-method due to the fact that a displacement of the equilibrium between the solid silver thiocyanate and the thiosulphate solution occurs when the concentration is increased. As far as the sensitivity of these methods is concerned, it is seen that the $^{110}AgSCN$-method is sensitive

to much lower contents than the ^{35}S-method. This comparison is of course based on the experimental procedures used as well as on the specific activities of the silver and sulphur which have been employed in this work.

Finally, it should be mentioned that the ^{35}S-method can be used for an indirect determination of thiosulphate. The sample is first oxidized with iodine after which the amount of tetrathionate formed is determined. In the presence of polythionates, it is necessary to perform two determinations, one before and one after the oxidation with iodine. This method has been tested for the determination of thiosulphate in spent liquors from the sulphite cellulose process. The results of these determinations will be published later.

Acknowledgements. The financial support of *Statens Tekniska Forskningsråd* is gratefully acknowledged.

REFERENCES

1. Kurtenacker, A. *Analytische Chemie der Sauerstoffsäuren des Schwefels*, Stuttgart 1938.
2. Goehring, M., Feldmann, U. and Helbing, W. *Z. anal. Chem.* **129** (1949) 346.
3. Schöön, N.-H. *Acta Chem. Scand.* **13** (1959) 525.
4. Schöön, N.-H. *Acta Chem. Scand.* **12** (1958) 1730.
5. Kurtenacker, A. and Matejka, K. *Z. anorg. u. allgem. Chem.* **193** (1930) 367.
6. Stamm, H., Siepold, O. and Goehring, M. *Z. anorg. u. allgem. Chem.* **247** (1941) 277.
7. Jay, R. R. *Anal. Chem.* **25** (1953) 288.
8. Larson, F. C., Maass, A. R., Robinson, C. V. and Gordon, E. S. *Anal. Chem.* **21** (1949) 1206.
9. Voge, H. H. *J. Am. Chem. Soc.* **61** (1939) 1032.

Received August 29, 1960.

ACTA CHEMICA SCANDINAVICA 14 (1960) 2021–2034

Benzaurinstudien

V. Gleichgewichte und Reaktionskinetik des 3,3′-Dimethoxy-benzaurins in wässrigen Lösungen

HANS GUSTAF HANSSON

Abteilung für anorganische und physikalische Chemie des Chemischen Instituts der Universität Lund, Schweden

In two previous papers [1,2] the equilibrium and kinetic conditions in aqueous solutions of benzaurin and three substituted benzaurins, 3,3′,5,5′-tetrabromo-benzaurin, 3,3′-dibromo-5,5′-dimethyl-benzaurin and 4″-chloro-benzaurin, were laid down in an equilibrium system that consists of three coloured "anhydrous" forms and three colourless "carbinolic" forms. The equilibrium constants of the protolytic reactions between the "anhydrous" or the "carbinolic" forms, and of the hydration reactions between corresponding "anhydrous" and "carbinolic" forms were determined through calculations on values, belonging together, of the light absorption E and the $[H^+]$. The velocity constants of the hydration reactions, which appear as a gradual fading of the colour of the solutions until equilibrium is reached, were determined by following E as a function of time.

In the present paper the corresponding investigation of the 3,3′-dimethoxy-benzaurin is presented according to the same scheme. The constants determined refer to the ionic strength 0.50 M, the temperature 20°C and a solvent with the composition 98 % water + 2 % acetone.

In zwei früheren Veröffentlichungen [1,2] wurde über Untersuchungen über die Gleichgewichtsverhältnisse in wässriger Lösung bei Benzaurin und drei substituierten Benzaurinen, nämlich 3,3′,5,5′-Tetrabrom-benzaurin, 3,3′-Dibrom-5,5′-dimethyl-benzaurin und 4″-Chlor-benzaurin, berichtet. Die zum Gleichgewichtsschema gehörenden Protolysen-, Hydratations- und Geschwindigkeitskonstanten wurden bestimmt. In der vorliegenden Arbeit werden die Resultate einer entsprechenden Untersuchung über 3,3′-Dimethoxy-benzaurin dargelegt. Wie erwartet können die Verhältnisse bei diesem Farbstoff mit demselben Schema beschrieben werden, das sich für die früher untersuchten Farbstoffe des Benzaurintypus [1,2] als gültig zeigte. Das Schema wird unten wiedergegeben, wobei die Konstanten in derselben Weise wie in den vorhergehenden Arbeiten definiert werden.

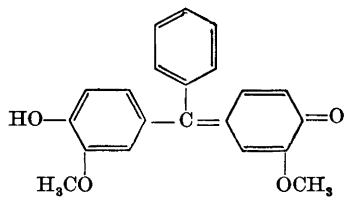

3,3′-Dimethoxy-benzaurin.
Anhydrid (G_1).

Die in das Schema * eingehenden Konstanten werden folgendermassen definiert:

Die Protolysenkonstanten:

$$K_1 = \frac{[G_1]}{[H^+] \cdot [R]} ; K_7 = \frac{[H^+] \cdot [G_1]}{[G_2];} ; K_3 = \frac{[H^+] \cdot [F_2]}{[F_1]} ; K_4 = \frac{[H^+] \cdot [F_3]}{[F_2]}$$

Die Hydratationskonstanten bei konstanter Wasseraktivität:

$$K_2 = \frac{[F_1]}{[G_1]} ; K_6 = \frac{[R]}{[F_2]}$$

Aus den Definitionen erigbt sich $K_1 \cdot K_2 \cdot K_3 \cdot K_6 = 1$.
Ferner wird $K_6/K_4 = K_5$ gesetzt.

Die Geschwindigkeitskonstanten:

k_1 für die Reaktion $G_1 + H_2O \rightarrow F_1$
k_2 für die Reaktion $F_1 \rightarrow G_1 + H_2O$
k_3 für die Reaktion $R + H_2O \rightarrow F_2$ einschliesslich $R + OH^- \rightarrow F_3$
k_4 für die Reaktion $F_2 \rightarrow R + H_2O$ einschliesslich $F_3 \rightarrow R + OH^-$

k_1 und k_3 enthalten die Aktivität des Wassers. Es gilt, dass $k_2 = k_1/K_2$ und $k_4 = k_3 \cdot K_6$ ist.

Es wird also angenommen, dass der Farbstoff in wässriger Lösung teils eine Reihe von gefärbten Formen (R, G_1 und G_2) bildet, die in momentanem Protonengleichgewicht mit einander stehen, teils eine Reihe von farblosen Formen (F_1, F_2 und F_3) bildet, die gleichfalls in momentanem Protonengleichgewicht mit einander stehen. Eine farblose Form entsteht aus der entsprechenden gefärbten durch Aufnahme von Wasser, ein reversibler Prozess, der meistens eine Zeitreaktion ist. Durch Auflösen des Farbstoffes (G_1) in wasserfreiem Aceton erhält man eine Stammlösung, die keine der F—Formen enthält. Beim Mischen einer solchen Stammlösung mit einem Puffer wird eine Lösung erhalten, deren Farbe wegen der fortlaufenden Hydratation aufhellt. Nachdem Gleichgewicht eingetreten ist, wird im allgemeinen ein konstanter Endwert,

* Ausgezogene Pfeile bezeichnen Momentanreaktionen, gestrichelte Pfeile Zeitreaktionen.

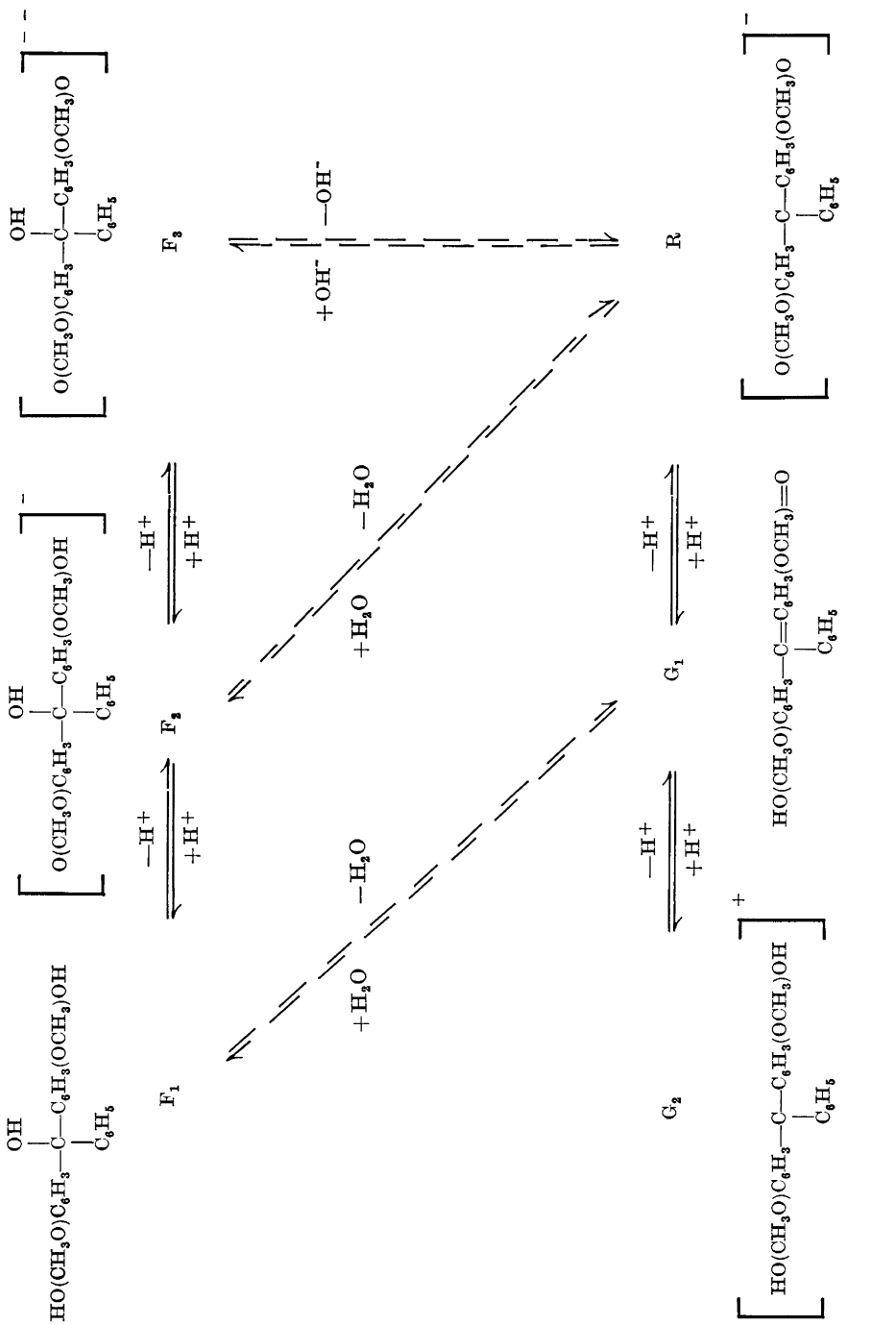

E_∞, der Lichtextinktion der Lösung erhalten. Aus zusammengehörigen Werten von E_∞ und $[H^+]$ können in geeignet gewählten pH-Intervallen die Konstanten K_2, K_3, K_4 und K_6, und in sauren Lösungen, wo sich das Gleichgewicht fast momentan einstellt, K_7 ermittelt werden. Dadurch dass der Verlauf der Aufhellung spektrophotometrisch verfolgt wird, werden die Geschwindigkeitskonstanten und (durch Extrapolation auf die Zeit $t = 0$) die Lichtextinktion, E_0, im Moment des Mischens bestimmt. Aus zusammengehörigen Werten von E_0 und $[H^+]$ wird K_1 bestimmt. Die Formeln für die Berechnung der verschiedenen Konstanten sind in den früheren Aufsätzen [1,2] abgeleitet worden und werden im Folgenden durch die Bezugszahlen in diesen Arbeiten gekennzeichnet. "Formel (10; III.)" bezieht sich folglich auf die Formel mit der Nummer (10) im Aufsatz "Benzaurinstudien III." [2].

Dimethoxy-benzaurin unterscheidet sich von den früher untersuchten Farbstoffen [1,2] vor allem dadurch, dass die Hydratations- (Aufhellungs-) Geschwindigkeit im ganzen in Frage kommenden pH-Gebiet wesentlich geringer ist. Die Wartezeit vor der Messung von E_∞ wird also länger und die störende Einwirkung evtl. irreversibler Verläufe stärker hervortretend. Die Reproduzierbarkeit bei Messung von E_∞ war aus dem Grunde weniger gut als bei den früheren Untersuchungen und die erhaltenen Werte der Konstanten demzufolge mit grösserer Unsicherheit behaftet.

MESSUNGEN UND ERGEBNISSE

Allgemeines. Apparatur und Methoden bei den Messungen waren die gleichen wie bei den früheren Untersuchungen [1,2]. Für die Messungen der Lichtextinktion wurde folglich ein Beckman-Quarz-Spektrophotometer, Modell DU, benutzt. Die Messungen von $[H^+]$ wurden mit Chinhydronelektroden für $pH \leq 8{,}2$ und mit Platin-Wasserstoffgaselektroden für $pH > 8{,}2$ ausgeführt. Als Vergleichs-Lösung wurde eine HCl-NaCl-Lösung mit bekannter $[H^+]$ verwendet.

Bei der Bereitung der Messlösungen wurden zu 49,0 ml Puffer 1,050 ml Stammlösung des Farbstoffes in Aceton mit einer Injektionsspritze hinzugefügt. Die Stammlösungen waren in Bezug auf den Farbstoff $1{,}8 \times 10^{-4}$ M. Um ihre Empfindlichkeit gegen Spuren von Wasser (Hydratation) zu verringern wurden sie mit Triäthylamin [3] zu einer ungefähren Konzentration von 5×10^{-3} M versetzt. Die Ionenstärke der Puffer war so bemessen, dass die Ionenstärke der Endlösungen 0,50 * betrug. Als Zusatzsalz wurde NaCl verwendet.

Die bestimmten Konstanten beziehen sich also auf ein Lösungsmittel von der Zusammensetzung 98 % Wasser + 2 % Aceton; Ionenstärke 0,50 M.

Die Temperatur im Küvetten-Haus des Beckman-Apparates betrug 20°C. Die Puffer und die Endlösungen für die Bestimmung von E_∞ wurden im Thermostaten bei 20°C aufbewahrt. Beim Mischen von 1 ml Aceton mit 49 ml Wasser (Puffer) steigt die Temperatur um etwa 0,5°. Folglich werden die Geschwindigkeitskonstanten zu Mittelwerten im Temperaturintervall 20,0° – 20,5°. Die für die Bestimmung von K_1 berechneten E_0-Werte beziehen sich auf die Temperatur 20,5°. Dasselbe gilt von den früheren Untersuchungen [1,2].

Die Geschwindigkeitskonstanten sind mit Brigg'schen Logarithmen berechnet worden; enthalten daher die Grösse $^{10}\log e$.

---

* Bei der Bestimmung von K_7 musste eine primäre Mess-serie bei der Ionenstärke 1,00 M ausgeführt werden.

Das verwendete Präparat des Farbstoffes war das in einer früheren Arbeit beschriebene Anhydrid [3]. Der Farbstoff wurde in den Gebieten $5{,}5 < \mathrm{pH} < 12{,}0$ und $0 \leq \mathrm{pH} < 1{,}1$ untersucht.

In sämtlichen untenstehenden Messungen war, bis auf einige nicht aufgeführte Kontrollmessungen, die Gesamtkonzentration C des Farbstoffes in der Messlösung $3{,}8 \times 10^{-6}$ M. Die eingeführten Bezeichnungen haben dieselbe Bedeutung wie früher [1,2]. Folglich stellt E_R (E_{G_1}, E_{G_2}) die Extinktion bei der jeweiligen Schichtdicke für eine Lösung dar, in der [R] ([G_1], [G_2]) gleich C ist.

Als *Puffersubstanzen* wurden Dinatriumhydrogenphosphat-Natriumhydroxyd, Borsäure-Natriumhydroxyd und Natriumdihydrogenphosphat-Dinatriumhydrogenphosphat in folgenden ungefähren pH-Intervallen verwendet: 9,8—11,6; 7,8—9,5; 5,5—7,8. Im Gebiet $0 \leq \mathrm{pH} < 1{,}1$ wurde [H^+] durch Zusatz von bestimmten Mengen HCl definiert. Im Gebiet $\mathrm{pH} > 11{,}6$ wurde [OH^-] durch Zusatz von bestimmten Mengen NaOH definiert. $K_w = [H^+] \cdot [OH^-]$ ist früher [1] zu $1{,}22 \times 10^{-14}$ bestimmt worden.

Die Lichtabsorptionskurven für die gefärbten Formen R, G_1 und G_2 finden sich in Fig. 1 wieder, die den molekularen Lichtextinktionskoeffizienten ε als Funktion der Wellenlänge λ in mμ zeigt.

Die Aufnahme der R-Kurve wurde in einer Lösung mit pH = 9,47 vorgenommen. Aus den gemessenen Extinktionen (E) wurde ε_R unter Berücksichtigung der Konzentrationen der übrigen Formen berechnet.

Die G_1-Kurve wurde in Lösungen mit pH = 5,59 aufgenommen. Da die Gleichgewichtsextinktionen (E_∞) klein sind, wurde E_0 durch Extrapolation ermittelt. Aus E_0 wurde auf dieselbe Weise wie früher [1,2] ε_{G_1} berechnet.

Die G_2-Kurve wurde in einer Lösung mit $[H^+] = 1{,}00$ M (Ionenstärke = 1,00 M) aufgenommen. Aus den erhaltenen E-Werten wurde ε_{G_2} in der früher beschriebenen Weise [2] mit $E_{G_2}/E = 4{,}2(1)$ berechnet.

Sämtliche Kurve wurden bei der Schichtdicke $d = 5$ cm aufgenommen.

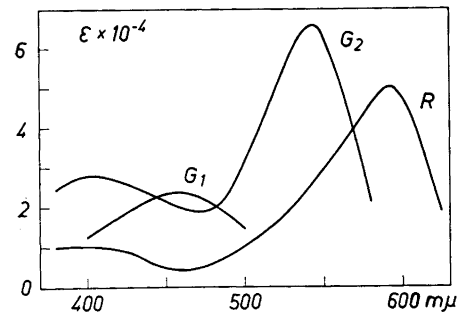

Fig. 1. Lichtabsorptionskurven. R ist das blaue Ion $[(O\ CH_3O\ C_6H_3)_2\ C(C_6H_5)]^+$; G_1 das gelbe Molekül $(HO\ CH_3O\ C_6H_3)C(C_6H_5)(C_6H_3\ CH_3O\ O)$ und G_2 das rote Ion $[(HO\ CH_3O\ C_6H_3)_2\ C(C_6H_5)]^+$.

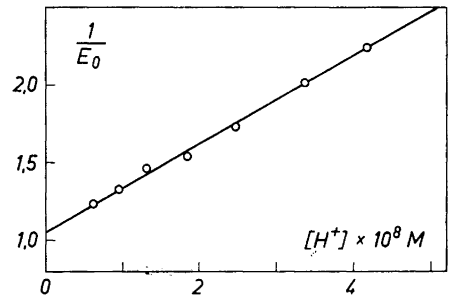

Fig. 2. $1/E_0$ als Funktion von $[H^+]$ für die Bestimmung von K_1 (und E_R). $\lambda = 592$ mμ und $d = 5$ cm.

Die Daten für die Maxima betrugen:

$(\varepsilon_R)_{max} = 5{,}0 \times 10^4$ bei $\lambda \approx 592$ mμ
$(\varepsilon_K)_{max} = 1{,}0 \times 10^4$ bei $\lambda \approx 400$ mμ
$(\varepsilon_{G_1})_{max} = 2{,}4 \times 10^4$ bei $\lambda \approx 458$ mμ
$(\varepsilon_{G_2})_{max} = 6{,}6 \times 10^4$ bei $\lambda \approx 544$ mμ
$(\varepsilon_{G_3})_{max} = 2{,}8 \times 10^4$ bei $\lambda \approx 404$ mμ

Bestimmung von K_1 im Intervall $7{,}3 < \text{pH} < 8{,}3$. Die Aufhellung der Messlösungen wurde extinktiometrisch bei $\lambda = 592$ mμ (Absorptionsmaximum von R) und mit $d = 5$ cm verfolgt. Durch Extrapolation auf die Zeit $t = 0$, wo nur die Formen R und G_1 vorliegen, wurde E_0 erhalten. In Fig. 2 ist $1/E_0$ als Funktion von $[H^+]$ aufgetragen. Man erhält eine Gerade laut Formel:

$$\frac{1}{E_0} = \frac{1}{E_R} + \frac{K_1 \cdot [H^+]}{E_R} \qquad (1;\ \text{II.})^1$$

Graphische Bestimmung ergab als Resultat:
$E_R = 0{,}95(5)$; $K_1 = 2{,}7(1) \times 10^7$; $1/K_1 = 3{,}7 \times 10^{-8}$.

Bestimmung von K_3K_6 *und* K_6 im Intervall $8{,}4 < \text{pH} < 9{,}4$. E_∞ wurde bei $\lambda = 592$ mμ mit $d = 5$ cm gemessen. Entsprechendes E_R wurde durch Extrapolation auf die Zeit $t = 0$ für fünf Lösungen im selben pH-Gebiet bestimmt. Aus den E_0-Werten wurde, nach Korrektion für $[G_1]$, $E_R = 0{,}949 \pm 0{,}004$ erhalten; der Wert stimmt gut überein mit dem oben erhaltenen bei der Bestimmung von K_1. Es gilt die folgende Formel:

$$\frac{1}{E_\infty} = \frac{1 + 1/K_6}{E_R} + \frac{1}{E_R \cdot K_3K_6} \cdot [H^+] \qquad (3;\ \text{II.})^1$$

Die gemessen E_∞-Werte wurden, wie früher beschrieben [1], korrigiert und zwar mit Rücksicht auf die geringen Konzentrationen von G_1 und F_3, die

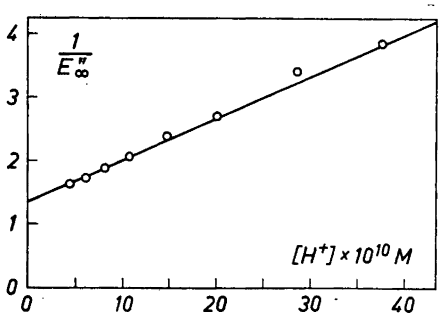

Fig. 3. $1/E''_\infty$ als Funktion von $[H^+]$ für die Bestimmung von K_3K_6 und K_6. $\lambda = 592$ mμ und $d = 5$ cm.

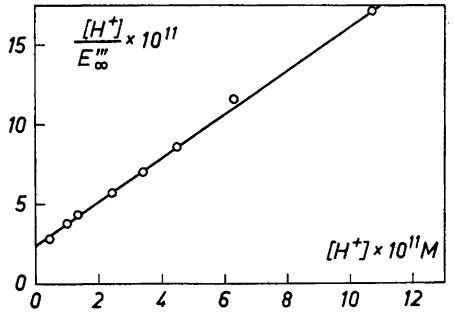

Fig. 4. $[H^+]/E'''_\infty$ als Funktion von $[H^+]$ für die Bestimmung von K_5 und K_6. $\lambda = 592$ mμ und $d = 5$ cm.

nicht ganz vernachlässigt werden können *. (Die Formel oben setzt voraus, dass $[G_1]$ und $[F_3]$ Null sind.) Aus den korrigierten Werten, E''_∞, ist in Fig. 3 $1/E''_\infty$ als Funktion von $[H^+]$ aufgetragen. Man erhält, nach Formel (3; II.) oben, eine Gerade. Die graphische Bestimmung ergab das Resultat:

$$K_6 = 3{,}6 \qquad K_3K_6 = 1{,}60 \times 10^{-9}$$

Bestimmung von $K_5 = K_6/K_4$ *und* K_6 im Intervall $9{,}8 < \mathrm{pH} < 11{,}4$. E_∞ wurde bei $\lambda = 592$ mμ mit $d = 5$ cm gemessen. Da die Stammlösung nicht dieselbe wie oben war, wurde die Bestimmung von E_R durch Extrapolation wiederholt. Aus sieben Versuchen im Intervall $9{,}8 < \mathrm{pH} < 10{,}9$ wurde $E_R = 0{,}983 \pm 0{,}003$ erhalten. Es gilt die folgende Formel:

$$\frac{[H^+]}{E_\infty} = \frac{1}{E_R \cdot K_5} + \frac{1 + 1/K_6}{E_R} \cdot [H^+] \qquad (4;\ \mathrm{II.})^1$$

Da die Formel voraussetzt, dass $[F_1]$ (und $[G_1]$) Null sind, wurden die gemessenen E_∞-Werte mit Rücksicht auf die kleine Menge F_1*, die nicht ganz zu vernachlässigen ist, korrigiert [1]. Aus den korrigierten Werten, E'''_∞, ist in Fig. 4 $[H^+]/E'''_\infty$ als Funktion von $[H^+]$ aufgetragen. Man erhält eine Gerade gemäss der Formel (4; II.). Durch graphische Bestimmung wurde das Resultat

$$K_6 = 2{,}9; \qquad K_5 = K_6/K_4 = 4{,}2(4) \times 10^{10}$$

erhalten.

Aus obenstehendem Ergebnis wurde

$$K_6 = 3{,}2(5); \qquad K_3 = 4{,}(93) \times 10^{-10}; \qquad K_4 = 7{,}(7) \times 10^{-11}$$

erhalten.

Bestimmung von $(E_\infty)max$. Im Gebiet $9{,}1 \leq \mathrm{pH} \leq 10{,}2$ kann E_∞ (nach Korrektion für $[G_1]$, falls dieses nicht vernachlässigt werden kann) als Funktion von $[H^+]$ mit der Formel

$$E_\infty = E_R \frac{K_6}{1 + K_6 + [H^+]/K_3 + K_4/[H^+]} \qquad (2;\ \mathrm{II.})^1$$

wiedergegeben werden.

Dann gilt ferner, dass

$$\frac{(E_\infty)_{max}}{E_R} = \frac{K_6}{1 + K_6 + 2 \cdot \sqrt{K_4/K_3}} \qquad (5;\ \mathrm{II.})^1$$

ist.

* Die Korrektionen betragen höchst 3—4 % von E_∞.

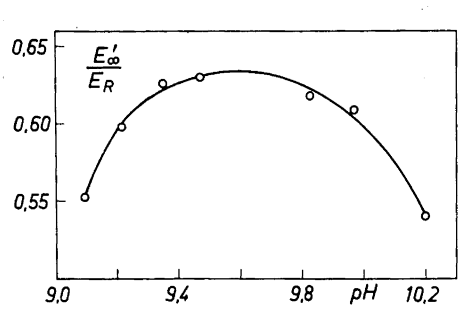

Fig. 5. E'_∞/E_R als Funktion von pH für die graphische Bestimmung von $(E_\infty/E_R)_{max}$. $\lambda = 592$ mμ und $d = 5$ cm. $(E'_\infty/E_R)_{max} = 0{,}63$.

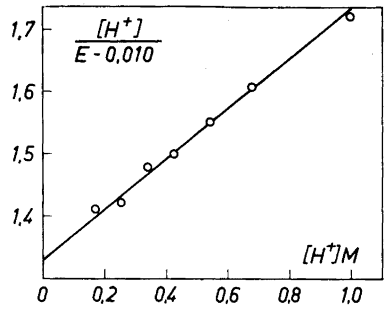

Fig. 6. $[H^+]/\left(E - \frac{E_{G_1}}{1+K_2}\right)$ als Funktion von $[H^+]$ für die Bestimmung von E_{G_1}. $\lambda = 542$ mμ und $d = 10$ cm.

E_∞ wurde wie oben bei $\lambda = 592$ mμ mit $d = 5$ cm gemessen. In Fig. 5 ist E'_∞/E_R* als Funktion von pH aufgetragen worden. Durch graphische Bestimmung wurde $(E'_\infty/E_R)_{max} = 0{,}63$ bei pH = 9,62 erhalten; die Berechnung des zweiten Gliedes in der Formel (5; II.) mit den oben erhaltenen Werten von K_3, K_4 und K_6 eingesetzt, ergab in guter übereinstimmung damit $(E_\infty)_{max}/E_R = 0{,}65$

Bestimmung von K_2 erfolgte im Intervall $7{,}8 < \text{pH} < 8{,}5$. E_∞ wurde bei $\lambda = 592$ mμ mit $d = 5$ cm gemessen. K_2 wurde aus

$$K_2 = \frac{E_R - E_\infty(1 + K_1[H^+] + 1/K_6)}{E_\infty \cdot K_1\,[H^+]} \qquad (6,\ \text{II.})^{1}$$

unter Einsetzen der oben bestimmten Werte von K_1 und K_6 berechnet. E_R war für die verwendete Stammlösung zu 0,949 bestimmt worden (siehe "Bestimmung von K_3K_6 und K_6" oben).

Folgende Resultate wurden erhalten:

$[H^+] \times 10^9$ M	13,1(2)	9,4(9)	6,18	3,77
E_∞	0,102(5)	0,137	0,196	0,253
K_2	21,4	20,9	20,1	23,0

Mittelwert: $K_2 = 21{,}(3)$.

Mit den oben erhaltenen Werten wird das Produkt $K_1 \cdot K_2 \cdot K_3 \cdot K_6 = 0{,}92$.

Bestimmung von K_7 erfolgte gemäss der früher beschriebenen Methodik [2] durch Messungen der Extinktion, E, im Intervall $0 \leq \text{pH} < 1{,}1$ **. E wurde

* E'_∞ = korrigiertes E.

** Das Gleichgewicht stellt sich hier zwischen den Formen F_1, G_1 und G_2 momentan ein.

bei $\lambda = 542$ mμ (Absorptionsmaximum von G_2) mit $d = 10$ cm gemessen. Zur Bestimmung von E_{G_2} wurde zuerst eine Mess-serie bei der Ionenstärke 1,00 M ausgeführt. $[H^+]$ variierte zwischen 0,17 und 1,00 M. Es gilt *, dass

$$\frac{[H^+]}{E - \frac{E_{G_1}}{1+K_2}} = \frac{K_7(1 + K_2)}{E_{G_2} - \frac{E_{G_1}}{1 + K_2}} + \frac{[H^+]}{E_{G_2} - \frac{E_{G_1}}{1 + K_2}} \quad (7;\ \text{III.})^2$$

ist.

In Fig. 6 ist $[H^+]/\left(E - \frac{E_{G_1}}{1 + K_2}\right)$ als Funktion von $[H^+]$ aufgetragen worden. Gemäss Formel (7; III.) erhält man eine Gerade. Durch graphische Bestimmung wurde das Resultat

$$E_{G_2} = 2{,}4(8); \qquad (K_7(1 + K_2) = 3{,}29)$$

erhalten.

Danach wurde eine Mess-serie bei der Ionenstärke 0,50 M (mit selbem λ und d wie oben) ausgeführt. $[H^+]$ variierte zwischen 0,085 und 0,49 M. Es gilt die folgende Formel **

$$\frac{E - \frac{E_{G_1}}{1 + K_2}}{E_{G_2} - E} = \frac{[H^+]}{K_7(1 + K_2)} \quad (8;\ \text{III.})^2$$

In Fig. 7 ist $\left(E - \frac{E_{G_1}}{1 + K_2}\right)/(E_{G_2} - E)$ als Funktion von $[H^+]$ aufgetragen. Man erhält nach Formel (8; III.) eine Gerade. Durch graphische Bestimmung wurde

$$K_7(1 + K_2) = 4{,}4(1) \text{ erhalten.}$$

Das Einsetzen von $K_2 = 21{,}3$ ergibt $K_7 = 0{,}19(8)$

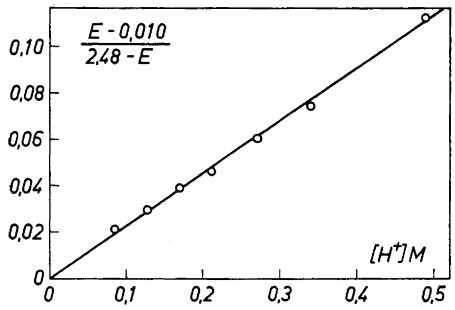

Fig. 7. $\left(E - \frac{E_{G_1}}{1 + K_2}\right)/(E_{G_2} - E)$ als Funktion von $[H^+]$ für die Bestimmung von K_7. $\lambda = 542$ mμ und $d = 10$ cm.

* $\frac{E_{G_1}}{1 + K_2}$ wird durch Messung der Extinktion in einem Puffer mit pH = 3,87 bestimmt.

** Es ist nicht vorteilhaft Formel (7;III.) hier zu verwenden, weil $[H^+]$ im Vergleich zum Produkt $K_7(1 + K_2)$ klein ist. In Formel (8; III.) wird das oben erhaltene E_{G_2} eingestezt.

Messung der Reaktions(Aufhellungs)-Geschwindigkeiten.

Die Geschwindigkeitskonstante k für den Aufhellungsverlauf wird aus den experimentellen Daten mit Hilfe der Formel

$$k = \frac{1}{t} \cdot \ln \frac{E_0 - E_\infty}{E - E_\infty} \qquad (7;\ \text{II.})^1$$

berechnet.
k wird aus den einzelnen Geschwindigkeitskonstanten nach Formel

$$k = \frac{k_2[H^+]^2 + k_4K_3[H^+]}{[H^+]^2 + K_3\,[H^+] + K_3\,K_4} + \frac{k_1K_1[H^+] + k_3}{1 + K_1\,[H^+]} \qquad (8;\ \text{II.})^1$$

zusammengesetzt.

k ist im Intervall $5{,}5 < \text{pH} < 12{,}0$ experimentell bestimmt worden. Die Extinktionsmessungen wurden durchgehend bei 5 cm Schichtdicke ausgeführt; für $7{,}3 < \text{pH} < 12{,}0$ bei $\lambda = 592$ mμ (Absorptionsmaximum für R) und für $5{,}5 < \text{pH} < 6{,}6$ bei $\lambda = 450$ mμ (ungefähres Absorptionsmaximum von G_1). Die Figuren 8 und 9 zeigen die kinetischen Verläufe in den sauren und alkalischen Lösungen, bei denen die Messungen der Berechnung von k_1 und k_2, bzw. k_3 und k_4 zu Grunde liegen. Fig. 10 zeigt k als Funktion vom pH-Wert, (vgl. Formel (8; II.) oben).

Bestimmung von k_1 und k_2. Im Gebiet $5{,}5 < \text{pH} \leq 6{,}5$, in dem die Reaktion $G_1 + H_2O \rightleftharpoons F_1$ dominiert und man die Reaktion $R + H_2O \rightleftharpoons F_2$ nicht zu berücksichtigen braucht, geht Formel (8; II.) in

$$k = k_1 \cdot \frac{K_1\,[H^+]}{1 + K_1\,[H^+]} + k_2 \qquad (9;\ \text{II.})^1$$

über.

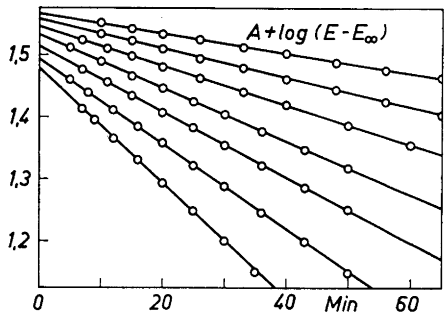

Fig. 8. Reaktionskinetik bei $\lambda = 450$ mμ und $d = 5$ cm. Für die Linien gelten in der Ordnung von oben nach unten die folgenden Daten:

A	2,00	1,97	1,95	1,93	1,91	1,89	1,87
pH	6,541	6,292	6,124	5,975	5,854	5,731	5,589

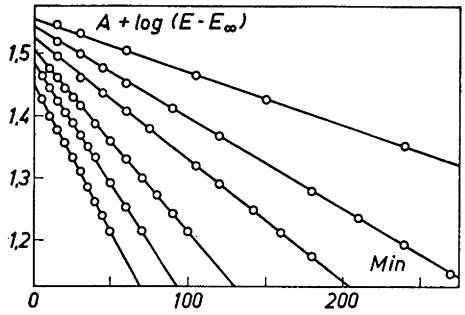

Fig. 9. Reaktionskinetik bei $\lambda = 592$ mμ und $d = 5$ cm. Für die Linien gelten in der Ordnung von oben nach unten die folgenden Daten:

A	1,70	1,63	1,59	1,57	1,54	1,50
pH	11,00(5)	11,33(5)	11,53]	11,69(5)	11,82	11,91(5)

Durch Einsetzen von zusammengehörigen experimentell bestimmten Werten von k und $[H^+]$ und der Beziehung $k_2 = k_1/K_2$ in (9; II.) wurde k_1 bei verschiedenen $[H^+]$-Werten berechnet. Wie bei den früher untersuchten Farbstoffen [1,2] zeigte es sich, dass k_1 eine lineare Funktion von $[H^+]$ ist, gemäss der Formel

$$k_1 = k_1^\circ + k_1' \, [H^+] \qquad (10; \text{ II.})^1$$

in der k_1^0 von Null verschieden ist. In Fig. 11 * ist k_1 als Funktion von $[H^+]$ aufgetragen worden. Durch graphische Bestimmung wurde $k_1^0 = 0{,}8(2) \times 10^{-3}$ und $k_1' = 3{,}1 \times 10^3$ ermittelt. Man erhält also

$$k_1 = 0{,}8(2) \times 10^{-3} + 3{,}1 \times 10^3 \, [H^+];$$
$$k_2 = 0{,}39 \times 10^{-4} + 1{,}4(7) \times 10^2 \, [H^+]; \; (\text{Min}^{-1}); \; [H^+] \text{ in Mol/l.}$$

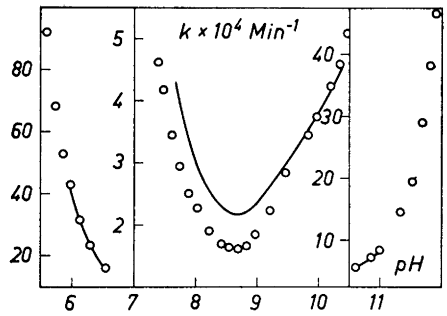

Fig. 10. Die Geschwindigkeitskonstante k als Funktion von pH. Die experimentellen Werte sind mit Kreisen ausgezeichnet. Die ausgezogene Kurve ist aus Formel (8; II.) berechnet.

* Die gestrichelte Abweichung wird später erläutert.

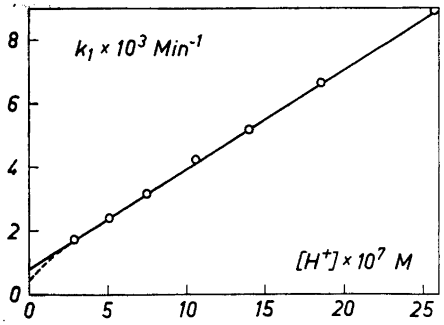

Fig. 11. Die Geschwindigkeitskonstante k_1 als Funktion von [H$^+$]. Zur Erläuterung der gestrichelten Abweichung, siehe den letzten Absatz im Text.

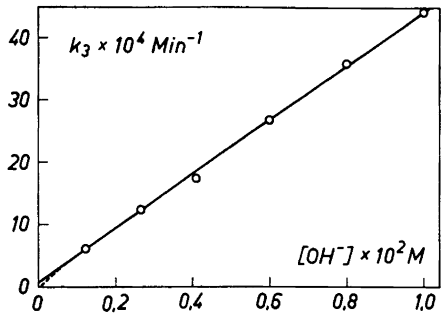

Fig. 12. Die Geschwindigkeitskonstante k_3 als Funktion von [OH$^-$]. Zur Erläuterung der gestrichelten Abweichung, siehe den letzten Absatz im Text.

Bestimmung von k_3 und k_4. Im Gebiet pH $\geq$ 11,0, wo die Reaktion $G_1 + H_2O \rightleftharpoons F_1$ vernachlässigt werden kann, geht Formel (8; II.) in

$$k = k_4 \cdot \frac{[H^+]}{[H^+] + K_4} + k_3 \qquad (12;\ II.)^1$$

über.

Durch Einsetzen von zusammengehörigen experimentellen Werten von k und [H$^+$] und der Beziehung $k_4 = k_3 \cdot K_6$ in (12; II.) wurde k_3 bei verschiedenen [H$^+$]-Werten berechnet. Man fand wie früher [1,2], dass k_3 eine lineare Funktion von [OH$^-$] nach der Formel

$$k_3 = k_3^0 + k_3' \ [OH^-] \qquad (13;\ II.)^1$$

ist, in der k_3^0 von Null verschieden ist. In Fig. 12 * ist k_3 als Funktion von [OH$^-$] aufgetragen worden. Die graphische Bestimmung ergab das Resultat:

$$k_3^0 \approx 0{,}8 \times 10^{-4}; \qquad k_3' = 0{,}43(4)$$

Weil die Linie die Ordinate nahe Origo schneidet, wird die Bestimmung von k_3^0 äusserst unsicher. Aus diesem Grunde wurde eine zusätzliche Bestimmung von k_3^0 bei niedrigerer [OH$^-$] gemacht. Durch Einsetzen von zusammengehörigen Werten von k und [H$^+$] und der Relation $k_4 = k_3 K_6$ in Formel (8; II.) wurde k_3 (mit den oben erhaltenen Werten für die übrigen in die Formel eingehenden Konstanten) für fünf Lösungen berechnet. Aus den erhaltenen k_3-Werten wurde $k_3^0 = k_3 - k_3' \ [OH^-]$ berechnet. Resultat:

[H$^+$] × 10^{10} M	0,449	0,629	1,07(2)	1,48(4)	3,37
$k \times 10^4$ Min^{-1}	4,60	4,24	3,75	3,45	2,84
$k_3^0 \times 10^4$ Min^{-1}	0,94	0,92	0,88	0,84	0,82

* Die gestrichelte Abweichung wird später erläutert.

Tabelle 1. Zusammenfassung der Ergebnisse. $[H^+]$ und $[OH^-]$ in Mol/l.

K_7	$1/K_1$	K_3	K_4	K_2	K_6
0,20	$3,7 \times 10^{-8}$	$4,(9) \times 10^{-10}$	$7,(7) \times 10^{-11}$	21	3,2

k_1 Min^{-1}	k_2 Min^{-1}
$0,8(2) \times 10^{-3} + 3,1 \times 10^{3} [H^+]$	$0,39 \times 10^{-4} + 14(7) [H^+]$

k_3 Min^{-1}	k_4 Min^{-1}
$0,8(8) \times 10^{-4} + 0,43 [OH^-]$	$2,8(7) \times 10^{-4} + 1,4(1) [OH^-]$

Mittelwert: $k_3^0 = 0,88 \times 10^{-4}$.
Man erhält also:
$k_3 = 0,8(8) \times 10^{-4} + 0,43\ [OH^-]$;
$k_4 = 2,8(7) \times 10^{-4} + 1,4(1)\ [OH^-]$; (Min^{-1}); $[OH^-]$ in Mol/l.

Wenn man mit den oben bestimmten Konstanten die Geschwindigkeitskonstante k für die Hydratation bei den verschiedenen $[H^+]$-Werten aus Formel (8; II.) berechnet, erhält man die ausgezogene Kurve in Fig. 10. Die Kurve schliesst sich selbstverständlich gut an die experimentell gefundenen Punkte in den sauren und alkalischen Randgebieten an, in denen k_1 und k_2, bzw. k_3 und k_4 aus den experimentell gefundenen Daten berechnet worden sind. Im Gebiet um das Minimum liegt dagegen eine verhältnissmässig grosse Abweichung (25—30 %) zwischen berechneten und experimentell gefundenen Werten vor. Die Ursache dieser Abweichung kann nicht mit Sicherheit festgestellt werden. Wie schon erwähnt, war die Reproduzierbarkeit bei der Messung von E_∞ weniger gut im vorliegenden Falle als in den früheren Untersuchungen [1,2]; daher wird die Unsicherheit in einigen von den berechneten Gleichgewichtskonstanten grösser als früher. Möglicherweise könnte die Abweichung links des Minimums einem zu grossen K_1-Wert entsprechen und die Abweichung rechts des Minimums einem zu hohen K_6-Wert entsprechen. Eine andere mögliche Erklärung ist auch die, dass k_1 und k_3 nicht, wie angenommen wurde, lineare Funktionen von $[H^+]$ bzw. $[OH^-]$ sind (bei *geringen* Werten derselben), sondern dass sie in der Nähe der Ordinate gemäss den gestrichelten Kurven in den Figuren 11 und 12 * abbiegen. Letzterer Hypothese wird nicht von dem Gang in den oben bestimmten Werten von k_3^0 widersprochen. Die Abbie-

* Die Grösse der Abweichungen ist in den Figuren mit Absicht übertrieben worden.

gung kann durch das Vorhandensein einer Nebenreaktion erklärt werden. Eine ähnliche, geringere Abweichung bei k_3 ist früher bei Untersuchungen von 3,3'-Dibrom-5,5'-dimethyl-benzaurin beobachtet worden [1].

Mein besonderer Dank gilt Herrn Professor Sven Bodforss, Herrn Professor Sture Fronæus und Herrn Dozent Rune Cigén, die mir durch guten Rat und wertvolle Diskussionen bei der Durchführung dieser Arbeit behilflich waren.

Die Untersuchung wurde mit finanzieller Hilfe von *Statens Naturvetenskapliga Forskningsråd* und *Kungliga Fysiografiska Sällskapet i Lund* ausgeführt.

Die Übersetzung ins Deutsche wurde von Fil.mag. Ingrid Wartenberg ausgeführt.

LITERATUR

1. Hansson, H. G. *Acta Chem. Scand.* **13** (1959) 1309 (= Benzaurinstudien II.).
2. Hansson, H. G. *Acta Chem. Scand.* **14** (1960) 407 (= Benzaurinstudien III.).
3. Hansson, H. G. und Nilsson, O. *Kgl. Fysiograf. Sällskap. Lund, Förh.* **30** (1960) No. 3 (= Benzaurinstudien IV.).

Eingegangen am 31. Mai 1960.

ACTA CHEMICA SCANDINAVICA 14 (1960) 2035–2045

New Methods for the Determination of Free Acid in the Presence of Large Amounts of Uranyl Salt

STEN AHRLAND*

Eurochemic, Mol-Donk, Belgium

Two new methods have been developed for the determination of free acid in solutions containing large amounts of uranyl salt. Both methods are based upon the weakening of the acidic properties of the uranyl ion which is brought about by its bonding to sulphate ions. By utilizing this complex formation it is in fact possible to arrive at a titration curve of two distinct steps. According to the first method, the free acid is determined by potentiometric titration to the well determinable point of inflexion between these steps. For low concentrations of acid, however, when a titration is not practical, the free acid is instead determined by direct measurement of pH, according to the second method described.

For all methods of aqueous reprocessing of irradiated uranium fuel, the concentration of free acid in the uranyl salt solutions to be treated is one of the most important process variables. Frequent and reliable determinations of this quantity are therefore wanted. On account of the acid properties of the uranyl ion, UO_2^{2+}, these cannot, however, be performed as simple alkalimetric titrations. Even if the concentration of uranyl salt, C_U, is fairly low, the hydrolysis of UO_2^{2+} will be appreciable before the free acid has been completely titrated [1]. Further, direct measurement of the pH of the process solutions by, *e.g.*, the glass electrode is not attractive as the reading will depend very much on C_U. In solutions of low acidity UO_2^{2+} will affect the pH both by acting as an acid and by influencing the activity coefficient of the hydrogen ions. The latter effect is present even in strongly acid solutions, where in any case direct pH measurements are not very suitable because of the large and variable liquid junction potentials.

With increasing C_U, the conditions for the determination of free acid grow worse at a rate much faster than would be expected from the simple rise in concentration of the hydrolyzable species UO_2^{2+}, on account of the increase in

* Present address: Department of Inorganic and Physical Chemistry, Chemical Institute, University of Lund, Lund, Sweden.

the degree of hydrolysis at a given pH which is a consequence of the formation of polynuclear aggregates in the solution [1].

In this connection it should be emphasized that the concentration of "free" acid to be determined is by definition the acidity of the solution when the uranium(VI) is present solely as the unhydrolysed ion UO_2^{2+} (or, of course, as complexes formed by this ion). If only anions of strong acids are present, (*e.g.* nitrate, chloride or perchlorate ions) this concentration of free acid, C_H, will be $= [H^+]$, the concentration of hydrogen ions. If however anions of weaker acids are also present (*e.g.* sulphate ions), C_H will be equal to the sum of $[H^+]$ and the concentrations of species of undissociated acid (*e.g.* HSO_4^-). In this latter case, the pH will, of course, depend very much upon the concentrations of the proton accepting anions. If these vary, the possibility of an accurate measurement of C_H by the pH is obviously less than in a solution containing only anions of very strong acids.

In practice, nitrate solutions are by far the most important and they will therefore be the main consideration of this work.

METHODS FOR MEASURING THE FREE ACID IN URANYL SALT SOLUTIONS

A number of methods have been used, or could be conceived, to avoid the interference of uranyl ions with the determination of free acid. However, by dividing according to the principle applied, they fall into a few classes only which are specified below, together with a discussion of their relative merits.

Measurements of pH in salt media, acid enough to prevent hydrolysis of UO_2^{2+}. As has already been stated, accurate values of C_H cannot be obtained by direct measurements of the pH of the process solutions. The position can be very much improved, however, by measuring in the presence of a high and approximately constant concentration of a neutral salt (*e.g.* sodium perchlorate or sodium nitrate). In such solutions, the liquid junction potentials are mostly suppressed and the activity conditions stay fairly constant even if C_U and C_H vary considerably, Thus the values of pH found will give true values of $[H^+]$, and this quantity equals C_H, as long as the hydrolysis of UO_2^{2+} is negligible. In order to determine the range of acidity where this condition is actually fulfilled, the measurements can be arranged as follows [2]. To a slightly acidified solution of a certain C_U, containing a high concentration of sodium salt, portions of a strongly acid solution of the same C_U and salt content are added. After each addition, the pH (*i.e.* $[H^+]$) of the resulting mixture is measured. If the uranyl salt preparation contains free acid, this value of $[H^+]$ will be higher than that calculated from the amount of strong acid deliberately added. At the beginning of the titration, however, still another rise in $[H^+]$ is likely to occur due to a partial hydrolysis of the uranyl salt. As the acidity of the mixture increases, the hydrolysis will be more and more suppressed, and finally its influence on $[H^+]$ will practically cease. As C_U is kept constant, and hence also the amount of acid coming from the original uranyl salt, the virtual suppression of the hydrolysis will be indicated by the appearance of a constant difference between the found and calculated values of $[H^+]$. The free acid contamination of the original uranyl preparation is easily calculated from this difference.

Once the acidity ensuring a complete suppression of hydrolysis is known as a function of the uranyl salt concentration, then the measurements can also be arranged in the following way. A solution is prepared which contains, as well as a high concentration of neutral salt, enough acid to prevent hydrolysis of uranyl ions even if added in considerable concentration. To this solution, another solution is added which has the same content of neutral salt and deliberately added acid, but also contains a fairly high concentration of uranyl salt. As long as the uranyl concentration of the mixture stays within a certain known limit, the increase of $[H^+]$ measured is due to the content of free acid of the original uranyl salt preparation. The increase should be proportional to C_U which gives a good check on the reliability of the measurements.

This method of determining C_H by measurement in solutions where it is simultaneously proved that no hydrolysis exists is certainly the least objectionable one from a theoretical point of view. On the other hand, the procedure cannot easily be adapted to very small samples, as several portions of uranyl solution have to be added in order to ensure a good result. The measurements also require a fair amount of care and time, as the value of pH has to be accurately determined for each point in the series of titration.

It is therefore preferable to use this as a reference method by which other methods more suited to routine work can be checked. As such it has been employed in the present investigation.

Precipitation of uranium(VI) with subsequent conventional alkalimetric titration of acid. As precipitating agents cyanoferrate(II)[3], iodate [4] and hydrogen peroxide [3] have been used. After precipitation, the solution is centrifuged and samples taken from the supernatant solution.

All precipitation methods depend on the assumption that the precipitate is strictly an uranyl compound, *i.e.* no hydrolysis of the group UO_2^{2+} must take place. Moreover, no occlusion of acid is supposed to occur within the precipitate. These conditions are, of course, serious weaknesses common to all precipitation methods. As to convenience, the centrifugation introduces an extra handling step.

Removal of uranium(VI) by means of ion exchange with subsequent conventional titration of acid. If the sample is passed through a cation exchange column, saturated with hydrogen ions, the uranyl ions will be exchanged for an equivalent amount of hydrogen ions. The pure acid solution thus obtained can then be titrated without complications, and C_H is found as the difference between the amount of acid thus found and the amount arising from the exchange which equals $2C_U$ (*cf.* Ref.[5]).

The method therefore presupposes that the C_U of each sample is accurately known. If this concentration is high relative to C_H, the latter quantity will however not be determined very precisely.

Suppression of the hydrolysis of the uranyl ion by means of complex formation, with subsequent potentiometric titration of the free acid. The formation of a metal complex in solution implies as a rule that one or more water molecules in the hydration shell of the metal ions are replaced by the complex forming ligand. The acid properties of the metal ion, which are due to the dissociation of hydrogen ions from the hydration shell, are therefore likely to decrease on complex formation, *i.e.* the hydrolysis at a given pH will generally be less

for the complex than for the simple hydrated ion. If the ligand is an anion, the decrease of ionic charge brought about by its association will further decrease the probability of hydrogen ion dissociation from the remaining water of hydration. In such cases the effect of complex formation upon the hydrolysis should thus be especially marked.

In order to be analytically useful for the determination of free acid in solutions of hydrolyzable ions, the effect brought about by the complex formation must be large enough to give a titration curve with two steps which are distinctly separated. In the case of uranyl salt solutions, this means a rather large displacement of the metal ion step. It is therefore necessary to add a ligand which binds practically all uranium(VI) into complexes which are not easily hydrolyzed. Unfortunately, most ligands forming strong complexes with the uranyl ion are also fairly basic and thus convert the strong acid of the solution into weaker acids, thereby displacing the acid steps towards a higher pH region as well. The crucial point is thus to find a ligand combining a strong affinity for UO_2^{2+} with as low a basicity as possible. Once a ligand has been found that really separates the acid step from the uranyl one, then the acid can be determined by a straightforward potentiometric titration. The simple procedure thus arrived at, demanding neither a separation of the uranium nor an exact knowledge of its concentration, makes the complex formation approach the most attractive one for removing the uranium interference. It therefore seems natural to choose this line for further development.

Up till now, oxalate [6-8] and fluoride [9] have been the most widely used complexing agents. The basicity of the oxalate ion is however unsuitably high so that the separation between the acid and uranyl steps is still rather poor. The inflexion point is therefore rather difficult to determine, and if the molar ratio C_U/C_H is high, the value of C_H tends to come out too high. This is especially the case at high uranium concentrations, as has also been shown in the present investigation. Thus if $C_U = 0.84$ M (= 200 g U/l), a significant deviation occurs if the molar ratio exceeds 3 (*cf.* tab. 1). Evidently, oxalate prevents interference from the uranyl hydrolysis only if the conditions are not very severe *. As to fluoride, the attack on glass by acid fluoride solutions will always make it impossible to perform reliable potentiometric titrations involving a glass electrode. One might resort to conductometric titration, though this method seems to work only for rather low concentrations of uranyl salt [9].

Among complexing agents which have so far not been used for the present purpose, the sulphate ion especially seems to be quite promising. Its basicity is fairly low, yet it forms rather strong complexes with the uranyl ion [10], without any tendency to precipitation at high ligand concentrations. In the last respect, the sulphate ion differs favourably from, *e.g.*, oxalate.

In the present investigation, a potentiometric titration method based upon sulphate complex formation has been worked out for the determination of free acid in the presence of even very large amounts of uranyl salt. In order to achieve as good a suppression of the hydrolysis as possible, a saturated ($\approx$ 4

* Oxalate works better at 0°C than at room temperature [8], but the cooling certainly means a complication in routine work.

M) solution of ammonium sulphate has been chosen as ionic medium, this salt being the most soluble of the readily available sulphates. In this medium, the free acid of samples containing as much as 400 g U/l can still be fairly correctly determined even at a molar concentration ratio uranyl/acid of 5 to 6, as will be described below in greater detail. This implies that acidities as low as 0.3 M can be determined in an almost saturated uranyl solution. For acidities below 0.3 M, the determined value is too low in solutions containing C_U = 400 g U/l, but correct at lower C_U. However the quantity of base required for the titration soon becomes inconveniently small for samples of the desired volume.

For samples of low acidity, a new approach, utilizing direct pH measurement in a complex forming medium, is therefore applied.

Measurement of pH in a salt medium where the hydrolysis has been extensively suppressed by means of complex formation. If the salt medium, which is in any case necessary for a successful direct measurement of pH, is chosen so that its anions form strong complexes with the uranyl ion, then it might be expected that the influence of the uranium on pH will be much less than in a non-complexing medium. Therefore, it should be possible to treat a value of pH determined in such a solution as a measure of the free acid content of the sample, even if the uranium/acid ratio is much too high for a successful direct measurement of pH in a medium where no complexes are formed. In the present investigation it has in fact been shown that fairly good values of C_H can be obtained in this way, even for solutions of rather unfavourable composition. As in the titration method just described, the sulphate ion was used as the complex forming ligand, and moreover the same medium, $\approx$ 4 M ammonium sulphate, was chosen. From the measured values of pH correct values of C_H (down to C_H = 25 mM) can be calculated directly if $C_U \lesssim$ 100 g U/l. For more concentrated uranyl solutions the method can still be used if empirical corrections are applied to the measured values of pH. At least up to C_U = 200 g U/l, the corrections are quite modest and presuppose only a very rough knowledge of C_U.

As a measured value of pH corresponds to one single value of C_H once the correction for the influence of uranium (if any) has been introduced, only one measurement is necessary in order to determine the acidity (once the glass electrode has been duly calibrated, as described below). No elaborate titrations with accurate determinations of several pH values are needed, contrary to what is the case if C_H is to be reliably determined by pH measurement in a non-complexing medium, according to the first method mentioned above. As only small samples are wanted ($\lesssim$ 0.2 ml) and a minimum of manipulation, the present method is especially well suited for highly active solutions. On the whole it is the most suitable method for all samples that contain so little acid that the otherwise more precise titration in sulphate medium is not feasible.

In the following, a detailed description will be given of the two new methods which have been developed in the present investigation. Each of them has so far been used successfully for more than 200 routine analyses.

THE TESTING OF REAGENTS FOR ACID IMPURITIES

Ideally, the salts used in the present investigation should have been free from acidic or basic impurities, but as this could not be guaranteed it was necessary to examine them and determine the exact concentration of any such impurities so that a correction could be made.

The *uranyl nitrate* (Hoboken "nucléairment pure") was tested by pH measurements in an approximately constant ionic medium, according to the first method given above. The second variant of the method was applied, *i.e.* the concentration of uranyl salt in the solution was increased at approximately constant concentration of acid. Titrations were performed at four acidities, ranging from 10 mM to 110 mM. The ionic strength of the medium was 2 M, sodium nitrate being used as the supplementary neutral salt. The temperature was kept constant at 25°C. As was also the case for all other measurements reported in this paper, the values of pH were determined by a glass electrode, in connection with the Radiometer pH Meter pHM 4. As reference, a saturated calomel electrode was used.

In fact, no free acid could be found in the uranyl nitrate preparation within the experimental error of the method applied. This means that the acid contamination, if any, is certainly < 2 % of the concentration of the uranyl ions.

Ammonium sulphate. The value of the pH of a saturated ammonium sulphate sclution of the correct stoicheiometric composition was found by potentiometric titration of a slightly acidified solution. Before titration the solution was freed from carbon dioxide by a stream of nitrogen gas.

The inflexion point, corresponding to equivalent amounts of NH_4^+ and SO_4^{2-}, was found at pH $= 5.2 \pm 0.1$. In fact, solutions having $5.0 <$ pH < 5.4 gave the same result when tried in actual titrations. If a preparation has a value of pH outside these limits, it must be adjusted by a small addition of strong base or acid. In order to arrive at a reasonably stoicheimetric composition it was necessary to dissolve the salt without heating the solution. From a solution that had been boiled, so much ammonia had been expelled that the pH afterwards was only 3.20.

No difficulties were met in the measurement of pH in this concentrated salt solution by the glass electrode in the experiments just described, nor in the later ones where uranyl salt was also present.

THE DETERMINATION OF FREE ACID IN AN URANYL SALT SOLUTION BY POTENTIOMETRIC TITRATION IN A SULPHATE MEDIUM

Trying out the most favourable complex forming medium. Preliminary experiments showed that weakly complexing agents, such as nitrate and chloride ions [11], could not create a sufficiently wide interval between the steps of strong acid and uranyl ion in the titration curve, in spite of the fact that such ions do not move the acid step at all toward higher pH. This is evident from Table 1 which gives the results of titrations of 0.2 ml samples of the composition stated, added to 15 ml of the salt media tried. Even in very concentrated salt solutions the found values of C_H are always too low.

As has already been mentioned, decidedly better results were obtained with the more strongly complex forming sulphate ion, in spite of the fact that this agent also moves the acid step towards higher pH. When a 2 M sodium sulphate medium was used, the error was considerably less than for 2 M nitrate, and still better was saturated ammonium sulphate.

Titrations in saturated ($\approx$ 4 M) ammonium sulphate medium. For this medium, an elaborate testing was carried out, using values of $C_U = 400$ and 200 g U/l. In each series, C_H was varied within wide limits. All titrations were performed as before with solutions prepared by adding 0.2 ml of the acid uranyl solution to 15 ml of the neutral salt medium. The concentration of the sodium hydroxide titrant was chosen so that 1 to 3 ml was used.

Table 1. Titrations of free acid in uranyl nitrate solution in nitrate, chloride and oxalate media.

C_U g U/l ⟶	400		200	
C_H M ⟶	1	0.3	1	0.3
Medium	% error			
2 M $NaNO_3$	−15	−30	...	...
4 M $NaNO_3$	− 7	...	−5	...
6 M $NaNO_3$	− 7	...	−4	...
4 M NaCl	−13	...	...	...
0.43 M $K_2C_2O_4$	+ 10	+ 16	−1	+ 5

Table 2. Determination of free acid in uranyl nitrate solutions by titration in saturated (= 4 M) ammonium sulphate solution.

C_U ⟶ g U/l	400			200		
C_H M	C_{Hd} M	δ %	δ_r %	C_{Hd} M	δ %	δ_r %
7.20				7.03	−2.4	2
4.80	4.60	−4.2	2			
	4.65	−3.1				
3.03	2.98	−1.7	2	3.02	−0.3	2
	2.93	−3.3				
2.02	2.04	+ 1.0	3			
	2.02	0.0				
1.00	0.98	−2.0	3	1.02	+ 2.0	3
	0.985	−1.5		0.995	−0.5	
0.500	0.485	−3.0	4			
	0.48	−4.0				
0.303	0.312	+ 3.0	5	0.308	+ 1.7	3
	0.302	−0.3				
	0.295	−2.7				
0.252	0.245	−2.8	5			
	0.245	−2.8				
	0.235	−6.8				
	0.246	−2.4				
0.202	0.195	−3.5	6	0.198	−2.0	4
	0.187	−7.4				
	0.187	−7.4				
	0.185	−8.4				
	0.185	−8.4				
	0.183	−8.9				
0.157	0.125	−17	7			
	0.153	+ 1				
	0.130	−14				

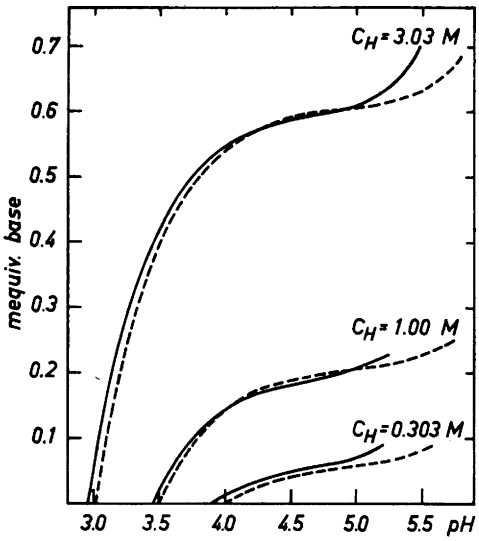

Fig. 1. Titration curves for samples of acid uranyl nitrate solutions in a large excess of saturated ammonium sulphate solution. Samples of 0.2 ml, with the concentrations of nitric acid indicated in the figure, have been added to 15 ml of the ammonium sulphate solution. Fulldrawn and dashed curves refer to samples containing 400 and 200 g U/l, respectively.

In Table 2, the concentrations of acid found, C_{Hd}, are given together with their deviations, δ, from the actual concentrations C_H. The maximum random errors, δ_r, expected to arise under the prevailing experimental conditions are also given. These errors are mainly due to (*i*) the uncertainty in the determination of the inflexion point of the titration curve and (*ii*) the error inherent in measuring the sample aliquot of 0.2 ml. The latter error might be estimated as 1—2 % while the former one varies with C_H and C_U. Its relative amount is roughly inversely proportional to C_H, as the slope of the titration curve is practically independent of C_H, and the absolute error (expressed in equivalents of base) in the determination of the inflexion point is therefore the same for all values of C_H. The error becomes larger with increasing C_U as the uranyl step then comes closer to the strong acid step which results in a steeper slope of the curve between them. In Fig. 1, some titration curves are given in order to illustrate these points.

As is evident from Table 2, the deviations found are of the same magnitude as the estimated values of δ_r down to $C_H = 0.3$ M for the series of $C_U = 400$ g U/l, though the negative deviations seem to preponderate somewhat over the positive ones. For values of $C_H = 0.3$ M, the negative deviations become significant. For such extremes of the ratio C_U/C_H, not even the strong complex formation in a concentrated sulphate solution is sufficient to ensure a good determination of C_H.

For $C_U = 200$ gU/l, the present method works well over the whole range of C_H investigated, down to $C_H = 0.2$ M (Table 2).

For comparison, some of the test solutions were also titrated according to the oxalate method mentioned above, which uses a 0.43 M oxalate solution (80 g $K_2C_2O_4 \cdot H_2O$/l) as complex forming medium. The results (Table 1) show that large positive deviations are found for solutions which are correctly determined by the sulphate method.

THE DETERMINATION OF FREE ACID IN AN URANYL SALT SOLUTION BY pH MEASUREMENTS IN A SULPHATE MEDIUM

A prerequisite for every reasonably accurate determination of C_H from pH measurements is careful calibration of the glass electrode. Preferably, the calibrations should be arranged in such a way that the electrode need not afterwards be transferred to another solution for the main measurement. Such a transfer, with accompanying partial drying *etc.*, is apt to cause small alterations in the asymmetry potential of the electrode, which encroach upon the precision of the measurement. In the present work, the following procedure was therefore adopted. To V ml saturated ammonium sulphate solution, v_1 ml of an a M nitric acid was added and the pH value of the resulting solution measured. As soon as a stable value ($= pH_O$) had been read for this calibration mixture, v_2 ml was added of the acid uranyl solution to be tested and the new value of pH ($= pH_U$) measured. The difference $\Delta pH = pH_O - pH_U$ is a function of the concentration of free acid of the uranyl solution, C_H, and to some degree also of C_U, if the hydrolysis of the uranyl group is not completely suppressed. If it is, the value of pH found should agree with that value which is calculated in the following way.

If $[H^+]_O$ and $[H^+]_U$ are the hydrogen ion concentrations of solutions after the addition of v_1 and v_2 respectively, then

$$\Delta pH = \log[([H^+]_U/[H^+]_O) \qquad (1)$$

Table 3. Calculation of free acid in uranyl nitrate solution from values of pH measured in saturated (= 4 M) ammonium sulphate solution.

	$C_U \rightarrow$ g U/l	0		50		100		200	
C_H mM	Δ pH calc.	δ	C_{Hd} mM	δ	C_{Hd} mM	δ	C_{Hd} mM	δ	C_{Hd} mM
		$v_1 = 1$ ml		$a = 20$ mM				$v_2 = 0.2$ ml	
25	0.091	0.000	25.0	−0.019	19.7	−0.004	23.9	0.033	34.9
50	0.170	0.000	50.0	−0.007	47.6	−0.010	46.5	0.019	57.0
100	0.295	−0.003	98.6	−0.008	96.3	0.006	103	0.020	109
150	0.392	−0.003	148	−0.020	139	0.010	156	0.029	167
200	0.471	0.010	207	0.000	200	−0.010	193	0.046	233
250	0.538	−0.011	241	−0.015	238	−0.012	240	...	...
	$C_U \rightarrow$ g U/l	0		200		400			
		$v_1 = 0{,}5$ ml		$a = 100$ mM		$v_2 = 0{,}5$ ml			
50	0.162	0.008	52.5	0.040	65	0.084	82		
100	0.287	0.009	104	0.036	117	0.081	141		
150	0.384	0.011	157	0.011	157	0.070	194		
200	0.463	0.015	210	0.044	231	0.048	235		

The corresponding total concentrations of acid (= $[H^+] + [HSO^-_4]$) are called C_{HO} and C_{HU}. As $V[SO^{2-}_4] \gg v_2\ C_H$, the concentration of sulphate ions is virtually constant during the measurements which implies that $[H^+]_U/[H+]_O = C_{HU}/C_{HO}$. As $C_{HO} = v_1a/(V + v_1)$ and $C_{HU} = (v_1a+v_2C_H)/(V + v_1 + v_2)$, the following expression for pH results:

$$\Delta\,\mathrm{pH} = \log \frac{(v_1a + v_2C_H)\ (V + v_1)}{v_1a\ (V + v_1 + v_2)} \qquad (2)$$

In the present experiments, a value of $V = 15$ ml has been chosen. As to a, v_1 and v_2, two different sets of values have been used, as stated in Table 3. In this table, the results of the tests performed are given in a summarized form. For each solution, only the mean value is stated out of at least two and often up to five measurements actually carried out. The table first contains the values of ΔpH, calculated according to eqn. (2) for each value of C_H used. Then the differences δ between the (mean) values of ΔpH actually measured and those calculated are tabulated for each solution, and finally C_{Hd}, the concentrations of acid found from the *measured* values of ΔpH. Two series have been performed with solutions free from uranium. From the values of δ found in these series, as well as from the reproducibility of pH for the individual solutions, it seems realistic to reckon an error of at least $\pm$ 0.015, or rather $\pm$ 0.020 units in the determination of pH. The error seems to be about the same in the whole range of C_H measured. The corresponding relative error in C_H depends upon the relation between the amounts of acid added for calibration, v_1a, and that added with the sample, v_2C_H. With the volumes and concentrations used here, an error of 5—7 % should be expected at $C_H = 250$ mM, increasing to $\approx$ 20 % for $C_H = 25$ mM.

The values of pH actually found for the series of $C_U = 50$ and 100 g U/l do not deviate more from those calculated than can be explained by the random errors. For unknown samples of $C_U \leqq 100$ g U/l, correct values of C_H can thus be calculated according to eqn. (2), direct from the measured value of pH, as has already been stated above. For $C_U = 200$ g U/l, however, a significant deviation of + 0.03 pH units appears. For $C_U = 400$ g U/l, a rather large deviation is found, evidently decreasing for increasing acidity of the solution, which is also to be expected.

The determination of nitric acid in a solution of uranyl nitrate in tributyl phosphate — kerosene. The direct measurement of the pH can be used also for the determination of acid in the TBP-kerosene solutions of the Purex process. Because of the small volume v_2 of the organic sample added, an almost complete extraction of the acid into the sulphate solution will always take place. Once extracted, the acid can be determined exactly in the same way as described above. The small amount of organic solvent present does not seem to impair the function of the electrodes.

I am indebted to the General Director of Eurochemic, Dr Erich Pohland, and to the Director of Research, Dr Rudolf Rometsch, for permission to publish this investigation. The experimental assistance of Mr Hanns-Peter Wichmann, Chemie-Ingenieur, and Mr Emil Vervecken is gratefully acknowledged. My thanks are also due to Dr George Gamlen, Manchester, for his linguistic revision of my manuscript.

REFERENCES

1. Ahrland, S., Hietanen, S. and Sillén, L. G. *Acta Chem. Scand.* **8** (1954) 1907.
2. Ahrland, S., Larsson, R. and Rosengren, K. *Acta Chem. Scand.* **10** (1956) 705.
3. *Analytical Chemistry of the Manhattan Project, NNES VIII—1,* New York 1950, p. 214.
4. Corpel, J. *Private communication.*
5. Ahrland, S. and Larsson, R. *Acta Chem. Scand.* **8** (1954) 137.
6. Booman, G. L., Elliott, M. C., Kimball, R. B., Cartan, F. O. and Rein, J. E. *IDO*-14387 (1956).
7. Sikes, J. H. and Rein, J. E. *IDO*-14316 (Suppl. 3, 1957).
8. Ryan, J. A., Sanderson, J. R. and Winsor, D. *SCS-R*-378 (1959).
9. Shepherd, M. J. Jr. and Rein, J. E. (Edit.) *IDO*-14316 (1955).
10. Ahrland, S. *Acta Chem. Scand.* **5** (1951) 1151.
11. Ahrland, S. *Acta Chem. Scand.* **5** (1951) 1271.

Received June 9, 1960.

ACTA CHEMICA SCANDINAVICA 14 (1960) 2046–2066

Short Communications

On the Half-Life of ^{33}P

INGRID FOGELSTRÖM-FINEMAN
and TORBJÖRN WESTERMARK

Division of Physical Chemistry, Royal Institute of Technology, Stockholm 70, Sweden

^{33}P was discovered by three teams independently, *viz.* Sheline *et al.*[1], Jensen *et al.*[2] and Westermark [3], but unfortunately there exists a discrepancy in the half-life determinations on this isotope. In his first experiments [3], Westermark found a half-life of 25 ± 2 days by studying the beta activity from a mixed sample of ^{32}P and ^{33}P and correcting for the amount of ^{32}P by using absorbers of aluminium. Later measurements [4], begun with a sample containing about 70 % ^{33}P and 30 % ^{32}P, gave 25.4 ± 0.3 days. Sheline *et al.*[1] give the value 25 ± 2 days, while Jensen and Nichols [2] in their first publication on the subject give 24.8 ± 0.5 days. Further experiments [5], where the amount of ^{33}P was determined from its area in a beta-spectrum from a mixture of ^{32}P and ^{33}P, gave a half-life of 24.4 ± 0.2 days.

Russell [6] found a half-life for ^{33}P of 25 ± 1 days by calculating it from an analysis of the decay curve of a $^{32}P-^{33}P$ mixture taken with a Lauritsen electroscope.

As can be seen there is a discrepancy between the two most accurate figures, namely those given by Westermark [4] and by Nichols and Jensen [5]. As ^{33}P will probably be important in the future [7], especially for biochemists, it is of interest to determine the half-life of ^{33}P with a greater accuracy.

In this laboratory it was found that ^{33}P was formed almost free from ^{32}P upon irradiating sulphur far out at the end of the thermal column in the Norwegian D_2O-reactor [8]. It was also found that large amounts of sulphur (1–10 kg) could be irradiated between the concrete wall and the reflector and that a P activity containing about 25 % ^{33}P was thereby formed.

Preparation of the ^{33}P samples. In order to produce a sample of ^{33}P with a low ^{32}P-content, two batches of sulphur were irradiated. A 200 g sample of sulphur was irradiated in the outmost part of the JENER reactor for one month and then left to age for about two months. Another sample consisting of 1 kg was irradiated between the reflector and the concrete wall for one month and then left to age for about six months.

The radioactive phosphorus was separated from the sulphur by dissolving in CS_2 and filtering through a filter paper. About 50 % of the P activity was then found in the amorphous sulphur lying on the filter paper as shown by earlier experiments in this laboratory [3,9]. The PO_4^{3-} was extracted from the amorphous sulphur by boiling with 5 N HNO_3 and PO_4^{3-} carrier. The phosphate was then precipitated from the filtered solution as a coprecipitate with lanthanum hydroxide formed by adding lanthanum nitrate and then ammonia. The lanthanum hydroxide (after filtering and washing) was dissolved in HCl and the solution purified, after evaporation and dissolution in 0.02 N HCl, by cation exchange and then by several evaporations with H_2O_2 and a final evaporation with H_2SO_4. The residue was then taken up in a small volume of water and transferred to a lucite cup which had been painted with graphite in ethanol (a commercial mixture of "aqua-dag") and evaporated to dryness. The cup was covered with pliofilm (thickness 0.36 mg/cm^2).

Activity measurements. Beta activity measurements were performed over a period of about half a year. During all measurements, which were made with an end window GM-tube (1.4 mg/cm^2), the cup containing the sample was connected electrically to ground. The distance between the cup and the window of the tube was about 3 cm. Measurements with absorbers consisting of 10.1 mg/cm^2 Al and 55.2 mg/cm^2 Al were also made. Each measurement involved more than 15 000 counts

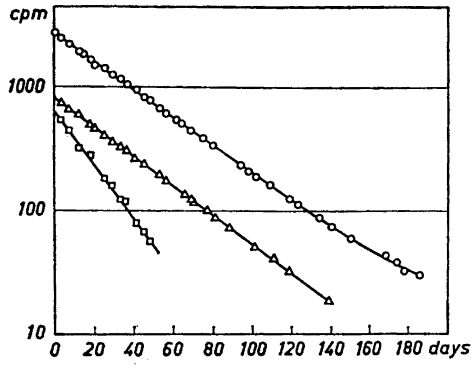

Fig. 1. Activity measurements of ^{33}P sample 2: O No aluminium absorber; △ 10.10 mg/cm² aluminium absorber; □ 55.22 mg/cm² aluminium absorber (scale raised by factor of 10).

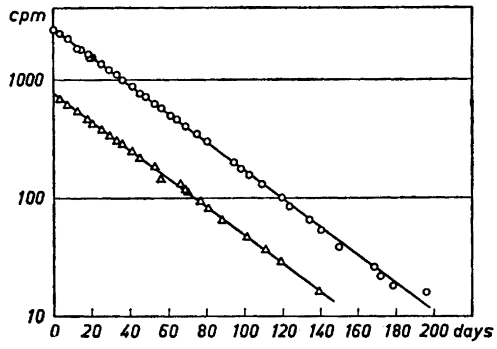

Fig. 2. Decay curves for ^{33}P sample 2: O No aluminium absorber; △ 10.10 mg/cm² aluminium absorber.

and usually more than 40 000. A non-aged ^{32}P source was measured both without any absorber and also with 10.1 mg/cm² Al and 55.2 mg/cm² Al absorbers in the same geometry as that for the ^{33}P-samples. The source was prepared from a carrier-free ^{32}P sample obtained from AERE, Harwell. This sample had been separated from sulphur shortly after the irradiation and probably contained some ^{33}P although not much. As a reference, a standard preparation of ^{60}Co was used.

Results. Fig. 1 shows the results obtained for sample 2 prepared from the 0.2 kg batch. It contained the largest fraction of ^{33}P (the rest being ^{32}P). The figures have been corrected for dead time losses and background. By means of the ^{60}Co standard which has a maximum beta energy (310 keV) not very far from that of ^{33}P (250 keV), corrections for changes in the apparatus, for instance due to changes in the GM-tube or the high voltage, and for changes in temperature and air pressure have been made. The activity measured with the absorber consisting of 55.2 mg/cm² Al should originate from ^{32}P alone since there is very little possibility of activities other than ^{32}P, ^{33}P and ^{35}S being present in the sample and since the ^{33}P and ^{35}S beta radiations have a shorter range than 55.2 mg/cm² apart from a small amount of bremsstrahlung. The measurements on the almost pure ^{32}P-sample (less than 1 % ^{33}P) with different absorbers gave a counting rate ratio $I_0/I_{55.2}$ (index refers to aluminium absorber used, index 0 means no absorber) of 1.218 and $I_{10.1}/I_{55.2}$ of 1.176. From the 55.2 mg/cm² curve for the sample and the above data, the GM response from the ^{32}P activity could be calculated and corrected for.

As can be seen in Fig. 1, the curve with no aluminium absorber for sample 2 bends off towards a longer half-life after about 150 days. It is very probable that this is

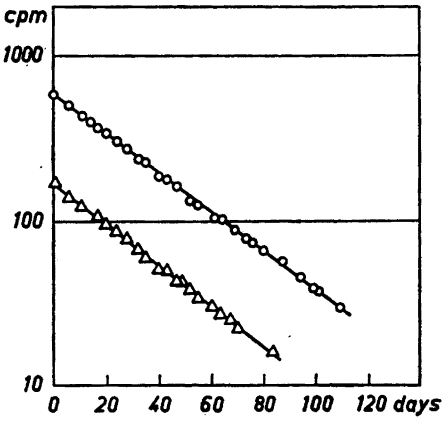

Fig. 3. Decay curves for ^{33}P sample 1: Q No aluminium absorber; △ 10.10 mg/cm² aluminium absorber.

caused by some ^{35}S being present in the sample despite the elaborate chemical procedures. The amount of ^{35}S giving rise to this longer half-life was calculated from the activity figures for the sample under the assumption that the half-life of ^{33}P is 25 days. It should be pointed out that this iterative procedure does not influence the main half-life determination because the correction for ^{35}S is rather small. From absorption curves for pure ^{35}S, corrections for ^{35}S could also be made for the 10.1 mg/cm^2 curve. The composition of the activity from the sample counted by the GM-tube with no aluminium absorber when the measurement started could thus be calculated to be: 95 % ^{33}P, 2.7 % ^{32}P and 2.2 % ^{35}S. The relative contributions of the radiation passing through the 10.1 mg/cm^2 absorber were 90 % ^{33}P, 9 % ^{32}P and 0.8 % ^{35}S.

Fig. 2 shows the ^{33}P decay curves, with no absorber and with 10.1 mg/cm^2 Al, obtained from Fig. 1 when corrections determined by means of the ^{60}Co standard and corrections for ^{32}P and ^{35}S had been made. The 10.1 mg/cm^2 curve gives, when evaluated with the least square method using the figures from 0—119 days, a half-life for ^{33}P of 25.36 $\pm$ 0.27 days with a confidence level of 95 %. The values from the decay curve with no absorber are rather scattered after about 100 days and a small error in the ^{35}S-correction might interfere with these figures. Therefore the half-life of ^{33}P has been calculated using this curve only from 0—98 days, *i.e.* about four half-lives. The value thus found was 25.34$\pm$0.22 days.

Sample 1, prepared from the 1 kg batch, produced a radiation composed of 87 % ^{33}P and 13 % ^{32}P when using no absorber and 69 % ^{33}P and 31 % ^{32}P when using a 10.1 mg/cm^2 absorber. Fig. 3 shows the decay curves obtained after correcting by means of the ^{60}Co standard and after correcting for ^{32}P. No indications of ^{35}S in the sample could be found. The values obtained for the half-life of ^{33}P were with no absorber 25.19 $\pm$ 0.23 days and with the 10.1 mg/cm^2 Al absorber 24.08 $\pm$ 0.46 days.

We feel that the results with sample 2 should be given about three times the weight of sample 2. A weighted mean would thus be 25.2 $\pm$ 0.2 days. This uncertainty includes counting statistics only. The accuracy of this half-life determination is further dependent on the uncertainty of the half-life of ^{35}S and of the ^{33}P content of the "fresh" sample. The final uncertainty is further dependent on the absorber procedure and might therefore be estimated conservatively to be half a day. Our final result is thus 25.2 $\pm$ 0.5 days.

The figure obtained is in accord with Westermark's determination [4] but is not in accord with that of Nichols and Jensen. The uncertainty is however still too high and a new determination would be desirable. Since a ^{35}S enrichment apparatus (based on ion exchange) is in operation here now, we hope to produce millicurie amounts of rather pure ^{33}P and to determine its decay properties, including the half-life, more accurately than has been possible with the rather weak samples studied hitherto.

Acknowledgements. We thank Professor Ole Lamm, Head of this institute, for promoting these studies and providing working facilities.

1. Sheline, R. K., Holtzman, R. B. and Fan, C. Y. *Bull. Am. Phys. Soc.* **26** (1951) 24; Sheline, R. K., Holtzman, R. B. and Fan, C. Y. *Phys. Rev.* **83** (1951) 919.
2. Jensen, E. N. and Nichols, R. T. *Bull. Am. Phys. Soc.* **26** (1951) 24; Jensen, E. N., Nichols, R. T., Clement, J. and Pohm, A. *Phys. Rev.* **85** (1952) 112.
3. Westermark, T. *Phys. Rev.* **88** (1952) 573.
4. Westermark, T. *Arkiv Fysik* **7** (1954) 87.
5. Nichols, R. T. and Jensen, E. N. *Phys. Rev.* **94** (1954) 369.
6. Russell, J. E. *Bull. Am. Phys. Soc.* Ser. II, **3** (1958) 61.
7. Westermark, E. G. T., Fogelström-Fineman, I. G. A. and Forberg, S. R., *Proc. 1st UNESCO Int. Conf. Paris 1957*, Pergamon Press London, Vol. 1, p. 19.
8. Fogelström-Fineman, I. and Westermark, T. *Nucleonics* **14** No. 2 (1956) 62.
9. Nilsson, G. *Acta Chem. Scand.* **10** (1956) 94.

Received October 18, 1960.

Note on the Preparation of Some 4-Amino-3,5-dimethyl- and 2-Amino-3-methyl-phenylurethanes

RICHARD DAHLBOM* and ALFONS MISIORNY

Research Laboratories, AB Astra, Södertälje, Sweden

Several amino- and methyl-substituted phenylurethanes (Types I and II) were required as starting material for certain syntheses in the field of local anesthetics.

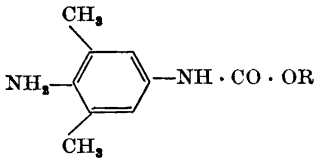

I

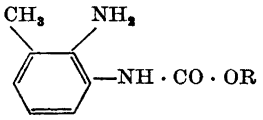

II

R = C_2H_5, *n*-C_3H_7, *n*-C_4H_9 and *n*-C_5H_{11}.

These compounds were obtained by the Curtius degradation of the appropriate nitro-substituted carboxylic acid.

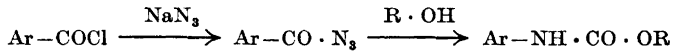

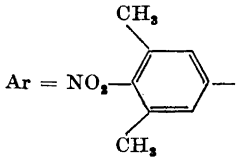

or

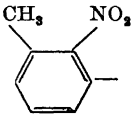

Degradation was followed by hydrogenation of the nitro group to the amino compound.

Experimental. *4-Nitro-3,5-dimethylbenzoyl chloride* was obtained from 4-nitro-3,5-dimethylbenzoic acid according to the method of Löfgren *et al.*[1]. B.p. 144–145°/9 mm, yield 86 %.

2-Nitro-3-methylbenzoyl chloride was similarly prepared by refluxing 2-nitro-3-methylbenzoic acid[2] (45 g, 0.25 mole) and thionyl chloride (89 g, 0.75 mole) for 4 h. The thionyl chloride was removed *in vacuo* and the residue (without purification) was used for further syntheses. An attempt to distill this compound *in vacuo* led to *a violent explosion.*

4-Nitro-3,5-dimethylbenzoyl azide. 4-Nitro-3,5-dimethylbenzoyl chloride (42.7 g, 0.2 mole) was dissolved in acetone (80 ml) and cooled to 10°. Sodium azide (14.3 g, 0.22 mole) in water (45 ml) was then added dropwise with stirring over a period of 15 min.; the temperature was maintained at 25° by external cooling. After one hour, water (100 ml) was added, and the reaction product which separated was collected and dried in a vacuum desiccator. Yield 40.8 g (93 %), m.p. 82–83° (decomp.). Without purification the product was used for further syntheses.

2-Nitro-3-methylbenzoyl azide was prepared as above. Yield 98 %, m.p. 86–87° (dec.).

4-Nitro-3,5-dimethyl- and *2-nitro-3-methyl-phenylurethanes.* A solution of the appropriate azide (0.05 mole) in an alcohol (50 ml) containing the desired alkyl group was heated on the water bath until nitrogen evolution had ceased (2 h). Excess of the alcohol was removed *in vacuo*, leaving an oil which in most instances quickly solidified. The resulting product, obtained in yields of 95–100 %, was practically pure. A sample was recrystallised for analysis.

The nitro compounds are listed in Table 1. The oils of the three compounds which did not

* Present address: Kungl. Farmaceutiska Institutet, Stockholm, Sweden.

Table 1. Nitro-substituted phenylurethanes, Ar-NH · CO · OR

Ar	R	M.p.°C	Recryst. solvent.[a]	Formula	Calc. %			Found %		
					C	H	N	C	H	N
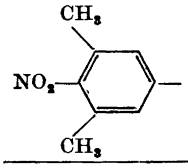	C_2H_5	77.5–78.5	L–B	$C_{11}H_{14}N_2O_4$	55.5	5.92	11.8	55.2	6.12	11.6
	n-C_3H_7	90.5–91.5	L–B	$C_{12}H_{16}N_2O_4$	57.1	6.39	11.1	57.0	6.63	10.9
	n-C_4H_9	104–105	L	$C_{13}H_{18}N_2O_4$	58.6	6.81	10.5	58.6	6.90	10.6
	n-C_5H_{11}	83–84	L–B	$C_{14}H_{20}N_2O_4$	60.0	7.19	10.0	60.1	7.10	9.90
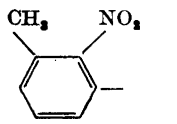	C_2H_5	86–87	L	$C_{10}H_{12}N_2O_4$	53.6	5.39	12.5	53.5	5.86	12.5
	n-C_3H_7	oil								
	n-C_3H_9	oil								
	n-C_5H_{11}	oil								

a Aq, water; B, benzene; L, ligroin; M, methanol; P, petroleum ether.

Table 2. Amino-substituted phenylurethanes, Ar-NH · CO · OR

Ar	R	M.p.°C	Recryst. solvent[a]	Formula	Calc. %			Found %		
					C	H	N	C	H	N
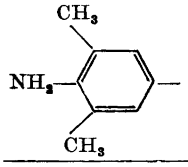	C_2H_5	97–98	M–Aq	$C_{11}H_{16}N_2O_2$	63.4	7.75	13.5	63.5	7.78	13.4
	n-C_3H_7	128–129	M–Aq	$C_{12}H_{18}N_2O_2$	64.8	8.16	12.6	64.9	8.14	12.5
	n-C_4H_9	117–118	M–Aq	$C_{13}H_{20}N_2O_2$	66.1	8.53	11.9	66.1	8.66	11.9
	n-C_5H_{11}	81–82	L–B	$C_{14}H_{22}N_2O_2$	67.2	8.86	11.2	67.7	9.10	10.9
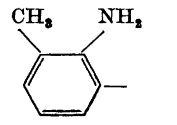	C_2H_5	75–76	L–B	$C_{10}H_{14}N_2O_2$	61.8	7.27	14.4	62.0	7.41	14.1
	n-C_3H_7	69–70	L–B	$C_{11}H_{16}N_2O_2$	63.4	7.75	13.5	63.5	7.59	13.2
	n-C_4H_9	71–72	L–B	$C_{12}H_{18}N_2O_2$	64.8	8.16	12.6	64.9	7.71	12.7
	n-C_5H_{11}	72–73	L–P	$C_{13}H_{20}N_2O_2$	66.1	8.53	11.9	66.1	8.60	11.8

a See Table 1.

crystallise were used directly in the next synthetic step.

4-Amino-3,5-dimethyl- and *2-Amino-3-methylphenylurethanes.* The appropriate nitro compund (0.05 mole) was dissolved in ethanol (50 ml). It was then hydrogenated over Raney nickel in a Parr hydrogenation apparatus for 2 h at about 55°C with a pressure of about 5 atm. The solvent was evaporated *in vacuo* and the crystalline residue (95–100 % of practically pure product) was recrystallised.

The amino compounds are listed in Table 2.

1. Löfgren, N., Tegnér, C., Willman, N. and Dahlbom, R. *Unpublished results.*
2. Tomisek, A., Graham, B., Griffith, A., Pease, C. S. and Christensen, B. E. *J. Am. Chem. Soc.* **68** (1946) 1587.

Received October 28, 1960.

Chromatographic Separation of Carotenes and Other Chloroplast Pigments on Aluminium Oxide-Containing Paper

ARNE JENSEN

Norwegian Institute of Seaweed Research, NTH, Trondheim, Norway

Whereas many of the hydroxylated carotenoids are readily separated by adsorption chromatography on kieselguhr-containing filter paper[1], the less polar carotenes showed too high mobilities to permit a good separation within the latter group of compounds. It is to be expected that a paper with a stronger adsorbent embedded in it might allow the desired separation to be carried out. On our request the filter paper manufacturers Carl Schleicher & Schüll, Dassel, West Germany, very promptly prepared a filter paper (No. 667) which contained approximately 20 % aluminium oxide. Circular chromatography on this paper using petroleum ether as solvent and following the technique previously described [1], gave satisfactory separation of a series of carotenes as seen from Table 1. It was observed that the separations of chloroplast pigments were generally better on this paper than on the kieselguhr-containing (SS No. 287) paper, the zones being narrower on the former. In addition several mixtures of carotenoids from *Viola tricolor* and from *Ranunculus acris* that exhibited similar R_F-values on the kieselguhr paper were readily separated on the aluminium oxide paper since their relative mobilities were different on this adsorbent.

As expected, the activity of the aluminium oxide-containing paper was dependent on its moisture content. The papers were generally heated at 150°C for 15 min. and then immediately used for the chromatographic separation. Activated papers which were left in the air for even short periods gradually lost their activity to a certain extent. The activation mentioned above secured reproduceable R_F-values and gave the paper an activity comparable to that of aluminium oxide, activity grade 2 of Brockmann and Schodder [2]. (R_F × 100 of azobenzene = 80 in petroleum ether containing 20 % benzene). It is recommended, however, always to add a reference compound, such as β-carotene or azobenzene, and to give the mobilities of the compounds in question relative to that of the test substance.

Table 1. R_F-values of carotenes on Schleicher & Schüll Paper No. 667. Activated at 150°C for 15 min. Solvent: Petroleum ether, boiling range 60–80°C.

Compound	R_F-value × 100	
	Petroleum ether	20 % Benzene
α-Carotene[a]	43	66
β-Carotene[b]	38	62
γ-Carotene[c]	5	15
Phytofluene[c]	77	88
ζ-Carotene[c,d]	36	60
Neurosporene[c,d]	15	25
Lycopene[b]	2	8

[a] From *Gigartina stellata* Batt.
[b] Synthetic product from Hoffman-La Roche & Co. Ltd., Switzerland.
[c] Kindly supplied by the Organic Chemistry Laboratories of The Norwegian Technical University, Trondheim.
[d] 2nd isomer [3].

1. Jensen, A. and Liaaen Jensen, S. *Acta Chem. Scand.* **13** (1959) 1863.
2. Brockmann, H. and Schodder, H. *Ber.* **74** (1941) 73.
3. Liaaen Jensen, S., Cohen-Bazire, G., Nakayama, T. O. M. and Stanier, R. Y. *Biochim. et Biophys. Acta* **29** (1958) 477.

Received October 25, 1960.

Alkaline Hydrolysis of Glycosidic Linkages

V *. The Action of Alkali on Some Methyl Furanosides

JAN JANSON and BENGT LINDBERG

Institutionen för Träkemi, Kungl. Tekn. Högskolan, Stockholm, Sweden

The aim of our studies on the alkaline hydrolysis of glycosidic linkages has been to illuminate possible reactions of the polysaccharides during the alkaline pulping

* Part IV. *Acta Chem. Scand.* **13** (1959) 138.

Table 1. Alkaline hydrolysis of some methyl glycosides in 10 % sodium hydroxide at 170°.

Sugar	Configuration	Relationship between OCH_3 and $C_{(2)}-OH$	Furanosides $10^3 \times k^a$	Pyranosides $10^3 \times k^a$
D-Glucose	α	*cis*		1.0
»	β	*trans*	>100	2.5
D-Galactose	α	*cis*	7.8	1.0
»	β	*trans*	28	5.7
D-Mannose	α	*trans*	30	2.8
»	β	*cis*		1.1
D-Xylose	α	*cis*	8.1	1.2
»	β	*trans*	>100	5.8
L-Arabinose	α	*trans*	32	10.0
»	β	*cis*		1.0

a) Rate constants are expressed in Brigg's logarithms and hours.

of wood. Previous communications have dealt with the hydrolysis of various types of pyranosidic linkages. The present investigation is concerned with the alkaline hydrolysis of several methyl furanosides which serve as model substances for the furanosidic residues found in wood hemicelluloses. The results are given in Table 1.

The rate constants for the alkaline hydrolysis of the corresponding pyranosides [1,2] are included in the table for comparison.

It can be seen that the furanosides are considerably more labile than the pyranosides. Furthermore, those furanosides containing the *trans*-configuration about C_1 and C_2 are hydrolysed at a much higher rate than the *cis*-isomers. This fact supports the mechanism which involves elimination of the aglycon group with the subsequent formation of a 1,2-anhydride. Somewhat unexpected is the very high reactivity of the β-gluco- and β-xylofuranosides compared to the other 1,2-*trans*-glycofuranosides studied. The corresponding pyranosidic glycosides of these sugars are the most stable of the hexosides and pentosides studied; this is to be expected because of their greater conformational stability compared to the other pyranosides.

In the case of all *trans*-glycofuranosides, small amounts of neutral products (other than the starting material) were detected in the reaction product. Thus, methyl-β-D-xylopyranoside and levoglucosan were isolated from the products obtained by alkaline treatment of methyl-β-D-xylofuranoside and methyl-β-D-glucofuranoside, respectively. They were formed in small quantities (about 2 %) and it is unknown whether they are reaction products or whether their presence is due to impurities in the non-crystalline starting materials. (It may be noted that small amounts of unidentified, neutral products were formed by alkaline treatments of the other *trans*-furanosides which were crystalline and highly purified).

Preliminary experiments on the alkaline hydrolysis of methyl-α- and -β-D-glucopyranosyl uronic acid have also been conducted. These substances, which were non-crystalline and incompletely characterised, are hydrolysed by alkali at even a higher rate than the furanosides.

Hamilton and co-workers [3] have recently studied the alkaline pulping of coniferous wood. These woods contain arabino-glucurono-xylans and they showed that the L-arabinofuranose residues were rather resistant, whereas the 4-*O*-methyl-D-glucopyranosyluronic acid residues were easily cleaved during the pulping operation. It is not known whether the L-arabinofuranosidic linkages in the polysaccharide have the α- or β-configuration. Only an α-arabinofuranoside was studied in the present investigation and it was found to be rather labile; the β-anomer would be expected to be more stable. The 4-*O*-methyl-D-glucopyranosyl uronic acid residue is known to be α-linked, and the corresponding model substance was found to be quite labile.

However, it should be stressed, that the reactivities of the arabinoglucuronoxylan and the model substances are not strictly comparable, for the reactivity of the furanosidic residues is undoubtedly influenced by its position in the polysaccharide molecule.

Experimental. All melting points are corrected. Distillations were carried out under reduced pressure. Paper chromatography was conducted on Whatman No. 1 filter paper using the following solvent systems:

A. Butanol-pyridine-water, 6 : 2 : 3

B. Butanone, saturated with water.

Substances. The D-xylo- and D-galacto-furanosides were prepared according to Augestad and Berner.[4] Methyl-α-D-mannofuranoside was prepared according to Haworth *et al*[6]. Methyl-α-L-arabinofuranoside was prepared as described for the corresponding D-form by Wright and Khorana[5]. It had m.p. 45–48° and $[\alpha]_D^{20}$ — 124°(water) in good agreement with reported values.

Methyl-β-D-glucofuranoside was prepared by a Fisher synthesis, following the technique devised by Augestad and Berner[4]. Glucose (60 g) was dissolved by stirring in 0.55 % methanolic hydrogen chloride; the solution was kept at room temperature overnight. The acid was removed by treatment with lead carbonate and the solution concentrated to a syrup. Paper chromatographic analysis of this syrup in solvent system B revealed the presence of four components: glucose; a mixture of α- and β-pyranosides, migrating as a single component; and the α- and β-furanosides, which were well separated. Part of the syrup (37 g) was added to the top of a cellulose column (6.4 × 130 cm) which was then eluted with solvent system B. Methyl β-D-glucofuranoside, the faster of the two anomers, was eluted between 18 000–30 000 ml. Concentration of this fraction gave methyl β-D-glucofuranoside as a chromatographically-pure syrup showing $[\alpha]_D^{20}$ −54° in water. Comparison with the reported value $[\alpha]_D$ −77°) indicated that the substance was incompletely dried.

Reaction of the glycosides with alkali was carried out as previously described[2]. In the case of the uronides, the following procedure was employed. After alkaline hydrolysis the reaction mixture was neutralised with hydrochloric acid and concentrated to dryness. The residue was dissolved in water and an aliquot concentrated and subjected to methoxyl analysis.

The authors are indebted to *Statens Tekniska Forskningsråd* for financial support.

1. Dryselius, E., Lindberg, B. and Theander, O. *Acta Chem. Scand.* **12** (1958) 340.
2. Janson, J. and Lindberg, B. *Acta Chem. Scand.* **13** (1959) 138.
3. Hamilton, J. K., Partlow, E. V. and Thompson, N. S. *Tappi* **14** (1958) 803.
4. Augestad, I. and Berner, E. *Acta Chem. Scand.* **8** (1954) 251.
5. Haworth, W. N., Hirst, E. L. and Webb, J. I. *J. Chem. Soc.* **1930**, 651.
6. Wright, R. S. and Khorana, H. G. *J. Am. Chem. Soc.* **80** (1958) 1994.

Received November 1, 1960.

Confirmation of the Structure of Ketomanoyl Oxide

C. ENZELL

Organisk-kemiska Institutionen, Kungl. Tekniska Högskolan, Stockholm, Sweden

Recent work in this laboratory has shown that hinokiol, hinokione[1] and totarolone[2] all have an oxygen function at C(3) (steroid numbering). The original assignment[3] of the keto group of ketomanoyl oxide to the 2-position has recently been questioned[4]*.

In connection with mass-spectrometric work on related substances[5] the mass-spectra of the tetra-deuterated and non-deuterated dihydroketomanoyl oxide were recorded (Figs. 1 and 2). A comparison of the two spectra shows clearly that 4 hydrogen atoms have been replaced by deuterium, since the peaks at *m/e* 307 (*M* + 1), 291 (*M*-15), and 277 (*M*-29) in the spectrum of dihydroketomanoyl oxide (Fig. 2) are found 4 mass units higher, at *m/e* 311, 295, and 281, in the spectrum of deuterated dihydroketomanoyl oxide (Fig. 1). These peaks are probably due to ions obtained from the molecule after addition of a proton (307 and 311), removal of a methyl group (291 and 295) and an ethyl group (277 and 281), respectively. The result shows that position 2, originally assigned to the oxo

* During the preparation of this manuscript a communication has appeared in which the same approach led to similar results. Grant, P.K. and Hodges, R. *Chem. & Ind. London* **1960** 1300.

Chromatographic Separation of Carotenes and Other Chloroplast Pigments on Aluminium Oxide-Containing Paper

ARNE JENSEN

Norwegian Institute of Seaweed Research, NTH, Trondheim, Norway

Whereas many of the hydroxylated carotenoids are readily separated by adsorption chromatography on kieselguhr-containing filter paper[1], the less polar carotenes showed too high mobilities to permit a good separation within the latter group of compounds. It is to be expected that a paper with a stronger adsorbent embedded in it might allow the desired separation to be carried out. On our request the filter paper manufacturers Carl Schleicher & Schüll, Dassel, West Germany, very promptly prepared a filter paper (No. 667) which contained approximately 20 % aluminium oxide. Circular chromatography on this paper using petroleum ether as solvent and following the technique previously described [1], gave satisfactory separation of a series of carotenes as seen from Table 1. It was observed that the separations of chloroplast pigments were generally better on this paper than on the kieselguhr-containing (SS No. 287) paper, the zones being narrower on the former. In addition several mixtures of carotenoids from *Viola tricolor* and from *Ranunculus acris* that exhibited similar R_F-values on the kieselguhr paper were readily separated on the aluminium oxide paper since their relative mobilities were different on this adsorbent.

As expected, the activity of the aluminium oxide-containing paper was dependent on its moisture content. The papers were generally heated at 150°C for 15 min. and then immediately used for the chromatographic separation. Activated papers which were left in the air for even short periods gradually lost their activity to a certain extent. The activation mentioned above secured reproduceable R_F-values and gave the paper an activity comparable to that of aluminium oxide, activity grade 2 of Brockmann and Schodder [2]. (R_F × 100 of azobenzene = 80 in petroleum ether containing 20 % benzene). It is recommended, however, always to add a reference compound, such as β-carotene or azobenzene, and to give the mobilities of the compounds in question relative to that of the test substance.

Table 1. R_F-values of carotenes on Schleicher & Schüll Paper No. 667. Activated at 150°C for 15 min. Solvent: Petroleum ether, boiling range 60–80°C.

Compound	R_F-value × 100	
	Petroleum ether	20 % Benzene
α-Carotene[a]	43	66
β-Carotene[b]	38	62
γ-Carotene[c]	5	15
Phytofluene[c]	77	88
ζ-Carotene[c,d]	36	60
Neurosporene[c,d]	15	25
Lycopene[b]	2	8

[a] From *Gigartina stellata* Batt.
[b] Synthetic product from Hoffman-La Roche & Co. Ltd., Switzerland.
[c] Kindly supplied by the Organic Chemistry Laboratories of The Norwegian Technical University, Trondheim.
[d] 2nd isomer [3].

1. Jensen, A. and Liaaen Jensen, S. *Acta Chem. Scand.* **13** (1959) 1863.
2. Brockmann, H. and Schodder, H. *Ber.* **74** (1941) 73.
3. Liaaen Jensen, S., Cohen-Bazire, G., Nakayama, T. O. M. and Stanier, R. Y. *Biochim. et Biophys. Acta* **29** (1958) 477.

Received October 25, 1960.

Alkaline Hydrolysis of Glycosidic Linkages

V *. The Action of Alkali on Some Methyl Furanosides

JAN JANSON and BENGT LINDBERG

Institutionen för Träkemi, Kungl. Tekn. Högskolan, Stockholm, Sweden

The aim of our studies on the alkaline hydrolysis of glycosidic linkages has been to illuminate possible reactions of the polysaccharides during the alkaline pulping

* Part IV. *Acta Chem. Scand.* **13** (1959) 138.

However, it should be stressed, that the reactivities of the arabinoglucuronoxylan and the model substances are not strictly comparable, for the reactivity of the furanosidic residues is undoubtedly influenced by its position in the polysaccharide molecule.

Experimental. All melting points are corrected. Distillations were carried out under reduced pressure. Paper chromatography was conducted on Whatman No. 1 filter paper using the following solvent systems:

A. Butanol-pyridine-water, 6 : 2 : 3

B. Butanone, saturated with water.

Substances. The D-xylo- and D-galacto-furanosides were prepared according to Augestad and Berner.[4] Methyl-α-D-mannofuranoside was prepared according to Haworth *et al*[6]. Methyl-α-L-arabinofuranoside was prepared as described for the corresponding D-form by Wright and Khorana[5]. It had m.p. 45–48° and $[\alpha]_D^{20}$ — 124°(water) in good agreement with reported values.

Methyl-β-D-glucofuranoside was prepared by a Fisher synthesis, following the technique devised by Augestad and Berner[4]. Glucose (60 g) was dissolved by stirring in 0.55 % methanolic hydrogen chloride; the solution was kept at room temperature overnight. The acid was removed by treatment with lead carbonate and the solution concentrated to a syrup. Paper chromatographic analysis of this syrup in solvent system B revealed the presence of four components: glucose; a mixture of α- and β-pyranosides, migrating as a single component; and the α- and β-furanosides, which were well separated. Part of the syrup (37 g) was added to the top of a cellulose column (6.4 × 130 cm) which was then eluted with solvent system B. Methyl β-D-glucofuranoside, the faster of the two anomers, was eluted between 18 000–30 000 ml. Concentration of this fraction gave methyl β-D-glucofuranoside as a chromatographically-pure syrup showing $[\alpha]_D^{20}$ −54° in water. Comparison with the reported value $[\alpha]_D$ −77°) indicated that the substance was incompletely dried.

Reaction of the glycosides with alkali was carried out as previously described[2]. In the case of the uronides, the following procedure was employed. After alkaline hydrolysis the reaction mixture was neutralised with hydrochloric acid and concentrated to dryness. The residue was dissolved in water and an aliquot concentrated and subjected to methoxyl analysis.

The authors are indebted to *Statens Tekniska Forskningsråd* for financial support.

1. Dryselius, E., Lindberg, B. and Theander, O. *Acta Chem. Scand.* **12** (1958) 340.
2. Janson, J. and Lindberg, B. *Acta Chem. Scand.* **13** (1959) 138.
3. Hamilton, J. K., Partlow, E. V. and Thompson, N. S. *Tappi* **14** (1958) 803.
4. Augestad, I. and Berner, E. *Acta Chem. Scand.* **8** (1954) 251.
5. Haworth, W. N., Hirst, E. L. and Webb, J. I. *J. Chem. Soc.* **1930**, 651.
6. Wright, R. S. and Khorana, H. G. *J. Am. Chem. Soc.* **80** (1958) 1994.

Received November 1, 1960.

Confirmation of the Structure of Ketomanoyl Oxide

C. ENZELL

Organisk-kemiska Institutionen, Kungl. Tekniska Högskolan, Stockholm, Sweden

Recent work in this laboratory has shown that hinokiol, hinokione[1] and totarolone[2] all have an oxygen function at C(3) (steroid numbering). The original assignment[3] of the keto group of ketomanoyl oxide to the 2-position has recently been questioned[4]*.

In connection with mass-spectrometric work on related substances[5] the mass-spectra of the tetra-deuterated and non-deuterated dihydroketomanoyl oxide were recorded (Figs. 1 and 2). A comparison of the two spectra shows clearly that 4 hydrogen atoms have been replaced by deuterium, since the peaks at *m/e* 307 (*M* + 1), 291 (*M*-15), and 277 (*M*-29) in the spectrum of dihydroketomanoyl oxide (Fig. 2) are found 4 mass units higher, at *m/e* 311, 295, and 281, in the spectrum of deuterated dihydroketomanoyl oxide (Fig. 1). These peaks are probably due to ions obtained from the molecule after addition of a proton (307 and 311), removal of a methyl group (291 and 295) and an ethyl group (277 and 281), respectively. The result shows that position 2, originally assigned to the oxo

* During the preparation of this manuscript a communication has appeared in which the same approach led to similar results. Grant, P.K. and Hodges, R. *Chem. & Ind. London* **1960** 1300.

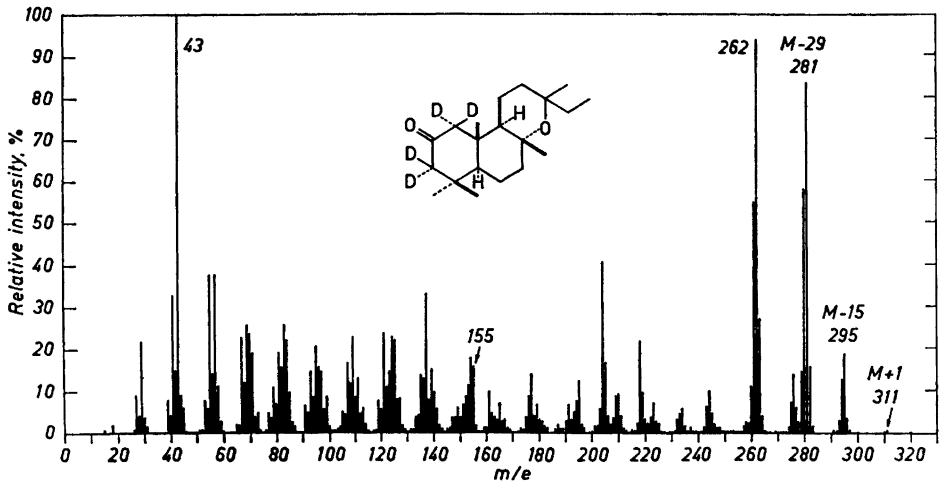

Fig. 1. Mass-spectrum of tetradeuterodihydroketomanoyl oxide.

group, is the only possible position for this group in ketomanoyl oxide.

The peak at *m/e* 151 in the spectrum of dihydroketomanoyl oxide, which occurs at *m/e* 155 in the spectrum of deuterated dihydroketomanoyl oxide, most probably is due to an ion originating from ring *A* by rupture of the C(6)—C(7) and C(9)—C(10) bonds and removal of a proton. Corresponding peaks have been observed in spectra of compounds with the same configuration as in ketomanoyl oxide at C(5), C(9), and C(10), *e.g.* torulosol, dihydrotorulosol, torulosal, manool, dihydromanool, manoyl oxide, agathadienecarbinolcarboxylic acid [5], methyl cryptopimarate and methyl pimarate [6] (dextropimarate) and are more fully discussed elsewhere [5].

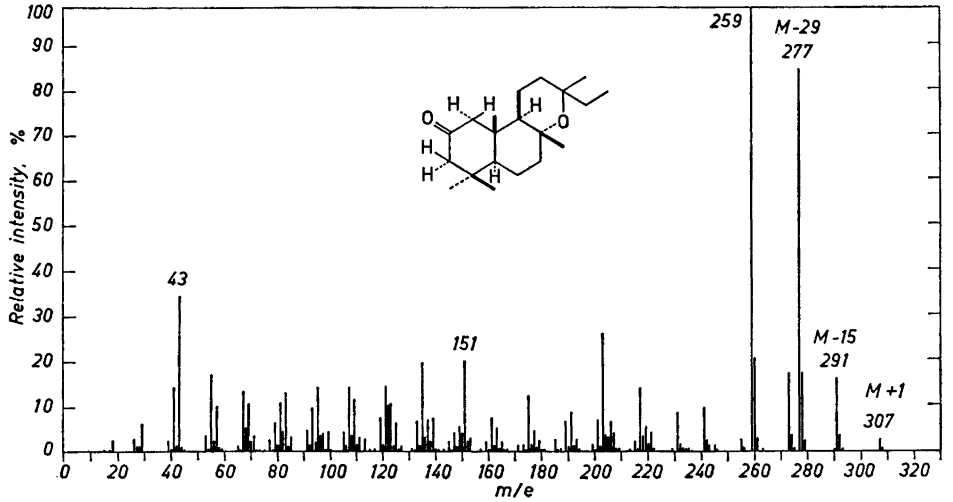

Fig. 2. Mass-spectrum of dihydroketomanoyl oxide.

Examination of the PMR-spectrum of dihydroketomanoyl oxide confirms the mass-spectrometric results. The intensity of the signal at 206 c/s (from internal benzene standard in dilute CCl_4 solution; 40 Mc/s) indicates the presence of four hydrogen atoms on the carbon atoms adjacent to the keto group.

Ketomanoyl oxide, in methanol solution, showed a comparatively [7,8] large positive Cotton effect ($[\alpha]_{600}$ + 400°; $[\alpha]_{313}$ + 3 300°; $[\alpha]_{275}$ −3 700°; $[\alpha]_{273}$ −3 600°), which, as in the case of 3-oxo terpenoid-type compounds, was not lowered on addition of hydrochloric acid [9]. The inability to form a hemiketal is probably caused by 1,3-interaction of the axial methyl substituents.

Deuterium exchange [10] was effected by boiling dihydroketomanoyl oxide [4], m.p. 91−92° (50 mg), with a solution obtained from sodium (7 mg), O-deuteromethanol (1.5 ml) and deuterium oxide (0.5 ml) under oxygen-free nitrogen for 10 min. followed by removal of the solvents. The proceedure was repeated three times with fresh solvents. Addition of deuterium oxide (3 ml) to the residue and extraction with dry ether gave, after drying, removal of the solvent and sublimation of the residue, tetradeuterodihydroketomanoyl oxide, m.p. 89 −92°.

Acknowledgements. I express my gratitude to Dr. I.R. McDonald, Wellington, for a sample of ketomanoyl oxide, to Dr. R. Ryhage, Karolinska Institutet, Stockholm, for the mass-spectrometric determinations, to Dr. W. Klyne, Post Graduate Medical School, London, for determining the RD-curves, to Dr. S. Forsén for measuring and interpreting the PMR-spectrum, to Dr. Y. L. Chow for valuable discussions, to Prof. H. Erdtman and Dr. E. Forslind for their interest. Thanks are offered to the *Swedish Technical Research Council* for financial support.

1. Chow, Y. L. and Erdtman, H. *Proc. Chem. Soc.* **1960** 174.
2. Chow, Y. L. and Erdtman, H. *Acta Chem. Scand.* **14** (1960) 1852.
3. Hoskings, J. R. and Brandt, C. W. *Ber.* **68** (1935) 286; *cf.* Simonsen, J. and Barton, D. H. R. *The Terpenes* (2nd Ed.) Vol. III, Cambridge 1951, p. 372.
4. Grant, P. K. *J. Chem. Soc.* **1959** 860.
5. Enzell, C. *Acta Chem. Scand.* **15** (1961). *In press.*
6. Bruun, H. H., Ryhage, R. and Stenhagen, E. *Acta Chem. Scand.* **12** (1958) 789.
7. Djerassi, C., Closson, W. and Lippman, A. E. *J. Am. Chem. Soc.* **78** (1956) 3163.
8. Djerassi, C., Osiecki, J. and Closson, W. *J. Am. Chem. Soc.* **81** (1959) 4587.
9. Djerassi, C., Mitscher, L. A. and Mitscher, B. J. *J. Am. Chem. Soc.* **81** (1959) 947.
10. Büchi, G., Schach v. Wittenau, M. and White, D. M. *J. Am. Chem. Soc.* **81** (1959) 1968.

Received November 4, 1960.

Inductive Effects on the Donor Strengths of Some Oxo Compounds

INGVAR LINDQVIST and BERT FJELLSTRÖM

Institute of Chemistry, University of Uppsala, Uppsala, Sweden

In a recent paper [1] it was reported that esters and ketones have almost equal donor strengths in reactions with $SbCl_5$. Passing from ketones to esters two main effects can be predicted. Thus the inductive effect would lead to a reduction of the donor strength owing to withdrawal of electrons from the carbonyl oxygen atom. This would be opposed, however, by delocalization of one of the lone pair of electrons of the ether oxygen atom. For the carbonyl oxygen atom the two effects seem to be of the same magnitude and on balance no appreciable difference is obtained. This is also reflected in the C=O bond lengths, which are almost equal in ketones and esters. On the other hand, in the presence of halogens, the inductive effect is dominant and the C=O bond lengths are shorter [2]. It has been shown moreover that halogen substitution has the same effect on the donor strengths of compounds containing S=O, Se=O and P=O bonds [1]. In this paper we report the effect of alkoxy substitution on the donor strengths of these compounds in order to determine the balance between the inductive and delocalization effects. The following esters have been studied: $(CH_3O)_2SeO$, $(CH_3O)_2SO$, $(CH_3O)(CH_3)SO_2$ and $(CH_3O)_3PO$.

Experimental. Dimethylselenite, $(CH_3O)_2SeO$, was prepared according to Michaelis and Landmann [3]. B.p. + 62−65°/11 mm.

Dimethyl sulfite, $(CH_3O)_2SO$, was prepared according to Woss [4]. B.p. + 125°.

Examination of the PMR-spectrum of dihydroketomanoyl oxide confirms the mass-spectrometric results. The intensity of the signal at 206 c/s (from internal benzene standard in dilute CCl_4 solution; 40 Mc/s) indicates the presence of four hydrogen atoms on the carbon atoms adjacent to the keto group.

Ketomanoyl oxide, in methanol solution, showed a comparatively [7,8] large positive Cotton effect ($[\alpha]_{600}$ + 400°; $[\alpha]_{313}$ + 3 300°; $[\alpha]_{275}$ −3 700°; $[\alpha]_{273}$ −3 600°), which, as in the case of 3-oxo terpenoid-type compounds, was not lowered on addition of hydrochloric acid [9]. The inability to form a hemiketal is probably caused by 1,3-interaction of the axial methyl substituents.

Deuterium exchange [10] was effected by boiling dihydroketomanoyl oxide [4], m.p. 91−92° (50 mg), with a solution obtained from sodium (7 mg), O-deuteromethanol (1.5 ml) and deuterium oxide (0.5 ml) under oxygen-free nitrogen for 10 min. followed by removal of the solvents. The proceedure was repeated three times with fresh solvents. Addition of deuterium oxide (3 ml) to the residue and extraction with dry ether gave, after drying, removal of the solvent and sublimation of the residue, tetradeuterodihydroketomanoyl oxide, m.p. 89 −92°.

Acknowledgements. I express my gratitude to Dr. I.R. McDonald, Wellington, for a sample of ketomanoyl oxide, to Dr. R. Ryhage, Karolinska Institutet, Stockholm, for the mass-spectrometric determinations, to Dr. W. Klyne, Post Graduate Medical School, London, for determining the RD-curves, to Dr. S. Forsén for measuring and interpreting the PMR-spectrum, to Dr. Y. L. Chow for valuable discussions, to Prof. H. Erdtman and Dr. E. Forslind for their interest. Thanks are offered to the *Swedish Technical Research Council* for financial support.

1. Chow, Y. L. and Erdtman, H. *Proc. Chem. Soc.* **1960** 174.
2. Chow, Y. L. and Erdtman, H. *Acta Chem. Scand.* **14** (1960) 1852.
3. Hoskings, J. R. and Brandt, C. W. *Ber.* **68** (1935) 286; *cf.* Simonsen, J. and Barton, D. H. R. *The Terpenes* (2nd Ed.) Vol. III, Cambridge 1951, p. 372.
4. Grant, P. K. *J. Chem. Soc.* **1959** 860.
5. Enzell, C. *Acta Chem. Scand.* **15** (1961). *In press.*
6. Bruun, H. H., Ryhage, R. and Stenhagen, E. *Acta Chem. Scand.* **12** (1958) 789.
7. Djerassi, C., Closson, W. and Lippman, A. E. *J. Am. Chem. Soc.* **78** (1956) 3163.
8. Djerassi, C., Osiecki, J. and Closson, W. *J. Am. Chem. Soc.* **81** (1959) 4587.
9. Djerassi, C., Mitscher, L. A. and Mitscher, B. J. *J. Am. Chem. Soc.* **81** (1959) 947.
10. Büchi, G., Schach v. Wittenau, M. and White, D. M. *J. Am. Chem. Soc.* **81** (1959) 1968.

Received November 4, 1960.

Inductive Effects on the Donor Strengths of Some Oxo Compounds

INGVAR LINDQVIST and BERT FJELLSTRÖM

Institute of Chemistry, University of Uppsala, Uppsala, Sweden

In a recent paper [1] it was reported that esters and ketones have almost equal donor strengths in reactions with $SbCl_5$. Passing from ketones to esters two main effects can be predicted. Thus the inductive effect would lead to a reduction of the donor strength owing to withdrawal of electrons from the carbonyl oxygen atom. This would be opposed, however, by delocalization of one of the lone pair of electrons of the ether oxygen atom. For the carbonyl oxygen atom the two effects seem to be of the same magnitude and on balance no appreciable difference is obtained. This is also reflected in the C=O bond lengths, which are almost equal in ketones and esters. On the other hand, in the presence of halogens, the inductive effect is dominant and the C=O bond lengths are shorter [2]. It has been shown moreover that halogen substitution has the same effect on the donor strengths of compounds containing S=O, Se=O and P=O bonds [1]. In this paper we report the effect of alkoxy substitution on the donor strengths of these compounds in order to determine the balance between the inductive and delocalization effects. The following esters have been studied: $(CH_3O)_2SeO$, $(CH_3O)_2SO$, $(CH_3O)(CH_3)SO_2$ and $(CH_3O)_3PO$.

Experimental. Dimethylselenite, $(CH_3O)_2SeO$, was prepared according to Michaelis and Landmann [3]. B.p. + 62−65°/11 mm.

Dimethyl sulfite, $(CH_3O)_2SO$, was prepared according to Woss [4]. B.p. + 125°.

Table 1. Relative donor strengths (decreasing from top to bottom). The magnitudes of the displacements between the molecules do not correspond to quantitative measurements.

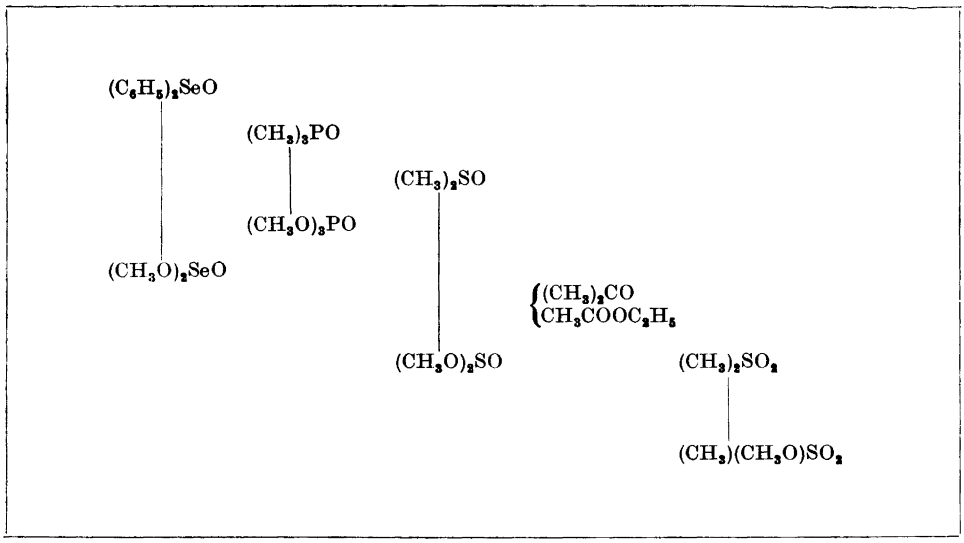

Methyl methansulfonate, $(CH_3O)(CH_3)SO_2$, was prepared according to Karbatow [5]. B.p. + 200–202°.

Trimethyl phosphate, $(CH_3O)_3PO$, was prepared according to Drushel [6]. B.p. 85–87°/12 mm.

All experiments were made in ethylene chloride solutions as described in an earlier paper [1].

Results and discussion. The relative donor strengths with $SbCl_5$ as acceptor molecule are given in Table 1. It is immediately clear that in all cases the substitution has produced quite a different result from that obtained for ketones. The inductive effect is obviously dominant. It is too early to conclude from the individual differences anything which would indicate particularly large inductive effects on the Se = O bond. Further structural and thermochemical work is needed.

In this connection, consideration of the consequence of adduct formation on the bonds in the oxo compounds shows that the inductive effect should be most pronounced. The weakening of the carbonyl bond in esters of carboxylic acids and the strengthening of the adjacent C–O bond can also be described primarily, as an inductive effect [7] further favoured by the delocalization effect. Thus by adduct formation the two effects reinforce giving a particularly large net effect in esters of carboxylic acids. However, by substitution (passing from ketone to ester) they are opposed, so that the net effect is almost negligible. In resonance language the effect of delocalization is expressed by the formulae $RO^+=C-O-Sb^-Cb^-Cl_5$ and $RO^+-C=O^-$.

A grant from the *Swedish Natural Science Research Council* is gratefully acknowledged. Finally we wish to thank Mrs. Zackrisson for valuable discussions and Professor Hägg for all facilities put at our disposal.

1. Lindqvist, I. and Zackrisson, M. *Acta Chem. Scand.* **14** (1960) 453.
2. Lindqvist, I. *Nova Acta Regiae Soc. Sci. Upsaliensis* (IV) **17** (1960) No. 11.
3. Michaelis, A. and Landmann, B. *Ann.* **241** (1887) 150.
4. Woss, W. *Chem. Zentr.* **1930:I**, 2006.
5. Karbatow, A. *Ann.* **173** (1874) 7.
6. Drushel, W. A. *Chem. Zentr.* **1916:I**, 1224.
7. Zackrisson, M. and Lindqvist, I. *J. Inorg. & Nuclear Chem. In the press.*

Received November 11, 1960.

The Determination of Small Proportions of Linolenic Acid in Vegetable Oils by Alkaline Isomerization

JENS G. NØRBY

Biokemisk Institut, Århus Universitet, Denmark

Brice and Swain [1] have devised a method for the accurate determination of small proportions of polyenoic fatty acids in vegetable oils based on the ultraviolet spectra of the oils before and after alkaline isomerization. The method, which includes corrections for background absorption, may be used on a variety of fatty acid mixtures containing conjugated and unconjugated dienoic and trienoic acids, but requires about 200 mg fatty acids for each analysis. The microisomerization method of Herb and Riemenschneider [2] has made it possible to use as little as 1—10 mg fatty acids. The present paper concerns the determination of small proportions of trienoic acid by the isomerization method of Herb and Riemenschneider [2] and the calculation method of Brice and Swain [1].

Reagents and methods are described by Nørby [3]. *Symbols:* k_{262}, k_{268}, and k_{274} are observed specific extinction coefficients ($E^{1g/l}_{1cm}$) before isomerization, the subscripts denoting the wave lengths. k'_{262}, k'_{268}, and k'_{274} are the same coefficients after isomerization. k_3 is the specific extinction coefficient before isomerization at 268 mμ (maximum for triene conjugation) after correction for bakground absorption according to eqn. II of Brice and Swain [1]. k'_3 is the same coefficient after isomerization.

Calculation of k'_3. Two equations can be used for the calculation of k'_3:

$$k'_3 = k'_{268} - k_{268} \quad \text{(I)}$$

$$k'_3 = 4.1\ [k'_{268} - \tfrac{1}{2}(k'_{274} + k'_{262})] - k_3 \quad \text{(II)}$$

As k'_3 is the specific extinction coefficient of the sample after isomerization due to triene conjugation produced by the isomerization, eqn. I is used when the background absorption is not changed during isomerization. In this case $k'_{268} - k_{268}$ is the increase due to triene conjugation.

If, however, isomerization increases the background absorption, $k'_{268} - k_{268}$ will be higher than k'_3, and eqn. I can not be used. Brice and Swain [1] have shown that if the increased background absorption is linear in the region 262—274 mμ, eqn. II will give the correct value for k'_3 (k_3 is zero if no conjugated material is present before isomerization). The correction factor 4.1 ($= F_3$) was derived from experiments on isomerized pure linolenic acid as:

$$F_3 = 4.1 = \frac{k'_{268}}{k'_{268} - \tfrac{1}{2}(k'_{274} + k'_{262})} \quad \text{(III)}$$

From the paper of Brice and Swain [1] it is seen that F_3 is the total height of the triene peak at 268 mμ divided by the height of the peak taken with a straight line between the minima at 262 and 274 as a base line. For a given sample the denominator will not change if a linear background absorption is added and hence II will give the correct k'_3 in such cases.

When k'_3 is known, % triene is $1.105 \cdot k'_3$ (Herb and Riemenschneider [2]).

Results. Determination of correction factor F_3 *for the method of Herb and Riemenschneider* [2]. Different amounts of two samples of linolenic acid (Hormel Foundation) and soybean oil (containing 51.8 % diene and 7.67 % triene) were isomerized and k'_{262}, k'_{268}, and k'_{274} determined. At the same time k_{262}, k_{268}, and k_{274} were determined on unisomerized samples. As all samples analyzed showed some absorption before isomerization, the following expression, which is a modification of that of Brice and Swain [1] (III), was used for the calculation of F_3:

$$F_3 = \frac{k'_{268} - k_{268}}{k'_{268} - k_{268} - \tfrac{1}{2}[(k'_{274} - k_{274}) + (k'_{262} - k_{262})]} \quad \text{(IV)}$$

In IV $k' - k$ is the increase in specific extinction coefficient due to isomerization of pure linolenic acid.

The value 4.12 found for F_3 (Table 1) agrees well with 4.1 found by Brice and Swain [1] for their method. F_3 did not vary with sample size in the range indicated in Table 1.

Determination of small amounts of triene. In the first experiment (Table 2) the specific extinction coefficients before and after isomerization were determined for five samples of linoleic acid (Hormel Foundation)

Table 1. Determination of correction factor F_3 for the method of Herb and Riemenschneider.

Sample	Sample weight mg	Number of determinations	F_3	SD
Linolenic acid I	2.3 – 3.5	9	4.124	0.012
" " II	0.08–12.2	22	4.112	0.013
Soybean oil	1.8 –40	19	4.123	0.018

Table 2. Determination of small amounts of triene calculated according to equation II and I.

Sample	Sample weight mg	% diene	% triene eqn. II	% triene eqn. I	F_3
Linoleic acid concentrate	1.16	99.2	1.18	2.19	7.47
" " "	1.86	99.4	1.09	1.85	6.82
" " "	2.61	99.2	1.07	1.21	4.68
" " "	4.39	97.2	1.20	1.44	4.91
" " "	9.04	98.1	1.20	1.48	5.06
Sunflower seed oil	4.5	58.2	0.13	0.27	8.36
" " "	4.7	58.9	0.11	0.27	8.00
" " "	5.6	60.0	0.09	0.37	13.60
" " "	9.4	59.2	0.10	0.27	11.04
" " "	17.8	56.5	0.10	0.25	10.81

Table 3. Determination of triene in mixtures of linoleic or linolenic acid and soybean oil after calculation of k'_3 by eqn. I or II (see text).

Sample	Sample weight mg	Calculated composition % diene	% triene	% triene found eqn. II	eqn. I	Recovery % eqn. II	eqn. I	F_3^{sample}
Soybeen oil	4.3	88.5	2.59	2.55	3.03	98.5	117.0	4.94
+ linoleic	3.0	82.4	3.44	3.40	3.91	98.8	113.7	4.78
acid	2.6	77.1	4.14	4.17	4.49	100.7	108.5	4.46
Soybean oil	8.9	47.5	15.2	15.6	15.3	102.6	100.7	4.05
+ linolenic	7.6	39.7	28.9	28.6	29.0	99.6	100.3	4.15
acid	5.5	24.5	55.6	54.6	55.6	98.2	100.0	4.19

Table 4. k'_{233} k'_{268} and F_3^{sample} for all experiments mentioned in the present paper.

Sample	k'_{233}	k'_{268}	k'_{233}/k'_{268}	F_3^{sample}
Sunflower seed oil	ca. 54	0.27–0.39	142–199	5.82–13.6
Linoleic acid	ca. 90	1.4 –1.8	50–64	4.7 –11.3
Soybean oil + linoleic acid	72–82	2.8 –4.2	17–29	4.4 – 4.9
Soybean oil	51	7	7.3	4.12
Soybean oil + linolenic acid	49–52	14–63	0.8–3.7	4.18
Linolenic acid	46	92	0.5	4.11

and sunflower seed oil. The content of triene was determined after calculation of k'_3 by eqn. I or eqn. II and F_3^{sample} was calculated by eqn. IV. It is seen that F_3^{sample} is consistently higher than 4.12 indicating that a background absorption has developed during isomerization. In accordance with this, calculation of k'_3 by eqn. I gives higher values than by eqn. II.

In order to determine whether the use of eqn. II, when F_3^{sample} is higher than 4.12, will give the *correct* value for % triene, a number of recovery experiments were carried out. Known mixtures of soybean oil and linoleic or linolenic acid were isomerized and % triene determined after calculation of k'_3 by eqn. I or II. F_3^{sample} was calculated by eqn. IV. The results in Table 3 confirm, that when F_3^{sample} is higher than 4.12, as seen in the isomerized mixtures of soybean oil and linoleic acid, calculation of k'_3 by eqn. II gives the correct value for % triene.

In conclusion it can be said that the value of F_3^{sample} will indicate which of the eqns. I or II will give the correct value for k'_3 and thereby the correct value for the triene content of the sample. If F_3^{sample} is higher than 4.12 eqn. II should be used, in all other cases eqn. I will give the correct k'_3.

In an attempt to standardize the spectrophotometric determination of polyenoic fatty acids and to simplify the calculations involved, Brice *et al.*[4] have recommended the use of eqn. II only when k'_{268} is lower than 1. In Table 4 the values for k'_{233} k'_{268}, k'_{233}/k'_{268} and F_3^{sample} found in the experiments described in this paper are collected. It is clearly seen that in several experiments, in which k'_{268} is greater than 1, eqn. II must be used since F_3^{sample} is higher than 4.12. From Table 4 it furthermore appears that if the ratio k'_{233}/k'_{268} is higher than 7, F_3^{sample} is higher than 4.12. Inspection of spectral curves for isomerized samples of this type clearly shows that the diene peak, with maximum at 233 mμ, contributes significantly to the absorption in the region 262—274 mμ. As this "tail absorption" is approximately linear, eqn. II will give the true k'_3 for these samples.

1. Brice, B. A. and Swain, M. L. *J. Opt. Soc. Am.* **35** (1945) 532.
2. Herb, S. F. and Riemenschneider, R. W. *Anal. Chem.* **25** (1953) 953.
3. Nørby, J. G. *Acta Chem. Scand. To be published.*
4. Brice, B. A., Swain, M. L., Herb, S. F., Nichols, P. L. and Riemenschneider, R. W. *J. Am. Oil. Chemists' Soc.* **29** (1952) 279.

Received November 1, 1960.

Studies on Rennin

IV. Chromatographic Fractionation of Rennin

BENT FOLTMANN

Carlsberg Laboratory, Copenhagen, Denmark

In previous papers of this series rennin was considered a rather homogeneous protein. Only one peak was observed on moving boundary electrophoresis at pH 5.8, and in a solubility test the enzyme behaved nearly as a single-component system (Foltmann [1,2]).

On the other hand, Ernstrom [3] reported that although rennin only showed one peak on electrophoresis in buffers of ionic strength 0.1—0.2, it would split up in 3—4 peaks on moving boundary electrophoresis in buffers of ionic strength 0.033 and pH 6.8. In a personal communication to the author, Ernstrom added that on zone-electrophoresis in buffers of ionic strength 0.033 he had observed a slight displacement of enzymatic activity as compared with optical density; however, no separation into discrete peaks was achieved by such zone-electrophoresis.

Jirgensons *et al.*[4] have reported chromatography of a commercial crystalline rennin on diethylaminoethylcellulose. They found that the rennin could be fractionated into one inactive and two active fractions. However, these experiments were carried out at pH 6.7, which is somewhat above the stability range of the enzyme (Foltmann [1]).

The present communication deals with fractionation at a more appropriate pH of rennin by chromatography on diethylaminoethylcellulose (DEAE-cellulose) as described by Peterson and Sober [5]. The ion-exchange cellulose used was a commercial

and sunflower seed oil. The content of triene was determined after calculation of k'_3 by eqn. I or eqn. II and F_3^{sample} was calculated by eqn. IV. It is seen that F_3^{sample} is consistently higher than 4.12 indicating that a background absorption has developed during isomerization. In accordance with this, calculation of k'_3 by eqn. I gives higher values than by eqn. II.

In order to determine whether the use of eqn. II, when F_3^{sample} is higher than 4.12, will give the *correct* value for % triene, a number of recovery experiments were carried out. Known mixtures of soybean oil and linoleic or linolenic acid were isomerized and % triene determined after calculation of k'_3 by eqn. I or II. F_3^{sample} was calculated by eqn. IV. The results in Table 3 confirm, that when F_3^{sample} is higher than 4.12, as seen in the isomerized mixtures of soybean oil and linoleic acid, calculation of k'_3 by eqn. II gives the correct value for % triene.

In conclusion it can be said that the value of F_3^{sample} will indicate which of the eqns. I or II will give the correct value for k'_3 and thereby the correct value for the triene content of the sample. If F_3^{sample} is higher than 4.12 eqn. II should be used, in all other cases eqn. I will give the correct k'_3.

In an attempt to standardize the spectrophotometric determination of polyenoic fatty acids and to simplify the calculations involved, Brice *et al.*[4] have recommended the use of eqn. II only when k'_{268} is lower than 1. In Table 4 the values for k'_{233} k'_{268}, k'_{233}/k'_{268} and F_3^{sample} found in the experiments described in this paper are collected. It is clearly seen that in several experiments, in which k'_{268} is greater than 1, eqn. II must be used since F_3^{sample} is higher than 4.12. From Table 4 it furthermore appears that if the ratio k'_{233}/k'_{268} is higher than 7, F_3^{sample} is higher than 4.12. Inspection of spectral curves for isomerized samples of this type clearly shows that the diene peak, with maximum at 233 mμ, contributes significantly to the absorption in the region 262—274 mμ. As this "tail absorption" is approximately linear, eqn. II will give the true k'_3 for these samples.

1. Brice, B. A. and Swain, M. L. *J. Opt. Soc. Am.* **35** (1945) 532.
2. Herb, S. F. and Riemenschneider, R. W. *Anal. Chem.* **25** (1953) 953.
3. Nørby, J. G. *Acta Chem. Scand. To be published.*
4. Brice, B. A., Swain, M. L., Herb, S. F., Nichols, P. L. and Riemenschneider, R. W. *J. Am. Oil. Chemists' Soc.* **29** (1952) 279.

Received November 1, 1960.

Studies on Rennin

IV. Chromatographic Fractionation of Rennin

BENT FOLTMANN

Carlsberg Laboratory, Copenhagen, Denmark

In previous papers of this series rennin was considered a rather homogeneous protein. Only one peak was observed on moving boundary electrophoresis at pH 5.8, and in a solubility test the enzyme behaved nearly as a single-component system (Foltmann [1,2]).

On the other hand, Ernstrom [3] reported that although rennin only showed one peak on electrophoresis in buffers of ionic strength 0.1—0.2, it would split up in 3—4 peaks on moving boundary electrophoresis in buffers of ionic strength 0.033 and pH 6.8. In a personal communication to the author, Ernstrom added that on zone-electrophoresis in buffers of ionic strength 0.033 he had observed a slight displacement of enzymatic activity as compared with optical density; however, no separation into discrete peaks was achieved by such zone-electrophoresis.

Jirgensons *et al.*[4] have reported chromatography of a commercial crystalline rennin on diethylaminoethylcellulose. They found that the rennin could be fractionated into one inactive and two active fractions. However, these experiments were carried out at pH 6.7, which is somewhat above the stability range of the enzyme (Foltmann [1]).

The present communication deals with fractionation at a more appropriate pH of rennin by chromatography on diethylaminoethylcellulose (DEAE-cellulose) as described by Peterson and Sober [5]. The ion-exchange cellulose used was a commercial

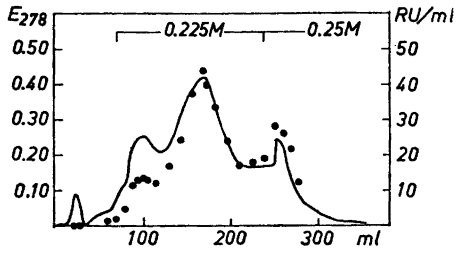

Fig. 1. Chromatography of dissolved rennin crystals on DEAE-cellulose, using stepwise elution with phosphate buffers pH 5.7; 0.20 M, 0.225 M and 0.25 M. Load 40 mg. Column 0.9 × 17 cm. Flow rate 13.5 ml/h, collected in fractions of 4.5 ml. ● milk-clotting activity (RU/ml). Experimental points have been omitted from the extinction curve (E_{278})for the sake of clarity.

product (Eastman-Kodak, lot no. 7392). The rennin was prepared and recrystallized as earlier described [1]. After the crystals had been dissolved by dialysis of the suspending medium (4 M NaCl), the sample was applied to a column of DEAE-cellulose previously equilibrated with 0.20 M phosphate buffer of pH 5.7. The elution was carried out by stepwise increase of the phosphate concentration to 0.225 M and 0.25 M. Fig. 1 illustrates one of the experiments. In the figures the concentration of protein is expressed by the optical density at 278 mμ. The enzymatic activity is expressed in rennin units (RU) according to Berridge [6].

The chromatogram shows a slight front peak of inactive material. After change of the buffer concentration to 0.225 and further to 0.25 M phosphate, a complex system of three peaks develops. Each of the three peaks contains milk-clotting activity, but the specific activity, *i.e.* the ratio RU/E_{278} is different for the three peaks. The component which is eluted last has the highest specific activity; RU/E_{278} equals about 125. This fraction is called the A-rennin. The main component which is called B-rennin has a specific activity of about 100, while the first eluted component, the C-rennin, has a specific activity of 55—60. The recovery of milk-clotting activity was 98 % and on an optical density basis the recovery was 102 %. Calculated from optical densities the first peak of inactive material represents *ca.* 3 % of the total, while the

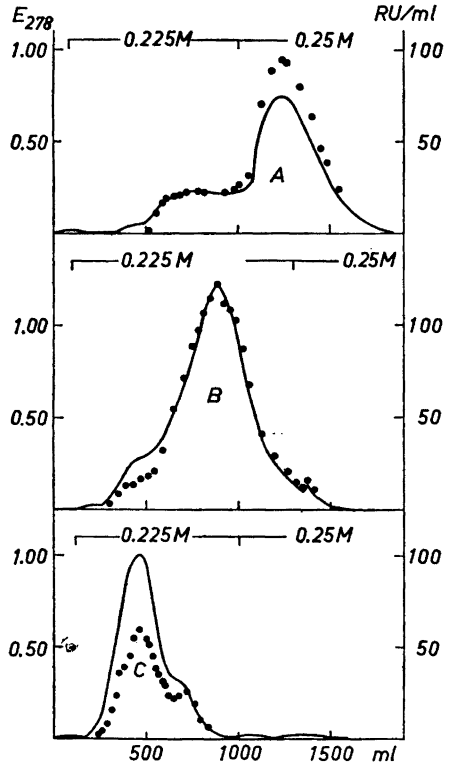

Fig. 2. Rechromatography of pooled fractions containing A, B, and C rennins, respectively. Columns of DEAE-cellulose 2 × 23 cm. Stepwise elution with phosphate buffers pH 5.7; 0.20 M, 0.225 M and 0.25 M. Load 160 to 300 mg per run. Flow rate 25—57 ml/h, three fractions collected per hour. ● milk-clotting activity (RU/ml). Solid line, optical density at 278 mμ.

A, B, and C peaks represent 22, 55, and 20 %, respectively.

For each of the three components, the corresponding fractions from several runs were pooled, and after concentration each component was further analysed and purified by rechromatography. Fig. 2 illustrates three such experiments involving rechromatography of pooled fractions. In these chromatograms the main peaks appear at three different positions corresponding to the A-, B-, and C-rennins, thus indicating that peak formation in the first

run with the crystalline material is not due to artefacts arising during chromatography. Furthermore the specific activities of the purified components also agree with those found in the peaks obtained in the first run of rennin crystals. In each of the A- and B-peaks, the specific activity is constant (within experimental error) across the peak, but over the C-peak there is a slight increase in specific activity. Whether this is due to overlapping contamination with B-rennin, or whether the C-rennin is a mixture itself is not yet clear.

The experiments indicate that the crystalline rennin investigated contains only small amounts of inactive material, and further that the crystals contain at least three components with different enzymatic activity.

Examination of the results of Jirgensons *et al.*[4] shows that the main component in their chromatogram has increasing specific activity over the peak, suggesting that this peak in fact represents a mixture of A- and B-rennins. This assumption is supported by the failure of attempts to separate A- and B-rennins by chromatography at pH 6.2 in this laboratory.

Full details of these experiments and further studies on the rennin fractions will appear in the *Comp. rend. trav. lab. Carlsberg.*

Acknowledgements. The author thanks Chr. Hansen's Laboratory, Ltd. for generous supply of material. The author is indebted to the staff of the Carlsberg Laboratory, especially to the head, Professor M. Ottesen, for valuable discussions.

1. Foltmann, B. *Acta Chem. Scand.* **13** (1959) 1927.
2. Foltmann, B. *Acta Chem. Scand.* **13** (1959) 1936.
3. Ernstrom, C. A. *J. Dairy Sci.* **41** (1958) 1663.
4. Jirgensons, B., Ikenaka, T. and Gorguraki, V. *Makromol. Chem.* **28** (1958) 96.
5. Peterson, E. A. and Sober, H. A. *J. Am. Chem. Soc.* **78** (1956) 751.
6. Berridge, N. J. *Biochem. J.* **39** (1945) 179.

Received November 4, 1960.

Enzymatic Hydrolysis of Bifunctional S-Substituted L-Cysteine Derivatives

SIGMUND SCHWIMMER* and SVEND E. HANSEN

*The Western Regional Research Laboratory **, Albany, California and Organic Chemical Laboratory of the Royal Veterinary and Agricultural College, Copenhagen, Denmark*

Previous publications [1,2] have reported that the C—S-lyase of the endosperm of the seeds of *Albizzia lophanta* can act on a variety of S-substituted cysteine and cysteine sulfoxide derivatives. Whereas a typical monofunctional derivative such as S-ethyl-L-cysteine can undergo complete hydrolysis to pyruvic acid [3], results presented in this communication show that the two bifunctional cysteine derivatives investigated, djenkolic acid and L-lanthionine sulfoxide, are not fully hydrolyzed. The extent of hydrolysis of djenkolic acid, as measured by formation of pyruvic acid, amounted to 66.0, 67.2, and 65 % at substrate concentrations of 1, 2, and 2.5 mM, respectively (Fig. 1). Thus the actual maximum amount of pyruvate formed was pro-

* Senior Postdoctoral Fellow, National Science Foundation, 1958—1959.

** A laboratory of the Western Utilization Research and Development Division, Agricultural Research Service, U. S. Department of Agriculture.

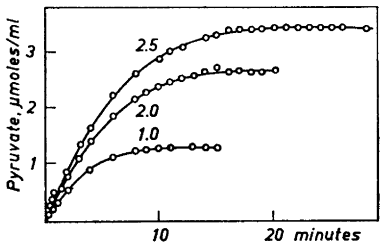

Fig. 1. Course of hydrolysis of djenkolic acid by *Albizzia* C—S-lyase. One ml of reaction mixture at 37° contained 35 μg of enzyme (specific acitivity = 200)[4], 40 μmoles of borate buffer, pH 8.0 and 0.02 μmole of pyridoxal phosphate. Micromoles per ml of djenkolic acid are indicated for each curve.

run with the crystalline material is not due to artefacts arising during chromatography. Furthermore the specific activities of the purified components also agree with those found in the peaks obtained in the first run of rennin crystals. In each of the A- and B-peaks, the specific activity is constant (within experimental error) across the peak, but over the C-peak there is a slight increase in specific activity. Whether this is due to overlapping contamination with B-rennin, or whether the C-rennin is a mixture itself is not yet clear.

The experiments indicate that the crystalline rennin investigated contains only small amounts of inactive material, and further that the crystals contain at least three components with different enzymatic activity.

Examination of the results of Jirgensons *et al.*[4] shows that the main component in their chromatogram has increasing specific activity over the peak, suggesting that this peak in fact represents a mixture of A- and B-rennins. This assumption is supported by the failure of attempts to separate A- and B-rennins by chromatography at pH 6.2 in this laboratory.

Full details of these experiments and further studies on the rennin fractions will appear in the *Comp. rend. trav. lab. Carlsberg.*

Acknowledgements. The author thanks Chr. Hansen's Laboratory, Ltd. for generous supply of material. The author is indebted to the staff of the Carlsberg Laboratory, especially to the head, Professor M. Ottesen, for valuable discussions.

1. Foltmann, B. *Acta Chem. Scand.* **13** (1959) 1927.
2. Foltmann, B. *Acta Chem. Scand.* **13** (1959) 1936.
3. Ernstrom, C. A. *J. Dairy Sci.* **41** (1958) 1663.
4. Jirgensons, B., Ikenaka, T. and Gorguraki, V. *Makromol. Chem.* **28** (1958) 96.
5. Peterson, E. A. and Sober, H. A. *J. Am. Chem. Soc.* **78** (1956) 751.
6. Berridge, N. J. *Biochem. J.* **39** (1945) 179.

Received November 4, 1960.

Enzymatic Hydrolysis of Bifunctional S-Substituted L-Cysteine Derivatives

SIGMUND SCHWIMMER* and SVEND E. HANSEN

*The Western Regional Research Laboratory **, Albany, California and Organic Chemical Laboratory of the Royal Veterinary and Agricultural College, Copenhagen, Denmark*

Previous publications [1,2] have reported that the C—S-lyase of the endosperm of the seeds of *Albizzia lophanta* can act on a variety of S-substituted cysteine and cysteine sulfoxide derivatives. Whereas a typical monofunctional derivative such as S-ethyl-L-cysteine can undergo complete hydrolysis to pyruvic acid [3], results presented in this communication show that the two bifunctional cysteine derivatives investigated, djenkolic acid and L-lanthionine sulfoxide, are not fully hydrolyzed. The extent of hydrolysis of djenkolic acid, as measured by formation of pyruvic acid, amounted to 66.0, 67.2, and 65 % at substrate concentrations of 1, 2, and 2.5 mM, respectively (Fig. 1). Thus the actual maximum amount of pyruvate formed was pro-

* Senior Postdoctoral Fellow, National Science Foundation, 1958—1959.

** A laboratory of the Western Utilization Research and Development Division, Agricultural Research Service, U. S. Department of Agriculture.

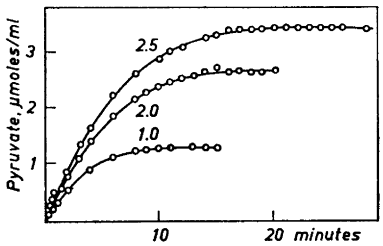

Fig. 1. Course of hydrolysis of djenkolic acid by *Albizzia* C—S-lyase. One ml of reaction mixture at 37° contained 35 μg of enzyme (specific acitivity = 200)[4], 40 μmoles of borate buffer, pH 8.0 and 0.02 μmole of pyridoxal phosphate. Micromoles per ml of djenkolic acid are indicated for each curve.

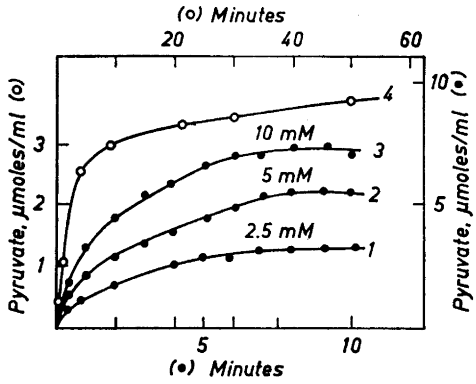

Fig. 2. Curves 1, 2, and 3-course of hydrolysis of L-lanthionine sulfoxide by *Albizzia* C—S-lyases at indicated substrate concentration under the same conditions as in Fig. 1. Curve 4,hydrolysis of mixture of 3,3-bis-(2-aminoethylthio)-*iso*butyric acid and 3-(2-carboxy-2-ethylaminothio)-3-hydroxybutyric acid by 172 μg/ml of enzyme. Concentration of substrate = 3.05 mg/ml, equivalent to 10 μmoles/ml of bisubstituted derivative.

portional to the substrate concentration, or the percentage hydrolysis was independent of the substrate concentration. On the other hand percent maximum hydrolysis of L-lanthionine sulfoxide was found to be dependent on the substrate concentration (Fig. 2). The three values found, 26 %, 22 %, and 14 % for substrate concentration 2.5, 5.0, and 10.0 mM fell on a straight line (in a substrate *vs* hydrolysis plot) which extrapolated to 30 % hydrolysis at zero substrate concentration.

It is suggested that the cessation of enzyme action prior to complete hydrolysis arises as a result of the inactivation of the enzyme by the highly reactive expected end products:

1. $R-S-CH_2-S-R + 2\ H_2O \longrightarrow S-CH_2-S + 2NH_3 + 2CH_3COCOOH$
2. $R-SO-R + 2\ H_2O \longrightarrow HSOH + 2NH_3 + 2CH_3COCOOH$

where $R = CH_2-CHNH_2-COOH$.
Thus djenkolic acid yields methylene dithiol and L-lanthionine sulfoxide yields the hypothetical sulfenic acid. Both of these sulfur-containing products could presumably react with the enzyme and inactivate it.

In addition to the above-mentioned difference between these two substrates, their course-of-hydrolysis curves appear to be quite distinct. Thus the course of hydrolysis of djenkolic acid is characterized by a linearity of rate for the first 20 to 30 % hydrolysis, followed by a progressive decrease in rate until the maximum is reached. The hydrolysis of L-lanthionine sulfoxide does not exhibit a distinct linear rate at the initial stages of the reaction. A linearity in rate at the later stage of hydrolysis prior to achievement of maximum hydrolysis was observed. In this respect, the course of hydrolysis resembles more closely that of a monosubstituted cysteine derivative (S-ethyl-L-cysteine [3]) and suggests that considerable product inhibition of the enzyme occurs during the reaction. The superimposition of product inhibition on product inactivation would then explain why the percent hydrolysis decreases with increasing substrate concentration.

Fig. 2 includes the course of hydrolysis of a preparation consisting mainly of 3,3'-bis-(2-carboxy-2-aminoethylthio)-*iso*butyric acid, which may be considered as an analogue of djenkolic acid [2]. The distinctly biphasic mode of the course of liberation of pyruvic acid probably arises from the presence of the impurity 3-(2-carboxy-2-aminoethylthio)-3-hydroxy*iso*butyric acid.

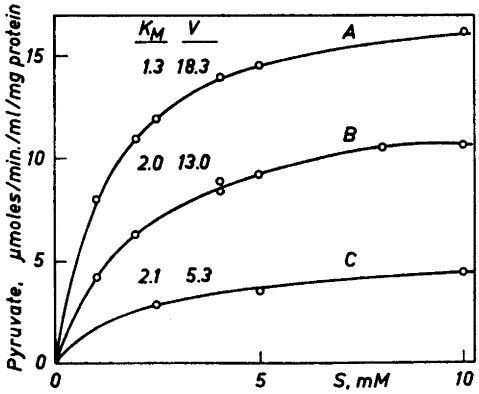

Fig. 3. Effect of substrate concentration on the initial rate of hydrolysis of djenkolic acid (A), S-ethyl-cysteine (B), and L-lanthionine sulfoxide (C) under the conditions of Fig. 1. The smooth curves were calculated from the classical Michaelis equation using values for the constants K_M and V shown in this figure. The points are the experimental values.

The ratio of the initial fast rate to the slow rate at the later stage of hydrolysis is equal to roughly about ten times the estimated ratio of the intensity of the ninhydrin spots on paper chromatograms of this preparation. This suggests that the mono-substituted cysteine derivative is much less susceptible to hydrolysis by the C—S-lyase than is the disubstituted derivative.

Fig. 3 shows the influence of substrate concentration on the rate of hydrolysis of djenkolic acid (A), S-ethyl-L-cysteine (B), and L-lanthionine sulfoxide (C). It will be noted that the Michaelis constants K_M vary considerably less than the values for V, the maximum rate when the enzyme is saturated with substrate. Let us assume as a first approximation, that K_M is a measure of the traditional steady-state constant $(k_{-1} + k_2)/k_1$ according to the usual formation $E + S \underset{k_{-1}}{\overset{k_1}{\rightleftharpoons}} ES \xrightarrow{k_2} E +$ product, and that V is a measure of the magnitude of k_2. If K_M remains constant while k_2 increases, then k_1 (the velocity constant for combination of enzyme with substrate) must also increase. This analysis corroborates the previous conclusion that the susceptibility to hydrolysis as function of the S-substituent depends upon the absence of structures in this substituent which would tend to interfere with hydrogen bond formation between the pyridoxal phosphate moiety of the enzyme and the substrate [2]. Such interference would tend to decrease the rate of formation of enzyme-substrate complex (k_1) and also decrease the rate of decomposition of the complex (k_2). This would tend to maintain K_M at a constant value, as was found experimentally.

1. Gmelin, R., Hasenmeier, G. and Strauss, G. *Z. Naturforsch.* **12b** (1957) 687.
2. Schwimmer, S. and Kjær, A. *Biochim. et Biophys. Acta* **42** (1960) 316.
3. Schwimmer, S. *Biochim. et Biophys. Acta. In press* (1961).
4. Hansen, S., Kjær, A. and Schwimmer, S. *Compt. rend. trav. lab. Carlsberg. Sér. chim.* **31** (1959) 193.

Received November 7, 1960.

Preparation and Properties of Human Thyroglobulin

CLAES WEIBULL and LARS LINDER

Central Bacteriological Laboratory of Stockholm City, Stockholm, Sweden

The preparation and properties of thyroglobulin of animal origin has been described by several investigators [1-5]. Some chemical and physico-chemical studies on human thyroglobulin will be described briefly in the following.

The thyroid glands were frozen, sliced and extracted with 0.15 M NaCl for about 20 h at 5°C. The mixture was then centrifuged and the sediment discarded. Neutralized, saturated ammonium sulphate was added to the supernatant at a final saturation of 33 %. The sediment was removed by centrifugation and additional ammonium sulphate was added to the supernatant at a final saturation of 50 %. The sediment was collected by centrifugation and dissolved in distilled water. The solution was dialyzed against distilled water, and the dialysate was treated with ammonium sulphate as described above. The protein fraction precipitated between 33 and 50 % salt saturation was collected and investigated chemically and physico-chemically.

The iodine content of the material isolated from the thyroid glands was determined according to Kendall [6]. Nitrogen was determined by the Kjeldahl method. Ultracentrifugal studies were performed using the Spinco analytical ultracentrifuge working at 59 780 rpm. The protein concentration in the samples used for the ultracentrifugal analyses was 1 % and the total salt concentration in these samples was 0.17 M (0.15 M NaCl and 0.02 M phosphate, pH 7.0).

The main part of the iodine of the thyroid extracts was recovered in the protein fraction precipitated between 33 and 50 % saturation of ammonium sulphate. Table 1 gives the results of the chemical analyses carried out on the proteinaceous material thus obtained. The values for iodine and nitrogen content agree with those reported previously for animal thyroglobulin [2,3].

Table 2 shows the results of the ultracentrifugal analyses. It can be seen that the main high molecular weight component of the analyzed solutions has a sedimentation constant ($S_{20,\,aq}$) of about 17 *S*. Similar

The ratio of the initial fast rate to the slow rate at the later stage of hydrolysis is equal to roughly about ten times the estimated ratio of the intensity of the ninhydrin spots on paper chromatograms of this preparation. This suggests that the mono-substituted cysteine derivative is much less susceptible to hydrolysis by the C—S-lyase than is the disubstituted derivative.

Fig. 3 shows the influence of substrate concentration on the rate of hydrolysis of djenkolic acid (A), S-ethyl-L-cysteine (B), and L-lanthionine sulfoxide (C). It will be noted that the Michaelis constants K_M vary considerably less than the values for V, the maximum rate when the enzyme is saturated with substrate. Let us assume as a first approximation, that K_M is a measure of the traditional steady-state constant $(k_{-1} + k_2)/k_1$ according to the usual formation $E + S \underset{k_{-1}}{\overset{k_1}{\rightleftharpoons}} ES \xrightarrow{k_2} E +$ product, and that V is a measure of the magnitude of k_2. If K_M remains constant while k_2 increases, then k_1 (the velocity constant for combination of enzyme with substrate) must also increase. This analysis corroborates the previous conclusion that the susceptibility to hydrolysis as function of the S-substituent depends upon the absence of structures in this substituent which would tend to interfere with hydrogen bond formation between the pyridoxal phosphate moiety of the enzyme and the substrate [2]. Such interference would tend to decrease the rate of formation of enzyme-substrate complex (k_1) and also decrease the rate of decomposition of the complex (k_2). This would tend to maintain K_M at a constant value, as was found experimentally.

1. Gmelin, R., Hasenmeier, G. and Strauss, G. *Z. Naturforsch.* **12b** (1957) 687.
2. Schwimmer, S. and Kjær, A. *Biochim. et Biophys. Acta* **42** (1960) 316.
3. Schwimmer, S. *Biochim. et Biophys. Acta. In press* (1961).
4. Hansen, S., Kjær, A. and Schwimmer, S. *Compt. rend. trav. lab. Carlsberg. Sér. chim.* **31** (1959) 193.

Received November 7, 1960.

Preparation and Properties of Human Thyroglobulin

CLAES WEIBULL and LARS LINDER

Central Bacteriological Laboratory of Stockholm City, Stockholm, Sweden

The preparation and properties of thyroglobulin of animal origin has been described by several investigators [1-5]. Some chemical and physico-chemical studies on human thyroglobulin will be described briefly in the following.

The thyroid glands were frozen, sliced and extracted with 0.15 M NaCl for about 20 h at 5°C. The mixture was then centrifuged and the sediment discarded. Neutralized, saturated ammonium sulphate was added to the supernatant at a final saturation of 33 %. The sediment was removed by centrifugation and additional ammonium sulphate was added to the supernatant at a final saturation of 50 %. The sediment was collected by centrifugation and dissolved in distilled water. The solution was dialyzed against distilled water, and the dialysate was treated with ammonium sulphate as described above. The protein fraction precipitated between 33 and 50 % salt saturation was collected and investigated chemically and physico-chemically.

The iodine content of the material isolated from the thyroid glands was determined according to Kendall [6]. Nitrogen was determined by the Kjeldahl method. Ultracentrifugal studies were performed using the Spinco analytical ultracentrifuge working at 59 780 rpm. The protein concentration in the samples used for the ultracentrifugal analyses was 1 % and the total salt concentration in these samples was 0.17 M (0.15 M NaCl and 0.02 M phosphate, pH 7.0).

The main part of the iodine of the thyroid extracts was recovered in the protein fraction precipitated between 33 and 50 % saturation of ammonium sulphate. Table 1 gives the results of the chemical analyses carried out on the proteinaceous material thus obtained. The values for iodine and nitrogen content agree with those reported previously for animal thyroglobulin [2,3].

Table 2 shows the results of the ultracentrifugal analyses. It can be seen that the main high molecular weight component of the analyzed solutions has a sedimentation constant ($S_{20,\,aq}$) of about 17 *S*. Similar

Table 1. Chemical composition of preparations of human thyroglobulin.

Preparation	Iodine content, % of dry weight	Nitrogen content, % of dry weight
I *	0.440	14.9
II **	0.324	14.5

* Preparation from thyroid tissue surgically removed from a case of nontoxic goiter.

** Preparation from normal thyroid glands obtained at autopsy.

Table 2. Ultracentrifugal analyses of preparations of human thyroglobulin.

Sedimentation const. ($S_{20, aq}$), of high molecular weight components in preparation		Amounts of components, expressed as per cent of total high molecular weight material in prep.	
Prep. I (*cf.* Table 1)	Prep. II	Prep. I	Prep. II
~ 7 *S*	6.9 *S*	3	3
11.6 "	11.7 "	11	6
17.8 "	17.1 "	81	86
23 "	26 "	5	5

values have been reported for thyroglobulin isolated from hog [4,7] and calf [5].

It therefore seems very probable that the main, high molecular weight component in the extracts studied by us represents human thyroglobulin.

The data given above suggest that the chemical and physico-chemical properties of human thyroglobulin are similar to those of thyroglobulin of animal origin.

We wish to thank Dr. A. Ehrenberg for carrying out the ultracentrifugal analyses.

1. Cavett, J. W. and Seljeskog, S. R. *J. Biol. Chem.* **100** (1933) XXVI.
2. Heidelberger, M. and Foster, W. W. *J. Biol. Chem.* **101** (1933) 433.
3. Derrien, Y., Michel, R. and Roche, J. *Biochim. et Biophys. Acta* **2** (1948) 454.
4. Shulman, S., Rose, N. R. and Witebsky, E. *J. Immunol.* **75** (1955) 291.
5. Edelhoch, H. *J. Biol. Chem.* **235** (1960) 1326.
6. Kendall, C. *J. Biol. Chem.* **43** (1920) 149.
7. Derrien, Y., Michel, R., Pedersen, K. O. and Roche, J. *Biochim. et Biophys. Acta* **3** (1949) 436.

Received November 11, 1960.

2,2′-Diphenyl-3,3′-diindolylmethane

EDWARD LEETE

School of Chemistry, University of Minnesota, Minneapolis 14, Minnesota, USA

In a recent paper [1] on the chemistry of 3-hydroxymethylindoles we reported on their self-condensation to 3,3′-diindolylmethanes on boiling with water or aqueous sodium hydroxide. An exception was 3-hydroxymethyl-2-phenylindole which yielded 2-phenylindole on refluxing with 10 % sodium hydroxide. The expected product, 2,2′-diphenyl-3,3′-diindolylmethane (I), was described by Dahlbom and Misiorny [2] who claimed to have obtained this compound from 2-phenylindole and formaldehyde. However, the melting point which

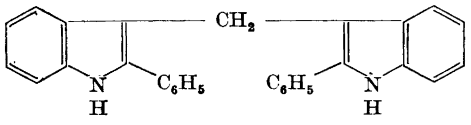

I

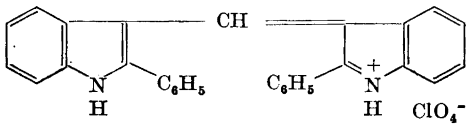

II

they reported (184—185°) for this substance seemed to be unusually low, since all the other known 3,3′-diindolylmethanes melt considerably above the corresponding indoles, as indicated in Table 1.

This led us to suggest that the compound, m.p. 184—185°, was not authentic 2,2′-

Table 1. Melting points of substituted indoles and 3,3′-diindolylmethanes. °C.

Substituent	Indole	3,3′-Diindolylmethane
None	52—53	167—168
1-Methyl	below 0	112.5—113
2-Methyl	62	237—238
1,2-Dimethyl	56	161.5—162.5
1-Methyl-2-phenyl	100—101	185—186
2-Phenyl	187—188	184—185

Table 1. Chemical composition of preparations of human thyroglobulin.

Preparation	Iodine content, % of dry weight	Nitrogen content, % of dry weight
I *	0.440	14.9
II **	0.324	14.5

* Preparation from thyroid tissue surgically removed from a case of nontoxic goiter.

** Preparation from normal thyroid glands obtained at autopsy.

Table 2. Ultracentrifugal analyses of preparations of human thyroglobulin.

Sedimentation const. ($S_{20, aq}$), of high molecular weight components in preparation		Amounts of components, expressed as per cent of total high molecular weight material in prep.	
Prep. I (*cf.* Table 1)	Prep. II	Prep. I	Prep. II
~ 7 *S*	6.9 *S*	3	3
11.6 "	11.7 "	11	6
17.8 "	17.1 "	81	86
23 "	26 "	5	5

values have been reported for thyroglobulin isolated from hog [4,7] and calf [5].

It therefore seems very probable that the main, high molecular weight component in the extracts studied by us represents human thyroglobulin.

The data given above suggest that the chemical and physico-chemical properties of human thyroglobulin are similar to those of thyroglobulin of animal origin.

We wish to thank Dr. A. Ehrenberg for carrying out the ultracentrifugal analyses.

1. Cavett, J. W. and Seljeskog, S. R. *J. Biol. Chem.* **100** (1933) XXVI.
2. Heidelberger, M. and Foster, W. W. *J. Biol. Chem.* **101** (1933) 433.
3. Derrien, Y., Michel, R. and Roche, J. *Biochim. et Biophys. Acta* **2** (1948) 454.
4. Shulman, S., Rose, N. R. and Witebsky, E. *J. Immunol.* **75** (1955) 291.
5. Edelhoch, H. *J. Biol. Chem.* **235** (1960) 1326.
6. Kendall, C. *J. Biol. Chem.* **43** (1920) 149.
7. Derrien, Y., Michel, R., Pedersen, K. O. and Roche, J. *Biochim. et Biophys. Acta* **3** (1949) 436.

Received November 11, 1960.

2,2′-Diphenyl-3,3′-diindolylmethane

EDWARD LEETE

School of Chemistry, University of Minnesota, Minneapolis 14, Minnesota, USA

In a recent paper [1] on the chemistry of 3-hydroxymethylindoles we reported on their self-condensation to 3,3′-diindolylmethanes on boiling with water or aqueous sodium hydroxide. An exception was 3-hydroxymethyl-2-phenylindole which yielded 2-phenylindole on refluxing with 10 % sodium hydroxide. The expected product, 2,2′-diphenyl-3,3′-diindolylmethane (I), was described by Dahlbom and Misiorny [2] who claimed to have obtained this compound from 2-phenylindole and formaldehyde. However, the melting point which

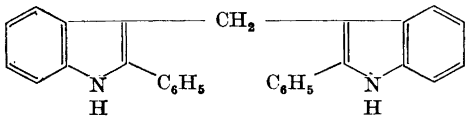

I

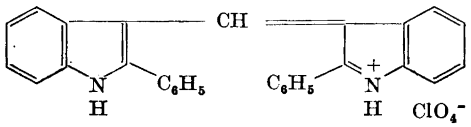

II

they reported (184—185°) for this substance seemed to be unusually low, since all the other known 3,3′-diindolylmethanes melt considerably above the corresponding indoles, as indicated in Table 1.

This led us to suggest that the compound, m.p. 184—185°, was not authentic 2,2′-

Table 1. Melting points of substituted indoles and 3,3′-diindolylmethanes. °C.

Substituent	Indole	3,3′-Diindolylmethane
None	52—53	167—168
1-Methyl	below 0	112.5—113
2-Methyl	62	237—238
1,2-Dimethyl	56	161.5—162.5
1-Methyl-2-phenyl	100—101	185—186
2-Phenyl	187—188	184—185

diphenyl-3,3′-diindolylmethane. Dahlbom and Misiorny were quick to reply [3] to our unworthy suggestion, and in the light of further work to be described here, we offer our sincere apologies to these authors for suggesting that they had failed to perform a mixed melting point between 2-phenylindole and the product, m.p. 184—185°.

In the present work 2-phenylindole was refluxed in ethanol, containing a trace of hydrochloric acid, with ethyl orthoformate for 24 h. The product was 2,2′-diphenyl-3,3′-diindolylmethene which was isolated as its perchlorate (II) according to the procedure of Harley-Mason and Bu'Lock [4]. Crystallization from acetic acid afforded orange-red prisms, m.p. 289—290° (decomp.) (Found: C 69.83; H 4.34; N 5.58. Calc. for $C_{29}H_{21}O_4N_2Cl$: C 70.09; H 4.26; N 5.64.) This methene salt was hydrogenated in ethanol in the presence of platinum oxide. Evaporation of the filtered solution yielded I which was obtained as colorless needles from ethanol, m.p. 188—189° (Found: C 87.50; H 5.77; N 6.78. Calc. for $C_{29}H_{22}N_2$: C 87.40; H 5.57; N 7.03). The di-1,3,5-trinitrobenzene complex of 2,2′-diphenyl-3,3′-diindolylmethane was obtained as reddish brown needles from methanol, m.p. 161—162°(Found: C 59.86; H 3.62; N 13.82. Calc. for $C_{29}H_{22}N_2 \cdot 2C_6H_3O_6N_3$: C 59.71; H 3.42; N 13.59). In order to confirm that we had obtained authentic I, the compound m.p. 188—189° was N-methylated according to the procedure of Potts and Saxton [5] to yield 1,1′-dimethyl-2,2′-diphenyl-3,3′-diindolylmethane, m.p. 185—186°, identical (mixed m.p., I.R. spectrum) with material previously obtained [1] by the self-condensation of 3-hydroxymethyl-1-methyl-2-phenylindole.

It is thus evident that Dahlbom and Misiorny obtained authentic I (the slight difference in our observed melting points for this compound is probably not significant) and it is remarkable that 2-phenylindole, 2,2′diphenyl-3,3′-diindolylmethane and its 1,1′-dimethyl derivative should melt so close together. We have also reinvestigated the self-condensation of 3-hydroxymethyl-2-phenylindole. In agreement with our previous results we obtained 2-phenylindole when this compound was refluxed with 10 % sodium hydroxide. However, when exactly neutral or slightly acidic conditions were used the product was in fact the diindolylmethane I. We suspect that traces of alkali caused the formation of 2-phenylindole when 3-hydroxymethyl-2-phenylindole was refluxed with water in our previous experiments.

This investigation was supported by a research grant CY-5336 from the *National Institutes of Health*, Public Health Service, U.S.A. The analyses were performed by Mrs. Olga Hamerston of the University of Minnesota.

1. Leete, E. *J. Am. Chem. Soc.* **81** (1959) 6023.
2. Dahlbom, R. and Misiorny, A. *Acta Chem. Scand.* **9** (1955) 1074.
3. Dahlbom, R. and Misiorny, A. *J. Am. Chem. Soc.* **82** (1960) 2397.
4. Harley-Mason, J. and Bu'Lock, J. D. *Biochem. J.* **51** (1952) 430.
5. Potts, K. T. and Saxton, J. E. *J. Chem. Soc.*, **1954** 2641.

Received November 14, 1960.

Acid Soluble Nucleotide Linked Peptides in Extracts of Ascites Tumor Cells

GUNNAR ÅGREN

From the Department of Medical Chemistry, University of Uppsala, Sweden

In a recent paper [1] it was reported that trichloroacetic acid (TCA) extracts of rabbit livers contained at least four ultra violet (UV) absorbing peaks with bound ninhydrin positive material. These four fractions were eluted immediately after adenosine diphosphate (ADP) and guanosine diphosphate (GDP) with a formic acid-ammonium formate system [2] from a Dowex 1 column. The positions on the elution curve of the UV-linked ninhydrin positive material were in the same region where we previously had found the uridine nucleotide bound peptides in *L. casei* [3]. Using a modification of the method of Strominger and Threnn [4] it was possible to isolate from the four fractions ten UV-absorbing spots. Seven of these contained from three up to seven amino acids, some of them at least bound to uridylic acid [5].

Since these data seemed to prove that animal tissues also contained acid soluble nucleotide bound peptides of a type previously only observed in extracts of different

diphenyl-3,3′-diindolylmethane. Dahlbom and Misiorny were quick to reply [3] to our unworthy suggestion, and in the light of further work to be described here, we offer our sincere apologies to these authors for suggesting that they had failed to perform a mixed melting point between 2-phenylindole and the product, m.p. 184—185°.

In the present work 2-phenylindole was refluxed in ethanol, containing a trace of hydrochloric acid, with ethyl orthoformate for 24 h. The product was 2,2′-diphenyl-3,3′-diindolylmethene which was isolated as its perchlorate (II) according to the procedure of Harley-Mason and Bu'Lock [4]. Crystallization from acetic acid afforded orange-red prisms, m.p. 289—290° (decomp.) (Found: C 69.83; H 4.34; N 5.58. Calc. for $C_{29}H_{21}O_4N_2Cl$: C 70.09; H 4.26; N 5.64.) This methene salt was hydrogenated in ethanol in the presence of platinum oxide. Evaporation of the filtered solution yielded I which was obtained as colorless needles from ethanol, m.p. 188—189° (Found: C 87.50; H 5.77; N 6.78. Calc. for $C_{29}H_{22}N_2$: C 87.40; H 5.57; N 7.03). The di-1,3,5-trinitrobenzene complex of 2,2′-diphenyl-3,3′-diindolylmethane was obtained as reddish brown needles from methanol, m.p. 161—162°(Found: C 59.86; H 3.62; N 13.82. Calc. for $C_{29}H_{22}N_2 \cdot 2C_6H_3O_6N_3$: C 59.71; H 3.42; N 13.59). In order to confirm that we had obtained authentic I, the compound m.p. 188—189° was N-methylated according to the procedure of Potts and Saxton [5] to yield 1,1′-dimethyl-2,2′-diphenyl-3,3′-diindolylmethane, m.p. 185—186°, identical (mixed m.p., I.R. spectrum) with material previously obtained [1] by the self-condensation of 3-hydroxymethyl-1-methyl-2-phenylindole.

It is thus evident that Dahlbom and Misiorny obtained authentic I (the slight difference in our observed melting points for this compound is probably not significant) and it is remarkable that 2-phenylindole, 2,2′diphenyl-3,3′-diindolylmethane and its 1,1′-dimethyl derivative should melt so close together. We have also reinvestigated the self-condensation of 3-hydroxymethyl-2-phenylindole. In agreement with our previous results we obtained 2-phenylindole when this compound was refluxed with 10 % sodium hydroxide. However, when exactly neutral or slightly acidic conditions were used the product was in fact the diindolylmethane I. We suspect that traces of alkali caused the formation of 2-phenylindole when 3-hydroxymethyl-2-phenylindole was refluxed with water in our previous experiments.

This investigation was supported by a research grant CY-5336 from the *National Institutes of Health*, Public Health Service, U.S.A. The analyses were performed by Mrs. Olga Hamerston of the University of Minnesota.

1. Leete, E. *J. Am. Chem. Soc.* **81** (1959) 6023.
2. Dahlbom, R. and Misiorny, A. *Acta Chem. Scand.* **9** (1955) 1074.
3. Dahlbom, R. and Misiorny, A. *J. Am. Chem. Soc.* **82** (1960) 2397.
4. Harley-Mason, J. and Bu'Lock, J. D. *Biochem. J.* **51** (1952) 430.
5. Potts, K. T. and Saxton, J. E. *J. Chem. Soc.*, **1954** 2641.

Received November 14, 1960.

Acid Soluble Nucleotide Linked Peptides in Extracts of Ascites Tumor Cells

GUNNAR ÅGREN

From the Department of Medical Chemistry, University of Uppsala, Sweden

In a recent paper [1] it was reported that trichloroacetic acid (TCA) extracts of rabbit livers contained at least four ultra violet (UV) absorbing peaks with bound ninhydrin positive material. These four fractions were eluted immediately after adenosine diphosphate (ADP) and guanosine diphosphate (GDP) with a formic acid-ammonium formate system [2] from a Dowex 1 column. The positions on the elution curve of the UV-linked ninhydrin positive material were in the same region where we previously had found the uridine nucleotide bound peptides in *L. casei* [3]. Using a modification of the method of Strominger and Threnn [4] it was possible to isolate from the four fractions ten UV-absorbing spots. Seven of these contained from three up to seven amino acids, some of them at least bound to uridylic acid [5].

Since these data seemed to prove that animal tissues also contained acid soluble nucleotide bound peptides of a type previously only observed in extracts of different

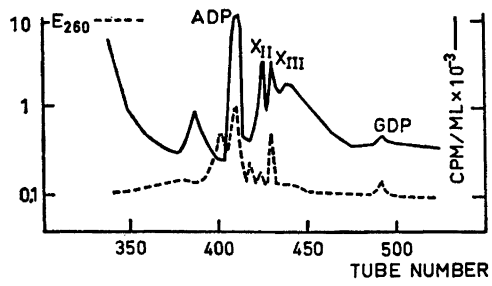

Fig. 1. Acid soluble nucleotides from 3.8 × 10^9 tetraploid tumor ascites cells. The nucleotides were separated on a 3 × 50 cm Dowex 1 formate column by gradient elution with reservoir content changed at the tubes numbered as follows: *72*, 1 N formic acid; *164*, 4 N formic acid; *390*, 0.2 M ammonium formate + 4 N formic acid; *510*, 0.4 M ammonium formate + 4 N formic acid. The continuous line represents radioactivity and the broken line represents optical density values at 260 mμ ($\bar{E}_{260}$).

microorganisms it was of interest to look for them in other animal cells. In connection with other experiments the TCA-extracts of ascites tumor cells were chromatographed in the usual way [3]. In Fig. 1 a section of an elution diagram is presented consisting of the peaks immediately before and after ADP. The tumor cells had been separated by counter-streaming centrifugation [6] (by prof. Lindahl) into mainly tetraploid (3.8 × 10^9) and octaploid cells (10.9 × 10^9) and incubated for 30 min. with ^{32}P in relation to cell numbers. The TCA extract in Fig. 1 was from the tetraploid cells. The TCA extract from the octaploid cells qualitatively gave a similar elution diagram. In view of the low UV-absorbtion values the X_{II} and X_{III} peaks from the tetraploid cells were taken together with the corresponding peaks from the octaploid cells. After charcoal-absorbtion and elution less than 0.5 mg material was obtained from each of the combined X_{II} and X_{III} peaks. No attempt was therefore made to separate the material on an electrophero-chromatogram. After acid hydrolysis all material was put on each of two papers for two dimensional paper chromatography. Both papers showed stronger spots in positions corresponding to glycine, serine, glutamic acid and aspartic acid. Weaker spots were obtained in the positions of leucine or *iso*leucine, lysine, arginine and threonine. At least four more unidentified spots were also observed on both papers.

Preliminary estimations of the specific activity calculated as counts per minute per μmole of nucleotide compound gave the following values:

	X_{II}	X_{III}
Tetraploid	40 × 10^5	8.9 × 10^5
Octaploid	11 × 10^5	3.0 × 10^5

The figures are of interest since the tetraploid cells are the more rapidly dividing of the two cell types [7] and nucleotide linked peptides in microorganisms have been claimed as precursors in the formation of cell wall proteins [8].

The investigation was supported by grants from the *Swedish Cancer Society*.

1. Ågren, G. *Acta Soc. Med. Upsaliensis* **65** (1960) 49.
2. Hurlbert, P. B., Schmitz, H., Brumm, A. F. and Potter, V. R. *J. Biol. Chem.* **209** (1954) 23.
3. de Verdier, C.-H. and Ågren, G. *Acta Chem. Scand.* **13** (1959) 1425.
4. Strominger, J. L. and Threnn, R. H. *Biochim. et Biophys Acta* **36** (1959) 83.
5. Ågren, G. *Acta Soc. Med. Upsaliensis. In press* (1960).
6. Lindahl, P. E. *Cancer Research* **20** (1960) 841.
7. Lindahl, P. E. *Personal communication.*
8. Park, J. T. and Strominger, J. L. *Science* **125** (1957) 99.

Received November 18, 1960.

ACTA CHEMICA SCANDINAVICA 14 (1960) 2067–2070

The Phase Diagram of the System $SrCl_2$—$BaCl_2$

A. SCHEI and H. FLOOD

Royal Norwegian Council for Scientific and Industrial Research, Institute of Silicate Science, Technical University of Norway, Trondheim, Norway

The liquidus curve of the system $SrCl_2$ – $BaCl_2$ was determined by thermal analysis and by high-temperature filtration, the solidus by a tracer technique previously described.[3] The system shows complete miscibility in both liquid and solid phases, with a freezing point minimum of 852.0°C at about 68 mole percent $SrCl_2$.

Assuming ideal behaviour of the liquid mixtures, and positive deviations with symmetrical activity coefficients of the type $RT \ln \gamma_A = b N_B^2$ for the solid mixtures, it is shown that with a value of $b \simeq 1$ kcal, a phase diagram can be calculated which gives fairly good agreement with the experimental values.

The binary system $SrCl_2$—$BaCl_2$ was investigated about 45 years ago by Vortisch[1], who also quotes the results of previous workers. More recently, Bergman and Bukhalova[2] checked the earlier results by means of a thermal visual method. According to Vortisch, the system shows complete miscibility in both liquid and solid phases. Our own investigation was aimed particularly at a more precise determination of the solidus curve.

RESULTS AND DISCUSSION

The results are given in Table 1 and in Fig. 1. A comparison between the present and earlier results is given in Table 2. The diagram (Fig. 1) is quite similar to that of Vortisch [1], although in his work, the solidus was largely estimated.

At the strontium chloride side of the diagram, the difference between the solidus and liquidus curves proved to be very small, so small in fact, that the separation of the two curves could not be effected by the present method.

The shape of the phase diagram indicates that the tendency towards forming a solution is weaker in the solid than in the liquid state. Hence the solid solutions will show more positive (or less negative) deviations from ideality than the liquid solutions. The scanty information available regarding the mixing behaviour of molten salt mixtures of the type AX_2 — BX_2 indicates that the deviations from ideality are generally smaller here than in the corre-

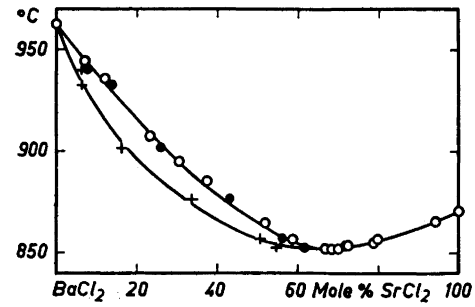

Fig. 1. The system $SrCl_2$ — $BaCl_2$. Open circles: Liquidus points determined by thermal analysis. Filled circles: Liquidus points determined from high-temperature filtration. Crosses: Solidus points determined with ^{134}Cs tracer.

sponding mixtures of the type A'X — B'X. From the phase diagram $CaCl_2$ — $FeCl_2$ it can be concluded that the liquid mixtures in this system show very nearly ideal behaviour.[5] It seems reasonable as a first approximation to assume ideal behaviour for the liquid $BaCl_2$ — $SrCl_2$ mixtures, and interpret the minimum of the liquidus curve as due to positive deviations from ideality in the solid solutions. It is then of interest to see whether the phase diagram can be interpreted by applying simple symmetrical expressions for the activity coefficients of the solid solutions.

A frequently applied set of expressions for the activity coefficients is

$$\begin{aligned} RT \ln \gamma_A &= b\ N_B^2 \\ RT \ln \gamma_B &= b\ N_A^2 \end{aligned} \qquad (1)$$

where γ is the activity coefficient, N the mole fraction and b is a constant. If the entropy of mixing is ideal (*i. e.*, the Sr^{++} and Ba^{++} ions are distributed at random over the cation positions, and the change in vibrational entropy

Table 1. Data of thermal analysis and high temperature filtration of the system $SrCl_2$ — $BaCl_2$.

Thermal analysis		Thermal analysis		High temperature filtration		
Total composition, mole % $SrCl_2$	Temp. of the first crystallization °C	Total composition, mole % $SrCl_2$	Temp. of the first crystallization °C	Equilibrium temperature °C	Composition of phases in equilibrium, mole % $SrCl_2$	
					liquid phase	solid phase
100.0	870.5	58.8	856.6	852.7	61.7	54.9
94.3	865.5	51.9	864.3	857.0	56.3	50.7
79.8	856.7	37.5	884.8	876.5	43.0	34.0
78.8	855.0	70.3	894.8			
72.3	853.7	23.3	907.8	901.8	25.8	16.1
71.9	853.7	12.1	935.6	932.7	13.6	6.5
69.9	852.0	7.1	944.2	940.0	7.6	6.6
68.2	852.0	0.0	962.3			
66.8	852.0					

Table 2. Minimum in the System $SrCl_2$ — $BaCl_2$.

	Temperature °C	Composition mole % $SrCl_2$
Vortisch	845	70
Sandonini	854	65
Bergman and Bukhalova	840	70
This paper	852	68

upon mixing is zero), then b is equal to the partial molar heat of solution of one component in the pure second component.

The equilibrium between solid and liquid phases may be expressed by the well-known equation (valid for both components)

$$\ln a_l - \ln a_s = \frac{\Delta H_m}{R}\left(\frac{1}{T_m} - \frac{1}{T}\right) \quad (2)$$

where the a's are the activities, ΔH_m is the heat of melting, assumed to be independent of temperature (Δc_p for the melting process is neglected) and T_m is the melting point of the pure component. Assuming ideal behaviour of the liquid, eqns. (1) and (2) are combined to give

$$RT \ln N_l/N_s = \Delta H_m\left(\frac{T}{T_m} - 1\right) + b\,(1 - N_s)^2 \quad (3)$$

which is also valid for both components. The heats of melting for $SrCl_2$ and $BaCl_2$ are taken as 4.1 and 5.4 kcal/mole, respectively, as estimated by Kelley[6] from phase diagrams.

The experimental data do not fit this equation too well, since the best-fit value of b differs for the two sides of the diagram; a value of about 1.2 kcal is found for the $SrCl_2$ side, 0.6 kcal for the $BaCl_2$. The uncertainty in these b-values is rather large, however, and application of the symmetrical equation (3) with a value of $b = 1.0$ kcal may be equally reasonable. Fig. 2 shows that this gives a phase diagram quite similar to the experimental (minimum at 847°C and 71 mole percent $SrCl_2$). The differences between calculated and

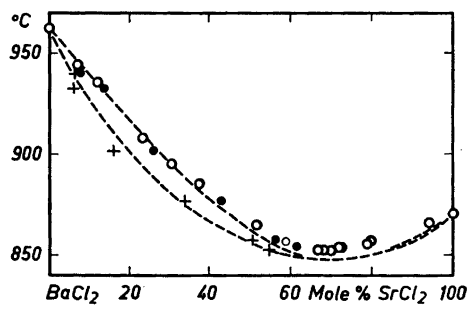

Fig. 2. The system $SrCl_2$ — $BaCl_2$. Dashed lines calculated (see text). Experimental points, same as in Fig. 1, shown for comparison.

experimental values seems not to be outside the possible errors caused by the approximations involved in eqn. (2) and by the probably inaccurate values for the heats of fusion.

EXPERIMENTAL

The liquidus of the system was determined by ordinary thermal analysis. A Pt/90 Pt 10 Rh thermocouple, with the bare leads dipping into the molten salt, was used for temperature measurement. The thermocouple was checked against the melting point of pure NaCl (800.4°C).

The solidus was determined by a method developed by Seltveit and Flood[3]. The principle is as follows: To a mixture of known composition within the system is added a small amount (*e.g.*, 0.05 %) of a radioactive third component which is soluble in the liquid, but insoluble in the solid phase of the system. The mixture is heated to complete fusion and the specific activity of this liquid is determined. Next, the mixture is cooled to a temperature where liquid and solid phases are coexistent, and kept at this temperature until equilibrium is established (usually overnight). A small sample of the liquid is then filtered off and its composition determined by chemical analysis. This analytical composition serves as a check on the liquidus obtained from thermal analysis. On another sample of the liquid, the specific activity is determined. From the increase in tracer content per gram of liquid (as compared to the content when the whole system was fused) the weight-ratio of liquid to solid can be determined, and thus the solidus.

The chemicals used were $BaCl_2$ *p.a.* and $SrCl_2$ *puriss. cryst.* (both from Merck A.G.) dried at 150°C. As tracer component was used $CsCl_2$ with a content of ^{134}Cs (half life 2.3 years) obtained from JENER, Lilleström, Norway. The assumption that the Cs^+ ion cannot enter the solid solutions of $SrCl_2$ — $BaCl_2$ was not proved by experiment. But it is known from previous work[3] that NaCl does not enter into solid solution in the $CaCl_2$ lattice, and the radius ratio r_{Cs+}/r_{Ba++} is more unfavourable than the ratio r_{Na+}/r_{Ca++} with respect to solid solution formation.

The salt mixtures were analyzed by conventional methods[4]. Barium was precipitated by an excess of potassium dichromate, and after filtration the excess of chromate was titrated with sodium thiosulphate. Strontium was taken as difference. As an extra check, the chloride content was determined by titration with silver nitrate, using chromate as indicator (after removal of barium by sulphate addition). The tracer activity was determined by an EKCO Scintillation Counter N 550.

Acknowledgement. Our investigations have been carried out with aid from *Statsminister Gunnar Knudsen og hustru Sophie f. Cappelen's Familjelegat (Borgestad Legat IV)* for which we wish to express our sincere gratitude.

REFERENCES

1. Vortisch, E. *Neues Jahrb. Mineral., Geol. Beilage* **38** (1914) 185.
2. Bergman, A. G. and Bukhalova, G. A. *J. Gen. Chem. USSR* **19** (1949) 553.
3. Seltveit, A. and Flood, H. *Acta Chem. Scand.* **12** (1958) 1030.
4. Scott, W. W. *Standard Methods of Chemical Analysis* Vol. I, 5th Ed. D. Van Nostrand Company, New York 1939, p. 128 and 272.
5. Flood, H., Cyvin, S. J. and Solli, O. *Unpublished work.*
6. Kelley, K. K. *Bureau of Mines, Bull.* **393** (1936) p. 20 and 117.

Received July 5, 1960.

ACTA CHEMICA SCANDINAVICA 14 (1960) 2071–2074

The Binding of the "Structural" Zinc Ions in Crystalline Insulin

K. MARCKER

Universitetets Fysisk-kemiske Institut, Copenhagen, Denmark

The site of binding of zinc in crystalline insulin has been investigated by determinations of the molecular weight of insulin which has been substituted on the N-terminal amino groups by phenyl-*iso*cyanate and of insulin in which all carboxyl groups have been methylated. It is shown that the N-terminal amino groups are essential for the zinc-binding capacity of insulin whereas the carboxyl groups are without importance as regards the binding of zinc to insulin. In conclusion it is made probable that the zinc is attached to the N-terminal amino group of phenylalanine.

It has long been known that insulin can only be crystallized in combination with a trace of zinc ions. The minimum amount of zinc ions sufficient for crystallization, *i.e.* the amount of zinc ions which belong to the crystal structure as an integral part was originally believed to be three atoms of zinc per unit cell. By repeated crystallization Schlichtkrull [2], however, demonstrated that the minimum amount of zinc sufficient for crystallization was only two atoms per unit cell. This result is in accordance with the work of Cunningham *et al.*[3] who studied the zinc-insulin system by the equilibrium dialysis technique at pH 7.3—7.6 in barbiturate-acetate buffer. These investigations demonstrated that 0.6—0.8 gram atom zinc per 12 000 g of insulin were bound so tightly to insulin that they could not be dialyzed away. This amount of zinc corresponds very closely to the two atoms of zinc per unit cell which were found by Schlichtkrull to have a structural significance in the crystal structure of insulin. The site of binding of these two zinc ions has been investigated by Tanford and Epstein [4], who obtained the hydrogen ion titration curves of zinc-free insulin and crystalline zinc-insulin. The crystalline insulin used was claimed to contain three atoms of zinc per unit cell. By comparison of the two titration curves obtained and by calculations in which the three zinc atoms were treated alike as being identically bound to insulin the authors concluded that each zinc atom is bound to two imidazole groups. To the author this conclusion seems not the only possible one. The titration data of Tanford and Epstein does not exclude the possibility of the participation of α-amino groups in the binding of zinc to insulin as also pointed out by Gurd and Wilcox [5]. As mentioned Tanford and Epstein in their calculations treated the zinc atoms as

being bound to identical sites. In view of the findings of Schlichtkrull and Cunningham *et al.* it remains questionable if this assumption is correct. It would seem that one of the three atoms of zinc is bound by a weaker force than the other two.

In a previous publication [6] a difference in the behaviour of zinc-free insulin from that of crystalline zinc-insulin was demonstrated. It was shown that in the entire pH range investigated, pH 2.10—9.10, zinc-free insulin is inhomogeneous with respect to molecular weight, which depended upon pH and insulin concentration of the solution. This is in contrast to crystalline zinc-insulin which at neutral and basic pH is monodisperse in solution having a molecular weight of 36 000. It is therefore possible to obtain information about the site of binding of zinc to insulin by using zinc-free substituted insulin and measure the molecular weights by means of osmometry with and without the addition of the calculated amount of zinc sufficient for crystallization (2 atoms per unit cell).

The determinations of the molecular weights were performed as described in a previous publication [6]. In this investigation two substituted insulins * were used: One being substituted by phenyl*iso*cyanate, and one in which the carboxyl groups have been esterified by methanol. The insulin substituted by phenyl*iso*cyanate (*Iso*insulin) was prepared according to Hallas-Møller [7]. In this procedure two groups are substituted. By chromatography according to the method of Andersen [8] it was shown that the groups substituted were the N-terminal amino groups of phenylalanine and glycine. Phenylhydantoins of glycine and phenylalanine which were prepared by the method of Mouneyrat [9], were used as standards.

The methylinsulin was prepared by the method of Mommaerts and Neurath [10]. The methylinsulin was shown to be biologically inactive. Its methoxyl content was determined at 3.27 % (theoretical 3.05 %). It can therefore be concluded that all six available carboxyl groups have been esterified. Both the *iso*insulin and the methylinsulin were prepared free of zinc.

The determinations of the molecular weights of the substituted insulins with and without zinc were first performed at neutral pH. On account of the solubility properties of *iso*insulin, methylinsulin, and crystalline zinc-insulin it is unfortunately impossible to measure all three insulins at the same pH. Therefore the methylinsulin was measured at pH 6.7 and *iso*insulin and crystalline zinc-insulin at pH 7.4. The buffer used was barbiturate-acetate adjusted to an ionic strength of 0.06. The results of these measurements are recorded in Fig. 1. The curves I and II represent the results obtained with zinc-free *iso*insulin and methylinsulin. It is seen that the shape of these curves in identical with that obtained for zinc-free insulin which was recorded in a previous publication [6]. By addition of the calculated amount of zinc (the zinc was added as the chloride) however, the curve representing the results obtained for zinc-free methylinsulin is transformed into curve III, which represents a monodisperse compound having a molecular weight of 36×10^3. By addition of the calculated amount of zinc to *iso*insulin it is seen that no effect could be demonstrated thus indicating that *iso*insulin is unable to bind zinc whereas the opposite is true of methylinsulin. Crystalline zinc-insulin containing two zinc atoms per unit cell is used as reference. The results obtained with this sample

* The substituted insulin was kindly prepared by "Novo Terapeutisk Laboratorium".

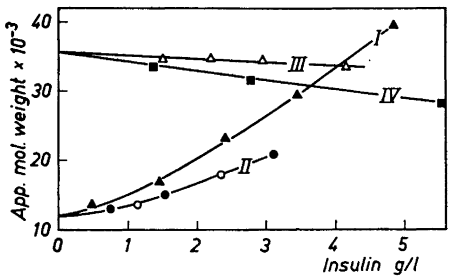

Fig. 1. Molecular weight determinations on *iso*insulin, methylinsulin and crystalline zinc-insulin. Ordinate: Apparent molecular weight; Abscissa: Concentration in g/l. I and III: Methylinsulin, ▲ without Zn^{++}, △ with Zn^{++}, pH = 6.7; II: *Iso*insulin, ● without Zn^{++}, ○ with Zn^{++}, pH = 7.4; IV: Crystalline zinc-insulin, pH = 7.4. All measurements performed in barbiturate-acetate buffer. I = 0.06 and temperature 20°C.

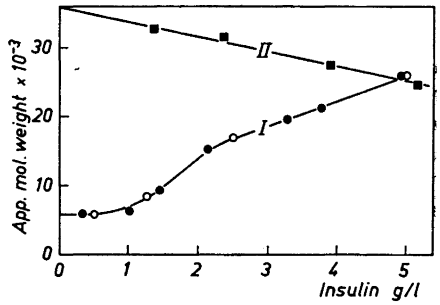

Fig. 2. Molecular weight determinations on *iso*insulin and crystalline zinc-insulin. I: *Iso*insulin, ● without Zn^{++}, ○ with Zn^{++}; II: Crystalline zinc-insulin. All measurements performed in barbiturate buffer. pH = 8.6, I = 0.2 and temperature 20°C.

are represented by curve IV, which indicates a monodisperse compound with a molecular weight of 36 × 10^3. The difference in the slopes of curve III and IV may be due to the difference in charges on methylinsulin and crystalline zinc-insulin.

In order to examine the behaviour of *iso*insulin more closely measurements were performed at pH = 8.6 in barbiturate buffer adjusted to the ionic strength 0.2 by addition of KCl. Crystalline zinc-insulin containing two zinc atoms per unit cell was again used as reference. The results are recorded in Fig. 2. It is clearly demonstrated that addition of the calculated amount of zinc has no effect on the behaviour of *iso*insulin.

From the experiments reported here one can safely conclude that the N-terminal amino groups of insulin are essential for the zinc-binding capacity of insulin, whereas the carboxyl groups seem to be without importance with respect to the binding of zinc to insulin. In insulin, however, there are two N-terminal amino groups, one from glycine and one from phenylalanine and the question still to be solved is the problem whether the zinc is bound to both amino groups or only to one of them. Support for the latter view comes from the experiments performed by Christensen [11] and especially from the work of Andersen [8]. Using the Edman procedure Christensen demonstrated that the N-terminal amino group of phenylalanine in crystalline zinc-insulin reacted to a much lesser extent than did the N-terminal amino group of glycine. By substitution of crystalline zinc-insulin with phenyl*iso*cyanate Andersen demonstrated that the first group to be substituted by this reagent was the N-terminal amino group of glycine. The N-terminal amino group of phenylalanine reacted more sluggishly with a considerably lower reaction rate. By column chromatography Andersen was able to separate two reaction products;

a mono-derivative which was substituted at the N-terminal amino group of glycine and a di-derivative which was substituted at both the available N-terminal amino groups. By sedimentation experiments performed with crystalline zinc-insulin and the mono- and di-derivatives of the substituted insulin Andersen [12] showed that crystalline zinc-insulin and the mono-derivative behaved identically in the ultracentrifuge as monodisperse compounds having a molecular weight of 36×10^3. The behaviour of the di-derivative in the ultracentrifuge was quite different from the behaviour of crystalline zinc-insulin and the mono-derivative. The di-derivative showed an inhomogeneous pattern and, under the experimental circumstances chosen, had a higher molecular weight than the crystalline zinc-insulin. This result is in complete agreement with the osmotic pressure data recorded here. Andersen interpreted his results in terms of interaction of non-polar groups, but in view of the findings herein presented a much more plausible explanation is possible. The explanation simply implies that the "structural" zinc is attached to the N-terminal amino group of phenylalanine. By assuming this it is readily understandable that the N-terminal amino group of glycine is the first to be substituted. Furthermore it is to be expected that substitution of this amino group will have no influence on the structure of the zinc-insulin complex, *i.e.* the substituted insulin should be monodisperse having a molecular weight of 36×10^3 in complete agreement with the findings of Andersen. By substitution also on the N-terminal amino group of phenylalanine, however, the structure of the insulin would be expected to deteriorate, since zinc is essential for the structure of the hexamer unit (mol.wt. 36×10^3). The behaviour of the di-substituted insulin should therefore be identical with the behaviour of zinc-free insulin in being polydisperse and having a molecular weight depending upon the insulin concentration and pH of the solution. This prediction is in complete accordance with the results obtained in this investigation and with the results obtained by Andersen. The above mentioned experiments therefore strongly support the view that in crystalline zinc-insulin the "structural" zinc is attached to the N-terminal amino group of phenylalanine.

Acknowledgements. The author wishes to thank Professor J. A. Christiansen and Dr. J. Schlichtkrull for their kind interest and many valuable suggestions. Financial support from "Statens Almindelige Videnskabsfond" is gratefully acknowledged.

REFERENCES

1. Scott, D. A. and Fischer, A. M. *Biochem. J.* **29** (1935) 1048.
2. Schlichtkrull, J. *Acta Chem. Scand.* **10** (1956) 1455.
3. Cunningham, L. W., Fischer, R. L. and Vestling, C. S. *J. Am. Chem. Soc.* **77** (1955) 5703.
4. Tanford, C. and Epstein, J. *J. Am. Chem. Soc.* **76** (1954) 2170.
5. Gurd, F. R. N. and Wilcox, P. E. *Advances in Protein Chem.* **11** (1956) 311.
6. Marcker, K. *Acta Chem. Scand.* **14** (1960) 194.
7. Hallas-Møller, K. *Chemical and Biological Insulin Studies* (Diss.) København 1945.
8. Andersen, W. *Compt. rend. trav. lab. Carlsberg, Sér. chim.* **30** (1956) 104.
9. Mouneyrat, A. *Ber.* **33** (1900) 2393.
10. Mommaerts, W. F. H. M. and Neurath, H. *J. Biol. Chem.* **185** (1950) 909.
11. Christensen, H. N. *Compt. rend. trav. lab. Carlsberg, Sér. chim.* **28** (1951) 265.
12. Andersen, W. *Compt. rend. trav. lab. Carlsberg, Sér. chim.* **30** (1956) 126.

Received July 11, 1960.

ACTA CHEMICA SCANDINAVICA 14 (1960) 2075–2080

The Reaction between *Iso*propoxy-methyl-phosphoryl Fluoride and Hydrogen Peroxide

GUNNAR AKSNES*

Norwegian Defence Research Establishment, Toxicological Group, Kjeller pr Lillestrøm, Norway

The reaction between *iso*propoxy-methyl-phosphoryl fluoride and hydrogen peroxide has been studied by measuring the amount of oxygen evolved during the reaction.
The mechanism of the decomposition reaction is discussed.

The bimolecular reaction between *iso*propoxy-methyl-phosphoryl fluoride and hydrogen peroxide has been studied by Larsson [1] by means of an automatic titration method. He concludes that the rate of the bimolecular reaction is proportional to the concentration of the anion of hydrogen peroxide. Gehauf *et al.*[2], Epstein *et al.*[3] and Larsson [1] suggest that the decomposition of the intermediately formed peroxyphosphorus acid is due to a bimolecular reaction of this acid with hydrogen peroxide. This last step is believed to be rate determining:

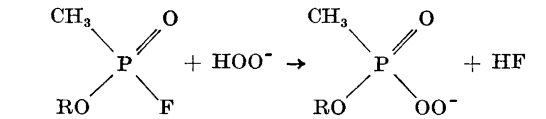

(1)

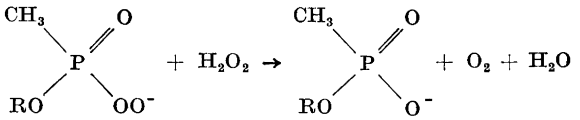

(2)

The kinetic of the second step of the above reactions has been the main interest of the present work. For this reason a volumetric method of measuring the oxygen evolution during the reaction has been developed.

* Present address: Chemical Institute, University of Bergen, Bergen, Norway.

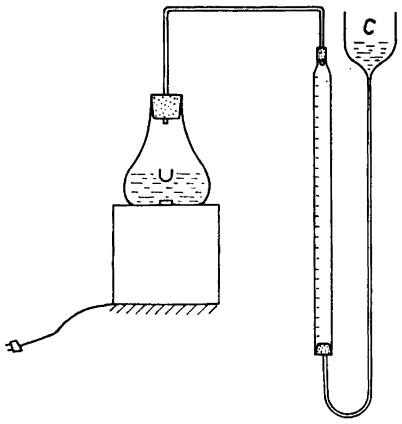

Fig. 1. Apparatus used for determination of the rate of oxygen evolution.

EXPERIMENTAL

*Materials. Iso*propoxy-methyl-phosphoryl fluoride was synthesized in this institute. Hydrogen peroxide was an E. Merck anal. reagent. The concentration of the hydrogen peroxide solutions was determined by titration with 0.1 N solution of potassium permanganate.

Kinetic measurements. The apparatus used for the study of the oxygen evolution is shown in Fig. 1. The oxygen is collected in a burette of 50 ml capacity connected by a glass tube to the reaction vessel. The reaction vessel consisted of a 100 ml Erlenmeyer flask. Fifty ml of hydrogen peroxide solution containing 0.2 M buffer was placed in the reaction vessel. The weighed sample of the fluorophosphorus compound was placed in a small conical glass vessel. The vessel was brought into the Erlenmeyer flask and placed on the surface of the hydrogen peroxide solution in floating position. The reaction is started by tipping the content of the conical flask into the solution. This is simply obtained by starting the magnetic stirrer whereupon the reaction vessel was placed. The amount of oxygen evolved is found by lowering of the level of the water in the container

Table 1. The reaction between *iso*propoxy-methyl-phosphoryl fluoride and hydrogen peroxide. Buffer: 0.2 M citrate — phosphate pH = 7.

0.000546 M fluorophosphorus compound +4.0 %H_2O_2 Temp. 18°C.	Time (min)	5	10	15	23	31	43	58	73	95	105	Calculated rate constant
	Oxygen evolved, cm^3(corr.)	(0.2)	(0.6)	1.8	2.9	3.2	4.4	5.0	6.0	6.1	6.2	0.026 min^{-1}
0.00160 M fluorophosphorus compound +4.0 %H_2O_2 Temp. 18°C.	Time (min)	9	19	26	32	44	54	65	73	100		Calculated rate constant
	Oxygen evolved cm^3(corr.)	(3.6)	7.5	9.5	10.0	13.3	14.8	16.3	16.9	17.8		0.026 min^{-1}

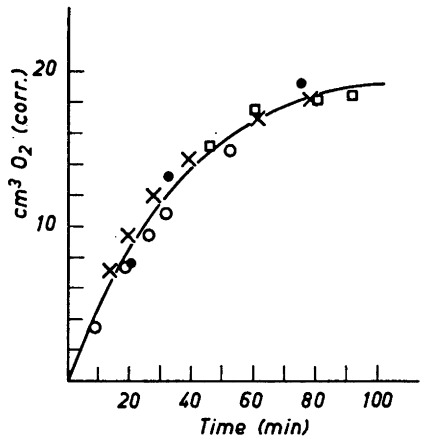

Fig. 2. The evolution of oxygen at different hydrogen peroxide concentration. Buffer 0.2 M citrate-phosphate, pH = 7.00. Temp. 18°C. Concentration of *iso*propoxy-methyl-phosphoryl fluoride: 0.0016 M. Hydrogen peroxide concentration: ×, 1.93 %; O, 2.98 %; ●, 3.94 %; □, 4.78 %.

C until the same level as the water in the burette. The water in the burette and the container is saturated with oxygen at room temperature. Correction was always made for the amount of oxygen evolved at the different pH studied due to the self-decomposition of the hydrogen peroxide solution. The self-decomposition was found to rise rapidly with increasing pH.

RESULTS

In Table 1 are recorded the experimental values of the oxygen evolution of two different concentrations of the fluorophosphorus compound when the hydrogen peroxide concentration is maintained constant. We find that the amount of oxygen evolved is proportional to the concentration of the fluorophosphorus compound.

In Fig. 2 are recorded the rates of oxygen evolution at four different concentrations of hydrogen peroxide. The concentration of the *iso*propoxy-methyl-

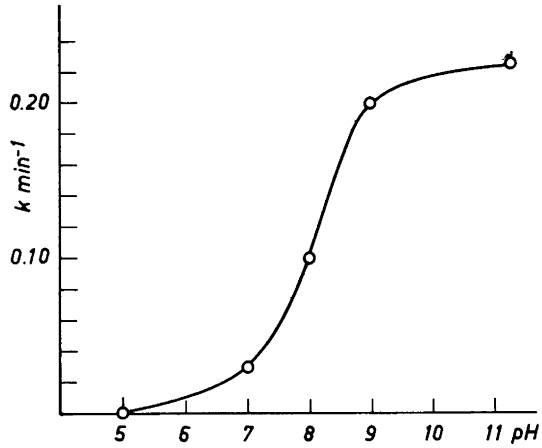

Fig. 3. The relation between the rate of oxygen evolution and pH of the solution. Buffers: 0.2 M citrate-phosphate (pH = 5, 7 and 8). 0.2 M boric acid-sodium hydroxide pH = 9. 0.2 M potassium dihydrogenphosphate-potassium hydroxide (pH = 11.3). Hydrogen peroxide concentration = 4 %.

phosphoryl fluoride is maintained constant. The full-drawn curve in Fig. 2 shows a first order reaction with a rate constant of 0.03 min^{-1}. The experimental points of the oxygen evolution at the four different hydrogen peroxide concentrations in Fig. 2 show average deviation of about 5 % from the first order reaction curve. This is within the limits of the experimental errors of the applied technique.

In Fig. 3 is plotted the rate constants of the oxygen evolution at five different pH (5, 7, 8, 9 and 11.3) as function of pH.

Some experiments were performed in order to determine the amount of hydrogen peroxide consumed when the decomposition reaction approached completion. When the initial concentration of hydrogen peroxide in the reaction solution varied between 0.010 M and 0.1 M the ratio between the hydrogen peroxide decomposed and the total concentration of fluorophosphorus compound varied between 1.5 and 1.9.

DISCUSSION

The first order rate of oxygen evolution which is observed under the conditions of the present experiments shows that the formation of the peroxyphosphorus acid according to eqn. (1) must be much more rapid than its decomposition, *i.e.* the decomposition of the peroxyphosphorus acid is the rate determining step. This observation is in agreement with the findings of Larsson [1]. From his calculated pseudo first order rate constant of the reaction between *iso*propoxy-methyl-phosphoryl fluoride and hydrogen peroxide at 25°C we may estimate that the pseudo first order reaction of the same step under the present conditions will be so rapid that the deviation of the second step from the first order reaction rate will not be observable.

The present results do not confirm the assumption of Gehauf *et al.*[2] and Epstein *et al.*[3] that the decomposition of the peroxyphosphorus acid is a true bimolecular reaction with hydrogen peroxide. If that had been so the ratio between the amount of hydrogen peroxide decomposed and the total concentration of fluorophosphorus compound should approach 2 at all concentrations of hydrogen peroxide. The present results and the observation of Larsson [1] are not in accordance with this reaction scheme. Another argument against this view is found in the results quoted in Fig. 2. The hydrogen peroxide in the four separate experiments is in sufficiently great excess as compared with the fluorophosphorus compound to give the postulated second order reaction between the peroxyphosphorus acid and hydrogen peroxide a pseudo first order character. The rate of oxygen evalution should therefore be expected to be proportional to the hydrogen peroxide concentration. On the contrary the results show nearly the same rate of oxygen evolution at the four different concentrations of hydrogen peroxide. It seems therefore reasonable to conclude that the hydrogen peroxide does not participate in the rate determining decomposition of the peroxyphosphorus acid. Larsson [1] has postulated a competing reaction between peroxyphosphorus acid and unreacted fluorophosphorus compound to explain the deviation of the second order kinetics of the decomposition of the peroxyphosphorus acid at low concentration of hydrogen peroxide. But it is difficult to explain the results quoted in Fig. 2

according to such a hypothesis. A more reasonable explanation seems therefore to be that the decomposition of the peroxyphosphorus acid is a rate-determining unimolecular reaction (perhaps influenced by the solvent or the glass wall) and that the oxidation of the hydrogen peroxide is a rapid process between "active oxygen" and hydrogen peroxide. The decreasing consumption of hydrogen peroxide with decreasing hydrogen peroxide concentration can then be explained to be due to a competing pairing formation of "active oxygen" to molecular oxygen:

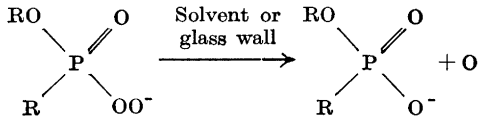

(1)

$$O + H_2O_2 \rightarrow O_2 + H_2O \text{ and } O + O \rightarrow O_2 \quad (2)$$

A support for this view may be found from different sources concerning the decomposition of peroxide compounds [6].

The S-shaped relation between the decomposition of the peroxyphosphorus acid and the pH of the solution suggest that the decomposition proceeds *via* the anion of the peroxy acid and that the pK of this acid may have a value of approximately 8. Everett *et al.*[4] have found that the pK values of peroxy fatty acids lie in the range of pK 7.1—8.3. By analogy to the difference between the pK values of fatty acids and substitued phosphorus acids (the last-mentioned are 2—3 pH-units lower) Larsson [1] assumes that the difference between the pK of the corresponding peroxyacids is of the same order of magnitude. This need not necessary be so because the stabilization effect due to the perfect resonance of the anions of the oxyacids do not exist in the peroxyacids. It seems therefore doubtful that the inductive mechanism which must be assumed to be the chief electronic effect operating in the peroxyacids is able to maintain the same difference between pK-values of different peroxyacids as between corresponding oxyacids This argument is strengthened by the observation of Everett *et al.*[4] that the differences in the inductive effects between H, CH_3, C_2H_5, *iso*-C_3H_7 which are clearly reflected in the differences between the pK-values of water and alcohols are almost absent in the same serie of hydroperoxides. It is also some reason to question the accuracy of the titrimetric method used by Everett *et al.*[4] for determination of the pK-values of peroxyacids. This method may be encumbered with error due to the instability of the peroxyacids. This decomposition which produces the corresponding oxyacids increases rapidly with the rise of pH and will give as result that the observed pK-value of the peroxyacid will lie below the actual one. The error will increase with increasing rate of decomposition and increasing length of time used to obtain the titration curve. In Holleman-Richters' textbook of organic chemistry [5] the dissociation constant of peroxyacetic acid is quoted as 4×10^{-10} (pK = 9.4). Unfortunately the authors give no reference to the original work from which this value is taken. It seems also worth while to mention that the pK of the bisulphate ion and its corresponding peroxyacid are 1.7 and 9.4, respectively [7].

REFERENCES

1. Larsson, L. *Acta Chem. Scand.* **12** (1958) 723.
2. Gehauf, B., Epstein, J., Wilson, G. B., Witten, B., Sass, S., Bauer, V. E. and Ruegge-berg, W. H. C. *Anal. Chem.* **29** (1957) 278.
3. Epstein, J., Demek, M. M. and Rosenblatt, D. H. *J. Org. Chem.* **21** (1956) 796.
4. Everett, A. J. and Minkoff, G. J. *Trans. Faraday Soc.* **49** (1953) 410.
5. Hollemann, A. F. and Richter, F. *Lehrbuch der Organischen Chemie.* W. de Gruyter and Co., Berlin 1953, p. 97.
6. Cyrkin, J. K. and Moiscev, I. I. *Uspekhi Khimii U.S.S.R.* **19** (1960) 425.
7. Fortnum, D. H., Battaglia, C. J., Cohen, S. R. and Edwards, J. O. *J. Am. Chem. Soc.* **82** (1960) 778.

Received July 12, 1960.

ACTA CHEMICA SCANDINAVICA 14 (1960) 2081–2088

Oxidation of 3-Hydroxy-Anthranilic Acid by Human Serum

GÖSTA EHRENSVÄRD*, JAN LILJEKVIST**, and ROBERT G. HEATH***

Institute of Biochemistry, University of Lund, Lund, Sweden, and Department of Psychiatry and Neurology, Tulane University School of Medicine, New Orleans, Louisiana, U.S.A.

The oxidation of 3-hydroxy-anthranilic acid by human serum has been investigated by fluorimetric techniques. The influence of some activators and inhibitors has been studied. By examination of approximately one hundred samples of sera from various origins, it has been found that the partial inhibition by cyanide is subject to a considerable variation. In sera from schizophrenic subjects the cyanide inhibition in per cent of total oxidation ranges from 0 to 6 %; in some cases there is a slight activation. In normal controls the corresponding range is from 6 to 20 %. The overlapping between the groups is about 15 %.

In the plethora of reactions involved in tryptophan metabolism 3-hydroxy-anthranilic acid (HOA) keeps a position as an intermediary metabolite. Its formation through enzymatic cleavage of 3-hydroxy-kynurenine has been demonstrated in a variety of organisms [1–4]. In man the main route for disposal of 3-hydroxykynurenine seems to involve its transformation *via* oxidative desamination and ringclosure to xanthurenic acid and derivatives of this compound [5]. Since, however, a minor fraction of tryptophan metabolized in man is providing part of his nicotinic acid supply [6,7], and this reaction in mammals has been demonstrated to involve an oxidative splitting and rearrangement of HOA [3–10] the existence of the latter compound in human organism is indirectly indicated. The demonstration by Wiss [3] of the presence of kynureninase in pig liver, catalyzing the conversion of 3-hydroxy-kynurenine to HOA, gives additional, although indirect, support to the assumption of HOA partaking in human metabolism as an intermediate. Another indication is the recent finding of conjugated derivatives of HOA in human urine [11,12].

* Chairman, Institute of Biochemistry, University of Lund; Visiting Professor to the Department of Psychiatry and Neurology and the Department of Biochemistry, Tulane University School of Medicine.

** Assistant, Institute of Biochemistry, University of Lund; Visiting Research Associate to the Department of Psychiatry and Neurology, Tulane University School of Medicine.

*** Professor and Chairman, Department of Psychiatry and Neurology, Tulane University School of Medicine.

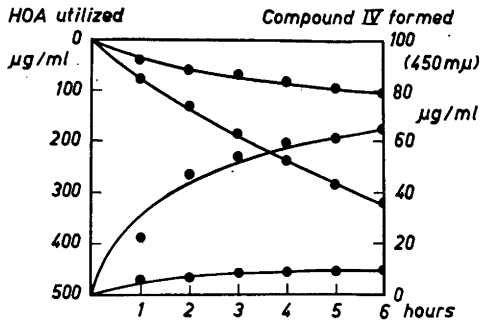

Fig. 1. Diagram of HOA-oxidation by human serum and the corresponding formation of compounds absorbing at 450 mµ. Figures in µg per ml of reaction mixture.

In view of the marked tendency of HOA to form a variety of oxidation products under various conditions, as shown by Butenandt *et al.*[13], it should be expected that a small fraction of HOA in circulation should give rise to similar products, related to phenyl-quinoneimides and phenoxazines. An indication of this is a finding that rat liver homogenate forms from HOA a red pigment, possibly related to the phenoxazines of Butenandt [14]. The present work is an investigation of the oxidation of HOA by human serum under different conditions.

As a preliminary experiment 2 ml of serum were incubated at 30°C with 2 ml of a 0.1 % solution of HOA in 0.02 M tris-buffer. At intervals 25 µl samples were taken and analyzed for HOA and compounds absorbing at 450 mµ; see Fig. 1. The result showed a rapid disappearance of HOA and a steady, but not stoichiometric rise of compounds absorbing at 450 mµ. The similar situation, but at a slower rate appears in a parallel run without serum; *i.e.* the result of pure autoxidation. Examination by paper chromatography of the formed reaction products showed the same distribution of spots, coloured and fluorescent in UV, for both runs, the solvent being butanol-propanol-water (1:2:1). The R_F-values and the colours of some of the spots indicate identity with Butenandt's "compounds III and IV" [14].

In order to elucidate some aspects of the serum factors involved in HOA-oxidation, a series of experiments with various inhibitors were performed. The results indicate that only a part of the total oxidation was sensitive to inhibitors, and thus could represent an enzymatic mechanism. In view of the fact that metal ions in combination with serum proteins could bring about a nonspecific oxidation of a variety of substances (for a general review of this subject see Ref.[15]) the influence of some metal ions upon the HOA-oxidation was studied with and without the presence of human serum. As a further development a comparative study of the HOA-oxidation in human serum from various sources was performed, with special reference to subjects with clinical symptoms of schizophrenia, and with normal healthy subjects as controls.

EXPERIMENTAL

For the determination of the rate of HOA-oxidation under various conditions the following procedure was used: To a series of 10 ml Erlenmeyer flasks 2 ml of serum, or 2 ml of a 0.9 % NaCl-solution, was added, followed by additional solutions of various activators and/or inhibitors in 100 μl quantities. (Corrections for these minor additions were made when necessary in order to keep the volumes constant.) When cyanide was used as inhibitor, the solution (0.4 M) was neutralized with HCl against phenol red. Thereafter 2 ml of a 0.1 % HOA-solution in 0.02 M tris-buffer, pH 7.5, were added and the flasks incubated at 30°C under gentle shaking. (Dubnoff Metabolic Shaking Incubator). At intervals, 25 μl samples were withdrawn and diluted with 2 ml of a 0.9 % NaCl-solution. These diluted samples were analyzed in an Aminco-Bowman Spectrophotofluorimeter, for their HOA-content; activation maximum 330 mμ fluorescence wave-length 415 mμ. The instrument was calibrated within the range used by a series of HOA-solutions of known concentrations with the same amount of serum added from a mixture of 2 ml of HOA-solution and 2 ml of serum, 25 μl were taken and diluted as above with 2 ml of saline solution.

The human sera were usually prepared from bloodsamples drawn in the early morning, before eating. They were immediately stored at + 2°C, and, as a rule, analyzed the same day. The schizophrenic patients providing the serum for this study were hospitalized on a special Tulane University research unit at the East Louisiana State Hospital at Jackson. These patients were under intensive observation on the unit for a minimum period of 3 years. Agreement on the diagnosis of schizophrenia had been reached by a minimum of 4 psychiatrists and 2 clinical psychologists. The various clinical subcategories of schizophrenia were represented almost equally, *i.e.*, catatonia, paranoia, hebephrenia, and chronic undifferentiated schizophrenia. All patients selected for these special wards were required to meet exacting clinical and laboratory criteria. They had been hospitalized for a minimum of 3 years without clinical remission. They were under 45 years of age

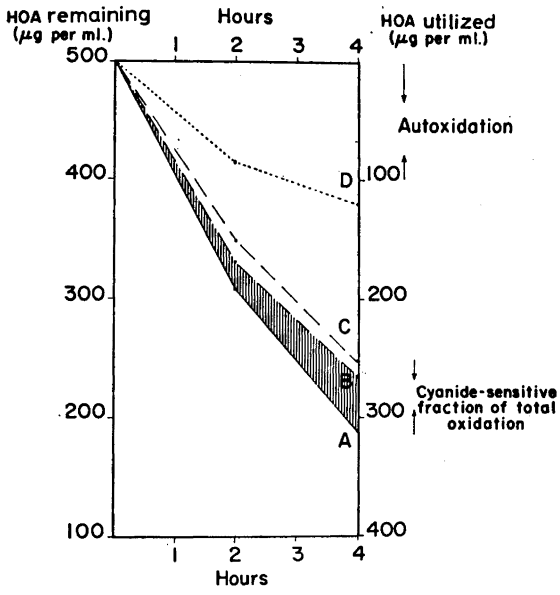

Fig. 2. Diagram of HOA-oxidation by human serum during 4-hour period, curve A. The curves B and C represent the rate of oxidation in the presence of 0.01 M NaCN, and 0.001 M NaN_3. The shaded region between curves A and B represents the cyanide-sensitive fraction of total oxidation. Curve D shows the oxidation rate without serum.

Table 1. Influence of Cu^{2+} and Mn^{2+} in a concentration of 0.0001 M upon the oxidation of HOA in the presence of human serum and without, 4 hours incubation at 30°C. Figures denote μg HOA consumed per ml of incubation mixture. Starting concentration 500 μg per ml.

	Without serum			With serum		
	0	Cu^{2+}	Mn^{2+}	0	Cu^{2+}	Mn^{2+}
+ 0.01 M NaCN	50	145	405	280	310	437
0	30	195	170	315	328	472
Difference:	+ 20	−50	+ 235	−35	−18	−35

completely negative on physical and neurological examinations and on a large number of routine laboratory tests, including a battery of liver tests. The minimal educational level for the group was 9th grade. A special diet was provided for the patients on these wards which included extra rations of meat and daily vitamin supplements.

The normal control group was composed of staff and faculty of the Tulane Department of Psychiatry and Neurology and carefully selected medical students. Each student was screened by a minimum of 2 members of the team of research psychiatrists after having been observed for a minimum of 3 weeks while on the psychiatric teaching block of the curriculum. All normal controls were required to have a negative family history for nervous and mental disease.

RESULTS

A comparison between the rate of HOA-oxidation by human serum and plain autoxidation gives an approximate ratio of 2:1 for a 2-hour period, and 2.5:1 for a 4-hour period; see Fig. 2. The influence of inhibitors is shown in curve B and C, depicting the oxidation rate in the presence of 0.01 M NaCN and 0.001 M NaN_3. As seen the inhibition is not very great, 15 % at the most for a 4-hour run. However, this percentage represents most likely the part of the total oxidation, which is connected with an enzymatic mechanism; the rest being a non-specific oxidation brought about by metal-protein complexes. For simplicity in the following, we will use the category type I- and type II-oxidations, of which type II represents the cyanide-azide-sensitive fraction.

In order to evaluate the influence of metal ions upon HOA-oxidation of type I and type II, experiments were carried out under the same standard conditions, with and without the presence of various metal ions at a total concentration of 0.0001 M. The result is shown in Table 1.

This experiment demonstrates the relative activating influence of copper and manganese ions upon the HOA-oxidation, whereby manganese exerts a stronger influence than copper. The activating effect of the manganese is especially marked in the presence of cyanide, without serum. In the presence of serum, the activating effect of manganese is not further enhanced by cyanide. Probably the effect of Mn^{2+} in the concentration used, both upon cyanide, 0.01 M, and serum, has a common denominator, namely a tendency to formation of a complex which would function as a HOA-"pseudo"-oxidase.

Table 2. Influence of Cu^{2+} and Mn^{2+} in a concentration of 0.0001 M upon the oxidation of HOA in the presence of coeruloplasmin, 300 μg per ml, 3 hours incubation at 30°C. Figures denote μg HOA consumed per ml of incubation mixture. Starting value 500 μg per ml.

	Without Coeruloplasmin		With Coeruloplasmin		
	Cu^{2+}	Mn^{2+}	0	Cu^{2+}	Mn^{2+}
+ 0.01 M NaCN	75	340	66	120	315
0	130	90	45	330	210
Difference:	−55	+ 250	+ 21	−210	+105

As both Cu^{2+} and Mn^{2+} are normal serum constituents, the former to some extent or possibly totally, protein bond as coeruloplasmin [16], it was appropriate to investigate the oxidation of HOA by this metal-protein alone, and in the presence of cyanide, with and without the addition of free Cu^{2+} and Mn^{2+} ions. For comparison, a similar set of experiments was carried out with the copper-containing enzyme ascorbic acid oxidase (AAO), isolated by Dawson [17]. The results of these two experiments are shown in Tables 2 and 3.*

As seen, the pattern of activation and inhibition of coeruloplasmin compared to AAO differs so far as AAO is a quite effective oxidase for HOA, whereas coeruloplasmin (CP) is a very sluggish enzyme against this substrate. With regard to inhibition AAO is almost completely inhibited by cyanide, in contrast to CP. The two Cu^{2+} enzymes differ also with regard to the activation. CP is strongly activated by Cu^{2+}, and to a less extent by Mn^{2+}, whereas the activity of AAO on the whole is not enhanced by Cu^{2+}, but is activated to some extent by Mn^{2+}. The intricate interplay between inhibition and activation is illustrated for instance in the case of AAO, where cyanide apparently does not

Table 3. Influence of Cu^{2+} and Mn^{2+} in a concentration of 0.0001 M upon the oxidation of HOA in the presence of ascorbic acid oxidase (AAO), 5 units per ml, 3 hours incubation at 30°C. Figures denote μg HOA consumed per ml of incubation mixture. Starting value 500 μg per ml.

	Without AAO		With AAO		
	$+Cu^{2+}$	Mn^{2+}	0	$+Cu^{2+}$	Mn^{2+}
+ 0.01 NaCN	100	332	30	85	330
0	150	80	225	230	320
Difference:	−50	+252	−195	−145	+10

* For highly purified sample of coeruloplasmin we wish to express our gratitude to KABI AB, Stockholm. Likewise we are greatly indebted to professor C. R. Dawson, Columbia University for a generous gift of crystalline ascorbic acid oxidase.

Table 4. Typical 4-hour run with serum from 4 normal (Nos. 1, 4, 7, 8) and 5 schizophrenic (Nos. 2, 3, 5, 6, 9) subjects. Figures denote μg HOA consumed per ml of incubation mixture. Starting concentration 500 μg HOA per ml.

	1	2	3	4	5	6	7	8	9
+ 0.01 M NaCN	299	305	296	292	322	335	309	287	310
0	311	336	311	327	334	316	330	322	300
Difference:	12	31	15	35	12	−19	21	35	−10
Δ %	3.9	9.2	4.9	10.7	3.5	−5.2	6.4	10.9	−3.3

inhibit the Mn^{2+}-activated enzyme. Yet the explanation could be that the cyanide inhibition of AAO (difference −225) is in this case counteracted by a pure cyanide-activation of Mn^{2+} as such (difference + 272). With regard to CP, it is evident that Cu^{2+} and, to a less extent Mn^{2+}, evoke a HOA-oxidase activity in this copper-protein complex, which may have a bearing to the HOA-oxidase activity in serum, of the cyanide sensitive type II.

DISCUSSION

As a tentative hypothesis we suggest that in human serum the cyanide sensitive part of HOA-oxidation — type II — is brought about by some combination of metal ions and some special proteins. Cu^{2+} and Mn^{2+} have been shown to exert an activating influence upon coeruloplasmin, in itself a copper-protein complex, still it is possible that another complex of similar kind, not implicating coeruloplasmin, could be involved in the HOA-oxidation, type II.

With regard to the absolute rate of HOA-oxidation in sera from various human subjects, it has been found that this rate varies from case to case. Examining the material from approximately one hundred HOA-oxidation tests, we found that on the whole the rate of oxidation is lower for sera from subjects with chronic schizophrenia as compared to sera from the groups of normal, healthy subjects. As seen from Table 4, the differences in oxidation rate between schizophrenics and normals is partly eliminated when cyanide or azide is added to the reaction.

Expressing the cyanide effect, Δ %, as $\frac{a-b}{a} \times 100$, where a is the total HOA consumed during a 4-hour period, and b is the corresponding amount of HOA consumed in the presence of cyanide, we find that the value for schizophrenics is encountered in the lower range −2→6, and the normal controls in the higher range 6→20; see Fig. 3.

These findings indicate that in serum from schizophrenics, the type II-oxidation of HOA constitutes a smaller fraction of the total HOA-oxidation, as compared with serum from the control group. In about 20 % of the schizophrenics type II-oxidation is virtually absent.

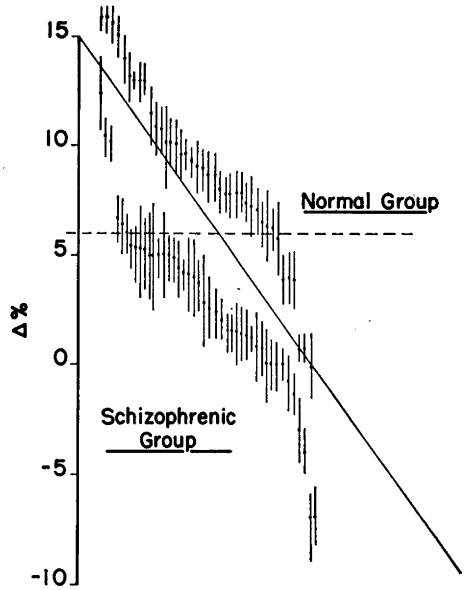

Fig. 3. Diagrammatic representation of Δ %-values for the cyanide effect on HOA-oxidation by serum from schizophrenic subjects as compared with the corresponding values for normal controls. Standard variations of individual test-runs are shown as verticals lines. Overlapping of the two groups less than 15 %. The division line at value 6 is arbitrarily taken as a boundary between the two groups.

Being aware of the fact that the rate of oxidation of various substrates by human serum could be influenced by various external factors, as well as internal, we have, whenever possible, tried to sample the sera examined from subjects on the same diet. With regard to different levels of ascorbic acid in sera, which previously has been shown to influence the rate of other oxidation reactions [18], we find that addition of 50 μg per ml serum before running a HOA test did not influence either the reaction rate or the cyanide effect. With regard to the general concept of diurnal variations under fasting and non-fasting conditions the results of a test series from two schizophrenics show slight variations in the Δ % values, the range being for one subject 1.4→1.6, for the other —4.8 → 2.3 (samples taken at 07.30 and 19.30). As comparison, two normal controls were tested in the same way, one showing the range 7.9→4.9, the other 15.0→3.8, thus considerable variation during the day. It should, however, be emphasized that the delta values recorded in Fig. 3 are all derived from morning samples of sera in order to eliminate diurnal variations. These data demonstrate a convincing difference between the two groups, the overlapping being less than 15 %. The question of the diurnal variations in normals, as well as the general problems of the relationship of the HOA oxidation to the clinical syndrome of schizophrenia, will be subject of continuing investigation.

REFERENCES

1. Jacoby, W. and Bonner, D. M. *J. Biol. Chem.* **205** (1953) 699, 709.
2. Miller, I. L. and Adelberg, E. A. *J. Biol. Chem.* **205** (1953) 691.
3. Wiss, O. *Helv. Chim. Acta* **32** (1949) 1694.
4. Wiss, O. *Z. physiol. Chem. Hoppe-Seyler's* **293** (1953) 106.

5. Price, J. M. and Dodge, L. W. *J. Biol. Chem.* **223** (1953) 699.
6. Dalgliesh, C. E. *Intern. Congr. Biochem. 4th Meeting Symposium* **11**.
7. Horwitt, M. K. *Am. J. Clin. Nutrition* **3** (1955) 244.
8. Bokman, A. H. and Schweigert, D. S. *Arch. Biochem. Biophys.* **33** (1951) 270.
9. Wiss, O. *Z. Naturforsch.* **9b** (1954) 740; **11b** (1956) 54.
10. Wiss, O. *Z. physiol. Chem. Hoppe-Seyler's* **304** (1956) 237.
11. Boyland, E. *Nature* **177** (1956) 837.
12. Boyland, E. *Biochem. J.* **64** (1956) 578.
13. Butenandt, A., Keck, J. and Neubert, G. *Ann.* **602** (1957) 61.
14. Viollier, G. and Süllmann, H. *Helv. Chim. Acta* **33** (1950) 776.
15. Massart, L. and Vercauteren, R. *Annual. Rev. Biochem.* **28** (1959) 527.
16. Holmberg, C. G. and Laurell, C. B. *Acta Chem. Scand.* **2** (1948) 550.
17. Dawson, C. R. and Tarpley, W. B. in Sumner, J. B. and Myrbäck, K. (eds) *The Enzymes*, vol. 2, p. 454. (Academic Press Inc. N.Y. 1951).
18. Åkerfeldt, S. *Science* **125** (1957) 117.

Received June 2, 1960.

ACTA CHEMICA SCANDINAVICA 14 (1960) 2089–2096

Dehydrogenation of Phenols

II. Dehydrogenation Polymers from Guaiacol

BENGT O. LINDGREN

Wood Chemistry Department, Swedish Forest Products Research Laboratory, Stockholm Ö, Sweden

The dehydrogenation polymers which are obtained from guaiacol by treatment with silver oxide, potassium ferricyanide, sodium persulphate and an oxygen-laccase system have been examined. The first two reagents gave polymers in which the phenol units were linked together with ether bonds (Formula II) while the other two reagents produced polymers with carbon-carbon bonds (Formulae III and IV).

It was shown in an earlier paper [1] that 2,6-dimethylphenol on dehydrogenation with silver oxide is transformed mainly into a polymer * with ether linked phenol units (I). In connection with studies on lignin, which is probably formed by dehydrogenation of coniferyl alcohol by an oxygen-laccase system [2], it seemed to be of interest to examine the dehydrogenation of guaiacol also. Silver oxide, potassium ferricyanide, persulphate catalysed with ferro-ions, and oxygen-laccase were used as oxidation systems.

Silver oxide dehydrogenation

The dominant product obtained on treating a benzene solution of guaiacol with silver oxide was a polymeric material. 3,3′-Dimethoxy-4,4′-dihydroxydiphenyl was also isolated but the yield was low. This compound has previously been obtained in low yield from guaiacol by electrolytic oxidation [3].

The polymeric material was an amorphous, light-coloured powder with the formula $[C_6H_3O(OCH_3)]_n$, where n is higher than 6. Its structure was determined mainly by using spectrophotometric methods.

The NMR spectrum of the polymer showed no peak for aliphatic or olefinic hydrogen except that for the hydrogen in methoxyl groups. The aromatic structure of at least the greater part of the guaiacol nuclei had therefore not been destroyed during the oxidation. The UV spectra in neutral (Fig. 1) and alkaline solutions differed only slightly showing that the proportion of phenolic groups present was low [4].

* See addendum p. 2096.

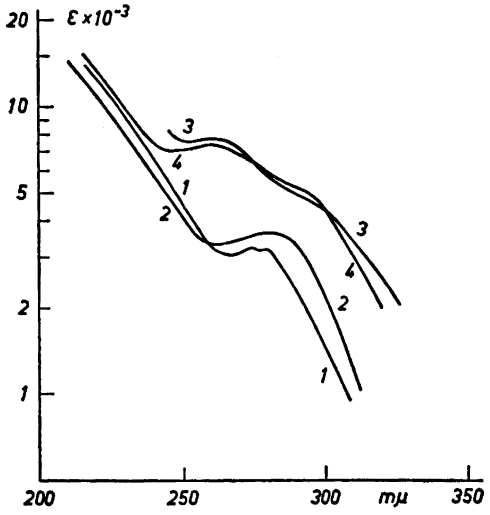

Fig. 1. UV spectra of guaiacol polymers. Oxidation reagents: 1) silver oxide, 2) potassium ferricyanide, 3) laccase plus oxygen, and 4) sodium persulphate plus ferro-ions. Solvent: ethanol. The ε values are calculated for one C_6-unit.

The IR spectrum of the polymer (Fig. 2) has no or, in some preparations, only weak carbonyl bands. Its hydroxyl content, determined by acetylation, was low. The two samples examined contained one hydroxyl group to 14 and to 5 C_6-units, respectively. The polymer contained no peroxide groups.

Most of its oxygen atoms must for these reasons be present in ether groups, and the polymer is therefore built up in the same way as the polymer from 2,6-dimethylphenol *i.e.* phenol units linked by ether bonds. Its formula is then (II).

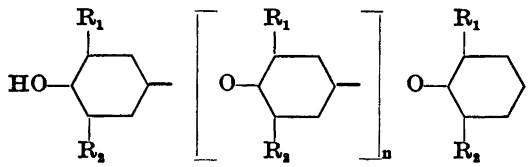

I. $R_1 = R_2 = CH_3$
II. $R_1 = OCH_3$, $R_2 = H$

It has been assumed that the ether bond links the carbon atom of guaiacol which in almost all reactions has the greatest reactivity, *i.e.* that in the *para* position to the phenolic group. Even if an *ortho* carbon linkage seems less likely it cannot however at present be excluded.

The dimeric compound (II, n = 0) could not be isolated from the oxidation mixture even though a considerable amount of guaiacol was recovered. This may be explained as in the dimethylphenol oxidation [1] by a faster rate of oxidation for the dimer than for guaiacol.

When the silver oxide dehydrogenation was done in a mixture of dimethylformamide and methyl iodide, veratrol and the polymer (II) were obtained, indicating that the methylation competed better with the oxidation of guaiacol than with the oxidation of the dimer. This is a further proof of the easier oxidation of the dimer than of the guaiacol.

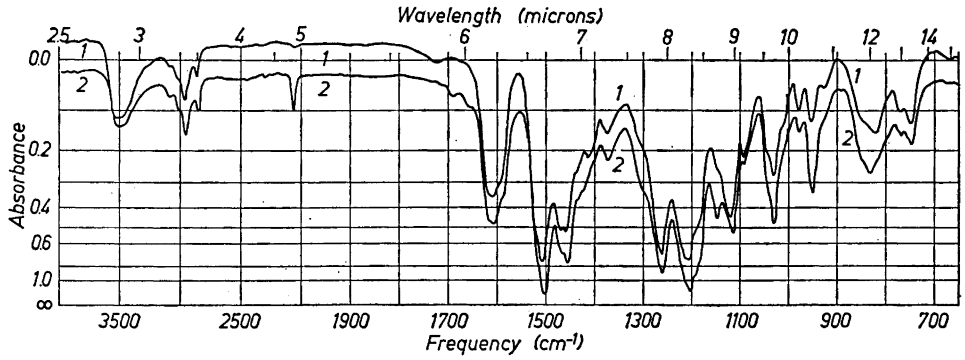

Fig. 2. IR spectra of guaiacol polymers. Oxidation reagents: 1) silver oxide, and 2) potassium ferricyanide. Potassium bromide disc.

Potassium ferricyanide dehydrogenation

Potassium ferricyanide in alkaline solution transformed guaiacol into a grey amorphous product, the UV and IR spectra of which (Figs. 1 and 2) agreed so closely with those of the silver oxide polymer that they must be structurally similar.

Laccase-oxygen dehydrogenation

Treatment of guaiacol with oxygen in the presence of laccase or peroxidase gives a bright red dehydrogenation polymer, which has been called "tetraguaiacoquinone" by Bertrand [5]. Booth and Saunders [6] in addition to "tetraguaiacoquinone" also obtained a very small amount of 2,2′-dihydroxy-3,3′-dimethoxy-diphenyl. Reductive acetylation of the polymer gave, also in a very low yield, the diacetate of 3,3′-dimethoxy-4,4′-dihydroxy-diphenyl. From this they concluded that "tetraguaiacoquinone" is a polymer of guaiacol units linked together with carbon-carbon bonds (III) and that the red colour is due to the oxidation of some units to diphenoquinone (IV) residues.

As the support for their assumption is rather indirect, a further examination was made of "tetraguaiacoquinone".

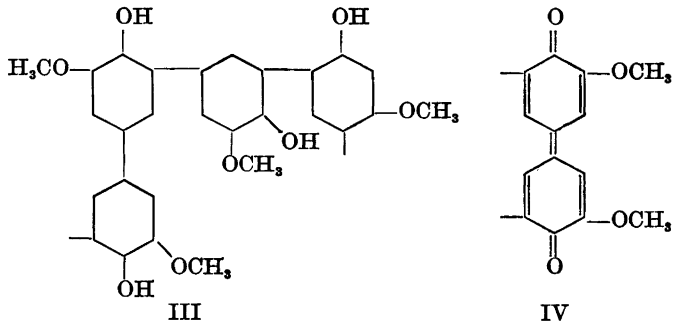

III IV

Analyses of the polymer gave the formula

$$C_6H_{2.4}O_{0.32}^{carbonyl}\ (OH)_{0.7}\ (OCH_3)_{1.0}$$

which is consistent with the assumption that (III) should be the predominant structural element. After reduction with sodium borohydride, which removed the red colour, the polymer did not react with dibromoquinone-monochloroimide. Evidently the *para* positions in the polymer were substituted. On the other hand, *p*-diazobenzenesulphonic acid gave a red colour with the reduced polymer and thus at least a part of the *ortho* positions (possibly those belonging to the end groups) are free.

Further support for the structure (III) was given by UV spectra, as shown below. The bonds from a benzene nucleus in the polymer to the two proximal nuclei are in *meta* position to each other. The largest mesomeric system in the polymer consists therefore of only two nuclei and the UV maximum should therefore be at the same wavelength as that of the corresponding diphenyl (*cf.* Ref[7].). Two guaiacyl nuclei can be linked in either *o,o'*-, *p,p'*- or *o,p'*-positions to the phenol groups. The *ortho*-substituents decreased the extinction value of the diphenyl maximum as is evident from the fact that the diphenyl maximum has a higher extinction value for 3,3'-dimethoxy-4,4'-dihydroxy-diphenyl than for 3,3'-dimethoxy-2,2'-dihydroxy-diphenyl (Table 1) (*cf.* Ref.[8]). A polymer (III) would therefore be expected to have a UV maximum reminiscent of that of 3,3'-dimethoxy-4,4'-dihydroxy-diphenyl. In reality it was found that even if there are some differences between the spectrum of "tetraquinone" and that of the diphenyl they are certainly of the same type (Table 1).

The presence of the diphenoquinone structure (IV) was supported by the IR spectrum of the polymer. The carbonyl band was at 1 625 cm^{-1}, close to the aromatic 1 600 cm^{-1} band (Fig. 3). This frequency, which is unusually low for a carbonyl band, agrees with that of diphenoquinones (diphenoquinone [9] at 1 626 cm^{-1}, its 3,3', 5,5'-tetramethyl derivative at 1 633 cm^{-1}, and the 3,3',5,5'-tetramethoxy derivative at 1 628 cm^{-1}). The carbonyl peaks of benzoquinones are in the vicinity of 1 650^{-1} cm (benzoquinone [10] at 1 667 cm^{-1}). In the visible part of the polymer spectrum there is a maximum at 475 mμ which was evidently due to the diphenoquinone groups since they absorb in this region.

Persulphate oxidation

Erdtman [11] has pointed out that a polymer similar to "tetraguaiacoquinone" is formed when guaiacol is treated with sodium persulphate in acidic aqueous solution containing a small amount of ferrosulphate. The results of analyses on material prepared here indicated a formula

$$C_6H_{2.3}O_{0.40}^{carbonyl}\ (OH)_{1.0}(OCH_3)_{0.75}$$

(This formula agrees reasonably well with data by Erdtman and Johanson [12]).

The persulphate polymer differed in several respects from "tetraguaiacoquinone". The lower methoxyl value showed that some methoxyl had been eliminated during the persulphate oxidation and that a part of the aromatic

Table 1. UV data for "tetraguaiacoquinone", the persulphate polymer, and two related diphenyl derivatives.

Substance	Neutral solution [1] Diphenyl maximum mμ	ε	Benzene maximum mμ	ε	Alkaline solution [2] mμ	ε
"Tetraguaiacoquinone"	257	7 520	300*	3 600	298	5 250
Reduced ditto	261	7 750	300*	4 300		
Persulphate polymer	258	6 900	295*	4 300	298	8 350
Reduced ditto	261	7 350	295*	5 000		
3,3′-Dimethoxy-4,4′-dihydroxy-diphenyl	268	7 800	291	6 600	308	11 200
3,3′-Dimethoxy-2,2′-dihydroxy-diphenyl [3]	247	4 100	283	2 500	304	3 650

Extinction values (ε) calculated per C_6-unit for both polymers and diphenyls. The maxima marked with * were noticeable only as inflections in the absorption curves

[1] Solvent: ethanol.

[2] Solvent: 0.1 N ethanolic potassium hydroxide solution.

[3] Synthesised according to Ref.[6]

nuclei might have been destroyed. Even though the IR spectra of the two polymers were of the same aromatic type (Fig. 3) they show distinct dissimilarities. For instance the spectrum of the persulphate polymer showed no diphenoquinone band in the vicinity of 1 625 cm^{-1} but, on the other hand, it had an absorption peak at 1 645 $cm,^{-1}$ which might be due to benzoquinone groups. The visible light spectrum also indicated differences between the carbonyl groups of the two polymers, the persulphate polymer having a maximum at

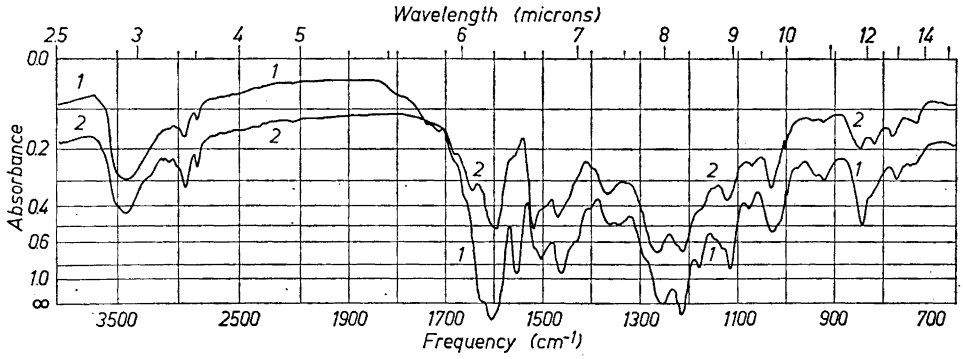

Fig. 3. IR spectra of guaiacol polymers. Oxidation reagents: 1) laccase plus oxygen, and 2) persulphate plus ferro-ions. Potassium bromide disc.

438 mμ, significantly different from the wavelength of that of "tetraguaiacoquinone" (475 mμ). It therefore seems probable that the greater part of the carbonyl groups in the persulphate polymer are benzoquinone groups formed by an Elbs persulphate reaction [13].

The UV spectra of the polymer (Table 1 and Fig. 1) closely resembled that of the "tetraquaiacoquinone". Furthermore the reduced persulphate polymer did not react with dibromo-quinone-monochloroimide and gave only a weak colour reaction with diazobenzene-sulphonic acid. Together with the general conformity of the IR spectra, these results indicated that the persulphate polymer contained a large proportion of the predominant structural elements in "tetraguaiacoquinone", *i.e.* (III).

DISCUSSION

It is apparent from these experiments that different types of dehydrogenation polymers are obtained from guaiacol depending on the type of oxidation reagent used. Polymers with ether-linked units are obtained when silver oxide and potassium ferricyanide are used while persulphate and the oxygen-laccase system link the units by carbon-carbon bonds.

The formation of both types of polymers can be explained according to the well known scheme for dehydrogenation of phenols (reviewed in Refs. [14,15]) in which the primary reaction products are considered to be phenoxyl radicals. These radicals may combine with each other or with phenol molecules. The formation of both oxygen bonds and carbon-carbon bonds can be accounted for by this process.

However, that the oxidation reagent should affect the manner of linking is not indicated in this simplified scheme; it might be explained in several ways. One alternative is that the radicals are never really free but form π-complexes with the oxidation reagents such as those assumed by Hammond and co-workers [16] to be the primary products obtained by reaction of peroxy radicals with phenols or amines (V).

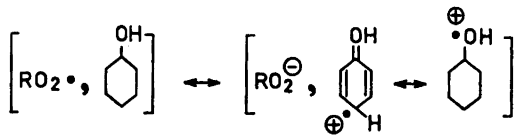

V

EXPERIMENTAL

Oxidation of guaiacol with silver oxide in benzene solution. Isolation of the polymer. Guaiacol (15 g) dissolved in benzene (140 ml) was shaken with silver oxide (16 g) for 48 h. Undissolved material (15 g) was removed and the filtrate was shaken with 2 N sodium hydroxide solution, which dissolved a part of the product. The benzene solution was dried and evaporated. The residue was dissolved in chloroform, and light petroleum was added to the solution. The white precipitate obtained was collected (1.4 g, Preparation A).

The alkaline solution was acidified and the solution decanted from the sticky precipitate, which was washed with water and dissolved in dioxane. The dioxane solution was

dried and evaporated. The residue (5.2 g) was precipitated from chloroform solution by addition of light petroleum, and the white precipitate obtained was collected (3.3 g, Preparation B).

The acidified aqueous solution was extracted with ether and the ether solution was combined with the chloroform-light petroleum filtrate. The combined solution was evaporated. The residue (10 g) yielded guaiacol (5 g) on distillation.

Examination of the polymeric preparations A and B. Analyses: Preparation A, found C 68.8; H 5.0; O 26.7; OCH_3 26.6; OH 1.1. Preparation B, found C 67.3, H 5.3, O 27.2, OCH_3 24.4, OH 2.7 peroxide [17] 0.0, molecular weight at least 750.

The hydroxyl content was determined by heating the preparations with acetic anhydride and pyridine for 3 h, precipitating the acetylated material by addition of water and determining the acetyl content of this material.

UV and IR spectra of the two preparations were the same. They are shown in Figs. 1 and 2, respectively.

NMR spectrum of preparation B in a benzene solution showed a peak at a shift of 3.7 p.p.m. relative to the benzene peak. The peak due to the hydrogen of the methoxyl group in guaiacol has a shift of 3.8 p.p.m.

Isolation of 3,3'-dimethoxy-4,4'-dihydroxy-diphenyl. Guaiacol (20 g) was treated with silver oxide (21 g) as described. The alkaline solution was acidified and extracted with benzene, which was then dried and evaporated. Distillation of the residue gave guaiacol (8.5 g) and a fraction, distilling at 0.3 mm Hg/160—180° (bath temperature). The latter partly crystallised and on recrystallisation from methanol gave a product (0.15 g), m.p. 153°, raised to 166—167° by further recrystallisation from methanol. (Found C 68.3; H 5.9. Calc. for $C_{14}H_{14}O_4$ (246): C 68.3; H 5.7.) UV data are given in Table 1. Its structure was determined by methylation to 3,3'4,4'-tetra-methoxy-diphenyl.

Methylation of 3,3'-dimethoxy-4,4'-dihydroxy-diphenyl. Dimethyl sulphate (1 ml) was added with vigorous agitation to a solution of the dimethoxy-dihydroxy-diphenyl (3.4 mg) in 3 N potassium hydroxide (1 ml). When the solution turned acidic 3 N potassium hydroxide (1 ml) was added. The treatment with dimethyl sulphate (1 ml) and 3 N potassium hydroxide (1 ml) was repeated once and then dimethyl sulphate (1 ml) and solid potassium hydroxide were added. The temperature was kept at about 80° during the whole methylation procedure. When all the dimethyl sulphate had reacted the crystals were removed from the solution and washed with water, m.p. 129—130°, undepressed by addition of 3,3'4,4'-tetramethoxy-diphenyl prepared by Ullman coupling of 3,4-dimethoxyphenyl iodide [18]. The IR spectrum of the methylation product was identical with that of the tetramethyl-diphenyl.

Oxidation of guaiacol with silver oxide in dimethylformamide-methyl iodide solution. Silver oxide (25 g) was added in portions during 1 h to a solution of guaiacol (10 g) in dimethylformamide (50 ml) and methyl iodide (30 ml). The mixture was then shaken for 17 h, undissolved material was removed and benzene was added to the filtrate. The precipitate obtained was removed and the benzene solution was extracted with 5 % sodium thiosulphate solution, then water, and dried. Light petroleum was added to the benzene solution. The white amorphous precipitate obtained was collected (3.2 g). (Found: C 68.9; H 5.0; O 25.6; OCH_3 27.1; OH 0.0.) IR and UV spectra were identical with those of the polymer preparations obtained by oxidations in benzene solution.

The light petroleum-benzene solution from the polymer precipitation was evaporated. The residue (2.2 g) distilled at 130° (bath temperature); the m.p. of the distillate, 22°, was undepressed by addition of veratrol. Its IR spectrum was identical with that of veratrol.

Oxidation of guaiacol with potassium ferricyanide. An aqueous solution of potassium ferricyanide (30 g in 100 ml) was added during 1 h to a solution of guaiacol (5 g) in $\frac{1}{4}$N sodium hydroxide solution (150 ml) which was strongly agitated (room temperature). The reaction mixture was agitated for a further 5 h and then extracted with chloroform. The chloroform solution was dried and evaporated. The residue (0.5 g) was reprecipitated from a chloroform solution by addition of light petroleum. Weight 0.3 g. (Found: C 66.2; H 5.3; O 25.1; OCH_3 22.8.)

The chloroform-extracted alkaline solution was acidified and extracted again with chloroform. The extract was dried and added to light petroleum. The precipitate obtained was collected (1.5 g). (Found: C 64.6; H 4.9; O 27.0.) UV and IR spectra are shown in Figs. 1 and 2, respectively.

Oxidation of guaiacol with sodium persulphate. The polymer was prepared as described by Erdtman [11]. (Found: C 65.4; H 4.4; O 28.4; OCH_3 18.2.)

The carbonyl group content was determined by sodium borohydride reduction according to Lindberg and Paju [19]. The reduction time was about half an hour. Found: 0.20 moles of hydrogen consumed per equivalent weight of 122. The UV and IR results are shown in Figs. 1 and 3 and in Table 1.

Reductive acetylation: A mixture of zinc powder (5 g), the polymer (2 g) and acetic anhydride-pyridine (10 ml, v/v) was heated on a boiling water bath for 1 h. Undissolved material was removed and water was added to the filtrate. The light brown precipitate obtained was collected and washed with water. Weight: 2.7 g. (Found: OCH_3 12.1, CH_3CO 26.3.) The formula given in the discussion was calculated on the assumption that the carbonyl groups are reduced to hydroxyl groups and then acetylated in this procedure.

"*Tetraguaiacoquinone*". A dialysed solution from a culture of *Polyporus versicolor* (3 ml) was added to guaiacol (1 g) dissolved in a 0.01 M acetic acid-sodium acetate buffer of pH 4.8 (80 ml). The solution was shaken for 24 h. The precipitate obtained was collected and washed with water. (This experiment was kindly performed by Dr. Gösta Fåhraeus and Mr. Hans Ljunggren). Weight 770 mg. (Found: C 67.8; H 4.9; O 25.8; OCH_3 25.4.) Carbonyl was determined as in the case of the persulphate polymer. Found: 0.16 moles of hydrogen consumed per equivalent weight of 122. Reductive acetylation was also carried out as with the persulphate polymer. (Found: OCH_3 18.7; CH_3CO 22.0.) UV and IR data are collected in Figs. 1 and 3 and in Table 1.

Acknowledgement. I wish to thank Miss Marit Goliath and Mr. Sigurd Söderberg for valuable experimental assistance. The IR spectra were recorded at the Department of Organic Chemistry, Royal Institute of Technology, by Miss Gurli Hammarberg, and the NMR spectrum were determined in the Department of Physical Chemistry at the same institute by Mr. Jan-Christer Eriksson to both of whom I am greatly indebted. I also wish to thank Dr. Gösta Fåhraeus and Mr. Hans Ljunggren, Royal Agricultural College of Sweden Ultuna, for their preparation of "tetraguaiacoquinone".

Added in proof. This polymer recently been synthesised by two other methods (Hay, A. S. *et al. J. Am. Chem. Soc.* **81** (1959) 6335, and Staffin, G. D. and Price, Ch. C. *ibid.* **82** (1960) 3632).

REFERENCES

1. Lindgren, B. O. *Acta Chem. Scand.* **14** (1960) 1203.
2. Freudenberg, K. and Grion, G. *Chem. Ber.* **92** (1959) 1355 and earlier papers.
3. Fichter, F. and Dietrich, W. *Helv. Chim. Acta* **7** (1924) 137.
4. Aulin-Erdtman, G. and Hegbom, L. *Svensk Papperstidn.* **60** (1957) 671.
5. Bertrand, G. *Compt. rend.* **137** (1903) 1270; *Bull. soc. chim. France* [3] **31** (1904) 187.
6. Booth, H. and Saunders, B. C. *J. Chem. Soc.* **1956** 940.
7. Gillam, A. E. and Hey, D. H. *J. Chem. Soc.* **1939** 1170.
8. Beaven, G. H. in *Steric Effects in Conjugated Systems* (Ed. Gray, G. W.), London 1958, p. 22.
9. Hadži, D. and Sheppard, N. *J. Am. Chem. Soc.* **73** (1951) 5460.
10. Josien, M. L., Fuson, N., Lebas, J. M. and Gregory, T. M. *J. Chem. Phys.* **21** (1953) 331.
11. Erdtman, H. *Svensk Kem. Tidskr.* **47** (1935) 225 (foot note).
12. Erdtman, H. and Johanson, L. *Unpublished results.*
13. Forrest, J. and Petrow, V. *J. Chem. Soc.* **1950** 2340; Baker, W. and Brown, N. C. *J. Chem. Soc.* **1948** 2303.
14. Barton, D. H. R. and Cohen, T. *Festschrift Arthur Stoll*, Basel 1957, p. 117.
15. Erdtman, H. and Wachtmeister, C. A. *Festschrift Arthur Stoll*, Basel 1957, p. 144.
16. Boozer, C. E., Hammond, G. S., Hamilton, C. E. and Sen, J. N. *J. Am. Chem. Soc.* **77** (1955) 3238.
17. Kokatnur, V. R. and Jelling, M. *J. Am. Chem. Soc.* **63** (1941) 1432.
18. Späth, E. and Gibian, K. *Monatsh.* **55** (1930) 348.
19. Lindberg, B. and Paju, J. *Svensk Kem. Tidskr.* **65** (1953) 9.

Received July 1, 1960.

ACTA CHEMICA SCANDINAVICA 14 (1960) 2097–2101

N-Substituted Alkyltriaminosilanes

IV. On Intermolecular Condensation

LEWI TANSJÖ

Department of Organic Chemistry, University of Lund, Lund, Sweden

Ammonolysis of methyl-, ethyl-, and *n*-propyltrichlorosilane gave no distillable products. Alkyltriaminosilanes were presumably first formed but condensed intermolecularly with evolution of ammonia to give polymers. The corresponding N-substituted alkyltriaminosilanes, however, were obtained in good yields. In the presence of a small amount of a proton donor also these compounds condensed intermolecularly, the reactivity being greatly depending upon the nature of the groups attached to the silicon and nitrogen atoms.

This paper describes the intermolecular condensation of some alkyltriaminosilanes and their N-substituted derivatives, which proceeds with evolution of ammonia or amine and the first stage of which would be according to the general equation

$$2RSi(NHR')_3 \longrightarrow \begin{matrix} & NHR' & & NHR' & \\ & | & & | & \\ RSi & -NR'- & Si & R & \end{matrix} + R'NH_2$$
$$\qquad\qquad\quad NHR' \qquad\quad NHR'$$

This reaction has been performed for R = H, CH_3, C_2H_5 and n-C_3H_7 and R′ = H, CH_3 and C_2H_5.

When methyl-, ethyl-, or *n*-propyltrichlorosilane reacted with ammonia, the monomeric alkyltriaminosilanes, $RSi(NH_2)_3$, were not obtained even if the reactions were performed in liquid ammonia. Presumably these compounds were first formed according to the equation

$$RSiCl_3 + 6H_3N \longrightarrow RSi(NH_2)_3 + 3H_4NCl$$

but they very easily condensed intermolecularly, as mentioned above, with the formation of ether-soluble polymeric silazanes with Si—NH—Si linkages, which, after evaporation of the solvent gave viscous oils. Upon heating of these, more ammonia was split out and high polymers with a three dimensional

network resulted. This is analogous to the ammonolysis of trichlorosilane [1] which gave a polymer, $HSi(NH)_{1.5}$, with a cross-linked structure and a very high degree of polymerization. Nor did Larsson [2] observe any low-molecular products from the ammonolysis of *n*-butoxitrichlorosilane. Chugunov [3], however, obtained a compound which appeared to be α-$C_{10}H_7Si(NH_2)_3$, by bubbling dry gaseous ammonia into an ether solution of α-naphthyltrifluorosilane, but no analyses or further studies of the compound were given to authorize the formula. It was mentioned only that the compound rapidly hydrolyzed in contact with moist air with evolution of ammonia. The bulky α-naphthyl-group can certainly be expected to exert a greater retarding influence on the intermolecular condensation than the R-groups investigated in this paper, but it seems not unlikely that what was interpreted as a hydrolysis may have been the first stages of a condensation of the type mentioned above.

It was reported in a previous paper [4] that *n*-propyltri-(methylamino)-silane and *n*-propyltri-(ethylamino)-silane are stable at their normal boiling points and it was now found that the corresponding methyl- and ethyl-compounds could be isolated without difficulty. This shows that organic groups on the nitrogen atoms effectively impede the tendency toward intermolecular condensation of the compounds compared with that of the unsubstituted alkyltriaminosilanes. Tri-(ethylamino)-silane, with the silicon bearing only a hydrogen atom beside the ethylamino groups, could also be isolated, but no uncondensed products were obtained from the reaction mixture of trichlorosilane and methylamine.

The accelerating effect of hydrogen ion on the reaction of N-substituted *n*-propyltriaminosilanes with primary and secondary amines was demonstrated in part II of this work [5]. As can be expected the intermolecular condensation, which is apparently of the same nature as the exchange reactions studied in the previous paper, is also catalyzed by the hydrogen ion. Thus, methyl-, ethyl- and *n*-propyltri-(methylamino)-silane all gave a vigorous evolution of methylamine far beneath their ordinary reflux temperatures when heated with a small amount of ammonium sulfate. The reaction mixtures, which were soluble in organic solvents, crystallized on cooling and gave good yields of compounds the analyses of which corresponded to the cyclic structure I.

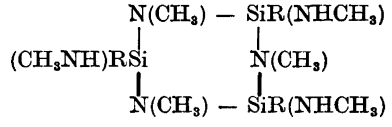

I

The building up of high-molecular-weight cross-linked structures from these by further condensation seems to be effectively sterically hindered for they could all be heated with ammonium sulfate present to 200°C for several hours without any noteworthy liberation of methylamine. However, when the mixture of low-molecular condensation products which was obtained from the reaction of trichlorosilane and methylamine was heated with a small amount of ammonium sulfate to the same temperature, a considerable evolution of methylamine occurred, and after a few hours there remained an insoluble hard and glassy mass, typical of cross-linked structures.

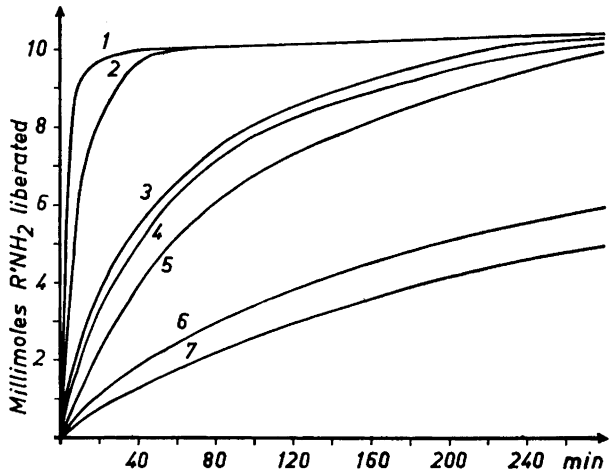

Fig. 1. Intermolecular condensation of $RSi(NHR')_3$. 1. $HSi(NHC_2H_5)_3$; 2. $CH_3Si(NHCH_3)_3$; 3. $C_2H_5Si(NHCH_3)_3$; 4. n-$C_3H_7Si(NHCH_3)_3$; 5. $CH_3SiNHC_2H_5)_3$; 6. $C_2H_5Si(NHC_2H_5)_3$; 7. n-$C_3H_7Si(NHC_2H_5)_3$.

In Fig. 1 are given the results of a series of experiments in which 0.01 mole of some substituted triaminosilanes, $RSi(NHR')_3$, were heated in the presence of a small amount of ammonium sulfate at 120°C and the liberated amine, $R'NH_2$, was titrated with standard acid. It appears that the rate of evolution of amine depends on the nature of R and R', being increased in the order R = n—C_3H_7, C_2H_5, CH_3, H and R' = C_2H_5, CH_3.
The physical constants and analyses of the following compounds are given in Table 1: I, $CH_3Si(NHCH_3)_3$; II, $CH_3Si(NHC_2H_5)_3$; III, $C_2H_5Si(NHCH_3)_3$; IV, $C_2H_5Si(NHC_2H_5)_3$.

EXPERIMENTAL

The method of the determination of the physical constants of the compounds and the analyses have been previously described [4]. The experiments, the results of which are given in Fig. 1, were performed in the following way. The triaminosilanes (0.01 mole) and 6 mg (5×10^{-5} mole) of ammonium sulfate were introduced into a 10 ml flask which was heated to 120 ± 0.5°C in a thermostat. The liberated amine was withdrawn by a weak, uniform stream of nitrogen, which had been carefully dried with conc. sulphuric acid and phos-

Table 1. Physical constants and analyses of $RSi(NHR')_3$

No.	M	B.p. °C	Pressure mm Hg	n_D^{20}	d^{20}	MR_D	% Si		Equiv. wt.	
							found	calc.	found	calc.
I	133.27	61	40	1.4339	0.8942	38.81	21.1	21.1	44.8	44.4
II	175.35	62–63	10	1.4300	0.8522	53.15	16.0	16.0	58.8	58.5
III	147.30	51–52	10	1.4410	0.8966	43.38	19.2	19.1	49.3	49.1
IV	189.38	78–79	10	1.4360	0.8581	57.70	14.9	14.8	63.4	63.1

phorus pentoxide, and had to pass a reflux condensor cooled with water before it was absorbed in a known volume of standard hydrochloric acid. The acid was added in small portions into the absorption vessel and the times of neutralization (methyl red as the indicator) were noted. All the investigated N-substituted alkyltriaminosilanes gave only a very slow evolution when heated without ammonium sulfate but tri-(ethylamino)-silane condensed rapidly even in the absence of the catalyst.

Ammonolysis of ethyltrichlorosilane. In a 500 ml three-necked flask immersed in a Dry Ice and acetone-bath were placed about 100 ml of liquid ammonia. From a dropping funnel, 16.4 g (0.1 mole) of ethyltrichlorosilane in 250 ml of ether was added dropwise during 2 h to the stirred ammonia. The temperature was slowly raised by the removal of the bath. After 2 h at room temperature most of the excess of ammonia had evaporated. Ether was distilled from the mixture until the distillation temperature reached 35°C and about 50 ml were removed at this temperature to take away most of the residual ammonia. Filtration left 16.0 g (calc. for the total exchange of chlorine 16.0 g) of ammonium chloride on the filter. No silicon was found in the precipitate so the reaction product was still quite ether soluble. The filtrate gave after the filtration only a weak odour of ammonia, but after standing for a few hours in a sealed bottle, an additional pressure, owing to free ammonia, had been formed. During the course of the distillation of ether ammonia continuously escaped, and after the last traces of ether had been removed at reduced pressure, there remained a viscous, colourless oil which could again be dissolved in ether and neutralized some acid when agitated with 0.1 N hydrochloric acid. Attempts to distil the oil at reduced pressure only caused more ammonia to evolve giving a residue of an amorphous plastic solid which on heating to about 200°C lost a little more ammonia and changed to a brittle, colourless resin. When treated with strong warm alcoholic potassium hydroxide, ammonia was set free in an amount corresponding to a nitrogen content of 26.0 %; calc. for $C_2H_5Si(NH)_{1.5}$ N 26.4. The silicon content was 34.2 against 35.3 for the formula above. The low silicon content points to incomplete condensation. Wagner *et al.*[6] found that brittle polymers obtained by hydrolysis of vinyltrichlorosilane contained as much as 9.5 % silanol hydroxyl so it is apparent that complete condensation is not necessary to give silicon polymers with a high degree of polymerization. That there was not found a corresponding increase of the nitrogen content of the product is probably due to partial hydrolysis.

The ammonolysis of *methyltrichlorosilane* and *n-propyltrichlorosilane* was performed in the same way and proceeded analogously to give insoluble, high-molecular-weight products as above.

Tri-(methylamino)-silane. 27.1 g (0.2 mole) of trichlorosilane in 100 ml of ether were added dropwise to an ice-cooled, stirred solution of 50 g (1.6 mole) of methylamine in 300 ml of ether. The temperature was then slowly raised by the removal of the ice-bath. Filtration of the reaction mixture left 40.3 g (calc. 40.5 g) of methylamine hydrochloride on the filter. On distillation of the filtrate, no distillate was obtained beneath 100°C (9 mm Hg) where tri-(methylamino)-silane can be supposed to distil. Between 125—175°C/9 mm, however, 8.0 g of an ether soluble product were obtained (Found: Equiv. wt. 43.8; Si 30.6. Calc. for $[HSi(NHCH_3)(NCH_3)]_n$: Equiv. wt. 44.1; Si 31.8.) On further heating of the distillation flask a vigorous evolution of methylamine took place and 5.5 g of an insoluble, hard and glassy residue were obtained.

When the distillate was heated to 200°C with a small amount of ammonium sulfate, methylamine was set free and after 3 h a high-molecular-weight product had been formed as above.

Tri-(ethylamino)-silane. 27.1 g (0.2 mole) of trichlorosilane in 100 ml of ether were added to 75 g (1.7 mole) of ethylamine in 400 ml of ether, cooled to 0°C. On filtration, 48.7 g (calc. 48.9 g) of ethylamine hydrochloride were left on the filter. On distillation of the filtrate, 8.0 g (25 %) of tri-(ethylamino)-silane were obtained, b.p. 62—63°/10 mm, (Found: Equiv. wt. 54.0; Si 17.5. Calc. for $HSi(NHC_2H_5)_3$: Equiv. wt. 53.8; Si 17.4.) On further heating a considerable amount of ethylamine escaped from the distillation flask. After the content had been heated for two hours at about 150°C the distillation was continued giving:

125—45°/0.5 mm: 2.0 g; equiv. wt. 57.5; Si 22.7;
145—60°/0.5 mm: 7.2 g; equiv. wt. 57.5; Si 22.9;
160—80°/0.5 mm: 4.2 g; equiv. wt. 58.1; Si 23.6.

Methyltri-(methylamino)-silane. To an ice-cooled, stirred solution of 30 g (1.0 mole) of methylamine in 300 ml of ether, a solution of 15.0 g (0.1 mole) of methyltrichlorosilane was added dropwise. The stirred mixture was heated to reflux temperature for 1 h and was then filtered giving 20.2 g (calc. 20.3 g) of methylamine hydrochloride on the filter. Distillation of the filtrate gave 9.5 g (71 %) of methyltri-(methylamino)-silane with the data given in Table 1.

5.8 g of the compound was heated for 5 h at 150°C with 10 mg of ammonium sulfate and gave a product which crystallized on cooling (m.p. 133—36°). Recrystallization from pentane at —20° gave 2.0 g, m.p. 136—38° (Found: Equiv. wt. 52.0, Si 27.9, *M* (in benzene) 320. Calc. for $[CH_3Si(NHCH_3)(NCH_3)]_3$ (I): Equiv. wt. 51.1, Si 27.5, M 307.)

Methyltri-(ethylamino)-silane. 11.1 g (0.074 mole) of methyltrichlorosilane in 50 ml of ether were added to 45 g (1.0 mole) of ethylamine in 300 ml of ether. The stirred mixture was refluxed for 1 h. Filtration left 18.0 g (calc. 18.1 g) of ethylamine hydrochloride on the filter. On distillation of the filtrate 10.1 g (78 %) of methyltri-(ethylamino)-silane were obtained.

Ethyltri-(methylamino)-silane (22.3 g; 76 %) was obtained in the same way as described for methyltri-(methylamino)-silane from 32.7 g (0.2 mole) of ethyltrichlorosilane and excess of methylamine. 6.0 g of it were heated for 5 h at 150°C with 10 mg of ammonium sulfate. The reaction mixture, which crystallized on cooling, was recrystallized from pentane at —20° and gave 2.2 g, m.p. 189—92° (Found: Equiv. wt. 59.0, Si 24.2, *M* 355. Calc. for $[C_2H_5Si(NHCH_3)(NCH_3)]_3$: Equiv. wt. 58.1, Si 24.2, *M* 349.)

Ethyltri-(ethylamino)-silane (33.5 g; 88 %) was obtained in the same way as was described for methyltri-(methylamino)-silane, from 32.7 g (0.2 mole) of ethyltrichlorosilane and excess of ethylamine.

The synthesis of *n-propyltri-(methylamino)-silane* and *n-propyltri-(ethylamino)-silane* was described in a previous paper[4].

16.1 g of *n*-propyltri-(methylamino)-silane were heated for 5 h at 180°C in the presence of 20 mg of ammonium sulfate. On distillation of the reaction mixture, no *n*-propyltri-(methylamino)-silane was removed. Between 167—75°/1 mm 11.1 g of a product were obtained which crystallized on cooling (m.p. 67—70°). Recrystallization from pentane at —20° gave 7.5 g, m.p. 69—70° (Found: Equiv. wt. 65.9, Si 21.6, *M* 404. Calc. for $[n\text{-}C_3H_7Si(NHCH_3)(NCH_3)]_3$: Equiv. wt. 65.1, Si 21.6, M 391.)

The author wishes to thank Professor E. Larsson for his kind interest in this work.

REFERENCES

1. Stoch, A. and Zeidler, F. *Ber.* **56** (1923) 986.
2. Larsson, E. *Acta Chem. Scand.* **8** (1954) 1084.
3. Chugunov, V. S. *Zhur. Obshchei Khim.* **23** (1953) 777.
4. Tansjö, L. *Acta Chem. Scand.* **11** (1957) 1613.
5. Tansjö, L. *Acta Chem. Scand.* **13** (1959) 29.
6. Wagner, G. H., Bailey, D. L., Pines, A. N., Dunham, M. L. and McIntire, D. B. *Ind. Eng. Chem.* **45** (1953) 367.

Received July 4, 1960.

ACTA CHEMICA SCANDINAVICA 14 (1960) 2102–2112

Betaine-Homocysteine-Methyl-Transferases

I. Distribution in Nature

L.-E. ERICSON

Division of Food Chemistry, Royal Institute of Technology, Stockholm 70, Sweden

Various types of living material have been homogenized and incubated with betaine and homocysteine in order to test their ability to form methionine by means of methyl group transfer. Enzymes that catalyze this reaction are called betaine-homocysteine-methyl-transferases and were found in the livers of all the vertebrates investigated, ranging from *Homo sapiens* to *Petromyzon fluviatilis*. These enzymes were not found in appreciable amounts in any other vertebrate organ except in the kidney of the guinea pig. The only non-vertebrate in which a betaine-homocysteine-methyl-transferase has been detected so far is the pond mussel *Anodonta cygnea* [4]. Methyl transferases were not found in plants and microorganisms.

The transferases were partially purified from some materials. Dimethyl-β-propiothetin but not choline could replace betaine as methyl group donor in all cases tested. Dimethylglycine but not choline markedly inhibited the transfer reaction. The methyl-transferase of human liver was much more stable to heat than that of pike liver. The apparent pH-optima of the transferases studied varied from about 7.0 for pike to about 8.5 for pond mussel. Only L-homocysteine seemed to be methylated.

In the present paper some observations are reported on the distribution in Nature of enzymes that catalyze the transfer of a methyl group form betaine (carboxymethyl-trimethyl-ammonium chloride) to homocysteine. These enzymes will be called betaine-homocysteine-methyl-transferases. A comparison of some of the properties of transferases of different origin will also be made. Methionine and dimethylglycine are produced in the enzymic reaction [1,2] and enzyme activity has been measured as the amount of methionine formed per hour.

Some of the results of this investigation have already been briefly mentioned elsewhere.[2–4] The existence of a betaine-homocysteine-methyl-transferase in *Anodonta cygnea*, for instance, has recently been reported from this laboratory [4] and will therefore not be dealt with in detail here.

EXPERIMENTAL

The material to be tested for betaine-homocysteine-methyl-transferase activity was homogenized in a Potter-Elvehjem-homogenizer (or crushed in a mortar and homogenized) in ice-cold 0.05 M phosphate buffer having a pH-value of 7.8. In some cases other pH-values were tried (see Table 1). Betaine hydrochloride (California Corporation for Biochemical Research, Cal., USA, or L. Light & Co., Ltd., England) and DL-homocysteine (Nutritional Biochemicals Corporation, Ohio, USA) were added to the homogenate and the mixture was incubated aerobically for 2—4 h at 37°C. Another mixture consisting of homogenate, DL-homocysteine and buffer was incubated under the same conditions and served as the blank.

Methionine was determined chemically by the method suggested by McCarthy and Sullivan [5] and modified by Borsook and Dubnoff [6] and others [7]. The red colour obtained upon addition of the hydrochloric-phosphoric acid mixture was developed overnight at 4°C [7]. The solution was then filtered and the light absorption at 5 100 Å was measured in a Beckman Model DU spectrophotometer. Also a microbiological method using *Leuconostoc mesenteroides* P-60 according to the procedure given by Steele *et al.*[8] was used for the estimation of methionine. Standard methionine solutions were prepared from L-methionine (Nutritional Biochemicals Corporation, Ohio, USA).

RESULTS

Distribution studies. Table 1 summarizes the results of the attempts to find betaine-homocysteine-methyl-transferase activity in various types of living material. Only when significant amounts of methionine could be detected by both the chemical and the microbiological methods of analysis was the presence in the incubation mixture of a methionine producing system considered as certain. A pig liver homogenate was always run at the same time as the unknown sample to ensure that the test system functioned. The data presented here de not permit a direct comparison of the concentrations of the transferases in the various materials, as the specific activity of the different transferases are not known. It is also probable [3] that the homogenates used contained inhibitors or activators. A very great variation in activity was furthermore encountered between different samples of the same test material, *e.g.* between different human livers.

With some organs the test was repeated many times. For instance, about forty human livers from patients suffering from various diseases were studied *. The data presented in Table 1 are the highest and the lowest values observed and give an indication of the variation in transferase activity that was encountered in these patients. In none of the cases could transferase activity be detected in the blood.

It can be seen in Table 1 that betaine-homocysteine-methyl-transferases were found in the livers of all vertebrate animals investigated ranging from *Homo sapiens* to *Petromyzon fluviatilis*. These enzymes could not be detected in any other organ of these animals except in the kidney of the guinea pig. Using dimethyl-β-propiothetin as the methyl donor, methyl group transfer was found to take place also in rat kidney homogenates. The pancreas, spleen, small intestine, lung, heart, striated muscle, testicles, cerebellum and cerebrum seemed to lack betaine-homocysteine-methyl-transferase activity.

* These samples were kindly supplied by Dr. W. Graf, St. Erik's Hospital, Stockholm.

Table 1. Distribution in Nature of betaine-homocysteine-methyl-transferases.

Name	Latin name	Material tested	pH of incubation mixture	Conc. in incubation mixture Bet.	Conc. in incubation mixture DL-Hcyst.	Transferase activity Chemical determ.	Transferase activity Microbiol. determ.
				mM	mM	μg L-methionine per g and h.	
Human	*Homo sapiens*	liver	7.8	110	24.6	125[a]	130
		»	7.8	110	24.6	690[b]	—
		blood	7.8	110	24.6	0	0
Monkey	*Macaca rhesus*	liver	7.8	5.5	12.3	510	450
		pancreas	7.8	5.5	12.3	0	40
		spleen	7.8	5.5	12.3	0	30
		small intestine	7.8	5.5	12.3	0	0
		cerebellum	7.8	5.5	12.3	0	0
		cerebrum	7.8	5.5	12.3	0	0
		liver	7.8	110	24.6	490	560
		pancreas	7.8	110	24.6	0	0
		spleen	7.8	110	24.6	0	0
		small intestine	7.8	110	24.6	0	0
		lung	7.8	110	24.6	0	0
		cerebellum	7.8	110	24.6	0	0
		cerebrum	7.8	110	24.6	0	0
Hedgehog	*Ecinaceus europaeus*	liver	7.8	110	12.3	2 600	2 650
Dog[c]	*Canis familiaris*	liver	7.8	5.5	12.3	250	250
		»	7.8	5.5	12.3	210	260
		kidney	7.8	5.5	12.3	0	0
		»	5.0	5.5	12.3	0	0
		pancreas	7.8	5.5	12.3	0	0
		»	5.0	5.5	12.3	0	0
		spleen	7.8	5.5	12.3	0	0
		»	5.0	5.5	12.3	0	0
		small intestine	7.8	5.5	12.3	0	0
		» »	5.0	5.5	12.3	0	0
Horse	*Equus caballus*	liver	7.8	110	24.6	1 200	1 450
		»	7.8	110	24.6	1 300	1 360
Pig	*Sus domesticus*	»	7.8	110	24.6	900	1 000
Calf	*Bos taurus juv.*	»	7.8	110	24.6	350	500
		»	7.8	110	24.6	400	400
Sheep	*Ovis aries*	»	7.8	110	24.6	170	180
Guinea pig	*Cavia cobaya*	liver	7.8	110	24.6	2 050	2 200
		kidney	7.8	110	24.6	1 000	1 100
		heart	7.8	110	24.6	—	0

[a] Lowest value observed. [b] Highest value observed. [c] (Alsatian) Police dog 7 years old.

Name	Latin name	Material tested	pH of incubation mixture	Conc. in incubation mixture Bet.	Conc. in incubation mixture DL-Hcyst.	Transferase activity Chemical determ.	Transferase activity Microbiol. determ.
				mM	mM	µg L-methionine per g and h.	
Rat	*Rattus norvegicus* (albino var.)	liver	7.8	110	24.6	750	850
		kidney	7.8	110	24.6	0	0[d]
		testicle	7.8	110	24.6	0	0
Rabbit	*Oryctologus cuniculus*	liver	7.8	110	24.6	800	850
Chicken	*Gallus domesticus* juv.	liver	7.8	5.5	12.3	125	—
		kidney	7.8	5.5	12.3	0	—
		pancreas	7.8	5.5	12.3	0	—
		liver	7.8	5.5	12.3	330	400
		kidney	7.8	5.5	12.3	0	10
		pancreas	7.8	5.5	12.3	20	0
		small intestine	7.8	5.5	12.3	0	40
		liver	7.8	110	24.6	780	810
Pigeon	*Columbia livia*	liver	7.8	110	24.6	530	650
Turkey	*Meleagris gallopavo*	liver	7.8	110	24.6	1 260	1 470
Grass snake	*Coronella austriaca*	liver	7.8	5.5	12.3	190	320
Frog	*Xenopus loevis*	liver	7.8	110	12.3	135	160
Pike	*Esox lucius*	liver	7.8	5.5	12.3	185	210
		roe	7.8	5.5	12.3	0	20
		muscle	7.8	5.5	12.3	20	35
		liver	7.8	5.5	12.3	185	310
		muscle	7.8	5.5	12.3	0	25
		liver	7.8	22	24.6	610	625
		muscle	7.8	22	24.6	0	0
Perch	*Perca fluviatilis*	liver	7.8	5.5	12.3	95	100
		soft roe	7.8	5.5	12.3	10	0
		muscle	7.8	5.5	12.3	0	0
		liver	7.8	5.5	12.3	170	250
		»	7.8	110	24.6	250	500
		»	7.8	110	24.6	540	620
Cod	*Cadus callarias*	liver	7.8	110	24.6	375	430
Burbot	*Lota lota*	liver	7.45	225	27.0	200	—
Lamprey	*Petromyzon fluviatilis*	liver	7.8	5.5	12.3	260	275
		rest	7.8	5.5	12.3	0	0

[d] Methionine was formed in kidney homogenates when dimethyl-β-propiothetin was used as methyl donor.

Name	Latin name	Material tested	pH of incubation mixture	Conc. in incubation mixture DL-Bet.	Conc. in incubation mixture DL-Hcyst.	Transferase activity Chemical determ.	Transferase activity Microbiol. determ.
				mM	mM	μg L-methionine per g and h.	
Ant	*Formica rufia*	whole	7.8	5.5	12.3	0	—
		»	4.5	5.5	12.3	—	20
		»	7.8	5.5	12.3	0	0
Bee	*Apis mellifica*	whole	7.8	5.5	12.3	0	0
		»	5.0	5.5	12.3	0	0
Banana fly	*Drosophila melanogaster*	whole	7.8	5.5	12.3	0	0
Spider	not identified	whole	7.8	5.5	12.3	0	0
Lobster	*Homarus gammarus*	intestine	7.8	22	12.3	0	65[e]
		»	6.0	22	12.3	0	40
		»	3.0	22	12.3	0	0
		liver	7.8	110	24.6	0	0
		»	6.0	110	24.6	0	0
		»	7.8	110	24.6	0	0[f]
Edible snail	*Helix pomatia*	liver	7.8	110	12.3	0	0
Cuttle-fish	*Eledone cyrrosa*	liver	7.8	110	24.6	0	0[e]
		»	6.0	110	24.6	60	0
		»	3.0	110	24.6	0	0
Sea mussel	*Mytilus edulis*	all except the shell	7.8	5.5	12.3	0	0
Mussel	*Cardium edule*	» »	7.8	5.5	12.3	0	0
Pond mussel	*Anodonta cygnea*	liver	7.8	110	12.3		g
Protozoa	*Tetrahymena pyriformis*	whole	7.8	110	24.6	0	0
Sugar beet	*Beta vulgaris* L. ssp. *esculenta* var. *altissima*	root	7.8	5.5	12.3	0	0
		»	2.7	5.5	12.3	0	0
		»	4.3	5.5	12.3	0	0
		»	6.4	5.5	12.3	0	0
		»	9.05	5.5	12.3	0	0

[e] Frozen to death.

[f] Liver excised while the animal was alive and immediately homogenized in ice-cold buffer and a portion of the homogenate pipetted into a solution of betaine and homocysteine.

[g] For results see Ericson, L.-E. *Nature* **185** (1960) 465.

Name	Latin name	Material tested	pH of incubation mixture	Conc. in incubation mixture Bet.	Conc. in incubation mixture DL-Hcyst.	Transferase activity Chemical determ.	Transferase activity Microbiol. determ.
				mM	mM	μg L-methionine per g and h.	
Oat	*Avena sativa*	seeds	7.8	5.5	12.3	0	0
Wheat	*Triticum sativum*	»	7.8	5.5	12.3	0	0
Mushroom	not identified	whole	7.8	5.5	12.3	25	7
»	*Pleurotus ostreatus* var. *pulmonarius*	cap with gills	7.8	5.5	12.3	0	0
Pea	*Pisum sativum*	pods + peas	7.8	5.5	12.3	0	15
Leek	*Allium porrum*	bulb	7.8	5.5	12.3	0	0
Birch	*Betula verrucosa*	leaves	7.8	5.5	12.3	0	—
		»	7.8	5.5	12.3	0	0
Elder	*Sambucus racemosa*	leaves	7.8	5.5	12.3	—	0
		»	7.8	5.5	12.3	0	0
Mountain-ash	*Sorbus aucuparia*	leaves	7.8	5.5	12.3	0	0
Potatoe	*Solanum tuberosum*	tuber + stem + leaves	7.8	5.5	12.3	0	0
Tomato	*Solanum esculentum* var. *ribesiforma*	stem + leaves	7.8	5.5	12.3	0	0
Tobacco	*Nicotiana rustica*	leaves	7.8	5.5	12.3	0	0
	Nicotiana silvestris	leaves	7.8	5.5	12.3	0	0[h]
		»	4.0	5.5	12.3	0	0
		»	9.0	5.5	12.3	0	0
Microorganisms	*Escherichia coli* 113—3	whole cells	7.8	110	12.3	0	0[i]
	Lactobacillus leichmannii	» »	7.8	110	12.3	0	0[i]
	Rhodotorula gracilis	» »	7.8	110	12.3	0	0[i]
	Saccharomyces carlbergensis	» »	7.8	110	12.3	0	0[i]
	Penicillium N_zA_{19}	» »	7.8	110	12.3	0	0[i]
	Streptomyces griseus	» »	7.8	110	12.3	0	0[i]

[h] Immediately after harvesting the leaves were put into ice-cold buffer to which betaine and homocysteine had been added.

[i] The cells were crushed in a mortar with sand and buffer at + 2°C.

With the method used betaine-homocysteine-methyl-transferase activity could not be detected in any non-vertebrate except in *Anodonta cygnea* [4]. Nor was it found in the plants or the microorganisms tested.

The chemical method of methionine determination gave in most cases slightly lower values than the microbiological method. The data indicate that only L-metionine was formed in the enzymic reaction and consequently that only L-homocysteine was methylated.

Some properties of the methyl-transferases from various sources. It has been shown by Sloane *et al.*[9] and from this laboratory [2-4,10] that dimethylglycine is a potent inhibitor of betaine-homocysteine-methyl-transferase. It is also well established that choline can not function as a donor of methyl groups with enzyme preparations lacking choline oxidase activity,[1,3,6,10-12] nor does choline interfere with the utilization of betaine.[2-4,10] It was considered of interest to determine whether the methyl-transferases of some of the organs investigated here fulfilled these criteria. Partially purified enzyme preparations were therefore made from human, monkey, chicken and pike livers and incubated with combinations of betaine, choline, dimethylglycine and homocysteine. The results, which are summarized in Table 2, indicate that dimethylglycine caused an almost complete inhibition of the methyl transfer when present in the incubation mixture at the same molar concentration as betaine. Choline had in no case an inhibitory effect nor did it act as a methyl donor. In other experiments, dimethyl-β-propiothetin was found to be an excellent methyl donor with these purified enzyme systems and with some liver homogenates from other animals.

Table 2. The influence of choline and dimethylglycine on the amount of methionine formed by betaine-homocysteine-methyl-transferases of different origin.

Enzyme purified from	Betaine 0.1 M	Choline 0.1 M	Dimethyl-glycine 0.1 M	DL-Homo-cysteine 0.015 M	Relative transferase activity %
Human liver	+	−	−	+	100
	−	+	−	+	0
	+	+	−	+	100
	+	−	+	+	0
Monkey liver	+	−	−	+	100
	−	+	−	+	0
	+	+	−	+	103
	+	−	+	+	5
Chicken liver	+	−	−	+	100
	−	+	−	+	0
	+	+	−	+	115
	+	−	+	+	7
Pike liver	+	−	−	+	100
	−	+	−	+	0
	+	+	−	+	102
	+	−	+	+	0

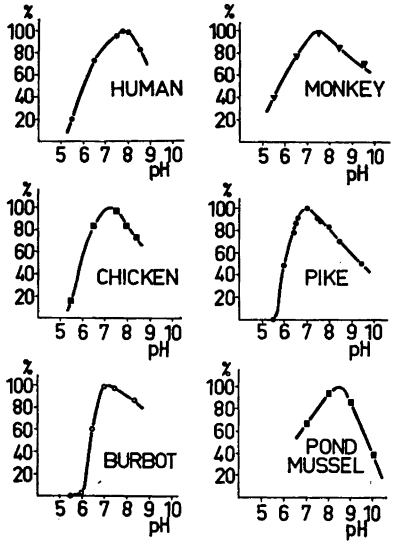

Fig. 1. Apparent activity-pH curves for betaine-homocysteine-methyl-transferases of different origin.

The apparent pH-optima of the transferases of human, monkey, chicken, pike and burbot livers were also determined. Fig. 1 shows the activity-pH curves for these enzymes and also, for the sake of comparison, the corresponding curve for the transferase of *Anodonta*-liver. The lowest apparent pH-optimum that was observed occurred at about 7 (pike) and the highest at 8.5 (pond mussel).

In connection with the purification of some of the transferases mentioned above it was noticed that the transferases of fish livers were much more *heat labile* than those of human, pig and rat livers. Crude and purified betaine-homocysteine-methyl-transferase of pig liver, for instance, could be kept at 80°C for several minutes without appreciable loss of activity (*cf.* Ref.[10]), whereas pike liver transferase suffered complete loss of activity from such treatment. This difference in heat stability is exemplified in Fig. 2. The curves shown in this figure were obtained with solutions of transferases purified from human liver and from pike liver containing approximately 0.5 % of protein and having a pH of 7.5. The solutions were heated at 60°C and the enzyme activity of samples taken at different time intervals was determined. The results show that the pike liver enzyme is much more sensitive to heat than the enzyme from human liver.

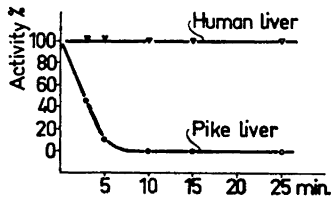

Fig. 2. A comparison of the temperature stability of betaine-homocysteine-methyl-transferase purified from human and from pike liver. The enzyme preparations were adjusted to pH 7.5 and kept at 60°C for various periods of time.

It might also be mentioned that the betaine-homocysteine-methyl-transferases of different origin behaved quite differently during the purification procedure. The transferase from human liver could be purified according to the first three steps used in the fractionation of the pig liver enzyme [10]. This was not possible with the transferase of pike liver. It was, as just mentioned, destroyed on heating at 80°C (step 2 in the fractionation of pig liver transferase [10]) and was not adsorbed on calcium phosphate gel under conditions which would retain the pig liver enzyme. The pike liver transferase was therefore purified by means of pH-adjustment and precipitation with ethanol.

DISCUSSION

The results of this investigation make it probable that betaine-homocysteine-methyl-transferases occur in the livers of all vertebrates. In other organs (*e.g.* kidneys) of vertebrates these transferases are encountered only occasionally.

A betaine-homocysteine-methyl-transferase has been found also in a member of the *Mollusca* [4]. This shows that formation of methionine by means of methyl group transfer does take place also in lower animals.

That betaine-homocysteine-methyl-transferases could not be observed in plants or in microorganisms must not be taken as conclusive evidence that they do not exist in such materials. It may only show that the method used was unsuitable for their detection. However, to the author's knowledge, no evidence for the transfer in plants or microorganism of an intact methyl group from betaine or from a thetin to homocysteine has yet been provided by any other research group. Dubnoff [13,14] found that in the presence of homocysteine, dimethyl-β-propiothetin but not betaine could replace the vitamin B_{12}-requirement of a mutant of *E. coli* but states [14] that "this reaction is not the simple methyl transfer demonstrated in animal tissues". Schlenk and De Palma [15] could not demonstrate any methyl group transfer from betaine, choline, dimethyl-acetothetin or dimethyl-β-propiothetin to homocysteine in *Torulopsis utilis*. Dimethyl-acetothetin and dimethyl-β-propiothetin are inactive as methyl donors also in *Aerobacter aerogenes*, *Saccharomyces cerevisiae* and some strains of *E. coli* [16]. Other examples of the inability of choline, betaine and the thetins to serve as donors of methyl groups in microorganisms have been cited.[17] — Challenger and his collaborators have isolated dimethyl-β-propiothetin from red [18] and green [19] algae but no evidence is as yet available indicating that this compound can donate its methyl groups to homocysteine in these or other plants. Dimethyl-acetothetin, although a potent methyl group donor in animal systems, has not been found to occur naturally.

On the other hand, methyl group transfers *from* methionine derivatives * to various acceptors take place in both microorganisms and plants as well as in animals. This has been amply demonstrated for microorganisms by Schlenk and De Palma [20], Shapiro [16,21,22], Alexander and Schwenk [23], Parks [24], Melville *et al.*[25], Birch *et al.*[26] and Remy [27], and for plants by Byerrum *et al.*[28–30],

* Dimethyl-β-propiothetin is here not considered as a derivative of methionine although it could be looked upon as a breakdown product of this amino acid.

Kirkwood *et al.*[31,32] and Mudd [33,34]. It is of interest to recall that in some of these reactions methionine is produced by methyl group transfer to homocysteine. Examples of such reactions are

S-methylmethionine + homocysteine → 2 methionine

and

S-adenosylmethionine + homocysteine → S-adenosyl homocysteine + + methionine

which have been studied in particular by Shapiro [16,21,22] and by Schlenk and De Palma [20]. S-Methylmethionine stimulated methionine formation also with the horse liver "thetin-homocysteine methylpherase" of Durell *et al.*[12], with the "thetin-homocysteine transmethylase" purified from rat liver by Maw [35] and with our betaine-homocysteine-methyl-transferase from pig liver [10]. For the moment it therefore seems that S-methylmethionine and betaine are interchangeable as methyl donors to homocystein in animal but not in microbial transferase reactions.

After this investigation had been completed and the results prepared for publication, a paper by Maw appeared [36] which dealt with the distribution of thetin-homocysteine transmethylase. The data presented here are in general agreement with the conclusions presented by Maw.

The author would like to express his thanks to Miss I. Frölich for technical assistance and to Dr. P. Lundberg for the biological classification of the material tested. The financial support of the *Medical Research Council* and the *Knut and Alice Wallenberg Foundation* is also acknowledged.

REFERENCES

1. Muntz, J. A. *J. Biol. Chem.* **182** (1950) 489.
2. Ericson, L.-E. IV. *International Congress of Biochemistry*, Vienna (1958), *Abstracts of Communications*, p. 45.
3. Ericson, L.-E. *Acta Chem. Scand.* **12** (1958) 1541.
4. Ericson, L.-E. *Nature* **185** (1960) 465.
5. Mc Carthy, T. E. and Sullivan, M. X. *J. Biol. Chem.* **141** (1941) 871.
6. Borsook, H. and Dubnoff, J. W. *J. Biol. Chem.* **169** (1947) 247.
7. Ericson, L.-E., Williams, J. N. and Elvehjem, C. A. *J. Biol. Chem.* **212** (1955) 537.
8. Steele, B. F., Sauberlich, H. E., Reynolds, M. S. and Baumann, C. A. *J. Biol. Chem.* **177** (1949) 533.
9. Sloane, N. H., Boggiano, E. M., Coulomb, B. and Hutchings, B. L. *Federation Proc.* **15** (1956) 357.
10. Ericson, L-E. *Acta Chem. Scand.* **14** (1960) 2113.
11. Sloane, N. H., Boggiano, E., Smith, B. and Hutchings, B. L. *Federation Proc.* **14** (1955) 915.
12. Durell, J., Anderson, D. G. and Cantoni, G. L. *Biochim. et Biophys. Acta* **26** (1957) 270.
13. Dubnoff, J. W. *Arch. Biochem. Biophys.* **37** (1952) 37.
14. Dubnoff, J. W. *Arch. Biochem. Biophys.* **52** (1954) 151.
15. Schlenk, F. and De Palma, R. E. *Federation Proc.* **15** (1956) 348.
16. Shapiro, S. K. *Biochim. et Biophys. Acta* **29** (1958) 405.
17. Challenger, F. *Quart. Revs.* **9** (1955) 255.
18. Challenger, F. and Simpson, M. J. *J. Chem. Soc.* **1948** 1591.
19. Challenger, F., Bywood, R., Thomas, P. and Hayward, B. J. *Arch. Biochem. Biophys.* **69** (1957) 514.

20. Schlenk, F. and De Palma, R. E. *Arch. Biochem. Biophys.* **57** (1955) 266.
21. Shapiro, S. K. *Biochim. et Biophys. Acta* **18** (1955) 134.
22. Shapiro, S. K. and Yphantis, D. A. *Biochim. et Biophys. Acta* **36** (1959) 241.
23. Alexander, G. J. and Schwenk, E. *J. Biol. Chem.* **232** (1958) 611.
24. Parks, L. W. *J. Am. Chem. Soc.* **80** (1958) 2023.
25. Melville, D. B., Ludwig, M. L., Inamine, E. and Rachele, J. R. *J. Biol. Chem.* **234** (1959) 1195.
26. Birch, A. J., English, R. J., Massy-Westropp, R. A., Slaytor, M. and Smith, H. *J. Chem. Soc.* **67** (1958) 365.
27. Remy, C. N. *J. Biol. Chem.* **234** (1959) 1485.
28. Byerrum, R. U., Flokstra, J. H., Dewey, L. J. and Ball, C. D. *J. Biol. Chem.* **210** (1954) 633.
29. Dewey, L. J., Byerrum, R. U. and Ball, C. D. *J. Am. Chem. Soc.* **76** (1954) 3997.
30. Sato, C. S., Byerrum, R. U., Albersheim, P. and Bonner, J. *J. Biol. Chem.* **233** (1958) 128.
31. Dubeck, M. and Kirkwood, S. *J. Biol. Chem.* **199** (1952) 307.
32. Sribney, M. and Kirkwood, S. *Nature* **171** (1953) 931.
33. Mudd, S. H. *Biochim. et Biophys. Acta* **37** (1960) 164.
34. Mudd, S. H. *Biochim. et Biophys. Acta* **38** (1960) 354.
35. Maw, G. A. *Biochem. J.* **70** (1958) 168.
36. Maw, G. A. *Biochem. J.* **72** (1959) 602.

Received June 2, 1960.

ACTA CHEMICA SCANDINAVICA 14 (1960) 2113–2126

Betaine-Homocysteine-Methyl-Transferases

II. Isolation and Properties of the Transferase of Pig Liver

L.-E. ERICSON

Division of Food Chemistry, Royal Institute of Technology, Stockholm 70, Sweden

Procedures for the purification of the betaine-homocysteine-methyl-transferase of pig liver are described and discussed. Using these procedures, an enzyme preparation was obtained which was essentially homogeneous, as judged by sedimentation, chromatography and electrophoresis experiments. The molecular weight of the transferase monomer was found to be about 270 000. The transferase did not appear to be a metalloenzyme and no bound co-factors related to vitamin B_{12}, vitamin B_6, folic or folinic acid could be detected in the purified enzyme. The transferase showed a single light absorption maximum near 276 mμ. The apparent pH-optimum of the reaction catalyzed by the enzyme was approximately 7.5. In this reaction one molecule of betaine and homocysteine gave one molecule of dimethylglycine and methionine. Reversibility could not be demonstrated.

Enzymes that catalyze the transfer of an intact methyl group from betaine or some thetins to homocysteine thereby making methionine seem to occur in the livers of most vertebrates.[1] Enzymes with this property have been purified from rat liver by Ericson *et al.*[2], Maw [3], and Fromm and Nordlie [4], and from horse liver by Durell *et al.*[5]

In this laboratory we have for some years been engaged in a study of procedures for the purification of betaine-homocysteine-methyl-transferases from a variety of sources. Most work has been devoted to the methyl-transferase of pig liver and we have in a previous publication reported a method for the purification of this enzyme [6]. Since then some modifications have been made in the fractionation procedure and it is the purpose of this paper to describe in detail the method now in use in our laboratory, as well as some of the properties of the purified enzyme.

EXPERIMENTAL

The pig livers were purchased from a slaughter-house. They were removed and packed in ice immediately after the animals had been killed and bled. In the laboratory the livers were kept frozen before use. No decrease in the betaine-homocysteine-methyl-transferase activity of frozen livers could be detected over a period of several months. The methyl-transferase activity of different fresh livers varied considerably, in extreme cases by a factor of four or five. A similar variation in activity has been observed for instance with human livers [1] as well as with the livers of rats given various diets [7-9].

The activity of the enzyme solutions obtained during the fractionation was estimated by determining the amount of methionine formed aerobically per hour at 37°C during the initial phase of the reaction. The volumes of the different enzyme solutions used in the tests were chosen so that approximatively the same amount of methionine (and of dimethylglycine) was formed per hour from each enzyme fraction. All incubation mixtures contained 0.11 M betaine hydrochloride (California Corporation for Biochemical Research, Cal., USA, or L. Light & Co., Ltd., England) and 0.025 M DL-homocysteine (Nutritional Biochemicals Corporation, Ohio, USA). Methionine was determined chemically [2,10] or microbiologically [11]. The protein content of the different enzyme preparations was estimated by the biuret reaction [12] or by the optical method suggested by Kalckar [13]. In some cases the results were checked with the Kjeldahl procedure of Perrin [14].

The fractionation procedure for the preparation of purified betaine-homocysteine-methyl-transferase comprised the following steps:

Step 1

Alternative 1. 200 g of pig liver were cut into pieces and homogenized in 600 ml ice-cold water in a Waring blender. The pH of the homogenate was 6.4—6.8. The homogenate was centrifuged in a Spinco Model L ultracentrifuge at 44 000 × *g* for 25 min. and the supernatant fluid was adjusted to approximatively pH 7.7. The precipitate was washed with 250 ml ice-cold water and again spun down at 44 000 × *g* for 25 min. The supernatant fluid was combined with the fluid obtained after the first centrifuging. The total volume of the enzyme solution was approximately 810 ml.

Alternative 2. 200 g of frozen pig liver were cut into pieces and homogenized in 600 ml ice-cold water in a Waring blender. The homogenate was kept at 0°C while the pH was adjusted to approximately 5.1 with 1 N H_2SO_4. The slurry obtained was centrifuged in a Spinco ultracentrifuge at 44 000 × *g* for 15 min. The pH of the supernatant fluid was immediately adjusted to 7.5—8.0 with 1 N NaOH. The precipitate was suspended in 250 ml of ice-cold water and homogenized in a Waring blender. The suspension was centrifuged at 44 000 × *g* for 15 min. and the supernatant fluid was added to the fluid obtained after centrifuging the homogenate. The total volume was generally of the order of 890 ml. As the enzyme is very labile at pH 5.1 it is essential to keep the temperature near 0°C and to work quickly.

Foaming can be controlled with a few drops of *iso*octyl alcohol.

Step 2

The material from step 1 was adjusted to pH 7.75 and poured into test tubes with a diameter of 17 mm. The tubes were put in a water bath having a temperature of 80°C and stirred for 80—90 sec. The manual stirring of all tubes simultanously was accomplished by means of a rake-like contrivance having two rows of prongs fitting into the two rows of test tubes. After the heating, the tubes were immediately transferred to an ice-bath where the stirring was continued for 2—3 min. The fluid was thereafter centrifuged at 44 000 × *g* for 15 min. The supernatant fluid contained the enzyme. The precipitate was washed with 100 ml of water in a Waring blender and again centrifuged at 44 000 × *g* for 15 min. The combined supernatant fluids had a volume of approximately 800 ml when alternative 1, step 1, was used, and over 870 ml when alternative 2, step 1, was employed.

At this stage of the purification the enzyme can be stored for many months in the frozen state without loss of activity.

Step 3

In this step the enzyme was first adsorbed on and then eluted from calcium phosphate gel.

The calcium phosphate gel was prepared according to Keilin and Hartree [15] and was stored at room temperature. The day before the gel was to be used it was washed three times with 0.01 M phosphate buffer pH 8.0 and finally centrifuged at 4 500 × *g* in an MSE "Major Refrigerator" centrifuge. The dry weight of the washed gel was determined after it had been heated at 105°C for 2 h.

Alternative 1. If in step 1 the enzyme had been purified according to alternative 1, the amount of gel added to the solution obtained in step 2 corresponded to 10 mg dry gel per ml. With the facilities at hand it was found convenient to treat only 200 ml enzyme solution at a time. The gel was suspended in the solution by means of an electric stirrer for 30 min at 0°C and was thereafter recovered by centrifuging at 4 500 × *g* for 2 min. (Table 1). The supernatant fluid which contained only a few per cent of the activity but more than 50 % of the protein of the step 2 material was discarded. The gel was washed three times at 0°C with a total of 100 ml 0.05 M sodium phosphate buffer pH 8.0. Between each washing, the suspension was centrifuged at 4 000—4 500 × *g* for a few minutes (Table 1). The supernatant fluids from the washings were also discarded. They generally contained 5—10 % of the activity and about 25 % of the protein.

The elution of the enzyme from the gel was accomplished by means of five successive washings at 0°C, the first two with 0.15 M sodium phosphate buffer pH 8.5, the following three with a solution containing 0.15 M sodium phosphate and 0.1 M sodium citrate at pH 8.5 (Table 1). Vigorous stirring was used in order to get an even suspension of the gel in the eluting agent. The first two elutions lasted 40 min, the third and the fourth 30 min and the last 10 min. The volumes of the buffer solutions used were 25, 25, 20, 20, and 20 ml, respectively. After each of the first two elutions the suspensions were centrifuged at 4 500 × *g*, after the third and the fourth at 26 000 × *g* and after the fifth at 105 000 × *g*. The volume of the eluate was 110—115 ml.

Alternative 2. When the alternative 2 of step 1 was used, the amount of gel added to the enzyme solution from step 2 corresponded to only 6.5 mg dry gel per ml. All other operations followed the procedure outlined in alternative 1 of step 3.

The conditions used for the adsorption and desorption of the transferase from the calcium-phosphate gel are summarized in Table 1. If necessary a few drops of *iso*octyl alcohol were added to control the foaming.

Table 1. The conditions used for the purification of the transferase by treatment with calciumphosphate gel. All procedures were carried out at 0°C.

Process	No.	Washing or eluting agents	Volume ml	pH	Time min	Gel recovered by centrifuging at
Adsorption			200	8.0	30	4 500 × *g* 2 min
Washing	1st	0.05 M phosphate	50	8.0	15	4 000 × *g* 2 min
	2nd	0 05 M »	30	8 0	10	4 000 × *g* 2 min
	3rd	0.05 M »	20	8.0	3	4 500 × *g* 10 min
Elution	1st	0.15 M phosphate	25	8.5	40	4 500 × *g* 2 min
	2nd	0.15 M »	25	8.5	40	4 500 × *g* 2 min
	3rd	0.15 M phosphate + 0.10 M citrate	20	8.5	30	26 000 × *g* 10 min
	4th	—»—	20	8.5	30	26 000 × *g* 10 min
	5th	—»—	20	8.5	10	105 000 × *g* 10 min

Step 4

Alternative 1. The pH of the step 3 eluate was adjusted to 7.80 and the material poured into a row of test tubes. These tubes were submerged into a water bath having a temperature of 80°C. Stirring was performed as in step 2. After 80 sec. the tubes were put in ice-water and the stirring was continued for 2—3 min. The precipitate was removed by centrifuging at 44 000 × *g*. It was washed with 10 ml of water and again spun down at 44 000 × *g*.

This fractionation step was used only with enzyme preparations purified according to the alternative 1 of the first and the third steps. No purification was obtained when it was applied to enzyme solutions made according to alternative 2.

The preparation was dialyzed over night at 2°C against 2 l of distilled water.

Alternative 2. The pH of the eluate from step 3, alternative 2, was adjusted to 7.2 and ice-cold acetone to a final concentration of 55 % was slowly added to the enzyme solution. The mixture was kept at 0°C for 1 h and then centrifuged at 4 500 × *g* for 15 min. The precipitate that contained the enzyme was transferred to a dialysis bag by washing with approximately 5 ml of water. The dialysis was carried out over night at 2°C against 2 l of a 0.0025 M sodium phosphate buffer having a pH of 8.2.

Step 5

Alternative 1. Any precipitate formed during the dialysis was removed by centrifuging at 20 000 × *g* for a few minutes. The pH of the supernatant was then adjusted to 7.2 and ice-cold acetone was added to a final concentration of 60 %. The mixture was kept at 0°C for 2—3 h and then centrifuged at 22 000 × *g* for 25 min. The precipitate was dissolved in 10—15 ml of 0.010 M sodium phosphate buffer at pH 8.0.

Alternative 2. The precipitate formed during the dialysis was removed by centrifuging at 20 000 × *g* for 10 min. The supernatant was adjusted to pH 8.0 before step 6 was carried out.

Step 6

In this step the enzyme was poured through a column of triethylaminoethyl cellulose (TEAE-cellulose) [16] under conditions which retained on the column the remaining impurities in the step 5 preparation but let most of the enzyme pass through. The cellulose ion exchanger was purchased from the Serva Laboratories, Heidelberg, Germany. It was suspended in 0.010 M sodium phosphate at pH 8.0 and after about 45 min. the smallest particles were removed by decanting. Approximately 1 g of TEAE-cellulose was used per 70 mg of protein. The suspension was deaerated before being used for making the column, which had an inner diameter of 17 mm. The material was poured into the column as a slurry and was allowed to settle on the glass filter disc at the bottom. When most of the material had come to rest, a flow of buffer was passed through the column until the pH of the effluent was 8.0. A filter paper disc was then put on the top of the column.

The enzyme solution from step 5 was let through the column at a rate of approximately 0.5 ml per min and at a temperature of about 2°C. The effluent, which was virtually colourless, was collected in fractions of 2 or 5 ml. Fractions containing a substantial amount of activity were freeze-dried. It was possible to store the enzyme in this state for many months at temperatures below 0°C without loss of activity. However, the enzyme was not stable at room temperature.

Tables 2 and 3 summarize the steps used and the yield and purification obtained in the fractionation of betaine-homocysteine-methyl-transferase from pig liver according to alternative 1 and 2 respectively.

Other fractionation experiments

It may be of interest to mention briefly some of the other fractionation methods that have been tried, although they have given less satisfactory results. Precipitation with ammonium sulfate or ammonium phosphate [17] has in our hands consistently given low yields. Fromm and Nordlie [4] had the same experience in attempts to purify thetin-homocysteine transmethylase from rat liver with ammonium sulfate. Durell *et al.*[5], on the

other hand, used ammonium sulfate fractionation successfully for the purification of the thetin homocysteine methylpherase from horse liver.

Organic solvents, *e.g.* methanol, ethanol, *n*-propanol, *iso*propanol, acetone, methylethylketone and dioxane were also tried for the precipitation of the methyl-transferase at different stages of the purification procedure. Although good results were occasionally obtained, particularly with methanol, ethanol and acetone, we had difficulties in obtaining reproduceable results. Only when an excess of the precipitating agent was used (which led to little or no increase in specific activity) as in step 5, alternative 1, could a good yield consistantly be obtained.

Chromatography on the cation exchange resin Amberlite XE-64, treated as recommended by Hirs [18], was also unsuccessful as the degree of separation was poor. Chromatography on a column of the calcium phosphate (hydroxylapatite) prepared by the method of Tiselius, Hjertén and Levin [19] failed, due to irreversible adsorption of the transferase. Also attempts to use this particular calcium phosphate preparation for batch-wise adsorption and desorption (as in step 3) were unsuccessful, as it was very difficult to elute the enzyme from the "gel". To improve the yield when eluting the transferase from this "gel" or the gel prepared according to Keilin and Hartree, we added betaine, homocysteine, sodium chloride or sodium pyrophosphate to the eluting agent without success. Increasing the temperature during the elution step lowered the yield.

Zone electrophoresis on starch [20] or on specially treated cellulose [21] was tried, but low yields were obtained in both cases, probably due to irreversible adsorption of the transferase to the column material. Paper electrophoresis was also unsuccessful for the same reason. Electrophoresis in a density gradient according to Svenson *et al.*[22] was possible and separated the partially purified (step 5) transferase from coloured impurities [6]. However, we consider this method more elaborate and much more time consuming than the TEAE-cellulose treatment of step 6. The latter procedure can moreover be adapted to larger quantities and it does not require that a person works in a cold-room for long periods of time.

It should be pointed out that our failure to use the above mentioned methods for the purification of betaine-homocysteine-methyl-transferase does not mean that they cannot be successfully applied for this purpose under different conditions.

RESULTS AND DISCUSSION

Comments on the fractionation procedure. It can be seen from Table 3 that the purification of the betaine-homocysteine-methyl-transferase of pig liver according to alternative 2 gave satisfactory results in a comparatively large number of cases. The experiments on which the data are based were carried out during 1956, 1957 and the first part of 1958. When the investigations on the transferase were resumed in the summer of 1959, we were surprised to find, on the one hand that the transferase activity of the pig livers then obtained was on the average about three times higher than previously, on the other hand that the purification method that we had successfully applied in earlier experiments failed. This was particularly so in step 1 but also steps 2 and 3 gave unsatisfactory results. As it was impossible to account for all the activity in the different fractions from these steps, it appeared that the methyl-transferase of the high-activity livers was more labile than that of the livers with low transferase activity. Thetin homocysteine methylpherase has been shown by Durell *et al.*[5,23] to consist of a mixture of polymers and this seems to be the case also with the enzyme described here. It is conceivable that in a liver with a high concentration of the betaine-homocysteine-methyl-transferase less depolymerization of the enzyme to the monomer form takes place. The more polymerized form may be more labile than the monomer. This speculation finds some support from the observation that oxidizing agents (iodine and air) were found to make the

Table 2. Data relevant to the purification of betaine-homocysteine-methyl-transferase according to alternative 1.

Step	Total protein (approx.)	Total volume (approx.)	Step to step recovery (approx.)	Over all recovery (approx.)	Over all purification (approx.)
	mg	ml	%	%	
Homogenate	40 000	760	100	100	1
1 Centrifuging at pH 6.4–6.8	20 000	810	85	85	1.7
2 Heating at 80°C	6 900	800	95	80	4.7
3 Treatment with calcium phosphate gel	400[1]	115[1]	70	57	14
4 Heating at 80°C and dialysis	220	115	90	50	23
5 Precipitation with acetone	97	15	75	38	39
6 TEAE-cellulose column	38	20	75	28	75

[1] Only 200 ml of the material from step 2 was treated at a time.

enzyme more heat labile than reducing agents (cysteine and homocysteine). This observation can, however, not be considered to prove the hypothesis as it is open to several objections, and the explanation for the above-mentioned phenomenon will have to await further and more eleborate experiments in which polymer and monomer forms are quantitatively prepared. It should also be mentioned that we have not yet been able to trace the cause of the increase in transmethylase activity of the pig livers between 1958 and 1959. It is possible that dietary factors play a part.*

The purification of betaine-homocysteine-methyl-transferase from pig liver according to alternative 1 (Table 2) has not been repeated as many times as alternative 2 (Table 3). However, when the procedure had been developed, a skilled technician was able to carry out the fractionation with satisfactory results (Table 2) in five consecutive experiments. The purification took four days. By using a fractionation procedure that is different from alternative 1 or 2, we have occassionally obtained reasonably pure transferase preparations in one day, but it has so far not been possible to get reproduceable results with this procedure.

Purity. The purity of transferase preparations obtained as described under Experimental (alternative 1) have been studied using sedimentation, chromatography and electrophoresis. Fig. 1 shows two photographs from a

* We have since learned from Dr. H. Fredholm of the Swedish Federation of Butchers, Stockholm, that the pigs slaughtered in 1959 and 1960 were on the average younger than in previous years.

Table 3. Data compiled from a number of attempts to purify betaine-homocysteine-methyl-transferase according to alternative 2.

Step	Total protein (approx)	Total volume (approx)	Step to step recovery Average ±standard error	Highest and lowest value	Over all recovery (approx)	Over all purification (approx)
Homogenate	mg 40 000	ml 760	% 100	% 100	% 100	1
1 Centrifuging at pH 5.1—5.2	15 900	890	83.5[2] ± 0.9	77.4—88.0	83.5	2.1
2 Heating at 80°C	3 700	870	98.5[3] ± 1.5	86 —100	82	8.9
3 Treatment with calcium phosphate gel	125[1]	115[1]	77.4[4] ± 1.3	61.5—89.0	64	51
4—5 Precipitation with acetone and dialysis	78	25	77.7[5] ± 3.8	51.5—100	49	64
6 TEAE-cellulose column	25	30	74[6]	53 —80	36	150

[1] Only 200 ml of the material from step 2 was treated at a time.
[2] Average for 12 runs over a period of 18 months.
[3] " " 20 " " " " " 24 "
[4] " " 26 " " " " " 18 "
[5] " " 13 " " " " " 18 "
[6] Only four runs performed.

sedimentation experiment in a Spinco Model A ultracentrifuge, taken after 32 and 64 min at 59 780 r.p.m. The enzyme was dissolved in a 0.01 M phosphate buffer having a pH of 8.0. The sedimentation constant s_{20} was approximatively 8.5 Svedberg units. Only if DL-homocysteine was added to the transferase solution was a sedimentation pattern with one peak obtained. In the absence of reducing agents, three peaks could be observed. This indicates that betaine-homocysteine-methyl-transferase can exist in monomer and polymer forms and that the ratio of monomer to polymer is influenced by reducing agents, *e.g.* SH-groups. This situation is analogues to the one discovered for thetin homocysteine methylpherase by Durell *et al.*[5,23], and suggests a close similarity between the two enzymes.

Fig. 2 shows the result of a *chromatography* experiment on a preparation of betaine-homocysteine-methyl-transferase using a TEAE column. In this experiment the enzyme was eluted with increasing concentrations of phosphate buffer at pH 8 and a careful analysis was made of the distribution of protein and enzyme in the effluent. It can be seen that the curves for protein content and enzyme activity are symetrical about the same fraction number. The enzyme activity was determined using either betaine or dimethyl-β-pro-

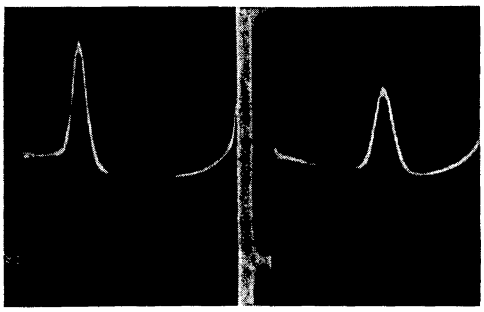

Fig. 1. Sedimentation pattern of purified betaine-homocysteine-methyl-transferase. The pictures were taken after 32 and 64 min at 59 780 r.p.m. in a Spinco Analytical Ultracentrifuge Model E.

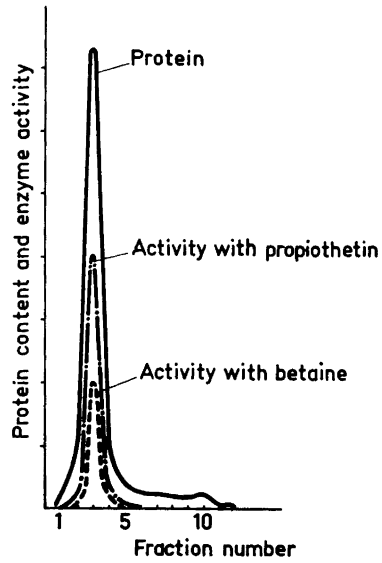

Fig. 2. Chromatography of purified betaine-homocysteine-methyl-transferase on a column of TEAE-cellulose. The units of protein concentration and of enzyme activity (measured either with betaine or dimethyl-β-propiothetin as methyl donor) are arbitrarily chosen to keep the three curves separate from each other.

piothetin as the methyl donor and it is noteworthy that there is no separation of the two activity curves.

In Fig. 3 the *electrophoretic* behaviour of the purified betaine-homocysteine-methyl-transferase is shown. The electrophoresis was carried out in the microcells of a Spinco Model H apparatus. A sodium borate buffer (pH = 9.36, $\mu = 0.1$) containing 1 mg DL-homocysteine per ml was used. Prior to the electrophoresis, the enzyme solution was dialysed against the same buffer, again in the presence of homocysteine.

Figs. 1—3 demonstrate, that although ultracentrifuging, chromatography and electrophoresis revealed minor impurities in the betaine-homocysteine-methyl-transferase purified from pig liver, the transferase protein seemed to dominate according to these criteria of purity.

Molecular weight. An attempt was made to estimate the molecular weight of the transferase monomer using the principle of centrifuging towards sedimentation equilibrium [24]. Calculations at the meniscus and at the cell bottom from a series of concentration gradient patterns, obtained in a run performed in 0.01 M sodium phosphate and at 8 000 r.p.m. in a Spinco Model A ultracentrifuge, gave a mean value of approximatively 270 000.

Absorption spectrum. The light absorption spectrum of a solution of purified betaine-homocysteine-methyl-transferase in a phosphate buffer pH 7.8

Fig. 3. Electrophoresis of purified betaine--homocysteine-methyl-transferase in a sodium borate buffer at pH 9.36, $\mu = 0.1$. The picture was taken after 261 min.

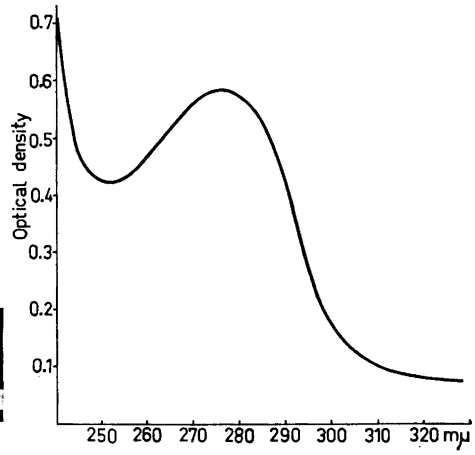

Fig. 4. Light absorption spectrum between 240 and 330 mμ of purified betaine-homocysteine-methyl-transferase.

was determined in a Beckmann Model DU spectrophotometer. The curve shown in Fig. 4 was obtained. This curve, that shows a single absorption peak at 276 mμ, does not suggest the presence of any bound co-factors of, for instance, a vitamin nature. In some preparations a small peak was noticed at 415 mμ. However, we believe that this was caused by an impurity as we have not been able to correlate it with the enzyme activity.

Content of vitamin B_{12}, folic- and folinic acid, and vitamin B_6. Several investigators have noticed that the betaine-homocysteine-methyl-transferase ("betaine-homocysteine-transmethylase") activity is lower in the livers from rats given a diet deficient in vitamin B_{12} than in the livers from normal rats. However, no determination of the vitamin B_{12} content of a purified methyl-transferase has ever been made. A solution of the betaine-homocysteine-methyl-transferase isolated from pig liver was therefore boiled for 10 min. at pH 6.0 in the presence of potassium cyanide in order to release bound vitamin B_{12} from the enzyme. The vitamin B_{12} content of the solution was thereafter determined using the mutant 113—3 of *E. coli* [25] in the medium suggested by Diding [26]. The result of this determination is given in Table 4. It should be mentioned that not only vitamin B_{12} (cyanocobalamin) itself but a large number of vitamin B_{12}-like compounds can support the growth of *E. coli* 113—3. The theoretical content of vitamin B_{12} (and of the other vitamins and growth factors studied, see Table 4) was calculated on the assumption of a one to one relationship between the "co-factor" and the monomer form of the protein moiety and on the basis of a molecular weight of 270 000 for this form of the transferase. It appears unlikely in view of the result of the microbiological assay (Table 4) that vitamin B_{12} or a vitamin B_{12} derivative is present in the betaine-homocysteine-methyl-transferase described here. The fact

Table 4. Calculated and experimentally determined concentrations of microbial growth factors related to vitamin B_{12}, folic- and folinic acid, and vitamin B_6 in solutions of purified betaine-homocysteine-methyl-transferase.

Vitamin or growth factor	Calculated concentration	Experimentally determined concentration
	mμg/ml	mμg/ml
Vitamin B_{12}	30	< 0.004
Folic acid	6	0*
» »	6	< 0.1 **
Folinic acid	6	< 0.3 *
» »	6	< 0.1 **
Vitamin B_6	30	< 1.0

* Direct determination.
** Determination after incubation with chicken pancreas conjugase.

that the enzyme is virtually colourless and that its absorption spectrum shows no maximum near 360 mμ also supports this conclusion. The effect of vitamin B_{12} deficiency on the transferase activity must consequently be indirect and is possibly mediated by certain metabolites, which have been shown to affect the enzyme activity *in vitro* [6].

Numerous studies indicate that an intimate relationship exists between the biological function of vitamin B_{12} and of "folic- and folinic acid". An example of this relationship is the series of reactions leading to the *synthesis* of methyl groups, in which both vitamin B_{12} and pteridine co-factors play a rôle. The function of various pteridine derivatives in the transfer of 1-C fragments at the oxidation level of formate or formaldehyde is well established. It was consequently considered of interest to assay the purified betaine-homocysteine-methyl-transferase for microbial growth factors related to folic- and folinic acid, especially in view of the recent findings by Sauberlich, which show a decrease in mouse liver transmethylase activity due to folic acid deficiency[27]. In order to release folic- and folinic acid factors from the enzyme and to obtain microbially active conjugates of these compounds, aliquots of the enzyme solutions were incubated for 20 h at pH 6.8 and 37°C with a chicken pancreas preparation prior to assay. *Streptococcus faecalis* ATCC 8043 and *Pediococcus cereviseae* (*Leuconostoc citrovorum*) ATCC 8081 were used as test organisms in the turbidimetric tube assay media described by Dr. A. Bolinder of this laboratory [28]. Pteroylglutamic acid and N^5-formyl-tetrahydro-pteroylglutamic acid (Leucovorin, Lederle Laboratories Division, Pearl River, N.J., USA) were used as reference substances. As can be seen from Table 4, the transferase could not replace these two substances as a growth factor for *S. faecalis* or *P. cereviseae* either before or after treatment with chicken pancreas. No evidence was thus obtained for the existence of a pteridine-like co-factor in the betaine-homocysteine-methyl-transferase of pig liver.

Fromm and Nordlie have suggested that pyridoxine is a tightly bound co-factor in the thetin homocysteine transmethylase of rat liver [4]. The sugges-

tion was based on the fact that their transmethylase preparations showed flourescence and absorption at 415 mμ. An attempt was therefore made to determine the vitamin B_6 content of the betaine-homocysteine-methyl-transferase of pig liver. A tube assay with *E. coli* 154—59L [29] was used[30]. This organism responds well to pyridoxine, pyridoxal and to a lesser degree also to pyridoxamine. The vitamin B_6 was released from the enzyme by boiling a solution of the transferase at pH 1.0 for 30 min or by autoclaving at pH 1.7 for 60 min. It was not possible to detect any compound in the enzyme solutions treated in this way that could support the growth of *E. coli* 154—59L (Table 4). In a separate experiment it was also shown that the acid treated transferase failed to stimulate the growth of the B_6-requiring *Saccharomyces carlsbergensis* [31]. As we have only occassionally been able to find an absorption maximum at 415 mμ in our transferase preparations (see above) our data do not provide any evidence for the participation of vitamin B_6 in this type of methyl group transfer. Ericson and Harper have previously shown that a vitamin B_6 deficiency does not decrease the transferase activity of rat liver[8].

Dependance on metals. Two solutions of purified betaine-homocysteine-methyl-transferase were dialysed at 2°C for 50 h, one solution against 0.025 M phosphate buffer pH 8.0, the other against 0.025 M phosphate buffer pH 8.0 containing 2×10^{-3} M EDTA (ethylenediamine tetraacetic acid). There was only a slight decrease but no difference in the transferase activity of these two enzyme solutions after the dialysis, which indicates that the activity is not dependent on bound metals. In other experiments it was found that the addition of potassium cyanide, sodium citrate, sodium pyrophosphate or 8-hydroxyquinoline to the incubation mixtures had no effect on the transferase activity. This is in accordance with the results from similar studies with the methyl transferases purified from rat [2,32] and horse liver [5]. Microbial transferases, on the other hand, appear to be metalloenzymes [33].

Activators and inhibitors. Although no evidence was found for the presence of bound co-factors in the betaine-homocysteine-methyl-transferase described in this communication, it can be shown that the activity of the enzyme is greatly influenced by a number compounds, *e.g.* organic acids, amino acids and peptides [6]. This phenomenon will not be further elaborated upon here, but the author hopes to return to the problem of activation and inhibition in connection with a study of some kinetic properties of the enzyme.

Apparent pH-optimum. Incubation mixtures containing betaine-homocysteine-methyl-transferase, betaine and DL-homocysteine in phosphate buffer were adjusted at 0°C to pH-values ranging from approximatively 5.5 to 9.5. They were thereafter kept at 37°C for 3 h whereupon their methionine content was determined. When the activity of the enzyme was plotted against the pH a curve of the type shown in Fig. 5 was obtained. This indicates that the apparent pH-optimum of the pig liver transferase is near 7.5. It should be mentioned that the apparent pH-optimum — as would be expected — is influenced by a number of factors, *e.g.* the type of buffer, the concentration of the components of the incubation mixture, *etc.*

Stoichiometry of the reaction. To study the stoichiometry of the reaction, betaine containing ^{14}C in one of the N-methyl groups was used. This compound was synthesized from dimethylglycine and ^{14}C-methyl iodide (Radio-

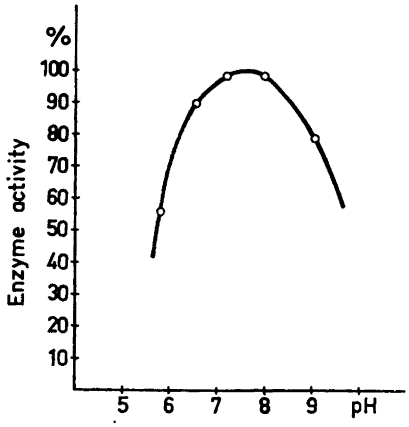

Fig. 5. The apparent pH-optimum of purified betaine-homocysteine-methyl-transferase.

chemical Center, Amersham, England). Carrier betaine was added to make possible crystallization of the product.

The ^{14}C-methyl betaine was incubated overnight together with the enzyme and an excess of DL-homocysteine at 37°C and pH 7.8. The reaction was terminated by boiling and the mixture clarified by centrifuging. The supernatant fluid was chromatographed in a solvent system containing methyl ethyl ketone: acetone: NH_3 (ca. 35 %) at a ratio of 60:27:13 for 30 h at 22°C. After drying, the radioactivity along the chromatogram was measured using a Tracerlab TGC2 Geiger-Müller tube and a LKB Scaler Type Nr 117. At the areas where betaine, dimethylglycine and methionine were located on the chromatogram the following net counts per minute were found in two separate experiments:

	betaine	dimethylglycine	methionine
Expt. 1	204	90	44
Expt. 2	360	180	89

These results show that the radioactivity in counts per min. was twice as high for dimethylglycine (that contains two methyl groups) as for methionine (that contains one methyl group). This suggests that for each molecule of dimethylglycine, one molecule of methionine is formed and that the reaction takes place according to the over all scheme:

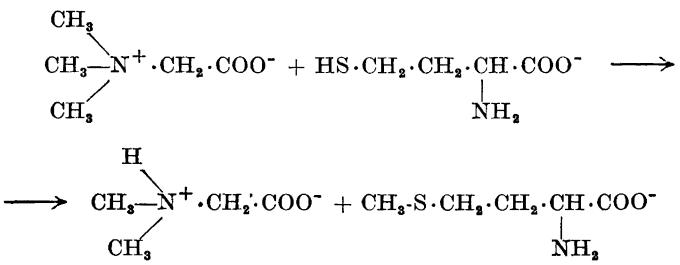

At the apparent pH-optimum of the reaction, dimethylglycine exists mainly in the "zwitterion" form shown above, as indicated by the pK_a and pK_b values determined by Bjerrum [34]. Only insignificant amounts of H_3O^+-ions therefore result from this reaction in contrast to the reaction in which a thetin serves as the donor of the methyl group [3,5].

An attempt was also made to determine whether the transferase reaction is reversible or not. L-Methionine containing ^{14}C in the methyl group (Radiochemical Center, Amersham, England), dimethylglycine and the transferase were incubated for several hours at 37°C and the reaction mixture was thereafter boiled, centrifuged and chromatographed. It was not possible to detect any radioactivity at the site of betaine on the chromatogram.

The skilled technical assistance of Miss I. Frölich is gratefully acknowledged. The author would also like to thank Drs. A. Hedbom and S. Åkesson most sincerely for their help with the ultracentrifugal and electrophoretic experiments. Financial support was provided by the *Medical Research Council* and the *Knut och Alice Wallenberg Foundation*.

REFERENCES

1. Ericson, L.-E. *Acta Chem. Scand.* **14** (1960) 2102.
2. Ericson, L.-E., Williams, J. N. and Elvehjem, C. A. *J. Biol. Chem.* **212** (1955) 537.
3. Maw, G. A. *Biochem. J.* **63** (1956) 116.
4. Fromm, H. J. and Nordlie, R. C. *Arch. Biochem. Biophys.* **81** (1959) 363.
5. Durell, J., Anderson, D. G. and Cantoni, G. L. *Biochim. et Biophys. Acta* **26** (1957) 270.
6. Ericson, L.-E. *Acta Chem. Scand.* **12** (1958) 1541.
7. Ericson, L.-E., Harper, A. E., Williams, J. N. and Elvehjem, C. A. *J. Biol. Chem.* **219** (1956) 59.
8. Ericson, L.-E. and Harper, A. E. *Proc. Soc. Exptl. Biol. Med.* **90** (1955) 298.
9. Harper, A. E., Ericson, L.-E., Boldt, R. E. and Elvehjem, C. A. *Am. J. Physiol.* **184** (1956) 457.
10. Mc Carthy, T. E. and Sullivan, M. X. *J. Biol. Chem.* **141** (1941) 871.
11. Steele, B. F., Sauberlich, H. E., Reynolds, M. S. and Baumann, C. A. *J. Biol. Chem.* **177** (1949) 533.
12. Johnson, B. C. and Swanson, A. M. *J. Dairy Science* **35** (1952) 823.
13. Kalckar, H. *J. Biol. Chem.* **167** (1947) 461.
14. Perrin, C. H. *Anal. Chem.* **25** (1953) 968.
15. Keilin, D. and Hartree, E. F. *Proc. Roy. Soc.* **B 124** (1938) 397.
16. Porath, J. *Arkiv Kemi* **11** (1957) 97.
17. Racker, E. *J. Biol. Chem.* **217** (1955) 855.
18. Hirs, C. H. W. In Colowick, S. P. and Kaplan, N. O. *Methods in Enzymology* **I** (1955) 113, Academic Press Inc., New York. 1955–1957.
19. Tiselius, A., Hjertén, S. and Levin, Ö. *Arch. Biochem. Biophys.* **65** (1956) 132.
20. Carlson, L. A. *Acta Chem. Scand.* **8** (1954) 357.
21. Flodin, P. and Kupke, D. W. *Biochim. et Biophys. Acta* **21** (1956) 368.
22. Svensson, H., Hagdahl, L. and Lerner, K.-D. *Science Tools* **4** (1957) 1.
23. Durell, J. and Cantoni, G. L. *Biochim. et Biophys. Acta* **35** (1959) 515.
24. Schachman, H. K. In Colowick, S. P. and Kaplan, N. O. *Methods in Enzymology*, **IV** (1957) 32, Academic Press Inc., New York 1955–1957.
25. Davis, B. D. and Mingioli, E. S. *J. Bacteriol.* **60** (1950) 17.
26. Diding, N. *Scand. J. Clin. Lab. Invest.* **3** (1951) 215.
27. Sauberlich, H. E. *J. Nutrition* **68** (1959) 141.

28. Bolinder, A. *Acta Chem. Scand. To be published.*
29. Davis, B. D. *Proc. Natl. Acad. Sci. U.S.* **35** (1949) 1.
30. Diding, N. *Svensk Farm. Tidskr.* **59** (1955) 321.
31. Snell, E. E. In Sebrell, W. H. jr. and Harris, R. S. *The Vitamins* **III** (1954) 253, Academic Press Inc., New York.
32. Maw, G. A. *Biochem. J.* **70** (1958) 168.
33. Shapiro, S. K. and Yphantis, D. A. *Arch. Biochem. Biophys.* **82** (1959) 477.
34. Bjerrum, N. *Z. physik. Chem. Leipzig* **104** (1923) 147.

Received June 2, 1960.

ACTA CHEMICA SCANDINAVICA 14 (1960) 2127–2134

Betaine-Homocysteine-Methyl-Transferases

III. The Methyl Donor Specificity of the Transferase Isolated from Pig Liver

L.-E. ERICSON

Division of Food Chemistry, Royal Institute of Technology, Stockholm 70, Sweden

Studies have been made on the specificity of the methyl donor requirement of a betaine-homocysteine-methyl-transferase purified from pig liver. It was found that a number of betaine derivatives and sulfonium compounds could replace betaine as methyl donor. No evidence was obtained for ethyl group transfer.

Many of the ammonium compounds tested as methyl donors interfered with the utilization of betaine, and betaine itself decreased the rate of methyl transfer from certain sulfonium compounds.

The data presented are tentatively interpreted and discussed.

In a previous communication [1] methods were reported for the preparation of a purified betaine-homocysteine-methyl-transferase from pig liver. It is the purpose of this article to describe some studies on the specificity of the methyl donor requirement of this enzyme preparation. The problem has already been discussed briefly in two earlier papers from this laboratory [2,3], and has been investigated also by other research groups [4,5].

The ability of the substances tested as methyl donors to compete with betaine (carboxymethyl-trimethyl-ammonium chloride) for the active donor site on the transferase was also studied in the investigation reported here.

EXPERIMENTAL

The enzyme preparation used in the experiments described below, was obtained from pig liver by the method given in Ref.[1] (alternative 1). As judged from electrophoretic and ultracentrifuge studies the transferase contributed approximatively 90 % of the total protein of the preparation. The protein content of the incubation mixtures was determined using the method suggested by Kalckar [6]. Enzyme activity was measured as the amount of methionine formed per hour during the initial phase of the reaction when the amount of dimethylglycine was small. The incubations were carried out aerobically at 37°C.

Methionine was determined microbiologically according to Steele *et al.*[7] The nitroprusside method [8] was found unsuitable for this purpose as many of the compounds tested

interfered with the colour formation. Ethionine, however, was measured chemically by determining the optical density at 520 mμ of the nitroprusside reaction product.

Of the compounds tested as methyl donors betaine, choline, dimethylglycine, acetyl choline, dimethyl-β-propiothetin, trimethylamine hydrochloride, methyl methionine sulfonium chloride, ergothioneine · HCl, and S-adenosyl methionine iodide were commercial products purchased from California Corporation for Biochemical Research, Cal., USA; L. Light & Co., England; Fluka AG, Switzerland, and Nutritionals Biochemicals Corporation, Ohio, USA. Betaine aldehyde; DL-carnitine, O-acetyl-DL-carnitine; muscarine iodide; N-trimethyl taurine; dimethyl acetothetin and trimethylsulfonium chloride were kindly supplied by Drs. D. R. Strength, S:t Louis University School of Medicine, USA; G. S. Fraenkel, University of Illinois, USA; F. Hoffman-La Roche & Co, Switzerland; D. Ackermann, University of Würzburg, Germany; F. Challenger, University of Leeds, England and G. A. Maw, A. Guinness, Son & Co, Ltd., Dublin, Eire.

The methyl and ethyl esters of betaine were synthesized from the methyl and ethyl esters of bromoacetic acid and trimethylamine [9]. The betaine amide was prepared from chloroacetamide and trimethylamine [9]. The nitrile corresponding to betaine was obtained by reacting dimethyl-amino-acetonitrile prepared according to von Braun [10] with methyl iodide. The betaine-like compounds that are formed when one, two or all three of the N-methyl groups are replaced by ethyl groups were prepared *via* dimethyl- or diethyl-amino-acetonitrile [10] and ethyl bromide or methyl iodide [11]. The nitriles were converted to the corresponding betaines according to Klages and Margolinsky [12]. The α-methyl betaine was synthesized by N-methylation of α-alanine with methyl iodide [11]. Propiobetaine was obtained from trimethylamine and propionic acid lactone [13] and butyrobetaine from α-amino buturic acid and methyl iodide [14]. All the compounds synthesized in the laboratory were recrystallized to constant melting points.

RESULTS AND DISCUSSION

It is obvious from the results presented in Tables 1 and 2 that the betaine-homocysteine-methyl-transferase of pig liver can use a variety of compounds as methyl group donors. However, neither choline nor betaine aldehyde can replace betaine in this function (Table 1). The methyl and ethyl esters of betaine, on the other hand, are excellent donors of methyl groups, being equally potent in this respect as betaine itself. This was found to be the case over a wide range of concentrations. It is of interest to notice in this connection the complete lack of donor activity of the betaine amide.

The "betaine nitrile" seems to possess some ability to donate methyl groups with the enzyme preparation used. This would suggest that the

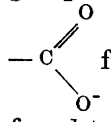

function, present in all the other compounds in Table 1 that were found to act as methyl donors, is not essential for donor activity.

If one of the three N-methyl groups of betaine is replaced by an ethyl groups, a compound is formed that has a methyl donor activity that is only 30 % of that of betaine. Replacement of two of the N-methyl groups by ethyl group lowers the donor activity to 6 %. Ethyl groups cannot apparently be handled by the enzyme, since no ethionine could be detected in incubation mixtures containing betaine derivatives in which one, two or all three of the N-methyl groups had been replaced by ethyl groups. Attempts to detect ethionine were made either by the nitroprusside method or by paper chromatography. It is of course possible that the amount of ethionine formed was too small to be detected by these methods.

Table 1. The ability of some nitrogenous compounds that are structurally related to betaine to serve as donors of methyl groups using a preparation of betaine-homocysteine-methyl-transferase. The enzyme activity is also given for incubation mixtures containing both the compound and betaine at the concentration ratio of 2:1. All incubation mixtures contained 0.025 M DL-homocysteine and approximatively 0.2 mg protein per ml. Anions are omitted in the formulae.

Name	Formula	Relative activity	
		0.05 M of the compound alone %	0.1 M of the compound + 0.05 M of betaine %
Betaine (carboxymethyl-trimethyl-ammonium chloride)	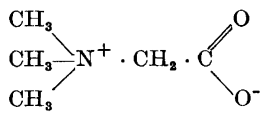	100	100
Choline	$(CH_3)_3N^+ \cdot CH_2 \cdot CH_2 - OH$	0	100
Betaine aldehyde	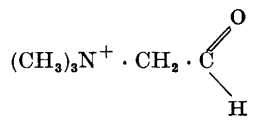	0	80
Betaine methyl ester	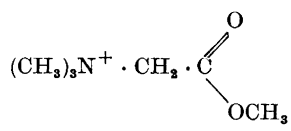	100	130
Betaine ethyl ester	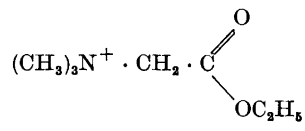	100	108
Betaine amide	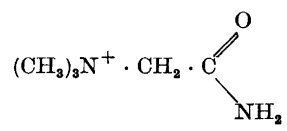	0	93 *
2-Acetonitrile-trimethyl-ammonium chloride	$(CH_3)_3N^+ \cdot CH_2 \cdot C \equiv N$	12	55
Dimethylglycine	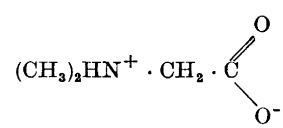	0	0

* Tested at 0.05 M together with 0.05 M betaine.

Table 1 (cont.)

Carboxymethyl-dimethyl-ethyl-ammonium chloride	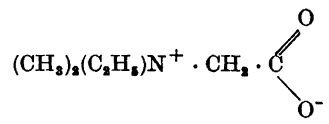	30	72
Carboxymethyl-diethyl-methyl-ammonium chloride	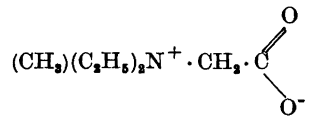	6	100
Carboxymethyl-triethyl-ammonium chloride	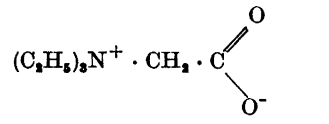	No ethionine	93
1-Carboxyethyl-trimethyl--ammonium chloride (α-methylbetaine)	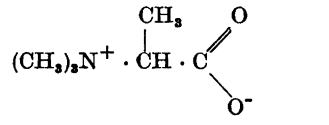	13	85
2-Carboxyethyl-trimethyl-ammonium chloride (propiobetaine)	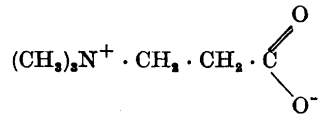	0	95
3-Carboxypropyl-trimethyl-ammonium chloride (butyrobetaine)	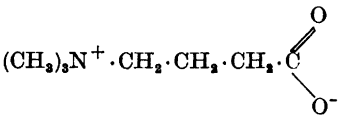	0	—
DL-Carnitine	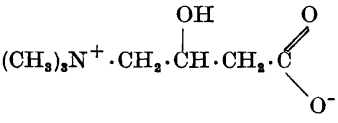	0	90
O-Acetyl-DL-carnitine	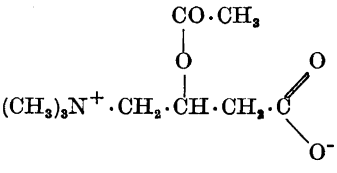	0	77
Acetyl choline	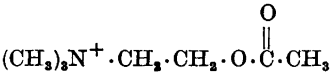	0	100

Table 1 (cont.)

L-Ergothioneine hydrochloride	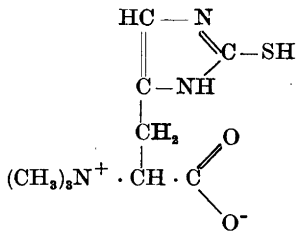	0	0 *
Muscarine iodide [18]	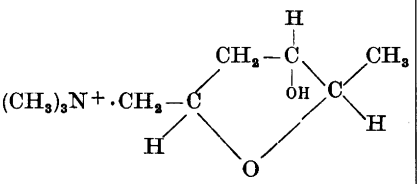	0	69
N-Trimethyl taurine	$(CH_3)_3N^+ \cdot CH_2 \cdot CH_2 \cdot SO_3^-$	0	115
Trimethyl-ammonium chloride	$(CH_3)_3N$	0	100

* When tested at a concentration of 0.01 M together with 0.05 M betaine the relative activity was 77 %.

In connection with a discussion on N-substituted betaines it is relevant to draw attention to the fact that dimethylglycine, which at the pH tested can be considered as a betaine molecule in which one of the N-methyl groups has been replaced by a hydrogen atom [15], cannot act as a donor of methyl groups although its affinity to the active center on the enzyme appears to be considerable.

With the purified betaine-homocysteine-methyl-transferase used in the present study, α-methyl betaine showed 13 % donor activity. The decrease in activity caused by the introduction of the α-methyl group in betaine is probably to a large extent due to steric hindrance. With a crude methyl-transferase from *Anodonta cygnea* the α-methyl betaine was found to have 45 % of the donor activity of betaine [3]. The reason for this discrepancy between the two enzyme preparations is not known. It is possible that the betaine-homocysteine-methyl-transferase of *Anodonta cygnea* has a different steric configuration around its active donor site than the betaine-homocysteine-methyl-transferase of pig liver. It is also conceivable that *Anodonta* liver contains more than one transferase. The difference between the results with the two enzyme preparations may of course be caused by the different degree of saturation at which the substrates were tested with the two transferases.

The latter explanation seems less plausible, however, as it has not been possible to increase appreciably the relative activity of α-methyl betaine for the transferase of pig liver by increasing its concentration in the incubation mixture several times above that used in Table 1.

Ergothioneine which has a larger substituent than the methyl radical in the α-position, can apparently not donate its methyl groups under the conditions of the test. It is of interest to notice, however, that ergothioneine is a very potent methyl-transferase inhibitor.

The length of the carbon chain of the ammonium compounds tested is obviously of vital importance for determining the ability to serve as a donor of methyl groups. Propiobetaine, butyrobetaine, carnitine and O-acetylcarnitine were all found to be completely inactive (Table 1). This is in contrast to the results obtained with the sulfonium compounds (Table 2). Not only dimethyl-acetothetin but also dimethyl-β-propiothetin and methyl methionine sulfonium chloride are excellent methyl group donors. Also the difference in behaviour of trimethyl ammonium chloride and trimethyl sulfonium chloride should be noted; the latter but not the former is able to act as methyl group donor.

Only a qualitative comparison can be made between the results reported here and those of other investigators. There is as far as this comparison is

Table 2. The ability of some sulfonium compounds to serve as donors of methyl groups using a preparation of betaine-homocysteine-methyl-transferase. The enzyme activity is also given for incubation mixtures containing both the test compound and betaine at the concentration ratios shown in the table. All incubation mixtures contained 0.025 M DL-homocysteine and 0.2 mg protein per ml.

Name	Relative activity		
	0.05 M of the compound alone	*x* M of the test compound and *y* M of betaine	
	%	%	*x* : *y*
Betaine	100	100	—
Dimethyl acetothetin	1 300	1 000 840	0.05 : 0.10 0.05 : 0.20
Dimethyl-β-propiothetin	850	200 170	0.05 : 0.10 0.05 : 0.20
Methyl methionine sulfonium chloride	1 200	350	0.05 : 0.20
S-Adenosyl-methionine iodide *	22	—	—
Trimethyl sulfonium chloride	500	125	0.05 : 0.10

* Tested at a concentration of 0.005 M.

possible, a general agreement between the methyl donor specificity of the horse liver thetin homocysteine methylpherase of Durell *et al.*[4], the rat liver thetin homocysteine transmethylase of Maw [5], the betaine-homocysteine-methyl-transferase from *Anodonta cygnea* [3] and the methyl transferase purified from pig liver. However, S-adenosyl-methionine was reported to be unable to donate its methyl group using the enzyme isolated from horse liver by Durell *et al.*[4] whereas this compound was found to possess donor activity with our pig liver transferase. Sufficient material has not been available to investigate further the reason for this difference in results. It should be mentioned that the S-adenosyl-methionine used by Durell *et al.*[4] was prepared by them, whereas the compound used in our studies was of commercial origin (California Corporation for Biochemical Research, Cal., USA). Shapiro [16,17] found that S-adenosyl-methionine prepared from yeast cells could donate its methyl group to homocysteine in cell free extracts from both rat liver and from some microorganisms.

Many betaine-like compounds that are not themselves methyl donors have the ability to inhibit the transfer of a methyl group from betaine to homocysteine (Table 1). This is for instance the case with dimethylglycine, betaine aldehyde, betaine amide, "triethyl betaine", propiobetaine, DL-carnitine, O-acetyl-DL-carnitine, ergothioneine, and muscarine [18]. The inhibition is most likely caused by competition between the inactive ammonium compounds and betaine for the active donor site on the transferase. Such a competition is probably also the reason for the decrease in transmethylase activity caused by some of the less potent methyl donors listed in Table 1, *e.g.* betaine nitrile, "mono- and diethylbetaine" and α-methyl betaine. The phenomenon is apparent also from the data in Table 2, where it is shown that betaine, which is less potent as a methyl donor than dimethyl-acetothetin, dimethyl-β-propiothetin, methyl methionine sulfonium chloride or trimethyl sulfonium chloride can markedly interfere with the methyl transfer from the latter compounds. In a previous communication from this laboratory [2] it was reported that all attempts have failed to separate the transferase that uses betaine as the methyl donor from a transferase that uses thetins. It was also observed at that time, that the conditions that altered the rate of transmethylation from betaine to homocysteine also altered in a similar manner the transfer of methyl groups from dimethyl-β-propiothetin to homocysteine [2]. All data accumulated so far therefore indicate that betaine and the thetins are bound to the same active center on the enzyme. However, further studies are necessary to prove conclusively that this is the case.

It appears likely from the observations presented in Table 1 that methyl donors of the ammonium type have to be bound at two (or more) points to the enzyme surface before they can perform their function.

It should be emphasized that the investigation described in this paper must be considered as being of an exploratory nature only. For a correct interpretation of the observations, the studies should be extended over a greater number of compounds. It is also necessary that the tests be performed under a variety of conditions to make possible kinetic evaluation of the data.

The author is indebted to Mr. Nils Walde and Miss I. Frölich for assistance and to Drs. D. Ackermann, F. Challenger, G. S. Fraenkel, G. A. Maw and D. R. Strength as well as F. Hoffman-La Roche & Co. for gifts of some of the compounds tested. He would also like to thank the *Medical Research Council* and the *Knut and Alice Wallenberg Foundation* for financial support.

REFERENCES

1. Ericson, L.-E. *Acta Chem. Scand.* **14** (1960) 2113.
2. Ericson, L.-E. *Acta Chem. Scand.* **12** (1958) 1541.
3. Ericson, L.-E. *Nature* **185** (1960) 465.
4. Durell, J., Anderson, D. G. and Cantoni, G. L. *Biochim. et Biophys. Acta* **26** (1957) 270.
5. Maw, G. A. *Biochem. J.* **70** (1958) 168.
6. Kalckar, H. *J. Biol. Chem.* **167** (1947) 461.
7. Steele, B. F., Sauberlich, H. E., Reynolds, M. S. and Baumann, C. A. *J. Biol. Chem.* **177** (1949) 533.
8. McCarthy, T. E. and Sullivan, M. X. *J. Biol. Chem.* **141** (1941) 871.
9. Renshaw, R. R. and Hotchkiss, H. T. *J. Am. Chem. Soc.* **48** (1926) 2698.
10. von Braun, J. *Ber* **40** (1907) 3933.
11. Griess, P. *Ber.* **5** (1872) 1036; **6** (1873) 585; **8** (1875) 1406.
12. Klages, A. and Margolinsky, S. *Ber.* **36** (1903) 4188.
13. Gresham, T. L., Jansen, J. E., Shaver, F. W., Bankart, R. A. and Fiedorek, F. T. *J. Am. Chem. Soc.* **73** (1951) 3168.
14. Willstätter, R. *Ber.* **35** (1902) 584.
15. Bjerrum, N. *Z. physik. Chem. Leipzig* **104** (1923) 147.
16. Shapiro, S. K. *Biochim. et Biophys. Acta* **29** (1958) 405.
17. Shapiro, S. K. and Yphantis, D. A. *Biochim. et Biophys. Acta* **36** (1959) 241.
18. Kögl, F., Cox, H. C. and Salemink, C. A. *Experientia* **13** (1957) 137.

Received June 2, 1960.

ACTA CHEMICA SCANDINAVICA 14 (1960) 2135–2138

Investigations on the Molecular Weight of Aqueous Solutions of Potato Amylose by Osmotic Pressure

B. B. JØRGENSEN and O. B. JØRGENSEN

*Department of Technical Biochemistry, Royal Technical University, Copenhagen *, and the University Institute of Physical Chemistry, Copenhagen, Denmark*

The colloid osmotic pressure of aqueous amylose solutions is measured. In concentrations of 0.2–0.6 % amylose the reduced osmotic pressure, p/c, is constant within the experimental error. The influence of heating in alkaline solution on the osmotic pressure and viscosity of amylose solutions is examined. The osmotic pressure of the potato amylose examined corresponds to a molecular weight $\sim 2.02-2.10 \times 10^5$ and to a D.P. $\sim 1\,250-1\,300$.

On account of the difficulties in making stable aqueous solutions of amylose most of the physical determinations of molecular weight of amylose are performed on amylose derivatives in a suitable solvent. Reviews on this subject are given by Greenwood [1] and Whelan [2].

By means of the inverted microosmometer described by Christiansen and Jensen [3] it is possible to measure small osmotic pressures in rather short times. The purpose of this investigation is to examine the possibility of measuring the osmotic pressure of aqueous solutions of amylose by means of the inverted microosmometer before retrogradation of amylose takes place. As the amylose was brought in solution in alkali it was necessary to examine how alkali treatment influenced the osmotic pressure of the amylose solution.

EXPERIMENTAL

Amylose. The amylose examined was prepared from potato starch by precipitation with thymol after the precipitation of the amylopectin as described by Hobson *et al.*[4] The amylose showed a "blue value" = 1.38.

Amylose solution. The amylose solutions were prepared by dissolving a suitable amount of amylose in 0.4 N KOH by shaking for 1 ½ h and filtering through a G4 sintered-glass filter. The solutions were then heated the time wanted (0–16 min) in a boiling water bath. During the shaking and heating the amylose solutions were protected against oxygen by an atmosphere of nitrogen. After the heating the solutions were cooled in running tap water. Immediately before the osmotic measurements a suitable volume of the solutions was neutralized with 0.4 N HCl and eventually diluted with 0.2 M KCl.

* Address: Odensegade 14, Copenhagen Ø.

The exact concentrations of amylose in the solutions were determined by acid hydrolysis according to Pirt and Whelan [5] followed by determination of glucose by the method of Somogyi [6] and Nelson [7].

Osmotic pressure measurements. The colloid osmotic pressures were measured by means of the inverted microosmometer described by Christiansen and Jensen [3]. The semipermeable membranes were prepared as described by Jensen and Marcker [8]. On account of the instability of neutral amylose solutions the measurements were started immediately after the equilibrium was established. The measurements were performed at 21°C. The outer liquid in the osmometer was 0.2 M KCl.

Viscosity measurements. The specific viscosities of the amylose solutions were measured at 25°C in an Ostwald viscosimeter. The measurements of the viscosity were made on the same alkaline solutions as were used for the osmotic measurements (heated different times) after dilution 1:10 with water.

RESULTS

Molecular weight calculations from osmotic pressures were made by means of the equation: $M = k\frac{c}{p}$, where c = concentration of amylose in g/ml and p = osmotic pressure in cm water column. At 21°C the value of k is 247.6×10^5 (Christiansen and Jensen [3]). D.P. = $M/162$.

It was examined how increasing heating times of the alkaline amylose solution influenced the osmotic pressure and the specific viscosity of the amylose solution, see Fig. 1.

Fig. 1 shows that the apparent D.P. obtains a rather constant value after heating of the amylose solution for about 5 min and only decreases slightly for longer heating times.

It is further seen from Fig. 1 that the specific viscosity of the solution, which was used for osmotic measurements but not neutralized after dilution

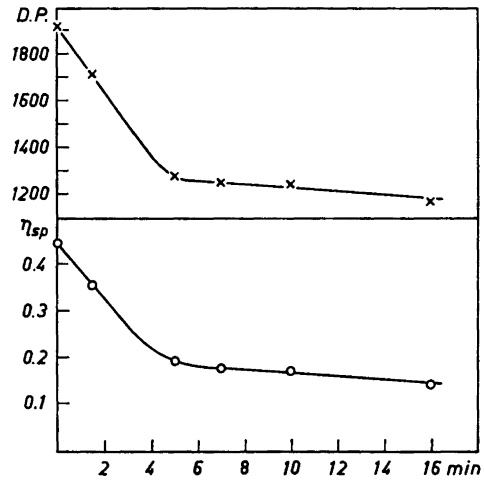

Fig. 1. The graph shows the relation between apparent D.P. and time of heating, t, of amylose in 0.4 N KOH, $c = 4.28 \times 10^{-3}$ g/ml after neutralisation, × — × — ×, and the relation between specific viscosity, η_{sp}, and time of heating of amylose in 0.4 N KOH, $c = 0.43 \times 10^{-3}$ g/ml 0.04 N KOH, ⊙—⊙—⊙.

Table 1. Experiments I—IV show the osmotic pressure of different dilutions of an amylose solution. Experiment V shows the osmotic pressure of the same amylose preparation but in another solution and with another membrane. Experiments VI and VII show the osmotic pressure of another preparation with a known D.P.
c is concentration of amylose in the neutral solution, p is osmotic pressure in cm water column, M is molecular weight and D.P. is degree of polymerisation.

Exp.	$c \times 10^3$ g/ml	p cm	p/c	$M \times 10^{-5}$	D.P.
I	2.15	0.30	140	1.77	1 090
II	2.86	0.41	143	1.73	1 070
III	4.29	0.60	140	1.77	1 090
IV	5.73	0.80	140	1.77	1 090
V	5.02	0.69	137	1.81	1 120
VI	5.14	0.62	121	2.05	1 270
VII	4.96	0.60	121	2.05	1 270

1:10 with water, shows a quite analogous variation. It was further found that η_{sp}/c was independent of c ($c \leq 0.43 \times 10^{-3}$ g/ml), the amylose concentration, by further dilution both in heated and in unheated solutions.

These results seem to show that it is necessary to heat the alkaline amylose solutions at least for 5 min before the osmotic pressure and the viscosity of the solutions are well defined.

It was examined if the proportion p/c, the so-called reduced osmotic pressure, was dependent on the concentration.

In Table 1 are shown the results of these measurements. The alkaline amylose solution was heated for 5 min (these experiments were performed without protection by N_2), and the concentration was varied from 0.215 % to 0.573 % by dilution (Expts. I—IV). It is seen from the table that p/c does not change with concentration in the range of concentration examined; accordingly the molecular weight can be calculated directly from p/c without extrapolating to $c = 0$. This means that the second virial coefficient is negligible at 21 °C in agreement with the light scattering measurements by Everett and Foster [11].

Experiment V, Table 1, shows an experiment, where the osmotic pressure of another solution of the same preparation is measured with another membrane than in experiments I—IV. It is seen that the measurements are reproducible.

The osmotic pressure was then determined of an amylose preparation, that kindly was placed at our disposal by dr. W. J. Whelan, and the D.P. of which was determined by dr. Whelan by periodate oxidation to 1 250. Our results of two independent measurements of the osmotic pressure (without use of N_2) are given as experiments VI and VII in Table 1.

DISCUSSION

It is seen from the reproducibility of the measurements that it is possible, with the technique used, to measure the osmotic pressure of neutral amylose solutions, before the amylose retrogrades.

Fig. 1 shows that the apparent D.P. falls very fast with the time of heating in alkali for the first short heating period, while further fall in apparent D.P.

for heating times longer than 5 min is very slight. As the amylose solutions were protected against oxygen by an atmosphere of nitrogen this effect is hardly due to oxidation. The slow fall for heating times longer than 5 min is possibly due to an alkaline degradation of amylose. The fast fall for shorter heating times may be due to another effect. Either the amylose contains a few very alkali-labile bonds — having eventually been introduced into the amylose during the preparation (Baum and Gilbert [9]) — or the heating in alkali causes a disaggregation of the associated amylose molecules, the amylose only being of molecular form after a heating time of about 5 min. Paschall and Foster [10] have shown that amylose disaggregates by standing in 1 N KOH at room temperature, but this effect is not pronounced for potato amylose. As the potato amylose in our examinations has been heated in alkali it is possible that the phenomenon may be explained as a disaggregation of the amylose.

The most well-defined molecular weight of amylose is found after a heating time of about 5—10 min in 0.4 N KOH under N_2. It is seen from Fig. 1 that D.P. of the amylose preparation examined under these conditions is about 1 250. Extrapolating to a heating time of 0 min a D.P. of about 1 300 is found.

Acknowledgements. We are gratefully indebted to Professor Holger Jørgensen for his interest of this work and to Professor J. A. Christiansen and the late Dr. C. E. Jensen, the University Institute of Physical Chemistry, Copenhagen, for their help in the performance of the osmotic measurements. Financial support from *Det teknisk-videnskabelige Forskningsråd* is gratefully acknowledged.

REFERENCES

1. Greenwood, C. T. *Advances in Carbohydrate Chem.* **11** (1956) 362.
2. Whelan, W. J. *Handbuch der Pflanzenphysiologie* (W. Ruhland Ed.) Springer Verlag, Wien 1958, p. 170.
3. Christiansen, J. A. and Jensen, C. E. *Acta Chem. Scand.* **7** (1953) 1247.
4. Hobson, P. N., Pirt, S. J., Whelan, W. J. and Peat, S. *J. Chem. Soc.* **1951** 801.
5. Pirt, S. J. and Whelan, W. J. *J. Sci. Food Agr.* **2** (1951) 224.
6. Somogyi, M. *J. Biol. Chem.* **195** (1952) 19.
7. Nelson, N. *J. Biol. Chem.* **153** (1944) 375.
8. Jensen, C. E. and Marcker, K. *Acta Chem. Scand.* **12** (1958) 855.
9. Baum, H. and Gilbert, G. A. *Chem. & Ind. London* **1954** 489.
10. Paschall, E. F. and Foster, J. F. *J. Polymer Sci.* **9** (1952) 73.
11. Everett, W. W. and Foster, J. F. *J. Am. Chem. Soc.* **81** (1959) 3459.

Received July 22, 1960.

ACTA CHEMICA SCANDINAVICA 14 (1960) 2139–2144

The Conformational Analysis of *cis*-1,4-Chlorobromo*cyclo*hexane

V. A. ATKINSON and K. LUNDE

Universitetets Kjemiske Institutt, Blindern — Oslo, Norway

Cis-1,4-chlorobromo*cyclo*hexane has been studied in the gaseous state by electron diffraction, and in the liquid and solid states by infra-red spectroscopy. The results show that the compound is all, or nearly all, in the *e*-chloro *a*-bromo conformation.

Some years ago it was found that when crystals of 1*e*,2*e*-dichloro-4*e*,5*e*-dibromo*cyclo*hexane were heated to the melting point they isomerized, and that when the melt cooled it consisted mainly of the 1*e*,2*e*-dichloro-4*a*,5*a*-dibromo isomer [1]. More surprising was the fact that neither infra-red [2] nor electron diffraction [3] investigations were able to establish the expected conformational equilibrium (*ee*Cl_2-*aa*Br_2 ⇌ *aa*Cl_2-*ee*Br_2) between the free molecules of this isomer. The only conformation detectable by both methods was that established by X-ray investigations [4] to exist in the crystal, *viz.* the conformation where the two bromine atoms occupy equatorial positions. These findings were hard to explain by simple steric considerations.

It is true that Kozima and Sakashita [5] did claim to have detected evidence of an equilibrium between the two possible conformations of this compound. However, their infra-red investigation used the KBr-disc method, with high temperatures. These are conditions which are more likely to facilitate an S_N2 reaction (such as the reversal of the isomerization [1]: *ee*Cl_2—*ee*Br_2 ⇌ *aa*Cl_2—*ee*Br_2) than the claimed shift in the conformational equilibrium.

In the circumstances, it seemed worthwhile to investigate another compound which might be expected to have a similar conformational oddity. We chose *cis*-1,4-chlorobromo*cyclo*hexane, which might exist as either of the two conformations shown in Fig. 1, or as a conformational equilibrium between them. To the best of our knowledge this compound has not been described before.

PREPARATION

During the preparation of the *trans*-1,4-chlorobromo*cyclo*-hexane from 4-chloro*cyclo*-hexanol and phosphorus tribromide, an oily fraction boiling between 62°C and 64°C (0.5 mm) was collected [6]. This fraction contains both isomers of 1,4-chlorobromo*cyclo*-hexane. Most of the *trans* isomer was precipitated upon cooling to 5°C. The cooling and

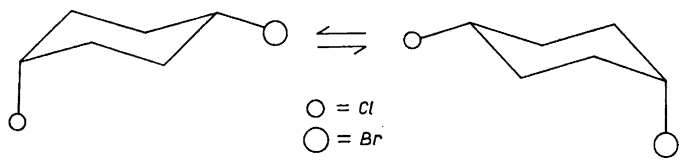

Fig. 1. The possible conformational equilibrium.

filtration was continued until no further crystals formed. Then the filtrate was distilled *in vacuo* in a spinning band column equivalent to 25 theoretical plates. After an appreciable forerun (presumably the remains of the *trans* compound, boiling at about 90°C, 11 mm), a fraction boiling constantly at 97°C (11 mm) was collected. The 97°C fraction solidified on being kept in a refrigerator for some time, and melted again at 21° to 21.5°C. Re-distillation yielded pure *cis*-1,4-chlorobromo*cyclo*hexane with a melting point of 22.0°C.

ELECTRON DIFFRACTION

The electron-diffraction measurements were carried out in the gas phase using the new Oslo apparatus [7] with distances of 19 and 48 cm between the nozzle and the photographic plates. The experimental intensity data, extending from $s = 1.5$ to $s = 45.0$, were treated in the manner described in a series of papers from this institute published after 1955. After appropriate corrections and the inclusion of a damping factor of 0.0024, the experimental intensity curve shown in Fig. 2 was obtained. This was subjected to a Fourier transform to give an initial $\sigma(r)/r$ radial ditribution curve which had substantially the same form as that shown in Fig. 3a.

Theoretical $\sigma(r)/r$ curves (Fig. 3b) were built up from Gauss curves for each of the two possible conformations. The internuclear distances in the two conformations were calculated from models in which the bond distances were: C—H = 1.074, C—C = 1.529, C—Cl = 1.824 and C—Br = 1.981 Å (obtained from the initial radial distribution curve), and the bond angles were C—C—C = 111.5°, C—C—X = 110.0° and X—C—X = 108.7° (obtained from the latest figures for *cyclo*hexane [8]). The models also included a slight distortion of the axial carbon-halogen bonds, suggested by previous work on related compounds [9]. The carbon-chlorine bond was bent outwards 6.3° from the axial position in the *a*-chloro *e*-bromo model, and the carbon-bromine bond was bent outwards 7.7° from the axial position in the *e*-chloro *a*-bromo model.

The two theoretical radial distribution curves were then Fourier transformed back to give two theoretical intensity curves directly comparable with the experimental intensity curve of Fig. 2. It can be seen at once that the theoretical intensity curve for the *e*-chloro *a*-bromo conformation gives the better agreement with the experimental curve. However, this does not eliminate the possibility that both conformations are present together, so a number of composite theoretical intensity curves were also calculated. The values of the dispersion of the standard error between these curves and the experimental intensity curve are given in Table 1. The steady decrease in the standard error as we proceed from 100 % *a*-chloro *e*-bromo to 100 % *e*-

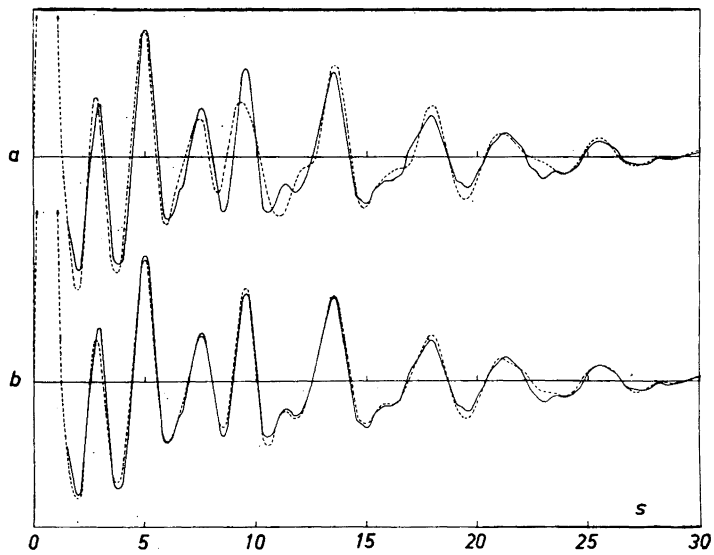

Fig. 2. The experimental intensity curve (full line) compared with the theoretical intensity curves (broken lines) for (a) 1*a*-chloro-4*e*-bromo*cyclo*hexane and (b) 1*e*-chloro-4*a*-bromo*cyclo*hexane. The heavily damped data for $s > 30$ has been omitted so that the figure should still be reasonably distinct after reduction.

chloro *a*-bromo shows that the compound must be all, or nearly all, in the latter conformation.

A final "experimental" radial distribution curve (Fig. 3a) was prepared using the experimental intensity data from $s = 1.5$ to $s = 45.0$, and theoretical intensity data from the *e*-chloro *a*-bromo curve for the experimentally unobtainable inner part from $s = 0$ to $s = 1.5$. It can be seen at once that this final $\sigma(r)/r$ curve agrees well with the theoretical curve for the *e*-chloro *a*-bromo conformation. The dispersion of the standard deviation in that part of the radial distribution curve of relevance for structural assessments ($r > 0.8$ Å) was found to be $\pm$ 8 %.

It is not easy to assess the accuracy of this conformational analysis. While electron diffraction is nowadays very useful in cases where two conformations are present in quantity, it is not very well adapted to the detection of a con-

Table 1. Standard deviation of theoretical intensity curves from the experimental intensity curve, in the range $1.5 < s < 45.0$.

Percentage of *e*-chloro *a*-bromo form in theoretical intensity curve	Percentage dispersion of standard error between theoretical and experimental curves.
0	41.7
25	34.5
50	27.8
70	23.4
90	20.3
95	19.7
100	19.4

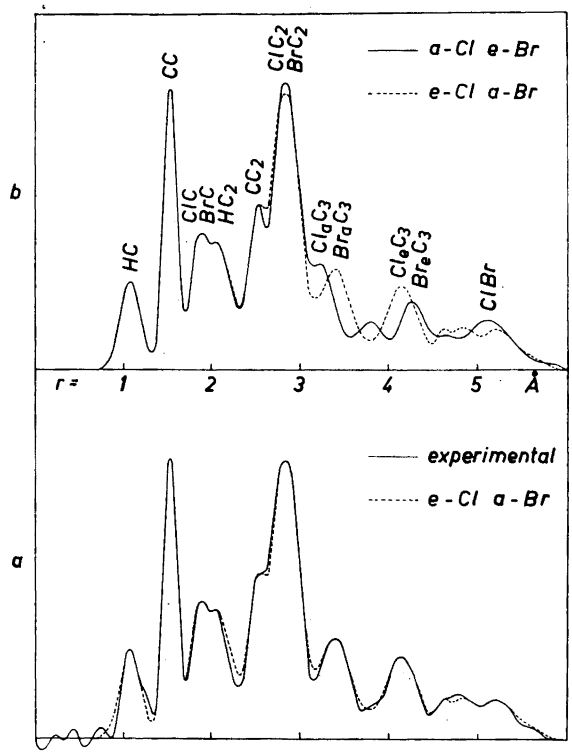

Fig. 3. Theoretical and experimental radial distribution curves for *cis*-1,4-chlorobromo-*cyclo*hexane. The internuclear distances responsible for the principal peaks are indicated.

formation present as a trace. A small quantity of the undetected conformation might easily be masked by the major component. However, we feel safe to conclude from this part of the work, that *at least* 90 % of the substance is in the *e*-chloro *a*-bromo form in the gaseous state. This means that the energy difference between the two conformations must exceed 1.2 kcal/mole.

INFRA-RED SPECTRA

The spectra were recorded on a Perkin-Elmer model 21 spectrometer using a sodium chloride cell which permitted work at high and low temperatures. The vapour pressure of *cis*-1,4-chlorobromo*cyclo*hexane is not high enough to give a satisfactory recording of the spectrum of the gas in a 1 m cell, so only the liquid and solid states could be investigated. No solvents were used. The liquid was pure, and crystallisation of the solid was always confirmed by inspection in polarised light.

Typical spectra of the liquid and solid states are reproduced in Fig. 4. It can be seen that the spectra are practically identical, and contain only such minor variations as might be expected as the effect on the vibrations of the changes of state and temperature. Other spectra, taken of samples with

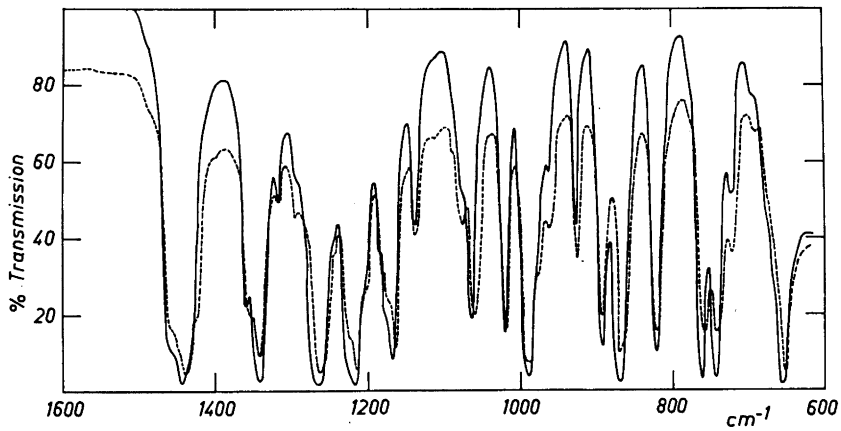

Fig. 4. Infrared spectra of *cis*-1,4-chlorobromo*cyclo*hexane: ———— liquid, at about 30°C; — — — — solid, at about 0°C.

different solidification times and recorded at temperatures down to —170°C, also show little or no variation in the relative intensities and positions of the spectral bands.

The probability of a simultaneous crystallisation of the two conformations, or an unchanging ratio between these conformations under various conditions of temperature and state, must be very low, for this would require not only similar melting points for the two conformations, but also identical lattice packing forces and even identical energy contents for the free molecules.

We therefore conclude that there is only one detectable conformation present in *cis*-1,4-chlorobromo*cyclo*hexane in both the liquid and solid states. This view is supported by our spectral assignments in the carbon-halogen stretching region.

In this region there are strong bands at 743 and 654 cm^{-1}, a weak band at 722 cm^{-1} and an inflection at about 690 cm^{-1}.

Previous work with monohalogeno-*cyclo*hexanes [10], *trans*-1,2-dihalogeno-*cyclo*hexanes [11], *cis*-1,4-dihalogeno-*cyclo*hexanes and the mono-conformational [12] crystals of *trans*-1,4-dihalogeno*cyclo*hexanes, has shown that the different carbon-halogen stretching vibrations are represented by bands which are always found within a few cm^{-1} of the following average frequencies:

C—Cl_e	740 cm^{-1}
C—Cl_a	685 cm^{-1}
C—Br_e	685 cm^{-1}
C—Br_a	655 cm^{-1}

The main bands of the *cis*-1,4-chlorobromo*cyclo*hexane in this region must therefor be assigned to the C—Cl_e and C—Br_a stretching vibrations, and it must be concluded that the compound exists mainly in the *e*-chloro *a*-bromo conformation in the solid and liquid states.

The inflection at 690 cm^{-1} could be assigned to the C—Cl_a and/or C—Br_e vibrations. However, it persists unchanged under all recording conditions,

and must therefore be regarded as doubtful evidence of a possible conformational equilibrium. Even if this inflection is taken as evidence of the existence of an *a*-chloro *e*-bromo form, it could hardly represent more than about 2 % of an equilibrium mixture. This would put the energy difference between the two forms up to at least 2.3 kcal/mole.

DISCUSSION

Only the *e*-chloro *a*-bromo conformation of *cis*-1,4-chlorobromo-*cyclo*hexane has been detected in the gas, liquid and solid states. The infra-red part of this investigation, which is better suited to the detection of traces of the other possible conformation, shows that if this form is present it must be less than 2 % of the whole.

The conclusion must therefore be either (a) there is a conformational equilibrium, but the *e*-chloro *a*-bromo form predominates overwhelmingly and the energy difference between the two forms exceeds 2.3 kcal/mole, or (b) there is no conformational equilibrium, no ring inversion, and the only form produced by our preparative route is the *e*-chloro *a*-bromo conformation. If the latter case is true, it may be that of the disubstituted *cyclo*hexanes only the *ee* forms can invert their rings. In this connection it is interesting to note that a systematic difference has recently been discovered between the proton magnetic resonance spectra of *ee* and *ea* disubstituted *cyclo*hexanes [13].

The preference for the *e*-chloro *a*-bromo conformation, rather than the other possibility, can not be explained on steric grounds. If steric forces were the only ones concerned, we would expect the bulkier bromine atom to prefer the more open equatorial position, as it seems to do in 1,2-dichloro-4,5 dibromo-*cyclo*hexane [2-4]. However, *cis*-1,4-bromomethyl*cyclo*hexane [14] provides another case where bromine is reported to be mainly in the sterically less-favoured axial position.

The authors are grateful to A. Almenningen who kindly made the electron diffraction plates, and to *Norges Teknisk-Naturvitenskapelige Forskningsråd* for a post-doctorate fellowship (to V.A.A.).

REFERENCES

1. Hassel, O., Wang Lund, E. and Lunde, K. *Acta Chem. Scand.* **6** (1952) 426.
2. Lunde, K. *Acta Chem. Scand.* **10** (1956) 690.
3. Bastiansen, O. and Hassel, O. *Acta Chem. Scand.* **5** (1951) 1404.
4. Hassel, O. and Wang Lund, E. *Acta Chem. Scand.* **6** (1952) 238.
5. Kozima, K. and Sakashita, K. *J. Chem. Phys.* **25** (1956) 177.
6. Hassel, O. and Lunde, K. *Acta Chem. Scand.* **6** (1952) 1126.
7. Bastiansen, O., Hassel, O. and Risberg, E. *Acta Chem. Scand.* **9** (1955) 232.
8. Davis, M. *To be published.*
9. Atkinson, V. A. and Hassel, O. *Acta Chem. Scand.* **13** (1959) 1737.
10. Klæboe, P., Lothe, J. L. and Lunde, K. *Acta Chem. Scand.* **10** (1956) 1465.
11. Klæboe, P., Lothe, J. L. and Lunde, K. *Acta Chem. Scand.* **11** (1957) 1677.
12. Kozima, K. and Yoshino, T. *J. Am. Chem. Soc.* **75** (1953) 166.
13. Brownstein, S. and Miller, R. *J. Org. Chem.* **24** (1959) 1886.
14. Eliel, E. L. and Haber, R. G. *J. Am. Chem. Soc.* **81** (1959) 1248; Eliel, E. L. *Chem. & Ind. London* **1959** 568.

Received August 25, 1960.

ACTA CHEMICA SCANDINAVICA 14 (1960) 2145–2151

The Crystal Structure of the 1:1 Addition Compound Formed by Benzyl Sulphide and Iodine

CHR. RØMMING

Universitetets Kjemiske Institutt, Blindern-Oslo, Norway

The crystal structure of a compound containing 1 molecule of benzyl sulphide and 1 molecule of iodine has been determined. The space group is *Pnma* with four molecules of $(C_6H_5CH_2)_2S \cdot I_2$ in the unit cell, the dimensions of which are: a = 9.86 Å; b = 16.86 Å; c = 9.36 Å. The investigation reveals a linear sulphur-iodine-iodine arrangement with the observed bond distances 2.78 Å for S-I and 2.82 Å for I-I.

In the course of an investigation of charge transfer complexes in the crystalline state, mainly between halogen molecules and organic electron donor molecules as ethers and amines carried out by Hassel and coworkers, it was found to be of interest to determine whether thioethers form similar compounds with halogen. The 1 : 1 compound benzyl sulphide-iodine was chosen as an object for this investigation. This compound was first prepared by Fromm[1], by whom it was regarded as a compound of quadrivalent sulphur with each of the halogen atoms linked to the sulphur atom. Feigl and Bondi[2], however, investigated further the chemical behaviour of the compound and concluded that it is to be regarded as a polyiodide.

Preliminary results of the present investigation have been reported in a survey article by Hassel[3].

EXPERIMENTAL

The crystals were prepared according to Feigl and Bondi [2] by mixing hot solutions of benzyl sulphide and iodine in glacial acetic acid and heating the mixture for a quarter of an hour at 120°C. By cooling, small dark red crystals of the addition compound (m.p. 63°C) separated. The crystals were approximately octahedral with the orthorhombic axes along the space diagonals. The dimensions were about 0.15 mm along the axes; the crystals were used without further preparations in the X-ray work.

Integrated Weissenberg photographs were taken with rotation about the three orthorhombic axes. The more intense reflections were measured photometrically; the others were estimated visually by comparison with a standard scale. Cu$K\alpha$-radiation was employed, and of the 114 $h0l$, 91 $0kl$ and 104 $hk0$ reflections attainable, 82, 78, and 51 were actually observed, respectively. The intensities were corrected for Lorentz- and polarisation effects, but no corrections for absorption were applied.

The atomic scattering factor used in the last stages of the calculations are given by the analytical approximation $f = A\exp(-ax^2) + B\exp(-bx^2) + C$ with the constants given by Forsyth and Wells[4].

CRYSTAL DATA

The crystals were found to be orthorhombic with the unit cell dimensions: $a = 9.86$ Å ; $b = 16.86$ Å ; $c = 9.36$ Å
The figures given are believed to be accurate to within 0.5 %. By flotation the density was found to be 1.95 g/cm^3, while the calculated value with four molecules per unit cell is 2.00 g/cm^3.

According to the systematically absent reflections the space group might be either *Pnma* or $Pn2_1a$. The former was assumed to be the correct one, and the structure analysis subsequently confirmed this. Since the number of equivalent positions is eight in the space group *Pnma*, the molecules must posess a center of symmetry or a mirror plane. Only the latter is possible in the present compound.

STRUCTURE DETERMINATION

The structure analysis was started with projection along the *b*-axis. This is the longest of the axes, but since the mirror planes of the space group are perpendicular to this axis a well resolved Fourier projection could be expected with ideal overlapping of some of the atoms. A Patterson synthesis showed clearly that the iodine atoms lie in a mirror plane. It indicated also strongly that the sulphur atom is lying in the mirror plane with one benzyl group on each side. The parameters of the iodine atoms were determined from the Patterson synthesis and a set of structure factors was calculated. On the basis of signs from these calculations and the observed data a Fourier synthesis (plane group *pgg*) was computed. The Fourier map not only showed the iodine atoms but also indicated the position of the benzyl sulphide molecule. It became quite clear that the S-I-I arrangement is nearly linear, and tentative parameters for the atoms in the benzyl sulphide group could be found. These were now included in the calculations, and a series of Fourier refinements were carried out. At the stage where no more signs shifted the reliability factor *R* had decreased to 20 %. It became obvious from the corresponding Fourier map, however, that the thermal vibrations of the »outer» iodine atom is anisotropic, the peak being elongated in a direction about normal to the I-I bond.

Now a least squares refinement was carried out, using a Ferranti Mercury computer[5]. Two cycles were computed with variation of the parameters with isotropic temperature functions, then a few cycles with an anisotropic temperature function for the »outer» iodine atom. During the first step the reliability factor decreased from 20 % to 15 %, after the anisotropic temperature function was introduced it dropped to 10.5 %. The positional parameters changed very little during the last cycles, however. The direction of the maximum vibration amplitude of the iodine atom in question as calculated from the constants in the expression for the temperature factor $\exp(-uh^2-vhk-wk^2)$ was found to be within 2° perpendicular to the direction of the I—I bond.

Table 1. Observed and calculated structure factors.

h k l	F_o	F_c	*h k l*	F_o	F_c	*h k l*	F_o	F_c
0 0 2	81	73	5 0 7	<30	− 11	12 0 2	19	24
0 0 4	<18	− 9	5 0 8	<28	− 18	0 2 0	211	277
0 0 6	112	114	5 0 9	<26	− 11	0 4 0	470	482
0 0 8	80	81	5 0 10	35	− 32	0 6 0	346	348
0 0 10	<26	10	6 0 0	34	24	0 8 0	266	252
1 0 1	92	117	6 0 1	35	− 31	0 10 0	320	277
1 0 2	171	221	6 0 2	137	128	0 12 0	240	209
1 0 3	<18	8	6 0 3	47	− 44	0 14 0	212	201
1 0 4	41	37	6 0 4	166	174	0 16 0	152	136
1 0 5	62	65	6 0 5	<27	− 11	0 18 0	122	120
1 0 6	21	10	6 0 6	<28	− 11	0 20 0	112	96
1 0 7	70	76	6 0 7	39	23	0 1 1	104	− 54
1 0 8	60	59	6 0 8	<27	18	0 3 1	87	− 83
1 0 9	44	41	6 0 9	<27	− 20	0 5 1	86	− 84
1 0 10	31	40	6 0 10	28	35	0 7 1	45	− 39
1 0 11	<20	− 6	7 0 1	50	39	0 9 1	92	− 63
2 0 0	114	90	7 0 2	56	− 52	0 11 1	<33	− 11
2 0 1	30	− 9	7 0 3	109	105	0 13 1	<40	− 14
2 0 2	140	−137	7 0 4	56	48	0 15 1	<40	3
2 0 3	103	103	7 0 5	51	54	0 17 1	<39	− 14
2 0 4	104	− 97	7 0 6	66	53	0 19 1	<30	12
2 0 5	21	− 16	7 0 7	33	27	0 2 2	190	−185
2 0 6	<23	− 8	7 0 8	<24	10	0 4 2	126	−116
2 0 7	<27	16	7 0 9	27	36	0 6 2	85	− 95
2 0 8	<28	− 11	7 0 10	11	11	0 8 2	95	−112
2 0 9	58	73	8 0 0	<27	− 16	0 10 2	101	− 93
2 0 10	<26	− 23	8 0 1	46	− 39	0 12 2	102	− 93
2 0 11	34	46	8 0 2	<28	8	0 14 2	105	− 97
3 0 1	154	−156	8 0 3	<28	− 11	0 16 2	78	− 63
3 0 2	178	179	8 0 4	<28	8	0 18 2	81	− 70
3 0 3	143	−152	8 0 5	29	43	0 20 2	49	− 50
3 0 4	51	− 45	8 0 6	30	− 32	0 1 3	<20	− 5
3 0 5	58	− 53	8 0 7	48	53	0 3 3	64	53
3 0 6	76	− 60	8 0 8	<21	1	0 5 3	61	41
3 0 7	100	− 84	9 0 1	52	− 51	0 7 3	33	21
3 0 8	54	56	9 0 2	54	− 49	0 9 3	41	42
3 0 9	53	− 53	9 0 3	53	− 45	0 11 3	<36	− 14
3 0 10	<24	11	9 0 4	38	41	0 13 3	<39	− 5
3 0 11	18	− 26	9 0 5	66	− 68	0 15 3	<40	1
4 0 0	204	−189	9 0 6	38	42	0 17 3	<37	− 13
4 0 1	46	47	9 0 7	22	− 27	0 19 3	<30	16
4 0 2	92	− 87	10 0 0	<25	− 7	0 2 4	39	− 34
4 0 3	38	28	10 0 1	31	− 26	0 4 4	31	34
4 0 4	<22	− 13	10 0 2	54	− 58	0 6 4	<30	10
4 0 5	72	− 61	10 0 3	<24	− 9	0 8 4	<34	0
4 0 6	97	− 93	10 0 4	80	− 78	0 10 4	59	60
4 0 7	53	− 50	10 0 5	<23	14	0 12 4	<39	5
4 0 8	49	− 41	10 0 6	31	− 30	0 14 4	40	39
4 0 9	32	− 11	10 0 7	21	− 15	0 16 4	57	50
4 0 10	<23	− 7	11 0 1	<23	9	0 18 4	32	27
5 0 1	70	− 63	11 0 2	<23	− 7	0 1 5	118	142
5 0 2	<21	10	11 0 3	19	− 26	0 3 5	111	134
5 0 3	82	75	11 0 4	10	− 10	0 5 5	115	110
5 0 4	61	− 59	11 0 5	<18	− 18	0 7 5	84	75
5 0 5	84	85	12 0 0	59	67	0 9 5	93	95
5 0 6	95	− 83	12 0 1	<18	− 2	0 11 5	93	79

h k l	F_o	F_c	h k l	F_o	F_c	h k l	F_o	F_c
0 13 5	61	57	0 10 8	57	77	4 13 0	144	−130
0 15 5	72	70	0 12 8	52	64	4 14 0	114	106
0 17 5	37	31	0 14 8	43	50	4 15 0	118	100
0 2 6	164	−171	0 1 9	56	35	4 16 0	112	− 98
0 4 6	139	−150	0 3 9	<39	14	4 17 0	96	− 90
0 6 6	137	−151	0 5 9	59	58	4 18 0	70	80
0 8 6	134	−150	0 7 9	37	27	4 19 0	70	72
0 10 6	86	−109	0 9 9	41	47	4 20 0	56	− 66
0 12 6	81	−106	2 1 0	92	− 60	8 1 0	194	182
0 14 6	85	− 82	2 3 0	62	40	8 3 0	204	−190
0 16 6	80	− 82	2 5 0	30	− 28	8 5 0	190	168
0 18 6	68	− 73	2 7 0	58	56	8 7 0	184	−174
0 1 7	94	−110	4 1 0	238	−266	8 9 0	150	140
0 3 7	101	−114	4 2 0	200	228	8 11 0	138	−134
0 5 7	93	−105	4 3 0	194	214	8 13 0	112	108
0 7 7	79	− 87	4 4 0	222	−220	8 15 0	110	− 98
0 9 7	88	− 96	4 5 0	228	−218	12 1 0	70	− 60
0 11 7	60	− 82	4 6 0	230	220	12 2 0	82	− 68
0 13 7	59	− 64	4 7 0	218	212	12 3 0	72	60
0 15 7	57	− 71	4 8 0	200	−176	12 4 0	70	70
0 2 8	89	95	4 9 0	182	−148	12 5 0	52	− 56
0 4 8	73	87	4 10 0	174	148	12 6 0	58	− 60
0 6 8	102	122	4 11 0	182	160			
0 8 8	64	78	4 12 0	138	−118			

A Fourier map of the projection along the *b*-axis based on the signs arrived at with the final set of parameters is reproduced in Fig. 1. Observed and calculated structure factors are listed in Table 1.

From a model of the benzyl sulphide molecule the *y*-coordinates could be estimated, the sulphur and iodine atoms lying in mirror planes.

A set of structure factors was then calculated for the 0*kl*-zone and the corresponding Fourier synthesis was worked out. The plane group of this projection is *cmm*, the origin being in (1/4, 1/4) relative to the origin of the original unit cell. The iodine peaks were found at the expected positions in the mirror plane at $y = 0$, and the benzyl sulphide molecule showed up clearly in the map. Some atoms from different molecules overlapped, however. After a few Fourier refinements the parameters of this projection were subjected to at least squares refinement. The »outer» iodine atom was not corrected for anisotropic thermal vibrations in this projection, this not being possible for an atom in a mirror plane with the present computer program. The discrepancies of the common parameters of the heavy atoms found in the (010)- and (100)-projections were 0.0005 for I_1, 0.0019 for I_2, and 0.004 for S. The final *R*-factor for the (100)-projection was 13.8 %; the corresponding Fourier map is shown in Fig. 2 and the observed and calculated structure factors (origin in (1/4, 1/4) of the cell given in *International Tables*) are listed in Table 1.

In the *hk*0-zone very few reflections other than the ones with $h = 4n$ were observed. The reason for this is of course the rather special positions of the iodine atoms in this projection, the projection having a pseudo translation 1/4 along the *a*-axis. One iodine atom overlaps with the sulphur atom in this projection, consequently rather few informations is to be had from these

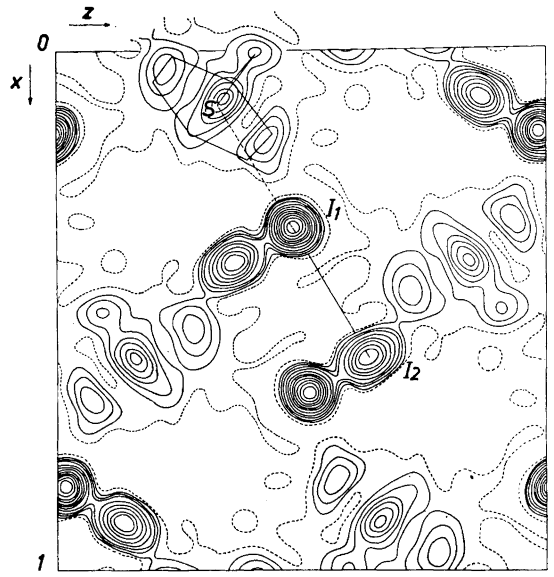

Fig. 1. Electron density projection along the *b*-axis. Contour intervals of 5 e.Å^{-2} up to 20 e.Å^{-2} and of 10 e.Å^{-2} from 30 to 100 e.Å^{-2}.

data. Only the *x*-parameter of the iodine atom nearest the sulphur atom was determined from this projection and it showed good agreement with the one found in the projection along *b*. The final *R*-factor for the *hk*0-zone was 10.4 %. The observed and the corresponding calculated structure factors are listed in Table 1.

DISCUSSION OF THE STRUCTURE

Benzyl sulphide-iodine crystallizes with a nearly linear S-I-I arrangement with a mirror plane through the sulphur and iodine atoms and between the benzyl groups. Figs. 1 and 2 show the electron density projections along the *b* and *a* axes, respectively. For the final parameters listed in Table 2, values from the projections along *b* were used for the sulphur and iodine atoms, whereas a mean value from all projections were used for the lighter atoms.

The distance between the iodine atoms in the iodine molecule is found to be 2.819 Å and between the sulphur atom and the nearest iodine atom 2.78 Å. The standard deviations[6] for these distances are 0.009 Å and 0.02 Å, respectively. The sulphur and iodine atoms are within the accuracy of the investigation lying on a straight line, the S-I-I angle being found equal to 179°.

The sulphur-methylene carbon distance was found to be 1.82 Å, in good agreement with the normal single bond value[7]. The distances between carbon atoms in the benzene ring are of course not well determined in a structure with heavy atoms like the present one, the mean value was found to be 1.38 Å for the nearest C-C distance with deviations of up to 0.1 Å. There is an angle

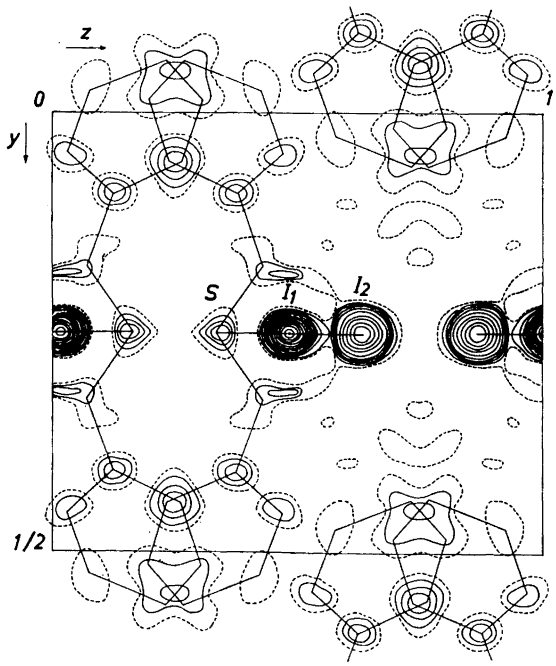

Fig. 2. Electron density projection along the *a*-axis. Contour intervals as in Fig. 1.

of 93° between the two sulphur-methylene carbon directions; the angle between the sulphur-iodine and the sulphur-methylene carbon directions is found to be 100°.

The nearest iodine-iodine approach between the molecules was 4.33 Å, corresponding closely to the van der Waals' distance given by Pauling [7]. The fact that the direction of maximum vibration of the »outer» iodine atom as observed in the projection along the *b*-axis is normal not only to the intramolecular I-I bond but also to the loose intermolecular I-I interaction in the mirror plane suggests that the anisotropy has some structural significance.

Table 2. Atomic coordinates as fractions of the cell edges.

Atom	*x*	*y*	*z*
I_1	0.3428	0.2500	0.4849
I_2	0.5893	0.2500	0.6374
S	0.1025	0.2500	0.3298
C_{methyl}	0.009	0.328	0.422
C_1	0.062	0.426	0.369
C_2	0.002	0.459	0.237
C_3	0.074	0.524	0.196
C_4	0.164	0.554	0.270
C_5	0.223	0.526	0.409
C_6	0.151	0.458	0.454

The investigation shows that organic sulphur compounds may act as electron donors to form molecular addition compounds in the same way as amines. The lengthening of the I-I bond (0.17 Å relative to the sum of the normal covalent radii [7]) is the same as found where an amine act as the electron donor [8]. It agrees also fairly well with the value given by McCullough *et al.* in the compound dithiane · $2I_2$. The lengthening of the S-I bond relative to the covalent bond distance is consistent with the corresponding values in compounds between amines and halogen, it is in very good agreement with the value given by McCullough.

This investigation has been sponsored by the *United States Air Force Development Command* under contract AF 61 (052)—71.

REFERENCES

1. Fromm, E. *Ann.* **396** (1913) 92.
2. Feigl, F. and Bondi, A. *Monatsh.* **53—54** (1929) 543.
3. Hassel, O. *Proc. Chem. Soc.* **1957** 250.
4. Forsyth, J. B. and Wells, M. *Acta Cryst.* **12** (1959) 412.
5. Curtis, A. R. *A.E.R.E. Mercury Autocode Program No. 29.*
6. Cruickshank, D. W. J. *Acta Cryst.* **2** (1949) 65.
7. Pauling, L. *The Nature of the Chemical Bond,* Cornell University Press, New York 1948.
8. Strømme, K. O. *Acta Chem. Scand.* **13** (1959) 268.
9. McCullough, J. D., Chao, G. Y. and Succaro, D. E. *Acta Cryst.* **12** (1959) 815.

Received July 6, 1960.

ACTA CHEMICA SCANDINAVICA 14 (1960) 2152–2160

Studies on the Chemistry of Lichens

III *. Long-Chain Tetrahydroxy Fatty Acids from Some Norwegian Lichens

YNGVE JOHANNES SOLBERG

Research Chemical Laboratory, Agricultural College of Norway, Vollebekk, Norway

Norwegian lichen species have been studied with regard to content of higher tetrahydroxy fatty acids. The lichens are found on the bark of trees, on rocks, and on the ground. The hydroxy acids isolated are of the same type as those previously recorded in *Haematomma ventosum*. Infra-red spectra of the acids in solid state have been obtained in the region from 4 000 to 700 cm^{-1} and confirm the similarity.

Semi-solid and solid fatty acids were obtained by reduction with hydrogen iodide and zinc. Paper chromatographic analysis of the products obtained by periodic acid oxidation of ventosic acid from *Haematomma ventosum* showed the presence of tetrahydroxy *heneicosanoic* acid ($C_{21}H_{42}O_6$) and tetrahydroxy *docosanoic* acid ($C_{22}H_{44}O_6$) in the lichen.

Work on *Parmelia centrifuga*, has pointed out the possibility of the presence of tetrahydroxy *tricosanoic* acid ($C_{23}H_{46}O_6$) in the lichen.

Systematic investigations of Norwegian lichen species were made during the period 1955 to 1959. The presence of higher tetrahydroxy fatty acids in some lichens was of special interest. In 1957 ventosic acid was obtained from *Haematomma ventosum* and reported [1] as a tetrahydroxy *docosanoic* acid with the composition $C_{22}H_{44}O_6$. Later uniform substances have been isolated from the lichen species *Parmelia centrifuga, Parmelia encausta, Parmelia furfuraceae, Parmelia physodes, Cetraria nivalis, Cetraria delisei, Cladonia alpestris, Alectoria ochroleuca*, and *Siphula ceratites*.

The plant material was collected in different parts of the country and before the extraction, the material was dried and ground into coarse powder. The extraction process was carried out first with ether for about 24 h, and subsequently with acetone for 48 h in a Soxhlet extractor designed to take 400—500 g of the material. As a rule the main portion of the acids were separated already

* Part II: *Acta Chem. Scand.* **11** (1957) 1477.

under the acetone extraction and could therefore easily be isolated in a pure condition.

After the solvents had been removed from these extracts, the highly coloured solids were examined separately in the usual manner [2,3]. Analytical data will be given only for those compounds for which values have not been reported in the literature. From *Parmelia centrifuga* a relatively larger portion of sugar alcohol and from *Siphula ceratites* a new lichen substance with the probable formula $C_{19}H_{21}O_6$ have been isolated. The investigations are being continued and complete data will be given in a forthcoming paper.

The hydroxy fatty acids which have been isolated so far, at once distinguished themselves by an especially low solubility in the common organic solvents. The acids are less soluble in alcohols, more soluble in warm dioxane, pyridine and glacial acetic acid. Glacial acetic acid has in all cases proved to be the most suitable recrystallization solvent, from which an easily filterable product has been obtained.

The hydroxy fatty acids are colourless, amorphous substances with melting points in the region 180—193° (*cf.* Table 1). Occasionally two different melting points for the same hydroxy acid have been observed. This is probably due to the presence of *cistrans* isomerism, and is otherwise known from tetrahydroxy stearic acid.

The lichen species *Haematomma ventosum* and *Parmelia centrifuga* are distinguished by a particularly high amount of these acids, a fact which gave rise to a further investigation. In both cases the hydroxy acids were reduced to the corresponding fatty acids. However, these seemed not to be identical, but differed with regard to solubility, melting points and by paper chromatographic analysis (Tables 2 and 3).

In *Parmelia physodes* hydroxy fatty acids have been established by means of solubility, X-ray, and infra-red spectra. However, the sample was contaminated with a tenacious impurity which rendered purification extremely difficult and wasteful. The yield of the crude product was too low and further analysis was not possible.

RESULTS AND DISCUSSION

In Table 1 a series of experimental results of the isolated hydroxy fatty acids, or acid-mixtures, from nine different lichen species are listed. The average composition is: C 66.33 %; H 11.05 %.

It is interesting to compare these results with those reported by Zellner [4,5], who isolated the lichen substances *Hypogymnole* I and II from *Parmelia physodes*.

Compound	M.p.	Found by Zellner	
Hypogymnole I	190°	C 64.39 %	H 11.12 %
Hypogymnole II	218°	C 63.64 %	H 11.16 %

Table 1. Analysis of the isolated tetrahydroxy fatty acids.

Lichen species	Yield of purified hydroxy acid, %	Melting point	Analysis, values obtained % C	% H	Characteristic strong peaks in the X-Ray diffraction pattern (Å)			
Haematomma ventosum	0.5	184°	65.29	10.88	32.5	—	4.55	4.05
Parmelia centrifuga	0.5	191°	64.77–64.37	10.84–10.68	31.6	20.5	4.54	4.04
Parmelia furfuraceae	0.2	191–193°	65.68–66.45	10.82–10.92	33.0	22.1	4.56	4.05
Parmelia encausta	—	180°	65.58	11.00	—	22.1	4.57	4.06
Cetraria nivalis	0.2	181°	66.16–66.78	11.02–11.02	—	—	—	—
Cetraria delisei	0.03	184–186°	66.98	11.23	—	—	—	—
Cladonia alpestris	0.2	191°	66.31–67.64	11.18–11.32	32.4	21.5	4.54	4.05
Siphula ceratites	0.1	182°	68.39	11.61	—	23.6	4.51	4.04
Alectoria ochroleuca	0.05	179°	67.06	11.21	33.2	23.2	4.54	4.04

In the present work the attempts made to resolve the acid-mixture from *Parmelia physodes* failed. Zellner indicated that these two compounds might be *higher aliphatic alcohols*. Today it is fairly obvious that Zellner's *Hypogymnoles* are identical with the isolated hydroxy fatty acids.

The X-ray diffraction patterns show two characteristic peaks at 4.54 and 4.05 Å. With the normal fatty acids the two corresponding peaks are found at 4.1 and 3.7 Å. The technique for the X-ray analysis has already been described in Part II of this series, and two diffraction patterns have been recorded in the same paper.

The infra-red absorption spectra of the hydroxy acids in Fig. 1 show a surprisingly close similarity. Bayzer [6] reported broad absorption bands at 3 200—3 300 cm^{-1} for C_{18}-hydroxy acids due to the valence bands of the OH-groups. The hydroxy acids in Fig. 1 show a broad unresolved OH-band around 3 270 cm^{-1}. Further, it is worth noting that this band shows a constant intensity, compared with the well known asymmetric carbon-hydrogen stretching band around 2 900 cm^{-1}. According to Bayzer, all isolated hydroxy acids should contain four OH-groups in the molecule. In all of the IR analyses carried out, the ratio of hydroxy acid to KBr has been nearly constant, 1.5 mg/200 mg. *Previously ventosic acid from Haematomma ventosum has been shown to contain four OH-groups.*

Susi [7] pointed out that the constant position of the 3 270 cm^{-1} band would be expected to depend on a similar position of the hydroxyl groups in the molecule. The associated carboxyl group exhibits a weak band at 2 700 cm^{-1}. The carboxyl band appears to be constant at 1 700 cm^{-1}.

The infra-red spectra are nearly identical above 1 500 cm^{-1}. Curiously enough only a few, effaced bands are found in the region 1 180—1 350 cm^{-1} compared with the spectra of sativic acid (No. 8, Fig. 1).

The bands at 1 465 cm^{-1} and at 715 cm^{-1} in the spectra are attributed to bending and rocking methylene vibrations [8,9].

Spectra of mono-, di-, tetra- and hexahydroxy stearic acid are reported by Bayzer. These spectra show a close similarity to those obtained in the present paper.

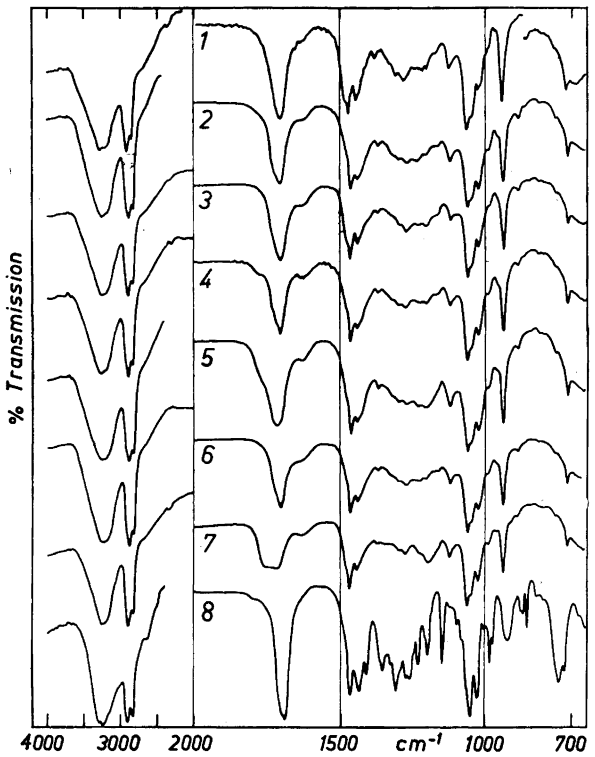

Figs. 1—8. Infrared spectra of tetrahydroxy acids from *Haematomma ventosum*(1), *Alectoria ochroleuca*(2), *Parmelia centrifuga*(3), *Cladonia alpestris*(4), *Cetraria nivalis*(5) *Cetraria delisei*(6), *Parmelia furfuraceae*(7) and *Sativic* acid(8). All substances are pressed in KBr-disks.

Several paper-chromatographic analyses of the hydroxy fatty acids have been tried without success.

Reduction to fatty acids. Upon treatment of ventosic acid from *Haematomma ventosum* and the hydroxy acid component from *Parmelia centrifuga* with hydrogen iodide and zinc, as described in the earlier publication, the com-

Table 2. Fatty acids obtained by the reduction of the hydroxy acids isolated from *Haematomma ventosum* (H.v.) and *Parmelia centrifuga* (P.c.).

Fatty acid and the related methyl ester	Melting point	Found by analysis C	H	CH_3O	Calculated C	H	CH_3O
Docosanoic acid (H.v.)	74—75°	77.54	12.82		77.55	13.02	
» » methyl ester	52—53°	78.10	13.01	9.89	77.90	13.08	8.75
Tricosanoic acid (P. c.)	69—70°	77.92	13.03		77.90	13.08	
» » methyl ester	53.5°	78.06	13.09	7.97	78.19	13.12	8.42

Table 3. Ascending paper chromatography of the fatty acids obtained by the reduction of hydroxy fatty acids from *Haematomma ventosum* (H.v.) and *Parmelia centrifuga* (P.c.). 50 μg of the fatty acid was chromatographed. The paper was impregnated with A) *n*-undecan (0.23), B) liquid paraffin (0.18), and C) liquid paraffin (0.16). Paper S & S 2043 b. Temperature 47°, 4 h.

Fatty acids	A	B	C
Autentic n-*docosanoic* acid	—	0.35	—
Docosanoic acid (H.v.)	0.18	0.35	0.45
Tricosanoic acid (P.c.)	0.13	0.27	0.35

pounds are converted into *n*-fatty acids. The fatty acids were white, crystalline substances and the elementary results are given in Table 2.

Paper chromatography of the fatty acids. During the period 1954 to 1958, Kaufman and Wagner [10–12] described some paper chromatographic methods for higher *n*-fatty acids. These methods have been useful in the present chromatographic investigations. The results, which are given in Table 3, confirm the fact that *n*-docosanoic acid (C_{22}) is the main component of the reduction products from ventosic acid. The reduction product from *Parmelia centrifuga* is the higher homologous tricosanoic acid (C_{23}). These observations are in agreement with the elementary analysis (Table 2).

Infra-red analysis of the fatty acids. The infra-red absorption spectra of the fatty acids are shown in Fig. 2. Examination of the spectra of the free acids by the potassium bromide disk technique has definite advantages, and the spectra recorded in this paper show distinctly that by the classical reduction of the hydroxy fatty acids with hydrogen iodide and zinc, long-chain normal fatty acids have been obtained.

The IR-spectra of long chain fatty acids as a class have certain characteristic features which have been discussed by other authors [9,13–16].

The carbonyl stretching band of the carboxyl acid group appeared at very nearly the same wave number, 1 700 cm^{-1}. The two strong bands at 2 900 and 2 830 cm^{-1} are attributable to the asymmetrical and symmetrical methylene stretching and vibrations, respectively.

Strong complex absorption occurs between 880 and 930 cm^{-1}. The bands at 1 460—1 470 cm^{-1} and at 720 cm^{-1} in the spectra of the fatty acids are attributed to bending and rocking methylene vibrations, respectively. The splitting of the 720 cm^{-1} rocking band into two components, in the solid phase spectra, is in accordance with the observations of Stein and Sutherland [17] for *n*-paraffins below the transition point. Some or all of the absorption bands occurring between 1 460 and 1 400 cm^{-1} can probably be attributed also to methylene bending vibrations.

Of particular interest for the study of the spectra is the absence of progression of bands between 1 180—1 350 cm^{-1} spaced at approximately equal intervals of 15—20 cm^{-1}, (compare with spectra of pure *n*-docosanoic acid in the same figure). The progression bands are almost certainly associated with

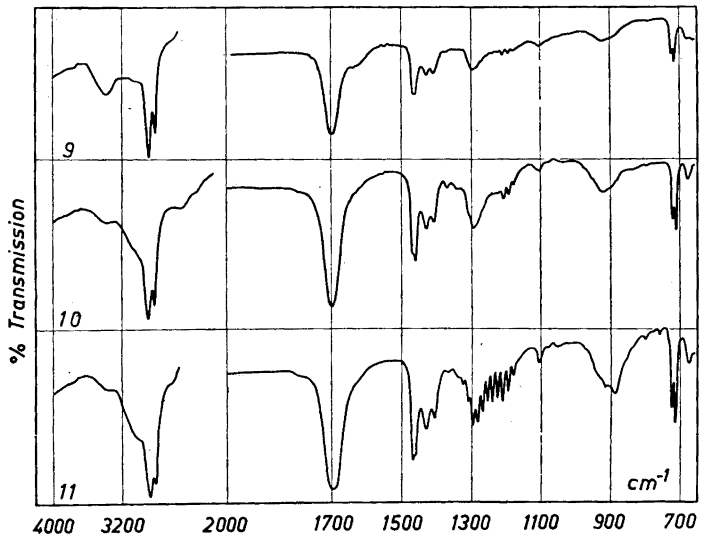

Figs. 9—11. Infrared spectra of *docosanoic* acid and reduced hydroxy acids from *Haematomma ventosum* and *Parmelia centrifuga*. All substances are pressed in KBr-disks.

methylene wagging and/or twisting vibrations. The introduction of substituents along the molecule-chain alters the appearance of these bands. If the degree of substitution is excessive, the characteristic appearance of the progression is lost. In this work, branched acids have not been established. Infrared spectra of monocarboxylic acids are fairly insensitive in relation to homologous. Therefore, the lack of bands in the region 1 180—1 350 cm^{-1} can scarcely be due to the presence of fatty acid mixtures.

Oxidation of ventosic acid from Haematomma ventosum. A sufficient amount of ventosic acid was available from *Haematomma ventosum* and enabling an

Table 4. R_x values of the 2,4-dinitrophenylhydrazones obtained with the aldehydes from the oxidation of the hydroxy compounds with HIO_4. Paper: S & S 2043b, impregnated with 2-phenoxyethanol. Solvent *n*-heptan and water.

2,4-Dinitrophenylhydrazone of	R_x		
Autentic *n*-decanal			1.00
n-Nonal from 9,10-dihydroxystearic acid		0.89	
n-Hexanal from 9,10,12,13-tetrahydroxy stearic acid	0.58		
Azelaic half-aldehyde ($OHC \cdot (CH_2)_7 \cdot COOH$) from 9,10-dihydroxy stearic acid	0.18		
Azelaic half-aldehyde from 9,10,12,13-tetrahydroxy stearic acid	0.19		
Oxidation products from ventosic acid (*Haematomma ventosum*)	0.17	0.86	1.02

examination of the products obtained by oxidation with HIO_4. In this way the position of the four OH-groups in the molecule were determined.

A sulphuric acid solution of KIO_4 was added to a suspension of ventosic acid in 96 % ethanol. Within a short time and by continuous shaking an almost clear solution with a characteristic smell of higher aldehydes was obtained. After concentration, the aqueous solution was steam distilled and the volatile aldehyde compounds converted into 2,4-dinitrophenylhydrazones. The main amount of the distillate proved to be *n*-decanal. However, small amounts of hydrazones were obtained by careful examination of the filtrate. By chromatographic analysis of the last fraction mentioned, the presence of *n*-nonal and azelaic-half-aldehyde was demonstrated.

For comparison by the chromatographic analysis, di- and tetrahydroxy stearic acid also were oxidized in the same manner, and the following substances were obtained:

Compound	Oxidation products
9,10-dihydroxy stearic acid	*n*-nonal azelaic half-aldehyde
9,10,12,13-tetrahydroxy-stearic acid	*n*-hexanal azelaic half-aldehyde

Chiefly the method of King [18] was used in the oxidation with HIO_4. The hydrazones were separated on paper S & S 2043b, impregnated with 2-phenoxyethanol, (Lynn [19]). The results are summarized in Table 4.

Polymerization products constituted the main part of the non-volatile matter produced under the steam distillation. They were not further examined.

All things considered the facts given in Tables 3 and 4 lend support to the conclusion that a mixture of 9,10,12,13-tetrahydroxy docosanoic acid ($C_{22}H_{44}O_6$) and 9,10,12,13-tetrahydroxy heneicosanoic acid ($C_{21}H_{42}O_6$) must be present in the lichen. By the reduction of the mixture of the two tetrahydroxy acids, and the repeated recrystallization of the reduction products, the heneicosanoic acid was lost. As already mentioned, only docosanoic acid has been recognized on the paper chromatogram. It is, therefore, likely that only a small amount of tetrahydroxy heneicosanoic acid is present in the lichen.

It is known that mixtures of the normal fatty acids C_{21} and C_{22} give melting points in the region 74.9—75.2° [20]. This is in agreement with the melting point found in the present work.

Nor has the reduction product of the tetrahydroxy acid from *Parmelia centrifuga* any distinct melting point. There are some indications that a mixture of two acids is present, with tricosanoic acid (C_{23}) as the main component.

Reduction of tetrahydroxy acids from the lichen species *Parmelia encausta*, *Parmelia furfuraceae*, *Cetraria nivalis* and *Cladonia alpestris* have also been made. Solubilities, melting points and paper chromatographic analysis undoubtedly indicated the presence of mixtures. Work is in progress with a view to establishing the different tetrahydroxy acids in these lichens.

At times it has been supposed that these tetrahydroxy fatty acids might be compounds caused by the extraction of the lichens. However, an intense research in this field, has yielded no facts supporting this hypothesis. It is therefore reasonable to assume that the acids may be a result of biochemical oxidations in the lichens. In 1932 oleic- and linoleic acid were isolated from *Alectoria ochroleuca* by Klima [21].

EXPERIMENTAL

Extraction and isolation of the lichen substances from the different lichen species were carried out according to the procedure described in Part II. The analytical results are summarized in Table 1.

In the same paper reduction with HI and Zn, and methylation of the fatty acids obtained are also described in detail. The analytical results of the fatty acids are given in Table 2.

Oxidation of ventosic acid. The double amount of KIO_4 in N H_2SO_4 (40°) was added to a suspension of ventosic acid in 96 % ethanol (20°), and the mixture shaken for 30 min. The reaction mixture was then filtered, diluted with the same volume of water, and extracted with ether. The ether extract was filtered, concentrated, and distilled with steam. Only polymerisation products could be detected in the distillation remainder.

The aldehydes in the distillate were converted into 2,4-dinitrophenylhydrazones. The crude adduct obtained was filtered off and recrystallized several times from hot 96 % ethanol. The pure hydrazone crystallized as yellow prisms; m.p. 104—105° undepressed when mixed with the authentic hydrazone of *n*-decanal. (Found: C, 7.01; H 7.31; N 16.70. Calc. for $C_{16}H_{24}O_4N_4$: C 57.13; H 57.19; N 16.66.)

The crude hydrazone product obtained by concentration of the filtrate above was crystallized, and melted in the 76—93° range. This mixture of hydrazones was subjected to chromatographic investigations. The results are summarized in Table 4.

The oxidation of di- and tetrahydroxy stearic acids was carried out according to the method described by King [18]. The oxidation products were converted into 2,4-dinitrophenylhydrazones, purified by extraction with petroleum ether (60—70°) and recrystallized from ethanol.

In the X-ray diffraction analysis, a Philips X-ray Geiger Counter Spectrometer with $CuK\alpha_1$ radiation was used.

The elementary analyses have been carried out by *Mikroanalyslaboratoriet, Medicinsk-Kemiska Institutionen, Uppsala Universitet,* and the IR spectra by *Sentralinstitutt for industriell forskning,* Oslo.

I have received a grant from *Nansenfondet,* Oslo, which is gratefully acknowledged.

The author also wishes to thank Dr. Eilif Dahl for his interest and assistance in collecting material.

REFERENCES

1. Solberg, Y. J. *Acta Chem. Scand.* **11** (1957) 1477.
2. Zopf, W. *Die Flechtenstoffe in Chemischer, botanischer, pharmakologischer und technischer Beziehung,* Jena 1907.
3. Asahina, Y. and Shibata, S. *Chemistry of Lichen Substances,* Japan Soc. for the Promotion of Science, Tokyo 1954.
4. Zellner, J. *Monatsh.* **64** (1934) 6.
5. Zellner, J. *Monatsh.* **66** (1935) 81.
6. Bayzer, H., Schauenstein, E. and Winsauer, K. *Monatsh.* **89** (1958) 15.
7. Susi, H. *Anal. Chem.* **37** (1959) 910.
8. Sinclair, R. G., McKay, A. F. and Norman Jones, R. *J. Am. Chem. Soc.* **74** (1952) 2570.
9. Celthup, N. B. *J. Opt. Soc. Am.* **40** (1950) 397.
10. Kaufmann, H. P. and Nitsch, W. H. *Fette, Seifen, Anstrichmitt.* **56** (1954) 154.

11. Wagner, H., Abisch, L. and Bernhard, K. *Helv. Chim. Acta* **38** (1955) 1536.
12. Kaufmann, H. P. and Mohr, E. *Fette, Seifen, Anstrichmitt.* **60** (1958) 165.
13. Freeman, N. K. *J. Am. Chem. Soc.* **74** (1952) 2523.
14. Norman Jones, R., McKay, A. F. and Sinclair, R. G. *J. Am. Chem. Soc.* **74** (1952) 2575.
15. Cross, A. D. *Introduction to Practical Infra-Red Spectroscopy*, Imperial College of Science & Technology, London 1960.
16. Fuchs, W. and Addicks, G. *Fette, Seifen, Anstrichmitt.* **60** (1958) 907.
17. Sutherland, G. B. B. M. *Discussions Faraday Soc.* **9** (1950) 274.
18. King, G. *J. Chem. Soc.* **1938** 1826.
19. Lynn, W. S., Steele, L. A. and Staple, E. *Anal. Chem.* **28** (1956) 132.
20. Francis, F., Piper, S. H. and Malkin, Th. *Proc. Roy. Soc. London*, **128 A** (1930) 214.
21. Klima, J. *Monatsh.* **62** (1932) 209.

Received July 23, 1960.

ACTA CHEMICA SCANDINAVICA 14 (1960) 2161–2168

Die Chemie der Natürlichen Ordnung Cupressales

XXXII *. Über die Inhaltsstoffe des Kernholzes von *Athrotaxis selaginoides* Don, *Athrotaxis cupressoides* Don und *Chamaecyparis pisifera* Sieb. et Zucc.

HOLGER ERDTMAN und HELMUT VORBRÜGGEN

Organisk-kemiska Institutionen, Kungl. Tekniska Högskolan, Stockholm, Schweden

Die Kernholzbestandteile von *Athrotaxis selaginoides* und *Athrotaxis cupressoides* sowie ein Neutralöl aus dem Kernholz von *Chamaecyparis pisifera* wurden untersucht. Aus dem wasserlöslichen Teil von *A. selaginoides* wurde L-Arabinose sowie eine neue phenolische Substanz $C_{17}H_{18}O_7$ isoliert. Die saure Fraktion enthielt kristalline höhere Fettsäuren. Die neutrale Hauptfraktion lieferte eine Cadinen- und eine Cadinolfraktion. Das ölige Cadinolgemisch konnte chromatographisch in kristallines α-, δ- und »x-Cadinol» aufgetrennt werden. Der Destillationsrückstand ergab Hinokiol und β-Sitosterol.

Aus *A. cupressoides* wurde analog L-Arabinose, höhere kristalline Fettsäuren, Cedren, Cadinen, die drei genannten kristallinen Cadinole und Hinokiol isoliert.

Das Neutralöl von *Ch. pisifera* enthielt Cadinene und die drei kristallinen Cadinole.

Zur sehr heterogenen Familie *Taxodiaceae*, die viele kleine Gattungen umfasst und bisher noch wenig untersucht worden ist, gehören drei *Athrotaxis* Arten, zwei Bäume und ein Strauch (*A. laxifolia* Hook.), die alle in Tasmanien heimisch sind. Botanisch nahestehend scheint besonders *Taiwania*, eine monotypische Gattung aus Yunnan und Formosa, zu sein.

In der vorliegenden Arbeit wurden die Kernhölzer zweier *Athrotaxis* Arten, *A. selaginoides* und *A. cupressoides*, genauer untersucht. Im Verlaufe dieser Arbeit konnte neben anderen Substanzen ein öliges Gemisch von Cadinolen isoliert werden, das sich leicht chromatographisch in drei kristallisierte reine Cadinole zerlegen liess. Diese chromatographische Methode wurde anschliessend auf ein Cadinolgemisch aus *Chamaecyparis pisifera* angewandt, um ihre allgemeine Anwendbarkeit zu zeigen.

* Teil XXXI, *Acta Chem. Scand.* 14 (1960) 1995.

Der Acetonextrakt des Kernholzes von *Athrotaxis selaginoides* wurde zuerst mit Äther und dann das ätherlösliche mit Leichtpetroleum gefällt. Aus dem wasserlöslichen Teil der Ätherfällung kristallisierte neben L-Arabinose eine phenolische Substanz, $C_{17}H_{18}O_7$, aus. Schmp. 285° u. Zers. (aus Äthanol) und Schmp. 185° (aus Wasser), $[\alpha]_D$ + 274°. Beide Kristallformen haben ein fast identisches IR-Spektrum (starke breite Bande bei 3 300 cm^{-1} sowie starke Bande bei 1 658 cm^{-1} und 1 610 cm^{-1}). Diese Substanz ist Gegenstand weiterer Untersuchungen.

Der in Leichtpetroleum lösliche Anteil wurde wie üblich in eine bikarbonatlösliche, eine alkalilösliche und eine neutrale Fraktion zerlegt.

Aus beiden sauren Fraktionen kristallisierten beim Stehen geringe Mengen höherer Fettsäuren vom Schmp. 80° bzw. 70—75°. Die charakteristische Serie von Banden zwischen 1 350 und 1 180 cm^{-1} weist auf Säuren im Bereich von C_{20}—C_{24} hin[1].

Der in Petroläther lösliche neutrale Anteil ergab bei der fraktionierten Destillation Kohlenwasserstoff- und Alkoholfraktionen. Die ersteren bildeten mit Chlorwasserstoff (—)-Cadinen-dihydrochlorid und enthalten deshalb Cadinene. Starke Banden im IR-Spektrum bei 890 cm^{-1} zeigten die Anwesenheit von Methylengruppen an.

Die viskosen, höher siedenden Sesquiterpenalkoholfraktionen lieferten ebenfalls mit Chlorwasserstoff (—)-Cadinen-dihydrochlorid und enthalten somit Cadinole. Da diese Öle auch bei längerem Aufbewahren nicht kristallisierten, wurden sie an Aluminiumoxyd chromatographiert. Die kristallinen Fraktionen lieferten bei wiederholter Sublimation und Umkristallisation drei reine kristallisierte Cadinole.

Die zuerst eluierte Substanz schmolz nach wiederholter Sublimation bei 78°, $[\alpha]_D$ — 86,2°, *p*-Nitrobenzoat, Schmp. 104°, und erwies sich als identisch mit dem von Šorm und Mitarbeitern[2] aus dem Beerenöl des Wacholders (*Juniperus communis*) isolierten Cadinol vom Schmp. 78,5—79°, $[\alpha]_D$ —89° (nach Reinigung über das *p*-Nitrobenzoat Schmp. 104°). Dieses Cadinol von unbekannter Struktur wird in dieser Arbeit als »x-Cadinol» bezeichnet.

Die zweite eluierte Substanz wurde nur in geringer Menge erhalten und erwies sich nach der Reinigung als δ-Cadinol (Pilgerol), Schmp. 139°, $[\alpha]_D$ —106°. Diese Substanz wurde kürzlich von Erdtman, Pelchowicz und Topliss[3] aus dem Kernholz von *Pilgerodendron uviferum* und ebenfalls von Šorm und Mitarbeitern[2] aus dem Öl von Wacholder-Beeren isoliert. Ein Vergleich mit einer Probe von Albicaulol[4], (Schmp. und Misch-Schmp. 139°, opt. Drehung und IR-Spektrum) aus *Pinus albicaulis* und *Pinus armandi* zeigte, dass auch diese Substanz mit δ-Cadinol identisch ist.

Die dritte eluierte Substanz schmolz bei 73—74° $[\alpha]_D$ —48,6°, *p*-Nitrobenzoat Schmp. 138° und wurde als α-Cadinol identifiziert.

Reines α-Cadinol, Schmp. 72—74°, $[\alpha]_D$ —39°, wurde zuerst aus Java citronellöl[5] und kürzlich aus *Chamaecyparis lawsoniana*[6] und *Juniperus communis*[2] über das *p*-Nitrobenzoat isoliert. Die Struktur von α-Cadinol sowie seine absolute Konfiguration klärten Šorm und Mitarbeiter[2] sowie Soffer und Mitarbeiter[7] auf.

Aus dem hoch siedenden neutralen Destillationsrückstand wurde eine geringe Menge eines viskosen Öls erhalten, das in seinen Eigenschaften mit dem später beschriebenen Öl aus *Athrotaxis cupressoides* identisch war und worüber weiter unter berichtet wird.

Verseifung des nicht-flüchtigen neutralen Destillationsrückstandes ergab eine Neutralfraktion, aus der beim Stehen mit Leichtpetroleum eine geringe Menge einer kristallinen Substanz ausfiel, Schmp. 195—215°, die nach Sublimation bei 238° schmolz, $[\alpha]_D$ +74,3°, und durch Mischschmp. und IR-Spektrum als Hinokiol[8] identifiziert wurde. Aus der Mutterlauge kristallisierte eine Substanz aus, die nach zwei Umkristallisationen bei 138° schmolz, $[\alpha]_D$ —31,5° und positive Digitoninreaktion zeigte. Die Substanz ist dem IR-Spektrum und den physikalischen Konstanten nach relativ reines β-Sitosterin.

Der Acetonextrakt von *Athrotaxis cupressoides* wurde direkt mit Leichtpetroleum gefällt. Aus dem wasserlöslichen Teil der Fällung kristallisierte L-Arabinose aus.

Beim Einengen der Leichtpetroleum-Lösung fielen schöne Kristalle aus, die durch Schmp., Mischschmp. optische Drehung und IR-Spektrum als Hinokiol identifiziert wurden.

Der in Leichtpetroleum lösliche Anteil wurde in bikarbonatlösliche, alkalilösliche und neutrale Fraktion zerlegt.

Aus der alkalilöslichen Fraktion fiel beim Stehen mit Methanol ein wenig Hinokiol aus. Der neutrale Hauptteil wurde nach einer Vordestillation sorgfältig im Vakuum fraktioniert. Die ersten Kohlenwasserstoff-Fraktionen enthielten nach physikalischen Konstanten und IR-Spektrum α-Cedren. Ozonisierung und Hypobromit-Oxydation lieferte reine Cedren-dicarbonsäure, Schmp. 183—184°, $[\alpha]_D$ —36,5°. Die höher siedenden Kohlenwasserstoff-Fraktionen bildeten mit Chlorwasserstoff (—)-Cadinen-dihydrochlorid und enthielten also Gemische von Cadinenen. Die IR-Spektren dieser Cadinen-Fraktionen stimmten mit den IR-Spektren der Cadinen-Fraktionen aus *Athrotaxis selaginoides* überein. Die Sesquiterpenalkohol-Fraktionen ergaben mit Chlorwasserstoff ebenfalls (—)-Cadinen-dihydrochlorid und wurden durch Chromatographie an Aluminiumoxyd in die drei bereits beschriebenen kristallinen Cadinole aufgetrennt. Cedrol, dessen Anwesenheit wegen des Vorkommens von Cedren erwartet wurde, konnte bisher nicht isoliert werden.

Aus den hochsiedenden, viskos-öligen Alkoholen, die auch aus *Athrotaxis selaginoides* isoliert worden waren und die im IR-Spektrum Hydroxyl-, Methyl-, Isopropylbanden sowie schwache Banden bei 1 675 cm^{-1} und 1 710 cm^{-1} zeigten, konnte bisher weder durch Chromatographie noch durch Acylierung und anschliessende Chromatographie irgendeine kristalline Substanz isoliert werden. Aus dem neutralem Destillationsrückstand wurde noch weiteres Hinokiol gewonnen.

Die oben beschriebene einfache Auftrennung der nicht kristallisierenden öligen Cadinolgemische legte die Annahme nahe, dass viele in der Literatur[9] beschriebene ölige sogenannte L-Cadinole mit einer optischen Drehung zwischen —30 und —80° Gemische von α, δ, und »x-Cadinol» darstellen, die sich leicht chromatographisch trennen lassen sollten. Um dies nachzuprüfen, wurde ein Neutralöl aus *Chamaecyparis pisifera*, in dem Nakatsuka und Hirose[10] Cadinene und (—)-Cadinol nachgewiesen hatten, sorgfältig fraktioniert und wie

beschrieben Cadinene und (—)-Cadinol erhalten. Chromatographie des (—)-Cadinols ergab die obigen drei kristallinen Cadinole in ähnlichen Mengenverhältnissen.

Interessanterweise enthält das Kernholz der mit *Athrotaxis* verwandten *Taiwania cryptomerioides* ebenfalls Cadinole »Taiwanol». Tropolone wurden in der Familie *Taxodiaceae* noch nicht aufgefunden[11].

EXPERIMENTELLER TEIL

Alle Schmelzpunkte wurden mit dem Heizmikroskop nach Kofler bestimmt und sind korrigiert. Die IR-Spektren wurden mit dem Perkin-Elmer Modell 21 aufgenommen (Für kristalline Substanzen Kaliumbromid-Scheiben; Flüssigkeiten als reine Öle in einer 0,025 mm Natriumchlorid Zelle oder in CCl_4 gelöst). Optische Drehungen wurden in Chloroform-Lösung gemessen.

Athrotaxis selaginoides

Extraktion. 16 kg trockenes gemahlenes Kernholz extrahierte man 36 Stunden im Heissextraktor mit Aceton und erhielt 1,955 kg rohen braunen Extrakt I. Der Extrakt wurde mit 300 ml Aceton verdünnt, auf 40° erwärmt und unter heftigem Rühren zu 20 l Äther getropft. Das dabei ausgefallene dunkelbraune, Äther-unlösliche Öl, II (700 g), löste sich grösstenteils in Aceton und ergab beim Filtrieren eine weisse Substanz. Diese wurde in heissem Wasser gelöst, Tierkohle zugesetzt, filtriert und das Filtrat im Vakuum eingedampft. Der Rückstand kristallisierte aus Alkohol und ergab 19 g reine L-Arabinose, Schmpt. 158—160°.

200 g der *Äther-unlöslichen Fraktion II* wurden in 250 ml heissem Aceton gelöst, langsam unter Rühren zu 2 l kochendem Wasser gegeben, vom braun-schwarzen Rückstand dekantiert und filtriert. Das Filtrat behandelte man heiss mit Tierkohle, filtrierte und engte im Vakuum stark ein. Vom ausgefallenen braunen Öl, IIA, wurde dekantiert und schliesslich der Rest des Wassers im Vakuum bei 50° entfernt, wobei ein brauner Syrup anfiel, IIB.

IIA zeigte eine stark positive Reaktion mit Eisen(III)-Chlorid in Äthanol, mit Mg und HCl in Methanol war die Reaktion negativ. Da die Substanz auch bei längerem Stehen im Eisschrank mit Methanol nicht kristallisierte, wurde sie nicht weiter untersucht.

Aus dem braunen Syrup IIB kristallisierte beim Stehen mit Methanol im Eisschrank eine schöne farblose Substanz aus. Schmp. 270—274° unter Zers. nach Absaugen, Waschen mit Methanol und Trocknen. Auf dem Papierchromatogramm (Äthylacetat: Essigsäure:Wasser, 3 : 1 : 1) war noch L-Arabinose nachzuweisen. Eine Umkristallisation aus Äthanol lieferte papierchromatographisch reine Substanz, Schmp. 285° unter Zers. $[\alpha]_D$ —274° (*c* 0,55, Dimethylformamid-Wasser, 1 : 1).

Aus Äthanol-Wasser kristallisiert die Substanz in schönen Nadeln, die bei 185° schmelzen, bei höherer Temperatur wieder teilweise kristallisieren, um dann vollständig bei ca. 280° zu schmelzen. (Getrocknet im Vakuum Gef. C 61,2 : H 5,6. Ber. für $C_{17}H_{18}O_7$: C 61,1; H 5,4). Beim Aufarbeiten des restlichen ätherunlöslichen Teils II wurde weitere Substanz erhalten. Totalausbeute 4,5 g. Beim Trocknen bei 120° wurde die Substanz purpurrot. Kochen mit Salzsäure ergab eine rotviolette Lösung.

Die ätherlösliche Fraktion III wurde konzentriert und unter lebhaftem Rühren in 12 l Leichtpetroleum eingetropft, wobei 400 g gelbliches, in Leichtpetroleum unlösliches Pulver IV ausfiel. Die lösliche Fraktion V wurde in einen bikarbonatlöslichen Teil VI, einen alkalilöslichen Teil VII einen und Neutralteil VIII aufgetrennt.

Die saure Fraktion VI (8,5 g) kristallisierte teilweise beim Stehen mit Methanol im Eisschrank. Filtration und Waschen der Kristalle mit eiskaltem Methanol ergab 0,7 g kristallisierte Fettsäuren, Schmp. 80°.

Die alkalilösliche Fraktion VII (61 g) lieferte wie Fraktion VI ca. 4 g eines Gemisches kristallisierter Fettsäuren, Schmp. 70—75°. Chromatographie des nicht kristallinen Teils an Eisen-freiem Silicagel und Elution mit Benzol, Benzol-Aceton und Benzol-Methanol-Gemischen ergab nur Spuren kristallisierter Fettsäuren.

Die neutrale Fraktion VIII wurde bei 0.2 — 0.3 mm Druck fraktioniert. 400 g Substanz ergaben folgende Fraktionen:

1. Sdp. 99—100°: 170 g, $[\alpha]_D$ −3,8°
2. Sdp. 100—110°: 69 g, $[\alpha]_D$ −26,3°
3. Sdp. 110—113°: 90 g, $[\alpha]_D$ −34,3°
4. Rückstand XI: 25 g

Fraktion 1 wurde in einer Füllkörper-Kolonne mit Vakuummantel (LKB) bei hohem Rückflussverhältnis destilliert. Folgende Fraktionen wurden erhalten:

Fraktion	Sdp./10 mm	Gewicht	n_D	$[\alpha]_D$
1 a	120—130°	8,44 g	1,5018	0°
1 b	130—133°	9,56 g	1,5064	0°
1 c	133—135°	66,16 g	1,5091	+50,9°
1 d	135—138°	8,06 g	1,5124	+58,1°
1 e	138—151,5°	7,47 g	1,5095	−9,95°
1 f	151.5—154°	6,90 g	1,5067	−52,6°
1 g	154—156°	24,29 g	1,5071	−51,1°
1 h	140—150°	13,43 g	1,5070	−50,0°

Bei Fraktion 1 h wurde der Druck auf 3—5 mm gesenkt.

Cadinene (IX). Einen kleinen Teil von Fraktion 1 c löste man in absolutem Äther und sättigte die Lösung mit trockenem Chlorwasserstoff. Verdampfen des Äthers im Vakuum, Umkristallisation des kristallinen Rückstandes aus Leicht-Petroleum und Sublimation bei 0.1 mm Druck ergab lange schöne Nadeln, Schmp. 117—118°, $[\alpha]_D$ −37,9° (*c* 2,8). Der Mischschmelzpunkt mit (−)-Cadinen-dihydrochlorid zeigte keine Erniedrigung.

Cadinole (X). 3,1 g von Fraktion 1 g wurden an Aluminiumoxyd (Brockmann, Aktivität II, 300 g) chromatographiert. Benzol (1 Liter) eluierte 135 mg Öl, weitere 1,5 Liter Benzol lieferten 1,6 g »x-Cadinol», das durch mehrfache Sublimation über einen Temperaturgradienten bei 0,1 mm Druck gereinigt wurde. Schmp. 78°, $[\alpha]_D$ −86,2° (*c* 1,5). Elution mit 3 Litern Benzol + 1 % Äther ergab zuerst 100 mg δ-Cadinol, das nach zweifacher Sublimation rein war. Schmp. 139°, $[\alpha]_D$ −106° (*c* 3,0). Darauf wurden 700 mg eines Gemisches von δ- und α-Cadinol eluiert, gefolgt von 400 mg reinem α-Cadinol. α-Cadinol zeigte nach zweifacher Destillation bei 0,1 mm einen Schmp. von 73—74°. $[\alpha]_D$ −48,6° *c*) 5,7). Die Identität aller drei Cadinole wurde durch Mischschmelzpunkt mit authentischen Substanzen bestätigt.

Aus dem Gemisch von δ- und α-Cadinol konnten durch Kristallisation aus Leichtpetroleum weitere Mengen δ-Cadinol gewonnen werden. Fraktion 1 g enthält ca 50 % »x-Cadinol», ca 10 % δ-Cadinol und ca. 30 % α-Cadinol. Animpfen des restlichen Teils von Fraktion 1 g mit δ-Cadinol und Aufbewahren im Eisschrank ergab weitere Mengen δ-Cadinol. Auch beim Animpfen mit »x-Cadinol» kristallisierte Fraktion 1 g, aber die Kristalle konnten nur sehr schwer vom anhaftenden Öl befreit werden, da »x-Cadinol» wie α-Cadinol mit Leichtpetroleum oder Methanol sofort ein Öl bildet.

Analoge Chromatographie der Destillat-Fraktionen 1h und 2 und 3 ergaben ca 60—70 % α-Cadinol und ca. 30—40 % »x-Cadinol», aber kein δ-Cadinol. δ-Cadinol wird also in den ersten Destillatfraktionen angereichert, was die Gewinnung grösserer Mengen reinen α-Cadinols aus den höher siedenden Destillat-Fraktionen sehr erleichtert.

Bereitung der p-Nitrobenzoate. 0,786 g rohes »x-Cadinol» wurde in 8 ml absolutem Pyridin gelöst und unter Kühlen mit 1,1 g reinem *p*-Nitro-benzoylchlorid versetzt. Nach 50 min. Erhitzen auf dem Dampfbad wurde mit Äther verdünnt, dreimal mit 1 N Salzsäure und dreimal mit 2 N Natriumcarbonatlösung gewaschen. Das nach Trocknen und Abdampfen erhaltene Rohprodukt wurde mit Äther extrahiert und die Lösung über eine kleine Säule von neutralem Aluminiumoxyd (0,7 × 8 cm, Merck) filtriert. Die erste schwach gelbe Zone lieferte nach Umkristallisation aus Leicht-Petroleum und Äthanol 200 mg reines *p*-Nitrobenzoat des »x-Cadinols», Schmp. und Misch-Schmp. 104—105°. Die Mutterlaugen ergaben weitere 250 mg vom Schmp. 102—104°.

Das *p*-Nitro-benzoat des α-Cadinols, Schmpt. 138°, wurde in analoger Weise erhalten.

Hochsiedendes neutrales Öl XI. Redestillation der Fraktionen VIII, 2, 3 und 4 (Seite 2165) bei 0,2—0,3 mm Druck über eine 30 cm lange Vigreux-Kolonne lieferte neben der Hauptmenge an Cadinolen ca. 8—9 g viskoses leicht gelbliches Öl vom Sdp. 132—154°, dessen optische Drehung und IR-Spektrum in CCl_4 praktisch identisch war mit dem hochsiedenden Öl aus *Athrotaxis cupressoides* (Seite 2167).

Neutraler Destillationsrückstand XII. 5,1 g des dunkelbraunen Destillationsrückstandes wurden 1,5 Std mit 5 g Natriumhydroxyd in 50 ml Äthanol auf dem Dampfbad verseift, darauf 50 ml Wasser zugesetzt und der Alkohol unter vermindertem Druck abgedampft. Die alkalische Lösung extrahierte man mit Äther, trocknete den Ätherextrakt mit Natriumsulfat und trieb das Lösungsmittel ab. Aus der Lösung der Substanz in Leichtpetroleum fielen beim Stehen im Eisschrank ca. 105 mg einer kristallinen Substanz aus, Schmp. 195—215°, die nach Sublimation bei 0.01 mm scharf bei 238° schmolz, $[\alpha]_D$ +74,3° (*c* 1,1), und durch Mischschmelzpunkt und IR-Spektrum als Hinokiol identifiziert wurde. Das Filtrat löste man nach Abdampfen des Leichtpetroleums in Methanol und bewahrte es im Kühlschrank auf, wobei 1,3 g einer kristallinen Substanz, Schmp. 122—132° ausfiel. Die Substanz schmolz nach zwei Umkristallisationen aus Äthanol scharf bei 138°, $[\alpha]_D$ −31,5° (*c* 1,9), zeigte eine positive Digitonin-Reaktion und stellt nach IR-Spektrum, Schmelzpunkt und optischer Drehung ziemlich reines β-Sitosterol dar.

Athrotaxis cupressoides

Extraktion. 4,45 kg trockenes, gemahlenes Kernholz extrahierte man 36 Stunden im Heissextraktor mit Aceton und erhielt nach Abdampfen des Lösungsmittels 262 g braunen Roh-Extrakt. Nach Lösen in ca. 200 ml Aceton wurde die Substanz unter lebhaftem Mischen mit einem Vibrator in ca. 5 l Leichtpetroleum eingetropft und noch ca. 2 Stunden vibriert (Fällung = I; Lösung = II.)

Leichtpetroleum-unlöslicher Anteil (I). Den ausgefallenen Niederschlag (I) filtrierte man ab, wusch mit Leichtpetroleum und löste die Substanz (136 g) in wenig Aceton. Nach Eintropfen der Acetonlösung in 2 l siedendes Wasser, Dekantieren und Filtration nach Kohlezusatz wurde die Lösung im Vakuum stark eingeengt, vom ausgefallenen Öl dekantiert und schliesslich der Rest des Lösungsmittels im Vakuum entfernt. Aus dem sirupösen Rückstand kristallisierten nach Zusatz von Methanol und Impfen 8 g reine L-Arabinose aus, Schmp. 158—160°. Animpfen mit der phenolischen Substanz aus *Athrotaxis selaginoides* lieferte keine Kristalle, auch nicht bei wochenlangem Aufbewahren der Substanz im Kühlschrank.

Leichtpetroleum-löslicher Anteil (II). Beim Einengen der Leichtpetroleumlösung II auf ca. 200 ml kristallisierten beim Stehen 2 g einer Substanz aus, (III) Schmp. 231—235°, die nach Sublimation bei 0,01 mm bei 238° schmolz, $[\alpha]_D$ +75,1°, und durch Mischschmelzpunkt und IR-Spektrum als Hinokiol erkannt wurde. Das Filtrat vom Hinokiol trennte man in üblicher Weise in eine bikarbonatlösliche Fraktion IV, eine alkalilösliche Fraktion V und einen Neutralteil VI auf.

Die bikarbonatlösliche, saure Fraktion IV (2.32 g) lieferte geringe Mengen höherer Fettsäuren, *die alkalilösliche Fraktion V* (9.0 g) etwa 100 mg Hinokiol.

Den Neutralteil VI (ca. 90 g) destillierte man bei 0,3 mm Druck und 150° Ölbadtemperatur, wobei 66,5 g flüchtige Substanz VII übergingen und 12,5 g im Rückstand verblieben VIII.

Den flüchtigen Neutralteil VII destillierte man bei hohem Rücklaufverhältnis in einer Füllkörperkolonne mit Vakuummantel (LKB).

Fraktion	Sdp./10 mm	Gewicht	n_D	*D*
VII : 1	90—122°	2,698 g	1,4800	−42,4°
VII : 2	122—126°	4,493 g	1,4978	−50,8°
VII : 3	126—130°	5,763 g	1,5013	−28,4°
VII : 4	130—134°	6,712 g	1,5053	+1,64°
VII : 5	134—138°	6,212 g	1,5078	+17,4°
VII : 6	138—148°	2,254 g	1,5074	+5,13°
VII : 7	148—152°	17,494 g	1,5078	−37,7°
VII : 8 Rückstand		22,0 g		

Cedren. Die physikalischen Daten von Fraktion VII : 1 — VII : 3 sowie ihre IR-Spektren stimmten gut mit α-Cedren überein.

Ozonisierung. Durch eine Lösung von 0,710 g von Fraktion VII : 2 in 10 ml Methylenchlorid leitete man 4 Std. bei −70° einen ca. 3—5 %-igen Ozon-Strom bis Blaufärbung eintrat. Darauf fügte man in der Kälte 5 ml 30 %-iges Wasserstoffperoxyd und 5 ml gesättigte Soda-Lösung hinzu und schüttelte über Nacht. Nach Extraktion mit 50 ml Äther wurde die wässrige Phase abgetrennt, 10 Min. gekocht, mit Eis gekühlt und vorsichtig mit einer Lösung von Natriumhypobromit aus 2 g Natriumhydroxyd und 1 ml Brom versetzt. Nach 3 Std. leitete man Schwefeldioxyd ein bis die Lösung farblos wurde und schüttelte die alkalische Lösung zweimal mit 50 ml Äther aus. Ansäuern der wässrigen Phase mit verd. Schwefelsäure fällte eine weisse Substanz aus, die nochmals in Äther aufgenommen und mit Bikarbonat extrahiert wurde. Nach Ansäuern der Bikarbonatlösung wurden 170 mg weisse Kristalle erhalten, Schmp. 173°. Nach Umkristallisation aus Äthanol-Wasser unter Zusatz von Tierkohle schmolz die Substanz bei 175—184°. Sublimation bei 140—150°/0,01 mm lieferte reine Cedrendicarbonsäure Schmp. 183—184°, $[\alpha]_D$ −35,5°. (*c* 1,9).

Cadinene. Aus Fraktion VII : 4 und in besserer Ausbeute aus Fraktion VII : 5 wurde mit Chlorwasserstoff reines (−) -Cadinen-dihydrochlorid erhalten. Schmp. 117—118°.

Cadinole. 6,2 g von Fraktion VII : 7 wurde wie auf Seite 000 beschrieben an 455 g Aluminiumoxyd chromatographiert und ergab ca. 50 % »x-Cadinol», ca. 15 % δ-Cadinol und ca. 25 % α-Cadinol, die nach Reinigung durch wiederholte Sublimation durch Mischprobe, optische Drehung und IR-Spektrum identifiziert wurden.

Der Rückstand VII : 8 wurde bei 0,3 mm Druck und 110—200° Ölbadtemperatur destilliert.

Fraktion	Sdp.	Gewicht	opt. Drehung
VII : 8 : 1	112—130°	0,66 g	
VII : 8 : 2	130—152°	19,01 g	−32,1°

Da Fraktion VII : 8 : 1 mit Chlorwasserstoff eine gute Ausbeute an (−)-Cadinen-dihydrochlorid lieferte, besteht diese Fraktion grösstenteils aus Cadinolen und wurde nicht weiter untersucht.

Fraktion VII : 8 : 2 ergab nur sehr wenig Cadinen-dihydrochlorid. Chromatographie von Fraktion VII : 8 : 2 an Aluminiumoxyd und aktiviertem Silicagel lieferte nur ölige Alkohole. Acetylierung mit Pyridin-Acetanhydrid und Chromatographie an neutralem Aluminiumoxyd ergab ebenfalls nur ölige Acetate.

Auch nach Reaktion von Fraktion VII : 8 : 2 mit *p*-Nitro-benzoyl-chlorid und Pyridin und nachfolgender Chromatographie an neutralem Aluminiumoxyd wurden keine kristallinen Derivative erhalten.

Der braune harte Destillationsrückstand kristallisierte mit Methanol und erbrachte weitere Mengen Hinokiol.

Chamaecyparis pisifera

Destillation. 81 g Wasserdampf-destilliertes neutrales Öl aus dem Kernholz von *Chamaecyparis pisifera* wurde bei 10 mm Druck in einer Füllkörperkolonne mit Vakuummantel (LKB) sorgfältig fraktioniert.

Fraktion	Sdp.	Gewicht	n_D	opt. Drehung
1	124—132°	8,62 g	1,5052	+9,24°
2	132—135°	9,34 g	1,5073	+28,9°
3	135—142°	13,135 g	1,5093	+50,2°
4	142—153°	5,13 g	1,5079	−15,8°
5	153—156°	26,42 g	1,5073	−39,3°
Rückstand		17,0 g		

Der dunkelbraune Rückstand wurde nicht weiter untersucht.

Cadinene. Aus Fraktion 2 und 3 wurde mit Chlorwasserstoff (−)-Cadinen-dihydrochlorid erhalten, Schmp. und Mischschmp. 117−118°.

Cadinole. 5,298 g von Fraktion 5 chromatographierte man wie auf Seite 2165 beschrieben an Aluminiumoxyd (420 g) und erhielt ca. 40 % »x-Cadinol», 5−10 % δ-Cadinol und 40 % α-Cadinol, die nach wiederholter Sublimation durch Mischschmp., opt. Drehung und IR-Spektrum identifiziert wurden.

Die Verfasser danken der *U.S. Army and Development Liaison Group* unter der Kontrakt Nr DA-91−508−EUC−288 für die finanzielle Unterstützung, welche einem von uns (*H.V.*) die Teilnahme an dieser Arbeit ermöglichte. Wir danken auch Professor W. Dauben für eine Probe von Albicaulol, sowie Professor F. Šorm für Proben von α- und »x-Cadinol».

Literaturverzeichnis

1. Bellamy, L. J. *The Infra-Red Spectra of Complex Molecules*, 1959, Seite 173.
2. Motl., O., Sykora, V., Herout, V. und Šorm, F. *Collection Czechoslov. Chem. Communs.* **23** (1958) 1297; Herout, V. und Sykora, V. *Tetrahedron* **4** (1958) 246.
3. Erdtman, H., Pelchowicz, Z. und Topliss, J. G. *Acta Chem. Scand.* **10** (1956) 1563.
4. Haagen-Smit, A. J., Wang, T. H. und Mirov, N. T. *J. Am. Pharm. Assoc. Sci. Ed.* **40** (1951) 557.
5. Plattner, P. A. und Markus, R. *Helv. Chim. Acta* **25** (1942) 1674.
6. Kritchevsky, G. und Anderson, A. B. *J. Am. Pharm. Assoc. Sci. Ed.* **44** (1955) 534.
7. Soffer, M. D., Brey, M. und Fournier, J. *Chem. & Ind. London* **1958** 19; *J. Am. Chem. Soc.* **81** (1959) 1678.
8. Simonsen, J. Barton, D. H. R. und Owen, L. N. *The Terpenes* (2nd Ed. 1952) Vol. III, Seite 365.
9. Simonsen, J., *Ibid.*, Seite 75.
10. Nakatsuka, T. und Hirose, Y. *J. Japan Forestry Soc.* **37** (1955) 452.
11. Kafuko, K. und Kato, R. *Bull. Chem. Soc. Japan* **6** (1931) 65.
12. Erdtman, H. *Fourth International Congress of Biochemistry.* Vol. II-Biochemistry of Wood. 1958.

Eingegangen am 28. Juni 1960.

ACTA CHEMICA SCANDINAVICA 14 (1960) 2169–2176

The Crystal Structure of $Ru_{11}B_8$

JAN ÅSELIUS

Institute of Chemistry, University of Uppsala, Uppsala, Sweden

The crystal structure of $Ru_{11}B_8$ has been determined by single crystal methods.

The orthorhombic unit cell has the following dimensions: $a = 11.60_9$ Å, $b = 11.34_2$ Å and $c = 2.83_6$ Å.

There are two formula units in the elementary cell and the space-group is $Pbam-(D_{2h}^9)$ No. 55.

The twentytwo ruthenium atoms are situated in one twofold position and five fourfold positions with two ruthenium atoms in 2(*a*), twelve ruthenium atoms in three fourfold positions 4(*g*): $x_{II} = 0.2844$ $y_{II} = 0.3913$, $x_{III} = 0.0429$ $y_{III} = 0.3952$, $x_{IV} = 0.1686$ $y_{IV} = 0.1740$ and eight ruthenium atoms in two fourfold positions 4(*h*): $x_V = 0.4636$ $y_V = 0.2962$, $x_{VI} = 0.3404$ $y_{VI} = 0.0616$.

The sixteen boron atoms are also situated in fourfold positions with four in 4(*g*): $x_{II} = 0.34_{79}$ $y_{II} = 0.21_{56}$, and twelve in 4(*h*): $x_I = 0.13_{98}$ $y_I = 0.01_{81}$, $x_{III} = 0.15_{23}$ $y_{III} = 0.32_{65}$, $x_{IV} = 0.27_{99}$ $y_{IV} = 0.25_{35}$.

Very little is known about the structures of the borides of the platinum metals.

Buddery and Welch [1] have prepared a number of such borides by direct combination of the elements.

Mooney and Welch [2] determined the crystal structure of Rh_2B from single crystal data. Later Aronsson [3] determined the crystal structures of Ru_7B_3 and Rh_7B_3 and Aronsson and co-workers [4] the crystal structures of RhB, PtB and IrB_{1-2}.

An X-ray investigation of the Ru—B system has been started at this Institute in order to establish the existence and compositions of the intermediate phases and to determine the crystal structures. In arc-melted ruthenium-boron alloys five intermediate phases can be identified, Ru_7B_3, $Ru_{11}B_8$, RuB, $RuB_{\sim 1.5}$, $RuB_{\sim 3}$.

The present paper gives an account of the crystal structure of the phase $Ru_{11}B_8$.

EXPERIMENTAL

Alloys were prepared by high frequency-melting ruthenium (claimed purity *ca.* 99.8 %, obtained from Heraeus, Hanau, Germany) and boron (claimed purity 99.0—99.7 %, kindly donated by Borax Consolidated, London). No chemical analyses were carried out and all compositions reported are nominal.

The reaction products were investigated with X-ray powder methods. Guinier-type cameras with Cu$K\alpha$-radiation were used. The unit cell dimensions were determined with CaF_2 as internal calibration standard, $a = 5.4630$ Å.

For the single-crystal work, a small, roughly spherical crystal fragment was selected from a crushed $Ru_{1.25}B$-alloy. Single crystal photographs were taken around the *c*-axis with an equi-inclination Weissenberg camera with niobium-filtered MoK radiation. The multiple film technique was employed with thin iron foil between successive films. The intensities were visually estimated with the aid of a standard intensity scale. The summation of the Fourier series and the structure factor calculations were made on the electronic digital computer BESK with programs (available at BESK) devised by M. Edstrand and Åsbrink *et al.*[5] In the structure factor calculations the atomic scattering factors were approximated to the following expression:

$$f_i = A_i \exp(-a_i/\lambda^2\sin^2\Theta) + B_i \exp(-b_i/\lambda^2\sin^2\Theta) + C_i \exp(-c_i/\lambda^2\sin^2\Theta) + D_i$$

The constants A_i, B_i, C_i and a_i, b_i, c_i have been calculated by Appel [6] on the basis of atomic scattering factor tables given by Tomas and Umeda [7] for ruthenium and by Ibers [8] for boron.

	A	B	C	a	b	c
Ruthenium	15.176	16.599	11.760	0.240	2.637	20.292
Boron	1.644	0.406	2.878	0.6069	4.5832	33.019

The real part of the dispersion correction for ruthenium (D_i in the expression above) was obtained from the table of Dauben and Templeton [9].

RESULTS

The powder photograph of the alloy from which the actual single-crystal specimen was selected, gave the following dimensions of the orthorhombic unit cell:

$$a = 11.60_9 \text{ Å}, \qquad b = 11.34_2 \text{ Å}, \qquad c = 2.83_6 \text{ Å and } U = 373.4 \text{ Å}^3.$$

Small variations of the lattice parameters (0.2 %) have been observed.

It is evident from powder and single-crystal data that $Ru_{11}B_8$ is orthorhombic. Since 0kl reflexions appear only for $k = 2n$, and $h0l$ reflexions only for $h = 2n$, and no limiting conditions are found for hkl,$hk0$ and $00l$ reflexions, the most probable space-groups are *Pbam* and *Pba*2. The distribution of intensities in the $hk0$ and $hk2$ zones are similar, apart from the normal decline. This distribution of intensities indicates that the ruthenium atoms are situated in planes perpendicular to the *c*-axis with a spacing of $c/2$. For that reason, only the $|F|^2$ values for $hk0$ and $hk1$ reflexions were necessary for evaluating the Patterson sections $P(UV0)$ and $P(UV\ 1/2)$. The analysis of these sections showed that the heights and positions of all large peaks in $P(UV0)$ and $P(UV\ 1/2)$ could be interpreted by assuming the space-group to be *Pbam* with twenty ruthenium atoms in five fourfold positions and two ruthenium atoms in a twofold position. If the twofold position 2(a) is chosen, twelve ruthenium atoms are situated in three fourfold positions 4(g) and eight ruthenium atoms in two

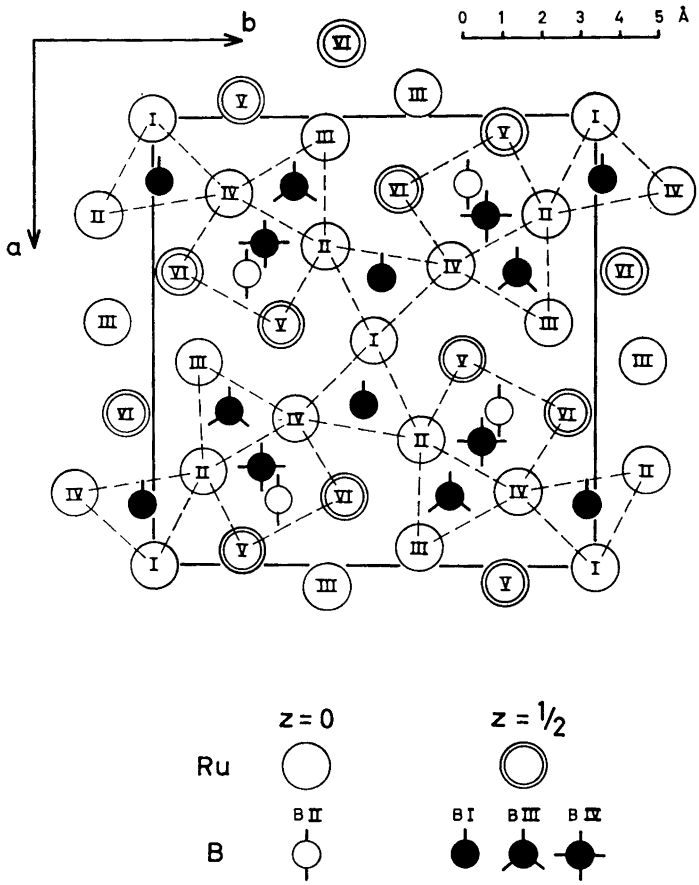

Fig. 1. The structure of $Ru_{11}B_8$ projected on the *ab*-plane.

fourfold positions 4(*h*). During the refinement of the structure nothing was found to contradict the choice of the space-group *Pbam*. (Small deviations from this symmetry for the boron positions cannot be excluded.)

Starting with the rough parameter values obtained from the Patterson maps, signs were calculated for the observed $F(hk0)$ values, and the electron density projection $\varrho\ (xy)$ was computed. The x and y coordinates of the ruthenium atoms were refined from successive difference syntheses. After the final refinement of the ruthenium coordinates, the R value 0.105 was obtained for the observed 310 independent $hk0$ reflexions when an empirical isotropic temperature factor with $B = 0.23_0$ Å^2 was applied. No corrections for absorption and extinction were made.

In the final difference synthesis map, in which all ruthenium atoms were subtracted, four rather well resolved boron maxima were visible. Three of

Table 1. Final atomic parameters of $Ru_{11}B_8$. Space-group *Pbam*. (The standard deviation for all Ru-coordinates is ± 0.0002.)

2 Ru_I	in 2(*a*)		
4 Ru_{II}	in 4(*g*)	$x_{II} = 0.2844$	$y_{II} = 0.3913$
4 Ru_{III}	in 4(*g*)	$x_{III} = 0.0429$	$y_{III} = 0.3952$
4 Ru_{IV}	in 4(*g*)	$x_{IV} = 0.1686$	$y_{IV} = 0.1740$
4 Ru_V	in 4(*h*)	$x_V = 0.4636$	$y_V = 0.2962$
4 Ru_{VI}	in 4(*h*)	$x_{VI} = 0.3404$	$y_{VI} = 0.0616$
4 B_I	in 4(*h*)	$x_I = 0.13_{98}$	$y_I = 0.01_{81}$
4 B_{II}	in 4(*g*)	$x_{II} = 0.34_{79}$	$y_{II} = 0.21_{56}$
4 B_{III}	in 4(*h*)	$x_{III} = 0.15_{23}$	$y_{III} = 0.32_{65}$
4 B_{IV}	in 4(*h*)	$x_{IV} = 0.27_{99}$	$y_{IV} = 0.25_{35}$

these maxima, corresponding to one 4(*g*) position and three 4(*h*) positions had about the same height, but the B_{IV} maxima was considerably lower and not symmetrical in shape. Only one other maximum of the same height as the boron maxima was found, but space considerations showed that this maximum could not be a boron maximum.

With the same temperature factor ($B = 0.23_0$ Å^2) and with all atoms subtracted, a final refinement cycle was made. The reliability index of the observed 310 independant *hk*0 reflexions was found to be 0.097. A list of calculated and observed structure factors can be obtained from this Institute on request.

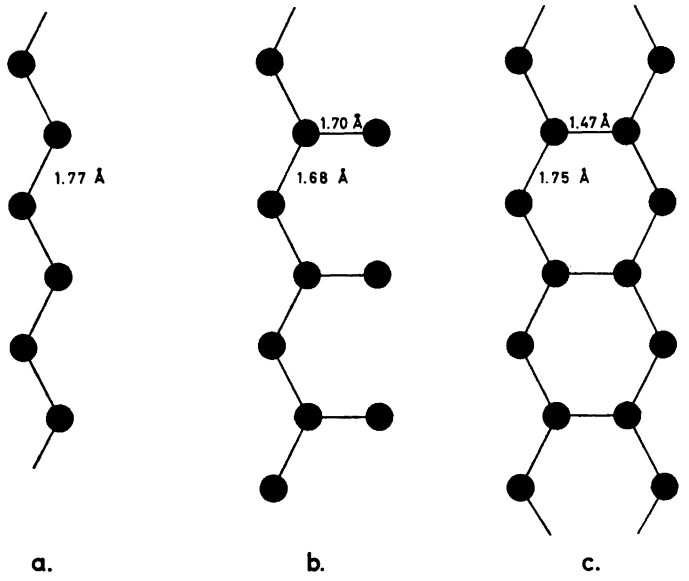

Fig. 2. Three different types of boron chains.
a. boron chain in FeB
b. boron chain in $Ru_{11}B_8$
c. boron chain in Mn_3B_4

Table 2. Interatomic distances (in Å) in $Ru_{11}B_8$. (Distances ≤ 3.25 Å listed. The standard deviations of Ru—Ru distances less than 0.01 Å.)

		Average			Average
Ru_I	$-2Ru_I$: 2.84(2)	2.78 Å	Ru_{II}	$-Ru_I$: 2.79	2.79 Å (nine shortest)
	$-2Ru_{II}$: 2.79(2)			$-2Ru_{II}$: 2.84(2)	
	$-2Ru_{IV}$: 2.78(2)			$-Ru_{III}$: 2.80	
	$-4Ru_V$: 2.74(4)			$-2Ru_{IV}$: 2.81; 3.25	
	$-4B_I$: 2.16(4)			$-2Ru_V$: 2.74(2)	
				$-2Ru_{VI}$: 2.80(2)	
				$-2B_I$: 2.20(2)	
				$-B_{II}$: 2.12	
				$-2B_{III}$: 2.21(2)	
				$-2B_{IV}$: 2.11(2)	
Ru_{III}	$-Ru_{II}$: 2.80	2.77 Å	Ru_{IV}	$-Ru_I$: 2.78	2.81 Å (nine shortest)
	$-3Ru_{III}$: 2.58; 2.84(2)			$-2Ru_{II}$: 2.81; 3.25	
	$-Ru_{IV}$: 2.90			$-Ru_{III}$: 2.90	
	$-2Ru_V$: 2.75(2)			$-2Ru_{IV}$: 2.84(2)	
	$-4Ru_{VI}$: 2.72(2);2.79(2)			$-4Ru_{VI}$: 2.76(2); 2.79(2)	
	$-B_{II}$: 2.59			$-2B_I$: 2.29(2)	
	$-2B_{III}$: 2.06(2)			$-B_{II}$: 2.13	
				$-2B_{III}$: 2.24(2)	
				$-2B_{IV}$: 2.12(2)	
Ru_V	$-2Ru_I$: 2.74(2)	2.79 Å	Ru_{VI}	$-2Ru_{II}$: 2.80(2)	2.80 Å
	$-2Ru_{II}$: 2.74(2)			$-4Ru_{III}$: 2.72(2); 2.79(2)	
	$-2Ru_{III}$: 2.75(2)			$-2Ru_{IV}$: 2.76(2)	
	$-2Ru_{IV}$: 2.79(2)			$-Ru_V$: 3.02	
	$-2Ru_V$: 2.84(2)			$-2Ru_{VI}$: 2.84(2)	
	$-Ru_{VI}$: 3.02			$-B_I$: 2.38	
	$-2B_I$: 2.79; 2.94			$-2B_{II}$: 2.25(2)	
	$-2B_{II}$: 2.16(2)			$-B_{III}$: 2.67	
	$-B_{III}$: 2.60			$-B_{IV}$: 2.29	
	$-B_{IV}$: 2.19				
B_I	$-2Ru_I$: 2.16(2)	2.22 Å (six shortest)	B_{II}	$-Ru_{II}$: 2.12	2.18 Å (six shortest)
	$-2Ru_{II}$: 2.20(2)			$-Ru_{III}$: 2.59	
	$-2Ru_{III}$: 2.29(2)			$-Ru_{IV}$: 2.13	
	$-2Ru_V$: 2.79; 2.94			$-2Ru_V$: 2.16(2)	
	$-Ru_{VI}$: 2.38			$-2Ru_{VI}$: 2.25(2)	
	$-2B_I$: 2.84(2)			$-2B_{II}$: 2.84(2)	
	$-B_{III}$: 3.25			$-2B_{III}$: 2.96(2)	
	$-2B_{IV}$: 3.13; 3.14			$-2B_{IV}$: 1.68(2)	
B_{III}	$-2Ru_{II}$: 2.21(2)	2.17 Å (six shortest)	B_{IV}	$-2Ru_{II}$: 2.11(2)	2.16 Å
	$-2Ru_{III}$: 2.06(2)			$-2Ru_{IV}$: 2.12(2)	
	$-2Ru_{IV}$: 2.24(2)			$-Ru_V$: 2.19	
	$-Ru_V$: 2.60			$-Ru_{VI}$: 2.29	
	$-Ru_{VI}$: 2.67			$-2B_I$: 3.13; 3.14	
	$-B_I$: 3.25			$-2B_{II}$: 1.68(2)	
	$-2B_{II}$: 2.96(2)			$-B_{III}$: 1.70	
	$-2B_{III}$: 2.84(2)			$-2B_{IV}$: 2.84(2)	
	$-B_{IV}$: 1.70				

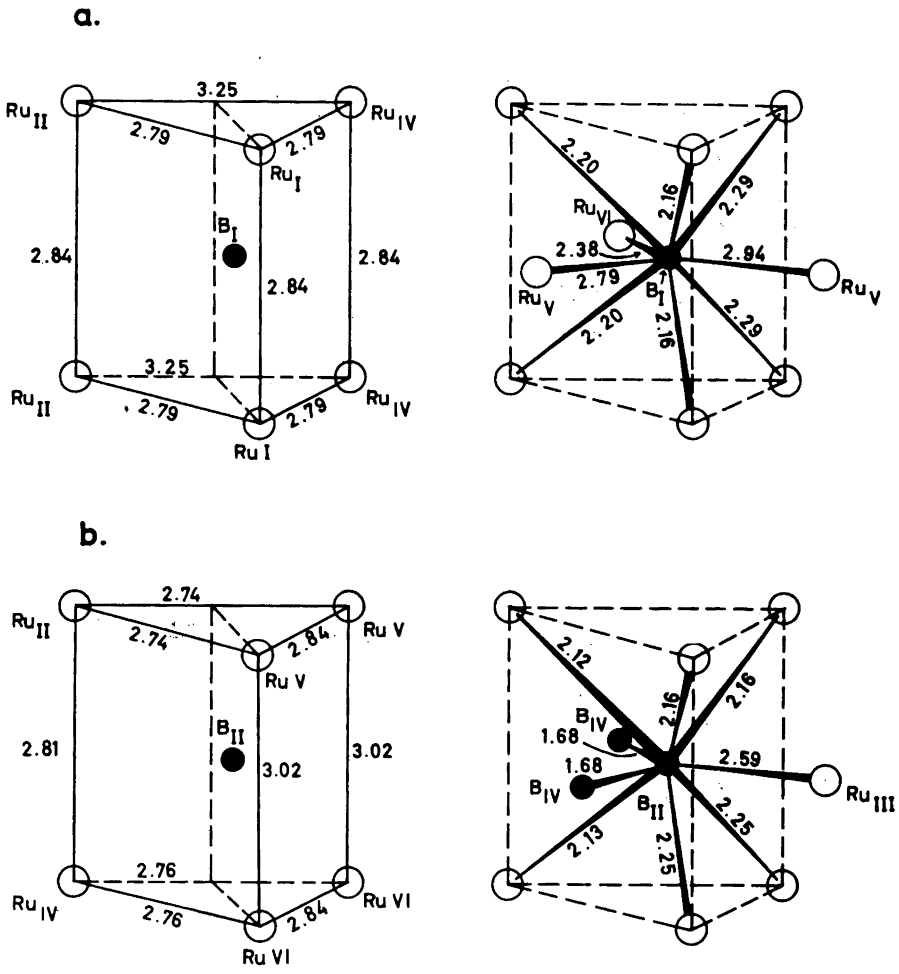

Fig. 3. The environment of the boron atoms in $Ru_{11}B_8$.
a. the environment of the B_I atoms
b. the environment of the B_{II} atoms

The final atomic parameters with standard deviations and interatomic distances are listed in Tables 1 and 2. (The standard deviations of the atomic parameters of ruthenium were estimated with Cruickshank's [10] formula.)

DESCRIPTION OF THE STRUCTURE

A projection of the structure on the *ab*-plane is shown in Fig. 1.

From the crystal-chemical point of view, the structure of $Ru_{11}B_8$ shows many resemblances to the orthorhombic Ni_4B_3 structure described by Rund-

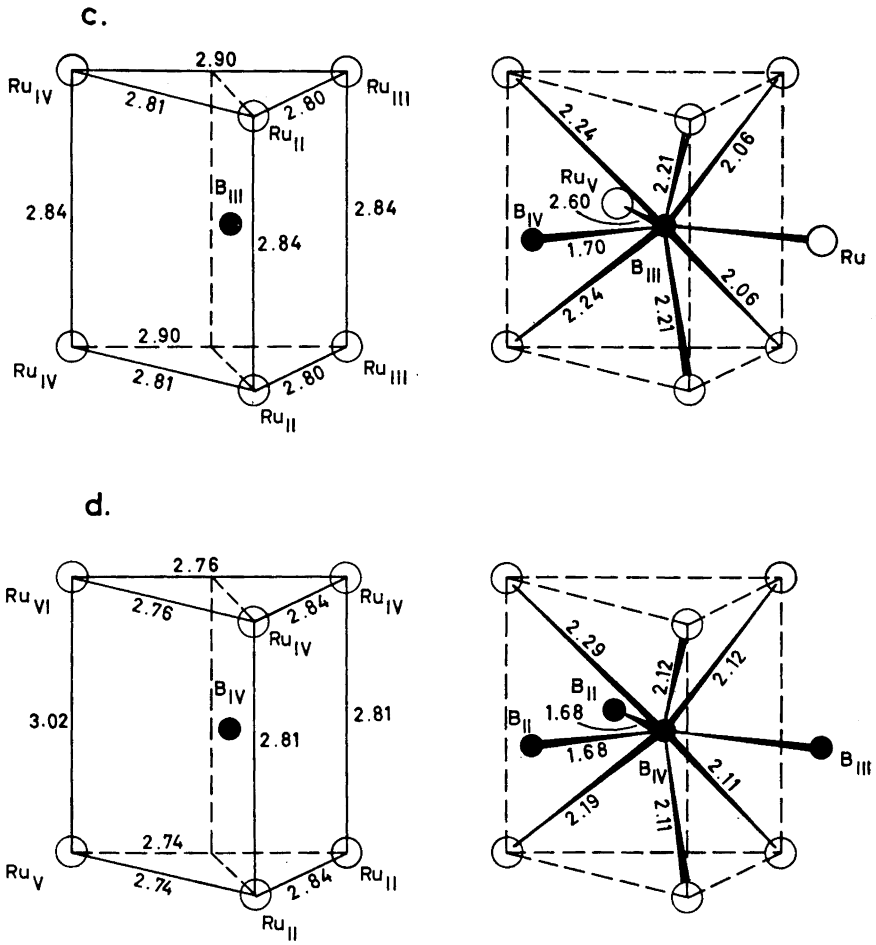

c. the environment of the B_{III} atoms
d. the environment of the B_{IV} atoms

qvist [11]. Both structures can be described as built-up by interconnected trigonal prisms of metal atoms, with the boron atoms situated in the centers of these prisms. The metal atoms have ten or eleven neighbours of their own kind, and the boron atoms have the usual triangular prismatic environment.

In both the structures the boron atoms are partly isolated without close boron contacts, partly connected to infinite zig-zag chains running throughout the structure in the direction of the shortest axis.

The boron chains in orthorhombic Ni_4B_3 are single zig-zag chains of the same type as the chains in the MeB-borides of the FeB-, MoB- and CrB-types [12]. Every boron atom in the chains is in close contact with two other boron atoms.

In the boron zig-zag chains in $Ru_{11}B_8$ every second boron atom is in close contact with two other boron atoms and every second boron atom is in close contact with three other boron atoms (see Fig. 2 b). In the borides of composition Me_3B_4[12] the boron atoms form double chains.

The boron chain in $Ru_{11}B_8$ can be looked upon as a transition type between a single chain and a double chain.

For comparison a single chain in FeB[13] and a double chain in Mn_3B_4[14] are shown in Figs. 2 a and 2 c.

The four types of trigonal ruthenium atom prisms are shown in Figs. 3 a, b, c and d together with the environments of the B_I, B_{II}, B_{III} and B_{IV} atoms.

The coordination number of the boron atoms is nine, the B_I atoms have nine ruthenium neighbours, the B_{III} atoms have eight ruthenium neighbours and one boron neighbour, the B_{II} atoms have seven ruthenium neighbours and two boron neighbours and the B_{IV} atoms have six ruthenium neighbours and three boron neighbours.

The metal-metal distances are normal with an average distance of 2.79 Å. The average of the twentyfour shortest ruthenium-boron distances is 2.18 Å. This value is in good agreement with the sum, 2.21 Å, of the normal atomic radius of boron, 0.87 Å (Kiessling [12]) and the atomic radius of ruthenium for coordination number 12, 1.34 Å.

Acknowledgements. I wish to thank Professor G. Hägg for his kind interest and for all facilities put at my disposal.

I also want to thank Drs. B. Aronsson, R. Hesse and S. Rundqvist for introducing me into this interesting field of science.

Thanks are also due Mr E. Stenberg for many stimulating discussions.

Financial support is gratefully acknowledged from the *Air Force Office of Scientific Research and Development Command, United States Air Force,* through its European Office under Contract No. AF 61(052)—40 and from the *Swedish Technical Science Research Council.* Facilities for use of the electronic digital computer BESK were given by the *Swedish Board for Computing Machinery.*

REFERENCES

1. Buddery, J. H. and Welch, A. J. E. *Nature* **167** (1951) 362.
2. Mooney, R. W. and Welch, A. J. E. *Acta Cryst.* **7** (1954) 49.
3. Aronsson, B. *Acta Chem. Scand.* **13** (1959) 109.
4. Aronsson, B., Stenberg, E. and Åselius, J. *Acta Chem. Scand.* **14** (1960) 733.
5. Åsbrink, S., Blomqvist, G. and Westman, S. *Arkiv Kemi* **14** (1959) 545.
6. Appel, K. *Technical Note from the Quantum Chemistry Group, University of Uppsala.*
7. Tomas, L. H. and Umeda, K. *J. Chem. Phys.* **26** (1957) 293.
8. Ibers, J. A. *Acta Cryst.* **10** (1957) 86.
9. Dauben, C. H. and Templeton, D. H. *Ibid.* **8** (1955) 841.
10. Cruickshank, D. W. J. *Ibid.* **2** (1949) 65.
11. Rundqvist, S. *Acta Chem. Scand.* **13** (1959) 1193.
12. Kiessling, R. *Ibid.* **4** (1950) 209.
13. Bjurström, T. *Arkiv Kemi, Mineral. Geol.* **11 A** (1933) No. 5.
14. Kiessling, R. *Acta Chem. Scand.* **4** (1950) 146.

Received July 12, 1960.

ACTA CHEMICA SCANDINAVICA 14 (1960) 2177–2190

Studies on the Coagulation of Chicken Blood

I. Factors which Limit Plasma Coagulation Rate during Vitamin K Deficiency and Treatment with Coumarin Drugs

ØYVIND SØRBYE* and INGER KRUSE

Department of Biochemistry and Nutrition, Polytechnic Institute, Copenhagen, Denmark

It is shown that the coagulation time of vitamin K-deficient and dicumarol or coumachlor plasmas is determined by the concentrations of three different types of factors ($\varkappa$-, δ- and φ-factors).

A method for assay of these factors is described. Coagulation tests with thromboplastin, RVV-cephalin or cephalin alone, are all sensitive to $\varkappa$- and δ-factors. The activity measured as φ-factor activity, in the three different coagulation systems, probably includes both system specific entities and entities, common to all three coagulation systems. The relation of these coagulation factors to well-established human coagulation factors is discussed.

In 1948 Dam and Søndergaard [1] observed that mixtures of plasmas from vitamin K-deficient and dicumarol-treated chickens had shorter thromboplastin coagulation times than either plasma alone. The existence of two coagulation factors, different from prothrombin, was assumed to account for the observation: one, which was especially low in vitamin K-deficient plasma, and another, which was especially low in dicumarol plasma. Prothrombin was assumed to be the third rate-limiting factor, lacking in both plasmas.

The factor in dicumarol plasma which accelerated the coagulation of vitamin K-deficient plasma was named δ (delta)-factor, and the factor in vitamin K-deficient plasma which accelerated the coagulation of dicumarol plasma was named $\varkappa$ (kappa)-factor by Sørbye *et al.*[2,3] The factors were concentrated from dicumarol plasma and vitamin K-deficient plasma, respectively.

A full account of the latter findings and recent progress in the study of coagulation factors, responsible for the phenomena described, is presented in this article. Since the first short communications [2,3] were published, our attention has been drawn to the new experimental possibilities offered by use of mixtures of vitamin K-deficient and anticoagulant drug plasmas as test substrates. It seems that this technique will permit more detailed studies of the

* Fellow of the Royal Norwegian Council for Scientific and Industrial Research.

coagulation entities in normal plasma, which are reduced below optimal levels during vitamin K deficiency and anticoagulant drug treatment. Great interest is attached to the possibility of correlating these coagulation entities with coagulation factors, known from studies of human blood. An established correlation between human and chicken coagulation factors will permit problems of human coagulation to be attacked through work on chicken coagulation factors, and *vice versa*.

MATERIALS AND METHODS

"*Normal plasma*". Blood was obtained from the carotid arteries or jugular veins of chickens, reared on a commercial diet [4] or on special diets (Table 1). The chickens were fasted not less than 4—5 h before blood samples were taken, to avoid turbidity in the centrifuged plasma. Nine parts of blood were drawn into one part of 0.15 M potassium oxalate or 0.10 M trisodium citrate and immediately centrifuged at 1 500 *g* for 20 min. After centrifugation the plasma could be poured off after immersion of the centrifuge tubes in ice-water for 5—10 min. It was completely clear and free from blood cells. In cases where the hematocrit value was abnormally low, the concentration of anticoagulant was adjusted to 18—21 mM oxalate or 12—14 mM citrate. Plasma was used fresh or after storage at —20°C.

Vitamin K-deficient plasma. Chickens were reared on a vitamin K-deficient diet [4] until they showed signs of subcutaneous hemorrhage. Blood was obtained as for "normal plasma". Deficiency in δ-factor was pronounced in plasmas with thromboplastin coagulation times more than 7—8 times the normal value.

Dicumarol plasma. Dicumarol was administered orally to chickens on the commercial diet as single dose (0.7—0.9 mg/g) 48—67 h before blood collection, or in two doses (0.7—0.8 and 0.3 mg/g) 50—58 and 24 h before blood collection. The plasmas obtained had thromboplastin coagulation times of 5—12 times the normal plasma value and showed pronounced κ-factor deficiency.

*Coumachlor * plasma.* Coumachlor was administered orally to chickens on the commercial diet in two doses, 44 and 20 h before blood collection. Usually 0.08 and 0.04 mg/g as first and second dose gave plasmas with thromboplastin times of 7—10 times the normal plasma value. Such plasmas had pronounced κ-factor deficiency. Coumachlor gave more uniform responses than dicumarol and was the preferred anticoagulant in the later part of this work. Coumachlor plasma has been shown to behave identically to dicumarol plasma in coagulation tests [5].

Thromboplastin. Chicken brains were carefully freed from blood and vessels and kept frozen in dry ice. For preparation they were dehydrated and ground with acetone and dried to a light powder in air at + 37°C or under vacuum. The powder was stored at —20°C. Of this powder, 0.15 g was triturated with 3 ml of veronal buffer for 30 min at + 37°C and centrifuged for 10 min at 900 *g* and + 2°C. The supernatant normally had optimal coagulation activity, when diluted with 4—5 ml veronal buffer.

Russel's viper venom (RVV). This product was obtained from the Wellcome Research Laboratories, Beckenham, England; it was dissolved in veronal buffer. Dilution 1:12 000 proved optimal in most cases.

Russel's viper venom-Ca (RVV-Ca). This reagent was prepared by dissolving RVV in 30 mM $CaCl_2$-solution (1:12 000).

$CaCl_2$. A stock solution of 100 mM $CaCl_2$ was prepared. This solution was diluted to optimal concentration (25—30 mM) before use.

Brain "cephalin". This phosphatide fraction was prepared from chicken brains, according to Milstone [6]. A 1 % suspension of "cephalin" in buffer was prepared and stored at —20°C. It was thawed and diluted to optimal concentration (0.06—0.09 %) before use.

Blood cell "cephalin". Packed chicken blood cells, separated by centrifugation of blood, were washed with 3 volumes of oxalated saline by suspension and centrifugation,

* 3-(α-*p*-Chlorphenyl-β-acetylethyl)-4-hydroxycoumarin, supplied by J. R. Geigy, Basle.

treated with 2—3 volumes of 96 % ethanol on a steam bath for one hour and filtered. To the filtrate was added 3 volumes of ether and 3 volumes of distilled water. The mixture was shaken and then allowed to stand for separation of the phases. The ether layer was evaporated to dryness with absolute alcohol under reduced pressure. The residue was washed twice with acetone and finally extracted with ether. The clear ether solution was evaporated, and the lipids were suspended in veronal buffer. The suspension was stored deep frozen. It was thawed and diluted to optimal concentration (0.008—0.06 %) before use.

Buffer. 550 ml of 0.1 M sodium barbiturate, 450 ml of 0.1 M HCl, and 5.8 g sodium chloride were mixed with 1 000 ml of 0.9 % sodium chloride. pH was 7.10—7.14. Usually a trace of potassium oxalate (0.009 %) was added.

Oxalated saline. 0.9 g sodium chloride and 0.009 g potassium oxalate in 1 000 ml distilled water.

Citrate-buffer. One part of 0.1 M trisodium citrate was mixed with seven parts of buffer. This solution had the same concentration of anticoagulant as citrate plasma.

Glassware. Thin-walled conical centrifuge glass tubes (15 ml) were used for coagulation time determinations. All glassware were rinsed in chromic-sulfuric acid, washed with tap water at least 10 times and with distilled water 3 times, finally with ethanol and dried at + 80°C.

Coagulation time determination. All reagents, except the trigger solution ($CaCl_2$ or RVV-Ca), were kept in ice-water during the experiment, mixed in desired proportions and placed in a water bath at + 37°C. Coagulation was started by blowing in prewarmed trigger solution with a syringe. Time for formation of a firm clot was noted by means of a stop watch. The glass was tilted slowly until 3—4 sec. before the expected coagulation time when a rapid, but yet cautious tilting began. With some experience and great accuracy it was possible to duplicate the coagulation times within 1/10 of a second for coagulation times up to 40—50 sec. and within half a second for coagulation times up to 2—3 min. A one-stage coagulation test was normally used:

Thromboplastin coagulation time (tpl.-time).

Coagulation system: 0.2 ml plasma or plasma mixture
0.2 ml thromboplastin solution
0—0.2 ml buffer or test solution
0.2 ml $CaCl_2$ (30 mM).

Thromboplastin time is known to depend on the concentration of prothrombin, proconvertin, Stuart factor and proaccelerin, and is said to be insensitive to variations in the levels of intrinsic factors *.

We have also made use of some modifications of this technique:

RVV-cephalin coagulation time (RVV-ceph.-time). Thromboplastin is replaced by cephalin, and $CaCl_2$ is replaced by RVV-Ca. The RVV-ceph.-time depends on the concentration of prothrombin, Stuart factor and proaccelerin, and is not influenced by the concentration of proconvertin or intrinsic factors.

Cephalin coagulation time (ceph.-time). Thromboplastin is replaced by cephalin. Ceph.-time is insensitive to the concentration of proconvertin, but depends on the concentration of intrinsic factors, Stuart factor, prothrombin and proaccelerin. On determination of ceph.-time, tilting of the glass was avoided. The glass was rotated instead. Time for formation of the first visible fibrin threads was noted.

Serum prothrombin activity.

Coagulation system: 0.2 ml serum or plasma
0.2 ml $SrCO_3$-adsorbed oxalated normal plasma
0.2 ml thromboplastin
0.2 ml $CaCl_2$ (50 mM).

A dilution curve was prepared with normal plasma. Dilutions were made with citrate-buffer. The prothrombin activities of serum, read from this curve, were not expected to

* The intrinsic factors include the antihemophilic factor-A, (AHF, factor VIII), antihemophilic factor-B (PTC, Christmas factor, factor IX), antihemophilic factor-C (PTA) and Hagemann factor.

be correct estimates of the prothrombin concentration, as the concentration of accessory factors (proconvertin, Stuart factor, *etc.*) relative to prothrombin generally is higher in serum than in plasma. However, the test is thought to give an idea of the extent of prothrombin consumption during coagulation.

Serum. Blood samples were collected without anticoagulant and allowed to clot at + 37°C. After 2 1/2—3 h the serum was separated and 1/6 volume of 0.1 M trisodium citrate was added. In this work the serum was examined shortly after citrate addition.

Adsorbed plasma. Plasma samples were stirred with the adsorbent for 15 min. at 0°C, centrifuged for 10 min at 1 500 *g* and + 2°C. The supernatant plasma was poured off and stored at 0°C until used.

Elution of adsorbed factors. The sedimented adsorbent, obtained in the procedure above, was first washed twice by stirring for 10 min. with oxalated saline at 0°C. The volume of washing fluid corresponded to the original volume of plasma. After centrifugation the supernatant was discarded. The adsorbed factors were eluted with citrate or phosphate buffers. The pH and molarity of the eluant will be indicated in the text (p. 000). Elution was done by stirring for 15 min. at 0°C, followed by centrifugation. The supernatant was dialyzed against distilled water, when the preparation subsequently was to be freeze-dried. When the preparation could be used immediately after dialysis, oxalated saline was used as dialysis fluid with buffer as the last change of outer phase.

Dialysis. Dialysis was carried out at + 1 — + 2°C for 40—44 h with 5—6 changes of outer phase.

EXPERIMENTS AND RESULTS

Coagulation times for mixtures of different sets of vitamin K-deficient and dicumarol plasmas are seen in Fig. 1 (A, B, C). It is apparent that replacement of small amounts of one plasma by the other causes some acceleration of the coagulation. This indicates the presence of relatively large amounts of a factor in vitamin K-deficient plasma, which is reduced below its optimal level in dicumarol plasma (*x*-factor), and relatively large amounts of a factor

Table 1. Composition of special diets.

F—6		F—7		F—8	
Ground barley	170	Ground barley	170	Ground barley	170
Ground oats	50	Ground oats	60	Ground oats	60
Wheat bran	55	Wheat bran	50	Wheat bran	50
Ground corn	70	Ground corn	90	Ground corn	100
Corn oil	50	Corn oil	25	Corn oil	20
Dried skimmed milk	50	Dried skimmed milk	55	Dried skimmed milk	65
Pancreas powder [1]	140	Pancreas powder [1]	130	Pancreas powder [1]	100
Casein [2]	220	Casein [2]	225	Casein [2]	240
Dried alfalfa	40	Dried alfalfa	40	Dried alfalfa	40
Salt mixture [1]	50	Salt mixture [1]	50	Salt mixture [1]	50
Vitamin mixture [3]	105	Vitamin mixture [3]	105	Vitamin mixture [3]	105
	1 000		1 000		1 000
Vitamins A and D[1]		Vitamins A and D[1]		Vitamins A and D[1]	

[1] As described by Dam and Søndergaard [4].

[2] From A/S Dansk Mejeri Industri & Export Kompagni, Stege, Møn, Denmark.

[3] This mixture contained: Thiamine hydrochloride, 6 mg; riboflavin, 8 mg; nicotinic acid, 100 mg; calcium pantothenate, 24 mg; pyridoxine, 7 mg; biotin, 0.2 mg; folic acid, 4 mg; choline chloride, 2 000 mg; inositol, 1 000 mg; *p*-aminobenzoic acid, 300 mg; DL-α-tocopheryl acetate (Ephynal, Roche), 100 mg; bicalcium 2-methyl-1,4-naphthoquinone biphosphate (Synkavit, Roche), 10 mg; mixed with sugar to make 105 g.

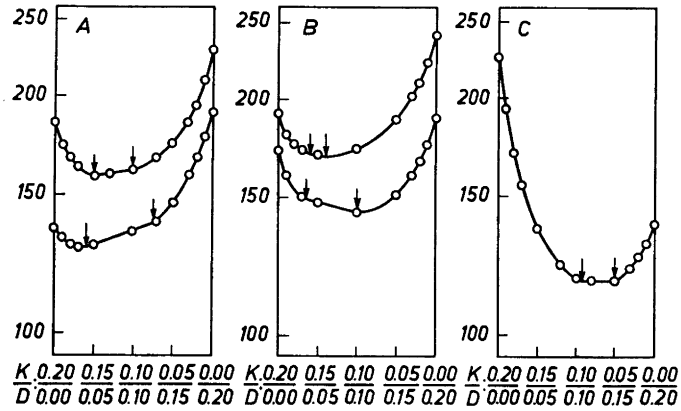

Fig. 1. (*A, B, C*). Coagulation times for plasma mixtures with thromboplastin and 0.2 ml buffer: K, vitamin K-deficient plasma; D, dicumarol plasma; Abscissæ, plasma mixtures in ml; Ordinates, coagulation time in min./100.

in dicumarol plasma, which is below its optimal concentration in vitamin K-deficient plasma (δ-factor). It should be especially noticed, that with increasing concentration of the other plasma in the mixtures a point is reached where the concentration of the factor, supplied by the other plasma, appears to become optimal. These points are indicated by arrows. In the range between the two points the curve appears to be straight-lined when drawn on semi-logarithmic paper.

If the interpretation given above is correct, then plasma mixtures within this range will contain $\varkappa$-factor and δ-factor in optimal amounts. The coagulation time will then depend on the concentration of factors — other than $\varkappa$-factor and δ-factor — which are depressed below optimal levels both in vitamin K-deficient and in dicumarol plasma. In previous reports [1–3] this "common deficiency" has been assumed to be a deficiency in prothrombin. We now prefer to call it a deficiency in φ (phi)-factor(s) until a proper identification with a known coagulation entity becomes possible.

Mixtures of different sets of dicumarol plasmas show no similar depression of the coagulation times (Fig. 2 A), indicating deficiencies in the same rate-limiting factors. The same is true for mixtures of two different vitamin K-deficient plasmas (Fig. 2 B).

These experiments confirm the original observations by Dam and Søndergaard [1].

On treatment of oxalated plasma with $BaCO_3$, all factors, able to shorten the coagulation time of vitamin K-deficient or dicumarol plasma, were removed from normal, vitamin K-deficient and dicumarol plasmas (Fig. 2 C).

It was thus evident that the $\varkappa$, δ- and φ-factors can be adsorbed from oxalated plasma by typical prothrombin adsorbers, such as $BaCO_3$ and $SrCO_3$.

Attempts were made to prepare concentrates of $\varkappa$- and δ-factor from oxalated vitamin K-deficient and dicumarol plasma, respectively, by treatment with

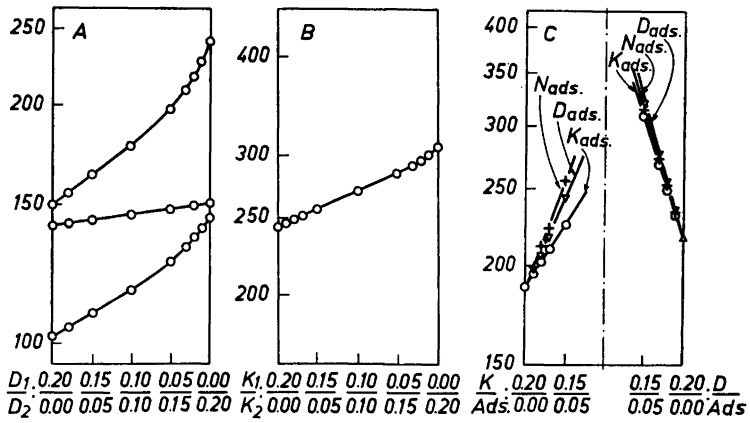

Fig. 2. (*A*, *B*, *C*). Coagulation time for plasma mixtures with thromboplastin and 0.2 ml buffer. *2 A:* D_1 and D_2, dicumarol plasmas; *2 B:* K_1 and K_2, vitamin K-deficient plasmas; *2 C:* K, vitamin K-deficient plasma; D, dicumarol plasma; N, normal plasma; Ads., $BaCO_3$-adsorbed plasma; Abscissæ, plasma mixtures in ml; Ordinates, coagulation time in min./100.

1 % $BaCO_3$, elution twice with 1/3 volume of 0.1 M sodium citrate followed by dialysis and lyophilization. The preparations were redissolved in buffer. Details of the various preparations used in this work are given in Table 2.

The effect of addition of the concentrates of $\varkappa$-factor and δ-factor on the coagulation time of mixtures of vitamin K-deficient and dicumarol plasmas is seen in Figs. 3 and 4.

Figs. 3 A and 4 A show the effect of addition of increasing amounts of δ-concentrates. Coagulation of the plasma mixtures was accelerated only in mixtures with high percentages of vitamin K-deficient plasma. There was no effect on mixtures with high percentages of dicumarol plasma. This proved that the latter mixtures already contained the added factor in optimal concentration. The range for optimal $\varkappa$- and δ-factor concentration (to be referred to

Table 2. Details of $\varkappa$- and δ-factor preparations.

Preparation	Original material			Final volume
	Volume	Plasma	tpl.-time min./100	
$\varkappa$-216	9 ml	vit. K-deficient	275	3 ml
$\varkappa$-420	13 »	vit. K-deficient	300	2 »
$\varkappa$-391	11 »	vit. K-deficient	310	2 »
$\varkappa$-611	10 »	vit. K-deficient	255	2 »
$\varkappa$-615	12 »	vit. K-deficient	435	3 »
δ-436	8 »	dicumarol	360	3 »
δ-427	20 »	dicumarol	470	6 »
δ-228	18 »	dicumarol	375	6 »

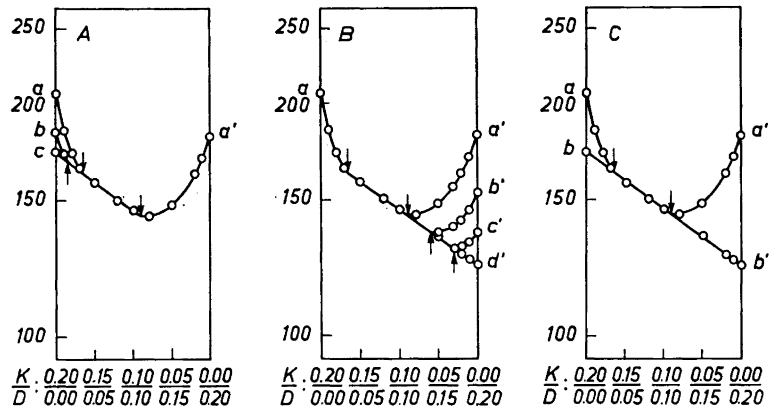

Fig. 3. (*A, B, C*). Coagulation time for plasma mixtures with thromboplastin. Effect of test solutions. Curves a—a', 0.20 ml buffer; *3 A:* Curve b—a', 0.05 ml δ-436 and 0.15 ml buffer; Curve c—a', 0.10 ml δ-436 and 0.10 ml buffer; *3 B:* Curve a—b', 0.10 ml ϰ-216 and 0.10 ml buffer; Curve a—c', 0.20 ml ϰ-216; Curve a—d', 0.10 ml ϰ-420 and 0.10 ml buffer; *3 C:* Curve b—b', 0.10 ml ϰ-420 and 0.10 ml δ-436; K, vitamin K-deficient plasma; D, dicumarol plasma; Abscissæ, plasma mixtures in ml; Ordinates, coagulation time in min./100.

as the optimal range) was extended to the left only, proportionally to the amount of δ-factor added. Full correction of the δ-factor deficiency for all mixtures occurred with 0.1 ml of preparation δ-436 (Fig. 3 A) and with 0.1

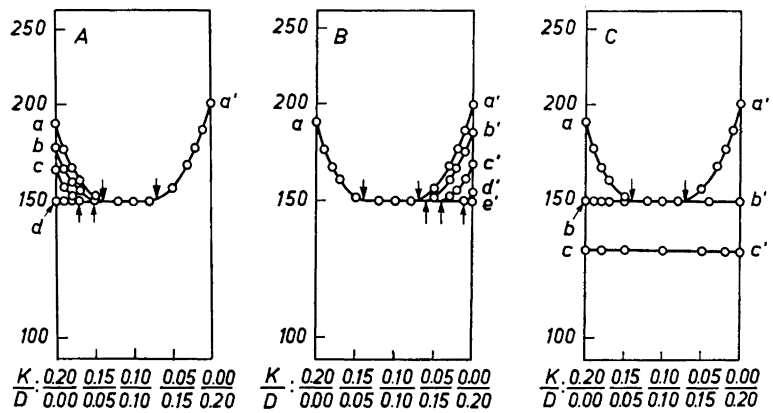

Fig. 4 (*A, B, C*). Coagulation time for plasma mixtures with thromboplastin. Effect of test solutions. Curves a—a': 0.20 ml buffer; *4 A*: Curve b—a', 0.02 ml δ-427 and 0.18 ml buffer; Curve c—a', 0.05 ml δ-427 and 0.15 ml buffer; Curve d—a', 0.10 ml δ-427 and 0.10 ml buffer. *4 B:* Curve a—b', 0.03 ml ϰ-615 and 0.17 ml buffer; Curve a—c', 0.10 ml ϰ-615 and 0.10 ml buffer; Curve a—d', 0.20 ml ϰ-615; Curve a—e', 0.10 ml ϰ-391 and 0.10 ml buffer; *4 C:* Curve b—b', 0.10 ml ϰ-391 and 0.10 ml δ-427; Curve c—c', 0.10 ml ϰ-611 and 0.10 ml δ-228; K, vitamin K-deficient plasma; D, dicumarol plasma; Abscissæ, plasma mixtures in ml; Ordinates, coagulation time in min./100.

ml of preparation δ-427 (Fig. 4 A). No $\varkappa$- or φ-factor activity could thus be demonstrated in these preparations.

Figs. 3 B and 4 B show the effect of addition of increasing amounts of $\varkappa$-concentrates. Coagulation time of the plasma mixtures was shortened only in mixtures with high percentages of dicumarol plasma. The lack of effect on mixtures with high percentages of vitamin K-deficient plasma proved that these mixtures already contained the added factor in optimal amounts. The optimal range was extended to the right only, proportionally to the amount of $\varkappa$-factor added. Full correction of the $\varkappa$-factor deficiency for all mixtures occurred with 0.1 ml of preparation $\varkappa$-420 (Fig. 3 B) and with 0.1 m l of prparation $\varkappa$-391 (Fig. 4 B). No measurable δ- or φ-factor activity was thus present in these preparations.

In Figs. 3 C and 4 C it is seen that simultaneous addition of sufficient amounts of $\varkappa$- and δ-factors completely wiped out every indication of deficiencies in these factors. The coagulation times were shortened only in mixtures with high percentages of either vitamin K-deficient or dicumarol plasma.

The coagulation times for mixtures within the optimal range were not affected. The curves were completely straightened out to give the expected picture of the coagulation time for mixtures of two plasmas with a slight difference in (Fig. 3 C) or identical amounts (Fig. 4 C) of the same rate-limiting factors.

In the lower curve of Fig. 4 C the $\varkappa$- and δ-factor deficiencies had also been corrected, but the entire curve was shifted to slightly shorter coagulation times, indicating the presence of small amounts of φ-factor in the preparations $\varkappa$-611, or δ-228, or both.

The present experiments very strongly support the original interpretation [1] of the "anomalous" coagulation time observed for mixtures of vitamin K-deficient and dicumarol plasmas. They also justify the more detailed interpretation given here (pp. 2080—2081). Furthermore it is evident that the effect of test solutions on the coagulation time of such mixtures can be used to distinguish sharply between $\varkappa$-, δ- and φ- factor type of activities.

Method for the assay of $\varkappa$-, δ- and φ-factors

The results above suggested the possibility that mixtures of vitamin K-deficient and 'dicumarol (or coumachlor) plasmas might be used as test substrates for individual determinations of $\varkappa$-, δ- and φ-factor levels in plasma. It could be expected that addition of a constant, small amount of plasma to all mixtures would shorten their coagulation times, thereby: 1) extending their optimal range to the left, proportionally to the amount of δ-factor, 2) extending their optimal range to the right, proportionally to the amount of $\varkappa$-factor, and 3) shifting the entire curve to shorter coagulation times, depending on the amount of φ-factor(s), in the plasma added.

These expectations were fully met, as seen in Figs. 5 A and 5 B. Strict proportionality was observed between the amount of added plasma and the extension of the optimal range to either side. Fig. 5 A shows the effect of addition of varying amounts of a plasma (N_1), which appeared to have a relatively high δ- and low $\varkappa$-factor level. The plasma was therefore used to

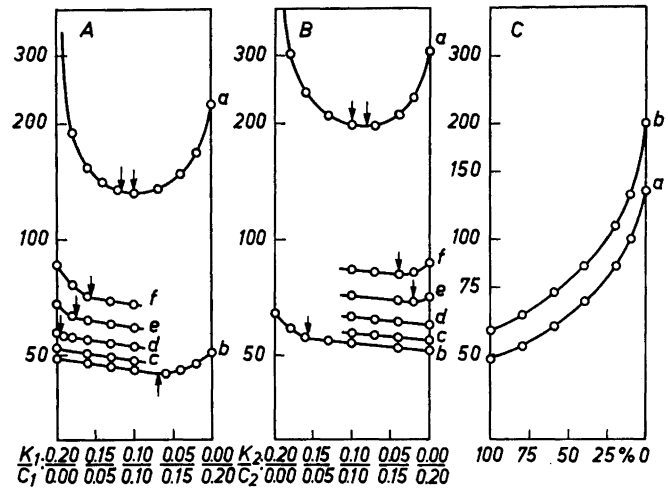

Fig. 5 (*A*, *B*). Coagulation time for plasma mixtures with thromboplastin. Effect of normal plasma.

5 A (*5 B*) Curves a, K_1/C_1 (K_2/C_2) and 0.010 ml buffer.
» b, » » » 0.012 » plasma N_1 (N_2).
» c, » » » 0.010 » »
» d, » » » 0.008 » and 0.002 ml buffer.
» e, » » » 0.006 » » » 0.004 » »
» f, » » » 0.004 » » » 0.006 » »

K_1 and K_2; vitamin K-deficient plasmas; C_1 and C_2, coumachlor plasmas; N_1 and N_2 normal plasmas; Abscissæ, plasma mixtures in ml; Ordinates, coagulation time in min./100.

Fig. 5 C. Dilution curves for φ-factor activity. Diluted normal (N) plasma (0.01 ml) added to a mixture of 0.10 ml vitamin K-deficient (K) and 0.10 ml coumachlor (C) plasma. Curve a, with N_1, K_1 and C_1; Curve b, with N_2, K_2 and C_2; Abscissa, concentration of normal plasma; Ordinate, coagulation time in min./100.

study the relation between amount of added plasma and extension of the optimal range to the left (δ-effect). The plasma, used in Fig. 5 B (N_2), appeared to have a high $\varkappa$- and a relatively low δ-factor level. It was therefore used to bring out the relation between amount of added plasma and extension of the optimal range to the right ($\varkappa$-effect).

The technique makes it possible to compare the $\varkappa$- and δ-factor levels of different plasmas by comparing the extension of the optimal range to either side, which occurs on addition of a constant, small amount of plasma to mixtures of vitamin K-deficient and anticoagulant drug plasmas.

Comparison of the φ-factor levels of different plasmas is also possible from the results of this type of experiments. Estimation of φ-factor(s) alone is, however, most easily done with a substrate of vitamin K-deficient and anticoagulant drug plasmas in proportion 1:1. Such mixtures normally contain optimal amounts of both $\varkappa$- and δ-factors, and the observed coagulation time depends only on the concentration of φ-factor(s). Fig. 5 C shows the rela-

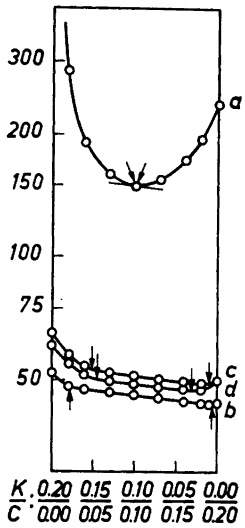

Fig. 6. Coagulation time for plasma mixtures with thromboplastin. Effect of different plasmas. Curve a, 0.010 ml buffer; Curve b, 0.010 ml plasma F-6; Curve c, 0.009 ml plasma F-7 and 0.001 ml buffer; Curve d, 0.010 ml plasma F-8; K, vitamin K-deficient plasma; C, coumachlor plasma; Abscissa, plasma mixtures in ml; Ordinate, coagulation time in min./100.

tion between concentration of added normal plasma (φ-factor(s)) and observed coagulation time with this special mixture of substrate plasmas. The normal plasma and substrate plasmas were the same as those used in Figs. 5 A and 5 B.

Fig. 6 shows the results of an assay of $\varkappa$-, δ- and φ-factor levels in plasmas from 3 different chickens. The chickens were given slightly different diets (Table 1). This experiment may serve as an example of evaluation of the $\varkappa$-, δ- and φ-factor activities of different plasmas. Optimal ranges were read

Table 3. $\varkappa$-, δ- and φ-factor levels in plasma.

Added to substrates		Optimal range $\left(\frac{K}{C}\right)$	Extension of the optimal range		Activity of factors		
Volume (v) ml	Material		to the left(d)	to the right(k)	$\delta\left(\frac{d}{v}\right)$	$\varkappa\left(\frac{k}{v}\right)$	φ*, %
0.010	buffer	$\frac{0.100}{0.100} - \frac{0.100}{0.100}$					
0.010	plasma F-6	$\frac{0.175}{0.025} - \frac{0.005}{0.195}$	0.075	0.095	7 1/2	9 1/2	100
0.009	plasma F-7	$\frac{0.150}{0.050} - \frac{0.010}{0.190}$	0.050	0.090	5 1/2	10	80
0.010	plasma F-8	$\frac{0.145}{0.055} - \frac{0.030}{0.170}$	0.045	0.070	4 1/2	7	84

* Read from a φ-factor dilution curve made with F-6 plasma.

from Fig. 6, and φ-factor activities of the other two plasmas were read from a dilution curve (similar to the curves of Fig. 5 C) made with F-6 plasma. The results are given in Table 3.

The variations in the activities of $\varkappa$-, δ- and φ-factors, observed in this experiment, suggest that the concentration of the factors may vary to some extent with the diet. Thus it seems possible that the formation of $\varkappa$-, δ- and φ-factors depends on dietary factors other than vitamin K. This is, however, an entirely new type of problem, which will receive further treatment in later publications.

Substitution of other Procoagulants for Thromboplastin

In all experiments reported so far, coagulation of the plasma mixtures was accelerated by addition of optimal amounts of chicken brain thromboplastin. It was therefore of interest to see if the deficiency symptoms, observed with thromboplastin as procoagulant, also could be observed in other coagulation systems, where thromboplastin was replaced by RVV-cephalin or by cephalin alone.

The results of two different experiments are seen in Figs. 7 (A, B, C). With all procoagulants the same type of curves was obtained. In all coagulation

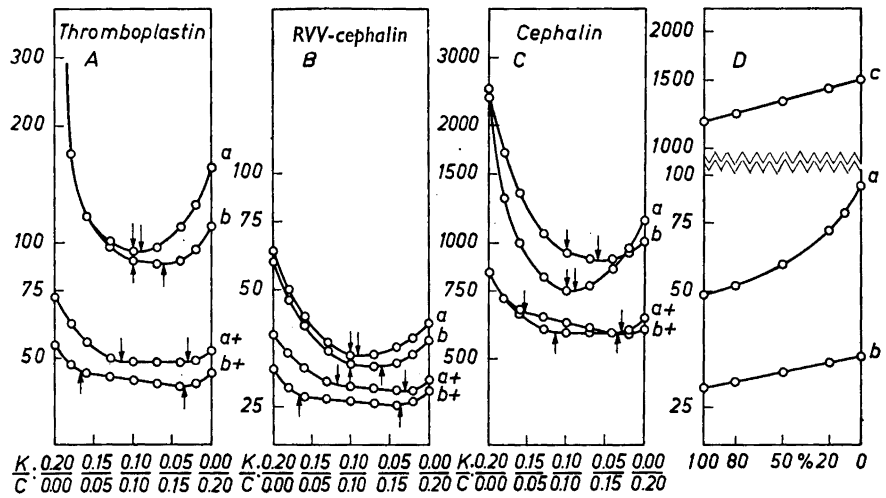

Fig. 7 (A, B, C). Coagulation time for plasma mixtures with thromboplastin (7 A), RVV-cephalin (7 B) and cephalin (7 C). Effect of normal plasma. Curves a, with K_1, C_1 and 0.01 ml buffer; Curves a+, with K_1, C_1 and 0.01 ml plasma N_1; Curves b, with K_2, C_2 and 0.01 ml buffer; Curves b+, with K_2, C_2 and 0.01 ml plasma N_2; K_1 and K_2, vitamin K deficient plasmas; C_1 and C_2, coumachlor plasmas; N_1 and N_2, normal plasmas; Abscissæ, plasma mixtures in ml; Ordinates, coagulation time in min./100.

Fig. 7 D. Dilution curves for φ-factor activity. Diluted normal (N) plasma (0.01 ml) added to a mixture of 0.10 ml vitamin K-deficient (K) and 0.10 ml coumachlor (C) plasma. Curve a, with thromboplastin; Curve b, with RVV-cephalin; Curve c, with cephalin; Abscissa, concentration of normal plasma; Ordinate, coagulation time in min./100.

systems both vitamin K-deficient plasma and coumachlor plasma seemed to contain relatively large amounts of a factor which was reduced below optimal levels in the other plasma. The range, where these factors appeared to be optimal, was, for each set of plasma mixtures, the same in all three coagulation systems (curves a and b). Furthermore, when an assay of the concentration of these factors in normal plasma was performed, according to the method suggested, identical results were obtained with the three different coagulation accelerators (curves a+ and b+).

Thus, it is apparent that $\varkappa$- and δ-factors are important in all three coagulation systems.

It is, however, not immediately clear, whether the activity, measured as φ-factor(s) in the three different coagulation systems, is due to the same factor(s), or if different entities are measured.

The dilution curves for φ-factor(s) appeared to be straight lines with RVV-cephalin and with cephalin, when plotted on semi-logarithmic paper, whereas the curve with thromboplastin was definitely curved (Fig. 7 D).

These findings suggest that the activity, referred to as φ-factor activity, may include one or more factors which are specific for the thromboplastin system. The possibility that the cephalin system may be sensitive to a φ-factor, which is without effect in the two other systems, must also be taken into consideration. The exact number of different entities, measured as φ-factors in the different coagulation systems, is thus still an unsolved problem.

Behavior of $\varkappa$- and δ-factor during coagulation

Comparison of plasma and its corresponding serum, obtained by spontaneous coagulation of blood at + 37°C, showed regularly that δ-factor disappeared during coagulation. The activity of $\varkappa$-factor was, on the contrary, increased. A typical experiment is summarized in Table 4.

The disappearance of δ-factor and activation of $\varkappa$-factor during spontaneous coagulation of blood at + 37°C was measured in all three coagulation systems. Identical results were obtained.

DISCUSSION

The experiments reported demonstrate that the "anomalous" coagulation times, observed for mixtures of vitamin K-deficient and anticoagulant drug plasmas, has been correctly interpreted. Particularly illustrating is the effect

Table 4. Behavior of $\varkappa$- and δ-factors during coagulation.

Activity of	Prothrombin %	δ-factor %	$\varkappa$-factor %
Plasma	100	100	100
Serum	25	0	172

of addition of concentrates, prepared from vitamin K-deficient and anticoagulant drug plasmas, on the coagulation time of such mixtures. The experiments prove that the accelerated coagulation, observed for mixtures of vitamin K-deficient and anticoagulant drug plasmas, is due to great differences in the concentrations of two factors ($\varkappa$- and δ-factors) in these plasmas. However, the prolonged coagulation time of vitamin K-deficient and anticoagulant drug plasmas cannot be completely accounted for by the reduced concentrations of these two factors alone. Three different types of coagulation factors ($\varkappa$-, δ- and φ-factors) are responsible for the prolonged coagulation time of plasma during severe vitamin K-deficiency and after short-time treatment with coumarin drugs.

It is evident that the proposed assay method, based on mixtures of vitamin K-deficient and anticoagulant drug plasmas as substrates, can only be sensitive to the concentration of factors which have been reduced *below optimal levels* in the substrate mixtures. The assay method can therefore not be expected to be sensitive to *all* coagulation factors, affected by vitamin K deficiency and coumarin drug treatment. The reduction of some of the affected factors may not be so extensive that their concentrations drop below optimal levels.

The method should, however, be of value for studies of the factors in normal plasma which are most highly affected by vitamin K deficiency and coumarin drug treatment.

The adsorbability, vitamin K dependence and anticoagulant drug sensitivity of $\varkappa$-, δ- and φ-factors exclude their identity with Hageman factor, PTA, AHF or proaccelerin.

It even seems impossible to identify $\varkappa$- or δ-factor with any of the adsorbable coagulation factors known from studies of human blood. As $\varkappa$-factor and δ-factor are important for the coagulation mechanisms, initiated by addition of thromboplastin, RVV-cephalin and cephalin, neither can be identified with proconvertin or PTC. (RVV-ceph.-time and ceph.-time are not proconvertin sensitive, and tpl.-time and RVV-ceph.-time are insensitive to PTC.) They cannot be identical to prothrombin, as no δ- and increased $\varkappa$-factor activity is found in fresh serum where the prothrombin activity is 25 % of that of plasma.

The possibility discussed by Dam and Søndergaard [7] that differences in ratio of prothrombin to proconvertin might account for the coagulation times of vitamin K-deficient plasma, anticoagulant drug plasma and mixtures of the two, has thus not been supported by the present experiments.

An identification of δ-factor with Stuart factor seems impossible, since this coagulation factor usually is found in serum with unchanged [8] or increased [9] activity. The rate and extent of decrease reported for Stuart factor during anticoagulant drug treatment [9,10], does not conform with the great sensitivity of $\varkappa$-factor to anticoagulant drugs.

Theoretically, it remains a possibility that proconvertin might be registered as a thromboplastin-specific φ-factor, that PTC might behave as a cephalin-specific φ-factor, and that Stuart factor and prothrombin could be measured as φ-factors, common to all three coagulation systems. All these factors are reduced during vitamin K deficiency and coumarin drug treatment, but we do not know if the reduction is so extensive and so rapid that they become

rate-limiting coagulation factors under the conditions described. Further experimentation is necessary to establish the nature and exact number of the different entities in normal plasma, that are measured as φ-factors in the three coagulation systems.

A better knowledge of, and control over, the $\varkappa$-, δ- and φ-factors should be of value for anticoagulant drug therapy, as they seem to control the coagulation rate of plasma during vitamin K deficiency and after treatment with coumarin drugs.

REFERENCES

1. Dam, H. and Søndergaard, E. *Biochim. et Biophys. Acta* **2** (1948) 409.
2. Sørbye, Ø., Kruse, I and Dam, H *Acta Chem Scand* **4** (1950) 549.
3 Sørbye, Ø., Kruse, I. and Dam, H. *Acta Chem. Scand.* **4** (1950) 831.
4. Dam, H. and Søndergaard, E. *Acta Pharmacol. Toxicol.* **9** (1953) 131.
5. Dam, H. and Søndergaard, E. *Acta Pharmacol. Toxicol.* **9** (1953) 137.
6. Milstone, J. H. *Yale J. Biol. and Med.* **22** (1950) 675.
7. Dam, H. and Søndergaard, E. *Acta Physiol. Scand.* **31** (1954) 376.
8. Johnston, Jr., C. L., Ferguson, J. H., O'Hanlon, F. A. and Black, W. L. *Thromb. et Diath. Haemorrhag.* **3** (1959) 367.
9. Bierstedt, P. *Z. ges. inn. Med. u. ihre Grenzgebiete.* **14** (1959) 16.
10. Koller, F. *Thromb. et Diath. Haemorrhag.* **2** (1958) 407.

Received July 22, 1960.

ACTA CHEMICA SCANDINAVICA 14 (1960) 2191–2195

Complex Dibenzofurans

II *. Synthesis of 2,2′,3′,2″-Dioxido-*p*-terphenyl

NILS E. STJERNSTRÖM

Organisk-kemiska Institutionen, Kungl. Tekniska Högskolan, Stockholm, Sweden

In a search for a convenient synthetic route to dioxidoterphenyls, Ebel's dibenzofuran synthesis was investigated. 2,2′,3′,2″-Dioxido-*p*-terphenyl (II) was obtained in good yield starting from the sodium salt of 4-hydroxydibenzofuran which reacted with 2-bromo*cyclo*hexanone to give the expected keto-ether. This was cyclised with polyphosphoric acid and the product dehydrogenated with palladium.

The dihydroxy-dioxidoterphenyl obtained by the action of strong sulphuric acid on *p*-benzoquinone has recently been related to similar polymerisation products from monoalkyl-*p*-benzoquinones [1]. These products have for obvious reasons been considered to be derivatives of *o*-terphenyl (Ia) [2] and the structure Ib has consequently been suggested for the phenolic terphenyl derivative from *p*-benzoquinone.

On zinc dust distillation the above *p*-benzoquinone polymerisation product gave a dioxidoterphenyl which accordingly should possess structure Ic. Other structures are of course theoretically possible and an unambigous synthesis of compound Ic is therefore a matter of interest.

Of the five theoretically possible dioxidoterphenyls, only two have been prepared by reliable methods, namely 2,2′, 5′,2″-dioxido-*p*-terphenyl [1,3,4] and 2,6′,4′,2″-dioxido-*m*-terphenyl [5]. During attempts to find convenient methods for the preparation of dioxidoterphenyls 2,2′,3′,2″-dioxido-*p*-terphenyl (II) has now been obtained.

Most of the methods of preparing dibenzofurans appear to be suitable for the synthesis of dioxidoterphenyls. The Pschorr synthesis (for a recent review see Ref.[6]) and the procedure of Ebel [7] seemed to be especially suitable since the starting material would already contain a dibenzofuran nucleus.

The possibility of using the Pschorr synthesis was investigated first. It was found impossible to prepare the intermediate ether from the sodium salt

* Part I. *Acta Chem. Scand.* **14** (1960) 1274.

of 4-hydroxydibenzofuran and 2-bromonitrobenzene under sufficiently mild conditions (employing solvents as nitrobenzene, mono- and diglyme), since it was intended later to introduce a blocking bromine group in the dibenzofuran moiety. Blocking groups such as this have been used previously in the synthesis of phenanthrene derivatives in order to affect the direction of ring closure [2].

Ebel's dibenzofuran synthesis has recently been used in this laboratory for the preparation of 2,2′,5′,2″-dioxido-*p*-terphenyl from hydroquinone and 2-bromo*cyclo*hexanone [1].

The disodium salt of catechol reacted with 2-chloro*cyclo*hexanone to give a compound $C_{12}H_{14}O_3$. The infrared spectrum of this substance indicated the presence of a hydroxyl group, a benzene nucleus carrying four adjacent hydrogen atoms and methylene and aryl ether groups. The compound was therefore assumed to be 1,2,3,4-tetrahydro-4a-hydroxydibenzo-*p*-dioxin (III) and this was shown to be correct. Conversion of compound III by treatment with phosphorus oxychloride in pyridine yielded 1,2,3,4-tetrahydrodibenzo-*p*-dioxin (IV) (the position of the double bond in the hydroaromatic ring is slightly uncertain), which was dehydrogenated to dibenzo-*p*-dioxin (V). This was shown to be identical with an authentic specimen [8].

A successful synthesis of compound II was achieved as follows. 4-Hydroxy-6,7,8,9-tetrahydrodibenzofuran (VI) was easily prepared from the known methyl ether [7] by demethylation with hydrobromic acid. Its sodium salt reacted with 2-bromo*cyclo*hexanone to give 4-(2-keto*cyclo*hexyloxy)-6,7,8,9-tetrahydrodibenzofuran (VII). This substance was cyclised with polyphosphoric acid to give what must be 3,4,5,6,3″,4″,5″,6″-octahydro-2,2′,3′,2′-dioxido-*p*-terphenyl (VIII), which was then dehydrogenated to 2,2′,3′,2″-dioxido-*p*-terphenyl (II). This substance was not identical with the dioxidoterphenyl Ic.

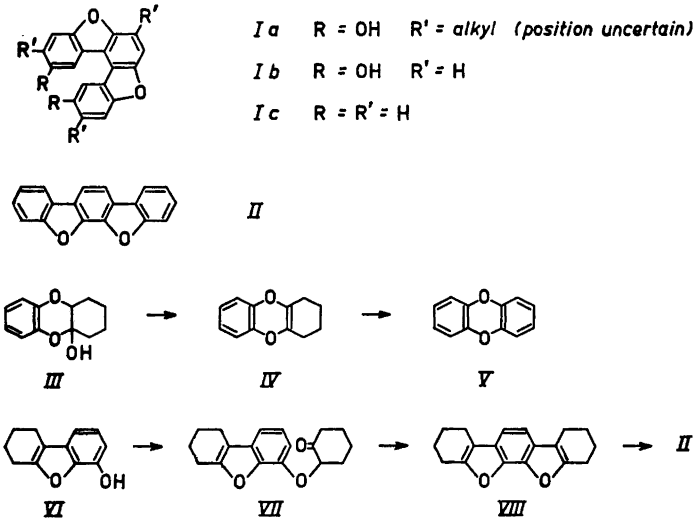

A more convenient route to compound II started with the easily available 4-hydroxydibenzofuran [9], the sodium salt of which reacted with 2-bromo*cyclo*hexanone to give 4-(2-keto*cyclo*hexyloxy)-dibenzofuran (VII, left hand ring also aromatic) in a good yield. This keto-ether was cyclised to 3,4,5,6-tetrahydro-2,2',3',2''-dioxido-*p*-terphenyl (VIII, two rings aromatic). The position of the double bond in the hydroaromatic ring of these compounds (VIII, tetrahydro- and octahydro-) is almost certainly that indicated in formula VIII (*cf.* Ebel [7]). The tetrahydro-compound on dehydrogenation with palladium furnished 2,2',3',2''-dioxido-*p*-terphenyl (II).

This method seems to be of general applicability for the synthesis of dioxidoterphenyls and experiments aiming at the synthesis of compound Ic are now in progress.

EXPERIMENTAL

All melting points are uncorrected

1,2,3,4-Tetrahydro-4a-hydroxydibenzo-p-*dioxin (III).* Sodium (2.3 g) was dissolved in absolute ethanol (40 ml) and a solution of cathechol (5.5 g) in absolute ethanol (20 ml) was added with stirring under a stream of dry oxygen-free nitrogen. The alcohol was evaporated under reduced pressure, care being taken to avoid oxidation. The dry catechol sodium salt, 2-chloro*cyclo*hexanone [10] (14.0 g) and dry toluene (100 ml) were stirred and heated under reflux in an atmosphere of nitrogen for 3 h. The reaction mixture was allowed to cool to room temperature and was extracted with sodium hydroxide solution (10 %). The toluene layer was washed with water and saturated sodium chloride solution and then dried over magnesium sulphate. After evaporation of the toluene, the residue, a yellow oil, was thoroughly triturated with boiling light petroleum (400 ml). The petroleum extract was cooled to −40°, precipitating a greasy oil (crop A). The mother liquor was evaporated to a smaller volume (25 ml) and a crystalline material (crop B, 1.1 g) deposited. Crop B was purified by recrystallisation from *n*-pentane and sublimation *in vacuo* (90°, 20 mm), m.p. 104−105°. (Found: C 70.1; H 6.7; mol. wt. (Rast) 192. Calc. for $C_{12}H_{14}O_3$: C 69.9; H 6.8; mol. wt. 206.)

The infrared spectrum of compound III (KBr) was recorded on a Perkin-Elmer No 21 instrument using a sodium chloride prism. Relevant absorption maxima: 3 400 cm^{-1} (s), 3 000 cm^{-1} (w), 2 900 cm^{-1} (m,s), 1 600 cm^{-1} (m), 1 500 cm^{-1} (vs), 1 455 cm^{-1} (m) and 740 cm^{-1} (vs).

Crop A did not crystallise. Chromotography on neutral alumina yielded only a small amount of compound III, eluted with benzene. The desired product 1,2-di-(2-keto*cyclo*hexyloxy)-benzene could not be traced.

1,2,3,4-Tetrahydrodibenzo-p-*dioxin (IV).* 1,2,3,4-Tetrahydro-4a-hydroxydibenzo-*p*-dioxin (300 mg) was dissolved in dry pyridine (4 ml) and freshly distilled phosphorus oxychloride (1 ml) was cautiously added under stirring and cooling under the water tap. The mixture was stirred for three days at room temperature and was then poured into ice-water. The ether extract was washed with dilute hydrochloric acid and water. After drying over magnesium sulphate the solvent was evaporated and the somewhat oily reaction product (225 mg) was collected. The substance was purified by recrystallisation from absolute methanol and sublimation *in vacuo*, m.p. 61−62.5°. (Found: C 76.4; H 6.5. Calc. for $C_{12}H_{12}O_2$: C 76.6; H 6.4.)

Dibenzo-p-*dioxin (V).* Compound IV (40 mg) was thoroughly mixed with a palladium-charcoal catalyst (10 % Pd, 30 mg) and the mixture was heated to 230° for 5 h in an atmosphere of nitrogen. The reaction product was extracted with hot ethanol (15 ml). After evaporation of the alcohol, the residue (28 mg) was purified by sublimation *in vacuo* and recrystallisation from ethanol (0.5 ml). Yield of pure compound 4 mg, m.p. 117−120.5°. A mixed melting point with a sample of dibenzo-*p*-dioxin prepared according to Gilman [8] (m.p. 120.5−121.5°) showed no depression (m.p. 118−121°). The infrared spectra of the two samples were identical.

4-Hydroxy-6,7,8,9-tetrahydrodibenzofuran (VI). The starting material, 4-methoxy-6,7,8,9-tetrahydrodibenzofuran, was prepared according to Ebel [7] by cyclisation of 1-

methoxy-2-(2-keto*cyclo*hexyloxy)-benzene. The use of polyphosphoric acid as condensing agent instead of sulphuric acid as recommended by Ebel, did not increase the yield. The methyl ether (9 g) was stirred and heated under reflux with constant boiling hydrobromic acid (150 ml) for 12 h in an atmosphere of nitrogen. The reaction mixture was diluted with water (300 ml) and the crude product (8.2 g, violet due to superficial oxidation) was collected, thoroughly washed with water and dried. The substance was recrystallised from *cyclo*hexane and sublimed *in vacuo*. Yield 5.8 g, m.p. 117—118°. (Found: C 77.1; H 6.6. Calc. for $C_{18}H_{18}O_2$: C 76.6; H 6.4.)

*4-(2-Keto*cyclo*hexyloxy)-6,7,8,9-tetrahydrodibenzofuran (VII).* Sodium (0.7 g) was dissolved in absolute methanol (20 ml) and compound VI (5.6 g) in absolute methanol (20 ml) was added, care being taken to exclude moisture and air. The methanol was removed under reduced pressure and 2-bromo*cyclo*hexanone [11] (5.3 g) in dry benzene (125 ml) was added with mechanical stirring. The mixture was stirred at room temperature for 0.5 h and at reflux temperature for further 2 h; it was then extracted with dilute sodium hydroxide and water. The benzene solution was dried over magnesium sulphate and the solvent was evaporated under reduced pressure. The remaining brown oil (6.4 g) was chromatographed on neutral alumina. The fractions eluted with benzene-light petroleum mixtures were collected (3.0 g) and made to crystallise by scratching. The substance was purified by recrystallisation from ligroin and distillation *in vacuo*, m.p. 85—87°. (Found: C 75.9; H 7.0. Calc. for $C_{18}H_{20}O_2$: C 76.0; H 7.1.)

*3,4,5,6,3'',4'',5'',6''-Octahydro-2,2',3',2''-dioxido-*p*-terphenyl (VIII).* Compound VII (1.0 g) was stirred with a mixture of phosphorus pentoxide (15 g) and phosphoric acid (*d* 1.7, 30 ml) for 2 h at 100°. The hot reaction mixture was poured into water. The precipitate was collected, washed and dried. The yield almost quantitative. The product was recrystallised from *cyclo*hexane and sublimed *in vacuo*, m.p. 163—164°. (Found: C 81.6; H 6.8. Calc. for $C_{18}H_{18}O_2$: C 81.2; H 6.8.)

*2,2',3',2''-Dioxido-*p*-terphenyl (II) from compound VIII.* Compound VIII (50 mg) was mixed with a palladium-charcoal catalyst (10 % Pd, 50 mg) and the mixture was heated to 230° for 5 h in an atmosphere of nitrogen. The reaction product (30 mg) that sublimed on the cool parts of the reaction vessel was recrystallised from *cyclo*hexane. Two crystalline forms were observed (long needles which gradually changed to leaflets at ~ 179°), m.p. 180—183°. A mixed melting point with a sample of 2,2',3',2''-dioxido-*p*-terphenyl, synthesised as described below, showed no depression (m.p. 179—182°). The infrared spectra of the two samples were identical.

*4-(2-Keto*cyclo*hexyloxy)-dibenzofuran.* The sodium salt of 4-hydroxydibenzofuran [9] (prepared as described above from 1.2 g sodium and 9.2 g phenol), freshly distilled 2-bromo*cyclo*hexanone (9.0 g) and dry benzene (100 ml) were stirred at room temperature for 18 h and heated under reflux for additional 2 h. The reaction mixture was treated with dilute sodium hydroxide and the benzene extract was thoroughly washed with water and saturated sodium chloride solution and then dried over magnesium sulphate. After evaporation of the solvent the reaction product, colourless crystals (11.7 g), was recrystallised from ethanol and sublimed *in vacuo*, m.p. 142—142.5°. (Found: C 77.1; H 5.7. Calc. for $C_{18}H_{16}O_3$: C 77.1; H 5.8.)

*3,4,5,6-Tetrahydro-2,2',3',2''-dioxido-*p*-terphenyl.* The preceding substance (1.0 g) was stirred with a mixture of phosphorus pentoxide (10 g) and phosphoric acid (*d* 1.7, 20 ml) at 100° for 3 h. The reaction mixture was poured into water (250 ml) and the crystalline precipitate was collected, washed with water and dried. The substance (0.8 g) was recrystallised from *n*-butanol and sublimed *in vacuo*, m.p. 149—150°. (Found: C 82.7; H 5.4. Calc. for $C_{18}H_{14}O_2$: C 82.4; H 5.4.)

*2,2',3',2''-Dioxido-*p*-terphenyl (II).* The tetrahydrocompound (300 mg) was thoroughly mixed with a palladium-charcoal catalyst (10 % Pd, 200 mg) and heated to 230° for 5 h in an atmosphere of nitrogen. The reaction mixture was extracted with boiling *cyclo*hexane. The dioxido-*p*-terphenyl (200 mg) crystallised on cooling. Two crystal forms were observed, needles m.p. 178—179° which changed to leaflets m.p. 183—184°. The substance was purified for analysis by sublimation *in vacuo*. (Found: C 84.2; H 3.9. Calc. for $C_{18}H_{10}O_2$: C 83.7; H 3.9.)

The author is thankful to Dr. Brian Thomas for checking the manuscript.

REFERENCES

1. Erdtman, H. and Stjernström, N. E. *Acta Chem. Scand.* **13** (1959) 653.
2. Erdtman, H. *Proc. Roy. Soc. London* **A 143** (1933) 228.
3. Schimmelschmidt, K. *Ann.* **566** (1950) 184.
4. Stjernström, N. E. *Acta Chem. Scand.* **14** (1960) 1274.
5. Stjernström, N. E. *Acta Chem. Scand. To be published.*
6. DeTar, D. F. *Org. Reactions* **9** (1957) 409.
7. Ebel, F. *Helv. Chim. Acta* **12** (1929) 3.
8. Gilman, H. and Stuckwisch, C. G. *J. Am. Chem. Soc.* **65** (1943) 1461.
9. Gilman, H., Cheney, L. C. and Willis, H. B. *J. Am. Chem. Soc.* **61** (1939) 951.
10. *Org. Syntheses Coll. Vol.* **3**, p. 188.
11. Allinger, J. and Allinger, N. L. *Tetrahedron* **2** (1958) 64.

Received July 13, 1960.

ACTA CHEMICA SCANDINAVICA 14 (1960) 2196–2215

The Crystal Structure of Hg_2O_2NaI Studied by X-Ray and Neutron Diffraction Methods

KARIN AURIVILLIUS

Institute of Inorganic and Physical Chemistry, University of Stockholm, Stockholm, Sweden; Joint Establishment for Nuclear Energy Research, Kjeller, Norway

The crystal structure of Hg_2O_2NaI has been studied by X-ray (single crystal) and neutron (powder) diffraction methods. The crystals are hexagonal (space group $P6_322$ ($P6_422$)) with the cell edges a = 6.667 Å and c = 10.054 Å. The unit cell contains three formula units. The mercury and oxygen atoms form infinite planar chains, -Hg-O-Hg-O-, lying perpendicularly to the c axis of the unit cell. The Hg-O distance is 2.03 Å and the angles O-Hg-O and Hg-O-Hg are 180° and 110°, respectively.

As earlier reported [1,2], the structures of the orthorhombic and hexagonal modifications of mercury(II)oxide are built up of infinite chains -O-Hg-O- which, in the orthorhombic modification, are of planar zig-zag type and, in the hexagonal modification, of spiral type. Every mercury atom is thus coordinated to two oxygen atoms and every oxygen atom to two mercury atoms. The aim of the present investigation was to find whether such chains -O-Hg-O- are fundamental constituents of other mercury(II)salts containing oxygen and whether this arrangement is independent of the other kinds of atoms occurring in the structure.

PREPARATION AND ANALYSIS

In connection with the preparation of the hexagonal modification of mercury(II)oxide, the complex compound Hg_2O_2NaI, earlier reported by Laruelle [3], was synthesized. The best way for preparing Hg_2O_2NaI is to mix one part of a cold solution of 0.1 M K_2HgI_4 containing an excess of KI with two parts of 10 M NaOH at about 0°C and to keep the solution at this temperature for about 100 h. The temperature was then slowly increased to room temperature and the substance obtained, which consisted of beautiful yellow pencil-shaped crystals, was then filtered off. Another way of preparing this compound is to heat equivalent quantities of mercury(II)oxide and sodium

iodide in a fused glass tube to 130°C for about 100 h. This method, however, did not give a pure sample.

Attempts were made to replace the sodium atoms in the compound with lithium, potassium, rubidium and caesium. However, these efforts have not yet been successful.

The compound Hg_2O_2NaI decomposes into orthorhombic HgO and NaI when heated in open air to higher temperatures. Thus, a powder diagram of the residue, after the substance had been heated to 200°C for 14 days, did not show any lines characteristic for Hg_2O_2NaI.

The compound is not stable if treated with water – it decomposes into other, not yet identified, phases. Upon exposure to light, the yellow crystals of the substance become dark green. To investigate this phenomenon more closely, a sample of Hg_2O_2NaI was exposed to U.V. light for a long time. X-Ray diagrams of the green substance showed only lines characteristic for Hg_2O_2NaI. A microscopic examination revealed, however, the presence of small drops of mercury.

The pure sample was analysed for Hg, Na, K, I and H_2O and was found to contain neither potassium nor water. The mercury analysis was performed using electrolysis [4], the sodium and potassium analyses flame spectrophotometrically using a Beckman D.U. spectrophotometer [5] and the iodine analysis by iodometric titration [6] after the sample had been brought into solution by melting with sodium hydroxide in a gold crucible. The water analysis was performed according to Penfield [7]. The results of the analyses are in fair agreement with the values calculated for Hg_2O_2NaI (Found %: Hg 67.9; Na 3.8; I 20.9. Calc. Hg 68.8; Na 3.9; I 21.8).

CELL DIMENSIONS AND SYMMETRY

The powder photographs were taken in a Guinier focusing camera of 80 mm diameter using Cu$K\alpha_1$ radiation and potassium chloride ($a = 6.2930$ Å[8]) as an internal standard. The powder pattern is given in Table 1. Heavily exposed photographs did not show any lines that were not visible in normally exposed ones. The powder pattern could be interpreted by means of a hexagonal unit cell with the following cell dimensions:

$$a = 6.667 \text{ Å} \qquad c = 10.054 \text{ Å} \qquad V = 387.0 \text{ Å}^3$$

The observed density, 7.0 gcm^{-3}, indicates a cell content of three formula units Hg_2O_2NaI (calculated density 7.5 gcm^{-3}). For the single crystal photographs, CuK and MoK radiations were used. Rotation diagrams were taken around the a and c axes and Weissenberg photographs were used to register the reflexions $h0l$-$h3l$ and $hk0$-$hk5$.

Since $|F(hk0)|^2$ was found throughout to be equal to $|F(hk3)|^2$, $|(F(hk1)|^2$ equal to $|F(hk4)|^2$ and $|F(hk2)|^2$ equal to $|F(hk5)|^2$ within the limits of experimental error, the heavy atoms of the structure must be situated at the planes normal to the c axis of the unit cell at the z values 0 and $\pm\frac{1}{3}$ or $\frac{1}{2}$ and $\pm\frac{1}{6}$. The coefficients

$$\sum_{l=-\infty}^{l=+\infty} |F(hkl)|^2$$

were thus approximated by the expressions

Table 1. Powder diagram (Guinier focusing camera) and powder diffractogram (Geiger Mueller diffractometer) of Hg_2O_2NaI. I_{calc} is normalized so as to give the best agreement with I_{obs}.

h k l	$10^4\sin^2\Theta_{obs}$ Guinier	$10^4\sin^2\Theta_{calc}$	I_{obs} Guinier	I^*_{calc} Guinier	I_{obs} Diffr.	I^{**}_{calc} Diffr.
1 0 0	178	178	st	540	218	236
1 0 1	237	237	m	165	52	59
1 0 2	413	413	w	105	35	31
0 0 3	529	528	vst	1072	376	415
1 1 0	534	534	m	276		
1 1 1	—	593	—	11	—	0
1 0 3	707	706	m	518	909	824
2 0 0	713	712	vst	2009		
1 1 2	769	769	vvw	8	—	3
2 0 1	—	771	—	0		
2 0 2	—	947	—	0	—	0
1 1 3	1062	1062	m	360	149	112
1 0 4	—	1117	—	26	—	8
2 0 3	1240	1240	vst	1587	569	530
2 1 0	1245	1246	m	158		
2 1 1	1304	1305	w	47	—	14
1 1 4	—	1473	—	5	—	13
2 1 2	1480	1481	w	41		
3 0 0	1601	1602	w	65	20	18
1 0 5	1648	1645	vw	17	—	6
2 0 4		1651		0		
3 0 1	—	1660	—	5		
2 1 3	1774	1774	st	346	100	93
3 0 2	—	1837	—	5	—	1
1 1 5	—	2001	—	4	—	1
0 0 6	2112	2113	m	196		
3 0 3	—	2130	—	147	258	227
2 2 0	2136	2136	m	553		
2 0 5	—	2179	—	0		
2 1 4	—	2185	—	25	—	6
2 2 1	—	2194	—	0		
1 0 6	2291	2291	w	63	34	32
3 1 0	2313	2314	w	64		
2 2 2	2370	2370	vvw	0	—	0
3 1 1		2372		20		
3 0 4	2544	2541	vvw	3	—	1
3 1 2		2548		20		
1 1 6	—	2647	—	71	188	178
2 2 3	2663	2664	st	748		
2 1 5	—	2713	—	19	—	4
2 0 6	2825	2825	st	759	275	269
3 1 3	—	2842	—	196		
4 0 0	2847	2848	st	426		
4 0 1	—	2906	—	0		
1 0 7	—	3054	—	8		
3 0 5	—	3069	—	3	—	—
2 2 4	—	3075	—	0		
4 0 2	—	3082	—	0		
3 1 4	—	3253	—	16	—	3
2 1 6	—	3359	—	109		
4 0 3	3377	3376	st	575	120	125
3 2 0	—	3381	—	45		

$h\,k\,l$	$10^4\sin^2\Theta_{obs}$ Guinier	$10^4\sin^2\Theta_{calc}$	I_{obs} Guinier	I^*_{calc} Guinier	I_{obs} Diffr.	I^{**}_{calc} Diffr.
1 1 7	—	3410	—	3	—	3
3 2 1	—	3440	—	14		
2 0 7	—	3588	—	0	—	2
2 2 5	—	3603	—	0		
3 2 2	—	3616	—	14	—	18
3 0 6	3713	3715	vvw	61		
4 1 0	3737	3737	vvw	60		
3 1 5	—	3781	—	16	—	3
4 0 4	—	3787	—	0		
4 1 1	—	3796	—	7		
3 2 3	3911	3910	m⁻	160	8	24
1 0 8	—	3935	—	8		
4 1 2	—	3972	—	7		
2 1 7	—	4122	—	19	—	—
2 2 6	4249	4249	st	844	89	116
4 1 3	4268	4266	m	215		
1 1 8	—	4291	—	4		
4 0 5	—	4315	—	0	—	2
3 2 4	—	4321	—	16		
3 1 6	4426	4427	w	119	—	12

$$I^*_{calc} = 10^{-4}p\varphi(\Theta)F^2; \quad \varphi(\Theta) = \frac{1 + \cos 2\alpha\cos^2 2\Theta}{\sin\Theta(1 + \cos 2\alpha)\cos^2(2\Theta - \beta)\sin 2\Theta} \qquad (cf.\ \text{Ref. 9}).$$

$$I^{**}_{calc} = 10^{-4}p\,\frac{1 + \cos^2\Theta}{\sin^2\Theta\cos\Theta}\,F^2$$

$$|F(hk0)|^2 + |F(hk3)|^2 + |F(hk1)|^2 + |F(hk4)|^2 + |F(hk2)|^2 + |F(hk5)|^2.$$

The Laue symmetry found from the Weissenberg photographs was $6/mmm$. In the powder and Weissenberg photographs, the following spectra were systematically missing: $h = 0$, $k = 0$, $l \neq 3n$ and h, k even, $l \neq 3n$ (n is an integer). This is characteristic for the enantiomorphous space groups [10] $P6_222$ (No. 180) and $P6_422$ (No. 181). Possible space groups are: $P6/mmm$ (No. 191), $P\bar{6}2m$ (No. 189), $P\bar{6}m2$ (No. 187), $P6mm$ (No. 183) and $P622$ (No. 177).

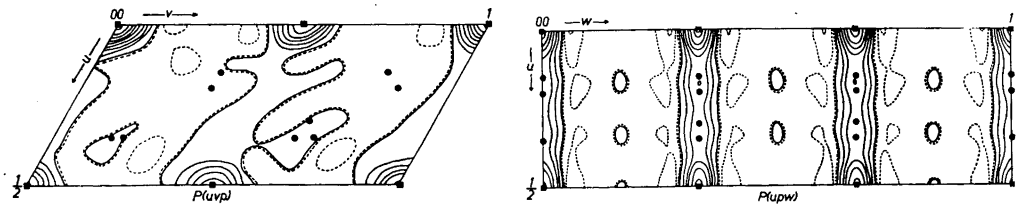

Fig. 1. The Patterson functions $P(uvp)$ and $P(upw)$. The vectors Hg—Hg (□), Hg-I (△) and Hg-O (●) for the final structure are indicated. Dashed lines indicate negative values.

THE POSITIONS OF THE MERCURY ATOMS

To locate the heavy metal atoms in the unit cell, the Patterson projections $P(uvp)$ and $P(upw)$ (Fig. 1) were calculated using F^2 values derived from the visually estimated intensities of the Weissenberg photographs.

Now in space group $P6_622$ (No. 180) and analogously for the enantiomorphous space group $P6_422$ (No. 181), it is possible for the six mercury atoms to occupy one of the sixfold point positions 6(j), 6(i), 6(h), 6(g), 6(f) and 6(e) or a combination of two threefold point positions 3(d), 3(c), 3(b) and 3(a). Since it is not possible to distinguish between the two characteristic space groups, one of them, *viz.* $P6_222$, is chosen arbitrarily.

$P6_222$:

6(j):	$\pm(x, 2x), \frac{1}{2}$;	$\pm(2x, x), \frac{1}{6}$	;	$\pm(x, \bar{x}), \frac{5}{6}$
6(i):	$\pm(x, 2x), 0$;	$\pm(2x, x), \frac{2}{3}$	;	$\pm(x, \bar{x}), \frac{1}{3}$
6(h):	$\pm x, 0, \frac{1}{2}$;	$0, \pm x, \frac{1}{6}$	;	$\pm(x, x), \frac{5}{6}$
6(g):	$\pm x, 0, 0$;	$0, \pm x, \frac{2}{3}$	;	$\pm(x, x), \frac{1}{3}$
6(f):	$\frac{1}{2}, 0, \pm z$;	$0, \frac{1}{2}, \frac{2}{3} \pm z$	;	$\frac{1}{2}, \frac{1}{2}, \frac{1}{3} \pm z$
6(e):	$0, 0, \pm z$;	$0, 0, \frac{1}{3} \pm z$	;	$0, 0, \frac{2}{3} \pm z$
3(d):	$\frac{1}{2}, 0, \frac{1}{2}$;	$0, \frac{1}{2}, \frac{1}{6}$	;	$\frac{1}{2}, \frac{1}{2}, \frac{5}{6}$
3(c):	$\frac{1}{2}, 0, 0$;	$0, \frac{1}{2}, \frac{2}{3}$	;	$\frac{1}{2}, \frac{1}{2}, \frac{1}{3}$
3(b):	$0, 0, \frac{1}{2}$;	$0, 0, \frac{5}{6}$	;	$0, 0, \frac{1}{6}$
3(a):	$0, 0, 0$;	$0, 0, \frac{1}{3}$	;	$0, 0, \frac{2}{3}$

The possible combinations of the threefold point positions are:

3(a) + 3(b); 3(a) + 3(c); 3(a) + 3(d); 3(b) + 3(c); 3(b) + 3(d) and 3(c) + 3(d).

On displacing the origin of the unit cell by $\frac{c}{2}$, however, the point position 6(j) becomes identical to 6(i), 6(h) to 6(g), 3(a) + 3(b) to 3(c) + 3(d), 3(a) + 3(c) to 3(b) + 3(d) and 3(a) + 3(d) to 3(b) + 3(c).

The Hg-Hg vectors u, v, w, required by these possibilities are given in Table 2. This table should be compared with Fig. 1.

The major maxima of the two Patterson projections should be mainly due to mercury-mercury vectors. The point positions 6(e) and 3(a) + 3(d) cannot explain the high maxima at $u = \frac{1}{2}$, $v = 0$; $u = 0$, $v = \frac{1}{2}$ and $u = \frac{1}{2}$, $v = \frac{1}{2}$ in $P(uvp)$ and can thus be excluded. Since there do not exist any heavy maxima at $u = \frac{1}{2}$, $v = \frac{1}{6}$ or $u = 0$, $v = \frac{1}{6}$ in $P(uvp)$, the combination 3(a) + 3(b) can also be ruled out. Nor was it possible to find an x parameter for the vectors u, v, w, of the point positions 6(j) and 6(h) which could satisfy the Patterson projections $P(uvp)$ and $P(upw)$. Thus the remaining possibilities for the positions of the six mercury atoms in $P6_222$ (No. 180) are: 6(f) with $z = 0.333$ or 3(a) + 3(c). By calculating the values of the structure factors $|F_{hkl}| = \sqrt{A^2 + B^2}$ for the two geometrically different arrangements of the six mercury atoms, it was found that they gave the same values. Thus, by evaluating the Patterson projections $P(uvp)$ and $P(upw)$ above, a homometric pair of arrangements for the mercury atoms was found. These two homometric mercury atom positions gave rise to six possible point positions for the three iodine atoms. The Patterson projections $P(uvp)$ and $P(upw)$ were then examined for these different possibilities.

Table 2. Required vectors Hg-Hg in the Patterson functions.

	u	v	w	Relative weight
6(*j*):	$\pm(3x, 3x)$		$\pm\frac{1}{3}$	4
	$\pm(x, \bar{x})$		$\pm\frac{1}{3}$	4
	0	$\pm 3x$	$\pm\frac{1}{3}$	4
	$\pm 3x$	0	$\pm\frac{1}{3}$	4
	$\pm(2x, x)$		$\pm\frac{1}{3}$	4
	$\pm(x, 2x)$		$\pm\frac{1}{3}$	4
	$\pm(4x, 2x)$		0	2
	$\pm(2x, 4x)$		0	2
	$\pm(2x, 2\bar{x})$		0	2
6(*h*):	$\pm(x, \bar{x})$		$\pm\frac{1}{3}$	4
	$\pm(x, x)$		$\pm\frac{1}{3}$	4
	$\pm(x, 2x)$		$\pm\frac{1}{3}$	4
	$\pm(2x, x)$		$\pm\frac{1}{3}$	4
	0	$\pm x$	$\pm\frac{1}{3}$	4
	$\pm x$	0	$\pm\frac{1}{3}$	4
	$\pm 2x$	0	0	2
	0	$\pm 2x$	0	2
	$\pm(2x, 2x)$		0	2
6(*f*):	$\frac{1}{2}$	0	$\pm\frac{1}{3}$	4
	0	$\frac{1}{2}$	$\pm\frac{1}{3}$	4
	$\frac{1}{2}$	$\frac{1}{2}$	$\pm\frac{1}{3}$	4
	0	0	$\pm 2z$	6
	$\frac{1}{2}$	0	$\pm(2z\pm\frac{1}{3})$	4
	0	$\frac{1}{2}$	$\pm(2z\pm\frac{1}{3})$	4
	$\frac{1}{2}$	$\frac{1}{2}$	$\pm 2(z\pm\frac{1}{3})$	4
6(*e*):	0	0	$\pm\frac{1}{3}$	12
	0	0	$\pm 2z$	6
	0	0	$\pm(2z\pm\frac{1}{3})$	8
	0	0	$\pm(2z\pm\frac{2}{3})$	4
3(*a*) + 3(*b*):	$\frac{1}{2}$	0	$\pm\frac{1}{6}$	4
	$\frac{1}{2}$	0	$\pm\frac{1}{3}$	4
	0	$\frac{1}{2}$	$\pm\frac{1}{6}$	4
	0	$\frac{1}{2}$	$\pm\frac{1}{3}$	4
	$\frac{1}{2}$	$\frac{1}{2}$	$\pm\frac{1}{6}$	4
	$\frac{1}{2}$	$\frac{1}{2}$	$\pm\frac{1}{3}$	4
3(*a*) + 3(*c*):	0	0	$\pm\frac{1}{3}$	6
	$\frac{1}{2}$	0	$\pm\frac{1}{3}$	6
	0	$\frac{1}{2}$	$\pm\frac{1}{3}$	6
	$\frac{1}{2}$	$\frac{1}{2}$	$\pm\frac{1}{3}$	6
	$\frac{1}{2}$	0	0	2
	0	$\frac{1}{2}$	0	2
	$\frac{1}{2}$	$\frac{1}{2}$	0	2
3(*a*) + 3(*d*):	0	0	$\pm\frac{1}{6}$	12
	0	0	$\pm\frac{1}{3}$	12
	0	0	$\frac{1}{2}$	6

Thus, if the mercury atoms occupy the combination of threefold point positions 3(*a*) and 3(*c*), the only possible point positions left for the three iodine atoms are 3(*b*) and 3(*d*) since a statistical distribution over a sixfold point

Table 3. Required and observed vectors Hg-Hg and Hg-I in the Patterson projection $P(upw)$. The structure possibility: 6 Hg in 3(*a*) + 3(*c*). The calculated relative weights of the maxima due to the Hg-Hg and Hg-I vectors were calculated using the expression $\nu \sum_{k,l} f_k f_l$ where ν denotes the frequence of the vector and f_k, f_l the scattering factors of the atoms.

u	w	Vectors Hg-Hg 6 Hg in 3(*a*) + 3(*c*)	Vectors Hg-I 3 I in 3(*b*)	Vectors Hg-I 3 I in 3(*d*)	calc. I	calc. II	obs.
0	$\frac{1}{6}$		4	2	75	37	$\overline{200}$
0	$\frac{1}{3}$	6			178	178	400
0	$\frac{1}{2}$		4	4	75	75	$\overline{200}$
$\frac{1}{2}$	0	2			59	59	310
$\frac{1}{2}$	$\frac{1}{6}$		2	4	37	75	20
$\frac{1}{2}$	$\frac{1}{3}$	6			178	178	310
$\frac{1}{2}$	$\frac{1}{2}$		2	2	37	37	0

position is very improbable. Now, in Table 3, there are listed the required vectors mercury-mercury and mercury-iodine (u, w) for the combinations:

6 Hg in 3(*a*) + 3(*c*), 3 I in 3(*b*) (I)
6 Hg in 3(*a*) + 3(*c*), 3 I in 3(*d*) (II)

From the calculated and observed heights of the maxima in this table, it is clearly seen that the possibilities I and II are inconsistent with the experimental data.

The arrangements I and II seem to be impossible also from space considerations. Case I gives a very short distance Hg-I of only 1.7 Å and case II offers 3 (*b*) as the only possible position for the three sodium atoms which results in the very short distance Hg-Na of 1.7 Å.

However, if the mercury atoms occupy the point position 6(*f*), then a point position for the iodine atoms can be found. This is explained in the following section.

The contribution of the iodine atoms to the X-ray intensities is relatively large and thus the observed Laue symmetry 6/*mmm* must be valid also for the iodine atoms. Attempts have been made to find a mercury arrangement equivalent to 3(*a*) + 3(*c*) in $P6_222$ and to derive possible iodine arrangements, satisfying the observed heights of the maxima of the Patterson projection $P(upw)$, in the possible space groups $P6/mmm$ (No. 191), $P\bar{6}2m$ (No. 189), $P\bar{6}m2$ (No. 187), $P6mm$ (No. 183) and $P622$ (No. 177). The results of these calculations were in no case satisfactory.

Thus, X-ray data were alone sufficient to make a decision between the two homometric mercury atom positions. The only possibility was, namely, the point position 6(*f*) in $P6_222$ (No. 180).

Table 4. Required vectors Hg-I in the Patterson functions. 6 Hg in 6(*f*) + 3 I in 3(*a*), 3(*b*), 3(*c*) or 3(*d*).

	u	*v*	*w*	Relative weight
6(*f*), 3(*a*):	0	$\frac{1}{2}$	0	2
	0	$\frac{1}{2}$	$\pm\frac{1}{3}$	4
	$\frac{1}{2}$	0	0	2
	$\frac{1}{2}$	0	$\pm\frac{1}{3}$	4
	$\frac{1}{2}$	$\frac{1}{2}$	0	2
	$\frac{1}{2}$	$\frac{1}{2}$	$\pm\frac{1}{3}$	4
6(*f*), 3(*b*):	0	$\frac{1}{2}$	$\pm\frac{1}{6}$	4
	0	$\frac{1}{2}$	$\frac{1}{2}$	2
	$\frac{1}{2}$	0	$\pm\frac{1}{6}$	4
	$\frac{1}{2}$	0	$\frac{1}{2}$	2
	$\frac{1}{2}$	$\frac{1}{2}$	$\pm\frac{1}{6}$	4
	$\frac{1}{2}$	$\frac{1}{2}$	$\frac{1}{2}$	2
6(*f*), 3(*c*):	0	0	$\pm\frac{1}{3}$	6
	0	$\frac{1}{2}$	0	2
	0	$\frac{1}{2}$	$\pm\frac{1}{3}$	2
	$\frac{1}{2}$	0	0	2
	$\frac{1}{2}$	0	$\pm\frac{1}{3}$	2
	$\frac{1}{2}$	$\frac{1}{2}$	0	2
	$\frac{1}{2}$	$\frac{1}{2}$	$\pm\frac{1}{3}$	2
6(*f*), 3(*d*):	0	0	$\pm\frac{1}{6}$	6
	0	$\frac{1}{2}$	$\pm\frac{1}{6}$	2
	0	$\frac{1}{2}$	$\frac{1}{2}$	2
	$\frac{1}{2}$	0	$\pm\frac{1}{6}$	2
	$\frac{1}{2}$	0	$\frac{1}{2}$	2
	$\frac{1}{2}$	$\frac{1}{2}$	$\pm\frac{1}{6}$	2
	$\frac{1}{2}$	$\frac{1}{2}$	$\frac{1}{2}$	2

THE POSITIONS OF THE IODINE ATOMS

Since the six mercury atoms occupy the point position 6(*f*) with $z = 0.333$, it is thus possible for the three iodine atoms to occupy one of the threefold point positions 3(*a*), 3(*b*), 3(*c*) or 3(*d*). The required mercury-iodine vectors *u*, *v*, *w* for the four different cases are listed in Table 4. From the Patterson projection $P(upw)$ (Fig. 1), it is seen that it is impossible for the relatively heavy iodine atoms to occupy one of the threefold point positions 3(*b*) or 3(*d*) because the projection does not show any maxima at $u = 0$, $w = \pm\frac{1}{6}$ or $u = 0$, $w = \frac{1}{2}$. On the other hand it is seen that the expected vectors Hg-I for the remaining possibilities for the iodine atoms 3(*a*) and 3(*c*) correspond to the calculated projection. However, the maximum of the projection $P(upw)$ at $u = 0$, $w = \frac{1}{3}$ is about 30 % higher than that at $u = \frac{1}{2}$, $w = \frac{1}{3}$. This can only be explained if the iodine atoms are situated in the point position 3(*c*) (Table 5).

To confirm that 3(*c*) is the actual point position for the iodine atoms, three-dimensional electron density calculations were performed using 860 reflexions (not independent) obtained with Cu*K* radiation. Theoretically, the Fourier projection $\varrho(xyp)$ should differentiate between the possibilities 3(*a*) and

Table 5. Required and observed vectors Hg-Hg and Hg-I in the Patterson projection $P(upw)$. The structure possibility: 6 Hg in 6(*f*). The calculations were performed as in Table 3.

u w	Vectors Hg-Hg 6 Hg in 6(*f*)	Vectors Hg-I 3 I in 3(*a*)	Vectors Hg-I 3 I in 3(*c*)	Rel. weight calc. 3(*a*), 6(*f*)	Rel. weight calc. 3(*c*), 6(*f*).	Rel. weight obs.
0 $\frac{1}{3}$	6	2	4	332	395	400
$\frac{1}{2}$ 0	4	4	4	298	298	310
$\frac{1}{2}$ $\frac{1}{3}$	6	4	2	395	332	310

3(*c*) but, as it is based on only a few reflexions, its exactness is much less than that of the sections of the three-dimensional electron density space. Hence, the electron density sections $\varrho(xyz)$ at $z = 0$, $\frac{1}{6}$, $\frac{1}{3}$, $\frac{1}{2}$ and $\frac{2}{3}$ were computed. The calculations were at first based on F values derived in the usual way from the visually estimated intensities of the reflexions and on the signs and values of the phase angles $\alpha_{hkl} = \text{arctg}\,(\frac{B}{A})_{hkl}$ determined from the mercury contributions for all reflexions except 54 of the weakest.

The sections show high maxima at $0\frac{1}{2}0$, $\frac{1}{2}\frac{1}{2}0$, $\frac{1}{2}0\frac{1}{3}$, $0\frac{1}{2}\frac{1}{3}$, $\frac{1}{2}0\frac{2}{3}$ and $\frac{1}{2}\frac{1}{2}\frac{2}{3}$ which is espected for mercury atoms occupying the point position 6(*f*) that was assumed when calculating the values of the phase angles. Moreover, maxima with a height correct for an iodine atom appear at $\frac{1}{2}00$, $\frac{1}{2}\frac{1}{2}\frac{1}{3}$ and and $0\frac{1}{2}\frac{2}{3}$, indicating that the iodine atoms are situated in the point position 3(*c*). Apart from these maxima, there are only small maxima in the sections $\varrho(xy0)$, $\varrho(xy\frac{1}{3})$ and $\varrho(xy\frac{2}{3})$ and they can be ascribed to diffraction effects from the mercury and iodine atoms and to sodium and oxygen atoms. The sections $\varrho(xy\frac{1}{6})$ and $\varrho(xy\frac{1}{2})$ show small peaks at $x = 0$, $y = 0$ (Fig. 2). Otherwise, these sections do not show any peaks with a height differing from the general background by more than that expected for diffraction effects from the heavy atoms. Using calculated F values (the contributions of the mercury atoms only being taken into account) and the same phase angles as above, the electron density sections $\varrho(xy0)$ and $\varrho(xy\frac{1}{3})$ were also computed. These sections did not show any maxima at $\frac{1}{2}00$ and $\frac{1}{2}\frac{1}{2}\frac{1}{3}$ — only the high maxima at $0\frac{1}{2}0$, $\frac{1}{2}\frac{1}{2}0$, $\frac{1}{2}0\frac{1}{3}$ and $0\frac{1}{2}\frac{1}{3}$. This further confirms that the point position of the iodine atoms is 3(*c*).

The electron density sections $\varrho(xy0)$, $\varrho(xy\frac{1}{3})$ (Fig. 2) and $\varrho(xy\frac{2}{3})$ were then recalculated using the observed F values and the signs and values of the phase angles determined from the contributions of the mercury and iodine atoms for all observed reflexions. There was no difference worth mentioning between these sections and those obtained by the previous calculations. To obtain further proof concerning the positions of the iodine atoms and if possible to get some information on the positions of the sodium and the oxygen atoms, first the mercury atoms and then both the mercury and iodine atoms (Fig. 2) were substracted from $\varrho(xy0)$ and $\varrho(xy\frac{1}{3})$. In this way, most of the diffraction

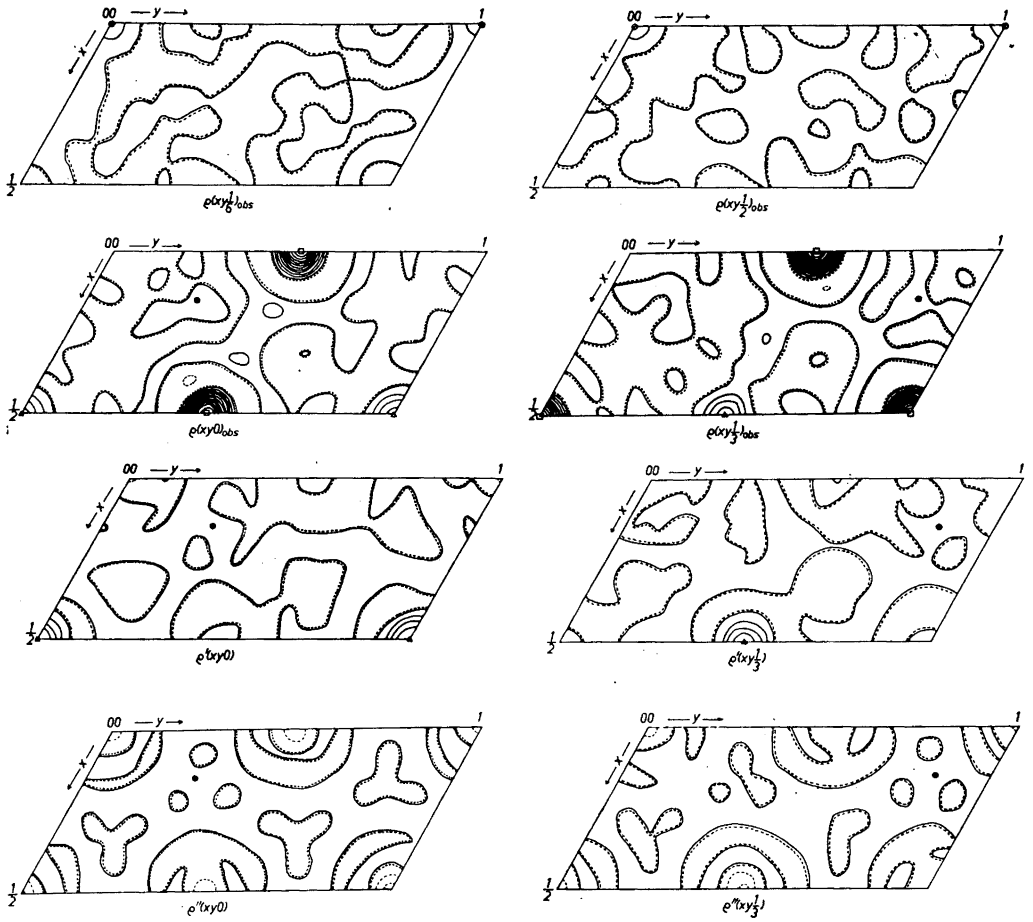

Fig. 2. The observed electron density sections $\varrho(xy\frac{1}{8})$, $\varrho(xy\frac{1}{2})$, $\varrho(xy0)$ and $\varrho(xy\frac{1}{3})$, the electron density sections $\varrho'(xy0)$ and $\varrho'(xy\frac{1}{3})$, where the contributions of the mercury atoms are substracted from $\varrho(xy0)$ and $\varrho(xy\frac{1}{3})$, and the electron density sections $\varrho''(xy0)$ and $\varrho''(xy\frac{1}{3})$, where the contributions of the mercury and of the iodine atoms have been substracted from $\varrho(xy0)$ and $\varrho(xy\frac{1}{3})$. The final mercury (□), iodine (△), oxygen (●) and sodium (○) atom positions are indicated. Dashed lines indicate negative values.

effects from the heavy atoms should disappear and only maxima indicating the iodine atoms and possibly small maxima indicating the sodium and oxygen atoms (Fig. 2) should be obtained. As expected, these calculations show clearly that the point position of the three iodine atoms is 3(*c*).

The temperature factor that should have been introduced in these calculations was found to be negligible when calculated by the ordinary procedure. Probably, it approximately cancels out with the absorption effects.

The positions for the sodium and oxygen atoms which could possibly be obtained from these sections would doubtless be rather uncertain. One reason is that the Fourier series has in fact been broken at $l = 5$, another one is the dominant scattering power for X-rays of the heavy atoms. No attempt was therefore made to utilize the information obtainable from these small maxima for the determination of the positions of the light atoms.

THE POSITIONS OF THE LIGHT ATOMS

The above discussion has shown that the six mercury atoms occupy the point position 6(*f*) and the three iodine atoms the point position 3(*c*) in the space group $P6_222$ (No. 180). Consequently the holes between these atoms must also possess the symmetry $P6_222$. It is therefore probable that the sodium and the oxygen atoms have the same symmetry — it will be seen later on that this is supported by the results of a neutron diffraction investigation. Now, in $P6_222$, the only positions left for the three sodium atoms are 3(*a*), 3(*b*) and 3(*d*) (see p. 2200). The position 3(*d*) would result in a very short distance Hg-Na of only 1.7 Å and can therefore be excluded. The remaining positions 3(*a*) and 3(*b*) are, with regard to the distances Hg-Na and I-Na, equally probable for the sodium atoms. In the unit cell, there are in addition six oxygen atoms. The positions left for them are therefore: 6(*i*), 6(*j*), 6(*h*), 6(*g*), 6(*f*), 6(*e*), the combinations of the threefold point positions 3(*a*) + 3(*d*) and 3(*b*) + 3(*d*) and the less probable arrangement of a statistical distribution over 12(*k*). The possibilities 3(*a*) + 3(*d*), 3(*b*) + 3(*d*), 6(*e*) and 6(*f*) would give a very short distance of 1.7 Å between Hg-O, O-O or I-O and can thus be ruled out. Hence, the possibilities for the oxygen atoms are limited to 6(*j*), 6(*i*), 6(*h*) and 6(*g*). To find the arrangement of the light atoms according to the possible point positions, it is necessary to consider the geometry of the holes in the structure. The following distances from the mercury, sodium and iodine atoms to the oxygen atoms were assumed when drawing *xy*-sections of the unit cell at different *z* values:

$$\text{Hg-O} \geq 2.0 \text{ Å}, \quad \text{Na-O} \geq 2.3 \text{ Å}, \quad \text{I-O} \geq 3.0 \text{ Å}.$$

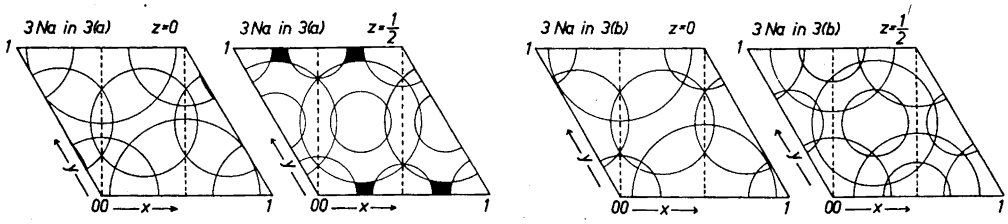

Fig. 3. Survey over the space which is free (black areas) for the oxygen atoms in the planes $z = 0$ and $z = 0.50$. The point position of the sodium atoms is assumed to be 3(*a*) and 3(*b*). The function $y = 2x$ is drawn with dashed lines.

The results are given in Fig. 3. From these figures, it can be concluded that the possible positions for the sodium and oxygen atoms are:

A: 3 Na in 3(*a*), 6 O in 6(*j*) with $x \sim 0.40$.
B: 3 Na in 3(*a*), 6 O in 6(*h*) with $0.30 \geq x \geq 0.20$.
C: 3 Na in 3(*b*), 6 O in 6(*i*) with $x \sim 0.15$.

The combinations A and B give rise to an arrangement for the mercury and the oxygen atoms which seems very unusual. Each mercury atom is coordinated to two oxygen atoms and each oxygen atom to two mercury atoms, giving an arrangement of isolated rhombs of the composition Hg_2O_2. The distances from the mercury and sodium atoms to the oxygen atoms are:

A: $x_0 = 0.40$, Hg-O = 2.6 Å, Na-O = 2.1 Å.
B: $x_0 = 0.25$, Hg-O = 2.4 Å, Na-O = 2.4 Å.

With the combination C, the arrangement of the mercury and oxygen atoms is made up of planar zig-zag chains -Hg-O-Hg- with all distances Hg-O equal to 2.0 Å, the oxygen parameter being 0.15. The structure of orthorhombic mercury(II)oxide described earlier[1] is built up of such chains with the same distance Hg-O and the same values for the angles O-Hg-O and Hg-O-Hg as given here for the possibility C. It seems therefore very probable that the combination C is the most applicable one for this structure problem.

In order to make possible an objective decision between the three geometrically possible structures, the investigation was supplemented by a neutron diffraction study.

NEUTRON DIFFRACTION STUDIES

The coherent scattering amplitudes of mercury, iodine, sodium and oxygen for neutrons and X-rays are given in the following table:

Scattering amplitude (10^{-12} cm), Ref.[11]

	Neutron	X-ray ($\Theta = 0°$)
Hg	1.31	22.5
I	0.52	15.0
Na	0.35	3.09
O	0.58	2.25

The amplitude values for neutrons are independent of the scattering angle while those for X-rays decrease with Θ and relatively more so for sodium and oxygen than for mercury and iodine. Therefore, it seems rather unlikely that one can locate these light atoms from the observed X-ray data but it is evident that neutron diffraction work would provide much better possibilities for the determination of the sites. Since it was impossible to get a crystal large enough for single crystal investigations with the apparatus available, the neutron diffraction work was carried out on a powder sample in a flat aluminium container. Since the cross section for true absorption is very large

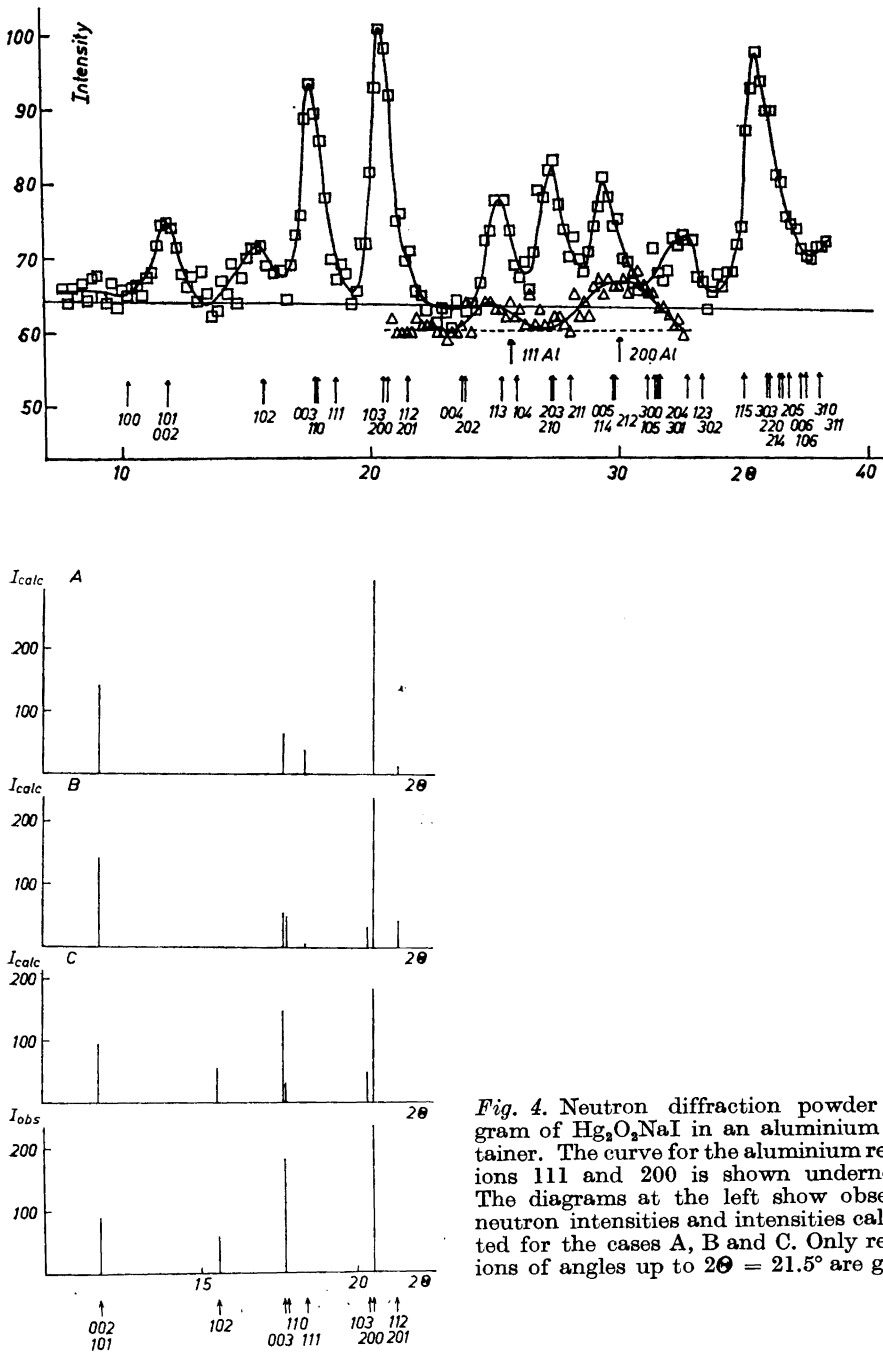

Fig. 4. Neutron diffraction powder diagram of Hg_3O_2NaI in an aluminium container. The curve for the aluminium reflexions 111 and 200 is shown underneath. The diagrams at the left show observed neutron intensities and intensities calculated for the cases A, B and C. Only reflexions of angles up to $2\Theta = 21.5°$ are given.

Table 6. Observed neutron intensities from a powdered sample of Hg_2O_2NaI. The intensities of the coinciding reflexions 113 and 104, from 005 to 212 and from 300 to 302 were corrected for the contributions of the aluminium reflexions 111 and 200. The intensities were calculated for the case C (3(*b*), 6(*i*)): I. neglecting the influence of the oxygen atoms and II. taking the influence of the oxygen atoms into account. $I\text{calc}_I$ and $I\text{calc}_{II}$ are normalized so as to give the best agreement with Iobs.

hkl	I_{obs}	I_{calc_I}	$I_{calc_{II}}$	*hkl*	I_{obs}	I_{calc_I}	$I_{calc_{II}}$
101	89	40	93	005			
002				114	66	20	39
				212			
102	59	23	54				
				300			
003				204			
110	182	116	176	105			
111				301	128	102	103
				123			
103				302			
200	235	404	227				
112							
201				115			
				303			
004	—	0	1	220			
202				221			
				214			
113	84	73	106	205	290	206	300
104				006			
				106			
203				310			
210	143	293	178	222			
211				311			

for mercury, the powder sample had to be thin and the observed neutron intensities were therefore low. The aluminium holder was chosen so that $\mu \cdot t = 0.439$ where μ is the linear absorption coefficient of the compound

Table 7. Observed neutron intensities from a powdered sample of Hg_2O_2NaI and intensities calculated for the structure possibility C. The parameter for the oxygen atom position was varied within the limits $0.10 \leq x_O \leq 0.20$.

hkl	*I* obs	*I* calc.				
		$x_O = 0.10$	$x_O = 0.13$	$x_O = 0.15$	$x_O = 0.17$	$x_O = 0.20$
101, 002	89	69	83	96	92	101
102	59	40	48	55	53	58
003, 110, 111	182	166	197	180	203	152
103, 200, 112, 201	235	290	237	233	217	254

Table 8. Calculated and observed structure factors *hkl* for Hg_2O_2NaI.

h k l	$\lvert F_{calc} \rvert$	$\lvert F_{obs} \rvert$	*h k l*	$\lvert F_{calc} \rvert$	$\lvert F_{obs} \rvert$
0 1 0	160	149	1 6 2	34	36
0 2 0	556	502	2 2 2	2	—
0 3 0	147	192	2 3 2	42	38
0 4 0	430	418	2 4 2	5	—
0 5 0	117	122	2 5 2	29	33
0 6 0	369	355	2 6 2	6	—
0 7 0	84	124	3 3 2	28	33
1 1 0	173	236	3 4 2	39	38
1 2 0	146	195	3 5 2	34	36
1 3 0	122	162	4 4 2	3	—
1 4 0	119	154	0 0 3	579	619
1 5 0	108	99	0 1 3	198	195
1 6 0	93	83	0 2 3	463	325
2 2 0	490	418	0 3 3	179	215
2 3 0	106	112	0 4 3	379	401
2 4 0	380	388	0 5 3	144	163
2 5 0	106	83	0 6 3	336	329
2 6 0	315	281	0 7 3	103	117
3 3 0	110	145	1 1 3	206	178
3 4 0	107	107	1 2 3	179	183
3 5 0	95	83	1 3 3	155	195
4 4 0	335	289	1 4 3	148	185
0 1 1	66	64	1 5 3	133	149
0 2 1	5	—	1 6 3	113	124
0 3 1	29	30	2 2 3	427	274
0 4 1	8	—	2 3 3	136	135
0 5 1	43	46	2 4 3	342	383
0 6 1	2	—	2 5 3	128	144
0 7 1	32	33	2 6 3	290	282
1 1 1	26	13	3 3 3	137	167
1 2 1	58	58	3 4 3	129	134
1 3 1	49	46	3 5 3	113	109
1 4 1	29	33	4 4 3	308	291
1 5 1	41	51	0 1 4	58	54
1 6 1	34	45	0 2 4	2	—
2 2 1	1	—	0 3 4	29	31
2 3 1	42	40	0 4 4	6	—
2 4 1	6	—	0 5 4	41	48
2 5 1	29	26	0 6 4	0	—
2 6 1	7	—	0 7 4	32	28
3 3 1	28	38	1 1 4	27	25
3 4 1	39	45	1 2 4	52	45
3 5 1	34	41	1 3 4	45	46
4 4 1	3	—	1 4 4	28	30
0 1 2	64	51	1 5 4	39	46
0 2 2	5	—	1 6 4	33	33
0 3 2	29	26	2 2 4	2	—
0 4 2	7	—	2 3 4	40	46
0 5 2	42	41	2 4 4	4	—
0 6 2	2	—	2 5 4	29	25
0 7 2	32	46	3 3 4	27	36
1 1 2	26	31	3 4 4	38	46
1 2 2	57	61	3 5 4	33	33
1 3 2	48	56	4 4 4	2	—
1 4 2	29	33			
1 5 2	41	50			

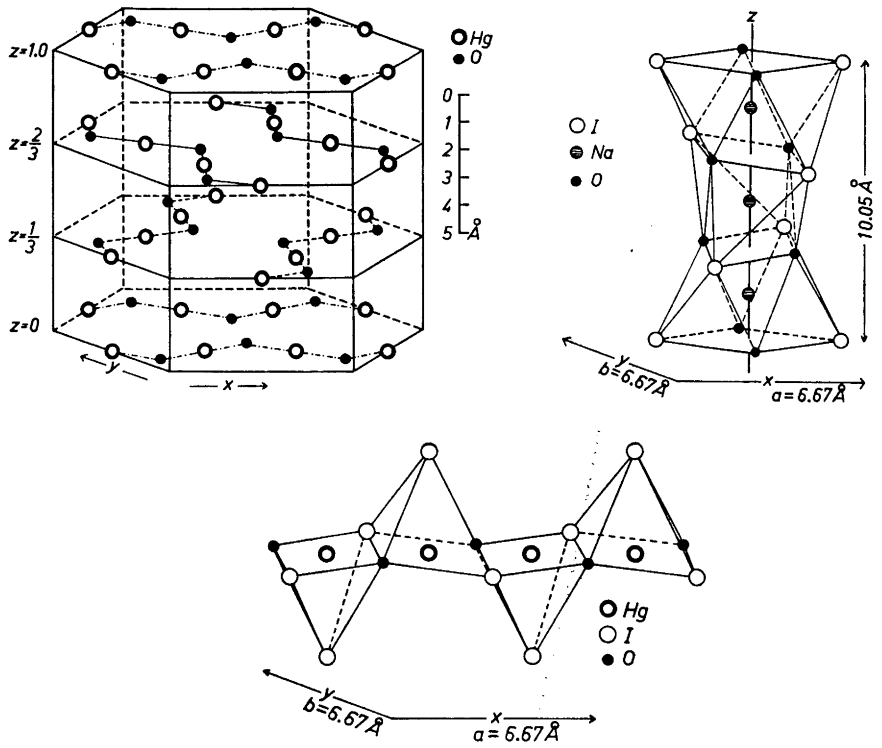

Fig. 5. Schematic drawings showing the infinite planar chains —O—Hg—O—Hg—, lying perpendicularly to the *c* axis at the heights $z = 0$, $\frac{1}{3}$ and $\frac{2}{3}$, showing a chain of deformed Archimedean square antiprisms, running parallel to the *c* axis and showing a chain of pyramids, lying perpendicularly to the *c* axis. Each Archimedean antiprism is made up of four iodine and four oxygen atoms with one sodium atom in its centre. Each pyramid is made up of three iodine and two oxygen atoms with one mercury atom in the centre of its base plane.

and t the length of the sample. The reactor was run at a level of 450 kW. The diffracted intensity was measured at intervals of 0.2° scattering angle, counts being taken during the time necessary for accumulating 500 000 neutron counts in the monitor for the incident neutron beam. The curve that was obtained by plotting the counts against the angles is given in Fig. 4. The observed intensities, obtained by measuring the areas under the peaks with a planimeter and correcting for the contribution of the aluminium reflexions 111 and 200 from the container, are given in Table 6. Due to serious overlapping, only the intensities of the reflexions at low Θ angles could be evaluated with accuracy. The neutron intensities of the observed reflexions were calculated for the structure possibilities A, B and C assuming the parameter values given above and were compared with the observed intensities in a neutron diffraction diagram. The result is given in Fig. 4, from which it is

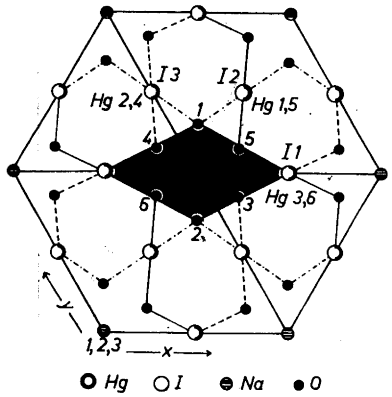

Fig. 6. The *xy* projection of the structure of Hg_2O_2NaI showing the coordination of the atoms. The infinite planar chain —O—Hg—O— at $z = 0$ is indicated by a dasheddotted line, that at $z = 0.33$ by a dotted line and that at $z = 0.67$ by a full line. The base plane of the deformed Archimedean antiprism at $z = 0$ is indicated by the black area.

Na 1	$z = 1/6$;	Hg 1,2	$z = 0$;	I 1	$z = 0$;	O 1,2	$z = 0$
Na 2	$z = 1/2$;	Hg 3,4	$z = 1/3$;	I 2	$z = 1/3$;	O 3,4	$z = 1/3$
Na 3	$z = 5/6$;	Hg 5,6	$z = 2/3$;	I 3	$z = 2/3$;	O 5,6	$z = 2/3$

clearly seen that the possibility C is the only one that is consistent with the experimental data. For the case C, a systematic variation of the parameter for the oxygen atom position gave the best agreement between observed and calculated intensities when $x_o = 0.15$ (Table 7). The neutron intensities of the reflexions were calculated according to Bacon [12], the influence of the temperature factor being, however, neglected.

CORRELATION OF X-RAY AND NEUTRON DIFFRACTION INTENSITIES

The point positions and parameters of the atoms having been determined, the X-ray structure factors of the reflexions *hkl* were then calculated and compared with the observed ones (*cf.* Table 8). The influence of the temperature factor was, however, neglected. The agreement between observed and calculated values was found to be good. To obtain a criterion of the correspondence, the reliability factor $R = \frac{\Sigma \, || F_{obs} | - | F_{calc} ||}{\Sigma \, | F_{obs} |}$ was calculated according to Booth [13] and found to be 13.7 % (absent reflexions included) or 13.0 % (absent reflexions not included), showing that the structure should be essentially correct as regards the heavy atoms.

To reduce the influence of orientation effects observed in the Guinier photogram (*e.g.* the reflexion 303), accurate values for the intensities of the X-ray powder reflexions were measured for a sample mixed with gum arabic (1 : 3) using a Geiger-Mueller diffractometer. The observed intensities obtained by measuring the areas under the peaks are given in Table 1. For overlapping reflexions, the sum of the intensities are given. As seen, the agreement between observed and calculated intensities is good (Table 1).

The calculated and observed neutron intensities for all reflexions that could be evaluated are given in Table 6. The accuracy of the observed reflexions

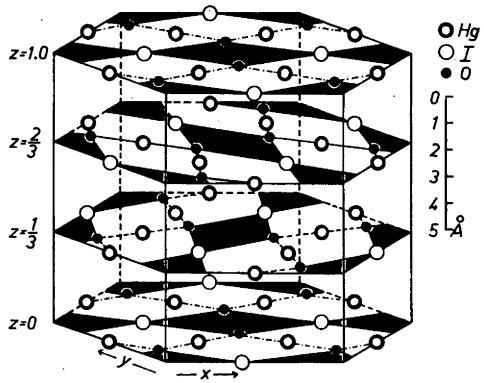

Fig. 7. A schematic drawing showing the connection between the infinite planar chains —O—Hg—O— and the base planes of the Archimedean antiprisms. The base planes are indicated by black areas.

Table 9. Interatomic distances in the structure of Hg_2O_2NaI. The atoms are named as in the *xy* projection (Fig. 6).

Hg_1-O_1,O_2	2.03 Å	Hg_1-Hg_2	3.33 Å
Hg_2-O_1,O_2	2.03 Å	Hg_1-Hg_5	3.35 Å
Hg_3-O_3,O_4	2.03 Å	Hg_2-Hg_4	3.35 Å
Hg_4-O_3,O_4	2.03 Å	Hg_3-Hg_4	3.33 Å
Hg_5-O_5,O_6	2.03 Å	Hg_3-Hg_6	3.35 Å
Hg_6-O_5,O_6	2.03 Å	Hg_5-Hg_6	3.33 Å
Na_1-O_1,O_2,O_3,O_4	2.41 Å	Na_1-Na_2	3.35 Å
Na_2-O_3,O_4,O_5,O_6	2.41 Å	Na_1-Na_3	3.35 Å
Na_3-O_1,O_2,O_5,O_6	2.41 Å	Na_2-Na_3	3.35 Å
Na_1-I_1,I_2	3.73 Å	I_1-I_2,I_3	4.73 Å
Na_2-I_2,I_3	3.73 Å	I_2-I_3	4.73 Å
Na_3-I_1,I_3	3.73 Å		
I_1-Hg_1,Hg_2	3.33 Å	O_1-O_2	3.46 Å*,4.06 Å**
I_1-Hg_3,Hg_6	3.35 Å	O_1-O_4,O_5	3.77 Å
I_2-Hg_3,Hg_4	3.33 Å	O_1-O_3,O_6	4.49 Å
I_2-Hg_1,Hg_5	3.35 Å	O_2-O_3,O_6	3.77 Å
I_3-Hg_3,Hg_6	3.33 Å	O_2-O_4,O_5	4.49 Å
I_3-Hg_2,Hg_4	3.35 Å	O_3-O_4	3.46 Å*,4.06 Å**
		O_3-O_5	3.77 Å
I_1-O_1,O_2	3.76 Å	O_3-O_6	4.49 Å
I_1-O_3,O_4,O_5,O_6	3.92 Å	O_4-O_5	4.49 Å
I_2-O_1,O_2,O_5,O_6	3.92 Å	O_4-O_6	3.77 Å
I_2-O_3,O_4	3.76 Å	O_5-O_6	3.46 Å*,4.06 Å**
I_3-O_5,O_6	3.76 Å		
I_3-O_1,O_2,O_3,O_4	3.92 Å	* within a chain —O—Hg—O—	
Na_1-Hg_1,Hg_2,Hg_3,Hg_4	3.73 Å	** between two chains —O—Hg—O—	
Na_2-Hg_3,Hg_4,Hg_5,Hg_6	3.73 Å		
Na_3-Hg_1,Hg_2,Hg_5,Hg_6	3.73 Å		

that had to be corrected for the contributions due to the aluminium reflexions is less than that of those peaks, at low 2 Θ values, which were not affected by these reflexions (Fig. 4). Taking this fact into consideration, it can be concluded that the agreement between calculated and observed intensities is satisfactory, thus showing that the structure should be principally correct also as regards the light atoms.

DESCRIPTION OF THE STRUCTURE

The following structure is therefore proposed for Hg_2O_2NaI:
Cell content: 3 Hg_2O_2NaI

Space croup: $P6_222$ (No. 180)
6 Hg in 6(f): $\frac{1}{2},0,\pm z$; $0,\frac{1}{2},\frac{2}{3}\pm z$; $\frac{1}{2},\frac{1}{2},\frac{1}{3}\pm z$; $z = 0.333$
3 I in 3(c): $\frac{1}{2},0,0$; $0,\frac{1}{2},\frac{2}{3}$; $\frac{1}{2},\frac{1}{2},\frac{1}{3}$
3 Na in 3(b): $0,0,\frac{1}{2}$; $0,0,\frac{5}{6}$; $0,0,\frac{1}{6}$
6 O in 6(i): $\pm(x, 2x), 0$; $\pm(2x, x), \frac{2}{3}$; $\pm(x, \bar{x}), \frac{1}{3}$; $x = 0.15$

A fundamental constituent of the structure is the series of infinite planar zig-zag chains -O-Hg-O-, lying perpendicularly to the c axis at the heights $z = 0,\frac{1}{3}$ and $\frac{2}{3}$ (Fig. 5). The distances Hg-O within the chains are 2.03 Å (Table 9) and the angles O-Hg-O 180° ± 3° and Hg-O-Hg 110° ± 1°. This Hg-O distance and the values of the angles (*cf.* Refs.[14,15]) suggest that the bond between Hg and O within the chains is mainly homopolar. Since the interatomic distances are considerably larger between the chains, the forces between them are far weaker.

Each mercury atom is, in addition to the two oxygen atoms at the close distance of 2.03 Å, also surrounded by three iodine atoms at the distances $\frac{a}{2} = 3.33$ Å and $\frac{c}{3} = 3.35$ Å, the two oxygen and the three iodine atoms thus forming a pyramid with the mercury atom in the centre of its base plane (Fig. 5).

Each iodine atom is octahedrally surrounded by six mercury atoms at the distances 3.33 and 3.35 Å. The calculated sum of the ionic radii is 3.26 Å (Ref.[16]).

Each sodium atom in the structure is surrounded by four oxygen and four iodine atoms, forming a deformed square Archimedean antiprism. These coordination polyhedra share their base planes to form infinite chains running along the c axis of the unit cell (Fig. 5). The interatomic distances in the polyhedra and between the polyhedra and the chains are listed in Table 9 (Fig. 6). The distances Na-I seem to be relatively long but the Na-O distances are close to the sum of the ionic radii (Ref. [16]):

	obs.	calc.		obs.	calc.
Na-I, (Å)	3.73	3.11	Na-O, (Å)	2.41	2.3€

The connection between the chains and the base planes of the Archimedean antiprism is shown clearly in Fig. 7.

The author is greatly indebted to Professor A. Ölander for his kind interest in this work and to Dr. A. Magnéli for many valuable discussions. Thanks are also due to Professor J. A. Goedkoop and Dr. A. F. Andresen for very valuable help in the neutron diffraction work. The author wishes to thank Miss Inga-Britt Carlsson and Miss Birgitta Malmros for valuable help in the chemical work and assistance in the calculations. Thanks are also due to the *Swedish Board for Computing Machinery* for the use of the calculator BESK for a considerable part of the calculating work involved in this investigation. The author is also indebted to G. Blomqvist, S. Westman and S. Åsbrink for access to the programs (*c.f.* Refs.[17,18]) used for calculations with BESK.

These studies form part of a research program on mercury(II)oxide salts, financially supported by the *Swedish Natural Science Research Council.*

REFERENCES

1. Aurivillius, K. *Acta Chem. Scand.* **10** (1956) 852.
2. Aurivillius, K. and Carlsson, I.-B. *Acta Chem. Scand.* **12** (1958) 1297.
3. Laruelle, M. P. *Compt. rend.* **241** (1955) 802.
4. Charlot, G. and Bézier, D. *Quantitative Inorganic Analysis*, 3rd ed. London, New York 1957, p. 486.
5. Barnes, R. B., Richardson, D., Berry, J. W. and Wood, R. L. *Ind. Eng. Chem. Anal. Ed.* **17** (1945) 605.
6. Kolthoff, I. M. and Sandell, E. B. *Textbook of Quantitative Inorganic Analysis*, 3rd ed. New York 1952, p. 599.
7. Kolthoff, I. M. and Sandell, E. B. *Textbook of Quantitative Inorganic Analysis*, 3rd ed. New York 1952, p. 717.
8. Hambling, P. G. *Acta Cryst.* **6** (1953) 98.
9. The abstract »Pulverfotogram» published at the Institute of Chemistry, University of Uppsala, Uppsala, Sweden; Berger, S. *Acta Chem. Scand.* **7** (1953) 612; Heller, E. *Z. Krist.* **106** (1954) 122.
10. *International Tables for X-ray Crystallography*, Vol. 1, Birmingham 1952.
11. Bacon, G. E. *Neutron Diffraction*, Oxford 1955, p. 28.
12. Bacon, G. E. *Neutron Diffraction*, Oxford 1955, p. 89.
13. Booth, A. D. *Fourier Technique in X-ray Organic Structure Analysis*, Cambridge 1948, p. 101.
14. Wells, A. F. *Structural Inorganic Chemistry*, Oxford 1950, p. 58.
15. Aurivillius, K. *Acta Chem. Scand.* **4** (1950) 1413.
16. Wells, A. F. *Structural Inorganic Chemistry*, Oxford 1950, p. 70.
17. Westman, S., Blomqvist, G. and Åsbrink, S. *Arkiv Kemi* **14** (1959) 535
18. Åsbrink, S., Blomqvist, G. and Westman, S. *Arkiv Kemi* **14** (1959) 545.

Received May 16, 1960.

ACTA CHEMICA SCANDINAVICA 14 (1960) 2216–2229

On the Stability of Nitrate and Chloride Complexes of Plutonium(IV)

INGMAR GRENTHE and BERTIL NORÉN

Department of Inorganic and Physical Chemistry, Chemical Institute, University of Lund, Lund, Sweden

The nitrate and chloride complexes of Pu^{4+} were studied in an acid perchlorate medium of ionic strength $I = 4$ M at a temperature of 20°C, using the cation-exchanger method of Fronæus [1-3]. The calculation method was extended to systems of the type $M^{4+}-A^{-}$, where the central ion, the first, second and third complexes can be sorbed on the ion-exchanger. The complexity constants obtained for the nitrate system were:

$\beta_1 = 5.5 \pm 0.2$ M^{-1}; $\beta_2 = 23.5 \pm 1$ M^{-2}; $\beta_3 = 15 \pm 10$ M^{-3}

and for the chloride system:

$\beta_1 = 1.4 \pm 0.2$ M^{-1}; $\beta_2 = 1.2 \pm 0.2$ M^{-2}; $\beta_3 = 0.1 \pm 0.1$ M^{-3}.

The nitrate and chloride complexes of Pu^{4+} have previously been studied by several authors [4-8] using ion-migration, spectrophotometric, electrometric and solvent extraction methods. Most of the work is of a qualitative nature and all the quantitative measurements are confined to the spectrophotometric and electrometric methods. In the electrometric measurements the variation of the redox potential for the couple Pu(IV)/Pu(III) has been studied. To evaluate the complexity constants for Pu^{4+} it is then necessary to know the corresponding complexity constants for Pu^{3+}. As these are not known with any degree of accuracy the result has a corresponding uncertainty in the magnitude of the Pu^{4+} constants. In addition mixed complexes of Pu^{4+} and Pu^{3+} are neglected.

The ion-exchanger method seems to be a more direct and accurate way of studying these complex systems than theother methods mentioned above.

The hydrolysis [9] and disproportionation [10] reactions of Pu^{4+} must be taken into consideration for work in water solutions. By using a medium with a hydrogen-ion concentration of 4 M, the hydrolysis can be sufficiently suppressed. The disproportionation reaction

$$3\ Pu^{4+} + 2\ H_2O \rightleftharpoons 2\ Pu^{3+} + PuO_2^{2+} + 4\ H^+$$

is also strongly displaced towards left at this high acidity. The disproportionation rate of Pu^{4+} decreases with decreasing plutonium concentration and at the concentrations used here ($< 1.2 \times 10^{-5}$ M) it is entirely negligible. The high acidity and the low plutonium concentration thus removes the complications that would arise because of the presence of hydrolysis-products and oxidation states other than + 4.

THEORETICAL

The calculation of the complexity constants is made according to a method developed by Fronæus [1-3]. In the derivation it is assumed that only mononuclear complexes are formed both in the solution and in the ion-exchanger. This assumption is reasonable because of the low total metal-ion concentration ($< 1.2 \times 10^{-5}$ M) and the high acidity (4 M) of the solution.

The following symbols and equations have been used:

C'_M, C'_A = the total concentrations of metal-ion and ligand in solution before addition of the ion-exchanger.

C_M, C_A = the total concentrations of metal-ion and ligand in the solution in equilibrium with the ion exchanger.

$[M^{4+}]$, $[MA_j^{4-j}]$, $[A^-]$ = equilibrium concentrations of the different species in solution.

$[M^{4+}]_R$, $[MA_j^{4-j}]_R$ = equilibrium concentrations of the different species in the resin phase.

β_j = the complexity constant for the complex MA_j^{4-j} in solution.

v = the volume of the solution before addition of ion-exchanger.

m = the weight in grammes of dried ion-exchanger.

δ = the swelling factor of the ion-exchanger.

$X_n = \sum_{j=n}^{N} \beta_j \cdot [A^-]^{j-n}$; $(\beta_o = 1)$

Using these notations following equations are obtained

$$C_M = [M^{4+}](1 + \sum_{j=1}^{N} \beta_j [A]^j) \tag{1}$$

$$C_{MR} = \sum_{j=0}^{3} [MA_j^{4-j}]_R \tag{2}$$

For each of the ions MA_j^{4-j} $(j \leq 3)$ exchanging for hydrogen-ions in the resin, the following equilibrium can be written

$$MA_j^{4-j} + (4-j)\ H_R^+ \rightleftharpoons MA_{jR}^{4-j} + (4-j)\ H^+$$

Applying the law of mass action gives the expression

$$\frac{[MA_j^{4-j}]_R}{[MA_j^{4-j}]} = k_j \frac{[H^+]_R^{4-j}}{[H^+]^{4-j}} = l_i;\ (j = 0, 1, 2, 3) \tag{3}$$

where the coefficients k_j and l_j are functions of the activity coefficients in resin and solution. In this case the activity coefficients in solution are kept constant by using a medium of constant ionic strength and in the ion-exchanger by having a constant value of C_{MR} and $[H^+]_R$[1,11]. $[H^+]_R$ is constant because the load, C_{MR}, is much smaller (1.2×10^{-7} moles/g) than the total exchange capacity of the resin. The constant C_{MR} is obtained from a determination of the distribution coefficient, φ, at several different C'_M. The original articles should be consulted for further details [1-3].

The distribution of the metal-ion between resin and solution is given by

$$\varphi = \frac{C_{MR}}{C_M} = l_0 \frac{1 + l'_1[A^-] + l'_2[A^-]^2 + l'_3[A^-]^3}{X} \tag{4}$$

where $l'_j = l_j \cdot \beta_j \cdot l_0^{-1}$, $(j = 1, 2, 3)$

and $l_0 = [M^{4+}]_R/[M^{4+}] = \lim_{[A^-] \to 0} \varphi$

Because of the impossibility of an accurate determination of the total metal-ion concentration in the resin phase, φ is obtained from a determination of C'_M and C_M.

Thus $v \cdot C'_M = v \cdot \delta \cdot C_M + m \cdot C_{MR}$

$$\varphi = \frac{C_{MR}}{C_M} = \frac{v}{m}\left(\frac{C'_M}{C_M} - \delta\right)$$

and because $C'_M \ll C'_A$ $\qquad [A^-] \approx C_A = C'_A/\delta$

In order to obtain the complexity constants from corresponding values of φ and $[A^-]$, three new functions φ_1, f and g are introduced.

$$\varphi_1 = \left(\frac{l_0}{\varphi} - 1\right) \cdot \frac{1}{[A^-]} \tag{6}$$

$$f = \left\{\frac{l_0}{\varphi}[(\beta_1 - l'_1)[A^-] - 1] + 1\right\} \cdot \frac{1}{[A^-]^2} \tag{7}$$

$$g = \left\{f - \beta_1 \varphi_1 + \frac{l_0}{\varphi}(\beta_2 - l'_2)\right\} \cdot \frac{1}{[A^-]} \tag{8}$$

By substitution of expression (4) in eqns. (6) and (7) the following limiting values are obtained

$$\lim_{[A^-] \to 0} \varphi_1 = \varphi_1^0 = \beta_1 - l'_1 \tag{9}$$

$$\lim_{[A^-] \to 0} f = f^\circ = \beta_1(\beta_1 - l'_1) - (\beta_2 - l'_2) \tag{10}$$

A combination of eqns. (4), (6) and (7) gives

$$f = \beta_1\varphi_1 - X_2 + (\varphi_1 \cdot [A^-] + 1)(l'_2 + l'_3 \cdot [A^-]) \tag{11}$$

In the same way eqn. (12) is obtained by a combination of eqns. (6), (9), (10) and (11).

$$\frac{\Delta f}{[A^-]} = \beta_1 \cdot \frac{\Delta \varphi_1}{[A^-]} + \varphi_1 (l_2' + l_3' \cdot [A^-]) + l_3' - X_3 \qquad (12)$$

where $\Delta f = f - f^\circ$ and $\Delta \varphi_1 = \varphi_1 - \varphi_1^0$

For small [A] eqn. (12) can be approximated to

$$\frac{\Delta f}{[A^-]} = \beta_1 \frac{\Delta \varphi_1}{[A^-]} + (\beta_1 - l_1') \cdot l_2' + l_3' - \beta_3 \qquad (13)$$

β_1 can thus be obtained by plotting $\Delta f/[A^-]$ against $\Delta \varphi_1/[A^-]$. When β_1 is known $(\beta_2 - l_2')$ can be calculated from eqn. (10). This makes it possible to calculate the function g.

By introducing the functions φ_1, f and g eqn. (4) can be written in the alternate form

$$g = \beta_2 \varphi_1 - X_3 + l_0 l_3' \varphi^{-1} \qquad (14)$$

At small ligand concentrations the last term in eqn. (14) is approximately equal to l_3' and X_3 equal to β_3. Thus g is a linear function of φ_1 with the slope β_2 and the intercept $-(\beta_3 - l_3')$.

It is desirable to know the magnitude of l_2'. This can be obtained from the expression [3]

$$\frac{\beta_1^2}{\beta_2} = \frac{(l_1')^2}{l_2'} \qquad (15)$$

If the term $l_3'[A^-]$ in eqn. (11) can be neglected in comparison with l_2' in a wide range of $[A^-]$ then the constants of higher complexes are obtained from corresponding values of [A] and X_3 using the approximation

$$X_3 = \beta_2 \varphi_1 - g \qquad (16)$$

which also is obtained from eqn. (14) if $l_0 l_3' \varphi^{-1}$ is neglected.

Eqn. (13) cannot always be used for graphical evaluation of β_1 because in some cases $\Delta f/[A^-]$ and $\Delta \varphi_1/[A^-]$ are nearly constant over the entire [A]-range investigated. In this case the quotient $\Delta f/\Delta \varphi_1$, can be used as a first approximation of β_1. Using this value the order of magnitude of β_2 and β_3 can be obtained from eqns. (10), (8) and (14). The approximate value of β_3 is then used for a better estimate of β_1, and so on until the β-values remain constant.

EXPERIMENTAL

A concentrated plutonium solution was prepared as before [12]. From this concentrated plutonium $-HNO_3$ solution, a stock solution of Pu(IV) was prepared by dilution with 4 M $HClO_4$. The final concentration of the stock-solution was $C_H = 4.25$ M, $C_{HNO_3} = 0.25$ M, $C_{Pu} = 0.5 \times 10^{-3}$ M.

More than 99.5 % of the total amount of plutonium was in the oxidation state + 4. Hydrochloric acid, nitric acid and perchloric acid were all of analytical grade. The ion-exchanger Dowex 50, 50—100 mesh, was converted to the hydrogen form by repeated shaking with 6 M HCl. After saturation it was washed with distilled water and finally dried for 15 h at 40°C. The ion-exchanger was then stored in a closed bottle to keep the water content of the resin constant.

The value of v/m was kept constant (4×10^{-2} l/g) in all measurements thus keeping the volume decrease of the solutions, caused by the swelling of the resin, constant. The swelling factor δ was determined by shaking 250 mg ion-exchanger with 10 ml of 4 M $HClO_4$ and 4 M HNO_3. From the change in hydrogen-ion concentration a value of $\delta = 0.99$ was obtained in both cases. The distribution coefficient, φ, was determined by shaking 5 ml of solutions of the following composition to equilibrium at 20° C.

$C_{HClO_4} = 4 - [A]$ M
C_{HNO_3} or $C_{HCl} = [A]$ M
$C_{Pu(IV)} = C'_M$ M
0.125 g Dowex 50

The time necessary for attainment of equilibrium was determined in a separate experiment. The results given in Table 1 show that equilibrium was established after 20 h. A shaking time of 40 h was nevertheless used in most of the experiments.

Table 1. Determination of φ as a function of the shaking time for $[NO_3^-] = 7$, 207 and 707 mM. $C_H = 4$ M, $T = 20$°C, $v/m = 4 \times 10^{-2}$ l/g, $C'_M = 2 \times 10^{-6}$ M

Hours	10	20	60
$[NO_3^-]$ mM	$\varphi \times 10^3$ l/g		
7	559	948	922
207	337	341	333
707	76	72	77

The plutonium concentration of the above solutions was determined by measuring the α-activity of 0.1 ml of the solution before addition of ion-exchanger and after equilibrium was attained. The analytical procedure has been described before [12]. Since the activity of the solution is proportional to the plutonium-concentration, φ can be calculated from the following expression

$$\varphi = 4 \times 10^{-2} \left(\frac{I_0}{I} - \delta \right)$$

where I_0 is the activity in cpm/0.1 ml of the solution before addition of ion-exchanger and I is the activty in the same units after equilibrium.

RESULTS

The plutonium(IV)-nitrate system

The distribution fucntion φ was determined at three different C'_M, Fig. 1. From these values φ, at a constant load, $C_{MR} = 1.2 \times 10^{-7}$ moles/g, was obtained by interpolation. Only a slight variation of φ with C_{MR} was obtained,

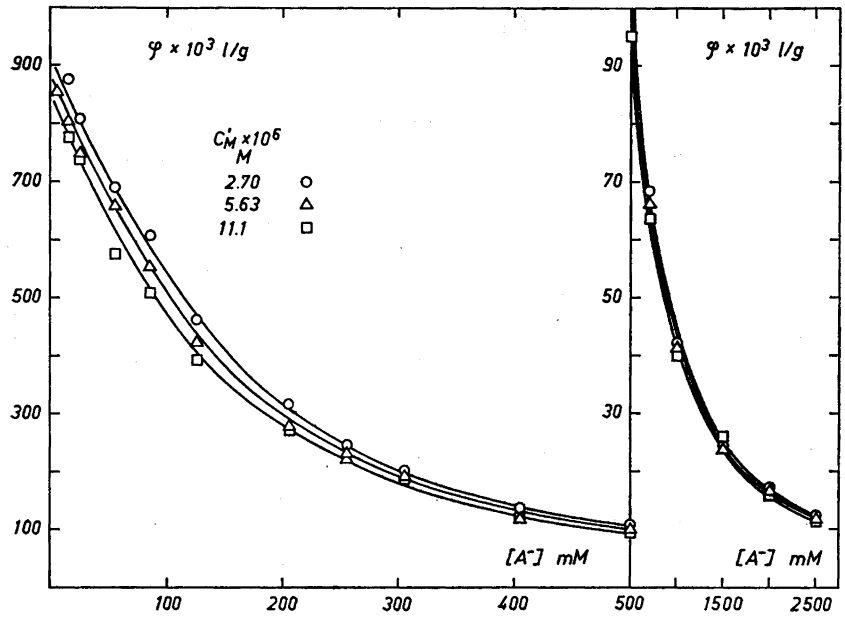

Fig. 1. φ for the nitrate complex system of plutonium(IV). The points refer to determination with different values of C'_M, as indicated by the scheme given in the figure. Note that the ordinate is expanded and the abscissa contracted for $[A^-] \geq 500$ mM. $C_H = 4$ M, $v/m = 4 \times 10^{-2}$ l/g, $T = 20°C$.

Table 2. In Table 3 the values of φ_1, f, g, $\Delta f/[A^-]$ and $\Delta\varphi_1/[A^-]$, valid for $C_{MR} = 1.2 \times 10^{-7}$ moles · g^{-1}, are given. l_0, φ_1^0 and $f°$ are determined with a fairly good accuracy by the graphical extrapolation shown in Figs. 2, 3 and 4. The values obtained are

$$l_0 = 0.92 \pm 0.02 \text{ g/l}$$
$$\varphi_1^0 = 5.3 \pm 0.2 \text{ M}^{-1}$$
$$f° = 6.0 \pm 0.5 \text{ M}^{-2}$$

In Fig. 5, $\Delta f/[A^-]$ has been plotted as a function of $\Delta\varphi_1/[A^-]$. A straight line with the slope $\beta_1 = 5.5 \pm 0.2$ M^{-1} is obtained. With known values of $f°$, β_1 and φ_1^0 a value of $(\beta_2 - l'_2) = 23 \pm 3$ M^{-2} is calculated from eqn. (10). Using this value the function g is determined. The results are given in Table 3. Fig. 6 gives a plot of g against φ_1. From the resulting straight line a value of of $\beta_2 = 23.5 \pm 1$ M^{-2} is obtained. The intercept gives a very uncertain value of $\beta_3 - l'_3 = 15 \pm 10$ M^{-3}, which can be put equal to β_3 since l_0 is much greater than l_3, *i.e.* Pu^{4+} is more strongly sorbed on the ion exchanger than $Pu(NO_3)_3^+$. Another value of β_3 is obtained from eqn. (16), Table 3, which gives $\beta_3 = 11 \pm 7$ M^{-3}.

Table 2. Corresponding values of [A], C_{MR} and φ for the nitrate system taken from Fig. 1. $C_H = 4$ M, $T = 20$°C.

[A] mM	$C_{MR} \times 10^7$ moles/g	$\varphi \times 10^3$ l/g	$C_{MR} \times 10^7$ moles/g	$\varphi \times 10^3$ l/g	$C_{MR} \times 10^7$ moles/g	$\varphi \times 10^3$ l/g
5	1.03	894	2.16	864	4.25	840
15	1.03	848	2.14	820	4.23	792
25	1.03	803	2.14	779	4.22	748
55	1.02	684	2.12	657	4.17	628
85	1.01	575	2.11	553	4.14	522
125	0.99	462	2.04	422	4.05	420
205	0.96	321	1.99	298	3.88	281
255	0.93	244	1.92	235	3.76	222
305	0.89	191	1.86	188	3.62	178
405	0.84	137	1.72	129	3.34	123
505	0.79	107	1.62	101	3.12	95
705	0.68	68	1.40	66	2.73	64
1 000	0.56	43.0	1.14	41.5	2.22	40.0
1 500	0.42	25.8	0.86	24.5	1.65	23.5
2 000	0.33	17.5	0.67	17.1	1.27	16.0
2 500	0.25	12.3	0.52	12.0	1.02	11.8

Table 3. Corresponding values of [A], φ, φ_1, f, g, $\Delta f/[A^-]$, $\Delta\varphi_1/[A]$ and X_3 for the nitrate system. X_3 is calculated according to eqn. (16). $C_H = 4$ M, $T = 20$°C, $C_{MR} = 1.2 \times 10^{-7}$ moles/g.

[A] mM	$\varphi \times 10^3$ l/g	φ_1 M^{-1}	f M^{-2}	g M^{-3}	$\Delta f/[A]$ M^{-3}	$\Delta\varphi_1/[A]$ M^{-2}	X_3 M^{-3}
0	*920*	*5.3*	*6.0*				
5	884						
15	840						
25	798						
55	680	6.4	14.5	189	155	20.0	(−39)
85	570	7.2	16.0	158	118	22.4	11
125	456	8.1	20.7	178	118	22.4	12
205	310	9.6	29.9	221	117	21.0	5
255	240	11.1	36.1	248	118	22.7	13
305	190	12.6	42.8	278	120	23.9	18
405	134	14.5	54.1	326	119	22.7	15
505	103	15.7	62.6	358	112	20.6	11
705	67	18.0	77.4	416	101	18.0	7
1 000	41.5	21.2	96.5	491	91	15.9	8
1 500	24.0	24.8	118.8	576	75	13.0	8
2 000	16.5	27.4	134.2	634	64	11.1	11
2 500	11.6	31.3	155.6	724	60	10.4	12

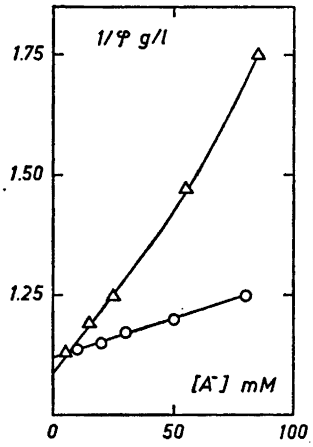

Fig. 2. $1/\varphi$ as a function of [A] for the nitrate △ and chloride ○ systems. C_H = 4 M, T = 20°C.

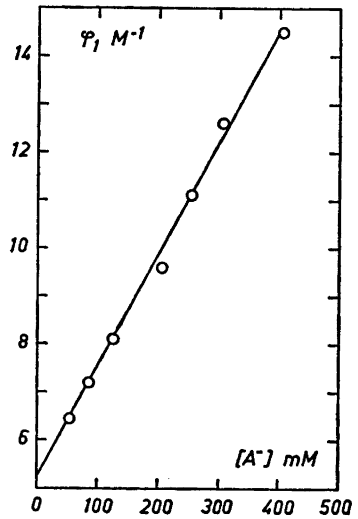

Fig. 3. φ_1 plotted against [A] for the plutonium(IV) nitrate system.

The value of $\beta_1 - l_1' = 5.3 \pm 0.2$ M^{-1} and $\beta_1 = 5.5 \pm 0.2$ M^{-1} gives an upper limit of $l_1' = 0.6$ M^{-1}. Another estimate can be obtained from eqn. (6) which for low values of [A^-] can be written as

$$\varphi_1 \approx (\beta_1 - l_1') + \{\beta_2 - l_2' - l_1' (\beta_1 - l_1')\} [A]$$

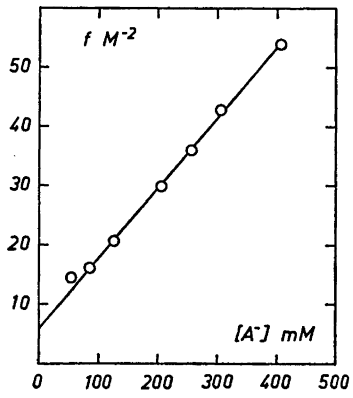

Fig. 4. The function f for the plutonium (IV) nitrate system.

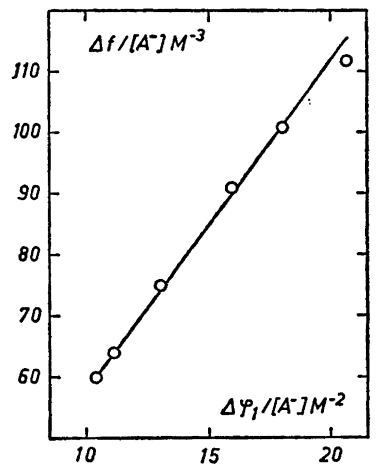

Fig. 5. Δf/[A] plotted against $\Delta \varphi_1$/[A] for the plutonium(IV) nitrate system.

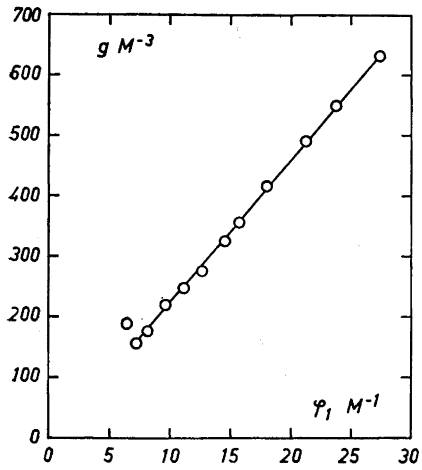

Fig. 6. g as a function of φ_1 for the plutonium(IV) nitrate system.

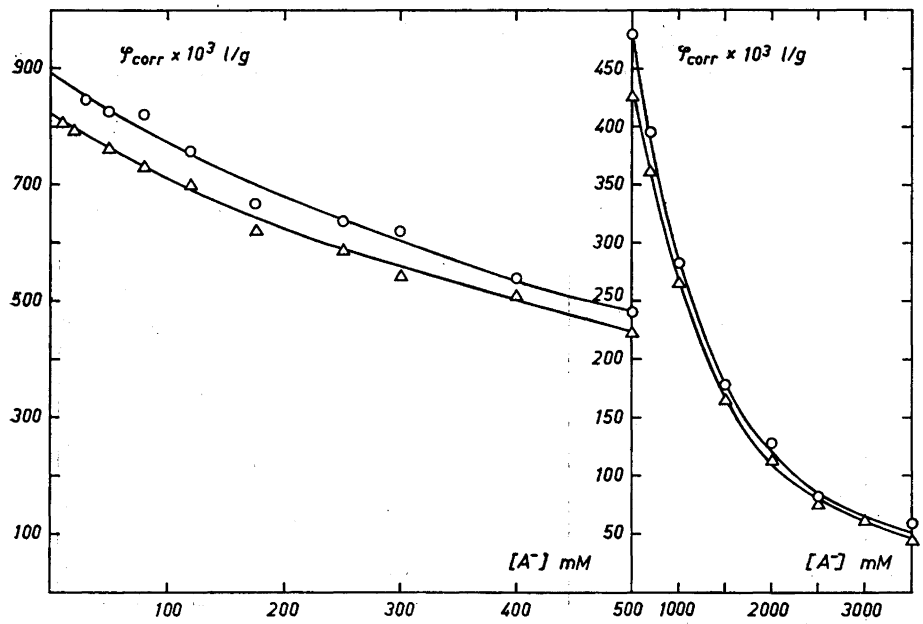

Fig. 7. φ_{corr} for the chloride complex system of plutonium(IV). Note that the ordinate is expanded and the abscissa contracted for $[A^-] \geq 500$ mM. $C'_M = 3.15 \times 10^{-6}$ M O, $C'_M = 6.30 \times 10^{-6}$ M △. $C_H = 4$ M, $v/m = 4 \times 10^{-2}$ l/g, $T = 20$°C.

Table 4. Corresponding values of [A], C_{MR}, and φ_{corr} for the chloride system taken from Fig. 7. $C_H = 4$ M, $T = 20°C$.

[A] mM	$C_{MR} \times 10^7$ moles/g	$\varphi \times 10^3$ l/g	$C_{MR} \times 10^7$ moles/g	$\varphi \times 10^3$ l/g
10	1.20	878	2.40	815
20	1.20	868	2.40	803
30	1.20	855	2.40	792
50	1.20	832	2.40	772
80	1.20	800	2.40	741
120	1.20	760	2.38	700
175	1.19	708	2.37	650
250	1.19	640	2.36	587
300	1.19	602	2.35	574
400	1.18	537	2.34	497
500	1.16	480	2.31	447
700	1.15	385	2.28	365
1 000	1.10	281	2.19	268
1 500	1.03	177	2.03	165
2 000	0.96	120	1.85	111
2 500	0.84	82	1.66	78
3 000	0.79	67	1.51	60
3 500	0.72	53	1.36	47

Table 5. Corresponding values of [A], $\varphi_{corr.}$, φ_1, f, g, $\Delta f/\Delta \varphi_1$ and X_3 for the chloride system. X_3 is calculated according to eqn. (16). $C_H = 4$ M, $T = 20°C$, $C_{MR} = 1.2 \times 10^{-7}$ moles/g.

[A] mM	$\varphi_{corr} \times 10^3$ l/g	φ_1 M^{-1}	f M^{-2}	g M^{-3}	$\Delta f/\Delta \varphi_1$ M^{-1}	X_3 M^{-3}
0	*892*	*1.25*	*0.56*			
10	878					
20	868					
30	855					
50	832					
80	800					
120	760					
175	708					
250	640					
300	602	1.61	0.82	1.13	0.72	0.8
400	536	1.66	1.05	1.80	1.20	0.2
500	480	1.72	1.21	2.04	1.38	0
700	384	1.89	1.45	2.27	1.39	0
1 000	280	2.19	1.80	2.56	1.32	0.1
1 500	174	2.75	2.44	3.16	1.25	0.1
2 000	118	3.28	3.08	3.77	1.24	0.2
2 500	80	4.06	3.95	4.65	1.21	0.2
3 000	64	4.31	4.37	5.01	1.25	0.2
3 500	51	4.71	4.90	5.50	1.25	0.2

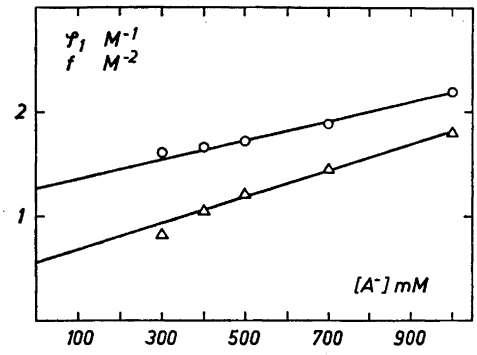

Fig. 8 φ_1 (O) and f (△) as functions of [A] for the plutonium(IV) chloride system.

i.e., φ_1 is a linear function of [A], *cf.* Fig. 3. The slope of the line gives a value of $(\beta_2—l_2')—l_1'$ $(\beta_1—l_1') = 23 \pm 2$ M^{-2} which together with the previously determined values of $\beta_2—l_2' = 23 \pm 3$ M^{-2} and $\beta_1—l_1' = 5.3 \pm 0.2$ M^{-1} gives $l_1' < 1$ M^{-1}. From (15) and the definion of l_i the maximum values of the coefficients l_1 and l_2 can be calculated to be $l_1 < 0.1$ l/g and $l_2 < 0.01$ l/g.

The plutonium(IV)-chloride system

φ was determined at two different C_M' (Fig. 7) and the interpolation to a constant load was made as before. In this case too, the variation of φ with C_{MR} was slight, Table 4. The measured φ-values must be corrected for the complex formation caused by the presence of nitrate ion in the Pu(IV) stock solution. This has been done in the following way: Because of the low nitrate ion concentration (≤ 0.010 M) in the solutions only the prescence of the first nitrate complex has to be considered.

$$\varphi = \frac{l_0\ (1 + l_1'[Cl^-] + l_2' \cdot [Cl^-]^2 + l_3' \cdot [Cl^-]^3 + l_1'^{(NO_3)}[NO_3^-]}{X_{Cl} + \beta_1^{(NO_3)} \cdot [NO_3^-]}$$

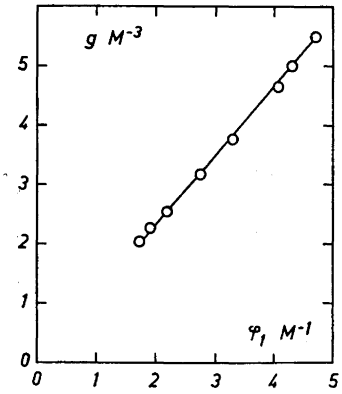

Fig. 9. g as function of φ_1 for the plutonium (IV) chloride system.

Table 6. Formation constants for nitrate and chloride complexes of Pu^{4+}.

	Reference	Medium	β_1 M^{-1}	β_2 M^{-2}	β_3 M^{-3}
NO_3^-	5	$I = 2$ M; 2 M $HClO_4$; $T = 25°C$	2.9		
	6	$I = 1$ M; 1 M $HClO_4$; $T = 25°C$	3.48		
	This work	$I = 4$ M; 4 M $[H^+]$; $T = 20°C$	5.5 ± 0.2	23.5 ± 1	15 ± 10
Cl^-	5	$I = 2$ M; 2 M HNO_3; $T = 25°C$	0.38		
	6	$I = 1$ M; 1 M $HClO_4$; $T = 25°C$	0.58		
	7	$I = 2$ M; 2 M $HClO_4$; $T = 25°C$	0.59		
	7	$I = 1$ M; 1 M $HClO_4$; $T = 25°C$	0.56		
	13	$I = 1$ M; 1 M $HClO_4$; $T = 25°C$	2.10		
	This work	$I = 4$ M; 4 M $[H^+]$ $T = 20°C$	1.4 ± 0.2	1.2 ± 0.2	0.1 ± 0.1

The term $l_1'^{(NO_3)} \cdot [NO_3^-]$ is $< 0.6 \times 0.01$ and is negligible compared with 1. In the denominator the term $\beta_1^{(NO_3)} \cdot [NO_3^-]$ varies from 0.03 to 0.06 and is not negligible for small values of $[Cl^-]$ when $X_{Cl} \approx 1$. Using the above approximation φ can be expressed as

$$\varphi = \frac{l_0 \cdot (1 + l_1'[Cl^-] + l_2' \cdot [Cl^-]^2 + l_3'[Cl]^3)}{X_{Cl}} \left(1 + \frac{5.5 \times [NO_3^-]}{X_{Cl}}\right)^{-1}$$

$$i.e., \varphi_{corr} = \varphi \cdot \left(1 + \frac{5.5[NO_3^-]}{X_{Cl}}\right)$$

where φ_{corr} is the distribution coefficient that would be obtained in abscence of nitrate. φ_{corr} was calculated using approximate values of $\beta_1 = 2$ M^{-1} and $\beta_2 = 10$ M^{-2} for the evaluation of X_{Cl} in the correction term. The φ-values obtained in the following calculation were then used to get a better estimate of φ_{corr} and better values of the complexity constants. The β-values obtained using the second φ_{corr} were the same as the ones obtained in the first approximation. Corresponding values of φ_{corr}, φ_1, f, $\Delta f/\Delta\varphi_1$ and [A] are given in Table 5. The graphical determination of l_0, φ_1^0 and f° are given in Figs. 2 and 8.

$$l_0 = 0.89 \pm 0.02 \text{ g/l} \quad \varphi_1^0 = 1.25 \pm 0.05 \text{ } M^{-1} \quad f^\circ = 0.56 \pm 0.06 \text{ } M^{-2}$$

In this case β_1 can not be determined graphically from the function $\Delta f/[A^-]$ because the values of $\Delta f/[A^-]$ and $\Delta\varphi_1/[A^-]$ are nearly constant over the entire $[A^-]$ range, Table 5. Instead β_1 is calculated from eqn. (9) using the approximate value of l_1 obtained from the nitrate system. In this way a value of $\beta_1 = 1.4 \pm 0.1$ M^{-1} is obtained. Using this value of β_1 the function g is calculated according to eqn. (8). From a plot of g as a function of φ_1, Fig. 9., β_2 is found to be 1.2 ± 0.2 M^{-2}. β_2 can also be determined from eqn. (10) if l_2' is neglected. We obtain in this case $\beta_2 = 1.2 \pm 0.2$ M^{-2}. X_3 calculated from eqn.

Table 7. The nitrate and chloride complexes of Zr^{4+}, Th^{+4} and U^{+4}.

	Metal ion	Ref.	Medium	β_1 M^{-1}	β_2 M^{-2}
NO_3^-	Zr^{4+}	14	2 M $HClO_4$ $T = 25°$	2.0	
		15	4 M $HClO_4$ $T = 20°C$	2.20	1.30
	Th^{4+}	16	2 M $HClO_4$ $T = 20°C$	6.0	13.0
		17, 18	5.97 M $NaClO_4$ $T = 25°C$	2.8	1.4
Cl^-	Zr^{4+}	14	2 M $HClO_4$ $T = 25°C$	2.0	
		15	6.54 M $HClO_4$ $T = 20°C$	8.4	21.0
	Th^{4+}	19	4 M $NaClO_4$ $T = 25°C$	1.7	0.16
		17	4 M $NaClO_4$ $T = 25°C$	1.3	0.11
	U^{4+}	20	1 M $NaClO_4$, $[H^+] = 0.6$ M $T = 20°C$	2.0	
		21	2 M $NaClO_4$ $[H^+] = 1$ M $T = 25°C$	1.8 * 1.2 *	1.15 *

* Alternative interpretation.

(16) gives a very approximative value of $\beta_3 = 0.1 \pm 0.1$ M^{-3}, Table 5. With this value of β_3 eqn. (13) gives, if l_3' is neglected, $\beta_1 = 1.4 \pm 0.2$ M^{-2} in good accordance with the value calculated from eqn. (9).

The distribution coefficients, l_j, show the sorption of the plutonium complexes to be very low compared with the sorption of the uncomplexed Pu^{4+}-ion.

$$l_0 = 0.9 \text{ l/g} \qquad l_1 < 0.1 \text{ l/g} \qquad l_2 < 0.01 \text{ l/g}$$

This means that the absolute decrease of φ will be so small when PuA_2^{2+} is converted into higher complexes that it is impossible to obtain the higher constants with any accuracy.

DISCUSSION

A comparison between the complexity constants obtained in this work and those obtained by other authors is given in Table 6. It is difficult to make any quantitative comparisons because of the differences in experimental conditions. No values of the higher constants have been previously reported in the literature.

It is also of interest to compare the complexity constants of Pu^{4+} with those of other four-valent ions. Values are given in the literature for nitrate and chloride complexes fo Zr^{4+}, Th^{4+} and U^{4+} but they have usually been measured under other conditions than in this work. The results are summarised in Table 7. The corresponding complexity constants of the four-valent actinide elements all have about the same magnitude. As to Zr^{4+} its chloride complexes are decidedly stronger than those of the actinides. This is to be

expected on account of the smaller ionic radius of Zr^{4+} if the complex formation is governed mainly by electrostatic forces which is very likely for complexes of this type. On the other hand, the nitrate complexes of Zr^{4+} seems to be weaker than the corresponding actinide complexes. This is rather unexpected and is possibly an indication of a somewhat different type of bond in these complexes [22].

This investigation has been supported by a grant from *AB Atomenergi*, Stockholm (the *Swedish Atomic Energy Company*).

With Professor Sture Fronæus, Dr Sten Ahrland and Dr Artur Sonesson we have had many fruitful discussions. The have given us views and information, which have strongly promoted our work.

REFERENCES

1. Fronæus, S. *Acta Chem. Scand.* **5** (1951) 859.
2. Fronæus, S. *Acta Chem. Scand.* **6** (1952) 1200.
3. Fronæus, S. *Svensk Kem. Tidskr.* **65** (1953) 19.
4. McLane, C. K., Dixon, J. S. and Hindman, J. C. *Natl. Nuclear Energy Ser.* **IV—14 B** (1949) p. 358.
5. Hindman, J. C. *Natl. Nuclear Energy Ser.* **IV—14 B** (1949) pp. 388 and 405.
6. Rabideau, S. W. and Lemon, J. F. *J. Am. Chem. Soc.* **73** (1951) 2895.
7. Rabideau, S. W. and Cowan, H. D. *J. Am. Chem. Soc.* **77** (1955) 6145.
8. Zebroski, E. L. and Newman, F. K. *U.S. Atomic Energy Commission Report* **KAPL—184** (1949).
9. Katz, J. J. and Seaborg, G. T. *The Chemistry of the Actinide Elements*, Methuen & Co Ltd, London 1957, p. 299.
10. Katz, J. J. and Seaborg, G. T. *The Chemistry of the Actinide Elements*, Methuen & Co Ltd, London 1957, p. 315.
11. Fronæus, S. *Acta Chem. Scand.* **7** (1953) 469.
12. Ahrland, S., Grenthe, I. and Norén, B. *Acta Chem. Scand.* **14** (1960) 1059.
13. Katz, J. J. and Seaborg, G. T. *The Chemistry of the Actinide Elements*, Methuen & Co Ltd, London 1957, p. 305.
14. Connick, R. E. and McVey, W. H. *J. Am. Chem. Soc.* **71** (1949) 3182.
15. Solovkin, A. S. *Zhur. Neorg. Khim.* **2** (1957) 611.
16. Fomin, V. V. and Maiorova, E. P. *Zhur. Neorg. Khim.* **1** (1956) 1703, 2749.
17. Zebroski, E. L., Alter, H. W. and Heuman, F. K. *J. Am. Chem. Soc.* **73** (1951) 5646.
18. Day, R. A. and Stoghton, R. W. *J. Am. Chem. Soc.* **72** (1950) 5662.
19. Waggener, W. C. and Stoughton, R. W. *J. Phys. Chem.* **56** (1952) 1.
20. Ahrland, S. and Larsson, R. *Acta Chem. Scand.* **8** (1954) 137.
21. Day, R. A. White, R. N. and Hamilton, F. D. *J. Am. Chem. Soc.* **77** (1955) 3180.
22. Katz, J. J. and Seaborg, G. T. *The Chemistry of the Actinide Elements*, Methuen & Co Ltd, London 1957, pp. 463—470.

Received July 4, 1960.

ACTA CHEMICA SCANDINAVICA 14 (1960) 2230–2235

Beiträge zur Chemie α-substituierter Sulfide. II *. Einige potentiell fungizide Verbindungen, die die Trichlormethylmerkaptogruppe enthalten

ALEXANDER SENNING und SVEN-OLOV LAWESSON

Institut für Organische Chemie der Universität Uppsala, Uppsala, Schweden

Um weiteres Material zum Substituenteneinfluss auf die Fungitoxizität der Trichlormethylarylsulfide zu sammeln, wurden die drei Methylmerkaptobenzoesäuren und deren Äthylester chloriert. Die *m*- und *p*-Verbindungen lieferten die erwarteten Trichlormethylmerkaptoderivate, während bei den *o*-Verbindungen Besonderheiten auftraten. Bei der Chlorierung der *o*-Methylmerkaptobenzoesäure führte ein Ringschluss zum 4-Thiaisochromanon-(1)-system. In einem Parallelversuch konnte die Muttersubstanz 4-Thiaisochromanon-(1) durch Kondensation von Thiosalizylsäure mit Formaldehyd dargestellt werden.

Die bekanntesten fungiziden Verbindungen dieses Typus tragen die Trichlormethylmerkaptogruppe an einem Stickstoff- oder Schwefelatom und gehören den beiden Typen

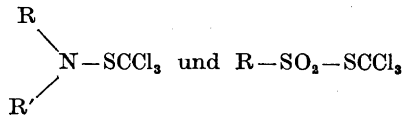

an. Diese Verbindungen werden vom Trichlormethansulfenylchlorid ausgehend dargestellt, dessen Chemie von Sosnovsky [1] in einem Übersichtsartikel eingehend behandelt wurde.

Egen [2] entdeckte, dass Trichlormethylphenylsulfid und kernsubstituierte Trichlormethylarylsulfide fungistatische Eigenschaften besitzen. Solche Verbindungen sind ganz allgemein durch Chlorierung der entsprechenden Methylarylsulfide zugänglich. Trichlormethylarylsulfide wurden zuerst von Zincke [3–5] und in neuerer Zeit von Egen [2] und Böhme [6] dargestellt. Böhme [6] hat auch

* I. Mitteilung: *Acta Chem. Scand.* 14 (1960) 1444.

den Mechanismus der α-Chlorierung der Thioäther aufgeklärt. Die von Sanna [7] beschriebene Darstellung des Trichlormethylphenylsulfids aus Trichlormethansulfenylchlorid und Phenylmagnesiumbromid lässt sich nicht nacharbeiten [8]. Ausserdem besitzen die von diesem Verfasser als Trichlormethylphenylsulfid und Trichlormethylphenylsulfon beschriebenen Verbindungen ganz andere physikalische Eigenschaften als die von Egen und Böhme dargestellten und sind mit diesen offensichtlich nicht identisch.

Die von Egen dargestellten und biologisch untersuchten Trichlormethylarylsulfide geben gewisse Hinweise auf den Substituenteneinfluss, jedoch ist das vorliegende Material zu unvollständig, um exakte Schlussfolgerungen zuzulassen. Um weiteres Material zum Substituenteneinfluss zu sammeln, wurde in der vorliegenden Arbeit unternommen, die Trichlormethylmerkaptobenzoesäuren und deren Äthylester darzustellen und auf ihre Fungitoxizität und Phytotoxizität zu undersuchen.

Es soll hier über den präparativen Teil der Arbeit berichtet werden. Die biologischen Versuchsergebnisse werden zu einem späteren Zeitpunkt veröffentlicht werden.

Als Ausgangsmaterial dienten *o*-, *m*- und *p*-Methylmerkaptobenzoesäure und deren Äthylester. *o*-Methylmerkaptobenzoesäure wurde nach D.R.P. 193 800 [9] dargestellt. *m*- und *p*-Methylmerkaptobenzoesäure wurden in Abwandlung des von Wiley [10] für die Merkaptosäuren beschriebenen Verfahrens durch direkte Methylierung des Hydrolysates der Xanthogenate erhalten. Die Säuren fallen in etwas unreinem Zustand an und lassen sich bei Bedarf über die Methyl- oder Äthylester reinigen. Zur Darstellung der Äthylester wurden die Säuren mit Hilfe eines Veresterungsaufsatzes verestert. *o*- und *m*-Methylmerkaptobenzoesäureäthylester sind unseres Wissens bisher noch nicht beschrieben worden.

Die Chlorierung der Verbindungen wurde nach der Vorschrift von Böhme [6] mit in Tetrachlorkohlenstoff oder Chloroform gelöstem Chlor durchgeführt.

Die *m*- und *p*-Trichlormethylmerkaptoderivate wurden in glatter Reaktion erhalten. Der *o*-Methylmerkaptobenzoesäureäthylester liess sich auch unter energischen Bedingungen nicht vollständig chlorieren. Das intensiv gelb gefärbte Chlorierungsprodukt, das in einem Siedepunktsintervall von wenigen Graden überging, hatte einen zu niedrigen Chlorgehalt und war nach dem Infrarotspektrum zu urteilen nicht einheitlich. Die Chlorierung der *o*-Methylmerkaptobenzoesäure führte zu einem Ringschluss und lieferte ein Produkt, dem wir auf Grund der Analysendaten folgende Struktur zuschreiben:

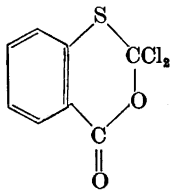

3,3-Dichlor-4-thiaisochromanon-(1)
(2,2-Dichlor-1,3-benzthioxan-4-on)

Im Infrarotspektrum des 3,3-Dichlor-4-thiaisochromanons-(1) war die Laktonkarbonylbande charakteristisch verschoben und lag bei 5,63 μ. Adler [11]

beobachtete eine entsprechende Verschiebung bei der 3,4-Dihydroisokumarin-karbonsäure-(3) (Laktonkarbonylbande bei 5,63 μ —5,69 μ).

Der Grundkörper, 4-Thiaisochromanon-(1), liess sich durch Einwirkung von trockenem Chlorwasserstoff auf eine siedende Lösung von Thiosalizylsäure und Paraformaldehyd in Eisessig darstellen:

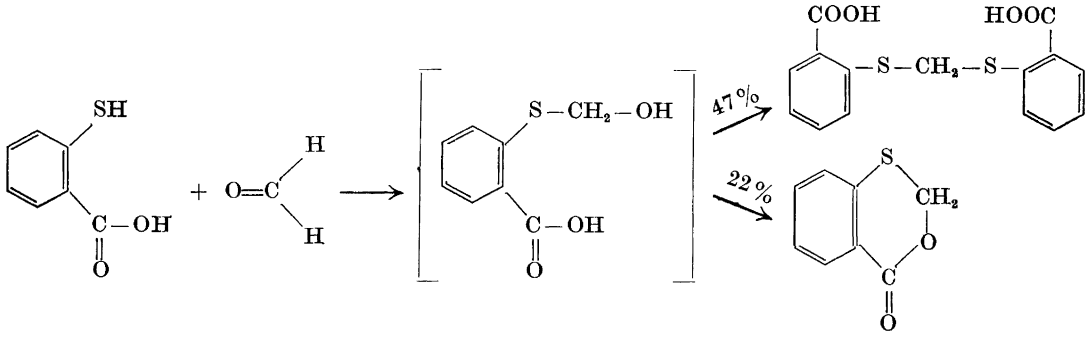

4-Thiaisochromanon-(1) selbst ist unseres Wissens noch nicht dargestellt worden. Dagegen sind Derivate der Tetrahydroverbindung beschrieben sowie eine Spiroverbindung, die das 1,3-Benzthioxanon-(4)-system enthält.

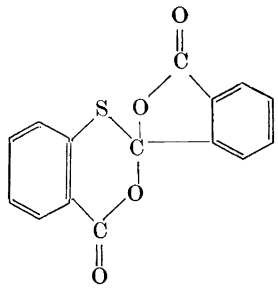

"Thiosalicylsäurephthalidenätherester" Spiro-[1,3-benzthioxan-2,1′(3′H)-isobenzofuran-4,3′-dion] [12]

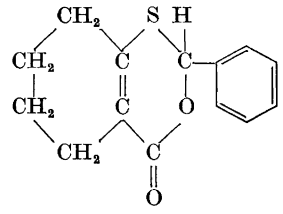

5,6,7,8-Tetrahydro-2-phenyl-1,3-benzthioxan-4-on [13]

Das Sauerstoffhomologe, 3-Oxachromanon-(4), ist von Calvet [14] und von Borsche [15] dargestellt worden. 1,3-Thioxan- bzw. 1,3-Oxthiophanderivate entstehen durch Umsetzung von Ketonen mit γ-Merkaptopropanol bzw. β-Merkaptoäthanol (Sjöberg [16], Djerassi [17], Marshall [18]), während α-Merkaptokarbonsäuren mit Aldehyden und Ketonen 1,3-Oxthiophanon-(5)-derivate liefern (Bistrzycki [19], Fredga [20]).

Die Untersuchungen in der Verbindungsklasse der Trichlormethylarylsulfide werden fortgesetzt. Gleichzeitig untersuchen wir den Mechanismus der Ringschlussreaktion der *o*-Methylmerkaptobenzoesäure sowie die Möglichkeiten zur Darstellung substituierter 4-Thiaisochromanone-(1).

BESCHREIBUNG DER VERSUCHE

Alle Schmelz- und Siedepunkte sind unkorrigiert. Infrarotspektrogramme wurden mit den Spektrographen Perkin-Elmer Modell 137 und Perkin-Elmer Modell 21 aufgenommen. Die Analysen wurden teils im Institut für Analytische Chemie der Universität Uppsala, teils von der Firma Alfred Bernhardt, Mülheim (Ruhr) ausgeführt.

o-*Methylmerkaptobenzoesäure.* 138,0 g Diphenyldisulfiddikarbonsäure-(2,2′) wurden in einer Lösung von 120,0 g Ätznatron in 750 ml Wasser gelöst und 1 1/2 Stunden mit 139,0 g Dimethylsulfat gekocht. Die *o*-Methylmerkaptobenzoesäure wurde über Nacht im Trockenschrank getrocknet, aus Benzol umkristallisiert und erneut im Trockenschrank getrocknet. Ausbeute: 87,6 g (58 % der Theorie). F: 168°—169° (Literatur: 168°—169°).

m-*Methylmerkaptobenzoesäure.* 109,5 g m-Aminobenzoesäure wurden nach Wiley [10] diazotiert, mit Kaliumxanthogenat umgesetzt und unter Stickstoff hydrolysiert. Anschliessend wurden 200 g Dimethylsulfat und 64 g Ätznatron, gelöst in 165 ml Wasser, zugetropft und anschliessend noch 1 Stunde gekocht. Das Produkt wurde im Trockenschrank bei 90° getrocknet und zur Entfernung anorganischer Verunreinigungen aus Alkohol und Wasser umgefällt. Die bei 90° im Trockenschrank getrocknete *m*-Methylmerkaptobenzoesäure schmolz zwischen 120° und 126° (Literatur: 129°) und wog 109,0 g (82 % der Theorie).

p-*Methylmerkaptobenzoesäure.* Diese Säure wurde analog der *m*-Säure dargestellt. Ausbeute 95 % der Theorie, F: 188°—192° (Literatur: 192°).

o-*Methylmerkaptobenzoesäureäthylester.* 50,0 g *o*-Methylmerkaptobenzoesäure wurden in 800 ml Benzol gelöst und mit Hilfe eines Veresterungsaufsatzes mit 200 ml Äthanol und 20 ml konzentrierter Schwefelsäure bis zur Beendigung der Wasserabscheidung gekocht (100 Stunden). Der Ester wurde auf die übliche Weise isoliert. Zwischen 161°/12 mm und 162°/12 mm gingen 42,3 g (72 % der Theorie) über. *o*-Methylmerkaptobenzoesäureäthylester ist eine farblose Flüssigkeit, Sdp. 129°/0,2 mm, n_D^{20} 1,5784. Der Ester wird im Kühlschrank fest, schmilzt aber unterhalb Zimmertemperatur. (Gef. C 61,02; H 5,89. Ber. für $C_{10}H_{12}O_2S$: C 61,20; H 6,16).

m-*Methylmerkaptobenzoesäureäthylester.* Dieser Ester wurde analog dem *o*-Ester dargestellt. Das Produkt ging zwischen 153°/16 mm und 157°/16 mm über. Ausbeute 61 % der Theorie. *m*-Methylmerkaptobenzoesäureäthylester ist eine farblose Flüssigkeit, Sdp. 121°/0,8 mm, n_D^{20} 1,5612. (Gef. C 61,31; H 6,13. Ber. für $C_{10}H_{12}O_2S$: C 61,20; H 6,16).

p-*Methylmerkaptobenzoesäureäthylester.* Dieser Ester wurde analog dem *o*-Ester dargestellt. Das Produkt ging zwischen 165°/16 mm und 171°/16 mm über. Ausbeute 59 % der Theorie. F: 23°—25° (Literatur: 28°).

m-*Trichlormethylmerkaptobenzoesäure.* 10,7 g (0,064 Mol) *m*-Methylmerkaptobenzoesäure (F: 125°—126°) wurden in 100 ml Chloroform suspendiert. Im Laufe von 15 Min. wurden unter Rühren 18,2 g (0,256 Mol) Chlor, gelöst in 400 ml Chloroform, zugegeben. Nach einigen Minuten ging die Säure in Lösung und es entwickelte sich unter mässiger Erwärmung Chlorwasserstoff. Nach weiteren 5 Min. wurde ein Wasserbad von 40° langsam auf 80° aufgeheizt. Nach insgesamt 2 1/2 Stunden war die Chlorwasserstoffentwicklung beendet. Der Kolbeninhalt wurde bis fast zur Trockne eingeengt, abfiltriert und mit wenig leichtsiedendem Petroläther gewaschen. Ausbeute 11,7 g (67 % der Theorie), F: 111°—117°. Das Produkt wurde im Soxhletapparat mit 200 ml leichtsiedendem Petroläther extrahiert und schmolz dann zwischen 119° und 122°. Nach mehrmaligem Umkristallisieren aus Chloroform und Trocknen im Vakuumexsikkator über Paraffin und Kalziumchlorid schmolz die Säure (farblose Rhomben) zwischen 125° und 127°. (Gef. C 35,00; H 1,87; Cl 39,10; S 11,46. Ber. für $C_8H_5Cl_3O_2S$: C 35,38; H 1,86; Cl 39,17; S 11,81).

p-*Trichlormethylmerkaptobenzoesäure.* 42,0 g (0,25 Mol) *p*-Methylmerkaptobenzoesäure wurden in 400 ml Chloroform suspendiert. Zu dieser Suspension wurden unter Rühren im Laufe von 25 Min. 71,0 g (1,00 Mol) Chlor, gelöst in 800 ml Chloroform, zugegeben. Nach weiteren 5 Min. wurde ein Wasserbad von 40° langsam auf 80° aufgeheizt. Nach 70 Min. war die Chlorwasserstoffentwicklung beendet. Nach dem Erkalten wurden 32,0 g Produkt vom Schmelzpunkt 192°—194° abfiltriert. Aus der Mutterlauge wurden durch Einengen weitere 20,0 g vom Schmelzpunkt 182°—188° erhalten. Ausbeute 52,0 g (77 % der Theorie). Nach mehrfachem Umkristallisieren aus Chloroform und Trocknen im Vakuumexsikkator über Paraffin und Kalziumchlorid schmolz die Säure

(feine Nadeln) zwischen 198° und 200° (unter leichter Zersetzung). (Gef. C 35,51 %; H 1,93 %; Cl 39,60 % S 11,69 %. Ber. für $C_8H_6Cl_3O_2S$: C 35,38; H 1,86; Cl 39,17; S 11,81).

m-*Trichlormethylmerkaptobenzoesäureäthylester.* 19,6 g (0,10 Mol) *m*-Methylmerkaptobenzoesäureäthylester wurden in 100 ml Tetrachlorkohlenstoff gelöst und im Laufe von 1/2 Stunde unter Rühren mit 25,5 g (0,36 Mol) Chlor, gelöst in 400 ml Tetrachlorkohlenstoff, versetzt. Darauf wurde 6 Stunden auf dem Wasserbad erwärmt. Das Lösungsmittel wurde abgezogen und der Ester destilliert. Zwischen 192° und 204° (16 mm) gingen 28,9 g (97 % der Theorie) über. *m*-Trichlormethylmerkaptobenzoesäureäthylester ist eine farblose Flüssigkeit (meist von einer schwer zu entfernenden gelben Verunreinigung begleitet), Sdp. 158°/0,6 mm, n_D^{20} 1,5692. (Gef. C 40,75; H 3,19; Cl 34,92; S 10,94. Ber. für $C_{10}H_9Cl_3O_2S$: C 40,09; H 3,03; Cl 35,50; S 10,70).

p-*Trichlormethylmerkaptobenzoesäureäthylester.* Dieser Ester wurde analog dem *m*-Ester dargestellt. Zwischen 160°/0,6 mm und 165°/0,6 mm gingen 24,8 g (83 % der Theorie) über. F: 50°—52°. Nach mehrmaligem Umkristallisieren aus leichtsiedendem Petroläther und Trocknen im Vakuumexsikkator über Paraffin und Kalziumchlorid schmolz der Ester (farblose Säulen) zwischen 55° und 57°. Gef. C 39,74; H 2,85; Cl 35,63; S 10,85. Ber. für $C_{10}H_9Cl_3O_2S$: C 40,09; H 3,03; Cl 35,50; S 10,70).

3,3-Dichlor-4-thiaisochromanon-(1). 27,8 g o-Methylmerkaptobenzoesäure (0,17 Mol) wurden in 100 ml Tetrachlorkohlenstoff suspendiert und unter Rühren mit 60,0 g (0,84 Mol) Chlor, gelöst in 850 ml Tetrachlorkohlenstoff, versetzt. Nach 8 Stunden Erwärmen auf dem Wasserbad war keine Chlorwasserstoffentwicklung mehr zu beobachten. Nach dem Abziehen des Lösungsmittels ging das Produkt zwischen 165°/16 mm und 170°/16 mm über. Ausbeute 25,2 g (65 % der Theorie). 3,3-Dichlor-4-thiaisochromanon-(1) ist eine gelbe Flüssigkeit, die im Kühlschrank fest wird, aber unterhalb Zimmertemperatur schmilzt, Sdp. 97°/0,03 mm, n_D^{20} 1,6196. (Gef. C 40,84; H 1,84; Cl 29,78; S 13,69. Ber. für $C_8H_4Cl_2O_2S$: C 40,87; H 1,72; Cl 30,16; S 13,64).

4-Thiaisochromanon-(1). 15,4 g (0,1 Mol) Thiosalizylsäure und 3,0 g (0,1 Mol) Paraformaldehyd wurden in 150 ml siedendem Eisessig gelöst. In die siedende Lösung wurde 3 Stunden lang trockener Chlorwasserstoff eingeleitet, wobei nach wenigen Minuten ein weisser Niederschlag ausfiel. Anschliessend wurde vom Niederschlag abfiltriert, das Filtrat in ca. 5 l kaltes Wasser gegossen und über Nacht stehen gelassen. Am nächsten Tag war das 4-Thiaisochromanon-(1) in groben Nadeln auskristallisiert. Es wurde abfiltriert, mit 2 %-iger Sodalösung gewaschen und getrocknet. Ausbeute 3,7 g (22 % der Theorie). F: 43°—45°. Nach mehrmaligem Umkristallisieren aus leichtsiedendem Petroläther schmolz die Substanz (farblose Rhomben) zwischen 45° und 47°. (Gef. C 57,74; H 3,66; S 19,24. Ber. für $C_8H_6O_2S$: C 57,81; H 3,64; S 19,29).

Der weisse Niederschlag war Methylen-bis-(*o*-karboxyphenylsulfid), 7,2 g (47 % der Theorie), F: 283°—285°. Nach Umfällen mit Sodalösung und Salzsäure schmolz die Substanz zwischen 286° und 288° (Literatur: 286°—288°). Stevenson und Mitarbeiter [21] haben Thiosalizylsäure und Formalin in Alkohol miteinander umgesetzt und das Merkaptal in 66 %-iger Ausbeute erhalten [22].

Wir danken Herrn Professor A. Fredga für das Interesse, das er unserer Arbeit entgegengebracht hat und für anregende Diskussionen. Wir sind Herrn Professor A. Fredga für die Überlassung des Arbeitsplatzes und *Jordbrukets Forskningsråd* für die finanzielle Unterstützung unserer Arbeit zu Dank verpflichtet.

LITERATUR

1. Sosnovsky, G. *Chem. Revs.* **58** (1958) 509.
2. Egen, R. *Diss.* Erlangen 1951; vgl. Pfleger, R. *Angew. Chem.* **65** (1953) 415.
3. Zincke, T. und Frohneberg, W. *Ber.* **43** (1910) 837.
4. Zincke, T. und Jörg, P. *Ber.* **43** (1910) 3443.
5. Zincke, T. und Müller, J. *Ber.* **46** (1913) 775.
6. Böhme, H. und Gran, H.-J. *Ann.* **581** (1953) 133.
7. Sanna, G. und Stefano, S. *Gazz. chim. ital.* **72** (1942) 305.
8. Senning, A. und Lawesson, S.-O. *Acta Chem. Scand.* **14** (1960) 1444.
9. Deutsches Patent 193800; *Chem. Zentr.* **1908:1**, 1003.

10. Wiley, P. F. *J. Org. Chem.* **16** (1951) 810.
11. Adler, E., Magnusson, R. und Berggren, B. *Acta Chem. Scand.* **14** (1960) 539.
12. Kaufmann, H. P. und Rossbach, E. *Ber.* **58** (1925) 1556.
13. Chandra, K., Chakrabarty, N. K. und Mitra, S. K. *J. Indian Chem. Soc.* **19** (1942) 139.
14. Calvet, F. und Carnero, C. *Anales soc. españ. fis. y quim.* **30** (1932) 445.
15. Borsche, W. und Berckhout, A. D. *Ann.* **330** (1903) 82.
16. Sjöberg, B. *Ber.* **75** (1942) 13.
17. Djerassi, C. und Gorman, M. *J. Am. Chem. Soc.* **75** (1953) 3704.
18. Marshall, J. R. und Stevenson, H. A. *J. Chem. Soc.* **1959** 2360.
19. Bistrzycki, A. und Brenken, B. *Helv. Chim. Acta* **3** (1920) 447.
20. Fredga, A. *Ber.* **71** (1938) 289.
21. Brookes, R. F., Cranham, J. E., Cummings, W. A. W., Greenwood, D., Jackson, B. S. und Stevenson, H. A. *J. Sci. Food Agr.* **1957** No. 1, 31.
22. Stevenson, H. A. *Private Mitteilung.*

Eingegangen am 22. Juli 1960.

ACTA CHEMICA SCANDINAVICA 14 (1960) 2236–2239

The Oxidation of Glycosides

XI *. Oxidation of Methyl β-D-xylopyranoside and Methyl β-D-ribopyranoside

EILEEN BRIMACOMBE, JOHN S. BRIMACOMBE and BENGT LINDBERG

Träkemiska avdelningen, Svenska Träforskningsinstitutet, Stockholm Ö, Sweden

Methyl β-D-xylopyranoside was oxidised with chromium trioxide in acetone and the resulting oxo-xylosides fractionated. The 2-oxo-, 3-oxo and 4-oxo-methylxylosides were isolated as amorphous materials. Platinum catalysed oxidation of methyl β-D-ribopyranoside gave methyl β-D-3-oxo-xylopyranoside (methyl β-D-3-oxo-ribopyranoside) as the principal oxidation product.

Oxidation of the anomeric methyl-6-*O*-trityl-D-glucopyranosides with chromium trioxide in acetone [1] yields mainly the 3-oxo-derivative (3—5 %) together with smaller amounts of the 2-oxo- and 4-oxo-derivatives (0.3—0.5 %). Similarly, oxidation of methyl β-D-glucopyranoside with this reagent [2] results in the aforementioned products together with a compound identified as methyl β-D-6-oxo-glucopyranoside (1.3 %). These oxidation studies have now been extended to glycosides of the pentoses and an attempt has been made to localise the oxidation by catalytic methods.

The oxidation procedure used with chromium trioxide in acetone was essentially that described by Theander [1]. The reaction mixture was shown by paper chromatography to contain at least seven products, the principal components of which were separated by chromatography on a carbon-Celite column. The 2-oxo- and 4-oxo-xylosides were eluted from the column together and in a fraction containing unreacted methyl β-D-xyloside. They were subfractionated on thick filter papers (see Experimental). As in the glucoside series [1,2] the 2-oxo- and 4-oxo-xylosides were more labile than the corresponding 3-oxo-xyloside at a pH near the neutral point and readily gave epimerisation and decomposition products. This was particularly noticeable in working up eluates from thick filter papers and in neither case was a chromatographically homogeneous product obtained. Methyl β-D-3-oxo-xylopyranoside, the principal product of the oxidation, was obtained as an amorphous powder ($[\alpha]_D$ −90°) but chromatographically and electrophoretically pure. The yield of oxo-derivatives was essentially the same as found by Theander [1] with methyl

* Part X. *Acta Chem. Scand.* **12** (1958) 1883.

Table 1. Oxo-xylosides; preparation and characteristics.

	Methyl β-D-oxo-xylopyranosides			Methyl β-D-xylopyranoside
	2-oxo	3-oxo	4-oxo	
Yield [a] (%)	0.4	3.5	0.4	43
Percentage of ethanol in the eluate when substance emerged from the column[b]	7.5	12.6	7.5	8.25
Paper chromatography $R_{glucose}$ values [b]				
Irrigant A	1.62	3.48	2.01	1.81
Irrigant B	1.44	2.14	1.63	2.10
Paper electrophoresis M_V values Buffer D at room temperature[b]	1.0	1.0	1.0	0
Products of reduction and hydrolysis	xylose lyxose	xylose ribose	xylose arabinose	

a. The yields are calculated as percentage of the amount of xyloside before oxidation.
b. Data of the carbon column separation and solvents and buffer used for paper chromatoraphy and electrophoresis are given in the Experimental section.

6-*O*-trityl-β-D-glucopyranoside and are recorded in Table 1. The structure of the oxo-xylosides was shown by identifying the sugars obtained on reduction (sodium amalgam) and hydrolysis (see Table 1 for details).

The oxo-xylosides formed strong complexes in hydrogen sulphite buffer at pH 4.7 and all had an M_v value = 1 (migration relative to that of vanillin). This contrasts with the results obtained in the glucoside series [3] where the various isomers showed significant differences in their rates of migration in hydrogen sulphite buffer. The M_v values and $R_{glucose}$ values of the oxo-xylosides are recorded in Table 1. The oxo-xylosides gave strong reducing reactions with silver nitrate-sodium ethoxide reagent and a characteristic yellow colouration (absorption in UV-light) with anisidine hydrogen chloride.

The dehydrogenation of polyols by treatment with oxygen in the presence of platinum catalysts has recently been reviewed by Heyns and Paulsen [4]. In the cyclitol series it has been found that axial hydroxyl groups are preferentially dehydrogenated. *myo*-Inositol has, for example, been selectively dehydrogenated to *myo*-inosose-2. These reactions are generally reversible as axial hydroxyl groups are preferentially formed by platinum catalysed hydrogenation of the corresponding ketones. Theander [5] has shown that platinum catalysed reduction of an oxo-glucoside results in a mixture of glycosides in which the epimer with the axial hydroxyl group predominates. Methyl β-D-ribopyranoside on treatment with oxygen over reduced Adams' catalyst gave a mixture of products, the main component of which was chromatographically indistinguishable from methyl β-D-3-oxo-xylopyranoside (methyl β-D-3-

oxo-ribopyranoside). Carbon column chromatography gave four main fractions (see Experimental) one of which contained relatively pure methyl β-D-3-oxo-xylopyranoside. Reduction of this fraction with sodium amalgam and subsequent hydrolysis gave two sugars indistinguishable from ribose and xylose in irrigants A—C. Another fraction, containing some 3-oxo-derivative together with much unreacted methyl β-D-ribopyranoside, was effectively separated by chromatography on a carbon-Celite column using sodium hydrogen sulphite elution [2]. The yield of methyl β-D-3-oxo-xylopyranoside (*ca.* 6 %) is limited by secondary oxidation and degradation reactions which occur on prolonged oxidation.

In the sterically favoured C-1 conformation of methyl β-D-ribopyranoside only the hydroxyl at $C_{(3)}$ is axially disposed and it seems, as in the cyclitol series, that preferential dehydrogenation occurs at this position. Other experiments, for example with methyl α-L-arabinopyranoside ($C_{(4)}$ hydroxyl group axial), indicated that dehydrogenation occurs at the axial hydroxyl group. This reaction is complicated by the ease of epimerisation and degradation of the initially form oxo-compounds at a pH near the neutral point. Methyl β-D-xylopyranoside (all hydroxyl groups equatorial) was largely unaffected under identical conditions but some slight oxidation was observed. This suggests that either some dehydrogenation occurs at the equatorial hydroxyl groups or that the molecule can react in a sterically unfavourable conformation.

EXPERIMENTAL

Melting points are corrected. All distillations were carried out under reduced pressure (bath temperature < 35°) or by freeze-drying. Whatman 1 filter papers were used for paper chromatography and electrophoresis except for preparative separations which were made on Whatman 3 MM filter papers previously washed thoroughly with water.

Irrigants and buffer used:

A. Ethyl acetate-acetic acid-water, 3:1:3 (upper phase)
B. Butanol-ethanol-water, 10:3:5
C. Ethyl acetate-pyridine-water, 2:1:2
D. Hydrogen sulphite buffer [3] pH 4.7, 0.1 M.

Oxidation of methyl β-D-xylopyranoside with chromium trioxide

The oxidation and fractionation procedures were essentially as described by Theander [1] and an abbreviated description only is given.

Methyl β-D-xylopyranoside (20.0 g) in acetone (1.2 l) was oxidised by treatment under reflux with chromium trioxide (18.3 g) in acetone (1.2 l) for 30 min. The brown chromium oxides were filtered from the oxidation mixture and boiled with acetone (4 × 400 ml) for 10 min with intermediate filtrations. The combined filtrates were evaporated to a dark brown clear solution, adjusted to 500 ml with acetone and treated with 0.5 N alcoholic hydrogen chloride (60 ml) at 25° for 30 min to reduce the chromium in solution to Cr^{3+}. The solution was adjusted (Ag_2CO_3) with agitation and cooling to pH 5. The silver precipitate was filtered, washed with acetone and water and the combined filtrate and washings evaporated to a small volume and deionised [Dowex 50(H^+) and Dowex 3(free base)]. The solution, which had a pH of 5, was evaporated to a semi-crystalline mass (13.6 g) which was fractionated on a carbon-Celite column (70 × 8 cm) using linear gradient elution technique (ethanol: 0—20 %, 16 l). The following main fractions were collected in 50 ml portions.

Fraction I (0.123 g), 120—130, contained a mixture of methyl 2- and 4-oxo-xylosides and was subfractionated on thick filter papers using irrigant A. As the oxo-compounds

were quite labile and further transformed to other products even at pH 4—7, eluates from the thick filter papers were evaporated by freeze-drying in silicone treated flasks.

Fraction II (9.45 g), 132—195, consisted mainly of methyl β-D-xyloside and traces of methyl 2- and 4-oxo-xylosides. The mother-liquors were fractionated on thick filter papers to give further small quantities of 2- and 4-oxo-xylosides after removal of the methyl β-D-xyloside by crystallisation. Fraction III (0.7 g) 202—242 contained methyl β-D-3-oxo-xyloside which was obtained as an amorphous powder $[\alpha]_D^{21.5}$ −90° (*c*, 1.0 in water) after removal of the solvent.

Characterisation of methyl β-oxo-xylosides

Methyl β-D-3-oxo-xylopyranoside (0.2 g) in water (5 ml) was treated over 2 h with 2.5 % sodium amalgam and pH 6 maintained by gradual addition of glacial acetic acid. After deionisation [Dowex 50(H^+) and Dowex 3(free base)] and concentration, the solution was hydrolysed with 0.5 N sulphuric acid for 16 h at 100°. The neutral (Dowex 3) solution was concentrated and the sugars formed were separated on thick filter papers using irrigant A. After elution and evaporation, ribose was obtained as a syrup which failed to crystallise but gave a crystalline 2,4-dinitrophenylhydrazone, m.p. and mixed m.p. 162—163°.

Methyl β-D-2-oxo-xylopyranoside (20 mg) gave on similar treatment two sugars chromatographically indistinguishable from xylose and lyxose in irrigants A—C.

Methyl β-D-4-oxo-xylopyranoside (20 mg) gave on reduction and hydrolysis two sugars chromatographically indistinguishable from xylose and arabinose in irrigants A—C.

Platinum catalysed oxidation of methyl β-D-ribopyranoside

A stream of hydrogen was passed through a suspension of platinum dioxide (2 g) in water (200 ml) in a 500 ml Kluyver flask until reduction was complete. Excess hydrogen was removed in a stream of nitrogen and oxygen then passed in a rapid stream until the metal was finely suspended; β-methyl-D-ribopyranoside (4 g) was added and oxidised at atmospheric pressure for 5 h at 20°. On paper chromatograms, run in irrigant A, the oxidised solution gave a strong spot with $R_{glucose}$ value 3.48, which showed a characteristic colour reaction with anisidine hydrogen chloride spray and was chromatographically indistinguishable from methyl β-D-3-oxo-xylopyranoside. The oxidised solution was shaken with Dowex 3(free base) to remove any acids produced, filtered and the filtrate concentrated under reduced pressure. The combined yield of two such treatments was chromatographed on a carbon-Celite column (70 × 8 cm) using the linear gradient elution technique (ethanol: 0—20 %, 16 l). The following fractions were collected in 50 ml portions.

Fraction I (0.3 g), 128—160, contained three components, the main component having $R_{glucose}$ value 1.58. This fraction was not further investigated.

Fraction II (0.38 g), 178—187, contained relatively pure methyl β-D-3-oxo-xylopyranoside. It was chromatographically indistinguishable from the methyl β-D-3-oxo-xylopyranoside obtained by chromium trioxide oxidation. Ribose and xylose were the only sugars formed on reduction and hydrolysis.

Fraction III (4.8 g), 188—244, contained a small amount of methyl β-D-3-oxo-xylopyranoside together with unreacted starting material. Separation of 2.3 g of this fraction on a carbon-Celite column (35 × 3 cm) using 0.1 N sodium hydrogen sulphite elution [2] gave a further quantity (42 mg) of the 3-oxo-derivative.

Fraction IV (1.8 g), 246—280, contained mainly methyl β-D-ribopyranoside which crystallised on removal of the solvent.

REFERENCES

1. Theander, O. *Acta Chem. Scand.* **11** (1957) 1557.
2. Assarsson, A. and Theander, O. *Acta Chem. Scand.* **12** (1958) 1507.
3. Theander, O. *Acta Chem. Scand.* **11** (1957) 717.
4. Heyns, K. and Paulsen, H. *Angew. Chem.* **69** (1957) 600.
5. Theander, O. *Acta Chem. Scand.* **12** (1958) 1883.

Received July 4, 1960.

ACTA CHEMICA SCANDINAVICA 14 (1960) 2240–2250

Short Communications

Studies on Carbamates
XIV. On the Catalytic Action of Metal Ammines on the Process "Carbon Dioxide ⇌ Carbonic Acid"

ERIK JOHANSEN and CARL FAURHOLT

The Royal Danish School of Pharmacy, Copenhagen, Denmark

In a previous investigation [1] from this laboratory it was shown that $Zn(NH_3)_4^{++}$ increases the rate of the process "$NH_2COONH_4 + H_2O = (NH_4)_2CO_3$" which was explained by assuming that the process "$CO_2 + H_2O = H_2CO_3$" is catalyzed by $Zn(NH_3)_4^{++}$.

In the present investigation it is shown that also $Cu(NH_3)_4^{++}$ has some catalytic effect, whereas $Co(NH_3)_6^{+++}$ has no effect.

Experiments with the carbamate of glycine show that the complex zinc glycinate acts as a catalyst to some degree, whereas the complex cupric glycinate has no significant catalytic effect.

1. *Studies on the ammonium carbamate.* In the previous investigation only a single experiment was carried out with $Cu(NH_3)_4^{++}$. The present investigation is supplementary to this experiment. The results of experiments carried out in the buffer 0.5 M NH_4Cl/0.05 M NH_3 are listed in Table 1. The experiments were carried out at 0°C, and the velocity constants were calculated by means of Briggs logarithms. It is seen that the catalytic action is small. Experiments with $Co(NH_3)_6^{+++}$ in the same buffer solution gave no significant effect.

2. *Studies on the carbamate of glycine.* The experiments are carried out in the buffer 0.5 M $+H_3NCH_2COO^-$/0.05 M $H_2NCH_2COO^-$ at 18°C. The reaction was started by addition of K_2CO_3.

The method of analysis was a slight modification of a complexometric titration described by Jørgensen [2].

The reaction was quenched by addition of sodium hydroxide. It was necessary to mask the added catalyst, *e.g.* zinc glycinate or cupric glycinate, in order to titrate excess barium ion. The masking was performed by means of potassium cyanide, since the complex ions, zinc cyanide ion

Table 1. Ca. 0.02 M NH_2COONH_4 in 0.50 M NH_4Cl/0.05 M NH_3 with and without $Cu(NH_3)_4^{++}$. 0°C.

	$c_{metal\ ammine}$	c_{CO_2} total millimole	% carbamate in eq.	$k_{amate} + k_{onate}$	k_{amate}	k_{onate}
$Cu(NH_3)_4^{++}$	0	20.5	15.0	0.0018	0.0015	0.00027
	0.01	20.8	14.5	0.0023	0.0020	0.00033
	0.02	22.9	14.5	0.0040	0.0034	0.00058
	0.04	22.8	12.5	0.0054	0.0047	0.00068
$Co(NH_3)_6^{+++}$	0.04	19.6	18.9	0.0013	0.0010	0.00025

Table 2. 0.02 M K_2CO_3 in 0.50 M $+H_3NCH_2COO^-$/0.05 M $H_2NCH_2COO^-$.

	$c_{metal\ glycinate}$	$c_{CO_3,\ total}$ millimole	% carbonate in eq.	$k_{amate} + k_{onate}$	k_{amate}	k_{onate}
Zinc glycinate	0	21.3	33.5	0.0047	0.0016	0.0031
	0.005	18.3	39.3	0.0058	0.0023	0.0035
	0.01	18.0	34.9	0.0065	0.0023	0.0042
	0.02	18.2	36.7	0.0085	0.0031	0.0054
Cupric glycinate	0.01	18.0	35.6	0.0048	0.0017	0.0031

and cupric cyanide ion, are not titrated together with excess barium ion.

The details are as follows:

20.00 ml of the specimen are run into a flask containing 2.00 ml of a mixture that is 6.4 M in sodium hydroxide and 2 M in potassium cyanide. 8.00 ml of this mixture are precipitated with barium chloride and analysed as described by Jørgensen. It was found that a faint blue colour appeared before the equivalence point was reached, but at the end point a distinct jump in colour intensity was observed.

The complexometric titration gives results which are identical to those obtained by the method previously used.

The experiments are listed in Table 2. It is seen, that the catalytic action of zinc glycinate is significant but it can not be compared in order of magnitude with the catalytic action of zinc tetrammine.

A corresponding experiment with 0.01 M cupric glycinate gave no significant effect.

1. Grønvald, M. and Faurholt, C. *Acta Chem. Scand.* **14** (1960) 1374.
2. Jørgensen, E. *Acta Chem. Scand.* **10** (1956) 747.

Received November 21, 1960.

Acid Soluble Cytidine Nuoleotide Linked Amino Acids in Extracts of Rabbit Liver

GUNNAR ÅGREN

From the Department of Medical Chemistry, University of Uppsala, Sweden

In recent papers [1,2] it was reported that ^{32}P-labeled trichloroacetic acid (TCA) extracts of liver and kidneys of the rat and rabbit contained an ultra violet (UV) absorbing peak (X_I) which contained ninhydrin positive substances. After purification by ionophoresis and paperchromatography the material from the peak still gave a ninhydrin positive reaction. A labeled UV-peak in the same position of the elution curve could also be observed in TCA extracts of ^{32}P-labeled tissue homogenates of rat kidneys. The nucleotide-amino acid complex exhibited changes in UV-absorbtion spectrum characteristic of cytidine nucleotide (CMP). Since CMP-linked amino acids do not seem to have been observed in animal cells previously some properties of the fraction will be described briefly.

In Fig. 1 a section of the elution diagram of the TCA extract is presented consisting of the peaks immediately before and after AMP (adenylic acid). The TCA extract of rabbit livers was eluted according to Hurlbert *et al.*[3] The two first labeled UV-peaks (X_I) appearing with formic acid concentration between 0 and 0.23 M were taken to dryness. At paper electropherograms in

Table 2. 0.02 M K_2CO_3 in 0.50 M $+H_3NCH_2COO^-$/0.05 M $H_2NCH_2COO^-$.

	$c_{metal\ glycinate}$	$c_{CO_3,\ total}$ millimole	% carbonate in eq.	$k_{amate} + k_{onate}$	k_{amate}	k_{onate}
Zinc glycinate	0	21.3	33.5	0.0047	0.0016	0.0031
	0.005	18.3	39.3	0.0058	0.0023	0.0035
	0.01	18.0	34.9	0.0065	0.0023	0.0042
	0.02	18.2	36.7	0.0085	0.0031	0.0054
Cupric glycinate	0.01	18.0	35.6	0.0048	0.0017	0.0031

and cupric cyanide ion, are not titrated together with excess barium ion.

The details are as follows:

20.00 ml of the specimen are run into a flask containing 2.00 ml of a mixture that is 6.4 M in sodium hydroxide and 2 M in potassium cyanide. 8.00 ml of this mixture are precipitated with barium chloride and analysed as described by Jørgensen. It was found that a faint blue colour appeared before the equivalence point was reached, but at the end point a distinct jump in colour intensity was observed.

The complexometric titration gives results which are identical to those obtained by the method previously used.

The experiments are listed in Table 2. It is seen, that the catalytic action of zinc glycinate is significant but it can not be compared in order of magnitude with the catalytic action of zinc tetrammine.

A corresponding experiment with 0.01 M cupric glycinate gave no significant effect.

1. Grønvald, M. and Faurholt, C. *Acta Chem. Scand.* **14** (1960) 1374.
2. Jørgensen, E. *Acta Chem. Scand.* **10** (1956) 747.

Received November 21, 1960.

Acid Soluble Cytidine Nuoleotide Linked Amino Acids in Extracts of Rabbit Liver

GUNNAR ÅGREN

From the Department of Medical Chemistry, University of Uppsala, Sweden

In recent papers [1,2] it was reported that ^{32}P-labeled trichloroacetic acid (TCA) extracts of liver and kidneys of the rat and rabbit contained an ultra violet (UV) absorbing peak (X_I) which contained ninhydrin positive substances. After purification by ionophoresis and paperchromatography the material from the peak still gave a ninhydrin positive reaction. A labeled UV-peak in the same position of the elution curve could also be observed in TCA extracts of ^{32}P-labeled tissue homogenates of rat kidneys. The nucleotide-amino acid complex exhibited changes in UV-absorbtion spectrum characteristic of cytidine nucleotide (CMP). Since CMP-linked amino acids do not seem to have been observed in animal cells previously some properties of the fraction will be described briefly.

In Fig. 1 a section of the elution diagram of the TCA extract is presented consisting of the peaks immediately before and after AMP (adenylic acid). The TCA extract of rabbit livers was eluted according to Hurlbert *et al.*[3] The two first labeled UV-peaks (X_I) appearing with formic acid concentration between 0 and 0.23 M were taken to dryness. At paper electropherograms in

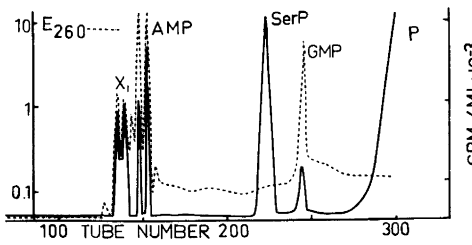

Fig. 1. Acid soluble nucleotides from 7 rabbit livers. The nucleotides were separated on a 6.5 × 45 cm Dowex 1 formate column by gradient elution with reservoir content changed at the tubes numbered as follows: *92*, 1 N formic acid; *250*, 4 N formic acid. The continuous line represents radioactivity and the broken line represents optical density values at 260 mμ.

1 M acetic acid most of the free amino acids were carried away leaving a labeled UV-spot which gave a positive ninhydrin reaction. In one dimensional paper chromatography with *iso*butyric acid and ammonia materials from both fractions behaved differently. Only with material from the second X_I peak one sharp spot with congruent UV, ^{32}P-labeling and positive ninhydrin reaction was obtained together with a ninhydrin negative UV-spot. All of the material from the second X_I peak was purified in this way. When this fraction was again run through a Dowex 1 formate column with a gradient 0 → 1 M formic acid concentration a sharp peak giving UV-absorbtion, activity and positive ninhydrin reaction was observed. Both compounds from X_I exhibited changes in their UV-absorbtion spectra characteristic of cytidine nucleotides; namely an absorbtion maximum in acid medium at 280 mμ with an absorption minimum at 240 mμ. The absorption maximum in neutral solution was located at 270 mμ and the minimum at 250 mμ [4]. Following hydrolysis in 0.1 N HCl for 3 min [5] the hydrolysate of the purified material from the second X_I fraction showed the following properties. In electropherograms in 1 N acetic acid a sharp, labeled ninhydrin positive spot with UV-absorbtion was still observed together with three ninhydrin positive spots slowly moving towards the anode and one spot towards the cathode. At pH 5 in 0.1 N pyridine acetate buffer a labeled, ninhydrin positive spot with UV-absorbtion could be observed together with one ninhydrin positive spot moving towards the anode and one to the cathode. After hydrolysis in sealed tubes for 20 h at 120°C the compound was completely hydrolyzed. Electropherograms in acetic acid showed at least seven ninhydrin positive spots all moving towards the cathode and one or two which did not move. Papers run at pH 5 showed two ninhydrin positive spots moving against the anode and several to the cathode. A two dimensional electrophero-chromatogram [5] showed spots corresponding to aspartic acid, glutamic acid, at least six neutral and one basic amino acid. Following hydrolysis in 1 N HCl for 7 min electropherograms in pyridine acetate showed four sharp, labeled spots giving UV-absorbtion and positive ninhydrin reaction. Two spots corresponding to one acid and one basic amino acid were also observed.

All these data taken together seem to prove that extracts from animal tissues contain amino acids linked to CMP-nucleotides probably in peptide combinations. The results with 7 min hydrolysis are rather complicated and do not exclude the possibility that the material may consist of a complex of CMP-nucleotides with adjacent amino acids linked to each other. The partial acid hydrolysis may produce free nucleotides, nucleotides with amino acids, peptides and free amino acids. So far we have not been able to isolate a substance with quite similar properties from *L. casei*.

This investigation was supported by grants from the *Swedish Medical Research Council.*

1. Ågren, G. *Acta Soc. Med. Upsaliensis* **65** (1960) 49.
2. Ågren, G. *Acta Soc. Med. Upsaliensis* **65** (1960) 55.
3. Hurlbert, P. B., Schmitz, H., Brumm, A. F. and Potter, V. R. *J. Biol. Chem.* **209** (1954) 23.
4. *Pabst Laboratories Circular OR-10*, Milwaukee 1956.
5. Strominger, J. L. and Threnn, R. H. *Biochim. et Biophys. Acta* **36** (1959) 83.

Received November 28, 1960.

Synthesis of Compounds Related to Muscarufin

V. Ethyl 5-(5-methoxy-*p*-benzoquinonyl)-valerate *

MARTIN NILSSON and TORBJÖRN NORIN

Organisk-kemiska Institutionen, Kungl. Tekniska Högskolan, Stockholm, Sweden

Alkyl radicals, obtained by thermal decomposition of diacyl peroxides, may react with quinones to give alkylated products [1,2]. However, no alkylation was observed when bis-(5-ethoxycarbonylvaleryl)-peroxide in acetic acid was thermally decomposed in the presence of dimethyl 2,2′-(*p*-benzoquinon-2,5-ylene)-dibenzoate[3]. Instead the quinone was reduced and converted into the dilactone of 2′,5′-dihydroxy-*p*-terphenyl-2,2″-dicarboxylic acid [3]. Also *p*-benzoquinone was found to be reduced under the same conditions.

However, a 32 % yield of ethyl 5-(5-methoxy-*p*-benzoquinonyl)-valerate was obtained by decomposition of the peroxide in toluene solution in the presence of 2-methoxy-*p*-benzoquinone. The structure of the alkylation product was established by reduction, methylation and oxidation to 2,4,5-trimethoxybenzoic acid. The intermediate 5-(2,4,5-trimethoxyphenyl)-valeric acid could also be obtained, in very good yield, by acylation of 1,2,4-trimethoxybenzene with glutaric anhydride using boron trifluoride as the catalyst, followed by catalytic hydrogenation.

During these studies on the synthesis of compounds related to muscarufin evidence has accumulated which casts some doubt on the correctness of the proposed structure. The work has therefore been discontinued.

Experimental. The melting points were determined on a Kofler block.

*Ethyl 5-(5-methoxy-*p*-benzoquinonyl)-valerate.* 2-Methoxy-*p*-benzoquinone [4] (0.025 mole) in toluene (100 ml, chosen as the solvent because of the sensitivity of the quinone to acids) was heated on a vigorously boiling water bath and a solution of bis(5-ethoxycarbonylvaleryl)-peroxide [2] (0.025 mole) in ether added slowly through a capillary extending to the bottom of the flask while the ether was distilled off. After addition of the peroxide the heating was continued until the evolution of carbon dioxide ceased. The solvent was removed under reduced pressure until the product started to sublime. The mixture was cooled and the crystalline mass collected and recrystallised from methanol, m.p. 100–101° and 112–113° (dimorphism) (yield 32 %). On sublimation the high-melting form was obtained. (Found: C 62.7; H 7.1. Calc. for $C_{14}H_{18}O_5$: C 63.1; H 6.8).

5-(2,4-5-Trimethoxyphenyl)-valeric acid. The quinone (0.27 g) was boiled with acetic anhydride, sodium acetate and zinc dust until the solution was colourless. The mixture was filtered and water was added to precipitate the ethyl 5-(2,5-diacetoxy-4-methoxyphenyl)-valerate, which was recrystallised from methanol, m.p. 41–42.5°. (Found: C 61.1; H 7.0. Calc. for $C_{18}H_{24}O_7$: C 61.4; H 6.9.) The acetate was dissolved in methanol and excess dimethyl sulphate and a concentrated solution of potassium hydroxide added under coal gas. The mixture was then heated to ensure complete saponification of the ester. The reaction product was precipitated and recrystallised from acetic acid-water. The trimethoxyphenylvaleric acid, m.p. 46–47° (0.1 g) was distilled at *ca.* 0.5 mm and then solidified as a higher melting form, m.p. 59–61°. (Found: C 62.7; H 7.4. Calc. for $C_{14}H_{20}O_5$: C 62.7; H 7.5.)

The acid was also prepared by another procedure: A solution of 1,2,4-trimethoxybenzene (0.01 mole) and glutaric anhydride (0.011 mole) in ether was saturated with boron trifluoride and left in the refrigerator for 3 days. The mixture was poured onto ice and the ether evaporated. The 4-(2,4,5-trimethoxybenzoyl-) butyric acid was collected and recrystallised from methanol, m.p. 164–165° (95 %). (Found: C 59.2; H 6.4. Calc. for $C_{14}H_{18}O_6$: C 59.6; H 6.4.)

The synthesis of this acid under somewhat different conditions has been reported but the yield then was lower [5]. A portion (1.03 g) was dissolved in ethanol and hydrogenated over palladised charcoal (0.33 g, 10 %) to absorb 2 mole of hydrogen in 15 h. The 5-(2,4,5-trimethoxyphenyl)-valeric acid was recrystallised from methanol, m.p. 46–48° alone or in admixture with the product obtained from the quinone (95 %). On distillation the same dimorphism was encountered.

Oxidation of 5-(2,4,5-trimethoxyphenyl)-valeric acid with potassium permanganate gave 2,4,5-trimethoxybenzoic acid in 30 % yield,

* Part IV. *Acta Chem. Scand.* **12** (1958) 1830. In the present communication the nomenclature has been changed from that previously used in this series to conform with current usage.

m.p. 144° alone or in admixture with an authentic specimen.

We thank Professor H. Erdtman for his interest in this work and Dr. I Wellings for checking the English.

1. Fieser, L. F. and Oxford, A. E. *J. Am. Chem. Soc.* **64** (1942) 2060.
2. Fieser, L. F., Berliner, E., Bondhus, F. J., Chang, F. C., Dauben, W. G., Ettlinger, M. G., Fawaz, G., Fields, M., Heidelberger, C., Heymann, H., Vaughan, W. R., Wilson, A. G., Wilson, E., Wu, M.-I., Leffler, M. T., Hamlin, K. E., Matson, E. J., Moore, E. E., Moore, M. B., and Zaugg, H. E. *J. Am. Chem. Soc.* **70** (1948) 3174, 3175.
3. Erdtman, H. and Nilsson, M. *Acta Chem. Scand.* **10** (1956) 735.
4. Erdtman, H. *Proc. Roy. Soc.* (*London*) **A 143** (1933) 177, p. 186.
5. Anderson, C. L., Horton, W. J., Walker, F. E. and Weiler, M. R. *J. Am. Chem. Soc.* **77** (1955) 598.

Received November 24, 1960.

The Crystal Structure of Hf_2Al_3

LARS-ERIK EDSHAMMAR

Institute of Inorganic and Physical Chemistry, University of Stockholm, Stockholm, Sweden

In the course of phase analyses and crystal structure determinations in the binary metal systems hafnium-aluminium [1-3] and zirconium-aluminium [1], a phase with the composition Hf_2Al_3 has been studied.

The structure has been determined from complete single crystal data using Patterson and electron density maps. The alloy was prepared by arc-melting and single crystals could be obtained from the crushed melt. The single crystal and Guinier powder data showed the structure to be orthorhombic with the following unit cell dimensions:

$a = 9.52_3$ Å $b = 13.76_3$ Å $c = 5.52_2$ Å

The following structure was derived:

Unit cell content: 8 Hf_2Al_3 (observed density 8.00, calculated density 8.04).

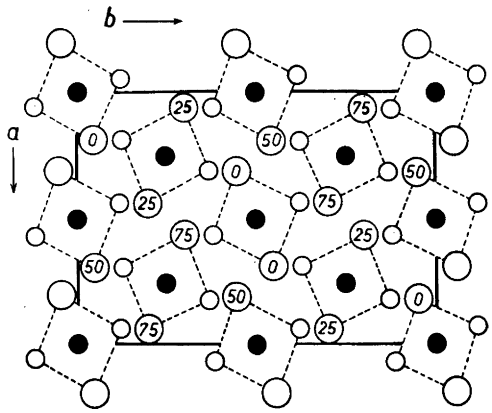

Fig. 1. The structure of Hf_2Al_3 seen along the *c*-axis. The figures in the large circles indicate the height of the Hf-atoms in percent of *c*. Small open circles: Al at *c*/4 above the Hf atoms in the pyramid. Small black circles: Al at 0.39 *c* below the Hf atoms in the pyramid.

Space-group: *Fdd*2 (No. 43).

16 Hf in 16(*b*): $x = 0.185$ $y = 0.052$ $z = 0.000$
16 Al in 16(*b*): $x = 0.185$ $y = 0.133$ $z = 0.500$
8 Al in 8(*a*): $x = 0$ $y = 0$ $z = 0.61$

The structure may be described as built up by triangular-bipyramids, Hf_2Al_3, with the hafnium-atoms forming the apices of the pyramids (*cf.* Fig. 1).

An examination of the zirconium-aluminium system shows the existence of an isotypic structure Zr_2Al_3.

Full details on these investigations and a discussion of the structures in the hafnium-aluminium system will be given elsewhere.

The author wishes to express his thanks to Dr. Arne Magnéli for his kind interest in this work.

1. Edshammar, L.-E. and Andersson, S. *Acta Chem. Scand.* **14** (1960) 223.
2. Edshammar, L.-E. *Acta Chem. Scand.* **14** (1960) 1220.
3. Edshammar, L.-E. *Acta Chem. Scand.* **15** (1961). *In press.*

Received November 26, 1960.

m.p. 144° alone or in admixture with an authentic specimen.

We thank Professor H. Erdtman for his interest in this work and Dr. I Wellings for checking the English.

1. Fieser, L. F. and Oxford, A. E. *J. Am. Chem. Soc.* **64** (1942) 2060.
2. Fieser, L. F., Berliner, E., Bondhus, F. J., Chang, F. C., Dauben, W. G., Ettlinger, M. G., Fawaz, G., Fields, M., Heidelberger, C., Heymann, H., Vaughan, W. R., Wilson, A. G., Wilson, E., Wu, M.-I., Leffler, M. T., Hamlin, K. E., Matson, E. J., Moore, E. E., Moore, M. B., and Zaugg, H. E. *J. Am. Chem. Soc.* **70** (1948) 3174, 3175.
3. Erdtman, H. and Nilsson, M. *Acta Chem. Scand.* **10** (1956) 735.
4. Erdtman, H. *Proc. Roy. Soc.* (*London*) **A 143** (1933) 177, p. 186.
5. Anderson, C. L., Horton, W. J., Walker, F. E. and Weiler, M. R. *J. Am. Chem. Soc.* **77** (1955) 598.

Received November 24, 1960.

The Crystal Structure of Hf_2Al_3

LARS-ERIK EDSHAMMAR

Institute of Inorganic and Physical Chemistry, University of Stockholm, Stockholm, Sweden

In the course of phase analyses and crystal structure determinations in the binary metal systems hafnium-aluminium [1-3] and zirconium-aluminium [1], a phase with the composition Hf_2Al_3 has been studied.

The structure has been determined from complete single crystal data using Patterson and electron density maps. The alloy was prepared by arc-melting and single crystals could be obtained from the crushed melt. The single crystal and Guinier powder data showed the structure to be orthorhombic with the following unit cell dimensions:

$a = 9.52_3$ Å $b = 13.76_3$ Å $c = 5.52_2$ Å

The following structure was derived:

Unit cell content: 8 Hf_2Al_3 (observed density 8.00, calculated density 8.04).

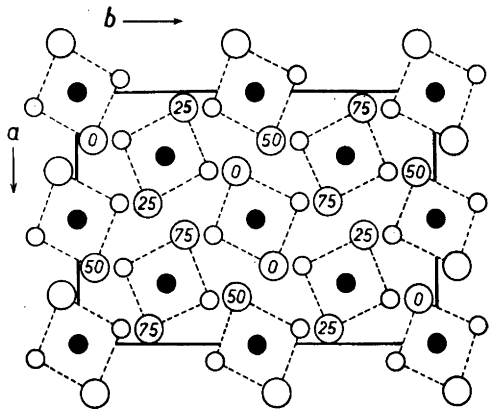

Fig. 1. The structure of Hf_2Al_3 seen along the *c*-axis. The figures in the large circles indicate the height of the Hf-atoms in percent of *c*. Small open circles: Al at *c*/4 above the Hf atoms in the pyramid. Small black circles: Al at 0.39 *c* below the Hf atoms in the pyramid.

Space-group: *Fdd*2 (No. 43).

16 Hf in 16(*b*): $x = 0.185$ $y = 0.052$ $z = 0.000$
16 Al in 16(*b*): $x = 0.185$ $y = 0.133$ $z = 0.500$
8 Al in 8(*a*): $x = 0$ $y = 0$ $z = 0.61$

The structure may be described as built up by triangular-bipyramids, Hf_2Al_3, with the hafnium-atoms forming the apices of the pyramids (*cf.* Fig. 1).

An examination of the zirconium-aluminium system shows the existence of an isotypic structure Zr_2Al_3.

Full details on these investigations and a discussion of the structures in the hafnium-aluminium system will be given elsewhere.

The author wishes to express his thanks to Dr. Arne Magnéli for his kind interest in this work.

1. Edshammar, L.-E. and Andersson, S. *Acta Chem. Scand.* **14** (1960) 223.
2. Edshammar, L.-E. *Acta Chem. Scand.* **14** (1960) 1220.
3. Edshammar, L.-E. *Acta Chem. Scand.* **15** (1961). *In press.*

Received November 26, 1960.

A Method for the Detection of Oxygen in Organic Compounds

BENGT SMITH and RAGNAR OHLSON

Institutionen för Organisk kemi, Chalmers Tekniska Högskola, Göteborg, Sweden

For the qualitative determination of elements in organic compounds the sodium fusion method of Lassaigne has since long been the most important one. It permits the detection of most common elements occurring in organic compounds. However, neither this nor any other method permits a reliable detection of oxygen, a fact which has been a considerable drawback in qualitative organic analysis. When studying methods for the detection of elements in organic compounds by gas chromatography we found that oxygen could be identified in a simple and reasonably reliable way by cracking the substance over a glowing platinum wire in an atmosphere of helium and analyzing the pyrolysis products for carbon oxide. The new method has been applied to a substantial number of organic compounds of various types including alcohols, phenols, ethers, aldehydes, ketones, carboxylic acids, esters, acetals, amides, anhydrides, carbohydrates, proteins, lignin, nitro compounds, sulphonic acids, oxygen-containing organosilicon compounds and oxygen-containing heterocyclic compounds.

The test was positive in every case. In the pyrolysis of oxygen-containing organosilicon compounds and nitro compounds, a large part of the oxygen was bound up in silicon dioxide and nitrogen oxides, respectively. However, enough carbon oxide was formed, if an adequate amount of substance was used. We have also investigated a number of oxygen-free organic compounds but have not obtained a positive test in any case.

The carbon oxide formed was identified using gel tubes, containing silica gel impregnated with a mixture of palladium sulphate and ammonium molybdate [1]. The yellow silico molybdato complex turns to green or blue in the presence of carbon oxide. Other reducing substances may give a similar test, but the silica gel layer (*cf.* below) placed before the indicating layer is stated to absorb interfering substances [1].

It is also possible to identify the carbon oxide by means of gas chromatography, *e.g.* using columns containing silica gel [2] or molecular sieves [3]. These methods will be discussed in a forthcoming paper, describing the detection of oxygen and other elements in organic compounds by means of gas chromatography.

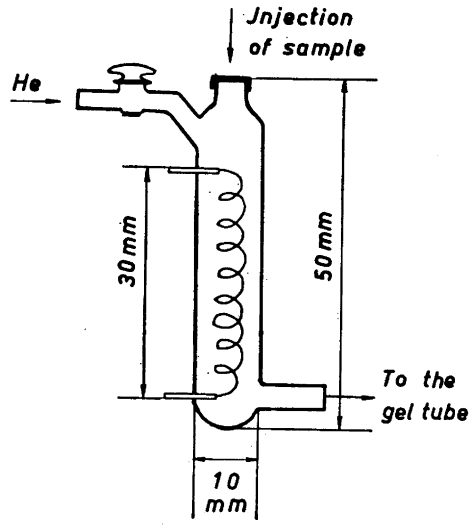

Fig. 1. Pyrolysis apparatus used for the detection of oxygen.

The apparatus used for the pyrolysis is shown in Fig. 1. It consisted of a pyrex glass tube containing a platinum glowing wire. The thin glowing wire (0.35 mm diam.) was welded to two thicker contact wires. The reactor was equipped with inlet and outlet tubes for helium and a tube covered by a serum cap for injecting liquid samples.

An experiment was performed in the following way. The gel tube was connected to the reactor and a stream of helium passed through for some minutes to sweep the air from the reactor. This done, the flow of helium through the reactor was interrupted by turning the three-way stopcock, and a voltage of 3—4 V was applied to the platinum wire causing it to glow. The liquid sample (1—5 μl) was injected through the serum cap and pyrolysed by the glowing wire. After 10 sec the flow of helium was resumed and the pyrolysis products swept through the gel tube. For solid substances the same procedure was followed except that the reactor was used in a horisontal position with the sample in the middle of the reactor at the start.

Instead of helium, oxygen-free nitrogen might be used.

The gel tube * was 100 mm long and had an outer diam. of 4 mm. It was packed to a length of 10 mm with the carbon oxide indicating gel (silica gel impregnated with a mixture of palladium sulphate and ammonium molybdate, *cf.* Ref.[1]). On the inlet side of the indicating layer was placed a 40 mm length and on the outlet side a 10 mm length of silica gel.

1. Shepherd, M. *Anal. Chem.* **19** (1947) 77.
2. Smith, R. N., Swinehart, J. and Lesnini, D. G. *Anal. Chem.* **30** (1958) 1217.
3. Brenner, N. and Ettre, L. S. *Anal. Chem.* **31** (1959) 1815.

Received November 30, 1960.

* We have used tubes manufactured and sold by LKB-Produkter Fabriksaktiebolag, Stockholm.

The Crystal Structure of Pd_3P

STIG RUNDQVIST and
LARS-OTTO GULLMAN

Institute of Chemistry, University of Uppsala, Uppsala, Sweden

An X-ray investigation of the palladium-phosphorus system was recently begun at this Institute. Preliminary results show that the system is far more complex than is indicated in the equilibrium diagram given by Wiehage *et al.*[1] It is especially noteworthy that at least four intermediate phases seem to exist in the range 0—25 atom % phosphorus. The existence of a phase near the composition Pd_3P, as observed by Wiehage *et al.*[1], was confirmed by our results. A single-crystal investigation showed that Pd_3P has the cementite ($D\,O_{11}$) structure. The homogeneity range, determined from alloys quenched from 740°C, was found to extend from approximately $Pd_3P_{0.75}$ to $Pd_3P_{1.0}$ with the following lattice parameters (accuracy ± 0.05 %): phosphorus-rich limit $a = 5.980$ Å; $b = 7.440$ Å; $c = 5.164$ Å and palladium-rich limit $a = 5.645$ Å; $b = 7.558$ Å; $c = 5.071$ Å.

The crystal structure was determined by examination of single-crystals selected from an alloy with the approximate composition $Pd_3P_{0.95}$. 62 $F(h0l)$-values and 63 $F(0kl)$-values were recorded with niobium-filtered MoK-radiation in a multiple-film Weissenberg camera with thin iron foils between successive films. Atomic parameters were refined from electron density projections and difference syntheses. Fourier summations and structure factor calculations were made on the electronic digital computer BESK with programs devised by Åsbrink *et al.*[2]

The final R-value for the recorded $F(h0l)$-values was 0.087, applying an isotropic temperature factor with $B = 0.72_4$ Å^2; the corresponding figures for the $F(0kl)$-values were $R = 0.088$, $B = 0.67$ Å^2. (The five largest $F(0kl)$-values, which were obviously weakened owing to extinction, were omitted in the final stages of refinement).

The following structural data for $Pd_3P_{0.95}$ were obtained: Space group $Pnma-(D_{2h}^{16})$; $Z = 4$. *(Table 1.)*

The standard deviations quoted were calculated using Cruickshank's formula [3].

Interatomic distances are listed in Table 2.

It is of interest to note that in addition to Pd_3P described above, the compounds Pd_3Si and Pd_3B also possess the cementite structure [4,5]. A case of isomorphism between a boride, a silicide and a phosphide of the same metal is thus demonstrated.

Further reports of the work on palladium phosphides will be published later in this journal.

Table 1. Structural data for $Pd_3P_{0.95}$.

$a = 5.947$ Å; $b = 7.451$ Å; $c = 5.170$ Å; $U = 229.1$ Å^3

		x	$\sigma(x)$	y	$\sigma(y)$	z	$\sigma(z)$
8 Pd_I	in 8(d)	0.1783	0.0002	0.0636	0.0003	0.3373	0.0003
4 Pd_{II}	in 4(c)	0.0264	0.0004	—	—	0.8700	0.0004
4 P	in 4(c)	0.8834	0.0011	—	—	0.4550	0.0011

Instead of helium, oxygen-free nitrogen might be used.

The gel tube * was 100 mm long and had an outer diam. of 4 mm. It was packed to a length of 10 mm with the carbon oxide indicating gel (silica gel impregnated with a mixture of palladium sulphate and ammonium molybdate, *cf.* Ref.[1]). On the inlet side of the indicating layer was placed a 40 mm length and on the outlet side a 10 mm length of silica gel.

1. Shepherd, M. *Anal. Chem.* **19** (1947) 77.
2. Smith, R. N., Swinehart, J. and Lesnini, D. G. *Anal. Chem.* **30** (1958) 1217.
3. Brenner, N. and Ettre, L. S. *Anal. Chem.* **31** (1959) 1815.

Received November 30, 1960.

* We have used tubes manufactured and sold by LKB-Produkter Fabriksaktiebolag, Stockholm.

The Crystal Structure of Pd_3P

STIG RUNDQVIST and
LARS-OTTO GULLMAN

Institute of Chemistry, University of Uppsala, Uppsala, Sweden

An X-ray investigation of the palladium-phosphorus system was recently begun at this Institute. Preliminary results show that the system is far more complex than is indicated in the equilibrium diagram given by Wiehage *et al.*[1] It is especially noteworthy that at least four intermediate phases seem to exist in the range 0—25 atom % phosphorus. The existence of a phase near the composition Pd_3P, as observed by Wiehage *et al.*[1], was confirmed by our results. A single-crystal investigation showed that Pd_3P has the cementite ($D\,O_{11}$) structure. The homogeneity range, determined from alloys quenched from 740°C, was found to extend from approximately $Pd_3P_{0.75}$ to $Pd_3P_{1.0}$ with the following lattice parameters (accuracy ± 0.05 %): phosphorus-rich limit $a = 5.980$ Å; $b = 7.440$ Å; $c = 5.164$ Å and palladium-rich limit $a = 5.645$ Å; $b = 7.558$ Å; $c = 5.071$ Å.

The crystal structure was determined by examination of single-crystals selected from an alloy with the approximate composition $Pd_3P_{0.95}$. 62 $F(h0l)$-values and 63 $F(0kl)$-values were recorded with niobium-filtered MoK-radiation in a multiple-film Weissenberg camera with thin iron foils between successive films. Atomic parameters were refined from electron density projections and difference syntheses. Fourier summations and structure factor calculations were made on the electronic digital computer BESK with programs devised by Åsbrink *et al.*[2]

The final R-value for the recorded $F(h0l)$-values was 0.087, applying an isotropic temperature factor with $B = 0.72_4$ Å^2; the corresponding figures for the $F(0kl)$-values were $R = 0.088$, $B = 0.67$ Å^2. (The five largest $F(0kl)$-values, which were obviously weakened owing to extinction, were omitted in the final stages of refinement).

The following structural data for $Pd_3P_{0.95}$ were obtained: Space group $Pnma-(D_{2h}^{16})$; $Z = 4$. *(Table 1.)*

The standard deviations quoted were calculated using Cruickshank's formula [3].

Interatomic distances are listed in Table 2.

It is of interest to note that in addition to Pd_3P described above, the compounds Pd_3Si and Pd_3B also possess the cementite structure [4,5]. A case of isomorphism between a boride, a silicide and a phosphide of the same metal is thus demonstrated.

Further reports of the work on palladium phosphides will be published later in this journal.

Table 1. Structural data for $Pd_3P_{0.95}$.

$a = 5.947$ Å; $b = 7.451$ Å; $c = 5.170$ Å; $U = 229.1$ Å^3

		x	$\sigma(x)$	y	$\sigma(y)$	z	$\sigma(z)$
8 Pd_I	in 8(d)	0.1783	0.0002	0.0636	0.0003	0.3373	0.0003
4 Pd_{II}	in 4(c)	0.0264	0.0004	—	—	0.8700	0.0004
4 P	in 4(c)	0.8834	0.0011	—	—	0.4550	0.0011

Table 2. Interatomic distances in $Pd_3P_{0.95}$ (Å). (Distances shorter than 3.5 Å listed).

	Pd_I	Pd_{II}	P
Pd_I	2.77_8, 2.85_1, $2.88_9(2)$,$3.10_7(2)$	2.83_9,2.92_5, 2.92_6,2.93_5, 3.21_0	2.30_9,2.39_4, 2.59_6
Pd_{II}	$2.83_9(2)$,$2.92_5(2)$ $2.92_6(2)$,$2.93_5(2)$ $3.21_0(2)$	$3.22_2(2)$	2.30_8,2.30_8 3.14_2
P	$2.30_9(2)$,$2.39_4(2)$ $2.59_6(2)$	2.30_8,2.30_8, 3.14_2	—

This work has been supported by the *Air Force Office of Scientific Research of the Air Research and Development Command, United States Air Force* through its European Office under Contract No. AF 61(052)-40 and by the *Swedish State Council for Technical Research.* Facilities for use of the digital computer BESK were granted by the *Swedish Board for Computing Machinery.*

1. Wiehage, G., Weibke, F., Biltz, W., Meisel, K. and Wiechmann, F. *Z. anorg. Chem.* **228** (1936) 357.
2. Åsbrink, S., Blomqvist, G. and Westman, S. *Arkiv Kemi* **14** (1959) 545.
3. Cruickshank, D. W. J. *Acta Cryst.* **2** (1949) 65.
4. Aronsson, B. and Nylund, A. *Acta Chem. Scand.* **14** (1960) 1011.
5. Stenberg, E. *Acta Chem. Scand.* **15** (1961). *In print.*

Received December 2, 1960.

Studies on Rennin

V. Chromatographic Purification of Prorennin

BENT FOLTMANN

Carlsberg Laboratory, Copenhagen, Denmark

The first paper in this series [1] described the preparation of partly purified prorennin obtained from dried calf stomachs by extraction with a 2 % solution of sodium bicarbonate. After clarification with aluminium sulphate and disodium hydrogen phosphate, the extract was precipitated twice by saturation with sodium chloride. Paper electrophoresis indicated that approximately 50 % of the protein in the second precipitate was prorennin, but attempts at further purification by salt fractionation failed.

The investigations have been continued by chromatographic fractionation of the partly purified prorennin on columns of diethylaminoethylcellulose (DEAE-cellulose) as described by Peterson and Sober [2].

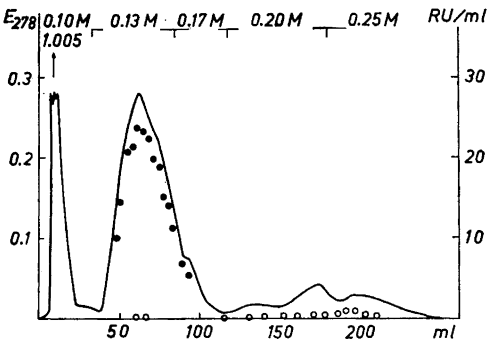

Fig. 1. Chromatography of partly purified prorennin on DEAE-cellulose involving stepwise elution with phosphate buffers of pH 5.8—5.7; 0.10 M, 0.13 M, 0.17 M, 0.20 M, and 0.25 M. Load 20 mg, column 0.9 × 11 cm. Flow rate 4 ml/h; fractions of 2 ml. ○ preformed milk-clotting activity (RU/ml). ● milk-clotting activity after activation. Experimental points have been omitted from the extinction curve of E_{278} for the sake of clarity.

Commercial products of DEAE-cellulose were used (Bio-Rad lot No. CXD $^{59-1}$ and Eastman-Kodak lot No. 7392). The partly purified prorennin was prepared as earlier described. After removal of the NaCl by dialysis the sample was applied to a column of DEAE-cellulose previously equilibrated with 0.10 M phosphate buffer of pH 5.8. Fig. 1 illustrates such an experiment with elution carried out by stepwise increase of the phosphate concentration from 0.10 to 0.25 M. The concentration of protein is expressed by the optical density at 278 mμ. For assay of the potential milk-clotting activity, 200 μl of each fraction was mixed with 200 μl 0.4 M acetate buffer of pH 4.1 and kept 24 h at 25°C to convert the prorennin to active enzyme before the

Table 2. Interatomic distances in $Pd_3P_{0.95}$ (Å). (Distances shorter than 3.5 Å listed).

	Pd_I	Pd_{II}	P
Pd_I	2.77_8, 2.85_1, $2.88_9(2)$,$3.10_7(2)$	2.83_9,2.92_5, 2.92_6,2.93_5, 3.21_0	2.30_9,2.39_4, 2.59_6
Pd_{II}	$2.83_9(2)$,$2.92_5(2)$ $2.92_6(2)$,$2.93_5(2)$ $3.21_0(2)$	$3.22_2(2)$	2.30_8,2.30_8 3.14_2
P	$2.30_9(2)$,$2.39_4(2)$ $2.59_6(2)$	2.30_8,2.30_8, 3.14_2	—

This work has been supported by the *Air Force Office of Scientific Research of the Air Research and Development Command, United States Air Force* through its European Office under Contract No. AF 61(052)-40 and by the *Swedish State Council for Technical Research.* Facilities for use of the digital computer BESK were granted by the *Swedish Board for Computing Machinery.*

1. Wiehage, G., Weibke, F., Biltz, W., Meisel, K. and Wiechmann, F. *Z. anorg. Chem.* **228** (1936) 357.
2. Åsbrink, S., Blomqvist, G. and Westman, S. *Arkiv Kemi* **14** (1959) 545.
3. Cruickshank, D. W. J. *Acta Cryst.* **2** (1949) 65.
4. Aronsson, B. and Nylund, A. *Acta Chem. Scand.* **14** (1960) 1011.
5. Stenberg, E. *Acta Chem. Scand.* **15** (1961). *In print.*

Received December 2, 1960.

Studies on Rennin

V. Chromatographic Purification of Prorennin

BENT FOLTMANN

Carlsberg Laboratory, Copenhagen, Denmark

The first paper in this series [1] described the preparation of partly purified prorennin obtained from dried calf stomachs by extraction with a 2 % solution of sodium bicarbonate. After clarification with aluminium sulphate and disodium hydrogen phosphate, the extract was precipitated twice by saturation with sodium chloride. Paper electrophoresis indicated that approximately 50 % of the protein in the second precipitate was prorennin, but attempts at further purification by salt fractionation failed.

The investigations have been continued by chromatographic fractionation of the partly purified prorennin on columns of diethylaminoethylcellulose (DEAE-cellulose) as described by Peterson and Sober [2].

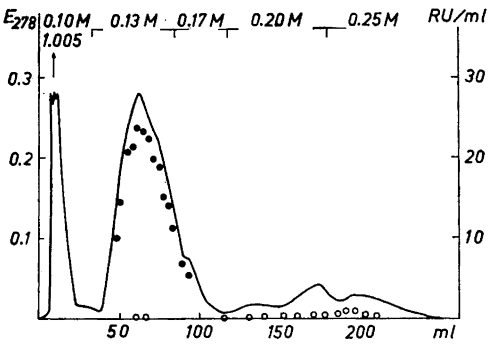

Fig. 1. Chromatography of partly purified prorennin on DEAE-cellulose involving stepwise elution with phosphate buffers of pH 5.8—5.7; 0.10 M, 0.13 M, 0.17 M, 0.20 M, and 0.25 M. Load 20 mg, column 0.9 × 11 cm. Flow rate 4 ml/h; fractions of 2 ml. ○ preformed milk-clotting activity (RU/ml). ● milk-clotting activity after activation. Experimental points have been omitted from the extinction curve of E_{278} for the sake of clarity.

Commercial products of DEAE-cellulose were used (Bio-Rad lot No. CXD $^{59-1}$ and Eastman-Kodak lot No. 7392). The partly purified prorennin was prepared as earlier described. After removal of the NaCl by dialysis the sample was applied to a column of DEAE-cellulose previously equilibrated with 0.10 M phosphate buffer of pH 5.8. Fig. 1 illustrates such an experiment with elution carried out by stepwise increase of the phosphate concentration from 0.10 to 0.25 M. The concentration of protein is expressed by the optical density at 278 mμ. For assay of the potential milk-clotting activity, 200 μl of each fraction was mixed with 200 μl 0.4 M acetate buffer of pH 4.1 and kept 24 h at 25°C to convert the prorennin to active enzyme before the

clotting test was performed. The milk-clotting activities of the activated fractions of prorennin and of preformed rennin are expressed in rennin units (RU) according to Berridge [3].

The chromatogram in Fig. 1 shows that most of the inert material from the partly purified prorennin passed the column as a high, narrow front peak. Without previous activation the peak which was developed after buffer shift to 0.13 and 0.17 M phosphate had only a faint milk-clotting activity (as these tests were carried out with a very high potential activity in the reaction mixture, the clotting observed might be due to activation taking place during the tests). After activation, however, the ratio between potential activity and optical density was constant (within experimental error) across the peak, approximately 90. After further change of the buffer concentration to 0.20 M and 0.25 M phosphate, smaller peaks containing preformed rennin were developed.

For preparation of larger amounts of prorennin, 425 mg freeze-dried, partly purified prorennin was dissolved in 5 ml 0.01 M phosphate buffer of pH 6.1 and applied to a column of DEAE-cellulose (2 × 15 cm) previously equilibrated with 0.1 M phosphate buffer of pH 5.8. The elution was started with 0.1 M phosphate buffer. As expected from the small scale experiment, most of the inert material passed the column in the first 150 ml of eluate. After 280 ml of eluate, the concentration of the eluent buffer was increased to 0.20 M. This rapid increase of the buffer concentration resulted in a very sharp peak with concentrations of prorennin up to 3 mg/ml. The fractions containing the prorennin were pooled, dialysed against 0.001 M phosphate buffer of pH 6.6, and freeze-dried. In this way about 150 mg chromatographically purified prorennin was prepared.

A 16.8 mg sample of this preparation was chromatographed on a column of DEAE-cellulose by the same technique as in the first experiment. The preparation proved to be slightly inhomogeneous, but about 85 % of the total optical density at 278 mμ is represented by the peak containing the prorennin activity (Fig. 2a). Another 13.7 mg of the chromatographically purified prorennin was dissolved in 2 ml of water, and 0.1 N HCl was added to a final pH of 2.1. After 1.5 h at 22°C, the sample was neutralised by addition of 0.1 ml 0.5 M disodium-hydrogenphosphate. The neutralised sample was applied to a column of DEAE-cellulose and chromatographed by the same technique as in the foregoing experiment. The results are illustrated in Fig. 2b.

From Fig. 2 it is seen that the front peak of inactive material is increased from 8 % of the

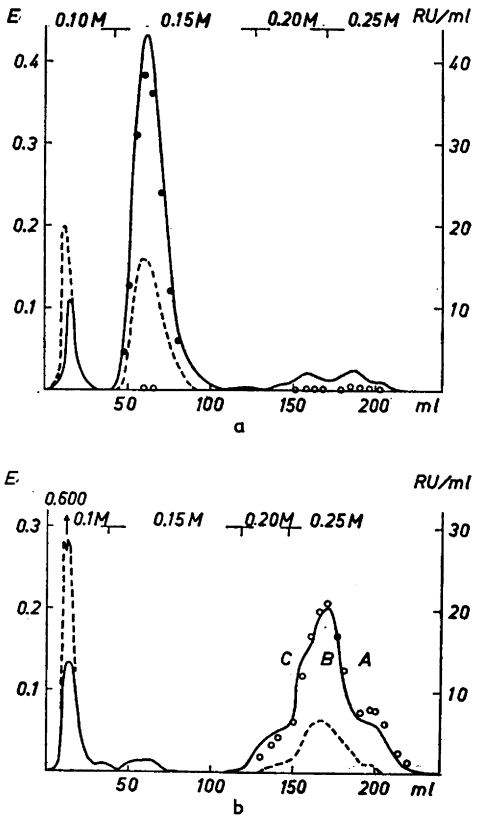

Fig. 2. a. Rechromatography of chromatographically purified prorennin. b. Chromatography of the same preparation after activation at pH 2.1. Columns of DEAE-cellulose (0.9 × 13 cm). Stepwise elution with phosphate buffers, pH 5.8 – 5.7; 0.10 M, 0.15 M, 0.20 M, and 0.25 M. Flow rate 6 ml/h; fractions of 3 ml. ○ milk-clotting activity (RU/ml). ● milk-clotting activity after activation. Solid line: optical density at 278 mμ. Dashed line: ninhydrin color according to Moore and Stein [7] (0.5 ml sample + 0.5 ml reagent diluted with 10 ml of ethanol).

total optical density of the unactivated prorennin (Fig. 2a) to 15 % in the activated sample (Fig. 2b), and further that the ninhydrin reaction of the same peak is much increased, suggesting that one or more tyrosine-containing peptides are split off from the prorennin during the activation.

The prorennin peak has disappeared in Fig. 2b, and in the peak which contains the rennin activity it is possible to recognize three components similar to the A, B, and C rennins obtained from rennin crystals. Furthermore, the specific activity (*i.e.* RU/ml/E_{278}) varies over the rennin peak in a similar way as in chromatography of rennin crystals (Foltmann [4]).

An experiment was carried out after only 15 min. of activation at pH 2. Chromatography of the reaction mixture thus obtained revealed approximately equal amounts of A and B rennins and only traces of C. On the basis of this experience it may be surmised that the different rennins are formed from the same prorennin, perhaps by consecutive reactions as in activation of chymotrypsinogen.

The chromatographically purified prorennin was labelled with fluorodinitrobenzene by the Sanger method [5]. After 7 h of hydrolysis in constant boiling, glass-distilled HCl at 110°C, the DNP-amino acids formed were analysed by paper chromatography according to Levy [6]. In this way alanine was found as NH_2-terminal. With the use of an internal standard of DNP-alanine which was treated in the same way as the DNP-prorennin, a semi-quantitative assay indicated 1 mole of DNP-alanine per 60 000 g of DNP-prorennin. Allowing for the weight increase due to DNP groups, this corresponds to a molecular weight of 40 000—50 000 for the prorennin.

In ultracentrifugation the chromatographically purified prorennin showed one slightly asymmetrical peak. The sedimentation constant was increased by increasing concentrations of prorennin, suggesting the formation of dimers in the more concentrated solutions. By extrapolation to zero concentration, $S_{20,w}$ was found to be 3.5.

The chromatographic behaviour of prorennin and rennin is consistent with the earlier observation (Foltmann [1]) that the isoelectric point of prorennin is higher than that of rennin since compounds with higher isoelectric points would be expected to be eluted first in the technique used.

Further studies on prorennin and its activation will appear in the *Compt. rend. trav. lab. Carlsberg.*

Acknowledgements. The author thanks Chr. Hansen's Laboratory, Ltd. for a generous supply of material. The author is indebted to the staff of the Carlsberg Laboratory, especially to the department head, Professor M. Ottesen, for valuable discussions.

1. Foltmann, B. *Acta Chem. Scand.* **12** (1958) 343.
2. Peterson, E. A. and Sober, H. A. *J. Am. Chem. Soc.* **78** (1958) 751.
3. Berridge, N. J. *Biochem. J.* **39** (1945) 179.
4. Foltmann, B. *Acta Chem. Scand.* **14** (1960) 2059.
5. Sanger, F. *Biochem. J.* **39** (1945) 507.
6. Levy, A. L. *Nature* **174** (1954) 126.
7. Moore, S. and Stein, W. H. *J. Biol. Chem.* **211** (1954) 907.

Received December 2, 1960.

Chromatographic Analysis of Sugars as Complex Borate Ions

ANUND HALLÉN

Chemistry Department II, Karolinska Institutet, Stockholm, Sweden

As demonstrated by Khym and Zill [1], neutral sugars can be separated chromatographically on an anion exchange resin as borate complexes, when elution is performed with dilute borate buffers. However, although they used small columns (0.5 × 11 cm) the effluent volumes of the monosaccharides became very large (500 — 1 500 ml). This is obviously a disadvantage in the analysis of small amounts of sugars. A modification involving elution at a higher ionic strength has therefore been worked out. Fig. 1 shows a typical chromatogram, including galacturonic acid and glucuronic acid, of which the separation has been reported by Khym and Doherty [2].

The components were obtained in 100 % yield (error of method ± 10 %). In parallel with the relative rates of migration of the sugar-borate complexes in high-voltage paper electrophoresis [3,4], lyxose was eluted together with mannose, ribose together with fucose, arabinose together with galactose, and xylose together with glucose. It thus seems necessary to use specific colour reactions [5,1] for the differential analysis of such sugar pairs. Keto sugars give a low colour yield in the aniline reaction used.

Experimental. The sugars (0.2—0.8 mg of each component) were dissolved in a total

The prorennin peak has disappeared in Fig. 2b, and in the peak which contains the rennin activity it is possible to recognize three components similar to the A, B, and C rennins obtained from rennin crystals. Furthermore, the specific activity (*i.e.* RU/ml/E_{278}) varies over the rennin peak in a similar way as in chromatography of rennin crystals (Foltmann [4]).

An experiment was carried out after only 15 min. of activation at pH 2. Chromatography of the reaction mixture thus obtained revealed approximately equal amounts of A and B rennins and only traces of C. On the basis of this experience it may be surmised that the different rennins are formed from the same prorennin, perhaps by consecutive reactions as in activation of chymotrypsinogen.

The chromatographically purified prorennin was labelled with fluorodinitrobenzene by the Sanger method [5]. After 7 h of hydrolysis in constant boiling, glass-distilled HCl at 110°C, the DNP-amino acids formed were analysed by paper chromatography according to Levy [6]. In this way alanine was found as NH_2-terminal. With the use of an internal standard of DNP-alanine which was treated in the same way as the DNP-prorennin, a semi-quantitative assay indicated 1 mole of DNP-alanine per 60 000 g of DNP-prorennin. Allowing for the weight increase due to DNP groups, this corresponds to a molecular weight of 40 000—50 000 for the prorennin.

In ultracentrifugation the chromatographically purified prorennin showed one slightly asymmetrical peak. The sedimentation constant was increased by increasing concentrations of prorennin, suggesting the formation of dimers in the more concentrated solutions. By extrapolation to zero concentration, $S_{20,w}$ was found to be 3.5.

The chromatographic behaviour of prorennin and rennin is consistent with the earlier observation (Foltmann [1]) that the isoelectric point of prorennin is higher than that of rennin since compounds with higher isoelectric points would be expected to be eluted first in the technique used.

Further studies on prorennin and its activation will appear in the *Compt. rend. trav. lab. Carlsberg.*

Acknowledgements. The author thanks Chr. Hansen's Laboratory, Ltd. for a generous supply of material. The author is indebted to the staff of the Carlsberg Laboratory, especially to the department head, Professor M. Ottesen, for valuable discussions.

1. Foltmann, B. *Acta Chem. Scand.* **12** (1958) 343.
2. Peterson, E. A. and Sober, H. A. *J. Am. Chem. Soc.* **78** (1958) 751.
3. Berridge, N. J. *Biochem. J.* **39** (1945) 179.
4. Foltmann, B. *Acta Chem. Scand.* **14** (1960) 2059.
5. Sanger, F. *Biochem. J.* **39** (1945) 507.
6. Levy, A. L. *Nature* **174** (1954) 126.
7. Moore, S. and Stein, W. H. *J. Biol. Chem.* **211** (1954) 907.

Received December 2, 1960.

Chromatographic Analysis of Sugars as Complex Borate Ions

ANUND HALLÉN

Chemistry Department II, Karolinska Institutet, Stockholm, Sweden

As demonstrated by Khym and Zill [1], neutral sugars can be separated chromatographically on an anion exchange resin as borate complexes, when elution is performed with dilute borate buffers. However, although they used small columns (0.5 × 11 cm) the effluent volumes of the monosaccharides became very large (500 — 1 500 ml). This is obviously a disadvantage in the analysis of small amounts of sugars. A modification involving elution at a higher ionic strength has therefore been worked out. Fig. 1 shows a typical chromatogram, including galacturonic acid and glucuronic acid, of which the separation has been reported by Khym and Doherty [2].

The components were obtained in 100 % yield (error of method ± 10 %). In parallel with the relative rates of migration of the sugar-borate complexes in high-voltage paper electrophoresis [3,4], lyxose was eluted together with mannose, ribose together with fucose, arabinose together with galactose, and xylose together with glucose. It thus seems necessary to use specific colour reactions [5,1] for the differential analysis of such sugar pairs. Keto sugars give a low colour yield in the aniline reaction used.

Experimental. The sugars (0.2—0.8 mg of each component) were dissolved in a total

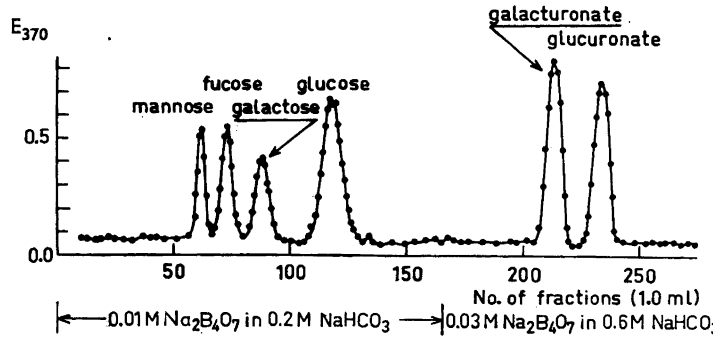

Fig. 1. Chromatography of monosaccharides on a 0.6 × 150 cm Dowex 2 column with borax-bicarbonate solutions. Test mixture: D-mannose (285 μg), L-fucose (298 μg), D-galactose (280 μg), D-glucose (544 μg), D-galacturonic acid (828 μg) and D-glucurone (795 μg).

volume of 0.3 ml of 0.05 M borax (19.1 g $Na_2B_4O_7 \cdot 10\ H_2O$ per liter), and put on the column in the usual way.

The resin, Dowex 2 X 8, 200–400 mesh, was treated with 2 M hydrochloric acid, 2 M sodium hydroxide, 2 M sodium carbonate, and finally 0.03 M borax in 0.60 M sodium bicarbonate, in which solution the resin was stored until used. It was then suspended in a suitable amount of 0.01 M borax in 0.20 M sodium bicarbonate, and was allowed to sediment spontaneously to form a 0.6 × 150 cm column. The column was washed overnight with 0.01 M borax in 0.20 M sodium bicarbonate before application of the sugar mixture. The air present in the solvents was removed by treatment in a suction flask under reduced pressure. Toluene was added to a concentration of 0.5 ml /liter to prevent growth of microorganisms.

The neutral sugars were eluted at room temperature with 0.01 M borax in 0.20 M sodium bicarbonate and, after the appearance of the last neutral sugar peak (glucose), the uronic acids were eluted with 0.03 M borax in 0.60 M sodium bicarbonate. The pH of both solutions was found to be 8.7. The flow rate was adjusted to 1.5 ml/h, and the effluent was collected in 1.0 ml fractions.

A set of standards was prepared for each component. The standards contained 10–100 (150) μg of sugar per ml, dissolved in 0.01 M borax in 0.20 M sodium bicarbonate.

Analysis was performed with a modification of Gardell's aldo sugar method [6]: 3 ml of a freshly prepared mixture of 10 ml of aniline (distilled) and 500 ml of acetic acid was added with an automatic pipette to unknowns and standards. After thorough shaking, the test tubes were provided with aluminium caps, heated for 20 min in a vigorously boiling water bath, and cooled with tap water. The yellow-brown colour was read at 370 mμ in a Beckman B spectrophotometer with water as a blank

The investigation was aided by grants from *Karolinska Institutets reservationsanslag.*

1. Khym, J. X. and Zill, L. P. *J. Am. Chem. Soc.* **73** (1951) 2399; **74** (1952) 2090.
2. Khym, J. X. and Doherty, D. G. *J. Am. Chem. Soc.* **74** (1952) 3199.
3. Foster, A. B. *Advances in Carbohydrate Chem.* **12** (1957) 81.
4. Frahn, J. L. and Mills, J. A. *Australian J. Chem.* **12** (1959) 65.
5. Dische, Z. in Glick, D. *Methods of Biochemical Analysis* **2** (1955) 313.
6. Gardell, S. *Acta Chem. Scand.* **5** (1951) 1011.

Received December 1, 1960.